26/1-24/pt.1

VOLUME 26
1988
ACC. NOS N88-10001 TO N88-30583

STAR

AN ABSTRACT JOURNAL

Scientific and Technical Aerospace Reports

Annual Index 1988

Part One
SUBJECT

PRODUCED BY THE
SCIENTIFIC AND TECHNICAL
INFORMATION
DIVISION

NASA

NATIONAL AERONAUTICS AND SPACE ADMINISTRATION

NAS 1.9/5:

WHAT YOU CAN DO FOR *STAR*

All users of this abstract service are urged to forward reports to be considered for announcement in *STAR*. This will aid NASA in its efforts to provide the fullest possible coverage of all scientific and technical publications that might support aeronautics and space research and development. If you have prepared relevant reports (other than those that you will transmit to NASA, DoD, or DOE through the usual contract- or grant-reporting channels), please send them for consideration to the NASA Scientific and Technical Information Facility, P.O. Box 8757, BWI Airport, Maryland 21240.

Reprints of journal articles, book chapters, and conference papers are also welcome. These will be considered for announcement in *STAR's* companion journal, *International Aerospace Abstracts*.

You may specify a particular source to be included in a report announcement if you wish; otherwise the report will be placed on public sale at the National Technical Information Service. Copyrighted publications will be announced but not distributed or sold.

PURCHASE OF *STAR*

The semimonthly issues are available to registered users on annual subscription for $99.00 from the NASA Scientific and Technical Information Facility, ATTN: Registration Services, P.O. Box 8757, BWI Airport, MD 21240. *STAR* is publically available on annual subscription for $99.00 from the Superintendent of Documents, U.S. Government Printing Office, Washington, DC 20402.

PUBLISHED BY:

UNITED STATES GOVERNMENT
NATIONAL AERONAUTICS AND SPACE ADMINISTRATION
SCIENTIFIC AND TECHNICAL INFORMATION DIVISION

Scientific and Technical Aerospace Reports, Volume 26, is prepared by the NASA Scientific and Technical Information Facility operated for the National Aeronautics and Space Administration by RMS Associates.

The Administrator of the National Aeronautics and Space Administration has determined that the publication of this periodical is necessary in the transaction of the public business required by law of this Agency. Use of funds for printing this periodical has been approved by the Director of the Office of Management and Budget through March 22, 1989.

US ISSN 0036-8741

SPECIAL NOTICE

The abstract sections of the semimonthly *STAR* journals can be bound separately. Individual abstracts can be located readily by means of the page numbers given at each entry, e.g., p 1753. To assist the user in binding *STAR* Volume 26, four (4) title pages are included in the back of Part 1 of the Annual Index.

For sale by the Superintendent of Documents, U.S. Government Printing Office
Washington, D.C. 20402

VOLUME 26 NUMBERS 1-24

Scientific and Technical Aerospace Reports

Annual Index (Part I) January - December 1988

TABLE OF CONTENTS

Page

PART I

Introduction iii

Subject Index A-1

PART II

Introduction iii

Personal Author Index B-1

Corporate Source Index C-1

Contract Number Index D-1

Report/Accession Number Index E-1

INTRODUCTION

WHAT STAR ANNUAL INDEXES ARE

This Annual Index is an edited consolidation of the indexes to the individual issues of *Scientific and Technical Aerospace Reports (STAR)* for the calendar year 1988 (Volume 26 Numbers 1 through 24). For the convenience of the user, it is divided into two parts, each bound separately. Part I contains the Subject Index. Part II contains the Personal Author Index, Corporate Source Index, Contract Number Index, and Report/Accession Number Index. The Annual Index supersedes the semimonthly indexes previously issued during 1988.

Each entry in this index includes a group of identifying numbers in the following form: 12 p 1680 N88-20043. The first two digits (12) identify the issue in which the document was announced. The "p" and the four digits that follow (1680) refer to the page number, in the designated issue, on which the abstract of the document appears. The next group of numbers (N88-20043) is the NASA Accession Number, a unique identification number assigned by NASA to each document that was acquired, indexed, and announced in *STAR* during the year.

In addition to these identifying numbers each entry in the Subject Index contains a title, or title and title extension. Each entry in the Personal Author and Corporate Source Indexes contains the title of the document.

At the beginning of each index in this cumulation, a typical listing is illustrated with each of its elements identified to assist the reader in using the different types of index entries.

HOW TO USE THE SUBJECT INDEX

Subject terms in this cumulative index are arranged alphabetically, and are supplemented with cross-references which are intended to serve as directions that will enable the user to modify, enlarge, or narrow his search in accordance with his specific interest. The subject headings have been selected from the latest revison of the *NASA Thesaurus*. Two types of cross-references are used:

1. Use (U) references direct the user to alternate headings under which materials on the subject may be found. For example:

   ANNULAR JETS
     U ANNULAR FLOW
     U JET FLOW
   COLUMBIUM
     U NIOBIUM

2. Narrower Term (NT) references refer the user to more specific headings in the same subject area, under which additional material on the subjects may be found. For example:

   EMISSION
     NT ELECTRON EMISSION
     NT NEUTRON EMISSION
     NT THERMAL EMISSION

Finally, a searcher should use the titles and title extensions in the index to narrow further his quest for particular items. This is because subject terms can readily refer to more than one class of document. For example:

CATHODES
  Cesium plasma cathodes as sources of high intensity electron beams
  Cathode material testing in electrochemical half cells

This illustrates a case where two references on different topics are listed under the same subject term.

HOW TO USE THE PERSONAL AUTHOR INDEX

All personal authors identified in the abstract-section citations in the individual *STAR* issues appear in this index. Differences in transliteration schemes may require multiple searching of the index for variants of an author's name. For example:

EMELIANOV, M. D.
YEMELYANOV, M. D.

HOW TO USE THE CORPORATE SOURCE INDEX

The corporate source index entries are abridged versions of the corporate sources used in the abstract-section citations in the individual issue supplements. The corporate source supplementary (organizational component) does not appear in the index. For example:

PRINCETON UNIV., N.J. DEPT. OF CHEMICAL ENGINEERING.
(Corporate source at citation)
PRINCETON UNIV., N.J.
(Corporate source index entry)

HOW TO USE THE CONTRACT NUMBER INDEX

All contract numbers that are identified in the abstract-section citations in the individual *STAR* issues appear in this index. Changes by agencies in the style in which contract numbers are presented may require multiple searching for variants. For example:

AF 33(615)-67-C-1758
F33615-67-C-1758

HOW TO USE THE REPORT/ACCESSION NUMBER INDEX

All report numbers that have been assigned by the corporate source, monitoring activity, or cataloging activity appear in this index. Variations in initial input may result in different report number series. For example:

TP-924
ONERA-TP-924

A COMPREHENSIVE INFORMATION SERVICE

The National Aeronautics and Space Administration makes the results of worldwide research and development activities in aeronautics, space, and supporting disciplines promptly available to participants in its program. NASA's scientific and technical information system now contains over two million documents, which are abstracted, indexed, and obtained through retrieval and dissemination services. These services which include the abstract journal, *Scientific and Technical Aerospace Reports (STAR)*, are described fully in a bulletin, *The NASA Scientific and Technical Information System... and How to Use It*, available at no charge from the NASA Scientific and Technical Information Facility, P.O. Box 8757, B.W.I. Airport, Maryland 21240.

AVAILABILITY OF DOCUMENTS

Information concerning the availability of documents announced in the *STAR* issues covered in this index is found in the introduction to the most currently issued semimonthly issue.

PUBLIC COLLECTIONS OF NASA DOCUMENTS

DOMESTIC: NASA and NASA-sponsored documents and a large number of aerospace publications are available to the public for reference purposes at the library maintained by the American Institute of Aeronautics and Astronautics, Technical Information Service, 555 West 57th Street, 12th Floor, New York, New York 10019

EUROPEAN: An extensive collection of NASA and NASA-sponsored publications is maintained by the British Library Lending Division, Boston Spa, Wetherby, Yorkshire, England for public access. The British Library Lending Division also has available many of the non-NASA publications cited in *STAR*. European requesters may purchase facsimile copy or microfiche of NASA and NASA-sponsored documents, those identified by both the symbols # and * from ESA - Information Retrieval Service European Space Agency, 8-10 rue Mario-Nikis, 75738 Paris CEDEX 15, France.

FEDERAL DEPOSITORY LIBRARY PROGRAM

In order to provide the general public with greater access to U.S. Government publications, Congress established the Federal Depository Library Program under the Government Printing Office (GPO), with 50 regional depositories responsible for permanent retention of material, inter-library loan, and reference services. At least one copy of nearly every NASA and NASA-sponsored publication, either in printed or microfiche format, is received and retained by the 50 regional depositories. A list of the regional GPO libraries, arranged alphabetically by state, appears on the inside back cover. These libraries are *not* sales outlets. A local library can contact a Regional Depository to help locate specific reports, or direct contact may be made by an individual.

SUBJECT INDEX

SCIENTIFIC AND TECHNICAL AEROSPACE REPORTS VOLUME 26 NUMBERS 1-24

Typical Subject Index Listing

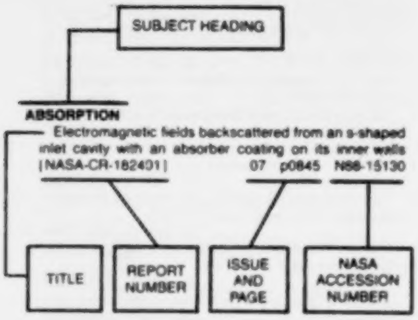
SUBJECT HEADING
ABSORPTION
Electromagnetic fields backscattered from an s-shaped inlet cavity with an absorber coating on its inner walls
[NASA-CR-182401] 07 p0845 N88-15130
TITLE
REPORT NUMBER
ISSUE AND PAGE
NASA ACCESSION NUMBER

The subject heading is the key to the subject content of the document. Titles, issues, page numbers, report numbers, and accession numbers of pertinent documents are provided under each subject heading. When the title is insufficiently descriptive of the document content, a title extension has been added, separated by three hyphens. The report number helps to indicate the type of document cited (e.g., NASA report, translation, NASA contractor report). The issue and page identify the *STAR* issue in which the document was announced and the page number on which the citation appears. The accession number denotes the number by which the citation is identified on that page. The titles are arranged under each subject heading in ascending accession number order. The subject headings have been selected from the latest revision of the *NASA Thesaurus* (NASA SP-7064).

A

A STARS
Generation and propagation of sound waves in a collapsing or anti-collapsing star with uniform density
[DE87-703034] 15 p2151 N88-22839
A-300 AIRCRAFT
The European Airbus A-300 10 p1308 N88-17824
A-320 AIRCRAFT
The A320 Airbus program
[SNIAS-872-111-105] 05 p0529 N88-13215
Electrical flight commands in transport aircraft
[SNIAS-872-111-108] 05 p0551 N88-13361
Overall descriptiun of the computer aided design and manufacturing systems associated with the A320 program at Aerospatiale and its partners
[SNIAS-872-111-104] 06 p0635 N88-13883
Presentation of SIGMA (Interactive Assisted Geometry System). A computer assisted shape design program developed at the Aerospatiale Aircraft Division
[SNIAS-872-111-110] 06 p0635 N88-13884
The use of simulation in the development of the Airbus 12 p1702 N88-20188
Design and implementation of contact ultrasonic sensors to assess internal damage
[I-177/87] 21 p2906 N88-27247
New generation of integrated monitoring systems for modern aircraft 22 p3035 N88-29015
ABEL FUNCTION
A construction of simple Abelian varieties
[ZW-8702] 06 p0642 N88-13929
Class of N-associative rings
[PB87-230421] 06 p0769 N88-14724
Theory of the generalized Abel integral equations
[ETN-88-91086] 09 p1229 N88-17362
On generalized lie-like algebras
[PREPRINT-574] 14 p1968 N88-21748
Retrieval of temperature and concentration profiles from a limited number of absorption measurements
21 p2947 N88-27501
ABERRATION
Aberrations: Their effect on off-axis beam steering
[AD-A189601] 13 p1840 N88-21008
ABILITIES
Exploiting auxiliary information about items in the estimation of Rasch item difficulty parameters
[AD-A184383] 03 p0372 N88-12341
Intelligent tutoring systems as tools for investigating individual differences in learning
09 p1204 N88-17216
Modeling incorrect responses to multiple-choice items with multilinear formula score theory
[AD-A187887] 11 p1522 N88-19090
Visual recognition training: Effectiveness of computer graphics
[AD-A188302] 12 p1669 N88-19997
A comparison of the Army's Project A: Cognitive and psychomotor tests to analogous Air Force and Navy tests
[AD-A188636] 12 p1670 N88-20002
Optimizing feedback utilization in motor skill training
[AD-A191559] 18 p2552 N88-25146
Skilled memory and expertise: Mechanisms of exceptional performance
[AD-A193829] 22 p3133 N88-28628
ABLATION
Time-resolved ablation measurements of imploding targets
[DE87-014464] 02 p0178 N88-11111
The Rayleigh-Taylor instability in ablatively accelerated targets with 1, 1/2 and 1/4 micrometers laser light
[AD-A185945] 07 p0858 N88-15208
Molecular dynamics of laser ablation of a polymer coating
[DE88-004337] 13 p1750 N88-20486
Analytic solutions to dynamic equations of plasma armature railguns
[DE88-006842] 15 p2023 N88-22057
Self-similar expansions in ion beam fusion
16 p2278 N88-23635
Spectroscopic study of helictron E plasmas: Stark profile, CXR, poloidal rotation and carbon coating
17 p2441 N88-24523
Use of a two-stage light-gas gun as an injector for electromagnetic railguns
[DE88-007200] 18 p2460 N88-24657
Systematics of excimer laser ablation: Thin film preparation of high T(sub c) material
[DE88-010569] 19 p2675 N88-25909
Why plasma armature railguns don't work (and what can be done about it)
[DE88-007900] 20 p2763 N88-26384
Absorption characteristics of Si3N4 ablation layer plasma 20 p2783 N88-26504
ABLATIVE NOSE CONES
Experimental investigation of hypersonic aerodynamics
[NASA-CR-182973] 18 p2458 N88-24591
ABM
U APOGEE BOOST MOTORS
ABNORMALITIES
Correlation between EEG abnormal activity and aircraft accidents: A long term observation
21 p2984 N88-27719
Detection of latent epilepsy in aircrew candidates
21 p2984 N88-27720
ABORT TRAJECTORIES
The effects of RCS jet firing on the isolated Orbiter and mated coast phases of the glide return to launch site maneuver at Mach number 6 (IA302B)
[NASA-CR-180223] 20 p2766 N88-26403
ABORTED MISSIONS
Destruction test of small scaled solid propellant motors
[ISAS-R-620] 03 p0278 N88-11752
RB-ARD: A proof of concept rule-based abort
06 p1065 N88-16435
ABRASION
Abrasion resistant porous silica antireflective coatings
[DE88-006230] 14 p1894 N88-21308
Stressed fabric abrasion test procedure for urethane coated fabric fuel tanks
[AD-A196327] 24 p3356 N88-29982
ABRASION RESISTANCE
Anti-abrasion protection with highly organized materials
[DE87-014236] 01 p0029 N88-10187
Coatings for Advanced Heat Engines Workshop: Book of abstracts
[DE87-012623] 02 p0180 N88-11121
Indentation damage in ceramics
[AD-A184686] 03 p0294 N88-11844
Synthesis and structure property studies of toughened epoxy resins via functionalized polysiloxanes. Friction and wear studies
[AD-A188258] 11 p1462 N88-18718
Abrasion and impact resistant coatings
[DE88-003562] 13 p1750 N88-20484
Study of the friction and wear-related properties of ceramic superconductors
[DE88-011844] 21 p3024 N88-27950
ABRASIVES
Some speculations on the mechanisms of abrasive grinding and polishing
[DE87-014242] 02 p0181 N88-11126
Surface conditioning products as tools for corrosion removal and corrosion prevention
17 p2320 N88-23856
ABSOLUTE ZERO
Zero temperature quark matter equation of state
[DE88-003408] 10 p1422 N88-18496
ABSORBERS
Toward a comprehensive theory for the sweeping of trapped radiation by inert orbiting matter
[NASA-CR-182584] 11 p1569 N88-19395
Comprehensive model for laser instability in a CO2 laser with gaseous saturable absorber
14 p1979 N88-21806
ABSORBERS (EQUIPMENT)
Fiber optics refractometer for absorption machines
[DE88-002296] 07 p0932 N88-15682
Variable response load limiting device
[NASA-CASE-LAR-12801-1] 17 p2346 N88-23982
ABSORBERS (MATERIALS)
NT ANTIRADAR COATINGS
NT RADAR ABSORBERS
Heat and mass transfer in laminar wavy film absorption with the presence of non-absorbable gases
21 p2947 N88-27502
ABSORPTION
Electromagnetic fields backscattered from an s-shaped inlet cavity with an absorber coating on its inner walls
[NASA-CR-182401] 07 p0845 N88-15130
Determination of aquo-complexes of chromium and iron in chromium plating and polishing solutions by ion chromatography
[AD-A190168] 15 p2039 N88-22148
Sources and levels of background noise in the NASA Ames 40- by 80-foot wind tunnel
[NASA-TM-100077] 17 p2395 N88-24239
ABSORPTION BANDS
U ABSORPTION SPECTRA
ABSORPTION COEFFICIENT
U ABSORPTIVITY
ABSORPTION COOLING
Technical evaluation of a solar-powered absorption cooling system (LiBr-H2O)
[PB87-108254] 04 p0463 N88-12867
Design and development of absorption heat pumps
[DE88-900082] 04 p0466 N88-12885
Self operating absorption cooling system using solar energy: Small power experimental plant
[DE88-900194] 07 p0874 N88-15299
Thermal energy storage by means of an absorption cycle
[ETN-88-91614] 09 p1186 N88-17108

ABSORPTION CROSS SECTIONS
Absorption, scattering, and thermal radiation by conductive fibers
[AD-A186105] 07 p0842 N88-15106
Absolute rate measurements of two-photon process of gases, liquids, and solids
[DE88-003800] 10 p1407 N88-18391
Rotational structure and absorption cross sections from 300 to 190 K of the Schumann-Runge bands
[AERONOMICA-ACTA-A-318-1987]
15 p2036 N88-22131
Ultraviolet absorption cross sections of methylbromide at stratospheric temperatures
[AERONOMICA-ACTA-A-320-1987]
15 p2036 N88-22132
Temperature dependence of ultraviolet absorption cross sections of chlorofluoroethanes
[AERONOMICA-ACTA-A-325-1987]
18 p2482 N88-24726
Nucleon-nucleus interaction data base: Total nuclear and absorption cross sections
[NASA-TM-4053] 20 p2852 N88-26935
Studies of HZE particle interactions and transport for space radiation protection purposes
[NASA-TM-101158] 20 p2886 N88-27142
Ultraviolet absorption cross sections of chloro- and chlorofluoromethanes at stratospheric temperatures
[AERONOMICA-ACTA-A-324-1988]
23 p3231 N88-29228
Aeronomic problems of molecular oxygen photodissociation. Part 2: Theoretical absorption cross sections of the Schumann-Runge bands at 79 K
[AERONOMICA-ACTA-A-331-1988]
24 p3344 N88-29907

ABSORPTION SPECTRA
NT FRAUNHOFER LINES
NT HERZBERG BANDS
Picosecond CO2 laser interactions with polyatomic molecules
[DE87-012072] 01 p0051 N88-10327
DSA RuO2/TiO2 electrode modeled by ion implantation: An in situ characterization by photoacoustic and photocurrent spectroscopy
[DE87-008129] 02 p0245 N88-11545
Photoluminescence studies of GaAs/AlAs superlattices
[DE87-013817] 02 p0245 N88-11548
Spectroscopy and nonthermal processes
02 p0252 N88-11584
A mode-locked ruby laser with chlorophyll d as saturable absorber 0. p0327 N88-12064
Investigations of extragalactic hydroxyl
03 p0389 N88-12441
Far infrared Fourier transform spectroscopy of semiconductors
[DE88-000188] 04 p0499 N88-13072
Titanium oxide absorption and spot sizes in II Peg, HR 1099 and UX Ari 04 p0508 N88-13126
A flash spectrum of Cl I, C I, N I, and N II absorption in 31 Cygni: A direct observation of the reversing layer
04 p0513 N88-13158
Sensitivity of the H alpha line to expansion, geometrical extent and temperature gradient in the G and K supergiant chromospheres 04 p0514 N88-13159
IUE observations of the hybrid K3 II star Iota Aurigae and constraints on the outer atmospheric structure
04 p0516 N88-13171
Pure dephasing of a vibrational adbond
[AD-A185222] 05 p0609 N88-13740
Proceedings of the Third Airborne Imaging Spectrometer Data Analysis Workshop
[NASA-CR-181552] 05 p0611 N88-13755
Preliminary results from an investigation of AIS-1 data over an area of epithermal alteration: Plateau, Northern Queensland, Australia 05 p0613 N88-13768
Causes of spurious features in spectral reflectance data 05 p0614 N88-13769
Automatic continuum analysis of reflectance spectra
05 p0614 N88-13770
Analysis of airborne imaging spectrometer data for the Ruby Mountains, Montana, by use of absorption-band-depth images 05 p0614 N88-13771
Mapping hydrothermally altered rocks in the Northern Grapevine Mountains, Nevada and California with the airborne imaging spectrometer 05 p0614 N88-13772
Analysis of SO2 signals in SBUV/TOMS data
05 p0618 N88-13794
Comparison of ground based and TOMS measurements of SO2 from volcanic emissions
05 p0618 N88-13795
A critical review of measurements of water vapor absorption in the 840 to 1100 cm(-1) spectral region
[NASA-CR-182361] 06 p0742 N88-14565
Use of lasers with F sub A(II)-color center KCl:Li crystals in the intraresonator laser spectroscopy method
06 p0769 N88-14729
Laboratory measurements of the ozone absorption coefficient in the wavelength region 339 to 362 nm at different temperatures
[NOTA-INTERNA-882] 07 p0878 N88-15324
Intracavity spectrum analyzer with NaF:F2(+):F3(-) crystal laser for long-wave IR wave band
07 p0919 N88-15564
Characterization of Er,Cr:YSGG
[AD-A185885] 07 p0932 N88-15659
Literature survey relating to the absorption properties of ozone in the near ultraviolet
[ESRO-SM-81] 09 p1190 N88-17129
Memory effects on infrared adsorbate spectra
[AD-A186976] 09 p1253 N88-17512
Guided-wave approaches to spectrally selective energy absorption
[NASA-CR-182532] 10 p1320 N88-17892
Absolute rate measurements of two-photon process of gases, liquids, and solids
[DE88-003800] 10 p1407 N88-18391
Simulation of infrared spectra
[AD-A187861] 11 p1453 N88-18658
Growth and characteristics of materials for tunable lasers in the near infrared spectral region
[NASA-CR-182501] 11 p1481 N88-18901
Laser raman studies related to liquid propellants: Structural characteristics inferred from the nitrate anion spectra
[AD-A188462] 12 p1612 N88-19641
Study of the vibrational modes of subsurface oxygen on Al (111) using diode laser infrared reflection-absorption spectroscopy
[AD-A188322] 12 p1632 N88-19769
Influence of nonlinear spectroscopic effects on atmospheric propagation of intense laser radiation at 10.6 microns wavelength 13 p1789 N88-20705
Effect of Mg impurity on local vibrations of U-centers in LiF lattice 14 p1969 N88-21753
Infrared reflection-absorption spectroscopy of hyperfine layers on surfaces of semiconductors and dielectrics
14 p1969 N88-21755
Single-laboratory evaluation of SW-846 methods 7090/7091 determination of beryllium by flame and furnace atomic absorption spectrophotometry
[PB88-171434] 16 p2175 N88-22963
A sup 57 Fe Mossbauer study of the superconductor YBa sub 2 (Fe sub x Cu sub 1-x) sub 3 O sub y
[DE88-701543] 16 p2262 N88-23661
Selective radiation absorption in aluminized composite propellant combustion 19 p2630 N88-25598
Absorption characteristics of Si3N4 ablation layer plasma 20 p2783 N88-26504
Raman and absorption spectrophotometric studies of selected lanthanide, californium-doped lanthanide, and actinide trihalides in the solid state
[DE88-008234] 20 p2874 N88-27061
Detection of absorption lines in the spectra of X-ray bursts from X1636-53
[ISAS-RN-390] 20 p2887 N88-27143
The 1985-86 measurements with the tunable diode laser absorption spectrometer
[PB88-214002] 23 p3231 N88-29226
Absorption spectra and energy levels of Gd(3+), Nd(3+) and Cr(3+) in the garnet Gd3Sc2Ga3O12
[AD-A193634] 23 p3282 N88-29589

ABSORPTION SPECTROSCOPY
Calorimetric Absorption Spectroscopy (CAS): A new method for the characterization of the optical properties of semiconductor systems
[ETN-87-90407] 01 p0088 N88-10645
Intracavity absorption spectroscopy with ring traveling-wave dye laser 03 p0300 N88-11890
Study of interactional effects in the chemisorbed layer by Infrared Reflection Absorption Spectroscopy (IRAS)
[DE88-001808] 06 p0680 N88-14164
Latitude coverage of observations of the middle atmosphere by solar absorption spectrometry from a heliosynchronous orbit
[AERONOMICA-ACTA-A-316-1987]
06 p0742 N88-14566
L2,3 XANES of the high T sub c superconductor YBa2Cu3O7 with variable oxygen content
[NOTA-INTERNA-889] 06 p0788 N88-14837
Lyman-alfa/OH-resonance-absorbtion measurements and simulation calculations for the investigation of the induction behavior of methane/ethane/oxygen mixtures in reflected shock waves
[ETN-88-90808] 07 p0831 N88-15042
Increasing time resolution of picosecond absorption spectrometer by selection of length of laser light pulses
07 p0919 N88-15579
Energy transfer studies with lasers
[DE88-004864] 10 p1337 N88-17991
Hot corrosion in gas turbines: A new, unique and informative technique is EASE (Electronic Absorption Spectroscopy Experiments)
[AD-A188508] 12 p1583 N88-19470
Resonance energy transfer between carbon monoxide and oxygen molecules using dye laser intracavity absorption spectroscopy
[AD-A188488] 12 p1689 N88-2010-
Infrared absorption spectroscopy and chemical kinetics of free radicals
[DE88-006536] 15 p2033 N88-22112
Diode laser spectroscopy of chemical moieties at surfaces
[AD-A190710] 15 p2036 N88-22127
Merit of Hadamard transform active absorption spectrometer described 15 p2053 N88-22232
Statistical fine structure in inhomogeneously broadened absorption lines in solids
[AD-A190341] 16 p2174 N88-22957
Methods and possibilities of biological action spectroscopy 16 p2272 N88-23597
Measurement of atmospheric OH with laser differential optical absorption spectroscopy (LDOAS)
18 p2539 N88-25068
Tropospheric OH measurements by long path absorption with rapid spectral concordance
18 p2539 N88-2506-
Isothermal measurement and thermal desorption using SAW devices 19 p2671 N88-25881
Laser spectroscopy of plasmas
[AD-A193009] 20 p2861 N88-26991

ABSORPTIVE INDEX
U ABSORPTIVITY

ABSORPTIVITY
Direct Absorption Receiver (DAR) systems assessment
[DE87-012277] 02 p0196 N88-11222
Enhancement of surface-atmosphere fluxes by desert-fringe vegetation through reduction of surface albedo and of soil heat flux
[NASA-CR-181442] 02 p0197 N88-11231
Laboratory evaluation and application of microwave absorption properties under simulated conditions for planetary atmospheres
[NASA-CR-181466] 02 p0254 N88-11606
Precise measurement of refractive index and absorption coefficient of near millimeter wave and far infrared materials
[AD-A184538] 03 p0293 N88-11840
Double-effect absorption heat pump: phase 3
[PB87-232195] 03 p0317 N88-12005
Thermal stress in the edge cladding of Nova glass laser disks
[DE88-000425] 04 p0448 N88-12780
Optical probe
[EP-PATENT-0-210-869-A1] 05 p0650 N88-13984
Laboratory measurements of the ozone absorption coefficient in the wavelength region 339 to 362 nm at different temperatures
[NOTA-INTERNA-882] 07 p0878 N88-15324
Instability of strong-absorption domain in semiconductor 08 p1077 N88-16495
Literature survey relating to the absorption properties of ozone in the near ultraviolet
[ESRO-SM-81] 09 p1190 N88-17129
Effect of translucence of engineering ceramics on heat transfer in diesel engines
[DE88-003732] 10 p1305 N88-17804
Photoacoustic measurements of atmospheric aerosol absorption coefficients at ultraviolet, visible and infrared wavelengths 11 p1512 N88-19036
Experimental research on skin reflection, transmission, absorption of light rays 16 p2187 N88-23039
Behavior, physiology and energy deposition in rats chronically exposed to 2450 MHz radiation
[PB88-171418] 16 p2237 N88-23383
Influence of refractive index and solar concentration on optical power absorption in slabs
[NASA-TM-4058] 19 p2726 N88-26190
Storage of thermal energy by means of an absorption cycle
[PB88-190814] 21 p2966 N88-27619
Atmospheric nitrogen oxides: Their detection and chemistry
[PB88-193057] 21 p2970 N88-27642
The effect of particle properties on radiative heat transfer 24 p3350 N88-29841

ABSTRACTS
Center for Electronics and Electrical Engineering Technical Progress Bulletin covering center programs, October to December 1986 with 1987 CEEE events calendar
[PB87-226890] 02 p0168 N88-11058

Center for Electronics and Electrical Engineering technical publication announcements covering center programs, July to September 1986 with 1987 CEEE events calendar
[PB87-223442] 02 p0168 N88-11059
FY 1985 scientific and technical reports, articles, papers and presentations
[NASA-TM-86521] 04 p0501 N88-13083
Strategic management of research and development: A literature search
[NASA-CR-182337] 06 p0780 N88-14847
USSR Space Life Sciences Digest index to issues 10-14
[NASA-CR-3922(17)] 07 p0883 N88-15361
The Shock and Vibration Digest, Volume 20, No. 1
08 p0975 N88-15897
USSR Space Life Sciences Digest, issue 14
[NASA-CR-3922(16)] 08 p1045 N88-16317
AGARD reports: A quarterly listing, 1 July through September 30, 1987
[AD-A186572] 08 p1093 N88-16579
NASA JSC neural network survey results
09 p1205 N88-17220
Engine structures: A bibliography of Lewis Research Center's research for 1980-1987
[NASA-TM-100842] 17 p2350 N88-24002
USSR Space Life Sciences Digest, issue 17
[NASA-CR-3922(20)] 17 p2381 N88-24155
The Shock and Vibration Digest, volume 20, no. 4
17 p2391 N88-24214
Infinite dimensional dynamical systems and their finite dimensional analogues
[AD-A192041] 18 p2563 N88-25216
USSR space life sciences digest, issue 18
[NASA-CR-3922(21)] 19 p2707 N88-26096
Reports of planetary geology and geophysics program, 1987
[NASA-TM-4041] 20 p2885 N88-27133
Aerospace applications studies, 1971-1987.
[AGARD-R-759] 21 p2889 N88-27147
Bibliography of Lewis Research Center technical publications announced in 1987
[NASA-TM-100910] 22 p3162 N88-28832
Nineteenth Lunar and Planetary Science Conference. Press abstracts
[NASA-CR-183037] 24 p3440 N88-30473

ABUNDANCE
Quasi-thermal models 02 p0253 N88-11600
Carbon abundances and C12/C13 ratios in M giants
04 p0515 N88-13167
Infrared excesses of barium stars
04 p0516 N88-13174
Galactic interstellar abundance surveys with IUE and IRAS 04 p0522 N88-13206
Abundance and distribution of ultramafic microbreccia in Moses Rock Dike: Quantitative application of AIS data
05 p0613 N88-13786
Primordial nucleosynthesis during the keV era
[DE88-002233] 08 p1104 N88-16623
Spectroscopic determinations of surface gravities of giant stars, and ultraviolet observations of RR Lyrae and X Arietis 11 p1569 N88-19391
Effects of galactic chemical evolution on thorium/neodymium cosmochronology
[DE88-003829] 11 p1570 N88-19397
HNC: A detector to study ultraheavy cosmic rays
12 p1713 N88-20252
Ground-based column abundance measurements of atmospheric hydroxyl
[NASA-CR-182676] 14 p1944 N88-21586
The relationship between low activity comets and more active comets 14 p1997 N88-21904
On the interpretation of the 3 micron emission feature in the spectrum of Comet Halley: Abundances in Comet Halley and in interstellar matter
14 p2002 N88-21935
On the forbidden red lines of oxygen in comets
14 p2006 N88-21963
Para-ortho abundance ratio of molecular hydrogen in NGC2023
[ISAS-RN-352] 18 p2573 N88-25286
Review of the theoretical changes of surface chemistry during massive star evolution
[SER-C-PREPUBL-FASC-17] 18 p2583 N88-25411
Fine-scale traverses in cumulate rocks, Stillwater Complex: A lunar analogue study
[NASA-CR-183086] 20 p2823 N88-26747
Probing the possibility of a (12)C/(13)C abundance gradient from observations of interstellar CH+
[DE88-008908] 20 p2884 N88-27125
Detection of abundant molecular gas in the UV-excess quasar Mrk 1014 22 p3164 N88-28842
An upper limit on the primordial He4 abundance from speckle interferometric observations of muon Cassiopeiae 23 p3298 N88-29641
Mars: Near-infrared comparative spectroscopy during the 1986 opposition 23 p3301 N88-29658

AC (CURRENT)
U ALTERNATING CURRENT

AC GENERATORS
Study of free-piston Stirling engine driven linear alternators
[NASA-CR-181425] 01 p0055 N88-10355
The ac power system testbed
[NASA-CR-175068] 03 p0308 N88-11948
Computer-aided modeling and prediction of performance of the modified Lundell class of alternators in space station solar dynamic power systems
[NASA-CR-182538] 11 p1507 N88-19000
Design of a superconducting alternator for space-based power generation 17 p2412 N88-24340

ACCELERATED LIFE TESTS
Improved cathode life testing
[REPT-3189-T] 02 p0168 N88-11056
Time-temperature-stress capabilities of composite materials for advanced supersonic technology application
[NASA-CR-178272] 06 p0677 N88-14144
Developing an accelerated endurance test for greases: A status report
[AD-A185963] 07 p0836 N88-15072
Robust prediction and interpolation for vector stationary processes, 2d enriched version
[AD-A185875] 07 p0865 N88-15247
Technical applications of solar energy. Project: Selective coatings
[BMFT-FB-T-86-213] 14 p1943 N88-21581
Examination of temperature effects on gate-to-drain avalanche breakdown in GaAs MESFETs (Metal-Semiconductor Field Effect Transistors) by measuring light emission under RF drive
[AD-A189634] 15 p2141 N88-22779
Development of a slip-ring system for energy transfer in space conditions. Space flight qualification and extended life tests
[BMFT-FB-W-88-019] 16 p2169 N88-22932
Brief evaluation of the alloy 17-4-PH (25 CNU 17-04). Semifinished product: 205 mm dia forged roller, test reports
[DF/NH-3616/84] 17 p2322 N88-23866
A statistical treatment of accelerated life test data for copper-water heat pipes 20 p2783 N88-26509
Analysis of debris from accelerated life test of the Hughes five-year Vuilleumier cryocooler
[AD-A193101] 21 p2931 N88-27430
Development of a test method to determine potential peroxide content in turbine fuels. Part 2
[AD-A192244] 23 p3199 N88-29042
Performance Prediction for Coatings. Proceedings of a Workshop
[AD-A188973] 24 p3354 N88-29966
Prediction of degradation of polymeric coating materials 24 p3354 N88-29970
Alternative immersion accelerated testing of coating systems for Naval shoreline facilities
24 p3355 N88-29977

ACCELERATION (PHYSICS)
NT ANGULAR ACCELERATION
NT DECELERATION
NT ELECTRON ACCELERATION
NT HIGH GRAVITY ENVIRONMENTS
NT IMPACT ACCELERATION
NT PARTICLE ACCELERATION
NT PLASMA ACCELERATION
NT SPIN REDUCTION
NT TRANSVERSE ACCELERATION
Acceleration to hypervelocities using minimum energy concepts
[DE87-011796] 01 p0089 N88-10583
Flame acceleration and transition to detonation in channels
[DE87-014193] 03 p0284 N88-11796
Fiber-optic accelerometer investigation
[AD-A185359] 05 p0584 N88-13561
Separable orthogonal coordinates and particle creation for an accelerating observer
[DE87-703356] 05 p0657 N88-14029
Steady waves in a nonlinear theory of viscoelasticity
[AD-A185546] 06 p0723 N88-14448
On a possibility of ion acceleration up to high energies in a high-current electron beam
[DE88-700532] 07 p0831 N88-15657
Looking for new gravitational forces with antiprotons
[DE88-003154] 09 p1192 N88-17142
Considerations of acceleration effects in relativistic kinematics 09 p1260 N88-17553
Research and development of surface skimming bulk wave devices for sensor applications
[AD-A187574] 11 p1470 N88-18766
Reference position vector 12 p1577 N88-19432
Fighter design for human load limits
12 p1580 N88-19451
Lower bounds on acceleration estimation accuracy
[AD-A188383] 12 p1619 N88-19661
Parametric study of acceleration-induced stresses and frequency changes in doubly-rotated crystal resonators
[AD-A189261] 13 p1761 N88-20532
An experimental investigation of decelerating flow about two-dimensional cambered plates
[DE88-008598] 13 p1766 N88-20567
Impact shock generator from explosively driven plates
[DE88-003596] 14 p1918 N88-21452
Analysis of head response to torso acceleration. Volume 1: Development of performance requirements
[PB88-156757] 14 p1953 N88-21640
Centrifugal acceleration of ions in the polar magnetosphere
[NASA-TM-101148] 17 p2374 N88-24120
Effects of Coriolis acceleration on the vibrations of spinning structures 18 p2522 N88-24966
Study of the structure of turbulence in accelerating transitional boundary layers
[AD-A191698] 19 p2663 N88-25837
Dynamics explorer data analysis
[NASA-CR-181428] 19 p2691 N88-25996
Gone with the solar wind: A study of protons accelerated by interplanetary shocks 19 p2743 N88-26283
An investigation of soft launch and instability breakup with a two-stage light gas gun
[DE88-010371] 21 p2901 N88-27218
Characterization of accelerating pipe flow
[AD-A193065] 21 p2943 N88-27481
Stochastic geologic effects on near-field ground motions in alluvium
[AD-A192315] 21 p2972 N88-27652
A study of mechanisms producing astrophysical jets
[AD-A194100] 23 p3300 N88-29649
Models of cerebral-body perfusion and cerebral chemical transport
[AD-A194945] 24 p3407 N88-30283

ACCELERATION STRESSES (PHYSIOLOGY)
Fighter design for human load limits
12 p1580 N88-19451
Liquid ventilation: New data and possible use in space medicine 12 p1654 N88-19908
Macaca rhesus tolerance to +Gz accelerations
19 p2704 N88-26080
Evoked potential analysis of impact acceleration experiments 21 p2981 N88-27709
EEG indices of G-induced Loss Of Consciousness (G-LOC) 21 p2982 N88-27706

ACCELERATION TOLERANCE
F-16 control stick response during +Gz-induced loss of consciousness
[AD-A184107] 04 p0400 N88-12431
Measurement and modification of sensorimotor system function during visual-motor performance
[AD-A186351] 07 p0889 N88-15387
Human and animal hypovolemic reactions to increasing +Gz accelerations 07 p0890 N88-15395
Karyometric evaluation of neuronal reactions of rat cerebral cortex to the combined effect of ionizing radiation, longitudinal accelerations and vibration
07 p0890 N88-15396
Improvement of human tolerance to head-pelvis (+Gz) accelerations by increasing hydration
10 p1364 N88-18153
Effect of cardioactive compounds on rat myocardium actomyosin following exposure to accelerations
10 p1365 N88-18161
Fighter design for human load limits
12 p1580 N88-19451
Analysis of head response to torso acceleration. Volume 2: Description of data retrieval, analysis and display software
[PB88-156765] 15 p2104 N88-22536
Macaca rhesus tolerance to +Gz accelerations
19 p2704 N88-26080
Significance of sensory signal phase mismatch in mechanisms of motion sickness development
20 p2830 N88-26797
Physiological monitoring methodology in the USAFSAM centrifuge 21 p2924 N88-27356
Detection of acceleration (+Gz) induced blackout by matched filtering of visual evoked potentials
21 p2982 N88-27710
Variation of carotid flow under load, studied by the Doppler echo method — acceleration tolerance
[REPT-1149] 23 p3240 N88-29282

ACCELERATORS
The impact of new computer technology on accelerator control
[DE87-014021] 02 p0219 N88-11376
GOLD: Integration of model-based control systems with artificial intelligence and workstations
[DE88-000506] 04 p0460 N88-12976

GOLD: Integration of model-based control systems with artificial intelligence and workstations
[DE88-000706] 04 p0483 N88-12977
An improved data reduction procedure for accelerometer centrifuge data 12 p1577 N88-19436

ACCELEROMETERS
NT STRAIN GAGE ACCELEROMETERS
Requirements for the calibration of mechanical shock transducers
[PB87-227591] 03 p0325 N88-12054
Fiber-optic accelerometer investigation
[AD-A185359] 05 p0584 N88-13561
Design and test of a spacecraft instrument shock isolator 08 p0998 N88-16044
An integration test for accelerometer evaluation
09 p1178 N88-17054
A quantitative method for evaluating sensor layouts
09 p1178 N88-17056
Strategic placement of accelerometers to measure forces by the sum of weighted accelerations
[DE88-002262] 10 p1333 N88-17968
Research and development of surface skimming bulk wave devices for sensor applications
[AD-A187504] 11 p1470 N88-18766
Thirteenth Biennial Guidance Test Symposium, volume 1
[AD-A185782] 12 p1576 N88-19427
Robotics applications in the testing of inertial sensors
12 p1577 N88-19433
GRADIO three-axis electrostatic accelerometers
12 p1645 N88-19849
Concept of an Opto-electronic Accelerometer System (OAS) 12 p1645 N88-19852
Surface wave accelerometer
[ETN-88-92000] 16 p2210 N88-23192
The optical accelerometer: A novel sensor for vertical flight guidance 18 p2518 N88-24935
Air loading effects on a capacitively sensed membrane supported silicon accelerometer
19 p2672 N88-25886
Wave structures in thermospheric density from satellite electrostatic triaxial accelerometer measurements
[AD-A194134] 23 p3233 N88-29240

ACCEPTABILITY
Automatically generated acceptance test: A software reliability experiment
[NASA-CR-181667] 17 p2347 N88-23984
Electromagnetic characterization and acceptance test of the electromagnetic pulse (EMP) simulator SPERANS
[FOA-C-30476-4.2] 22 p3071 N88-28230

ACCEPTANCE
U ACCEPTABILITY

ACCEPTOR MATERIALS
Wittig synthesis of conductive segmented block polymer compositions
[AD-A184018] 03 p0295 N88-11850
Excimer laser-assisted deposition of GaAs, AlAs and (Al,Ga)As from Lewis acid-base adducts
[AD-A184588] 03 p0329 N88-12081
Donor acceptor polymerization chemistry as a vehicle to low energy cure matrix resins
[AD-A190119] 15 p2044 N88-22179
Modeling the primary events of photosynthesis using chlorophyll containing fixed distance donor-acceptor molecules
[DE88-010033] 20 p2831 N88-26793

ACCESS CONTROL
The varieties of capabilities in Flex
[RSRE-MEMO-4042] 01 p0078 N88-10500
Usage analysis of user files in UNIX
[NASA-CR-181561] 05 p0633 N88-13868
Channel access protocols for multihop packet radio networks
[AD-A186074] 07 p0842 N88-15105
Media independent interface
[NASA-CR-172033] 08 p1066 N88-16446
Media independent interface. Interface control document
[NASA-CR-172032] 08 p1067 N88-16447
On proving register atomicity
[CWI-CS-R8707] 13 p1818 N88-20862
Two queues with alternating service and switching times
[CWI-OS-R8712] 13 p1831 N88-20949
Impact of blocking policies in closed, exponential and symmetrical ring networks
[FUB-8-1986] 14 p1960 N88-21693
Protection and security mechanisms in the SMITE capability computer
[RSRE-MEMO-4117] 17 p2384 N88-24167
Computer resource management technology program (PE 64740F). Task no. 9: Advanced user authentication
[PB88-183066] 18 p2555 N88-25163
L-band and SHF multiple access schemes for the MSAT system 19 p2650 N88-25734
Using common subexpressions to optimize multiple queries
[DE88-008210] 20 p2844 N88-26877
A state-of-the-art survey of low-cost security in local area networks
[NPL-DITC-113/88] 22 p3141 N88-28678
Formal specification of a secure document control system for SMITE
[RSRE-88002] 23 p3245 N88-29309
Performance analysis of FDDI
[NASA-CR-183206] 24 p3413 N88-30321

ACCESSORIES
Stability analysis of a rigid body with a flexible attachment using the energy-casimir method
[AD-A185646] 06 p0723 N88-14449
Software modifications to total data reporting accessory for metabolic measurement cart
[AD-A193641] 22 p3132 N88-28623

ACCIDENT INVESTIGATION
NT AIRCRAFT ACCIDENT INVESTIGATION
Detection of hyperventilation of parachutists
[DFVLR-FB-87-11] 01 p0075 N88-10482
Aircraft accident reports: Brief format, US Civil and Foreign Aviation, Issue Number 4 of 1986 accidents
[PB87-916906] 06 p0666 N88-14086
Aircraft accident report: Grand Canyon Airlines, Inc., and Helitech, Inc., midair collision over Grand Canyon National Park, June 19, 1986
[PB87-910403] 06 p0666 N88-14087
Aircraft accident/incident, Newark, New Jersey, November 13, 1986
[NTSB/AAR-87/04-SUMM] 10 p1276 N88-17639
Space shuttle accident: NASA's actions to address the Presidential Commission report
[PB88-135306] 15 p2024 N88-22059

ACCIDENT PREVENTION
Detection of hyperventilation of parachutists
[DFVLR-FB-87-11] 01 p0075 N88-10482
Report of the helicopter human factors working group --- accident prevention
[CAA-PAPER-87007] 03 p0361 N88-12274
Protected areas with enhanced bird-aircraft collision risk in the Federal Republic of Germany
[GEOPHYSBDBW-FM-209] 11 p1437 N88-18576
Rotorcraft TCAS (traffic alert and collision avoidance system) evaluation: Group 3 results
[AD-A191719] 18 p2461 N88-24614

ACCIDENTS
NT BIRD-AIRCRAFT COLLISIONS
NT LOSS OF COOLANT
Cost savings possible with Air Force conversion to JP-8 as its primary fuel
[AD-A183784] 01 p0030 N88-10192
Measurements of gas velocities and temperatures in a large open pool fire
[DE87-005853] 03 p0261 N88-11641
Structural analysis of a bolted joint concept for the space shuttle's solid rocket motor casing
[NASA-TM-89092] 04 p0407 N88-12531
Visualization of an aircraft accident based on digital flight data recorder information 05 p0538 N88-13276
Aircraft accident report: Grand Canyon Airlines, Inc., and Helitech, Inc., midair collision over Grand Canyon National Park, June 18, 1986
[PB87-910403] 06 p0666 N88-14087
Post-Challenger evaluation of space shuttle risk assessment and management
[NASA-CR-182461] 12 p1705 N88-20202
Potential off-normal events and associated radiological source terms for the compact ignition tokamak: Fusion Safety Program
[DE88-004112] 13 p1842 N88-21024
Chronic stress as a factor in aircraft mishaps
16 p2239 N88-23376
Acute stress 16 p2239 N88-23377
Critical nuclear launch issues: A perspective from the State of Florida 17 p2423 N88-24412
A novel plant protection strategy for transient reactors
17 p2425 N88-24423
Evaluation of UN fuel pin failure modes and motion of fuel during severe accidents for reactors in space
17 p2425 N88-24424
Reactor core coolability with reduced power levels
17 p2425 N88-24425
Analysis of a nuclear orbital transfer vehicle reentry accident 17 p2425 N88-24426
Health and environmental consequences of the Chernobyl nuclear power plant accident
[DOE/ER-0332] 19 p2689 N88-25985
Book analysis. Challenger: A major malfunction
[AD-A192458] 20 p2764 N88-26388
The role and the place of insurance of large space projects 22 p3161 N88-28826

ACCLIMATIZATION
NT ALTITUDE ACCLIMATIZATION
NT COLD ACCLIMATIZATION
NT HEAT ACCLIMATIZATION
Physicochemical correlates of human adaptation to extreme environments 06 p0750 N88-14607
Medical problems related to altitude in: Human performance physiology and environmental medicine at terrestrial extremes, chapter 14
[AD-A188340] 12 p1666 N88-19989
Acute mountain sickness at 4500 m is not altered by repeated eight-hour exposures to 3200-3550 m normobaric hypoxic equivalent
[AD-A188358] 12 p1666 N88-19990

ACCOMMODATION
Evaluation of a cryogenic refrigerator for cooling focal plane instrumentation. Appendix B: Accommodation study --- satellite instruments
[BAE-TP-8095-VOL-2] 05 p0572 N88-13486
Gradiometer accommodation on board a drag-free satellite 12 p1645 N88-19850

ACCOUNTING
A general approach to error propagation
[DE87-014287] 02 p0224 N88-11412
A comparison of the Cray-2 performance before and after the installation of memory pseudo-banking
[NASA-CR-177462] 09 p1215 N88-17287
Monitoring the usage of a computer system
[DE88-004310] 15 p2106 N88-22542
Financial reporting: NASA (National Aeronautics and Space Administration) can improve compliance with GAO (General Accounting Office) standards and treasury requirements
[PB88-172523] 18 p2567 N88-25373
Aircraft avionics and missile system installation cost study. Volume 2: Appendices F and G
[AD-A195372] 24 p3325 N88-29801

ACCRETION
U DEPOSITION

ACCRETION DISKS
Gravitational accretion of hot dark matter
03 p0386 N88-12439
X-ray pulsars: Accretion flow deceleration
03 p0390 N88-12451
Disk accretion during the early stages of stellar evolution 04 p0505 N88-13106
The contribution of accretion luminosity to the infrared spectra of T Tauri stars: A possible test
04 p0518 N88-13183
EXOSAT guest observer program. Binary parameters of the X-ray Pulsar 4U1626-67
[NASA-CR-182374] 06 p0802 N88-14905

ACCUMULATIONS
Ultra-low power digital filter
[AD-A184485] 03 p0310 N88-11959

ACCUMULATORS
NT DUST COLLECTORS
NT SOLAR COLLECTORS
Wet deposition and snowpack monitoring operations and quality assurance manual
[PB87-212817] 01 p0064 N88-10413
The use of alloy 117 as a liquid metal current collector
[AD-A185740] 06 p0698 N88-14281
Performance of a small, graphite electrode, multistage depressed collector with a 500-W, continuous wave, 4.8- to 9.6-GHz traveling wave tube
[NASA-TP-2788] 07 p0848 N88-15146
A dynamic model for the aft accumulator in the TE SP-100 system 17 p2414 N88-24354

ACCURACY
NT GEODETIC ACCURACY
NT GEOMETRIC ACCURACY
Impact of turbulence modeling on numerical accuracy and efficiency of compressible flow simulations
[NASA-TM-88333] 02 p0173 N88-11088
Performance and operating envelope of imaging and scattering particle sizing instruments
[NASA-CR-180859] 03 p0323 N88-12042
Dynamic positioning at sea using the global positioning system
[AD-A184453] 04 p0397 N88-12476
Optimization of dilatometer test procedures
[DE87-014998] 04 p0447 N88-12769
Accuracy potential of non-metric cameras in close-range photogrammetry 04 p0463 N88-12862
Lower bounds on bearing accuracy for closely spaced sources
[AD-A184258] 04 p0486 N88-12997
Contribution to the improvement of the guidance accuracy of automatic pilots
[ETN-88-90607] 05 p0551 N88-13360
Operating envelopes of particle sizing instrumentation used for icing research
[NASA-CR-180870] 05 p0566 N88-13573
Timing variation in dual loop benchmarks
[AD-A185697] 06 p0707 N88-14336

Robot accuracy improvement through kinematic parameter identification 06 p0712 N88-14363

Limiting accuracy of scatterometer determination of wind speed over ocean from satellite
08 p1007 N88-16107

Successful mixed formulation for axisymmetric shell analysis employing discontinuous stress fields of the same order as the displacement field
[DE88-700021] 09 p1178 N88-17052

The accuracy of the radiation parameterization in mesoscale models
[DFVLR-IB-553-85/11] 09 p1190 N88-17133

The empirical accuracy of uncertain inference models
09 p1208 N88-17243

On precision and accuracy (bias) statements for measurement procedures
[DE88-004434] 10 p1402 N88-18359

Total Variation Diminishing (TVD) schemes of uniform accuracy
[NASA-TM-100552] 11 p1436 N88-18566

Effects of stress on judgement and decision making in dynamic tasks
[AD-A188203] 11 p1523 N88-19092

Lower bounds on acceleration estimation accuracy
[AD-A188383] 12 p1619 N88-19681

Measuring accuracy of 3-dimensional bodies by the GOMER-1 device
[DE87-703230] 12 p1628 N88-19744

Cramer-Rao bounds on the accuracy of location and velocity estimations using CCD optical sensors
[AD-A188481] 12 p1629 N88-19748

Experience with and ways to upgrade accuracy of hydromagnetic surveys in ocean
13 p1787 N88-20692

Density measurements on solids and liquids
[PB88-164934] 15 p2036 N88-22129

Effect of friction and control parameters on the tracking accuracy of a target seeker
[AD-A190010] 15 p2058 N88-22257

Analysis of a range estimator which uses MLS angle measurements
[NASA-CR-182896] 16 p2160 N88-22884

Accuracy versus convergence rates for a three dimensional multistage Euler code
[NASA-CR-181665] 16 p2261 N88-23519

Mapping from LANDSAT and SPOT satellite imagery
17 p2352 N88-24018

Limits of accuracy and range of laser radars
18 p2517 N88-24934

DMSP-SSM/1 NASA algorithm validation using primarily LANDSAT and secondarily DMSP and/or AVHRR visible and thermal infrared satellite imagery
[NASA-CR-182979] 18 p2532 N88-25024

Portable implementation of a generic exponential function in Ada
[DE88-007609] 19 p2715 N88-26117

Basic research for the geodynamics program
[NASA-CR-183149] 21 p2973 N88-27662

Global-scale temperature changes to August 1987 and a comparison of satellite and conventional data
22 p3125 N88-28572

Another approach for forecasting forecast skill
22 p3126 N88-28580

Experimental 30-day forecasts from several spectral general circulation models 22 p3126 N88-28582

Dependence of medium range forecast errors upon the large-scale initial state 22 p3126 N88-28585

Aerodynamic data accuracy and quality: Requirements and capabilities in wind tunnel testing
[AGARD-AR-254] 23 p3173 N88-28893

Accuracy of satellite data navigation
[AD-A195877] 24 p3322 N88-29787

Precision measurement of the Fresnel drag coefficient using a ring laser
[AD-A196025] 24 p3366 N88-30043

Increasing accuracy in evaluating vector of state under conditions of incomplete observability of expanded system 24 p3446 N88-30511

ACEE PROGRAM

Department of Housing and Urban Development-Independent Agencies Appropriations for fiscal year 1988, Friday, 10 April 1987: National Aeronautics and Space Administration
03 p0386 N88-12425

SR-7A aeroelastic model design report
[NASA-CR-174791] 23 p3179 N88-28928

ACETIC ACID

Changes in functional parameters of animals during long-term inhalation of acetic acid
07 p0895 N88-15423

Effect of long-term inhalation of acetic acid vapor on some functional parameters of man
19 p2705 [illegible]8-26084

ACETONE

Characterization of catalysts with metal-support effects and of the species adsorbed on their surfaces
[DE87-014636] 04 p0414 N88-12564

Boundary layer flow visualization for flight testing
17 p2297 N88-23742

Liquid-phase oxidation of acetone with hydrogen peroxide on oxide catalysts 19 p2706 N88-26091

ACETONITRILE

Electrochemistry in near-critical and supercritical fluids. 6: The electrochemistry of ferrocene and phenazine in acetonitrile between 25C and 300C
[AD-A192171] 18 p2482 N88-24723

ACETYL COMPOUNDS

Process for the preparation of acyl halides
[GB-PATENT-2-133-792-A] 01 p0020 N88-10124

The photochemistry of some possible cometary CN parent species 14 p1997 N88-21905

ACETYLENE

Ethynylated aromatics as high temperature matrix resins
[NASA-TM-89829] 11 p1450 N88-18640

Polymerization of fluorinated diacetylenes
[AD-A188051] 11 p1462 N88-18716

The photochemistry of some possible cometary CN parent species 14 p1997 N88-21905

Large ionic species in sooting acetylene and benzene flames 24 p3348 N88-29932

ACHONDRITES

Ureilites are not igneous differentiates
24 p3441 N88-30477

ACID BASE EQUILIBRIUM

Acid-base equilibrium and some rat blood parameters following exposure to hyperbaric oxygenation
07 p0894 N88-15420

ACID RAIN

Spatial characterization of acid rain stress in Canadian Shield Lakes
[NASA-CR-181136] 01 p0067 N88-10430

Spatial characterization of acid rain stress in Canadian Shield Lakes
[NASA-CR-180577] 01 p0067 N88-10431

Simulation of global wet and dry deposition of nitric acid in a three-dimensional chemistry-transport model
[DE87-009847] 09 p1188 N88-17116

Acid rain: Delays and management changes in the Federal research program
[GAO/RCED-87-89] 19 p2690 N88-25988

Acid Precipitation: A current awareness bulletin
[DE88-007987] 20 p2821 N88-26738

Atmospheric science issues in Congress
22 p3125 N88-28573

Regional environmental studies using national data bases and GIS (Geographic Information System)
[DE88-008368] 23 p3230 N88-29225

ACIDITY

Photon stimulated desorption from oxidized [illegible](110)
[DE88-002209] 06 p0787 N88-[illegible]4826

ACIDS

NT ACETIC ACID
NT ACRYLIC ACID
NT AMINO ACIDS
NT BORIC ACIDS
NT CARBOXYLIC ACIDS
NT CHROMIC ACID
NT DEOXYRIBONUCLEIC ACID
NT DICARBOXYLIC ACIDS
NT GLUTAMIC ACID
NT GLUTAMINE
NT HYDROCHLORIC ACID
NT HYDROFLUORIC ACID
NT NICOTINIC ACID
NT NITRIC ACID
NT NUCLEIC ACIDS
NT PHOSPHORIC ACID
NT RIBONUCLEIC ACIDS
NT SULFONIC ACID
NT SULFURIC ACID
NT THYMINE

Synthesis of novel acid electrolytes for phosphoric acid fuel cells
[PB87-221305] 01 p0066 N88-10426

Compilation and analysis of air quality data in support of acid deposition research
[DE87-014428] 02 p0196 N88-11226

Wear of iron and nickel in corrosive liquid environments
[NASA-TM-100246] 03 p0289 N88-11817

Corrosion strength of niobium and its alloys
[DE87-703693] 04 p0416 N88-12578

Electroformation: Principle electrochemical process of electrodeposition and electroformation of copper
[INPE-4374-NTE/274] 06 p0969 N88-15863

Copper electroforming from acid sulfate baths: Preliminary studies
[INPE-4375-RPE/554] 06 p0969 N88-15864

Active sites and roles of solid acid base catalysts
[NASA-TT-20333] 24 p3345 N88-29909

ACOUSTIC ATTENUATION

NT SHOCK WAVE ATTENUATION

Active minimisation of acoustic fields. A review of research into the active control of sound undertaken at ISVR from 1983 to 1986
[ISVR-TR-146] 01 p0091 N88-10593

AFAR (Azores Fixed Acoustic Range) measurements of intensity and intensity moments
[AD-A184431] 03 p0355 N88-12237

Theoretical and practical aspects of the functional absorber method of arranging sound absorbing panels
[BBC-RD-1987/15] 05 p0646 N88-13955

Attenuation of ultrasonic waves in nonmagnetized magnetic fluids 09 p1234 N88-17398

Measured and calculated acoustic attenuation rates of tuned resonator arrays for two surface impedance distribution models with flow
[NASA-TP-2766] 09 p1241 N88-17440

High frequency acoustic underwater communication with low probability of being traced
[REPT-4-87] 09 p1242 N88-17447

Silencium resonators (Silators) for the attenuation and elimination of sound
[MBB-Z-546/83] 10 p1312 N88-17841

An application of dimensionless Eigenvalues to underwater acoustic ducts
[AD-A188167] 11 p1542 N88-19219

Sound propagation through a turbulent atmosphere: Experimental techniques and data analysis
[AD-A188891] 12 p1686 N88-20094

Overground Excess Sound Attenuation (ESA). Volume 1: Experimental study for flat grassy terrains
[AD-A191289] 16 p2265 N88-23549

Reflection of sound in open ended ducts
[PB88-103478] 21 p3012 N88-27870

Acoustic propagation in the lower atmosphere
[ISL-R-126/87] 21 p3013 N88-27878

Experiments on the dissipation of sound by separated flow at an edge
[ISVR-TR-151] 23 p3279 N88-29522

A comparison of simple analytical models for representing propeller aircraft structural and acoustic responses
[ISVR-TR-153] 23 p3279 N88-29523

ACOUSTIC COMBUSTION

U COMBUSTION STABILITY

ACOUSTIC DUCTS

An application of dimensionless Eigenvalues to underwater acoustic ducts
[AD-A188167] 11 p1542 N88-19219

ACOUSTIC EMISSION

Fracture mode research of boron aluminum composite materials by Acoustic Emission (AE)
[NAL-TR-927] 02 p0142 N88-10891

An acoustic emission digital data acquisition workstation
[DE87-012425] 02 p0191 N88-11191

Transply crack density detection by acousto-ultrasonics
[NASA-TM-100224] 03 p0279 N88-11758

Development of an acoustic emission monitor and monitoring techniques for long-term monitoring of U-0.8Ti electron-beam weldments for postweld cracking
[DE88-000819] 04 p0453 N88-12804

Contribution of acoustic analysis to assess damage in fluid storage tanks under high pressure --- composite materials, filament winding
[SNIAS-872-430-119] 05 p0559 N88-13407

The Shock and Vibration Digest, Volume 19, No. 12
05 p0610 N88-13746

Experimental studies on acoustic emission monitoring of crack propagation in offshore structures. A literature survey 05 p0610 N88-13748

Acoustic emissions at an open crack
[DE88-001504] 05 p0611 N88-13751

Theory of transient thermal self-focusing of sound beams 09 p1234 N88-17401

Nonlinear and diffraction effects in sound beams with random transverse structure 09 p1235 N88-17402

Laboratory studies related to in-flight acoustic emission monitoring
[AD-A186714] 09 p1242 N88-17445

The acoustic-electric field analysis of multilayered surface acoustic wave devices
[ETN-88-91592] 09 p1242 N88-17446

Acoustic emission-microstructural relations in ferritic steels. Part 3: The effect of inclusion content
[AERE-R-12041] 10 p1341 N88-18015

Acoustic emission measurements of PWR weld materials with inserted defects
[AERE-R-12386] 10 p1341 N88-18016

Institute for Materials Science and Engineering, nondestructive evaluation: Technical activities 1987
[PB88-153655] 10 p1342 N88-18020

STA-2A NDT testing
[NASA-CR-178301] 11 p1497 N88-18937
Ultrasonic measurements research: Progress in 1987
[AD-A188506] 12 p1667 N88-20092
Application of ISRM testing methods to fracture toughness testing of graphite 13 p1747 N88-20446
A study of the dynamics of high temperature brittle intergranular fracture by acoustic emission
[AERE-R-12479] 13 p1780 N88-20650
Study of strength characteristics of glass-reinforced plastic by acoustic emissions method
14 p1865 N88-21268
Acoustic emission frequency discrimination
[NASA-CASE-MSC-20467-1] 17 p2342 N88-23966
Frequency Analysis of Acoustic Emission - Application to machining and welding
[DE88-701478] 18 p2570 N88-25262
An analysis of the efficiency and directivity of the sound generated by a moving laser source
[AD-A192220] 20 p2849 N88-26914
On the possibility of the soliton description of acoustic emission during plastic deformation of crystals
[DE88-701878] 20 p2876 N88-27075
Acoustic emission calibration instrumentation
[DE88-010817] 21 p2951 N88-27526
Application of pattern recognition techniques to the identification of aerospace acoustic sources
[NASA-CR-183116] 21 p3013 N88-27877
Proceedings of the French-German Colloquium on Helicopter Detection
[ISL-R-104/87] 22 p3147 N88-28723
Acoustic direction finding of flying helicopters
22 p3148 N88-28728
Examples of the application of acoustics for the detection and classification of targets 22 p3148 N88-28729
The development of acoustic emission for structural integrity monitoring of aircraft
[AD-A196264] 24 p3427 N88-30396

ACOUSTIC EXCITATION
Active control of jet flowfields
[AD-A186736] 08 p0969 N88-15969
Characteristics of thermooptical sound excitation in metals 08 p1076 N88-16486
Performance of linear vertical antenna in refractive multimode waveguide 08 p1076 N88-16489
On the correlation of plume centerline velocity decay of turbulent acoustically excited jets
[NASA-TM-100193] 09 p1114 N88-16681
Coupled FE and HIE method for exterior acoustics of axisymmetric shells — finite element (FE) Helmholtz integral equation (HIE)
[ARE-TM(UHA)-87506] 09 p1243 N88-17448
Transient sound radiation from infinite thin plate
[ARE-TM(UHA)-87508] 09 p1243 N88-17449
Acoustic radiation from line- and point-loaded plates: Uniformly asymptotic solutions
[AD-A189367] 13 p1834 N88-20969
Enhanced viscous flow drag reduction using acoustic excitation
[NASA-CR-182734] 15 p2062 N88-22295
Acoustically excited heated jets. 1: Internal excitation
[NASA-CR-4129-PT-1] 17 p2298 N88-23751
Acoustically excited heated jets. 2: In search of a better understanding
[NASA-CR-4129-PT-2] 17 p2299 N88-23752
Acoustically excited heated jets. 3: Mean flow data
[NASA-CR-4129-PT-3] 17 p2299 N88-23753

ACOUSTIC FATIGUE
Abrasion and impact resistant coatings
[DE88-003562] 13 p1750 N88-20464

ACOUSTIC FREQUENCIES
NT AUDIO FREQUENCIES
Describing the source created by turbulent flow over orifices and louvers
[AD-A190254] 15 p2130 N88-22706

ACOUSTIC GENERATORS
U SOUND GENERATORS

ACOUSTIC IMPEDANCE
Development of a new method of measuring the characteristic impedance and complex wave number of a porous acoustic material
[AD-A185038] 05 p0646 N88-13957
Measured and calculated acoustic attenuation rates of tuned resonator arrays for two surface impedance distribution models with flow
[NASA-TP-2786] 09 p1241 N88-17440
Evaluation of a multi-point method for determining acoustic impedance
[NASA-TM-100637] 20 p2849 N88-26913
Arctic ice attenuation model study
[AD-A193362] 22 p3146 N88-28715

ACOUSTIC INSTABILITY
Low-disturbance wind tunnels
07 p0811 N88-14937
Characterizing particle combustion in a Rijke burner
[AD-A186157] 08 p0966 N88-15847

Propagation of acoustic disturbances in transonic flow fields of lifting wings
[DFVLR-FB-88-13] 21 p3013 N88-27880

ACOUSTIC LEVITATION
Single mode levitation and translation
[NASA-CASE-NPO-16675-1-CU]
17 p2395 N88-24241
Program for the feasibility of developing a high pressure acoustic levitator
[NASA-CR-182154] 20 p2782 N88-26486
Combustion studies of acoustically suspended liquid droplets
[AD-A193892] 23 p3192 N88-28998

ACOUSTIC MEASUREMENT
NT NOISE MEASUREMENT
Investigation of the suitability of the 8ft x 8ft transonic wind-tunnel for aeroacoustic research on propellers
[RAE-TM-AERO-2090] 01 p0008 N88-10041
A new method for determining acoustic properties of the seabed from the ambient noise field in the ocean
[RAE-TR-86035] 01 p0090 N88-10580
Experimental study of the propagation of an acoustic wave in the low atmosphere
[ISL-R-111/86] 02 p0231 N88-11454
AFAR (Azores Fixed Acoustic Range) measurements of intensity and intensity moments
[AD-A184431] 03 p0355 N88-12237
Development of an acoustic echosounder for detection of lower level atmospheric turbulence
[AD-A184677] 05 p0626 N88-13631
Measuring the annoyance of aircraft noise
[AD-A185454] 06 p0777 N88-14770
Transient classifier systems and man-machine interface research
[AD-A186213] 07 p0899 N88-15446
Comprehensive inflight vibration and acoustic testing
08 p0999 N88-16052
Wind tunnel investigations of periodic vortex separation on rough-surface circular cylinders using acoustic measuring methods
[DFVLR-FB-87-24] 09 p1112 N88-16665
Recommendations for organising the calibration of pure-tone audiometers
[NPL-AC-112] 09 p1167 N88-16999
Payload bay atmospheric vent airflow testing at the Vibration and Acoustic Test Facility
[NASA-TM-100460] 11 p1437 N88-18572
The estimation of target trajectory parameters from Closest Point of Approach (CPA) time measurements in a field of acoustic sensors
[FB-3-87] 11 p1439 N88-18586
Acoustic measurements from a rotor blade-vortex interaction noise experiment in the German-Dutch Wind Tunnel (DNW)
[NASA-TM-4024] 11 p1542 N88-19218
Analysis of in-flight acoustic data for a twin-engined turboprop airplane
[NASA-CR-178389] 11 p1543 N88-19220
Application of ISRM testing methods to fracture toughness testing of graphite 13 p1747 N88-20446
Method for determination of the wind velocity and direction
[NASA-TT-20233] 13 p1802 N88-20769
Survey of acoustic techniques for monitoring El Nino
[PB88-157615] 13 p1804 N88-20783
Measurement and analysis of the noise radiated by low Mach numbers centrifugal blowers
[AD-A189226] 13 p1833 N88-20966
Method for determining the coordinates of sound sources by means of a sound measurement system
[NASA-TT-20242] 13 p1834 N88-20972
Method for determining artillery position
[NASA-TT-20238] 13 p1834 N88-20973
Space time processing, environmental-acoustic effects
[AD-A190764] 15 p2130 N88-22708
Acoustic propagation in the low atmosphere. Experimental study and modeling by the radius method
[ISL-CO-247/86] 15 p2131 N88-22713
Simulated measurement of power flow in structures near to simple sources and simple boundaries
[NASA-TM-89124] 19 p2722 N88-26166
Sound power measurements in situ using a reference sound source
[PB88-182571] 20 p2849 N88-26910
Evaluation of a multi-point method for determining acoustic impedance
[NASA-TM-100637] 20 p2849 N88-26913
Acoustic propagation in the lower atmosphere
[ISL-R-126/87] 21 p3013 N88-27878
Application of acoustic-Doppler current profiler and expendable bathythermograph measurements to the study of the velocity structure and transport of the Gulf Stream
[NASA-CR-183188] 22 p3129 N88-28605

ACOUSTIC MICROSCOPES
Imaging subtle microstructural variations in ceramics with precision ultrasonic velocity and attenuation measurements
[NASA-TM-100129] 07 p0867 N88-15257
Cryogenic acoustic microscopy
[AD-A187274] 10 p1299 N88-17767
Interface control using low frequency (3 to 20 MHz) acoustic microscopy
[REPT-48-411/F] 21 p2959 N88-27577
Application of nondestructive testing techniques to materials testing
[AD-A195716] 24 p3381 N88-30136

ACOUSTIC PROPAGATION
Application of ray theory to propagation of low frequency noise from wind turbines
[NASA-CR-178367] 03 p0373 N88-12349
Compressor large bandwidth noise emission mechanisms
[ETN-88-91177] 05 p0646 N88-13959
The acoustic source created by turbulent flow over orifices and louvers
[REPT-87674] 06 p0776 N88-14764
Model-scale sound propagation experiment
[NASA-TM-100602] 15 p2130 N88-22709
Acoustic propagation in the low atmosphere. Experimental study and modeling by the radius method
[ISL-CO-247/86] 15 p2131 N88-22713
Study of the convergence of a finite difference scheme for acoustic propagation in the atmosphere in a parabolic approximation. Statistical calculation of the sound field in the presence of kinematic turbulence
[ONERA-RS-8/3641-PY-160-P]
17 p2394 N88-24235
The calculation of casually constrained optima in the active control of sound
[ISVR-TR-147] 17 p2395 N88-24237
Investigation of intensity and phase fluctuations of an acoustic wave after crossing thermal turbulence
[ETN-88-92542] 17 p2395 N88-24238
Linear and nonlinear acoustic wave propagation in the atmosphere
[NASA-CR-4157] 18 p2571 N88-25268
Sound propagation over uneven ground and irregular topography
[NASA-CR-182956] 20 p2849 N88-26911
Acoustic propagation in the lower atmosphere
[ISL-R-126/87] 21 p3013 N88-27878

ACOUSTIC PROPERTIES
NT ACOUSTIC IMPEDANCE
NT ACOUSTIC INSTABILITY
NT ACOUSTIC SCATTERING
NT ACOUSTIC VELOCITY
NT REVERBERATION
NT SOUND INTENSITY
First article test noise survey of the A/F32T-9 large turbo fan engine enclosed noise suppressor system, Sky Harbor IAP (International Airport), Phoenix, Arizona
[AD-A183799] 01 p0090 N88-10586
Development of a new method of measuring the characteristic impedance and complex wave number of a porous acoustic material
[AD-A185038] 05 p0646 N88-13957
Aerodynamic and acoustic characteristics of an advanced propeller under take-off and landing conditions
[NAL-TR-935] 09 p1243 N88-17453
The temporal and spatial acoustical response of a point-driven fluid-loaded plate
[AD-A188504] 12 p1636 N88-19794
Low frequency ocean ambient noise: Measurements and theory
[AD-A191188] 16 p2237 N88-23362
Acoustic characteristics of 1/20-scale model helicopter rotors
[NASA-CR-177355] 16 p2265 N88-23548
Remote sensing of acoustic properties of shallow water sediments: A review
[AD-A192107] 18 p2570 N88-25267
Ray scattering from a collection of ice keels
[AD-A191757] 19 p2722 N88-26163
The acoustic field scattered from some approximate pressure release materials
[AD-A194768] 23 p3278 N88-29515

ACOUSTIC RADIATION
U SOUND WAVES

ACOUSTIC SCATTERING
NT REVERBERATION
Underwater acoustic backscatter from a model of arctic ice open leads and pressure ridges
[AD-A184693] 03 p0354 N88-12234
On a boundary data operator and generalized exterior Robin problems for the Helmholtz equation
[AD-A185124] 05 p0640 N88-13915

Research on acoustical scattering, diffraction catastrophes, optics of bubbles, photoacoustics, and acoustical phase conjugation
[AD-A185785] 06 p0776 N88-14761
Acoustic scattering from composite wind-wave surfaces 3: Forward scatter intensities and spatial coherence at low and high frequencies and small grazing angles for Bubble-free regimes
[AD-A185908] 07 p0881 N88-15345
Ultrasonic testing of near-surface zones using scattered signals
[ETN-88-90813] 07 p0929 N88-15642
Acoustic backscattering from bottom sediment at normal incidence in the laboratory
[AD-A186905] 09 p1242 N88-17443
Comparison of the rough surface reflection coefficient with specularly scattered acoustic data
[AD-A187086] 09 p1242 N88-17444
Scattering of impulsive acoustic waves by a semi-infinite crack in the plane interface of a half-space and a layer
[PB88-126396] 10 p1405 N88-18377
Inversion of parabolic and paraboloidal projections
[AD-A187538] 10 p1405 N88-18380
Estimation of sea surface wave spectra using acoustic tomography
[AD-A187837] 11 p1516 N88-19057
Observations of the upper ocean using a multi-beam Doppler sonar
[AD-A188596] 12 p1648 N88-19678
Sound propagation through a turbulent atmosphere: Experimental techniques and data analysis
[AD-A188891] 12 p1686 N88-20094
Ray scattering from a collection of ice keels
[AD-A191757] 19 p2722 N88-26163
Quantitative particle characterization by scattered ultrasound 20 p2846 N88-26908
Studying materials using acoustic waves
[AD-A192234] 20 p2850 N88-26915
The covariance of scalar fields scattered by pressure-release randomly rough surfaces
[AD-A192489] 22 p3146 N88-28714
Arctic ice attenuation model study
[AD-A193382] 22 p3146 N88-28715
The acoustic field scattered from some approximate pressure release materials
[AD-A194768] 23 p3278 N88-29515
Reflection and scattering of acoustic rays computed for parabolic ice keel models
[AD-A193898] 23 p3278 N88-29517

ACOUSTIC SOUNDING
Remote acoustic sounding of ferromanganese nodules
06 p0727 N88-14471
Nonlinear acoustic parameter and its application in ultrasonic imaging 14 p1902 N88-21364
Remote sensing of temperature profiles. Performance test of PASS
[DE88-753108] 20 p2826 N88-26768

ACOUSTIC STABILITY
U FREQUENCY STABILITY

ACOUSTIC VELOCITY
Noncontact temperature measurements of hot steel bodies using an electromagnetic acoustic transducer (EMAT)
[DE88-000560] 04 p0446 N88-12765
Coupled acoustic and ocean thermodynamic model
[AD-A184357] 04 p0472 N88-12911
A modified version of the phase sensitive technique for measurements of absolute sound velocity in solids
[DE88-002303] 10 p1405 N88-18378
Ultrasonic-velocity studies of composite and heterogeneous materials
[AD-A189000] 12 p1604 N88-19595
On the possibility of high velocity deflagration front propagation by radiative energy transfer
[AD-A189022] 12 p1613 N88-19645
Target localization in an inhomogeneous medium
[AD-A190008] 15 p2130 N88-22703
Low frequency ocean ambient noise: Measurements and theory
[AD-A191188] 16 p2237 N88-23362
Operational noise data for CH-47D and AH-64 army helicopters
[AD-A191059] 18 p2570 N88-25263
Evaluation of the biot coefficients
[AD-A191643] 18 p2570 N88-25265
The high pressure sound velocity and equation of state of aqueous solutions of hydroxylammonium nitrate and triethanolammonium nitrate
[AD-A191740] 18 p2570 N88-25266
Thermophysical properties of argon
[DE86-010376] 18 p2613 N88-25509
Dynamics and stability of combustion driven self oscillations in presence of various frequencies. Extensive stability criteria
[ETN-88-92123] 20 p2771 N88-26432
Ultrasonic studies of stresses and plastic deformation in steel during tension and compression
[AD-A192308] 21 p2912 N88-27280
Metal halide optical glasses
[AD-A193794] 23 p3198 N88-29032
Calculation of non-stationary aerodynamic forces in the near sonic range
[NASA-TT-20310] 24 p3322 N88-29782

ACOUSTIC VIBRATIONS
U SOUND WAVES

ACOUSTICS
NT AERODACOUSTICS
NT GEOMETRICAL ACOUSTICS
NT MAGNETOACOUSTICS
NT PSYCHOACOUSTICS
NT UNDERWATER ACOUSTICS
Activities report of the Institute of Sound and Vibration Research
[ETN-87-90685] 01 p0090 N88-10589
Design, construction, activation, and operation of a high intensity acoustic test chamber
02 p0137 N88-10864
A digital control system for high level acoustic noise generation 02 p0138 N88-10865
Nonsteady-state vibrations in acoustic medium of elastic elliptical shell subjected to instantaneously applied uniform pressure 02 p0160 N88-11000
Evaluation of a scale-model experiment to investigate long-range acoustic propagation
[NASA-TP-2748] 02 p0230 N88-11450
A hybrid numerical technique for predicting the aerodynamic and acoustic fields of advanced turboprops
[NASA-CR-174926] 03 p0374 N88-12352
Excitation of natural oscillations of a boundary layer by an external acoustic field 04 p0425 N88-12634
Nonlinear acoustics
[AD-A184271] 04 p0488 N88-13004
Development of an acoustic echosounder for detection of lower level atmospheric turbulence
[AD-A184877] 05 p0626 N88-13831
Application of Vandermonde decomposition to directional and modal analysis of broadband transients
[AD-A185007] 05 p0646 N88-13956
Longitudinal mode combustion instabilities in air breathing engines 06 p0680 N88-14166
JPRS report: Science and technology. USSR: Physics and mathematics
[JPRS-UPM-87-008] 06 p0769 N88-14727
Dependence of acoustical characteristics of laser-induced breakdown in dielectric materials on shape of inelastic region 06 p0774 N88-14753
Acoustical phase conjugation
[PREPRINT-561] 06 p0777 N88-14768
Development of rotorcraft interior noise control concepts. Phase 2: Full scale testing, revision 1
[NASA-CR-172594-REV-1] 06 p0777 N88-14769
Study on arc sound in TIG and plasma welding processes and the possibility of its application in practice
[PB87-143947] 07 p0863 N88-15238
On the convergence of the p-version of the boundary element Galerkin method
[AD-A186198] 07 p0910 N88-15514
Solid mechanics research for quantitative non-destructive evaluation
[AD-A186599] 08 p0993 N88-16010
JPRS report: Science and technology. USSR: Physics and mathematics
[JPRS-UPM-87-010] 08 p1075 N88-16485
Recent Langley helicopter acoustics contributions
09 p1109 N88-16646
The assessment of the sound insulation requirements for a large broadcasting studio, using a scale model: Theoretical considerations
[BBC-RD-1987/20] 09 p1155 N88-16921
Qualification by analysis of IUS plume deflectors
09 p1179 N88-17063
JPRS report: Science and technology. USSR: Physics and mathematics
[JPRS-UPM-87-009] 09 p1233 N88-17395
Investigation of thermoacoustic heat transport using a thermoacoustic couple
[AD-A186689] 09 p1242 N88-17442
Acoustic backscattering from bottom sediment at normal incidence in the laboratory
[AD-A186905] 09 p1242 N88-17443
The acoustic-electric field analysis of multilayered surface acoustic wave devices
[ETN-88-91592] 09 p1242 N88-17446
Wind turbine acoustics research bibliography with selected annotation
[NASA-TM-100528] 09 p1243 N88-17450
Bearing detection in the presence of two sources of varying coherence using the complex cepstrum
[NASA-CR-181605] 09 p1243 N88-17451
Speech recognition: Acoustic-phonetic knowledge acquisition and representation
[AD-A187293] 10 p1320 N88-17893
An application of dimensionless Eigenvalues to underwater acoustic ducts
[AD-A188167] 11 p1542 N88-19219
Linear and nonlinear acoustics with nonuniform entropy in combustion chambers 12 p1607 N88-19609
The temporal and spatial acoustical response of a point-driven fluid-loaded plate
[AD-A188504] 12 p1636 N88-19794
Structural-acoustic interior noise modeling and analysis from experimental data
[PB88-141775] 12 p1667 N88-20088
Three-dimensional scattering of impulsive acoustic waves by a semi-infinite crack in the plane interface of a half space and a layer
[PB88-146996] 12 p1687 N88-20089
A study of methods to predict and measure the transmission of sound through the walls of light aircraft
[NASA-CR-182656] 12 p1687 N88-20090
Acoustic phonons, surface plasmons and surface acoustic plasmons in a superlattice and their nonreciprocal device applications
[AD-A188918] 12 p1698 N88-20163
Invariant characteristics of acoustic field in stratified ocean 13 p1788 N88-20698
Survey of acoustic techniques for monitoring El Nino
[PB88-157615] 13 p1804 N88-20783
Flow/acoustic interaction in duct inflow
[AD-A189264] 13 p1833 N88-20967
Mixing fuel particles for space combustion research using acoustics
[NASA-TM-100295] 14 p1872 N88-21186
Additional peak of light scattering by sound under conditions of acoustic instability
14 p1968 N88-21752
Nondestructive evaluation by acousto-ultrasonics
15 p2082 N88-22412
Flaw characterization in structural ceramics using scanning laser acoustic microscopy
15 p2082 N88-22415
Nondestructive evaluation of sintered ceramics
15 p2083 N88-22416
Mechanisms mediating perception of complex acoustic patterns
[AD-A189765] 15 p2102 N88-22520
Mechanisms mediating the perception of complex acoustic patterns
[AD-A190112] 15 p2130 N88-22705
Space time processing, environmental-acoustic effects
[AD-A190764] 15 p2130 N88-22708
Thin superconducting film characterization by surface acoustic waves
[AD-A190417] 15 p2143 N88-22791
Applications research studies of microtubules
[AD-A190855] 16 p2182 N88-23005
Utilization of dense packed planar acoustic echosounders to identify turbulence structure in the lowest levels of the atmosphere
[AD-A191006] 16 p2233 N88-23335
Advanced turboprop aircraft flyover noise: Annoyance to counter-rotating-propeller configurations with an equal number of blades on each rotor, preliminary results
[NASA-TM-100612] 16 p2265 N88-23547
Control of combustion and acoustically coupled fluid dynamic instabilities 17 p2318 N88-23843
The exact calculation of quadrupole sources for some incompressible flows
[NASA-TM-100623] 17 p2395 N88-24240
Acoustic convective system
[NASA-CASE-NPO-17278-1-CU]
18 p2498 N88-24818
Identification and acoustic characterization of seamounts
[AD-A192204] 18 p2548 N88-25123
Remote sensing of acoustic properties of shallow water sediments: A review
[AD-A192107] 18 p2570 N88-25267
Effects of Mach number on acoustic-vortex interactions in a ramjet 19 p2625 N88-25573
Acousto-ultrasonic input-output characterization of unidirectional fiber composite plate by P waves
[NASA-CR-4162] 19 p2678 N88-25923
Local free-space mapping and path guidance for mobile robots
[AD-A192970] 20 p2810 N88-26674
Acoustic diffraction by an absorbing finite strip in a moving fluid
[PB88-191382] 20 p2849 N88-26912
An analysis of the efficiency and directivity of the sound generated by a moving laser source
[AD-A192220] 20 p2849 N88-26914
Studying materials using acoustic waves
[AD-A192234] 20 p2850 N88-26915

Robust methods for array signal processing
[AD-A192854] 21 p3012 N88-27871
Publications on acoustics research at the Langley Research Center during 1980-1986
[NASA-TM-100590] 21 p3013 N88-27881
Development of a nitrile rubber for dynamic damping
[AD-A194080] 22 p3058 N88-28145
Theory of acoustoplasticity and ultrasonic measurements of residual stresses
22 p3087 N88-28328
Computer-controlled measurements of nonlinear standing waves
[AD-A193840] 22 p3147 N88-28717
Large aperture multi-dimensional laser radar testbed
[AD-A193447] 23 p3218 N88-29155
Asymptotic modal analysis and statistical energy analysis
[NASA-CR-183077] 23 p3278 N88-29514
ASKA-acoustics: Theory and applications --- vibro acoustics
[FFA-TN-1988-13] 23 p3279 N88-29519
Overview of computational vibro acoustics. State of the art and future development
[FFA-TN-1988-17] 23 p3279 N88-29521

ACOUSTO-OPTICS
Discussion on the modelling and processing of signals from an acousto-optic spectrum analyzer
[AD-A185639] 06 p0694 N88-14257
Research on acoustical scattering, diffraction catastrophes, optics of bubbles, photoacoustics, and acoustical phase conjugation
[AD-A185785] 06 p0776 N88-14761
A continued study of optical sound generation and amplification
[AD-A188362] 12 p1691 N88-20116
Bathymetric hazard survey test
[AD-A189150] 13 p1803 N88-20775
Solid-state ring laser with acoustooptical phase nonreciprocity of opposing waves
14 p1970 N88-21761
The effect of internal relaxation on optoacoustic conversion in liquids
[AD-A191307] 16 p2176 N88-22970
Fast acting optical beam detection and deflection system
[AD-A192161] 18 p2521 N88-24954
A high dynamic range acousto-optic image correlator for real-time pattern recognition
[DE88-0079[illegible]3] 19 p2726 N88-26191
Studies of coherent beam processing concepts, phase 1
[AD-A194749] 22 p3083 N88-28306
Approximate and numerical methods in acousto-optics. Part 1: Normal incidence of the light
[AD-A194294] 22 p3152 N88-28755
Acoustic-optical detector of gravitational waves based on high-quality crystals
[DE88-702459] 23 p3232 N88-29232
Acoustooptic processing of two-dimensional signals using temporal and spatial integration
[AD-A194803] 24 p3359 N88-29999

ACQUISITION
NT DATA ACQUISITION
NT TARGET ACQUISITION
Speech recognition: Acoustic-phonetic knowledge acquisition and representation
[AD-A185897] 07 p0840 N88-15097
Systems integrated human engineering on the Navy's rapid acquisition of manufactured parts/test and integration facility 09 p1206 N88-17226
Avionics acquisition, trends and future approaches
12 p1702 N88-20184
Performance of a rapid carrier acquisition circuit for satellite ground terminal modems
[RSRE-TEST-REPORT-87/CC3/2]
22 p3071 N88-28227
Artificial intelligence software acquisition program, volume 2
[AD-A194239] 22 p3141 N88-28680
Estimating reliability with discrete growth models
[AD-A193845] 22 p3143 N88-28692
Artificial intelligence software acquisition program, volume 1
[AD-A194104] 23 p3267 N88-29447
Scattering impulse response synthesis using random noise illumination: Initial concept evaluation
[AD-A195086] 24 p3364 N88-30034

ACRYLATES
Interactions in miscible polymer blends
[AD-A193824] 22 p3058 N88-28144
Dissolution rates of polymers and copolymers based on methyl, ethyl and butyl methacrylate
[AD-A194713] 23 p3197 N88-29027

ACRYLIC ACID
Polyacrylic acid electrolyte-modified zinc phosphate conversion coatings for corrosion protection of steel
[DE88-004878] 19 p2617 N88-25527

ACRYLIC RESINS
High-molecular compounds (selected articles)
[AD-A184668] 03 p0293 N88-11842
Polymer material for heat sensors
06 p0676 N88-14142
Group contribution analysis of the damping behavior of homopolymers, statistical copolymers and interpenetrating polymer networks based on acrylic, vinyl and styrenic mers
[AD-A185904] 07 p0836 N88-15070
The adhesive bonding of thermoplastic composites
[AD-A190994] 16 p2173 N88-22953
Modification of polymers by photografting processes
17 p2323 N88-23871
Polyacrylic acid electrolyte-modified zinc phosphate conversion coatings for corrosion protection of steel
[DE88-004878] 19 p2617 N88-25527
Interactions in miscible polymer blends
[AD-A193824] 22 p3058 N88-28144

ACRYLONITRILES
Interfacial shear strength of pitch and high strain pan fibers in an epoxy matrix
[AD-A185966] 07 p0826 N88-15011
Method of obtaining of fire resistant polyacrylonitrile fiber or cloth from it
[AD-A18594[illegible]] 07 p0836 N88-15071

ACTINIDE SERIES
NT LAWRENCIUM
NT NEPTUNIUM
NT PLUTONIUM ISOTOPES
NT PLUTONIUM 238
NT THORIUM
NT URANIUM
NT URANIUM ISOTOPES
NT URANIUM 238

ACTINIDE SERIES COMPOUNDS
NT CALIFORNIUM COMPOUNDS
NT URANIUM COMPOUNDS
NT URANIUM FLUORIDES
Bulk superconductivity in La2CuO4
[DE88-002509] 09 p1254 N88-17516

ACTINOMETERS
NT ADVANCED VERY HIGH RESOLUTION RADIOMETER
NT DICKE RADIOMETERS
NT INFRARED DETECTORS
NT INFRARED RADIOMETERS
NT INFRARED SCANNERS
NT INFRARED SPECTROMETERS
NT INFRARED SPECTROPHOTOMETERS
NT MICROWAVE RADIOMETERS
NT RADIOMETERS
NT SOLAR SPECTROMETERS
NT SPECTROHELIOGRAPHS
NT SPECTROPHOTOMETERS
NT SPECTRORADIOMETERS
NT TOTAL OZONE MAPPING SPECTROMETER
NT ULTRAVIOLET SPECTROMETERS
NT ULTRAVIOLET SPECTROPHOTOMETERS

ACTIVATION
Oxide-bound transition metal complexes for methane activation
[PB88-169719] 14 p1887 N88-21277
Determination of Tafel constants in nonlinear polarization curves
[AD-A192335] 21 p2912 N88-27282
The design of methane activation catalysts
[DE88-002265] 23 p3199 N88-29043

ACTIVATION (BIOLOGY)
Influence of general vertical vibration on relationships between mediators in various segments of brain
06 p0751 N88-14613
Toward a mathematical formalism of performance, task difficulty, and activation 16 p2239 N88-23372
Effect of microgravity on lymphocyte activation --- Spacelab D1 mission 22 p3061 N88-28163

ACTIVATION ANALYSIS
NT NEUTRON ACTIVATION ANALYSIS

ACTIVATION ENERGY
Flammability limits in cocurrent smoldering combustion
[DE87-014102] 03 p0284 N88-11785
Precipitation in alumina-rich spinel: A transformation-toughened ceramic single crystal
[DE87-012380] 06 p0785 N88-14815
Insights into the mechanisms of chemical reactions: Reaction paths for chemical reactions
[DE88-003041] 10 p1297 N88-17755
Diffusion studies in amorphous NiZr alloys
[DE88-003009] 10 p1301 N88-17781
Novel catalysts for methane activation
[DE88-003637] 13 p1738 N88-20390
Kinetics of polymer decomposition
[DE88-005500] 13 p1749 N88-20460
Dissolution rates of polymers and copolymers based on methyl, ethyl and butyl methacrylate
[AD-A194713] 23 p3197 N88-29027

ACTIVE CONTROL
Flutter suppression and gust load alleviation. Part 1: Results of phase 1 to 3. Part 2: Description of the Garteur model
[MBB/LKE-292/S/PUB/191] 01 p0007 N88-10038
Augmenting the control of a flexible manipulator with passive mechanical damping 01 p0055 N88-10350
Active minimisation of acoustic fields. A review of research into the active control of sound undertaken at ISVR from 1963 to 1986
[ISVR-TR-146] 01 p0091 N88-10593
A preliminary investigation into the feasibility of implementing a direct sideforce control system on the Astra Hawk by means of an active control surface --- aircraft control
[ETN-87-90924] 02 p0126 N88-10795
Investigation of control law for active flutter suppression
[NASA-TT-20126] 02 p0130 N88-10818
Active control of helicopter vibration using multiloop self-adaptive control 03 p0264 N88-11660
Minimisation of helicopter vibration through active control of structural response 03 p0264 N88-11662
Modeling and control of large flexible vehicles in the atmosphere and space
[AD-A185368] 05 p0555 N88-13377
Cartesian path control of a two-degree-of-freedom robot manipulator
[NASA-CR-182331] 05 p0639 N88-13906
Design verification and fabrication of active control systems for the DAST ARW-2 high aspect ratio wing, part 1
[NASA-CR-177959-PT-1] 06 p0669 N88-14101
Design verification and fabrication of active control systems for the DAST ARW-2 high aspect ratio wing. Part 2: Appendices
[NASA-CR-177959-PT-2] 06 p0669 N88-14102
Active control of flexural vibrations in beams
06 p0794 N88-14866
Handling qualities of a wide-body transport airplane utilizing Pitch Active Control Systems (PACS) for relaxed static stability application
[NASA-TP-2482] 07 p0821 N88-14987
Active control of jet flowfields
[AD-A186736] 08 p0989 N88-15989
Analytical study of the effect of early warning on optimal shock isolation 08 p0998 N88-16047
Sensitivity of active vibration control to structural changes and model reduction 10 p1284 N88-17683
Active control technology with adaptive control concept in the aircraft construction
[MBB/LKE-294/S/PUB/295] 10 p1313 N88-17845
La Recherche Aerospatiale, bimonthly bulletin, number 1987-2, 237/March April
[ESA-TT-1074] 11 p1433 N88-18550
An application of active surface heating for augmenting lift and reducing drag of an airfoil
[NASA-TM-100563] 11 p1436 N88-18570
Structural design requirements for aircraft incorporating active control technology 12 p1580 N88-19453
Active vibration control of a cantilevered beam with three elastic coordinates
[AD-A188824] 12 p1636 N88-19797
Control augmented structural synthesis
[NASA-CR-4132] 13 p1721 N88-20290
Practical considerations for structural control: System uncertainty, system time delay and truncation of small control forces
[PB88-163738] 14 p1933 N88-21526
Sensitivity of control-augmented structure obtained by a system decomposition method
[NASA-TM-100535] 14 p1954 N88-21647
Instrumentation to provide an active control capability for distributed parameter systems
[AD-A190043] 15 p2076 N88-22375
Active control and system identification of rotordynamic structure 16 p2218 N88-23230
Integrated Application of Active Controls (IAAC) technology to an advanced subsonic transport project: Program review
[NASA-CR-3880] 17 p2301 N88-23763
Vibration and control of flexible rotor supported by magnetic bearings
[NASA-TM-100888] 17 p2345 N88-23977
The calculation of casually constrained optima in the active control of sound
[ISVR-TR-147] 17 p2395 N88-24237
Low authority control of large space structures using a constrained threshold control formulation
18 p2472 N88-24667

Experimental study of active vibration control
[AD-A191454] 18 p2526 N88-24989

Vibration protection of inelastic structures by means of active and passive control 18 p2528 N88-25001

Analysis of a closed-kinematic chain robot manipulator
[NASA-CR-183031] 18 p2561 N88-25206

Active control of 2-D instability waves on an axisymmetric body
[AD-A191578] 19 p2663 N88-25835

Active phase compensation system for fiber optic holography
[NASA-TM-101295] 20 p2805 N88-26641

Direct-solution techniques for viscous flows and their control
[AD-A194775] 23 p3211 N88-29114

A comparison of simple analytical models for representing propeller aircraft structural and acoustic responses
[ISVR-TR-153] 23 p3279 N88-29523

ACTIVE GALACTIC NUCLEI

Image sharpening observations of active galactic nuclei 01 p0098 N88-10643

Spherical models of QSO/AGN emission line clouds
06 p0806 N88-14921

The radio structure of active nuclei in edge-on spiral and Seyfert galaxies 09 p1264 N88-17576

Prediction and analysis of basic gravitational microlensing phenomena 11 p1550 N88-19272

Speckle imaging of active galactic nuclei: NGC 1068 and NGC 4151 18 p2592 N88-25407

Activities in astrophysics
[INPE-4582-PRE/1316] 24 p3456 N88-30570

ACTIVE GALAXIES
NT RADIO GALAXIES
NT SEYFERT GALAXIES

The imaging of extra-galactic low-energy gamma-ray sources prospects, techniques, and instrumentation
[NASA-CR-182536] 12 p1713 N88-20251

Variable spectra of active galaxies
[NASA-CR-182694] 13 p1853 N88-21091

ACTIVE GLACIERS
U GLACIERS

ACTIVE MAGNETO PARTICLE TRACER EXPLORERS
U AMPTE (SATELLITES)

ACTIVE VOLCANOES
U VOLCANOES

ACTIVITY (BIOLOGY)

Biophysical applications of solid state and tritium NMR
[DE88-005328] 13 p1806 N88-20806

Biological processes in the water column of the South Atlantic bight: Zooplankton responses
[DE88-004811] 14 p1951 N88-21630

Methods and possibilities of biological action spectroscopy 16 p2272 N88-23597

ACTIVITY CYCLES (BIOLOGY)

Pharmacological resetting of the Circadian sleep-wake cycle
[AD-A186194] 07 p0889 N88-15385

Biological rhythms, sleep, and wakefulness in prolonged confinement 19 p2696 N88-26022

ACTS

Communication satellite technology trends
01 p0015 N88-10088

An examination of the Advanced Communications Technology Satellite (ACTS) and its application to the Defense Data Network (DDN)
[AD-A184003] 03 p0276 N88-11742

A laser communication experiment utilizing the ACT satellite and an airborne laser transceiver
[NASA-TM-100792] 11 p1492 N88-18910

Space communication link propagation data for selected cities within the multiple beam and steerable antenna coverage areas of the advanced communications technology satellite
[NASA-TM-100861] 16 p2191 N88-23070

Service offerings and interfaces for the ACTS network of Earth stations
[NASA-TM-100809] 18 p2471 N88-24663

Experiments applications guide: Advanced Communications Technology Satellite (ACTS)
[NASA-TM-100265] 22 p3048 N88-28082

A statistical rain attenuation prediction model with application to the advanced communication technology satellite project. 1: Theoretical development and application to yearly predictions for selected cities in the United States
[NASA-CR-179498] 23 p3205 N88-29077

ACTUATION

Wind-tunnel investigation of actuated forebody strakes for yaw control at high angles of attack
17 p2299 N88-23754

ACTUATOR DISKS

Calculation of the damage of highly loaded gas turbine disks under real flight conditions
[ETN-87-90416] 01 p0007 N88-10036

Linear and nonlinear theories of flow through an actuator disk --- windpowered pumps
[R-803-A] 03 p0316 N88-11995

ACTUATORS

Minimisation of helicopter vibration through active control of structural response 03 p0264 N88-11662

On the root locus method applied to flexural vibration control systems 03 p0320 N88-12022

An evaluation plan of bus architectures and protocols using the NASA Ames intelligent redundant actuation system
[NASA-CR-177458] 04 p0398 N88-12482

Design of feedback control systems for stable plants with saturating actuators
[NASA-CR-182613] 12 p1681 N88-20050

Design of a linear actuator and breadboard test result --- far IR telescope 14 p1877 N88-21217

Photoelastic model tests of the Dornier linear actuator --- far IR telescope 14 p1877 N88-21218

Fine adjustment mechanism for FIRST
14 p1878 N88-21219

A joint actuator design for a robotic manipulator
14 p1879 N88-21232

The 22nd Aerospace Mechanisms Symposium
[NASA-CP-2506] 14 p1924 N88-21468

The 15-meter diameter hoop/column antenna surface control actuator system 14 p1924 N88-21469

High output paraffin actuators: Utilization in aerospace mechanisms 14 p1924 N88-21470

Servo-actuator control for sampled-data feedback disturbance rejection --- helicopters
[ESA-TT-1002] 16 p2163 N88-22903

Evaluation of a high-torque backlash-free roller actuator 16 p2219 N88-23239

The LDCM actuator for vibration suppression
[NASA-CR-182898] 17 p2335 N88-23940

Linear force device
[NASA-CASE-MSC-20549-2] 18 p2516 N88-24927

Toggle release
[NASA-CASE-MSC-21354-1] 18 p2523 N88-24969

SRB/SLEEC (Solid Rocket Booster/Shingle Lap Extendible Exit Cone) feasibility study, volume 2. Appendix A: Design study for a SLEEC actuation system
[NASA-CR-178974] 23 p3187 N88-28965

Semiconductor bridge (SCB) igniter studies. 1: Comparison of SCB and hot-wire pyrotechnic actuators
[DE88-008802] 23 p3200 N88-29046

Thermocouple for heating and cooling of memory metal actuators
[NASA-CASE-NPO-17068-1-CU]
23 p3217 N88-29151

Feasibility study of a microprocessor controlled actuator test mechanism
[AD-A194654] 23 p3249 N88-29337

Sensor and actuator selection for large space structure control
[AD-A194912] 24 p3333 N88-29842

A standard architecture for controlling robots
[AD-A195929] 24 p3423 N88-30371

ACUITY
NT VISUAL ACUITY

ADA (PROGRAMMING LANGUAGE)

Data Management Working Group report
01 p0016 N88-10097

Petri nets as a support to symbolic execution of concurrent Ada programs
[REPT-87-007] 01 p0082 N88-10529

Praxis: The programming language: An advanced overview
[DE87-014319] 02 p0220 N88-11388

ADAMEASURE: An implementation of the Halstead and Henry metrics
[AD-A184005] 03 p0365 N88-12299

PROVER: A first-order logic system in Ada
[DE88-000220] 04 p0479 N88-12951

A review and analysis of Fortran 8x
[DE88-001320] 04 p0479 N88-12955

An Ada graphical tool to support software development
[DE87-014854] 05 p0636 N88-13891

A plan for collecting ada software development cost, schedule and environment data
[AD-A185905] 07 p0902 N88-15460

Version description document for the Ada compiler validation capability (version 1.9) (for microcomputer)
[AD-A186390] 07 p0903 N88-15471

Can space station software be specified through Ada?
07 p0925 N88-15622

Ada (trade name) compiler validation summary report. Systems designers' PLC SD Ada-plus VAX/VMS x MC68020. Version 2B.00. Host: VAX 8600. Target: Motorola MC68020. Completion of on-site testing
[AD-A186571] 08 p1053 N88-16356

The Ada compiler: On the design and implementation of an Ada compiler
[ETN-88-91594] 09 p1215 N88-17284

Rationale for the design of the Ada (tradename) programming language
[AD-A187106] 09 p1217 N88-17297

Implementation of elementary functions in Ada
[CWI-NM-R8709] 09 p1218 N88-17303

Design and implementation of elementary functions in Ada
[CWI-NM-R8710] 09 p1218 N88-17304

Description of a limited VAX-Ada program support environment developed within UDP division version 1.0
[ARE-TM(UDP)-87103] 09 p1219 N88-17308

Contributions to a numerical library in Ada
[NPL DITC-98/87] 09 p1219 N88-17309

Occam/Ada parallel programming system
[ISAL-IDI1-87-11] 09 p1219 N88-17312

The implementation and use of Ada on distributed systems with high reliability requirements
[NASA-CR-182461] 09 p1221 N88-17326

Factors causing unexpected variations in Ada benchmarks
[AD-A187231] 10 p1388 N88-18291

VAXELN experimentation: Programming a real-time clock and interrupt handling using VAXELN Ada 1.1
[AD-A188100] 11 p1525 N88-19107

Applicability of Ada (trademark) tasking for avionics executives
[AD-A188827] 12 p1578 N88-19445

Design method for Ada programs
[ESA-CR(P)-2528] 14 p1958 N88-21671

Ada tasking in Ten15
[RSRE-MEMO-4074] 14 p1958 N88-21676

Examination of the effects of using Ada (trade name) in flight control software
[AD-A189679] 14 p1959 N88-21683

Ada (Trademark) compiler validation summary report. ALSYS: AlsyCOMP-013, V2.0 HOST: IBM PC AT. Target: IBM 370 3084Q
[AD-A189640] 15 p2106 N88-22546

Ada user library
[FOA-C-20657-2.7] 16 p2246 N88-23418

Proposal for standard mathematical packages in Ada
[CWI-NM-R8718] 16 p2249 N88-23439

Simulation: A simulation system in Ada
[FOA-A-20043-2.7] 17 p2385 N88-24176

Dialog design: General requirements and analysis of an Ada system --- user interface design
[FOA-C-20691-2.7] 17 p2385 N88-24177

New York TRACON demonstration of program recoding requirements analysis document
[DOT/FAA/CT-87/34] 18 p2462 N88-24622

Beyond Ada: Generating Ada code from equational specifications
[AD-A191866] 18 p2557 N88-25176

Portable implementation of a generic exponential function in Ada
[DE88-007699] 19 p2715 N88-26117

Ada (trade name) compiler validation summary report: Verdix Corporation VAda-010-03315, version 5.5 MicroVAX 2 host ISBC 386/20P Intel target
[AD-A193226] 21 p2997 N88-27774

Ada (trade name) compiler validation summary report: Verdix corporation VAda-010-13125, version 5.41 Sun Microsystems Sun-3/160 host microbar GPC68020 target
[AD-A193415] 21 p2997 N88-27777

Ada (trade name) compiler validation summary report: Verdix Corporation VAda-010-0101, version 5.41 VAX-11/750
[AD-A193414] 22 p3136 N88-28645

Ada (trade name) compiler validation summary report: Verdix Corporation VAda-010-03205, version 5.42 MicroVAX 2 host and national DB32000 (NS32032 target
[AD-A193485] 23 p3247 N88-29326

Level 1 Ada/SQL (Structured Query Language) database language interface user's guide
[AD-A194490] 23 p3249 N88-29335

ADAPTATION
NT ACCLIMATIZATION
NT ALTITUDE ACCLIMATIZATION
NT COLD ACCLIMATIZATION
NT DARK ADAPTATION
NT HEAT ACCLIMATIZATION
NT LIGHT ADAPTATION

System adaptivity and the modelling of stereotypes --- human-computer interaction
[NPL-DITC-91/87] 01 p0077 N88-10494

Wall interference tests of a CAST 10-2/DOA 2 airfoil in an adaptive-wall test section
[NASA-TM-4015] 02 p0122 N88-10772

The role of adaptive supplemental visual cuing in flight simulation
[AD-A185932] 07 p0822 N88-14992

Long-term adaptation of the otolith organs
07 p0886 N88-15375

Physiological and immunological aspects of human adaptation to temperature elevation in a closed environment 07 p0895 N88-15424

Adaptive finite difference methods in fluid dynamics 08 p0985 N88-15958

General biological character of adaptive capacity of mammalian metabolism in response to diverse and extreme environmental factors 08 p1047 N88-16324

Group adaptation and individual adjustment in antarctica: A summary of recent research
[AD-A186605] 08 p1051 N88-16347

Adaptive finite element methods for parabolic systems in one- and two-space dimensions
[AD-A186534] 08 p1073 N88-16475

Brain potentials and personality: A new look at stress susceptibility
[AD-A186931] 09 p1199 N88-17189

Physiological and ecological implications of coupled heat- and water-transport mechanisms of endotherms and vegetation
[DE88-004170] 10 p1352 N88-18081

Polar worker adaptability to Antarctic high altitudes 10 p1366 N88-18165

NASA Workshop on Biological Adaptation
[NASA-TM-89468] 10 p1368 N88-18174

Analysis and synthesis of adaptive neural elements
[AD-A187047] 10 p1395 N88-18316

Human adaptation to various hypercapnic conditions in relation to salivary electrolyte dynamics and renal function 12 p1664 N88-19977

A multiple model adaptive tracking algorithm against airborne targets
[AD-A190619] 15 p2057 N88-22263

Adaptive neural network architecture
[AD-A190114] 15 p2104 N88-22533

Implementation of a distributed adaptive routing algorithm on the Intel iPSC (Intel Personal Super-Computer)
[AD-A189849] 15 p2109 N88-22567

Development of adaptive grid schemes based on Poisson grid generators
[AD-A190953] 16 p2262 N88-23528

Adaptive segmentation evaluation
[AD-A190965] 16 p2274 N88-23609

Adaptive local grid refinement in computational fluid mechanics
[AD-A192215] 18 p2510 N88-24890

Method of assessing changes in biorhythmological structure of human physiological functions 19 p2706 N88-26088

The human element in space: Lessons from Antarctica
[AD-A193440] 21 p2988 N88-27741

Adaptive identification by systolic arrays
[AD-A193532] 23 p3266 N88-29444

An adaptive overlapping local grid refinement method for two-dimensional parabolic systems
[AD-A193560] 23 p3271 N88-29464

On adaptive cell-averaging CFAR (Constant False-Alarm Rate) radar signal detection
[AD-A196286] 24 p3360 N88-30009

ADAPTIVE CONTROL
NT ACTIVE CONTROL
NT LEARNING MACHINES
NT MODEL REFERENCE ADAPTIVE CONTROL
NT SELF ADAPTIVE CONTROL SYSTEMS

A method for the calculation of transonic flows for the control of adaptive wind tunnels
[ETN-87-90411] 01 p0003 N88-10015

Model adaptation and imbalance compensation in rotors with active magnetic bearings
[ETN-87-90440] 01 p0056 N88-10361

Adaptive control of hydraulic devices
[FB-1/85] 01 p0084 N88-10543

Improvements to the adaptive maneuvering logic program
[NASA-CR-3985] 03 p0262 N88-11648

Minimisation of helicopter vibration through active control of structural response 03 p0264 N88-11662

Adaptive control of Large Space Structure (LSS)
[ISAS-R-621] 03 p0276 N88-11740

Correction of inertial navigation system drift errors for an autonomous land vehicle using optical radar terrain data
[AD-A184973] 05 p0544 N88-13311

A Multipurpose Adaptive Controller (MAC) for real time digital regulation
[REPT-87-028] 06 p0762 N88-14673

Dynamics, control and sensor issues pertinent to robotic hands for the EVA retriever system 06 p0796 N88-14876

Pulsed plasma arc welding process with double closed-loop adaptive penetration control system
[PB87-143780] 07 p0863 N88-15236

Solid modelling for the manipulative robot arm (power) and adaptive vision control for space station missions 08 p1061 N88-16409

Adaptive proximate time-optimal servomechanisms 09 p1175 N88-17043

Real-time artificial intelligence issues in the development of the adaptive tactical navigator 09 p1211 N88-17260

Systolic array adaptive beamforming
[AD-A187496] 10 p1385 N88-18260

Adaptive control of a manipulator with a flexible link
[NASA-CR-181637] 11 p1476 N88-18807

An evaluation in a modern wind tunnel of the transonic adaptive wall adjustment strategy developed by NPL in the 1940's
[NASA-CR-181623] 12 p1575 N88-19417

Speed control of a missile with throttleable ducted rocket propulsion 12 p1597 N88-19561

A wind tunnel model with dynamic control
[BU-352] 13 p1724 N88-20310

Estimation-correlation, modeling, and identification in adaptive array processors
[AD-A189130] 13 p1757 N88-20512

Adaptive algorithms for HF antenna arrays
[AD-A189329] 13 p1761 N88-20534

Wall interference assessment and corrections for transonic adaptive wall airfoil data 14 p1863 N88-21129

Flexiwall 3 SO: A second order predictive strategy for rapid wall adjustment in two-dimensional compressible flow
[NASA-CR-181662] 15 p2015 N88-22018

Model selection for the multiple model adaptive algorithm for in-flight simulation
[AD-A189715] 15 p2016 N88-22022

Multivariable control law design for the AFTI/F-16 with a failed control surface using a parameter-adaptive controller
[AD-A189848] 15 p2020 N88-22040

Multiple model parameter adaptive control for in-flight simulation
[AD-A190568] 15 p2021 N88-22044

Optimal control and identification of space structures
[AD-A190033] 15 p2025 N88-22065

Moving-bank multiple model adaptive estimation applied to flexible spacestructure control
[AD-A190761] 15 p2026 N88-22071

Aerofoil testing in a self-streamlining flexible walled wind tunnel
[NASA-CR-4128] 16 p2156 N88-22865

Automatic control of robot motion
[AD-A191012] 16 p2215 N88-23218

Accurate positioning of long, flexible ARM's (Articulated Robotic Manipulator) 16 p2219 N88-23243

Contribution to the adaptive dynamic control of a robot manipulator
[LAAS-87-350] 16 p2255 N88-23475

Genetic algorithms for adaptive real-time control in space systems 17 p2388 N88-24195

Generalized predictive control of multivariable systems
[OUEL-1640/86] 17 p2391 N88-24209

An adaptive load-following control system for a space nuclear power system 17 p2406 N88-24307

Accurate multigrid solution of the Euler equations on unstructured and adaptive meshes
[NASA-CR-181679] 18 p2460 N88-24606

Parameter-adaptive model-following for in-flight simulation
[AD-A190567] 18 p2467 N88-24645

Kinematics, dynamics and control of a closed chain mechanism manipulator 18 p2523 N88-24967

Robust adaptive regulation without persistent excitation
[NASA-TM-100571] 18 p2561 N88-25204

The experimental verification of wall movement influence coefficients for an adaptive walled test section
[NASA-CR-181681] 19 p2598 N88-25439

Empty test section streamlining of the transonic self-streamlining wind tunnel fitted with new walls
[NASA-CR-181680] 19 p2598 N88-25442

Adaptive residual mode filter control of distributed parameter systems for large space structure applications 19 p2719 N88-26143

Experiments in adaptive control of a very flexible one link manipulator 20 p2842 N88-26865

Asymptotically efficient adaptive allocation schemes for controlled Markov chains: Finite parameter space
[AD-A192228] 20 p2846 N88-26893

An h-p adaptive finite element method for steady compressible flow 21 p2941 N88-27467

Control of free-flying space robot manipulator systems
[NASA-CR-183104] 21 p2957 N88-27563

Unified multilevel adaptive finite element methods for elliptic problems
[DE88-011938] 21 p3007 N88-27840

Dual adaptive control: Design principles and applications
[NASA-CR-177485] 22 p3038 N88-28038

Experimental investigations for the generation of phase modes for adaptive antennas
[REPT-10-87] 23 p3205 N88-29074

Adaptive computational methods for aerothermal heating analysis
[NASA-CR-181636] 23 p3212 N88-29115

Motion planning with obstacles and dynamic constraints 23 p3222 N88-29175

Identification and control of time-varying flexible structures: An artificial intelligence approach 23 p3265 N88-29437

Computer-Aided-Control Engineering (CACE) primitives for robust and adaptive control systems, phase 1
[AD-A192446] 23 p3265 N88-29439

Topics in adaptive control and inference
[AD-A194718] 23 p3266 N88-29443

Adaptive identification by systolic arrays
[AD-A193532] 23 p3266 N88-29444

Adaptive mesh generation for viscous flows using Delaunay triangulation
[NASA-CR-181699] 24 p3316 N88-29749

Supersonic wall adaptation in the rubber tube test section of the DFVLR Goettingen
[IB-222-87-A-08] 24 p3330 N88-29824

Adaptive control in positioning a rigid-flexible robot arm
[AD-A195194] 24 p3422 N88-30367

ADAPTIVE CONTROL SYSTEMS
U ADAPTIVE CONTROL

ADAPTIVE FILTERS

Estimation filters with adaptive scanning time for flying target tracking
[ETN-87-90401] 01 p0036 N88-10232

An adaptive lattice algorithm for spectral line estimation
[AD-A184970] 05 p0634 N88-13876

A generalization of order statistic filters: The alpha-trimmed linear filter
[AD-A186125] 07 p0842 N88-15107

An adaptive filtering technique for removing periodic noise from modal response data
[DE88-002347] 10 p1322 N88-17903

A Gram-Schmidt space-time adaptive canceller using adaptive lattice filters
[AD-A189684] 14 p1959 N88-21684

Active control of 2-D instability waves on an axisymmetric body
[AD-A191578] 19 p2663 N88-25835

Sidelobe level of an adaptive array using the SMI (Sampled Matrix Inversion) algorithm
[AD-A193131] 21 p2932 N88-27409

CryoSQUID: A SQUID-based magnetic field sensor
[AD-A194237] 23 p3239 N88-29275

Topics in adaptive control and inference
[AD-A194718] 23 p3266 N88-29443

ADAPTIVE OPTICS

Performances of an Actively Stabilized Stellar Interferometer (ASSI): Faint magnitudes, low fringe contrast measurements and operationality 01 p0097 N88-10641

Wavefront error sensing
[NASA-CR-181504] 03 p0321 N88-12030

Develop techniques for ion implantation of (lead-lanthanum-zirconate-titanate) for adaptive optics
[DE88-000642] 05 p0650 N88-13986

Research in the optical sciences
[AD-A192175] 18 p2575 N88-25297

ADDITION RESINS
NT ACRYLIC RESINS
NT VINYL COPOLYMERS

ADDITIVES
NT ADMIXTURES
NT ANTIKNOCK ADDITIVES
NT ANTIOXIDANTS
NT OIL ADDITIVES
NT PLASTICIZERS
NT PROPELLANT ADDITIVES
NT PROPELLANT BINDERS
NT SOLID ROCKET BINDERS

Effect of high-temperature annealing on the microstructure and thermoelectric properties of GaP doped SiGe
[NASA-TM-100164] 01 p0029 N88-10188

The effect of additives on the reactivity of palladium surfaces for the chemisorption and hydrogenation of carbon monoxide: A surface science and catalytic study
[DE87-014885] 02 p0145 N88-10909

Polymer modified binders for bituminous or asphaltic paving layers
[PC-5] 02 p0153 N88-10958

Boundary lubrication. Experiments with boundary lubrication and plain bearings at +60...-60 deg C temperatures
[DE87-752869] 02 p0180 N88-11124
Slip casting and extruding shapes of rhemium with metal oxide additives. Part 2: Development of grain stabilized rhenium parts for resistojets
[NASA-CR-180851] 03 p0278 N88-11749
Mechanical properties of an acicular ferrite steel microalloyed to niobium and vanadium
[DE87-703547] 04 p0415 N88-12574
Partial substitution of vanadium by niobium in AISI H13 steel
[DE87-703548] 04 p0415 N88-12575
Analysis of free cutting brass by A.C. polarography
[PD-MT-8726] 04 p0417 N88-12587
Investigation of fuel additive effects on sooting flames
[AD-A186403] 07 p0829 N88-15026
Diagonal and off-diagonal disorder in doped quantum wells
[INPE-4255-PRE/1128] 08 p1089 N88-16556
Effects of additives on fire properties of polyethylene
[AD-A187064] 09 p1146 N88-16871
IRAC test report. Gallium doped silicon band 2: Read noise and dark current
[NASA-TM-87813] 09 p1159 N88-16945
Electron Spin Resonance (ESR) measurements on intermediate-valence Cer compounds doped with paramagnetic ions: CeOs2:Gd ion and CePd3:Mn-ion
[ETN-88-91081] 09 p1258 N88-17526
Silicon and indium doping of GaAs: Measurements of the effect of doping on mechanical behavior and relation with dislocation formation
[DE88-003862] 11 p1554 N88-19303
A review of approaches to the study of turbulence modification by means of non-Newtonian additives
[AD-A188799] 12 p1627 N88-19734
Lattice relaxation of the DX centers in Ga/sub 1-x/Al/sub x/As and of the pressure-induced deep donors in GaAs
[DE88-005452] 13 p1846 N88-21061
Development of a laboratory test for multiport injector deposits: Approaches 1 and 2
[AD-A190697] 15 p2048 N88-22203
Improved properties of SiGe/GaP alloys
[NASA-CASE-NPO-17259-1-CU]
18 p2585 N88-25358
Grain boundary structure in Ni3Al
[DE88-009164] 20 p2773 N88-26444
Alternate/modified binders for airfield pavements
[AD-A192781] 21 p2899 N88-27206
Processing and additive effects of ZrO2 on microstructure and dielectric porperties of BaTiO3 ceramics
[AD-A193126] 21 p2917 N88-27316
Relative flow rates of explosive powders
[DE88-010767] 21 p2923 N88-27350
Numerical calculations of dopent diffusion involving flashlamp heating of silicon 21 p2929 N88-27384
Influence of dispersed additives reinforcement on the wear reinforcement mechanisms of the alumina-steel couple. Macroscopic and structural aspects
[ECL-88-01] 22 p3059 N88-28148

ADDRESSING
Protection and security mechanisms in the SMITE capability computer
[RSRE-MEMO-4117] 17 p2384 N88-24167

ADDUCTS
Excimer laser-assisted deposition of GaAs, AlAs and (Al,Ga)As from Lewis acid-base adducts
[AD-A184588] 03 p0329 N88-12081

ADENOSINE TRIPHOSPHATE
Electron cytochemical detection of Ca(2)+-ATPase in protonema of moss funaria hygrometrica (H e d w.) under hypogravitation 06 p0749 N88-14602
Myosin Ca sup (2+), Mg sup (2+)-adenosine triphosphatase activity in ray myocardium following 30-day expose to 1.1 and 2.0 G 10 p1362 N88-18141

ADENOSINES
NT ADENOSINE TRIPHOSPHATE
Role of adenosine analogs and growth hormone in waking and sleep
[AD-A187897] 11 p1519 N88-19070

ADHEROMETERS
U ADHESION TESTS

ADHESION
Adhesion properties of polyelectrolyte-chemisorbed zinc phosphate conversion coatings
[DE87-012489] 01 p0029 N88-10186
Variational and nonvariational theory of frictionless adhesive contact between bodies
[REPT-87-11] 01 p0054 N88-10345
The effect of sulfur and zirconium Co-doping on the oxidation of NiCrAl
[NASA-TM-100209] 02 p0150 N88-10940
Ion plating: Fundamental processing studies and synthesis of high performance coatings
[AD-A184766] 03 p0303 N88-11908
Interfacial strength development in thermoplastic resins and fiber-reinforced thermoplastic composites
[NASA-CR-181525] 04 p0411 N88-12549
Tribological studies on high speed steel cutting tools
[DE88-002550] 07 p0864 N88-15246
Mechanical properties of steel-to-steel adhesive bonds
[PB88-111299] 08 p0971 N88-15877
Effect of peel angle on peel force
[AD A186117] 08 p0972 N88-15878
Adhesion, friction and micromechanical properties of ceramics
[NASA-TM-100782] 10 p1305 N88-17801
Adhesion of vapour phase deposited ultra-thin polyimide films on polycrystalline silver
[AD-A187930] 10 p1306 N88-17810
Adhesion of PVD titanium coatings to beryllium substrates
[DE88-005147] 11 p1463 N88-18721
Factors affecting the sticking of insects on modified aircraft wings
[NASA-CR-182615] 12 p1575 N88-19421
Generalized Levinson's theorem and quantum sticking coefficients at O K
[AD-A189371] 12 p1699 N88-20171
Interfacial adhesion: Theory and experiment
[NASA-TM-100830] 13 p1742 N88-20417
Development of a torsion balance for adhesion measurements
[NASA-TM-100799] 13 p1748 N88-20454
Mechanical design of a ultrahigh gravity UHV facility to launch and recover a low-speed projectile tested on board KC 135 14 p1877 N88-21216
Laser enhanced adhesion of copper films to sapphire substrates
[DE88-006802] 15 p2038 N88-22144
Fracture toughness of silicon nitride-silicon nitride joints bonded with oxynitride glass
[DE88-005548] 15 p2043 N88-22172
Development of a high-temperature resistant (700 F), corrosion-preventive organic coating
[AD-A191407] 16 p2182 N88-23009
Interface characterization of Cu-Cu and Cu-Ag-Cu low temperature solid state bonds
[AD-A191015] 16 p2263 N88-23667
Adhesion between polystyrene and polymethylmethacrylate
[AD-A192050] 18 p2492 N88-24785
Environmental integrity of coating/metal interface
[AD-A192184] 18 p2492 N88-24786
The adherence of nickel oxide on nickel during high temperature oxidation
[DE88-011194] 20 p2774 N88-26450
Reducing adhesion and agglomeration within a cloud of combustible particles
[NASA-TM-100902] 20 p2788 N88-26539
An IETS (Inelastic Electron Tunneling Spectroscopy) study of surface reactions applicable to adhesion
[AD-A192274] 21 p2909 N88-27261
Improved adhesion for SiO2 particles in silica substrates using helium-ion irradiation
[DE88-008915] 21 p2920 N88-27332
Plasma treatment of polymers for improved adhesion
[DE88-011623] 21 p2921 N88-27334
Dry adhesive friction of elastomers: A study of the fundamental mechanical aspects
[ETN-88-92903] 23 p3198 N88-29036
Ultrasonic detection of diffusion and adhesion loss
24 p3354 N88-29967
Semi-microdroplet assay for cell adhesion molecules
[NASA-CR-183139] 24 p3406 N88-30274
Scanning electron microscopy study of adhesion in sea urchin blastulae
[NASA-CR-183136] 24 p3406 N88-30275

ADHESION TESTS
Study of surface treatment before bonding of light alloys
[DCQ/L-48-287/F] 06 p0682 N88-14181
Composite/metal jointing technology for vehicle weight reduction
[DE88-900228] 08 p0992 N88-16005
Mechanical design of a ultrahigh gravity UHV facility to launch and recover a low-speed projectile tested on board KC 135 14 p1877 N88-21216
The use of micromachined structures for the management of mechanical properties and adhesion of thin films 19 p2674 N88-25899
Study of surface treatments before adhesive bonding of light alloys --- aircraft industry
[ETN-88-92743] 21 p2916 N88-27308
Adhesion of hydrated silicate films
[DE88-011250] 21 p2920 N88-27333
Semi-microdroplet assay for cell adhesion molecules
[NASA-CR-183139] 24 p3406 N88-30274

ADHESIVE BONDING
Pressure sensitive adhesives
[EP-PATENT-0-183-495-A1] 01 p0026 N88-10164
Polyitaconic acid macromolecule primer for adhesive bonding and corrosion control of aluminum
[DE87-013306] 01 p0027 N88-10173
Effect of adhesive layers on impact damage and dynamic response in composite laminates
02 p0141 N88-10887
Durability (lifetime) predictions adhesively bonded structures
[AD-A184069] 03 p0335 N88-12110
Influence of bonding shop moisture on metal-honeycomb junctions bonded with ultra-thin adhesive films
[SNIAS-872-422-112] 05 p0558 N88-13399
Water disbondment characterization of organic Coating/metal substrate systems
[AD-A184847] 05 p0567 N88-13454
Computation of bonded assemblies. Elastoplastic adhesives, first part
[SNIAS-NT-18926/AQET] 05 p0569 N88-13467
First International Week of Adhesive Bonding and Assembling
[SNIAS-872-430-106] 05 p0569 N88-13468
Flexibilized copolyimide adhesives
[NASA-TM-89303] 05 p0570 N88-13474
Bending of a bonded beam as a test method for adhesive properties
[AD-A184813] 05 p0609 N88-13736
Study of surface treatment before bonding of light alloys
[DCQ/L-48-287/F] 06 p0682 N88-14181
Study of selection criteria for adhesives used in aircraft structure bonding
[ETN-88-91619] 08 p0971 N88-15875
Synthesis of high molecular weight peptide polymers and copolymers containing L-dope residues
[AD-A186462] 08 p0973 N88-15887
Composite/metal jointing technology for vehicle weight reduction
[DE88-900228] 08 p0992 N88-16005
Adhesive bond strengths on aluminium alloys as a function of surface topographies and their wetting properties
[ARE-TM(UMM)-87403] 09 p1148 N88-16880
The failure and fracture analysis of adhesive bonds
[ETN-87-90713] 09 p1181 N88-17077
A finite element analysis of adhesively bonded composite joints including geometric nonlinearity, nonlinear viscoelasticity moisture diffusion and delayed failure
[AD-A187455] 10 p1298 N88-17747
The effect on initial bond strength and durability of a Phosphoric Acid Dip (PAD) following chromic acid anodising of aluminum
[ARE-TM(UMM)-87402] 10 p1300 N88-17772
New scientific findings on the morphology of aluminum oxide layers, serving as an adhesive basis
[MBB-Z-137/86] 10 p1312 N88-17840
Theoretical analysis of adhesive fracture and crack-damage interactions 10 p1343 N88-18030
Cavitation in model elastomeric composites
[AD-A187401] 11 p1447 N88-18625
Finite element analysis of adhesively bonded composite joints including geometric nonlinearity, nonlinear viscoelasticity, moisture diffusion and delayed failure
[PB88-147822] 11 p1451 N88-18648
Shelf life degradation of selected anaerobic threadlocking adhesives at various storage temperatures
[AD-A187712] 11 p1461 N88-18711
An interdisciplinary approach to predictive modeling of structural adhesive bonding: Factors affecting the durability of titanium/epoxy bonds
[AD-A189503] 12 p1611 N88-19636
Detection of bondline delaminations in multilayer structures with lossy components
[NASA-CR-182716] 14 p1883 N88-21256
Increasing strength of graphite/epoxy bolted joints by introducing an adhesively bonded metallic insert
[FFA-TN-1987-45] 15 p2088 N88-22442
The adhesive bonding of thermoplastic composites
[AD-A190994] 16 p2173 N88-22953
A modified sulphuric acid anodising process used as a pretreatment for the adhesive bonding of aluminum alloys
[ARE-TM(UMM)-87410] 16 p2177 N88-22974
Evaluation of a thermoplastic polyimide (422) for bonding GR/PI composite
[NASA-TM-100584] 16 p2182 N88-23003
Polyitaconic acid macromolecule primer for adhesive bonding and corrosion control of aluminum
17 p2319 N88-23849

Water based primers for structural adhesive bonding of aircraft 17 p2321 N88-23862

Thermographic detection of buried debonds
[AD-A192115] 18 p2475 N88-24680

Calculation of assemblies bonded with quasi-elastic adhesives
[REPT-47-632/F] 18 p2493 N88-24793

Study of surface treatments before adhesive bonding of light alloys --- aircraft industry
[ETN-88-92743] 21 p2916 N88-27308

Adhesion of hydrated silicate films
[DE88-011250] 21 p2920 N88-27333

Chemistry of adhesion at the polyimide-metal interface
[AD-A194647] 22 p3056 N88-28143

A study of the floating roller peel test for adhesives
[AD-A194114] 23 p3198 N88-29034

Criteria for matrix dominated failure
[AD-A196263] 24 p3341 N88-29887

Method of attaching strain gauges to various materials
[NASA-CASE-LAR-13797-1] 24 p3376 N88-30106

ADHESIVES

NT PASTES

Pressure sensitive adhesives
[EP-PATENT-0-183-495-A1] 01 p0026 N88-10164

Low extractable wipers for cleaning space flight hardware 02 p0137 N88-10863

Contribution to the study of composite materials and their damage
[NASA-TT-20107] 02 p0143 N88-10897

Process for the production of a thermoplastic elastomer composition
[EP-PATENT-0-202-782-A2] 05 p0569 N88-13465

Flexibilized copolyimide adhesives
[NASA-TM-89303] 05 p0570 N88-13474

High temperature adhesive
[PB87-109229] 06 p0683 N88-14186

Viscoelastic properties of EA951 adhesive: A source of creep deformations of a strongback
[DE88-001561] 06 p0685 N88-14197

Effect of peel angle on peel force
[AD-A186117] 08 p0972 N88-15878

Composite/metal jointing technology for vehicle weight reduction
[DE88-900226] 08 p0992 N88-16005

Evaluation of high temperature structural adhesives for extended service, phase 5
[NASA-CR-178176] 09 p1149 N88-16884

Initial adhesive screening of novel polyamide-imides and their copolymers
[NASA-TM-100641] 20 p2779 N88-26481

Conductivity mechanism and operating behavior of electrically conductive adhesives on the example of a power transistor
[ETN-88-92355] 21 p2940 N88-27464

A study of the floating roller peel test for adhesives
[AD-A194114] 23 p3198 N88-29034

Criteria for matrix dominated failure
[AD-A196263] 24 p3341 N88-29887

Predicting the durability of adhesives and coatings by remote detection of hidden defects and coating-thickness irregularities: A theoretical and numerical study 24 p3355 N88-29972

Primerless RTV silicones
[BDX-613-3807] 24 p3356 N88-29980

ADI METHODS

U ALTERNATING DIRECTION IMPLICIT METHODS

ADIABATIC CONDITIONS

Monte Carlo simulation of primitive atom-transfer reactions in solution
[AD-A183977] 03 p0375 N88-12360

Adiabatic diesel engine component development: Reference engine for on-highway applications
[NASA-CR-179531] 03 p0386 N88-12428

Adiabatic supernova expansion into the circumstellar medium
[DE87-014241] 03 p0387 N88-12433

Variation of wave action: Modulations of the phase shift for strongly nonlinear dispersive waves with weak dissipation. A new adiabatic invariant involving the modulated phase shift for strongly nonlinear, slowly varying, and weakly damped oscillators. The modulated phase shift for weakly dissipated nonlinear oscillatory waves of the Korteweg-de vries type
[AD-A185630] 06 p0765 N88-14702

Model for plasma equilibrium configuration evolution in a tokamak with adiabatic compression
[DE88-700354] 07 p0936 N88-15684

Review of the state of the art and projected technology of low heat rejection engines
[PB88-131255] 11 p1496 N88-18934

On stress collapse in adiabatic shear bands
[AD-A187185] 11 p1498 N88-18942

Adiabatic representation of three-body problem in hyperspherical coordinates. Statement of the problem
[DE88-701162] 15 p2126 N88-22678

Analysis for high compressible supersonic flow in converging nozzle
[IPPJ-860] 16 p2157 N88-22869

ADIABATIC DEMAGNETIZATION COOLING

Research on high-specific-heat dielectrics
[AD-A187246] 11 p1461 N88-18710

ADIABATIC EQUATIONS

Adiabatic formation of large-scale models of the atmosphere 14 p1935 N88-21541

ADIPOSE TISSUES

Role of body fat in the prediction of the metabolic response for immersion in cold water
[AD-A186914] 09 p1198 N88-17182

Prediction of physical fitness: Estimated percent body fat using body circumferences versus weight-height measures
[AD-A190233] 15 p2103 N88-22526

ADJOINTS

The adjoint process in stochastic optimal control
[AD-A189720] 15 p2116 N88-22605

ADJUSTING

Method for joint adjustment of satellite and surface geodetic networks 08 p1007 N88-16105

Possibilities for on-line surge suppression by fast guide vane adjustment in axial compressors 10 p1283 N88-17674

The significance of orientation unknowns in station and net adjustments 11 p1506 N88-18994

Fine adjustment mechanism for FIRST 14 p1878 N88-21219

ADJUSTMENT

U ADJUSTING

ADMINISTRATION

U MANAGEMENT

ADMITTANCE

U ELECTRICAL IMPEDANCE

ADMIXTURES

Structure of stably stratified atmospheric surface layer in presence of heat-releasing admixture 04 p0462 N88-12856

Development of an equation of state for computation of supercompressibility factors, critical flow factors and other properties for wet, sour natural gases, synthetic gases and admixtures
[PB88-202676] 20 p2798 N88-26602

ADRENAL GLAND

Effect of external electrostatic field on catecholamine secretion by rat adrenals 10 p1366 N88-18166

Hypothalamic-pituitary-adrenal responses to short duration high intensity cycle exercise
[AD-A192597] 21 p2985 N88-27727

ADRENALINE

U EPINEPHRINE

ADRENERGICS

Distinctions and mechanisms of effects of epinephrine and norepinephrine on cardiac pumping function under hypokinetic conditions 07 p0891 N88-15399

Propranolol and the compensatory circulatory responses to orthostasis at high altitude
[AD-A192675] 22 p3131 N88-28618

ADRIATIC SEA

Preliminary report of hydrological measurements carried out in the southern Adriatic Sea: Palma 86 campaign
[PREPRINT-555] 06 p0748 N88-14597

ADSORBENTS

Characterization and fundamental studies on CuO sorbent materials to determine attrition mechanisms on substrate gamma alumina
[DE88-003674] 13 p1749 N88-20456

ADSORPTION

NT CHEMISORPTION

Kinetics of CO adsorption on nickel using time resolved vibration spectroscopy
[ETN-87-90615] 03 p0289 N88-11814

Study of field adsorption using pulsed-laser field ion microscopy
[DE88-000310] 03 p0330 N88-12085

Characterization of catalysts with metal-support effects and of the species adsorbed on their surfaces
[DE87-014636] 04 p0414 N88-12564

The structure of adsorbed sulfur and carbon on molybdenum and rhenium single crystal surfaces, and their influence on carbon monoxide and hydrocarbon chemisorption
[DE88-001393] 04 p0499 N88-13073

Pure dephasing of a vibrational adbond
[AD-A185222] 05 p0609 N88-13740

Extending the range of Low Energy Electron Diffraction (LEED) surface structure determination: Co-adsorbed molecules, incommensurate overlayers and alloy surface order studied by new video and electron counting LEED techniques
[DE88-001401] 06 p0786 N88-14820

Coverage dependence of adsorbate-substrate bond lengths: Chlorine and caesium adsorbed on silver single crystals
[PB87-125142] 06 p0788 N88-14833

Use of hydrophilic polymer coatings for control of electroosmosis and protein adsorption 07 p0925 N88-15620

Memory effects on infrared adsorbate spectra
[AD-A186976] 09 p1253 N88-17512

Proceedings of the 19th DOE/NRC Airborne Waste Management and Air Cleaning Conference
[NUREG/CP-0086-VOL-2] 11 p1509 N88-19019

Scanning tunneling microscopy of silver, gold, and aluminium monomers and small clusters on graphite
[DE88-003671] 11 p1562 N88-19349

In-situ vibrational spectroscopy of specifically adsorbed azide on silver electrodes
[AD-A188511] 12 p1605 N88-19600

Some applications of surface Raman and infrared spectroscopies to mechanistic electrochemistry involved adsorbed species
[AD-A188777] 12 p1606 N88-19602

Electrosorptive detection based on double-layer capacitance for selective anion monitoring in ion chromatography. Part 1: Mercury electrodes
[AD-A188780] 12 p1606 N88-19603

FTIR (Fourier Transform Infrared) and FTNMR (Fourier Transform Nuclear Magnetic Resonance) study of organophosphorus surface reactions
[AD-A188337] 12 p1609 N88-19625

Electrosorptive detection of simple organic compounds in liquid chromatography
[AD-A188757] 13 p1736 N88-20376

Measuring thin film properties using SAW (Surface Acoustic Wave) devices: Diffusivity and surface area
[DE88-002216] 13 p1834 N88-20970

Recent progress in structure determination by LEED (Low-Energy Electron Diffraction) measure the properties of the deep donors (DX-cent)
[DE88-003851] 13 p1846 N88-21048

Millimeter-wave pulse distortion by a single adsorption line simulating the terrestrial atmosphere
[PB88-161237] 14 p1906 N88-21388

Mass transfer mechanisms for water adsorbed on silica gel
[DE88-005993] 15 p2032 N88-22107

Molecular dynamics of materials possessing high energy content
[AD-A190034] 15 p2034 N88-22118

Dilution refrigerator with non-valve adsorption system of sup 3/He circulation
[DE88-700974] 15 p2050 N88-22209

Theory of the dissociation dynamics of small molecules on metal surfaces: Finite temperature studies
[DE88-006495] 15 p2132 N88-22716

Anomalies in the heat-capacity signatures of submonolayer adsorbates with attractive lateral interactions
[AD-A190736] 15 p2147 N88-22817

UV-Laser reactions of molecular adsorbates
[AD-A190796] 16 p2212 N88-23201

Preferential surface adsorption in miscible blends of polystyrene and poly(vinyl methyl ether)
[AD-A191451] 18 p2490 N88-24769

The electrokinetic behavior of calcium oxalate monohydrate in macromolecular solutions
[NASA-TM-101144] 18 p2493 N88-24791

Heat pump augmented radiator for low-temperature space applications
[DE88-008369] 20 p2765 N88-26393

Fundamental optical studies of competitive adsorption and thin film phenomena
[DE88-008780] 20 p2875 N88-27068

Theory of the dissociation dynamics of small molecules on metal surfaces: Finite temperature studies
[DE88-007763] 21 p3013 N88-27882

Modification of YBa2Cu3O(7-x) ceramics by adsorbed water and other gases
[DE88-011518] 22 p3057 N88-28140

Correlations between wettability and structure in monolayers of alkanethiols adsorbed on gold
[AD-A194348] 23 p3191 N88-28991

ADSORPTIVITY

Coadsorption of H2O and CO2 on the Martian surface 23 p3307 N88-29702

ADVANCED COMMUNICATIONS TECHNOLOGY SAT

U ACTS

ADVANCED VERY HIGH RESOLUTION RADIOMETER

AVHRR/HIRS (Advanced Very High Resolution Radiometer/High Resolution Infra-Red Sounder) operational method for satellite based sea surface temperature determination
[PB88-107594] 06 p0708 N88-14340

Sea surface current estimates off central California as derived from enhanced AVHRR (Advanced Very High Resolution Radiometer) infrared images
[AD-A186867] 09 p1194 N88-17155
General determination of Earth surface type and cloud amount using multispectral AVHRR data
[NOAA-TR-NESDIS-39] 11 p1506 N88-18997
Pre-launch calibration of channels 1 and 2 of the advanced very high resolution radiometer
[PB88-157169] 14 p1913 N88-21427
The absolute radiometric calibration of the advanced very high resolution radiometer
[NASA-CR-182755] 14 p1941 N88-21584
Calibration and processing of AVHRR data for temperature estimation
[INPE-4493-PRE/1257] 15 p2095 N88-22485
Navigation system from AVHRR data from NOAA series satellites 17 p2359 N88-24054
DMSP-SSM/1 NASA algorithm validation using primarily LANDSAT and secondarily DMSP and/or AVHRR visible and thermal infrared satellite imagery
[NASA-CR-182979] 18 p2532 N88-25024
An objective technique for Arctic cloud analysis using multispectral AVHRR (Advanced Very High Resolution Radiometer) satellite imagery
[AD-A194732] 23 p3235 N88-29250

ADVANCED X RAY ASTROPHYSICS FACILITY
U X RAY ASTROPHYSICS FACILITY

ADVANCING GLACIERS
U GLACIERS

ADVECTION
A study of numerical methods for hyperbolic conservation laws with stiff source terms
[NASA-TM-100075] 10 p1399 N88-18343
Coherent structure-reflective turbulent viscous flow modeling
[AD-A188339] 13 p1765 N88-20556
Open cell associated with warm advection
17 p2351 N88-24010
A zoomable and adaptable hidden fine-mesh approach to solving advection-dispersion equations
[DE88-006174] 21 p3004 N88-27816

AE-C SATELLITE
U EXPLORER 51 SATELLITE

AE-D SATELLITE
U EXPLORER 54 SATELLITE

AE-E SATELLITE
U EXPLORER 55 SATELLITE

AERIAL EXPLOSIONS
Australian structures response evaluation: Ground shock and air blast measurements for site investigation survey
[MRL-TN-526] 20 p2813 N88-26685

AERIAL IMAGERY
U AERIAL PHOTOGRAPHY

AERIAL PHOTOGRAPHY
Matching segments from a map and an aerial image using relaxation techniques
[SNIAS-872-422-103] 05 p0620 N88-13809
Application of remote sensing to agricultural field trials
[ISBN-90-6754-089-7] 06 p0729 N88-14483
Model-based building verification in aerial photographs
[AD-A188010] 07 p0870 N88-15278
The aerophotogrammetric determination of Earth surface deformations
[SER-C-321] 07 p0872 N88-15288
Photogrammetric principles for combining remote sounding and three-dimensional mapping
08 p1012 N88-16135
Three-dimensional image generation from an aerial photograph
[AD-A188039] 11 p1503 N88-18979
Automatic knowledge acquisition for aerial image interpretation
[AD-A188616] 12 p1638 N88-19810
A texture analysis approach to computer vision for identification of roads in aerial photographs
[AD-A189340] 12 p1639 N88-19815
Marginal Ice Zone Experiment (MIZEX) 1984 VARAN-S data set
[ETN-88-92032] 14 p1950 N88-21625
Updating land-use of the Sao Jose dos Campos municipality through remote sensing data
[INPE-4479-RPE/562] 16 p2287 N88-23693
Latin American Symposium on Remote Sensing. 4th Brazilian Remote Sensing Symposium and 6th SELPER Plenary Meeting, volume 1 17 p2352 N88-24013
Remote sensing techniques in the estimation of the area cultivated with beans, corn, and castor beans in the Irece County (Bahia State) 17 p2358 N88-24045
Structure and dynamics of vegetation in the middle semi-arid tropics. Quixaba's Caatinga (PE): Terrain analysis of MSS/LANDSAT data 17 p2358 N88-24049
Remote sensing and structural rupture: Application examples in the study of tectonics
17 p2359 N88-24050
Analysis and interpretation of image lithostructure: An application of the multiconcept in the metamorphic belt of Sul de Santana da Boa Vista (RS)
17 p2359 N88-24051
Tornado tracks in Southwestern Brazil, Eastern Paraguay, and Northwestern Argentina
17 p2362 N88-24071
Interpretation of MSS/LANDSAT data for evaluation of physical distribution of mangroves in Cananeia-Iguape (SP) 17 p2363 N88-24072
Low altitude remote sensing data in the implementation of a mathematical model for the planning of urban equipment networks 17 p2363 N88-24074
Evaluation of the mangrove area at the Piaui River (SE) through remote sensing 17 p2365 N88-24086
The 35 mm vertical aerial photographs for mapping stands of bracatinga in different age classes
17 p2366 N88-24087
The breaked anticlines, cuesta and crest homoclines, ortoclinal valleys, and other forms of relief outcrops delineated with the help of remote sensing imagery
17 p2366 N88-24089
Stereoscopic photographs, ground and aerial, of trees used in the arborization of Curitiba (PR)
17 p2366 N88-24091
Preliminary study on the application of digital processing of TM-LANDSAT data in the mapping of apple orchards in Fraiburgo (SC) 17 p2367 N88-24093
Characteristics of drainage determinations in aerial photographs and relief determination on different scales planialtimetric charts for three soils in the state of Sao Paulo 17 p2367 N88-24095
Criteria for planimetric and altimetric correction of maps restituted from aerial photographs in 1:100,000 scale
17 p2367 N88-24097
National Meeting on Remote Sensing Applied to Municipal Planning 19 p2681 N88-25939
Application of remote sensing in the conservation of natural areas: Ribeira Valley 19 p2683 N88-25949
Use of remote sensing in the study of superficial formation certifying the development of integrated economy-case example: Rio Claro (SP) region
19 p2683 N88-25950
Application of 35mm EM aerial reconnaissance photographic format of the municipality of Ubatuba (SP)
19 p2684 N88-25953
Aerial photography as an instrument of atmospheric analysis: Maps of the middle atmosphere and its dynamics, Baixada Santista (SP) 19 p2684 N88-25955
Aerial photography as an instrument of municipal and regional planning: Metropolitan area of Sao Paulo (SP)
19 p2684 N88-25957
New duplicating paper with high resolution for aerial photography
[PB87-228706] 19 p2685 N88-25962
Automatic line network extraction from aerial imagery of urban areas through knowledge based image analysis
[AD-A193067] 21 p2965 N88-27615
Automatic line network extraction from aerial imagery of urban areas through knowledge-based image analysis
[AD-A192399] 23 p3227 N88-29208

AERIAL RECONNAISSANCE
Earth resources: A continuing bibliography with indexes (supplement 56)
[NASA-SP-7041(56)] 10 p1347 N88-18051
Hydrographic data from the OPTOMA (Ocean Prediction Through Observation, Modeling and Analysis) program: OPTOMA 23, 9-19 November 1986
[AD-A189868] 15 p2099 N88-22506
Air-to-air radar flight testing
[AGARD-AG-300-VOL-7] 21 p2932 N88-27406

AEROACOUSTICS
Investigation of the suitability of the 8ft x 6ft transonic wind-tunnel for aeroacoustic research on propellers
[RAE-TM-AERO-2093] 01 p0008 N88-10041
Noise of a model high speed counterrotation propeller at simulated takeoff/approach conditions (F7/A7)
[NASA-TM-100206] 01 p0091 N88-10592
Fluctuating pressure loads under high speed boundary layers
[NASA-TM-100517] 05 p0647 N88-13962
Flow induced pulsations in pipe systems
[ETN-88-91367] 06 p0702 N88-14307
NASA/Army Rotorcraft Technology. Volume 2: Materials and Structures, Propulsion and Drive Systems, Flight Dynamics and Control, and Acoustics
[NASA-CP-2495-VOL-2] 09 p1106 N88-16632
A decade of aeroacoustic research at NASA Ames Research Center 09 p1109 N88-16648
Aeroacoustic research programs at the Army Aviation Research and Technology Activity
09 p1109 N88-16649
An experimental investigation of the chopping of helicopter main rotor tip vortices by the tail rotor. Part 2: High speed photographic study
[NASA-CR-177457] 09 p1114 N88-16678
Investigation of aeroacoustic mechanisms by remote thermal imaging
[DE88-002612] 15 p2021 N88-22046
Aerodynamic noise of wind turbines
[PB88-165188] 16 p2265 N88-23546
Research investigation of helicopter main rotor/tail rotor interaction noise
[NASA-CR-4143] 19 p2722 N88-26165
Outdoor sound propagation, its implications for unattended ground sensors
[FEL-1986-64] 20 p2850 N88-26917
The influence of surface rounding on trailing edge noise
[AD-A193387] 21 p3012 N88-27876
Acoustic propagation in the lower atmosphere
[ISL-R-126/87] 21 p3013 N88-27878
The role of acoustic resonances in unsteady turbomachinery aerodynamics
[PNR90455] 22 p3147 N88-28720

AEROASSIST
Aeroassisted-vehicle design studies for a manned Mars mission
[NASA-TM-100031] 03 p0271 N88-11700
Aeroassisted manned transfer vehicle (TAXI) for advanced Mars Transportation: NASA/USRA 1987 Senior Design Project
[NASA-CR-181478] 03 p0275 N88-11736
An analysis of the effect of aeroassist maneuvers on orbital transfer vehicle performance
[NASA-TM-89117] 06 p0672 N88-14116
Effect of transition aerodynamics on aeroassist flight experiment trajectories
[NASA-TM-100546] 11 p1446 N88-18620
Aeroassisted orbit transfer vehicle trajectory analysis
[NASA-TM-89138] 12 p1599 N88-19575
Aeroassist flight experiment guidance Quiet Time
[NASA-TM-100556] 14 p1881 N88-21244
Orbital transfer vehicle: Concept definition and system analysis study
[NASA-CR-179315] 15 p2024 N88-22060

AEROBIOLOGY
Project Explorer takes its second step: GAS-608 in engineering development 10 p1288 N88-17707

AEROBRAKING
Aeroassisted-vehicle design studies for a manned Mars mission
[NASA-TM-100031] 03 p0271 N88-11700
Aeroassisted manned transfer vehicle (TAXI) for advanced Mars Transportation: NASA/USRA 1987 Senior Design Project
[NASA-CR-181478] 03 p0275 N88-11736
New concepts for atmospheric braking deceleration in planetary atmosphere entry
[SNIAS-CAS-DECE-P003-DPAA]
16 p2168 N88-22923

AEROCAPTURE
A technique for capture analysis of low thrust missions in a planetary system
[AD-A188934] 12 p1594 N88-19544
A design study of onboard navigation and guidance during aerocapture at Mars
[NASA-CR-172053] 18 p2469 N88-24654

AERODYNAMIC AXIS
U AERODYNAMIC BALANCE

AERODYNAMIC BALANCE
The effects of rotor unbalance on the vertical response of a soft-mounted block 08 p1000 N88-16057

AERODYNAMIC BRAKES
NT DRAG CHUTES
NT LEADING EDGE FLAPS
NT TRAILING EDGE FLAPS
NT VORTEX FLAPS
NT WING FLAPS

AERODYNAMIC BUZZ
U FLUTTER

AERODYNAMIC CENTER
U AERODYNAMIC BALANCE

AERODYNAMIC CHARACTERISTICS
NT AERODYNAMIC BALANCE
NT AERODYNAMIC DRAG
NT AERODYNAMIC STABILITY
NT INTERFERENCE DRAG
NT INTERFERENCE LIFT
NT JET LIFT
NT LIFT
NT STATIC AERODYNAMIC CHARACTERISTICS
NT SUPERSONIC DRAG
NT ZERO LIFT
Integration of dynamic, aerodynamic and structural optimization of helicopter rotor blades
[NASA-CR-181441] 01 p0002 N88-10012
Diagnosis of flow channel in aircraft gas-turbine engines on basis of vibration spectrum characteristics
02 p0159 N88-10993

An experimental evaluation of advanced rotorcraft airfoils in the NASA Ames eleven-foot transonic wind tunnel
[NASA-CR-166587] 03 p0261 N88-11640

Improvements to the adaptive maneuvering logic program
[NASA-CR-3985] 03 p0262 N88-11648

An aerodynamic performance evaluation of the NASA/Ames Research Center advanced concepts flight simulator
[NASA-TM-89659] 03 p0268 N88-11685

Fin gaps and body slots of guided projectiles: Effects, data correlation and modeling
[AD-A184440] 03 p0270 N88-11698

Technical evaluation report on the Fluid Dynamics Panel Symposium on aerodynamic and related hydrodynamic studies using water facilities
[AGARD-AR-225] 03 p0312 N88-11968

A hybrid numerical technique for predicting the aerodynamic and acoustic fields of advanced turboprops
[NASA-CR-174926] 03 p0374 N88-12352

Planform effects on the supersonic aerodynamics of multibody configurations
[NASA-TP-2762] 04 p0393 N88-12454

A method for the efficient calculation of elastic rotor blade dynamic response in forward flight
04 p0394 N88-12460

An integrated study of structures, aerodynamics and controls on the forward swept wing X-29A and the oblique wing research aircraft
[NASA-CR-181548] 04 p0399 N88-12486

Calculation of aerodynamic characteristics of three-dimensional finite span wings in potential incompressible flow 04 p0425 N88-12631

Conical wing with maximum lift-to-drag ratio in supersonic gas flow 04 p0425 N88-12633

Aerodynamics of Hypersonic Lifting Vehicles
[AGARD-CP-428] 05 p0529 N88-13219

The drag of slender axisymmetric cones in rarefied hypersonic flow 05 p0531 N88-13229

Low Reynolds number influence on aerodynamic performance of hypersonic lifting vehicles
05 p0531 N88-13230

Hypersonic airbreathing propulsion: Evolution and opportunities 05 p0531 N88-13231

Hypersonic aerodynamics: Applications for HOTOL
05 p0535 N88-13252

A perspective of computational fluid dynamics
05 p0538 N88-13279

Computational methods for problems in aerodynamics and large space structure using parallel and vector architectures
[AD-A185401] 05 p0541 N88-13294

An experimental investigation of the aerodynamics of a NACA 64A010 airfoil-flap combination with and without flap oscillations. Part 1: Steady-state characteristics
[NASA-TM-88217] 05 p0542 N88-13305

Nonlinear lift control at high speed and high angle of attack using vortex flow technology
05 p0545 N88-13319

Aircraft dynamics: Aerodynamic aspects and wind tunnel techniques 05 p0545 N88-13320

Full-envelope aerodynamic modeling of the Harrier aircraft
[NASA-TM-88376] 05 p0552 N88-13363

Vortical Flows Research Program of the Fluid Dynamics Research Branch
[NASA-TM-88332] 05 p0582 N88-13549

On the parabolized Navier-Stokes equations without sublayer assumptions
[AD-A186127] 07 p0849 N88-15152

Chemical reactions in turbulent mixing flows
[AD-A186141] 07 p0849 N88-15153

A note on the aerodynamic design of thin parallel-sided aerofoil sections
[ARL-AERO-TM-388] 09 p1114 N88-16677

A flight-test methodology for identification of an aerodynamic model for a V/STOL aircraft
[NASA-TM-100067] 09 p1117 N88-16694

Aerodynamic and acoustic characteristics of an advanced propeller under take-off and landing conditions
[NAL-TR-935] 09 p1243 N88-17453

Investigation of the influence of wind shear on the aerodynamic characteristics of aircraft using a vortex-lattice method 10 p1274 N88-17619

The aerodynamic design optimisation of a forward swept wing fighter aircraft
[CAR-87-18] 11 p1433 N88-18553

Aerodynamic characteristics of wings designed with a combined-theory method to cruise at a Mach number of 4.5
[NASA-TP-2799] 12 p1575 N88-19420

Australian aerodynamic design codes for aerial tow bodies
[AD-A189045] 13 p1715 N88-20258

Nonaxisymmetric body supersonic, aerodynamic prediction
[AD-A189336] 13 p1716 N88-20259

A correlation study of X-29A aircraft and associated analytical development
[NASA-CR-183103] 13 p1722 N88-20296

Lateral and longitudinal stability and control parameters for the space shuttle discovery as determined from flight test data
[NASA-TM-100555] 13 p1724 N88-20309

Investigation into the effects of flap end modifications on the performance of a wing with a single slotted flap
[BU-357] 14 p1866 N88-21148

Oscillating airfoils: Achievements and conjectures
[AD-A190490] 15 p2014 N88-22008

Improvements to tilt rotor performance through passive blade twist control
[NASA-TM-100583] 15 p2086 N88-22434

Design method for laminar flow control of two-dimensional airfoils in incompressible flow. Numerical study of LFC design concepts
[DE88-751809] 16 p2155 N88-22859

The structure of sonic underexpanded turbulent air jets in still air
[AD-A190856] 16 p2157 N88-22870

Propfan model wind tunnel aeroelastic research results 16 p2220 N88-23246

High Reynolds number tests of a Douglas DLBA 032 airfoil in the Langley 0.3-meter transonic cryogenic tunnel
[NASA-TM-87663] 17 p2296 N88-23734

Boundary layer flow visualization for flight testing
17 p2297 N88-23742

Natural laminar flow and airplane stability and control
17 p2298 N88-23747

The exact calculation of quadrupole sources for some incompressible flows
[NASA-TM-100623] 17 p2395 N88-24240

Experiment investigation on longitudinal characteristics of the forward swept wing
[AD-A191553] 18 p2456 N88-24582

High speed and high angle of attack aerodynamic characteristics of winged space vehicle
[ISSN-0285-6808] 18 p2459 N88-24599

Numerical solutions of the Euler equations for the flow field around counter-rotating propellers
19 p2636 N88-25638

Influence of wind shear on the aerodynamic characteristics of airplanes
[NASA-TP-2827] 20 p2755 N88-26344

Airbus 1987: Success in Europe
[ETN-88-92099] 20 p2758 N88-26364

Surface disturbances produced by low-level, subsonic B-1 aircraft
[AD-A192257] 20 p2824 N88-26752

Wind tunnel tests of elliptical missile body configurations at Mach numbers 0.4 to 5.0
[AD-A193525] 22 p3038 N88-28040

Effects of independent variation of Mach and Reynolds numbers on the low-speed aerodynamic characteristics of the NACA 0012 airfoil section
[NASA-TM-4074] 23 p3170 N88-28879

Aerodynamic data accuracy and quality: Requirements and capabilities in wind tunnel testing
[AGARD-AR-254] 23 p3173 N88-28893

Technology for pressure-instrumented thin airfoil models
[NASA-CR-4173] 23 p3180 N88-28933

Interactive plotting of NASTRAN aerodynamic models using NPLOT and DISSPLA
[AD-A194115] 23 p3226 N88-29204

Aircraft dynamics: Aerodynamic aspects and wind tunnel techniques 24 p3313 N88-29731

Survey on nonlinear effects 24 p3317 N88-29757

Semi-empirical methods for conventional and unconventional missiles 24 p3318 N88-29758

Air intake aerodynamics 24 p3318 N88-29762

A new computational capability for ramjet projectiles
[AD-A196061] 24 p3327 N88-29812

AERODYNAMIC CHORDS
U AIRFOIL PROFILES

AERODYNAMIC COEFFICIENTS

International Conference on the Aerodynamics at Low Reynolds Numbers between 10(4) and 10(6)
[ONRL-7-023-C] 01 p0002 N88-10010

Investigations of separated flow states on wings of medium aspect ratio taking into account the wind tunnel interference problem
[ETN-87-90437] 01 p0003 N88-10016

An experimental evaluation of advanced rotorcraft airfoils in the NASA Ames eleven-foot transonic wind tunnel
[NASA-CR-166587] 03 p0261 N88-11640

Improvements to the adaptive maneuvering logic program
[NASA-CR-3985] 03 p0262 N88-11648

Semiempirical method for prediction of aerodynamic forces and moments on a steadily spinning light airplane
[NASA-TM-4009] 04 p0393 N88-12456

Aerodynamic sensitivities from subsonic, sonic and supersonic unsteady, nonplanar lifting surface theory
[NASA-TM-100502] 04 p0394 N88-12459

Numerical calculations of the flowfield around propellers 05 p0536 N88-13261

Characteristics of a separating confluent boundary layer and the downstream wake
[NASA-TM-100046] 06 p0704 N88-14323

Computer program for the calculation of the profile-vortices interactions (two dimensional inviscid incompressible flow with point singularities)
[ISL-R-124/86] 08 p0987 N88-15982

Friction drag reduction (a speculative essay)
[INPE-4278-PRE/1150] 08 p0988 N88-15985

Experimental rotordynamic coefficient results for honeycomb seals
[NASA-CR-182440] 08 p0993 N88-16007

Wind tunnel modeling techniques
[KU-SFB-210/E/33] 09 p1121 N88-16711

Investigation of the influence of wind shear on the aerodynamic characteristics of aircraft using a vortex-lattice method 10 p1274 N88-17619

Finite element calculations for aerodynamic coefficients of a 3-dimensional body in subsonic flow using Green's function method
[NASA-TT-20208] 13 p1718 N88-20272

Constructing Gloved wings for aerodynamic studies
[NASA-TM-100440] 14 p1863 N88-21126

Data processing method for high angle of attack testing with rolling angle 14 p1864 N88-21134

New definition of pressure-center coefficient of reentry craft with asymmetrical configuration
14 p1864 N88-21138

New airfoil sections for straight bladed turbine
[DE88-701075] 14 p1942 N88-21586

Submunitions simulations, volume 2
[TR-CR-RD-SS-87-7-VOL-2] 19 p2641 N88-25669

A preliminary investigation of drag reduction and mechanism for a blunt body of revolution with slanted base
[NASA-TT-20349] 24 p3317 N88-29753

Accuracy criteria for evaluating supersonic aerodynamic coefficient predictions 24 p3317 N88-29756

Computational aerodynamic analysis for a range-limited 25mm training round
[AD-A185270] 24 p3320 N88-29772

AERODYNAMIC CONFIGURATIONS
NT WING NACELLE CONFIGURATIONS

Problem and solution formulations for the generation of 3D block-structured grids --- aircraft design
[NLR-MP-86020-U] 01 p0005 N88-10028

The aerothermodynamic environment for holes in hypersonic configurations
[DE87-014651] 02 p0121 N88-10767

Aerodynamic design and performance of a bent-axis geometry vehicle
[DE87-013726] 02 p0124 N88-10786

An aerodynamic performance evaluation of the NASA/Ames Research Center advanced concepts flight simulator
[NASA-TM-89659] 03 p0268 N88-11685

Numerical simulation of the hypersonic flow around lifting vehicles 05 p0532 N88-13234

Lifting bodies: An attractive aerodynamic configuration choice for hypervelocity vehicles
05 p0534 N88-13248

General aerodynamic-aerothermodynamic concepts for Hermes 05 p0535 N88-13251

Numerical analysis of supersonic flows using panel method 05 p0537 N88-13266

Tip aerodynamics from wind tunnel test of semi-span wing
[NASA-TM-88253] 05 p0540 N88-13290

Fundamentals of fighter aircraft design
05 p0544 N88-13316

Nonlinear aerodynamic wing design
[NASA-CR-3950] 06 p0665 N88-14079

Large-Scale Advanced Prop-Fan (LAP) blade design
[NASA-CR-174790] 06 p0668 N88-14097

Design verification and fabrication of active control systems for the DAST ARW-2 high aspect ratio wing, part 1
[NASA-CR-177959-PT-1] 06 p0669 N88-14101

Design verification and fabrication of active control systems for the DAST ARW-2 high aspect ratio wing. Part 2: Appendices
[NASA-CR-177959-PT-2] 06 p0669 N88-14102

Aerodynamic design of first stage turbines for small aero engines 06 p0713 N88-14370

Aerodynamic testing of small turbines
06 p0713 N88-14371

Langley Symposium on Aerodynamics, volume 1
[NASA-CP-2397] 07 p0809 N88-14926

Computational fluid dynamics overview 07 p0809 N88-14927

Finite-volume scheme for transonic potential flow about airfoils and bodies in an arbitrarily shaped channel 07 p0809 N88-14928

Application of a full potential method for analysis of complex aircraft geometries 07 p0809 N88-14930

Three-dimensional unsteady flow elicited by finite wings and complex configurations [AD-A186464] 08 p0951 N88-15770

An overview of key technology thrusts at Bell Helicopter Textron 09 p1111 N88-16657

Burst vortex/boundary layer interaction [NASA-CR-182510] 10 p1268 N88-17583

The intelligent wing. Aerodynamic development direction for future passenger aircraft [MBB-UT-006/87] 10 p1313 N88-17848

Aerodynamic aspects of the configurational systems layout of a dispenser [MBB-UA-1047/87] 10 p1315 N88-17863

A performance index approach to aerodynamic design with the use of analysis codes only [NASA-TP-2805] 11 p1433 N88-18552

Analysis of shear-layer probe data for holes in hypersonic configurations [DE88-003992] 11 p1435 N88-18564

Computer program for conceptual tandem rotor helicopter design [AD-A187832] 11 p1439 N88-18584

Generation of surface grids through elliptic partial differential equations for aircraft and missile configurations [AD-A186631] 11 p1535 N88-19169

A multigrid full potential transonic code for arbitrary configurations --- aircraft 11 p1539 N88-19195

A review of technologies applicable to low-speed flight of high-performance aircraft investigated in the Langley 14- x 22-foot subsonic tunnel [NASA-TP-2796] 13 p1717 N88-20264

New definition of pressure-center coefficient of reentry craft with asymmetrical configuration 14 p1864 N88-21138

An investigation into the effect of canard location on the aerodynamics of the close-coupled canard configuration [BU-361] 14 p1866 N88-21149

Designs of profiles for cascades [NASA-TT-20161] 15 p2067 N88-22326

Experimental investigation of the hypersonic flow over a six finned configuration [AD-A190870] 16 p2157 N88-22871

Qualification of a water tunnel for force measurements on aeronautical models 16 p2200 N88-23128

An experimental study to determine the flow and the subsonic static and dynamic stability characteristics of aircraft operating at high angles-of-attack 16 p2201 N88-23129

It's time to reinvent the general aviation airplane 17 p2294 N88-23726

Full potential methods for analysis/design of complex aerospace configurations [NASA-CR-3982] 17 p2296 N88-23736

Preliminary aerodynamic design considerations for advanced laminar flow aircraft configurations 17 p2297 N88-23746

Flight testing a V/STOL aircraft to identify a full-envelope aerodynamic model [NASA-TM-100996] 17 p2301 N88-23762

Multi-body aircraft with an all-movable center fuselage actively controlling fuselage pressure drag [NASA-CASE-LAR-13511-1] 17 p2301 N88-23765

An analytic model for aerodynamic shapes [AD-A191573] 18 p2456 N88-24583

Wind tunnel investigation of wing and control panel loads at transonic and supersonic speeds on some schematic cruciform missile configurations [FFA-TN-1986-43] 18 p2457 N88-24585

Incompressible Euler solution on a multiblock grid around a car configuration [FFA-TN-1987-65] 18 p2457 N88-24586

Summary of low-speed wind tunnel results of several high-speed counterrotation propeller configurations [NASA-TM-100945] 18 p2458 N88-24597

High speed and high angle of attack aerodynamic characteristics of winged space vehicle [ISSN-0285-6808] 18 p2459 N88-24599

Actuated forebody strakes [NASA-CASE-LAR-13983-1] 18 p2464 N88-24628

Application of advanced grid generation techniques for flow field computations about complex configurations [NASA-CR-183049] 18 p2515 N88-24922

Aerodynamics of lifting bodies with combined transverse and longitudinal curvature 19 p2598 N88-25436

A low speed wind tunnel investigation of Reynolds number effects on a 60-deg swept wing configuration with leading and trailing edge flaps [NASA-CR-181684] 19 p2598 N88-25441

Proceedings of the 5th NAL Symposium on Aircraft Computational Aerodynamics [NAL-SP-8] 19 p2635 N88-25630

Numerical simulations of aerodynamic contribution of flows about a space-plane-type configuration 19 p2635 N88-25632

Aerodynamic simulation for complete ASKA aircraft configuration 19 p2637 N88-25641

Numerical simulation of viscous flows over transonic aircraft configurations 19 p2637 N88-25642

Calculations of unsteady aerodynamics for a full aircraft configuration using boundary element method 19 p2637 N88-25643

Ludwig Prandtl collected treatises on applied mechanics, hydro- and aerodynamics, part 1 [NASA-TT-20316] 20 p2752 N88-26337

Wind tunnel tests of the influence of airfoil-thickness on normal force and pitching moment of two slender wings at transonic and supersonic Mach numbers [DFVLR-FB-88-17] 21 p2893 N88-27171

AGARD standard aeroelastic configurations for dynamic response. 1: Wing 445.6 [AGARD-R-765] 21 p2896 N88-27193

Wind tunnel tests of elliptical missile body configurations at Mach numbers 0.4 to 5.0 [AD-A193525] 22 p3038 N88-28040

Delta wing configurations 23 p3167 N88-28860

Complex configurations 23 p3167 N88-28861

Transport-type configurations 23 p3169 N88-28867

Combat aircraft 23 p3169 N88-28868

Three dimensional grid generation for complex configurations: Recent progress [AGARD-AG-309] 23 p3245 N88-29313

Component adaptive grid generation for aircraft configurations 23 p3246 N88-29316

Experience with three dimensional composite grids 23 p3247 N88-29324

Space shuttle phase B wind tunnel model and test information. Volume 3: Launch configuration [NASA-CR-178416-VOL-3-PT-2] 24 p3315 N88-29744

Space shuttle phase B wind tunnel model and test information. Volume 1: Booster configuration [NASA-CR-178414-VOL-1-PT-1] 24 p3315 N88-29745

Special Course on Missile Aerodynamics [AGARD-R-754] 24 p3317 N88-29755

Prediction of dynamic derivatives 24 p3318 N88-29761

Next generation missile design 24 p3319 N88-29766

AERODYNAMIC DRAG

NT SUPERSONIC DRAG

The contraction of satellite orbits under the influence of air drag. Part 8: Orbital lifetime in an oblate atmosphere, when perigee distance is perturbed by odd zonal harmonics in the geopotential [RAE-TR-86069-PT-8] 01 p0010 N88-10058

Planform effects on the supersonic aerodynamics of multibody configurations [NASA-TP-2762] 04 p0393 N88-12454

Numerical study of supersonic flow around blunt bodies with extended needle nose 04 p0425 N88-12635

Studies of unsteadiness in boundary layers [AD-A185662] 06 p0703 N88-14315

Investigation of the feasibility of an analytical method of accounting for the effects of atmospheric drag on satellite motion 07 p0923 N88-15608

Full scale and wind tunnel surface pressure measurements on the T.R.R.L. spray dispersion programme vehicles [REPT-8623] 09 p1114 N88-16676

Transonic wind tunnel calibration 1986: Force measurements on three ONERA-C5 models and three half sphere cylinder calibration bodies in the F + W transonic test section [F + W-FO-1854] 09 p1122 N88-16714

Verification of a micro-thrusting model to maintain satellites in low orbit [AD-A186874] 09 p1133 N88-16793

Wind tunnel studies of circulation control elliptical airfoils 10 p1270 N88-17598

Preliminary design of the ORION attitude control system [AD-A187179] 10 p1292 N88-17729

Determination of the drag of missiles with variable lateral acceleration possibility [REPT-FM15] 10 p1310 N88-17831

Flight tests of external modifications used to reduce blunt base drag [NASA-TM-100433] 13 p1719 N88-20279

Frozen orbit analysis in the Martian system [AD-A189574] 13 p1856 N88-21106

Comparison of pressure distributions on model and full-scale NACA 64-621 airfoils with ailerons for wind turbine application [NASA-TM-100802] 14 p1943 N88-21593

Computational fluid dynamics drag prediction: Results from the Viscous Transonic Airfoil Workshop [NASA-TM-100095] 15 p2014 N88-22009

Zero-lift drag predictions in supersonic flow for complex configurations 15 p2054 N88-22246

Boundary layer measurements using hot-film sensors 17 p2297 N88-23743

Calibration of averaging total pressure flight wake rake and natural-laminar-flow airfoil drag certification [NASA-CR-181630] 19 p2599 N88-25443

Theoretical and experimental investigations of a vortex drag behind a wing profile with spoiler [ISL-PU-309/87] 21 p2892 N88-27169

A preliminary investigation of drag reduction and mechanism for a blunt body of revolution with slanted base [NASA-TT-20349] 24 p3317 N88-29753

AERODYNAMIC FORCES

NT AERODYNAMIC DRAG
NT AERODYNAMIC INTERFERENCE
NT AERODYNAMIC LOADS
NT BLAST LOADS
NT GUST LOADS
NT INTERFERENCE LIFT
NT JET LIFT
NT LIFT
NT SUPERSONIC DRAG
NT WING LOADING
NT ZERO LIFT

Semiempirical method for prediction of aerodynamic forces and moments on a steadily spinning light airplane [NASA-TM-4009] 04 p0393 N88-12456

Numerica calculation in the Laplace domain for subsonic unsteady aerodynamic forces acting on a finite wing 05 p0535 N88-13256

Computational methods for problems in aerodynamics and large space structure using parallel and vector architectures [AD-A185401] 05 p0541 N88-13294

Calculated unsteady aerodynamics of wings [AD-A189608] 12 p1574 N88-19415

Unsteady aerodynamics of a Wortmann FX-63-137 wing in a fluctuating wind field [AD-A190128] 15 p2013 N88-22006

Influence of unsteady aerodynamic forces on dynamic response of variable sweep aircraft 15 p2054 N88-22245

Measurements of aerodynamic forces on unsteadily moving bluff parachute canopies 16 p2202 N88-23137

Reduced order models for nonlinear aerodynamics 16 p2220 N88-23248

Nonlinear programming extensions to rational function approximation methods for unsteady aerodynamic forces [NASA-TP-2776] 18 p2463 N88-24623

A characteristic method for calculating the generalized flat flutter aerodynamic forces [NASA-TT-20300] 19 p2598 N88-25438

Contamination and distortion of steady flow field induced by discrete frequency disturbances in aircraft gas engines [AD-A195440] 24 p3370 N88-30069

AERODYNAMIC HEAT TRANSFER

Calculation of aerodynamic heat transfer for blunt-nosed thin wings at different angles of attack at supersonic speeds [NASA-TT-20127] 02 p0123 N88-10776

AERODYNAMIC HEATING

NT SHOCK HEATING

Thermal stress analysis of space shuttle orbiter subjected to reentry aerodynamic heating [NASA-TM-88286] 01 p0061 N88-10389

The aerodynamics of supersonic parachutes [DE87-014846] 04 p0395 N88-12464

Parachute materials [DE87-014845] 04 p0411 N88-12550

Atmospheric entry heating of cosmic dust 06 p0794 N88-14865

High-temperature properties of ceramic fibers and insulations for thermal protection of atmospheric entry and hypersonic cruise vehicles [NASA-TM-100059] 10 p1295 N88-17743

Trajectory characteristics and heating of hypervelocity projectiles having large ballistic coefficients [NASA-TP-2614] 12 p1574 N88-19412

Fluid-thermal-structural study of aerodynamically heated leading edges [NASA-TM-100579] 13 p1783 N88-20666

Nuclear-powered space debris sweeper 17 p2418 N88-24380

Aerodynamic heating of missiles
24 p3319 N88-29764
AERODYNAMIC INTERFERENCE
A transonic model representation for two-dimensional wall interference assessment
[NLR-TR-86026-U] 01 p0001 N88-10006
Wall interference tests of a CAST 10-2/DOA 2 airfoil in an adaptive-wall test section
[NASA-TM-4015] 02 p0122 N88-10772
A 0.15-scale study of configuration effects on the aerodynamic interaction between main rotor and fuselage
[NASA-CR-166577] 04 p0395 N88-12462
Computation of nacelle interference using boundary element method 05 p0537 N88-13267
Determination of the drag of missiles with variable lateral acceleration possibility
[REPT-FM15] 10 p1310 N88-17831
An investigation into the effect of canard location on the aerodynamics of the close-coupled canard configuration
[BU-361] 14 p1866 N88-21149
Porous wind tunnel corrections for counterrotation propeller testing
[NASA-TM-100873] 15 p2015 N88-22019
Multi-body aircraft with an all-movable center fuselage actively controlling fuselage pressure drag
[NASA-CASE-LAR-13511-1] 17 p2301 N88-23765
Submunitions simulations, volume 2
[TR-CR-RD-SS-87-7-VOL-2] 19 p2641 N88-25669
The present status and the future of missile aerodynamics
[NASA-TM-100063] 24 p3320 N88-29773
AERODYNAMIC LIFT
U LIFT
AERODYNAMIC LOADS
NT BLAST LOADS
NT GUST LOADS
Stability of mechanical joints in launching vehicles: Local and global stationary values of energy density
03 p0270 N88-11696
Numerical optimization of conical flow waveriders including detailed viscous effects
05 p0533 N88-13245
Aeroelastic analysis of modern transport aircraft
05 p0550 N88-13352
Wing divergence of trimmed aircraft
05 p0550 N88-13354
Measurement of model deformation in wind tunnels
05 p0551 N88-13358
Crack growth prediction in 3D structures under aeronautical-type spectrum loadings
05 p0602 N88-13666
Static force and moment test of the Holloman narrow-gage rocket sled at Mach numbers from 3.5 to 5.5
[AD-A186291] 07 p0822 N88-14995
A review of research in rotor loads
09 p1106 N88-16629
Loads and aeroelasticity division research and technology accomplishments for FY 1987 and plans for FY 1988
[NASA-TM-100534] 09 p1114 N88-16680
X-wing potential for Navy applications
10 p1271 N88-17604
Cornering characteristics of the main-gear tire of the space shuttle orbiter
[NASA-TP-2790] 11 p1436 N88-18583
Some aspects of aircraft dynamic loads due to flow separation
[AGARD-R-750] 11 p1439 N88-18586
Testing of a one-bladed 30-meter-diameter rotor on the DOE/NASA Mod-O wind turbine
[NASA-TM-100274] 11 p1509 N88-19014
Calculated unsteady aerodynamics of wings
[AD-A189608] 12 p1574 N88-19415
Workshop on Design Loads for Advanced Fighters
[AGARD-R-746] 12 p1579 N88-19449
The development of manoeuvre load criteria for agile aircraft 12 p1579 N88-19450
Structural design requirements for aircraft incorporating active control technology 12 p1580 N88-19453
The relationship between operational flight manoeuvre parameters and design parameters
12 p1580 N88-19454
Manoeuvres by default, by demand and by design
12 p1580 N88-19455
Design loads for Swedish military aircraft in a twenty years' perspective 12 p1580 N88-19456
Nonaxisymmetric body supersonic, aerodynamic prediction
[AD-A189338] 13 p1716 N88-20259
Calculation of the distributed loads on the blades of individual multiblade propellers in axial flow using linear and nonlinear lifting surface theories
[NASA-TT-20173] 13 p1719 N88-20278
Determination of canopy loads for a light aircraft by wind tunnel testing and computer modelling
[BU-353] 14 p1869 N88-21167
A numerical model of unsteady, subsonic aeroelastic behavior
[NASA-TM-101126] 16 p2156 N88-22862
The 2-D and 3-D time marching transonic potential flow method for propfans 16 p2220 N88-23245
Certification aspects of airplanes which may operate with significant natural laminar flow 17 p2298 N88-23749
An initial investigation into methods of computing transonic aerodynamic sensitivity coefficients
[NASA-CR-183061] 20 p2752 N88-26332
In-flight load measurements of the Robot-X canards
[AD-A193428] 21 p2895 N88-27187
Unsteady flow past an NACA 0012 airfoil at high angles of attack
[AD-A194650] 23 p3172 N88-28886
Stress intensity factors for cracked metallic structures under rapid thermal loading
[AD-A191219] 23 p3193 N88-29004
Matching P.S.D.: Design loads
24 p3312 N88-29720
A summary of methods for establishing airframe design loads from continuous gust design criteria
24 p3312 N88-29721
Status review of atmosphere turbulence and aircraft response 24 p3312 N88-29726
A summary of atmospheric turbulence measurements with specially-equipped aircraft in the US
24 p3312 N88-29727
Calculation of non-stationary aerodynamic forces in the near sonic range
[NASA-TT-20313] 24 p3322 N88-29782
Empirical flutter prediction method
[AD-A195699] 24 p3327 N88-29810
AERODYNAMIC MOMENTS
U STABILITY DERIVATIVES
AERODYNAMIC NOISE
NT BLADE SLAP NOISE
Rotorcraft flight research with emphasis on rotor systems 09 p1111 N88-16656
Laboratory studies related to in-flight acoustic emission monitoring
[AD-A186714] 09 p1242 N88-17445
Measurement and analysis of the noise radiated by low Mach numbers centrifugal blowers
[AD-A189226] 13 p1833 N88-20966
Structureborne noise measurements on a small twin-engine aircraft
[NASA-CR-4137] 16 p2265 N88-23545
Aerodynamic noise of wind turbines
[PB88-165188] 16 p2265 N88-23546
Analytical modeling of the structureborne noise path on a small twin-engine aircraft
[NASA-CR-4136] 17 p2394 N88-24233
First article noise survey of the A/F32T-9 large turbo fan engine enclosed noise suppressor system, far-field noise, Ellsworth AFB, South Dakota
[AD-A191938] 19 p2602 N88-25457
Research investigation of helicopter main rotor/tail rotor interaction noise
[NASA-CR-4143] 19 p2722 N88-26165
Theory of sound production by vortex-airfoil interaction
[AD-A193386] 21 p3012 N88-27875
The influence of surface rounding on trailing edge noise
[AD-A193387] 21 p3012 N88-27876
Noise generation and boundary layer effects in vortex-airfoil interaction and methods of digital hologram analysis for these flow fields
[AD-A194191] 23 p3171 N88-28883
AERODYNAMIC STABILITY
On the prediction of the aeroelastic behavior of lifting systems due to flow separation
[ESA-TT-1043] 03 p0259 N88-11633
Effects of the installation and operation of jet-exhaust yaw vanes on the longitudinal and lateral-directional characteristics of the F-14 airplane
[NASA-TP-2769] 04 p0393 N88-12455
Predictions of F-111 TACT aircraft buffet response and correlations of fluctuating pressures measured on aluminum and steel models and the aircraft
[NASA-CR-4069] 05 p0529 N88-13218
Analysis and test evaluation of the dynamic response and stability of three advanced turboprop models at low forward speed
[NASA-CR-175026] 06 p0668 N88-14096
Flap-lag-torsion aeroelastic stability of a circulation control rotor in forward flight 10 p1271 N88-17600
An application of eigenspace methods to symmetric flutter suppression
[NASA-CR-181618] 10 p1284 N88-17684
Special flight mechanical features of the bearingless helicopter rotor
[MBB-FM-315/O] 10 p1309 N88-17825
A correlation study of X-29A aircraft and associated analytical development
[NASA-CR-183103] 13 p1722 N88-20296
Unsteady aerodynamics of a Wortmann FX-63-137 wing in a fluctuating wind field
[AD-A190128] 15 p2013 N88-22006
Preliminary airworthiness evaluation of the UH-60A with Advanced Digital Optical Control System (ADOCS)
[AD-A190674] 15 p2018 N88-22030
The application of linear maximum likelihood estimation of aerodynamic derivatives for the Bell-205 and Bell-206
[AD-A191279] 16 p2161 N88-22894
Stability and control methodology for conceptual aircraft design. Volume 1: Methodology manual
[AD-A191314] 16 p2164 N88-22906
Actuated forebody strakes
[NASA-CASE-LAR-13983-1] 18 p2464 N88-24626
Integrated Technology Rotor Methodology Assessment Workshop
[NASA-CP-10007] 21 p2889 N88-27148
A comparison of the various helicopter mathematical models used in the methodology assessment
21 p2889 N88-27149
A comparison of theory and experiment for aeroelastic stability of a hingeless rotor model in hover
21 p2889 N88-27150
A comparison of theory and experiment for coupled rotor-body stability of a hingeless rotor model in hover under simulated vacuum conditions
21 p2889 N88-27151
A comparison of theory and experiment for coupled rotor-body stability of a hingeless rotor model in hover
21 p2889 N88-27152
A comparison of theory and experiment for the aeroelastic stability of a bearingless model rotor in hover
21 p2890 N88-27153
A comparison of theory and experiment for coupled rotor body stability of a bearingless rotor model in hover and forward flight 21 p2890 N88-27154
The importance of steady and dynamic inflow on the stability of rotor-body systems 21 p2890 N88-27156
Effects of static equilibrium and higher-order nonlinearities on rotor blade stability in hover
21 p2890 N88-27157
Aeroelastic modeling of rotor blades with spanwise variable elastic axis offset: Classic issues revisited and new formulations 21 p2890 N88-27158
Comparison of experimental rotor damping data-reduction techniques 21 p2891 N88-27159
Comparison of experimental coupled helicopter rotor/body stability results with a simple analytical model
21 p2891 N88-27160
Aeromechanical stability analysis of COPTER
21 p2891 N88-27161
The present status and the future of missile aerodynamics
[NASA-TM-100063] 24 p3320 N88-29773
AERODYNAMIC STALLING
Measurements and calculations of aerodynamic torques for a vertical-axis wind turbine
[DE88-001763] 04 p0465 N88-12876
Unsteady stall penetration experiments at high Reynolds number
[AD-A186120] 07 p0814 N88-14958
The development of CFD methods for rotor applications 09 p1105 N88-16627
Investigation of dynamic stall using LDV (Laser Doppler Velocimetry): Mean flow studies
[AD-A187629] 10 p1272 N88-17611
Modeling of limit cycle stall flutter oscillations
12 p1583 N88-19472
Effect of spatial inlet temperature and pressure distortion on turbofan engine stability
[NASA-TM-100850] 14 p1868 N88-21162
Performance optimization of a cruise missile using dynamic-stall induced lift augmentation
[AD-A190497] 15 p2017 N88-22027
Development of aeroelastic analysis methods for turborotors and propfans, including mistuning
16 p2219 N88-23244
Application of Navier-Stokes analysis to stall flutter
16 p2220 N88-23249
Stall flutter analysis of propfans
16 p2221 N88-23256
Preliminary aerodynamic design considerations for advanced laminar flow aircraft configurations
17 p2297 N88-23746
E3 10C compressor test analysis of high-speed post-stall data
[NASA-CR-179521] 23 p3179 N88-28929
AERODYNAMIC VEHICLES
U AIRCRAFT

AERODYNAMICS
NT AEROTHERMODYNAMICS
NT ROTOR AERODYNAMICS
NT SUPERSONICS
NT UNSTEADY AERODYNAMICS

Aeronautical engineering: A continuing bibliography with indexes (supplement 218)
[NASA-SP-7037(218)] 01 p0001 N88-10002

The Green's function method for fully unsteady aerodynamics around three-dimensional bodies and its application to flutter analysis
[UTIAS-298] 03 p0260 N88-11639

Modeling XV-15 tilt-rotor aircraft dynamics by frequency and time-domain identification techniques
03 p0263 N88-11657

New aerodynamic design of the fenestron for improved performance 03 p0264 N88-11664

The Proceedings of the Symposium on Mechanics for Space Flight
[ISAS-SP-5] 03 p0317 N88-12006

Aeronautical engineering: A continuing bibliography with indexes (supplement 219)
[NASA-SP-7037(219)] 04 p0396 N88-12470

Proceedings of the 4th NAL Symposium on Aircraft Computational Aerodynamics
[NAL-SP-7] 05 p0535 N88-13253

Unsteady aerodynamics of an oscillating cascade in a compressible flow field
[NASA-TM-100219] 05 p0549 N88-13346

Aeronautical engineering: A continuing bibliography with indexes (supplement 220)
[NASA-SP-7037(220)] 06 p0663 N88-14065

Development of an unsteady wake theory appropriate for aeroelastic analyses of rotors in hover and forward flight
[NASA-CR-182357] 06 p0664 N88-14075

Development of transonic speed cascade design method using Euler code and inverse solution
06 p0676 N88-14139

Aeronautical engineering. A continuing bibliography with indexes, supplement 221
[NASA-SP-7037(221)] 08 p0949 N88-15758

Unsteady three-dimensional flow separation
[NASA-CR-182412] 08 p0949 N88-15761

Realization of the immediate objectives of the Aero-Gas Dynamics and Vibration Laboratory (LAGG) at the National Center for Research, Science and Technology (PUSPIPTEK) at Serpong, Java (Indonesia). Project TTA-79
[GG/OPR-10] 08 p1092 N88-16572

Aeronautical engineering: A continuing bibliography with indexes (supplement 223)
[NASA-SP-7037(223)] 09 p1111 N88-16661

Computational unsteady aerodynamics for aeroelastic analysis
[NASA-TM-100523] 09 p1112 N88-16668

Method of iterative coupling between periodic aerodynamic and dynamic fields
[PB87-169934] 09 p1113 N88-16669

Mach number effects on transonic aeroelastic forces and flutter characteristics
[NASA-TM-100547] 09 p1113 N88-16675

Methods for evaluating the quality and reliability of aerodynamic software programs
[PB87-169793] 09 p1219 N88-17314

Application of empirical and linear methods to VSTOL powered-lift aerodynamics
[NASA-TM-100048] 10 p1267 N88-17581

Fixed wing CCW aerodynamics with and without supplementary thrust deflection
10 p1272 N88-17607

Supersonic aerodynamics of delta wings
[NASA-TP-2771] 10 p1273 N88-17615

A research program on the aerodynamics of a highly loaded turbine stage 10 p1280 N88-17655

Design and aerodynamic performance of a small mixed-flow gas generator turbine
10 p1281 N88-17662

Aerodynamic performance of a scale-model, counter-rotating unducted fan 10 p1282 N88-17666

Numerical methods for propeller aerodynamics and acoustics at DFVLR 10 p1282 N88-17668

Analysis of highspeed propellers aerodynamics
10 p1282 N88-17669

Effect of transition aerodynamics on aeroassist flight experiment trajectories
[NASA-TM-100546] 11 p1446 N88-18620

Aeronautical engineering: A cumulative index to a continuing bibliography
[NASA-SP-7037(222)] 12 p1574 N88-19416

JPRS report: Science and technology. Europe and Latin America
[JPRS-ELS-88-001] 12 p1614 N88-19649

Aeronautical engineering: A continuing bibliography with indexes (supplement 224)
[NASA-SP-7037(224)] 13 p1715 N88-20254

Australian aerodynamic design codes for aerial tow bodies
[AD-A189048] 13 p1715 N88-20258

Activities report of the Lille Institute of Fluid Mechanics
[ETN-88-91983] 13 p1771 N88-20597

Activities report of the Aerodynamics Department
[ETN-88-91979] 14 p1862 N88-21123

Aeronautical engineering: A continuing bibliography with indexes (supplement 225)
[NASA-SP-7037(225)] 14 p1863 N88-21126

Aeronautical engineering: A continuing bibliography with indexes (supplement 226)
[NASA-SP-7037(226)] 16 p2155 N88-22857

Oil flow patterns on a series of capsule-type re-entry vehicles at hypersonic speeds
[DE88-751805] 16 p2155 N88-22858

Aerofoil testing in a self-streamlining flexible walled wind tunnel
[NASA-CR-4128] 16 p2156 N88-22865

Computer tomography and hybrid optical/digital methods for aerodynamic measurements
[AD-A190909] 16 p2157 N88-22872

Aircraft flight dynamics research in past decade reviewed 16 p2186 N88-23031

Aerodynamic and Related Hydrodynamic Studies Using Water Facilities
[AGARD-CP-413] 16 p2200 N88-23125

Application of high speed holography to aerodynamic and hydrodynamic three-dimensional velocimetry
16 p2203 N88-23144

Use of water towing tanks for aerodynamics and hydrodynamics 16 p2204 N88-23149

A new laminar water tunnel to study the transition process in a blasius layer and in a separation bubble and a new tool for industrial aerodynamics and hydrodynamic research 16 p2204 N88-23150

Reduced order models for nonlinear aerodynamics
16 p2220 N88-23248

Model forced response of propfans in yawed flow
16 p2221 N88-23253

Joint University Program for Air Transportation Research, 1986
[NASA-CP-2502] 17 p2293 N88-23715

The effects of inlet turbulence and rotor/stator interactions on the aerodynamics and heat transfer of a large-scale rotating turbine model. Part 4: Aerodynamic data tabulation
[NASA-CR-179469] 17 p2339 N88-23956

Aeronautical engineering: A continuing bibliography with indexes (supplement 227)
[NASA-SP-7037(227)] 18 p2456 N88-24578

Some rotorcraft applications of computational fluid dynamics
[NASA-TM-100066] 18 p2459 N88-24601

A decade of computer simulations for space shuttle aerodynamics
[NASA-TM-100990] 18 p2459 N88-24603

Nonlinear programming extensions to rational function approximation methods for unsteady aerodynamic forces
[NASA-TP-2776] 18 p2463 N88-24623

Nonlinear flying quality parameters based on dynamic inversion
[AD-A192146] 18 p2464 N88-24627

Internal fluid dynamics within a nonspinning partially liquid-filled shell due to burster rupture
[AD-A191055] 18 p2507 N88-24874

NAS: The first year
[NASA-TM-101006] 18 p2560 N88-25196

Aerodynamics of lifting bodies with combined transverse and longitudinal curvature 19 p2598 N88-25436

Aerodynamic focusing of particles and heavy molecules
[DE88-007145] 19 p2598 N88-25440

Aerodynamic analysis of natural laminar flow airfoil
19 p2634 N88-25624

Accurate, productive aerodynamic simulation on patched mesh systems
[AD-A192040] 19 p2714 N88-26110

Ludwig Prandtl collected treatises on applied mechanics, hydro- and aerodynamics, part 2. IV interfaces and resistance
[NASA-TT-20315] 20 p2752 N88-26336

A two-point aerodynamic model for identification
20 p2786 N88-26526

Parametric estimation of aerodynamic nonlinearities in rolling moment due to sideslip using maximum likelihood method 20 p2786 N88-26528

Aeronautical engineering: A continuing bibliography with indexes
[NASA-SP-7037(229)] 21 p2891 N88-27163

Analysis of experimental data for cast 10-2/DOA2 supercritical airfoil at high Reynolds numbers
[AD-A192827] 21 p2892 N88-27166

An experimental study of the effect of pitch rate on delta wing aerodynamics and stability
[NASA-CR-183159] 21 p2893 N88-27173

Design of a mechanism to control wind tunnel turbulence 21 p2926 N88-27370

Aerodynamics of Hypersonic Lifting Vehicles: Fluid Dynamics Panel AGARD Symposium
[AGARD-AR-246] 21 p2943 N88-27480

Aeronautical engineering: A continuing bibliography with indexes
[NASA-SP-7037(228)] 22 p3037 N88-28031

Three-dimensional zonal grids about arbitrary shapes by Poisson's equation
[NASA-TM-101018] 22 p3039 N88-28042

The role of acoustic resonances in unsteady turbomachinery aerodynamics
[PNR90455] 22 p3147 N88-28720

Theoretical aerodynamics, transonic flow
[AD-A196247] 24 p3321 N88-29777

AEROELASTIC RESEARCH WINGS

Analytic investigation of helicopter rotor blade appended aeroelastic devices
[NASA-CR-166525] 03 p0266 N88-11676

Prediction of wing aeroelastic effects on aircraft life and pitching moment characteristics
05 p0551 N88-13356

AEROELASTICITY

The history of aeroelasticity research in Germany from the beginning until 1945 --- airframes
[DFVLR-MITT-86-25] 01 p0001 N88-10003

Analytical modeling of helicopter static and dynamic induced velocity in GRASP
[NASA-TM-100026] 02 p0123 N88-10777

AGARD standard aeroelastic configurations for dynamic response. Candidate configuration I.-wing 445.6
[NASA-TM-100492] 02 p0192 N88-11202

On the prediction of the aeroelastic behavior of lifting systems due to flow separation
[ESA-TT-1043] 03 p0259 N88-11633

Linearized aeroelastic analysis of a wind turbine with a two-bladed rotor
[ETN-87-90600] 03 p0347 N88-12192

The effect of mass, wind angle and erection technique on the aeroelastic behaviour of a cable-stayed bridge model
[NAE-AN-46] 04 p0455 N88-12819

Numerica calculation in the Laplace domain for subsonic unsteady aerodynamic forces acting on a finite wing
05 p0535 N88-13256

Aeroelasticity and optimization in fighter aircraft design
05 p0546 N88-13324

Aeroelastic analysis of modern transport aircraft --- European Airbus
[SNIAS-872-111-102] 05 p0546 N88-13329

Velocity scaled aeroelastic testing of an unducted fan
[GTL-191] 05 p0548 N88-13337

Static Aeroelastic Effects on High Performance Aircraft
[AGARD-CP-403] 05 p0550 N88-13348

Examples of static aeroelastic effects on present combat aircraft projects 05 p0550 N88-13349

Trends in aeroelastic analysis of combat aircraft
05 p0550 N88-13350

Static aeroelastic considerations in the definition of design loads for fighter airplanes
05 p0550 N88-13351

Static aeroelastic effects on the flutter of a supercritical wing 05 p0550 N88-13353

The use of aeroelastic wind tunnel models to prove structural design 05 p0551 N88-13355

Prediction of wing aeroelastic effects on aircraft life and pitching moment characteristics
05 p0551 N88-13356

Influence of the static deformation on a wing in the unsteady aerodynamic 05 p0551 N88-13357

Solution procedure for the Navier-Stokes equations applied to rotors 05 p0579 N88-13533

A numerical model of unsteady, subsonic aeroelastic behavior
[NASA-TM-100487] 06 p0663 N88-14064

Modern wing flutter analysis by computational fluid dynamics methods
[NASA-TM-100531] 07 p0816 N88-14365

Unsteady transonic algorithm improvements for realistic aircraft applications
[NASA-TM-100516] 08 p0949 N88-15760

NASA/Army Rotorcraft Technology. Volume 1: Aerodynamics, and Dynamics and Aeroelasticity
[NASA-CP-2495-VOL-1] 09 p1105 N88-16625

Rotorcraft aeroelastic stability
09 p1106 N88-16631

Rotorcraft flight research with emphasis on rotor systems 09 p1111 N88-16656

Computational unsteady aerodynamics for aeroelastic analysis
[NASA-TM-100523] 09 p1112 N88-16668

Mach number effects on transonic aeroelastic forces and flutter characteristics
[NASA-TM-100547] 09 p1113 N88-16675
Loads and aeroelasticity division research and technology accomplishments for FY 1987 and plans for FY 1988
[NASA-TM-100534] 09 p1114 N88-16680
Experimental study on the effect of fiber orientation on flutter characteristics of high-aspect-ratio transport wing
[NAL-TR-936] 09 p1120 N88-16708
Flap-lag-torsion aeroelastic stability of a circulation control rotor in forward flight 10 p1271 N88-17600
Prediction of aeroelastic response of a model X-wing rotor 10 p1271 N88-17603
Using frequency-domain methods to identify XV-15 aeroelastic modes
[NASA-TM-100033] 10 p1277 N88-17646
The application of modern aeroelastic developments for future projects
[MBB-UT-007/87] 10 p1313 N88-17850
Vibration and flutter characteristics of the SR7L large-scale propfan
[NASA-TM-100272] 10 p1344 N88-18036
A discretization of the integral equation for the time dependent linearized subsonic potential flow over a wing
[AD-A188534] 12 p1574 N88-19411
Unsteady transonic small-disturbance theory including entropy and vorticity effects
[NASA-TM-100568] 12 p1575 N88-19418
Structural design requirements for aircraft incorporating active control technology 12 p1580 N88-19453
Design of an aeroelastic composite wing wind tunnel model
[AD-A188855] 12 p1582 N88-19466
An experimental investigation of the flap-lag-torsion aeroelastic stability of a small-scale hingeless helicopter rotor in hover
[NASA-TP-2546] 13 p1715 N88-20257
Application of a nonisentropic full potential method to AGARD standard airfoils
[NASA-TM-100560] 13 p1716 N88-20263
Aeroelastic models in aircraft design
[MBB/LKE-294/S/PUB/249] 13 p1722 N88-20298
Activities report of the Structures Department
[ETN-88-91986] 13 p1783 N88-20672
Scale model development for aeroelasticity studies
[ETN-88-91887] 14 p1868 N88-21164
Shape sensitivity analysis of wing static aeroelastic characteristics
[NASA-TP-2808] 15 p2018 N88-22031
A numerical model of unsteady, subsonic aeroelastic behavior
[NASA-TM-101126] 16 p2156 N88-22862
Lewis Structures Technology, 1988. Volume 1: Structural Dynamics
[NASA-CP-3003-VOL-1] 16 p2217 N88-23226
Development of aeroelastic analysis methods for turborotors and propfans, including mistuning
16 p2219 N88-23244
The 2-D and 3-D time marching transonic potential flow method for propfans 16 p2220 N88-23245
Aeroelastic forced response analysis of turbomachinery 16 p2220 N88-23247
Vibration and flutter analysis of the SR-7L large-scale propfan 16 p2221 N88-23254
Unsteady pressure and structural response measurements of an elastic supercritical wing
[NASA-TM-100591] 17 p2299 N88-23756
Control law parameterization for an aeroelastic wind-tunnel model equipped with an active roll control system and comparison with experiment
[NASA-TM-100593] 17 p2308 N88-23807
Aircraft aeroelasticity and structural dynamics research at the NASA Langley Research Center: Some illustrative results
[NASA-TM-100627] 18 p2459 N88-24598
Integrated Technology Rotor Methodology Assessment Workshop
[NASA-CP-10007] 21 p2889 N88-27148
A comparison of theory and experiment for aeroelastic stability of a hingeless rotor model in hover
21 p2889 N88-27150
A comparison of theory and experiment for coupled rotor-body stability of a hingeless rotor model in hover
21 p2889 N88-27152
A comparison of theory and experiment for the aeroelastic stability of a bearingless model rotor in hover
21 p2890 N88-27153
Effects of static equilibrium and higher-order nonlinearities on rotor blade stability in hover
21 p2890 N88-27157
Aeroelastic modeling of rotor blades with spanwise variable elastic axis offset: Classic issues revisited and new formulations 21 p2890 N88-27158
Comparison of experimental rotor damping data-reduction techniques 21 p2891 N88-27159
Comparison of experimental coupled helicopter rotor/body stability results with a simple analytical model
21 p2891 N88-27160
Aeromechanical stability analysis of COPTER
21 p2891 N88-27161
Aeroelastic characteristics of the AH-64 bearingless tail rotor 21 p2891 N88-27162
AGARD standard aeroelastic configurations for dynamic response. 1: Wing 445.6
[AGARD-R-765] 21 p2896 N88-27193
Prediction of the aeroelastic behavior of tuned blades. Application to aircraft engines
[ISAL-87-0046] 21 p2897 N88-27199
Nonlinear stochastic interaction in aeroelastic structures
[AD-A193427] 21 p2961 N88-27589
Experimental investigation of propfan aeroelastic response in off-axis flow with mistuning
[NASA-TM-101320] 22 p3089 N88-28344
SR-7A aeroelastic model design report
[NASA-CR-174791] 23 p3179 N88-28928
Application of unsteady aerodynamic methods for transonic aeroelastic analysis
[NASA-TM-100665] 24 p3317 N88-29754
History of aeroelasticity in Germany from the beginning to 1945
[ESA-TT-1082] 24 p3319 N88-29767
Recent advances in transonic computational aeroelasticity
[NASA-TM-100663] 24 p3321 N88-29778
Aeroelastic response of metallic and composite propfan models in yawed flow
[NASA-TM-100964] 24 p3326 N88-29807

AEROEMBOLISM
Space cabin atmosphere and extracurricular sortie --- embolisms 19 p2696 N88-26023

AEROLOGY
Statistical structure of temperature field over South Pacific Ocean 06 p0726 N88-14465
Acoustic propagation in the lower atmosphere
[ISL-R-126/87] 21 p3013 N88-27878

AEROMAGNETO FLUTTER
U FLUTTER

AERONAUTICAL ENGINEERING
Aeronautical engineering: A continuing bibliography with indexes (supplement 218)
[NASA-SP-7037(218)] 01 p0001 N88-10002
Color display programming for aviation
[DFVLR-MITT-87-03] 01 p0006 N88-10031
USSR Report: Engineering and Equipment
[JPRS-UEQ-87-007] 02 p0157 N88-10985
On the occasion of the 50th anniversary of the death of Professor Hugo Junkers
[MBB/LW-3016/S/PUB/201] 02 p0257 N88-11627
Status of titanium alloys R and D described
03 p0298 N88-11876
JPRS Report: Science and Technology. China
[JPRS-CST-87-033] 03 p0326 N88-12062
Aeronautical engineering: A continuing bibliography with indexes (supplement 219)
[NASA-SP-7037(219)] 04 p0396 N88-12470
JPRS report: Science and technology. Japan
[JPRS-JST-87-025] 04 p0403 N88-12502
USSR report: Engineering and equipment
[JPRS-UEQ-87-008] 04 p0423 N88-12621
Fundamentals of fighter aircraft design
05 p0544 N88-13316
Astronautics and aeronautics, 1978: A chronology
[NASA-SP-4023] 05 p0662 N88-14062
Aeronautical engineering: A continuing bibliography with indexes (supplement 220)
[NASA-SP-7037(220)] 06 p0663 N88-14065
Low frequency VLBI in space using GAS-Can satellites: Report on the May 1987 JPL Workshop
[NASA-CR-182362] 06 p0801 N88-14904
Aeronautical engineering. A continuing bibliography with indexes, supplement 221
[NASA-SP-7037(221)] 08 p0949 N88-15758
Aeronautical engineering: A continuing bibliography with indexes (supplement 223)
[NASA-SP-7037(223)] 09 p1111 N88-16661
Impact and promise of NASA aeropropulsion technology 09 p1118 N88-16698
Aeronautical engineering. A cumulative index to a continuing bibliography
[NASA-SP-7037(222)] 12 p1574 N88-19416
Research and technology, 1987
[NASA-TM-100323] 12 p1713 N88-20253
Aeronautical engineering: A continuing bibliography with indexes (supplement 224)
[NASA-SP-7037(224)] 13 p1715 N88-20254
Aeronautics and space report of the President: 1986 activities 13 p1852 N88-21087
Aeronautical engineering: A continuing bibliography with indexes (supplement 225)
[NASA-SP-7037(225)] 14 p1863 N88-21126
External tank gamma ray imaging telescope study. Final review, phase 2
[NASA-CR-179320] 15 p2150 N88-22834
Research and technology
[NASA-TM-100172] 15 p2153 N88-22851
Aeronautical engineering: A continuing bibliography with indexes (supplement 226)
[NASA-SP-7037(226)] 16 p2155 N88-22857
The use of the NRC/NAE water facilities in Canadian aeronautical research and development
16 p2201 N88-23132
The ONERA water tunnels test possibilities for flow visualization in aeronautical and Naval domains
16 p2202 N88-23139
Aeronautical engineering: A continuing bibliography with indexes (supplement 227)
[NASA-SP-7037(227)] 18 p2456 N88-24578
NASA history data book. Volume 1: NASA resources 1958-1968
[NASA-SP-4012-VOL-1] 18 p2596 N88-25428
The role of computational fluid dynamics in aeronautical engineering (5). Improvements and applications of implicit TVD finite volume code 19 p2638 N88-25653
Flight research and testing
[NASA-TM-100439] 20 p2758 N88-26361
Aeronautical engineering: A continuing bibliography with indexes
[NASA-SP-7037(229)] 21 p2891 N88-27163
Aeronautical engineering: A continuing bibliography with indexes
[NASA-SP-7037(228)] 22 p3037 N88-28031
Development and design of windtunnel and test facility for RPV (Remote Piloted Vehicle) enhancement devices
[AD-A194842] 24 p3329 N88-29822

AERONAUTICS
Langley aerospace test highlights, 1987
[NASA-TM-100595] 15 p2153 N88-22853
NASA historical data book. Volume 2: Programs and projects 1958-1968
[NASA-SP-4012-VOL-2] 18 p2596 N88-25429
NASA historical data book. Volume 3: Programs and projects 1969-1978
[NASA-SP-4012-VOL-3] 18 p2596 N88-25430
Activities report of the Department of Aerospace Engineering
[ETN-88-91607] 24 p3460 N88-30582

AERONOMY
Computer simulation procedure for designing airborne aerometric monitoring programs
[DE88-011896] 21 p2975 N88-27674
Aeronomic problems of the molecular oxygen photodissociation. Part 3: Solar spectral irradiances in the region of the O2 Herzberg continuum, Schumann-Runge bands and continuum
[AERONOMICA-ACTA-A-332-1988]
24 p3343 N88-29897
Aeronomic problems of molecular oxygen photodissociation. Part 2: Theoretical absorption cross sections of the Schumann-Runge bands at 79 K
[AERONOMICA-ACTA-A-331-1988]
24 p3344 N88-29907
Aeronomic problems of molecular oxygen photodissociation. Part 4: The various parameters for the Herzberg continuum
[AERONOMICA-ACTA-A-333-1988]
24 p3352 N88-29955

AEROPHYSICS
U ATMOSPHERIC PHYSICS

AEROSOLS
NT FOG
Aerosol sensor: Real time determination of aerosol mass size distributors using filtering quartz oscillators
[ETN-87-90397] 01 p0049 N88-10311
Comparison of three aerosol sampling techniques and the differences in the nitrate determined by each
[DE87-011456] 03 p0348 N88-12200
Plume mechanics and aerosol growth processes
[AD-A184467] 04 p0442 N88-12742
Thermophoresis of spherical aerosol particle at arbitrary Knudsen numbers 04 p0461 N88-12850
Theory of heat and moisture exchange between finely disperse storm-generated spray and turbulent air flow
04 p0461 N88-12851
Multiwave laser soundings of atmospheric aerosol: Experimental research (review)
04 p0461 N88-12852
Structure of stably stratified atmospheric surface layer in presence of heat-releasing admixture
04 p0462 N88-12856
Altered and enhanced iodargyrite with bismuth triiodide for use in precipitation enhancement operations
[AD-A185229] 05 p0561 N88-13419
Comparison of ground based and TOMS measurements of SO2 from volcanic emissions
05 p0618 N88-13795

Short-term in vitro screening studies related to the inhalation toxicology of potentially toxic aerosols
[AD-A184815] 05 p0629 N88-13845
Airborne particulate matter in spacecraft
[NASA-CP-2499] 06 p0753 N88-14623
Nonuniformity of electromagnetic field at Lambda = 10 6 micron wavelength inside atmospheric aerosol particles
06 p0772 N88-14743
Aerosol optical depth and ratios of diffuse-sky to total solar irradiance measured from aircraft following the eruption of El Chichon
[PB88-100789] 07 p0878 N88-15326
Atmospheric heating from optical absorption by aerosols
[DE88-002654] 07 p0878 N88-15327
Atmospheric science 07 p0883 N88-15357
Mechanisms of cloud layer formation in Venusian atmosphere 08 p1004 N88-16087
Mesoscale aerosol clouds 08 p1013 N88-16140
Characteristics and climatic relevance of the atmospheric aerosol components
08 p1017 N88-16164
An aureolar radiometer for the determination of aerosol size distribution 08 p1018 N88-16174
Aerosol size distribution from measurements of the radiance in the solar aureole 08 p1019 N88-16176
Remote measurement of aerosol stream velocity with continuous-wave CO2-laser 08 p1079 N88-16506
Aerosols in Martian Atmosphere and Natural Dust Observation (AMANDO). Proposal for the Mars orbiter balloon and rover to study the Martian atmosphere, its thermal content, and its interaction with the soil
[IFSI-87-9] 08 p1100 N88-16619
Comparison of UNL laser imaging and sizing system and a phase/Doppler system for analyzing sprays from a NASA nozzle
[NASA-CR-182437] 09 p1161 N88-16956
Design and characteristics of a liquid aerosol generator
[AD-A186942] 09 p1174 N88-17034
Radon Research Program, FY-1987
[DE88-002633] 09 p1186 N88-17120
Induced turbulence in aerosol-loaded atmospheres, Jun. 1987
[DE87-014724] 09 p1192 N88-17141
Statistics of breakdown centers appearing during propagation of laser radiation through turbulent atmosphere 09 p1236 N88-17411
Christiansen effect in infrared spectra of soil-derived atmospheric dusts
[AD-A187071] 09 p1248 N88-17479
Meteorological and aerosol measurements from the NOAA WP-3D aircraft during WATOX-86, January 4-9, 1986
[PB88-120860] 10 p1352 N88-18079
Measurement of combustion aerosol size distributions with multistage inertial impactors
[DE88-751101] 11 p1454 N88-18669
Optical characterization of tropospheric aerosols
[AD-A187839] 11 p1511 N88-19029
Photoacoustic measurements of atmospheric aerosol absorption coefficients at ultraviolet, visible and infrared wavelengths 11 p1512 N88-19036
Air quality and human performance, chapter 16
[AD-A188335] 12 p1666 N88-19988
Fibrous glass aerosols: A literature review
[AD-A188420] 12 p1672 N88-20008
Vertical structure of Venusian cloud layer at landing sites of Vega-1 and Vega-2 vehicles
13 p1725 N88-20317
Roentgenoradiometric analysis of aerosol in Venusian clouds by Vega-1 and Vega-2 automatic interplanetary stations 13 p1726 N88-20319
Determining chemical composition of aerosol in Venusian cloud layer on Vega-1 automatic interplanetary station using Malakhit mass spectrum analyzer
13 p1726 N88-20321
Observations on electrostatic effects in a filter test system
[AD-A186797] 13 p1736 N88-20378
Application of laser-induced fluorescence in an atmospheric-pressure boron-seeded flame
[AD-A189631] 14 p1889 N88-21267
Combined aerodynamic size, charge-to-mass, and velocity measurements of aerosol particles
[ST-REPT-VOL-5-NO-4] 14 p1944 N88-21599
Corrections for differential scattering by aerosols in the measurement of ozone by DIAL --- differential absorption lidar (DIAL)
[NPL-QU-78] 14 p1945 N88-21603
Optical properties of Southern Hemisphere aerosols: Report of the joint CSIRO/NASA study
[NASA-CR-179287] 14 p1945 N88-21605
Analysis of meteorological conditions and haze distribution for the Second Arctic Gas and Aerosol Sampling Program (AGASP 2), March-April 1986
[PB88-164140] 14 p1948 N88-21616
Aerosol lidar for environment protection and meteorology
[DFVLR-FB-87-43] 14 p1982 N88-21828
Study of mean free path effects on growth of ultrafine metallic aerosols
[AD-A190206] 15 p2039 N88-22149
The optical properties of aerosols
[AD-A191420] 16 p2176 N88-22972
Understanding CO2 and climate
[PB88-167655] 16 p2234 N88-23341
SAGE 1 and SAM 2 measurements of 1 micron aerosol extinction in the free troposphere
[NASA-CR-182945] 17 p2374 N88-24121
High-energy laser-assisted imaging through vaporizing aerosols
[DE88-007911] 18 p2521 N88-24957
Information analysis of integral equations in remote sensing of atmospheric aerosols
18 p2532 N88-25022
SAM 2 data user's guide
[NASA-RP-1200] 18 p2543 N88-25094
Aerodynamic focusing of particles and heavy molecules
[DE88-007145] 19 p2598 N88-25440
Laser-RDX aerosol pyrolysis with matrix isolation of unstable intermediates 19 p2632 N88-25614
Composite, meso-gamma scale diagnostic modeling
[DE88-008169] 19 p2689 N88-25983
Studies of the mechanisms and rates with which nitrogen species are incorporated into cloud water and precipitation
[PB88-193065] 20 p2826 N88-26764
Cloud simulation warm cloud experiments: Droplet growth and aerosol scavenging
[AD-A192944] 21 p2974 N88-27666
Interpretation of the polarimetric observations of Jupiter
[DE88-702414] 21 p3031 N88-27991
South Pole lidar: Brief description of the instrument
[NOTA-INTERNA-907] 22 p3083 N88-28308
IR (infrared) sky radiance distributions in the marine boundary layer
[AD-A193683] 22 p3119 N88-28531
Stratocumulus and cloud-free reflectance from multi-spectral satellite measurements
[AD-A193899] 22 p3128 N88-28599
Real-time measurements of the size fractionation of ambient black carbon aerosols at elevated humidities
[DE88-010870] 23 p3215 N88-29138
High energy and high intensity laser effects on aerosols: Changes in droplet morphology, surrounding temperature and vapor concentration
[AD-A193825] 23 p3220 N88-29164
Forty-eight-inch lidar aerosol measurements taken at the Langley Research Center, May 1974 to December 1987
[NASA-RP-1209] 23 p3232 N88-29234
European validation of SAGE-2 aerosol profiles
[AERONOMICA-ACTA-A-327-1988]
23 p3234 N88-29243
Microphysical processes in cloud layers of Venus
24 p3448 N88-30522
Possibilities of determining vertical profiles of microphysical characteristics of stratospheric aerosol using space measurements of transparency and solar halo 24 p3449 N88-30526
Volatiles on Mars
[NASA-CR-183113] 24 p3456 N88-30571

AEROSPACE ENGINEERING
NT AERONAUTICAL ENGINEERING
Numerical simulation system
04 p0404 N88-12511
Astronautics and aeronautics, 1978: A chronology
[NASA-SP-4023] 05 p0662 N88-14062
NAL news updated: FY87 business plan, developments 06 p0675 N88-14135
Research and technology objectives and plans. Summary, Fiscal Year 1986
[NASA-TM-87504] 06 p0800 N88-14894
Activities report in aircraft design and astronautics
[ETN-88-90618] 07 p0809 N88-14925
Investigation of design concepts for large space structures to support military applications
[AD-A186098] 07 p0824 N88-15000
Internal fluid mechanics research on supercomputers for aerospace propulsion systems
[NASA-TM-100289] 07 p0854 N88-15188
FY87 scientific and technical reports, articles, papers, and presentations
[NASA-TM-100316] 08 p1093 N88-16578
Environment assisted degradation mechanisms in aluminum-lithium alloys
[NASA-CR-182482] 10 p1301 N88-17782
Messerschmitt-Boelkow-Blohm: A company with a tradition 10 p1316 N88-17866
JPRS report: Science and technology. Europe and Latin America
[JPRS-ELS-88-003] 11 p1468 N88-18754
JPRS report: Science and technology. China
[JPRS-CST-87-029] 11 p1468 N88-18755
JPRS report: Science and technology: Europe and Latin America
[JPRS-ELS-87-054] 12 p1573 N88-19406
JPRS report: Science and technology: Europe and Latin America
[JPRS-ELS-87-055] 12 p1686 N88-20086
JPRS report: Science and technology. USSR: Space
[JPRS-USP-88-002] 13 p1724 N88-20312
JPRS report: Science and technology. China
[JPRS-CST-88-003] 13 p1755 N88-20495
JPRS report: Science and technology. China
[JPRS-CST-87-030] 13 p1756 N88-20501
Aeronautics and space report of the President: 1986 activities 13 p1852 N88-21087
Wave propagation and dynamics of lattice structures
[AD-A190611] 15 p2025 N88-22069
JPRS report: Science and technology. Japan
[JPRS-JST-88-001] 15 p2051 N88-22218
JPRS report: Science and technology. Japan
[JPRS-JST-87-029] 15 p2052 N88-22228
Life and reliability of rotating disks
15 p2085 N88-22426
JPRS report: Science and technology. Japan
[JPRS-JST-87-030] 16 p2185 N88-23026
JPRS report: Science and technology. China
[JPRS-CST-88-009] 16 p2186 N88-23030
A low dimensional dynamical system for the wall layer
16 p2194 N88-23088
Technology development program for twenty-first century aerospace vehicles 17 p2302 N88-23768
Soviet spacecraft engineering research
[FASAC-TAR-3090] 17 p2311 N88-23823
Effects of spatial resolution in CARS measurements
[PB88-121900] 18 p2482 N88-24727
Marine techniques: R and D axes, identification of areas of common interest with space techniques
19 p2609 N88-26047
Aerospace applications studies, 1971-1987
[AGARD-R-759] 21 p2889 N88-27147
Damping characteristics of metal matrix composites
[AD-A193144] 21 p2904 N88-27233
The 1988 Goddard Conference on Space Applications of Artificial Intelligence
[NASA-CP-3009] 24 p3415 N88-30330
Activities report of the Department of Aerospace Engineering
[ETN-88-91607] 24 p3460 N88-30582

AEROSPACE ENVIRONMENTS
NT EARTH ORBITAL ENVIRONMENTS
NT INTERPLANETARY SPACE
NT INTERSTELLAR SPACE
TIROS-N/NOAA A-J space environment monitor subsystem
[PB87-203996] 01 p0015 N88-10083
The combined release and radiation effects satellite, a joint NASA/DOD program 02 p0135 N88-10851
High temperature metal matrix composites for future aerospace systems
[NASA-TM-100212] 02 p0149 N88-10938
Effects of long term storage on aerospace nickel cadmium cell performance 02 p0165 N88-11035
Space Environment Technology --- conference
[ISBN-2-85428-170-5] 03 p0271 N88-11702
Irradiations. Accumulated doses. Heavy ions --- space environment 03 p0272 N88-11708
Low Earth orbit environmental effects on the space station photovoltaic power generation systems
[NASA-TM-100230] 03 p0387 N88-12429
Mechanistic studies of polymeric samples exposed aboard STS 8
[NASA-CR-182364] 06 p0686 N88-14202
Comparative anatomic analysis of seedling organs of pisum sativum (fabaceae) cultivated under space flight conditions 06 p0749 N88-14503
Airborne particulate matter in spacecraft
[NASA-CP-2499] 06 p0753 N88-14623
Space environmental effects on polymeric materials
[NASA-CR-182418] 07 p0838 N88-15082
Exobiology and life science 07 p0883 N88-15358
Resolution of holograms produced by the fluid experiment system and the holography ground system
07 p0923 N88-15609
Space environmental effects on polymeric materials
[NASA-CR-182454] 09 p1148 N88-16879
Space station integrated wall damage and penetration damage control. Task 5: Space debris measurement, mapping and characterization system
[NASA-CR-179281] 10 p1285 N88-17688

USSR Space Life Sciences Digest, issue 15
[NASA-CR-3922(18)] 10 p1368 N88-18175
Radiation and temperature effects on the time-dependent response of T300/934 graphite/epoxy
[NASA-CR-182603] 11 p1451 N88-18646
Oxidation and protection of fiberglass-epoxy composite masts for photovoltaic arrays in the low Earth orbital environment
[NASA-TM-100839] 11 p1465 N88-18734
Microgravity and Materials Processing Facility study (MMPF): Requirements and Analyses of Commercial Operations (RACO) preliminary data release
[NASA-CR-179309] 11 p1466 N88-18742
Study of industry requirements that can be fulfilled by combustion experimentation aboard space station
[NASA-CR-180654] 11 p1566 N88-19377
Space utilization plans 15 p2051 N88-22219
Microgravity robotics technology program
[NASA-TM-100898] 16 p2215 N88-23219
EnviroNET: An interactive space-environment information resource
[NASA-TM-101137] 17 p2309 N88-23812
Space spider crane
[NASA-CASE-LAR-13411-1-SB]
17 p2312 N88-23826
Turbomachinery in space 17 p2408 N88-24321
Electromagnetic damping and vibration isolation of space structures
[AD-A191492] 18 p2471 N88-24665
Technologies applicable to space tethers
[NASA-CR-183055] 19 p2606 N88-25471
Application of AI to space systems
19 p2634 N88-25626
Evaluation of the ion trap mass spectrometer for potential application in the space station
[DE88-008940] 19 p2674 N88-25902
Microgravity science and applications bibliography, 1987 revision
[NASA-TM-4067] 22 p3062 N88-28171
Optimization of low gravity materials processing experiments using expert systems
23 p3252 N88-29361

AEROSPACE INDUSTRY
NT AIRCRAFT INDUSTRY
Aerospace research at the National Aerospace Laboratory (NLR)
[ETN-87-90821] 01 p0107 N88-10697
Implementation of finite element quality assurance in a commercial industrial organisation
[PNR90393] 02 p0183 N88-11137
Fundamentals of fighter aircraft design
05 p0544 N88-13316
Requirements and recommendations for the development of theoretical codes and experimental facilities in the near future 05 p0546 N88-13327
Measurements in an electromagnetic test laboratory
[SNIAS-872-430-102] 05 p0575 N88-13507
Operational groups at the Aerospatiale Aircraft Division
[SNIAS-872-111-107] 05 p0658 N88-14036
Activities report in aircraft design and astronautics
[ETN-88-90618] 07 p0809 N88-14925
Wind shear detection. Forward-looking sensor technology
[NASA-CP-10004] 07 p0817 N88-14970
The appropriate use of contract types in development contracts (a systems approach with emphasis on the European space sector)
[ESA-STR-222] 08 p1092 N88-16573
The ESA centralized management system for satellite electronic test and checkout instrumentation
09 p1124 N88-16731
European industrial consortia, for space projects: Their origins, development and possible evolution
09 p1128 N88-16765
Research, development, and growth strategy
10 p1309 N88-17820
Cooperation know-how in high-tech products
[MBB-Z-101/86] 10 p1311 N88-17833
The prospects of space utilization
[MBB-UR-931/86] 10 p1314 N88-17856
Messerschmitt-Boelkow-Blohm: A company with a tradition 10 p1316 N88-17866
Messerschmitt-Boelkow-Blohm: Biography and history of a company 10 p1316 N88-17867
Messerschmitt-Boelkow-Blohm, the company today. Data, numbers and facts 10 p1316 N88-17868
JPRS report: Science and Technology. Europe and Latin America
[JPRS-ELS-88-002] 10 p1316 N88-17870
A comparison of projection methods in the forecasting of overhead costs for seven government aerospace contractors
[AD-A1[illegible]7572] 10 p1425 N88-18514
The judgement and evaluation of long-term investments demonstrated by means of a civil aircraft program
12 p1701 N88-20180
Time and cost reduction through computer integrated manufacture 12 p1703 N88-20191
Acceleration of prototype development and reduction of cost by multidisciplinary integration
12 p1704 N88-20199
Quality and productivity drive innovation and improvement at United Technologies Aerospace Operations, Inc.
[NASA-CR-182944] 18 p2525 N88-24983
Air Force technical objective document, FY89
[AD-A193110] 21 p2896 N88-27194
Managing and controling change
[PNR90419] 22 p3159 N88-28801
Aircraft airframe cost estimating relationships: Study approach and conclusions
[R-3255-AF] 24 p3324 N88-29795
Study on industrial organization for European Ground Support Equipment (EGSE) to support European space programs. Volume 1: Technical reports
[SD-RP-AI-009-VOL-1] 24 p3435 N88-30446
Study on industrial organization for European Ground Support Equipment (EGSE) to support European space programs. Volume 2: Technical reports
[SD-RP-AI-009-VOL-2] 24 p3435 N88-30448

AEROSPACE MEDICINE
NT AVIATION PSYCHOLOGY
NT SPACE PSYCHOLOGY
Aerospace medicine and biology: A continuing bibliography with indexes
[NASA-SP-7011(303)] 02 p0217 N88-11367
Summary report of the history and events pertinent to the Civil Aeromedical Institute's evaluation of providing smoke/fume protective breathing equipment for airline passenger use
[AD-A184499] 03 p0261 N88-11645
Motion and space sickness 04 p0404 N88-12510
JPRS report: Science and technology. USSR: Life sciences
[JPRS-ULS-87-009] 04 p0473 N88-12915
Study of certain biological characteristics of bacteria during the French-Soviet CYTOS-2 space experiment
04 p0473 N88-12917
Aerospace medicine and biology: A continuing bibliography with indexes
[NASA-SP-7011(304)] 04 p0474 N88-12922
Human respiratory responses during high performance flight
[AGARD-AG-312] 04 p0474 N88-12923
JPRS report: Science and technology. USSR: Life sciences
[JPRS-ULS-87-011] 06 p0749 N88-14601
Electron cytochemical detection of Ca(2)+-ATPase in protonema of moss funaria hygrometrica (Hedw.) under hypogravitation 06 p0749 N88-14602
Comparative anatomic analysis of seedling organs of pisum sativum (fabaceae) cultivated under space flight conditions 06 p0749 N88-14603
Aerospace medicine and biology: A continuing bibliography with indexes (supplement 305)
[NASA-SP-7011(305)] 06 p0752 N88-14616
JPRS report: Science and technology. USSR: Space Biology and Aerospace Medicine, volume 21, no. 3, May - June 1987
[JPRS-USB-88-001] 07 p0889 N88-15389
JPRS report: Science and technology. USSR: Space Biology and Aerospace Medicine, volume 21, no. 4, July - August 1987
[JPRS-USB-88-002] 07 p0893 N88-15412
Use of bifidumbacterin for correction of intestinal dysbacteriosis 07 p0895 N88-15427
Bibliography of space biology and medicine
07 p0897 N88-15435
JPRS report: Science and technology. USSR: Space
[JPRS-USP-87-006] 08 p1001 N88-16063
Space biology and medicine 08 p1006 N88-16096
USSR Space Life Sciences Digest, issue 14
[NASA-CR-3922(16)] 08 p1045 N88-16317
USSR report: Life sciences. Biomedical and behavioral sciences
[JPRS-UBB-86-022] 08 p1046 N88-16318
Preliminary evaluation of a micro-based repeated measures testing system
[NASA-CR-172036] 08 p1048 N88-16331
Aerospace medicine and biology: A continuing bibliography with indexes (supplement 307)
[NASA-SP-7011(307)] 08 p1049 N88-16332
Sudden in-flight incapacitation in general aviation
[AD-A187044] 09 p1115 N88-16682
JPRS Report: Science and Technology. USSR: Space Biology and Aerospace Medicine, volume 21, no. 5, September - October 1987
[JPRS-USB-88-003] 10 p1359 N88-18122
Medical and psychological problems of assuring flight safety under present conditions
10 p1359 N88-18123
Isotope methods of determining distribution and movement of blood in the body
10 p1362 N88-18138
Discrete adaptation to sensory conflict
10 p1363 N88-18146
JPRS Report: Science and Technology. USSR: Space Biology and Aerospace Medicine, volume 21, no. 6, November - December 1987
[JPRS-USB-88-004] 10 p1364 N88-18150
Present stage of space medicine
10 p1364 N88-18151
Improvement of human tolerance to head-pelvis (+Gz) accelerations by increasing hydration
10 p1364 N88-18153
Aerospace medicine and biology: A cumulative index to a continuing bibliography (supplement 306)
[NASA-SP-7011(306)] 10 p1369 N88-18180
Aerospace medicine and biology: A continuing bibliography with indexes (supplement 308)
[NASA-SP-7011(308)] 10 p1369 N88-18183
JPRS report: Science and technology. USSR: Life sciences
[JPRS-ULS-88-001] 11 p1520 N88-19079
Summary of Payload Integration Plan (PIP) for Starlab-1 flight experiment, enclosure 3
[NASA-TM-89713] 11 p1522 N88-19086
Full scale architectural simulation techniques for space stations 12 p1651 N88-19867
Life science techonology --- space applications
12 p1653 N88-19900
Liquid ventilation: New data and possible use in space medicine 12 p1654 N88-19908
Medilab: A project of a medical laboratory in space
12 p1660 N88-19946
Gastric emptying assessment by echography after a stress (rotating chair) 12 p1661 N88-19955
USSR report: Life sciences. Biomedical and behavioral sciences
[JPRS-UBB-87-008] 12 p1662 N88-19966
Selected aspects of triazolam in relation to aviator performance in naval flight operations
[AD-A189322] 12 p1667 N88-19996
Aerospace medicine and biology: A continuing bibliography with indexes (supplement 309)
[NASA-SP-7011(309)] 13 p1810 N88-20814
USSR Space Life Sciences Digest, issue 16
[NASA-CR-3922(19)] 15 p2101 N88-22515
Aerospace medicine and biology: A continuing bibliography with indexes (supplement 310)
[NASA-SP-7011(310)] 16 p2238 N88-23369
USSR Space Life Sciences Digest, Issue 17
[NASA-CR-3922(20)] 17 p2381 N88-24155
Aerospace medicine and biology: A continuing bibliography with indexes (supplement 311)
[NASA-SP-7011(311)] 17 p2382 N88-24161
Aerospace medicine and biology: A continuing bibliography with indexes (supplement 312)
[NASA-SP-7011(312)] 18 p2551 N88-25141
JPRS report: Science and technology. USSR: Space Biology and Aerospace Medicine, volume 22, no. 1, January - February 1988
[JPRS-USB-88-005] 19 p2702 N88-26069
Results of medical research conducted in 1985 during long-term spaceflights 19 p2702 N88-26070
USSR space life sciences digest, issue 18
[NASA-CR-3922(21)] 19 p2707 N88-26096
JPRS report: Science and technology. USSR: Life sciences
[JPRS-ULS-88-009] 20 p2829 N88-26785
Does dihydroergotamine used in therapeutical doses influence the physical and psychomotor performance of young pilots or other traffic drivers subjected to hypotonia?
[ETN-88-92136] 20 p2832 N88-26799
Aerospace medicine and biology: A continuing bibliography with indexes (supplement 313)
[NASA-SP-7011(313)] 20 p2832 N88-26800
Electric and Magnetic Activity of the Central Nervous System: Research and Clinical Applications in Aerospace Medicine
[AGARD-CP-432] 21 p2977 N88-27683
Simulator sickness in the AH-64 Apache combat mission simulator
[AD-A193419] 21 p2988 N88-27739
Aerospace Medicine and Biology: A continuing bibliography with indexes (supplement 314)
[NASA-SP-7011(314)] 21 p2988 N88-27742
Activities report in aerospace medicine
[ETN-88-92906] 23 p3240 N88-29283
Central serous chorioretinopathy in USAF aviators: A review
[AD-A195697] 24 p3407 N88-30280

Aerospace medicine and biology: A continuing bibliography with indexes (supplement 315)
[NASA-SP-7011(315)] 24 p3407 N88-30281

AEROSPACE PLANES
NT HOTOL LAUNCH VEHICLE
NT X-30 VEHICLE
National aero-space plane: A technology development and demonstration program to build the X-30
[GAO/NSIAD-88-122] 17 p2301 N88-23764
Review of convectively cooled structures for hypersonic flight
[NASA-TM-87740] 17 p2310 N88-23817
Heat transfer in aurospace propulsion
[NASA-TM-100874] 17 p2339 N88-23957
A system status monitor for the National Aerospace Plane
[AD-A190681] 18 p2463 N88-24624
Guidance and control strategies for aerospace vehicles
[NASA-CR-183032] 18 p2467 N88-24644
High speed and high angle of attack wind tunnel test results of the winged space vehicle C-2
[ISAS-RN-623] 20 p2751 N88-26329
Ascent guidance for a winged boost vehicle
[NASA-CR-172083] 24 p3334 N88-29846
A study of the critical factors controlling the synthesis of ceramic matrix composites from preceramic polymers
[AD-A195405] 24 p3340 N88-29881

AEROSPACE SAFETY
Report of the helicopter human factors working group --- accident prevention
[CAA-PAPER-87007] 03 p0361 N88-12274
Civil aeronautics
[ETN-88-90616] 05 p0543 N88-13309
Safety philosophy, policy, and requirements for manned spaceflight. Volume 1: Executive summary
[HEG-0886/1036-VOL-1] 06 p0962 N88-15826
Parachute for in-flight training on parachute ejection
[REPT-87-11] 18 p2458 N88-24593

AEROSPACE SCIENCES
Trends in research and development in the Netherlands. The influence of national science policy between 1973 and 1986
[B8701588] 08 p1094 N88-16580
Activities report in aerospace
[ETN-88-91978] 14 p1991 N88-21866
USSR Space Life Sciences Digest, issue 16
[NASA-CR-3922(19)] 15 p2101 N88-22515
NASA scientific and technical publications: A catalog of Special Publications, Reference Publications, Conference Publications, and Technical Papers, 1987
[NASA-SP-7063(02)] 15 p2149 N88-22830
Issues and recommendations associated with distributed computation and data management systems for the space sciences
[NASA-CR-183026] 20 p2881 N88-27108
JPRS report: Science and technology. USSR: Space
[JPRS-USP-88-001] 24 p3444 N88-30498

AEROSPACE SYSTEMS
Design of a condenser-boiler for a binary mercury-organic Rankine cycle solar dynamic space power system
[AD-A184188] 03 p0348 N88-12198
An approach to implementing state space searches on heterogeneous systems of multiprocessors
[DE88-001321] 04 p0482 N88-12967
Initial dynamic load estimates during configuration design 05 p0593 N88-13621
AGARD: The NATO Advisory Group for Aerospace Research and Development
[AD-A185062] 05 p0662 N88-14063
Maximum entropy/optimal projection design synthesis for decentralized control of large space structures
[AD-A186359] 07 p0824 N88-15003
An inference engine for embedded diagnostic systems
08 p1056 N88-16367
KBS V and V as related to automation of space station subsystems: Rationale for a KBS lifecycle
08 p1057 N88-16375
Case-based reasoning for space applications: Utilization of prior experience in knowledge-based systems
08 p1065 N88-16433
Relating service doctrine to space system requirements
[AD-A186620] 08 p1074 N88-16483
AGARD reports: A quarterly listing, 1 July through September 30, 1987
[AD-A186572] 08 p1093 N88-16579
Verification of a micro-thrusting model to maintain satellites in low orbit
[AD-A186874] 09 p1133 N88-16793
Multipurpose corrosion inhibitors for aerospace materials in Naval environments
[AD-A186728] 09 p1143 N88-16853
High-resolution Real-Time Radiography (RTR) system design
[AD-A187107] 09 p1166 N88-16992
Dynamic stress at critical locations of a structure as a criterion for mathematical model modification
09 p1180 N88-17066
Advanced decision aiding techniques applicable to space 09 p1209 N88-17250
The evolution of naval warfare technology and the impact of space systems
[AD-A186900] 09 p1233 N88-17392
A strategy for space warfare
[AD-A186658] 09 p1233 N88-17394
AFAL (Air Force Astronautics Laboratory) technical objective document FY89
[AD-A187861] 11 p1567 N88-19378
Hot corrosion in gas turbines: A new, unique and informative technique is EASE (Electronic Absorption Spectroscopy Experiments)
[AD-A188508] 12 p1583 N88-19470
Activities report of the Systems Department
[ETN-88-91987] 13 p1756 N88-20505
Vapor-mist for lightweight high voltage space insulation systems
[DE87-011704] 13 p1762 N88-20538
Compatibility in space reactor fuel systems
[DE88-005698] 13 p1839 N88-21004
JPRS report: Science and technology. China
[JPRS-CST-87-023] 14 p1863 N88-21130
On the danger of redundancies in some aerospace mechanisms 14 p1925 N88-21475
Technologies applicable to space tethers
[NASA-CR-183055] 19 p2606 N88-25471
Application of AI to space systems
19 p2634 N88-25626
Army space systems for terrestrial applications
[AD-A192735] 21 p2965 N88-27613
Electronic combat roadmap for space
[AD-A194282] 22 p3146 N88-28709
Intelligent test integration system
23 p3254 N88-29371
Sensor and actuator selection for large space structure control
[AD-A194912] 24 p3333 N88-29842

AEROSPACE TECHNOLOGY TRANSFER
Spinoff, 1987
[NASA-TM-89652] 02 p0250 N88-11577
AGARD: The NATO Advisory Group for Aerospace Research and Development
[AD-A185062] 05 p0662 N88-14063
Cooperation know-how in high-tech products
[MBB-Z-101/86] 10 p1311 N88-17833
Langley aerospace test highlights, 1987
[NASA-TM-100595] 15 p2153 N88-22853

AEROSPACE VEHICLES
NT AEROSPACE PLANES
NT FLEXIBLE SPACECRAFT
NT HOTOL LAUNCH VEHICLE
NT X-30 VEHICLE
Computational methods for problems in aerodynamics and large space structure using parallel and vector architectures
[AD-A185401] 05 p0541 N88-13294
Guidance and control strategies for aerospace vehicles
[NASA-CR-181579] 05 p0643 N88-13935
Hypervelocity Technology (HVT) crew escape
09 p1214 N88-17280
Rainfall rates and drop-size distributions for environmental testing
[AD-A191342] 16 p2236 N88-23354
Study of the influence of metallurgical factors on fatigue and fracture of aerospace structural materials
[AD-A192909] 20 p2774 N88-26452
Knowledge-based fault diagnosis on future space vehicles 23 p3254 N88-29374
Dynamics of articulated aerospace structures
[AD-A195685] 24 p3324 N88-29794
Automated early fatigue damage sensing system
[AD-A195717] 24 p3382 N88-30143

AEROSTATICS
Static Aeroelastic Effects on High Performance Aircraft
[AGARD-CP-403] 05 p0550 N88-13348

AEROSTATS
U AIRSHIPS

AEROTHERMOCHEMISTRY
Summary of discussions at the Ninth Meeting of the Sandia Cooperative Group on the Aerothermochemistry of Turbulent Combustion
[DE88-002281] 06 p0680 N88-14165
Summary of discussions at the Tenth Meeting of the Sandia Cooperative Group on the Aerothermochemistry of Turbulent Combustion
[DE88-008467] 21 p2910 N88-27269

AEROTHERMODYNAMICS
The aerothermodynamic environment for holes in hypersonic configurations
[DE87-014651] 02 p0121 N88-10767
Aerothermal modeling program, phase 2
02 p0185 N88-11149
A 3-D Euler solution for hypersonic Mach numbers
05 p0533 N88-13240
Aerothermodynamics research at NASA Ames
05 p0533 N88-13242
The off-design performance of hypersonic waveriders
05 p0533 N88-13244
General aerodynamic-aerothermodynamic concepts for Hermes 05 p0535 N88-13251
HOST turbine heat transfer program summary
[NASA-TM-100280] 06 p0704 N88-14320
Computational fluid dynamics and aerothermodynamics
[NASA-CR-182490] 09 p1166 N88-16989
Shock wave/turbulent boundary layer interaction in high-Reynolds-number hypersonic flows
[AD-A188029] 11 p1434 N88-18555
Assessment, development and application of combustor aerothermal models
[NASA-TM-100290] 12 p1582 N88-19469
Activities report of the Toulouse Research Center
[ETN-88-91988] 13 p1850 N88-21077
Aerothermal tests of quilted dome models on a flat plate at a Mach number of 6.5
[NASA-TP-2804] 15 p2067 N88-22325
Review and assessment of the HOST turbine heat transfer program 15 p2086 N88-22431
Experimental measurements of heat transfer from an iced surface during artificial and natural cloud icing conditions
[AIAA-PAPER-86-1352] 17 p2293 N88-23718
Application of integrated fluid-thermal-structural analysis methods
[NASA-TM-100625] 17 p2350 N88-24001
Analysis of gas turbine test cell number 1, Lemoore Naval Air Station, California
[AD-A192870] 20 p2762 N88-26380
Adaptive computational methods for aerothermal heating analysis
[NASA-CR-181636] 23 p3212 N88-29115
Numerical models for analytical predictions of combustor aerothermal performance characteristics
24 p3349 N88-29935
Impact of ETO propellants on the aerothermodynamic analyses of propulsion components
[NASA-TM-101303] 24 p3374 N88-30094

AFC (CONTROL)
U AUTOMATIC FREQUENCY CONTROL

AFCS (CONTROL SYSTEM)
U AUTOMATIC FLIGHT CONTROL

AFFINITY
NT ELECTRON AFFINITY

AFRICA
Desertification in the Sahelian and Sudanian Zones of West Africa
[PB87-217063] 03 p0345 N88-12183
Environmental processes and spectral reflectance characteristics associated with soil erosion in desert fringe regions
[NASA-CR-182332] 05 p0620 N88-13811
Northern Hemisphere circulation and the principal components of subsequent summer patterns in North America and West Africa 13 p1801 N88-20765
Using space photography of the Earth in the classroom: Drought in Africa
[NASA-CR-182948] 19 p2685 N88-25960
Westward moving atmospheric wave disturbances over the African tropics: Dynamic and energetic aspects
[MITT-57] 20 p2827 N88-26774
Monitoring of agricultural production in West Africa. The need to integrate different satellite platforms
22 p3096 N88-28383
Modes of interannual climate variability and Sahel rainfall anomalies 22 p3121 N88-28547
ENSO, sea-surface temperatures and African rainfall
22 p3122 N88-28550
Sub-Saharan rainfall anomalies and global sea-surface temperature relationships for the recent fifteen year (1970-1984) period 22 p3122 N88-28552
Simulation studies of the influence of sea-surface temperature anomalies on the Sahelian circulation and rainfall 22 p3122 N88-28553
An observational study of interaction between large scale tropical cumulus convection and the equatorial circulation anomalies 22 p3124 N88-28564

AFRICAN RIFT SYSTEM
Geologic results obtained from the use of SPOT imagery along plate boundaries. Examples in the East African rift and of the northern-Caribbean collision
22 p3105 N88-28437

AFTERBODIES
Comparison of wind tunnel and flight test afterbody and nozzle pressures for a twin-jet fighter aircraft at transonic speeds
[NASA-TP-2588] 02 p0121 N88-10785
Effect of empennage arrangement on single-engine nozzle/afterbody static pressures at transonic speeds
[NASA-TP-2753] 02 p0122 N88-10771
A calculation method for the propulsive jet and its aerodynamic interaction with an afterbody
[ESA-TT-1039] 03 p0259 N88-11632
A dynamic model for the aft accumulator in the TE SF-100 system 17 p2414 N88-24354
Variable Mach number wall jets for control/propulsion on hypervelocity projectiles/interceptors: Tests with an existing model
[AD-A192645] 21 p2892 N88-27167
AFTERBURNERS
U AFTERBURNING
AFTERBURNING
Kinetic mechanisms for ionization and afterburning suppression
[AD-A189219] 13 p1737 N88-20383
High performance turbofan afterburner systems
24 p3347 N88-29922
AGB STARS
U ASYMPTOTIC GIANT BRANCH STARS
AGE DETERMINATION
U CHRONOLOGY
AGE FACTOR
Drosophila geotaxis as a tool for the study of aging
10 p1288 N88-17706
Age, alcohol, and simulated altitude: Effects on performance and breathalyzer scores
[AD-A190642] 15 p2103 N88-22531
Biological patterns of growth in postnatal ontogenesis of lower primates 19 p2705 N88-26087
AGE HARDENING
U PRECIPITATION HARDENING
AGGLOMERATION
Measurement of agglomerate strength distributions in agglomerated powders
[DE87-013605] 01 p0090 N88-10591
Comparison of calculated and measured ignition times for boron agglomerates 19 p2624 N88-25563
Reducing adhesion and agglomeration within a cloud of combustible particles
[NASA-TM-100902] 20 p2788 N88-26539
AGGREGATES
Planetary science 07 p0883 N88-15356
Cometary nucleus as aggregate of planetesimals
[ISAS-RN-364] 19 p2741 N88-26275
AGING (BIOLOGY)
Drosophila geotaxis as a tool for the study of aging
10 p1288 N88-17706
Biological patterns of growth in postnatal ontogenesis of lower primates 19 p2705 N88-26087
AGING (MATERIALS)
NT AGING (METALLURGY)
Rheological and aging characterization of elastomers
[DE87-009598] 02 p0151 N88-10944
Pyrotechnic component development at Sandia National Laboratory
[DE87-006899] 02 p0154 N88-10967
PRAAGE: An interactive IBM-PC code for unreliability/aging analysis
[DE87-012124] 04 p0453 N88-12803
Theoretical bases of polymer photodegradation and photooxidation
[AD-A186533] 08 p0974 N88-15889
Evaluation of bituminous materials used in pavement recycling projects at Tyndall, MacDill, and Hurlburt Air Force Bases
[AD-A188068] 10 p1317 N88-17871
Effects of thermal and thermo-mechanical treatments on the mechanical properties of centrifugally cast alloy 718
[AD-A188195] 11 p1458 N88-18690
Experimental and mathematical investigation of response characteristics and aging phenomena in safety fuse elements
[ETN-88-91478] 11 p1480 N88-18832
Aging properties of cable polmers (2)
[NASA-TT-20228] 13 p1752 N88-20479
Partial discharges and the electrical aging of cross linked polyethene (XLPE) cable insulation
[EUT-86-E-160] 14 p1892 N88-21300
Pressure induced ageing of polymers
14 p1929 N88-21504
Effect of moisture level in PBXW-109(E) (plastic-bonded explosive) mixes on the aging of the cured explosive
[AD-A190200] 15 p2048 N88-22202
Elementary characterization of Fibredux 913 CTS 5 34 percent preimpregnated carbon-epoxy from Ciba Geigy
[M-484300] 16 p2171 N88-22941
Investigation of the long term effects of aging on carbon epoxy composites exposed naturally to the weather under cyclic loads. (Results of sampling after 2.5 years). Test report M1-641300
[CEAT-39/M/79-C-M1-641300]
17 p2316 N88-23834
Aging of carbon fibers
[SNPE-NT-10/86/CRB/NP] 18 p2479 N88-24707
Evaluation of the chromium oxide arc spraying treatment on solar energy collectors
[ETN-88-92564] 18 p2537 N88-25053
High temperature resins for injection. High temperature pre-impregnated
[RC-648676] 20 p2780 N88-26486
Aging of CFRP due to longterm storage in heated air
[DFVLR-FB-88-05] 21 p2922 N88-27345
Degradation of fiber composites during storage
[FOA-C-20702-2.6] 22 p3051 N88-28102
Prediction of long-term creep in polypropylene from short-term tests
[NPL-DMA(A)-156] 22 p3068 N88-28337
Stress corrosion of ceramic materials
[AD-A191979] 23 p3195 N88-29016
Development of a test method to determine potential peroxide content in turbine fuels. Part 2
[AD-A192244] 23 p3199 N88-29042
AGING (METALLURGY)
The aging behavior of types 308 and 308CRE stainless steels and its effect on mechanical properties
[DE87-012541] 04 p0417 N88-12590
Influence of microstructure and aging condition on the fatigue crack propagation in age hardened aluminium alloys 05 p0599 N88-13659
Role of interstitials and precipitates in initiation and propagation of L.C.F. cracks in austenitic stainless steels
06 p0718 N88-14411
Shear failure in round bar tensile tests of Al-Zn-Mg-Cu alloys
[PB87-143632] 07 p0869 N88-15271
Kinetics and mechanism of thermal aging embrittlement of duplex stainless steels
[DE88-002987] 08 p0969 N88-15866
Long-term-aging embrittlement of cast duplex stainless steels: Mechanism and kinetics
[DE88-002929] 09 p1145 N88-16861
Long-term aging of cast stainless steels: Mechanisms and resulting properties
[DE88-002888] 09 p1145 N88-16864
Characterization of duplex stainless steel by TEM (Transmission Electron Micrpscopy), SANS (Small-Angle Neutron Scattering) and APFIM (Atom-Probe Field Ion Microscopy) techniques
[DE88-002916] 09 p1145 N88-16865
Aging degradation of cast stainless steels: Effects on mechanical properties
[DE88-003053] 09 p1145 N88-16866
Effect of low-temperature aging on the mechanical properties of cast stainless steels
[DE88-002872] 10 p1300 N88-17774
Brief evaluation of the alloy 17-4-PH (Z5 CNU 17-04). Semifinished product: 205 mm dia forged roller, test reports
[DF/NH-3616/84] 17 p2322 N88-23866
On the reversion phenomena of Cu-3 percent Ti alloys
[NASA-TT-20170] 18 p2488 N88-24762
On the abnormal phenomena observed in the electrical resistivity measurement during the decomposition process of saturated Cu-Fe alloys
[NASA-TT-20183] 18 p2507 N88-24869
Aging behavior of Au-based ohmic contacts to GaAs
[NASA-CR-182146] 19 p2662 N88-25831
AGREEMENTS
High resolution satellite imagery simulation --- treaty verification
[FOA-C-30462-3.3,9.3] 05 p0620 N88-13810
The impact of independent research and development regulations on companies not required to negotiate advanced independent research and development agreements
[AD-A190007] 15 p2147 N88-22818
Department of Defense Statement on the Balanced Technology Initiative to the Committee on Armed Services, United States Senate, 100th Congress, second session
[AD-A191841] 18 p2568 N88-25378
Monitoring space weaponry: Detection and verification issues
[DE88-008726] 20 p2847 N88-26900
AGRICULTURAL AIRCRAFT
AN-30M cloud-seeding airplane in international exhibition 06 p0725 N88-14456
AGRICULTURE
A comparative thematic mapping analysis of SPOT data: The Vientiane Plain (Laos) 03 p0343 N88-12168
SPOT: A tool for agricultural statistics
03 p0344 N88-12170
JPRS report: Science and technology. USSR: Life sciences
[JPRS-ULS-87-009] 04 p0473 N88-12915
Application of remote sensing to agricultural field trials
[ISBN-90-6754-089-7] 06 p0729 N88-14483
Crop forecasting in Brazil: A short history of productivity models
[INPE-4150-PRE/1056] 12 p1637 N88-19801
USSR report: Life sciences. Biomedical and behavioral sciences
[JPRS-UBB-87-010] 12 p1651 N88-19889
USSR report: Life sciences. Biomedical and behavioral sciences
[JPRS-UBB-87-008] 12 p1662 N88-19966
Food Irradiation Newsletter, Vol. 11, No. 1
[DE88-700608] 12 p1671 N88-20004
Global mixed-layer natural and anthropogenic fluxes
13 p1807 N88-20803
Assessment of crop loss from air pollutants: Meteorology-atmospheric chemistry and long range transport
[PB88-146857] 15 p2089 N88-22448
Thailand in maps. Application of the mapping system THEMAK2 for specific purpose atlas preparation
16 p2226 N88-23295
Earth resources: A continuing bibliography with indexes (issue 57)
[NASA-SP-7041(57)] 16 p2229 N88-23314
Estimation of an area cultivated with wheat from LANDSAT data through a two-phase sampling method
17 p2357 N88-24041
National Meeting on Remote Sensing Applied to Municipal Planning 19 p2681 N88-25939
Mapping of land use in Sao Jose dos Campos municipality by remote sensing, an aid for the elaboration of its PDDI 19 p2681 N88-25940
Technique to obtain the agricultural ownership limits by satellite imagery, to approve control, and to accompany agricultural activity 19 p2682 N88-25943
The use of satellite imagery for municipal conditions in rural recording in Pereira Barreto (SP)
19 p2682 N88-25944
The impact of hemp production on the development of the municipalities of Araras, Leme, Santa Cruz da Conceicao and Pirassununga 19 p2683 N88-25948
Application of interactive graphic system (CAD/CAM) in the determination of process evolution in land use in the Ribeirao Preto municipality 19 p2684 N88-25956
Water resources and agricultural land use investigations in northeastern Gujarat (India) 22 p3091 N88-28355
Application of SPOT to agricultural information systems in temperate regions 22 p3093 N88-28369
On the modes of growing-season precipitation over central North America 22 p3124 N88-28567
Study of the spectral response of soybeans
[INPE-4592-PRE/1322] 24 p3387 N88-30174
AGRISTARS PROJECT
Potential use of SPOT satellite data for the national resources inventory 22 p3093 N88-28370
Monitoring of agricultural production in West Africa. The need to integrate different satellite platforms
22 p3096 N88-28383
AGROMETEOROLOGY
Nowcasting for the national economy needs
02 p0199 N88-11241
Automatic data acquisition system utilizing microcomputers: Automatic Meteorological Stations (AMS)
[INPE-4215-PRE/1096] 12 p1646 N88-19859
LANDSAT TM and agrometeorological data for wheat yield estimation at the farm level
[INPE-4591-PRE/1321] 24 p3388 N88-30180
AH-64 HELICOPTER
Apache for the battlefield of today and the 21st century 03 p0265 N88-11670
Operational noise data for CH-47D and AH-64 army helicopters
[AD-A191059] 18 p2570 N88-25263
Aeroelastic characteristics of the AH-64 bearingless tail rotor 21 p2891 N88-27162
Test of an 0.8-scale model of the AH-64 Apache in the NASA Langley full-scale wind tunnel
[AD-A196129] 24 p3319 N88-29768
AILERONS
Comparison of pressure distributions on model and full-scale NACA 64-621 airfoils with ailerons for wind turbine application
[NASA-TM-100802] 14 p1943 N88-21593
AIR
NT ALVEOLAR AIR
NT HIGH TEMPERATURE AIR
Fuel-injector/air-swirl characterization
02 p0185 N88-11150
Dilution jet mixing program, phase 3
02 p0185 N88-11153

Flame acceleration and transition to detonation in channels
[DE87-014193] 03 p0284 N88-11786
Millimeter-wave studies of moist air
[AD-A184681] 03 p0306 N88-11935
The atomic weight and isotopic composition of oxygen and their variation in nature
[DE87-014397] 04 p0413 N88-12558
On the meteor trail spectra 06 p0737 N88-14533
Fuel-injector/air-swirl characterization
[NASA-CR-180864] 07 p0820 N88-14985
A rapid method for the computation of equilibrium chemical composition of air to 15000 K
[NASA-TP-2792] 09 p1140 N88-16830
NF85: A three-dimensional, air-dynamics computer code for analyzing explosions in structures
[DE88-005085] 10 p1331 N88-17953
J85-21 fuel nozzle atomization tests
[AD-A189394] 12 p1613 N88-19647
Two-dimensional electron fluid computer calculations of nanosecond pulse, low pressure microwave air breakdown in a rectangular waveguide and their verification by experimental measurement
[DE88-004407] 12 p1618 N88-19678
Ion content and infrared absorption of moist atmospheric air
[AD-A188839] 12 p1643 N88-19838
An interferometric investigation of the diffraction of planar shock waves over a half-diamond cylinder in air
[UTIAS-322] 3 p1768 N88-20575
Observation of anomalous low J-value Stokes and anti-Stokes lines in stimulated rotational Raman scattering over long air paths
[DE88-003756] 14 p1911 N88-21418
Simplified curve fits for the transport properties of equilibrium air
[NASA-CR-178411] 18 p2513 N88-24911
Numerical simulation of ignition of hydrogen jet in hot air 19 p2637 N88-25647
Air loading effects on a capacitively sensed membrane supported silicon accelerometer
19 p2672 N88-25886
Heat and mass transfer in laminar wavy film absorption with the presence of non-absorbable gases
21 p2947 N88-27502

AIR BEARINGS
U GAS BEARINGS

AIR BLASTS
U AERIAL EXPLOSIONS

AIR BREATHING ENGINES
NT CONVERTIBLE FAN-SHAFT ENGINES
NT GAS TURBINE ENGINES
NT J-57 ENGINE
NT JET ENGINES
NT RAMJET ENGINES
NT SUPERSONIC COMBUSTION RAMJET ENGINES
NT TURBOFAN ENGINES
NT TURBOJET ENGINES
NT TURBOPROP ENGINES
Longitudinal mode combustion instabilities in air breathing engines 06 p0680 N88-14166

AIR CARGO
Aircraft accident reports, brief format, US civil and foreign aviation. Issue number 1: 1986 accidents
[PB87-916903] 02 p0123 N88-10781

AIR CONDITIONING
Life-cycle cost analysis of residential heat pumps and alternative HVAC (Heating, Ventilating and Air-Conditioning) systems
[DE88-003701] 07 p0839 N88-15090
Use of a general control simulation program to evaluate HVAC control stability
[DE88-000476] 08 p0975 N88-15896
Research on fluid dynamic energy separation
[DE88-002776] 10 p1339 N88-18001
Enhanced emergency smoke venting
[DOT/FAA/CT-88/22] 20 p2756 N88-26350

AIR CONDITIONING EQUIPMENT
Plant Growth Module (PGM) conceptual design
05 p0631 N88-13855
Experimental studies of heat and mass exchange in parallel-passage rotary desiccant dehumidifiers for solar cooling applications
[DE88-001119] 10 p1350 N88-18069
Perspectives in microclimate cooling involving protective clothing in hot environments
[AD-A188370] 12 p1671 N88-20007
Pressurizing systems and air conditioning systems
[MBB/LKE-312/S/PUB/246] 13 p1812 N88-20828
The effects of different combinations of inlet air conditions used for cooling as measured on a heated manikin
[AD-A191116] 18 p2552 N88-25151

AIR COOLING
The influence of high free stream turbulence, intensive cooling and wake on the external heat transfer of convectively cooled gas turbine blades
[ETN-87-90432] 01 p0056 N88-10360
National Aerospace Laboratory experiment
04 p0404 N88-12509
Cooling electronic equipment at simulated high altitude in hypobaric chambers
[AD-A185196] 05 p0584 N88-13560
Portable, ambient air microclimate cooling in simulated desert and tropic conditions
[AD-A186457] 08 p1050 N88-16338
Perspectives in microclimate cooling involving protective clothing in hot environments
[AD-A188370] 12 p1671 N88-20007
Acoustic convective system
[NASA-CASE-NPO-17278-1-CU]
18 p2498 N88-24818
The effects of different combinations of inlet air conditions used for cooling as measured on a heated manikin
[AD-A191116] 18 p2552 N88-25151
Computational study on thermal efficiency of ceramic gas turbine
[DE88-753114] 20 p2809 N88-26667
Study on the heat resisting and cooling property of the ceramics-metal hybrid stator vanes
[DE88-753117] 20 p2810 N88-26668

AIR CURRENTS
NT JET STREAMS (METEOROLOGY)
NT MERIDIONAL FLOW
NT VERTICAL AIR CURRENTS
Cross flow in the Alps and flat foehn during the experiment MERKUR --- mesoscale experiment
08 p1013 N88-16142
Study of passages of cross-equatorial current during southern monsoon 14 p1900 N88-21347

AIR CUSHION VEHICLES
U GROUND EFFECT MACHINES

AIR DATA SYSTEMS
Proceedings of the 14th Symposium on Aircraft Integrated Monitoring Systems
[DFVLR-MITT-88-04] 22 p3033 N88-28001
German Air Force requirements for the on-board life monitoring system (OLMOS) on Tornado
22 p3033 N88-28007
Event monitoring functions introduced by the Onboard Life Monitoring System (OLMOS) into a German aircraft
22 p3034 N88-28008
Onboard Life Monitoring System (OLMOS), hardware equipment onboard and on ground
22 p3034 N88-28009
A solution to improve a military aircraft's Onboard-Checkout-And-Monitoring-System (OCAMS)
22 p3034 N88-28013
Japan Air Line's Aircraft Integrated Monitoring System (AIMS) activities 22 p3034 N88-28014
New generation of integrated monitoring systems for modern aircraft 22 p3035 N88-28015
Proposal for the on-board part of a future aircraft integrated monitoring system 22 p3035 N88-28016
Planning for AIMS on the next generation 7J7 aircraft
22 p3035 N88-28017
Faultfinder: A diagnostic expert system with graceful degradation for onboard aircraft applications
22 p3035 N88-28018
The Sundstrand B747-400 data management unit
22 p3035 N88-28021
The use of AIMS data for operational and research purposes in atmospheric sciences
22 p3036 N88-28025
On-board data processing of navigation data at high latitudes in Antarctica 22 p3036 N88-28027
Interface techniques and systems for standard aircraft data buses 22 p3036 N88-28028
A guide to good magnetic tape management practice for MODAS users --- modular airborne data acquisition system (MODAS)
[RAE-TM-IT-212] 22 p3162 N88-28834

AIR DEFENSE
NT ANTIMISSILE DEFENSE
Automation strategy and results for an airbase command and control information system
[NLR-MP-86031-U] 01 p0035 N88-10223
A piloted simulation investigating handling qualities and performance requirements of a single-pilot helicopter in air combat employing a helmet-driven turreted gun
[AD-A186878] 09 p1116 N88-16689
MOAOPS and BOOM-MAP computer programs for sonic boom research, volume 1
[AD-A189548] 12 p1574 N88-19414
Aircrew training devices: Utility and utilization of advanced instructional features, phase 4
[AD-A188418] 12 p1670 N88-20000
Simulation of effect of anti-radar stealth principle
13 p1755 N88-20496
Task listing: Visually assisted and visually dependent tasks for fighter aircraft
[AD-A191041] 16 p2244 N88-23404
Modeling and evaluation of variable structure organizations
[AD-A191947] 18 p2588 N88-25381
Proposal for a new aggressor aircraft
[AD-A194311] 22 p3041 N88-28056
Inflight rearming
[AD-A193564] 23 p3176 N88-28909
Typical weather months in the past (1973-1983) in Central Europe
[AD-A194701] 23 p3235 N88-29249
Integration of LANTIRN (Low Altitude Navigation and Targeting Infrared for Night) into operational fighter training
[AD-A194906] 24 p3325 N88-29799
LANTIRN simulator training in the F-16C
[AD-A195201] 24 p3330 N88-29826

AIR DROP OPERATIONS
Developmental airdrop testing techniques and devices
[AGARD-AG-300-VOL-6] 04 p0398 N88-12481
Control systems for platform landings cushioned by air bags
[AD-A196154] 24 p3358 N88-29996

AIR DUCTS
Reflection of sound in open ended ducts
[PB88-103478] 21 p3012 N88-27870

AIR FILTERS
Comparison of three aerosol sampling techniques and the differences in the nitrate determined by each
[DE87-011456] 03 p0348 N88-12200
Computer code simulations of explosions in flow networks and comparison with experiments
[DE88-001946] 05 p0573 N88-13491
Characteristics of pressure loss during filtration using a porous ceramic filter
[DE88-752547] 20 p2798 N88-26604

AIR FLOW
NT AIR CURRENTS
NT JET STREAMS (METEOROLOGY)
NT MERIDIONAL FLOW
NT VERTICAL AIR CURRENTS
Boundary layer profile investigations downstream of an aero-engine intake anti-icing air exhaust slot
[PNR90378] 02 p0171 N88-11080
The generation of nearly isotropic turbulence by means of grids
[PNR90411] 02 p0172 N88-11084
The air flow on hills from models and experiments
[BMFT-FB-T-86-175] 02 p0198 N88-11236
On the role of snow in the redistribution of precipitation by small scale topography 02 p0203 N88-11267
A real-data numerical study and four-dimensional data assimilation application for mesobeta-scale flow in complex terrain 02 p0212 N88-11329
On the scheme dependency of the three-dimensional Euler solutions 03 p0318 N88-12010
National Aerospace Laboratory experiment
04 p0404 N88-12509
Practical application of two-dimensional viscous flow computation 05 p0535 N88-13257
The development and evaluation of three-dimensional models of cold flow in internal combustion engines
[DE88-900077] 05 p0589 N88-13594
Controlled ecological life support systems: Development of a plant growth module 05 p0630 N88-13854
Foam generation and air entrainment near a free surface
[AD-A185986] 07 p0848 N88-15149
Typhoon structural evolution
[AD-A186090] 07 p0879 N88-15333
Portable, ambient air microclimate cooling in simulated desert and tropic conditions
[AD-A186457] 08 p1050 N88-16338
Preliminary experiments on surface flow visualization in the cryogenic wind tunnel by use of condensing or freezing gases
[NASA-CR-181634] 11 p1442 N88-18602
Perspectives in microclimate cooling involving protective clothing in hot environments
[AD-A188370] 12 p1671 N88-20007
Air-jet spoiler
[BU-364] 13 p1722 N88-20299
Control of structure in turbulent flows: Bifurcating and blooming jets
[AD-A189607] 13 p1766 N88-20562
The pressure drag and momentum flux during a cold frontal passage over the Alps 13 p1800 N88-20763
Determination of canopy loads for a light aircraft by wind tunnel testing and computer modelling
[BU-353] 14 p1869 N88-21167

Visualization of the air flowing through a dynamic model of the vocal folds
[ISVR-TR-154] 14 p1952 N88-21634

The development of a microanemometer. New possibilities for measuring very low air velocities
[ETN-88-92244] 16 p2210 N88-23191

The role of vortex structure in tropical cyclone motion
[AD-A190961] 16 p2235 N88-23351

Acoustic convective system
[NASA-CASE-NPO-17278-1-CU] 18 p2496 N88-24818

Noise generation by air bubbles in water: An experimental study of creation and splitting
[AD-A192063] 19 p2664 N88-25839

A numerical study of the test time in a hypersonic shock tunnel
[AD-A194057] 23 p3172 N88-28888

A calculation of the turbulent boundary layer on a slender ellipsoid at low incidence
[FFA-TN-1988-02] 23 p3213 N88-29126

Nozzle airflow influences on fuel patternation
24 p3346 N88-29916

AIR FREIGHT
U AIR CARGO

AIR INLETS
U AIR INTAKES

AIR INTAKES
NT ENGINE INLETS
NT SUPERSONIC INLETS

The role of computation fluid dynamics in aeronautical engineering (4). The development and applications of implicit TVD finite volume code
05 p0536 N88-13259

Calibration of the ARL (Aeronautical Research Laboratories) rain and icing facility
[AD-A186776] 09 p1121 N88-16710

Details of low speed intake test facility at the Warton (United Kingdom) 2.7m x 2.1m wind tunnel
[AXM-127] 14 p1970 N88-21174

Equipment for mass flow measurements in the low-speed wind tunnel at DFVLR in Brunswick, West Germany
[DFVLR-MITT-88-02] 21 p2900 N88-27212

AIR JETS

Experimental study of three-dimensional turbulent jet-solid boundary interaction 01 p0046 N68-10293

The numerical simulation of the mesoscale characteristics associated with Baiu front. Part 1: Structure, low-level jet and radiation characteristics
02 p0203 N88-11272

Interaction of the cold conveyor belt with polar jet streaks
[AD-A186774] 09 p1192 N88-17145

Air-jet spoiler
[BU-384] 13 p1722 N88-20299

The structure of sonic underexpanded turbulent air jets in still air
[AD-A190856] 16 p2157 N88-22870

AIR LAND INTERACTIONS

Validation of a three dimensional numerical model of the sea breeze in complex terrain
02 p0211 N88-11325

An introduction to the parameterization of land-surface processes 14 p1937 N88-21554

Continental surface processes and water cycle
14 p1937 N88-21555

Sensitivity of general circulation models to surface processes 14 p1937 N88-21556

AIR LAUNCHING

Automatic routing module 09 p1210 N88-17251

Store separation and missile firing from aircraft: Experimental methods for trajectory projection
[NASA-TT-20214] 11 p1439 N88-18589

AIR LOCKS

HERMES Program: Airlock swimming pool tests
12 p1591 N88-19525

AIR MASSES

Operational practice of an air mass transformation model 02 p0208 N88-11308

Development and testing of an air-mass transformation trajectory model 02 p0209 N88-11309

Model calculations of the behavior of orographically influenced cold fronts 08 p1015 N88-16155

Parametric methodologies of cloud vertical transport for acid deposition models
[PB88-191374] 20 p2825 N88-26762

Energy budget and ground temperatures in hot regions
[AD-A196298] 24 p3404 N88-30268

AIR NAVIGATION
NT ALL-WEATHER AIR NAVIGATION
NT AREA NAVIGATION
NT NAP-OF-THE-EARTH NAVIGATION

Generating diagnostic knowledge from a structural and functional description 02 p0129 N88-10813

Proceedings of a Workshop on Innovative Solutions for Safety in Air Transportation
[ILR-MITT-178(1987)] 11 p1437 N88-18573

Activities report in air traffic control
[ETN-88-91092] 11 p1438 N88-18581

Integrated avionics reliability 17 p2294 N88-23723

A comparison of integrated and separate systems for flight control and navigation 17 p2303 N88-23779

A positioning system based on NAVSAT
[NLR-MP-87018-U] 20 p2757 N88-26356

Electrical load and power source capacity report for the C-130 aircraft Self Contained Navigation System (SCNS): LSI model 6216A, 6216B, 6216C, revision
[AD-A193079] 21 p2895 N88-27186

Observed track-keeping performance of DC10 aircraft equipped with the Collins AINS-70 area navigation system: Karlsruhe and Masstricht UACs (Upper Area Control centres)
[EEC-202] 24 p3323 N88-29788

Integration of LANTIRN (Low Altitude Navigation and Targeting Infrared for Night) into operational fighter training
[AD-A194906] 24 p3325 N88-29799

AIR POLLUTION
NT GLOBAL AIR POLLUTION
NT INDOOR AIR POLLUTION

NBS (National Bureau of Standards) research reports (April 1987)
[PB87-210258] 01 p0018 N88-10111

Investigations of the dispersion of spontaneously released heavy gases
[WA-81] 01 p0066 N88-10427

Carbon monoxide (CO) concentration in the air as a purity parameter
[INPE-4232-PRE/1107] 01 p0067 N88-10429

An instrument for the quasi-continuous determination of atmospheric soot content
[DFVLR-FB-87-04] 01 p0068 N88-10433

Investigation of large scale impact of air pollution components on forest ecosystems in Bavaria, West Germany
[DFVLR-FB-87-17] 01 p0068 N88-10434

Mid infrared LHS system packaging using flexible waveguides
[NASA-CR-181192] 01 p0093 N88-10607

Opportunities for nowcasting air pollution episodes and accidental toxic and radioactive releases
02 p0210 N88-11317

Real-time evaluation and prediction of coastal dispersion near the SW tip of Africa --- effluents
02 p0210 N88-11318

Aircraft engine exhaust plume dynamics
[AD-A184238] 04 p0400 N88-12488

Emerging environmental constraints on the use of gasoline and diesel fuel and tradeoffs associated with the use of alternative fuels
[DE87-011504] 04 p0422 N88-12614

The use of TOMS data for tropospheric ozone studies
05 p0616 N88-13784

AN-30M cloud-seeding airplane in international exhibition 06 p0725 N88-14456

On-site meteorological program guidance for regulatory modeling applications
[PB87-227542] 06 p0731 N88-14498

Pollution from motor vehicles and aircraft at Stapleton International Airport (abbreviated report), revision 2
[AD-A185916] 07 p0875 N88-15307

Use of back air trajectories in interpreting atmospheric chemistry data: A review and bibliography
[PB88-102108] 07 p0876 N88-15312

Fuel nitrogen conversion in a supercharged spark ignition engine
[DE88-003739] 08 p0974 N88-15893

A review of methanol vehicles and air quality impacts
[DE88-002846] 08 p1023 N88-16194

Current issues in atmospheric change
[NASA-CR-182406] 08 p1039 N88-16267

Estimation of aerial deposition and foliar uptake of xenobiotics: Assessment of current models
[DE88-000993] 09 p1188 N88-17117

A comparison of multi-layer meso-alpha MLAM model results with surface and aircraft observations from CAPTEX
[DE88-000549] 09 p1188 N88-17118

Model investigations of atmospheric ammonia scavenging
[DE88-002337] 09 p1194 N88-17153

The role of repowering in America's power generation future
[DOE/FE-0096] 10 p1351 N88-18076

Meteorological and aerosol measurements from the NOAA WP-3D aircraft during WATOX-86, January 4-9, 1986
[PB88-120860] 10 p1352 N88-18079

The role of analytical chemistry in assessing atmospheric effects of combustion
[DE88-003909] 10 p1352 N88-18082

Developments in National Weather Service meteorological data collection programs as related to EPA (Environmetal Protection Agency) air pollution models
[PB88-130240] 10 p1356 N88-18104

Using SIR (Scientific Information Retrival) system for data management during a field program
[DE88-001555] 10 p1424 N88-18508

Computer architecture for research in meteorology and atmospheric chemistry
[PB88-145313] 11 p1510 N88-19020

Optimal sampling to provide user-specific climate information 11 p1515 N88-19051

Proceedings of the Forest-Atmosphere Interaction Workshop
[CONF-8510250] 12 p1641 N88-19824

Air quality and human performance, chapter 16
[AD-A188335] 12 p1686 N88-19988

Computer simulation of tropospheric chemistry
[JUEL-2144] 13 p1798 N88-20756

Carbon dioxide and climate 14 p1936 N88-21545

Assessment of crop loss from air pollutants: Meteorology-atmospheric chemistry and long range transport
[PB88-146857] 15 p2089 N88-22448

A theoretical model of the washout of trace gases by raindrops in the atmosphere 17 p2375 N88-24125

Air pollution: Ozone attainment requires long-term solutions to solve complex problems
[PB88-167275] 18 p2538 N88-25060

Ozone in the atmosphere 18 p2539 N88-25064

Motor vehicles as sources of compounds important to tropospheric and stratospheric ozone
[PB88-195219] 18 p2540 N88-25076

Photointerpretation with instrumentation for evaluation of environmental impact: Mata Atlantica in Cubatao
19 p2683 N88-25946

Study of evolution of vegetal cover and slide scars in the Cubatao municipality-Sao Paulo
19 p2683 N88-25947

A primer on greenhouse gases
[DE88-007576] 19 p2689 N88-25981

Composite, meso-gamma scale diagnostic modeling
[DE88-008189] 19 p2689 N88-25983

Pollutant formation in heterogeneous mixtures of fuel drops and air
[DOE/CE-50052/H1] 19 p2689 N88-25986

Sulfur dioxide-hydrogen peroxide relationships in clean air, clouds, and precipitation
[DE88-006352] 19 p2690 N88-25990

Overview of the PRECP (processing of emissions by clouds and precipitation) Program
[DE88-008205] 20 p2822 N88-26741

An efficient model for changes of global climate and composition of the atmosphere due to human activities
[ETN-88-92359] 20 p2827 N88-26775

National air toxics information clearinghouse: NATICH data base users guide for data viewing, February 1988
[PB88-197470] 21 p2970 N88-27645

National ambient Volatile Organic Compounds (VOCs) data base update, documentation
[PB88-195631] 21 p2971 N88-27646

Photochemical oxidant formation: Overview of current knowledge and emerging issues
[PB88-195235] 21 p2971 N88-27647

Foliar nitrate reductase: A marker for assimilation of atmospheric nitrogen oxides
[DE88-010453] 21 p2971 N88-27648

Atmospheric science issues in Congress
22 p3125 N88-28573

Effects of air polution on human exercise performance
[AD-A192660] 22 p3131 N88-28617

The 1985-86 measurements with the tunable diode laser absorption spectrometer
[PB88-214002] 23 p3231 N88-29226

Investigation of the large-scale impact of air pollution components on forest ecosystems in Bavaria
[ESA-TT-1087] 24 p3390 N88-30187

AIR PURIFICATION

Operation of an experimental algal gas exchanger for use in a CELSS 03 p0358 N88-12255

Non-conventional approaches to food processing in CELSS, 1. Algal proteins: Characterization and process optimization 03 p0358 N88-12256

Preliminary experimental results of gas recycling subsystems except carbon dioxide concentration
03 p0359 N88-12261

Airborne particulate matter in spacecraft
[NASA-CP-2499] 06 p0753 N88-14823

Proceedings of the 19th DOE/NRC Airborne Waste Management and Air Cleaning Conference
[NUREG/CP-0086-VOL-1] 11 p1509 N88-19018

Proceedings of the 19th DOE/NRC Airborne Waste Management and Air Cleaning Conference
[NUREG/CP-0086-VOL-2] 11 p1509 N88-19019

AIR QUALITY

Carbon monoxide (CO) concentration in the air as a purity parameter
[INPE-4232-PRE/1107] 01 p0067 N88-10429

Compilation and analysis of air quality data in support of acid deposition research
[DE87-014428] 02 p0196 N88-11226

Aircraft engine exhaust plume dynamics
[AD-A184238] 04 p0400 N88-12488

Airborne particulate matter in spacecraft
[NASA-CP-2499] 06 p0753 N88-14623

Pollution from motor vehicles and aircraft at Stapleton International Airport (abbreviated report), revision 2
[AD-A185916] 07 p0875 N88-15307

Impacts of world development on selected characteristics of the atmosphere: An integrative approach. Volume 1: Main report
[DE88-001495] 07 p0875 N88-15309

Impacts of world development on selected characteristics of the atmosphere: An integrative approach. Volume 2: Appendices
[DE88-001496] 07 p0875 N88-15310

A review of methanol vehicles and air quality impacts
[DE88-002846] 08 p1023 N88-16194

Evaluation of regional-scale air quality models: Chairmen reports from four workshops
[DE88-001397] 10 p1352 N88-18080

Tropospheric ultraviolet radiation: Assessment of existing data and effect on ozone formation
[PB88-130133] 10 p1354 N88-18095

Air quality and human performance, chapter 16
[AD-A188335] 12 p1666 N88-19988

Air pollution: Ozone attainment requires long-term solutions to solve complex problems
[PB88-167275] 18 p2538 N88-25060

NOAA (National Oceanic and Atmospheric Administration) Meteorology Division support to the Environmental Protection Agency
[PB88-179866] 19 p2689 N88-25980

Sulfur dioxide-hydrogen peroxide relationships in clean air, clouds, and precipitation
[DE88-006352] 19 p2690 N88-25990

Meteorological aspects of wet deposition in Southern Finland
[FMI-3] 19 p2693 N88-26007

Regional environmental studies using national data bases and GIS (Geographic Information System)
[DE88-008368] 23 p3230 N88-29225

AIR SAMPLING

Detection of vapors of flammable liquids in air by atmospheric sampling mass spectrometry/mass spectrometry
[DE88-000030] 02 p0196 N88-11227

Comparison of three aerosol sampling techniques and the differences in the nitrate determined by each
[DE87-011456] 03 p0348 N88-12200

Method for sampling of methyl salicylate vapor in air using passivated stainless steel syringes and analysis by gas chromatography
[AD-A187838] 11 p1447 N88-18624

Proceedings of the 19th DOE/NRC Airborne Waste Management and Air Cleaning Conference
[NUREG/CP-0086-VOL-2] 11 p1509 N88-19019

Optimal sampling to provide user-specific climate information 11 p1515 N88-19051

Fibrous glass aerosols: A literature review
[AD-A188420] 12 p1672 N88-20008

Aircraft emissions characterization: TF41-A2, TF30-P103 and TF30-P109 engines
[AD-A192053] 18 p2466 N88-24638

AIR SEA ICE INTERACTIONS

Report of the second session of the working group on sea ice and climate
[WCP-128] 06 p0745 N88-14580

AIR SEA INTERACTIONS

U AIR WATER INTERACTIONS

AIR SICKNESS

U MOTION SICKNESS

AIR START

Propulsion analysis and application potential of air breathing combined propulsion for ballistic space transporter
[ETN-88-92369] 21 p2903 N88-27227

AIR TO AIR MISSILES

Advances in Air-Launched Weapon Guidance and Control
[AGARD-CP-431] 12 p1596 N88-19553

Effects of closing speed uncertainty on optimal guidance 12 p1597 N88-19556

Guidance and control of air-launched armaments: An aeroengineer's perspective 12 p1597 N88-19557

Future air-to-air training for the RF-4
[AD-A194363] 23 p3240 N88-29284

Approximations and implementations of nonlinear filtering schemes
[AD-A194885] 23 p3271 N88-29462

AIR TO AIR REFUELING

Aircraft refueling demonstrator using a microbot alpha 2 robot 21 p2926 N88-27367

Low altitude: A new dimension in air refueling
[AD-A193819] 23 p3176 N88-28910

AIR TO AIR ROCKETS

U AIR TO AIR MISSILES

AIR TO SURFACE MISSILES

A study into the effects and viability of applying lateral force control to an air to ground rocket
[ETN-87-90925] 02 p0131 N88-10821

Advances in Air-Launched Weapon Guidance and Control
[AGARD-CP-431] 12 p1596 N88-19553

Guidance and control of air-launched armaments: An aeroengineer's perspective 12 p1597 N88-19557

The use of hardware-in-the-loop-techniques in the development of a modern air-to-surface missile system
12 p1597 N88-19562

AIR TRAFFIC

Activities report in flight and space travel
[ISSN-0070-3966] 14 p2012 N88-22000

FAA (Federal Aviation Administration) technical center: Mission and role in natinal airspace system plan implementation
[PB88-169818] 18 p2460 N88-24609

AIR TRAFFIC CONTROL

Knowledge Based Concepts and Artificial Intelligence: Applications to Guidance and Control
[AGARD-LS-155] 02 p0128 N88-10806

An expert system for aircraft conflict resolution in dense airspaces 02 p0129 N88-10810

A rule-based system for arrival sequencing and scheduling in air traffic control 02 p0129 N88-10815

Nowcasting for the national economy needs
02 p0199 N88-11241

Experimental use of artificial intelligence for (future) ATC systems
[PB87-106449] 04 p0482 N88-12970

Flightpath reconstruction and systematic radar error estimation from multiradar range-azimuth measurements
[NLR-MF-85064-U] 06 p0693 N88-14251

FAA air traffic control operations concepts. Volume 1: ATC background and analysis methodology
[AD-A185979] 07 p0818 N88-14973

FAA air traffic control operations concepts. Volume 2: ACF/ACCC (Area Control Facility/Area Control Computer Complex) terminal and en route controllers
[AD-A185980] 07 p0818 N88-14974

FAA air traffic control operations concepts. Volume 3: ISSS (Initial Sector Suite System) en route controllers
[AD-A185981] 07 p0818 N88-14975

FAA air traffic control operations concepts. Volume 4: TAAS (Terminal Advanced Automation System) terminal controllers
[AD-A185982] 07 p0818 N88-14976

FAA air traffic control operations concepts. Volume 5: ATCT/TCCC (Airport Traffic Control Tower/Tower Control Computer Complex) tower controllers
[AD-A185983] 07 p0818 N88-14977

Chicago's O'Hare Runway Configuration Management System (RCMS). Volume 2: Users guide
[AD-A186222] 08 p0953 N88-15783

Cockpit data management
[NASA-CR-178407] 11 p1438 N88-18579

Cockpit data management
[NASA-CR-178407-SUPPL] 11 p1438 N88-18580

Activities report in air traffic control
[ETN-88-91092] 11 p1438 N88-18581

Air traffic control
[FAA-ORDER-7110.65E] 12 p1576 N88-19426

Estimates of potential increases in airport capacity through ATC (Air Traffic Control) system improvements in the airport and terminal areas
[AD-A188533] 12 p1578 N88-19444

Activities report in civil aeronautics
[ETN-88-91344] 13 p1715 N88-20255

A method and measures to evaluate trackers for air traffic control
[NLR-TR-86072-U] 13 p1720 N88-20287

Electronics and communications in air traffic control: The Presidential Address
[ETN-88-92057] 14 p1865 N88-21146

Aircraft accident report: North Star Aviation, Inc., PA-32 RT-300, N39614 and Alameda Aero Club Cessna 172, N75584, Oakland, California, March 31, 1987
[PB87-910412] 15 p2016 N88-22021

An evaluation of the effects of high visual taskload on the separate behaviors involved in complex monitoring performance
[AD-A190641] 15 p2105 N88-22538

Integrated multisensor navigation systems
17 p2294 N88-23722

Space based radar application to air traffic control
17 p2399 N88-24262

FAA (Federal Aviation Administration) technical center: Mission and role in natinal airspace system plan implementation
[PB88-169818] 18 p2460 N88-24609

Optimization of the dilation characteristic on the control jurisdiction of an area control facility
[AD-A191720] 18 p2461 N88-24615

World-wide aeronautical satellite communications
19 p2644 N88-25688

Statistical properties of real time events in an ATC (Air Traffic Control) system
[PB88-118781] 20 p2756 N88-26353

Analysis of ATCRBS (Air Traffic Control Radar Beacon System), mode select (Mode S) in combat operations
[AD-A193140] 22 p3040 N88-28050

Fine resolution errors in secondary surveillance radar altitude reporting
[RSRE-87019] 23 p3175 N88-28906

AIR TRAFFIC CONTROLLERS (PERSONNEL)

An expert system for aircraft conflict resolution in dense airspaces 02 p0129 N88-10810

A rule-based system for arrival sequencing and scheduling in air traffic control 02 p0129 N88-10815

FAA air traffic control operations concepts. Volume 1: ATC background and analysis methodology
[AD-A185979] 07 p0818 N88-14973

Air traffic control
[FAA-ORDER-7110.65E] 12 p1576 N88-19426

The program Kennedy Approach as an experimental design of a dynamic computerized air traffic control test
[DFVLR-FB-87-50] 16 p2159 N88-22881

AIR TRANSPORTATION

Issues in air transport and airport management
[PB87-204509] 02 p0124 N88-10782

V/STOL aircraft configurations and opportunities in the Pacific Basin
[NASA-TM-100005] 03 p0261 N88-11644

Airline safety: A comparative analysis
[AD-A185358] 05 p0543 N88-13308

Digest of the annual report of the Lufthansa German Airlines
[ISSN-0415-603X] 08 p0952 N88-15779

TECOM's research efforts in the dynamic environments 08 p0999 N88-16048

Proceedings of a Workshop on Innovative Solutions for Safety in Air Transportation
[ILR-MITT-178(1987)] 11 p1437 N88-18573

Activities report in civil aeronautics
[ETN-88-91344] 13 p1715 N88-20255

FAA aviation forecasts fiscal years 1988-1999
[AD-A191711] 18 p2455 N88-24576

AIR WATER INTERACTIONS

NT AIR SEA ICE INTERACTIONS

Study on propagation and inverse scattering --- sea studies
[ESA-CR(P)-2394] 01 p0063 N88-10405

Contribution of bubbles and waves to air-sea CO2 flux, with implications for remote sensing
[PB87-203980] 01 p0073 N88-10467

Vertical profiles of wind-induced current --- North Sea
[IOS-238] 02 p0193 N88-11207

Properties of the atmospheric boundary layer above a subtropical oceanic front
[AD-A184006] 03 p0351 N88-12215

Influence of stratification in near-surface water layer on intensity of gas exchange between atmosphere and water 04 p0459 N88-12841

Studies of thin surface films aim at seeing deep ocean processes 04 p0460 N88-12847

Theory of heat and moisture exchange between finely disperse storm-generated spray and turbulent air flow
04 p0461 N88-12851

Interactions between the Asian monsoons, the tropical Pacific and the southern hemisphere extratropics
04 p0470 N88-12907

Reactions of porphyrins in surfactant assemblies, microemulsions and in solutions
[AD-A184797] 05 p0560 N88-13412

Estimation of marine boundary layer depth and relative humidity with multispectral satellite measurements
[AD-A184881] 05 p0620 N88-13804

Influence of gas exchange between ocean and atmosphere on formation of atmospheric pressure field
06 p0726 N88-14467

Acoustic scattering from composite wind-wave surfaces 3: Forward scatter intensities and spatial coherence at low and high frequencies and small grazing angles for Bubble-free regimes
[AD-A185908] 07 p0881 N88-15345

The ocean heat budget
[AD-A186130] 07 p0881 N88-15346

WOCE Core Project 2 Planning Meeting: The Southern Ocean
[WCP-138] 07 p0882 N88-15348

Report of the Workshop on Space Systems Possibilities for a Global Energy and Water Cycle Experiment
[WCP-137] 09 p1193 N88-17147

Moving ionospheric perturbations induced by wave trains propagating through ocean 09 p1239 N88-17427

NASA Oceanic Processes Program
[NASA-TM-4025] 10 p1357 N88-18109

Numerical simulations of the California current: Filament formation as related to baroclinic instability
[AD-A187573] 10 p1358 N88-18115

On the barotropic model of the ocean circulation
[AD-A188148] 10 p1358 N88-18118

Variation of the wind stress related to frontal passages during FASINEX (Frontal Air-Sea Interaction Experiment) 1986
[AD-A187180] 11 p1514 N88-19042

Numerical simulation of the ocean front response to the mesoscale atmospheric forcing
[INPE-4473-TDL/324] 12 p1648 N88-19868

Estimates of ocean-atmosphere thermal interaction in Gulf Stream energy-active test range in winter of 1984
13 p1785 N88-20679

Sample models of steady and low frequency circulations in the tropical atmosphere, with application to tropical air-sea interactions 13 p1801 N88-20764

Dynamics of the Oceanic Surface Mixed Layer
[AD-A188348] 13 p1804 N88-20785

Structures and fluxes in a deep convecting mixed layer 13 p1804 N88-20786

On the zonal momentum balance at the equator
13 p1805 N88-20788

The mixed layer of the western equatorial Pacific Ocean
[HIG-1861] 13 p1805 N88-20789

Unsteady shallowing mixed layer
13 p1805 N88-20791

Some effects of heating on the wind-driven velocity in the upper ocean 13 p1805 N88-20792

Mixed-layer shear related to wind stress in the central equatorial Pacific 13 p1805 N88-20793

Wind forcing and observed oceanic wavenumber spectra 13 p1806 N88-20797

Energy and momentum fluxes through the sea surface
13 p1806 N88-20798

Radiative processes affecting ocean mixed-layer heat content and their monitoring from satellite
13 p1806 N88-20800

The Hapex-Mobilhy program 14 p1938 N88-21560

Equatorial dynamics and ocean-atmosphere coupling
14 p1938 N88-21565

An improved wind input source term for third generation ocean wave modeling
[KNMI-WR-87-8] 14 p1950 N88-21624

Mass, heat and nutrient fluxes in the Atlantic Ocean determined by inverse methods
[NASA-CR-180535] 14 p1950 N88-21626

Changes in the California current system observed off northern California during July-August 1986
[AD-A190027] 15 p2100 N88-22510

Noise generation by air bubbles in water: An experimental study of creation and splitting
[AD-A192063] 19 p2664 N88-25839

US participation in the TOGA (Tropical Ocean and the Global Atmosphere) Program: A research strategy
[DE88-010986] 19 p2681 N88-25938

A study of the dynamics of the Intertropical Convergence Zone (ITCZ) in a symmetric atmosphere-ocean model
[NASA-TM-86220] 19 p2693 N88-26005

Physical oceanography and tracer chemistry of the southern ocean
[DE88-006852] 20 p2828 N88-26779

Air-sea interaction in the vicinity of a land-sea boundary in the presence of upwelling 21 p2973 N88-27661

Zonal wind observations at Christmas Island (2 deg N, 157 deg W) during the 1986-1987 El-Nino
22 p3120 N88-28539

Atlantic SST variability and high latitude climate fluctuations 22 p3122 N88-28551

Simulation studies of the influence of sea-surface temperature anomalies on the Sahelian circulation and rainfall 22 p3122 N88-28553

Recent secular changes in the wintertime circulation of the Southern Hemisphere 22 p3122 N88-28555

On the energy source of 1982-83 ENSO episode simulated by the NCAR community climate model
22 p3122 N88-28556

Some evidence for a Northern Hemispheric extratropic trigger mechanism of ENSO events
22 p3123 N88-28558

A system for determination of wind fields from cloud tracks: INPE experiment
[INPE-4492-PRE/1256] 22 p3128 N88-28594

Genesis of Atlantic lows experiment NASA electra boundary layer flights data report
[NASA-TM-100703] 22 p3128 N88-28597

Observational/numerical study of the upper ocean response to hurricanes
[AD-A193592] 22 p3128 N88-28598

A bulk model for the unstable planetary boundary layer over the sea. A sensitivity investigation
[DM-51] 22 p3129 N88-28600

Doppler radar analysis of coastal marine atmospheric boundary layer structure during a cold air outbreak
[AD A196023] 24 p3403 N88-30261

Analysis of environmental parameters from the Panama City tower radar experiment
[AD-A194994] 24 p3404 N88-30264

AIRBORNE EQUIPMENT

NT AIRBORNE/SPACEBORNE COMPUTERS

Airborne lidar experiments at the Savannah River Plant
[NASA-TM-4007] 02 p0194 N88-11209

Efficiency analysis of airborne Electronic CounterMeasures (ECM) systems
[AD-A184606] 03 p0306 N88-11934

Definition and use of sensors for measuring electrical conductivity in thunderclouds
[ESA-TT-1047] 03 p0352 N88-12222

Study of an airborne Doppler radar: Project Asterix
[BLL-MO-TRANS-1667-(9022.552)]
04 p0432 N88-12675

Airborne Visible/Infrared Imaging Spectrometer (AVIRIS). A description of the sensor, ground data processing facility, laboratory calibration, and first results
[NASA-CR-182365] 06 p0705 N88-14325

A system overview of the Airborne Visible/Infrared Imaging Spectrometer (AVIRIS)
06 p0705 N88-14326

First results from the Airborne Visible/Infrared Imaging Spectrometer (AVIRIS) 06 p0707 N88-14335

BARS-1M meteorological complex carried on IL-18 airplane 06 p0725 N88-14458

Uses of airborne laser Chayka-1 for probing water, land surfaces 06 p0725 N88-14461

Airborne tracking sunphotometer apparatus and system
[NASA-CASE-ARC-11622-1] 06 p0730 N88-14492

Helicopters as test carriers for avionics systems (HETAS)
[DFVLR-IB-112-85/18] 09 p1116 N88-16692

Airborne Wind Shear Detection and Warning Systems: First Combined Manufacturers' and Technologists' Conference
[NASA-CP-10006] 10 p1273 N88-17616

Airborne Doppler lidar detection of wind shear. Results of performance analysis 10 p1275 N88-17627

Forward looking wind shear detection
10 p1275 N88-17629

Crew interface with windshear systems
10 p1275 N88-17631

Feasibility study for a 2nd generation system for airborne maritime pollution surveillance
[ETN-88-92108] 15 p2092 N88-22466

Users guide to CAESAR
[BCRS-87-04] 16 p2228 N88-23306

Preparation and execution of calibration measurements for handling of airborne SAR data (AGRISAR)
[ETN-88-92338] 17 p2333 N88-23926

Airborne and spaceborne radar images for geologic and environmental mapping in the Amazon rain forest, Brazil
17 p2353 N88-24021

Trajectory measurement of the Fokker 100 aircraft during autoland testing
[NLR-MP-86010-U] 20 p2758 N88-26366

Computer simulation procedure for designing airborne aerometric monitoring programs
[DE88-011696] 21 p2975 N88-27674

Maintenance support for military aircraft by intelligent on-board maintenance data panel
22 p3034 N88-28012

On experiences with two hot-wire instruments for measuring the liquid water content in clouds
[ESA-TT-1085] 23 p3236 N88-29255

Airborne radar technology for windshear detection
[NASA-CR-183203] 23 p3236 N88-29257

AIRBORNE LASERS

A study of the performance of airborne laser radar systems and techniques
[ETN-87-90928] 02 p0179 N88-11117

Atmospheric backscatter at 10.6 microns: a compendium of measurements made outside the United Kingdom by the airborne LATAS coherent laser radar velocimeter
[RSRE-87002] 12 p1631 N88-19763

AIRBORNE SURVEILLANCE RADAR

Airborne bistatic radar applications
[ETN-87-90930] 02 p0163 N88-11020

A study of the performance of airborne laser radar systems and techniques
[ETN-87-90928] 02 p0179 N88-11117

Air-to-air radar flight testing
[AGARD-AG-300-VOL-7] 21 p2932 N88-27406

AIRBORNE/SPACEBORNE COMPUTERS

Data Management Working Group report
01 p0016 N88-10097

A129 advanced solutions for meeting today's combat helicopter requirement 03 p0265 N88-11669

Electrical flight commands in transport aircraft
[SNIAS-872-111-108] 05 p0551 N88-13361

Study of fault tolerant techniques for satellite data handling
[FTT/REP/0001/SAAB] 05 p0632 N88-13860

AVIRIS onboard data handling and control
06 p0706 N88-14332

The feasibility of using TAE as the UIL for the space station and for other internal NASA tasks and projects
07 p0925 N88-15618

Modeling of architecture of a problem-oriented on-board processor 08 p1008 N88-16114

An inference engine for embedded diagnostic systems
08 p1056 N88-16367

Embedded expert system for space shuttle main engine maintenance 08 p1058 N88-16382

ESSAA: Embedded system safety analysis assistant
08 p1060 N88-16396

Intelligent man/machine interfaces on the space station 08 p1063 N88-16418

Space languages 08 p1063 N88-16420

Knowledge representation by connection matrices: A method for the on-board implementation of large expert systems 08 p1065 N88-16434

Prototype space station automation system delivered and demonstrated at NASA 08 p1066 N88-16442

Applications of expert systems for satellite autonomy
08 p1066 N88-16443

Introducing new technology into onboard handling systems 09 p1124 N88-16733

Verifying shuttle onboard software using expert systems 09 p1207 N88-17237

Airworthiness considerations
10 p1276 N88-17636

An expert system to support the verification/validation of flight-critical software
[MBB-UT-102/87] 10 p1314 N88-17852

The RVD mission: The on-board data processing requirements 12 p1586 N88-19495

Advances in Air-Launched Weapon Guidance and Control
[AGARD-CP-431] 12 p1596 N88-19553

Computer aided tactics for air combat
12 p1597 N88-19559

The use of hardware-in-the-loop-techniques in the development of a modern air-to-surface missile system
12 p1597 N88-19562

Microprocessors in space instrumentation
[RR-321] 14 p1955 N88-21655

Architecture and role of the Sensor Subsystem in future aircraft weapon systems 17 p2302 N88-23770

Development of a generic architecture
17 p2303 N88-23774

Test philosophy of the EH101 integrated avionic
17 p2303 N88-23775

Modeling of functional specifications for onboard software: Experience with the Rafale avionics system
17 p2303 N88-23777

The avionics software architecture impact on system architecture 17 p2303 N88-23778

Design for interoperability (interchangeability)
17 p2305 N88-23789

Development of an airborne facility for advanced avionics research 17 p2307 N88-23801

Workshops for the design of avionics systems and the development of onboard software
17 p2307 N88-23802

A timing evaluator for C programs generated by the model system
[AD-A191204] 17 p2385 N88-24174

Development of an airborne facility for advanced avionics research
[NLR-MP-87012-U] 20 p2760 N88-26368

A cockpit natural language study - selected transcripts
[AD-A192972] 20 p2834 N88-26808

Airborne remote operated device
[DE88-010324] 21 p2895 N88-27188

Aircraft component health monitoring: An effective approach 22 p3033 N88-28006

Event monitoring functions introduced by the Onboard Life Monitoring System (OLMOS) into a German aircraft
22 p3034 N88-28008

Reliable onboard computing for critical space systems
[RR-670-I] 22 p3135 N88-28641

Computers in weapons systems: A look at the F-15
[AD-A194498] 23 p3178 N88-28920

Feasibility study of a microprocessor controlled actuator test mechanism
[AD-A194654] 23 p3249 N88-29337

Knowledge-based fault diagnosis on future space vehicles 23 p3254 N88-29374

An expert systems application to space base data processing 23 p3256 N88-29384

Development and demonstration of an on-board mission planner for helicopters
[NASA-CR-177482] 24 p3328 N88-29817

AIRBUS

U EUROPEAN AIRBUS

AIRCRAFT

Steering mechanism --- vehicles
[EP-PATENT-0-181-700-A1] 01 p0053 N88-10338

Bibliography of icing on aircraft (status 1987)
[DFVLR-MITT-87-18] 16 p2158 N88-22876

AIRCRAFT ACCIDENT INVESTIGATION

Aircraft accident/incident summary reports: Unalaska, Alaska, September 25, 1985; Jenkinsburg, Georgia, September 29, 1985; Boston, Massachusetts, December 15, 1985; Dekalb, Texas, December 31, 1985; and Erie, Pennsylvania, February 21, 1986
[PB87-910406] 02 p0123 N88-10780

Aircraft accident reports, brief format, US civil and foreign aviation. Issue number 1: 1986 accidents
[PB87-916903] 02 p0123 N88-10781

Aircraft accident reports: Brief format, US Civil and Foreign Aviation, Issue Number 5 of 1986 accidents
[PB87-916907] 08 p0952 N88-15780

Aircraft accident reports: Brief format, US Civil and Foreign Aviation, Issue Number 7 of 1986 accidents
[PB87-916909] 08 p0952 N88-15781

Aircraft accident reports: Brief format, US Civil and Foreign Aviation, Issue Number 8 of 1986 accidents
[PB87-916910] 08 p0953 N88-15782

Aircraft accident/incident summary reports, Des Moines, Iowa, November 25, 1985; Chicago, Illinois, August 10, 1986
[PB88-910411] 09 p1115 N88-16685

Aircraft accident report: Midair collision of Cessna-340A, N8716K, and North American SNJ-4N, N711SQ, Orlando, Florida, May 1, 1987
[PB88-910402] 13 p1720 N88-20282

Aircraft accident reports, brief format, US civil and foreign aviation, issue number 10 of 1986 accidents
[PB87-916912] 15 p2016 N88-22020

Aircraft accident report: North Star Aviation, Inc., PA-32 RT-300, N39614 and Alameda Aero Club Cessna 172, N75584, Oakland, California, March 31, 1987
[PB87-910412] 15 p2016 N88-22021

Aircraft accident report: Midair collision of US Army U-21A, Army 18061 and Sachs Electric Company Piper PA-31-350, N60SE, Independence, Missouri, January 20, 1987
[PB88-910401] 16 p2159 N88-22877

Aircraft accident/incident summary reports: Modena, Pennsylvania, March 17, 1986; Redwater, Texas, April 4, 1986
[PB88-910403] 16 p2159 N88-22878

Aircraft accident/incident, Copperhill, Tennessee, February 22, 1986
[PB88-910407] 18 p2461 N88-24612

Aircraft accident report: Northwest Airlines, Inc., McDonnell Douglas DC-9-82, N312RC, Detroit Metropolitan Wayne County Airport, Romulus, Michigan, August 16, 1987
[PB88-910406] 19 p2601 N88-25449

Aircraft accident report: Air New Orleans, DBA continental express flight 962 British Aerospace 3101 (Jetstream 31), N331CY, New Orleans International Airport, Kenner, Louisiana, May 26, 1987
[PB88-910408] 19 p2601 N88-25450

Aircraft accident report: Joe Foster Excavating, Inc., Bell 206B, N49606, in-flight collision with trees, Alamo, California, August 3, 1986
[PB88-910405] 20 p2755 N88-26345

Aircraft accident report: Midair collision of SkyWest Airlines Swearingen METRO 2, N163SW, and Mooney M20, N6485U, Kearns, Utah, January 15, 1987
[PB88-910404] 20 p2755 N88-26346

The role played by FDRs in understanding the windshear phenomenon 22 p3036 N88-28023

Centralized class A flight mishap investigation
[AD-A194397] 24 p3322 N88-29786

AIRCRAFT ACCIDENTS

NT BIRD-AIRCRAFT COLLISIONS

Aircraft accidents
[JB-84] 01 p0004 N88-10020

Full-scale transport controlled impact demonstration program
[NASA-TM-89642] 01 p0004 N88-10021

Summary report of the history and events pertinent to the Civil Aeromedical Institute's evaluation of providing smoke/fume protective breathing equipment for airline passenger use
[AD-A184499] 03 p0261 N88-11645

Aircraft fire safety research 04 p0406 N88-12526

Airline safety: A comparative analysis
[AD-A185358] 05 p0543 N88-13306

Aircraft accident reports: Brief format, US Civil and Foreign Aviation, Issue Number 4 of 1986 accidents
[PB87-916906] 06 p0666 N88-14086

Annual review of aircraft accident data: US air carrier operations calendar year 1985
[PB88-135843] 10 p1276 N88-17638

Aircraft accident/incident, Newark, New Jersey, November 13, 1986
[NTSB/AAR-87/04-SUMM] 10 p1276 N88-17639

Aircraft accident report: Midair collision of Cessna-340A, N8716K, and North American SNJ-4N, N711SQ, Orlando, Florida, May 1, 1987
[PB88-910402] 13 p1720 N88-20282

Aircraft accident report: Midair collision of US Army U-21A, Army 18061 and Sachs Electric Company Piper PA-31-350, N60SE, Independence, Missouri, January 20, 1987
[PB88-910401] 16 p2159 N88-22877

Peak Acceleration Device (PAD)
[AD-A191639] 18 p2461 N88-24611

Improved procedure for impact probability computation of aircraft crash based on Balfanz model
[JUEL-SPEZ-425] 21 p2894 N88-27176

Correlation between EEG abnormal activity and aircraft accidents: A long term observation
21 p2984 N88-27719

Smoke hoods: Net safety benefit analysis --- aircraft accidents
[CAA-PAPER-87017] 23 p3174 N88-28896

Visual related accidents/incidents
23 p3242 N88-29293

Failure analysis for gas turbines
[NLR-MP-87037-U] 24 p3326 N88-29808

AIRCRAFT ANTENNAS

A conformal aircraft phased array antenna for airplane satellite communication in the L band
[ESA-TT-1057] 03 p0305 N88-11926

Air gap testing using Trailing Wire Antenna (TWA) waveform
[AD-A187639] 11 p1477 N88-18812

MSAT-X phased array antenna adaptions to airborne applications 19 p2647 N88-25713

Airborne measurement of low frequency atmospheric noise ALFAN 1
[AD-A193056] 21 p2931 N88-27405

AIRCRAFT BASES

U MILITARY AIR FACILITIES

AIRCRAFT BRAKES

NT TRAILING EDGE FLAPS

NT WING FLAPS

Aircraft and ground vehicle friction correlation test results obtained under winter runway conditions during joint FAA/NASA Runway Friction Program
[NASA-TM-100506] 11 p1438 N88-18582

AIRCRAFT CABINS

U AIRCRAFT COMPARTMENTS

AIRCRAFT CARRIERS

Simulator evaluation of lineup visual landing aids for night carrier landing
[AD-A191212] 18 p2468 N88-24648

Multiple-Purpose Subsonic Naval Aircraft (MPSNA): Multiple Application Propfan Study (MAPS)
[NASA-CR-175104] 23 p3177 N88-28917

AIRCRAFT COMMUNICATION

Optimizing HF antenna systems on the Dolphin and Sea Hawk helicopters
[AD-A186552] 09 p1152 N88-16901

Information transfer in the National Airspace System
10 p1275 N88-17634

Electronics and communications in air traffic control: The Presidential Address
[ETN-88-92057] 14 p1865 N88-21146

Operation and performance of an integrated helicopter communication system 17 p2305 N88-23787

Developing a global aeronautical satellite system
19 p2644 N88-25687

World-wide aeronautical satellite communications
19 p2644 N88-25688

Design, development and trials of an airline passenger telephone system 19 p2646 N88-25704

Performance of the ICAO standard core service modulation and coding techniques
19 p2648 N88-25723

Development of an 8000 bps voice codec for AvSat
19 p2653 N88-25755

Airborne measurement of low frequency atmospheric noise ALFAN 1
[AD-A193056] 21 p2931 N88-27405

AIRCRAFT COMPARTMENTS

Test results and predictions for the response of near-ceiling sprinkler links in a full-scale compartment fire
[NBSIR-87/3633] 01 p0033 N88-10209

Research simulators for helicopters
03 p0263 N88-11656

Aircraft fire safety research 04 p0406 N88-12526

A hybrid fibreglass-CFRP cloth for new furnishings --- aircraft cabins
[SNIAS-872-111-109] 05 p0558 N88-13396

Development of rotorcraft interior noise control concepts. Phase 3: Development of noise control concepts
[NASA-CR-178172] 06 p0776 N88-14762

Man rating the b-1B molecular sieve oxygen generation system
[AD-A186275] 07 p0899 N88-15447

Analysis of in-flight acoustic data for a twin-engined turboprop airplane
[NASA-CR-178389] 11 p1543 N88-19220

Pressurizing systems and air conditioning systems
[MBB/LKE-312/S/PUB/246] 13 p1812 N88-20828

Aircraft interior noise reduction by alternate resonance tuning
[NASA-CR-182540] 20 p2849 N88-26909

Analysis of the transmission of sound into the passenger compartment of a propeller aircraft using the finite element method
[FFA-TN-1988-15] 23 p3273 N88-29520

A field study on soft contact lens wear in USAF military transport aircraft
[AD-A195962] 24 p3407 N88-30285

AIRCRAFT CONFIGURATIONS

Intergration effects of D-shaped, underwing, aft-mounted, separate-flow, flow-through nacelles on a high-wing transport
[NASA-TM-4018] 02 p0122 N88-10773

Civil applications of high-speed rotorcraft and powered-lift aircraft configurations
[NASA-TM-100035] 03 p0261 N88-11643

Planform effects on the supersonic aerodynamics of multibody configurations
[NASA-TP-2762] 04 p0393 N88-12454

A 0.15-scale study of configuration effects on the aerodynamic interaction between main rotor and fuselage
[NASA-CR-166577] 04 p0395 N88-12462

Analytical method for generating computational grids about complete aircraft configurations
05 p0540 N88-13287

Navier-Stokes simulation of transonic transportation aircraft configurations. 1: Flow-field simulation over wing-fuselage combinations 05 p0540 N88-13288

Computation of transonic flows with nacelle simulation
[SNIAS-872-111-117] 05 p0542 N88-13300

A simulation study of the flight dynamics of elastic aircraft. Volume 2: Data
[NASA-CR-4102-VOL-2] 08 p0959 N88-15813

Predicting dynamic separation characteristics of general configurations
[AD-A186689] 09 p1116 N88-16691

An examination of the impact of potential advances in component technology for future military engines
10 p1279 N88-17650

The aerodynamic design optimisation of a forward swept wing fighter aircraft
[CAR-87-18] 11 p1433 N88-18553

Presentation of Class 1 designs for a family of commuter airplanes
[NASA-CR-182563] 11 p1439 N88-18587

Generation of surface grids through elliptic partial differential equations for aircraft and missile configurations
[AD-A186631] 11 p1535 N88-19169

A multigrid full potential transonic code for arbitrary configurations --- aircraft 11 p1539 N88-19195

Steady and unsteady transonic small disturbance analysis of realistic aircraft configurations
[NASA-TM-100557] 13 p1717 N88-20269

CODAC (Cockpit Oriented Display of Aircraft Configurations) version 1.4 user's guide
[NASA-CR-181650] 13 p1718 N88-20273

Configuration management issues and objectives for a real-time research flight test support facility
[NASA-TM-100437] 13 p1813 N88-20832

Oscillating airfoils: Achievements and conjectures
[AD-A190490] 15 p2014 N88-22006

Trends in Computational Fluid Dynamics (CFD) for aeronautical 3D steady applications: The Dutch situation
[NLR-MP-86074-U] 15 p2015 N88-22017

The application of linear maximum likelihood estimation of aerodynamic derivatives for the Bell-205 and Bell-206
[AD-A191279] 16 p2161 N88-22894

Water facilities in retrospect and prospect: An illuminating tool for vehicle design
16 p2200 N88-23126

Flow visualization study of vortex manipulation on fighter configurations at high angles of attack
16 p2201 N88-23130

Aircraft aeroelasticity and structural dynamics research at the NASA Langley Research Center: Some illustrative results
[NASA-TM-100627] 18 p2459 N88-24598
Applications of the Navier-Stokes equations to wings and complex configurations using a zonal approach
[NASA-TM-100080] 18 p2459 N88-24602
Actuated forebody strakes
[NASA-CASE-LAR-13983-1] 18 p2464 N88-24628
Computational design of low aspect ratio wing-winglet configurations for transonic wind-tunnel tests
[NASA-CR-183021] 18 p2464 N88-24630
Application of advanced grid generation techniques for flow field computations about complex configurations
[NASA-CR-183049] 18 p2515 N88-24922
Calculation of aerodynamic characteristics of airplane configurations at high angles of attack
[NASA-CR-4182] 23 p3172 N88-28891
Three dimensional grid generation for complex configurations: Recent progress
[AGARD-AG-309] 23 p3245 N88-29313
Lessons learned in the mesh generation for PN/S calculations 23 p3245 N88-29314
Component adaptive grid generation for aircraft configurations 23 p3246 N88-29316
Generation of multiple block grids for arbitrary 3D geometries 23 p3246 N88-29317
Grid generation on and about a cranked-wing fighter aircraft configuration 23 p3246 N88-29318
Grid generation for an advanced fighter aircraft
23 p3246 N88-29319
Algebraic grid generation for fighter type aircraft
23 p3246 N88-29320
Composite grid generation for aircraft configurations with the EAGLE code 23 p3246 N88-29321
Analytical surfaces and grids
23 p3247 N88-29322
Mesh generation for industrial application of Euler and Navier Stokes solvers 23 p3247 N88-29323
Grid generation around transport aircraft configurations using a multi-block structured computational domain
23 p3247 N88-29325
Recent advances in transonic computational aeroelasticity
[NASA-TM-100663] 24 p3321 N88-29778
Generation of surface grids through elliptic partial differential equations for aircraft and missile configurations
[AD-A195639] 24 p3424 N88-30378

AIRCRAFT CONSTRUCTION
U AIRCRAFT STRUCTURES

AIRCRAFT CONSTRUCTION MATERIALS
NT AIRFRAME MATERIALS
The fatigue properties of aerospace steels under constant amplitude and flight-by-flight simulated loading
[BAE-MSM-R-GEN-0566] 01 p0059 N88-10377
Review of investigations of aeronautical fatigue in the Federal Republic of Germany
[LBF-S-178] 02 p0192 N88-11201
The use of aeroelastic wind tunnel models to prove structural design 05 p0551 N88-13355
A hybrid fibreglass-CFRP cloth for new furnishings --- aircraft cabins
[SNIAS-872-111-109] 05 p0558 N88-13396
Paints required for aeronautical construction
[SNIAS-872-551-102] 05 p0569 N88-13470
Flammability test on aircraft seats equipped with fire barrier fabrics for the Porcher company
[CEAT-M5-525200] 06 p0666 N88-14084
Time-temperature-stress capabilities of composite materials for advanced supersonic technology applicaion
[NASA-CR-178272] 06 p0677 N88-14144
Study of the evolution of short cracks in fatigue analysis --- aircraft construction materials
[DCQ/L-46-555] 06 p0722 N88-14442
Roughness and waviness requirements for laminar flow surfaces 07 p0813 N88-14953
Moisture plotting of carbon fiber composite in flight operations
[MBB-UT-119/87] 09 p1138 N88-16823
Multipurpose corrosion inhibitors for aerospace materials in Naval environments
[AD-A186728] 09 p1143 N88-16853
Modern materials for light constructions --- aircraft
[MBB-Z-136/86] 10 p1312 N88-17839
Viscoelastic behavior of a polyetheretherketone (PEEK) composite
[AD-A189545] 13 p1734 N88-20368
Environmental effects on the post-impact compressive strength of CFC
[RAE-TM-MAT-STR-1088] 14 p1884 N88-21258
Experimental comparison of lightning simulation techniques to CV-580 airborne lightning strike measurements
[AD-A190576] 15 p2098 N88-22496
Elementary characterization of Fibredux 913 CTS 5 34 percent preimpregnated carbon-epoxy from Ciba Geigy
[M-484300] 16 p2171 N88-22941
Investigation into the operation of the new special drills for drilling holes in thin components made of composite materials --- aircraft components
[LR-519] 16 p2215 N88-23215
Detection sensitivity in thick assemblies --- eddy currents, light alloys, aircraft construction materials
[REPT-48-912/F] 16 p2216 N88-23221
Application of the ONERA model to the life estimation under fatigue cracking of a Al-Li alloy. Parameter identification and test-experiment comparison under FALSTAFF loading
[ONERA-RT-32/7169-RY-063-R]
16 p2222 N88-23264
Crack retardation under load spectra. Experimental study and numerical simulation using the simplified K constant model --- light alloys, aircraft construction materials
[ONERA-RT-30/7169-RY-054-R]
16 p2222 N88-23266
Certification aspects of airplanes which may operate with significant natural laminar flow 17 p2298 N88-23749
Characterization of the 2219 Cegedur alloy. Data acquisition of the fracture mechanics --- aircraft construction materials
[REPT-48-442/F] 18 p2487 N88-24751
Characterization of 7090 and 7091 profiles made with Cegedur powder --- powder metallurgy, aircraft construction materials
[REPT-48-441/F] 18 p2487 N88-24752
Aluminum alloy
[NASA-CASE-LAR-13924-1-CU]
18 p2487 N88-24753
Energy dissipation in a rolling aircraft tire
[NASA-CR-182978] 19 p2676 N88-25913
Prediction of fatigue life of notched specimens under aircraft loading and importance of the relative method in the case of local strain approach, part 2
[TAE-595-PT-2] 19 p2680 N88-25934
Factors affecting strength in composite materials used for aircraft
[DT-212/87] 21 p2907 N88-27248
The composite aeroengine
[PNR90451] 22 p3045 N88-28070

AIRCRAFT CONTROL
NT HELICOPTER CONTROL
Measurements in the functional mock up test of the NAL QSTOL aircraft control system
[NAL-TR-928] 02 p0126 N88-10793
A survey of aircraft integrated control technology
[AR-004-561] 02 p0126 N88-10794
A preliminary investigation into the feasibility of implementing a direct sideforce control system on the Astra Hawk by means of an active control surface --- aircraft control
[ETN-87-90924] 02 p0126 N88-10795
The application of emulation techniques in the analysis of highly reliable, guidance and control computer systems 02 p0127 N88-10796
Knowledge Based Concepts and Artificial Intelligence: Applications to Guidance and Control
[AGARD-LS-155] 02 p0128 N88-10806
Overview of AGARD Lecture Series No. 155: Knowledge-based concepts and artificial intelligence applications to guidance and control
02 p0128 N88-10807
AI expert system technology issues for guidance and control applications 02 p0128 N88-10808
Application of knowledge-based techniques to aircraft trajectory generation and control
02 p0129 N88-10811
Towards the unmanned cockpit
02 p0129 N88-10812
Approach trajectory planning system for maximum concealment
[NASA-TM-88258] 02 p0227 N88-11435
Mission-oriented flying qualities criteria for helicopter design via in-flight simulation 03 p0263 N88-11652
Effects of the installation and operation of jet-exhaust yaw vanes on the longitudinal and lateral-directional characteristics of the F-14 airplane
[NASA-TP-2769] 04 p0393 N88-12455
An integrated study of structures, aerodynamics and controls on the forward swept wing X-29A and the oblique wing research aircraft
[NASA-CR-181548] 04 p0399 N88-12486
Structural optimization in the design process --- aircraft
[SNIAS-872-111-115] 05 p0635 N88-13685
Flaps-up takoff performance of the OV-1D aircraft with YT53-L-704 engine installed
[AD-A185960] 07 p0819 N88-14979
Fiber optics for controls 08 p0956 N88-15798
A flight-test methodology for identification of an aerodynamic model for a V/STOL aircraft
[NASA-TM-100067] 09 p1117 N88-16694
Aircraft flight test trajectory control
[NASA-CR-179428] 09 p1120 N88-16707
Proceedings of the Circulation-Control Workshop, 1986
[NASA-CP-2432] 10 p1268 N88-17586
The impact of circulation control on rotary aircraft controls systems 10 p1271 N88-17601
A potential flight evaluation of an upper-surface-blowing/circulation-control-wing concept
10 p1272 N88-17609
Airborne Wind Shear Detection and Warning Systems: First Combined Manufacturers' and Technologists' Conference
[NASA-CP-10006] 10 p1273 N88-17616
Investigation of the influence of wind shear on the aerodynamic characteristics of aircraft using a vortex-lattice method 10 p1274 N88-17619
Simulator investigation of wind shear recovery techniques 10 p1275 N88-17630
Active control technology with adaptive control concept in the aircraft construction
[MBB/LKE-294/S/PUB/295] 10 p1313 N88-17845
Workshop on Design Loads for Advanced Fighters
[AGARD-R-746] 12 p1579 N88-19449
Structural design requirements for aircraft incorporating active control technology 12 p1580 N88-19453
The relationship between operational flight manoeuvre parameters and design parameters
12 p1580 N88-19454
Output aiming control
[AD-A188463] 12 p1583 N88-19473
Rotorcraft flight-propulsion control integration: An eclectic design concept
[NASA-TP-2815] 12 p1584 N88-19475
F-16 simulator for man-in-the-loop testing of aircraft control systems (SIMTACS)
[AD-A189675] 14 p1870 N88-21178
Design of an integrated control system for flutter margin augmentation and gust load alleviation, tested on a dynamic windtunnel model
[PB88-149885] 15 p2020 N88-22038
Expanded envelope concepts for aircraft control-element failure detection and identification
[NASA-CR-181664] 16 p2160 N88-22886
Conceptual final paper on the preliminary design of an oblique flying wing SST
[NASA-CR-182879] 16 p2161 N88-22891
Stability and control methodology for conceptual aircraft design. Volume 1: Methodology manual
[AD-A191314] 16 p2164 N88-22906
Joint University Program for Air Transportation Research, 1986
[NASA-CP-2502] 17 p2293 N88-23715
Investigation of air transportation technology at Princeton University, 1986 17 p2294 N88-23724
Flight penetration of wind shear: Control strategies
17 p2294 N88-23727
Natural laminar flow and airplane stability and control
17 p2298 N88-23747
Wind-tunnel investigation of actuated forebody strakes for yaw control at high angles of attack
17 p2299 N88-23754
Optimization of the dilation characteristic on the control jurisdiction of an area control facility
[AD-A191720] 18 p2461 N88-24615
Actuated forebody strakes
[NASA-CASE-LAR-13983-1] 18 p2464 N88-24628
Overview of NASA research in fiber optics for aircraft controls
[NASA-TM-100919] 19 p2603 N88-25458
Influence of wind shear on the aerodynamic characteristics of airplanes
[NASA-TP-2827] 20 p2755 N88-26344
Propfan test assessment testbed aircraft stability and control/performance 1/9-scale wind tunnel tests
[NASA-CR-182121] 20 p2757 N88-26360
Low-speed wind-tunnel test of a STOL supersonic-cruise fighter concept
[NASA-TM-4050] 20 p2761 N88-26374
Nonlinear identification of an aircraft for the direct calculation of an anticipatory control
20 p2787 N88-26535
Investigations of aircraft control with jet spoilers
[ISL-R-112/87] 21 p2898 N88-27202
Computer system for the primary fly-by-wire control of civil transport aircraft (experimental system)
[FBW-TB-2086/88] 21 p2898 N88-27204
Optimal control of the wing rock phenomenon
21 p2927 N88-27373
High performance forward swept wing aircraft
[NASA-CASE-ARC-11636-1] 23 p3177 N88-28914

Variable wing camber control systems for the future Airbus program
[MBB-UT-104/88] 23 p3180 N88-28932

Comparison of the influence of different gust models on structural design 24 p3312 N88-29722

Pilot modeling 24 p3314 N88-29736

Pilot modeling applications 24 p3314 N88-29737

Advances in flying qualities. Concepts and criteria for a mission oriented flying qualities specification
24 p3314 N88-29739

A second look at MIL prime flying qualities requirements 24 p3314 N88-29740

The role of simulation in flying qualities and flight control system related development 24 p3315 N88-29742

Angle of attack and sideslip estimation using an inertial reference platform
[AD-A194876] 24 p3319 N88-29769

A fiber optic collective flight control system for helicopters
[AD-A195406] 24 p3328 N88-29818

Controlled degradation of resolution of high-quality flight simulator images for training effectiveness evaluation
[AD-A196189] 24 p3330 N88-29823

Numerical simulation of nozzle flows
[AD-A195144] 24 p3369 N88-30064

Four-axis side-arm flight control simulator investigation
[AD-A196026] 24 p3409 N88-30294

Prediction and measurement of human pilot dynamic characteristics in a manned rotorcraft simulation
[NASA-CR-183246] 24 p3410 N88-30297

AIRCRAFT DESIGN

NT HELICOPTER DESIGN

International Conference on the Aerodynamics at Low Reynolds Numbers between 10(4) and 10(6)
[ONRL-7-023-C] 01 p0002 N88-10010

Design principles and practices for implementation of MIL-STD-1760 in aircraft and stores
[AD-A183724] 01 p0005 N88-10027

Problem and solution formulations for the generation of 3D block-structured grids --- aircraft design
[NLR-MP-86020-U] 01 p0005 N88-10028

Aerospace research at the National Aerospace Laboratory (NLR)
[ETN-87-90821] 01 p0107 N88-10697

Ensuring the service life of designs (experience in aircraft construction) 02 p0157 N88-10966

On the occasion of the 50th anniversary of the death of Professor Hugo Junkers
[MBB/LW-3016/S/PUB/201] 02 p0257 N88-11627

Rotorcraft Design for Operations
[AGARD-CP-423] 03 p0262 N88-11649

The influence of operational requirements on LHX concept formulation 03 p0262 N88-11650

Design requirements for future commercial operations
03 p0262 N88-11651

Mission-oriented flying qualities criteria for helicopter design via in-flight simulation 03 p0263 N88-11652

MBB simulation facilities applied for rotorcraft research 03 p0263 N88-11655

Impacts of rotor hub design criteria on the operational capabilities of rotorcraft systems
03 p0264 N88-11663

New aerodynamic design of the fenestron for improved performance 03 p0264 N88-11664

Rotorcraft designs for the year 2000
03 p0264 N88-11665

Apache for the battlefield of today and the 21st century 03 p0265 N88-11670

The EH-101 integrated project: A naval, utility and commercial helicopter system 03 p0265 N88-11672

Flight propulsion control integration for V/STOL aircraft
[NASA-TM-100226] 03 p0267 N88-11680

Flap-lag equations of motion of rigid, articulated rotor blades with three hinge sequences
[NASA-TM-100023] 04 p0401 N88-12495

A reliability concept for optimizing aircraft design
04 p0423 N88-12622

Renewed interest in airships for industry use discussed 04 p0424 N88-12628

The A320 Airbus program
[SNIAS-872-111-105] 05 p0529 N88-13215

Validation elements of the computation methods and measurement techniques for high lift aerodynamic systems
[SNIAS-872-111-101] 05 p0541 N88-13299

Special Course on Fundamentals of Fighter Aircraft Design
[AGARD-R-740] 05 p0544 N88-13315

Fundamentals of fighter aircraft design
05 p0544 N88-13316

Mission requirements and aircraft sizing
05 p0545 N88-13317

Design of wings and wing/body configurations for transonic and supersonic speeds
05 p0545 N88-13318

Aircraft dynamics: Aerodynamic aspects and wind tunnel techniques 05 p0545 N88-13320

Fundamentals of fighter aircraft design: Engine intake and afterbody 05 p0545 N88-13322

Aeroelasticity and optimization in fighter aircraft design
05 p0546 N88-13324

Materials for fighter aircraft 05 p0546 N88-13325

Requirements and recommendations for the development of theoretical codes and experimental facilities in the near future 05 p0546 N88-13327

Aeroelastic analysis of modern transport aircraft --- European Airbus
[SNIAS-872-111-102] 05 p0546 N88-13329

Damage considerations in sizing aircraft cells. Life predictions
[SNIAS-872-111-116] 05 p0546 N88-13330

Static Aeroelastic Effects on High Performance Aircraft
[AGARD-CP-403] 05 p0550 N88-13348

Static aeroelastic considerations in the definition of design loads for fighter airplanes
05 p0550 N88-13351

The use of aeroelastic wind tunnel models to prove structural design 05 p0551 N88-13355

Surface treatment problems found in new aircraft designed using structural composites
[SNIAS-872-111-113] 05 p0558 N88-13397

Utilization of a high rate vector computer in computational fluid mechanics for aeronautics
[ETN-88-91171] 05 p0581 N88-13547

Overall description of the computer aided design and manufacturing systems associated with the A320 program at Aerospatiale and its partners
[SNIAS-872-111-104] 05 p0635 N88-13883

Presentation of SIGMA (Interactive Assisted Geometry System). A computer assisted shape design program developed at the Aerospatiale Aircraft Division
[SNIAS-872-111-110] 05 p0635 N88-13884

Structural optimization in the design process --- aircraft
[SNIAS-872-111-115] 05 p0635 N88-13885

Operational groups at the Aerospatiale Aircraft Division
[SNIAS-872-111-107] 05 p0658 N88-14036

Damage tolerance of stiffened-skin structures: Prediction and experimental verification
[NLR-MP-86041-U] 06 p0667 N88-14091

A simulation study of the flight dynamics of elastic aircraft. Volume 1: Experiment, results and analysis
[NASA-CR-4102] 06 p0669 N88-14099

NAL news updated: FY87 business plan, developments 06 p0675 N88-14135

Activities report in aircraft design and astronautics
[ETN-88-90618] 07 p0809 N88-14925

Langley Symposium on Aerodynamics, volume 1
[NASA-CP-2397] 07 p0809 N88-14926

Application of a full potential method for analysis of complex aircraft geometries 07 p0809 N88-14930

Viscous vortex flows 07 p0810 N88-14934

Flight research on natural laminar flow
07 p0813 N88-14950

Design and experimental evaluation of a swept supercritical Laminar Flow Control (LFC) airfoil
07 p0813 N88-14951

The NASA aircraft icing research program
08 p0957 N88-15803

Overview of NASA PTA propfan flight test program
08 p0957 N88-15805

NASA/Army Rotorcraft Technology. Volume 2: Materials and Structures, Propulsion and Drive Systems, Flight Dynamics and Control, and Acoustics
[NASA-CP-2495-VOL-2] 09 p1106 N88-16632

NASA's rotorcraft icing research program
09 p1108 N88-16641

Rotorcraft flight-propulsion control integration
09 p1108 N88-16643

Aeroacoustic research programs at the Army Aviation Research and Technology Activity
09 p1109 N88-16649

NASA/Army Rotorcraft Technology. Volume 3: Systems Integration, Research Aircraft, and Industry
[NASA-CP-2495-VOL-3] 09 p1110 N88-16650

Integrated diagnostics 09 p1111 N88-16655

McDonnell Douglas Helicopter Company independent research and development: Preparing for the future
09 p1111 N88-16660

Testing of a schematic transport plane model in several European windtunnels
[PB87-170270] 09 p1113 N88-16671

The wind tunnel as a yardstick for aircraft design
[NLR-MP-85032-U] 09 p1121 N88-16712

Computational fluid dynamics and aerothermodynamics
[NASA-CR-182490] 09 p1166 N88-16969

Development of vertical takeoff aircraft with turbojet engines in Germany 10 p1309 N88-17822

Variable sweep wings 10 p1309 N88-17823

The European Airbus A-300 10 p1309 N88-17824

Purposes and tasks of high-performance aircraft construction
[MBB/LK-S/PUB/296] 10 p1312 N88-17842

Presentation of Class 1 designs for a family of commuter airplanes
[NASA-CR-182563] 11 p1439 N88-18587

Counter-Rotating Integrated Shrouded Propfan (CRISP): The MTU propfan program --- Motoren und Turbinen Union (MTU)
[ETN-88-91023] 11 p1441 N88-18597

Chinese 7760 CAD/CAMM software system introduced 11 p1468 N88-18756

Aerodynamic characteristics of wings designed with a combined-theory method to cruise at a Mach number of 4.5
[NASA-TP-2799] 12 p1575 N88-19420

Workshop on Design Loads for Advanced Fighters
[AGARD-R-746] 12 p1579 N88-19449

The development of manoeuvre load criteria for agile aircraft 12 p1579 N88-19450

Changes in USAF structural loads requirements
12 p1580 N88-19452

Structural design requirements for aircraft incorporating active control technology 12 p1580 N88-19453

The relationship between operational flight manoeuvre parameters and design parameters
12 p1580 N88-19454

Manoeuvres by default, by demand and by design
12 p1580 N88-19455

Design loads for Swedish military aircraft in a twenty years' perspective 12 p1580 N88-19456

Determination of design loads for modern combat aircraft 12 p1580 N88-19457

Interaction between structural considerations and system design in advanced flight controls
12 p1580 N88-19458

Manned simulation: Helpful means to determine and improve structural load criteria 12 p1581 N88-19459

Use of demonstration/validation prototypes: Impact on total development costs and times
12 p1703 N88-20194

The design of aircraft using the decision support problem technique
[NASA-CR-4134] 13 p1721 N88-20291

How to generate equal probability design load conditions --- aircraft design
[NLR-TR-86060-U] 13 p1722 N88-20295

Aeroelastic models in aircraft design
[MBB/LKE-294/S/PUB/249] 13 p1722 N88-20298

Activities report in aeronautics and astronautics
[ETN-88-91332] 13 p1859 N88-21115

Computer aided design of aircraft structures
[ETN-88-91353] 14 p1867 N88-21154

The NASA integrated test facility and its impact on flight research
[NASA-TM-100418] 14 p1870 N88-21177

Trends in Computational Fluid Dynamics (CFD) for aeronautical 3D steady applications: The Dutch situation
[NLR-MP-86074-U] 15 p2015 N88-22017

Activities report in aerospace
[ETN-88-91566] 16 p2155 N88-22856

The initial calculation of range and mission fuel during conceptual design --- aircraft design
[LR-525] 16 p2161 N88-22889

Basic design of a flight director system for NAL STOL research aircraft
[DE88-751806] 16 p2162 N88-22897

Stability and control methodology for conceptual aircraft design. Volume 1: Methodology manual
[AD-A191314] 16 p2164 N88-22906

Water facilities in retrospect and prospect: An illuminating tool for vehicle design
16 p2200 N88-23126

The use of the NRC/NAE water facilities in Canadian aeronautical research and development
16 p2201 N88-23132

It's time to reinvent the general aviation airplane
17 p2294 N88-23726

Full potential methods for analysis/design of complex aerospace configurations
[NASA-CR-3982] 17 p2296 N88-23736

Laminar Flow Aircraft Certification
[NASA-CP-2413] 17 p2296 N88-23737

Boundary-layer stability and airfoil design
17 p2296 N88-23738

High-flaps for natural laminar flow airfoils
17 p2296 N88-23739

Computational wing design studies relating to natural laminar flow 17 p2297 N88-23740

Preliminary aerodynamic design considerations for advanced laminar flow aircraft configurations
17 p2297 N88-23746

Multi-body aircraft with an all-movable center fuselage actively controlling fuselage pressure drag
[NASA-CASE-LAR-13511-1] 17 p2301 N88-23765
Sensitivity analysis and multidisciplinary optimization for aircraft design: Recent advances and results
[NASA-TM-100630] 17 p2302 N88-23766
The specification and design of a future maritime reconnaissance aircraft 17 p2303 N88-23772
A structured approach to weapon system design
17 p2303 N88-23773
Acta aeronautica et astronautica sinica (selected articles)
[AD-A191552] 18 p2455 N88-24575
A transonic small disturbance wing design methodology 18 p2457 N88-24590
Class 2 design update for the family of commuter airplanes
[NASA-CR-182681] 18 p2464 N88-24629
Current fire safety design aspects of commuter aircraft
[DOT/FAA/CT-87/32] 19 p2600 N88-25448
Proceedings of the 5th NAL Symposium on Aircraft Computational Aerodynamics
[NAL-SP-8] 19 p2635 N88-25630
Numerical calculation of supersonic flow by the PNS equations 19 p2636 N88-25636
Aerodynamic simulation for complete ASKA aircraft configuration 19 p2637 N88-25641
Calculations of unsteady aerodynamics for a full aircraft configuration using boundary element method
19 p2637 N88-25643
An initial investigation into methods of computing transonic aerodynamic sensitivity coefficients
[NASA-CR-183061] 20 p2752 N88-26332
Flight research and testing
[NASA-TM-100439] 20 p2758 N88-26361
Flight Mechanics Panel Symposium on Rotorcraft Design for Operations: Technical evaluation report
[AGARD-AR-243] 20 p2758 N88-26362
A new method for the estimation of aircraft inertia characteristics 20 p2787 N88-26530
Concept development of a Mach 3.0 high-speed civil transport
[NASA-TM-4058] 21 p2895 N38-27182
Supersonic transport/hypersonic transport (SST/HST) development
[REPT-881-111-101] 21 p2896 N88-27192
Development of direct-inverse 3-D methods for applied transonic aerodynamic wing design and analysis
[NASA-CR-183127] 22 p3037 N88-28033
Complex configurations 23 p3167 N88-28861
Transport-type configurations
23 p3169 N88-28867
Combat aircraft 23 p3169 N58-28868
Variable Sweep Transition Flight Experiment (VSTFE)-parametric pressure distribution boundary layer stability study and wing glove design task
[NASA-CR-3992] 23 p3173 N88-28894
A contribution to the quantitative analysis of the influence of design parameters on the optimal design of passenger aircraft
[ETN-88-92979] 23 p3176 N88-28912
Critical joints in large composite primary aircraft structures. Volume 2: Technology demonstration test report
[NASA-CR-172587] 23 p3177 N88-28915
Critical joints in large composite primary aircraft structures. Volume 3: Ancillary test results
[NASA-CR-172588] 23 p3177 N88-28916
Vision through aircraft transparencies
23 p3242 N88-29294
The Flight of Flexible Aircraft in Turbulence: State-of-the-Art in the Description and Modelling of Atmospheric Turbulence
[AGARD-R-734-ADD] 24 p3311 N88-29717
Current and proposed gust criteria and analysis methods: An FAA overview 24 p3311 N88-29718
Matching P.S.D.: Design loads
24 p3312 N88-29720
A summary of methods for establishing airframe design loads from continuous gust design criteria
24 p3312 N88-29721
Comparison of the influence of different gust models on structural design 24 p3312 N88-29722
Measured and predicted responses of the Nord 260 aircraft to the low altitude atmospheric turbulence
24 p3312 N88-29723
A review of measured gust responses in the light of modern analysis methods 24 p3312 N88-29724
Aircraft dynamics: Aerodynamic aspects and wind tunnel techniques 24 p3313 N88-29731
Compression pylon
[NASA-CASE-LAR-13777-1] 24 p3323 N88-29789

AIRCRAFT DETECTION
Acta aeronautica et astronautica sinica (selected articles)
[AD-A191552] 18 p2455 N88-24575
Surface disturbances produced by low-level, subsonic B-1 aircraft
[AD-A192257] 20 p2624 N88-26752
Proceedings of the French-German Colloquium on Helicopter Detection
[ISL-R-104/87] 22 p3147 N88-28723
Acoustic detection of helicopters: Experiments
22 p3148 N88-28727
Examples of the application of acoustics for the detection and classification of targets 22 p3148 N88-28729
Detection of helicopters using ground-controlled microphones 22 p3148 N88-28730
Correlation method and sensors adapted to the environment 22 p3149 N88-28732
Acoustic-seismic helicopter detection
22 p3149 N88-28734
Helicopter Warning Sensor (HWS)
22 p3149 N88-28735
The VHF experimental radar LARA. A long-wavelength radar for helicopter detection 22 p3149 N88-28738
The radar detection of hovering helicopters
22 p3150 N88-28739

AIRCRAFT ENERGY EFFICIENCY PROGRAM
U ACEE PROGRAM

AIRCRAFT ENGINES
NT CONVERTIBLE FAN-SHAFT ENGINES
NT HELICOPTER ENGINES
NT TF-30 ENGINE
NT TF-34 ENGINE
Noise emission of civil and military aero-engines. Sources of generation and measures for attenuation
[ETN-87-91021] 01 p0091 N88-10595
Turbines with counterrotating runners for aircraft power plants 02 p0158 N88-10992
Diagnosis of flow channel in aircraft gas-turbine engines on basis of vibration spectrum characteristics
02 p0159 N88-10993
Transmission efficiency in advanced aerospace powerplant
[PNR90391] 02 p0182 N88-11133
The use of Kevlar on aero-engine fan containment casings
[PNR90410] 02 p0182 N88-11134
Development of heat flux sensors for turbine airfoils
02 p0184 N88-11143
The flight evaluation of an advanced engine display and monitoring system 03 p0264 N88-11659
A129 advanced solutions for meeting today's combat helicopter requirement 03 p0265 N88-11669
Crack initiation and propagation due to cyclic thermal gradients --- aircraft turbine blades
[ESA-TT-1023] 03 p0336 N88-12114
Aircraft engine exhaust plume dynamics
[AD-A184238] 04 p0400 N88-12488
Aircraft classification by type of propulsive devices. Determination of type and number of carrying solutions
04 p0424 N88-12626
Dynamics of reverse flows at pump inlet
04 p0425 N88-12636
Calculation of the tribological properties of surfaces by semi-empirical methods
[AD-A184283] 04 p0450 N88-12791
A numerical investigation on wing/nacelle interferences 05 p0535 N88-13258
Correlation of air pressure drop and flame arrestor characteristics for explosion suppression materials
[AD-A184960] 05 p0548 N88-13340
Performance of supersonic impingement radial turbines 06 p0712 N88-14367
Conclusions from a research program on mixed flow gas generator turbines 06 p0713 N88-14368
Aerodynamic design of first stage turbines for small aero engines 06 p0713 N88-14370
Flaps-up takoff performance of the OV-1D aircraft with YT53-L-704 engine installed
[AD-A185960] 07 p0819 N88-14979
Pollution from motor vehicles and aircraft at Stapleton International Airport (abbreviated report), revision 2
[AD-A185916] 07 p0875 N88-15307
Technology developments for a compound cycle engine 09 p1107 N88-16637
Small gas turbine engine technology
09 p1107 N88-16638
Creep and fatigue research efforts on advanced materials 09 p1119 N88-16701
Turbine engine monitoring systems: Can they benefit component improvement program management?
[AD-A186992] 09 p1120 N88-16706
Calibration of the ARL (Aeronautical Research Laboratories) rain and icing facility
[AD-A186776] 09 p1121 N88-16710
Development of a shell system for DS moulds at RR precision casting facility --- directional solidification (DS)
[PNR90400] 09 p1151 N88-16893
Advanced Technology for Aero Gas Turbine Components
[AGARD-CP-421] 10 p1279 N88-17647
The coming revolution in turbine engine technology
10 p1279 N88-17648
Optimisation of military compressors for weight and volume 10 p1279 N88-17649
An examination of the impact of potential advances in component technology for future military engines
10 p1279 N88-17650
Specification of an engine and its components starting from a consideration of aircraft missions
10 p1279 N88-17651
Application of highly loaded single-stage mixed-flow compressors in small jet-engines
10 p1280 N88-17652
A research program on the aerodynamics of a highly loaded turbine stage 10 p1280 N88-17655
Design and aerodynamic performance of a small mixed-flow gas generator turbine
10 p1281 N88-17662
Development of a plenum chamber burner system for an advanced VTOL engine 10 p1281 N88-17664
Aerodynamic performance of a scale-model, counter-rotating unducted fan 10 p1282 N88-17666
Gear systems for advanced turboprops
10 p1282 N88-17667
Ceramic bearings for use in gas turbine engines
[NASA-TM-100288] 10 p1340 N88-18007
Sampling intervals
[AD-A189445] 12 p1573 N88-19408
Elevated temperature crack growth studies of advanced titanium aluminides
[AD-A189025] 12 p1608 N88-19618
Optimizing powerplant design and development cycles
12 p1701 N88-20183
Engine flow simulation for wind tunnel testing at NLR
[NLR-MP-87011-U] 13 p1723 N88-20305
Aircraft corrosion problems and research in the Netherlands
[NLR-MP-86066-U] 13 p1744 N88-20427
Investigation of the misfueling of reciprocating piston aircraft engines
[NASA-TP-2803] 14 p1865 N88-21144
Research as part of the Air Force in aero propulsion technology (AFRAPT) program
[AD-A190336] 15 p2019 N88-22036
AFRAPT (Air Force Research in Aero Propulsion Technology) trainee program
[AD-A190525] 15 p2035 N88-22123
Lewis Structures Technology, 1988. Volume 2: Structural Mechanics
[NASA-CP-3003-VOL-2] 15 p2077 N88-22382
Structural analyses of engine wall cooling concepts and materials 15 p2081 N88-22405
Engine structures: A bibliography of Lewis Research Center's research for 1980-1987
[NASA-TM-100842] 17 p2350 N88-24002
Prediction of the aeroelastic behavior of tuned blades. Application to aircraft engines
[ISAL-87-0046] 21 p2897 N88-27199
Engine condition monitoring civil requirements: A British Airways view 22 p3033 N88-28002
Background to the UK military requirements for engine usage, condition and maintenance management systems
22 p3033 N88-28004
Recent advances in engine health management
22 p3033 N88-28005
Aircraft component health monitoring: An effective approach 22 p3033 N88-28006
The design and testing of aero engines to minimise hazard from birds
[PNR90436] 22 p3040 N88-28049
Applications of fatigue analyses: Aircraft engines
[PNR90439] 22 p3044 N88-28066
Trends in civil aircraft propulsion
[PNR90441] 22 p3044 N88-28067
Future trends in aviation propulsion
[PNR90443] 22 p3044 N88-28068
RB211 developments
[PNR90444] 22 p3045 N88-28069
The composite aeroengine
[PNR90451] 22 p3045 N88-28070
A review of non-contacting displacement measurement techniques used to monitor the movement of rotor blades in gas turbine aero engines
[PNR90457] 22 p3045 N88-28071
Holographic interferometry for flow visualization studies in high speed fans
[PNR90459] 22 p3045 N88-28072
Use of penetrating radiations for the dynamic examination of aero gas turbines
[PNR90470] 22 p3045 N88-28073
AGARD engine disc cooperative test programme
[AGARD-R-766] 23 p3179 N88-28926

Developing the Rolls-Royce Tay
[PNR90447] 24 p3327 N88-29609
Fuel effects on flame radiation and hot-section durability 24 p3347 N88-29925
Contamination and distortion of steady flow field induced by discrete frequency disturbances in aircraft gas engines
[AD-A195440] 24 p3370 N88-30069

AIRCRAFT EQUIPMENT
NAVSIM 2: A computer program for simulating aided-inertial navigation for aircraft
[NASA-CR-177438] 04 p0398 N88-12478
Lightning discharge protection rod
[NASA-CASE-LAR-13470-1] 06 p0666 N88-14083
Information transfer in the National Airspace System
10 p1275 N88-17634
Electrical/pneudraulic design considerations
[AD-A188097] 12 p1581 N88-19462
Equipment test methods for externally produced electromagnetic transients
[RAE-TM-FS(F)-457] 14 p1865 N88-21140
Recommended test specification for the electromagnetic compatibility of aircraft equipment
[RAE-TM-FS(F)-510] 14 p1867 N88-21155
Basic design studies for the realization of liquid crystal display systems in aircraft
[VA-87-001] 16 p2163 N88-22900
Aircraft field degradation and electromagnetic compatibility
[PB88-183975] 19 p2602 N88-25456
Tactical Rubidium Frequency Standard (TRFS), volume 1
[AD-A192981] 20 p2805 N88-26640
A cockpit natural language study - selected transcripts
[AD-A192972] 20 p2834 N88-26808
Electrical load and power source capacity report for the C-130 aircraft Self Contained Navigation System (SCNS): LSI model 6216A, 6216B, 6216C, revision
[AD-A193079] 21 p2895 N88-27186
The Flight of Flexible Aircraft in Turbulence: State-of-the-Art in the Description and Modelling of Atmospheric Turbulence
[AGARD-R-734] 24 p3312 N88-29725
A summary of atmospheric turbulence measurements with specially-equipped aircraft in the US
24 p3312 N88-29727
Standard fatigue specimens for fastener evaluation --- aircraft components
[FFA-TN-1987-68] 24 p3384 N88-30157

AIRCRAFT FUEL SYSTEMS
Pumping systems and flow interfaces for rapid response electronic reheat controls 10 p1282 N88-17665

AIRCRAFT FUELS
Correlation of air pressure drop and flame arrestor characteristics for explosion suppression materials
[AD-A184960] 05 p0548 N88-13340
Study of electrostatic modulation of fuel sprays to enhance combustion performance in an aviation gas turbine
[AD-A184967] 05 p0548 N88-13341
Effects of aviation fluids on fiber composite material
[FOA-C-20674-2.6] 08 p0965 N88-15840
Large-Scale Advanced Prop-Fan (LAP)
[NASA-CR-182112] 13 p1723 N88-20306
Aviation turbine fuels from tar sands bitumen and heavy oils. Part 3: Laboratory sample production
[AD-A189278] 13 p1753 N88-20484
Feasibility of producing jet fuel from GPGP (Great Plains Gasification Plant) by-products
[DE88-010233] 20 p2781 N88-26492
Biodegradation of JP-5 aviation fuel by subsurface microbial communities
[AD-A192743] 20 p2781 N88-26493
Combustion and fuels in gas turbine engines
[AGARD-CP-422] 24 p3345 N88-29910

AIRCRAFT GUIDANCE
The application of emulation techniques in the analysis of highly reliable, guidance and control computer systems 02 p0127 N88-10798
Knowledge Based Concepts and Artificial Intelligence: Applications to Guidance and Control
[AGARD-LS-155] 02 p0128 N88-10806
Overview of AGARD Lecture Series No. 155: Knowledge-based concepts and artificial intelligence applications to guidance and control
02 p0128 N88-10807
Some data processing requirements for precision Nap-Of-the-Earth (NOE) guidance and control of rotorcraft
[NASA-CR-177453] 04 p0401 N88-12493
Contribution to the improvement of the guidance accuracy of automatic pilots
[ETN-88-90607] 05 p0551 N88-13360
Simulator investigation of wind shear recovery techniques 10 p1275 N88-17630
Airworthiness considerations
10 p1276 N88-17636
Commonality in the design and production of the H-423 (F3) and H-770 (F-15) RLG inertial navigation systems
12 p1577 N88-19431
Flight simulations of MLS interception procedures applicable to laterally segmented approach paths
[NLR-MP-86037-U] 13 p1721 N88-20288
Joint University Program for Air Transportation Research, 1986
[NASA-CP-2502] 17 p2293 N88-23715
Investigation of air transportation technology at Princeton University, 1986 17 p2294 N88-23724
Optics: Perspectives for Measurement Techniques and Signal Processing for Flight Guidance --- conference
[DFVLR-MITT-87-21] 18 p2516 N88-24928
Laboratory tests of laser gyroscopes for future utilization in multifunction systems for precision navigation and flight guidance 18 p2517 N88-24932
Limits of accuracy and range of laser radars
18 p2517 N88-24934
The optical accelerometer: A novel sensor for vertical flight guidance 18 p2518 N88-24935

AIRCRAFT HAZARDS
Test results and predictions for the response of near-ceiling sprinkler links in a full-scale compartment fire
[NBSIR-87/3633] 01 p0033 N88-10209
Aircraft fire safety research 04 p0406 N88-12526
TOMS and the NOAA/FAA volcano support plan
05 p0618 N88-13796
NASA wind shear model: Summary of model analyses
10 p1273 N88-17617
Response of wind shear warning systems to turbulence with implication of nuisance alerts
10 p1274 N88-17618
Forward looking wind shear detection
10 p1275 N88-17629
Crew interface with windshear systems
10 p1275 N88-17631
Aviation weather: Status of FAA's (Federal Aviation Administration's) new hazardous weather detection and dissemination systems
[PB88-115910] 11 p1513 N88-19041
Lapwings and birdstrikes. The biology of the lapwing Vanellus vanellus in relation to the birdstrike hazard it presents
[CAA-PAPER-87015] 14 p1865 N88-21142
An experimental and theoretical study of the ice accretion process during artificial and natural icing conditions
[NASA-CR-182119] 14 p1865 N88-21143
Heat transfer from a negatively buoyant wall jet
[NBS/GCR-88/541] 15 p2050 N88-22206
In-flight measurement of ice growth on an airfoil using an array of ultrasonic transducers
[AIAA-PAPER-87-0178] 17 p2293 N88-23717
Experimental measurements of heat transfer from an iced surface during artificial and natural cloud icing conditions
[AIAA-PAPER-86-1352] 17 p2293 N88-23718
National plans for aircraft icing and improved aircraft icing forecasts and associated warning services
18 p2546 N88-25113
Flight-management strategies for escape from microburst encounters
[NASA-TM-4057] 19 p2603 N88-25461
Intelligent guidance and control for wind shear encounter
[NASA-CR-183060] 20 p2755 N88-26347
Extinguishing agent for magnesium fire, phases 5 and 6
[AD-A192436] 21 p2930 N88-27398
TDWR (Terminal Doppler Weather Radar) PRF (Pulse Repetition Frequency) selection criteria
[AD-A193089] 21 p2932 N88-27407
Extreme gusts distribution 24 p3314 N88-29734

AIRCRAFT INDUSTRY
Purposes and tasks of high-performance aircraft construction
[MBB/LK-S/PUB/296] 10 p1312 N88-17842
The use of simulation in the development of the Airbus 12 p1702 N88-20188
Prototype manufacturing techniques for reducing cost, schedule, and technical risk 12 p1702 N88-20189
Activities report in aerospace
[ETN-88-91566] 16 p2155 N88-22856
FAA aviation forecasts fiscal years 1988-1999
[AD-A191711] 18 p2455 N88-24576
Class 2 design update for the family of commuter airplanes
[NASA-CR-182681] 18 p2464 N88-24629
China's acquisition and use of foreign aviation technology
[AD-A194827] 24 p3440 N88-30471

AIRCRAFT INSTRUMENTS
NT AUTOMATIC PILOTS
NT FLIGHT RECORDERS
Boeing 727 MLS (Microwave Landing System) terminal instrument procedures (TERPS) approach data collection and processing, data report
[AD-A185523] 06 p0667 N88-14090
Quantifying some information processing aspects of the pilot's instrument crosscheck
[AD-A186114] 07 p0898 N88-15443
A comparison of keyboard designs for cockpit applications
[AD-A187775] 12 p1581 N88-19460

AIRCRAFT INTERIORS
U AIRCRAFT COMPARTMENTS

AIRCRAFT LANDING
NT CRASH LANDING
NT DITCHING (LANDING)
Global positioning satellite-based automatic landing system and wind estimated feedback for the AH-64 helicopter 02 p0124 N88-10784
A rule-based system for arrival sequencing and scheduling in air traffic control 02 p0129 N88-10815
Additional investigations in landing process of aircraft: Test distributions
[DFVLR-MITT-87-13] 09 p1115 N88-16686
An investigation of classical dynamic scaling techniques applied to an oleo-pneumatic landing gear strut
[AD-A187664] 13 p1721 N88-20292
Simulator evaluation of lineup visual landing aids for night carrier landing
[AD-A191212] 18 p2468 N88-24648
Additional investigations into the aircraft landing process: Test distributions
[ESA-TT-1099] 23 p3177 N88-28913

AIRCRAFT MAINTENANCE
A project of an intelligent system to help on-line trouble shooting --- aircraft maintenance
[SNIAS-872-111-106] 05 p0529 N88-13216
Design and control of repairs of carbon fiber lift augmentation flaps in the ATR42 aircraft
[SNIAS-872-111-112] 05 p0529 N88-13217
Simulated service test behavior of various internal and external coatings applied on CF6-50 first stage turbine blades
[NLR-MP-86018-U] 05 p0549 N88-13343
Investigation of the nature and concentration of vapor and mist during the cleaning of aircraft
[PML-1985-29] 05 p0623 N88-13817
Damage tolerance of stiffened-skin structures: Prediction and experimental verification
[NLR-MP-86041-U] 06 p0667 N88-14091
Field evaluation of interactive simulation for maintenance training: SH-3 helicopter electro-mechanical bladefold system
[AD-A185923] 07 p0821 N88-14991
Supportability in aircraft systems through technology and acquisition strategy applications
[AD-A186465] 08 p0949 N88-15759
A model for estimating depot maintenance costs for Air Force fighter and attack aircraft
[AD-A187097] 09 p1105 N88-16624
IMIS: Integrated Maintenance Information System. A maintenance information delivery concept
09 p1203 N88-17207
Knowledge based jet engine diagnostics
09 p1203 N88-17210
Tutoring electronic troubleshooting in a simulated maintenance work environment
09 p1204 N88-17215
Army maintenance: Actions to reduce the likelihood of helicopter gear failures
[PB88-135256] 11 p1433 N88-18551
Sampling intervals
[AD-A189445] 12 p1573 N88-19408
The design of aircraft using the decision support problem technique
[NASA-CR-4134] 13 p1721 N88-20291
Development of a flexible and economic helicopter engine monitoring system
[PB88-165147] 16 p2160 N88-22887
Development of a high-temperature resistant (700 F), corrosion-preventive organic coating
[AD-A191407] 16 p2182 N88-23005
Preventing aircraft corrosion by predictive corrosion modeling 17 p2321 N88-23863
Composite repair of cracked aluminum alloy aircraft structure
[AD-A190514] 18 p2455 N88-24573
Predictive corrosion modeling, volume 1
[AD-A191229] 18 p2485 N88-24739
Proceedings of the 14th Symposium on Aircraft Integrated Monitoring Systems
[DFVLR-MITT-88-04] 22 p3033 N88-28001

Background to the UK military requirements for engine usage, condition and maintenance management systems
22 p3033 N88-28004
Recent advances in engine health management
22 p3033 N88-28005
Tornado: Airframe fatigue life monitoring
22 p3034 N88-28011
Maintenance support for military aircraft by intelligent on-board maintenance data panel
22 p3034 N88-28012
A solution to improve a military aircraft's Onboard-Checkout-And-Monitoring-System (OCAMS)
22 p3034 N88-28013
Proposal for the on-board part of a future aircraft integrated monitoring system 22 p3035 N88-28016
Development of a maintenance data bus monitor and recorder 22 p3036 N88-28022
The impact of increased aircraft reliability on maintenance facility design
[AD-A194395] 22 p3042 N88-28057

AIRCRAFT MANEUVERS
Global positioning satellite-based automatic landing system and wind estimated feedback for the AH-64 helicopter 02 p0124 N88-10784
Improvements to the adaptive maneuvering logic program
[NASA-CR-3985] 03 p0262 N88-11648
Developmental airdrop testing techniques and devices
[AGARD-AG-300-VOL-6] 04 p0398 N88-12481
Trends in aeroelastic analysis of combat aircraft
05 p0550 N88-13350
Overlooked potential of systems with Markovian coefficients
[NLR-MP-86049-U] 05 p0552 N88-13366
Langley Symposium on Aerodynamics, volume 1
[NASA-CP-2397] 07 p0809 N88-14926
Unsteady stall penetration experiments at high Reynolds number
[AD-A186120] 07 p0814 N88-14958
Rotorcraft flight-propulsion control integration
09 p1108 N88-16643
Rotorcraft handling-qualities design criteria development 09 p1109 N88-16645
Predicting dynamic separation characteristics of general configurations
[AD-A186689] 09 p1116 N88-16691
Future fighter maneuverability for air combat
[MBB/LKE-1/S/PUB/120] 10 p1312 N88-17843
MOAOPS and BOOM-MAP computer programs for sonic boom research, volume 1
[AD-A189548] 12 p1574 N88-19414
Workshop on Design Loads for Advanced Fighters
[AGARD-R-746] 12 p1579 N88-19449
The development of manoeuvre load criteria for agile aircraft 12 p1579 N88-19450
Fighter design for human load limits
12 p1580 N88-19451
The relationship between operational flight manoeuvre parameters and design parameters
12 p1580 N88-19454
Manoeuvres by default, by demand and by design
12 p1580 N88-19455
Design loads for Swedish military aircraft in a twenty years' perspective 12 p1580 N88-19456
Manned simulation: Helpful means to determine and improve structural load criteria 12 p1581 N88-19459
Task listing: Visually assisted and visually dependent tasks for fighter aircraft
[AD-A191041] 16 p2244 N88-23404
Full potential methods for analysis/design of complex aerospace configurations
[NASA-CR-3982] 17 p2296 N88-23736
Flight-management strategies for escape from microburst encounters
[NASA-TM-4057] 19 p2603 N88-25461
Flight simulator: Field of view utilized in performing tactical maneuvers
[AD-A192412] 20 p2762 N88-26379
Structural dynamics of maneuvering aircraft
[AD-A192376] 23 p3176 N88-28906
Variation of carotid flow under load, studied by the Doppler echo method --- acceleration tolerance
[REPT-1149] 23 p3240 N88-29282
An interim comparison of operational CG records in turbulence on small and large civil aircraft
24 p3313 N88-29729

AIRCRAFT MODELS
Improvements to the adaptive maneuvering logic program
[NASA-CR-3985] 03 p0262 N88-11648
Measurement of model deformation in wind tunnels
05 p0551 N88-13358
Aeroelastic models in aircraft design
[MBB/LKE-294/S/PUB/249] 13 p1722 N88-20298
Activities report of the Lille Institute of Fluid Mechanics
[ETN-88-91983] 13 p1771 N88-20597
Measurements on a helicopter rotor
[R-764-S] 14 p1861 N88-21119
Design, simulation and laboratory testing of an inertial system for measuring the attitude and narrow-spaced motions
[DFVLR-FB-87-42] 14 p1912 N88-21426
User's manual for LINEAR, a FORTRAN program to derive linear aircraft models
[NASA-TP-2768] 14 p1967 N88-21740
Model selection for the multiple model adaptive algorithm for in-flight simulation
[AD-A189715] 15 p2016 N88-22022
K-pulse estimation from incomplete multiple-frequency scattering data and target identification
[AD-A190827] 16 p2190 N88-23061
Nonlinear flying quality parameters based on dynamic inversion
[AD-A192146] 18 p2464 N88-24627
A two-point aerodynamic model for identification
20 p2786 N88-26526
Estimation of aircraft parameters using filter error methods and extended Kalman filter
[DFVLR-FB-88-15] 23 p3176 N88-28911
Interactive plotting of NASTRAN aerodynamic models using NPLOT and DISSPLA
[AD-A194115] 23 p3226 N88-29204
Analysis of the transmission of sound into the passenger compartment of a propeller aircraft using the finite element method
[FFA-TN-1988-15] 23 p3279 N88-29520
A comparison of simple analytical models for representing propeller aircraft structural and acoustic responses
[ISVR-TR-153] 23 p3279 N88-29523
Computer programs for generation of NASTRAN and VIBRA-6 aircraft models
[AD-A195467] 24 p3322 N88-29737

AIRCRAFT NOISE
NT BLADE SLAP NOISE
NT JET AIRCRAFT NOISE
NT SONIC BOOMS
Noise of a model high speed counterrotation propeller at simulated takeoff/approach conditions (F7/A7)
[NASA-TM-100206] 01 p0091 N88-10592
Noise levels from propeller-driven aircraft measured at ground level and at 1.2 m above the ground
[NPL-AC-110] 01 p0091 N88-10594
Noise emission of civil and military aero-engines. Sources of generation and measures for attenuation
[ETN-87-91021] 01 p0091 N88-10595
Results of the 1986 NASA/FAA/DFVLR main rotor test entry in the German-Dutch wind tunnel (DNW)
[NASA-TM-100507] 04 p0487 N88-13003
Aircraft interior noise reduction by alternate resonance tuning
[NASA-CR-181530] 04 p0488 N88-13005
Development of rotorcraft interior noise control concepts. Phase 3: Development of noise control concepts
[NASA-CR-178172] 06 p0776 N88-14762
Development of rotorcraft interior noise control concepts. Phase 2: Full scale testing, revision 1
[NASA-CR-172594-REV-1] 06 p0777 N88-14769
Measuring the annoyance of aircraft noise
[AD-A185494] 06 p0777 N88-14770
Recent Langley helicopter acoustics contributions
09 p1109 N88-16646
Identification and proposed control of helicopter transmission noise at the source
09 p1109 N88-16647
A decade of aeroacoustic research at NASA Ames Research Center 09 p1109 N88-16648
Aeroacoustic research programs at the Army Aviation Research and Technology Activity
09 p1109 N88-16649
Laboratory studies related to in-flight acoustic emission monitoring
[AD-A186714] 09 p1242 N88-17445
Supersonic and subsonic aircraft noise effects on animals: A literature survey
[AD-A186922] 10 p1404 N88-18373
Sound transmission through the walls of light aircraft. An investigation of structure-borne noise in a Handley Page 137 Jetstream 3 aircraft
[NASA-CR-182509] 10 p1405 N88-18376
Comparison of two transonic noise prediction formulations using the aircraft noise prediction program
[NASA-CR-181609] 12 p1688 N88-20095
Activities report of the Physics Department
[ETN-88-91985] 13 p1833 N88-20964
Noise assessment of unsuppressed TF-34-GE-100A engine at Warfield ANG, Baltimore, Maryland
[AD-A189966] 15 p2129 N88-22702
Structureborne noise measurements on a small twin-engine aircraft
[NASA-CR-4137] 16 p2265 N88-23545
Advanced turboprop aircraft flyover noise: Annoyance to counter-rotating-propeller configurations with an equal number of blades on each rotor, preliminary results
[NASA-TM-100612] 16 p2265 N88-23547
Analytical modeling of the structureborne noise path on a small twin-engine aircraft
[NASA-CR-4136] 17 p2394 N88-24233
Advisory circular: Noise certification handbook
[FAA-AC-36-4B] 17 p2394 N88-24234
Research investigation of helicopter main rotor/tail rotor interaction noise
[NASA-CR-4143] 19 p2722 N88-26165
Simulated measurement of power flow in structures near to simple sources and simple boundaries
[NASA-TM-89124] 19 p2722 N88-26166
Helicopter main-rotor noise: Determination of source contributions using scaled model data
[NASA-TP-2825] 20 p2848 N88-26907
Application of pattern recognition techniques to the identification of aerospace acoustic sources
[NASA-CR-183116] 21 p3013 N88-27877
Aeroacoustic investigation on the noise from ultralight aircraft
[DFVLR-FB-88-03] 21 p3013 N88-27879
Aircraft noise: A review
[PNR90450] 22 p3147 N88-28719
Aircraft noise prediction program propeller analysis system IBM-PC version user's manual version 2.0
[NASA-CR-181689] 24 p3428 N88-30399

AIRCRAFT NOISE PREDICTION
U NOISE PREDICTION (AIRCRAFT)

AIRCRAFT PARTS
Operational load measurements on service helicopters
03 p0263 N88-11658
Lewis materials research and technology: An overview
09 p1119 N88-16699
High temperature polymer matrix composites
09 p1119 N88-16700
Validation of GEMACS (General Electromagnetic Model for the Analysis of Complex Systems) for modeling lightning-induced electromagnetic fields
[AD-A188822] 12 p1620 N88-19687
Design and test of a new coaxial air joints
[DE88-751808] 16 p2164 N88-22908
Simulation of moisture diffusion of fiber reinforced components of aircraft for general air transportation
[IFL-IB-87-05] 21 p2807 N88-27253
Stress corrosion of C ring specimen in salt spray tests
[I-186/87] 21 p2916 N88-27307

AIRCRAFT PERFORMANCE
NT HELICOPTER PERFORMANCE
Helicopter (performance) management
03 p0264 N88-11666
Analytic investigation of helicopter rotor blade appended aeroelastic devices
[NASA-CR-166525] 03 p0266 N88-11676
The A320 Airbus program
[SNIAS-872-111-105] 05 p0529 N88-13215
Aircraft dynamics: Aerodynamic aspects and wind tunnel techniques 05 p0545 N88-13320
Techniques for performance optimisation in cruise and manoeuverability 05 p0545 N88-13321
Requirements and recommendations for the development of theoretical codes and experimental facilities in the near future 05 p0546 N88-13327
Aeroelastic analysis of modern transport aircraft
05 p0550 N88-13352
Influence of Environmental Factors on Aircraft Wing Performance
[VKI-LS-1987-03] 08 p0951 N88-15771
The influence of wind shear, downdraft, and turbulence in aircraft performance 08 p0952 N88-15773
The potential influence of rain on airfoil performance
08 p0952 N88-15774
Effects of wing simulated ground frost on aircraft performance 08 p0952 N88-15775
Effects of aircraft deicing/anticing fluids on airfoil characteristics 08 p0952 N88-15776
Low altitude windshear threat to commercial aircraft
08 p0952 N88-15777
Effects of enviromentally imposed roughness on airfoil performance 08 p0952 N88-15778
Directions in propulsion control
08 p0956 N88-15799
SWAN: An expert system with natural language interface for tactical air capability assessment
09 p1210 N88-17253
Development of vertical takeoff aircraft with turbojet engines in Germany 10 p1309 N88-17822
Variable sweep wings 10 p1309 N88-17823
Purposes and tasks of high-performance aircraft construction
[MBB/LK-S/PUB/296] 10 p1312 N88-17842

Flight testing of fighter aircraft
[MBB/LKE-62/S/PUB/292] 10 p1312 N88-17844
Performance survey of airfoil profiles
[ETN-88-91093] 11 p1436 N88-18568
Investigations of the laminar-turbulent boundary layer transition for the improvement of the performance of powered glider aircraft profiles
[ETN-88-91094] 11 p1436 N88-18569
Aircraft and ground vehicle friction correlation test results obtained under winter runway conditions during joint FAA/NASA Runway Friction Program
[NASA-TM-100506] 11 p1438 N88-18582
Structural shape optimization in multidisciplinary system synthesis
[NASA-TM-100538] 12 p1614 N88-19650
Aquila remotely piloted vehicle: Its potential battlefield contribution still in doubt
[PB88-120241] 13 p1721 N88-20289
Development of a real-time aeroperformance analysis technique for the X-29A advanced technology demonstrator
[NASA-TM-100432] 14 p1866 N88-21151
Performance improvements of an F-15 airplane with an integrated engine-flight control system
[NASA-TM-100431] 14 p1867 N88-21159
Parametric study of supersonic STOVL flight characteristics
[NASA-CR-177330] 16 p2161 N88-22893
Airplane runway performance monitoring system
[NASA-CASE-LAR-13854-1-CU]
18 p2432 N88-24621
Method for prediction and determination of takeoff performance for vectored thrust vehicles
[AD-A191809] 18 p2463 N88-24626
Propfan test assessment testbed aircraft stability and control/performance 1/9-scale wind tunnel tests
[NASA-CR-182121] 20 p2757 N88-26360
Proceedings of the 14th Symposium on Aircraft Integrated Monitoring Systems
[DFVLR-MITT-88-04] 22 p3033 N88-28001
Japan Air Line's Aircraft Integrated Monitoring System (AIMS) activities 22 p3034 N88-28014
The exploitation of Aircraft Integrated Monitoring System (AIMS) data in height-keeping studies for aircraft operating above FL 290 22 p3036 N88-28026
High performance forward swept wing aircraft
[NASA-CASE-ARC-11636-1] 23 p3177 N88-28914
Measured and predicted responses of the Nord 260 aircraft to the low altitude atmospheric turbulence
24 p3312 N88-29723
Status review of atmosphere turbulence and aircraft response 24 p3312 N88-29726
Aircraft dynamics: Aerodynamic aspects and wind tunnel techniques 24 p3313 N88-29731

AIRCRAFT PILOTS
Application of knowledge-based techniques to aircraft trajectory generation and control
02 p0129 N88-10811
Human respiratory responses during high performance flight
[AGARD-AG-312] 04 p0474 N88-12923
Sitting posture of helicopter pilots of the Royal Netherlands Air Force: preliminary recommendations
[IZF-1986-16] 05 p0631 N88-13857
Does the knife open perspectives for the myopic pilot?
[ETN-87-90166] 09 p1199 N88-17187
Sitting posture of pilots in the Boelkow 105c helicopter
[IZF-1986-22] 09 p1202 N88-17202
Crew interface with windshear systems
10 p1275 N88-17631
Trends in the distribution of tasks between commercial pilots and flight control systems
[MBB-UT-008/87] 10 p1314 N88-17851
Realtime pilot model parameter identification
[AD-A188873] 12 p1584 N88-19476
Selected aspects of triazolam in relation to aviator performance in naval flight operations
[AD-A189322] 12 p1667 N88-19996
Relationship of encoding speed and memory tests to flight training performance
[AD-A190670] 15 p2105 N88-22539
Personality, attitudes, and pilot training performance: Preliminary analysis
[AD-A193102] 21 p2981 N88-27746
Stress/fatigue and the ARNG (Army National Guard) aviator
[AD-A194184] 22 p3132 N88-28621
Central serous chorioretinopathy in USAF aviators: A review
[AD-A195697] 24 p3407 N88-30280

AIRCRAFT POWER SOURCES
U AIRCRAFT ENGINES

AIRCRAFT POWER SUPPLIES
Aerospace energy systems laboratory: Requirements and design approach
[NASA-TM-100423] 17 p2390 N88-24206

AIRCRAFT PRODUCTION
Advanced organic composite materials for aircraft structures: Future program
[NASA-CR-181467] 06 p0678 N88-14155
Product planning in civil aircraft construction
[MBB-UT-002/87] 10 p1313 N88-17849
The application of modern aeroelastic developments for future projects
[MBB-UT-007/87] 10 p1313 N88-17850
Flight Vehicle Development Time and Cost Reduction
[AGARD-CP-424] 12 p1700 N88-20173
Risk reduction cost avoidance for full scale development begins with concept formulation
12 p1700 N88-20174
Development savings through parametric modeling of program costs 12 p1700 N88-20175
Picking winners: Parametric cost estimating and project management 12 p1700 N88-20176
Parametric study of the total cost of aircraft modernization in terms of development and equipment series costs 12 p1700 N88-20177
The increased time and cost of development: Causes and (some) remedies 12 p1701 N88-20178
The judgement and evaluation of long-term investments demonstrated by means of a civil aircraft program
12 p1701 N88-20180
Development cost reduction using integrated CAE-CAD-CAM techniques 12 p1701 N88-20182
Structural materials: The changing scene
12 p1703 N88-20190
Schedule and cost control of development
12 p1704 N88-20196
People, procedures, performance: The keys to improving the development environment 12 p1704 N88-20197
The effects of two Carlucci initiatives concurrency and streamlining, on the test and evaluation phase of system acquisitions 12 p1704 N88-20198
Acceleration of prototype development and reduction of cost by multidisciplinary integration
12 p1704 N88-20199
Organization of helicopter development activities with a view toward reduction of costs and cycles
12 p1704 N88-20200
The influence of infrastructure on the costs and timescales of collaborative programmes
12 p1704 N88-20201
Activities report in aerospace
[ETN-88-91566] 16 p2155 N88-22856

AIRCRAFT PRODUCTION COSTS
Advanced composite airframe program: Today's technology 09 p1107 N88-16636
Product planning in civil aircraft construction
[MBB-UT-002/87] 10 p1313 N88-17849

AIRCRAFT RELIABILITY
Ensuring the service life of designs (experience in aircraft construction) 02 p0157 N88-10986
Reliability of finite element methods in North America
[AGARD-R-748] 02 p0184 N88-11139
The Shock and Vibration Digest, Volume 19, No. 11
03 p0265 N88-11673
Airworthiness of long-life jet transport structures
03 p0265 N88-11674
Damage tolerance of stiffened-skin structures: Prediction and experimental verification
[NLR-MP-86041-U] 06 p0667 N88-14091
Preliminary airworthiness evaluation of a UH-1 equipped with a terrain mapping receiver antenna
[AD-A186274] 07 p0819 N88-14980
Airworthiness considerations
10 p1276 N88-17636
An evaluation of perceptions of form, fit, function (F3) standardization on the Standard Inertial Navigation Unit (STD INU) program
[AD-A188955] 12 p1579 N88-19446
The development of manoeuvre load criteria for agile aircraft 12 p1579 N88-19450
Preliminary airworthiness evaluation of the UH-60A equipped with the XM-139 VOLCANO mine dispensing system
[AD-A190604] 15 p2018 N88-22029
Preliminary airworthiness evaluation of the UH-60A with Advanced Digital Optical Control System (ADOCS)
[AD-A190674] 15 p2018 N88-22030
Airworthiness and flight characteristics test of a ski assembly for the UH-60A Black Hawk helicopter
[AD-A191414] 16 p2162 N88-22895
Semi-Markov adjunction to the Computer-Aided Markov Evaluator (CAME)
[NASA-CR-181645] 19 p2678 N88-25924
The impact of increased aircraft reliability on maintenance facility design
[AD-A194395] 22 p3042 N88-28057
The Flight of Flexible Aircraft in Turbulence: State-of-the-Art in the Description and Modelling of Atmospheric Turbulence
[AGARD-R-734-ADD] 24 p3311 N88-29717
Current and proposed gust criteria and analysis methods: An FAA overview 24 p3311 N88-29718
Re-assessment of gust statistics using CAADRP data
24 p3313 N88-29732
Acquisition of gust statistics from AIDS-recorded data
24 p3313 N88-29733
Preliminary airworthiness evaluation of the UH-60A/ESSS (External Stores Support System) with HELLFIRE launcher installed
[AD-A196187] 24 p3323 N88-29793
The development of acoustic emission for structural integrity monitoring of aircraft
[AD-A196264] 24 p3427 N88-30398

AIRCRAFT SAFETY
Some approaches to the design of high integrity software 02 p0127 N88-10799
Reliability of finite element methods in North America
[AGARD-R-748] 02 p0184 N88-11139
Experimental evidence for modifying the current physical model for ice accretion on aircraft surfaces
[NASA-TM-87184] 04 p0397 N88-12473
Airline safety: A comparative analysis
[AD-A185358] 05 p0543 N88-13308
Theoretical analysis of the electrical aspects of the basic electro-impulse problem in aircraft de-icing applications
[NASA-CR-180845] 05 p0543 N88-13310
Corrosion in avionics and associated equipment; cause, effect and prevention 05 p0547 N88-13335
A flow visualization study of the leading edge separation bubble on a NACA 0012 airfoil with simulated glaze ice
[NASA-CR-180846] 07 p0816 N88-14966
Sudden in-flight incapacitation in general aviation
[AD-A187044] 09 p1115 N88-16682
Annual review of aircraft accident data: US air carrier operations calendar year 1985
[PB88-135843] 10 p1276 N88-17638
Aircraft accident/incident, Newark, New Jersey, November 13, 1986
[NTSB/AAR-87/04-SUMM] 10 p1276 N88-17639
Aviation weather: Status of FAA's (Federal Aviation Administration's) new hazardous weather detection and dissemination systems
[PB88-115910] 11 p1513 N88-19041
The development of manoeuvre load criteria for agile aircraft 12 p1579 N88-19450
Atmospheric electrical modeling in support of the NASA F-106 storm hazards project
[NASA-CR-181639] 13 p1799 N88-20758
Proceedings of the Workshop on the Assessment of Crew Workload Measurements Methods, Techniques and Procedures. Volume 1: Preliminary Selection of Measures
[AD-A189004] 13 p1812 N88-20827
Equipment test methods for externally produced electromagnetic transients
[RAE-TM-FS(F)-457] 14 p1865 N88-21140
Activities report in flight and space travel
[ISSN-0070-3966] 14 p2012 N88-22000
Soft-ground aircraft arresting systems
[AD-A190838] 16 p2165 N88-22912
Variable response load limiting device
[NASA-CASE-LAR-12801-1] 17 p2346 N88-23982
Study of benefits of passenger protective breathing equipment from analysis of past accidents
[DOT/FAA/CT-88/03] 18 p2461 N88-24610
Development of a multipurpose smart recorder for general aviation aircraft
[NASA-CR-168353] 18 p2465 N88-24637
Current fire safety design aspects of commuter aircraft
[DOT/FAA/CT-87/32] 19 p2600 N88-25448
Enhanced emergency smoke venting
[DOT/FAA/CT-88/22] 20 p2756 N88-26350
Corrosion in aircraft structures. Part 1: Text
[LR-527-PT-1] 20 p2775 N88-26458
Corrosion in aircraft structures. Part 2: Figures
[LR-527-PT-2] 20 p2775 N88-26459
The Flight of Flexible Aircraft in Turbulence: State-of-the-Art in the Description and Modelling of Atmospheric Turbulence
[AGARD-R-734-ADD] 24 p3311 N88-29717

AIRCRAFT SPECIFICATIONS
The European Airbus A-300 10 p1309 N88-17624

AIRCRAFT SPIN
Contribution to the numerical solution of airplane spin motion
[ETN-88-92368] 21 p2896 N88-27190

AIRCRAFT STABILITY
Decoupling and stabilization of speed and height in F4 Phantom aircraft using output feedback
[ETN-87-90926] 02 p0125 N88-10787
Local-optimal control in systems with delay
04 p0424 N88-12627
Examples of static aeroelastic effects on present combat aircraft projects 05 p0550 N88-13349

Integration of a supersonic unsteady aerodynamic code into the NASA FASTEX system
[NASA-CR-182329] 06 p0663 N88-14068

General Rotorcraft Aeromechanical Stability Program (GRASP) version 1.03: User's manual
[NASA-TM-100043] 09 p1219 N88-17313

Some aspects of aircraft dynamic loads due to flow separation
[AGARD-R-750] 11 p1439 N88-18586

A flight test investigation into flow separation and structural response for a transport aircraft at buffet onset
[RAE-TR-87006] 14 p1867 N88-21156

The effects of torque response and time delay on rotorcraft vertical axis handling qualities
[AD-A189873] 15 p2017 N88-22023

Influence of unsteady aerodynamic forces on dynamic response of variable sweep aircraft
15 p2054 N88-22245

Natural laminar flow and airplane stability and control
17 p2298 N88-23747

Propfan test assessment testbed aircraft stability and control/performance 1/9-scale wind tunnel tests
[NASA-CR-182121] 20 p2757 N88-26360

Low-speed wind-tunnel test of a STOL supersonic-cruise fighter concept
[NASA-TM-4050] 20 p2761 N88-26374

High performance forward swept wing aircraft
[NASA-CASE-ARC-11636-1] 23 p3177 N88-28914

A second look at MIL prime flying qualities requirements 24 p3314 N88-29740

AIRCRAFT STRUCTURES
NT AIRFRAMES
NT FUSELAGES
NT PLASTIC AIRCRAFT STRUCTURES

The influence of load cycle reconstitution on fatigue behaviour
[ARL-STRUC-R-424] 02 p0192 N88-11198

A reliability concept for optimizing aircraft design
04 p0423 N88-12622

Aircraft dynamic response calculation based on discrete-continual model 04 p0424 N88-12624

Aircraft classification by type of propulsive devices. Determination of type and number of carrying solutions
04 p0424 N88-12626

Materials for fighter aircraft 05 p0546 N88-13325

Surface treatment problems found in new aircraft designed using structural composites
[SNIAS-872-111-113] 05 p0558 N88-13397

Philosophy and practice of nondestructive tests of composite material structures at Aerospatiale Aquitaine
[SNIAS-872-430-105] 05 p0559 N88-13400

Measurement and control of damage in composite materials: Nondestructive controls by thermography, holography, and radiography
[SNIAS-872-430-110] 05 p0559 N88-13403

Structural optimization in the design process --- aircraft
[SNIAS-872-111-115] 05 p0635 N88-13685

Damage tolerance of stiffened-skin structures: Prediction and experimental verification
[NLR-MP-86041-U] 06 p0667 N88-14091

Numerical simulation of flight body circumference flow
06 p0676 N88-14137

Study of surface treatment before bonding of light alloys
[DCQ/L-48-287/F] 06 p0682 N88-14181

Study of selection criteria for adhesives used in aircraft structure bonding
[ETN-88-91619] 08 p0971 N88-15875

Experimental study on the effect of fiber orientation on flutter characteristics of high-aspect-ratio transport wing
[NAL-TR-936] 09 p1120 N88-16708

Evaluation of high temperature structural adhesives for extended service, phase 5
[NASA-CR-178176] 09 p1149 N88-16884

Modern materials for light constructions --- aircraft
[MBB-Z-136/86] 10 p1312 N88-17839

Purposes and tasks of high-performance aircraft construction
[MBB/LK-S/PUB/296] 10 p1312 N88-17842

The application of modern aeroelastic developments for future projects
[MBB-UT-007/87] 10 p1313 N88-17850

Sound transmission through the walls of light aircraft. An investigation of structure-borne noise in a Handley Page 137 Jetstream 3 aircraft
[NASA-CR-182509] 10 p1405 N88-18376

High performance composites research at NASA-Langley
[NASA-TM-100518] 11 p1450 N88-18642

Automatic riveting machine for spherically-formed airframe structures
[ETN-88-91024] 11 p1495 N88-18924

Factors affecting the sticking of insects on modified aircraft wings
[NASA-CR-182615] 12 p1575 N88-19421

Changes in USAF structural loads requirements
12 p1580 N88-19452

Manoeuvres by default, by demand and by design
12 p1580 N88-19455

Advanced durability analysis. Volume 1: Analytical methods
[AD-A188341] 12 p1635 N88-19789

Structural materials: The changing scene
12 p1703 N88-20190

Standardized environmental fatigue sequence for the evaluation of composite components in combat aircraft (ENSTAFF = ENvironmental falSTAFF)
[LBF-FB-179] 13 p1722 N88-20300

European approaches in standard spectrum development --- aircraft load spectra
[NLR-MP-87007-U] 13 p1782 N88-20661

Activities report of the Structures Department
[ETN-88-91966] 13 p1783 N88-20672

Activities report in aeronautics and astronautics
[ETN-88-91332] 13 p1859 N88-21115

Computer aided design of aircraft structures
[ETN-88-91353] 14 p1867 N88-21154

A flight test investigation into flow separation and structural response for a transport aircraft at buffet onset
[RAE-TR-87006] 14 p1867 N88-21156

A study of damage tolerance in curved composite panels
[AD-A190617] 15 p2029 N88-22092

Activities report in aerospace
[ETN-88-91566] 16 p2155 N88-22856

Design studies of primary aircraft structures in ARALL laminates
[LR-520] 16 p2160 N88-22888

User's manual for EULER3DS
[AD-A191048] 16 p2206 N88-23177

Investigation into the operation of the new special drills for drilling holes in thin components made of composite materials --- aircraft components
[LR-519] 16 p2215 N88-23215

Structureborne noise measurements on a small twin-engine aircraft
[NASA-CR-4137] 16 p2265 N88-23545

Fuel containment, lightning protection and damage tolerance in large composite primary aircraft structures
[NASA-CR-3875] 17 p2317 N88-23839

Water based primers for structural adhesive bonding of aircraft 17 p2321 N88-23862

Analytical modeling of the structureborne noise path on a small twin-engine aircraft
[NASA-CR-4136] 17 p2394 N88-24233

Simulated measurement of power flow in structures near to simple sources and simple boundaries
[NASA-TM-89124] 19 p2722 N88-26166

Sensitivity to crack initiation in thick assemblies. Test report 48-444
[REPT-48-444] 20 p2758 N88-26365

Corrosion in aircraft structures. Part 1: Text
[LR-527-PT-1] 20 p2775 N88-26458

Corrosion in aircraft structures. Part 2: Figures
[LR-527-PT-2] 20 p2775 N88-26459

Design manual for impact damage tolerant aircraft structure, addendum
[AGARD-AG-238-ADD] 21 p2895 N88-27185

Design and implementation of contact ultrasonic sensors to assess internal damage
[I-177/87] 21 p2906 N88-27247

Nonlinear vibrations of periodically stiffened plates
21 p2963 N88-27598

Critical joints in large composite primary aircraft structures. Volume 2: Technology demonstration test report
[NASA-CR-172587] 23 p3177 N88-28915

Critical joints in large composite primary aircraft structures. Volume 3: Ancillary test results
[NASA-CR-172588] 23 p3177 N88-28916

Asymptotic modal analysis and statistical energy analysis
[NASA-CR-183077] 23 p3278 N88-29514

A comparison of simple analytical models for representing propeller aircraft structural and acoustic responses
[ISVR-TR-153] 23 p3279 N88-29523

Dynamics of articulated aerospace structures
[AD-A195685] 24 p3324 N88-29794

Aircraft airframe cost estimating relationships: Study approach and conclusions
[R-3255-AF] 24 p3324 N88-29795

AIRCRAFT SURVIVABILITY

Efficiency analysis of airborne Electronic CounterMeasures (ECM) systems
[AD-A184606] 03 p0306 N88-11934

SWAN: An expert system with natural language interface for tactical air capability assessment
09 p1210 N88-17253

A computer graphics simulation of the endgame in aircraft combat survivability
[AD-A187826] 11 p1541 N88-19214

Threat expert system technology advisor
[NASA-CR-177479] 24 p3328 N88-29816

AIRCRAFT TIRES

Aircraft and ground vehicle friction correlation test results obtained under winter runway conditions during joint FAA/NASA Runway Friction Program
[NASA-TM-100506] 11 p1438 N88-18582

Static mechanical properties of 30 x 11.5 - 14.5, type 8 aircraft tires of bias-ply and radial-belted design
[NASA-TP-2810] 14 p1867 N88-21157

Energy dissipation in a rolling aircraft tire
[NASA-CR-182978] 19 p2676 N88-25913

A critical speed study for aircraft bias ply tires
[AD-A193616] 22 p3084 N88-28313

AIRCRAFT WAKES
NT PROPELLER SLIPSTREAMS
NT SLIPSTREAMS

Dispersion in the wake of aircraft: An investigation of the effects of a ground plane on trailing vortices. Literature survey
[IC-AERO-REP-86-04] 01 p0003 N88-10014

Predicting dynamic separation characteristics of general configurations
[AD-A186689] 09 p1116 N88-16691

Propulsive performance of a lifting flapping wing
17 p2295 N88-23733

Laser-Doppler measurements of turbulence structures in free streams behind flat and rotation symmetrical profiles
[ETN-88-92336] 21 p2948 N88-27510

AIRCREWS
U FLIGHT CREWS

AIRDROPS

Control systems for platform landings cushioned by air bags
[AD-A196154] 24 p3358 N88-29996

AIRFIELD SURFACE MOVEMENTS

A new look at the use of linear methods to predict aircraft dynamic response to taxi over bomb damaged and repaired airfields 09 p1180 N88-17069

Airport surface traffic automation study
[AD-A194553] 23 p3181 N88-28934

AIRFIELDS
U AIRPORTS

AIRFOIL CHARACTERISTICS
U AIRFOILS

AIRFOIL OSCILLATIONS
NT WING OSCILLATIONS

A natural low frequency oscillation in the wake of an airfoil near stalling conditions
[NASA-TM-100213] 02 p0123 N88-10779

Active feedback interaction with a shear layer
[AD-A188525] 12 p1573 N88-19410

Wing flutter calculations with the CAP-TSD unsteady transonic small disturbance program
[NASA-TM-100580] 12 p1575 N88-19419

Application of a nonisentropic full potential method to AGARD standard airfoils
[NASA-TM 100560] 13 p1716 N88-20263

Development of drive mechanism for an oscillating airfoil 14 p1926 N88-21482

Unsteady flow field measurements using LDV (Laser Doppler Velocimetry)
[AD-A189907] 15 p2063 N88-22298

Control and use of unsteady flows: Insect use of various wing kinematics and related pressure measurements using a pitching airfoil 21 p2926 N88-27366

Liquid crystals for unsteady surface shear stress visualization
[DE88-010570] 21 p2951 N88-27527

AIRFOIL PROFILES
NT WING PROFILES
NT WING SPAN

A critical assessment of wind tunnel results for the NACA 0012 airfoil
[NASA-TM-100019] 03 p0260 N88-11636

Breakdown of the conservative potential equation
07 p0809 N88-14929

Computer program for the calculation of the profile-vortices interactions (two dimensional inviscid incompressible flow with point singularities)
[ISL-R-124/86] 08 p0987 N88-15982

Flow field measurements using hotwire anemometry
[AD-A187029] 09 p1160 N88-16951

The further development of circulation control airfoils
10 p1270 N88-17594

Circulation control STOL aircraft design aspects
10 p1272 N88-17610

Performance survey of airfoil profiles
[ETN-88-91093] 11 p1436 N88-18568

Investigations of the laminar-turbulent boundary layer transition for the improvement of the performance of powered glider aircraft profiles
[ETN-88-91094] 11 p1436 N88-18569

An experimental-computational investigation of transonic shock wave-turbulent boundary layer interaction in a curved test section
[CWI-NM-R8716] 14 p1909 N88-21408

New airfoil sections for straight bladed turbine
[DE88-701075] 14 p1942 N88-21588

High Reynolds number, low Mach number, steady flow field calculations over a NACA 0012 airfoil using Navier-Stokes and interactive boundary layer theory
[AD-A189871] 15 p2013 N88-22005

Computational fluid dynamics drag prediction: Results from the Viscous Transonic Airfoil Workshop
[NASA-TM-100095] 15 p2014 N88-22009

Designs of profiles for cascades
[NASA-TT-20161] 15 p2067 N88-22326

Short duration flow establishment on a profile in a Water-Ludwieg-Tunnel 16 p2201 N88-23134

Computation of flow around NACA0012 airfoil at high angle of attack 19 p2636 N88-25640

Parallelization on a multiprocessor system of a solution method for the unsteady Navier-Stokes equations at high Reynolds numbers
[ONERA-NT-1987-8] 20 p2803 N88-26632

Treatment of the separated flow around profiles (nonviscous, incompressible, two dimensionel flow) by the singularities method
[ISL-R-106/87] 20 p2803 N88-26633

Wind tunnel tests of the influence of airfoil-thickness on normal force and pitching moment of two slender wings at transonic and supersonic Mach numbers
[DFVLR-FB-88-17] 21 p2893 N88-27171

Theory of sound production by vortex-airfoil interaction
[AD-A193386] 21 p3012 N88-27875

The influence of surface rounding on trailing edge noise
[AD-A193387] 21 p3012 N88-27876

An efficient patched grid Navier-Stokes solution for multiple bodies, phase 1
[AD-A194166] 23 p3211 N88-29110

Effects of precipitation on wind turbine performance
[DE88-001144] 23 p3228 N88-29211

AIRFOIL SECTIONS
U AIRFOIL PROFILES

AIRFOIL THICKNESS
U AIRFOIL PROFILES

AIRFOILS
NT AEROELASTIC RESEARCH WINGS
NT AILERONS
NT ARROW WINGS
NT BEARINGLESS ROTORS
NT CAMBERED WINGS
NT CIRCULATION CONTROL AIRFOILS
NT CIRCULATION CONTROL ROTORS
NT CRUCIFORM WINGS
NT DELTA WINGS
NT FIXED WINGS
NT FLAPS (CONTROL SURFACES)
NT JET FLAPS
NT LAMINAR FLOW AIRFOILS
NT LEADING EDGE FLAPS
NT LOW ASPECT RATIO WINGS
NT OBLIQUE WINGS
NT PROPELLER BLADES
NT RIGID ROTORS
NT ROTARY WINGS
NT SLENDER WINGS
NT SPOILERS
NT SUPERCRITICAL AIRFOILS
NT SUPERCRITICAL WINGS
NT SUPERSONIC AIRFOILS
NT SWEPT FORWARD WINGS
NT SWEPT WINGS
NT SWEPTBACK WINGS
NT TABS (CONTROL SURFACES)
NT THIN AIRFOILS
NT THIN WINGS
NT TILTING ROTORS
NT TRAILING EDGE FLAPS
NT UPPER SURFACE BLOWN FLAPS
NT VARIABLE SWEEP WINGS
NT VORTEX FLAPS
NT WING FLAPS
NT WINGS
NT X WING ROTORS

Analyses and assessments of span wise gust gradient data from NASA B-57B aircraft
[NASA-CR-178288] 01 p0002 N88-10007

The structure of separated flow regions occurring near the leading edge of airfoils including transition
[NASA-CR-181434] 01 p0002 N88-10011

Wall interference tests of a CAST 10-2/DOA 2 airfoil in an adaptive-wall test section
[NASA-TM-4015] 02 p0122 N88-10772

Development of heat flux sensors for turbine airfoils
02 p0184 N88-11143

Film cooling heat transfer on a turbine airfoil
02 p0186 N88-11156

Measurement of airfoil heat transfer coefficients on a turbine stage 02 p0188 N88-11158

Coolant passage heat transfer with rotation
02 p0186 N88-11160

Thermal barrier coating life prediction model development 02 p0190 N88-11183

Thermal barrier coating life prediction model development 02 p0190 N88-11185

Local heat/mass transfer and pressure drop in a two-pass rib-roughened channel for turbine airfoil cooling
[NASA-CR-179635] 03 p0322 N88-12039

Theoretical and practical aspects of multigrid methods in boundary element calculations
[NLR-MP-85021-U] 03 p0370 N88-12328

Investigation of low-speed turbulent separated flow around airfoils
[NASA-CR-177450] 04 p0396 N88-12471

NCSU code: Validation and extension on NAL's UNIVAC 1100/60 system
[PD-FM-8716] 04 p0476 N88-12931

Measurement of velocity and vorticity fields in the wake of an airfoil in periodic pitching motion
[NASA-TP-2780] 04 p0487 N88-13002

Computation of dynamic stall of NACA0012 airfoil by block pentadiagonal matrix scheme
05 p0535 N88-13255

Practical application of two-dimensional viscous flow computation 05 p0535 N88-13257

The role of computation fluid dynamics in aeronautical engineering (4). The development and applications of implicit TVD finite volume code
05 p0536 N88-13259

Application of discrete vortex method to analysis of separated flow around aerofoils
05 p0537 N88-13268

Navier-Stokes analysis of laminar flow control of a two-dimensional airfoil 05 p0540 N88-13286

A swept wing panel in a low speed flexible walled test section
[NASA-CR-4106] 05 p0540 N88-13292

The development of a computer code (U2DIIF) for the numerical solution of unsteady, inviscid and incompressible flow over an airfoil
[AD-A185033] 05 p0541 N88-13293

Computation of rime ice accretion on airfoils
[FFA-TN-1987-08] 05 p0542 N88-13301

An experimental investigation of the aerodynamics of a NACA 64A010 airfoil-flap combination with and without flap oscillations. Part 1: Steady-state characteristics
[NASA-TM-88217] 05 p0542 N88-13305

Measurement of local convective heat transfer coefficients from a smooth and roughened NACA-0012 airfoil: Flight test data
[NASA-TM-100284] 05 p0582 N88-13552

Potential flow around two-dimensional airfoils using a singular integral method
[NASA-CR-182345] 06 p0664 N88-14070

Investigation of viscous/inviscid interaction in transonic flow over airfoils with suction 06 p0664 N88-14074

A zonal approach for the solution of coupled Euler and potential solutions of flows with complex geometries
[AD-A185465] 06 p0702 N88-14310

Characteristics of a separating confluent boundary layer and the downstream wake
[NASA-TM-100046] 06 p0704 N88-14323

Computational fluid dynamics overview
07 p0809 N88-14927

Finite-volume scheme for transonic potential flow about airfoils and bodies in an arbitrarily shaped channel
07 p0809 N88-14928

A multistage time-stepping scheme for the thin-layer Navier-Stokes equations 07 p0810 N88-14932

Boundary layer transition 07 p0811 N88-14942

Separated flow 07 p0812 N88-14944

Advanced natural laminar flow airfoil with high lift to drag ratio 07 p0812 N88-14947

Airfoil large eddy breakup devices for turbulent drag reduction 07 p0814 N88-14956

Unsteady stall penetration experiments at high Reynolds number
[AD-A186120] 07 p0814 N88-14958

A flow visualization study of the leading edge separation bubble on a NACA 0012 airfoil with simulated glaze ice
[NASA-CR-180846] 07 p0816 N88-14986

An experimental mapping of the flow field behind a glaze ice shape on a NACA 0012 airfoil
[NASA-CR-180847] 08 p0950 N88-15766

Three-dimensional unsteady flow elicited by finite wings and complex configurations
[AD-A186464] 08 p0951 N88-15770

Effects of enviromentally imposed roughness on airfoil performance 08 p0952 N88-15778

Theoretical and experimental studies of the transonic flow field and associated boundary conditions near a longitudinally-slotted wind-tunnel wall
[NASA-CR-181169] 08 p0959 N88-15815

Experimental investigation of shock-induced disturbances on transonic airfoils
[DFVLR-FB-87-28] 09 p1112 N88-16666

A note on the aerodynamic design of thin parallel-sided aerofoil sections
[ARL-AERO-TM-388] 09 p1114 N88-16677

Navier-Stokes solutions for laminar incompressible flow over a NACA 0012 airfoil and a backward facing step
[FFA-TN-1987-50] 09 p1162 N88-16966

Well-posedness and spectral estimation for infinite dimensional systems
[AD-A187621] 10 p1401 N88-18354

Pressure distributions from high Reynolds number transonic tests of an NACA 0012 airfoil in the Langley 0.3-meter transonic cryogenic tunnel
[NASA-TM-100526] 11 p1435 N88-18565

High Reynolds number transonic tests on a NACA 0012 airfoil in the Langley 0.3-meter transonic cryogenic tunnel
[NASA-TM-100527] 11 p1436 N88-18571

Status of the special-purpose airfoil families
[DE88-001124] 11 p1506 N88-18998

A generalisation of Hall's scheme for solving the Euler equations for two-dimensional flows
11 p1537 N88-19188

Application of a nonisentropic full potential method to AGARD standard airfoils
[NASA-TM-100560] 13 p1716 N88-20263

On the Kutta condition for flows around lifting airfoils and wings
[DFVLR-FB-87-40] 13 p1717 N88-20268

Constructing Gloved wings for aerodynamic studies
[NASA-TM-100440] 14 p1863 N88-21128

Wall interference assessment and corrections for transonic adaptive wall airfoil data
14 p1863 N88-21129

Comparison of pressure distributions on model and full-scale NACA 64-621 airfoils with ailerons for wind turbine application
[NASA-TM-100802] 14 p1943 N88-21593

High Reynolds number, low Mach number, steady flow field calculations over a NACA 0012 airfoil using Navier-Stokes and interactive boundary layer theory
[AD-A189871] 15 p2013 N88-22005

Oscillating airfoils: Achievements and conjectures
[AD-A190490] 15 p2014 N88-22008

Aerofoil testing in a self-streamlining flexible walled wind tunnel
[NASA-CR-4128] 16 p2156 N88-22865

An integral equation for the linearized supersonic flow over a wing
[AD-A191408] 16 p2158 N88-22875

The transonic wind tunnel (TWB) at DFVLR, Brunswick (Federal Republic of Germany)
[DFVLR-MITT-88-01] 16 p2164 N88-22909

Reduced order models for nonlinear aerodynamics
16 p2220 N88-23248

Application of Navier-Stokes analysis to stall flutter
16 p2220 N88-23249

In-flight measurement of ice growth on an airfoil using an array of ultrasonic transducers
[AIAA-PAPER-87-0178] 17 p2293 N88-23717

High Reynolds number tests of a Douglas DLBA 032 airfoil in the Langley 0.3-meter transonic cryogenic tunnel
[NASA-TM-87683] 17 p2296 N88-23734

Boundary-layer stability and airfoil design
17 p2296 N88-23738

Wind tunnel testing of low-drag airfoils
17 p2297 N88-23741

Flight experiences with laminar flow
17 p2297 N88-23744

Preliminary aerodynamic design considerations for advanced laminar flow aircraft configurations
17 p2297 N88-23746

Natural laminar flow and airplane stability and control
17 p2298 N88-23747

Passive shock wave-boundary layer control for the Bell FX69-H-098 airfoil 18 p2457 N88-24588

Prediction of laminar and turbulent flows past single and twin airfoils 18 p2457 N88-24589

Two dimensional hyperbolic grid generation
[VKI-TN-162] 18 p2511 N88-24897

Characteristics of merging shear layers and turbulent wakes of a multi-element airfoil
[NASA-TM-100053] 18 p2511 N88-24900

Manipulation of the structure of a turbulent boundary layer 18 p2512 N88-24901
Computational Fluid Mechanics
[NASA-CR-183022] 18 p2514 N88-24915
A characteristic method for calculating the generalized flat flutter aerodynamic forces
[NASA-TT-20300] 19 p2598 N88-25438
Finite element analysis of incompressible viscous flow around multi-element aerofoils 19 p2635 N88-25634
Wall interference assessment/correction of data from tests of a CAST 10-2/DOA 2 airfoil in the Langley 0.3-m transonic cryogenic tunnel 20 p2751 N88-26331
Improved potential flow computational methods with Euler corrections for airfoil and wing/body design
[AD-A192303] 20 p2752 N88-26334
Effects of numerical dissipation on finite-volume solutions of compressible flow problems
[AD-A193173] 21 p2944 N88-27485
Investigation of viscous/inviscid interaction in transonic flow over airfoils with suction
[NASA-CR-183112] 21 p2945 N88-27490
Determination of the local heat-transfer characteristics on glaze ice accretions on a cylinder and a NACA 0012 airfoil 21 p2946 N88-27500
An experimental investigation of two 15 percent-scale wind tunnel fan-blade designs
[NASA-TM-88256] 22 p3046 N88-28076
Thermal barrier coating life-prediction model development
[NASA-CR-179507] 22 p3058 N88-28142
Computational tools for simulation methodologies
23 p3168 N88-28865
Effects of independent variation of Mach and Reynolds numbers on the low-speed aerodynamic characteristics of the NACA 0012 airfoil section
[NASA-TM-4074] 23 p3170 N88-28879
Noise generation and boundary layer effects in vortex-airfoil interaction and methods of digital hologram analysis for these flow fields
[AD-A194191] 23 p3171 N88-28883
Unsteady flow past an NACA 0012 airfoil at high angles of attack
[AD-A194650] 23 p3172 N88-28886
The effects of inlet turbulence and rotor/stator interactions on the aerodynamics and heat transfer of a large-scale rotating turbine model. Volume 3: Heat transfer data tabulation 65 percent axial spacing
[NASA-CR-179468] 23 p3180 N88-28930
The use of hot-film technique for boundary layer studies on a 21 percent thick airfoil
[NAE-AN-45] 24 p3321 N88-29781
The effects of inlet turbulence and rotor/stator interactions on the aerodynamics and heat transfer of a large-scale rotating turbine model. Volume 2: Heat transfer data tabulation. 15 percent axial spacing
[NASA-CR-179467] 24 p3326 N88-29804
Studies of gas turbine heat transfer airfoil surface and end-wall cooling effects
[AD-A195165] 24 p3326 N88-29805

AIRFRAME MATERIALS
Composite structural materials
[NASA-CR-181416] 02 p0190 N88-11186

AIRFRAMES
The history of aeroelasticity research in Germany from the beginning until 1945 --- airframes
[DFVLR-MITT-86-25] 01 p0001 N88-10003
Reduced complexity structural modeling for automated airframe synthesis
[NASA-CR-177440] 04 p0393 N88-12453
Fundamentals of fighter aircraft design: Engine intake and afterbody 05 p0545 N88-13322
Advanced composite airframe program: Today's technology 09 p1107 N88-16636
Durability and damage tolerance of aluminum castings
[AD-A186444] 10 p1341 N88-18013
Aircraft corrosion problems and research in the Netherlands
[NLR-MP-86066-U] 13 p1744 N88-20427
A study of damage tolerance in curved composite panels
[AD-A190617] 15 p2029 N88-22092
Propulsion and airframe aerodynamic interactions of supersonic V/STOL configurations. Volume 4: Summary
[NASA-CR-177343-VOL-4] 16 p2157 N88-22868
Design manual for impact damage tolerant aircraft structure, addendum
[AGARD-AG-238-ADD] 21 p2895 N88-27165
Tornado: Airframe fatigue life monitoring
22 p3034 N88-28011
Crash simulation calculations and component idealization for an airframe. Computer code KRASH 79
[ETN-88-92971] 23 p3174 N88-28899
Stress intensity factors for cracked metallic structures under rapid thermal loading
[AD-A191219] 23 p3193 N88-29004
A summary of methods for establishing airframe design loads from continuous gust design criteria
24 p3312 N88-29721
Aircraft airframe cost estimating relationships: Study approach and conclusions
[R-3255-AF] 24 p3324 N88-29795
Evaluation of bond testing equipment for inspection of Army advanced composite airframe structures
[AD-A195795] 24 p3341 N88-29885

AIRGLOW
NT GEOCORONAL EMISSIONS
NT NIGHTGLOW
The nonlinear thermodynamics of meteors, noctilucent clouds, enhanced airglow and global atmospheric circulation 06 p0738 N88-14538
Vehicle glow observed on the SONDA 3
[INPE-4297-PRE/1168] 12 p1600 N88-19581
Ground-based facility for spectrophotometric studies of the airflow and aurora
[AP-29] 22 p3119 N88-28532

AIRLINE OPERATIONS
Issues in air transport and airport management
[PB87-204509] 02 p0124 N88-10782
Civil aeronautics
[ETN-88-90616] 05 p0543 N88-13309
Digest of the annual report of the Lufthansa German Airlines
[ISSN-0415-613X] 08 p0952 N88-15779
Analysis of bird strikes to UK registered aircraft 1985 (civil aircraft over 5700 kg maximum weight
[CAA-PAPER-87012] 09 p1115 N88-16684
Annual review of aircraft accident data: US air carrier operations calendar year 1985
[PB88-135843] 10 p1276 N88-17638
Estimates of potential increases in airport capacity through ATC (Air Traffic Control) system improvements in the airport and terminal areas
[AD-A188533] 12 p1578 N88-19444
Engine condition monitoring civil requirements: A British Airways view 22 p3033 N88-28002
RB211 developments
[PNR90444] 22 p3045 N88-28069

AIRPORT PLANNING
Issues in air transport and airport management
[PB87-204509] 02 p0124 N88-10782
Measuring airport landside capacity
[PB88-102637] 06 p0670 N88-14107
Analyses of heliport system plans
[DOT/FAA/PM-87/31] 17 p2308 N88-23610
FAA aviation forecasts fiscal years 1988-1999
[AD-A191711] 18 p2455 N88-24576
Airport surface traffic automation study
[AD-A194553] 23 p3181 N88-28934

AIRPORT SECURITY
Aviation security: FAA (Federal Aviation Administration) needs preboard passenger screening performance standards
[PB87-216800] 02 p0124 N88-10783

AIRPORT TOWERS
FAA air traffic control operations concepts. Volume 3: ISSS (Initial Sector Suite System) en route controllers
[AD-A185981] 07 p0818 N88-14975
FAA air traffic control operations concepts. Volume 4: TAAS (Terminal Advanced Automation System) terminal controllers
[AD-A185982] 07 p0818 N88-14976
FAA air traffic control operations concepts. Volume 5: ATCT/TCCC (Airport Traffic Control Tower/Tower Control Computer Complex) tower controllers
[AD-A185983] 07 p0818 N88-14977

AIRPORTS
NT HELIPORTS
First article test noise survey of the A/F32T-9 large turbo fan engine enclosed noise suppressor system, Sky Harbor IAP (International Airport), Phoenix, Arizona
[AD-A183799] 01 p0090 N88-10588
ZEUS: A knowledge-based expert system that assists in predicting visibility at airbases
[AD-A184197] 05 p0626 N88-13829
Measuring airport landside capacity
[PB88-102637] 06 p0670 N88-14107
Measuring the annoyance of aircraft noise
[AD-A185494] 06 p0777 N88-14770
Pollution from motor vehicles and aircraft at Stapleton International Airport (abbreviated report), revision 2
[AD-A185916] 07 p0875 N88-15307
NASA wind shear model: Summary of model analyses
10 p1273 N88-17617
Radar backscatter from airports and surrounding areas 10 p1274 N88-17623
Radar returns from ground clutter in vicinity of airports
10 p1274 N88-17624
Status of FAA terminal Doppler weather radar programs 10 p1275 N88-17632
The advanced low-level windshear alert system operational demonstration results, Summer, 1987, Denver Stapleton International Airport 10 p1275 N88-17633
Evaluation of bituminous materials used in pavement recycling projects at Tyndall, MacDill, and Hurlburt Air Force Bases
[AD-A188068] 10 p1317 N88-17871
Micro PAVER concept and development airport pavement management system
[AD-A187360] 11 p1441 N88-18598
Estimates of potential increases in airport capacity through ATC (Air Traffic Control) system improvements in the airport and terminal areas
[AD-A188533] 12 p1578 N88-19444
Noise assessment of unsuppressed TF-34-GE-100A engine at Warfield ANG, Baltimore, Maryland
[AD-A189966] 15 p2129 N88-22702
Microwave landing system mathematical modeling study for Midway Airport Runway 22L, Chicago, Illinois
[AD-A191721] 18 p2462 N88-24616
An analysis of time and space requirements for aircraft turnrounds
[TT-8705] 24 p3322 N88-29783

AIRSHIPS
A heat transfer model for a heated helium airship
[AD-A183786] 03 p0259 N88-11629
Renewed interest in airships for industry use discussed 04 p0424 N88-12628

AIRSPACE
Information transfer in the National Airspace System
10 p1275 N88-17634

AIRSPEED
An observer approach to the estimation of helicopter airspeed
[DFVLR-FB-87-13] 01 p0005 N88-10029
Decoupling and stabilization of speed and height in F4 Phantom aircraft using output feedback
[ETN-87-90926] 02 p0125 N88-10787
MOAOPS and BOOM-MAP computer programs for sonic boom research, volume 1
[AD-A189548] 12 p1574 N88-19414

AIRWORTHINESS
U AIRCRAFT RELIABILITY

AIRWORTHINESS REQUIREMENTS
U AIRCRAFT RELIABILITY

ALABAMA
Hypocenters (1977-1984) around the Richton Dome and the Melvin, Alabama, 1978 earthquake
[DE87-014336] 03 p0351 N88-12214

ALARMS
U WARNING SYSTEMS

ALASKA
Solar Energy Meteorological Research and Training Site, Alaska
[DE87-013706] 01 p0069 N88-10440
Coastal winds of the southeast Alaska Peninsula
[PB87-206173] 02 p0215 N88-11354
Thematic mapper study of Alaskan ophiolites
[NASA-CR-182554] 11 p1504 N88-18984
Alaska Loran C probe test results
[AD-A189131] 13 p1720 N88-20284
Influence of the Yukon River on the Bering Sea
[NASA-CR-182802] 17 p2376 N88-24126

ALBEDO
NT EARTH ALBEDO
Estimating scattered and absorbed radiation in plant canopies by remote sensing
[NASA-CR-181390] 02 p0193 N88-11205
Enhancement of surface-atmosphere fluxes by desert-fringe vegetation through reduction of surface albedo and of soil heat flux
[NASA-CR-181442] 02 p0197 N88-11231
Preliminary estimation of color inhomogeneities on the surface of Venus according to the television images obtained by the VENERA-13 and VENERA-14 automated space probes
[NASA-TT-20114] 02 p0254 N88-11606
Estimation of broadband planetary albedo from operational narrowband satellite measurements
[PB88-107644] 07 p0945 N88-15748
Research project on CO-induced climate change
[DE88-002352] 08 p1023 N88-16193
Higher frequency ambient noise in the arctic ocean
[AD-A192203] 18 p2547 N88-25122
Ultraviolet geometric albedo of Uranus
[NASA-CR-183099] 20 p2885 N88-27136
Differences in radiation budget parameters over Asia in relation to contrasting Indian monsoons
22 p3125 N88-28574
Energy budget and ground temperatures in hot regions
[AD-A196298] 24 p3404 N88-30268

ALCOHOLS
NT ETHYL ALCOHOL
NT GLYCOLS
NT ISOPROPYL ALCOHOL

NT METHYL ALCOHOL
NT PHENOLS
NT POLYVINYL ALCOHOL
Compendium of significant events in the recent development of alcohol fuels in the United States
[DE87-013355] 01 p0032 N88-10202
Preparation of polymer polyols
[EP-PATENT-0-162-589-A1] 01 p0102 N88-10665
Experimental and theoretical study of condensation in multicomponent mixtures
[DE88-002715] 07 p0830 N88-15033
Status of alcohol fuels utilization technology for highway transportation: A 1986 perspective. Volume 2: Compression ignition engines
[DE88-006059] 13 p1753 N88-20485
Comparison of isopropyl alcohol and trichloroethylene in removing solder flux
[DE88-005556] 14 p1889 N88-21288
Age, alcohol, and simulated altitude: Effects on performance and breathalyzer scores
[AD-A190642] 15 p2103 N88-22531
ALDEHYDES
NT FORMALDEHYDE
Characterization of catalysts with metal-support effects and of the species adsorbed on their surfaces
[DE87-014636] 04 p0414 N88-12564
ALDOSTERONE
Effects of anti-g suit inflation on renin and aldosterone response physical exercise 12 p1656 N88-19944
Plasma cortisol, renin and aldosterone during an intense heat acclimation program
[AD-A189387] 13 p1809 N88-20810
ALERTNESS
An evaluation of the effects of high visual taskload on the separate behaviors involved in complex monitoring performance
[AD-A190641] 15 p2105 N88-22538
Pupil measures of alertness and mental load
16 p2239 N88-23378
Physiological measures and mental-state assessment
16 p2242 N88-23392
The application of non-stationary data analysis techniques in the identification of changes in the electroencephalogram associated with the onset of drowsiness 21 p2978 N88-27688
ALEUTIAN ISLANDS (US)
Geological evolution and analysis of confirmed or suspected gas hydrate localities. Volume 10: Basin analysis, formation and stability of gas hydrates of the Aleutian Trench and the Bering Sea
[DE88-001008] 10 p1346 N88-18048
ALFVEN WAVES
U MAGNETOHYDRODYNAMIC WAVES
ALGAAS
U ALUMINUM GALLIUM ARSENIDES
ALGAE
NT BLUE GREEN ALGAE
NT CHLORELLA
NT MICROCYSTIS
Controlled Ecological Life Support System: Regenerative Life Support Systems in Space
[NASA-CP-2480] 03 p0357 N88-12251
Biomass recycle as a means to improve the energy efficiency of CELSS algal culture systems
03 p0358 N88-12254
Operation of an experimental algal gas exchanger for use in a CELSS 03 p0358 N88-12255
Non-conventional approaches to food processing in CELSS. 1: Algal proteins: Characterization and process optimization 03 p0358 N88-12256
Sunlight supply and gas exchange systems in microalgal bioreactor 03 p0359 N88-12258
Research on a solar biotechnology based on the culture of photosynthetic cells
[DE88-900129] 10 p1359 N88-18120
Ecological algal system in microgravity conditions: Preliminary results 12 p1655 N88-19915
Regenerative life support system research
[NASA-CR-182606] 12 p1671 N88-20006
An outdoor test facility for the large-scale production of microalgae
[DE88-001146] 21 p2984 N88-27723
The biological clock of Chlamydomonas reinhardii in space 22 p3061 N88-28162
ALGAL BLOOM
U ALGAE
ALGEBRA
NT ADJOINTS
NT AUTOMORPHISMS
NT BANACH SPACE
NT BINOMIALS
NT CANONICAL FORMS
NT CUBIC EQUATIONS
NT DETERMINANTS
NT DYADICS
NT EIGENVALUES
NT EIGENVECTORS
NT GROUP THEORY
NT HERMITIAN POLYNOMIAL
NT HESSIAN MATRICES
NT HILBERT SPACE
NT LIE GROUPS
NT LINEAR EQUATIONS
NT LINEAR TRANSFORMATIONS
NT MATRICES (MATHEMATICS)
NT NONLINEAR EQUATIONS
NT NONLINEAR EVOLUTION EQUATIONS
NT POLYNOMIALS
NT QUADRATIC EQUATIONS
NT RICCATI EQUATION
NT STATE VECTORS
NT STIFFNESS MATRIX
NT STRESS TENSORS
NT TENSORS
NT VECTOR SPACES
NT VECTORS (MATHEMATICS)
NT VORTICITY
A system of three-dimensional complex variables
[NASA-TM-88318] 05 p0645 N88-13951
Fast algorithms for structural optimization and least squares
[AD-A185766] 06 p0724 N88-14452
Embedding topological median algebras in products of dendrons
[PB88-100888] 06 p0767 N88-14713
Class of N-associative rings
[PB87-230421] 06 p0769 N88-14724
Scientific data manipulation in a relational database system
[PB87-124400] 06 p0791 N88-14850
Stability analysis of finite difference schemes for hyperbolic systems, and problems in applied and computational linear algebra
[AD-A185824] 07 p0908 N88-15499
Algebraic specification of process algebra, including two examples
[PB88-106729] 07 p0912 N88-15531
Annotated algebraic specification of the static semantics of pool
[PB88-106695] 07 p0912 N88-15533
Recent developments in the numerical solution of differential/algebraic systems
[DE88-001885] 07 p0912 N88-15535
Prospectus for the development of a linear algebra library for high-performance computers
[DE88-003715] 08 p1068 N88-16457
Strong convergence and convergence rates of approximating solutions for algebraic Riccati equations in Hilbert spaces
[AD-A180190] 08 p1072 N88-16464
Symbolic, algebraic, and numeric solutions to heat conduction problems using Green's functions
09 p1165 N88-16987
An algebraic approach to a calculus of functional differences: Fixed differences and integrals
[AD-A187079] 09 p1227 N88-17346
An applicative programmer's approach to matrix algebra, lessons for hardware and software
10 p1382 N88-18251
The impact of hierarchical memory systems on linear algebra algorithm design
[DE88-003574] 10 p1385 N88-18274
Programming methodology and performance issues for advanced computer architectures
[DE88-003098] 10 p1387 N88-18287
Leapfrog variants of iterative methods for linear algebra equations
[NASA-CR-181616] 10 p1398 N88-18332
Vector bundles over real algebraic varieties
[PB88-126677] 10 p1398 N88-18335
A new approach for shaping of dual-reflector antennas
[NASA-CR-182581] 11 p1476 N88-18806
Generating the states of a probabilistic system
[AD-A187896] 11 p1540 N88-19208
Supporting valid time: An historical algebra
[AD-A187740] 11 p1565 N88-19368
An evaluation of historical algebras
[AD-A188350] 12 p1684 N88-20067
New representation for kinematics of manipulator
[DE88-751446] 14 p1917 N88-21445
Tutorial on GAMS (Generalized Algebraic Modeling System): A modeling language for optimization
[AD-A189867] 15 p2109 N88-22568
Design of an algorithm to translate nested relational algebra queries to GENESIS trace manager commands
[AD-A190502] 15 p2112 N88-22581
Numerical solution of nonlinear algebraic equations in stiff ODE solving
[DE88-006634] 15 p2118 N88-22622
About disequations simplification
[RR-645-I-IMAG-55-LIFIA] 15 p2119 N88-22624
Research on algebraic manipulation
[AD-A190149] 15 p2120 N88-22634
The algebraic structure of convolutional codes
[AD-A190280] 15 p2120 N88-22635
Complexity of some problems in module algebra
[PB88-165386] 15 p2122 N88-22648
Super Virasoro algebra and solvable supersymmetric quantum field theories
[DE88-752299] 15 p2127 N88-22681
A new block solver for large, full, unsymmetric, complex systems of linear algebraic equations
[AD-A190590] 16 p2256 N88-23483
Mahler's method in transcendence theory
17 p2393 N88-24227
Nonlinear conformal transformations and Clifford algebras
[PB87-225942] 19 p2719 N88-26147
Flexible valued algebras of four-dimensions
[ETN-88-92382] 21 p3008 N88-27844
Algebraic grid generation for fighter type aircraft
23 p3246 N88-29320
Composite grid generation for aircraft configurations with the EAGLE code 23 p3246 N88-29321
Polynomial definition of discrete field points of map of diffusion equation, part 1
[AD-A193697] 23 p3271 N88-29467
ALGORITHMS
NT PARSING ALGORITHMS
NT SIMPLEX METHOD
Feature selection applied to radar target identification
[AD-A183880] 01 p0034 N88-10215
Simulations using the pseudo-current algorithm
[DE87-012403] 01 p0040 N88-10255
Accurate, stable, explicit solution of the parabolized Navier-Stokes equations 01 p0043 N88-10276
Development of response models for the Earth Radiation Budget Experiment (ERBE) sensors. Part 4: Preliminary nonscanner models and count conversion algorithms
[NASA-CR-178295] 01 p0050 N88-10317
Description of NCAR (National Center for Atmospheric Research) Community Climate Model (CCM1)
[PB87-203782] 01 p0072 N88-10462
Fronts propagating with curvature dependent speed: Algorithms based on Hamilton-Jacobi formulations
[NASA-CR-178382] 01 p0077 N88-10495
Study, design and evaluation of data reduction by encoding or information extraction. Part 3: Algorithm design --- multispectral satellite imagery
[NLR-TR-85094-L-PT-3] 01 p0079 N88-10503
Study, design and evaluation of data reduction by encoding or information extraction. Part 4: Performance demonstration --- multispectral satellite imagery
[NLR-TR-85094-L-PT-4] 01 p0079 N88-10504
Study, design and evaluation of data reduction by encoding or information extraction. Part 5: Algorithm implementation aspects --- multispectral satellite imagery
[NLR-TR-85094-L-PT-5] 01 p0079 N88-10505
A nonmythical generalization of Dekker's algorithm and its ramifications --- mutually exclusive processes
[CS-8702] 01 p0080 N88-10513
The box method for linear programming. Part 1: Basic theory
[DE87-011029] 01 p0080 N88-10515
A graphical tool for observing the behavior of parallel logic programs
[DE87-011467] 01 p0080 N88-10516
A look at the evolution of mathematical software for dense matrix problems over the past fifteen years
[DE87-011485] 01 p0081 N88-10517
Adaptive line of sight algorithms
[DE87-014275] 01 p0081 N88-10523
EVA reference manual
[DE87-014073] 01 p0082 N88-10526
Strategies for concurrent processing of complex algorithms in data driven architectures
[NASA-CR-181435] 01 p0082 N88-10527
Development of a line-drawing algorithm
[CS-8701] 01 p0082 N88-10530
Digital algorithms for the control and dynamic decoupling of industrial robot axes
[ETN-87-90441] 01 p0084 N88-10546
Computing the bounded region determined by finitely many lines in the plane
[CS-8703] 01 p0086 N88-10558
S-step iterative methods for symmetric linear systems
[DE87-010819] 01 p0086 N88-10559
Parallel computation of a domain decomposition method
[DE87-011444] 01 p0086 N88-10560
PROGRESS: A program for robust regression analysis on the IBM PC
[REPT-85-14] 01 p0088 N88-10576
Numerical computation of transonic potential flow about 3-dimensional inlets
[NAL-TR-924] 02 p0122 N88-10770

Automated detection of severe thunderstorms using geosynchronous infrared data 02 p0201 N88-11257

Statistical remote sensing algorithm development: A complementary process to mesoscale numerical models
02 p0206 N88-11292

Numerical simulation of Tokamaks: Ideal MHD equilibrium and stability
[DE87-013452] 02 p0218 N88-11373

A preliminary taxonomy of visible surface algorithms
[DE87-013559] 02 p0220 N88-11386

Concurrent algorithms for transient nonlinear FE analysis
[NASA-CR-181455] 02 p0221 N88-11389

Using MINOS (Modular in-core Nonlinear Optimization System) as a subroutine for decomposition
[DE87-013086] 02 p0221 N88-11390

Projection-space iterative interpolation for limited-angle tomography in parallel- and fan-beam geometry, part 1
[DE87-013965] 02 p0221 N88-11391

Weighted decoding of block codes and some topics on decoding complexity
[ENST-87E005] 02 p0221 N88-11394

Finite elements for 2D elliptic equations with moving nodes
[DE87-013501] 02 p0224 N88-11410

Iterative solution of a nonlinear system arising in phase change problems
[DE87-014672] 02 p0226 N88-11426

BIMOND3: Monotone piecewise bicubic Hermite interpolation code
[DE87-014612] 02 p0229 N88-11442

QUICKSILVER: A 3D, electromagnetic, PIC code
[DE87-013013] 02 p0245 N88-11547

Efficient numerical approaches for predicting supersonic flows with viscous/inviscid interaction
03 p0260 N88-11637

An antenna array processing system for multiple source bearing estimation 03 p0305 N88-11927

Application of an upwind algorithm to the parabolized Navier-Stokes equations 03 p0316 N88-12000

An algorithmic approach to crustal deformation analysis
[NASA-CR-181497] 03 p0349 N88-12203

Study of microburst detection performance during 1985 in Memphis, Tennessee
[AD-A184013] 03 p0354 N88-12231

SBNR (Signed Binary Number Representations) digital signal processor architecture
[AD-A184603] 03 p0364 N88-12290

Token execution strategies for distributed algorithms: Simulation studies
[AD-A184792] 03 p0365 N88-12294

Algorithms and hardware for efficient image smoothing
[TR-149] 03 p0365 N88-12296

End of year report for parallel vision algorithm design and implementation
[AD-A184327] 03 p0366 N88-12301

The structure-mapping engine: Algorithm and examples
[AD-A184042] 03 p0368 N88-12315

Numerical solution of bound constrained problems
[DE88-000653] 03 p0371 N88-12334

Solution of the two-dimensional Euler equations on unstructured triangular meshes
04 p0396 N88-12469

Two dimensional path planning with obstacles and shadows
[AD-A184075] 04 p0397 N88-12474

Autonomous Land Vehicle (ALV) planning and navigation system
[AD-A184243] 04 p0397 N88-12475

GPS vertical axis performance enhancement for helicopter precision landing approach
[NASA-CR-177443] 04 p0397 N88-12477

New feedback design methodologies for large space structures: A multi-criterion optimization approach
04 p0408 N88-12535

On M-ARY sequential hypotheses testing for the classification of radar signals
[AD-A184094] 04 p0430 N88-12666

Design of source coders and joint source/channel coders for noisy channels
[NASA-CR-181547] 04 p0432 N88-12678

A simplified procedure for correcting both errors and erasures of a Reed-Solomon code using the Euclidean algorithm 04 p0435 N88-12698

On the VLSI design of a pipeline Reed-Solomon decoder using systolic arrays 04 p0436 N88-12700

A modern control theory based algorithm for control of the NASA/JPL 70-meter antenna axis servos
04 p0436 N88-12706

Programmable Logic Arrays (PLA's) design for testability
[PB87-102935] 04 p0438 N88-12718

Studies of pressure-velocity coupling schemes for analysis of incompressible and compressible flows
[NASA-CR-181526] 04 p0443 N88-12748

Optimization of explicit time-stepping algorithms and Stream-Function-Coordinate (SFC) concept for fluid dynamics problems 04 p0445 N88-12762

Tracking through turbulence at the Tonopah Test Range
[DE88-001448] 04 p0446 N88-12766

An algorithmic approach to crustal deformation analysis 04 p0468 N88-12891

Coupled acoustic and ocean thermodynamic model
[AD-A184357] 04 p0472 N88-12911

Comparing barrier algorithms
[NASA-CR-178377] 04 p0476 N88-12934

A tight upper bound for the speed-up of parallel best-first branch-and-bound algorithms
[AD-A184246] 04 p0477 N88-12939

A characterization of separating pairs and triplets in a graph
[AD-A184278] 04 p0477 N88-12941

Numerical studies of the dual HEMT/algorithm development and numerical studies of Schrodinger's equation
[AD-A184471] 04 p0478 N88-12946

Statistical inference: Computer oriented algorithmic approach
[DE87-013874] 04 p0478 N88-12948

Methods for design and evaluation of integrated hardware/software systems for concurrent computation
[NASA-CR-181522] 04 p0479 N88-12953

Parallelization of hydrocodes on the Intel Hypercube, part 2
[DE88-001591] 04 p0480 N88-12957

Development of the non-equilibrium reactive chemical transport code CHMTRNS
[DE88-000682] 04 p0481 N88-12964

On operator splitting for unsteady boundary value problems
[AD-A184281] 04 p0484 N88-12981

A comparison of adaptive refinement techniques for elliptic problems
[DE88-000805] 04 p0485 N88-12987

The finite element method for electronic structure
[DE88-001708] 04 p0485 N88-12989

Driving mechanism of unsteady separation shock motion in hypersonic interactive flow 05 p0530 N88-13226

Numerical prediction of turbulent flows in dump diffusers 05 p0537 N88-13265

Programming techniques for high-speed processing of large scale numerical simulation on supercomputers
05 p0537 N88-13269

Vectorizing the FFTs on supercomputer SX system
05 p0537 N88-13270

Tridiagonal approximate factorization method: A preconditioning technique for solving nonsymmetric linear systems suitable to supercomputers
05 p0537 N88-13271

MODTRAN: A moderate resolution model for LOWTRAN
[AD-A185384] 05 p0574 N88-13503

Model-based motion estimation and its application to restoration and interpolation of motion pictures
[AD-A185054] 05 p0584 N88-13558

Free Lagrange reconnection algorithms for hydrocodes using a quadrilateral mesh
[DE88-001580] 05 p0611 N88-13752

Automatic continuum analysis of reflectance spectra
05 p0614 N88-13770

Learning a color algorithm from examples
[AD-A184385] 05 p0632 N88-13862

Approximating multivariate normal orthant probabilities using the Clark algorithm
[AD-A184855] 05 p0634 N88-13873

An adaptive lattice algorithm for spectral line estimation
[AD-A184970] 05 p0634 N88-13876

Indirect solution of static problems using concurrent vector processing computers
[DE87-012105] 05 p0636 N88-13889

The maximum likelihood estimator method of image reconstruction: Its fundamental characteristics and their origin
[DE88-000462] 05 p0636 N88-13892

Research and development of finite elements and iterative algorithms for elliptic partial differential equations
[DE88-001381] 05 p0643 N88-13934

Restoration of particle pitch angle distribution functions by a maximum entropy algorithm
[ATR-86(7098)-3] 05 p0648 N88-13969

Molecular dynamics studies of aromatic hydrocarbon liquids
[DE88-001473] 05 p0648 N88-13973

Supercomputing at Florida State University (FSU)
[DE87-013900] 05 p0654 N88-14009

Range imagery algorithms for the detection of obstacles by autonomous vehicles
[AD-A185421] 05 p0659 N88-14045

A fully redundant double difference algorithm for obtaining minimum variance estimates from GPS observations
[NASA-CR-182363] 06 p0667 N88-14089

Study of synthetic aperture radar data compression and encoding. Part 3: Performance evaluation of speckle suppression and data compression algorithms
[NLR-TR-85085-L-PT-3] 06 p0692 N88-14248

Study of synthetic aperture radar data compression and encoding. Part 4: Algorithm implementation aspects
[NLR-TR-85085-L-PT-4] 06 p0692 N88-14249

On real-time systems using local area networks
[AD-A185475] 06 p0694 N88-14256

Vectorization of a multigrid method for the compressible Navier-Stokes equations
[PB87-230496] 06 p0698 N88-14284

Computational methods for complex flowfields
[AD-A185793] 06 p0703 N88-14317

Fast algorithms for structural optimization and least squares
[AD-A185766] • 06 p0724 N88-14452

Numerical modeling of troposphere-induced gravity wave propagation 06 p0735 N88-14522

Report of the International Satellite Cloud Climatology Project (ISCCP) workshop on cloud algorithms in the polar regions
[WCP-131] 06 p0745 N88-14581

Optimal pre-scheduling of problem remappings
[NASA-CR-178378] 06 p0756 N88-14633

Parallel algorithms for unconstrained and constrained nonlinear optimization
[PB87-230454] 06 p0756 N88-14634

Parallel algorithms for polynomials
[PB87-226304] 06 p0756 N88-14635

Algorithms and programming tools for image processing on the MPP 3
[NASA-CR-182349] 06 p0757 N88-14641

A computer decision-making process for the elimination of noise from data
[AD-A185746] 06 p0759 N88-14659

Parallel pivoting combined with parallel reduction
[NASA-CR-178422] 06 p0760 N88-14662

Adaptive grid for polyhedral visibility in object space: An implementation
[PB88-100938] 06 p0760 N88-14663

A Multipurpose Adaptive Controller (MAC) for real time digital regulation
[REPT-87-028] 06 p0762 N88-14673

Scanline algorithms on a grid
[PB88-103379] 06 p0766 N88-14710

Digital signal processing algorithms for automatic voice recognition 06 p0793 N88-14862

Some vision algorithms 06 p0795 N88-14871

An engineering study of hybrid adaptation of wind tunnel walls for three-dimensional testing
[NASA-CR-178374] 07 p0814 N88-14957

Experimental design of a piloted helicopter off-axis-tracking simulation using a helmet mounted display
[AD-A186228] 07 p0820 N88-14982

Catalog of compartment fire model algorithms and associated computer subroutines
[PB88-110861] 07 p0839 N88-15087

Study of synthetic aperture radar data compression and encoding. Part 2: SAR image speckle suppression and data compression algorithms
[NLR-TR-85085-L-PT-2] 07 p0843 N88-15116

Multipath time-delay estimation via the EM algorithm
[PB88-106851] 07 p0845 N88-15124

Multitasked embedded multigrid for three-dimensional flow simulation
[NASA-CR-182398] 07 p0852 N88-15173

An efficient algorithm for computing the crossovers in satellite altimetry
[NASA-CR-182369] 07 p0871 N88-15286

Middle atmospheric wind measurements using a medium frequency radar
[AD-A185931] 07 p0879 N88-15330

Improvements in profiler wind estimates using smoothed data in the spectrum finder algorithm
[PB88-102181] 07 p0881 N88-15342

Parallel algorithms for computer vision on the connection machine
[AD-A185842] 07 p0901 N88-15456

Program translation via abstraction and reimplementation
[AD-A185845] 07 p0901 N88-15458

Investigation and implementation of an algorithm for computing optimal search paths
[AD-A185927] 07 p0902 N88-15461

A multicut algorithm for two-stage stochastic linear programs
[AD-A186148] 07 p0903 N88-15466

Image processing language development
[AD-A186251] 07 p0903 N88-15467

Tracking procedure for non-normally distributed measurement errors
[AD-A186287] 07 p0903 N88-15468

Parallel LU-factorization algorithms for dense matrices
[DE88-002179] 07 p0904 N88-15478

Algorithm and program for recognition of compactly positioned vertices of events for the HPD minimum guidance system
[DE88-700542] 07 p0905 N88-15482

Monte Carlo photon transport on vector and parallel supercomputers
[DE88-002503] 07 p0905 N88-15486

Simplified self-tuning control algorithms
[OUEL-1657/86] 07 p0907 N88-15494

An O(n3L) interior point algorithm for convex quadratic programming
[AD-A186001] 07 p0909 N88-15504

Correctness proofs for systolic algorithms. Palindromes and sorting
[PB88-106075] 07 p0912 N88-15534

Investigation of candidate data structures and search algorithms to support a knowledge based fault diagnosis system 07 p0923 N88-15606

Monte Carlo simulation of triangulated random surfaces in grand canonical ensemble
[DE88-700378] 07 p0941 N88-15718

Unsteady transonic algorithm improvements for realistic aircraft applications
[NASA-TM-100516] 08 p0949 N88-15760

Attitude determination of artificial satellites through joint application of static and dynamic optimal estimation techniques
[INPE-4415-TDL/306] 08 p0963 N88-1[illegible]32

Numerical arc segmentation algorithm for a radio conference-NASARC (version 2.0) technical manual
[NASA-TM-100160] 08 p0977 N88-15910

The design and implementation of surface acoustic wave devices for linear FM and a new non-linear FM pulse compression technique for radar applications
[AD-A186741] 08 p0980 N88-15922

Assessment of VAS-derived products created by a simultaneous algorithm on a convectively active day
[AD-A186158] 08 p1054 N88-16359

Orbital navigation, docking and obstacle avoidance as a form of three dimensional model-based image understanding 08 p1061 N88-16406

Iterative deepening heuristic search for optimal and semi-optimal resource allocation
08 p1062 N88-16410

The power of neural nets 08 p1064 N88-16430

A data structure and algorithm for fault diagnosis
08 p1065 N88-16432

A parallel algorithm for the general LU-factorization
[DE88-002177] 08 p1066 N88-16444

A note on the partitioning shortest path algorithm
[CWI-OS-R8703] 08 p1067 N88-16451

Short data length effects in an asymptotically efficient ARMA (AutoRegressive Moving Average) spectral estimator
[AD-A186561] 08 p1068 N88-16458

Adaptive exponential stabilization of a first order continuous-time system
[CWI-OS-R8705] 08 p1069 N88-16461

Control variate selection for multiresponse simulation
[AD-A186637] 08 p1069 N88-16463

High performance VLSI algorithms and architectures for digital signal processing 09 p1155 N88-16926

Numerical arc segmentation algorithm for a radio conference-NASARC, version 2.0. User's manual
[NASA-TM-100161] 09 p1156 N88-16928

Mesospheric dynamics and chemistry from SME data
[NASA-CR-182465] 09 p1191 N88-17139

Implementing clips on a parallel computer
09 p1211 N88-17259

Vision technology/algorithms for space robotics applications 09 p1212 N88-17267

Calibration of neural networks using genetic algorithms, with application to optimal path planning
09 p1214 N88-17277

Supercomputers for solving PDE (Partial Differantial Equations) problems
[AD-A186583] 09 p1215 N88-17283

Nested transactions, conflict-based locking, and dynamic atomicity
[AD-A187033] 09 p1217 N88-17294

Multicolor numbering of irregular triangular meshes
[AD-A186559] 09 p1217 N88-17298

Algorithm design for scientific computation for highly parallel multiprocessor systems
[AD-A186713] 09 p1217 N88-17299

Algorithms for transitive reduction of an acyclic graph
[PB87-162822] 09 p1220 N88-17317

A comparison of algorithms for the analysis of images generated by two-dimensional electrophoresis
[DE88-003730] 09 p1220 N88-17319

A fast bottom-up algorithm for computing the cut sets of noncoherent fault trees
[DE88-003741] 09 p1220 N88-17320

A raster scan algorithm for generating visible parametric surfaces
[DE88-003222] 09 p1220 N88-17321

Multiple-object motion estimation by maximal matching of 3-D point and line features 09 p1220 N88-17322

Acceleration techniques for decoupling algorithms in semiconductor simulation
[DE88-003593] 09 p1221 N88-17323

A parallel block cyclic reduction algorithm for the fast solution of elliptic equations
[DE88-003595] 09 p1221 N88-17324

A state space approach to the problem of adaptive pole assignment
[CWI-OS-R8704] 09 p1224 N88-17339

Experiments with the back propagation algorithm: A systematic look at a small problem
[RSRE-MEMO-4049] 09 p1224 N88-17340

On line search termination criteria for and convergence of conic algorithms for minimization
[DE88-002844] 09 p1227 N88-17351

Advances in reliable numerical computation: A summary --- conference
[NPL-DITC-102/87] 09 p1229 N88-17367

Navier-Stokes simulation of wind-tunnel flow using LU-ADI factorization algorithm
[NASA-TM-100042] 10 p1268 N88-17584

Formulation methods of rigid multibody systems for large space structures and some results of computer simulation
[NAL-TR-942] 10 p1293 N88-17730

Designing variable-length codes with good error-recovery properties
[BBC-RD-1987/19] 10 p1317 N88-17876

Recursive forward dynamics for multiple robot arms moving a common task object
[NASA-CR-182526] 10 p1340 N88-18008

The arithmetic cube and its associated algorithms
10 p1374 N88-18195

Hardware implementation for special functions. An application for combat simulation
10 p1374 N88-18197

Role of broadcasting in multiprocessor systems
10 p1374 N88-18201

The mapping of parallel algorithms to reconfigurable parallel architectures 10 p1376 N88-18209

A comparative study of heurstic algorithms for task assignment in distributed computing systems
10 p1376 N88-18211

Distributed control of large parallel computers
10 p1376 N88-18215

Strategies for concurrent processing of complex algorithms 10 p1379 N88-18236

Investigations on the usefulness of the Massively Parallel Processor for study of electronic properties of atomic and condensed matter systems
[NASA-CR-182514] 10 p1383 N88-18259

Parameter identification and sensitivity analysis for a robotic manipulator arm
[NASA-CR-181608] 10 p1385 N88-18272

The impact of hierarchical memory systems on linear algebra algorithm design
[DE88-003574] 10 p1385 N88-18274

PSolve: A concurrent algorithm for solving sparse systems of linear equations
[DE88-003584] 10 p1386 N88-18275

Introduction to a system for implementing neural net connections on SIMD architectures
[NASA-CR-181612] 10 p1386 N88-18279

Graph transformation algorithms for array memory optimization in applicative languages
[DE88-004727] 10 p1387 N88-18283

Experiences with serial and parallel algorithms for channel routing using simulated annealing
[NASA-CR-182530] 10 p1388 N88-18289

Semantics of EqL
[AD-A188151] 10 p1389 N88-18297

Implementation and analysis of a Navier-Stokes algorithm on parallel computers
[NASA-CR-181614] 10 p1390 N88-18301

A parallel quasi-Newton method for partially separable large scale minimization
[DE88-003592] 10 p1393 N88-18309

Performance studies of a parallel processor for large linear programming problems
[PB88-121611] 10 p1393 N88-18310

Application of a multigrid method to a buoyancy-induced flow problem
[DE88-003961] 10 p1397 N88-18326

Quasigroup approach to solution of linear algebraic equation systems
[DE88-700595] 10 p1398 N88-18330

Straightening and the Stanley decomposition for the (2;n)-nilpotent vectorfield
[PB88-126685] 10 p1398 N88-18336

The hybrid Monte Carlo Algorithm and the chiral transition
[DE88-004305] 10 p1399 N88-18341

A computer simulation study of an expert system for walking machine motion planning
[AD-A187907] 11 p1438 N88-18577

Further results on finite-state codes
11 p1472 N88-18782

New mode switching algorithm for the JPL 70-meter antenna servo controller 11 p1474 N88-18791

A hydrodynamic analysis of fluid flow between meshing spur gear teeth
[AD-A187671] 11 p1482 N88-18844

Three-dimensional flow fields past reentry vehicles
11 p1484 N88-18858

A new computational technique for generating algorithms, with application to the solution of the time-dependent incompressible Navier-Stokes equations
11 p1485 N88-18964

Real-time kinematic and dynamic analysis and adaptive model following control of manipulator arms
11 p1495 N88-18927

Symmetries in nonlinear control systems and their applications 11 p1496 N88-18929

Contour-to-grid interpolation with nonlinear finite elements: A feasibility study
[AD-A188108] 11 p1503 N88-18980

A spectral method for computing complete synthetic seismograms
[AD-A187663] 11 p1510 N88-19024

Ground clutter processing for wind measurements with airport surveillance radars
[AD-A187708] 11 p1514 N88-19044

Visual integration and detection of discontinuities: The key role of intensity edges
[AD-A188012] 11 p1520 N88-19076

Approaches to the automatic generation and control of finite element meshes 11 p1526 N88-19113

A hierarchical structure for automatic meshing and adaptive FEM analysis 11 p1527 N88-19119

Digital control of the Czochralski growth of Gallium arsenide-controller software reference manual
[AD-A187210] 11 p1528 N88-19127

The roll back chip: Hardware support for distributed simulation using time warp
[AD-A187823] 11 p1529 N88-19132

Performance measurements of distributed simulation strategies
[AD-A187824] 11 p1529 N88-19133

A theory of program correctness, and algorithms for proofs
[ANL-87-4] 11 p1531 N88-19146

An exact pseudo polynomial algorithm for the 0-1 linear diophantine equation
[INPE-4289-PRE/1160] 11 p1531 N88-19148

Algorithmic alternatives
[DE88-003905] 11 p1531 N88-19149

A tool for the analysis of quasi-Newton methods with application to unconstrained minimization
[DE88-005783] 11 p1532 N88-19153

A shared memory algorithm and proof for the alternative construct in CSP (Communicating Sequential Processes)
[AD-A187820] 11 p1533 N88-19156

Two new frameworks for learning
[AD-A187723] 11 p1534 N88-19162

Learning functions from examples
[AD-A187725] 11 p1534 N88-19163

Implementation of multigrid in SOLA algorithm --- fluid flow 11 p1538 N88-19191

Solution of a rotating Navier-Stokes problem by a nonlinear multigrid algorithm 11 p1538 N88-19194

Application of the multigrid technique to the pressure-correction equation for the SIMPLE algorithm --- Semi-Implicit Method for Pressure Linked Equations (SIMPLE) 11 p1539 N88-19196

Discretizations for multigrid methods
11 p1539 N88-19198

Estimation in linear models with censored data
[AD-A187209] 11 p1540 N88-19203

Generating the states of a probabilistic system
[AD-A187896] 11 p1540 N88-19208

Connection between general observers and Lanczos potential
[DE88-700139] 11 p1563 N88-19354

A traveling-salesman-based approach to aircraft scheduling in the terminal area
[NASA-TM-100062] 12 p1576 N88-19424

Calibration of a ring laser gyro inertial navigation system 12 p1576 N88-19428

Realtime pilot model parameter identification
[AD-A188873] 12 p1584 N88-19476
Preliminary orbit determination algorithms: Application to the Brazilian satellite
[INPE-4411-NTE/276] 12 p1594 N88-19546
Identification of microwave line-of-sight multipath components 12 p1616 N88-19665
Optimum filters and smoothers design for carrier phase and frequency tracking
[NASA-CR-182654] 12 p1618 N88-19679
An efficient numerical algorithm for solving scattering and inverse scattering problems of electromagnetic waves
[AD-A188479] 12 p1619 N88-19684
Evaluating the performance of the LPC (Linear Predictive Coding) 2.4 kbps (kilobits per second) processor with bit errors using a sentence verification task
[AD-A188573] 12 p1620 N88-19686
A numerical study of automated dynamic relaxation for nonlinear static tensioned structures
[AD-A188372] 12 p1635 N88-19790
An intelligent allocation algorithm for parallel processing
[NASA-CR-182648] 12 p1675 N88-20014
Computer architecture for efficient algorithmic executions in real-time systems: New technology for avionics systems and advanced space vehicles
[NASA-CR-182650] 12 p1675 N88-20016
Some questions of using coding theory and analytical calculation methods on computers
[DE88-700905] 12 p1676 N88-20021
A variant of the ISODATA algorithm for application to agricultural targets
[INPE-4436-PRE/1235] 12 p1676 N88-20023
Research on algorithms for nonlinear programming
[AD-A188326] 12 p1677 N88-20024
Analysis, estimation, and control for perturbed and singular systems and for systems subject to discrete events
[AD-A188496] 12 p1677 N88-20026
Experimental analysis of algorithms
[AD-A188528] 12 p1677 N88-20028
Research on automatic verification of finite-state concurrent systems
[AD-A188618] 12 p1677 N88-20029
An emulation tool for simulating matrix operations on an SIMD (Single Instruction Multiple Data stream) multiprocessor
[AD-A188654] 12 p1678 N88-20030
Analysis of simulated annealing type algorithms
[AD-A189382] 12 p1679 N88-20037
MOBICALC: An integrated and interactive system for development of administrative models
[INPE-4335-TDL/291] 12 p1679 N88-20038
A computer code for the solution of large scale network reliability analysis problems
[AD-A188455] 12 p1680 N88-20042
Support for concurrent computing environments
[AD-A188498] 12 p1680 N88-20043
OPS83: Style guide for high performance
[AD-A188505] 12 p1681 N88-20051
Method of reduction of polynomially nonlinear equations to linear equations
[DE88-700922] 12 p1683 N88-20064
Further refinement and applications of the mixed computational algorithm for plane elastic contact problems
[AD-A188308] 12 p1683 N88-20065
Object-oriented design in numerical linear algebra
[AD-A189427] 12 p1685 N88-20073
Task allocation for efficient performance of a decentralized organization
[AD-A188699] 12 p1705 N88-20204
Development of a dependency theory toolbox for database design
[AD-A188872] 12 p1707 N88-20216
Analysis of pre-flight modulator voltage calibration data for the Voyager plasma science experiment
[NASA-CR-182577] 12 p1710 N88-20236
An L-U implicit multigrid algorithm to solve the Euler equations for transonic flow in rotating turbomachinery passages 13 p1718 N88-20270
A method and measures to evaluate trackers for air traffic control
[NLR-TR-86072-U] 13 p1720 N88-20287
Material parameter measurements at high temperatures
[NASA-CR-182707] 13 p1739 N88-20397
Adaptive control of scientific balloon-borne gondola attitude 13 p1755 N88-20497
Statistical signal processing using a class of iterative estimation algorithms
[AD-A189050] 13 p1757 N88-20511
Adaptive algorithms for HF antenna arrays
[AD-A189329] 13 p1761 N88-20534
Systems near the onset and in the well-developed regimes of turbulence
[DE88-005365] 13 p1766 N88-20585
Finite element methods for quasi-prismatic bodies with application to gears 13 p1779 N88-20644
Numerical modeling of wave migration of seismic data 13 p1786 N88-20684
Stratospheric trace gas distributions from fair infrared thermal emission spectroscopy 13 p1797 N88-20749
A new algorithm for general multiobjective optimization
[NASA-TM-100536] 13 p1813 N88-20830
The physical structure of concurrent problems and concurrent computers
[DE88-005812] 13 p1814 N88-20835
Parallel image compression
[NASA-CR-180758] 13 p1814 N88-20837
Broadband correlation analysis
[AD-A188732] 13 p1814 N88-20839
On relaxation algorithms based on Markov random fields
[AD-A189043] 13 p1814 N88-20840
Passive DF: A tutorial, part 1
[NASA-CR-182669] 13 p1815 N88-20846
Two dimensional uncorrelated bias in fix algorithms
[NASA-CR-182683] 13 p1815 N88-20847
Preconditioned conjugate gradient algorithms and software for solving large sparse linear systems
[DE88-002180] 13 p1816 N88-20849
Conic algorithms for unconstrained minimization with special consideration of problems with large sparse Hessians: A summary of research performed
[DE88-002549] 13 p1816 N88-20850
Algorithms with conic termination for nonlinear optimization
[DE88-005893] 13 p1816 N88-20851
Method to evaluate image-recovery algorithms based on task performance
[DE88-005382] 13 p1816 N88-20853
Experimental verification of a finite-difference time-domain thin slot algorithm
[DE88-005572] 13 p1817 N88-20859
Approximation algorithms for scheduling unrelated parallel machines
[CWI-OS-R8714] 13 p1817 N88-20861
Verification of a systolic algorithm for string comparison
[CWI-CS-R8734] 13 p1819 N88-20873
Interpolation algorithms for digital terrain models
[INPE-4373-PRE/1196] 13 p1820 N88-20877
Spectral element methods: Algorithms and architectures
[NASA-CR-182701] 13 p1820 N88-20878
A report on the study of algorithms to enhance vector computer performance for the discretized one-dimensional time-dependent heat conduction equation: EPIC research, phase 1
[DE88-005642] 13 p1820 N88-20880
An implementation of the OPS5 language for computers compatible with IBM-PC
[INPE-4291-PRE/1162] 13 p1821 N88-20882
On the design of parallel numerical methods in message passing and shared memory environments
[DE88-003566] 13 p1822 N88-20888
An amoeba replicated service organisation --- Amoeba operating system
[CWI-CS-R8723] 13 p1822 N88-20892
Robustifying the Kalman filter
[AD-A189240] 13 p1825 N88-20907
A study of data compactation using numerical methods
[INPE-4317-TDL/284] 13 p1828 N88-20929
Local search for constrained routing problems --- traveling salesman
[CWI-OS-R8711] 13 p1830 N88-20948
Passive autonomous infrared sensor technology
[AD-A188698] 13 p1839 N88-21005
Optics for large telescope 13 p1840 N88-21014
On the role of complete reducibility in general competitive equilibrium models
[DE88-005693] 13 p1851 N88-21083
JPRS report. Science and technology. China
[JPRS-CST-87-023] 14 p1863 N88-21130
Finite element explicit algorithm for solving temporal temperature fields 14 p1899 N88-21339
Advances in contact algorithms and their application to tires
[NASA-TP-2781] 14 p1922 N88-21456
Modeling the viscoplastic behavior of Inconel 718 at 1200 F 14 p1929 N88-21502
Classification of small image areas by digital correlation for the connection of different images in photogrammetry and long-range reconnaissance
[ETN-88-91506] 14 p1940 N88-21578
Development and testing of the gust front algorithm
[AD-A189722] 14 p1949 N88-21622
Verification of an algorithm for log-time sorting by square comparison
[CWI-CS-R8729] 14 p1956 N88-21656
Multiextremal optimization via adaptive partition algorithms
[REPT-87-44] 14 p1957 N88-21664
On the design of some systolic algorithms
[CS-8705] 14 p1957 N88-21666
Monte Carlo modified method for Green function. Algorithm and computer code for calculations in equal mass many-body system
[DE88-701114] 14 p1957 N88-21667
A parallel algorithm for computing the singular value decomposition of a matrix
[DE88-007059] 14 p1958 N88-21673
Identification of nonlinear output-affine systems using an orthogonal least squares algorithm
[RR-313] 14 p1958 N88-21678
A prediction-error estimation algorithm for nonlinear output-affine systems
[RR-314] 14 p1959 N88-21679
Identification of nonlinear rational systems using a prediction-error estimation algorithm
[RR-317] 14 p1959 N88-21680
A Gram-Schmidt space-time adaptive canceller using adaptive lattice filters
[AD-A189684] 14 p1959 N88-21684
Implementing embedded artificial intelligence rules within algorithmic programming languages
[NASA-CR-178393] 14 p1959 N88-21686
Parallel algorithms for mapping pipelined and parallel computations
[NASA-CR-181655] 14 p1960 N88-21687
A state-space approach to super optimal H sup infinity control problems
[OUEL-1690/87] 14 p1962 N88-21702
An orthogonal parameter estimation algorithm for nonlinear stochastic systems
[RR-307] 14 p1966 N88-21736
Model selection for the multiple model adaptive algorithm for in-flight simulation
[AD-A189715] 15 p2016 N88-22022
Moving-bank multiple model adaptive estimation applied to flexible spacestructure control
[AD-A190761] 15 p2026 N88-22071
Identification of a star field from a spinning satellite
[CNES-NT-120] 15 p2026 N88-22074
A multiple model adaptive tracking algorithm against airborne targets
[AD-A190619] 15 p2057 N88-22263
Motion sickness: Quantitative, algorithmic malaise indication in real time
[AD-A189674] 15 p2101 N88-22518
The visit problem: Visibility graph-based solution
[DE88-000343] 15 p2108 N88-22556
Consistent estimates of autoregressive parameters for autoregressive moving average models
[RR-663-I] 15 p2109 N88-22564
Implementation of a distributed adaptive routing algorithm on the Intel iPSC (Intel Personal Super-Computer)
[AD-A189849] 15 p2109 N88-22567
Memory efficient evaluations of nonlinear stochastic equations and C3 applications
[AD-A189872] 15 p2110 N88-22569
An analysis of multiple grain CHiP architectures
[AD-A189942] 15 p2110 N88-22570
Extension of computer based algorithms by operator analysts
[NASA-CR-182798] 15 p2111 N88-22575
Transformations of concurrent algorithms for highly parallel systems: A one year project summary report
[AD-A190236] 15 p2111 N88-22576
Design and implementation of VLSI prime factor algorithm processor
[AD-A190483] 15 p2112 N88-22580
Design of an algorithm to translate nested relational algebra queries to GENESIS trace manager commands
[AD-A190502] 15 p2112 N88-22581
SEARCH: An interactive computer program for optimizing two-variable, unconstrained experiments or simulation
[AD-A190593] 15 p2112 N88-22583
Cholesky downdating on a hypercube
[DE88-006780] 15 p2113 N88-22586
Implementation and performance analysis of parallel assignment algorithms on a hypercube computer
[AD-A190678] 15 p2115 N88-22600
Finding texture boundaries in images
[AD-A190554] 15 p2117 N88-22609
Multi-disciplinary techniques for understanding time-varying space-based imagery
[AD-A190711] 15 p2117 N88-22610
Development and application of the p-version of the finite element method
[AD-A190036] 15 p2120 N88-22633

The algebraic structure of convolutional codes
[AD-A190280] 15 p2120 N88-22635
Non-rigid motion and Regge calculus
[AD-A190387] 15 p2121 N88-22640
Trust regions and projected gradients
[DE88-005829] 15 p2122 N88-22646
Structural decomposition of multiple time scale Markov processes
[AD-A189739] 15 p2123 N88-22657
Approximation methods for the identification and control of distributed parameter systems
[AD-A190201] 15 p2124 N88-22662
Target localization in an inhomogeneous medium
[AD-A190008] 15 p2130 N88-22703
Expanded envelope concepts for aircraft control-element failure detection and identification
[NASA-CR-181664] 16 p2160 N88-22886
Numerical arc segmentation algorithm for a radio conference: A software tool for communication satellite systems planning
[NASA-TM-100789] 16 p2167 N88-22919
Algorithms and architectures for acoustic phonetical detection of continuous speech
[ENST-87E016] 16 p2189 N88-23054
Strategies for concurrent processing of complex algorithms in data driven architectures
[NASA-CR-181657] 16 p2193 N88-23083
Test code for the assessment and improvement of Reynolds stress models 16 p2197 N88-23105
Fast algorithms for Euler and Navier-Stokes simulations
[AD-A190897] 16 p2208 N88-23175
Multigrid for structures analysis
16 p2218 N88-23232
Parallel computer methods for eigenvalue extraction
16 p2218 N88-23233
Microgravity manipulator demonstration
16 p2219 N88-23242
Results of the testing of the segmentation program on RESEDA
[BCRS-87-01] 16 p2228 N88-23304
Validate algorithms for the determination of rainfall rates from SSM/I microwave satellite imagery
[AD-A191337] 16 p2236 N88-23353
Efficient and fast data compression codes for discrete sources with memory
[ETN-88-92233] 16 p2246 N88-23420
HIFI: A design method for implementing signal processing algorithms on VLSI processor arrays
[ETN-88-92238] 16 p2247 N88-23421
Synthesis and simulation of systolic algorithms
[ETN-88-92183] 16 p2247 N88-23423
Correctness proofs for systolic algorithms: A palindrome recognizer
[CWI-CS-R8747] 16 p2248 N88-23434
A very simple construction for atomic multiwriter register
[CWI-CS-R8751] 16 p2249 N88-23436
A queueing network model for analyzing a class of branch and bound algorithms on a master-slave architecture
[CWI-OS-R8717] 16 p2249 N88-23441
Approximate agreement
[AD-A191030] 16 p2251 N88-23455
Fast Algorithm Simulation and Test (FAST) facility
[AD-A191183] 16 p2252 N88-23457
On 2-D versus 3-D: Sine of squared angular error and weighted perpendicular fixing
[NASA-CR-182899] 16 p2252 N88-23458
Algorithms and intuition
[NASA-CR-182900] 16 p2252 N88-23459
Compilation of preprints
[AD-A191245] 16 p2252 N88-23460
An algorithm for random access communication over a noisy channel
[AD-A191315] 16 p2252 N88-23461
Simulation of FELIN logics: Polynomials roots simultaneous computation algorithms
[ETN-88-92182] 16 p2253 N88-23464
Parallelization of Gauss-Seidel algorithms as an example of parallel iterative equation solving
[REPT-87-76] 16 p2254 N88-23471
Parallel artificial intelligence search techniques for real time applications
[AD-A190683] 16 p2255 N88-23473
Systolic algorithm for matrix-vector multiplication
[PB88-165394] 16 p2256 N88-23484
Computation of a complete elliptic integral of the first kind using q-expansion 16 p2257 N88-23490
New stable, vectorisable Kalman filter algorithms based on orthogonal transformations
[DFVLR-FB-87-52] 16 p2258 N88-23494
Formal solution of differential linear systems in the proximity of a singularity
[ETN-88-92190] 16 p2258 N88-23495
Approximation and representation of explicit surfaces in the presence of singularities
[ETN-88-92191] 16 p2258 N88-23496
Convergence qualification of partition algorithms in global optimization
[REPT-87-61] 16 p2259 N88-23505
Algorithm for accounting the conditions in infinity for two-dimensional magnetostatics problems
[DE88-701673] 16 p2264 N88-23541
Adaptive segmentation evaluation
[AD-A190965] 16 p2274 N88-23609
Automated database design technology and tools
[NASA-CR-182875] 16 p2286 N88-23687
A three dimensional assignment method in the time space
[REPT-87-49] 16 p2287 N88-23690
Experimental evaluation of algorithms for connected speech recognition using hidden Markov models
[RSRE-MEMO-4099] 17 p2333 N88-23928
An efficient parallel algorithm for the simulation of three-dimensional compressible transition on a 20 processor Flex/32 multicomputer
[NASA-CR-178340] 17 p2337 N88-23943
Shape detection in remote sensing through graph isomorphism 17 p2354 N88-24028
Digital processing of infrared and visible images from the GOES satellite and its integration with meteorological radar data 17 p2360 N88-24057
Generation of thematic maps for updating aeronautical pilot charts utilizing LANDSAT-TM images
17 p2361 N88-24062
Low altitude remote sensing data in the implementation of a mathematical model for the planning of urban equipment networks 17 p2363 N88-24074
Research on enhancing the utilization of digital multispectral data and geographic information systems in global habitability studies
[NASA-CR-182799] 17 p2368 N88-24101
Cloud cover determination in polar regions from satellite imagery
[NASA-CR-182906] 17 p2375 N88-24123
The multi-disciplinary design study: A life cycle cost algorithm
[NASA-CR-4156] 17 p2385 N88-24172
On the efficient implementation of the fast multipole algorithm
[AD-A191167] 17 p2385 N88-24173
Parallel processors and nonlinear structural dynamics algorithms and software
[NASA-CR-182925] 17 p2387 N88-24187
Genetic algorithms for adaptive real-time control in space systems 17 p2388 N88-24195
An algorithm for super-optimal H sup inf design: The 2-block case
[OUEL-1711/87] 17 p2391 N88-24210
A control technique for improved robot performance
17 p2391 N88-24212
Small particle bed reactors: Sensitivity to Brayton cycle parameters 17 p2435 N88-24487
A feedback linearization approach to spacecraft control using momentum exchange devices
[NASA-CR-172057] 18 p2472 N88-24668
Dynamics of a flexible orbiting platform with MRMS
[ISSN-0285-6808] 18 p2473 N88-24673
Geodesy by radio interferometry: Optimization of wet path delay algorithms using microwave radiometer data
[PB88-167739] 18 p2498 N88-24820
Delay-doppler radar imaging
[AD-A191509] 18 p2499 N88-24826
A method for discrimination of radar targets using complex natural resonances
[AD-A191848] 18 p2500 N88-24832
Information and stochastic systems
[AD-A192167] 18 p2501 N88-24838
Identification of cascaded microwave circuits with moderate reflections using reflections and transmission measurements
[PB88-171921] 18 p2503 N88-24849
Fast algorithm development for large-eddy simulation of circular-jet turbulence
[AD-A192044] 18 p2509 N88-24887
SOLA-DM: A numerical solution algorithm for transient three-dimensional flows
[DE88-007159] 18 p2514 N88-24913
The coordination of multiple robotic manipulators
[AD-A190869] 18 p2522 N88-24963
Dynamic response of plates to moving loads: Structural impedance and finite element methods
18 p2528 N88-25000
Advanced development of the boundary element method for elastic and inelastic thermal stress analysis
18 p2529 N88-25002
Multishaker modal testing
[NASA-CR-179355] 18 p2530 N88-25010
DMSP-SSM/1 NASA algorithm validation using primarily LANDSAT and secondarily DMSP and/or AVHRR visible and thermal infrared satellite imagery
[NASA-CR-182979] 18 p2532 N88-25024
Analysis of lightning field changes during active thunderstorms in Florida 18 p2545 N88-25103
A multiprocessor data flow accelerator module
[DE88-007587] 18 p2554 N88-25161
Multi-sensor integration on the NCUBE hypercube computer
[DE88-007472] 18 p2554 N88-25162
A mixed-integer linear programming problem which is efficiently solvable
[AD-A191028] 18 p2556 N88-25168
Decomposition of linear programs using parallel computation
[AD-A191718] 18 p2556 N88-25173
An electrostatic potential comparator
[AD-A192051] 18 p2557 N88-25177
A centered projective algorithm for linear programming
[AD-A192100] 18 p2557 N88-25178
Making progress during a stall in the simplex algorithm
[DE88-007120] 18 p2558 N88-25182
An improved simulated annealing algorithm for standard cell placement
[NASA-CR-182952] 18 p2558 N88-25183
Algorithms and software for solving finite element equations on serial and parallel architectures
[NASA-CR-183027] 18 p2559 N88-25191
Gram-Schmidt implementation of a linearly constrained adaptive array
[AD-A191651] 18 p2560 N88-25198
Robot navigation using simple sensor fusion
[DE88-006184] 18 p2561 N88-25203
A concurrent neural network algorithm for the traveling salesman problem
[DE88-006981] 18 p2562 N88-25208
Algorithms and data structures for an expanded family of matroid intersection problems
[AD-A191482] 18 p2562 N88-25213
A primal-dual algorithm for the computation of the minimum of a convex function on the intersection of convex functions, and its application in data analysis
[RR-638-M] 18 p2563 N88-25217
Multigrid methods for elliptic Partial Differential Equations (PDEs)
[CWI-NM-R8722] 18 p2566 N88-25242
A constraint algorithm for maintaining rigid bonds in molecular dynamics simulations of large molecules
[AD-A191663] 18 p2572 N88-25277
Dendritic growth in the presence of convection
18 p2580 N88-25328
Modem for the land mobile satellite channel
19 p2649 N88-25727
Rearrangement procedures in regenerative multibeammobile communications satellites with frequency reuse 19 p2650 N88-25735
Speech coding at 4800 bps for mobile satellite communications 19 p2652 N88-25749
A 4.8 kbps code-excited linear predictive coder
19 p2652 N88-25750
Robust vector quantization for noisy channels
19 p2653 N88-25754
Analysis and improvement of the vector quantization in SELP (Stochastically Excited Linear Prediction)
19 p2653 N88-25756
The solution of the Elrod algorithm for a dynamically loaded journal bearing using multigrid techniques
[NASA-TM-100941] 19 p2666 N88-25854
Automatic calibration of space based manipulators and mechanisms
[NASA-CR-182804] 19 p2676 N88-25912
A concurrent on-board vision system for a mobile robot
[DE88-007475] 19 p2676 N88-25914
Model-based computed tomography for nondestructive evaluation: An overview and proposal
[DE88-010600] 19 p2679 N88-25926
Updating of municipal official register of real estate through the geographical information system
19 p2684 N88-25952
Algorithmic generation of feasible system architectures
[AD-A191722] 19 p2713 N88-26106
Intermediate level computer vision processing algorithm development for the content addressable array parallel processor
[AD-A192086] 19 p2714 N88-26111
Automatic routing in symbolic IC design environment
19 p2714 N88-26112
Efficient parallel algorithm for the connected component problem and its implementation on the DPP84 (Delft Parallel Processor)
[PB87-225959] 19 p2715 N88-26118

An extension of the Hopfield-Tank model for solution of the multiple traveling salesmen problem
[DE88-008377] 19 p2715 N88-26122
Hybrid simulations
[DE88-009125] 19 p2715 N88-26123
Distributed mathematics in a heterogeneous environment
[DE88-009128] 19 p2716 N88-26124
Gaussian techniques on shared-memory multiprocessors
[DE88-010594] 19 p2716 N88-26126
QR factorization of a dense matrix on a hypercube multiprocessor
[DE88-009187] 19 p2716 N88-26129
Fault diagnosis in distributed computer networks
[AD-A192406] 19 p2718 N88-26140
SLAPP: A special multiprocessor array for signal processing and linear algebra
[AD-A191587] 19 p2719 N88-26146
Some supraconvergent schemes for hyperbolic equations on irregular grids
[DE88-009113] 19 p2720 N88-26151
Calculating the self-intersections of Bezier curves
[AD-A192371] 19 p2721 N88-26156
Digital control of the czochralski growth of gallium arsenide. System reference manual. Valid for Czochralski growth controller software version 2.4
[AD-A191997] 19 p2732 N88-26227
Simple 2-D navigation for wheeled vehicles
[DE88-007115] 20 p2756 N88-26351
Microwave image understanding and its application to radar cross section management
20 p2788 N88-26542
Multi-target tracking algorithms for cluttered environments 20 p2789 N88-26543
A random access algorithm for environments with capture and limited feedback capabilities
[AD-A192233] 20 p2790 N88-26552
Effects of atmospheric model layering on LOWTRAN 6 calculations of 8-12 micrometers near-horizon sky radiances
[AD-A192969] 20 p2791 N88-26559
Improved 3-D turbomachinery CFD algorithm
[NASA-CR-179364] 20 p2801 N88-26619
Parallelization on a multiprocessor system of a solution method for the unsteady Navier-Stokes equations at high Reynolds numbers
[ONERA-NT-1987-8] 20 p2803 N88-26632
Optimization of performance criteria with bounded joint velocities for robots with one degree of redundancy
[DE88-003915] 20 p2810 N88-26670
An assessment of modelling techniques for the finite element analysis of reinforced concrete plate and shell structures
[AD-A192263] 20 p2814 N88-26697
Image pyramid motion detection applied to sea ice
20 p2817 N88-26713
Computer science research, 1987: Computation Directorate
[DE88-008637] 20 p2834 N88-26812
Tuning a major part of a clustering algorithm
[AD-A191446] 20 p2836 N88-26821
SEGMERGE: A scanline visible surface algorithm with adaptive span selection and inexpensive antialiasing
[DE88-009186] 20 p2836 N88-26826
Computing small singular values of bidiagonal matrices with guaranteed high relative accuracy: LAPACK working note number 3
[DE88-008465] 20 p2837 N88-26829
A practical shifted Adams algorithm
[DE88-008573] 20 p2837 N88-26830
Conditions for finite convergence of algorithms for nonlinear programs and variational inequalities
[AD-A192355] 20 p2838 N88-26834
A matroid algorithm and its application to the efficient solution of two optimization problems on graphs, revision
[AD-A192709] 20 p2838 N88-26838
A new trajectory following polynomial-time algorithm for the linear programming problem
[REPT-87-87] 20 p2840 N88-26846
Algorithm for generating the minimal cycle basis of a graph
[PB88-126610] 20 p2846 N88-26891
A new approach to machine-based perception of monocular images
[DE88-002418] 20 p2853 N88-26942
Methods for indirect imaging through the atmosphere
[ONERA-NT-1987-4] 20 p2884 N88-27124
Processing and analysis of images transmitted by Vega space probes over Halley's comet
[ETN-88-92291] 20 p2885 N88-27131
Three-dimensional scene analysis using stero based imaging
[AD-A193120] 21 p2894 N88-27178
Automatic omega station and LOP (Line Of Position) selection
[AD-A193302] 21 p2894 N88-27179
Numerical optimization, system theoretic and software tools for the integrated design of flexible structures and their control systems
[AD-A192927] 21 p2895 N88-27183
The integration of decision support problems into feature modeling based design 21 p2927 N88-27372
Optimal control of the wing rock phenomenon
21 p2927 N88-27373
Calibration and data reduction techniques for the AFGL infrared array spectrometer 21 p2927 N88-27374
Creating aspect graphs for use in object recognition
21 p2928 N88-27379
Optical interconnections for digital image coding
21 p2928 N88-27381
TDWR (Terminal Doppler Weather Radar) PRF (Pulse Repetition Frequency) selection criteria
[AD-A193089] 21 p2932 N88-27407
Sidelobe level of an adaptive array using the SMI (Sampled Matrix Inversion) algorithm
[AD-A193131] 21 p2932 N88-27409
A numerically efficient digital matched filter for periodic and windowed periodic radar waveforms
[AD-A193132] 21 p2932 N88-27410
Effects of numerical dissipation on finite-volume solutions of compressible flow problems
[AD-A193173] 21 p2944 N88-27485
Higher order vortex methods with rezoning
[DE88-010777] 21 p2947 N88-27505
Dexterous hands: Optimizing grasp by design and planning 21 p2958 N88-27572
A lubrication study of engine bearings
21 p2958 N88-27574
Three-dimensional aspects of fatigue crack closure
[AD-A192296] 21 p2960 N88-27581
Photon limited image processing in the space-time domain
[AD-A193142] 21 p2972 N88-27655
Validate algorithms for the determination of rainfall rates from SSM/I microwave satellite imagery
[AD-A192299] 21 p2974 N88-27664
Full analysis of a powerful window random access algorithm
[AD-A192437] 21 p2995 N88-27763
Synchronizable series expressions. Part 2: Overview of the theory and implementation
[AD-A192783] 21 p2996 N88-27768
Distributed algorithms for probabilistic solution of computational vision problems
[AD-A193150] 21 p2997 N88-27773
Computer aided design for linear control State Variable System (SVS)
[AD-A193282] 21 p2997 N88-27775
Verification of flight software written in C using ACSL
[DE88-006100] 21 p2998 N88-27779
The sub-implicit method: New multiprocessor algorithms for old implicit codes
[DE88-011345] 21 p2999 N88-27785
Maximum entropy signal restoration with linear programming
[DE88-011740] 21 p2999 N88-27787
A hidden-surface removal algorithm for structures defined by triangular and rectangular surface patches
[DFVLR-MITT-88-03] 21 p3000 N88-27792
Performability analysis: Measures, an algorithm and a case study
[AD-A192477] 21 p3001 N88-27800
A modular proof of correctness for a network synchronizer
[AD-A192726] 21 p3002 N88-27802
Improving the performance of AI algorithms
[AD-A192848] 21 p3003 N88-27809
Parallel quasi-Newton methods for unconstrained optimization
[AD-A193250] 21 p3003 N88-27812
Parallel solutions to geometric problems on the scan model of computation
[AD-A192321] 21 p3004 N88-27819
Finding minimum-cost circulations by successive approximation
[AD-A192724] 21 p3005 N88-27824
Finding minimum-cost circulations by canceling negative cycles
[AD-A192727] 21 p3005 N88-27825
Numerical optimization
[AD-A193032] 21 p3005 N88-27827
A review of parallel methods for solving sets of linear equations and their application within optimisation algorithms
[AD-A193137] 21 p3006 N88-27830
The computation of stationary distributions on Markov chains through perturbations
[AD-A193191] 21 p3009 N88-27855
A comparison of generators for pseudo-random normal deviates
[DE88-011711] 21 p3010 N88-27859
Robust methods for array signal processing
[AD-A192854] 21 p3012 N88-27871
Satellite attitude determination using a CCD (Charge-Coupled-Device) star camera
[AD-A192662] 22 p3046 N88-28080
Efficient multiplication algorithms over the finite fields GF(q sup m), where q equals 3,5
22 p3066 N88-28191
A wideband, high-resolution spectrum analyzer
22 p3066 N88-28194
Surface tension and viscosity with Lagrangian hydrodynamics on a triangular mesh
[AD-A194120] 22 p3075 N88-28258
Interferometric tomography of continuous fields with incomplete projections
[NASA-CR-183181] 22 p3081 N88-28295
Applications of an exponential finite difference technique
[NASA-TM-100939] 22 p3084 N88-28312
An analytical investigation of geared system dynamics containing spur and helical gears
22 p3085 N88-28317
Parameter identification of material constants in a composite shell structure
[DE88-008115] 22 p3086 N88-28326
A systolic array for efficient execution of the Faddeev algorithm
[DE88-011330] 22 p3135 N88-28635
VAXGAP: A code for the routine analysis of gamma-ray pulse-height spectra on a VAX computer
[DE88-011702] 22 p3137 N88-28648
Importance sampling for stochastic simulations
[AD-A193585] 22 p3138 N88-28654
A fast algorithm for the numerical evaluation of conformal mappings
[AD-A193903] 22 p3138 N88-28658
Rational Newton algorithms to compute formal solutions of linear differential equations in an irregular singular point
[RR-704-M] 22 p3140 N88-28670
Random pseudo-polynomial algorithms and exact problems
[REPT-87-014] 22 p3140 N88-28672
Fitting an ellipse to data
[NPL-DITC-95/87] 22 p3143 N88-28693
Second order differential equations in the complex domain
[RR-674-M] 22 p3144 N88-28695
Random number generation
[USIP-87-15] 22 p3145 N88-28707
Time minimal computation of feedback control schemes for optimal guidance problems used in space flight
[ETN-88-92959] 23 p3184 N88-28953
An overview of technology for spoken interaction with machines
[AD-A194153] 23 p3202 N88-29058
Random-access algorithms for environments with capture
[AD-A194303] 23 p3203 N88-29060
Automatic classification of digitally modulated signals
[AD-A194623] 23 p3203 N88-29064
Hierarchical organization for large, dynamic radio networks
[AD-A193942] 23 p3204 N88-29067
An efficient patched grid Navier-Stokes solution for multiple bodies, phase 1
[AD-A194166] 23 p3211 N88-29110
Vortex dynamics of coherent and chaotic structures (including algorithms for computer simulations and diagnosis)
[AD-A193580] 23 p3212 N88-29117
Analysis of the effect of faulty spares on the performance of diagnostic algorithms in reliable systems
[AD-A193526] 23 p3223 N88-29186
The gradient method for interface tracking
[AD-A194477] 23 p3248 N88-29334
Some learnability results for analogical generation
[AD-A193669] 23 p3250 N88-29342
An algorithm for determining the location of points in computer simulations
[AD-A193713] 23 p3250 N88-29343
A fast parametric maximum flow algorithm, revision
[AD-A194026] 23 p3250 N88-29345
Faster algorithms for the shortest path problem
[AD-A194031] 23 p3250 N88-29347
Faster scaling algorithms for network problems
[AD-A194032] 23 p3251 N88-29348
Analyst-centered models for systems design, analysis, and development 23 p3253 N88-29364
Mathematical algorithms for approximate reasoning
23 p3262 N88-29418

Optimisation algorithms for highly parallel computer architectures. The performance of the truncated Newton, conjugate gradient algorithm in FORTRAN and Ada
[AD-A193940] 23 p3265 N88-29435

The complexity of AI algorithms
[AD-A193494] 23 p3265 N88-29438

MACSYMA program for the painleve test of nonlinear ordinary and partial differential equations
[AD-A194293] 23 p3270 N88-29458

On Wiener-Masani's algorithm for finding the generating function of multivariate stochastic processes
[NASA-CR-182905] 23 p3273 N88-29481

SDI (Strategic Defense Initiative) battle management/C3 (Command, Control and Communications) algorithms technology program plan
[AD-A194357] 23 p3275 N88-29495

A streamwise upwind algorithm for the Euler and Navier-Stokes equations applied to transonic flows
[NASA-TM-101019] 24 p3316 N88-29751

An improved spherical earth diffraction algorithm for SEKE
[AD-A195847] 24 p3360 N88-30005

Transient interaction of electromagnetic pulses in dielectrics and microwave biophysics
[AD-A195687] 24 p3360 N88-30008

Reducing the parallel solution time of sparse circuit matrices using reordered Gaussian elimination and relaxation
[AD-A195152] 24 p3366 N88-30045

LANDSAT-TM data to map flooded areas
[INPE-4594-PRE/1324] 24 p3387 N88-30177

Validate algorithms for the determination of rainfall rates from SSM/I microwave satellite imagery
[AD-A195428] 24 p3404 N88-30270

Algorithms for nonlinear least-squares problems
[AD-A196071] 24 p3411 N88-30305

Range data description based on multiple characteristics 24 p3419 N88-30351

Statistical analysis of the LMS (Last Mean Squares) and modified stochastic gradient
[AD-A195497] 24 p3424 N88-30376

Kalman filter-based algorithms for estimating depth from image sequences
[AD-A195816] 24 p3424 N88-30380

Reconstruction of multidimensional signals from multiple level threshold crossings
[AD-A195561] 24 p3425 N88-30383

Design and performance analysis of a relational replicated database system
[AD-A196290] 24 p3437 N88-30456

The guide star catalog
[NASA-CR-183253] 24 p3452 N88-30547

ALIGNMENT
NT SELF ALIGNMENT

An optoelectronic alignment telescope for straightness measurements
[ETN-87-90383] 01 p0093 N88-10609

Recognizing rigid objects by aligning them with an image
[AD-A184253] 03 p0368 N88-12318

Carbon-fiber reinforced plastics
04 p0403 N88-12506

Optical alignment of Centaur's inertial guidance system
[NASA-TM-88844] 04 p0405 N88-12515

Alignment and assembly tool for very large diameter cylinders
[NASA-CASE-MFS-28001-2] 06 p0711 N88-14360

Development and study of fibre-optic link lines on the basis of the KEM-8-4PD. KEM-8-4PR quantum-electronic modules
[DE88-700372] 07 p0932 N88-15663

Demonstration of efficient full aperture Type 1/Type 2 third harmonic conversion on Nova
[DE88-003834] 14 p1914 N88-21438

Particle beam alignment system for single event upset-Van de Graaf experiments
[AD-A189695] 15 p2132 N88-22721

Thermal compensating mount
[NASA-CASE-LAR-13794-1] 18 p2519 N88-24942

Precise beam alignment He-Ne laser tubes
[PB87-228334] 19 p2675 N88-25906

Precise rotational alignment of X-ray transmission diffraction gratings
[DE88-010599] 21 p2911 N88-27273

ALIPHATIC HYDROCARBONS
NT ACETYLENE
NT ALKANES
NT ALKENES
NT BUTADIENE
NT BUTANES
NT BUTENES
NT CETANE
NT ETHANE
NT ETHYLENE
NT METHANE
NT OXYACETYLENE
NT PARAFFINS
NT POLYBUTADIENE
NT PROPANE
NT PROPYLENE
NT VINYLIDENE

ALKALI HALIDES
NT CESIUM IODIDES
NT SODIUM CHLORIDES
NT SODIUM FLUORIDES

ALKALI METALS
NT CESIUM
NT LIQUID LITHIUM
NT LIQUID POTASSIUM
NT LIQUID SODIUM
NT LITHIUM
NT LITHIUM ISOTOPES
NT POTASSIUM
NT RUBIDIUM
NT RUBIDIUM ISOTOPES
NT SODIUM
NT SODIUM VAPOR

Valence bond cluster studies of alkali metal/semiconductor bonding
[AD-A184276] 04 p0496 N88-13054

Tetrahedral carbon and interstitial electrons in Li cluster: CLi4 and (LiCH3)4
[AD-A184277] 04 p0496 N88-13055

Solar pumped, alkali vapor laser
[AD-A187156] 09 p1170 N88-17016

Clusters: Link between molecules and solids
[AD-A188170] 11 p1543 N88-19224

Kinetic mechanisms for ionization and afterburning suppression
[AD-A189219] 13 p1737 N88-20383

AMTEC electrode development
17 p2409 N88-24324

Thermochemical analysis of mass transfer in a NB-1ZR-potassium heat pipe 17 p2412 N88-24346

Review of alkali metal and refractory alloy compatibility for Rankine cycle applications 17 p2428 N88-24447

Alkali metal thermoelectric converter design for space power systems applications 17 p2437 N88-24499

A capillary pumped SHE/AMTEC system
17 p2437 N88-24500

High power density electrodes for AMTEC
17 p2437 N88-24501

Performance of vapor-fed sodium heat engine/AMTEC systems 17 p2437 N88-24502

C-CAMP: A closed cycle alkali metal power system
[DE88-009715] 19 p2688 N88-25975

A fundamental understanding of the interfacial compatibility in hybrid material systems
[AD-A192921] 21 p2909 N88-27264

Model for bimetallic interfaces, part 2
[DE88-702672] 22 p3157 N88-28787

ALKALIES
NT LITHIUM HYDROXIDES
NT SODIUM HYDROXIDES

DTA/DSC studies of phase equilibria in binary mixtures of barium carbonate with alkali carbonates
[DE87-001195] 02 p0194 N88-11213

Mechanisms of intergranular attack and stress corrosion cracking of alloy 600 by high-temperature caustic solutions containing impurities
[DE87-012820] 10 p1300 N88-17773

The band systems of alkali vapors
[NASA-TT-20206] 10 p1417 N88-18462

ALKALINE BATTERIES

A new concept in an electrically rechargeable zinc-air alkaline battery
[DE88-003858] 13 p1762 N88-20539

Alkaline fuel cell performance investigation
[NASA-TM-100937] 21 p2909 N88-27267

Regenerative fuel cell energy storage system for a low earth orbit space station
[NASA-CR-174802] 24 p3389 N88-30184

ALKALINE EARTH METALS

Group 2A metastable collision complexes: Spectroscopy and behavior in intense radiation fields
[AD-A186737] 08 p1082 N88-16524

Evaluation and compilation of thermodynamic properties of high temperature chemical species
[AD-A187509] 11 p1452 N88-18654

Electronic energy transfer processes in the alkali/alkaline earth metal vapors
[AD-A190035] 15 p2034 N88-22119

Thermochemistry and high temperature thermodynamic properties of rare earth-alkaline earth-copper oxide superconductors
[DE88-005976] 15 p2140 N88-22770

Multiphoton ionization of alkaline earth atoms in an intense laser field
[DE88-008078] 21 p3014 N88-27884

ALKALINE EARTH OXIDES
NT BARIUM OXIDES
NT BERYLLIUM OXIDES
NT CALCIUM OXIDES
NT MAGNESIUM OXIDES

Activated metal oxide surfaces as highly basic and reducing environments
[AD-A184958] 05 p0561 N88-13417

ALKALINITY

Corrosion strength of niobium and its alloys
[DE87-703693] 04 p0416 N88-12578

ALKALOIDS
NT ATROPINE
NT CAFFEINE
NT ERGOTAMINE
NT MORPHINE

ALKANES
NT BUTANES
NT CETANE
NT ETHANE
NT METHANE
NT PARAFFINS
NT PROPANE

Organic molecules on meteoritic solid substrates
[NASA-CR-181570] 05 p0560 N88-13411

Photolytic formation of free radicals and their effect on hydrocarbon pyrolysis chemistry in a concentrated solar environment
[DE88-004129] 13 p1794 N88-20730

ALKENES
NT BUTENES
NT ETHYLENE
NT PROPYLENE
NT VINYLIDENE

Chemical activation of molecules by metals: Experimental studies of electron distributions and bonding
[DE88-004465] 10 p1407 N88-18393

Photolytic formation of free radicals and their effect on hydrocarbon pyrolysis chemistry in a concentrated solar environment
[DE88-004129] 13 p1794 N88-20730

Evaluation of the acute toxicity of a synthetic polyalphaolefin-based hydraulic fluid
[AD-A190412] 15 p2045 N88-22184

ALKYL COMPOUNDS

Separation of anionic from nonionic alkoxy compounds using silica gel
[GB-PATENT-2-140-415-A] 01 p0020 N88-10122

Surface catalytic degradation study of two linear perfluoropolyalkylethers at 345 C
[NASA-TP-2774] 04 p0410 N88-12543

Improved perfluoroalkylether fluid development
[NASA-CR-180872] 08 p0967 N88-15851

The performance of perfluoropolyalkylether oils under boundary lubrication conditions
[AD-A191057] 17 p2323 N88-23869

A study of solvent effects on the synthesis of pure component and composite ceramic powders by metal alkoxide hydrolysis
[DE88-008381] 20 p2777 N88-26470

ALKYLATION

Evaluation of direct methane conversion to higher hydrocarbons and oxygenates
[DE88-003812] 15 p2049 N88-22204

ALKYNES
NT ACETYLENE
NT OXYACETYLENE

ALL-WEATHER AIR NAVIGATION

Rotor SAR (ROSAR): A new high-resolution all-weather vision method for helicopters
[MBB-UA-1046/87] 10 p1314 N88-17855

ALLOCATIONS
NT RESOURCE ALLOCATION

An allotment planning concept and related computer software for planning the fixed satellite service at the 1988 space WARC
[NASA-TM-100244] 03 p0308 N88-11944

Architecture for dynamic task allocation in a man-robot symbiotic system
[DE87-013872] 03 p0362 N88-12277

Engineering calculations for the Delta S method of solving the orbital allotment problem
[NASA-CR-182372] 06 p0671 N88-14110

Dynamic function allocation in fighter cockpits
[AD-A185397] 09 p1201 N88-17199

Task allocation in a distributed computing system
09 p1206 N88-17230

Allocation of database files across parallel stores for efficient processing of partial-match queries
[AD-A188196] 11 p1565 N88-19371

An intelligent allocation algorithm for parallel processing
[NASA-CR-182648] 12 p1675 N88-20014

On two-stage allocation procedures for selection problems
[AD-A190766] 15 p2126 N88-22675
Topics in adaptive control and inference
[AD-A194718] 23 p3266 N88-29443

ALLOYING
De-alloying
[DE87-012488] 01 p0022 N88-10139
A study of surface tension driven segregation in monotectic alloy systems
[NASA-CR-182894] 16 p2178 N88-22983
Ion beam alloying of aluminum for corrosion resistance 17 p2321 N88-23860
Shape memory alloys: New materials for future engineering
[NASA-TT-20193] 20 p2775 N88-26455

ALLOYS
NT ALUMINUM ALLOYS
NT ANTIMONY ALLOYS
NT ASTROLOY (TRADEMARK)
NT AUSTENITIC STAINLESS STEELS
NT BAINITIC STEEL
NT BEARING ALLOYS
NT BERYLLIUM ALLOYS
NT BINARY ALLOYS
NT BORON ALLOYS
NT BRASSES
NT BRONZES
NT CARBON STEELS
NT CAST ALLOYS
NT CHROMIUM ALLOYS
NT CHROMIUM STEELS
NT COBALT ALLOYS
NT COPPER ALLOYS
NT EUTECTIC ALLOYS
NT FERRITIC STAINLESS STEELS
NT GERMANIUM ALLOYS
NT GOLD ALLOYS
NT HASTELLOY (TRADEMARK)
NT HEAT RESISTANT ALLOYS
NT HIGH STRENGTH ALLOYS
NT HIGH STRENGTH STEELS
NT INCONEL (TRADEMARK)
NT INDIUM ALLOYS
NT IRON ALLOYS
NT LEAD ALLOYS
NT LIGHT ALLOYS
NT LIQUID ALLOYS
NT LITHIUM ALLOYS
NT LOW CARBON STEELS
NT MAGNESIUM ALLOYS
NT MANGANESE ALLOYS
NT MARAGING STEELS
NT MARTENSITIC STAINLESS STEELS
NT MOLYBDENUM ALLOYS
NT MONOTECTIC ALLOYS
NT NICKEL ALLOYS
NT NICKEL STEELS
NT NIMONIC ALLOYS
NT NIOBIUM ALLOYS
NT NITINOL ALLOYS
NT QUATERNARY ALLOYS
NT RARE EARTH ALLOYS
NT REFRACTORY METAL ALLOYS
NT RHENIUM ALLOYS
NT SHAPE MEMORY ALLOYS
NT SILICON ALLOYS
NT SILVER ALLOYS
NT SOLDERS
NT STAINLESS STEELS
NT STEELS
NT TANTALUM ALLOYS
NT TELLURIUM ALLOYS
NT TERNARY ALLOYS
NT THALLIUM ALLOYS
NT TIN ALLOYS
NT TITANIUM ALLOYS
NT TUNGSTEN ALLOYS
NT URANIUM ALLOYS
NT VANADIUM ALLOYS
NT ZINC ALLOYS
NT ZIRCONIUM ALLOYS
A physical metallurgical basis for heat-affected zone and base-plate properties of a microalloyed HSLA steel
[AD-A180200] 01 p0022 N88-10137
De-alloying
[DE87-012488] 01 p0022 N88-10139
Equations for determining CVD tungsten-rhenium alloy composition and plating rate
[DE87-008831] 01 p0024 N88-10152
Formation of amorphous alloys by solid state reactions
[DE87-013175] 02 p0146 N88-10918
Investigation of the structure of coatings of self fluxing alloys fused by laser energy
[BLL-M-37301-(5828.4)] 02 p0148 N88-10930
Elevated temperature strain gages
02 p0184 N88-11144
Creep fatigue life prediction for engine hot section materials (isotropic): Third year progress review
02 p0186 N88-11173
Life prediction and constitutive models for engine hot section anisotropic materials program
02 p0188 N88-11175
Effects of surface chemistry on hot corrosion life
02 p0189 N88-11180
Modelling and theories of alloy phase behavior
[DE87-014399] 03 p0287 N88-11804
A fundamental study of the mechanical and microstructural response of elevated temperature PM aluminum-titanium alloys 03 p0289 N88-11819
Ultra-fine grained alloy material
[AD-A184500] 03 p0290 N88-11820
Progress in the development of niobium alloyed high speed steel
[DE87-703549] 04 p0415 N88-12576
An expert system for materials design
[DE88-000191] 04 p0483 N88-12974
The mechanism by which sigma-phase forms in Fe-Cr-Ni system alloys
[BLL-M-37380-(5828.4)] 05 p0564 N88-13437
Corrosion resistance of sintered alloy steels
[BLL-M-37363-(5828.4)] 05 p0564 N88-13438
Projects within the Center for Advanced Materials
[PB88-123054] 06 p0677 N88-14143
Study of the embedded atom method of atomistic calculations for metals and alloys
[DE88-002798] 07 p0835 N88-15065
Rare earth elements in heat treatable steels
[PB87-144002] 08 p0968 N88-15858
Mechanisms of intergranular attack and stress corrosion cracking of alloy 600 by high-temperature caustic solutions containing impurities
[DE87-012820] 10 p1300 N88-17773
Transmission electron microscopy studies of titanium-containing braze/alumina seals
[DE88-005243] 10 p1303 N88-17792
Strength and structure of Ga sub 1-xIn sub xAs alloys
[AD-A188092] 10 p1303 N88-17795
Electronic structure of random alloys and the theory of ordering processes
[DE88-004476] 10 p1407 N88-18394
Tight binding theory of semiconductors
10 p1415 N88-18447
Corrosion performance of high damping alloys in 3.5 percent sodium chloride environment
[AD-A188048] 11 p1457 N88-18687
Institute for Materials Science and Engineering, Metallurgy: Technical activities 1987
[PB88-157722] 11 p1460 N88-18702
National Center for Small-Angle Scattering Research: Reports on measurements carried out by users of the facilities of the NCSASR, December 1, 1985-September 30, 1987
[DE88-003754] 11 p1462 N88-18719
Electron paramagnetic resonance studies of Mn(2+) in 2-6 semiconductor alloys 11 p1560 N88-19340
Electronic structure and phase stability of alloys
[DE88-004574] 11 p1562 N88-19350
JPRS report: Science and technology. USSR: Materials science
[JPRS-UMS-87-009] 14 p1884 N88-21261
Electrical resistivities of some compound forming liquid metal alloys
[PB88-145172] 15 p2037 N88-22137
Bithermal fatigue: A simplified alternative to thermomechanical fatigue 15 p2084 N88-22424
Protective coatings on metals, volume 10
[PB88-174461] 16 p2181 N88-23000
Noncontact temperature measurement. Requirements and applications for metals and alloys research
17 p2326 N88-23899
Predictive corrosion modeling, volume 1
[AD-A191229] 18 p2485 N88-24739
Effect of size of precipitates on recrystallization temperatures in Cu-Cr, Cu-Zr, and Cu-Zr-Cr alloys
[NASA-TT-20166] 18 p2489 N88-24763
On quench sensitivity of Cu-Cr alloys
[NASA-TT-20174] 18 p2489 N88-24765
Solid-state combustion synthesis of ceramics and alloys in reduced gravity
[NASA-CR-4163] 19 p2608 N88-25479
Plastic deformation and roughness of free metal surfaces
[PB88-196621] 20 p2772 N88-26439
EXAFS studies of the microstructure of semiconductor alloys, defects and semiconductor-metal interfaces
20 p2868 N88-27031
Non-equilibrium phases and phase diagrams
[DE88-008896] 20 p2880 N88-27098
On the systematics of phase transformation in metallic alloys
[DE88-008041] 21 p2913 N88-27288
Theoretical predictions of precipitate shapes in cubic alloys
[DE88-010856] 21 p2914 N88-27291
Oxidation-erosion of metals and alloys: Models, verification, and prediction
[DE88-010016] 21 p2915 N88-27300
Refractory metal alloys and composites for space power systems
[NASA-TM-100946] 21 p2916 N88-27310
Thermal conductivity of isotopically pure semiconductors, superlattices, semiconductor alloys and semiconductors as a function of temperature; control of the segregation coefficient in LEC crystal growth; and photo-Hall measurements of GaAs
21 p2927 N88-27375
Significance of the local electrode potential within pits, crevices and cracks
[AD-A192482] 21 p2935 N88-27432
Study of the erosion corrosion of alloys and coatings
[AD-A194337] 22 p3055 N88-28128
Equipment for the pressure welding of metals and alloys utilising the effects of superplasticity
[RAE-TRANS-2162] 22 p3055 N88-28129
The VPE-hydride technique with alloy source: Equilibrium analysis
[AD-A194036] 22 p3157 N88-28784
Influence of local volume forces on surface relaxation of pure metals and alloys: Applications to Ni, Al, Ni3Al
[DE88-702718] 23 p3195 N88-29014

ALLUVIUM
Stochastic geologic effects on near-field ground motions in alluvium
[AD-A192315] 21 p2972 N88-27652

ALMUCANTAR
U ELEVATION ANGLE

ALOHA SYSTEM
Spatial distribution of traffic in a cellular mobile data network
[EUT-87-E-168] 14 p1904 N88-21378
L-band and SHF multiple access schemes for the MSAT system 19 p2650 N88-25734
Integrated voice/data protocols for satellite channels
19 p2651 N88-25739

ALOUETTE SATELLITES
Alouette-ISIS program summary
[NASA-CR-180747] 08 p1023 N88-16195

ALPHA DECAY
Modeling of irradiation-induced amorphization in a titanate ceramic
[DE87-014751] 03 p0292 N88-11833

ALPHA PARTICLES
Feasibility of alpha particle measurement in a magnetically confined plasma by CO2 laser Thomson scattering
[DE88-000039] 02 p0241 N88-11522
Theoretical plasma physics
[DE88-001475] 04 p0492 N88-13029
Slowing down tail enhanced, neoclassical and classical alpha particle fluxes in tokamak reactors
[DE88-001930] 06 p0783 N88-14806
Long-term-aging embrittlement of cast duplex stainless steels: Mechanism and kinetics
[DE88-002929] 09 p1145 N88-16861
Influence of fast alpha diffusion and thermal alpha buildup on Tokamak reactor performance
[DE88-003661] 09 p1251 N88-17496
Problems in modeling TF ripple loss of fast alphas from a tokamak reactor
[DE88-000612] 11 p1553 N88-19296
Simulation of nuclear collisions at high energies in the frames of quark-gluon string model
[DE88-700914] 12 p1690 N88-20113
The calibration of photographic and spectroscopic films: The response of 2aO film to small dosages of alpha particles from 3/10th's rad to 8 rads at energy levels 153 MeV, 79 MeV and 47 MeV
[NASA-CR-177630] 13 p1773 N88-20608
Spectroscopic data relevant to alpha particle diagnostics 17 p2442 N88-24527
Infrared and far-infrared laser development for plasma diagnostics at Oak Ridge National Laboratory
[DE88-007262] 19 p2674 N88-25904
Design and calibration of a two-channel low-noise heterodyne receiver for use in a CO2 laser Thomson scattering alpha particle diagnostic
[DE88-007866] 19 p2728 N88-26201
A CO2 laser Thomson scattering diagnostic for fusion product alpha particle measurement
[DE88-007683] 20 p2857 N88-26965
The distribution of some chemical elements between dissolved and particulate phases in the ocean
[DE88-010181] 21 p2977 N88-27682

Measure of hydrogen concentration profile in materials by resonant nuclear reactions
[DE88-702599] 23 p3193 N88-28999
ALPHA RADIATION
U ALPHA PARTICLES
ALPHABETS
Errors associated with Russian name transliteration
[DE87-011717] 02 p0248 N88-11566
ALPHANUMERIC CHARACTERS
NT BINARY DIGITS
NT DIGITS
Comparison of alphanumeric data entry methods for advanced helicopter cockpits
[AD-A186934] 09 p1201 N88-17201
A comparison of two chord keyboard coding systems for alphanumeric data entry
[AD-A189230] 13 p1813 N88-20834
ALPINE METEOROLOGY
The 54-hours continuous post-frontal precipitation north of the Alpine mountain barrier, 22-25 August 1975
02 p0203 N88-11268
Study of isolated convective clouds in the lower Alps in summer 1984, using radar and a simple Weinstein numerical model
[ESA-TT-1061] 03 p0353 N88-12224
Research work at the Meteorological Institute of the University of Munich (Federal Republic of Germany)
[MITT-56] 08 p1013 N88-16141
Cross flow in the Alps and flat foehn during the experiment MERKUR --- mesoscale experiment
08 p1013 N88-16142
Energy balance and discharge of an Alpine glacier, illustrated by Mount Vernagtferner in the Oetzal Alps, Tyrol 08 p1014 N88-16145
Results of the experiment MERKUR: Structural change of a weak cold front in the sphere of influence of the Alps --- mesoscale experiment 08 p1014 N88-16146
Vertical sounding of th air layer close to a glacier on Mount Vernagferner in the Oetzal Alps, Tyrol (experiment LUZIVER 1983) 08 p1015 N88-16152
Simulation of a lee cyclogenesis using a numerical model 08 p1016 N88-16162
Simulations of thermally induced winds and cross flow situations
[MITT-57] 09 p1193 N88-17148
An analytical method for the determination of the average horizontal wind velocities across two-dimensional hills
[ISBN-3-923624-06-9] 11 p1515 N88-13048
The German Front Experiment 1987: Experimental design
[DFVLR-MITT-87-24] 16 p2234 N88-23343
ALPS MOUNTAINS (EUROPE)
Energy balance and discharge of an Alpine glacier, illustrated by Mount Vernagtferner in the Oetzal Alps, Tyrol 08 p1014 N88-16145
Results of the experiment MERKUR: Structural change of a weak cold front in the sphere of influence of the Alps --- mesoscale experiment 08 p1014 N88-16146
Statistics of two-dimensional structure elements of mountainous ranges (mosaic model) for calculating three-dimensional reflection functions
[DFVLR-FB-87-33] 09 p1185 N88-17099
The Monte Generoso-Zimmerwald (Switzerland) baseline from satellite laser ranging data using various analysis techniques
[LR-533] 14 p1940 N88-21576
The German Front Experiment 1987: Experimental design
[DFVLR-MITT-87-24] 16 p2234 N88-23343
SPOT image exploitation for glacial mass balance fluctuation monitoring in the French Alps
22 p3090 N88-28350
ALTERATION
U REVISIONS
ALTERNATING CURRENT
Evaluation of stand-alone inverters for remote applications
[DE87-010957] 01 p0040 N88-10257
Comparison of costs and benefits for dc and ac transmission
[DE87-008774] 02 p0167 N88-11052
Output power enhancement of AC Raman free-electron laser
[DE88-000503] 04 p0449 N88-12786
Sliding charge density waves and related problems
[AD-A186720] 09 p1157 N88-16934
The theory and implementation of a high quality pulse width modulated waveform synthesiser applicable to voltage FED inverters
[ETN-87-90712] 09 p1157 N88-16937
Application of ac-impedance method on determination of corrosion rate of metals
[DE88-750307] 10 p1300 N88-17771
Advanced capacitor development
[AD-A189985] 15 p2059 N88-22276
AC impedance analysis of corrosion fatigue in naval aircraft alloys
[AD-A190822] 17 p2322 N88-23865
Some equivalent circuit models for AC impedance analysis of pyrite/solution interface
[DE88-010574] 21 p2939 N88-27452
ALTERNATING CURRENT GENERATORS
U AC GENERATORS
ALTERNATING DIRECTION IMPLICIT METHODS
A finite-element alternating method for two-dimensional Mode-1 crack configurations
[NASA-TM-100616] 16 p2224 N88-23276
ALTERNATIVES
Compendium of significant events in the recent development of alcohol fuels in the United States
[DE87-013355] 01 p0032 N88-10202
Alternative fuels: Information on DOD's (Department of Defense's) methanol vehicle program
[PB87-213328] 02 p0156 N88-10976
Application of electronic fuel injection to the optimum engine for methanol utilization
[PB87-201950] 02 p0180 N88-11120
A systems analysis of fire suppression alternatives for the US space station
[AD-A189847] 15 p2025 N88-22064
ALTERNATORS (GENERATORS)
U AC GENERATORS
ALTIMETERS
NT LASER ALTIMETERS
NT RADIO ALTIMETERS
The global positioning system as an aid to the testing of inertial navigation units (volume 1, addendum 1)
[AD-A185783] 12 p1578 N88-19443
Integrated multisensor navigation systems
17 p2294 N88-23722
ALTIMETRY
NT SATELLITE ALTIMETRY
Considering refraction in leveling with laser plane
04 p0462 N88-12857
Tidal estimation in the Pacific with application to SEASAT altimetry
[NASA-TM-100694] 13 p1803 N88-20780
Criteria for planimetric and altimetric correction of maps restituted from aerial photographs in 1:100,000 scale
17 p2367 N88-24097
ALTITUDE
NT FLIGHT ALTITUDE
NT HIGH ALTITUDE
NT LOW ALTITUDE
NT SEA LEVEL
Analysis of the inter-layer independence of stellar scintillometer profiles of Cn2
[AD-A189372] 12 p1645 N88-19854
A model of the ionosphere in the altitude interval 50 to 4000 km. Part 1: Atomic ions (H(+), He(+), N(+), O(+))
[DFVLR-FB-88-11-PT-1] 23 p3233 N88-29241
ALTITUDE ACCLIMATIZATION
Differentiation of hemopoietic stem cells during adaptation to high altitude 07 p0893 N88-15410
Mononuclear phagocytes during adaptation of essentially healthy people to high altitudes
07 p0896 N88-15432
Biorhythmic aspects of intercontinental Antarctic adaptation 08 p1046 N88-16321
Dexamethasone as prophylaxis for acute mountain sickness: Effect of dose level
[AD-A185848] 08 p1047 N88-16325
Status of microcirculation in high-altitude blood loss
12 p1663 N88-19973
Depressed sweating during exercise at altitude
[AD-A192603] 22 p3130 N88-28609
Human acclimatization and physical performance at high altitude
[AD-A192651] 22 p3130 N88-28611
Influence of altitude and caffeine during rest and exercise on plasma levels of proenkephalin peptide F
[AD-A192659] 22 p3131 N88-28616
Biomedical aspects of military operations at high altitude
[AD-A192677] 22 p3132 N88-28619
Alterations in upper extremity motor function in soldiers during acute high altitude exposure
[AD-A192676] 23 p3238 N88-29272
ALTITUDE CONTROL
Magnetic emissions testing of the space station engineering model resistojet
[NASA-TM-100788] 10 p1292 N88-17728
The exploitation of Aircraft Integrated Monitoring System (AIMS) data in height-keeping studies for aircraft operating above FL 290 22 p3036 N88-28026
ALTITUDE SICKNESS
Dexamethasone as prophylaxis for acute mountain sickness: Effect of dose level
[AD-A185848] 08 p1047 N88-16325
Medical problems related to altitude in: Human performance physiology and environmental medicine at terrestrial extremes, chapter 14
[AD-A188340] 12 p1666 N88-19989
Acute mountain sickness at 4500 m is not altered by repeated eight-hour exposures to 3200-3550 m normobaric hypoxic equivalent
[AD-A188358] 12 p1666 N88-19990
Human acclimatization and physical performance at high altitude
[AD-A192651] 22 p3130 N88-28611
Alterations in cutaneous vasomotor regulation during acute and chronic hypoxia
[AD-A192653] 22 p3131 N88-28612
Biomedical aspects of military operations at high altitude
[AD-A192677] 22 p3132 N88-28619
Alterations in upper extremity motor function in soldiers during acute high altitude exposure
[AD-A192676] 23 p3238 N88-29272
ALTITUDE SIMULATION
Cooling electronic equipment at simulated high altitude in hypobaric chambers
[AD-A185196] 05 p0584 N88-13560
Oxygen transport during exercise at extreme simulated altitude: Operation Everest 2
[AD-A185720] 06 p0752 N88-14620
Operation Everest 2: Comparison of four instruments for measuring blood oxygen saturation
[AD-A186456] 08 p1049 N88-16337
Altitude simulation testing of Ariane's second-stage engine 09 p1126 N88-16747
Experimental evaluation of turning vane designs for high-speed and coupled fan-drive corners of 0.1-scale model of NASA Lewis Research Center's proposed altitude wind tunnel
[NASA-TP-2681] 10 p1285 N88-17686
Age, alcohol, and simulated altitude: Effects on performance and breathalyzer scores
[AD-A190642] 15 p2103 N88-22531
Techniques utilized in the simulated altitude testing of a 2D-CD vectoring and reversing nozzle
[NASA-TM-100872] 19 p2604 N88-25464
Analysis of clinical symptoms of human decompression sickness during altitude chamber studies
19 p2703 N88-26074
ALTITUDE TESTS
Measured performance of the heat exchanger in the NASA icing research tunnel under severe icing and dry-air conditions
[NASA-TM-100116] 04 p0451 N88-12796
Techniques utilized in the simulated altitude testing of a 2D-CD vectoring and reversing nozzle
[NASA-TM-100872] 19 p2604 N88-25464
ALTITUDE TOLERANCE
Effect of pyrocetam on mouse resistance to hypoxic hypoxia 2-3 months after exposure to X-radiation
07 p0895 N88-15425
Operation Everest 2: Alterations in the immune system at high altitude
[AD-A188011] 11 p1520 N88-19075
Analysis of clinical symptoms of human decompression sickness during altitude chamber studies
19 p2703 N88-26074
ALU (COMPUTER COMPONENTS)
U ARITHMETIC AND LOGIC UNITS
ALUMINA
U ALUMINUM OXIDES
ALUMINATES
Conductivity studies on hydroxide ion conductors in the Li-Al-O-H system at intermediate temperatures
[AD-A185714] 06 p0697 N88-14279
Phase behavior in the Li-Al-O-H system at intermediate temperatures
[AD-A185732] 06 p0697 N88-14280
ALUMINIDES
Advances in processing techniques for nickel aluminides
[DE87-014571] 05 p0566 N88-13449
Development of iron aluminides
[AD-A185190] 05 p0568 N88-13461
Elevated temperature crack growth studies of advanced titanium aluminides
[AD-A189025] 12 p1608 N88-19618
Chemical compatibility between silicon carbide and a nickel aluminide
[DE88-006188] 18 p2479 N88-24708
Hot isostatic pressing of nickel aluminide powders
[DE88-009677] 19 p2617 N88-25525
Nickel aluminides: A new family of nickel + aluminum alloys featuring simple composition, low density, excellent oxidation resistance and high yield strength that increases with temperature
[DE88-010692] 20 p2776 N88-26461

A fundamental understanding of the interfacial compatibility in hybrid material systems
[AD-A192921] 21 p2909 N88-27264

ALUMINIZING
U ALUMINUM COATINGS

ALUMINUM

Large-strain softening of aluminum at elevated temperature
[DE87-011559] 01 p0024 N88-10153

Observations of localized grain boundary dislocations in series of (001) and (110) symmetrical tilt boundaries in aluminum
[DE87-014011] 01 p0025 N88-10156

Polyitaconic acid macromolecule primar for adhesive bonding and corrosion control of aluminum
[DE87-013306] 01 p0027 N88-10173

Relation between shock strength and strain-rate plasticity at maximum deviatoric stress
[DE87-011736] 01 p0061 N88-10390

Accurate ab initio calculations which demonstrate a 3 Pi u ground state for Al2
[NASA-TM-89302] 01 p0102 N88-10666

A simulation study of interfaces in Ni, Al and Ni3Al with and without boron
[DE87-013156] 01 p0102 N88-10667

Mathematical modelling of solar ultraviolet radiation induced optical degradation in anodized aluminum
02 p0135 N88-10846

Factors determining the morphology of precipitation in aluminum-germanium and aluminum-silicon alloys
[DE87-014682] 03 p0287 N88-11806

The infiltration kinetics of aluminum in silicon carbide compacts
[AD-A184682] 03 p0290 N88-11823

Aluminum oxynitride spinel (ALON): A review
[AD-A184753] 03 p0294 N88-11845

Defect characterization in quartz and related materials
[AD-A184754] 03 p0294 N88-11846

Carbon-fiber reinforced aluminum
04 p0403 N88-12507

Data base on the high heat flux behaviour of metals and carbon materials for plasma facing components: Experiments at the 10 MW neutral beam injection test stand of the IPP Nagoya
[IPPJ-AM-53] 04 p0492 N88-13031

Microstructural change of Al on H implantation
[IPPJ-847] 04 p0493 N88-13036

Plasticity of aluminum and iron at high shear strain rate and high pressure 05 p0563 N88-13430

X-ray analysis of polycrystalline aluminium subjected to fatigue cycling
[NAL-TM-MT-8706] 05 p0564 N88-13434

The growth of persistent slip bands
05 p0597 N88-13648

Temperature dependent mechanical properties of an alumina fiber reinforced aluminum composite
06 p0677 N88-14147

Bending properties of aluminum base composite with CVD-fiber
[PB87-130878] 06 p0678 N88-14156

The effect of temperature on fatigue crack initiation from aluminosilicate inclusions 06 p0720 N88-14427

Chromic acid anodizing of aluminum foil
[NASA-CR-178417] 07 p0837 N88-15077

J-estimation procedure based on moire interferometry data
[AD-A185965] 07 p0867 N88-15256

Nb3Al formation in sputter-deposited Nb/Al mutli-layer samples
[DE88-003192] 08 p0970 N88-15868

Investigation on diffusion reaction brazing of aluminium
[PB87-143368] 08 p0992 N88-16001

The effect on initial bond strength and durability of a Phosphoric Acid Dip (PAD) following chromic acid anodising of aluminum
[ARE-TM(UMM)-87402] 10 p1300 N88-17772

Investigation of materials for inert electrodes in aluminum electrodeposition cells
[DE88-003380] 10 p1323 N88-17906

Strategic placement of accelerometers to measure forces by the sum of weighted accelerations
[DE88-002262] 10 p1333 N88-17968

Durability and damage tolerance of aluminum castings
[AD-A186444] 10 p1341 N88-18013

Evaluation and compilation of thermodynamic properties of high temperature chemical species
[AD-A187509] 11 p1452 N88-18654

Dynamical properties of aluminium from experimental dispersion relations
[DE88-700240] 11 p1459 N88-18697

Study of the vibrational modes of subsurface oxygen on Al (111) using diode laser infrared reflection-absorption spectroscopy
[AD-A188322] 12 p1632 N88-19769

X-ray source model for Z-pinch aluminum plasmas
[AD-A189509] 12 p1696 N88-20148

The effect of microstructure on the fatigue crack growth resistance of nickel base superalloys
[AD-A189526] 13 p1741 N88-20414

Aluminum-air battery development
[DE88-006617] 13 p1762 N88-20542

Aluminum-air battery development
[DE88-006618] 13 p1762 N88-20543

Development of a manufacturing unit for selective coating of solar absorbers made out of aluminum
[BMFT-FB-T-86-204] 14 p1942 N88-21580

Fabrication and electrical characterization of multilevel aluminum interconnects used to achieve silicon-hybrid wafer-scale integration
[AD-A190519] 15 p2060 N88-22282

Polyitaconic acid macromolecule primer for adhesive bonding and corrosion control of aluminum
17 p2319 N88-23849

The variation of torsional ductility of high-purity aluminum with temperature and strain rate
[DE88-005618] 18 p2487 N88-24755

Plate response analysis using shock tube
[AD-A190828] 18 p2526 N88-24987

A numerical study of Rayleigh-Taylor instability in aluminum and steel plates
[DE88-010475] 20 p2774 N88-26449

A finite element analysis for the hydroforming of aluminum
[DE88-008050] 20 p2784 N88-26516

Crystallization of aluminum hydroxide in the aluminum-air battery: Literature review, crystalizer design and results of integrated system tests
[DE88-010510] 20 p2797 N88-26594

Ultraviolet-visible spectroscopy of laser-produced aluminum plasmas
[AD-A193004] 20 p2860 N88-26990

Electronic and geometric structure of silver and palladium on aluminum (111) in monoatomic surface layers
[ETN-88-92120] 20 p2879 N88-27093

Evaluation of explosive bonding for patching aluminum with aluminum
[AD-A193303] 21 p2913 N88-27285

Nuclear magnetic resonance spectrometer
[AD-A192928] 21 p2950 N88-27523

Growth and characterization of CuGaS2, CuAlS2 and CuGa0.9Al0.1S2 single crystals
[AD-A192963] 21 p3021 N88-27930

The 2D Rydberg series in Al I
[NASA-TM-101189] 22 p3150 N88-28740

Initiation of explosive molten aluminum-water interactions at wet or underwater surfaces
[DE88-004686] 23 p3194 N88-29006

Relation between strength, creep and relaxation behavior in Cu and Al at room temperature
[ETN-88-92982] 23 p3195 N88-29015

Muon-spin rotation experiment (micro + SR) on aluminum and indium after low temperature electron irradiation
[ETN-88-92985] 23 p3294 N88-29617

Fatigue crack growth characteristics of ARALL (trademark)-1
[AD-A196185] 24 p3341 N88-29889

High frequency GaAlAs modulator and photodetector for phased array antenna applications
[NASA-TM-101328] 24 p3367 N88-30048

Development of graded reference radiographs for aluminum welds, phase 1
[AD-A195594] 24 p3381 N88-30140

ALUMINUM ALLOYS

Contribution to the study of the Ti-Al phase diagram by conventional and high resolution electron microscopy
[ESA-TT-1021] 01 p0023 N88-10143

Evaluation of cracking in aluminum cylinders
[PB87-201398] 01 p0024 N88-10149

Crack propagation behavior of the materials StE 460 and AlMg 4.5Mn
[FD-1/1986] 01 p0058 N88-10373

Monte Carlo calculations for the simulation of channeling experiments on irradiated aluminum alloys. Calculation of angle-dependent efficiency curves
[HMI-B-433] 01 p0092 N88-10597

An investigation of the high strain rate deformation of SiCw/2124 Al composite
[OUEL-1675/87] 02 p0142 N88-10895

Development of a pilot plant for the production of rapidly solidified aluminum alloy powders
[BMFT-FB-T-86-153] 02 p0146 N88-10914

Study of the microscopic mechanisms of cyclic deformation. Development of a new approach: The case of aluminum
[ISAL-87-0003] 02 p0149 N88-10936

Coating life prediction 02 p0189 N88-11161

Corrosion resistance of silver-plated carbon-aluminum composite 03 p0285 N88-11793

A fundamental study of the mechanical and microstructural response of elevated temperature PM aluminum-titanium alloys 03 p0289 N88-11819

Gas tungsten arc welding of Al-10Fe-5Ce
[AD-A184202] 03 p0334 N88-12104

Corrosion behavior of P/M mechanically alloyed IN-9052.1: An electro-chemical investigation
[AD-A184191] 04 p0414 N88-12567

Weldability of 2219-T851 and 2519-T87 aluminum armor alloys for use in Army vehicle systems
[AD-A184296] 04 p0451 N88-12792

Investigation by differential scanning calorimetry of microstructure in a superplastic Al-Mg-Zr alloy
[AD-A184902] 05 p0564 N88-13439

A fundamental study of P/M processed elevated temperature aluminum alloys
[AD-A185393] 05 p0565 N88-13445

Phase diagram and thermochemical properties of the Al-Cu system
[ETN-88-91015] 05 p0566 N88-13447

An investigation of unipolar arcing at atmospheric pressure in aluminum 2024 and aluminum coated glass slides
[AD-A184903] 05 p0577 N88-13521

The effect of ion beam mixed Ni-Al surface layers on PSB extrusion morphology in fatigued nickel
05 p0598 N88-13652

The evolution of local mechanical properties of Al 2219-T851 during fatigue 05 p0598 N88-13653

Cyclic deformation of an extruded AlMgSi alloy
05 p0598 N88-13654

Closure behavior under constant effective stress intensity loading conditions 05 p0598 N88-13656

Growth of short fatigue cracks in a squeeze formed aluminum alloy 05 p0598 N88-13658

Influence of microstructure and aging condition on the fatigue crack propagation in age hardened aluminium alloys 05 p0599 N88-13659

Fatigue crack growth behavior of A356-T6 cast aluminum alloy 05 p0599 N88-13660

Behavior of short cracks in a 2024 aluminum alloy sheet tested at several stress ratios 05 p0600 N88-13669

The effect of microstructure on the surface crack length: Crack depth relationship for short cracks
05 p0600 N88-13670

On the role of crack tip shielding in influencing the behavior of long and small fatigue cracks in aluminum-lithium alloy 2090 05 p0600 N88-13671

The influence of microstructure and residual stresses on the initiation and propagation of short surface cracks on AlMgSi1 05 p0601 N88-13674

An experimental study of closure behavior of naturally initiated small cracks 05 p0601 N88-13676

Propagation of small fatigue cracks in 2024-T3 aluminum alloy 05 p0601 N88-13678

Fatigue crack retardation in aluminium alloys
05 p0602 N88-13681

Observations on the effect of overloads on fatigue crack growth 05 p0602 N88-13684

Crack growth in contrasting titanium alloys under the conjoint action of high and low cycle fatigue
05 p0602 N88-13686

Variable amplitude fatigue crack growth in aluminum alloys 2090-T8E41 and 7075-T651
05 p0602 N88-13687

Effects of MN dispersoids on near threshold fatigue crack growth in 2134 type alloys
05 p0603 N88-13692

Fatigue mechanisms in ARALL, a fatigue resistant hybrid aluminum aramid composite material
05 p0605 N88-13711

A comparison of plastic work energy and external input for fatigue crack propagation 05 p0607 N88-13722

X-ray fatigue failure prediction based on plasticity response to microcracks 05 p0607 N88-13725

Environmentally assisted fatigue crack growth
05 p0608 N88-13731

Fatigue crack growth 05 p0608 N88-13734

Characterization of the microstructures of various materials
[AD-A184961] 05 p0655 N88-14017

Study of surface treatment before bonding of light alloys
[DCQ/L-48-287/F] 06 p0682 N88-14181

The effect of shear lips on fatigue crack growth in Al-2024 sheet material 06 p0718 N88-14408

Study of the evolution of short cracks in fatigue analysis --- aircraft construction materials
[DCQ/L-46-555] 06 p0722 N88-14442

Effect of overload ratios on fatigue crack growth behavior in Ti-6Al-4V alloy
[PB87-147062] 07 p0833 N88-15055

Study on the square wave alternating plasma arc welding for aluminum alloys
[PB87-143772] 07 p0863 N88-15239

Examination of the physical processes associated with the keyhole region of variable polarity plasma arc welds in aluminum alloy 2219 07 p0927 N88-15634

X-ray measurements of phason distortion in ion-implanted Al-Mn
[DE87-014566] 07 p0937 N88-15694

Investigation of microstructural factors that cause low fracture toughness in silicon carbide whisker/Al alloy composites
[AD-A186443] 09 p1137 N88-16817

Multipurpose corrosion inhibitors for aerospace materials in Naval environments
[AD-A186728] 09 p1143 N88-16853

Adhesive bond strengths on aluminium alloys as a function of surface topographies and their wetting properties
[ARE-TM(UMM)-87403] 09 p1148 N88-16880

Micro-mechanisms of deformation in SiC/Al composites
[AD-A188282] 10 p1296 N88-17749

Environment assisted degradation mechanisms in aluminum-lithium alloys
[NASA-CR-182482] 10 p1301 N88-17782

Corrosion behavior of sputter-deposited aluminum-based alloys exposed to chloride solutions
[AD-A187262] 10 p1303 N88-17794

The metallurgical database of Aladin: An alloy de sign system
[AD-A187724] 11 p1457 N88-18682

Study of the effects of metallurgical factors on the growth of fatigue microcracks
[AD-A188475] 12 p1608 N88-19615

Development of metastable processing paths for high temperature alloys
[AD-A188682] 12 p1608 N88-19617

Thermal-mechanical fatigue testing of a titanium-aluminide alloy
[AD-A189555] 12 p1609 N88-19620

Composites strengthening
[AD-A189258] 13 p1734 N88-20364

Threshold fatigue crack growth in Ti-6Al-2Sn-4Zr-6Mo
[AD-A189560] 13 p1741 N88-20415

A calorimetric determination of the enthalpy of formation and a description of the defect structure of the ordered beta-phase /Ni, Cu/ /1-x/ Al/x/
[NASA-TT-20157] 13 p1745 N88-20434

Processing of glass to aluminum (low melting metals) seals via an injection molding technique
[DE88-004689] 13 p1751 N88-20468

Processing, physical metallurgy and creep of NiAl + Ta and NiAl + Nb alloys
[NASA-CR-182113] 14 p1890 N88-21295

Electron diffraction evidence for the ordering of excess nickel atoms by relation to stoichiometry in nickel-rich beta NiAl formation of a nickel-aluminum (Ni2Al) superlattices
[NASA-TT-20177] 14 p1890 N88-21297

Diffusion welding of aluminomagnesium alloys to ceramics 14 p1898 N88-21333

The effect of strain rate on the strength and ductility of SiCw/2124 Al composite
[OUEL-1692/87] 14 p1924 N88-21466

Effect of loading conditions on environment-sensitive fracture
[BR102697] 14 p1934 N88-21533

Joints in fiber-reinforced aluminum alloys
[NASA-TT-20160] 15 p2031 N88-22104

Processing, microstructure, and mechanical properties of silicon carbide particulate reinforced aluminum alloys
[AD-A188981] 15 p2037 N88-22136

The effective fracture toughness of aluminum at rapid heating rates
[AD-A189745] 15 p2038 N88-22146

The age hardening response of thermomechanically processed Al-Mg-Li alloys
[AD-A189870] 15 p2039 N88-22147

Investigation and synthesis of high temperature and increased stiffness RSP aluminum alloys
[AD-A190407] 15 p2039 N88-22151

Response of aluminum alloys to erosive particle impacts
[DE88-005910] 15 p2041 N88-22159

The corrosion resistance of an aluminum alloy coated with polysilazane derived ceramics
[AD-A190703] 15 p2046 N88-22189

Aluminum-air battery development
[DE88-006620] 15 p2061 N88-22287

A modified sulphuric acid anodising process used as a pretreatment for the adhesive bonding of aluminum alloys
[ARE-TM(UMM)-87410] 16 p2177 N88-22974

Fatigue crack growth under full-scale cyclic plasticity
[DFVLR-FB-87-48] 16 p2222 N88-23263

Environment effects on crack propagation with tensile stress
[GKSS-87/E/46] 16 p2223 N88-23267

Stress corrosion cracking properties of Al-Li alloys
17 p2320 N88-23853

AC impedance analysis of corrosion fatigue in naval aircraft alloys
[AD-A190822] 17 p2322 N88-23865

Strain hardening at large strains in aluminum alloys
[DE88-007415] 18 p2484 N88-24737

Improving knowledge of the corrosion behavior of aluminum alloys of the 7XXX series
[REPT-48-451/F] 18 p2486 N88-24750

Characterization of the 2219 Cegedur alloy: Data acquisition of the fracture mechanics --- aircraft construction materials
[REPT-48-442/F] 18 p2487 N88-24751

Aluminum alloy
[NASA-CASE-LAR-13924-1-CU]
18 p2487 N88-24753

Martensitic transformation and microstructures in sintered NiAl alloys
[NASA-TT-20178] 18 p2488 N88-24761

Rapidly solidified lightweight durable disk material
[AD-A191697] 18 p2491 N88-24775

Nondestructive evaluation methods for determination of thermal history and mechanical properties of aluminum-lithium alloys
[DE88-007352] 19 p2615 N88-25516

Effect of Zr or Cr content on the fracture toughness of the high purity Al-Zn-Mg alloys
[NASA-TT-20294] 19 p2616 N88-25518

Extended ductility of Al and alpha-Fe alloys through dynamic recovery mechanisms
[DE88-008679] 19 p2616 N88-25522

Prediction of fatigue life of notched specimens under aircraft loading and importance of the relative method in the case of local strain approach, part 2
[TAE-595-PT-2] 19 p2680 N88-25934

Precipitation study by electrical resistivity measurement in Ni-Al alloys
[DE88-701877] 20 p2773 N88-26440

Grain boundary structure in Ni3Al
[DE88-009164] 20 p2773 N88-26444

Optimizing superplastic response in lithium containing aluminum-magnesium alloys
[AD-A192217] 20 p2774 N88-26451

Fatigue of lithium-aluminum alloys: An example of localization of the plastic deformation
[ETN-88-92309] 20 p2775 N88-26456

Analysis of the perforation of monolithic and simple laminate aluminium targets as a test of analytical deformation models
[MRL-R-1111] 20 p2813 N88-26686

A fundamental understanding of the interfacial compatibility in hybrid material systems
[AD-A192921] 21 p2909 N88-27264

A method for determining the solubility of hydrogen in molten aluminum-lithium alloys
[DE88-009807] 21 p2910 N88-27270

Thermomechanical processing of Al alloy 2090 for grain refinement and superplasticity
[AD-A192333] 21 p2912 N88-27281

Analysis of grain refinement and superplasticity in aluminum-magnesium alloys
[AD-A193029] 21 p2912 N88-27283

Processing and properties of advanced aluminum alloys
[AD-A193224] 21 p2912 N88-27284

Constant amplitude fatigue life data for notched and unnotched annealed Ti-6Al-4V sheet
[AD-A193420] 21 p2913 N88-27287

Study of surface treatments before adhesive bonding of light alloys --- aircraft industry
[ETN-88-92743] 21 p2916 N88-27308

Study of feasibility and optimization conditions of laser treatments: Application of the local recrystallization of aluminum
[ISAL-87-0048] 21 p2916 N88-27309

Kinetic of oxidation to air of a Fe-Al-Mn alloy system at 600-800(sup 0)C temperature range
[DE88-702309] 21 p2920 N88-27330

Influence of microstructure and microdamage processes on fracture at high loading rates
[AD-A192957] 21 p2960 N88-27583

Stress relaxation of a titanium (Ti-6Al-4V) threaded joint
[DE88-010102] 21 p2961 N88-27590

Stress corrosion evaluation of powder metallurgy aluminum alloy 7091 with the breaking load test method
22 p3053 N88-28115

Corrosion of aluminium alloys by IRFNA
[AD-A194319] 22 p3055 N88-28127

Study of fatigue cracks in aluminum alloys. Influence of microstructure
[REPT-48-553] 22 p3056 N88-28134

A fundamental study of P/M processed elevated temperature aluminum alloys
[AD-A192958] 23 p3194 N88-29005

An investigation into the metallurgical aspects of joining rapidly-solidified aluminum alloys
[AD-A194677] 23 p3194 N88-29009

Structural relationship between icosahedral and Frank-Kasper phases of Al-Li-Cu
[AD-A193768] 23 p3195 N88-29011

Passive damping concepts for free and forced member and grillage vibration
[NASA-CR-183114] 23 p3225 N88-29196

Some effects of nitrates on the tensile properties of Al 7075-T7351
[AD-A195116] 24 p3354 N88-29965

ALUMINUM ARSENIDES

Photoluminescence studies of GaAs/AlAs superlattices
[DE87-013817] 02 p0245 N88-11548

Excimer laser-assisted deposition of GaAs, AlAs and (Al,Ga)As from Lewis acid-base adducts
[AD-A184588] 03 p0329 N88-12081

Photoluminescence studies of InGaAlAs quaternary alloys
[DE88-007197] 20 p2674 N88-27062

Investigations on the MBE (Molecular Beam Epitaxy) growth and properties of Al(sub y)Ga(sub y)In(sub 1-x-y)AsInP and InGaAs-InAlAs superlattices
[DE88-009105] 21 p3022 N88-27941

ALUMINUM BORON COMPOSITES

Fracture mode research of boron aluminum composite materials by Acoustic Emission (AE)
[NAL-TR-927] 02 p0142 N88-10891

Analytical and experimental characterization of damage processes in composite laminates
[AD-A187221] 10 p1296 N88-17746

Structure and strength of boron-aluminum composites
14 p1885 N88-21264

Influence of heat treatment on the properties of boroaluminum 14 p1886 N88-21270

ALUMINUM CARBIDES

Research and development on high strength ceramic heaters discussed 04 p0404 N88-12508

ALUMINUM COATINGS

Ion plating for corrosion control
[AD-A185061] 05 p0565 N88-13442

Studies on hot-dip zinc-aluminum coated sheet steels
[ETN-88-92217] 15 p2042 N88-22166

ALUMINUM COMPOUNDS
NT ALUMINATES
NT ALUMINIDES
NT ALUMINUM ARSENIDES
NT ALUMINUM CARBIDES
NT ALUMINUM FLUORIDES
NT ALUMINUM NITRIDES
NT ALUMINUM OXIDES
NT ALUMINUM SILICATES
NT ANDESITE
NT SAPPHIRE

Application of sol-gel procedures to ceramic composites
[ETN-88-92741] 21 p2921 N88-27338

ALUMINUM FLUORIDES

High temperature solar electrothermal processing-3. Zinc from zinc oxide at 1200-1675K using a non-consumable anode
[AD-A186600] 09 p1141 N88-16836

ALUMINUM GALLIUM ARSENIDES

Numerical studies of the dual HEMT/algorithm development and numerical studies of Schrodinger's equation
[AD-A184471] 04 p0478 N88-12946

Resonant level lifetime in GaAs/ AlGaAs double-barrier structures
[AD-A185376] 05 p0655 N88-14020

Radiant power degradation of silicon-doped gallium arsenide and gallium aluminum arsenide infrared light-emitting diodes
[AD-A186726] 09 p1157 N88-16935

AlGaAs heterojunction lasers
[NASA-CR-4119] 09 p1171 N88-17020

Superlattice photodetectors
[AD-A186956] 09 p1253 N88-17511

The physics of very small structures
[AD-A187672] 11 p1556 N88-19311

Comparison of low temperature photoluminescence of bulk MBE (Molecular Beam Epitaxy) grown AlGaAs and GaAs using a graphite generated dimer versus a standard tetramer arsenic group-V source
[DE88-004939] 11 p1558 N88-19329

Pressure-dependent DLTS (Deep Level Transient Spectroscopy) experiments on Si-doped AlGaAs
[DE88-003842] 13 p1846 N88-21047

Optical nonlinearities in GaAs/GaAlAs multiple quantum wells fabricated by metalorganic chemical vapor deposition for use in optical signal processing
[AD-A191558] 18 p2582 N88-25337

Nonlinear optical properties and subpicosecond dynamics of excitons and electron-hole plasmas in multiple quantum well structures
[AD-A191926] 19 p2727 N88-26196

Far-infrared studies of doped AlGaAs/GaAs multiple-quantum-well structures
20 p2862 N88-26998

Electro-optical studies of Al(x)Ga(1-x)As/GaAs coupled quantum wells 20 p2862 N88-26999

Quantum wells and bulk AlGaAs under hydrostatic pressure 20 p2862 N88-27000

Ultrafast physics in semiconductor microstructures
[AD-A193300] 21 p3022 N88-27936

A high frequency GaAlAs travelling wave electro-optic modulator at 0.82 micrometers
[NASA-TM-100970] 22 p3073 N88-28240

Spectroscopic studies with multiple quantum well materials with applications to optical signal processing at room temperature
[AD-A194171] 24 p3429 N88-30409

ALUMINUM GRAPHITE COMPOSITES

Effect of interface on mechanical properties of graphite/201 aluminum composites
05 p0606 N88-13717

Interface characteristics and the mechanical properties of metal matrix composites
[AD-A186441] 08 p0966 N88-15845

Elastoplastic response of unidirectional graphite/aluminum under combined tension-compression cyclic loading
[CCMS-88-01] 11 p1451 N88-18647

A piecewise quadratic strength tensor theory for composites
[AD-A190929] 16 p2173 N88-22952

Temperature-dependent tensile and shear response of graphite/aluminum
[NASA-CR-182914] 19 p2609 N88-25484

ALUMINUM NITRIDES

Ceramic substrates for semiconductor applications reported: AlN substrates 19 p2633 N88-25621

AlN substrate applications 19 p2634 N88-25622

Low temperature film growth of the oxides of zinc, aluminum and vanadium (and related systems, oxides of gold and germanium, nitrides of aluminum and tungsten) by reactive sputter deposition
[AD-A193497] 23 p3191 N88-28986

ALUMINUM OXIDES

NT SAPPHIRE

Toughening of alpha-alumina: Preliminary results
[DE87-702776] 01 p0028 N88-10178

Studies of alumina additions in zirconia - magnesia
[DE87-703500] 04 p0419 N88-12602

T.E.M. study of boehmite gels and of their transformation into alpha-alumina
[SNIAS-872-430-121] 05 p0656 N88-14023

Temperature dependent mechanical properties of an alumina fiber reinforced aluminum composite
06 p0677 N88-14147

The effect of texture on the crack growth resistance of alumina
[NASA-TM-100250] 06 p0686 N88-14206

The dc conductivity studies of an hydroxide ion conductor at intermediate temperatures
[AD-A186044] 07 p0847 N88-15142

Static and dynamic determination of aluminum oxide toughness
[PB87-146999] 07 p0869 N88-15275

Tunable Al2O3:Ti3 + -laser with optical pumping
09 p1237 N88-17415

The influence of the heating procedure on the oxidation behaviour of NiAl studied by XPS
[AERE-R-12498] 10 p1300 N88-17776

The migration of grain boundaries in ceramic materials with particular reference to the sintering process
[DE86-004065] 10 p1306 N88-17808

New scientific findings on the morphology of aluminum oxide layers, serving as an adhesive basis
[MBB-Z-137/86] 10 p1312 N88-17840

The soft/hard wet anodization of aluminum oxide and its use in a thin film multilayered capacitor
[AD-A187575] 10 p1325 N88-17919

Deactivation of alumina based catalysts
11 p1455 N88-18673

Study of adherent oxide scales
[AD-A187368] 11 p1456 N88-18680

The YAlO(sub 3):Er laser
[PB88-130877] 11 p1493 N88-18911

Preparation and characterization of thin films of alumina by metalorganic chemical vapor deposition
[AD-A188366] 12 p1608 N88-19614

Contact and current noise in beta alumina and Nasicon ceramics
[AD-A189168] 12 p1611 N88-19635

Characterization and fundamental studies on CuO sorbent materials to determine attrition mechanisms on substrate gamma alumina
[DE88-003674] 13 p1749 N88-20456

Recommendations on developing polycrystalline alumina fiber 13 p1756 N88-20502

Analytically modeling the carbothermic reduction of alumina in a thermal plasma
[DE88-005535] 13 p1841 N88-21020

Crack resistance of multilayer ceramic-based composite material 14 p1885 N88-21265

Oxide-bound transition metal complexes for methane activation
[PB88-169719] 14 p1887 N88-21277

Nonlinearly tunable wideband emission of infrared radiation by Al2O3:Ti laser 14 p1970 N88-21758

Microwave sintering of alumina-SiC composites at 2.45 and 60 GHz
[DE88-006455] 15 p2030 N88-22095

Processing defects and strength of alumina substrates
[W-10/87] 15 p2087 N88-22441

The kinetics of contact noise in NaBeta alumina
[AD-A190651] 15 p2130 N88-22707

Synthesis and characterization of high-T(sub c) screen-printed Y-Ba-Cu-O films on alumina
[NASA-TM-100860] 15 p2146 N88-22805

High-strength ceramic based on tetragonal ZrO2 with Al2O3 admixture 16 p2180 N88-22996

Thermal conductivity of hard anodized coatings on aluminum
[AD-A191755] 18 p2492 N88-24784

Effect of process conditions on aluminum oxide thin film used in pH ISFET 19 p2673 N88-25892

The protonic Beta double prime aluminas: Preparation, stability, conductivity and structure
[DE88-008442] 20 p2768 N88-26415

Application of controlled interfacial pore structures to kinetic studies in alumina
[DE88-010894] 21 p2919 N88-27326

Preparation and characterization of ceramic materials based on Al2O3 reinforced with a ZrO2 dispersion
[ISAL-87-0041] 21 p2922 N88-27340

Comparison of sol-gel procedures for zircon and alumina
[REPT-881-430-108] 21 p2922 N88-27342

Study of the erosion corrosion of alloys and coatings
[AD-A194337] 22 p3055 N88-28128

Influence of dispersed additives reinforcement on the wear reinforcement mechanisms of the alumina-steel couple. Macroscopic and structural aspects
[ECL-88-01] 22 p3059 N88-28148

Laser crystallized silicon films on alumina ceramic substrates and application to thin film c-Si solar cells
[PB88-131966] 22 p3116 N88-28515

The high temperature creep deformation of Si3N4-6Y2O3-2Al2O3
[NASA-CR-183204] 23 p3190 N88-28981

Low temperature film growth of the oxides of zinc, aluminum and vanadium (and related systems, oxides of gold and germanium, nitrides of aluminum and tungsten) by reactive sputter deposition
[AD-A193497] 23 p3191 N88-28986

Al2O3-TiO2 and Al2TiO5 ceramic materials
[SNIAS-881-430-122] 23 p3199 N88-29038

ALUMINUM SILICATES

NT ANDESITE

The effect of temperature on fatigue crack initiation from aluminosilicate inclusions
[PNR90377] 02 p0154 N88-10962

Structure and mechanical properties of metal matrix composites made using semi-solid processes: The case of the system Al-Si/SiC
[ETN-88-92299] 17 p2316 N88-23836

Mechanical and structural characterization of aluminum ceramic fibers
[ETN-88-92168] 17 p2323 N88-23870

ALVEOLAR AIR

Biofeedback control of alveolar carbon dioxide tension to eliminate hypocapnia in man in the presence of hypoxia 07 p0892 N88-15405

Breath-by-breath measurement of alveolar gas exchange 12 p1653 N88-19905

ALVEOLI

Breath-by-breath measurement of alveolar gas exchange 12 p1653 N88-19905

Liquid ventilation: New data and possible use in space medicine 12 p1654 N88-19906

AMAZON REGION (SOUTH AMERICA)

Project CODEAMA/FUNCATE (test-area of Barreinnha-AM): Field report
[INPE-4500-RPE/563] 15 p2090 N88-22455

Surface CO results from the ABLE-2B expedition to Amazonia
[INPE-4501-PRE/1258] 15 p2093 N88-22469

Surface ozone and ozonesounding results from the ABLE-2B expedition to Amazonia
[INPE-4523-PRE/1275] 15 p2095 N88-22484

Aerodynamic aspects of the Amazon Forest
[INPE-4445-TDL/313] 15 p2098 N88-22501

Detection, monitoring and analysis of some environmental effects of fires in the Amazon region through utilization of NOAA and LANDSAT satellite imagery and aircraft data
[INPE-4503-TDL/326] 16 p2230 N88-23322

Oxidation and reduction rates for organic carbon in the Amazon mainstream tributary and floodplain, inferred from distributions of dissolved gases
[NASA-CR-182943] 18 p2538 N88-25062

Recent measurements of ozone in the Amazon forests
[INPE-4494-PRE/1258] 24 p3389 N88-30185

AMBIENCE

Vertical directionality of ambient noise at 32 deg N as a function of longitude: Tape number 86180
[AD-A193228] 21 p3012 N88-27872

AMBIENT TEMPERATURE

GAS eleven node thermal model (GEM)
10 p1289 N88-17712

Polymeric electrolytes for ambient temperature lithium batteries
[DE88-004896] 13 p1763 N88-20547

Ambient temperature secondary lithium batteries using LiAl lithium insertion anodes
[DE88-008394] 20 p2793 N88-26574

AMBIPOLAR DIFFUSION

Evolution of poloidal variation of impurity density and ambipolar potential in rotating tokamak plasma, part 2
[DE88-009882] 19 p2731 N88-26218

AMBIT

U FIELD THEORY (PHYSICS)

AMBULANCES

Satellite communications experiment for the Ontario air ambulance service 19 p2646 N88-25705

AMIDES

NT POLYIMIDES
NT UREAS

A 13C and 15N solid state NMR characterization of aramid-containing nylon-6 polymers synthesized by in situ polymerization of caprolactam with benzoyl caprolactam derivatives
[AD-A187067] 09 p1147 N88-16672

Synthesis and characterization of 1,2-cyclobutenedicarboxamides: Thermally generated polymers and Diels-Alder adducts
[AD-A188591] 12 p1611 N88-19633

AMINES

NT DIAMINES
NT EPINEPHRINE
NT ERGOTAMINE
NT GUANIDINES
NT NOREPINEPHRINE
NT SEROTONIN
NT TETRYL

High-molecular compounds (selected articles)
[AD-A184668] 03 p0293 N88-11842

Studies on syntheses of amine-carboxyboranes (boron analogues of amino acids) and derivatives
[AD-A184838] 05 p0557 N88-13386

Thermally stable aromatic structures from acyclic precursors. 1: Para polyphenylene model compounds from 3-Dimethyl amino hex-5-EN-1-YNES
[AD-A185300] 05 p0568 N88-13462

Modification of polymers by photografting processes
17 p2323 N88-23871

Aromatic cyclotriphosphazenes
[NASA-CASE-ARC-11428-3] 18 p2477 N88-24692

Structural study of impregnating resins of TGMDA/DDS type
[ETN-88-92167] 20 p2780 N88-26486

AMINO ACIDS

NT GLUTAMIC ACID
NT GLUTAMINE

Observing effect of laser radiation of low-frequency Raman scattering of light 06 p0772 N88-14742

A program for the study of skeletal muscle catabolism following physical trauma
[AD-A189771] 15 p2102 N88-22521

Studies of model ion channels in defect-free multibilayers of phospholipids
[AD-A188740] 16 p2238 N88-23365

Fast atom bombardment study on interaction of anticodonic nucleotides and their cognate amino acid
[ISAS-RN-355] 20 p2850 N88-26918

Precise ultraviolet absorbance study of the interaction of amino acids and mononucleosides in aqueous solution
[ISAS-RN-356] 21 p2908 N88-27256

AMMONIA

NT LIQUID AMMONIA

Ruthenium catalysts and their use in ammonia production
[GB-PATENT-2-136-704-A] 01 p0020 N88-10123
JPRS report: Science and technology. China
[JPRS-CST-87-031] 03 p0299 N88-11880
XeCl excimer laser induced multiphoton ionization of ammonia molecule 03 p0299 N88-11883
Model investigations of atmospheric ammonia scavenging
[DE88-002337] 09 p1194 N88-17153
Human blood glutamic acid level with exposure to high ambient concentrations of ammonia
10 p1361 N88-18134
Electrochemistry in near-critical and supercritical fluids. 5: The dimerization of quinoline and acridine radical anions and dianions in ammonia from -70 C to 150 C
[AD-A190858] 16 p2175 N88-22967
Microwave spectroscopy and gravitational collapse
18 p2594 N88-25413
Interaction of vinylidene fluoride: Tetrafluoroethylene copolymer with ammonia
[NASA-TT-20292] 19 p2620 N88-25542
Employment of porous polytetrafluoroethylene Membrane with a hydrophilic and hydrophobic stratal structure for construction of an enzyme electrode
[NASA-TT-20296] 19 p2620 N88-25543

AMMONIUM COMPOUNDS
NT AMMONIUM NITRATES
NT AMMONIUM PERCHLORATES
Development of microencapsulated DNBM quaternary ammonium inhibitors for paints
17 p2319 N88-23851

AMMONIUM NITRATES
An infra-red investigation of HAN (Hydroxylammonium Nitrate)-based liquid propellants
[AD-A187226] 10 p1307 N88-17815
The burning of HAN-based (hydroxylammonium nitrate) liquid propellants
[DE88-006863] 18 p2494 N88-24800
Electrical ignition of HAN-based liquid propellants
[AD-A191349] 18 p2495 N88-24801
The high pressure sound velocity and equation of state of aqueous solutions of hydroxylammonium nitrate and triethanolammonium nitrate
[AD-A191740] 18 p2570 N88-25266
Titrimetric analysis of HAN-based liquid propellants
[AD-A196225] 24 p3357 N88-29990

AMMONIUM PERCHLORATES
Equilibrium calculations of ionization in tracer flames
[PB87-104154] 04 p0412 N88-12555
A general qualitative study of point and extended defects and their interactions in non-metallic systems
[AD-A191687] 19 p2618 N88-25532
Descriptive characterization of propellant particles
[AD-A195176] 24 p3356 N88-29985

AMMONOLYSIS
Process for preparing transition metal nitrides and transition metal carbonitrides and their reaction intermediates
[DE88-000849] 06 p0679 N88-14162

AMMUNITION
NT INCENDIARY AMMUNITION
Control and stabilization mechanisms of submunitions
[DFVLR-IB-111-86/9] 03 p0259 N88-11630
Thermoplastic elastomers as LOVA (Low Vulnerability Ammunition) binders
[AD-A184350] 04 p0419 N88-12599
Calculation evaluation of the boundary conditions of autoinflammation of propulsive charges
[PB87-139044] 08 p0974 N88-15890
Real time AI expert system for robotic applications
08 p1061 N88-16408
Dependence of the expectancy of hitting on the number of spread shots. Determination of the expectancy of hitting using a spread salvo
[REPT-FM6] 10 p1310 N88-17829
Splinter generator
[MBB-UA-1048/87] 11 p1491 N88-18897

AMOEBA
How does Physarum polycephalum perceive and use gravity? 12 p1655 N88-19918

AMORPHOUS MATERIALS
NT AMORPHOUS SILICON
Construction and characterization of amorphous-silicon test structures
[DE87-013595] 01 p0029 N88-10182
Formation of amorphous alloys by solid state reactions
[DE87-013175] 02 p0146 N88-10918
EXELFS (Extended Electron Energy Loss Fine Structure) of amorphous and crystalline SiC
[DE87-013551] 02 p0151 N88-10948
Corrosion-resistant amorphous metallic coatings. Engineering development
[NASA-CR-181487] 03 p0287 N88-11802
Modeling of irradiation-induced amorphization in a titanate ceramic
[DE87-014751] 03 p0292 N88-11833
Microstructure of amorphous and crystalline zirconium alloys rapidly solidified
[DE87-703700] 05 p0564 N88-13432
Structural investigations of some metallic glasses
[ECN-198] 06 p0686 N88-14203
Structural relaxation and mechanical properties of amorphous Fe-Zr alloys 07 p0840 N88-15094
Study of molecular mobility of noncrystalline polymer alloys of different compatibility using mechanical spectrometry
[ISAL-87-0032] 09 p1149 N88-16883
Diffusion studies in amorphous NiZr alloys
[DE88-003009] 10 p1301 N88-17781
The soft/hard wet anodization of aluminum oxide and its use in a thin film multilayered capacitor
[AD-A187575] 10 p1325 N88-17919
Laboratory amorphous carbon: A possible analog of cometary dust 14 p2009 N88-21981
Fast ion conducting glasses
[AD-A191412] 16 p2183 N88-23010
Long-time tunneling in amorphous metals at helium temperatures
[DE88-701150] 16 p2281 N88-23654
Electrodeposition of amorphous Ni-Cr-P alloys
[DE88-006868] 19 p2616 N88-25521
Hydrogenated amorphous silicon-germanium alloys
[DE88-001147] 19 p2620 N88-25546
Study of Staebler-Wronsky degradation effect in a Si:H based P-I-N solar cells
[NASA-CR-182564] 19 p2687 N88-25970
Glass forming ranges of amorphous alloys
[DE88-007897] 20 p2772 N88-26438
Plasma deposition: Investigations on a new approach
[ETN-88-92619] 20 p2861 N88-26992
Formation of metastable structures and amorphous phases in Cu-W alloys using the triod sputtering technique
[DE88-009051] 21 p2915 N88-27298
PECVD of amorphous nickel--phosphorus films
[DE88-011086] 21 p2915 N88-27299
Influence of the interface on the crystallization of amorphous Ge in Pb/Ge multilayers
[DE88-010072] 22 p3156 N88-28776

AMORPHOUS SEMICONDUCTORS
NT AMORPHOUS SILICON
Amorphous or microcrystalline semiconductor memory device
[EP-PATENT-0-162-529-A1] 01 p0026 N88-10167
Preparation of amorphous silicon semiconductors
[GB-PATENT-2-176-054-A] 05 p0656 N88-14022
Defects and disorder in amorphous and damaged silicon
[AD-A192277] 20 p2879 N88-27089
Influence of the temperature-dependence of recombination life-time of free carriers in amorphous semiconductors on thermostimulated photocurrent spectra
[DE88-702728] 23 p3293 N88-29609
Thermostimulated conductivity in amorphous semiconductors with non-exponential density of localized states
[DE88-702737] 23 p3293 N88-29612
Ultrafast processes and spectroscopy with free electron lasers
[AD-A195248] 24 p3379 N88-30126

AMORPHOUS SILICON
Detection of minimum-ionizing particles in hydrogenated amorphous silicon
[DE88-002769] 07 p0837 N88-15081
Research on high-efficiency, stacked, multijunction, amorphous silicon alloy thin-film solar cells
[DE88-001108] 13 p1793 N88-20723
Progress of amorphous silicon based solar cells and modules
[DE88-004666] 13 p1794 N88-20733
Investigations of the origins of metastable, light-induced changes in hydrogenated amorphous silicon
[DE88-001117] 13 p1846 N88-21051
Defects and disorder in amorphous and damaged silicon
[AD-A192277] 20 p2879 N88-27089
Amorphous silicon solar cells using a metal substrate
[PB88-131941] 21 p2968 N88-27628
Rapid thermal annealing of silicon layers amorphized by ion implantation
[DE88-702307] 23 p3290 N88-29591

AMPERAGE
U ELECTRIC CURRENT

AMPHIBIA
NT FROGS
Limb regeneration in amphibians, a suitable model for investigations of the effects of weightlessness as regards evolution and modifications 07 p0885 N88-15369
Changes in the morphological and molecular biological processes during early embryo development in amphibians under micro-g conditions 07 p0885 N88-15371
Embryonic development of the newt Cynops pyrrhogaster in very weak magnetic fields
[ISAS-RN-357] 19 p2702 N88-26068

AMPHIBOLES
Origin of SNC kaersutitic amphibole: Experimental data 23 p3306 N88-29693
Reappraisal of the geology of Kangimut Sammisoq, Ameralik Fjord, Southern West Greenland: Crustal structure and interpretation of isotopic data
24 p3398 N88-30234

AMPLIFICATION
NT POWER GAIN
NT SOUND AMPLIFICATION
NT WAVE AMPLIFICATION
Gain evaluation for an idealized curtain array antenna
[PB87-210290] 02 p0161 N88-11006
Investigation of two laser beam coupling and amplification in Ce-doped SBN single crystals
03 p0327 N88-12069
Increased gain of channel intensifier tubes by pulsed biasing
[DE88-000512] 04 p0490 N88-13019
A focussed MCP (microchannel plate) image intensifier type for high speed gating
[DE88-000480] 05 p0583 N88-13555
Narrow linewidth gain measurements in a KrF excimer amplifier pumped longitudinally by a high-power electron beam
[DE88-001365] 05 p0586 N88-13575
Signal processing studies program optical signal amplification, volume 2
[AD-A188054] 10 p1320 N88-17896
Signal processing studies program optical signal amplification, volume 1
[AD-A188055] 10 p1321 N88-17897
A cause of divergence in the Kalman gain equation
12 p1578 N88-19438
Some measurements of height gain at V.H.F.
12 p1617 N88-19671
Solid-state travelling wave amplifiers based on multi-stream instability
[AD-A189566] 12 p1624 N88-19718
Fiber-coupled external-cavity semiconductor high power laser
[AD-A188454] 13 p1774 N88-20611
Wavelength scaling of lithium-like recombination scheme for X-UV gain production --- X-ray lasers
[ETN-88-92002] 13 p1778 N88-20634
Effect of off-axis radiation in amplified spontaneous emission
[DE88-007001] 14 p1915 N88-21440
Amplification of signals in fiber optics using the stimulated Raman effect
[AD-A190281] 15 p2133 N88-22727
Analysis and design of gain scheduled control systems
[NASA-CR-182867] 16 p2163 N88-22904
Model for pulse amplification by a gaseous laser amplifier
[DE88-011729] 20 p2808 N88-26657
On the small signal gain of free electron lasers in the low-current regime
[DFVLR-FB-88-10] 21 p2955 N88-27552
Optoelectronic gain control of a microwave single stage GaAs MESFET amplifier
[NASA-CR-182201] 24 p3368 N88-30055

AMPLIFICATION FACTOR
U AMPLIFICATION

AMPLIFIER DESIGN
Phase 2 development of a 12 GHz MMIC FET amplifier
[IM-I86-1010] 01 p0038 N88-10240
Construction of a 60 GHz Traveling Wave Tube (TWT) for intersatellite link on geostationary orbit (ISL/TWT)
[BMFT-FB-W-86-015] 16 p2192 N88-23076

AMPLIFIERS
NT BROADBAND AMPLIFIERS
NT CYCLOTRON RESONANCE DEVICES
NT DISTRIBUTED AMPLIFIERS
NT FLUID AMPLIFIERS
NT LIGHT AMPLIFIERS
NT MICROWAVE AMPLIFIERS
NT PARAMETRIC AMPLIFIERS
NT PHOTOMULTIPLIER TUBES
NT POWER AMPLIFIERS
NT PREAMPLIFIERS
NT TRANSISTOR AMPLIFIERS
NT TRAVELING WAVE AMPLIFIERS
NT VOLTAGE AMPLIFIERS
Traveling-wave maser closed-cycle refrigerator data acquisition and display system 04 p0437 N88-12708
Power density measurements in the near field of the DSS 13 26-meter antenna 04 p0437 N88-12711

Narrow linewidth gain measurements in a KrF excimer amplifier pumped longitudinally by a high-power electron beam
[DE88-001365] 05 p0586 N88-13575
Integrated photo-responsive metal oxide semiconductor circuit
[NASA-CASE-GSC-12782-1] 06 p0696 N88-14271
Conceptual designs of a 50 NM FEL (Free-Electron Laser) oscillator and a 20-40 NM SASE (Self-Amplified Spontaneous Emission) amplifier
[DE88-003150] 10 p1334 N88-17974
New generation imager system
[NASA-CR-180464] 10 p1408 N88-18398
Design and fabrication of advanced hybrid circuits for high energy physics
[DE88-004392] 11 p1479 N88-18825
Ballistic deficits in pulse shaping amplifiers
[DE88-003908] 11 p1481 N88-18840
Pulse-train amplification of subnanosecond near-transform-limited KrF laser pulses
[DE88-004460] 12 p1631 N88-19764
Phase preservation cleanup in a double-pass Raman amplifier SBS (Stimulated Brillouin Scattering) conjugator
[AD-A189428] 13 p1761 N88-20536
Advanced components for spaceborne infrared astronomy
[NASA-CR-177470] 13 p1772 N88-20601
Wiggler taper optimization for free-electron-laser amplifiers with moderate space-charge effects
[DE88-003758] 13 p1775 N88-20618
Generating squeezed microwave radiation with a Josephson parametric amplifier
14 p1976 N88-21805
Characterization of a 30-GHz IMPATT solid state amplifier
[NASA-TM-100876] 18 p2503 N88-24847
Aurora status and plans
[DE88-006476] 18 p2521 N88-24955
Reducing sensitivity to errors in free electron laser amplifiers
[DE88-007017] 18 p2522 N88-24960
Thermionic integrated circuit program
[DE88-010119] 19 p2662 N88-25833
A 2.3-GHz low-noise cryo-FET amplifier
22 p3066 N88-28195
Theoretical and experimental study of a mode-converting coupler for application to a harmonic gyrotron amplifier
[AD-A193760] 22 p3081 N88-28294

AMPLITUDE DISTRIBUTION ANALYSIS
Four-wave mixing used in optical amplitude encoding
03 p0376 N88-12366
Near optimal blind deconvolution
[REPT-87-016] 15 p2123 N88-22655

AMPLITUDE MODULATION
Four-wave mixing used in optical amplitude encoding
03 p0376 N88-12366
Fast autotuning of a hydrogen maser by cavity Q modulation 04 p0436 N88-12707
Axial anisotropy of the intensity of the cosmic ray nuclear component
[IFSI-87-7] 05 p0662 N88-14061
Phase phenomena in parametric generators and amplifiers of ultrashort light pulses
07 p0918 N88-15576
Magnet strength fluctuations in the SSC (Superconducting Super Collider) lattice. Part 2: Frequency modulation
[DE88-006491] 15 p2141 N88-22774
A study on the co- and adjacent channel protection requirements for mobile satellite ACSSB modulation
19 p2650 N88-25732
Basic causes of amplitude modulation in climatic/weather parameters
[DE88-702743] 23 p3236 N88-29254

AMPLITUDE PROBABILITY ANALYSIS
U AMPLITUDE DISTRIBUTION ANALYSIS

AMPLITUDES
NT PULSE AMPLITUDE
NT SCATTERING AMPLITUDE
The giant spot on II Peg in 1986
04 p0508 N88-13120
Fatigue 87, volume 1
[AD-A184045] 05 p0597 N88-13645
A dislocation model for fatigue crack propagation under variable amplitude loading 05 p0602 N88-13683
The how and why of variable amplitude testing
05 p0603 N88-13690
Regional wave attenuation and seismic moment from the inversion of NORESS spectra
[AD-A187399] 11 p1510 N88-19023
Envelope and phase statistics for non-Gaussian noise and resulting error probabilities for digital communications systems 12 p1617 N88-19672
Passive DF: A tutorial, part 1
[NASA-CR-182669] 13 p1815 N88-20846
Constant amplitude fatigue life data for notched and unnotched annealed Ti-6Al-4V sheet
[AD-A193420] 21 p2913 N88-27287

AMPTE (SATELLITES)
A fluid simulation of the AMPTE lithium gas releases in the solar wind
[TRITA-EPP-87-06] 05 p0661 N88-14056
Nature and the nonlinear evolution of electrostatic waves associated with the AMPTE (Active Magnetosphere Particle Tracer Explorers) solar wind releases
[AD-A185471] 06 p0806 N88-14920
AMPTE-UKS ion observations at a quasi-parallel bow shock 08 p1095 N88-16589
An unusual magnetopause encounter by AMPTE-UKS
08 p1097 N88-16602
Observations of small scale structures using data from the wave experiment on the AMPTE-UKS spacecraft
08 p1099 N88-16612
Deployable booms and antennas on AMPTE-IRM
14 p1874 N88-21196
Magnetic cavity formation at Comet Halley and at the AMPTE Li release 14 p1996 N88-21898
Observation of nonlinear wave decay processes in the solar wind by the AMPTE IRM plasma wave experiment
[AD-A191409] 16 p2290 N88-23713
Attitude and orbit control for the AMPTE-UKS (Active Magnetospheric Particle Tracer Explores-UK Subsatellite): Evaluation of the in-flight performance
[PB87-225199] 19 p2604 N88-25467
Plasma of earth's magnetosphere ring currents. Model compared with results of AMPTE/CCE experiment
24 p3447 N88-30515

ANAEROBES
A process study of the biothermal conversion of water hyacinths to methane
[DE88-000554] 06 p0730 N88-14488
Shelf life degradation of selected anaerobic threadlocking adhesives at various storage temperatures
[AD-A187712] 11 p1461 N88-18711

ANALOG CIRCUITS
DEDALE: An expert system for analog circuit maintenance 02 p0128 N88-10809

ANALOG COMPUTERS
Specification for IBM/IBM compatible 3480 tape cartridge
[NASA-TM-100702] 17 p2384 N88-24168

ANALOG DATA
Statistical very short-range forecasting via analogues
02 p0206 N88-11290
The design and testing of an analog optical communication link capable of the simultaneous transmission of four frequency division multiplexed audio signals
[AD-A184695] 03 p0307 N88-11936
Signal chain for the Airborne Visible/Infrared Imaging Spectrometer (AVIRIS) 06 p0706 N88-14331
Massively parallel implementations of theories for apparent motion
[AD-A185841] 07 p0901 N88-15455
Emerging technologies program 3-5: Microelectronics Panel report
[AD-A189463] 12 p1624 N88-19716
Visual display representation of multidimensional systems: The effect of information correlation and display integrality
[AD-A188655] 12 p1672 N88-20010
An overview of the development of a linear broadband analog fiber-optic link
[DE88-008668] 20 p2854 N88-26945

ANALOG SIMULATION
Modeling of environmentally-induced transients within satellites. Part 2: Discharge coupling transients
03 p0273 N88-11722
Modelling of a hydraulic motor and servo-valve to produce a desired system response using analogue and digital compensation techniques
[ETN-88-92079] 14 p1899 N88-21337
Development of a hybrid simulator for robotic manipulators
[AD-A193119] 21 p2956 N88-27557

ANALOG TO DIGITAL CONVERTERS
Digital to analog and analog to digital conversion using pulse duration modulation
[ETN-87-90415] 01 p0078 N88-10499
Measurements in the functional mock up test of the NAL QSTOL aircraft control system
[NAL-TR-928] 02 p0126 N88-10793
Digitization functions in computer graphics
[ETN-88-91363] 05 p0635 N88-13887
Life sciences flight experiments microcomputer
06 p0792 N88-14857
Multilayer holographic functional element in analog-digital converter 07 p0921 N88-15593
Method for set-up for researching signal curve development
[NASA-TT-20235] 13 p1760 N88-20526
Fast analog-to-digital converter
[DE88-701488] 15 p2106 N88-22543
Mass digitization of topographic-cartographic information 16 p2226 N88-23288
Digitizing the traffic network of JOG 250 by scanning --- JOG 250 map 18 p2533 N88-25029
Tests for the automatic pattern recognition of building surfaces by the TK 50 18 p2533 N88-25030
Development of a mobile satellite communication unit
19 p2646 N88-25701
Baseband assembly analog-to-digital converter board
22 p3067 N88-28201
Multichannel data transmission through a fiber optic cable
[AD-A193842] 22 p3070 N88-28221

ANALOGIES
Geometrically nonlinear rod mechanism analogy of axisymmetrically loaded spherical shells based on a comprehensive approach to the stability of circular arches
[ETN-87-90419] 01 p0062 N88-10398
Analogical inference and analogical access
[AD-A184345] 03 p0369 N88-12321
Similarity networks as a knowledge representation for space applications 08 p1062 N88-16411
Some learnability results for analogical generation
[AD-A193669] 23 p3250 N88-29342

ANALOGS
Studies on syntheses of amine-carboxyboranes (boron analogues of amino acids) and derivatives
[AD-A184838] 05 p0557 N88-13386
Infinite dimensional dynamical systems and their finite dimensional analogues
[AD-A192041] 18 p2563 N88-25216
Space station habitability recommendations based on a systematic comparative analysis of analogous conditions
[NASA-CR-3943] 18 p2587 N88-25372
Superconductive analogue of spin glasses
[DE88-702059] 19 p2733 N88-26233
Operational multifield analog forecasting of US seasonal temperatures for non-winter seasons
22 p3127 N88-26592
Rifts of deeply eroded Hawaiian basaltic shields: A structural analog for large Martian volcanoes
24 p3443 N88-30494

ANALYSIS (MATHEMATICS)
NT ABEL FUNCTION
NT ANALYTIC FUNCTIONS
NT APPROXIMATION
NT ASYMPTOTES
NT ASYMPTOTIC SERIES
NT BANACH SPACE
NT BESSEL FUNCTIONS
NT BIHARMONIC EQUATIONS
NT BINARY INTEGRATION
NT BOREL SETS
NT BORN APPROXIMATION
NT BORN-OPPENHEIMER APPROXIMATION
NT BOUNDARY INTEGRAL METHOD
NT BURGER EQUATION
NT CALCULUS
NT CALCULUS OF VARIATIONS
NT CAUCHY INTEGRAL FORMULA
NT CAUCHY-RIEMANN EQUATIONS
NT CHEBYSHEV APPROXIMATION
NT COLLINEARITY
NT COMBINATIONS (MATHEMATICS)
NT COMBINATORIAL ANALYSIS
NT COMPLEX VARIABLES
NT COMPUTATIONAL CHEMISTRY
NT COMPUTATIONAL FLUID DYNAMICS
NT CONFORMAL MAPPING
NT CONJUGATE GRADIENT METHOD
NT CONTINUITY (MATHEMATICS)
NT CONVOLUTION INTEGRALS
NT COPLANARITY
NT COSINE SERIES
NT CUBIC EQUATIONS
NT DELTA FUNCTION
NT DIFFERENCE EQUATIONS
NT DIFFERENTIAL EQUATIONS
NT EINSTEIN EQUATIONS
NT ELLIPTIC DIFFERENTIAL EQUATIONS
NT ELLIPTIC FUNCTIONS
NT ENTIRE FUNCTIONS
NT ERROR ANALYSIS
NT EULER-CAUCHY EQUATIONS
NT EXISTENCE THEOREMS
NT EXPONENTIAL FUNCTIONS
NT EXTREMUM VALUES
NT FAST FOURIER TRANSFORMATIONS
NT FINITE DIFFERENCE THEORY
NT FINITE ELEMENT METHOD
NT FINITE VOLUME METHOD
NT FLUX VECTOR SPLITTING

NT FOKKER-PLANCK EQUATION
NT FOURIER ANALYSIS
NT FOURIER TRANSFORMATION
NT FOURIER-BESSEL TRANSFORMATIONS
NT FREDHOLM EQUATIONS
NT FUNCTION SPACE
NT FUNCTIONAL ANALYSIS
NT GAUSS EQUATION
NT GREEN'S FUNCTIONS
NT HALF PLANES
NT HALF SPACES
NT HANKEL FUNCTIONS
NT HARMONIC ANALYSIS
NT HARTREE APPROXIMATION
NT HELMHOLTZ VORTICITY EQUATION
NT HILBERT SPACE
NT HILBERT TRANSFORMATION
NT HYPERBOLIC DIFFERENTIAL EQUATIONS
NT HYPERBOLIC FUNCTIONS
NT HYPERGEOMETRIC FUNCTIONS
NT HYPERPLANES
NT INTEGRAL CALCULUS
NT INTEGRAL EQUATIONS
NT INTEGRAL TRANSFORMATIONS
NT INTERPOLATION
NT ITERATION
NT ITERATIVE SOLUTION
NT J INTEGRAL
NT JACOBI MATRIX METHOD
NT KERNEL FUNCTIONS
NT LAGUERRE FUNCTIONS
NT LAPLACE TRANSFORMATION
NT LEAST SQUARES METHOD
NT LEBESGUE THEOREM
NT LIAPUNOV FUNCTIONS
NT LIMITS (MATHEMATICS)
NT LINEAR EQUATIONS
NT LIOUVILLE THEOREM
NT LIPSCHITZ CONDITION
NT LOGARITHMS
NT MAXIMA
NT MEAN SQUARE VALUES
NT MEASURE AND INTEGRATION
NT MEROMORPHIC FUNCTIONS
NT MINIMA
NT MONTE CARLO METHOD
NT NEUMANN PROBLEM
NT NEWTON METHODS
NT NEWTON-RAPHSON METHOD
NT NONLINEAR EQUATIONS
NT NONLINEAR EVOLUTION EQUATIONS
NT NUMERICAL ANALYSIS
NT NUMERICAL INTEGRATION
NT ORTHOGONAL FUNCTIONS
NT PADE APPROXIMATION
NT PARABOLIC DIFFERENTIAL EQUATIONS
NT PARTIAL DIFFERENTIAL EQUATIONS
NT PARTICLE IN CELL TECHNIQUE
NT PARTITIONS (MATHEMATICS)
NT PERIODIC FUNCTIONS
NT PERMUTATIONS
NT PHASE-SPACE INTEGRAL
NT POISSON EQUATION
NT POWER SERIES
NT QUADRATIC EQUATIONS
NT RAYLEIGH-RITZ METHOD
NT REAL VARIABLES
NT RELAXATION METHOD (MATHEMATICS)
NT RICCATI EQUATION
NT RITZ AVERAGING METHOD
NT RUNGE-KUTTA METHOD
NT SERIES (MATHEMATICS)
NT SINGULAR INTEGRAL EQUATIONS
NT SINGULARITY (MATHEMATICS)
NT SPHERICAL HARMONICS
NT STURM-LIOUVILLE THEORY
NT TANGENTS
NT TAYLOR SERIES
NT TRIGONOMETRIC FUNCTIONS
NT TRUNCATION ERRORS
NT VECTOR ANALYSIS
NT VLASOV EQUATIONS
NT VOLTERRA EQUATIONS
NT VORTICITY
NT VORTICITY EQUATIONS
NT WALSH FUNCTION
NT WEIERSTRASS FUNCTIONS
NT WEIGHTING FUNCTIONS
NT ZONAL HARMONICS

Transactions of the 4th Army Conference on Applied Mathematics and Computing
[AD-A183544] 01 p0085 N88-10547

Mathematics applied to nuclear geophysics
[INPE-4234-PRE/1109] 01 p0086 N88-10561

Summaries of the FY 1987 applied mathematical sciences research program
[DE87-014447] 02 p0225 N88-11416
A collection of test problems for ordinary differential equation solvers which have provisions for rootfinding
[DE88-000045] 02 p0226 N88-11428
Mathematical techniques for system realization and identification
[AD-A186352] 07 p0915 N88-15557
Strong representation of weak convergence
[AD-A186433] 07 p0916 N88-15563
Numerical resolution of the equations of three-dimensional stable compressible transonic flows
[PB87-168415] 09 p1113 N88-16673
Practical applicability of exact and approximate forms of the randomization test for two independent samples
[AD-A188815] 09 p1231 N88-17381
The mathematization of the military sciences
[MBB-Z-139/87] 10 p1311 N88-17834
International Conference on Industrial and Applied Mathematics
[AD-A188251] 11 p1483 N88-18851
Cumulative reports and publications through December 31, 1987
[NASA-CR-181624] 11 p1524 N88-19099
A unified approach for digital image processing problems: Mathematical morphology
[INPE-4311-TDL/278] 11 p1537 N88-19183
Analysis of simulated annealing type algorithms
[AD-A189382] 12 p1679 N88-20037
Analiticity in fourth order wave equations
[DE88-700837] 12 p1686 N88-20080
Research in applied mathematics related to identification of noisy systems
[AD-A189355] 13 p1825 N88-20908
Computation and graphics in mathematical research
[DE88-005796] 13 p1831 N88-20953
Aero/structural tailoring of engine blades (AERO/STAEBL)
[NASA-CR-180805] 14 p1959 N88-21682
Nonlinear analysis and optimal design of dynamic mechanical systems for spacecraft application
[AD-A190644] 15 p2026 N88-22070
The analysis of non-linear dynamic behavior (including snap-through) of postbuckled plates by simple analytical solution
[NASA-TM-89165] 15 p2087 N88-22439
Symmetry and global bifurcation in nonlinear solid mechanics
[AD-A190521] 15 p2121 N88-22642
Analytical sensor redundancy assessment
[NASA-CR-182892] 16 p2163 N88-22901
Analytical orbit propagation of artificial satellites
[INPE-4454-TDL/315] 16 p2166 N88-22915
Generalizing the structure of explanations in explanation-based learning
[AD-A191327] 16 p2256 N88-23461
On 1/n-expansion and wave functions
[DE88-701639] 16 p2260 N88-23509
Application of chaos theory to 1/f noise
[AD-A191150] 17 p2334 N88-23935
Activities of the Institute for Computer Applications in Science and Engineering (ICASE)
[NASA-CR-181666] 17 p2384 N88-24166
Analytical modeling of the structureborne noise path on a small twin-engine aircraft
[NASA-CR-4136] 17 p2394 N88-24233
On a class of functionals invariant under a Z(sup n) action
[AD-A193474] 23 p3269 N88-29451
Finite element analysis of steady and transiently moving/rolling nonlinear viscoelastic structure. Part 1: Theory
[NASA-CR-179886] 23 p3273 N88-29480
Theoretical aerodynamics, transonic flow
[AD-A196247] 24 p3321 N88-29777
ANALYSIS OF VARIANCE
A heteroscedastic hierarchical model
[AD-A184256] 03 p0372 N88-12340
Annotated computer output for split plot design: GENSTAT ANOVA
[AD-A187120] 10 p1385 N88-18271
The statistical characterization of tensile strengths for a nuclear-type graphite 13 p1746 N88-20440
Exact tests for variance component models with unequal cell frequencies in the last stage
[AD-A191645] 18 p2568 N88-25253
ANALYTIC FUNCTIONS
NT ENTIRE FUNCTIONS
A system of three-dimensional complex variables
[NASA-TM-88318] 05 p0645 N88-13951
Using Clifford algebras for the geometry of a tube domain (and its corresponding bounded domain) in the complexified Minkowski space of arbitrary dimension
[REPT-87-64] 16 p2264 N88-23540

N = 2 supergravity in superspace: Solution to the constraints
[DE88-702135] 19 p2741 N88-26272
N = 2 supergravity in superspace: The invariant action
[DE88-702136] 19 p2741 N88-26273
Holomorphic geometry of interacting string
[DE88-702714] 23 p3295 N88-29627
Track performance considerations for monopulse radars
[AD-A196232] 24 p3360 N88-30007
ANALYTIC GEOMETRY
NT CATENARIES
NT CIRCUMFERENCES
NT CONICS
NT ELLIPSES
NT OBLATE SPHEROIDS
NT PARABOLAS
NT PROLATE SPHEROIDS
NT QUADRANTS
NT S CURVES
NT TANGENTS
NT TORUSES
Steps into a geometer's workbench
[CWI-CS-R8726] 13 p1819 N88-20870
Geometry and graphics applied to robotics
[CWI-CS-R8727] 13 p1824 N88-20903
ANALYTICAL CHEMISTRY
The development of a new and novel Hadamard transform infrared spectrometer for analytical chemistry
[DE87-014804] 02 p0175 N88-11094
A prototype expert system for separation science
[DE87-013542] 03 p0371 N88-12333
Atomic and molecular gas phase spectrometry
[AD-A187562] 11 p1452 N88-18655
Analytical Chemistry Division
[DE88-701236] 16 p2174 N88-22956
ANALYZERS
NT ENGINE ANALYZERS
NT SIGNAL ANALYZERS
Multi-channel communications system analyzer
[AD-A184756] 03 p0307 N88-11937
Multichannel scaling analyzer
[DE88-700541] 07 p0905 N88-15481
A comparison of measurements from the A/E35U-3 and PWMA (Portable Wear Metal Analyzer) spectrometers
[AD-A186855] 09 p1177 N88-17047
Diagnostics for research in atomization and turbulent two-phase flows
[AD-A187338] 11 p1482 N88-18843
Some applications of surface Raman and infrared spectroscopies to mechanistic electrochemistry involved adsorbed species
[AD-A188777] 12 p1606 N88-19602
Hercules: A power analyzer for MOS VLSI circuits
[AD-A188702] 12 p1623 N88-19706
A production-quality UNIX Very High Speed Integrated Circuit (VHSIC) Hardware Description Language (VHDL) subset analyzer
[AD-A188832] 12 p1623 N88-19710
Instrumentation for the characterization and development of millimeter wave components compatible with monolithic integration
[AD-A189724] 15 p2059 N88-22275
FLOSIN: A fluid loop analyzer for SINDA
15 p2066 N88-22321
Two papers on a symbolic analyzer for MOS (Metal-Oxide Semiconductors) circuits
[AD-A188617] 15 p2139 N88-22761
Computer-aided writing
[AD-A192516] 20 p2838 N88-26837
An investigation of the uses of time domain capable vector network analyzers as a diagnostic for helix traveling-wave circuits
[AD-A192460] 21 p2935 N88-27430
Calibration of the portable wear metal analyzer
[AD-A192971] 21 p2950 N88-27524
ANATOMY
NT ADRENAL GLAND
NT ALVEOLI
NT AORTA
NT ARM (ANATOMY)
NT ARTERIES
NT AUTONOMIC NERVOUS SYSTEM
NT BONE MARROW
NT BONES
NT BRAIN
NT CAPILLARIES (ANATOMY)
NT CARDIAC VENTRICLES
NT CARDIOVASCULAR SYSTEM
NT CENTRAL NERVOUS SYSTEM
NT CEREBELLUM
NT CEREBRAL CORTEX
NT CEREBRUM
NT CHEMORECEPTORS
NT CIRCULATORY SYSTEM
NT COCHLEA

NT COLLAGENS
NT CORNEA
NT EAR
NT EFFERENT NERVOUS SYSTEMS
NT EYE (ANATOMY)
NT FINGERS
NT FOVEA
NT GASTROINTESTINAL SYSTEM
NT GLOTTIS
NT GRAVIRECEPTORS
NT HAND (ANATOMY)
NT HEAD (ANATOMY)
NT HEART
NT HIPPOCAMPUS
NT HUMAN BODY
NT HYPOTHALAMUS
NT INTESTINES
NT JOINTS (ANATOMY)
NT KIDNEYS
NT LARYNX
NT LEG (ANATOMY)
NT LIMBS (ANATOMY)
NT LIVER
NT LUNGS
NT MIDDLE EAR
NT MUSCLES
NT MUSCULOSKELETAL SYSTEM
NT MYOCARDIUM
NT NECK (ANATOMY)
NT NERVES
NT NERVOUS SYSTEM
NT OCULOMOTOR NERVES
NT OTOLITH ORGANS
NT PHOTORECEPTORS
NT PITUITARY GLAND
NT PROPRIOCEPTORS
NT PUPILS
NT RESPIRATORY SYSTEM
NT RETINA
NT SEMICIRCULAR CANALS
NT SENSE ORGANS
NT SKIN (ANATOMY)
NT SKULL
NT SPINAL CORD
NT SPLEEN
NT STOMACH
NT SYMPATHETIC NERVOUS SYSTEM
NT TESTES
NT THALAMUS
NT TIBIA
NT TORSO
NT VEINS
NT VESTIBULES
NT WRIST

ANDES MOUNTAINS (SOUTH AMERICA)
SPOT imagery as an aid to understanding volcanism and tectonics: Examples from the Chilean Andes and the Tibetan Plateau 22 p3103 N88-28427

ANDESITE
Does subduction zone magmatism produce average continental crust 24 p3394 N88-30214

ANDROMEDA GALAXY
Stars, gas and dust in the Andromeda galaxy
[B8679680] 16 p2289 N88-23708

ANECHOIC CHAMBERS
Anechoic Chamber test of the Electromagnetic Measurement System ground test unit
[DE87-012998] 01 p0035 N88-10226
New main reflector, subreflector and dual chamber concepts for compact range applications
[NASA-CR-181506] 04 p0402 N88-12498
Acoustic characteristics of 1/20-scale model helicopter rotors
[NASA-CR-177355] 16 p2265 N88-23548
Almond test body --- for microwave anechoic chambers
[NASA-CASE-LAR-13747-1] 18 p2502 N88-24845

ANELASTICITY
Anelastic behaviour of materials under multiaxial strains. Part 3: Order-disorder transition, Shoek effect and Poisson's ratio in AISI-1080 steel
[DE87-703087] 02 p0191 N88-11193
Effect of hydrogen, deuterium and oxygen on the anelastic properties of refractory alloys
[DE88-007349] 18 p2484 N88-24736

ANEMIAS
Hypoxic hypoxia as a stimulus of erythropoiesis in vivo and in vitro 07 p0885 N88-15373
Role of hemoglobin affinity for oxygen in efficiency of blood respiratory function 07 p0892 N88-15406
Hemolysis in runners as evidenced by low serum haptoglobin: Implications for preflight monitoring of astronauts
[NASA-TM-100304] 11 p1516 N88-19067

ANEMOMETERS
NT HOT-FILM ANEMOMETERS
NT HOT-WIRE ANEMOMETERS
NT LASER ANEMOMETERS
Measurement of gas flow velocities near obstacles: Analysis and optimization of an optical barrier velocimeter. Associated signal processing
[ESA-TT-1056] 03 p0315 N88-11991
Comparative testing of wind measuring equipment. Part 1: Inventory and selection
[R-814-D-PT-1] 03 p0325 N88-12053
Simulating high-resolution vertical plane array wind characteristics using lower-spatial-resolution wind measurements
[DE88-005626] 13 p1800 N88-20761
The development of a microanemometer. New possibilities for measuring very low air velocities
[ETN-88-92244] 16 p2210 N88-23191
Thermal remote anemometer system
[NASA-CASE-LAR-13508-1] 17 p2342 N88-23962
A microcomputer based frequency-domain processor for laser Doppler anemometry
[NASA-TM-100998] 20 p2603 N88-26634

ANEMOMETRY
U VELOCITY MEASUREMENT

ANGLE OF ATTACK
Calculation of aerodynamic heat transfer for blunt-nosed thin wings at different angles of attack at supersonic speeds
[NASA-TT-20127] 02 p0123 N88-10776
Optimum take-off run of aircraft on ground airfields 04 p0423 N88-12623
Low speed wind tunnel investigation of propeller slipstream aerodynamic effects on different nacelle/wing combinations. Part 1: Total forces and moments and pressure distributions on nacelle/wing at different angles of attack and yaw and at different thrust coefficients
[FFA-TN-1987-22] 05 p0542 N88-13302
Predicting dynamic separation characteristics of general configurations
[AD-A186689] 09 p1116 N88-16691
Measurement of forces and moments on, and velocity about a body of revolution with an attached fin at angles of attack
[AD-A187796] 11 p1433 N88-18554
Modeling of limit cycle stall flutter oscillations 12 p1583 N88-19472
Surface flow visualization of separated flows on the forebody of an F-18 aircraft and wind-tunnel model
[NASA-TM-100436] 14 p1863 N88-21127
Data processing method for high angle of attack testing with rolling angle 14 p1864 N88-21134
An experimental study to determine the flow and the subsonic static and dynamic stability characteristics of aircraft operating at high angles-of-attack 16 p2201 N88-23129
Flow visualization study of vortex manipulation on fighter configurations at high angles of attack 16 p2201 N88-23130
Investigation on the movement of vortex burst position with dynamically changing angle of attack for a schematic deltawing in a watertunnel with correlation to similar studies in windtunnel 16 p2204 N88-23152
Experiments to investigate the vortices shed from a submarine-like body of revolution 16 p2205 N88-23156
Wind-tunnel investigation of actuated forebody strakes for yaw control at high angles of attack 17 p2299 N88-23754
Computation of flow around NACA0012 airfoil at high angle of attack 19 p2636 N88-25640
High speed and high angle of attack wind tunnel test results of the winged space vehicle C-2
[ISAS-RN-623] 20 p2751 N88-26329
The effect of a turbulent airstream on a vertically-launched missile at high angles of attack
[AD-A192408] 20 p2758 N88-26363
Calculation of aerodynamic characteristics of airplane configurations at high angles of attack
[NASA-CR-4182] 23 p3172 N88-28891
Angle of attack and sideslip estimation using an inertial reference platform
[AD-A194876] 24 p3319 N88-29769
Computer programs for calculation of sting pitch and roll angles required to obtain angles of attack and sideslip on wind tunnel models
[NASA-TM-100659] 24 p3329 N88-29820

ANGLES (GEOMETRY)
NT ANGLE OF ATTACK
NT BRAGG ANGLE
NT DIHEDRAL ANGLE
NT ELEVATION ANGLE
NT LEADING EDGE SWEEP
NT SWEEP ANGLE
NT SWEEPBACK
Effects of free stream turbulence, Reynolds number and incidence angle on axial turbine cascade performance 05 p0548 N88-13339
The effect of collision angle on mach reflection
[AD-A185798] 06 p0704 N88-14319
Acoustic scattering from composite wind-wave surfaces 3: Forward scatter intensities and spatial coherence at low and high frequencies and small grazing angles for Bubble-free regimes
[AD-A185908] 07 p0881 N88-15345
An investigation of oblique hypervelocity impact 07 p0927 N88-15629
The angular reflectance signature of the canopy hot spot in the optical regime
[DE88-005385] 11 p1505 N88-18991
Reduction of erosion in elbows due to flow modifications, phase 1
[DE88-001028] 13 p1769 N88-20584
A symmetric set of Euler angles and oblique orientation space sections
[DE88-005317] 13 p1847 N88-21056
Universal precision sine bar attachment
[NASA-CASE-MFS-28253-1] 18 p2523 N88-24971
Joint angle sensors for closed-loop control 19 p2673 N88-25891

ANGULAR ACCELERATION
Laser gyroscopes using the rate-bias technique 18 p2517 N88-24930

ANGULAR CORRELATION
Perturbed angular correlations in zirconia ceramics
[DE88-004117] 11 p1464 N88-18731
Angular position measurements at high temperatures and high radiation environments 17 p2434 N88-24479

ANGULAR DISTRIBUTION
Analysis of relativistic nucleus-nucleus interactions in emulsion chambers 07 p0926 N88-15624
Mode pattern of field generated by parametric radiator in acoustic waveguide 08 p1076 N88-16488
Equation of gravitational-gyroscopic waves. Angular potential and its applications 08 p1079 N88-16504
Research relative to angular distribution of snow reflectance/snow cover characterization and microwave emission
[NASA-CR-182733] 14 p1941 N88-21582
Angular resolved energy analysis of (69)Ga + ions from a gallium liquid metal ion source
[AERE-R-12649] 15 p2139 N88-22760
Angular radiation models for Earth-atmosphere system. Volume 1: Shortwave radiation
[NASA-RP-1184] 21 p2976 N88-27677

ANGULAR MOMENTUM
Angular momentum evolution of young stars 04 p0504 N88-13099
Post-zero-age main sequence rotation 04 p0504 N88-13100
Relation of wave energy and momentum with the plasma dispersion relation in an inhomogeneous plasma
[DE88-002305] 08 p1084 N88-16530
Application of state-multipole Heisenberg equations to Raman excitation dynamics
[DE88-003828] 10 p1335 N88-17977
State-to-state dynamics of molecular energy transfer
[DE88-003282] 10 p1406 N88-18382
Positron-annihilation 2D-ACAR studies of disordered and defected alloys
[DE88-003118] 10 p1416 N88-18454
Parametric dependence in the equilibrium dynamics of rotating structures
[AD-A187817] 11 p1498 N88-18945
Modelling and control of an annular momentum control device
[NASA-CR-4138] 13 p1754 N88-20491
Collective rotation of molecules driven by the angular momentum of light in a nematic film
[FUB-6-1986] 15 p2131 N88-22714
Nutational stability of a satellite equipped with an active magnetic momentum wheel 20 p2784 N88-26513
Mass transfer instabilities due to angular momentum flows in close binaries --- stars
[MPE-PREPRINT-113] 22 p3165 N88-28849
Atmospheric angular momentum and length of day
[AD-A194505] 23 p3233 N88-29238

ANGULAR MOTION
U ANGULAR VELOCITY

ANGULAR RESOLUTION
CERGA high angular resolution optical network --- astronomical interferometry 01 p0096 N88-10633
Diagnostics of solar coronal loops at interferometric angular resolution 01 p0098 N88-10642
Galactic nuclei and quasars at high angular resolution 01 p0098 N88-10644
New results from high angular resolution observations of alpha Ori 04 p0514 N88-13161
The angular diameter of alpha Scorpii in the near-infrared Ca II triplet 04 p0514 N88-13162

Analysis of a range estimator which uses MLS angle measurements
[NASA-CR-182896] 16 p2160 N88-22884
ANGULAR VELOCITY
Spin-up and spin-down on the way to the main sequence 04 p0518 N88-13181
Investigation of the spin stability of the NPS (Naval Postgraduate School) mini-satellite (Orion)
[AD-A187781] 11 p1445 N88-18613
A LQG regulator for the angular motion of the rotor at a tuned gyroscope
[INPE-4280-PRE/1152] 12 p1631 N88-19759
Automatic feedback control of a rigid body for finite displacements 18 p2473 N88-24674
ANHYDRIDES
NT PEROXIDES
Synthesis of energetic materials
[AD-A189115] 13 p1753 N88-20482
ANIMALS
NT AMOEBA
NT AMPHIBIA
NT ARTEMIA
NT BIRDS
NT CATS
NT CHICKENS
NT DOGS
NT DROSOPHILA
NT FISHES
NT FROGS
NT HUMAN BEINGS
NT INSECTS
NT INVERTEBRATES
NT MAMMALS
NT MICE
NT MOLLUSKS
NT MONKEYS
NT PARAMECIA
NT PRIMATES
NT RATS
NT SEA URCHINS
NT SNAILS
NT VERTEBRATES
NT WATERFOWL
A plethysmograph for measuring pulmonary ventilation in small animals
[AD-A184978] 05 p0629 N88-13846
Space station accommodations for life sciences research facilities. Phase 1: Conceptual design and programmatics studies for Missions SAAX0307, SAAX0302 and the transition from SAAX0307 to SAAX0302. Volume 2: Study results
[NASA-CR-179244] 08 p0962 N88-15829
Supersonic and subsonic aircraft noise effects on animals: A literature survey
[AD-A186922] 10 p1404 N88-18373
Five New South Wales barrier lagoons: Their macrobenthic fauna and seagrass communities
11 p1517 N88-19059
Space station accommodations for life sciences research facilities: Phase A conceptual design and programmatics studies for Missions SAAX0307, SAAX0302 and the transition from SAAX0307 to SAAX0302. Volume 1: Executive summary
[NASA-CR-179267] 12 p1599 N88-19571
Animal research on the Space Station
12 p1662 N88-19964
A neuronal model of classical conditioning
[AD-A188378] 12 p1670 N88-19999
A cardiostimulant protein from the Australian Red Waratah Sea anemone, Actinia tenebrosa
18 p2550 N88-25138
USAF hyperbaric animal transfer chamber system
[AD-A193633] 23 p3237 N88-29265
ANIMATION
NT COMPUTER ANIMATION
ANIONS
Separation of anionic from nonionic alkoxy compounds using silica gel
[GB-PATENT-2-140-415-A] 01 p0020 N88-10122
The mechanism of stereo regulation during anionic polymerization of polar monomers
[AD-A186530] 08 p0973 N88-15888
A simple interpretation of the Fe2(-, photoelectron spectrum
[NASA-CR-182553] 11 p1543 N88-19225
Electrosorptive detection based on double-layer capacitance for selective anion monitoring in ion chromatography. Part 1: Mercury electrodes
[AD-A188780] 12 p1606 N88-19603
Electronic structure and stability of small cation and anion hydrogen clusters 16 p2267 N88-23562
ANISOTROPIC FLUIDS
Study of one-dimensional spectral dynamic equations of the Reynolds stresses in homogeneous anisotropic turbulence: Application to split-spectrum modeling
16 p2196 N88-23095
Modeling scalar flux and the energy and dissipation equations 16 p2196 N88-23096
ANISOTROPIC MEDIA
NT ANISOTROPIC FLUIDS
Mechanics of anisotropic media. Study of the boundary conditions --- stratified composites
[SNIAS-872-430-112] 05 p0559 N88-13404
Time-domain reciprocity theorems for electromagnetic fields in dispersive media
[PB88-126925] 10 p1319 N88-17886
Subroutines for solving the equation of diffusion in media with anisotropic properties
[DE88-700743] 11 p1536 N88-19179
An improved boundary force method for analyzing cracked anisotropic materials
[NASA-TM-101495] 24 p3340 N88-29879
ANISOTROPIC PLATES
A refined nonlinear analysis of laminated composite plates and shells
[AD-A184436] 04 p0454 N88-12811
Postbuckling of laminated anisotropic panels
[NASA-TM-100509] 08 p0994 N88-16011
The buckling and vibration of composite plates using the Levy method considering shear deformation and rotary inertia
[AD-A189743] 15 p2076 N88-22374
On the calculation of stresses in pin-loaded anisotropic plates
[ETN-88-92239] 16 p2222 N88-23261
On the calculation of stresses in pin-loaded anisotropic plates
[LR-529] 16 p2223 N88-23268
ANISOTROPIC SHELLS
A refined nonlinear analysis of laminated composite plates and shells
[AD-A184436] 04 p0454 N88-12811
ANISOTROPY
NT ELASTIC ANISOTROPY
Life prediction and constitutive models for engine hot section anisotropic materials program
02 p0188 N88-11175
Deviatoric constitutive relationship for anisotropic materials
[AD-A184332] 03 p0295 N88-11854
Experimental perspectives on heavy electron metals
[DE87-014766] 04 p0416 N88-12583
Structure of thermotropic polyesters with large substituents
[AD-A184086] 04 p0418 N88-12595
Velocity scaled aeroelastic testing of an unducted fan
[GTL-191] 05 p0548 N88-13337
Molecular and supramolecular orientation in conducting polymers
[DE88-000533] 05 p0569 N88-13472
Axial anisotropy of the intensity of the cosmic ray nuclear component
[IFSI-87-7] 05 p0662 N88-14061
Nonlinear relaxation and ergodicity breakdown in random anisotropy spin glasses
[PREPRINT-565] 06 p0764 N88-14693
Dipole component of relict radiation determined from Relikt experiment data 08 p1002 N88-16070
Nonequilibrium ionization of pregalactic plasma and lessening of relic radiation anisotropy
08 p1002 N88-16071
The role of anisotropy in the long range reconnaissance of the albedo of land surfaces 08 p1017 N88-16169
The anisotropy of reflected solar radiation over several types of land surface 08 p1018 N88-16171
Transversely anisotropic curved optical fibres: Variational analysis of a nonstandard Eigenproblem
[PB88-112966] 08 p1083 N88-16528
An analytical study of the effects of transverse shear deformation and anisotropy on natural vibration frequencies of laminated cylinders
[NASA-TM-100554] 10 p1295 N88-17739
Bias, internal stress and substrate effects on the microstructure and properties of PVD-wear resistant coatings
[AERE-R-12360] 10 p1304 N88-17798
The mechanism of anisotropic silicon etching and its relevance for micromachinings
[MBB-UA-1013/86] 10 p1311 N88-17838
The physics of metallic superlattices: An experimental point of view
[DE88-003080] 10 p1416 N88-18452
A sky temperature survey at 19.2 GHz using a balloon borne Dicke radiometer for anisotropy tests of the cosmic microwave background 11 p1571 N88-19403
Brillouin scattering from collective spin waves in magnetic superlattices
[DE88-005347] 12 p1697 N88-20154
Observations of the large scale anisotropy in the cosmic background radiation at 3 mm
[INPE-4425-PRE/1229] 12 p1712 N88-20249
Anisotropy of microstructural eddy motion in surface layer during calm 13 p1784 N88-20677
Electrical characteristics of MBE (Molecular Beam Epitaxyl)-grown GaAs/sub 1-x/Sb/sub x on InP and correlation with film microstructure
[DE88-003841] 13 p1847 N88-21053
Early reheating and cosmic strings
13 p1855 N88-21103
A model of the anisotropic structure of the neutral gas coma of a comet 14 p1999 N88-21918
Anisotropic emission from comets: Fans versus jets. 1: Concept and modeling 14 p2001 N88-21927
Anisotropic emission from comets: Fans versus jets. 2: Periodic Comet Tempel 2 14 p2001 N88-21928
Improvements to tilt rotor performance through passive blade twist control
[NASA-TM-100583] 15 p2086 N88-22434
Electrical anisotropy of layered semiconductor ZrSe2
16 p2257 N88-23488
Shape stability in composites
18 p2479 N88-24706
Changes in seismic velocity and apparent attenuation due to isotropic and anisotropic scattering: Results from physical modeling 19 p2691 N88-25997
Peturbational analysis of the curved anisotropic optical fiber for the birefringence due to the geometry
[PB88-171848] 19 p2726 N88-26189
Stress concentration around circular hole in a composite material specimen representative of the X-29A forward-swept wing aircraft
[NASA-CR-179435] 20 p2814 N88-26694
Anisotropic characteristic lengths in single crystal YBa2Cu3O(sub 7-Delta)
[DE88-009959] 20 p2877 N88-27080
Anisotropy of the lower critical field in YBa2Cu3O(sub 7-Delta)
[DE88-009971] 20 p2877 N88-27081
Probabilistic anisotropic failure criteria for composite materials
[AD-A193046] 21 p2904 N88-27232
An anisotropic continuum damage model for creep-dominated, multiaxial loading histories
21 p2964 N88-27608
On plasma stability under anisotropic random electric field influence
[DE88-702422] 21 p3019 N88-27918
Investigation of magnetic anisotropy and spin wave modes in transition metal multilayers
[DE88-009007] 22 p3154 N88-28765
Anisotropic constitutive modeling for nickel-base single crystal superalloys
[NASA-CR-182157] 24 p3353 N88-29961
ANNEALING
NT LASER ANNEALING
NT PULSE HEATING
Effect of high-temperature annealing on the microstructure and thermoelectric properties of GaP doped SiGe
[NASA-TM-100164] 01 p0029 N88-10188
Hydrogen annealing of P(sub) b and E prime defect centers in oxidized silicon wafers
[DE87-014293] 02 p0152 N88-10951
Defect characterization in quartz and related materials
[AD-A184754] 03 p0294 N88-11846
Dynamics of atoms in low-symmetry systems
[AD-A184318] 03 p0375 N88-12361
On the stressing of annealed NITINOL: The electrical resistance and calorimetric effects
[AD-A184465] 04 p0414 N88-12569
Threshold stress for fatigue crack initiation from a small crack 05 p0601 N88-13675
Structural characterization of ion implanted beta-SiC thin films
[DE87-014567] 05 p0656 N88-14027
Ion mixing and surface modification in metal-semiconductor systems
[DE88-001702] 06 p0786 N88-14823
Effect of high pressure oxygen loading on the superconductivity of La2CuO4
[DE88-002108] 06 p0787 N88-14827
Kinetics and mechanism of thermal aging embrittlement of duplex stainless steels
[DE88-002987] 08 p0969 N88-15866
Influence of post-anneal cooling treatments on suppression of cryogenic intergranular fracture in experimental Ni-free high-Mn austenitic steels
[DE88-002766] 09 p1145 N88-16863
Neutron- and X-ray-small angle scattering with Fe-base metallic glasses
[DE88-002538] 09 p1147 N88-16876
Forward-biased current annealing of radiation damaged gallium arsenide and silicon solar cells
[AD-A186904] 09 p1186 N88-17105
Growth of HgZnTe layers by LPE technique
[AD-A186723] 09 p1255 N88-17520

X-ray diffraction study of thermotropic liquid crystalline polyesters and diester model compounds
[AD-A186788] 09 p1255 N88-17521

Low temperature reactivity of chars towards oxygen, appendix E2
[DE88-004088] 10 p1298 N88-17760

Experiences with serial and parallel algorithms for channel routing using simulated annealing
[NASA-CR-182530] 10 p1388 N88-18289

High temperature processing of superconducting Y1Ba2Cu3O6.9
[DE88-003002] 10 p1416 N88-18449

Improved magnetization for YBa2Cu3O/sub 7-delta annealed in oxygen above 1000 C
[DE88-003934] 10 p1418 N88-18469

Processing relationships in YBa2Cu3O(7-x) superconductors
[DE88-005137] 11 p1559 N88-19330

Radiation response of thin oxides grown by rapid thermal oxidation and rapid thermal annealing techniques
[DE88-003632] 11 p1561 N88-19347

An in situ annealing study of lead implanted single crystal calcium titanate
[DE88-005435] 11 p1562 N88-19351

Analysis of simulated annealing type algorithms
[AD-A189382] 12 p1679 N88-20037

Study of defects in metals by positron annihilation
[DE88-701042] 13 p1745 N88-20432

Optical study of germanium, germanium plus arsenic, and germanium plus gallium implants in gallium arsenide
[AD-A189600] 13 p1845 N88-21045

Structure and strength of boron-aluminum composites
14 p1885 N88-21264

Dynamical optimization techniques for the calculation of electronic structure in solids
[DE88-006010] 15 p2140 N88-22768

The effect of elevated temperature on irradiated MOS devices 17 p2406 N88-24308

A study on the precipitation and reversion behaviors of Cu-0.3 percent Cr alloy by the step annealing method
[NASA-TT-20169] 18 p2489 N88-24764

An improved simulated annealing algorithm for standard cell placement
[NASA-CR-182952] 18 p2558 N88-25183

Electrical study of metal/group 3-5 semiconductor interfaces: Comparison with the atomic-level studies
20 p2674 N88-27059

NDP (Neutron Depth Profiling) evaluations of boron-implanted compound semiconductors
[AD-A192306] 21 p2934 N88-27425

Short pulse X-ray diffraction studies of shocked and annealed crystals using the JANUS research laser
[DE88-011329] 23 p3288 N88-29579

An HVEM study of displacement cascade damage in Nb3Sn at 13 K
[DE88-009997] 23 p3289 N88-29584

Rapid thermal annealing of silicon layers amorphized by ion implantation
[DE88-702307] 23 p3290 N88-29591

ANNIHILATION REACTIONS

NT POSITRON ANNIHILATION

Basic physics program for a low energy antiproton source in North America
[DE88-003148] 08 p1082 N88-16522

Event classification in (anti)neutrino experiments using an Internal Picket Fence-External Muon Identifier (IPF-EMI) detector system
[NIKHEF-H/87-6] 09 p1245 N88-17457

Beta limitation of matter-antimatter boundary layers
[TRITA-EPP-87-11] 09 p1250 N88-17490

A study of the magnetic field annihilation process in the magnetosphere and some geotechnical applications
[DE88-004165] 10 p1355 N88-18096

Nuclear structure at intermediate energies
[DE88-002796] 10 p1407 N88-18390

Advanced space propulsion study - antiproton and beamed power propulsion
[AD-A189218] 13 p1732 N88-20355

Proton/antiproton yields W(+/-)boson gamma X as a test of the quark charges
[NIKHEF-H/87-11] 13 p1836 N88-20987

New limits on charged Higgs boson mass with CELLO at Petra (Italy) and status of the neutral Higgs boson search
[NOTA-INTERNA-897] 14 p1980 N88-21817

Annihilation momentum density of positrons trapped at vacancy-type defects in metals and alloys
[DE88-005936] 15 p2144 N88-22797

Prospects for antiproton production and propulsion
16 p2267 N88-23556

Stable, heavy, neutral particles in the sun and in toponium decay 17 p2452 N88-24568

Research in theoretical particle physics
[DE88-008230] 20 p2851 N88-26927

Study of the production of Ko mesons in proton antiproton interactions at 630 GeV
[NOTA-INTERNA-908] 21 p3015 N88-27892

ANNOTATIONS

Annotated algebraic specification of the static semantics of pool
[PB88-106695] 07 p0912 N88-15533

ANNUAL VARIATIONS

Spatial characterization of acid rain stress in Canadian Shield Lakes
[NASA-CR-181136] 01 p0067 N88-10430

Spatial characterization of acid rain stress in Canadian Shield Lakes
[NASA-CR-180577] 01 p0067 N88-10431

Theoretical and lidar studies of the seasonal and nocturnal variations of the mesospheric sodium layer at Urbana, Illinois 01 p0068 N88-10435

Atlas of wide-field-of-view outgoing longwave radiation derived from Nimbus 7 Earth radiation budget data set - November 1978 to October 1985
[NASA-RP-1186] 01 p0070 N88-10451

Short reference year
[PB87-107470] 03 p0352 N88-12221

Environmental processes and spectral reflectance characteristics associated with soil erosion in desert fringe regions
[NASA-CR-182332] 05 p0620 N88-13811

The lower thermosphere wind regime from simultaneous observations over Euroasia (Collm, Dushanbe, Frunze)
06 p0733 N88-14510

On the interconnection of dynamic processes in the lower thermosphere with meteorological phenomena in the tropostratosphere 06 p0734 N88-14512

Characteristics of atmospheric disturbances with a quasi-two day period 06 p0734 N88-14515

Lower thermosphere wind regime according to radiometeor measurements in Kazan
06 p0736 N88-14526

Density variations of meteor flux along the Earth's orbit 06 p0739 N88-14545

Structural peculiarities of the Quadrantid meteor shower 06 p0740 N88-14552

The global climate system: Autumn 1984 to spring 1985
[CSM-R84/86] 06 p0745 N88-14583

Neurophysiological analysis of hypothalamic regulation mechanisms of primary sleep and hypobiosis
06 p0751 N88-14611

Seasonal cycling of sulfur and iron in porewaters of a Delaware salt marsh
[NASA-CR-182385] 07 p0876 N88-15311

The solar radiation incident at the top of the atmosphere of Uranus and Neptune
[AERONOMICA-ACTA-A-317-1987]
07 p0878 N88-15323

SEQUAL (seasonal Equatorial Atlantic) meteorological data from Moorings S2, S5 and S6 (March 1983 - March 1985)
[PB88-108048] 07 p0880 N88-15337

Long-term variation of total ozone
[INPE-4307-PRE/1173] 08 p1023 N88-16192

Effect of storage thermal behavior in seasonal storage solar heating systems
[PB88-114236] 10 p1350 N88-18067

Spatial-temporal variability of North Pacific sea surface temperature anomaly patterns 11 p1516 N88-19058

Seasonal variations and excitation mechanisms of the equatorially trapped waves 13 p1798 N88-20751

Computer simulation of tropospheric chemistry
[JUEL-2144] 13 p1798 N88-20756

Northern Hemisphere circulation and the principal components of subsequent summer patterns in North America and West Africa 13 p1801 N88-20765

Analysis of winter season precipitation bands over the Southern Plains 14 p1947 N88-21609

Seasonal variation for structural strength value
[PB88-169248] 16 p2222 N88-23260

Latitudinal and seasonal variation of the cloud characteristic parameters and their affects on the cloud classification 17 p2351 N88-24005

Sea ice kinematics: Space and time scales
[AD-A191162] 17 p2376 N88-24128

Examples of ice pack rigidity and mobility characteristics determined from ice motion
[AD-A191163] 17 p2377 N88-24129

The seasonal exchange of carbon dioxide between the atmosphere and the terrestrial biosphere: Extrapolation from site-specific models to regional models
[DE88-007870] 20 p2822 N88-26740

Circulation statistics from seasonal and perpetual January and July simulations with the NCAR (National Center for Atmospheric Research) Community Climate Model (CCM1):R15
[PB88-192620] 20 p2823 N88-26748

The 1985 Meteorological Yearbook of Ispra (27th)
[PB88-125729] 20 p2828 N88-26777

Following the seasonal evolution of a natural environment in a humid tropical region. Preliminary Evaluation of SPOT (PEPS) number 186: Bangui, Central Africa 22 p3093 N88-28368

Variations in spectral reflectance signature in healthy stands of pine and spruce
[FOA-C-30468-3.1] 22 p3116 N88-28512

Proceedings of the Twelfth Annual Climate Diagnostics Workshop
[PB88-191747] 22 p3119 N88-28534

Indian monsoon rainfall, 1986-1987
22 p3120 N88-28536

Zonal wind observations at Christmas Island (2 deg N, 157 deg W) during the 1986-1987 El-Nino
22 p3120 N88-28539

Intraseasonal variability in atmospheric surface pressure and relationship to polar motion
22 p3120 N88-28540

The dynamics and thermodynamics of a 30-60 day oscillation 22 p3121 N88-28543

Complex EOF analysis of intraseasonal tropical wind fluctuations 22 p3121 N88-28544

Some diagnostic results concerning the tropical 40-50 day oscillation 22 p3121 N88-28546

Tropospheric biennial variability and its relationship to the southern oscillation 22 p3121 N88-28549

Recent secular changes in the wintertime circulation of the Southern Hemisphere 22 p3122 N88-28555

Northern Hemisphere 700 mb teleconnections based on half-monthly mean anomaly data stratified by season and by sign 22 p3123 N88-28561

Interannual variability of 850 mb temperatures during the Northern Hemisphere winter
22 p3123 N88-28562

The active layer of the upper Atlantic Ocean
22 p3124 N88-28566

Operational multifield analog forecasting of US seasonal temperatures for non-winter seasons
22 p3127 N88-28592

Observed normal mode structure of low frequency oscillations 22 p3128 N88-28595

ANNULAR DUCTS

Determination of the dynamic parameters of annular clearances with turbulent flow and incompressible media
[ETN-87-90434] 01 p0047 N88-10303

Use of a local heat source for determining temperature of inlet heat section in ring channels
[DE88-700332] 07 p0854 N88-15187

Entrance and exit region friction factor models for annular seal analysis
[NASA-CR-183084] 19 p2678 N88-25921

ANNULAR FLOW

Experimental and theoretical studies of vertical annular liquid jets
[DE87-013907] 01 p0047 N88-10299

The numerical and analytical study of bifurcation and multicellular flow instability due to natural convection between narrow horizontal isothermal cylindrical annuli at high Rayleigh numbers
[AD-A186113] 07 p0849 N88-15151

An experimental investigation of straight and curved annular wall jets
[NASA-CR-182546] 11 p1434 N88-18557

Experimental and numerical study of liquid distribution in dispersive-annular flow
[DE88-700844] 14 p1909 N88-21406

Interaction of a two-dimensional bluff body and incompressible jet and annulus flows
[AD-A190503] 15 p2064 N88-22310

Investigation of annular flow at high evaporation rates in view of liquid film cooling
[DFVLR-FB-88-08] 21 p2949 N88-27517

ANNULAR NOZZLES

Wake interaction effects on the transition process on turbine blades
[AD-A188020] 10 p1332 N88-17962

ANNULAR PLATES

A finite element procedure for interference-fit and cold-working problems with limited yielding
[AR-004-517] 04 p0485 N88-12992

Analyses of annular microstrip antennas for hyperthermic applicators
[PB88-181508] 19 p2643 N88-25679

ANNULAR SUSPENSION AND POINTING SYSTEM

Synchronous response modelling and control of an annular momentum control device
[NASA-CR-4166] 24 p3358 N88-29995

ANNULI

The numerical and analytical study of bifurcation and multicellular flow instability due to natural convection between narrow horizontal isothermal cylindrical annuli at high Rayleigh numbers 10 p1329 N88-17937

Embedded minimal sufaces with an infinite number of ends
[DE88-006429] 15 p2126 N88-22680

Nonlinear elliptic problems with critical exponent in shrinking annuli
[W-02/87] 23 p3273 N88-29477

ANODES

NT CELL ANODES

Impedance of passive lithium anodes in SOCl2 solutions under low-field polarization
[DE88-000922] 04 p0439 N88-12728

Internal reforming development for solid oxide fuel cells
[DE87-006518] 04 p0464 N88-12871

Investigation of materials for inert electrodes in aluminum electrodeposition cells
[DE88-003380] 10 p1323 N88-17906

Anodic behavior of Ni-P and Ni-Cr-P metallic glasses
[DE88-005334] 11 p1463 N88-18722

Aluminum-air battery development
[DE88-006617] 13 p1762 N88-20542

Generation of high brightness ion beam from insulated anode PED 16 p2278 N88-23637

Research on anode plasma behavior of flashover pulsed ion sources 16 p2279 N88-23640

Time-resolved spectroscopic measurement of anode plasma in magnetically-insulated diode
16 p2279 N88-23641

Study on the flashover ion diode with cryogenic anode
16 p2279 N88-23642

Sulfur-tolerant anode materials
[DE88-001034] 18 p2537 N88-25054

Ambient temperature secondary lithium batteries using LiAl lithium insertion anodes
[DE88-008394] 20 p2793 N88-26574

ANODIC COATINGS

Corrosion behavior of high density tungsten alloys
[AD-A187108] 09 p1143 N88-16852

The soft/hard wet anodization of aluminum oxide and its use in a thin film multilayered capacitor
[AD-A187575] 10 p1325 N88-17919

An interdisciplinary approach to predictive modeling of structural adhesive bonding: Factors affecting the durability of titanium/epoxy bonds
[AD-A189503] 12 p1611 N88-19636

ONR Far East Scientific Bulletin, volume 12, number 3, July-September 1987
[AD-A188554] 13 p1851 N88-21081

AC impedance analysis of corrosion fatigue in naval aircraft alloys
[AD-A190822] 17 p2322 N88-23865

Thermal conductivity of hard anodized coatings on aluminum
[AD-A191755] 18 p2492 N88-24784

ANODIZING

Mathematical modelling of solar ultraviolet radiation induced optical degradation in anodized aluminum
02 p0135 N88-10846

Chromic acid anodizing of aluminum foil
[NASA-CR-178417] 07 p0837 N88-15077

The effect on initial bond strength and durability of a Phosphoric Acid Dip (PAD) following chromic acid anodising of aluminum
[ARE-TM(UMM)-87402] 10 p1300 N88-17772

A modified sulphuric acid anodising process used as a pretreatment for the adhesive bonding of aluminum alloys
[ARE-TM(UMM)-87410] 16 p2177 N88-22974

ANOMALIES

NT GEOTHERMAL ANOMALIES

NT GRAVITY ANOMALIES

NT MAGNETIC ANOMALIES

BRASILSAT A2: Ground and in-orbit anomalies
02 p0164 N88-11032

Effects of long term storage on aerospace nickel cadmium cell performance 02 p0165 N88-11035

Test summary for advanced H2 cycle Ni-CD cell
02 p0165 N88-11040

Anomalies in gauge theories
[DE87-014087] 02 p0229 N88-11444

Covariant Lorentz anomalies in higher dimensional space
[DE87-753021] 02 p0230 N88-11448

Chiral U(1) anomaly in D = 4 super Yang-Mills theory coupled to supergravity
[DE87-753022] 02 p0252 N88-11591

Analytical average model of studies on orbital resonance 03 p0269 N88-11689

On air-drag perturbation of transit satellite and selection of parameters in orbit improvement
03 p0269 N88-11691

Electrostatic discharges in geostationary orbit: The case of Telecom 1 03 p0275 N88-11733

The interpretation of crustal dynamics data in terms of plate motions and regional deformation near plate boundaries
[NASA-CR-181475] 03 p0349 N88-12205

Failure control techniques for the SSME
[NASA-CR-179224] 04 p0409 N88-12537

J = O Task Force
[DE88-001326] 04 p0450 N88-12788

On the interannual variability of South American climate and the Southern Oscillation 04 p0470 N88-12905

Anomalous phonon behavior of superconductor Y-Ba-Cu-O
[DE87-703401] 05 p0654 N88-14010

Role of anomalous currents in formation of ocean surface temperature field 06 p0727 N88-14474

Anomalies in electromagnetic absorption of circularly polarized ultrasonic waves by tungsten within Doppler-shifted cyclotron resonance range
06 p0775 N88-14756

Anomalous scaling laws in multifractal objects
[NOTA-INTERNA-883] 07 p0916 N88-15565

Variations of tropical circulation and associated rainfall anomalies, during 2 years of contrast
[INPE-4359-TDL/300] 08 p1039 N88-16286

Space shuttle main engine anomaly data and inductive knowledge based systems: Automated corporate expertise 08 p1060 N88-16398

A generalized description of the anomalous Doppler resonance and the stabilizing role of ion dynamics
[INPE-4384-PRE/1204] 08 p1081 N88-16513

F-layer polar cap arcs
[AD-A186592] 09 p1190 N88-17127

Persistence characteristics of 500 mb blocking and zonal flows in the mid-latitudes of the Northern and Southern Hemispheres 10 p1353 N88-18088

Spatial-temporal variability of North Pacific sea surface temperature anomaly patterns 11 p1516 N88-19058

NAVARES: A prototype expert system for NAVSTAR anomaly resolution
[AD-A189491] 12 p1600 N88-19579

Ion content and infrared absorption of moist atmospheric air
[AD-A188839] 12 p1643 N88-19838

SUSY anomaly in quantum-mechanical systems
[DE88-700890] 12 p1699 N88-20170

Anomalous shock sensitivity/density relationship for RDX-polyethylene wax and related formulations from MRL Small Scale Gap Test (SSGT) measurements
[MRL-R-1099] 13 p1739 N88-20399

Sample models of steady and low frequency circulations in the tropical atmosphere, with application to tropical air-sea interactions 13 p1801 N88-20764

Computerised measurement of human horizontal smooth pursuit eye movements
13 p1811 N88-20819

Sea surface temperatures of winter 1982-83 and their effect on atmospheric circulation
14 p1936 N88-21546

Aerodynamic aspects of the Amazon Forest
[INPE-4445-TDL/313] 15 p2098 N88-22501

Tropical circulations and the associated rainfall anomalies during two contrasting years
[INPE-4506-PRE/1261-REV] 15 p2098 N88-22502

Recent developments in the path integral approach to anomalies
[DE87-703032] 15 p2118 N88-22616

Anomalies in the vegetation in the Alto Xingu - MT
17 p2357 N88-24043

Remote sensing and structural rupture: Application examples in the study of tectonics
17 p2359 N88-24050

Electrical conduction in thin film carbons
[AD-A191726] 18 p2491 N88-24780

Anomalous temperature-dependent negative magnetoresistance in pregraphitic carbons
[AD-A191725] 19 p2619 N88-25535

Electron tunneling in junctions doped with semiconductors and metals 19 p2734 N88-26236

A severe spacecraft-charging event on SCATHA in September 1982
[AD-A193007] 20 p2765 N88-26396

Drift wave vortices and anomalous transport
[DE88-009562] 20 p2859 N88-26982

The 1986-87 Pacific warm episode: Oceanic and Atmospheric features 22 p3120 N88-28535

Modes of interannual climate variability and Sahel rainfall anomalies 22 p3121 N88-28547

Tropospheric biennial variability and its relationship to the southern oscillation 22 p3121 N88-28549

Sub-Saharan rainfall anomalies and global sea-surface temperature relationships for the recent fifteen year (1970-1984) period 22 p3122 N88-28552

Simulation studies of the influence of sea-surface temperature anomalies on the Sahelian circulation and rainfall 22 p3122 N88-28553

Northern Hemisphere 700 mb teleconnections based on half-monthly mean anomaly data stratified by season and by sign 22 p3123 N88-28561

An observational study of interaction between large scale tropical cumulus convection and the equatorial circulation anomalies 22 p3124 N88-28564

Factors influencing summer temperatures and precipitation in the southwest 22 p3124 N88-28565

Global-scale temperature changes to August 1987 and a comparison of satellite and conventional data
22 p3125 N88-28572

The impact of the El Nino event on the ECMWF model performance 22 p3125 N88-28576

Determination of most probable predicted 50 kPa pattern by empirical orthogonal functions
22 p3128 N88-28593

Global gauge anomaly of classical groups in even dimension
[DE88-008572] 22 p3158 N88-28797

One equatorial anomaly in nighttime ionospheric F region 24 p3447 N88-30517

Evolutionary helium and CNO anomalies in the atmospheres and winds of massive hot stars
[NASA-CR-183254] 24 p3452 N88-30550

ANORTHOSITE

The tectonic setting of Archean anorthosites
24 p3397 N88-30231

Crustal underplating in the North American Craton: Evidence from the Petrogenesis of anorthositic rocks in the Middle Proterozoic Midcontinent Rift System
24 p3400 N88-30252

ANTARCTIC ENVIRONMENT

U ICE ENVIRONMENTS

ANTARCTIC OCEAN

Physical oceanography and tracer chemistry of the southern ocean
[DE88-006852] 20 p2828 N88-26779

ANTARCTIC REGIONS

NT ROSS ICE SHELF

Antarctic field tests of SARSAT personal locater beacons
[NASA-TM-4006] 01 p0063 N88-10403

Contributions to geodesy, photogrammetry, and cartography. Series 2, number 45
[ISSN-0469-4244] 01 p0065 N88-10416

Digital Name Data Base Antarctic as a component of a landscape data base of the Antarctic
01 p0065 N88-10419

Kinetics investigations of atmospheric chemical reactions
[PB87-213351] 01 p0069 N88-10439

Human adaptation to isolated and confined environments
[NASA-CR-181502] 03 p0357 N88-12248

TOMS: The Antarctic ozone hole and ozone trends
05 p0615 N88-13775

USSR report: Earth sciences
[JPRS-UES-87-004] 06 p0725 N88-14455

Ferromanganese nodules of Antarctic sector in Pacific Ocean 06 p0727 N88-14472

A review of atmospheric ozone and current thinking on the Antarctic ozone hole
[AD-A185608] 06 p0732 N88-14501

The distribution of evaporitic weathering products on Antarctic meteorites 06 p0798 N88-14888

WOCE Core Project 2 Planning Meeting: The Southern Ocean
[WCP-138] 07 p0882 N88-15348

Biorhythmic aspects of intercontinental Antarctic adaptation 08 p1046 N88-16321

Group adaptation and individual adjustment in antarctica: A summary of recent research
[AD-A186605] 08 p1051 N88-16347

Physical and structural characteristics of Weddell Sea pack ice
[AD-A188189] 10 p1358 N88-18119

Observations and analyses of summer whistlers at the Great Wall Station of Antarctica
11 p1469 N88-18759

Feasibility report: Operation of light air cushion vehicle at McMurdo Sound, Antarctica
[AD-A189057] 13 p1755 N88-20494

The 1987 Airborne Antarctic Ozone Experiment: The Nimbus-7 TOMS data atlas
[NASA-RP-1201] 13 p1791 N88-20714

Activities and objectives of the Polar Research Board
[DE88-004543] 13 p1797 N88-20747

Radon-222 in the Antarctic Peninsula
[INPE-4486-PRE/1251] 15 p2092 N88-22468

Ionospheric research in Antarctica
[INPE-4521-PRE/1273] 16 p2232 N88-23331

Changes in the Antarctic atmosphere due to the reduction of stratospheric ozone
[ETN-88-92565] 18 p2540 N88-25074

ECC (Electrochemical Concentration Cell) ozonesonde observations at South Pole, Antarctica during 1987
[PB88-202015] 21 p2970 N88-27644

On-board data processing of navigation data at high latitudes in Antarctica 22 p3036 N88-28027

South Pole lidar: Brief description of the instrument
[NOTA-INTERNA-907] 22 p3083 N88-28308

Topography of an Antartic ice stream
22 p3092 N88-28361

An evaluation of SPOT imagery for Earth science studies in the Antarctic. Preliminary Evaluation Program (PEPS) 289 for SPOT 22 p3103 N88-28430

Changes in stratospheric ozone: Observations and theories
[AERONOMICA-ACTA-A-334-1988]
24 p3390 N88-30188

Antarctic Meteorite Newsletter, Volume 11, Number 2, August 1988
[NASA-TM-89801] 24 p3457 N88-30573

ANTARCTICA

U ANTARCTIC REGIONS

ANTENNA ARRAYS

NT LINEAR ARRAYS

NT STEERABLE ANTENNAS

The application of group radiators for the determination of tension crack corrosion
[BAM-08264] 01 p0022 N88-10141

Gain evaluation for an idealized curtain array antenna
[PB87-210290] 02 p0161 N88-11006

A conformal aircraft phased array antenna for airplane-satellite communication in the L band
[ESA-TT-1057] 03 p0305 N88-11926

An antenna array processing system for multiple source bearing estimation 03 p0305 N88-11927

Analysis of the ICE combiner for multiple antenna arraying 04 p0436 N88-12704

The use of coaxial transmission line elements in log-periodic dipole arrays
[AD-A184864] 05 p0574 N88-13499

An evaluation of equivalent models for design of rectangular microstrip antennas
[FOA-C-30451-3.2] 08 p0977 N88-15905

Investigation of design considerations for Telemetry, Tracking and Command (TT and C) antenna system on Naval Postgraduate School Orion mini-satellite
[AD-A187130] 10 p1291 N88-17718

Compensation of relector antenna surface distortion using an array feed
[NASA-TM-100286] 11 p1476 N88-18805

Deformations in VLBI antennas
[NASA-TM-100696] 11 p1502 N88-18970

Large-aperture sparse array antenna systems of moderate bandwidth for multiple emitter location
[AD-A188409] 12 p1619 N88-19683

Investigation of surface wave blindness in microstrip phased array antennas
[AD-A189326] 12 p1621 N88-19696

Estimation-correlation, modeling, and identification in adaptive array processors
[AD-A189130] 13 p1757 N88-20512

Adaptive algorithms for HF antenna arrays
[AD-A189329] 13 p1761 N88-20534

Conformal microstrip slot antenna and antenna array
[AD-A189623] 15 p2055 N88-22252

Case study of active array feed compensation with sidelobe control for reflector surface distortion
[NASA-TM-100287] 16 p2192 N88-23073

Gram-Schmidt implementation of a linearly constrained adaptive array
[AD-A191651] 18 p2560 N88-25198

An adaptive array antenna for mobile satellite communications 19 p2647 N88-25710

MSAT mobile electronically steered phased array antenna development 19 p2647 N88-25711

MSAT-X phased array antenna adaptions to airborne applications 19 p2647 N88-25713

Simple, low-profile, circularly polarized arrays
19 p2647 N88-25716

Antenna technology for advanced mobile communication systems 19 p2651 N88-25743

A microstrip array feed for MSAT spacecraft reflector antenna 19 p2652 N88-25747

Active feed array compensation for reflector antenna surface distortions
[NASA-TM-100826] 19 p2654 N88-25762

Array trade-off study using multilayer parasitic subarrays
[NASA-TM-101321] 22 p3070 N88-28222

A novel method to correct radiation pattern distortion of conformal antennas
[AD-A193675] 23 p3204 N88-29066

Development of a general software package for the analysis and synthesis of planar antenna arrays for space applications
[S-247-02] 24 p3359 N88-30000

High frequency GaAlAs modulator and photodetector for phased array antenna applications
[NASA-TM-101328] 24 p3367 N88-30048

ANTENNA COMPONENTS

NT ANTENNA FEEDS

NT DIPLEXERS

Gain evaluation for an idealized curtain array antenna
[PB87-210290] 02 p0161 N88-11006

Studies of the structural dynamic behavior of satellite antenna system
[AD-A185526] 06 p0673 N88-14121

Development of a magnetically suspended, tetrahedron-shaped antenna pointing system
14 p1926 N88-21478

Features and applications of the integrated composites analyzer (ICAN) code 15 p2078 N88-22391

Sidelobe level of an adaptive array using the SMI (Sampled Matrix Inversion) algorithm
[AD-A193131] 21 p2932 N88-27409

ANTENNA COUPLERS

NT DIPLEXERS

ANTENNA DESIGN

Study of advanced satellite concept using a multifeed reconfigurable antenna
[ESA-CR(P)-2406-VOL-1] 01 p0013 N88-10073

Study of advanced satellite concept using a multifeed reconfigurable antenna. Detailed report on mission definition, coverage analysis and performance requirements, antenna geometry
[ITS-TR-014.C/85] 01 p0013 N88-10074

Study of advanced satellite concept using a multifeed reconfigurable antenna. Detailed report on Polarization Sensitive Reflector (PSR) and offset parabolic antennas, Appendix 1
[ESA-CR(P)-2406-VOL-3] 01 p0013 N88-10075

. Study of advanced satellite concept using a multifeed reconfigurable antenna. Appendix 3 : Feeding network, final performance analysis, study of reconfiguration possibilities
[ITS-TR-032/85] 01 p0014 N88-10076

Telemetry, Tracking, and Control Working Group report 01 p0016 N88-10096

Mechanical properties characterization of composite sandwich materials intended for space antenna applications
[NASA-TM-88893] 01 p0020 N88-10121

Realization of a conical four-part antenna for the scanning of interference fields
[REPT-13-86] 01 p0034 N88-10216

Shape optimization of linear antennas
[ETN-87-90413] 01 p0036 N88-10233

Data Relay Satellite antenna subsystem study
[ESA-CR(P)-2435-VOL-2] 02 p0162 N88-11014

Study of antenna configuration for Data Relay Satellite (DRS) user spacecraft
[A5/516/86] 02 p0162 N88-11018

DRS (Data Relay Satellite) antenna subsystem study
[ESA-CR(P)-2435-VOL-1] 02 p0162 N88-11019

New main reflector, subreflector and dual chamber concepts for compact range applications
[NASA-CR-181506] 04 p0402 N88-12498

Band 2 VHF antenna for home construction
[BBC-RD-1987/13] 04 p0432 N88-12677

Capacitive resonant transducer for the Frascati gravitational antenna
[IFSI-86-9] 05 p0578 N88-13528

Studies of the structural dynamic behavior of satellite antenna system
[AD-A185526] 06 p0673 N88-14121

Theory of displaced phase center antenna for space based radar applications
[PB87-229837] 06 p0690 N88-14227

National Aeronautics and Space Administration (NASA)/American Society for Engineering Education (ASEE) Summer Faculty Fellowship Program, 1987. Volume 2
[NASA-CR-172009-VOL-2] 06 p0796 N88-14874

Automatic antenna switching design for Extra Vehicular Activity (EVA) communication system
06 p0797 N88-14883

Interaction between a module cluster and a plasma in a magnetic field
[PB87-148276] 07 p0934 N88-15675

An evaluation of equivalent models for design of rectangular microstrip antennas
[FOA-C-30451-3.2] 08 p0977 N88-15905

A simplified approach to axisymmetric dual-reflector antenna design
[NASA-TP-2797] 09 p1111 N88-16662

European developments in antenna technology
09 p1123 N88-16725

Multisurface control mechanism for a deployable antenna: Far Infrared and Submillimeter Space Telescope (FIRST) technology study
[RP-FA-D003] 09 p1135 N88-16807

Optimizing HF antenna systems on the Dolphin and Sea Hawk helicopters
[AD-A186552] 09 p1152 N88-16901

Study of dual beam antenna systems for the data relay satellite, volume 1
[S-272-02-VOL-1] 09 p1152 N88-16905

Study of dual beam antenna systems for the data relay satellite. Volume 2: Executive summary
[S-272-03-VOL-2] 09 p1153 N88-16906

Study on a double reflector compact range --- satellite antennas
[S-201-05] 09 p1153 N88-16908

Evaluation of CWMS (Continuous-Wave Measurement System) single-wire dipole antenna
[DE88-003979] 09 p1155 N88-16920

Investigation of design considerations for Telemetry, Tracking and Command (TT and C) antenna system on Naval Postgraduate School Orion mini-satellite
[AD-A187130] 10 p1291 N88-17718

User's guide for the HF (High Frequency) broadcast antenna design and validation summary programs
[PB88-116124] 10 p1317 N88-17875

Capacitor analysis for RF antennas
[DE88-004178] 10 p1318 N88-17883

Observation model and parameter partials for the JPL VLBI parameter estimation software MASTERFIT-1987
[NASA-CR-182524] 10 p1427 N88-18523

Improved backfire antenna using circular dipole
11 p1468 N88-18757

The characteristics of two broadband (2 MHz to 10 MHz) switched vee antennas
[AD-A187874] 11 p1471 N88-18770

The Telecommunications and Data Acquisition Report
[NASA-CR-182545] 11 p1471 N88-18774

An optimal structure for a 34-meter millimeter-wave center-fed BWG antenna: The Cross-Box concept
11 p1472 N88-18778

A 2.3-GHz maser at Usuda, Japan, for TDRSS-orbiting VLBI experiment 11 p1472 N88-18779

A noise-adding radiometer for the Parkes antenna
11 p1473 N88-18788

X-band system performance of the very large array
11 p1473 N88-18789

DSS 14 64-meter antenna S- and X-band efficiency and system noise temperature calibrations, September 1987
11 p1473 N88-18790

New mode switching algorithm for the JPL 70-meter antenna servo controller 11 p1474 N88-18791

Optical links in the angle-data assembly of the 70-meter antennas 11 p1474 N88-18792

Seventy-meter antenna performance predictions: GTD analysis compared with traditional ray-tracing methods
11 p1474 N88-18793

A new approach for shaping of dual-reflector antennas
[NASA-CR-182581] 11 p1476 N88-18806

Deformations in VLBI antennas
[NASA-TM-100696] 11 p1502 N88-18970

Large-aperture sparse array antenna systems of moderate bandwidth for multiple emitter location
[AD-A188409] 12 p1619 N88-19683

Aerospatiale unfurlable reflector and associated mechanisms 14 p1875 N88-21203

Multiple-beam ground station reflector antenna system: A preliminary study
[EUT-87-E-171] 14 p1904 N88-21379

Optically interconnected phased arrays
[NASA-TM-100855] 14 p1908 N88-21400

The 15-meter diameter hoop/column antenna surface control actuator system 14 p1924 N88-21469

Short experiment study of four-wire helical antennas (half turn half wave)
[CNES-CT/DRT/TIT/AN-249-T]
15 p2058 N88-22266

Simple, low-profile, circularly polarized arrays
19 p2647 N88-25716

Omni-directional L-band antenna for mobile communications 19 p2648 N88-25717

The 15-meter antenna performance optimization using an interdisciplinary approach 19 p2652 N88-25746

Technologies for antenna shape and vibration control
19 p2652 N88-25748

A role for high frequency superconducting devices in free space power transmission systems
[NASA-TM-100971] 19 p2662 N88-25830

Radar cross section studies/compact range research
[NASA-CR-183124] 20 p2792 N88-26565

Experiments applications guide: Advanced Communications Technology Satellite (ACTS)
[NASA-TM-100265] 22 p3048 N88-28082

Strawman Optical Reception Development Antenna (SORDA) 22 p3065 N88-28187

DSS 13 microprocessor antenna controller
22 p3066 N88-28192

An 8.4-GHz dual maser front end for Parkes reimplementation 22 p3066 N88-28197

X-band noise temperature near the Sun at a 34-meter high efficiency antenna 22 p3067 N88-28200

Investigations on multiport antennas for polarimetric and modal field scanning
[REPT-5-87] 23 p3205 N88-29073

Experimental investigations for the generation of phase modes for adaptive antennas
[REPT-10-87] 23 p3205 N88-29074

Development of a multiport-hybrid-mode exciter for use in antennas for polarimetric field measurements
[REPT-12-87] 23 p3205 N88-29075

Development of a general software package for the analysis and synthesis of planar antenna arrays for space applications
[S-247-02] 24 p3359 N88-30000

Fields and waves 24 p3363 N88-30025

A 30/20 GHz multibeam array antenna suitable for future high rate TDMA European satellite networks
[ETN-88-93079] 24 p3365 N88-30037

ANTENNA FEEDS

Study of advanced satellite concept using a multifeed reconfigurable antenna
[ESA-CR(P)-2406-VOL-1] 01 p0013 N88-10073

Study of advanced satellite concept using a multifeed reconfigurable antenna. Detailed report on mission definition, coverage analysis and performance requirements, antenna geometry
[ITS-TR-014.C/85] 01 p0013 N88-10074

Study of advanced satellite concept using a multifeed reconfigurable antenna. Detailed report on Polarization Sensitive Reflector (PSR) and offset parabolic antennas, Appendix 1
[ESA-CR(P)-2406-VOL-3] 01 p0013 N88-10075

Study of advanced satellite concept using a multifeed reconfigurable antenna. Appendix 3 : Feeding network, final performance analysis, study of reconfiguration possibilities
[ITS-TR-032/85] 01 p0014 N88-10076

An analysis of simplified feed architectures for MMIC (Monolithic Microwave Integrated Circuit; T/R (Transmit/Receive) module arrays
[AD-A185474] 06 p0697 N88-14275

Compensation of relector antenna surface distortion using an array feed
[NASA-TM-100286] 11 p1476 N88-18805

Modification of parabolic dish antenna pattern using two symmetrically placed circular flat plates
[AD-A189543] 13 p1758 N88-20517

Development of 20 GHz monolithic transmit modules
[NASA-CR-182134] 17 p2445 N88-24539

A MININEC model of the miniloop antenna
[AD-A191759] 18 p2500 N88-24830

Active feed array compensation for reflector antenna surface distortions
[NASA-TM-100826] 19 p2654 N88-25762

ANTENNA FIELDS

U ANTENNA RADIATION PATTERNS

ANTENNA RADIATION PATTERNS

NT SIDELOBES

Study of advanced satellite concept using a multifeed reconfigurable antenna. Appendix 3 : Feeding network, final performance analysis, study of reconfiguration possibilities
[ITS-TR-032/85] 01 p0014 N88-10076

Realization of a conical four-part antenna for the scanning of interference fields
[REPT-13-86] 01 p0034 N88-10216

Effects on electromagnetic wave propagation at frequencies over 10 GHz due to inhomogeneities of the complex refraction index
[REPT-86-025] 01 p0036 N88-10228

NBS (National Bureau of Standards) calibration procedures for horizontal dipole antennas (25 to 1000 MHz)
[PB87-210233] 03 p0305 N88-11922

New main reflector, subreflector and dual chamber concepts for compact range applications
[NASA-CR-181506] 04 p0402 N88-12498

Overestimation of on-axis power density by the Fraunhofer (far-field) approximation
[AD-A186399] 07 p0843 N88-15111

The ESTEC Mini Compact Antenna Test Range
[ESA-CR(P)-2475] 08 p0977 N88-15907

Diagnostic concept of the resonance cone technique and its application in ground and space experiments
08 p1027 N88-16222

Resonance cones in nonthermal plasmas: Laboratory experiments 08 p1027 N88-16223

Performance of linear vertical antenna in refractive multimode waveguide 08 p1076 N88-16[illegible]9

A simplified approach to axisymmetric dual-reflector antenna design
[NASA-TP-2797] 09 p1111 N88-16662

Exact image principle in electromagnetic field computation
[EL-57] 09 p1153 N88-16907

Modification of parabolic dish antenna pattern using two symmetrically placed circular flat plates
[AD-A189543] 13 p1758 N88-20517

Multiple-beam ground station reflector antenna system: A preliminary study
[EUT-87-E-171] 14 p1904 N88-21379

Exact image method for Gaussian beam problems involving a planar interface
[NASA-CR-182702] 14 p1905 N88-21380

Short experiment study of four-wire helical antennas (half turn half wave)
[CNES-CT/DRT/TIT/AN-249-T]
15 p2058 N88-22266

Analysis and experiments concerning the performance and calibration of compact antenna-test ranges
[PB88-169263] 16 p2188 N88-23047

Analysis and experiments concerning the performance and calibration of compact antenna-test ranges
[ISBN-9-09-001727-5] 16 p2188 N88-23048

Determination of characteristic radiation properties of a torus antenna: Integral equation method
[DFVLR-FB-87-46] 16 p2188 N88-23049

A diagnostic technique used to obtain cross range radiation centers from antenna patterns
[NASA-CR-182903] 16 p2192 N88-23071

A MININEC model of the miniloop antenna
[AD-A191759] 18 p2500 N88-24830

Analysis of annular microstrip antennas for hyperthermic applicators
[PB88-181508] 19 p2643 N88-25679

An adaptive array antenna for mobile satellite communications 19 p2647 N88-25710

Evaluation of vertical monopole antennas with elevated radials
[DE88-008339] 19 p2654 N88-25760

Active feed array compensation for reflector antenna surface distortions
[NASA-TM-100826] 19 p2654 N88-25762

Antenna heights for the optimum utilization of the oceanic evaporation duct. Part 3: Results from the Mediterranean measurements, volume 2
[AD-A192311] 20 p2791 N88-26554

Antenna heights for the optimum utilization of the oceanic evaporation duct. Part 1: Results from the Pacific measurements. Part 2: Results from the Key West measurements, volume 1
[AD-A192358] 20 p2791 N88-26555

Analytical approximation of a distorted reflector surface defined by a discrete set of points
[NASA-TM-101323] 21 p2934 N88-27424

Polynomials with restricted coefficients and their applications
[AD-A192589] 23 p3202 N88-29055

A novel method to correct radiation pattern distortion of conformal antennas
[AD-A193675] 23 p3204 N88-29066

Application of sampling techniques to near-field far-field transformation
[ESA-CR(P)-2546] 24 p3359 N88-30002

The focal plane reception pattern calculation for a paraboloidal antenna with a nearby fence
[NASA-TM-100691] 24 p3365 N88-30039

ANTENNAS

NT AIRCRAFT ANTENNAS
NT BACKFIRE ANTENNAS
NT DIPOLE ANTENNAS
NT DIRECTIONAL ANTENNAS
NT FURLABLE ANTENNAS
NT GRAVITATIONAL WAVE ANTENNAS
NT HELICAL ANTENNAS
NT HOOP COLUMN ANTENNAS
NT LOG PERIODIC ANTENNAS
NT LOOP ANTENNAS
NT MICROSTRIP ANTENNAS
NT MICROWAVE ANTENNAS
NT MONOPOLE ANTENNAS
NT OMNIDIRECTIONAL ANTENNAS
NT PARABOLIC ANTENNAS
NT PLASMA ANTENNAS
NT RADIO ANTENNAS
NT REFLECTOR ANTENNAS
NT SATELLITE ANTENNAS
NT SLOT ANTENNAS
NT SPACECRAFT ANTENNAS
NT STEERABLE ANTENNAS
NT TWO REFLECTOR ANTENNAS
NT WAVEGUIDE ANTENNAS

Numerical modeling: Integral equation method
03 p0304 N88-11919

Experiments: Test range facilities, part 2
03 p0305 N88-11921

Low-frequency VLBI in space and interstellar refraction
[PB87-127643] 06 p0696 N88-14267

Preliminary airworthiness evaluation of a UH-1 equipped with a terrain mapping receiver antenna
[AD-A186274] 07 p0819 N88-14980

Treatment of small wire loops in the method of moments code NEC (Numerical Electromagnetics Code)
[DE88-002995] 07 p0846 N88-15136

Optimizing HF antenna systems on the Dolphin and Sea Hawk helicopters
[AD-A186552] 09 p1152 N88-16901

Space-time processing of field produced by moving source 09 p1234 N88-17399

The design of impedance- matching networks for broadband antennas
[AD-A187600] 10 p1320 N88-17895

The coaxial colinear antenna: Theoretical and experimental models 11 p1475 N88-18803

Optically controlled phased-array antenna technology for space communication systems
[NASA-TM-100852] 11 p1476 N88-18809

The complex point spread function of the RSRE SAR (Synthetic Aperture Radar)
[AD-A189011] 12 p1621 N88-19693

The evaluation and selection of a 5th ground antenna site for the global positioning system
[AD-A189495] 13 p1720 N88-20286

Electromagnetic scattering from and natural resonances of the circular strip 13 p1759 N88-20523

Optical RF distribution links for MMIC phased array antennas
[NASA-TM-100841] 13 p1764 N88-20555

Optically interconnected phased arrays
[NASA-TM-100855] 14 p1908 N88-21400

Nonlinear wave and diffusion equations
[AD-A191421] 16 p2265 N88-23544

Practical VLF/LF radio test system
[AD-A191768] 18 p2500 N88-24831

IGUANA: Interactive graphics utility for automated NEC analysis
[AD-A191760] 18 p2556 N88-25174

The new MININEC (version 3): A mini-numerical electromagnetic code
[AD-A191778] 19 p2642 N88-25675

Adaptive interference techniques for mobile antennas
19 p2647 N88-25714

On 3-5 transistors for MM-wave applications
[AD-A191580] 19 p2661 N88-25825

Antenna heights for the optimum utilization of the oceanic evaporation duct. Part 3: Results from the Mediterranean measurements, volume 2
[AD-A192311] 20 p2791 N88-26554

Antenna heights for the optimum utilization of the oceanic evaporation duct. Part 1: Results from the Pacific measurements. Part 2: Results from the Key West measurements, volume 1
[AD-A192358] 20 p2791 N88-26555

A model for insulated wires in the method of moments code NEC (Numerical Electromagnetics Code)
[DE88-008920] 20 p2794 N88-26577

The feasibility of the disturbance accommodating controller for precision antenna pointing
22 p3064 N88-28182

HPM (High Power Microwave) simulation fidelity studies
[DE88-012229] 22 p3068 N88-28209

Improvements in techniques of microwave thermography
[AD-A193620] 23 p3239 N88-29276

ANTHRACENE

Statistical fine structure in the inhomogeneously broadened electronic origin of pentacene in p-terphenyl
[AD-A191211] 16 p2176 N88-22968

Electronic and ionic transport in polymers
[AD-A191642] 18 p2490 N88-24772

ANTHROPOMETRY

Physiological determinants of load bearing capacity
[AD-A184977] 05 p0629 N88-13848

ANTIAIRCRAFT MISSILES

Dependence of the expectancy of hitting on the number of spread shots. Determination of the expectancy of hitting using a spread salvo
[REPT-FM6] 10 p1310 N88-17829

Investigation of several spread shot conditions
[REPT-TR-164] 10 p1310 N88-17830

POLYPHEM, a universal defensive missile with optical waveguides guidance
[MBB-UA-1045/87] 10 p1315 N88-17862

ANTIBIOTICS

Study of certain biological characteristics of bacteria during the French-Soviet CYTOS-2 space experiment
04 p0473 N88-12917

Antibiotic activity in space, results and hypothesis
12 p1660 N88-19952

The Antibio experiment --- Spacelab D1 mission
22 p3060 N88-28159

ANTICLINES

The breaked anticlines, cuesta and crest homoclines, ortoclinal valleys, and other forms of relief outcrops delineated with the help of remote sensing imagery
17 p2366 N88-24089

Diapirs of the Mediterranean ridge: The tectonic regime of an incipient accreted terrane
24 p3396 N88-30224

ANTICLINORIA
U ANTICLINES
ANTICONVULSANTS
Carbamates, atropine, and diazepam: Effects on performance in the running rat
[AD-A188009] 11 p1517 N88-19062
ANTICYCLONES
Synoptic perturbations and climate
08 p1016 N88-16158
ANTIFERROMAGNETISM
Experimental perspectives on heavy electron metals
[DE87-014766] 04 p0416 N88-12583
A mechanism for symmetry breaking in antiferromagnetic Heisenberg systems
[ETN-88-91320] 05 p0657 N88-14031
Structural properties of high-T/sub c/ oxide super conductors
[DE88-002974] 08 p1090 N88-16563
Comparison between muon spin rotation and neutron scattering studies on the 3-dimensional magnetic ordering of La2CuO(4-y) 17 p2396 N88-24244
Ground state properties and electronic structure of high T sub c superconductors
[DE88-007485] 18 p2585 N88-25360
Self energy corrections to the ab initio band structures: Chromium
[DE88-701825] 21 p3020 N88-27927
Static and dynamic behavior of a quasi one-dimensional Heisenberg antiferromagnet in the long-range ordered state. A nuclear magnetic resonance study performed with a He3-He4 dilution refrigerator
[B8705564] 23 p3281 N88-29533
Theory of superconductivity in oxides
[AD-A195647] 24 p3433 N88-30432
Theoretical model of high temperature superconductors
[DE88-702707] 24 p3434 N88-30441
ANTIFRICTION BEARINGS
NT BALL BEARINGS
NT ROLLER BEARINGS
Corrosion-wear process under rolling-sliding motion
[AD-A189603] 13 p1778 N88-20635
On the computation of stationary deterministic behavior of nonlinear dynamic systems with applications to rotor-bearing structures
[ETN-88-92241] 16 p2214 N88-23213
ANTIGENS
A solid phase enzyme-linked immunosorbent assay for the antigenic detection of Legionella pneumophila (serogroup 1): A compliment for the space station diagnostic capability 06 p0795 N88-14868
ANTIGRAVITY
Non-minimal interaction of gravity with other physical fields: An overview
[DE87-703362] 05 p0624 N88-13819
ANTIKNOCK ADDITIVES
Detailed kinetic modeling of autoignition chemistry
[DE87-013226] 03 p0283 N88-11782
ANTIMATTER
NT ANTINEUTRINOS
NT ANTINUCLEONS
NT ANTIPARTICLES
NT ANTIPROTONS
NT POSITRONS
A matter-antimatter propulsion system for manned interstellar flight
[DE87-013311] 02 p0141 N88-10885
Solid antimatter
[PB87-166146] 09 p1259 N88-17549
Antimatter: Its history and its properties
[DE88-004306] 10 p1423 N88-18498
Proceedings of the Cooling, Condensation, and Storage of Hydrogen Cluster Ions Workshop
[AD-A189857] 16 p2266 N88-23555
Atomic processes in matter-antimatter interactions
[DE88-008911] 19 p2723 N88-26172
ANTIMISSILE DEFENSE
Mathematical models for the S.D.I.
[AD-A184667] 03 p0373 N88-12345
Investigation of design concepts for large space structures to support military applications
[AD-A186098] 07 p0824 N88-15000
Feasibility of software built-in test for SDI (Strategic Defense Initiative) applications
[AD-A185750] 07 p0917 N88-15572
The impact of deployment rates on the effectiveness of strategic defenses
[AD-A186907] 09 p1233 N88-17393
Signal and data processing for IR sensors
10 p1374 N88-18199
Strategic Defense Initiative Program: Status of space surveillance and tracking system
[PB88-150436] 14 p1967 N88-21739
Real-time stressed channel simulator
[AD-A190223] 15 p2025 N88-22067
Constellation sizing for modest directed energy platforms
[DE88-007033] 15 p2070 N88-22343
MPD (magnetoplasmadynamic) thruster advanced pumping system concepts
[AD-A190513] 15 p2138 N88-22756
The Oak Ridge National Laboratory strategic defense initiative shield optimization program
[DE88-008946] 19 p2721 N88-26160
The Oak Ridge National Laboratory strategic defense initiative shield optimization program: Executive summary
[DE88-008016] 20 p2847 N88-26899
SDI: Myth or reality
[DE88-009121] 20 p2847 N88-26901
The strategic defense initiative: Strategic implications
[AD-A192341] 20 p2847 N88-26902
Future SDI (Strategic Defense Initiative) decision making
[AD-A192794] 21 p3010 N88-27860
Comparative analysis of the space power architecture studies
[NASA-TM-100977] 22 p3049 N88-28090
SDI (Strategic Defense Initiative): A policy analysis
[AD-A194240] 23 p3275 N88-29493
Strategic defense initiative architecture dataflow modeling technique version 1.5
[AD-A194356] 23 p3275 N88-29494
SDI (Strategic Defense Initiative) battle management/C3 (Command, Control and Communications) algorithms technology program plan
[AD-A194357] 23 p3275 N88-29495
SDI (Strategic Defense Initiative): Where do we go from here
[AD-A194544] 23 p3275 N88-29497
Nonlinear analysis of non-neutral plasmas
[AD-A192506] 23 p3284 N88-29556
Report to congress on the strategic defense system architecture
[AD-A195476] 24 p3426 N88-30393
ANTIMISSILE MISSILES
A simulation of post boost vehicle deployment of multiple reentry vehicles
[DE88-009537] 20 p2764 N88-26391
Looking beyond the strategic defense initiative
[AD-A195079] 24 p3427 N88-30394
ANTIMISTING FUELS
Antimisting kerosene: Low temperature degradation and blending
[NASA-CR-182725] 20 p2781 N88-26495
ANTIMONIDES
NT INDIUM ANTIMONIDES
ANTIMONY ALLOYS
MBE growth of InAsSb strained-layer superlattices
[DE88-000365] 05 p0654 N88-14011
Nonlinear absorption of CO2 laser radiation in p-type InSb
[DE88-004055] 11 p1492 N88-18906
Electrical characteristics of MBE (Molecular Beam Epitaxyl)-grown GaAs/sub 1-x/Sb/sub x on InP and correlation with film microstructure
[DE88-003841] 13 p1847 N88-21053
The influence of solute segregation on the dislocation structure of small and large angle (001) twist boundaries in Fe-Sb alloys
[DE88-009166] 22 p3155 N88-28770
ANTIMONY COMPOUNDS
NT INDIUM ANTIMONIDES
Activities of As, Sb, Bi and Pb in copper mattes and their effects on impurity elimination
[TKK-V-A10(1988)] 15 p2041 N88-22165
ANTINEUTRINOS
Wrong helicity events induced by the CERN-SPS wide band muonic (anti)neutrino beam
[NIKHEF-H/87-2] 06 p0779 N88-14779
Properties of nuclei and elementary particles at low and intermediate energies
[DE88-001913] 09 p1244 N88-17456
Event classification in (anti)neutrino experiments using an Internal Picket Fence-External Muon Identifier (IPF-EMI) detector system
[NIKHEF-H/87-6] 09 p1245 N88-17457
ANTINUCLEONS
Theoretical studies in few-body intermediate energy physics
[DE88-004101] 12 p1689 N88-20106
ANTIOXIDANTS
Experimental study of protective effect of antioxidant enzymes-superoxide dismutase and catalase-when using intermittent toxic modes of hyperbaric oxygenation
19 p2707 N88-26094
ANTIPARTICLES
NT ANTINEUTRINOS
NT ANTINUCLEONS
NT ANTIPROTONS
NT POSITRONS
Formation and reactivity of small hydrogen cluster ions 16 p2267 N88-23560
Infrared spectroscopy of H3(+)
16 p2268 N88-23565
The role of electron-ion recombination in bulk antimatter production 16 p2268 N88-23567
First capture of antiprotons in an ion trap and the possibility of antihydrogen 16 p2268 N88-23569
Magnetic traps for an anti-hydrogen gas
16 p2269 N88-23572
Production of heavy antinuclei: Review of experimental results 16 p2269 N88-23574
Atomic processes in matter-antimatter interactions
[DE88-008911] 19 p2723 N88-26172
ANTIPROTONS
A program to study antiprotons in the cosmic rays: Arizona collaboration
[NASA-CR-180702] 01 p0120 N88-10764
Experimental studies of elementary particle interactions at high energies
[DE88-000804] 05 p0648 N88-13971
Basic physics program for a low energy antiproton source in North America
[DE88-003148] 08 p1082 N88-16522
Looking for new gravitational forces with antiprotons
[DE88-003154] 09 p1192 N88-17142
Nuclear structure at intermediate energies
[DE88-002796] 10 p1407 N88-18390
Initial operation of the Tevatron collider
[FNAL-TM-1449] 11 p1547 N88-19252
Advanced space propulsion study - antiproton and beamed power propulsion
[AD-A189218] 13 p1732 N88-20355
Prospects for antiproton production and propulsion
16 p2267 N88-23556
First capture of antiprotons in an ion trap and the possibility of antihydrogen 16 p2268 N88-23569
The cluster ion approach to the condensation and storage of antihydrogen 16 p2269 N88-23575
Analysis of containerless condensation of polyatomic hydrogen ions, with emphasis on H3(+,-) association channels and a future workshop to study related topics
16 p2269 N88-23576
ANTIRADAR COATINGS
Radar ECCM's new area: Anti-STEALTH and anti-ARM 03 p0299 N88-11881
ANTIREFLECTION COATINGS
On 1064 nm and 350 nm laser damage thresholds of high index oxide films deposited from organic solutions and sols
[DE88-001636] 07 p0859 N88-15217
Abrasion resistant porous silica antireflective coatings
[DE88-006230] 14 p1894 N88-21308
Oxide optical coatings prepared by metal-organic vapor deposition
[DE88-006809] 15 p2043 N88-22175
Optical coatings for high average power XeF lasers
[DE88-011356] 20 p2807 N88-26656
Improved adhesion for SiO2 particles in silica substrates using helium-ion irradiation
[DE88-008915] 21 p2920 N88-27332
Survey of material for an infrared-opaque coating
[NASA-TM-88204] 22 p3153 N88-28757
ANTISHIP MISSILES
Utilization of dynamic characteristics of materials to optimize military explosive charges. Application to antiship devices
[SNIAS-872-320-101] 05 p0610 N88-13743
ANTISTATIC DEVICES
U STATIC DISCHARGERS
ANTISUBMARINE WARFARE
Investigation and implementation of an algorithm for computing optimal search paths
[AD-A185927] 07 p0902 N88-15461
ANTISUBMARINE WARFARE AIRCRAFT
NT P-3 AIRCRAFT
ANTITANK MISSILES
An investigation of steep descent guidance for terminally-guided sub-munitions
12 p1596 N88-19555
ANXIETY
Selecting the right crew for future space stations: An analysis of selection research on offshore divers, aviation pilots and other high risk groups in Scandinavia
19 p2696 N88-26021
AO-1 AIRCRAFT
U OV-1 AIRCRAFT
AORTA
Morphometric analysis of rat aorta endothelium during long-term hypokinesia 07 p0894 N88-15417
APATITES
U MINERALS
APERTURES
NT SYNTHETIC APERTURES

An excitation-term modification for a certain class of electromagnetic aperture-coupling problems
[DE88-000260] 04 p0437 N88-12713

Overestimation of on-axis power density by the Fraunhofer (far-field) approximation
[AD-A186399] 07 p0843 N88-15111

Aberrations: Their effect on off-axis beam steering
[AD-A189601] 13 p1840 N88-21008

Demonstration of efficient full aperture Type 1/Type 2 third harmonic conversion on Nova
[DE88-003834] 14 p1914 N88-21438

Experimental determination of the coefficients of the hydraulic resistance of apertures in the rotary disks
[AD-A190627] 15 p2066 N88-22317

Improvements in techniques of microwave thermography
[AD-A193620] 23 p3239 N88-29276

APL (PROGRAMMING LANGUAGE)

Report outline of a programming variable and application through example
[INPE-4211-PRE/1092] 01 p0081 N88-10521

APNEA

U RESPIRATION

APOGEE BOOST MOTORS

ESA Bulletin No. 8
[ETN-87-90513] 09 p1122 N88-16718

A European apogee boost motor for GEOS
09 p1123 N88-16719

APPENDAGES

NT ARM (ANATOMY)
NT FINGERS
NT HAND (ANATOMY)
NT LEG (ANATOMY)

An experimental investigation of appendage-flat plate junction flow. Volume 2: Elliptical nose appendage data base
[AD-A184974] 05 p0580 N88-13539

Numerical calculation of appendage, flat plate junction flow
[AD-A186371] 07 p0850 N88-15158

APPLICATION

U UTILIZATION

APPLICATIONS OF MATHEMATICS

Toward a mathematical formalism of performance, task difficulty, and activation 16 p2239 N88-23372

APPLICATIONS PROGRAMS (COMPUTERS)

NT NASTRAN

Integration of dynamic, aerodynamic and structural optimization of helicopter rotor blades
[NASA-CR-181441] 01 p0002 N88-10012

Collection and analysis of specific ELINT Signal Parameters
[NASA-CR-181419] 01 p0033 N88-10213

High-efficiency silicon solar cells: Numerical modeling, transient measurements, efficiency goals, and v-shaped grooves
[DE87-012842] 01 p0066 N88-10423

A study of carbon monoxide distribution determinations for a global transport model
[NASA-CR-181423] 01 p0067 N88-10432

A reference guide for IGVIEW: An IGES-compatible geometry system
[DE87-013441] 01 p0083 N88-10534

An interactive computer program for materials analysis by means of ion scattering
[MRL-R-1040] 01 p0091 N88-10596

RE-1000 free-piston Stirling engine hydraulic output system description
[NASA-TM-100185] 01 p0108 N88-10700

Recent advances in structural dynamics of large space structures
[NASA-TM-100513] 02 p0138 N88-10867

Computer simulation of thermal modeling of primary lithium cells 02 p0163 N88-11022

Pinhole occulter experiment
[NASA-CR-179206] 02 p0235 N88-11481

Vectorization of MHD equilibrium and stability codes
[DE87-753013] 02 p0240 N88-11516

Limit of possible operation of crescent and bean shaped Tokamaks
[IPPJ-837] 02 p0242 N88-11532

A heat transfer model for a heated helium airship
[AD-A183786] 03 p0259 N88-11629

Improvements to the adaptive maneuvering logic program
[NASA-CR-3985] 03 p0262 N88-11648

Analytic investigation of helicopter rotor blade appended aeroelastic devices
[NASA-CR-166525] 03 p0266 N88-11676

Electromagnetic scattering by a thick strip on a half-space
[PB87-227096] 03 p0306 N88-11926

Bearing loads in slider crank mechanisms
[PB87-216495] 03 p0332 N88-12089

Issues in image processing software development for a multi-user, multi-programming environment
[DE88-000358] 03 p0365 N88-12298

Stochastic model of the NASA/MSFC ground facility for large space structures with uncertain parameters: The maximum entropy approach
[NASA-CR-181488] 03 p0372 N88-12343

A hybrid numerical technique for predicting the aerodynamic and acoustic fields of advanced turboprops
[NASA-CR-174926] 03 p0374 N88-12352

Solution of the two-dimensional Euler equations on unstructured triangular meshes
04 p039[illegible] N88-12469

An integrated study of structures, aerodynamics and controls on the forward swept wing X-29A and the oblique wing research aircraft
[NASA-CR-181548] 04 p0399 N88-12486

Microgravity nucleation and particle coagulation experiments support
[NASA-CR-181540] 04 p0423 N88-12618

Higher order theory analysis of a modified free-edge delamination specimen 04 p0455 N88-12820

Applications of the hybrid automated reliability predictor
[NASA-TP-2760] 04 p0475 N88-12928

The ISI (Information Sciences Institute) grapher: A portable tool for displaying graphs pictorially
[AD-A184354] 04 p0478 N88-12944

Methods for design and evaluation of integrated hardware/software systems for concurrent computation
[NASA-CR-181522] 04 p0479 N88-12953

Monocrystal sputtering by the computer simulation code ACOCT
[IPPJ-848] 04 p0493 N88-13035

Cosmological applications of singular hypersurfaces in general relativity 04 p0521 N88-13202

Experiences using the Mark IV supersonic hypersonic arbitrary body program 05 p0534 N88-13249

Practical application of two-dimensional viscous flow computation 05 p0535 N88-13257

The role of computation fluid dynamics in aeronautical engineering (4). The development and applications of implicit TVD finite volume code
05 p0536 N88-13259

Practical and modern simulation by systematic connection of the LU-ADI code and the solution adaptive grid program 05 p0536 N88-13260

Development of the computer program for turbulent boundary layers 05 p0536 N88-13264

Numerical analysis of supersonic flows using panel method 05 p0537 N88-13266

Computation of nacelle interference using boundary element method 05 p0537 N88-13267

Computer graphics for computational aerodynamics
05 p0538 N88-13276

A numerical study of the effects of curvature and convergence on dilution jet mixing
[NASA-TM-89878] 05 p0549 N88-13347

MODTRAN: A moderate resolution model for LOWTRAN
[AD-A185384] 05 p0574 N88-13503

Integration of a supersonic unsteady aerodynamic code into the NASA FASTEX system
[NASA-CR-182329] 06 p0663 N88-14068

Transonic Navier-Stokes computations of strake-generated vortex interactions for a fighter-like configuration 06 p0664 N88-14073

Documentation of computer programs for optimization and simulation of multicarrier SAW-based demodulator
[PB87-134532] 06 p0693 N88-14252

Virtual image processor: A prototype implementation
[AD-A185580] 06 p0758 N88-14652

Interactive nonlinear least squares program
[PB88-109855] 06 p0760 N88-14661

Computational fluid dynamics overview
07 p0809 N88-14927

Research study for materials/properties test results database
[NASA-CR-178923] 07 p0861 N88-15222

Accomplishments at NASA Langley Research Center in rotorcraft aerodynamics technology
09 p1105 N88-16626

Comprehensive rotorcraft analysis methods
09 p1106 N88-16630

A jet in a crossflow
[NASA-CR-182469] 09 p1113 N88-16674

Numerical modeling of multidimensional flow in seals and bearings used in rotating machinery
[NASA-TM-100779] 09 p1165 N88-16988

Algorithm design for scientific computation for highly parallel multiprocessor systems
[AD-A186713] 09 p1217 N88-17299

SURE reliability analysis: Program and mathematics
[NASA-TP-2764] 09 p1231 N88-17380

Two-phase reduced gravity experiments for a space reactor design
[DE86-015530] 09 p1247 N88-17475

Data reduction and analysis of HELIOS plasma wave data
[NASA-CR-182466] 09 p1264 N88-17572

Vibration and flutter characteristics of the SR7L large-scale propfan
[NASA-TM-100272] 10 p1344 N88-18036

Evaluation of surface energy and radiation balance systems on the Konza Prairie
[NASA-CR-182534] 10 p1355 N88-18097

SAGE: The Clemson University Systolic Array Generating Engine 10 p1379 N88-18235

Parameter identification and sensitivity analysis for a robotic manipulator arm
[NASA-CR-181608] 10 p1385 N88-18272

Benchmarks of neutral beam injection codes for stellarators
[DE88-003786] 10 p1412 N88-18426

On the stability of the supersonic boundary layer
11 p1435 N88-18561

Documentation for computer code NACL
[LBL-21859] 11 p1531 N88-19145

ZAP user's manual
[LBL-21270] 11 p1546 N88-19248

Predictive wall adjustment strategy for two-dimensional flexible walled adaptive wind tunnel: A detailed description of the first one-step method
[NASA-CR-181635] 12 p1573 N88-19409

Calculation of flow about posts and powerhead model
[NASA-CR-179305] 12 p1625 N88-19722

Analysis of pre-flight modulator voltage calibration data for the Voyager plasma science experiment
[NASA-CR-182577] 12 p1710 N88-20236

Dynamics of high-speed mechanisms with elastic members 13 p1779 N88-20643

Computer software for the computation of the scattered field and the optical microscope image of line objects patterned in thick layers
[PB88-153705] 13 p1814 N88-20838

Accuracy requirements and benchmark experiments for CFD validation
[NASA-TM-100087] 14 p1911 N88-21423

Monolithic ceramic analysis using the SCARE program
15 p2061 N88-22409

Continuous fiber ceramic matrix composites for heat engine components 15 p2082 N88-22411

Numerical arc segmentation algorithm for a radio conference: A software tool for communication satellite systems planning
[NASA-TM-100789] 16 p2167 N88-22919

Thermoviscoelastic characterization and predictions of Kevlar/epoxy composite laminates
[NASA-CR-182878] 16 p2172 N88-22946

Two-equation low-Reynolds-number turbulence modeling of transitional boundary layer flows characteristic of gas turbine blades
[NASA-CR-4145] 16 p2209 N88-23185

POPEYE: A production rule-based model of multitask supervisory control (POPCORN)
16 p2240 N88-23384

Development of Electromagnetic PIC code for LIB diode 16 p2276 N88-23622

Stability requirement FOT ignition and high gain implosion = 2-D simulation for high neutron yield experiment = 16 p2278 N88-23633

The application of Rutherford backscattering for analyzing multilayered structure change induced by pulsed ion beam bombardment 16 p2278 N88-23638

Numerical simulation of scramjet inlet flow fields
[NASA-TP-2517] 17 p2296 N88-23735

Testing complex avionics software: A practical experience 17 p2306 N88-23794

Theoretical studies of Resonance Enhanced Stimulated Raman Scattering (RESRS) of frequency doubled Alexandrite laser wavelength in cesium vapor
[NASA-CR-182871] 17 p2317 N88-23841

Electromagnetic scattering from nonlinear anisotropic cylinders 17 p2333 N88-23930

Manual for obscuration code with space station applications
[NASA-CR-178099] 17 p2334 N88-23931

Numerical modelling of flows using phoenics
17 p2339 N88-23955

Theory of neutron moisture probes and interpretation of measurements in complex soil and water systems
17 p2342 N88-23965

A proposal of adaptation of a knowledge-based scene analysis model to some remote sensing problems
17 p2354 N88-24026

The SAGE geographic analysis system
17 p2361 N88-24063

COMTAL vision one/20 programming processor system from the VAX 11/780 17 p2364 N88-24079

A control technique for improved robot performance 17 p2331 N88-24212
Novel silicon Schottky barrier infrared imaging arrays 17 p2439 N88-24510
A benchmark for galactic cosmic ray transport codes [NASA-TM-101157] 17 p2453 N88-24571
Prediction of laminar and turbulent flows past single and twin airfoils 18 p2457 N88-24589
Dynamics of a flexible orbiting platform with MRMS [ISSN-0285-6808] 18 p2473 N88-24673
Shape stability in composites 18 p2479 N88-24706
Kinematics, dynamics and control of a closed chain mechanism manipulator 18 p2523 N88-24967
Dynamic response of plates to moving loads: Structural impedance and finite element methods 18 p2528 N88-25000
Advanced development of the boundary element method for elastic and inelastic thermal stress analysis 18 p2529 N88-25002
Automated cartographic generalization for linear map features 18 p2532 N88-25021
Computer and model changes at National Meteorological Center (NWC) 18 p2547 N88-25116
SYMBL: A new Boolean compiler 18 p2554 N88-25160
The Environment for Application Software Integration and Execution (EASIE), version 1.0. Volume 3: Program execution guide [NASA-TM-100575] 18 p2556 N88-25184
Phase diagrams in materials science and the use of the computer in their calculation [PB88-155262] 18 p2586 N88-25364
The development of a user friendly thermodynamic code for the personal computer 19 p2623 N88-25559
Development of a generic combustion stability code for liquid propellant rocket engines 19 p2626 N88-25576
Anatomy of group burning mode transitions in spray group combustion 19 p2626 N88-25578
A computer program for performance prediction of tripropellant rocket engines with tangential slot injection 19 p2627 N88-25581
Boundary layer simulator (BLIMPJ) improvement 19 p2627 N88-25582
Analysis of microwave burner measurement system using a microwave network analysis computer program 19 p2631 N88-25604
Solid rocket motor performance: A workshop report 19 p2631 N88-25607
Evaluation of techniques for direct measurement of burning rates in nozzleless motors 19 p2631 N88-25609
On the NAL numerical simulator system 19 p2635 N88-25631
Rarefied gas numerical wind tunnel 3. Universal code for three dimensional bodies 19 p2637 N88-25644
The new MININEC (version 3): A mini-numerical electromagnetic code [AD-A191778] 19 p2642 N88-25675
Semi-Markov adjunction to the Computer-Aided Markov Evaluator (CAME) [NASA-CR-181645] 19 p2678 N88-25924
Prediction of fatigue life of notched specimens under aircraft loading and importance of the relative method in the case of local strain approach, part 2 [TAE-595-PT-2] 19 p2680 N88-25934
Improved method for stress and compatibility analysis of multicomponent rotating systems [NASA-TM-100884] 19 p2680 N88-25935
The impact of disorganized occupation of urban sub-basins: Sub-basin of the Cabucu River, metropolitan area of Sao Paulo (SP) 19 p2682 N88-25945
Updating of municipal official register of real estate through the geographical information system 19 p2684 N88-25952
MM4 (Penn State/NCAR (National Center for Atmospheric Research)) mesoscale model version 4 documentation [PB88-173232] 19 p2688 N88-25979
BOLETIM: An expert system for weather forecasting [INPE-4538-TDL/329] 19 p2693 N88-26011
Stability of spheromak against current driven modes: Effects of flux hole on stability [IPPJ-868] 19 p2730 N88-26211
Intelligent guidance and control for wind shear encounter [NASA-CR-183080] 20 p2755 N88-26347
Determination of Tafel constants in nonlinear polarization curves [AD-A192335] 21 p2912 N88-27282

APPROACH
NT INSTRUMENT APPROACH
Noise of a model high speed counterrotation propeller at simulated takeoff/approach conditions (F7/A7) [NASA-TM-100206] 01 p0091 N88-10592
GPS vertical axis performance enhancement for helicopter precision landing approach [NASA-CR-177443] 04 p0397 N88-12477
Effect of motion cues during complex curved approach and landing tasks: A piloted simulation study [NASA-TP-2773] 04 p0398 N88-12480

APPROACH CONTROL
Report of safety survey: Human integration of approach charts [DOT/FAA/PM-87/15] 01 p0076 N88-10488
Approach trajectory planning system for maximum concealment [NASA-TM-88258] 02 p0227 N88-11435
The role of adaptive supplemental visual cuing in flight simulation [AD-A185932] 07 p0822 N88-14992
Space vehicle approach velocity judgments under simulated visual space conditions [NASA-TM-89437] 11 p1523 N88-19094
Flight simulations of MLS interception procedures applicable to laterally segmented approach paths [NLR-MP-86037-U] 13 p1721 N88-20288

APPROPRIATIONS
Budget reimbursements: The National Aeronautics and Space Administration's reimbursable work [PB87-207296] 01 p0107 N88-10696
Department of Housing and Urban Development, and Certain Independent Agencies Appropriations, 1988, Part 2 [S-HRG-100-106-PT-2] 03 p0365 N88-12423
The 1986 National Aeronautics and Space Administration (NASA) authorization [GPO-76-600] 06 p0792 N88-14854
Department of Housing and Urban Development independent agencies appropriations for 1989. Part 7: National Aeronautics and Space Administration [GPO-85-166] 16 p2286 N88-23689
Department of Defense statement on defense agency research and development to the Subcommittee on Defense of the Committee on Appropriations, United States House of Representatives, 100th Congress, second session [AD-A191840] 18 p2586 N88-25377
The Department of Defense report on the merit review process for competitive selection of university research projects and an analysis of the potential for expanding the geographic distribution of research for the Committees on Appropriations, United States Congress [AD-A191842] 18 p2586 N88-25379

APPROXIMATION
NT BORN APPROXIMATION
NT BORN-OPPENHEIMER APPROXIMATION
NT CHEBYSHEV APPROXIMATION
NT FINITE DIFFERENCE THEORY
NT FINITE ELEMENT METHOD
NT HARTREE APPROXIMATION
NT LEAST SQUARES METHOD
NT MEAN SQUARE VALUES
NT NEWTON METHODS
NT NEWTON-RAPHSON METHOD
NT PADE APPROXIMATION
NT PARTICLE IN CELL TECHNIQUE
NT RAYLEIGH-RITZ METHOD
NT RELAXATION METHOD (MATHEMATICS)
NT RITZ AVERAGING METHOD
Correction to a single higher order theory of elastic plates [ETN-87-90676] 01 p0062 N88-10397
Approximate polynomial preconditioning applied to biharmonic equations on vector supercomputers [NASA-TM-100217] 01 p0087 N88-10563
Wake shield 03 p0298 N88-11871
Relaxation effect of stark split levels for two-level system interacting with symmetrical strong resonant bichromatic field 03 p0299 N88-11882
Polynomial compensation, inversion, and approximation of discrete time linear systems [NASA-TM-100027] 03 p0372 N88-12344
Finite deformations of shell with rigid inclusion 04 p0426 N88-12639
Solution of three-dimensional inverse problem of gravimetry in contact surfaces class by local corrections method 04 p0460 N88-12848
An adaptive subdivision method with crack prevention for rendering beta-spline objects [AD-A184249] 04 p0477 N88-12940
Back-of-the-envelope problems [AD-A184105] 04 p0484 N88-12980
Tridiagonal approximate factorization method: A preconditioning technique for solving nonsymmetric linear systems suitable to supercomputers 05 p0537 N88-13271
Master plots for predicting the case-depth in laser surface treatments [PB87-221875] 05 p0586 N88-13574
Approximating multivariate normal orthant probabilities using the Clark algorithm [AD-A184855] 05 p0634 N88-13873
Stability properties of spline approximations for retarded systems [PB87-220919] 05 p0639 N88-13910
Numerical and analytical methods in nonlinear partial differential equations [AD-A185210] 05 p0641 N88-13918
Approximate solutions for the momentum transport in turbulent flows in narrow rod array bundles using the finite element method [ETN-88-90810] 06 p0701 N88-14306
Errors in retrieving hydrological fields and fields of their differential characteristics by method of approximation by orthogonal functions 06 p0727 N88-14475
Distributed infimum approximation [PB87-234969] 06 p0764 N88-14695
Diffusion first passage times: Approximations and related differential equations [AD-A185592] 06 p0765 N88-14700
Stochastic approximation and large deviations: General results for w.p.l. Convergence [AD-A185818] 06 p0768 N88-14721
Relativistic stellar pulsations 06 p0801 N88-14902
Error assessments of widely-used orbit error approximations in satellite altimetry [NASA-CR-182390] 07 p0823 N88-14998
On the approximation of the output process of multi-user random access communication networks [AD-A186197] 07 p0842 N88-15108
Overestimation of on-axis power density by the Fraunhofer (far-field) approximation [AD-A186399] 07 p0843 N88-15111
Bounding the expectation of convex functions with limited distribution information [AD-A186147] 07 p0910 N88-15512
Estimation and testing in truncated and nontruncated linear median-regression models [AD-A186317] 07 p0911 N88-15522
On stochastic optimality of policies in first passage problems [AD-A186293] 07 p0915 N88-15554
Propagation of radiation along a constricting optical waveguide 07 p0920 N88-15590
The application of vector diffraction to the scalar anomalous diffraction approximation of Van de Hulst [AD-A185930] 07 p0929 N88-15643
A semianalytical solution of the heat conduction equation for several boundary conditions 08 p1014 N88-16148
Short data length effects in an asymptotically efficient ARMA (AutoRegressive Moving Average) spectral estimator [AD-A186561] 08 p1068 N88-16458
Strong convergence and convergence rates of approximating solutions for algebraic Riccati equations in Hilbert spaces [AD-A186190] 08 p1072 N88-16464
A study of the free energy of the Lenz-Ising model using the cluster variation method of Morita [AD-A186023] 08 p1073 N88-16476
Approximation of noncorrelated reflections in problem of sound propagation through waveguide with rough boundary 08 p1076 N88-16487
Active and passive remote sensing of ice [AD-A186685] 09 p1195 N88-17162
Applications of nonlinear systems theory to control design [NASA-CR-182485] 09 p1231 N88-17377
Random truncation models and Markov processes [CWI-MS-R8702] 09 p1232 N88-17389
Fully Lagrangian Renormalized Approximation theory of fluid turbulence [DE88-004960] 10 p1330 N88-17952
Explicit approximations for strictly nonlinear oscillators with slowly varying parameters with applications to free electron lasers [DE88-004116] 10 p1336 N88-17984
A unified framework for approximation in inverse problems for distributed parameter systems [NASA-CR-181621] 10 p1400 N88-18346
Eigenvalue problems [AD-A188069] 10 p1401 N88-18356
Advances in calculating macroionic solution structure [DE88-003799] 10 p1409 N88-18406
The application of the hybrid iterative method to scattering by perfectly conducting bodies of revolution 11 p1475 N88-18802
Approximate method for predicting the permanent set in a beam in vacuo and in water subject to a shock wave 11 p1500 N88-18957
Accurate efficient evaluation of Bessel transform: Programs and error analysis [AD-A187718] 11 p1536 N88-19174

WKBJ method and strained coordinates for high frequency inertial wave filtering
[INPE-4214-PRE/1095] 11 p1537 N88-19186

Core-core and core-valence correlation
[NASA-CR-182552] 11 p1544 N88-19226

Theoretical studies of the potential surface for the F - H2 greater than HF + H reaction
[NASA-CR-182551] 11 p1557 N88-19319

Approximation algorithms for scheduling unrelated parallel machines
[CWI-OS-R8714] 13 p1817 N88-20861

Predicting oscillatory finite difference solutions to the heat equation: A comparative study of the coefficient and matrix methods
[AD-A189591] 13 p1825 N88-20911

What do multistep methods approximate
[PB88-148838] 13 p1828 N88-20932

Nonstationary solution in random vibration theory
[PB88-163746] 14 p1933 N88-21529

The NPL data approximation subroutine library: Current and planned facilities
[NPL-DITC-104/87] 14 p1959 N88-21681

On the Edgeworth expansion and the bootstrap approximation for a Studentized U-statistic
[CWI-MS-R8706] 14 p1965 N88-21728

Deterministic approximations of probability inequalities
[REPT-87-43] 14 p1966 N88-21732

A posterior error estimation in a finite element method for parabolic partial differential equations
[AD-A190296] 15 p2120 N88-22636

An approximation technique for solving a system of Fredholm integral equations for asymmetric detector response functions
[AD-A190577] 15 p2121 N88-22645

Constructive version of the approximation induction principle
[PB88-165477] 15 p2122 N88-22647

Approximations in extreme value theory
[AD-A189817] 15 p2124 N88-22659

Approximation methods for the identification and control of distributed parameter systems
[AD-A190201] 15 p2124 N88-22662

Extreme value for dependent sequences via the Stein-Chen method of poisson approximation
[AD-A190325] 15 p2125 N88-22668

Efficiency of some computational techniques for electromagnetic scattering problems
[PB88-148895] 16 p2187 N88-23043

On local approximations of the pressure-strain term in turbulence models 16 p2197 N88-23102

Approximation and representation of explicit surfaces in the presence of singularities
[ETN-88-92191] 16 p2258 N88-23496

Jacobi polynomials as generalized Faber polynomials
[CWI-PM-R8706] 16 p2258 N88-23498

An approximation theory for the identification of nonlinear distributed parameter systems
[NASA-CR-181658] 16 p2260 N88-23510

Introduction to nilpotent approximation filtering
[CWI-PM-R8709] 16 p2262 N88-23524

Complex space monofilar approximation of diffraction currents on a conducting half plane
[NASA-CR-182883] 16 p2273 N88-23605

A new collocation-type method for the numerical solution of Hammerstein equations 17 p2393 N88-24226

An evaluation of energy-independent heavy ion transport coefficient approximations
[NASA-TM-101158] 17 p2397 N88-24251

Nonlinear programming extensions to rational function approximation methods for unsteady aerodynamic forces
[NASA-TP-2776] 18 p2463 N88-24623

A feedback linearization approach to spacecraft control using momentum exchange devices
[NASA-CR-172057] 18 p2472 N88-24668

Axisymmetric viscid-inviscid interaction by a frozen vorticity approximation
[AD-A191743] 18 p2503 N88-24885

Construction of approximations to acoustic Green's functions for nonhomogeneous oceans using transmutation
[PB88-185384] 18 p2548 N88-25126

Open or closed curves by regularized B-splines
[RR-652-M] 18 p2563 N88-25218

A mixed min-max control problem governed by integral equations 18 p2564 N88-25228

Numerical solution of linear integral equations with random forcing terms 18 p2565 N88-25237

On a biorthogonal system associated with uniform asymptotic expansions
[CWI-AM-R8709] 18 p2566 N88-25240

Galerkin approximation for inverse problems for nonautonomous nonlinear distributed systems
[NASA-CR-181676] 18 p2567 N88-25246

Optimal discrete-time LQR problems for parabolic systems , with unbounded input: Approximation and convergence
[NASA-CR-181673] 18 p2567 N88-25247

Curvature of blended rolled edge reflectors at the shadow boundary contour
[NASA-CR-182974] 18 p2576 N88-25300

Non equilibrium expansion of a radiating gas in a channel of varying section
[DE88-702063] 19 p2665 N88-25845

Solution of Faddeev-Yakubovsky differential equations by the finite-dimensional approximation method for four spinless particles in the 1 + 3 scattering problem
[DE87-702983] 19 p2719 N88-26145

Semi-discrete approximations to nonlinear systems of conservation laws; consistency and L(infinity)-stability imply convergence
[NASA-CR-181683] 19 p2721 N88-26157

Finite element approximation to a model problem of transonic flow
[DE88-701835] 20 p2752 N88-26333

L(sub infinity symbol)-approximations of complex functions and robust controllers for large flexible space structures
[PB88-186226] 20 p2764 N88-26390

Finite-dimensional approximation for optimal fixed-order compensation of distributed parameter systems
[NASA-CR-181674] 20 p2843 N88-26873

Prolongation, restriction and coarse grid approximation in a three-dimensional cell-centered multigrid method
[REPT-88-02] 20 p2846 N88-26889

Analytical approximation of a distorted reflector surface defined by a discrete set of points
[NASA-TM-101323] 21 p2934 N88-27424

A fast vortex code for computing 2-D flow in a box
[DE88-011732] 21 p2946 N88-27498

Approximation problems of the Hilbert transform to identify minimum phase linear systems
[FUB-42-1986] 21 p2999 N88-27790

Modeling and approximate performance analysis of multiuser computer systems
[ETN-88-92137] 21 p3002 N88-27806

Approximations of stochastic equations driven by predictable processes
[AD-A192714] 21 p3005 N88-27823

Finding minimum-cost circulations by successive approximation
[AD-A192724] 21 p3005 N88-27824

Asymptotic of Peanokerns of finite fixed order
[ETN-88-92381] 21 p3008 N88-27843

Approximations and optimal control for the pathwise average cost per unit time and discounted problems for wideband noise driven systems
[AD-A192712] 21 p3008 N88-27847

Evaluation of quantum mechanics path integrals by the approximations exact on a class of polynomial functionals
[DE88-702434] 21 p3011 N88-27865

Perturbation expansions generated by an approximate propagator
[DE88-702435] 21 p3011 N88-27866

Steady-state approximations in Raman excitation equations
[DE88-011759] 21 p3014 N88-27889

Approximate and numerical methods in acousto-optics. Part 1: Normal incidence of the light
[AD-A194294] 22 p3152 N88-28755

Stability of semidiscrete approximations for hyperbolic initial-boundary-value problems: Stationary modes
[NASA-TM-100994] 23 p3270 N88-29455

Canonical forms in the control of DPS
[AD-A194671] 23 p3270 N88-29461

Approximations and implementations of nonlinear filtering schemes
[AD-A194685] 23 p3271 N88-29462

Finding minimum-cost circulations by successive approximation
[AD-A194028] 23 p3272 N88-29469

Numerical modelling of premixed flames in gaseous media 24 p3350 N88-29944

Approximation of viscoelastic stresses from Newtonian turbulent kinematics
[AD-A194317] 24 p3371 N88-30077

Automatic qualitative analysis of ordinary differential equations using piecewise linear approximations
[AD-A196310] 24 p3424 N88-30379

Convergence of Galerkin approximations for operator Riccati equations: A nonlinear evolution equation approach
[NASA-CR-181706] 24 p3425 N88-30386

Image focusing in space and time
[AD-A195839] 24 p3429 N88-30410

APPROXIMATION METHODS
U APPROXIMATION

APSIDES
NT PERIGEES
NT PERIHELIONS

APT (PICTURE TRANSMISSION)
U AUTOMATIC PICTURE TRANSMISSION

APTITUDE

A comparison of the Army's Project A: Cognitive and psychomotor tests to analogous Air Force and Navy tests
[AD-A188636] 12 p1670 N88-20002

Properties of some Bayesian scoring procedures for computerized adaptive tests
[AD-A189925] 15 p2124 N88-22660

Validity of the academic aptitude composite of the Air Force Officer Qualifying Test (AFOQT)
[AD-A194753] 23 p3240 N88-29286

Reliability and construct validity of reaction time, inspection time and machine-paced tests of cognitive speed
[AD-A193779] 23 p3241 N88-29289

AQUARID METEOROIDS

Results of observations of the Eta Aquarid and Orionid meteor showers in 1980-1984 06 p0740 N88-14548

The structure of the Halley meteor stream and the orbital history of the comet 14 p2008 N88-21975

AQUATIC PLANTS
NT PHYTOPLANKTON

AQUEOUS SOLUTIONS

Reduction of CO2 to methanol and methane by photo and dark reactions on semiconductor and metal electrodes
[PB87-226825] 02 p0156 N88-10975

Organic molecules on meteoritic solid substrates
[NASA-CR-181570] 05 p0560 N88-13411

Coagulation in stirred tanks
[B8711373] 05 p0562 N88-13420

Observing effect of laser radiation of low-frequency Raman scattering of light 06 p0772 N88-14742

Excess thermodynamic properties of aqueous electrolytes to high temperatures and pressures
[DE88-001768] 07 p0940 N88-15712

Precipitation of surfactants and surfactant mixtures in aqueous solutions
[DE88-003333] 10 p1298 N88-17763

A review of pitting corrosion in high temperature aqueous solutions
[DE88-003547] 10 p1302 N88-17787

An experimental investigation of the hydrodynamic and heat-transfer behavior of aqueous foam in laminar tube flow
[DE88-004954] 11 p1483 N88-18855

The influence of strain on hydrogen entry, transport, and embrittlement of a high strength steel in aqueous sodium chloride solution
[AD-A189302] 12 p1608 N88-19619

Velocity and concentration fields over a crystal growing in a water solution. Experimental study and numerical simulation 14 p1987 N88-21856

Corrosion and fatique properties of FeCrB/Si metallic glass wires in aqueous environments
17 p2320 N88-23855

The high pressure sound velocity and equation of state of aqueous solutions of hydroxylammonium nitrate and triethanolammonium nitrate
[AD-A191740] 18 p2570 N88-25266

Precise ultraviolet absorbance study of the interaction of amino acids and mononucleosides in aqueous solution
[ISAS-RN-356] 21 p2908 N88-27256

AQUICULTURE

Aquarack: Aims and Possible Research Projects
[DFVLR-MITT-87-01] 01 p0073 N88-10469

The Aquarack as a potential instrument for basic research work in space biology: Inventory and scientific dispositions 01 p0073 N88-10470

Investigations of the survey of the reproductive biology of Xiphophorus in an Aquarack
01 p0074 N88-10471

The usefulness of microalgal structures as an element of closed ecological systems like Aquarack and CELSS — Controlled Ecological Life Support System (CELSS)
01 p0074 N88-10476

Use of SPOT images for coastal development and inventory of aquacultural sites in New Caledonia (ALIAS project). First results 03 p0344 N88-12175

SPOT: A tool to aid preselection of sites favorable for aquiculture. Evaluation and perspectives of the Preliminary Evaluation Program for SPOT (PEPS) ALIAS Caledonie
22 p3108 N88-28456

AQUIFERS

Field experience with aquifer thermal energy storage
[DE88-007075] 18 p2538 N88-25058

ARABSAT

Prevention of radiation induced degradations and of electrostatic perturbations on the Arabsat spacecraft in flight results 03 p0275 N88-11734

ARC CLOUDS
Convective scale interaction: Arc cloud lines and the development and evolution of deep convection
[NASA-CR-181469] 02 p0215 N88-11357
ARC DISCHARGES
Introduction to the problem of environmentally induced discharges 03 p0273 N88-11717
Modeling of environmentally-induced transients within satellites. Part 2: Discharge coupling transients
03 p0273 N88-11722
In-flight diagnosis: Analysis of spurious events --- spacecraft 03 p0274 N88-11724
Low-current behavior and current chopping of vacuum arcs
[ISBN-90-9001649-X] 05 p0578 N88-13529
Some investigations of electrical discharges at the surfaces of solid cathodes immersed in aqueous electrolyte solutions
[PB87-168209] 09 p1159 N88-16946
Arcs in cesium seeded noble gases resulting from a magnetically induced electric field
[EUT-87-E-177] 13 p1843 N88-21028
Study of surface discharges
[ONERA-12/7236-PY] 15 p2026 N88-22073
Arcing and rf signal generation during target irradiation by a high-energy, pulsed neutral particle beam
[DE88-007169] 18 p2471 N88-24664
Multiply stripped ion generation in the metal vapor vacuum arc
[DE88-008418] 19 p2725 N88-26179
ARC HEATING
Rocket nozzle thermal shock tests in an arc heater facility 02 p0133 N88-10832
Spectroscopic investigations and measurements of certain ARC jet parameters 06 p0796 N88-14877
Upgrading of NASA-Ames high-energy hypersonic facilities: A Study
[NASA-CR-182475] 09 p1122 N88-16717
Numerical investigations in three-dimensional internal flows
[NASA-CR-183108] 23 p3210 N88-29106
ARC JET ENGINES
A low-power arcjet cyclic lifetest
[NASA-TM-100233] 03 p0278 N88-11748
Advanced electric propulsion and space plasma contactor research
[NASA-CR-180862] 06 p0674 N88-14126
Performance-limiting factors in MPD thrusters
[AD-A185605] 06 p0674 N88-14128
Arcjet thruster research and technology
[NASA-CR-180865] 10 p1293 N88-17732
An experimental investigation of an arcjet thruster exhaust using Langmuir probes
[NASA-TM-100258] 14 p1883 N88-21253
MPD (magnetoplasmadynamic) thrust chamber flow dynamics
[AD-A189940] 15 p2137 N88-22751
Advanced electric propulsion research
[NASA-CR-182130] 16 p2170 N88-22937
Arcjet thruster research and technology, phase 1
[NASA-CR-182107] 17 p2314 N88-23830
Electric propulsion options for the SP-100 reference mission 17 p2404 N88-24296
Status of high power electric propulsion technology
17 p2428 N88-24443
Performance and long duration test of a 30 kw thermal arcjet engine
[AD-A190962] 18 p2474 N88-24677
Evaluation of the communications impact of a low power arcjet thruster
[NASA-TM-100926] 18 p2475 N88-24682
An extended life and performance test of a low-power arcjet
[NASA-TM-100942] 18 p2476 N88-24687
Arcjet power supply and start circuit
[NASA-CASE-LEW-14374-1] 23 p3161 N88-28939
Performance and lifetime assessment of MPD arc thruster technology
[NASA-TM-101293] 24 p3336 N88-29860
Unified study of plasma/surface interactions for space power and propulsion
[AD-A195971] 24 p3338 N88-29870
ARC LAMPS
Arc lamp power supply using a voltage multiplier
[NASA-CASE-LAR-13202-1] 17 p2335 N88-23942
ARC MELTING
Growth and deformation mechanisms of refractory alloy hybrid materials
[AD-A190492] 15 p2039 N88-22152
Evaporation characteristics of elements during vacuum arc remelting of alloy A-286 15 p2055 N88-22248
ARC SPRAYING
Evaluation of the chromium oxide arc spraying treatment on solar energy collectors
[ETN-88-92564] 18 p2537 N88-25053
ARC WELDING
NT GAS TUNGSTEN ARC WELDING
NT PLASMA ARC WELDING
A physical metallurgical basis for heat-affected zone and base-plate properties of a microalloyed HSLA steel
[AD-A180200] 01 p0022 N88-10137
Process and equipment capabilities materials joining laboratory, 1987
[DE87-014534] 02 p0180 N88-11122
The nature of metallurgical reactions in underwater welding
[AD-A184464] 04 p0414 N88-12568
Optical seam tracking in robotic arc welding
[VTT-RR-463] 06 p0713 N88-14376
Study on the cryogenic toughness of stainless steel weld metals
[PB87-143830] 07 p0834 N88-15057
Synchronous multi-image high speed photography of welding arc by optical fibers
[PB87-143939] 07 p0857 N88-15202
Electronic imaging technique for welding and other high-luminosity processes
[DE88-002199] 07 p0862 N88-15227
Microcomputer controlled arc welding power source: Its steady state and transient performance
[PB87-143921] 07 p0863 N88-15233
MIG welding with pulsed wire feed
[PB87-143582] 07 p0863 N88-15234
Study of welding arc control in China
[PB87-143350] 07 p0863 N88-15235
Study on arc sound in TIG and plasma welding processes and the possibility of its application in practice
[PB87-143947] 07 p0863 N88-15238
A numerical thermal model of the rapid solidification parameters in the capacitor discharge welding process
[DE88-002206] 07 p0864 N88-15244
Submerged arc flux welding with CaF2-CaO-SiO2 fluxes: Possible electrochemical effects on weld metal
[DE88-003107] 08 p0992 N88-16004
A detailed microstructural examination of the cause of HAZ cracking in type 316 steel
[AERE-R-12428] 10 p1301 N88-17777
A generalized method for automatic downhand and wirefeed control of a welding robot and positioner
[NASA-TP-2807] 10 p1316 N88-17869
Microstructural characterization of HSLA-100 GMA-weldments
[AD-A187782] 11 p1457 N88-18683
Microstructural characterization of the heat affected zone of HSLA (High Strength Low Alloy)-100 steel GMA (Gas Metal Arc)-weldment
[AD-A187825] 11 p1457 N88-18686
Ensuring higher stability of immersed-arc welding of structural aluminum alloys and magnesium alloys
14 p1898 N88-21331
The effect of surface tension in the weld pool on seam formation when welding thin sheet with light rays
14 p1898 N88-21334
Welding torch gas cup extension
[NASA-CASE-MFS-29252-1] 17 p2345 N88-23980
Trailer shield assembly for a welding torch
[NASA-CASE-MFS-29260-1] 18 p2524 N88-24972
Ultrasonic and video computerized data acquisition for automated welding
[DE88-006741] 19 p2677 N88-25918
Physical-chemical reactions at welding arc/molten pool interfaces
[DE88-007717] 20 p2808 N88-26662
ARC length control for plasma welding
[NASA-CASE-MSC-20900-1] 24 p3380 N88-30131
ARCHAEOLOGY
Subsurface morphology and geoarchaeology revealed by spaceborne and airborne radar
17 p2353 N88-24022
Utilization of LANDSAT-TM , for aiding in the localization of archeological sites in the state of Sao Paulo
17 p2362 N88-24069
ARCHES
Reinforced cocnrete arches under blast and shock environments 09 p1180 N88-17065
ARCHITECTURE
Maximum entropy/optimal projection design synthesis for decentralized control of large space structures
[AD-A186359] 07 p0824 N88-15003
Helicopter crashworthiness research program
09 p1107 N88-16635
Finely grained parallelism in an applicative architecture
10 p1383 N88-18256
Introduction to a system for implementing neural net connections on SIMD architectures
[NASA-CR-181612] 10 p1386 N88-18279
Space Station Human Factors Research Review. Volume 3: Space Station Habitability and Function: Architectural Research
[NASA-CP-2426-VOL-3] 12 p1650 N88-19883
Space station architectural elements model study
[REPT-31799] 12 p1650 N88-19885
Real-time stressed channel simulator
[AD-A190223] 15 p2025 N88-22067
A direct-execution parallel architecture for the Advanced Continuous Simulation Language (ACSL)
[NASA-CR-182809] 15 p2115 N88-22602
Space station architectural elements and issues definition study
[NASA-CR-3941] 18 p2587 N88-25371
Comparative analysis of the space power architecture studies
[NASA-TM-100977] 22 p3049 N88-28090
Microsupercomputers: Design and implementation
[AD-A194712] 22 p3135 N88-28638
The triangle: A multiprocessor architecture for fast curve and surface generation
[AD-A195882] 24 p3414 N88-30324
Report to congress on the strategic defense system architecture
[AD-A195476] 24 p3426 N88-30393
Monte-Carlo estimation of the influence of plant architecture parameters on spectral brightness
24 p3450 N88-30533
ARCHITECTURE (COMPUTERS)
Digital system bus integrity
[NASA-CR-181446] 01 p0006 N88-10030
The varieties of capabilities in Flex
[RSRE-MEMO-4042] 01 p0078 N88-10500
Strategies for concurrent processing of complex algorithms in data driven architectures
[NASA-CR-181435] 01 p0082 N88-10527
A unified approach to parallel computation: Performance evaluation and architecturally independant parallel programming
[DE87-012519] 01 p0084 N88-10540
Fault tolerant considerations and methods for guidance and control systems
[AGARD-AG-289] 02 p0126 N88-10796
An expert system for aircraft conflict resolution in dense airspaces 02 p0129 N88-10810
An embedded multiprocessor computer for proof-of-principle testing of exploratory systems concepts
[DE87-012735] 02 p0218 N88-11372
Benchmarking the Connection Machine
[DE87-013500] 02 p0218 N88-11374
Memory systems for single bus multiprocessor architecture. Application to the SCQM system
[ENST-86E022] 02 p0219 N88-11379
Multi-processor architectures for artificial intelligence processing
[OUEL-1671/87] 02 p0219 N88-11380
Some 2-D WSI array architectures --- wafer scale integration (WSI)
[OUEL-1672/87] 02 p0219 N88-11381
Implementation of preconditioned s-step conjugate gradient methods on a multiprocessor system with memory hierarchy
[DE87-014401] 02 p0222 N88-11400
Summaries of the FY 1987 applied mathematical sciences research program
[DE87-014447] 02 p0225 N88-11416
Methodology of performance evaluation of real time distributed systems
[ENST-87D003] 02 p0228 N88-11440
The warp computer: Architecture, implementation, and performance
[AD-A184329] 03 p0363 N88-12286
SBNR (Signed Binary Number Representations) digital signal processor architecture
[AD-A184603] 03 p0364 N88-12290
Layering central authentication on the interactive services of an existing homogeneous distributed system
[DE87-011544] 03 p0366 N88-12304
Delft parallel processor 84/16
[PB87-226254] 03 p0366 N88-12305
Interfacing distributed operating systems
[AD-A184489] 03 p0366 N88-12306
Network reconstitution protocol
[AD-A184755] 03 p0367 N88-12309
A survey of artificial neural systems
[AD-A184759] 03 p0368 N88-12312
An object-oriented architecture for intelligent tutoring systems
[AD-A184790] 03 p0368 N88-12314
Low-level vision on warp and the apply programming model
[AD-A184330] 03 p0369 N88-12320
Implementation of the Runge-Kutta-Fehlberg method for solution of ordinary differential equations on a parallel processor
[AD-A184660] 03 p0370 N88-12331
Autonomous Land Vehicle (ALV) planning and navigation system
[AD-A184243] 04 p0397 N88-12475

An evaluation plan of bus architectures and protocols using the NASA Ames intelligent redundant actuation system
[NASA-CR-177458] 04 p0398 N88-12482

Programmable real-time digital video image processing
[PB87-104162] 04 p0430 N88-12661

On the VLSI design of a pipeline Reed-Solomon decoder using systolic arrays 04 p0436 N88-12700

Research in VLSI (Very Large Scale Integration) systems
[AD-A184089] 04 p0438 N88-12721

Center for Supercomputing Research and Development (CEDAR)
[DE88-000807] 04 p0475 N88-12930

Methods for design and evaluation of integrated hardware/software systems for concurrent computation
[NASA-CR-181522] 04 p0479 N88-12953

Parallelization of hydrocodes on the Intel Hypercube, part 2
[DE88-001591] 04 p0480 N88-12957

Utilization of a high rate vector computer in computational fluid mechanics for aeronautics
[ETN-88-91171] 05 p0581 N88-13547

Test and evaluation of the transputer in a multi-transputer system
[AD-A184969] 05 p0631 N88-13859

Arrays for discrete Fourier transform
[REPT-87-019] 05 p0632 N88-13861

XCUT: A rule-based expert system for the automated process planning of machined parts
[DE87-011638] 05 p0639 N88-13905

On real-time systems using local area networks
[AD-A185475] 06 p0694 N88-14256

Fast algorithms for structural optimization and least squares
[AD-A185766] 06 p0724 N88-14452

Objects architecture: A comprehensive design approach for real-time, distributed, fault-tolerant, reactive operating systems
[AD-A185476] 06 p0755 N88-14631

A taxonomy of analytical computer performance models for computer design
[AD-A185561] 06 p0755 N88-14632

Set of multi-process primitives for stack based machines
[PB87-234381] 06 p0756 N88-14636

Benchmarking and evaluation of hardware description languages for design of VLSI systems
[PB87-134557] 06 p0758 N88-14648

Wide-area communication under Amoeba
[PB87-234431] 06 p0760 N88-14665

Computer architectures for artificial intelligence
[PB87-123824] 06 p0761 N88-14671

National Aeronautics and Space Administration (NASA)/American Society for Engineering Education (ASEE) Summer Faculty Fellowship Program, 1987, Volume 2
[NASA-CR-172009-VOL-2] 06 p0796 N88-14874

A general architecture for intelligent training systems
06 p0796 N88-14875

Fault-tolerant computer architecture based on INMOS transputer processor 06 p0797 N88-14880

Study of communication options in a distributed data handling system and survey of advanced man machine communications schemes. Work package 1: Interprocess communication
[ESA-CR(P)-2447] 07 p0843 N88-15114

Reliability modelling for fault-tolerant parallel processor
[AD-A185867] 07 p0900 N88-15451

An interactive visual interface for Fastbus diagnostics
[DE88-002569] 07 p0900 N88-15453

UNITY: A framework for study of parallel programming problem-solving
[AD-A185616] 07 p0906 N88-15490

Image understanding by Image-Seeking Adaptive Networks (ISAN)
[AD-A186214] 07 p0906 N88-15492

Integration of symbolic and algorithmic hardware and software for the automation of space station subsystems
[NASA-TM-89705] 07 p0907 N88-15497

Correctness proofs for systolic algorithms: Palindromes and sorting
[PB88-106075] 07 p0912 N88-15534

Modeling of architecture of a problem-oriented on-board processor 08 p1008 N88-16114

An easy-to-use diagnostic system development shell
08 p1055 N88-16366

A distributed architecture for intelligent monitoring and anomaly diagnosis of the Hubble Space Telescope
08 p1057 N88-16379

Development of a task-level robot programming and simulation system 08 p1058 N88-16387

A multiprocessing architecture for real-time monitoring
08 p1059 N88-16390

Application of parallel distributed processing to space based systems 08 p1059 N88-16393

Knowledge-based simulation
08 p1061 N88-16404

Similarity networks as a knowledge representation for space applications 08 p1062 N88-16411

Conceptual information processing: A robust approach to KBS-DBMS integration 08 p1063 N88-16422

Neural networks as a possible architecture for the distributed control of space systems
08 p1064 N88-16431

A learning apprentice for software parts composition
08 p1065 N88-16436

Information handling architecture and software for CIM (Computer Integrated Manufacturing)
[PB88-105820] 08 p1067 N88-16453

Prospectus for the development of a linear algebra library for high-performance computers
[DE88-003715] 08 p1068 N88-16457

High performance VLSI algorithms and architectures for digital signal processing 09 p1155 N88-16926

First Annual Workshop on Space Operations Automation and Robotics (SOAR 87)
[NASA-CP-2491] 09 p1203 N88-17206

Design of a neural network simulator on a transputer array 09 p1205 N88-17221

Communications patterns in a symbolic multiprocessor
[AD-A186896] 09 p1215 N88-17282

Supercomputers for solving PDE (Partial Differential Equations) problems
[AD-A186583] 09 p1215 N88-17283

High performance data buses: Progress and evolution
[DE88-002570] 09 p1215 N88-17285

Rationale for the design of the Ada (tradename) programming language
[AD-A187106] 09 p1217 N88-17297

A multithreaded processor architecture for parallel symbolic computation
[AD-A187034] 09 p1222 N88-17327

A type-oriented approach to knowledged-based systems
[MA-47] 09 p1222 N88-17329

Horizontal estimation and information fusion in multitarget and multisensor environments
[AD-A186935] 09 p1224 N88-17336

Proceedings of the Workshop on Future Directions in Computer Architecture and Software
[AD-A184949] 10 p1373 N88-18191

Some further observations about reduced instruction set computers 10 p1373 N88-18192

An empirical analysis of the Lilith instruction set
10 p1373 N88-18193

High-performance CPU implementation of the nebula instruction set architecture 10 p1373 N88-18194

The arithmetic cube and its associated algorithms
10 p1374 N88-18195

Automatically reconfigurable computer architecture
10 p1375 N88-18204

A large-grain dataflow architecture
10 p1375 N88-18207

A distributed system architecture based on macro dataflow model 10 p1376 N88-18210

Future directions in computer architecture and software: The year 2000 10 p1377 N88-18218

An investigation of parallelism in rule based systems
10 p1377 N88-18223

A parallel computer based on cube connected cycles
10 p1378 N88-18227

Performance evaluation of a loop interconnection structure 10 p1378 N88-18229

Aspects of a multiprocessor architecture
10 p1379 N88-18232

Strategies for concurrent processing of complex algorithms 10 p1379 N88-18236

Parallel architectures for logic programming
10 p1380 N88-18241

Real time artificial intelligence architecture
10 p1380 N88-18242

Future directions in computer architecture
10 p1383 N88-18257

Future directions in computer architecture and software workshop 10 p1383 N88-18258

A performance analysis of architectural scalability
[DE88-003537] 10 p1383 N88-18261

Emerging supercomputer architectures
[DE88-003539] 10 p1384 N88-18262

Supercomputer performance: The theory, practice, and results
[DE88-004697] 10 p1384 N88-18266

Systolic array adaptive beamforming
[AD-A187496] 10 p1385 N88-18269

MICRO system for control, acquisition and processing of experimental data
[DE88-700724] 10 p1386 N88-18278

Using program structure to achieve prefetching for cache memories
[DE88-003599] 10 p1387 N88-18282

CUEMAP: A tool for generating hierarchical charts and dataflow diagrams
[DE88-004778] 10 p1387 N88-18284

Programming methodology and performance issues for advanced computer architectures
[DE88-003098] 10 p1387 N88-18287

Implementation and analysis of a Navier-Stokes algorithm on parallel computers
[NASA-CR-181614] 10 p1390 N88-18301

A framework for evaluating computer architectures to support systems with security requirements, with applications
[AD-A187082] 10 p1392 N88-18303

An Ethernet local area network controller with supporting operating system software
[DE88-003534] 10 p1392 N88-18304

Dynamic processor self-scheduling for general parallel nested loops
[DE88-003572] 10 p1393 N88-18311

Parallel garbage collection on a virtual memory system
[DE88-003567] 10 p1396 N88-18317

The implementation of artificial intelligence in control systems
[DE88-003497] 10 p1396 N88-18318

Performance and evaluation at the Center for Supercomputing Research and Development
[DE88-003563] 10 p1417 N88-18456

Center for Supercomputing Research and Development
[DE88-003564] 10 p1418 N88-18466

Fuzzy logic inference processor for real time control: A second generation full custom design
[AD-A188155] 11 p1471 N88-18773

A comparison of VLSI architectures for time and transform domain decoding of Reed-Solomon codes
11 p1472 N88-18783

Modules of nanosecond logic electronics system with computer control
[DE88-700190] 11 p1479 N88-18828

Computer architecture for research in meteorology and atmospheric chemistry
[PB88-145313] 11 p1510 N88-19020

Optical symbolic processor for expert system execution
[AD-A187882] 11 p1525 N88-19103

Measurement and analysis of memory conflicts on vector multiprocessors
[AD-A188206] 11 p1525 N88-19104

Modular CAMAC system, 2
[DE88-700237] 11 p1525 N88-19106

Feasibility study of generating plans and strategies for software testing by knowledge based system
[AD-A187834] 11 p1529 N88-19134

Parallel processing in nonlinear programming
[INPE-4298-PRE/1169] 11 p1533 N88-19158

Object recognition on a systolic array
[AD-A187726] 11 p1534 N88-19164

Performance of a multigrid method on parallel architecture 11 p1539 N88-19200

Theory and practice of fault tolerance in distributed systems
[AD-A187559] 11 p1540 N88-19204

Optical computing research
[AD-A187862] 11 p1549 N88-19264

VSLI design generators
[AD-A188706] 12 p1623 N88-19707

Architecture with parallel processing for incremental computation
[INPE-4326-PRE/1178] 12 p1675 N88-20012

Efficient parallel architecture for highly coupled real-time linear system applications
[NASA-CR-182649] 12 p1675 N88-20015

Computer architecture for efficient algorithmic executions in real-time systems: New technology for avionics systems and advanced space vehicles
[NASA-CR-182650] 12 p1675 N88-20016

BLITZ: Blitzen's micron-code assembly language design document, version 1.0
[TR88-14] 12 p1676 N88-20019

An emulation tool for simulating matrix operations on an SIMD (Single Instruction Multiple Data stream) multiprocessor
[AD-A188654] 12 p1678 N88-20030

A laboratory facility for research in parallel computation
[AD-A188499] 12 p1680 N88-20044

Northeast Artificial Intelligence Consortium (NAIC) administrative matters and ancillary functions, volume 1
[AD-A189466] 12 p1682 N88-20055

NAVLAB: An autonomous navigation testbed
[AD-A189049] 13 p1720 N88-20283

Architecture specification for PAVE PILLAR avionics
[AD-A188722] 13 p1723 N88-20303

Analysis for architecture for image processing
[INPE-4294-PRE/1165] 13 p1791 N88-20715

Spectral element methods: Algorithms and architectures
[NASA-CR-182701] 13 p1820 N88-20876

Distributed transaction processing and the Camelot system
[AD-A188614] 13 p1821 N88-20885

A simulation study of a parallel processor with unbalanced loads
[AD-A189573] 13 p1822 N88-20887

On the design of parallel numerical methods in message passing and shared memory environments
[DE88-003566] 13 p1822 N88-20888

Locality, communication and interconnect length in multicomputers
[CWI-CS-R8708] 13 p1822 N88-20890

Soar: An architecture for general intelligence
[AD-A188742] 13 p1823 N88-20898

Towards a tribology information system: The results of a Planning Workshop held at the National Bureau of Standards, July-August 1985
[PB88-168604] 14 p1918 N88-21448

Activities and operations of the Advanced Computing Research Facility, October 1986-October 1987
[DE88-006223] 14 p1955 N88-21653

Proposal for a parallel system with image processing applications
[INPE-4293-PRE/1164] 14 p1961 N88-21696

Adaptive neural network architecture
[AD-A190114] 15 p2104 N88-22533

Parallel memory addressing using coincident optical pulses
[AD-A189767] 15 p2106 N88-22547

Multiple-transform pipelines for image coding
[REPT-87-038] 15 p2108 N88-22561

An analysis of multiple grain CHiP architectures
[AD-A189942] 15 p2110 N88-22570

Transformations of concurrent algorithms for highly parallel systems: A one year project summary report
[AD-A190236] 15 p2111 N88-22576

Inference engine for expert systems
[INPE-4465-TDL/321] 15 p2113 N88-22590

Modeling a parallel architecture for image processing
[RR-646-I] 15 p2114 N88-22593

Simulation of fault tolerance in a hypercube arrangement of discrete processors
[AD-A189682] 15 p2114 N88-22594

The modeling, simulation and comparison of interconnection networks for parallel processing
[AD-A190571] 15 p2115 N88-22599

Design and implementation of a parallel computer for expert system applications
[DE88-005288] 15 p2115 N88-22601

Concurrent algorithms for a mobile robot vision system
[DE88-005850] 15 p2117 N88-22614

High speed transcendental elementary function architecture in support of the Vector Wave Equation (VWE)
[AD-A189746] 15 p2119 N88-22627

Space-variant optical systems
[AD-A189967] 15 p2133 N88-22724

Application of new technologies to DTIC document processing
[AD-A189778] 15 p2148 N88-22823

A methodolgy, based on analytical modeling, for the design of parallel and distributed architectures for relational database query processors
[AD-A189844] 15 p2149 N88-22825

New generation knowledge processing, volume 1
[AD-A190165] 15 p2149 N88-22826

Algorithms and architectures for acoustic phonetical detection of continuous speech
[ENST-87E016] 16 p2189 N88-23054

Strategies for concurrent processing of complex algorithms in data driven architectures
[NASA-CR-181657] 16 p2193 N88-23083

Parallel computer methods for eigenvalue extraction
16 p2213 N88-23233

Microgravity manipulator demonstration
16 p2219 N88-23242

Fundamentals of microprocessor-based design: A tutorial, second edition
[DE88-006761] 16 p2244 N88-23406

Design of high yield microprocessors
[ETN-88-92184] 16 p2245 N88-23410

Synthesis and simulation of systolic algorithms
[ETN-88-92183] 16 p2247 N88-23423

Intelligent systems interconnection: What should come after open systems interconnection?
[CWI-CS-R8742] 16 p2253 N88-23465

New generation knowledge processing, volume 2
[AD-A190166] 16 p2285 N88-23681

Architecture and role of the Sensor Subsystem in future aircraft weapon systems 17 p2302 N88-23770

Rapid prototyping of complex avionic system architectures 17 p2302 N88-23771

Development of a generic architecture
17 p2303 N88-23774

Test philosophy of the EH101 integrated avionic
17 p2303 N88-23775

The avionics software architecture impact on system architecture 17 p2303 N88-23778

A software life cycle support environment
17 p2306 N88-23800

Evolution of a family of image processing systems at INPE 17 p2361 N88-24065

Integration of symbolic and algorithmic hardware and software for the automation of space station subsystems
17 p2387 N88-24190

TALOS: A distributed architecture for intelligent monitoring and anomaly diagnosis of the Hubble Space Telescope 17 p2388 N88-24193

Models and metrics for software management and engineering
[NASA-CR-182953] 17 p2389 N88-24200

A five-layer Open Systems Interconnection (OSI) implementation 17 p2390 N88-24204

Adaptive local grid refinement in computational fluid mechanics
[AD-A192215] 18 p2510 N88-24890

Tutorial on computer control
[DE88-006185] 18 p2554 N88-25157

The -mdoc macro package: A software tool to support computer documentation standards
[DE88-000500] 18 p2559 N88-25188

Algorithms and software for solving finite element equations on serial and parallel architectures
[NASA-CR-183027] 18 p2559 N88-25191

Network architecture for OPS5
[DE88-002802] 18 p2560 N88-25194

The ATF (Advanced Toroidal Facility) Data M Management System
[DE88-007265] 18 p2589 N88-25385

SAMS: The synchronization and monitoring system for ATF (Advanced Toroidal Facility) data acquisition provides unified data access for ATF data acquisition
[DE88-007268] 18 p2589 N88-25386

Signal processing computational needs
[AD-A191756] 19 p2642 N88-25674

Algorithmic generation of feasible system architectures
[AD-A191722] 19 p2713 N88-26106

Multidimensional nodal transport methods for multiple-instruction multiple-data distributed memory machines
[DE88-004732] 19 p2713 N88-26108

Intermediate level computer vision processing algorithm development for the content addressable array parallel processor
[AD-A192086] 19 p2714 N88-26111

Effective communication between a microVAX and a specialized high-speed subprocessor
[DE88-007967] 19 p2714 N88-26115

Logic and fault simulation on the Mach1000 hardware accelerator
[DE88-009794] 19 p2717 N88-26130

Analysis and synthesis of decision-making organizations
[AD-A191948] 19 p2738 N88-26258

The UMAC simulator 20 p2834 N88-26811

Research in VLSI computer systems
[AD-A192915] 20 p2835 N88-26816

Design of high performance microcomputers for numerical data processing
[ETN-88-92371] 20 p2835 N88-26818

The scaled-sized model: A revision of Amdahl's law
[DE88-008114] 20 p2844 N88-26875

An investigation of performance improvement in knowledge-based control systems
21 p2928 N88-27382

Computational fluid dynamics on parallel processors
[AD-A192397] 21 p2941 N88-27469

A demonstration of retro-traverse using a semi-autonomous land vehicle
[DE88-009851] 21 p2957 N88-27568

Assessing and enhancing human performance: Utility of a workstation network
[AD-A192840] 21 p2991 N88-27743

MINIAC: A small embedded computer
[DE88-008142] 21 p2994 N88-27757

Research into the architecture of CAD based robot vision systems
[AD-A193330] 21 p2997 N88-27776

Software engineering guidelines for RASP and ANDECS: Requirements and architectural design
[DFVLR-MITT-88-07] 21 p3000 N88-27793

FORTRAN 77 implementation of abstract datatype models
[DFVLR-MITT-88-08] 21 p3000 N88-27794

Image processing using a parallel architecture
[AD-A192833] 21 p3002 N88-27803

Notes on operating system requirements for the next millennium
[DE88-010712] 21 p3002 N88-27805

Neural network research: A personal perspective
[AD-A192717] 21 p3003 N88-27808

Parallel quasi-Newton methods for unconstrained optimization
[AD-A193250] 21 p3003 N88-27812

What have we learnt from using real parallel machines to solve real problems
[DE88-011227] 22 p3135 N88-28636

Configuration control in compiler construction
[AD-A193916] 22 p3135 N88-28639

Survey of neural net paradigms for specification of discrete networks
[AD-A192682] 22 p3141 N88-28674

Dynamic resource allocation in a hierarchical multiprocessor system: A preliminary study
[NASA-CR-183177] 22 p3141 N88-28675

Method for Veterbi decoding of large constraint length convolutional codes
[NASA-CASE-NPO-17310-1-CU]
23 p3183 N88-28946

Hierarchical organization for large, dynamic radio networks
[AD-A193942] 23 p3204 N88-29067

Systolic array fault tolerance performance analysis
[AD-A193521] 23 p3244 N88-29306

Nanosequencer digital logic controller
[NASA-CASE-NPO-16116-2] 23 p3245 N88-29310

Solving the symmetric tridiagonal eigenvalue problem on the hypercube
[AD-A193905] 23 p3250 N88-29344

Issues on the use of meta-knowledge in expert systems 23 p3252 N88-29357

DAISY-DAMP: A distributed AI system for the dynamic allocation and management of power
23 p3254 N88-29373

ARGES: An expert system for fault diagnosis within space-based ECLS systems 23 p3255 N88-29380

SCARES: A Spacecraft Control Anomaly Resolution Expert System 23 p3256 N88-29381

Programming model for distributed intelligent systems
23 p3257 N88-29390

Blackboard architectures and their relationship to autonomous space systems 23 p3261 N88-29414

Validation of expert systems 23 p3262 N88-29416

Semantic based man-machine interface for real-time communication 23 p3262 N88-29421

Networking and AI systems: Requirements and benefits 23 p3263 N88-29425

Expert system technology as a data processing tool
23 p3263 N88-29427

A performance study of the hypercube architecture
[AD-A194361] 23 p3264 N88-29433

Optimisation algorithms for highly parallel computer architectures. The performance of the truncated Newton, conjugate gradient algorithm in FORTRAN and Ada
[AD-A193940] 23 p3265 N88-29435

Adaptive identification by systolic arrays
[AD-A193532] 23 p3266 N88-29444

Strategic defense initiative architecture dataflow modeling technique version 1.5
[AD-A194356] 23 p3275 N88-29494

A multiprocessor avionics system for an unmanned research vehicle
[AD-A194806] 24 p3325 N88-29800

N-version software demonstration for digital flight controls
[NASA-CR-181483] 24 p3328 N88-29815

Acoustooptic processing of two-dimensional signals using temporal and spatial integration
[AD-A194803] 24 p3359 N88-29999

A model for architectural comparison
[AD-A195993] 24 p3411 N88-30302

The design of an intelligent multidisk control module for VME bus based systems
[AD-A195587] 24 p3411 N88-30303

Scheme86: A system for interpreting SCHEME
[AD-A195931] 24 p3413 N88-30319

Automated satellite control in Ada
24 p3416 N88-30336

MOORE: A prototype expert system for diagnosing spacecraft problems 24 p3418 N88-30343

A standard architecture for controlling robots
[AD-A195929] 24 p3423 N88-30371

Architecture for optical digital computers
[AD-A195477] 24 p3430 N88-30416

Integrating information systems in a major decentralized international organization, volume 7
[AD-A195856] 24 p3439 N88-30468

ARCS
Numerical arc segmentation algorithm for a radio conference: A software tool for communication satellite systems planning
[NASA-TM-100789] 16 p2167 N88-22919
ARCTIC ENVIRONMENTS
U ICE ENVIRONMENTS
ARCTIC OCEAN
Eastern - western Arctic Sea ice analysis 1986
[AD-A184016] 03 p0355 N88-12235
Physical and structural characteristics of Weddell Sea pack ice
[AD-A188189] 10 p1358 N88-18119
Predictions and studies with a one-dimensional ice/ocean model
[AD-A189158] 13 p1803 N88-20776
Microwave and structural properties of saline ice
[AD-A189307] 13 p1803 N88-20779
Higher frequency ambient noise in the arctic ocean
[AD-A192203] 18 p2547 N88-25122
Arctic ice island and sea ice movements and mechanical properties
[DE88-004267] 20 p2829 N88-26782
Arctic ice attenuation model study
[AD-A193382] 22 p3146 N88-28715
Sea ice processes
[AD-A193980] 23 p3237 N88-29262
ARCTIC REGIONS
On the surging potential of polar ice streams. Antarctic surges: A clear and present danger
[DE87-013980] 02 p0216 N88-11363
Underwater acoustic backscatter from a model of arctic ice open leads and pressure ridges
[AD-A184693] 03 p0354 N88-12234
Huurre expedition to the North Pole in 1984
[PB87-220935] 04 p0462 N88-12858
Disturbance and recovery of Arctic Alaskan tundra terrain. A review of recent investigations
[AD-A184442] 04 p0467 N88-12887
USSR report: Earth sciences
[JPRS-UES-87-004] 06 p0725 N88-14455
A 1,000-watt solar power unit for Far North
06 p0728 N88-14481
Neogene paleoclimate in Pacific Ocean subarctic region determined from study of diatoms
08 p1010 N88-16125
Rocket experiments and payloads for Super CAMP --- Cold Arctic Mesopause Project (CAMP)
08 p1034 N88-16271
Physical and structural characteristics of Weddell Sea pack ice
[AD-A188189] 10 p1358 N88-18119
Activities and objectives of the Polar Research Board
[DE88-004543] 13 p1797 N88-20747
Analysis of meteorological conditions and haze distribution for the Second Arctic Gas and Aerosol Sampling Program (AGASP 2), March-April 1986
[PB88-164140] 14 p1948 N88-21618
Real-time environmental Arctic monitoring (R-TEAM)
[AD-A189948] 15 p2099 N88-22508
An investigation of Soviet capabilities in extended range arctic ice forecasting
[AD-A191082] 17 p2376 N88-24127
Sea ice kinematics: Space and time scales
[AD-A191162] 17 p2376 N88-24128
Higher frequency ambient noise in the arctic ocean
[AD-A192203] 18 p2547 N88-25122
A modal approach to Arctic noise modelling with implied vertical coherence
[AD-A192966] 20 p2850 N88-26916
Arctic ice attenuation model study
[AD-A193382] 22 p3146 N88-28715
The spatial and temporal variability of the arctic atmospheric boundary layer and its effect on electromagnetic (EM) propagation
[AD-A193958] 23 p3204 N88-29068
An objective technique for Arctic cloud analysis using multispectral AVHRR (Advanced Very High Resolution Radiometer) satellite imagery
[AD-A194732] 23 p3235 N88-29250
Reflection and scattering of acoustic rays computed for parabolic ice keel models
[AD-A193898] 23 p3278 N88-29517
AREA
Computer modeling for surface properties of carbon fibers 21 p2928 N88-27383
Determination of the specific area of liquid gas and the velocity of weak pressure waves in aqueous foams
[NASA-TT-20347] 24 p3373 N88-30087
AREA NAVIGATION
Observed track-keeping performance of DC10 aircraft equipped with the Collins AINS-70 area navigation system: Karlsruhe and Masstricht UACs (Upper Area Control centres)
[EEC-202] 24 p3323 N88-29788
ARGON
NT ARGON ISOTOPES
Comparative tests of high temperature creep-rupture behavior of the austenitic CrNi steel DIN W.NR.1.4970 in argon and steam
[KFK-4261] 01 p0063 N88-10402
Extreme ultraviolet beam-foil spectroscopy of highly ionized neon and argon
[AD-A185197] 05 p0561 N88-13418
Rovibrational spectroscopy of ArCO van der Waals complex
[DE88-004291] 10 p1406 N88-18387
Two-photon (VUV and visible) resonant ionization spectroscopy of atoms and molecules
[DE88-004332] 10 p1407 N88-18388
Electron stimulated desorption and coherent electron scattering
[AD-A189091] 13 p1605 N88-20978
Kinetics of slow electrons in excimer laser with electron-beam pumping 14 p1970 N88-21760
Question on the measurement of the metal work function in an electron spectrometer by the secondary-electron emission threshold method
[NASA-TT-20190] 16 p2178 N88-22979
Thermophysical properties of argon
[DE88-010376] 19 p2613 N88-25509
ARGON ISOTOPES
Prospects for large dynamic range isotope analysis using photon burst mass spectrometry
[DE88-009110] 19 p2613 N88-25505
ARGON LASERS
Photocurrent generation from basic metals, utilizing a short pulsed ArF excimer laser
[AD-A184928] 05 p0587 N88-13579
Mirrors for high-power continuous-wave Ar-lasers
09 p1235 N88-17404
Psychophysical, biochemical and histological studies of spectrally selective photic damage to primate retina
[AD-A188115] 11 p1517 N88-19063
Resonator coupling of two ring cavity, argon-ion lasers
[AD-A189558] 13 p1775 N88-20616
Doubly periodic output from a dye laser pumped by a free-running argon laser
[DE88-005027] 13 p1778 N88-20633
The interaction of small particles with laser beams
[AD-A190716] 15 p2072 N88-22354
Design and preliminary evaluation of an underwater laser-based imaging system
[DE88-010560] 19 p2675 N88-25908
ARGON PLASMA
Investigations on an RF plasma related to plasma etching
[ETN-88-91366] 06 p0784 N88-14809
Laser thermal propulsion
[AD-A186407] 07 p0933 N88-15666
Electron temperature measurements in an argon/cesium plasma diode
[AD-A188835] 12 p1695 N88-20141
Modeling of atomic processes in X-ray laser plasmas
[AD-A194118] 23 p3286 N88-29567
Energy conversion measurements in laser-sustained argon plasmas for application to rocket propulsion
[AD-A194931] 24 p3337 N88-29861
ARGOS SYSTEM
Mini-station for VHF reception. Argos system simplified description
[INPE-4551-NTE/279] 19 p2655 N88-25764
ARGUMENTS (MATHEMATICS)
U INDEPENDENT VARIABLES
ARIANE LAUNCH VEHICLE
Telemetry conditioning units for the European launcher Ariane 01 p0012 N88-10068
Study of advanced satellite concept using a multifeed reconfigurable antenna
[ESA-CR(P)-2406-VOL-1] 01 p0013 N88-10073
Study of advanced satellite concept using a multifeed reconfigurable antenna. Detailed report on mission definition, coverage analysis and performance requirements, antenna geometry
[ITS-TR-014.C/85] 01 p0013 N88-10074
Study of advanced satellite concept using a multifeed reconfigurable antenna. Appendix 3 : Feeding network, final performance analysis, study of reconfiguration possibilities
[ITS-TR-032/85] 01 p0014 N88-10076
Introduction to local area network design on Ariane 5 and future launchers
[SNIAS-872-422-102] 05 p0635 N88-13886
Aerodynamic design and test performance of supersonic turbines for the Vulcain rocket engine
06 p0713 N88-14373
Ariane localization technique by Data Relay Satellite (DRS)
[SES/ENG/TN-548/86] 08 p0961 N88-15821
The TV-SAT/TDF/TELE-X pyrotechnical system
[CNES-87/CT/DRT/TVE/IL/358]
08 p0974 N88-15891
Ariane 4, long version: Pressure distribution measurements on two models of different scale of the Ariane 4 nose fairings in the transonic tunnel of F+W Emmen (Switzerland) with varying tunnel configurations. Comparison with measurements taken at Modane (France) and with calculations after the Euler method
[F+W-TF-1878] 09 p1122 N88-16716
Launch vehicle vibration: Measures taken to avoid pogo on ESA's Ariane launch vehicle
09 p1123 N88-16727
ESA Bulletin No. 15: Ariane, the European launcher for the 1980's
[ESA-BULLETIN-NO-15] 09 p1125 N88-16741
The Ariane launcher and its progress
09 p1125 N88-16742
Ariane launch performance 09 p1125 N88-16743
Increased performance for Ariane
09 p1125 N88-16744
SYLDA: A dual-launch system for Ariane
09 p1125 N88-16745
The Ariane launch base 09 p1126 N88-16746
Altitude simulation testing of Ariane's second-stage engine 09 p1126 N88-16747
Mechanical in-flight environment of Ariane payloads
09 p1126 N88-16748
Dynamic tests of the Ariane launch vehicle
09 p1126 N88-16749
Integration testing of the propulsion system of Ariane's first stage 09 p1126 N88-16751
Stage separation testing of Ariane
09 p1126 N88-16752
The HM-7 engine of Ariane's third stage
09 p1126 N88-16753
The Ariane fairing and its separation systems
09 p1126 N88-16754
ESA Bulletin No. 25
[ISSN-0376-4265] 09 p1128 N88-16767
The Ariane-3 program 09 p1128 N88-16771
Ariane 4 pyrotechnics system: Definition of the chains and pyrotechnic devices
[CNES-88/CT/DRT/TVE/IL/25]
17 p2310 N88-23816
Reaching for the skies: The Ariane family story and beyond. An introduction to Europe's successful series of space transportation systems
[ESA-BR-42] 22 p3046 N88-28078
The Ariane line 22 p3161 N88-28828
The Ariane 5 program management specifications
22 p3162 N88-28829
Ariane 5, HERMES and European vehicles for space station servicing
[SNIAS-881-422-102] 23 p3183 N88-28943
Simulation of Vulcain engine operation at low inlet pressure
[ETN-88-93083] 24 p3339 N88-29875
ARID LANDS
Remote Sensing-Arid Lands Workshop, Page, Arizona, June 10-12, 1986
[DE87-012368] 01 p0064 N88-10412
The use of SPOT images for water resources surveys. The examples of the Kasserine area (Tunisia) and the Jebel Amour (Algeria) 03 p0345 N88-12179
Desertification in the Sahelian and Sudanian Zones of West Africa
[PB87-217063] 03 p0345 N88-12183
Semi-arid ecosystem development as a function of resource processing and allocation
[DE88-000890] 07 p0875 N88-15306
Improved canopy reflectance modeling and scene inference through improved understanding of scene pattern
[NASA-CR-182488] 10 p1347 N88-18049
Preliminary analyses of SPOT HRV multispectral products for arid and temperate environments
22 p3099 N88-28407
ARIP (IMPACT PREDICTION)
U COMPUTERIZED SIMULATION
U IMPACT PREDICTION
ARITHMETIC
NT FLOATING POINT ARITHMETIC
Implementation of a digital optical matrix-vector multiplier using a holographic look-up table and residue arithmetic
[NASA-CR-180431] 01 p0078 N88-10496
A programmable global system for the manipulation of residue numbers
[ETN-88-91476] 11 p1530 N88-19139
ARITHMETIC AND LOGIC UNITS
The arithmetic cube and its associated algorithms
10 p1374 N88-18195
The design of ultra high-speed numeric intensive systems (having fault tolerant and load balancing capabilities) 10 p1374 N88-18196

Fast serial input-serial output pipelined inner product units
[REPT-87-031] 11 p1530 N88-19142

ARIZONA

A Workshop on Desert Processes, September 24-28, 1984: Report on the conference
[AD-A184599] 03 p0345 N88-12184

ARM (ANATOMY)

Determination of the effect of walking on the forced convective heat transfer coefficient using an articulated mannikin
[AD-A186452] 08 p1049 N88-16335

Free boundary problems arising in the control of a flexible robot arm
[AD-A189124] 12 p1634 N88-19781

A three dimensional non-singular modelling of rigid manipulators
[AD-A189707] 15 p2116 N88-22604

ARMATURES

Exact solutions to the governing dynamic equations of plasma armature electromagnetic railguns
[DE87-014442] 01 p0011 N88-10063

The method of rigid armature flux orientation for the field-oriented control of highly dynamic drives with synchronous machines
[ETN-87-90405] 01 p0042 N88-10269

On the glitches in the force transmitted by an electrodynamic exciter to a structure
05 p0594 N88-13624

A laboratory railgun for terminal ballistics and arc armature research studies
[AD-A187225] 11 p1442 N88-18603

Structural integrity of metallic armature rail guns
[AD-A188735] 13 p1728 N88-20333

Analytic solutions to dynamic equations of plasma armature railguns
[DE88-006842] 15 p2023 N88-22057

Fundamental limits to the velocity of solid armatures in railguns 18 p2469 N88-24656

Why plasma armature railguns don't work (and what can be done about it)
[DE88-007900] 20 p2763 N88-26384

Plasma armature formation in high-pressure, high-velocity hydrogen
[DE88-008347] 20 p2857 N88-26967

ARMED FORCES

NT ARMED FORCES (FOREIGN)
NT ARMED FORCES (UNITED STATES)
NT NAVY

Land campaign force assessment. Methods used in Central-Europe-study
[FOA-C-10288-9.3] 06 p0768 N88-14723

ARMED FORCES (FOREIGN)

Corrosion in avionics and associated equipment; cause, effect and prevention 05 p0547 N88-13335

Soviet military power, 1987 13 p1858 N88-21114

Fire retardant coatings for military equipment: A review
[MRL-R-1104] 19 p2619 N88-25540

ARMED FORCES (UNITED STATES)

Military needs and forecast, 2
01 p0015 N88-10087

Cost savings possible with Air Force conversion to JP-8 as its primary fuel
[AD-A183784] 01 p0030 N88-10192

Transactions of the 4th Army Conference on Applied Mathematics and Computing
[AD-A183544] 01 p0085 N88-10547

Turbine engine supportability study for Army Aviation Systems Command (AVSCOM)
[DE88-002339] 07 p0820 N88-14984

Relating service doctrine to space system requirements
[AD-A186620] 08 p1074 N88-16483

Brain potentials and personality: A new look at stress susceptibility
[AD-A186931] 09 p1199 N88-17189

IMIS: Integrated Maintenance Information System. A maintenance information delivery concept
09 p1203 N88-17207

Evaluating software testing methods to reduce testing duplication in US Army communications equipment acquisition
[AD-A186961] 09 p1216 N88-17292

Sampling intervals
[AD-A189445] 12 p1573 N88-19408

Digital Topographic Support System (DTSS)
[AD-A188304] 12 p1638 N88-19808

Soft maps for US Army electronic map background applications
[AD-A188427] 12 p1638 N88-19809

Implementing information systems/office automation in an Air Force environment
[AD-A188956] 12 p1707 N88-20218

An overview of the army GIS (Geographic Information Systems) Research Program
[AD-A189711] 14 p1992 N88-21871

The Engineer Studies Center guide to research and data collection
[AD-A189971] 16 p2285 N88-23680

Defense Small Business Innovation Research Program (SBIR). Volume 3: Air Force abstracts of phase 1 awards, 1987 17 p2448 N88-24548

Management and the executive
[AD-A190778] 18 p2587 N88-25374

Department of Defense Statement on the Technology Base to the Subcommittee on Defense Industry and Technology of the Committee on Armed Services, United States Senate, 100th Congress, second session
[AD-A191839] 18 p2588 N88-25376

The Army's role in space: Support for the battlefield commander
[RAND-P-7396] 19 p2721 N88-26159

Army space systems for terrestrial applications
[AD-A192735] 21 p2965 N88-27613

Stress/fatigue and the ARNG (Army National Guard) aviator
[AD-A194184] 22 p3132 N88-28621

Tactical air force night/adverse weather training
[AD-A194243] 22 p3133 N88-28625

Stress and the military pilot
[AD-A194313] 22 p3133 N88-28626

Proposed improvements to the USAF flight screening program
[AD-A194506] 23 p3240 N88-29285

Validity of the academic aptitude composite of the Air Force Officer Qualifying Test (AFOQT)
[AD-A194753] 23 p3240 N88-29286

Reliability and construct validity of reaction time, inspection time and machine-paced tests of cognitive speed
[AD-A193779] 23 p3241 N88-29289

SSTS (Space Surveillance and Tracking System): The importance of early test and evaluation organizational participation
[AD-A193745] 23 p3276 N88-29499

Centralized class A flight mishap investigation
[AD-A194397] 24 p3322 N88-29786

ARMOR

Weldability of 2219-T851 and 2519-T87 aluminum armor alloys for use in Army vehicle systems
[AD-A184296] 04 p0451 N88-12792

Numerical simulations of impact tests on a rigid wall --- armor steel
[SNIAS-872-320-102] 05 p0610 N88-13744

Short fiber reinforced thermoplastic composites for armor applications: Interfacial bonding
[DE88-004007] 10 p1295 N88-17742

Crack arrest fracture toughness of armor steels
[AD-A187711] 11 p1456 N88-18681

Hydrogen induced cracks in armor steel weldments fabricated with austenitic filler alloys
[AD-A188733] 13 p1740 N88-20406

Texture profile in thermomechanically processed 2-inch-thick 5 Ni-steel armor plate
[AD-A189275] 13 p1741 N88-20410

Fit evaluation of female body armor
[AD-A188721] 14 p1953 N88-21638

Armoured vehicle track elastomers: Research and development at MRL
[MRL-GD-0012] 19 p2620 N88-25541

Ballistic evaluation of applique armours: Presentation and interpretation of ballistic data
[MRL-TN-527] 19 p2635 N88-25629

AROMATIC COMPOUNDS

Ethynylated aromatics as high temperature matrix resins
[NASA-TM-89829] 11 p1450 N88-18640

ARRAYS

NT ANTENNA ARRAYS
NT LINEAR ARRAYS
NT PHASED ARRAYS
NT SOLAR ARRAYS
NT STEERABLE ANTENNAS
NT SYNTHETIC ARRAYS
NT SYSTOLIC ARRAYS

Methodology for control and operation of wind arrays in utility systems
[DE87-013129] 01 p0039 N88-10248

The fundamentals of photovoltaic system electrical design
[DE87-009061] 02 p0194 N88-11214

Some 2-D WSI array architectures --- wafer scale integration (WSI)
[OUEL-1672/87] 02 p0219 N88-11381

Programmable Logic Arrays (PLA's) design for testability
[PB87-102935] 04 p0438 N88-12718

Chemically modified microelectrode arrays: New kinds of electronic devices
[AD-A184389] 04 p0439 N88-12724

Arrays for discrete Fourier transform
[REPT-87-019] 05 p0632 N88-13861

Low frequency VLBI in space using GAS-Can satellites: Report on the May 1987 JPL Workshop
[NASA-CR-182362] 06 p0801 N88-14904

Thin film electret boundary layer transition detector: A feasibility study
[AD-A185675] 07 p0856 N88-15199

Strong laws of large numbers for arrays of orthogonal random variables
[AD-A186159] 07 p0910 N88-15513

A study of the TCAS 2 collision avoidance system mounted on a Boeing 737 aircraft
[NASA-CR-182457] 09 p1116 N88-16687

IRAC test report. Gallium doped silicon band 2: Read noise and dark current
[NASA-TM-87813] 09 p1159 N88-16945

A combined cosmic ray muon spectrometer and high energy air shower arrays
[DE88-003057] 09 p1264 N88-17574

A deep-water OBS (Ocean Bottom Seismometer) array with real-time telemetry
[AD-A187404] 10 p1357 N88-18112

Massive fine-grain parallelism in array computation: A data flow solution 10 p1382 N88-18254

Implementing dynamic arrays: A challenge for high-performance machines
[AD-A188142] 11 p1533 N88-19157

Piezoelectric polymer tactile sensor arrays for robotics
[AD-A188852] 12 p1634 N88-19780

Phase transitions in two-dimensional superconducting arrays in a transverse magnetic field
[INPE-4457-RPE/559] 12 p1697 N88-20157

Control strategies and hardware used in solar thermal applications
[DE88-004631] 13 p1794 N88-20731

Simulating high-resolution vertical plane array wind characteristics using lower-spatial-resolution wind measurements
[DE88-005626] 13 p1800 N88-20761

GADL: A gate array description language
[EUT-87-E-165] 14 p1907 N88-21396

Electromagnetic sensor arrays for nondestructive evaluation and robot control
[AD-A190210] 15 p2056 N88-22260

Coupled high power waveguide laser research
[AD-A189800] 15 p2071 N88-22345

Today's photovoltaic systems: An evaluation of their performance
[DE88-006926] 15 p2090 N88-22457

Self-checking logic arrays
[RR-656-I] 15 p2106 N88-22545

A computer model investigation of a half square log-periodic array
[AD-A190955] 16 p2190 N88-23062

Derivative arrays, geometric control theory and realizations of linear descriptor systems
[AD-A190882] 16 p2260 N88-23513

Spectral radiation measurement using a photodiode array as receiver 16 p2271 N88-23591

Joint services electronics program
[AD-A191749] 18 p2504 N88-24853

Null steering applications of polynomials with unimodular coefficients
[AD-A191087] 18 p2562 N88-25211

The XRD (X-Ray Diode) array, the grazing incidence spectrometer and the X-ray imaging camera on PBFA 2
[DE88-007282] 19 p2728 N88-26200

Development of 30 micrometers extrinsic silicon multiplexed infrared deterctor array
[NASA-CR-177446] 22 p3082 N88-28301

Recent advances in optical spectroscopy using high performance array detectors
[AD-A194219] 22 p3152 N88-28753

Natural convection immersion cooling of an array of simulated chips in an enclosure filled with dielectric liquid
[AD-A193594] 23 p3207 N88-29088

SQUID (superconducting quantum interference device) arrays for simultaneous magnetic measurements: Calibration and source localization performance
[AD-A193815] 23 p3216 N88-29143

Nonlinear dynamics of coupled oscillator arrays
[AD-A194888] 24 p3367 N88-30053

Development of a unit cell for a Ge:Ga detector array
[NASA-CR-177445] 24 p3375 N88-30100

Tolerances for phase locking of semiconductor laser arrays
[AD-A195974] 24 p3378 N88-30120

ARRESTING GEAR

Analysis of head response to torso acceleration. Volume 1: Development of performance requirements
[PB88-156757] 14 p1953 N88-21640

Soft-ground aircraft arresting systems
[AD-A190838] 16 p2165 N88-22912

ARRHYTHMIA

Vagal tone as an index of mental state
16 p2239 N88-23373

Estimating the cost of mental loading in a bimodal divided-attention task: Combining reaction time, heart-rate variability and signal-detection theory
16 p2241 N88-23385

ARRIVALS

On the direction of arrival estimation
[AD-A186031] 07 p0914 N88-15546

ARROW WINGS

Parametric flutter studies of an arrow-wing configuration: Some early results
[NASA-TM-100608] 19 p2599 N88-25444

ARSENIC

Comparison of low temperature photoluminescence of bulk MBE (Molecular Beam Epitaxy) grown AlGaAs and GaAs using a graphite generated dimer versus a standard tetramer arsenic group-V source
[DE88-004939] 11 p1558 N88-19329

Optical study of germanium, germanium plus arsenic, and germanium plus gallium implants in gallium arsenide
[AD-A189600] 13 p1845 N88-21045

Raman characterization of AsF5-intercalated vapor grown graphite fibers
[AD-A191709] 18 p2491 N88-24778

ARSENIC COMPOUNDS

NT ALUMINUM ARSENIDES
NT ALUMINUM GALLIUM ARSENIDES
NT ARSENIDES
NT GALLIUM ARSENIDES
NT INDIUM ARSENIDES

The first gallium-arsenic compound containing a single Ga3As unit: Isolation and crystal structure of ((thf)Br2Ga)3As (thf = tetrahydrofuran)
[AD-A187457] 11 p1555 N88-19309

ARSENIDES

NT ALUMINUM ARSENIDES
NT ALUMINUM GALLIUM ARSENIDES
NT GALLIUM ARSENIDES
NT INDIUM ARSENIDES

Chemical vapor deposition of B6P and B6As films
[DE87-009288] 02 p0151 N88-10942

The synthesis and characterization of some rare earth arsenides
[AD-A186445] 08 p0965 N88-15839

Non-linear materials (TAS)
[AD-A189197] 12 p1633 N88-19775

Activities of As, Sb, Bi and Pb in copper mattes and their effects on impurity elimination
[TKK-V-A10(1988)] 15 p2041 N88-22165

Recent data on Si:As impurity band conduction multiplexed arrays
[AD-A191752] 18 p2582 N88-25340

ARTEMIA

Effect of spaceflight factors on biological material flown aboard Cosmos-1514 biosatellite
10 p1364 N88-18154

ARTERIES

NT AORTA

Distinctive changes in arterial pressure and blood flow in common carotid artery of monkeys flown aboard Cosmos-1514 biosatellite 07 p0892 N88-15404

Operation Everest 2: Comparison of four instruments for measuring blood oxygen saturation
[AD-A186456] 08 p1049 N88-16337

Hemodynamic effects of beta-adrenergic blocking with obsidan in clinostatic and orthostatic positions
10 p1367 N88-18171

Models of cerebral-body perfusion and cerebral chemical transport
[AD-A194945] 24 p3407 N88-30283

ARTHROPODS

NT ARTEMIA
NT DROSOPHILA
NT INSECTS

ARTIFICIAL CLOUDS

NT BARIUM ION CLOUDS
NT CHEMICAL CLOUDS

ARTIFICIAL GRAVITY

Preliminary analysis of an integrated logistics system for OSSA payloads. Volume 4: Supportability analysis of the 1.8m centrifuge 12 p1584 N88-19481

Analysis of a rotating advanced-technology space station for the year 2025
[NASA-CR-178345] 12 p1600 N88-19580

Some operational aspects of a rotating advanced-technology space station for the year 2025
[NASA-CR-181617] 20 p2765 N88-26397

ARTIFICIAL INTELLIGENCE

NT EXPERT SYSTEMS

Space Station Mission Planning System (MPS) development study. Volume 1: Executive summary
[NASA-CR-179202] 01 p0009 N88-10047

Space Station Mission Planning System (MPS) development study. Volume 2
[NASA-CR-179200] 01 p0009 N88-10048

Space Station Mission Planning Study (MPS) development study. Volume 3: Software development plan
[NASA-CR-179203] 01 p0009 N88-10049

A methodology for dynamic task allocation in a man-machine system
[DE87-007373] 01 p0077 N88-10492

Workshop on AI (Artificial Intelligence) and Simulation (2nd) held in Seattle, Washington on 14 July 1987
[AD-A183736] 01 p0084 N88-10542

Language modelling for automatic speech recognition: A review
[RSRE-MEMO-4038] 01 p0084 N88-10544

Multimedia sensory systems for the solution of the error recovery problem --- robots
[REPT-87-010] 01 p0084 N88-10545

Application of knowledge-based techniques to aircraft trajectory generation and control
02 p0129 N88-10811

Multi-processor architectures for artificial intelligence processing
[OUEL-1671/87] 02 p0219 N88-11380

Semantic network processing systems --- artificial intelligence
[OUEL-1677/87] 02 p0223 N88-11401

Robotics and Intelligent Systems Program
[DE87-014561] 02 p0223 N88-11404

Knowledge acquisition issues encountered during the development of an estimating expert system
[DE87-013320] 02 p0248 N88-11568

Diagnostics aid for mass spectrometer trouble-shooting
[DE88-000350] 03 p0324 N88-12049

The user's guide to the BACK system --- knowledge representation
[KIT-42] 03 p0367 N88-12310

A survey of artificial neural systems
[AD-A184759] 03 p0368 N88-12312

Antithesis: A study in clause combining and discourse structure
[AD-A184789] 03 p0368 N88-12313

An object-oriented architecture for intelligent tutoring systems
[AD-A184790] 03 p0368 N88-12314

The structure-mapping engine: Algorithm and examples
[AD-A184042] 03 p0368 N88-12315

Performance evaluation of artificial intelligence systems
[AD-A184054] 03 p0368 N88-12316

Potential applications of expert systems and operations research to space station logistics functions
[NASA-CR-180473] 03 p0372 N88-12342

Advanced techniques for the storage and use of very large, heterogeneous spatial databases. The representation of geographic knowledge: Toward a universal framework --- relations (mathematics)
[NASA-CR-181517] 03 p0385 N88-12421

A tight upper bound for the speed-up of parallel best-first branch-and-bound algorithms
[AD-A184246] 04 p0477 N88-12939

Experimental use of artificial intelligence for (future) ATC systems
[PB87-106449] 04 p0482 N88-12970

An expert system for materials design
[DE88-000191] 04 p0483 N88-12974

A model of functional knowledge and insight
[AD-A184113] 04 p0483 N88-12975

GOLD: Integration of model-based control systems with artificial intelligence and workstations
[DE88-000506] 04 p0483 N88-12976

GOLD: Integration of model-based control systems with artificial intelligence and workstations
[DE88-000706] 04 p0483 N88-12977

A project of an intelligent system to help on-line trouble shooting --- aircraft maintenance
[SNIAS-872-111-106] 05 p0529 N88-13216

Towards building a team of intelligent robots
[NASA-CR-181538] 05 p0589 N88-13595

Collision-free motion of two robot arms in a common workspace
[CSE-87-00002] 05 p0589 N88-13596

Dealing with unanticipated events in autonomous navigation
[DE88-000590] 05 p0590 N88-13602

ZEUS: A knowledge-based expert system that assists in predicting visibility at airbases
[AD-A184197] 05 p0626 N88-13829

Diagnostic reasoning in digital systems
[NASA-CR-181564] 05 p0633 N88-13871

Behavioral Architecture Robot Control System (BARCS): A new way of building robots
[REPT-87-036] 05 p0638 N88-13902

LISP: A language for stratified design
[AD-A185606] 06 p0759 N88-14654

A computer decision-making process for the elimination of noise from data
[AD-A185746] 06 p0759 N88-14659

USSR report: Cybernetics, computers and automation technology
[JPRS-UCC-86-014] 06 p0761 N88-14669

Artificial intelligence systems
06 p0761 N88-14670

Computer architectures for artificial intelligence
[PB87-123824] 06 p0761 N88-14671

Genie inference engine rule writer's guide
[AD-A185709] 06 p0762 N88-14675

A general architecture for intelligent training systems
06 p0796 N88-14875

Dynamics, control and sensor issues pertinent to robotic hands for the EVA retriever system
06 p0796 N88-14876

Tools and technologies for expert systems: A human factors perspective 06 p0797 N88-14882

Development of a prototype H-46 helicopter diagnostic expert system
[AD-A186077] 07 p0809 N88-14924

Expert system study for spacecraft management
[TL-2699-ISS-1] 07 p0824 N88-15004

Improved input representation for enhancement of neural network performance
[DE88-001830] 07 p0907 N88-15496

Proceedings of the Second International Symposium on Methodologies for Intelligent Systems. Colloquia program
[DE88-001490] 07 p0907 N88-15498

Expert system technology 07 p0926 N88-15628

DoD Gateway Information System (DGIS) common command language: The first prototyping and the decision for artificial intelligence
[AD-A185950] 07 p0942 N88-15725

Directions in propulsion control
08 p0956 N88-15799

A knowledge-based object recognition system for applications in the space station
[NASA-CR-182411] 08 p0989 N88-15991

Deriving descriptions of the mind
[AD-A186647] 08 p1052 N88-16349

Methodology for testing and validating knowledge bases 08 p1055 N88-16364

Clips as a knowledge based language
08 p1055 N88-16365

MTK: An AI tool for model-based reasoning
08 p1056 N88-16372

KBS V and V as related to automation of space station subsystems: Rationale for a KBS lifecycle
08 p1057 N88-16375

Monitoring of space station life support systems with miniature mass spectrometry and artificial intelligence
08 p1057 N88-16376

Automatic mathematical modeling for space application 08 p1060 N88-16402

Knowledge-based simulation
08 p1061 N88-16404

Rapid prototyping and AI programming environments applied to payload modeling 08 p1061 N88-16405

Iterative-deepening heuristic search for optimal and semi-optimal resource allocation
08 p1062 N88-16410

Similarity networks as a knowledge representation for space applications 08 p1062 N88-16411

Discovery and problem solving: Triangulation as a weak heuristic 08 p1062 N88-16412

Planning and scheduling for robotic assembly
08 p1062 N88-16416

Intelligent man/machine interfaces on the space station 08 p1063 N88-16418

Space languages 08 p1063 N88-16420

The intelligent user interface for NASA's advanced information management systems
08 p1063 N88-16424

An AI approach for scheduling space-station payloads at Kennedy Space Center 08 p1064 N88-16425

Neural network based speech synthesizer: A preliminary report 08 p1064 N88-16429

The power of neural nets 08 p1064 N88-16430

Neural networks as a possible architecture for the distributed control of space systems
08 p1064 N88-16431

Application of artificial intelligence to impulsive orbital transfers 08 p1066 N88-16439

Substructure discovery in executed action sequences
[AD-A186446] 08 p1069 N88-16462

Tutoring electronic troubleshooting in a simulated maintenance work environment
09 p1204 N88-17215

An intelligent tutor for the space domain
09 p1204 N88-17217

Neural network based architectures for aerospace applications 09 p1204 N88 17218

NASA JSC neural network survey results 09 p1205 N88-17220

Design of a neural network simulator on a transputer array 09 p1205 N88-17221

Cooperative analysis expert situation assessment research 09 p1206 N88-17228

Teaching artificial neural systems to drive: Manual training techniques for autonomous systems 09 p1207 N88-17238

A situation-response model for intelligent pilot aiding 09 p1208 N88-17241

A human performance modelling approach to intelligent decision support systems 09 p1208 N88-17242

Artificial Intelligence (AI), Operations Research (OR), and Decision Support Systems (DSS): A conceptual framework 09 p1209 N88-17245

Range and mission scheduling automation using combined AI and operations research techniques 09 p1209 N88-17249

Robotic air vehicle. Blending artificial intelligence with conventional software 09 p1210 N88-17252

A conceptual framework for intelligent real-time information processing 09 p1211 N88-17257

Real-time artificial intelligence issues in the development of the adaptive tactical navigator 09 p1211 N88-17260

Implementation of a robotic flexible assembly system 09 p1212 N88-17265

System integration of a Telerobotic Demonstration System (TDS) testbed 09 p1212 N88-17266

Mathematical structures for speech recognition [AD-A187063] 09 p1217 N88-17295

Horizontal estimation and information fusion in multitarget and multisensor environments [AD-A186935] 09 p1224 N88-17336

Parallel architectures for logic programming 10 p1380 N88-18241

Real time artificial intelligence architecture 10 p1380 N88-18242

Analysis and synthesis of adaptive neural elements [AD-A187047] 10 p1395 N88-18316

Parallel garbage collection on a virtual memory system [DE88-003567] 10 p1396 N88-18317

The implementation of artificial intelligence in control systems [DE88-003497] 10 p1396 N88-18318

The representation of knowledge within model-based control systems [DE88-004863] 10 p1396 N88-18319

Visual integration and detection of discontinuities: The key role of intensity edges [AD-A188012] 11 p1520 N88-19076

Research in knowledge representation for natural language communication and planning assistance [AD-A187355] 11 p1522 N88-19087

Effects of stress on judgement and decision making in dynamic tasks [AD-A188203] 11 p1523 N88-19092

TYPICAL: A knowledge representation system for automated discovery and inference [AD-A187483] 11 p1533 N88-19160

The choice of learning strategy in an autonomous system [AD-A187707] 11 p1534 N88-19161

Two new frameworks for learning [AD-A187723] 11 p1534 N88-19162

Learning functions from examples [AD-A187725] 11 p1534 N88-19163

Error detection and recovery for robot motion planning with uncertainty [AD-A187746] 11 p1534 N88-19165

Concepts and nomenclature in the world modeling system (a lesson in applied metaphysics) [AD-A188246] 11 p1534 N88-19166

Optical computing research [AD-A187862] 11 p1549 N88-19264

Autonomous Liquid Encapsulated Czochralski (LEC) growth of single crystal GaAs by intelligent digital control [AD-A187211] 11 p1555 N88-19305

Robotic intelligence issues for space manipulator monitoring, control programming 12 p1588 N88-19504

Mobile robot activity model for autonomous free flying platforms 12 p1588 N88-19507

Low cost mobile robot [AD-A188507] 12 p1633 N88-19778

A knowledge acquisition tool for the intelligent processing of materials [AD-A188982] 12 p1679 N88-20036

Knowledge-based system analysis and control [AD-A188163] 12 p1681 N88-20049

OPS83: Style guide for high performance [AD-A188505] 12 p1681 N88-20051

Learning by experimentation [AD-A188912] 12 p1681 N88-20053

Physics for robots [AD-A189056] 12 p1682 N88-20054

Northeast Artificial Intelligence Consortium (NAIC): administrative matters and ancillary functions, volume 1 [AD-A189466] 12 p1682 N88-20055

The integration of artificial intelligence techniques to improve the effectiveness of electronic countermeasure strategies in a tactical environment [AD-A189483] 12 p1682 N88-20056

Towards a solution to the proper integration of a logic programming system and a large knowledge based management system [AD-A188949] 12 p1705 N88-20207

Intelligent control of robot manipulators in hazardous environments [DE88-003305] 13 p1778 N88-20638

An implementation of the OPS5 language for computers compatible with IBM-PC [INPE-4291-PRE/1162] 13 p1821 N88-20882

The use of an automated flight test management system in the development of a rapid-prototyping flight research facility [NASA-TM-100435] 13 p1823 N88-20896

Mathematic modeling of visual perception problems [INPE-4355-PRE/1186] 13 p1823 N88-20897

Soar: An architecture for general intelligence [AD-A188742] 13 p1823 N88-20898

Knowledge retrieval as specialized inference [AD-A189042] 13 p1823 N88-20899

A Darwinian approach to artificial neural systems [DE87-013184] 13 p1824 N88-20900

Quality enhancement with machine intelligence [DE88-005639] 13 p1824 N88-20901

Aspects and applications of primary processing of visual information [INPE-4290-PRE/1161] 13 p1841 N88-21015

Application of expert systems in project management decision aiding [NASA-CR-180762] 13 p1850 N88-21074

Implementing embedded artificial intelligence rules within algorithmic programming languages [NASA-CR-178393] 14 p1959 N88-21686

Representing knowledge in two distinct descriptions: Extensional vs. intensional [CWI-CS-R8728] 14 p1961 N88-21699

Perfect knowledge and beyond --- chess endgames [REPT-87-37] 14 p1967 N88-21738

Comparative analysis [AD-A190556] 15 p2065 N88-22313

Instrumentation for scientific computing in neural networks, information science, artificial intelligence and applied mathematics [AD-A189981] 15 p2106 N88-22549

A probabilistic approach to low-level vision [AD-A189041] 15 p2107 N88-22553

An intelligent simulation model generator [REPT-87-053] 15 p2109 N88-22562

Inference engine for expert systems [INPE-4465-TDL/321] 15 p2113 N88-22590

Memory-based expert systems [AD-A190203] 15 p2116 N88-22606

Synapses that compute motion [AD-A190389] 15 p2116 N88-22607

Multi-disciplinary techniques for understanding time-varying space-based imagery [AD-A190711] 15 p2117 N88-22610

Discrete event simulation in the artificial intelligence environment [DE88-004296] 15 p2117 N88-22613

Multivariate analysis and its application [AD-A189983] 15 p2124 N88-22661

Rigidity and smoothness of motion [AD-A190555] 15 p2128 N88-22694

ROVER: A prototype active vision system [AD-A189246] 15 p2133 N88-22722

Autonomous control system for Czochralski growth of LEC GaAs [AD-A189726] 15 p2141 N88-22779

The Scientific and Technical Information Network (STINET): Foundation for evolution [AD-A189750] 15 p2148 N88-22822

Data base design and implementation [AD-A190414] 15 p2149 N88-22827

Extending problem solver capabilities through case-based inference [AD-A191332] 16 p2243 N88-23401

Design as a formal, knowledge engineered activity [CWI-CS-R8744] 16 p2248 N88-23431

Knowledge engineering in design [CWI-CS-R8745] 16 p2248 N88-23432

STRUTEX: A prototype knowledge-based system for initially configuring a structure to support point loads in two dimensions [NASA-TM-100613] 16 p2250 N88-23448

Parallel artificial intelligence search techniques for real time applications [AD-A190683] 16 p2255 N88-23473

Automatic control of an industrial process and computer aided process control by means of an expert system [LAAS-88-004] 16 p2255 N88-23476

Parallelism in a Prolog knowledge base machine [ETN-88-92187] 16 p2255 N88-23477

Capitalizing on failure through case-based inference [AD-A190927] 16 p2255 N88-23480

Rule-based fault-tolerant flight control 17 p2294 N88-23725

Fiber waveguide sensors for intelligent materials [NASA-CR-183028] 17 p2343 N88-23968

A proposal of adaptation of a knowledge-based scene analysis model to some remote sensing problems 17 p2362 N88-24068

Linguistic definition of generic models in computer vision [RSRE-MEMO-4110] 17 p2386 N88-24182

MTK: An AI tool for model-based reasoning 17 p2387 N88-24189

Simultaneous use of artificial intelligence and Petri nets. Application to the monitoring of a fabrication plan [LAAS-87-354] 17 p2390 N88-24207

Notes on artificial intelligence. Part 1: Technical forecast [FOA-C-30448-3.3-PT-1] 17 p2390 N88-24208

Energy optimal trajectory planning for robot manipulators and autonomous vehicles 17 p2437 N88-24497

A system status monitor for the National Aerospace Plane [AD-A190681] 18 p2463 N88-24624

Timesharing performance as an indicator of pilot mental workload [NASA-CR-182807] 18 p2552 N88-25150

A computational model of motor behavior [AD-A191179] 18 p2553 N88-25152

LispSEI: The programmer's manual [AD-A191632] 18 p2556 N88-25172

Representation and decision mechanisms in artificial intelligence [AD-A191083] 18 p2560 N88-25197

The ISI (Information Sciences Institute) grapher manual [AD-A192198] 18 p2561 N88-25200

Modeling of geometric reasoning for robot programming [ETN-88-92290] 18 p2561 N88-25202

Robot navigation using simple sensor fusion [DE88-006184] 18 p2561 N88-25203

Application of flight systems methodologies to the validation of knowledge-based systems [NASA-TM-100442] 18 p2561 N88-25207

Automatic discovery of optimal classes [NASA-TM-101174] 18 p2566 N88-25238

JPRS report: Science and technology. Japan [JPRS-JST-88-005] 19 p2633 N88-25619

Application of AI to space systems 19 p2634 N88-25626

The development of an intelligent interface to a computational fluid dynamics flow-solver code [NASA-TM-100908] 19 p2716 N88-26127

An expert system model using predicate transition nets [AD-A191953] 19 p2718 N88-26141

Modeling and evaluation of expert systems in decisionmaking organizations [AD-A191951] 19 p2739 N88-26260

A cockpit natural language study - selected transcripts [AD-A192972] 20 p2834 N88-26808

Direct manipulation and the design of user interfaces [PB88-126354] 20 p2834 N88-26810

SIMS: Single Interface to Multiple Systems [AD-A192264] 20 p2837 N88-26832

Building an artificial intelligence capability at Los Alamos [DE88-009155] 20 p2842 N88-26866

Expert system application education project [NASA-CR-183089] 20 p2843 N88-26867

Narrative domain implementation [AD-A192265] 20 p2843 N88-26868

NEXT: An expert system development tool to support engineering design [NLR-MP-86070-U] 20 p2843 N88-26871

Qualitative reasoning for physicists [PB88-116298] 20 p2848 N88-26906

Challenge equality problems in lattice theory [DE88-010094] 20 p2876 N88-27072

EXSAT: Expert system to configure telecommunication satellites [SNIAS-881-440-101] 21 p2902 N88-27223

Mitsubishi Electric Advance (R and D Edition), Volume 41 [PB88-194162] 21 p2929 N88-27388

Computer-Aided Engineering (CAE) for engineering design 21 p2929 N88-27390

The MELCOM PSI 2 AI workstation
21 p2930 N88-27395

Motor-response learning at a process control panel by an autonomous robot
[DE88-005055] 21 p2955 N88-27554

Block Oriented Simulation System (BOSS)
[NASA-CR-182947] 21 p2995 N88-27760

Synchronizable series expressions. Part 2: Overview of the theory and implementation
[AD-A192783] 21 p2996 N88-27768

The programmer's apprentice project: A research overview
[AD-A192784] 21 p2996 N88-27769

Improving the performance of AI algorithms
[AD-A192848] 21 p3003 N88-27809

Faultfinder: A diagnostic expert system with graceful degradation for onboard aircraft applications
22 p3035 N88-28018

Heat exchanger demonstration expert system
22 p3066 N88-28193

Artificial intelligence software acquisition program, volume 2
[AD-A194239] 22 p3141 N88-28680

Stereo and eye movement
[AD-A193588] 22 p3142 N88-28681

Loglisp programming system users manual
[AD-A193933] 22 p3142 N88-28682

Connectionist models and artificial intelligence
[RR-684-I-IMAG-66-LIFIA] 22 p3142 N88-28684

Uncertainty analysis in automatic robot programming
[RR-695-I-IMAG-68-LIFIA] 22 p3142 N88-28685

Motion planning for legged locomotion systems on uneven terrain 23 p3221 N88-29170

Automatic line network extraction from aerial imagery of urban areas through knowledge-based image analysis
[AD-A192399] 23 p3227 N88-29208

Artificial intelligence applied to process signal analysis
23 p3252 N88-29359

DAISY-DAMP: A distributed AI system for the dynamic allocation and management of power
23 p3254 N88-29373

Intelligent resource management for local area networks: Approach and evolution
23 p3256 N88-29385

Distributed cooperating processes in a mobile robot control system 23 p3256 N88-29386

Programming model for distributed intelligent systems
23 p3257 N88-29390

AI and simulation: What can they learn from each other 23 p3257 N88-29391

Reasoning about fault diagnosis for the space station common module thermal control system
23 p3258 N88-29395

Intelligent interface design and evaluation
23 p3260 N88-29405

The concurrent common Lisp development environment 23 p3263 N88-29422

AI tools in computer based problem solving
23 p3263 N88-29424

Networking and AI systems: Requirements and benefits 23 p3263 N88-29425

Radial basis functions, multi-variable functional interpolation and adaptive networks
[RSRE-MEMO-4148] 23 p3265 N88-29436

Identification and control of time-varying flexible structures: An artificial intelligence approach
23 p3265 N88-29437

The complexity of AI algorithms
[AD-A193494] 23 p3265 N88-29438

A model of information growth
23 p3265 N88-29440

Artificial intelligence software acquisition program, volume 1
[AD-A194104] 23 p3267 N88-29447

Design of a feeling-thinking machine
[AD-A194107] 23 p3267 N88-29448

Active explanation reduction: An approach to the multiple explanations problem
[AD-A194127] 23 p3276 N88-29501

Distributed knowledge base systems for diagnosis and information retrieval
[AD-A193107] 23 p3296 N88-29633

Corner extraction from radar images
[AD-A194857] 24 p3362 N88-30020

Path planning and path following for the Amsterdam autonomous cart
[FVI-86-22] 24 p3380 N88-30133

The design of an intelligent multidisk control module for VME bus based systems
[AD-A195587] 24 p3411 N88-30303

Quality measures and assurance for AI (Artificial Intelligence) software
[NASA-CR-4187] 24 p3411 N88-30304

Reification without evaluation
[AD-A195928] 24 p3414 N88-30326

The 1988 Goddard Conference on Space Applications of Artificial Intelligence
[NASA-CP-3009] 24 p3415 N88-30330

An intelligent training system for space shuttle flight controllers 24 p3415 N88-30331

Artificial intelligence costs, benefits, risks for selected spacecraft ground system automation scenarios
24 p3416 N88-30332

A shared-world conceptual model for integrating space station life sciences telescience operations
24 p3416 N88-30333

Artificial intelligence in a mission operations and satellite test environment 24 p3416 N88-30334

Automated satellite control in Ada
24 p3416 N88-30336

Contingency rescheduling of spacecraft operations
24 p3416 N88-30337

Knowledge based tools for Hubble Space Telescope planning and scheduling: Constraints and strategies
24 p3417 N88-30338

The proposal entry processor: Telescience applications for Hubble Space Telescope science operations
24 p3417 N88-30339

Candidate functions for advanced technology implementation in the Columbus mission planning environment 24 p3417 N88-30340

A rule-based systems approach to spacecraft communications configuration optimization
24 p3417 N88-30341

MOORE: A prototype expert system for diagnosing spacecraft problems 24 p3418 N88-30343

Low level image processing techniques using the pipeline image processing engine in the flight telerobotic servicer 24 p3418 N88-30346

Autonomous image data reduction by analysis and interpretation 24 p3418 N88-30347

Parallel and distributed computation for fault-tolerant object recognition 24 p3419 N88-30350

The second generation intelligent user interface for the crustal dynamics data information system
24 p3419 N88-30352

Spacelab data processing facility (SLDPF) Quality Assurance (QA)/Data Accounting (DA) expert systems: Transition from prototypes to operational systems
24 p3420 N88-30353

Automated cataloging and characterization of space-derived data 24 p3420 N88-30354

A design for a ground-based data management system 24 p3420 N88-30355

Automatic mathematical modeling for real time simulation system 24 p3420 N88-30356

A simulation engine: Combining an expert system with a simulation language 24 p3421 N88-30358

Verification and validation of rulebased systems for Hubble Space Telescope ground support
24 p3421 N88-30361

The need for a comprehensive expert system development methodology 24 p3421 N88-30362

The combinatorics of object recognition in cluttered environments using constrained search
[AD-A196224] 24 p3422 N88-30364

Study of software requirements and artificial intelligence techniques for robotics
[TL-3333] 24 p3422 N88-30365

Research on problem-solving systems
[AD-A195154] 24 p3423 N88-30370

Knowledge based simulation: An artificial intelligence approach to system modeling and automating the simulation life cycle
[AD-A195838] 24 p3423 N88-30372

Theories of comparative analysis
[AD-A196328] 24 p3427 N88-30395

Optical symbolic computing
[AD-A195690] 24 p3429 N88-30406

Information retrieval systems evolve-advances for easier and more successful use 24 p3438 N88-30462

ARTIFICIAL RESPIRATION
U RESUSCITATION

ARTIFICIAL SATELLITES
NT ACTS
NT ALOUETTE SATELLITES
NT AMPTE (SATELLITES)
NT ARABSAT
NT ASTRONOMICAL SATELLITES
NT AZUR SATELLITE
NT BIOSATELLITES
NT COLUMBUS SPACE STATION
NT COMMUNICATION SATELLITES
NT COS-B SATELLITE
NT COSMIC BACKGROUND EXPLORER SATELLITE
NT COSMOS SATELLITES
NT COSPAS
NT DIRECT BROADCAST SATELLITES
NT DMSP SATELLITES
NT DYNAMICS EXPLORER 1 SATELLITE
NT ERS-1 (ESA SATELLITE)
NT ESA SATELLITES
NT EUROPEAN COMMUNICATIONS SATELLITE
NT EXOSAT SATELLITE
NT EXPLORER SATELLITES
NT EXPLORER 47 SATELLITE
NT EXPLORER 51 SATELLITE
NT EXPLORER 54 SATELLITE
NT EXPLORER 55 SATELLITE
NT FRENCH SATELLITES
NT GAMMA RAY OBSERVATORY
NT GEODETIC SATELLITES
NT GEOPHYSICAL SATELLITES
NT GEOPOTENTIAL RESEARCH MISSION
NT GEOS SATELLITES (ESA)
NT GEOS 2 SATELLITE
NT GEOSAT SATELLITES
NT GOES SATELLITES
NT HEAO 2
NT HELIOS SATELLITES
NT HELIOS 1
NT HELIOS 2
NT HIPPARCOS SATELLITE
NT HUBBLE SPACE TELESCOPE
NT INFRARED ASTRONOMY SATELLITE
NT INFRARED SPACE OBSERVATORY (ISO)
NT INTERCOSMOS SATELLITES
NT INTERNATIONAL SUN EARTH EXPLORER 3
NT INTERNATIONAL SUN EARTH EXPLORERS
NT ISIS SATELLITES
NT IUE
NT L-SAT
NT LAGEOS (SATELLITE)
NT LANDSAT SATELLITES
NT LANDSAT 5
NT MAGSAT SATELLITES
NT MARECS MARITIME SATELLITES
NT MARISAT SATELLITES
NT MARITIME SATELLITES
NT METEOROLOGICAL SATELLITES
NT METEOSAT SATELLITE
NT MIR SPACE STATION
NT NAVIGATION SATELLITES
NT NAVSTAR SATELLITES
NT NIMBUS 7 SATELLITE
NT NOAA SATELLITES
NT NOAA 7 SATELLITE
NT PASSIVE SATELLITES
NT PEGASUS SATELLITES
NT PROGNOZ SATELLITES
NT ROSAT MISSION
NT SAGE SATELLITE
NT SALYUT SPACE STATION
NT SARSAT
NT SAS
NT SCATHA SATELLITE
NT SCIENTIFIC SATELLITES
NT SEASAT SATELLITES
NT SHUTTLE PALLET SATELLITES
NT SOLAR MESOSPHERE EXPLORER
NT SOLAR POWER SATELLITES
NT SPACE INFRARED TELESCOPE FACILITY
NT SPACE STATION POLAR PLATFORMS
NT SPACE STATIONS
NT SPOT (FRENCH SATELLITE)
NT SYNCHRONOUS SATELLITES
NT TETHERED SATELLITES
NT TIROS N SERIES SATELLITES
NT TIROS SATELLITES
NT UK SATELLITES
NT X RAY ASTROPHYSICS FACILITY

The combined release and radiation effects satellite, a joint NASA/DOD program 02 p0135 N88-10851

Evaluation and certification of heater assemblies developed for thermal vacuum acceptance testing
02 p0136 N88-10853

Design, construction, activation, and operation of a high intensity acoustic test chamber
02 p0137 N88-10864

Computational method for orbit improvement for short arc observations of artificial satellites
03 p0269 N88-11690

Estimates of satellite EHF communication outages due to attenuation by rain
[AD-A183969] 03 p0307 N88-11941

Satellite autonomous navigation with SHAD (Stellar Horizon Atmospheric Dispersion)
[AD-A184988] 05 p0544 N88-13313

MAXIE 1 (Magnetospheric Atmospheric X-ray Imaging Experiment) Program
[AD-A185878] 07 p0877 N88-15317

Supportability in aircraft systems through technology and acquisition strategy applications
[AD-A186465] 08 p0949 N88-15759

An evaluation of semianalytical satellite theory against long arcs of real data for highly eccentric orbits
[AD-A185825] 08 p0960 N88-15819
Attitude determination of artificial satellites through joint application of static and dynamic optimal estimation techniques
[INPE-4415-TDL/306] 08 p0963 N88-15832
Attitude dynamics for satellites stabilized through spin
[INPE-4403-NTE/275] 08 p0963 N88-15833
SAMSS: An in-progress review of the Spacecraft Assembly, Maintenance, and Servicing Study
08 p0981 N88-15930
Development of on-orbit fluid gaging techniques
08 p0982 N88-15936
Selection of efficient correcting motor for an artificial Earth satellite 08 p1007 N88-16102
Space applications in geography
08 p1007 N88-16104
Applications of expert systems for satellite autonomy
08 p1066 N88-16443
Verification of a micro-thrusting model to maintain satellites in low orbit
[AD-A186874] 09 p1133 N88-16793
Formulation methods of rigid multibody systems for large space structures and some results of computer simulation
[NAL-TR-942] 10 p1293 N88-17730
Five-diagonal weighting scheme for geoidal profiles
[AD-A188033] 10 p1347 N88-18054
Project SKYLITE: A design exploration
[AD-A187906] 11 p1511 N88-19030
Optimal selection of global positioning system set to minimize emitter location errors
[AD-A189559] 12 p1579 N88-19447
Customer concerns regarding satellite servicing
12 p1587 N88-19503
Analysis of the sensitivity of the attitude control system of an artificial satellite
[INPE-4285-PRE/1157] 12 p1599 N88-19573
Electromagnetic modeling of a control valve
[INPE-4140-PRE/1048] 12 p1622 N88-19700
Zoom versus full-field sensitivity at the ETS (Experimental Test System)
[AD-A188162] 12 p1628 N88-19742
Dynamics of small and large scale irregularities at sub-auroral latitudes
[AD-A189052] 12 p1645 N88-19853
Utilization of strapdown inertial and non-inertial sensors in determination of satellite attitude by Kalman filters
[INPE-4313-TDL/280] 13 p1731 N88-20349
Aeronautics and space report of the President: 1986 activities 13 p1852 N88-21087
Comparison of methods for the calculation of thermal contact resistance of the first Brazilian satellite
[NASA-TT-20180] 14 p1880 N88-21239
MAXIE 1
[AD-A189688] 14 p1882 N88-21247
Numerical orbit propagation methods for earth artificial satellites
[INPE-4405-RPE/556] 15 p2023 N88-22053
Chronology of China's successful satellite launchings
15 p2053 N88-22234
Analytical orbit propagation of artificial satellites
[INPE 4454-TDL/315] 16 p2166 N88-22915
Review of power requirements for satellite remote sensing systems 17 p2419 N88-24387
Design considerations for the ORION satellite: Structure, propulsion and attitude control subsystems for a small, general purpose spacecraft
[AD-A193837] 22 p3048 N88-28086
The 44/20 GHz ground terminal
[AD-A194002] 23 p3204 N88-29069
Long haul communications in the HF spectrum utilizing high speed modems
[AD-A194683] 24 p3360 N88-30003
DATATRAN: Datum transformation software
[AD-A195723] 24 p3387 N88-30175
Space systems cost study
[AD-A196024] 24 p3439 N88-30469
Orbital evolution of distant artificial earth satellites
24 p3445 N88-30506
Families of periodic solutions in problem of solid body rotation at triangular libration point in restricted three-body problem 24 p3446 N88-30508

ARTILLERY
Method for determining artillery position
[NASA-TT-20238] 13 p1834 N88-20973
Method for determining artillery position
[NASA-TT-20237] 13 p1834 N88-20974
Method for determining artillery position
[NASA-TT-20236] 14 p1979 N88-21813

ARTS
NT ABILITIES
NT COMPUTER ANIMATION
NT GRAPHIC ARTS

ARYABHATA
U INDIAN SPACECRAFT

ARYL COMPOUNDS
U AROMATIC COMPOUNDS

ASBESTOS
Environmental projects. Volume 4: Asbestos survey
[NASA-CR-182527] 10 p1353 N88-18083

ASCENT
NT CLIMBING FLIGHT
Analysis of clinical symptoms of human decompression sickness during altitude chamber studies
19 p2703 N88-26074

ASCENT PROPULSION SYSTEMS
Propulsion analysis and application potential of air breathing combined propulsion for ballistic space transporter
[ETN-88-92369] 21 p2903 N88-27227
Ascent guidance for a winged boost vehicle
[NASA-CR-172083] 24 p3334 N88-29846

ASCENT TRAJECTORIES
A study to evaluate STS heads-up ascent trajectory performance employing a minimum-Hamiltonian optimization strategy
[NASA-TP-2793] 08 p0960 N88-15820
Optimal thrust vector control of coplanar orbital evasive maneuvers
[AD-A189544] 13 p1730 N88-20346
Wind measurements by electromagnetic probes
[NASA-TM-4066] 23 p3236 N88-29256
Ascent guidance for a winged boost vehicle
[NASA-CR-172083] 24 p3334 N88-29846

ASHES
TOMS and the NOAA/FAA volcano support plan
05 p0618 N88-13796
Energy efficient continuous flow ash lockhopper
[NASA-CASE-NPO-16985-1-CU]
18 p2497 N88-24814

ASIA
Conceptual models of Baiu front and Baiu frontal disturbances in multiscale characteristics --- East Asia
02 p0203 N88-11271
The numerical simulation of the mesoscale characteristics associated with Baiu front. Part 1: Structure, low-level jet and radiation characteristics
02 p0203 N88-11272
Tropical and monsoonal studies
[AD-A188387] 14 p1947 N88-21611

ASPECT RATIO
NT HIGH ASPECT RATIO
NT LOW ASPECT RATIO
Investigations of separated flow states on wings of medium aspect ratio taking into account the wind tunnel interference problem
[ETN-87-90437] 01 p0003 N88-10016
On tokamak equilibrium
[DE87-014811] 02 p0239 N88-11507
The effect of microstructure on the surface crack length: Crack depth relationship for short cracks
05 p0600 N88-13670
Experimental model of halo plasma observed in small-aspect FRC plasma
[INPE-4159-PRE/1061] 08 p1085 N88-16534
Conceptual design of a radio-frequency driven compact tokamak
[INPE-4364-PRE/1190] 08 p1085 N88-16535
High Rayleigh number convection in rectangular enclosures with differentially heated vertical walls and aspect ratios between zero and unity
[NASA-TM-100277] 12 p1628 N88-19739
The aspect ratio dependence of the attractor dimension in Taylor-Couette flow
[AD-A196297] 24 p3369 N88-30065

ASPHALT
A laboratory study of asphalt concrete mix designs for high-contact pressure aircraft traffic
[AD-A185753] 06 p0670 N88-14106
Comparative study of nondestructive pavement testing, MacDill Air Force Base, Florida
[AD-A186082] 07 p0822 N88-14993
Investigation of the inter-relationship between base pavement stiffness and asphalt overlay compaction
[DOT/FAA/ES-88/1] 14 p1869 N88-21170

ASPHALTENES
Application of high performance liquid chromatography to the fast determination of bitumen generic composition
[PC-2] 02 p0145 N88-10911

ASPIRATION
U VACUUM

ASSAULTING
U ATTACKING (ASSAULTING)

ASSAYING
Experience of developing an integrated nondestructive assay system
[DE88-003149] 09 p1184 N88-17092
Methods and techniques of NDA (nondestructive assay)
[DE88-009145] 20 p2812 N88-26682

ASSEMBLIES
NT SUBASSEMBLIES
NT TAIL ASSEMBLIES
Fast shock tube assemblies
[DE87-011732] 01 p0008 N88-10042
The effect of different packagings on the vibration behavior and the coupling factors of steam turbine blading
[ETN-87-90425] 01 p0056 N88-10357
Reactions of porphyrins in surfactant assemblies, microemulsions and in solutions
[AD-A184797] 05 p0560 N88-13412
Computation of bonded assemblies. Elastoplastic adhesives, first part
[SNIAS-NT-18926/AQET] 05 p0569 N88-13467

ASSEMBLING
NT ORBITAL ASSEMBLY
Space Assembly, Maintenance, and Servicing Study (SAMSS) 01 p0015 N88-10089
Space station assembly/servicing capabilities
01 p0016 N88-10100
Structural Assembly Demonstration Experiment (SADE)
[NASA-CR-179205] 02 p0138 N88-10868
Experimental assembly of structures in EVA: Hardware morphology and development issues
02 p0139 N88-10872
Access flight hardware design and development
02 p0139 N88-10873
Marshall Space Flight Center's role in EASE/ACCESS mission management 02 p0139 N88-10875
Research and development at the Marshall Space Flight Center Neutral Buoyancy Simulator
02 p0139 N88-10878
A synopsis of the EVA training conducted on EASE/ACCESS for STS-61-B 02 p0140 N88-10879
Results of the ACCESS experiment
02 p0140 N88-10880
Overview of crew member energy expenditure during Shuttle Flight 61-8 EASE/ACCESS task performance
02 p0140 N88-10882
Design and assembly sequence analysis of option 3 for CETF reference space station
[NASA-TM-100503] 05 p0553 N88-13369
RETE experiment Assembly, Integration, and Verification (AIV) activities
[IFSI-87-6] 05 p0555 N88-13380
Planning and scheduling for robotic assembly
08 p1062 N88-16416
Implementation of a robotic flexible assembly system
09 p1212 N88-17265
Robotic assembly and testing of rotary solenoids
[BDX-613-3663] 11 p1480 N88-18834
The space station assembly phase: Flight telerobotic servicer feasibility, volume 1
[NASA-CR-182689] 13 p1731 N88-20351
The space station assembly phase: Flight telerobotic servicer feasibility. Volume 2: Methodology and case study
[NASA-CR-182690] 13 p1731 N88-20352
Recognizing and locating partially occluded planar objects for assembly routines
[LAAS-87-360] 16 p2247 N88-23422
Assembly Test Article (ATA)
[NASA-CR-179361] 21 p2903 N88-27226
Study of the assembly, integration and verification programs of telecommunication satellites applicable to other satellite programs
[MATRA-100/CC/MLG/031/87]
24 p3334 N88-29847

ASSEMBLY
Alignment and assembly tool for very large diameter cylinders
[NASA-CASE-MFS-28001-2] 06 p0711 N88-14360

ASSEMBLY LANGUAGE
High-speed assembly language (80386/80387) programming for laser spectra scan control and data acquisition providing improved resolution water vapor spectroscopy
[NASA-CR-4117] 08 p1053 N88-16355
Efficient instruction level simulation of computers
[AD-A187821] 11 p1529 N88-19130

ASSESSMENTS
NT DAMAGE ASSESSMENT
NT TECHNOLOGY ASSESSMENT
Land campaign force assessment. Methods used in Central-Europe-study
[FOA-C-10288-9.3] 06 p0768 N88-14723

ASSIGNMENT
U ALLOCATIONS

ASSIMILATION
A real-data numerical study and four-dimensional data assimilation application for mesobeta-scale flow in complex terrain 02 p0212 N88-11329
Assimilation of meteorological observations
14 p1936 N88-21544
ASSOCIATION REACTIONS
Overview of hydrogen clusters
16 p2267 N88-23557
Associative two-body condensation in laser-cooled sodium and hydrogen 16 p2267 N88-23559
Formation and reactivity of small hydrogen cluster ions 16 p2267 N88-23560
Analysis of containerless condensation of polyatomic hydrogen ions, with emphasis on H3(+,-) association channels and a future workshop to study related topics
16 p2269 N88-23576
ASSOCIATIONS
U ORGANIZATIONS
ASSOCIATIVE PROCESSING (COMPUTERS)
The associative memory ME7
[ESA-TT-1033] 01 p0079 N88-10506
Estimation of the position and orientation of objects using associative memories
[ESA-TT-1034] 01 p0079 N88-10507
General potential surfaces and neural networks
[AD-A184484] 03 p0367 N88-12311
Optical Conceptual Computing and Associative Memory (OCCAM)
[AD-A190030] 15 p2107 N88-22550
Rapid feature extraction via the radon transform
[AD-A190032] 15 p2110 N88-22573
Optical computing based on neuronal models
[AD-A191481] 18 p2575 N88-25293
Optical data processing
[AD-A193024] 20 p2839 N88-26841
Content-addressable memory storage by neural networks: A general model and global Liapunov method
[AD-A192716] 21 p3002 N88-27807
ASSURANCE
Implementation of finite element quality assurance in a commercial industrial organisation
[PNR90393] 02 p0183 N88-11137
ESTEC's product assurance activities
09 p1125 N88-16739
Quality assurance of ceramic materials and gas turbine components
[IZFP-850303-TW] 11 p1465 N88-18735
Case study: The Hermes program product assurance
22 p3162 N88-28831
ASTEROID BELTS
NT ASTEROIDS
On the possible origin of meteoroid generating asteroid orbits 06 p0740 N88-14553
ASTEROID CAPTURE
Design study for asteroidal exploitation
03 p0389 N88-12445
ASTEROID MISSIONS
Design study for asteroidal exploitation
03 p0389 N88-12445
The comet rendezvous asteroid flyby mission
14 p2005 N88-21956
ASTEROIDS
Design study for asteroidal exploitation
03 p0389 N88-12445
Speckle interferometry of asteroids
[NASA-CR-180438] 15 p2151 N88-22843
ASTHMA
Mathematical modelling of the heat and water vapour transport in the human respiratory tract
17 p2382 N88-24160
ASTRO MISSIONS (STS)
IPS guidestar selection for stellar mode (ASTRO)
[NASA-TM-100336] 21 p2894 N88-27181
ASTROBIOLOGY
U EXOBIOLOGY
ASTRODYNAMICS
The kinematics of late-type supergiants
[SER-C-PREPUBL-FASC-28] 24 p3454 N88-30560
ASTROLOY (TRADEMARK)
The effect of temperature on fatigue crack initiation from aluminosilicate inclusions 06 p0720 N88-14427
ASTROMASTS
U LONGERONS
ASTROMETRY
Test of the Hipparcos payload in the Liege vacuum facility focal 02 p0135 N88-10850
Phase-coherent astrometric interferometry
[AD-A184428] 04 p0439 N88-12725
An astrometric search for a stellar companion to the sun 04 p0520 N88-13195
Performance considerations for the astrometric telescope facility on the phase 1 space station
[NASA-TM-100040] 06 p0800 N88-14898
Preparation of photometric measurements on a million stars in the framework of the satellite project HIPPARCOS/TYCHO
[ETN-88-91502] 13 p1853 N88-21093
Apparent brightness of stars and lasers
22 p3065 N88-28188
An upper limit on the primordial He4 abundance from speckle interferometric observations of muon Cassiopeiae 23 p3298 N88-29641
ASTRONAUT LOCOMOTION
Results of research with biological satellites
08 p1006 N88-16097
ASTRONAUT MANEUVERING EQUIPMENT
NT MANNED MANEUVERING UNITS
Personnel occupied woven envelope robot
23 p3260 N88-29408
ASTRONAUT PERFORMANCE
Results of the ACCESS experiment
02 p0140 N88-10880
EASE (Experimental Assembly of Structures in EVA) overview of selected results 02 p0140 N88-10881
Overview of crew member energy expenditure during Shuttle Flight 61-B EASE/ACCESS task performance
02 p0140 N88-10882
Implications of shiftwork in space for human physiology experiments 12 p1659 N88-19942
Hypnosis: Possible applications for cosmonauts
12 p1665 N88-19984
NASA-Ames workload research program
17 p2380 N88-24151
ASTRONAUT TRAINING
A synopsis of the EVA training conducted on EASE/ACCESS for STS-61-B 02 p0140 N88-10879
The relationship between preflight underwater training and space motion sickness 19 p2696 N88-26025
Marintek's ocean basin, a training facility for extravehicular activity? 19 p2698 N88-26041
ASTRONAUTICS
Soviet space transport systems
13 p1727 N88-20328
Activities report of the Department of Aerospace Engineering
[ETN-88-91607] 24 p3460 N88-30582
ASTRONAUTS
NT ORBITAL WORKERS
Radiation effects in space
[DE87-012529] 01 p0075 N88-10479
Assessment of intercompartment fluid shifts by blood densitometry in astronauts 12 p1661 N88-19958
Studies of the vestibulo-ocular reflex on STS 4, 5 and 6
[NASA-TM-100461] 12 p1666 N88-19987
Incorporation of privacy elements in space station design
[NASA-CR-182748] 14 p1881 N88-21242
Design, development and evaluation of Stanford/Ames EVA prehensors
[NASA-CR-182688] 15 p2105 N88-22540
An investigation of conformable antennas for the astronaut backpack communication system
[NASA-CR-182908] 17 p2333 N88-23929
Bi-stem gripping apparatus
[NASA-CASE-MFS-28185-1] 17 p2345 N88-23979
Human performance issues arising from manned space station missions
[NASA-CR-3942] 18 p2553 N88-25156
Selection of isolated space crews
19 p2697 N88-26028
ASTRONOMICAL CATALOGS
Rigorous compilation of the Northern International Reference Stars (NIRS) 03 p0387 N88-12431
Catalogue of chromospherically active binaries
04 p0520 N88-13192
Catalog of infrared observations. Part 1: Data
[NASA-RP-1196-PT-1-ED-2] 07 p0944 N88-15738
Color-magnitude diagrams of star clusters in the Magellanic clouds from wide-field electronography. Part 3: NGC 1841
[PUBL-SER-C-FASC-14] 07 p0944 N88-15740
Catalog of infrared observations. Part 2: Appendixes
[NASA-RP-1196-PT-2-ED-2] 08 p1099 N88-16615
Global properties of star formation in spiral galaxies
14 p1994 N88-21883
Far infrared supplement: Catalog of infrared observations, second edition
[NASA-RP-1205] 24 p3452 N88-30545
A new determination of the Geneva photometric passbands and their absolute calibration
[SER-C-PREPUBL-FASC-26] 24 p3452 N88-30546
The guide star catalog
[NASA-CR-183253] 24 p3452 N88-30547
ASTRONOMICAL MAPS
Long-baseline astrometric interferometers
[AD-A188474] 12 p1713 N88-20250
Solar microwave radiation maps measured at Metsaehovi Radio Research Station in 1978-1979
[PB88-127543] 13 p1857 N88-21108
The guide star catalog
[NASA-CR-183253] 24 p3452 N88-30547
ASTRONOMICAL MODELS
NT DENSITY WAVE MODEL
NT STELLAR MODELS
On the degree of generality of inflationary solutions in cosmological models with a scalar field
[DE87-703079] 02 p0251 N88-11586
Cosmology with decaying vacuum energy
[DE88-000698] 03 p0389 N88-12443
A re-examination of the corona-wind dividing line: Diagnostics of non-coronal atmospheres
04 p0504 N88-13101
The acceleration of winds by MHD waves in open magnetic structures 04 p0506 N88-13109
Large scale solar and stellar magnetic fields
04 p0507 N88-13117
Comments on H. Arp The persistent problem of spiral galaxies
[TRITA-EPP-87-05] 05 p0660 N88-14052
The archiving of meteor research information
06 p0732 N88-14505
Neutron stars observations as astrophysical probes
06 p0800 N88-14896
Mars: High resolution VLA observations at wavelengths of 2 and 6 cm and derived properties
06 p0804 N88-14909
Spherical models of QSO/AGN emission line clouds
06 p0806 N88-14921
Number count-redshift relation in a perturbed Friedmann universe
[DE88-750302] 07 p0945 N88-15743
HEAO-1 observations of gamma-ray bursts
07 p0947 N88-15756
Comparative analysis of ultraviolet observations of Halley's comet on ASTRON astrophysical station before and after perihelion 08 p1004 N88-16086
Magnetic field of planet Uranus: Predictions, measurements, interpretations 08 p1005 N88-16094
Observations and modeling of the prominence/corona transition region 08 p1094 N88-16585
Beta limitation of matter-antimatter boundary layers
[TRITA-EPP-87-11] 09 p1250 N88-17490
Prediction and analysis of basic gravitational microlensing phenomena 11 p1550 N88-19272
Spectral images and multi-component models of the chromospheres of AR Lacertae
11 p1568 N88-19384
The TempIS Project: Performance analysis of temporal queries
[AD-A188354] 12 p1706 N88-20213
Models of recombination lines in radio H2 regions
[INPE-4302-TDL/277] 12 p1710 N88-20232
Data analysis of an observation of the quasar 3C 273 in the high-energy X-ray range, and the significance for astrophysical models
[ETN-88-91493] 14 p1993 N88-21878
Radiation transport in planetary nebulae
[ETN-88-91500] 14 p1993 N88-21880
Time dependent MHD models for the cometary magnetosphere 14 p1997 N88-21900
Cometary MHD and chemistry: Application to Halley
14 p2000 N88-21922
Crustal models of the evolving comet nucleus
14 p2005 N88-21953
Three approaches to the modeling of Comet Halley's motion over long periods of time
14 p2010 N88-21992
The thermal evolution of the jets in SS433 --- galactic object
[MPE-PREPRINT-107] 16 p2289 N88-23705
Stochasticity in elliptical galaxies
[SER-C-PREPUBL-FASC-20] 17 p2450 N88-24556
On the magnetic structure and energy balance of EUV-emitting plasma in the quiet Sun
17 p2452 N88-24567
Observation of a point source in Cygnus constellation with the underground detector at Frejus (France)
[PITHA-87/02] 20 p2884 N88-27122
Gamma radiation from center of the galaxy of the order of MeV values
[MPE-207] 21 p3032 N88-27999
On the dynamics of the metagalaxy
[TRITA-EPP-88-05] 22 p3166 N88-28852
Clustering of galaxies and clusters of galaxies in a decaying-particle cosmological model with a massive decay product
[DE88-753434] 23 p3298 N88-29642
Molecular hydrogen in galaxies
23 p3299 N88-29645
The interaction of Io with the plasma torus
23 p3308 N88-29704

Workshop on the Origins of Solar Systems
[NASA-CR-183025] 24 p3451 N88-30536
Comparisons of solar nebula models
24 p3451 N88-30539
The atmospheres of the earth and the other planets: Origin, evolution and composition
24 p3452 N88-30544

ASTRONOMICAL OBSERVATORIES
NT ASTRONOMICAL SATELLITES
NT GAMMA RAY OBSERVATORY
NT HEAO 2
NT HUBBLE SPACE TELESCOPE
NT INFRARED ASTRONOMY SATELLITE
NT INFRARED SPACE OBSERVATORY (ISO)
NT IUE
NT ROSAT MISSION
NT SAS
NT SPACE INFRARED TELESCOPE FACILITY
NT X RAY ASTROPHYSICS FACILITY
Ground-based optical interferometry
01 p0096 N88-10631
Activities report in astronomy
[ISSN-0531-4496] 01 p0108 N88-10701
A near-earth optical communications terminal with a corevolving planetary sun shield
04 p0434 N88-12693
Automatic telescope operations
04 p0519 N88-13190
LDR structural experiment definition
[NASA-TM-100618] 17 p2312 N88-23826

ASTRONOMICAL PHOTOGRAPHY
A search for X-ray luminous late type stars in NIPSS data 04 p0511 N88-13143
Further development of a stellar camera following the rotation-modulation-collimator principle for balloon-borne observations in the X-ray range
[ETN-88-91496] 14 p1913 N88-21428
Study of the ionic and neutral species in the coma of Comet Halley with an image intensifier camera
14 p2006 N88-21962
Memoirs of the Faculty of Science, Kyoto University. Series of Physics, Astrophysics, Geophysics and Chemistry, volume 37, no. 2
[ISSN-0368-9689] 16 p2287 N88-23694
Narrow-band photographic observations of the HII Region S296 in Canis Major 16 p2288 N88-23696
Dust and C2-contents in the coma of Halley's Comet (1986III) 16 p2288 N88-23697
Photographic observations of the large scale features of Comet Halley 16 p2288 N88-23698
Methods for indirect imaging through the atmosphere
[ONERA-NT-1987-4] 20 p2884 N88-27124
Satellite attitude determination using a CCD (Charge-Coupled-Device) star camera
[AD-A192662] 22 p3046 N88-28080

ASTRONOMICAL PHOTOMETRY
NT STELLAR SPECTROPHOTOMETRY
Extragalactic VLBI objects: Candidates for optical interferometry? 01 p0094 N88-10616
Automatic telescope operations
04 p0519 N88-13190
A processing method and results of meteor shower radar observations 06 p0738 N88-14539
The Valec fireball and predicted meteorite fall
06 p0739 N88-14547
Conception and realization of components for a microchannel-plate detector, and testing of the detector system in the laboratory and in astronomical use
[ETN-88-91495] 11 p1491 N88-18899
Memoirs of the Faculty of Science, Kyoto University. Series of Physics, Astrophysics, Geophysics and Chemistry, volume 37, no. 2
[ISSN-0368-9689] 16 p2287 N88-23694
Method of digital surface photometry of galaxies and its application to the edge-on galaxy NGC 5907
16 p2287 N88-23695
Surface photometric investigations for spiral galaxies of large dimension structures in edge-on gemetry
[ETN-88-92126] 21 p3030 N88-27985

ASTRONOMICAL SATELLITES
NT GAMMA RAY OBSERVATORY
NT HEAO 2
NT HUBBLE SPACE TELESCOPE
NT INFRARED ASTRONOMY SATELLITE
NT INFRARED SPACE OBSERVATORY (ISO)
NT IUE
NT SAS
NT SPACE INFRARED TELESCOPE FACILITY
NT X RAY ASTROPHYSICS FACILITY
An autonomous, closed-loop pointing system for use with satellite optics
[DE87-012011] 02 p0235 N88-11483
Infrared astronomy: Why and how?
09 p1123 N88-16722
Integrated focal plane star sensor
[OG-RT/86-0156] 09 p1262 N88-17562
Observation model and parameter partials for the JPL VLBI parameter estimation software MASTERFIT-1987
[NASA-CR-182524] 10 p1427 N88-18523
Deep space target location with Hubble Space Telescope (HST) and Hipparcos data
[NASA-CR-182520] 10 p1427 N88-18524
Study of a safe attitude for the Infrared Space Observatory (ISO) during perigee pass
[SNIAS-881-440-113] 23 p3185 N88-28954
Far infrared spectroscopy telescope (FIRST) inflatable thermal shield, phase 1
[SR/FIS/108(87)CZ] 24 p3453 N88-30552

ASTRONOMICAL SPECTROSCOPY
Microcomputer control of spectroscopic instruments
[ATR-86(8431)-4] 03 p0326 N88-12058
A 23 hour EXOSAT observation of the X-ray pulsar 1E2259+586 and the associated supernova remnant G109.1-1.0
[MPE-PREPRINT-99] 14 p1994 N88-21882
The observability of carbon monoxide in planetary nebulae
[ETN-88-91498] 14 p2011 N88-21994
Multiple object redshift determinations in clusters of galaxies using OCTOPUS
[INPE-4528-PRE/1278] 15 p2150 N88-22835
Fabry-Perot etalons as prefilters for astronomical far infrared Fourier transform spectroscopy
[MPE-205] 16 p2273 N88-23603
A spectroscopic study of absorption and emission features of interstellar dust components
[B8681462] 16 p2289 N88-23706
The high-throughput X-ray spectroscopy mission E6889478 MN513835 -- ESA program
[ESA-SP-1092] 17 p2450 N88-24554
Radial velocities monitoring of a sample of barium and S stars using CORAVEL: Towards an evolutionary link between barium and S stars?
[SER-C-PREPUBL-FASC-19] 18 p2593 N88-25410
Analysis of emission features in IRAS LRS spectra
21 p2928 N88-27380
The high-throughput X-ray spectroscopy mission: The mission-science report
[ESA-SP-1097] 24 p3453 N88-30557

ASTRONOMICAL TELESCOPES
U TELESCOPES

ASTRONOMY
NT GAMMA RAY ASTRONOMY
NT INFRARED ASTRONOMY
NT RADIO ASTRONOMY
NT SPACEBORNE ASTRONOMY
NT ULTRAVIOLET ASTRONOMY
NT X RAY ASTRONOMY
NT X RAY BINARIES
NT X RAY SOURCES
Activities report in astronomy
[ISSN-0531-4496] 01 p0108 N88-10701
National Science Foundation
[PB87-228375] 03 p0384 N88-12410
Method for determining atmospheric temperature profiles from observations of astronomical refraction of stars 08 p1013 N88-16139
On the time delay of the ultrahigh-energy radiation signal from the source Cygnus X-3
[DE88-700649] 10 p1431 N88-18547
Research and technology, 1987
[NASA-TM-100323] 12 p1713 N88-20253
Advice for astronomical research
[ISBN-9-03-460977-4] 16 p2289 N88-23703
Computing basic solar and lunar data from the Air Almanac
[AD-A190777] 16 p2290 N88-23710
NASA thesaurus: Astronomy vocabulary
[NASA-SP-7069] 17 p2450 N88-24553
Digital image processing from speckle interferograms by correlation methods: Application in atmospheric optics, astronomy, and biology
[ETN-88-92125] 20 p2855 N88-26953
Reports of planetary astronomy, 1988
[NASA-TM-4063] 22 p3163 N88-28835
Amateur astronomy in the space age
[RAE-TM-SS-4] 22 p3163 N88-28836
On the dynamics of the metagalaxy
[TRITA-EPP-88-05] 22 p3166 N88-28852
Automated generation of spacecraft activity plans
23 p3258 N88-29396
Catalog of open clusters and associated interstellar matter
[NASA-RP-1202] 23 p3300 N88-29652
Activities report in astronomy
[ISSN-0531-4496] 24 p3451 N88-30535
Workshop on the Origins of Solar Systems
[NASA-CR-183025] 24 p3451 N88-30536

ASTROPHYSICS
NT NUCLEAR ASTROPHYSICS
NT SOLAR PHYSICS
NT STELLAR PHYSICS
USSR report: Space
[JPRS-USP-87-003] 01 p0009 N88-10050
X-ray astronomy instruments to operate on Mir station
01 p0009 N88-10052
Institute of Geophysics and Planetary Physics at Lawrence Livermore National Laboratory
[DE87-014618] 02 p0251 N88-11583
Calibration on the Sun for stellar magnetic fields
04 p0506 N88-13113
Variations of the vertical and horizontal velocities of the small-scale structures and the physical problems related to overshoot layers 04 p0507 N88-13115
Photon counting image sensor development for astronomical applications
[NASA-CR-181507] 05 p0660 N88-14049
Astrophysics observatory in Byurakan
[AD-A185144] 05 p0660 N88-14050
Neutron stars observations as astrophysical probes
06 p0800 N88-14896
Interface between astrophysical datasets and distributed database management systems (DAVID)
[NASA-CR-182394] 07 p0942 N88-15731
Nonlinear, relativistic Langmuir waves in astrophysical magnetospheres
[NASA-CR-182422] 08 p1024 N88-16197
An introduction to nuclear astrophysics
[DE88-002761] 08 p1100 N88-16618
Quark matter in astrophysics and cosmology
[DE88-003406] 10 p1429 N88-18534
Measurements of astrophysical reaction rates for radioactive samples
[DE88-004309] 10 p1429 N88-18537
An adaptive grid finite difference method for time-dependent Magnetohydrodynamic (MHD) flows and its astrogeophysical applications
11 p1553 N88-19294
Photohydrodynamical processes near compact objects
11 p1569 N88-19390
Research and technology, 1987
[NASA-TM-100323] 12 p1713 N88-20253
Physics of condensed matter at extreme conditions
[DE88-006232] 13 p1832 N88-20958
Very high energy gamma ray astrophysics
[DE88-005821] 13 p1854 N88-21095
Particle cosmology comes of age
[DE88-006998] 15 p2151 N88-22844
Memoirs of the Faculty of Science, Kyoto University. Series of Physics, Astrophysics, Geophysics and Chemistry, volume 37, no. 2
[ISSN-0368-9689] 16 p2287 N88-23694
Narrow-band photographic observations of the HII Region S296 in Canis Major 16 p2288 N88-23696
Research and Technology, 1987, Goddard Space Flight Center
[NAS 1.15:101097] 17 p2453 N88-24572
Research in particle and gamma-ray astrophysics
[NASA-CR-183111] 20 p2887 N88-27146
The classical nova outburst
[DE88-009138] 21 p3030 N88-27987
A study of mechanisms producing astrophysical jets
[AD-A194100] 23 p3300 N88-29649
A coded mask telescope for observations of X and gamma ray sources in the southern sky
[INPE-4580-PRE/1314] 24 p3453 N88-30551
Research in particle and gamma-ray astrophysics
[NASA-CR-183126] 24 p3455 N88-30566
Activities in astrophysics
[INPE-4582-PRE/1316] 24 p3456 N88-30570

ASYMMETRY
Two classes of preconditioners computed using block matrix factorization techniques
[DE88-001313] 04 p0485 N88-12988
Asymmetry and variations of solar limb darkening along the diameter defined by diurnal motion in April 1981
04 p0506 N88-13111
Dynamic behavior of dissymmetric rotor bearings modelled with a periodic coefficient large system
05 p0596 N88-13640
Geometric nonlinear analysis of asymmetric thin-walled members
[PB87-133856] 06 p0723 N88-14446
Solar Dynamics and G-modes
[NASA-CR-180737] 06 p0805 N88-14911
The effect of asymmetric heating on flow stability and heat transfer for flow in a vertical tube
[DE88-003242] 07 p0855 N88-15193
Typhoon structural evolution
[AD-A186090] 07 p0879 N88-15333
Calculation of symmetric and asymmetric vortex seperation on cones and tangent ogives based on discrete vortex models
[NASA-CR-4122] 08 p0950 N88-15768
Evaluation of magnetic coordinates in finite-beta, asymmetric plasmas
[DE88-003665] 10 p1412 N88-18424

Asymmetric double Langmuir probe for fast and automatic measurements of plasma temperature
[DE88-004773] 10 p1414 N88-18436
Multiple scattering from nonspherical targets
[AD-A189939] 15 p2133 N88-22723
Stable, heavy, neutral particles in the sun and in toponium decay 17 p2452 N88-24568
Employment of porous polytetrafluoroethylene Membrane with a hydrophilic and hydrophobic stratal structure for construction of an enzyme electrode
[NASA-TT-20296] 19 p2620 N88-25543
Three-dimensional vortex interactions
[AD-A194066] 23 p3172 N88-28889

ASYMPTOTES
Asymptotic error bounds for power approximations to multinomial tests of fit
[MEMO-640] 08 p1072 N88-16470
On 1/n-expansion and wave functions
[DE88-701639] 16 p2260 N88-23509
Asymptotics for a system of nonlinearly coupled wave equations with an application to the galloping oscillations of overhead transmission lines
[REPT-87-78] 17 p2348 N88-23991
The two isotropic asymptotes of fiber composites
[AD-A192305] 21 p2904 N88-27231

ASYMPTOTIC GIANT BRANCH STARS
Neutron capture nucleosynthesis in low mass AGB stars 04 p0517 N88-13178
AGB (Asymptotic Giant Branch): Star evolution
[DE88-001829] 07 p0945 N88-15742
Asymptotic giant branch populations in composite stellar systems 13 p1854 N88-21098

ASYMPTOTIC METHODS
An asymptotic theory for a class of initial-boundary value problems for weakly nonlinear wave equations with an application to a model of the galloping oscillations of overhead transmission lines
[REPT-87-12] 01 p0086 N88-10556
Parallel computation of a domain decomposition method
[DE87-011444] 01 p0086 N88-10560
Asymptotics of the effective potentials and wave functions of a three-body problem in suitable coordinates
[DE87-703323] 03 p0370 N88-12326
Extrema of skewed stable processes
[AD-A185422] 05 p0642 N88-13925
Asymptotic normality of poly-t densities with Bayesian applications
[AD-A185718] 06 p0768 N88-14719
Sound propagation over uneven ground and irregular topography
[NASA-CR-182352] 06 p0776 N88-14763
Detecting and interval estimation about a slope change point
[AD-A186030] 07 p0909 N88-15509
Maximum likelihood principle and model selection when the true model is unspecified
[AD-A186027] 07 p0914 N88-15544
A note on extended quasi-likelihood
[AD-A186318] 07 p0915 N88-15555
Short data length effects in an asymptotically efficient ARMA (AutoRegressive Moving Average) spectral estimator
[AD-A186561] 08 p1068 N88-16458
Numerical analysis of motion of solid bodies in atmosphere 08 p1079 N88-16505
Steady ship waves at low Froude numbers, part 2
[AD-A176805] 09 p1160 N88-16953
On some asymptotics of laminar flow in a coiled pipe
10 p1328 N88-17936
Joint moments of the maximum in a critical branching process
[AD-A188157] 11 p1541 N88-19209
Extrema of Gaussian process by simulation
11 p1541 N88-19211
Analysis, estimation, and control for perturbed and singular systems and for systems subject to discrete events
[AD-A188496] 12 p1677 N88-20026
Steps into a geometer's workbench
[CWI-CS-R8726] 13 p1819 N88-20870
Estimation of convolution tails
[AD-A190323] 15 p2125 N88-22666
Asymptotically efficient adaptive allocation schemes for controlled Markov chains: Finite parameter space
[AD-A192228] 20 p2846 N88-26893
A simple explanation of the Stokes phenomenon
[AD-A193253] 21 p3006 N88-27832
Asymptotic normality of minimum L1-norm estimates in linear models
[AD-A193399] 21 p3006 N88-27835
Thickness effects on the stability of shell like structures 23 p3224 N88-29192
An asymptotic evaluation of the tail of a multiple symmetric alpha-stable integral
[AD-A194570] 23 p3270 N88-29460
Asymptotic modal analysis and statistical energy analysis
[NASA-CR-183077] 23 p3278 N88-29514

ASYMPTOTIC PROPERTIES
Asymptotically stable all-pass transfer functions: Canonical form, parametrization and realization
[PB87-123972] 06 p0763 N88-14684
AGB (Asymptotic Giant Branch): Star evolution
[DE88-001829] 07 p0945 N88-15742
Adaptive exponential stabilization of a first order continuous-time system
[CWI-OS-R8705] 08 p1069 N88-16461
A state space approach to the problem of adaptive pole assignment
[CWI-OS-R8704] 09 p1224 N88-17339

ASYMPTOTIC SERIES
Concurrent algorithms for transient nonlinear FE analysis
[NASA-CR-181455] 02 p0221 N88-11389
Elastodynamic ray theory and asymptotic methods for direct and inverse scattering problems
03 p0335 N88-12108
Asymptotic form of stationary solutions of the Navier-Stokes equations for large Reynolds numbers
04 p0459 N88-12838
Asymptotic analysis of a turbulent boundary layer in a strong adverse pressure gradient
[AD-A185406] 05 p0581 N88-13543
Diffusion first passage times: Approximations and related differential equations
[AD-A185592] 06 p0765 N88-14700
Testing and interval estimation in a change-point model allowing at most one change
[AD-A185525] 06 p0767 N88-14716
Parameter estimation for the Dirichlet-Multinomial Distribution (DMD) using supplementary beta-binomial data
[AD-A186335] 07 p0911 N88-15524
Maximum likelihood principle and model selection when the true model is unspecified
[AD-A186027] 07 p0914 N88-15544
Variable selection in logistic regression
[AD-A186032] 07 p0914 N88-15547
On the asymptotic joint distributions of the eigenvalues of random matrices which arise under components of covariance model
[AD-A186387] 07 p0915 N88-15558
Dynamic observers as asymptotic limits of recursive filters: Special cases
[AD-A187578] 10 p1397 N88-18324
Asymptotic expansions for large deviation probabilities in the strong law of large numbers
[AD-A187432] 10 p1402 N88-18361
Estimation of the probability of a long time to the first entrance to a state in a semi-Markov model
[AD-A188960] 12 p1685 N88-20074
Survival analysis using additive risk models
[AD-A189053] 13 p1825 N88-20906
Acoustic radiation from line- and point-loaded plates: Uniformly asymptotic solutions
[AD-A189367] 13 p1834 N88-20969
On the Edgeworth expansion and the bootstrap approximation for a Studentized U-statistic
[CWI-MS-R8708] 14 p1965 N88-21728
On 2-D versus 3-D: Sine of squared angular error and weighted perpendicular fixing
[NASA-CR-182899] 16 p2252 N88-23458
Asymptotic theory for weighted least squares estimators in Aalen's additive risk model
[AD-A191085] 18 p2562 N88-25210
On a biorthogonal system associated with uniform asymptotic expansions
[CWI-AM-R8709] 18 p2566 N88-25240
Asymptotic of Peanokerns of finite fixed order
[ETN-88-92381] 21 p3008 N88-27843
Statistical analysis of dyadic stationary processes
[AD-A193057] 21 p3009 N88-27853
Joint asymptotic distribution of marginal quantiles and quantile functions in samples from a multivariate population
[AD-A193385] 21 p3010 N88-27856
Asymptotic orders of reachability in perturbed linear systems
[AD-A192718] 22 p3143 N88-28688
Mathematical problems of nonlinear wave propagation and of waves in heterogeneous media
[AD-A195970] 24 p3368 N88-30057

ASYNCHRONOUS MOTORS
Study on the dynamics of executive electromechanism with thyristor commutator for cryogenic systems
[DE87-703209] 12 p1622 N88-19702
Industrial electric motors and controllers
[PB88-139589] 14 p1907 N88-21394

ATHODYDS
U RAMJET ENGINES

ATLANTIC OCEAN
An illustrative example of the nowcasting challenge
02 p0199 N88-11243
Summary of 1987 Atlantic tropical cyclone activity and verification of author's seasonal forecast
02 p0215 N88-11356
On the interannual variability of South American climate and the Southern Oscillation 04 p0470 N88-12905
Tectonics and magmatism of Walvis Ridge and Discovery Rise (Atlantic Ocean)
06 p0726 N88-14463
Geophysical-geomorphological statistical regionalization of North Atlantic
06 p0726 N88-14466
Tectonics of sedimentary cover and basement of Labrador Sea 06 p0726 N88-14468
Mathematical-cartographic modeling of economic utilization of Atlantic Ocean 06 p0726 N88-14469
Hydrochemical structure of Gulf Stream frontal zone waters 06 p0727 N88-14476
Modes of surface circulation and climate over the tropical Atlantic, Eastern Pacific, and Indian Oceans
06 p0742 N88-14564
Annual data summary and climatological evaluation, CERC (Coastal Engineering Research Center) field research facility, 1985, volume 2, appendix C
[AD-A185894] 07 p0881 N88-15344
Nature of Western Pacific transition zone
08 p1010 N88-16122
New data on structure of earth's crust and seismicity of basins in Atlantic and Indian Oceans
08 p1010 N88-16123
Hurricane climatology for the Atlantic and Gulf coasts of the United States
[PB88-114657] 08 p1039 N88-16288
Annual data summary and climatological evaluation CERC (Coastal Engineering Research Center) field research facility, 1985. Volume 1. Main text and appendixes A and B
[AD-A186442] 08 p1039 N88-16289
Predictability of ice concentration in the high-latitude North Atlantic from statistical analysis of SST (Sea Surface Temperature) and ice concentration data
[AD-A186621] 08 p1045 N88-16315
Hydrographic and current measurements in the North-East Atlantic Ocean. Data report on F.S. Meteor cruises 69/5 and 69/6, October to November 1984
[REPT-166] 09 p1196 N88-17164
Analysis of low frequency current fluctuations in the North-East Atlantic Ocean
[REPT-170] 09 p1196 N88-17165
Meteorological and aerosol measurements from the NOAA WP-3D aircraft during WATOX-86, January 4-9, 1986
[PB88-120860] 10 p1352 N88-18079
Trace element geochemistry of the South Atlantic Bight
[DE88-003515] 10 p1356 N88-18108
Current velocity and hydrographic observations in the Straits of Florida, the Caribbean Sea and offshore of the Antillean Archipelago: Subtropical Atlantic climate studies (STACS) 1984 and 1985
[PB88-149299] 12 p1649 N88-19874
Propagation of subsurface salinity maximum in tropical Atlantic 13 p1786 N88-20686
The use of a barotropic finite element model for the study of circulation on the continental shelf of the southeast coast of Brazil
[INPE-4401-PRE/1218] 13 p1802 N88-20774
Oceanographic export system development, year 1
[AD-A189134] 14 p1950 N88-21623
Current velocity and hydrographic observations in the Straits of Florida, the Caribbean Sea and offshore of the Antillean Archipelago: Subtropical Atlantic Climate Studies (STACS) 1986
[PB88-160767] 14 p1951 N88-21628
Forecast of Atlantic seasonal hurricane activity for 1988 15 p2098 N88-22500
SeaSoar profiles in the Iceland-Scotland area, May 1987
[IOS-253] 18 p2548 N88-25124
Determination of mesoscale variability of sea surface temperature and attenuation in the North Atlantic from satellite measurement
[REPT-162] 18 p2548 N88-25127
Meteorological satellite product support and research for project GALE
[NASA-CR-180989] 19 p2727 N88-26193
Interannual variability in the Atlantic and Indian Oceans and its relationship to the southern oscillation
22 p3121 N88-28548
Atlantic SST variability and high latitude climate fluctuations 22 p3122 N88-28551

Sub-Saharan rainfall anomalies and global sea-surface temperature relationships for the recent fifteen year (1970-1984) period 22 p3122 N88-28552
Low frequency variability of SST and its relationship to atmospheric forcing 22 p3122 N88-28554
The active layer of the upper Atlantic Ocean
22 p3124 N88-28566

ATMOSPHERE EXPLORER C
U EXPLORER 51 SATELLITE

ATMOSPHERE EXPLORER D
U EXPLORER 54 SATELLITE

ATMOSPHERE EXPLORER E
U EXPLORER 55 SATELLITE

ATMOSPHERES
MAXIE 1
[AD-A189688] 14 p1882 N88-21247

ATMOSPHERIC ABSORPTION
U ATMOSPHERIC ATTENUATION

ATMOSPHERIC ATTENUATION
An instrument for the quasi-continuous determination of atmospheric soot content
[DFVLR-FB-87-04] 01 p0068 N88-10433
Development of a climatic map of rainfall attenuation for Europe
[REPT-372] 02 p0216 N88-11359
Experimental study of the propagation of an acoustic wave in the low atmosphere
[ISL-R-111/86] 02 p0231 N88-11454
Estimates of satellite EHF communication outages due to attenuation by rain
[AD-A183969] 03 p0307 N88-11941
Absorption of far IR-radiation by H_2O-N_2 complexes under atmospheric conditions 04 p0462 N88-12855
Method of determining atmospheric moisture content by measurement of upward radiation intensity in near IR
08 p1007 N88-16106
Radiation absorption in the infrared spectral range: A comparison between laboratory measurements and theoretical calculation illustrated by a H_2O 2.7 micrometer 08 p1018 N88-16170
Literature survey relating to the absorption properties of ozone in the near ultraviolet
[ESRO-SM-81] 09 p1190 N88-17129
Remote sensing of atmospheric optical thickness and sea-water attenuation when submerged: Wavelength selection and anticipated errors
[AD-A187609] 11 p1548 N88-19262
MM-wave propagation and application in military communication systems 12 p1617 N88-19669
Distortion of wideband carbon dioxide laser radar waveforms due to atmospheric dispersion and absorption
[AD-A188687] 12 p1632 N88-19771
Calibration of the solar radiation estimation method by satellites
[INPE-4349-PRE/1185] 12 p1646 N88-19861
Atmospheric attenuation of near infrared radiation propagating through fog 14 p1899 N88-21342
Corrections for differential scattering by aerosols in the measurement of ozone by DIAL --- differential absorption lidar (DIAL)
[NPL-OU-78] 14 p1945 N88-21603
Space communication link propagation data for selected cities within the multiple beam and steerable antenna coverage areas of the advanced communications technology satellite
[NASA-TM-100861] 16 p2191 N88-23070
Study of the convergence of a finite difference scheme for acoustic propagation in the atmosphere in a parabolic approximation. Statistical calculation of the sound field in the presence of kinematic turbulence
[ONERA-RS-8/3641-PY-160-P]
17 p2394 N88-24235
Atmospheric propagation of laser beams
[AD-A191447] 18 p2520 N88-24952
Development and validation of transmission measurements techniques of image contrast, utilizing existing IR imagers
[AD-A191471] 18 p2541 N88-25079
Ground level hydroxyl (OH) concentration measurements by long path differential optical laser absorption
[ETN-88-92124] 20 p2855 N88-26952
An evaluation of two millimeter wave propagation models for horizontal atmospheric attenuation at 70-115 GHZ
[AD-A192699] 21 p2931 N88-27403
Sound propagation at low altitude
22 p3148 N88-28725
Evaluation of atmospheric effects for operational tactical decision aid
[AD-A194205] 23 p3232 N88-29236
European validation of SAGE-2 aerosol profiles
[AERONOMICA-ACTA-A-327-1988]
23 p3234 N88-29243

ATMOSPHERIC BOUNDARY LAYER
The air flow on hills from models and experiments
[BMFT-FB-T-86-175] 02 p0198 N88-11236
Forecasting boundary layer clouds and fog: A review of operational numerical models
02 p0208 N88-11307
Evaluation of a mesoscale prediction system with surface weather observations and comparison with a large-scale prediction system 02 p0210 N88-11319
Development and testing of a vertically-nested regional prediction system --- weather forecasting
02 p0210 N88-11322
A preliminary demonstration of the use of boundary-layer models of flow in complex terrain for high resolution surface wind forecasting 02 p0212 N88-11330
Visualization of the flow field around a generic destroyer model in a simulated turbulent atmospheric boundary layer
[AD-A184658] 03 p0320 N88-12023
Properties of the atmospheric boundary layer above a subtropical oceanic front
[AD-A184006] 03 p0351 N88-12215
A model for the convective atmospheric boundary layer during the winter in the Khartoum Region (Sudan)
[R-822-A] 03 p0353 N88-12225
Heat and moisture transport in the atmospheric boundary layer
[AD-A184222] 04 p0470 N88-12904
Estimation of marine boundary layer depth and relative humidity with multispectral satellite measurements
[AD-A184881] 05 p0620 N88-13804
A method to obtain a wind model for the boundary layer in a representative tropical region
[R-818-D] 06 p0743 N88-14569
Facilities for research and weather observations on the 213 m tower at Cabauw (Netherlands) and at remote locations
[KNMI-WR-87-5] 06 p0746 N88-14587
A semianalytical solution of the heat conduction equation for several boundary conditions
08 p1014 N88-16148
Wind tunnel modeling techniques
[KU-SFB-210/E/33] 09 p1121 N88-16711
Correction of the wind field measured by the NCAR electra during FASINEX (Frontal Air-Sea Interaction Experiment) for inertial navigation system drifts
[AD-A187780] 11 p1514 N88-19045
Similarity theories and microturbulence in the atmospheric mixed layer 13 p1806 N88-20802
Modeling surface exchanges: The soil-vegetation-atmosphere continuum
14 p1937 N88-21553
An introduction to the parameterization of land-surface processes 14 p1937 N88-21554
Continental surface processes and water cycle
14 p1937 N88-21555
Sensitivity of general circulation models to surface processes 14 p1937 N88-21556
Unsteady aerodynamics of a Wortmann FX-63-137 wing in a fluctuating wind field
[AD-A190128] 15 p2013 N88-22006
Spectral measurements in a disturbed boundary layer over snow
[AD-A190217] 15 p2097 N88-22494
Ground level hydroxyl (OH) concentration measurements by long path differential optical laser absorption
[ETN-88-92124] 20 p2855 N88-26952
Genesis of Atlantic lows experiment NASA electra boundary layer flights data report
[NASA-TM-100703] 22 p3128 N88-28597
The spatial and temporal variability of the arctic atmospheric boundary layer and its effect on electromagnetic (EM) propagation
[AD-A193958] 23 p3204 N88-29068
The surface evaporative duct height product: An evaluation
[AD-A195918] 24 p3392 N88-30199
Doppler radar analysis of coastal marine atmospheric boundary layer structure during a cold air outbreak
[AD-A196023] 24 p3403 N88-30261

ATMOSPHERIC CHEMISTRY
A study of carbon monoxide distribution determinations for a global transport model
[NASA-CR-181423] 01 p0067 N88-10432
Diagnostics of atmospheric chemistry through ozone measurement
[INPE-4230-PRE/1105] 01 p0068 N88-10437
Kinetics investigations of atmospheric chemical reactions
[PB87-213351] 01 p0069 N88-10439
Status of the solar and infrared radiation submodels in the LLNL 1-D and 2-D chemical-transport models
[DE87-014320] 01 p0069 N88-10441
Description of the Mountain Cloud Chemistry Program version of the PLUVIUS MOD 5.0 reactive storm simulation model
[DE87-012846] 01 p0070 N88-10450
The combined release and radiation effects satellite, a joint NASA/DOD program 02 p0135 N88-10851
Production of NO by galactic cosmic rays and lightning
[DE87-014613] 02 p0197 N88-11230
The effects of minor trace gases on the transfer of thermal infrared radiation through the Earth's atmosphere 04 p0468 N88-12893
Scientific and Operational Requirements for TOMS Data
[NASA-CP-2497] 05 p0615 N88-13774
The use of TOMS data for tropospheric ozone studies
05 p0616 N88-13784
The polar ionosphere and interplanetary field
[AD-A185386] 05 p0624 N88-13822
First flight of the ATMOS instrument during the Spacelab 3 Mission, April 29 through May 6, 1985
[NASA-CR-182360] 06 p0728 N88-14482
Use of lasers with F sub A(II)-color center KCl:Li crystals in the intraresonator laser spectroscopy method
06 p0769 N88-14729
Nonuniformity of electromagnetic field at Lambda = 10.6 micron wavelength inside atmospheric aerosol particles
06 p0772 N88-14743
Use of back air trajectories in interpreting atmospheric chemistry data: A review and bibliography
[PB88-102108] 07 p0876 N88-15312
Characteristics and climatic relevance of the atmospheric aerosol components
08 p1017 N88-16164
Investigations of the influence of chemical reactions of the vertical flow of gaseous and particulate compounds
08 p1017 N88-16165
The sodium layer at 69 N latitude in wintertime
08 p1027 N88-16218
Lidar metal density measurements in the upper atmosphere 08 p1027 N88-16219
Current issues in atmospheric change
[NASA-CR-182406] 08 p1039 N88-16287
Measurement of vertical distributions of halogenated hydrocarbons in the stratosphere
[ETN-88-91065] 09 p1191 N88-17135
Investigation of OH reaction products. Excimer laser photolysis/slab laser fluorescence under tropospheric conditions
[REPT-8] 09 p1191 N88-17137
Mesospheric dynamics and chemistry from SME data
[NASA-CR-182465] 09 p1191 N88-17139
Model investigations of atmospheric ammonia scavenging
[DE88-002337] 09 p1194 N88-17153
Gas phase pulse radiolysis
[DE88-002981] 10 p1296 N88-17751
Evaluation of regional-scale air quality models: Chairmen reports from four workshops
[DE88-001397] 10 p1352 N88-18080
The role of analytical chemistry in assessing atmospheric effects of combustion
[DE88-003909] 10 p1352 N88-18082
Initial results with the LLNL 2-D chemical-radiative-transport model of the troposphere and stratosphere
[DE88-004355] 11 p1512 N88-19033
Reports and contributions of the Max-Planck Institute of Chemistry (Otto Hahn Institute)
[REPT-1/87] 11 p1570 N88-19398
Ion content and infrared absorption of moist atmospheric air
[AD-A188839] 12 p1643 N88-19838
Evaluation of chemical and atmospheric sciences research
[AD-A188468] 12 p1687 N88-20091
Gas-chromatographic analysis of products of thermal reactions of aerosol in Venusian cloud layer on Vega-1 and Vega-2 automatic interplanetary stations
13 p1725 N88-20318
Roentgenoradiometric analysis of aerosol in Venusian clouds by Vega-1 and Vega-2 automatic interplanetary stations 13 p1726 N88-20319
Effect of nitrogen dioxide release on thermosphere
13 p1789 N88-20704
Activities report in meteorology
[AR-86-87] 13 p1798 N88-20755
Computer simulation of tropospheric chemistry
[JUEL-2144] 13 p1798 N88-20756
Local meteorological processes and air mass origin during a cloud chemical field experiment on Areskutan, Sweden, in summer 1986
[AP-28] 14 p1948 N88-21615
Observational and theoretical studies of greenhouse climate effects
[DE88-006237] 14 p1948 N88-21621

The role of water in the thermal balance of the coma
14 p1999 N88-21916

Atmospheric carbon dioxide and the global carbon cycle: The key uncertainties
[DE88-005059] 15 p2092 N88-22465

Effect of vibrational excitation on rate parameters of atmospheric reactions
[AD-A190464] 15 p2094 N88-22477

Surface ozone and ozonesounding results from the ABLE-2B expedition to Amazonia
[INPE-4523-PRE/1275] 15 p2095 N88-22484

Study of polyatomic dynamics in the atmosphere
[AD-A190964] 16 p2233 N88-23334

A theoretical model of the washout of trace gases by raindrops in the atmosphere 17 p2375 N88-24125

Ozone in the atmosphere 18 p2539 N88-25064

Laboratory experiments on atmospheric OH reactions
18 p2539 N88-25066

Effect of carbohydrate oxidation on the tropospheric HOx-system 18 p2539 N88-25067

Measurement of atmospheric OH with laser differential optical absorption spectroscopy (LDOAS)
18 p2539 N88-25068

Tropospheric OH measurements by long path absorption with rapid spectral concordance
18 p2539 N88-25069

Determination of tropospheric H concentrations by a double-pulsed UV laser method
18 p2539 N88-25070

Tropospheric OH measurement by Laser Induced Fluorescence (LIF) 18 p2540 N88-25071

Development of continuous wave laser frequency modulation of OH in tropospheric concentrations range
18 p2540 N88-25073

A primer on greenhouse gases
[DE88-007576] 19 p2689 N88-25981

Sulfur dioxide-hydrogen peroxide relationships in clean air, clouds, and precipitation
[DE88-006352] 19 p2690 N88-25990

The rate of volcanism on Venus
[NASA-CR-183039] 19 p2742 N88-26281

The solar flare of 18 August 1979: Incoherent scatter radar data and photochemical model comparisons
[DE88-007616] 19 p2743 N88-26286

Overview of the PRECP (processing of emissions by clouds and precipitation) Program
[DE88-008205] 20 p2822 N88-26741

Studies of the mechanisms and rates with which nitrogen species are incorporated into cloud water and precipitation
[PB88-193065] 20 p2826 N88-26764

Ground level hydroxyl (OH) concentration measurements by long path differential optical laser absorption
[ETN-88-92124] 20 p2855 N88-26952

Atmospheric nitrogen oxides: Their detection and chemistry
[PB88-193057] 21 p2970 N88-27642

Large-eddy simulations of concentration fluctuations
[DE88-009480] 21 p2973 N88-27660

Low density real gas flows about hypersonic vehicles
[AD-A194251] 22 p3075 N88-28253

Investigations into the properties, conditions and effects of the ionosphere
[AD-A194245] 22 p3118 N88-28528

Photochemistry of ionospheric D-region with injection of nitrogen oxides 24 p3444 N88-30499

ATMOSPHERIC CIRCULATION

NT ZONAL FLOW (METEOROLOGY)

A baroclinic wavy basic state model: Description and preliminary experiments
[KNMI-WR-87-1] 01 p0068 N88-10436

Description of NCAR (National Center for Atmospheric Research) Community Climate Model (CCM1)
[PB87-203782] 01 p0072 N88-10462

Detailed analysis of a mesoscale convective complex situation in the Carpathian Basin (Europe)
02 p0207 N88-11296

Operational practice of an air mass transformation model 02 p0208 N88-11308

Development and testing of an air-mass transformation trajectory model 02 p0209 N88-11309

An isentropic coordinate model used in a mesoscale data assimilation system 02 p0212 N88-11333

Convective scale interaction: Arc cloud lines and the development and evolution of deep convection
[NASA-CR-181469] 02 p0215 N88-11357

Heat and moisture transport in the atmospheric boundary layer
[AD-A184222] 04 p0470 N88-12904

Systematic stratospheric-tropospheric exchange viewed from isentropic coordinates 05 p0615 N88-13777

Insights into the general circulation of the lower stratosphere from TOMS 05 p0616 N88-13780

Lower-stratospheric/upper-tropospheric exchange processes associated with tropical cyclones as observed by TOMS 05 p0616 N88-13782

Environmental and convective influence on tropical cyclone development versus non-development
[AD-A185231] 05 p0627 N88-13835

Global atmospheric circulation statistics: Four year averages
[NASA-TM-100690] 05 p0628 N88-13842

Atmosphere dynamics in the equatorial meteor zone
06 p0733 N88-14508

Circulation in the mesosphere and lower thermosphere during the MAP (Middle Atmosphere Program)/WINE (Winter in the Northern Europe) period
06 p0734 N88-14514

On connection between evolution of troposphere fronts and changes of circulation regime in meteor zone
06 p0735 N88-14519

The nonlinear thermodynamics of meteors, noctilucent clouds, enhanced airglow and global atmospheric circulation 06 p0738 N88-14538

Interim review of the possibilities and opportunities for the ONR tropical cyclone motion research initiative
[AD-A185679] 06 p0746 N88-14592

The global balance of dynamic vorticity in relation to heat sources and sinks 07 p0876 N88-15316

Thunderstorms with snow: A comprehensive, empirical study of their occurrence, development and structure
[AD-A185929] 07 p0879 N88-15329

Middle atmospheric wind measurements using a medium frequency radar
[AD-A185931] 07 p0879 N88-15330

Feasibility studies of optical processing of image bandwidth compression schemes
[AD-A186073] 07 p0932 N88-15660

Orographically influenced cold fronts in a spectral approach 08 p1016 N88-16161

Numerical simulation of the flow about New Zealand
08 p1017 N88-16163

Long-term variation of total ozone
[INPE-4307-PRE/1173] 08 p1023 N88-16192

Research project on CO-induced climate change
[DE88-002352] 08 p1023 N88-16193

Large-scale dynamics of the mean flow breakdown in the stratosphere and mesosphere during the winter 1983/84 08 p1028 N88-16228

Variations of tropical circulation and associated rainfall anomalies, during 2 years of contrast
[INPE-4359-TDL/300] 08 p1039 N88-16286

Meteosat tracks Karman vortex streets in the atmosphere 09 p1128 N88-16770

Simulation of global wet and dry deposition of nitric acid in a three-dimensional chemistry-transport model
[DE87-009847] 09 p1188 N88-17116

Numerical investigation of orographically enhanced instability
[AD-A186841] 09 p1189 N88-17125

The effects of a geomagnetic storm on thermospheric circulation
[AD-A186638] 09 p1190 N88-17128

Numerical simulation of thermally generated mountain-foreland circulation
[DFVLR-FB-87-30] 09 p1190 N88-17132

Interaction of the cold conveyor belt with polar jet streaks
[AD-A186774] 09 p1192 N88-17145

Development of a physically-based general circulation model parameterization of clouds and their radiative interactions
[DE88-004060] 09 p1194 N88-17154

Persistence characteristics of 500 mb blocking and zonal flows in the mid-latitudes of the Northern and Southern Hemispheres 10 p1353 N88-18088

Application of satellite data in observational and theoretical studies of the evolving structure of baroclinic waves
[NASA-CR-179277] 10 p1354 N88-18091

Northern winter circulations for the period 1974-1983
[AD-A187779] 11 p1511 N88-19028

Analysis of quasi-geostrophic forcing during the AIMCS (Airborne Investigations of Mesoscale Convective System) Project. Volume 1: Discussion
[PB88-133095] 12 p1646 N88-19860

Sound propagation through a turbulent atmosphere: Experimental techniques and data analysis
[AD-A188891] 12 p1688 N88-20094

Negative viscosity in global circulations
13 p1786 N88-20685

Low-order spectral models of atmospheric circulation: A survey
[CWI-AM-R8705] 13 p1797 N88-20748

Seasonal variations and excitation mechanisms of the equatorially trapped waves 13 p1798 N88-20751

Model validation research: Comparison of simulated and observed climate patterns for the past 18,000 years
[DE88-004945] 13 p1800 N88-20759

Sample models of steady and low frequency circulations in the tropical atmosphere, with application to tropical air-sea interactions 13 p1801 N88-20764

Northern Hemisphere circulation and the principal components of subsequent summer patterns in North America and West Africa 13 p1801 N88-20765

Planetary scale barotropic spectral model
13 p1801 N88-20766

Study of passages of cross-equatorial current during southern monsoon 14 p1900 N88-21347

Introduction to the dynamics of the ocean and the atmosphere 14 p1935 N88-21537

The atmosphere as a component of the climate system: Structure and variability 14 p1935 N88-21540

Adiabetic formation of large-scale models of the atmosphere 14 p1935 N88-21541

Representation of physical processes in global atmospheric models 14 p1935 N88-21542

Parameterization of radiation in a general circulation model 14 p1935 N88-21543

Sea surface temperatures of winter 1982-83 and their effect on atmospheric circulation
14 p1936 N88-21546

Lidar active remote sensing: Applications to the atmosphere 14 p1936 N88-21547

Wind and buoyancy driven ocean circulation
14 p1938 N88-21564

Tropical and monsoonal studies
[AD-A188387] 14 p1947 N88-21611

Stellar scintillometer atmospheric optical turbulence profiling experiment: A qualitative comparison of two identical instruments at AMOS (Air Force Maui Optical Station), 1985
[AD-A190589] 15 p2094 N88-22479

Aerodynamic aspects of the Amazon Forest
[INPE-4445-TDL/313] 15 p2098 N88-22501

Tropical circulations and the associated rainfall anomalies during two contrasting years
[INPE-4506-PRE/1261-REV] 15 p2098 N88-22502

Ocean general circulation models: Report on proceedings of a meeting of ocean and climate modelers
[DE88-005530] 15 p2099 N88-22504

Utilization of dense packed planar acoustic echosounders to identify turbulence structure in the lowest levels of the atmosphere
[AD-A191006] 16 p2233 N88-23335

Global atmospheric circulation statistics, 1000-1 mb
[PB83-168240] 16 p2234 N88-23340

Nonlinear normal mode initialization of the NCAR (National Center for Atmospheric Research) CCM (Community Climate Model)
[PB88-171814] 16 p2235 N88-23347

The role of vortex structure in tropical cyclone motion
[AD-A190961] 16 p2235 N88-23351

Geostrophic flow in the central Bering Sea, Fall 1986 and Summer 1987
[PB88-174354] 16 p2237 N88-23360

Open cell associated with warm advection
17 p2351 N88-24010

A system for determination of wind fields using geostationary meterological satellites
17 p2360 N88-24056

On regime selection in global atmospheric flow
17 p2374 N88-24119

Cloud cover determination in polar regions from satellite imagery
[NASA-CR-182906] 17 p2375 N88-24123

Analysis of a six-component barotropic spectral model: Chaotic motion, predictability and vacillation --- atmospheric circulation
[CWI-AM-R8710] 18 p2542 N88-25090

Cluster analysis of multiple planetary flow regimes
[NASA-CR-182931] 18 p2594 N88-25418

US participation in the TOGA (Tropical Ocean and the Global Atmosphere) Program: A research strategy
[DE88-010986] 19 p2681 N88-25938

ECMWF (European Centre for Medium Range Weather Forecasts) global analyses 1979-1986: Circulation statistics and data evaluation
[PB88-178165] 19 p2692 N88-26001

Tracer water transport and subgrid precipitation variation within atmospheric general circulation models
[NASA-CR-182897] 20 p2823 N88-26745

Circulation statistics from seasonal and perpetual January and July simulations with the NCAR (National Center for Atmospheric Research) Community Climate Model (CCM1):R15
[PB88-192620] 20 p2823 N88-26748

Photon limited image processing in the space-time domain
[AD-A193142] 21 p2972 N88-27655

Intercomparison of NMC (National Meteorological Center) and ECMWF (European Centre for Medium Range Weather Forecasts) global analyses: 1980-1986
[PB88-196548] 21 p2974 N88-27668

Surface energy balance of three general circulation models: Current climate and response to increasing atmospheric CO2 [DE88-010967] 21 p2975 N88-27673

Beaufort sea mesoscale circulation study: Hydrography helicopter operations, April 1987 [PB88-203658] 21 p2976 N88-27681

The 1986-87 Pacific warm episode: Oceanic and Atmospheric features 22 p3120 N88-28535

The observed dynamical structure of low frequency variabilities 22 p3120 N88-28541

Climatology of various synoptic systems over the tropical North Pacific 22 p3121 N88-28542

The dynamics and thermodynamics of a 30-60 day oscillation 22 p3121 N88-28543

Aspects of the 30-60 day oscillation in a GCM simulation 22 p3121 N88-28545

Some diagnostic results concerning the tropical 40-50 day oscillation 22 p3121 N88-28546

Low frequency variability of SST and its relationship to atmospheric forcing 22 p3122 N88-28554

Recent secular changes in the wintertime circulation of the Southern Hemisphere 22 p3122 N88-28555

On the energy source of 1982-83 ENSO episode simulated by the NCAR community climate model 22 p3122 N88-28556

Variations in the atmosphere associated with the 11-year solar cycle 22 p3122 N88-28557

Some evidence for a Northern Hemispheric extratropic trigger mechanism of ENSO events 22 p3123 N88-28558

Persistence of North Pacific Sea surface temperature and atmospheric flow patterns 22 p3123 N88-28559

On the impact of low-latitude anomalous forcing on local and remote circulation: Winters(DJF) 1978/79 to 1986/87 22 p3123 N88-28560

Northern Hemisphere 700 mb teleconnections based on half-monthly mean anomaly data stratified by season and by sign 22 p3123 N88-28561

An observational study of interaction between large scale tropical cumulus convection and the equatorial circulation anomalies 22 p3124 N88-28564

Factors influencing summer temperatures and precipitation in the southwest 22 p3124 N88-28565

Another approach for forecasting forecast skill 22 p3126 N88-28580

Theoretical and practical limits of predictability of the NMC medium-range model 22 p3127 N88-28586

On climate prediction for India 22 p3127 N88-28590

Characteristics of regression equations for specifying monthly precipitation amounts over the United States from the field of concurrent mean 700 mb heights 22 p3127 N88-28591

Observed normal mode structure of low frequency oscillations 22 p3128 N88-28595

Development of an adjustable buoyancy balloon tracer of atmospheric motion. Phase 3: Refinement of the operational prototype system [PB88-190764] 23 p3231 N88-29230

Atmospheric angular momentum and length of day [AD-A194505] 23 p3233 N88-29238

Regional intercomparisons of General Circulation Model predictions and historical climate data: CO2 [DE88-010416] 23 p3235 N88-29248

ATMOSPHERIC COMPOSITION

NT ATMOSPHERIC MOISTURE

NT IONOSPHERIC COMPOSITION

NBS (National Bureau of Standards) research reports (April 1987) [PB87-210258] 01 p0018 N88-10111

Carbon monoxide (CO) concentration in the air as a purity parameter [INPE-4232-PRE/1107] 01 p0067 N88-10429

An instrument for the quasi-continuous determination of atmospheric soot content [DFVLR-FB-87-04] 01 p0068 N88-10433

Diagnostics of atmospheric chemistry through ozone measurement [INPE-4230-PRE/1105] 01 p0068 N88-10437

Kinetics investigations of atmospheric chemical reactions [PB87-213351] 01 p0069 N88-10439

Airborne lidar studies of Arctic polar stratospheric clouds 01 p0069 N88-10443

Contribution of bubbles and waves to air-sea CO2 flux, with implications for remote sensing [PB87-203980] 01 p0073 N88-10467

ECC (Electrochemical Concentration Cell) ozonesonde observations at South Pole, Antarctica during 1986 [PB87-207502] 02 p0197 N88-11228

Stratospheric particles: Synchrotron X-ray fluorescence determination of trace element contents [DE87-012482] 02 p0198 N88-11234

Convective cross section analysis [PB87-204566] 02 p0216 N88-11361

Spectroscopic and retrieval studies in support of SCRIBE (Stratospheric Cryogenic Interferometer Balloon Experiment) [AD-A184037] 03 p0351 N88-12216

Preliminary experimental results of gas recycling subsystems except carbon dioxide concentration 03 p0359 N88-12261

Spacecraft Fire Safety [NASA-CP-2476] 04 p0406 N88-12520

Inerting and atmospheres 04 p0406 N88-12524

Fire-related medical science 04 p0406 N88-12525

Spacecraft material flammability testing and configurations 04 p0407 N88-12529

OH(A-X) fluorescence from photodissociative excitation of HO2 at 157.5 nm [NASA-CR-181580] 05 p0563 N88-13429

TOMS: The Antarctic ozone hole and ozone trends 05 p0615 N88-13775

October lower stratospheric Antarctic temperature and total ozone from 1979-1985 05 p0615 N88-13776

Photochemical ozone overburden correction 05 p0615 N88-13778

Analysis of the breakdown of the Antarctic circumpolar vortex using TOMS ozone data 05 p0615 N88-13779

Insights into the general circulation of the lower stratosphere from TOMS 05 p0616 N88-13780

Lower-stratospheric/upper-tropospheric exchange processes associated with tropical cyclones as observed by TOMS 05 p0616 N88-13782

Volcanic eruption detection with TOMS 05 p0618 N88-13793

Analysis of SO2 signals in SBUV/TOMS data 05 p0618 N88-13794

Comparison of ground based and TOMS measurements of SO2 from volcanic emissions 05 p0618 N88-13795

Use of satellite data in volcano monitoring 05 p0618 N88-13797

Complementary information between UV and IR for remote sensing of total ozone 05 p0619 N88-13800

First flight of the ATMOS instrument during the Spacelab 3 Mission, April 29 through May 6, 1985 [NASA-CR-182360] 06 p0728 N88-14482

A review of atmospheric ozone and current thinking on the Antarctic ozone hole [AD-A185608] 06 p0732 N88-14501

Lidar investigations of M-zone 06 p0741 N88-14558

Description of data on the Nimbus 7 LIMS map archive tape: Water vapor and nitrogen dioxide [NASA-TP-2761] 06 p0744 N88-14572

Use of back air trajectories in interpreting atmospheric chemistry data: A review and bibliography [PB88-102108] 07 p0876 N88-15312

Hydrogen chloride measurements in launch-vehicle exhaust clouds [DE87-011552] 08 p0964 N88-15837

Mechanisms of cloud layer formation in Venusian atmosphere 08 p1004 N88-16087

Atmosphere of Venus in north polar area based on radio transmission data from Venera-15 and Venera-16 spacecraft 08 p1005 N88-16090

Characteristics and climatic relevance of the atmospheric aerosol components 08 p1017 N88-16164

Lidar metal density measurements in the upper atmosphere 08 p1027 N88-16219

An advanced visible-UV spectrometer for atmospheric composition measurements 08 p1029 N88-16231

Current issues in atmospheric change [NASA-CR-182406] 08 p1039 N88-16287

A rapid method for the computation of equilibrium chemical composition of air to 15000 K [NASA-TP-2792] 09 p1140 N88-16830

An infrared grating spectrometer for GIRL [ETN-88-91071] 09 p1167 N88-16997

Concept, construction, and experimental testing of a polychromator for a Raman lidar for the simultaneous telemetering of carbon dioxide and water vapor, relative to oxygen [GKSS-87/E/20] 09 p1191 N88-17134

Model investigations of atmospheric ammonia scavenging [DE88-002337] 09 p1194 N88-17153

Tropospheric ultraviolet radiation: Assessment of existing data and effect on ozone formation [PB88-130133] 10 p1354 N88-18095

Gas-phase photoelectron spectroscopy of metals and metal oxides of importance in the upper atmosphere [AD-A187771] 11 p1511 N88-19027

The influence of atmospheric thermal tides on diurnal variations in chemical constituents in the mesosphere 11 p1512 N88-19035

Vega-1 and Vega-2 automatic stations: Functioning of landing modules in Venusian atmosphere 13 p1725 N88-20313

Research on absorption of UV radiation in Venusian atmosphere from Vega-1 and Vega-2 landing modules 13 p1725 N88-20316

Gas-chromatographic analysis of products of thermal reactions of aerosol in Venusian cloud layer on Vega-1 and Vega-2 automatic interplanetary stations 13 p1725 N88-20318

Chemical composition and structure of Venusian clouds determined from results of roentgenoradiometric experiments carried out by landing modules of Vega-1 and Vega-2 automatic interplanetary stations 13 p1726 N88-20320

Effect of nitrogen dioxide release on thermosphere 13 p1789 N88-20704

An automated ozone photometer [NASA-TM-100064] 14 p1908 N88-21404

Lidar active remote sensing Applications to the atmosphere 14 p1936 N88-21547

Report of Atmospheric-Canopy Exchange Panel [DE88-004478] 14 p1944 N88-21597

Ground-based column abundance measurements of atmospheric hydroxyl [NASA-CR-182676] 14 p1944 N88-21598

Analysis of meteorological conditions and haze distribution for the Second Arctic Gas and Aerosol Sampling Program (AGASP 2), March-April 1986 [PB88-164140] 14 p1948 N88-21618

Assessment of crop loss from air pollutants. Meteorology-atmospheric chemistry and long range transport [PB88-146857] 15 p2089 N88-22448

Surface CO results from the ABLE-2B expedition to Amazonia [INPE-4501-PRE/1258] 15 p2093 N88-22469

Study of polyatomic dynamics in the atmosphere [AD-A190964] 16 p2233 N88-23334

Understanding CO2 and climate [PB88-167655] 16 p2234 N88-23341

Information analysis of integral equations in remote sensing of atmospheric aerosols 18 p2532 N88-25022

Oxidation and reduction rates for organic carbon in the Amazon mainstream tributary and floodplain, inferred from distributions of dissolved gases [NASA-CR-182943] 18 p2538 N88-25062

Trace gas measurements in the troposphere using tunable diode lasers 18 p2540 N88-25072

Stratospheric positive ion composition measurements and acetonitrile detection: A consistent picture [AERONOMICA-ACTA-A-326-1987] 18 p2542 N88-25084

A primer on greenhouse gases [DE88-007576] 19 p2689 N88-25981

Diagnostic studies of the HxOy-NzOy-O3 photochemical system using data from NASA GTE field expeditions [NASA-CR-183038] 19 p2689 N88-25984

Meteorological aspects of wet deposition in Southern Finland [FMI-3] 19 p2693 N88-26007

Physiological effects on man of long duration confinement in a carbon dioxide enriched environment 19 p2695 N88-26017

Measurement of HO2 and other trace gases in the stratosphere using a high resolution far-infrared spectrometer at 28 KM [NASA-CR-180400] 20 p2821 N88-26737

Wavenumber spectra from THIR 6.7 micron water vapor data 20 p2824 N88-26756

An efficient model for changes of global climate and composition of the atmosphere due to human activities [ETN-88-92359] 20 p2827 N88-26775

Space infrared telescope facility project [NASA-CR-183058] 20 p2883 N88-27121

Ultraviolet geometric albedo of Uranus [NASA-CR-183099] 20 p2885 N88-27136

ECC (Electrochemical Concentration Cell) ozonesonde observations at South Pole, Antarctica during 1987 [PB88-202015] 21 p2970 N88-27644

National air toxics information clearinghouse: NATICH data base users guide for data viewing, February 1988 [PB88-197470] 21 p2970 N88-27645

National ambient Volatile Organic Compounds (VOCs) data base update, documentation [PB88-195631] 21 p2971 N88-27646

Photochemical oxidant formation: Overview of current knowledge and emerging issues [PB88-195235] 21 p2971 N88-27647

Atmospheric deposition of nitrate to the ocean surface 23 p3231 N88-29227

Forty-eight-inch lidar aerosol measurements taken at the Langley Research Center, May 1974 to December 1987 [NASA-RP-1209] 23 p3232 N88-29234

Laboratory evaluation and application of microwave absorption properties under simulated conditions for planetary atmospheres
[NASA-CR-182443] 23 p3300 N88-29653
Recent measurements of ozone in the Amazon forests
[INPE-4494-PRE/1258] 24 p3389 N88-30185
Recent observations of carbon monoxide in the Amazon Rain Forest
[INPE-4478-PRE/1245] 24 p3390 N88-30186

ATMOSPHERIC CONDITIONS
U METEOROLOGY

ATMOSPHERIC CONDUCTIVITY
The influence of conductivities consistent with field-aligned currents on high-latitude convection patterns
[TRITA-EPP-88-02] 22 p3119 N88-28533

ATMOSPHERIC CORRECTION
The absolute radiometric calibration of the advanced very high resolution radiometer
[NASA-CR-182755] 14 p1941 N88-21584
Atmospheric corrections for in-flight satellite radiometric calibration
[AD-A196124] 24 p3391 N88-30194

ATMOSPHERIC DENSITY
Models of high spatial frequency thermal blooming instabilities
[DE87-014280] 01 p0052 N88-10330
Mesoscale density variability in the mesosphere and thermosphere: Effects of vertical flow accelerations
06 p0736 N88-14529
Aerosol optical depth and ratios of diffuse-sky to total solar irradiance measured from aircraft following the eruption of El Chichon
[PB88-100789] 07 p0878 N88-15326
Investigation of the feasibility of an analytical method of accounting for the effects of atmospheric drag on satellite motion 07 p0923 N88-15608
Atmosphere of Venus in southern polar area
08 p1005 N88-16088
Atmosphere of Venus in south polar area based on radio transmission data 08 p1005 N88-16089
Density flows at the mountain edge
08 p1016 N88-16156
Improved resolution atmospheric density measurements based on simulations 08 p1027 N88-16221
A method of atmospheric density measurements during space shuttle entry using ultraviolet-laser Rayleigh scattering
[NASA-TM-100056] 15 p2069 N88-22337
A survey of denser-than-air atmospheric dispersion models
[DE88-006626] 15 p2092 N88-22467
Three-dimensional temperature fields in the atmosphere up to 50 km altitude
[ETN-88-92150] 18 p2542 N88-25089
Wave structures in thermospheric density from satellite electrostatic triaxial accelerometer measurements
[AD-A194134] 23 p3233 N88-29240
Approximation of atmospheric density by Chebyshev polynomials in predicting motion of low artificial earth satellites 24 p3445 N88-30503

ATMOSPHERIC DIFFUSION
Opportunities for nowcasting air pollution episodes and accidental toxic and radioactive releases
02 p0210 N88-11317
Real-time evaluation and prediction of coastal dispersion near the SW tip of Africa --- effluents
02 p0210 N88-11318
A computer code to calculate line by line atmospheric transmission spectra on a microcomputer
[NASA-TM-100686] 05 p0554 N88-13372
Atmospheric diffusion at coastal site in presence of sea-breeze
[DE88-700038] 07 p0876 N88-15314
Development of an atmospheric diffusion evaluation method incorporating topographical effects. Part 1: Literature review of atmospheric diffusion models incorporating terrain effects
[DE88-753104] 20 p2822 N88-26742
Wind tunnel study of atmospheric diffusion in unstable stratified boundary layer. Part 2: Characteristic scale and diffusion
[DE88-753109] 20 p2823 N88-26749
Global vertical mass transport by clouds: A two-dimensional model study
[CM-74] 24 p3391 N88-30192

ATMOSPHERIC EFFECTS
Analysis of free molecular effects on the attitude of satellites in geostationary transfer orbit. Part 2: Force and torque measurement in free molecular wind tunnel tests
[DFVLR-IB-222-86-A/07] 01 p0014 N88-10078
Object-dependent atmospheric influence on LANDSAT recordings 01 p0065 N88-10420
Computational method for orbit improvement for short arc observations of artificial satellites
03 p0269 N88-11690
The atmosphere of Mars and optical communications
04 p0434 N88-12692
Considering refraction in leveling with laser plane
04 p0462 N88-12857
The effect of environment on low cycle fatigue properties in HSLA steel 05 p0605 N88-13705
Fatigue crack propagation in Al-Zn-Mg bicrystals and its dependence on the environment
05 p0605 N88-13707
Environmental fracture toughness and static fatigue crack propagation of silica glass
05 p0606 N88-13716
Environmentally assisted fatigue crack growth
05 p0608 N88-13731
AIS-2 radiometry and a comparison of methods for the recovery of ground reflectance
05 p0611 N88-13757
Calibrating AIS images using the surface as a reference 05 p0612 N88-13760
Causes of spurious features in spectral reflectance data 05 p0614 N88-13769
Results on the low elevation angle propagation experiment, part 1
[TUD-R-328] 06 p0693 N88-14250
Induced turbulence in aerosol-loaded atmospheres, Jun. 1987
[DE87-014724] 09 p1192 N88-17141
User's guide for the HF (High Frequency) broadcast antenna design and validation summary programs
[PB88-116124] 10 p1317 N88-17875
The role of analytical chemistry in assessing atmospheric effects of combustion
[DE88-003909] 10 p1352 N88-18082
Proceedings of the Forest-Atmosphere Interaction Workshop
[CONF-8510250] 12 p1641 N88-19824
Analysis of spectral reflectance characteristics of targets under satellites and automatic cloud recognition
13 p1755 N88-20498
The spreading and mixing of dense gas clouds in still air
[KNMI-WR-87-12] 16 p2230 N88-23320
The effects of solar cycle and latitude dependence on the formation of ionospheric C layer
[INPE-4342-TDL/293] 16 p2232 N88-23332
Spectral measurements for correcting LANDSAT data for atmospheric effects 17 p2353 N88-24020
Spectral measurements for correcting LANDSAT data for atmospheric effects 17 p2362 N88-24066
Analysis of the parameters responsible for the variations of the illumination conditions in the LANSAT data
17 p2362 N88-24070
Evaluation of atmospheric effects for operational tactical decision aid
[AD-A194205] 23 p3232 N88-29236

ATMOSPHERIC ELECTRICITY
NT AURORAL ELECTROJETS
NT EQUATORIAL ELECTROJET
NT IONOSPHERIC CURRENTS
F-layer polar cap arcs
[AD-A186592] 09 p1190 N88-17127
The growth potential of corona discharges from aircraft flying in precipitation
[AD-A190507] 15 p2094 N88-22478
Atmospheric Science and Remote Sensing Laboratory
[NASA-CR-179290] 16 p2236 N88-23355
Finite element simulation of the atmosphere's electromagnetic response to charge perturbations associated with lightning 17 p2375 N88-24124

ATMOSPHERIC EMISSION
U AIRGLOW

ATMOSPHERIC ENTRY
NT HYPERSONIC REENTRY
NT REENTRY
NT SPACECRAFT REENTRY
Guidance and control strategies for aerospace vehicles
[NASA-CR-181579] 05 p0643 N88-13935
Atmospheric entry heating of cosmic dust
06 p0794 N88-14865
A simplified streamline swallowing procedure for the windward meridian of axisymmetric blunt bodies
[AD-A188413] 12 p1626 N88-19732
Guidance and control strategies for aerospace vehicles
[NASA-CR-183032] 18 p2467 N88-24644
A design study of onboard navigation and guidance during aerocapture at Mars
[NASA-CR-172053] 18 p2469 N88-24654
Investigation of the validity of the non-rotating planet assumption for three-dimensional earth atmospheric entry
[AD-A194877] 24 p3331 N88-29829

ATMOSPHERIC HEAT BUDGET
Climatology and space observations
[ISBN-2-85-428179-9] 14 p1935 N88-21536
Introduction to the dynamics of the ocean and the atmosphere 14 p1935 N88-21537
Parameterization of radiation in a general circulation model 14 p1935 N88-21543
Carbon dioxide and climate 14 p1936 N88-21545
The Earth radiation budget and its spatial and temporal variations 14 p1936 N88-21548
The role of radiation transfer in climate modification
14 p1936 N88-21549
Continental surface processes and water cycle
14 p1937 N88-21555
Sensitivity of general circulation models to surface processes 14 p1937 N88-21556

ATMOSPHERIC HEATING
Possible dynamical mechanisms for the Martian polar warming phenomenon
[NASA-CR-181454] 02 p0254 N88-11605
Structure of stably stratified atmospheric surface layer in presence of heat-releasing admixture
04 p0462 N88-12856
Flux tube dynamics and solar/stellar redshift measurements 04 p0503 N88-13095
Observational constraints and evidence for saturation
04 p0503 N88-13097
Heating of stellar chromospheres and coronae: Evidence for non-magnetic basal heating
04 p0503 N88-13098
Atmospheres of stars in the limits of thin and thick convection zones: The M dwarfs
04 p0505 N88-13104
Magnetic flux tubes as sources of wave generation
04 p0505 N88-13108
Statistical properties of small high-velocity events in the solar transition region 04 p0506 N88-13112
Atmospheric heating from optical absorption by aerosols
[DE88-002654] 07 p0878 N88-15327
The role of anabatic winds in the heating of valleys
08 p1014 N88-16144
The role of water in the thermal balance of the coma
14 p1999 N88-21916
Extratropical response to tropical heating as a function of period of model integrations
22 p3125 N88-28577
Observed normal mode structure of low frequency oscillations 22 p3128 N88-28595
Ionosonde studies of field-aligned irregularities during high-power HF heating at Arecibo
[AD-A195848] 24 p3401 N88-30256

ATMOSPHERIC IMPURITIES
U AIR POLLUTION

ATMOSPHERIC IONIZATION
NT AURORAL IONIZATION
Satellite environment: Polar orbits
03 p0272 N88-11713
Elementary process and meteor train spectra
06 p0732 N88-14504
Meteor matter interaction with the Earth's atmosphere and the ionospheric E-region structure
06 p0738 N88-14537
Meteor velocity distribution and an optimum monitoring mathematical model 06 p0739 N88-14546
TOTAL: A new instrument to study turbulent parameters in the mesosphere and lower thermosphere
08 p1029 N88-16234
Theoretical plasma physics research of active space experiments
[AD-A192075] 18 p2577 N88-25309

ATMOSPHERIC LASERS
Atmospheric backscatter at 10.6 microns; a compendium of measurements made outside the United Kingdom by the airborne LATAS coherent laser radar velocimeter
[RSRE-87002] 12 p1631 N88-19763
Distortion of wideband carbon dioxide laser radar waveforms due to atmospheric dispersion and absorption
[AD-A188687] 12 p1632 N88-19771
Atmospheric propagation of laser beams
[AD-A191447] 18 p2520 N88-24952

ATMOSPHERIC LOADING
U POLLUTION TRANSPORT

ATMOSPHERIC MODELS
NT REFERENCE ATMOSPHERES
A study of carbon monoxide distribution determinations for a global transport model
[NASA-CR-181423] 01 p0067 N88-10432
A baroclinic wavy basic state model. Description and preliminary experiments
[KNMI-WR-87-1] 01 p0068 N88-10436
Description of NCAR (National Center for Atmospheric Research) Community Climate Model (CCM1)
[PB87-203782] 01 p0072 N88-10462

ATMOSPHERIC MODELS

Contribution of bubbles and waves to air-sea CO2 flux, with implications for remote sensing
[PB87-203980] 01 p0073 N88-10467
The air flow on hills from models and experiments
[BMFT-FB-T-86-175] 02 p0198 N88-11236
Mesoscale Analysis and Forecasting: Incorporating Nowcasting
[ESA-SP-282] 02 p0199 N88-11239
On the role of snow in the redistribution of precipitation by small scale topography 02 p0203 N88-11267
Conceptual models of Baiu front and Baiu frontal disturbances in multiscale characteristics --- East Asia
02 p0203 N88-11271
A one-dimensional model of thermally-driven coastal front evolution 02 p0204 N88-11274
The role of low-level cooling in a conceptual model of the Australian summertime cool change: Implications for very-short-range forecasting 02 p0204 N88-11275
On the interaction between radar and satellite image nowcasting systems and mesoscale numarical models
02 p0204 N88-11277
Satellite imagery and conceptual models in mesoscale forecasting 02 p0205 N88-11282
Simplified models for use in an operational short range forecasting system 02 p0206 N88-11289
The studies of physical models on hailstorms and their applications in nowcasting 02 p0207 N88-11300
Forecasting boundary layer clouds and fog: A review of operational numerical models
02 p0208 N88-11307
Operational practice of an air mass transformation model 02 p0208 N88-11308
Development and testing of an air-mass transformation trajectory model 02 p0209 N88-11309
Two-dimensional numerical modeling of the life cycle of fog 02 p0209 N88-11311
The Norwegian mesoscale Numerical Weather Prediction (NWP) system 02 p0210 N88-11320
Preliminary results from real data experiments with the NRL mesoscale numerical model
02 p0211 N88-11323
Validation of a three dimensional numerical model of the sea breeze in complex terrain
02 p0211 N88-11325
The mesoscale numerical model for heavy rainfall forecasting in Yangtze River Valley, China
02 p0211 N88-11326
The impact on short-term precipitation forecast skill of time-dependent lateral and lower boundary conditions within a meso-beta numerical cloud prediction model
02 p0211 N88-11327
Mesoscale analysis and nowcasting via a numerical model coupled with satellite sounder data
02 p0211 N88-11328
A preliminary demonstration of the use of boundary-layer models of flow in complex terrain for high resolution surface wind forecasting 02 p0212 N88-11330
An isentropic coordinate model used in a mesoscale data assimilation system 02 p0212 N88-11333
Strategies for using mesoscale data in an operational mesoscale model 02 p0212 N88-11335
Methods of incorporating satellite data into mesoscale numerical forecast models 02 p0212 N88-11336
Toward optimizing the use of data for operational mesoscale forecasting at the National Meteorological Center 02 p0213 N88-11337
Assimilation of high resolution TOVS data into a mesoscale NWP model --- numerical weather prediction (NWP) 02 p0213 N88-11338
Impact of a direct assimilation of satellite-inferred precipitation rates into a regional meteorological model
02 p0213 N88-11342
Initialization experiments with the NMC nested grid model --- National Meteorological Center (NMC)
02 p0213 N88-11343
The future of data in mesoscale numerical models
02 p0214 N88-11344
Simulation of mesoscale satellite sounder data from a mesoscale numerical model 02 p0214 N88-11345
The challenge of using mesoscale data in mesoscale numerical models 02 p0214 N88-11346
The challenge of using mesoscale data in mesoscale numerical models: A position paper
02 p0214 N88-11347
Comments on the challenge of using mesoscale data in mesoscale numerical models
02 p0214 N88-11348
Four-dimensional initialization of mesoscale models
02 p0214 N88-11349
Windfield simulations from a hierarchy of nested meso- and micrometeorological models
02 p0215 N88-11351
Documentation of the regional climate model based on FITNAH
[DFVLR-MITT-87-07] 02 p0216 N88-11358
Thermal atmospheric models
02 p0253 N88-11599
Quasi-thermal models 02 p0253 N88-11600
M dwarfs: Theoretical work 02 p0253 N88-11602
A model for the convective atmospheric boundary layer during the winter in the Khartoum Region (Sudan)
[R-822-A] 03 p0353 N88-12225
Structure of stably stratified atmospheric surface layer in presence of heat-releasing admixture
04 p0462 N88-12856
Banded ion morphology 04 p0468 N88-12892
User's guide to NCAR (National Center for Atmospheric Research) CCM1
[PB87-224366] 04 p0469 N88-12899
A review of parameterizations of microphysical processes in clouds for application in models of regional atmospheric deposition
[DE88-000451] 04 p0471 N88-12909
Application of dynamic atmosphere models to the analysis of angular diameter observations of Mira variables 04 p0515 N88-13168
Analysis of geophysical data bases and models for spacecraft interactions
[AD-A184809] 05 p0555 N88-13375
MODTRAN: A moderate resolution model for LOWTRAN
[AD-A185384] 05 p0574 N88-13503
Ozone, jet streaks and severe weather
05 p0616 N88-13781
Application of TOMS data to weather analysis models
05 p0617 N88-13787
The polar ionosphere and interplanetary field
[AD-A185386] 05 p0624 N88-13822
On-site meteorological program guidance for regulatory modeling applications
[PB87-227542] 06 p0731 N88-14498
A method to obtain a wind model for the boundary layer in a representative tropical region
[R-818-D] 06 p0743 N88-14569
Integrated systems with applications to the multi-phases of the ephemerides, physics and methematics of the upper atmosphere
[AD-A185748] 06 p0743 N88-14570
An Earth radiation budget climate model
[NASA-CR-182368] 06 p0744 N88-14578
Report of the second session of the CAS/JSC working group on numerical experimentation --- weather forecasting
[WMO/TD-168] 06 p0745 N88-14579
A survey study of energy distribution in component stars of Algol-type binary systems 06 p0801 N88-14901
Dynamics Explorer guest investigator
[NASA-CR-181494] 07 p0878 N88-15325
An introduction to single point closure methodology
08 p0986 N88-15973
Turbulence models for practical applications
08 p0986 N88-15974
Examples of turbulence-model applications
08 p0987 N88-15975
Direct and large eddy simulation of turbulence. Summary of the state of art 1987 08 p0987 N88-15977
Synoptic perturbations and climate
08 p1016 N88-16158
Numerical modeling of radiation fog
08 p1017 N88-16166
Research project on CO-induced climate change
[DE88-002352] 08 p1023 N88-16193
A comparison of multi-layer meso-alpha MLAM model results with surface and aircraft observations from CAPTEX
[DE88-000549] 09 p1188 N88-17118
Numerical investigation of orographically enhanced instability
[AD-A186841] 09 p1189 N88-17125
The effects of a geomagnetic storm on thermospheric circulation
[AD-A186638] 09 p1190 N88-17128
The accuracy of the radiation parameterization in mesoscale models
[DFVLR-IB-553-85/11] 09 p1190 N88-17133
Simulations of thermally induced winds and cross flow situations
[MITT-57] 09 p1193 N88-17148
A Lagrangian model of dry thermals
[DM-50] 09 p1193 N88-17150
Development of an engineering model atmosphere for Mars
[NASA-CR-182462] 09 p1263 N88-17568
Theoretical and observational problems with Holes in the far UV dayglow
[AD-A188190] 10 p1355 N88-18100
Minimum Energy Routing through Interactive Techniques (MERIT) modeling
[NASA-CR-182535] 10 p1356 N88-18105
A spherical, non-LTE, blanketed model stellar atmosphere for Phi Cas (FOIa)
10 p1428 N88-18528
Computer architecture for research in meteorology and atmospheric chemistry
[PB88-145313] 11 p1510 N88-19020
Initial results with the LLNL 2-D chemical-radiative-transport model of the troposphere and stratosphere
[DE88-004355] 11 p1512 N88-19033
The influence of atmospheric thermal tides on diurnal variations in chemical constituents in the mesosphere
11 p1512 N88-19035
An analytical method for the determination of the average horizontal wind velocities across two-dimensional hills
[ISBN-3-923624-06-9] 11 p1515 N88-19048
Model of limited area of 5 layers for numerical weather forcasting
[INPE-4324-RPE/551] 11 p1516 N88-19053
Comparison of simulation modeling and satellite techniques for monitoring ecological processes
[NASA-CR-182592] 12 p1641 N88-19825
Enhancements to the atmospheric transmittance/radiance program FASCODE
[AD-A188863] 12 p1643 N88-19839
National Severe Storms Laboratory, fiscal year 1987
[PB88-140108] 12 p1647 N88-19863
Spatial and temporal monitoring of the Jovian atmosphere 12 p1711 N88-20240
A polarimetric rain backscatter model developed for coherent polarization diversity radar applications
13 p1759 N88-20520
Low-order spectral models of atmospheric circulation: A survey
[CWI-AM-R8705] 13 p1797 N88-20748
Dynamical modeling of marine boundary layer convection 13 p1797 N88-20750
Computer simulation of tropospheric chemistry
[JUEL-2144] 13 p1798 N88-20756
Model validation research: Comparison of simulated and observed climate patterns for the past 18,000 years
[DE88-004945] 13 p1800 N88-20759
Sample models of steady and low frequency circulations in the tropical atmosphere, with application to tropical air-sea interactions 13 p1801 N88-20764
Similarity theories and microturbulence in the atmospheric mixed layer 13 p1806 N88-20802
Model of Jovian F region ionosphere
[NASA-CR-182587] 13 p1855 N88-21105
Millimeter-wave properties of the atmosphere: Laboratory studies and propagation modeling
[PB88-164215] 14 p1905 N88-21387
Climatology and space observations
[ISBN-2-85-428179-9] 14 p1935 N88-21536
Adiabetic formation of large-scale models of the atmosphere 14 p1935 N88-21541
Representation of physical processes in global atmospheric models 14 p1935 N88-21542
Parameterization of radiation in a general circulation model 14 p1935 N88-21543
Assimilation of meteorological observations
14 p1936 N88-21544
Carbon dioxide and climate 14 p1936 N88-21545
Sea surface temperatures of winter 1982-83 and their effect on atmospheric circulation
14 p1936 N88-21546
The role of radiation transfer in climate modification
14 p1936 N88-21549
Net radiative flux at the Earth surface: Estimation from satellite observations 14 p1936 N88-21550
Satellite estimations of the solar radiation flux at the surface 14 p1936 N88-21551
Satellite retrieval of cloud cover parameters and the International Satellite Cloud Climatology Program (ISCCP) 14 p1937 N88-21552
An introduction to the parameterization of land-surface processes 14 p1937 N88-21554
Sensitivity of general circulation models to surface processes 14 p1937 N88-21556
The Hapex-Mobilhy program 14 p1938 N88-21560
Nonlinear normal mode initialization of a limited area model using nonstationary Rossby modes --- numerical weather forecasting
[KNMI-WR-87-10] 14 p1947 N88-21614
A model of the anisotropic structure of the neutral gas coma of a comet 14 p1999 N88-21918
Derivation of consistent surface fixed fields for use in a global NWP model
[AD-A190131] 15 p2093 N88-22475
A study on electric fields and conductivity associated with electrified clouds in the region of South America
[INPE-4487-TDL/325] 15 p2096 N88-22486

Ocean general circulation models: Report on proceedings of a meeting of ocean and climate modelers
[DE88-005530] 15 p2099 N88-22504

WAVFLD: A program to compute ionospheric height gain functions and field strengths at VLF
[AD-A191159] 16 p2191 N88-23066

Nonlinear normal mode initialization of the NCAR (National Center for Atmospheric Research) CCM (Community Climate Model)
[PB88-171814] 16 p2235 N88-23347

Chemical kinetics and photochemical data for use in stratospheric modeling evaluation Number 8
[NASA-CR-182919] 17 p2351 N88-24012

On regime selection in global atmospheric flow
17 p2374 N88-24119

Cloud cover determination in polar regions from satellite imagery
[NASA-CR-182906] 17 p2375 N88-24123

The precipitation of energetic heavy ions into the upper atmosphere of Jupiter
[NASA-TM-101155] 17 p2452 N88-24565

Changes in the Antarctic atmosphere due to the reduction of stratospheric ozone
[ETN-88-92565] 18 p2540 N88-25074

Brunt-Doppler ducting of buoyancy waves in a temperature- and wind-stratified atmosphere
18 p2542 N88-25086

Analysis of a six-component barotropic spectral model: Chaotic motion, predictability and vacillation --- atmospheric circulation
[CWI-AM-R8710] 18 p2542 N88-25090

Photochemical and thermal modeling in the early atmosphere of the earth
[NASA-CR-183029] 18 p2543 N88-25093

Adaptive grid refinement for numerical weather prediction
[AD-A192172] 18 p2544 N88-25101

Bracknell Meteorological Office
18 p2545 N88-25107

Applications products of aviation forecast models
18 p2546 N88-25109

Comparative verification between GEM model and official aviation terminal forecasts
18 p2546 N88-25115

Computer and model changes at National Meteorological Center (NWC) 18 p2547 N88-25116

MM4 (Penn State/NCAR (National Center for Atmospheric Research)) mesoscale model version 4 documentation
[PB88-173232] 19 p2688 N88-25979

NOAA (National Oceanic and Atmospheric Administration) Meteorology Division support to the Environmental Protection Agency
[PB88-179866] 19 p2689 N88-25980

A study of the dynamics of the Intertropical Convergence Zone (ITCZ) in a symmetric atmosphere-ocean model
[NASA-TM-86220] 19 p2693 N88-26005

Verification of regional climates of GISS GCM. Part 1: Winter
[NASA-TM-100695] 19 p2694 N88-26012

Effects of atmospheric model layering on LOWTRAN 6 calculations of 8-12 micrometers near-horizon sky radiances
[AD-A192969] 20 p2791 N88-26559

Rocket measurements within a polar cap arc: Ionospheric modelling
[AD-A192381] 20 p2824 N88-26754

Diffusion of slight solar induced disturbances in the middle atmosphere
[MITT-53] 20 p2825 N88-26758

The NASA Marshall engineering thermosphere model
[NASA-CR-179359] 20 p2825 N88-26760

Influence of stable stratification on atmospheric turbulence: An experimental contribution
[ETN-88-92292] 20 p2827 N88-26772

Photochemical oxidant formation: Overview of current knowledge and emerging issues
[PB88-195235] 21 p2971 N88-27647

Approximate analytical formulae for electron density and collision frequency in the natural and nuclear-disturbed ionosphere and inner magnetosphere
[AD-A193129] 21 p2972 N88-27654

Development of radiation and cloud parameterization programs for AFGL (Air Force Geophysics Laboratory) global models
[AD-A193369] 21 p2973 N88-27658

Air-sea interaction in the vicinity of a land-sea boundary in the presence of upwelling 21 p2973 N88-27661

Surface energy balance of three general circulation models: Current climate and response to increasing atmospheric CO2
[DE88-010967] 21 p2975 N88-27673

Another approach for forecasting forecast skill
22 p3126 N88-28580

A bulk model for the unstable planetary boundary layer over the sea. A sensitivity investigation
[DM-51] 22 p3129 N88-28600

Atmospheric deposition of nitrate to the ocean surface
23 p3231 N88-29227

A model of the ionosphere in the altitude interval 50 to 4000 km. Part 1: Atomic ions (H(+), He(+), N(+), O(+))
[DFVLR-FB-88-11-PT-1] 23 p3233 N88-29241

A model of the ionosphere in the altitude interval 50 to 4000 km. Part 2: Molecular ions (N2(+), NO(+), O2(+)) and electron density
[DFVLR-FB-88-12-PT-2] 23 p3234 N88-29242

Snapshots of high-latitude electrodynamics using Viking and DMSP/F7 observations
[TRITA-EPP-88-01] 23 p3234 N88-29244

Investigations on the entropy of cloudy air
[ESA-TT-1060] 23 p3234 N88-29245

Global vertical mass transport by clouds: A two-dimensional model study
[CM-74] 24 p3391 N88-30192

Ionosonde studies of field-aligned irregularities during high-power HF heating at Arecibo
[AD-A195848] 24 p3401 N88-30256

Cloud/mesoscale model development and application studies
[AFGL-TR-87-0219] 24 p3404 N88-30269

Using nonstationary models of the atmosphere to describe satellite drag 24 p3445 N88-30502

Model representation of electron concentration distribution in outer middle-latitude ionosphere using data from Intercosmos-19 artificial earth satellite
24 p3447 N88-30513

ATMOSPHERIC MOISTURE

Diagnosing short term changes in temperature and moisture profiles from single Doppler radar
02 p0200 N88-11251

Structure and modification of winter mountain clouds in the Sierra Nevada: Nowcasting/forecasting the onset of supercooled liquid water 02 p0202 N88-11263

Effects of the large scale motion and horizontal inhomogeneity of the moist static instability on development of the mesoscale convective systems in the midlatitudes 02 p0207 N88-11297

The effect of enhanced conventional and VAS moisture analysis on RAFS short-range precipitation forecasts --- Regional Analysis and Forecasting System (RAFS)
02 p0215 N88-11352

Lidar-radiometric method for determining liquid-water content of cirrus clouds 04 p0461 N88-12854

Influence of bonding shop moisture on metal-honeycomb junctions bonded with ultra-thin adhesive films
[SNIAS-872-422-112] 05 p0558 N88-13399

Investigation of effect of silver compounds on microflora in water reclaimed from atmospheric moisture condensate in a closed environment 07 p0892 N88-15407

Method of determining atmospheric moisture content by measurement of upward radiation intensity in near IR
08 p1007 N88-16106

Characteristics and climatic relevance of the atmospheric aerosol components
08 p1017 N88-16164

Report of the Workshop on Space Systems Possibilities for a Global Energy and Water Cycle Experiment
[WCP-137] 09 p1193 N88-17147

Determination of atmospheric moisture structure from high resolution MAMS radiance data
11 p1515 N88-19049

Climatology and space observations
[ISBN-2-85-428179-9] 14 p1935 N88-21536

ATMOSPHERIC OPTICS

Object-dependent atmospheric influence on LANDSAT recordings 01 p0065 N88-10420

An instrument for the quasi-continuous determination of atmospheric soot content
[DFVLR-FB-87-04] 01 p0068 N88-10433

Effect of clarifying the atmosphere in relation to quasi-monochromatic CO2 laser radiation
06 p0709 N88-14348

Aerosol optical depth and ratios of diffuse-sky to total solar irradiance measured from aircraft following the eruption of El Chichon
[PB88-100789] 07 p0878 N88-15326

Influence of nonlinear spectroscopic effects on atmospheric propagation of intense laser radiation at 10.6 microns wavelength 13 p1789 N88-20705

Activities report of the Division of Optical Technology
[FOA-C-30477-3] 18 p2576 N88-25299

ATMOSPHERIC PHYSICS

NT CLOUD PHYSICS

Morphology of the Earth's environment
03 p0272 N88-11706

Ionosphere and plasmasphere
03 p0272 N88-11709

USSR report: Earth sciences
[JPRS-UES-86-006] 04 p0458 N88-12831

Analysis of geophysical data bases and models for spacecraft interactions
[AD-A184809] 05 p0555 N88-13375

USSR report: Earth sciences
[JPRS-JES-87-004] 06 p0725 N88-14455

Polar Geophysical Institute's studies of magnetosphere, ionosphere 06 p0728 N88-14480

Integrated systems with applications to the multi-phases of the ephemerides, physics and methematics of the upper atmosphere
[AD-A185748] 06 p0743 N88-14570

The ocean heat budget
[AD-A186130] 07 p0881 N88-15346

USSR report: Earth sciences
[JPRS-UES-87-003] 08 p1009 N88-16119

Electrodynamics of the high latitude middle atmosphere 08 p1028 N88-16225

Rayleigh lidar observations of gravity wave activity in the stratosphere and lower mesosphere
[NASA-CR-182384] 09 p1189 N88-17123

AFGL (Air Force Geophysics Laboratory) fiscal year 1988 Air Force technical objectives document
[AD-A187701] 11 p1503 N88-18977

Enhancements to the atmospheric transmittance/radiance program FASCODE
[AD-A188863] 12 p1643 N88-19839

Analysis of the inter-layer independence of stellar scintillometer profiles of Cn2
[AD-A189372] 12 p1645 N88-19854

Evaluation of chemical and atmospheric sciences research
[AD-A188468] 12 p1687 N88-20091

JPRS report: Science and technology. USSR: Earth sciences
[JPRS-UES-88-001] 13 p1784 N88-20674

Activities report in meteorology
[AR-86-87] 13 p1798 N88-20755

Plasmapause formation
[AERONOMICA-ACTA-A-319-1987]
15 p2138 N88-22759

NOAA-ERL-ARL (National Oceanic and Atmospheric Administration-Environmental Research Laboratories-Air Resources Laboratory) solar UV radiation and climate research project: Program description
[PB88-169396] 16 p2233 N88-23339

Theoretical plasma physics research of active space experiments
[AD-A192075] 18 p2577 N88-25309

Atmospheric Lidar Experiment In Space (ALEXIS)
[DFVLR-MITT-88-10] 22 p3118 N88-28526

Investigations into the properties, conditions and effects of the ionosphere
[AD-A194245] 22 p3118 N88-28528

Atmospheric science issues in Congress
22 p3125 N88-28573

Investigations of magnetosphere-ionosphere coupling relevant to operational systems
[AD-A195972] 24 p3391 N88-30195

ATMOSPHERIC PRESSURE

KR+ laser excitation of NH2 in atmospheric pressure flames
[AD-A183421] 01 p0050 N88-10322

Detection of CO2-induced climate change
[DE87-013127] 01 p0071 N88-10457

Regime dependent analysis experiments --- sea level pressure field 02 p0209 N88-11314

Mesoscale surface field analysis from routine observations --- pressure, wind fields
02 p0209 N88-11315

High resolution determination of true surface winds at sea from wind and pressure data
02 p0210 N88-11316

An improved method of analyzing surface geostrophic winds and pressure 02 p0212 N88-11334

On the interannual variability of South American climate and the Southern Oscillation 04 p0470 N88-12905

An investigation of unipolar arcing at atmospheric pressure in aluminum 2024 and aluminum coated glass slides
[AD-A184903] 05 p0577 N88-13521

An analysis of tropopause pressure and total ozone correlations 05 p0617 N88-13789

The use of TOMS-modified VAS data for large-scale NWP 05 p0618 N88-13791

Cosmic ray NM-64 neutron monitor data 14, Rome, Italy, January - December 1985
[IFSI-87-8] 05 p0661 N88-14060

Influence of gas exchange between ocean and atmosphere on formation of atmospheric pressure field
06 p0726 N88-14467

Observations of a midlatitude squall line boundary layer wake
[AD-A185609] 06 p0746 N88-14589

Atmosphere of Venus in southern polar area
08 p1005 N88-16088
Atmosphere of Venus in south polar area based on radio transmission data 08 p1005 N88-16089
The structure and dynamics of monsoon depressions
10 p1355 N88-18102
Moscow USSR. Limited surface observations climatic summary (LISOCS), parts A-F
[AD-A188080] 11 p1514 N88-19046
Application of laser-induced fluorescence in an atmospheric-pressure boron-seeded flame
[AD-A189631] 14 p1889 N88-21287
Premixed turbulent flame propagation
[AD-A192955] 21 p2909 N88-27265
Intraseasonal variability in atmospheric surface pressure and relationship to polar motion
22 p3120 N88-28540
Observed normal mode structure of low frequency oscillations 22 p3128 N88-28595

ATMOSPHERIC RADIATION
NT AIRGLOW
NT AURORAL ARCS
NT AURORAS
NT DAYGLOW
NT GEOCORONAL EMISSIONS
NT IONOSPHERIC NOISE
NT NIGHTGLOW
NT SKY RADIATION
NT STRATOSPHERE RADIATION
NT TROPOSPHERIC RADIATION
NT WHISTLERS
The accuracy of the radiation parameterization in mesoscale models
[DFVLR-IB-553-85/11] 09 p1190 N88-17133
Microscopic control of metallization stability
[AD-A187553] 10 p1421 N88-18487
Radon-222 in the Antarctic Peninsula
[INPE-4486-PRE/1251] 15 p2092 N88-22468
Estimation of total Outgoing Longwave Radiation (OLR) flux from geostationary meteorological satellite infrared window radiance 17 p2351 N88-24006
Observations of wave number dependent spectral line ratio fluctuations in the atmospheric emissions
[IRF-PREPRINT-101] 18 p2542 N88-25085
Radiation safety in commercial air traffic
[NASA-TM-101156] 19 p2600 N88-25447
Review of methods for remote sensing of atmospheric emissions from stationary sources
[PB88-190483] 20 p2821 N88-26739
A control program for global radiation measurements
[KNMI-TR-100] 20 p2824 N88-26757

ATMOSPHERIC REFRACTION
NT RADIO WAVE REFRACTION
Microwave refractive index structure function profiles (Cn2) measured from a small aircraft
[AD-A184343] 04 p0431 N88-12670
Use of electron beam instruments to determine fluctuations in vertical refraction partial angle
04 p0461 N88-12853
Considering refraction in leveling with laser plane
04 p0462 N88-12857
Satellite autonomous navigation with SHAD (Stellar Horizon Atmospheric Dispersion)
[AD-A184988] 05 p0544 N88-13313
An investigation of millimeter wave propagation in the atmosphere: Measurement program
[AD-A184837] 05 p0574 N88-13498
Method for determining atmospheric temperature profiles from observations of astronomical refraction of stars 08 p1013 N88-16139
An evaluation of the impact of variable temporal and spatial data resolution upon IREPS (Integrated Refractive Effects Prediction System)
[AD-A187764] 11 p1470 N88-18769
Propagation in longitudinally varying ducts, with emphasis on guiding to antiguiding transitions
12 p1615 N88-19658
The correlation between methodological and low-level angle-of-arrival measurements 12 p1617 N88-19668
The spatial and temporal variability of the arctic atmospheric boundary layer and its effect on electromagnetic (EM) propagation
[AD-A193958] 23 p3204 N88-29068

ATMOSPHERIC SCATTERING
NT TROPOSPHERIC SCATTERING
Study on propagation and inverse scattering --- sea studies
[ESA-CR(P)-2394] 01 p0063 N88-10405
Statistical model of interaction of electromagnetic waves with natural objects being sensed
08 p1008 N88-16112
Atmospheric backscatter at 10.6 microns; a compendium of measurements made outside the United Kingdom by the airborne LATAS coherent laser radar velocimeter
[RSRE-87002] 12 p1631 N88-19763
Ozone sonde and Dobson spectrometer data obtained during the MAP/GLOBUS 1983 campaign over Western Europe
[BPT-5/87] 13 p1802 N88-20771
Temporal analysis of the changes in Parque Estadual de Jacupiranga vegetation through digital treatment of LANDSAT imagery 17 p2367 N88-24094

ATMOSPHERIC SHELLS
U ATMOSPHERIC STRATIFICATION

ATMOSPHERIC SOUNDING
GOES observations for the FIRE/SRB Wisconsin experiment region from October 11 through November 2, 1986
[NASA-TM-100485] 01 p0071 N88-10453
Parachute characteristics of Titan descent modules --- planetary probe
[BF-3/86-B] 02 p0122 N88-10774
Thunderstorm nowcasting using Doppler radar and soundings 02 p0200 N88-11248
Diagnosing short term changes in temperature and moisture profiles from single Doppler radar
02 p0200 N88-11251
VAS products as indices of thunderstorms and severe local storm potential --- Visible and Infrared Spin Scan Radiometer Atmospheric Sounder (VAS)
02 p0201 N88-11253
Horizontal shape matching applied to VAS data --- Visible and Infrared Spin Scan Radiometer Atmospheric Sounder (VAS) 02 p0201 N88-11254
Analysis of thickness fields retrieved from NOAA-7 observations through the 3I (Improved Initialization Inversion) method. Interest for weather forecasting
02 p0201 N88-11255
Assimilation of high resolution TOVS data into a mesoscale NWP model --- numerical weather prediction (NWP) 02 p0213 N88-11338
A VAS-numerical model impact study using the Gal-Chen variational approach --- Visible Infrared Spin-Scan Radiometer Atmospheric Sounder (VAS)
02 p0213 N88-11339
High latitude problems to be studied by incoherent scatter radars
[DMI-GEOPHYS-PAPERS-R-77]
03 p0350 N88-12211
Spectroscopic and retrieval studies in support of SCRIBE (Stratospheric Cryogenic Interferometer Balloon Experiment)
[AD-A184037] 03 p0351 N88-12216
Multiwave laser soundings of atmospheric aerosol: Experimental research (review)
04 p0461 N88-12852
Development of a data analysis system for the detection of lower level atmospheric turbulence with an acoustic sounder
[AD-A184972] 05 p0624 N88-13821
Development of an acoustic echosounder for detection of lower level atmospheric turbulence
[AD-A184877] 05 p0626 N88-13831
Statistical structure of temperature field over South Pacific Ocean 06 p0726 N88-14465
Latitude coverage of observations of the middle atmosphere by solar absorption spectrometry from a heliosynchronous orbit
[AERONOMICA-ACTA-A-316-1987]
06 p0742 N88-14566
Facilities for research and weather observations on the 213 m tower at Cabauw (Netherlands) and at remote locations
[KNMI-WR-87-5] 06 p0746 N88-14587
High-spatial-resolution TOVS observations for the FIRE/SRB Wisconsin experiment region from October 14 through November 2, 1986
[NASA-TM-100522] 06 p0747 N88-14593
Vertical sounding of th air layer close to a glacier on Mount Vernagferner in the Oetzal Alps, Tyrol (experiment LUZIVER 1983) 08 p1015 N88-16152
Telescope design for Michelson Interferometer for Passive Atmospheric Sounding (MIPAS) B
08 p1017 N88-16167
Proceedings of the 8th ESA Symposium on European Rocket and Balloon Programs and Related Research
[ESA-SP-270] 08 p1024 N88-16201
The German scientific balloon and sounding rocket program 08 p1024 N88-16202
The French balloon and sounding rocket space program 08 p1025 N88-16203
The Norwegian scientific balloon and sounding rocket program 1987-1990 08 p1025 N88-16204
The Swedish sounding rocket and balloon program
08 p1025 N88-16205
Swiss scientific balloon and sounding rocket experiments 1985-1987 08 p1025 N88-16206
New techniques for rocket and balloon-borne instrumentation for investigations of the structure, dynamics and electrodynamics of the middle atmosphere 08 p1027 N88-16220
An advanced visible-UV spectrometer for atmospheric composition measurements 08 p1029 N88-16231
In-situ stratospheric water vapor measurements on board long duration balloons 08 p1029 N88-16232
TOTAL: A new instrument to study turbulent parameters in the mesosphere and lower thermosphere
08 p1029 N88-16234
Developments in instrumental techniques for observations of magnetospheric and ionospheric shaped charge releases 08 p1031 N88-16248
The Cryogenic Infrared Spectrometer and Telescope for the Atmosphere (CRISTA) experiment on Astro-SPAS
08 p1034 N88-16270
Rocket experiments and payloads for Super CAMP --- Cold Arctic Mesopause Project (CAMP)
08 p1034 N88-16271
Future developments of auroral D-region research using the EISCAT VHF incoherent scatter radar
08 p1035 N88-16278
Assessment of VAS-derived products created by a simultaneous algorithm on a convectively active day
[AD-A186158] 08 p1054 N88-16359
Technical assessment of the joint CSIRO/Bureau of Meteorology proposal for a geostationary imager/sounder over the Australian region
[RTP-15] 09 p1135 N88-16811
Report of the Workshop on Space Systems Possibilities for a Global Energy and Water Cycle Experiment
[WCP-137] 09 p1193 N88-17147
Analysis of quasi-geostrophic forcing during the AIMCS (Airborne Investigations of Mesoscale Convective Systems) Project. Volume 2: Results for June 14 through July 16, 1984
[PB88-123807] 10 p1354 N88-18092
Roys and radiosondes in the region
[INPE-4362-PRE/1188] 13 p1796 N88-20743
Lidar active remote sensing. Applications to the atmosphere 14 p1936 N88-21547
Aerosol lidar for environment protection and meteorology
[DFVLR-FB-87-43] 14 p1982 N88-21828
Coordinated Auroral Experiments using Scatter And Rocket investigations (CAESAR investigations)
[MPAE-W-47-87-13] 15 p2096 N88-22487
A multivariate variational objective analysis-assimilation method. Part 1: Development of the basic model
[NASA-CR-182651] 15 p2097 N88-22491
Geochemistry of the middle and lower atmosphere: Environmental impact through the deterioration of the ozone layer
[INPE-4477-PRE/1241] 16 p2230 N88-23321
Ozonesonde observations at Lauder, New Zealand during the Spring and early Summer of 1986
[PB88-173273] 16 p2232 N88-23328
Spectroradiometry in meteorology
16 p2272 N88-23599
Tiros operational vertical sounder (TOVS) and radiosonding in the region 17 p2360 N88-24059
Stratospheric positive ion composition measurements and acetonitrile detection: A consistent picture
[AERONOMICA-ACTA-A-326-1987]
18 p2542 N88-25084
MRS-3000 meteorological rocket probe for the MMR-06 dart integrated meteorological rocket system
[NASA-TT-20303] 19 p2693 N88-26010
High latitude ionospheric radio studies
[AD-A192270] 20 p2824 N88-26753
Influence of stable stratification on atmospheric turbulence: An experimental contribution
[ETN-88-92292] 20 p2827 N88-26772
Components of an atmospheric lidar system
[AD-A193366] 21 p2953 N88-27539
ECC (Electrochemical Concentration Cell) ozonesonde observations at South Pole, Antarctica during 1987
[PB88-202015] 21 p2970 N88-27644
The use of AIMS data for operational and research purposes in atmospheric sciences
22 p3036 N88-28025
South Pole lidar: Brief description of the instrument
[NOTA-INTERNA-907] 22 p3083 N88-28308
European validation of SAGE-2 aerosol profiles
[AERONOMICA-ACTA-A-327-1988]
23 p3234 N88-29243
Microwave instrument for planetary mission (Titan/CASSINI mission orbiter spacecraft)
[BAE-CS/TP-8359] 24 p3375 N88-30102
Spaceborne lidar: Development of a laboratory test system
[BF-R-66.090-1] 24 p3378 N88-30118
Possibilities of determining vertical profiles of microphysical characteristics of stratospheric aerosol using space measurements of transparency and solar halo 24 p3449 N88-30526

ATMOSPHERIC STRATIFICATION

Analysis of thickness fields retrieved from NOAA-7 observations through the 3I (Improved Initialization Inversion) method. Interest for weather forecasting
02 p0201 N88-11255

General theory of radio propagation through a stratified atmosphere
[PB87-226197] 04 p0430 N88-12662

Structure of stably stratified atmospheric surface layer in presence of heat-releasing admixture
04 p0462 N88-12856

Systematic stratospheric-tropospheric exchange viewed from isentropic coordinates 05 p0615 N88-13777

Mechanisms of cloud layer formation in Venusian atmosphere 08 p1004 N88-16087

Atmosphere of Venus in north polar area based on radio transmission data from Venera-15 and Venera-16 spacecraft 08 p1005 N88-16090

Distribution of electron concentration in nightime atmosphere of Venus based on radio transmission data
08 p1005 N88-16092

Chemical composition and structure of Venusian clouds determined from results of roentgenoradiometric experiments carried out by landing modules of Vega-1 and Vega-2 automatic interplanetary stations
13 p1726 N88-20320

Influence of stable stratification on atmospheric turbulence: An experimental contribution
[ETN-88-92292] 20 p2827 N88-26772

ATMOSPHERIC TEMPERATURE

NT AURORAL TEMPERATURE

NT IONOSPHERIC TEMPERATURE

A device for measuring fast temperature fluctuations --- atmospheric temperature
[KNMI-TR-92] 01 p0070 N88-10449

Detection of CO2-induced climate change
[DE87-013127] 01 p0071 N88-10457

Diagnosing short term changes in temperature and moisture profiles from single Doppler radar
02 p0200 N88-11251

Mesoscale MOS forecast support for 1988 winter Olympics ski events --- model output statistics (MOS)
02 p0209 N88-11312

Short range forecast of the daily maximum temperature 02 p0209 N88-11313

Spectroscopic and retrieval studies in support of SCRIBE (Stratospheric Cryogenic Interferometer Balloon Experiment)
[AD-A184037] 03 p0351 N88-12216

Contributions of lidar measurements to the study of long term variations of the middle atmosphere
[ETN-88-91237] 05 p0625 N88-13824

Statistical structure of temperature field over South Pacific Ocean 06 p0726 N88-14465

Influence of gas exchange between ocean and atmosphere on formation of atmospheric pressure field
06 p0726 N88-14467

Particle-gas temperature differentials resulting from time-dependent radiative-conductive heat flux divergences in the tenuous dust-laden atmosphere of mars
[AD-A185888] 07 p0945 N88-15747

Atmosphere of Venus in southern polar area
08 p1005 N88-16088

Atmosphere of Venus in south polar area based on radio transmission data 08 p1005 N88-16089

Method for determining atmospheric temperature profiles from observations of astronomical refraction of stars 08 p1013 N88-16139

Development of a Doppler wind lidar system for atmospheric wind measurements
08 p1027 N88-16217

Revised uniform summary of surface weather observations. Parts A-F: Carswell AFB, Texas
[AD-A186820] 09 p1192 N88-17144

Statistical studies of low frequency oscillations in satellite-observed stratospheric temperatures
10 p1353 N88-18086

Air temperature shield tests
[AD-A187459] 11 p1514 N88-19043

Moscow USSR. Limited surface observations climatic summary (LISOCS), parts A-F
[AD-A188080] 11 p1514 N88-19046

Thermal structure of Venusian Atmosphere determined from results of measurements from Vega-2 landing module 13 p1725 N88-20315

Roys and radiosondes in the region
[INPE-4362-PRE/1188] 13 p1796 N88-20743

A study of satellite emission computed tomography
[AD-A189567] 13 p1797 N88-20745

Tropic heat MR (Meteorological Recorder) meteorological data (April 1984 - June 1985)
[PB88-161286] 14 p1948 N88-21620

Ultraviolet absorption cross sections of methylbromide at stratospheric temperatures
[AERONOMICA-ACTA-A-320-1987]
15 p2036 N88-22132

Tiros operational vertical sounder (TOVS) and radiosonding in the region 17 p2360 N88-24059

Three-dimensional temperature fields in the atmosphere up to 50 km altitude
[ETN-88-92150] 18 p2542 N88-25089

Effects of moderate cold and heat stress on the potential work performance of industrial workers. Part 6: The effects of increasing vapour pressure at four air temperatures on the performance and physiology of white females
[PB88-124854] 18 p2550 N88-25137

Satellite remote sensing of the wet bulb globe temperature heat stress index, phase 2
[AD-A192798] 20 p2818 N88-26717

Our climate in danger
[DE88-701824] 20 p2822 N88-26743

An efficient model for changes of global climate and composition of the atmosphere due to human activities
[ETN-88-92359] 20 p2827 N88-26775

Investigations on Mie and Rayleigh scattering as basis for the development of Rayleigh temperature lidars with aid of Michelson interferometry
[GKSS-87/E/62] 21 p2976 N88-27675

Proceedings of the Twelfth Annual Climate Diagnostics Workshop
[PB88-191747] 22 p3119 N88-28534

The 1986-87 Pacific warm episode: Oceanic and Atmospheric features 22 p3120 N88-28535

Prolonged periods of above-normal temperatures in Canada, 1986/87 22 p3120 N88-28538

Atlantic SST variability and high latitude climate fluctuations 22 p3122 N88-28551

Northern Hemisphere 700 mb teleconnections based on half-monthly mean anomaly data stratified by season and by sign 22 p3123 N88-28561

Interannual variability of 850 mb temperatures during the Northern Hemisphere winter
22 p3123 N88-28562

Urbanization: Its detection and effect in the United States climate record 22 p3125 N88-28571

Global-scale temperature changes to August 1987 and a comparison of satellite and conventional data
22 p3125 N88-28572

DERF forecasts of thickness
22 p3126 N88-28579

Some screening experiments in objective prediction of monthly mean temperature over the United States during the winter season 22 p3127 N88-28589

Operational multifield analog forecasting of US seasonal temperatures for non-winter seasons
22 p3127 N88-28592

Determination of most probable predicted 50 kPa pattern by empirical orthogonal functions
22 p3128 N88-28593

Soot and radiation in a gas turbine combustor
[AD-A191991] 23 p3179 N88-28924

Energy budget and ground temperatures in hot regions
[AD-A196298] 24 p3404 N88-30268

ATMOSPHERIC TIDES

Meteor observation by the Kyoto meteor radar
06 p0733 N88-14507

Variations of the semi-diurnal tidal wind in the meteor region with periods of about 27 and 13.5 days
06 p0734 N88-14516

Tidal activity in the meteor zone over Budrio, Italy
06 p0734 N88-14517

Some aspects of metallic ion chemistry and dynamics in the mesosphere and thermosphere
06 p0737 N88-14534

Solar tides in the upper equatorial thermosphere: A comparison between AE-E data and the NCAR thermospheric general circulation model
[AD-A186160] 08 p1023 N88-16196

ATMOSPHERIC TURBULENCE

NT CLEAR AIR TURBULENCE

NT GUSTS

NT LOW LEVEL TURBULENCE

The atmosphere of Mars and optical communications
04 p0434 N88-12692

Development of a data analysis system for the detection of lower level atmospheric turbulence with an acoustic sounder
[AD-A184972] 05 p0624 N88-13821

Development of an acoustic echosounder for detection of lower level atmospheric turbulence
[AD-A184877] 05 p0626 N88-13831

Introduction to the Modeling of Turbulence
[VKI-LS-81-06] 08 p0986 N88-15972

An introduction to single point closure methodology
08 p0986 N88-15973

Turbulence models for practical applications
08 p0986 N88-15974

Examples of turbulence-model applications
08 p0987 N88-15975

Numerical implementation and performance of Reynolds stress closures in finite volume computations of recirculating and strongly swirling flows
08 p0987 N88-15976

Observational evidence for saturation of gravity waves and the production of turbulence in the mesosphere
08 p1028 N88-16229

TOTAL: A new instrument to study turbulent parameters in the mesosphere and lower thermosphere
08 p1029 N88-16234

VAWT (Vertical-Axis Wind Turbine) stochastic loads produced by atmospheric turbulence
[DE88-001355] 09 p1187 N88-17110

Statistics of breakdown centers appearing during propagation of laser radiation through turbulent atmosphere 09 p1236 N88-17411

Comparison of a few methods of restoring images distorted by atmospheric turbulence
[ESA-TT-1065] 09 p1248 N88-17481

Response of wind shear warning systems to turbulence with implication of nuisance alerts
10 p1274 N88-17618

Similarity theories and microturbulence in the atmospheric mixed layer 13 p1806 N88-20802

Effect of atmospheric turbulence on the bit error probability of a space to ground near infrared laser communications link using binary pulse position modulation and an avalanche photodiode detector
[NASA-TM-100699] 14 p1873 N88-21189

JPRS report: Science and technology. China
[JPRS-CST-87-042] 14 p1899 N88-21338

Intermittency of atmospheric turbulence--applicatin of Lyapunov exponents and fractional dimension
14 p1900 N88-21348

Stellar scintillometer atmospheric optical turbulence profiling experiment: A qualitative comparison of two identical instruments at AMOS (Air Force Maui Optical Station), 1985
[AD-A190589] 15 p2094 N88-22479

The potential impact on atmospheric ozone and temperature of increasing trace gas concentrations
[NASA-CR-182965] 17 p2373 N88-24112

Study of the convergence of a finite difference scheme for acoustic propagation in the atmosphere in a parabolic approximation. Statistical calculation of the sound field in the presence of kinematic turbulence
[ONERA-RS-8/3641-PY-160-P]
17 p2394 N88-24235

Aircraft/lidar turbulence comparison
18 p2546 N88-25111

Influence of stable stratification on atmospheric turbulence: An experimental contribution
[ETN-88-92292] 20 p2827 N88-26772

Atmospheric turbulence research at DFVLR
[AGARD-R-752] 21 p2975 N88-27669

Performance analysis of a noncoherently combined large aperture optical heterodyne receiver
22 p3065 N88-28189

The Flight of Flexible Aircraft in Turbulence: State-of-the-Art in the Description and Modelling of Atmospheric Turbulence
[AGARD-R-734-ADD] 24 p3311 N88-29717

Current and proposed gust criteria and analysis methods: An FAA overview 24 p3311 N88-29718

Flight test equipment for the on-board measurement of wind turbulence 24 p3311 N88-29719

Measured and predicted responses of the Nord 260 aircraft to the low altitude atmospheric turbulence
24 p3312 N88-29723

The Flight of Flexible Aircraft in Turbulence: State-of-the-Art in the Description and Modelling of Atmospheric Turbulence
[AGARD-R-734] 24 p3312 N88-29725

Status review of atmosphere turbulence and aircraft response 24 p3312 N88-29726

A summary of atmospheric turbulence measurements with specially-equipped aircraft in the US
24 p3312 N88-29727

The NAE atmospheric research aircraft
24 p3313 N88-29730

Extreme gusts distribution 24 p3314 N88-29734

A digital simulation technique for the Dryden atmospheric model
[NASA-TT-20342] 24 p3404 N88-30266

Microphysical processes in cloud layers of Venus
24 p3448 N88-30522

ATMOSPHERIC WINDOWS

Filling of the atmospheric transmission window due to emission from very high rotational levels of NO and O3
[AD-A194670] 23 p3233 N88-29239

Molecular line shape effects on atmospheric window absorption
[AD-A196316] 24 p3342 N88-29894

ATMOSPHERICS

NT WHISTLERS

ATOLL REEFS
U CORAL REEFS
ATOMIC BATTERIES
U RADIOISOTOPE BATTERIES
ATOMIC BEAMS
High intensity 5 eV O-atom exposure facility for material degradation studies 02 p0135 N88-10847
Materials preparation and longevity in hyperthermal atomic oxygen 03 p0297 N88-11862
Atomic beam studies of the interaction of hydrogen with transition metal surfaces
[DE88-000208] 05 p0648 N88-13970
Atomic beam study of crystalline order and precipitation in nickel based alloys
[ETN-88-91994] 16 p2177 N88-22975
Laboratory experiments of relevance to the space station environment 18 p2592 N88-25402
Fast atom bombardment study on interaction of anticodonic nucleotides and their cognate amino acid
[ISAS-RN-355] 20 p2850 N88-26918
ATOMIC CLOCKS
On-orbit frequency stability analysis of the GPS NAVSTAR 8 rubidium clock and NAVSTARs 9 and 10 cesium clocks
[AD-A184984] 05 p0544 N88-13312
Study and construction of a compact hydrogen maser with a high-degree of frequency stability
[PB87-151122] 07 p0859 N88-15216
Atomic clocks research: An overview
[AD-A185567] 07 p0930 N88-15648
Ultrahigh coherent semiconductor lasers and their applications to Rb atomic clock
14 p1976 N88-21789
Tactical Rubidium Frequency Standard (TRFS), volume 2
[AD-A191190] 18 p2503 N88-24850
Quartz crystal resonators and oscillators for frequency control and timing applications
[AD-A193310] 21 p2937 N88-27443
A three-dimensional model of the gas-cell atomic frequency standard
[AD-A193218] 21 p3011 N88-27868
ATOMIC COLLISIONS
Proceedings of the Workshop on Opportunities for Atomic Physics Using Slow, Highly-Charged Ions
[DE87-013991] 02 p0231 N88-11457
Final (n,l) state-resolved electron capture by multiply charged ions from neutral atoms
[IPPJ-AM-54] 04 p0492 N88-13030
Monocrystal sputtering by the computer simulation code ACOCT
[IPPJ-848] 04 p0493 N88-13035
Total and partial cross sections for electron capture for C(q+) (q=6-2) and O(q+) (q=8-2) ions in collisions with H, H2 and He atoms
[IPPJ-AM-56] 09 p1252 N88-17501
Correlated processes in atomic collisions
[DE88-003508] 10 p1406 N88-18383
Negative-energy quanta
[DE88-700904] 12 p1689 N88-20101
Memoirs of the Faculty of Science, Kyoto University. Series of Physics, Astrophysics, Geophysics and Chemistry, volume 37, no. 2
[ISSN-0368-9689] 16 p2287 N88-23694
Theoretical studies of dynamics combustion
[DE88-007565] 19 p2611 N88-25495
Theoretical atomic and molecular physics
[DE88-007122] 19 p2724 N88-26175
Atomic physics of strongly correlated systems
[DE88-007789] 19 p2724 N88-26177
Recoil saturation of the self-energy in atomic systems
[DE88-010450] 20 p2851 N88-26930
ATOMIC ENERGY
U NUCLEAR ENERGY
ATOMIC ENERGY LEVELS
The influence of polymer structure on triplet luminescence
[DE87-014431] 02 p0152 N88-10952
Migration and transfer of triplet energy in selected polymer systems
[DE87-014432] 02 p0152 N88-10953
Wavelengths of the 3p-3d transitions of the Co- and Fe-like ions: The effects of electron correlation
[DE88-000219] 04 p0498 N88-13067
The angular diameter of alpha Scorpii in the near-infrared Ca II triplet 04 p0514 N88-13162
Localization of Cu 3d levels in the high Tc superconductor YBa2Cu3O approximately 7 by Cu2p X-ray photoelectron spectroscopy
[NOTA-INTERNA-887] 07 p0939 N88-15710
Nuclear excitation via the motion of electrons in a strong laser field
[AD-A187166] 09 p1171 N88-17017
Light absorption by an atom moving inside a spherical box
[AD-A187241] 10 p1407 N88-18395
Systematics on neutron-induced isomeric cross-section ratios at 14.5 MeV
[ECN-200] 14 p1980 N88-21815
Electronic energy transfer processes in the alkali/alkaline earth metal vapors
[AD-A190035] 15 p2034 N88-22119
Stark effect in intense field. Perturbation theory and 1/n-expansion
[DE87-702947] 16 p2266 N88-23550
ATOMIC EXCITATIONS
The study of excited oxygen molecule gas species production and quenching on thermal protection system materials
[NASA-CR-172027] 02 p0233 N88-11470
Low-power photolytically pumped lasers
[DE88-002448] 08 p0991 N88-15998
New branch of solid-state physics
08 p1079 N88-16508
Resonance excitation in gamma gamma collisions at LEP200
[NIKHEF-H/87-3] 08 p1081 N88-16514
Kinetic studies following state-selective laser excitation
[DE88-004094] 10 p1335 N88-17981
Nuclear transitions induced by atomic excitations
[DE88-004311] 11 p1545 N88-19239
Quantum Monte Carlo study of the MIES associated with H2(X 1 sigma g +) and H2(B 1 sigma u +)
16 p2268 N88-23564
Density diagnostics by hydrogen line intensity ratios: Excitation cross section between excited states
17 p2441 N88-24522
Cascade fluorescences from laser-excited lithium atom for plasma diagnostics 17 p2442 N88-24526
Distorted-wave-method calculation of electron-impact excitation of atomic ions 17 p2443 N88-24532
Monte Carlo investigation of hot photoexcited electron relaxation in GaAs 19 p2659 N88-25805
High-speed phenomena in GaAs multiple-quantum-wells 19 p2660 N88-25812
Excitation of single-mode glass fiber by partially coherent sources
[ETN-88-92121] 20 p2854 N88-26951
ATOMIC EXPLOSIONS
U NUCLEAR EXPLOSIONS
ATOMIC GASES
U MONATOMIC GASES
ATOMIC INTERACTIONS
NT ATOMIC COLLISIONS
A simple interpretation of the Fe2(-) photoelectron spectrum
[NASA-CR-182553] 11 p1543 N88-19225
Competing interactions in metallic superlattices
[DE88-005344] 13 p1847 N88-21057
Contribution to the study of order effects in the Ising model framework: Ground states and phase diagrams
[ONERA-NT-1987] 20 p2880 N88-27095
Determination of quantum corrections for electrical conductivity mechanism of three dimensional, perturbed copper coatings. Weak localization and electron-electron interaction
[ETN-88-92378] 21 p2941 N88-27466
ATOMIC MASS
U ATOMIC WEIGHTS
ATOMIC PHYSICS
Proceedings of the Workshop on Opportunities for Atomic Physics Using Slow, Highly-Charged Ions
[DE87-013991] 02 p0231 N88-11457
Atomic physics with highly charged ions
[DE88-000894] 05 p0648 N88-13972
Theoretical atomic and molecular physics
[DE88-001625] 05 p0649 N88-13974
Application of ECR ion source beams in atomic physics
[DE88-003767] 10 p1406 N88-18384
Research and technology, 1987
[NASA-TM-100323] 12 p1713 N88-20253
Simulation code for ICF including radiative energy transfer 16 p2277 N88-23627
Finite ion-relaxation and nonequilibrium radiation effects on laser-driven implosions 16 p2278 N88-23636
Atomic processes in matter-antimatter interactions
[DE88-006911] 19 p2723 N88-26172
Theoretical atomic and molecular physics
[DE88-007122] 19 p2724 N88-26175
Atomic physics of strongly correlated systems
[DE88-007789] 19 p2724 N88-26177
Modeling of atomic processes in X-ray laser plasmas
[AD-A194118] 23 p3286 N88-29567
ATOMIC RECOMBINATION
NT OXYGEN RECOMBINATION
Nascent vibrational/rotational distribution produced by hydrogen atom recombination
[AD-A193005] 20 p2852 N88-26933
ATOMIC SPECTRA
Atomic frequency standards for ultra-high-frequency stability 04 p0433 N88-12685
Hydrogen and deuterium in the local interstellar medium 04 p0521 N88-13204
Atomic and molecular gas phase spectrometry
[AD-A187562] 11 p1452 N88-18655
Theory of two-photon emission from atomic inner shells
[AD-A187742] 11 p1543 N88-19223
Single-laboratory evaluation of SW-846 methods 7090/7091 determination of beryllium by flame and furnace atomic absorption spectrophotometry
[PB88-171434] 16 p2175 N88-22963
Array detectors for plasma spectrochemistry
[AD-A194220] 22 p3052 N88-28105
The electromagnetic spectrum: The information mine
[AD-A194316] 22 p3069 N88-28215
Determination of impurities in silicon carbide by ICP AES (inductively coupled plasma atomic emission spectrometry) after coprecipitation with lanthanum hydroxide
[NASA-TT-20332] 23 p3193 N88-29003
Modeling of atomic processes in X-ray laser plasmas
[AD-A194118] 23 p3286 N88-29567
ATOMIC STRUCTURE
Some electronic factors influencing superconductivity in some rare-Earth-like elements and the beginning of rare-Earth series
[DE87-702582] 01 p0102 N88-10668
Electronic structure of crystalline NaSn
[DE87-702583] 01 p0102 N88-10669
Elastic moduli of copper under compression
[DE87-013137] 02 p0147 N88-10922
Small-Angle Neutron Scattering (SANS) from polymers and colloids
[DE87-013548] 02 p0151 N88-10946
Dynamics of atoms in low-symmetry systems
[AD-A184318] 03 p0375 N88-12361
Interatomic Auger rates for the sodium fluoride crystal
[DE87-013012] 03 p0382 N88-12401
Experimental perspectives on heavy electron metals
[DE87-014766] 04 p0416 N88-12583
The finite element method for electronic structure
[DE88-001708] 04 p0485 N88-12989
Nuclear techniques in studies of condensed matter
[NASA-RP-1195] 04 p0489 N88-13015
Tetrahedral carbon and interstitial electrons in Li cluster: CLi4 and (LiCH3)4
[AD-A184277] 04 p0496 N88-13055
Atomic and electronic structure of surfaces and chemisorbed layers
[DE87-014987] 04 p0498 N88-13065
Wavelengths of the 3p-3d transitions of the Co- and Fe-like ions: The effects of electron correlation
[DE88-000219] 04 p0498 N88-13067
The role of electronic structure calculation in mechanistic analysis of electron transfer reactions in the liquid phase
[DE87-014395] 05 p0647 N88-13963
Structural investigations of some metallic glasses
[ECN-198] 06 p0686 N88-14203
Electronic band structure and photoemission: A review and projection
[DE88-002236] 06 p0787 N88-14829
Study of the embedded atom method of atomistic calculations for metals and alloys
[DE88-002798] 07 p0835 N88-15065
Embedded cluster models for electronic structure and energetics of complex oxides
[DE88-003097] 07 p0938 N88-15702
Soft X-ray absorption and emission spectra and the electronic structure of the Ba2YCu3O/sub 7-x/ superconductor
[DE88-002609] 08 p1090 N88-16559
Structural properties of high-T/sub c/ oxide super conductors
[DE88-002974] 08 p1090 N88-16563
Activities report in nuclear physics
[ETN-88-91609] 09 p1245 N88-17458
Electronic and chemical structure of 3-5/metal and Si/metal interfaces
[AD-A186579] 09 p1254 N88-17518
Electronic structure calculations and binding analyses for selected binary and ternary metal hydrides
[ETN-88-91087] 09 p1256 N88-17527
Surface and interface electronic structure
[DE88-003363] 09 p1258 N88-17545
Insights into the mechanisms of chemical reactions: Reaction paths for chemical reactions
[DE88-003041] 10 p1297 N88-17755
Investigations on the usefulness of the Massively Parallel Processor for study of electronic properties of atomic and condensed matter systems
[NASA-CR-182514] 10 p1383 N88-18259
Energy-related atomic and molecular structure and scattering studies
[DE88-004246] 10 p1406 N88-18386

Semiempirical studies of atomic structure
[DE88-004096] 10 p1407 N88-18392
Electronic structure of random alloys and the theory of ordering processes
[DE88-004476] 10 p1407 N88-18394
The electronic structure of YBa2Cu3O/sub 7-delta/ above and below T/sub c/
[DE88-003495] 10 p1420 N88-18479
Calculations of rate constants for the three-body recombination of H2 in the presence of H2
[NASA-CR-182548] 11 p1454 N88-18664
Gas-phase photoelectron spectroscopy of metals and metal oxides of importance in the upper atmosphere
[AD-A187771] 11 p1511 N88-19027
A simple interpretation of the Fe2(-) photoelectron spectrum
[NASA-CR-182553] 11 p1543 N88-19225
Atomic-scale simulation in materials science
[DE88-005204] 11 p1544 N88-19230
Symmetry and equivalence restrictions in electronic structure calculations
[NASA-TM-89252] 11 p1557 N88-19320
Spatial distribution of carbon and native defects in large-diameter bulk grown GaAs
[DE88-003870] 11 p1562 N88-19348
Electronic properties of semiconductor inversion layers in sub-micron structures
[AD-A188635] 12 p1698 N88-20161
Tungsten-carbon multilayer system studied with X-ray scattering
[DE88-005749] 13 p1735 N88-20373
Model catalyst studies of SMSI (Strong Metal/Support Interactions) and the role of D-electrons in chemisorption and catalysis
[DE88-004518] 13 p1738 N88-20393
Properties of reactively sputtered WNx films Zhao, X. -A.
[AD-A188711] 13 p1835 N88-20976
Theoretical studies on the electronic structure and properties of complex ceramic crystals and glasses
[DE88-005837] 13 p1846 N88-21049
Research on stable processible conducting polymers for electronic applications
[AD-A190246] 15 p2044 N88-22180
Dynamical optimization techniques for the calculation of electronic structure in solids
[DE88-006010] 15 p2140 N88-22768
First-principles calculations of quasiparticle energies at surfaces and interfaces: Semiconductor surface-state spectra and band offsets
[DE88-006340] 15 p2141 N88-22773
Experimental studies on electronic properties of HgTe/CdTe and Hg sub 1-z Cd sub x Te/CdTe heterostructures and superlattices
[AD-A189826] 15 p2142 N88-22783
Electronic structure of matter at high compression: Isostructural transitions and approach of the Fermi-gas limit
[MPQ-124] 16 p2266 N88-23551
The H5(+) potential energy hypersurface: Characterization of ten distinct energetically low-lying stationary points 16 p2267 N88-23561
Electronic structure and stability of small cation and anion hydrogen clusters 16 p2267 N88-23562
Point defects in irradiated silicates
17 p2408 N88-24319
The theory of random alloys
[DE88-006408] 18 p2487 N88-24756
Silicon-sapphire waveguides
[AD-A191754] 18 p2504 N88-24854
Electronic structure, elementary excitations, optical and transport properties of semiconductor superlattices
[AD-A190795] 18 p2581 N88-25333
Transition probabilities in OH A 2 sigma + - X 2 pi i: Bands with v prime = 0 and 1, v double prime = 0 to 4
[NASA-CR-182946] 18 p2584 N88-25353
Ground state properties and electronic structure of high T sub c superconductors
[DE88-007485] 18 p2585 N88-25360
Electronic structure of Zintl phase compounds by nonlinear optimization
[DE88-009998] 19 p2613 N88-25508
Half collision studies of inelastic energy transfer processes
[DE88-008096] 19 p2724 N88-26178
Calculation of the line shapes of radiators immersed in plasma 19 p2729 N88-26210
All-electron local density theory of electronic structure and superconductivity in YBa2Cu3O7 and YBa2Cu3O6
[DE88-009944] 19 p2735 N88-26246
Structural and magnetic properties of Fe impurities in YBa2Cu3O(sub 7-delta)
[DE88-009961] 19 p2735 N88-26247
The electronic structure of condensed molecular systems
[DE88-007823] 20 p2851 N88-26923
Piezoelectric effects in strained layer superlattices
20 p2863 N88-27002
Electronic structure of quantum-well states revealed under high pressures 20 p2870 N88-27038
Ordering transitions of ternary alloys A(1-x)B(x)C
20 p2873 N88-27054
Discrete variational methods and their application to electronic structures
[DE88-702215] 21 p3014 N88-27888
Probing the electronic and defect structure of perovskite superconductors
[DE88-008349] 21 p3022 N88-27939
The 2D Rydberg series in Al I
[NASA-TM-101189] 22 p3150 N88-28740
Atomistic simulation of silicon grain boundaries
[DE88-009925] 22 p3155 N88-28771
Influence of local volume forces on surface relaxation of pure metals and alloys: Applications to Ni, Al, Ni3Al
[DE88-702718] 23 p3195 N88-29014
Possible mechanism for high-temperature superconductivity in the BaSr-La(Y)-CuO systems
[DE88-702060] 23 p3288 N88-29576
Band electronic structures and crystal packing forces
[DE88-010247] 23 p3289 N88-29585

ATOMIC THEORY
NT HEISENBERG THEORY

ATOMIC WEIGHTS
The atomic weight and isotopic composition of nitrogen and their variation in nature
[DE87-012867] 02 p0144 N88-10902
The atomic weight and isotopic composition of oxygen and their variation in nature
[DE87-014397] 04 p0413 N88-12558
Measurement of Beta-decay energies of short-lived neutron-rich nuclei in the vicinity of mass number between 101 and 106, and A = 109
[ETN-88-92376] 21 p3014 N88-27890
Diamond like carbon coatings: Categorization by atomic number density
[NASA-CR-174895] 22 p3059 N88-28151

ATOMIZATION
U ATOMIZING

ATOMIZERS
Calculation on film preparation and film motion of a swirl atomizer
[DFVLR-FB-87-25] 09 p1162 N88-16962
Laboratory scale inert gas atomizer for producing rapidly solidified powders
[DE88-006734] 18 p2497 N88-24812
Analysis of the flow through double swirl airblast atomizers 24 p3351 N88-29949

ATOMIZING
NT GAS ATOMIZATION
NT LIQUID ATOMIZATION
Study of electrostatic modulation of fuel sprays to enhance combustion performance in an aviation gas turbine
[AD-A184967] 05 p0548 N88-13341
Military jet fuels, 1944-1987
[AD-A186752] 09 p1150 N88-16890
Design and characteristics of a liquid aerosol generator
[AD-A186942] 09 p1174 N88-17034
J85-21 fuel nozzle atomization tests
[AD-A189394] 12 p1613 N88-19647
Atomization in a turbulent shear layer: Preliminary measurements 19 p2624 N88-25565
Liquid Engine Jet Atomization Workshop report
19 p2627 N88-25584
Pulsed spray structure and atomisation techniques
[AD-A192280] 20 p2800 N88-26614
Small-droplet spray measurements with a scattered-light scanner
[NASA-TM-100973] 20 p2806 N88-26645

ATOMS
NT HELIUM ATOMS
NT HYDROGEN ATOMS
NT METASTABLE ATOMS
NT NEUTRAL ATOMS
NT NITROGEN ATOMS
NT OXYGEN ATOMS
Theory of atoms in strong, pulsed electromagnetic fields. 2: A free electron and a harmonically bound electron
[DE87-012571] 01 p0035 N88-10225
Field ion microscope studies of surface reconstructions
[DE87-014644] 02 p0147 N88-10924
Quantum-mechanical aspects of classically chaotic driven systems
[DE87-013152] 02 p0178 N88-11106
Quantum electrodynamics based on self-energy: Spontaneous emission in cavities
[DE87-703071] 02 p0232 N88-11461
Materials preparation and longevity in hyperthermal atomic oxygen 03 p0297 N88-11862
Theory of atomic additivity in molecular hyperpolizabilities 03 p0297 N88-11867
Production of atom flows at materials evaporation by laser radiation
[DE87-703327] 03 p0328 N88-12074
Theory of multiphoton ionization of atoms by strong, short pulsed lasers
[DE88-000963] 05 p0588 N88-13588
Photoionization of atoms and ions: Application of time-dependent response method within the density functional theory
[AD-A185686] 07 p0930 N88-15649
Correlation effects on double electron capture in highly-charged, low-energy ion-atom collisions
[DE87-013179] 07 p0930 N88-15651
Status of cross section data for photon scattering by atoms
[DE87-011281] 08 p1081 N88-16517
Depth of origin of sputtered atoms: Experimental and theoretical study of Cu/Ru(0001)
[DE88-002848] 08 p1082 N88-16520
Light absorption by an atom moving inside a spherical box
[AD-A187241] 10 p1407 N88-18395
Electron tunneling microscopy
[AD-A187426] 11 p1452 N88-18652
Atomistic simulation of low-energy beam deposition
[DE88-004344] 11 p1544 N88-19228
Laser measurements of state-resolved Ga and in atom sticking and desorption on metal and semiconductor surfaces
[AD-A187644] 11 p1555 N88-19310
Theory of laser cooling and spectroscopy of harmonically trapped single atoms
[AD-A189576] 13 p1775 N88-20617
Spontaneous decay and atomic fluorescence near a metal surface of an absorbing dielectric
[AD-A187508] 13 p1835 N88-20975
Optical cooling and trapping 14 p1974 N88-21782
Macroscopic quantum jumps in a single atom
14 p1975 N88-21784
Squeezed states of light 14 p1976 N88-21791
Clusters of transition metal atoms
[AD-A191265] 16 p2270 N88-23579
Theoretical calculations of XeF ground state kinetics
[AD-A191398] 16 p2270 N88-23580
Sources of polarized ions and atoms
[DE88-010910] 20 p2852 N88-26931
Multiphoton ionization of alkaline earth atoms in an intense laser field
[DE88-008078] 21 p3014 N88-27884
Soot and radiation in a gas turbine combustor
[AD-A191991] 23 p3179 N88-28924
Infrared detection using Rydberg atoms
[AD-A194308] 23 p3191 N88-28990
Cooperative effects and intrinsic optical bistability in collections of atoms
[AD-A193993] 23 p3280 N88-29530
Modeling of atomic processes in X-ray laser plasmas
[AD-A194118] 23 p3286 N88-29567
Cluster beam studies
[AD-A195182] 24 p3434 N88-30443

ATP
U ADENOSINE TRIPHOSPHATE

ATROPHY
Investigation of rat skeletal muscles following short-term spaceflight aboard Cosmos-1667 biosatellite
10 p1365 N88-18157
Evaluation of the endogenous glucocorticoid hypothesis of denervation atrophy
[NASA-CR-182848] 17 p2381 N88-24157

ATROPINE
Carbamates, atropine, and diazepam: Effects on performance in the running rat
[AD-A188009] 11 p1517 N88-19062
Low doses of atropine sulfate impair retention of a well-learned spatial task
[AD-A194065] 23 p3237 N88-29266

ATTACHMENTS
U ACCESSORIES

ATTACK AIRCRAFT
NT AH-64 HELICOPTER
NT B-1 AIRCRAFT
NT B-57 AIRCRAFT
NT B-70 AIRCRAFT
NT BOMBER AIRCRAFT
NT F-4 AIRCRAFT
NT F-14 AIRCRAFT
NT F-15 AIRCRAFT
NT F-16 AIRCRAFT
NT F-18 AIRCRAFT
NT F-27 AIRCRAFT
NT F-106 AIRCRAFT
NT F-111 AIRCRAFT
NT FIGHTER AIRCRAFT

NT HARRIER AIRCRAFT
NT MIG AIRCRAFT
NT MIRAGE AIRCRAFT
NASA supersonic STOVL propulsion technology program
[NASA-TM-100227] 06 p0668 N88-14093
A model for estimating depot maintenance costs for Air Force fighter and attack aircraft
[AD-A187097] 09 p1105 N88-16624
Task listing: Visually assisted and visually dependent tasks for fighter aircraft
[AD-A191041] 16 p2244 N88-23404

ATTACKING (ASSAULTING)
A strategy for space warfare
[AD-A186658] 09 p1233 N88-17394
Computer aided tactics for air combat
12 p1597 N88-19559
Task listing: Visually assisted and visually dependent tasks for fighter aircraft
[AD-A191041] 16 p2244 N88-23404
Determination of the hydroperoxide potential of jet fuels
[AD-A195975] 24 p3357 N88-29991

ATTENTION
Effects of divided attention on identity and semantic priming
[AD-A184269] 03 p0357 N88-12250
Latency differences and effects of selective attention to gratings in the central and right visual fields: 2
[DE87-014730] 04 p0473 N88-12918
Research on visual information processing with special reference to oculomotor behavior in the areas of exploration, recognition and search
[AD-A186598] 08 p1051 N88-16346
Visual evoked potentials
[AD-A187942] 11 p1519 N88-19071
Two attentional models of classical conditioning: Variations in CS effectiveness revisited
[AD-A187697] 11 p1522 N88-19088
Construction of a multidimensional questionnaire to determine interindividual differences in controlling attention
[DFVLR-FB-87-45] 14 p1952 N88-21637
Selective mechanisms in auditory and bimodal signal processing
[AD-A190529] 15 p2103 N88-22530
Vagal tone as an index of mental state
16 p2239 N88-23373
Probe-evoked event-related potential techniques for evaluating aspects of attention and information processing 16 p2240 N88-23379
Estimating the cost of mental loading in a bimodal divided-attention task: Combining reaction time, heart-rate variability and signal-detection theory
16 p2241 N88-23385
Attention, effort, and fatigue: Neuropsychological perspectives 16 p2241 N88-23387
Processing deficits in monitoring analog and digital displays: Implications for attentional theory and mental-state estimation research
16 p2241 N88-23389
Eye and head response to an attention cue in a dual task paradigm
[AD-A191052] 18 p2551 N88-25143
A model for visual attention
[AD-A193061] 21 p2991 N88-27744
Divided attention revisited: Selection based on location or pitch
[AD-A193814] 22 p3133 N88-28627
Visual motion perception and visual attentive processes
[AD-A193640] 23 p3241 N88-29288
Central adrenergic receptors as mediators of central response to stress: Study with Positron Emission Tomography (PET)
[AD-A194947] 24 p3407 N88-30284
Comparative aspects of multiple processes of attention
[AD-A195805] 24 p3408 N88-30291

ATTENUATION
NT ACOUSTIC ATTENUATION
NT ATMOSPHERIC ATTENUATION
NT MICROWAVE ATTENUATION
NT RADIO ATTENUATION
NT SHOCK WAVE ATTENUATION
NT SIDELOBE REDUCTION
NT WAVE ATTENUATION
Radiation-induced transient attenuation of optical fibers at 800 and 1300 nm
[DE87-013165] 02 p0235 N88-11485
A statistical rain attenuation prediction model with application to the advanced communication technology satellite project. Part 2: Theoretical development of a dynamic model and application to rain fade durations and tolerable control delays for fade countermeasures
[NASA-TM-100242] 03 p0308 N88-11945
Ferromagnetic mitigation of electromagnetic pulse effects
[AD-A185685] 06 p0694 N88-14258
Chapter 2: Threshold for Raman conversion of FEL laser pulses in the atmosphere
[DE88-002470] 07 p0859 N88-15215
Theory of transient thermal self-focusing of sound beams 09 p1234 N88-17401
Formulation of a general technique for predicting pneumatic attenuation errors in airborne pressure sensing devices
[NASA-TM-100430] 13 p1723 N88-20302
Phase velocity and attenuation of plane elastic waves in a particle-reinforced composite medium
[AD-A189414] 13 p1734 N88-20366
Some models for rain and cloud attenuation of millimeter waves
[PB88-160809] 14 p1948 N88-21616
Fog, rain and aerosol attenuation in the atmosphere
[AD-A190867] 16 p2235 N88-23350
Theoretical basis for an experimental test with regard to the origin of VHF (Very High Frequency) radiation from natural lightning
[DE88-007535] 18 p2544 N88-25102
Determination of mesoscale variability of sea surface temperature and attenuation in the North Atlantic from satellite measurement
[REPT-162] 18 p2548 N88-25127
Propagation measurements for an Australian land mobile satellite system 19 p2645 N88-25697
Influence of scattering on seismic waves: Physical mechanisms contributing to attenuation in the crust
[AD-A191699] 19 p2690 N88-25992
Changes in seismic velocity and apparent attenuation due to isotropic and anisotropic scattering: Results from physical modeling 19 p2691 N88-25997
Poloidal field measurements using laser enhanced attenuation of an energetic lithium beam
[DE88-008360] 20 p2856 N88-26963
A statistical rain attenuation prediction model with application to the advanced communication technology satellite project. 1: Theoretical development and application to yearly predictions for selected cities in the United States
[NASA-CR-179498] 23 p3205 N88-29077
Finite-difference simulations of Rayleigh-wave scattering by shallow heterogeneity
[AD-A194961] 24 p3402 N88-30259

ATTENUATION COEFFICIENTS
Transport coefficients close to the mobility edge and nonlinear sigma model composite operators --- electron transport
[PREPRINT-541] 06 p0777 N88-14767
The analytical exponential decay coefficient of the submarine light field
[AD-A187215] 11 p1548 N88-19261
Remote sensing of acoustic properties of shallow water sediments: A review
[AD-A192107] 18 p2570 N88-25267
Metal halide optical glasses
[AD-A193794] 23 p3198 N88-29032

ATTENUATORS
NT POTENTIOMETERS (RESISTORS)
NT RESISTORS
NT THERMISTORS

ATTITUDE (INCLINATION)
NT PITCH (INCLINATION)
NT ROLL
NT SATELLITE ORIENTATION
NT YAW
Observations of localized grain boundary dislocations in series of (001) and (110) symmetrical tilt boundaries in aluminum
[DE87-014011] 01 p0025 N88-10156
Long-term adaptation of the otolith organs
07 p0886 N88-15375
Attitude determination of artificial satellites through joint application of static and dynamic optimal estimation techniques
[INPE-4415-TDL/306] 08 p0963 N88-15832
Numerical simulations of buoyancy driven flows in cylinders and cavities for vapor crystal growth
14 p1987 N88-21854
Minimal parameter solution of the orthogonal matrix differential equation
[NASA-TM-4043] 17 p2383 N88-24165
Improvement of head-up display standards. Volume 2: Evaluation of head-up displays to enhance unusual attitude recovery
[AD-A194601] 23 p3178 N88-28921

ATTITUDE CONTROL
NT DIRECTIONAL CONTROL
NT LATERAL CONTROL
NT LONGITUDINAL CONTROL
NT SATELLITE ATTITUDE CONTROL
NT THRUST VECTOR CONTROL
Attitude Control Working Group report
01 p0016 N88-10099
Improvements to the precision pan and tilt head
[RSRE-MEMO-3996] 01 p0057 N88-10365
Predictive momentum management for a space station measurement and computation requirements
[NASA-CR-172026] 02 p0138 N88-10866
USSR Report: Engineering and Equipment
[JPRS-UEQ-87-007] 02 p0157 N88-10985
Equal-modulus vector programmed frequency control of minimally redundant structure of powered, single-degree-of-freedom gyroscopes for spacecraft attitude control system 02 p0159 N88-10994
Effect of void gas lying between fluid slugs in nutation dampers 03 p0319 N88-12015
On the root locus method applied to flexural vibration control systems 03 p0320 N88-12022
Attitude dynamics for satellites stabilized through spin
[INPE-4403-NTE/275] 08 p0963 N88-15833
Analysis, design, construction and testing of a reaction wheel model for space applications
[INPE-4358-TDL/299] 08 p0963 N88-15834
Guidance of high-altitude sounding rockets using the S19 and Spinning Rocket Altitude Control (SPINRAC) systems 08 p1034 N88-16273
Development of a coupled expert system for the spacecraft attitude control problem
09 p1205 N88-17223
A fiber optic gyro strapdown reference system for guided weapons 12 p1597 N88-19560
Analysis of the sensitivity of the attitude control system of an artificial satellite
[INPE-4285-PRE/1157] 12 p1599 N88-19573
Separation dynamics for the last stage of a launch vehicle and satellite
[INPE-4281-PRE/1153] 12 p1601 N88-19582
Electromagnetic modeling of a control valve
[INPE-4140-PRE/1048] 12 p1622 N88-19700
Characterization of integrated photovoltaic detectors for MECB solar sensors
[INPE-4408-PRE/1221] 12 p1630 N88-19754
Laser gyro attitude control system feasibility
[AD-A189368] 13 p1720 N88-20285
Utilization of strapdown inertial and non-inertial sensors in determination of satellite attitude by Kalman filters
[INPE-4313-TDL/280] 13 p1731 N88-20349
A feedback double path compensating control structure for the attitude control of a flexible spacecraft
[INPE-4464-PRE/1239] 14 p1880 N88-21240
Multivariable control law design for the AFTI/F-16 with a failed control surface using a parameter-adaptive controller
[AD-A189848] 15 p2020 N88-22040
Three axis attitude control system
[NASA-CASE-GSC-12970-1] 17 p2308 N88-23808
Attitude control laws for gas-jet spacecraft
18 p2467 N88-24643
Attitude and orbit control for the AMPTE-UKS (Active Magnetospheric Particle Tracer Explores-UK Subsatellite): Evaluation of the in-flight performance
[PB87-225199] 19 p2604 N88-25467
Spacecraft applications of advanced global positioning system technology
[NASA-CR-172063] 20 p2757 N88-26359
Spacecraft applications of advanced global positioning system technology
[NASA-CR-172055] 21 p2894 N88-27180
Airborne remote operated device
[DE88-010324] 21 p2895 N88-27188
Simulation of attitude and maneuvers for the Brazilian spin-stabilized satellite
[INPE-4271-PRE/1143] 22 p3046 N88-28079
SIRTF nod maneuvers
[NASA-TM-101007] 22 p3048 N88-28085
Angle of attack and sideslip estimation using an inertial reference platform
[AD-A194876] 24 p3319 N88-29769
Synchronous response modelling and control of an annular momentum control device
[NASA-CR-4136] 24 p3358 N88-29995
Robust design of distributed controllers for large flexible space structures
[NASA-CR-183202] 24 p3380 N88-30134
MOORE: A prototype expert system for diagnosing spacecraft problems 24 p3418 N88-30343

ATTITUDE GYROS
Equal-modulus vector programmed frequency control of minimally redundant structure of powered, single-degree-of-freedom gyroscopes for spacecraft attitude control system 02 p0159 N88-10994
Advanced gyros in spacecraft control. Digital capture loops for dry tuned gyros
[LITEF-120046] 08 p0962 N88-15827

Design, simulation and laboratory testing of an inertial system for measuring the attitude and narrow-spaced motions
[DFVLR-FB-87-42] 14 p1912 N88-21426

ATTITUDE INDICATORS
Calibration of attitude control sensors
02 p0159 N88-10995

ATTITUDE STABILITY
NT DIRECTIONAL STABILITY
NT GYROSCOPIC STABILITY
NT LATERAL STABILITY
NT LONGITUDINAL STABILITY

ATTRACTION
Weak convergence of sums of moving averages in the alpha-stable domain of attraction
[AD-A186430] 07 p0912 N88-15529

ATTRITION (MATERIALS)
U COMMINUTION

AUDIO EQUIPMENT
NT MICROPHONES
Acoustic backscattering from bottom sediment at normal incidence in the laboratory
[AD-A186905] 09 p1242 N88-17443

AUDIO FREQUENCIES
Complementary satellite sound broadcasting systems: A NASA assessment for the Voice of America
[NASA-TM-100300] 10 p1321 N88-17899
Performance of single and multiple system AM stereo decoder receivers
[PB88-168307] 15 p2057 N88-22265
Auditory pattern memory: Mechanisms of tonal sequence discrimination by human observers
[AD-A190337] 15 p2104 N88-22534
Use of optical disk technology at the Air Command and Staff College
[AD-A192424] 21 p3027 N88-27969
Divided attention revisited: Selection based on location or pitch
[AD-A193814] 22 p3133 N88-28627

AUDIO SIGNALS
A digital audio link to the Channel Islands in the UHF television band: Preliminary experimental results
[BBC-RD-1987/9] 02 p0161 N88-11011

AUDIO VISUAL EQUIPMENT
U TRAINING DEVICES
U VISUAL AIDS

AUDIOLOGY
Activities report of the Institute of Sound and Vibration Research
[ETN-87-90685] 01 p0090 N88-10589
Further investigation of tests for susceptibility to noise-induced hearing loss
[ISVR-TR-149] 14 p1952 N88-21633

AUDIOMETRY
Recommendations for organising the calibration of pure-tone audiometers
[NPL-AC-112] 09 p1167 N88-16999
Auditory evoked magnetic fields in man
[PB88-193446] 20 p2831 N88-26796

AUDITORY PERCEPTION
Recognition of isolated non-speech sounds
[AD-A184600] 03 p0306 N88-11933
Speech recognition: Acoustic-phonetic knowledge acquisition and representation
[AD-A185897] 07 p0840 N88-15097
Long-term adaptation of the otolith organs
07 p0886 N88-15375
Morphology and development of the inner ear of Anurans 07 p0886 N88-15378
Computing support for basic research in perception and cognition
[AD-A186192] 07 p0897 N88-15437
Further investigation of tests for susceptibility to noise-induced hearing loss
[ISVR-TR-149] 14 p1952 N88-21633
Mechanisms mediating perception of complex acoustic patterns
[AD-A189765] 15 p2102 N88-22520
Complex sound processing: An interdisciplinary approach
[AD-A189782] 15 p2102 N88-22523
Perception of complex auditory patterns
[AD-A190218] 15 p2102 N88-22524
Auditory perception of complex sounds
[AD-A190528] 15 p2103 N88-22529
Mechanisms mediating the perception of complex acoustic patterns
[AD-A190112] 15 p2130 N88-22705
Motor theory of auditory perception
[AD-A192095] 18 p2550 N88-25136
Contra- and ipsilateral auditory stimuli produce different activation patterns at the human auditory cortex: A neuromagnetic study
[PB88-181490] 19 p2708 N88-26098
Demodulation processes in auditory perception
[AD-A193421] 21 p2988 N88-27740
Divided attention revisited: Selection based on location or pitch
[AD-A193814] 22 p3133 N88-28627

AUDITORY SIGNALS
Multipath time-delay estimation via the EM algorithm
[PB88-106851] 07 p0845 N88-15124
Complex sound processing: An interdisciplinary approach
[AD-A189782] 15 p2102 N88-22523
Auditory perception of complex sounds
[AD-A190528] 15 p2103 N88-22529
Selective mechanisms in auditory and bimodal signal processing
[AD-A190529] 15 p2103 N88-22530
Auditory pattern memory: Mechanisms of tonal sequence discrimination by human observers
[AD-A190337] 15 p2104 N88-22534
Time-frequency representations for speech signals
[AD-A188661] 18 p2498 N88-24819
Motor theory of auditory perception
[AD-A192095] 18 p2550 N88-25136

AUDITORY STIMULI
Further investigation of tests for susceptibility to noise-induced hearing loss
[ISVR-TR-149] 14 p1952 N88-21633
Complex sound processing: An interdisciplinary approach
[AD-A189782] 15 p2102 N88-22523
Auditory pattern memory: Mechanisms of tonal sequence discrimination by human observers
[AD-A190337] 15 p2104 N88-22534
Motor theory of auditory perception
[AD-A192095] 18 p2550 N88-25136
Contra- and ipsilateral auditory stimuli produce different activation patterns at the human auditory cortex: A neuromagnetic study
[PB88-181490] 19 p2708 N88-26098
Auditory evoked magnetic fields in man
[PB88-193446] 20 p2831 N88-26796
The interaction of thalamo-cortical systems in the 40 Hz following response 21 p2979 N88-27694
Divided attention revisited: Selection based on location or pitch
[AD-A193814] 22 p3133 N88-28627
Human auditory and visual continuous evoked potentials 23 p3238 N88-29269

AUGER EFFECT
Interatomic Auger rates for the sodium fluoride crystal
[DE87-013012] 03 p0382 N88-12401

AUGER SPECTROSCOPY
Auger electron spectroscopy of oxidized titanium overlayers: Speciation of homogeneous and heterogeneous samples
[KFK-4221] 02 p0146 N88-10913
Metal modification for improved glass-ceramic to metal seals. 1. Auger results on ion implantation and vapor deposition films
[DE88-005244] 10 p1339 N88-18006
The intergranular segregation of boron in substoichiometric Ni3Al
[DE88-004783] 11 p1462 N88-18720
An electron spectroscopic investigation of high-temperature superconducting oxides
[DE88-003807] 11 p1558 N88-19325
An interpretation of the ethylenic, carbidic, and graphite auger lineshapes of chemisorbed carbon species
[AD-A189092] 13 p1736 N88-20379
Quantitative AES: The establishment of a standard reference spectrum for the accurate determination of spectrometer transmission functions
[NPL-DMA(A)-151] 14 p1887 N88-21279
Auger electron spectroscopy of contrast-forming layers on metals
[NASA-TT-20182] 16 p2178 N88-22980
Initial stages of molecular beam heteroepitaxial growth in GaAs-(Ca,Sr)F2 and GaAs/Si systems
[LAAS-87-355] 16 p2281 N88-23658
Interface characterization of Cu-Cu and Cu-Ag-Cu low temperature solid state bonds
[AD-A191015] 16 p2283 N88-23667
Application of Auger electron spectroscopy to the study of trace element effects on weldability
[DE88-010457] 21 p2915 N88-27301

AUGMENTATION
NT STABILITY AUGMENTATION
NT THRUST AUGMENTATION
Optical sizing of soot in gas turbine combustors and exhaust augmentor tubes
[AD-A183785] 01 p0006 N88-10034
Method estimating integral mean value of enhancement factor and path latitude for whistlers below magnetic latitude 10 deg 03 p0300 N88-11885
Improvements to a UHF rebroadcast television link suffering tidal fading: Countisbury UHF relay station
[BBC-RD-1987/14] 05 p0573 N88-13495
Software enhancements and modifications to Program FDTD executable on the Cray X-MP computer
[DE88-001877] 07 p0904 N88-15476
Improved input representation for enhancement of neural network performance
[DE88-001830] 07 p0907 N88-15496
Enhancement of computer system for applications software branch 07 p0923 N88-15610
New technique for enhancing helium production in ferritic materials
[DE88-003048] 09 p1142 N88-16847
Suppression of the mass enhancement in CeB6 in high magnetic fields
[DE88-002946] 09 p1241 N88-17439
Observation of enhanced electric field in an RF-plugged sheet plasma in the RFC-XX-M open-ended machine
[IPPJ-857] 09 p1252 N88-17503
Design for performance enhancement in feedback control systems with multiple saturating nonlinearities
[NASA-CR-182614] 11 p1535 N88-19168
Investigations into shock-induced enhancement of mixing and combustion in supersonic burners
[AD-A189609] 12 p1607 N88-19608
Sensitivity of control-augmented structure obtained by a system decomposition method
[NASA-TM-100535] 14 p1954 N88-21647
Real-time flight test data distribution and display
[NASA-TM-100424] 15 p2022 N88-22050
Theoretical studies of Resonance Enhanced Stimulated Raman Scattering (RESRS) of frequency-doubled Alexandrite laser wavelength in cesium vapor
[NASA-CR-182870] 15 p2036 N88-22133
Data management and language enhancement for generalized set theory computer language for operation of large relational databases
[NASA-CR-182868] 16 p2250 N88-23446
Enhanced backscattering from rough surfaces
[AD-A191089] 16 p2274 N88-23610
Saturation and the limit of jet mixing enhancement by single frequency plane wave excitation: Experiment and theory
[NASA-TM-100882] 17 p2295 N88-23732
Application of its transformation in color enhancement of LANDSAT imagery 17 p2365 N88-24082
Enhancement of volume H(-) production by vibrationally pre-exciting the hydrogen molecules
[DE88-010783] 20 p2853 N88-26937
Vapor Compression Distillation Subsystem (VCDS) component enhancement, testing and expert fault diagnostics development, volume 2
[NASA-CR-172076] 21 p2994 N88-27755

AURIGA CONSTELLATION
A flash spectrum of Cl I, C I, N I, and Ni II absorption in 31 Cygni: A direct observation of the reversing layer
04 p0513 N88-13158

AURORAL ACTIVITY
U AURORAS

AURORAL ARCS
Electrodynamics of midnight sector of auroral oval in period of slight disturbance 08 p1003 N88-16077
Characteristics of particle acceleration at high latitude
08 p1026 N88-16210
First results from the Viking associated Aureld-VIP rocket and EISCAT campaign --- auroras: Swedish satellite
08 p1026 N88-16211
CAESAR investigations --- Coordinated Auroral Experiment using Scatter And Rockets (CAESAR)
08 p1031 N88-16249
EISCAT measurements of ion velocities during Coordinated Auroral Experiment using Scatter And Rockets (CAESAR) campaign 08 p1031 N88-16251
Remote and in-situ plasma measurements during the Coordinated Auroral Experiment using Scatter And Rockets (CAESAR) flight 08 p1032 N88-16252
Low frequency electrostatic waves observed on board the Coordinated Auroral Experiment using Scatter And Rockets (CAESAR) 2 payload 08 p1032 N88-16253
A multiple-satellite observation of the high-latitude auroral activity on 11 January 1983
[AD-A175170] 09 p1189 N88-17122
Coordinated Auroral Experiments using Scatter And Rocket investigations (CAESAR investigations)
[MPAE-W-47-87-13] 15 p2096 N88-22487
Dynamics explorer data analysis
[NASA-CR-181428] 19 p2691 N88-25996

AURORAL ELECTROJETS
Simultaneous observation of upward moving field aligned energetic electrons and ions on auroral zone field lines
[IRF-PREPRINT-102] 16 p2231 N88-23326

AURORAL IONIZATION
Spectrophotometric remote sensing of the diffuse aurora
[AD-A188599] 12 p1643 N88-19837

AURORAL SPECTROSCOPY

Auroral X-ray images during a pulsation event
08 p1026 N88-16214

Ground-based facility for spectrophotometric studies of the airflow and aurora
[AP-29] 22 p3119 N88-28532

AURORAL TEMPERATURE

Support for FY87 midlatitude electron-density calibration campaign
[AD-A190174] 15 p2094 N88-22476

AURORAL ZONES

Electric field measurements on Viking: First results
[TRITA-EPP-87-04] 05 p0625 N88-13826

Balloon measurement of magnetic field during substorms in auroral zone 08 p1026 N88-16213

Future developments of auroral D-region research using the EISCAT VHF incoherent scatter radar
08 p1035 N88-16278

Preliminary results from the dc electric field experiment on Viking --- Swedish satellite
[TRITA-EPP-87-03] 09 p1190 N88-17130

On the conjugacy of the aurora: High and low latitudes
[AD-A193008] 20 p2824 N88-26755

AURORAS

NT AURORAL ARCS

Relativistic electron precipitations in a pulsating aurora
04 p0488 N88-12894

Viking quick look plots: A short description --- Swedish satellite 06 p0692 N88-14243

Polar Geophysical Institute's studies of magnetosphere, ionosphere 06 p0728 N88-14480

Dynamics Explorer guest investigator
[NASA-CR-181494] 07 p0878 N88-15325

Holes in OI 130 nm emission fields of upper atmosphere during day 08 p1004 N88-16082

Viking: The first Swedish satellite
08 p1025 N88-16207

Global views of the aurora from the Viking satellite --- Swedish satellite 08 p1025 N88-16208

Instantaneous pictures of the high-latitude electrodynamics using Viking and DMSP/F7 observations --- Swedish satellite
08 p1025 N88-16209

Report on ground-based activity at Andoya (Norway) in relation to the Aureld-VIP high rocket and to the Viking satellite --- Swedish satellite 08 p1026 N88-16212

Auroral X-ray images during a pulsation event
08 p1026 N88-16214

First results of balloon-borne X-ray and electric field observations near the footprint of the Viking satellite
08 p1026 N88-16215

A new technique for rocket and space-borne investigations of time-dependant auroral morphology
08 p1030 N88-16241

Wave acceleration of auroral electrons
08 p1031 N88-16245

Acceleration of auroral particles by magnetic field-aligned electric fields 08 p1031 N88-16246

Observations of field-aligned current structures during the Coordinated Auroral Experiment using Scatter And Radar (CAESAR) flight 2 08 p1031 N88-16250

AURIO: A proposal for flying auroral imaging observatory on the Polar Platform in the Space Station/Columbus program 08 p1034 N88-16268

The rocket and scatter experiment ROSE: Presentation of the scientific payload 08 p1034 N88-16269

Microphysics of the auroral acceleration region of other regions of the magnetosphere 08 p1096 N88-16592

Acceleration/heating processes on auroral field lines as observed by the Viking spacecraft
08 p1096 N88-16596

Low frequency waves and small scale solitary structures observed by Viking --- Swedish satellite; auroras
08 p1099 N88-16611

Acceleration of auroral particles by magnetic field-aligned electric fields
[TRITA-EPP-87-08] 09 p1190 N88-17131

Spectrophotometric remote sensing of the diffuse aurora
[AD-A186599] 12 p1643 N88-19837

Dynamics of small and large scale irregularities at sub-auroral latitudes
[AD-A189052] 12 p1645 N88-19853

Waves and static electric fields in the aurora acceleration region 12 p1646 N88-19856

On the acceleration of electrons and positive ions in the same direction along magnetic field lines by parallel electric fields
[IRF-PREPRINT-103] 15 p2096 N88-22488

A proposal for the establishment of a center of excellence in theoretical geoplasma research
[AD-A189742] 16 p2231 N88-23327

The Jovian aurora: Electron or ion precipitation
[NASA-TM-101153] 17 p2452 N88-24566

Dynamics Explorer-2 measurements during an isolated auroral substorm
[AD-A191202] 18 p2543 N88-25091

Superthermal electron processes in the upper atmosphere of Uranus: Aurora and electroglow
[NASA-TM-101150] 18 p2594 N88-25417

Dynamics explorer data analysis
[NASA-CR-181428] 19 p2691 N88-25996

Investigation of the Sun-aligned F-region walls and related phenomena in the auroral latitude range
[AFGL-TR-87-0248] 19 p2692 N88-26000

High latitude ionospheric radio studies
[AD-A192270] 20 p2824 N88-26753

The low-latitude auroral boundary: Steady-state and time-dependent representations
[AD-A193200] 21 p2972 N88-27656

On the dynamics of the auroral ionosphere during the breakup of a substorm
[AD-A193368] 21 p2972 N88-27657

Snapshots of high-latitude electrodynamics using Viking and DMSP/F7 observations
[TRITA-EPP-88-01] 23 p3234 N88-29244

Five channel auroral photometer
[REPT-112] 24 p3375 N88-30101

Structural dynamics of high-latitude magnetosphere determined from solar electron data
24 p3444 N88-30500

X- and gamma-ray background observations in Antarctic
[INPE-4583-PRE/1317] 24 p3459 N88-30578

AUSTENITE

Fatigue, fracture and strain hardening of high carbon hardened alloy steel
[AD-A186101] 07 p0831 N88-15043

Sliding-wear properties of retained austenite in carburized layer
[PB87-149092] 07 p0833 N88-15054

The effect of deformation rate on JBK-75 staniess steel forgings
[DE88-001696] 07 p0834 N88-15061

The influence of grain boundary chemistry and structure on the intergranular attack and intergranular stress corrosion cracking of austenitic alloys
[DE88-002436] 07 p0835 N88-15063

Response of Fe-Cr-Mn austenitic alloys to thermal aging neutron irradiation
[DE88-003415] 10 p1302 N88-17765

Hydrogen induced cracks in armor steel weldments fabricated with austenitic filler alloys
[AD-A188733] 13 p1740 N88-20406

Ultrasonic studies of stresses and plastic deformation in steel during tension and compression
[AD-A192308] 21 p2912 N88-27280

Kinetic of martensitic transformations induced by hydrogen in the austenite
[DE88-701623] 23 p3194 N88-29007

AUSTENITIC STAINLESS STEELS

Development of creep resistant austenitic stainless steels for advanced steam cycle superheater application
[DE87-012929] 01 p0023 N88-10147

Comparative tests of high temperature creep-rupture behavior of the austenitic CrNi steel DIN W.NR.1.4970 in argon and steam
[KFK-4261] 01 p0063 N88-10402

Study of stainless steel time-temperature sensitization diagrams, part 1
[ETN-87-90762] 03 p0289 N88-11815

Effect of helium on irradiation creep in an austenitic stainless steel
[DE87-013754] 03 p0290 N88-11824

Modified 14Cr-16Ni stainless steels with improved creep resistance at 700 C due to tailored precipitate microstructures
[DE87-014788] 03 p0290 N88-11825

Influence of some parameters on the stress corrosion of a ABNT 304 stainless steel in MgCl/sub 2/
[DE87-703707] 04 p0416 N88-12580

Method for the ultrasonic inspection of the soundness of the metal in weld joints in two-ply pipes
[BLL-CE-TRANS-8265-(9022.09)]
04 p0453 N88-12805

Ultrasonic method of inspecting austenitic weld joints in nuclear power station equipment
[BLL-CE-TRANS-8281-(9022.09)]
04 p0453 N88-12806

Welded joint fatigue of a AISI 304 L type stainless steel
[DE87-703530] 05 p0592 N88-13607

Role of interstitials and precipitates in initiation and propagation of L.C.F. cracks in austenitic stainless steels
06 p0718 N88-14411

Elevated temperature fatigue crack propagation
06 p0720 N88-14424

Sliding-wear properties of retained austenite in carburized layer
[PB87-149092] 07 p0833 N88-15054

Evolution of radiation-induced voids and dislocations at low temperature
[DE88-700350] 07 p0939 N88-15704

Effects of a regenerating heat treatment on the creep behavior and the lifetime during creep test loading
[ETN-88-91063] 09 p1144 N88-16855

Influence of post-anneal cooling treatments on suppression of cryogenic intergranular fracture in experimental Ni-free high-Mn austenitic steels
[DE88-002766] 09 p1145 N88-16863

The role of composition and microstructure gradients on weld metal properties and behavior
[DE88-004956] 10 p1303 N88-17791

Thermal fatigue of stainless steel
[DE88-004146] 11 p1458 N88-18694

Properties fo seals made with Li2O-Al2O3-SiO2-glass ceramics and aluminum-containing austenitic stainless steels
[DE88-004688] 12 p1633 N88-19776

The fatigue behavior of ferritic and austenitic steels at elevated temperatures
[DE88-006304] 13 p1744 N88-20431

Improved glass-ceramic to metal seals in actuator and detonator applications with an aluminum-containing austenitic stainless steel
[DE88-004691] 13 p1749 N88-20458

Investigation of the use of horizontally polarised shear waves for TOFD studies on austenitic steel
[AERE-R-12145] 13 p1780 N88-20649

Fracture toughness characterization of SA508 and Sa533B RPB steels
[CISE-3908] 14 p1889 N88-21292

Effect of protective coatings on high-temperature fatigue of heat-resistant alloys 14 p1895 N88-21314

Dependence of hydrogen embrittlement of austenitic stainless steels on structural state of grain boundaries
14 p1896 N88-21316

Reduced-activation austenitic stainless steels: The Fe-Cr-C system
[DE88-008091] 20 p2773 N88-26442

Helium induced degradation in the weldability of an austenitic stainless steel
[DE88-009062] 20 p2773 N88-26443

Controlling phase formation and stability to improve the high temperature creep resistance of austenitic stainless steels
[DE88-011401] 21 p2914 N88-27293

AUSTRALIA

The role of low-level cooling in a conceptual model of the Australian summertime cool change: Implications for very-short-range forecasting 02 p0204 N88-11275

Australian East Coast cyclones 3: Case study of the storm of August 1986 02 p0204 N88-11276

Analysis of the reliability of Royal Australian Air force non-destructive inspection
[AD-A186979] 09 p1177 N88-17049

Mesoscale coastal ocean dynamics
11 p1517 N88-19060

Sixteenth AINSE Plasma Physics Conference. Conference handbook
[DE88-700825] 11 p1552 N88-19290

Recommended replacements for tetryl in Australian production fuzes and related ordnance
[MRL-R-1089] 13 p1754 N88-20489

Some properties of Australian produced explosive composition H-6
[MRL-TN-525] 13 p1754 N88-20490

Fire retardant coatings for military equipment: A review
[MRL-R-1104] 19 p2619 N88-25540

Propagation measurements for an Australian land mobile satellite system 19 p2645 N88-25697

AUTOCLAVES

The 700 F properties of autoclave cured PMR-2 composites
[NASA-TM-100923] 18 p2480 N88-24712

AUTOCLAVING

Determination of lumped-mass thermal properties associated with autoclave curing of graphite/epoxy composites 21 p2925 N88-27364

AUTOCOLLIMATORS

U COLLIMATORS

AUTOCORRELATION

The circular serial autocorrelation computer program
[AD-A184795] 03 p0365 N88-12295

Autocorrelation of control points on 11-band multispectral imagery
[AD-A188185] 10 p1348 N88-18056

The display of multivariate information: The effects of auto- and cross-correlation, reliability and heterogeneity
[AD-A191070] 16 p2243 N88-23398

Picosecond optical autocorrelation experiments on fast photodetectors 19 p2659 N88-25802

AUTOIONIZATION

Two-laser resonance enhanced photoionization spectrum of gas phase benzene
03 p0300 N88-11889

Correlation effects on double electron capture in highly-charged, low-energy ion-atom collisions
[DE87-013179] 07 p0930 N88-15651

Photoionization dynamics of excited molecular states
[DE88-002982] 09 p1245 N88-17468

Theoretical studies of atomic transitions
[DE88-004719] 10 p1407 N88-18389

Contributions of autoionizing resonances to the electron collisional excitation rates for Be-like ions
[AD-A190924] 18 p2572 N88-25275

Autoionization for lower level detrapping in X-ray lasers
[AD-A195845] 24 p3379 N88-30123

AUTOMATA THEORY

USSR report: Cybernetics, computers and automation technology
[JPRS-UCC-86-014] 06 p0761 N88-14669

Management of complex information in support of evolving autonomous expert systems
[AD-A186680] 09 p1224 N88-17337

Connectionist models and artificial intelligence
[RR-684-I-IMAG-66-LIFIA] 22 p3142 N88-28684

A proof of the Kahn principle for input/output automata
[AD-A194454] 23 p3248 N88-29333

The complexity of AI algorithms
[AD-A193494] 23 p3265 N88-29438

AUTOMATIC CONTROL

NT ACTIVE CONTROL
NT ADAPTIVE CONTROL
NT AUTOMATIC FLIGHT CONTROL
NT AUTOMATIC FREQUENCY CONTROL
NT AUTOMATIC LANDING CONTROL
NT CASCADE CONTROL
NT DYNAMIC CONTROL
NT FEEDBACK CONTROL
NT FEEDFORWARD CONTROL
NT LEARNING MACHINES
NT LINEAR QUADRATIC GAUSSIAN CONTROL
NT LINEAR QUADRATIC REGULATOR
NT MODEL REFERENCE ADAPTIVE CONTROL
NT NUMERICAL CONTROL
NT OFF-ON CONTROL
NT OPTIMAL CONTROL
NT SELF ADAPTIVE CONTROL SYSTEMS
NT SELF ALIGNMENT
NT SEQUENTIAL CONTROL
NT TIME OPTIMAL CONTROL

Test results and predictions for the response of near-ceiling sprinkler links in a full-scale compartment fire
[NBSIR-87/3633] 01 p0033 N88-10209

Hardware fault insertion and instrumentation system: Mechanization and validation
[NASA-CR-181445] 01 p0078 N88-10497

Optimization of a controlled two-server maintenance system
[INPE-4202-PRE/1083] 01 p0107 N88-10694

Synthesizing controllers for uncertain systems by a quantitative pole-placement
[PB87-195590] 02 p0223 N88-11403

Real time analysis of the results from mechanized ultrasonic testing
[DE87-752511] 03 p0334 N88-12107

CNET (Chief of Naval Education and Training) Program Automated Tracking System (CPATS): A comprehensive study
[AD-A184694] 03 p0385 N88-12416

Some data processing requirements for precision Nap-Of-the-Earth (NOE) guidance and control of rotorcraft
[NASA-CR-177453] 04 p0401 N88-12493

Failure control techniques for the SSME
[NASA-CR-179224] 04 p0409 N88-12537

Robust statistical methods for automated outlier detection 04 p0433 N88-12681

GOLD: Integration of model-based control systems with artificial intelligence and workstations
[DE88-000506] 04 p0483 N88-12976

On the next generation of reliability analysis tools
[NASA-CR-178380] 04 p0487 N88-13000

Ground vehicle convoying
[DE88-000360] 04 p0502 N88-13086

Automatic telescope operations
04 p0519 N88-13190

Automated design of controlled diffusion blades
[NASA-TM-100251] 05 p0542 N88-13304

Study of welding arc control in China
[PB87-143350] 07 p0863 N88-15235

Study on arc sound in TIG and plasma welding processes and the possibility of its application in practice
[PB87-143947] 07 p0863 N88-15236

Intelligent controllers
[DE88-001862] 07 p0904 N88-15475

Modelling of clustering effects in point processes: An application to failures in SPC-systems (stored program control-systems)
[PB87-149241] 07 p0904 N88-15480

Integration of symbolic and algorithmic hardware and software for the automation of space station subsystems
[NASA-TM-89705] 07 p0907 N88-15497

Investigation of candidate data structures and search algorithms to support a knowledge based fault diagnosis system 07 p0923 N88-15606

Microprocessor control and networking for the amps breadboard 07 p0924 N88-15615

NASA (National Aeronautics and Space Administration) ADP (Automated Data Processing) system: Information on the automated mission and the payload tracking system
[PB88-104989] 07 p0942 N88-15730

Advancing automation and robotics technology for the space station and for the US economy: Submitted to the United States Congress October 1, 1987
[NASA-TM-100777] 08 p0959 N88-15816

Advancing automation and robotics technology for the space station and for the US economy: Submitted to the United States Congress May 15, 1987
[NASA-TM-89811] 08 p0959 N88-15817

Advancing automation and robotics technology for the space station and for the US economy: Submitted to the United States Congress October 1, 1986
[NASA-TM-89190] 08 p0960 N88-15818

Preliminary evaluation of a micro-based repeated measures testing system
[NASA-CR-172038] 08 p1048 N88-16331

Integration of symbolic and algorithmic hardware and software for the automation of space station subsystems
08 p1056 N88-16373

KBS V and V as related to automation of space station subsystems: Rationale for a KBS lifecycle
08 p1057 N88-16375

Artificial intelligence and space power systems automation 08 p1058 N88-16381

Prototype space station automation system delivered and demonstrated at NASA 08 p1066 N88-16442

Hydrogen maser
[PB87-171617] 09 p1172 N88-17025

Computer control of a microgravity mammalian cell bioreactor 09 p1197 N88-17172

First Annual Workshop on Space Operations Automation and Robotics (SOAR 87)
[NASA-CP-2491] 09 p1203 N88-17206

Teaching artificial neural systems to drive: Manual training techniques for autonomous systems
09 p1207 N88-17238

Autonomous control procedures for shuttle rendezvous proximity operations 09 p1208 N88-17244

Automatic routing module 09 p1210 N88-17251

A conceptual framework for intelligent real-time information processing 09 p1211 N88-17257

Implementation of a robotic flexible assembly system
09 p1212 N88-17265

System integration of a Telerobotic Demonstration System (TDS) testbed 09 p1212 N88-17266

Regulation of nonlinear and generalized linear systems
[AD-A186706] 09 p1224 N88-17338

A smart, mapping, charting and geodesy control generator, phase 1
[AD-A188184] 10 p1347 N88-18055

A collaborative program of research in engineering sciences
[DE88-003383] 10 p1423 N88-18504

Robotic assembly and testing of rotary solenoids
[BDX-613-3663] 11 p1480 N88-18834

Toward automatic finite element analysis
11 p1527 N88-19120

Autonomous Liquid Encapsulated Czochralski (LEC) growth of single crystal GaAs by intelligent digital control
[AD-A187211] 11 p1555 N88-19305

Calibration of a ring laser gyro inertial navigation system 12 p1576 N88-19428

Research on flow control
[AD-A189014] 12 p1627 N88-19736

Automatic data acquisition system utilizing microcomputers: Automatic Meteorological Stations (AMS)
[INPE-4215-PRE/1096] 12 p1646 N88-19859

The automated symbolic derivation of state equations for dynamic systems
[DE88-005222] 12 p1683 N88-20060

RIAR automated research and management systems
[DE88-700934] 12 p1706 N88-20209

AVSCOM'S modifications to Teledyne Systems Company's air-to-air fire control system simulation model
[AD-A189136] 13 p1722 N88-20294

Analysis of spectral reflectance characteristics of targets under satellites and automatic cloud recognition
13 p1755 N88-20498

The evaluation of automatic barometers, illustrated by the Nakaasa barometer
[KNMI-TR-95] 13 p1774 N88-20610

The use of an automated flight test management system in the development of a rapid-prototyping flight research facility
[NASA-TM-100435] 13 p1823 N88-20896

The automated symbolic derivation of state equations for dynamic systems
[DE88-000968] 13 p1830 N88-20945

Development and flight test of an experimental maneuver autopilot for a highly maneuverable aircraft
[NASA-TP-2618] 14 p1867 N88-21153

An automated ozone photometer
[NASA-TM-100064] 14 p1908 N88-21404

Autonomous control system for Czochralski growth of LEC GaAs
[AD-A189726] 15 p2141 N88-22779

The necessity of automation in Brazil
[INPE-4346-PRE/1183] 15 p2150 N88-22832

A computational procedure for automated flutter analysis 15 p2220 N88-23250

Automatic control of an industrial process and computer aided process control by means of an expert system
[LAAS-88-004] 16 p2255 N88-23476

Automated database design technology and tools
[NASA-CR-182875] 16 p2286 N88-23687

Operation and performance of an integrated helicopter communication system 17 p2305 N88-23787

Development of an airborne facility for advanced avionics research 17 p2307 N88-23801

A design analysis for an automated robotic workpiece manipulator 17 p2344 N88-23975

Integration of symbolic and algorithmic hardware and software for the automation of space station subsystems
17 p2387 N88-24190

Connecting remote systems for demonstration of automation technologies 17 p2387 N88-24191

Knowledge based system verification and validation as related to automation of space station subsystems: Rationale for a knowledge based system lifecycle
17 p2387 N88-24192

Automatic program generation from specifications using PROLOG 17 p2388 N88-24196

An optimal disturbance rejection control system for multimegawatt space nuclear power systems
17 p2436 N88-24495

Energy optimal trajectory planning for robot manipulators and autonomous vehicles 17 p2437 N88-24497

A general approach for automating source code verification
[AD-A191461] 18 p2556 N88-25170

Development of the field-induced electron injection and impact ionization (F4I) technique for radiation hardness testing of MOS (Metal-Oxide-Semiconductor) gate insulators
[AD-A192114] 18 p2583 N88-25345

Technical feasibility study of applying auto-control methods to plating process solutions
[DE88-008014] 19 p2641 N88-25670

Technical instructions for a control operating system of the gas flow installation for the solid fuel combustion chamber
[LR-507] 20 p2788 N88-26537

Automated measurement of crack length and load line displacement at elevated temperature
[AGARD-R-751] 20 p2814 N88-26695

Feasibility study of a microprocessor controlled actuator test mechanism
[AD-A194654] 23 p3249 N88-29337

Second Conference on Artificial Intelligence for Space Applications
[NASA-CP-3007] 23 p3251 N88-29351

Space station as a vital focus for advancing the technologies of automation and robotics
[IAF-86-62] 23 p3251 N88-29352

Machine vision for real time orbital operations
23 p3253 N88-29367

Automatic object recognition
23 p3254 N88-29368

Failure modes and effects analysis automation
23 p3254 N88-29370

A plan for time-phased incorporation of automation and robotics on the US space station
23 p3255 N88-29377

Software development without languages
23 p3257 N88-29392

Utilization of artificial intelligence techniques for the Space Station power system 23 p3261 N88-29412

Spray automated balancing of rotors: Methods and materials
[NASA-CR-182151] 24 p3330 N88-29825

best copy available

Artificial intelligence costs, benefits, risks for selected spacecraft ground system automation scenarios
24 p3416 N88-30332
Automated space vehicle control for rendezvous proximity operations 24 p3416 N88-30335
An automated computerized vision technique for determination of three-dimensional object geometry
24 p3419 N88-30346
AUTOMATIC CONTROL VALVES
NT PRESSURE REGULATORS
AUTOMATIC DATA PROCESSING
U DATA PROCESSING
AUTOMATIC FLIGHT CONTROL
NT AUTOMATIC LANDING CONTROL
Assessment of software quality for the AIRBUS A310 automatic pilot 02 p0128 N88-10604
Design verification and fabrication of active control systems for the DAST ARW-2 high aspect ratio wing. Part 2: Appendices
[NASA-CR-177959-PT-2] 06 p0869 N88-14102
Study on a unidirectional ring laser gyro. Part 1: Proposition of the principle and studies on the components
[NAL-TR-933] 09 p1160 N88-17010
Expert system applications in spacecraft subsystem controllers 09 p1210 N88-17254
Automatic flight control system for modern helicopters
12 p1597 N88-19558
Preliminary airworthiness evaluation of the UH-60A with Advanced Digital Optical Control System (ADOCS)
[AD-A190674] 15 p2018 N88-22030
Automation tools for demonstration of goal directed and self-repairing flight control systems
[NASA-CR-179433] 19 p2715 N88-26121
Automatic landing by computer vision
[ETN-88-92991] 23 p3175 N88-28905
AUTOMATIC FREQUENCY CONTROL
State of tuning
[NASA-TT-20195] 18 p2561 N88-25205
AUTOMATIC LANDING CONTROL
Trajectory measurement of the Fokker 100 aircraft during autoland testing
[NLR-MP-86010-U] 20 p2758 N88-26366
Automatic landing by computer vision
[ETN-88-92991] 23 p3175 N88-28905
AUTOMATIC PATTERN RECOGNITION
U PATTERN RECOGNITION
AUTOMATIC PICTURE TRANSMISSION
A low cost automatic Earth observation satellite tracking ground receiving station 17 p2309 N88-23815
AUTOMATIC PILOTS
Assessment of software quality for the AIRBUS A310 automatic pilot 02 p0128 N88-10604
Towards the unmanned cockpit
02 p0129 N88-10612
A linear quadratic Gaussian with loop transfer recovery proximity operations autopilot for spacecraft
[NASA-CR-172029] 02 p0227 N88-11433
Contribution to the improvement of the guidance accuracy of automatic pilots
[ETN-88-90607] 05 p0551 N88-13360
Reduced order optimal command applied to longitudinal automatic pilots
[SNIAS-872-111-114] 05 p0552 N88-13362
An autopilot design for the United States Marine Corps' airborne remotely operated device
[AD-A186379] 07 p0820 N88-14983
Integrated autopilot/autothrottle based on a total energy control concept: Design and evaluation of additional autopilot modes
[NASA-CR-4131] 13 p1724 N88-20308
Development and flight test of an experimental maneuver autopilot for a highly maneuverable aircraft
[NASA-TP-2618] 14 p1867 N88-21153
Low altitude: A new dimension in air refueling
[AD-A193819] 23 p3176 N88-28910
AUTOMATIC ROCKET IMPACT PREDICTORS
U COMPUTERIZED SIMULATION
U IMPACT PREDICTION
AUTOMATIC TEST EQUIPMENT
Rivista Tecnica Selenia, volume 10, number 2
[ETN-87-90763] 01 p0011 N88-10064
The ISA test system: A catalog of automatic support facilities 01 p0012 N88-10067
Ultrasonic examination of high performance polymer composites
[DRIC-T-7862] 01 p0027 N88-10170
Automated microwave dielectric constant measurement
[AD-A184182] 04 p0431 N88-12667
Survey of electronic measurement needs below 10 MHz
[PB88-110366] 07 p0844 N88-15121
Computer aided testing procedure for stress corrosion cracking investigations
[GKSS-86/E/63] 11 p1460 N88-18706
Rocketdyne automated dynamics data analysis and management system 11 p1499 N88-18954
Systems for the 21st century
17 p2302 N88-23769
Automated measurement of crack length and load line displacement at elevated temperature
[NLR-MP-87049-U] 20 p2816 N88-26706
Results of the use of an automated electrical measuring instrument calibration system
[SNIAS-881-430-107] 23 p3217 N88-29146
AUTOMATIC WEATHER STATIONS
Very short range statistical forecasting of automated weather observations
[AD-A190803] 16 p2235 N88-23349
AUTOMATION
Technology requirements for telerobotic satellite servicing in space 12 p1592 N88-19536
Principles of lazy and incremental program generation
[CWI-CS-R8749] 16 p2249 N88-23435
Automation of surface observations program
18 p2545 N88-25106
Enumeration, comments and discussion concerning papers presented during the Conference on Computer Applications in Production and Engineering (CAPE) 87
[NLR-MP-87015-U] 20 p2839 N88-26844
Advanced manufacturing management current and forthcoming technologies
[PNR90445] 22 p3159 N88-28802
AUTOMOBILE ENGINES
Japanese industrial research on lean combustion: A case study: International Research Monitoring Program
[DE87-013839] 02 p0144 N88-10904
Development of a light duty gas engine for cogeneration service
[PB87-221297] 02 p0180 N88-11119
Application of electronic fuel injection to the optimum engine for methanol utilization
[PB87-201950] 02 p0180 N88-11120
Automotive Stirling engine: Mod 2 design report
[NASA-CR-175106] 02 p0250 N88-11578
Hot piston ring tests
[NASA-TM-100256] 06 p0729 N88-14486
Advanced Gas Turbine (AGT) Technology Development Project, ceramic component developments
[NASA-CR-180871] 12 p1709 N88-20229
Advanced Gas Turbine (AGT) technology development project
[NASA-CR-180891] 12 p1709 N88-20230
Motor vehicles as sources of compounds important to tropospheric and stratospheric ozone
[PB88-195219] 18 p2540 N88-25076
The influence of foreign particles on bearing metals
[NASA-TT-20155] 20 p2775 N88-26454
Phase 1 results from the Stirling-powered vehicle project
[NASA-TM-100978] 21 p3029 N88-27980
Testing of a variable-stroke Stirling engine
[NASA-TM-100899] 24 p3440 N88-30472
AUTOMOBILE FUELS
Alternative fuels: Information on DOD's (Department of Defense's) methanol vehicle program
[PB87-213328] 02 p0156 N88-10976
Detailed kinetic modeling of autoignition chemistry
[DE87-013226] 03 p0283 N88-11782
Models for conducting economic analysis of alternative fuel vehicles
[AD-A184028] 03 p0334 N88-12103
Technical highlights of the Alternative Fuels Utilization Program
[DE88-005064] 15 p2049 N88-22205
AUTOMOBILES
NT ELECTRIC AUTOMOBILES
Steering mechanism --- vehicles
[EP-PATENT-0-181-700-A1] 01 p0053 N88-10338
Identifying areas of leading edge Japanese science and technology: Patent activity and citation analysis using US POC (Patent Office Classification) classification
[PB87-204095] 02 p0249 N88-11575
A simulation study of a speed control system for autonomous on-road operation of automotive vehicles
[AD A184030] 03 p0362 N88-12279
Computational study of three-dimensional wake structures
[REPT-2] 05 p0539 N88-13261
Applications of fatigue analyses: Transportation
05 p0608 N88-13733
Development, features of roller rocker arm reported
06 p0689 N88-14219
Report to Congress on the Automotive Technology Development Program
[DE88-003742] 07 p0864 N88-15242
Experimental investigation on the bending fatigue performance of gas carbonitrided and carburized gears
[PB87-147997] 08 p0992 N88-16003
Ergonomics of car controls for disabled people, phase 1. Part 1: Chapters 1-7. Part 2: Appendices. Part 3: References
[ISBN-0-947767-82-7] 09 p1202 N88-17204
JPRS report: Science and technology. Japan
[JPRS-JST-87-026] 16 p2184 N88-23018
Present, future of automotive hybrid IC applications discussed 16 p2185 N88-23024
The integration of digital maps in vehicle navigation systems 16 p2225 N88-23286
Incompressible Euler solution on a multiblock grid around a car configuration
[FFA-TN-1987-65] 18 p2457 N88-24586
Navigation system for land vehicles
[NASA-CASE-LAR-13322-1] 18 p2462 N88-24620
Digital maps for an electronic traffic guide
18 p2534 N88-25033
Unified methods of accelerated laboratory tests of the preparations for temporary protection of cars
[NASA-TT-20298] 21 p2921 N88-27336
A demonstration of retro-traverse using a semi-autonomous land vehicle
[DE88-009851] 21 p2957 N88-27568
AUTOMORPHISMS
A construction of simple Abelian varieties
[ZW-8702] 05 p0642 N88-13929
Mathematical morphology: An algebraic approach
[CWI-AM-R8707] 16 p2258 N88-23497
AUTONOMIC NERVOUS SYSTEM
NT SYMPATHETIC NERVOUS SYSTEM
Motion and space sickness 04 p0404 N88-12510
Direct interaction between autonomic nerves and the immune system
[AD-A188576] 12 p1667 N88-19991
AUTONOMOUS NAVIGATION
Dynamic image interpretation for autonomous vehicle navigation
[AD-A184043] 03 p0262 N88-11647
The 3-D world modeling for an autonomous robot
[DE87-013878] 03 p0333 N88-12102
A simulation study of a speed control system for autonomous on-road operation of automotive vehicles
[AD-A184030] 03 p0362 N88-12279
Autonomous Land Vehicle (ALV) planning and navigation system
[AD-A184243] 04 p0397 N88-12475
Expert robots in nuclear plants
[DE87-014839] 04 p0452 N88-12800
Satellite autonomous navigation with SHAD (Stellar Horizon Atmospheric Dispersion)
[AD-A184988] 05 p0544 N88-13313
Dealing with unanticipated events in autonomous navigation
[DE88-000590] 05 p0590 N88-13602
Range imagery algorithms for the detection of obstacles by autonomous vehicles
[AD-A185421] 05 p0656 N88-14045
A demonstration of autonomous navigation and machine vision using the HERMIES-2B robot
[DE88-002298] 07 p0862 N88-15226
Proceedings of Image Understanding Workshop, volume 2
[AD-A186104] 07 p0902 N88-15464
Real-time artificial intelligence issues in the development of the adaptive tactical navigator
09 p1211 N88-17260
An overview of vision-based navigation for autonomous land vehicles 1986
[AD-A186186] 10 p1276 N88-17640
A computer simulation study of an expert system for walking machine motion planning
[AD-A187907] 11 p1438 N88-18577
Search problems in mission planning and navigation of autonomous aircraft
[NASA-CR-182666] 12 p1579 N88-19448
Low cost mobile robot
[AD-A188507] 12 p1633 N88-19778
NAVLAB: An autonomous navigation testbed
[AD-A189049] 13 p1720 N88-20283
Local free-space mapping and path guidance for mobile robots
[AD-A192970] 20 p2810 N88-26674
A feasibility study in path planning using optimization techniques
[AD-A193030] 21 p2894 N88-27177
Three-dimensional scene analysis using stero based imaging
[AD-A193120] 21 p2894 N88-27178
A demonstration of retro-traverse using a semi-autonomous land vehicle
[DE88-009851] 21 p2957 N88-27568
Assessments of maneuverability with the TeleOperated Vehicle (TOV)
[AD-A191584] 21 p2993 N88-27751

AUTONOMY
An autonomous, closed-loop pointing system for use with satellite optics
[DE87-012011] 02 p0235 N88-11483
Expert system study for spacecraft management
[TL-2699-ISS-1] 07 p0824 N88-15004
Intelligent Mobile Autonomous System (IMAS)
[AD-A193181] 21 p3003 N88-27811
Study of standard generic approach for spacecraft (S/C) autonomy and automation (phase 3). Book A: Autonomy concept description
[ESA-CR(P)-2555-VOL-1] 23 p3185 N88-28955
Study of standard generic approach for spacecraft (S/C) autonomy and automation (phase 3). Book B: Autonomy concept application example
[ESA-CR(P)-2555-VOL-2] 23 p3185 N88-28956
Study of standard generic approach for spacecraft (S/C) autonomy and automation (phase 3). Book C: Autonomy concept summary
[ESA-CR(P)-2555-VOL-3] 23 p3185 N88-28957
Knowledge elicitation for an operator assistant system in process control tasks 23 p3253 N88-29366
Expert systems for MSFC power systems
23 p3255 N88-29375
Blackboard architectures and their relationship to autonomous space systems 23 p3261 N88-29414
Path planning and path following for the Amsterdam autonomous cart
[FVI-86-22] 24 p3380 N88-30133
Integrating information systems in a major decentralized international organization, volume 7
[AD-A195856] 24 p3439 N88-30468

AUTOPILOTS
U AUTOMATIC PILOTS

AUTORADIOGRAPHY
High resolution electron and ion microscopy
[AERE-R-12502] 10 p1297 N88-17754
Optimization of the southern electrophoretic transfer method
[DE88-004527] 10 p1299 N88-17765

AUTOREGRESSIVE PROCESSES
Least squares linear lags and limited memory filters
[NASA-CR-178381] 03 p0372 N88-12339
Application of lattice filtering techniques to CW measured time domain data
[AD-A184351] 04 p0431 N88-12671
Identifiability of multivariate ARMA models
[AD-A187384] 10 p1400 N88-18350
Identification of microwave line-of-sight multipath components 12 p1616 N88-19865
Application of the NARMAX method to nonlinear frequency response estimation
[RR-319] 14 p1964 N88-21721
Parametric methods of analysing linear and nonlinear systems
[RR-318] 14 p1967 N88-21741
Consistent estimates of autoregressive parameters for autoregressive moving average models
[RR-663-I] 15 p2109 N88-22564
Autoregressive moving average modeling of radar target signatures
[AD-A194612] 22 p3069 N88-28218
Strong law for mixing sequence
[AD-A193615] 23 p3274 N88-29490

AUXILIARY EQUIPMENT (COMPUTERS)
U PERIPHERAL EQUIPMENT (COMPUTERS)

AUXILIARY POWER SOURCES
NT FISSION ELECTRIC CELLS
NT NUCLEAR AUXILIARY POWER UNITS
NT SNAP
NT SNAP 19
NT SPACE POWER REACTORS
Design and testing of a small radial turbine for auxiliary power units 10 p1281 N88-17661

AUXILIARY PROPULSION
An 8-cm ion thruster characterization
[NASA-CR-180819] 01 p0017 N88-10106
Auxiliary propulsion system flight package
[NASA-CR-180828] 02 p0141 N88-10686
Auxiliary propulsion technology for advanced Earth-to-orbit vehicles
[NASA-TM-100237] 06 p0674 N88-14127
Component data base for space station resistojet auxiliary propulsion
[NASA-CR-180834] 10 p1293 N88-17731
A cyclic ground test of an ion auxiliary propulsion system: Description and operational considerations
[NASA-TM-100870] 17 p2313 N88-23629
Successful completion of a cyclic ground test of a mercury ion auxiliary propulsion system
[NASA-TM-101351] 24 p3330 N88-29873

AV-8A AIRCRAFT
U HARRIER AIRCRAFT

AV-8B AIRCRAFT
U HARRIER AIRCRAFT

AVAILABILITY
Resilient procedures: A structured replication approach 10 p1381 N88-18245

AVALANCHE DIODES
V-band IMPATT power amplifier
[NASA-CR-180711] 01 p0042 N88-10267
Optically tuned MM-wave IMPATT source
[AD-A185250] 05 p0577 N88-13523
Optical communication with semiconductor laser diodes
[NASA-CR-182464] 09 p1154 N88-16918
Superlattice photodetectors
[AD-A186956] 09 p1253 N88-17511
Effect of atmospheric turbulence on the bit error probability of a space to ground near infrared laser communications link using binary pulse position modulation and an avalanche photodiode detector
[NASA-TM-100699] 14 p1873 N88-21189
Examination of temperature effects on gate-to-drain avalanche breakdown in GaAs MESFETs (Metal-Semiconductor Field Effect Transistors) by measuring light emission under RF drive
[AD-A189634] 15 p2141 N88-22778
Study for the determination of general and specific properties of wide energy-band gap HgCdTe in the 1 to 2 micrometer wavelength range
[AD-A191091] 17 p2334 N88-23934
Characterization of a 30-GHz IMPATT solid state amplifier
[NASA-TM-100876] 18 p2503 N88-24847

AVALANCHES
Gas flow effects in pulse avalanche discharge XeCl excimer lasers 03 p0328 N88-12070

AVERAGE
NT MEAN
Causes of spurious features in spectral reflectance data 05 p0614 N88-13769
Weak convergence of sums of moving averages in the alpha-stable domain of attraction
[AD-A186430] 07 p0912 N88-15529
Weighted averaging method for image smoothing reported 14 p1901 N88-21352

AVHRR
U ADVANCED VERY HIGH RESOLUTION RADIOMETER

AVIATION
U AERONAUTICS

AVIATION METEOROLOGY
Meteorological systems support to critical shuttle requirements on the Eastern Test Range --- STS
02 p0205 N88-11281
Study of microburst detection performance during 1985 in Memphis, Tennessee
[AD-A184013] 03 p0354 N88-12231
Eighth Session of the Commission for Aeronautical Meteorology (abridged)
[WMO-673] 06 p0745 N88-14585
Characterization of meteorological phenomena influencing aircraft operations 08 p0951 N88-15772
AEV local verification for aviation, precipitation and temperature programs: AV, REL, TEM (September 1987 revision)
[PB88-115662] 10 p1355 N88-18101
Power spectral density analysis of wind-shear turbulence for related flight simulations
[NASA-CR-182721] 13 p1802 N88-20773
Meteorological and Environmental Inputs to Aviation Systems
[NASA-CP-2498] 18 p2545 N88-25105
Automation of surface observations program
18 p2545 N88-25106
Bracknell Meteorological Office
18 p2545 N88-25107
Special observations 18 p2545 N88-25108
Applications products of aviation forecast models
18 p2546 N88-25109
General-aviation's view of progress in the aviation weather system 18 p2546 N88-25110
Objective detection and forecasting of Clear-Air Turbulence (CAT): A status report
18 p2546 N88-25114
Comparative verification between GEM model and official aviation terminal forecasts
18 p2546 N88-25115
Denver ARTCC evaluation of PROFS (Prototype Regional Observations and Forecast System) mesoscale weather products 18 p2547 N88-25117
The Federal Aviation Administration/Massachusetts Institute of Technology (FAA/MIT) Lincoln Laboratory Doppler weather radar program
18 p2547 N88-25118

AVIATION PSYCHOLOGY
Some aspects of sociopsychological screening of flying school applicants 07 p0890 N88-15392
JPRS report: Science and technology. USSR: Space Biology and Aerospace Medicine, volume 21, no. 4, July - August 1987
[JPRS-USB-88-002] 07 p0893 N88-15412
New US book on aviation psychology reviewed
07 p0896 N88-15433
Temperament Structure Scales (TSS). Test manual
[ESA-TT-1069] 09 p1201 N88-17197

AVIATORS
U AIRCRAFT PILOTS

AVIONICS
Digital system bus integrity
[NASA-CR-181446] 01 p0006 N88-10030
The ISA test system: A catalog of automatic support facilities 01 p0012 N88-10067
AI expert system technology issues for guidance and control applications 02 p0128 N88-10808
Soviet aviation technology's state of the art SU-27 fighter
[AD-A184121] 03 p0259 N88-11628
The flight evaluation of an advanced engine display and monitoring system 03 p0264 N88-11659
Helicopter (performance) management
03 p0264 N88-11666
The Avionics Flight Evaluation System (AFES) of the DFVLR
[ESA-TT-1037] 03 p0266 N88-11677
Assessment of existing specifications against the design-philosophy for grounding and inter-unit wiring (EMCR 20/85)
[EMCR-22/85] 03 p0310 N88-11956
Electronic system reliability and effectiveness
[AD-A184522] 03 p0311 N88-11961
Workshop on Avionics Corrosion Control
[AGARD-R-733] 05 p0547 N88-13331
Avionic corrosion 05 p0547 N88-13332
Corrosion of electronic components
05 p0547 N88-13333
US Naval Air Force avionic and electrical system corrosion prevention and control maintenance
05 p0547 N88-13334
Avionics and corrosion 05 p0547 N88-13336
Error propagation in a digital avionic mini processor
[NASA-CR-181565] 05 p0633 N88-13872
Diagnostic emulation: Implementation and user's guide
[NASA-CR-178391] 06 p0756 N88-14638
Supportability in aircraft systems through technology and acquisition strategy applications
[AD-A186465] 08 p0949 N88-15759
Avionics systems integration technology
09 p1110 N88-16654
Helicopters as test carriers for avionics systems (HETAS)
[DFVLR-IB-112-85/18] 09 p1116 N88-16692
Neural network based architectures for aerospace applications 09 p1204 N88-17218
Helicopter activities in Germany
[MBB-UD-487/86] 10 p1314 N88-17853
Navigation recovery block design description
[NASA-CR-182473] 10 p1342 N88-18022
Applicability of Ada (trademark) tasking for avionics executives
[AD-A188827] 12 p1578 N88-19445
An evaluation of perceptions of form, fit, function (F3) standardization on the Standard Inertial Navigation Unit (STD INU) program
[AD-A188955] 12 p1579 N88-19446
Computer architecture for efficient algorithmic executions in real-time systems: New technology for avionics systems and advanced space vehicles
[NASA-CR-182650] 12 p1675 N88-20016
Avionics acquisition, trends and future approaches
12 p1702 N88-20184
Reducing time required for the development of avionic systems 12 p1702 N88-20185
Architecture specification for PAVE PILLAR avionics
[AD-A188722] 13 p1723 N88-20303
Advanced avionics system analysis. Modular avionics cost benefit study formulation
[AD-A189019] 14 p1867 N88-21158
General aviation activity and avionics survey: 1986 data
[AD-A189986] 15 p2013 N88-22003
Reliability analysis within a Computer Aided Engineering (CAE) infrastructure
[NLR-MP-86059-U] 15 p2074 N88-22369
Information systems for quality. Experience at the Nerviano Aeritalia plant. Avionic systems and equipment group
[ETN-88-92274] 15 p2148 N88-22821
Rapid prototyping of complex avionics system architectures
[ETN-88-92275] 16 p2162 N88-22898
The use of rule induction to assist in the diagnosis of avionic circuit board defects
[ETN-88-92077] 16 p2162 N88-22899

Digital avionics design and reliability analyzer
[NASA-CR-181641] 16 p2254 N88-23472
Joint University Program for Air Transportation Research, 1986
[NASA-CP-2502] 17 p2293 N88-23715
Integrated avionics reliability 17 p2294 N88-23723
Integrated Application of Active Controls (IAAC) technology to an advanced subsonic transport project: Program review
[NASA-CR-3880] 17 p2301 N88-23763
The Design, Development and Testing of Complex Avionics Systems
[AGARD-CP-417] 17 p2302 N88-23767
Technology development program for twenty-first century aerospace vehicles 17 p2302 N88-23768
Systems for the 21st century
17 p2302 N88-23769
Rapid prototyping of complex avionic system architectures 17 p2302 N88-23771
The specification and design of a future maritime reconnaissance aircraft 17 p2303 N88-23772
A structured approach to weapon system design
17 p2303 N88-23773
Development of a generic architecture
17 p2303 N88-23774
Test philosophy of the EH101 integrated avionic
17 p2303 N88-23775
Systems engineering technique
17 p2303 N88-23776
Modeling of functional specifications for onboard software: Experience with the Rafale avionics system
17 p2303 N88-23777
The avionics software architecture impact on system architecture 17 p2303 N88-23778
A comparison of integrated and separate systems for flight control and navigation 17 p2303 N88-23779
Development and testing of a predictive methodology for optimization of man-machine interface in future avionics systems 17 p2304 N88-23780
Crewstation Information and Development System (CIDS) 17 p2304 N88-23781
Managing advanced avionic system design
17 p2304 N88-23733
Psychosensory cockpit ergonomics, advantages of intelligent information systems 17 p2304 N88-23784
Advanced development of a cockpit automation design support system 17 p2304 N88-23785
Design and development of an avionics system adapted to helicopter missions 17 p2305 N88-23786
Operation and performance of an integrated helicopter communication system 17 p2305 N88-23787
Designing for design effectiveness of complex avionics systems 17 p2305 N88-23788
Design for interoperability (interchangeability)
17 p[illegible] N88-23789
The electromagnetic threat to future a[illegible]stems
17 p2305 [illegible]790
The integration, characterisation and trialling of a modern complex airborne radar 17 p2305 N88-23791
Experience in the integration of human engineering effort with avionics systems development
17 p2305 N88-23793
Testing complex avionics software: A practical experience 17 p2306 N88-23794
A look toward the future of complex avionics systems development using the USAF Test Pilot School's avionics systems test training aircraft 17 p2306 N88-23797
Software engineering for the British Aerospace Experimental Aircraft Programme (EAP)
17 p2306 N88-23798
Avionics systems: Development method and computer tools 17 p2306 N88-23799
Development of an airborne facility for advanced avionics research 17 p2307 N88-23801
Workshops for the design of avionics systems and the development of onboard software
17 p2307 N88-23802
Coherent functional development: Key to successful future system integration 17 p2307 N88-23803
Development of complex avionics systems: Experience from French military programs 17 p2307 N88-23804
User's guide to the Fault Inferring Nonlinear Detection System (FINDS) computer program
[NASA-CR-178410] 18 p2462 N88-24619
Development of an airborne facility for advanced avionics research
[NLR-MP-87012-U] 20 p2760 N88-26368
A cockpit natural language study - selected transcripts
[AD-A192972] 20 p2834 N88-26808
Air Force technical objective document, FY89
[AD-A193110] 21 p2896 N88-27194
Computation of ECM (Electronic Counter-Measures) war reserve materiel spare requirements
[AD-A193301] 21 p2897 N88-27195
The impact of increased aircraft reliability on maintenance facility design
[AD-A194395] 22 p3042 N88-28057
Avionic and electrical system corrosion prevention and control maintenance 22 p3054 N88-28119
Electronic failure analysis-corrosion of avionics
22 p3054 N88-28122
Avionics system design for high energy fields: A guide for the designer and airworthiness specialist
[NASA-CR-181590] 23 p3178 N88-28919
Aircraft avionics and missile system installation cost study. Volume 1: Technical report and appendices A through E
[AD-A194605] 23 p3178 N88-28923
Avionic expert systems 23 p3253 N88-29365
Contribution of expert systems to avionics advance. Application on AS30 laser weapon system
[SNIAS-881-320-103] 23 p3267 N88-29449
The OFP (Operational Flight Program) update cycle needs you
[AD-A194910] 24 p3325 N88-29798
Aircraft avionics and missile system installation cost study. Volume 2: Appendices F and G
[AD-A195372] 24 p3325 N88-29801

AVOIDANCE
NT COLLISION AVOIDANCE
Windshear training aid. Volume 1: Overview, pilot guide, training program
[PB88-127196] 10 p1276 N88-17637

AXAF
U X RAY ASTROPHYSICS FACILITY

AXES (COORDINATES)
U COORDINATES

AXES (REFERENCE LINES)
NT AXES OF ROTATION
NT EARTH AXIS

AXES OF ROTATION
NT EARTH AXIS
Resources, confusions and compatibility in dual axis tracking: Displays, controls and dynamics
[AD-A185871] 07 p0898 N88-15440
Data acquisition and analysis system for the Sandia 34-meter Vertical Axis Wind Turbine
[DE88-002417] 09 p1187 N88-17112
Study on a rotor speed control system for a horizontal axis windmill
[NAL-TR-931] 10 p1349 N88-18062

AXIAL COMPRESSION LOADS
Elastoplastic response of unidirectional graphite/aluminum under combined tension-compression cyclic loading
[CCMS-88-01] 11 p1451 N88-18647
Fracture criterion of reactor graphite under multiaxial stresses 13 p1746 N88-20442
Local delamination buckling in layered structures
18 p2480 N88-24711

AXIAL COMPRESSORS
U TURBOCOMPRESSORS

AXIAL FLOW
Experimental study of interacting vortex rings
03 p0318 N88-12007
Gas dynamic characteristics in past axial flow CO2 laser 03 p0327 N88-12067
Application of modified loss and deviation correlations to transonic axial compressors
[AGARD-R-745] 05 p0549 N88-13344
Highlights from a research program on a very highly loaded axial gas generator turbine
06 p0713 N88-14369
Computation of secondary flows in an axial multistage compressor 10 p1284 N88-17681
Boundary effects on the drag of a cylinder in axial motion at low Reynolds number 13 p1768 N88-20578
Supersonic axial-flow fan flutter
16 p2221 N88-23255
Hydrogen turbines for space power systems: A simplified axial flow gas turbine model 17 p2419 N88-24385
Solid rocket motor aft field joint flow field analysis
[NASA-CR-179288] 18 p2474 N88-24675
Experimental investigation of propfan aeroelastic response in off-axis flow with mistuning
[NASA-TM-101320] 22 p3089 N88-28344
Nonequilibrium flow of a radiating gas in a vertical channel with axial temperature variation
[DE88-702535] 23 p3212 N88-29120
Studies of unsteady axial-compressor functioning
24 p3380 N88-30129

AXIAL FLOW COMPRESSORS
U TURBOCOMPRESSORS

AXIAL FLOW PUMPS
NT TURBINE PUMPS
High Reynolds number pump facility for cavitation research
[AD-A189310] 13 p1765 N88-20558
Rotor self lubricating axial stop
[NASA-CASE-MFS-28273-1] 17 p2344 N88-23974

AXIAL FLOW TURBINES
Modal testing of a very flexible 110 m wind turbine structure
[DE88-003796] 10 p1351 N88-18072
Visualization of flows in turbomachinery
[AD-A189927] 15 p2063 N88-22299
Visualisation of the flow at the tip of a high speed axial flow turbine rotor
[AD-A189928] 15 p2063 N88-22300
Visualisation of the flow at the tip of a high speed axial flow turbine rotor: An assessment of flow visualisation techniques and the requirement of the experimental turbine
[AD-A189929] 15 p2063 N88-22301
Experimental vibration damping characteristics of the third-stage rotor of a three-stage transonic axial-flow compressor
[NASA-TM-100948] 18 p2466 N88-24642
Hydrogen turbines for space power systems: A simplified axial flow gas turbine model
[DE88-009585] 19 p2677 N88-25920

AXIAL LOADS
NT AXIAL COMPRESSION LOADS
The use of Hencky's equations for the estimation of multiaxial elastic-plastic notch stresses and strains
[FB-3/1986] 01 p0060 N88-10383
Stress-strain analysis and life predictions of a notched shaft under multiaxial loading
[FB-5/1986] 01 p0060 N88-10384
Application of fracture mechanics theory in the reliability analysis of structural ceramics in multiaxial loading
03 p0335 N88-12113
Analysis and testing of predamaged shell structures
04 p0428 N88-12653
Micromechanics of fatigue crack initiation under axial and torsional loadings 06 p0719 N88-14413
Residual stress effect on stability of axially loaded columns
[PB87-143889] 08 p0996 N88-16032
An experimental and numerical study of notch sensitivity of ARALL laminates
[CCMS-88-04] 11 p1450 N88-18644
Fracture criterion of reactor graphite under multiaxial stresses 13 p1746 N88-20442
Notch sensitivity of graphite materials for VHTR
13 p1747 N88-2044[illegible]
Cyclic uniaxial and biaxial hardening of type 304 stainless steel modeled by the viscoplasticity theory based on overstress 14 p1931 N88-21514
Damage models for delamination and transverse fracture
[AD-A189652] 15 p2029 N88-22086
Numerical and experimental research on propagation of elastic stress waves in conical shell under axial impulsive loading 15 p2053 N88-22238
JPRS report: Science and technology. USSR: Materials science
[JPRS-UMS-88-006] 16 p2179 N88-22988
Effect of uniaxial compression on physical and mechanical properties of ferroelectric ceramic material
16 p2180 N88-22993
Effects of axial load on elastomeric isolation bearings
[PB88-179015] 16 p2223 N88-23269
Integrated polysilicon tactile sensor
19 p2669 N88-25863
Forces and moments on a slender, cavitating body
[DE88-007208] 21 p2945 N88-27491
Stress relaxation of a titanium (Ti-6Al-4V) threaded joint
[DE88-010102] 21 p2961 N88-27590
Development of a biaxial test system for thin-walled metal tubes using tensile-compressive axial load and internal-external pressure
[DE88-011279] 21 p2962 N88-27592
An experimental and analytical evaluation of a biaxial test for determining shear properties of composite materials
[NASA-CR-182928] 21 p2962 N88-27593
An anisotropic continuum damage model for creep-dominated, multiaxial loading histories
21 p2964 N88-27608
Failure analysis of quasi-isotropic composite laminates with free edges under off-axis loading
22 p3049 N88-28092
Determination of multiaxial flow surfaces at elevated temperatures using the concept of dissipation potential
[ORNL/TM-10787] 24 p3383 N88-30149

AXIAL MODES
Generating soft X-ray spectra using the SPEED pentaxial diode
[DE87-013591] 01 p0098 N88-10647
Aerodynamic design and performance of a bent-axis geometry vehicle
[DE87-013728] 02 p0124 N88-10786

Permanent magnet excitation of axial flow synchronous machines with high rotation moment
[ETN-88-92385] 20 p2796 N88-26592

AXIAL STRAIN
On the relations between cyclic contraction ratio, flow stress, and deformation mechanisms in bainitic CrMoV steels
[VTT-36] 01 p0025 N88-10158
Fatigue oxidation interaction in low cycle fatigue
06 p0719 N88-14420
Effect of uniaxial stress on the Raman spectra of graphite fibers
[AD-A191730] 18 p2492 N88-24783
Uniaxial tensile strain measurement for ceramic testing at elevated temperature: Requirements, problems and solutions
[DE88-008090] 19 p2621 N88-25550

AXIAL STRESS
Ion-implantation-induced stress in glasses: Variation of damage mode efficiency with changes in glass structure
[DE87-013523] 01 p0028 N88-10175
Life prediction of steel cords
06 p0715 N88-14386
An investigation of the failure response of laminates under biaxial stress
[AD-A190039] 15 p2029 N88-22090
J-integral measurement using moire interferometry
[AD-A193751] 23 p3226 N88-29202

AXIOMS
Using design axioms and topology to model database semantics
[CWI-CS-R8711] 13 p1818 N88-20863
Algebra of Communicating Processes (ACP)tau: A universal axiom system for process specification
[CWI-CS-R8725] 13 p1819 N88-20869
A convergence theorem in process algebra
[CWI-CS-R8733] 13 p1827 N88-20920
Pairwise complete regularity as a seperation axiom
[REPT-87-57] 16 p2264 N88-23539
Fixpoint representations of characteristic sets of linear-time temporal formulas
[CWI-CS-R8754] 20 p2840 N88-26849

AXISYMMETRIC BODIES
Numerical study of supersonic flow around blunt bodies with extended needle nose 04 p0425 N88-12635
The drag of slender axisymmetric cones in rarefied hypersonic flow 05 p0531 N88-13229
Hypersonic static and dynamic stability of axisymmetric shapes: A comparison of prediction methods and experiment 05 p0534 N88-13246
The role of computation fluid dynamics in aeronautical engineering (4). The development and applications of implicit TVD finite volume code
05 p0536 N88-13259
Development of the computer program for turbulent boundary layers 05 p0536 N88-13264
Rarefied gas numerical wind tunnel. 2: Two-dimensional and axially symmetric bodies 05 p0538 N88-13273
Coupled FE and HIE method for exterior acoustics of axisymmetric shells --- finite element (FE) Helmholtz integral equation (HIE)
[ARE-TM(UHA)-87506] 09 p1243 N88-17448
A simplified streamline swallowing procedure for the windward meridian of axisymmetric blunt bodies
[AD-A188413] 12 p1626 N88-19732
Nonaxisymmetric body supersonic, aerodynamic prediction
[AD-A189338] 13 p1716 N88-20259
Static performance of an axisymmetric nozzle with post-exit vanes for multiaxis thrust vectoring
[NASA-TP-2800] 13 p1719 N88-20280
Active control of 2-D instability waves on an axisymmetric body
[AD-A191578] 19 p2663 N88-25835
Influence of rear body geometry on the velocity characteristics of the near wake
[ISL-R-113/87] 20 p2753 N88-26139

AXISYMMETRIC DEFORMATION
U AXIAL STRAIN

AXISYMMETRIC FLOW
NT ANNULAR FLOW
Effect of empennage arrangement on single-engine nozzle/afterbody static pressures at transonic speeds
[NASA-TP-2753] 02 p0122 N88-10771
Numerical analysis of axisymmetric flow with H2-O2 reactions 05 p0538 N88-13272
Method of calculations for flow of ideal gas through plane and axisymmetric nozzles with broken-line contour
06 p0771 N88-14737
New techniques in computational aerodynamics
[AD-A186719] 09 p1112 N88-16664
Numerical simulation of axisymmetric turbulent flow in combustors and diffusors
[NASA-CR-4115] 10 p1268 N88-17582
On the interaction of Tollmein-Schlichting waves in axisymmetric supersonic flows
[NASA-CR-181619] 10 p1331 N88-17955
Visualisation of the flow at the tip of a high speed axial flow turbine rotor
[AD-A189928] 15 p2063 N88-22500
An investigation of ducted propellers in axisymmetric shear flow 16 p2202 N88-23136
Initial condition effect on pressure waves in an axisymmetric jet
[NASA-TM-100915] 16 p2209 N88-23184
Saturation and the limit of jet mixing enhancement by single frequency plane wave excitation: Experiment and theory
[NASA-TM-100882] 17 p2295 N88-23732
Solid rocket motor aft field joint flow field analysis
[NASA-CR-179288] 18 p2474 N88-24675
Nonaxisymmetric viscous lower branch modes in axisymmetric supersonic flows
[NASA-CR-181687] 21 p2891 N88-27164
Velocity measurements and flow visualization in turbulent three-dimensional supersonic flows using oxygen flow tagging
[AD-A192551] 21 p2892 N88-27165
Coupled experimental and theoretical investigations of instability, chaos and turbulence in an axisymmetric jet flow
[AD-A192943] 21 p2942 N88-27476
Fellowships in hypersonic aerodynamics
[AD-A194265] 23 p3172 N88-28885

AXISYMMETRY
U SYMMETRY

AXLES
U SHAFTS (MACHINE ELEMENTS)

AZIDES (INORGANIC)
In-situ vibrational spectroscopy of specifically adsorbed azide on silver electrodes
[AD-A188511] 12 p1605 N88-19600

AZIDES (ORGANIC)
Polyazidoesters as energetic polymers and copolymer components with fluoro derivatives
[AD-A194236] 23 p3199 N88-29039

AZIMUTH
Optical alignment of Centaur's inertial guidance system
[NASA-TM-88844] 04 p0405 N88-12515
An optimal structure for a 34-meter millimeter-wave center-fed BWG antenna: The Cross-Box concept
11 p1472 N88-18778
The orientation of global satellite networks
11 p1506 N88-18996
Analysis of a range estimator which uses MLS angle measurements
[NASA-CR-182896] 16 p2160 N88-22884
Small scale mixing in the initial region of a jet
[AD-A193500] 23 p3192 N88-28994

AZO COMPOUNDS
NT HMX
NT RDX

AZOLES
NT CARBAZOLES
NT PYRROLES
Ordered polymers for space applications
[AD-A188460] 12 p1610 N88-19630

AZULENE
Energy transfer studies with lasers
[DE88-004864] 10 p1337 N88-17991
The effect of oriented defects on long-range ordering of hydrocarbon films: Azulene on Pt(111)
[AD-A196089] 24 p3344 N88-29904

AZUR SATELLITE
AZUR, the first German research satellite 625-A, 1964-1969 10 p1310 N88-17827

B

B STARS
A helium flare on the active G5 dwarf Kappa Ceti
04 p0519 N88-13189
Consistent spherical Nonlocal Thermal Equilibrium (NLTE) models for objects with B-star-like luminosities
[ETN-88-90601] 06 p0800 N88-14897
A spherical, non-LTE, blanketed model stellar atmosphere for Phi Cas (FOIa)
10 p1426 N88-18528
The effects of rotation on the winds from hot stars
11 p1569 N88-19393

B-1 AIRCRAFT
Surface disturbances produced by low-level, subsonic B-1 aircraft
[AD-A192257] 20 p2824 N88-26752

B-57 AIRCRAFT
Analyses and assessments of span wise gust gradient data from NASA B-57B aircraft
[NASA-CR-178268] 01 p0002 N88-10007

B-70 AIRCRAFT
An experimental investigation of dynamic ground effect
[NASA-CR-4105] 04 p0394 N88-12458

BAC AIRCRAFT
NT VC-10 AIRCRAFT

BACILLUS
Growth and differentiation of Bacillus subtilis under microgravity conditions 22 p3060 N88-28158

BACK INJURIES
Sitting posture of pilots in the Boelkow 105c helicopter
[IZF-1986-22] 09 p1202 N88-17202

BACKFIRE ANTENNAS
Improved backfire antenna using circular dipole
11 p1468 N88-18757

BACKGROUND NOISE
The assessment of the sound insulation requirements for a large broadcasting studio, using a scale model: Practical details
[BBC-RD-1987/21] 10 p1318 N88-17878
Determination of distributed resistance of base of bipolar transistors measuring noise spectral densities
[DE88-700197] 11 p1479 N88-18829
Stellar scintillometer atmospheric optical turbulence profiling experiment: A qualitative comparison of two identical instruments at AMOS (Air Force Maui Optical Station), 1985
[AD-A190589] 15 p2094 N88-22479
Sources and levels of background noise in the NASA Ames 40- by 80-foot wind tunnel
[NASA-TM-100077] 17 p2395 N88-24239
Effect of hypoxia on speech recognition in noise
[AD-A193943] 23 p3240 N88-29280

BACKGROUND RADIATION
Quantification of the background signal to solar neutrino detection from cosmogenic activation of the atmosphere
[DE87-013830] 01 p0119 N88-10762
Particle physics and cosmology
[DE87-005400] 03 p0387 N88-12432
Dipole component of relict radiation determined from Relikt experiment data 08 p1002 N88-16070
The origin of the diffuse X-ray background and the formation of galaxies and voids
10 p1428 N88-18527
A sky temperature survey at 19.2 GHz using a balloon borne Dicke radiometer for anisotropy tests of the cosmic microwave background 11 p1571 N88-19403
An attempt to measure the diffuse brightness of the sky at submillimeter wavelengths
12 p1710 N88-20233
Measurements of the cosmic background radiation
[NASA-CR-182637] 12 p1712 N88-20248
Observations of the large scale anisotropy in the cosmic background radiation at 3 mm
[INPE-4425-PRE/1229] 12 p1712 N88-20249
Specification for an infrared satellite surveillance system for the detection of aircraft
[AD-A189592] 13 p1797 N88-20746
A low-frequency measurement of the spectrum of the cosmic microwave background radiation
13 p1858 N88-21112
A map of the cosmic background radiaton at 3 millimeters
[INPE-4529-PRE/1279] 15 p2152 N88-22850
The two-dimensional one component plasma in a doubly periodic background: Exact results
[AD-A191260] 16 p2280 N88-23650
Sky radiance distributions for thermal imaging backgrounds
[AD-A191135] 17 p2373 N88-24115

BACKSCATTERING
Investigation of lidar backscatter including depolarization and higher scattering orders
[ETN-87-90431] 01 p0052 N88-10334
Airborne lidar studies of Arctic polar stratospheric clouds 01 p0069 N88-10443
Underwater acoustic backscatter from a model of arctic ice open leads and pressure ridges
[AD-A184693] 03 p0354 N88-12234
Measurement of cirrus cloud optical properties by high spectral resolution lidar 04 p0470 N88-12906
Large bandwidth ground scattering model --- radar scattering
[FOA-C-30458-3.2] 05 p0576 N88-13511
Electromagnetic wave probing of Earth's environment
[NASA-CR-182358] 06 p0690 N88-14232
The inverse back scattering problem for the Schroedinger equation in two space dimensions
[AD-A185603] 06 p0765 N88-14701
Research on acoustical scattering, diffraction catastrophes, optics of bubbles, photoacoustics, and acoustical phase conjugation
[AD-A185785] 06 p0776 N88-14761
Backscatter from a periodic rough surface at near grazing incidence
[NASA-CR-182397] 07 p0845 N88-15126

Electromagnetic fields backscattered from an s-shaped inlet cavity with an absorber coating on its inner walls
[NASA-CR-182401] 07 p0645 N88-15130

Design of the Backscatter Spectroscopy System for the Nova Laser Facility
[DE88-001880] 07 p0859 N88-15214

A backscatter lidar proposed for the second German Spacelab mission 08 p1018 N88-16173

Backscattering signal analysis concerning a three-dimensional object configuration on the basis of object motion
[ESA-TT-1044] 09 p1154 N88-16915

Focused ultrasonic backscatter technique for near-surface flaw detection in structural ceramics
[DE88-003112] 09 p1183 N88-17091

Acoustic backscattering from bottom sediment at normal incidence in the laboratory
[AD-A186905] 09 p1242 N88-17443

Composition and thickness of multilayer foils using MeV ion-beam techniques
[DE88-004360] 11 p1448 N88-18629

Backscatter from flaws in fiber-reinforced composites
11 p1450 N88-18639

Backscattering from three dimensional conducting bodies
[AD-A187570] 11 p1470 N88-18768

Depolarized infrared reflectance from dry and wetted surfaces
[AD-A188213] 11 p1492 N88-18903

Atmospheric backscatter at 10.6 microns; a compendium of measurements made outside the United Kingdom by the airborne LATAS coherent laser radar velocimeter
[RSRE-87002] 12 p1631 N88-19763

Observations of the upper ocean using a multi-beam Doppler sonar
[AD-A188896] 12 p1649 N88-19878

A polarimetric rain backscatter model developed for coherent polarization diversity radar applications
13 p1759 N88-20520

Radial track of moving objects determined by HF backscatter technique 14 p1901 N88-21354

Corrections for differential scattering by aerosols in the measurement of ozone by DIAL --- differential absorption lidar (DIAL)
[NPL-QU-78] 14 p1945 N88-21603

Space-time structure of ultrashort light pulses formed during stimulated backscattering of laser beam
14 p1972 N88-21767

Enhanced backscattering from rough surfaces
[AD-A190995] 16 p2190 N88-23063

Enhanced backscattering from rough surfaces
[AD-A191089] 16 p2274 N88-23610

The application of Rutherford backscattering for analyzing multilayered structure change induced by pulsed ion beam bombardment 16 p2278 N88-23638

Radar penetration in the Amazonian rain forest
17 p2358 N88-24044

Multiple scattering of waves in discrete random media
[AD-A191069] 18 p2499 N88-24823

Radio-wave scintillations and ionospheric irregularities at high latitudes
[AD-A192140] 18 p2501 N88-24837

Center for thin film studies
[AD-A191906] 19 p2732 N88-26226

Sources of scattering in vegetarian and other surfaces and objects
[NASA-CR-182975] 20 p2816 N88-26710

ZT imaging system for layered thin wall structures
[AD-A195468] 24 p3352 N88-29954

The effect of equatorial ionospheric irregularities on the performance of a south-looking OTH-B (Over-The-Horizon-Backscatter) radar
[AD-A195090] 24 p3362 N88-30016

Measurement and interpretation of North Atlantic Ocean marine radar sea scatter
[AD-A196239] 24 p3364 N88-30036

Spaceborne lidar: Development of a laboratory test system
[BF-R-66.090-1] 24 p3378 N88-30118

BACKWARD FACING STEPS

Numerical solution of turbulent flow past a backward facing step using a nonlinear K-epsilon model
[NASA-CR-178421] 07 p0854 N88-15189

Navier-Stokes solutions for laminar incompressible flow over a NACA 0012 airfoil and a backward facing step
[FFA-TN-1987-50] 09 p1162 N88-16966

Modeling the stability of a turbulent premixed flame, downstream from a step by a Lagrangian method
24 p3350 N88-29943

BACKWARD WAVES

JPRS report: Science and technology. China
[JPRS-CST-87-034] 03 p0301 N88-11897

New physical explanation of phase-conjugate waves produced in backward stimulated scattering
03 p0302 N88-11900

BACTERIA

NT BACILLUS
NT ESCHERICHIA
NT PSEUDOMONAS
NT STAPHYLOCOCCUS

Application of photosynthetic N(2)-fixing cyanobacteria to the CELSS program 03 p0358 N88-12257

Study of certain biological characteristics of bacteria during the French-Soviet CYTOS-2 space experiment
04 p0473 N88-12917

Investigation of effect of silver compounds on microflora in water reclaimed from atmospheric moisture condensate in a closed environment 07 p0892 N88-15407

Possible use of plasmids for study of effect of space flight factors on biological objects
08 p1046 N88-16319

Analysis of gases in the earth's crust
[PB88-141619] 10 p1354 N88-18093

Antibiotic activity in space, results and hypothesis
12 p1660 N88-19952

Production and turnover of suspended organic detritus in the coastal water of the southeastern continental shelf
[DE88-005118] 14 p1951 N88-21631

Saccharification of cellulose by combined fungal and bacterial preparations 17 p2316 N88-23833

The synthesis of polyphenylene from a CIS-dihydrocatechol biologically produced monomer
18 p2478 N88-24699

Biodegradation of JP-5 aviation fuel by subsurface microbial communities
[AD-A192743] 20 p2781 N88-26493

Genetic effects of low level microwave radiation
[AD-A192687] 21 p2984 N88-27722

BACTERIAL DISEASES

A solid phase enzyme-linked immunosorbent assay for the antigenic detection of Legionella pneumophila (serogroup 1): A compliment for the space station diagnostic capability 06 p0795 N88-14868

Use of bifidumbacterin for correction of intestinal dysbacteriosis 07 p0895 N88-15427

BACTERIOLOGY

Study of certain biological characteristics of bacteria during the French-Soviet CYTOS-2 space experiment
04 p0473 N88-12917

BAFFLES

Computational studies of wave-shaping in a blast simulator by perforated plates in the driver
[AD-A188200] 11 p1483 N88-18850

BAGS

NT GAS BAGS

BAINITIC STEEL

On the relations between cyclic contraction ratio, flow stress, and deformation mechanisms in bainitic CrMoV steels
[VTT-36] 01 p0025 N88-10158

Activities report in metal manufacturing
[ISSN-0524-7705] 07 p0839 N88-15086

On the relations between cyclic contraction ratio flowstress and deformation mechanisms in bainitic CrMoV steels
[DE87-753043] 08 p0968 N88-15856

BALANCE

Energy balance in laser-irradiated vaporizing droplets
[DE88-000525] 04 p0449 N88-12782

A GaAs MESFET balanced mixer with very low intermodulation
[AD-A184848] 05 p0655 N88-14015

An empirical investigation of load indices for load balancing applications
[AD-A185763] 06 p0724 N88-14451

Functional development of gravity receptors in insects and amphibians 07 p0886 N88-15376

An analysis of DREO's (Defence Research Establishment Ottawa) analog rebalance loops for the CSG-2 (Canadian Strapdown Gyroscope) tuned-rotor gyroscope
[AD-A188577] 12 p1629 N88-19749

The effect of sting interference at low speeds on the drag coefficient of an ellipsoidal body using a magnetic suspension and balance system
[NASA-CR-181611] 13 p1718 N88-20274

Development of a torsion balance for adhesion measurements
[NASA-TM-100799] 13 p1748 N88-20454

Stability of uncapsulated weight cells with thin film elongation measurement bands under influence of humidity, temperature and operation voltage
[ETN-88-92383] 21 p2951 N88-27531

BALANCE EQUATIONS

U EQUATIONS

BALANCING

Balancing strain gauge bridges
[GB-PATENT-2-129-587-A] 01 p0048 N88-10307

Model adaptation and imbalance compensation in rotors with active magnetic bearings
[ETN-87-90440] 01 p0056 N88-10361

Botany Facility: Considerations and analyses of the balancing system: philosophy proposed for the BF centrifuge
[SIRA-A/7373/WP110/PWF001]
17 p2378 N88-24139

Spray automated balancing of rotors: Methods and materials
[NASA-CR-182151] 24 p3330 N88-29825

BALL BEARINGS

Investigation of instability, dynamic forces, and effect of dynamic loading on strength of cages for the bearings in the high pressure oxygen turbopumps for the space shuttle main engine
[NASA-CR-176[illegible]70] 06 p0714 N88-14378

Mechanisms of rolling contact spalling
[NASA-CR-178243] 06 p0714 N88-14380

Models for steady and nonsteady Coulomb torque in ball bearings 14 p1876 N88-21208

Ball bearings with chemical vapor deposition (CVD)-TiC coated components 14 p1876 N88-21210

Experience with duplex bearings in narrow angle oscillating applications 14 p1926 N88-21484

On the torque and wear behavior of selected thin film MOS2 lubricated gimbal bearings
14 p1926 N88-21485

Titanium carbide coatings for aerospace ball bearings
14 p1927 N88-21486

Two gimbal bearing case studies: Some lessons learned 14 p1927 N88-21487

Investigation of rolling contact fatigue of ball bearings
[NASA-TT-20196] 19 p2678 N88-25922

Evaluation of transfer films of Salox M on 440C for HPOTP bearing cage applications, task 119
[NASA-CR-179020] 23 p3223 N88-29184

BALLISTIC MISSILES

Rocket and airjet propulsion for ballistic and aerodynamic space probes
[REPT-TR-527] 10 p1310 N88-17826

Where directed energy stands in strategic defense
[DE88-005092] 10 p1403 N88-18365

BALLISTIC RANGES

Design and implementation of the ESL compact range underhung bridge crane
[NASA-CR-182396] 07 p0862 N88-15231

BALLISTIC TRAJECTORIES

Ballistic Single Stage Carrier Vehicle (BETA): A single stage reusable ballistic space shuttle concept
[MBB-UR-949/70] 10 p1310 N88-17828

Trajectory characteristics and heating of hypervelocity projectiles having large ballistic coefficients
[NASA-TP-2814] 12 p1574 N88-19412

Motion in a random gyrotropic environment in D dimensions
[PB87-170650] 12 p1585 N88-20079

Aerodynamic possibilities for the realization of trajectory corrections
[ISL-CO-251/86] 14 p1862 N88-21120

Distribution of neutral gas molecules at large distances from Halley's comet 14 p1999 N88-21914

BALLISTICS

NT HYDROBALLISTICS
NT INTERIOR BALLISTICS
NT TERMINAL BALLISTICS

High pressure strand burn rate tests of polyvinylnitrate/nitramine propellants
[AD-A184178] 04 p0422 N88-12615

Composite materials applications program at the US Army Ballistic Research Laboratory: Work in progress
04 p0428 N88-12651

An ultra-high-speed cinematographic method for the study of wakes in hypersonic ballistic ranges
05 p0531 N88-13228

Production of flows for aeroballistic investigation in the shock tubes of the Franco-German Research Institute (ISL), Saint-Louis (France)
[ISL-R-113/86] 05 p0541 N88-13295

Optoelectronic measurement methods for ballistic experiments
[PB87-110706] 05 p0583 N88-13554

Computer simulations of ballistic experiments
[DE87-005835] 07 p0862 N88-15226

Critical analysis of the dynamic behavior laws for metallic materials --- ballistics
[ISL-NB-401/86] 08 p0969 N88-15862

A continuous oxidizer regression model for the combustion of composite solid propellants
[AD-A186742] 08 p0974 N88-15894

Study on cineradiography
[ISL-R-120/86] 08 p0990 N88-15994

Ballistic deficits in pulse shaping amplifiers
[DE88-003908] 11 p1481 N88-18840

A simplified computer code for reduction to burning rates of closed bomb pressure-time data (MINICB)
[AD-A189112] 13 p1736 N88-20380
Experimental investigation of hypersonic aerodynamics
[NASA-CR-182973] 18 p2458 N88-24591
Ballistic transport and hot electron spectroscopy in Tunneling Hot Electron Transfer Amplifier (THETA)
19 p2659 N88-25808
Contact force history and dynamic response due to the impact of a soft projectile
[NASA-TM-100961] 20 p2811 N88-26679
Proof-of-principle high speed electronic imaging system, phase 2
[AD-A193798] 23 p3181 N88-28937
Combustion diagnostics of propellant with new grain geometries
[AD-A194944] 24 p3342 N88-29895

BALLISTOCARDIOGRAPHY
Cardiac contractility in weightlessness according to spatial ballistocardiography 07 p0890 N88-15393
Ballistocardiography in weightlessness research
11 p1521 N88-19080

BALLOON FLIGHT
Large balloon development and trans-Mediterranean flights 08 p1030 N88-16239
Instrumentation utilisation for risk control in safety operations --- balloons and rockets
08 p1030 N88-16240
Contribution of stratospheric balloon flights in space biology 08 p1033 N88-16266
Future plans for the NASA suborbital program
08 p1034 N88-16267
Results of the 1987 NASA/JPL balloon flight solar cell calibration program
[NASA-CR-182617] 12 p1574 N88-19413
On the dynamic behavior of balloon during its launch; application of panel method and extension to unsteady problem
[ISAS-RN-622] 20 p2751 N88-26330
Development of an adjustable buoyancy balloon tracer of atmospheric motion. Phase 3: Refinement of the operational prototype system
[PB88-190764] 23 p3231 N88-29230

BALLOON SOUNDING
Balloon-based infrared solar occultation measurements of stratospheric O3, H2O, HNO3 and CFC-12
[NOAA-TR-NESDIS-34] 01 p0068 N88-10438
Spectroscopic and retrieval studies in support of SCRIBE (Stratospheric Cryogenic Interferometer Balloon Experiment)
[AD-A184037] 03 p0351 N88-12216
The German scientific balloon and sounding rocket program 08 p1024 N88-16202
The French balloon and sounding rocket space program 08 p1025 N88-16203
The Norwegian scientific balloon and sounding rocket program 1987-1990 08 p1025 N88-16204
The Swedish sounding rocket and balloon program
08 p1025 N88-16205
Swiss scientific balloon and sounding rocket experiments 1985-1987 08 p1025 N88-16206
Balloon measurement of magnetic field during substorms in auroral zone 08 p1026 N88-16213
First results of balloon-borne X-ray and electric field observations near the footprint of the Viking satellite
08 p1026 N88-16215
How ground-based observations contribute to rocket, balloon and space shuttle experiments: Experience from the past and outlook for the future
08 p1026 N88-16216
New techniques for rocket and balloon-borne instrumentation for investigations of the structure, dynamics and electrodynamics of the middle atmosphere 08 p1027 N88-16220
In-situ stratospheric water vapor measurements on board long duration balloons 08 p1029 N88-16232
Aerosols in Martian Atmosphere and Natural Dust Observation (AMANDO). Proposal for the Mars orbiter balloon and rover to study the Martian atmosphere, its thermal content, and its interaction with the soil
[IFSI-87-9] 08 p1100 N88-16619
Stratospheric positive ion composition measurements and acetonitrile detection: A consistent picture
[AERONOMICA-ACTA-A-326-1987]
18 p2542 N88-25084

BALLOON-BORNE INSTRUMENTS
Balloon-based infrared solar occultation measurements of stratospheric O3, H2O, HNO3 and CFC-12
[NOAA-TR-NESDIS-34] 01 p0068 N88-10438
Forecasting and nowcasting cumulus convection with soundings released from a storm-intercept vehicle
02 p0202 N88-11262
Max '91: Flare research at the next solar maximum
[NASA-TM-89700] 06 p0806 N88-14919
A new liquid helium-cooled Fabry-Perot spectrometer used in a far infrared astronomical balloon experiment
08 p1028 N88-16224
An advanced visible-UV spectrometer for atmospheric composition measurements 08 p1029 N88-16231
Justification and prospects of observations of interstellar, far-infrared emission lines, using a small-sized balloon-borne telescope 08 p1032 N88-16254
PRONAOS: A submillimeter facility --- astronomical balloon 08 p1032 N88-16255
Solar ultraviolet spectrum obtained from a balloon gondola 08 p1032 N88-16258
Contribution of stratospheric balloon flights in space biology 08 p1033 N88-16266
Balloon-borne three-meter telescope for far-infrared and submillimeter astronomy
[NASA-CR-182310] 09 p1262 N88-17565
Mars Lander/Rover vehicle development: An advanced space design project for USRA and NASA/OAST
[NASA-CR-182571] 12 p1709 N88-20227
Further development of a stellar camera following the rotation-modulation-collimator principle for balloon-borne observations in the X-ray range
[ETN-88-91496] 14 p1913 N88-21428
Far-infrared (120-300 micron) observations of the Carina Nebula 14 p1993 N88-21876
Balloon-borne three-meter telescope for far-infrared and submillimeter astronomy
[NASA-CR-182924] 17 p2449 N88-24550
Utilization of the IR telescope gimbaling system as a stabilized pointing platform for balloon payloads. Volume 1: Technical results
[NASA-CR-179339] 18 p2522 N88-24962
Estimation of balloon position from wind data
[DE88-008968] 19 p2597 N88-25434
Modeling, designing and simulating a pointing control system for balloon-borne solar experiments
[NASA-TM-100337] 22 p3082 N88-28300

BALLOONING MODES
Limit of possible operation of crescent and bean shaped Tokamaks
[IPPJ-837] 02 p0242 N88-11532
Ballooning modes or Fourier modes in a toroidal plasma?
[AD-A184299] 04 p0491 N88-13022

BALLOONS
NT HIGH ALTITUDE BALLOONS
NT JIMSPHERE BALLOONS
Proceedings of the 8th ESA Symposium on European Rocket and Balloon Programs and Related Research
[ESA-SP-270] 08 p1024 N88-16201
Operational activity and improvements in the services and facilities of the balloon launch centers in France
08 p1030 N88-16238
Large balloon development and trans-Mediterranean flights 08 p1030 N88-16239
Balloon-borne three-meter telescope for far-infrared and submillimeter astronomy
[NASA-CR-182310] 09 p1262 N88-17565
Adaptive control of scientific balloon-borne gondola attitude 13 p1755 N88-20497
Utilization of the IR telescope gimbaling system as a stabilized pointing platform for balloon payloads. Volume 1: Technical results
[NASA-CR-179339] 18 p2522 N88-24962

BALLS
Film thicknesses in circular elastohydrodynamic contacts
[PB87-123725] 06 p0710 N88-14354

BALMER SERIES
Excess emission in the wings of the Hydrogen Balmer lines during a flare on the late-type dMe star YZ CMi
04 p0511 N88-13146

BANACH SPACE
NT HILBERT SPACE
Spectral and structural properties of nonnegative reducible operators in Banach relations
[ETN-87-90402] 01 p0089 N88-10581
Spectral dilation of L(B,H)-valued measures and its application to stationary dilation for Banach space valued processes
[NASA-CR-182388] 07 p0913 N88-15536
Series representations of infinitely divisible random vectors and a generalized shot noise in Banach spaces
[AD-A186429] 07 p0918 N88-15574
Series representations of infinitely divisible random vectors and a generalized shot noise in banach spaces
[AD-A186502] 08 p1073 N88-16474
Some aspects of control for semilinear distributed parameter systems
[INPE-4147-PRE/1054] 08 p1075 N88-16484
Feedback stabilization of distributed systems
[AD-A187111] 09 p1222 N88-17328
Perturbation theory for dual semigroups. 2. Time-dependent perturbations in the sun-reflexive case
[PB88-113097] 09 p1230 N88-17369
Critical values of functionals on Banach surfaces
[DE88-702735] 23 p3272 N88-29472

BAND STRUCTURE OF SOLIDS
Electronic band structure and photoemission: A review and projection
[DE88-002236] 06 p0787 N88-14829
The band systems of alkali vapors
[NASA-TT-20206] 10 p1417 N88-18462
Electronic structure of matter at high compression: Isostructural transitions and approach of the Fermi-gas limit
[MPQ-124] 16 p2266 N88-23551
Non-effective-mass matching in superlattices
20 p2872 N88-27049
Self energy corrections to the ab initio band structures: Chromium
[DE88-701825] 21 p3020 N88-27927
Study of superconducting properties in some many valley semiconductors
[DE88-702325] 23 p3291 N88-29593

BANDGAP
U ENERGY GAPS (SOLID STATE)

BANDPASS FILTERS
NT TRACKING FILTERS
Implementation of an FIR band pass filter using a bit-slice processor
[AD-A184895] 05 p0634 N88-13875
Computer aided filter design
[AD-A193959] 23 p3208 N88-29093
Band pass with cavity resonators by use of three oscillation types
[ETN-88-92984] 23 p3209 N88-29096

BANDSTOP FILTERS
A notch filter instrument for measuring ELF (Extremely Low Frequency) MSK (Minimum Shift Keying) signals
[AD-A193324] 21 p2933 N88-27414
Confirmation of slow-waves in a crosstie overlay coplanar waveguide and its application to band-reject gratings and reflectors
[AD-A194981] 24 p3361 N88-30011

BANDWIDTH
NT BROADBAND
NT NARROWBAND
NT SPECTRAL LINE WIDTH
Bandwidth efficient block codes for M-ary PSK modulation
[NASA-CR-181543] 04 p0437 N88-12712
Performance optimization of electronic networks in the frequency domain
[PB87-123873] 04 p0438 N88-12720
Feasibility studies of optical processing of image bandwidth compression schemes
[AD-A186073] 07 p0932 N88-15660
Considerations concerning the basic bandwidth reduction of high definition television systems (HDTV) component signals, based on psychophysiological properties of the eye
[IRT-B-83/87] 09 p1153 N88-16909
Large-aperture sparse array antenna systems of moderate bandwidth for multiple emitter location
[AD-A188409] 12 p1619 N88-19683
High speed, bandpass sampling of digital communications waveforms
[AD-A189842] 15 p2056 N88-22254
Monolithic phase shifter study
[AD-A190213] 15 p2059 N88-22278
A fiber optic beamforming processor for wideband direction finding
[AD-A194862] 24 p3428 N88-30404
Ultra-wideband direction finding using a fiber optic beamforming processor
[AD-A194861] 24 p3430 N88-30413

BANG-BANG CONTROL
U OFF-ON CONTROL

BARANY CHAIR
Gastric emptying assessment by echography after a stress (rotating chair) 12 p1661 N88-19955

BARCHANS
U DUNES

BARDEEN APPROXIMATION
U BARRIER LAYERS
U ELECTRICAL PROPERTIES
U SURFACE PROPERTIES

BARIUM
Magnetic anomalies in the rare earth oxide superconductors GdBa2Cu3O(7-x) and YbBa2Cu3O(7-x)
[AD-A190713] 15 p2144 N88-22793
Synthesis and characterization of high-T(sub c) screen-printed Y-Ba-Cu-O films on alumina
[NASA-TM-100860] 15 p2146 N88-22805
High temperature superconductivity
[AD-A190259] 16 p2281 N88-23655
Effects of 67.5 MeV electron irradiation on Y-Ba-Cu-O and Gd-Ba-Cu-O high-temperature superconductors
[AD-A191271] 16 p2283 N88-23669

Radial velocities monitoring of a sample of barium and S stars using CORAVEL: Towards an evolutionary link between barium and S stars?
[SER-C-PREPUBL-FASC-19] 18 p2593 N88-25410
Electron irradiation effects in YBa2Cu3O7-Delta single crystals
[DE88-010050] 20 p2878 N88-27085
Generation of Adlam-Allen waves by plasma release experiments in the solar wind
[PB88-106000] 20 p2886 N88-27140

BARIUM COMPOUNDS
NT BARIUM OXIDES
NT BARIUM TITANATES
DTA/DSC studies of phase equilibria in binary mixtures of barium carbonate with alkali carbonates
[DE87-001195] 02 p0194 N88-11213
Resistivity of EuBa2(Cu/sub 1-y/Zn/sub y/)3O/sub x/ as a ffunction of temperature, magnetic field, pressure and Zn concentration
[DE87-014740] 04 p0499 N88-13069
Effect of a weak magnetic field on high temperature superconductivity in Y-Ba-Cu-O ceramics
[DE88-702192] 19 p2733 N88-26235
All-electron local density theory of electronic structure and superconductivity in YBa2Cu3O7 and YBa2Cu3O6
[DE88-009944] 19 p2735 N88-26246
Anharmonic model for high-Tc superconductors
[DE88-702196] 21 p3020 N88-27924
Superconducting properties of LaBa2Cu3O(sub x) and YBa2Cu3O(sub y)
[DE88-012038] 21 p3024 N88-27952
Magnetic phase transitions in 90-K superconductors Ho1Ba2Cu3O(7-delta) and Gd1Ba2Cu3O(7-delta) observed by ZF-muon(+)SR
[DE88-752611] 23 p3290 N88-29588

BARIUM ION CLOUDS
Deployable booms and antennas on AMPTE-IRM
14 p1874 N88-21196

BARIUM OXIDES
High temperature stability of superconducting YBa2Cu3O subx as characterized by X-ray diffraction
[DE88-001856] 06 p0787 N88-14824
Atomic-level studies of superconducting YBa2Cu3O sub 7-x
[DE88-002522] 06 p0788 N88-14831
Low field characterization of YBa2Cu3O sub 7-delta single crystals
[DE88-002895] 07 p0938 N88-15700
Fabrication of YBa2Cu3O7 superconducting ceramics
[DE88-003012] 07 p0938 N88-15701
Magnetic investigations of superconductive, polycrystalline (RE)1Ba2Cu3O(7-x) compounds (RE = Y, Gd, Ho, Dy)
[DE88-002537] 08 p1090 N88-16558
Soft X-ray absorption and emission spectra and the electronic structure of the Ba2YCu3O/sub 7-x/ superconductor
[DE88-002609] 08 p1090 N88-16559
High temperature superconductivity research at Argonne National Laboratory
[DE88-003055] 09 p1258 N88-17541
The structure and properties of twin boundaries in superconducting YBa2Cu3O7
[DE88-003864] 10 p1418 N88-18468
Improved magnetization for YBa2Cu3O/sub 7-delta annealed in oxygen above 1000 C
[DE88-003934] 10 p1418 N88-18469
Freestanding films of YBa2Cu3O/sub 6.9/
[DE88-003905] 10 p1419 N88-18471
Grain boundaries, planar defects and superconducting properties of YBa2Cu3O7
[DE88-003477] 10 p1419 N88-18475
Superconductivity and phase stability in the heavy rare earth quaternary compounds RBa2Cu3O7 (R = Ho, Er, Tm, Yb, Lu)
[DE88-003478] 10 p1419 N88-18476
Superconducting properties and structural characterization of high T/sub c/ oxides
[DE88-003479] 10 p1420 N88-18477
Penetration depth measurements of YBa2Cu3O/sub 7-delta/ at 4 MHz
[DE88-003493] 10 p1420 N88-18478
The electronic structure of YBa2Cu3O/sub 7-delta/ above and below T/sub c/
[DE88-003495] 10 p1420 N88-18479
Simulation and processing of high resolution images of defects and interfaces in superconducting YBa2Cu3O7
[DE88-003856] 10 p1420 N88-18480
High-resolution X-ray microstructural study of single crystals of YBa2Cu3O/sub 7-y/
[DE88-004858] 10 p1421 N88-18484
Atom probe microanalysis of superconducting YBa2Cu3O(sub 7-x)
[DE88-003203] 11 p1557 N88-19322
Processing relationships in YBa2Cu3O(7-x) superconductors
[DE88-005137] 11 p1559 N88-19330
Mass transport and chemical demixing of Y-Ba-Cu-O compounds during sintering in temperature gradients
[DE88-004887] 12 p1696 N88-20151
Properties of superconductors with strong electron-phonon interaction 14 p1974 N88-21779
Ordered structures in YBa2Cu3O/sub 7-y/, La2Cu3O/sub 7-y/, La/sub 2-x/Sr/sub x/CuO/sub 4-par. delta/ and related perovskites
[DE88-006461] 14 p1987 N88-21851
Melt processing ceramic YBa2Cu3O(sub 6.9)
[DE88-007039] 15 p2047 N88-22199
Superconductivity and the tailoring of lattice parameters of the compound YBa2Cu3O(sub x)
[DE88-005904] 15 p2140 N88-22769
High temperature superconductors in the La(sub 1+x)Ba(sub 2-x)Cu O(sub y system
[DE88-006367] 15 p2145 N88-22802
Material degradation in a barium hydroxide latent heat storage pilot unit
[DFVLR-FB-87-49] 16 p2175 N88-22961
A sup 57 Fe Mossbauer study of the superconductor YBa sub 2 (Fe sub x Cu sub 1-x) sub 3 O sub y
[DE88-701543] 16 p2282 N88-23661
Vacancy ordering in the basal plane of YBa2Cu3O(sub)z
[DE88-004572] 18 p2583 N88-25348
Mass spectrometric high temperature measurements of the barium oxide-zirconium dioxide system and the determination of thermodynamic data for barium zirconate. Clarification of the counter-stopping capacity of coated particles for solid fission products by zirconium dioxide addition
[NASA-TT-20187] 19 p2611 N88-25496
Effects of grain boundary composition on properties of YBa2Cu3O/sub 7-x/
[DE88-007679] 20 p2875 N88-27064
The superconducting transition in oxygen deficient YBa2Cu3O(sub 7-Delta)
[DE88-009957] 20 p2877 N88-27079
Anisotropic characteristic lengths in single crystal YBa2Cu3O(sub 7-Delta)
[DE88-009959] 20 p2877 N88-27080
Anisotropy of the lower critical field in YBa2Cu3O(sub 7-Delta)
[DE88-009971] 20 p2877 N88-27081
Preparation of high-T(sub)c Y1Ba2CuGO(sub 7-Delta) superconducting thin films by MBE (Molecular-Beam-Epitaxy) techniques
[DE88-009999] 20 p2877 N88-27082
Oxygen vacancy ordering and superconductivity in YBa2Cu3O(sub 7-x)
[DE88-010005] 20 p2877 N88-27083
Pure metallic bridge and point-contact tunneling into single- and polycrystal YBa2Cu3O(sub 7-y)
[DE88-010030] 20 p2878 N88-27084
Phase transformations and thermodynamic behavior of the YBa2Cu3O(sub)x system via EMF measurements
[DE88-010054] 20 p2878 N88-27086
Ceramic processing of high-T(sub)c superconductors
[DE88-010090] 20 p2878 N88-27087
Compilation of NRL publications on high temperature superconductivity
[AD-A189137] 21 p3019 N88-27921
Thermodynamics of oxygen-vacancy ordering in YBa2Cu3O(sub z)
[DE88-009816] 21 p3022 N88-27940
Preparation and characterization of isotopic oxygen-enriched yttrium barium copper oxide
[DE88-010939] 22 p3154 N88-28766
High Tc superconducting HoBa2Cu(sub 1-x)Fe(sub x)3O(sub 7-y)
[DE88-006909] 22 p3155 N88-28768
Superconducting properties of oxygen deficient YBa2Cu3O(sub 7-delta)
[DE88-009969] 22 p3155 N88-28774
Effect of neutron irradiation on critical magnetization current in single crystal YBa2Cu3O(sub 7-delta)
[DE88-009970] 22 p3156 N88-28775
Effects of metal substitutions (Fe and Ga) in YBa2Cu3O7 on its superconducting properties and microstructures
[DE88-007393] 23 p3287 N88-29572
Possible mechanism for high-temperature superconductivity in the BaSr-La(Y)-CuO systems
[DE88-702060] 23 p3288 N88-29576
Preparation of superconducting YBa2Cu3O(sub 7-x) films by magnetron sputtering
[DE88-009977] 23 p3289 N88-29583

BARIUM TITANATES
Determination of the origin of self-pumped phase conjugation in barium titanate
[AD-A184607] 03 p0377 N88-12372
Manufacturing of a barium titanate with high dielectric coefficient by decomposition of precipitates of double oxalates
[ISAL-IDI1-88-02] 21 p2911 N88-27278

BAROCLINIC INSTABILITY
Numerical model of Rayleigh instability and spin-off eddies on fronts 13 p1788 N88-20696

BAROCLINIC WAVES
A baroclinic wavy basic state model: Description and preliminary experiments
[KNMI-WR-87-1] 01 p0068 N88-10436
Application of satellite data in observational and theoretical studies of the evolving structure of baroclinic waves
[NASA-CR-179277] 10 p1354 N88-18091
Westward moving atmospheric wave disturbances over the African tropics: Dynamic and energetic aspects
[MITT-57] 20 p2827 N88-26774
Rossby waves in mid-latitude oceans
24 p3405 N88-30273

BAROCLINITY
A study of finite differgnce and finite element vertical discretization schemes for baroclinic prediction equations
[AD-A186617] 08 p1040 N88-16291
North Pacific Ocean. Subtropical front north of Hawaii, R/V Thomas G. Thompson: 7 January - 10 February 1974. CTD data report
[AD-A186565] 08 p1044 N88-16310
North Pacific Ocean. Subarctic front central Pacific, R/V Thomas G. Thompson: 8 September - 9 October 1975. CTD data report
[AD-A186567] 08 p1044 N88-16312
North Pacific Ocean. Northwest Pacific Transition Zone, R/V Thomas G. Thompson: 19 March - 1 May 1971. STD data report
[AD-A186568] 08 p1044 N88-16313
North Pacific Ocean. Gulf of Alaska, R/V Thomas G. Thompson: 1 February - 8 March 1967. STD data report
[AD-A186569] 08 p1045 N88-16314
North Pacific Ocean. Central Pacific Transition Zone, R/V Thomas G. Thompson: 25 March - 3 May 1968. STD data report
[AD-A186570] 09 p1195 N88-17160
Sampling strategies for Monte-Carlo forecasting methods 22 p3126 N88-28583

BAROMETERS
The evaluation of automatic barometers, illustrated by the Nakaasa barometer
[KNMI-TR-95] 13 p1774 N88-20610

BAROMETRIC PRESSURE
U ATMOSPHERIC PRESSURE

BAROTROPIC FLOW
Properties of the atmospheric boundary layer above a subtropical oceanic front
[AD-A184006] 03 p0351 N88-12215
Mesoscale eddy dynamics by the method of point vortices 04 p0463 N88-12863
The role of vortex structure in tropical cyclone motion
[AD-A190961] 16 p2235 N88-23351
Analysis of a six-component barotropic spectral model: Chaotic motion, predictability and vacillation --- atmospheric circulation
[CWI-AM-R8710] 18 p2542 N88-25090
Cluster analysis of multiple planetary flow regimes
[NASA-CR-182931] 18 p2594 N88-25418

BAROTROPISM
NT PLANETARY WAVES
On the barotropic model of the ocean circulation
[AD-A188148] 10 p1358 N88-18118
The use of a barotropic finite element model for the study of circulation on the continental shelf of the southeast coast of Brazil
[INPE-4401-PRE/1218] 13 p1802 N88-20774

BARRED GALAXIES
Kinematics and dynamics of barred spiral galaxies
03 p0388 N88-12440

BARRELS (CONTAINERS)
Numerical computations of natural convection heat transfer in irregular geometries
[DE88-002358] 07 p0852 N88-15178

BARRICADES
U BARRIERS

BARRIER LAYERS
Ytterbium monolayer diffusion barriers at Hg(1-x)Cd(x)Te/Al junctions
[AD-A188013] 10 p1299 N88-17768
Calculating depletion region carrier concentrations with capacitance-voltage measurements and etching
[AD-A189630] 15 p2141 N88-22777
A review of diffusion barrier technology for application in SP-100 fuel pins 17 p2410 N88-24328
Fabrication of SP-100 fuel barrier structures by chemical vapor deposition 17 p2416 N88-24371

A 10 microns photoexcited avalanche gain due to electron impact ionization from GaAs quantum well superlattices 20 p2867 N88-27026

Resonant tunneling in InGaAs-InP double-barrier structures and superlattices 20 p2871 N88-27047

Containment of a silicone fluid free surface in reduced gravity using barrier coatings
[NASA-TM-101314] 24 p3371 N88-30072

BARRIERS

Flammability test on aircraft seats equipped with fire barrier fabrics for the Porcher company
[CEAT-M5-525200] 06 p0666 N88-14084

Macroscopic quantum effects in a Josephson tunnel junction
[DE88-002239] 06 p0787 N88-14830

Verification of obstacle accountability areas using a simple mathematical model. Part 1: Description of general model and application for a specific case --- engine failure at takeoff
[NLR-TR-85069-U] 09 p1115 N88-16683

A program for the calculation of radio-wave transmission loss over the spherical earth and over obstacles
12 p1616 N88-19662

BARS

NT ELASTIC BARS

Exact finite element method analysis of viscoelastic tapered structures to transient loads
05 p0595 N88-13632

Bar code document accountability system performance update
[DE88-002256] 06 p0791 N88-14849

On the dissipative response due to discontinuous strains in bars of unstable elastic material
[AD-A188114] 11 p1498 N88-18947

Delamination stresses in semicircular laminated composite bars
[NASA-TM-4026] 13 p1735 N88-20375

Vibration frequencies of tapered bars with nonclassical boundary conditions
[NASA-CR-183059] 20 p2813 N88-26686

Wide range stress intensity factor expression for an edge-cracked round bar bend specimen
[AD-A196285] 24 p3382 N88-30147

BARYCENTER

U CENTER OF GRAVITY

BARYONS

Scalar densities and baryon mass differences in lattice QCD with Wilson fermions
[PREPRINT-544] 06 p0778 N88-14773

BRYNTRN: A baryon transport computer code, computation procedures and data base
[NASA-TM-4037] 16 p2290 N88-23714

BASALT

Petrogenesis of basalts from the Archean Matachewan Dike Swarm Superior Province of Canada
06 p0796 N88-14878

BASE FLOW

Influence of base modifications on in-flight base drag in the presence of jet exhaust for Mach numbers from 0.7 to 1.5
[NASA-TP-2802] 11 p1488 N88-18881

Efficient, high resolution computations of projectile and missile flow fields
[AD-A191086] 16 p2158 N88-22873

Study of a system for reducing base drag by controling vortices
[REPT-87/43] 17 p2295 N88-23730

BASE PRESSURE

Empirical formulas for the base pressure of missile bodies with a central propulsive jet
[ESA-TT-1046] 03 p0270 N88-11694

Base pressure measurements on a missile body with cruciform tail
[ESA-TT-1062] 03 p0270 N88-11695

Flight and wind-tunnel measurements showing base drag reduction provided by a trailing disk for high Reynolds number turbulent flow for subsonic and transonic Mach numbers
[NASA-TP-2638] 06 p0701 N88-14299

Flight tests of external modifications used to reduce blunt base drag
[NASA-TM-100433] 13 p1719 N88-20279

An experimental investigation of rocket ramjet nozzle assembly base pressures
[AD-A189714] 15 p2027 N88-22076

BASES

Improved description of base dynamics in the modeling of bipolar transistors
[PB88-181516] 19 p2732 N88-26229

Active sites and roles of solid acid base catalysts
[NASA-TT-20333] 24 p3345 N88-29909

BASES (CHEMICAL)

NT ALKALIES
NT ATROPINE
NT CAFFEINE
NT ERGOTAMINE
NT LITHIUM HYDROXIDES
NT MORPHINE
NT PYRIDINES
NT QUINOLINE
NT SODIUM HYDROXIDES
NT URACIL

BASES (FOUNDATIONS)

U FOUNDATIONS

BASIC (PROGRAMMING LANGUAGE)

Computer program in BASIC language for computation of spectrochemical analytical data
[DE88-701229] 15 p2032 N88-22106

BASINS

U STRUCTURAL BASINS

BASINS (CONTAINERS)

Marintek's ocean basin, a training facility for extravehicular activity? 19 p2698 N88-26041

BATCH PROCESSING

Scale-up of a batch-type chemical powder preparation process for high field varistor fabrication
[DE88-006601] 13 p1782 N88-20541

MVS (Multiple Virtual Storage) batch computing and data management at ANL
[DE88-007342] 19 p2718 N88-26137

Fabrication of bulk superconducting ceramics
[DE88-009956] 22 p3155 N88-28773

BATHING

Analysis of water recovered after being used for washing by men and women 10 p1361 N88-18135

The effects of normal and therapeutic baths on the central vascular organs of persons with healthy hearts, as measured by X-ray
[NASA-TT-20252] 13 p1811 N88-20818

BATHOLITHS

Pluton emplacement and magmatic arc construction: A model from the Patagonian batholith
24 p3393 N88-30206

Genesis of archean granitoids in the Pilbara block and implications for crustal growth 24 p3394 N88-30210

BATHS

A rapid electrochemical technique for determining the current efficiency for cadmium plating
[AD-A193679] 22 p3056 N88-28130

BATHYMETERS

Airborne electromagnetic sounding of sea ice thickness and sub-ice bathymetry
[AD-A188939] 12 p1649 N88-19879

Bathymetric hazard survey test
[AD-A189150] 13 p1803 N88-20775

Inversion algorithms for geophysical problems
[AD-A189252] 13 p1815 N88-20845

The representation of the sea-bottom in deep sea areas by the Digital Terrain Model (DTM) program TASH
16 p2226 N88-23293

To relate measurements of gravity and geoid anomalies over the oceans to near surface density distributions
[AD-A192168] 18 p2547 N88-25120

Identification and acoustic characterization of seamounts
[AD-A192204] 18 p2548 N88-25123

Bathymetry estimation by analyzing swell on SPOT images 19 p2701 N88-26062

Study of the Arachon (France) underwater delta using Thematic Mapper data 19 p2702 N88-26064

Evaluation of the contribution of SPOT in the framework of the mineral exploration program of the Aitutaki Atoll (Cook Islands). Preliminary study of the impact of the passage of Hurricane Sally 22 p3109 N88-28463

BATHYMETRY

U BATHYMETERS

BATHYTHERMOGRAPHS

JEDA (Joint Environmental Data Analysis) Center report on tropical Pacific subsurface thermal data management, 1986
[PB88-140090] 12 p1649 N88-19875

Editing master oceanographic observation data set 4
[AD-A188405] 12 p1649 N88-19876

Expendable conductivity, temperature and depth system (XCTD) development program
[AD-A192182] 18 p2547 N88-25121

Application of acoustic-Doppler current profiler and expendable bathythermograph measurements to the study of the velocity structure and transport of the Gulf Stream
[NASA-CR-183188] 22 p3129 N88-28605

BATTERIES

U ELECTRIC BATTERIES

BATTERY CHARGERS

Overcharge protection in Li-alloy/metal disulfide cells
[DE87-011364] 01 p0041 N88-10260

A novel class of positive electrodes for rechargeable batteries
[DE88-004559] 13 p1763 N88-20545

Development of a total electric vehicle drive system
[DE88-900367] 14 p1917 N88-21446

GTE battery management system: State of charge indicator evaluation
[DE88-006800] 15 p2058 N88-22272

Aircraft battery state of charge and charge control system
[AD-A194979] 24 p3367 N88-30052

BATTERY SEPARATORS

U SEPARATORS

BAYES THEOREM

Comparing hard and soft prior bounds in geophysical inverse problems
[NASA-CR-181557] 05 p0624 N88-13820

A unified mathematical approach to image analysis
[AD-A185719] 06 p0765 N88-14703

Asymptotic normality of poly-t densities with Bayesian applications
[AD-A185718] 06 p0768 N88-14719

A three-parameter generalisation of the beta-binomial distribution with applications
[AD-A185733] 06 p0768 N88-14720

On determining the weight for obtaining a large number of items
[AD-A186181] 07 p0915 N88-15553

A prototype of pilot knowledge evaluation by an intelligent CAI (Computer-Aided Instruction) system using a Bayesian diagnostic model
[AD-A186080] 08 p1054 N88-16358

De Finetti's approach to group decision making
[AD-A188074] 11 p1538 N88-19177

Signal-filter design and system performance for polarimetric radar
[AD-A189257] 13 p1758 N88-20514

Admissibility in fair Bayes prediction problems. Part 1: General theory
[CWI-MS-R8703] 14 p1965 N88-21725

Sequential tests for the drift of a Wiener process with a smooth prior and the heat equation
[AD-A190322] 15 p2121 N88-22638

Properties of some Bayesian scoring procedures for computerized adaptive tests
[AD-A189925] 15 p2124 N88-22660

Admissible Bayes tests for structural relationship
[AD-A190326] 15 p2125 N88-22669

Empirical and hierarchical Bayes competitors of preliminary test estimators in two sample problems
[AD-A190327] 15 p2125 N88-22670

On two-stage allocation procedures for selection problems
[AD-A190786] 15 p2126 N88-22675

Bayesian solutions to a 2 x 2 decision matrix using interval scaled payoffs with an application to foreign policy decisions
[AD-A190863] 16 p2260 N88-23511

Knowledge acquisition tool implementation
[AD-A190415] 18 p2555 N88-25164

Automatic discovery of optimal classes
[NASA-TM-101174] 18 p2566 N88-25238

An application of the Bayesian method to the estimation and forecast of system hardware components MTBF
22 p3068 N88-28211

Topics in adaptive control and inference
[AD-A194718] 23 p3266 N88-29443

Selecting the best binomial population: Parametric empirical Bayes approach
[AD-A193341] 23 p3269 N88-29450

Easy Bayes estimation for Rasch-type models
[AD-A193628] 23 p3274 N88-29491

Dirichlet prior in Bayesian estimation of item response curves
[AD-A195311] 24 p3426 N88-30392

BAYESIAN STATISTICS

U BAYES THEOREM

BAYS (STRUCTURAL UNITS)

Redistribution of particulates in shuttle bay during launch 02 p0133 N88-10837

Centaur G Prime modal test 09 p1181 N88-17075

Payload bay atmospheric vent airflow testing at the Vibration and Acoustic Test Facility
[NASA-TM-100460] 11 p1437 N88-18572

Moving-bank multiple model adaptive estimation applied to flexible spacestructure control
[AD-A190761] 15 p2026 N88-22071

FEB structural analysis, revision H
[AD-A192302] 20 p2814 N88-26698

BAYS (TOPOGRAPHIC FEATURES)

NT DELAWARE BAY (US)

Tide- and wind-forced currents in Buzzards Bay, Massachusetts
[PB88-110580] 07 p0882 N88-15350

Continental shelf processes affecting the oceanography of the South Atlantic Bight
[DE88-004102] 09 p1196 N88-17166

Biological processes in the water column of the South Atlantic bight: Zooplankton responses
[DE88-004811] 14 p1951 N88-21630

Relevance of a thematic map (SPOT data) with regards to the real flora and structure of the vegetation covering of salt marshes (Mont Saint Michel Bay, France)
22 p3109 N88-25468

BCC LATTICES
U BODY CENTERED CUBIC LATTICES

BEACONS
NT RADAR BEACONS
NT RADIO BEACONS
COSPAS/SARSAT 406-MHz emergency beacon digital controller
[NASA-TM-100859] 20 p2792 N88-26566

BEADS
Examination of the physical processes associated with the keyhole region of variable polarity plasma arc welds in aluminum alloy 2219 07 p0927 N88-15634
Unsteady flow about cambered plates
[AD-A191226] 17 p2337 N88-23945
Analysis of a feed device for the pneumatic transport of noncohesive particles
[VKI-TM-44] 24 p3369 N88-30062

BEAM CURRENTS
Use of polarimetry to measure the current profile in MTX
[DE87-013835] 02 p0237 N88-11495
Stabilized X-ray generator power supply
[DE88-700297] 07 p0830 N88-15034
Neutral beam propagation through the atmosphere
[AD-A188984] 12 p1681 N88-20115
Requirements for neutral beam current drive in tokamaks
[DE88-006180] 20 p2859 N88-26980
A millimeter-wave tunneLadder TWT
[NASA-CR-182184] 22 p3072 N88-28239

BEAM INJECTION
Improvement of energy confinement of neutral beam heated plasma by lower hybrid current drive in JT-60
[DE87-752983] 02 p0239 N88-11509
Two dimensional neutral transport analysis in tokamak plasma
[DE87-752984] 02 p0239 N88-11510
Transport analysis of OH and NBI heated discharges in JT-60
[DE87-752985] 02 p0239 N88-11511
Reactivity for DT plasma with beam-induced tail in magnetic confinement system
[DE87-753017] 02 p0240 N88-11517
Fusion reactivity enhancement due to ion tail formation by beam and ion cyclotron heating
[DE87-753018] 02 p0240 N88-11518
Volume produced H(-),D(-) ion source for proton accelerator and thermo-nuclear fusion research by sheet plasma (III)
[IPPJ-838] 02 p0242 N88-11531
Effects of injection of free electron lasers on axial velocity spread of beams 03 p0299 N88-11878
Negative ion beams for heating and current-drive in NET
[AD-A184390] 04 p0489 N88-13012
Coherent emission from relativistic beam-plasma interactions 04 p0493 N88-13039
Method of plasma diagnostics by a heavy ion beam for the T-15 tokamak
[DE88-700342] 07 p0935 N88-15678
Simple model for hot ion plasmas
[DE88-750045] 07 p0936 N88-15686
Electrostatic VLF emission determined from rocket and satellite experiments 08 p1002 N88-16068
Absorption of cyclotron radiation in skin layer in Araks experiment 08 p1003 N88-16076
Preliminary injector, accelerator, and beamline design for rf-linac-driven XUV free-electron lasers
[DE88-003185] 10 p1336 N88-17983
The numerical simulation of accelerator components
[DE87-011587] 10 p1412 N88-18423
Benchmarks of neutral beam injection codes for stellarators
[DE88-003788] 10 p1412 N88-18428
Effects of X irradiation and high field electron injection on the electrical properties of rapid thermal oxides
[DE88-002642] 10 p1417 N88-18461
Corpuscular plasma diagnostics complex on a tokamak with a strong field
[DE88-701576] 16 p2279 N88-23646
Ion temperature profile measurement using charge exchange recombination spectroscopy on JIPP T-IIU
17 p2440 N88-24518
Spectroscopic measurements of ion temperature, rotation speed and beam deposition profile on DIII-D
17 p2440 N88-24519
Spectroscopic study of heliotron E plasmas: Stark profile, CXR, poloidal rotation and carbon coating
17 p2441 N88-24523
REFLEX: An energy deposition code that models the effects of electron reflection during electron beam heating tests
[DE88-009789] 19 p2726 N88-26186
Pseudospark switches
[DE88-702227] 23 p3207 N88-29085
Initial operation and edge plasma studies in ATF (Advanced Toroidal Facility)
[DE88-011400] 23 p3285 N88-29562

BEAM INTERACTIONS
Transverse focussing using plasma wake fields
[DE87-011503] 01 p0099 N88-10652
Investigation of two laser beam coupling and amplification in Ce-doped SBN single crystals
03 p0327 N88-12069
Coherent emission from relativistic beam-plasma interactions 04 p0493 N88-13039
Atomic beam studies of the interaction of hydrogen with transition metal surfaces
[DE88-000208] 05 p0648 N88-13970
Experimental research of electron beam instability on the Doppler anomalous effect
[DE88-700565] 07 p0932 N88-15658
Two dimensional simulations of multipass beam breakup
[CEBAF-PR-87-008] 11 p1547 N88-19254
Observation of anomalous low J-value Stokes and anti-Stokes lines in stimulated rotational Raman scattering over long air paths
[DE88-003756] 14 p1911 N88-21418
Crossed molecular beam studies of substitution and exchange reactions
[DE88-006322] 14 p1980 N88-21814
Gamma rays from Cygnus X-1: Modeling and nonthermal pair production
[DE88-006830] 18 p2596 N88-25426

BEAM SPLITTERS
Advances in X-ray optics, 1987
[DE88-003298] 11 p1549 N88-19268
Soft X-ray beamsplitters and highly dispersive multilayer mirrors for use as soft X-ray laser cavity components
[DE88-004003] 11 p1549 N88-19270
Space infrared telescope facility wide field and diffraction limited array camera (IRAC)
[NASA-CR-182704] 13 p1853 N88-21092
Detecting squeezed states by cross-correlation
14 p1978 N88-21806
Modulated-splitting-ratio fiber-optic temperature sensor
[NASA-TM-101332] 22 p3042 N88-28062
Four-frame gated optical imager with 120-ps resolution
[DE88-011735] 22 p3080 N88-28288

BEAM SWITCHING
Investigations on beam quality of high frequency excited CO2 high performance lasers
[ETN-88-92363] 21 p2954 N88-27550

BEAM WAVEGUIDES
A millimeter-wave tunneLadder TWT
[NASA-CR-182184] 22 p3072 N88-28239
Analytical and experimental studies of beam waveguide absorbers for structural damping
[AD-A195085] 24 p3382 N88-30144

BEAMS (RADIATION)
NT ATOMIC BEAMS
NT ELECTRON BEAMS
NT ION BEAMS
NT LASER BEAMS
NT LIGHT BEAMS
NT MOLECULAR BEAMS
NT NEUTRAL BEAMS
NT NEUTRINO BEAMS
NT NEUTRON BEAMS
NT PARTICLE BEAMS
NT PHONON BEAMS
NT PHOTON BEAMS
NT PROTON BEAMS
NT RADAR BEAMS
NT RELATIVISTIC ELECTRON BEAMS
The nature of beamstrahlung
[DE87-012837] 02 p0234 N88-11474
Interactive Design of Accelerators (IDA)
[DE87-013298] 02 p0234 N88-11476
Determination of the origin of self-pumped phase conjugation in barium titanate
[AD-A184697] 03 p0377 N88-12372
Phenomena at a focus in a laser system
[AD-A185442] 05 p0586 N88-13585
Current status of high power microwave effects and simulation
[DE87-004112] 06 p0751 N88-14615
Investigation of the performance of a novel double crystal X-ray monochromator measurements
[PB87-125167] 06 p0788 N88-14834
Cage mode propagation experiments
[AD-A186019] 07 p0841 N88-15100
Microsecond beam propagation in air
[DE88-002221] 07 p0845 N88-15127
Explosive absorption of laser beam of finite diameter
07 p0921 N88-15597
Analysis of the decomposition of transparent polymer materials (blocks) under the action of laser beams in free generation mode
[AD-A187090] 09 p1147 N88-16873
Theory of transient thermal self-focusing of sound beams 09 p1234 N88-17401
Nonlinear and diffraction effects in sound beams with random transverse structure 09 p1235 N88-17402
A ring model of the lasertron
[DE88-004656] 10 p1323 N88-17908
Correcting ray field failures caused by focusing in an inhomogeneous duct: A critical look at the Gaussian beam method 12 p1616 N88-19663
Multipass beam breakup in recirculating linacs
[CEBAF-PR-87-007] 12 p1690 N88-20111
Multimode-waveguide laser beam deflector
[DE88-006222] 13 p1776 N88-20622
Practical constraints on sources for pulsed beam lithographies
[DE88-006594] 13 p1776 N88-20623
Studies of compound states of negative ions using laser beams
[DE88-004708] 13 p1777 N88-20627
Aberrations: Their effect on off-axis beam steering
[AD-A189601] 13 p1840 N88-21006
Observation of anomalous low J-value Stokes and anti-Stokes lines in stimulated rotational Raman scattering over long air paths
[DE88-003756] 14 p1911 N88-21418
Optical cooling and trapping 14 p1974 N88-21782
Laser cooling of neon metastable states
14 p1975 N88-21785
Quantum nondemolition detection and squeezing in optical fibers 14 p1976 N88-21793
Variable-energy positron studies on liquids and liquid-solid interfaces
[DE88-006356] 15 p2033 N88-22109
The interaction of small particles with laser beams
[AD-A190716] 15 p2072 N88-22354
Ultrasonic beam distortion in transversely isotropic media
[DE88-005937] 15 p2129 N88-22699
Optical switching and control techniques using nonlinear optical wave mixing
[AD-A190467] 15 p2134 N88-22730
TDWR (Terminal Doppler Weather Radar) clutter residue map generation and usage
[AD-A191148] 16 p2235 N88-23352
Fast acting optical beam detection and deflection system
[AD-A192161] 18 p2521 N88-24954
Heavy ion fusion system assessment: Final focus and transport model
[LBL-23040] 19 p2725 N88-26183
Electron-acoustic waves in a beam-plasma system
[DE88-702053] 19 p2729 N88-26207
Time-Optimal Adaptive Shaped Torque (TOAST) technical note
[AD-A192719] 20 p2843 N88-26869
Distortion functions
[DE88-752634] 21 p3015 N88-27696
Guided radiation beams in free electron lasers
[AD-A194525] 22 p3062 N88-28305
Beam optics test stand
[AD-A193901] 23 p3216 N88-29144

BEAMS (SUPPORTS)
NT BOX BEAMS
NT CANTILEVER BEAMS
NT CURVED BEAMS
NT I BEAMS
NT TIMOSHENKO BEAMS
An experimental and theoretical study of the bending behavior of Kevlar 49/epoxy beams and rings
[DE87-010430] 01 p0061 N88-10394
Assessment of structural integrity from forced vibration testing
[DE87-014642] 02 p0191 N88-11195
Shape optimization of damping layers
05 p0595 N88-13635
An examination of chaotic motion for the buckled beam 05 p0597 N88-13644
Optimal control of large space structures via generalized inverse matrix
[NASA-CR-182336] 05 p0639 N88-13907
Beam and column buckling under directed loading
[PB87-124004] 06 p0722 N88-14436
Buckling of braced monosymmetric cantilevers: Timoshenko energy approach
[PB87-133849] 06 p0723 N88-14445
Effects of fabrication on the fatigue capacity of welded steel structures
[PB87-144226] 08 p0995 N88-16021

FABSTRAN: A computer program for frame and beam static and transient response analysis (nonlinear)
[ARE-TR-86205] 09 p1182 N88-17079
Composite materials for rail transit systems
[NASA-CR-178401] 10 p1294 N88-17738
Strategic placement of accelerometers to measure forces by the sum of weighted accelerations
[DE88-002262] 10 p1333 N88-17968
Robust controller design for flexible structures
[AD-A187217] 10 p1340 N88-18009
Some aspects of the mechanics and mechanisms of dynamic brittle fracture 10 p1343 N88-18028
Piezoelectric laminates for torsional and bending model control: Theory and experiment
10 p1343 N88-18029
Experimental set-up and mathematical modeling of H-shaped beam type structure
[AD-A187196] 11 p1466 N88-18743
Approximate method for predicting the permanent set in a beam in vacuo and in water subject to a shock wave 11 p1500 N88-18957
The Euler-Bernoulli beam equation with boundary energy dissipation
[AD-A189517] 13 p1765 N88-20560
Component mode synthesis using experimental modes enhanced by mass loading
[DE88-006097] 13 p1781 N88-20657
Finite element methodology for nonlinear free and harmonic forced vibrations of beam and plate structures
13 p1782 N88-2066[illegible]
Design graphs for the first two bending Eigenvibration forms of rotating beams consisting of two beam points
[IW-86006R] 13 p1783 N88-20670
The X-beam as a deployable boom for the space station 14 p1925 N88-21473
Motion synchronization of a mechanism to deploy and restow a truss beam 14 p1925 N88-21474
Creep rupture analysis of a beam resting on high temperature foundation 14 p1930 N88-21509
Stabilization and control problems in structural dynamics
[AD-A190197] 15 p2073 N88-22361
Coupled bending-torsion steady-state response of pretwisted, nonuniform rotating beams using a transfer-matrix method
[NASA-TM-100596] 15 p2086 N88-22435
Bi-stem gripping apparatus
[NASA-CASE-MFS-28185-1] 17 p2345 N88-23979
Dynamic characteristics of a vibrating beam with periodic variation in bending stiffness
[NASA-TP-2697] 17 p2348 N88-23986
Space station architectural elements model study
[NASA-CR-4027] 18 p2464 N88-24632
Estimation and control of distributed models for certain elastic systems arising in large space structures
[AD-A192120] 18 p2472 N88-24686
On the bending response of Kevlar 49/epoxy beams and rings
[DE88-006824] 18 p2530 N88-25012
Mobile remote manipulator system for a tetrahedral truss
[NASA-CASE-MSC-20985-1] 20 p2765 N88-26398
Optimal design of viscoelastic structures
21 p2959 N88-27579
Coupled thermal vibrations of beams with temperature-dependent properties
21 p2963 N88-27601
Tripping of stiffened plates using a refined beam theory
[AD-A193989] 22 p3087 N88-28333
Damage initiation in the short beam shear test of composite materials using stiffness reduction
[AD-A194880] 24 p3340 N88-29863
Vibrational power flow analysis of rods and beams
[NASA-CR-183166] 24 p3383 N88-30151

BEAMSHAPING
U COLLIMATION

BEARING (DIRECTION)
Lower bounds on bearing accuracy for closely spaced sources
[AD-A184258] 04 p0486 N88-12997
Visual attention effects on discrimination of line orientation and line arrangement
[AD-A187013] 09 p1200 N88-17190
Bearing detection in the presence of two sources of varying coherence using the complex cepstrum
[NASA-CR-181605] 09 p1243 N88-17451
Composite ceramic superconducting filaments for superconducting cable
[AD-A187833] 11 p1556 N88-19312
A comparison of terrain association and resection as methods of position location
[AD-A189480] 13 p1790 N88-20710
Method for determining artillery position
[NASA-TT-20236] 14 p1979 N88-21813
Determination of beam orientation of optical diagnostics of excited 200-MeV hydrogen atoms resulting from photodetachment of H(-)ions
[AD-A189976] 14 p1981 N88-21823
Relative orientation
[AD-A190385] 15 p2089 N88-22449
Deflection of a circular liquid jet on a flat plate perpendicular to the flow direction
[NASA-TT-20278] 16 p2207 N88-23173

BEARING ALLOYS
The influence of foreign particles on bearing metals
[NASA-TT-20155] 20 p2775 N88-26454

BEARINGLESS ROTORS
An overview of key technology thrusts at Bell Helicopter Textron 09 p1111 N88-16657
Special flight mechanical features of the bearingless helicopter rotor
[MBB-FM-315/O] 10 p1309 N88-17825
Testing of a tail rotor system in a fiber composite type of construction
[MBB-UD-472/86] 10 p1314 N88-17854
Comprehensive analysis of helicopters with bearingless rotors
[NASA-CR-182537] 10 p1390 N88-18300
Design, manufacture and spin test of high contact ratio helicopter transmission utilizing Self-Aligning Bearingless Planetary (SABP)
[NASA-CR-4155] 18 p2524 N88-24975
A comparison of theory and experiment for the aeroelastic stability of a bearingless model rotor in hover
21 p2890 N88-27153
A comparison of theory and experiment for coupled rotor body stability of a bearingless rotor model in hover and forward flight 21 p2890 N88-27154
A comparison of theory and flight test of the BO 105/BMR in hover and forward flight
21 p2890 N88-27155
Aeromechanical stability analysis of COPTER
21 p2891 N88-27161
Aeroelastic characteristics of the AH-64 bearingless tail rotor 21 p2891 N88-27162

BEARINGS
NT ANTIFRICTION BEARINGS
NT BALL BEARINGS
NT FOIL BEARINGS
NT GAS BEARINGS
NT JOURNAL BEARINGS
NT MAGNETIC BEARINGS
NT ROLLER BEARINGS
Composite bearing materials containing solid lubricant in filamentary form, stages 3 and 4
[IRD-87/2] 01 p0054 N88-10344
Boundary lubrication. Experiments with boundary lubrication and plain bearings at +60...-60 deg C temperatures
[DE87-752869] 02 p0180 N88-11124
Bearing loads in slider crank mechanisms
[PB87-216495] 03 p0332 N88-12089
Coatings for high-temperature bearings and seals
[NASA-TM-100249] 05 p0567 N88-13453
Dynamic behavior of dissymmetric rotor bearings modelled with a periodic coefficient large system
05 p0596 N88-13640
Developing an accelerated endurance test for greases: A status report
[AD-A185963] 07 p0836 N88-15072
Evaluation of load tracks and wear of two sets of bearings from space shuttle main engine high pressure oxygen turbopumps
[NASA-CR-178969] 07 p0861 N88-15223
A variational formulation of a hydrodynamic lubrication problem
[MEMO-642] 08 p0987 N88-15979
Results of NASA/Army transmission research
09 p1108 N88-16640
Self-lubricating coatings for high-temperature applications 09 p1119 N88-16703
Numerical modeling of multidimensional flow in seals and bearings used in rotating machinery
[NASA-TM-100779] 09 p1165 N88-16988
Optimal design and parameter identification of flexible rotor-bearing systems 10 p1339 N88-18002
Numerical and analytical study of fluid dynamic forces in seals and bearings
[NASA-TM-100268] 11 p1485 N88-18867
Computer-aided design analysis of 57-mm, angular-contact, cryogenic turbopump bearings
[NASA-TP-2816] 11 p1496 N88-18933
Ply-level failure analysis of a graphite/epoxy laminate under bearing-bypass loading
[NASA-TM-100578] 13 p1735 N88-20372
Performance of elastomeric bearings
[PB88-159470] 14 p1918 N88-21450
The 22nd Aerospace Mechanisms Symposium
[NASA-CP-2506] 14 p1924 N88-21468
Mode 2 fracture mechanics 15 p2083 N88-22418
Active control and system identification of rotordynamic structure 16 p2218 N88-23230
Effects of axial load on elastomeric isolation bearings
[PB88-179015] 16 p2223 N88-23269
The flying characteristics of the membrane slider bearing 18 p2522 N88-24965
The 000 stage equipment bearing performance with a lower viscosity lubricant
[DE88-011827] 21 p2957 N88-27566

BEAT
U SYNCHRONISM

BEAT FREQUENCIES
Energy cascading in the beat-wave accelerator
[DE87-014727] 03 p0377 N88-12374
Heating efficiency of beat wave excitation in a density gradient
[AD-A193066] 21 p3017 N88-27905

BEAUFORT SEA (NORTH AMERICA)
Examples of ice pack rigidity and mobility characteristics determined from ice motion
[AD-A191163] 17 p2377 N88-24129
MIZPAC (marginal ice zone Pacific) 84-86 CTD (Conductivity, Temperature, Depth) data report
[AD-A192478] 21 p2976 N88-27679
Beaufort sea mesoscale circulation study: Hydrography helicopter operations, April 1987
[PB88-203658] 21 p2976 N88-27681

BED REST
Prevention of disuse osteoporosis: Effect of sodium fluoride during five weeks of bed rest
[NASA-CR-172018] 01 p0075 N88-10483
Regulation of calcium metabolism during prolonged antiorthostatic hypokinesia
[NASA-TT-20219] 11 p1521 N88-19085
P-31 Magnetic Resonance Spectroscopy (MRS) of limb muscles during bedrest with exercise countermeasures
12 p1656 N88-19925
Some reflections on the standardization of bed-rest procedures for weightlessness simulation (cardiovascular and endocrine apsects) 12 p1662 N88-19961
Noninvasive examination of bones during long-term hypokinesia 19 p2704 N88-26077
Physiology of prolonged bed rest
[NASA-TM-101010] 22 p3130 N88-28607
Interplanetary travel: Is gravity needed to close the loop
[NASA-TM-101013] 22 p3132 N88-28622

BEDROCK
NT BATHOLITHS
Preliminary estimation of color inhomogeneities on the surface of Venus according to the television images obtained by the VENERA-13 and VENERA-14 automated space probes
[NASA-TT-20114] 02 p0254 N88-11606
Structure of Southwestern Michipicoten Greenstone Belt, Ontario: Evidence for Archean accretion
24 p3397 N88-30228

BEDS (PROCESS ENGINEERING)
Theoretical prediction of single phase turbulent flow distribution in particulate bed reactors
17 p2419 N88-24386

BEER LAW
The analytical exponential decay coefficient of the submarine light field
[AD-A187215] 11 p1548 N88-19261

BEHAVIOR
NT HUMAN BEHAVIOR
Assessment of fatigue in aviation crews
[AD-A184129] 03 p0356 N88-12245
Supertracks: The building blocks of chaos
[DE88-001513] 04 p0522 N88-13207
Quantifying some information processing aspects of the pilot's instrument crosscheck
[AD-A186114] 07 p0898 N88-15443
Innovation and creativity: A critical linkage
[DE88-003309] 10 p1426 N88-18515
Experiments concerning gravisensitivity of protozoa
12 p1660 N88-19949
Describing constraints on a digital circuit's behavior
[AD-A189200] 13 p1761 N88-20531
An evaluation of the effects of high visual taskload on the separate behaviors involved in complex monitoring performance
[AD-A190641] 15 p2105 N88-22538
Program profiling in Cedar
[AD-A190883] 16 p2250 N88-23449
The behavior of drop-containing turbulent eddies
[AD-A191669] 18 p2509 N88-24883
Behavioral response of rats exposed to high-power microwave radiation
[AD-A192199] 18 p2548 N88-25128
Motor theory of auditory perception
[AD-A192095] 18 p2550 N88-25136
Modeling and evaluation of variable structure organizations
[AD-A191947] 18 p2568 N88-25381

Anomalous temperature-dependent negative magnetoresistance in pregraphitic carbons
[AD-A191725] 19 p2619 N88-25535
Behavioral, psychological and demographic predictors of physical fitness
[AD-A192697] 21 p2986 N88-27730
The dynamic behavior of a turbulent boundary layer subjected to a shock-induced separation
[AD-A194164] 22 p3075 N88-28252
Optical bistable behavior of a planar quasi-waveguide interferometer made with a conjugated organic polymer film
[AD-A194349] 22 p3152 N88-28756
Elastic behavior of a rubber layer bonded between two rigid spheres
[AD-A193698] 23 p3198 N88-29030

BELGIUM
Analysis of SPOT multispectral data concerning a border zone between two geographical regions in southern Belgium 22 p3100 N88-28411

BELL AIRCRAFT
NT UH-1 HELICOPTER
NT XV-15 AIRCRAFT

BELLMAN THEORY
Normed Bellman equation with degenerate diffusion coefficients and its application to differential equations
[AD-A190319] 15 p2120 N88-22637

BELTRAMI FLOW
Weak interactions and local order in strong turbulence
09 p1159 N88-16948

BENCHES
U SEATS

BEND TESTS
Investigation on ductile fracture behavior of 3-inch diameter Type 304 stainless steel pipe with a circumferential through-wall crack
[DE87-753016] 02 p0191 N88-11196
Crack initiation studies in hydrogen embrittled spring steel strip 05 p0605 N88-13710
An optical interferometry technique to evaluate closure along a crack front 05 p0607 N88-13726
Experimental investigation on the bending fatigue performance of gas carbonitrided and carburized gears
[PB87-147997] 08 p0992 N88-16003

BENDING
NT ELASTIC BENDING
An experimental and theoretical study of the bending behavior of Kevlar 49/epoxy beams and rings
[DE87-010430] 01 p0061 N88-10394
Aerodynamic design and performance of a bent-axis geometry vehicle
[DE87-013726] 02 p0124 N88-10786
Hardening of metal during production of bent shapes
[BLL-M-37250-(5828.4)] 02 p0148 N88-10928
Generalized hybrid variational principle, corresponding finite element model 03 p0301 N88-11895
Compactness of quasi-conforming element spaces, convergence of quasi-conforming element method
03 p0301 N88-11896
Analysis and testing of predamaged shell structures
04 p0428 N88-12653
Kinematic formulation of finite elements for plate bending 04 p0455 N88-12821
Crack growth prediction in 3D structures under aeronautical-type spectrum loadings
05 p0602 N88-13688
Bending properties of aluminum base composite with CVD-fiber
[PB87-130878] 06 p0678 N88-14156
Developments in electronics ceramics reported
06 p0684 N88-14192
Life prediction of steel cords
06 p0715 N88-14386
Multiaxial fatigue failure criterion: A new approach
06 p0719 N88-14418
Bending analysis of thin plates with openings
[PB87-143400] 07 p0869 N88-15274
Study of the temperature dependence of the mechanical characteristics of the steels GX 5 CrNi 13 4 and GGG 40 in tensile and bending tests
[DE88-001460] 09 p1143 N88-16850
Piezoelectric laminates for torsional and bending modal control: Theory and experiment
10 p1343 N88-18029
Benchmark computation and finite element performance evaluation for a rhombic plate bending problem
[AD-A187402] 10 p1345 N88-18041
Mechanisms in thermal mechanical forming of plates
[AD-A187797] 11 p1486 N88-18744
Mathematical modeling of the postbuckling behavior of structural elements 11 p1500 N88-18860
An efficient Mindlin finite strip plate element based on assumed strain distribution 15 p2081 N88-22407
Coupled bending-torsion steady-state response of pretwisted, nonuniform rotating beams using a transfer-matrix method
[NASA-TM-100596] 15 p2086 N88-22435
Non-rigid motion and Regge calculus
[AD-A190387] 15 p2121 N88-22640
Effects of axial load on elastomeric isolation bearings
[PB88-179015] 16 p2223 N88-23269
Dynamic characteristics of a vibrating beam with periodic variation in bending stiffness
[NASA-TP-2697] 17 p2348 N88-23988
On the bending response of Kevlar 49/epoxy beams and rings
[DE88-006824] 18 p2530 N88-25012
MHD bending waves in a current sheet
[NASA-TM-101149] 18 p2579 N88-25323
Static analysis of thin plates using the finite strip-element method 19 p2679 N88-25931
Vertical ship motions and sea loads considering nonlinear effects
[TAE-592] 20 p2784 N88-26515
Improved finite strip Mindlin plate bending element using assumed shear strain distributions
[NASA-TM-100928] 23 p3225 N88-29195

BENDING DIAGRAMS
Design graphs for the first two bending Eigenvibration forms of rotating beams consisting of two beam points
[IW-88006R] 13 p1783 N88-20670

BENDING FATIGUE
Bending of a bonded beam as a test method for adhesive properties
[AD-A184813] 05 p0609 N88-13736
Experimental investigation on the bending fatigue performance of gas carbonitrided and carburized gears
[PB87-147997] 08 p0992 N88-16003

BENDING MOMENTS
Computation of the tensile and bending restraint intensities of welded specimens by finite element method
[PB87-143798] 08 p0995 N88-16024
The Euler-Bernoulli beam equation with boundary energy dissipation
[AD-A189517] 13 p1785 N88-20560

BENDING VIBRATION
Dynamic characteristics of a vibrating beam with periodic variation in bending stiffness
[NASA-TP-2697] 17 p2348 N88-23988

BENDS (PHYSIOLOGY)
U DECOMPRESSION SICKNESS

BENZENE
Detailed mechanism of benzene oxidation
[NASA-TM-100202] 03 p0282 N88-11775
Two-laser resonance enhanced photoionization spectrum of gas phase benzene
03 p0300 N88-11889
Detailed mechanism of toluene oxidation and comparison with benzene
[NASA-TM-100261] 05 p0563 N88-13428
Ordered polymers for space applications
[AD-A188460] 12 p1610 N88-19630
Size effects in the electrical resistivity of benzene-derived carbon fibers
[AD-A191708] 18 p2491 N88-24777
Microstructure of thin intercalated benzene derived graphite fibers
[AD-A191724] 19 p2618 N88-25534
Large ionic species in sooting acetylene and benzene flames 24 p3348 N88-29032

BERING SEA
Navarin Basin Ice Drift Program
[PB88-104021] 06 p0748 N88-14599
Geostrophic flow in the central Bering Sea, Fall 1986 and Summer 1987
[PB88-174354] 16 p2237 N88-23360
Influence of the Yukon River on the Bering Sea
[NASA-CR-182802] 17 p2376 N88-24126

BERNOULLI EQUATION
U BERNOULLI THEOREM

BERNOULLI THEOREM
Subcritical branching processes in a two state random environment, and a percolation problem on trees
[PB87-230439] 06 p0762 N88-14677
A Prohorov bound for a Poisson process and a Bernoulli process
[CWI-MS-R8701] 09 p1232 N88-17388

BERNSTEIN ENERGY PRINCIPLE
ICRF launcher studies
[DE88-001710] 04 p0495 N88-13046
Ion Bernstein modes in current-carrying plasmas
21 p3017 N88-27903

BERYLLIUM
Shielding analysis of a small compact space nuclear reactor
[AD-A185566] 06 p0779 N88-14784
Phenomenological model of superconductivity of heavy fermions in U(sub 1-x)ThsubxBesub13
09 p1238 N88-17423
Evaluation and compilation of thermodynamic properties of high temperature chemical species
[AD-A187509] 11 p1452 N88-18654
Adhesion of PVD titanium coatings to beryllium substrates
[DE88-005147] 11 p1463 N88-18721
Single-laboratory evaluation of SW-846 methods 7090/7091 determination of beryllium by flame and furnace atomic absorption spectrophotometry
[PB88-171434] 16 p2175 N88-22963
Contributions of autoionizing resonances to the electron collisional excitation rates for Be-like ions
[AD-A190924] 18 p2572 N88-25275
Studies of internal stresses and surface roughness of sputtered Be and BeB films
[DE88-011737] 22 p3086 N88-28327

BERYLLIUM ALLOYS
High velocity erosion of metal interfaces
[DE87-013937] 01 p0025 N88-10155
Joining of dissimilar materials with the pulsed Nd-YAG laser
[DE88-003757] 11 p1458 N88-18693

BERYLLIUM COMPOUNDS
NT BERYLLIUM OXIDES

BERYLLIUM OXIDES
Gas core reactors for direct nuclear propulsion
17 p2428 N88-24442

BESSEL FUNCTIONS
NT HANKEL FUNCTIONS
Frozen-field, rigid-beam, uniform-conductivity-channel tracking force calculation
[DE87-012510] 02 p0190 N88-11190
Accurate efficient evaluation of Bessel transform: Programs and error analysis
[AD-A187718] 11 p1536 N88-19174
Expressing mathematical subroutines constructively
[AD-A190559] 15 p2121 N88-22644
Distributions of quadratic forms
[AD-A190224] 15 p2124 N88-22663
Exact image theory for the problem of dielectric/magnetic slab
[NASA-CR-182865] 16 p2189 N88-23055
On the nucleonics component of cosmic radiation in the atmosphere
[DE88-702493] 22 p3166 N88-28854

BETA FACTOR
Beta limitation of matter-antimatter boundary layers
[TRITA-EPP-87-11] 09 p1250 N88-17490
Formation of high-Beta plasmas in various modes of operation in TPE-2 12 p1693 N88-20132
Flux coordinate studies of elongated plasmas at high Beta 12 p1694 N88-20134
Shear Alfven spectrum of analytic high-Beta equilibria
12 p1694 N88-20136

BETA INTERACTIONS
U WEAK INTERACTIONS (FIELD THEORY)

BETA PARTICLES
Nuclear beta decay after Les Houches
[DE87-014921] 04 p0489 N88-13011
Double beta decay and nuclear structure
[DE88-001986] 07 p0931 N88-15652
Theory of double beta decay
[DE88-002285] 07 p0931 N88-15653
Plasma separation process: Betacell (BCELL) code, user's manual
[DE88-006955] 20 p2859 N88-26981
Measurement of Beta-decay energies of short-lived neutron-rich nuclei in the vicinity of mass number between 101 and 106, and A = 109
[ETN-88-92376] 21 p3014 N88-27890

BETATRONS
Betatron oscillations in a free electron laser
[DE88-004859] 10 p1337 N88-17990
Optical guiding in the separable beam limit
[AD-A192452] 21 p2952 N88-27534
Distortion functions
[DE88-752634] 21 p3015 N88-27896

BIAS
NT RESPONSE BIAS
Increased gain of channel intensifier tubes by pulsed biasing
[DE88-000512] 04 p0490 N88-13019
Conditionally unbiased bounded influence robust regression with applications to generalized linear models
[AD-A186319] 07 p0915 N88-15556
On precision and accuracy (bias) statements for measurement procedures
[DE88-004434] 10 p1402 N88-18359
Simultaneous estimation and detection of bias shifts for inertial navigation systems 12 p1576 N88-19429
Homogenizing surface and satellite observations of cloud. Aspects of bias in surface data
[AD-A188523] 12 p1648 N88-19869

Two dimensional uncorrelated bias in fix algorithms
[NASA-CR-182683] 13 p1815 N88-20847
Bias reduction when there is no unbiased estimate
[AD-A189407] 13 p1829 N88-20937
Min-max bias robust regression
[AD-A191345] 16 p2263 N88-23529
A critical speed study for aircraft bias ply tires
[AD-A193616] 22 p3084 N88-28313
Urbanization: its detection and effect in the United States climate record 22 p3125 N88-28571
Systematic behavior of NMC medium range forecasts and the effect of model changes 1985-87
22 p3125 N88-28575
Two biased estimation techniques in linear regression: Application to aircraft
[NASA-TM-100649] 23 p3274 N88-29489

BIBLIOGRAPHIES
Aeronautical engineering: A continuing bibliography with indexes (supplement 218)
[NASA-SP-7037(218)] 01 p0001 N88-10002
Standard reference data publications, 1985-1986
[PB87-210241] 01 p0021 N88-10128
Earth resources: A continuing bibliography with indexes (issue 55)
[NASA-SP-7041(55)] 01 p0085 N88-10415
Problems in integrating geographic data
[DE87-012880] 01 p0106 N88-10689
A physico-chemical study of some areas of fundamental significance to biophysics
[DE87-013457] 02 p0217 N88-11365
Aerospace medicine and biology: A continuing bibliography with indexes
[NASA-SP-7011(303)] 02 p0217 N88-11367
Using bibliographic databases in technology transfer
[NASA-CR-181403] 02 p0222 N88-11399
Current experiments in elementary particle physics
[DE87-013961] 02 p0231 N88-11456
Publications and final reports on contracts and grants, 1986 (National Environmental Satellite, Data and Information Service)
[PB87-220810] 03 p0352 N88-12218
Health hazards of video display terminals: A comprehensive annotated bibliography on a critical issue of workplace health and safety with sources for obtaining items and list of terminal suppliers
[RSI-IAS-4] 03 p0355 N88-12240
Aeronautical engineering: A continuing bibliography with indexes (supplement 219)
[NASA-SP-7037(219)] 04 p0386 N88-12470
Internal reforming development for solid oxide fuel cells
[DE87-008518] 04 p0464 N88-12871
Aerospace medicine and biology: A continuing bibliography with indexes
[NASA-SP-7011(304)] 04 p0474 N88-12922
Research papers and publications (1981-1987): Workload research program
[NASA-TM-100016] 04 p0474 N88-12924
Literature review of solid lubrication mechanisms
[AD-A185010] 05 p0567 N88-13456
Aeronautical engineering: A continuing bibliography with indexes (supplement 220)
[NASA-SP-7037(220)] 06 p0683 N88-14065
Aerospace medicine and biology: A continuing bibliography with indexes (supplement 305)
[NASA-SP-7011(305)] 06 p0752 N88-14616
Precipitation in alumina-rich spinel: A transformation-toughened ceramic single crystal
[DE87-012380] 06 p0785 N88-14815
University program management information system, fiscal year 1985
[NASA-TM-88381] 06 p0790 N88-14848
Bibliographic relationships: Toward a conceptual structure of bibliographic information used in cataloging
06 p0791 N88-14852
Bibliography of textbooks on fibre reinforced plastics (212 books)
[PB87-148080] 07 p0827 N88-15017
Annotated bibliography on reliable system design
[PB88-108848] 07 p0866 N88-15254
USSR Space Life Sciences Digest index to issues 10-14
[NASA-CR-3922(17)] 07 p0883 N88-15361
Bibliography of space biology and medicine
07 p0897 N88-15435
A summary of the Naval Postgraduate School research program
[AD-A186362] 07 p0942 N88-15727
Index of USA-CERL publications for October 1984 - June 1987
[AD-A186375] 07 p0942 N88-15728
NASA patent abstracts bibliography: A continuing bibliography. Section 1: Abstracts (supplement 32)
[NASA-SP-7039(32)-SECT-1-ABST]
07 p0943 N88-15732
Catalog of infrared observations. Part 1: Data
[NASA-RP-1196-PT-1-ED-2] 07 p0944 N88-15738
Aeronautical engineering. A continuing bibliography with indexes, supplement 221
[NASA-SP-7037(221)] 08 p0949 N88-15758
Aerospace medicine and biology: A continuing bibliography with indexes (supplement 307)
[NASA-SP-7011(307)] 08 p1049 N88-16332
Aeronautical engineering: A continuing bibliography with indexes (supplement 223)
[NASA-SP-7037(223)] 09 p1111 N88-16661
Publications of the exobiology program for 1986: A special bibliography
[NASA-TM-4029] 09 p1203 N88-17205
Wind turbine acoustics research bibliography with selected annotation
[NASA-TM-100528] 09 p1243 N88-17450
Earth resources: A continuing bibliography with indexes (supplement 56)
[NASA-SP-7041(56)] 10 p1347 N88-18051
Aerospace medicine and biology: A cumulative index to a continuing bibliography (supplement 306)
[NASA-SP-7011(306)] 10 p1369 N88-18180
Aerospace medicine and biology: A continuing bibliography with indexes (supplement 308)
[NASA-SP-7011(308)] 10 p1369 N88-18183
Recent progress in the dynamic applications of piezoelectric crystals 10 p1417 N88-18460
NASA patent abstracts bibliography: A continuing bibliography. Section 2: Indexes (supplement 32)
[NASA-SP-7039(32)-SECT-2] 10 p1425 N88-18511
Spacecraft fire detection and extinguishment: A bibliography
[NASA-CR-180880] 11 p1444 N88-18612
Cumulative reports and publications through December 31, 1987
[NASA-CR-181624] 11 p1524 N88-19099
Aeronautical engineering: A cumulative index to a continuing bibliography
[NASA-SP-7037(222)] 12 p1574 N88-19416
The Shock and Vibration Digest, volume 20, no. 3
12 p1635 N88-19786
Aeronautical engineering: A continuing bibliography with indexes (supplement 224)
[NASA-SP-7037(224)] 13 p1715 N88-20254
Aerospace medicine and biology: A continuing bibliography with indexes (supplement 309)
[NASA-SP-7011(309)] 13 p1810 N88-20814
Aeronautical engineering: A continuing bibliography with indexes (supplement 225)
[NASA-SP-7037(225)] 14 p1863 N88-21126
Management: A bibliography for NASA managers
[NASA-SP-7500(22)] 14 p1991 N88-21867
Artificial neural networks: An introduction with an annotated bibliography
[DE88-007003] 15 p2116 N88-22603
Aeronautical engineering: A continuing bibliography with indexes (supplement 226)
[NASA-SP-7037(226)] 16 p2155 N88-22857
Enhanced backscattering from rough surfaces
[AD-A190995] 16 p2190 N88-23063
Earth resources: A continuing bibliography with indexes (issue 57)
[NASA-SP-7041(57)] 16 p2229 N88-23314
Aerospace medicine and biology: A continuing bibliography with indexes (supplement 310)
[NASA-SP-7011(310)] 16 p2236 N88-23369
Engine structures: A bibliography of Lewis Research Center's research for 1980-1987
[NASA-TM-100842] 17 p2350 N88-24002
Aerospace medicine and biology: A continuing bibliography with indexes (supplement 311)
[NASA-SP-7011(311)] 17 p2382 N88-24161
Aeronautical engineering: A continuing bibliography with indexes (supplement 227)
[NASA-SP-7037(227)] 18 p2456 N88-24578
Electromagnetic field penetration into structures
[AD-A192127] 18 p2501 N88-24836
Bibliography of Soviet laser developments, number 83, May - June 1986
[AD-A190968] 18 p2520 N88-24950
Aerospace medicine and biology: A continuing bibliography with indexes (supplement 312)
[NASA-SP-7011(312)] 18 p2551 N88-25141
Management and the executive
[AD-A190778] 18 p2587 N88-25374
NASA patent abstracts bibliography: A continuing bibliography. Section 1: Abstracts
[NASA-SP-7039(33)] 18 p2580 N88-25386
Wind tunnel wall interference (January 1980 - May 1988): A selected, annotated bibliography
[NASA-TM-4061] 19 p2604 N88-25486
Ocean, Wave, and Tidal Energy Systems: Current abstracts
[DE88-008299] 19 p2687 N88-25973
Proceedings of the Workshop on the Assessment of Crew Workload Measurement Methods, Techniques and Procedures. Volume 2: Library references
[AD-A191209] 19 p2710 N88-26101
A bibliography and author index for electrical discharges in vacuum (1897-1986)
[DE88-008744] 20 p2794 N88-26579
Aerospace medicine and biology: A continuing bibliography with indexes (supplement 313)
[NASA-SP-7011(313)] 20 p2832 N88-26800
Aeronautical engineering: A continuing bibliography with indexes
[NASA-SP-7037(229)] 21 p2891 N88-27163
Technology for large space systems: A bibliography with indexes (supplement 18)
[NASA-SP-7046(18)] 21 p2901 N88-27214
Photovoltaic Energy. Electricity from Sunlight: A current awareness bulletin
[DE88-008289] 21 p2969 N88-27634
Aerospace Medicine and Biology: A continuing bibliography with indexes (supplement 314)
[NASA-SP-7011(314)] 21 p2988 N88-27742
Aeronautical engineering: A continuing bibliography with indexes
[NASA-SP-7037(228)] 22 p3037 N88-28031
Microgravity science and applications bibliography, 1987 revision
[NASA-TM-4067] 22 p3062 N88-28171
The anatomy of the gyroscope
[AGARD-AG-313] 22 p3079 N88-28287
Bibliography on tropical rain forests and the global carbon cycle. Volume 1: An introduction to the literature
[DE88-010761] 22 p3118 N88-28523
Bibliography of Lewis Research Center technical publications announced in 1987
[NASA-TM-100910] 22 p3162 N88-28832
Literature review: Validity and potential usefulness of psychomotor ability tests for personnel selection and classification
[AD-A193558] 23 p3241 N88-29287
Multicriteria integer programming for problems involving linear and nonlinear utility functions
[AD-A194530] 23 p3249 N88-29336
Topics in adaptive control and inference
[AD-A194718] 23 p3266 N88-29443
Bibliography of Soviet laser developments, number 88, March - April 1987
[AD-A195978] 24 p3378 N88-30116
Aerospace medicine and biology: A continuing bibliography with indexes (supplement 315)
[NASA-SP-7011(315)] 24 p3407 N88-30281
Publications of the Jet Propulsion Laboratory 1987
[NASA-CR-181198] 24 p3436 N88-30453

BICARBONATES
U CARBONATES

BICRYSTALS
Fatigue crack propagation in Al-Zn-Mg bicrystals and its dependence on the environment
05 p0605 N88-13707
Fatigue crack growth and fracture of copper-bismuth bicrystals 06 p0715 N88-14385
Free energy calculation via MD (molecular dynamics): Methodology and application to bicrystals
[DE88-002902] 09 p1256 N88-17532
Molecular dynamics study of high-temperature grain-boundary stability in a (100) sigma = 29 bicrystal model
[DE88-002955] 09 p1258 N88-17546

BIDIRECTIONAL REFLECTANCE
Cloud cover determination in polar regions from satellite imagery
[NASA-CR-181544] 04 p0471 N88-12908
Summary of along-track data from the Earth radiation budget satellite for several major desert regions
[NASA-RP-1197] 13 p1802 N88-20772
Determination and application of bidirectional solar-optical properties of fenestration systems
[DE88-010364] 20 p2820 N88-26727
Angular radiation models for Earth-atmosphere system. Volume 1: Shortwave radiation
[NASA-RP-1184] 21 p2976 N88-27677
Comparison of the bidirectional reflectance distribution function of various surfaces
[NASA-TM-101317] 22 p3153 N88-28760

BIFURCATION (MATHEMATICS)
U BRANCHING (MATHEMATICS)

BIG BANG COSMOLOGY
Particle physics and cosmology
[DE87-006400] 03 p0387 N88-12432
New cosmological scenario
[DE87-703357] 04 p0520 N88-13198
Cosmology in the plasma universe
[TRITA-EPP-87-07] 05 p0660 N88-14053
Big Bang Nucleosynthesis: Accelerator tests and can (UC OMEGA)(sub B) really be large
[DE88-003405] 11 p1570 N88-19386

Particle physics and cosmology
[DE88-004944] 13 p1854 N88-21096
BIGHTS
U BAYS (TOPOGRAPHIC FEATURES)
BIHARMONIC EQUATIONS
Approximate polynomial preconditioning applied to biharmonic equations on vector supercomputers
[NASA-TM-100217] 01 p0087 N88-10563
Grid generation for an advanced fighter aircraft
23 p3246 N88-29319
BIMETALS
Model for bimetallic interfaces, part 2
[DE88-702672] 22 p3157 N88-28787
BINARY ALLOYS
Electronic structure of crystalline NaSn
[DE87-702583] 01 p0102 N88-10609
Superconductivity of pseudobinary compounds A15 (V-Cr)3Si, (V-MO)3Si, Mo3(Si-Re), bombarded with fast neutrons 03 p0285 N88-11792
Structural analysis using X-ray scattering and neutron scattering on binary amorphous (Co,Cu)Ti alloys
[ETN-88-91487] 11 p1459 N88-18699
Processing, structure and properties of heavily deformed in situ composites
[AD-A189611] 13 p1742 N88-20416
Erosion in dual-phase microstructures
[DE88-004507] 13 p1743 N88-20421
On the theory of the conversion of metallic mixed phases 5: Fluctuations and nucleation in sub-cooled phases
[NASA-TT-20249] 14 p1890 N88-21296
Fundamental studies on high temperature deformation recrystallization, and grain growth of two-phase materials
[AD-A189725] 15 p2038 N88-22145
Corrosion and electrochemical behavior of binary magnesium alloys
[AD-A190624] 15 p2040 N88-22154
BINARY CODES
Bandwidth efficient block codes for M-ary PSK modulation
[NASA-CR-181543] 04 p0437 N88-12712
Parallel binary and parallel coded decimal time code formats
[AD-A190126] 17 p2384 N88-24170
BINARY DATA
SBNR (Signed Binary Number Representations) digital signal processor architecture
[AD-A184603] 03 p0364 N88-12290
Distributed fault tolerant embeddings of binary trees in hypercubes
[AD-A192929] 20 p2839 N88-26840
Use of a coherent square wave reference to demodulate BPSK (Binary Phase Shift Keying) carriers and a visual indicator of the quality of received QPSK (Quadrature Phase Shift Keying) carriers
[AD-A193528] 23 p3204 N88-29065
BINARY DIGITS
Extraction and evaluation of Boolean relations for the solution of linear programs in 0-1 variables, volume 1
[ENST-88E023-VOL-1] 02 p0227 N88-11430
Extraction and evaluation of Boolean relations for the solution of linear programs in 0-1 variables, volume 2
[ENST-88E023-VOL-2] 02 p0227 N88-11431
BINARY INTEGRATION
Very thin VLSI-layouts (Very Large Scale Integration-Layouts) of complete binary trees
[PB88-100847] 06 p0789 N88-14841
Analysis of binarized Hartley phase-only filter performance with respect to stochastic noise
[DE88-007604] 18 p2519 N88-24945
BINARY MIXTURES
NT EUTECTIC ALLOYS
NT EUTECTICS
DTA/DSC studies of phase equilibria in binary mixtures of barium carbonate with alkali carbonates
[DE87-001195] 02 p0194 N88-11213
Thermodynamic properties for natural gas binaries
[PB87-226833] 04 p0500 N88-13074
Laval nozzle flow of a binary, retrograde mixture
[MPIS-1/1987] 11 p1486 N88-18862
Exciton relaxation phenomena in a disordered system
14 p1978 N88-21802
BINARY STARS
NT CATACLYSMIC VARIABLES
NT DWARF NOVAE
NT ECLIPSING BINARY STARS
NT NEMESIS (STAR)
NT X RAY BINARIES
Binary Star Explorer 01 p0095 N88-10624
The nucleus of LT-5: An unusual triple system? --- planetary nebula
[PUBL-SER-C-FASC-11] 03 p0388 N88-12436
Differential B and V light curves of the bright BY Draconis star HD80715 04 p0509 N88-13130
Asynchronous rotation in close binary systems with circular orbits 04 p0509 N88-13131
PG 0308 + 096: A short-period white dwarf + dM binary with strongly modulated H-alpha emission
04 p0509 N88-13132
The Parkes radio survey of active chromosphere stars
04 p0511 N88-13141
IRAS and near IR observations of active binaries
04 p0518 N88-13186
Radio emission from RS CVn binaries: A 5 GHz VLA survey of 93 systems 04 p0519 N88-13191
Catalogue of chromospherically active binaries
04 p0520 N88-13192
A survey study of energy distribution in component stars of Algol-type binary systems 06 p0801 N88-14901
Mapping stellar surface features
09 p1262 N88-17564
The formation of single millisecond pulsars in globular clusters
[MPE-PREPRINT-97] 10 p1428 N88-18525
Very high energy gamma ray astrophysics
[DE88-005821] 13 p1854 N88-21095
The X-ray properties of AM Her stars
[MPE-PREPRINT-106] 16 p2289 N88-23704
A model for the X-ray binary 4U1820-30
[NASA-TM-101143] 17 p2451 N88-24562
Colliding stellar winds in the eclipsing Wolf-Rayet binary V444 Cygni
[NASA-CR-182937] 17 p2451 N88-24563
Duplicity in the solar neighborhood. Part 3: New spectroscopic elements for nine solar-type binary stars
[SER-C-PREPUBL-FASC-18-PT-3]
18 p2582 N88-25405
EXOSAT observations of Hercules X-1
[MPE-PREPRINT-119] 22 p3164 N88-28841
Mass transfer instabilities due to angular momentum flows in close binaries --- stars
[MPE-PREPRINT-113] 22 p3165 N88-28849
An upper limit on the primordial He4 abundance from speckle interferometric observations of muon Cassiopeiae 23 p3298 N88-29641
Binary star measurements using digital speckle interferometer of 6-m telescope
24 p3448 N88-30521
Duplicity in the solar neighborhood. Part 4: Spectroscopic orbits for four dwarf M stars
[SER-C-PREPUBL-FASC-21] 24 p3454 N88-30561
Duplicity in the solar neighborhood. Part 5: Spectroscopic orbit for the nearby double-lined solar-type star HR 8581
[SER-C-PREPUBL-FASC-23] 24 p3455 N88-30562
Activities in astrophysics
[INPE-4582-PRE/1316] 24 p3456 N88-30570
BINARY SYSTEMS (DIGITAL)
U DIGITAL SYSTEMS
BINARY SYSTEMS (MATERIALS)
NT BINARY ALLOYS
NT BINARY MIXTURES
NT EUTECTIC ALLOYS
NT EUTECTICS
Investigation of the deformation behavior of ferritic two-phase Fe-Ni-Al alloys with high concentrations of the intermetallic (Fe, Ni)Al phase at high temperatures
[ETN-87-90605] 03 p0288 N88-11812
The correlation between microstructure and thermomechanical properties of two-phase materials and porous sintered materials
[KFK-4205] 03 p0292 N88-11835
Retention processes in supercritical fluid chromatography
[DE88-000079] 04 p0413 N88-12559
Thermodynamic properties of supercritical mixtures
[DE88-000809] 04 p0413 N88-12562
Boundary effects on the drag of an oscillating sphere. Applications to the magnetic sphere rheometer. Attenuation and dispersion of acoustic waves in nematic liquid crystals 04 p0488 N88-13007
Electronic structure calculations and binding analyses for selected binary and ternary metal hydrides
[ETN-88-91087] 09 p1256 N88-17527
Demixing of aqueous polymer two-phase systems in low gravity
[NASA-TM-101141] 16 p2496 N88-24809
BINDERS (ADHESIVES)
U ADHESIVES
BINDERS (MATERIALS)
NT PROPELLANT BINDERS
NT SOLID ROCKET BINDERS
Polymer modified binders for bituminous or asphaltic paving layers
[PC-5] 02 p0153 N85-10958
Thermoplastic elastomers as LOVA (Low Vulnerability Ammunition) binders
[AD-A184350] 04 p0419 N88-12599
The use of NMR imaging to measure porosity and binder distributions in green-state and partially sintered ceramics
[DE88-003099] 08 p0972 N88-15881
Mechanism of and particle size effects on shock sensitivity of heterogeneous pressed explosives: Preliminary assessment of binderless RDX in fuze trains
[MRL-R-1077] 09 p1150 N88-16892
Thermoplastic elastomers as LOVA binders
[AD-A186563] 10 p1304 N88-17797
NMR (Nuclear Magnetic Resonance) imaging for detecting binder/plasticizers in green-state structural ceramics
[DE88-003111] 10 p1304 N88-17800
High yield synthesis of B4C/BN ceramic materials by pyrolysis of polymeric Lewis base adducts of decaborane(14)
[AD-A188154] 11 p1462 N88-18717
Increasing the rate at which ceramic castings undergo preliminary heat-treatment in an ultra-high frequency magnetic field 14 p1886 N88-21275
Effect of moisture level in PBXW-109(E) (plastic-bonded explosive) mixes on the aging of the cured explosive
[AD-A190200] 15 p2048 N88-22202
Determination of binder distributions in green-state ceramics by NMR imaging
[DE88-009990] 20 p2778 N88-26474
Alternate/modified binders for airfield pavements
[AD-A192781] 21 p2899 N88-27206
BINDING
Relativistic corrections for one- and two-photon matrix elements of weakly-bound systems
[NOTA-INTERNA-884] 07 p0929 N88-15645
Electronic structure calculations and binding analyses for selected binary and ternary metal hydrides
[ETN-88-91087] 09 p1256 N88-17527
Tight binding theory of semiconductors
10 p1415 N88-18447
BINOCULAR VISION
Biorhythms of binocular vision
20 p2830 N88-26788
BINOMIALS
A three-parameter generalisation of the beta-binomial distribution with applications
[AD-A185733] 06 p0768 N88-14720
Selecting the best binomial population: Parametric empirical Bayes approach
[AD-A193341] 23 p3269 N88-29450
Relaxed heaps: An alternative to fibonacci heaps
[AD-A194030] 23 p3272 N88-29470
BIOASSAY
DNA damage and repair in human skin in situ
[DE87-014288] 03 p0356 N88-12241
Superoxide dismutase assays
[AD-A183972] 03 p0356 N88-12242
Methods of quantifying and enhancing reactive oxygen species production 21 p2924 N88-27357
Genetic effects of low level microwave radiation
[AD-A192687] 21 p2984 N88-27722
BIOASTRONAUTICS
Lung function in simulated microgravity
12 p1654 N88-19907
BIOCHEMISTRY
NT BIOGEOCHEMISTRY
NT ENZYMOLOGY
NT PHYSIOCHEMISTRY
JPRS report: Science and technology. USSR: Life sciences
[JPRS-ULS-87-009] 04 p0473 N88-12915
JPRS report: Science and technology. USSR: Life sciences
[JPRS-ULS-87-011] 06 p0749 N88-14601
Human physical fields 06 p0750 N88-14609
A learning model as a basis for investigations of the effects of gravity on the learning processes and memory formulation 07 p0886 N88-15374
Experiments with rats flown aboard Cosmos-1667 biosatellite (main objectives, conditions and results)
07 p0893 N88-15414
Acid-base equilibrium and some rat blood parameters following exposure to hyperbaric oxygenation
07 p0894 N88-15420
Changes in functional parameters of animals during long-term inhalation of acetic acid
07 p0895 N88-15423
Neurochemical changes in hibernation
08 p1046 N88-16372
Biophysical and biochemical mechanisms in synaptic transmitter release
[AD-A187059] 09 p1199 N88-17184
Molecular mechanisms of neuronal responsivity
[AD-A187061] 09 p1199 N88-17185
Project Explorer takes its second step: GAS-608 in engineering development 10 p1288 N88-17707
Human blood glutamic acid level with exposure to high ambient concentrations of ammonia
10 p1361 N88-18134
New book on metabolic aspects of spaceflight stress
10 p1367 N88-18172

USSR report: Life sciences. Biomedical and behavioral sciences
[JPRS-UBB-87-010] 12 p1651 N88-19889
Survival under space vacuum: Biochemical aspects
12 p1657 N88-19930
USSR report: Life sciences. Biomedical and behavioral sciences
[JPRS-UBB-87-008] 12 p1662 N88-19966
Improved methods for high resolution electron microscopy
[DE88-005731] 13 p1774 N88-20609
JPRS report: Science and technology. USSR: Life sciences
[JPRS-ULS-88-004] 13 p1810 N88-20815
Technology '87. Research and Development Laboratory Technology Transfer Program
[DE88-003142] 13 p1852 N88-21084
Diagnostic studies of the HxOy-NzOy-O3 photochemical system using data from NASA GTE field expeditions
[NASA-CR-183038] 19 p2689 N88-25984
JPRS report: Science and technology. USSR: Life sciences
[JPRS-ULS-88-009] 20 p2829 N88-26785
Regulatory biochemical and metabolic responses in photoreceptors
[AD-A192898] 20 p2831 N88-26794
Methods of quantifying and enhancing reactive oxygen species production 21 p2924 N88-27357

BIOCONTROL SYSTEMS
Motion sickness: Quantitative, algorithmic malaise indication in real time
[AD-A189674] 15 p2101 N88-22518
The biomorphic model of the human operator controlling a single or a double integrator
[LR-505] 16 p2243 N88-23402

BIOCONVERSION
ECUT (Energy Conversion and Utilization Technologies) program: Biocatalysis Project
[NASA-CR-182917] 17 p2370 N88-24110

BIODEGRADATION
Shelf life degradation of selected anaerobic threadlocking adhesives at various storage temperatures
[AD-A187712] 11 p1461 N88-18711
Degradation of jet and missile fuels by aquatic microbial communities
[AD-A188065] 11 p1465 N88-18737
Biodegradation of JP-5 aviation fuel by subsurface microbial communities
[AD-A192743] 20 p2781 N88-26493

BIODYNAMICS
Facilitory effects of voluntary movements on vestibulomotor reaction 12 p1664 N88-19976
Analysis of head response to torso acceleration. Volume 2: Description of data retrieval, analysis and display software
[PB88-156765] 15 p2104 N88-22536
Using IMSL mathematical and statistical computer subroutines in physiological and biomechanical research
[AD-A192594] 21 p2995 N88-27765
Hierarchical structure in polymeric solids and its influence on properties
[AD-A194720] 23 p3197 N88-29029

BIOELECTRIC POTENTIAL
Electroencephalographic changes during equilibrium test in the presence of rhythmic photic interference
19 p2703 N88-26075

BIOELECTRICITY
Local human skin potential: Spatial distribution, magnitude and origin
[DE87-012882] 01 p0075 N88-10480
Critical phenomena and electromagnetic effects in biological membranes
[AD-A188156] 11 p1518 N88-19064
Changes in blood conductivity during immersion
12 p1663 N88-19969
Brain activity during tactical decision-making. Part 2: Probe-evoked potentials and workload
[AD-A188688] 12 p1667 N88-19954
Studies of the intact human brain: Implications for performance 21 p2977 N88-27684
CEEG dynamic brain mapping. A new method to evaluate brain function in different psychological and drug conditions 21 p2977 N88-27685
Fourth generation neurocognitive pattern analysis system 21 p2977 N88-27686
The application of non-stationary data analysis techniques in the identification of changes in the electroencephalogram associated with the onset of drowsiness 21 p2978 N88-27688
Neurophysiological patterns of operational fatigue: Preliminary results 21 p2981 N88-27703
Fighter pilot performance during airborne and simulator missions: Physiological comparisons
21 p2981 N88-27704
Event-related and steady potential changes in the brain related to workload during tracking
21 p2981 N88-27705
Neurophysiological precursors of accurate visuomotor performance 21 p2981 N88-27706
The neuroelectric selection of Naval aviation personnel: An evaluation 21 p2981 N88-27707
Evoked potential analysis of impact acceleration experiments 21 p2981 N88-27708
EEG indices of G-induced Loss Of Consciousness (G-LOC) 21 p2982 N88-27709
Detection of acceleration (+Gz) induced blackout by matched-filtering of visual evoked potentials
21 p2982 N88-27710
Electroencephalographic correlates of pilot performance: Simulation and in-flight studies
21 p2982 N88-27711
Motion evoked vestibular potentials
21 p2982 N88-27712
Measurement and classification of the mode of action of antidepressant drugs 21 p2983 N88-27714
Measurement of electrical activity in the CNS with cortical evoked potentials and EEG: Efficacy profiles of drugs using factor analysis 21 p2983 N88-27715
An approach to studying the effects of psychostimulants on cerebral electrical activity in the non-human primate
21 p2983 N88-27716
Spontaneous cerebral electrical activity during prolonged hypoglycemia: A quantitative study in humans
21 p2983 N88-27717
Correlation between EEG abnormal activity and aircraft accidents: A long term observation
21 p2984 N88-27719
Cytochrome electron transfer and biomolecular electronics
[AD-A195482] 24 p3406 N88-30277

BIOENGINEERING
NT ANTHROPOMETRY
NT BALLISTOCARDIOGRAPHY
NT BIOINSTRUMENTATION
NT BIOMETRICS
NT BIOTELEMETRY
NT BODY MEASUREMENT (BIOLOGY)
NT ECHOCARDIOGRAPHY
NT ELECTROCARDIOGRAPHY
NT ELECTROENCEPHALOGRAPHY
NT ELECTRORETINOGRAPHY
NT MAGNETOCARDIOGRAPHY
NT PLETHYSMOGRAPHY
ECUT (Energy Conversion and Utilization Technologies) program: Biocatalysis Project
[NASA-CR-182917] 17 p2370 N88-24110

BIOFEEDBACK
NT SENSORY FEEDBACK
Biofeedback control of alveolar carbon dioxide tension to eliminate hypocapnia in man in the presence of hypoxia 07 p0892 N88-15405
The effects of increased cognitive demands on autonomic self-regulation: An indicator of parallel processing in the brain 21 p2925 N88-27362

BIOGENESIS
U BIOLOGICAL EVOLUTION

BIOGENY
Exobiology and life science 07 p0883 N88-15358

BIOGEOCHEMISTRY
Biogeochemical cycling in the ocean. Part 1: Introduction to the effects of upwelling along the west coast of North America
[NASA-TM-88230] 07 p0882 N88-15349
International geosphere-biosphere program: A study of global change
[PB88-142393] 11 p1510 N88-19021
Global mixed-layer natural and anthropogenic fluxes
13 p1807 N88-20803

BIOGRAPHY
On the occasion of the 50th anniversary of the death of Professor Hugo Junkers
[MBB/LW-3016/S/PUB/201] 02 p0257 N88-11627
Messerschmitt-Boelkow-Blohm: Biography and history of a company 10 p1216 N88-17867

BIOINSTRUMENTATION
NT BIOTELEMETRY
High polymer sensor materials discussed
06 p0676 N88-14140
Vital signs rate meter
[AD-A187015] 09 p1198 N88-17183
Clinical applications of computerized thermography
17 p2330 N88-23915
Electrical and chemical sensors for biological cell research 19 p2669 N88-25866
Silver multi-layers for planar Ag/AgCl reference electrodes 19 p2672 N88-25883

BIOLOGICAL ACTIVITY
U ACTIVITY (BIOLOGY)

BIOLOGICAL ANALYSIS
U BIOASSAY

BIOLOGICAL CELLS
U CELLS (BIOLOGY)

BIOLOGICAL CLOCKS
U RHYTHM (BIOLOGY)

BIOLOGICAL EFFECTS
NT DESYNCHRONIZATION (BIOLOGY)
NT JET LAG
Master index for the carbon dioxide research state-of-the-art report series
[DE87-012757] 01 p0072 N88-10459
The photophysics and chemistry of PAH (Polycyclic Aromatic Hydrocarbons) compounds
[DE87-014455] 02 p0153 N88-10954
Photocatalytic electrochemistry at a biological-membrane metal-colloid interface
[DE87-009122] 02 p0166 N88-11041
Aerospace medicine and biology: A continuing bibliography with indexes
[NASA-SP-7011(303)] 02 p0217 N88-11367
Aerospace medicine and biology: A continuing bibliography with indexes
[NASA-SP-7011(304)] 04 p0474 N88-12922
TOMS as a monitor of the ultraviolet radiation environment: Applications to photobiology
05 p0617 N88-13785
Research for electric energy systems
[DE88-001733] 06 p0695 N88-14265
Aerospace medicine and biology: A continuing bibliography with indexes (supplement 305)
[NASA-SP-7011(305)] 06 p0752 N88-14616
Semi-arid ecosystem development as a function of resource processing and allocation
[DE88-000890] 07 p0875 N88-15308
Biogeochemical cycling in the ocean. Part 1: Introduction to the effects of upwelling along the west coast of North America
[NASA-TM-88230] 07 p0882 N88-15349
JPRS report: Science and technology. USSR: Space Biology and Aerospace Medicine, volume 21, no. 3, May - June 1987
[JPRS-USB-88-001] 07 p0889 N88-15389
Karyometric evaluation of neuronal reactions of rat cerebral cortex to the combined effect of ionizing radiation, longitudinal accelerations and vibration
07 p0890 N88-15396
Nystagmometric distinctions of individuals regularly exposed to vibration 07 p0891 N88-15401
Distinctive changes in arterial pressure and blood flow in common carotid artery of monkeys flown aboard Cosmos-1514 biosatellite 07 p0892 N88-15404
Investigation of energy metabolism of biological systems in weightlessness 07 p0893 N88-15409
Third Soviet-French Symposium on Space Cytology
07 p0893 N88-15411
Simulation of effect on biological systems of impact wave from heavy charged particle track
07 p0896 N88-15429
New book on space ecology reviewed
07 p0897 N88-15434
Possible use of plasmids for study of effect of space flight factors on biological objects
08 p1046 N88-16319
Zero gravity and living organism
08 p1046 N88-16320
Aerospace medicine and biology: A continuing bibliography with indexes (supplement 307)
[NASA-SP-7011(307)] 08 p1049 N88-16332
Rapid hypothermia subsequent to oral nicotinic acid and immersion in warm (30C) water
[AD-A186458] 08 p1050 N88-16339
Radon Research Program, FY-1987
[DE88-002633] 09 p1188 N88-17120
Kinetic toxic aspect of potential use of sulfur hexafluoride in closed environments 10 p1362 N88-18142
Effect of external electrostatic field on catecholamine secretion by rat adrenals 10 p1366 N88-18166
Aerospace medicine and biology: A cumulative index to a continuing bibliography (supplement 306)
[NASA-SP-7011(306)] 10 p1369 N88-18180
Aerospace medicine and biology: A continuing bibliography with indexes (supplement 308)
[NASA-SP-7011(308)] 10 p1369 N88-18183
The ESA facility Biorack 12 p1652 N88-19897
Survival under space vacuum: Biochemical aspects
12 p1657 N88-19930
Cellular effects of heavy ions: Experimental results and theoretical approaches — space radiation
12 p1658 N88-19933
Radiation problems in manned space flight with a view to the Space Station 12 p1658 N88-19934
Effects of cosmic heavy ion radiation and space microgravity on plant systems 12 p1658 N88-19936
Organs and tissues regeneration in amphibia under the space flight conditions 12 p1660 N88-19951

Biorack experiments in Spacelab D-1 and TML-1: Further developments in gravitational biology
12 p1661 N88-19953
Nitrogen's biological effect on oxygen transport through hematoparenchymal barrier 12 p1662 N88-19967
Effects of whole-body irradiation with low-intensity microwaves on morphological, functional and cytochemical characteristics of leukocytes 12 p1663 N88-19971
Aerospace medicine and biology: A continuing bibliography with indexes (supplement 309)
[NASA-SP-7011(309)] 13 p1810 N88-20814
Protection against laser damage to human body reviewed 15 p2053 N88-22237
Behavior, physiology and energy deposition in rats chronically exposed to 2450 MHz radiation
[PB88-171418] 16 p2237 N88-23363
Aerospace medicine and biology: A continuing bibliography with indexes (supplement 310)
[NASA-SP-7011(310)] 16 p2238 N88-23369
Spectroradiometry in industrial safety
16 p2272 N88-23600
Aerospace medicine and biology: A continuing bibliography with indexes (supplement 311)
[NASA-SP-7011(311)] 17 p2382 N88-24161
A cardiostimulant protein from the Australian Red Waratah Sea anemone, Actinia tenebrosa
18 p2550 N88-25138
Aerospace medicine and biology: A continuing bibliography with indexes (supplement 312)
[NASA-SP-7011(312)] 18 p2551 N88-25141
Extremely Low Frequency (ELF) communications program: Non-ionizing electromagnetic radiation literature evaluation and assessment, 1986-1987 literature review
[AD-A192024] 19 p2642 N88-25677
Effect of long-term inhalation of acetic acid vapor on some functional parameters of man
19 p2705 N88-26084
Validation of maximum permissible concentration of urea in reclaimed potable water and evaluation of its biological effect 19 p2705 N88-26086
Interaction of biological systems with static and ELF electric and magnetic fields
[DE88-007951] 20 p2831 N88-26792
Aerospace medicine and biology: A continuing bibliography with indexes (supplement 313)
[NASA-SP-7011(313)] 20 p2832 N88-26800
Aerospace Medicine and Biology: A continuing bibliography with indexes (supplement 314)
[NASA-SP-7011(314)] 21 p2988 N88-27742
Physiological effects of extremely low frequency electric and magnetic fields
[DE88-752814] 22 p3132 N88-28620
Study of biological effects and radiation protection to future European manned space flights
[DGT-33061] 23 p3281 N88-29535
Bioeffects of electromagnetic waves
24 p3364 N88-30032
Aerospace medicine and biology: A continuing bibliography with indexes (supplement 315)
[NASA-SP-7011(315)] 24 p3407 N88-30281

BIOLOGICAL EVOLUTION
Analysis of laser extracted volatiles in carbonaceous chondrites 06 p0793 N88-14861
Publications of the exobiology program for 1986: A special bibliography
[NASA-TM-4029] 09 p1203 N88-17205
The evolution of glutathione metabolism in phototrophic microorganisms
[NASA-CR-182902] 19 p2695 N88-26015
LSU scientists discover evidence of large meteorite impacts on the early earth 24 p3441 N88-30480

BIOLOGICAL MODELS
U BIONICS

BIOLOGICAL MODELS (MATHEMATICS)
A functional interpretation of the logistic equation
[REPT-87-037] 05 p0645 N88-13946
A theoretical concept for state changes and shape changes in weightlessness 07 p0884 N88-15365
Random truncation models and Markov processes
[CWI-MS-R8702] 09 p1232 N88-17389
Regulation of hemodynamics upon imitation of the transition to weightlessness (mathematical modeling)
13 p1810 N88-20817
Validation of mathematical model predictions of immersion survival times
[IAM-652] 14 p1952 N88-21635
Further development of a mathematical model for the specification of immersion clothing insulation
[IAM-653] 14 p1954 N88-21644
Models describing muscle behavior and control
[LR-522] 16 p2238 N88-23368
The biomorphic model of the human operator controlling a single or a double integrator
[LR-505] 16 p2243 N88-23402

BIOLOGICAL RHYTHM
U RHYTHM (BIOLOGY)

BIOLOGY
JPRS report: Science and technology. China
[JPRS-CST-88-003] 13 p1755 N88-20495

BIOLUMINESCENCE
Vanfront 3 expedition data report (USNS DE STEIGUER CRUISE 1202-82). Bioluminescence, hydrographic, nutrient, and satellite data from the Gulf of California (November-December 1981)
[AD-A185011] 05 p0620 N88-13805

BIOMAGNETISM
An innovative workstation 08 p1063 N88-16421
Auditory evoked magnetic fields in man
[PB88-193446] 20 p2831 N88-26796
SQUID (superconducting quantum interference device) arrays for simultaneous magnetic measurements: Calibration and source localization performance
[AD-A193815] 23 p3216 N88-29143
Methods and instrumentation for biomagnetism
[AD-A193811] 23 p3239 N88-29278

BIOMASS
Wheat production in controlled environments
[UAES-PAPER-3324] 03 p0361 N88-12270
Design concepts for bioreactors in space
09 p1198 N88-17179
Vegetation mapping using high resolution MSS (multispectral scanner) data: Canopy reflectance and shadow problems encountered and possible solutions
[DE88-004273] 14 p1939 N88-21574
The use of SLAR and SIRA imageries for the classification of forest types in tropical rain forests
17 p2356 N88-24036
Production costs of hydrocarbon fuels from biomass
[DE88-006667] 18 p2495 N88-24804
Proceedings of the 1987 Biomass Thermochemical Conversion Contractors' Review Meeting
[DE88-006730] 18 p2535 N88-25041
An advanced extruder-feeder biomass liquefaction reactor system 18 p2535 N88-25042
Molecular-beam, mass-spectrometric studies of wood vapor and model compounds over HZSM-5 catalyst
18 p2535 N88-25044
Low-temperature thermochemical conversion of high moisture biomass feedstocks 18 p2536 N88-25047
Evaluation of the grassy biomass in the Sahelian zone in the South Tamesna region (Niger): Prospects and limits of use of SPOT data 22 p3092 N88-28359
Study of the spectral response of soybeans
[INPE-4592-PRE/1322] 24 p3387 N88-30174

BIOMASS ENERGY PRODUCTION
Biomass recycle as a means to improve the energy efficiency of CELSS algal culture systems
03 p0358 N88-12254
A process study of the biothermal conversion of water hyacinths to methane
[DE88-000554] 06 p0730 N88-14486
Alternative Energy in the Midwest: Research and Applications. Conference Proceedings, Rosemont, Illinois, March 19-20, 1987
[PB88-142278] 11 p1509 N88-19015
Proceedings of the 1987 Biomass Thermochemical Conversion Contractors' Review Meeting
[DE88-006730] 18 p2535 N88-25041
An advanced extruder-feeder biomass liquefaction reactor system 18 p2535 N88-25042
Low pressure entrained flow pyrolysis of biomass to produce liquid fuels 18 p2535 N88-25043
Molecular-beam, mass-spectrometric studies of wood vapor and model compounds over HZSM-5 catalyst
18 p2535 N88-25044
Upgrading pyrolysis vapors to aromatic gasoline with zeolite catalysis at atmospheric pressure
18 p2536 N88-25045
Low-temperature thermochemical conversion of high moisture biomass feedstocks 18 p2536 N88-25047
Technical and economic evaluation of emerging biomass pyrolysis processes for gasoline production
18 p2536 N88-25048
Bench-scale studies on fluid-bed pyrolysis of wood using different contact gases 18 p2536 N88-25049
An outdoor test facility for the large-scale production of microalgae
[DE88-001146] 21 p2984 N88-27723

BIOMECHANICS
U BIODYNAMICS

BIOMEDICAL DATA
Human respiratory responses during high performance flight
[AGARD-AG-312] 04 p0474 N88-12923
USSR report: Life sciences. Biomedical and behavioral sciences
[JPRS-UBB-87-010] 12 p1651 N88-19889
Results of medical research conducted in 1985 during long-term spaceflights 19 p2702 N88-26070
Use of principal component method for analysis of multidimensional quantitative data in biomedical investigations 19 p2706 N88-26089
Biomedical aspects of military operations at high altitude
[AD-A192677] 22 p3132 N88-28619

BIOMETRICS
NT ANTHROPOMETRY
NT BALLISTOCARDIOGRAPHY
NT BODY MEASUREMENT (BIOLOGY)
NT ECHOCARDIOGRAPHY
NT ELECTROCARDIOGRAPHY
NT ELECTROENCEPHALOGRAPHY
NT ELECTRORETINOGRAPHY
NT MAGNETOCARDIOGRAPHY
NT PLETHYSMOGRAPHY
Air quality and human performance, chapter 16
[AD-A188335] 12 p1666 N88-19988
Mental-State Estimation, 1987
[NASA-CP-2504] 16 p2239 N88-23370
An overview of current approaches and future challenges in physiological monitoring
16 p2239 N88-23371
Toward a mathematical formalism of performance, task difficulty, and activation 16 p2239 N88-23372
Vagal tone as an index of mental state
16 p2239 N88-23373
Challenges of physiological monitoring in a Navy operational setting 16 p2239 N88-23374
Attention, effort, and fatigue: Neuropsychological perspectives 16 p2241 N88-23387
C3 generic workstation: Performance metrics and applications 16 p2242 N88-23397
Computer resource management technology program (PE 64740F). Task no. 9: Advanced user authentication
[PB88-183066] 18 p2555 N88-25163
Method for measuring absolute linear parameters of chromosomes 19 p2707 N88-26095

BIONICS
Multiaperture optical system research
[AD-A188211] 11 p1549 N88-19267
Complex sound processing: An interdisciplinary approach
[AD-A189782] 15 p2102 N88-22523

BIOPHYSICS
NT HEALTH PHYSICS
NT PUBLIC HEALTH
A physico-chemical study of some areas of fundamental significance to biophysics
[DE87-013457] 02 p0217 N88-11365
JPRS report: Science and technology. USSR: Life sciences
[JPRS-ULS-87-013] 06 p0750 N88-14608
Biophysical and biochemical mechanisms in synaptic transmitter release
[AD-A187059] 09 p1199 N88-17184
Long term synaptic plasticity and learning in neuronal networks
[AD-A186834] 09 p1199 N88-17186
Evaluation of spare room in cerebrospinal system using noninvasive methods 10 p1361 N88-18137
Two-dimensional static otolith model
10 p1367 N88-18167
Critical phenomena and electromagnetic effects in biological membranes
[AD-A188156] 11 p1518 N88-19064
USSR report: Life sciences. Biomedical and behavioral sciences
[JPRS-UBB-87-008] 12 p1662 N88-19966
Biophysical applications of solid state and tritium NMR
[DE88-005328] 13 p1808 N88-20806
JPRS report: Science and technology. USSR: Life sciences
[JPRS-ULS-88-004] 13 p1810 N88-20815
Synapses that compute motion
[AD-A190389] 15 p2116 N88-22607
JPRS report: Science and technology. USSR: Life sciences
[JPRS-ULS-88-009] 20 p2829 N88-26785
Transient interaction of electromagnetic pulses in dielectrics and microwave biophysics
[AD-A195687] 24 p3360 N88-30008

BIOPOLYMER DENATURATION
Estimations of gravitational effects on thermal denaturation process in a biopolymer
03 p0318 N88-12013

BIOPOLYMERS
NT CARBONIC ANHYDRASE
NT CATALASE
NT CHOLINESTERASE
NT CYTOCHROMES
NT DEOXYRIBONUCLEIC ACID
NT ENZYMES
NT FIBRINOGEN
NT HEMOGLOBIN
NT NUCLEIC ACIDS
NT PROTEINS
NT RIBONUCLEIC ACIDS

Estimations of gravitational effects on thermal denaturation process in a biopolymer
03 p0318 N88-12013
Calculation of far infrared absorption in B poly(dA) poly(dT)
[AD-A193128] 21 p2918 N88-27318

BIOPROCESSING
Space Bioreactor Science Workshop
[NASA-CP-2485] 09 p1196 N88-17168
Design concepts for bioreactors in space
09 p1198 N88-17179
Cell culture experiments planned for the space bioreactor 09 p1198 N88-17180
Cell cultures in space From basic research to biotechnology 2 12 p1660 N88-19948
French evaluation of Japanese biosensors
16 p2184 N88-23020
Separation of biological materials in microgravity
[NASA-TM-101142] 17 p2331 N88-23916

BIOREACTORS
Sunlight supply and gas exchange systems in microalgal bioreactor 03 p0359 N88-12258
Space Bioreactor Science Workshop
[NASA-CP-2485] 09 p1196 N88-17168
Suspension cell culture in microgravity and development of a space bioreactor 09 p1196 N88-17169
Space bioreactor Design/process flow
09 p1197 N88-17170
Bioreactor design concepts 09 p1197 N88-17171
Computer control of a microgravity mammalian cell bioreactor 09 p1197 N88-17172
Shear and mixing effects on cells in agitated microcarrier tissue culture reactors 09 p1197 N88-17173
Some process control/design considerations in the development of a microgravity mammalian cell bioreactor 09 p1197 N88-17174
Nutrient requirements and other factors involved in the culture of human kidney cells on microcarrier beads
09 p1197 N88-17176
Potential use of the bioreactor to determine effects of microgravity and other environmental parameters on growth of hybridoma cells 09 p1198 N88-17178
Design concepts for bioreactors in space
09 p1198 N88-17179
Aspects of bioregenerative life support systems
12 p1655 N88-19917

BIOREGENERATION
U REGENERATION (PHYSIOLOGY)

BIOREGENERATIVE LIFE SUPPORT SYSTEMS
U CLOSED ECOLOGICAL SYSTEMS

BIORHYTHMS
U RHYTHM (BIOLOGY)

BIOSATELLITES
Space biology and medicine 08 p1006 N88-16098

BIOSENSORS
U BIOINSTRUMENTATION

BIOSIMULATION
U BIONICS

BIOSPHERE
Remote sensing of the biosphere
[NASA-CR-182382] 07 p0871 N88-15281
New book on space ecology reviewed
07 p0897 N88-15434
International geosphere-biosphere program A study of global change
[PB88-142393] 11 p1510 N88-19021
The seasonal exchange of carbon dioxide between the atmosphere and the terrestrial biosphere Extrapolation from site-specific models to regional models
[DE88-007870] 20 p2822 N88-26740

BIOSYNTHESIS
Synthesis of high molecular weight peptide polymers and copolymers containing L-dopa residues
[AD-A186462] 08 p0973 N88-15687
Life sciences experiments on stratospheric balloons and sounding rockets 08 p1033 N88-16262

BIOT METHOD
Evaluation of the biot coefficients
[AD-A191643] 18 p2570 N88-25265

BIOTECHNOLOGY
Preliminary study of a biotechnology research facility for microgravity, executive summary
[MATRA-EPT/AS/VT209/246/NT]
01 p0032 N88-10204
JPRS report Science and technology USSR Life sciences
[JPRS-ULS-87-012] 03 p0355 N88-12238
Biotechnology in western Europe
[PB88-105687] 07 p0883 N88-15360
Safety guidelines and procedures for bioscience-based industry and other applied microbiology
[PB87-140521] 08 p1045 N88-16316
Space Bioreactor Science Workshop
[NASA-CP-2485] 09 p1196 N88-17168
Advanced utilization of solar energy Utilization for biotechnology
[DE88-770031] 12 p1640 N88-19819
USSR report Life sciences Biomedical and behavioral sciences
[JPRS-UBB-87-010] 12 p1651 N88-19889
BIOTEX, a project for biotechnological basic experiments under microgravity --- Spacelab
12 p1652 N88-19899
Cell cultures in space From basic research to biotechnology 2 12 p1660 N88-19948
USSR report Life sciences Biomedical and behavioral sciences
[JPRS-UBB-87-008] 12 p1662 N88-19966
JPRS report Science and technology USSR Life sciences
[JPRS-ULS-88-002] 12 p1665 N88-19982
JPRS report Science and technology USSR Life sciences
[JPRS-ULS-88-004] 13 p1810 N88-20815
JPRS report Science and technology Japan
[JPRS-JST-88-001] 15 p2051 N88-22218
JPRS report Science and technology Japan
[JPRS-JST-87-026] 16 p2184 N88-23018
French evaluation of Japanese biosensors
16 p2184 N88-23020
North Carolina Biomolecular Engineering and Materials Applications Center (NC-BEMAC)
[AD-A190923] 16 p2237 N88-23364
Non-contact temperature measurements for biotechnology discipline working group
17 p2329 N88-23904
Proceedings of the American Society for Composites
[AD-A189861] 18 p2477 N88-24693
Carbon matrix composites prospective roles for biotechnology 18 p2477 N88-24694
Current and future molecular structures of aerospace organic matrix resins 18 p2477 N88-24695
Industrial perspective on current and future needs in aerospace matrix resin chemistry
18 p2477 N88-24696
Applications of biotechnology to synthetic chemistry for aerospace matrix resins development
18 p2478 N88-24697
The application of hydrocarbon bioconversion technology to aerospace materials production
18 p2478 N88-24698
Ecological risk factors related to environmental uses of genetically engineered organisms
[DE88-006674] 18 p2549 N88-25132
Research and development programs on advanced structural ceramics in Korea 19 p2633 N88-25620

BIOTELEMETRY
An innovative workstation 08 p1063 N88-16421

BIOTITE
An integrated study of the Alto Paranaiba Kimberlite Province, Minas Gerais, Brazil A possible tool for diamond exploration 17 p2355 N88-24031
The petrogenesis of oceanic kimberlites and included mantle megacrysts The Malaitan alnoite
24 p3397 N88-30232

BIPOLAR TRANSISTORS
On the choice of a element low-noise preamplifier on bipolar transistors
[DE88-700639] 10 p1322 N88-17904
Development of a planar heterojunction bipolar transistor for very high speed logic
[AD-A188137] 11 p1478 N88-18820
Determination of distributed resistance of base of bipolar transistors measuring noise spectral densities
[DE88-700197] 11 p1479 N88-18829
Microelectronic applications of the conductor-thin insulator-semiconductor (CIS) structure
11 p1560 N88-19341
Technology development of a planar BiPolar transistor
[AD-A188761] 12 p1623 N88-19708
Solid-state traveling wave amplifiers based on multi-stream instability
[AD-A189566] 12 p1624 N88-19718
Quartz oscillator analysis
[DE88-005886] 13 p1764 N88-20550
Neutron effects on the electrical and switching characteristics of NPN bipolar power transistors
17 p2431 N88-24463
Joint services electronics program research in electronics
[AD-A192206] 18 p2504 N88-24857
Improved description of base dynamics in the modeling of bipolar transistors
[PB88-181516] 19 p2732 N88-26229
Resonant tunneling transistors and resonant tunneling hot electron spectroscopy 20 p2866 N88-27018

BIPOLARITY
Small scale bipolar nickel-hydrogen testing
[NASA-TM-100936] 18 p2538 N88-25059

BIPROPELLANTS
U LIQUID ROCKET PROPELLANTS

BIRD-AIRCRAFT COLLISIONS
Analysis of bird strikes to UK registered aircraft 1985 (civil aircraft over 5700 kg maximum weight
[CAA-PAPER-87012] 09 p1115 N88-16684
Protected areas with enhanced bird-aircraft collision risk in the Federal Republic of Germany
[GEOPHYSBDBW-FM-209] 11 p1437 N88-18576
Lapwings and birdstrikes The biology of the lapwing Vanellus vanellus in relation to the birdstrike hazard it presents
[CAA-PAPER 87015] 14 p1865 N88-21142
The design and testing of aero engines to minimise hazard from birds
[PNR90436] 22 p3040 N88-28049

BIRDS
NT CHICKENS
NT WATERFOWL
Compilation of 1986 annual reports of the Navy ELF (Extremely Low Frequency) communications system ecological monitoring program, volume 3
[AD-A184563] 03 p0306 N88-11932
Lapwings and birdstrikes The biology of the lapwing Vanellus vanellus in relation to the birdstrike hazard it presents
[CAA-PAPER-87015] 14 p1865 N88-21142
Motor theory of auditory perception
[AD-A192095] 18 p2550 N88-25136
Survey for least bell's vireo in riparian habitat on Vandenberg Air Force Base, Santa Barbara County, California
[NASA-TM-100984] 20 p2822 N88-26744

BIREFRINGENCE
NT KERR ELECTROOPTICAL EFFECT
Improper ferroelectricity A theoretical and experimental study
[AD-A184614] 03 p0381 N88-12397
Spectral contents readout of birefringent sensors
[NASA-CR-179430] 13 p1784 N88-20673
Multiple scattering of polarized light in cirrus clouds
13 p1801 N88-20768
Peturbational analysis of the curved anisotropic optical fiber for the birefringence due to the geometry
[PB88-171848] 19 p2726 N88-26189
Theory of acoustoplasticity and ultrasonic measurements of residual stresses
22 p3087 N88-28328

BISMUTH
Fatigue crack growth and fracture of copper-bismuth bicrystals 06 p0715 N88-14385

BISMUTH COMPOUNDS
NT BISMUTH OXIDES
NT BISMUTH SULFIDES
Altered and enhanced iodargyrite with bismuth triiodide for use in precipitation enhancement operations
[AD-A185229] 05 p0561 N88-13419
Photorefractive damage mechanism in electro-optic materials
[AD-A194560] 23 p3282 N88-29543

BISMUTH OXIDES
Holographically correcting synthetic aperture aberrations
[AD-A189510] 12 p1692 N88-20123
Properties of superconductors with strong electron-phonon interaction 14 p1974 N88-21779

BISMUTH SULFIDES
Activities of As, Sb, Bi and Pb in copper mattes and their effects on impurity elimination
[TKK-V-A10(1988)] 15 p2041 N88-22165

BISTABLE CIRCUITS
Applications of optical computing to problems with symbolic computations
[AD-A189772] 15 p2106 N88-22548
Optical bistable behavior of a planar quasi-waveguide interferometer made with a conjugated organic polymer film
[AD-A194349] 22 p3152 N88-28756

BISTATIC RADAR
U MULTISTATIC RADAR

BISTATIC REFLECTIVITY
Active and passive remote sensing of ice
[AD-A186685] 09 p1195 N88-17162

BIT ERROR RATE
Program description of FIBRAM A radiation attenuation model for optical fibers
[PB87-230686] 06 p0690 N88-14229
Implementation of encoders and decoders for Reed-Solomon codes
[PB88-126628] 10 p1387 N88-18286
Digital bit error rate estimator for telemetry links
[INPE-4351-TDL/295] 12 p1598 N88-19563
Evaluating the performance of the LPC (Linear Predictive Coding) 2.4 kbps (kilobits per second) processor with bit errors using a sentence verification task
[AD-A188573] 12 p1620 N88-19686

Effect of atmospheric turbulence on the bit error probability of a space to ground near infrared laser communications link using binary pulse position modulation and an avalanche photodiode detector
[NASA-TM-100699] 14 p1873 N88-21189
Direct bit detection receiver noise performance analysis for 32-PSK and 64-PSK modulated signals
[AD-A190009] 15 p2056 N88-22256
The bit-error rate performance of a satellite microwave matrix switch
[NASA-TM-100285] 16 p2167 N88-22920
Interleaver design for trellis-coded differential 8-PSK modulation with non-coherent detection
19 p2648 N88-25719
An error floor in tone calibrated transmission
19 p2649 N88-25729
Error performance of voice band data signals with an overloaded delta modulator
[FEL-1987-05] 20 p2792 N88-26562
A new code for Galileo 22 p3065 N88-28186

BIT SYNCHRONIZATION
Direct bit detection receiver performance analyses for 8-DPSK (Differential Phase Shift Keyed) modulated signals operating with improper carrier phase synchronization
[AD-A193839] 22 p3070 N88-28220

BITS
Digital video bit-rate reduction: DPCM for sub-Nyquist PAL
[BBC-RD-1987/16] 05 p0573 N88-13494
Direct bit detection receiver noise performance analysis for 32-PSK and 64-PSK modulated signals
[AD-A190009] 15 p2056 N88-22256

BITUMENS
Application of high performance liquid chromatography to the fast determination of bitumen generic composition
[PC-2] 02 p0145 N88-10911
Colloidal structure of bitumens. Relationship between composition-structure behavior
[PC-4] 02 p0146 N88-10912
Polymer modified binders for bituminous or asphaltic paving layers
[PC-5] 02 p0153 N88-10958
Aviation turbine fuels from tar sands bitumen and heavy oils. Part 2: Laboratory sample production
[AD-A185744] 06 p0687 N88-14211
Evaluation of bituminous materials used in pavement recycling projects at Tyndall, MacDill, and Hurlburt Air Force Bases
[AD-A188068] 10 p1317 N88-17871
Aviation turbine fuels from tar sands bitumen and heavy oils. Part 3: Laboratory sample production
[AD-A189278] 13 p1753 N88-20484
Turbine fuels from tar sands bitumen and heavy oil. Volume 2, phase 3: Process design specifications for a turbine fuel refinery charging San Ardo heavy crude oil
[AD-A190120] 16 p2163 N88-23011

BIVARIATE ANALYSIS
On the extreme points of the set of all 2xn bivariate positive quadrant dependent distributions with fixed marginals and some applications
[AD-A186316] 07 p0911 N88-15521
Measuring the dependence between two point processes through confidence intervals for the second order distribution
[AD-A186735] 08 p1074 N88-16481
An APL function for bivariate normal probabilities
[AD-A186535] 09 p1232 N88-17382

BL LACERTAE OBJECTS
Relativistic jet models for the BL Lacertae object Mrk 421 during three epochs of observation
[NASA-TM-89727] 13 p1853 N88-21090

BLACK AND WHITE PHOTOGRAPHY
Use of SPOT panchromatic imagery to update forest maps of northern Quebec, Canada
03 p0344 N88-12172
Application of 35mm EM aerial reconnaissance photographic format of the municipality of Ubatuba (SP)
19 p2684 N88-25953

BLACK BODY RADIATION
Numerical calculations of dopent diffusion involving flashlamp heating of silicon 21 p2929 N88-27384
Overview and future direction for blackbody solar-pumped lasers
[NASA-TM-100621] 21 p2955 N88-27553

BLACK BRANT SOUNDING ROCKETS
Past, present and future role of Black Brant rocket systems to support international space science programs 08 p1034 N88-16272

BLACK HOLES (ASTRONOMY)
Photohydrodynamical processes near compact objects
11 p1569 N88-19390

BLACK SEA
Geological evolution and analysis of confirmed or suspected gas hydrate localities. Volume 2: Basin analysis, formation and stability of gas hydrates in the Black Sea
[DE88-001052] 18 p2532 N88-25023

BLACKOUT (PHYSIOLOGY)
F-16 control stick response during +Gz-induced loss of consciousness
[AD-A184107] 04 p0400 N88-12491
Detection of acceleration (+Gz) induced blackout by matched-filtering of visual evoked potentials
21 p2982 N88-27710

BLADDERS (MECHANICS)
U DIAPHRAGMS (MECHANICS)

BLADE SLAP
U BLADE-VORTEX INTERACTION

BLADE SLAP NOISE
Helicopter main-rotor noise: Determination of source contributions using scaled model data
[NASA-TP-2825] 20 p2848 N88-26907

BLADE TIPS
Modeling and measurement of heat transfer on turbine blade tips 01 p0006 N88-10032
Heat transfer in the tip region of a rotor blade simulator 02 p0186 N88-11159
The physics and mathematical description of the Achilles heel of stationary wind turbine aerodynamics: The tip flow
[R-812-D] 03 p0260 N88-11635
Calculation of helicopter rotor blade/vortex interaction by Navier-Stokes procedures
[NASA-CR-177441] 05 p0540 N88-13291
Aerodynamic design of first stage turbines for small aero engines. 06 p0713 N88-14370
An experimental investigation of the chopping of helicopter main rotor tip vortices by the tail rotor. Part 2 High speed photographic study
[NASA-CR-177457] 09 p1114 N88-16678
Inflow measurements made with a laser velocimeter on a helicopter model in forward flight. Volume 4: Tapered planform blades at an advance ratio of 0.15
[NASA-TM-100544] 16 p2156 N88-22863
Recent advances in capacitance type of blade tip clearance measurements
[NASA-TM-101291] 19 p2603 N88-25460
Investigation of helicopter rotor blade/wake interactive impulsive noise
[NASA-CR-177435] 23 p3171 N88-28882
Computational methods for the problems of the tip vortex
[NASA-CR-181436] 24 p3320 N88-29/75

BLADE-VORTEX INTERACTION
Results of the 1986 NASA/FAA/DFVLR main rotor test entry in the German-Dutch wind tunnel (DNW)
[NASA-TM-100507] 04 p0487 N88-13003
Calculation of helicopter rotor blade/vortex interaction by Navier-Stokes procedures
[NASA-CR-177441] 05 p0540 N88-13291
Lift distribution and velocity field measurements for a three-dimensional, steady blade/vortex interaction
[NASA-TM-100013] 07 p0815 N88-14962
The development of CFD methods for rotor applications 09 p1105 N88-16627
Recent Langley helicopter acoustics contributions
09 p1109 N88-16646
An experimental investigation of the chopping of helicopter main rotor tip vortices by the tail rotor. Part 2: High speed photographic study
[NASA-CR-177457] 09 p1114 N88-16678
Acoustic measurements from a rotor blade-vortex interaction noise experiment in the German-Dutch Wind Tunnel (DNW)
[NASA-TM-4024] 11 p1542 N88-19218
Advancing-side directivity and retreating-side interactions of model rotor blade-vortex interaction noise
[NASA-TP-2784] 15 p2131 N88-22710
Theory of sound production by vortex-airfoil interaction
[AD-A193386] 21 p3012 N88-27875
Transonic blade-vortex interactions
22 p3037 N88-28035
Investigation of helicopter rotor blade/wake interactive impulsive noise
[NASA-CR-177435] 23 p3171 N88-28882

BLADES
Euler solution of multiblade rotor flow
[NASA-TM-100014] 06 p0704 N88-14322
A multistage mesh generator for solving the average-passage equation system
[NASA-CR-179539] 08 p0951 N88-15769
Vibration and flutter characteristics of the SR7L large-scale propfan
[NASA-TM-100272] 10 p1344 N88-18036
Analysis of rotating flexible blades using MSC/NASTRAN 16 p2222 N88-23259
Cascades with harmonically oscillating blades in supersonic flow
[NASA-TT-20323] 19 p2599 N88-25446

BLANKETS (FUSION REACTORS)
Technical evaluation of major candidate blanket systems for fusion power reactor
[DE87-752989] 02 p0239 N88-11512
Physics modeling support contract
[DE88-004039] 10 p1335 N88-17980
MHD (magnetohydrodynamic) thermal hydraulic analysis of three-dimensional liquid metal flows in fusion blanket ducts
[DE88-009929] 19 p2731 N88-26219
Blanket technology experiments at Argonne National Laboratory
[DE88-010006] 19 p2731 N88-26220
Reactor applications of the Compact Fusion Advanced Rankine (CFAR) cycle for a D-T tokamak fusion reactor
[DE88-011351] 22 p3153 N88-28762

BLASIUS FLOW
A new laminar water tunnel to study the transition process in a blasius layer and in a separation bubble and a new tool for industrial aerodynamics and hydrodynamic research 16 p2204 N88-23150

BLAST LOADS
Composite materials applications program at the US Army Ballistic Research Laboratory: Work in progress
04 p0428 N88-12651
A summary of experimental results on square plates and stiffened panels subjected to air-blast loading
09 p1178 N88-17057
Mechanical impact: Theoretical simulation and correlation 09 p1179 N88-17060
Misty picture weather-watch and microbarograph project: Experiments 9412-14-18
[DE88-003949] 11 p1514 N88-19047
Buckling of blast loaded cylinder
[AD-A190124] 15 p2076 N88-22376

BLASTOFF
U ROCKET LAUNCHING

BLEED-OFF
U PRESSURE REDUCTION

BLENDS
U MIXTURES

BLINDNESS
NT FLASH BLINDNESS
Maps for the blind and methods of their production
16 p2227 N88-23296

BLOCH BAND
Bloch oscillations in small Josephson junctions: Their manifestation in switching effects
14 p1969 N88-21756

BLOCK DIAGRAMS
A new state space model for the NASA/JPL 70-meter antenna servo controls 04 p0436 N88-12702

BLOCKING
Adaptive line of sight algorithms
[DE87-014275] 01 p0081 N88-10523
Persistence characteristics of 500 mb blocking and zonal flows in the mid-latitudes of the Northern and Southern Hemispheres 10 p1353 N88-18088
Impact of blocking policies in closed, exponential and symmetrical ring networks
[FUB-8-1986] 14 p1960 N88-21693

BLOCKS
Analysis of the decomposition of transparent polymer materials (blocks) under the action of laser beams in free generation mode
[AD-A187090] 09 p1147 N88-16873
A new block solver for large, full, unsymmetric, complex systems of linear algebraic equations
[AD-A190590] 16 p2256 N88-23483

BLOOD
NT FIBRINOGEN
Scotopic sensitivity with 10 percent oxygen
[AD-A183973] 03 p0356 N88-12243
An assessment of clinical chemical sensing technology for potential use in space station health maintenance facility
[NASA-CR-172013] 04 p0475 N88-12926
Oxygen transport during exercise at extreme simulated altitude: Operation Everest 2
[AD-A185720] 06 p0752 N88-14620
Physiological and biochemical aspects of toxic effects of oxidants in man's environment (air, water)
07 p0890 N88-15391
Cosmonauts' hormonal responses after brief spaceflights 07 p0890 N88-15394
Role of hemoglobin affinity for oxygen in efficiency of blood respiratory function 07 p0892 N88-15406
Operation Everest 2: Comparison of four instruments for measuring blood oxygen saturation
[AD-A186456] 08 p1049 N88-16337
Significance of nutrition to change in human carbohydrate and lipid metabolism under emotional stress 19 p2703 N88-26073

BLOOD CELLS
NT ERYTHROCYTES
NT LEUKOCYTES
NT LYMPHOCYTES
Blood redistribution in man with lower body negative pressure 07 p0891 N88-15397

BLOOD CIRCULATION
NT BRAIN CIRCULATION
NT CORONARY CIRCULATION
NT PERIPHERAL CIRCULATION
NT PULMONARY CIRCULATION
Polycythemia and hydration status: Effects on blood volume and thermoregulation during exercise-heat stress [AD-A185946] 07 p0888 N88-15383
Human and animal hypovolemic reactions to increasing +Gz accelerations 07 p0890 N88-15395
Blood redistribution in man with lower body negative pressure 07 p0891 N88-15397
Human metabolism and peripheral circulation during antiorthostatic hypokinesia 07 p0891 N88-15398
Distinctive changes in arterial pressure and blood flow in common carotid artery of monkeys flown aboard Cosmos-1514 biosatellite 07 p0892 N88-15404
Changes in regional and central hemodynamics during seven-day water immersion 07 p0895 N88-15421
Exercise thermoregulation after prolonged wakefulness [AD-A186224] 08 p1048 N88-16327
Late radiation damage in bone, bone marrow and brain vasculature, with particular emphasis upon fractionation models [DE87-753039] 08 p1048 N88-16330
Effect of spaceflight factors on primate's blood circulation 10 p1359 N88-18124
Isotope methods of determining distribution and movement of blood in the body 10 p1362 N88-18138
Comparative evaluation of orthostatic stability following immersion in horizontal and vertical positions 10 p1363 N88-18143
Effect of antiorthostatic position and different illumination on sensitivity of skin in upper half of the body to ultraviolet radiation 10 p1363 N88-18145
Improvement of human tolerance to head-pelvis (+Gz) accelerations by increasing hydration 10 p1364 N88-18153
Effect of exogenous cardiosynchronized counterpulsation on human regional and central hemodynamics 10 p1366 N88-18163
Response of coronary blood flow to step changes in plasma protein concentration in the isolated rat heart 12 p1651 N88-19892
Load and control of the cardiocirculatory system in weightlessness 12 p1656 N88-19922
Neuro-reflex mechanisms of circulation regulation in simulated microgravity 12 p1656 N88-19923
Physiological reactions upon controlled changes of blood distribution in humans 12 p1656 N88-19924
Nitrogen's biological effect on oxygen transport through hematoparenchymal barrier 12 p1662 N88-19967
Status of microcirculation in high-altitude blood loss 12 p1663 N88-19973
Effects of intense, time-constrained mental effort on hemodynamics and cardiovascular function 12 p1664 N88-19975
The effects of normal and therapeutic baths on the central vascular organs of persons with healthy hearts, as measured by X-ray [NASA-TT-20252] 13 p1811 N88-20818
Contribution of ultrasonic Doppler detection of circulating bubbles to human interventions under the sea and in space 19 p2697 N88-26029
Human hemodynamics during water immersion as related to position during submersion 19 p2703 N88-26071
Hemostasis parameters of individuals with neurocirculatory dystonia submitted to dry immersion 19 p2703 N88-26072
Respiration and oxygen tension in the blood of animals exposed to high pressures 20 p2830 N88-26790
The impact of hyperthermia and hypohydration on circulation, strength, endurance and health [AD-A192657] 22 p3131 N88-28615
Propranolol and the compensatory circulatory responses to orthostasis at high altitude [AD-A192675] 22 p3131 N88-28518
Variation of carotid flow under load, studied by the Doppler echo method --- acceleration tolerance [REPT-1149] 23 p3240 N88-29232

BLOOD COAGULATION
Role of carbon dioxide in correction of coagulation hemostasis under hypoxic conditions 10 p1365 N88-18160
Changes in hemostasis system of animals under conditions of granulocytopoiesis inhibition under effect of decreased barometric pressure 12 p1651 N88-19890
Distinctive features in blood clotting and fibrinolytic properties under effect of epinephrine in presence of hypoxia and hypercapnia 19 p2705 N88-26082
Hemorrhages and hemostasis in guinea pigs exposed to radiation at high altitude 19 p2705 N88-26083

BLOOD FLOW
Studies of the processing of single words using positron tomographic measures of cerebral blood flow change [AD-A184058] 03 p0356 N88-12244
Assessment of intercompartment fluid shifts by blood densitometry in astronauts 12 p1661 N88-19958
Potential applications of computational fluid dynamics to biofluid analysis [NASA-TM-100089] 14 p1911 N88-21422

BLOOD PLASMA
Polycythemia and hydration status: Effects on blood volume and thermoregulation during exercise-heat stress [AD-A185946] 07 p0888 N88-15383
Human and animal hypovolemic reactions to increasing +Gz accelerations 07 p0890 N88-15395
Role of testing total gas (O2 and CO2) tension of blood plasma in the study of human gas homeostasis 07 p0894 N88-15419
Response of coronary blood flow to step changes in plasma protein concentration in the isolated rat heart 12 p1651 N88-19892
Assessment of intercompartment fluid shifts by blood densitometry in astronauts 12 p1661 N88-19958
Changes in blood conductivity during immersion 12 p1663 N88-19969
Plasma cortisol, renin and aldosterone during an intense heat acclimation program [AD-A189387] 13 p1809 N88-20810
Hemostasis parameters of individuals with neurocirculatory dystonia submitted to dry immersion 19 p2703 N88-26072
Plasma volume expansion in rats: Effects on thermoregulation and exercise [AD-A192656] 22 p3130 N88-28606
Influence of altitude and caffeine during rest and exercise on plasma levels of proenkephalin peptide F [AD-A192659] 22 p3131 N88-28616

BLOOD PRESSURE
NT HYPERTENSION
NT LOWER BODY NEGATIVE PRESSURE
Distinctive changes in arterial pressure and blood flow in common carotid artery of monkeys flown aboard Cosmos-1514 biosatellite 07 p0892 N88-15404

BLOOD VESSELS
NT AORTA
NT ARTERIES
NT CAPILLARIES (ANATOMY)
NT VEINS

BLOOD VOLUME
Polycythemia and hydration status: Effects on blood volume and thermoregulation during exercise-heat stress [AD-A185946] 07 p0888 N88-15383
Human and animal hypovolemic reactions to increasing +Gz accelerations 07 p0890 N88-15395
Blood redistribution in man with lower body negative pressure 07 p0891 N88-15397
Distinctive changes in arterial pressure and blood flow in common carotid artery of monkeys flown aboard Cosmos-1514 biosatellite 07 p0892 N88-15404
Is ANF implied in the night attenuated renal response to central hypervolemia? 12 p1659 N88-19945
Plasma cortisol, renin and aldosterone during an intense heat acclimation program [AD-A189387] 13 p1809 N88-20810
Leg volume change under Lower Body Negative Pressure (LBNP) in dependence on stratification [DFVLR-FB-87-47] 16 p2238 N88-23367
Validation of a modified one-step rebreathing technique for non-invasive measurement of submaximal cardiac output [AD-A192852] 21 p2987 N88-27735
Plasma volume expansion in rats: Effects on thermoregulation and exercise [AD-A192656] 22 p3130 N88-28606
Alterations in cutaneous vasomotor regulation during acute and chronic hypoxia [AD-A192653] 22 p3131 N88-28612

BLOWDOWN WIND TUNNELS
The 0.6m x 0.6m trisonic test section (TMK) of DFVLR in Cologne-Porz, Federal Republic of Germany (status 1986) [ESA-TT-1052] 03 p0267 N88-11681
The vertical test section (VMK) of DFVLR in Cologne-Porz, Federal Republic of Germany (status 1986) [ESA-TT-1053] 03 p0267 N88-11682
The design and preliminary calibration of a boundary-layer flow channel [NASA-CR-178399] 04 p0394 N88-12457
The 30 x 30 inch wind tunnel [IC-AERO-87-01] 14 p1869 N88-21168
The transonic wind tunnel (TWB) at DFVLR, Brunswick (Federal Republic of Germany) [DFVLR-MITT-88-01] 16 p2164 N88-22909

BLOWERS
An experimental comparison of two designs of mercury propellant tank for use with an electric propulsion engine [RAE-TR-75109] 01 p0018 N88-10109
Measurement and analysis of the noise radiated by low Mach numbers centrifugal blowers [AD-A189226] 13 p1833 N88-20966

BLOWING
NT SPANWISE BLOWING
Experimental investigations on blunt bodies and corner configurations in hypersonic flow 05 p0530 N88-13225
Dimensions of ignition zones in blow-outs of combustible gases from rectangular and circular ports 07 p0918 N88-15577
An aerodynamic comparison of blown and mechanical high lift airfoils 10 p1272 N88-17606
Numerical study of delta wing leading edge blowing [NASA-CR-183101] 20 p2752 N88-26335

BLUE GREEN ALGAE
NT MICROCYSTIS
The usefulness of microalgal structures as an element of closed ecological systems like Aquarack and CELSS --- Controlled Ecological Life Support System (CELSS) 01 p0074 N88-10476
Food production and gas exchange system using blue-green alga (spirulina) for CELSS 03 p0358 N88-12253

BLUFF BODIES
Computational study of three-dimensional wake structures [REPT-2] 05 p0539 N88-13281
Wakes of two dimensional bluff bodies in subsonic flow. Influence of a separating plate and of a pulsed injection of momentum [IMFL-4200-86/75] 05 p0541 N88-13297
Separated flow 07 p0812 N88-14944
Numerical solutions of three-dimensional Navier-Stokes equations for closed-bluff bodies [NASA-CR-182359] 09 p1166 N88-1[illegible]
Experimental study of two-dimensional vortex patterns for impulsively started bodies in comparison with other configurations 11 p1435 N88-18562
Research on flow around bluff bodies, flow induced vibrations 14 p1864 N88-21135
Interaction of a two-dimensional bluff body and incompressible jet and annulus flows [AD-A190503] 15 p2064 N88-22310
Oscillating flow over bluff bodies in a U-shaped water tunnel 16 p2201 N88-23131
Measurements of aerodynamic forces on unsteadily moving bluff parachute canopies 16 p2202 N88-23137
Incompressible Euler solution on a multiblock grid around a car configuration [FFA-TN-1987-65] 18 p2457 N88-24586
Vortex methods for separated flows [NASA-TM-100068] 20 p2753 N88-26342

BLUNT BODIES
Calculation of aerodynamic heat transfer for blunt-nosed thin wings at different angles of attack at supersonic speeds [NASA-TT-20127] 02 p0123 N88-10776
Numerical study of supersonic flow around blunt bodies with extended needle nose 04 p0425 N88-12635
Experimental investigations on blunt bodies and corner configurations in hypersonic flow 05 p0530 N88-13225
The effects of sweep and bluntness on a glancing shock wave turbulent boundary layer interaction 05 p0531 N88-13227
A spatial marching technique for the inviscid blunt body problem 05 p0533 N88-13239
The role of computation fluid dynamics in aeronautical engineering (4). The development and applications of implicit TVD finite volume code 05 p0536 N88-13259
Studies of unsteadiness in boundary layers [AD-A185662] 06 p0703 N88-14315
The simulation of three-dimensional viscous supersonic flow past blunt bodies with a hybrid implicit/explicit finite difference method [DFVLR-FB-87-32] 08 p0950 N88-15765
Hypersonic blunt body computations including real gas effects [NASA-TM-100074] 10 p1400 N88-18344
A simplified streamline swallowing procedure for the windward meridian of axisymmetric blunt bodies [AD-A188413] 12 p1626 N88-19732
Nonaxisymmetric body supersonic aerodynamic prediction [AD-A189338] 13 p1716 N88-20259
Flight tests of external modifications used to reduce blunt base drag [NASA-TM-100433] 13 p1719 N88-20279

Interaction of a two-dimensional bluff body and incompressible jet and annulus flows
[AD-A190503] 15 p2064 N88-22310
Numerical study of unsteady viscous hypersonic blunt body flows with an impinging shock
[NASA-TM-100096] 15 p2122 N88-22650
High-resolution shock-capturing schemes for inviscid and viscous hypersonic flows
[NASA-TM-100097] 15 p2122 N88-22651
Relaxation scheme for compressible flows
19 p2640 N88-25663
The modified-fluid-in-cell method to which adaptive mesh and multigrid were applied
19 p2640 N88-25664
Navier-Stokes code NS3D for blunt bodies. Part 1: Analysis, results and verification
[DE88-010105] 19 p2666 N88-25855
A preliminary investigation of drag reduction and mechanism for a blunt body of revolution with slanted base
[NASA-TT-20349] 24 p3317 N88-29753

BMC
U BONE MINERAL CONTENT

BO-105 HELICOPTER
Test equipment with fiber optic data bus and laser gyro strapdown system LTN-90 for the helicopter BO-105
[ESA-TT-1038] 01 p0005 N88-10025
Sitting posture of pilots in the Boelkow 105c helicopter
[IZF-1986-22] 09 p1202 N88-17202
Helicopter main-rotor noise: Determination of source contributions using scaled model data
[NASA-TP-2825] 20 p2848 N88-26907

BODIES OF REVOLUTION
NT CONCENTRIC SPHERES
NT CONICAL BODIES
NT CYLINDRICAL BODIES
NT FALLING SPHERES
NT PARABOLIC BODIES
NT ROTATING CYLINDERS
NT ROTATING SPHERES
NT SLENDER CONES
NT SPHERES
NT TORUSES
Solution of geometrically nonlinear problem for reinforced shell of revolution having arbitrary shape
04 p0426 N88-12637
Similar solutions for viscous hypersonic flow over a slender three-fourths-power body of revolution
[NASA-TM-100205] 04 p0443 N88-12752
Numerical analysis of motion of solid bodies in atmosphere 08 p1079 N88-16505
Measurement of forces and moments on, and velocity about a body of revolution with an attached fin at angles of attack
[AD-A187796] 11 p1433 N88-18554
The Hamiltonian structure of nonlinear elasticity: The convective representation of solids, rods, and plates
[AD-A187200] 11 p1498 N88-18943
The effect of sting interference at low speeds on the drag coefficient of an ellipsoidal body using a magnetic suspension and balance system
[NASA-CR-181611] 13 p1718 N88-20274
Experiments to investigate the vortices shed from a submarine-like body of revolution
16 p2205 N88-23156
The use of fins to reduce the pressure drop in a rotating cavity with a radial flow
[PNR90465] 22 p3079 N88-28292
A preliminary investigation of drag reduction and mechanism for a blunt body of revolution with slanted base
[NASA-TT-20349] 24 p3317 N88-29753

BODY CENTERED CUBIC LATTICES
Computer simulations of knock-on processes in bcc Ta crystal
[DE87-752980] 02 p0246 N88-11554
Computer simulation of pencil glide in B.C.C. metals
[DE88-001802] 07 p0834 N88-15062

BODY FLUIDS
NT BLOOD
NT CEREBROSPINAL FLUID
NT FIBRINOGEN
NT SALIVA
NT URINE
Effect of spaceflight factors on primate hydration homeostasis 10 p1360 N88-18126
The precision of limits on bodily fluids when using beta-expectation inner tolerance limits
[AD-A187966] 10 p1369 N88-18185
Fluid volume changes in astronauts: How they fit our understanding of physiology 12 p1655 N88-19919
Estimation of body fluid shift by electrical impedance in various postures 12 p1661 N88-19956
Use of principal component method for analysis of multidimensional quantitative data in biomedical investigations 19 p2706 N88-26089

BODY KINEMATICS
Numerical solution of multibody systems in space applications 14 p1875 N88-21200

BODY MEASUREMENT (BIOLOGY)
NT ANTHROPOMETRY
Estimating the cost of mental loading in a bimodal divided-attention task: Combining reaction time, heart-rate variability and signal-detection theory
16 p2241 N88-23385
Physiological measures and mental-state assessment
16 p2242 N88-23392
Improvements in techniques of microwave thermography
[AD-A194613] 23 p3203 N88-29062
Improvements in techniques of microwave thermography
[AD-A193620] 23 p3239 N88-29276

BODY SWAY TEST
Electroencephalographic changes during equilibrium test in the presence of rhythmic photic interference
19 p2703 N88-26075

BODY TEMPERATURE
Human thermoregulatory model for whole body immersion in water at 20 and 28 C
[AD-A185052] 05 p0629 N88-13849
Infradian biorhythms of human vital signs
06 p0750 N88-14606
Biorhythmic aspects of intercontinental Antarctic adaptation 08 p1046 N88-16321
Influence of skeletal muscle glycogen on passive rewarming after hypothermia
[AD-A186451] 08 p1049 N88-16334
Rapid hypothermia subsequent to oral nicotinic acid and immersion in warm (30C) water
[AD-A186458] 08 p1050 N88-16339
Role of body fat in the prediction of the metabolic response for immersion in cold water
[AD-A186914] 09 p1198 N88-17182
The role of hydration on peripheral response to cold
[AD-A186448] 09 p1199 N88-17186
Vestibular response to caloric stimulation during orbital flight 12 p1658 N88-19939
Plasma cortisol, renin and aldosterone during an intense heat acclimation program
[AD-A189387] 13 p1809 N88-20810

BODY TEMPERATURE (NON-BIOLOGICAL)
U TEMPERATURE

BODY TEMPERATURE REGULATION
U THERMOREGULATION

BODY WEIGHT
Operation Everest 2: Nutrition and body composition
[AD-A186449] 08 p1049 N88-16333
Variability in intake and dehydration in young men during a simulated desert walk
[AD-A192654] 22 p3131 N88-28613

BODY-WING AND TAIL CONFIGURATIONS
Design of wings and wing/body configurations for transonic and supersonic speeds
05 p0545 N88-13318
Investigation of the influence of wind shear on the aerodynamic characteristics of aircraft using a vortex-lattice method 10 p1274 N88-17619
The determination of the topological structure of skin friction lines on a rectangular wing-body combination
[NASA-CR-4168] 20 p2753 N88-26343

BODY-WING CONFIGURATIONS
Numerical simulation of the hypersonic flow around lifting vehicles 05 p0532 N88-13234
Vortex formation over delta, double-delta and wave rider configurations at supersonic speeds
05 p0533 N88-13243
The RAE experimental data-base for missiles at high Mach number and its use in assessing CFD methods
05 p0534 N88-13250
Low speed wind tunnel investigation of propeller slipstream aerodynamic effects on different nacelle/wing combinations. Part 1: Total forces and moments and pressure distributions on nacelle/wing at different angles of attack and yaw and at different thrust coefficients
[FFA-TN-1987-22] 05 p0542 N88-13302
Compressible Euler solution on a multiblock grid around a wing-fuselage configuration
[FFA-TN-1987-46] 05 p0542 N88-13303
Transonic Navier-Stokes computations of strake-generated vortex interactions for a fighter-like configuration 06 p0664 N88-14073
Aerodynamic and propeller performance characteristics of a propfan-powered, semispan model
[NASA-TM-86705] 06 p0667 N88-14092
Testing of a schematic transport plane model in several European windtunnels
[PB87-170270] 09 p1113 N88-16671
Design of an aeroelastic composite wing wind tunnel model
[AD-A188855] 12 p1582 N88-19466
Transonic Navier-Stokes computations of strake-generated vortex interactions for a fighter-like configuration
[NASA-TM-100009] 15 p2014 N88-22010
Laser velocimeter measurements in a wing-fuselage type juncture
[NASA-TM-100586] 15 p2014 N88-22012
A transonic small disturbance wing design methodology 18 p2457 N88-24590
Improved potential flow computational methods with Euler corrections for airfoil and wing/body design
[AD-A192303] 20 p2752 N88-26334
VSAERO analysis of tip planforms for the free-tip rotor
[NASA-CR-177487] 22 p3038 N88-28036
Analytical surfaces and grids
23 p3247 N88-29322

BOEING AIRCRAFT
NT BOEING 737 AIRCRAFT
NT BOEING 747 AIRCRAFT
NT C-135 AIRCRAFT
NT CH-46 HELICOPTER
Prototype manufacturing techniques for reducing cost, schedule, and technical risk 12 p1702 N88-20189
Planning for AIMS on the next generation 7J7 aircraft
22 p3035 N88-28017

BOEING MILITARY AIRCRAFT
U MILITARY AIRCRAFT

BOEING 737 AIRCRAFT
Simulation of an enhanced TCAS 2 system in operation
[NASA-CR-181545] 04 p0398 N88-12479
A study of the TCAS 2 collision avoidance system mounted on a Boeing 737 aircraft
[NASA-CR-182457] 09 p1116 N88-16687

BOEING 747 AIRCRAFT
Acquisition of gust statistics from Aircraft Integrated Data Systems (AIDS) recorded data
[NLR-MP-86048-U-ISS-2] 06 p0745 N88-14586
The intelligent QAR and its cost effective role in new generation AIMS --- quick access recorder (QAR); aircraft integrated monitoring systems (AIMS)
22 p3035 N88-28020
The Sundstrand B747-400 data management unit
22 p3035 N88-28021
RB211 developments
[PNR90444] 22 p3045 N88-28069

BOGOLIUBOV THEORY
Bogolyubov transformation in relativistic theory of gravitation
[DE88-701592] 16 p2232 N88-23329

BOGS
U MARSHLANDS

BOHR THEORY
Inelastic two composite particle systems scattering at high energy
[DE88-701841] 20 p2851 N88-26928

BOILERS
Design of a condenser-boiler for a binary mercury-organic Rankine cycle solar dynamic space power system
[AD-A184188] 03 p0348 N88-12198
Proceedings of the 1987 International Symposium on Condensing Heat Exchangers
[DE88-005230] 13 p1766 N88-20564

BOILING
NT FILM BOILING
NT NUCLEATE BOILING
Review of nucleation and incipient boiling under pool and forced convection conditions
08 p0982 N88-15938
A model for stationary and dynamic impression of undercooled boiling in coupled thermohydraulic and neutron physics calculations of nuclear reactors
[IKE-6-171] 09 p1247 N88-17472
Prediction of high-temperature thermodynamic properties of mixed electrolyte solutions including solubility equilibria, vapor pressure depression and boiling point elevation
[DE88-006344] 13 p1849 N88-21069
Analysis and interpretation of low gravity boiling experiments in the KC-135 17 p2432 N88-24466
Ammonia boiling in long tubes. Heat transfer and charge loss in vertical and horizontal tubes
[NASA-TT-20313] 19 p2667 N88-25858
Investigation on refrigerant R12 critical boiling point in narrow flow pipes considered as model fluid
[ETN-88-92374] 20 p2802 N88-26626
Effects of surface tension and contact angle on sensible heating and boiling incipience in dielectric falling films
[DE88-007057] 21 p2945 N88-27492

BOILING WATER REACTORS
The dishomogeneity of the degree of sensitization in large recirculation pipes in Boiling Water Reactor (BWR) power plants
[CISE-3955] 09 p1247 N88-17473

BOLIDES
The end height of fireball as a function of their residual kinetic energy 06 p0737 N88-14535
The Valec fireball and predicted meteorite fall 06 p0739 N88-14547

BOLKOW AIRCRAFT
NT BO-105 HELICOPTER

BOLOGRAMS
U BOLOMETERS

BOLOMETERS
An adiabatic demagnetization cooled bolometer system for millimeter continuum astronomy 07 p0943 N88-15735
Preparing the Alcator C bolometer system for use on MTX (Microwave Tokamak Experiment)
[DE88-006724] 15 p2134 N88-22733

BOLTED JOINTS
Structural analysis of a bolted joint concept for the space shuttle's solid rocket motor casing
[NASA-TM-89092] 04 p0407 N88-12531
Nonlinear axial stiffness characteristics of axisymmetric bolted joints 04 p0452 N88-12799
Behavior of bolted joints in composite laminates 06 p0677 N88-14148
Device for measuring hole elongation in a bolted joint
[NASA-CASE-LAR-13453-1] 06 p0712 N88-14361
Comparison of the strength of single and multiple bolted joints in CFRP
[PB87-123766] 06 p0722 N88-14438
Experimental and theoretical investigation of mechanically fastened composites
[AD-A185896] 07 p0826 N88-15008
Simplified procedures for designing composite bolted joints
[NASA-TM-100281] 07 p0828 N88-15020
Experimental investigation of damping characteristics of bolted structural connections for plates and shells
[AD-A186075] 07 p0867 N88-15259
Detection sensitivity in thick assemblies --- eddy currents, light alloys, aircraft construction materials
[REPT-48-912/F] 16 p2216 N88-23221
Experimental investigation of the effects of underwater exposure on the damping characteristics of bolted structural connections for plates and shells
[AD-A194486] 23 p3226 N88-29200
Clevis joint for deployable space structures
[NASA-CASE-LAR-13898-1] 24 p3380 N88-30130

BOLTS
Joints in carbon fibre reinforced composites
[BR99969] 01 p0019 N88-10114
Fastening high resistance bolts in real assemblies
[CRIF-MT-171] 07 p0861 N88-15221
Increasing strength of graphite/epoxy bolted joints by introducing an adhesively bonded metallic insert
[FFA-TN-1987-45] 15 p2068 N88-22442
On the calculation of stresses in pin-loaded anisotropic plates
[ETN-88-92239] 16 p2222 N88-23261
Bearing-bypass material system test
[NASA-CASE-LAR-13458-1] 17 p2342 N88-23967
FEB structural analysis, revision H
[AD-A192302] 20 p2814 N88-26698

BOLTZMANN DISTRIBUTION
A moment approach to modeling negative ion sources
[AD-A186858] 12 p1691 N88-20114
Para-ortho abundance ratio of molecular hydrogen in NGC2023
[ISAS-RN-352] 18 p2573 N88-25286
Extension of Boltzmann's theory to a liquid
[DE88-009153] 20 p2880 N88-27097
Boltzmann equation approach to two-phase flow turbulence
[AD-A196153] 24 p3373 N88-30086

BOLTZMANN TRANSPORT EQUATION
The physics of charge separation preceding lightning strokes in thunderclouds
[NASA-CR-178371] 01 p0071 N88-10452
Boltzmann-Fokker-Planck calculations using standard discrete-ordinates codes
[DE88-005393] 11 p1537 N88-19135
Simulation of the plasma interaction with thin dust clouds 11 p1552 N88-19261
The development of KENO and the calculation of differential parameters with KENO
[DE88-006176] 18 p2555 N88-25166
On microphysical principles of thermofluid dynamics
[ETN-88-92095] 20 p2801 N88-26620
Feedback control of a hyperbolic partial-differential equation with viscoelastic damping
[AD-A192896] 21 p3003 N88-27810

BOMB CALORIMETERS
Determination of the melting and decomposition points of different materials in an oxygen stream
[INFORME-I-158/86] 09 p1142 N88-16844

BOMBER AIRCRAFT
NT B-1 AIRCRAFT
NT B-57 AIRCRAFT
NT B-70 AIRCRAFT
Store separation of nuclear weapons
[DE87-010778] 02 p0124 N88-10785
Use of demonstration/validation prototypes: Impact on total development costs and times 12 p1703 N88-20194
A study of Radar Cross Section (RCS) characteristics and their application in future weapon systems
[ETN-88-92081] 14 p1906 N88-21390
Pilot report: AFTI (Advanced Fighter Technology Integration) F-111
[AD-A192937] 21 p2895 N88-27184
The Soviet Stealth fighter: Check or checkmate
[AD-A195200] 24 p3323 N88-29791
Human factors report on information management requirements for next-generation manned bombers
[AD-A195870] 24 p3409 N88-30296

BOMBS (ORDNANCE)
A simplified computer code for reduction to burning rates of closed bomb pressure-time data (MINICB)
[AD-A189112] 13 p1736 N88-20380
Descriptive characterization of propellant particles
[AD-A195176] 24 p3356 N88-29985

BOMBS (PRESSURE GAGES)
U PRESSURE GAGES

BOMBS (SAMPLERS)
U SAMPLERS

BOND GRAPHS
An interactive-graphics method for dynamic system modelling, applying consistency rules 09 p1181 N88-17072

BONDING
NT ADHESIVE BONDING
NT CERAMIC BONDING
NT EXPLOSIVE WELDING
NT INERTIA BONDING
NT METAL BONDING
NT METAL-METAL BONDING
NT REACTION BONDING
NT RESIN BONDING
Low-pressure eutectic bonding of depleted uranium to copper
[DE87-014625] 02 p0181 N88-11128
Bond character at a silicon/copper surface
[AD-A184167] 03 p0295 N88-11851
Superconductivity as a synchronous spatial alternation of valence bonds
[AD-A184208] 03 p0382 N88-12405
Tool and process for miniature explosive joining of tubes
[NASA-CASE-LAR-13662-1] 06 p0711 N88-14359
Mechanical properties of steel-to-steel adhesive bonds
[PB88-111299] 08 p0971 N88-15877
Tight binding theory of semiconductors 10 p1415 N88-18447
Interfacial adhesion: Theory and experiment
[NASA-TM-100830] 13 p1742 N88-20417
An investigation of the infrared emission spectra of carbon condensates 14 p1886 N88-21272
Fracture toughness of silicon nitride-silicon nitride joints bonded with oxynitride glass
[DE88-005548] 15 p2043 N88-22172
The inspection of electronic metallurgical bonds
[AD-A192197] 18 p2486 N88-24745
Molecular characterization of structure and bonding in thin film materials
[DE88-006811] 18 p2584 N88-25351
Fracture physics of delamination of composite materials
[AD-A192021] 19 p2609 N88-25482
Molecular orbital studies of the bonding in heavy element organometallics: Progress report
[DE88-007765] 19 p2723 N88-26168
Effect of the matrix on the creep-behavior of carbon-carbon composite
[AD-A193211] 21 p2905 N88-27235
An IETS (Inelastic Electron Tunneling Spectroscopy) study of surface reactions applicable to adhesion
[AD-A192274] 21 p2909 N88-27261
Method for maintaining precise suction strip porosities
[NASA-CASE-LAR-13638-1] 23 p3201 N88-29051
Evaluation of bond testing equipment for inspection of Army advanced composite airframe structures
[AD-A195795] 24 p3341 N88-29885

BONE DEMINERALIZATION
Prevention of disuse osteoporosis: Effect of sodium fluoride during five weeks of bed rest
[NASA-CR-172018] 01 p0075 N88-10483
Histomorphometric analysis of rat bones after spaceflight aboard Cosmos-1667 biosatellite 10 p1360 N88-18128
NASA Workshop on Biological Adaptation
[NASA-TM-89468] 10 p1368 N88-18174
Disuse condition stimulates bone resorption in organ culture 12 p1656 N88-19926
Noninvasive examination of bones during long-term hypokinesia 19 p2704 N88-26077
Effect of different doses of alpha-hydroxydimethyl-gamma-aminopropylidene phonate on rat bones 19 p2704 N88-26078

BONE MARROW
Late radiation damage in bone, bone marrow and brain vasculature, with particular emphasis upon fractionation models
[DE87-753039] 08 p1048 N88-16330

BONE MINERAL CONTENT
Disuse condition stimulates bone resorption in organ culture 12 p1656 N88-19926
An in vitro model system to study the effect of microgravity and loading conditions on the mineralization and resorption of skeletal tissues 12 p1657 N88-19927
Use of diphosphonates to correct disorders in calcium metabolism and mineral composition of bone tissue with 60-day hypokinesia in rats
[NASA-TT-20220] 13 p1809 N88-20807
Noninvasive examination of bones during long-term hypokinesia 19 p2704 N88-26077
Effect of different doses of alpha-hydroxydimethyl-gamma-aminopropylidene phonate on rat bones 19 p2704 N88-26078

BONES
NT SKULL
NT TIBIA
Histomorphometric analysis of rat bones after spaceflight aboard Cosmos-1667 biosatellite 10 p1360 N88-18128
Morphological study of early changes in rat bones in simulated weightlessness 10 p1365 N88-18158

BOOLEAN ALGEBRA
NT BOOLEAN FUNCTIONS
Search rearrangement backtracking often requires exponential time to verify unsatisfiability
[AD-A186121] 07 p0909 N88-15511
A graph separator theorem and its application to Gaussian elimination to optimize Boolean expressions for parallel evaluation
[AD-A188527] 14 p1962 N88-21706
Two papers on a symbolic analyzer for MOS (Metal-Oxide Semiconductors) circuits
[AD-A188617] 15 p2139 N88-22761

BOOLEAN FUNCTIONS
Extraction and evaluation of Boolean relations for the solution of linear programs in 0-1 variables, volume 1
[ENST-86E023-VOL-1] 02 p0227 N88-11430
Extraction and evaluation of Boolean relations for the solution of linear programs in 0-1 variables, volume 2
[ENST-86E023-VOL-2] 02 p0227 N88-11431
The geometry of the Karnaugh map --- Boolean expressions
[ETN-87-90961] 02 p0227 N88-11432
A complexity transform for NP-complete problems
[OUEL-1708/87] 14 p1962 N88-21703
A graph separator theorem and its application to Gaussian elimination to optimize Boolean expressions for parallel evaluation
[AD-A188527] 14 p1962 N88-21706
Technology mapping from Boolean expressions to standard cells
[EUT-87-E-174] 14 p1963 N88-21709
SYMBL: A new Boolean compiler 18 p2554 N88-25160
Investigation of the potential impact of new photonic materials on optical processing systems 21 p2924 N88-27359

BOOMS (EQUIPMENT)
Pinhole occulter experiment
[NASA-CR-179206] 02 p0235 N88-11481
Development of the Extendable and Retractable Mast (ERM). Design phase 2. Volume 1 --- spacecraft payloads
[RP-2010-0000-DS/09] 11 p1467 N88-18750
Some highlights on ROSAT mechanisms 14 p1874 N88-21195
The CTM program of masts and the CTM engineering model --- spacecraft mechanism 14 p1874 N88-21196
Deployable/retrievable boom: One application to tethered satellite 14 p1874 N88-21197
Deployable booms and antennas on AMPTE-IRM 14 p1874 N88-21198
The EURECA antenna deployment and retraction mechanisms 14 p1878 N88-21225
Required operational capacity for a 7-1/2 ton capacity, Air Mobile Crane (AMC)
[AD-A192023] 19 p2601 N88-25451

BOOST
U ACCELERATION (PHYSICS)
BOOSTER RECOVERY
A two stage launch vehicle for use as an advanced space transportation system for logistics support of the space station
[NASA-CR-182572] 11 p1443 N88-18606
BOOSTER ROCKET ENGINES
NT APOGEE BOOST MOTORS
NT SPACE SHUTTLE BOOSTERS
A two stage launch vehicle for use as an advanced space transportation system for logistics support of the space station
[NASA-CR-182572] 11 p1443 N88-18606
BOOSTERS (EXPLOSIVES)
A study of diverging detonation in high-explosive systems
[DE87-006070] 01 p0031 N88-10194
BORANES
Dynamics of production and oxidation of boranes
[AD-A188988] 12 p1606 N88-19605
BORATES
Structure of sol-gel-derived inorganic polymers. 2: Silicates and borates
[DE87-013068] 01 p0027 N88-10172
BORAZON (TRADEMARK)
U BORON NITRIDES
BOREHOLES
Cryogenic cell --- neutron borehole logging
[GB-PATENT-2-139-745-A] 01 p0048 N88-10308
Geophysical diffraction tomography for imaging isolated subsurface inclusions
[DE88-003918] 11 p1505 N88-18990
Evaluation of a miniature horizontal pendulum tilt transducer 12 p1577 N88-19435
Theoretical and numerical solution of the forward-scattering problem in a circularly cylindrical configuration
[PB88-173489] 16 p2189 N88-23056
Finite elements for the computation of three-dimensional electromagnetic fields in inhomogeneous media (revised)
[PB88-173471] 16 p2190 N88-23057
Reaming experiments for the lethality test system
[DE88-007902] 20 p2763 N88-26383
BOREL SETS
Volume functions in the general theory of relativity
[ETN-87-90408] 01 p0089 N88-10582
BORES
U CAVITIES
BORESCOPES
U ENDOSCOPES
BORIC ACIDS
Boronium complexes as polymer catalysts
[GB-PATENT-2-161-475-A] 01 p0026 N88-10166
BORIDES
NT TITANIUM BORIDES
A synthetic plasma source
[TRITA-EPP-86-15] 05 p0652 N88-13995
High-current density, high-brightness electron beams from large-area lanthanum hexaboride cathodes
[AD-A187700] 11 p1477 N88-18813
The relationship of the chemical bonding topology of high critical temperature copper oxide superconductors to that of the chevrel phases and the ternary lanthanide rhodium borides
[AD-A189255] 13 p1845 N88-21042
The combustion synthesis of boride composites
[DE88-005474] 15 p2028 N88-22084
Boron-containing organosilane polymers and ceramic materials thereof
[NASA-CASE-ARC-11649-1-SB]
23 p3199 N88-29040
BORN APPROXIMATION
Inversion of parabolic and paraboloidal projections
[AD-A187538] 10 p1405 N88-18380
Seismic inversion by a RMS (Root-Mean-Square) Born approximation in the space-time domain
[PB88-165402] 15 p2131 N88-22711
Born-type reconstruction of material parameters of an inhomogeneous, lossy dielectric slab from reflected-field data
[PB88-188358] 18 p2569 N88-25261
Time-domain far-field scattering of plane electromagnetic waves by a penetrable object in the Born approximation
[PB87-176129] 24 p3365 N88-30040
BORN-MAYER EQUATION
U BORN APPROXIMATION
BORN-OPPENHEIMER APPROXIMATION
Systematic studies of molecular vibrational anharmonicity and vibration-rotation interaction by self-consistent-field higher derivative methods: Applications to asymmetric and symmetric top and linear polyatomic molecules
[DE87-014691] 02 p0232 N88-11465
BORON
NT BORON ISOTOPES
A simulation study of interfaces in Ni, Al and Ni3Al with and without boron
[DE87-013156] 01 p0102 N88-10667
Analytical electron microscopy characterization of boron in sintered alpha-SiC
[DE87-012532] 02 p0142 N88-10889
Influence of boron on porosity in nickel-base superalloy castings 03 p0299 N88-11877
Studies on syntheses of amine-carboxyboranes (boron analogues of amino acids) and derivatives
[AD-A184838] 05 p0557 N88-13386
Basic energy sciences research in the Metals and Ceramics Division of Oak Ridge National Laboratory
[DE87-013538] 06 p0681 N88-14171
Evaluation and compilation of thermodynamic properties of high temperature chemical species
[AD-A187509] 11 p1452 N88-18654
The intergranular segregation of boron in substoichiometric Ni3Al
[DE88-004783] 11 p1462 N88-18720
Feasibility studies of the growth of 3-5 compounds of boron by MOCVD
[NASA-CR-181622] 11 p1561 N88-19343
The unique characteristics of the structure of composite materials made on a base of sphalerite-analogous boron nitride 14 p1886 N88-21273
The structure of the boron-hydrogen complex in silicon
[DE88-005433] 15 p2144 N88-22795
Comparison of calculated and measured ignition times for boron agglomerates 19 p2624 N88-25563
Grain boundary structure in Ni3Al
[DE88-009164] 20 p2773 N88-26444
NDP (Neutron Depth Profiling) evaluations of boron-implanted compound semiconductors
[AD-A192306] 21 p2934 N88-27425
Paramagnetic point defects in boron-implanted HgO.7CdO.3Te
[AD-A193276] 21 p3021 N88-27934
BORON ALLOYS
Investigations of crystallization velocity and boron diffusion in glassy iron-boron alloys and of activity coefficients of boron in crystalline iron-boron alloys
[ETN-87-90613] 03 p0381 N88-12393
BORON CARBIDES
Analytical electron microscopy characterization of boron in sintered alpha-SiC
[DE87-012532] 02 p0142 N88-10889
Shielding analysis of a small compact space nuclear reactor
[AD-A185566] 06 p0779 N88-14784
Wire-cut electrical discharge machinability of ceramics
[AD-A186989] 09 p1146 N88-16870
High yield synthesis of B4C/BN ceramic materials by pyrolysis of polymeric Lewis base adducts of decaborane(14)
[AD-A188154] 11 p1462 N88-18717
Microdesigning of lightweight/high strength ceramic materials
[AD-A188526] 12 p1610 N88-19631
The combustion synthesis of boride composites
[DE88-005474] 15 p2028 N88-22084
Electrical properties of materials for elevated temperature resistance strain gage application
[NASA-CR-182214] 24 p3376 N88-30106
BORON CHLORIDES
Advanced B and Al combustion kinetics over wide temperature ranges
[AD-A190752] 15 p2036 N88-22128
BORON COMPOUNDS
NT BORANES
NT BORATES
NT BORIC ACIDS
NT BORIDES
NT BORON CARBIDES
NT BORON CHLORIDES
NT BORON HYDRIDES
NT BORON NITRIDES
NT BORON OXIDES
NT BORON PHOSPHIDES
NT TITANIUM BORIDES
Boron-containing organosilane polymers and ceramic materials thereof
[NASA-CASE-ARC-11649-1-SB]
23 p3199 N88-29040
BORON FIBERS
Analytical and experimental characterization of damage processes in composite laminates
[AD-A187221] 10 p1296 N88-17746
BORON HYDRIDES
NT BORANES
New synthetic approaches to boron hydride transformations
[AD-A193872] 22 p3052 N88-28108
BORON ISOTOPES
Studies of boron implantation through photochemically deposited SiO2 films on Hg(sub 1-x)Cd(sub x)Te
[SD-TR-87-26] 19 p2621 N88-25548
BORON NITRIDES
Investigation of BN CO2 wave guide laser
03 p0302 N88-11905
High yield synthesis of B4C/BN ceramic materials by pyrolysis of polymeric Lewis base adducts of decaborane(14)
[AD-A188154] 11 p1462 N88-18717
A segmented calorimeter for low-energy particle beams in space
[DE88-001806] 13 p1838 N88-20997
Hermetic coating of optical fibers
[AD-A189886] 15 p2044 N88-22177
BORON OXIDES
Application of laser-induced fluorescence in an atmospheric-pressure boron-seeded flame
[AD-A189631] 14 p1889 N88-21287
BORON PHOSPHIDES
Chemical vapor deposition of B6P and B6As films
[DE87-009288] 02 p0151 N88-10942
BORON REINFORCED MATERIALS
NT ALUMINUM BORON COMPOSITES
NT BORON-EPOXY COMPOSITES
Fracture mode research of boron aluminum composite materials by Acoustic Emission (AE)
[NAL-TR-927] 02 p0142 N88-10891
Joints in fiber-reinforced aluminum alloys
[NASA-TT-20160] 15 p2031 N88-22104
BORON-EPOXY COMPOSITES
Composite repair of cracked aluminum alloy aircraft structure
[AD-A190514] 18 p2455 N88-24573
BOROSILICATE GLASS
Homogeneity of glasses: Experiment WL-IHF-05 in D1 mission --- Spacelab
[ETN-88-92339] 21 p2924 N88-27353
BOSE GEOMETRY
Method of two-time Green functions in molecular hydrodynamics of superfluid liquid
06 p0771 N88-14735
BOSE-EINSTEIN STATISTICS
U QUANTUM STATISTICS
BOSON FIELDS
Searches for forces weaker than gravity
[DE88-003579] 13 p1832 N88-20959
BOSONS
NT ALPHA PARTICLES
NT KAONS
NT MESON RESONANCE
NT MESONS
NT MUONS
NT PHOTONS
NT PIONS
W decays
[NOTA-INTERNA-877] 05 p0648 N88-13966
Vector boson pair production in e(+)e(-) collisions
[PREPRINT-549] 06 p0778 N88-14774
Single weak gauge boson production at CLIC
[PREPRINT-550] 06 p0778 N88-14775
Searches for forces weaker than gravity
[DE88-003579] 13 p1832 N88-20959
Proton/antiproton yields W(+/-)boson gamma X as a test of the quark charges
[NIKHEF-H/87-11] 13 p1836 N88-20987
New limits on charged Higgs boson mass with CELLO at Petra (Italy) and status of the neutral Higgs boson search
[NOTA-INTERNA-897] 14 p1980 N88-21817
Einstein metrics and Brans-Dicke superfields
[DE88-006992] 15 p2146 N88-22809
Involution-dependent constants and the cancellation of divergences in the 1-loop open string amplitude
[DE88-006537] 15 p2146 N88-22811
Stable, heavy, neutral particles in the sun and in toponium decay 17 p2452 N88-24568
Superfluidity of a two dimensional Boson Coulomb gas
[DE88-009827] 19 p2735 N88-26244
Production of pi(0) mesons and charged hadrons in nu bar neon and nu neon charges current interactions
[MPI-PAE/EXP.EL.188] 22 p3150 N88-28743
The ground state of the bosonic string
[USIP-88-01] 22 p3151 N88-28746
The Hilbert space of the closed bosonic string
[USIP-88-04] 22 p3151 N88-28747
Open bosonic string in background electromagnetic field
[DE88-702140] 23 p3201 N88-29053
The Hilbert space of the open bosonic string
[USIP-88-02] 23 p3295 N88-29628
BOTANY
NT GEOBOTANY
Exobiology and botany facilities for EURECA
12 p1652 N88-19898

Botany Facility pre-phase C/D. Core payload for EURECA, volume 2
[BF-RP-ER-015-VOL-2] 17 p2377 N88-24130

Life Support Subsystem (LSS). Concept for the Botany Facility --- EURECA
[TN-RB524-107/86] 17 p2377 N88-24131

Impact of control errors on the volume/weight demand of the Ventilation and Dryer (VAD) concept --- EURECA Botany Facility
[TN-RB524-006/87] 17 p2377 N88-24132

Summary of the activities performed during the Botany Facility (BF) predevelopment phase for the Life Support S/S (LSS)
[TB-RB524-002/87] 17 p2378 N88-24133

Botany Facility. Thermal Control (TC) subsystem test report on experiment container of laboratory model and breadboard centrifuge
[BF-TN-ER-061/86] 17 p2378 N88-24135

Botany Facility: Test report on breadboard tests for the determination of the heat transfer at the glass disk and of the temperature distribution in the fluorescent tube
[BF-TN-ER-053] 17 p2378 N88-24136

Botany Facility: Breadboarding results of the illumination system
[SIRA-A/7373/WP110/MAC003]
17 p2378 N88-24137

Botany Facility: Magnetic fluid seal considerations for the centrifuge
[SIRA-A/7373/WP110/MAC004]
17 p2378 N88-24138

Botany Facility: Considerations and analyses of the balancing system philosophy proposed for the BF centrifuge
[SIRA-A/7373/WP110/PWF001]
17 p2378 N88-24139

Botany Facility: The problems of plant fixation
[SIRA-A/7373/WP220/RJS/001]
17 p2379 N88-24140

Botany Facility: Problems of water supply, plant nutrients and soil in the Botany Facility
[SIRA-A/7373/WP220/RJS/003]
17 p2379 N88-24141

Supply and distribution of plant nutrients in the Botany Facility
[SIRA-A/7373/WP220/RJS/004]
17 p2379 N88-24142

EURECA Botany Facility. Technical note: Removal of phytotoxins
[SIRA-A/7373/WP220/RJS/005]
17 p2379 N88-24143

Botany Facility pre-phase C/D. Core payload for EURECA, volume 1
[BF-RP-ER-015-VOL-1] 17 p2379 N88-24144

BOUNDARIES
NT FLUID BOUNDARIES
NT FREE BOUNDARIES
NT GRAIN BOUNDARIES
NT LIQUID-LIQUID INTERFACES
NT LIQUID-SOLID INTERFACES
NT LIQUID-VAPOR INTERFACES

Some investigations of electrical discharges at the surfaces of solid cathodes immersed in aqueous electrolyte solutions
[PB87-168209] 09 p1159 N88-16946

Image chunking: Defining spatial building blocks for scene analysis
[AD-A187072] 09 p1200 N88-17191

Boundary stabilization of thin elastic plates
[AD-A187123] 10 p1343 N88-18025

Numerical studies of propagation of Lg waves across ocean continent boundaries using the Representation Theorem (RT) 10 p1353 N88-18085

Probability bounds for M-Skorohod oscillations
[AD-A187981] 10 p1404 N88-18371

Finding texture boundaries in images
[AD-A190554] 15 p2117 N88-22609

The theory of flotation
[NASA-TT-20278] 16 p2207 N88-23172

Transmitting boundary for finite-difference calculations with finite modeling of an infinite medium
[AD-A191441] 18 p2570 N88-25264

Curvature of blended rolled edge reflectors at the shadow boundary contour
[NASA-CR-182974] 18 p2576 N88-25300

On the use of convergent beam electron diffraction for identification of antiphase boundaries in GaAs grown on Si
[DE88-008220] 18 p2585 N88-25362

Seismic body waves and the earth's inner core
[DE88-007395] 19 p2691 N88-25994

Physical mechanisms in shock-induced turbulent separated flow
[AD-A193165] 21 p2944 N88-27484

Computational boundary conditions for the incompressible Navier-Stokes equations in channels and pipes
[AD-A193356] 21 p2944 N88-27487

The low-latitude auroral boundary: Steady-state and time-dependent representations
[AD-A193200] 21 p2972 N88-27656

Indian Ocean validation
[AD-A194458] 23 p3175 N88-28902

BOUNDARY ELEMENT METHOD

Calculation of the eigenvibrations of axisymmetric fluid configurations with a singularity method, taking into account surface tension effects under reduced gravity
[ETN-87-90438] 01 p0048 N88-10304

Characteristics and boundary elements for three dimensional nonstationary Navier Stokes flows
[PREPRINT-1051] 02 p0172 N88-11086

An integral equation analysis of inelastic shells
03 p0336 N88-12118

Theoretical and practical aspects of multigrid methods in boundary element calculations
[NLR-MP-85021-U] 03 p0370 N88-12328

Computation of nacelle interference using boundary element method 05 p0537 N88-13267

Significance of foundation-soil separation in dynamic soil-structure interaction 05 p0596 N88-13641

Studies on fluid-structural vibration using boundary element method
[PB87-129508] 06 p0699 N88-14291

Boundary element analysis for dynamic loading of a circular plate on an elastic medium
[CI-86] 06 p0722 N88-14443

On the convergence of the p-version of the boundary element Galerkin method
[AD-A186198] 07 p0910 N88-15514

Boundary elements combined with singular fields for three-dimensional cracked solids
[RAE-TR-87038] 09 p1183 N88-17088

A viscoelastic BEM (Boundary Element Method) for modeling oxidation
[AD-A187490] 11 p1452 N88-18653

An analysis of large deformation axisymmetric inelastic problems by finite element and boundary element methods 13 p1782 N88-20664

Three-dimensional mesh-generation and plotting routines for use with a boundary element program (BIE3D)
[AD-A188079] 14 p1958 N88-21675

A note on the analyticity of the Neumann Kernel and an associated quadrature problem in two-dimensional boundary element methods
[ETN-88-92054] 14 p1964 N88-21719

Boundary element method for three-dimensional magnetostatic fields in terms of vector variables
[EL-61] 15 p2122 N88-22649

Calculations of unsteady aerodynamics for a full aircraft configuration using boundary element method
19 p2637 N88-25643

Boundary element method for contact heat transfer
[DE88-011013] 20 p2800 N88-26613

Time-domain boundary element analysis of dynamic near-tip fields for impact-loaded collinear cracks
[AD-A192930] 20 p2815 N88-26700

Off-boundary approach to the boundary element method
[AD-A192931] 20 p2815 N88-26701

Parallel implementation of the boundary element method
[DE88-011846] 21 p3007 N88-27839

An improved boundary force method for analyzing cracked anisotropic materials
[NASA-TM-101495] 24 p3340 N88-29879

BOUNDARY INTEGRAL METHOD

A user's guide for BIE3D: A boundary integral equation computer program for three-dimensional elastostatic analysis
[RAE-TM-MAT-STR-1078] 01 p0079 N88-10509

Boundary integral technique for performing analysis of two-dimensional volumes of revolution
[DE87-013053] 01 p0082 N88-10524

Numerical modeling: Finite methods
03 p0304 N88-11918

Boundary integral analysis of flow and deformation of long bubbles in capillaries
[DE88-002110] 10 p1326 N88-17927

Boundary-integral-equation method for computing the three-dimensional flow of groundwater
[PB88-126891] 10 p1330 N88-17951

Fast Poisson solver on irregular regions by boundary integral-based domain decomposition methods
[DE88-003583] 10 p1399 N88-18340

Three-dimensional mesh-generation and plotting routines for use with a boundary element program (BIE3D)
[AD-A188079] 14 p1958 N88-21675

A note on the analyticity of the Neumann Kernel and an associated quadrature problem in two-dimensional boundary element methods
[ETN-88-92054] 14 p1964 N88-21719

A new boundary integral equation formulation for elastodynamic and elastostatic crack analysis
[AD-A192967] 20 p2815 N88-26702

BOUNDARY LAYER CONTROL

Investigations on a transonic airfoil with a 30 mm wide perforation/cavity arrangement
[ESA-TT-1072] 03 p0260 N88-11634

Navier-Stokes analysis of laminar flow control of a two-dimensional airfoil 05 p0540 N88-13286

Study of the effect of mass transfer on a transonic boundary layer. Application to flow relaminarization
[ETN-88-91169] 05 p0541 N88-13296

Structural tests and development of a laminar flow control wing surface composite chordwise joint
[NASA-CR-172462] 06 p0663 N88-14066

Turbulence, turbulence control, and drag reduction
[AD-A185643] 06 p0665 N88-14080

Numerical simulation of a controlled boundary layer
07 p0810 N88-14933

Wind tunnel wall interference
07 p0811 N88-14938

Boundary layer transition 07 p0811 N88-14942

Separated flow 07 p0812 N88-14944

Vortex dynamics 07 p0812 N88-14945

Overview of the Langley viscous drag reduction program 07 p0812 N88-14946

Flight research on natural laminar flow
07 p0813 N88-14950

Design and experimental evaluation of a swept supercritical Laminar Flow Control (LFC) airfoil
07 p0813 N88-14951

Laminar flow integration: Flight tests status and plans
07 p0813 N88-14952

Roughness and waviness requirements for laminar flow surfaces 07 p0813 N88-14953

Secondary subharmonic instability of boundary layers with pressure gradient and suction
[NASA-CR-4112] 07 p0848 N88-15148

Control of vortical separation on conical bodies
10 p1267 N88-17580

Reduction of tilt rotor download using circulation control 10 p1271 N88-17605

Structure of shear flow turbulence and its control
[AD-A187909] 11 p1482 N88-18846

Research on flow control
[AD-A189014] 12 p1627 N88-19736

Development of disturbances in swept wing flows
[NASA-CR-182675] 13 p1768 N88-20574

The NASA Langley Laminar-Flow-Control (LFC) experiment on a swept, supercritical airfoil: Design overview
[NASA-TP-2809] 14 p1861 N88-21117

Application of hybrid laminar flow control to global range military transport aircraft
[NASA-CR-181638] 14 p1862 N88-21124

Control of laminar flow around of the wing in free-air conditions
[AD-A187479] 15 p2013 N88-22004

Modifications to the Langley 8-foot transonic pressure tunnel for the laminar flow control experiment
[NASA-TM-4032] 15 p2021 N88-22047

Investigation of boundary layer disturbances caused by periodic heating of a thin ribbon
[AD-A190572] 15 p2065 N88-22314

Design method for laminar flow control of two-dimensional airfoils in incompressible flow: Numerical study of LFC design concepts
[DE88-751809] 16 p2155 N88-22859

An assessment of the drag reduction properties of riblets and the penalties of off-design conditions
[RAE-TM-AERO-2113] 17 p2295 N88-23731

Boundary-layer stability and airfoil design
17 p2296 N88-23738

Wind tunnel testing of low-drag airfoils
17 p2297 N88-23741

Operational considerations for laminar flow aircraft
17 p2298 N88-23748

Pressure distributions from subsonic tests of an advanced laminar-flow-control wing with leading- and trailing-edge flaps
[NASA-TM-4040-PT-1] 17 p2300 N88-23758

Passive shock wave-boundary layer control for the Bell FX69-H-098 airfoil 18 p2457 N88-24588

A new method of calculating the boundary layer characteristics downstream of manipulators. Part 1: Boundary layer integral parameters
[PNR90455] 22 p3078 N88-28279

A new method of calculating the boundary layer characteristics downstream of manipulators. Part 2: Skin friction and net drag reduction
[PNR90456] 22 p3078 N88-28280

Boundary layer simulation and control in wind tunnels [AGARD-AR-224] 23 p3167 N88-28857
High-aspect-ratio wings 23 p3167 N88-28859
Techniques for boundary layer tripping and control 23 p3168 N88-28863
Environmental effects on transition and boundary layer characteristics 23 p3170 N88-28876
A mapping of the viscous flow behavior in a controlled diffusion compressor cascade using laser Doppler velocimetry and preliminary evaluation of codes for the prediction of stall [AD-A194490] 23 p3211 N88-29112
Pressure distributions from subsonic tests of an advanced laminar-flow-control wing with leading- and trailing-edge flaps [NASA-TM-4040-PT-2] 24 p3321 N88-29776

BOUNDARY LAYER EQUATIONS
Breakdown of steady and unsteady interacting boundary layers [NLR-MP-86047-U] 01 p0045 N88-10284
Development and testing of a vertically-nested regional prediction system — weather forecasting 02 p0210 N88-11322
Introduction to Computational Fluid Dynamics [VKI-LS-1987-02] 06 p0701 N88-14300
Boundary layer equations and methods of solution 06 p0701 N88-14302
Three-dimensional structure of boundary layers in transition to turbulence [AD-A185466] 06 p0702 N88-14311
The numerical and analytical study of bifurcation and multicellular flow instability due to natural convection between narrow horizontal isothermal cylindrical annuli at high Rayleigh numbers [AD-A186113] 07 p0849 N88-15151
Pseudo-stationary oblique-shock-wave reflections in low gamma gases: Isobutene and sulphur hexafluoride [UTIAS-TN-267] 13 p1768 N88-20576
General fuselage coordinates for the calculation of three-dimensional boundary layers [MBB/LKE-122/S/PUB/244] 13 p1771 N88-20596
The sensitivity of boundary layer instability growth rates to compliant wall properties [AD-A190433] 15 p2064 N88-22309
Composite reduced Navier-Stokes procedures for flow problems with strong pressure interactions [AD-A191127] 18 p2508 N88-24875
Transient particle deposition in a boundary layer of impulsive flow over a flat plate [AD-A191537] 18 p2508 N88-24880
Cross stream differencing for integral boundary layer equations [AD-A191744] 18 p2509 N88-24886
Boundary layer solutions for the free-edge problem in composite laminates 21 p2904 N88-27229
A study of the vortex sheet method for solving the Prandtl boundary layer equations [DE88-011346] 22 p3074 N88-28249

BOUNDARY LAYER FLOW
NT BOUNDARY LAYER SEPARATION
NT REATTACHED FLOW
NT SECONDARY FLOW
NT SEPARATED FLOW
Measurement techniques in low-speed turbulent flows: A report on EUROMECH 202 [NLR-MP-86038-U] 01 p0045 N88-10283
Breakdown of steady and unsteady interacting boundary layers [NLR-MP-86047-U] 01 p0045 N88-10284
Numerical solution of Euler equations for compressible fluids by the finite element method, volume 3 [ETN-87-90650] 02 p0170 N88-11070
Boundary layer profile investigations downstream of an aero-engine intake anti-icing air exhaust slot [PNR90378] 02 p0171 N88-11080
Vertical profiles of wind-induced current --- North Sea [IOS-238] 02 p0193 N88-11207
Theoretical analysis of primary instabilities in three dimensional boundary layer flows [ESA-TT-1063] 03 p0315 N88-11992
Visualization of the flow field around a generic destroyer model in a simulated turbulent atmospheric boundary layer [AD-A184658] 03 p0320 N88-12023
The design and preliminary calibration of a boundary-layer flow channel [NASA-CR-178399] 04 p0394 N88-12457
Total linearisation method for solving viscous free boundary flow problems by the finite element method [PB87-222337] 04 p0441 N88-12737
Active and passive plume distribution models in the convective boundary layer using a large eddy simulation model [KNMI-TR-90] 05 p0581 N88-13546
Combined riblet and lebu drag reduction system [NASA-CASE-LAR-13286-1] 06 p0664 N88-14071
Characteristics of a separating confluent boundary layer and the downstream wake [NASA-TM-100046] 06 p0704 N88-14323
Upwind relaxation algorithms for Euler/Navier-Stokes equations 07 p0810 N88-14931
Vortex dynamics 07 p0812 N88-14945
Computational design of natural laminar flow wings for transonic transport application 07 p0813 N88-14948
On the parabolized Navier-Stokes equations without sublayer assumptions [AD-A186127] 07 p0849 N88-15152
A method for the approximate calculation of the skin friction coefficient of horizontal wavy plates [VKI-TN-160] 07 p0851 N88-15172
Acta Aerodynamica Sinica (selected articles) [AD-A185723] 08 p0949 N88-15757
Numerical simulation of heat transfer turbulence, volume 2 [AD-A185130] 08 p0983 N88-15947
Numerical simulation of turbulent spots in channel and boundary layer flows 08 p0983 N88-15948
A theory for turbulent curved wall jets 10 p1269 N88-17590
The further development of circulation control airfoils 10 p1270 N88-17594
Boundary-layer and wake measurements on a swept, circulation-control wing 10 p1270 N88-17597
Boundary integral analysis of flow and deformation of long bubbles in capillaries [DE88-002110] 10 p1326 N88-17927
Shock wave/turbulent boundary layer interaction in high-Reynolds-number hypersonic flows [AD-A188029] 11 p1434 N88-18555
Radial mixing in turbomachines [AD-A188028] 11 p1482 N88-18847
Effects of waves on the boundary layer of a surface-piercing flat plate: Experiment and theory [AD-A188356] 12 p1626 N88-19731
A simplified streamline swallowing procedure for the windward meridian of axisymmetric blunt bodies [AD-A188413] 12 p1626 N88-19732
The design and use of a temperature-compensated hot-film anemometer system for boundary-layer flow transition detection on supersonic aircraft [NASA-TM-100421] 13 p1723 N88-20304
Numerical experiments on the stability of controlled boundary layers [NASA-CR-181649] 13 p1771 N88-20591
General fuselage coordinates for the calculation of three-dimensional boundary layers [MBB/LKE-122/S/PUB/244] 13 p1771 N88-20596
Surface flow visualization of separated flows on the forebody of an F-18 aircraft and wind-tunnel model [NASA-TM-100436] 14 p1863 N88-21127
Boundary-layer and wake measurements on a swept, circulation-control wing [NASA-TM-89426] 15 p2014 N88-22013
Visualization of flows in turbomachinery [AD-A189927] 15 p2063 N88-22299
Cavitation inception in rectangular two-dimensional slots [AD-A190677] 15 p2066 N88-22318
Theoretical investigation of secondary instability of three-dimensional boundary-layer flows with application to the DFVLR-F5 model wing [DFVLR-FB-87-44] 15 p2068 N88-22330
Shear-layer structures in near-wall turbulence 16 p2196 N88-23110
Conditionally-averaged structures in wall-bounded turbulent flows 16 p2198 N88-23112
Nonlinear wave interactions in swept wing flows [NASA-CR-4142] 16 p2206 N88-23160
Solution of the compressible Navier-Stokes equations of motion by Chebyshev polynomials for laminar shock-boundary layer flow [AD-A191033] 16 p2208 N88-23176
Simulation of laminar-turbulent transition in the vicinity of a wall [AD-A191380] 16 p2208 N88-23180
Two-equation low-Reynolds-number turbulence modeling of transitional boundary layer flows characteristic of gas turbine blades [NASA-CR-4145] 16 p2209 N88-23185
Single phase liquid immersion cooling of discrete heat sources in a vertical channel [AD-A191224] 17 p2337 N88-23944
Unsteady flow about cambered plates [AD-A191226] 17 p2337 N88-23945
Surface curvature and pressure gradient effects on turbulent flow: An assessment based on numerical solution of the Reynolds equations 17 p2338 N88-23954
Transient particle deposition in a boundary layer of impulsive flow over a flat plate [AD-A191537] 18 p2508 N88-24880
Hypersonic turbulent wall boundary layer computations [NASA-CR-182147] 18 p2514 N88-24917
Correlations of velocity and temperature fluctuations in the stagnation-point flow of circular cylinder in turbulent flow [NASA-TM-100930] 19 p2597 N88-25435
Boundary layer development as a function of chamber pressure in the NASA Lewis 1030:1 area ratio rocket nozzle [NASA-TM-100917] 19 p2664 N88-25841
The heat transfer and fluid dynamics of concave surface curvature [AD-A193064] 21 p2943 N88-27479
A simple, analytic 3-dimensional downburst model based on boundary layer stagnation flow [NASA-TM-100632] 22 p3042 N88-28058
Flow dynamics stimulated by hairpin-like vortices in initially laminar boundary layers [AD-A194253] 22 p3075 N88-28254
Noise generation and boundary layer effects in vortex-airfoil interaction and methods of digital hologram analysis for these flow fields [AD-A194191] 23 p3171 N88-28883
The use of hot-film technique for boundary layer studies on a 21 percent thick airfoil [NAE-AN-45] 24 p3321 N88-29781

BOUNDARY LAYER NOISE*
U AERODYNAMIC NOISE
U BOUNDARY LAYERS

BOUNDARY LAYER PLASMAS
The formation of boundary layers by the entry of low-energy electrons and energetic ions into the Earth's magnetosphere 08 p1095 N88-16590
Fundamental studies on MPD thrusters [AD-A190307] 15 p2137 N88-22753
Plasma behavior in the boundary layer near a railgun surface [DE88-008889] 21 p3017 N88-27909

BOUNDARY LAYER SEPARATION
Calculation of three-dimensional stationary turbulent boundary layer on root section of wing ignoring compressibility 04 p0424 N88-12630
Numerical simulation of unsteady separated flows [AD-A184132] 04 p0442 N88-12741
Study of the effect of mass transfer on a transonic boundary layer. Application to flow relaminarization [ETN-88-91169] 05 p0541 N88-13296
Delta wing in incompressible flow. Experimental study in F2 [ONERA-RT-36/1147-AN-249-G] 05 p0541 N88-13298
Vortical Flows Research Program of the Fluid Dynamics Research Branch [NASA-TM-88332] 05 p0582 N88-13549
Post stall behavior in axial-flow compressors [AD-A185712] 06 p0665 N88-14081
Separated flow 07 p0812 N88-14944
Advanced natural laminar flow airfoil with high lift to drag ratio 07 p0812 N88-14947
Design and experimental evaluation of a swept supercritical Laminar Flow Control (LFC) airfoil 07 p0813 N88-14951
Three-dimensional unsteady flow elicited by finite wings and complex configurations [AD-A186464] 08 p0951 N88-15770
High-speed inlet research program and supporting analyses 08 p0958 N88-15811
A computationally efficient modelling of laminar separation bubbles [NASA-CR-182417] 08 p0984 N88-15949
Wind tunnel investigations of periodic vortex separation on rough-surface circular cylinders using acoustic measuring methods [DFVLR-FB-87-24] 09 p1112 N88-16665
Burst vortex/boundary layer interaction [NASA-CR-182510] 10 p1268 N88-17583
A theory for turbulent curved wall jets 10 p1269 N88-17590
Pressure distributions and oil-flow patterns for a swept circulation-control wing 10 p1270 N88-17596
Experimental research on swept shock wave/boundary layer interactions [AD-A187250] 10 p1331 N88-17957
Effects of waves on the boundary layer of a surface-piercing flat plate: Experiment and theory [AD-A188356] 12 p1626 N88-19731
Interaction between two-dimensional sonic jets and supersonic flow to model heat addition in a supersonic combustor [AD-A189572] 13 p1716 N88-20261
Coherent structure-reflective turbulent viscous flow modeling [AD-A188339] 13 p1765 N88-20556
A flight test investigation into flow separation and structural response for a transport aircraft at buffet onset [RAE-TR-87006] 14 p1867 N88-21156

Unsteady flow about cambered plates
[AD-A191226] 17 p2337 N88-23945

Accounting for the effects of unsteady, separated boundary layers in transonic two dimensional calculations
[ONERA-RT-30/3064-RY-063-R] 17 p2338 N88-23952

Instability of laminar separation bubbles: Causes and effects
[AD-A191168] 18 p2508 N88-24876

Computation of the turbulent boundary layer downstream of vortex generators
[AD-A191544] 18 p2508 N88-24881

Experimental study of unsteady separating turbulent boundary layers
[AD-A192997] 21 p2943 N88-27477

Physical mechanisms in shock-induced turbulent separated flow
[AD-A193165] 21 p2944 N88-27484

Study of three-dimensional transonic flow separations
[AD-A193018] 22 p3037 N88-28032

The dynamic behavior of a turbulent boundary layer subjected to a shock-induced separation
[AD-A194164] 22 p3075 N88-28252

Missiles, fuselage and similar bodies
23 p3167 N88-28858

Empirical tools for simulation methodologies
23 p3168 N88-28866

Calculation of aerodynamic characteristics of airplane configurations at high angles of attack
[NASA-CR-4182] 23 p3172 N88-28891

A study of the effect of random input motion on low Reynolds number flows
[AD-A195559] 24 p3316 N88-29747

The effects of incoming boundary layer thickness on unsteady shock-induced turbulent separations induced by cylinders
[AD-A196190] 24 p3368 N88-30060

BOUNDARY LAYER STABILITY

Experience about the application and valuation of roughness strips for boundary layer transition control in wind tunnel tests in the high-speed range
[ESA-TT-1028] 01 p0044 N88-10278

Theoretical analysis of primary instabilities in three dimensional boundary layer flows
[ESA-TT-1063] 03 p0315 N88-11992

Time-dependent hypersonic viscous interactions
[AD-A185764] 06 p0665 N88-14082

Low-disturbance wind tunnels
07 p0811 N88-14937

Boundary layer transition 07 p0811 N88-14942

Advanced natural laminar flow airfoil with high lift to drag ratio 07 p0812 N88-14947

Laminar flow integration: Flight tests status and plans
07 p0813 N88-14952

Secondary subharmonic instability of boundary layers with pressure gradient and suction
[NASA-CR-4112] 07 p0848 N88-15148

Calculation evaluation of the boundary conditions of autoinflammation of propulsive charges
[PB87-139044] 08 p0974 N88-15890

Oscillating airfoils: Achievements and conjectures
[AD-A190490] 15 p2014 N88-22008

The sensitivity of boundary layer instability growth rates to compliant wall properties
[AD-A190433] 15 p2064 N88-22309

Investigation of boundary layer disturbances caused by periodic heating of a thin ribbon
[AD-A190572] 15 p2065 N88-22314

Theoretical investigation of secondary instability of three-dimensional boundary-layer flows with application to the DFVLR-F5 model wing
[DFVLR-FB-87-44] 15 p2068 N88-22330

Spectral measurements in a disturbed boundary layer over snow
[AD-A190217] 15 p2097 N88-22494

Boundary-layer stability and airfoil design
17 p2296 N88-23739

Wind tunnel testing of low-drag airfoils
17 p2297 N88-23741

Cross stream differencing for integral boundary layer equations
[AD-A191744] 18 p2509 N88-24886

Active control of 2-D instability waves on an axisymmetric body
[AD-A191578] 19 p2663 N88-25835

Stability and drag reduction in a boundary layer with microbubbles
[AD-A191975] 23 p3209 N88-29099

A singular perturbation analysis of the weakly nonlinear evolution of long and short water waves and waves in boundary layers 23 p3209 N88-29102

BOUNDARY LAYER TRANSITION

The structure of separated flow regions occurring near the leading edge of airfoils including transition
[NASA-CR-181434] 01 p0002 N88-10011

Excitation of natural oscillations of a boundary layer by an external acoustic field 04 p0425 N88-12634

Numerical optimization of conical flow waveriders including detailed viscous effects
05 p0533 N88-13245

Hypersonic static and dynamic stability of axisymmetric shapes: A comparison of prediction methods and experiment 05 p0534 N88-13246

JPRS report: Science and technology. Japan
[JPRS-JST-87-028] 06 p0675 N88-14130

Visible boundary layer transition points through flight tests 06 p0675 N88-14136

Three-dimensional structure of boundary layers in transition to turbulence
[AD-A185466] 06 p0702 N88-14311

Low-disturbance wind tunnels
07 p0811 N88-14937

Flow diagnostics and visualization in wind tunnels and flight 07 p0811 N88-14940

Boundary layer transition 07 p0811 N88-14942

Advanced natural laminar flow airfoil with high lift to drag ratio 07 p0812 N88-14947

Computational design of natural laminar flow wings for transonic transport application 07 p0813 N88-14948

Natural laminar flow nacelle for transport aircraft
07 p0813 N88-14949

Design and experimental evaluation of a swept supercritical Laminar Flow Control (LFC) airfoil
07 p0813 N88-14951

Roughness and waviness requirements for laminar flow surfaces 07 p0813 N88-14953

Thin film electret boundary layer transition detector: A feasibility study
[AD-A185675] 07 p0856 N88-15199

Wake interaction effects on the transition process on turbine blades
[AD-A188020] 10 p1332 N88-17962

Investigations of the laminar-turbulent boundary layer transition for the improvement of the performance of powered glider aircraft profiles
[ETN-88-91094] 11 p1436 N88-18569

Structure of shear flow turbulence and its control
[AD-A187909] 11 p1482 N88-18846

Development of disturbances in swept wing flows
[NASA-CR-182675] 13 p1768 N88-20574

Preliminary in-flight boundary layer transition measurements on a 45 deg swept wing at Mach Numbers between 0.9 and 1.8
[NASA-TM-100412] 13 p1772 N88-20598

Turbulent transfer of momentum and heat in boundary layer of fluid beyond an obstacle. 1: Hydrodynamic characteristics 13 p1787 N88-20690

Propagation of artificial disturbances immersed in thick turbulent boundary layer 14 p1864 N88-21136

Control of laminar flow around of the wing in free-air conditions
[AD-A187479] 15 p2013 N88-22004

The sensitivity of boundary layer instability growth rates to compliant wall properties
[AD-A190433] 15 p2064 N88-22309

Theoretical investigation of secondary instability of three-dimensional boundary-layer flows with application to the DFVLR-F5 model wing
[DFVLR-FB-87-44] 15 p2068 N88-22330

Inflectional instabilities in the wall region of bounded turbulent shear flows 16 p2199 N88-23114

Two-equation low-Reynolds-number turbulence modeling of transitional boundary layer flows characteristic of gas turbine blades
[NASA-CR-4145] 16 p2209 N88-23185

Experimental study of bypass transition in a boundary layer
[NASA-TM-100913] 16 p2209 N88-23186

Boundary layer measurements using hot-film sensors
17 p2297 N88-23743

Natural laminar flow and airplane stability and control
17 p2298 N88-23747

Certification aspects of airplanes which may operate with significant natural laminar flow 17 p2298 N88-23749

Crossflow vorticity sensor
[NASA-CASE-LAR-13436-1-CU] 17 p2300 N88-23759

Boundary layer transition
[CERT-OA-37/5018-AYD] 18 p2458 N88-24595

Numerical simulation of transition to turbulence in plane Poiseuille flow by a spectral method
19 p2640 N88-25661

Study of the structure of turbulence in accelerating transitional boundary layers
[AD-A191698] 19 p2663 N88-25837

Boundary layer development as a function of chamber pressure in the NASA Lewis 1030:1 area ratio rocket nozzle
[NASA-TM-100917] 19 p2664 N88-25841

Numerical simulation studies of laminar-turbulent transition in the plan channel 19 p2665 N88-25850

Turbulence transition in a circular pipe
20 p2782 N88-26503

Empirical tools for simulation methodologies
23 p3168 N88-28866

Missiles, fuselages and similar bodies
23 p3169 N88-28869

Introduction and critical flow phenomena
23 p3169 N88-28870

Boundary layer development and transition
23 p3169 N88-28871

Classical separation, trailing-edge flows and buffeting
23 p3170 N88-28874

Environmental effects on transition and boundary layer characteristics 23 p3170 N88-28876

Boundary layer manipulation 23 p3170 N88-28877

Variable Sweep Transition Flight Experiment (VSTFE)-parametric pressure distribution boundary layer stability study and wing glove design task
[NASA-CR-3992] 23 p3173 N88-28894

On the generation of mean flows by the interaction of Goertler vortices and Tollmien-Schlichting waves in curved channel flows
[NASA-CR-181690] 24 p3315 N88-29743

Techniques used in the F-14 variable-sweep transition flight experiment
[NASA-TM-100444] 24 p3374 N88-30093

BOUNDARY LAYERS

NT ATMOSPHERIC BOUNDARY LAYER
NT COMPRESSIBLE BOUNDARY LAYER
NT HYPERSONIC BOUNDARY LAYER
NT INCOMPRESSIBLE BOUNDARY LAYER
NT LAMINAR BOUNDARY LAYER
NT PLANETARY BOUNDARY LAYER
NT SUPERSONIC BOUNDARY LAYERS
NT THERMAL BOUNDARY LAYER
NT THREE DIMENSIONAL BOUNDARY LAYER
NT TURBULENT BOUNDARY LAYER
NT TWO DIMENSIONAL BOUNDARY LAYER

Vortex/boundary-layer interactions: Data report, volume 1
[NASA-CR-181462] 02 p0121 N88-10768

Vortex/boundary-layer interactions: Data report, volume 2
[NASA-CR-181463] 02 p0122 N88-10769

Numerical simulation of a supersonic chemically reacting mixing layer 02 p0143 N88-10900

The four spot time-of-flight laser anemometer
02 p0184 N88-11145

Heat transfer in a real engine environment
02 p0186 N88-11155

Film cooling heat transfer on a turbine airfoil
02 p0186 N88-11156

Flow field measurements in a 90 degree turning duct
02 p0186 N88-11157

A flash spectrum of Cl I, C I, N I, and Ni II absorption in 31 Cygni: A direct observation of the reversing layer
04 p0513 N88-13158

Numerical simulation of boundary layers. Part 3: Turbulence and relaminarization in sink flows
[NASA-TM-88220] 06 p0698 N88-14283

An investigation of the effects of the propeller slipstream on a wing boundary layer 06 p0700 N88-14293

Experimental investigation of heterogeneous compressible shear layers 06 p0700 N88-14294

Studies of unsteadiness in boundary layers
[AD-A185662] 06 p0703 N88-14315

Modern concept concerning transport of bottom sediments in abyssal regions of world ocean
06 p0728 N88-14478

Observations of a midlatitude squall line boundary layer wake
[AD-A185609] 06 p0746 N88-14589

Spectral methods: Analysis and applications to flow problems
[AD-A186265] 07 p0850 N88-15156

Consistent boundary conditions for Reduced Navier-Stokes (RNS) scheme applied to 3-dimensional internal viscous flows
[NASA-CR-180874] 08 p0950 N88-15762

Friction drag reduction (a speculative essay)
[INPE-4278-PRE/1150] 08 p0988 N88-15995

Influence of the wall boundary layer on force measurements on half models in the transonic wind tunnel
[F+W-TF-1876] 09 p1122 N88-16715

Use of boundary-layer method for problem of sound propagation through channel with variable cross-section containing stream of fluid 09 p1233 N88-17396

Beta limitation of matter-antimatter boundary layers
[TRITA-EPP-87-11] 09 p1250 N88-17490

Free-surface flow phenomena ahead of a two-dimensional body in a viscous fluid
10 p1329 N88-17944

Experimental research on swept shock wave/boundary layer interactions
[AD-A187250] 10 p1331 N88-17957

On the stability of the supersonic boundary layer
11 p1435 N88-18561

Analysis of shear-layer probe data for holes in hypersonic configurations
[DE88-003992] 11 p1435 N88-18564

Thermal cracking and variable properties effects on free boundary layer diffusion flames
[NBS/GCR-88/542] 12 p1614 N88-19652

Effects of waves on the boundary layer of a surface-piercing flat plate: Experiment and theory
[AD-A188356] 12 p1626 N88-19731

A finite-amplitude analysis of the buoyant instability of a highly viscous film over a less viscous half-space
13 p1769 N88-20581

Dynamical modeling of marine boundary layer convection 13 p1797 N88-20750

Proceedings of the Seminar on Hydrodynamics and Crystal Growth
[ETN-88-92025] 14 p1987 N88-21853

Transport processes during directional solidification and crystal growth: Scaling and experimental study
14 p1988 N88-21857

High Reynolds number, low Mach number, steady flow field calculations over a NACA 0012 airfoil using Navier-Stokes and interactive boundary layer theory
[AD-A189871] 15 p2013 N88-22005

Coherent structure 16 p2199 N88-23117

Coherent structures and modeling: Some background comments 16 p2199 N88-23120

High Reynolds number tests of a Douglas DLBA 032 airfoil in the Langley 0.3-meter transonic cryogenic tunnel
[NASA-TM-87663] 17 p2296 N88-23734

Boundary layer measurements using hot-film sensors
17 p2297 N88-23743

Unsteady flow about cambered plates
[AD-A191226] 17 p2337 N88-23945

A formulation for the boundary-layer equations in general coordinates
[NASA-TM-100079] 18 p2459 N88-24600

Flame spread mechanisms over PMMA surfaces
[NASA-TT-20284] 19 p2612 N88-25500

Ignition and flammability characteristics of solid fuel ramjets 19 p2626 N88-25575

Boundary layer simulator (BLIMPJ) improvement
19 p2627 N88-25582

Numerical investigation of acoustic energy exchange through flow turning 19 p2629 N88-25593

Investigation of Rossby-number similarity in the neutral boundary layer using large-eddy simulation
[DE88-008910] 19 p2666 N88-25851

A domain decomposition method for boundary layer problems
[DE88-008917] 19 p2666 N88-25852

Prediction of continental shelf sediment transport using a theoretical model of the wave-current boundary layer
[AD-A192272] 20 p2829 N88-26783

Solution of the Orr-Sommerfeld equation for the Blausius boundary-layer documentation of program ORRBL and a test case
[NASA-CR-4169] 20 p2841 N88-26858

The diffusion of vorticity from a plane boundary
[AD-A192706] 21 p2942 N88-27474

IR (infrared) sky radiance distributions in the marine boundary layer
[AD-A193883] 22 p3119 N88-28531

Shock boundary layer interaction
23 p3170 N88-28873

Three-dimensional laser Doppler velocimeter studies of flow in a 90 deg curved duct having a square cross-section 23 p3209 N88-29101

Polynomial definition of discrete field points of map of diffusion equation, part 1
[AD-A193697] 23 p3271 N88-29467

Temperature profile construction methods: An evaluation
[AD-A195919] 24 p3403 N88-30262

BOUNDARY LUBRICATION

The performance of perfluoropolyalkylether oils under boundary lubrication conditions
[AD-A191057] 17 p2323 N88-23869

Perfluoropolyalkylether lubricants under boundary conditions: Iron catalysis of lubricant degradation
[AD-A193241] 21 p2956 N88-27580

Evaluation of transfer films of Salox M on 440C for HPOTP bearing cage applications, task 119
[NASA-CR-179020] 23 p3223 N88-29184

BOUNDARY VALUE PROBLEMS

NT CAUCHY PROBLEM
NT DIRICHLET PROBLEM
NT NEUMANN PROBLEM

Inhomogeneous conditions at open boundaries for wave propagation problems
[AD-A183847] 01 p0033 N88-10214

An exact theory of elastic plates
[ETN-87-90675] 01 p0062 N88-10396

Regularity properties of a doubly degenerate equation in hydrology
[REPT-87-07] 01 p0084 N88-10409

An asymptotic theory for a class of initial-boundary value problems for weakly nonlinear wave equations with an application to a model of the galloping oscillations of overhead transmission lines
[REPT-87-12] 01 p0086 N88-10556

Computing the bounded region determined by finitely many lines in the plane
[CS-8703] 01 p0086 N88-10558

Effect of dissipation on propagation of spherical detonation shock wave 02 p0159 N88-10996

Analysis of thickness fields retrieved from NOAA-7 observations through the 3I (Improved Initialization Inversion) method. Interest for weather forecasting
02 p0201 N88-11255

Strategies for using mesoscale data in an operational mesoscale model 02 p0212 N88-11335

Toward optimizing the use of data for operational mesoscale forecasting at the National Meteorological Center 02 p0213 N88-11337

Initialization experiments with the NMC nested grid model --- National Meteorological Center (NMC)
02 p0213 N88-11343

Four-dimensional initialization of mesoscale models
02 p0214 N88-11349

Preconditioned iterative methods applied to singularly perturbed elliptic boundary value problems: Volume 2
[DE87-014337] 02 p0225 N88-11415

The method of lines for time dependent free boundary problems
[DE87-013929] 02 p0226 N88-11423

IMPSOR: A fully vectorized FORTRAN code for three dimensional moving boundary problems with Dirichlet or Neumann boundary conditions
[DE87-014964] 02 p0226 N88-11427

A collection of test problems for ordinary differential equation solvers which have provisions for rootfinding
[DE88-000045] 02 p0226 N88-11428

Stability of semidiscrete approximations for hyperbolic initial-boundary-value problems: An eigenvalue analysis
[NASA-TM-88328] 02 p0227 N88-11434

Numerical modeling: Finite methods
03 p0304 N88-11916

Dynamics of the von Karman vortex street
03 p0316 N88-11998

The diffusion-convection vortex method for solving two-dimensional incompressible Navier-Stokes equation
03 p0317 N88-12001

Nonlinear thermoviscoelastic analysis of metallic plane curved beams 03 p0336 N88-12119

Numerical solution of bound constrained problems
[DE88-000653] 03 p0371 N88-12334

Numerical prediction of propeller performance by vortex lattice method
[UTIAS-TN-265] 04 p0400 N88-12489

Three-dimensional, free-Lagrange hydrodynamics
[DE88-000494] 04 p0443 N88-12749

Analytical studies of axially symmetric motion of an incompressible viscous fluid between two concentric rotating spheres 04 p0444 N88-12757

Higher order theory analysis of a modified free-edge delamination specimen 04 p0455 N88-12820

On operator splitting for unsteady boundary value problems
[AD-A184281] 04 p0484 N88-12981

Solution of some 3-D viscous and inviscid supersonic flow problems by finite-volume space-marching schemes
05 p0532 N88-13235

Numerical experiments with hypersonic flows beneath a cone-delta-wing combination 05 p0532 N88-13238

Development of an integrated BEM approach for hot fluid structure interaction
[NASA-CR-181577] 05 p0556 N88-13384

Mechanics of anisotropic media. Study of the boundary conditions --- stratified composites
[SNIAS-872-430-112] 05 p0559 N88-13404

An examination of chaotic motion for the buckled beam 05 p0597 N88-13644

On a boundary data operator and generalized exterior Robin problems for the Helmholtz equation
[AD-A185124] 05 p0640 N88-13915

Guidance and control strategies for aerospace vehicles
[NASA-CR-181579] 05 p0643 N88-13935

Boundary layer equations and methods of solution
06 p0701 N88-14302

Modified quantum mechanics of small composite systems
[NIKHEF-H/87-1] 06 p0790 N88-14845

Stability analysis of finite difference schemes for hyperbolic systems, and problems in applied and computational linear algebra
[AD-A185824] 07 p0906 N88-15499

Perturbative coherence in field theory
[DE88-700366] 07 p0941 N88-15717

A semianalytical solution of the heat conduction equation for several boundary conditions
08 p1014 N88-16148

Adaptive finite element methods for parabolic systems in one- and two-space dimensions
[AD-A186534] 08 p1073 N88-16475

Equation of gravitational-gyroscopic waves: Angular potential and its applications 08 p1079 N88-16504

An initial investigation into methods of computing transonic aerodynamics sensitivity coefficients
[NASA-CR-182444] 09 p1112 N88-16663

Investigation of iterative and spectral Galerkin techniques for solving electromagnetic boundary value problems 09 p1155 N88-16925

Steady ship waves at low Froude numbers, part 2
[AD-A176805] 09 p1160 N88-16953

A guide to the transient three phase porous flow model implemented in the two-dimensional CRAY-TENSOR code: Physics, numerics, and code description
[DE88-003709] 09 p1165 N88-16983

A quasi-three-dimensional calculation procedure for the prediction of flow and heat transfer in heat exchanger passages 09 p1165 N88-16985

Feedback stabilization of distributed systems
[AD-A187111] 09 p1222 N88-17328

Note on boundary stabilization of wave equations
[AD-A187113] 09 p1227 N88-17348

Boundary value problems for ordinary differential equations with multiple turning points
[CWI-AM-R8701] 09 p1228 N88-17354

Numerical solutions of two moving boundary problems by both finite difference and finite element methods with applications
[DE88-002867] 09 p1230 N88-17374

An experimental investigation of pressure driven three-dimensional turbulent boundary layers
10 p1327 N88-17934

Free-surface flow phenomena ahead of a two-dimensional body in a viscous fluid
10 p1329 N88-17944

The h-p version of the finite element method for problems with nonhomogeneous essential boundary condition
[AD-A187356] 10 p1400 N88-18348

Boundary value problems for differential and functional differential equations
[AD-A187378] 10 p1400 N88-18349

On an overdetermined Neumann problem
[AD-A187451] 10 p1401 N88-18352

Time delays and boundary feedback stabilization in one-dimensional viscoelasticity, appendices A through H
[AD-A187534] 10 p1401 N88-18353

Integral equations with modified fundamental solutions for exterior boundary value problems from electromagnetic wave theory
[ETN-88-91483] 11 p1475 N88-18800

On the dissipative response due to discontinuous strains in bars of unstable elastic material
[AD-A188114] 11 p1498 N88-18947

Spatial-temporal variability of North Pacific sea surface temperature anomaly patterns 11 p1516 N88-19058

Parallel pseudospectral domain decomposition techniques
[NASA-CR-181629] 11 p1524 N88-19101

Estimates of green tensors for certain boundary value problems
[NASA-TT-20203] 11 p1535 N88-19172

Accurate boundary conditions for exterior problems in gas dynamics
[NASA-TM-100607] 11 p1537 N88-19182

Accelerating the computation of steady state solutions for non-equilibrium, chemically reacting flow fields
12 p1625 N88-19724

Mesoscale monitoring of the soil freeze/thaw boundary from orbital microwave radiometry
[NASA-CR-182659] 12 p1645 N88-19855

Error questions in the computation of solution manifolds of parametrized equations
[AD-A188648] 12 p1684 N88-20068

Study of inhomogeneously filled cylindrical resonant cavities by the finite integration technique
[PB88-133707] 12 p1697 N88-20156

Predicting oscillatory finite difference solutions to the heat equation: A comparative study of the coefficient and matrix methods
[AD-A189591] 13 p1825 N88-20911

Convergence of Runge-Kutta methods on classes of stiff initial value problems
[CWI-NM-R8717] 13 p1827 N88-20924

Double layer polarization of nonconducting spheroidal particles and its application to Kerr effect
[ISSN-0208-5658] 13 p1832 N88-20960

Solutions for direct and indirect problems in free surface flows
[REPT-87-35] 14 p1909 N88-21409

Nonlinear normal mode initialization of a limited area model using nonstationary Rossby modes -- numerical weather forecasting
[KNMI-WR-87-10] 14 p1947 N88-21614

A spline collocation method for integral equations of the first kind with logarithmic singularity -- boundary value problems
[REPT-87-39] 14 p1963 N88-21712

On a class of similarity solutions of the equation u sub t = (absolute value of u sup m-1 u sub x) sub x with m greater than -1
[REPT-87-54] 14 p1963 N88-21713

Some maximum norm estimates for the finite element method applied to nonlinear two dimensional boundary value problems
[ETN-88-91505] 14 p1964 N88-21715

Boundary stabilization of the reaction-diffusion equation with unilateral conditions
[RR-315] 14 p1964 N88-21720

Global spatial periodic solutions to the Ginzburg-Landau equations
[DE88-006424] 15 p2119 N88-22623

Numerical methods for singularly perturbed differential equations with applications
[AD-A189786] 15 p2119 N88-22628

Pointwise stabilization for coupled quasilinear and linear wave equations
[AD-A190031] 15 p2120 N88-22632

Sequential tests for the drift of a Wiener process with a smooth prior and the heat equation
[AD-A190322] 15 p2121 N88-22638

Stopping rules and observed significance levels
[AD-A190320] 15 p2124 N88-22664

Some numerical methods for the computation of capillary free boundaries governed by the Navier-Stokes equations
[REPT-87-69] 16 p2206 N88-23167

Modeling and estimation of a low degree geopotential model from terrestrial gravity data
[NASA-CR-182808] 16 p2232 N88-23330

Continuous decoupling transformations for linear boundary value problems
[ETN-88-92248] 16 p2258 N88-23493

Spectral analyses in the linear geodetic boundary value problem
[B8735056] 16 p2259 N88-23502

Algorithm for accounting the conditions in infinity for two-dimensional magnetostatics problems
[DE88-701673] 16 p2264 N88-23541

Nonlinear wave and diffusion equations
[AD-A191421] 16 p2265 N88-23544

Analysis for fuel implosion in ICF target and pellet gain 16 p2276 N88-23620

Parameter estimation for boundary value problems by integral equations of the second kind
[NASA-CR-181660] 17 p2332 N88-23918

The calculation of transonic flow over the shuttle orbiter using slender body theory 18 p2460 N88-24606

Computation and characteristics of pulsatile multi-bifurcation flow 18 p2483 N88-24729

Nonlinear waves
[AD-A192148] 18 p2510 N88-24889

Duct flow nonuniformities for Space Shuttle Main Engine (SSME)
[NASA-CR-179338] 18 p2511 N88-24899

Advanced development of the boundary element method for elastic and inelastic thermal stress analysis
18 p2529 N88-25002

NFEARS: A nonlinear adaptive finite element solver, part 1
[AD-A191823] 18 p2563 N88-25215

Solving time-dependent two-dimensional eddy current problems
[NASA-TM-100875] 18 p2566 N88-25239

Stability and convergence of the Peaceman-Rachford ADI method for initial-boundary value problems
[CWI-NM-R8724] 18 p2566 N88-25243

On bunch lengthening using the fourth harmonic cavity in the NSLS VUV ring
[DE88-007392] 18 p2574 N88-25288

Characterization of a modified Rijke burner for measurement of distributed combustion
19 p2628 N88-25587

Static analysis of thin plates using the finite strip-element method 19 p2679 N88-25931

Modelling and forecasting deep ocean and near surface mesoscale eddies: Hindcasting and forecasting with, and coupling a surface boundary layer model to, the Harvard quasigeostrophic model 19 p2694 N88-26013

Initial value problems for nonlinear heat equations
[DE88-702021] 19 p2737 N88-26251

Vortex methods for separated flows
[NASA-TM-100068] 20 p2753 N88-26342

Vibration frequencies of tapered bars with nonclassical boundary conditions
[NASA-CR-183059] 20 p2813 N88-26688

Off-boundary approach to the boundary element method
[AD-A192831] 20 p2815 N88-26701

Thermo-viscoelastic analysis of composite materials, volume 1
[NASA-CR-183048-VOL-1] 21 p2904 N88-27230

Investigation of viscous/inviscid interaction in transonic flow over airfoils with suction
[NASA-CR-183112] 21 p2945 N88-27490

Initial boundary value problems of nonlinear wave equations in an exterior domain
[DE88-701883] 21 p3026 N88-27962

Development of direct-inverse 3-D methods for applied transonic aerodynamic wing design and analysis
[NASA-CR-183127] 22 p3037 N88-28033

Optimum-Path-to-Go guidance of command adjusted trajectory projectiles
[AD-A193377] 22 p3040 N88-28051

Non-reflecting boundary conditions for computations of unsteady flows in turbomachines
[PNR90469] 22 p3079 N88-28284

Regularity of solutions for nonlinear degenerate elliptic boundary value problems
[DE88-702646] 22 p3146 N88-28710

The influence of numerical boundary conditions on transonic flow
[DFVLR-FB-88-06] 23 p3172 N88-28890

Computation of the eigenvalues for perturbations of Poiseuille flow using a two-point boundary value method
[AD-A193479] 23 p3210 N88-29104

Nonlinear dynamic analysis and optimal control of shallow shells 23 p3224 N88-29191

Thickness effects on the stability of shell like structures 23 p3224 N88-29192

Stability of semidiscrete approximations for hyperbolic initial-boundary-value problems: Stationary modes
[NASA-TM-100994] 23 p3270 N88-29455

Canonical forms in the control of DPS
[AD-A194671] 23 p3270 N88-29461

Stability and convergence in the numerical solution of stiff initial value problems
[B8681480] 23 p3272 N88-29474

Nonlinear elliptic problems with critical exponent in shrinking annuli
[W-02/87] 23 p3273 N88-29477

Elliptic equations with nearly critical growth
[W-16-87] 23 p3273 N88-29478

The acoustic field scattered from some approximate pressure release materials
[AD-A194768] 23 p3278 N88-29515

Theory of filtering and control with application to control of large space structures
[AD-A195500] 24 p3335 N88-29851

Initial value problems in viscoelasticity
[AD-A196052] 24 p3382 N88-30145

Stability, stochastic stationarity and generalized Lyapunov equations for two-point boundary-value descriptor systems
[AD-A195645] 24 p3425 N88-30385

Multiple solutions and bifurcation for a class of nonlinear Sturm-Liouville eigenvalue problems on an unbounded domain
[AD-A195854] 24 p3426 N88-30389

BOW SHOCK WAVES

U BOW WAVES

U SHOCK WAVES

BOW WAVES

Slow-mode shocks in the earth's magnetosphere
[DE88-000483] 04 p0468 N88-12895

On the numerical simulation of three-dimensional hypersonic flow 05 p0532 N88-13237

The off-design performance of hypersonic waveriders
05 p0533 N88-13244

AMPTE-UKS ion observations at a quasi-parallel bow shock 08 p1095 N88-16589

On the start up of supersonic underexpanded jets -- Mach disks 11 p1435 N88-18563

To what extent is mass loading responsible for the Venus bowshock precursor?
[NASA-TM-89307] 12 p1711 N88-20239

The foreshock region upstream from the Comet Halley bow shock 14 p1995 N88-21893

BOX BEAMS

Design procedures for fiber composite box beams
[NASA-TM-100296] 09 p1139 N88-16828

BOXES (CONTAINERS)

Cage mode propagation experiments
[AD-A186019] 07 p0841 N88-15100

FEB (Multifilter Electronics Box) lifting device analysis, revision A
[AD-A192313] 21 p2935 N88-27427

BRACKETS

Mechanical design of the ac bracket package for the RETE experiment
[IFSI-87-4] 05 p0555 N88-13379

Partially braced [illegible] beam buckling experiments
[PB87-133831] 06 p0723 N88-14444

Locking hinge
[NASA-CASE-MSC-21056-1] 17 p2312 N88-23827

BRAGG ANGLE

Distributed feedback effects in lasers and high gain laser instabilities in optically pumped CH3F
03 p0329 N88-12079

Models for electromagnetic scattering from the sea at extremely low grazing angles
[AD-A190472] 15 p2057 N88-22261

BRAIN

NT CEREBELLUM

NT CEREBRAL CORTEX

NT CEREBRUM

NT HIPPOCAMPUS

NT HYPOTHALAMUS

NT THALAMUS

Latency differences and effects of selective attention to gratings in the central and right visual fields: 2
[DE87-014730] 04 p0473 N88-12918

Influence of general vertical vibration on relationships between mediators in various segments of brain
06 p0751 N88-14613

Dimensional analysis of nonlinear oscillations in brain, heart and muscle
[DE87-014749] 06 p0751 N88-14614

Model based monitoring of human sleep stages
[ISBN-90-9001448-9] 06 p0752 N88-14618

Brain morphogenesis in rats developing in weightlessness 07 p0894 N88-15415

Evoked brain activity and personnel performance
[AD-A185922] 07 p0897 N88-15436

Neurochemical changes in hibernation
08 p1046 N88-16322

Effects of extreme hypoxia on phospholipid metabolism in subcellular structures of rat brain
08 p1046 N88-16323

Late radiation damage in bone, bone marrow and brain vasculature, with particular emphasis upon fractionation models
[DE87-753039] 08 p1048 N88-16330

Changing the layers of mind
[AD-A186648] 08 p1052 N88-16350

An innovative workstation 08 p1063 N88-16421

Knowledge representation by connection matrices: A method for the on-board implementation of large expert systems 08 p1065 N88-16434

Probabilistic neural networks: In or out of equilibrium
[DE88-002907] 09 p1201 N88-17198

Development and experimentation of an eye/brain/task testbed 09 p1205 N88-17219

Effect of exogenous cardiosynchronized counterpulsation on human regional and central hemodynamics 10 p1366 N88-18163

Center for nonlinear dynamics of the brain
[AD-A187245] 11 p1518 N88-19068

Three-dimensional computer graphics brain-mapping project
[AD-A187202] 11 p1528 N88-19126

Effects of intense, time-constrained mental effort on hemodynamics and cardiovascular function
12 p1664 N88-19975

Protection from stress 12 p1664 N88-19978

Risk of hypertension and functional cerebral laterality in oil expedition works in far north
12 p1665 N88-19980

Brain activity during tactical decision-making. Part 2: Probe-evoked potentials and workload
[AD-A188688] 12 p1667 N88-19994

Neurocognitive predictions of performance
[AD-A188323] 12 p1669 N88-19998

Neurophysiological predictors of quality of performance 16 p2242 N88-23391

The event-related brain potential as an index of information processing and cognitive activity: A program of basic research
[AD-A191244] 16 p2243 N88-23400

Role of opioid peptides in pathogenesis of vestibulovegetative disorders 19 p2704 N88-26079

Effect of low-frequency whole-body vertical vibration on the serotoninergic system of the brain and spinal cord
19 p2704 N88-26081

Effect of weightlessness on brain development (results of flight of pregnant rats on Kosmos-1514 biosatellite and study of subsequent development of their progeny on earth 20 p2829 N88-26786

Studies of the intact human brain: Implications for performance 21 p2977 N88-27684

CEEG dynamic brain mapping: A new method to evaluate brain function in different psychological and drug conditions 21 p2977 N88-27685

Fourth generation neurocognitive pattern analysis system 21 p2977 N88-27686

Normative developmental equations for the EEG and their sensitivity to neurological and psychiatric disorders
21 p2977 N88-27687
Squid instrumentation for neuromagnetic study of complex brain activity 21 p2978 N88-27691
Electric and magnetic brain activity related to cognitive performance 21 p2979 N88-27692
Neuromagnetic evidence of place mechanisms for frequency and intensity coding in the human auditory cortex 21 p2979 N88-27693
A study of sources in the human brain associated with stereopsis 21 p2979 N88-27695
Event-related brain potentials as indices of mental workload and attentional allocation
21 p2979 N88-27696
Using ERPS to study human information processing
21 p2980 N88-27698
Cognitive task demands as reflected in physiological measures 21 p2980 N88-27699
The effect of endogenous alpha on hemispheric asymmetries and the relationship of frontal theta to sustained attention 21 p2980 N88-27701
Fighter pilot performance during airborne and simulator missions: Physiological comparisons
21 p2981 N88-27704
Event-related and steady potential changes in the brain related to workload during tracking
21 p2981 N88-27705
EEG indices of G-induced Loss Of Consciousness (G-LOC) 21 p2982 N88-27709
Motion evoked vestibular potentials
21 p2982 N88-27712
The effect of mild hypoxia on the vestibular evoked response 21 p2982 N88-27713
An approach to studying the effects of psychostimulants on cerebral electrical activity in the non-human primate
21 p2983 N88-27716
Spontaneous cerebral electrical activity during prolonged hypoglycemia: A quantitative study in humans
21 p2983 N88-27717
Correlation between EEG abnormal activity and aircraft accidents: A long term observation
21 p2984 N88-27719
Cognitive and neural bases of skilled performance
[AD-A193392] 21 p2992 N88-27747
Content-addressable memory storage by neural networks: A general model and global Liapunov method
[AD-A192716] 21 p3002 N88-27807
New method for the study of spontaneous brain activity
[AD-A193813] 22 p3132 N88-28624
SQUID (superconducting quantum interference device) arrays for simultaneous magnetic measurements: Calibration and source localization performance
[AD-A193815] 23 p3216 N88-29143
Methods and instrumentation for biomagnetism
[AD-A193811] 23 p3239 N88-29278
Design of a feeling-thinking machine
[AD-A194107] 23 p3267 N88-29448
Central adrenergic receptors as mediators of central response to stress: Study with Positron Emission Tomography (PET)
[AD-A194947] 24 p3407 N88-30284

BRAIN CIRCULATION
Fast dynamic studies with PC384-7B; system improvements and development of an automated blood sampling system --- tomography
[USIP-87-05] 01 p0075 N88-10481
Studies of the processing of single words using positron tomographic measures of cerebral blood flow change
[AD-A184058] 03 p0356 N88-12244
Change in functional activity of cortical brain structures and their blood supply in alert rabbits in response to rocking 04 p0473 N88-12916
Circulatory response of males 45-52 years of age to antiorthostatic hypokinesia 07 p0894 N88-15416
Models of cerebral-body perfusion and cerebral chemical transport
[AD-A194945] 24 p3407 N88-30283

BRAIN DAMAGE
Neuropeptides in experimental head injury
[AD-A188067] 11 p1520 N88-19077
Three-dimensional computer graphics brain-mapping project
[AD-A187202] 11 p1526 N88-19126

BRAKES
Preloaded brake disc
[NASA-CASE-MSC-21132-1] 23 p3223 N88-29181

BRAKES (FOR ARRESTING MOTION)
NT AIRCRAFT BRAKES
NT DRAG CHUTES
NT LEADING EDGE FLAPS
NT TRAILING EDGE FLAPS
NT VORTEX FLAPS
NT WING FLAPS
Developing an accelerated endurance test for greases: A status report
[AD-A185963] 07 p0836 N88-15072
Aerodynamic and thermal modeling of electromagnetic brakes. Evaluation of convective exchange coefficients and friction losses in the rough wall channels
[ISAL-ITC1-87-02] 16 p2215 N88-23214

BRAKING
Flaps-up takoff performance of the OV-1D aircraft with YT53-L-704 engine installed
[AD-A185960] 07 p0819 N88-14979

BRANCHING (MATHEMATICS)
NT PERIOD DOUBLING
Fully developed turbulence via Feigenbaum's period-doubling bifurcations
[DE88-000242] 04 p0441 N88-12739
Application of the Von Karman equation to the bifurcation theory
[NOTA-INTERNA-891] 05 p0642 N88-13927
Transient periodic behavior related to a saddle-node bifurcation
[ETN-88-91321] 05 p0642 N88-13928
Tutorial on elementary bifurcation theory
[DE87-014849] 05 p0642 N88-13932
Subcritical branching processes in a two state random environment, and a percolation problem on trees
[PB87-230439] 06 p0762 N88-14677
Global bifurcation of periodic solutions with symmetry
[AD-A185881] 07 p0908 N88-15501
Local bifurcation control
[AD-A187435] 10 p1324 N88-17915
Joint moments of the maximum in a critical branching process
[AD-A188157] 11 p1541 N88-19209
Problems in fluid dynamics
[NASA-CR-182678] 14 p1909 N88-21410
Bifurcations in unsteady aerodynamics-implications for testing
[NASA-TM-100083] 15 p2015 N88-22014
Symmetry and global bifurcation in nonlinear solid mechanics
[AD-A190521] 15 p2121 N88-22642
Research in nonlinear partial differential equations and bifurcation theory
[AD-A190986] 16 p2260 N88-23514
Generalized Jordan chains and two bifurcation theorems of Krasnoselskii
[AD-A192353] 21 p3008 N88-27845
Bifurcations of periodic solutions of non-integrable Hamiltonians with two degrees of freedom: Numerical and analytical results
[DE88-702747] 23 p3272 N88-29473

BRANCHING (PHYSICS)
W decays
[NOTA-INTERNA-877] 05 p0648 N88-13966
The numerical and analytical study of bifurcation and multicellular flow instability due to natural convection between narrow horizontal isothermal cylindrical annuli at high Rayleigh numbers 10 p1328 N88-17937
Systematics on neutron-induced isomeric cross-section ratios at 14.5 MeV
[ECN-200] 14 p1980 N88-21815
Gluino branching ratio effects on the search for supersymmetry
[PREPRINT-572] 14 p1981 N88-21821

BRASSES
Analysis of free cutting brass by A.C. polarography
[PD-MT-8728] 04 p0417 N88-12587
Materials dependence of deformation texture development in various deformation modes
[DE88-004312] 14 p1922 N88-21457

BRAVAIS CRYSTALS
Equilibria, lattices and chaotic dynamics of point vortices 04 p0444 N88-12758

BRAYTON CYCLE
The Goddard Space Flight Center mechanical cooler program 08 p0983 N88-15944
Design features of small Brayton cycles for autonomous underwater vehicles
[AD-A187799] 11 p1506 N88-18999
Gas-cooled reactor power systems for space
[DE88-005220] 11 p1545 N88-19240
Comparison of entropy generation and conventional design methods for heat exchangers
[AD-A190256] 15 p2064 N88-22306
Speculations on future opportunities to evolve Brayton powerplants aboard the space station
17 p2398 N88-24258
Characteristics of the closed Brayton cycle for dynamic isotope power systems 17 p2422 N88-24401
Dynamic isotope power system critical component verification 17 p2425 N88-24421
SNAP-DYN: Proven technology for wear-term, higher power in space 17 p2425 N88-24422
The closed Brayton cycle. An energy conversion system for near-term military space missions
17 p2435 N88-24488
The effect of operating temperature and turbine blade cooling on Brayton cycle space power systems
17 p2435 N88-24489
A combined Rankine/Brayton pulse power cycle
17 p2435 N88-24490
Energy conversion system optimization study for multimegawatt space nuclear power application
17 p2436 N88-24492
Advanced energy system program
[PB88-183025] 19 p2686 N88-25965

BRAZIL
Impacts of world development on selected characteristics of the atmosphere: An integrative approach. Volume 1: Main report
[DE88-001495] 07 p0875 N88-15309
Actual performance and economic feasibility of residential solar water heaters
[INPE-4399-RPE/555] 08 p1023 N88-16191
Conditions and mechanisms of the process of technological innovation in Brazil: The role of research institutes
[INPE-4175-TDL/274] 11 p1567 N88-19383
Crop forecasting in Brazil. A short history of productivity models
[INPE-4150-PRE/1056] 12 p1637 N88-19801
Mapping of the mangroves of the Guanabarra Bay through the utilization of remote sensing techniques
[INPE-3942-TDL/229] 12 p1637 N88-19804
High altitude chemical release systems for project BIME (Brazilian Ionospheric Modification Experiments) project IMS (Ionospheric Modification Studies) project PIIE (Polar Ionospheric Irregularities Experiment) project polar arcs
[AD-A188299] 12 p1642 N88-19833
The use of a barotropic finite element model for the study of circulation on the continental shelf of the southeast coast of Brazil
[INPE-4401-PRE/1218] 13 p1802 N88-20774
Radon-222 in the Antarctic Peninsula
[INPE-4486-PRE/1251] 15 p2092 N88-22468
The necessity of automation in Brazil
[INPE-4346-PRE/1183] 15 p2150 N88-22832
The 1985 mutual phenomena of Jupiter's satellites observed in Brazil
[INPE-4526-PRE/1276] 15 p2152 N88-22848

BRAZILIAN SPACE PROGRAM
BRASILSAT A2: Ground and in-orbit anomalies
02 p0164 N88-11032
Vehicle glow observed on the SONDA 3
[INPE-4297-PRE/1168] 12 p1600 N88-19581
Multilayer thermal insulation tests
[INPE-4475-PRE/1243] 12 p1626 N88-19729
Report of the participation in the International Training Course: Remote Sensing in Village Forestry
[INPE-4476-NTE/278] 12 p1637 N88-19802
Solar cell experiment on the first satellite of the Brazilian complete space mission
[INPE-4248-PRE/1121] 14 p1880 N88-21238
INPE position paper on the CCSDS standardized method of link budget computation
[INPE-4533-NTE/279] 15 p2148 N88-22820

BRAZING
Process and equipment capabilities materials joining laboratory, 1987
[DE87-014534] 02 p0180 N88-11122
Low-pressure eutectic bonding of depleted uranium to copper
[DE87-014625] 02 p0181 N88-11128
Investigation on diffusion reaction brazing of aluminum
[PB87-143368] 08 p0992 N88-16001
Transmission electron microscopy studies of titanium-containing braze/alumina seals
[DE88-005243] 10 p1303 N88-17792
Technology for pressure-instrumented thin airfoil models
[NASA-CR-4173] 23 p3180 N88-28933

BREADBOARD MODELS
Design, manufacture and testing of an elegant breadboard model communications processor
[D/2244] 01 p0034 N88-10217
Coherent infrared detection, volume D --- CO2 laser intersatellite data link
[ESA-CR(P)-2392-VOL-2] 01 p0034 N88-10219
Microprocessor control and networking for the amps breadboard 07 p0924 N88-15615
High-resolution Real-Time Radiography (RTR) system design
[AD-A187107] 09 p1166 N88-16992
Design of a linear actuator and breadboard test result --- far IR telescope 14 p1877 N88-21217
Docking/berthing subsystem: Design and breadboard test 14 p1879 N88-21233

Mid infrared multichannel focal plane breadboard --- pushbroom sensors
[RT-87/014] 14 p1982 N88-21827

Nondestructive evaluation of large scale composite components
[AD-A190998] 16 p2173 N88-22954

Botany Facility. Thermal Control (TC) subsystem test report on experiment container of laboratory model and breadboard centrifuge
[BF-TN-ER-061/86] 17 p2378 N88-24135

Botany Facility: Test report on breadboard tests for the determination of the heat transfer at the glass disk and of the temperature distribution in the fluorescent tube
[BF-TN-ER-053] 17 p2378 N88-24136

Botany Facility: Breadboarding results of the illumination system
[SIRA-A/7373/WP110/MAC003]
17 p2378 N88-24137

MSAT mobile electronically steered phased array antenna development 19 p2647 N88-25711

AC power system breadboard
[NASA-CR-179369] 22 p3049 N88-28091

Biosample: Preservation, handling and observation system synthesis and breadboarding --- Spacelab
[ESA-CR(P)-2609] 24 p3336 N88-29857

Breadboard RL10-2B low-thrust operating mode (second iteration) test report
[NASA-CR-182160] 24 p3338 N88-29867

The dc power control for a liquid-fed resistojet
[NASA-TM-101326] 24 p3338 N88-29869

BREAKAWAY

U BOUNDARY LAYER SEPARATION

BREAKDOWN

Dependence of acoustical characteristics of laser-induced breakdown in dielectric materials on shape of inelastic region 06 p0774 N88-14753

BREAKERS (ELECTRIC)

U CIRCUIT BREAKERS

BREAKING

Buckling and breakdown problems in structural mechanics. Failure of prestressed double-walled containers or rings
[MBB-UR-E-956/87] 13 p1783 N88-20671

Stress corrosion evaluation of powder metallurgy aluminum alloy 7091 with the breaking load test method
22 p3053 N88-28115

BREAKWATERS

Breaking wave forces on vertical cylinders
[RR-CE71] 03 p0338 N88-12126

Technology Reports of Kyushu University, volume 61, no. 2
[ISSN-0023-2718] 16 p2256 N88-23485

BREATHING

Life in a hyperbaric environment. A new O2-H2 breathing mixture for industrial diving 19 p2695 N88-26019

BREATHING APPARATUS

NT OXYGEN MASKS

Summary report of the history and events pertinent to the Civil Aeromedical Institute's evaluation of providing smoke/fume protective breathing equipment for airline passenger use
[AD-A184499] 03 p0261 N88-11645

A plethysmograph for measuring pulmonary ventilation in small animals
[AD-A184978] 05 p0629 N88-13846

Man rating the b-1B molecular sieve oxygen generation system
[AD-A186275] 07 p0899 N88-15447

Acute mountain sickness at 4500 m is not altered by repeated eight-hour exposures to 3200-3550 m normobaric hypoxic equivalent
[AD-A188358] 12 p1666 N88-19990

Study of benefits of passenger protective breathing equipment from analysis of past accidents
[DOT/FAA/CT-88/03] 18 p2461 N88-24610

BRECCIA

Abundance and distribution of ultramafic microbreccia in Moses Rock Dike: Quantitative application of AIS data
05 p0613 N88-13766

BREEDER REACTORS

NT EXPERIMENTAL BREEDER REACTOR 2

NT LIQUID METAL FAST BREEDER REACTORS

Three dimensional Monte Carlo simulation of molecular movement and heat radiation in vacuum devices: Computer code MOVAK3D --- fusion reactors
[KFK-4292] 09 p1246 N88-17471

Outlook for the fusion hybrid and tritium-breeding fusion reactors
[PB88-149281] 13 p1843 N88-21029

Development of fast breeder reactors in China
16 p2186 N88-23032

BREMSSTRAHLUNG

Generating soft X-ray spectra using the SPEED pentaxial diode
[DE87-013591] 01 p0098 N88-10647

LLE Review, volume 30
[DE87-014469] 02 p0178 N88-11109

The Hermes-3 program
[DE87-012132] 02 p0234 N88-11473

The nature of beamstrahlung
[DE87-012837] 02 p0234 N88-11474

Relativistic plasma concentration measuring by Bremsstrahlung
[DE88-700560] 07 p0836 N88-15685

Spectrophotometric remote sensing of the diffuse aurora
[AD-A188599] 12 p1643 N88-19837

Measurements of Z(sub eff) profile with a visible bremsstrahlung continuum detector array
17 p2443 N88 24529

Spectral modelling of the soft gamma ray repeater
[DE88-007027] 17 p2453 N88-24570

Intense ion beam diagnostics for particle beam fusion experiments on PBFA 2
[DE88-007279] 18 p2577 N88-25308

Bremsstrahlung from high Z impurities in hot plasmas
[DE88-011755] 20 p2861 N88-26994

Proof of the feasibility of coherent and incoherent schemes for pumping a gamma-ray laser
[AD-A193856] 23 p3220 N88-29165

X- and gamma-ray background observations in Antarctic
[INPE-4583-PRE/1317] 24 p3459 N88-30578

BRIDGES (STRUCTURES)

The effect of mass, wind angle and erection technique on the aeroelastic behaviour of a cable-stayed bridge model
[NAE-AN-46] 04 p0455 N88-12819

Design and implementation of the ESL compact range underhung bridge crane
[NASA-CR-182396] 07 p0862 N88-15231

Deformation induced cracking in steel girder bridges and retrofit guidelines
[PB88-102710] 07 p0868 N88-15265

Dynamic analysis of plane frames by microcomputer
11 p1531 N88-19143

Propagation modeling for land mobile satellite systems
19 p2645 N88-25694

Multi-metallic galvanic corrosion
[AD-A195995] 24 p3353 N88-29963

BRIDGMAN METHOD

Numerical analysis of Marangoni convection in Bridgman method 03 p0319 N88-12014

MCT crystal growth
[NASA-CR-179297] 11 p1557 N88-19318

Analysis of low gravity tolerance of model experiments for space station: Preliminary results for directional solidification
[NASA-CR-182657] 12 p1614 N88-19648

BRIGHTNESS

Compact electron storage rings
[DE87-013301] 02 p0234 N88-11477

Eyesight trainer for pilots 03 p0355 N88-12239

The closest solar analogs in the bright star catalogue
04 p0506 N88-13110

Performance characteristics of magnesium-sodium nitrate flares in oxygen-nitrogen atmospheres
[AD-A185274] 05 p0570 N88-13476

AIS-2 spectra of California wetland vegetation
05 p0613 N88-13763

Monte Carlo method calculation of spectral brightness coefficient of vegetation cover as function of illumination conditions 08 p1008 N88-16113

Bright source lasers and experiments at very high irradiance
[DE88-004317] 10 p1337 N88-17988

Relaxing the brightness constancy assumption in computing optical flow
[AD-A187437] 10 p1410 N88-18410

An attempt to measure the diffuse brightness of the sky at submillimeter wavelengths
12 p1710 N88-20233

Research on influence of individual sea water components on spectral brightness coefficient of outgoing radiation 13 p1785 N88-20682

IUE program SUGSD: Varability time scale of H Ly-alpha from Uranus
[NASA-CR-182706] 13 p1856 N88-21107

The absolute total magnitudes of periodic comets and their variations 14 p1994 N88-21887

Comparison of active regions on the nucleus of Comet Halley 14 p2004 N88-21948

Comparison of Halley's monochromatic comae with others 14 p2006 N88-21965

Dynamic properties of human brightness perception
[ETN-88-92243] 16 p2238 N88-23366

Generation of high brightness ion beam from insulated anode PED 16 p2278 N88-23637

Study on the flashover ion diode with cryogenic anode
16 p2279 N88-23642

Dust and C2-contents in the coma of Halley's Comet (1986III) 16 p2288 N88-23697

Mapping soil and rock variation from satellite images in the Sahel 17 p2354 N88-24023

Space station contamination study: Assessment of contaminant spectral brightness
18 p2591 N88-25395

Apparent brightness of stars and lasers
22 p3065 N88-28188

Preliminary analysis of recent 2.2-4.2 micrometers telescopic observations of Elysium, Mars: Implications for crystallinity and hydration state of surface materials
23 p3306 N88-29692

Astron observations of supernova 1987A in large magellanic cloud 24 p3445 N88-30504

BRIGHTNESS DISCRIMINATION

Laser flash effects on chromatic discrimination in monkeys
[AD-A187703] 11 p1517 N88-19061

BRIGHTNESS DISTRIBUTION

Observations of the brightness temperature distribution of the quiet solar corona at decametric wavelengths
01 p0114 N88-10729

Doppler snapshots 04 p0508 N88-13125

Application of correlation method of reception of direct and reflected cosmic radiation to study of plasmaspheres of planet and distribution of radiation brightness
08 p1004 N88-16085

Comparative analysis of ultraviolet observations of Halley's comet on ASTRON astrophysical station before and after perihelion 08 p1004 N88-16086

Some periodicities in motion of Halley's Comet relative to center of mass 13 p1726 N88-20324

Spectral reflective characteristics of sea surface
13 p1784 N88-20676

BRIGHTNESS TEMPERATURE

Observations of the brightness temperature distribution of the quiet solar corona at decametric wavelengths
01 p0114 N88-10729

Mars: High resolution VLA observations at wavelengths of 2 and 6 cm and derived properties
06 p0804 N88-14909

LANDSAT thematic mapper radiometric calibration study
[NASA-CR-182410] 07 p0872 N88-15287

Statistical studies of low frequency oscillations in satellite-observed stratospheric temperatures
10 p1353 N88-18086

Mesoscale monitoring of the soil freeze/thaw boundary from orbital microwave radiometry
[NASA-CR-182659] 12 p1645 N88-19855

Validate algorithms for the determination of rainfall rates from SSM/I microwave satellite imagery
[AD-A188769] 16 p2233 N88-23337

The NBS scale of radiance temperature
17 p2326 N88-23897

BRILLOUIN EFFECT

Stimulated Mandelstam-Brillouin scattering during forward scattering of light 08 p1078 N88-16499

Brillouin scattering from collective spin waves in magnetic superlattices
[DE88-005347] 12 p1697 N88-20154

Phase preservation cleanup in a double-pass Raman amplifier SBS (Stimulated Brillouin Scattering) conjugator
[AD-A189428] 13 p1761 N88-20536

Experimental studies of elastic properties of crystals by Brillouin scattering
[DE88-005923] 14 p1986 N88-21848

Brillouin scattering and transmission electron microscopy studies of radiation-induced elastic softening, disordering and amorphization of intermetallic compounds
[DE88-005927] 14 p1987 N88-21850

Computer modeling of time dependent SBS (Stimulated Brillouin Scattering) in two and three dimensions
[DE88-008922] 19 p2720 N88-26150

BRILLOUIN ZONES

Positron-annihilation 2D-ACAR studies of disordered and defected alloys
[DE88-003116] 10 p1416 N88-18454

Center for thin film studies
[AD-A191996] 19 p2732 N88-26226

Calculation of far infrared absorption in B poly(dA).poly(dT)
[AD-A193126] 21 p2918 N88-27318

BRINES

Porosity influence on the strength and elasticity of first-year sea ice
[AD-A184493] 03 p0354 N88-12233

Geochemistry of freezing brines, low-temperature properties of sodium chloride
[AD-A185751] 06 p0680 N88-14168

The effect of H2S concentration and pH on hydrogen permeation in AISI 410 stainless steel in 5 percent NaCl
[NPL-DMA(A)-148] 14 p1890 N88-21293

The effect of H2S concentration and pH on the cracking resistance of AISI 410 stainless steel in 5 percent brine
[NPL-DMA(A)-149] 14 p1890 N88-21294

BRITISH COLUMBIA
Longer-duration post-frontal precipitation at Vancouver International Airport, 1953-1983
02 p0203 N88-11269

BRITTLE MATERIALS
Strength and toughness of a brittle material
[VTT-RR-479] 09 p1183 N88-17089
A fractal analysis of brittle fracture
[AD-A188334] 12 p1635 N88-19788
Bimodular behavior and crack closure in compression in a brittle material
[AD-A191267] 16 p2224 N88-23275
Loading rate sensitivity of open hole composites in compression
[NASA-TM-100634] 19 p2610 N88-25490
Size effects in linear elastic fracture mechanics
21 p2964 N88-27609

BRITTLENESS
A probabilistic model of brittle crack formation
[AD-A184423] 03 p0338 N88-12129
Effects of stress-relieving on the mechanical properties and the structure of specimens of high-temperature fine-grained structural steels heat-treated to simulate welding
[BLL-CE-TRANS-8258-(9022.09)]
04 p0417 N88-12586
Evaluation method of the brittle fracture strength in structurally stress-concentrated regions
[PB87-129490] 06 p0721 N88-14435
New mechanism of the high temperature (reversible) temper brittleness of alloy steels
[PB87-143954] 07 p0833 N88-15056
The development of test methodology for testing glassy materials 07 p0927 N88-15633
Some aspects of the mechanics and mechanisms of dynamic brittle fracture 10 p1343 N88-18028
Brittle to ductile transition to cleavage fracture
[DE88-004074] 10 p1420 N88-18481
A fractal analysis of brittle fracture
[AD-A188334] 12 p1635 N88-19788
A study of the dynamics of high temperature brittle intergranular fracture by acoustic emission
[AERE-R-12479] 13 p1780 N88-20650
Guidelines for estimation and characterization of the thermo-mechanical properties of new optical materials
[DE88-004359] 13 p1840 N88-21010
The Nordic J-R curve round robin test program --- reactor steel
[VTT-RR-510] 14 p1923 N88-21459
High-performance polymeric materials
[AD-A190708] 15 p2046 N88-22190
Strength and microstructure of ceramics
[AD-A190712] 15 p2046 N88-22191
Fracture technology for brittle materials
15 p2083 N88-22417
Bimodular behavior and crack closure in compression in a brittle material
[AD-A191267] 16 p2224 N88-23275
Some design considerations for ceramic components in heat engine applications 17 p2323 N88-23875
Rapidly solidified lightweight durable disk material
[AD-A191687] 18 p2491 N88-24775
Self-consistent model for the brittle response of solids
18 p2528 N88-24999
Ductile-brittle transition of cutting behavior in diamond turning of single crystal Si
[DE88-008890] 20 p2809 N88-26664

BROADBAND
Design and analysis of a broadband TM(sub 01) mode generator in cylindrical waveguide
[DE87-011308] 01 p0038 N88-10243
Experiments: Test range facilities, part 2
03 p0305 N88-11921
Lewis Information Network (LINK): Background and overview
[NASA-TM-100162] 03 p0305 N88-11925
NBS (National Bureau of Standards) wideband sampling wattmeter
[PB87-210324] 03 p0323 N88-12041
Band 2 VHF antenna for home construction
[BBC-RD-1987/13] 04 p0432 N88-12677
Broadband linear polarization and chromospheric Call H and K line emission in late-type main sequence stars
04 p0511 N88-13140
Application of Vandermonde decomposition to directional and modal analysis of broadband transients
[AD-A185007] 05 p0646 N88-13956
A study of rotor broadband noise mechanisms and helicopter tail rotor noise 06 p0777 N88-14766
Design, production, and characterization of broadband optical waveguides
[DFVLR-FB-85-52] 06 p0780 N88-14791
Determination of cloud base height and emissivity from downwelling angular radiances
[AD-A185965] 07 p0879 N88-15331
Estimation of broadband planetary albedo from operational narrowband satellite measurements
[PB88-107644] 07 p0945 N88-15748
Crosstalk analysis of a broadband data communications system
[DE88-003652] 09 p1156 N88-16927
Signal processing for an optical wide band data transmission system
[DE88-003854] 10 p1319 N88-17888
Wide band data transmission system using optical fibers
[DE88-004555] 10 p1319 N88-17889
The design of impedance matching networks for broadband antennas
[AD-A187600] 10 p1320 N88-17895
Low-noise cryogenically cooled broad-band microwave preamplifiers
[DE88-004561] 10 p1324 N88-17912
Nonlinear optics with broad-band lasers
[DE88-005026] 10 p1337 N88-17992
CARS measurements of combustion. 2: Gas species concentration measurements
[NAL-TR-940] 11 p1453 N88-18663
Distortion of wideband carbon dioxide laser radar waveforms due to atmospheric dispersion and absorption
[AD-A188687] 12 p1632 N88-19771
Bragg-cell receiver study
[NASA-CR-182684] 13 p1761 N88-20535
Broadband correlation analysis
[AD-A188732] 13 p1814 N88-20839
Optimal and conventional space-time processing in flow noise
[AD-A189104] 13 p1833 N88-20965
New wide-band transducer developed
14 p1901 N88-21353
Nonlinearly tunable wide band emission of infrared radiation by Al2O3 Ti laser 14 p1970 N88-21758
A very wide frequency band pulsed/IF radar system
[NASA-CR-182889] 16 p2190 N88-23059
A mixed-modem solution for sensitive data segregation on a broadband network
[DE88-001765] 19 p2718 N88-26139
Approximations and optimal control for the pathwise average cost per unit time and discounted problems for wideband noise driven systems
[AD-A192712] 21 p3008 N88-27847
SERI standard broadband format: A solar and meteorological data archival format
[DE88-001145] 21 p3028 N88-27975
Effects of tectonic release on broadband regional distance bodywaves
[AD-A194247] 22 p3119 N88-28529
On broadband matching of multiport electrical networks with applications
[AD-A194224] 23 p3207 N88-29086
The effect of equatorial ionospheric irregularities on the performance of a south-looking OTH-B (Over-The-Horizon-Backscatter) radar
[AD-A195090] 24 p3362 N88-30018
Scattering impulse response synthesis using random noise illumination: Initial concept evaluation
[AD-A195086] 24 p3364 N88-30034
A fiber optic beamforming processor for wideband direction finding
[AD-A194862] 24 p3428 N88-30404
Ultra-wideband direction finding using a fiber optic beamforming processor
[AD-A194861] 24 p3430 N88-30413

BROADBAND AMPLIFIERS
Wide band gyrotron traveling wave amplifier analysis
[AD-A194260] 23 p3216 N88-29139

BROADCASTING
Monitoring of harmful interference to the HF (High Frequency) broadcasting service. 3: Results of the June 1986 coordinated monitoring period
[PB87-210274] 01 p0036 N88-10229
HF (High Frequency) broadcasting planning model: A comparison of two versions
[PB87-210282] 01 p0036 N88-10230
The criterion of equal integrated quality: An improved method of planning DBS systems
[BBC-RD-1987/10] 02 p0161 N88-11012
Theory and methods for design of pulse shapes for broadcast teletext
[CRC-1405] 02 p0162 N88-11013
Band 2 VHF antenna for home construction
[BBC-RD-1987/13] 04 p0432 N88-12677
Improvements to a UHF rebroadcast television link suffering tidal fading: Countisbury UHF relay station
[BBC-RD-1987/14] 05 p0573 N88-13495
SAHAYOG: A testbed for load sharing under failure
[AD-A186615] 08 p1069 N88-16460
The assessment of the sound insulation requirements for a large broadcasting studio, using a scale model: Theoretical considerations
[BBC-RD-1987/20] 09 p1155 N88-16921
Experimental Radio Data System (RDS): A survey of reception reliability in the UK
[BBC-RD-1987/17] 09 p1155 N88-16922
Future television systems: Comparison of sequential and interlaced scanning
[BBC-RD-1987/18] 09 p1155 N88-16923
User's guide for the HF (High Frequency) broadcast antenna design and validation summary programs
[PB88-116124] 10 p1317 N88-17875
The assessment of the sound insulation requirements for a large broadcasting studio, using a scale model: Practical details
[BBC-RD-1987/21] 10 p1318 N88-17878
Complementary satellite sound broadcasting systems: A NASA assessment for the Voice of America
[NASA-TM-100300] 10 p1321 N88-17899
Role of broadcasting in multiprocessor systems
10 p1374 N88-18201
Datacast: The transmission system
[BBC-RD-1988/1] 14 p1905 N88-21385
Performance study of a unipole antenna with conventional and elevated radial wire ground screens
[AD-A193283] 21 p2933 N88-27413

BROKEN SYMMETRY
Abrikosov vortex motion and elementary pinning force in a SNS Josephson junction
[DE87-013607] 01 p0105 N88-10683
Spontaneous symmetry breaking in N = 2 supergravity
[DE87-702749] 01 p0109 N88-10704
Spontaneous symmetry breaking in N = 3 supergravity
[DE87-702753] 01 p0109 N88-10705
A mechanism for symmetry breaking in antiferromagnetic Heisenberg systems
[ETN-88-91320] 05 p0657 N88-14031
Breaking of supersymmetry degeneracy and phenomenological conditions
[PREPRINT-559] 06 p0790 N88-14843
Chiral symmetry breaking in finite quantum electrodynamics
[DE88-700860] 12 p1699 N88-20169
Diffraction theory in QCD and beyond
[DE88-005958] 13 p1837 N88-20992
Measurement of the sup 4He(gamma, p)sup 3H total cross section and charge symmetry
[NOTA-INTERNA-902] 14 p1981 N88-21820
Research in theoretical particle physics
[DE88-008230] 20 p2851 N88-26927

BROMIDES
NT POTASSIUM BROMIDES
Technical evaluation of a solar-powered absorption cooling system (LiBr-H2O)
[PB87-108254] 04 p0463 N88-12867
Organic metal (ET)4Hg3Br8A quasi-two-dimensional superconductor 14 p1974 N88-21778
Ultraviolet absorption cross sections of methylbromide at stratospheric temperatures
[AERONOMICA-ACTA-A-320-1987]
15 p2036 N88-22132

BROMINATION
The effect of bromination of carbon fibers on the coefficient of thermal expansion of graphite fiber-epoxy composites
[NASA-TM-100236] 02 p0143 N88-10899
Improving the interlaminar shear strength of carbon fiber-epoxy composites through carbon fiber bromination
[NASA-TM-100248] 07 p0827 N88-15018
Brominated graphite fibers and method of producing the same
[NASA-CASE-LEW-14698-1] 24 p3341 N88-29888

BROMINE
NT BROMINE ISOTOPES

BROMINE COMPOUNDS
NT BROMIDES
NT POTASSIUM BROMIDES
Impact on ozone attainment of CFC (chlorofluorocarbon) controls used to prevent future depletion of stratospheric ozone
[PB88-195177] 19 p2690 N88-25989

BROMINE ISOTOPES
Development and applications of new technical advances to problems of fluid/electrolyte/mineral imbalance in military personnel
[AD-A186437] 07 p0889 N88-15386

BROMINE 82
U BROMINE ISOTOPES

BROMINE 87
U BROMINE ISOTOPES

BRONZES
Progress toward a crystal streak camera using tungsten bronze crystals for the electrooptic material
[DE87-013110] 03 p0323 N88-12044

The effects of various conductor components on Nb3Sn filament prestrain in cable-in-conduit conductors [DE88-003956] 11 p1479 N88-18824

BROWNIAN MOVEMENTS

Detecting and interval estimation about a slope change point [AD-A186030] 07 p0909 N88-15509

Green's function for a ball [AD-A186239] 07 p0910 N88-15516

Decoupling identities and predictable transformations in exchangeability [AD-A186013] 07 p0913 N88-15540

Remark on the multiple Wiener integral [AD-A186015] 07 p0913 N88-15541

Techniques in linear and nonlinear partial differential equations [AD-A187109] 09 p1227 N88-17347

Filtering of jump processes [AD-A189701] 15 p2123 N88-22656

BRUCETON TEST

U STATISTICAL TESTS

BRYOPHYTES

Electron cytochemical detection of Ca(2)+-ATPase in protonema of moss funaria hygrometrica (H e d w.) under hypogravitation 06 p0749 N88-14602

BUBBLE CHAMBERS

Scanning and measuring peculiarities with high-space resolution objects recorded at the Gabor holograms [DE88-700373] 07 p0857 N88-15203

Analysis of relativistic nucleus-nucleus interactions in emulsion chambers 07 p0926 N88-15624

Optical system of laser illuminated streamer chamber [DE88-702127] 18 p2577 N88-25306

BUBBLE MEMORY DEVICES

High density ion implanted contiguous disk bubble technology [AD-A190169] 15 p2143 N88-22789

BUBBLE TECHNIQUE

High density ion implanted contiguous disk bubble technology [AD-A190169] 15 p2143 N88-22789

BUBBLES

The structure of separated flow regions occurring near the leading edge of airfoils including transition [NASA-CR-181434] 01 p0002 N88-10011

An inviscid model of planar, separated flows of finite extent [RAE-TR-86070] 01 p0044 N88-10279

The dynamics of bubble growth for Rayleigh-Taylor unstable interfaces [AD-A184752] 03 p0321 N88-12027

Cosmological applications of singular hypersurfaces in general relativity 04 p0521 N88-13202

Heat transfer investigations in a slurry bubble column [DE88-001445] 06 p0699 N88-14286

Bubble expansion and collapse studies [DE88-002377] 06 p0699 N88-14290

New equilibrium forms of free surface of confined magnetic fluid 06 p0770 N88-14734

Research on acoustical scattering, diffraction catastrophes, optics of bubbles, photoacoustics, and acoustical phase conjugation [AD-A185785] 06 p0776 N88-14761

A flow visualization study of the leading edge separation bubble on a NACA 0012 airfoil with simulated glaze ice [NASA-CR-180846] 07 p0816 N88-14966

Foam generation and air entrainment near a free surface [AD-A185986] 07 p0848 N88-15149

A computationally efficient modelling of laminar separation bubbles [NASA-CR-182417] 08 p0984 N88-15949

Cavitation inception scale effects. 1: Nuclei distributions in natural waters. 2: Cavitation inception in a turbulent shear flow [AD-A186553] 08 p0988 N88-15987

Experimental and theoretical study on cavitation inception and bubbly flow dynamics. Part 1: Design, development and operation of a cavitation susceptibility meter. Part 2: Linearized dynamics of bubbly and cavitating flows with bubble dynamics effects [AD-A187133] 09 p1160 N88-16952

Boundary integral analysis of flow and deformation of long bubbles in capillaries [DE88-002110] 10 p1326 N88-17927

Mechanistic model for void distribution in flashing flow [DE88-002948] 10 p1326 N88-17928

Mass transport phenomena between bubbles and dissolved gases in liquids under reduced gravity conditions [NASA-TM-100273] 11 p1455 N88-18672

Analytical and numerical analysis of finite amplitude Rayleigh-Taylor instability [DE88-004056] 11 p1474 N88-18797

Optically stimulated sound from gas bubbles in water 12 p1686 N88-20087

Cavitation inception [AD-A189220] 13 p1765 N88-20557

Some problems of the theory of bubble growth and condensation in bubble chambers [NASA-TT-20232] 13 p1771 N88-20593

Detecting the gas bubbles in a liquid metal coolant by means of magnetic flowmeters [DE88-701427] 15 p2062 N88-22294

The elliptic Sinh-Gordon equation and the construction of toroidal soap bubbles [DE88-006426] 15 p2113 N88-22585

Generation and coalescence of bubbles and stability of foams under microgravity conditions [BMFT-FB-W-86-020] 16 p2184 N88-23017

A new laminar water tunnel to study the transition process in a blasius layer and in a separation bubble and a new tool for industrial aerodynamics and hydrodynamic research 16 p2204 N88-23150

Some visualization studies on turbulent boundary layers using multiwire hydrogen bubble generation 16 p2204 N88-23153

Low frequency ocean ambient noise: Measurements and theory [AD-A191188] 16 p2237 N88-23362

The structure and stability of spherically expanding flames 17 p2318 N88-23842

Instability of laminar separation bubbles: Causes and effects [AD-A191168] 18 p2508 N88-24876

Dynamical properties of a collapsing spherical cavity 19 p2623 N88-25562

Noise generation by air bubbles in water: An experimental study of creation and splitting [AD-A192063] 19 p2664 N88-25839

Contribution of ultrasonic Doppler detection of circulating bubbles to human interventions under the sea and in space 19 p2697 N88-26029

Stability and drag reduction in a boundary layer with microbubbles [AD-A191975] 23 p3209 N88-29099

A multiple-scales partial solution of the pulse-forced Rayleigh-Plesset equation of cavitation bubble dynamics [AD-A193733] 23 p3212 N88-29118

Fluid physics double rack --- Spacelab [SD-TN-AI-012] 24 p3358 N88-29992

Studies on pressure response of gas bubbles contributions of condensed droplets in bubbles generated by a uniform nucleation [NASA-TT-20343] 24 p3370 N88-30068

BUCKLING

NT CREEP BUCKLING

NT ELASTIC BUCKLING

NT THERMAL BUCKLING

Interactive buckling effects in stiffened FRP panels [ARE-TM(UMS)-87204] 01 p0059 N88-10378

Buckling of viscoelastic columns 02 p0190 N88-11187

An analytical study of the effects of transverse shear deformation and anisotropy on buckling loads of laminated cylinders [NASA-TM-100508] 05 p0557 N88-13387

An examination of chaotic motion for the buckled beam 05 p0597 N88-13644

Beam and column buckling under directed loading [PB87-124004] 06 p0722 N88-14436

Distortional buckling formulae for thin-walled channel columns [PB87-124012] 06 p0722 N88-14437

Partially braced inelastic beam buckling experiments [PB87-133831] 06 p0723 N88-14444

Buckling of braced monosymmetric cantilevers: Timoshenko energy approach [PB87-133849] 06 p0723 N88-14445

Contribution to the study of wrinkling in metal stamping [ISAL-IDI1-87-08] 08 p0976 N88-15900

Postbuckling of laminated anisotropic panels [NASA-TM-100509] 08 p0994 N88-16011

Accuracies of southwell and force/stiffness methods in the prediction of buckling strength of hypersonic aircraft wing tubular panels [NASA-TM-88295] 09 p1183 N88-17090

Determination of the ultimate loads for corrugated-steel, barrel-type shell structures [AD-A187716] 11 p1498 N88-18944

Mathematical modeling of the postbuckling behavior of structural elements 11 p1500 N88-18960

Buckling and breakdown problems in structural mechanics. Failure of prestressed double-walled containers or rings [MBB-UR-E-956/87] 13 p1783 N88-20671

Unrestrained out-of-plane buckling of monosymmetric rings [PB88-155213] 14 p1923 N88-21458

Postbuckling delamination of a stiffened composite panel using finite element methods [NASA-CR-182603] 15 p2030 N88-22098

Cubic spline solution of symmetric buckling problems of clamped shallow spherical shells 15 p2053 N88-22239

The buckling and vibration of composite plates using the Levy method considering shear deformation and rotary inertia [AD-A189743] 15 p2076 N88-22374

Buckling of blast loaded cylinder [AD-A190124] 15 p2076 N88-22376

The analysis of non-linear dynamic behavior (including snap-through) of postbuckled plates by simple analytical solution [NASA-TM-89165] 15 p2087 N88-22439

Local buckling and crippling of composite stiffener sections [NASA-TM-101133] 17 p2317 N88-23840

Forced motion of initially stressed shells and plates 18 p2529 N88-25005

Three-dimensional analysis of a postbuckled embedded delamination [NASA-TP-2823] 20 p2812 N88-26684

A study of fluid-structure problems 21 p2941 N88-27468

Nonlinear interaction between overall and local buckling of stiffened panels with symmetric cross-sections [PB88-104054] 21 p2960 N88-27580

Adaptive finite element methods for shells [AD-A193221] 21 p2960 N88-27585

Tripping of stiffened plates using a refined beam theory [AD-A193989] 22 p3087 N88-28333

BUDGETING

High energy experimental physics [DE87-013516] 03 p0376 N88-12363

CNET (Chief of Naval Education and Training) Program Automated Tracking System (CPATS): A comprehensive study [AD-A184694] 03 p0385 N88-12418

Budget and programs for 1986 research [IFSI-86-16] 05 p0660 N88-14048

Department of Defense statement on defense agency research and development to the Subcommittee on Defense of the Committee on Appropriations, United States House of Representatives, 100th Congress, second session [AD-A191840] 18 p2588 N88-25377

Department of Defense Statement on the Balanced Technology Initiative to the Committee on Armed Services, United States Senate, 100th Congress, second session [AD-A191841] 18 p2588 N88-25378

Economic impact of space flight activities in West Germany. Influence of allocations of Bundesministerium fuer Forschung und Technologie [ETN-88-92106] 21 p2901 N88-27215

BUDGETS

Budget reimbursements: The National Aeronautics and Space Administration's reimbursable work [PB87-207296] 01 p0107 N88-10696

Feasibility study of a carbon dioxide observational platform system. Volume 2: Programmatics [NASA-CR-180404] 06 p0672 N88-14114

INPE position paper on the CCSDS standardized method of link budget computation [INPE-4533-NTE/279] 15 p2148 N88-22820

BUFFER STORAGE

A review of the semiconductor storage of television signals. Part 2: Applications 1975-1986 [BBC-RD-1987/6] 02 p0161 N88-11009

Throughput analysis of a flow-contoured communication network with buffer space limitations [CWI-OS-R8702] 08 p0977 N88-15908

Effective buffering schemes for performing matrix operations for numerical databases 21 p3027 N88-27968

BUFFERS

Effects of emission energy transient in periodic-pulse XeCl excimer laser of approximately 400 W average power 14 p1971 N88-21763

BUFFETING

On the prediction of the aeroelastic behavior of lifting systems due to flow separation [ESA-TT-1043] 03 p0259 N88-11633

A modular BLSS simulation model 03 p0359 N88-12260

Predictions of F-111 TACT aircraft buffet response and correlations of fluctuating pressures measured on aluminum and steel models and the aircraft [NASA-CR-4069] 05 p0529 N88-13218

Experimental investigation of shock-induced disturbances on transonic airfoils [DFVLR-FB-87-28] 09 p1112 N88-16666

Some aspects of aircraft dynamic loads due to flow separation
[AGARD-R-750] 11 p1439 N88-18588
A flight test investigation into flow separation and structural response for a transport aircraft at buffet onset
[RAE-TR-87006] 14 p1867 N88-21156
Numerical method for unsteady viscous-inviscid interaction to calculate buffeting
[ONERA-RSF-02/3617-AY-008-A]
17 p2338 N88-23949
Classical separation, trailing-edge flows and buffeting
23 p3170 N88-28874
BUILDING MATERIALS
U CONSTRUCTION MATERIALS
BUILDING STRUCTURES
U BUILDINGS
BUILDINGS
Measuring the annoyance of aircraft noise
[AD-A185494] 06 p0777 N88-14770
A proposed metric for assessing the potential of community annoyance from wind turbine low-frequency noise emissions
[DE88-001113] 08 p1022 N88-16187
Experimental studies of heat and mass exchange in parallel-passage rotary desiccant dehumidifiers for solar cooling applications
[DE88-001119] 10 p1350 N88-18069
Computer assisted generalization of buildings for digital landscape models by classification methods
16 p2226 N88-23294
BULK MODULUS
Ground state properties and electronic structure of high T sub c superconductors
[DE88-007485] 18 p2585 N88-25360
BUMPY TORUSES
Long wavelength vortices of low frequency interchange modes
[IPPJ-844] 02 p0241 N88-11525
BUNA (TRADEMARK)
Fracture morphologies of carbon-black-loaded SBR (Styrene-Butadiene Rubber) subjected to low-cycle, high-stress fatigue
[DE88-006808] 16 p2181 N88-23002
BUNCHING
NT ELECTRON BUNCHING
A qualitative study of wake fields for very short bunches
[DE88-002565] 09 p1164 N88-16980
BUOYANCY
Numerical computations of natural convection heat transfer in irregular geometries
[DE88-002358] 07 p0852 N88-15178
A payload for investigating the influence of convection on GaAs crystal growth 10 p1288 N88-17702
Application of a multigrid method to a buoyancy-induced flow problem
[DE88-003961] 10 p1397 N88-18326
Wind and buoyancy driven ocean circulation
14 p1938 N88-21564
Heat transfer from a negatively buoyant wall jet
[NBS/GCR-88/541] 15 p2050 N88-22208
Direct numerical simulation of buoyantly driven turbulence 16 p2196 N88-23097
Brunt-Doppler ducting of buoyancy waves in a temperature- and wind-stratified atmosphere
18 p2542 N88-25086
Nonlinear equation of state effects and the momentum-dilution trade-off in a turbulent buoyant jet
[DE88-701839] 20 p2799 N88-26610
Development of an adjustable buoyancy balloon tracer of atmospheric motion. Phase 3: Refinement of the operational prototype system
[PB88-190764] 23 p3231 N88-29230
BUOYS
Navarin Basin Ice Drift Program
[PB88-104021] 06 p0748 N88-14599
SEQUAL (seasonal Equatorial Atlantic) meteorological data from Moorings S2, S5 and S6 (March 1983 - March 1985)
[PB88-108048] 07 p0880 N88-15337
A deep-water OBS (Ocean Bottom Seismometer) array with real-time telemetry
[AD-A187404] 10 p1357 N88-18112
Comparison of surface current determined from satellite-tracked buoy with shipboard wind data during the 4th Brazilian antarctic expedition, 10-14 March, 1986
17 p2354 N88-24024
Near surface current determined from INPE's satellite-tracked buoy, during 6-26 November, 1985
17 p2360 N88-24058
Descriptions of HF and VHF Loran-C buoys and evaluations as potential datum marker buoys
[AD-A192069] 18 p2462 N88-24618
Arctic ice island and sea ice movements and mechanical properties
[DE88-004267] 20 p2829 N88-26782
KOSPAS-SARSAT satellites used for ocean current study 24 p3450 N88-30534
BURGER EQUATION
Vectorization of the odd-even hopscotch scheme and the alternating direction implicit scheme for the two-dimensional Burgers' equations
[CWI-NM-R8720] 16 p2249 N88-23440
BURKINA
Evaluation of SPOT data for crop inventory and monitoring in Sudanian Africa. Example of Bane area (Burkina Faso) 22 p3096 N88-28388
BURN-IN
Burn-in with mixed populations
[AD-A194651] 22 p3085 N88-28321
BURNERS
Turbulent Bunsen burner flames
[ETN-87-90433] 01 p0021 N88-10134
Correlation of velocity and velocity-density turbulence in the exhaust of an atmospheric burner
02 p0185 N88-11147
Experimental verification of vapor deposition rate theory in high velocity burner rigs 02 p0189 N88-11179
Effects of surface chemistry on hot corrosion life
02 p0189 N88-11160
Oxygen enriched combustion system performance study
[DE88-001500] 05 p0562 N88-13424
Development of a plenum chamber burner system for an advanced VTOL engine 10 p1281 N88-17664
Investigations into shock-induced enhancement of mixing and combustion in supersonic burners
[AD-A189609] 12 p1607 N88-19608
Dual Stokes cars measurements in supersonic combusting flow 19 p2625 N88-25569
Evidences for distributed combustion
19 p2628 N88-25586
Characterization of a modified Rijke burner for measurement of distributed combustion
19 p2628 N88-25587
Nonlinear mechanisms of solid propellant combustion instability 19 p2628 N88-25588
Analysis of microwave burner measurement system using a microwave network analysis computer program
19 p2631 N88-25604
Dynamics and stability of combustion driven self oscillations in presence of various frequencies. Extensive stability criteria
[ETN-88-92123] 20 p2771 N88-26432
Flame stabilization in a reheat combustor
24 p3346 N88-29921
BURNING
U COMBUSTION
BURNING PROCESS
U COMBUSTION
BURNING RATE
High pressure strand burn rate tests of polyvinylnitrate/nitramine propellants
[AD-A184178] 04 p0422 N88-12615
Performance characteristics of magnesium-sodium nitrate flares in oxygen-nitrogen atmospheres
[AD-A185274] 05 p0570 N88-13476
A continuous oxidizer regression model for the combustion of composite solid propellants
[AD-A186742] 08 p0974 N88-15894
The correlation of HMX (cyclotetramethylenetetranitramine) particle characterization techniques to propellant burn rate
[AD-A187119] 09 p1140 N88-16833
Speed control of a missile with throttleable ducted rocket propulsion 12 p1597 N88-19561
A simplified computer code for reduction to burning rates of closed bomb pressure-time data (MINICB)
[AD-A189112] 13 p1736 N88-20380
Crack opening and extension in inert solid propellant. An experimental study
[AD-A189608] 15 p2048 N88-22201
Chemical kinetics of nitramine propellant combustion
[AD-A191556] 18 p2495 N88-24802
Effect of thickness on downward flame spread over paper
[NASA-TT-20282] 19 p2612 N88-25501
Measurement of burning rates of NOSOL-363 propellants under cross-flow and strand burner conditions using real-time X-ray radiography
19 p2623 N88-25560
Burning rate measurements of Non-Newtonian Liquid Propellant (NNLP) 19 p2623 N88-25561
Combustion rate limits of hydrogen plus hydrocarbon fuel: Air diffusion flames from an opposed jet burner technique 19 p2624 N88-25567
Anatomy of group burning mode transitions in spray group combustion 19 p2626 N88-25578
Effect of burn-path tortuosity on the burn rate of composite propellants 19 p2630 N88-25602
Analysis of microwave burner measurement system using a microwave network analysis computer program
19 p2631 N88-25604
Modeling and experimental measurements of solid propellant flame structure 19 p2631 N88-25605
Pressure differential scanning calorimetry (DSC) evaluation of solid rocket propellant burn rate mod
19 p2631 N88-25606
Evaluation of techniques for direct measurement of burning rates in nozzleless motors
19 p2631 N88-25609
Combustion diagnostics of propellant with new grain geometries
[AD-A194944] 24 p3342 N88-29895
Descriptive characterization of propellant particles
[AD-A195176] 24 p3356 N88-29985
Discovery of a low temperature form of TAGN (Triaminoguanidinium Nitrate)
[AD-A196059] 24 p3357 N88-29989
BURNOUT
Computer calculations of PIN diode limiter characteristics
[AD-A185563] 06 p0697 N88-14277
Investigation of fuel additive effects on sooting flames
[AD-A186403] 07 p0829 N88-15026
BURST TESTS
Hydroburst test of a carbon-carbon involute exit cone
[NASA-TP-2556] 06 p0671 N88-14112
BURSTS
NT GAMMA RAY BURSTS
NT RADIO BURSTS
NT SOLAR RADIO BURSTS
NT TYPE 3 BURSTS
Nowcasting microbursts using Doppler radar in a forecaster-computer environment
02 p0200 N88-11246
Three-wave parametric resonance in plasma of relativistic electron flux 14 p1972 N88-21772
Analysis of the coma outburst of Comet Halley, March 24 to 25 (UT), 1986 14 p2000 N88-21920
Outburst of Halley's comet 14 p2007 N88-21967
Prospects for large dynamic range isotope analysis using photon burst mass spectrometry
[DE88-009110] 19 p2613 N88-25505
Detection of absorption lines in the spectra of X-ray bursts from X1608-52
[ISAS-RN-360] 20 p2887 N88-27143
The hard X-ray burst spectrometer event listing 1980-1987
[NASA-TM-4036] 20 p2887 N88-27144
BURUNDI
Analysis of the multispectral content and of SPOT subscenes in two regions of Burundi. Lithologic and tectonic interpretations 22 p3105 N88-28439
BUS CONDUCTORS
Digital system bus integrity
[NASA-CR-181446] 01 p0006 N88-10030
Lightweight power bus for a baseload nuclear reactor in space 17 p2438 N88-24505
BUSINESS MANAGEMENT
U INDUSTRIAL MANAGEMENT
BUTADIENE
Polymerization of azaethylenes (imines) and aza-1,3-dienes: Potential reactive monomers
[AD-A194717] 23 p3197 N88-29026
BUTANES
The role of low temperature chemistry in the autoignition of n-butane
[DE88-002385] 07 p0829 N88-15031
Pseudo-stationary oblique-shock-wave reflections in low gamma gases: Isobutane and sulphur hexafluoride
[UTIAS-TN-267] 13 p1768 N88-20576
Dissolution rates of polymers and copolymers based on methyl, ethyl and butyl methacrylate
[AD-A194713] 23 p3197 N88-29027
BUTENES
Synthesis and characterization of 1,2-cyclobutenedicarboxamides: Thermally generated polymers and Diels-Alder adducts
[AD-A188591] 12 p1611 N88-19633
High-temperature thermosets derived from the Diels-Alder polymerization of bisbenzocyclobutenes and bimaleimides
[AD-A188800] 13 p1747 N88-20449
BUTT JOINTS
Plasma joining of metal matrix composites
[AD-A188559] 12 p1604 N88-19593
BUTYLENE
U BUTENES
BY-PRODUCTS
Production of jet fuels from coal derived liquids. Volume 1: Market assessment for liquid by-products from the Great Plains gasification plant
[AD-A184846] 05 p0570 N88-13475

CELSS Program Meeting 05 p0630 N88-13853

Controlled ecological life support systems: Development of a plant growth module 05 p0630 N88-13854

Upgrading pyrolysis vapors to aromatic gasoline with zeolite catalysis at atmospheric pressure
18 p2536 N88-25045

Feasibility of producing jet fuel from GPGP (Great Plains Gasification Plant) by-products
[DE88-010233] 20 p2781 N88-26492

BYPASS RATIO

Experimental study of bypass transition in a boundary layer
[NASA-TM-100913] 16 p2209 N88-23186

C

C (PROGRAMMING LANGUAGE)

Mixing Microsoft C and Microsoft FORTRAN program modules on the IBM Personal Computer
[DE88-001947] 05 p0637 N88-13895

C-GKS, a C implementation of GKS, the graphical kernel system
[CWI-CS-R8753] 16 p2249 N88-23438

VPC: A proposal for a vector parallel C programming language
[AD-A190885] 16 p2251 N88-23451

A timing evaluator for C programs generated by the model system
[AD-A191204] 17 p2385 N88-24174

FASTRUN phase sequencer descriptor language (PDL)
[DE88-007966 20 p2837 N88-26828

C STARS

U CARBON STARS

C-M DIAGRAM

U COLOR-MAGNITUDE DIAGRAM

C-130 AIRCRAFT

Electrical load and power source capacity report for the C-130 aircraft Self Contained Navigation System (SCNS): LSI model 6216A, 6216B, 6216C, revision
[AD-A193079] 21 p2895 N88-27186

C-135 AIRCRAFT

Reduced-gravity two phase flow experiments in the NASA KC-135 17 p2431 N88-24465

Analysis and interpretation of low gravity boiling experiments in the KC-135 17 p2432 N88-24466

The Marshall Space Flight Center KC-135 microgravity test program for FY84-86
[NASA-TM-4059] 22 p3056 N88-28136

CABIN ATMOSPHERES

NT SPACECRAFT CABIN ATMOSPHERES

Northwest Airlines flight experiments
05 p0617 N88-13786

Advancements in oxygen generation and humidity control by water vapor electrolysis
[NASA-CR-172073] 22 p3134 N88-28633

CABLES

Development and study of fibre-optic link lines on the basis of the KEM-8-4PD, KEM-8-4PR quantum-electronic modules
[DE88-700372] 07 p0932 N88-15663

CABLES (ROPES)

BASIC desk-top computer program for the three-dimensional static configuration of an extensible flexible cable in a uniform stream
[AD-A184852] 05 p0609 N88-13737

The Shock and Vibration Digest, Volume 19, No. 12
05 p0610 N88-13746

Dynamics of cables and chains
05 p0610 N88-13747

Life prediction of steel cords
06 p0715 N88-14386

CAD (DESIGN)

U COMPUTER AIDED DESIGN

CADASTRAL MAPPING

The Systeme d'Analyse Geographique (SAGE) geographic analysis system 17 p2353 N88-24019

The SAGE geographic analysis system
17 p2361 N88-24063

Tests for the automatic pattern recognition of building surfaces by the TK 50 18 p2533 N88-25030

Recent developments in software and hardware by Scitex Co. --- computer aided mapping
18 p2535 N88-25038

Technique to obtain the agricultural ownership limits by satellite imagery, to approve control, and to accompany agricultural activity 19 p2682 N88-25943

Updating of municipal official register of real estate through the geographical information system
19 p2684 N88-25952

Aerial photography as an instrument of municipal and regional planning: Metropolitan area of Sao Paulo (SP)
19 p2684 N88-25957

CADMIUM

Effects of cadmium electrode properties on nickel-cadmium cell performance
[AD-A191394] 16 p2193 N88-23081

A rapid electrochemical technique for determining the current efficiency for cadmium plating
[AD-A193679] 22 p3056 N88-28130

CADMIUM COMPOUNDS

NT CADMIUM SELENIDES
NT CADMIUM SULFIDES
NT CADMIUM TELLURIDES

CADMIUM MERCURY TELLURIDES

U MERCURY CADMIUM TELLURIDES

CADMIUM NICKEL BATTERIES

U NICKEL CADMIUM BATTERIES

CADMIUM SELENIDES

Ultrafast physics in semiconductor microstructures
[AD-A193300] 21 p3022 N88-27936

CADMIUM SULFIDES

Physico-chemical studies on copper sulfide behavior in the CdS-Cu2S solar cell
[ETN-88-91068] 09 p1187 N88-17109

Investigation of the subsequent treatment and the stability of CuxS-CdS thin-film solar cells
[ETN-88-91488] 11 p1507 N88-19006

CADMIUM TELLURIDES

Preparation and properties of evaporated CdTe films
[DE87-012270] 02 p0195 N88-11216

Population inversion in gapless semiconductors as result of interband pumping 06 p0770 N88-14732

CdTe(110)-Mn interface reaction and the formation of non-equilibrium ternary semimagnetic semiconductor alloys
[AD-A187593] 10 p1422 N88-18491

Metal contacts to cadmium telluride (CdTe)
[AD-A188306] 12 p1698 N88-20159

CdZnTe as a wide-band-gap absorber for a tandem, thin-film solar cell
[DE88-001114] 13 p1793 N88-20724

Research on single-crystal CdTe solar cells
[DE88-001115] 13 p1793 N88-20725

Thin-film cadmium telluride solar cells
[DE88-001107] 13 p1846 N88-21050

Electrical and optical properties of Hg/sub 1-x/Cd/sub x/Te doped layers grown by Liquid Phase Epitaxy (LPE)
[DE88-701023] 16 p2281 N88-23653

MBE growth of HgTe/CdTe superlattices on Si(100) substrates 20 p2869 N88-27033

Type 3 - type 1 transition and strain effect in Hg(1-x)Cd(x)Te-CdTe and Hg(1-x)Zn(x)Te-CdTe superlattices 20 p2872 N88-27052

Tunnelling currents in reverse biased CMT photodiodes
[RSRE-MEMO-4137] 23 p3209 N88-29097

CAFFEINE

Influence of altitude and caffeine during rest and exercise on plasma levels of proenkephalin peptide F
[AD-A192659] 22 p3131 N88-28616

CAI

U COMPUTER ASSISTED INSTRUCTION

CALCITE

Kinetics of thermochemical gas-solid reactions important in the Venus sulfur cycle
[NASA-CR-182963] 19 p2742 N88-26280

CALCIUM

NT CALCIUM ISOTOPES

Simultaneous, cospatial imaging of the Sun in cyanogen and singly-ionized calcium 04 p0507 N88-13114

The angular diameter of alpha Scorpii in the near-infrared Ca II triplet 04 p0514 N88-13162

Lidar metal density measurements in the upper atmosphere 08 p1027 N88-16219

High temperature superconductivity
[AD-A190259] 16 p2281 N88-23655

CALCIUM CARBONATES

NT CALCITE

Characterization of the dimensions of colloidal calcium carbonate dispersions in toluene with neutron small-angle scattering
[ECN-197] 06 p0680 N88-14167

Nucleation and growth of calcium carbonate crystals on surface-modified polyethylene and polystyrene
[DE88-005126] 11 p1485 N88-18733

CALCIUM COMPOUNDS

NT CALCITE
NT CALCIUM CARBONATES
NT CALCIUM FLUORIDES
NT CALCIUM OXIDES
NT CALCIUM SILICATES
NT PEROVSKITES

Electron cytochemical detection of Ca(2)+-ATPase in protonema of moss funaria hygrometrica (H e d w.) under hypogravitation 06 p0749 N88-14602

An in situ annealing study of lead implanted single crystal calcium titanate
[DE88-005435] 11 p1562 N88-19351

CALCIUM FLUORIDES

Submerged arc flux welding with CaF2-CaO-SiO2 fluxes: Possible electrochemical effects on weld metal
[DE88-003107] 08 p0992 N88-16004

High temperature solar electrothermal processing-3. Zinc from zinc oxide at 1200-1675K using a non-consumable anode
[AD-A186600] 09 p1141 N88-16836

CALCIUM ISOTOPES

The elastic scattering of intermediate energy protons from (40)Ca and (208)Pb 01 p0092 N88-10599

CALCIUM METABOLISM

Prevention of disuse osteoporosis: Effect of sodium fluoride during five weeks of bed rest
[NASA-CR-172018] 01 p0075 N88-10483

Regulation of calcium metabolism during prolonged antiorthostatic hypokinesia
[NASA-TT-20219] 11 p1521 N88-19085

Use of diphosphonates to correct disorders in calcium metabolism and mineral composition of bone tissue with 60-day hypokinesia in rats
[NASA-TT-20220] 13 p1809 N88-20807

CALCIUM OXIDES

Submerged arc flux welding with CaF2-CaO-SiO2 fluxes: Possible electrochemical effects on weld metal
[DE88-003107] 08 p0992 N88-16004

Nuclear magnetic ordering and paramagnetic relaxation of diatomic molecules in Ca (OH)2
[B8681469] 23 p3281 N88-29532

CALCIUM SILICATES

Development of highly porous calcium silicate hydrate materials with extremely low thermal conductivity
[BMFT-FB-T-86-164] 02 p0150 N88-10941

CALCIUM 45

U CALCIUM ISOTOPES

CALCULATION

U COMPUTATION

CALCULATORS

Langlie Test Method Program for use with the HP-41CV/X calculator
[DE88-001935] 06 p0687 N88-14210

CALCULUS

NT ASYMPTOTIC SERIES
NT COLLINEARITY
NT CONTINUITY (MATHEMATICS)
NT COPLANARITY
NT COSINE SERIES
NT FOURIER-BESSEL TRANSFORMATIONS
NT INTEGRAL CALCULUS
NT LIMITS (MATHEMATICS)
NT PADE APPROXIMATION
NT POWER SERIES
NT SERIES (MATHEMATICS)
NT TAYLOR SERIES
NT VECTOR ANALYSIS
NT VORTICITY

Formalizing reusable software components in the programmer's apprentice
[AD-A185843] 07 p0901 N88-15457

Martingale representation and the Malliavin calculus
[AD-A189721] 15 p2119 N88-22626

Non-rigid motion and Regge calculus
[AD-A190387] 15 p2121 N88-22640

Filtering of jump processes
[AD-A189701] 15 p2123 N88-22656

Unique normal forms for lambda calculus with surjective pairing
[PB88-173539] 16 p2260 N88-23508

Practical higher-order functional and logic programming based on lambda-calculus and set-abstraction
[AD-A193645] 23 p3271 N88-29466

CALCULUS OF VARIATIONS

A VAS-numerical model impact study using the Gal-Chen variational approach --- Visible Infrared Spin-Scan Radiometer Atmospheric Sounder (VAS)
02 p0213 N88-11339

The method of lines for time dependent free boundary problems
[DE87-013929] 02 p0226 N88-11423

The role of computation fluid dynamics in aeronautical engineering (4): The development and applications of implicit TVD finite volume code
05 p0536 N88-13259

A study of the free energy of the Lenz-Ising model using the cluster variation method of Morita
[AD-A186023] 08 p1073 N88-16476

A substructure method for dynamic simulation of flexible mechanical systems with geometric nonlinearities
09 p1176 N88-17044

Studies in finite time thermodynamics
[DE88-004531] 10 p1423 N88-18500

Total Variation Diminishing (TVD) schemes of uniform accuracy
[NASA-TM-100552] 11 p1436 N88-18566

On exterior variational calculus
[DE88-700861] 12 p1683 N88-20062

Inversion algorithms for geophysical problems
[AD-A189252] 13 p1815 N88-20845
Nonlinear differential equations
[DE88-006047] 13 p1826 N88-20933
The inverse power method for semilinear elliptic equations
[DE88-006427] 15 p2118 N88-22620
Discrete variational methods and their application to electronic structures
[DE88-702215] 21 p3014 N88-27888
On the distribution equations
[DE88-7022[illegible]7] 23 p3270 N88-29454
On the Nash point equilibria in the calculus of variations
[AD-A194959] 24 p3424 N88-30381

CALDERAS
Gravity and fault structures, Long Valley Caldera, California
[DE87-014117] 02 p0197 N88-11229
Mid-tertiary volcano-tectonic development of the Southwestern Cordillera of North America
06 p0797 N88-14879
A three-dimensional gravity model of the geologic structure of Long Valley caldera
[DE88-006331] 16 p2231 N88-23324
A core hole into the hydrothermal system of the Long Valley caldera
[DE88-006335] 16 p2231 N88-23325

CALENDARS
Calendar of selected aeronautical and space meetings
[AGARD-CAL-87/1] 05 p0657 N88-14033
Calendar of selected aeronautical and space meetings
[AGARD-CAL-88/1] 05 p0658 N88-14037

CALIBRATING
NT WIND TUNNEL CALIBRATION
Development of response models for the Earth Radiation Budget Experiment (ERBE) sensors. Part 2: Analysis of the ERBE integrating sphere ground calibration
[NASA-CR-178293] 01 p0049 N88-10316
Wet deposition and snowpack monitoring operations and quality assurance manual
[PB87-212817] 01 p0064 N88-10413
Spectrometric test of a linear array sensor
[NASA-TM-100676] 01 p0064 N88-10414
NBS (National Bureau of Standards) calibration services users guide: Fee schedule
[PB87-210654] 01 p0090 N88-10586
Monitored background radiometer
02 p0133 N88-10831
Calibration of attitude control sensors
02 p0159 N88-10995
The absolute radiometric calibration of space-based sensors 03 p0277 N88-11744
Mass transport by diffusion 03 p0297 N88-11864
NBS (National Bureau of Standards) calibration procedures for horizontal dipole antennas (25 to 1000 MHz)
[PB87-210233] 03 p0305 N88-11922
Requirements for the calibration of mechanical shock transducers
[PB87-227591] 03 p0325 N88-12054
NBS (National Bureau of Standards) measurement services: Radiometric standards in the vacuum ultraviolet
[PB87-227625] 03 p0325 N88-12055
Calibration standard for metallographic microscopes
[RFP-3956-REV] 03 p0326 N88-12057
Absolute and interband calibration --- SPOT
03 p0341 N88-12152
The correspondence of surface climate parameters with satellite and terrain data
[NASA-CR-181515] 03 p0346 N88-12185
Lyman alpha SMM/UVSP absolute calibration and geocoronal correction
[NASA-TM-100314] 03 p0389 N88-12446
The design and preliminary calibration of a boundary-layer flow channel
[NASA-CR-178399] 04 p0394 N88-12457
Performance optimization of electronic networks in the frequency domain
[PB87-123873] 04 p0438 N88-12720
Evaluation of the sensidyne toxic gas sensor for HF (Hydrogen Fluoride) vapor
[DE88-000647] 04 p0446 N88-12767
Accuracy potential of non-metric cameras in close-range photogrammetry 04 p0463 N88-12862
Radiometric calibration of the Earth observing system's imaging sensors
[NASA-CR-181542] 04 p0463 N88-12865
Calibration on the Sun for stellar magnetic fields
04 p0506 N88-13113
Development of response models for the Earth Radiation Budget Experiment (ERBE) sensors. Part 3: ERBE scanner measurement accuracy analysis due to reduced housekeeping data
[NASA-CR-178294] 05 p0583 N88-13553
Fabricate, calibrate and test a dosimeter for integration into the CRRES (Combined Release and Radiation Effects Satellite) satellite
[AD-A185439] 05 p0585 N88-13564
Improvement of modal scaling factors using mass additive technique 05 p0593 N88-13620
AIS-2 radiometry and a comparison of methods for the recovery of ground reflectance
05 p0611 N88-13757
Calibrating AIS images using the surface as a reference 05 p0612 N88-13760
Causes of spurious features in spectral reflectance data 05 p0614 N88-13769
Analysis of SO2 signals in SBUV/TOMS data
05 p0618 N88-13794
Media calibrations of the Doppler signal for a gravitational wave experiment --- interplanetary medium
[IFSI-86-13] 05 p0625 N88-13825
Area detectors for X-ray spectroscopy
[DE88-001429] 06 p0679 N88-14163
Picosecond cable calibrator: Beam Research Program
[DE88-002375] 06 p0695 N88-14266
Computer simulation of the L/sub 3/-edge densitometer
[DE88-001944] 06 p0705 N88-14324
Airborne Visible/Infrared Imaging Spectrometer (AVIRIS). A description of the sensor, ground data processing facility, laboratory calibration, and first results
[NASA-CR-182365] 06 p0705 N88-14325
Spectral and radiometric calibration of the Airborne Visible/Infrared Imaging Spectrometer
06 p0707 N88-14334
Robot accuracy improvement through kinematic parameter identification 06 p0712 N88-14363
Self calibration of motion and stereo vision for mobile robot navigation
[AD-A185602] 06 p0781 N88-14794
Calibration constants for the 1986 BGO crystals matrix
[NOTA-INTERNA-886] 07 p0856 N88-15197
LANDSAT thematic mapper radiometric calibration study
[NASA-CR-182410] 07 p0872 N88-15267
The results of the 1984/1985 Round-Robin Calibration of Reference Solar Cells for the Summit Working Group on Technology, Growth and Employment
[DE88-900215] 07 p0874 N88-15303
Problems and possible solutions involved in hard target calibration of coherent Doppler lidar
07 p0922 N88-15602
Research sensors 08 p0955 N88-15795
Optical measurement systems
08 p0955 N88-15796
High Resolution Picture Transmission (HRPT) data processing from NOAA series satellites
[INPE-4372-PRE/1195] 08 p0963 N88-15831
Temperature Metrology '86
[DE88-700236] 08 p0989 N88-15990
Calibration of the ARL (Aeronautical Research Laboratories) rain and icing facility
[AD-A186776] 09 p1121 N88-16710
Tensorial calibration. 2. Second order tensorial calibration
[AD-A186614] 09 p1167 N88-16994
Tensorial calibration. Part 1: First order tensorial calibration
[AD-A186706] 09 p1167 N88-16995
The superconducting gravimeter: Application, calibration, and further development
[SER-C-329] 09 p1167 N88-16998
Recommendations for organising the calibration of pure-tone audiometers
[NPL-AC-112] 09 p1167 N88-16999
Hydrogen maser
[PB87-171617] 09 p1172 N88-17025
Finite element analysis for the calculation of calibration curves of fracture mechanics specimen for semicircular surface cracks with several starting depths, for the crack depth measurement following the dc potential method
[GKSS-87/E/19] 09 p1183 N88-17086
Calibration of neural networks using genetic algorithms, with application to optimal path planning
09 p1214 N88-17277
Strong consistency of certain information theoretic criteria for model selection in calibration, discriminant analysis and canonical correlation analysis
[AD-A186584] 09 p1232 N88-17385
Error modeling and confidence interval estimation for inductively coupled plasma calibration curves
[AD-A186711] 09 p1250 N88-17486
Signal processing studies program optical signal amplification, volume 2
[AD-A188054] 10 p1320 N88-17896
Johnson noise thermometer for high radiation and high temperature environments
[DE88-003770] 10 p1323 N88-17911
A technique for low level, wide range CW microwave power meter calibrations
[DE88-004147] 10 p1333 N88-17966
NBS (National Bureau of Standards) measurement services: Spectral irradiance calibrations
[PB88-123781] 10 p1408 N88-18401
Source and event selection for radio-planetary frame-tie measurements using the Phobos Landers
11 p1471 N88-18775
Using ridge regression in systematic pointing error corrections 11 p1472 N88-18777
Phase calibration generator 11 p1473 N88-18785
DSS 14 64-meter antenna S- and X-band efficiency and system noise temperature calibrations, September 1987
11 p1473 N88-18790
Calibration of a Harwood DWT-1000 controlled-clearance piston gauge
[DE88-004496] 11 p1489 N88-18888
Calibration of beam power monitors for laser welding
[DE88-004687] 11 p1492 N88-18908
Thirteenth Biennial Guidance Test Symposium, volume 1
[AD-A185782] 12 p1576 N88-19427
Calibration of a ring laser gyro inertial navigation system 12 p1576 N88-19428
The complex point spread function of the RSRE SAR (Synthetic Aperture Radar)
[AD-A189011] 12 p1621 N88-19693
Zoom versus full-field sensitivity at the ETS (Experimental Test System)
[AD-A188162] 12 p1628 N88-19742
DIRBE External Calibrator (DEC)
[NASA-CR-180761] 12 p1631 N88-19760
Long term measurement network for FIFE
[NASA-CR-182491] 12 p1646 N88-19857
Ultrasonic measurements research: Progress in 1987
[AD-A188506] 12 p1687 N88-20092
Investigations of high resolution imaging through the Earth's atmosphere using speckle interferometry
[AD-A189295] 12 p1692 N88-20121
An attempt to measure the diffuse brightness of the sky at submillimeter wavelengths
12 p1710 N88-20233
Analysis of pre-flight modulator voltage calibration data for the Voyager plasma science experiment
[NASA-CR-182577] 12 p1710 N88-20236
The Joint NASA/Goddard-University of Maryland Research Program in Charged Particle and High Energy Photon Detector Technology
[NASA-CR-182612] 12 p1712 N88-20247
The imaging of extra-galactic low-energy gamma-ray sources prospects, techniques, and instrumentation
[NASA-CR-182536] 12 p1713 N88-20251
A low-frequency measurement of the spectrum of the cosmic microwave background radiation
13 p1858 N88-21112
NBS (National Bureau of Standards) measurement services. GOES (Geostationary Operational Environmental Satellite) time code dissemination: Description and operation
[PB88-168760] 14 p1880 N88-21235
Quantitative AES: The establishment of a standard reference spectrum for the accurate determination of spectrometer transmission functions
[NPL-DMA(A)-151] 14 p1887 N88-21279
Pre-launch calibration of channels 1 and 2 of the advanced very high resolution radiometer
[PB88-157169] 14 p1913 N88-21427
Calibration of a hot-wire/hot-film anemometer over a range of temperatures, velocities and pressures
[AD-A189717] 14 p1913 N88-21430
The Spring 1985 high precision baseline test of the JPL GPS-based geodetic system
[NASA-CR-182686] 14 p1940 N88-21577
The absolute radiometric calibration of the advanced very high resolution radiometer
[NASA-CR-182755] 14 p1941 N88-21584
High energy cosmic muons and the calibration of the L3 electromagnetic calorimeter
[NOTA-INTERNA-895] 14 p2011 N88-21999
A 150,000 pounds per square inch dynamic pressure calibrator
[AD-A190659] 15 p2069 N88-22335
Support for FY87 midlatitude electron-density calibration campaign
[AD-A190174] 15 p2094 N88-22476
Stellar scintillometer atmospheric optical turbulence profiling experiment: A qualitative comparison of two identical instruments at AMOS (Air Force Maui Optical Station), 1985
[AD-A190589] 15 p2094 N88-22479
Computer grading of extensometers (BS 3846)
[NPL-DMA(A)-152] 15 p2108 N88-22560
Design, fabricate, calibrate, test and deliver two satellite electron flux detectors
[AD-A190799] 16 p2169 N88-22930

Analysis and experiments concerning the performance and calibration of compact antenna-test ranges
[PB88-169263] 16 p2188 N88-23047
Analysis and experiments concerning the performance and calibration of compact antenna-test ranges
[ISBN-9-09-001727-5] 16 p2188 N88-23048
Enhanced backscattering from rough surfaces
[AD-A190995] 16 p2190 N88-23063
Radiation standards 16 p2272 N88-23592
Reflection standards for spectroradiometry. Realization and calibration 16 p2272 N88-23595
Preparation and execution of calibration measurements for handling of airborne SAR data (AGRISAR)
[ETN-88-92338] 17 p2333 N88-23926
A control technique for improved robot performance
17 p2391 N88-24212
Johnson noise thermometer for high-radiation and high-temperature environments
17 p2434 N88-24480
Intensity calibration of a VUV system by branching line pairs 17 p2443 N88-24533
Expendable conductivity, temperature and depth system (XCTD) development program
[AD-A192182] 18 p2547 N88-25121
Calibration of averaging total pressure flight wake rake and natural-laminar-flow airfoil drag certification
[NASA-CR-181630] 19 p2599 N88-25443
An error floor in tone calibrated transmission
19 p2649 N88-25729
Automatic calibration of space based manipulators and mechanisms
[NASA-CR-182804] 19 p2676 N88-25912
Design and calibration of a two-channel low-noise heterodyne receiver for use in a CO2 laser Thomson scattering alpha particle diagnostic
[DE88-007666] 19 p2728 N88-26201
Time-resolved doubly bent crystal X-ray spectrometer
[DE88-007899] 20 p2805 N88-26637
Microwave calibration system 2
[AD-A192976] 20 p2805 N88-26639
Fiber optic sensors with internal referencing
[NASA-TM-100893] 20 p2806 N88-26644
Surface disturbances produced by low-level, subsonic B-1 aircraft
[AD-A192257] 20 p2824 N88-26752
Calibration and data reduction techniques for the AFGL infrared array spectrometer 21 p2927 N88-27374
Calibration of the portable wear metal analyzer
[AD-A192971] 21 p2950 N88-27524
Acoustic emission calibration instrumentation
[DE88-010817] 21 p2951 N88-27528
Validate algorithms for the determination of rainfall rates from SSM/I microwave satellite imagery
[AD-A192299] 21 p2974 N88-27664
Test and calibration system for monitoring the Advanced Technologies Testing Aircraft System (ATTAS) data acquisition system 22 p3037 N88-28029
Apparent brightness of stars and lasers
22 p3065 N88-28188
A digitally implemented phase-locked loop detection scheme for analysis of the phase and power stability of a calibration tone 22 p3066 N88-28196
DSS 14 antenna calibrations for GSSR/VLA Saturn radar experiments 22 p3068 N88-28207
Calibration technique and study on metrological characteristics of a high-voltage inverse square-law function generator
[DE88-702101] 22 p3072 N88-28236
Calibration of a triple wire probe for turbulence measurements
[AD-A193956] 22 p3081 N88-28296
Calibration of quartz load cells: An in-situ procedure for instrumented falling weight impact machines
[NPL-DMA(A)-155] 22 p3081 N88-28297
Langley Research Center Metrology Program status for fiscal year 1987
[NASA-TM-100651] 22 p3086 N88-28324
Research and development objectives: Installation, startup, and test operation of a remote and program controlled measuring table for the calibration of EGRET experiment
[ETN-88-92105] 22 p3152 N88-28752
SQUID (superconducting quantum interference device) arrays for simultaneous magnetic measurements: Calibration and source localization performance
[AD-A193815] 23 p3216 N88-29143
Results of the use of an automated electrical measuring instrument calibration system
[SNIAS-881-430-107] 23 p3217 N88-29146
Development of an adjustable buoyancy balloon tracer of atmospheric motion. Phase 3: Refinement of the operational prototype system
[PB88-190764] 23 p3231 N88-29230
NBS (National Bureau of Standards) measurement services: The NBS photodetector spectral response calibration transfer program
[PB88-201595] 24 p3376 N88-30109
Atmospheric corrections for in-flight satellite radiometric calibration
[AD-A196124] 24 p3391 N88-30194
A new determination of the Geneva photometric passbands and their absolute calibration
[SER-C-PREPUBL-FASC-26] 24 p3452 N88-30546

CALIFORNIA
North Pacific Ocean. Tradewind region east of Hawaii, R/V Thomas G Thompson: 25 September - 1 November 1972. STD data report
[AD-A186566] 08 p1044 N88-16311
CTD observations in the coastal transition zone off northern California, 16-25 February 1987
[AD-A187283] 10 p1357 N88-18111
Numerical simulations of the California current: Filament formation as related to baroclinic instability
[AD-A187573] 10 p1358 N88-18115
Hydrographic data from the OPTOMA (Ocean Prediction Through Observation, Modeling and Analysis) program: OPTOMA 23, 9-19 November 1986
[AD-A189868] 15 p2099 N88-22506
Soil erosion and causative factors at Vandenberg Air Force Base, California
[NASA-TM-100981] 17 p2381 N88-24156
Survey for least bell's vireo in riparian habitat on Vandenberg Air Force Base, Santa Barbara County, California
[NASA-TM-100984] 20 p2822 N88-26744

CALIFORNIUM COMPOUNDS
Raman and absorption spectrophotometric studies of selected lanthanide, californium-doped lanthanide, and actinide trihalides in the solid state
[DE88-008234] 20 p2874 N88-27061

CALORIC REQUIREMENTS
Significance of nutrition to change in human carbohydrate and lipid metabolism under emotional stress 19 p2703 N88-26073

CALORIC STIMULI
Nystagmometric distinctions of individuals regularly exposed to vibration 07 p0891 N88-15401

CALORIMETERS
NT BOMB CALORIMETERS
Calorimetric Absorption Spectroscopy (CAS): A new method for the characterization of the optical properties of semiconductor systems
[ETN-87-90407] 01 p0098 N88-10645
Application of prediction of equilibrium to servo-controlled calorimetry measurements
[DE87-013745] 03 p0324 N88-12046
Simultaneous TG/DSC (thermogravimetry/Differential Scanning Calorimetry) and TG/MS (thermogravimetry/Mass Spectrometry) analyses of polymeric and energetic materials
[DE88-000727] 04 p0413 N88-12561
Investigation by differential scanning calorimetry of microstructure in a superplastic Al-Mg-Zr alloy
[AD-A184902] 05 p0564 N88-13439
An automated flow calorimeter for heat capacity and enthalpy measurements at elevated temperatures and pressures
[DE88-002357] 07 p0857 N88-15206
A calorimeter for measuring the neutral beam power reaching the plasma
[DE88-001412] 07 p0937 N88-15691
The high resolution spaghetti hadron calorimeter
[NIKHEF-H/87-7] 08 p0990 N88-15993
DSC (Differential Scanning Calorimeter) stability test for liquid propellants: A preliminary report
[AD-A187115] 09 p1150 N88-16888
Design and fabrication of advanced hybrid circuits for high energy physics
[DE88-004392] 11 p1479 N88-18825
High resolution hadron calorimetry
[NIKHEF-H/87-8] 13 p1773 N88-20605
Energy loss of particles in dense matter-calorimetry
[NIKHEF-H/87-12] 13 p1836 N88-20988
A segmented calorimeter for low-energy particle beams in space
[DE88-001806] 13 p1838 N88-20997
High energy cosmic muons and the calibration of the L3 electromagnetic calorimeter
[NOTA-INTERNA-895] 14 p2011 N88-21999
Calorimetric technique for measuring liquid helium flow rate
[DE88-701308] 16 p2200 N88-23123
Calorimetry applied to nucleus-nucleus collisions at ultrarelativistic energies
[DE88-006173] 18 p2573 N88-25282
Pressure differential scanning calorimetry (DSC) evaluation of solid rocket propellant burn rate mod
19 p2631 N88-25606

CALORIMETRY
U HEAT MEASUREMENT

CAM (MANUFACTURING)
U COMPUTER AIDED MANUFACTURING

CAMBER
NT WING CAMBER
Unsteady flow about cambered plates
[AD-A184725] 03 p0320 N88-12025
An experimental investigation of decelerating flow about two-dimensional cambered plates
[DE88-006596] 13 p1766 N88-20567
Discrete vortex analysis of unsteady flow about two-dimensional cambered plates
[DE88-006597] 14 p1909 N88-21407

CAMBERED WINGS
Aerodynamic characteristics of wings designed with a combined-theory method to cruise at a Mach number of 4.5
[NASA-TP-2799] 12 p1575 N88-19420

CAMERA SHUTTERS
Analysis of spectral reflectance characteristics of targets under satellites and automatic cloud recognition
13 p1755 N88-20496

CAMERA TUBES
NT IMAGE DISSECTOR TUBES
NT VIDICONS

CAMERAS
NT DIFFRACTION LIMITED CAMERAS
NT FAINT OBJECT CAMERA
NT FRAMING CAMERAS
NT HIGH SPEED CAMERAS
NT MULTISPECTRAL BAND CAMERAS
NT PINHOLE CAMERAS
NT STREAK CAMERAS
NT TELEVISION CAMERAS
Study of a payload for Columbus Polar Platform Earth observation demonstration mission, executive summary
[ESA-CR(P)-2412] 01 p0014 N88-10079
Use of a 35mm camera for remote surface cleanliness verification 02 p0133 N88-10835
Programmable 10 MHz optical fiducial system for hydrodiagnostic cameras
[DE87-013223] 02 p0175 N88-11091
Cineradiography
[DE87-013158] 03 p0324 N88-12045
Accuracy potential of non-metric cameras in close-range photogrammetry 04 p0463 N88-12862
The technical evolution of the Wilson camera: The beginnings (1895-1925)
[NOTA-INTERNA-876] 05 p0585 N88-13568
Electronic imaging technique for welding and other high-luminosity processes
[DE88-002199] 07 p0862 N88-15227
Object detection in images from outdoor scenes using evidential reasoning
[FOA-C-30461-3.3] 08 p1020 N88-16183
Space infrared telescope facility wide field and diffraction limited array camera (IRAC)
[NASA-CR-182704] 13 p1853 N88-21092
Cryogenic mechanism for ISO camera
14 p1878 N88-21221
Analysis of contamination data recorded by the IECM camera/photometer
[NASA-TM-100324] 14 p1882 N88-21246
Further development of a stellar camera following the rotation-modulation-collimator principle for balloon-borne observations in the X-ray range
[ETN-88-91496] 14 p1913 N88-21428
ROVER: A prototype active vision system
[AD-A189246] 15 p2133 N88-22722
An investigation of the crystalchemistry and thermochemistry of selected mineral systems
[AD-A189758] 15 p2142 N88-22781
An investigation into the precision of a digital camera
[B8735054] 16 p2210 N88-23193
Obtaining information on cloud particles by a commercial miniature camera
[DFVLR-MITT-87-19] 16 p2234 N88-23342
The modeling of error budget analysis and tolerance specifications for BRESEX multiband linear array CCD camera 17 p2355 N88-24029
The XRD (X-Ray Diode) array, the grazing incidence spectrometer and the X-ray imaging camera on PBFA 2
[DE88-007262] 19 p2728 N88-26200
Stress analysis using infrared thermography
[ETN-88-92169] 20 p2816 N88-26705
The FEL CCD-camera: Experimental system for camera and image processing research
[FEL-1987-34] 21 p2952 N88-27532
Satellite attitude determination using a CCD (Charge-Coupled-Device) star camera
[AD-A192662] 22 p3046 N88-28080
Four-frame gated optical imager with 120-ps resolution
[DE88-011735] 22 p3080 N88-28288

PLZT (Lead-Lathanium-Zirconium-Titanium) electro-optic photographic system
[AD-A193473] 23 p3215 N88-29137
Kalman filter-based algorithms for estimating depth from image sequences
[AD-A195818] 24 p3424 N88-30380

CAMOUFLAGE
A Workshop on Desert Processes, September 24-28, 1984: Report on the conference
[AD-A184599] 03 p0345 N88-12184
Cleanability of aircraft polyurethane topcoats
[AD-A193456] 23 p3170 N88-28678

CAMS
AVIRIS scan drive design and performance
06 p0706 N88-14330

CANADA
NT BRITISH COLUMBIA
Corrosion in avionics and associated equipment; cause, effect and prevention 05 p0547 N88-13335
Petrogenesis of basalts from the Archean Matachewan Dike Swarm Superior Province of Canada
06 p0796 N88-14878
Northern lights: The economic and practical potential of imported power from Canada
[DE88-006026] 15 p2093 N88-22473
Mobile satellite service for Canada
19 p2643 N88-25683
International and domestic regulator issues facing the Canadian MSAT system 19 p2644 N88-25692
An evaluation of the applicability of SPOT stereoscopic imagery to the Canada Land Use Monitoring Program (CLUMP) 22 p3099 N88-28403
Prolonged periods of above-normal temperatures in Canada, 1986/87 22 p3120 N88-28538

CANADIAN SPACE PROGRAM
The Canadian SPOT program
03 p0340 N88-12147
Canadian activities and goals in remote sensing of ocean colour and fluorescence from space
08 p1043 N88-16300
Multi-axis control of telemanipulators
12 p1593 N88-19539
System and concept design of the SSRMS latching end effector --- Space Station 14 p1875 N88-21204

CANADIAN SPACECRAFT
NT ALOUETTE SATELLITES

CANARD CONFIGURATIONS
Examples of static aeroelastic effects on present combat aircraft projects 05 p0550 N88-13349
An investigation into the effect of canard location on the aerodynamics of the close-coupled canard configuration
[BU-361] 14 p1866 N88-21149
Preliminary aerodynamic design considerations for advanced laminar flow aircraft configurations
17 p2297 N88-23746
Flow around a delta wing with or without a canard control surface (phi BA = 60 deg). Part 1: Hydrodynamic visualization in permanent regime
[ONERA-RT-10/2891-AN-101-A-PT-1]
21 p2892 N88-27170
In-flight load measurements of the Robot-X canards
[AD-A193428] 21 p2895 N88-27187

CANBERRA BOMBER
U B-57 AIRCRAFT

CANCELLATION
A Gram-Schmidt space-time adaptive canceller using adaptive lattice filters
[AD-A189684] 14 p1959 N88-21684

CANCER
DNA damage and repair in human skin in situ
[DE87-014288] 03 p0356 N88-12241
Analysis of annular microstrip antennas for hyperthermic applicators
[PB88-181508] 19 p2643 N88-25679

CANISTERS
U CANS

CANNONS
U GUNS (ORDNANCE)

CANONICAL FORMS
Canonical transformations and exact invariants for dissipative systems
[DE87-703663] 04 p0485 N88-12985
Asymptotically stable all-pass transfer functions: Canonical form, parametrization and realization
[PB87-123972] 06 p0763 N88-14684
Canonical coordinates for partial differential equations
[NASA-CR-182486] 11 p1535 N88-19170
Introduction to classical mechanics of systems with constraints, part 1
[DE88-701055] 13 p1832 N88-20957
Introduction to classical mechanics of systems with constraints, part 3
[DE88-701057] 13 p1850 N88-21073
Bogolyubov transformation in relativistic theory of gravitation
[DE88-701592] 16 p2232 N88-23329
Perturbation theory for dual semigroups. Part 4: The intertwining formula and the canonical pairing
[CWI-AM-R8802-PT-4] 18 p2569 N88-25258
Canonical construction of differential operators intertwining representations of real semisimple Lie groups
[DE88-701852] 20 p2845 N88-26882
Canonical forms in the control of DPS
[AD-A194671] 23 p3270 N88-29461
Canonical variables and canonical integrals for motion in near-circular orbits 24 p3446 N88-30512

CANOPIES
Resistance of canopy materials against chemicals
[PML-1985-22] 05 p0569 N88-13466
Determination of canopy loads for a light aircraft by wind tunnel testing and computer modelling
[BU-353] 14 p1869 N88-21167
Measurements of aerodynamic forces on unsteadily moving bluff parachute canopies
16 p2202 N88-23137
Vision through aircraft transparencies
23 p3242 N88-29294

CANOPIES (VEGETATION)
Moisture determinations in and under vegetation canopies. Part 2: Results after parameterization of the CLOUD model
[FEL-1986-63] 01 p0064 N88-10410
Estimating scattered and absorbed radiation in plant canopies by remote sensing
[NASA-CR-181390] 02 p0193 N88-11205
Proceedings of the Third Airborne Imaging Spectrometer Data Analysis Workshop
[NASA-CR-181552] 05 p0611 N88-13755
The use of airborne imaging spectrometer data to determine experimentally induced variation in coniferous canopy chemistry 05 p0612 N88-13761
Toward detecting California shrubland canopy chemistry with AIS data 05 p0613 N88-13764
Analysis of airborne imaging spectrometer data for the Ruby Mountains, Montana, by use of absorption-band-depth images 05 p0614 N88-13771
Application of remote sensing to agricultural field trials
[ISBN-90-6754-089-7] 06 p0729 N88-14483
Monte Carlo method calculation of spectral brightness coefficient of vegetation cover as function of illumination conditions 08 p1008 N88-16113
Detection of soil erosion with Thematic Mapper (TM) satellite data within Pinyon-Juniper woodlands
[NASA-CR-182476] 09 p1185 N88-17103
Improved canopy reflectance modeling and scene inference through improved understanding of scene pattern
[NASA-CR-182488] 10 p1347 N88-18049
The angular reflectance signature of the canopy hot spot in the optical regime
[DE88-005385] 11 p1505 N88-18991
Proceedings of the Forest-Atmosphere Interaction Workshop
[CONF-8510250] 12 p1641 N88-19824
Remote sensing of earth terrain
[NASA-CR-182677] 13 p1790 N88-20711
Modeling surface exchanges: The soil-vegetation-atmosphere continuum
14 p1937 N88-21553
Report of Atmospheric-Canopy Exchange Panel
[DE88-004478] 14 p1944 N88-21597
Surface CO results from the ABLE-2B expedition to Amazonia
[INPE-4501-PRE/1258] 15 p2093 N88-22469
Use of energy emission for detecting the necessity of irrigation in wheat in field conditions
[INPE-4461-TDL/318] 16 p2229 N88-23315
Radar penetration in the Amazonian rain forest
17 p2352 N88-24015
Radar penetration in the Amazonian rain forest
17 p2358 N88-24044
Structure and dynamics of vegetation in the middle semi-arid tropics. Quixaba's Caatinga (PE): Terrain analysis of MSS/LANDSAT data 17 p2358 N88-24049
History of wildland fires on Vandenberg Air Force Base, California
[NASA-TM-100983] 18 p2549 N88-25134
The use of satellite imagery for municipal conditions in rural recording in Pereira Barreto (SP)
19 p2682 N88-25944
Study of evolution of vegetal cover and slide scars in the Cubatao municipality-Sao Paulo
19 p2683 N88-25947
Remote sensing technique applied to vegetation as an aid to municipal planning 19 p2683 N88-25951
Canopy reflectance modeling in a tropical wooded grassland
[NASA-CR-182981] 19 p2685 N88-25961
Hydrologic models for land-atmosphere retrospective studies of the use of LANDSAT and AVHRR data
[NASA-CR-182862] 20 p2818 N88-26716
Foliar nitrate reductase: A marker for assimilation of atmospheric nitrogen oxides
[DE88-010453] 21 p2971 N88-27648

CANS
Modal analyses of the Kernville diagnostic canister
[DE88-003268] 07 p0870 N88-15277
CRRES chemical release mechanisms
14 p1874 N88-21192
Optimization of mechanical/corrosion properties of TI-CODE 12 plate and sheet. Part 2: Thermomechanical processing effects
[DE88-007493] 19 p2616 N88-25517

CANT
U SLOPES

CANTILEVER BEAMS
The matrix exponential in transient structural analysis
05 p0593 N88-13619
Bending of a bonded beam as a test method for adhesive properties
[AD-A184813] 05 p0609 N88-13736
Beam and column buckling under directed loading
[PB87-124004] 06 p0722 N88-14436
Active control of flexural vibrations in beams
06 p0794 N88-14866
A fiber-resin micromechanics analysis of the delamination front in a DCB specimen
[NASA-TM-100540] 10 p1294 N88-17737
Research and development of surface skimming bulk wave devices for sensor applications
[AD-A187504] 11 p1470 N88-18766
Active vibration control of a cantilevered beam with three elastic coordinates
[AD-A188824] 12 p1636 N88-19797

CANTILEVER MEMBERS
NT CANTILEVER BEAMS
Buckling of braced monosymmetric cantilevers: Timoshenko energy approach
[PB87-133849] 06 p0723 N88-14445
A parametric study of embedded cantilever retaining walls: The results of a finite element study
[RR-CE83] 24 p3383 N88-30152

CANTILEVER WINGS
U WINGS

CAPACITANCE
Development of a repetitive 1-MV, 22-kJ Marx generator
[DE87-011286] 01 p0038 N88-10242
Improper ferroelectricity: A theoretical and experimental study
[AD-A184614] 03 p0381 N88-12397
Polymer materials for pressure sensors
06 p0676 N88-14141
Extraction of MOS VLSI (Very-Large-Scale-Integrated) circuit models including critical interconnect parasitics
[AD-A185847] 08 p0979 N88-15914
Minimum necessary intensity of source of preionization for stabilization of a self-sustaining laser discharge with mean power raised by electron beam or X-rays
[PB87-178158] 09 p1171 N88-17024
Design of a charge sensitive preamplifier on high resistivity silicon
[DE88-003491] 10 p1323 N88-17907
Capacitive charge division in centroid finding cathode readouts in MWPCs
[DE88-003545] 10 p1333 N88-17969
Electrosorptive detection based on double-layer capacitance for selective anion monitoring in ion chromatography. Part 1: Mercury electrodes
[AD-A188780] 12 p1606 N88-19603
Recent advances in capacitance type of blade tip clearance measurements
[NASA-TM-101291] 19 p2603 N88-25460
Noise in piezoresistive and capacitive sensors
19 p2670 N88-25874
Air loading effects on a capacitively sensed membrane supported silicon accelerometer
19 p2672 N88-25886
Defects in high-mobility semiconductor systems
[AD-A192298] 20 p2879 N88-27090
Ice detector
[NASA-CASE-LAR-13776-1] 23 p3217 N88-29149

CAPACITANCE-VOLTAGE CHARACTERISTICS
Calculating depletion region carrier concentrations with capacitance-voltage measurements and etching
[AD-A189630] 15 p2141 N88-22777

CAPACITORS
Investigations into the design of multi-terawatt magnetic switches
[DE87-012014] 01 p0040 N88-10254
The role of hydrogen in radiation-induced defect formation in polysilicon gate MOS devices
[DE87-012374] 06 p0785 N88-14814

Radiation hardness evaluation of thin film ferroelectric capacitors
[DE88-001357] 07 p0848 N88-15147
A numerical thermal model of the rapid solidification parameters in the capacitor discharge welding process
[DE88-002206] 07 p0864 N88-15244
Capacitor analysis for RF antennas
[DE88-004178] 10 p1318 N88-17883
Pulsed current transformer for low inductive loads
[AD-A187224] 10 p1324 N88-17913
The soft/hard wet anodization of aluminum oxide and its use in a thin film multilayered capacitor
[AD-A187575] 10 p1325 N88-17919
Radiation response of thin oxides grown by rapid thermal oxidation and rapid thermal annealing techniques
[DE88-003632] 11 p1561 N88-19347
Advanced capacitor development
[AD-A189965] 15 p2059 N88-22276
The application of high temperature superconductors to space electrical power distribution components
[NASA-TM-100901] 16 p2171 N88-22939
Joint angle sensors for closed-loop control
19 p2673 N88-25891
High power pulse energy system concept
[AD-A192440] 21 p2935 N88-27429
Development of inductive storage pulsed power generators
[AD-A193878] 22 p3117 N88-28521
Stress corrosion of ceramic materials
[AD-A191979] 23 p3195 N88-29016
In-house capacitor technology program
[AD-A194804] 24 p3367 N88-30049

CAPE HATTERAS (NC)
Research on the physical oceanography of the Gulf Stream
[AD-A188512] 12 p1649 N88-19877

CAPE KENNEDY LAUNCH COMPLEX
Short-term forecasting of lightning based on the surface wind field at Kennedy Space Center
02 p0208 N88-11306
Short range forecasting of sea breeze generated thunderstorms at the Kennedy Space Center: A real-time experiment using a primitive equation mesoscale numerical model 02 p0211 N88-11324

CAPES (LANDFORMS)
NT CAPE HATTERAS (NC)

CAPILLARIES (ANATOMY)
Models of cerebral-body perfusion and cerebral chemical transport
[AD-A194945] 24 p3407 N88-30283

CAPILLARY CIRCULATION
U CAPILLARY FLOW

CAPILLARY FLOW
Experimental study of thermocapillary flows in a thin liquid layer with heat fluxes imposed on the free surface
[NASA-TM-100252] 04 p0445 N88-12763
Computation of free boundaries
[PB87-226023] 06 p0763 N88-14680
Study of helium transfer technology for STICCR: Fluid management
[NASA-CR-177463] 10 p1291 N88-17720
Continual capillary viscosimetry using extrusiograph techniques
[PB88-166293] 15 p2046 N88-22195
Instrumental aspects of capillary supercritical fluid chromatography
[ETN-88-92242] 16 p2174 N88-22960
Some numerical methods for the computation of capillary free boundaries governed by the Navier-Stokes equations
[REPT-87-69] 16 p2206 N88-23167
Liquid motions in partially filled containers: Preliminary results of the D-1 mission --- Spacelab
[NLR-MP-86042-U] 20 p2802 N88-26629
Polymeric heat pipe wick
[NASA-CASE-GSC-13019-1] 23 p3214 N88-29133

CAPILLARY TUBES
Boundary integral analysis of flow and deformation of long bubbles in capillaries
[DE88-002110] 10 p1326 N88-17927

CAPILLARY WAVES
NT BAROCLINIC WAVES
NT GRAVITY WAVES
NT RIPPLES
Dispersion equation for plane capillary-gravity wave on free surface of viscous incompressible fluid
04 p0459 N88-12842
Influence of surfactants on damping of gravity-capillary waves. 1: Frequency dependence
04 p0459 N88-12843

CAPTIVE TESTS
NT STATIC FIRING
NT STATIC TESTS

CAPTURE CROSS SECTIONS
U ABSORPTION CROSS SECTIONS

CAPTURE EFFECT
On symmetric TVD schemes
19 p2639 N88-25659

CARBAMATES (TRADENAME)
NT URETHANES
Carbamates, atropine, and diazepam: Effects on performance in the running rat
[AD-A188009] 11 p1517 N88-19062

CARBAZOLES
Research on stable processible conducting polymers for electronic applications
[AD-A190246] 15 p2044 N88-22180

CARBIDES
NT ALUMINUM CARBIDES
NT BORON CARBIDES
NT CHROMIUM CARBIDES
NT NIOBIUM CARBIDES
NT SILICON CARBIDES
NT TITANIUM CARBIDES
NT TUNGSTEN CARBIDES
Surface chemistry of transition metal carbides: A theoretical analysis
[AD-A184237] 03 p0291 N88-11829
JPRS report: Science and technology. Japan
[JPRS-JST-87-028] 06 p0675 N88-14130
Effects of ion implantation on cavitation erosion of a cobalt based metal/carbide alloy
[AD-A187239] 10 p1303 N88-17793
A comparison of uranium nitride and mixed carbide fuels swelling 17 p2435 N88-24485
Development of fine-grained carbide-particle hardened Hadfield manganese steels
[DE88-008919] 19 p2617 N88-25523

CARBOHYDRATE METABOLISM
NT HYPOGLYCEMIA
Significance of nutrition to change in human carbohydrate and lipid metabolism under emotional stress 19 p2703 N88-26073
Physiology of prolonged bed rest
[NASA-TM-101010] 22 p3130 N88-28607

CARBOHYDRATES
NT CELLULOSE
NT GLUCOSE
NT GLYCOGENS
NT NUCLEOSIDES
NT STARCHES
Manipulation of muscle glycogen concentrations using high and low carbohydrate diets and exercise
[AD-A187732] 11 p1519 N88-19069
Workshop on Atmospheric OH
[BPT-7/87] 18 p2538 N88-25063
Effect of carbohydrate oxidation on the tropospheric HOx-system 18 p2539 N88-25067

CARBON
NT CARBON 12
NT CARBON 13
Theory of the carbon phase diagram at high pressures and temperatures
[DE87-012245] 01 p0028 N88-10180
Materials preparation and longevity in hyperthermal atomic oxygen 03 p0297 N88-11862
Carbon abundances and C12/C13 ratios in M giants
04 p0515 N88-13167
The initiation and growth of fatigue cracks in carburised 9Cr1Mo steel 05 p0603 N88-13696
Studies of metal/carbon surface chemistry
[DE87-009545] 07 p0829 N88-15029
Non-steady group combustion of a cloud of char particles
[DE87-010773] 08 p0966 N88-15849
The influence of yellow substances on remote sensing of sea-water constituents from space
08 p1044 N88-16308
Total and partial cross sections for electron capture for C(q+) (q=6-2) and O(q+) (q=8-2) ions in collisions with H, H2 and He atoms
[IPPJ-AM-56] 09 p1252 N88-17501
Clusters: Link between molecules and solids
[AD-A188170] 11 p1543 N88-19224
Spectroscopic studies of a laser-produced carbon plasma in the near and extreme ultraviolet
11 p1553 N88-19292
Carbon residue studies of polyphenyl ethers and ester-based lubricants using a microcarbon residue tester
[AD-A188585] 12 p1611 N88-19632
Tungsten-carbon multilayer system studied with X-ray scattering
[DE88-005749] 13 p1735 N88-20373
An interpretation of the ethylenic, carbidic, and graphite auger lineshapes of chemisorbed carbon species
[AD-A189092] 13 p1736 N88-20379
Improved methods for high resolution electron microscopy
[DE88-005731] 13 p1774 N88-20809
Microprobe examination of composite materials produced by burning of Ti, Cr, C powders with powder of any one Fe-group metal 14 p1886 N88-21269
An investigation of the infrared emission spectra of carbon condensates 14 p1886 N88-21272
Laboratory amorphous carbon: A possible analog of cometary dust 14 p2009 N88-21981
Hermetic coating of optical fibers
[AD-A189886] 15 p2044 N88-22177
Characterization of precipitates in a niobium-zirconium-carbon alloy
[NASA-TM-100848] 16 p2178 N88-22981
Fracture morphologies of carbon-black-loaded SBR (Styrene-Butadiene Rubber) subjected to low-cycle, high-stress fatigue
[DE88-006808] 16 p2181 N88-23002
High temperature solid lubrication by catalytically generated carbon
[AD-A190804] 16 p2182 N88-23004
Interface characterization of Cu-Cu and Cu-Ag-Cu low temperature solid state bonds
[AD-A191015] 16 p2283 N88-23667
Krypton based adsorption type cryogenic refrigerator
[NASA-CASE-NPO-17334-1-CU]
17 p2331 N88-23917
Cryogenic regenerator including saran-carbon heat conduction matrix
[NASA-CASE-NPO-17291-1-CU]
17 p2337 N88-23946
Liquid carbon
[AD-A191707] 18 p2491 N88-24776
Electrical conduction in thin film carbons
[AD-A191726] 18 p2491 N88-24780
Electron-Rayleigh wave interaction in thin film carbons
[AD-A191727] 18 p2492 N88-24781
Anomalous temperature-dependent negative magnetoresistance in pregraphitic carbons
[AD-A191725] 19 p2619 N88-25535
Zero-dimensional calculation for ZT-H
[DE88-009175] 19 p2731 N88-26217
Carbon analysis in natural olivine crystals of deep origin
[NASA-TT-20311] 19 p2734 N88-26239
Reduced-activation austenitic stainless steels: The Fe-Cr-C system
[DE88-008091] 20 p2773 N88-26442
Carbon deposition model for oxygen-hydrocarbon combustion, volume 1
[NASA-CR-179375] 21 p2908 N88-27254
Carbon deposition model for oxygen-hydrocarbon combustion, volume 2
[NASA-CR-179376] 21 p2908 N88-27255
Refractory films from spin-cast carbon
[DE88-011251] 21 p2919 N88-27327
Erosion/redeposition modeling and calculations for carbon
[DE88-010382] 22 p3057 N88-28139
A study of the interaction of NO2 with carbon particles
[DE88-010778] 22 p3118 N88-28524
High spatial resolution observations of neutral atomic carbon in the molecular clouds M17 and W51
[MPE-PREPRINT-109] 22 p3164 N88-28846
Real-time measurements of the size fractionation of ambient black carbon aerosols at elevated humidities
[DE88-010870] 23 p3215 N88-29138

CARBON COMPOUNDS
NT ALUMINUM CARBIDES
NT BORON CARBIDES
NT CALCITE
NT CALCIUM CARBONATES
NT CARBIDES
NT CARBON DIOXIDE
NT CARBON MONOXIDE
NT CARBONATES
NT CHLOROCARBONS
NT CHROMIUM CARBIDES
NT FLUOROCARBONS
NT NIOBIUM CARBIDES
NT POLYCARBONATES
NT SILICON CARBIDES
NT TITANIUM CARBIDES
NT TUNGSTEN CARBIDES

CARBON CYCLE
Carbon dioxide and climate: Summaries of research in FY 1987
[DE88-000916] 06 p0744 N88-14574
Atmospheric carbon dioxide and the global carbon cycle: The key uncertainties
[DE88-005059] 15 p2092 N88-22465
Simulation analysis of moored fluorometer time series from the Mid-Atlantic Bight
[DE88-006066] 15 p2099 N88-22505
Bibliography on tropical rain forests and the global carbon cycle. Volume 1: An introduction to the literature
[DE88-010761] 22 p3118 N88-28523

CARBON DIOXIDE

Detection of CO2-induced climate change
[DE87-013127] 01 p0071 N88-10457

Testimony to the US Senate on the greenhouse effect
[DE87-013995] 01 p0071 N88-10458

Master index for the carbon dioxide research state-of-the-art report series
[DE87-012757] 01 p0072 N88-10459

Contribution of bubbles and waves to air-sea CO2 flux, with implications for remote sensing
[PB87-203980] 01 p0073 N88-10467

Reduction of CO2 to methanol and methane by photo and dark reactions on semiconductor and metal electrodes
[PB87-226825] 02 p0156 N88-10975

High temperature CO2 study: Anti-Stokes coherent Raman diffusion and infrared spectroscopy
[ESA-TT-1048] 03 p0282 N88-11777

Kinetics of CO adsorption on nickel using time resolved vibration spectroscopy
[ETN-87-90615] 03 p0289 N88-11814

Carbon dioxide treatment for scale removal and control in potable water systems
[AD-A184346] 04 p0412 N88-12556

Organic molecules on meteoritic solid substrates
[NASA-CR-181570] 05 p0560 N88-13411

Controlled ecological life support systems: Development of a plant growth module 05 p0630 N88-13854

Interpretation of our present terrestrial climatic record
[DE88-000223] 06 p0744 N88-14573

The carbon dioxide chaperon efficiency for the reaction H + O2 + M yields HO2 + M from ignition delay times behind reflected shock waves
[NASA-TM-100125] 07 p0830 N88-15036

Welding in high pressure CO2 atmosphere --- underwater welding
[PB87-144044] 07 p0862 N88-15232

Concept, construction, and experimental testing of a polychromator for a Raman lidar for the simultaneous telemetering of carbon dioxide and water vapor, relative to oxygen
[GKSS-87/E/20] 09 p1191 N88-17134

Mesospheric dynamics and chemistry from SME data
[NASA-CR-182465] 09 p1191 N88-17139

Energy transfer studies with lasers
[DE88-004864] 10 p1337 N88-17991

Role of carbon dioxide in correction of coagulation hemostasis under hypoxic conditions
10 p1365 N88-18160

Effects of breathing air containing contaminants such as CO2, CO and hydrocarbons at 1 and 5 atmospheres
[PB88-132915] 11 p1521 N88-19084

Solar-assisted hydrogen generation by photoelectrocatalysis
[PB88-160932] 12 p1605 N88-19597

Carbon dioxide and climate 14 p1936 N88-21545

Observational and theoretical studies of greenhouse climate effects
[DE88-006237] 14 p1948 N88-21621

Sublimation characteristics of H2O comet nucleus with CO2 impurities 14 p2010 N88-21988

Atmospheric carbon dioxide and the global carbon cycle: The key uncertainties
[DE88-005059] 15 p2092 N88-22465

A laser-based photoacoustic spectrometer for direct breath C-13O2/C-12O2 measurement
[DE88-004915] 15 p2101 N88-22516

A glossary for carbon dioxide and climate
[DE88-007885] 19 p2689 N88-25982

A shock-tube experiment on gases mixing processes associated with CO2/N2 mixing gasdynamic laser
[ISAS-RN-350] 20 p2797 N88-26598

The seasonal exchange of carbon dioxide between the atmosphere and the terrestrial biosphere: Extrapolation from site-specific models to regional models
[DE88-007870] 20 p2822 N88-26740

Catalytic activation of carbon dioxide by metal complexes
[AD-A192310] 21 p2909 N88-27262

Surface energy balance of three general circulation models: Current climate and response to increasing atmospheric CO2
[DE88-010967] 21 p2975 N88-27673

Validation of a modified one-step rebreathing technique for non-invasive measurement of submaximal cardiac output
[AD-A192852] 21 p2987 N88-27735

Regional intercomparisons of General Circulation Model predictions and historical climate data: CO2
[DE88-010416] 23 p3235 N88-29248

Miniature respiratory sensor
[AD-A193430] 23 p3243 N88-29300

Coadsorption of H2O and CO2 on the Martian surface
23 p3307 N88-29702

CARBON DIOXIDE CONCENTRATION

Master index for the carbon dioxide research state-of-the-art report series
[DE87-012757] 01 p0072 N88-10459

Carbon Dioxide observational platform system (CO-OPS) Feasibility Study
[NASA-CR-179225] 06 p0671 N88-14113

Carbon dioxide and climate: Summaries of research in FY 1987
[DE88-000916] 06 p0744 N88-14574

Model validation research: Comparison of simulated and observed climate patterns for the past 18,000 years
[DE88-004945] 13 p1800 N88-20759

Atmospheric carbon dioxide and the global carbon cycle: The key uncertainties
[DE88-005059] 15 p2092 N88-22465

Surface CO results from the ABLE-2B expedition to Amazonia
[INPE-4501-PRE/1258] 15 p2093 N88-22469

Understanding CO2 and climate
[PB88-167655] 16 p2231 N88-23341

Physiological effects on man of long duration confinement in a carbon dioxide enriched environment
19 p2695 N88-26017

Visual sensitivities under reduced oxygen
[AD-A195628] 24 p3406 N88-30279

CARBON DIOXIDE LASERS

Picosecond CO2 laser interactions with polyatomic molecules
[DE87-012072] 01 p0051 N88-10327

Feasibility of alpha particle measurement in a magnetically confined plasma by CO2 laser Thomson scattering
[DE88-000039] 02 p0241 N88-11522

Investigation of BN CO2 wave guide laser
03 p0302 N88-11905

Gas dynamic characteristics in past axial flow CO2 laser 03 p0327 N88-12067

Methods for a coherent CO2 laser heterodyne radar system
[ESA-TT-1035] 03 p0328 N88-12076

USSR report: Physics and mathematics
[JPRS-UPM-87-006] 06 p0708 N88-14344

Compensation of small-scale phase distortions by means of a Fourier phase corrector
06 p0708 N88-14345

Repetitively pulsed and continuous wave CO2 lasers pumped by a pulsed self-sustained discharge for thermal processing 06 p0709 N88-14346

Effect of clarifying the atmosphere in relation to quasi-monochromatic CO2 laser radiation
06 p0709 N88-14348

NO2 heterodyne frequency measurements with a tunable diode laser, a CO laser transfer oscillator and CO2 laser standards
[NASA-CR-182393] 06 p0710 N88-14353

Strategic Defense Initiative Organization/DARPA (Defense Advanced Research Projects Agency) workshop on laser propulsion. Volume 1: Executive summary
[DE87-003254] 06 p0768 N88-14722

Production-process CO2 laser with amplified pulse-repetition operation 06 p0771 N88-14739

Nonuniformity of electromagnetic field at Lambda = 10.6 micron wavelength inside atmospheric aerosol particles
06 p0772 N88-14743

Dynamic restructuring of pulsed CO2 laser frequency and multiple-peak generation in a cell with IR-absorbing gas in the resonator 07 p0919 N88-15580

Study of vibration relaxation in active medium of CO2-laser using phase-absorption method
07 p0919 N88-15582

Laser thermal propulsion
[AD-A186407] 07 p0933 N88-15666

Study of combination type CO2 laser welding system
[PB87-143764] 08 p0992 N88-16002

Remote measurement of aerosol stream velocity with continuous-wave CO2-laser 08 p1079 N88-16506

Continuously frequency-tunable high-pressure CO2-laser with plasmatic cathode
09 p1238 N88-17418

Airborne Doppler lidar detection of wind shear. Results of performance analysis 10 p1275 N88-17627

Experiments for the high resolution detection of moving targets using a CO2 laser radar
[MBB-UA-1044/87] 10 p1316 N88-17864

Operation of electron-beam controlled CO2 laser at 6 atmospheres 11 p1468 N88-18758

Nonlinear absorption of CO2 laser radiation in p-type InSb
[DE88-004055] 11 p1492 N88-18906

Coherent laser radar system theory
[AD-A188759] 13 p1774 N88-20612

Influence of nonlinear spectroscopic effects on atmospheric propagation of intense laser radiation at 10.6 microns wavelength 13 p1789 N88-20705

Characteristics of welds joining parts of high-strength pipe steels and produced by beam of continuous-wave CO2-laser 14 p1897 N88-21325

Laser technology: CO2 lasers and laser optics
[ETN-88-91469] 14 p1915 N88-21441

Comprehensive model for laser instability in a CO2 laser with gaseous saturable absorber
14 p1979 N88-21808

Laser processing-status, perspectives
15 p2050 N88-22211

Compound ceramic processing
15 p2050 N88-22212

Single crystal growth by laser CVD
15 p2050 N88-22213

Hard ceramic film by laser PVD
15 p2051 N88-22216

Coupled high power waveguide laser research
[AD-A189800] 15 p2071 N88-22345

Laser evaporation studies
[AD-A189815] 15 p2071 N88-22346

Engineering planetary lasers for interstellar communication
[NASA-CR-180780] 17 p2311 N88-23825

An optical preamplifier for detection of CO2 laser radiation
[AD-A190790] 18 p2520 N88-24949

High power axial flow CO2 laser
[ETN-88-91951] 18 p2521 N88-24959

Design of catalytic monoliths for closed-cycle carbon dioxide lasers
[NASA-CR-182983] 18 p2558 N88-25185

A two-wavelength infrared interferometer/polarimeter system for CIT (Compact Ignition Tokamak)
[DE88-007681] 18 p2579 N88-25321

Design and calibration of a two-channel low-noise heterodyne receiver for use in a CO2 laser Thomson scattering alpha particle diagnostic
[DE88-007866] 19 p2728 N88-26201

Alternative analysis of CO2-laser-produced plasma waves
[DE88-008434] 19 p2730 N88-26215

A CO2 laser Thomson scattering diagnostic for fusion product alpha particle measurement
[DE88-007683] 20 p2857 N88-26965

Investigations on beam quality of high frequency excited CO2 high performance lasers
[ETN-88-92363] 21 p2954 N88-27550

Transverse CO2 laser two-dimensional gain distributions
[AD-A196240] 24 p3378 N88-30119

CARBON DIOXIDE REMOVAL

Electrochemical carbon dioxide concentrator subsystem development
[NASA-CR-177411] 08 p1053 N88-16353

Advanced EMU electrochemically regenerable CO2 and moisture absorber module breadboard
[NASA-CR-172054] 21 p2993 N88-27754

CARBON DIOXIDE TENSION

NT HYPERCAPNIA
NT HYPOCAPNIA

Human adaptation to various hypercapnic conditions in relation to salivary electrolyte dynamics and renal function 12 p1664 N88-19977

CARBON FIBER REINFORCED PLASTICS

Joints in carbon fibre reinforced composites
[BR99969] 01 p0019 N88-10114

Theoretical investigation of stress concentrations in damaged carbon fibre reinforced plastic plate structures. Volume 1: Main text
[BR99872-VOL-1] 03 p0280 N88-11761

Theoretical investigation of stress concentrations in damaged carbon fibre reinforced plastic plate structures. Volume 2: Tables, figures and plates
[BR99873-VOL-2] 03 p0280 N88-11762

Investigation of reliability of strength values measured on CFRP test bars by statistical methods. Part 1: Probability distributions for strength analysis
[ESA-TT-1036] 03 p0336 N88-12115

Solar converging method 04 p0403 N88-12504

Carbon-fiber reinforced plastics
04 p0403 N88-12506

Design and control of repairs of carbon fiber lift augmentation flaps in the ATR42 aircraft
[SNIAS-872-111-112] 05 p0529 N88-13217

A hybrid fibreglass-CFRP cloth for new furnishings --- aircraft cabins
[SNIAS-872-111-109] 05 p0558 N88-13396

Determination of the fiber ratio in carbon fiber/resin composites by means of image analysis
[SNIAS-872-422-101] 05 p0558 N88-13398

Measurement and control of damage in composite materials: Nondestructive controls by thermography, holography, and radiography
[SNIAS-872-430-110] 05 p0559 N88-13403

Comparison of fire resistance of metallic and nonmetallic structures
[SNIAS-872-551-101] 05 p0572 N88-13489
Study of damage in carbon fiber-epoxy composite materials. Utilization to assess broken specimens
[DCQ/L-45-650/F] 06 p0678 N88-14152
Flaw effects: Behavior in operation of delamination in a crossed multilayer composite specimen
[DCQ/L-47-363/F] 06 p0678 N88-14153
Measurement of mechanical parameters to define damage criteria in delamination of crossed stratified layers
[DCQ/L-47-361/F] 06 p0678 N88-14154
Comparison of the strength of single and multiple bolted joints in CFRP
[PB87-123766] 06 p0722 N88-14438
Hybrid FEM (Finite Element Method) approach to stress distribution in the vicinity of a notch in non-homogeneous materials
[PB87-143392] 07 p0868 N88-15268
Effects of aviation fluids on fiber composite material
[FOA-C-20674-2.6] 08 p0965 N88-15840
The effect of thermal shock on carbon fiber epoxy composites
[FOA-C-20675-2.6] 08 p0965 N88-15841
Fatigue and damage tolerance design data for carbon fibre composites
[BAE-MSM-R-GEN-0454] 09 p1138 N88-16818
Moisture plotting of carbon fiber composite in flight operations
[MBB-UT-119/87] 09 p1138 N88-16823
Integrity control of carbon fiber reinforced plastics (CFRP) structural elements. Conclusion with respect to the control methodology of CFRP primary structures in manned space flight and the implications to the design, analysis and testing of CFRP structural elements, executive summary
[MBB-TR-RB517-014/85] 09 p1139 N88-16824
Mechanical properties of carbon fiber reinforced thermoplastic matrix composites
[NAL-TR-934] 09 p1139 N88-16827
Ultrasonic inspection of advanced CFRP structures by computer-controlled, pulse-echo technique
[ETN-88-91665] 09 p1177 N88-17051
To determine the stress distribution in the vicinity of GRP end pads where the specimen is held and loaded (CFC coupon specimens) --- glass reinforced plastic (GRP) carbon fiber composite (CFC)
[BAE-WST-R-RES-CFC-12023]
09 p1182 N88-17080
Further tests to determine the stress distribution in the vicinity of GRP end pads where the specimen is held and loaded (CFC coupon specimens) --- glass reinforced plastic (GRP) carbon fiber composite (CFC)
[BAE-WST-R-RES-CFC-12023-ADD-1]
09 p1182 N88-17081
Colloquium on damage mechanics of graphite/expoxy laminates during fatigue
[DFVLR-MITT-87-08] 11 p1448 N88-18630
Influence of different parameters on damage development --- carbon fiber reinforced plastics
11 p1448 N88-18632
Initiation and propagation of damage in notched unidirectional and multidirectional CFRE resin laminates
11 p1449 N88-18633
Statistical evaluation of experimental results from fatigue strength tests on CFRP composite materials
11 p1449 N88-18635
Damage mechanisms of CFRP riveted joints
11 p1449 N88-18636
Damage mechanisms and fatigue life prediction of graphite/epoxy laminates 11 p1449 N88-18637
Reinforcing of thermoplastic polycarbonate and polysulfone with carbon fibers: Production and characteristics of UD-compound objects
[NASA-TT-20158] 13 p1735 N88-20374
Studies of traverse impact damage in composite materials using a Hopkinson pressure-bar technique
[OUEL-1706/87] 14 p1883 N88-21255
An investigation of the mechanical properties of improved carbon fibre composite materials
[RAE-TR-86021] 14 p1884 N88-21259
Stress-strain behaviour of a bolt hole in carbon fibre composite plates
[BU-354] 14 p1923 N88-21460
Fractography of composite delamination
[NASA-CR-182757] 15 p2030 N88-22096
Elementary characterization of Fibredux 913 CTS 5 34 percent preimpregnated carbon-epoxy from Ciba Geigy
[M-484300] 16 p2171 N88-22941
Delamination analysis in crossed layer composites
[REPT-48-447/F] 16 p2171 N88-22942
Fatigue damage development of various CFRP-laminates
[NASA-TT-20247] 16 p2172 N88-22945
Investigation of the long term effects of aging on carbon epoxy composites exposed naturally to the weather under cyclic loads. (Results of sampling after 2.5 years). Test report M1-641300
[CEAT-39/M/79-C-M1-641300]
17 p2316 N88-23834
GARTEUR TP-037: Impact damage tolerance of carbon fiber and hybrid laminates
[RAE-TR-87057] 17 p2316 N88-23837
Elementary characterization of preimpregnated carbon epoxy T400H/DA0506 from STRUCTIL. Test report M6-577100
[CEAT-047426] 18 p2478 N88-24703
Detecting delaminations in CFRP specimens using X-ray techniques
[FFA-TN-1988-04] 18 p2479 N88-24704
High temperature resins for injection. High temperature pre-impregnated
[RC-648676] 20 p2780 N88-26486
Rocket motor case materials. An evaluation of new fibers for composites
[FOA-C-20696-2.1] 21 p2906 N88-27245
Determination of the glass transition temperature of cured composite materials
[DT-87/62-R] 21 p2906 N88-27246
Design and implementation of contact ultrasonic sensors to assess internal damage
[I-177/87] 21 p2906 N88-27247
Relation between the mechanical characteristics of carbon-resin composites and their impact strength
[REPT-48-284/F] 21 p2907 N88-27249
Aging of CFRP due to longterm storage in heated air
[DFVLR-FB-88-05] 21 p2922 N88-27345
Use of microwave measuring systems for the nondestructive control of resins and composites
[REPT-881-430-123] 21 p2959 N88-27576
Nondestructive tests and high performance composite structures
[SNIAS-881-430-119] 23 p3188 N88-28969
Investigations on the modification of structural reliability by substitution of aluminum by carbon fiber reinforced plastics in aircraft construction
[ILR-MITT-195] 24 p3339 N88-29877
Thermal stress analysis in PMR-15 carbon fibre laminates
[ETN-88-93123] 24 p3341 N88-29886
Rupture of carbon fiber reinforced plastics (T300-914) composite materials. Influence of initial first ply failures on the fatigue behavior
[SNIAS-881-422-103] 24 p3342 N88-29892
Evaluation of the potential health hazards associated with the machining of carbon fiber composites
[AD-A194835] 24 p3408 N88-30286

CARBON FIBERS
Anti-abrasion protection with highly organized materials
[DE87-014238] 01 p0029 N88-10187
Electron beam irradiation effects on carbon fiber reinforced PEEK composite
[DE87-753001] 02 p0142 N88-10890
The effect of bromination of carbon fibers on the coefficient of thermal expansion of graphite fiber-epoxy composites
[NASA-TM-100236] 02 p0143 N88-10899
Composite structural materials
[NASA-CR-181416] 02 p0190 N88-11186
Carbon-fiber reinforced aluminum
04 p0403 N88-12507
Carbon fiber reinforced glass matrix composites for space based applications
[AD-A184355] 04 p0410 N88-12546
Study of zero CTE (Coefficients of Thermal Expansion) of graphite/epoxy composites
[DE87-013557] 04 p0412 N88-12554
The use of aeroelastic wind tunnel models to prove structural design 05 p0551 N88-13355
Interfacial shear strength of pitch and high strain pan fibers in an epoxy matrix
[AD-A185966] 07 p0826 N88-15011
Macroscopic distribution of fiber finish
[DCQ/L-48-283/F] 07 p0827 N88-15013
Improving the interlaminar shear strength of carbon fiber-epoxy composites through carbon fiber bromination
[NASA-TM-100248] 07 p0827 N88-15018
Effects of processing variables on the behavior of E-glass/913 and XAS carbon fibre/913 laminates subjected to hot/wet environmental conditions
[BR101940] 09 p1138 N88-16820
The strength of hybrid composites
[BR101991] 09 p1138 N88-16821
Effect of post-cure heat-treatment on static and fatigue behaviour of XAS-914C carbon fibre composite
[AD-A186943] 10 p1294 N88-17735
Structure and surface characterizations of high strength carbon fibers
[AD-A189642] 15 p2029 N88-22087
Interfacial structure-property relationships at the fiber-matrix interphase in advanced composites
[AD-A190649] 15 p2030 N88-22093
Thermal expansion behavior of randomly oriented short carbon fiber reinforced copper composites
[NASA-TT-20175] 15 p2031 N88-22099
Reciprocating sliding wear characteristics of copper-carbon fiber composites
[NASA-TT-20176] 15 p2031 N88-22100
Eddy current nondestructive inspection of graphite epoxy using ferrite cup core probes
[AD-A189823] 15 p2074 N88-22365
Thermal conductivity, electrical conductivity and specific heat of copper-carbon fiber composite
[NASA-TT-20172] 16 p2172 N88-22948
Surface and interfacial properties of carbon fibers
[NASA-CR-182890] 16 p2173 N88-22951
High-temperature thermal conductivity of a carbon-bonded carbon-fiber insulation
17 p2402 N88-24281
Aging of carbon fibers
[SNPE-NT-10/86/CRB/NP] 18 p2479 N88-24707
Size effects in the electrical resistivity of benzene-derived carbon fibers
[AD-A191708] 18 p2491 N88-24777
Photoconductivity in carbon fibers
[AD-A191728] 18 p2492 N88-24782
Effect of uniaxial stress on the Raman spectra of graphite fibers
[AD-A191730] 18 p2492 N88-24783
Influence of carbon fiber surface treatment
[ETN-88-92536] 18 p2492 N88-24787
Electronic and structural studies of carbon/carbon composites
[AD-A191729] 19 p2609 N88-25481
Observation of metallic conductivity in liquid carbon
[AD-A191723] 19 p2618 N88-25533
Microstructure of thin intercalated benezene derived graphite fibers
[AD-A191724] 19 p2618 N88-25534
Thermoplastic coating of carbon fibers
[NASA-CR-183067] 20 p2767 N88-26407
The crystallization of tough thermoplastic resins in the presence of carbon fibers
[NASA-CR-182984] 20 p2776 N88-26464
Effect of the matrix on the creep-behavior of carbon-carbon composite
[AD-A193211] 21 p2905 N88-27235
Effects of electron beam irradiation on mechanical properties at low and high temperature of fiber reinforced composites using PEEK as matrix material
[DE88-753134] 21 p2905 N88-27239
Fabrication of SiC fiber reinforced glass matrix by extrusion process and investigation of its mechanical properties
[ETN-88-92367] 21 p2906 N88-27244
Refractory fibers surface treatment
[REPT-47-803/F] 21 p2922 N88-27339
Computer modeling for surface properties of carbon fibers 21 p2928 N88-27383
Effects of applied stress and temperature on the nonlinear elastic properties of graphite fibers
[AD-A194469] 22 p3050 N88-28093
An investigation of some basic properties of hybrid composite materials
[AD-A194136] 23 p3189 N88-28975
A test for interfacial effects and stress transfer in ceramic matrix composites
[NASA-CR-182873] 24 p3340 N88-29880
Brominated graphite fibers and method of producing the same
[NASA-CASE-LEW-14698-1] 24 p3341 N88-29888
Transverse expansion of individual carbon and graphite filaments
[AD-A195073] 24 p3342 N88-29891
Evaluation of the potential health hazards associated with the machining of carbon fiber composites
[AD-A194835] 24 p3408 N88-30286

CARBON ISOTOPES
NT CARBON 12
NT CARBON 13

CARBON MONOXIDE
Carbon monoxide (CO) concentration in the air as a purity parameter
[INPE-4232-PRE/1107] 01 p0067 N88-10429
A study of carbon monoxide distribution determinations for a global transport model
[NASA-CR-181423] 01 p0067 N88-10432
The effect of additives on the reactivity of palladium surfaces for the chemisorption and hydrogenation of carbon monoxide: A surface science and catalytic study
[DE87-014685] 02 p0145 N88-10909
Surface chemistry of transition metal carbides: A theoretical analysis
[AD-A184237] 03 p0291 N88-11829

Characterization of catalysts with metal-support effects and of the species adsorbed on their surfaces
[DE87-014636] 04 p0414 N88-12564

K-CO on transition metals: A local ionic interaction
[AD-A184342] 04 p0496 N88-13056

The structure of adsorbed sulfur and carbon on molybdenum and rhenium single crystal surfaces, and their influence on carbon monoxide and hydrocarbon chemisorption
[DE88-001393] 04 p0499 N88-13073

The delta upsilon = 1 fundamental bands of carbon monoxide in late-type stars 04 p0517 N88-13177

Carbon monoxide and turbulence-chemistry interactions: Blowoff and extinction of turbulent diffusion flames
[AD-A186276] 07 p0828 N88-15025

Energy transfer studies with lasers
[DE88-004864] 10 p1337 N88-17991

Investigation of effects of short-term exposure to high concentrations of carbon monoxide on operator's psychophysiological functions 10 p1361 N88-18133

Effects of breathing air containing contaminants such as CO2, CO and hydrocarbons at 1 and 5 atmospheres
[PB88-132915] 11 p1521 N88-19084

Resonance energy transfer between carbon monoxide and oxygen molecules using dye laser intracavity absorption spectroscopy
[AD-A188488] 12 p1689 N88-20104

Determination of the content of CO(+) and H2O(+) ions in the tail of Comet Giacobini-Zinner and Comet Halley 14 p2006 N88-21964

The observability of carbon monoxide in planetary nebulae
[ETN-88-91498] 14 p2011 N88-21994

Kinetics of CO oxidation over a deactivated Rh(111) single crystal catalyst
[DE88-003000] 19 p2613 N88-25504

The response of ultrathin palladium gate sensors to hydrogen and carbon monoxide
19 p2672 N88-25885

Mechanism of the nitric oxide-carbon monoxide-oxygen reaction over a single crystal rhodium catalyst
[DE88-006274] 21 p2910 N88-27268

Effects of air polution on human exercise performance
[AD-A192660] 22 p3131 N88-28617

Modelling of CO oxidation in dilution jet flows
24 p3351 N88-29947

Recent observations of carbon monoxide in the Amazon Rain Forest
[INPE-4478-PRE/1245] 24 p3390 N88-30186

CARBON MONOXIDE LASERS

NO2 heterodyne frequency measurements with a tunable diode laser, a CO laser transfer oscillator and CO2 laser standards
[NASA-CR-182393] 06 p0710 N88-14353

CARBON STARS

Analysis of the carbon star G77-61
[ETN-87-90422] 01 p0109 N88-10707

Basic properties and variability
02 p0252 N88-11593

Spectroscopy and nonthermal processes
02 p0252 N88-11594

Circumstellar chemistry 02 p0253 N88-11598

Thermal atmospheric models
02 p0253 N88-11599

Synthetic spectra for the N-type carbon star TX Psc
04 p0516 N88-13173

Water masers associated with 2 carbon stars: EU Andromedae and V778 Cygni 04 p0517 N88-13176

Low mass stars with mass loss and low-luminosity carbon star formation 06 p0801 N88-14900

Asymptotic giant branch populations in composite stellar systems 13 p1854 N88-21098

CARBON STEELS

NT LOW CARBON STEELS

A quantitative statistical model for cleavage fracture initiation in carbide strengthened steels
[ETN-87-90735] 01 p0025 N88-10157

Laminated ferrous composites based on ultrahigh carbon (UHC) steels
[AD-A184617] 03 p0280 N88-11764

Method for the ultrasonic inspection of the soundness of the metal in weld joints in two-ply pipes
[BLL-CE-TRANS-8265-(9022.09)]
04 p0453 N88-12805

Crack initiation studies in hydrogen embrittled spring steel strip 05 p0605 N88-13710

Fatigue thresholds of C.Mn steels in saline environments 06 p0717 N88-14403

Fatigue, fracture and strain hardening of high carbon hardened alloy steel
[AD-A186101] 07 p0831 N88-15043

Weldability of a leaded carbon steel
[PB88-110341] 07 p0861 N88-15225

Propagation of fatigue crack in the medium-carbon steel containg both martensite and ferrite
[PB87-143962] 07 p0869 N88-15273

Development of a constitutive equation for HSLA (High-Strength Low-Alloy)-100 at cryogenic temperatures
[AD-A189243] 13 p1740 N88-20408

Environmental integrity of coating/metal interface
[AD-A192184] 18 p2492 N88-24786

Diffusion and solubility of some interstitial impurities in deformed metals
[DE88-701859] 21 p2914 N88-27296

Multi-metallic galvanic corrosion
[AD-A195995] 24 p3353 N88-29963

CARBON 12

Carbon abundances and C12/C13 ratios in M giants
04 p0515 N88-13167

Probing the possibility of a (12)C/(13)C abundance gradient from observations of interstellar CH+
[DE88-008908] 20 p2884 N88-27125

Dispersion effects in elastic electron scattering from C12
[B8805297] 23 p3281 N88-29536

CARBON 13

Solid state C-13 NMR characterization of textiles: Qualitative and quantitative analysis
[AD-A184349] 04 p0419 N88-12598

Carbon abundances and C12/C13 ratios in M giants
04 p0515 N88-13167

Probing the possibility of a (12)C/(13)C abundance gradient from observations of interstellar CH+
[DE88-008908] 20 p2884 N88-27125

CARBON-CARBON COMPOSITES

Carbon-carbon compositus and Aerospatiale. State of the art and prospects
[SNIAS-872-430-108] 05 p0559 N88-13401

Hydroburst test of a carbon-carbon involute exit cone
[NASA-TP-2556] 06 p0671 N88-14112

Stress rupture behavior of silicon carbide coated, low modulus carbon/carbon composites
[NASA-CR-180863] 06 p0678 N88-14150

Interface characteristics and the mechanical properties of metal matrix composites
[AD-A186441] 08 p0966 N88-15845

A study of the mechanical behavior of a 2-D carbon-carbon composite 11 p1449 N88-18638

Study of the mechanical behavior of a 2-D carbon-carbon composite
[NASA-CR-182594] 11 p1451 N88-18649

Nondestructive evaluation of carbon-carbon coatings
[AD-A189524] 13 p1748 N88-20453

Strength and failure rate of composite materials with carbon in ceramic matrix 16 p2180 N88-22995

Composite piston
[NASA-CASE-LAR-13435-1] 17 p2346 N88-23981

Electronic and structural studies of carbon/carbon composites
[AD-A191729] 19 p2609 N88-25481

Electrical resistivity of carbon-carbon composites
[AD-A193006] 20 p2768 N88-26410

High temperature testing of C/C (Carbon/Carbon) composites
[AD-A193012] 20 p2768 N88-26411

Effect of the matrix on the creep-behavior of carbon-carbon composite
[AD-A193211] 21 p2905 N88-27235

Studies in support of oxidation-resistant composite materials
[AD-A193320] 21 p2905 N88-27238

On the electrical properties of carbon/carbon composites densified by chemical deposit in vapor phase
[SNIAS-881-430-117] 21 p2907 N88-27252

Soot and radiation in a gas turbine combustor
[AD-A191991] 23 p3179 N88-28924

Spallation and dynamic fracture as an effect of laser induced shock-waves
[AD-A193513] 23 p3188 N88-28971

Ultrafine microstructure composites prepared by chemical vapor deposition
[AD-A193849] 23 p3189 N88-28973

Very high temperature materials for mechanical application
[SNIAS-881-430-106] 23 p3189 N88-28978

Creep of carbon yarn and carbon-carbon composites at high temperatures and high stresses
[AD-A195224] 24 p3340 N88-29878

CARBONACEOUS CHONDRITES

Analysis of laser extracted volatiles in carbonaceous chondrites 06 p0783 N88-14861

Noble gases, C,N, and Si isotopes in interstellar SiC form the Murchison carbonaceous chondrite
24 p3442 N88-30483

CARBONACEOUS MATERIALS

NT GRAPHITE

NT PYROLYTIC GRAPHITE

CARBONACEOUS METEORITES

Organic molecules on meteoritic solid substrates
[NASA-CR-181570] 05 p0560 N88-134

CARBONACEOUS ROCKS

NT COAL

Effective use of principal component analyses with hi resolution remote sensing data to delineate hydrotherm alteration and carbonate rocks 05 p0612 N88-137

CARBONATES

NT CALCITE

NT CALCIUM CARBONATES

NT POLYCARBONATES

DTA/DSC studies of phase equilibria in binary mixture of barium carbonate with alkali carbonates
[DE87-001195] 02 p0194 N88-112

Determination of optimum electrolyte composition fo molten carbonate fuel cells literature review
[DE88-001015] 10 p1348 N88-1805

Evaluation and compilation of thermodynamic propertie of high temperature chemical species
[AD-A187509] 11 p1452 N88-1865

Composite ceramic superconducting filaments fo superconducting cable
[AD-A187833] 11 p1556 N88-1931

Studies on the use of propylene carbonate as a high-voltage insulator
[DE88-011786] 22 p3057 N88-26141

CARBONIC ANHYDRASE

North Carolina Biomolecular Engineering and Materials Applications Center (NC-BEMAC)
[AD-A190923] 16 p2237 N88-23364

CARBONIZATION

Process for preparing transition metal nitrides and transition metal carbonitrides and their reaction intermediates
[DE88-000849] 06 p0679 N88-14162

Disclination structures in carbon and graphite
[AD-A191056] 17 p2322 N88-23868

Influence of carbon fiber surface treatment
[ETN-88-92536] 18 p2492 N88-24787

CARBONYL COMPOUNDS

Surface modification by metal deposition and laser irradiation 01 p0023 N88-10146

The spectroscopy and reaction kinetics of coordinatively unsaturated metal carbonyls
[AD-A190533] 15 p2035 N88-22124

CARBOXYL GROUP

High-molecular compounds (selected articles)
[AD-A184668] 03 p0293 N88-11842

Studies on syntheses of amine-carboxyboranes (boron analogues of amino acids) and derivatives
[AD-A184838] 05 p0557 N88-13386

The radiation sensitivity of select metal chelate polymers: Mechanistic changes at higher energies
[AD-A193467] 23 p3196 N88-29019

CARBOXYLATES

Carboxylate formation at the interface between a polyimide coating and cobalt 17 p2320 N88-23859

CARBOXYLIC ACIDS

NT ACETIC ACID

NT ACRYLIC ACID

NT DICARBOXYLIC ACIDS

NT NICOTINIC ACID

Organic molecules on meteoritic solid substrates
[NASA-CR-181570] 05 p0560 N88-13411

CARBURETORS

A study of the interaction of laser light with liquid propellant drops
[AD-A185117] 05 p0587 N88-13582

CARBURIZING

A theoretical analysis of the deactivation of metal surfaces upon carburization
[AD-A184556] 03 p0290 N88-11821

Wear of hard steel in rolling lubricated contact
[RP-699] 03 p0332 N88-12094

Sliding-wear properties of retained austenite in carburized layer
[PB87-149092] 07 p0833 N88-15054

Effects of ion implantation on cavitation erosion of a cobalt based metal/carbide alloy
[AD-A187239] 10 p1303 N88-17793

Surface fatigue life of CBN and vitreous ground carburized and hardened AISI 9310 spur gears
[NASA-TM-100960] 19 p2677 N88-25916

CARCINOGENS

Toxic effects of man-made mineral fibers with particular reference to ceramic fibers
[AD-A187949] 11 p1519 N88-19072

CARCINOMA

U CANCER

CARDIAC VENTRICLES

Diagnostic value of some load tests in evaluation of nonspecific electrocardiographic changes
07 p0805 N88-15426

CARDIOGRAPHY
NT BALLISTOCARDIOGRAPHY
NT ECHOCARDIOGRAPHY
NT ELECTROCARDIOGRAPHY
NT MAGNETOCARDIOGRAPHY
CARDIOLOGY
The use of heart rate in the prescription and evaluation of exercise programs [AD-A186454] 08 p1049 N88-16336
Challenges of physiological monitoring in a Navy operational setting 16 p2239 N88-23374
CARDIOVASCULAR SYSTEM
NT AORTA
NT ARTERIES
NT CAPILLARIES (ANATOMY)
NT CARDIAC VENTRICLES
NT HEART
NT MYOCARDIUM
NT VEINS
Cardiac contractility in weightlessness according to spatial ballistocardiography 07 p0890 N88-15393
Changes in regional and central hemodynamics during seven-day water immersion 07 p0895 N88-15421
Diagnostic value of some load tests in evaluation of nonspecific electrocardiographic changes 07 p0895 N88-15426
The use of heart rate in the prescription and evaluation of exercise programs [AD-A186454] 08 p1049 N88-16336
Respiratory and cardiovascular responses to cold stress following repeated cold water immersion [AD-A186480] 08 p1050 N88-16340
Forecasting complications of cardiovascular disease in flight personnel 10 p1361 N88-18136
JPRS Report: Science and Technology. USSR: Space Biology and Aerospace Medicine, volume 21, no. 6, November - December 1987 [JPRS-USB-88-004] 10 p1364 N88-18150
Results of long-term electrocardiographic monitoring of cosmonauts 10 p1364 N88-18152
Effect of hypercapnic-hypoxic test on cardiorespiratory parameters of individuals with neurocirculatory dystonia 10 p1367 N88-18169
Cardiovascular adaptation to zero-g during a long term flight (237 days) on board the Salyut 7 Soviet space station (1984) 12 p1655 N88-19920
Cardiac and peripheral circulation assessment by ultrasound on 3 astronauts during two 7-day space flights (1982 Salyut-7 - 1985 STS 51G) 12 p1656 N88-19921
Load and control of the cardiocirculatory system in weightlessness 12 p1656 N88-19922
Renal effects of anti-gravity suit inflation in man in relation to cardiovascular and hormonal changes 12 p1661 N88-19959
Effects of intense, time-constrained mental effort on hemodynamics and cardiovascular function 12 p1664 N88-19975
The effects of normal and therapeutic baths on the central vascular organs of persons with healthy hearts, as measured by X-ray [NASA-TT-20252] 13 p1811 N88-20818
Cardiovascular effects of weightlessness and ground-based simulation [NASA-TM-88314] 18 p2551 N88-25140
JPRS report: Science and technology. USSR: Space Biology and Aerospace Medicine, volume 22, no. 1, January - February 1988 [JPRS-USB-88-005] 19 p2702 N88-26069
Results of medical research conducted in 1985 during long-term spaceflights 19 p2702 N88-26070
Hemostasis parameters of individuals with neurocirculatory dystonia submitted to dry immersion 19 p2703 N88-26072
Models of cerebral-body perfusion and cerebral chemical transport [AD-A194945] 24 p3407 N88-30283
CARDS
The effects of data structure on total time on test plots [AD-A187628] 10 p1389 N88-18298
Optical memory cards: A comparison with other current technologies and potential military applications [AD-A187287] 10 p1425 N88-18512
The mechanical properties of card measured by photographic Moire [NPL-DMOM-87] 14 p1923 N88-21463
CARGO
NT AIR CARGO
Developmental airdrop testing techniques and devices [AGARD-AG-300-VOL-6] 04 p0398 N88-12481
Analysis of shock and vibration environments for cargo on C9B transport aircraft 08 p0999 N88-16051
Centaur G Prime modal test 09 p1181 N88-17075
Steps toward lunar settlement [DE88-009141] 21 p2900 N88-27213
CARGO AIRCRAFT
NT C-130 AIRCRAFT
NT C-135 AIRCRAFT
NT F-27 AIRCRAFT
General equilibrium characteristics of a dual-lift helicopter system [NASA-TP-2615] 12 p1573 N88-19407
CARGO SPACECRAFT
Design study for asteroidal exploitation 03 p0389 N88-12445
STS propellant scavenging systems study. Part 2, volume 2: Cost and WBS/dictionary [NASA-CR-179276] 10 p1290 N88-17717
CARIBBEAN REGION
Caribbean and Central America wind energy assessment [DE88-005134] 11 p1507 N88-19002
The role of aviation technology in the Caribbean Basin [NASA-CR-183069] 20 p2745 N88-26289
Geologic results obtained from the use of SPOT imagery along plate boundaries: Examples in the East African rift and of the northern-Caribbean collision 22 p3105 N88-28437
CARIBBEAN SEA
Current velocity and hydrographic observations in the Straits of Florida, the Caribbean Sea and offshore of the Antillean Archipelago: Subtropical Atlantic Climate Studies (STACS) 1986 [PB88-160767] 14 p1951 N88-21628
CAROTENE
Cross section of resonant Raman scattering of light by polyenes 07 p0920 N88-15591
CARPATHIAN MOUNTAINS (EUROPE)
Detailed analysis of a mesoscale convective complex situation in the Carpathian Basin (Europe) 02 p0207 N88-11296
CARRIER DENSITY (SOLID STATE)
First report on InGaAs hall device 14 p1903 N88-21372
Free carrier nonlinear optics 14 p1977 N88-21796
High density femtosecond excitation of nonthermal carrier distributions in intrinsic and modulation doped GaAs quantum wells 14 p1977 N88-21798
Dynamical aspects of carrier tunneling in semiconductor superlattices 14 p1977 N88-21799
Femtosecond studies in hot carrier relaxation in GaAs and AlGaAs 14 p1977 N88-21801
Development of a model procedure for the determination of volume diffusion lengths by transient measurements on monocrystal silicon solar cells [ETN-88-92119] 20 p2821 N88-26733
Auger recombination in GaSb/AlSb-multi quantum well heterostructures 20 p2862 N88-27001
CARRIER FREQUENCIES
Performance of a rapid carrier acquisition circuit for satellite ground terminal modems [RSRE-TEST REPORT-87/CC3/2] 22 p3071 N88-28227
CARRIER INJECTION
The qualitative determination of high injection effects in flux-loaded P-I-N diodes using the recombination radiation measuring method [ETN-88-91475] 11 p1580 N88-19336
Neutron radiation tolerance of Au-activated silicon 17 p2408 N88-24316
Direct subpicosecond measurement of carrier mobility of photoexcited electrons in GaAs 19 p2659 N88-25803
Longitudinally localized optical carrier injection for femtosecond transport studies 19 p2659 N88-25806
CARRIER LIFETIME
An investigation of the equivalent circuit and carrier lifetimes of Si/SiGe heterostructure p-n diodes for frequencies between 0.5 and 18.5 MHz [FOA-C-30469-3.2] 09 p1256 N88-17529
Carrier lifetime versus ion-implantation dose in Silicon On Sapphire 19 p2658 N88-25791
Auger recombination in GaSb/AlSb-multi quantum well heterostructures 20 p2862 N88-27001
Control of carrier lifetime in PbTe nipi superlattices by external photoinjection 20 p2863 N88-27006
CARRIER MOBILITY
NT ELECTRON MOBILITY
NT HOLE MOBILITY
First report on InGaAs hall device 14 p1903 N88-21372
Radiation effects in silicon [DE88-006642] 16 p2282 N88-23659
Direct subpicosecond measurement of carrier mobility of photoexcited electrons in GaAs 19 p2659 N88-25803
Picosecond carrier transport in GaAs quantum wells 19 p2660 N88-25813
High power storage system based on thin film solid ionics [AD-A193623] 23 p3291 N88-29598
Temperature dependence of conductivity and of Hall coefficients for noble metal films [ETN-88-92981] 23 p3294 N88-29616
CARRIER MODULATION
U MODULATION
CARRIER ROCKETS
U LAUNCH VEHICLES
CARRIER TO NOISE RATIOS
Optimized tracking of RF carriers with phase noise, including Pioneer 10 results 04 p0434 N88-12694
High frequency acoustic underwater communication with low probability of being traced [REPT-4-87] 09 p1242 N88-17447
The relationship between vision carrier-to-noise ratio and picture signal-to-noise ratio in a System I television receiver [BBC-RD-1987/23] 10 p1318 N88-17377
CARRIER TRANSPORT (SOLID STATE)
A flux analysis of the solar cells [INPE-4247-PRE/1120] 08 p1022 N88-16186
Picosecond carrier transport in GaAs quantum wells 19 p2660 N88-25813
Carrier transport in semiconductor magnetic sensors under nonuniform fields 19 p2672 N88-25888
CARRIER WAVES
Optimum filters and smoothers design for carrier phase and frequency tracking [NASA-CR-182654] 12 p1618 N88-19679
CARRINGTON ROTATION
U SOLAR ROTATION
CARTAN SPACE
Torsion as a source of expansion in a Bianchi type I universe in the self-consistent Einstein-Cartan theory of a perfect fluid with spin density [AD-A184200] 03 p0322 N88-12037
Raychaudhuri equation in the self-consistent Einstein-Cartan theory with spin-density [NASA-TM-101145] 17 p2447 N88-24546
Inflation in Einstein-Cartan theory with energy-momentum tensor with spin [NASA-TM-101164] 17 p2447 N88-24547
Inevitable inflation in Einstein-Cartan theory with improved energy-momentum tensor with spin [NASA-TM-101146] 18 p2586 N88-25365
CARTESIAN COORDINATES
Fundamentals of turbulence for turbulence modeling and simulation 03 p0312 N88-11971
Point processes in the plane [AD-A186017] 07 p0913 N88-15542
Supporting valid time: An historical algebra [AD-A187740] 11 p1565 N88-19368
COMESH: A corner mesh finite difference code to solve multigroup diffusion equations in multidimensions [DE88-701248] 15 p2108 N88-22555
A multigrid approach for the solution of a nonlinear diffusion equation in a time-dependent area using Cartesian coordinates [GMD-STUDIEN-122] 16 p2257 N88-23491
A formulation for the boundary-layer equations in general coordinates [NASA-TM-100079] 18 p2459 N88-24600
QN3D: A 3-dimensional quasi-neutral hybrid particle-in-cell code with applications to the tilt mode instability in field reversed configurations 18 p2580 N88-25325
Spatial dynamics of deformable multibody systems with variable kinematic structure 20 p2813 N88-26687
Application of rectangular co-ordinates to the problem of laminar combined convection in a straight horizontal tube whose circumference is heated nonuniformly [PDR/CFDU/IC/33] 22 p3076 N88-28263
CARTOGRAPHY
U MAPPING
CARTRIDGE ACTUATED DEVICES
U ACTUATORS
U EXPLOSIVE DEVICES
CARTS
Software modifications to total data reporting accessory for metabolic measurement cart [AD-A193641] 22 p3132 N88-28623
CASCADE CONTROL
Closed-loop system analysis using Lyapunov stability theory 04 p0483 N88-12978
Description and analysis of a cascade control of fluid flow [PB87-112686] 06 p0698 N88-14282
Robust design of cascade control [REPT-88-006] 22 p3142 N88-28687
CASCADE FLOW
Experimental determination of the oscillatory forces on two turbine blade profiles [ETN-87-90417] 01 p0007 N88-10037
Theoretical investigations of three turbine cascades using a two dimensional time marching procedure [DFVLR-FB-87-02] 01 p0057 N88-10362

Navier-Stokes cascade analysis with a stiff Kappa-Epsilon turbulence solver
[NASA-TM-100218] 02 p0123 N88-10778

Numerical analysis of cascade flow solving Navier-Stokes equations 05 p0536 N88-13262

Inverse design method for two-dimensional transonic cascades 05 p0536 N88-13263

Effects of free stream turbulence, Reynolds number and incidence angle on axial turbine cascade performance
05 p0548 N88-13339

Unsteady aerodynamics of an oscillating cascade in a compressible flow field
[NASA-TM-100219] 05 p0549 N88-13346

Post stall behavior in axial-flow compressors
[AD-A185712] 06 p0665 N88-14081

The unsteady gas flow through stator and rotor of a turbomachine 10 p1281 N88-17660

Transonic blade design on rotational stream surfaces
10 p1282 N88-17671

Investigation of dihedral effects in compressor cascades 10 p1282 N88-17672

Flow patterns induced by vortices
[NAL-TR-932] 10 p1332 N88-17963

Mixed direct-inverse problem of transonic cascade
15 p2054 N88-22244

Effect of freestream turbulence on a two dimensional cascade, with different surface roughness, at high Reynolds number
[AD-A190615] 15 p2065 N88-22316

Designs of profiles for cascades
[NASA-TT-20161] 15 p2067 N88-22326

Theoretical investigations of three turbine cascades using a 2-D time marching procedure
[ESA-TT-1077] 16 p2207 N88-23170

Development of a method of calculating unstable flows of cascades seperated at the leading edge
[PB87-228714] 19 p2596 N88-25437

Cascades with harmonically oscillating blades in supersonic flow
[NASA-TT-20323] 19 p2599 N88-25446

Numerical analysis of three dimensional cascade flow by solving Navier-Stokes equations
19 p2638 N88-25650

Application of computational fluid dynamics to design of compressor cascade 19 p2639 N88-25655

A Navier-Stokes solver for cascade flows
[NASA-CR-181682] 19 p2666 N88-25856

A Navier-Stokes study of cascade flow fields including inlet distortion and rotating stall
[AD-A193109] 21 p2943 N88-27483

Investigation of oscillating cascade aerodynamics by an experimental influence coefficient technique
[NASA-TM-101313] 22 p3039 N88-28041

Modeling of momentum transport of axially parallel turbulent flows in rod cascades
[ETN-88-92978] 23 p3214 N88-29131

Numerical solutions of unsteady inviscid transonic turbine cascade flows
[AD-A196111] 24 p3316 N88-29748

Aerodynamics in ground effect and predicted landing ground roll of a fighter configuration with a secondary-nozzle thrust reverser
[NASA-TP-2834] 24 p3317 N88-29752

Three-dimensional elliptic grid generation technique with application to turbomachinery cascades
[NASA-TM-101330] 24 p3372 N88-30078

CASCADE WIND TUNNELS

Hot-wire measurements of compressor blade wakes in a cascade wind tunnel
[AD-A194737] 23 p3181 N88-28936

CASCADES

On helicity fluctuations and the energy cascade in turbulence
[NASA-CR-178403] 03 p0321 N88-12028

CASCADES (FLUID DYNAMICS)

U FLUID DYNAMICS

CASCODE MOSFET

U FIELD EFFECT TRANSISTORS

CASES (CONTAINERS)

NT ROCKET ENGINE CASES

Structural frequency functions for an impulsive, distributed forcing function 05 p0594 N88-13627

Low temperature storage container for transporting perishables to space station
[NASA-CASE-MFS-28248-1] 16 p2498 N88-24817

CASKS

U BARRELS (CONTAINERS)

CASSEGRAIN OPTICS

Optical photometer for the Tirgo telescope
[IFSI-87-5] 05 p0650 N88-13985

Design, fabrication and delivery of a miniature Cassegrainian concentrator solar array system
[NASA-CR-179237] 06 p0730 N88-14493

CASSINI MISSION

Study of a Radio Relay Link (RRL). Cassini mission. Data package for final presentation
[ESA-CR(P)-2472] 07 p0847 N88-15138

CAST ALLOYS

Influence of boron on porosity in nickel-base superalloy castings 03 p0299 N88-11677

Fatigue crack growth behavior of A356-T6 cast aluminum alloy 05 p0599 N88-13660

Durability and damage tolerance of aluminum castings
[AD-A186444] 10 p1341 N88-18013

Effects of thermal and thermo-mechanical treatments on the mechanical properties of centrifugally cast alloy 718
[AD-A188195] 11 p1458 N88-18690

Processing, physical metallurgy and creep of NiAl + Ta and NiAl + Nb alloys
[NASA-CR-182113] 14 p1890 N88-21295

CASTING

NT CENTRIFUGAL CASTING

NT INVESTMENT CASTING

NT SLIP CASTING

Activities at government research laboratories reported 04 p0403 N88-12503

Development of advanced fiber reinforced ceramics
[DE88-000779] 04 p0420 N88-12604

Advances in processing techniques for nickel aluminides
[DE87-014571] 05 p0566 N88-13449

Cyclic deformation behaviour of cast irons with various graphite shapes in the temperature range 20 C less than or = T less than or = 500 C 06 p0715 N88-14384

Selection of polymer materials for manufacturing optical parts
[AD-A185898] 07 p0836 N88-15069

Fabrication of YBa2Cu3O7 superconducting ceramics
[DE88-003012] 07 p0938 N88-15701

Development of a shell system for DS moulds at RR precision casting facility --- directional solidification (DS)
[PNR90400] 09 p1151 N88-15893

Materials development for JPL oxygen plant
[DE88-003067] 10 p1297 N88-17752

Cast iron-base alloy for cylinder/regenerator housing
[NASA-CR-182116] 12 p1608 N88-19613

SBIR-Long fluoride fiber
[AD-A188595] 13 p1754 N88-20492

Structure and mechanical properties of metal matrix composites made using semi-solid processes: The case of the system Al-Si/SiC
[ETN-88-92299] 17 p2316 N88-23836

Compositional redistribution during casting of Hg sub 0.8 Cd sub 0.2 Te alloys
[NASA-TM-101151] 17 p2326 N88-23893

Fabrication of reactor shields at the Y-12 plant
17 p2402 N88-24283

Fluid flow modeling in casting processes and its implications
[DE88-010009] 20 p2810 N88-26671

Spatial organization of homopolymer chains inside spherical polybutadiene domains of SB diblock copolymers
[AD-A193390] 21 p2918 N88-27321

Preliminary investigation of flow modeling during solid propellant processing
[AD-A196168] 24 p3357 N88-29987

CASTING SOLVENTS

U PLASTICIZERS

CASTINGS

NT INGOTS

Studies on estimation of nickel in zinc base die casting by D.C. polarography
[PD-MT-8729] 04 p0417 N88-12588

Hydrogen induced cracks in armor steel weldments fabricated with austenitic filler alloys
[AD-A188733] 13 p1740 N88-20406

Increasing the rate at which ceramic castings undergo preliminary heat-treatment in an ultra-high frequency magnetic field 14 p1886 N88-21275

CAT SCANNER

U COMPUTER AIDED TOMOGRAPHY

CATABOLISM

Long duration confinement of aquatic organisms in weightlessness (aquaspace) 07 p0887 N88-15380

A program for the study of skeletal muscle catabolism following physical trauma
[AD-A189771] 15 p2102 N88-22521

CATACLYSMIC VARIABLES

Ultraviolet observations of AM Her --- cataclysmic variable
[MPE-PREPRINT-92] 02 p0250 N88-11581

The hard X-ray eclipse in the intermediate polar EX Hydrae
[MPE-PREPRINT-95] 02 p0251 N88-11582

The Parkes radio survey of active chromosphere stars
04 p0511 N88-13141

SW UMa and V426 Oph: EXOSAT surprises
19 p2740 N88-26269

EXO033319-2554.2: A 55-MG eclipsing AM Herculis binary
[MPE-PREPRINT-114] 22 p3163 N88-28838

Intermediate polars observed in Brazil in the last eight years
[INPE-4567-PRE/1308] 24 p3454 N88-30559

Activities in astrophysics
[INPE-4582-PRE/1316] 24 p3456 N88-30570

CATALASE

Experimental study of protective effect of antioxidant enzymes-superoxide dismutase and catalase-when using intermittent toxic modes of hyperbaric oxygenation
19 p2707 N88-26094

CATALOGS

Source hierarchy list. Volume 1: A through D
[AD-A185900] 07 p0941 N88-15722

Component data base for space station resistojet auxiliary propulsion
[NASA-CR-180834] 10 p1293 N88-17731

Catalog of open clusters and associated interstellar matter
[NASA-RP-1202] 23 p3300 N88-29652

CATALOGS (PUBLICATIONS)

NT ASTRONOMICAL CATALOGS

Source header list. Volume 1: A through K
[AD-A184000] 04 p0501 N88-13086

Bibliographic relationships: Toward a conceptual structure of bibliographic information used in cataloging
06 p0791 N88-14852

Catalog of compartment fire model algorithms and associated computer subroutines
[PB88-110861] 07 p0839 N88-15087

NASA scientific and technical publications: A catalog of Special Publications, Reference Publications, Conference Publications, and Technical Papers, 1987
[NASA-SP-7063(02)] 15 p2149 N88-22830

Report on the Second Catalog Interoperability Workshop
[NASA-TM-100701] 19 p2718 N88-26135

CATALYSIS

Catalytic processes for space station waste conversion
[NASA-CR-177423] 01 p0077 N88-10491

A surface science investigation of potential intermediates, catalysts, and promoters in the synthesis of higher alcohols by metals
[DE87-014186] 02 p0144 N88-10906

The effect of additives on the reactivity of palladium surfaces for the chemisorption and hydrogenation of carbon monoxide: A surface science and catalytic study
[DE87-014685] 02 p0145 N88-10909

Photocatalytic electrochemistry at a biological-membrane metal-colloid interface
[DE87-009122] 02 p0166 N88-11041

The applicability of the catalytic wet-oxidation to CELSS 03 p0360 N88-12264

Surface catalytic degradation study of two linear perfluoropolyalkylethers at 345 C
[NASA-TP-2774] 04 p0410 N88-12543

Surface mediated photocatalysis
[AD-A188882] 12 p1603 N88-19589

Chromatographic and related reactors
[AD-A188452] 12 p1605 N88-19599

The redox chemistry of some peroxo and superoxo metal ion complexes
[AD-A189159] 12 p1606 N88-19606

Model catalyst studies of SMSI (Strong Metal/Support Interactions) and the role of D-electrons in chemisorption and catalysis
[DE88-004518] 13 p1738 N88-20393

On copper peroxide
[NASA-TT-20263] 15 p2037 N88-22135

Improvements to Raney copper zinc methanol synthesis catalysts 17 p2318 N88-23844

ECUT (Energy Conversion and Utilization Technologies) program: Biocatalysis Project
[NASA-CR-182917] 17 p2370 N88-24110

A scientific basis for an alternate cathode architecture
[AD-A191498] 18 p2481 N88-24717

An improved external recycle reactor for determining gas-solid reaction kinetics
[NASA-TM-101160] 19 p2611 N88-25492

Catalytic activation of carbon dioxide by metal complexes
[AD-A192310] 21 p2909 N88-27262

Precursor chemistry and the structure of silica aerogels
[DE88-011253] 21 p2920 N88-27328

Perfluoropolyalkylether lubricants under boundary conditions: Iron catalysis of lubricant degradation
[AD-A193241] 21 p2956 N88-27560

CATALYSTS

NT ELECTROCATALYSTS

Ruthenium catalysts and their use in ammonia production
[GB-PATENT-2-136-704-A] 01 p0020 N88-10123
Boronium complexes as polymer catalysts
[GB-PATENT-2-161-475-A] 01 p0026 N88-10166
A surface science investigation of potential intermediates, catalysts, and promoters in the synthesis of higher alcohols by metals
[DE87-014188] 02 p0144 N88-10906
A life test of a 22-Newton (5-lbf) hydrazine rocket
[NASA-TM-100232] 03 p0278 N88-11750
A theoretical analysis of the deactivation of metal surfaces upon carburization
[AD-A184556] 03 p0290 N88-11821
Surface coatings and catalyst production by electrodeposition 03 p0297 N88-11863
Mass transport by diffusion 03 p0297 N88-11864
Characterization of catalysts with metal-support effects and of the species adsorbed on their surfaces
[DE87-014636] 04 p0414 N88-12564
Phase purity of NiCo2O4, a catalyst candidate for electrolysis of water
[NASA-TM-100239] 05 p0556 N88-13385
Activated metal oxide surfaces as highly basic and reducing environments
[AD-A184958] 05 p0561 N88-13417
Catalytic combustion of methane
[PB88-123112] 07 p0829 N88-15028
Studies of metal/carbon surface chemistry
[DE87-009545] 07 p0829 N88-15029
Model Cu/ZnO catalysts for methanol synthesis: The role of surface structure
[DE88-002354] 07 p0830 N88-15037
Studies of supported metal catalysts
[DE88-002546] 07 p0831 N88-15038
Deactivation of alumina based catalysts
11 p1455 N88-18673
Properties of lanthanide oxides as supports for transition metal catalysts
[DE88-004520] 11 p1456 N88-18678
Electron microscopy study of morphology and composition of a ferrisilicate catalyst
[DE88-005754] 11 p1562 N88-19352
Surface mediated photocatalysis
[AD-A188882] 12 p1603 N88-19589
Chromatographic and related reactors
[AD-A188452] 12 p1605 N88-19599
Novel catalysts for methane activation
[DE88-003637] 13 p1738 N88-20390
A new polymer-based hydrogen getter
[DE88-004538] 13 p1751 N88-20467
Evaluation of direct methane conversion to higher hydrocarbons and oxygenates
[DE88-003812] 15 p2049 N88-22204
Improvements to Raney copper zinc methanol synthesis catalysts 17 p2318 N88-23844
Catalytic ignition of hydrogen and oxygen propellants
[NASA-TM-100957] 18 p2476 N88-24689
Surface composition-reactivity relationships in heterogeneous catalysis
[DE88-006679] 18 p2480 N88-24714
Update of low temperature catalyst development
[DE88-007032] 18 p2480 N88-24715
Molecular-beam, mass-spectrometric studies of wood vapor and model compounds over HZSM-5 catalyst
18 p2535 N88-25044
Upgrading pyrolysis vapors to aromatic gasoline with zeolite catalysis at atmospheric pressure
18 p2536 N88-25045
Research on hydrotreating catalysts to hydrodeoxygenate biocrude oils
18 p2536 N88-25046
Sulfur-tolerant anode materials
[DE88-001034] 18 p2537 N88-25054
Liquid-phase oxidation of acetone with hydrogen peroxide on oxide catalysts 19 p2706 N88-26091
Alkaline fuel cell performance investigation
[NASA-TM-100937] 21 p2909 N88-27267
Preparation and development of advanced battery catalysts
[AD-A193208] 21 p2937 N88-27441
The design of methane activation catalysts
[DE88-002265] 23 p3199 N88-29043
Active sites and roles of solid acid base catalysts
[NASA-TT-20333] 24 p3345 N88-29909
CATALYTIC ACTIVITY
A review of methanol vehicles and air quality impacts
[DE88-002846] 08 p1023 N88-16194
Surface composition-reactivity relationships in heterogeneous catalysis
[DE87-003450] 09 p1140 N88-16834
Copper peroxide
[NASA-TT-20245] 14 p1888 N88-21282
Design of catalytic monoliths for closed-cycle carbon dioxide lasers
[NASA-CR-182983] 18 p2558 N88-25185
Production of powdered sodium hydride with large specific surface by the catalyzed reaction of molten sodium with hydrogen-1
[NASA-TT-20185] 20 p2776 N88-26462
CATCHMENT AREAS
U WATERSHEDS
CATECHOLAMINE
NT EPINEPHRINE
NT NOREPINEPHRINE
CATEGORIES
The distribution of evaporitic weathering products on Antarctic meteorites 06 p0798 N88-14888
CATENARIES
Strain gages in engineering geodesy
[SER-C-320] 01 p0048 N88-10309
CATHODE RAY TUBES
Generation of specific chromaticities on CRT monitors
[AD-A187739] 11 p1440 N88-18590
Human efficiency for visual detection of targets on CRT displays using a two-level multiple channel time history format
[AD-A188419] 12 p1670 N88-20001
Design and testing of a luminance and chrominance stabilization system for a computer-controlled color display
[AD-A191922] 18 p2554 N88-25159
Display system image quality
23 p3242 N88-29298
Use of color CRTs (Cathode Ray Tubes) in aircraft cockpit: A literature search, revision B
[AD-A195062] 24 p3324 N88-29797
CATHODES
NT CELL CATHODES
NT HOLLOW CATHODES
NT PHOTOCATHODES
NT THERMIONIC CATHODES
NT TUBE CATHODES
Synergism of electroplating and vacuum processes
[DE87-013496] 01 p0033 N88-10211
Plasma thruster development
[AD-A184173] 04 p0408 N88-12536
Raman scattering as a diagnostic technique for cathode characterization
[AD-A184434] 04 p0439 N88-12726
Some investigations of electrical discharges at the surfaces of solid cathodes immersed in aqueous electrolyte solutions
[PB87-168209] 09 p1159 N88-16946
Continuously frequency-tunable high-pressure CO2-laser with plasmatic cathode
09 p1238 N88-17418
Investigation of materials for inert electrodes in aluminum electrodeposition cells
[DE88-003380] 10 p1323 N88-17906
Capacitive charge division in centroid finding cathode readouts in MWPCs
[DE88-003545] 10 p1333 N88-17969
A novel class of positive electrodes for rechargeable batteries
[DE88-004559] 13 p1763 N88-20545
Theoretical model of the cathode spot on a unipolar arc
[AD-A190109] 15 p2059 N88-22277
Aluminum-air battery development
[DE88-006620] 15 p2061 N88-22287
A scientific basis for an alternate cathode architecture
[AD-A191498] 18 p2481 N88-24717
Basic processes of plasma propulsion
[AD-A192117] 18 p2577 N88-25310
Degradation of beam brightness by field emission from a cathode shroud
[DE88-008345] 20 p2794 N88-26576
Alkaline fuel cell performance investigation
[NASA-TM-100937] 21 p2909 N88-27267
Long-pulse, high-power vircator experiments
[DE88-011787] 21 p2940 N88-27458
Electrocatalytic reduction of oxygen on modified oxide surfaces
[NASA-TM-101333] 24 p3352 N88-29952
CATHODIC COATINGS
The influence of cathodic protection on erosion-corrosion of metals and model alloys
[AD-A191613] 18 p2465 N88-24742
Extinction behavior of low voltage switching arc under consideration of cathodic coatings and dynamic arc column
[ETN-88-92384] 20 p2796 N88-26591
CATIONS
Impedance of passive lithium anodes in SOCl2 solutions under low-field polarization
[DE88-000922] 04 p0439 N88-12728
Precipitation of surfactants and surfactant mixtures in aqueous solutions
[DE88-003333] 10 p1298 N88-17763
Study of cations in the precipation of Estacao Antartica Comandante Ferraz
[INPE-4377-PRE/1197] 12 p1644 N88-19843
Universal detection of ions by replacement-ion chromatography employing an anion-replacement method and an ultraviolet-visible spectrophotometric detector
[AD-A191326] 16 p2176 N88-22971
Electronic structure and stability of small cation and anion hydrogen clusters 16 p2267 N88-23562
Computer simulation of uphill diffusion in ternary ionic system
[NASA-TT-20194] 18 p2573 N88-25285
Possible mechanism for high-temperature superconductivity in the BaSr La(Y)-CuO systems
[DE88-702060] 23 p3288 N88-29576
CATS
Emetic mechanism in acute radiation sickness
[AD-A194102] 23 p3238 N88-29267
CAUCHY INTEGRAL FORMULA
A quadrature formula for a double-pole singular integral
[PD-FM-8725] 04 p0485 N88-12990
A method for the numerical solution of random Cauchy singular integral equation 18 p2565 N88-25234
CAUCHY PROBLEM
Cauchy problem for linearized system of Navier-Stokes equations considering compressibility
04 p0459 N88-12837
Computation of flow past conical hypersonic wings using a second order Godunov method
05 p0533 N88-13241
The Eckhaus Partial Differential Equation (PDE) I psi t + psi xx + 2(psi/sq)x psi + 2(/psi/) to the 4th power psi = 0
[PREPRINT-546] 06 p0763 N88-14686
A fast Riemann solver with constant covolume applied to the random choice method
[CAR-87-19] 09 p1231 N88-17375
Detection of signals in non-Gaussian correlated noise derived from Cauchy processes
[AD-A187488] 10 p1320 N88-17894
On the equivalence of four-dimensional self-duality equations to continual analog of the main chiral field problem
[DE88-700871] 12 p1686 N88-20083
Further extensions of the choquet-deny and deny theorems with applications in characterization theory
[AD-A193358] 21 p3006 N88-27834
Cauchy problem for the nonlinear Schroedinger equation
[DE88-702454] 21 p3011 N88-27867
Backlund transformations associated with a Riemann-Hilbert spectral problem
[PREPRINT-596] 22 p3146 N88-28712
A limiting viscosity approach to the Riemann problem for materials exhibiting change of phase
[AD-A193477] 23 p3210 N88-29103
CAUCHY-RIEMANN EQUATIONS
On the Fefferman class of metrics associated with a 3-dimensional Cauchy-Riemann (CR) space
[PREPRINT-579] 14 p1991 N88-21865
CAUSTIC LINES
Analytical caustic surfaces
[NASA-TM-87805] 02 p0168 N88-11060
CAUSTICS
U ALKALIES
CAUSTICS (OPTICS)
Analytical caustic surfaces
[NASA-TM-87805] 02 p0168 N88-11060
CAVITATION
U CAVITATION FLOW
CAVITATION CORROSION
Simulated service test behavior of various internal and external coatings applied on CF6-50 first stage turbine blades
[NLR-MP-86018-U] 05 p0549 N88-13343
Effects of ion implantation on cavitation erosion of a cobalt based metal/carbide alloy
[AD-A187239] 10 p1303 N88-17793
CAVITATION FLOW
Investigations of creep cavitation in Type 304 stainless steel
[DE87-014198] 03 p0287 N88-11803
Some stochastic aspects of intergranular creep cavitation
[DE88-000065] 04 p0416 N88-12581
Gas diffusion studies in steady and nonsteady cavities
[AD-A185795] 06 p0704 N88-14318
Cavitation inception scale effects. 1: Nuclei distributions in natural waters. 2: Cavitation inception in a turbulent shear flow
[AD-A186553] 08 p0988 N88-15987

Experimental and theoretical study on cavitation inception and bubbly flow dynamics. Part 1: Design, development and operation of a cavitation susceptibility meter. Part 2: Linearized dynamics of bubbly and cavitating flows with bubble dynamics effects
[AD-A187133] 09 p1160 N88-16952
Effects of ion implantation on cavitation erosion of a cobalt based metal/carbide alloy
[AD-A187239] 10 p1303 N88-17793
The use of multigrid techniques in the solution of the Elrod algorithm for a dynamically loaded journal bearing
[NASA-CR-180873] 10 p1331 N88-17954
Cavitation inception
[AD-A189220] 13 p1765 N88-20557
High Reynolds number pump facility for cavitation research
[AD-A189310] 13 p1765 N88-20558
Cavitation inception in rectangular two-dimensional slots
[AD-A190677] 15 p2066 N88-22318
Modeling of cavitation phenomena in homogeneous flow in transitory regimes in pipes
[ISAL-IDI1-87-15] 17 p2337 N88-23948
Superplasticity: A fundamental investigation on deformation mechanism and cavitation phenomena
[AD-A191548] 18 p2485 N88-24741
Gas diffusion studies in steady and nonsteady cavities
18 p2512 N88-24902
Noise generation by air bubbles in water: An experimental study of creation and splitting
[AD-A192063] 19 p2664 N88-25839
Pulsed spray structure and atomisation techniques
[AD-A192280] 20 p2800 N88-26614
Forces and moments on a slender, cavitating body
[DE88-007208] 21 p2945 N88-27491
Cavitation inception in a turbulent shear flow
[DE88-011486] 21 p2946 N88-27497
A multiple-scales partial solution of the pulse-forced Rayleigh-Plesset equation of cavitation bubble dynamics
[AD-A193733] 23 p3212 N88-29118
An investigation of acoustic cavitation produced by pulsed ultrasound
[AD-A193523] 23 p3278 N88-29516
Beam combining by phase transition nonlinear media
[AD-A194116] 23 p3283 N88-29547
Studies on pressure response of gas bubbles contributions of condensed droplets in bubbles generated by a uniform nucleation
[NASA-TT-20343] 24 p3370 N88-30068

CAVITIES
Development of response models for the Earth Radiation Budget Experiment (ERBE) sensors. Part 2: Analysis of the ERBE integrating sphere ground calibration
[NASA-CR-178293] 01 p0049 N88-10316
Quantum electrodynamics based on self-energy: Spontaneous emission in cavities
[DE87-703071] 02 p0232 N88-11461
Investigations on a transonic airfoil with a 30 mm wide perforation/cavity arrangement
[ESA-TT-1072] 03 p0260 N88-11634
Inertial confinement fusion reactor cavity analysis
[DE88-000788] 04 p0492 N88-13028
Program to development an optical transistor and switch
[AD-A185666] 06 p0697 N88-14278
Gas diffusion studies in steady and nonsteady cavities
[AD-A185795] 06 p0704 N88-14318
Electromagnetic fields backscattered from an s-shaped inlet cavity with an absorber coating on its inner walls
[NASA-CR-182401] 07 p0845 N88-15130
Review of nucleation and incipient boiling under pool and forced convection conditions
08 p0982 N88-15938
Evaluation of spare room in cerebrospinal system using noninvasive methods 10 p1361 N88-18137
Cavitation in model elastomeric composites
[AD-A187401] 11 p1447 N88-18625
Investigation of a ray-mode representation of the Green's function in a rectangular cavity
[PB88-131677] 11 p1469 N88-18763
Structural-acoustic interior noise modeling and analysis from experimental data
[PB88-141775] 12 p1687 N88-20088
Tunable condensed-media laser with antiresonant ring cavity 14 p1971 N88-21764
Observation of energetic particles (E greater than 30 keV) by the Giotto experiment EPA in the magnetic cavity of Comet Halley 14 p1997 N88-21903
Observation of synchronously transient pumped mode-locking dye laser under negative cavity detuning
16 p2187 N88-23041
Research in electromagnetic shielding theory. Part1: Shielding by rectangular enclosures
[AD-A192881] 20 p2791 N88-26557
Rf cavity primer for cyclic proton accelerators
[DE88-010655] 20 p2853 N88-26938
A critical review of IR drops and electrode potentials within pits, crevices and cracks
[AD-A192481] 21 p2935 N88-27431
Thermo-mechanical cracking in coated media with a cavity by a moving asperity friction
[AD-A193311] 21 p2961 N88-27586
The use of fins to reduce the pressure drop in a rotating cavity with a radial flow
[PNR90465] 22 p3079 N88-28282
Solar energy absorption efficiency of an ellipsoidal receiver-reactor with specularly reflecting walls
[AD-A193726] 22 p3117 N88-28520
Navier-Stokes calculations of transonic flows past cavities
[NASA-CR-180484] 23 p3212 N88-29116
Effects on the resonant frequencies caused by loading a spherical cavity with a dielectric sphere
[AD-A193864] 23 p3277 N88-29511
Studies on pressure response of gas bubbles contributions of condensed droplets in bubbles generated by a uniform nucleation
[NASA-TT-20343] 24 p3370 N88-30068

CAVITY RESONATORS
Theoretical and experimental investigation of electron beam acceleration and sub-millimeter wave generation in cyclotron resonant cavities
[AD-A184806] 05 p0649 N88-13975
Initial operation of a high-power whispering-gallery-mode gyrotron
[DE88-002500] 07 p0857 N88-15207
High-sensitivity recording of weak reflected or scattered radiation by method of coherent intracavity reception with YAG:Nd(3+) laser 08 p1078 N88-16502
Photodetachment neutralizer development: Laser window design study. Volume 2: Window design details
[DE88-000783] 09 p1170 N88-17014
Measured and calculated acoustic attenuation rates of tuned resonator arrays for two surface impedance distribution models with flow
[NASA-TP-2766] 09 p1241 N88-17440
Measurement technique for characterization of the gyrotron
[INPE-4322-RPE/550] 12 p1630 N88-19758
Study of inhomogeneously filled cylindrical resonant cavities by the finite integration technique
[PB88-133707] 12 p1697 N88-20156
Progress in diagnostic techniques for SC cavities
[CEBAF-PR-88-003] 13 p1772 N88-20600
Resonator coupling of two ring cavity, argon-ion lasers
[AD-A189558] 13 p1775 N88-20616
Status of RF superconductivity at Argonne National Laboratory
[DE88-005913] 15 p2144 N88-22796
Fluxons and order in long Josephson junctions
[AD-A190879] 16 p2282 N88-23665
On bunch lengthening using the fourth harmonic cavity in the NSLS VUV ring
[DE88-007392] 18 p2574 N88-25288
Superconducting rf and beam-cavity interactions
[DE88-008598] 20 p2852 N88-26936
Rf cavity primer for cyclic proton accelerators
[DE88-010655] 20 p2853 N88-26938
Progress in diagnostic techniques for SC (superconducting) cavities
[DE88-008600] 20 p2876 N88-27077
Laser CO2/TEA frequency-stabilized by phase conjugation 22 p3082 N88-28303
Qualitative characteristics of open waveguide resonator spectra
[DE88-702387] 23 p3202 N88-29056
Band pass with cavity resonators by use of three oscillation types
[ETN-88-92984] 23 p3209 N88-29096
Free electron lasers with small period wigglers
[DE88-011627] 23 p3218 N88-29156

CCD
U CHARGE COUPLED DEVICES

CD-ROM
U OPTICAL DISKS
U READ-ONLY MEMORY DEVICES

CDC COMPUTERS
NT CDC CYBER 205 COMPUTER

CDC CYBER 205 COMPUTER
An efficient sparse matrix multiplication scheme for the CYBER 205 computer
[NASA-TM-4028] 10 p1390 N88-18302
Optimization of the real level 2 BLAS on the Cyber 205
[CWI-NM-R8715] 14 p1956 N88-21657
Solving bidiagonal systems of linear equations on the CDC CYBER 205
[CWI-NM-R8725] 18 p2558 N88-25187

CDMA
U CODE DIVISION MULTIPLE ACCESS

CEILINGS (ARCHITECTURE)
Test results and predictions for the response of near-ceiling sprinkler links in a full-scale compartment fire
[NBSIR-87/3633] 01 p0033 N88-10209

CEILOMETERS
U CLOUD HEIGHT INDICATORS

CELESTIAL BODIES
NT A STARS
NT ACHONDRITES
NT ACTIVE GALAXIES
NT ANDROMEDA GALAXY
NT AQUARID METEOROIDS
NT ASTEROID BELTS
NT ASTEROIDS
NT ASYMPTOTIC GIANT BRANCH STARS
NT B STARS
NT BARRED GALAXIES
NT BINARY STARS
NT BL LACERTAE OBJECTS
NT BLACK HOLES (ASTRONOMY)
NT BOLIDES
NT CARBON STARS
NT CARBONACEOUS CHONDRITES
NT CARBONACEOUS METEORITES
NT CATACLYSMIC VARIABLES
NT CEPHEID VARIABLES
NT CHONDRITES
NT COMET HEADS
NT COMET NUCLEI
NT COMET TAILS
NT COMETS
NT COOL STARS
NT CRAB NEBULA
NT DEIMOS
NT DISK GALAXIES
NT DOUBLE STARS
NT DWARF NOVAE
NT DWARF STARS
NT EARLY STARS
NT EARTH (PLANET)
NT ECLIPSING BINARY STARS
NT ELLIPTICAL GALAXIES
NT ENCKE COMET
NT EXTRAGALACTIC RADIO SOURCES
NT F STARS
NT FAINT OBJECTS
NT FLARE STARS
NT G STARS
NT GALACTIC CLUSTERS
NT GALAXIES
NT GAS GIANT PLANETS
NT GEMINID METEOROIDS
NT GIACOBINI-ZINNER COMET
NT GIANT STARS
NT GLOBULAR CLUSTERS
NT GRIGG-SKJELLERUP COMET
NT H II REGIONS
NT HALLEY'S COMET
NT HERBIG-HARO OBJECTS
NT HERCULES NOVA
NT HOT STARS
NT INFRARED SOURCES (ASTRONOMY)
NT INFRARED STARS
NT IO
NT IRON METEORITES
NT IRREGULAR GALAXIES
NT JUPITER (PLANET)
NT JUPITER SATELLITES
NT K STARS
NT LATE STARS
NT LOCAL GROUP (ASTRONOMY)
NT M STARS
NT MAGELLANIC CLOUDS
NT MAGNETIC STARS
NT MAIN SEQUENCE STARS
NT MARS (PLANET)
NT METEORITES
NT METEOROID SHOWERS
NT METEOROIDS
NT MICROMETEOROIDS
NT MILKY WAY GALAXY
NT MIRA VARIABLES
NT MOON
NT NATURAL SATELLITES
NT NEBULAE
NT NEMESIS (STAR)
NT NEPTUNE (PLANET)
NT NEUTRON STARS
NT NOVAE
NT O STARS
NT ORION NEBULA
NT ORIONID METEOROIDS
NT PERSEID METEOROIDS
NT PHOBOS
NT PLANETARY NEBULAE

NT PLANETARY RINGS
NT PRE-MAIN SEQUENCE STARS
NT PROTOPLANETS
NT PROTOSTARS
NT PULSARS
NT QUADRANTID METEOROIDS
NT QUASARS
NT RADIO GALAXIES
NT RADIO JETS (ASTRONOMY)
NT RADIO SOURCES (ASTRONOMY)
NT RADIO STARS
NT RED DWARF STARS
NT RED GIANT STARS
NT REFERENCE STARS
NT S STARS
NT SATURN RINGS
NT SATURN SATELLITES
NT SEYFERT GALAXIES
NT SOLAR SYSTEM
NT SPIRAL GALAXIES
NT SPORADIC METEOROIDS
NT STAR CLUSTERS
NT STARBURST GALAXIES
NT STARS
NT STELLAR SYSTEMS
NT SUBGIANT STARS
NT SUN
NT SUPERGIANT STARS
NT SUPERMASSIVE STARS
NT SUPERNOVA 1987A
NT SUPERNOVAE
NT T TAURI STARS
NT TAURID METEOROIDS
NT TEMPEL 2 COMET
NT TERRESTRIAL PLANETS
NT TITAN
NT TITANIA
NT URANUS (PLANET)
NT URANUS RINGS
NT URANUS SATELLITES
NT VARIABLE STARS
NT VENUS (PLANET)
NT VIRGO GALACTIC CLUSTER
NT WEST COMET
NT WHITE DWARF STARS
NT WOLF-RAYET STARS
NT X RAY BINARIES
NT X RAY STARS
NT ZODIACAL DUST

CELESTIAL GEODESY
New possibilities for using gravity data in developing geodetic coordinate systems 08 p1009 N88-16116
Study of modern instrumentation and methods for astronomic positioning in the field
[AD-A196173] 24 p3452 N88-30548

CELESTIAL MECHANICS
Propagation of random initial conditions in time
04 p0486 N88-12993
Periodic orbits around a satellite modelled as a triaxial ellipsoid
[AD-A190592] 15 p2022 N88-22051
A standard library for modeling satellite orbits on a microcomputer
[AD-A195759] 24 p3331 N88-29830

CELESTIAL OBSERVATION
U ASTRONOMY

CELL ANODES
Morphological changes in polymer electrolyte cells
[AD-A195821] 24 p3368 N88-30054

CELL CATHODES
New materials for electrochemical cells
[AD-A183659] 01 p0037 N88-10238

CELL DIVISION
Potential use of the bioreactor to determine effects of microgravity and other environmental parameters on growth of hybridoma cells 09 p1198 N88-17178
Gravisensing in lentil seedling roots grown in space (Spacelab D-1 mission) 12 p1654 N88-19911

CELLS (BIOLOGY)
NT BLOOD CELLS
NT EGGS
NT ERYTHROCYTES
NT EUKARYOTES
NT LEUKOCYTES
NT LYMPHOCYTES
NT NEURONS
NT PROKARYOTES
NT PROTOPLASTS
Superoxide dismutase assays
[AD-A183972] 03 p0356 N88-12242
Electron cytochemical detection of Ca(2)+ ATPase in protonema of moss funaria hygrometrica (H e d w.) under hypogravitation 06 p0749 N88-14602
Review of cytoskeleton research in cell differentiation and development
[AD-A185832] 07 p0882 N88-15353
Investigations of Paramecium cells analyzed under microgravity conditions 07 p0884 N88-15367
Possible use of plasmids for study of effect of space flight factors on biological objects
08 p1046 N88-16319
Zero gravity and living organism
08 p1046 N88-16320
Effects of extreme hypoxia on phospholipid metabolism in subcellular structures of rat brain
08 p1046 N88-16323
Space Bioreactor Science Workshop
[NASA-CP-2485] 09 p1196 N88-17168
Suspension cell culture in microgravity and development of a space bioreactor 09 p1196 N88-17169
Space bioreactor: Design/process flow
09 p1197 N88-17170
Computer control of a microgravity mammalian cell bioreactor 09 p1197 N88-17172
Shear and mixing effects on cells in agitated microcarrier tissue culture reactors 09 p1197 N88-17173
Some process control/design considerations in the development of a microgravity mammalian cell bioreactor 09 p1197 N88-17174
Plant cell technologies in space: Background, strategies and prospects 09 p1198 N88-17177
Potential use of the bioreactor to determine effects of microgravity and other environmental parameters on growth of hybridoma cells 09 p1198 N88-17178
Cell culture experiments planned for the space bioreactor 09 p1198 N88-17180
Histomorphometric analysis of rat bones after spaceflight aboard Cosmos-1667 biosatellite
10 p1360 N88-18128
Effect of weightlessness on replicative function of rat hepatocyte DNA 10 p1360 N88-18129
Morphological and functional state of the hypothalamo-hypophyseal neurosecretory system of rats flown aboard Cosmos-1667 10 p1365 N88-18156
Interactions of cultured human endothelial cells with polymeric surfaces
[PB88-112255] 10 p1369 N88-18178
Critical phenomena and electromagnetic effects in biological membranes
[AD-A188156] 11 p1518 N88-19064
Cell cultures in space: From basic research to biotechnology 2 12 p1660 N88-19948
Cyropreservation of isolated rat hepathocytes for future use in Spacelab experiments: Preliminary results
12 p1660 N88-19950
Electrical and chemical sensors for biological cell research 19 p2669 N88-25866
Genetic effects of low level microwave radiation
[AD-A192687] 21 p2984 N88-27722
Contraction behavior and protoplasmic streaming in the slime mold Physarum polycephalum (Physarum kinetics) --- Spacelab D1 mission 22 p3060 N88-28160

CELLULAR MATERIALS (NON BIOLOGICAL)
U FOAMS

CELLULOSE
Saccharification of cellulose by combined fungal and bacterial preparations 17 p2316 N88-23833

CEMENTS
Open-graded bases for airfield pavements
[AD-A184461] 04 p0402 N88-12500
A laboratory study of asphalt concrete mix designs for high-contact pressure aircraft traffic
[AD-A185753] 06 p0670 N88-14106
Development of strength in cements
[PB87-232971] 06 p0684 N88-14189
Comparative study of nondestructive pavement testing, MacDill Air Force Base, Florida
[AD-A186082] 07 p0822 N88-14993
Use of reinforced inorganic cement materials for spark wire and drift chamber wire frames
[NASA-CR-180759] 13 p1746 N88-20438
The effect of Ca(OH)2-treated ceramic microspheres on the mechanical properties of high-temperature lightweight cement composites
[DE88-004590] 13 p1749 N88-20457
Cement paste matrix composite materials center
[AD-A188657] 15 p2028 N88-22083

CENSORED DATA (MATHEMATICS)
Further studies in estimation of life distribution characteristics from censored data
[AD-A184862] 05 p0643 N88-13937
A modified kernel quantile estimator under censoring
[AD-A186364] 07 p0911 N88-15525
Estimation and comparison of changes in the presence of information right censoring by modeling the censoring process
[AD-A186320] 08 p1074 N88-16478
A generalized quantile estimator under censoring
[AD-A188280] 10 p1402 N88-18364
Estimation in linear models with censored data
[AD-A187209] 11 p1540 N88-19203
Survival analysis, or what to do with upper limits in astronomical surveys
[NASA-CR-182936] 17 p2449 N88-24551

CENTAUR LAUNCH VEHICLE
The 250AH/90A active lithium-thionyl chloride cell for Centaur-G application 02 p0163 N88-11023
Zero-G thermodynamic vent system for shuttle/Centaur 06 p0983 N88-15943
Centaur G Prime modal test 09 p1181 N88-17075
Centaur operations at the space station
[NASA-CR-179593] 19 p2606 N88-25473
Centaur operations at the space station: Cost and transportation analysis
[NASA-CR-182128] 24 p3332 N88-29835

CENTAUR VEHICLE
U CENTAUR LAUNCH VEHICLE

CENTER OF GRAVITY
Effect of permissible variations of center-of-gravity locations of cargo airplane on its mass
04 p0424 N88-12625
A new method for the estimation of aircraft inertia characteristics 20 p2787 N88-26530

CENTER OF MASS
Numerical analysis of motion of solid bodies in atmosphere 08 p1079 N88-16505
An improved data reduction procedure for accelerometer centrifuge data 12 p1577 N88-19436
Some periodicities in motion of Halley's Comet relative to center of mass 13 p1726 N88-20324

CENTER OF PRESSURE
Experimental research on center of pressure of slender body with two pointed ends 14 p1864 N88-21137
New definition of pressure-center coefficient of reentry craft with asymmetrical configuration
14 p1864 N88-21138

CENTERBODIES
Multi-body aircraft with an all-movable center fuselage actively controlling fuselage pressure drag
[NASA-CASE-LAR-13511-1] 17 p2301 N88-23765

CENTIMETER WAVES
Utilization of microwave measuring systems for nondestructive control of composite materials
[SNIAS-872-430-109] 05 p0559 N88-13402
Recent observations of the OH radio lines in comets
14 p1999 N88-21917

CENTRAL AMERICA
Geological evolution and analysis of confirmed or suspected gas hydrate localities. Volume 9: Formation and stability of gas hydrates of the Middle America Trench
[DE88-001007] 10 p1347 N88-18050
Caribbean and Central America wind energy assessment
[DE88-005134] 11 p1507 N88-19002

CENTRAL EUROPE
Land campaign force assessment. Methods used in Central-Europe-study
[FOA-C-10288-9.3] 06 p0768 N88-14723
Typical weather months in the past (1973-1983) in Central Europe
[AD-A194701] 23 p3235 N88-29249

CENTRAL NERVOUS SYSTEM
NT BRAIN
NT CEREBELLUM
NT CEREBRAL CORTEX
NT CEREBRUM
NT HIPPOCAMPUS
NT HYPOTHALAMUS
NT SPINAL CORD
NT THALAMUS
Functional plasticity of the nervous system of vertebrates 01 p0074 N88-10474
Discrete adaptation to sensory conflict
10 p1363 N88-18146
Combined effect of ionizing radiation and altered gas atmosphere on central nervous system
10 p1367 N88-18168
Neuropeptides in experimental head injury
[AD-A188067] 11 p1520 N88-19077
Models describing muscle behavior and control
[LR-522] 16 p2238 N88-23368
Vagal tone as an index of mental state
16 p2239 N88-23373
The N2-P3 complex of the evoked potential and human performance 16 p2241 N88-23388
Effect of different modes of voluntary control of breathing on human electroencephalogram with exposure to acute hypoxic hypoxia 19 p2707 N88-26093
Measurement and classification of the mode of action of antidepressant drugs 21 p2983 N88-27714
Measurement of electrical activity in the CNS with cortical evoked potentials and EEG: Efficacy profiles of drugs using factor analysis 21 p2983 N88-27715

CENTRAL PROCESSING UNITS
NT ARITHMETIC AND LOGIC UNITS

Design, manufacture and testing of an elegant breadboard model communications processor
[D/2244] 01 p0034 N88-10217
Study and design of a communication processor unit
[RIDU/TREP/1002/SAAB] 01 p0083 N88-10538
File usage analysis and resource usage prediction: A measurement-based study
[NASA-CR-181553] 05 p0633 N88-13867
Predictability of process resource usage: A measurement-based study of UNIX
[NASA-CR-181562] 05 p0633 N88-13869
High-performance CPU implementation of the nebula instruction set architecture 10 p1373 N88-18194
Implementation of a buddy failure recovery concept in the NOVAC system 10 p1375 N88-18205
Simulation: A simulation system in Ada
[FOA-A-20043-2.7] 17 p2385 N88-24176
Computers in weapons systems: A look at the F-15
[AD-A194498] 23 p3178 N88-28920
The LTPP communication processor --- Columbus and Hermes
[CL/CP/SES/FR/004] 24 p3415 N88-30328

CENTRIFUGAL CASTING
Effects of thermal and thermo-mechanical treatments on the mechanical properties of centrifugally cast alloy 718
[AD-A188195] 11 p1458 N88-18690

CENTRIFUGAL COMPRESSORS
Flow in Centrifugal Compressors --- conference
[VKI-LS-1987-01] 07 p0850 N88-15160
Measurements in centrifugal compressors
07 p0850 N88-15161
Centrifugal compressors 07 p0850 N88-15162
The technology of centrifugal compressors: A design approach and new goals for research
07 p0850 N88-15163
Identification and avoidance of instabilities in high performance turbomachinery 07 p0850 N88-15164
Blade vibration problems in centrifugal compressors. Fundamental considerations 07 p0851 N88-15165
Flow in volutes and the influence on the flow in centrifugal compressors 07 p0851 N88-15169
Numerical study of a centrifugal impeller response to a downstream static pressure perturbation
07 p0851 N88-15170
The Goddard Space Flight Center mechanical cooler program 08 p0983 N88-15944
The advantage of variable geometry for turbine engines at low power 10 p1280 N88-17653
Secondary flow measurements with L2F-technique in centrifugal compressors 10 p1283 N88-17676
Method for predicting performance limits of centrifugal compressors 10 p1283 N88-17677
Open-cycle centrifugal vapor-compression heat pump
[PB88-157391] 11 p1488 N88-18885

CENTRIFUGAL FORCE
Two-dimensional static otolith model
10 p1367 N88-18167
Measurement and analysis of the noise radiated by low Mach numbers centrifugal blowers
[AD-A189226] 13 p1833 N88-20966
Centrifugal acceleration of ions in the polar magnetosphere
[NASA-TM-101148] 17 p2374 N88-24120

CENTRIFUGAL PUMPS
Operating experiences and test results of six cold helium compressors
[DE87-012115] 02 p0157 N88-10982
Rotor dynamic behavior of centrifugal pumps
08 p0975 N88-15898
Ames Research Center cryogenics program
08 p0981 N88-15927
Open-cycle centrifugal vapor-compression heat pump
[PB88-157391] 11 p1488 N88-18885

CENTRIFUGES
NT HUMAN CENTRIFUGES
Plasma centrifuge development at INPE
[INPE-4243-PRE/1117] 08 p1087 N88-16546
An improved data reduction procedure for accelerometer centrifuge data 12 p1577 N88-19436
Control test and validation for a large diameter high stability centrifuge 12 p1577 N88-19437
Preliminary analysis of an integrated logistics system for OSSA payloads
[NASA-CR-4114] 12 p1584 N88-19477
Preliminary analysis of an integrated logistics system for OSSA payloads. Volume 4: Supportability analysis of the 1.8m centrifuge 12 p1584 N88-19481
Vacuum-arc plasma centrifuge experiment
[INPE-4509-PRE/1263] 15 p2138 N88-22758
Botany Facility. Thermal Control (TC) subsystem test report on experiment container of laboratory model and breadboard centrifuge
[BF-TN-ER-061/86] 17 p2378 N88-24135
Botany Facility: Magnetic fluid seal considerations for the centrifuge
[SIRA-A/7373/WP110/MAC004]
17 p2378 N88-24138
Botany Facility: Considerations and analyses of the balancing system philosophy proposed for the BF centrifuge
[SIRA-A/7373/WP110/PWF001]
17 p2378 N88-24139
Computation of flow and diffusion process in gas centrifuges
[ETN-88-92366] 21 p2949 N88-27514

CEPHEID VARIABLES
The pulsation modes of CO Aur
[PUBL-SER-C-FASC-10] 03 p0387 N88-12430
Membership of Cepheids and red giants in 8 open clusters: NGC 129, 6067, 6649, 6664, IC 4725, Ly 6, Ru 79
[PUBL-SER-C-FASC-13] 07 p0944 N88-15739
Near-infrared observations of cepheids: The distance to M33 15 p2152 N88-22846

CEPSTRAL ANALYSIS
Some properties of the Hilbert transform
[DE88-002465] 09 p1227 N88-17350
Bearing detection in the presence of two sources of varying coherence using the complex cepstrum
[NASA-CR-181605] 09 p1243 N88-17451

CERAMAL PROTECTIVE COATINGS
U CERMETS
U PROTECTIVE COATINGS

CERAMALS
U CERMETS

CERAMIC BONDING
Analysis of end stresses in glass-metal bimaterial strips
[DE87-007848] 05 p0610 N88-13750
Behavior of metal ceramic interfaces
[PB87-147500] 07 p0837 N88-15076
Composite piston
[NASA-CASE-LAR-13435-1] 17 p2346 N88-23981

CERAMIC COATINGS
Thermal barrier coating life prediction model development 02 p0190 N88-11185
Ceramic-ceramic shell tile thermal protection system and method thereof
[NASA-CASE-ARC-11641-1] 11 p1448 N88-18628
Titanium carbide coatings for aerospace ball bearings
14 p1927 N88-21486
The corrosion resistance of an aluminum alloy coated with polysilazane derived ceramics
[AD-A190703] 15 p2046 N88-22183
Evaluation of ceramic thermal barrier coatings for gas turbine engine components
[ETN-88-91947] 16 p2181 N88-22998
Recent advances in metallic/ceramic coatings for corrosion control in military applications
17 p2320 N88-23858
Vanadic hot corrosion of gas turbine blade coating materials 17 p2321 N88-23864
An investigation of ceramic coatings for protection of SiC from high-temperature corrosion
[DE88-007873] 18 p2493 N88-24790
Development of protective coatings for ceramic tubular components
[PB88-197165] 20 p2776 N88-26463
Effects of ceramic surfaces on autoignition in a constant volume combustion apparatus
[AD-A193055] 21 p2909 N88-27266

CERAMIC FIBERS
Processing and properties of SiC/Nicalon composites
[DE87-013885] 03 p0279 N88-11757
High-temperature properties of ceramic fibers and insulations for thermal protection of atmospheric entry and hypersonic cruise vehicles
[NASA-TM-100059] 10 p1295 N88-17743
High yield synthesis of B4C/BN ceramic materials by pyrolysis of polymeric Lewis base adducts of decaborane(14)
[AD-A188154] 11 p1462 N88-18717
Toxic effects of man-made mineral fibers with particular reference to ceramic fibers
[AD-A187949] 11 p1519 N88-19072
Contemporary ceramics and the new technological revolution 14 p1902 N88-21363
High-T(sub c) superconducting wire fabrication and testing
[DE88-005989] 15 p2144 N88-22798
Mechanical and structural characterization of aluminum ceramic fibers
[ETN-88-92168] 17 p2323 N88-23870
SiC fiber analysis 17 p2326 N88-23891
SiC fiber reinforced reaction-bonded Si3N4 composites 17 p2326 N88-23892
Development of materials for fabric radiators
17 p2429 N88-24448
Auger analysis of a fiber/matrix interface in a ceramic matrix composite
[NASA-TM-100892] 19 p2610 N88-25487
Studies in support of oxidation-resistant composite materials
[AD-A193320] 21 p2905 N88-27238

CERAMIC MATRIX COMPOSITES
Ceramic-Ceramic Composites Meeting in Belgium
[ONRL-7-020-R] 01 p0019 N88-10118
Structural reliability and damage tolerance of ceramic composites for high-temperature applications
[PB87-208310] 01 p0019 N88-10119
Carbon fiber reinforced glass matrix composites for space based applications
[AD-A184355] 04 p0410 N88-12546
Study of ceramic-fiber/ceramic sol-gel based matrix composites
[SNIAS-872-430-120] 05 p0569 N88-13469
Thermo-mechanical behavior of high temperature fiber composites 06 p0678 N88-14149
High temperature tensile testing of ceramic composites
[NASA-CR-180888] 08 p0990 N88-15996
Activities report of the Materials Department
[ETN-88-91984] 13 p1745 N88-20436
Contemporary ceramics and the new technological revolution 14 p1902 N88-21363
Fracture toughness testing of a ceramic matrix composite
[AD-A189846] 15 p2029 N88-22089
A test for interfacial effects and stress transfer in ceramic matrix composites
[NASA-CR-182758] 15 p2046 N88-22194
Continuous fiber ceramic matrix composites for heat engine components 15 p2082 N88-22411
Fracture technology for brittle materials
15 p2083 N88-22417
Strength and failure rate of composite materials with carbon in ceramic matrix 16 p2180 N88-22995
Ceramic matrix composites 17 p2325 N88-23888
Carbon matrix composites prospective roles for biotechnology 18 p2477 N88-24694
Auger analysis of a fiber/matrix interface in a ceramic matrix composite
[NASA-TM-100892] 19 p2610 N88-25487
Manufacturing of a ceramic-ceramic composite matrix using the sol-gel procedure
[ETN-88-92157] 20 p2768 N88-26414
Theoretical and experimental analysis of the toughening behavior of whisker reinforcement in ceramic matrix composites
[DE88-011841] 21 p2906 N88-27241
Contribution to the development of coated fiber ceramic insolation material
[ETN-88-92361] 21 p2906 N88-27243
Very high temperature materials for mechanical application
[SNIAS-881-430-106] 23 p3189 N88-28978
A test for interfacial effects and stress transfer in ceramic matrix composites
[NASA-CR-182873] 24 p3340 N88-29880
A study of the critical factors controlling the synthesis of ceramic matrix composites from preceramic polymers
[AD-A195405] 24 p3340 N88-29881
Processing technology research in composites
[AD-A195693] 24 p3341 N88-29890

CERAMIC NUCLEAR FUELS
Cermet-fueled reactors for advanced space applications
[DE88-005528] 13 p1839 N88-21002
Cermet fuel thermal conductivity
17 p2410 N88-24329
Monolithic fuel cell based power source for burst power generation 17 p2429 N88-24450

CERAMICS
NT CERAMIC NUCLEAR FUELS
X-ray tomography and nuclear magnetic resonance imaging applications for advanced ceramic materials
[DE87-011534] 01 p0027 N88-10171
Use of sol-gels in the application of ceramic oxide thin films
[DE87-013610] 01 p0028 N88-10176
Toughening of alpha-alumina: Preliminary results
[DE87-702776] 01 p0028 N88-10178
Physics and chemistry of packing fine ceramic powders
[DE87-013709] 01 p0029 N88-10183
Ceramic composites by chemical vapor infiltration
[DE87-009128] 01 p0029 N88-10185
Simple instrumentation for testing of ceramic superconductors
[DE87-013849] 01 p0103 N88-10672
Studies on surface chemical states of some metals and ceramics bombarded with energetic light-ions
[DE87-752975] 02 p0145 N88-10910

Needs assessment for NDT and characterization of ceramics: Assessment of inspection technology for green state and sintered ceramics
[DE87-013550] 02 p0151 N88-10947

Needs assessment for nondestructive testing and materials characterization for improved reliability in structural ceramics for heat engines
[DE88-000040] 02 p0153 N88-10957

Study of the micromechanical behavior of a SiO2-Al2O3-Li2O glass ceramic and its relation to the microstructure
[ISAL-ITC1-87-01] 02 p0153 N88-10960

Crack behavior in ceramic materials under static, slowly increasing, and cyclic loading conditions
[KFK-4209] 02 p0154 N88-10964

NDE (Nondestructive Evaluation) of advanced structural ceramics
[DE87-014417] 03 p0292 N88-11832

Modeling of irradiation-induced amorphization in a titanate ceramic
[DE87-014751] 03 p0292 N88-11833

The behavior of plastic, ceramic masses in compression tests
[ETN-87-90603] 03 p0292 N88-11836

High temperature characterization of ceramic materials
[REPT-NT-3403] 03 p0292 N88-11837

Structure and grain coarsening during the processing of engineering ceramics
[NASA-TM-100235] 03 p0293 N88-11838

Indentation damage in ceramics
[AD-A184686] 03 p0294 N88-11844

Aluminum oxynitride spinel (ALON): A review
[AD-A184753] 03 p0294 N88-11845

Investigation of BN CO2 wave guide laser
03 p0302 N88-11905

The Shock and Vibration Digest, Volume 19, No. 10
03 p0335 N88-12112

Application of fracture mechanics theory in the reliability analysis of structural ceramics in multiaxial loading
03 p0335 N88-12113

Adiabatic diesel engine component development: Reference engine for on-highway applications
[NASA-CR-179531] 03 p0386 N88-12428

JPRS report: Science and technology. Japan
[JPRS-JST-87-025] 04 p0403 N88-12502

Ceramics thin film 04 p0403 N88-12505

Research and development on high strength ceramic heaters discussed 04 p0404 N88-12508

Effect of time and temperature on transformation toughened zirconias
[AD-A184356] 04 p0419 N88-12600

Molecular engineering of ceramics
[DE88-000174] 04 p0420 N88-12603

Development of advanced fiber reinforced ceramics
[DE88-000779] 04 p0420 N88-12604

Ceramic technology for advanced heat engines project
[DE88-001520] 04 p0420 N88-12605

Real-time Raman detection of molecular changes in ceramics undergoing sliding friction
[DE88-000558] 04 p0421 N88-12609

Statistical process control applied to the liquid-fed ceramic melter process
[DE88-000271] 05 p0569 N88-13471

Process for preparing transition metal nitrides and transition metal carbonitrides and their reaction intermediates
[DE88-000849] 06 p0679 N88-14162

Ceramic technology for advanced heat engines
[PB87-232997] 06 p0683 N88-14188

JPRS report: Science and technology. Japan
[JPRS-JST-87-023] 06 p0684 N88-14191

Developments in electronics ceramics reported
06 p0684 N88-14192

Electron microscopy studies of tensile cyclic fatigue-tested silicon nitride ceramics
[DE88-001438] 06 p0685 N88-14196

Cyclic fatigue of ceramics at high temperatures
[PB87-127700] 06 p0685 N88-14200

Exploitation of the sol-gel route in processing of ceramics and composites
[AD-A185482] 06 p0686 N88-14204

Characterization of mechanical damage mechanisms in ceramic composite materials
[AD-A185549] 06 p0686 N88-14205

The effect of texture on the crack growth resistance of alumina
[NASA-TM-100250] 06 p0686 N88-14206

Hitachi develops ceramic superconducting device
06 p0688 N88-14214

The consequences of intergrain Josephson coupling in ceramic high-temperature superconductors
[DE87-013713] 06 p0785 N88-14816

Interface effects on the mechanical properties of ceramic composites
[AD-A185899] 07 p0826 N88-15009

Assessment of electroceramics research in Europe and the Middle East
[AD-A186377] 07 p0836 N88-15074

A comparison of film-based tomography and computed tomography for advanced ceramic materials
[DE88-003114] 07 p0837 N88-15079

Techniques for ceramic sintering using microwave energy
[DE88-001416] 07 p0837 N88-15080

Imaging subtle microstructural variations in ceramics with precision ultrasonic velocity and attenuation measurements
[NASA-TM-100129] 07 p0867 N88-15257

Fabrication of YBa2Cu3O7 superconducting ceramics
[DE88-003012] 07 p0938 N88-15701

Nondestructive characterization of ceramic composite whiskers with neutron diffraction and ultrasonic techniques
[DE88-003075] 08 p0965 N88-15844

Processing and interfacial analysis of glass-ceramic to metal seals
[DE88-002999] 08 p0971 N88-15873

The use of NMR imaging to measure porosity and binder distributions in green-state and partially sintered ceramics
[DE88-003099] 08 p0972 N88-15881

Steady-state deformation of some lithium ceramics
[DE88-003116] 08 p0972 N88-15882

Aeropropulsion '87. Session 1: Aeropropulsion Materials Research
[NASA-CP-10003-SESS-1] 09 p1118 N88-16697

Ceramics for engines 09 p1119 N88-16704

Microstructures and properties of SiC whisker-reinforced mullite composites
[DE88-002611] 09 p1139 N88-16826

Nondestructive evaluation of structural ceramics by photoacoustic microscopy
[NASA-CR-180858] 09 p1146 N88-16868

Wire-cut electrical discharge machinability of ceramics
[AD-A186989] 09 p1146 N88-16870

Image correlation on an IBM-PC for characterization of advanced ceramics
[DE88-002829] 09 p1149 N88-16885

LFCM (Liquid-Fed Ceramic Melter) vitrification technology
[DE88-003441] 09 p1149 N88-16887

Focused ultrasonic backscatter technique for near-surface flaw detection in structural ceramics
[DE88-003112] 09 p1183 N88-17091

Application of high temperature ceramic superconductors (CSC) to commercial tokamak reactors
[DE88-003973] 09 p1257 N88-17538

Fabrication and materials evaluation of high performance aligned ceramic fibre reinforced glass matrix composite
[AERE-R-12517] 10 p1294 N88-17736

Materials development for JPL oxygen plant
[DE88-003067] 10 p1297 N88-17752

Friction and wear of monolithic and fiber reinforced silicon-ceramics sliding against IN-718 alloy at 25 to 800 C in atmospheric air at ambient pressure
[NASA-TM-10[illegible]94] 10 p1304 N88-17796

NMR (Nuclear Magnetic Resonance) imaging for detecting binder/plasticizers in green-state structural ceramics
[DE88-003111] 10 p1304 N88-17800

Adhesion, friction and micromechanical properties of ceramics
[NASA-TM-100782] 10 p1305 N88-17801

Tribology of ceramics: Report of the Committee on Tribology of Ceramics
[NASA-CR-182506] 10 p1305 N88-17802

Effect of translucence of engineering ceramics on heat transfer in diesel engines
[DE88-003732] 10 p1305 N88-17804

Fabrication, phase transformation studies and characterization of SiC-AlN-Al2OC ceramics
[DE88-004053] 10 p1306 N88-17807

The migration of grain boundaries in ceramic materials with particular reference to the sintering process
[DE88-004085] 10 p1306 N88-17808

Metal modification for improved glass-ceramic to metal seals. 1: Auger results on ion implantation and vapor deposition films
[DE88-005244] 10 p1339 N88-18006

Ceramic bearings for use in gas turbine engines
[NASA-TM-100288] 10 p1340 N88-18007

Fundamental studies of corrosion of nonoxide structural ceramics
[PB88-141536] 11 p1461 N88-18709

Research on high-specific-heat dielectrics
[AD-A187248] 11 p1461 N88-18710

High yield synthesis of B4C/BN ceramic materials by pyrolysis of polymeric Lewis base adducts of decaborane(14)
[AD-A188154] 11 p1462 N88-18717

Tribological properties of alumina-boria-silicate fabric from 25 to 850 C
[NASA-TM-100806] 11 p1464 N88-18726

Application of X-ray computed tomography to ceramic/ceramic composites
[DE88-002903] 11 p1464 N88-18728

Ceramic technology for advanced heat-engines program data base
[DE88-003922] 11 p1464 N88-18730

Perturbed angular correlations in zirconia ceramics
[DE88-004117] 11 p1464 N88-18731

Ceramic decomposition under irradiation
[DE88-004327] 11 p1464 N88-18732

Quality assurance of ceramic materials and gas turbine components
[IZFP-850303-TW] 11 p1465 N88-18735

Slip casting of advanced ceramics and composites
[DE88-003424] 11 p1467 N88-18746

Prototype thin-film thermocouple/heat-flux sensor for a ceramic-insulated diesel engine
[NASA-TM-100798] 11 p1490 N88-18892

Review of the state of the art and projected technology of low heat rejection engines
[PB88-131255] 11 p1496 N88-18934

Reliability based analysis of contact problems
[NASA-CR-182117] 11 p1503 N88-18975

Composite ceramic superconducting filaments for superconducting cable
[AD-A187833] 11 p1556 N88-19312

Research briefing on high-temperature superconductivity
[PB88-133004] 11 p1561 N88-19344

The preparation of titanium nitride and titanium carbonitride by the preceramic polymer route
[AD-A188357] 12 p1610 N88-19626

Microdesigning of lightweight/high strength ceramic materials
[AD-A188526] 12 p1610 N88-19631

Contact and current noise in beta alumina and Nasicon ceramics
[AD-A189168] 12 p1611 N88-19635

Properties to seals made with Li2O-Al2O3-SiO2-glass ceramics and aluminum-containing austenitic stainless steels
[DE88-004688] 12 p1633 N88-19776

Basic research in ceramic and semiconductor science at selected Japanese laboratories, based on a September 1986 visit: Highlights, summary and overview and detailed notes from selected Japanese laboratories
[DOE/ER-0314] 12 p1696 N88-20150

Advanced Gas Turbine (AGT) Technology Development Project, ceramic component developments
[NASA-CR-180871] 12 p1709 N88-20229

A new process for synthesis of silicon nitride powders for advanced ceramics
[AD-A189354] 13 p1748 N88-20451

Development of a torsion balance for adhesion measurements
[NASA-TM-100799] 13 p1748 N88-20454

The effect of Ca(OH)2-treated ceramic microspheres on the mechanical properties of high-temperature lightweight cement composites
[DE88-004590] 13 p1749 N88-20457

Improved glass-ceramic to metal seals in actuator and detonator applications with an aluminum-containing austenitic stainless steel
[DE88-004691] 13 p1749 N88-20458

Ultrasonic characterization of non-uniform porosity distributions in SiC ceramic
[DE88-004814] 13 p1749 N88-20459

Interfacial chemistry-structure and fracture of ceramic composites
[DE88-005516] 13 p1750 N88-20461

PNL-1 improved ceramic composites through controlled fiber matrix interaction
[DE88-005680] 13 p1750 N88-20462

Abrasion and impact resistant coatings
[DE88-003562] 13 p1750 N88-20464

Advances in X-ray line profile analysis to determine microstructure information about ceramics
[DE88-003938] 13 p1750 N88-20465

Micromechanical and microstructural studies of ceramic superplasticity
[DE88-005793] 13 p1751 N88-20472

Recent developments in nondestructive evaluation for structural ceramics
[DE88-005889] 13 p1751 N88-20473

X-ray computed tomography for structural ceramic applications: Beam hardening corrections
[DE88-005891] 13 p1752 N88-20474

Processing of nanophase ceramics
[DE88-005985] 13 p1752 N88-20475

Theory and experiments of fracture in cyclic compression: Single phase ceramics, transforming ceramics and ceramic composites
[DE88-005792] 13 p1781 N88-20659
Fracture criteria for discontinuously reinforced metal matrix composites
[NASA-CR-182665] 13 p1782 N88-20662
Theoretical studies on the electronic structure and properties of complex ceramic crystals and glasses
[DE88-005837] 13 p1846 N88-21049
A hydroxycarbonate route to superconductor precursor powders
[DE88-003638] 13 p1846 N88-21052
ONR Far East Scientific Bulletin, volume 12, number 3, July-September 1987
[AD-A188554] 13 p1851 N88-21081
Fabric space radiators
[DE88-005569] 14 p1880 N88-21237
JPRS report: Science and technology. USSR: Materials science
[JPRS-UMS-87-009] 14 p1884 N88-21261
Crack resistance of multilayer ceramic-based composite material 14 p1885 N88-21265
A dense and strong ceramic material made from zirconium dioxide 14 p1886 N88-21274
Increasing the rate at which ceramic castings undergo preliminary heat-treatment in an ultra-high frequency magnetic field 14 p1886 N88-21275
Ceramic materials from preceramic organometallic copolymers
[DE88-006067] 14 p1892 N88-21301
Interface structure and properties of alumina/glass ceramic composites
[DE88-006219] 14 p1892 N88-21302
Processing, texture and mechanical properties of sintered silicon carbide
[NASA-TT-20253] 14 p1893 N88-21305
Effect of oxidation on strength and thermal stability of material based on Si3N4 14 p1896 N88-21319
Diffusion welding of aluminomagnesium alloys to ceramics 14 p1898 N88-21333
Interfacial structure-property relationships at the fiber-matrix interphase in advanced composites
[AD-A190649] 15 p2030 N88-22093
Specimen preparation techniques for the examination of ceramic and metal-matrix composites
[DE88-005157] 15 p2030 N88-22094
Thermal conductivity of oxide ceramics
[DE88-005842] 15 p2042 N88-22169
Ultrasonic characterization of ceramic joints
[DE88-005844] 15 p2043 N88-22173
Temperature-dependent conductivity of oxygen-depleted YBCO ceramics
[AD-A190340] 15 p2044 N88-22182
Transformation toughening of ceramics
[AD-A190399] 15 p2045 N88-22183
Stress corrosion of ceramic materials
[AD-A190501] 15 p2045 N88-22187
High-performance polymeric materials
[AD-A190708] 15 p2046 N88-22190
Strength and microstructure of ceramics
[AD-A190712] 15 p2046 N88-22191
High temperature corrosion of ceramics
[DE88-006567] 15 p2046 N88-22193
Hafnia-rich mixed oxide ceramics of the system HfO2-ZrO2-TiO2 for heaters and heat exchangers in electrothermal thrusters: The effects of titania on selected electrical and mechanical properties of Hafnia-rich mixed oxides in the system Hafnia-Zirconia-Titania, volume 1
[NASA-CR-182800-VOL-1] 15 p2047 N88-22197
Gamma-ray densitometry: Nondestructive analysis of density evolution during ceramic powder processing
[DE88-006671] 15 p2047 N88-22198
Melt processing ceramic YBa2Cu3O(sub 6.9)
[DE88-007039] 15 p2047 N88-22199
JPRS report: Science and technology. Japan
[JPRS-JST-88-002] 15 p2050 N88-22210
Compound ceramic processing
15 p2050 N88-22212
Hard ceramic film by laser PVD
15 p2051 N88-22216
Function of Japan Fine Ceramics Center described
15 p2052 N88-22227
JPRS report: Science and technology. Japan
[JPRS-JST-87-029] 15 p2052 N88-22228
Developments in ceramic superconducting materials
15 p2052 N88-22229
An evaluation of nondestructive methods for ceramic heat exchanger applications
[DE88-006731] 15 p2068 N88-22328
Monolithic ceramic analysis using the SCARE program
15 p2081 N88-22409
Whisker-reinforced ceramic composites for heat engine components 15 p2082 N88-22410
Nondestructive evaluation of sintered ceramics
15 p2083 N88-22416
Magnetic anomalies in the rare earth oxide superconductors GdBa2Cu3O(7-x) and YbBa2Cu3O(7-x)
[AD-A190713] 15 p2144 N88-22793
Synthesis and characterization of high-T(sub c) screen-printed Y-Ba-Cu-O films on alumina
[NASA-TM-100860] 15 p2146 N88-22805
Design and test of a new coaxial air joints
[DE88-751808] 16 p2164 N88-22908
JPRS report: Science and technology. USSR: Materials science
[JPRS-UMS-88-006] 16 p2179 N88-22988
Strength and cracking resistance of ceramics. Report 3: SiC ceramics 16 p2180 N88-22994
High-strength ceramic based on tetragonal ZrO2 with Al2O3 admixture 16 p2180 N88-22996
JPRS report: Science and technology. Japan
[JPRS-JST-87-026] 16 p2184 N88-23018
Government research on ceramics coating technology
16 p2184 N88-23019
Status, trends in research on internal combustion engines 16 p2185 N88-23027
Bimodular behavior and crack closure in compression in a brittle material
[AD-A191267] 16 p2224 N88-23275
Structural Ceramics
[NASA-CP-2427] 17 p2323 N88-23872
Ceramics for turbine engines
17 p2323 N88-23873
Friction and wear of ceramics
17 p2323 N88-23874
Some design considerations for ceramic components in heat engine applications 17 p2323 N88-23875
Nondestructive evaluation of structural ceramics
17 p2324 N88-23876
Fracture mechanics 17 p2324 N88-23877
Structural ceramics research
17 p2324 N88-23878
Nondestructive Evaluation (NDE) of structural ceramics by photoacoustic microscopy 17 p2325 N88-23884
Molten salt corrosion of SiC and Si3N4
17 p2325 N88-23885
Thermal cyclic durability testing of ceramic materials for turbine engines 17 p2325 N88-23886
Fractographic and microstructural evaluation of 3500-hour durability specimens
17 p2325 N88-23887
Polymer precursors for ceramic composites
17 p2326 N88-23890
Fabric radiators 17 p2427 N88-24435
Ceramic electrical insulator development for thermoelectric SACE power system
17 p2430 N88-24459
Apparatus for the measurement of resistivity of glasses and ceramics 17 p2431 N88-24460
Thrust chamber thermal barrier coating techniques
[NASA-TM-100933] 18 p2476 N88-24690
Role of cracks in the creep of structural polycrystalline ceramics
[AD-A191485] 18 p2490 N88-24770
Environmental effects on slow crack growth in silicon nitride
[DE88-007206] 18 p2494 N88-24795
The stress analysis of ceramic, polymeric, and metallic composite systems by the finite element method
18 p2529 N88-25004
Solid-state combustion synthesis of ceramics and alloys in reduced gravity
[NASA-CR-4163] 19 p2608 N88-25479
Metals and Ceramics Division
[DE88-008955] 19 p2618 N88-25530
Paramagnetic spins in oxygen-loaded ceramic La2CuO4/sub 4+delta/
[DE88-007114] 19 p2619 N88-25539
Assessment of opportunities for gas-fired sintering in the advanced ceramics and powdered metals industries
[PB88-197157] 19 p2620 N88-25545
Uniaxial tensile strain measurement for ceramic testing at elevated temperature: Requirements, problems and solutions
[DE88-008090] 19 p2621 N88-25550
An assessment of the state of the art in predicting the failure of ceramics
[DE88-008998] 19 p2621 N88-25551
JPRS report: Science and technology. Japan
[JPRS-JST-88-005] 19 p2633 N88-25619
Research and development programs on advanced structural ceramics in Korea 19 p2633 N88-25620
Ceramic substrates for semiconductor applications reported: AlN substrates 19 p2633 N88-25621
AlN substrate applications 19 p2634 N88-25622
Effect of a weak magnetic field on high temperature superconductivity in Y-Ba-Cu-O ceramics
[DE88-702192] 19 p2733 N88-26235
Application of electron microscopy for the analysis of the mechanical behavior of advanced ceramics
[DE88-005049] 20 p2777 N88-26469
A study of solvent effects on the synthesis of pure component and composite ceramic powders by metal alkoxide hydrolysis
[DE88-008381] 20 p2777 N88-26470
Observations on residual stresses in ceramic composites by neutron diffraction techniques
[DE88-009937] 20 p2778 N88-26472
Application of magnification xeroradiography to advanced ceramics
[DE88-009965] 20 p2778 N88-26473
Determination of binder distributions in green-state ceramics by NMR imaging
[DE88-009990] 20 p2778 N88-26474
The outlook for ceramics in heat engines, 1990-2010: Results of a worldwide Delphi survey
[DE88-010075] 20 p2778 N88-26475
Factors influencing the toughening behavior of whisker reinforced ceramics
[DE88-011396] 20 p2779 N88-26479
Fracture resistance of a TiB2 particle/SiC matrix composite at elevated temperature
[NASA-TM-100967] 20 p2779 N88-26482
Ceramic Technology for Advanced Heat Engines Program data base
[DE88-008954] 20 p2780 N88-26489
Characteristics of pressure loss during filtration using a porous ceramic filter
[DE88-752547] 20 p2798 N88-26604
Computational study on thermal efficiency of ceramic gas turbine
[DE88-753114] 20 p2809 N88-26667
Study on the heat resisting and cooling property of the ceramics-metal hybrid stator vanes
[DE88-753117] 20 p2810 N88-26668
Ceramic processing of high-T(sub)c superconductors
[DE88-010090] 20 p2878 N88-27087
Polymer-ceramic composites
[AD-A193244] 21 p2905 N88-27237
Studies in support of oxidation-resistant composite materials
[AD-A193320] 21 p2905 N88-27238
Theoretical and experimental analysis of the toughening behavior of whisker reinforcement in ceramic matrix composites
[DE88-011841] 21 p2906 N88-27241
Preparation and properties of new inorganic glasses and gel-derived solids
[AD-A192922] 21 p2917 N88-27315
Processing and additive effects of ZrO2 on microstructure and dielectric porperties of BaTiO3 ceramics
[AD-A193126] 21 p2917 N88-27316
Preparation and properties of high Q microwave dielectrics in the (CA, SR, BA) zirconate system
[AD-A193127] 21 p2918 N88-27317
Ceramic technology for advanced heat engines project
[DE88-008945] 21 p2919 N88-27323
Studies of dynamic contact of ceramics and alloys for advanced heat engines
[DE88-008996] 21 p2919 N88-27324
Effects of near interfacial microstructure on toughness and subcritical crack growth in ceramic/metal systems
[DE88-009842] 21 p2919 N88-27325
Data compilation for radiation damage on ceramic insulators. Revised with updated data and reviews
[DE88-753426] 21 p2920 N88-27329
Application of sol-gel procedures to ceramic composites
[ETN-88-92741] 21 p2921 N88-27338
Preparation and characterization of ceramic materials based on Al2O3 reinforced with a ZrO2 dispersion
[ISAL-87-0041] 21 p2922 N88-27340
Study of the friction and wear-related properties of ceramic superconductors
[DE88-011844] 21 p3024 N88-27950
Ceramic fabrication technology for high-T(sub)c materials
[DE88-012060] 21 p3024 N88-27953
The High Temperature Materials Laboratory: A new research and user facility at the Oak Ridge National Laboratory
[DE88-010792] 22 p3057 N88-28138
Modification of YBa2Cu3O(7-x) ceramics by adsorbed water and other gases
[DE88-011518] 22 p3057 N88-28140
Influence of dispersed additives reinforcement on the wear reinforcement mechanisms of the alumina-steel couple. Macroscopic and structural aspects
[ECL-88-01] 22 p3059 N88-28148
Optimization of nondestructive control of ceramic pieces for aeronautical turbines
[ETN-88-92684] 22 p3059 N88-28149

Development of sensors for ceramic components in advanced propulsion systems: Survey and evaluation of measurement techniques for temperature, strain and heat flux for ceramic components in advanced propulsion systems
[NASA-CR-182111] 22 p3081 N88-28299
Laser crystallized silicon films on alumina ceramic substrates and application to thin film c-Si solar cells
[PB88-131966] 22 p3116 N88-28515
Fabrication of bulk superconducting ceramics
[DE88-009956] 22 p3155 N88-28773
Ultrafine microstructure composites prepared by chemical vapor deposition
[AD-A193849] 23 p3189 N88-28973
A fundamental study of P/M processed elevated temperature aluminum alloys
[AD-A192958] 23 p3194 N88-29005
Stress corrosion of ceramic materials
[AD-A191979] 23 p3195 N88-29016
Wave and fracture phenomena in impacted ceramics
[AD-A192946] 23 p3196 N88-29020
Development of creep fracture modelling in ceramics
[PB88-202825] 23 p3196 N88-29021
The mechanical behavior of surface modified ceramics
[DE88-010564] 23 p3196 N88-29022
Sinterable ceramic powders from laser-heated gases
[AD-A194162] 23 p3197 N88-29024
The sol-gel synthesis of ceramics
[SNIAS-881-430-114] 23 p3199 N88-29037
Al2O3-TiO2 and Al2TiO5 ceramic materials
[SNIAS-881-430-122] 23 p3199 N88-29038
Boron-containing organosilane polymers and ceramic materials thereof
[NASA-CASE-ARC-11649-1-SB]
23 p3199 N88-29040
Development of planar geometry solid oxide fuel cell technology, phase 1
[PB88-210356] 23 p3229 N88-29215
Electron microscopy of ceramic superconductors
[DE88-006446] 23 p3288 N88-29580
Fluctuations of order parameters in the high T(sub c) superconductors
[DE88-702549] 23 p3292 N88-29603
A study of the critical factors controlling the synthesis of ceramic matrix composites from preceramic polymers
[AD-A195405] 24 p3340 N88-29881
Processing technology research in composites
[AD-A195693] 24 p3341 N88-29890
Polymer-ceramic composites
[AD-A195789] 24 p3356 N88-29983
Piezoelectric and electrostrictive materials for transducer applications, volume 1
[AD-A194957] 24 p3374 N88-30096

CEREBELLUM
Growth and differentiation of cells in organotypical rat embryo cerebellar culture developing in weightlessness
19 p2703 N88-26076

CEREBRAL CORTEX
Change in functional activity of cortical brain structures and their blood supply in alert rabbits in response to rocking 04 p0473 N88-12916
Large-scale neuronal circuits for selective storage and recognition of complex stimuli, a pilot study
[AD-A184134] 04 p0474 N88-12920
Sleep induced in cat by electric stimulation of acoustic and motor areas in brain cortex
06 p0751 N88-14612
Karyometric evaluation of neuronal reactions of rat cerebral cortex to the combined effect of ionizing radiation, longitudinal accelerations and vibration
07 p0890 N88-15396
Retinotopic mapping of the human visual system with magnetoencephalography
[AD-A189557] 13 p1810 N88-20811
A systems engineering based methodology for analyzing human electrocortical responses
[AD-A190809] 18 p2550 N88-25135
Growth and differentiation of cells in organotypical rat embryo cerebellar culture developing in weightlessness
19 p2703 N88-26076
Method for observing changes in functional state of human operator 20 p2830 N88-26789

CEREBROSPINAL FLUID
Evaluation of spare room in cerebrospinal system using noninvasive methods 10 p1361 N88-18137

CEREBRUM
NT CEREBRAL CORTEX
Studies of the processing of single words using positron tomographic measures of cerebral blood flow change
[AD-A184058] 03 p0356 N88-12244
Models of cerebral-body perfusion and cerebral chemical transport
[AD-A194945] 24 p3407 N88-30283

CERENKOV COUNTERS
A program to study antiprotons in the cosmic rays: Arizona collaboration
[NASA-CR-180702] 01 p0120 N88-10764
The application of an image intensifier to atmospheric Cerenkov gamma ray astronomy
[MPE-PREPRINT-115] 22 p3163 N88-28839

CERENKOV EFFECT
U CERENKOV RADIATION

CERENKOV RADIATION
Cerenkov radiation field analysis due to a passing electron beam
[AD-A184870] 05 p0649 N88-13976
Energy distribution of Cerenkov radiation for finite frequency intervals
[AD-A186901] 09 p1244 N88-17454
An analysis of whistler-mode radiation from the Spacelab-2 electron beam, revision
[AD-A188228] 11 p1552 N88-19287
The application of imaging to the atmospheric Cerenkov technique: Observations of the Crab nebula
20 p2884 N88-27126
Effects of charge distribution within a particle beam on the sub-Cerenkov radiation
[AD-A193992] 22 p3150 N88-28742
Diffraction transition radiation from periodic electron bunches
[AD-A193593] 23 p3280 N88-29528

CERIUM
Gas tungsten arc welding of Al-10Fe-5Ce
[AD-A184202] 03 p0334 N88-12104

CERIUM COMPOUNDS
NT CERIUM OXIDES
Heavy Fermions and coherence in Kondo lattices: Specific heat of low energy excitation in Cer systems
[ETN-88-91080] 09 p1255 N88-17525
Electron Spin Resonance (ESR) measurements on intermediate-valence Cer compounds doped with paramagnetic ions: CeOs2:Gd ion and CePd3:Mn-ion
[ETN-88-91081] 09 p1256 N88-17526
Coexisting static magnetic ordering and superconductivity in CeCu2.1Si2 found by muon spin relaxation 17 p2396 N88-24245
Static magnetic ordering of CeCu2.1Si2 found by muon spin relaxation 17 p2396 N88-24246

CERIUM OXIDES
Thermodynamic and conductivity studies of nonstoichiometric cerium dioxide by Coulometric titration: A simultaneous measurement
[DE88-003054] 08 p1091 N88-16566

CERMETS
Internal reforming development for solid oxide fuel cells
[DE87-006518] 04 p0464 N88-12871
Cermet-fueled reactors for advanced space applications
[DE88-005528] 13 p1839 N88-21002
Molybdenum-base cermet fuel development
[DE88-005529] 13 p1839 N88-21003
Technical applications of solar energy. Project: Selective coatings
[BMFT-FB-T-86-213] 14 p1943 N88-21591
Direct conversion of solar energy to thermal energy
[BMFT-FB-T-86-220] 14 p1943 N88-21592
Cermet fuel thermal conductivity
17 p2410 N88-24329
Molybdenum-base cermet fuel development
17 p2434 N88-24481

CERTIFICATION
Computerized certification of digital ultrasonic instrumentation
[DE88-000820] 04 p0488 N88-13008
Airworthiness considerations
10 p1276 N88-17636
Utility NDE personnel qualification/certification: Enhanced personnel qualification requirements for ASME (American Society for Mechanical Engineers) Code Section 11 examinations
[DE88-006748] 16 p2216 N88-23222
Laminar Flow Aircraft Certification
[NASA-CP-2413] 17 p2296 N88-23737
Certification aspects of airplanes which may operate with significant natural laminar flow 17 p2298 N88-23749
US civil airmen statistics, 1987
[AD-A191714] 18 p2455 N88-24577
Calibration of averaging total pressure flight wake rake and natural-laminar-flow airfoil drag certification
[NASA-CR-181630] 19 p2599 N88-25443
Zero/zero rotorcraft certification issues. Volume 1: Executive summary
[NASA-CR-177483-VOL-1] 19 p2602 N88-25453
Zero/zero rotorcraft certification issues. Volume 2: Plenary session presentations
[NASA-CR-177483-VOL-2] 19 p2602 N88-25454
Zero/zero rotorcraft certification issues. Volume 3: Working group results
[NASA-CR-177483-VOL-3] 19 p2602 N88-25455
Materials qualification in oceanology and the offshore industry 19 p2700 N88-26050
The design and testing of aero engines to minimise hazard from birds
[PNR90436] 22 p3040 N88-28049

CESIUM
Coverage dependence of adsorbate-substrate bond lengths: Chlorine and caesium adsorbed on silver single crystals
[PB87-125142] 06 p0788 N88-14833
Atomic clocks research. An overview
[AD-A185567] 07 p0930 N88-15648
Arcs in cesium seeded noble gases resulting from a magnetically induced electric field
[EUT-87-E-177] 13 p1843 N88-21028
Theoretical studies of Resonance Enhanced Stimulated Raman Scattering (RESRS) of frequency doubled Alexandrite laser wavelength in cesium vapor
[NASA-CR-182871] 17 p2317 N88-23841

CESIUM COMPOUNDS
NT CESIUM IODIDES
Suppression of the mass enhancement in CeB6 in high magnetic fields
[DE88-002946] 09 p1241 N88-17439

CESIUM HALIDES
NT CESIUM IODIDES

CESIUM IODIDES
Heterogeneous isotope exchange between solid cesium iodide and gaseous methyl iodide
[ETN-88-91085] 09 p1141 N88-16840

CESIUM IONS
Photoionization of atoms and ions: Application of time-dependent response method within the density functional theory
[AD-A185686] 07 p0930 N88-15649

CESIUM PLASMA
Electron temperature measurements in an argon/cesium plasma diode
[AD-A188835] 12 p1695 N88-20141

CESSNA MILITARY AIRCRAFT
U MILITARY AIRCRAFT

CETANE
Cetane scale evaluation and possible modification
[AD-A189730] 15 p2048 N88-22200
Diesel combustion fundamentals, phase 1, volume 1
[AD-A193831] 22 p3052 N88-28107

CEYLON
U SRI LANKA

CFRP
U CARBON FIBER REINFORCED PLASTICS

CH-113 HELICOPTER
U CH-46 HELICOPTER

CH-46 HELICOPTER
An independent evaluation of the CH-46 Safety Reliability and Maintainability Program (SR and M)
[AD-A186310] 07 p0817 N88-14971

CHAD
Using space photography of the Earth in the classroom: Drought in Africa
[NASA-CR-182948] 19 p2685 N88-25960

CHAINS
Trajectory control of robot manipulators with closed-kinematic chain mechanism
[NASA-TM-89305] 05 p0591 N88-13605
The Shock and Vibration Digest, Volume 19, No. 12
05 p0610 N88-13746
Dynamics of cables and chains
05 p0610 N88-13747
Distribution of chain ends inside the polybutadiene microspheres of SB diblock copolymers
[AD-A191257] 16 p2182 N88-23007
Kinematics, dynamics and control of a closed chain mechanism manipulator 18 p2523 N88-24967
Analysis of a closed-kinematic chain robot manipulator
[NASA-CR-183031] 18 p2561 N88-25206
Spatial organization of homopolymer chains inside spherical polybutadiene domains of SB diblock copolymers
[AD-A193390] 21 p2918 N88-27321

CHAIRS
U SEATS

CHALCOGENIDES
NT ALKALINE EARTH OXIDES
NT ALUMINUM OXIDES
NT ANHYDRIDES
NT BARIUM OXIDES
NT BERYLLIUM OXIDES
NT BISMUTH OXIDES
NT BISMUTH SULFIDES
NT BORON OXIDES
NT CADMIUM SELENIDES
NT CADMIUM SULFIDES
NT CADMIUM TELLURIDES

NT CALCIUM OXIDES
NT CARBON DIOXIDE
NT CARBON MONOXIDE
NT CERIUM OXIDES
NT CHROMIUM OXIDES
NT COBALT OXIDES
NT COPPER OXIDES
NT COPPER SELENIDES
NT COPPER SULFIDES
NT DIOXIDES
NT DISULFIDES
NT HAFNIUM OXIDES
NT HEMATITE
NT HYDROGEN PEROXIDE
NT HYDROGEN SULFIDE
NT IRON OXIDES
NT LANTHANUM OXIDES
NT LANTHANUM TELLURIDES
NT LEAD OXIDES
NT LEAD SULFIDES
NT LEAD TELLURIDES
NT LITHIUM OXIDES
NT MAGNESIUM OXIDES
NT MANGANESE OXIDES
NT MERCURY TELLURIDES
NT METAL OXIDES
NT MOLYBDENUM DISULFIDES
NT MOLYBDENUM OXIDES
NT MOLYBDENUM SULFIDES
NT NICKEL OXIDES
NT NIOBIUM OXIDES
NT NITROGEN DIOXIDE
NT NITROGEN OXIDES
NT NITROUS OXIDES
NT OXIDES
NT PEROXIDES
NT POLYSULFIDES
NT PYRITES
NT QUARTZ
NT RUTILE
NT SAPPHIRE
NT SELENIDES
NT SILICON DIOXIDE
NT SILICON OXIDES
NT SULFIDES
NT SULFUR DIOXIDES
NT TANTALUM OXIDES
NT TIN OXIDES
NT TIN TELLURIDES
NT TITANIUM OXIDES
NT VANADIUM OXIDES
NT YTTRIUM OXIDES
NT ZINC OXIDES
NT ZINC SELENIDES
NT ZINC SULFIDES
NT ZINC TELLURIDES
NT ZIRCONIUM OXIDES
Photoinduced low-temperature changes in optical losses in fiber optics based on chalcogenide glasses
06 p0770 N88-14731

CHALLENGER (ORBITER)
Structural analysis of a bolted joint concept for the space shuttle's solid rocket motor casing
[NASA-TM-89092] 04 p0407 N88-12531
Space shuttle accident: NASA's actions to address the Presidential Commission report
[PB88-135306] 15 p2024 N88-22059

CHANCE-VOUGHT MILITARY AIRCRAFT
U MILITARY AIRCRAFT

CHANGE DETECTION
High polymer sensor materials discussed
06 p0676 N88-14140
Real-time image difference detection using a polarization rotation spacial light modulator
[NASA-CASE-NPO-17144-1-CU]
18 p2576 N88-25305
Monitoring urban land cover changes at the urban fringe from SPOT HRV imagery in south-east England
22 p3099 N88-28406

CHANNEL CAPACITY
Coding for spread-spectrum communications networks
[AD-A185667] 07 p0844 N88-15119
Information and coding capacities of mismatched Gaussian channels
[AD-A190321] 15 p2124 N88-22665
Coding capacity of generalized additive channels
[AD-A190315] 15 p2127 N88-22685
Information capacity of Gaussian channels
[AD-A190316] 15 p2127 N88-22686
Conditions for information capacity of the discrete-time Gaussian channel to be increased by feedback
[AD-A190317] 15 p2127 N88-22687
Coding capacity of discrete-time Gaussian and non-Gaussian channels
[AD-A190318] 15 p2127 N88-22688
On the capacity of channels with unknown interference
[AD-A191160] 16 p2191 N88-23067
Communications using channels formed by meteor bursts
[AD-A192088] 18 p2501 N88-24834
Information and stochastic systems
[AD-A192167] 18 p2501 N88-24838
Evaluation of CDMA system capacity for mobile satellite system applications 19 p2651 N88-25740

CHANNEL FLOW
NT OPEN CHANNEL FLOW
Reynolds number effects on the small scale structure of a turbulent channel flow 01 p0001 N88-10004
MHD (magnetohydrodynamics) channel development
[DE87-014126] 02 p0237 N88-11498
Structural characteristics of dean vortices in a curved channel
[AD-A184724] 03 p0320 N88-12024
The design and preliminary calibration of a boundary-layer flow channel
[NASA-CR-178399] 04 p0394 N88-12457
A numerical investigation on wing/nacelle interferences 05 p0535 N88-13258
High resolution simulation of turbulent flow in a channel
[AD-A186022] 07 p0848 N88-15150
Reynolds-stress and dissipation rate budgets in a turbulent channel flow
[NASA-TM-89451] 07 p0852 N88-15174
Numerical simulation of heat transfer turbulence, volume 2
[AD-A185130] 08 p0983 N88-15947
Numerical simulation of turbulent spots in channel and boundary layer flows 08 p0983 N88-15948
Weak interactions and local order in strong turbulence
09 p1159 N88-16948
Numerical and physical aspects of large eddy simulation of turbulent flows
[ETN-88-91611] 09 p1162 N88-16965
Use of boundary-layer method for problem of sound propagation through channel with variable cross-section containing stream of fluid 09 p1233 N88-17396
Instability and transition in curved channel flow
10 p1328 N88-17938
Wavenumber - frequency structure of turbulent flow in a channel from a direct simulation
[AD-A189079] 12 p1627 N88-19737
Investigation of supersonic chemically reacting and radiating channel flow
[NASA-CR-182726] 14 p1862 N88-21125
Stochastic estimation of conditional eddies in turbulent channel flow 16 p2194 N88-23087
Self similarity of two point correlations in wall bounded turbulent flows 16 p2195 N88-23089
Ejection mechanisms in the sublayer of a turbulent channel 16 p2195 N88-23090
Modeling scalar flux and the energy and dissipation equations 16 p2196 N88-23096
Modeling of turbulent transport as a volume process
16 p2196 N88-23099
On local approximations of the pressure-strain term in turbulence models 16 p2197 N88-23102
Test code for the assessment and improvement of Reynolds stress models 16 p2197 N88-23105
Shear-layer structures in near-wall turbulence
16 p2198 N88-23110
Conditionally-averaged structures in wall-bounded turbulent flows 16 p2198 N88-23112
Active layer model for wall-bounded turbulence
16 p2199 N88-23115
A variational finite element method for three-dimensional, steady, compressible, viscous flows
18 p2512 N88-24904
Theoretical analysis of laminar incompressible flow in slender channels
[VTH-LR-517] 18 p2513 N88-24909
Numerical simulation studies of laminar-turbulent transition in the plan channel 19 p2665 N88-25850
Computational boundary conditions for the incompressible Navier-Stokes equations in channels and pipes
[AD-A193356] 21 p2944 N88-27487
Unsteady water channel
[AD-A194231] 23 p3171 N88-28884
Computation of the eigenvalues for perturbations of Poiseuille flow using a two-point boundary value method
[AD-A193479] 23 p3210 N88-29104
The strong nonlinear interaction of Tollmien-Schlichting waves and Taylor-Goertler vortices in curved channel flow
[NASA-CR-181697] 24 p3311 N88-29716
On the generation of mean flows by the interaction of Goertler vortices and Tollmien-Schlichting waves in curved channel flows
[NASA-CR-181690] 24 p3315 N88-29743

CHANNEL NOISE
Performance analysis of coded frequency-hopped spread-spectrum systems with unknown interference
[AD-A186069] 07 p0841 N88-15103
Information capacity of Gaussian channels
[AD-A190316] 15 p2127 N88-22686
An algorithm for random access communication over a noisy channel
[AD-A191315] 16 p2252 N88-23461
Outliner resistant filtering and smoothing: 2D version
[AD-A193319] 21 p3012 N88-27874

CHANNELS
Channeling and dechanneling at high energy
[DE88-003989] 11 p1548 N88-19259
Pre-launch calibration of channels 1 and 2 of the advanced very high resolution radiometer
[PB88-157169] 14 p1913 N88-21427
A study of a meteor burst communication system
21 p2934 N88-27421

CHANNELS (DATA TRANSMISSION)
Test equipment with fiber optic data bus and laser gyro strapdown system LTN-90 for the helicopter BO-105
[ESA-TT-1038] 01 p0005 N88-10025
Digital bus unit engineering model: Design, manufacture and test
[MRM/TREP/1003/SAAB] 01 [illegible]0083 N88-10537
An evaluation plan of bus architectures and protocols using the NASA Ames intelligent redundant actuation system
[NASA-CR-177458] 04 p0398 N88-12482
Design of source coders and joint source/channel coders for noisy channels
[NASA-CR-181547] 04 p0432 N88-12678
Increased gain of channel intensifier tubes by pulsed biasing
[DE88-000512] 04 p0490 N88-13019
An exact analysis and performance of framed ALOHA with capture
[AD-A185006] 05 p0574 N88-13500
Channel access protocols for multihop packet radio networks
[AD-A186074] 07 p0842 N88-15105
Coding for spread-spectrum communications networks
[AD-A185667] 07 p0844 N88-15119
High performance data buses: Progress and evolution
[DE88-002570] 09 p1215 N88-17285
Multiple-bus interconnection for future multiprocessor systems 10 p1375 N88-18203
Experiences with serial and parallel algorithms for channel routing using simulated annealing
[NASA-CR-182530] 10 p1388 N88-18289
Air Force Institute of Technology (AFIT) Local Area Network (LAN) performance evaluation model: An analytic model for assessing the impact of changing LAN hardware and software configurations
[AD-A187191] 11 p1469 N88-18764
An application of dimensionless Eigenvalues to underwater acoustic ducts
[AD-A188167] 11 p1542 N88-19219
DATAC bus monitor 17 p2294 N88-23721
Design for interoperability (interchangeability)
17 p2305 N88-23789
Communications using channels formed by meteor bursts
[AD-A192088] 18 p2501 N88-24834
Selection and effects of channels in distributed communication and decision making tasks: A theoretical review and a proposed research paradigm
[AD-A191807] 18 p2587 N88-25375
A study on the co- and adjacent channel protection requirements for mobile satellite ACSSB modulation
19 p2650 N88-25732
Development of a maintenance data bus monitor and recorder 22 p3036 N88-28022
Interface techniques and systems for standard aircraft data buses 22 p3036 N88-28028
Multichannel data transmission through a fiber optic cable
[AD-A193842] 22 p3070 N88-28221
Coding for meteor-burst communications channel and side information for channels with block-interference
23 p3202 N88-29054
Optics and symbolic computing
[AD-A195119] 24 p3360 N88-30004
Performance of DS/SSMA communications in impulsive channels. Part 1: Correlation receivers
[AD-A195712] 24 p3362 N88-30021

CHAOS
Dimension densities for turbulent systems with spatially decaying correlation functions
[DE87-010119] 02 p0169 N88-11066
IR laser excitation in molecules: Chaos and diffusive energy growth
[DE87-013147] 02 p0178 N88-11105

Quantum-mechanical aspects of classically chaotic driven systems
[DE87-013152] 02 p0178 N88-11106
Special Course on Modern Theoretical and Experimental Approaches to Turbulent Flow Structure and its Modelling
[AGARD-R-755] 03 p0312 N88-11970
Dynamics and routes to chaos from quasiperiodicity
03 p0312 N88-11974
A deterministic approach to turbulence: Chaos in Rayleigh-Benard convection 03 p0313 N88-11975
Determination of fractal dimension, connection of space and temporal chaos and application to experimental results 03 p0313 N88-11977
Fully developed turbulence via Feigenbaum's period-doubling bifurcations
[DE88-000242] 04 p0441 N88-12739
Supertracks: The building blocks of chaos
[DE88-001513] 04 p0522 N88-13207
Chaos: Chto Delat? (What is to be done?)
[DE88-000513] 05 p0643 N88-13933
Theoretical investigations of chaotic dynamics
[AD-A186404] 07 p0867 N88-15261
Studies of nonlinear and chaotic phenomena in solid state systems
[DE88-002330] 09 p1254 N88-17515
Instabilities and chaos in a multimode, standing-wave, CW dye laser
[DE88-005028] 10 p1337 N88-17993
Travelling waves and chaos in double-diffusive convection 11 p1484 N88-18857
Chaos, mappings and spatial complexity in fluids
11 p1484 N88-18860
Relative chaos in stellar systems
[DE88-700148] 12 p1710 N88-20234
Stochastic and chaotic oscillations
[CWI-AM-R8704] 13 p1829 N88-20940
Chaotic diffusion across magnetic field in a model of electrostatic turbulent plasma
[PREPRINT-566] 14 p1965 N88-21839
Electrical resistivity as quantum chaos
[DE88-007026] 16 p2284 N88-23675
Application of chaos theory to 1/f noise
[AD-A191150] 17 p2334 N88-23935
Stationary, wave type, and chaos type convection in spherical symmetry geometries
[ETN-88-92358] 20 p2801 N88-26625
Coupled experimental and theoretical investigations of instability, chaos and turbulence in an axisymmetric jet flow
[AD-A192943] 21 p2942 N88-27476
Statistical description of stochastic dynamics
[AD-A192924] 21 p3009 N88-27852
Regular and chaotic motion of fluid particles in a two dimensional fluid
[PREPRINT-591] 22 p3078 N88-28278
Vortex dynamics of coherent and chaotic structures (including algorithms for computer simulations and diagnosis)
[AD-A193580] 23 p3212 N88-29117
Chaotic behaviour in quantum dynamics
[AD-A193936] 23 p3295 N88-29623
Pierce diode with external circuit. Part 3: Chaotic behavior
[AD-A194837] 24 p3365 N88-30041

CHAOTIC CLOUD PATTERNS
U CLOUDS (METEOROLOGY)

CHAPMAN SHEAR LAYER
U SHEAR LAYERS

CHAPMAN-JOUGET FLAME
U CHEMICAL EQUILIBRIUM
U DETONATION
U FLAME PROPAGATION

CHARACTER RECOGNITION
Application of new technologies to DTIC document processing
[AD-A189778] 15 p2148 N88-22823

CHARACTERISTIC EQUATIONS
U EIGENVALUES
U EIGENVECTORS

CHARACTERISTIC FUNCTIONS
U EIGENVALUES
U EIGENVECTORS

CHARACTERISTIC METHOD
U METHOD OF CHARACTERISTICS

CHARACTERIZATION
Mechanical properties characterization of composite sandwich materials intended for space antenna applications
[NASA-TM-88893] 01 p0020 N88-10121
Elevated temperature strain gages
02 p0184 N88-11144
Characterization and thermal conductivity of hot-pressed silicon carbide
[DKG-25] 03 p0292 N88-11834
Synthesis and characterization of block copolymers
[AD-A184405] 03 p0295 N88-11855
Perturbation and characterization of nonlinear processes
[DE87-014580] 03 p0369 N88-12322
The characterization of diagnostic tasks for engineering systems
[DE88-000093] 04 p0483 N88-12973
Molecular-level synthesis and characterization of metal-polymer interfaces
[AD-A184956] 05 p0567 N88-13455
Characterization of the microstructures of various materials
[AD-A184961] 05 p0655 N88-14017
Study of damage in carbon fiber-epoxy composite materials. Utilization to assess broken specimens
[DCQ/L-45-650/F] 06 p0678 N88-14152
Design, production, and characterization of broadband optical waveguides
[DFVLR-FB-85-52] 06 p0780 N88-14791
Characterization of meteorological phenomena influencing aircraft operations 08 p0951 N88-15772
Study of selection criteria for adhesives used in aircraft structure bonding
[ETN-88-91619] 08 p0971 N88-15875
Comparison of UNL laser imaging and sizing system and a phase/Doppler system for analyzing sprays from a NASA nozzle
[NASA-CR-182437] 09 p1161 N88-16956
System characterization in nonlinear random vibration
09 p1180 N88-17071
Fracture mechanics characterization of crack growth under creep and fatigue conditions
[W-2/87] 09 p1183 N88-17087
Automatic prober for the dc characterization of gallium arsenide devices. Part 1: The measurement facility
[AD-A187583] 11 p1560 N88-19337
Preparation and characterization of thin films of alumina by metalorganic chemical vapor deposition
[AD-A188366] 12 p1608 N88-19614
Development of a CCD characterization system
[INPE-4361-TDL/301] 12 p1623 N88-19712
Microstructure characterization with a pulsed laser ultrasonic source
[DE88-005207] 12 p1632 N88-19766
The synthesis, characterization and structural studies of In(C5H4Me) by X-ray diffraction and electron diffraction techniques and a reinvestigation of the crystaline state of In(C5H5) by X-ray diffraction studies
[AD-A189110] 13 p1844 N88-21038
Fracture toughness characterization of SA508 and Sa533B RPB steels
[CISE-3906] 14 p1889 N88-21292
Research relative to angular distribution of snow reflectance/snow cover characterization and microwave emission
[NASA-CR-182733] 14 p1941 N88-21582
Fabrication and characterization of semiconductor lasers of Pb(1-x)Sn(x)Te
[INPE-4253-PRE/1126] 15 p2072 N88-22357
Spectrum fatigue testing for materials characterization
[VTT-RR-502] 15 p2088 N88-22443
Synthesis and characterization of high-T(sub c) screen-printed Y-Ba-Cu-O films on alumina
[NASA-TM-100860] 15 p2146 N88-22805
Characterization of precipitates in a niobium-zirconium-carbon alloy
[NASA-TM-100848] 16 p2178 N88-22981
The integration, characterisation and trialling of a modern complex airborne radar 17 p2305 N88-23791
Mechanical and structural characterization of aluminum ceramic fibers
[ETN-88-92168] 17 p2323 N88-23870
High frequency ultrasonic characterization of sintered SiC
[NASA-TM-100825] 17 p2347 N88-23985
Aircraft emissions characterization: TF41-A2, TF30-P103 and TF30-P109 engines
[AD-A192053] 18 p2466 N88-24638
Elementary characterization of preimpregnated carbon epoxy T400H/DA0506 from STRUCTIL. Test report M6-577100
[CEAT-047426] 18 p2478 N88-24703
Characterization of a 30-GHz IMPATT solid state amplifier
[NASA-TM-100876] 18 p2503 N88-24847
A characteristic method for calculating the generalized flat flutter aerodynamic forces
[NASA-TT-20300] 19 p2598 N88-25438
GTAW characterization for weld penetration on 304L stainless steel
[DE88-010611] 20 p2810 N88-26672
Techniques for characterizing damage zones in composite materials 21 p2905 N88-27240
Preparation and characterization of ceramic materials based on Al2O3 reinforced with a ZrO2 dispersion
[ISAL-87-0041] 21 p2922 N88-27340

CHARACTERS
U SYMBOLS

CHARGE CARRIERS
NT FREE ELECTRONS
NT HOLES (ELECTRON DEFICIENCIES)
NT MINORITY CARRIERS
The role of hydrogen in radiation-induced defect formation in polysilicon gate MOS devices
[DE87-012374] 06 p0785 N88-14814
Improving the method of calculating electronic properties of narrow bandgap semiconductors
07 p0926 N88-15627
Interpretation of the temperature dependence of conductivity in superconducting oxides
[DE88-003028] 08 p1091 N88-16565
Growth of HgZnTe layers by LPE technique
[AD-A186723] 09 p1255 N88-17520
Electronic structure, charge transfer excitations and high temperature superconductivity
[DE88-003096] 10 p1416 N88-18453
New method of examining micrononhomogeneity of local centers in high-resistivity semiconductor materials under scanning electron microscope 14 p1969 N88-21754
Free carrier nonlinear optics 14 p1977 N88-21796
Breathing mode lattice relaxation associated with carrier emission and capture by deep electronic levels in silicon
[DE88-003844] 14 p1985 N88-21842
Calculating depletion region carrier concentrations with capacitance-voltage measurements and etching
[AD-A189630] 15 p2141 N88-22777
Radiation effects in silicon
[DE88-006642] 16 p2282 N88-23659
Systematic variation of magnetic-field penetration depth in high-T(c) superconductors studied by muon spin relaxation 17 p2396 N88-24243
Picosecond optoelectronic sampling of electrical waveforms produced by an optically excited field effect transistor
[AD-A192384] 21 p2935 N88-27428
A study of electronic transport and breakdown in SiO2
[AD-A194258] 22 p3156 N88-28780

CHARGE COUPLED DEVICES
Photon counting image sensor development for astronomical applications
[NASA-CR-181507] 05 p0660 N88-14049
Vertical charge transport in junction charge-coupled devices
[ETN-88-91613] 09 p1255 N88-17523
New generation imager system
[NASA-CR-180464] 10 p1408 N88-18398
Development of a CCD characterization system
[INPE-4361-TDL/301] 12 p1623 N88-19712
Cramer-Rao bounds on the accuracy of location and velocity estimations using CCD optical sensors
[AD-A188481] 12 p1629 N88-19748
ROVER: A prototype active vision system
[AD-A189246] 15 p2133 N88-22722
Space-variant optical systems
[AD-A189967] 15 p2133 N88-22724
An investigation into the precision of a digital camera
[B8735054] 16 p2210 N88-23193
Users guide to CAESAR
[BCRS-87-04] 16 p2226 N88-23306
Novel silicon Schottky barrier infrared imaging arrays
17 p2439 N88-24510
Simple high speed camera with CCD-sensor
[MPIS-8/1987] 18 p2518 N88-24940
The FEL CCD-camera: Experimental system for camera and image processing research
[FEL-1987-34] 21 p2952 N88-27532
Satellite attitude determination using a CCD (Charge-Coupled-Device) star camera
[AD-A192662] 22 p3046 N88-28080
Array detectors for plasma spectrochemistry
[AD-A194220] 22 p3052 N88-28105
Molecular fluorescence measurements with a charge-coupled device detector
[AD-A194221] 22 p3080 N88-28291
High performance charge transfer device detectors
[AD-A194409] 23 p3192 N88-28993
Molecular fluorescence measurements with a charge-coupled device detector
[AD-A194437] 23 p3216 N88-29141

CHARGE DISTRIBUTION
The physics of charge separation preceding lightning strokes in thunderclouds
[NASA-CR-178371] 01 p0071 N88-10452
Capacitive charge division in centroid finding cathode readouts in MWPCs
[DE88-003545] 10 p1333 N88-17969
Application of ECR ion source beams in atomic physics
[DE88-003767] 10 p1406 N88-18384

Electron current effect on stability of plasma channel
16 p2276 N88-23825
Measurements of Z(sub eff) profile with a visible bremsstrahlung continuum detector array
17 p2443 N88-24529
The electrokinetic behavior of calcium oxalate monohydrate in macromolecular solutions
[NASA-TM-101144] 18 p2493 N88-24791
Analysis of lightning field changes during active thunderstorms in Florida 18 p2545 N88-25103
Effects of charge distribution within a particle beam on the sub-Cerenkov radiation
[AD-A193992] 22 p3150 N88-28742
Nuclear and ionic charge distribution experiment on ISEE-1 and ISEE-3
[NASA-CR-180776] 23 p3183 N88-28947
Charge composition of primary cosmic ray nuclei with z greater than or equal to 2 in energy region greater than or equal to 2 TeV 24 p3448 N88-30519

CHARGE EFFICIENCY
Real time charge efficiency monitoring for nickel electrodes in NICD and NIH2 cells
02 p0165 N88-11038
Nickel hydrogen cell positive-electrode studies: Cobalt segregation in reducing environments
[AD-A193025] 20 p2796 N88-26587
Computer controlled procedures for traction battery power performance tests
[ETN-88-92352] 20 p2796 N88-26589
Results from life test in progress on eagle-picher nickel cadmium cells
[AD-A192815] 21 p2936 N88-27434

CHARGE EXCHANGE
NT RESONANCE CHARGE EXCHANGE
Interpretation of the temperature dependence of conductivity in superconducting oxides
[DE88-003028] 08 p1091 N88-16565
Modeling considerations for selected rf-plasma edge effects
[DE88-003285] 09 p1252 N88-17500
Charge exchange in low energy (keV) and hyperthermal energy (10-100 eV) ion scattering
[AD-A187643] 11 p1543 N88-19222
Pion nucleus single charge exchange reactions above the delta(1232) resonance
[LA-11004-T] 11 p1544 N88-19231
Ion temperature profile measurement using charge exchange recombination spectroscopy on JIPP T-IIU
17 p2440 N88-24518
Spectroscopic measurements of ion temperature, rotation speed and beam deposition profile on DIII-D
17 p2440 N88-24519
Spectroscopic study of heliotron E plasmas: Stark profile, CXP, poloidal rotation and carbon coating
17 p2441 N88-24523

CHARGE SEPARATION
U POLARIZATION (CHARGE SEPARATION)

CHARGE TRANSFER
Synthesis, NMR characterization and electrical properties of siloxane-based polymer electrolytes
[AD-A184184] 04 p0418 N88-12596
Final (n,l) state-resolved electron capture by multiply charged ions from neutral atoms
[IPPJ-AM-54] 04 p0492 N88-13030
Comparison of 2D memory SEU transport simulation with experiments
[ATR-88(8139)-2-REV-A] 05 p0656 N88-14025
Vertical charge transport in junction charge-coupled devices
[ETN-88-91613] 09 p1255 N88-17523
Electronic structure, charge transfer excitations and high temperature superconductivity
[DE88-003096] 10 p1416 N88-18453
Mode priming in an overmoded gyrotron oscillator
[AD-A189151] 13 p1772 N88-20602
Characteristics of the positive lighting flash
[DE88-005854] 13 p1800 N88-20760
The kinetics of charge-transfer reactions on passive lithium electrodes
[DE88-009256] 21 p2939 N88-27454
Array detectors for plasma spectrochemistry
[AD-A194220] 22 p3052 N88-28105
Molecular fluorescence measurements with a charge-coupled device detector
[AD-A194221] 22 p3080 N88-28291
Applications of charge transfer devices in spectroscopy
[AD-A194408] 23 p3192 N88-28992

CHARGE TRANSFER DEVICES
NT CHARGE COUPLED DEVICES
Applications of charge transfer devices in spectroscopy
[AD-A194408] 23 p3192 N88-28992
High performance charge transfer device detectors
[AD-A194409] 23 p3192 N88-28993

CHARGED PARTICLES
NT ALPHA PARTICLES
NT ANTIPROTONS
NT ARGON PLASMA
NT BETA PARTICLES
NT BOUNDARY LAYER PLASMAS
NT CESIUM PLASMA
NT COLD PLASMAS
NT COLLISIONAL PLASMAS
NT COLLISIONLESS PLASMAS
NT CONDUCTION ELECTRONS
NT COSMIC PLASMA
NT CYLINDRICAL PLASMAS
NT DENSE PLASMAS
NT DEUTERIUM PLASMA
NT DEUTERONS
NT ELECTRON PLASMA
NT ELECTRONS
NT ENERGETIC PARTICLES
NT EVEN-EVEN NUCLEI
NT FREE ELECTRONS
NT HEAVY NUCLEI
NT HELIUM PLASMA
NT HIGH ENERGY ELECTRONS
NT HIGH TEMPERATURE PLASMAS
NT HOT ELECTRONS
NT HYDROGEN PLASMA
NT HYPERNUCLEI
NT INNER RADIATION BELT
NT IONIZED GASES
NT LASER PLASMAS
NT MAGNETIC CLOUDS
NT MAGNETICALLY TRAPPED PARTICLES
NT METALLIC PLASMAS
NT NITROGEN PLASMA
NT NONEQUILIBRIUM PLASMAS
NT NONUNIFORM PLASMAS
NT NUCLEI (NUCLEAR PHYSICS)
NT ODD-ODD NUCLEI
NT OXYGEN PLASMA
NT PARTONS
NT PHOTOELECTRONS
NT PLASMA CLOUDS
NT PLASMA FOCUS
NT PLASMA JETS
NT PLASMA LAYERS
NT PLASMA SHEATHS
NT PLASMAS (PHYSICS)
NT POLARONS
NT POSITRONS
NT PROTONS
NT RADIATION BELTS
NT RADIO JETS (ASTRONOMY)
NT RELATIVISTIC ELECTRON BEAMS
NT RELATIVISTIC PLASMAS
NT ROTATING PLASMAS
NT SEMICONDUCTOR PLASMAS
NT SOLAR ELECTRONS
NT SOLAR PROTONS
NT SOLAR WIND
NT SPACE PLASMAS
NT SPHERICAL PLASMAS
NT STELLAR WINDS
NT STRONGLY COUPLED PLASMAS
NT THERMAL PLASMAS
NT TOROIDAL PLASMAS
NT TRITONS
TIROS-N/NOAA A-J space environment monitor subsystem
[PB87-203998] 01 p0015 N88-10083
On the interaction of a planar metal surface with a charge and with a molecule
[DE87-703083] 02 p0147 N88-10920
Heavy-particle collisions in the plasma edge
[DE87-012928] 02 p0237 N88-11493
Complex scattering dynamics and the integer quantum Hall effect
[DE87-011790] 02 p0243 N88-11536
A simplified approach to the dynamics of charged particles in the magnetosphere
03 p0273 N88-11718
Defect characterization in quartz and related materials
[AD-A184754] 03 p0294 N88-11846
Development and evaluation of a Monte Carlo code system for analysis of ionization chamber responses
[AD-A183970] 03 p0375 N88-12359
Future directions in interplays between particle and nuclear physics: Summary session
[DE87-011791] 04 p0489 N88-13013
Cosmic-ray nuclear event with an anomalously strong concentration of energy and particles in the central region
[DE87-703376] 04 p0526 N88-13213
An electric field meter based upon a new principle: A dummy displacement electrode. Application to aerospace vehicles
[SNIAS-872-422-106] 05 p0585 N88-13567
Mechanistic studies of polymeric samples exposed aboard STS 8
[NASA-CR-182364] 06 p0686 N88-14202
Research in elementary particle physics
[DE88-002130] 06 p0777 N88-14771
Optimization of charged particle acceleration rate over wave parameters in the scheme with acceleration by surface electromagnetic waves
[DE88-700320] 07 p0846 N88-15134
Atmospheric science 07 p0883 N88-15357
Multiply charged particles in primary cosmic rays with energy less than or equal to 2 TeV
07 p0921 N88-15596
Analysis of relativistic nucleus-nucleus interactions in emulsion chambers 07 p0926 N88-15624
Performance and optimization of direct implicit time integration schemes for use in electrostatic particle simulation codes
[DE88-003254] 10 p1406 N88-18381
Forces on neutral atoms due to electromagnetic fields
[AD-A187461] 10 p1408 N88-18396
Boltzmann-Fokker-Planck calculations using standard discrete-ordinates codes
[DE88-005393] 11 p1537 N88-19185
Presentations to the SuperHILAC Program Advisory Committee
[DE88-003853] 11 p1547 N88-19256
On (e,e'N) reactions
[CEBAF-PR-87-028] 12 p1690 N88-20109
Velocity and concentration measurements in flowing suspensions by nuclear magnetic resonance
[DE88-006225] 13 p1770 N88-20589
Modeling the effects of heavy charged particles on MOSFETs (Metal-Oxide-Semiconductor Field Effect Transistors)
[AD-A190575] 15 p2143 N88-22792
A proposal for the establishment of a center of excellence in theoretical geoplasma research
[AD-A189742] 16 p2231 N88-23327
Nonlinear dynamics of interaction between charged particles modulated beam and bounded plasma regular oscillations
[DE88-701681] 16 p2280 N88-23648
Color charge motion in non-Abelian fields
[DE88-701306] 19 p2642 N88-25672
Electron-positron physics at 1 TeV
[DE88-009019] 19 p2725 N88-26180
Mechanisms for particle acceleration: Possibilities and constraints
[PB88-102538] 19 p2725 N88-26184
JFET/SOS (Junction Field-Effect Transistor/Silicon-on-Sapphire) devices: Gamma-radiation-induced effects
[AD-A193001] 20 p2795 N88-26586
Charged pion production and projectile breakup in 85A MeV(sup)12C induced heavy ion reactions
[LUIP-8802] 20 p2850 N88-26920
Neoclassical diffusion due to trapping/detrapping orbits in stellarators
[DE88-008566] 20 p2857 N88-26968
Optical guiding in the separable beam limit
[AD-A192452] 21 p2952 N88-27534
Self-energies and the interactions of particles with surfaces
[DE88-010451] 21 p3014 N88-27885
Propagation of charged particle beams in the atmosphere
[AD-A193185] 21 p3014 N88-27887
Solar flares and magnetospheric particles: Investigations based upon the ONR-602 and ONR-604 experiments
[AD-A193396] 21 p3031 N88-27994
Difficulties with interpretation of underground muons from Cygnus X-3
[DE88-701645] 23 p3309 N88-29710

CHARGING
Chemical analysis of charged Li/SO(sub)2 cells
02 p0163 N88-11026

CHARM (PARTICLE PHYSICS)
An introduction to charm and heavy quark physics
[DE87-013589] 02 p0231 N88-11455
On charm decays: Present status and future goals
[DE87-013586] 03 p0375 N88-12356
High energy experimental physics
[DE87-013516] 03 p0376 N88-12363
A method for the analysis of heavy flavor decays
[NOTA-INTERNA-909] 22 p3150 N88-28744

CHARPY IMPACT TEST
Fractographic and microstructural aspects of fracture toughness testing in irradiated 304 stainless steel
[DE88-000795] 06 p0681 N88-14172

Aging degradation of cast stainless steels: Effects on mechanical properties
[DE88-003053] 09 p1145 N88-16866
Influence of neutron irradiation on the Charpy impact properties of V-15Cr-5Ti
[DE88-003430] 11 p1458 N88-18692
The effect of notch root radius on the determination of toughness in ultrahigh strength steel friction welds
[AD-A195952] 24 p3384 N88-30156

CHARRING
Non-steady group combustion of a cloud of char particles
[DE87-010773] 08 p0966 N88-15849
Low temperature reactivity of chars towards oxygen, appendix E2
[DE88-004086] 10 p1298 N88-17760

CHARTS
NT BOND GRAPHS
NT FLOW CHARTS
NT GRAPHS (CHARTS)
NT METEOROLOGICAL CHARTS
NT NAUTICAL CHARTS
Control charts when the observations are correlated
[AD-A186388] 07 p0866 N88-15253
Evaluation of a parallel chart parser
[AD-A189172] 14 p1959 N88-21685

CHASSIS
Corrosion control by composite material substitution with application to the M-939 5-ton truck
04 p0428 N88-12654
Articulated suspension system
[NASA-CASE-NPO-17354-1-CU]
18 p2524 N88-24973
Unified methods of accelerated laboratory tests of the preparations for temporary protection of cars
[NASA-TT-20298] 21 p2921 N88-27336

CHEBYSHEV APPROXIMATION
An adaptive pseudo-spectral method for reaction diffusion problems
[NASA-CR-178394] 02 p0224 N88-11414
A vectorized Poisson solver over a spherical shell and its application to the quasi-geostrophic omega-equation
[NASA-CR-4116] 08 p1039 N88-16285
Electromagnetic scattering from and natural resonances of the circular strip 13 p1759 N88-20523
A study of data compactation using numerical methods
[INPE-4317-TDL/284] 13 p1828 N88-20929
Solution of the compressible Navier-Stokes equations of motion by Chebyshev polynomials for laminar shock-boundary layer flow
[AD-A191033] 16 p2208 N88-23176
Approximate solution of random differential equation
18 p2565 N88-25233
A comparative study of Chebyshev acceleration and residue smoothing in the solution of nonlinear elliptic difference equations
[CWI-NM-R8723] 18 p2569 N88-25259
Solution of the Orr-Sommerfeld equation for the Blausius boundary-layer documentation of program ORRBL and a test case
[NASA-CR-4169] 20 p2841 N88-26858
Solution to the compressible Navier-Stokes equations of motion by Chebyshev polynomials with implicit time stepping
[AD-A194119] 22 p3075 N88-28257
Approximation of atmospheric density by Chebyshev polynomials in predicting motion of low artificial earth satellites 24 p3445 N88-30503

CHECKOUT
Design and implementation of a debugger for an abstract machine
[AD-A184691] 03 p0363 N88-12283
Software reliability perspectives
[NASA-CR-181523] 04 p0479 N88-12952
A project of an intelligent system to help on-line trouble shooting --- aircraft maintenance
[SNIAS-872-111-106] 05 p0529 N88-13216
The ESA centralized management system for satellite electronic test and checkout instrumentation
09 p1124 N88-16731
The KATE shell: An implementation of model-based control, monitor and diagnosis 09 p1210 N88-17255
Debugging FORTRAN on a shared memory machine
[DE88-003589] 10 p1386 N88-18276

CHECKOUT EQUIPMENT
U TEST EQUIPMENT

CHELATE COMPOUNDS
U CHELATES

CHELATES
Soluble metal chelate polymers of coordination numbers six, seven and eight
[AD-A185094] 05 p0568 N88-13459
Chromatographic and mass spectrometric separation and analysis
[AD-A190113] 16 p2174 N88-22958
Soluble metal chelate polymers of coordination numbers six, seven and eight
[AD-A192485] 21 p2917 N88-27314

CHEMICAL ANALYSIS
NT CHROMATOGRAPHY
NT ELECTROPHOTOMETRY
NT GAS ANALYSIS
NT GAS CHROMATOGRAPHY
NT LIQUID CHROMATOGRAPHY
NT MICROANALYSIS
NT NEUTRON ACTIVATION ANALYSIS
NT OZONOMETRY
NT POTENTIOMETRIC ANALYSIS
NT QUALITATIVE ANALYSIS
NT QUANTITATIVE ANALYSIS
NT SPECTROSCOPIC ANALYSIS
NT VOLUMETRIC ANALYSIS
Real time analysis of detonation products
[DE87-007453] 01 p0031 N88-10195
Theoretical approaches to chemical dynamics in highly compressed fluids
[DE87-012242] 01 p0046 N88-10296
The development of a new and novel Hadamard transform infrared spectrometer for analytical chemistry
[DE87-014804] 02 p0175 N88-11094
Multidimensional elemental analysis with the Sandia nuclear microprobe
[DE87-014158] 02 p0183 N88-11136
Multidimensional elemental analysis with the Sandia nuclear microprobe
[DE87-014158] 02 p0183 N88-11136
Mass spectroscopic facility 03 p0296 N88-11861
Thin films for geothermal sensing
[DE88-000154] 03 p0326 N88-12061
Simultaneous TG/DSC (thermogravimetry/Differential Scanning Calorimetry) and TG/MS (thermogravimetry/Mass Spectrometry) analyses of polymeric and energetic materials
[DE88-000727] 04 p0413 N88-12561
Analysis of free cutting brass by A.C. polarography
[PD-MT-8728] 04 p0417 N88-12587
An assessment of clinical chemical sensing technology for potential use in space station health maintenance facility
[NASA-CR-172013] 04 p0475 N88-12926
The analysis of metal finishing solutions by ion chromatography
[AD-A184812] 05 p0561 N88-13414
Chemical analysis for excimer laser systems
[DE88-001941] 05 p0589 N88-13591
Evaluation of AIS-2 (1986) data over hydrothermally altered granitoid rocks of the Singatse Range (Yerington) Nevada and comparison with 1985 AIS-1 data
05 p0613 N88-13767
Development of FTMS methods for the detection of trace chemical species and development of FTMS methods for the analysis of various chemical species
[AD-A185857] 07 p0828 N88-15023
Specific organic compounds in excreta
07 p0895 N88-15422
The effect of propane on atomic spectrometric signals in the direct current plasma
[DE88-002457] 07 p0934 N88-15676
The synthesis and characterization of some rare earth arsenides
[AD-A186445] 08 p0965 N88-15839
Study of selection criteria for adhesives used in aircraft structure bonding
[ETN-88-91619] 08 p0971 N88-15875
Improved silicon nitride for advanced heat engines
[NASA-CR-175006] 08 p0973 N88-15886
Vapor generation of fuels
[PB88-109897] 08 p0974 N88-15892
Operation Everest 2: Comparison of four instruments for measuring blood oxygen saturation
[AD-A186456] 08 p1049 N88-16337
Ion chromatography in the manufacture of multilayer circuit boards
[DE88-002428] 10 p1322 N88-17902
The role of analytical chemistry in assessing atmospheric effects of combustion
[DE88-003909] 10 p1352 N88-18082
Analysis of gases in the earth's crust
[PB88-141619] 10 p1354 N88-18093
Analysis of water recovered after being used for washing by men and women 10 p1361 N88-18135
Synthesis and characterization of 1,2-cyclobutenedicarboxamides: Thermally generated polymers and Diels-Alder adducts
[AD-A188591] 12 p1611 N88-19633
Critical comparison of moving average and cumulative summation control charts for trace analysis data
[AD-A188312] 12 p1705 N88-20203
Fuels combustion research
[AD-A189114] 13 p1736 N88-20381
Development and evaluation of supercritical fluid chromatography-mass spectrometry
[DE88-005122] 13 p1738 N88-20394
Improved methods for high resolution electron microscopy
[DE88-005731] 13 p1774 N88-20609
Plasma cortisol, renin and aldosterone during an intense heat acclimation program
[AD-A189387] 13 p1809 N88-20810
On the structure of pulsed plasma jets
13 p1843 N88-21030
Measurement of species concentrations in flames by laser-induced fluorescence
[DE88-007096] 14 p1889 N88-21286
Analysis of explosives. 1: Computer programs for processing of X-ray powder deffraction data
[PB88-156898] 14 p1894 N88-21309
Spatial and temporal distribution of precipitation chemistry across Maryland in 1984, volume 1
[PB88-148929] 14 p1943 N88-21595
Isotopic and chemical studies of early crustal metasedimentary rocks
[NASA-CR-182711] 14 p1944 N88-21601
Structure and surface characterizations of high strength carbon fibers
[AD-A189642] 15 p2029 N88-22087
Spectrographic detection of nitrogen impurity in helium
[DE88-752301] 15 p2033 N88-22111
On copper peroxide
[NASA-TT-20263] 15 p2037 N88-22135
NMR analysis of a fluorocarbon copolymer
[DE88-002364] 15 p2043 N88-22170
Simulation analysis of moored fluorometer time series from the Mid-Atlantic Bight
[DE88-006066] 15 p2099 N88-22505
The adhesive bonding of thermoplastic composites
[AD-A190994] 16 p2173 N88-22953
Analytical Chemistry Division
[DE88-701236] 16 p2174 N88-22956
Chromatographic and mass spectrometric separation and analysis
[AD-A190113] 16 p2174 N88-22958
Identification of hydroxypropyl starch hydrolysate components 17 p2315 N88-23832
Analysis of thermal and radiation effects in materials using the GEMAT process 17 p2408 N88-24318
Thermochemical analysis of mass transfer in a NB-1ZR-potassium heat pipe 17 p2412 N88-24346
Selective detection in gas chromatography
[AD-A191499] 18 p2481 N88-24718
Synthesis and characterization of new phosphazene polymers
[AD-A191508] 18 p2490 N88-24771
Geological evolution and analysis of confirmed or suspected gas hydrate localities. Volume 2: Basin analysis, formation and stability of gas hydrates in the Black Sea
[DE88-001052] 18 p2532 N88-25023
Fundamental studies of separation processes
[DE88-007487] 19 p2611 N88-25494
Alternate techniques for noble-gas detection
[DE88-009471] 19 p2613 N88-25507
Carbon analysis in natural olivine crystals of deep origin
[NASA-TT-20311] 19 p2734 N88-26239
Surface phases and their influence on metal-oxide interfaces
[DE88-007938] 20 p2769 N88-26420
Microchemical analysis of polycrystalline Ni3Al and other ordered alloys using the field-ion microscope atom probe
[DE88-011519] 21 p2914 N88-27294
The electromagnetic spectrum: The information mine
[AD-A194316] 22 p3069 N88-28215
Noncontact photo-thermal sensing
[AD-A195450] 24 p3344 N88-29905
Geochronological and lead-isotope evidences for rapid crust formation in middle-proterozoic time: The Labrador example 24 p3398 N88-30239
Lithospheric evolution of the Northern Arabian Shield: Chemical and isotopic evidence from basalts, xenoliths and granites 24 p3399 N88-30242
Evidence of the in situ decay of Al-26 in a Semarkona chondrule 24 p3441 N88-30479

CHEMICAL ATTACK
NT INTERGRANULAR CORROSION
Corrosion resistance of silver-plated carbon-aluminum composite 03 p0285 N88-11793
Resistance of canopy materials against chemicals
[PML-1985-22] 05 p0569 N88-13466
Corrosion of tungsten alloys in marine environments
17 p2320 N88-23854

CHEMICAL BONDS
NT HYDROGEN BONDS
Polymer chain segment orientation during stress relaxation
[DE87-013392] 01 p0027 N88-10174

Accurate ab initio calculations which demonstrate a 3 Pi u ground state for Al2
[NASA-TM-89302] 01 p0102 N88-10666

Bonding and coupling of C sub 1 fragments on metal surfaces
[AD-A184186] 03 p0295 N88-11852

Free radical detection and reactions in the decomposition of energetic materials
[AD-A184677] 03 p0296 N88-11858

The itinerant resonating-valence-bond model for superconductivity
[DE87-014794] 03 p0380 N88-12391

Superconductivity as a synchronous spatial alternation of valence bonds
[AD-A184208] 03 p0382 N88-12405

Topological aspects of infinite metal clusters and superconductors
[AD-A184104] 04 p0495 N88-13049

Measurement of the electron density and the attachment rate coefficient in silane/helium discharges
[AD-A184268] 04 p0496 N88-13051

Valence bond theory and superconductivity
[AD-A184274] 04 p0496 N88-13052

The chemical bond and superconductivity
[AD-A184275] 04 p0496 N88-13053

Valence bond cluster studies of alkali metal/semiconductor bonding
[AD-A184276] 04 p0496 N88-13054

Tetrahedral carbon and interstitial electrons in Li cluster: CLi4 and (LiCH3)4
[AD-A184277] 04 p0496 N88-13055

Effect of sidechain length and crosslinking on ionic conductivity in polyphosphazene solid electrolytes
[AD-A184419] 04 p0497 N88-13058

Pure dephasing of a vibrational adbond
[AD-A185222] 05 p0609 N88-13740

Reactions and bonding between glasses and titanium
[DE88-000603] 06 p0685 N88-14195

The tribological properties of MoS2 coatings in vacuum, low relative humidity and high relative humidity environments
[DE88-001611] 06 p0711 N88-14356

X-ray structure analyses and molecular mechanics analyses of dense energetic materials
[AD-A185462] 06 p0779 N88-14781

Coverage dependence of adsorbate-substrate bond lengths: Chlorine and caesium adsorbed on silver single crystals
[PB87-125142] 06 p0788 N88-14833

Diffraction by glasses with a layer structure
[DE88-003059] 07 p0837 N88-15078

Feasibility of a complex compound heat pump
[PB88-113022] 07 p0853 N88-15183

The Coupled Cluster Single and Double excitation (CCSD) method in quantum chemistry: An efficient formulation of the theory and application to closed shell molecular systems
[DE88-000475] 07 p0930 N88-15650

Cohesive energies of transition metal silicides and phosphides --- Knudsen effusion
[AD-A186691] 09 p1254 N88-17519

Copper oxidation states, vacancy ordering and their effect on high temperature superconductivity
[DE88-003079] 09 p1258 N88-17542

Basic research on macromolecular dynamics
[PB88-141643] 10 p1305 N88-17805

Rovibrational spectroscopy of ArCO van der Waals complex
[DE88-004291] 10 p1406 N88-18387

Chemical activation of molecules by metals: Experimental studies of electron distributions and bonding
[DE88-004465] 10 p1407 N88-18393

Coupling of vibrational modes of adsorbates: Application to field induced shifts for CO and CN on Cu(100)
[AD-A187891] 11 p1453 N88-18659

A simple interpretation of the Fe2(-) photoelectron spectrum
[NASA-CR-182553] 11 p1543 N88-19225

An interdisciplinary approach to predictive modeling of structural adhesive bonding: Factors affecting the durability of titanium/epoxy bonds
[AD-A189503] 12 p1611 N88-19636

Properties of molecular solids and fluids at high pressure and temperature
[DE88-004195] 13 p1738 N88-20391

Improved glass-ceramic to metal seals in actuator and detonator applications with an aluminum-containing austenitic stainless steel
[DE88-004691] 13 p1749 N88-20458

The relationship of the chemical bonding topology of high critical temperature copper oxide superconductors to that of the chevrel phases and the ternary lanthanide rhodium borides
[AD-A189255] 13 p1845 N88-21042

Vapor phase deposition and growth of polyimide films on copper
[AD-A189969] 15 p2044 N88-22178

Synthesis and properties of novel cluster phases
[DE88-006816] 16 p2175 N88-22964

Distribution of chain ends inside the polybutadiene microspheres of SB diblock copolymers
[AD-A191257] 16 p2182 N88-23007

Polyitaconic acid macromolecule primer for adhesive bonding and corrosion control of aluminum
17 p2319 N88-23849

Liquid carbon
[AD-A191707] 18 p2491 N88-24776

A constraint algorithm for maintaining rigid bonds in molecular dynamics simulations of large molecules
[AD-A191663] 18 p2572 N88-25277

Molecular orbital studies of the bonding in heavy element organometallics: Progress report
[DE88-007765] 19 p2723 N88-26168

Fundamental studies of elastomers
[DE88-009679] 20 p2778 N88-26471

Structural studies of (Ga,In)(As,P) alloys and (InAs) sub m (GaAs) sub n strained-layer superlattices by fluorescence-detected EXAFS 20 p2872 N88-27051

Structure of bound states in polynomial potentials
[DE88-702437] 21 p3007 N88-27837

Discrete variational methods and their application to electronic structures
[DE88-702215] 21 p3014 N88-27888

Deep level defects in semiconductors: Stress and pressure studies
[DE88-010855] 21 p3024 N88-27948

On the bond distance in methane
[NASA-CR-181436] 22 p3150 N88-28741

Hydrogen storage by molecular polyhydrides
[AD-A194207] 23 p3191 N88-28989

Potential induced structural transformations of the Au(100) and Au(111) surfaces
[DE88-005446] 23 p3287 N88-29571

CHEMICAL CLEANING

Chemical cleaning of metal surfaces in vacuum systems by exposure to reactive gases
[AD-A188588] 12 p1608 N88-19616

Ammonia cleanup of lithium containing components
17 p2403 N88-24287

Cleanability of aircraft polyurethane topcoats
[AD-A193456] 23 p3170 N88-28878

CHEMICAL CLOUDS

NT BARIUM ION CLOUDS

A fluid simulation of the AMPTE lithium gas releases in the solar wind
[TRITA-EPP-87-06] 05 p0661 N88-14056

A modeling analysis program for the JPL table mountain Io sodium cloud data
[NASA-CR-182555] 11 p1570 N88-19400

High altitude chemical release systems for project BIME (Brazilian Ionospheric Modification Experiments) project IMS (Ionospheric Modification Studies) project PIIE (Polar Ionospheric Irregularities Experiment) project polar arcs
[AD-A188299] 12 p1642 N88-19833

CRRES chemical release mechanisms
14 p1874 N88-21192

Magnetic cavity formation at Comet Halley and at the AMPTE Li release 14 p1996 N88-21898

CHEMICAL COMPOSITION

NT CARBON DIOXIDE CONCENTRATION

NT STELLAR COMPOSITION

Optimizing the application of high temperature corrosion resistant aluminium-silicon-base coatings
[BLL-M-37222-(5828.4)] 01 p0018 N88-10112

Equations for determining CVD tungsten-rhenium alloy composition and plating rate
[DE87-008831] 01 p0024 N88-10152

The effect of RDX particle size on the shock sensitivity of cast PBX formulations. 2: Bimodal compositions
[DE87-009581] 01 p0031 N88-10198

Gases released by surface flashover of insulators
[DE87-013851] 01 p0039 N88-10249

Addition polyimide composition
[EP-PATENT-0-167-304-A1] 01 p0053 N88-10337

Contribution of bubbles and waves to air-sea CO2 flux, with implications for remote sensing
[PB87-203980] 01 p0073 N88-10467

The atomic weight and isotopic composition of nitrogen and their variation in nature
[DE87-012867] 02 p0144 N88-10902

Application of high performance liquid chromatography to the fast determination of bitumen generic composition
[PC-2] 02 p0145 N88-10911

A geometrical model for determining the physicochemical properties of ternary metallic systems
[BLL-M-37303-(5828.4)] 02 p0149 N88-10931

Study of the morphology of thermosetting matrices
[ONERA-RT-5/3346-M] 02 p0153 N88-10961

Composition, structure and chemistry of interstellar dust
[NASA-TM-88350] 02 p0253 N88-11603

Heavy element compositions and energy spectra of galactic and solar cosmic rays 03 p0272 N88-11714

Joining of silicon carbide reinforced ceramics
[DE87-014881] 03 p0294 N88-11847

JPRS report: Science and technology. China
[JPRS-CST-87-025] 03 p0300 N88-11888

The nature of metallurgical reactions in underwater welding
[AD-A184464] 04 p0414 N88-12568

Polymer composition --- cable insulation
[EP-PATENT-0-199-444-A1] 04 p0418 N88-12594

Raman scattering as a diagnostic technique for cathode characterization
[AD-A184434] 04 p0439 N88-12726

Nuclear techniques in studies of condensed matter
[NASA-RP-1195] 04 p0489 N88-13015

A mathematical model of high alloy nickel base high temperature alloys
[BLL-M-37381-(5828.4)] 05 p0564 N88-13436

Ion plating for corrosion control
[AD-A185061] 05 p0565 N88-13442

The use of airborne imaging spectrometer data to determine experimentally induced variation in coniferous canopy chemistry 05 p0612 N88-13761

Toward detecting California shrubland canopy chemistry with AIS data 05 p0613 N88-13764

High energy molecules of high symmetry
[AD-A185385] 05 p0647 N88-13965

Ferromanganese nodules of Antarctic sector in Pacific Ocean 06 p0727 N88-14472

Hydrochemical structure of Gulf Stream frontal zone waters 06 p0727 N88-14476

Progress in the measurement of salinity and oxygen at the Woods Hole Oceanographic Institution
[PB88-108089] 06 p0748 N88-14598

Atlas of atomic spectral lines of neptunium emitted by an inductively coupled plasma
[DE88-000640] 06 p0782 N88-14796

Metallurgical processes in multi-component rare earth-transition metal permanent magnet alloys
[AD-A186401] 07 p0832 N88-15045

Exobiology and life science 07 p0883 N88-15358

The use of chlorophyll fluorescence measurements from space for separating constituents of sea water
08 p1043 N88-16307

A rapid method for the computation of equilibrium chemical composition of air to 15000 K
[NASA-TP-2792] 09 p1140 N88-16830

The effects of fuel composition on ignition delay in homogeneous charge and direct injection compression ignition engines
[DE88-003691] 09 p1143 N88-16849

Influence of post-anneal cooling treatments on suppression of cryogenic intergranular fracture in experimental Ni-free high-Mn austenitic steels
[DE88-002766] 09 p1145 N88-16863

Electronic and chemical structure of 3-5/metal and Si/metal interfaces
[AD-A186579] 09 p1254 N88-17518

Application of inverse gas chromatography to fluidity studies
[DE88-002896] 10 p1296 N88-17750

The measurement of chemical compositon with high spatial resolution using a dedicated scanning transmission electron microscope
[AERE-R-12317] 10 p1297 N88-17753

Electrically conducting polymer-copper sulphide composite films, preparation by treatment of polymer-copper (2) acetate composites with hydrogen sulfide
[NASA-TT-20204] 10 p1305 N88-17803

Acoustic emission-microstructural relations in ferritic steels. Part 3: The effect of inclusion content
[AERE-R-12041] 10 p1341 N88-18015

Determination of optimum electrolyte composition for molten carbonate fuel cells literature review
[DE88-001015] 10 p1348 N88-18058

Normal and superconducting state properties of La2-xSr/sub x/CuO4
[DE88-003013] 10 p1416 N88-18450

Composition and thickness of multilayer foils using MeV ion-beam techniques
[DE88-004360] 11 p1448 N88-18629

S-glass analysis by X-ray spectroscopy
[DE88-004636] 11 p1454 N88-18666

Electron microscopy study of morphology and composition of a ferrisilicate catalyst
[DE88-005754] 11 p1562 N88-19352

Mass loss from evolved stars
11 p1569 N88-19354

Analysis of model fuels and their compatibility with selected elastomers, part 1
[AD-A188361] 12 p1612 N88-19639

High altitude chemical release systems for project BIME (Brazilian Ionospheric Modification Experiments) project IMS (Ionospheric Modification Studies) project PIIE (Polar Ionospheric Irregularities Experiment) project polar arcs
[AD-A188299] 12 p1642 N88-19833

Fast protonic conducting solid electrolytes
[AD-A188524] 12 p1698 N88-20160

Gas-chromatographic analysis of products of thermal reactions of aerosol in Venusian cloud layer on Vega-1 and Vega-2 automatic interplanetary stations
13 p1725 N88-20318

Roentgenoradiometric analysis of aerosol in Venusian clouds by Vega-1 and Vega-2 automatic interplanetary stations 13 p1726 N88-20319

Determining chemical composition of aerosol in Venusian cloud layer on Vega-1 automatic interplanetary station using Malakhit mass spectrum analyzer
13 p1726 N88-20321

Elemental composition of Venusian rocks in northeastern part of Terra Aphrodite (determined using data from Vega-2 landing module)
13 p1726 N88-20322

Content of natural radioactive elements in Venusian rocks determined using data from Vega-1 and Vega-2 stations 13 p1726 N88-20323

Results of infrared spectrometer experiment. 1: Infrared radiation of parent molecules in Halley's Comet
13 p1726 N88-20325

The effect of microstructure on the fatigue crack growth resistance of nickel base superalloys
[AD-A189526] 13 p1741 N88-20414

On the structure of pulsed plasma jets
13 p1843 N88-21030

Microprobe examination of composite materials produced by burning of Ti, Cr, C powders with powder of any one Fe-group metal 14 p1886 N88-21269

The unique characteristics of the structure of composite materials made on a base of sphalerite-analogous boron nitride 14 p1886 N88-21273

Ground-based column abundance measurements of atmospheric hydroxyl
[NASA-CR-182676] 14 p1944 N88-21598

Diversity and similarity of comets
14 p1994 N88-21885

Photometry of P/Halley (1982i): Is what we have learned useful for other comets? 14 p1998 N88-21909

Composition of cometary dust particles --- Halley
14 p2001 N88-21932

Isotopic composition of Halley dust
14 p2002 N88-21933

Nature of Comet Halley's organic grains inferred from infrared spectra 14 p2007 N88-21973

Segregation effects in welded stainless steels
[DE88-701224] 15 p2037 N88-22139

Stability of the high-temperature G-16 primer composition
[DE88-006201] 15 p2049 N88-22206

Understanding CO2 and climate
[PB88-167655] 16 p2234 N88-23341

A sup 57 Fe Mossbauer study of the superconductor YBa sub 2 (Fe sub x Cu sub 1-x) sub 3 O sub y
[DE88-701543] 16 p2282 N88-23661

Dust and C2-contents in the coma of Halley's Comet (1986III) 16 p2288 N88-23697

Identification of hydroxypropyl starch hydrolysate components 17 p2315 N88-23832

Hydrogen embrittlement susceptibility of high strength ESR 4340 steel alloys for ballistically resistant/tolerant components 17 p2319 N88-23848

Compositional redistribution during casting of Hg sub 0.8 Cd sub 0.2 Te alloys
[NASA-TM-101151] 17 p2326 N88-23893

Aging of carbon fibers
[SNPE-NT-10/86/CRB/NP] 18 p2479 N88-24707

Surface composition-reactivity relationships in heterogeneous catalysis
[DE88-006679] 18 p2480 N88-24714

Rapidly solidified lightweight durable disk material
[AD-A191697] 18 p2491 N88-24775

Geological evolution and analysis of confirmed or suspected gas hydrate localities. Volume 2: Basin analysis, formation and stability of gas hydrates in the Black Sea
[DE88-001052] 18 p2532 N88-25023

Selective radiation absorption in aluminized composite propellant combustion 19 p2630 N88-25598

The structure and properties of grain boundaries in B2 ordered alloys
[DE88-009890] 20 p2773 N88-26447

Nickel aluminides: A new family of nickel + aluminum alloys featuring simple composition, low density, excellent oxidation resistance and high yield strength that increases with temperature
[DE88-010692] 20 p2776 N88-26461

Physical-chemical reactions at welding arc/molten pool interfaces
[DE88-007717] 20 p2808 N88-26662

Fine-scale traverses in cumulate rocks, Stillwater Complex: A lunar analogue study
[NASA-CR-183066] 20 p2823 N88-26747

Effects of grain boundary composition on properties of YBa2Cu3O/sub 7-x/
[DE88-007679] 20 p2875 N88-27064

Defect characterization of the redox behavior and stability of conducting oxides
[DE88-010799] 20 p2878 N88-27088

Space infrared telescope facility project
[NASA-CR-183058] 20 p2883 N88-27121

Initial testing of the tunable diode laser absorption spectrometer for measuring HNO3 in diesel engine exhaust, stage 2
[PB88-193073] 21 p2970 N88-27641

The distribution of some chemical elements between dissolved and particulate phases in the ocean
[DE88-010181] 21 p2977 N88-27682

Structure of bound states in polynomial potentials
[DE88-702437] 21 p3007 N88-27837

Evolution of heavy-element abundances in the galactic halo and disk
[DE88-011736] 22 p3164 N88-28845

Surface composition of Mars: A Viking multispectral view 23 p3300 N88-29655

Elemental composition of the Martian surface
23 p3302 N88-29665

Lava flow-field morphology: A case study from Mount Etna, Sicily 23 p3303 N88-29676

How dirty is Mars' North Polar cap, and why isn't it black 23 p3303 N88-29677

Some probable characteristics of the Martian regolith
23 p3303 N88-29678

What SNC meteorites tell us about Martian magmatism 23 p3303 N88-29679

Spectral reflectance of SNC meteorites: Relationships to Martian surface composition
23 p3304 N88-29683

The surface composition of Mars from earthbased observations 23 p3306 N88-29696

Martian surface analogs: Laboratory spectral studies in the mid infrared 23 p3307 N88-29699

The characterizatin of combustion by fuel composition: Measurements in a small conventional combustor
24 p3346 N88-29920

The performance of a surrogate blend in simulating JP-4 in a spray-fueled combustor 24 p3347 N88-29926

The effect of particle properties on radiative heat transfer 24 p3350 N88-29941

Bibliography of Soviet laser developments, number 88, March - April 1987
[AD-A195978] 24 p3378 N88-30116

Archean crustal evolution of the northern North China Craton 24 p3398 N88-30235

The complexity, depth, and rapidity of processes that formed the lunar crust 24 p3398 N88-30237

Lithospheric evolution of the Northern Arabian Shield: Chemical and isotopic evidence from basalts, xenoliths and granites 24 p3399 N88-30242

Growth of planetary crusts 24 p3400 N88-30247

Non-atmospheric noble gases from CO(sub 2) well ga
24 p3441 N88-30476

Star formation and molecular clouds
24 p3451 N88-30537

CHEMICAL ELEMENTS
NT ALKALI METALS
NT ALKALINE EARTH METALS
NT ALUMINUM
NT AMORPHOUS SILICON
NT ARGON
NT ARGON ISOTOPES
NT ARSENIC
NT BARIUM
NT BERYLLIUM
NT BISMUTH
NT BORON
NT BORON ISOTOPES
NT BROMINE ISOTOPES
NT CADMIUM
NT CALCIUM
NT CALCIUM ISOTOPES
NT CARBON
NT CARBON 12
NT CARBON 13
NT CERIUM
NT CESIUM
NT CHLORINE
NT CHROMIUM
NT COBALT
NT COBALT 60
NT COPPER
NT DEUTERIUM
NT DYSPROSIUM
NT ERBIUM
NT EUROPIUM
NT FLUORINE
NT GADOLINIUM
NT GALLIUM
NT GERMANIUM
NT GOLD
NT HAFNIUM
NT HEAVY ELEMENTS
NT HELIUM
NT HELIUM ISOTOPES
NT HOLMIUM
NT HYDROGEN
NT HYDROGEN ISOTOPES
NT INDIUM
NT IODINE
NT IODINE ISOTOPES
NT IRIDIUM
NT IRIDIUM ISOTOPES
NT IRON
NT IRON ISOTOPES
NT IRON 57
NT ISOTOPES
NT KRYPTON
NT KRYPTON ISOTOPES
NT LANTHANUM
NT LAWRENCIUM
NT LEAD (METAL)
NT LEAD ISOTOPES
NT LIQUID HELIUM
NT LIQUID HELIUM 2
NT LIQUID HYDROGEN
NT LIQUID LITHIUM
NT LIQUID NITROGEN
NT LIQUID OXYGEN
NT LIQUID POTASSIUM
NT LIQUID SODIUM
NT LITHIUM
NT LITHIUM ISOTOPES
NT MAGNESIUM
NT MAGNESIUM ISOTOPES
NT MANGANESE
NT MERCURY (METAL)
NT MERCURY ISOTOPES
NT MERCURY VAPOR
NT MOLYBDENUM
NT NEODYMIUM
NT NEODYMIUM ISOTOPES
NT NEON
NT NEPTUNIUM
NT NICKEL
NT NIOBIUM
NT NIOBIUM ISOTOPES
NT NITROGEN
NT NITROGEN ISOTOPES
NT NUCLIDES
NT OSMIUM
NT OXYGEN
NT OXYGEN ISOTOPES
NT PALLADIUM
NT PHOSPHORUS
NT PLATINUM
NT PLATINUM ISOTOPES
NT PLUTONIUM ISOTOPES
NT PLUTONIUM 238
NT POTASSIUM
NT RADIOACTIVE ISOTOPES
NT RADON
NT RADON ISOTOPES
NT RARE EARTH ELEMENTS
NT RARE GASES
NT RHENIUM
NT RHENIUM ISOTOPES
NT RHODIUM
NT RUBIDIUM
NT RUBIDIUM ISOTOPES
NT RUTHENIUM
NT SAMARIUM ISOTOPES
NT SELENIUM
NT SILICON
NT SILVER
NT SODIUM
NT SODIUM VAPOR
NT STRONTIUM
NT SULFUR
NT TANTALUM
NT TELLURIUM
NT THORIUM
NT TIN
NT TITANIUM
NT TRITIUM
NT TUNGSTEN
NT URANIUM
NT URANIUM ISOTOPES
NT URANIUM 238
NT VANADIUM
NT XENON
NT YTTERBIUM

NT YTTRIUM
NT ZINC
NT ZIRCONIUM
Multidimensional elemental analysis with the Sandia nuclear microprobe
[DE87-014158] 02 p0183 N88-11136
Compilation of temperature factors of cubic elements
[PB88-108170] 21 p2908 N88-27260
Diamond like carbon coatings: Categorization by atomic number density
[NASA-CR-174895] 22 p3059 N88-28151

CHEMICAL ENERGY
NT ENERGY OF FORMATION
Application of solar technology to fuel production chemical processing, and thermochemical energy transport: Status and future
[DE87-014172] 03 p0346 N88-12189
Cohesive energies of transition metal silicides and phosphides --- Knudsen effusion
[AD-A186601] 09 p1254 N88-17519
Molecular collision processes in gases and at surfaces
[AD-A189518] 13 p1836 N88-20982
A chemical method for achieving acceleration of macroparticles to ultrahigh velocities
[DE88-006377] 15 p2128 N88-22695
Thermodynamic analysis of chemical heat storage system for heat pump
[DE88-753121] 20 p2820 N88-26728
Prediction of deep levels and equilibrium concentrations of defects in semiconductors 21 p3023 N88-27945

CHEMICAL ENGINEERING
Process for the preparation of acyl halides
[GB-PATENT-2-133-792-A] 01 p0020 N88-10124
A process for producing phenolic foams
[EP-PATENT-0-170-357-A1] 01 p0026 N88-10162
Novel conductive polymers
[EP-PATENT-0-182-548-A2] 01 p0026 N88-10163
Pressure sensitive adhesives
[EP-PATENT-0-183-495-A1] 01 p0026 N88-10164
Crosslinkable elastomeric materials
[EP-PATENT-0-181-735-A1] 01 p0026 N88-10165
Boronium complexes as polymer catalysts
[GB-PATENT-2-161-475-A] 01 p0026 N88-10166
Bulletin of the Yamagata University (Engineering), Volume 20, No. 1, January 1988
[ISSN-0085-834X] 07 p0839 N88-15091
Rust converters
[AD-A188767] 14 p1891 N88-21299

CHEMICAL EQUILIBRIUM
NT ACID BASE EQUILIBRIUM
Chemical equilibrium calculations for the high pressure and temperature dissociation of liquid nitrogen
[DE87-013788] 01 p0021 N88-10135
Study of improved methods for predicting chemical equilibria
[DE87-014647] 02 p0145 N88-10906
Study of improved methods for predicting chemical equilibria
[DE87-014647] 02 p0145 N88-10908
Equilibrium calculations of ionization in tracer flames
[PB87-104154] 04 p0412 N88-12555
A rapid method for the computation of equilibrium chemical composition of air to 15000 K
[NASA-TP-2792] 09 p1140 N88-16830
Stability and uniqueness in nonlinear continuum mechanics
[AD-A189616] 12 p1699 N88-20172
NNEPEQ: Chemical equilibrium version of the Navy/NASA Engine Program
[NASA-TM-100851] 14 p1868 N88-21161
Energy storage and transport by reversible chemical reactions
[DE88-900370] 14 p1942 N88-21587
Thermochemical analysis of mass transfer in a NB-1ZR-potassium heat pipe 17 p2412 N88-24346

CHEMICAL EVOLUTION
Analysis of laser extracted volatiles in carbonaceous chondrites 06 p0793 N88-14861
Effects of galactic chemical evolution on thorium/neodymium cosmochronology
[DE88-003829] 11 p1570 N88-19397
Isotopic and chemical studies of early crustal metasedimentary rocks
[NASA-CR-182711] 14 p1944 N88-21601
Diversity and similarity of comets
14 p1994 N88-21885

CHEMICAL EXPLOSIONS
NT GAS EXPLOSIONS
Hot-spot reaction in unsustained shocks
[DE87-011781] 01 p0044 N88-10277
Experimental measurements and numerical simulations of metal spallation by detonating solid explosives
[DE87-013227] 01 p0054 N88-10347
Misty picture weather-watch and microbarograph project: Experiments 9412-14-18
[DE88-003949] 11 p1514 N88-19047
Shock initiation studies on heterogeneous explosives
[DE88-008681] 21 p2923 N88-27351
Diode laser ignition of high explosives and pyrotechnics
[DE88-008771] 21 p2923 N88-27352

CHEMICAL EXTINGUISHERS
U FIRE EXTINGUISHERS

CHEMICAL FRACTIONATION
A prototype expert system for separation science
[DE87-013542] 03 p0371 N88-12333
Mathematical models of continuous flow electrophoresis: Electrophoresis technology
[NASA-CR-179241] 07 p0826 N88-15021
Fundamental studies of separation processes
[DE88-007487] 19 p2611 N88-25494

CHEMICAL FUELS
NT AIRCRAFT FUELS
NT ANTIMISTING FUELS
NT AUTOMOBILE FUELS
NT CRUDE OIL
NT DIESEL FUELS
NT GASOHOL (FUEL)
NT GASOLINE
NT HYDROCARBON FUELS
NT HYDROGEN FUELS
NT JET ENGINE FUELS
NT JP-4 JET FUEL
NT JP-5 JET FUEL
NT JP-8 JET FUEL
NT KEROSENE
NT LIQUEFIED NATURAL GAS
NT LIQUID FUELS
NT NATURAL GAS
NT SYNTHETIC FUELS
Technical instructions for a control operating system of the gas flow installation for the solid fuel combustion chamber
[LR-507] 20 p2788 N88-26537

CHEMICAL KINETICS
U REACTION KINETICS

CHEMICAL LASERS
Distributed feedback effects in lasers and high gain laser instabilities in optically pumped CH3F
03 p0329 N88-12079
Computer simulation of cw HF chemical laser unstable resonator performance
[AD-A185059] 05 p0587 N88-13581
An experimental study of CW HF chemical laser amplifier performance and zero power gain
[AD-A185241] 05 p0588 N88-13584
Nitrogen scale-up
[AD-A185702] 06 p0709 N88-14351
Feasibility of chemical lasers based on chain reaction involving hydrogen fluorination with thermal branching mechanism 09 p1238 N88-17420
A chemical precursor to optical damage. Studies by laser ionization mass spectrometry
[DE88-004321] 10 p1409 N88-18408
Project SKYLITE: A design exploration
[AD-A187906] 11 p1511 N88-19030
Effects of translational and rotational nonequilibrium on CW (Continuous Wave) chemical laser performance
[AD-A191425] 16 p2214 N88-23210
Overview of the SDI (Strategic Defense Initiative) Program in short wavelength chemical lasers
[DE88-007912] 21 p3010 N88-27861
Chemically-produced N2(A) to NO(X) energy transfer in a supersonic flow
[AD-A192501] 22 p3082 N88-28302
NF (a 1 delta) production in a supersonic flow using N2F4 + H2 in a BCL-16 nozzle
[AD-A194478] 22 p3082 N88-28304
Frequency doubling at 1.315 micrometers
[AD-A193902] 23 p3206 N88-29092
Preliminary studies of NF3 + H2 production of N2(A3 sigma(+)u) in a supersonic flow
[AD-A194479] 23 p3219 N88-29162
N2(A3epsilon u +) by reaction of N2F4 + H2 in a supersonic flow
[AD-A194493] 23 p3219 N88-29163
Bibliography of Soviet laser developments, number 88, March - April 1987
[AD-A195978] 24 p3378 N88-30116

CHEMICAL PROPERTIES
NT ACIDITY
NT HEAT OF COMBUSTION
NT HEAT OF FORMATION
NT HEAT OF FUSION
NT LATENT HEAT
NT SALINITY
NT THERMOCHEMICAL PROPERTIES
Standard reference data publications, 1985-1986
[PB87-210241] 01 p0021 N88-10128
Products of the neutralization of hydrazine fuels with hypochlorite, 2
[DE87-011454] 01 p0030 N88-10193
Theoretical approaches to chemical dynamics in highly compressed fluids
[DE87-012242] 01 p0046 N88-10296
Chemical vapor deposition of B6P and B6As films
[DE87-009288] 02 p0151 N88-10942
Contrast between the chemical, structural and electronic properties of thin films of Cu and Ni on the Ru(0001) surface
[DE88-002380] 07 p0938 N88-15696
Chemical activation of molecules by metals: Experimental studies of electron distributions and bonding
[DE88-004465] 10 p1407 N88-18393
Utilization of the JANAF (Joint Army Navy Air Force) database for chemical thermodynamic calculations
[DE88-004571] 10 p1423 N88-18501
Properties of lanthanide oxides as supports for transition metal catalysts
[DE88-004520] 11 p1456 N88-18678
Characteristics and use of lubricating greases
[DE88-751103] 11 p1463 N88-18723
Structure of sol-gel silica
[DE88-006870] 15 p2033 N88-22114
Diode laser spectroscopy of chemical moieties at surfaces
[AD A190710] 15 p2036 N88-22127
Chemical compatibility between silicon carbide and a nickel aluminide
[DE88-006188] 18 p2479 N88-24708
Pollutant formation in heterogeneous mixtures of fuel drops and air
[DOE/CE-50052/H1] 19 p2689 N88-25986
Synthesis of model polymers and related structures in support of vinyl monomer grafting studies
[DE88-010245] 20 p2778 N88-26476
Refractory Materials of Zirconate. Part 2: Synthesis and some properties of strontium, zirconate, calcium zirconate and barium zirconate
[NASA-TT-20186] 20 p2779 N88-26483
Scanning tunneling microscopy as a surface chemical probe
[AD-A192710] 21 p2909 N88-27263
Energy distribution and transfer in flowing hydrogen microwave plasmas 21 p3019 N88-27919
Growth and characterization of CuGaS2, CuAlS2 and CuGa0.9Al0.1S2 single crystals
[AD-A192963] 21 p3021 N88-27930
Thermodynamic data bases for multivalent elements: An example for ruthenium
[DE88-004395] 23 p3190 N88-28984
Laser induced chemical vapor epitaxial growth of gallium arsenide films
[AD-A194254] 23 p3291 N88-29595
Chemical and spectroscopic characterization of a suite of Mars soil analogs 23 p3302 N88-29667
Attenuated total reflectance FT-IR spectroscopy to measure interfacial reaction kinetics at silica surfaces
[AD-A196330] 24 p3344 N88-29908

CHEMICAL PROPULSION
NT HYBRID PROPULSION
Space station onboard propulsion system: Technology study
[NASA-CR-179233] 07 p0825 N88-15006
Prospects for antiproton production and propulsion
16 p2267 N88-23556
Comparison of a direct thrust nuclear engine, nuclear electric engine and a chemical engine for future space missions 17 p2418 N88-24379
Recent advances in low-thrust propulsion technology
[NASA-TM-100959] 18 p2569 N88-25260

CHEMICAL REACTIONS
NT ALKYLATION
NT AMMONOLYSIS
NT ASSOCIATION REACTIONS
NT ATOMIC RECOMBINATION
NT BROMINATION
NT CARBONIZATION
NT CHLORINATION
NT COPOLYMERIZATION
NT CRACKING (CHEMICAL ENGINEERING)
NT DESULFURIZING
NT DIELS-ALDER REACTIONS
NT ELECTROCHEMICAL OXIDATION
NT ENDOTHERMIC REACTIONS
NT EXOTHERMIC REACTIONS
NT FERMENTATION
NT FLUORINATION
NT HALOGENATION
NT HYDROCRACKING
NT HYDROGENATION
NT HYDROLYSIS
NT ION RECOMBINATION
NT METAL-WATER REACTIONS
NT NITRATION
NT NITRIDING
NT NITROGENATION

NT OXIDATION
NT OXIDATION-REDUCTION REACTIONS
NT OXYGEN RECOMBINATION
NT OXYGENATION
NT PHOSPHORYLATION
NT PHOTOCHEMICAL REACTIONS
NT PHOTOCHROMISM
NT PHOTODECOMPOSITION
NT PHOTOLYSIS
NT PHOTOOXIDATION
NT PHOTOSYNTHESIS
NT PYROHYDROLYSIS
NT PYROLYSIS
NT RADIOLYSIS
NT REDUCTION (CHEMISTRY)
NT RUSTING
NT SULFIDATION
NT THERMAL DECOMPOSITION
NT THERMAL DISSOCIATION
NT TITRATION

Overcharge protection in Li-alloy/metal disulfide cells
[DE87-011364] 01 p0041 N88-10260

Chemical analysis of charged Li/SO(sub)2 cells
02 p0163 N88-11026

Voltammetric investigation of porous silicon for integrated circuit applications
[DE87-009287] 02 p0166 N88-11042

Shock-chemistry in natural materials and evolution of planetary surfaces
[DE87-012737] 02 p0254 N88-11604

Superfluid He4 as a solar neutrino detector
[DE87-014477] 02 p0257 N88-11625

The calculation of thermal rate constants for gas-phase and heterogeneous reactions in combustion processes
[AD-A184435] 03 p0284 N88-11788

Stress corrosion cracking of high-strength steels in aqueous environments 03 p0289 N88-11818

Numerical simulation of internal combustion engine flows: Development and users guide for MAGIC radial-azimuthal version
[DE87-014453] 03 p0332 N88-12091

Development of the non-equilibrium reactive chemical transport code CHMTRNS
[DE88-000682] 04 p0481 N88-12964

Hypersonic laminar boundary layer. Parametric study for the representation of real gas effects
05 p0532 N88-13236

Numerical analysis of axisymmetric flow with H2-O2 reactions 05 p0538 N88-13272

Plasma joining of metal matrix composites
[AD-A184828] 05 p0557 N88-13390

Fabrication of composites by chemical vapor deposition
[DE87-014565] 05 p0559 N88-13408

Shock compression of solids as a physical-chemical-mechanical process
[DE88-001674] 05 p0563 N88-13427

Modeling the effect of sulfur on the threshold environmental cracking rate of steels in high temperature water 05 p0604 N88-13703

The role of electronic structure calculation in mechanistic analysis of electron transfer reactions in the liquid phase
[DE87-014395] 05 p0647 N88-13963

Numerical study of chemically reacting flows using an LU scheme
[NASA-CR-180882] 06 p0668 N88-14094

Reactions and bonding between glasses and titanium
[DE88-000603] 06 p0685 N88-14195

Nitrogen scale-up
[AD-A185702] 06 p0709 N88-14351

Ozone formation due to interaction of meteoroids with Earth's atmosphere 06 p0738 N88-14536

Studies of metal/carbon surface chemistry
[DE87-009545] 07 p0829 N88-15029

SRB combustion dynamics analysis computer program (CDA-1)
[NASA-CR-182404] 07 p0830 N88-15032

Surface chemistry of chemically sensitive field effect transistors
[AD-A185917] 07 p0847 N88-15139

Chemical reactions in turbulent mixing flows
[AD-A186141] 07 p0849 N88-15153

Mixing in variable density, isothermal turbulent flows and implications for chemically reacting turbulent flows
[PB88-110044] 07 p0852 N88-15176

The KIVA-2 computer program for transient multidimensional chemically reactive flows with sprays
[DE88-000502] 07 p0854 N88-15191

Biogeochemical cycling in the ocean. Part 1: Introduction to the effects of upwelling along the west coast of North America
[NASA-TM-88230] 07 p0882 N88-15349

Physiological and biochemical aspects of toxic effects of oxidants in man's environment (air, water)
07 p0890 N88-15391

Atomic oxygen effects on metals
07 p0924 N88-15617

Aeropropulsion '87. Session 3: Internal Fluid Mechanics Research
[NASA-CP-10003-SESS-3] 08 p0954 N88-15790

Chemical reacting flows 08 p0955 N88-15793

Structural study of the impregnating resins of the type TGMDA/DDS --- expoxy resins
[ETN-88-91616] 08 p0965 N88-15842

An analytical study of the hydrogen-air reaction mechanism with application to scramjet combustion
[NASA-TP-2791] 08 p0966 N88-15846

Processing and interfacial analysis of glass-ceramic to metal seals
[DE88-002999] 08 p0971 N88-15873

Investigations of the influence of chemical reactions of the vertical flow of gaseous and particulate compounds
08 p1017 N88-16165

Feasibility of chemical lasers based on chain reaction involving hydrogen fluorination with thermal branching mechanism 09 p1238 N88-17420

Gas phase pulse radiolysis
[DE88-002981] 10 p1296 N88-17751

Insights into the mechanisms of chemical reactions. Reaction paths for chemical reactions
[DE88-003041] 10 p1297 N88-17755

Precipitation of surfactants and surfactant mixtures in aqueous solutions
[DE88-003333] 10 p1298 N88-17763

The chemistry of the hypochlorite neutralization of hydrazine fuels
[DE88-002971] 10 p1307 N88-17812

Laser studies of the dynamics of free radical reactions
[DE88-004431] 10 p1337 N88-17989

Chemical activation of molecules by metals: Experimental studies of electron distributions and bonding
[DE88-004465] 10 p1407 N88-18393

Reactions of some thiol collectors at noble-metal and pyrite electrodes
[PB88-138318] 11 p1455 N88-18674

Voltammetric investigation of porous silicon for integrated circuit applications
[DE88-004024] 11 p1456 N88-18677

Gas phase reactions of electrons, negative ions and free-radicals with transition metal complexes
11 p1560 N88-19339

Thermodynamics of wetting by liquid metals
[DE88-003634] 11 p1563 N88-19360

Chromatographic and related reactors
[AD-A188452] 12 p1605 N88-19599

The redox chemistry of some peroxo and superoxo metal ion complexes
[AD-A189159] 12 p1606 N88-19606

Picosecond laser studies of excited state processes
[AD-A189606] 12 p1607 N88-19607

Thermal cracking and variable properties effects on free boundary layer diffusion flames
[NBS/GCR-88/542] 12 p1614 N88-19652

A new parabolized Navier-Stokes code for chemically reacting flow fields 12 p1625 N88-19721

MOPAC manual: A general molecular orbital package, fourth edition
[AD-A188623] 13 p1733 N88-20362

Combustion theory and related questions
[AD-A189160] 13 p1737 N88-20382

Kinetic mechanisms for ionization and afterburning suppression
[AD-A189219] 13 p1737 N88-20383

Potassium cuprate (3)
[NASA-TT-20246] 13 p1739 N88-20401

Scale-up of a batch-type chemical powder preparation process for high field varistor fabrication
[DE88-006601] 13 p1762 N88-20541

Experimental and theoretical constraints on the origin of mid-ocean ridge geothermal fluids
13 p1804 N88-20784

Solid-state electrochemical processes in dye films
[AD-A188756] 13 p1844 N88-21036

Investigation of supersonic chemically reacting and radiating channel flow
[NASA-CR-182726] 14 p1862 N88-21125

Copper peroxide
[NASA-TT-20245] 14 p1888 N88-21282

Techniques for studying fast reactions in liquids
[DE88-005917] 14 p1888 N88-21285

Energy storage and transport by reversible chemical reactions
[DE88-900370] 14 p1942 N88-21587

Numerical simulation of turbulent flames using vortex methods
[AD-A189813] 15 p2034 N88-22116

An investigation of flow structure, mixing and chemical reaction in combusting turbulent flows
[AD-A189980] 15 p2034 N88-22117

Investigation of combustion in large vortices
[AD-A190406] 15 p2035 N88-22121

AFRAPT (Air Force Research in Aero Propulsion Technology) trainee program
[AD-A190525] 15 p2035 N88-22123

Evaluation of direct methane conversion to higher hydrocarbons and oxygenates
[DE88-003812] 15 p2049 N88-22204

The numerical simulation of viscous flows with change of phase and chemical reaction
[DE88-003204] 15 p2062 N88-22292

Chemically reacting turbulent flow
[AD-A190522] 15 p2065 N88-22311

The kinetics of contact noise in NaBeta alumina
[AD-A190651] 15 p2130 N88-22707

Synthesis and properties of novel cluster phases
[DE88-006616] 16 p2175 N88-22964

Analysis of non-premixed turbulent reacting flows
16 p2196 N88-23100

Advanced chemical heat pumps using liquid-vapor reactions
[DE88-006760] 16 p2205 N88-23159

Energy transfer processes in free radicals: A collaborative experimental and theoretical investigation
[AD-A191264] 16 p2269 N88-23578

Preventing aircraft corrosion by predictive corrosion modeling 17 p2321 N88-23863

Chemical kinetics and photochemical data for use in stratospheric modeling evaluation Number 8
[NASA-CR-182919] 17 p2351 N88-24012

Chemical compatibility between silicon carbide and a nickel aluminide
[DE88-006188] 18 p2479 N88-24708

Electrochemistry in liquid crystals
[AD-A191554] 18 p2481 N88-24719

Analysis of molecular mixing and chemical reaction in mixing layer
[AD-A191600] 18 p2482 N88-24721

Structural study of the TGMDA-DDS system --- epoxy system
[ONERA-RT-4/3346-M] 18 p2493 N88-24792

Study of mixing and reaction in the field of a vortex
[AD-A191489] 18 p2508 N88-24878

Numerical solutions of the complete Navier-Stokes equations
[NASA-CR-183023] 18 p2514 N88-24914

Workshop on Atmospheric OH
[BPT-7/87] 18 p2538 N88-25063

Ozone in the atmosphere 18 p2539 N88-25064

Laboratory experiments on atmospheric OH reactions
18 p2539 N88-25066

Characterization of yttrium aluminum garnet/YAG/using 14 MeV neutron activation
[AD-A191925] 18 p2582 N88-25342

Surface interactions relevant to space station contamination problems 18 p2592 N88-25401

Theoretical studies of the chemical reactions involved in the ignition of nitramines 19 p2632 N88-25615

Direct simulations of chemically reacting turbulent mixing layers, part 2
[NASA-CR-180853] 19 p2667 N88-25857

The 1986 IEEE Solid-State Sensor Workshop
[AD-A190922] 19 p2668 N88-25860

Thin-membrane Lamb-mode acoustic oscillators for chemical detection 19 p2673 N88-25895

Kinetics of thermochemical gas-solid reactions important in the Venus sulfur cycle
[NASA-CR-182963] 19 p2742 N88-26280

The rate of volcanism on Venus
[NASA-CR-183039] 19 p2742 N88-26281

The protonic Beta double prime aluminas: Preparation, stability, conductivity and structure
[DE88-008442] 20 p2768 N88-26415

Structural study of impregnating resins of TGMDA/DDS type
[ETN-88-92167] 20 p2780 N88-26488

Freely expanding detonation products: Scaling of rate processes
[DE88-007827] 20 p2799 N88-26606

Physical-chemical reactions at welding arc/molten pool interfaces
[DE88-007717] 20 p2808 N88-26662

Ion and electron interactions of atmospheric importance
[AD-A192255] 20 p2824 N88-26751

On the chemistry of superconductivity
[DE88-010714] 20 p2880 N88-27096

A study of the interaction of diffusion flames with a vortex pair flowfield 21 p2908 N88-27258

Mechanism of the nitric oxide-carbon monoxide-oxygen reaction over a single crystal rhodium catalyst
[DE88-006274] 21 p2910 N88-27268

Numerical computation of space shuttle orbiter flow field
[NASA-CR-183193] 22 p3040 N88-28048

Modification of YBa2Cu3O(7-x) ceramics by adsorbed water and other gases
[DE88-011518] 22 p3057 N88-28140
A study of the interaction of NO2 with carbon particles
[DE88-010778] 22 p3118 N88-28524
Radiative heat transfer to chemically reacting flow between concentric rotating spheres
[DE88-702538] 22 p3118 N88-28525
Theoretical investigations of nitrocubane decomposition
[AD-A194556] 23 p3200 N88-29047
Method of dispensing reagent chemicals in space
[NASA-CASE-LAR-13607-1-CU] 23 p3200 N88-29048
Laser induced chemical vapor epitaxial growth of gallium arsenide films
[AD-A194254] 23 p3291 N88-29595
Computed potential energy surfaces for chemical reactions
[NASA-CR-183168] 24 p3342 N88-29893
Design criteria for extraction with chemical reaction and liquid membrane permeation
[NASA-TT-20352] 24 p3343 N88-29899
Gas phase combustion chemistry of nitramine propellants
[AD-A195082] 24 p3344 N88-29902
Attenuated total reflectance FT-IR spectroscopy to measure interfacial reaction kinetics at silica surfaces
[AD-A196330] 24 p3344 N88-29908
Recent observations of carbon monoxide in the Amazon Rain Forest
[INPE-4478-PRE/1245] 24 p3390 N88-30186

CHEMICAL REACTORS
Mechanistic model for void distribution in flashing flow
[DE88-002948] 10 p1326 N88-17928
Research on hydrotreating catalysts to hydrodeoxygenate biocrude oils
18 p2536 N88-25046
Low-temperature thermochemical conversion of high moisture biomass feedstocks 18 p2536 N88-25047
An improved external recycle reactor for determining gas-solid reaction kinetics
[NASA-TM-101160] 19 p2611 N88-25492
Integrated solar reforming for thermochemical energy transport
[DE88-005010] 19 p2686 N88-25967
C-CAMP: A closed cycle alkali metal power system
[DE88-009715] 19 p2688 N88-25975

CHEMICAL RELAXATION
U MOLECULAR RELAXATION

CHEMICAL RELEASE MODULES
The combined release and radiation effects satellite, a joint NASA/DOD program 02 p0135 N88-10851

CHEMICAL SHIFT
U CHEMICAL EQUILIBRIUM

CHEMICAL TESTS
NT CHEMICAL ANALYSIS
NT CHROMATOGRAPHY
NT ELECTROPHOTOMETRY
NT GAS ANALYSIS
NT GAS CHROMATOGRAPHY
NT LIQUID CHROMATOGRAPHY
NT MICROANALYSIS
NT NEUTRON ACTIVATION ANALYSIS
NT OZONOMETRY
NT POTENTIOMETRIC ANALYSIS
NT QUALITATIVE ANALYSIS
NT QUANTITATIVE ANALYSIS
NT SALT SPRAY TESTS
NT SPECTROSCOPIC ANALYSIS
NT VOLUMETRIC ANALYSIS
Viscosity measurements at high temperatures on a standard reference material supplied by BCR --- Bureau Communite de Reference (BCR)
[NPL-DMA(A)-146] 01 p0020 N88-10126
Material degradation in a barium hydroxide latent heat storage pilot unit
[DFVLR-FB-87-49] 16 p2175 N88-22961

CHEMICAL VAPOR DEPOSITION
U VAPOR DEPOSITION

CHEMICAL WARFARE
Advanced development waste processing unit for combat vehicles, phase 2
[AD-A193793] 23 p3243 N88-29302
Four-axis side-arm flight control simulator investigation
[AD-A196026] 24 p3409 N88-30204

CHEMILUMINESCENCE
Laser probes of natural gas ignition chemistry
[PB87-209599] 01 p0021 N88-10129
The kinetics and dynamics of iodine monofluoride formation in gas-phase collisions
[AD-A185715] 06 p0709 N88-14352
Methods of quantifying and enhancing reactive oxygen species production 21 p2924 N88-27357

CHEMISORPTION
Separation of anionic from nonionic alkoxy compounds using silica gel
[GB-PATENT-2-140-415-A] 01 p0020 N88-10122
Adhesion properties of polyelectrolyte-chemisorbed zinc phosphate conversion coatings
[DE87-012489] 01 p0029 N88-10186
The effect of additives on the reactivity of palladium surfaces for the chemisorption and hydrogenation of carbon monoxide: A surface science and catalytic study
[DE87-014685] 02 p0145 N88-10909
Ro-vibrational laser spectroscopy of ESD neutrals from chemisorbed species
[DE87-013011] 04 p0447 N88-12770
Atomic and electronic structure of surfaces and chemisorbed layers
[DE87-014987] 04 p0498 N88-13065
The structure of adsorbed sulfur and carbon on molybdenum and rhenium single crystal surfaces, and their influence on carbon monoxide and hydrocarbon chemisorption
[DE88-001393] 04 p0499 N88-13073
The influence of crack conditions on hydrogen uptake by steels 05 p0604 N88-13702
Oxygen chemisorption cryogenic refrigerator
[NASA-CASE-NPO-16734-1-CU] 06 p0689 N88-14223
Extending the range of Low Energy Electron Diffraction (LEED) surface structure determination: Co-adsorbed molecules, incommensurate overlayers and alloy surface order studied by new video and electron counting LEED techniques
[DE88-001401] 06 p0786 N88-14820
Surface composition-reactivity relationships in heterogeneous catalysis
[DE87-003450] 09 p1140 N88-16834
Low temperature reactivity of chars towards oxygen, appendix E2
[DE88-004088] 10 p1298 N88-17760
Coupling of vibrational modes of adsorbates: Application to field induced shifts for CO and CN on Cu(100)
[AD-A187891] 11 p1453 N88-18659
Laser-induced desorption determinations of surface diffusion on Rh(111)
[DE88-005159] 11 p1454 N88-18667
An interpretation of the ethylenic, carbidic, and graphite auger lineshapes of chemisorbed carbon species
[AD-A189092] 13 p1736 N88-20379
Model catalyst studies of SMSI (Strong Metal/Support Interactions) and the role of D-electrons in chemisorption and catalysis
[DE88-004518] 13 p1738 N88-20393
First-principles calculations of quasiparticle energies at surfaces and interfaces: Semiconductor surface-state spectra and band offsets
[DE88-006340] 15 p2141 N88-22773

CHEMONUCLEAR PROPULSION
U CHEMICAL PROPULSION
U NUCLEAR PROPULSION

CHEMORECEPTORS
Central adrenergic receptors as mediators of central response to stress: Study with Positron Emission Tomography (PET)
[AD-A194947] 24 p3407 N88-30284

CHEMOTHERAPY
Effect of different doses of alpha-hydroxydimethyl-gamma-aminopropylidene phonate on rat bones 19 p2704 N88-26078

CHICKENS
Combined effect of microwaves and ionizing radiation
07 p0893 N88-15413

CHILDREN
A study of the performance of automatic speech recognisers with speech impaired children
[RSRE-MEMO-4040] 01 p0076 N88-10486

CHILLING
U COOLING

CHIMES
U AUDITORY SIGNALS

CHINA
A review of the analysis forecasting and research about severe local storms in Guangdong province (China)
02 p0207 N88-11298
The mesoscale numerical model for heavy rainfall forecasting in Yangtze River Valley, China
02 p0211 N88-11326
JPRS report: Science and technology. China
[JPRS-CST-87-031] 03 p0299 N88-11880
JPRS report: Science and technology. China
[JPRS-CST-87-034] 03 p0301 N88-11897
LISP as a rapid prototyping environment: The chinese tutor
[AD-A184328] 03 p0369 N88-12319
JPRS report: Science and technology. China
[JPRS-CST-87-032] 03 p0376 N88-12365
Technology transfer to China
[PB87-223418] 04 p0502 N88-13087
An evaluation of effectiveness of PTFE (polytetrafluoroethylene) type friction reducers on reducing friction and wear
[AD-A187440] 10 p1340 N88-18010
JPRS report: Science and technology. China
[JPRS-CST-87-030] 13 p1756 N88-20501
Technology transfer to China. Volume 2: Working papers, part 1
[PB88-158704] 14 p1992 N88-21872
Technology transfer to China. Volume 2: Working papers, part 2
[PB88-158712] 14 p1992 N88-21873
Rate of slip on the Altin Dagh Fault (North Tibet, China) 22 p3102 N88-28420
Archean crustal evolution of the northern North China Craton 24 p3398 N88-30235

CHINA (COMMUNIST) MAINLAND
U CHINA

CHINESE PEOPLES REPUBLIC
U CHINA

CHINESE SPACE PROGRAM
JPRS report: Science and technology. China
[JPRS-CST-87-023] 14 p1863 N88-21130
PRC space satellite achievements highlighted
14 p1863 N88-21131

CHIPS (ELECTRONICS)
Low noise-low power monolithic multiplexing readout electronics for silicon strip detectors
[MPI-PAE/EXP.EL.178] 02 p0168 N88-11057
Ultra-low power digital filter
[AD-A184485] 03 p0310 N88-11959
Integrated circuit design
[AD-A184486] 03 p0311 N88-11960
The design plan of a VLSI single chip (255, 223) Reed-Solomon decoder 04 p0435 N88-12697
Research in VLSI (Very Large Scale Integration) systems
[AD-A184089] 04 p0438 N88-12721
Technology upgrade of a silicon compiler
[AD-A184873] 05 p0655 N88-14016
On systolic architectures for interpolation and integration 10 p1382 N88-18250
Cryocooler systems demonstration
[AD-A188025] 11 p1467 N88-18745
Fuzzy logic inference processor for real time control: A second generation full custom design
[AD-A188155] 11 p1471 N88-18773
RELIC: A reliability simulator for integrated circuits
[AD-A187493] 11 p1477 N88-18811
The roll back chip: Hardware support for distributed simulation using time warp
[AD-A187823] 11 p1529 N88-19132
Parts-R-Us
[AD-A188621] 12 p1622 N88-19705
Computer aided fast turnaround laboratory for research in VLSI (Very Large Scale Integration)
[AD-A189451] 12 p1624 N88-19715
Reliability analyses of a surface mounted package using finite element simulation
[AD-A189488] 12 p1624 N88-19717
Laser programming integrated circuits
[AD-A189590] 13 p1762 N88-20537
Gridless routing for generalized cell assemblies: Report and user manual
[EUT-87-E-180] 13 p1764 N88-20549
Modulatable thin film field emission space gun
[AD-A189279] 13 p1845 N88-21043
A new approach on test generation for array structures using the behavior of the system --- VLSI chips
[INF-87-27] 14 p1907 N88-21397
French Multiproject Chip (MPC) activity report, 1986
[RR-650-I] 15 p2059 N88-22273
An expert system for discrete component digital circuit design
[AD-A189680] 15 p2059 N88-22274
An analysis of multiple grain CHiP architectures
[AD-A189942] 15 p2110 N88-22570
Design and implementation of VLSI prime factor algorithm processor
[AD-A190483] 15 p2112 N88-22580
High density ion implanted contiguous disk bubble technology
[AD-A190169] 15 p2143 N88-22789
A 30 GHz monolithic receive module technology assessment
[NASA-CR-180825] 16 p2194 N88-23084
A five-layer Open Systems Interconnection (OSI) implementation 17 p2390 N88-24204
Development of 20 GHz monolithic transmit modules
[NASA-CR-182134] 17 p2445 N88-24539
Defect detection and classification in VLSI pattern inspection 18 p2507 N88-24871

An improved simulated annealing algorithm for standard cell placement
[NASA-CR-182952] 18 p2558 N88-25183
An integrated on-chip pressure sensor for accurate control applications 19 p2671 N88-25880
Natural convection immersion cooling of an array of simulated chips in an enclosure filled with dielectric liquid
[AD-A193594] 23 p3207 N88-29088
Reliability assessment of Surface Mount Technology (SMT)
[AD-A193759] 23 p3208 N88-29089
Design of a self-timed VLSI multicomputer communication controller
[AD-A194567] 24 p3361 N88-30014
Circuit design criteria for stable lateral inhibition neural networks
[AD-A195066] 24 p3366 N88-30046

CHIPS (MEMORY DEVICES)
MINIAC: A small embedded computer
[DE88-008142] 21 p2994 N88-27757

CHIRAL DYNAMICS
Light scattering by oriented and randomly dispersed chiral particles
[DE87-014758] 03 p0376 N88-12368
Determination of the neutral current chiral coupling constants u sublsq, u subrsq, d sublsq and d subrsq from an (anti)neutrino-deuterium experiment
[B8715857] 06 p0779 N88-14780
The hybrid Monte Carlo Algorithm and the chiral transition
[DE88-004305] 10 p1399 N88-18341
Comment on the Adler Bardeen theorem and related problems
[DE88-751051] 10 p1403 N88-18367
On the equivalence of four-dimensional self-duality equations to continual analog of the main chiral field problem
[DE88-700871] 12 p1686 N88-20083
Chiral symmetry in the path integral approach
[DE88-700833] 12 p1699 N88-20168
Chiral symmetry breaking in finite quantum electrodynamics
[DE88-700860] 12 p1699 N88-20169
N = 2 supergravity in superspace: The invariant action
[DE88-702136] 19 p2741 N88-26273
Theoretical particle physics
[DE88-011499] 23 p3295 N88-29621

CHIRP
The chirped-pulse free-electron laser
[DE88-009289] 20 p2807 N88-26651

CHLORELLA
Environmental life support system technology study — space flight
[ESA-CR(P)-2432] 02 p0218 N88-11371

CHLORIDES
NT BORON CHLORIDES
NT COPPER CHLORIDES
NT DICHLORIDES
NT HYDROCHLORIC ACID
NT HYDROGEN CHLORIDES
NT LITHIUM CHLORIDES
NT MAGNESIUM CHLORIDES
NT SILVER CHLORIDES
NT SODIUM CHLORIDES
Process for the preparation of acyl halides
[GB-PATENT-2-133-792-A] 01 p0020 N88-10124
The 250AH/90A active lithium-thionyl chloride cell for Centaur-G application 02 p0163 N88-11023
Corrosion susceptibility study of candidate pin materials for ALTC (Active Lithium/Thionyl Chloride) batteries
[DE88-001449] 04 p0440 N88-12734
Corrosion behavior of sputter-deposited aluminum-based alloys exposed to chloride solutions
[AD-A187262] 10 p1303 N88-17794
Rare Gas Halide (RGH) kinetics
[AD-A192352] 20 p2770 N88-26425
Effect of thermal cycling on CSPL (Chloride Silent Power Ltd.) sodium/sulfur cells
[DE88-011205] 21 p2939 N88-27455
Post-test observations on CSPL (Chloride Silent Power Limited) cells
[DE88-011975] 21 p2940 N88-27461
Advanced calcium-thionyl chloride high-power battery
[AD-A194401] 22 p3072 N88-28238
Some effects of nitrates on the tensile properties of Al 7075-T7351
[AD-A195118] 24 p3354 N88-29965

CHLORINATION
Crossed molecular beam studies of substitution and exchange reactions
[DE88-006322] 14 p1980 N88-21814

CHLORINE
Coverage dependence of adsorbate-substrate bond lengths: Chlorine and caesium adsorbed on silver single crystals
[PB87-125142] 06 p0788 N88-14833
The spreading and mixing of dense gas clouds in still air
[KNMI-WR-87-12] 16 p2230 N88-23320
Electronic states of the Xe(sub n)HCl systems in gas and condensed phases
[AD-A193881] 23 p3192 N88-28997

CHLORINE COMPOUNDS
NT AMMONIUM PERCHLORATES
NT BORON CHLORIDES
NT CHLORIDES
NT CHLORINE FLUORIDES
NT CHLOROCARBONS
NT COPPER CHLORIDES
NT DICHLORIDES
NT HYDROCHLORIC ACID
NT LITHIUM CHLORIDES
NT LITHIUM PERCHLORATES
NT MAGNESIUM CHLORIDES
NT SILVER CHLORIDES
NT SODIUM CHLORIDES
Magnetic investigations of the one-dimensional Heisenberg magnet Gd2Cl3
[ETN-88-91083] 09 p1241 N88-17438
Decomposition of hypochlorite in the presence of copper in a homogeneous medium
[NASA-TT-20199] 13 p1740 N88-20403

CHLORINE FLUORIDES
Temperature dependence of ultraviolet absorption cross sections of chlorofluoroethanes
[AERONOMICA-ACTA-A-325-1987] 18 p2482 N88-24726

CHLOROAROMATICS
Crossed molecular beam studies of substitution and exchange reactions
[DE88-006322] 14 p1980 N88-21814

CHLOROCARBONS
The potential impact on atmospheric ozone and temperature of increasing trace gas concentrations
[NASA-CR-182965] 17 p2373 N88-24112
Impact on ozone attainment of CFC (chlorofluorocarbon) controls used to prevent future depletion of stratospheric ozone
[PB88-195177] 19 p2690 N88-25989
Ultraviolet absorption cross sections of chloro- and chlorofluoromethanes at stratospheric temperatures
[AERONOMICA-ACTA-A-324-1988] 23 p3231 N88-29228

CHLOROETHYLENE
Comparison of isopropyl alcohol and trichloroethylene in removing solder flux
[DE88-005556] 14 p1889 N88-21288

CHLOROPHYLLS
A mode-locked ruby laser with chlorophyll d as saturable absorber 03 p0327 N88-12064
Vanfront 3 expedition data report (USNS DE STEIGUER CRUISE 1202-82): Bioluminescence, hydrographic, nutrient, and satellite data from the Gulf of California (November-December 1981)
[AD-A185011] 05 p0620 N88-13805
The use of chlorophyll fluorescence measurements from space for separating constituents of sea water. Volume 1: Summary
[ESA-CR(P)-2444-VOL-1] 07 p0873 N88-15294
The use of chlorophyll fluorescence measurements from space for separating constituents of sea water. Volume 2: Appendices
[ESA-CR(P)-2444-VOL-2] 07 p0873 N88-15295
Artificial photosynthesis using chlorophyll based carotenoid-quinone triads
[DE88-001660] 07 p0884 N88-15362
The use of chlorophyll fluorescence measurements from space for separating constituents of sea water 08 p1043 N88-16307
Remote determination of chlorophyll concentration in the ocean using an optical pulse radar
[NASA-TT-20301] 19 p2694 N88-26014
Mechanisms of photochemical energy conversion by chlorophyll
[DE88-008763] 20 p2819 N88-26725
Modeling the primary events of photosynthesis using chlorophyll containing fixed distance donor-acceptor molecules
[DE88-010033] 20 p2831 N88-26793

CHOICE
U SELECTION

CHOKES
Parametric study of choke flutter with a linear theory 10 p1283 N88-17673

CHOKES (RESTRICTIONS)
Geometric analysis of ensemble of solutions in two-phase flow and complete resolution of problem of choking
[DE88-001687] 04 p0445 N88-12764

CHOLESKY FACTORIZATION
Data traffic reduction schemes for sparse Cholesky factorizations
[NASA-CR-181626] 13 p1813 N88-20831
Cholesky downdating on a hypercube
[DE88-006780] 15 p2113 N88-22586

CHOLINESTERASE
Carbamates, atropine, and diazepam: Effects on performance in the running rat
[AD-A188009] 11 p1517 N88-19062
Low doses of atropine sulfate impair retention of a well-learned spatial task
[AD-A194065] 23 p3237 N88-29266

CHONDRITES
NT CARBONACEOUS CHONDRITES
NT CARBONACEOUS METEORITES
Stratospheric particles: Synchrotron X-ray fluorescence determination of trace element contents
[DE87-012482] 02 p0198 N88-11234
Organic molecules on meteoritic solid substrates
[NASA-CR-181570] 05 p0560 N88-13411
Cometary evolution: Clues from chondritic interplanetary dust particles 14 p2002 N88-21934
New type of primitive meteorite found in Antarcitca 24 p3441 N88-30478
Nebular processes recorded in chondritic meteorites 24 p3451 N88-30541

CHONDRULE
Astrophysics and the solar nebula 07 p0883 N88-15355
Evidence of the in situ decay of Al-26 in a Semarkona chondrule 24 p3441 N88-30479
Physical processes and timescales in planet and small-body accretion 24 p3451 N88-30540

CHOPPERS (ELECTRIC)
U ELECTRIC CHOPPERS

CHROMATES
Recent advances in metallic/ceramic coatings for corrosion control in military applications 17 p2320 N88-23858

CHROMATOGRAPHY
NT GAS CHROMATOGRAPHY
NT LIQUID CHROMATOGRAPHY
Supercritical fluid chromatography/supersonic jet spectroscopy
[DE88-000297] 03 p0282 N88-11774
Retention processes in supercritical fluid chromatography
[DE88-000079] 04 p0413 N88-12559
The analysis of metal finishing solutions by ion chromatography
[AD-A184812] 05 p0561 N88-13414
High energy molecules of high symmetry
[AD-A185385] 05 p0647 N88-13965
Ion chromatography in the manufacture of multilayer circuit boards
[DE88-002428] 10 p1322 N88-17902
Electrosorptive detection based on double-layer capacitance for selective anion monitoring in ion chromatography. Part 1: Mercury electrodes
[AD-A188780] 12 p1606 N88-19603
Fuels combustion research
[AD-A189114] 13 p1736 N88-20381
Determination of aquo-complexes of chromium and iron in chromium plating and polishing solutions by ion chromatography
[AD-A190168] 15 p2039 N88-22148
Universal detection of ions by replacement-ion chromatography employing an anion-replacement method and an ultraviolet-visible spectrophotometric detector
[AD-A191326] 16 p2176 N88-22971
Supercritical fluid chromatography/supersonic jet spectroscopy
[DE88-007935] 19 p2614 N88-25511

CHROME
U CHROMIUM

CHROMIC ACID
Chromic acid anodizing of aluminum foil
[NASA-CR-178417] 07 p0837 N88-15077
The effect on initial bond strength and durability of a Phosphoric Acid Dip (PAD) following chromic acid anodising of aluminum
[ARE-TM(UMM)-87402] 10 p1300 N88-17772

CHROMIUM
The mechanism by which sigma phase forms in Fe-Cr-Ni system alloys
[BLL-M-37380-(5828.4)] 05 p0564 N88-13437
Determination, by X-ray fluorescence, of platinum, palladium, ruthenium, iron and chromium in special steels
[PB87-132114] 06 p0683 N88-14183

Reaction mechanism of sulfur dioxide with single crystal cobalt and chromium and CoCrAlY coatings
[AD-A185989] 09 p1253 N88-17509
Microprobe examination of composite materials produced by burning of Ti, Cr, C powders with powder of any one Fe-group metal 14 p1886 N88-21269
Secondary electron emission characteristics improved by ion implantation 14 p1903 N88-21370
On quench sensitivity of Cu-Cr alloys
[NASA-TT-20174] 18 p2489 N88-24765
Effect of Zr or Cr content on the fracture toughness of the high purity Al-Zn-Mg alloys
[NASA-TT-20294] 19 p2616 N88-25518
Superconductivity of Cr/V superlattices
20 p2874 N88-27057
Self energy corrections to the ab initio band structures: Chromium
[DE88-701625] 21 p3020 N88-27927
Absorption spectra and energy levels of Gd(3+), Nd(3+) and Cr(3+) in the garnet Gd3Sc2Ga3O12
[AD-A193634] 23 p3292 N88-29599
An experimental study of biaxial yield in modified 9Cr-1Mo steel at room temperature
[NASA-CR-175012] 24 p3385 N88-30164

CHROMIUM ALLOYS
NT ASTROLOY (TRADEMARK)
NT CHROMIUM STEELS
The effect of sulfur and zirconium Co-doping on the oxidation of NiCrAl
[NASA-TM-100209] 02 p0150 N88-10940
Investigation of creep crack growth in heat resistant tube steels
[ETN-87-90606] 03 p0288 N88-11813
A comparison of high damping shape memory alloys with Cu-Mn-based and Fe-Cr-based alloys
[AD-A184110] 04 p0414 N88-12566
Model for ultrasonic attenuation and elastic constant in chromium and its alloys
[DE87-703478] 04 p0415 N88-12570
Microstructure and magnetic properties of cobalt-chromium alloys
[DE88-002762] 07 p0835 N88-15064
Reaction mechanism of sulfur dioxide with single crystal cobalt and chromium and CoCrAlY coatings
[AD-A185989] 09 p1253 N88-17509
Response of Fe-Cr-Mn austenitic alloys to thermal aging neutron irradiation
[DE88-003415] 10 p1302 N88-17785
The role of composition and microstructure gradients on weld metal properties and behavior
[DE88-004956] 10 p1303 N88-17791
Study of adherent oxide scales
[AD-A187368] 11 p1456 N88-18680
High temperature oxidation studies on alloys containing dispersed phase particles and clarification of the mechanism of growth of SiO2
[AD-A188158] 11 p1457 N88-18688
Corrosion resistance of electrodeposited amorphous Ni-Cr-P alloys
[DE88-005116] 11 p1459 N88-18695
Anodic behavior of Ni-P and Ni-Cr-P metallic glasses
[DE88-005334] 11 p1463 N88-18722
Effect of P implantation on the corrosion behavior of Fe-Cr alloys
[DE88-005732] 15 p2040 N88-22158
Characterization of an explosively consolidated rapidly solidified Fe-16Ni-9Cr-5Mo-2Cu alloy powder
[DE88-006733] 15 p2041 N88-22162
Fundamental studies of beta phase decomposition modes in titanium alloys
[AD-A191495] 18 p2485 N88-24740
The precipitation processes of Cu-Zr-Cr alloys
[NASA-TT-20168] 18 p2488 N88-24758
High temperature embrittleness of Cu-Cr alloy
[NASA-TT-20184] 18 p2488 N88-24759
Electrodeposition of amorphous Ni-Cr-P alloys
[DE88-006868] 19 p2616 N88-25521
Reduced-activation austenitic stainless steels: The Fe-Cr-C system
[DE88-008091] 20 p2773 N88-26442
The T-T-T curve in Cu-Cr alloy
[NASA-TT-20167] 20 p2774 N88-26453

CHROMIUM CARBIDES
Sputtered silver films to improve chromium carbide based solid lubricant coatings for use to 900 C
[NASA-TM-100783] 08 p0973 N88-15885

CHROMIUM COMPOUNDS
NT CHROMATES
NT CHROMIC ACID
NT CHROMIUM CARBIDES
NT CHROMIUM OXIDES

CHROMIUM OXIDES
Point defect structure of Cr2O3
[AD-A187620] 11 p1556 N88-19317
Evaluation of the chromium oxide arc spraying treatment on solar energy collectors
[ETN-88-92564] 18 p2537 N88-25053

CHROMIUM STEELS
On the relations between cyclic contraction ratio, flow stress, and deformation mechanisms in bainitic CrMoV steels
[VTT-36] 01 p0025 N88-10158
Modified 14Cr-16Ni stainless steels with improved creep resistance at 700 C due to tailored precipitate microstructures
[DE87-014788] 03 p0290 N88-11825
Reduced-activation ferritic steels: A comparison with Cr-Mo steels
[DE88-000332] 03 p0290 N88-11826
Impact behavior of 9-Cr and 12-Cr ferritic steels after low-temperature irradiation
[DE88-000333] 03 p0291 N88-11827
Tensile properties of extrusion consolidated Type 304 SS rapidly solidified powders
[DE87-014875] 05 p0566 N88-13450
Low cycle fatigue life predictions of a 1CrMoV steel in terms of a J-controlled short crack growth model
05 p0599 N88-13665
The influence of temper embrittlement on fatigue crack growth in hydrogen 05 p0605 N88-13709
Influence of stress ratio R on fatigue threshold delta K(th) for 40Cr steel 06 p0718 N88-14405
The effect of non-metallic inclusions on fatigue and fatigue thresholds of 25Mn-5Cr-1Ni steel
06 p0718 N88-14410
Low-chromium reduced-activation ferritic steels
[DE88-009060] 19 p2617 N88-25524
Investigation of structure and surface state effect on hydrogen embrittlement of steels, under consideration of acoustic emission analysis
[ETN-88-92350] 20 p2775 N88-26457

CHROMOSOMES
Changes in the morphological and molecular biological processes during early embryo development in amphibians under micro-g conditions 07 p0885 N88-15371
Method for measuring absolute linear parameters of chromosomes 19 p2707 N88-26095
Genetic effects of low level microwave radiation
[AD-A192687] 21 p2984 N88-27722
Effects of pulsed and CW (Continuous Wave) 2450 MHz radiation on transformation and chromosomes of human lymphocytes in vitro
[AD-A193104] 21 p2987 N88-27736

CHROMOSPHERE
Quasi-thermal models 02 p0253 N88-11600
Active region flows 02 p0255 N88-11611
High-resolution continuum observations of the Sun
02 p0255 N88-11614
Simultaneous, cospatial imaging of the Sun in cyanogen and singly-ionized calcium 04 p0507 N88-13114
Spectroscopic monitoring of RS CVn stars at Kitt Peak using the Penn State fiber optic echelle
04 p0509 N88-13127
X-rays, color, and the Vaughan-Preston gap
04 p0510 N88-13135
Relations between chromospheric and coronal structure, flux-flux correlations and convective zone properties
04 p0510 N88-13138
Broadband linear polarization and chromospheric CaII H and K line emission in late-type main sequence stars
04 p0511 N88-13140
The onset of chromospheric activity among the A- and F- type stars 04 p0511 N88-13144
Sensitivity of the H alpha line to expansion, geometrical extent and temperature gradient in the G and K supergiant chromospheres 04 p0514 N88-13159
The Wilson-Bappu relationship: A barometric effect
04 p0516 N88-13170
Synthetic spectra for the N-type carbon star TX Psc
04 p0516 N88-13173
Chromospheric variability mechanisms affecting pre-main sequence stars 04 p0517 N88-13180
Chromospheric and coronal heating in a bias-free sample of K dwarfs 04 p0518 N88-13184
Catalogue of chromospherically active binaries
04 p0520 N88-13192
A comprehensive exploration of late-type stars in the far-ultraviolet 04 p0520 N88-13194
Hydrogen and deuterium in the local interstellar medium 04 p0521 N88-13204
Observations of the solar chromosphere in Kunming
[PB87-143319] 07 p0944 N88-15737
Proceedings of the 21st ESLAB Symposium on Small Scale Processes in the Chromosphere/Corona, Interplanetary Medium and Planetary Magnetospheres
[ESA-SP-275] 08 p1094 N88-16582
Gasflows in the transition region above sunspot
08 p1095 N88-16586
Flux tubes and loops in the solar chromosphere and corona 08 p1095 N88-16591
Spectral images and multi-component models of the chromospheres of AR Lacertae
11 p1568 N88-19384

CHRONOBIOLOGY
U RHYTHM (BIOLOGY)

CHRONOLOGY
NT GEOCHRONOLOGY
Astronautics and aeronautics, 1978: A chronology
[NASA-SP-4023] 05 p0662 N88-14062
Data-base of Antarctic pre-Pleistocene sediment cores
[PB88-124151] 10 p1354 N88-18094
Effects of galactic chemical evolution on thorium/neodymium cosmochronology
[DE88-003629] 11 p1570 N88-19397
Early reheating and cosmic strings
13 p1855 N88-21103
Chronology of KSC and KSC related events for 1987
[NASA-CR-182754] 14 p2012 N88-22002
Marshall Space Flight Center 1960-1985: 25th anniversary report
[NASA-TM-100328] 15 p2153 N88-22852
Chronology of early lunar crust
24 p3394 N88-30212
Lewis Cliff 86010, a unique Antarctic meteorite: Possible new clues to the early history of the solar system
24 p3442 N88-30482

CHRONOTRONS
U TIME LAG

CHUGGING
U COMBUSTION STABILITY

CINEFLUOROGRAPHY
U MOTION PICTURES
U RADIOGRAPHY

CINEMATOGRAPHY
Flow measurements in a water tunnel using a holocinematographic velocimeter
16 p2203 N88-23141

CINERADIOGRAPHY
U MOTION PICTURES
U RADIOGRAPHY

CIRCADIAN RHYTHMS
Sleep and wakefulness: Handbook for flight medical officers, second edition
[AGARD-AG-270(E)] 02 p0217 N88-11366
Effect of night watches and intermittent sleep on state of circadian rhythms of physiological functions of fishermen 06 p0750 N88-14610
Pharmacological resetting of the Circadian sleep-wake cycle
[AD-A186194] 07 p0889 N88-15385
Biorhythmic aspects of intercontinental Antarctic adaptation 08 p1046 N88-16321
Inflight simian circadian rhythms and temperature homeostasis aboard Cosmos-1514 biosatellite
10 p1359 N88-18125
Center for the study of rhythmic processes
[AD-A188204] 11 p1520 N88-19078
Implications of shiftwork in space for human physiology experiments 12 p1659 N88-19942
Desynchronization of heart rate and breathing frequency after transmeridional flight across three time zones
12 p1663 N88-19968
Biological rhythms, sleep, and wakefulness in prolonged confinement 19 p2696 N88-26022
Biorhythms of binocular vision
20 p2830 N88-26788
The biological clock of Chlamydomonas reinhardii in space 22 p3061 N88-28162

CIRCLES (GEOMETRY)
Numerical arc segmentation algorithm for a radio conference-NASARC (version 2.0) technical manual
[NASA-TM-100160] 08 p0977 N88-15910
Fitting a circle to radially suppressed data
[NPL-DITC-103/87] 17 p2392 N88-24223
Linear programming in R sup 3 and the skeleton and largest incircle of a convex polygon
[PB88-124664] 20 p2846 N88-26892

CIRCUIT BOARDS
Ion chromatography in the manufacture of multilayer circuit boards
[DE88-002428] 10 p1322 N88-17902
VAXELN experimentation: Programming a real-time clock and interrupt handling using VAXELN Ada 1.1
[AD-A188100] 11 p1525 N88-19107
The inspection of electronic metallurgical bonds
[AD-A192197] 18 p2486 N88-24745
Procedures for identification and handling of Printed Circuit Boards (PCBs)
[AD-A191177] 23 p3206 N88-29078
Natural convection immersion cooling of an array of simulated chips in an enclosure filled with dielectric liquid
[AD-A193594] 23 p3207 N88-29086

CIRCUIT BREAKERS
Measuring technical and mathematical investigation of multiple reignitions at the switching of a motor using vacuum circuit breakers
[ETN-87-90406] 01 p0042 N88-10270
A simple self-breaking 2 MV gas switch
[DE87-014346] 02 p0166 N88-11047
Low-current behavior and current chopping of vacuum arcs
[ISBN-90-9001649-X] 05 p0578 N88-13529
CIRCUIT DIAGRAMS
Extraction of MOS VLSI (Very-Large-Scale-Integrated) circuit models including critical interconnect parasitics
[AD-A185847] 08 p0979 N88-15914
Data acquisition and processing for surface plate calibration
[AD-A187264] 11 p1564 N88-19366
ECP (Electrical Circuitry Program): A proposed program for electrical circuitry analysis
[AD-A190494] 15 p2060 N88-22280
Defect detection and classification in VLSI pattern inspection 18 p2507 N88-24871
Rule-based circuit optimization for CMOS VLSI
22 p3137 N88-28649
CIRCUIT PROTECTION
The 8.4-GHz low-noise maser pump source assembly
04 p0436 N88-12705
Trip electrical circuit of the gyrotron
[INPE-4336-NTE/273] 12 p1622 N88-19701
Metal oxide varistor polarization from an initial transient
[AD-A189012] 12 p1623 N88-19711
CIRCUIT RELIABILITY
DEDALE: An expert system for analog circuit maintenance 02 p0128 N88-10809
An integrated pressure sensor for in-vivo use
10 p1333 N88-17965
A methodology for hardware verification based on logic simulation
[AD-A188553] 12 p1622 N88-19704
Time domain wave propagation in multilayered integrated circuits
[AD-A193821] 22 p3073 N88-28241
CIRCUITS
NT ANALOG CIRCUITS
NT BISTABLE CIRCUITS
NT COINCIDENCE CIRCUITS
NT COMPARATOR CIRCUITS
NT COUPLING CIRCUITS
NT DELAY CIRCUITS
NT DIGITAL ELECTRONICS
NT DIPLEXERS
NT DISCRIMINATORS
NT ELECTRIC BRIDGES
NT ENCAPSULATED MICROCIRCUITS
NT EQUIVALENT CIRCUITS
NT FLUIDIC CIRCUITS
NT FREQUENCY DISCRIMINATORS
NT GATES (CIRCUITS)
NT HYBRID CIRCUITS
NT INTEGRATED CIRCUITS
NT ITERATIVE NETWORKS
NT LARGE SCALE INTEGRATION
NT LINEAR CIRCUITS
NT LINEAR INTEGRATED CIRCUITS
NT LOGIC CIRCUITS
NT MAGNETIC CIRCUITS
NT MATRICES (CIRCUITS)
NT MICROWAVE CIRCUITS
NT MIXING CIRCUITS
NT OHMS LAW
NT PHASE DETECTORS
NT PHASE SHIFT CIRCUITS
NT POWER SUPPLY CIRCUITS
NT PRINTED CIRCUITS
NT RC CIRCUITS
NT SCALERS
NT SWITCHING CIRCUITS
NT TRANSISTOR CIRCUITS
NT TRIGGER CIRCUITS
NT VARACTOR DIODE CIRCUITS
NT VERY LARGE SCALE INTEGRATION
NT VHSIC (CIRCUITS)
An optically strobed sample and hold circuit
[DE87-011877] 01 p0038 N88-10245
A tutorial on Rogowski coil theory and operation
[DE88-000006] 02 p0230 N88-11449
Electromagnetic effects of a discharge on circuitry --- spacecraft 03 p0274 N88-11726
The Pierce diode with an external circuit. Part 1: Simulations in the linear regime
[DE88-000413] 04 p0440 N88-12731
Radiation performance of AlGaAs concentrator cells and expected performance of cascade structures
[NASA-TM-100145] 04 p0465 N88-12878
Diagnostic reasoning in digital systems
[NASA-CR-181564] 05 p0633 N88-13871
The numerical and analytic of implicit differential equations and their application to control and circuit problems
[AD-A185404] 05 p0641 N88-13922
Signal processing for an optical wide band data transmission system
[DE88-003854] 10 p1319 N88-17688
Ballistic deficits in pulse shaping amplifiers
[DE88-003906] 11 p1481 N88-18840
Electrophoretically deposited styrene-acrylate coatings for suppression of internal electromagnetic pulse effects
[DE88-003820] 12 p1609 N88-19621
Research on automatic verification of finite-state concurrent systems
[AD-A188618] 12 p1677 N88-20029
Analysis of induction motors based on the numerical solution of the magnetic field and circuit equations
[EL-59] 14 p1907 N88-21398
ECP (Electrical Circuitry Program): A proposed program for electrical circuitry analysis
[AD-A190494] 15 p2060 N88-22280
A fully abstract semantics for event-based simulation
[AD-A190560] 15 p2060 N88-22283
Electrical circuit modeling of reversed field pinches
[DE88-006942] 15 p2136 N88-22745
Compilation of preprints
[AD-A191245] 16 p2252 N88-23460
Use of magnetic materials in excimer laser circuits
[DE88-006449] 19 p2674 N88-25903
RCL model for the development of hysteresis in superconductors
[DE88-702061] 19 p2733 N88-26234
An investigation of the uses of time domain capable vector network analyzers as a diagnostic for helix traveling-wave circuits
[AD-A192460] 21 p2935 N88-27430
A fiber optic synchronous detector using sample-and-hold circuits
[DE88-010973] 21 p3016 N88-27899
A millimeter-wave tunneLadder TWT
[NASA-CR-182184] 22 p3072 N88-28239
The p-well or n-well CMOS technology for advanced SEU-hard SRAMs
[DE88-006845] 22 p3156 N88-28777
Arcjet power supply and start circuit
[NASA-CASE-LEW-14374-1] 23 p3181 N88-28939
Distortions in processed signals and their application in electronic design. Part 1: Basic and general formulations
[DE88-702731] 23 p3204 N88-29070
Distortions in processed signals and their application in electronic design. Part 3: An automated generator of communication jamming signals
[DE88-702733] 23 p3205 N88-29072
Power supply conditioning circuit
[NASA-CASE-NPO-17233-1-CU]
23 p3208 N88-29095
Confirmation of slow-waves in a crosstie overlay coplanar waveguide and its application to band-reject gratings and reflectors
[AD-A194981] 24 p3361 N88-30011
Reducing the parallel solution time of sparse circuit matrices using reordered Gaussian elimination and relaxation
[AD-A195152] 24 p3366 N88-30045
CIRCULAR CYLINDERS
Effect of viscosity on a vertical cylinder due to surface waves
[ETN-87-90960] 02 p0171 N88-11075
The hybrid wavefront resonance method
03 p0303 N88-11913
The diffusion-convection vortex method for solving two-dimensional incompressible Navier-Stokes equation
03 p0317 N88-12001
Wind tunnel investigations of periodic vortex separation on rough-surface circular cylinders using acoustic measuring methods
[DFVLR-FB-87-24] 09 p1112 N88-16665
A large strain thermomechanical forming model for elastic-viscoplastic behavior in metals
10 p1301 N88-17780
Time-resolved heat transfer measurements and analysis in the wage region of a cylinder in crossflow
10 p1328 N88-17939
Nonaxisymmetric body supersonic, aerodynamic prediction
[AD-A189338] 13 p1716 N88-20259
Body tensor formalism in finite deformation elasticity and application to the torsion of a circular cylinder
13 p1780 N88-20651
Theoretical and numerical solution of the forward-scattering problem in a circularly cylindrical configuration
[PB88-173489] 16 p2189 N88-23056
Finite elements for the computation of three-dimensional electromagnetic fields in inhomogeneous media (revised)
[PB88-173471] 16 p2190 N88-23057
Oscillating flow over bluff bodies in a U-shaped water tunnel 16 p2201 N88-23131
Correlations of velocity and temperature fluctuations in the stagnation-point flow of circular cylinder in turbulent flow
[NASA-TM-100930] 19 p2597 N88-25435
Liquid motions in partially filled containers: Preliminary results of the D-1 mission --- Spacelab
[NLR-MP-86042-U] 20 p2802 N88-26629
Natural frequencies and stability of circular cylindrical immiscible liquid systems
[LRT-WE-9-FB-3(1987)] 22 p3062 N88-28172
Heat transport in a parabolic tube of circular cross-section
[LRT-WE-9-FB-2(1988)] 22 p3078 N88-28274
The effects of incoming boundary layer thickness on unsteady shock-induced turbulent separations induced by cylinders
[AD-A196190] 24 p3368 N88-30060
CIRCULAR ORBITS
NT STATIONARY ORBITS
Canonical variables and canonical integrals for motion in near-circular orbits 24 p3446 N88-30512
CIRCULAR PLATES
Unsteady flow about cambered plates
[AD-A184725] 03 p0320 N88-12025
On the instability of thin circular shear layers
04 p0395 N88-12467
Vibration and parametric excitation in rotating asymmetric circular plates 04 p0456 N88-12823
Boundary element analysis for dynamic loading of a circular plate on an elastic medium
[CI-86] 06 p0722 N88-14443
Experimental investigation of the effects of underwater exposure on the damping characteristics of bolted structural connections for plates and shells
[AD-A194486] 23 p3226 N88-29200
CIRCULAR POLARIZATION
An investigation on Faraday rotators and quarter-wave plates of a 35 GHz radar signature system
[DFVLR-FB-87-14] 01 p0037 N88-10236
Relativistic electromagnetic waves in an electron-ion plasma
[NASA-CR-182421] 08 p1085 N88-16532
Mode priming in an overmoded gyrotron oscillator
[AD-A189151] 13 p1772 N88-20602
Polarization properties of SiO masers
13 p1858 N88-21113
Linear and circular polarization of Comet Halley light
14 p2009 N88-21982
Research on Faraday rotators and quarter-wave plates of a 35-GHz radar signature system
[ESA-TT-1081] 16 p2189 N88-23052
CIRCULAR TUBES
Numerical study of the entrance flow and its transition in a circular pipe (2) 03 p0318 N88-12011
CIRCULAR WAVEGUIDES
Analysis of electromagnetic wave propagation in slightly inhomogeneous hollow waveguides
[DFVLR-FB-87-23] 09 p1152 N88-16904
CIRCULATION
NT ATMOSPHERIC CIRCULATION
NT BLOOD CIRCULATION
NT BRAIN CIRCULATION
NT COASTAL CURRENTS
NT CONGESTION
NT CORONARY CIRCULATION
NT EL NINO
NT GULF STREAM
NT LOMONOSOV CURRENT
NT OCEAN CURRENTS
NT PERIPHERAL CIRCULATION
NT PULMONARY CIRCULATION
NT WATER CIRCULATION
NT WATER CURRENTS
NT ZONAL FLOW (METEOROLOGY)
Influence of the friction coefficients, the power and the flowrate on the two-phase flow instabilities in natural circulation
[DE88-700036] 08 p0983 N88-15946
Solidification with natural circulation
[DE88-011197] 22 p3074 N88-28248
Finding minimum-cost circulations by canceling negative cycles
[AD-A194027] 23 p3271 N88-29468
Finding minimum-cost circulations by successive approximation
[AD-A194028] 23 p3272 N88-29469
Experimental and analytical study of two-phase flow in zero gravity
[AD-A195223] 24 p3358 N88-29993

An analysis of results of a high-resolution world ocean circulation model
[AD-A195760] 24 p3405 N88-30272

CIRCULATION CONTROL AIRFOILS
NT CIRCULATION CONTROL ROTORS

Proceedings of the Circulation-Control Workshop, 1986
[NASA-CP-2432] 10 p1268 N88-17586

Navier-Stokes calculations and turbulence modeling in the trailing edge region of a circulation control airfoil
10 p1268 N88-17587

Wall jet analysis for circulation control aerodynamics. Part 1: Fundamental CFD and turbulence modeling concepts 10 p1269 N88-17588

Investigations of a circulation control airfoil flowfield using an advanced laser velocimeter
10 p1269 N88-17589

Evaluation of a research circulation control airfoil using Navier-Stokes methods 10 p1269 N88-17591

Navier-Stokes computations for circulation control airfoils 10 p1269 N88-17592

Wall jet analysis for circulation control aerodynamics. Part 2: Zonal modeling concepts for wall jet/potential flow coupling 10 p1269 N88-17593

The further development of circulation control airfoils
10 p1270 N88-17594

On the effect of leading edge blowing on circulation control airfoil aerodynamics 10 p1270 N88-17595

Pressure distributions and oil-flow patterns for a swept circulation-control wing 10 p1270 N88-17596

Boundary-layer and wake measurements on a swept, circulation-control wing 10 p1270 N88-17597

Wind tunnel studies of circulation control elliptical airfoils 10 p1270 N88-17598

An aerodynamic comparison of blown and mechanical high lift airfoils 10 p1272 N88-17606

Fixed wing CCW aerodynamics with and without supplementary thrust deflection
10 p1272 N88-17607

Development of circulation control technology for powered-lift STOL aircraft 10 p1272 N88-17608

A potential flight evaluation of an upper-surface-blowing/circulation control-wing concept
10 p1272 N88-17609

Circulation control STOL aircraft design aspects
10 p1272 N88-17610

Boundary-layer and wake measurements on a swept, circulation-control wing
[NASA-TM-89426] 15 p2014 N88-22013

On the validation of a code and a turbulence model appropriate to circulation control airfoils
[NASA-TM-100090] 16 p2156 N88-22864

CIRCULATION CONTROL ROTORS

Proceedings of the Circulation-Control Workshop, 1986
[NASA-CP-2432] 10 p1268 N88-17586

Flap-lag-torsion aeroelastic stability of a circulation control rotor in forward flight 10 p1271 N88-17600

The impact of circulation control on rotary aircraft controls systems 10 p1271 N88-17601

Analysis of a fixed-pitch X-wing rotor employing lower surface blowing 10 p1271 N88-17602

Prediction of aeroelastic response of a model X-wing rotor 10 p1271 N88-17603

X-wing potential for Navy applications
10 p1271 N88-17604

Reduction of tilt rotor download using circulation control 10 p1271 N88-17605

Analysis of a fixed-pitch X-wing rotor employing lower surface blowing
[AD-A187379] 24 p3321 N88-29779

CIRCULATION DISTRIBUTION

On estimating the basin-scale ocean circulation from satellite altimetry. Part 1: Straightforward spherical harmonic expansion
[NASA-CR-182387] 07 p0882 N88-15352

Northern winter circulations for the period 1974-1983
[AD-A187779] 11 p1511 N88-19028

CIRCULATORY SYSTEM
NT AORTA
NT ARTERIES
NT CAPILLARIES (ANATOMY)
NT CARDIAC VENTRICLES
NT CARDIOVASCULAR SYSTEM
NT HEART
NT MYOCARDIUM
NT VEINS

Circulatory response of males 45-52 years of age to antiorthostatic hypokinesia 07 p0894 N88-15416

Oxidative enzyme activity in healthy subjects and individuals with neurocirculatory dystonia during graded exercise 10 p1367 N88-18170

Macaca rhesus tolerance to +Gz accelerations
19 p2704 N88-26080

CIRCUMFERENCES

Numerical simulation of flight body circumference flow
06 p0676 N88-14137

CIRCUMSTELLAR MATTER
U STELLAR ENVELOPES

CIRRUS CLOUDS

Lidar-radiometric method for determining liquid-water content of cirrus clouds 04 p0461 N88-12854

Measurement of cirrus cloud optical properties by high spectral resolution lidar 04 p0470 N88-12906

Galactic interstellar abundance surveys with IUE and IRAS 04 p0522 N88-13206

The collection of statistics on the frequency of cloud cover over North America
[AD-A190456] 15 p2097 N88-22495

The collection of statistics on the frequency of cloud cover over North America
[AD-A193093] 21 p2974 N88-27667

Cloud/mesoscale model development and application studies
[AFGL-TR-87-0219] 24 p3404 N88-30269

CITIES

A diffraction based theoretical model for prediction of UHF path loss in cities 12 p1616 N88-19661

Urban cartography: A book review
16 p2227 N88-23297

Remote sensing technique applied to vegetation as an aid to municipal planning 19 p2683 N88-25951

Application of 35mm EM aerial reconnaissance photographic format of the municipality of Ubatuba (SP)
19 p2684 N88-25953

Aerial photography as an instrument of municipal and regional planning: Metropolitan area of Sao Paulo (SP)
19 p2684 N88-25957

Spread of large tropical conurbations
22 p3098 N88-28398

Integration of SPOT data into a geocoded information system 22 p3098 N88-28400

Mapping and urban multi-experimental assessment of SPOT: Mapping results 22 p3112 N88-28483

Urbanization: Its detection and effect in the United States climate record 22 p3125 N88-28571

CIVIL AVIATION

Aircraft accident reports, brief format, US civil and foreign aviation. Issue number 1: 1986 accidents
[PB87-916903] 02 p0123 N88-10781

Civil applications of high-speed rotorcraft and powered-lift aircraft configurations
[NASA-TM-100035] 03 p0261 N88-11643

Design requirements for future commercial operations
03 p0262 N88-11651

The EH-101 integrated project: A naval, utility and commercial helicopter system 03 p0265 N88-11672

Airline safety: A comparative analysis
[AD-A185358] 05 p0543 N88-13308

Civil aeronautics
[ETN-88-90616] 05 p0543 N88-13309

Aircraft accident reports: Brief format, US Civil and Foreign Aviation, Issue Number 4 of 1986 accidents
[PB87-916906] 06 p0666 N88-14086

Aircraft accident report: Grand Canyon Airlines, Inc., and Helitech, Inc., midair collision over Grand Canyon National Park, June 18, 1986
[PB87-910403] 06 p0666 N88-14087

Eighth Session of the Commission for Aeronautical Meteorology (abridged)
[WMO-673] 06 p0745 N88-14585

Digest of the annual report of the Lufthansa German Airlines
[ISSN-0415-603X] 08 p0952 N88-15779

Aircraft accident reports: Brief format, US Civil and Foreign Aviation, Issue Number 5 of 1986 accidents
[PB87-916907] 08 p0952 N88-15780

Aircraft accident reports: Brief format, US Civil and Foreign Aviation, Issue Number 7 of 1986 accidents
[PB87-916909] 08 p0952 N88-15781

Aircraft accident reports: Brief format, US Civil and Foreign Aviation, Issue Number 8 of 1986 accidents
[PB87-916910] 08 p0953 N88-15782

Product planning in civil aircraft construction
[MBB-UT-002/87] 10 p1313 N88-17849

Minimum Energy Routing through Interactive Techniques (MERIT) modeling
[NASA-CR-182535] 10 p1356 N88-18105

JPRS report: Science and technology. Europe and Latin America
[JPRS-ELS-88-001] 12 p1614 N88-19649

The judgement and evaluation of long-term investments demonstrated by means of a civil aircraft program
12 p1701 N88-20180

Activities report in civil aeronautics
[ETN-88-91344] 13 p1715 N88-20255

Availability and cost estimate of a high naphthene, modified aviation turbine fuel
[NASA-TM-100823] 13 p1749 N88-20455

General aviation activity and avionics survey: 1986 data
[AD-A189986] 15 p2013 N88-22003

Aircraft accident reports, brief format, US civil and foreign aviation, issue number 10 of 1986 accidents
[PB87-916912] 15 p2016 N88-22020

JPRS report: Science and technology. Japan
[JPRS-JST-88-001] 15 p2051 N88-22218

Activities report of Lufthansa
[ISSN-0176-5086] 16 p2155 N88-22855

The challenges and opportunities of supersonic transport propulsion technology
[NASA-TM-100921] 17 p2307 N88-23806

Competitive assessment of the U.S. civil helicopter industry
[PB88-186325] 18 p2455 N88-24574

FAA aviation forecasts fiscal years 1988-1999
[AD-A191711] 18 p2455 N88-24576

US civil airmen statistics, 1987
[AD-A191714] 18 p2455 N88-24577

General-aviation's view of progress in the aviation weather system 18 p2546 N88-25110

Radiation safety in commercial air traffic
[NASA-TM-101156] 19 p2600 N88-25447

Trends in civil aircraft propulsion
[PNR90441] 22 p3044 N88-28067

An interim comparison of operational CG records in turbulence on small and large civil aircraft
24 p3313 N88-29729

Re-assessment of gust statistics using CAADRP data
24 p3313 N88-29732

An analysis of time and space requirements for aircraft turnrounds
[TT-8705] 24 p3322 N88-29783

Report to Congress on the effectiveness of the Civil Aviation Security Program
[AD-A195282] 24 p3322 N88-29784

CLADDING

Comparative tests of high temperature creep-rupture behavior of the austenitic CrNi steel DIN W.NR 1.4970 in argon and steam
[KFK-4261] 01 p0063 N88-10402

Thermal stress in the edge cladding of Nova glass laser disks
[DE88-000425] 04 p0448 N88-12780

Development of composite polymer-glass edge claddings for Nova laser disks
[DE88-002389] 07 p0860 N88-15220

Beneficial and detrimental effects of silica in the high temperature oxidation of 20Cr/25Ni/Nb stainless steel
[AERE-R-12667] 10 p1301 N88-17779

Effects of commercial cladding on the fracture behavior of pressure vessel steel plates
[DE88-004333] 10 p1303 N88-17790

Composite ceramic superconducting filaments for superconducting cable
[AD-A187833] 11 p1556 N88-19312

SBIR-Long fluoride fiber
[AD-A188595] 13 p1754 N88-20492

Development program for 1.93-micron lasers
[NASA-CR-4148] 16 p2212 N88-23198

Laser cladding of Ni, Nb and Mg alloys for improved environmental resistance at high temperature
[AD-A191274] 16 p2213 N88-23208

Parametric analyses of the TE SP-100 system performance 17 p2415 N88-24358

The application of high-rate biaxial testing to the design of containment vessels for radioisotope heat sources
17 p2426 N88-24428

SNAP fuel performance 17 p2435 N88-24484

CLARK Y AIRFOIL
U AIRFOIL PROFILES

CLASSICAL MECHANICS
NT ASTRODYNAMICS
NT CELESTIAL MECHANICS
NT KEPLER LAWS
NT ORBITAL MECHANICS

Institute for Computational Mechanics in Propulsion (ICOMP) first year summary
[NASA-TM-100225] 03 p0370 N88-12330

Composite mechanics for engine structures
[NASA-TM-100176] 04 p0411 N88-12552

Existence of absolutely closed universe
08 p1080 N88-16509

Institute for Computational Mechanics in Propulsion (ICOMP)
[NASA-TM-100790] 11 p1540 N88-19202

Introduction to classical mechanics of systems with constraints, part 1
[DE88-701055] 13 p1832 N88-20957

Introduction to classical mechanics of systems with constraints, part 2
[DE88-701056] 13 p1849 N88-21072

Introduction to classical mechanics of systems with constraints, part 3
[DE88-701057] 13 p1850 N88-21073

Galilei relativity principle in classical electrodynamics
[DE87-703203] 14 p1904 N88-21376
Singular Lagrangians. Classical dynamics and quantization. Lectures for young scientists
[DE88-701158] 15 p2146 N88-22806
On the quantization of constrained generalized dynamics
[DE88-702223] 23 p3277 N88-29505

CLASSIFICATIONS
NT HIERARCHIES
NT INDEXES (DOCUMENTATION)
Clustering by means of medoids
[REPT-87-03] 01 p0085 N88-10551
Theoretical Aspects of Target Classification
[AGARD-LS-152] 03 p0303 N88-11909
Theoretical aspects of target classification: Physical optics and radon transform methods
03 p0304 N88-11915
Parametrization in scattering models
03 p0304 N88-11916
Input signal shaping: K-pulse
03 p0304 N88-11917
Computer-controlled testing of visual-spatial ability
[AD-A183971] 03 p0357 N88-12249
Aircraft classification by type of propulsive devices. Determination of type and number of carrying solutions
04 p0424 N88-12626
Cloud cover determination in polar regions from satellite imagery
[NASA-CR-181544] 04 p0471 N88-12908
The classification problem of finite rings by computable means
[AD-A185869] 07 p0908 N88-15500
Membership of Cepheids and red giants in 8 open clusters: NGC 129, 6067, 6649, 6664, IC 4725, Ly 6, Ru 79
[PUBL-SER-C-FASC-13] 07 p0944 N88-15739
Estimation of broadband planetary albedo from operational narrowband satellite measurements
[PB88-107644] 07 p0945 N88-15748
The power of neural nets 08 p1064 N88-16430
Event classification in (anti)neutrino experiments using an Internal Picket Fence-External Muon Identifier (IPF-EMI) detector system
[NIKHEF-H/87-6] 09 p1245 N88-17457
Rapid underway sediment classification by electrical methods
[AD-A187477] 10 p1357 N88-18114
Radar descriptors for the classification of terrain features
[AD-A188145] 11 p1504 N88-18983
Multisource context classification methods in remote sensing 11 p1504 N88-18985
Environmental gradient analysis, ordination, and classification in environmental impact assessments
[AD-A187294] 11 p1509 N88-19016
Mathematical modeling of two-state classification technology transfer summary and user's guide
[DE88-003849] 11 p1526 N88-19110
Terrain classification from digital elevation data using slope and curvature information
[AD-A188940] 12 p1639 N88-19812
Asymptotic giant branch populations in composite stellar systems 13 p1854 N88-21098
Land-use classification in a region north-west of Wuerzburg (Federal Republic of Germany) using digital, multispectral LANDSAT 5 Thematic Mapper data
[DFVLR-FB-87-37] 14 p1940 N88-21579
Classification of comets recorded in ancient China (300 BC - 1800 AD) and statistics of type-1 tails
14 p2008 N88-21976
High temperature materials: What's available
[AERE-R-12632] 15 p2028 N88-22081
On categorizing sounds
[AD-A189784] 15 p2129 N88-22700
Computer assisted generalization of buildings for digital landscape models by classification methods
16 p2226 N88-23294
Software development for the reconstruction of source parameters using research and development arrays
[REPT-840445-TW] 16 p2246 N88-23417
Adaptive segmentation evaluation
[AD-A190965] 16 p2274 N88-23609
Latitudinal and seasonal variation of the cloud characteristic parameters and their effects on the cloud classification 17 p2351 N88-24005
The use of SLAR and SIRA imageries for the classification of forest typen in tropical rain forests
17 p2356 N88-24036
Utilization of TM/LANDSAT images in the implanted forests mapping in the Mogi-Guacu Region (SP-Brazil)
17 p2357 N88-24042
Generation of thematic maps for updating aeronautical pilot charts utilizing LANDSAT-TM images
17 p2361 N88-24062
Study of methods of post-processing applied to a problem of standard classification
17 p2362 N88-24067
Research on enhancing the utilization of digital multispectral data and geographic information systems in global habitability studies
[NASA-CR-182799] 17 p2368 N88-24101
A method for discrimination of radar targets using complex natural resonances
[AD-A191848] 18 p2500 N88-24832
Automatic discovery of optimal classes
[NASA-TM-101174] 18 p2566 N88-25238
Mechanisms for particle acceleration: Possibilities and constraints
[PB88-102538] 19 p2725 N88-26184
Interpreting forest biome productivity and cover utilizing nested scales of image resolution and biogeographical analysis
[NASA-CR-183036] 20 p2817 N88-26711
Topics in quasicrystallography
21 p3023 N88-27947
Discrimination methods of traditional fields in a humid tropical region (Shaba, Zaire) using digital classification on SPOT data 22 p3096 N88-28387
Accuracy of land use classification for SPOT image data 22 p3100 N88-28410
Rendering of surfaces from volume data
[AD-A193649] 22 p3143 N88-28689
Detection of helicopters using ground-controlled microphones 22 p3148 N88-28730
Spectral classification of Low Mass X-ray Binaries (LMXB) energy spectra with color-color diagrams
[MPE-PREPRINT-111] 22 p3163 N88-28837
Literature review: Validity and potential usefulness of psychomotor ability tests for personnel selection and classification
[AD-A193558] 23 p3241 N88-29287
Relief effect correction on LANDSAT imagery for forest applications using digital terrain models
[INPE-4611-PRE/1334] 24 p3388 N88-30179
Lava thicknesses: Implications for rheological and crustal development 24 p3443 N88-30490

CLASSIFYING
Transient classifier systems and man-machine interface research
[AD-A186213] 07 p0899 N88-15446
Method for determining the coordinates of sound sources by means of a sound measurement system
[NASA-TT-20242] 13 p1834 N88-20972

CLAYS
NT VERMICULITE
Surface mediated photocatalysis
[AD-A188882] 12 p1603 N88-19589
Chemical and spectroscopic characterization of a suite of Mars soil analogs 23 p3302 N88-29667

CLEAN ROOMS
Use of a 35mm camera for remote surface cleanliness verification 02 p0133 N88-10835
Design, construction, activation, and operation of a high intensity acoustic test chamber
02 p0137 N88-10864

CLEANERS
NT AIR FILTERS
Low extractable wipers for cleaning space flight hardware 02 p0137 N88-10863

CLEANING
NT BATHING
NT CHEMICAL CLEANING
NT HOUSEKEEPING (SPACECRAFT)
NT STERILIZATION
NT WASHING
Fourteenth Space Simulation Conference: Testing for a Permanent Presence in Space
[NASA-CP-2446] 02 p0132 N88-10829
Shear stress cleaning for surface departiculation
02 p0134 N88-10838
Low extractable wipers for cleaning space flight hardware 02 p0137 N88-10863
Investigation of the nature and concentration of vapor and mist during the cleaning of aircraft
[PML-1985-29] 05 p0623 N88-13817
Gas cleaning at high temperatures and pressures for gas turbines
[DE88-751171] 11 p1440 N88-18593
Evaluation of solder flux solvents in a vapor-degreasing application for hybrid microcircuits
[BDX-613-3638] 11 p1468 N88-18752
Thermal oxide growth on silicon: Intrinsic stress and silicon cleaning effects
[AD-A188790] 13 p1736 N88-20377
In-situ reactive of X-ray optics by glow discharge
[DE88-009840] 20 p2854 N88-26947

CLEANLINESS
NT HOUSEKEEPING (SPACECRAFT)
Use of a 35mm camera for remote surface cleanliness verification 02 p0133 N88-10835
Redistribution of particulates in shuttle bay during launch 02 p0133 N88-10837
Cleanliness tests with the Omega Meter: A comparative study for solder flux removal
[DE88-004634] 11 p1460 N88-18704
Electronic failure analysis-corrosion of avionics
22 p3054 N88-28122

CLEAR AIR TURBULENCE
Northwest Airlines flight experiments
05 p0617 N88-13786
Infrared low-level wind shear work
10 p1275 N88-17628
Objective detection and forecasting of Clear-Air Turbulence (CAT): A status report
18 p2546 N88-25114
Utilization of a single clear-air Doppler radar beam to measure vertical divergence
[AD-A195543] 24 p3405 N88-30271

CLEARANCES
Recent advances in capacitance type of blade tip clearance measurements
[NASA-TM-101291] 19 p2603 N88-25460

CLEAVAGE
A quantitative statistical model for cleavage fracture initiation in carbide strengthened steels
[ETN-87-90735] 01 p0025 N88-10157
On cleavage in fatigue for rail steels
06 p0716 N88-14388
Influence of cleavage on fatigue propagation rates in a low carbon steel 06 p0716 N88-14389
Brittle to ductile transition to cleavage fracture
[DE88-004074] 10 p1420 N88-18481
Small-scale cleavage test of polymer products
[PB88-165360] 16 p2181 N88-23001

CLIMATE
Atlas of wide field-of-view outgoing longwave radiation derived from Nimbus 7 Earth radiation budget data set - November 1978 to October 1985
[NASA-RP-1186] 01 p0070 N88-10451
Detection of CO2-induced climate change
[DE87-013127] 01 p0071 N88-10457
Testimony to the US Senate on the greenhouse effect
[DE87-013995] 01 p0071 N88-10458
Description of NCAR (National Center for Atmospheric Research) Community Climate Model (CCM1)
[PB87-203782] 01 p0072 N88-10462
Understanding passive cooling systems
[PB87-210464] 02 p0194 N88-11211
Development of a climatic map of rainfall attenuation for Europe
[REPT-372] 02 p0216 N88-11359
The correspondence of surface climate parameters with satellite and terrain data
[NASA-CR-181515] 03 p0346 N88-12185
On the interannual variability of South American climate and the Southern Oscillation 04 p0470 N88-12905
New method of estimating continentality of climate on global scale 06 p0725 N88-14460
The climatic wind regime in the lower thermosphere from meteor radar observations 06 p0733 N88-14506
Modes of surface circulation and climate over the tropical Atlantic, Eastern Pacific, and Indian Oceans
06 p0742 N88-14564
Report of the Joint Scientific Commitee Ad Hoc Working Group on Radiative Flux Measurements --- Earth radiation budget
[WCP-136] 06 p0742 N88-14567
Carbon dioxide and climate: Summaries of research in FY 1987
[DE88-000916] 06 p0744 N88-14574
Report of the second session of the working group on sea ice and climate
[WCP-128] 06 p0745 N88-14580
Report of the first session of the International Working Group on Data Management for the Global Precipitation Climatology project
[WCP-132] 06 p0745 N88-14582
The global climate system: Autumn 1984 to spring 1986
[CSM-R84/86] 06 p0745 N88-14583
Recent Colorado State University tropical cyclone research of interest to forecasters
[AD-A185996] 07 p0879 N88-15332
Annual data summary and climatological evaluation. CERC (Coastal Engineering Research Center) field research facility, 1985, volume 2, appendix C
[AD-A185894] 07 p0881 N88-15344
Greatest volcanic eruptions in world during 17th-18th centuries and weather anomalies in Eurasian middle latitudes 08 p1012 N88-16134
Synoptic perturbations and climate
08 p1016 N88-16158
Characteristics and climatic relevance of the atmospheric aerosol components
08 p1017 N88-16164

.Parameterization of radiative transfer in the Earth's atmosphere with specific applications to clouds 10 p1353 N88-18087
Optimal sampling to provide user-specific climate information 11 p1515 N88-19051
An investigation of terrain related variables for predicting the multipath fade depth distribution on terrestrial microwave lines 12 p1615 N88-19654
Refractive index, meteorology and fading in line-of-sight transmission paths 12 p1616 N88-19666
Worldwide distributions of shipboard surface meteorological observations for EM propagation analysis [AD-A188771] 12 p1648 N88-19871
Predictions and studies with a one-dimensional ice/ocean model [AD-A189158] 13 p1803 N88-20776
The World Climate Research Program 14 p1935 N88-21538
Observational and theoretical studies of greenhouse climate effects [DE88-006237] 14 p1948 N88-21621
Seasonal variation for structural strength value [PB88-169248] 16 p2222 N88-23260
Nonlinear normal mode initialization of the NCAR (National Center for Atmospheric Research) CCM (Community Climate Model) [PB88-171814] 16 p2235 N88-23347
Our climate in danger [DE88-701824] 20 p2822 N88-26743
Circulation statistics from seasonal and perpetual January and July simulations with the NCAR (National Center for Atmospheric Research) Community Climate Model (CCM1):R15 [PB88-192620] 20 p2823 N88-26748
Vegetation studies on Vandenberg Air Force Base, California [NASA-TM-100985] 20 p2831 N88-26795
Proceedings of the Twelfth Annual Climate Diagnostics Workshop [PB88-191747] 22 p3119 N88-28534
Prolonged periods of above-normal temperatures in Canada, 1986/87 22 p3120 N88-28538
Modes of interannual climate variability and Sahel rainfall anomalies 22 p3121 N88-28547
Simulation studies of the influence of sea-surface temperature anomalies on the Sahelian circulation and rainfall 22 p3122 N88-28553
Low frequency variability of SST and its relationship to atmospheric forcing 22 p3122 N88-28554
Persistence of North Pacific Sea surface temperature and atmospheric flow patterns 22 p3123 N88-28559
The relationship between polar sea ice and the position of the near equatorial convergence zone 22 p3123 N88-28563
Evaluation of global data sets for climate studies 22 p3124 N88-28569
Differences in radiation budget parameters over Asia in relation to contrasting Indian monsoons 22 p3125 N88-28574
Extratropical response to tropical heating as a function of period of model integrations 22 p3125 N88-28577
On climate prediction for India 22 p3127 N88-28590
Characteristics of regression equations for specifying monthly precipitation amounts over the United States from the field of concurrent mean 700 mb heights 22 p3127 N88-28591
Regional environmental studies using national data bases and GIS (Geographic Information System) [DE88-008368] 23 p3230 N88-29225
Regional intercomparisons of General Circulation Model predictions and historical climate data: CO2 [DE88-010416] 23 p3235 N88-29248
Activities report of the World Meteorological Organization [WMO-669] 24 p3404 N88-30265

CLIMATE CHANGE
Master index for the carbon dioxide research state-of-the-art report series [DE87-012757] 01 p0072 N88-10459
Global environmental change research [S-HRG-100-301] 03 p0348 N88-12199
On regime selection in global atmospheric flow 17 p2374 N88-24119
Geophysical monitoring for climatic change, number 15 [PB88-180146] 19 p2692 N88-26003

CLIMATOLOGY
NT MICROCLIMATOLOGY
NT PALEOCLIMATOLOGY
Venusian surface and crust 01 p0010 N88-10054
Cloud climatology derived from the AFGWC (Air Force Global Weather Central) 3D-nephanalysis for January and July 1979 [AD-A183686 01 p0070 N88-10446
Documentation of NCAR (National Center for Atmospheric Research) CCM1 program modules [PB87-213567] 03 p0352 N88-12220
Ocean model processor for climate studies [PB87-224713] 03 p0353 N88-12226
Inventory of weather stations. Climatological data from Dutch stations, no. 26 [KNMI-150-26] 05 p0628 N88-13841
New method of estimating continentality of climate on global scale 06 p0725 N88-14460
Interpretation of our present terrestrial climatic record [DE88-000223] 06 p0744 N88-14573
An Earth radiation budget climate model [NASA-CR-182368] 06 p0744 N88-14578
CTD/02 measurements during 1984 and 1985 as part of the Equatorial Pacific Ocean Climate Studies (EPOCS) [PB88-102082] 06 p0748 N88-14600
Recent Colorado State University tropical cyclone research of interest to forecasters [AD-A185996] 07 p0879 N88-15332
Objective prediction of monthly mean surface temperature and climatological relationships to mid-tropospheric heights [DE88-000908] 07 p0880 N88-15340
Annual data summary and climatological evaluation, CERC (Coastal Engineering Research Center) field research facility, 1985, volume 2, appendix C [AD-A185894] 07 p0881 N88-15344
Research work at the Meteorological Institute of the University of Munich (Federal Republic of Germany) [MITT-56] 08 p1013 N88-16141
Research project on CO-induced climate change [DE88-002352] 08 p1023 N88-16193
Hurricane climatology for the Atlantic and Gulf coasts of the United States [PB88-114657] 08 p1039 N88-16288
Annual data summary and climatological evaluation CERC (Coastal Engineering Research Center) field research facility, 1985. Volume 1. Main text and appendixes A and B [AD-A186442] 08 p1039 N88-16289
Revised uniform summary of surface weather observations. Parts A-F: Carswell AFB, Texas [AD-A186820] 09 p1192 N88-17144
US Navy climatic study of the Mediterranean Sea [AD-A188264] 10 p1356 N88-18107
Moscow USSR. Limited surface observations climatic summary (LISOCS), parts A-F [AD-A188080] 11 p1514 N88-19046
Wind energy resource survey of New Zealand: National resource assessment [PB88-139365] 12 p1640 N88-19822
A paper on horizontal deformation in the frontogenesis in south Brazil [INPE-4469-TDL/322] 12 p1647 N88-19867
JPRS report: Science and technology. USSR: Earth sciences [JPRS-UES-88-001] 13 p1784 N88-20674
Sample models of steady and low frequency circulations in the tropical atmosphere, with application to tropical air-sea interactions 13 p1801 N88-20764
Predictions and studies with a one-dimensional ice/ocean model [AD-A189158] 13 p1803 N88-20776
Climatology and space observations [ISBN-2-85-428179-9] 14 p1935 N88-21536
Space projects for the 90's relevant to climatology 14 p1935 N88-21539
The atmosphere as a component of the climate system: Structure and variability 14 p1935 N88-21540
The Earth radiation budget and its spatial and temporal variations 14 p1936 N88-21548
The role of radiation transfer in climate modification 14 p1936 N88-21549
Satellite retrieval of cloud cover parameters and the International Satellite Cloud Climatology Program (ISCCP) 14 p1937 N88-21552
Continental surface processes and water cycle 14 p1937 N88-21555
The International Satellite Land-Surface Climatology Project (ISLSCP) 14 p1937 N88-21558
Hydrological models 14 p1937 N88-21559
The Hapex-Mobilhy program 14 p1938 N88-21560
Climatic summaries of ocean weather stations [PB88-162920] 14 p1948 N88-21617
Current velocity and hydrographic observations in the Straits of Florida, the Caribbean Sea and offshore of the Antillean Archipelago: Subtropical Atlantic Climate Studies (STACS) 1986 [PB88-160767] 14 p1951 N88-21628
CTD/O2 data collected in 1985 and 1986 for EPOCS (Equatorial Pacific Ocean Climate Studies) [PB88-160775] 14 p1951 N88-21629
A multivariate variational objective analysis-assimilation method. Part 1: Development of the basic model [NASA-CR-182651] 15 p2097 N88-22491
Monthly mean global climatology of temperature, wind, geopotential height, and pressure for 0 - 120 km [NASA-TM-100697] 15 p2099 N88-22503
NOAA-ERL-ARL (National Oceanic and Atmospheric Administration-Environmental Research Laboratories-Air Resources Laboratory) solar UV radiation and climate research project: Program description [PB88-169396] 16 p2233 N88-23339
Understanding CO2 and climate [PB88-167655] 16 p2234 N88-23341
Outline of the GPCP strategy 17 p2351 N88-24007
Research and Technology, 1987, Goddard Space Flight Center [NAS 1.15:101097] 17 p2453 N88-24572
Territorial management program 19 p2682 N88-25942
A glossary for carbon dioxide and climate [DE88-007885] 19 p2689 N88-25982
Last spring frosts and first autumn frosts in Finland [FMI-6] 19 p2693 N88-26008
Verification of regional climates of GISS GCM. Part 1: Winter [NASA-TM-100695] 19 p2694 N88-26012
An efficient model for changes of global climate and composition of the atmosphere due to human activities [ETN-88-92359] 20 p2827 N88-26775
Evaluation of surface energy and radiation balance systems for FIFE [NASA-CR-183118] 20 p2828 N88-26778
Development of radiation and cloud parameterization programs for AFGL (Air Force Geophysics Laboratory) global models [AD-A193369] 21 p2973 N88-27658
Air-sea interaction in the vicinity of a land-sea boundary in the presence of upwelling 21 p2973 N88-27661
Intercomparison of NMC (National Meteorological Center) and ECMWF (European Centre for Medium Range Weather Forecasts) global analyses: 1980-1986 [PB88-196548] 21 p2974 N88-27668
Surface energy balance of three general circulation models: Current climate and response to increasing atmospheric CO2 [DE88-010967] 21 p2975 N88-27673
Space shuttle natural environment analysis [NASA-CR-179337] 21 p2976 N88-27676
Proceedings of the Twelfth Annual Climate Diagnostics Workshop [PB88-191747] 22 p3119 N88-28534
Climatology of various synoptic systems over the tropical North Pacific 22 p3121 N88-28542
Aspects of the 30-60 day oscillation in a GCM simulation 22 p3121 N88-28545
Evaluation of global data sets for climate studies 22 p3124 N88-28569
A method to adjust climatological time series for discontinuous inhomogeneities 22 p3124 N88-28570
Urbanization: Its detection and effect in the United States climate record 22 p3125 N88-28571
Systematic behavior of NMC medium range forecasts and the effect of model changes 1985-87 22 p3125 N88-28575
The impact of the El Nino event on the ECMWF model performance 22 p3125 N88-28576
DERF forecasts of thickness 22 p3126 N88-28579
Experimental 30-day forecasts from several spectral general circulation models 22 p3126 N88-28582
Dependence of medium range forecast errors upon the large-scale initial state 22 p3126 N88-28585
On climate prediction for India 22 p3127 N88-28590
Meteorological features during the marginal ice zone experiment from 20 March to 10 April 1987 [AD-A193960] 23 p3235 N88-29251
Episodic vs. epochal release of SO2 on Mars 23 p3305 N88-29688
Energy budget and ground temperatures in hot regions [AD-A196298] 24 p3404 N88-30268

CLIMBING FLIGHT
Improvement of head-up display standards. Volume 2: Evaluation of head-up displays to enhance unusual attitude recovery [AD-A194601] 23 p3178 N88-28921

CLINICAL MEDICINE
JPRS report: Science and technology. USSR: Life sciences [JPRS-ULS-87-012] 03 p0355 N88-12238
JPRS report: Science and technology. USSR: Life sciences [JPRS-ULS-87-009] 04 p0473 N88-12915

An assessment of clinical chemical sensing technology for potential use in space station health maintenance facility
[NASA-CR-172013] 04 p0475 N88-12926
JPRS report: Science and technology. USSR: Life sciences
[JPRS-ULS-87-013] 06 p0750 N88-14608
Diagnostic value of some load tests in evaluation of nonspecific electrocardiographic changes
07 p0895 N88-15426
Preliminary evaluation of a micro-based repeated measures testing system
[NASA-CR-172038] 08 p1048 N88-16331
Relationships between coronary heart disease risk factors and serum ionized calcium in Kennedy Space Center Cohort
[NASA-TM-100379] 10 p1368 N88-18177
Basic results of medical studies during prolonged manned flights on-board the Salyut-7/Soyuz-T orbital complex
[NASA-TT-20217] 10 p1369 N88-18182
Minutes of the meeting of the Indo-US Subcommission on Science and Technology (8th) held at Washington, D.C. on September 22-24, 1986
[PB88-130158] 10 p1423 N88-18503
Full scale architectural simulation techniques for space stations 12 p1651 N88-19887
Technology '87: Research and Development Laboratory Technology Transfer Program
[DE88-003142] 13 p1852 N88-21084
Lasers: Invention to application
[PB88-161583] 14 p1914 N88-21436
Clinical measurements using fiber optic sensors
[DE88-005624] 15 p2134 N88-22731
Clinical applications of computerized thermography
17 p2330 N88-23915
Design considerations for the development of an implantable sensor for the continuous measurement of glucose in the diabetic patient 17 p2382 N88-24159
Vanderbilt free electron laser project in biomedical and materials research
[AD-A195961] 24 p3378 N88-30121

CLOCKS
NT ATOMIC CLOCKS
The navigation experiment NAVEX: Experimental results of clock synchronization
[DFVLR-MITT-87-05] 03 p0271 N88-11701
Ultra-low power digital filter
[AD-A184485] 03 p0310 N88-11959
On real-time systems using local area networks
[AD-A185475] 06 p0694 N88-14256
Timing variation in dual loop benchmarks
[AD-A185697] 06 p0707 N88-14338
The navigation experiment NAVEX: Experimental results of clock synchronization
[ESA-TT-1084] 09 p1132 N88-16791
VAXELN experimentation: Programming a real-time clock and interrupt handling using VAXELN Ada 1.1
[AD-A188100] 11 p1525 N88-19107
A survey of provably correct fault-tolerant clock synchronization techniques
[NASA-TM-100553] 13 p1823 N88-20894
An investigation of a distributed clock for local area networks with ring topology 18 p2516 N88-24924

CLOSED BASINS
U STRUCTURAL BASINS

CLOSED CYCLES
A comparison of open and closed multimegawatt space power and weapon systems
[DE87-012975] 01 p0089 N88-10579
A cold ejector for closed-cycle helium refrigerators
04 p0434 N88-12690
Traveling-wave maser closed-cycle refrigerator data acquisition and display system 04 p0437 N88-12708
Design features of small Brayton cycles for autonomous underwater vehicles
[AD-A187799] 11 p1506 N88-18999
Analysis of closed cycle megawatt class space power systems with nuclear reactor heat sources
17 p2413 N88-24351
Comparison of open and closed multimegawatt space power systems 17 p2414 N88-24353
Characteristics of the closed Brayton cycle for dynamic isotope power systems 17 p2422 N88-24401
Design of catalytic monoliths for closed-cycle carbon dioxide lasers
[NASA-CR-182983] 18 p2558 N88-25185
Analysis of a closed-kinematic chain robot manipulator
[NASA-CR-183031] 18 p2561 N88-25206
C-CAMP: A closed cycle alkali metal power system
[DE88-009715] 19 p2688 N88-25975
CryoSQUID: A SQUID-based magnetic field sensor
[AD-A194237] 23 p3239 N88-29275

CLOSED ECOLOGICAL SYSTEMS
Aquarack: Aims and Possible Research Projects
[DFVLR-MITT-87-01] 01 p0073 N88-10469
The Aquarack as a potential instrument for basic research work in space biology: Inventory and scientific dispositions 01 p0073 N88-10470
The usefulness of microalgal structures as an element of closed ecological systems like Aquarack and CELSS --- Controlled Ecological Life Support System (CELSS)
01 p0074 N88-10476
Catalytic processes for space station waste conversion
[NASA-CR-177423] 01 p0077 N88-10491
Environmental life support system technology study --- space flight
[ESA-CR(P)-2432] 02 p0218 N88-11371
Controlled Ecological Life Support System: Regenerative Life Support Systems in Space
[NASA-CP-2480] 03 p0357 N88-12251
Progress in European CELSS activities
03 p0358 N88-12252
Food production and gas exchange system using blue-green alga (spirulina) for CELSS
03 p0358 N88-12253
Biomass recycle as a means to improve the energy efficiency of CELSS algal culture systems
03 p0358 N88-12254
Operation of an experimental algal gas exchanger for use in a CELSS 03 p0358 N88-12255
Non-conventional approaches to food processing in CELSS. 1: Algal proteins: Characterization and process optimization 03 p0358 N88-12256
Application of photosynthetic N(2)-fixing cyanobacteria to the CELSS program 03 p0358 N88-12257
Sunlight supply and gas exchange systems in microalgal bioreactor 03 p0359 N88-12258
A review of recent activities in the NASA CELSS program 03 p0359 N88-12259
A modular BLSS simulation model
03 p0359 N88-12260
Preliminary experimental results of gas recycling subsystems except carbon dioxide concentration
03 p0359 N88-12261
Fundamental study on gas monitoring in CELSS
03 p0359 N88-12263
The applicability of the catalytic wet-oxidation to CELSS 03 p0360 N88-12264
A large-scale perspective on ecosystems
03 p0360 N88-12265
Design of an elemental analysis system for CELSS research 03 p0360 N88-12266
An overview of Japanese CELSS research activities
03 p0360 N88-12267
Utilization of potatoes in bioregenerative life support systems 03 p0360 N88-12268
Wheat production in controlled environments
[UAES-PAPER-3324] 03 p0361 N88-12270
The effect of radiation on the long term productivity of a plant based CELSS 03 p0361 N88-12271
Mass balances for a biological life support system simulation model 03 p0361 N88-12272
Controlled Ecological Life Support System: Design, Development, and Use of a Ground-Based Plant Growth Module
[NASA-CP-2479] 05 p0630 N88-13852
CELSS Program Meeting 05 p0630 N88-13853
Controlled ecological life support systems: Development of a plant growth module 05 p0630 N88-13854
Plant Growth Module (PGM) conceptual design
05 p0631 N88-13855
Controlled Ecological Life Support Systems (CELSS) conceptual design option study
[NASA-CR-177421] 06 p0754 N88-14625
Controlled Ecological Life Support Systems (CELSS) physiochemical waste management systems evaluation
[NASA-CR-177422] 06 p0754 N88-14626
Modeling the growth dynamics of four candidate crops for Controlled Ecological Life Support Systems (CELSS)
06 p0799 N88-14889
Space station accommodations for life sciences research facilities. Phase 1: Conceptual design and programmatics studies for Missions SAAX0307, SAAX0302 and the transition from SAAX0307 to SAAX0302. Volume 2: Study results
[NASA-CR-179244] 08 p0962 N88-15829
Electrochemical carbon dioxide concentrator subsystem development
[NASA-CR-177411] 08 p1053 N88-16353
Design concepts for bioreactors in space
09 p1198 N88-17179
Kinetic toxic aspect of potential use of sulfur hexafluoride in closed environments 10 p1362 N88-18142
Ecological algal system in microgravity conditions. Preliminary results 12 p1655 N88-19915
Closed system physiology: Role of oxygen in the development of wheat 12 p1655 N88-19916
Regenerative life support system research
[NASA-CR-182606] 12 p1671 N88-20006

CLOSED FAULTS
U GEOLOGICAL FAULTS

CLOSED LOOP SYSTEMS
U FEEDBACK CONTROL

CLOSING
New concepts for high current self-sustained diffuse discharge closing switches
[DE87-011678] 01 p0040 N88-10252

CLOSURE LAW
Homogeneous turbulence two-point closures and applications to one-point closures
03 p0312 N88-11973
Reynold stress closure in jet flows using wave models
[NASA-CR-182662] 12 p1628 N88-19741
EDQNM closure: A homogeneous simulation to support it. A quasi-homogeneous simulation to disprove it
16 p2195 N88-23091
Angular distribution of turbulence in wave space
16 p2195 N88-23093
Study of one-dimensional spectral dynamic equations of the Reynolds stresses in homogeneous anisotropic turbulence: Application to split-spectrum modeling
16 p2196 N88-23095
Reynolds stress models of homogeneous turbulence
16 p2197 N88-23106

CLOSURES
Conditional second order closure for turbulent shear flows
[AD-A185369] 05 p0581 N88-13542
Quick actuating closure and handling system
14 p1925 N88-21476
Development of a more general Reynolds stress closure for swirling flow
[AD-A195121] 24 p3374 N88-30092
Syntactic closures
[AD-A195921] 24 p3412 N88-30311

CLOTH
U FABRICS

CLOTHING
NT EXTRAVEHICULAR MOBILITY UNITS
NT FLIGHT CLOTHING
NT GLOVES
NT GOGGLES
NT PRESSURE SUITS
NT PROTECTIVE CLOTHING
NT SPACE SUITS
Loss of performance due to military clothing and equipment
[IZF-1986-13] 01 p0077 N88-10490
An investigation of some basic properties of hybrid composite materials
[AD-A194136] 23 p3189 N88-28975

CLOUD CHAMBERS
Microgravity nucleation and particle coagulation experiments support
[NASA-CR-181540] 04 p0423 N88-12618
The technical evolution of the Wilson camera: The beginnings (1895-1925)
[NOTA-INTERNA-876] 05 p0585 N88-13568

CLOUD COVER
Cloud climatology derived from the AFGWC (Air Force Global Weather Central) 3D-nephanalysis for January and July 1979
[AD-A183686] 01 p0070 N88-10446
GOES observations for the FIRE/SRB Wisconsin experiment region from October 11 through November 2, 1986
[NASA-TM-100485] 01 p0071 N88-10453
Operational cloud-clearing techniques of VAS radiance data --- Visible and Infrared Spin Scan Radiometer Atmospheric Sounder (VAS) 02 p0201 N88-11256
The impact on short-term precipitation forecast skill of time-dependent lateral and lower boundary conditions within a meso-beta numerical cloud prediction model
02 p0211 N88-11327
Development of the SPOT commercial service: Preliminary conclusions after six months of operations
03 p0340 N88-12144
Cloud cover determination in polar regions from satellite imagery
[NASA-CR-181544] 04 p0471 N88-12906
Mesoscale applications of high resolution imagery
[AD-A185039] 05 p0627 N88-13833
Modeling cloudy and clear interval length probabilities using space shuttle imagery
[AD-A185290] 05 p0627 N88-13837
Automated satellite cloud analysis: A multispectral approach to the problem of snow/cloud discrimination
[AD-A185672] 06 p0746 N88-14591
Application of satellite data in observational and theoretical studies of the evolving structure of baroclinic waves
[NASA-CR-179277] 10 p1354 N88-18091
General determination of Earth surface type and cloud amount using multispectral AVHRR data
[NOAA-TR-NESDIS-39] 11 p1506 N88-18997

Homogenizing surface and satellite observations of cloud. Aspects of bias in surface data
[AD-A188523] 12 p1648 N88-19869

Satellite estimations of the solar radiation flux at the surface 14 p1936 N88-21551

Satellite retrieval of cloud cover parameters and the International Satellite Cloud Climatology Program (ISCCP) 14 p1937 N88-21552

Revised Uniform Summary of Surface Weather Observations, Loring AFB, Maine, Parts A - F
[AD-A188201] 14 p1947 N88-21610

Some models for rain and cloud attenuation of millimeter waves
[PB88-160809] 14 p1948 N88-21616

The collection of statistics on the frequency of cloud cover over North America
[AD-A190456] 15 p2097 N88-22495

Use of energy emission for detecting the necessity of irrigation in wheat in field conditions
[INPE-4461-TDL/318] 16 p2229 N88-23315

Comparison of the solar radiation estimation method by satellites 17 p2360 N88-24055

Restrictions in activity monitoring through remote sensing 17 p2365 N88-24084

Cloud cover determination in polar regions from satellite imagery
[NASA-CR-182906] 17 p2375 N88-24123

Development of radiation and cloud parameterization programs for AFGL (Air Force Geophysics Laboratory) global models
[AD-A193369] 21 p2973 N88-27658

The collection of statistics on the frequency of cloud cover over North America
[AD-A193093] 21 p2974 N88-27667

A system for determination of wind fields from cloud tracks: INPE experiment
[INPE-4492-PRE/1256] 22 p3128 N88-28594

CLOUD DISPERSAL

Numerical simulation of near-surface environments and particulate clouds generated by large-area fires
[AD-A188375] 12 p1641 N88-19828

CLOUD GLACIATION

Conception and discussion of a model describing ice formation on various obstacles
[ONERA-NT-1986-6] 01 p0072 N88-10460

The dependence of the normalized ice accretion thickness on cloud-physical parameters
[DFVLR-FB-87-08] 01 p0072 N88-10464

Obtaining information on cloud particles by a commercial miniature camera
[DFVLR-MITT-87-19] 16 p2234 N88-23342

Standardized ice accretion thickness as a function of cloud physics parameters
[ESA-TT-1080] 16 p2234 N88-23346

Experimental measurements of heat transfer from an iced surface during artificial and natural cloud icing conditions
[AIAA-PAPER-86-1352] 17 p2293 N88-23718

CLOUD HEIGHT INDICATORS

Determination of cloud base height and emissivity from downwelling angular radiances
[AD-A185985] 07 p0879 N88-15331

The visioceilometer and its tactical applications
[AD-A188216] 12 p1647 N88-19866

CLOUD PHOTOGRAPHY

The importance of mesoscale waves in the upper troposphere for formation of cloud and precipitation areas 02 p0203 N88-11273

Report of the International Satellite Cloud Climatology Project (ISCCP) workshop on cloud algorithms in the polar regions
[WCP-131] 06 p0745 N88-14581

Meteosat tracks Karman vortex streets in the atmosphere 09 p1128 N88-16770

Obtaining information on cloud particles by a commercial miniature camera
[DFVLR-MITT-87-19] 16 p2234 N88-23342

Enhanced infra-red picture of LR-FAX for spring and autumn seasons 17 p2351 N88-24011

CLOUD PHYSICS

The dependence of the normalized ice accretion thickness on cloud-physical parameters
[DFVLR-FB-87-08] 01 p0072 N88-10464

Structure and modification of winter mountain clouds in the Sierra Nevada: Nowcasting/forecasting the onset of supercooled liquid water 02 p0202 N88-11263

Detailed analysis of a mesoscale convective complex situation in the Carpathian Basin (Europe)
02 p0207 N88-11296

Effects of the large scale motion and horizontal inhomogeneity of the moist static instability on development of the mesoscale convective systems in the midlatitudes 02 p0207 N88-11297

Cumulus and thunderstorm initiation by mountains
02 p0207 N88-11301

The impact on short-term precipitation forecast skill of time-dependent lateral and lower boundary conditions within a meso-beta numerical cloud prediction model
02 p0211 N88-11327

Definition and use of sensors for measuring electrical conductivity in thunderclouds
[ESA-TT-1047] 03 p0352 N88-12222

Study of isolated convective clouds in the lower Alps in summer 1984, using radar and a simple Weinstein numerical model
[ESA-TT-1061] 03 p0353 N88-12224

Computer modeling aids studies of precipitation formation 04 p0458 N88-12832

The application of doubly-truncated hydrometeor distributions to numerical cloud models
[AD-A185273] 05 p0627 N88-13836

Report of the International Satellite Cloud Climatology Project (ISCCP) workshop on cloud algorithms in the polar regions
[WCP-131] 06 p0745 N88-14581

Automated satellite cloud analysis: A multispectral approach to the problem of snow/cloud discrimination
[AD-A185672] 06 p0746 N88-14591

Thunderstorms with snow: A comprehensive, empirical study of their occurrence, development and structure
[AD-A185929] 07 p0879 N88-15329

Anthropogenic effects on the droplet formation process, and ion concentrations in droplets --- clouds
08 p1018 N88-16175

Rocket experiments and payloads for Super CAMP --- Cold Arctic Mesopause Project (CAMP)
08 p1034 N88-16271

Layered-capacitor method for dielectric bridge measurements. Algorithms for inversion and parameter fitting: Documentation, verification, data analysis
[PB88-131479] 11 p1505 N88-18989

Cloud physics studies in SCPP (Sierra Cooperative Pilot Project) from 1977-87
[PB88-136924] 11 p1516 N88-19054

Research and development to acquire and reduce melting layer cloud physics and evaluate a prototype M-meter
[AD-A188390] 12 p1648 N88-19873

Gas-chromatographic analysis of products of thermal reactions of aerosol in Venusian cloud layer on Vega-1 and Vega-2 automatic interplanetary stations
13 p1725 N88-20318

Bibliography of icing on aircraft (status 1987)
[DFVLR-MITT-87-18] 16 p2158 N88-22876

Standardized ice accretion thickness as a function of cloud physics parameters
[ESA-TT-1080] 16 p2234 N88-23346

Studies of the mechanisms and rates with which nitrogen species are incorporated into cloud water and precipitation
[PB88-193065] 20 p2826 N88-26764

Present status of artificial rain making
[DE88-701823] 20 p2826 N88-26769

Dynamic interaction of convective cumulus with large-scale environment
[MITT-55] 20 p2827 N88-26773

Cloud simulation warm cloud experiments: Droplet growth and aerosol scavenging
[AD-A192944] 21 p2974 N88-27666

Stratocumulus and cloud-free reflectance from multi-spectral satellite measurements
[AD-A193899] 22 p3128 N88-28599

Investigations on the entropy of cloudy air
[ESA-TT-1060] 23 p3234 N88-29245

An objective technique for Arctic cloud analysis using multispectral AVHRR (Advanced Very High Resolution Radiometer) satellite imagery
[AD-A194732] 23 p3235 N88-29250

Global vertical mass transport by clouds: A two-dimensional model study
[CM-74] 24 p3391 N88-30192

Microphysical processes in cloud layers of Venus
24 p3448 N88-30522

CLOUD SEEDING

Altered and enhanced iodargyrite with bismuth triiodide for use in precipitation enhancement operations
[AD-A185229] 05 p0561 N88-13419

AN-30M cloud-seeding airplane in international exhibition 06 p0725 N88-14456

Present status of artificial rain making
[DE88-701823] 20 p2826 N88-26769

CLOUDS

Aqueous-phase reactions in clouds
[DE86-005249] 01 p0069 N88-10445

A review of parameterizations of microphysical processes in clouds for application in models of regional atmospheric deposition
[DE88-000451] 04 p0471 N88-12909

Volcanic eruption detection with TOMS
05 p0618 N88-13793

Analysis of SO2 signals in SBUV/TOMS data
05 p0618 N88-13794

The determination of exhaust cloud dimensions from films of space shuttle launches
[NASA-CR-4103] 06 p0732 N88-14500

Mesoscale aerosol clouds 08 p1013 N88-16140

Three-dimensional trajectory analyses of two drop sizing instruments: PMS OAP and PMS FSSP
[NASA-CR-4113] 11 p1437 N88-18574

Numerical simulation of near-surface environments and particulate clouds generated by large-area fires
[AD-A188375] 12 p1641 N88-19828

Polar mesospheric cloud experiment
[AD-A188936] 12 p1648 N88-19872

Chemical composition and structure of Venusian clouds determined from results of roentgenoradiometric experiments carried out by landing modules of Vega-1 and Vega-2 automatic interplanetary stations
13 p1726 N88-20320

Determining chemical composition of aerosol in Venusian cloud layer on Vega-1 automatic interplanetary station using Malakhit mass spectrum analyzer
13 p1726 N88-20321

Synchronous measurements of effective photon path length in visible and near-IR spectral regions in real cloud systems 13 p1790 N88-20706

The spreading and mixing of dense gas clouds in still air
[KNMI-WR-87-12] 16 p2230 N88-23320

SAM 2 data user's guide
[NASA-RP-1200] 18 p2543 N88-25094

Overview of the PRECP (processing of emissions by clouds and precipitation) Program
[DE88-008205] 20 p2822 N88-26741

Studies of the mechanisms and rates with which nitrogen species are incorporated into cloud water and precipitation
[PB88-193065] 20 p2826 N88-26764

Cloud simulation warm cloud experiments: Droplet growth and aerosol scavenging
[AD-A192944] 21 p2974 N88-27666

Distribution of hydroxyl clouds in the galaxy
[DE88-702415] 22 p3164 N88-28844

On experiences with two hot-wire instruments for measuring the liquid water content in clouds
[ESA-TT-1085] 23 p3236 N88-29255

CLOUDS (METEOROLOGY)

NT ARC CLOUDS
NT BARIUM ION CLOUDS
NT CHEMICAL CLOUDS
NT CIRRUS CLOUDS
NT CONVECTION CLOUDS
NT CUMULUS CLOUDS
NT NOCTILUCENT CLOUDS
NT STRATOCUMULUS CLOUDS
NT STRATUS CLOUDS

Solar Energy Meteorological Research and Training Site Alaska
[DE87-013706] 01 p0069 N88-10440

Airborne lidar studies of Arctic polar stratospheric clouds 01 p0069 N88-10443

Cloud climatology derived from the AFGWC (Air Force Global Weather Central) 3D-nephanalysis for January and July 1979
[AD-A183686] 01 p0070 N88-10446

Description of the Mountain Cloud Chemistry Program version of the PLUVIUS MOD 5.0 reactive storm simulation model
[DE87-012846] 01 p0070 N88-10450

The physics of charge separation preceding lightning strokes in thunderclouds
[NASA-CR-178371] 01 p0071 N88-10452

Estimation from satellite imagery of summertime rainfall over varied space and time scales
[PB87-203246] 01 p0071 N88-10454

Forecasting boundary layer clouds and fog: A review of operational numerical models
02 p0208 N88-11307

Measurements of vapor flux, liquid water contents, precipitation rates and riming in a Utah mountain cloud system
[PB87-224945] 04 p0469 N88-12900

Cloud cover determination in polar regions from satellite imagery
[NASA-CR-181544] 04 p0471 N88-12908

Tropical easterly jet located using TOMS data
05 p0616 N88-13783

BARS-1M meteorological complex carried on IL-18 airplane 06 p0725 N88-14458

Report of the International Satellite Cloud Climatology Project (ISCCP) workshop on cloud algorithms in the polar regions
[WCP-131] 06 p0745 N88-14581

Research project on CO-induced climate change
[DE88-002352] 08 p1023 N88-16193

Parameterization of radiative transfer in the Earth's atmosphere with specific applications to clouds
10 p1353 N88-18087
Homogenizing surface and satellite observations of cloud Aspects of bias in surface data
[AD-A188523] 12 p1648 N88-19869
Martian Clouds Data Workshop
[NASA-CR-182431] 12 p1711 N88-20238
Analysis of spectral reflectance characteristics of targets under satellites and automatic cloud recognition
13 p1755 N88-20498
Local meteorological processes and air mass origin during a cloud chemical field experiment on Areskutan, Sweden, in summer 1986
[AP-28] 14 p1948 N88-21615
Latitudinal and seasonal variation of the cloud characteristic parameters and their effects on the cloud classification 17 p2351 N88-24005
A system for determination of wind fields using geostationary meterological satellites
17 p2360 N88-24056
The rate of volcanism on Venus
[NASA-CR-183039] 19 p2742 N88-26281
The patterns of tropical convection during the 1986-87 ENSO 22 p3120 N88-28537

CLUMPS
Simulation studies for surfaces and materials strength
[NASA-CR-181535] 04 p0412 N88-12557
Supersonic beam observations of semiconductor clusters
[AD-A184991] 05 p0655 N88-14018
Clusters of transition metal atoms
[AD-A191265] 16 p2270 N88-23579
Submillimeter and far infrared line observations of M17 SW: A clumpy molecular cloud penetrated by UV radiation
[NASA-CR-182866] 16 p2288 N88-23701

CLUSTER ANALYSIS
Clustering by means of medoids
[REPT-87-03] 01 p0085 N88-10551
Annotated computer output for illustrative examples of clustering using the mixture method and two comparable methods from SAS
[AD-A184687] 03 p0364 N88-12292
Simulation of the layer-growth dynamics in silver films: Dynamics of adatom clusters and vacancy clusters on Ag(100)
[DE87-014764] 03 p0380 N88-12390
A study of the free energy of the Lenz-Ising model using the cluster variation method of Morita
[AD-A186023] 08 p1073 N88-16476
Environmental gradient analysis, ordination, and classification in environmental impact assessments
[AD-A187294] 11 p1509 N88-19016
The coordination cluster theory for metallic solutions
[DE88-005934] 13 p1738 N88-20389
A likelihood based grouping method for multidimensional observations: An interactive method used on large transportation data bases
[REPT-87-74] 16 p2286 N88-23685
Cluster analysis of multiple planetary flow regimes
[NASA-CR-182931] 18 p2594 N88-25418
Tuning a major part of a clustering algorithm
[AD-A191446] 20 p2836 N88-26821
Mutually exclusive alternatives by clustering
[DE88-007707] 20 p2882 N88-27115
To the opportunities of cluster analysis of light curves of supernovae
[DE88-701642] 21 p3030 N88-27982

CLUSTERS
Physics and chemistry 07 p0883 N88-15359
Transition metal cluster chemistry
[AD-A188731] 13 p1740 N88-20405

CLUTTER
Detection of targets in the presence of clutter using target echo modulations caused by rotating structures
[REPT-12-86] 01 p0036 N88-10231
Theory of displaced phase center antenna for space based radar applications
[PB87-229837] 06 p0690 N88-14227
Active and passive remote sensing of ice
[AD-A186685] 09 p1195 N88-17162
Radar backscatter from airports and surrounding areas 10 p1274 N88-17623
Radar returns from ground clutter in vicinity of airports
10 p1274 N88-17624
The maximum entropy method for the analysis of radar echoes from hovering helicopters in clutter
[FB-2/87] 11 p1475 N88-18799
Ground clutter processing for wind measurements with airport surveillance radars
[AD-A187708] 11 p1514 N88-19044
Computation of LMS (Least-Mean-Square) and matched digital filters for optical clutter suppression
[AD-A188885] 12 p1687 N88-20093
Signal-filter design and system performance for polarimetric radar
[AD-A189257] 13 p1758 N88-20514
A preliminary assessment of thunderstorm outflow wind measurement with airport surveillance radars
[AD-A189064] 13 p1799 N88-20757
Analysis, suppression of land clutter characteristics reported 14 p1903 N88-21369
The effects of better environmental inputs in estimating sea clutter
[AD-A192058] 19 p2643 N88-25678
Multi-target tracking algorithms for cluttered environments 20 p2789 N88-26543
Method and apparatus for measuring distance
[NASA-CASE-MSC-20912-1] 20 p2793 N88-26568
Rivista Tecnica Selenia, volume 10, no. 3, 1987
[ETN-88-92717] 22 p3068 N88-28210
Non-Gaussian models for surface clutter
22 p3068 N88-28212
The effect of equatorial ionospheric irregularities on the performance of a south-looking OTH-B (Over-The-Horizon-Backscatter) radar
[AD-A195090] 24 p3362 N88-30018

CMOS
Integrated circuit design
[AD-A184486] 03 p0311 N88-11960
Dramatically improved radiation hardness for CMOS silicon gate integrated circuits even down to cryogenic temperatures
[AD-A184672] 03 p0381 N88-12396
A study of charged particles/radiation damage to VLSI device materials
[NASA-CR-172036] 05 p0577 N88-13518
New breakthrough in Chinese integrated circuits: Successful development of high-speed CMOS circuits
[AD-A185381] 05 p0578 N88-13525
Effect of the gate oxide thickness on the speed of MOS integrated circuits
[PB88-155783] 10 p1323 N88-17910
Latent failures and coverage in fault-tolerant systems. A VLSI CMOS circuit design technique to aid test generation
[AD-A187615] 10 p1325 N88-17921
High density CMOS technology
11 p1561 N88-19342
Shorts in self-checking circuits
[RR-657-I] 14 p1908 N88-21402
An optimal CMOS structure for the design of a cell library
[EUT-87-E-166] 14 p1985 N88-21841
French Multiproject Chip (MPC) activity report, 1986
[RR-650-I] 15 p2059 N88-22273
Design of the Detector 2: A CMOS gate array for the study of concurrent error detection techniques
[AD-A191247] 16 p2193 N88-23079
Microelectronics the next fifteen years
17 p2305 N88-23792
Joint services electronics program
[AD-A190239] 18 p2503 N88-24848
Hot carrier effects in CMOS field effect transistors at cryogenic temperatures 19 p2662 N88-25829
Silver multi-layers for planar Ag/AgCl reference electrodes 19 p2672 N88-25883
Rule-based circuit optimization for CMOS VLSI
22 p3137 N88-28649
The p-well or n-well CMOS technology for advanced SEU-hard SRAMs
[DE88-006845] 22 p3156 N88-28777
The effects of total dose on the SEU sensitivity of CMOS static RAMS --- single event upset (SEU), satellite components
[AERE-R-12779] 24 p3428 N88-30401
A system study with an infrared sensitive microelectronic image sensor
[FOA-C-30481-3 1] 24 p3429 N88-30407

CN EMISSION
JHK photometry of CN-rich field giants
04 p0516 N88-13175

COAGULATION
NT BLOOD COAGULATION
Coagulation in stirred tanks
[B8711373] 05 p0562 N88-13420
Astrophysics and the solar nebula
07 p0883 N88-15355
Molecular composites processing and properties, 1
[AD-A194113] 23 p3189 N88-28974

COAL
Production of jet fuels from coal derived liquids. Volume 1: Market assessment for liquid by-products from the Great Plains gasification plant
[AD-A184846] 05 p0570 N88-13475
Application of inverse gas chromatography to fluidity studies
[DE88-002896] 10 p1296 N88-17750
High-density jet fuels from coal syncrudes, appendix 4
[DE88-003132] 10 p1307 N88-17813
The role of repowering in America's power generation future
[DOE/FE-0096] 10 p1351 N88-18076
Character of five selected LANDSAT lineaments in southwestern Pennsylvania: Report of investigations, 1987
[PB88-133517] 11 p1505 N88-18988
Coal particle behaviour in a counter-current combustor
[TAE-606] 19 p2612 N88-25498
Experiments on densely-loaded non-Newtonian slurries in laminar and turbulent pipe flows
[DE88-010579] 20 p2800 N88-26612

COAL DERIVED LIQUIDS
Production of jet fuels from coal derived liquids. Volume 1: Market assessment for liquid by-products from the Great Plains gasification plant
[AD-A184846] 05 p0570 N88-13475
Development and evaluation of supercritical fluid chromatography-mass spectrometry
[DE88-005122] 13 p1738 N88-20394

COAL GASIFICATION
Low temperature reactivity of chars towards oxygen, appendix E2
[DE88-004088] 10 p1298 N88-17760

COAL LIQUEFACTION
High-density jet fuels from coal syncrudes, appendix 4
[DE88-003132] 10 p1307 N88-17813

COALESCENCE
U COALESCING

COALESCING
Atmospheric science 07 p0883 N88-15357
Loop coalescing: A compiler transformation for parallel machines
[DE88-003571] 10 p1392 N88-18307
Effects of irradiation on thermal coalescence of pores in real crystals
[DE88-701683] 16 p2282 N88-23663

COANDA EFFECT
Proceedings of the Circulation-Control Workshop, 1986
[NASA-CP-2432] 10 p1268 N88-17586
Design of supersonic Coanda jet nozzles
10 p1270 N88-17599

COARSENESS
Structure and grain coarsening during the processing of engineering ceramics
[NASA-TM-100235] 03 p0293 N88-11838

COASTAL CURRENTS
Current velocity and hydrographic observations in the Straits of Florida, the Caribbean Sea and offshore of the Antillean Archipelago: Subtropical Atlantic climate studies (STACS) 1984 and 1985
[PB88-149299] 12 p1649 N88-19874
The use of a barotropic finite element model for the study of circulation on the continental shelf of the southeast coast of Brazil
[INPE-4401-PRE/1218] 13 p1802 N88-20774
Influence of the Yukon River on the Bering Sea
[NASA-CR-182802] 17 p2376 N88-24126

COASTAL DUNES
U DUNES

COASTAL ECOLOGY
NOAA's (National Oceanic and Atmospheric Administration's) Northeast Monitoring Program (NEMP): A report on progress of the first five years (1979-84) and a plan for the future
[PB87-210100] 02 p0196 N88-11225
Contribution of SPOT data to the physiographic study of coastal environment: La Pointe d'Arcay and l'Anse de l'Aiguillon (France) 03 p0344 N88-12176
Mapping of the mangroves of the Guanabarra Bay through the utilization of remote sensing techniques
[INPE-3942-TDL/229] 12 p1637 N88-19804

COASTAL MARSHLANDS
U MARSHLANDS

COASTAL PLAINS
Use of SPOT images for coastal development and inventory of aquacultural sites in New Caledonia (ALIAS project). First results 03 p0344 N88-12175

COASTAL WATER
Satellite and synoptic studies of chemical fronts in the California current and coastal upwelling zone
[AD-A183909] 01 p0073 N88-10466
Coastal winds of the southeast Alaska Peninsula
[PB87-206173] 02 p0215 N88-11354
Marine minerals: Exploring our new ocean frontier
[PB87-217725] 02 p0216 N88-11364
Contribution of SPOT data to the physiographic study of coastal environment: La Pointe d'Arcay and l'Anse de l'Aiguillon (France) 03 p0344 N88-12176
Coastal dynamics of the mouth of the Saloum (Senegal) --- SPOT imagery 03 p0345 N88-12177
The use of chlorophyll fluorescence measurements from space for separating constituents of sea water. Volume 1: Summary
[ESA-CR(P)-2444-VOL-1] 07 p0873 N88-15294

The use of chlorophyll fluorescence measurements from space for separating constituents of sea water. Volume 2: Appendices
[ESA-CR(P)-2444-VOL-2] 07 p0873 N88-15295

An investigation of offshore circulation using satellite data and feature tracking techniques
[AD-A186271] 07 p0881 N88-15347

Biogeochemical cycling in the ocean. Part 1: Introduction to the effects of upwelling along the west coast of North America
[NASA-TM-88230] 07 p0882 N88-15349

Ocean colour applications in ocean dynamics and coastal processes 08 p1042 N88-16297

Circulation and exchange processes on the South Atlantic Bight Continental Shelf
[DE88-003330] 13 p1804 N88-20781

Mechanical properties of sea ice and sea ice deformation in the near-shore zone
[PB88-147889] 13 p1804 N88-20782

Mixed-layer fronts in the California current
13 p1805 N88-20794

Production and turnover of suspended organic detritus in the coastal water of the southeastern continental shelf
[DE88-005118] 14 p1951 N88-21631

Changes in the California current system observed off northern California during July-August 1986
[AD-A190027] 15 p2100 N88-22510

Numerical simulation of coastal upwelling phenomena in Cabo Frio (RJ) through a two layer finite element model
[INPE-4502-RPE/561] 16 p2237 N88-23361

Influence of the Yukon River on the Bering Sea
[NASA-CR-182802] 17 p2376 N88-24126

Contribution of spaceborne high resolution radiometers to mapping of precoastal depths
19 p2701 N88-26063

The monitoring of sediment transport, water circulation and mixing in estuaries and coastal waters
22 p3108 N88-28457

Evaluation of SPOT data for remote sensing of physical and biological properties of estuaries and coastal zones
22 p3108 N88-28458

COASTAL ZONE COLOR SCANNER

Update of NASA's ocean colour activities
08 p1042 N88-16295

NIMBUS-7 CZCS. Coastal Zone Color Scanner imagery for selected coastal regions. North America - Europe. South America - Africa - Antarctica. Level 2 photographic product
[NASA-CR-180755] 15 p2089 N88-22447

COASTS

A one-dimensional model of thermally-driven coastal front evolution 02 p0204 N88-11274

An hourly analysis, updating and short-range forecasting system --- numerical weather forecasting
02 p0206 N88-11288

Real-time evaluation and prediction of coastal dispersion near the SW tip of Africa --- effluents
02 p0210 N88-11318

Contribution of SPOT data to the physiographic study of coastal environment: La Pointe d'Arcay and l'Anse de l'Aiguillon (France) 03 p0344 N88-12176

Coastal dynamics of the mouth of the Saloum (Senegal) --- SPOT imagery 03 p0345 N88-12177

East coast gravity validation study
[AD-A184292] 03 p0351 N88-12217

Hurricane Elena storm surge data
[AD-A184573] 03 p0353 N88-12228

The development of low level coastal flow fields when solar radiation is blocked by smoke
[DE87-014348] 03 p0354 N88-12230

Vanfront 3 expedition data report (USNS DE STEIGUER CRUISE 1202-82). Bioluminescence, hydrographic, nutrient, and satellite data from the Gulf of California (November-December 1981)
[AD-A185011] 05 p0620 N88-13805

Atmospheric diffusion at coastal site in presence of sea-breeze
[DE88-700038] 07 p0876 N88-15314

Hurricane climatology for the Atlantic and Gulf coasts of the United States
[PB88-114657] 08 p1039 N88-16288

Annual data summary and climatological evaluation CERC (Coastal Engineering Research Center) field research facility, 1985. Volume 1. Main text and appendixes A and B
[AD-A186442] 08 p1039 N88-16289

Nearshore wave transformation study of sites near Port Canaveral Inlet, Florida
[AD-A186965] 09 p1195 N88-17159

CTD observations in the coastal transition zone off northern California, 16-25 February 1987
[AD-A187283] 10 p1357 N88-18111

Numerical simulations of the California current: Filament formation as related to baroclinic instability
[AD-A187573] 10 p1358 N88-18115

A propagation campaign in a marine environment utilizing a digital system at 36 GHz 12 p1618 N88-19675

Relationships between remotely-sensed surface properties and subsurface structure in the ocean
[AD-A189317] 12 p1650 N88-19881

SPOT investigations of estuaries and coastal zones: An overview 22 p3107 N88-28455

The use of SPOT data in mapping coastal areas
22 p3108 N88-28461

Physiography and kinematics of the western coast of the province of Huelva (Andalousia, Spain)
22 p3109 N88-28465

Meteorological features during the marginal ice zone experiment from 20 March to 10 April 1987
[AD-A193960] 23 p3235 N88-29251

Doppler radar analysis of coastal marine atmospheric boundary layer structure during a cold air outbreak
[AD-A196023] 24 p3403 N88-30261

COATING

NT ANODIZING
NT ELECTROPLATING
NT ENCAPSULATING
NT METALLIZING

Molecular dynamics of laser ablation of a polymer coating
[DE88-004337] 13 p1750 N88-20466

COATINGS

NT ALUMINUM COATINGS
NT ANODIC COATINGS
NT ANTIRADAR COATINGS
NT ANTIREFLECTION COATINGS
NT CATHODIC COATINGS
NT CERAMIC COATINGS
NT ELECTROPLATING
NT ENAMELS
NT ENCAPSULATING
NT GLASS COATINGS
NT GLAZES
NT METAL COATINGS
NT METALLIZING
NT NICKEL COATINGS
NT PAINTS
NT PLASTIC COATINGS
NT PRIMERS (COATINGS)
NT PROTECTIVE COATINGS
NT REFRACTORY COATINGS
NT SPRAYED COATINGS
NT THERMAL CONTROL COATINGS
NT ZINC COATINGS

Synergism of electroplating and vacuum processes
[DE87-013496] 01 p0033 N88-10211

JPRS report: Science and technology. USSR: Materials science
[JPRS-UMS-87-006] 03 p0285 N88-11791

Consortium for Materials Development in Space. Technical section
[NASA-CR-181508] 03 p0296 N88-11859

Surface coatings and catalyst production by electrodeposition 03 p0297 N88-11863

Mass transport by diffusion 03 p0297 N88-11864

Advanced natural gas fueled engine development. Part 2: Materials investigation
[PB87-223160] 03 p0331 N88-12088

Long-range pulselength scaling of 351nm laser damage thresholds
[DE87-014754] 04 p0448 N88-12777

Thermomechanical cracking in coated media due to high speed asperity excitation
[AD-A184176] 04 p0454 N88-12809

Effectiveness of electrodeposited coatings in reducing atmospheric corrosion of copper substrates
[DE87-013651] 05 p0566 N88-13448

Raman microprobe characterization of dielectric films following high-energy pulsed laser irradiation
[DE88-000559] 05 p0588 N88-13587

Fatigue characteristics of ion treated surfaces
05 p0606 N88-13713

Fractographic study of fiber composites
06 p0677 N88-14146

Effects of hydrolysis on metallo-organic solution deposition of PZT films
[ATR-86(8443)-1] 06 p0679 N88-14160

The tribological properties of MoS2 coatings in vacuum, low relative humidity and high relative humidity environments
[DE88-001611] 06 p0711 N88-14356

Electromagnetic fields backscattered from an s-shaped inlet cavity with an absorber coating on its inner walls
[NASA-CR-182401] 07 p0845 N88-15130

Tribological studies on high speed steel cutting tools
[DE88-002550] 07 p0864 N88-15246

TiN coatings on M2 steel produced by plasma assisted chemical vapor deposition
[DE88-003189] 08 p0970 N88-15867

Sputtered silver films to improve chromium carbide based solid lubricant coatings for use to 900 C
[NASA-TM-100783] 08 p0973 N88-15885

Self-lubricating coatings for high-temperature applications 09 p1119 N88-16703

Organic coatings to improve the storageability and safety of pyrotechnic compositions
[AD-A187158] 09 p1150 N88-16889

Los Alamos optical materials reliability, maintainability, and exposure testing program
[DE88-001953] 10 p1409 N88-18404

Protecting old oil tanks made of steel against internal corrosion using organic coatings
[DE88-751089] 11 p1459 N88-18698

Electrochromic thin films
[DE88-751099] 11 p1559 N88-19334

Electrophoretically deposited styrene-acrylate coatings for suppression of internal electromagnetic pulse effects
[DE88-003820] 12 p1609 N88-19621

Investigations of surface coatings based on silicon and nitrogen: From amorphous Si to silicon nitride
[DE88-004995] 12 p1609 N88-19622

The influence of the fiber-matrix bond on the mechanical behavior of NICALON/SiC composites
[DE88-006155] 13 p1734 N88-20369

Optimization of binary pigment coatings
[AD-A189103] 13 p1748 N88-20450

PNL-1 improved ceramic composites through controlled fiber matrix interaction
[DE88-005680] 13 p1750 N88-20462

Causes of damage in multilayer dielectric coatings exposed to high average power visible laser radiation
[DE88-005363] 13 p1775 N88-20619

Fatigue damage modeling for coated single crystal superalloys 15 p2085 N88-22427

Present, future of automotive hybrid IC applications discussed 16 p2185 N88-23024

Thin film research diagnostics instrumentation
[AD-A191240] 16 p2213 N88-23207

Implications of the trapping-desorption and direct inelastic scattering channels on Dicke-narrowed lineshapes
[AD-A191410] 16 p2270 N88-23581

Boundary layer flow visualization for flight testing
17 p2297 N88-23742

Predictive corrosion modeling, volume 1
[AD-A191229] 18 p2485 N88-24739

Environmental integrity of coating/metal interface
[AD-A192184] 18 p2492 N88-24786

Design and demonstration of a system for the deposition of atomic-oxygen durable coatings for reflective solar dynamic power system concentrators
[NASA-CR-4158] 19 p2606 N88-25474

Thermoplastic coating of carbon fibers
[NASA-CR-183067] 20 p2767 N88-26407

Interface modification in Nicalon (trademark)/SiC composites
[DE88-009708] 20 p2767 N88-26409

The effects of Hertzian stress and test ambient on the friction coefficient of MsS2 coatings
[DE88-008118] 20 p2777 N88-26467

Characterization of coating wear phenomena in nitride and carbide coated tool inserts
[DE88-011196] 20 p2779 N88-26478

Contribution to the development of coated fiber ceramic insolation material
[ETN-88-92361] 21 p2906 N88-27243

PECVD of amorphous nickel-phosphorus films
[DE88-011088] 21 p2915 N88-27299

Radiative heat transfer and selective emission in planar slab coatings on hot emissive substrates
[AD-A193133] 21 p2918 N88-27319

Thermo-mechanical cracking in coated media with a cavity by a moving asperity friction
[AD-A193311] 21 p2961 N88-27586

Thin film coatings for space electrical power system applications
[NASA-TM-101325] 23 p3187 N88-28966

Thin film-residual stress assessment
[AD-A193205] 23 p3196 N88-29018

The diamond as a new electronic material
[NASA-TT-20354] 23 p3209 N88-29098

The acoustic field scattered from some approximate pressure release materials
[AD-A194768] 23 p3278 N88-29515

Indium-coated rhenium thrusters by CVD
[NASA-TM-101309] 24 p3339 N88-29874

Ultrasonic detection of diffusion and adhesion loss
24 p3354 N88-29967

Photoacoustic Fourier transform infrared spectroscopy: An early detection technique for coatings degradation
24 p3354 N88-29968

Predicting the durability of adhesives and coatings by remote detection of hidden defects and coating-thickness irregularities: A theoretical and numerical study
24 p3355 N88-29972
An electrochemical impedance spectroscopy study of reactions at the metal/coating interface
24 p3355 N88-29975
Containment of a silicone fluid free surface in reduced gravity using barrier coatings
[NASA-TM-101314] 24 p3371 N88-30072

COAXIAL CABLES
Crosstalk in braided shield coaxial cables
01 p0035 N88-10224
The use of coaxial transmission line elements in log-periodic dipole arrays
[AD-A184864] 05 p0574 N88-13499
Picosecond cable calibrator: Beam Research Program
[DE88-002375] 06 p0695 N88-14266
Coaxial cable connector
[NASA-CASE-NPO-16764-1-CU]
06 p0696 N88-14270
Shielding effectiveness against electromagnetic interference
[DE88-003664] 07 p0846 N88-15131
Measurement of shielding effectiveness of different cable and shielding configurations by mode-stirred techniques
[PB88-155791] 10 p1319 N88-17885
The coaxial colinear antenna: Theoretical and experimental models 11 p1475 N88-18803
The preparation, assembly and mounting of RF coaxial cables
[ESA-PSS-01-718-ISSUE-1] 13 p1756 N88-20504
Power transmission studies for tethered SP-100
[NASA-TM-100864] 14 p1883 N88-21251

COAXIAL FLOW
Experimental study of interacting vortex rings
03 p0318 N88-12007
Numerical solutions of the complete Navier-Stokes equations
[NASA-CR-183023] 18 p2514 N88-24914

COAXIAL TRANSMISSION
U COAXIAL CABLES
U TRANSMISSION

COBALT
NT COBALT 60
Microstructure and magnetic properties of cobalt-chromium alloys
[DE88-002762] 07 p0835 N88-15064
Reaction mechanism of sulfur dioxide with single crystal cobalt and chromium and CoCrAlY coatings
[AD-A185989] 09 p1253 N88-17509
Studies of the electron spectrum with reference to the clean surfaces of iron, cobalt and nickel and their subsequent exposure to oxygen
11 p1459 N88-18700
Carboxylate formation at the interface between a polyimide coating and cobalt 17 p2320 N88-23859
Nickel hydrogen cell positive-electrode studies: Cobalt segregation in reducing environments
[AD-A193025] 20 p2796 N88-26587

COBALT ALLOYS
NT ASTROLOY (TRADEMARK)
Reaction mechanism of sulfur dioxide with single crystal cobalt and chromium and CoCrAlY coatings
[AD-A185989] 09 p1253 N88-17509
Effects of ion implantation on cavitation erosion of a cobalt based metal/carbide alloy
[AD-A187239] 10 p1303 N88-17793
New super alloys used in turbochargers
19 p2634 N88-25628

COBALT COMPOUNDS
NT COBALT OXIDES
Growth of high quality CoSi2/Si superstructures on Si(111) 20 p2869 N88-27034

COBALT ISOTOPES
NT COBALT 60

COBALT OXIDES
Phase purity of NiCo2O4, a catalyst candidate for electrolysis of water
[NASA-TM-100239] 05 p0556 N88-13385

COBALT 60
Evaluation of silicon-on-insulator MOS (Metal-Oxide-Semiconductor) transistor response to 10-keV X-ray and cobalt-60 irradiation
[DE88-006102] 23 p3206 N88-29082

COBE
U COSMIC BACKGROUND EXPLORER SATELLITE

COBOL
COBOL Analysis System (CAS) users manual
[PB88-171442] 16 p2250 N88-23445

COCHLEA
Assessment of cochlear damage after microwave irradiation
[AD-A193237] 21 p2987 N88-27737

COCKPIT SIMULATORS
Investigation of pilot behavior in a training program for assessing handling qualities using a ground simulator
[ESA-TT-999] 03 p0357 N88-12247
Status of NASA/Army rotorcraft research and development piloted flight simulation
09 p1110 N88-16651
An enumeration of research to determine the optimal design and use of Army flight training simulators
[AD-A191242] 18 p2468 N88-24649

COCKPITS
MBB simulation facilities applied for rotorcraft research 03 p0263 N88-11655
Helicopter (performance) management
03 p0264 N88-11666
Effects of combining vertical and horizontal information into a primary flight display
[NASA-TP-2783] 04 p0399 N88-12487
Advanced helicopter cockpit and control configurations for helicopter combat missions
[NASA-TM-100017] 07 p0821 N88-14988
An inexpensive real-time interactive three dimensional flight simulation system
[AD-A184868] 07 p0821 N88-14989
Dynamic function allocation in fighter cockpits
[AD-A185397] 09 p1201 N88-17199
Comparison of alphanumeric data entry methods for advanced helicopter cockpits
[AD-A186934] 09 p1201 N88-17201
Cockpit data management
[NASA-CR-178407] 11 p1438 N88-18579
Cockpit data management
[NASA-CR-178407-SUPPL] 11 p1438 N88-18580
A comparison of keyboard designs for cockpit applications
[AD-A187775] 12 p1581 N88-19460
User perceptions of side-arm flight control in rotary-wing aircraft
[AD-A188519] 12 p1672 N88-20009
CODAC (Cockpit Oriented Display of Aircraft Configurations) version 1.4 user's guide
[NASA-CR-181650] 13 p1718 N88-20273
Geometric modeling of flight information for graphical cockpit display
[AD-A190484] 15 p2021 N88-22043
Psychosensory cockpit ergonomics, advantages of intelligent information systems 17 p2304 N88-23784
Advanced development of a cockpit automation design support system 17 p2304 N88-23785
Software engineering for the British Aerospace Experimental Aircraft Programme (EAP)
17 p2306 N88-23798
Checklist interruption and resumption: A linguistic study
[NASA-CR-177460] 20 p2756 N88-26348
A cockpit natural language study - selected transcripts
[AD-A192972] 20 p2834 N88-26808
Cockpit and cabin crew coordination
[AD-A192445] 21 p2993 N88-27752
A cockpit natural language study: Vocabulary and grammar analyses
[AD-A133289] 21 p2993 N88-27753
Visual related accidents/incidents
23 p3242 N88-29293
General operational and training visual concerns
23 p3242 N88-29295
Night lighting and night vision goggle compatibility
23 p3242 N88-29297
Future visual environment and concerns
23 p3242 N88-29299
Use of color CRTs (Cathode Ray Tubes) in aircraft cockpit: A literature search, revision B
[AD-A195062] 24 p3324 N88-29797

COD (CRACKS)
U CRACK OPENING DISPLACEMENT

CODE DIVISION MULTIPLE ACCESS
Code division multiple access applied to fiber optic data transmission
[AD-A186873] 09 p1247 N88-17477
Mobilestar field test program
19 p2646 N88-25707
Comparison of CDMA and FDMA for the MobileStar(sm) system 19 p2649 N88-25724
Evaluation of CDMA system capacity for mobile satellite system applications 19 p2651 N88-25740

CODERS
Design of source coders and joint source/channel coders for noisy channels
[NASA-CR-181547] 04 p0432 N88-12678
Experience with Omega: Implementation of a prototype programming environment, part 6
[AD-A187080] 10 p1385 N88-18270
A hybrid transform/DPCM encoder for data compression
[DE87-014852] 13 p1758 N88-20518
Speech coding at 4800 bps for mobile satellite communications 19 p2652 N88-25749
A 4.8 kbps code-excited linear predictive coder
19 p2652 N88-25750
Real-time speech encoding based on Code-Excited Linear Prediction (CELP) 19 p2653 N88-25751
Development of an 8000 bps voice codec for AvSat
19 p2653 N88-25755

CODING
NT AMPLITUDE MODULATION
NT DECODING
NT DELTA MODULATION
NT DIFFERENTIAL PULSE CODE MODULATION
NT FREQUENCY MODULATION
NT FREQUENCY SHIFT KEYING
NT PHASE MODULATION
NT PHASE SHIFT KEYING
NT PULSE AMPLITUDE MODULATION
NT PULSE CODE MODULATION
NT PULSE DURATION MODULATION
NT PULSE MODULATION
NT PULSE POSITION MODULATION
NT REDUNDANCY ENCODING
NT SIGNAL ENCODING
Study, design, and evaluation of data reduction by encoding or information extraction. Part 1: Data generation analysis --- multispectral satellite imagery
[NLR-TR-85094-L-PT-1] 01 p0078 N88-10501
Study, design and evaluation of data reduction by encoding or information extraction. Part 2: Operational considerations --- multispectral satellite imagery
[NLR-TR-85094-L-PT-2] 01 p0079 N88-10502
Study, design and evaluation of data reduction by encoding or information extraction. Part 3: Algorithm design --- multispectral satellite imagery
[NLR-TR-85094-L-PT-3] 01 p0079 N88-10503
Study, design and evaluation of data reduction by encoding or information extraction. Part 4: Performance demonstration --- multispectral satellite imagery
[NLR-TR-85094-L-PT-4] 01 p0079 N88-10504
Study, design and evaluation of data reduction by encoding or information extraction. Part 5: Algorithm implementation aspects --- multispectral satellite imagery
[NLR-TR-85094-L-PT-5] 01 p0079 N88-10505
Computations of hypervelocity impact using the CTH shock wave physics code
[DE87-013067] 02 p0169 N88-11062
IMPSOR: A fully vectorized FORTRAN code for three dimensional moving boundary problems with Dirichlet or Neumann boundary conditions
[DE87-014964] 02 p0226 N88-11427
BIMOND3: Monotone piecewise bicubic Hermite interpolation code
[DE87-014612] 02 p0229 N88-11442
A relativistic Monte Carlo binary collision model for use in plasma particle simulation codes
[DE87-013287] 02 p0237 N88-11494
The evolution of HOBO
[DE87-014742] 03 p0313 N88-11980
Studies of the processing of single words using positron tomographic measures of cerebral blood flow change
[AD-A184058] 03 p0356 N88-12244
Los Alamos National Laboratory computer benchmarking 1986
[LA-10898-MS] 03 p0363 N88-12285
Development and evaluation of a Monte Carlo code system for analysis of ionization chamber responses
[AD-A183970] 03 p0375 N88-12359
Competition Analysis Model (CAM). Volume 2: Computer manual
[AD-A184017] 03 p0384 N88-12411
Tau ranging revisited 04 p0437 N88-12710
INS3D: An incompressible Navier-Stokes code in generalized three-dimensional coordinates
[NASA-TM-100012] 04 p0485 N88-12991
A computer code to process and plot laser altimetry data interactively on a microcomputer
[NASA-TM-100687] 05 p0554 N88-13371
A computer code to calculate line by line atmospheric transmission spectra on a microcomputer
[NASA-TM-100688] 05 p0554 N88-13372
Hanford Meteorological Station computer codes. Volume 5: The TOWER computer code
[DE88-001610] 05 p0628 N88-13843
Some distance problems in coding theory
[B8711398] 05 p0635 N88-13888
Numerical study of chemically reacting flows using an LU scheme
[NASA-CR-180882] 06 p0668 N88-14094
Correction method for Barker-coded modulation
06 p0691 N88-14240
Methods for reducing computational costs of typical finite element unsteady hydrodynamic models
[AD-A185499] 06 p0702 N88-14312

Evaluation of a satellite laser ranging technique using pseudonoise code modulated laser diodes
[NASA-CR-182347] 06 p0708 N88-14343
Local and global techniques for the tracking of periodic solutions of parameter-dependent functional differential equations
[AD-A185756] 06 p0766 N88-14704
Plasma parameters for alternate operating modes of TIBER-2
[DE88-001890] 06 p0783 N88-14802
Bar code document accountability system performance update
[DE88-002256] 06 p0791 N88-14849
Analysis and performance prediction of scramjet inlets utilizing a three-dimensional Navier-Stokes code
07 p0811 N88-14936
Modern wing flutter analysis by computational fluid dynamics methods
[NASA-TM-100531] 07 p0816 N88-14965
Performance analysis of coded frequency-hopped spread-spectrum systems with unknown interference
[AD-A186069] 07 p0841 N88-15103
Coding for spread-spectrum communications networks
[AD-A185667] 07 p0844 N88-15119
Treatment of small wire loops in the method of moments code NEC (Numerical Electromagnetics Code)
[DE88-002995] 07 p0846 N88-15136
User manual for ATILA, a finite-element code for modeling piezoelectric transducers
[AD-A185948] 07 p0847 N88-15141
Local versus global minima in visual pattern completion
[PB87-234803] 07 p0897 N88-15439
TeXting the FORMULARY: A collection of examples of the use of TeX to produce ruled tables and displayed equations
[AD-A185920] 07 p0921 N88-15598
Verification of FANTASTIC integrated code
07 p0924 N88-15613
Neural network based speech synthesizer: A preliminary report 08 p1064 N88-16429
Absorption of electron cyclotron waves by superthermal electron velocity distributions in tokamak plasmas
[INPE-4385-PRE/1205] 08 p1086 N88-16539
New techniques in computational aerodynamics
[AD-A186719] 09 p1112 N88-16664
Outlier resistant predictive source encoding for a Gaussian stationary nominal source
[AD-A186725] 09 p1232 N88-17387
A transonic-small-disturbance wing design methodology
[NASA-TP-2806] 10 p1273 N88-17614
Designing variable-length codes with good error-recovery properties
[BBC-RD-1987/19] 10 p1317 N88-17876
The design of trellis codes for fading channels
[NASA-CR-182523] 10 p1320 N88-17891
Orthogonal patterns in binary neural networks
[NASA-TM-100060] 10 p1396 N88-18320
A performance index approach to aerodynamic design with the use of analysis codes only
[NASA-TP-2805] 11 p1433 N88-18552
The Telecommunications and Data Acquisition Report
[NASA-CR-182545] 11 p1471 N88-18774
A labeling procedure for linear finite-state codes
11 p1472 N88-18781
Further results on finite-state codes
11 p1472 N88-18782
A comparison of VLSI architectures for time and transform domain decoding of Reed-Solomon codes
11 p1472 N88-18783
A simplified, general-purpose deep-space ranging correlator design 11 p1473 N88-18786
VAXELN experimentation: Programming a real-time clock and interrupt handling using VAXELN Ada 1.1
[AD-A188100] 11 p1525 N88-19107
Spire based speaker-independent continuous speech recognition using mixed feature sets
[AD-A188834] 12 p1620 N88-19688
A concatenated coded modulation scheme for error control
[NASA-CR-182639] 12 p1621 N88-19697
A new parabolized Navier-Stokes code for chemically reacting flow fields 12 p1625 N88-19721
Some questions of using coding theory and analytical calculation methods on computers
[DE88-700905] 12 p1676 N88-20021
Trajectory code studies, 1987
[DE88-006216] 13 p1728 N88-20335
A comparison of two chord keyboard coding systems for alphanumeric data entry
[AD-A189230] 13 p1813 N88-20834
MASPLT: A one-dimensional graphics post processor for wave propagation codes
[DE88-005506] 13 p1817 N88-20856
CSQPLT: A graphics post processor for multidimensional wave propagation codes
[DE88-005508] 13 p1817 N88-20858
An integrated data description language for coding design knowledge
[CWI-CS-R8731] 13 p1819 N88-20871
Accuracy requirements and benchmark experiments for CFD validation
[NASA-TM-100087] 14 p1911 N88-21423
Tabulation of Mie scattering calculation results for microwave radiative transfer modeling
[NASA-CR-4130] 14 p1947 N88-21612
Performance of data compression codes in channels with errors
[AD-A189667] 15 p2055 N88-22253
Status of electric vehicle simulation programs at the INEL: Summer 1987
[DE88-006745] 15 p2058 N88-22271
Selective mechanisms in auditory and bimodal signal processing
[AD-A190529] 15 p2103 N88-22530
Multiple-transform pipelines for image coding
[REPT-87-038] 15 p2108 N88-22561
The algebraic structure of convolutional codes
[AD-A190280] 15 p2120 N88-22635
Information and coding capacities of mismatched Gaussian channels
[AD-A190321] 15 p2124 N88-22665
Coding capacity of generalized additive channels
[AD-A190315] 15 p2127 N88-22685
OCR vision system, an alternative to bar code
[DE88-003761] 15 p2149 N88-22828
On the validation of a code and a turbulence model appropriate to circulation control airfoils
[NASA-TM-100090] 16 p2156 N88-22864
A computer model investigation of a half square log-periodic array
[AD-A190955] 16 p2190 N88-23062
Mass digitization of opographic-cartographic information 16 p2226 N88-23288
Efficient and fast data compression codes for discrete sources with memory
[ETN-88-92233] 16 p2246 N88-23420
Error control techniques for satellite and space communications
[NASA-CR-182886] 17 p2332 N88-23922
Preliminary 2-D shell analysis of the space shuttle solid rocket boosters
[NASA-TM-100515] 17 p2348 N88-23989
Parallel binary and parallel coded decimal time code formats
[AD-A190126] 17 p2384 N88-24170
The Lewis heat pipe code with application to SP-100 GES heat pipes 17 p2421 N88-24395
Analytic and numerical modeling of heat and material transport in electrical hypervelocity guns
[AD-A192178] 18 p2469 N88-24655
Joint services electronics program
[AD-A190239] 18 p2503 N88-24848
Adaptive local grid refinement in computational fluid mechanics
[AD-A192215] 18 p2510 N88-24890
Duct flow nonuniformities for Space Shuttle Main Engine (SSME)
[NASA-CR-179338] 18 p2511 N88-24899
Narrative compression coding for a channel with errors
[AD-A191577] 19 p2642 N88-25673
Trellis-coded CPM for satellite-based mobile communications 19 p2648 N88-25718
Interleaver design for trellis-coded differential 8-PSK modulation with non-coherent detection
19 p2648 N88-25719
Codes for QPSK modulation with invariance under 90 degrees rotation 19 p2648 N88-25720
Trellis-coded MPSK modulation techniques for MSAT-X(sup)1 19 p2648 N88-25721
Modulation and coding for fast fading mobile satellite communication channels 19 p2648 N88-25722
Performance of the ICAO standard core service modulation and coding techniques
19 p2648 N88-25723
A 4.8 kbps code-excited linear predictive coder
19 p2652 N88-25750
Sinusoidal transform coding 19 p2653 N88-25752
Analysis and improvement of the vector quantization in SELP (Stochastically Excited Linear Prediction)
19 p2653 N88-25756
The development of an intelligent interface to a computational fluid dynamics flow-solver code
[NASA-TM-100908] 19 p2716 N88-26127
A VLSI single-chip (225,223) Reed-Solomon encoder with interleaver
[NASA-CASE-NPO-17280-1-CU]
21 p2902 N88-27220
SARLAC: A relativistic electron beam code
[AD-A193134] 21 p2932 N88-27411
Numerical computation of space shuttle orbiter flow field
[NASA-CR-183193] 22 p3040 N88-28048
Efficient multiplication algorithms over the finite fields GF(q sup m), where q equals 3,5
22 p3066 N88-28191
Numerical modeling results for mode propagation in a wedge
[AD-A193998] 22 p3147 N88-28718
Fine resolution errors in secondary surveillance radar altitude reporting
[RSRE-87019] 23 p3175 N88-28906
Method for Veterbi decoding of large constraint length convolutional codes
[NASA-CASE-NPO-17310-1-CU]
23 p3183 N88-28946
Coding for meteor-burst communications channel and side information for channels with block-interference
23 p3202 N88-29054
An overview of technology for spoken interaction with machines
[AD-A194153] 23 p3202 N88-29058
Hierarchical organization for large, dynamic radio networks
[AD-A193942] 23 p3204 N88-29067
A computer program package for introductory one-dimensional digital signal processing applications
[AD-A194656] 23 p3249 N88-29338

COEFFICIENT OF FRICTION
A method for the approximate calculation of the skin friction coefficient of horizontal wavy plates
[VKI-TN-160] 07 p0851 N88-15172
Influence of the friction coefficients, the power and the flowrate on the two-phase flow instabilities in natural circulation
[DE88-700036] 08 p0983 N88-15946
Tribological properties of alumina-boria-silicate fabric from 25 to 850 C
[NASA-TM-100806] 11 p1464 N88-18726
Evaluation of centrifugal barrel tumbling process for impregnation of molybdenum disulfide powder lubricant
[BDX-613-3696] 11 p1464 N88-18727
Compressible friction coefficients in a simulated heat pipe
[AD-A188818] 12 p1627 N88-19735
The effects of Hertzian stress and test ambient on the friction coefficient of MsS2 coatings
[DE88-008118] 20 p2777 N88-26467

COEFFICIENTS
NT AERODYNAMIC COEFFICIENTS
NT ATTENUATION COEFFICIENTS
NT COEFFICIENT OF FRICTION
NT CORRELATION COEFFICIENTS
NT COUPLING COEFFICIENTS
NT DIFFUSION COEFFICIENT
NT DISCHARGE COEFFICIENT
NT FLOW COEFFICIENTS
NT HEAT TRANSFER COEFFICIENTS
NT INFLUENCE COEFFICIENT
NT IONIZATION COEFFICIENTS
NT NOZZLE THRUST COEFFICIENTS
NT RECOMBINATION COEFFICIENT
NT REGRESSION COEFFICIENTS
NT SCATTERING COEFFICIENTS
NT STRUCTURAL INFLUENCE COEFFICIENTS
NT VIRIAL COEFFICIENTS
NT WIGNER COEFFICIENT
Reactive sticking coefficients of silane on silicon
[DE88-000601] 05 p0570 N88-13473
Concentration coefficients of elements in ferromanganese nodules relative to ocean sediments
06 p0726 N88-14464
Estimation of broadband planetary albedo from operational narrowband satellite measurements
[PB88-107644] 07 p0945 N88-15748
Cornering characteristics of the main-gear tire of the space shuttle orbiter
[NASA-TP-2790] 11 p1438 N88-18583
Calibration of a ring laser gyro inertial navigation system 12 p1576 N88-19428
Determination of the partition coefficients of organophosphorus compounds using high-performance liquid chromatography
[AD-A189276] 13 p1737 N88-20385
Transformation coefficient in wave-field acceleration scheme
[DE88-700158] 13 p1757 N88-20507
Predicting oscillatory finite difference solutions to the heat equation: A comparative study of the coefficient and matrix methods
[AD-A189591] 13 p1825 N88-20911
Experimental determination of the coefficients of the hydraulic resistance of apertures in the rotary disks
[AD-A190627] 15 p2066 N88-22317

Solving singular systems using orthogonal functions
[AD-A190881] 16 p2260 N88-23512
Evaluation of the biot coefficients
[AD-A191643] 18 p2570 N88-25265
Polynomials with restricted coefficients and their applications
[AD-A192589] 23 p3202 N88-29055

COENZYMES
NT ADENOSINE TRIPHOSPHATE
NT GLUTATHIONE

COFFEE
SPOT applications on Columbia's coffee zone
22 p3097 N88-28395

COGENERATION
Development of a light duty gas engine for cogeneration service
[PB87-221297] 02 p0180 N88-11119
Development of fast breeder reactors in China
16 p2186 N88-23032
Design of nuclear heat, power co-generation plant detailed 16 p2186 N88-23033
Advanced energy system program
[PB88-183025] 19 p2686 N88-25965

COGNITION
Studies of the processing of single words using positron tomographic measures of cerebral blood flow change
[AD-A184058] 03 p0356 N88-12244
Effects of divided attention on identity and semantic priming
[AD-A184289] 03 p0357 N88-12250
Evoked brain activity and personnel performance
[AD-A185922] 07 p0897 N88-15436
Computing support for basic research in perception and cognition
[AD-A186192] 07 p0897 N88-15437
Cirrus: An automated protocol analysis tool
[AD-A186646] 08 p1052 N88-16348
Deriving descriptions of the mind
[AD-A186647] 08 p1052 N88-16349
Changing the layers of mind
[AD-A186648] 08 p1052 N88-16350
Intelligent tutoring systems as tools for investigating individual differences in learning
09 p1204 N88-17216
A hypertext writing environment and its cognitive basis
[AD-A188179] 10 p1389 N88-18298
Effects of stress on judgement and decision making in dynamic tasks
[AD-A188203] 11 p1523 N88-19092
The construction of a pedagogy to promote meaningful learning of strategies and tactics for solving problems of elementary combinatorics
[AD-A187928] 11 p1542 N88-19216
Night Vision: Current Research and Future Directions, symposium proceedings
[PB88-132006] 11 p1550 N88-19274
Effects of intense, time-constrained mental effort on hemodynamics and cardiovascular function
12 p1664 N88-19975
Neurocognitive predictions of performance
[AD-A188323] 12 p1669 N88-19998
A comparison of the Army's Project A: Cognitive and psychomotor tests to analogous Air Force and Navy tests
[AD-A188636] 12 p1670 N88-20002
Expert systems: Their impact on performance and cognitive strategies in diagnostic inference
[AD-A188518] 12 p1677 N88-20027
Management information systems design implications: The effect of cognitive style and information presentation on problem solving
[AD-A188850] 12 p1705 N88-20205
A personalized and prescriptive decision aid for choice from a database of options
[AD-A188726] 13 p1811 N88-20820
Mental models of mechanical systems: Individual differences in qualitative and quantitative reasoning
[AD-A189035] 13 p1812 N88-20823
Human problem solving in dynamic environments: Understanding and supporting operators in large-scale, complex systems
[AD-A189539] 13 p1812 N88-20826
Online aiding for human-computer interfaces
[AD-A189239] 13 p1815 N88-20842
Soar: An architecture for general intelligence
[AD-A188742] 13 p1823 N88-20898
Conflict resolution in cooperative systems
[AD-A190351] 15 p2104 N88-22535
Relationship of encoding speed and memory tests to flight training performance
[AD-A190670] 15 p2105 N88-22539
The N2-P3 complex of the evoked potential and human performance 16 p2241 N88-23388
Processing deficits in monitoring analog and digital displays: Implications for attentional theory and mental-state estimation research
16 p2241 N88-23389
Problem solving in a natural task as a function of experience
[AD-A191180] 16 p2243 N88-23399
The event-related brain potential as an index of information processing and cognitive activity: A program of basic research
[AD-A191244] 16 p2243 N88-23400
Capitalizing on failure through case-based inference
[AD-A190927] 16 p2255 N88-23480
Extracting information from problem solving experience
[AD-A191331] 16 p2286 N88-23688
Spatial cognition 17 p2380 N88-24152
Induction of models under uncertainty
[NASA-TM-101173] 17 p2394 N88-24230
A systems engineering based methodology for analyzing human electrocortical responses
[AD-A190809] 18 p2550 N88-25135
Performance effectiveness and the work/rest cycle
[AD-A191448] 18 p2551 N88-25145
Models of incremental concept formation
[AD-A191597] 18 p2552 N88-25147
A computational model of motor behavior
[AD-A191179] 18 p2553 N88-25152
Selection and effects of channels in distributed communication and decision making tasks: A theoretical review and a proposed research paradigm
[AD-A191807] 18 p2587 N88-25375
Generalization and the backward propagation neural network
[AD-A191634] 19 p2710 N88-26100
Direct manipulation and the design of user interfaces
[PB88-126354] 2[illegible]2834 N88-26810
The effects of increased cog[illegible] demands on autonomic self-regulation: An indicator of parallel processing in the brain 21 p2925 N88-27362
Electric and magnetic brain activity related to cognitive performance 21 p2979 N88-27692
The effects of hypoxia on P300 and reaction time
[DCIEM-87-RR-12] 21 p2979 N88-27697
Cognitive task demands as reflected in physiological measures 21 p2980 N88-27699
Event-related and steady potential changes in the brain related to workload during tracking
21 p2981 N88-27705
Cognitive and neural bases of skilled performance
[AD-A193392] 21 p2992 N88-27747
Conjunctive measurement theory: Cognitive research prospects
[AD-A193627] 23 p3239 N88-29277
Reliability and construct validity of reaction time, inspection time and machine-paced tests of cognitive speed
[AD-A193779] 23 p3241 N85-29289
Expertise and reasoning with possibility: An explanation of modal logic and expert systems
23 p3253 N88-29363
Advancement of latent trait theory
[AD-A194302] 24 p3408 N88-30289
Contributions to engineering models of human-computer interaction, volume 1
[AD-A195590] 24 p3409 N88-30295
The bounded rationality constraint: Experimental and analytical results
[AD-A195897] 24 p3413 N88-30318

COGNITIVE PSYCHOLOGY
Gender and cognitive style differences at the human-computer interface
[NPL-DITC-90/87] 01 p0077 N88-10493
Determinants of dual-task interference and resource theories in cognitive psychology
[DFVLR-FB-88-14] 21 p2992 N88-27748

COHERENCE
A fast bottom-up algorithm for computing the cut sets of noncoherent fault trees
[DE88-003741] 09 p1220 N88-17320
Bearing detection in the presence of two sources of varying coherence using the complex cepstrum
[NASA-CR-181605] 09 p1243 N88-17451
Vortex dynamics of coherent and chaotic structures (including algorithms for computer simulations and diagnosis)
[AD-A193580] 23 p3212 N88-29117

COHERENT ANTI-STOKES RAMAN SPECTROSCOPY
U RAMAN SPECTROSCOPY

COHERENT ELECTROMAGNETIC RADIATION
NT COHERENT LIGHT
NT LASER BEAMS
Fluctuations in frequency of coherent radio signals in solar plasma according to Venera-15 and Venera-16 data 08 p1003 N88-16079
Emission angles for soft X-ray coherent transition radiation
[AD-A186851] 09 p1151 N88-16896

COHERENT LIGHT
Effect of optical inhomogeneities on space coherence of radiation emitted by laser with unstable resonator
06 p0771 N88-14738
Problems and possible solutions involved in hard target calibration of coherent Doppler lidar
07 p0922 N88-15602
Excitation of single-mode glass fiber by partially coherent sources
[ETN-88-92121] 20 p2854 N88-26951
Studies of coherent beam processing concepts, phase 1
[AD-A194749] 22 p3083 N88-28306

COHERENT RADAR
Distortion of wideband carbon dioxide laser radar waveforms due to atmospheric dispersion and absorption
[AD-A188687] 12 p1632 N88-19771
Coherent laser radar system theory
[AD-A188759] 13 p1774 N88-20612
Preliminary study of a coherent radar
[BCRS-86-03] 16 p2189 N88-23051

COHERENT RADIATION
NT COHERENT ELECTROMAGNETIC RADIATION
NT COHERENT LIGHT
NT LASER BEAMS
Coherent infrared detection, volume B --- CO2 laser intersatellite data link
[ESA-CR(P)-2392-VOL-1] 01 p0034 N88-10218
Coherent infrared detection, volume D --- CO2 laser intersatellite data link
[ESA-CR(P)-2392-VOL-2] 01 p0034 N88-10219
Brightness and coherence of radiation from undulators and high-gain free electron lasers
[DE87-011093] 02 p0177 N88-11102
Generation of IR stimulated radiation, UV visible violet coherent radiation by two-photon resonance pumping in K vapor 03 p0301 N88-11892
Methods for a coherent CO2 laser heterodyne radar system
[ESA-TT-1035] 03 p0328 N88-12076
Center for X-Ray Optics, 1986
[DE88-000715] 04 p0449 N88-12783
Coherent emission from relativistic beam-plasma interactions 04 p0493 N88-13039
Coherence, propagation and fluctuations of light: A generalized ray approach
[DE88-001669] 06 p0780 N88-14786
Formation of high-coherence radiation in free-running mode ruby laser for pulse holography
08 p1077 N88-16497
Coherent VUV source at 130 nm: Theory and modeling
[DE88-003874] 11 p1549 N88-19269
Nonclassical lights 14 p1979 N88-21810
Particle acceleration to high energies and amplification of coherent radiation by electromagnetic interactions in plasmas
[DE88-701020] 15 p2135 N88-22737
Generation of tunable coherent radiation in 3 micrometers-5 micrometers region using semiconductor lasers in external cavities
[AD-A190860] 16 p2212 N88-23202
Long duration coherent Lyman-alpha sources
16 p2268 N88-23571
Fast acting optical beam detection and deflection system
[AD-A192161] 18 p2521 N88-24954
Progress toward a soft X-ray FEL
[DE88-007669] 19 p2675 N88-25905
Interferometric recording of holographic optical elements using partially coherent light
20 p2805 N88-26636

COHERENT SCATTERING
Acoustic scattering from composite wind-wave surfaces 3: Forward scatter intensities and spatial coherence at low and high frequencies and small grazing angles for Bubble-free regimes
[AD-A185908] 07 p0881 N88-15345
A search for medium energy gamma ray pulsars
11 p1568 N88-19385
Characteristics of coherent and incoherent waves in snow at microwave and millimeter wave frequencies
[AD-A188990] 12 p1620 N88-19692
Electron stimulated desorption and coherent electron scattering
[AD-A189091] 13 p1835 N88-20978
Image charge, coherent scattering, and symmetry effects in electron stimulated desorption: O(-) from O sub 2 condensed on metals
[AD-A189093] 13 p1835 N88-20979
Ionospheric radio and propagation: Waves in plasmas
24 p3364 N88-30030

COHERENT SOURCES
U COHERENT RADIATION
U RADIATION SOURCES
COHERENT TRANSMISSION
U COHERENT RADIATION
COHESION
An explanation of the fractography of near-threshold fatigue in FCC metals 06 p0716 N88-14395
A comparison of the effects of group dynamics on individuals assigned to integral and non-integral aircrews
[AD-A186467] 08 p1051 N88-16345
Cohesive energies of transition metal silicides and phosphides --- Knudsen effusion
[AD-A186691] 09 p1254 N88-17519
COINCIDENCE CIRCUITS
Coincidence counting corrections under conditions used by A. DeVolpi
[NPL-RS(EXT)-90] 17 p2393 N88-24224
Some unsolved problems in modelling self-timed circuits using Petri Nets, series B, number 2
[PB88-161466] 18 p2507 N88-24872
COLD ACCLIMATIZATION
Biorhythmic aspects of intercontinental Antarctic adaptation 08 p1046 N88-16321
Respiratory and cardiovascular responses to cold stress following repeated cold water immersion
[AD-A186460] 08 p1050 N88-16340
Effects of moderate cold and heat stress on the potential work performance of industrial workers. Part 6: The effects of increasing vapour pressure at four air temperatures on the performance and physiology of white females
[PB88-124854] 18 p2550 N88-25137
COLD CATHODE TUBES
NT PHOTOMULTIPLIER TUBES
An experimental and theoretical investigation of optogalvanic effects
[AD-A189618] 12 p1625 N88-19720
COLD FLOW TESTS
The development and evaluation of three-dimensional models of cold flow in internal combustion engines
[DE88-900077] 05 p0589 N88-13594
COLD FORMING
U COLD WORKING
COLD FRONTS
The combined use of diagnosed mesoscale frontogenesis and satellite imagery in forecasting squall line formation 02 p0201 N88-11258
Structure and modification of winter mountain clouds in the Sierra Nevada: Nowcasting/forecasting the onset of supercooled liquid water 02 p0202 N88-11263
The role of low-level cooling in a conceptual model of the Australian summertime cool change: Implications for very-short-range forecasting 02 p0204 N88-11275
Results of the experiment MERKUR: Structural change of a weak cold front in the sphere of influence of the Alps --- mesoscale experiment 08 p1014 N88-16146
Model calculations of the behavior of orographically influenced cold fronts 08 p1015 N88-16155
Density flows at the mountain edge
08 p1016 N88-16156
Orographically influenced cold fronts in a spectral approach 08 p1016 N88-16161
Numerical investigation of orographically enhanced instability
[AD-A186841] 09 p1189 N88-17125
Scientific Colloquium in Honor of Prof. Dr. Rer. Nat. Hermann L. Jordan
[DFVLR-MITT-87-11] 09 p1240 N88-17432
The retardation of cold fronts at high mesoscale mountains 09 p1241 N88-17437
Variation of the wind stress related to frontal passages during FASINEX (Frontal Air-Sea Interaction Experiment) 1986
[AD-A187180] 11 p1514 N88-19042
Numerical simulation of the ocean front response to the mesoscale atmospheric forcing
[INPE-4473-TDL/324] 12 p1648 N88-19868
The German Front Experiment 1987: Experimental design
[DFVLR-MITT-87-24] 16 p2234 N88-23343
COLD GAS
The effect of heat transfer on the dispersion of cold dense gases
[OUEL-1688/87] 02 p0171 N88-11076
Cold gas jet system for satellite attitude control-modeling and simulation
[INPE-4279-PRE/1150] 12 p1601 N88-19583
COLD PLASMAS
Ionosphere and plasmasphere
03 p0272 N88-11709
Nonlinear, relativistic Langmuir waves in astrophysical magnetospheres
[NASA-CR-182422] 08 p1024 N88-16197
Resonance cones in nonthermal plasmas: Laboratory experiments 08 p1027 N88-16223
Hydromagnetic cavity eigenmodes in a non-uniform plasma 08 p1098 N88-16610
Nonlinear resonance of two-dimensional ion layers
[AD-A188890] 12 p1695 N88-20145
Experimental studies of plasma heating due to the parametric decay of a large amplitude pump into lower hybrid waves 13 p1841 N88-21017
Consistency between current ramp-up/recharging scenario by non-inductive current drive and dense and cold divertor plasma. Conceptual design study of FY86 FER
[DE88-751438] 14 p1984 N88-21833
COLD PRESSING
Preparation of oxide superconductors
[DE88-009136] 20 p2675 N88-27063
COLD SURFACES
Interaction of the cold conveyor belt with polar jet streaks
[AD-A186774] 09 p1192 N88-17145
COLD TOLERANCE
The effects of acute cold exposure on exercise performance
[AD-A192650] 22 p3130 N88-28610
Alterations in cutaneous vasomotor regulation during acute and chronic hypoxia
[AD-A192653] 22 p3131 N88-28612
COLD TRAPS
Magnetic trapping of neutral atoms
[AD-A188473] 12 p1689 N88-20103
Spontaneous force optical traps
[AD-A196103] 24 p3377 N88-30114
COLD WALLS
U COLD SURFACES
U WALLS
COLD WATER
Rational considerations for modelling human thermoregulation during cold water immersion
[AD-A186226] 08 p1048 N88-16329
Role of body fat in the prediction of the metabolic response for immersion in cold water
[AD-A186914] 09 p1198 N88-17182
COLD WEATHER
Attitudes towards the cold: Effects on psychological mood and subjective reports of illness during cold weather training
[AD-A194777] 23 p3239 N88-29274
COLD WEATHER TESTS
Huurre expedition to the North Pole in 1984
[PB87-220935] 04 p0462 N88-12858
Calibration of the ARL (Aeronautical Research Laboratories) rain and icing facility
[AD-A186776] 09 p1121 N88-16710
Flight testing under extreme environmental conditions
[AGARD-AG-300-VOL-8] 21 p2951 N88-27525
COLD WORKING
NT EXPLOSIVE FORMING
A finite element procedure for interference-fit and cold-working problems with limited yielding
[AR-004-517] 04 p0485 N88-12992
Interrelation and measurement of formability, strengthening, and thermomechanical processing under metalworking conditions
[DE86-002485] 08 p0967 N88-15850
Computed stress and strain distributions under interference fit and after coldworking
[AD-A186950] 10 p1342 N88-18024
Effects of cold working on precipitation in age hardenable alloys: On the copper alloys
[NASA-TT-20164] 16 p2177 N88-22973
Cold worked reinforcing bars in tensile test under high loading rate and low temperatures
[DE88-752993] 21 p2964 N88-27610
COLLAGENS
Hierarchical structure in polymeric solids and its influence on properties
[AD-A194720] 23 p3197 N88-29029
COLLAPSE
Radiation induced collapse of the crystalline structure
[DE87-014407] 04 p0498 N88-13064
Bubble expansion and collapse studies
[DE88-002377] 06 p0699 N88-14290
Generation and propagation of sound waves in a collapsing or anti-collapsing star with uniform density
[DE87-703034] 15 p2151 N88-22839
Dynamical properties of a collapsing spherical cavity
19 p2623 N88-25562
COLLECTION
Techniques utilized in the simulated altitude testing of a 2D-CD vectoring and reversing nozzle
[NASA-TM-100872] 19 p2604 N88-25464
The Hanford meteorological data collection system and data base
[DE88-006632] 21 p2975 N88-27672
Cooperative effects and intrinsic optical bistability in collections of atoms
[AD-A193993] 23 p3280 N88-29530
COLLECTORS
U ACCUMULATORS
COLLEGES
U UNIVERSITIES
COLLIMATION
Development of a computer model for missile simulation, or simulation of a kinetic coverage area for a collimation guided missile
[FOA-C-20667-2.5] 08 p1067 N88-16450
Systolic array adaptive beamforming
[AD-A187496] 10 p1385 N88-18269
Ion generator and ion application system
[NASA-CASE-MFS-28122-1] 17 p2397 N88-24253
COLLIMATORS
Optical links in the angle-data assembly of the 70-meter antennas 11 p1474 N88-18792
COLLINEARITY
Time-domain boundary element analysis of dynamic near-tip fields for impact-loaded collinear cracks
[AD-A192930] 20 p2815 N88-26700
Two biased estimation techniques in linear regression: Application to aircraft
[NASA-TM-100649] 23 p3274 N88-29489
COLLISION AVOIDANCE
UK airmiss statistics
[CAP-530] 03 p0261 N88-11642
Handling qualities criterion for very low visibility rotorcraft 03 p0263 N88-11654
Simulation of an enhanced TCAS 2 system in operation
[NASA-CR-181545] 04 p0398 N88-12479
Towards building a team of intelligent robots
[NASA-CR-181538] 05 p0589 N88-13595
Collision-free motion of two robot arms in a common workspace
[CSE-87-00002] 05 p0589 N88-13596
A study of the TCAS 2 collision avoidance system mounted on a Boeing 737 aircraft
[NASA-CR-182457] 09 p1116 N88-16687
Safe rendezvous approach to a space station by impulsive transfers and continuous thrust arcs
12 p1585 N88-19486
UK airmiss statistics
[REPT-3/87] 14 p1865 N88-21141
Aircraft accident report: Midair collision of US Army U-21A, Army 18061 and Sachs Electric Company Piper PA-31-350, N60SE, Independence, Missouri, January 20, 1987
[PB88-910401] 16 p2159 N88-22877
UK airmiss statistics
[CAA-1/87] 17 p2300 N88-23761
Orbital navigation, docking and obstacle avoidance as a form of three dimensional model-based image understanding 17 p2388 N88-24194
Nuclear-powered space debris sweeper
17 p2418 N88-24380
Rotorcraft TCAS (traffic alert and collision avoidance system) evaluation: Group 3 results
[AD-A191719] 18 p2461 N88-24614
The avoidance of collisions for Newtonian bodies with hidden variables
[RSRE-87013] 22 p3041 N88-28053
Fine resolution errors in secondary surveillance radar altitude reporting
[RSRE-87019] 23 p3175 N88-28906
UK airmisses involving commercial air transport
[CAA-1/88] 23 p3176 N88-28907
Airport surface traffic automation study
[AD-A194553] 23 p3181 N88-28934
On the collision hazard of colocated geostationary satellites
[DFVLR-FB-88-02] 23 p3184 N88-28952
COLLISION PARAMETERS
NT COLLISION RATES
Heavy-particle collisions in the plasma edge
[DE87-012928] 02 p0237 N88-11493
Total and partial cross sections for electron capture for C(q+) (q=6-2) and O(q+) (q=8-2) ions in collisions with H, H2 and He atoms
[IPPJ-AM-56] 09 p1252 N88-17501
Atomic data for hydrogens in collisions with electrons: Addenda
[IPPJ-AM-55-ADD] 09 p1252 N88-17502
Study of the production of Ko mesons in proton antiproton interactions at 630 GeV
[NOTA-INTERNA-908] 21 p3015 N88-27892
On the degenerate Ferrari-Ibanez solution for colliding plane gravitational waves
[MATH-REPT-209] 23 p3296 N88-29630
COLLISION RATES
Helical ripple transport in stellarators at low collision frequency
[DE88-006431] 13 p1843 N88-21031
Contributions of autoionizing resonances to the electron collisional excitation rates for Be-like ions
[AD-A190924] 18 p2572 N88-25275

Approximate analytical formulae for electron density and collision frequency in the natural and nuclear-disturbed ionosphere and inner magnetosphere
[AD-A193129] 21 p2972 N88-27654

COLLISION WARNING DEVICES
U COLLISION AVOIDANCE
U WARNING SYSTEMS

COLLISIONAL PLASMAS
NT STRONGLY COUPLED PLASMAS
Computer models for kinetic equations of magnetically confined plasmas
[DE87-011571] 02 p0236 N88-11492
Variable collision frequency effects on hose and sausage instabilities in relativistic electron beams
[AD-A184206] 04 p0490 N88-13021
The effects of a dc electric field on the current driven ion cyclotron instability
[AD-A188877] 12 p1695 N88-20142
Parallel gradient effects on ICRH (Ion Cyclotron Resonance Heating) in tokamaks
[DE88-009038] 19 p2730 N88-26216
Modulational instability of electric helicons in a magnetized collisional plasma
[DE88-701885] 20 p2858 N88-26976

COLLISIONLESS PLASMAS
Computer models for kinetic equations of magnetically confined plasmas
[DE87-011571] 02 p0236 N88-11492
Particle injection and cosmic ray acceleration at collisionless parallel shocks
[DE88-000507] 04 p0430 N88-12665
A study of single and binary ion plasma expansion into laboratory-generated plasma wakes
[NASA-CR-4125] 10 p1412 N88-18427
Plasma theory and simulation
[DE88-003620] 10 p1414 N88-18437
A quadratic-form analysis of the collisionless tearing mode
[AD-A188886] 12 p1695 N88-20144
Helical ripple transport in stellarators at low collision frequency
[DE88-006431] 13 p1843 N88-21031

COLLISIONS
NT ATOMIC COLLISIONS
NT BIRD-AIRCRAFT COLLISIONS
NT COULOMB COLLISIONS
NT INELASTIC COLLISIONS
NT IONIC COLLISIONS
NT METEORITE COLLISIONS
NT MIDAIR COLLISIONS
NT MOLECULAR COLLISIONS
NT PARTICLE COLLISIONS
Heavy-particle collisions in the plasma edge
[DE87-012928] 02 p0237 N88-11493
The Conference on the Dynamics of Molecular Collisions held in Oglebay Park, Wheeling, West Virginia on 12-17 July 1987
[AD-A184690] 03 p0374 N88-12354
Analytic model of an imploding Z-pinch plasma colliding inelastically with a thin-shelled cylindrical target
[DE88-000051] 03 p0378 N88-12379
A study of the interaction of laser light with liquid propellant drops
[AD-A185117] 05 p0587 N88-13582
The effect of collision angle on mach reflection
[AD-A185798] 06 p0704 N88-14319
Tool and process for miniature explosive joining of tubes
[NASA-CASE-LAR-13662-1] 06 p0711 N88-14359
Analysis and interpretation of satellite fragmentation data 06 p0798 N88-14885
Electronic energy transfer processes in the alkali/alkaline earth metal vapors
[AD-A190035] 15 p2034 N88-22119
Colliding stellar winds in the eclipsing Wolf-Hayet binary V444 Cygni
[NASA-CR-182937] 17 p2451 N88-24563
The multistring model VENUS for ultrarelativistic heavy ion collisions
[DE88-007666] 18 p2573 N88-25284
Atomic processes in matter-antimatter interactions
[DE88-008911] 19 p2723 N88-26172
Approximate analytical formulae for electron density and collision frequency in the natural and nuclear-disturbed ionosphere and inner magnetosphere
[AD-A193129] 21 p2972 N88-27654

COLLOCATION
Domain decomposition preconditioners for the spectral collocation method
[NASA-CR-181620] 10 p1400 N88-18345
A spline collocation method for integral equations of the first kind with logarithmic singularity --- boundary value problems
[REPT-87-39] 14 p1963 N88-21712
Periodic response of nonlinear systems
16 p2217 N88-23228
A new collocation-type method for the numerical solution of Hammerstein equations 17 p2393 N88-24226
On the collision hazard of colocated geostationary satellites
[DFVLR-FB-88-02] 23 p3184 N88-28952

COLLOIDING
Colloidal structure of bitumens. Relationship between composition-structure behavior
[PC-4] 02 p0146 N88-10912

COLLOIDS
NT AEROSOLS
NT FOG
Small-Angle Neutron Scattering (SANS) from polymers and colloids
[DE87-013548] 02 p0151 N88-10946
Photocatalytic electrochemistry at a biological-membrane metal-colloid interface
[DE87-009122] 02 p0166 N88-11041
Colloidal stability of oxidized silicon particles in ethanolic and aqueous media
[DE87-014783] 05 p0562 N88-13421
Characterization of the dimensions of colloidal calcium carbonate dispersions in toluene with neutron small-angle scattering
[ECN-197] 06 p0680 N88-14167
Electron transfer to iron(3) oxide colloids
[DE88-002885] 10 p1416 N88-18448
Colloidal characterization of silicon nitride and silicon carbide 17 p2325 N88-23883
Preliminary investigation of flow modeling during solid propellant processing
[AD-A196168] 24 p3357 N88-29987

COLOMBIA
SPOT applications on Columbia's coffee zone
22 p3097 N88-28395

COLONIES
Remote sensing applied to integrated regional development programs 19 p2685 N88-25958

COLOR
NT WATER COLOR
Development of a line-drawing algorithm
[CS-8701] 01 p0082 N88-10530
Preliminary estimation of color inhomogeneities on the surface of Venus according to the television images obtained by the VENERA-13 and VENERA-14 automated space probes
[NASA-TT-20114] 02 p0254 N88-11608
Performance and preference with various VDT (Video Display Terminal) phosphors
[AD-A184085] 04 p0475 N88-12925
On color polynomials of Fibonacci graphs
[AD-A184133] 04 p0486 N88-12996
X-rays, color, and the Vaughan-Preston gap
04 p0510 N88-13135
The use of color in electronic maps. Part 1: Generation and analysis of color on the Gould/DeAnza image processing system
[IZF-1986-32] 05 p0635 N88-13882
Fast, colour displays of digital terrain elevation data
[AD-A185596] 06 p0729 N88-14485
Use of colour on electronic data displays (second study)
[PB87-126744] 06 p0754 N88-14627
Use of lasers with F sub A(II)-color center KCl:Li crystals in the intraresonator laser spectroscopy method
06 p0769 N88-14729
Total light flux and colour of solar corona
[PB87-143335] 07 p0946 N88-15754
Status and prospects of the Joint Research Commitee (JRC) work on the application of ocean colour monitoring from space 08 p1043 N88-16299
Canadian activities and goals in remote sensing of ocean colour and fluorescence from space
08 p1043 N88-16300
Research in Switzerland on ocean and inland-water colour monitoring 08 p1043 N88-16301
Image chunking: Defining spatial building blocks for scene analysis
[AD-A187072] 09 p1200 N88-17191
Multicolor numbering of irregular triangular meshes
[AD-A186559] 09 p1217 N88-17298
Color shadow methods of analyzing reconstructed wave front 09 p1236 N88-17407
Excimer plasma displays
[AD-A186731] 09 p1250 N88-17489
The Quick Response Multicolor Printer (QRMP) system
[AD-A188140] 11 p1504 N88-18982
Laser flash effects on chromatic discrimination in monkeys
[AD-A187703] 11 p1517 N88-19061
Graphics and flow visualization of computer generated flow fields
[NASA-CR-182679] 13 p1767 N88-20573
Application of its transformation in color enhancement of LANDSAT imagery 17 p2365 N88-24082
Evaluation of TM false color composites for crop discrimination 17 p2367 N88-24096
CIMAG2: The computer program to generate color images
[AD-A191847] 18 p2557 N88-25175
Color charge motion in non-Abelian fields
[DE88-701306] 19 p2642 N88-25672
Cleanability of aircraft polyurethane topcoats
[AD-A193456] 23 p3170 N88-28878
Use of color CRTs (Cathode Ray Tubes) in aircraft cockpit: A literature search, revision B
[AD-A195062] 24 p3324 N88-29797

COLOR (PARTICLE PHYSICS)
U QUANTUM CHROMODYNAMICS

COLOR CENTERS
400-nm photoluminescence of a color center in undoped YAG grown under reducing atmosphere
[DE88-001760] 07 p0858 N88-15213
Anisotropy of light absorption by color centers in waveguides produced on photochromic glasses by diffusion 14 p1896 N88-21320
Dependence of formation of radiative color centers in optical glass fibers on technological factors
14 p1896 N88-21321
Infrared absorption spectroscopy and chemical kinetics of free radicals
[DE88-006536] 15 p2033 N88-22112

COLOR CODING
Generation of specific chromaticities on CRT monitors
[AD-A187739] 11 p1440 N88-18590
Utilization of space color transformation, linear contrast and filtration for enhancement of colored digital images
[INPE-4310-PRE/1176] 14 p1983 N88-21831
Comparative utilization of analog and digital processes in the treatment of MSS-LANDSAT data for studying the national parks of Brazil
[INPE-4011-TDL/240] 15 p2090 N88-22456
Visual enhancement of digital color imagery utilizing transformation in color coordinates (IHS transformation)
[INPE-4482-PRE/1248] 16 p2273 N88-23606
Use of color CRTs (Cathode Ray Tubes) in aircraft cockpit: A literature search, revision B
[AD-A195062] 24 p3324 N88-29797

COLOR ENHANCEMENT
U COLOR CODING

COLOR PERCEPTION
U COLOR VISION

COLOR PHOTOGRAPHY
Conversational Analysis of Color Images (CAICOU): An interactive development system for the analysis of color images
[RR-641-I-IMAG-39-LIFIA] 17 p2342 N88-23964
Anomalies in the vegetation in the Alto Xingu - MT
17 p2357 N88-24043
Remote sensing techniques in the estimation of the area cultivated with beans, corn, and castor beans in the Irece County (Bahia State) 17 p2358 N88-24045

COLOR VISION
Learning a color algorithm from examples
[AD-A184385] 05 p0632 N88-13862
Psychophysical, biochemical and histological studies of spectrally selective photic damage to primate retina
[AD-A188115] 11 p1517 N88-19063
Running head: What color is it
[NASA-CR-182600] 11 p1551 N88-19280
Design and testing of a luminance and chrominance stabilization system for a computer-controlled color display
[AD-A191922] 18 p2554 N88-25159
Central serous chorioretinopathy in USAF aviators: A review
[AD-A195697] 24 p3407 N88-30280
Eye movements and spatial pattern vision
[AD-A195496] 24 p3408 N88-30290

COLOR-MAGNITUDE DIAGRAM
Color-magnitude diagrams of star clusters in the Magellanic clouds from wide-field electronography. Part 3: NGC 1841
[PUBL-SER-C-FASC-14] 07 p0944 N88-15740

COLORATION
U COLOR

COLORIMETRY
Color fluctuations in the inner coma of Comet Halley as measured from VEGA-2 14 p2000 N88-21925
Near-infrared imaging of Comet Halley: Discovery of a color gradient in the inner coma
14 p2009 N88-21980
Note on the double crystal method of measuring heat transfer coefficient
[OUEL-1710/87] 17 p2338 N88-23950
Spectral classification of Low Mass X-ray Binaries (LMXB) energy spectra with color-color diagrams
[MPE-PREPRINT-111] 22 p3163 N88-28837

COLUMBIUM
U NIOBIUM

COLUMBUS SPACE STATION
Metallurgy laboratory for Columbus, executive summary
[SNIAS-813-CA/TS] 02 p0157 N88-10980
Thermophysical Properties Measurement Facility (TPMF) --- Columbus space station
[ESA-CR(P)-2417] 02 p0157 N88-10981
A preliminary study of a fluid science laboratory for space station (Columbus). Part 4: Executive summary
[NLR-TR-87023-L-PT-4] 02 p0170 N88-11072
Considerations concerning a thermal joint for a deployable or steerable battery radiator for the Columbus Polar Platform
[NLR-TR-86055-U] 03 p0276 N88-11739
Commercial Opportunities for Remote Sensing with Polar Platforms
[ESA-SP-269] 03 p0339 N88-12131
Possible commercial use of the polar platforms --- Columbus 03 p0339 N88-12132
Payload configurations and serviceability --- Columbus Polar Platforms 03 p0339 N88-12133
Legal protection of the Polar Platform's users
03 p0339 N88-12135
Confidentiality of data --- Columbus Polar Platforms
03 p0339 N88-12136
X-band SAR for a European remote sensing payload
03 p0340 N88-12142
Astromag: A particle spectrometer for the Space Station
[PREPRINT-557] 06 p0707 N88-14336
Columbus pressurized module utilization study, executive summary
[CS-RP-AI-027] 07 p0825 N88-15005
Allowable gravity-levels for Spacelab, Columbus and EURECA --- materials science
[BF-R-66.525-2] 07 p0838 N88-15084
Docking/Berthing Subsystem (DBS). Development part 1: Latching analysis --- Columbus
[ESA-CR(P)-2479] 08 p0962 N88-15825
Scientific objectives and functional requirements of life sciences in the Space Station 08 p1033 N88-16264
AURIO: A proposal for flying auroral imaging observatory on the Polar Platform in the Space Station/Columbus program 08 p1034 N88-16268
Technical aspects of future ocean colour remote sensing 08 p1042 N88-16298
Polar platform element of Space Station: Mission objectives, European priorities, candidate instrumentation and selection procedure 09 p1129 N88-16779
Space station overview 09 p1129 N88-16780
Use of Space Station for space science
09 p1129 N88-16782
Microgravity payloads and missions for Space Station: Some issues affecting compatibility with other payloads
09 p1129 N88-16783
The Columbus program, an overview
09 p1130 N88-16784
Coorbiting Platform Utilization Study (CPLUS), executive summary --- Columbus
[SN-WP-4000-DOC-6609/85/F]
09 p1133 N88-16798
Columbus feasibility studies. Volume 1: Requirements and system concept
[ETN-88-91073] 09 p1134 N88-16799
Columbus feasibility studies. Volume 2: Element constituents, mechanical
[ETN-88-91074] 09 p1134 N88-16800
Columbus feasibility studies. Volume 3: Avionics, systems
[ETN-88-91075] 09 p1134 N88-16801
Columbus feasibility studies. Volume 5: Programmatics
[ETN-88-91076] 09 p1134 N88-16802
Model of space platform electromagnetic (EMC) configuration
[ESA-CR(P)-2500] 09 p1135 N88-16809
Study on long term evolution towards European manned space flight. Volume 1: Executive summary
[MBB-RA3-004/87-VOL-1] 10 p1286 N88-17689
Project management in astronautics: From Spacelab to Columbus
[MBB-URE-943/87] 10 p1315 N88-17858
Columbus feasibility studies. Volume 4: Integration, test, and operations
[ETN-88-90576] 11 p1445 N88-18614
Man-Tended Free Flyer operational design features
12 p1585 N88-19485
Mission profiles of the MTFF co-orbiting with the US Space Station 12 p1585 N88-19487
Cost-effective orbit transfer modes for satellite retrieval and servicing --- Space Station
12 p1586 N88-19489
Assembly of user systems at Space Station
12 p1586 N88-19490
Analysis of RVD operations in manned space missions
12 p1586 N88-19494
On a knowledge based assisted system for highly autonomous control of experiment-manipulators in the Man-Tended Free Flyer 12 p1588 N88-19505
Promising concepts for ground-to-orbit experiment teleoperation --- Columbus 12 p1590 N88-19518
Columbus Simulation Facility (CSF)
12 p1590 N88-19522
External payload servicing: Operational requirements and technology 12 p1593 N88-19541
Microgravity User Support Center (MUSC) for EURECA, Spacelab and Columbus missions
12 p1660 N88-19947
Animal research on the Space Station
12 p1662 N88-19964
Feasibility demonstration of a sensor for high-quality two-phase flow --- Space Station
[NLR-TR-87009-U] 13 p1767 N88-20569
System and concept design of the SSRMS latching end effector --- Space Station 14 p1875 N88-21204
Colombus feasibility studies, executive summary
[ETN-88-92334] 17 p2311 N88-23820
Study on long-term evolution towards European manned spaceflight. Volume 1: Executive summary
[ERNO-OX1-002/88-VOL-1] 24 p3330 N88-29827
Studies on rocket exhaust plumes and impingement effects related to the Columbus Space Station program: Executive summary
[DFVLR-IB-222-88-A-12] 24 p3337 N88-29862
The LTPP, communication processor --- Columbus and Hermes
[CL/CP/SES/FR/004] 24 p3415 N88-30328
Candidate functions for advanced technology implementation in the Columbus mission planning environment 24 p3417 N88-30340
COLUMNS
Beam and column buckling under directed loading
[PB87-124004] 06 p0722 N88-14436
Distortional buckling formulae for thin-walled channel columns
[PB87-124012] 03 p0722 N88-14437
COLUMNS (SUPPORTS)
Buckling of viscoelastic columns
02 p0190 N88-11187
Residual stress effect on stability of axially loaded columns
[PB87-143889] 08 p0996 N88-16032
COMBAT
Loss of performance due to military clothing and equipment
[IZF-1986-13] 01 p0077 N88-10490
Improvements to the adaptive maneuvering logic program
[NASA-CR-3985] 03 p0262 N88-11648
Apache for the battlefield of today and the 21st century 03 p0265 N88-11670
Impact of flying qualities on mission effectiveness for helicopter air combat, volume 1
[NASA-CR-166568] 06 p0669 N88-14100
Advanced helicopter cockpit and control configurations for helicopter combat missions
[NASA-TM-100017] 07 p0821 N88-14988
A piloted simulation investigating handling qualities and performance requirements of a single-pilot helicopter in air combat employing a helmet-driven turreted gun
[AD-A186878] 09 p1116 N88-16689
Future fighter maneuverability for air combat
[MBB/LKE-1/S/PUB/120] 10 p1312 N88-17843
Hardware implementation for special functions. An application for combat simulation
10 p1374 N88-18197
Future directions in computer architecture
10 p1383 N88-18257
State of the art of natural language processing
[AD-A188112] 11 p1530 N88-19136
A computer graphics simulation of the endgame in aircraft combat survivability
[AD-A187826] 11 p1541 N88-19214
Manned simulation: Helpful means to determine and improve structural load criteria 12 p1581 N88-19459
Computer aided tactics for air combat
12 p1597 N88-19559
Predicting Air Combat Maneuvering (ACM) performance: Fleet fighter ACM readiness program grades as performance criteria
[AD-A191605] 19 p2710 N88-26099
Realistic planning scenarios
[AD-A191640] 19 p2740 N88-26267
Computation of ECM (Electronic Counter-Measures) war reserve materiel spare requirements
[AD-A193301] 21 p2897 N88-27195
Analysis of ATCRBS (Air Traffic Control Radar Beacon System), mode select (Mode S) in combat operations
[AD-A193140] 22 p3040 N88-28050
Proposal for a new aggressor aircraft
[AD-A194311] 22 p3041 N88-28056
Design guidelines for prevention of corrosion in combat and tactical vehicles
[AD-A194172] 22 p3055 N88-28126
Stress and the military pilot
[AD-A194313] 22 p3133 N88-28626
Electronic combat roadmap for space
[AD-A194282] 22 p3146 N88-28709
Future air-to-air training for the RF-4
[AD-A194363] 23 p3240 N88-29284
SDI (Strategic Defense Initiative) battle management/C3 (Command, Control and Communications) algorithms technology program plan
[AD-A194357] 23 p3275 N88-29495
COMBINATIONS (MATHEMATICS)
On perfect hash functions
[ENST-86D006] 01 p0087 N88-10565
COMBINATORIAL ANALYSIS
NT COMBINATIONS (MATHEMATICS)
NT PARTITIONS (MATHEMATICS)
NT PERMUTATIONS
An exact analysis and performance of framed ALOHA with capture
[AD-A185006] 05 p0574 N88-13500
Search rearrangement backtracking often requires exponential time to verify unsatisfiability
[AD-A186121] 07 p0909 N88-15511
The perfectly matchable subgraph polytope of an arbitrary graph
[AD-A185993] 07 p0913 N88-15539
Polyhedral combinatorics
[CWI-OS-R8701] 08 p1072 N88-16466
The construction of a pedagogy to promote meaningful learning of strategies and tactics for solving problems of elementary combinatorics
[AD-A187928] 11 p1542 N88-19216
Analysis of simulated annealing type algorithms
[AD-A189382] 12 p1679 N88-20037
The clique polytope of a graph
[MEMO-663] 14 p1963 N88-21710
Parallel computing in combinatorial optimization
[CWI-OS-R8720] 16 p2254 N88-23468
Algorithms and data structures for an expanded family of matroid intersection problems
[AD-A191482] 18 p2562 N88-25213
Challenge problems focusing on equality and combinatory logic: Evaluating automated theorem-proving programs
[DE88-010057] 20 p2844 N88-26879
The combinatorics of object recognition in cluttered environments using constrained search
[AD-A196224] 24 p3422 N88-30364
COMBINED STRESS
Estimation multiaxial elastic-plastic notch stresses and strains in combined loading
[FB-2/1986] 01 p0060 N88-10382
The use of Hencky's equations for the estimation of multiaxial elastic-plastic notch stresses and strains
[FB-3/1986] 01 p0060 N88-10383
Design procedures for fiber composite box beams
[NASA-TM-100296] 09 p1139 N88-16828
COMBUSTIBILITY
U FLAMMABILITY
COMBUSTIBLE FLOW
Flame driving of longitudinal instabilities in liquid fueled dump combustors
[AD-A183536] 01 p0006 N88-10033
European reacting flow research: A final assessment
[AD-A185833] 07 p0828 N88-15022
Effects of turbulence on stationary and non-stationary processes in C-systems
[AD-A186215] 07 p0849 N88-15154
Turbulence interactions in single- and multi-phase turbulent mixing and combustion processes
[AD-A187505] 10 p1332 N88-17960
Measurement of rate constants of elementary gas reactions of importance to upper atmosphere and combustion systems
[AD-A189432] 13 p1737 N88-20386
An investigation of flow structure, mixing and chemical reaction in combusting turbulent flows
[AD-A189980] 15 p2034 N88-22117
Advanced diagnostics for reacting flows
[AD-A190485] 15 p2035 N88-22122
Chemically reacting turbulent flow
[AD-A190522] 15 p2065 N88-22311
Ignition and flame spread of PMMA
[NASA-TT-20290] 20 p2771 N88-26431
Experimental research of combustion systems
21 p2927 N88-27371
Modeling and experimental study of a reactive flow confined with wall injection 24 p3351 N88-29946
COMBUSTION
NT AFTERBURNING
NT DEFLAGRATION
NT EROSIVE BURNING
NT FUEL COMBUSTION

NT HYDROCARBON COMBUSTION
NT METAL COMBUSTION
NT NUCLEAR FUEL BURNUP
NT PROPELLANT COMBUSTION
NT SOLID PROPELLANT COMBUSTION
NT SOLID PROPELLANT IGNITION
NT SPONTANEOUS COMBUSTION
NT SUPERSONIC COMBUSTION
Laser probes of natural gas ignition chemistry
[PB87-209599] 01 p0021 N88-10129
Improved numerical methods for turbulent viscous recirculating flows 02 p0185 N88-11148
An adaptive pseudo-spectral method for reaction diffusion problems
[NASA-CR-178394] 02 p0224 N88-11414
Combustion control with smart sensors
[DE87-013688] 03 p0281 N88-11768
Flammability limits in cocurrent smoldering combustion
[DE87-014102] 03 p0284 N88-11785
Flame acceleration and transition to detonation in channels
[DE87-014193] 03 p0284 N88-11786
Numerical simulation of turbulent premixed combustion and decay of turbulent swirling flow
[DE87-014253] 03 p0284 N88-11787
Techniques for fire detection
04 p0406 N88-12521
Fire-related standards and testing
04 p0406 N88-12522
Fire-related medical science 04 p0406 N88-12525
Space station internal environmental and safety concerns 04 p0407 N88-12527
Microgravity combustion fundamentals
04 p0407 N88-12528
Ignition and combustion of metals in oxygen
04 p0407 N88-12530
Combustion related shear-flow dynamics in elliptic supersonic jets 05 p0531 N88-13232
Correlation of air pressure drop and flame arrestor characteristics for explosion suppression materials
[AD-A184960] 05 p0548 N88-13340
Turbulence generation in combustion
[AD-A184810] 05 p0561 N88-13413
A study of the interaction of laser light with liquid propellant drops
[AD-A185117] 05 p0587 N88-13582
Summary of discussions at the Ninth Meeting of the Sandia Cooperative Group on the Aerothermochemistry of Turbulent Combustion
[DE88-002281] 06 p0680 N88-14165
Mixing and combustion of pulsed gas jets
[PB88-112834] 06 p0680 N88-14169
Mixing and combustion of pulsed gas jets
[PB88-108014] 06 p0680 N88-14170
Catalytic combustion of methane
[PB88-123112] 07 p0829 N88-15028
Dimensions of ignition zones in blow-outs of combustible gases from rectangular and circular ports
07 p0918 N88-15577
An analytical study of the hydrogen-air reaction mechanism with application to scramjet combustion
[NASA-TP-2791] 08 p0966 N88-15846
The effect of microgravity on flame spread over a thin fuel
[NASA-TM-100195] 08 p0967 N88-15853
Diffusion description of flame propagation due to the translational motion of burning reaction products
[DE88-700676] 10 p1297 N88-17757
The role of analytical chemistry in assessing atmospheric effects of combustion
[DE88-003909] 10 p1352 N88-18082
Fire tests on loose-fill insulation materials
[DE88-751182] 11 p1467 N88-18748
Investigations into shock-induced enhancement of mixing and combustion in supersonic burners
[AD-A189609] 12 p1607 N88-19608
The effect of combustion gas flow on the rotational dynamics of a spinning solid fuel rocket
13 p1732 N88-20358
Combustion theory and related questions
[AD-A189160] 13 p1737 N88-20382
Uncertainties in hydrogen combustion
[DE88-005354] 13 p1739 N88-20395
Microprobe examination of composite materials produced by burning of Ti, Cr, C powders with powder of any one Fe-group metal 14 p1886 N88-21269
Kinetics of combustion of finely divided solid fuel in granules
[BLL-M-37626-(5828.4)] 14 p1888 N88-21283
Numerical simulation of turbulent premixed combustion and decay of turbulent swirling flow
[DE88-006588] 14 p1888 N88-21284
The combustion synthesis of boride composites
[DE88-005474] 15 p2028 N88-22084
Cetane scale evaluation and possible modification
[AD-A189730] 15 p2048 N88-22200
Premixed turbulent flame calculation
16 p2196 N88-23098
Soviet combustion research
[PB88-182324] 18 p2483 N88-24730
The thermodynamic properties of quinoline and isoquinoline
[DE88-001218] 18 p2484 N88-24735
Evaluation of manure as a feedstock for gas turbines
18 p2536 N88-25050
Solid-state combustion synthesis of ceramics and alloys in reduced gravity
[NASA-CR-4163] 19 p2608 N88-25479
Theoretical studies of dynamics combustion
[DE88-007565] 19 p2611 N88-25495
Measurement of the radiative properties of gas and oil flames
[NASA-TT-20299] 19 p2612 N88-25502
Atomization in a turbulent shear layer: Preliminary measurements 19 p2624 N88-25565
Recent advances in photochemical techniques for ignition and combustion enhancement
19 p2625 N88-25570
Anatomy of group burning mode transitions in spray group combustion 19 p2626 N88-25578
Modelling of premixed combustion using a thin flame sheet and the effect of the hydrodynamic instability
[DE88-009467] 20 p2770 N88-26423
Asynchronous optical sampling for laser-based combustion diagnostics in high pressure flames
[AD-A192920] 20 p2770 N88-26428
Pulsed spray structure and atomisation techniques
[AD-A192280] 20 p2800 N88-26614
Premixed turbulent flame propagation
[AD-A192955] 21 p2909 N88-27265
Summary of discussions at the Tenth Meeting of the Sandia Cooperative Group on the Aerothermochemistry of Turbulent Combustion
[DE88-008467] 21 p2910 N88-27269
Theoretical study and numerical simulation of flame fronts
[PB88-122932] 22 p3051 N88-28104
Diesel combustion fundamentals, phase 1, volume 1
[AD-A193831] 22 p3052 N88-28107
Particle sizing in combustion systems, using scattered laser light
[AD-A196231] 24 p3352 N88-29953
Optical measurements of soot and temperature profiles in premixed propane-oxygen flames
[NASA-TM-101343] 24 p3358 N88-29997

COMBUSTION CHAMBERS
NT DUMP COMBUSTORS
Optical sizing of soot in gas turbine combustors and exhaust augmentor tubes
[AD-A183785] 01 p0006 N88-10034
On the modelling of non-reactive and reactive turbulent combustor flows 02 p0169 N88-11061
Turbine Engine Hot Section Technology, 1985
[NASA-CP-2405] 02 p0184 N88-11140
Aerothermal modeling program, phase 2
02 p0185 N88-11149
Fuel-injector/air-swirl characterization
02 p0185 N88-11150
Combustor-diffuser interaction program
02 p0185 N88-11152
Dilution jet mixing program, phase 3
02 p0185 N88-11153
On the mixing of a row of jets with a confined crossflow 02 p0185 N88-11154
3D inelastic analysis methods for hot section components 02 p0187 N88-11164
3-D inelastic analysis methods for hot section components 02 p0187 N88-11165
SCRAM JET (Supersonic Combustion Ramjet) combustion experiments 04 p0404 N88-12512
Longitudinal mode combustion instabilities in air breathing engines 06 p0680 N88-14166
Recent advances in high temperature instrumentation for hot section applications
[NASA-TM-100282] 06 p0707 N88-14339
Nitrogen scale-up
[AD-A185702] 06 p0709 N88-14351
Effects of turbulence on stationary and non-stationary processes in C-systems
[AD-A186215] 07 p0849 N88-15154
Design of a solid fuel combustion chamber
[VTH-LR-447] 09 p1141 N88-16837
Investigation of the flow and combustion behavior in a solid fuel combustion chamber, including the measuring program
[VTH-LR-460] 09 p1141 N88-16838
Design of a gas mass flow control system for the gas inlet installation of a solid fuel combustion chamber
[VTH-LR-471] 09 p1141 N88-16839
Solid fuel combustion chamber
[VTH-LR-515] 09 p1141 N88-16842
Numerical simulation of axisymmetric turbulent flow in combustors and diffusors
[NASA-CR-4115] 10 p1268 N88-17582
Numerical simulation of diffuser/combustor dome interaction 10 p1281 N88-17663
Measurements of gas turbine combustor and engine augmentor tube sooting characteristics
[AD-A187831] 11 p1440 N88-18592
Unsteady heat transfer in turbine blade ducts: Focus on combustor sources
[NASA-TM-100815] 11 p1486 N88-18870
Error evaluation of some practical thermocouple probes for gas turbine combustor tests
[NAL-TR-938] 11 p1489 N88-18886
Assessment, development and application of combustor aerothermal models
[NASA-TM-100290] 12 p1582 N88-19469
Linear and nonlinear acoustics with nonuniform entropy in combustion chambers 12 p1607 N88-19609
Interaction between two-dimensional sonic jets and supersonic flow to model heat addition in a supersonic combustor
[AD-A189572] 13 p1716 N88-20261
Finite area combustor theoretical rocket performance
[NASA-TM-100785] 14 p1883 N88-21252
High-temperature combustor liner tests in structural component response test facility
15 p2077 N88-22383
Life assessment of combustor liner using unified constitutive models 15 p2077 N88-22384
Combustion of a double base fuel in the presence of inert gases
[INPE-4516-RPE/564] 16 p2170 N88-22936
Water flow visualisation of a ramrocket combustion chamber 16 p2202 N88-23138
An empirical model of the effects of curvature and convergence on dilution jet mixing
[NASA-TM-100896] 18 p2466 N88-24640
Thrust chamber thermal barrier coating techniques
[NASA-TM-100933] 18 p2476 N88-24690
Combustion behavior of the vitiator. Experimental results of a second test series
[VTH-LR-509] 18 p2484 N88-24734
Evaluation of manure as a feedstock for gas turbines
18 p2536 N88-25050
Low frequency pressure oscillations in a model ramjet combustor 19 p2625 N88-25571
The pressure field generated in a cold-flow side-dump ramjet combustor 19 p2625 N88-25572
Numerical grid generation and flow simulation in SSME thrust chamber 19 p2626 N88-25577
A multiple chamber volume-filling model for prediction of transient solid rocket motor ballistic performance
19 p2633 N88-25618
An efficient computational tool for ramjet combustor research
[DE88-010034] 20 p2760 N88-26369
Dynamics and stability of combustion driven self oscillations in presence of various frequencies. Extensive stability criteria
[ETN-88-92123] 20 p2771 N88-26432
Technical instructions for a control operating system of the gas flow installation for the solid fuel combustion chamber
[LR-507] 20 p2788 N88-26537
Effects of ceramic surfaces on autoignition in a constant volume combustion apparatus
[AD-A193055] 21 p2909 N88-27266
Investigation of annular flow at high evaporation rates in view of liquid film cooling
[DFVLR-FB-88-08] 21 p2949 N88-27517
Experimental validation of a zero-dimensional computer model for spark-ignition engines
[DE88-009034] 21 p2957 N88-27565
Application of laser diffraction techniques to particle sizing in solid propellant rocket motors
[AD-A193841] 22 p3049 N88-28089
A study of flame spreading and combustion phenomena of stick propellants
[AD-A193598] 22 p3052 N88-28106
Numerical investigations in three-dimensional internal flows
[NASA-CR-183108] 23 p3210 N88-29106
Preliminary studies of NF3 + H2 production of N2(A3 sigma(+)u) in a supersonic flow
[AD-A194479] 23 p3219 N88-29162
Automatic data retrieval from rocket motor holograms
[AD-A195586] 24 p3337 N88-29864
Combustion and fuels in gas turbine engines
[AGARD-CP-422] 24 p3345 N88-29910
Comparison of the performance of a reverse flow annular combustion chamber under low and high pressure conditions 24 p3347 N88-29923
Flow characteristics of a model annular combustor
24 p3347 N88-29924

Particle size measurements in sooting combustion systems 24 p3348 N88-29931
Numerical models for analytical predictions of combustor aerothermal performance characteristics 24 p3349 N88-29935
Gas turbine combustion modeling 24 p3349 N88-29936
Three-dimensional gas turbine combustor modelling 24 p3349 N88-29937
Numerical modeling of combustion processes in gas turbines 24 p3350 N88-29939
Three-dimensional combustor predictors: A comparison of equilibrium and laminar flamelet chemistry models 24 p3350 N88-29940
The effect of particle properties on radiative heat transfer 24 p3350 N88-29941
Analysis of the flow through double swirl airblast atomizers 24 p3351 N88-29949
The behaviour of synthetic fuels in a small transparent combustor 24 p3351 N88-29950
A small annular combustor of high power density, wide operating range and low manufacturing cost 24 p3351 N88-29951
Transition mixing study empirical model report [NASA-CR-182139] 24 p3371 N88-30076

COMBUSTION CHEMISTRY
Development of many-body methods for flame chemistry and large molecule applications [AD-A184451] 03 p0284 N88-11789
Laser probes of propellant combustion chemistry [AD-A184854] 05 p0561 N88-13415
Detailed mechanism of toluene oxidation and comparison with benzene [NASA-TM-100261] 05 p0563 N88-13428
Carbon monoxide and turbulence-chemistry interactions: Blowoff and extinction of turbulent diffusion flames [AD-A186276] 07 p0828 N88-15025
Non-steady group combustion of a cloud of char particles [DE87-010773] 08 p0966 N88-15849
Combustion mechanisms [AD-A187979] 11 p1453 N88-18660
Combustion and performance characteristics of methanol plus higher alcohols in a spark ignition engine [PB88-147962] 14 p1918 N88-21451
Laser spectroscopy and dynamics of combustion intermediates [DE88-006541] 15 p2033 N88-22110
Theoretical studies of dynamics combustion [DE88-007565] 19 p2611 N88-25495
Minimum ignition energy measurements using laser induced spark initiation 19 p2632 N88-25610
Theoretical studies of the chemical reactions involved in the ignition of nitramines 19 p2632 N88-25615
Temperature and species profiles in propellant ignition and combustion 19 p2633 N88-25616
Experiments and modeling of multi-component fuel behavior in combustion [AD-A195011] 24 p3343 N88-29896
Gas phase combustion chemistry of nitramine propellants [AD-A195082] 24 p3344 N88-29902

COMBUSTION CONTROL
Combustion control with smart sensors [DE87-013688] 03 p0281 N88-11768
Study of industry requirements that can be fulfilled by combustion experimentation aboard space station [NASA-CR-180854] 11 p1566 N88-19377
Control of combustion and acoustically coupled fluid dynamic instabilities 17 p2318 N88-23843
A study of flame spreading and combustion phenomena of stick propellants [AD-A193598] 22 p3052 N88-28106

COMBUSTION EFFICIENCY
Performance and combustion characteristics of direct-injection stratified-charge rotary engines [NASA-TM-100134] 04 p0400 N88-12490
Study of electrostatic modulation of fuel sprays to enhance combustion performance in an aviation gas turbine [AD-A184967] 05 p0548 N88-13341
Oxygen enriched combustion system performance study [DE88-001500] 05 p0562 N88-13424
Small engine technology programs 08 p0956 N88-15801
An investigation into the feasibility of using a dual-combustion mode ramjet in a high Mach number tactical missile [AD-A186906] 09 p1119 N88-16705
Finite area combustor theoretical rocket performance [NASA-TM-100785] 14 p1883 N88-21252
Research as part of the Air Force in aero propulsion technology (AFRAPT) program [AD-A190336] 15 p2019 N88-22036
Advanced B and Al combustion kinetics over wide temperature ranges [AD-A190752] 15 p2036 N88-22128
Measurement data processing system based on personal computer: For scramjet combustion test [DE88-751807] 16 p2174 N88-22959
Characteristic time correlations to liquid fuel ramjet combustion efficiency 19 p2624 N88-25566
Mach 2 combustion characteristics of hydrogen/hydrocarbon fuel mixtures 19 p2625 N88-25568
Basic research in supersonic combustion 19 p2634 N88-25623
Atomization of alternative fuels 24 p3345 N88-29913
Spray performance of a vaporizing fuel injector 24 p3346 N88-29919
The characterizatin of combustion by fuel composition: Measurements in a small conventional combustor 24 p3346 N88-29920
High performance turbofan afterburner systems 24 p3347 N88-29922
Comparison of the performance of a reverse flow annular combustion chamber under low and high pressure conditions 24 p3347 N88-29923

COMBUSTION HEAT
U HEAT OF COMBUSTION

COMBUSTION INSTABILITY
U COMBUSTION STABILITY

COMBUSTION PHYSICS
Combustion in turbulent jets and buoyant flames [PB87-232674] 03 p0283 N88-11779
The calculation of thermal rate constants for gas-phase and heterogeneous reactions in combustion processes [AD-A184435] 03 p0284 N88-11788
Spacecraft Fire Safety [NASA-CP-2476] 04 p0406 N88-12520
Microgravity combustion fundamentals 04 p0407 N88-12528
Spacecraft material flammability testing and configurations 04 p0407 N88-12529
Combustion characteristics of gas turbine alternative fuels [NASA-TM-100247] 05 p0548 N88-13338
SRB combustion dynamics analysis computer program (CDA-1) [NASA-CR-182404] 07 p0830 N88-15032
The carbon dioxide chaperon efficiency for the reaction H + O2 + M yields HO2 + M from ignition delay times behind reflected shock waves [NASA-TM-100125] 07 p0830 N88-15036
Combustion mechanisms [AD-A187979] 11 p1453 N88-18660
A study of combustion and flow behaviour in solid-propellant rocket motors [UTIAS-280] 13 p1732 N88-20357
Advanced B and Al combustion kinetics over wide temperature ranges [AD-A190752] 15 p2036 N88-22128
Microgravity combustion discipline working group summary of requirements for noncontact temperature measurements 17 p2328 N88-23902
Requirements for temperature and species concentration measurements in microgravity combustion experiments 17 p2329 N88-23903
Laser Diagnostics for combustion temperature and species measurements 17 p2330 N88-23912
On the structure, propagation, extinction and stability of laminar premixed flames in dissociation equilibrium 18 p2483 N88-24728
Combustion of PMMA, PE and PS in a ramjet [VTH-LR-514] 18 p2484 N88-24733
CFD benefits, goals, stepping-stones and techniques. Proposals for the scientific programme of the European Reserch Centre on flow, turbulence and combustion --- computational fluid dynamics [CFDU/88/1] 18 p2510 N88-24894
Next-generation fire extinguishing agent. Phase 1: Suppression concepts [AD-A192279] 19 p2614 N88-25514
Driving of axial acoustic fields by side-wall stabilized premixed flames 19 p2629 N88-25592
Basic research in supersonic combustion 19 p2634 N88-25623
Study of the local behavior of a flame [ETN-88-92300] 20 p2771 N88-26433
A study of flame spreading and combustion phenomena of stick propellants [AD-A193598] 22 p3052 N88-28106
Soot and radiation in a gas turbine combustor [AD-A191991] 23 p3179 N88-28924
Combustion dynamics and thermal structure of a planar spray flame 23 p3190 N88-28985
Numerical modeling of combustion processes in gas turbines 24 p3350 N88-29939
Modeling the stability of a turbulent premixed flame, downstream from a step by a Lagrangian method 24 p3350 N88-29943
Modeling and experimental study of a reactive flow confined with well injection 24 p3351 N88-29946

COMBUSTION PRODUCTS
Real time analysis of detonation products [DE87-007453] 01 p0031 N88-10195
The equation of state of PETN detonation products [DE87-013796] 02 p0155 N88-10971
Experimental verification of vapor deposition rate theory in high velocity burner rigs 02 p0189 N88-11179
Laser probes of propellant combustion chemistry [AD-A184854] 05 p0561 N88-13415
Pulsed plasma jet igniters: Species measurements in methane combustion [DE88-001389] 05 p0562 N88-13422
Formation and destruction of nitrous oxide in lean premixed combustion [DE88-001390] 05 p0562 N88-13423
Impacts of world development on selected characteristics of the atmosphere: An integrative approach. Volume 1: Main report [DE88-001495] 07 p0875 N88-15309
Ionic mechanisms of soot formation in flames [AD-A186195] 08 p0966 N88-15848
CARS measurements of combustion. 1: Precision of thermometry [NAL-TR-939] 10 p1299 N88-17769
The role of analytical chemistry in assessing atmospheric effects of combustion [DE88-003909] 10 p1352 N88-18082
Gas cleaning at high temperatures and pressures for gas turbines [DE88-751171] 11 p1440 N88-18593
Measurements of particulates in solid propellant rocket motors [AD-A187777] 11 p1446 N88-18621
Simulation of infrared spectra [AD-A187881] 11 p1453 N88-18658
Measurement of combustion aerosol size distributions with multistage inertial impactors [DE88-751101] 11 p1454 N88-18669
Fuels combustion research [AD-A189114] 13 p1736 N88-20381
Burning characteristics and flammability of PVC cables in groups [NASA-TT-20226] 14 p1893 N88-21303
Development of a laboratory test for multiport fuel injector deposits - evaluation of the Jet Fuel Thermal Oxidation Test apparatus (JFTOT) [AD-A191313] 16 p2183 N88-23015
Evaluation of manure as a feedstock for gas turbines 18 p2536 N88-25050
Measurement of particulate size in solid propellant rocket motors 19 p2630 N88-25599
Temperature and species profiles in propellant ignition and combustion 19 p2633 N88-25616
Freely expanding detonation products: Scaling of rate processes [DE88-007827] 20 p2799 N88-26606
Carbon deposition model for oxygen-hydrocarbon combustion, volume 1 [NASA-CR-179375] 21 p2908 N88-27254
Carbon deposition model for oxygen-hydrocarbon combustion, volume 2 [NASA-CR-179376] 21 p2908 N88-27255
Finite-rate water condensation in combustion-heated wind tunnels [NASA-TP-2833] 22 p3046 N88-28075
Automatic data retrieval from rocket motor holograms [AD-A195586] 24 p3337 N88-29864
Gas turbine smoke measurement: A smoke generator for the assessment of current and future techniques 24 p3348 N88-29930
Rates of formation of soot from hydrocarbon flames and its destruction 24 p3349 N88-29933
The influence of pressure on soot formation 24 p3349 N88-29934

COMBUSTION STABILITY
NT FLAME STABILITY
Flame driving of longitudinal instabilities in liquid fueled dump combustors [AD-A183536] 01 p0006 N88-10033
Longitudinal mode combustion instabilities in air breathing engines 06 p0680 N88-14166
European reacting flow research: A final assessment [AD-A185833] 07 p0828 N88-15022
Catalytic combustion of methane [PB88-123112] 07 p0829 N88-15028
Characterizing particle combustion in a Rijke burner [AD-A186157] 08 p0966 N88-15847
Basic instability mechanisms in chemically reacting subsonic and supersonic flows [AD-A190101] 15 p2034 N88-22120

Investigation of combustion in large vortices
[AD-A190406] 15 p2035 N88-22121
AFRAPT (Air Force Research in Aero Propulsion Technology) trainee program
[AD-A190525] 15 p2035 N88-22123
Control of combustion instabilities in ramjet motors
19 p2625 N88-25574
Development of a generic combustion stability code for liquid propellant rocket engines
19 p2626 N88-25576
Liquid Engine Jet Atomization Workshop report
19 p2627 N88-25584
The 24th JANNAF Combustion Meeting, volume 1
[AD-A190163] 19 p2627 N88-25585
Evidences for distributed combustion
19 p2628 N88-25586
Characterization of a modified Rijke burner for measurement of distributed combustion
19 p2628 N88-25587
Nonlinear mechanisms of solid propellant combustion instability 19 p2628 N88-25588
Propellant combustion response to oscillatory radiant heat flux 19 p2628 N88-25589
Motor test data comparisons with laboratory data and stability predictions 19 p2629 N88-25594
One person's view of velocity-coupled instability
19 p2629 N88-25595
Measurement of particulate size in solid propellant rocket motors 19 p2630 N88-25599
Basic research in supersonic combustion
19 p2634 N88-25623
Dynamics and stability of combustion driven self oscillations in presence of various frequencies. Extensive stability criteria
[ETN-88-92123] 20 p2771 N88-26432
Study of the local behavior of a flame
[ETN-88-92300] 20 p2771 N88-26433
Evaluation and improvement of liquid propellant rocket chugging analysis techniques. Part 1: A one-dimensional analysis of low frequency combustion instability in the fuel preburner of the space shuttle main engine
[NASA-CR-183106] 21 p2903 N88-27224
Evaluation and improvement of liquid propellant rocket chugging analysis techniques. Part 2: A study of low frequency combustion instability in rocket engine preburners using a heterogeneous stirred tank reactor model
[NASA-CR-182724] 21 p2903 N88-27225
Small scale mixing in the initial region of a jet
[AD-A193500] 23 p3192 N88-28994
High performance turbofan afterburner systems
24 p3347 N88-29922

COMBUSTION TEMPERATURE
Ignition and flame propagation in sprays
[AD-A184679] 03 p0283 N88-11781
Flow characteristics of a model annular combustor
24 p3347 N88-29924

COMBUSTION WAVES
U FLAME PROPAGATION

COMBUSTION WIND TUNNELS
Finite-rate water condensation in combustion-heated wind tunnels
[NASA-TP-2833] 22 p3046 N88-28075

COMBUSTORS
U COMBUSTION CHAMBERS

COMET HEADS
Spatial distribution of O(supra 1D) from Comet Halley
14 p1999 N88-21913

COMET NUCLEI
Dynamics of meteor streams
06 p0732 N88-14503
Results of infrared spectrometer experiment. 1: Infrared radiation of parent molecules in Halley's Comet
13 p1726 N88-20325
Results of infrared spectrometer experiment. 2: Infrared radiometry of nucleus of Halley's Comet
13 p1727 N88-20326
Calculation of the shape of the contact surface at Comet Halley 14 p1995 N88-21892
Plasma phenomena in the vicinity of the closest approach of VEGA-1, 2 spacecraft to the Comet Halley nucleus 14 p1996 N88-21899
Photometry of P/Halley (1982i): Is what we have learned useful for other comets? 14 p1998 N88-21909
Water vapor and hydroxyl distributions in the inner coma of Comet Halley measured by the VEGA-2 three channel spectrometer TKS 14 p1998 N88-21910
Narrow-band photometry of Comet P/Giacobini-Zinner at the time of ICE encounter 14 p1998 N88-21911
CCD-observations of gas and dust jets in the coma of Comet Halley 14 p1998 N88-21912
Analysis of the coma outburst of Comet Halley, March 24 to 25 (UT), 1986 14 p2000 N88-21920
Color fluctuations in the inner coma of Comet Halley as measured from VEGA-2 14 p2000 N88-21925
Anisotropic emission from comets: Fans versus jets. 1: Concept and modeling 14 p2001 N88-21927
Anisotropic emission from comets: Fans versus jets. 2: Periodic Comet Tempel 2 14 p2001 N88-21928
Comet P/Halley's near-nucleus jet activity
14 p2001 N88-21929
Dust photometry in the near nucleus region of Comet Halley from VEGA-2 observations
14 p2001 N88-21930
The dust around the nucleus of Comet Halley
14 p2003 N88-21942
The nucleus of Comet Halley
14 p2004 N88-21947
Comparison of active regions on the nucleus of Comet Halley 14 p2004 N88-21948
Reconstruction of the orientation and shape of the nucleus of Comet Halley 14 p2004 N88-21949
Estimates of masses, volumes and densities of short-period comet nuclei 14 p2004 N88-21950
Porosity and fractality of a cometary nucleus
14 p2004 N88-21951
Properties of the nucleus of P/Halley
14 p2004 N88-21952
Crustal models of the evolving comet nucleus
14 p2005 N88-21953
Simulation of cometary nuclei
14 p2005 N88-21954
Diversity of comets, synergic temperature effects and the stability of organic compounds in icy nuclei
14 p2005 N88-21955
Rosetta: A mission to sample the nucleus of a comet
14 p2005 N88-21958
Retrieving samples from comet nuclei
14 p2006 N88-21959
P/Halley activity in November 1985
14 p2006 N88-21966
Different trapping mechanisms of gases by water ice and their relevance for comet nuclei
14 p2007 N88-21970
On the periodic southward jets of Comet Halley before perihelion passage 14 p2008 N88-21978
Dust tail streamers and Halley's nucleus rotation
14 p2008 N88-21979
Near-infrared imaging of Comet Halley: Discovery of a color gradient in the inner coma
14 p2009 N88-21980
The light curve of P/Halley and the rotation of its nucleus 14 p2009 N88-21984
Temperature of the nucleus of Comet Halley
14 p2009 N88-21985
Consequences of the size determination of P/Halley by space probes on the scale of sizes of cometary nuclei
14 p2009 N88-21986
Physical-mechanical properties of matrices on the comet nuclei surface models 14 p2010 N88-21987
Sublimation characteristics of H2O comet nucleus with CO2 impurities 14 p2010 N88-21988
The splitting of Comet Halley 1986
14 p2010 N88-21989
Photographic observations of the large scale features of Comet Halley 16 p2288 N88-23698
The evolution of cometary activity
18 p2594 N88-25416
Cometary nucleus as aggregate of planetesimals
[ISAS-RN-364] 19 p2741 N88-26275
Study of comet nucleus gamma-ray spectrometer penetration system
[NASA-CR-177393] 20 p2883 N88-27120
Processing and analysis of images transmitted by Vega space probes over Halley's comet
[ETN-88-92291] 20 p2885 N88-27131

COMET TAILS
Comparative plasma tails of Venus and comets
01 p0116 N88-10742
Plasma-tail activity and the interplanetary medium at Halley's Comet during Armada Week: 6-14 March 1986
01 p0118 N88-10752
Occultation of compact radio sources by the ion tail of Halley's Comet 01 p0118 N88-10753
Analysis of the ICE combiner for multiple antenna arraying 04 p0436 N88-12704
The striae in the dust tails of great comets: A formal comparison of the goodness of fit by various theories, and a new proposal 14 p2002 N88-21937
The origin of low mass particles within and beyond the dust coma envelopes of Comet Halley
14 p2002 N88-21938
Plasma tail of Comet Halley in January 1986
14 p2006 N88-21960
Determination of the content of CO(+) and H2O(+) ions in the tail of Comet Giacobini-Zinner and Comet Halley 14 p2006 N88-21964
The dust tail of Comet Halley
14 p2008 N88-21974
Classification of comets recorded in ancient China (300 BC - 1800 AD) and statistics of type-1 tails
14 p2008 N88-21976
Dust tail streamers and Halley's nucleus rotation
14 p2008 N88-21979
Dust and C2-contents in the coma of Halley's Comet (1986III) 16 p2288 N88-23697
Photographic observations of the large scale features of Comet Halley 16 p2288 N88-23698

COMETARY ATMOSPHERES
Study of pickup of cometary ions in turbulent solar winds 01 p0113 N88-10725
The global interaction of comets with the solar wind
01 p0117 N88-10746
Solar wind effects on the outer ion coma of Comet Halley 01 p0117 N88-10750
The solar wind interaction with comets: A post encounter view 01 p0118 N88-10751
Plasma-tail activity and the interplanetary medium at Halley's Comet during Armada Week: 6-14 March 1986
01 p0118 N88-10752
Extended atmospheres of outer planet satellites and comets
[NASA-CR-181449] 10 p1430 N88-18540
A mass spectrometer evolved gas analysis experiment for in-situ analysis of cometary dust volatiles
13 p1854 N88-21097
Proceedings of the International Symposium on the Diversity and Similarity of Comets
[ESA-SP-278] 14 p1994 N88-21884
Variability of Comet Halley's coma: VEGA-1 and VEGA-2 magnetic field observations 14 p1995 N88-21891
Calculation of the shape of the contact surface at Comet Halley 14 p1995 N88-21892
Physical processes in the vicinity of the cometopause interpreted on the basis of plasma, magnetic field and plasma wave data measured on board VEGA-2 spacecraft --- Halley's comet 14 p1996 N88-21894
Plasma phenomena in the vicinity of the closest approach of VEGA-1, 2 spacecraft to the Comet Halley nucleus 14 p1996 N88-21899
Time dependent MHD models for the cometary magnetosphere 14 p1997 N88-21900
Halley's environments by the Japanese Suisei spacecraft 14 p1999 N88-21915
The role of water in the thermal balance of the coma
14 p1999 N88-21916
A model of the anisotropic structure of the neutral gas coma of a comet 14 p1999 N88-21918
Profiles of the major gas emissions and distribution of dust particles in the inner coma (0 to 10,000 km) of Comet Halley 14 p1999 N88-21919
Comparison of Halley's monochromatic comae with others 14 p2006 N88-21965
Interaction mechanisms of comets with the zodiacal dust cloud 14 p2008 N88-21977
Dust and C2-contents in the coma of Halley's Comet (1986III) 16 p2288 N88-23697
Modeling of a cometary dust coma
[ETN-88-92980] 23 p3300 N88-29651
Extended atmospheres of outer planet satellites and comets
[NASA-CR-183157] 24 p3457 N88-30572

COMETARY MAGNETOSPHERES
Time dependent MHD models for the cometary magnetosphere 14 p1997 N88-21900

COMETS
NT COMET HEADS
NT COMET NUCLEI
NT COMET TAILS
NT ENCKE COMET
NT GIACOBINI-ZINNER COMET
NT GRIGG-SKJELLERUP COMET
NT HALLEY'S COMET
NT TEMPEL 2 COMET
NT WEST COMET
STIP Symposium on Physical Interpretation of Solar/Interplanetary and Cometary Intervals
[NASA-CR-181201] 01 p0110 N88-10709
Was the eclipse comet of 1893 a disconnected coronal transient? 01 p0115 N88-10733
Solar wind-cometary interaction at the ionopause and associated phenomena 01 p0117 N88-10748
Exobiology and life science 07 p0883 N88-15358
Laser simulation of light and plasma action on comets and planets 09 p1237 N88-17413
Proceedings of the International Symposium on the Diversity and Similarity of Comets
[ESA-SP-278] 14 p1994 N88-21884
Diversity and similarity of comets
14 p1994 N88-21885
The absolute total magnitudes of periodic comets and their variations 14 p1994 N88-21887
Cometary magnitude distribution: The tabulated data
14 p1995 N88-21888

The comet flux and the 15 Myr galactic cycle
14 p1995 N88-21889
The relationship between low activity comets and more active comets 14 p1997 N88-21904
The photochemistry of some possible cometary CN parent species 14 p1997 N88-21905
Polarization of molecular fluorescence bands in comets: Recent observations and interpretation
14 p1998 N88-21907
Photodissociation lifetimes of CH and CD radicals in comets 14 p1998 N88-21908
Objective-prism spectra of the Comets Honda (1968 e), Hartley-Good (1985 l) and Halley
14 p2000 N88-21924
Cometary evolution: Clues from chondritic interplanetary dust particles 14 p2002 N88-21934
The striae in the dust tails of great comets: A formal comparison of the goodness of fit by various theories, and a new proposal 14 p2002 N88-21937
Similarity and diversity of the polarization of comets
14 p2003 N88-21940
Particles injected by comets 14 p2003 N88-21944
Diversity of comets, synergic temperature effects and the stability of organic compounds in icy nuclei
14 p2005 N88-21955
On the forbidden red lines of oxygen in comets
14 p2006 N88-21963
On the interpretation of the CH cometary spectrum
14 p2007 N88-21969
The role of hydrogen thermalization in shaping the Lyman-alpha coma --- comets 14 p2007 N88-21971
Classification of comets recorded in ancient China (300 BC - 1800 AD) and statistics of type-1 tails
14 p2008 N88-21976
Interaction mechanisms of comets with the zodiacal dust cloud 14 p2008 N88-21977
The mass loss rates of periodic comets
14 p2010 N88-21991
The evolution of cometary activity
18 p2594 N88-25416
Did the greenhouse effect kill the dinosaurs
24 p3442 N88-30484

COMFORT
Improvement of the construction of protective clothing for better wearability and comfort --- rainwear
[IZF-1986-26] 07 p0899 N88-15448
Habitability of the Space Station: From vehicle to living space 19 p2697 N88-26033
Study of human factors engineering criteria for Extra Vehicular Activity (EVA) systems, volume 2
[STF23-F87025-VOL-2] 24 p3409 N88-30293

COMMAND AND CONTROL
Automation strategy and results for an airbase command and control information system
[NLR-MP-86031-U] 01 p0035 N88-10223
Using concept mapping to define problems and identify key kernels during the development of a decision support system
[AD-A185636] 06 p0762 N88-14674
An approach to validation and verification of the communications load model with supporting user's guide
[AD-A185926] 07 p0840 N88-15098
Case-based reasoning for space applications: Utilization of prior experience in knowledge-based systems
08 p1065 N88-16433
Relating service doctrine to space system requirements
[AD-A186620] 08 p1074 N88-16483
POCC capabilities document. Payload support capabilities description: MCC, JSC POCC, remote POCC interface
[NASA-TM-89708] 09 p1260 N88-17555
Future directions in computer architecture
10 p1383 N88-18257
Fuzzy logic inference processor for real time control: A second generation full custom design
[AD-A188155] 11 p1471 N88-18773
Aircrew training devices: Utility and utilization of advanced instructional features, phase 4
[AD-A188418] 12 p1670 N88-20000
Variable speed optimal control of a wind turbine generator
[LAAS-87-358] 16 p2229 N88-23316
Decision aiding and coordination in decision-making organizations
[AD-A191950] 19 p2738 N88-26259
Real time data base management
[AD-A191758] 19 p2739 N88-26265
An evaluation methodology for dependable multiprocessors
[AD-A192799] 20 p2842 N88-26863
Launch operations to support future space forces
[AD-A192679] 20 p2881 N88-27107
A virtual statistical mechanical neural computer
[AD-A193962] 22 p3139 N88-28660
LO-CO-GRAF (low cost graphics): Generating maps to support command and control/crisis management using small computers
[AD-A193964] 22 p3139 N88-28661
Distributed cooperating processes in a mobile robot control system 23 p3256 N88-29386
Strategic defense initiative architecture dataflow modeling technique version 1.5
[AD-A194356] 23 p3275 N88-29494
Definition of common support equipment and space station interface requirements for IOC model technology experiments
[NASA-TM-100656] 24 p3336 N88-29856
The design of an intelligent multidisk control module for VME bus based systems
[AD-A195587] 24 p3411 N88-30303
Automated satellite control in Ada
24 p3416 N88-30336

COMMAND GUIDANCE
Reduced order optimal command applied to longitudinal automatic pilots
[SNIAS-872-111-114] 05 p0552 N88-13362
Optimum-Path-to-Go guidance of command adjusted trajectory projectiles
[AD-A193377] 22 p3040 N88-28051
Air Force Systems Command software independent verification and validation implementation analysis and guidance
[AD-A194309] 22 p3137 N88-28653

COMMAND LANGUAGES
NT QUERY LANGUAGES
DOD Gateway Information System (DGIS) common command language: Prolog knowledge base profile. Common command language report no. 3
[AD-A186150] 08 p1092 N88-16574
A robotic language for cooperative multi-robots
17 p2387 N88-24186

COMMAND MODULES
Optimization techniques applied to passive measures for in-orbit spacecraft survivability
[NASA-CR-179216] 04 p0408 N88-12532

COMMAND SYSTEMS
U COMMAND GUIDANCE

COMMAND-CONTROL
U COMMAND AND CONTROL

COMMERCE
An overview of remote sensing users' requirements
03 p0340 N88-12139
A study of federal technology transfer to the commercial sector
[AD-A187017] 09 p1262 N88-17560
Status of emerging technologies: An economic/technological assessment to the year 2000
[PB88-155775] 11 p1567 N88-19381
Safety study: Commercial emergency medical service helicopter operation
[PB88-917001] 12 p1575 N88-19422
Spin off businesses as mechanisms for transferring technologies
[DE88-005640] 13 p1852 N88-21085
Datacast: The transmission system
[BBC-RD-1988/1] 14 p1905 N88-21385
Technology transfer to China. Volume 2: Working papers, part 2
[PB88-158712] 14 p1992 N88-21873
International commercialization of remote sensing
[BCRS-87-14] 16 p2228 N88-23310

COMMERCIAL AIRCRAFT
NT A-300 AIRCRAFT
NT A-320 AIRCRAFT
NT BOEING 737 AIRCRAFT
NT BOEING 747 AIRCRAFT
NT DC 9 AIRCRAFT
NT EUROPEAN AIRBUS
NT VC-10 AIRCRAFT
Design requirements for future commercial operations
03 p0262 N88-11651
Design and control of repairs of carbon fiber lift augmentation flaps in the ATR42 aircraft
[SNIAS-872-111-112] 05 p0529 N88-13217
Airline safety: A comparative analysis
[AD-A185358] 05 p0543 N88-13308
A study of the utilization of advanced composites in fuselage structures of commercial aircraft
[NASA-CR-172405] 06 p0679 N88-14157
Low altitude windshear threat to commercial aircraft
08 p0952 N88-15777
Aircraft accident reports: Brief format, US Civil and Foreign Aviation, Issue Number 7 of 1986 accidents
[PB87-916909] 08 p0952 N88-15781
Presentation of Class 1 designs for a family of commuter airplanes
[NASA-CR-182563] 11 p1439 N88-18587
High performance composites research at NASA-Langley
[NASA-TM-100518] 11 p1450 N88-18642
First encounters of the close kind: The formation process of airline flight crews
[AD-A187977] 11 p1523 N88-19091
NASA advanced turboprop research and concept validation program
[NASA-TM-100891] 16 p2163 N88-22902
Manufacturing requirements 17 p2297 N88-23745
From turboprop aircraft to multi-engined jet aircraft Aircraft Integrated Monitoring Systems (AIMS)
22 p3033 N88-28003
Critical joints in large composite primary aircraft structures. Volume 1: Technical summary
[NASA-CR-3914] 23 p3190 N88-28983
Report to Congress on the effectiveness of the Civil Aviation Security Program
[AD-A195282] 24 p3322 N88-29784

COMMERCIAL AVIATION
U CIVIL AVIATION
U COMMERCIAL AIRCRAFT

COMMERCIAL ENERGY
Heat pump and appliance research
[PB88-102462] 07 p0853 N88-15184

COMMINUTION
Planetary science 07 p0883 N88-15356
Characterization and fundamental studies on CuO sorbent materials to determine attrition mechanisms on substrate gamma alumina
[DE88-003674] 13 p1749 N88-20456

COMMON BUSINESS ORIENTED LANGUAGE
U COBOL

COMMONALITY
Expert system development for commonality analysis in space programs 07 p0928 N88-15635
Study of reconfigurable payloads for direct broadcast satellites, summary
[DBS87-0004] 09 p1135 N88-16808
Presentation of Class 1 designs for a family of commuter airplanes
[NASA-CR-182563] 11 p1439 N88-18587
Presentation of structural component designs for the family of commuter airplanes
[NASA-CR-182568] 12 p1581 N88-19463
A class 2 weight assessment for the implementation of commonality and preliminary structural designs for the family of commuter airplanes
[NASA-CR-182565] 12 p1581 N88-19464
Advanced propfan analysis for the family of commuter airplanes
[NASA-CR-182566] 12 p1582 N88-19468
Presentation of flight control design and handling quality commonality by separate surface stability augmentation for the family of commuter airplanes
[NASA-CR-182567] 12 p1583 N88-19471
A cost analysis for the implementation of commonality in the family of commuter airplanes, revised
[NASA-CR-182569] 12 p1708 N88-20221
Class 2 design update for the family of commuter airplanes
[NASA-CR-182681] 18 p2464 N88-24629

COMMUNICATING
NT AIRCRAFT COMMUNICATION
NT INFORMATION DISSEMINATION
NT MESSAGES
NT VERBAL COMMUNICATION
Online aiding for human-computer interfaces
[AD-A189239] 13 p1815 N88-20842

COMMUNICATION
NT FACSIMILE COMMUNICATION
NT LINE OF SIGHT COMMUNICATION
NT OPTICAL COMMUNICATION
NT UNDERWATER COMMUNICATION
Meteor-burst communications: Is this what the Navy needs?
[AD-A184433] 04 p0431 N88-12672
The SUPRENUM communications subroutine library for grid-oriented problems
[DE88-000137] 04 p0479 N88-12950
Program description of FIBRAM: A radiation attenuation model for optical fibers
[PB87-230686] 06 p0690 N88-14229
An approach to validation and verification of the communications load model with supporting user's guide
[AD-A185926] 07 p0840 N88-15098
Algebraic specification of process algebra, including two examples
[PB88-106729] 07 p0912 N88-15531
Space languages 08 p1063 N88-16420
POCC capabilities document. Payload support capabilities description: MCC, JSC POCC, remote POCC interface
[NASA-TM-89708] 09 p1260 N88-17555
Helsinki University of Technology Communications Laboratory
[PB88-112974] 10 p1318 N88-17881
The design of trellis codes for fading channels
[NASA-CR-182523] 10 p1320 N88-17891

Future directions in computer architecture
10 p1383 N88-18257
Networking requirements and future alternatives
[NASA-TM-89711] 10 p1426 N88-18517
The design and implementation of the Technical Facilities Controller (TFC) for the Goldstone deep space communications complex 11 p1474 N88-18794
Optimum filters and smoothers design for carrier phase and frequency tracking
[NASA-CR-182654] 12 p1618 N88-19679
Lasers: Invention to application
[PB88-161583] 14 p1914 N88-21436
Research and technology
[NASA-TM-100172] 15 p2153 N88-22851
The relationship between group process and performance 17 p2448 N88-24549
Evaluation of the communications impact of a low power arcjet thruster
[NASA-TM-100926] 18 p2475 N88-24682
Communication training for aircrews: A review of theoretical and pragmatic aspects of training program design
[NASA-CR-177459] 20 p2756 N88-26349
A study of a meteor burst communication system
21 p2934 N88-27421
Coding for meteor-burst communications channel and side information for channels with block-interference
23 p3202 N88-29054
An OKQPSK modem incorporating numerically controlled carrier synthesis
[DE88-009536] 23 p3244 N88-29304
Dynamic analysis of computer and communications sytems: Semi-Markov approach
23 p3244 N88-29305
Barriers to Information Transfer and Approaches Toward Their Reduction
[AGARD-CP-430] 24 p3437 N88-30458
Linguistic and cultural barriers to the transfer of information 24 p3437 N88-30459
Political and economic barriers to information transfer
24 p3437 N88-30460

COMMUNICATION CABLES
NT BEAM WAVEGUIDES
NT CIRCULAR WAVEGUIDES
NT COAXIAL CABLES
NT OPTICAL FIBERS
NT OPTICAL WAVEGUIDES
NT PLASMAGUIDES
NT RECTANGULAR WAVEGUIDES
NT WAVEGUIDES
Soliton mode of propagation of light pulses through single-mode optical fibers and problems of its experimental realization 07 p0920 N88-15592
Failure-resistant Fibre-Optical Communication Line (FOCL)
[DE88-700470] 10 p1408 N88-18400
Aging properties of cable polmers (2)
[NASA-TT-20228] 13 p1752 N88-20479
Burning characteristics and flammability of PVC cables in groups
[NASA-TT-20226] 14 p1893 N88-21303

COMMUNICATION EQUIPMENT
NT DIPLEXERS
NT RADIO RECEIVERS
NT SATELLITE TELEVISION
NT SUPERHETERODYNE RECEIVERS
NT TRANSMITTER RECEIVERS
Multi-channel communications system analyzer
[AD-A184756] 03 p0307 N88-11937
SBNR (Signed Binary Number Representations) digital signal processor architecture
[AD-A184603] 03 p0364 N88-12290
Automatic antenna switching design for Extra Vehicular Activity (EVA) communication system
06 p0797 N88-14883
Validation of a stochastic model to determine failure rates for communication-electronic systems
[AD-A186536] 08 p0980 N88-15920
Team problem solving: Effects of communication and function overlap
[AD-A187010] 09 p1152 N88-16898
Evaluating software testing methods to reduce testing duplication in US Army communications equipment acquisition
[AD-A186961] 09 p1216 N88-17292
Information and stochastic systems
[AD-A192167] 18 p2501 N88-24838
Digital communication transmitter and receiver test procedures
[AD-A191218] 20 p2788 N88-26540
Event-related brain potentials as indices of mental workload and attentional allocation
21 p2979 N88-27696
The Telecommunications and Data Acquisition Report
[NASA-CR-183131] 22 p3063 N88-28178
Doppler-corrected differential detection system
[NASA-CASE-NPO-16987-1-CU]
24 p3359 N88-30001

COMMUNICATION NETWORKS
NT ALOHA SYSTEM
NT LOCAL AREA NETWORKS
Design, manufacture and testing of an elegant breadboard model communications processor
[D/2244] 01 p0034 N88-10217
Study of a coding and modulation system for the V32 call of the CCITT
[ENST-87E007] 02 p0162 N88-11015
Modeling and performance evaluation of the DPS25 packet switching multiprocessor system --- communication networks
[ENST-87E009] 02 p0162 N88-11016
Contribution to the study of circuit switched networks: Modeling and numerical solutions
[LAAS-87-174] 02 p0162 N88-11017
The role of spread spectrum in packet radio networks
[AD-A184511] 03 p0306 N88-11929
The design and testing of an analog optical communication link capable of the simultaneous transmission of four frequency division multiplexed audio signals
[AD-A184695] 03 p0307 N88-11936
Multi-channel communications system analyzer
[AD-A184756] 03 p0307 N88-11937
Network reconstitution protocol
[AD-A184755] 03 p0367 N88-12309
Multicast gateway design considerations
[PB87-219960] 04 p0430 N88-12663
Heterogeneous multi-trunking queueing systems
[AD-A184255] 04 p0431 N88-12668
An interactive computer graphics network monitor for a tactical communications network
[AD-A184131] 04 p0477 N88-12938
Contribution to optimal flow in networks. A experimental multiprocessor for asynchronous iteration implementation
[LAAS-87-269] 05 p0576 N88-13510
Communications payload concepts for geostationary facilities
[NASA-TM-100154] 05 p0576 N88-13513
An evolutionary communications scenario for Mars exploration
[NASA-TM-100263] 05 p0576 N88-13515
Connecting RPC (Remote Procedure Call)-based distributed systems using wide-area networks
[PB87-234423] 05 p0658 N88-14041
Land mobile satellite transmission measurements at 869 MHz. A comparison of error probabilities for various message block durations and fade margins as a function of vegetation shadowing
[NASA-CR-179929] 06 p0693 N88-14255
On real-time systems using local area networks
[AD-A185475] 06 p0694 N88-14256
Wide-area communication under Amoeba
[PB87-234431] 06 p0760 N88-14665
Development of a graphical display on the DMS test bed 06 p0794 N88-14864
High data rate modem simulation for the space station multiple-access communications system
06 p0795 N88-14870
An approach to validation and verification of the communications load model with supporting user's guide
[AD-A185926] 07 p0840 N88-15098
On the approximation of the output process of multi-user random access communication networks
[AD-A186197] 07 p0842 N88-15106
Reliability and survivability of communication networks
[AD-A186248] 07 p0842 N88-15109
Round table on the future of satellite communications and broadcasting in Europe
[ESA-STR-221] 07 p0843 N88-15112
Coding for spread-spectrum communications networks
[AD-A185667] 07 p0844 N88-15119
Throughput analysis of a flow-contoured communication network with buffer space limitations
[CWI-OS-R8702] 08 p0977 N88-15908
Waiting times in discrete-time cyclic-service systems --- communication networks
[CWI-OS-R8707] 08 p0977 N88-15909
Approximating the size of a dynamically growing asynchronous distributed network
[AD-A187011] 09 p1152 N88-16899
Adaptive spread spectrum networks
[AD-A187154] 09 p1152 N88-16900
Transient electromagnetic scattering from heterogeneous lossy spheres
[AD-A186669] 09 p1152 N88-16903
An introduction to military satellite communications
[RSRE-MEMO-3976] 09 p1153 N88-16911
Communications patterns in a symbolic multiprocessor
[AD-A186896] 09 p1215 N88-17282
Terrestrial Propagation Characteristics in Modern Systems of Communications, Surveillance, Guidance and Control
[AGARD-CP-407] 12 p1614 N88-19653
MM-wave propagation and application in military communication systems 12 p1617 N88-19669
Spread spectrum radio networks
[AD-A188914] 12 p1620 N88-19689
Static and dynamic jamming of networks
[AD-A188921] 12 p1620 N88-19690
Evaluation of network communication multiprocessor fault tolerance
[INPE-4305-PRE/1171] 12 p1674 N88-20011
An intelligent allocation algorithm for parallel processing
[NASA-CR-182648] 12 p1675 N88-20014
Knowledge-based system analysis and control
[AD-A188163] 12 p1681 N88-20049
Design methodology for allocating data in a distributed database
[AD-A188826] 12 p1706 N88-20215
Alternative force structuring strategies for military satellite communication systems
[AD-A189492] 13 p1758 N88-20516
Human problem solving in dynamic environments. Understanding and supporting operators in large-scale, complex systems
[AD-A189539] 13 p1812 N88-20826
Spatial distribution of traffic in a cellular mobile data network
[EUT-87-E-168] 14 p1904 N88-21378
A packet-switched wide-area communication network simulator
[FUB-3-1986] 14 p1905 N88-21381
On-board processing for mobile satellite communications
[ESA-CR(P)-2519] 14 p1905 N88-21382
Real-time stressed channel simulator
[AD-A190223] 15 p2025 N88-22067
NASA and the challenge of ISDN: The role of satellites in an ISDN world
[NASA-CR-182749] 15 p2126 N88-22676
Discrete generalized networks: Application to integer constrained flow problems
[AD-A190823] 16 p2190 N88-23060
Multiple address facility for packet radio: An investigation of performance/complexity trade off
[AD-A191043] 16 p2190 N88-23064
Problems in integrated networks
[AD-A191391] 16 p2191 N88-23069
Near-real-time TOMS, telecommunications and meteorological support for the 1987 Airborne Antarctic Ozone Experiment
[NASA-CR-4133] 16 p2233 N88-23338
Alpha structure based B-HIVE multicomputer
[AD-A188708] 16 p2244 N88-23405
Reasoning about networks with many identical finite-state processes
[AD-A188743] 16 p2245 N88-23413
IPC for modular software requires a third party connect
[AD-A189199] 16 p2246 N88-23414
Modeling, filtering and control of stochastic processes --- communication networks
[ENST-87E021] 17 p2333 N88-23925
MSAT-X: A technical introduction and status report
[NASA-CR-182921] 17 p2334 N88-23933
Connecting remote systems for demonstration of automation technologies 17 p2387 N88-24191
Propagation management for no-acknowledge HF communications links 18 p2502 N88-24843
Human problem solving in complex dynamic environments
[AD-A190788] 18 p2551 N88-25142
The AMSC mobile satellite system
19 p2643 N88-25681
NASA's mobile satellite development program
19 p2643 N88-25682
Mobile satellite service for Canada
19 p2643 N88-25683
A satellite system for land-mobile communications in Europe 19 p2643 N88-25685
Developing a global aeronautical satellite system
19 p2644 N88-25687
World-wide aeronautical satellite communications
19 p2644 N88-25688
An overview of the OmniTRACS: The first operational mobile Ku-band satellite communications
19 p2644 N88-25689
International and domestic mobile satellite regulatory proceedings: A comparison of outcomes and discussion of implications 19 p2644 N88-25690
International and domestic regulator issues facing the Canadian MSAT system 19 p2644 N88-25692
Development of the network architecture of the Canadian MSAT system 19 p2646 N88-25702

System architecture for the Canadian interim mobile satellite system 19 p2646 N88-25703
Design mobile satellite system architecture as an integral part of the cellular access digital network
19 p2650 N88-25736
An access alternative for mobile satellite networks
19 p2651 N88-25737
Satellites at sea --- INMARSAT
19 p2700 N88-26054
The contribution of space to maritime activities
19 p2700 N88-26055
Analysis and synthesis of decision-making organizations
[AD-A191948] 19 p2738 N88-26258
The performance of Eurocom error correction schemes for data communications
[FEL-1987-56] 20 p2792 N88-26563
An integrated circuit for error protection in modern data communication systems conforming to Eurocom specifications
[FEL-1987-48] 20 p2796 N88-26593
Extensible networks. Part 1: Principles and constructions
[REPT-87-91-PT-1] 20 p2842 N88-26864
The MELMUX MX-7100 series high-speed digital multiplexers 21 p2930 N88-27396
Activities report of the Communications Department
[ENST-88D003] 21 p2931 N88-27401
Utilization of a satellite communication system to protect the national communication network
[FUB-33-1986] 21 p2934 N88-27423
The Frequency Division Multiple Access/Time Domain Multiplex (FDMA/TDM) system reviewed
22 p3069 N88-28214
Determination of satcom access power levels within the ground segment
[RSRE-MEMO-4097] 22 p3070 N88-28226
Performance of a rapid carrier acquisition circuit for satellite ground terminal modems
[RSRE-TEST-REPORT-87/CC3/2]
22 p3071 N88-28227
Hierarchical organization for large, dynamic radio networks
[AD-A193942] 23 p3204 N88-29067
Performance analysis of k-ary n-cube interconnection networks
[AD-A195542] 24 p3361 N88-30010
Design of a self-timed VLSI multicomputer communication controller
[AD-A194567] 24 p3361 N88-30014
Comparative analysis of passive communications satellites employing the SHF and HF spectrum for use in a strategic role
[AD-A194682] 24 p3362 N88-30019
Integrating images, applications, and communications networks, volume 5
[AD-A195854] 24 p3436 N88-30452

COMMUNICATION SATELLITES
NT ACTS
NT DIRECT BROADCAST SATELLITES
NT EUROPEAN COMMUNICATIONS SATELLITE
NT L-SAT
NT MARECS MARITIME SATELLITES
Communication satellite technology trends
01 p0015 N88-10088
Study of mobile communications payload for Columbus Polar Platforms
[ITS-TR-056A/86] 01 p0034 N88-10220
Electrostatic discharges in geostationary orbit: The case of Telecom 1 03 p0275 N88-11733
An examination of the Advanced Communications Technology Satellite (ACTS) and its application to the Defense Data Network (DDN)
[AD-A184003] 03 p0276 N88-11742
Engineering calculations for the Delta S method of solving the orbital allotment problem
[NASA-CR-182372] 06 p0671 N88-14110
Propagation effects on satellite systems at frequencies below 10 GHz: A handbook for satellite systems design
[NASA-RP-1108/2] 06 p0690 N88-14226
Numerical arc segmentation algorithm for a radio conference-NASARC (version 2.0) technical manual
[NASA-TM-100160] 08 p0977 N88-15910
Communications satellite systems operations with the space station. Volume 3: Supplementary technical report
[NASA-CR-180875] 09 p1133 N88-16794
Multicarrier demodulator design, volume 1 --- communication satellites
[ESA-CR(P)-2468-VOL-1] 09 p1158 N88-16941
Multicarrier demodulator design. Volume 2: Executive summary --- communication satellites
[ESA-CR(P)-2468-VOL-2] 09 p1158 N88-16942
Satellite interference analysis and simulation using personal computers
[NASA-CR-182522] 10 p1319 N88-17890
High efficiency, long life traveling wave tubes for future communications satellites
[NASA-TM-100837] 12 p1598 N88-19565
Communication satellites: Guidelines for a strategic plan
[NASA-TM-89306] 12 p1599 N88-19569
PRC space satellite achievements highlighted
14 p1863 N88-21131
RF-switches: Application and design --- satellite communication 14 p1877 N88-21215
Qualification testing of the EUROSTAR Solar Array Drive Mechanism (SADM) 14 p1879 N88-21229
NASA and the challenge of ISDN: The role of satellites in an ISDN world
[NASA-CR-182749] 15 p2126 N88-22676
Numerical arc segmentation algorithm for a radio conference: A software tool for communication satellite systems planning
[NASA-TM-100789] 16 p2167 N88-22919
The bit-error rate performance of a satellite microwave matrix switch
[NASA-TM-100285] 16 p2167 N88-22920
MSAT-X: A technical introduction and status report
[NASA-CR-182921] 17 p2334 N88-23933
Experimental radio frequency link for Ka-band communications applications
[NASA-TM-100824] 18 p2470 N88-24659
Simulations of the electrostatic charging of ESA communications satellites
[ESA-STM-239] 18 p2472 N88-24670
Proceedings of the Mobile Satellite Conference
[NASA-CR-182964] 19 p2643 N88-25680
The AMSC mobile satellite system
19 p2643 N88-25681
NASA's mobile satellite development program
19 p2643 N88-25682
Mobile satellite service for Canada
19 p2643 N88-25683
AUSSAT mobile satellite services
19 p2643 N88-25684
A satellite system for land-mobile communications in Europe 19 p2643 N88-25685
Developing a global aeronautical satellite system
19 p2644 N88-25687
An overview of the OmniTRACS: The first operational mobile Ku-band satellite communications
19 p2644 N88-25689
Mobile satellite services: International co-ordination, co-operation and competition 19 p2644 N88-25691
International and domestic regulator issues facing the Canadian MSAT system 19 p2644 N88-25692
Land mobile satellite propagation results
19 p2645 N88-25698
Development of a mobile satellite communication unit
19 p2646 N88-25701
System architecture for the Canadian interim mobile satellite system 19 p2646 N88-25703
Satellite communications experiment for the Ontario air ambulance service 19 p2646 N88-25705
Land mobile satellite demonstration system
19 p2646 N88-25706
The JPL MSAT mobile laboratory and the pilot field experiments 19 p2646 N88-25708
Technical characteristics of the OmniTRACS: The first operation mobile Ku-band satellite communications system 19 p2647 N88-25709
An adaptive array antenna for mobile satellite communications 19 p2647 N88-25710
MSAT mobile electronically steered phased array antenna development 19 p2647 N88-25711
MSAT-X electronically steered phased array antenna system 19 p2647 N88-25712
MSAT-X phased array antenna adaptions to airborne applications 19 p2647 N88-25713
Adaptive interference techniques for mobile antennas
19 p2647 N88-25714
The JPL mechanically steered antenna
19 p2647 N88-25715
Simple, low-profile, circularly polarized arrays
19 p2647 N88-25716
Codes for QPSK modulation with invariance under 90 degrees rotation 19 p2648 N88-25720
Modulation and coding for fast fading mobile satellite communication channels 19 p2648 N88-25722
Performance of the ICAO standard core service modulation and coding techniques
19 p2648 N88-25723
Comparison of CDMA and FDMA for the MobileStar(sm) system 19 p2649 N88-25724
An 8-DPSK TCM modem for MSAT-X
19 p2649 N88-25725
Modem for the land mobile satellite channel
19 p2649 N88-25727
Pilot-aided modulation for narrow-band satellite communications 19 p2649 N88-25728
A study on the co- and adjacent channel protection requirements for mobile satellite ACSSB modulation
19 p2650 N88-25732
A framework for implementing data services in multi-service mobile satellite systems
19 p2650 N88-25733
L-band and SHF multiple access schemes for the MSAT system 19 p2650 N88-25734
Rearrangement procedures in regenerative multibeammobile communications satellites with frequency reuse 19 p2650 N88-25735
Design mobile satellite system architecture as an integral part of the cellular access digital network
19 p2650 N88-25736
An access alternative for mobile satellite networks
19 p2651 N88-25737
An operational open-end file transfer protocol for mobile satellite communications 19 p2651 N88-25738
Integrated voice/data protocols for satellite channels
19 p2651 N88-25739
Evaluation of CDMA system capacity for mobile satellite system applications 19 p2651 N88-25740
Considerations for spacecraft design for MSAT
19 p2651 N88-25741
Antenna system for MSAT mission
19 p2651 N88-25742
Antenna technology for advanced mobile communication systems 19 p2651 N88-25743
Frequency addressable beams for land mobile communications 19 p2652 N88-25744
Large antenna experiments aboard the space shuttle: Application of nonuniform sampling techniques
19 p2652 N88-25745
A microstrip array feed for MSAT spacecraft reflector antenna 19 p2652 N88-25747
Technologies for antenna shape and vibration control
19 p2652 N88-25748
Real-time speech encoding based on Code-Excited Linear Prediction (CELP) 19 p2653 N88-25751
Mobile satellite communications in the Forest Service
19 p2654 N88-25757
Mobile satellite service in the United States
19 p2654 N88-25758
EXSAT: Expert system to configure telecommunication satellites
[SNIAS-881-440-101] 21 p2902 N88-27223
Utilization of a satellite communication system to protect the national communication network
[FUB-33-1986] 21 p2934 N88-27423
PSDE/SAT 2: Preliminary spacecraft configuration study, executive summary
[ESA-CR(P)-2618] 24 p3333 N88-29840
Comparative analysis of passive communications satellites employing the SHF and HF spectrum for use in a strategic role
[AD-A194682] 24 p3362 N88-30019

COMMUNICATION SYSTEMS
U TELECOMMUNICATION

COMMUNICATION THEORY
NT SYLLABLES
NT WORDS (LANGUAGE)
Embedded expert system for space shuttle main engine maintenance 08 p1058 N88-16382
The use and generation of illustrative examples in computer-based instructional systems
08 p1060 N88-16400
Intelligent man/machine interfaces on the space station 08 p1063 N88-16418
Interfacing the expert: Characteristics and requirements for the user interface in expert systems
08 p1063 N88-16419
Space languages 08 p1063 N88-16420
Activities report of the Department of Systems and Communications
[ENST-87D004] 16 p2189 N88-23053
DAISY-DAMP: A distributed AI system for the dynamic allocation and management of power
23 p3254 N88-29373

COMMUNITIES
Remote sensing techniques applied to the study of metropolitan regions: The west sector of the Sao Paulo metropolitan area 19 p2681 N88-25941

COMMUTATION
Determination of the commutation and angle and load response for a continuous-current, single phase controlled rectifier
[AD-A190602] 15 p2060 N88-22285
Reduced order modeling of grid-connected photovoltaic inverter systems
[DE88-010603] 21 p2969 N88-27635

COMMUTATORS
Study on the dynamics of executive electromechanism with thyristor commutator for cryogenic systems
[DE87-703209] 12 p1622 N88-19702

Loss evaluation of self-commutated power conditioner for battery energy storage system
[DE88-752075] 20 p2794 N88-26575

COMMUTER AIRCRAFT
U GENERAL AVIATION AIRCRAFT
U PASSENGER AIRCRAFT

COMPACT DISK READ-ONLY MEMORY DEVICES
U OPTICAL DISKS
U READ-ONLY MEMORY DEVICES

COMPACTING
Physics and chemistry of packing fine ceramic powders
[DE87-013709] 01 p0029 N88-10183
Effects of cure pressure on resin flow, voids, and mechanical properties
[AD-A184267] 03 p0295 N88-11853
A note on compactifications of products of semigroups
[CWI-PM-R8701] 08 p1072 N88-16469
Dynamic consolidation of metal powders
[AD-A192126] 18 p2485 N88-24744
Sintering of the heterogeneous MgO compacts
[DE88-010357] 20 p2767 N88-26408
Superconductor consolidation
[DE88-010938] 21 p3024 N88-27949

COMPACTNESS
U VOID RATIO

COMPANION STARS
NT NEMESIS (STAR)

COMPARATOR CIRCUITS
Timing for subnanosecond pulses
[DE88-701390] 16 p2192 N88-23074

COMPARATORS
Multi-channel communications system analyzer
[AD-A184756] 03 p0307 N88-11937
An electrostatic potential comparator
[AD-A192051] 18 p2557 N88-25177
Measurement of the thermal conductivity of dielectric thin solid films with a thermal comparator
[DE88-008468] 21 p3016 N88-27898

COMPARISON
Problem specifications and collated solutions of the two-phase numerical-benchmark exercise 1986-7 -- two phase flow
[CFDU/87/1] 01 p0047 N88-10300
Modeling of human judgement in multicriteria analysis using pairwise comparison
[REPT-87-01] 01 p0076 N88-10484
Comparison of measured temperatures, thermal stresses and creep residues with predictions on a built-up titanium structure
[NASA-TM-86814] 03 p0337 N88-12125
Glassy GeO2 obtained by the gel process
[NASA-TT-20125] 06 p0685 N88-14201
Calculations of the turbulent wake behind a slender self-propelled double-body and comparisons with experiment
[AD-A185661] 06 p0703 N88-14314
Summary of comparison between experimental and analytical (including empirical) results for initiation of crack growth for surface cracks
[DE88-001604] 06 p0721 N88-14433
Some performance comparisons for a fluid dynamics code
[PB88-113709] 07 p0852 N88-15175
A comparison of experimental and theoretical results for labyrinth gas seals with honeycomb stators
[NASA-CR-182441] 08 p0993 N88-16006
A performance comparison of the Cray-2 and the Cray X-MP
[NASA-CR-177461] 09 p1216 N88-17288
Evaluating software testing methods to reduce testing duplication in US Army communications equipment acquisition
[AD-A186961] 09 p1216 N88-17292
A comparison of fitting techniques for the cumulative average learning curves with historical lot cost data
[AD-A187127] 09 p1227 N88-17349
Supercomputer performance: The theory, practice, and results
[DE88-004697] 10 p1384 N88-18266
Parallels between control PDE's (Partial Differential Equations) and systems of ODE's (Ordinary Differential Equations)
[NASA-CR-182487] 10 p1398 N88-18331
A comparison of projection methods in the forecasting of overhead costs for seven government aerospace contractors
[AD-A187572] 10 p1425 N88-18514
A comparative assessment of US and UK explosives qualified as replacements for tetryl
[MRL-R-1094] 13 p1754 N88-20486
A comparison of terrain association and resection as methods of position location
[AD-A189480] 13 p1790 N88-20710
Stochastic comparisons of order statistics, with applications in reliability
[AD-A189408] 13 p1829 N88-20938
Comparison of pressure distributions on model and full-scale NACA 64-621 airfoils with ailerons for wind turbine application
[NASA-TM-100802] 14 p1943 N88-21593
Stellar scintillometer atmospheric optical turbulence profiling experiment: A qualitative comparison of two identical instruments at AMOS (Air Force Maui Optical Station), 1985
[AD-A190589] 15 p2094 N88-22479
Comparative analysis of multistage interconnection networks
[AD-A190436] 15 p2115 N88-22598
Groundwater sapping valleys: Experimental studies, geological controls and implications to the interpretation of valley networks on Mars
[NASA-CR-182718] 15 p2152 N88-22847
Qualification of a water tunnel for force measurements on aeronautical models 16 p2200 N88-23128
A comparative study of vortex flows in wind and water tunnels 16 p2204 N88-23151
Investigation on the movement of vortex burst position with dynamically changing angle of attack for a schematic deltawing in a watertunnel with correlation to similar studies in windtunnel 16 p2204 N88-23152
A description of an automated database comparison program
[NASA-TM-100609] 16 p2253 N88-23463
Comparison of a direct thrust nuclear engine, nuclear electric engine and a chemical engine for future space missions 17 p2418 N88-24379
Space station habitability recommendations based on a systematic comparative analysis of analogous conditions
[NASA-CR-3943] 18 p2587 N88-25372
Five-point form of the nodal diffusion method and comparison with finite-difference
[DE88-004141] 19 p2720 N88-26154
The influence of uncompensated solution resistance on the determination and standard electrochemical rate constants using cyclic voltammetry and some comparisons with AC voltammetry
[AD-A192825] 20 p2770 N88-26427
Comparison theorems and their use in the analysis of some nonlinear diffusion problems
[DE88-010032] 20 p2845 N88-26884
A comparison of generators for pseudo-random normal deviates
[DE88-011711] 21 p3010 N88-27859
Comparison of the bidirectional reflectance distribution function of various surfaces
[NASA-TM-101317] 22 p3153 N88-28760
Regional intercomparisons of General Circulation Model predictions and historical climate data: CO2
[DE88-010416] 23 p3235 N88-29248
A model for architectural comparison
[AD-A195993] 24 p3411 N88-30302
Design and performance analysis of a relational replicated database system
[AD-A196290] 24 p3437 N88-30456
Plasma of earth's magnetosphere ring currents. Model compared with results of AMPTE/CCE experiment
24 p3447 N88-30515

COMPARTMENTATION
U COMPARTMENTS

COMPARTMENTS
NT AIR LOCKS
NT AIRCRAFT COMPARTMENTS
NT ANECHOIC CHAMBERS
NT COMMAND MODULES
NT HYPERBARIC CHAMBERS
NT PRESSURE CHAMBERS
NT PRESSURIZED CABINS
NT REVERBERATION CHAMBERS
NT SPACECRAFT CABINS
NT TEST CHAMBERS
NT VACUUM CHAMBERS
Cryogenic cell --- neutron borehole logging
[GB-PATENT-2-139-745-A] 01 p0048 N88-10308

COMPATIBILITY
NT ELECTROMAGNETIC COMPATIBILITY
NT SYSTEMS COMPATIBILITY
Compatability of dispersion-strengthened platinum with resistojet propellants
[NASA-TP-2765] 04 p0409 N88-12538
Compatibility of explosives: A data base system
[PB87-234464] 06 p0687 N88-14208
Geographic application of the relational data base system Cantor
[PB87-120945] 06 p0791 N88-14851
Resources, confusions and compatibility in dual axis tracking: Displays, controls and dynamics
[AD-A185871] 07 p0898 N88-15440
Microgravity payloads and missions for Space Station: Some issues affecting compatibility with other payloads
09 p1129 N88-16783
Microgravity experiments in space: Compatibility with dynamic perturbing effects 09 p1241 N88-17435
High-temperature thermosets derived from the Diels-Alder polymerization of bisbenzocyclobutenes and bimaleimides
[AD-A188800] 13 p1747 N88-20449
Compatibility in space reactor fuel systems
[DE88-005698] 13 p1839 N88-21004
The PC/AT compatible computer as a mission control center display processor at Ames-Dryden Flight Research Facility
[NASA-TM-100426] 14 p1955 N88-21654
Chemical compatibility between silicon carbide and a nickel aluminide
[DE88-006188] 18 p2479 N88-24708
A compatible encapsulant for explosives
[DE88-007212] 18 p2495 N88-24806
Sulfur-tolerant anode materials
[DE88-001034] 18 p2537 N88-25054
Improved method for stress and compatibility analysis of multicomponent rotating systems
[NASA-TM-100884] 19 p2680 N88-25935
A fundamental understanding of the interfacial compatibility in hybrid material systems
[AD-A192921] 21 p2909 N88-27264
Capitalizing on experience with intelligence gateway software
[AD-A193362] 21 p3028 N88-27971

COMPENSATION
Polynomial compensation, inversion, and approximation of discrete time linear systems
[NASA-TM-100027] 03 p0372 N88-12344
Transport delay compensation for computer-generated imagery systems
[NASA-TM-100084] 10 p1277 N88-17645
Covariance analysis and post-processing of gravity compensation effects for aided multi-state navigation systems
[PAPER-87-13] 12 p1577 N88-19430
Case study of active array feed compensation with sidelobe control for reflector surface distortion
[NASA-TM-100287] 16 p2192 N88-23073

COMPENSATORS
Pinhole occulter experiment
[NASA-CR-179206] 02 p0235 N88-11481
Defect characterization in quartz and related materials
[AD-A184754] 03 p0294 N88-11846
Investigation, development, and application of optimal output feedback theory. Volume 3: The relationship between dynamic compensators and observers and Kalman filters
[NASA-CR-4107] 05 p0638 N88-13900
Design of a velocity and position control laboratory servo system
[AD-A186596] 08 p0990 N88-15997
A Prohorov bound for a Poisson process and a Bernoulli process
[CWI-MS-R8701] 09 p1232 N88-17388
Analysis and synthesis of two degrees of freedom control systems 11 p1495 N88-18928
Modelling of a hydraulic motor and servo-valve to produce a desired system response using analogue and digital compensation techniques
[ETN-88-92079] 14 p1899 N88-21337
Time-Optimal Adaptive Shaped Torque (TOAST) technical note
[AD-A192719] 20 p2843 N88-26869

COMPENSATORY TRACKING
Resources, confusions and compatibility in dual axis tracking: Displays, controls and dynamics
[AD-A185871] 07 p0898 N88-15440

COMPETITION
Space station: Leadership for the future
[NASA-PAM-509/8-87] 01 p0013 N88-10072
A role for national laboratories in enhancing economic competitiveness. The example of high-temperature superconductors: CNSS papers, No. 1
[DE87-013633] 03 p0379 N88-12386
New theory for competing interactions and microstructures in partially-ordered (liquid-crystalline) phases
[DE87-014739] 03 p0380 N88-12389
Competition Analysis Model (CAM). Volume 2: Computer manual
[AD-A184017] 03 p0384 N88-12411
Competing interactions in metallic superlattices
[DE88-005344] 13 p1847 N88-21057
Competition: Issued on establishing and using Federally funded research and development centers
[PB88-178884] 23 p3296 N88-29632

COMPILATION (COMPUTERS)
U COMPILERS

COMPILER PROGRAMS
U COMPILERS
COMPILERS
FORTRAN compiler performance benchmarks for the IBM personal computer
[LA-10883-MS] 03 p0363 N88-12284
Mixing Microsoft C and Microsoft FORTRAN program modules on the IBM Personal Computer
[DE88-001947] 05 p0637 N88-13895
Technology upgrade of a silicon compiler
[AD-A184873] 05 p0655 N88-14016
Microprocessor emulating the intermediate code for FORTRAN compiler
[DE88-700540] 07 p0900 N88-15452
Program translation via abstraction and reimplementation
[AD-A185845] 07 p0901 N88-15456
Version description document for the Ada compiler validation capability (version 1.9) (for microcomputer)
[AD-A186390] 07 p0903 N88-15471
Ada (trade name) compiler validation summary report. Systems designers' PLC SD Ada-plus VAX/VMS x MC68020. Version 2B.00. Host: VAX 8600. Target: Motorola MC68020. Completion of on-site testing
[AD-A186571] 08 p1053 N88-16356
The Ada compiler: On the design and implementation of an Ada compiler
[ETN-88-91594] 09 p1215 N88-17284
Types and effects towards the integration of functional and imperative programming
[AD-A186930] 09 p1216 N88-17290
Rationale for the design of the Ada (tradename) programming language
[AD-A187106] 09 p1217 N88-17297
Description of a limited VAX-Ada program support environment developed within UDP division version 1.0
[ARE-TM(UDP)-87103] 09 p1219 N88-17308
Programming language translation for multicomputers
10 p1381 N88-18244
Design for a TPL complier system: A system for retargeting high level language programs
10 p1381 N88-18248
Factors causing unexpected variations in Ada benchmarks
[AD-A187231] 10 p1388 N88-18291
Loop coalescing: A compiler transformation for parallel machines
[DE88-003571] 10 p1392 N88-18307
Performance and evaluation at the Center for Supercomputing Research and Development
[DE88-003563] 10 p1417 N88-18456
Efficient instruction level simulation of computers
[AD-A187821] 11 p1529 N88-19130
Applicability of Ada (trademark) tasking for avionics executives
[AD-A188827] 12 p1578 N88-19445
Automatic restructuring of FORTRAN programs for parallel execution
[DE88-003585] 12 p1676 N88-20018
Building software systems economically with mechanized logic: Initial design proposal
[AD-A188791] 12 p1678 N88-20031
Higher levels of a silicon compiler
[EUT-86-E-163] 14 p1955 N88-21650
Iteration of transformation passes over attributed program trees --- compilers
[INF-87-28] 14 p1956 N88-21661
Ada tasking in Ten15
[RSRE-MEMO-4074] 14 p1958 N88-21676
Examination of the effects of using Ada (trade name) in flight control software
[AD-A189679] 14 p1959 N88-21683
Ada (Trademark) compiler validation summary report. ALSYS: AlsyCOMP-013, V2.0 HOST: IBM PC AT. Target: IBM 370 3084Q
[AD-A189640] 15 p2106 N88-22546
ONTIC: A knowledge representation system for mathematics
[AD-A190553] 15 p2121 N88-22643
Automatic layout generation of data processing sections of VLSI microprocessor-like circuits
[ETN-88-92185] 16 p2245 N88-23411
Silicon compilers: Application to the compilation of the control area
[ETN-88-92188] 16 p2247 N88-23425
A timing evaluator for C programs generated by the model system
[AD-A191204] 17 p2385 N88-24174
EPL (Equational Programing Language) system design: Intermediate processing steps
[AD-A191203] 18 p2556 N88-25169
Nebula support software
[AD-A192281] 20 p2837 N88-26833
Programmer-friendly LL(1) parser generator
[PB88-126933] 20 p2841 N88-26857
Ada (trade name) compiler validation summary report: Verdix Corporation VAda-010-03315, version 5.5 MicroVAX 2 host ISBC 386/20P Intel target
[AD-A193226] 21 p2997 N88-27774
Ada (trade name) compiler validation summary report: Verdix corporation VAda-010-13125, version 5.41 Sun Microsystems Sun-3/160 host microbar GPC68020 target
[AD-A193415] 21 p2997 N88-27777
Configuration control in compiler construction
[AD-A193916] 22 p3135 N88-28639
Ada (trade name) compiler validation summary report: Verdix Corporation VAda-010-0101, version 5.41 VAX-11/750
[AD-A193414] 22 p3136 N88-28645
Subset-logic programming: Application and implementation
[AD-A193647] 22 p3138 N88-28655
Modularity in the PASCAL model compiler
[NPL-DITC-111/88] 22 p3139 N88-28664
Loglisp programming system users manual
[AD-A193933] 22 p3142 N88-28682
The SMITE modular compilation system
[RSRE-MEMO-4145] 23 p3244 N88-29307
Ada (trade name) compiler validation summary report: Verdix Corporatiun VAda-010-03205, version 5.42 MicroVAX 2 host and national DB32000 (NS32032 target
[AD-A193485] 23 p3247 N88-29326
A computer program package for introductory one-dimensional digital signal processing applications
[AD-A194656] 23 p3249 N88-29338
COMPLEMENTARY METAL OXIDE SEMICONDUCTORS
U CMOS
COMPLEMENTS (MATHEMATICS)
On serial-input multipliers for two-complement numbers
[REPT-86-035] 11 p1536 N88-19181
COMPLETENESS
Introduction to logic programming
[CWI-CS-R8741] 16 p2248 N88-23430
COMPLEX COMPOUNDS
Topological aspects of infinite metal clusters and superconductors
[AD-A184104] 04 p0495 N88-13049
An investigation of metal complexes of some 2-substituted and 2,6-disubstituted pyridine N-oxides
11 p1460 N88-18701
The structure of the boron-hydrogen complex in silicon
[DE88-005433] 15 p2144 N88-22795
Synthesis and properties of novel cluster phases
[DE88-006816] 16 p2175 N88-22964
Catalytic activation of carbon dioxide by metal complexes
[AD-A192310] 21 p2909 N88-27262
Structure and function of the manganese complex involved in photosynthetic oxygen evolution determined by X-ray adsorption spectroscopy and electron paramagnetic resonance spectroscopy
[DE88-010360] 21 p2985 N88-27725
Functional study of the Si/SiO2 structures Application to the implementation of an integrated ion sensor
[ECL-87-16] 22 p3073 N88-28246
Charge storage and switching phenomena in metal complexes
[AD-A193778] 23 p3192 N88-28996
Polymeric electrolytes
[AD-A193766] 23 p3198 N88-29031
COMPLEX SYSTEMS
Implementation and performance of a complex vision system on a systolic array machine
[AD-A184331] 04 p0482 N88-12971
Pattern-recognition software detecting the onset of failures in complex systems
[DE88-002861] 09 p1220 N88-17318
On the sensitivity of complex, internally coupled systems
[NASA-TM-100537] 13 p1813 N88-20829
KOMPOT Program complex for the calculation of spatial magnetostatic fields of electromagnetic systems
[DE88-701691] 16 p2192 N88-23072
Matched index laser anemometry systems for flow studies in complex geometries 16 p2203 N88-23145
A new block solver for large, full, unsymmetric, complex systems of linear algebraic equations
[AD-A190590] 16 p2256 N88-23483
Systems engineering technique
17 p2303 N88-23776
Accurate multigrid solution of the Euler equations on unstructured and adaptive meshes
[NASA-CR-181679] 18 p2460 N88-24608
Application of advanced grid generation techniques for flow field computations about complex configurations
[NASA-CR-183049] 18 p2515 N88-24922
Human problem solving in complex dynamic environments
[AD-A190788] 18 p2551 N88-25142
COMPLEX VARIABLES
NT ANALYTIC FUNCTIONS
NT BESSEL FUNCTIONS
NT CAUCHY INTEGRAL FORMULA
NT CONFORMAL MAPPING
NT ELLIPTIC FUNCTIONS
NT ENTIRE FUNCTIONS
NT EXPONENTIAL FUNCTIONS
NT HANKEL FUNCTIONS
NT HYPERBOLIC FUNCTIONS
NT HYPERGEOMETRIC FUNCTIONS
NT LAGUERRE FUNCTIONS
NT LIOUVILLE THEOREM
NT LOGARITHMS
NT MEROMORPHIC FUNCTIONS
NT ORTHOGONAL FUNCTIONS
NT SINGULARITY (MATHEMATICS)
NT SPHERICAL HARMONICS
Polynomials with restricted coefficients and their applications
[AD-A192589] 23 p3202 N88-29055
COMPLEXITY
NT TASK COMPLEXITY
Weighted decoding of block codes and some topics on decoding complexity
[ENST-87E005] 02 p0221 N88-11394
Diagonalisation methods in polynomial setting
[PB87-138616] 06 p0769 N88-14726
Machine models and simulations
[PB88-118690] 10 p1386 N88-18280
COMPLIANCE (ELASTICITY)
U MODULUS OF ELASTICITY
COMPLICATION
U COMPLEXITY
COMPONENT RELIABILITY
Fracture mechanism of fine grain graphite under high heat fluxes
[IPPJ-842] 02 p0242 N88-11527
The Shock and Vibration Digest, Volume 19, No. 11
03 p0265 N88-11673
The Shock and Vibration Digest, Volume 19, No. 10
03 p0335 N88-12112
PRAAGE: An interactive IBM-PC code for unreliability/aging analysis
[DE87-012124] 04 p0453 N88-12803
Extremum methods of structural analysis for system reliability assessment 04 p0456 N88-12824
Conservatism implications of shock test tailoring for multiple design environments 05 p0592 N88-13611
Small space reactor power systems for unmanned solar system exploration missions
[NASA-TM-100228] 05 p0660 N88-14054
Estimating system reliability: Monte Carlo methods, sensitivity and errors in input parameters
[AD-A186182] 07 p0865 N88-15248
How errors in component reliability affect system reliability
[AD-A186264] 07 p0865 N88-15249
Small engine technology programs
08 p0956 N88-15801
Results of NASA/Army transmission research
09 p1108 N88-16640
Ceramics for engines 09 p1119 N88-16704
A strategy for failure prediction
10 p1380 N88-18243
Design and dynamic testing of an instrumented spacecraft component 11 p1499 N88-18952
Random vibration (stress screening) of printed wiring assemblies 11 p1499 N88-18953
Optimal arrangement of components via pairwise rearrangements
[AD-A187633] 11 p1541 N88-19213
A computer code for the solution of large scale network reliability analysis problems
[AD-A188455] 12 p1680 N88-20042
Estimating system and component reliabilities under partial information on cause of failure
[AD-A189107] 13 p1780 N88-20653
Power components for the space station 20-kHz power distribution system
[NASA-TM-100866] 14 p1904 N88-21374
On the danger of redundancies in some aerospace mechanisms 14 p1925 N88-21475
Monolithic ceramic analysis using the SCARE program
15 p2081 N88-22409
Continuous fiber ceramic matrix composites for heat engine components 15 p2082 N88-22411
Cumulative fatigue damage models
15 p2084 N88-22422
Life and reliability of rotating disks
15 p2085 N88-22428

Incorporating reliability into the design of experimental fusion facilities
[DE88-006767] 16 p2275 N88-23618

Pioneer 10 and 11 RTG performance update
17 p2405 N88-24301

Dynamic isotope power system critical component verification 17 p2425 N88-24421

Small scale bipolar nickel-hydrogen testing
[NASA-TM-100936] 18 p2538 N88-25059

Determining system maintainability as a probability
[DE88-007722] 19 p2679 N88-25927

Probabilistic structural analysis to quantify uncertainties associated with turbopump blades
[NASA-TM-100278] 22 p3050 N88-28094

An application of the Bayesian method to the estimation and forecast of system hardware components MTBF
22 p3068 N88-28211

COMPONENTS

Commonality analysis as a knowledge acquisition problem 08 p1062 N88-16413

Vapor Compression Distillation Subsystem (VCDS) component enhancement, testing and expert fault diagnostics development, volume 2
[NASA-CR-172076] 21 p2994 N88-27755

Development of sensors for ceramic components in advanced propulsion systems: Survey and evaluation of measurement techniques for temperature, strain and heat flux for ceramic components in advanced propulsion systems
[NASA-CR-182111] 22 p3081 N88-28299

COMPOSITE MATERIALS

NT ALUMINUM BORON COMPOSITES
NT ALUMINUM GRAPHITE COMPOSITES
NT BORON REINFORCED MATERIALS
NT BORON-EPOXY COMPOSITES
NT CARBON FIBER REINFORCED PLASTICS
NT CARBON-CARBON COMPOSITES
NT CERAMIC MATRIX COMPOSITES
NT CERMETS
NT COMPOSITE PROPELLANTS
NT EPOXY MATRIX COMPOSITES
NT EUTECTIC COMPOSITES
NT FIBER COMPOSITES
NT GLASS FIBER REINFORCED PLASTICS
NT GRAPHITE-EPOXY COMPOSITES
NT GRAPHITE-POLYIMIDE COMPOSITES
NT LAMINATES
NT METAL MATRIX COMPOSITES
NT POLYMER MATRIX COMPOSITES
NT REINFORCED PLASTICS
NT RESIN MATRIX COMPOSITES
NT THREE DIMENSIONAL COMPOSITES
NT WHISKER COMPOSITES

Structures and Materials Working Group report
01 p0016 N88-10093

Ceramic-Ceramic Composites Meeting in Belgium
[ONRL-7-020-R] 01 p0019 N88-10118

Mechanical properties characterization of composite sandwich materials intended for space antenna applications
[NASA-TM-88893] 01 p0020 N88-10121

Ceramic composites by chemical vapor infiltration
[DE87-009128] 01 p0029 N88-10185

Anti-abrasion protection with highly organized materials
[DE87-014238] 01 p0029 N88-10187

Composite bearing materials containing solid lubricant in filamentary form, stages 3 and 4
[IRD-87/2] 01 p0054 N88-10344

An experimental and theoretical study of the bending behavior of Kevlar 49/epoxy beams and rings
[DE87-010430] 01 p0061 N88-10394

Contribution to the study of composite materials and their damage
[NASA-TT-20107] 02 p0143 N88-10897

Damping characteristics of a composite-reinforced stainless-steel tube
[DE87-012455] 02 p0191 N88-11192

Energy changes in transforming solids
[DE87-011257] 02 p0191 N88-11194

Composite materials in western Europe
[PB87-102943] 03 p0279 N88-11759

Effects of solvent exposures on poly(etheretherketone) (PEEK) and PEEK-fiberglass composites
[MLM-3405] 03 p0281 N88-11766

JPRS report: Science and technology. USSR: Materials science
[JPRS-UMS-87-006] 03 p0285 N88-11791

GSSR powder metallurgy research, production expanding 03 p0286 N88-11797

Joining of silicon carbide reinforced ceramics
[DE87-014881] 03 p0294 N88-11847

Fabrication and testing of fire resistant graphite composite panels
[NASA-CR-177397] 04 p0397 N88-12472

JPRS report: Science and technology. Japan
[JPRS-JST-87-025] 04 p0403 N88-12502

Activities at government research laboratories reported 04 p0403 N88-12503

Carbon-fiber reinforced aluminum
04 p0403 N88-12507

Failure analysis of composite structure materials
[AD-A184468] 04 p0410 N88-12548

Composite mechanics for engine structures
[NASA-TM-100176] 04 p0411 N88-12552

A creep measurement of unidirectional epoxy-fiberglass rod
[DE87-014812] 04 p0411 N88-12553

Thermoplastic elastomers as LOVA (Low Vulnerability Ammunition) binders
[AD-A184350] 04 p0419 N88-12599

Work-in-progress presented at the Army Symposium on Solid Mechanics, 1986: Lightening of the Force
[AD-A184791] 04 p0427 N88-12644

Composite materials applications program at the US Army Ballistic Research Laboratory: Work in progress
04 p0428 N88-12651

Damping characteristics of a composite-reinforced stainless-steel plate
[DE88-000303] 04 p0457 N88-12828

Materials for fighter aircraft 05 p0546 N88-13325

Fabrication of composites by chemical vapor deposition
[DE87-014565] 05 p0559 N88-13408

Bending of a bonded beam as a test method for adhesive properties
[AD-A184813] 05 p0609 N88-13736

Damping analysis of flexural waves in fluid-loaded single and constrained plates
[AD-A185116] 05 p0609 N88-13739

An element of a multilayer shell for the computation of composite structures
[ONERA-RT-14/3542-RY-051-R]
05 p0610 N88-13742

Development of an impact- and solvent-resistant thermoplastic composite matrix, phase 4
[NASA-CR-178413] 06 p0677 N88-14145

Behavior of bolted joints in composite laminates
06 p0677 N88-14148

Sintering and densification of particulate composites: Inclusion size and clustering
[DE88-002230] 06 p0685 N88-14199

Exploitation of the sol-gel route in processing of ceramics and composites
[AD-A185482] 06 p0686 N88-14204

Characterization of mechanical damage mechanisms in ceramic composite materials
[AD-A185549] 06 p0686 N88-14205

Interface effects on the mechanical properties of ceramic composites
[AD-A185899] 07 p0826 N88-15009

Composite reliability enhancement via preloading
[AD-A185938] 07 p0826 N88-15010

Characterization of microstructure in metallic and composite materials
[AD-A186193] 07 p0826 N88-15012

Simplified procedures for designing composite bolted joints
[NASA-TM-100281] 07 p0828 N88-15020

Thermoplastic elastomers as LOVA binders
[AD-A185864] 07 p0835 N88-15067

Thermoplastic elastomers as LOVA binders
[AD-A185865] 07 p0835 N88-15068

Contribution to modeling flexion fatigue damage in unidirectional composite materials
[ECL-87-12] 08 p0965 N88-15843

Nondestructive characterization of ceramic composite whiskers with neutron diffraction and ultrasonic techniques
[DE88-003075] 08 p0965 N88-15844

Transparent metal model study of the use of a cellular growth front to form aligned monotectic composite materials
[NASA-CR-182414] 08 p0969 N88-15861

Composite/metal jointing technology for vehicle weight reduction
[DE88-900228] 08 p0992 N88-16005

Failure modes of laminate structures
[DE88-002579] 08 p0996 N88-16033

Advanced composite airframe program: Today's technology 09 p1107 N88-16636

Recent Sikorsky R and D progress
09 p1111 N88-16659

Review of thermal properties of graphite composite materials
[NASA-TM-100049] 09 p1139 N88-16825

Finite element analysis of damaged cross-ply composite laminates
[CCMS-87-10] 09 p1139 N88-16829

Residual stiffness and strength of Kevlar/epoxy laminated impulsively loaded to 7.9 ktaps
[DE88-003724] 09 p1149 N88-16886

Automated Composites, First International Conference, September 10-12, 1986, University of Nottingham, England
[PB87-126199] 10 p1294 N88-17734

Composite materials for rail transit systems
[NASA-CR-178401] 10 p1294 N88-17738

Short fiber reinforced thermoplastic composites for armor applications: Interfacial bonding
[DE88-004007] 10 p1295 N88-17742

A finite element analysis of adhesively bonded composite joints including geometric nonlinearity, nonlinear viscoelasticity moisture diffusion and delayed failure
[AD-A187455] 10 p1296 N88-17747

The analysis of deformations and strains in composites by moire interferometry
[AD-A187482] 10 p1345 N88-18043

Ultrasonic characterization of layered composite systems 10 p1404 N88-18374

The effect of magnetic impurities and barriers on the magnetization and critical current of fine filament NbTi composites
[DE88-004443] 10 p1419 N88-18472

Quantitative non-destructive evaluation of porous composite materials based on ultrasonic wave propagation
[NASA-CR-182544] 11 p1447 N88-18627

High performance composites research at NASA-Langley
[NASA-TM-100518] 11 p1450 N88-18642

Analysis of composite laminates with matrix cracks
[CCMS-88-03] 11 p1451 N88-18645

Creep behavior of tungsten/niobium and tungsten/niobium-1 percent zirconium composites
[NASA-TM-100804] 11 p1460 N88-18707

Application of X-ray computed tomography to ceramic/ceramic composites
[DE88-002903] 11 p1464 N88-18728

Nucleation and growth of calcium carbonate crystals on surface-modified polyethylene and polystyrene
[DE88-005126] 11 p1465 N88-18733

Slip casting of advanced ceramics and composites
[DE88-003424] 11 p1467 N88-18746

The place for thermoplastic composites in structural components
[AD-A189149] 12 p1604 N88-19596

Experimental and analytical investigation on a proposed embedded fiber optic displacement sensor
[AD-A189030] 12 p1630 N88-19756

Comparison of ultrasonic flaw detection analysis for spherical composite test specimens using two data acquisition techniques
[DE88-005002] 12 p1634 N88-19782

The Shock and Vibration Digest, volume 20, no. 3
12 p1635 N88-19786

A continuum damage model for viscoelastic materials
[AD-A189426] 12 p1637 N88-19800

Compression of composite materials: A review
[AD-A189272] 13 p1734 N88-20365

Phase velocity and attenuation of plane elastic waves in a particle-reinforced composite medium
[AD-A189414] 13 p1734 N88-20366

The influence of the fiber-matrix bond on the mechanical behavior of NICALON/SiC composites
[DE88-006155] 13 p1734 N88-20369

Delamination stresses in semicircular laminated composite bars
[NASA-TM-4026] 13 p1735 N88-20375

The effect of $Ca(OH)_2$-treated ceramic microspheres on the mechanical properties of high-temperature lightweight cement composites
[DE88-004590] 13 p1749 N88-20457

PNL-1 improved ceramic composites through controlled fiber matrix interaction
[DE88-005680] 13 p1750 N88-20462

Micromechanical and microstructural studies of ceramic superplasticity
[DE88-005793] 13 p1751 N88-20472

Theory and experiments of fracture in cyclic compression: Single phase ceramics, transforming ceramics and ceramic composites
[DE88-005792] 13 p1781 N88-20659

Activities report in aeronautics and astronautics
[ETN-88-91332] 13 p1859 N88-21115

Detection of bondline delaminations in multilayer structures with lossy components
[NASA-CR-182716] 14 p1883 N88-21256

JPRS report: Science and technology. USSR: Materials science
[JPRS-UMS-87-009] 14 p1884 N88-21261

Microprobe examination of composite materials produced by burning of Ti, Cr, C powders with powder of any one Fe-group metal 14 p1886 N88-21269

The unique characteristics of the structure of composite materials made on a base of sphalerite-analogous boron nitride
14 p1886 N88-21273

JPRS report: Science and technology. USSR: Materials science
[JPRS-UMS-87-007] 14 p1895 N88-21312

Phenomenological piercing characteristics of composite materials
14 p1895 N88-21315

Mathematical stress analysis of composite materials
14 p1900 N88-21349

Cement paste matrix composite materials center
[AD-A188657] 15 p2028 N88-22083

The combustion synthesis of bonde composites
[DE88-005474] 15 p2028 N88-22084

Superplastic flow of mullite-zirconia composites
[DE88-005905] 15 p2028 N88-22085

Microplasticity phenomena in graphite/magnesium metal matrix composites
[DE88-006772] 15 p2029 N88-22086

Structure and surface characterizations of high strength carbon fibers
[AD-A189642] 15 p2029 N88-22087

An investigation of the failure response of laminates under biaxial stress
[AD-A190039] 15 p2029 N88-22090

A study of damage tolerance in curved composite panels
[AD-A190617] 15 p2029 N88-22092

Microwave sintering of alumina-SiC composites at 2.45 and 60 GHz
[DE88-006455] 15 p2030 N88-22095

Interlaminar fracture toughness of thermoplastic composites
[NASA-TM-100532] 15 p2030 N88-22097

Application of copper-carbon fiber composites to power semiconductor devices
[NASA-TT-20171] 15 p2031 N88-22101

Mechanical behaviour of particle filled thermoplastics
[PB88-169297] 15 p2047 N88-22196

Eddy current nondestructive inspection of graphite epoxy using ferrite cup core probes
[AD-A189823] 15 p2074 N88-22365

Biaxial experiments supporting the development of constitutive theories for advanced high-temperature materials
15 p2078 N88-22386

Structural analyses of engine wall cooling concepts and materials
15 p2081 N88-22405

Ultrasonic beam distortion in transversely isotropic media
[DE88-005937] 15 p2129 N88-22699

Towards a damage tolerance philosophy for composite materials and structures
[NASA-TM-100548] 16 p2173 N88-22949

A piecewise quadratic strength tensor theory for composites
[AD-A190929] 16 p2173 N88-22952

Nondestructive evaluation of large scale composite components
[AD-A190998] 16 p2173 N88-22954

New method of grafting crystals
16 p2180 N88-22992

Investigation of non-linear optical behavior of semiconductors for optical switching, volume 1
[AD-A191297] 16 p2274 N88-23611

Strain intensity factor approach for predicting the strength of continuously reinforced metal matrix composites
[NASA-TM-100617] 17 p2317 N88-23838

Local buckling and crippling of composite stiffener sections
[NASA-TM-101133] 17 p2317 N88-23840

Cryogenic regenerator including saran-carbon heat conduction matrix
[NASA-CASE-NPO-17291-1-CU]
17 p2337 N88-23946

Mixed-mode fracture of uniaxial fiber reinforced composites
[AD-A191629] 18 p2478 N88-24700

Interfacial shear phenomena in graphite epoxy composites under impact loading using dynamic moire interferometry
[DE88-006773] 18 p2479 N88-24709

Functional and mechanical analysis of continuous media-application to the study of elastic composites with periodic structure: Homogenization
[NASA-TT-20188] 18 p2480 N88-24710

The 700 F properties of autoclave cured PMR-2 composites
[NASA-TM-100923] 18 p2480 N88-24712

Status and prognosis for alternative engine materials
[NASA-TM-100903] 18 p2486 N88-24749

New polyisoimides An approach to in situ rigid-rod polyimide formation
[AD-A191665] 18 p2490 N88-24773

High strength/sigh modulus aromatic heterocyclic ABA block copolymers
[AD-A191666] 18 p2491 N88-24774

Nondestructive testing using ultrahigh frequencies
[CERT-5/1333-MO] 18 p2526 N88-24984

Improved structural polymer alloys and composites
[AD-A192092] 19 p2619 N88-25538

Fire retardant coatings for military equipment: A review
[MRL-R-1104] 19 p2619 N88-25540

Effect of a weak magnetic field on high temperature superconductivity in Y-Ba-Cu-O ceramics
[DE88-702192] 19 p2733 N88-26235

Instability-related delamination growth of embedded and edge delaminations 20 p2767 N88-26406

Interface modification in Nicalon (trademark)/SiC composites
[DE88-009708] 20 p2767 N88-26409

A micromechanics model of the stiffness and strength of laminates with fiber waviness
[NASA-CR-181670] 20 p2768 N88-26413

Observations on residual stresses in ceramic composites by neutron diffraction techniques
[DE88-009937] 20 p2778 N88-26472

Stress concentration around circular hole in a composite material specimen representative of the X-29A forward-swept wing aircraft
[NASA-CR-179435] 20 p2814 N88-26634

Boundary layer solutions for the free-edge problem in composite laminates 21 p2904 N88-27229

Thermo-viscoelastic analysis of composite materials, volume 1
[NASA-CR-183048-VOL-1] 21 p2904 N88-27230

Probabilistic anisotropic failure criteria for composite materials
[AD-A193046] 21 p2904 N88-27232

Analysis of transverse strength of composites using percolation theory
[AD-A193204] 21 p2904 N88-27234

Far- and mid-infrared properties of metal-insulator composite materials
[AD-A193227] 21 p2905 N88-27236

Polymer-ceramic composites
[AD-A193244] 21 p2905 N88-27237

Techniques for characterizing damage zones in composite materials 21 p2905 N88-27240

Characterization of elastic-plastic properties of AS4/APC-2 thermoplastic composite
[NASA-CR-183145] 21 p2906 N88-27242

Preparation and properties of new inorganic glasses and gel-derived solids
[AD-A192922] 21 p2917 N88-27315

Application of sol-gel procedures to ceramic composites
[ETN-88-92741] 21 p2921 N88-27338

Effects of applied stress and temperature on the nonlinear elastic properties of graphite fibers
[AD-A194469] 22 p3050 N88-28093

Durability of continuous fiber reinforced metal matrix composites
[AD-A193868] 22 p3050 N88-28097

Micromechanics of composite laminate compression failures
[NASA-CR-183179] 22 p3050 N88-28098

A transversely isotropic thermoelastic theory
[NASA-TM-101302] 22 p3087 N88-28332

Mixed finite element methods to compute stress in a load composite specimen with holes: Numerical results
[ONERA-RT-37/4242-RY-062-R]
22 p3088 N88-28336

Laboratory feasibility study of a composite embedded fiber optic sensor for measurement of structural vibrations
[AD-A194270] 22 p3152 N88-28754

Molecular composites processing and properties, 1
[AD-A194113] 23 p3189 N88-28974

Microwave frequency nondestructive control
[CERT-2/1355-MO] 23 p3189 N88-28976

Finite Element Composite Analysis Program (FECAP) for microcomputer
[NASA-TM-100670] 23 p3190 N88-28982

Creep of carbon yarn and carbon-carbon composites at high temperatures and high stresses
[AD-A195224] 24 p3340 N88-29878

An improved boundary force method for analyzing cracked anisotropic materials
[NASA-TM-101495] 24 p3340 N88-29879

ZT imaging system for layered thin wall structures
[AD-A195466] 24 p3352 N88-29954

Polymer-ceramic composites
[AD-A195789] 24 p3356 N88-29983

Piezoelectric and electrostrictive materials for transducer applications, volume 1
[AD-A194957] 24 p3374 N88-30096

Experimental aspects of using time-averaged holographic interferometry to detect barely visible impact damage in a graphite/epoxy composite plate
[AD-A194418] 24 p3375 N88-30097

Application of nondestructive testing techniques to materials testing
[AD-A195716] 24 p3381 N88-30138

An organometallic route to micron-sized whiskers of zinc sulfide
[AD-A195889] 24 p3430 N88-30414

COMPOSITE PROPELLANTS

A continuous oxidizer regression model for the combustion of composite solid propellants
[AD-A186742] 08 p0974 N88-15894

Laser ignition of nitramine composite propellants and crack propagation and branching in burning solid propellants
[AD-A189260] 13 p1753 N88-20483

Nonlinear mechanisms of solid propellant combustion instability 19 p2628 N88-25588

Selective radiation absorption in aluminized composite propellant combustion 19 p2630 N88-25598

Effect of burn-path tortuosity on the burn rate of composite propellants 19 p2630 N88-25602

Thermomechanical computations for GAP, a high energy binder for composite propellants
[FOA-C-20718-2.1] 24 p3357 N88-29988

COMPOSITE STRUCTURES

NT LAMINATES

Structures and Materials Working Group report
01 p0016 N88-10093

Compendium of post-failure analysis techniques for composite materials
[AD-A183783] 01 p0018 N88-10113

The analysis of moisture absorption in multi-layered media
[NPL-DMA(A)-147] 01 p0019 N88-10115

A mixed finite element method for the computation of stress in a composite with loaded holes
[ONERA-RT-34/4242-RY-054-R]
01 p0062 N88-10395

Models of degradation of stratified composite structures
[ONERA-RT-13/3542-RY-061-R]
02 p0142 N88-10892

Properties of Nb3Sn superconductor wires with composite cores
[KFK-4263] 02 p0246 N88-11557

Three-dimensional finite element based, interative approach for analysis of laminated composites
03 p0280 N88-11763

Durability (lifetime) predictions adhesively bonded structures
[AD-A184069] 03 p0335 N88-12110

Materials studies for magnetic fusion energy applications at low temperatures-X
[PB87-232575] 03 p0381 N88-12395

Failure analysis of composite structure materials
[AD-A184468] 04 p0410 N88-12548

Composite mechanics for engine structures
[NASA-TM-100176] 04 p0411 N88-12552

Corrosion control by composite material substitution with application to the M-939 5-ton truck
04 p0428 N88-12654

Characterization of thin layers for optics
[PB87-217949] 04 p0490 N88-13017

Surface treatment problems found in new aircraft designed using structural composites
[SNIAS-872-111-113] 05 p0558 N88-13397

Philosophy and practice of nondestructive tests of composite material structures at Aerospatiale Aquitaine
[SNIAS-872-430-105] 05 p0559 N88-13400

Measurement and control of damage in composite materials. Nondestructive controls by thermography, holography, and radiography
[SNIAS-872-430-110] 05 p0559 N88-13403

Mechanics of anisotropic media Study of the boundary conditions --- stratified composites
[SNIAS-872-430-112] 05 p0559 N88-13404

Micromechanics of the degradation of composite materials
[SNIAS-872-430-113] 05 p0559 N88-13405

The structures of large wound propulsion shells --- carbon fiber composites filament winding
[SNIAS-872-430-118] 05 p0559 N88-13406

Design and test of high performance composite tubes for use in deep water drilling and production systems
[SNIAS-872-430-107] 05 p0572 N88-13487

High performance composite tubes for offshore applications
[SNIAS-872-430-116] 05 p0572 N88-13488

Strain-energy-release rate analysis of the end-notched flexure specimen using the finite-element method
[NASA-TM-100494] 05 p0608 N88-13735

Bending of a bonded beam as a test method for adhesive properties
[AD-A184813] 05 p0609 N88-13736
Structural tests and development of a laminar flow control wing surface composite chordwise joint
[NASA-CR-172462] 06 p0663 N88-14066
A study of the utilization of advanced composites in fuselage structures of commercial aircraft
[NASA-CR-172405] 06 p0679 N88-14157
Ceramic technology for advanced heat engines
[PB87-232997] 06 p0683 N88-14188
Study on utilization of advanced composites in fuselage structures of large transports
[NASA-CR-172406] 07 p0827 N88-15014
Impact of solids on composite materials
[NASA-CR-182395] 07 p0827 N88-15015
Delamination durability of composite materials for rotorcraft 09 p1107 N88-16634
Helicopter crashworthiness research program
09 p1107 N88-16635
Experimental study on the effect of fiber orientation on flutter characteristics of high-aspect-ratio transport wing
[NAL-TR-936] 09 p1120 N88-16708
Space station structures development
[NASA-CR-179261] 09 p1133 N88-16792
Sublaminate damage mechanisms in composite structures
[AD-A186807] 09 p1137 N88-16815
The strength of hybrid composites
[BR101991] 09 p1138 N88-16821
Integrity control of carbon fiber reinforced plastics (CFRP) structural elements. Conclusion with respect to the control methodology of CFRP primary structures in manned space flight and the implications to the design, analysis and testing of CFRP structural elements, executive summary
[MBB-TR-RB517-014/85] 09 p1139 N88-16824
Mechanical properties of carbon fiber reinforced thermoplastic matrix composites
[NAL-TR-934] 09 p1139 N88-16827
Ultrasonic inspection of advanced CFRP structures by computer-controlled, pulse-echo technique
[ETN-88-91665] 09 p1177 N88-17051
Rotorcraft weight trends in light of structural material characteristics
[AD-A186576] 10 p1276 N88-17642
A finite element analysis of adhesively bonded composite joints including geometric nonlinearity, nonlinear viscoelasticity moisture diffusion and delayed failure
[AD-A187455] 10 p1296 N88-17747
La Recherche Aerospatiale, bimonthly bulletin, number 1987-1, 236/January-February
[ESA-TT-1055] 11 p1433 N88-18549
Finite element analysis of adhesively bonded composite joints including geometric nonlinearity, nonlinear viscoelasticity, moisture diffusion and delayed failure
[PB88-147822] 11 p1451 N88-18648
Slip casting of advanced ceramics and composites
[DE88-003424] 11 p1467 N88-18746
Wave propagation in laminated composite plates
[AD-A188999] 12 p1604 N88-19594
The place for thermoplastic composites in structural components
[AD-A189149] 12 p1604 N88-19596
Standardized environmental fatigue sequence for the evaluation of composite components in combat aircraft (ENSTAFF = ENvironmental falSTAFF)
[LBF-FB-179] 13 p1722 N88-20300
A preliminary investigation of finite-element modeling for composite rotor blades
[NASA-TM-100559] 13 p1781 N88-20656
Hygrothermomechanical fiber composite fatigue: Computational simulation
[NASA-TM-100840] 14 p1884 N88-21257
Structural and material testing of a composite microlite wing model
[BU-355] 14 p1923 N88-21461
The effect of strain rate on the strength and ductility of SiCw/2124 Al composite
[OUEL-1692/87] 14 p1924 N88-21466
Thermally stable deployable structure
14 p1925 N88-21472
A study of damage tolerance in curved composite panels
[AD-A190617] 15 p2029 N88-22092
Postbuckling delamination of a stiffened composite panel using finite element methods
[NASA-CR-182803] 15 p2030 N88-22098
Features and applications of the integrated composites analyzer (ICAN) code 15 p2078 N88-22391
Computational simulation methods for composite fracture mechanics 15 p2079 N88-22396
Thermal stress in high temperature cylindrical fasteners
[NASA-TM-100611] 15 p2087 N88-22438
Experimental comparison of lightning simulation techniques to CV-580 airborne lightning strike measurements
[AD-A190576] 15 p2098 N88-22496
Towards a damage tolerance philosophy for composite materials and structures
[NASA-TM-100548] 16 p2173 N88-22949
A piecewise quadratic strength tensor theory for composites
[AD-A190929] 16 p2173 N88-22952
Nondestructive evaluation of large scale composite components
[AD-A190998] 16 p2173 N88-22954
Durability of compound cylinder under static internal-pressure repeat load of long duration
16 p2180 N88-22991
Investigation into the operation of the new special drills for drilling holes in thin components made of composite materials --- aircraft components
[LR-519] 16 p2215 N88-23215
A nonlinear computation for composite structures
[ONERA-RT-15/3542-RY-062-R]
16 p2222 N88-23265
Insert design handbook
[ESA-PSS-03-1202-ISSUE-1] 17 p2311 N88-23822
Composite piston
[NASA-CASE-LAR-13435-1] 17 p2346 N88-23981
Interaction of ultrasonic waves with composite plates
[AD-A191879] 18 p2478 N88-24702
Shape stability in composites
18 p2479 N88-24706
The stress analysis of ceramic, polymeric, and metallic composite systems by the finite element method
18 p2529 N88-25004
Microlaminate composite structures by low pressure plasma spray deposition
[DE88-006453] 19 p2610 N88-25488
The construction of composite grids for general three-dimensional regions 20 p2843 N88-26872
Balance of X-ray radioscopy application to nondestructive tests of composite materials
[SNIAS-881-430-110] 21 p2907 N88-27250
Two-dimensional sequential and concurrent finite element analysis of unstiffened and stiffened aluminum and composite panels with hole
[NASA-CR-183083] 22 p3086 N88-28325
Parameter identification of material constants in a composite shell structure
[DE88-008115] 22 p3086 N88-28326
Critical joints in large composite primary aircraft structures. Volume 2: Technology demonstration test report
[NASA-CR-172587] 23 p3177 N88-28915
Critical joints in large composite primary aircraft structures. Volume 3: Ancillary test results
[NASA-CR-172588] 23 p3177 N88-28916
Elastic wave dispersion in laminated composite plate
[AD-A192289] 23 p3188 N88-28967
Nondestructive tests and high performance composite structures
[SNIAS-881-430-119] 23 p3188 N88-28969
Effect of fiber diameter on the reliability of composites - automated laser diffraction implementation
[AD-A193524] 23 p3188 N88-28972
Critical joints in large composite primary aircraft structures. Volume 1: Technical summary
[NASA-CR-3914] 23 p3190 N88-28983
Damage initiation in the short beam shear test of composite materials using stiffness reduction
[AD-A194880] 24 p3340 N88-29883
Evaluation of bond testing equipment for inspection of Army advanced composite airframe structures
[AD-A195795] 24 p3341 N88-29885
Experimental aspects of using time-averaged holographic interferometry to detect barely visible impact damage in a graphite/epoxy composite plate
[AD-A194418] 24 p3375 N88-30097

COMPOSITES
U COMPOSITE MATERIALS

COMPOSITION (PROPERTY)
NT ATMOSPHERIC COMPOSITION
NT ATMOSPHERIC MOISTURE
NT CARBON DIOXIDE CONCENTRATION
NT CHEMICAL COMPOSITION
NT CONCENTRATION (COMPOSITION)
NT GAS COMPOSITION
NT IONOSPHERIC COMPOSITION
NT METEORITIC COMPOSITION
NT METEOROID CONCENTRATION
NT MOISTURE CONTENT
NT PLANETARY COMPOSITION
NT STELLAR COMPOSITION

COMPOUND HELICOPTERS
Rotorcraft designs for the year 2000
03 p0264 N88-11665

COMPRESSED GAS
NT HIGH PRESSURE OXYGEN
Shock wave compression and metallization of simple molecules
[DE88-008031] 20 p2851 N88-26925

COMPRESSIBILITY
Shock measurements on explosives in the supra compressive region
[DE87-008423] 01 p0031 N88-10196
Nonlinear and nonparallel stability problems
[AD-A186406] 07 p0850 N88-15159
Compression of composite materials: A review
[AD-A189272] 13 p1734 N88-20365
Unsteady flow field measurements using LDV (Laser Doppler Velocimetry)
[AD-A189907] 15 p2063 N88-22298
Effects of axial load on elastomeric isolation bearings
[PB88-179015] 16 p2223 N88-23269
Bimodular behavior and crack closure in compression in a brittle material
[AD-A191267] 16 p2224 N88-23275
Nickel hydroxide active material densities
[AD-A191411] 16 p2230 N88-23319
The effects of thin compressive films on indentation fracture toughness measurements
[AD-A192243] 20 p2779 N88-26480
Development of an equation of state for computation of supercompressibility factors, critical flow factors and other properties for wet, sour natural gases, synthetic gases and admixtures
[PB88-202676] 20 p2798 N88-26602
Quantitative particle characterization by scattered ultrasound 20 p2848 N88-26908
Temperature, moisture and strain rate effects on the compressive mechanical behavior of Nylon 6/6
[DE88-010734] 21 p2961 N88-27591
Survey on nonlinear effects 24 p3317 N88-29757
Compression pylon
[NASA-CASE-LAR-13777-1] 24 p3323 N88-29789

COMPRESSIBILITY EFFECTS
Investigation of dihedral effects in compressor cascades 10 p1282 N88-17672

COMPRESSIBLE BOUNDARY LAYER
Secondary instability of compressible boundary layer to subharmonic three-dimensional disturbances
[NASA-CR-4144] 16 p2200 N88-23122
Theoretical investigation of 3-D shock wave-turbulent boundary layer interactions, part 6
[AD-A191546] 18 p2509 N88-24882
Spatial stability of a compressible mixing layer
[NASA-CR-181671] 18 p2514 N88-24915
Compressible boundary layers --- atmospheric reentry
[CERT-OA-13/5005-AYD] 20 p2801 N88-26623

COMPRESSIBLE FLOW
NT TRANSONIC FLOW
Rayleigh-Taylor instability in compressible fluids
[DE87-013494] 01 p0047 N88-10297
Numerical solution of Euler equations for compressible fluids by the finite element method, volume 3
[ETN-87-90650] 02 p0170 N88-11070
Impact of turbulence modeling on numerical accuracy and efficiency of compressible flow simulations
[NASA-TM-88333] 02 p0173 N88-11088
JPRS report: Science and technology. China
[JPRS-CST-87-034] 03 p0301 N88-11897
Analysis of compressible flow on high-velocity jet penetration 03 p0302 N88-11898
A free-Lagrange method for 2-D compressible flows
[DE88-000216] 04 p0442 N88-12745
Studies of pressure-velocity coupling schemes for analysis of incompressible and compressible flows
[NASA-CR-181526] 04 p0443 N88-12748
TOPAZ: The transient one-dimensional pipe flow analyzer: An update on code improvements and increased capabilities
[DE88-001781] 04 p0443 N88-12751
Cauchy problem for linearized system of Navier-Stokes equations considering compressibility
04 p0459 N88-12837
An analysis of the compressible-viscous flow field around a 3D-oscillating wing 05 p0535 N88-13254
Computation of dynamic stall of NACA0012 airfoil by block pentadiagonal matrix scheme
05 p0535 N88-13255
Computations of compressible viscous flows over multiple-bodies 05 p0539 N88-13282
Relaxation method for the compressible Navier-Stokes equations using upwind schemes
05 p0539 N88-13283
Interferometric data for a shock-wave/boundary-layer interaction
[NASA-TM-88227] 05 p0543 N88-13306
Unsteady aerodynamics of an oscillating cascade in a compressible flow field
[NASA-TM-100219] 05 p0549 N88-13346

A note on the use of symmetric line Gauss-Seidel for the steady upwind differenced Euler equations
[AD-A185223] 05 p0580 N88-13540

Evolution of mean square magnetic vector potential in compressible, two-dimensional, magnetofluid turbulence
[AD-A184985] 05 p0651 N88-13990

Vectorization of a multigrid method for the compressible Navier-Stokes equations
[PB87-230496] 06 p0698 N88-14284

Experimental investigation of heterogeneous compressible shear layers 06 p0700 N88-14294

A direct calculation method for perturbation fields of moving bodies in compressible media at subsonic Mach numbers
[ETN-88-90808] 06 p0701 N88-14305

On the subgrid-scale modeling of compressible turbulence
[NASA-CR-178420] 06 p0702 N88-14309

Rayleigh-Taylor instability in compressible fluids
[DE88-002473] 07 p0852 N88-15179

Finite element methods for compressible flows
08 p0984 N88-15956

Turbulence modeling for compressible flows
08 p0987 N88-15978

Modeling the unsteady flow found in axial turbomachinery
[ECL-87-07] 08 p0987 N88-15980

New techniques in computational aerodynamics
[AD-A186719] 09 p1112 N88-16664

Numerical resolution of the equations of three-dimensional stable compressible transonic flows
[PB87-168415] 09 p1113 N88-16673

Dynamic modelling by finite element method of an elasto-acoustic beam with due consideration of flow and viscosity
[PB87-178166] 09 p1164 N88-16978

Lifting-surface theory of oscillating propellers in compressible flow
[NAL-TR-943] 10 p1273 N88-17613

A numerical study of unsteady two-dimensional subsonic compressible base flow 10 p1327 N88-17931

On the stability of the supersonic boundary layer
11 p1435 N88-18561

A hydrodynamic analysis of fluid flow between meshing spur gear teeth
[AD-A187671] 11 p1482 N88-18844

A simplified streamline swallowing procedure for the windward meridian of axisymmetric blunt bodies
[AD-A188413] 12 p1626 N88-19732

Compressible friction coefficients in a simulated heat pipe
[AD-A188818] 12 p1627 N88-19735

Computational technique for compressible vortex flows using the integral equation solution
[NASA-CR-182695] 13 p1718 N88-20271

Slip velocity method for three-dimensional compressible turbulent boundary layers
[NASA-TM-100586] 13 p1771 N88-20592

Splitting of inviscid fluxes for real gases
[NASA-TM-100856] 14 p1964 N88-21717

Flexiwall 3 SO: A second order predictive strategy for rapid wall adjustment in two-dimensional compressible flow
[NASA-CR-181662] 15 p2015 N88-22018

Turbulent reacting flows and supersonic combustion
[AD-A189690] 15 p2034 N88-22115

Theoretical model and numerical solution for compressible viscous vortex cores
15 p2054 N88-22243

Transient compressible flow in porous materials
[DE88-006685] 15 p2067 N88-22324

Analysis for high compressible supersonic flow in converging nozzle
[IPPJ-860] 16 p2157 N88-22869

Solution of the compressible Navier-Stokes equations of motion by Chebyshev polynomials for laminar shock-boundary layer flow
[AD-A191033] 16 p2208 N88-23176

Noncondensing round turbulent gas jets in liquids
[AD-A191191] 16 p2208 N88-23179

Laser Doppler anemometry
[NASA-TM-100072] 16 p2210 N88-23187

Detailed transient model of a liquid-metal heat pipe
17 p2412 N88-24345

Boundary layer transition
[CERT-OA-37/5018-AYD] 18 p2458 N88-24595

Compressible flow in a pie-shaped cylinder rotating about the vertex 18 p2460 N88-24604

Accurate multigrid solution of the Euler equations on unstructured and adaptive meshes
[NASA-CR-181679] 18 p2460 N88-24608

Internal fluid dynamics within a nonspinning partially liquid-filled shell due to burster rupture
[AD-A191055] 18 p2507 N88-24874

A variational finite element method for three-dimensional, steady, compressible, viscous flows
18 p2512 N88-24904

Numerical simulation of compressible homogeneous turbulence: Effects of fluid compressibility
[PB88-127154] 19 p2597 N88-25433

Relaxation scheme for compressible flows
19 p2640 N88-25663

The modified-fluid-in-cell method to which adaptive mesh and multigrid were applied
19 p2640 N88-25664

Experimental and analytical studies of compressible vortices 19 p2665 N88-25848

An h-p adaptive finite element method for steady compressible flow 21 p2941 N88-27467

Implicit finite-difference simulation of an internal flow on a hypercube
[AD-A192474] 21 p2942 N88-27471

Solution to the compressible Navier-Stokes equations of motion by Chebyshev polynomials with implicit time stepping
[AD-A194119] 22 p3075 N88-28257

Analysis method for the production of Reynolds stresses in compressible turbulent flow (fluid mechanics)
[NASA-TT-20330] 24 p3373 N88-30088

Development of a more general Reynolds stress closure for swirling flow
[AD-A195121] 24 p3374 N88-30092

COMPRESSIBLE FLUIDS

Rayleigh-Taylor instability in compressible fluids
[DE87-013494] 01 p0047 N88-10297

Effect of dissipation on propagation of spherical detonation shock wave 02 p0159 N88-10998

Dispersion equation for plane capillary-gravity wave on free surface of viscous incompressible fluid
04 p0459 N88-12842

Rayleigh-Taylor instability in compressible fluids
[DE88-002473] 07 p0852 N88-15179

A compressible vapor flux model for transient heat pipe analysis 17 p2412 N88-24343

Implicit finite-difference simulation of an internal flow in a nozzle: An example of a physical application on a hypercube
[AD-A192475] 21 p2942 N88-27472

COMPRESSING

NT PLASMA COMPRESSION

NT SPEECH BASEBAND COMPRESSION

Optimum size of staged flux compression generators
[DE87-011741] 01 p0038 N88-10244

Theoretical approaches to chemical dynamics in highly compressed fluids
[DE87-012242] 01 p0046 N88-10296

A new compression method with fast searching on large databases
[DE87-010986] 01 p0106 N88-10691

Design of source coders and joint source/channel coders for noisy channels
[NASA-CR-181547] 04 p0432 N88-12678

Shock compression of solids as a physical-chemical-mechanical process
[DE88-001674] 05 p0563 N88-13427

Threshold and crack-growth tests on pre-cracked specimens produced in cyclic compression
06 p0718 N88-14412

Theory and experiments of fracture in cyclic compression: Single phase ceramics, transforming ceramics and ceramic composites
[DE88-005792] 13 p1781 N88-20659

Parallel image compression
[NASA-CR-180758] 13 p1814 N88-20837

Dynamic range compression/expansion of light beams by photorefractive crystals
[NASA-CASE-NPO-17140-1-CU]
17 p2438 N88-24508

Dynamic shear band development in plane strain
[AD-A190915] 18 p2526 N88-24988

The electronic structure of condensed molecular systems
[DE88-007823] 20 p2851 N88-26923

Ultrasonic studies of stresses and plastic deformation in steel during tension and compression
[AD-A192308] 21 p2912 N88-27280

An endochronic rate-sensitive constitutive equation for metals, application to generalized creep and large deformations
[AD-A194167] 22 p3055 N88-28125

Nonlinear stress-strain and inelastic rebound with exponential stiffness
[AD-A195667] 24 p3384 N88-30159

COMPRESSION LOADS

NT AXIAL COMPRESSION LOADS

NT IMPACT LOADS

Cumulative fatigue and life prediction of fibre composites. Part 2: Experimental techniques and results
[BR101014] 02 p0142 N88-10894

Experimental molecular spectroscopy in shock-compressed materials
[DE87-013139] 02 p0144 N88-10903

Analysis and testing of predamaged shell structures
04 p0428 N88-12653

Shock compression of solids as a physical-chemical-mechanical process
[DE88-001674] 05 p0563 N88-13427

Effect of compressive portion of loading cycles on the near threshold fatigue closure behavior
06 p0717 N88-14398

Mixed mode fatigue crack growth using the Brasilian disc 06 p0719 N88-14416

A loading system for creep testing under constant compressive stress
[NASA-TT-20119] 06 p0722 N88-14441

Equation of state of condensed materials physical principles and applications
[NASA-TT-20007] 08 p0968 N88-15855

An in vitro model system to study the effect of microgravity and loading conditions on the mineralization and resorption of skeletal tissues
12 p1657 N88-19927

Geodetic measurement of deformation east of the San Andreas fault in Central California
[NASA-CR-182709] 13 p1798 N88-20754

Effect of uniaxial compression on physical and mechanical properties of ferroelectric ceramic material
16 p2180 N88-22993

Investigation of the effect of minimum loads and compression of load spectra on the prediction capacities of the ONERA crack model --- wings
[ONERA-RTS-33/7169-RY-064-R]
18 p2527 N88-24994

Air loading effects on a capacitively sensed membrane supported silicon accelerometer
19 p2672 N88-25886

Compression creep of filamentary composites
[NASA-CR-182550] 20 p2798 N88-26601

Micromechanics of composite laminate compression failures
[NASA-CR-183179] 22 p3050 N88-28098

The effect of compression on individual pressure vessel nickel/hydrogen components
[NASA-TM-101312] 22 p3052 N88-28109

Load interaction effects on compression fatigue crack growth in ductile solids
[FFA-TN-1988-12] 22 p3089 N88-28342

Critical joints in large composite primary aircraft structures. Volume 3: Ancillary test results
[NASA-CR-172588] 23 p3177 N88-28916

COMPRESSION RATIO

Variable-compression-ratio pistons for high power output diesel engines 22 p3084 N88-28316

COMPRESSION TESTERS

U COMPRESSION TESTS

COMPRESSION TESTS

The behavior of plastic, ceramic masses in compression tests
[ETN-87-90603] 03 p0292 N88-11836

A loading system for creep testing under constant compressive stress
[NASA-TT-20119] 06 p0722 N88-14441

Compression of composite materials: A review
[AD-A189272] 13 p1734 N88-20365

Notch sensitivity of graphite materials for VHTR
13 p1747 N88-20447

An investigation of the mechanical properties of improved carbon fibre composite materials
[RAE-TR-86021] 14 p1884 N88-21259

Electronic structure of matter at high compression: Isostructural transitions and approach of the Fermi-gas limit
[MPQ-124] 16 p2266 N88-23551

Bearing-bypass material system test
[NASA-CASE-LAR-13458-1] 17 p2342 N88-23967

Fuel containment and damage tolerance in large composite primary aircraft structures. Phase 2: Testing
[NASA-CR-172519] 19 p2601 N88-25452

An experimental and analytical evaluation of a biaxial test for determining shear properties of composite materials
[NASA-CR-182928] 21 p2962 N88-27593

The effect of compression on individual pressure vessel nickel/hydrogen components
[NASA-TM-101312] 22 p3052 N88-28109

COMPRESSION WAVES

Observations of an ion acoustic oscillation near a pulsed sheath
[INPE-4386-PRE/1206] 08 p0979 N88-15915

COMPRESSIVE STRENGTH

Face compression yield strength of the copper-Inconel composite specimen
[DE87-011974] 01 p0019 N88-10116

Effects of cure pressure on resin flow, voids, and mechanical properties
[AD-A184267] 03 p0295 N88-11853
Effect of interface on mechanical properties of graphite/201 aluminum composites
05 p0606 N88-13717
Characterization of mechanical damage mechanisms in ceramic composite materials
[AD-A185549] 06 p0686 N88-14205
Effect of low velocity impact on compression strength of a quasi-isotropic laminate
[FFA-TN-1987-38] 09 p1138 N88-16822
Effect of post-cure heat-treatment on static and fatigue behaviour of XAS-914C carbon fibre composite
[AD-A186943] 10 p1294 N88-17735
Strength and structure of Ga sub 1-xIn sub xAs alloys
[AD-A188092] 10 p1303 N88-17795
Statistical considerations of graphite strength for assessing design allowable stresses
13 p1746 N88-20441
Effects of high temperature neutron irradiation on the physical, chemical and mechanical properties of fine-grained isotropic graphite 13 p1747 N88-20444
The effect of Ca(OH)2-treated ceramic microspheres on the mechanical properties of high-temperature lightweight cement composites
[DE88-004590] 13 p1749 N88-20457
Environmental effects on the post-impact compressive strength of CFC
[RAE-TM-MAT-STR-1088] 14 p1884 N88-21258
High-strength ceramic based on tetragonal ZrO2 with Al2O3 admixture 16 p2180 N88-22996
High strength/sigh modulus aromatic heterocyclic ABA block copolymers
[AD-A191666] 18 p2491 N88-24774
Fuel containment and damage tolerance in large composite primary aircraft structures. Phase 2: Testing
[NASA-CR-172519] 19 p2601 N88-25452
Properties of two composite materials made of toughened epoxy resin and high-strain graphite fiber
[NASA-TP-2826] 19 p2609 N88-25480
Loading rate sensitivity of open hole composites in compression
[NASA-TM-100634] 19 p2610 N88-25490
A micromechanics model of the stiffness and strength of laminates with fiber waviness
[NASA-CR-181670] 20 p2768 N88-26413
Compression creep of filamentary composites
[NASA-CR-182550] 20 p2798 N88-26601
Development of a biaxial test system for thin-walled metal tubes using tensile-compressive axial load and internal-external pressure
[DE88-011279] 21 p2962 N88-27592

COMPRESSOR BLADES
Advanced turboprop wing installation effects measured by unsteady blade pressure and noise
[NASA-TM-100200] 01 p0002 N88-10008
Automated design of controlled diffusion blades
[NASA-TM-100251] 05 p0542 N88-13304
Operation of gas turbine engines in dust-laden environments 10 p1280 N88-17654
Radial compressor design using an Euler solver
10 p1283 N88-17675
Secondary flow measurements with L2F-technique in centrifugal compressors 10 p1283 N88-17676
Design and testing of a front stage for an advanced high pressure compressor 10 p1283 N88-17679
Experimental investigation of a supercritical compressor rotor blade section 10 p1284 N88-17680
Computation of secondary flows in an axial multistage compressor 10 p1284 N88-17681
Aero/structural tailoring of engine blades (AERO/STAEBL)
[NASA-CR-180805] 14 p1959 N88-21682
Research on aero-thermodynamic distortion induced structural dynamic response of multi-stage compressor blading
[AD-A192169] 18 p2456 N88-24584
Hot-wire measurements of compressor blade wakes in a cascade wind tunnel
[AD-A194737] 23 p3181 N88-28936
Empirical flutter prediction method
[AD-A195699] 24 p3327 N88-29810

COMPRESSOR EFFICIENCY
Process support compressor motor electromagnetic design summary
[DE87-014359] 02 p0167 N88-11048
Small engine technology programs
08 p0956 N88-15801
Method for predicting performance limits of centrifugal compressors 10 p1283 N88-17677
Analysis of the performance of an air-water heat pump: Regulation of intrinsic performances
[DE88-900241] 10 p1349 N88-18061
Efficiency characteristics of speed modulated drives at predicted torque conditions for air-to-air heat pumps
[DE88-005846] 13 p1770 N88-20588
Experimental and theoretical study of the dynamic operational behavior of a three stage radial compressor
[ETN-88-92129] 20 p2811 N88-26676

COMPRESSOR ROTORS
Three-dimensional calculation in high subsonic axial compressor rotor and its comparison with L2F velocity measurement 03 p0300 N88-11886

COMPRESSORS
NT CENTRIFUGAL COMPRESSORS
NT SUPERCHARGERS
NT SUPERSONIC COMPRESSORS
NT TRANSONIC COMPRESSORS
NT TURBOCOMPRESSORS
Process support compressor motor electromagnetic design summary
[DE87-014359] 02 p0167 N88-11048
Design verification tests for an axial gap permanent magnet compressor motor
[DE87-014360] 02 p0167 N88-11049
Combustor-diffuser interaction program
02 p0185 N88-11152
XeCl excimer laser with magnetic compressor
03 p0299 N88-11879
Application of modified loss and deviation correlations to transonic axial compressors
[AGARD-R-745] 05 p0549 N88-13344
Compressor large bandwidth noise emission mechanisms
[ETN-88-91177] 05 p0646 N88-13959
Oxygen chemisorption cryogenic refrigerator
[NASA-CASE-NPO-16734-1-CU]
06 p0689 N88-14223
Tests of cold helium compressors at Fermilab
[DE88-00283[illegible]] 07 p0862 N88-15230
Air Force cryocooler development for spacecraft
08 p0983 N88-15945
Computation of secondary flows in an axial multistage compressor 10 p1284 N88-17681
RF pulse compression development
[DE88-004818] 11 p1479 N88-18826
Free-piston Stirling engine diaphragm-coupled heat-actuated heat pump component technology program, phase 1B
[DE88-003653] 11 p1483 N88-18854
Experimental vibration damping characteristics of the third-stage rotor of a three-stage transonic axial-flow compressor
[NASA-TM-100948] 18 p2466 N88-24642
Forced response unsteady aerodynamics in a multistage compressor 18 p2512 N88-24903
Application of computational fluid dynamics to design of compressor cascade 19 p2639 N88-25655
Fluid dynamics of high performance turbomachines
[AD-A192073] 19 p2664 N88-25840
Experimental and theoretical study of the dynamic operational behavior of a three stage radial compressor
[ETN-88-92129] 20 p2811 N88-26676
JTDE 1 XTE34 materials research and development report
[AD-A194268] 22 p3044 N88-28063
Erosion of metals exposed to hot, dense gases
[AD-A193708] 22 p3056 N88-28131
AGARD (Advisory Group for Aerospace Research and Development) engine disc material cooperative test (supplementary program)
[AD-A193678] 23 p3179 N88-28925
E3 10C compressor test analysis of high-speed post-stall data
[NASA-CR-179521] 23 p3179 N88-28929
A mapping of the viscous flow behavior in a controlled diffusion compressor cascade using laser Doppler velocimetry and preliminary evaluation of codes for the prediction of stall
[AD-A194490] 23 p3211 N88-29112
Reduction in mill air compressor power requirements through installation of a variable frequency speed control
[DE88-008493] 23 p3221 N88-29171
Development of the Simplified Compressor Model (SCM) for performance analysis of gaseous diffusion compressors
[DE88-009066] 23 p3221 N88-29173

COMPTON EFFECT
The development of diagnostic fuses
[SAND-86-0395] 03 p0311 N88-11963
Relativistic corrections for one- and two-photon matrix elements of weakly-bound systems
[NOTA-INTERNA-884] 07 p0929 N88-15645
A search for medium energy gamma ray pulsars
11 p1568 N88-19385
Experimental set-up for measurements of Compton scattering cross section on light nuclei
[DE88-700161] 12 p1688 N88-20097
Three-wave parametric resonance in plasma of relativistic electron flux 14 p1972 N88-21772
Waves and instabilities in an electron-positron plasma in an ultra-strong magnetic field
23 p3283 N88-29551

COMPUTATION
NT COMPUTATIONAL GEOMETRY
NT ORBIT CALCULATION
A parallel model of the kinetic depth effect using local computations
[AD-A181945] 01 p0083 N88-10536
Computational methods and software for differential equations and their applications
[DE87-014601] 02 p0226 N88-11424
Deviatoric constitutive relationship for anisotropic materials
[AD-A184332] 03 p0295 N88-11854
Combined calculation of deformation and stress for the body and sabot of an APFSDS
03 p0302 N88-11899
Institute for Computational Mechanics in Propulsion (ICOMP) first year summary
[NASA-TM-100225] 03 p0370 N88-12330
Aircraft dynamic response calculation based on discrete-continual model 04 p0424 N88-12624
Calculation of three-dimensional stationary turbulent boundary layer on root section of wing ignoring compressibility 04 p0424 N88-12630
Back-of-the-envelope problems
[AD-A184105] 04 p0484 N88-12980
Calculation of helicopter rotor blade/vortex interaction by Navier-Stokes procedures
[NASA-CR-177441] 05 p0540 N88-13291
Efficient computation of periodic Green's functions with application to grating structures
[AD-A184853] 05 p0640 N88-13912
Computer calculations of PIN diode limiter characteristics
[AD-A185563] 06 p0697 N88-14277
Methods for reducing computational costs of typical finite element unsteady hydrodynamic models
[AD-A185499] 06 p0702 N88-14312
Fast algorithms for structural optimization and least squares
[AD-A185766] 06 p0724 N88-14452
Optimal pre-scheduling of problem remappings
[NASA-CR-178378] 06 p0756 N88-14633
Development of symbolic computation methods for nonlinear dynamics
[AD-A185562] 06 p0758 N88-14653
Computing block-angular Karmarker projections with applications to stochastic programming, revision
[AD-A185647] 06 p0759 N88-14656
Diffusion first passage times: Approximations and related differential equations
[AD-A185592] 06 p0765 N88-14700
An efficient algorithm for computing the crossovers in satellite altimetry
[NASA-CR-182389] 07 p0871 N88-15286
Stability analysis of finite difference schemes for hyperbolic systems, and problems in applied and computational linear algebra
[AD-A185824] 07 p0908 N88-15499
The classification problem of finite rings by computable means
[AD-A185869] 07 p0908 N88-15500
Explicit construction and analysis of some efficient empirical production functions in data envelopment analysis
[AD-A185907] 07 p0908 N88-15502
Recent developments in the numerical solution of differential/algebraic systems
[DE88-001885] 07 p0912 N88-15535
Computers in theoretical physics
[DE88-700516] 07 p0941 N88-15720
Acta Aerodynamica Sinica (selected articles)
[AD-A185723] 08 p0949 N88-15757
Calculation evaluation of the boundary conditions of autoinflammation of propulsive charges
[PB87-139044] 08 p0974 N88-15890
Computational prediction of propellant reorientation
08 p0982 N88-15940
New directions for multivariate statistical computation and data analysis
[AD-A186523] 08 p1074 N88-16480
A rapid method for the computation of equilibrium chemical composition of air to 15000 K
[NASA-TP-2792] 09 p1140 N88-16830
Computational analysis of propagation properties of integrated-optical waveguides using a domain integral equation
[PB87-163358] 09 p1154 N88-16917
An efficient method for computing leading Eigenvalues and Eigenvectors of large asymmetric matrices
09 p1159 N88-16949

Design of a neural network simulator on a transputer array 09 p1205 N88-17221

A fast bottom-up algorithm for computing the cut sets of noncoherent fault trees
[DE88-003741] 09 p1220 N88-17320

A multithreaded processor architecture for parallel symbolic computation
[AD-A187034] 09 p1222 N88-17327

A note on computing robust regression estimates via iteratively reweighted least squares
[AD-A186709] 09 p1227 N88-17352

Advances in reliable numerical computation: A summary --- conference
[NPL-DITC-102/87] 09 p1229 N88-17367

On exact solutions of multidimensional Schroedinger equation with polynomial potentials
[DE88-700460] 09 p1230 N88-17373

Calculating measurement imprecision and uncertainty
[DE88-003981] 09 p1233 N88-17391

A computational study of thrust augmenting ejectors based on a viscous-inviscid approach
10 p1326 N88-17929

Annotated computer output for split plot design: GENSTAT ANOVA
[AD-A187120] 10 p1385 N88-18271

Machine models and simulations
[PB88-118690] 10 p1386 N88-18280

The effects of data structure on total time on test plots
[AD-A187628] 10 p1389 N88-18296

Recent progress in the p and h-p version on the finite element method
[AD-A187254] 10 p1400 N88-18347

International Conference on Industrial and Applied Mathematics
[AD-A188251] 11 p1483 N88-18851

A semianalytical technique for sensitivity analysis of unsteady aerodynamic computations
[NASA-TM-100810] 11 p1503 N88-18976

Institute for Computational Mechanics in Propulsion (ICOMP)
[NASA-TM-100790] 11 p1540 N88-19202

Theory and practice of fault tolerance in distributed systems
[AD-A187559] 11 p1540 N88-19204

Core-core and core valence correlation
[NASA-CR-182552] 11 p1544 N88-19226

Theoretical studies of the potential surface for the F - H2 greater than HF + H reaction
[NASA-CR-182551] 11 p1557 N88-19319

Spire based speaker-independent continuous speech recognition using mixed feature sets
[AD-A188834] 12 p1620 N88-19688

Support for concurrent computing environments
[AD-A188498] 12 p1680 N88-20043

Uncertain knowledge in distributed systems
[AD-A189017] 12 p1685 N88-20076

Computation of LMS (Least-Mean-Square) and matched digital filters for optical clutter suppression
[AD-A188885] 12 p1687 N88-20093

Pion absorption in nuclei: The pion(+ or -),proton reactions
[LA-10997-T] 12 p1688 N88-20098

A cost analysis for the implementation of commonality in the family of commuter airplanes, revised
[NASA-CR-182569] 12 p1708 N88-20221

Application of a flux vector splitting methodology towards the solution of unsteady transonic flows, with future emphasis on the blade flutter problem
[AD-A189500] 13 p1716 N88-20260

Implementation of a 3-D nonlinear MHD (magnetohydrodynamics) calculation on the Intel hypercube
[DE88-000625] 13 p1816 N88-20848

Computing with structured connections networks
[AD-A189244] 13 p1821 N88-20886

Numerical solution of ill posed problems in partial differential equations
[AD-A189383] 13 p1825 N88-20909

Algebraic specifications for parameterized data types: The case of minimal computable algebras and parameters with equality
[CWI-CS-R8714] 13 p1826 N88-20916

Computation and graphics in mathematical research
[DE88-005796] 13 p1831 N88-20953

A low-frequency measurement of the spectrum of the cosmic microwave background radiation
13 p1858 N88-21112

Comparison of methods for the calculation of thermal contact resistance of the first Brazilian satellite
[NASA-TT-20180] 14 p1880 N88-21239

On the theory of the conversion of metallic mixed phases. 5: Fluctuations and nucleation in sub-cooled phases
[NASA-TT-20249] 14 p1890 N88-21296

Computational aspects of sensitivity calculations in transient structural analysis
[NASA-TM-100589] 14 p1924 N88-21467

Measurements of optical nonlinearities in MOCVD-grown GaAs/GaAlAs multiple quantum wells
14 p1975 N88-21787

Calibration and processing of AVHRR data for temperature estimation
[INPE-4493-PRE/1257] 15 p2095 N88-22485

Optical Conceptual Computing and Associative Memory (OCCAM)
[AD-A190030] 15 p2107 N88-22550

Rapid feature extraction via the radon transform
[AD-A190032] 15 p2110 N88-22573

Microvax networked computer system
[AD-A190308] 15 p2114 N88-22596

High speed transcendental elementary function architecture in support of the Vector Wave Equation (VWE)
[AD-A189746] 15 p2119 N88-22627

Numerical methods for linear and nonlinear optimization
[AD-A190029] 15 p2120 N88-22631

Research on algebraic manipulation
[AD-A190149] 15 p2120 N88-22634

A physically consistent model for artificial dissipation in transonic potential flow computations
[NASA-TM-100846] 15 p2122 N88-22652

Interface formation and precursory dynamics
[AD-A190741] 15 p2144 N88-22794

INPE position paper on the CCSDS standardized method of link budget computation
[INPE-4533-NTF/279] 15 p2148 N88-22820

KOMPOT Program complex for the calculation of spatial magnetostatic fields of electromagnetic systems
[DE88-701691] 16 p2192 N88-23072

Coherent structure 16 p2199 N88-23117

Coherent structures: Comments on mechanisms
16 p2199 N88-23118

Multigrid for structures analysis
16 p2218 N88-23232

A computational procedure for automated flutter analysis 16 p2220 N88-23250

Approximate agreement
[AD-A191030] 16 p2251 N88-23455

Generalizing the structure of explanations in explanation-based learning
[AD-A191327] 16 p2256 N88-23481

Computation of a complete elliptic integral of the first kind using q-expansion 16 p2257 N88-23490

BRYNTRN: A baryon transport computer code, computation procedures and data base
[NASA-TM-4037] 16 p2290 N88-23714

Scientific computing environments
[AD-A191239] 17 p2385 N88-24175

The exact calculation of quadrupole sources for some incompressible flows
[NASA-TM-100623] 17 p2395 N88-24240

Quench detection by fluid dynamic means in cable-in-conduit superconductors
[DE88-007269] 18 p2585 N88-25359

Comment on non-renormalization theorem in the four dimensional superstrings
[DE88-752551] 18 p2586 N88-25367

Two-dimensional viscous flow computations of hypersonic scramjet nozzle flowfields at design and off-design conditions
[NASA-CR-182150] 19 p2603 N88-25459

Material void opening computation using particle method
[DE88-010950] 19 p2680 N88-25936

High speed inlet calculations with real gas effects
[NASA-CR-182167] 20 p2752 N88-26336

Off-boundary approach to the boundary element method
[AD-A192931] 20 p2815 N88-26701

Numerical model for the computation of radiance distributions in natural waters with wind-roughened surfaces
[PB88-192703] 20 p2826 N88-26765

Fully implicit splitting method for accurate tidal computations
[PB88-183637] 20 p2828 N88-26781

The role of working memory in language comprehension
[AD-A192721] 20 p2833 N88-26805

A computational analysis of under-expanded jets in the hypersonic regime
[NASA-TM-101319] 21 p2893 N88-27174

Numerical simulation of fuel droplet interactions and breakup
[AD-A192431] 21 p2941 N88-27470

Numerical experiments on turbulent mixing
[AD-A192572] 21 p2942 N88-27473

Computational boundary conditions for the incompressible Navier-Stokes equations in channels and pipes
[AD-A193356] 21 p2944 N88-27487

Numerical treatment of the pressure singularity at a re-entrant corner
[AD-A193357] 21 p2944 N88-27488

Neural network research: A personal perspective
[AD-A192717] 21 p3003 N88-27808

Parallel solutions to geometric problems on the scan model of computation
[AD-A192321] 21 p3004 N88-27819

Computing partial correlations from the data matrix
[AD-A193904] 22 p3138 N88-28659

On the computation of finite invariant sets of mappings
[AD-A193670] 22 p3143 N88-28690

Computation of the eigenvalues for perturbations of Poiseuille flow using a two-point boundary value method
[AD-A193479] 23 p3210 N88-29104

Solving the symmetric tridiagonal eigenvalue problem on the hypercube
[AD-A193905] 23 p3250 N88-29344

The history of Martian volcanism determined from a revised relative chronology 23 p3301 N88-29657

Calculation of non-stationary aerodynamic forces in the near sonic range
[NASA-TT-20310] 24 p3322 N88-29782

A new computational capability for ramjet projectiles
[AD-A196061] 24 p3327 N88-29812

Multilevel computational theory of stereoscopic visual image processing
[AD-A195331] 24 p3408 N88-30288

A model for architectural comparison
[AD-A195993] 24 p3411 N88-30302

Nonequilibrium flow computations. 1: An analysis of numerical formulations of conservation laws
[NASA-CR-177489] 24 p3425 N88-30384

Regularity and numerical solution of eigenvalue problems with piecewise analytic data
[AD-A194993] 24 p3425 N88-30387

Instrumentation for computational statistical research
[AD-A195887] 24 p3426 N88-30390

COMPUTATIONAL CHEMISTRY

A quantum theoretical study of polyimides
[NASA-CR-181495] 03 p0292 N88-11831

COMPUTATIONAL FLUID DYNAMICS

Rayleigh-Benard convection in a Hele-Shaw cell: A numerical study
[KFK-4212] 01 p0044 N88-10280

Generation of body-fitted grids for two dimensional interior domains by the solution of a system of Poisson equations using multigrid techniques
[GMD-246] 01 p0044 N88-10281

Mean flow structure of a turbulent junction vortex
[PB87-206231] 01 p0047 N88-10301

Numerical calculation of the turbulent flow about a cubic body
[ETN-87-90418] 01 p0047 N88-10302

Application of new conformal solution of theories
[PB87-214557] 01 p0105 N88-10684

Numerical computation of transonic potential flow about 3-dimensional inlets
[NAL-TR-924] 02 p0122 N88-10770

Calculation of aerodynamic heat transfer for blunt-nosed thin wings at different angles of attack at supersonic speeds
[NASA-TT-20127] 02 p0123 N88-10776

FDM-FEM zonal method for viscous flow computations over multiple-bodies
[NAL-TR-925T] 02 p0170 N88-11069

Computational fluid dynamics in the United Kingdom
[RAE-TM-AERO-2098] 02 p0171 N88-11073

Numerical simulation of transient two-phase flow
[CFDU/87/4] 02 p0171 N88-11077

Comparison between numerical solutions and measurements for a high speed turbine blade
[PNR90402] 02 p0172 N88-11082

Coolant passage heat transfer with rotation
02 p0186 N88-11160

The spatially nonuniform convergence of the numerical solution of flows
[NASA-TM-100037] 02 p0226 N88-11429

A supersonic potential gradient method for the calculation of unsteady aerodynamic pressures on harmonically oscillating wings
[ESA-TT-930] 03 p0259 N88-11631

Efficient numerical approaches for predicting supersonic flows with viscous/inviscid interaction
03 p0260 N88-11637

Analytic investigation of helicopter rotor blade appended aeroelastic devices
[NASA-CR-166525] 03 p0266 N88-11676

Analysis of compressible flow on high-velocity jet penetration 03 p0302 N88-11898

Turbulence modelling through one point closures-applications-enlightening by large eddy simulation 03 p0312 N88-11972

Numerical calculation of two dimensional fluid flow with strong shocks
[KFK-4191] 03 p0314 N88-11986

The Proceedings of the Symposium on Mechanics for Space Flight
[ISAS-SP-5] 03 p0317 N88-12006

On the scheme dependency of the three-dimensional Euler solutions 03 p0318 N88-12010

Numerical study of the entrance flow and its transition in a circular pipe (2) 03 p0318 N88-12011

Solution of the two-dimensional Euler equations on unstructured triangular meshes
04 p0396 N88-12469

Experimental aerothermodynamic research of hypersonic aircraft
[NASA-CR-181533] 04 p0399 N88-12483

USSR report: Engineering and equipment
[JPRS-UEQ-87-008] 04 p0423 N88-12621

Some asymptotic modes of transonic vortex flow
04 p0425 N88-12632

Numerical study of supersonic flow around blunt bodies with extended needle nose 04 p0425 N88-12635

Studies of pressure-velocity coupling schemes for analysis of incompressible and compressible flows
[NASA-CR-181526] 04 p0443 N88-12748

Optimization of explicit time-stepping algorithms and Stream-Function-Coordinate (SFC) concept for fluid dynamics problems 04 p0445 N88-12762

Cauchy problem for linearized system of Navier-Stokes equations considering compressibility
04 p0459 N88-12837

Asymptotic form of stationary solutions of the Navier-Stokes equations for large Reynolds numbers
04 p0459 N88-12838

Aerodynamics of Hypersonic Lifting Vehicles
[AGARD-CP-428] 05 p0529 N88-13219

Numerical simulation of the hypersonic flow around lifting vehicles 05 p0532 N88-13234

On the numerical simulation of three-dimensional hypersonic flow 05 p0532 N88-13237

Aerothermodynamics research at NASA Ames
05 p0533 N88-13242

The RAE experimental data-base for missiles at high Mach number and its use in assessing CFD methods
05 p0534 N88-13250

Proceedings of the 4th NAL Symposium on Aircraft Computational Aerodynamics
[NAL-SP-7] 05 p0535 N88-13253

An analysis of the compressible-viscous flow field around a 3D-oscillating wing 05 p0535 N88-13254

Computation of dynamic stall of NACA0012 airfoil by block pentadiagonal matrix scheme
05 p0535 N88-13255

Numerical calculation in the Laplace domain for subsonic unsteady aerodynamic forces acting on a finite wing
05 p0535 N88-13256

Practical application of two-dimensional viscous flow computation 05 p0535 N88-13257

A numerical investigation on wing/nacelle interferences 05 p0535 N88-13258

The role of computation fluid dynamics in aeronautical engineering (4). The development and applications of implicit TVD finite volume code
05 p0536 N88-13259

Practical and modern simulation by systematic connection of the LU-ADI code and the solution adaptive grid program 05 p0536 N88-13260

Numerical calculations of the flowfield around propellers 05 p0536 N88-13261

Numerical analysis of cascade flow solving Navier-Stokes equations 05 p0536 N88-13262

Inverse design method for two-dimensional transonic cascades 05 p0536 N88-13263

Development of the computer program for turbulent boundary layers 05 p0536 N88-13264

Numerical prediction of turbulent flows in dump diffusers 05 p0537 N88-13265

Numerical analysis of supersonic flows using panel method 05 p0537 N88-13266

Computation of nacelle interference using boundary element method 05 p0537 N88-13267

Application of discrete vortex method to analysis of separated flow around aerofoils
05 p0537 N88-13268

Programming techniques for high-speed processing of large scale numerical simulation on supercomputers
05 p0537 N88-13269

Vectorizing the FFTs on supercomputer SX system
05 p0537 N88-13270

Tridiagonal approximate factorization method: A preconditioning technique for solving nonsymmetric linear systems suitable to supercomputers
05 p0537 N88-13271

Numerical analysis of axisymmetric flow with H2-O2 reactions 05 p0538 N88-13272

Rarefied gas numerical wind tunnel. 2: Two-dimensional and axially symmetric bodies 05 p0538 N88-13273

Numerical analysis of flow characteristics of supersonic free-jets 05 p0538 N88-13274

Numerical simulation of splash of droplet at unit gravity 05 p0538 N88-13275

Computer graphics for computational aerodynamics
05 p0538 N88-13276

Flow visualization in computational fluid dynamics
05 p0538 N88-13277

Visualization of an aircraft accident based on digital flight data recorder information 05 p0538 N88-13278

A perspective of computational fluid dynamics
05 p0538 N88-13279

Three-dimensional flow past a two-dimensional body
05 p0539 N88-13280

Computational study of three-dimensional wake structures
[REPT-2] 05 p0539 N88-13281

Computations of compressible viscous flows over multiple-bodies 05 p0539 N88-13282

Relaxation method for the compressible Navier-Stokes equations using upwind schemes
05 p0539 N88-13283

Computation of flow around 2-D circular cylinder
05 p0539 N88-13284

Time-marching finite-difference methods for the three-dimensional Euler equations of contravariant velocity components 05 p0539 N88-13285

Navier-Stokes analysis of laminar flow control of a two-dimensional airfoil 05 p0540 N88-13286

Analytical method for generating computational grids about complete aircraft configurations
05 p0540 N88-13287

Navier-Stokes simulation of transonic transportation aircraft configurations. 1: Flow-field simulation over wing-fuselage combinations 05 p0540 N88-13288

Numerical simulation of transonic aircraft in comparison to wind tunnel test 05 p0540 N88-13289

Validation elements of the computation methods and measurement techniques for high lift aerodynamic systems
[SNIAS-872-111-101] 05 p0541 N88-13299

Compressible Euler solution on a multiblock grid around a wing-fuselage configuration
[FFA-TN-1987-46] 05 p0542 N88-13303

The role of experimental investigation and computational fluid dynamics during fighter aircraft design
05 p0546 N88-13326

A numerical study of the effects of curvature and convergence on dilution jet mixing
[NASA-TM-89878] 05 p0549 N88-13347

A note on the use of symmetric line Gauss-Seidel for the steady upwind differenced Euler equations
[AD-A185223] 05 p0580 N88-13540

Utilization of a high rate vector computer in computational fluid mechanics for aeronautics
[ETN-88-91171] 05 p0581 N88-13547

Physical analysis and numerical simulation of coherent turbulent structures in mixed layers, jets, and wakes
[ETN-88-91183] 05 p0581 N88-13548

Vortical Flows Research Program of the Fluid Dynamics Research Branch
[NASA-TM-88332] 05 p0582 N88-13549

Numerical analysis, computing and fundamental studies in fluid mechanics
[DE88-001912] 05 p0582 N88-13550

Low thrust viscous nozzle flow fields prediction
[NASA-CR-182334] 05 p0582 N88-13551

SHARP simulation of discontinuities in highly convective steady flow
[NASA-TM-100240] 05 p0642 N88-13931

Transonic Navier-Stokes computations of strake-generated vortex interactions for a fighter-like configuration 06 p0664 N88-14073

Numerical study of chemically reacting flows using an LU scheme
[NASA-CR-180882] 06 p0668 N88-14094

Analysis of internal flows relative to the space shuttle main engine
[NASA-CR-179240] 06 p0674 N88-14125

Computation of turbulent flow of air through smooth and rough pipes using a two-equation turbulence model
06 p0700 N88-14298

Introduction to Computational Fluid Dynamics
[VKI-LS-1987-02] 06 p0701 N88-14300

Introduction 06 p0701 N88-14301

Boundary layer equations and methods of solution
06 p0701 N88-14302

Finite element techniques 06 p0701 N88-14303

Implicit time dependent methods for inviscid and viscous compressible flows 06 p0701 N88-14304

Computational methods for complex flowfields
[AD-A185793] 06 p0703 N88-14317

Small High Pressure Ratio Turbines --- conference
[VKI-LS-1987-07] 06 p0712 N88-14364

Computation of free boundaries
[PB87-226023] 06 p0763 N88-14680

Method of calculations for flow of ideal gas through plane and axisymmetric nozzles with broken-line contour
06 p0771 N88-14737

Langley Symposium on Aerodynamics, volume 1
[NASA-CP-2397] 07 p0809 N88-14926

Computational fluid dynamics overview
07 p0809 N88-14927

Finite-volume scheme for transonic potential flow about airfoils and bodies in an arbitrarily shaped channel
07 p0809 N88-14928

Breakdown of the conservative potential equation
07 p0809 N88-14929

Application of a full potential method for analysis of complex aircraft geometries 07 p0809 N88-14930

A multistage time-stepping scheme for the thin-layer Navier-Stokes equations 07 p0810 N88-14932

Numerical simulation of a controlled boundary layer
07 p0810 N88-14933

Viscous vortex flows 07 p0810 N88-14934

A theory for the core flow of leading-edge vortices
07 p0810 N88-14935

Analysis and performance prediction of scramjet inlets utilizing a three-dimensional Navier-Stokes code
07 p0811 N88-14936

Wind tunnel wall interference
07 p0811 N88-14938

Separated flow 07 p0812 N88-14944

Modern wing flutter analysis by computational fluid dynamics methods
[NASA-TM-100531] 07 p0816 N88-14965

Numerical methods for fluid flow problems
[DE88-000156] 07 p0854 N88-15190

Unsteady transonic algorithm improvements for realistic aircraft applications
[NASA-TM-100516] 08 p0949 N88-15760

Consistent boundary conditions for Reduced Navier-Stokes (RNS) scheme applied to 3-dimensional internal viscous flows
[NASA-CR-180874] 08 p0950 N88-15762

Chemical reacting flows 08 p0955 N88-15793

High-speed inlet research program and supporting analyses 08 p0958 N88-15811

Numerical simulation of heat transfer turbulence, volume 2
[AD-A185130] 08 p0983 N88-15947

A computationally efficient modelling of laminar separation bubbles
[NASA-CR-182417] 08 p0984 N88-15949

Computational Fluid Dynamics
[VKI-LS-1987-04] 08 p0984 N88-15951

Characteristic flux averaging approach to the solution of Euler's equations 08 p0984 N88-15955

Finite element methods for compressible flows
08 p0984 N88-15956

Adaptive finite difference methods in fluid dynamics
08 p0985 N88-15958

Finite element fundamentals, part 1
08 p0985 N88-15961

Finite element method computer implementation
08 p0985 N88-15963

Finite Element Calculation Methods and Their Application to Turbomachinery, volume 2
[VKI-LS-1987-05-VOL-2] 08 p0985 N88-15965

Inviscid flows, part 2 08 p0985 N88-15966

Mesh generation 08 p0986 N88-15971

Introduction to the Modeling of Turbulence
[VKI-LS-81-06] 08 p0986 N88-15972

Turbulence models for practical applications
08 p0986 N88-15974

Modeling the unsteady flow found in axial turbomachinery
[ECL-87-07] 08 p0987 N88-15980

Comparative performance of the conjugate gradient and SOR (Successive Over Relaxation) methods for computational thermal hydraulics
[DE88-002553] 08 p0988 N88-15986

Spectral analysis of an orographically structured area in the forefield of mesoscale flow simulations
08 p1016 N88-16160

NASA/Army Rotorcraft Technology. Volume 1: Aerodynamics, and Dynamics and Aeroelasticity
[NASA-CP-2495-VOL-1] 09 p1105 N88-16625

The development of CFD methods for rotor applications 09 p1105 N88-16627

A summary of recent NASA/Army contributions to rotorcraft vibrations and structural dynamics technology
09 p1105 N88-16628

A review of research in rotor loads
09 p1106 N88-16629

Comprehensive rotorcraft analysis methods
09 p1106 N88-16630

Rotorcraft aeroelastic stability
09 p1106 N88-16631

A decade of aeroacoustic research at NASA Ames Research Center 09 p1109 N88-16648

Aeroacoustic research programs at the Army Aviation Research and Technology Activity
09 p1109 N88-16649

An initial investigation into methods of computing transonic aerodynamics sensitivity coefficients
[NASA-CR-182444] 09 p1112 N88-16663

New techniques in computational aerodynamics
[AD-A186719] 09 p1112 N88-16664

Computational unsteady aerodynamics for aeroelastic analysis
[NASA-TM-100523] 09 p1112 N88-16668

CFD validation experiments for internal flows
[NASA-TM-100797] 09 p1114 N88-16679

Solid fuel combustion chamber
[VTH-LR-515] 09 p1141 N88-16842

The viscous flow on surfaces with streamwise riblets
[DFVLR-FB-87-21] 09 p1162 N88-16961

Calculation on film preparation and film motion of a swirl atomizer
[DFVLR-FB-87-25] 09 p1162 N88-16962

Numerical and physical aspects of large eddy simulation of turbulent flows
[ETN-88-91611] 09 p1162 N88-16965

Calculation of the flow through a single-sided sudden expansion with the Computer Program for Parabolic and Elliptic Flows (COPPEF) computer program
[VTH-LR-523] 09 p1163 N88-16973

The dynamics of heat transfer at a turbulent pipe flow
[OEFZS-4400] 09 p1164 N88-16975

A guide to the transient three phase porous flow model implemented in the two-dimensional CRAY-TENSOR code: Physics, numerics, and code description
[DE88-003709] 09 p1165 N88-16983

Computational fluid dynamics and aerothermodynamics
[NASA-CR-182490] 09 p1166 N88-16989

Scientific Colloquium in Honor of Prof. Dr. Rer. Nat. Hermann L. Jordan
[DFVLR-MITT-87-11] 09 p1240 N88-17432

Numerical fluid mechanics 09 p1240 N88-17434

Solution of the three-dimensional Navier-Stokes equations for transonic flow using a multigrid method
10 p1267 N88-17579

Application of empirical and linear methods to VSTOL powered-lift aerodynamics
[NASA-TM-100048] 10 p1267 N88-17581

Wall jet analysis for circulation control aerodynamics. Part 1: Fundamental CFD and turbulence modeling concepts 10 p1269 N88-17588

Transonic blade design on rotational stream surfaces
10 p1282 N88-17671

Computation of secondary flows in an axial multistage compressor 10 p1284 N88-17681

Shuttle rocket booster computational fluid dynamics
[NASA-CR-182518] 10 p1293 N88-17733

Boundary layer calculation using digital computers
[REPT-MM-4] 10 p1309 N88-17821

Zonal solutions for viscous flow problems. Finite approximations in fluid mechanics
[MBB/LKE-122/S/PUB/226] 10 p1313 N88-17846

The use of multigrid techniques in the solution of the Elrod algorithm for a dynamically loaded journal bearing
[NASA-CR-180873] 10 p1331 N88-17954

A visual programming environment for the Navier-Stokes computer
[NASA-CR-181615] 10 p1390 N88-18299

Hypersonic blunt body computations including real gas effects
[NASA-TM-100074] 10 p1400 N88-18344

A code development system for computational fluid dynamics
[AD-A188050] 11 p1482 N88-18848

Specialized instrumentation for computational fluid dynamics research
[AD-A188160] 11 p1482 N88-18849

Finite element methods of analysis for high speed viscous flows
[NASA-CR-182529] 11 p1483 N88-18852

Chaos, mappings and spatial complexity in fluids
11 p1484 N88-18860

Theoretical and experimental analysis of pressure pulse transmission in non-Newtonian pipe flow
11 p1485 N88-18863

A posteriori error estimates in computational fluid mechanics 11 p1486 N88-18869

Topology and grid adaption for high-speed flow computations
[NASA-CR-182586] 11 p1487 N88-18875

Turbulence modeling in non-inertial frames of reference
[NASA-CR-181646] 11 p1488 N88-18880

Application of advanced computational technology to propulsion CFD
[NASA-TM-100843] 11 p1525 N88-19102

Generation of surface grids through elliptic partial differential equations for aircraft and missile configurations
[AD-A186631] 11 p1535 N88-19169

A numerical procedure for conformal mapping of the exterior of a circle onto the exterior of a wing profile with a spoiler
[ISL-R-110/86] 11 p1536 N88-19180

Multigrid methods: Special topics and applications --- conference
[GMD-120] 11 p1537 N88-19187

A generalisation of Hall's scheme for solving the Euler equations for two-dimensional flows
11 p1537 N88-19188

A multigrid solver for two-dimensional transonic full potential flow calculations 11 p1538 N88-19189

Implementation of multigrid in SOLA algorithm --- fluid flow 11 p1538 N88-19191

Solution of the Euler equations: Explicit schemes acceleration by a multigrid method
11 p1538 N88-19192

Unstructured multigrid methods
11 p1538 N88-19193

Solution of a rotating Navier-Stokes problem by a nonlinear multigrid algorithm 11 p1538 N88-19194

Application of the multigrid technique to the pressure-correction equation for the SIMPLE algorithm --- Semi-Implicit Method for Pressure Linked Equations (SIMPLE) 11 p1539 N88-19196

Calculation of flow about posts and powerhead model
[NASA-CR-179305] 12 p1625 N88-19722

Accelerating the computation of steady state solutions for non-equilibrium, chemically reacting flow fields
12 p1625 N88-19724

Time-accurate simulations of a shear layer forced at a single frequency
[NASA-TM-100836] 12 p1628 N88-19740

Reynold stress closure in jet flows using wave models
[NASA-CR-182662] 12 p1628 N88-19741

Application of a nonisentropic full potential method to AGARD standard airfoils
[NASA-TM-100560] 13 p1716 N88-20263

Computational technique for compressible vortex flows using the integral equation solution
[NASA-CR-182695] 13 p1718 N88-20271

Mixing of viscous fluids: Behavior of microstructures and chaos
[DE88-006287] 13 p1766 N88-20566

Three-dimensional shear layer experiments and their use as test cases for calculation methods
[NLR-MP-86036-U] 13 p1767 N88-20570

Solution of two-dimensional Euler equations: Experience with a finite volume code
[DFVLR-FB-87-41] 13 p1767 N88-20572

Graphics and flow visualization of computer generated flow fields
[NASA-CR-182679] 13 p1767 N88-20573

Pseudo-stationary oblique-shock-wave reflections in low gamma gases: Isobutane and sulphur hexafluoride
[UTIAS-TN-267] 13 p1768 N88-20576

Calculations of viscous flows with a multigrid method
13 p1769 N88-20580

General fuselage coordinates for the calculation of three-dimensional boundary layers
[MBB/LKE-122/S/PUB/244] 13 p1771 N88-20596

Activities report of the Lille Institute of Fluid Mechanics
[ETN-88-91983] 13 p1771 N88-20597

Comparison between computed and measured swirl and turbulence in reciprocating engines
[PDR/CFDU/IC/32] 13 p1779 N88-20647

Activities report of the Aerodynamics Department
[ETN-88-91979] 14 p1862 N88-21123

Utilization of parallel processing in solving the inviscid form of the average-passage equation system for multistage turbomachinery
[NASA-TM-89845] 14 p1868 N88-21160

Discrete vortex analysis of unsteady flow about two-dimensional cambered plates
[DE88-006597] 14 p1909 N88-21407

An experimental-computational investigation of transonic shock wave-turbulent boundary layer interaction in a curved test section
[CWI-NM-R8716] 14 p1909 N88-21408

Solutions for direct and indirect problems in free surface flows
[REPT-87-35] 14 p1909 N88-21409

Problems in fluid dynamics
[NASA-CR-182678] 14 p1909 N88-21410

An explicit method for the solution of the Euler equations applied to unsteady two-dimensional flows
[MBB/LKE-121/S/PUB/257] 14 p1910 N88-21411

High-speed flow calculations past 3-D configurations based on the Reynolds averaged Navier-Stokes equations
[NASA-TM-100082] 14 p1911 N88-21421

Potential applications of computational fluid dynamics to biofluid analysis
[NASA-TM-100089] 14 p1911 N88-21422

Accuracy requirements and benchmark experiments for CFD validation
[NASA-TM-100087] 14 p1911 N88-21423

One dimensional calculation model for laser produced plasmas expanding in vacuum
[ISL-R-128/86] 14 p1984 N88-21836

Computational fluid dynamics drag prediction: Results from the Viscous Transonic Airfoil Workshop
[NASA-TM-100095] 15 p2014 N88-22009

Trends in Computational Fluid Dynamics (CFD) for aeronautical 3D steady applications: The Dutch situation
[NLR-MP-86074-U] 15 p2015 N88-22017

Split-coefficient matrix solution and experimental study of axisymmetric underexpanded exhaust plumes
15 p2054 N88-22242

Theoretical model and numerical solution for compressible viscous vortex cores
15 p2054 N88-22243

Mixed direct-inverse problem of transonic cascade
15 p2054 N88-22244

Zero-lift drag predictions in supersonic flow for complex configurations 15 p2054 N88-22246

A panel method based on velocity potential to compute harmonically oscillating lift surface systems
[ETN-88-91886] 15 p2061 N88-22290

Duct flow nonuniformities: Effect of struts in SSME HGM II(+)
[NASA-CR-179285] 15 p2062 N88-22296

Theoretical investigation of secondary instability of three-dimensional boundary-layer flows with application to the DFVLR-F5 model wing
[DFVLR-FB-87-44] 15 p2068 N88-22330

Numerical study of unsteady viscous hypersonic blunt body flows with an impinging shock
[NASA-TM-100096] 15 p2122 N88-22650

High-resolution shock-capturing schemes for inviscid and viscous hypersonic flows
[NASA-TM-100097] 15 p2122 N88-22651

A multilifting line method and its application in design and analysis of nonplanar wing configurations
[DFVLR-FB-87-51] 16 p2155 N88-22860

Numerical analysis of critical penetration velocity for jet perpendicular penetration 16 p2186 N88-23037

Ejection mechanisms in the sublayer of a turbulent channel 16 p2195 N88-23090

EDQNM closure: A homogeneous simulation to support it. A quasi-homogeneous simulation to disprove it
16 p2195 N88-23091

Validation of EDQNM for subgrid and supergrid models 16 p2195 N88-23092

Angular distribution of turbulence in wave space
16 p2195 N88-23093

Premixed turbulent flame calculation
16 p2196 N88-23098

Analysis of non-premixed turbulent reacting flows
16 p2196 N88-23100

A statistical investigation of the single-point pdf of velocity and vorticity based on direct numerical simulations 16 p2196 N88-23101

On local approximations of the pressure-strain term in turbulence models 16 p2197 N88-23102

Local structure of intercomponent energy transfer in homogeneous turbulent shear flow
16 p2197 N88-23103

A general form for the dissipation length scale in turbulent shear flows 16 p2197 N88-23104

Test code for the assessment and improvement of Reynolds stress models 16 p2197 N88-23105

Evaluation of a theory for pressure-strain rate
16 p2198 N88-23108

Relations between two-point correlations and pressure strain terms 16 p2198 N88-23109

The simulation of coherent structures in a laminar boundary layer 16 p2198 N88-23111

Conditionally-averaged structures in wall-bounded turbulent flows 16 p2198 N88-23112

Coherent structures --- in turbulent flows
16 p2199 N88-23121

La Recherche Aerospatiale, bimonthly bulletin, number 1987-3, 238/May-June
[ESA-TT-1075] 16 p2206 N88-23161

Numerical treatment of Navier-Stokes equations
[REPT-87-22] 16 p2206 N88-23162

On the use of nonstaggered pressure-velocity arrangement for the numerical solution of incompressible flows
[KU-SFB-210/T/35] 16 p2206 N88-23165

A small concentration expansion for the effective heat conductivity of a random disperse two-component material; an assessment of Batchelor's renormalization method [REPT-87-71] 16 p2207 N88-23168
Investigation of subgrid models in homogeneous incompressible turbulence [ONERA-RSF-13/3419-AY-106-A] 16 p2209 N88-23183
Two-equation low-Reynolds-number turbulence modeling of transitional boundary layer flows characteristic of gas turbine blades [NASA-CR-4145] 16 p2209 N88-23185
Aeroelastic forced response analysis of turbomachinery 16 p2220 N88-23247
Methodology for matching experimental and computational aerodynamic data [NASA-TM-100592] 17 p2295 N88-23728
Numerical simulation of scramjet inlet flow fields [NASA-TP-2517] 17 p2296 N88-23735
An efficient parallel algorithm for the simulation of three-dimensional compressible transition on a 20 processor Flex/32 multicomputer [NASA-CR-178340] 17 p2337 N88-23943
Numerical method for unsteady viscous-inviscid interaction to calculate buffeting [ONERA-RSF-02/3617-AY-008-A] 17 p2338 N88-23949
Development and improvement of a code to calculate small, three dimensional, unsteady transonic perturbations [ONERA-RTS-31/3064-RY-062-R] 17 p2338 N88-23951
Accounting for the effects of unsteady, separated boundary layers in transonic two dimensional calculations [ONERA-RT-30/3064-RY-063-R] 17 p2338 N88-23952
Surface curvature and pressure gradient effects on turbulent flow: An assessment based on numerical solution of the Reynolds equations 17 p2338 N88-23954
Numerical modelling of flows using phoenics 17 p2339 N88-23955
Progress and future directions in computational fluid dynamics [NASA-TM-100091] 18 p2456 N88-24579
Prediction of laminar and turbulent flows past single and twin airfoils 18 p2457 N88-24589
A transonic small disturbance wing design methodology 18 p2457 N88-24590
A formulation for the boundary-layer equations in general coordinates [NASA-TM-100079] 18 p2459 N88-24600
Some rotorcraft applications of computational fluid dynamics [NASA-TM-100066] 18 p2459 N88-24601
Applications of the Navier-Stokes equations to wings and complex configurations using a zonal approach [NASA-TM-100080] 18 p2459 N88-24602
A decade of computer simulations for space shuttle aerodynamics [NASA-TM-100990] 18 p2459 N88-24603
Simulations of a missile with liquid payload under launch conditions [AD-A191479] 18 p2463 N88-24625
Internal fluid dynamics within a nonspinning partially liquid-filled shell due to burster rupture [AD-A191055] 18 p2507 N88-24874
Adaptive local grid refinement in computational fluid mechanics [AD-A192215] 18 p2510 N88-24890
Computational fluid dynamics applied to the prediction of the heat-transfer, mechanical and thermal-stress behavior of heat exchangers [CFDU/87/7] 18 p2510 N88-24893
CFD benefits, goals, stepping-stones and techniques. Proposals for the scientific programme of the European Reserch Centre on flow, turbulence and combustion --- computational fluid dynamics [CFDU/88/1] 18 p2510 N88-24894
Three dimensional spectral energy measurement on turbulence subjected to a high degree of plane deformation [ETN-88-92537] 18 p2511 N88-24896
Two dimensional hyperbolic grid generation [VKI-TN-162] 18 p2511 N88-24897
Duct flow nonuniformities for Space Shuttle Main Engine (SSME) [NASA-CR-179338] 18 p2511 N88-24899
Improving the performance of a finite element method using vector analysis on CRAY 1 [ETN-88-92153] 18 p2513 N88-24907
Theoretical analysis of laminar incompressible flow in slender channels [VTH-LR-517] 18 p2513 N88-24909
Review of numerical methods for radionuclide transport in three-dimensional porous media, at high Peclet numbers [CFDU/87/10] 18 p2538 N88-25061
NAS: The first year [NASA-TM-101006] 18 p2560 N88-25196
The 24th JANNAF Combustion Meeting, volume 2 [AD-A190164] 19 p2622 N88-25554
Dual Stokes cars measurements in supersonic combusting flow 19 p2625 N88-25569
Numerical grid generation and flow simulation in SSME thrust chamber 19 p2626 N88-25577
A computer program for performance prediction of tripropellant rocket engines with tangential slot injection 19 p2627 N88-25581
Proceedings of the 5th NAL Symposium on Aircraft Computational Aerodynamics [NAL-SP-8] 19 p2635 N88-25630
On the NAL numerical simulator system 19 p2635 N88-25631
Numerical simulations of flow around shuttle orbiter 19 p2635 N88-25633
Finite element analysis of incompressible viscous flow around multi-element aerofoils 19 p2635 N88-25634
Numerical simulations of astrophysical jets 19 p2636 N88-25635
Numerical calculation of supersonic flow by the PNS equations 19 p2636 N88-25636
Computation of flow around NACA0012 airfoil at high angle of attack 19 p2636 N88-25640
Aerodynamic simulation for complete ASKA aircraft configuration 19 p2637 N88-25641
Numerical simulation of viscous flows over transonic aircraft configurations 19 p2637 N88-25642
Calculations of unsteady aerodynamics for a full aircraft configuration using boundary element method 19 p2637 N88-25643
Rarefied gas numerical wind tunnel 3. Universal code for three dimensional bodies 19 p2637 N88-25644
A numerical analysis of flow characteristics in laser propulsion system 19 p2637 N88-25645
Numerical simulation of the shock tube flows by TVD scheme 19 p2638 N88-25648
Numerical calculation of three dimensional flow by TVD scheme 19 p2638 N88-25649
Numerical analysis of three dimensional cascade flow by solving Navier-Stokes equations 19 p2638 N88-25650
Simulation of axisymmetric flow with H2O2 reactions 19 p2638 N88-25651
The role of computational fluid dynamics in aeronautical engineering (5). Improvements and applications of implicit TVD finite volume code 19 p2638 N88-25653
Extensive verification of blade-to-blade flow code based on Denton scheme 19 p2638 N88-25654
Application of computational fluid dynamics to design of compressor cascade 19 p2639 N88-25655
On the accuracy of upwind biased finite volume method 19 p2639 N88-25656
On symmetric TVD schemes 19 p2639 N88-25659
Numerical simulation of transition to turbulence in plane Poiseuille flow by a spectral method 19 p2640 N88-25661
Numerical simulation of turbulent flow using the exponential expression of k-Epsilon equation 19 p2640 N88-25662
Relaxation scheme for compressible flows 19 p2640 N88-25663
The modified-fluid-in-cell method to which adaptive mesh and multigrid were applied 19 p2640 N88-25664
Grid generation of a helicopter rotary-wing 19 p2640 N88-25665
The development of an intelligent interface to a computational fluid dynamics flow-solver code [NASA-TM-100908] 19 p2716 N88-26127
Acoustic wave dispersion in a viscous, compressible, liquid-filled cylindrical elastic tube 19 p2722 N88-26164
An initial investigation into methods of computing transonic aerodynamic sensitivity coefficients [NASA-CR-183061] 20 p2752 N88-26332
The Proceedings of the Symposium on Mechanics for Space Flight 1987 [ISAS-SP-6] 20 p2782 N88-26499
Use of direct solvers for multidimensional fluid flow computations [DE88-010063] 20 p2799 N88-26611
Three-dimensional viscous flow computations of a circular jet in subsonic and supersonic cross flow [NASA-CR-182153] 20 p2800 N88-26616
A study of flow separation in transonic flow using inviscid and viscous computational fluid dynamics (CFD) schemes [NASA-CR-183119] 20 p2801 N88-26618
Improved 3-D turbomachinery CFD algorithm [NASA-CR-179364] 20 p2801 N88-26619
Study of a water-steam two phase flow in a T-branch [ETN-88-92306] 20 p2801 N88-26624
Preliminary design and analysis of procedures for the numerical generation of 3D block-structured grids [NLR-TR-86102-U] 20 p2802 N88-26628
Parallelization on a multiprocessor system of a solution method for the unsteady Navier-Stokes equations at high Reynolds numbers [ONERA-NT-1987-8] 20 p2803 N88-26632
Hybrid procedure for dynamic measurements in transonic wind tunnels: Demonstrated by pitch oscillation [DFVLR-FB-88-19] 21 p2900 N88-27211
Computational fluid dynamics on parallel processors [AD-A192397] 21 p2941 N88-27469
Aerodynamics of Hypersonic Lifting Vehicles: Fluid Dynamics Panel AGARD Symposium [AGARD-AR-246] 21 p2943 N88-27480
A Navier-Stokes study of cascade flow fields including inlet distortion and rotating stall [AD-A193109] 21 p2943 N88-27483
Numerical computation of three-dimensional turbulent flow in tightly curved ducts and spiral turbine casings [ETN-88-92362] 21 p2948 N88-27511
Method to predict external store carriage characteristics at transonic speeds [NASA-CR-4170] 22 p3037 N88-28034
Transonic blade-vortex interactions 22 p3037 N88-28035
An improved version of NCOREL: A computer program for 3-D nonlinear supersonic potential flow computations [NASA-CR-4165] 22 p3038 N88-28039
Field methods for computing high Reynolds number viscous flow [FFA-TN-1988-01] 22 p3039 N88-28046
Advanced computational methods for turbomachinery blade design [PNR90438] 22 p3044 N88-28065
The calculation of the flow through a two-dimensional faired diffuser [PNR90433] 22 p3076 N88-28259
Application of rectangular co-ordinates to the problem of laminar combined convection in a straight horizontal tube whose circumference is heated nonuniformly [PDR/CFDU/IC/33] 22 p3076 N88-28263
A new method of calculating the boundary layer characteristics downstream of manipulators. Part 1: Boundary layer integral parameters [PNR90455] 22 p3078 N88-28279
A new method of calculating the boundary layer characteristics downstream of manipulators. Part 2: Skin friction and net drag reduction [PNR90456] 22 p3078 N88-28280
Numerical predictions for the flow induced by an enclosed rotating disc [PNR90463] 22 p3078 N88-28281
Non-reflecting boundary conditions for computations of unsteady flows in turbomachines [PNR90469] 22 p3079 N88-28284
Boundary layer simulation and control in wind tunnels [AGARD-AR-224] 23 p3167 N88-28857
Complex configurations 23 p3167 N88-28861
Computational tools for simulation methodologies 23 p3168 N88-28865
Empirical tools for simulation methodologies 23 p3168 N88-28866
Transport-type configurations 23 p3169 N88-28867
Combat aircraft 23 p3169 N88-28868
Missiles, fuselages and similar bodies 23 p3169 N88-28869
Introduction and critical flow phenomena 23 p3169 N88-28870
Boundary layer manipulation 23 p3170 N88-28877
An unsteady helicopter rotor: Fuselage interaction analysis [NASA-CR-4178] 23 p3171 N88-28880
Accurate solutions, parameter studies and comparisons for the Euler and potential flow equations [NASA-TM-100664] 23 p3173 N88-28892
Variable Sweep Transition Flight Experiment (VSTFE)-parametric pressure distribution boundary layer stability study and wing glove design task [NASA-CR-3992] 23 p3173 N88-28894
Steady and unsteady internal flow computations via the solution of the compressible Navier Stokes equations for low Mach numbers 23 p3209 N88-29100
Three-dimensional laser Doppler velocimeter studies of flow in a 90 deg curved duct having a square cross-section 23 p3209 N88-29101
Numerical investigations in three-dimensional internal flows [NASA-CR-183108] 23 p3210 N88-29106

Navier-Stokes calculations of transonic flows past cavities
[NASA-CR-180484] 23 p3212 N88-29116

Computational fluid dynamics methods for low Reynolds number precessing/spinning incompressible flows
[AD-A193891] 23 p3212 N88-29119

A calculation of the turbulent boundary layer on a slender ellipsoid at low incidence
[FFA-TN-1988-02] 23 p3213 N88-29126

European research program on viscous flows
[DFVLR-AVA-IB-227-87-A-15] 23 p3214 N88-29129

Three dimensional grid generation for complex configurations: Recent progress
[AGARD-AG-309] 23 p3245 N88-29313

Experience with three dimensional composite grids
23 p3247 N88-29324

Overview of computational vibro acoustics. State of the art and future development
[FFA-TN-1988-17] 23 p3279 N88-29521

The computation of flow past an oblique wing using the thin-layer Navier-Stokes equations
[NASA-TM-88317] 24 p3320 N88-29774

Computational methods for the problems of the tip vortex
[NASA-CR-181438] 24 p3320 N88-29775

Recent advances in transonic computational aeroelasticity
[NASA-TM-100663] 24 p3321 N88-29778

Gas turbine combustion modeling
24 p3349 N88-29936

Numerical modeling of combustion processes in gas turbines 24 p3350 N88-29939

Numerical simulation of nozzle flows
[AD-A195144] 24 p3369 N88-30064

The viscous flow on surfaces with streamline riblets
[ESA-TT-1091] 24 p3370 N88-30067

Knowledge-based flow field zoning
[NASA-TM-101023] 24 p3412 N88-30314

Convergence acceleration for vector sequences and applications to computational fluid dynamics
[NASA-TM-101327] 24 p3424 N88-30377

COMPUTATIONAL GEOMETRY

Scanline algorithms on a grid
[PB88-103379] 06 p0766 N88-14710

Computer aided geometric design
[AD-A187324] 10 p1389 N88-18293

Steps into a geometer's workbench
[CWI-CS-R8726] 13 p1819 N88-20870

Geometry and graphics applied to robotics
[CWI-CS-R8727] 13 p1824 N88-20903

COMPUTATIONAL GRIDS

Problem and solution formulations for the generation of 3D block-structured grids --- aircraft design
[NLR-MP-86020-U] 01 p0005 N88-10028

Generation of body-fitted grids for two dimensional interior domains by the solution of a system of Poisson equations using multigrid techniques
[GMD-246] 01 p0044 N88-10281

Computational fluid dynamics in the United Kingdom
[RAE-TM-AERO-2098] 02 p0171 N88-11073

Development and testing of a vertically-nested regional prediction system --- weather forecasting
02 p0210 N88-11322

Differencing the diffusion equation on a mesh of triangles and quadrilaterals
[DE87-011550] 02 p0224 N88-11408

Finite elements for 2D elliptic equations with moving nodes
[DE87-013501] 02 p0224 N88-11410

FLIP (Fluid-Implicit-Particle): A low-dissipation, particle-in-cell method for fluid flow
[DE87-014745] 03 p0313 N88-11981

Numerical solution of partial differential equations on irregular grids
[DE87-014760] 03 p0369 N88-12324

Theoretical and practical aspects of multigrid methods in boundary element calculations
[NLR-MP-85021-U] 03 p0370 N88-12328

Solution of the two-dimensional Euler equations on unstructured triangular meshes
04 p0396 N88-12469

Generating meshes for finite-difference analysis using a solid modeler
[DE88-001458] 04 p0439 N88-12729

Parallel superconvergent multigrid
[DE87-013153] 04 p0480 N88-12960

High resolution finite volume methods on arbitrary grids via wave propagation
[NASA-CR-178397] 04 p0484 N88-12979

The finite element method for electronic structure
[DE88-001708] 04 p0485 N88-12989

Numerical simulation of the hypersonic flow around lifting vehicles 05 p0532 N88-13234

Computation of dynamic stall of NACA0012 airfoil by block pentadiagonal matrix scheme
05 p0535 N88-13255

Practical and modern simulation by systematic connection of the LU-ADI code and the solution adaptive grid program 05 p0536 N88-13260

A perspective of computational fluid dynamics
05 p0538 N88-13279

Computation of flow around 2-D circular cylinder
05 p0539 N88-13284

Analytical method for generating computational grids about complete aircraft configurations
05 p0540 N88-13287

Compressible Euler solution on a multiblock grid around a wing-fuselage configuration
[FFA-TN-1987-46] 05 p0542 N88-13303

A Cartesian finite-volume method for the Euler equations 05 p0579 N88-13532

Finite-element grid improvement by minimization of stiffness matrix trace
[NASA-TM-100255] 05 p0591 N88-13604

Free Lagrange reconnection algorithms for hydrocodes using a quadrilateral mesh
[DE88-001580] 05 p0611 N88-13752

Vectorization of a multigrid method for the compressible Navier-Stokes equations
[PB87-230496] 06 p0698 N88-14284

Finite element techniques 06 p0701 N88-14303

A zonal approach for the solution of coupled Euler and potential solutions of flows with complex geometries
[AD-A185465] 06 p0702 N88-14310

Computational methods for complex flowfields
[AD-A185793] 06 p0703 N88-14317

Adaptive grid for polyhedral visibility in object space: An implementation
[PB88-100938] 06 p0760 N88-14663

Scanline algorithms on a grid
[PB88-103379] 06 p0766 N88-14710

Shuttle computational grid generation
06 p0794 N88-14863

Multitasked embedded multigrid for three-dimensional flow simulation
[NASA-CR-182398] 07 p0852 N88-15173

Local uniform mesh refinement for partial differential equations
[AD-A186312] 07 p0910 N88-15519

The k-grid Fourier analysis of multigrid-type iterative methods
[AD-A186315] 07 p0910 N88-15520

Nacelle-wing interactions (studies 1986) development of a finite element code in a multi-domain version
[ONERA-RTS-10/3417-AY-308A]
08 p0950 N88-15764

A multistage mesh generator for solving the average-passage equation system
[NASA-CR-179539] 08 p0951 N88-15769

Finite element methods for compressible flows
08 p0984 N88-15956

Finite element method computer implementation
08 p0985 N88-15963

Finite Element Calculation Methods and Their Application to Turbomachinery, volume 2
[VKI-LS-1987-05-VOL-2] 08 p0985 N88-15965

Mesh generation 08 p0986 N88-15971

Adaptive finite element methods for parabolic systems in one- and two-space dimensions
[AD-A186534] 08 p1073 N88-16475

Review of fatigue and fracture research at NASA Langley Research Center 09 p1106 N88-16633

An automatic finite element mesh generator
[AD-A186939] 09 p1216 N88-17291

Finite element mesh generation and isoparametric elements
[NPL-DITC-97/87] 09 p1229 N88-17365

Modification of a successive corrections objective analysis for improved higher order calculations
[NASA-CR-182467] 09 p1230 N88-17370

Implicit solution of the incompressible Navier-Stokes equations in primitive variables on non-staggered grids
10 p1326 N88-17930

The use of multigrid techniques in the solution of the Elrod algorithm for a dynamically loaded journal bearing
[NASA-CR-180873] 10 p1331 N88-17954

Schwarz splitting and template operators
[AD-A187956] 10 p1404 N88-18370

A new computational technique for generating algorithms, with application to the solution of the time-dependent incompressible Navier-Stokes equations
11 p1485 N88-18864

Topology and grid adaption for high-speed flow computations
[NASA-CR-182586] 11 p1487 N88-18875

Numerical fracture mechanics using finite element method 11 p1501 N88-18966

Computer-aided modeling and prediction of performance of the modified Lundell class of alternators in space station solar dynamic power systems
[NASA-CR-182536] 11 p1507 N88-19000

Workshop on the Integration of Finite Element Modeling with Geometric Modeling
[NASA-CR-182515] 11 p1526 N88-19111

Approaches to the automatic generation and control of finite element meshes 11 p1526 N88-19113

Integration of geometric modeling and advanced finite element preprocessing 11 p1526 N88-19114

Finite element meshing of ANSYS (trademark) solid models 11 p1526 N88-19115

Solid/FEM integration at SNLA
[SAND-87-0882A] 11 p1526 N88-19116

Octree based automatic meshing from CSG models
11 p1527 N88-19117

Geometrical and topological issues in octree based automatic meshing 11 p1527 N88-19118

A hierarchical structure for automatic meshing and adaptive FEM analysis 11 p1527 N88-19119

Toward automatic finite element analysis
11 p1527 N88-19120

Finite octree meshing through topologically driven geometric operators 11 p1527 N88-19121

Multigrid methods: Special topics and applications --- conference
[GMD-120] 11 p1537 N88-19187

A generalisation of Hall's scheme for solving the Euler equations for two-dimensional flows
11 p1537 N88-19188

A multigrid solver for two-dimensional transonic full potential flow calculations 11 p1538 N88-19189

Multigrid methods in convex optimization
11 p1538 N88-19190

Implementation of multigrid in SOLA algorithm --- fluid flow 11 p1538 N88-19191

Solution of the Euler equations: Explicit schemes acceleration by a multigrid method
11 p1538 N88-19192

Unstructured multigrid methods
11 p1538 N88-19193

Solution of a rotating Navier-Stokes problem by a nonlinear multigrid algorithm 11 p1538 N88-19194

A multigrid full potential transonic code for arbitrary configurations --- aircraft 11 p1539 N88-19195

Application of the multigrid technique to the pressure-correction equation for the SIMPLE algorithm --- Semi-Implicit Method for Pressure Linked Equations (SIMPLE) 11 p1539 N88-19196

A signal processing approach to the numerical solution of parabolic differential equations
11 p1539 N88-19197

Discretizations for multigrid methods
11 p1539 N88-19198

Incorporation of multigrid in accelerator software --- particle accelerators 11 p1539 N88-19199

Applications of a multigrid finite volume method with Runge-Kutta time integrations for solving the Euler and Navier-Stokes equations 11 p1539 N88-19201

An L-U implicit multigrid algorithm to solve the Euler equations for transonic flow in rotating turbomachinery passages 13 p1718 N88-20270

The construction of a three-dimensional finite volume grid generator for a wing in a wind tunnel with application to Navier-Stokes flow solvers
[FFA-TN-1987-58] 13 p1719 N88-20277

An adaptive grid technique for solution of the Euler equations 13 p1768 N88-20579

Calculations of viscous flows with a multigrid method
13 p1769 N88-20580

Multigrid solution of the Euler equations
13 p1769 N88-20582

Data traffic reduction schemes for sparse Cholesky factorizations
[NASA-CR-181626] 13 p1813 N88-20831

A knowledge system for automatic finite element mesh generation: AMEKS
[DE87-014894] 13 p1826 N88-20914

A Lagrangian moving grid scheme for one-dimensional evolutionary partial differential equations
[CWI-NM-R8713] 13 p1827 N88-20922

Conservative finite volume solutions of a linear hyperbolic transport equation in two and three dimensions using multiple grids
[NASA-CR-182715] 13 p1828 N88-20934

Three-dimensional mesh-generation and plotting routines for use with a boundary element program (BIE3D)
[AD-A188079] 14 p1958 N88-21675

COMESH: A corner mesh finite difference code to solve multigroup diffusion equations in multidimensions
[DE88-701248] 15 p2108 N88-22555

Efficient, high resolution computations of projectile and missile flow fields
[AD-A191086] 16 p2158 N88-22873

Validation of EDQNM for subgrid and supergrid models 16 p2195 N88-23092

Application of a multigrid method for solving the Navier-Stokes equation in two-dimensional flow problems
[KU-SFB-210/T/32] 16 p2206 N88-23164

Fast algorithms for Euler and Navier-Stokes simulations
[AD-A190897] 16 p2208 N88-23175

Mixed finite element formulation applied to shape optimization 16 p2221 N88-23252

Development of adaptive grid schemes based on Poisson grid generators
[AD-A190953] 16 p2262 N88-23528

Incompressible Euler solution on a multiblock grid around a car configuration
[FFA-TN-1987-65] 18 p2457 N88-24586

Accurate multigrid solution of the Euler equations on unstructured and adaptive meshes
[NASA-CR-181679] 18 p2460 N88-24608

Adaptive local grid refinement in computational fluid mechanics
[AD-A192215] 18 p2510 N88-24890

Two dimensional hyperbolic grid generation
[VKI-TN-162] 18 p2511 N88-24897

Application of advanced grid generation techniques for flow field computations about complex configurations
[NASA-CR-183049] 18 p2515 N88-24922

DOD 1985 world magnetic model: Charts and grid values
[AD-A191484] 18 p2541 N88-25080

Adaptive grid refinement for numerical weather prediction
[AD-A192172] 18 p2544 N88-25101

Multigrid methods for elliptic Partial Differential Equations (PDEs)
[CWI-NM-R8722] 18 p2566 N88-25242

Aerodynamic simulation for complete ASKA aircraft configuration 19 p2637 N88-25641

The role of computational fluid dynamics in aeronautical engineering (5). Improvements and applications of implicit TVD finite volume code 19 p2638 N88-25653

On the accuracy of upwind biased finite volume method 19 p2639 N88-25656

The modified-fluid-in-cell method to which adaptive mesh and multigrid were applied
19 p2640 N88-25664

The solution of the Elrod algorithm for a dynamically loaded journal bearing using multigrid techniques
[NASA-TM-100941] 19 p2666 N88-25854

Automatic routing in symbolic IC design environment
19 p2714 N88-26112

A diagonally inverted LU implicit multigrid scheme
[NASA-TM-100911] 20 p2753 N88-26340

Numerical solution of weak forms of conservation laws on optimal unstructured triangular grids
20 p2797 N88-26597

Multigrid computation of practical fluid flows and heat transfer
[DE88-010064] 20 p2799 N88-26609

Preliminary design and analysis of procedures for the numerical generation of 3D block-structured grids
[NLR-TR-86102-U] 20 p2802 N88-26628

The construction of composite grids for general three-dimensional regions 20 p2843 N88-26872

Prolongation, restriction and coarse grid approximation in a three-dimensional cell-centered multigrid method
[REPT-88-02] 20 p2846 N88-26889

Creating aspect graphs for use in object recognition
21 p2928 N88-27379

Three-dimensional zonal grids about arbitrary shapes by Poisson's equation
[NASA-TM-101018] 22 p3039 N88-28042

High performance solutions of the Stokes problem using mini-elements, self-adaptive grids, and multigrid methods: Applications
[ECL-87-15] 22 p3077 N88-28266

Partitioning of regular computation on multiprocessor systems
[NASA-CR-183176] 22 p3141 N88-28676

An efficient patched grid Navier-Stokes solution for multiple bodies, phase 1
[AD-A194166] 23 p3211 N88-29110

Adaptive computational methods for aerothermal heating analysis
[NASA-CR-181636] 23 p3212 N88-29115

Three dimensional grid generation for complex configurations: Recent progress
[AGARD-AG-309] 23 p3245 N88-29313

Lessons learned in the mesh generation for PN/S calculations 23 p3245 N88-29314

Three-dimensional elliptic grid generation for an F-16
23 p3246 N88-29315

Component adaptive grid generation for aircraft configurations 23 p3246 N88-29316

Generation of multiple block grids for arbitrary 3D geometries 23 p3246 N88-29317

Grid generation on and about a cranked-wing fighter aircraft configuration 23 p3246 N88-29318

Grid generation for an advanced fighter aircraft
23 p3246 N88-29319

Algebraic grid generation for fighter type aircraft
23 p3246 N88-29320

Composite grid generation for aircraft configurations with the EAGLE code 23 p3246 N88-29321

Analytical surfaces and grids
23 p3247 N88-29322

Experience with three dimensional composite grids
23 p3247 N88-29324

Grid generation around transport aircraft configurations using a multi-block structured computational domain
23 p3247 N88-29325

An adaptive overlapping local grid refinement method for two-dimensional parabolic systems
[AD-A193560] 23 p3271 N88-29464

The computation of flow past an oblique wing using the thin-layer Navier-Stokes equations
[NASA-TM-88317] 24 p3320 N88-29774

Knowledge-based flow field zoning
[NASA-TM-101023] 24 p3412 N88-30314

Generation of surface grids through elliptic partial differential equations for aircraft and missile configurations
[AD-A195639] 24 p3424 N88-30378

COMPUTER AIDED DESIGN

Problem and solution formulations for the generation of 3D block-structured grids --- aircraft design
[NLR-MP-86020-U] 01 p0005 N88-10028

Shape optimization of linear antennas
[ETN-87-90413] 01 p0036 N88-10233

An interactive optimization procedure for the computer aided dimensioning of integrated circuits
[ETN-87-90414] 01 p0082 N88-10531

A reference guide for IGVIEW: An IGES-compatible geometry system
[DE87-013441] 01 p0083 N88-10534

A preliminary investigation into the feasibility of implementing a direct sideforce control system on the Astra Hawk by means of an active control surface --- aircraft control
[ETN-87-90924] 02 p0126 N88-10795

Heat transfer in a real engine environment
02 p0186 N88-11155

Contribution to the development of smart design techniques for VLSI integrated circuits --- CMOS
[LAAS-87-181] 02 p0221 N88-11395

Computer aided engineering/manufacturing at Rolls-Royce
[PNR90395] 02 p0222 N88-11397

Development of standard cells in NMOS technology for the design of digital integrated circuits
[FI-62-TB-6] 03 p0310 N88-11953

Double-effect absorption heat pump, phase 3
[PB87-232195] 03 p0317 N88-12005

The structure-mapping engine: Algorithm and examples
[AD-A184042] 03 p0368 N88-12315

The impact of information technology on research in science and engineering
[DE88-000342] 03 p0385 N88-12417

Digital-flight-control-system software written in automated-engineering-design language: A user's guide of verification and validation tools
[NASA-TM-88313] 04 p0401 N88-12494

Numerical simulation system
04 p0404 N88-12511

New feedback design methodologies for large space structures: A multi-criterion optimization approach
04 p0408 N88-12535

Interactions between science and precision engineering
[DE87-010873] 04 p0426 N88-12643

A procedural method for the efficient implementation of full-custom VLSI designs 04 p0436 N88-12701

A new state space model for the NASA/JPL 70-meter antenna servo controls 04 p0436 N88-12702

Large change-of-curvature effects in quadratic finite elements for CAD of membrane structures
04 p0480 N88-12958

Computer-aided X-ray image system design and evaluation
[DE88-000997] 04 p0481 N88-12965

Numerical simulation applied to the development of a pyrotechnical system
[SNIAS-872-430-115] 05 p0571 N88-13479

Applications of fatigue analyses: Transportation
05 p0608 N88-13733

An extension to the multilevel logic simulator for microcomputers
[AD-A185032] 05 p0634 N88-13879

Overall description of the computer aided design and manufacturing systems associated with the A320 program at Aerospatiale and its partners
[SNIAS-872-111-104] 05 p0635 N88-13883

Presentation of SIGMA (Interactive Assisted Geometry System). A computer assisted shape design program developed at the Aerospatiale Aircraft Division
[SNIAS-872-111-110] 05 p0635 N88-13884

Structural optimization in the design process --- aircraft
[SNIAS-872-111-115] 05 p0635 N88-13885

XCUT: A rule-based expert system for the automated process planning of machined parts
[DE87-011638] 05 p0639 N88-13905

Using hierarchically structured problem-solving knowledge in a rule-based process planning system
[DE87-011639] 05 p0639 N88-13906

Computer modeling of complete IC fabrication process
[AD-A184807] 05 p0654 N88-14012

Benchmarking and evaluation of hardware description languages for design of VLSI systems
[PB87-134557] 06 p0758 N88-14648

Scanline algorithms on a grid
[PB88-103379] 06 p0766 N88-14710

Computational design of natural laminar flow wings for transonic transport application 07 p0813 N88-14948

Fault tree reliability analysis of the Naval Postgraduate School mini-satellite (ORION)
[AD-A186283] 07 p0866 N88-15250

Computer aided design for Petri Nets
[AD-A186109] 07 p0902 N88-15465

Extraction of MOS VLSI (Very-Large-Scale-Integrated) circuit models including critical interconnect parasitics
[AD-A185847] 08 p0979 N88-15914

Pulse width modulator controller design for a brushless DC motor position servo
[AD-A186618] 08 p0980 N88-15921

HSTDEK: Developing a methodology for construction of large-scale, multi-use knowledge bases
08 p1057 N88-16377

FMEAssist: A knowledge-based approach to Failure Modes and Effects Analysis 08 p1060 N88-16395

Automatic mathematical modeling for space application 08 p1060 N88-16402

A learning apprentice for software parts composition
08 p1065 N88-16436

Automatic program generation from specifications using Prolog 08 p1065 N88-16437

On acquisition of programming knowledge
08 p1065 N88-16438

System analysis in rotorcraft design: The past decade
09 p1110 N88-16652

Kinematic optimization of mechanisms, a finite element approach
[ISBN-90-370-0012-6] 09 p1175 N88-17039

Optimized structure design using reanalysis techniques 09 p1180 N88-17067

First Annual Workshop on Space Operations Automation and Robotics (SOAR 87)
[NASA-CP-2491] 09 p1203 N88-17206

The use of computer graphic simulation in the development of robotic systems
09 p1214 N88-17275

Interfacing slave designs to Fastbus: Practical experience
[DE88-002807] 09 p1215 N88-17286

Methodological and structural principles for flexible geometric modeling in computer aided design
[MA-48] 09 p1218 N88-17306

A raster scan algorithm for generating visible parametric surfaces
[DE88-003222] 09 p1220 N88-17321

A generalized method for automatic downhand and wirefeed control of a welding robot and positioner
[NASA-TP-2807] 10 p1316 N88-17869

Optimal design and parameter identification of flexible rotor-bearing systems 10 p1339 N88-18002

Directions in computer graphics architecture
10 p1379 N88-18233

Computer aided geometric design
[AD-A187324] 10 p1389 N88-18293

Development of tokamak reactor system analysis code NEW-TORSAC
[DE88-751067] 10 p1411 N88-18417

Computer-Aided Design Information System (CADIS): User's manual
[DE88-004365] 10 p1424 N88-18509

Computer program for conceptual tandem rotor helicopter design
[AD-A187832] 11 p1439 N88-18584

Probabilistic and reliability design procedures for flexible airfield pavements: Elastic layered method
[AD-A187533] 11 p1442 N88-18600

Chinese 7760 CAD/CAMM software system introduced 11 p1468 N88-18756

Computer-aided design analysis of 57-mm, angular-contact, cryogenic turbopump bearings
[NASA-TP-2816] 11 p1496 N88-18933
Computer-aided modeling and prediction of performance of the modified Lundell class of alternators in space station solar dynamic power systems
[NASA-CR-182538] 11 p1507 N88-19000
Computer Applications in Geotechnical Engineering (CAGE) and Geotechnical aspects of the Computer-Aided Structural Engineering (G-CASE) projects. User's guide. UTEXAS2 slope-stability package. Volume 1: User's manual
[AD-A187674] 11 p1511 N88-19025
A multigrid full potential transonic code for arbitrary configurations --- aircraft 11 p1539 N88-19195
Incorporation of multigrid in accelerator software --- particle accelerators 11 p1539 N88-19199
Columbus Simulation Facility (CSF)
12 p1590 N88-19522
An EHF telecommunication system engineering model
12 p1618 N88-19674
Parts-R-Us
[AD-A188621] 12 p1622 N88-19705
Hercules: A power analyzer for MOS VLSI circuits
[AD-A188702] 12 p1623 N88-19706
A digital circuit design environment
[AD-A188831] 12 p1623 N88-19709
An automatic system for extraction of information from a Computer Aided Design (CAD), selection, sequencing, and execution of turning processes
[INPE-4350-TDL/294] 12 p1676 N88-20020
Twenty-fourth Industrial Associates Review
12 p1679 N88-20039
Development cost reduction using integrated CAE-CAD-CAM techniques 12 p1701 N88-20182
Time and cost reduction through computer integrated manufacture 12 p1703 N88-20191
Development of a dependency theory toolbox for database design
[AD-A188872] 12 p1707 N88-20216
Australian aerodynamic design codes for aerial tow bodies
[AD-A189048] 13 p1715 N88-20258
Computer-aided transformation of descriptive mode of mathematical models of a control system
13 p1756 N88-20503
Gridless routing for generalized cell assemblies: Report and user manual
[EUT-87-E-180] 13 p1764 N88-20549
On the sensitivity of complex, internally coupled systems
[NASA-TM-100537] 13 p1813 N88-20829
MacCAD (Macintosh Computer Aided Design), computer aided design tool for system analysis
[AD-A189241] 13 p1815 N88-20843
Computer aided surface representation
[DE88-005408] 13 p1817 N88-20854
The concept of intelligent integrated interactive CAD systems
[CWI-CS-R8717] 13 p1818 N88-20865
Organization of design knowledge in an intelligent CAD environment
[CWI-CS-R8720] 13 p1819 N88-20868
An integrated data description language for coding design knowledge
[CWI-CS-R8731] 13 p1819 N88-20871
GM: A gate matrix layout generator
[EUT-87-E-179] 13 p1820 N88-20875
Finite State Tables for general computer programming applications
[DE88-006254] 13 p1820 N88-20881
Computer aided design of aircraft structures
[ETN-88-91353] 14 p1867 N88-21154
A sequentially deployable structure for space applications 14 p1875 N88-21202
GADL: A gate array description language
[EUT-87-E-165] 14 p1907 N88-21396
Higher levels of a silicon compiler
[EUT-86-E-163] 14 p1955 N88-21650
Generating layouts for random logic: Cell generation schemes
[EUT-86-E-164] 14 p1956 N88-21658
ESKISS: A program for optimal state assignment
[EUT-87-E-167] 14 p1956 N88-21659
Supercomputer-aided generalized mixer analysis and optimization
[FUB-15-1986] 14 p1957 N88-21668
Activities report of the Computer Science Department
[ETN-88-91980] 14 p1958 N88-21672
Representing knowledge in two distinct descriptions: Extensional vs. intensional
[CWI-CS-R8726] 14 p1961 N88-21699
Technology mapping from Boolean expressions to standard cells
[EUT-87-E-174] 14 p1963 N88-21709
An optimal CMOS structure for the design of a cell library
[EUT-87-E-166] 14 p1985 N88-21841
Characteristics of LSI-wiring expert system discussed
15 p2052 N88-22226
Reliability analysis within a Computer Aided Engineering (CAE) infrastructure
[NLR-MP-86059-U] 15 p2074 N88-22369
Investigation into the development of computer aided design software for space based sensors
[NASA-CR-180772] 15 p2107 N88-22552
Software structuring principles for VLSI CAD
[AD-A190386] 15 p2112 N88-22579
A graphics editor for structured analysis with a data dictionary
[AD-A190618] 15 p2112 N88-22584
High speed transcendental elementary function architecture in support of the Vector Wave Equation (VWE)
[AD-A189746] 15 p2119 N88-22627
Rapid prototyping of complex avionics system architectures
[ETN-88-92275] 16 p2162 N88-22898
Status of CAD/CAM in medium-sized industries described 16 p2184 N88-23022
Automatic layout generation of data processing sections of VLSI microprocessor-like circuits
[ETN-88-92185] 16 p2245 N88-23411
Computer aided design tools for integrated silicon system structures
[ETN-88-92186] 16 p2247 N88-23424
Silicon compilers: Application to the compilation of the control area
[ETN-88-92188] 16 p2247 N88-23425
Contribution to the automatic generation of floor plan placing --- integrated circuit design
[ETN-88-92193] 16 p2247 N88-23426
Design as a formal, knowledge engineered activity
[CWI-CS-R8744] 16 p2248 N88-23431
Knowledge engineering in design
[CWI-CS-R8745] 16 p2248 N88-23432
Correctness proofs for systolic algorithms: A palindrome recognizer
[CWI-CS-R8747] 16 p2248 N88-23434
Piecewise linear approach for timing simulation of VLSI (Very-Large-Scale-Integrated) circuits on serial and parallel computers
[AD-A191328] 16 p2252 N88-23462
Data base management in CAD/CAM systems: Requirements for CAD/CAM data bases, actual market offer, advice for an efficient data base management, development tendencies
[MBB/LWD-11/S/PUB/254] 16 p2285 N88-23683
It's time to reinvent the general aviation airplane
17 p2294 N88-23726
Computational wing design studies relating to natural laminar flow 17 p2297 N88-23740
The Design, Development and Testing of Complex Avionics Systems
[AGARD-CP-417] 17 p2302 N88-23767
Rapid prototyping of complex avionic system architectures 17 p2302 N88-23771
The avionics software architecture impact on system architecture 17 p2303 N88-23778
Managing advanced avionic system design
17 p2304 N88-23783
Advanced development of a cockpit automation design support system 17 p2304 N88-23785
Design and development of an avionics system adapted to helicopter missions 17 p2305 N88-23786
Developing systems using state-of-the-art CAD/CAM technology 17 p2306 N88-23795
Interfacing and integrating hardware and software design systems 17 p2306 N88-23796
Avionics systems: Development method and computer tools 17 p2306 N88-23799
A software life cycle support environment
17 p2306 N88-23800
Coherent functional development: Key to successful future system integration 17 p2307 N88-23803
A software design tool for the analysis of robot dynamics properties
[NLR-MP-86064-U] 17 p2385 N88-24171
Simulation and computer aided engineering (the necessity of an integrated approach)
[NLR-MP-86050-U] 17 p2386 N88-24178
Expert systems approach to modeling systems with the ATHENA thermal-hydraulics code
17 p2416 N88-24365
An OOD (Object-Oriented Design) paradigm for flight simulators
[AD-A191097] 18 p2467 N88-24647
Computer aided design of monolithic microwave and millimeter wave integrated circuits and subsystems
[AD-A191593] 18 p2503 N88-24852
Calculation of root-mean-square loads
[BLL-M-37776-(5828.4)] 18 p2531 N88-25015
The Environment for Application Software Integration and Execution (EASIE), version 1.0. Volume 3: Program execution guide
[NASA-TM-100575] 18 p2558 N88-25184
The Sizing and Optimization Language, (SOL): Computer language for design problems
[NASA-TM-100565] 18 p2559 N88-25190
Extensive verification of blade-to-blade flow code based on Denton scheme 19 p2638 N88-25654
Semi-Markov adjunction to the Computer-Aided Markov Evaluator (CAME)
[NASA-CR-181645] 19 p2678 N88-25924
Improved method for stress and compatibility analysis of multicomponent rotating systems
[NASA-TM-100884] 19 p2680 N88-25935
Fault diagnosis in distributed computer networks
[AD-A192406] 19 p2718 N88-26140
Research in VLSI computer systems
[AD-A192915] 20 p2835 N88-26816
The knowledge based automatic extraction of the machinable surfaces for automatic CAD-CAM system
[INPE-4542-PRE/1288] 20 p2836 N88-26824
Enumeration, comments and discussion concerning papers presented during the Conference on Computer Applications in Production and Engineering (CAPE) 87
[NLR-MP-87015-U] 20 p2839 N88-26844
A survey of freeform solid modeling methods
[REPT-87-81] 20 p2839 N88-26847
Interaction management in CAD systems with a history mechanism
[CWI-CS-R8756] 20 p2840 N88-26851
NEXT: An expert system development tool to support engineering design
[NLR-MP-86070-U] 20 p2843 N88-26871
Programs for preliminary design of composite materials which were developed by the design group of Aerospatiale Aquitaine
[REPT-881-430-112] 21 p2907 N88-27251
Investigation of expert system design approaches for electronic design environments
21 p2926 N88-27365
The integration of decision support problems into feature modeling based design 21 p2927 N88-27372
Mitsubishi Electric Advance (R and D Edition), Volume 41
[PB88-194162] 21 p2929 N88-27388
Computer-Aided Engineering (CAE) for engineering design 21 p2929 N88-27390
STAR: Sandia Timing Analyzer Routine
[DE88-012412] 21 p2940 N88-27463
Optimization of planetary gears
[ETN-88-92375] 21 p2958 N88-27573
Computer aided design for linear control State Variable System (SVS)
[AD-A193282] 21 p2997 N88-27775
Research into the architecture of CAD based robot vision systems
[AD-A193330] 21 p2997 N88-27776
Benefits of an object approach in a computer aided design environment
[SNIAS-881-440-102] 21 p3000 N88-27791
A PRELUDE (analysis and design of control systems-preliminary utilities depository). A data-based interactive system of control software, user's guide
[DFVLR-MITT-88-12] 21 p3000 N88-27795
Large-signal modeling of gallium arsenide field-effect transistors 22 p3073 N88-28242
Advanced manufacturing management current and forthcoming technologies
[PNR90445] 22 p3159 N88-28802
Structural dynamics of maneuvering aircraft
[AD-A192376] 23 p3176 N88-28908
Computer aided filter design
[AD-A193959] 23 p3208 N88-29093
Interactive plotting of NASTRAN aerodynamic models using NPLOT and DISSPLA
[AD-A194115] 23 p3226 N88-29204
Second Conference on Artificial Intelligence for Space Applications
[NASA-CP-3007] 23 p3251 N88-29351
Hologram representation of design data in an expert system knowledge base 23 p3251 N88-29354
The use of computer graphic simulation in the development of robotic systems
23 p3257 N88-29388
Computer-Aided-Control Engineering (CACE) primitives for robust and adaptive control systems, phase 1
[AD-A192446] 23 p3265 N88-29439
Plasma torch design codes package
[SNIAS-881-430-115] 23 p3286 N88-29569
Special Course on Missile Aerodynamics
[AGARD-R-754] 24 p3317 N88-29755
Semiempirical methods for airbreathing missiles
24 p3318 N88-29763

Study on conceptual design of spacecraft using Computer Aided Engineering (CAE) [SNIAS-920-CA/TS] 24 p3333 N88-29841

MANIP --- spacecraft modeling program [MANIP-217A] 24 p3335 N88-29855

Development of a general software package for the analysis and synthesis of planar antenna arrays for space applications [S-247-02] 24 p3359 N88-30000

Computer-Aided Structural Engineering (CASE) project. Development of design formulas for ribbed mat foundations on expansive soils [AD-A194807] 24 p3412 N88-30307

Computer-Aided Structural Engineering (CASE) project. Computer program for analysis of planar grid structures (CGRID), user's guide [AD-A195977] 24 p3413 N88-30317

Geometric modeling for computer aided design [NASA-CR-183161] 24 p3413 N88-30320

The triangle: A multiprocessor architecture for fast curve and surface generation [AD-A195882] 24 p3414 N88-30324

The P-3 Scheduling Support System (P-3 S3) [AD-A194824] 24 p3436 N88-30450

COMPUTER AIDED ENGINEERING

U COMPUTER AIDED DESIGN

COMPUTER AIDED MANUFACTURING

Automatic seam welding with infrared sensor feedback [DE87-013556] 01 p0055 N88-10352

A CAMAC system controlled by an IBM AT computer for time-resolved spectroscopy [DE87-010111] 01 p0080 N88-10514

A reference guide for IGVIEW: An IGES-compatible geometry system [DE87-013441] 01 p0083 N88-10534

Computer aided engineering/manufacturing at Rolls-Royce [PNR90395] 02 p0222 N88-11397

Interactions between science and precision engineering [DE87-010873] 04 p0426 N88-12643

Overall description of the computer aided design and manufacturing systems associated with the A320 program at Aerospatiale and its partners [SNIAS-872-111-104] 05 p0635 N88-13883

XCUT: A rule-based expert system for the automated process planning of machined parts [DE87-011638] 05 p0639 N88-13905

Using hierarchically structured problem-solving knowledge in a rule-based process planning system [DE87-011639] 05 p0639 N88-13906

Computer modeling of complete IC fabrication process [AD-A184807] 05 p0654 N88-14012

Selected aspects of microelectronics technology and applications: Numerically controlled machine tools. Technology trends series no. 2 [PB87-132973] 06 p0696 N88-14268

Robot accuracy improvement through kinematic parameter identification 06 p0712 N88-14363

LISP based simulation generators for modeling complex space processes 08 p1061 N88-16403

Information handling architecture and software for CIM (Computer Integrated Manufacturing) [PB88-105820] 08 p1067 N88-16453

The use of computer graphic simulation in the development of robotic systems 09 p1214 N88-17275

A generalized method for automatic downhand and wirefeed control of a welding robot and positioner [NASA-TP-2807] 10 p1316 N88-17869

Chinese 7760 CAD/CAMM software system introduced 11 p1468 N88-18756

An automatic system for extraction of information from a Computer Aided Design (CAD), selection, sequencing, and execution of turning processes [INPE-4350-TDL/294] 12 p1676 N88-20020

Development cost reduction using integrated CAE-CAD-CAM techniques 12 p1701 N88-20182

Prototype manufacturing techniques for reducing cost, schedule, and technical risk 12 p1702 N88-20189

Time and cost reduction through computer integrated manufacture 12 p1703 N88-20191

Status of CAD/CAM in medium-sized industries described 16 p2184 N88-23022

Recognizing and locating partially occluded planar objects for assembly routines [LAAS-87-360] 16 p2247 N88-23422

Automatic control of an industrial process and computer aided process control by means of an expert system [LAAS-88-004] 16 p2255 N88-23476

Data base management in CAD/CAM systems: Requirements for CAD/CAM data bases, actual market offer, advice for an efficient data base management, development tendencies [MBB/LWD-11/S/PUB/254] 16 p2285 N88-23683

Developing systems using state-of-the-art CAD/CAM technology 17 p2306 N88-23795

Simulation and computer aided engineering (the necessity of an integrated approach) [NLR-MP-86050-U] 17 p2386 N88-24178

The knowledge based automatic extraction of the machinable surfaces for automatic CAD-CAM system [INPE-4542-PRE/1288] 20 p2836 N88-26824

Enumeration, comments and discussion concerning papers presented during the Conference on Computer Applications in Production and Engineering (CAPE) 87 [NLR-MP-87015-U] 20 p2839 N88-26844

A survey of freeform solid modeling methods [REPT-87-81] 20 p2839 N88-26847

Advanced manufacturing management current and forthcoming technologies [PNR90445] 22 p3159 N88-28802

The use of computer graphic simulation in the development of robotic systems 23 p3257 N88-29388

The concurrent common Lisp development environment 23 p3263 N88-29422

Utilizing dynamic stability of orient parts [AD-A195730] 24 p3427 N88-30397

COMPUTER AIDED MAPPING

The program DSMME: Digital Situation Model, Measurement --- mapping 01 p0065 N88-10418

Detection of critical points: The first step to automatic line generalization 05 p0619 N88-13803

Matching segments from a map and an aerial image using relaxation techniques [SNIAS-872-422-103] 05 p0620 N88-13809

The use of color in electronic maps. Part 1: Generation and analysis of color on the Gould/DeAnza image processing system [IZF-1986-32] 05 p0635 N88-13882

The digital landmass simulation production overview [AD-A187978] 11 p1503 N88-18978

Three-dimensional computer graphics brain-mapping project [AD-A187202] 11 p1528 N88-19126

The US Army Electronic Map Data (EMD) initiative [AD-A188209] 11 p1565 N88-19372

Development of a digital terrain modeling system for microcomputers [INPE-4406-TDL/303] 12 p1639 N88-19816

Computer aided cartographic representation of traffic data: The traffic intensity maps of Baden-Wuerttemberg (Federal Republic of Germany) 16 p2225 N88-23282

Computer-assisted symbolization by raster data processing --- mapping 16 p2225 N88-23284

Computer based modeling of thematic mapping 16 p2225 N88-23285

Extraction of texts and symbols from unstructured vector data --- mapping 16 p2225 N88-23287

Mass digitization of topographic-cartographic information 16 p2226 N88-23288

Computer-assisted cartography research and development report of the Federal Republic of Germany 1984 - 1986 16 p2226 N88-23289

The representation of the sea-bottom in deep sea areas by the Digital Terrain Model (DTM) program TASH 16 p2226 N88-23293

Computer assisted generalization of buildings for digital landscape models by classification methods 16 p2226 N88-23294

Thailand in maps. Application of the mapping system THEMAK2 for specific purpose atlas preparation 16 p2226 N88-23295

Presentation of map information on a color display [FOA-C-20687-2.7] 17 p2368 N88-24103

Coupling of satellite remote sensing to digitized topographic map to detect changes in land use [B8735129] 17 p2369 N88-24104

Digital monoplotting, part 1 [B8735122-PT-1] 17 p2369 N88-24106

Digital monoplotting, part 2 [B8735122-PT-2] 17 p2369 N88-24107

Reports on cartography and geodesy. Series 1, no. 99 [ETN-88-92387] 18 p2533 N88-25025

West German Geodetic Working Group: Official topographic-cartographic information system (ATKIS), content description 18 p2533 N88-25026

West German Geodetic Working Group: Official topographic-cartographic information system (ATKIS), technical conception 18 p2533 N88-25027

Vector graphics and raster data processing for spatial information systems 18 p2533 N88-25028

Digitizing the traffic network of JOG 250 by scanning --- JOG 250 map 18 p2533 N88-25029

Tests for the automatic pattern recognition of building surfaces by the TK 50 18 p2533 N88-25030

Creation of digital topographic models with the ALK-GIAP. The DLM 25 as an example 18 p2534 N88-25031

Topographic data processing for environmental planning 18 p2534 N88-25032

Digital maps for an electronic traffic guide 18 p2534 N88-25033

Development in data structures in PHOCUS for digital mapping 18 p2534 N88-25034

State of development of ALK (October 1986) 18 p2534 N88-25035

Vectorization of raster algorithms for elevation data processing 18 p2534 N88-25036

Geometric rectangular data file (GERD): An aid to the rapid access to position data 18 p2534 N88-25037

Recent developments in software and hardware by Scitex Co. --- computer aided mapping 18 p2535 N88-25038

Personal computer as a workstation in a cartographic automation system? 18 p2535 N88-25039

Use of modern scanner techniques in cartography 18 p2535 N88-25040

The transition from traditional to modern map reproduction [B8735128] 20 p2818 N88-26718

Graphical communication and symbolism in a computerized cartography and map compilation system [PB88-124672] 20 p2818 N88-26720

Development of automatic names placement software [AD-A192786] 21 p2996 N88-27770

COMPUTER AIDED TOMOGRAPHY

X-ray tomography and nuclear magnetic resonance imaging applications for advanced ceramic materials [DE87-011534] 01 p0027 N88-10171

Fast dynamic studies with PC384-7B; system improvements and development of an automated blood sampling system --- tomography [USIP-87-05] 01 p0075 N88-10481

Study of the distribution of a multi-electrode circular system sensitivity for the reconstruction of bioelectrical impedance images [ISAL-IDI1-87-01] 02 p0217 N88-11368

Projection-space iterative interpolation for limited-angle tomography in parallel- and fan-beam geometry, part 1 [DE87-013965] 02 p0221 N88-11391

Computed neutron tomography and coded aperture holography from real time neutron images 04 p0427 N88-12645

A comparison of film-based tomography and computed tomography for advanced ceramic materials [DE88-003114] 07 p0837 N88-15079

The development of emission tomography for the nuclear industry [AERE-R-12319] 10 p1341 N88-18014

Application of X-ray computed tomography to ceramic/ceramic composites [DE88-002903] 11 p1464 N88-18728

South African Association of Physicists in Medicine and Biology: 26th Annual Congress [DE88-700824] 11 p1521 N88-19082

Nondestructive testings of HTGR graphites 13 p1747 N88-20448

Recent developments in nondestructive evaluation for structural ceramics [DE88-005889] 13 p1751 N88-20473

X-ray computed tomography for structural ceramic applications: Beam hardening corrections [DE88-005891] 13 p1752 N88-20474

A hardware/software system for implementing geophysical diffraction tomography [DE88-006411] 15 p2094 N88-22480

Computer tomography and hybrid optical/digital methods for aerodynamic measurements [AD-A190909] 16 p2157 N88-22872

Model-based computed tomography for nondestructive evaluation: An overview and proposal [DE88-010600] 19 p2679 N88-25926

Turbulent flow field visualization with integral interferometric imaging and computed tomography 21 p2950 N88-27521

Direct visualization of surfaces from computed tomography data [AD-A193646] 22 p3153 N88-28758

COMPUTER ANIMATION

Visualization of an aircraft accident based on digital flight data recorder information 05 p0538 N88-13278

Dynamics of high-speed mechanisms with elastic members 13 p1779 N88-20643

Investigation into the use of texturing for real-time computer animation [AD-A191008] 16 p2251 N88-23454

COMPUTER ARCHITECTURE

U ARCHITECTURE (COMPUTERS)

COMPUTER ASSISTED INSTRUCTION

An object-oriented architecture for intelligent tutoring systems [AD-A184790] 03 p0368 N88-12314

LISP as a rapid prototyping environment: The chinese tutor
[AD-A184328] 03 p0369 N88-12319
The pros and cons of using a CAI package on a central computer as opposed to a microprocessor: What's your CAI MO, mainframe or micro
[DE87-011123] 04 p0475 N88-12929
Stress effects and the optimum format of a scrolling seven-line VDT text window
[AD-A185559] 06 p0758 N88-14651
Field evaluation of interactive simulation for maintenance training: SH-3 helicopter electro-mechanical bladefold system
[AD-A185923] 07 p0821 N88-14991
Finite element method computer implementation
08 p0985 N88-15963
A prototype of pilot knowledge evaluation by an intelligent CAI (Computer-Aided instruction) system using a Bayesian diagnostic model
[AD-A186080] 08 p1054 N88-16358
The use and generation of illustrative examples in computer-based instructional systems
08 p1060 N88-16400
Training in satellite ground system operations
09 p1129 N88-16775
IMIS: Integrated Maintenance Information System. A maintenance information delivery concept
09 p1203 N88-17207
An intelligent training system for payload-assist module deploys 09 p1204 N88-17214
Tutoring electronic troubleshooting in a simulated maintenance work environment
09 p1204 N88-17215
An intelligent tutor for the space domain
09 p1204 N88-17217
The desktop interface in intelligent tutoring systems
09 p1205 N88-17225
Computer assisted instruction: Two decades in perspective
[AD-A186813] 09 p1216 N88-17289
Computer aided design of aircraft structures
[ETN-88-91353] 14 p1867 N88-21154
Tutorial on GAMS (Generalized Algebraic Modeling System): A modeling language for optimization
[AD-A189867] 15 p2109 N88-22568
Development of training implying man-machine interface: From the aircraft to the spacecraft
19 p2700 N88-26052
Computer-aided writing
[AD-A192516] 20 p2838 N88-26837
Script editor: An editor for the specification phase in the development of computer based learning
[REPT-87-68] 20 p2839 N88-26846
The sine and cosine function for class 4-VWO. Exploration of possible bottlenecks
[REPT-87-72] 20 p2881 N88-27105
Design and development of courseware for goniometry
[REPT-87-73] 20 p2881 N88-27106

COMPUTER CODES
U COMPUTER PROGRAMS

COMPUTER COMPONENTS
Chips: A tool for developing software interfaces interactively
[AD-A187499] 10 p1389 N88-18295
Real time pipelined system for forming the sum of products in the processing of video data
[NASA-CASE-NPO-16462-1-CU]
17 p2384 N88-24169

COMPUTER DESIGN
Multi-processor architectures for artificial intelligence processing
[OUEL-1671/87] 02 p0219 N88-11380
A taxonomy of analytical computer performance models for computer design
[AD-A185561] 06 p0755 N88-14632
Annotated computer output for split plot design: GENSTAT ANOVA
[AD-A187120] 10 p1385 N88-18271
Design and implementation of a parallel computer for expert system applications
[DE88-005288] 15 p2115 N88-22601
Coding for write-unidirectional memories and conflict resolution
[ENST-87C005] 16 p2245 N88-23408
Locality, communication and interconnect length in multicomputers
[CWI-CS-R8743] 16 p2254 N88-23466
Optical computer and optical methods for data processing 18 p2518 N88-24939
Design of high performance microcomputers for numerical data processing
[ETN-88-92371] 20 p2835 N88-26818

COMPUTER GRAPHICS
NT COMPUTER ANIMATION

Recording multiple signals on a single waveform recorder
[DE87-011632] 01 p0049 N88-10313
Input devices for tasks using interactive video
[NPL-DITC-87/87] 01 p0080 N88-10510
A graphical tool for observing the behavior of parallel logic programs
[DE87-011467] 01 p0080 N88-10516
TIPS-1 user's manual: Cray-1 version
[DE87-013297] 01 p0081 N88-10522
Boundary integral technique for performing analysis of two-dimensional volumes of revolution
[DE87-013053] 01 p0082 N88-10524
DETOUR: A deformed mesh/contour plot program
[DE87-013119] 01 p0082 N88-10525
A reference guide for IGVIEW: An IGES-compatible geometry system
[DE87-013441] 01 p0083 N88-10534
An interactive computer program for materials analysis by means of ion scattering
[MRL-R-1040] 01 p0091 N88-10596
Nowcasting microbursts using Doppler radar in a forecaster-computer environment
02 p0200 N88-11246
The impact of new computer technology on accelerator control
[DE87-014021] 02 p0219 N88-11376
Illustrations of a density-equalizing map projection technique
[DE87-013992] 03 p0339 N88-12130
A scientific workstation operator-interface for accelerator control
[DE87-014689] 03 p0362 N88-12278
A simulation study of a speed control system for autonomous on-road operation of automotive vehicles
[AD-A184030] 03 p0362 N88-12279
The Macintosh computer as a tool for rapid data analysis and for producing camera ready viewgraphs/publications
[DE87-014350] 03 p0362 N88-12280
Technology applications branch graphics projects
[AD-A184621] 03 p0364 N88-12291
Issues in image processing software development for a multi-user, multi-programming environment
[DE88-000358] 03 p0365 N88-12298
End of year report for parallel vision algorithm design and implementation
[AD-A184327] 03 p0366 N88-12301
Layering central authentication on the interactive services of an existing homogeneous distributed system
[DE87-011544] 03 p0366 N88-12304
Low-level vision on warp and the apply programming model
[AD-A184330] 03 p0369 N88-12320
An inexpensive real-time interactive three-dimensional flight simulation system
[AD-A184340] 04 p0432 N88-12499
NACHOS 2: A finite element computer program for incompressible flow problems. Part 2: User's manual
[DE88-001451] 04 p0443 N88-12750
CGI delay compensation
[NASA-TM-86703] 04 p0476 N88-12932
An interactive computer graphics network monitor for a tactical communications network
[AD-A184131] 04 p0477 N88-12938
The ISI (Information Sciences Institute) grapher: A portable tool for displaying graphs pictorially
[AD-A184354] 04 p0478 N88-12944
Implementation and performance of a complex vision system on a systolic array machine
[AD-A184331] 04 p0482 N88-12971
GOLD: Integration of model-based control systems with artificial intelligence and workstations
[DE88-000506] 04 p0483 N88-12976
GOLD: Integration of model-based control systems with artificial intelligence and workstations
[DE88-000706] 04 p0483 N88-12977
Computer graphics for computational aerodynamics
05 p0538 N88-13276
Flow visualization in computational fluid dynamics
05 p0538 N88-13277
Visualization of an aircraft accident based on digital flight data recorder information 05 p0538 N88-13278
Implementation of an FIR band pass filter using a bit-slice processor
[AD-A184895] 05 p0634 N88-13875
The use of color in electronic maps. Part 1: Generation and analysis of color on the Gould/DeAnza image processing system
[IZF-1986-32] 05 p0635 N88-13882
Digitization functions in computer graphics
[ETN-88-91363] 05 p0635 N88-13887
An Ada graphical tool to support software development
[DE87-014854] 05 p0636 N88-13891
A general solution to the silhouette problem
[NASA-TP-2695] 06 p0755 N88-14629
Window system: A toolbox for interactive computer graphics
[PB87-234282] 06 p0756 N88-14637
The Wilson-Fowler spline in a global IGES (Initial Graphics Exchange Specification) coordinate frame
[DE88-001942] 06 p0757 N88-14640
Nonconformity testing for the Graphical Kernel System (GKS)
[GMD/VAL-86-104] 06 p0757 N88-14644
Virtual image processor: A prototype implementation
[AD-A185560] 06 p0758 N88-14652
Interaction of different modules in depth perception: Stereo and shading
[AD-A185607] 06 p0759 N88-14655
Adaptive grid for polyhedral visibility in object space: An implementation
[PB88-100938] 06 p0760 N88-14663
Development of a graphical display on the DMS test bed 06 p0794 N88-14864
An inexpensive real-time interactive three dimensional flight simulation system
[AD-A184868] 07 p0821 N88-14989
TRACKER: A 3-D radio ray tracing code
[DE88-003267] 07 p0847 N88-15137
Creating title blocks for vehicle animations
[AD-A185620] 07 p0904 N88-15473
After ten years of metafiles: Where does the Computer Graphics Metafile fit
[DE88-001840] 07 p0904 N88-15474
GENLPLOT: An interactive program for display and analysis of data, user's manual
[DE88-002292] 07 p0905 N88-15485
Methodology for testing and validating knowledge bases 08 p1055 N88-16364
Development of a task-level robot programming and simulation system 08 p1058 N88-16387
FMEAssist: A knowledge-based approach to Failure Modes and Effects Analysis 08 p1060 N88-16395
TOPP: A post-processor for TOPAZ, the one dimensional pipe flow analysis code
[DE88-003711] 09 p1164 N88-16981
An interactive-graphics method for dynamic system modeling, applying consistency rules
09 p1181 N88-17072
Vision algorithms and psychophysics
[AD-A186773] 09 p1200 N88-17193
The use of computer graphic simulation in the development of robotic systems
09 p1214 N88-17275
Fractal images: Procedure and theory
[AD-A187014] 09 p1217 N88-17293
Mathematical structures for speech recognition
[AD-A187063] 09 p1217 N88-17295
Interactive generation of fractal objects
[CWI-CS-R8706] 09 p1218 N88-17302
Solid modelling with faceted primitives
[ETN-88-91593] 09 p1218 N88-17305
Methodological and structural principles for flexible geometric modeling in computer aided design
[MA-48] 09 p1218 N88-17306
A raster scan algorithm for generating visible parametric surfaces
[DE88-003222] 09 p1220 N88-17321
Directions in computer graphics architecture
10 p1379 N88-18233
Personal computers and All-In-1: Document transfer and translation
[DE88-003760] 10 p1384 N88-18264
Graph transformation algorithms for array memory optimization in applicative languages
[DE88-004727] 10 p1387 N88-18283
CUEMAP: A tool for generating hierarchical charts and dataflow diagrams
[DE88-004778] 10 p1387 N88-18284
Chips: A tool for developing software interfaces interactively
[AD-A187499] 10 p1389 N88-18295
Development of tokamak reactor system analysis code NEW-TORSAC
[DE88-751067] 10 p1411 N88-18417
A computer simulation study of an expert system for walking machine motion planning
[AD-A187907] 11 p1436 N88-18577
Motion planning and control of robot manipulators via application of a computer graphics animated display
11 p1496 N88-18932
Brightness contrast and character height of five flat panel computer displays
[AD-A187743] 11 p1524 N88-19096
Workshop on the Integration of Finite Element Modeling with Geometric Modeling
[NASA-CR-182515] 11 p1526 N88-19111
Integration of finite element modeling with solid modeling through a dynamic interface 11 p1526 N88-19112
Approaches to the automatic generation and control of finite element meshes 11 p1525 N88-19113

Finite element meshing of ANSYS (trademark) solid models 11 p1526 N88-19115

Octree based automatic meshing from CSG models
11 p1527 N88-19117

Geometrical and topological issues in octree based automatic meshing 11 p1527 N88-19118

Toward automatic finite element analysis
11 p1527 N88-19120

Design modeling for shape optimization
11 p1527 N88-19122

Shape optimization of three-dimensional stamped and solid automotive components
[GMR-5166] 11 p1528 N88-19123

Postprocessing techniques for 3D non-linear structures 11 p1528 N88-19124

Geometric versus finite element modeling current and future trends at Northrop 11 p1528 N88-19125

Three-dimensional computer graphics brain-mapping project
[AD-A187202] 11 p1528 N88-19126

Distributed computation of graphics primitives on a transputer network
[NASA-TM-100814] 11 p1531 N88-19147

A computer graphics simulation of the endgame in aircraft combat survivability
[AD-A187826] 11 p1541 N88-19214

Visual recognition training: Effectiveness of computer graphics
[AD-A188302] 12 p1669 N88-19997

Twenty-fourth Industrial Associates Review
12 p1679 N88-20039

An interactive user-friendly approach to surface-fitting three-dimensional geometries
[NASA-CR-4126] 12 p1682 N88-20058

CODAC (Cockpit Oriented Display of Aircraft Configurations) version 1.4 user's guide
[NASA-CR-181650] 13 p1718 N88-20273

Western aeronautical test range real-time graphics software package MAGIC
[NASA-TM-100425] 13 p1757 N88-20506

Graphics and flow visualization of computer generated flow fields
[NASA-CR-182679] 13 p1767 N88-20573

Analysis for architecture for image processing
[INPE-4294-PRE/1165] 13 p1791 N88-20715

Logical input devices and interaction --- computer graphics
[CWI-CS-R8738] 13 p1814 N88-20836

MASPLT: A one-dimensional graphics post processor for wave propagation codes
[DE88-005506] 13 p1817 N88-20856

HISPLT: A history graphics post processor for wave propagation codes
[DE88-005507] 13 p1817 N88-20857

CSQPLT: A graphics post processor for multidimensional wave propagation codes
[DE88-005508] 13 p1817 N88-20858

A model for graphical interaction --- computer graphics
[CWI-CS-R8718] 13 p1818 N88-20866

Parallel graphical output from dialogue cells
[CWI-CS-R8719] 13 p1818 N88-20867

Steps into a geometer's workbench
[CWI-CS-R8726] 13 p1819 N88-20870

Dynamic run-time graphics
[DE87-008997] 13 p1820 N88-20879

Geometry and graphics applied to robotics
[CWI-CS-R8727] 13 p1824 N88-20903

Computation and graphics in mathematical research
[DE88-005796] 13 p1831 N88-20953

Definition and display of profiled sweep-objects --- computer graphics
[REPT-87-45] 14 p1957 N88-21665

Error reduction in two-dimensional pulse-area modulation, with application to computer-generated transparencies --- optical field synthesis
[EUT-87-E-172] 14 p1982 N88-21825

DataViews: A personalizable, interactive, data display system for the decisionmaker
[AD-A188509] 14 p1991 N88-21868

Effects of update and refresh rates on flight simulation visual displays
[NASA-TM-100415] 15 p2018 N88-22033

Geometric modeling of flight information for graphical cockpit display
[AD-A190484] 15 p2021 N88-22043

Investigation into the development of computer aided design software for space based sensors
[NASA-CR-180772] 15 p2107 N88-22552

The visit problem: Visibility graph-based solution
[DE88-000343] 15 p2108 N88-22556

Computer graphics tools for the study of minimal surfaces
[DE88-006421] 15 p2108 N88-22557

PLOT3D (version-5): A computer code for drawing three dimensional graphs, maps and histograms, in single or multiple colours, for mono or stereoscopic viewing
[DE88-701410] 15 p2108 N88-22558

A graphics editor for structured analysis with a data dictionary
[AD-A190618] 15 p2112 N88-22584

The elliptic Sinh-Gordon equation and the construction of toroidal soap bubbles
[DE88-006426] 15 p2113 N88-22585

Two-dimensional graphics tools for a transputer based display board
[NASA-TM-100820] 15 p2113 N88-22591

Rapid prototyping of simulations in artificial intelligence environments
[DE88-004295] 15 p2117 N88-22612

Discrete event simulation in the artificial intelligence environment
[DE88-004296] 15 p2117 N88-22613

Higher order crossings
[AD-A190489] 15 p2121 N88-22641

The program Kennedy Approach as an experimental design of a dynamic computerized air traffic control test
[DFVLR-FB-87-50] 16 p2159 N88-22881

Multiprocessor graphics computation and display using transputers 16 p2218 N88-23236

The integration of digital maps in vehicle navigation systems 16 p2225 N88-23286

Resource management in dialog cell specification (DICE) method
[CWI-CS-R8746] 16 p2248 N88-23433

C-GKS, a C implementation of GKS, the graphical kernel system
[CWI-CS-R8753] 16 p2249 N88-23438

PLOT300: A Tektronics PLOT10 emulator for HP 9000 series 200/300 computers
[NASA-TM-100606] 16 p2250 N88-23447

Editfont: an interactive font editing system
[AD-A191007] 16 p2251 N88-23453

Investigation into the use of texturing for real-time computer animation
[AD-A191008] 16 p2251 N88-23454

The geometric workstation, a new approach for geometric corrections of remotely sensed data
17 p2352 N88-24017

The Systeme d'Analyse Geographique (SAGE) geographic analysis system 17 p2353 N88-24019

Evolution of a family of image processing systems at INPE 17 p2361 N88-24065

Automatic registration of satellite imagery
17 p2364 N88-24080

Visualization of digital terrain models
17 p2364 N88-24081

Presentation of map information on a color display
[FOA-C-20687-2.7] 17 p2368 N88-24103

Graphics software tool for VT terminals (VTGRAPH)
[NASA-TM-100331] 17 p2389 N88-24201

Description of graphics translation software between Intergraph and Tektronix systems
[NASA-TM-100335] 17 p2389 N88-24202

An analytic model for aerodynamic shapes
[AD-A191573] 18 p2456 N88-24583

Airplane runway performance monitoring system
[NASA-CASE-LAR-13854-1-CU]
18 p2462 N88-24621

The coordination of multiple robotic manipulators
[AD-A190869] 18 p2522 N88-24963

Vector graphics and raster data processing for spatial information systems 18 p2533 N88-25028

Personal computer as a workstation in a cartographic automation system? 18 p2535 N88-25039

Knowledge acquisition tool implementation
[AD-A190415] 18 p2555 N88-25164

IGUANA: interactive graphics utility for automated NEC analysis
[AD-A191760] 18 p2556 N88-25174

A graphical, intelligent interface for discrete-event simulations
[DE88-000522] 18 p2557 N88-25181

Considerations involved in the display of finite element results using animation
[DE88-307581] 18 p2559 N88-25189

The ISI (Information Sciences Institute) grapher manual
[AD-A192198] 18 p2561 N88-25200

Engineering drawings and changes: Storing and controlling by the tens of terrabytes
[DE88-007605] 18 p2589 N88-25387

Cellular Array Processor (CAP) and its application to computer graphics 19 p2641 N88-25667

Application of interactive graphic system (CAD/CAM) in the determination of process evolution in land use in the Ribeirao Preto municipality 19 p2664 N88-25956

Graphical Multiprocessing Analysis Tool (GMAT)
[DE88-008019] 19 p2715 N88-26116

Checkout system software for INPE satellites
[INPE-4554-PRE/1297] 19 p2715 N88-26120

RAGS (Realtime Acquisition and Graphics System): An off-the-shelf hardware and system software small data acquisition computer
[DE88-008399] 19 p2716 N88-26128

Logic and fault simulation on the Mach1000 hardware accelerator
[DE88-009794] 19 p2717 N88-26130

GRAPHICS MANAGER (GFXMGR): An interactive graphics software program for the Advanced Electronics Design (AED) graphics controller, Model 767
[DE88-010370] 19 p2717 N88-26131

The transition from traditional to modern map reproduction
[B8735128] 20 p2818 N88-26718

Graphical communication and symbolism in a computerized cartography and map compilation system
[PB88-124672] 20 p2818 N88-26720

XDATAP
[DE88-007161] 20 p2837 N88-26827

Interactive computer programme for the analysis of a two-way Wilkinson divider/combiner
[PB88-105424] 20 p2837 N88-26831

Editfont: An interactive font editing system
[AD-A192373] 20 p2838 N88-26836

A survey of freeform solid modeling methods
[REPT-87-81] 20 p2839 N88-26847

An expeditious technique for keyboard input of information to FORTRAN computer programs
[DE88-009617] 20 p2840 N88-26855

Three-dimensional scene analysis using stero based imaging
[AD-A193120] 21 p2894 N88-27178

An aspect graph-based control strategy for 3-D object recognition 21 p2927 N88-27377

Creating aspect graphs for use in object recognition
21 p2928 N88-27379

The effect of input device on user performance with a menu-based natural language interface
[AD-A193095] 21 p2996 N88-27772

A menu-driven menu editor and associated menu system
[DE88-008026] 21 p2998 N88-27781

TRANSL: A PATRAN translator subroutine library
[DE88-010976] 21 p2998 N88-27784

Contribution to almost realistic picture processing by a computer graphics procedure
[ETN-88-92372] 21 p2999 N88-27789

A hidden-surface removal algorithm for structures defined by triangular and rectangular surface patches
[DFVLR-MITT-88-03] 21 p3000 N88-27792

User's manual for the two-dimensional transputer graphics toolkit
[NASA-TM-100974] 21 p3001 N88-27799

LO-CO-GRAF (low cost graphics): Generating maps to support command and control/crisis management using small computers
[AD-A193964] 22 p3139 N88-28661

Rendering of surfaces from volume data
[AD-A193649] 22 p3143 N88-28689

Interactive, networked moving platform simulators
[AD-A192374] 23 p3182 N88-28940

Interactive plotting of NASTRAN aerodynamic models using NPLOT and DISSPLA
[AD-A194115] 23 p3226 N88-29204

The use of computer graphic simulation in the development of robotic systems
23 p3257 N88-29388

Numerical simulation of nozzle flows
[AD-A195144] 24 p3369 N88-30064

Implementation of the NCAR (National Centre for Atmospheric Research) graphics package at ARL (Aeronautical Research Laboratory)
[AD-A195163] 24 p3391 N88-30193

Geometric modeling for computer aided design
[NASA-CR-183161] 24 p3413 N88-30320

COMPUTER INFORMATION SECURITY

New technologies and intellectual property: An economic analysis
[N-2601-NSF] 01 p0107 N88-10695

Confidentiality of data --- Columbus Polar Platforms
03 p0339 N88-12136

A classified bibliography on publications relevant to data security in LANs --- local area networks (LANS)
[NPL-DITC-99/87] 09 p1223 N88-17331

A framework for evaluating computer architectures to support systems with security requirements, with applications
[AD-A187062] 10 p1392 N88-18303

Defending secrets, sharing data: New locks and keys for electronic information
[PB88-143185] 12 p1706 N88-20210

The TEMPIS project: Current status
[AD-A188963] 12 p1707 N88-20220

best copy available

Monitoring the usage of a computer system
[DE88-004310] 15 p2106 N88-22542

Protection and security mechanisms in the SMITE capability computer
[RSRE-MEMO-4117] 17 p2384 N88-24167

Development environment for secure software
[RSRE-87015] 17 p2386 N88-24179

Separability and security models --- software
[RSRE-87020] 17 p2386 N88-24180

Computer resource management technology program (PE 64740F). Task no. 9: Advanced user authentication
[PB88-183066] 18 p2555 N88-25163

A mixed-modem solution for sensitive data segregation on a broadband network
[DE88-001765] 19 p2718 N88-26139

An evaluation methodology for dependable multiprocessors
[AD-A192799] 20 p2842 N88-26863

A state-of-the-art survey of low-cost security in local area networks
[NPL-DITC-113/88] 22 p3141 N88-28678

The SMITE modular compilation system
[RSRE-MEMO-4145] 23 p3244 N88-29307

COMPUTER METHODS
U COMPUTER PROGRAMS

COMPUTER NETWORKS
NT LOCAL AREA NETWORKS

HF (High Frequency) broadcasting planning model: A comparison of two versions
[PB87-210282] 01 p0036 N88-10230

EAGLES: An interactive environment for scientific computing
[DE87-013564] 01 p0064 N88-10541

Semantic network processing systems --- artificial intelligence
[OUEL-1677/87] 02 p0223 N88-11401

An examination of the Advanced Communications Technology Satellite (ACTS) and its application to the Defense Data Network (DDN)
[AD-A184003] 03 p0276 N88-11742

The network queueing system
[NASA-CR-177433] 03 p0365 N88-12297

Center for Supercomputing Research and Development (CEDAR)
[DE88-000807] 04 p0475 N88-12930

A data analysis environment for HP (Hewlett-Packard) 1000 computers
[DE87-010511] 04 p0477 N88-12936

A survey of object oriented languages in programming environments
[AD-A184127] 04 p0477 N88-12937

A network definition and solution of simulation problems
[DE88-000675] 04 p0481 N88-12962

Managing distributed derived data: A preliminary proposal
[DE88-000714] 04 p0481 N88-12966

An approach to implementing state space searches on heterogeneous systems of multiprocessors
[DE88-001321] 04 p0482 N88-12967

Relational data handling system for scientists
[PB87-223426] 05 p0656 N88-14038

Connecting RPC (Remote Procedure Call)-based distributed systems using wide-area networks
[PB87-234423] 05 p0658 N88-14041

Distribution of records on a ring of processors
[PB87-235784] 06 p0758 N88-14649

Wide-area communication under Amoeba
[PB87-234431] 06 p0760 N88-14665

USSR report: Cybernetics, computers and automation technology
[JPRS-UCC-86-014] 06 p0761 N88-14669

Distributed infimum approximation
[PB87-234969] 06 p0764 N88-14695

Image understanding by Image-Seeking Adaptive Networks (ISAN)
[AD-A186214] 07 p0906 N88-15492

Compilation and development of K-6 aerospace materials for implementation in NASA spacelink electronic information system 07 p0922 N88-15605

Enhancement of computer system for applications software branch 07 p0923 N88-15610

Short pseudorandom test sequences
[AD-A185883] 08 p1054 N88-16357

Integration of symbolic and algorithmic hardware and software for the automation of space station subsystems
08 p1056 N88-16373

Foundation: Transforming data bases into knowledge bases 08 p1063 N88-16423

The European space physics analysis network
08 p1089 N88-16613

NASA JSC neural network survey results
09 p1205 N88-17220

Description of a limited VAX-Ada program support environment developed within UDP division version 1.0
[ARE-TM(UDP)-87103] 09 p1219 N88-17306

Interdisciplinary research in applied mathematics
[AD-A186793] 09 p1226 N88-17344

Multiple-bus interconnection for future multiprocessor systems 10 p1375 N88-18203

An anlysis of the reliability of tree-structured interconnection networks 10 p1378 N88-18228

A strategy for failure prediction
10 p1380 N88-18243

Future directions in computer architecture and software workshop 10 p1383 N88-18258

Personal computers and All-In-1: Document transfer and translation
[DE88-003760] 10 p1384 N88-18264

An Ethernet local area network controller with supporting operating system software
[DE88-003534] 10 p1392 N88-18304

The Lambda network: A new permutation network
[DE88-003568] 10 p1392 N88-18305

Shared workspaces for real-time collaboration in distributed networks: Concepts, techniques, problems
[AD-A188150] 10 p1394 N88-18315

Guidelines for exchanging computerized information
[DE88-004736] 10 p1425 N88-18510

Networking requirements and future alternatives
[NASA-TM-89711] 10 p1426 N88-18517

Optical symbolic processor for expert system execution
[AD-A187882] 11 p1525 N88-19103

Distributed computation of graphics primitives on a transputer network
[NASA-TM-100814] 11 p1531 N88-19147

District information system of National Information Centre
[PB88-134739] 11 p1565 N88-19373

MOBICALC: An integrated and interactive system for development of administrative models
[INPE-4335-TDL/291] 12 p1679 N88-20038

A prototype for remotely shered textual workspaces
[AD-A188352] 2 p1679 N88-20040

Experience with Berkeley UNIX interprocess communications
[AD-A188353] 12 p1680 N88-20041

National Informatics Centre: Profile of services
[PB88-134135] 12 p1706 N88-20211

Computing with structured connections networks
[AD-A189244] 13 p1821 N88-20886

A fully abstract semantics for data flow nets
[CWI-CS-R8724] 13 p1822 N88-20893

Two queues with alternating service and switching times
[CWI-OS-R8712] 13 p1831 N88-20949

A menu-driven knowledge retrieval system accessing ASCII data
[DE88-001742] 13 p1851 N88-21079

Activities and operations of the Advanced Computing Research Facility, October 1986-October 1987
[DE88-006223] 14 p1955 N88-21653

Deadlock-free message routing in processor networks
[CS-8706] 14 p1960 N88-21691

Sigma system: Overview, prospects
15 p2052 N88-22230

Project Monitoring Package (PMP): A package for project activity monitoring
[DE88-701234] 15 p2107 N88-22554

Logarithmically connected, repetitive computer networks and numerical applications
[DE88-006632] 15 p2114 N88-22592

Multiprocessor graphics computation and display using transputers 16 p2218 N88-23236

A queueing network model for analyzing a class of branch and bound algorithms on a master-slave architecture
[CWI-OS-R8717] 16 p2249 N88-23441

Reference nuclear data for space applications
[DE88-007041] 16 p2270 N88-23583

Network architecture for OPS5
[DE88-002602] 18 p2560 N88-25194

A mixed-modem solution for sensitive data segregation on a broadband network
[DE88-001765] 19 p2718 N88-26139

Fault diagnosis in distributed computer networks
[AD-A192406] 19 p2718 N88-26140

Computer science research, 1987: Computation Directorate
[DE88-008637] 20 p2834 N88-26812

A linear-programming method inspired by the neural networks framework
[DE88-008688] 20 p2842 N88-26852

Optical interconnections for digital image coding
21 p2928 N88-27381

Implementing direct, spatially isolated problems on transputer networks
[NASA-TM-101297] 21 p3000 N88-27796

A modular proof of correctness for a network synchronizer
[AD-A192726] 21 p3002 N88-27802

Improving the performance of AI algorithms
[AD-A192848] 21 p3003 N88-27809

Finding minimum-cost circulations by canceling negative cycles
[AD-A192727] 21 p3005 N88-27825

Survey of neural net paradigms for specification of discrete networks
[AD-A192682] 22 p3141 N88-28674

Queueing network models for parallel processing of task systems: An operational approach
[NASA-CR-183174] 22 p3141 N88-28677

Process migration in UNIX environments
[NASA-CR-182951] 23 p3245 N88-29311

Issues on the use of meta-knowledge in expert systems 23 p3252 N88-29357

Intelligent test integration system
23 p3254 N88-29371

Knowledge based programming environments: A perspective 23 p3258 N88-29383

Two implementations of the Expert System for the Flight Analysis System (ESFAS) project
23 p3259 N88-29400

Mathematical algorithms for approximate reasoning
23 p3262 N88-29418

The concurrent common Lisp development environment 23 p3263 N88-29422

Networking and AI systems: Requirements and benefits 23 p3263 N88-29425

Radial basis functions, multi-variable functional interpolation and adaptive networks
[RSRE-MEMO-4148] 23 p3265 N88-29436

Improved time bounds for the maximum flow problem
[AD-A194034] 23 p3272 N88-29471

Signals and systems 24 p3363 N88-30026

Telescience testbed pilot program
[NASA-CR-183207] 24 p3412 N88-30309

Performance analysis of FDDI
[NASA-CR-183206] 24 p3413 N88-30321

The LTPP communication processor --- Columbus and Hermes
[CL/CP/SES/FR/004] 24 p3415 N88-30328

Knowledge-based integrated information systems engineering: Highlights and bibliography. Knowledge-Based Integrated Information Systems Engineering (KBIISE) Project, volume 1
[AD-A195850] 24 p3435 N88-30449

Integrating images, applications, and communications networks, volume 5
[AD-A195854] 24 p3436 N88-30452

Knowledge-Based Integrated Information Systems Development Methodologies Plan. Knowledge-Based Integrated Information Systems Engineering (KBIISE) report, volume 2
[AD-A195851] 24 p3436 N88-30455

COMPUTER PROGRAM INTEGRITY

Computing systems dependability and fault tolerance: Basic concepts and terminology
02 p0127 N88-10797

Some approaches to the design of high integrity software 02 p0127 N88-10798

ISAURE: Integration of security and fault tolerance in the REALITE 2000 system 02 p0127 N88-10802

ADAMEASURE: An implementation of the Halstead and Henry metrics
[AD-A184005] 03 p0365 N88-12298

Approaches to the verification of rule-based expert systems 09 p1206 N88-17232

Evaluating software testing methods to reduce testing duplication in US Army communications equipment acquisition
[AD-A186961] 09 p1216 N88-17282

Methodology for software reliability prediction, volume 1
[AD-A190018] 15 p2110 N88-22571

Methodology for software reliability prediction, volume 3
[AD-A190019] 15 p2110 N88-22572

Introduction to logic programming
[CWI-CS-R8741] 16 p2248 N88-23430

Development environment for secure software
[RSRE-87015] 17 p2386 N88-24179

Separability and security models --- software
[RSRE-87020] 17 p2386 N88-24180

Nebula support software
[AD-A192281] 20 p2837 N88-26833

COMPUTER PROGRAMMING
NT LANGUAGE PROGRAMMING
NT LOGIC PROGRAMMING
NT MICROPROGRAMMING
NT PARALLEL PROGRAMMING
NT SYMBOLIC PROGRAMMING

Space Station Mission Planning System (MPS) development study. Volume 2
[NASA-CR-179200] 01 p0009 N88-10048

Space Station Mission Planning Study (MPS) development study. Volume 3: Software development plan
[NASA-CR-179203] 01 p0009 N88-10049

Report outline of a programming variable and application through example
[INPE-4211-PRE/1092] 01 p0081 N88-10521

On perfect hash functions
[ENST-86D008] 01 p0087 N88-10565

File management using balanced trees
[ENST-87D001] 01 p0106 N88-10693

Knowledge Based Concepts and Artificial Intelligence: Applications to Guidance and Control
[AGARD-LS-155] 02 p0128 N88-10806

How to use PROLOG for expert system programming
02 p0129 N88-10816

Knowledge acquisition issues encountered during the development of an estimating expert system
[DE87-013320] 02 p0248 N88-11568

Hardware-assisted multiprocessor performance measurements
[PB87-226908] 03 p0363 N88-12282

Integrating syntax, semantics, and discourse DARPA (Defense Advanced Research Projects Agency) Natural Language Understanding Program
[AD-A184505] 03 p0364 N88-12289

A survey of object oriented languages in programming environments
[AD-A184127] 04 p0477 N88-12937

Guidelines for preparing software user documentation
[NASA-CR-181550] 04 p0480 N88-12959

COLA2: A computer program for the structural synthesis of two components using general modal coordinates
[DE88-001457] 04 p0481 N88-12963

Programming techniques for high-speed processing of large scale numerical simulation on supercomputers
05 p0537 N88-13269

Vectorizing the FFTs on supercomputer SX system
05 p0537 N88-13270

An APL workspace for conducting nonparametric statistical inference
[AD-A184971] 05 p0634 N88-13877

Digitization functions in computer graphics
[ETN-88-91363] 05 p0635 N88-13887

Some distance problems in coding theory
[B8711398] 05 p0635 N88-13888

A requirements specification for a software design support system
[NASA-CR-182333] 05 p0637 N88-13896

Presentation of a computer program permitting the exploitation of tests designed to determine the sensitivity of one shot devices to a parameter. Application to a degenerate one shot sequence
[SNIAS-872-430-117] 05 p0644 N88-13945

Objects architecture: A comprehensive design approach for real-time, distributed, fault-tolerant, reactive operating systems
[AD-A185476] 06 p0755 N88-14631

Set of multi-process primitives for stack based machines
[PB87-234381] 06 p0756 N88-14636

Learning to program methodically. 3: The newly designed course of the elementary programming
[PB87-119871] 06 p0757 N88-14643

Data processing of the JPA instrument. Part 1: Data management
[FSI-86-15-PT-1] 06 p0757 N88-14645

Development of symbolic computation methods for nonlinear dynamics
[AD-A185562] 06 p0758 N88-14653

Research study for materials/properties test results database
[NASA-CR-178923] 07 p0861 N88-15222

Formalizing reusable software components in the programmer's apprentice
[AD-A185843] 07 p0901 N88-15457

Documentation in a software maintenance environment
[AD-A185892] 07 p0901 N88-15459

FORTRAN 77 programming guidelines
[DFVLR-MITT-87-10] 07 p0905 N88-15487

AFL-1: A programming language for massively concurrent computers
[AD-A186422] 07 p0906 N88-15489

Nacelle-wing interactions (studies 1986) development of a finite element code in a multi-domain version
[ONERA-RTS-10/3417-AY-308A]
08 p0950 N88-15764

Adaptive finite difference methods in fluid dynamics
08 p0985 N88-15958

Finite element method computer implementation
08 p0985 N88-15963

Solution in vibration problems of rectangular plates with spline function
[PB87-143459] 08 p0996 N88-16029

Changing the layers of mind
[AD-A186648] 08 p1052 N88-16350

An easy-to-use diagnostic system development shell
08 p1055 N88-16366

Development of a task-level robot programming and simulation system 08 p1058 N88-16387

Rapid prototyping and AI programming environments applied to payload modeling 08 p1061 N88-16405

On acquisition of programming knowledge
08 p1065 N88-16438

Standardization of software development
[INPE-4330-NTE/272] 08 p1068 N88-16455

Replication and reconfiguration in a distributed mail repository
[AD-A186967] 09 p1151 N88-16897

Application of satellite data in variational analysis for global cyclonic systems
[NASA-CR-182468] 09 p1193 N88-17152

Simplifying the construction of domain-specific automatic programming systems: The NASA automated software development workstation project
09 p1204 N88-17212

The knowledge-based software assistant
09 p1204 N88-17213

Task-level robot programming: Integral part of evolution from teleoperation to autonomy
09 p1214 N88-17279

Types and effects towards the integration of functional and imperative programming
[AD-A186930] 09 p1216 N88-17290

FORTRAN 77 guidelines for the software projects RASP and ANDECS
[DFVLR-MITT-87-09] 09 p1218 N88-17301

Methodological and structural principles for flexible geometric modeling in computer aided design
[MA-48] 09 p1218 N88-17306

Concept of a programmable maintenance processor applicable to multiprocessing systems
[NASA-TM-100406] 09 p1223 N88-17333

Development of an engineering model atmosphere for Mars
[NASA-CR-182462] 09 p1263 N88-17568

Data reduction and analysis of HELIOS plasma wave data
[NASA-CR-182466] 09 p1264 N88-17572

Image texture classification with an optical crossbar interconnected processor 10 p1375 N88-18202

Predicate analysis for parallel program generation
10 p1377 N88-18222

Software support for heterogeneous machines
10 p1378 N88-18224

Semi-applicative programming
10 p1380 N88-18239

An applicative programmer's approach to matrix algebra, lessons for hardware and software
10 p1382 N88-18251

Implementing logical variables on a graph reduction architecture 10 p1382 N88-18252

Experience with Omega: Implementation of a prototype programming environment, part 6
[AD-A187080] 10 p1385 N88-18270

Using program structure to achieve prefetching for cache memories
[DE88-003599] 10 p1387 N88-18282

Programming methodology and performance issues for advanced computer architectures
[DE88-003098] 10 p1387 N88-18287

Development of a graphics based two-attribute utility assessment program with application to mission planning
[AD-A187276] 10 p1388 N88-18292

Deriving abstractions from a software object network
[AD-A187472] 10 p1389 N88-18294

Performance studies of a parallel processor for large linear programming problems
[PB88-121611] 10 p1393 N88-18310

SETI data controllers 11 p1474 N88-18795

KR: An efficient knowledge representation system
[AD-A187705] 11 p1529 N88-19129

Compact high order schemes for the Euler equations
[NASA-CR-181625] 11 p1530 N88-19138

An IBM PC version of ASENT
[DE88-004244] 11 p1532 N88-19150

Evaluating expert system tools: A framework and methodology-workshops
[AD-A187190] 11 p1533 N88-19159

The SAS (Statistical Analysis System) by forms: Putting statistical power into the hands of an end-user
[DE88-002217] 11 p1541 N88-19212

Progress toward a cosmic dust collection facility on space station
[NASA-CR-182427] 12 p1598 N88-19566

BLITZ: Blitzen's micron-code assembly language design document, version 1.0
[TR88-14] 12 p1676 N88-20019

EqL's user's guide
[AD-A188351] 12 p1677 N88-20025

Research on automatic verification of finite-state concurrent systems
[AD-A188618] 12 p1677 N88-20029

Building software systems economically with mechanized logic: Initial design proposal
[AD-A188791] 12 p1678 N88-20031

A knowledge acquisition tool for the intelligent processing of materials
[AD-A188982] 12 p1679 N88-20036

ARCTIC: Programmer's manual and tutorial
[AD-A188619] 12 p1680 N88-20047

OPS83: Style guide for high performance
[AD-A188505] 12 p1681 N88-20051

KREME (Knowledge Representation, Editing and Modeling Environment): A user's introduction, phase 1
[AD-A188906] 12 p1681 N88-20052

Object-oriented design in numerical linear algebra
[AD-A189427] 12 p1685 N88-20073

Towards a solution to the proper integration of a logic programming system and a large knowledge based management system
[AD-A188949] 12 p1705 N88-20207

Intergrated circuit design, phase 2
[AD-A189060] 13 p1760 N88-20530

Laser programming integrated circuits
[AD-A189590] 13 p1762 N88-20537

Finite State Tables for general computer programming applications
[DE88-006254] 13 p1820 N88-20881

Expert system techniques and decision support system: A case study (Dec. 1985 - Jun. 1986)
[ETN-88-91347] 13 p1821 N88-20884

Research in applied mathematics ralated to identification of noisy systems
[AD-A189355] 13 p1825 N88-20906

Oceanographic export system development, year 1
[AD-A189134] 14 p1950 N88-21623

Description of ground motion data processing codes, volume 2
[DE88-007137] 15 p2095 N88-22481

Tutorial on GAMS (Generalized Algebraic Modeling System): A modeling language for optimization
[AD-A189867] 15 p2109 N88-22568

Contour interactive extraction using image numerical treatment
[ISL-R-114/86] 15 p2113 N88-22587

Inference engine for expert systems
[INPE-4465-TDL/321] 15 p2113 N88-22590

Numerical methods for linear and nonlinear optimization
[AD-A190029] 15 p2120 N88-22631

PLASMOR: A laser-plasma simulation code, part 2
[DE88-701289] 15 p2135 N88-22736

New generation knowledge processing, volume 1
[AD-A190165] 15 p2149 N88-22826

Adapting high-level language programs for parallel processing using data flow 16 p2218 N88-23234

Principles of lazy and incremental program generation
[CWI-CS-R8749] 16 p2249 N88-23435

COBOL Analysis System (CAS) users manual
[PB88-171442] 16 p2250 N88-23445

Program profiling in Cedar
[AD-A190883] 16 p2250 N88-23449

Concurrency efficiency user's manual
[AD-A190884] 16 p2251 N88-23450

Supercomputer programming environments
[AD-A190887] 16 p2251 N88-23452

Unique normal forms for lambda calculus with surjective pairing
[PB88-173539] 16 p2260 N88-23508

New generation knowledge processing, volume 2
[AD-A190166] 16 p2285 N88-23681

New generation knowledge processing, volume 3
[AD-A190167] 16 p2285 N88-23682

Mapping from LANDSAT and SPOT satellite imagery
17 p2352 N88-24018

The SAGE geographic analysis system
17 p2361 N88-24063

The Environment for Application Software Integration and Execution (EASIE) version 1.0. Volume 4: System installation and maintenance guide
[NASA-TM-100576] 17 p2386 N88-24185

An OOD (Object-Oriented Design) paradigm for flight simulators
[AD-A191097] 18 p2467 N88-24647

Calculation of assemblies bonded with quasi-elastic adhesives
[REPT-47-632/F] 18 p2493 N88-24793

Automated cartographic generalization for linear map features 18 p2532 N88-25021

LispSEI: The programmer's manual
[AD-A191632] 18 p2556 N88-25172

CIMAG2: The computer program to generate color images [AD-A191847] 18 p2557 N88-25175

Beyond Ada: Generating Ada code from equational specifications [AD-A191866] 18 p2557 N88-25176

System overview: Teragon 4000, an image processing equipment at FOA 3 [FOA-C-30465-3.3] 18 p2557 N88-25179

KA-PROLOG. KAP-computer: Computer model and instructions set [ETN-88-91948] 18 p2558 N88-25186

The Sizing and Optimization Language, (SOL): Computer language for design problems [NASA-TM-100565] 18 p2559 N88-25190

Introduction to compliance in programming of robots [ETN-88-92189] 18 p2561 N88-25201

Modeling of geometric reasoning for robot programming [ETN-88-92290] 18 p2561 N88-25202

Design of partially replicated distributed database systems: An integrated methodology 18 p2589 N88-25383

The scaling of the threshold conditions for solid propellant erosive burning 19 p2630 N88-25601

Theory of numerical information environment and its applications 19 p2640 N88-25666

The new MININEC (version 3): A mini-numerical electromagnetic code [AD-A191778] 19 p2642 N88-25675

Accurate, productive aerodynamic simulation on patched mesh systems [AD-A192040] 19 p2714 N88-26110

A comparative study of project estimating tools [DE88-009059] 19 p2740 N88-26266

Research in computer science 1985/6 [PB88-113840] 20 p2835 N88-26815

Nebula support software [AD-A192281] 20 p2837 N88-26833

Why is it difficult to program in von Neumann languages [AD-A192630] 20 p2838 N88-26839

Directions for programming in FORTRAN 77 [NASA-TT-20317] 20 p2839 N88-26842

Diagnosing faults in autonomous robot plan execution [NASA-CR-182480] 20 p2841 N88-26859

Definition of an auxiliary processor dedicated to real-time operating system kernels [NASA-CR-183070] 20 p2841 N88-26860

PAX ECONOPACK economic analysis package users manual [AD-A192949] 20 p2883 N88-27117

Linear programming for Air Force decision aiding 21 p2926 N88-27378

A programmable systolic array for factorial analysis. Part 2: The symmetric eigenvalue problem [AD-A192396] 21 p2995 N88-27762

Inspection methods in programming: Cliches and plans [AD-A192782] 21 p2996 N88-27767

Synchronizable series expressions. Part 2: Overview of the theory and implementation [AD-A192783] 21 p2996 N88-27768

The programmer's apprentice project: A research overview [AD-A192784] 21 p2996 N88-27769

Contribution to almost realistic picture processing by a computer graphics procedure [ETN-88-92372] 21 p2999 N88-27789

FORTRAN 77 implementation of abstract datatype models [DFVLR-MITT-88-08] 21 p3000 N88-27794

Improving the performance of AI algorithms [AD-A192848] 21 p3003 N88-27809

Literal dynamic modeling [REPT-861-440-114] 22 p3048 N88-28083

Loading and linking in a modular language, an exercise in verification by unification [INF-87 30] 22 p3136 N88-28642

Optimization techniques for relational database systems 22 p3137 N88-28650

Loglisp programming system users manual [AD-A193933] 22 p3142 N88-28682

Uncertainty analysis in automatic robot programming [RR-695-I-IMAG-68-LIFIA] 22 p3142 N88-28685

ADP (Automated Data Processing) requirements definition and documentation through user-developed prototypes [AD-A194407] 23 p3248 N88-29332

Level 1 Ada/SQL (Structured Query Language) database language interface user's guide [AD-A194480] 23 p3249 N88-29335

Analyst-centered models for systems design, analysis, and development 23 p3253 N88-29364

Archetyping: A software generation and management methodology 23 p3256 N88-29382

Programming model for distributed intelligent systems 23 p3257 N88-29390

Knowledge based programming environments: A perspective 23 p3258 N88-29393

A standard library for modeling satellite orbits on a microcomputer [AD-A195759] 24 p3331 N88-29830

Syntactic closures [AD-A195921] 24 p3412 N88-30311

COMPUTER PROGRAMS

NT APPLICATIONS PROGRAMS (COMPUTERS)
NT COMPILERS
NT COMPUTER SYSTEMS PROGRAMS
NT EDITING ROUTINES (COMPUTERS)
NT INPUT/OUTPUT ROUTINES
NT MERGING ROUTINES
NT NASTRAN
NT OBJECT PROGRAMS
NT OPERATING SYSTEMS (COMPUTERS)
NT SUBROUTINE LIBRARIES (COMPUTERS)
NT SUBROUTINES

Transonic analysis and design of axisymmetric bodies in nonuniform flow [NASA-CR-4101] 01 p0003 N88-10013

Satellite orbits: Plot routines [UIO-SR-87-02] 01 p0011 N88-10060

NASA-VOF3D: A three-dimensional computer program for incompressible flows with free surfaces [DE87-011849] 01 p0045 N88-10288

A brief discussion of formally based approaches to rapid prototyping [BAE-WAA-RP-RES-SWE-440] 01 p0079 N88-10508

A graphical tool for observing the behavior of parallel logic programs [DE87-011467] 01 p0080 N88-10516

A look at the evolution of mathematical software for dense matrix problems over the past fifteen years [DE87-011485] 01 p0081 N88-10517

Boundary integral technique for performing analysis of two-dimensional volumes of revolution [DE87-013053] 01 p0082 N88-10524

Blade loss transient dynamics analysis, volume 1. Task 2: TETRA 2 theoretical development [NASA-CR-179632] 02 p0125 N88-10791

Computer modeling of two-phase flow [CFDU/87/5] 02 p0171 N88-11078

Computation of transonic separated wing flows using an Euler/Navier-Stokes zonal approach [NASA-TM-88311] 02 p0173 N88-11089

Combustor-diffuser interaction program 02 p0185 N88-11152

[illegible] transfer in a real engine environment 02 p0186 N88-11155

Hanford Meteorological Station computer codes. Volume 2: The PROD computer code [DE87-014807] 02 p0215 N88-11355

Software reliability models for fault-tolerant avionics computers and related topics [NASA-CR-181440] 02 p0220 N88-11382

Tutorial and hands-on demonstration of a fluent interpreter for CARE 3 [NASA-TM-4011] 02 p0220 N88-11383

Implementation and evaluation of several continuously imbedded methods of Sarafyan [DE88-000025] 02 p0221 N88-11393

IMPSOR: A fully vectorized FORTRAN code for three dimensional moving boundary problems with Dirichlet or Neumann boundary conditions [DE87-014964] 02 p0226 N88-11427

BIMOND3: Monotone piecewise bicubic Hermite interpolation code [DE87-014612] 02 p0229 N88-11442

Interactive Design of Accelerators (IDA) [DE87-013298] 02 p0234 N88-11476

A relativistic Monte Carlo binary collision model for use in plasma particle simulation codes [DE87-013287] 02 p0237 N88-11494

QUICKSILVER: A 3D, electromagnetic, PIC code [DE87-013013] 02 p0245 N88-11547

Dynamic image interpretation for autonomous vehicle navigation [AD-A184043] 03 p0262 N88-11647

Combined calculation of deformation and stress for the body and sabot of an APFSDS 03 p0302 N88-11899

Application of an upwind algorithm to the parabolized Navier-Stokes equations 03 p0316 N88-12000

NBS (National Bureau of Standards) wideband sampling wattmeter [PB87-210324] 03 p0323 N88-12041

A microwave FEL (Free Electron Laser) code using waveguide modes [DE88-000225] 03 p0330 N88-12084

Optical laser technology, specifically CD-ROM (Compact Disc - Read Only Memory) and its application to the storage and retrieval of information [AD-A184111] 03 p0330 N88-12086

Reliability-based optimal structural and mechanical design 03 p0335 N88-12109

Balloon track data analysis [AD-A184750] 03 p0350 N88-12213

Documentation of NCAR (National Center for Atmospheric Research) CCM1 program modules [PB87-213567] 03 p0352 N88-12220

FORTRAN compiler performance benchmarks for the IBM personal computer [LA-10883-MS] 03 p0363 N88-12284

A FORTRAN code for the calculation of probe volume geometry changes in a laser anemometry system caused by window refraction [NASA-TM-100210] 03 p0364 N88-12288

Technology applications branch graphics projects [AD-A184621] 03 p0364 N88-12291

Annotated computer output for illustrative examples of clustering using the mixture method and two comparable methods from SAS [AD-A184687] 03 p0364 N88-12292

The circular serial autocorrelation computer program [AD-A184795] 03 p0365 N88-12295

The network queueing system [NASA-CR-177433] 03 p0365 N88-12297

UNIX benchmark system [AD-A184492] 03 p0367 N88-12308

A prototype expert system for separation science [DE87-013542] 03 p0371 N88-12333

NAVSIM 2: A computer program for simulating aided-inertial navigation for aircraft [NASA-CR-177438] 04 p0398 N88-12478

Aircraft dynamic response calculation based on discrete-continual model 04 p0424 N88-12624

Automated microwave dielectric constant measurement [AD-A184182] 04 p0431 N88-12667

A simplified procedure for correcting both errors and erasures of a Reed-Solomon code using the Euclidean algorithm 04 p0435 N88-12698

Departmental report on program EMTP-machine windings surge transients: Travelling wave method [PB87-123733] 04 p0438 N88-12719

TOPAZ: The transient one-dimensional pipe flow analyzer: An update on code improvements and increased capabilities [DE88-001781] 04 p0443 N88-12751

NCSU code: Validation and extension on NAL's UNIVAC 1100/60 system [PD-FM-8716] 04 p0476 N88-12931

A data analysis environment for HP (Hewlett-Packard) 1000 computers [DE87-010511] 04 p0477 N88-12936

Software reliability perspectives [NASA-CR-181523] 04 p0479 N88-12952

INS3D: An incompressible Navier-Stokes code in generalized three-dimensional coordinates [NASA-TM-100012] 04 p0485 N88-12991

The development of a computer code (U2DIIF) for the numerical solution of unsteady, inviscid and incompressible flow over an airfoil [AD-A185033] 05 p0541 N88-13293

Development of an interface for an ultrareliable fault-tolerant control system and an electronic servo-control unit [NASA-TM-88236] 05 p0553 N88-13367

A computer code to process and plot laser altimetry data interactively on a microcomputer [NASA-TM-100687] 05 p0554 N88-13371

A computer code to calculate line by line atmospheric transmission spectra on a microcomputer [NASA-TM-100686] 05 p0554 N88-13372

Stress intensity factors for cracking metal structures under rapid thermal loading, phase 1 [AD-A184112] 05 p0591 N88-13606

BASIC desk-top computer program for the three-dimensional static configuration of an extensible flexible cable in a uniform stream [AD-A184852] 05 p0609 N88-13737

RADSPHERE: A computer program for calculating the steady-state, axially symmetric, forced response and radiation field of a submerged spherical shell [AD-A185025] 05 p0609 N88-13738

Development of a data analysis system for the detection of lower level atmospheric turbulence with an acoustic sounder [AD-A184972] 05 p0624 N88-13821

Media calibrations of the Doppler signal for a gravitational wave experiment — interplanetary medium [IFSI-86-13] 05 p0625 N88-13825

ZEUS: A knowledge-based expert system that assists in predicting visibility at airbases [AD-A184197] 05 p0626 N88-13829

Hanford Meteorological Station computer codes. Volume 5: The TOWER computer code
[DE88-001610] 05 p0628 N88-13843
Usage analysis of user files in UNIX
[NASA-CR-181561] 05 p0633 N88-13868
Performability modeling based on real data: A casestudy
[NASA-CR-181563] 05 p0633 N88-13870
A prototype ray tracer
[AD-A184863] 05 p0634 N88-13874
Implementation of an FIR band pass filter using a bit-slice processor
[AD-A184895] 05 p0634 N88-13875
Software design for an airborne gravity measurement system
[AD-A185000] 05 p0634 N88-13878
Illustrative examples of principal component analysis using BMDP/4M
[AD-A185179] 05 p0635 N88-13881
Sandia software guidelines: Software quality planning
[DE88-001931] 05 p0636 N88-13894
Illustrative examples of principal component analysis using GENSTAT/PCP
[AD-A185085] 05 p0644 N88-13941
Modeling and generating input processes
[DE87-013162] 05 p0645 N88-13948
Technology upgrade of a silicon compiler
[AD-A184873] 05 p0655 N88-14016
Approaches and possible improvements in the area of multibody dynamics modeling
[NASA-CR-179227] 06 p0663 N88-14067
Program description of FIBRAM: A radiation attenuation model for optical fibers
[PB87-230686] 06 p0690 N88-14229
An investigation of fatigue crack growth in a ductile material at high growth rates 06 p0715 N88-14383
Fast, colour displays of digital terrain elevation data
[AD-A185596] 06 p0729 N88-14485
Integrated systems with applications to the multi-phases of the ephemerides, physics and mathematics of the upper atmosphere
[AD-A185748] 06 p0743 N88-14570
Atmospheric electricity
[NASA-CR-179239] 06 p0744 N88-14575
How to estimate the total number of errors in a software system
[PB87-132130] 06 p0758 N88-14647
Stress effects and the optimum format of a scrolling seven-line VDT text window
[AD-A185559] 06 p0758 N88-14651
Interaction of different modules in depth perception: Stereo and shading
[AD-A185607] 06 p0759 N88-14655
Estimating the distribution of fault latency in a digital processor
[NASA-TM-100521] 06 p0760 N88-14666
Genie inference engine rule writer's guide
[AD-A185709] 06 p0762 N88-14675
Solution of non-symmetric linear systems by biconjugate gradients or conjugate gradients squared
[PB87-226387] 06 p0763 N88-14679
Plasma parameters for alternate operating modes of TIBER-2
[DE88-001890] 06 p0783 N88-14802
Geographic application of the relational data base system Cantor
[PB87-120945] 06 p0791 N88-14851
Shuttle computational grid generation
06 p0794 N88-14863
Development of a graphical display on the DMS test bed 06 p0794 N88-14864
Modern wing flutter analysis by computational fluid dynamics methods
[NASA-TM-100531] 07 p0816 N88-14965
Microwave Landing System (MLS) mathematical model installation manual
[AD-A185612] 07 p0819 N88-14978
An autopilot design for the United States Marine Corps' airborne remotely operated device
[AD-A186379] 07 p0820 N88-14983
A space transportation system operations model
[NASA-TM-100481] 07 p0823 N88-14999
Some performance comparisons for a fluid dynamics code
[PB88-113709] 07 p0852 N88-15175
Internal fluid mechanics research on supercomputers for aerospace propulsion systems
[NASA-TM-100289] 07 p0854 N88-15188
The KIVA-2 computer program for transient multidimensional chemically reactive flows with sprays
[DE88-000502] 07 p0854 N88-15191
An interactive visual interface for Fastbus diagnostics
[DE88-002569] 07 p0900 N88-15453
Formalizing reusable software components in the programmer's apprentice
[AD-A185843] 07 p0901 N88-15457
Program translation via abstraction and reimplementation
[AD-A185845] 07 p0901 N88-15458
A plan for collecting ada software development cost, schedule and environment data
[AD-A185905] 07 p0902 N88-15460
Investigation and implementation of an algorithm for computing optimal search paths
[AD-A185927] 07 p0902 N88-15461
A software planning and development methodology with resource allocation capability
[AD-A186088] 07 p0902 N88-15462
Parallel logic programming and ZMOB and parallel systems software and hardware
[AD-A186300] 07 p0903 N88-15470
Automated program recognition
[AD-A186421] 07 p0903 N88-15472
Creating title blocks for vehicle animations
[AD-A185620] 07 p0904 N88-15473
Modelling of clustering effects in point processes: An application to failures in SPC-systems (stored program control-systems)
[PB87-149241] 07 p0904 N88-15480
Algorithm and program for recognition of compactly positioned vertices of events for the HPD minimum guidance system
[DE86-700542] 07 p0905 N88-15482
A multiple node software development environment
[DE87-010995] 07 p0905 N88-15484
Sublinear upper bounds for stochastic programs with recourse, revision
[AD-A186436] 07 p0916 N88-15564
Feasibility of software built-in test for SDI (Strategic Defense Initiative) applications
[AD-A185750] 07 p0917 N88-15572
TeXting the FORMULARY: A collection of examples of the use of TeX to produce ruled tables and displayed equations
[AD-A185920] 07 p0921 N88-15598
Investigation of candidate data structures and search algorithms to support a knowledge based fault diagnosis system 07 p0923 N88-15606
Verification of FANTASTIC integrated code
07 p0924 N88-15613
The feasibility of using TAE as the UIL for the space station and for other internal NASA tasks and projects
07 p0925 N88-15618
The determination of equivalent bearing loading for the BSMT that simulate SSME high pressure oxidizer turbopump conditions using the SHABERTH/SINDA computer programs 07 p0925 N88-15623
Analysis of relativistic nucleus-nucleus interactions in emulsion chambers 07 p0926 N88-15624
Thermodynamic values from computer summation of group additivity data
[AD-A1861[illegible]1] 07 p0940 N88-15711
Self-adaptive data bases
[AD-A186414] 07 p0942 N88-15729
Rotorcraft transmission 08 p0956 N88-15802
Attitude determination of artificial satellites through joint application of static and dynamic optimal estimation techniques
[INPE-4415-TDL/306] 08 p0963 N88-15832
Scanning finite element calculation method
[PB87-143442] 08 p0995 N88-16017
Investigation of vibration problems with heterodyne holographic interferometer 08 p1000 N88-16058
Vertical atmospheric sounding
[INPE-4370-PRE/1195] 08 p1036 N88-16283
Preliminary evaluation of a micro-based repeated measures testing system
[NASA-CR-172038] 08 p1048 N88-16331
Deriving descriptions of the mind
[AD-A186647] 08 p1052 N88-16349
Third Conference on Artificial Intelligence for Space Applications, part 1
[NASA-CP-2492-Pt-1] 08 p1055 N88-16360
Verification issues for rule-based expert systems
08 p1055 N88-16361
Temporal and contextual knowledge in model-based expert systems 08 p1055 N88-16363
KBS V and V as related to automation of space station subsystems: Rationale for a KBS lifecycle
08 p1057 N88-16375
Automatic mathematical modeling for space application 08 p1060 N88-16402
Similarity networks as a knowledge representation for space applications 08 p1062 N88-16411
Qualitative models for planning: A gentle introduction
08 p1062 N88-16414
Intelligent man/machine interfaces on the space station 08 p1063 N88-16418
A data structure and algorithm for fault diagnosis
08 p1065 N88-16432
A learning apprentice for software parts composition
08 p1065 N88-16436
Automatic program generation from specifications using Prolog 08 p1065 N88-16437
Application of artificial intelligence to impulsive orbital transfers 08 p1066 N88-16439
TES: A modular systems approach to expert system development for real time space applications
08 p1066 N88-16441
Digital image processing: A summary of main techniques
[INPE-4404-PRE/1220] 08 p1068 N88-16454
Replication and reconfiguration in a distributed mail repository
[AD-A186967] 09 p1151 N88-16897
Symbolic, algebraic, and numeric solutions to heat conduction problems using Green's functions
09 p1165 N88-16987
Sea surface current estimates off central California as derived from enhanced AVHRR (Advanced Very High Resolution Radiometer) infrared images
[AD-A186867] 09 p1194 N88-17155
Simplifying the construction of domain-specific automatic programming systems: The NASA automated software development workstation project
09 p1204 N88-17212
The knowledge-based software assistant
09 p1204 N88-17213
User interface devices for mission control
09 p1205 N88-17224
The IDEAL (Integrated Design and Engineering Analysis Languages) modeling methodology: Capabilities and Applications 09 p1206 N88-17227
Expert system verification concerns in an operations environment 09 p1207 N88-17234
Robotic air vehicle. Blending artificial intelligence with conventional software 09 p1210 N88-17252
The KATE shell: An implementation of model-based control, monitor and diagnosis 09 p1210 N88-17255
An automatic finite element mesh generator
[AD-A186939] 09 p1216 N88-17291
Recovery using virtual memory
[AD-A187098] 09 p1217 N88-17296
FORTRAN 77 guidelines for the software projects RASP and ANDECS
[DFVLR-MITT-87-09] 09 p1218 N88-17301
Methods for evaluating the quality and reliability of aerodynamic software programs
[PB87-169793] 09 p1219 N88-17314
Software program validity: A survey
[PB87-170593] 09 p1219 N88-17315
A methodology for the synthesis of robust feedback systems
[NASA-CR-182455] 09 p1225 N88-17342
Examples of nonconservatism in the CARE 3 program
[NASA-TM-100524] 09 p1233 N88-17390
Overview of heat transfer and fluid flow problem areas encountered in Stirling engine modeling
[NASA-TM-100131] 09 p1262 N88-17561
Investigation of dynamic stall using LDV (Laser Doppler Velocimetry): Mean flow studies
[AD-A187629] 10 p1272 N88-17611
A transonic-small-disturbance wing design methodology
[NASA-TP-2806] 10 p1273 N88-17614
Transport delay compensation for computer-generated imagery systems
[NASA-TM-100084] 10 p1277 N88-17645
Shuttle rocket booster computational fluid dynamics
[NASA-CR-182518] 10 p1293 N88-17733
Satellite interference analysis and simulation using personal computers
[NASA-CR-182522] 10 p1319 N88-17890
A ring model of the lasertron
[DE88-004856] 10 p1323 N88-17906
Signal processing studies program VLSI designs for unary functions
[AD-A188053] 10 p1325 N88-17922
NF85: A three-dimensional, air-dynamics computer code for analyzing explosions in structures
[DE88-005085] 10 p1331 N88-17953
AEV local verification for aviation, precipitation and temperature programs: AV, REL, TEM (September 1987 revision)
[PB88-115662] 10 p1355 N88-18101
Proceedings of the Workshop on Future Directions in Computer Architecture and Software
[AD-A184949] 10 p1373 N88-18191
Why reusable software isn't 10 p1376 N88-18212
Future directions in computer architecture and software: The year 2000 10 p1377 N88-18218
Systolic array adaptive beamforming
[AD-A187496] 10 p1385 N88-18269
Annotated computer output for split plot design: GENSTAT ANOVA
[AD-A187120] 10 p1385 N88-18271

CUEMAP: A tool for generating hierarchical charts and dataflow diagrams
[DE88-004778] 10 p1387 N88-18284

Semantics of EqL
[AD-A188151] 10 p1389 N88-18297

The Lambda network: A new permutation network
[DE88-003568] 10 p1392 N88-18305

Development of tokamak reactor system analysis code NEW-TORSAC
[DE88-751067] 10 p1411 N88-18417

A performance index approach to aerodynamic design with the use of analysis codes only
[NASA-TP-2805] 11 p1433 N88-18552

Computer program for conceptual tandem rotor helicopter design
[AD-A187832] 11 p1439 N88-18584

Procedures for quantitative sensitivity and performance validation studies of a deterministic fire safety model
[NBS/GCR-88/544] 11 p1469 N88-18762

An evaluation of the impact of variable temporal and spatial data resolution upon IREPS (Integrated Refractive Effects Prediction System)
[AD-A187764] 11 p1470 N88-18769

GERA computer code for calculation of two-dimensional electromagnetic fields in resonators and electron-optical systems by the finite element method
[DE88-700678] 11 p1480 N88-18831

Digital control of the Czochralski growth of Gallium arsenide-controller software reference manual
[AD-A187210] 11 p1528 N88-19127

Report on desktop publishing
[AD-A187698] 11 p1528 N88-19128

Dynamic analysis of plane frames by microcomputer
11 p1531 N88-19143

A theory of program correctness, and algorithms for proofs
[ANL-87-4] 11 p1531 N88-19146

A maximum likelihood parameter estimation program for general non-linear systems
[ARL-AERO-TM-392] 11 p1532 N88-19154

Accurate efficient evaluation of Bessel transform: Programs and error analysis
[AD-A187718] 11 p1536 N88-19174

ICF special studies
[DE88-004057] 11 p1551 N88-19261

Structural design requirements for aircraft incorporating active control technology 12 p1580 N88-19453

Computer aided deflection measurement of an aircraft wing
[AD-A187778] 12 p1581 N88-19461

Relative motion of two satellites in close-elliptical orbits
[AD-A188851] 12 p1594 N88-19543

Calculation of eclipses for elliptical orbits
[INPE-4412-NTE/277] 12 p1594 N88-19545

HELIOS modelling of point-focusing solar concentrators
[DE88-004933] 12 p1640 N88-19820

Enhancements to the atmospheric transmittance/radiance program FASCODE
[AD-A188863] 12 p1643 N88-19839

Aircrew training devices: Utility and utilization of advanced instructional features, phase 4
[AD-A188418] 12 p1670 N88-20000

A computer code for the solution of large scale network reliability analysis problems
[AD-A188455] 12 p1680 N88-20042

A laboratory facility for research in parallel computation
[AD-A188499] 12 p1680 N88-20044

HP-41CX programs for HgCdTe detectors and IR systems
[AD-A188935] 12 p1692 N88-20120

Fully-coupled analysis of jet mixing problems. Three-dimensional PNS model, SCIP3D
[NASA-CR-4139] 13 p1715 N88-20256

Australian aerodynamic design codes for aerial tow bodies
[AD-A189048] 13 p1715 N88-20258

CODAC (Cockpit Oriented Display of Aircraft Configurations) version 1.4 user's guide
[NASA-CR-181650] 13 p1718 N88-20273

Documentation and installation of the hypersonic arbitrary-body computer program (Mark 3 version) of A.E. Gentry on the IBM computer system
[MBB/LKE-127/S/PUB/256] 13 p1719 N88-20276

Architecture specification for PAVE PILLAR avionics
[AD-A188722] 13 p1723 N88-20303

Trajectory code studies, 1987
[DE88-006218] 13 p1728 N88-20335

MOPAC manual: A general molecular orbital package, fourth edition
[AD-A188623] 13 p1733 N88-20362

A simplified computer code for reduction to burning rates of closed bomb pressure-time data (MINICB)
[AD-A189112] 13 p1736 N88-20380

Interactive automated system for testing analog units of digital seismic stations 13 p1789 N88-20702

MacCAD (Macintosh Computer Aided Design), computer aided design tool for system analysis
[AD-A189241] 13 p1815 N88-20843

Preconditioned conjugate gradient algorithms and software for solving large sparse linear systems
[DE88-002180] 13 p1816 N88-20849

A report on the study of algorithms to enhance vector computer performance for the discretized one-dimensional time-dependent heat conduction equation: EPIC research, phase 1
[DE88-005642] 13 p1820 N88-20880

Distributed transaction processing and the Camelot system
[AD-A188614] 13 p1821 N88-20885

Local refinement of stress field by finite element method
[INPE-4321-TDL/288] 13 p1826 N88-20930

A novel method for sputter-deposition of high T(sub c) superconductor films via a computer-controlled mass analyzed ion beam
[DE88-006001] 13 p1848 N88-21064

NNEPEQ: Chemical equilibrium version of the Navy/NASA Engine Program
[NASA-TM-100851] 14 p1868 N88-21161

The quasi-static contact problem with friction for three dimensional elastic bodies
[REPT-87-51] 14 p1918 N88-21447

CARE 3 User's Workshop
[NASA-CP-10011] 14 p1954 N88-21646

Applicability of nonlinear programming in decision support systems: Realization of user-friendly software
[REPT-87-42] 14 p1957 N88-21663

Monte Carlo modified method for Green function. Algorithm and computer code for calculations in equal mass many-body system
[DE88-701114] 14 p1957 N88-21667

Examination of the effects of using Ada (trade name) in flight control software
[AD-A189679] 14 p1959 N88-21683

User's manual for LINEAR, a FORTRAN program to derive linear aircraft models
[NASA-TP-2768] 14 p1967 N88-21740

Basic research on flame radiation
[PB88-168372] 15 p2032 N88-22105

Computer program in BASIC language for computation of spectrochemical analytical data
[DE88-701229] 15 p2032 N88-22106

Status of electric vehicle simulation programs at the INEL: Summer 1987
[DE88-006745] 15 p2058 N88-22271

An improved method for calculating power density in the Fresnel region of circular parabolic reflector antennas
[AD-A190569] 15 p2060 N88-22284

Traction model development
[AD-A188450] 15 p2073 N88-22359

Development of a computer code CRACK for elastic and elastoplastic fracture mechanics analysis of 2-D structures by finite element technique
[DE88-701231] 15 p2075 N88-22370

The composite blade structural analyzer (COBSTRAN)
15 p2078 N88-22390

Three-dimensional inelastic approximate analysis code (MOMM) 15 p2079 N88-22392

Specialty three-dimensional finite element analysis codes 15 p2079 N88-22393

MHOST: An efficient finite element program for inelastic analysis of solids and structures
15 p2079 N88-22394

METCAN: The metal matrix composite analyzer
15 p2079 N88-22395

Computational simulation methods for composite fracture mechanics 15 p2079 N88-22396

Probabilistic structural analysis computer code (NESSUS) 15 p2079 N88-22397

Structural tailoring of high-speed turbine blades (SSME/STAEBL) 15 p2080 N88-22398

Computational structural mechanics for engine structures 15 p2080 N88-22399

Structural tailoring of advanced turboprops
15 p2080 N88-22400

Geometric restoration of satellite image data
[AD-A190462] 15 p2089 N88-22450

Satellite UV image processing
[AD-A190466] 15 p2089 N88-22451

Updating of the municipal official register of real estate through a geographical information system
[INPE-4459-PRE/1238] 15 p2090 N88-22453

A survey of denser-than-air atmospheric dispersion models
[DE88-006626] 15 p2092 N88-22467

A hardware/software system for implementing geophysical diffraction tomography
[DE88-006411] 15 p2094 N88-22480

Motion sickness: Quantitative, algorithmic malaise indication in real time
[AD-A189674] 15 p2101 N88-22518

Analysis of head response to torso acceleration. Volume 2: Description of data retrieval, analysis and display software
[PB88-156765] 15 p2104 N88-22536

Project Monitoring Package (PMP): A package for project activity monitoring
[DE88-701234] 15 p2107 N88-22554

COMESH: A corner mesh finite difference code to solve multigroup diffusion equations in multidimensions
[DE88-701248] 15 p2108 N88-22555

PLOT3D (version-5): A computer code for drawing three dimensional graphs, maps and histograms, in single or multiple colours, for mono or stereoscopic viewing
[DE88-701410] 15 p2108 N88-22558

Computer grading of extensometers (BS 3846)
[NPL-DMA(A)-152] 15 p2108 N88-22560

Methodology for software reliability prediction, volume 1
[AD-A190018] 15 p2110 N88-22571

Methodology for software reliability prediction, volume 3
[AD-A190019] 15 p2110 N88-22572

Transformations of concurrent algorithms for highly parallel systems: A one year project summary report
[AD-A190236] 15 p2111 N88-22576

CK-LOG system conversion (user's manual and user interface)
[AD-A190273] 15 p2111 N88-22577

Software verification using partition analysis
[AD-A190570] 15 p2112 N88-22582

Memory-based expert systems
[AD-A190203] 15 p2116 N88-22606

ONTIC: A knowledge representation system for mathematics
[AD-A190553] 15 p2121 N88-22643

An approximation technique for solving a system of Fredholm integral equations for asymmetric detector response functions
[AD-A190577] 15 p2121 N88-22645

Analysis and testing of the SURE program
[NASA-TP-2817] 15 p2123 N88-22653

A chemical method for achieving acceleration of macroparticles to ultrahigh velocities
[DE88-006377] 15 p2128 N88-22695

Sources of digital spatial data for geographic information systems
[AD-A189786] 15 p2148 N88-22824

KOMPOT Program complex for the calculation of spatial magnetostatic fields of electromagnetic systems
[DE88-701691] 16 p2192 N88-23072

Computerized life and reliability modelling for turboprop transmissions
[NASA-TM-100918] 16 p2215 N88-23220

Multiprocessor graphics computation and display using transputers 16 p2218 N88-23236

Vibration and flutter analysis of the SR-7L large-scale propfan 16 p2221 N88-23254

Supersonic axial-flow fan flutter
16 p2221 N88-23255

Integrated multidisciplinary analysis tool IMAT users' guide
[NASA-TM-100605] 16 p2223 N88-23273

Extending problem solver capabilities through case-based inference
[AD-A191332] 16 p2243 N88-23401

Alpha structure based B-HIVE multicomputer
[AD-A188708] 16 p2244 N88-23405

The good, the bad and the ugly: Comparing high-speed computer systems
[DE88-007498] 16 p2245 N88-23412

Digital filter unit for selection of spectrometric information
[DE87-702890] 16 p2246 N88-23415

Portability of software. The use of software in the hardware mixture
[MBB/LWD-11/S/PUB/253] 16 p2246 N88-23416

Investigation into the use of texturing for real-time computer animation
[AD-A191008] 16 p2251 N88-23454

The PAWS and STEM reliability analysis programs
[NASA-TM-100572] 16 p2262 N88-23526

Computer program for parameterization of nucleus-nucleus electromagnetic dissociation cross sections
[NASA-TM-4038] 16 p2270 N88-23584

BRYNTRN: A baryon transport computer code, computation procedures and data base
[NASA-TM-4037] 16 p2290 N88-23714

PAN AIR analysis of the NASA/MCAIR 279-3: An advanced supersonic V/STOL fighter/attack aircraft
[NASA-TM-88838] 17 p2298 N88-23750

Modeling of functional specifications for onboard software: Experience with the Rafale avionics system
17 p2303 N88-23777

The avionics software architecture impact on system architecture
17 p2303 N88-23778

Workshops for the design of avionics systems and the development of onboard software
17 p2307 N88-23802

EnviroNET: An interactive space-environment information resource
[NASA-TM-101137] 17 p2309 N88-23812

Preventing aircraft corrosion by predictive corrosion modeling
17 p2321 N88-23863

Preliminary 2-D shell analysis of the space shuttle solid rocket boosters
[NASA-TM-100515] 17 p2348 N88-23989

The multi-disciplinary design study: A life cycle cost algorithm
[NASA-CR-4156] 17 p2385 N88-24172

A timing evaluator for C programs generated by the model system
[AD-A191204] 17 p2385 N88-24174

MIPS: The good, the bad and the useful
[NASA-CR-182893] 17 p2386 N88-24184

A robotic language for cooperative multi-robots
17 p2387 N88-24186

Third Conference on Artificial Intelligence for Space Applications, part 2
[NASA-CP-2492-PT-2] 17 p2387 N88-24188

Automatic program generation from specifications using PROLOG
17 p2388 N88-24196

TES: A modular systems approach to expert system development for real-time space applications
17 p2388 N88-24197

Mentat: An object-oriented macro data flow system
[NASA-TM-101165] 17 p2388 N88-24199

Description of graphics translation software between Intergraph and Tektronix systems
[NASA-TM-100335] 17 p2389 N88-24202

Cermet fuel thermal conductivity
17 p2410 N88-24329

ATHENA simulation of the 300 kW SP-100
17 p2414 N88-24357

Expert systems approach to modeling systems with the ATHENA thermal-hydraulics code
17 p2416 N88-24365

SP-100 system modeling: SNPSAM update
17 p2417 N88-24372

The Lewis heat pipe code with application to SP-100 GES heat pipes
17 p2421 N88-24395

HTPIPE: A steady state heat pipe analysis program
17 p2421 N88-24396

The THROHPUT code: Thermohydraulic heat pipe modeling
17 p2421 N88-24399

MACRAD: A mass analysis code for radiators
17 p2424 N88-24418

Energy storage evaluation for burst power applications
17 p2426 N88-24430

Space Power Reference Source (SPRS): A user's guide to SDI Space Power Technology Programs
17 p2427 N88-24440

Transient analyses of multimegawatt space reactors
17 p2430 N88-24456

A system status monitor for the National Aerospace Plane
[AD-A190881] 18 p2463 N88-24624

An OOD (Object-Oriented Design) paradigm for flight simulators
[AD-A191097] 18 p2467 N88-24647

Automated test device for FASR (Fixed Array Surveillance Radar) beam steering componentry
[AD-A191650] 18 p2500 N88-24829

Practical VLF/LF radio test system
[AD-A191768] 18 p2500 N88-24831

Transient particle deposition in a boundary layer of impulsive flow over a flat plate
[AD-A191537] 18 p2508 N88-24880

SOLA-DM: A numerical solution algorithm for transient three-dimensional flows
[DE88-007159] 18 p2514 N88-24913

The development of KENO and the calculation of differential parameters with KENO
[DE88-006176] 18 p2555 N88-25166

Annotated computer output for split plot design: SAS GLM
[AD-A190800] 18 p2555 N88-25167

A general approach for automating source code verification
[AD-A191461] 18 p2556 N88-25170

Research in enumeration and graph theory with applications to computer science
[AD-A191567] 18 p2556 N88-25171

IGUANA: Interactive graphics utility for automated NEC analysis
[AD-A191760] 18 p2556 N88-25174

CIMAG2: The computer program to generate color images
[AD-A191847] 18 p2557 N88-25175

An electrostatic potential comparator
[AD-A192051] 18 p2557 N88-25177

Design of catalytic monoliths for closed-cycle carbon dioxide lasers
[NASA-CR-182963] 18 p2558 N88-25185

KA-PROLOG. KAP-computer: Computer model and instructions set
[ETN-88-91948] 18 p2558 N88-25186

The ISI (Information Sciences Institute) grapher manual
[AD-A192198] 18 p2561 N88-25200

State of tuning
[NASA-TT-20195] 18 p2561 N88-25205

PAFEC level 6.2 application program
[AD-A191037] 18 p2562 N88-25209

NFEARS: A nonlinear adaptive finite element solver, part 1
[AD-A191823] 18 p2563 N88-25215

A perspective of PC-based probabilistic risk assessment
[DE88-006715] 18 p2568 N88-25251

QN3D: A 3-dimensional quasi-neutral hybrid particle-in-cell code with applications to the tilt mode instability in field reversed configurations
18 p2580 N88-25325

Department of Defense statement on the X-ray Lithography Program to the Research and Development Subcommittee of the House Armed Services Committee of 100th Congress, second session
[AD-A191854] 18 p2582 N88-25341

Defense Technical Information Center cataloging guidelines
[AD-A192200] 18 p2589 N88-25382

Submunitions simulations, volume 2
[TR-CR-RD-SS-87-7-VOL-2] 19 p2641 N88-25669

Codes for QPSK modulation with invariance under 90 degrees rotation.
19 p2648 N88-25720

Navier-Stokes code NS3D for blunt bodies. Part 1: Analysis, results and verification
[DE88-010105] 19 p2666 N88-25855

Hydrogen turbines for space power systems: A simplified axial flow gas turbine model
[DE88-009585] 19 p2677 N88-2[illegible]20

The development of an intelligent interface to a computational fluid dynamics flow-solver code
[NASA-TM-100908] 19 p2716 N88-26127

The MAFIA approach to solving Maxwell's equations in three dimensions
[DE88-007826] 19 p2720 N88-26155

Digital control of the czochralski growth of gallium arsenide. System reference manual. Valid for Czochralski growth controller software version 2.4
[AD-A191997] 19 p2732 N88-26227

Real time data base management
[AD-A191758] 19 p2739 N88-26265

High speed inlet calculations with real gas effects
[NASA-CR-182167] 20 p2752 N88-26336

An interactive computer code for preliminary design of solid propellant rocket motors
[AD-A192869] 20 p2766 N88-26399

Experimental and theoretical analysis of the radiative transfer within a sooty pool fire
[DE88-007099] 20 p2769 N88-26419

A numerical study of Rayleigh-Taylor instability in aluminum and steel plates
[DE88-010475] 20 p2774 N88-26449

Vertical ship motions and sea loads considering nonlinear effects
[TAE-592] 20 p2784 N88-26515

Parameter identification of the passenger simulation model MADYMO: Methods and experience
20 p2788 N88-26536

MAXWELL3: A 3D finite element electromagnetic modeling code
[DE88-010602] 20 p2790 N88-26551

The Oak Ridge Heat Pump Design Model: Mark 3 version program documentationon
[DE88-007863] 20 p2799 N88-26607

A study of flow separation in transonic flow using inviscid and viscous computational fluid dynamics (CFD) schemes
[NASA-CR-183119] 20 p2801 N88-26618

Improved 3-D turbomachinery CFD algorithm
[NASA-CR-179364] 20 p2801 N88-26619

A general-purpose approach to computer-aided dynamic analysis of a flexible helicopter
[NASA-TM-101002] 20 p2816 N88-26709

A control program for global radiation measurements
[KNMI-TR-100] 20 p2824 N88-26757

Computer controlled data acquisition system for the NASA 1988 Rocket Triggered Lightning Program
[DE88-008335] 20 p2826 N88-26766

Managing microcomputer applications: A primer and guide to good practice
[AD-A192992] 20 p2835 N88-26817

Common Data Format (CDF) to store images
[NASA-CR-179366] 20 p2836 N88-26825

XDATAP
[DE88-007161] 20 p2837 N88-26827

Interactive computer programme for the analysis of a two-way Wilkinson divider/combiner
[PB88-105424] 20 p2837 N88-26831

SIMS: Single Interface to Multiple Systems
[AD-A192264] 20 p2837 N88-26832

Nebula support software
[AD-A192281] 20 p2837 N88-26833

Computer programs for high-current beam transport in accelerators
[AD-A192356] 20 p2838 N88-26835

Computer-aided writing
[AD-A192516] 20 p2838 N88-26837

Colored stochastic Petri nets. Application to real time distributed systems
[ENST-87E017] 20 p2839 N88-26843

An expeditious technique for keyboard input of information to FORTRAN computer programs
[DE88-009617] 20 p2840 N88-26855

An evaluation methodology for dependable multiprocessors
[AD-A192799] 20 p2842 N88-26863

The construction of composite grids for general three-dimensional regions 20 p2843 N88-26872

Qualitative reasoning for physicists
[PB88-116298] 20 p2848 N88-26906

Recent applications of Monte Carlo methods for semiconductor microdevice simulation
20 p2871 N88-27046

Knowledge-based cost estimating vs traditional software cost models
[DE88-009707] 20 p2883 N88-27116

A comparison of the various helicopter mathematical models used in the methodology assessment
21 p2889 N88-27149

Aeromechanical stability analysis of COPTER
21 p2891 N88-27161

FORTRAN programs for computation of time dependent sea levels and trajectory errors from satellite altimeter data
[BONN-MITT-73] 21 p2901 N88-27216

Evaluation and improvement of liquid propellant rocket chugging analysis techniques. Part 1: A one-dimensional analysis of low frequency combustion instability in the fuel preburner of the space shuttle main engine
[NASA-CR-183106] 21 p2903 N88-27224

Evaluation and improvement of liquid propellant rocket chugging analysis techniques. Part 2: A study of low frequency combustion instability in rocket engine preburners using a heterogeneous stirred tank reactor model
[NASA-CR-182724] 21 p2903 N88-27225

Programs for preliminary design of composite materials which were developed by the design group of Aerospatiale Aquitaine
[REPT-881-430-112] 21 p2907 N88-27251

Hole diameters in plates impacted by projectiles
21 p2929 N88-27386

Control of free-flying space robot manipulator systems
[NASA-CR-183017] 21 p2956 N88-27562

Development of a biaxial test system for thin-walled metal tubes using tensile-compressive axial load and internal-external pressure
[DE88-011279] 21 p2962 N88-27592

IEMIS (Integrated Emergency Management Information System) floodplain mapping based on a LIDAR derived data set
[AD-A193071] 21 p2966 N88-27616

Validate algorithms for the determination of rainfall rates from SSM/I microwave satellite imagery
[AD-A192295] 21 p2974 N88-27664

Vision research. A national plan: 1983-1987, 1987 evaluation and update
[PB88-192604] 21 p2985 N88-27726

A cockpit natural language study. Vocabulary and grammar analyses
[AD-A193289] 21 p2993 N88-27753

Full analysis of a powerful window random access algorithm
[AD-A192437] 21 p2995 N88-27763

Using IMSL mathematical and statistical computer subroutines in physiological and biomechanical research
[AD-A192594] 21 p2995 N88-27765

Development of automatic names placement software
[AD-A192786] 21 p2996 N88-27770

The effect of input device on user performance with a menu-based natural language interface
[AD-A193095] 21 p2996 N88-27772

Computer aided design for linear control State Variable System (SVS)
[AD-A193282] 21 p2997 N88-27775
Synopsis of a computer program designed to interface a personal computer with the fast data acquisition system of a time-of-flight mass spectrometer
[NASA-CR-177474] 21 p3001 N88-27798
The SAS System by forms: Putting statistical power into the hands of an end-user
[DE88-010512] 21 p3010 N88-27857
Comparison of results based on a deterministic versus a statistical uncertainty analysis
[DE88-010751] 21 p3010 N88-27858
Development of direct-inverse 3-D methods for applied transonic aerodynamic wing design and analysis
[NASA-CR-183127] 22 p3037 N88-28033
VSAERO analysis of tip planforms for the free-tip rotor
[NASA-CR-177487] 22 p3038 N88-28036
An improved version of NCOREL: A computer program for 3-D nonlinear supersonic potential flow computations
[NASA-CR-4165] 22 p3038 N88-28039
Numerical computation of space shuttle orbiter flow field
[NASA-CR-183193] 22 p3040 N88-28048
Large-signal modeling of gallium arsenide field-effect transistors 22 p3073 N88-28242
Surface tension and viscosity with Lagrangian hydrodynamics on a triangular mesh
[AD-A194120] 22 p3075 N88-28258
What's on the menu? Friendlier computers
[AD-A194393] 22 p3135 N88-28637
Walter user's manual (Version 1.0)
[AD-A192542] 22 p3136 N88-28644
Software quality measurement demonstration project (1)
[AD-A193429] 22 p3136 N88-28646
VAXGAP: A code for the routine analysis of gamma-ray pulse-height spectra on a VAX computer
[DE88-011702] 22 p3137 N88-28648
Air Force Systems Command software independent verification and validation implementation analysis and guidance
[AD-A194309] 22 p3137 N88-28653
Computers in weapons systems: A look at the F-15
[AD-A194498] 23 p3178 N88-28920
Hot-wire measurements of compressor blade wakes in a cascade wind tunnel
[AD-A194737] 23 p3181 N88-28936
Evaluation of atmospheric effects for operational tactical decision aid
[AD-A194205] 23 p3232 N88-29236
Atmospheric angular momentum and length of day
[AD-A194505] 23 p3233 N88-29238
Electrochemical and optical studies of model photosynthetic systems
[DE88-009291] 23 p3237 N88-29264
Process migration in UNIX environments
[NASA-CR-182951] 23 p3245 N88-29311
Composite grid generation for aircraft configurations with the EAGLE code 23 p3246 N88-29321
Waveform analysis on the IBM PC
[AD-A194249] 23 p3248 N88-29330
OMV docking simulator 23 p3255 N88-29379
Archetyping: A software generation and management methodology 23 p3256 N88-29382
Generic supervisor: A knowledge-based tool for control of space station on-board systems
23 p3257 N88-29389
Software development without languages
23 p3257 N88-29392
Automated software development workstation
23 p3263 N88-29423
Programming language concepts for multiprocessors
[AD-A193465] 23 p3264 N88-29430
MACSYMA program for the painleve test of nonlinear ordinary and partial differential equations
[AD-A194293] 23 p3270 N88-29458
Space marching Euler solvers
24 p3316 N88-29759
Prediction of dynamic derivatives
24 p3318 N88-29761
Prediction of base-flows 24 p3319 N88-29765
Computer programs for generation of NASTRAN and VIBRA-6 aircraft models
[AD-A195467] 24 p3323 N88-29792
A new computational capability for ramjet projectiles
[AD-A196061] 24 p3327 N88-29812
N-version software demonstration for digital flight controls
[NASA-CR-181483] 24 p3328 N88-29815
Computer programs for calculation of sting pitch and roll angles required to obtain angles of attack and sideslip on wind tunnel models
[NASA-TM-100659] 24 p3329 N88-29820
Development of computer-controlled thermogravimetric instrumentation for measurement of environmental and high temperature volatilization and desorption of contaminants from polymeric materials
[AD-A195934] 24 p3343 N88-29900
Scattering impulse response synthesis using random noise illumination: Initial concept evaluation
[AD-A195086] 24 p3364 N88-30034
DATATRAN: Datum transformation software
[AD-A195723] 24 p3387 N88-30175
Computer-Aided Structural Engineering (CASE) project. Computer program for analysis of planar grid structures (CGRID), user's guide
[AD-A195977] 24 p3413 N88-30317
The eivaN: A forward-looking interactive orbital trajectory plotting tool for use with proximity operations (PROX OPS) and other maneuvers: Description and user's manual
[NASA-CR-177490] 24 p3414 N88-30327
Automatic qualitative analysis of ordinary differential equations using piecewise linear approximations
[AD-A196310] 24 p3424 N88-30379
Linguistic-technical aspects of machine translation
24 p3436 N88-30461

COMPUTER SECURITY
U COMPUTER INFORMATION SECURITY

COMPUTER SIMULATION
U COMPUTERIZED SIMULATION

COMPUTER STORAGE DEVICES
NT BUBBLE MEMORY DEVICES
NT BUFFER STORAGE
NT MAGNETIC DISKS
NT MAGNETIC TAPES
NT OPTICAL DISKS
NT RANDOM ACCESS MEMORY
NT READ-ONLY MEMORY DEVICES
NT REGISTERS (COMPUTERS)
Amorphous or microcrystalline semiconductor memory device
[EP-PATENT-0-162-529-A1] 01 p0026 N88-10167
The associative memory ME7
[ESA-TT-1033] 01 p0079 N88-10506
Estimation of the position and orientation of objects using associative memories
[ESA-TT-1034] 01 p0079 N88-10507
Implementation of preconditioned s-step conjugate gradient methods on a multiprocessor system with memory hierarchy
[DE87-014401] 02 p0222 N88-11400
QUICKSILVER: A 3D, electromagnetic, PIC code
[DE87-013013] 02 p0245 N88-11547
Documentation of NCAR (National Center for Atmospheric Research) CCM1 program modules
[PB87-213567] 03 p0352 N88-12220
Electronic Records Administration at the Savannah River Plant
[DE87-014842] 03 p0384 N88-12415
Storing photomicrographs on optical laser disks
[DE87-013747] 04 p0449 N88-12785
Center for Supercomputing Research and Development (CEDAR)
[DE88-000807] 04 p0475 N88-12930
Some distance problems in coding theory
[B8711398] 05 p0635 N88-13888
Distribution of records on a ring of processors
[PB87-235784] 06 p0758 N88-14649
Online monitoring of laserpulses using the GPIB-interface of a Tektronix 2430 Digital Storage Oscilloscope
[DE88-002836] 07 p0856 N88-15201
UNITY: A framework for study of parallel programming problem-solving
[AD-A185616] 07 p0906 N88-15490
Communications patterns in a symbolic multiprocessor
[AD-A186696] 09 p1215 N88-17282
Recovery using virtual memory
[AD-A187098] 09 p1217 N88-17296
An efficient sparse matrix multiplication scheme for the CYBER 205 computer
[NASA-TM-4028] 10 p1390 N88-18302
Performance and evaluation at the Center for Supercomputing Research and Development
[DE88-003563] 10 p1417 N88-18456
Optical memory cards: A comparison with other current technologies and potential military applications
[AD-A187287] 10 p1425 N88-18512
Modular CAMAC system, 2
[DE88-700237] 11 p1525 N88-19106
OPS83: Style guide for high performance
[AD-A188505] 12 p1681 N88-20051
An interface between object-oriented systems
[AD-A189245] 13 p1815 N88-20644
Application of static memory for data acquisition and transmission into a computer
[DE88-701491] 15 p2106 N88-22544
Parallel memory addressing using coincident optica pulses
[AD-A189767] 15 p2106 N88-22547
Memory efficient evaluations of nonlinear stochastic equations and C3 applications
[AD-A189672] 15 p2110 N88-2256
Design of an algorithm to translate nested relationa algebra queries to GENESIS trace manager comma
[AD-A190502] 15 p2112 N88-22581
Microvax networked computer system
[AD-A190308] 15 p2114 N88-2258
The modeling, simulation and comparison o interconnection networks for parallel processing
[AD-A190571] 15 p2115 N88-2258
The algebraic structure of convolutional codes
[AD-A190280] 15 p2120 N88-2263
Coding for write-unidirectional memories and conflic resolution
[ENST-87C005] 16 p2245 N88-2340
IPC for modular software requires a third par connect
[AD-A189199] 16 p2246 N88-23414
A computational model of motor behavior
[AD-A191179] 18 p2553 N88-25152
The role of working memory in languag comprehension
[AD-A192721] 20 p2833 N88-2680
Common Data Format (CDF) to store images
[NASA-CR-179366] 20 p2836 N88-2682
Implementation of an OPS5 derivative on the Nova RISC processor
[DE88-011392] 21 p2994 N88-2775
Content-addressable memory storage by neura networks: A general model and global Liapunov metho
[AD-A192716] 21 p3002 N88-2780
Research on wide area workstations
[AD-A192529] 22 p3136 N88-2864
Programming language concepts for multiprocessors
[AD-A193465] 23 p3264 N88-29430
Laser sensing for identification and control of distribut parameter systems
[AD-A195886] 24 p3379 N88-30124

COMPUTER SYSTEMS DESIGN
The program DSMME: Digital Situation Model. Measurement — mapping 01 p0065 N88-1041
System adaptivity and the modelling of stereotypes – human-computer interaction
[NPL-DITC-91/87] 01 p0077 N88-1049
Digital bus unit engineering model: Design, manufactur and test
[MRM/TREP/1003/SAAB] 01 p0083 N88-1053
Study and design of a communication processor uni
[RIDU/TREP/1002/SAAB] 01 p0083 N88-1053
The application of emulation techniques in the analys of highly reliable, guidance and control computer systems 02 p0127 N88-1079
ISAURE: Integration of security and fault tolerance in the REALITE 2000 system 02 p0127 N88-1080
A mini system for nowcasting
02 p0204 N88-1127
FRONTIERS: An operational system for nowcasting precipitation 02 p0204 N88-1127
The impact of new computer technology on accelerator control
[DE87-014021] 02 p0219 N88-1137
Memory systems for single bus multiprocessor architecture. Application to the SCOM system
[ENST-86E022] 02 p0219 N88-1137
A design methodology for the utilization of metrics within various phases of software lifecycle models
[DE87-010519] 02 p0220 N88-1138
Praxis: The programming language: An advanced overview
[DE87-014319] 02 p0220 N88-1138
Design and development of a database for spectral data and analysis results
[DE87-011323] 02 p0247 N88-1158
Delft parallel processor 84/16
[PB87-226254] 03 p0366 N88-1230
Methods for design and evaluation of integrated hardware/software systems for concurrent computation
[NASA-CR-181522] 04 p0479 N88-1295
User interface for a partially incompatible system software environment with non-ADP users
[DE88-001518] 04 p0482 N88-1296
Study of fault tolerant techniques for satellite data handling
[FTT/REP/0001/SAAB] 05 p0632 N88-1386
Introduction to local area network design on Ariane 5 and future launchers
[SNIAS-872-422-102] 05 p0635 N88-1388
Conceptual issues in measuring the behavior of a distributed real-time process-control computer system
[DE87-009748] 05 p0638 N88-1389

Connecting RPC (Remote Procedure Call)-based distributed systems using wide-area networks
[PB87-234423] 05 p0658 N88-14041

Study of synthetic aperture radar data compression and encoding. Part 4: Algorithm implementation aspects
[NLR-TR-85065-L-PT-4] 06 p0692 N88-14249

Diagnostic emulation: Implementaion and user's guide
[NASA-CR-178391] 06 p0756 N88-14638

Software-implemented fault insertion: An FTMP example
[NASA-CR-178423] 06 p0761 N88-14668

A Multipurpose Adaptive Controller (MAC) for real time digital regulation
[REPT-87-028] 06 p0762 N88-14673

Life sciences flight experiments microcomputer
06 p0792 N88-14857

Expert system study for spacecraft management
[TL-2699-ISS-1] 07 p0824 N88-15004

Packet telecommand. System performance assessment study --- onboard data handling
[PTC/TNOT/0015/SAAB] 07 p0843 N88-15113

Annotated bibliography on reliable system design
[PB88-109848] 07 p0866 N88-15254

DOE data exchange format specification, mechanical products/drafting. Version 1.2.2: CADCAM-045
[DE88-001923] 07 p0904 N88-15477

Facility design validation of the information systems laboratory
[AD-A186309] 07 p0906 N88-15488

AFL-1: A programming language for massively concurrent computers
[AD-A186422] 07 p0906 N88-15489

Enhancement of computer system for applications software branch 07 p0923 N88-15610

Can space station software be specified through Ada?
07 p0925 N88-15622

Reliability issues in distributed operating systems
[PB88-100870] 08 p0993 N88-16009

Interactive knowledge acquisition tools
08 p1060 N88-16401

Proposal of a methodology for the conceptual design of the Distributed Data Base
[INPE-4315-TDL/282] 08 p1093 N88-16576

Experiment control and data system for an infrared detector array with maximum sensitivity
[ETN-88-91497] 09 p1136 N88-16813

User engineering: A new look at system engineering
09 p1206 N88-17231

The implementation and use of Ada on distributed systems with high reliability requirements
[NASA-CR-182481] 09 p1221 N88-17326

A type-oriented approach to knowledged-based systems
[MA-47] 09 p1222 N88-17329

A proposal for a feasibility study on the design of software interfaces in large systems
[NPL-DITC-89/87] 09 p1222 N88-17330

An advanced microcomputer design for processing of semiconductor materials 10 p1288 N88-17703

Inexpensive solution for the mass distribution of satellite images
[PB88-114038] 10 p1317 N88-17873

Proceedings of the Workshop on Future Directions in Computer Architecture and Software
[AD-A184949] 10 p1373 N88-18191

Some further observations about reduced instruction set computers 10 p1373 N88-18192

An empirical analysis of the Lilith instruction set
10 p1373 N88-18193

High-performance CPU implementation of the nebula instruction set architecture 10 p1373 N88-18194

The design of ultra high-speed numeric intensive systems (having fault tolerant and load balancing capabilities) 10 p1374 N88-18196

Research and development trends for memory hierarchies --- cache memories
10 p1374 N88-18198

On parallelism in software/hardware design tools
10 p1374 N88-18200

A large-grain dataflow architecture
10 p1375 N88-18207

Towards reusable software designs and implementations 10 p1376 N88-18213

The case for a shared address space
10 p1378 N88-18225

Design for a TPL compiler system: A system for retargeting high level language programs
10 p1381 N88-18248

Cumulative reports and publications through December 31, 1987
[NASA-CR-181624] 11 p1524 N88-19099

Application of knowledge based systems to the maintenance of inertial system electronics
12 p1578 N88-19441

The RVD mission: The on-board data processing requirements 12 p1586 N88-19495

EUROSIM: A design concept for an in-orbit operations simulator 12 p1589 N88-19517

Definition of the EUROSIM simulation subsystem
12 p1592 N88-19532

The concept of intelligent integrated interactive CAD systems
[CWI-CS-R8717] 13 p1818 N88-20865

Organization of design knowledge in an intelligent CAD environment
[CWI-CS-R8720] 13 p1819 N88-20868

The German processing and archiving facility for ERS-1
[ESA-CR(P)-2531] 13 p1851 N88-21082

Software quality assurance workstation
[P-1124/RT-14791] 14 p1957 N88-21670

Distributed operating systems: An overview
[INF-87-29] 14 p1960 N88-21688

Conception of a knowledge-based system for designing distributed systems
[DFVLR-MITT-87-16] 14 p1961 N88-21694

Passive coupler, network adapter, and network acquisition procedure for optical local networks
[ETN-88-92130] 14 p1961 N88-21695

Sigma system: Overview, prospects
15 p2052 N88-22230

An intelligent simulation model generator
[REPT-87-053] 15 p2109 N88-22562

Transformations of concurrent algorithms for highly parallel systems: A one year project summary report
[AD-A190236] 15 p2111 N88-22576

Strategies for concurrent processing of complex algorithms in data driven architectures
[NASA-CR-181657] 16 p2193 N88-23083

Fundamentals of microprocessor-based design: A tutorial, second edition
[DE88-006761] 16 p2244 N88-23406

The PAWS and STEM reliability analysis programs
[NASA-TM-100572] 16 p2262 N88-23526

Automated database design technology and tools
[NASA-CR-182875] 16 p2286 N88-23687

Activities of the Institute for Computer Applications in Science and Engineering (ICASE)
[NASA-CR-181666] 17 p2334 N88-24166

Protection and security mechanisms in the SMITE capability computer
[RSRE-MEMO-4117] 17 p2384 N88-24167

Simulation and computer aided engineering (the necessity of an integrated approach)
[NLR-MP-86050-U] 17 p2386 N88-24178

MIPS: The good, the bad and the useful
[NASA-CR-182893] 17 p2386 N88-24184

Interconnection of high-speed local area networks
17 p2390 N88-24205

A multiprocess operating system for 16 bit microcomputers or porting Unix (trademark) to a NS32016 with enhancements 20 p2836 N88-26822

Computer science and technology: Knowledge-based system for physical database design
[PB88-193289] 20 p2862 N88-27109

An integrated, multi-vendor distributed data acquisition system
[DE88-008900] 20 p2882 N88-27113

Computer system for the primary fly-by-wire control of civil transport aircraft (experimental system)
[FBW-TB-2086/88] 21 p2898 N88-27204

MINIAC: A small embedded computer
[DE88-008142] 21 p2994 N88-27757

A menu-driven menu editor and associated menu system
[DE88-008026] 21 p2998 N88-27781

Notes on operating system requirements for the next millennium
[DE88-010712] 21 p3002 N88-27805

Event monitoring functions introduced by the Onboard Life Monitoring System (OLMOS) into a German aircraft
22 p3034 N88-28008

Proposal for the on-board part of a future aircraft integrated monitoring system 22 p3035 N88-28016

Faultfinder: A diagnostic expert system with graceful degradation for onboard aircraft applications
22 p3035 N88-28018

The Sundstrand B747-400 data management unit
22 p3035 N88-28021

Interface techniques and systems for standard aircraft data buses 22 p3036 N88-28028

Microsupercomputers: Design and implementation
[AD-A194712] 22 p3135 N88-28638

Reliable onboard computing for critical space systems
[RR-670-I] 22 p3135 N88-28641

V2500 Condition Monitoring and Performance Analysis Software System (COMPASS): Overview of system --- aircraft engine
[PNR90418] 22 p3139 N88-28666

On eclecticism in specifications: A case study centered around Petri nets --- software engineering
[REPT-87-008] 22 p3140 N88-28671

Use of Markov probability and reliability model generation methods in the analysis of reliability of a fault tolerant hardware and software based system with flexible repair policies
[PNR90467] 22 p3145 N88-28706

The SMITE modular compilation system
[RSRE-MEMO-4145] 23 p3244 N88-29307

The SMITE object oriented backing store
[RSRE-MEMO-4147] 23 p3244 N88-29308

Formal specification of a secure document control system for SMITE
[RSRE-88002] 23 p3245 N88-29309

Computer systems for the representation and manipulation of mathematical knowledge
[AD-A193547] 23 p3249 N88-29340

A software engineering approach to expert system design and verification 23 p3252 N88-29356

Issues on the use of meta-knowledge in expert systems 23 p3252 N88-29357

An approach to combining heuristic and qualitative reasoning in an expert system 23 p3253 N88-29362

Expertise and reasoning with possibility: An explanation of modal logic and expert systems
23 p3253 N88-29363

DAISY-DAMP: A distributed AI system for the dynamic allocation and management of power
23 p3254 N88-29373

Requirements for a tool to aid in the development of expert systems for space station applications
23 p3258 N88-29398

Life-span knowledge engineering for space operations
23 p3259 N88-29401

Intelligent interface design and evaluation
23 p3260 N88-29405

Design consideration in constructing high performance embedded Knowledge-Based Systems (KBS)
23 p3261 N88-29415

A nonlinear filtering process diagnostic system for the Space Station 23 p3262 N88-29417

A flexible search strategy for production systems
23 p3262 N88-29420

Central user and browse service --- ERS-1 ground segment
[CU-PG-MDA-SY-0005] 23 p3297 N88-29637

Telescience testbed pilot program
[NASA-CR-183207] 24 p3412 N88-30309

Scheme86: A system for interpreting SCHEME
[AD-A195931] 24 p3413 N88-30319

The LTPP communication processor --- Columbus and Hermes
[CL/CP/SES/FR/004] 24 p3415 N88-30328

The P-3 Scheduling Support System (P-3 S3)
[AD-A194824] 24 p3436 N88-30450

COMPUTER SYSTEMS PERFORMANCE

High performance clause indexing
[DE87-011399] 01 p0106 N88-10688

Short range forecast of the daily maximum temperature 02 p0209 N88-11313

Evaluating computers and their performance: Perspectives, pitfalls, and paths
[DE87-014264] 02 p0218 N88-11375

Layering central authentication on the interactive services of an existing homogeneous distributed system
[DE87-011544] 03 p0366 N88-12304

Applications of the hybrid automated reliability predictor
[NASA-TP-2760] 04 p0475 N88-12928

Parallelization of hydrocodes on the Intel Hypercube, part 2
[DE88-001591] 04 p0480 N88-12957

Towards automated consulting: Design feedback from the performance of online documentation
[DE87-012243] 04 p0501 N88-13082

An empirical investigation of load indices for load balancing applications
[AD-A185763] 06 p0724 N88-14451

A taxonomy of analytical computer performance models for computer design
[AD-A185561] 06 p0755 N88-14632

Nonconformity testing for the Graphical Kernel System (GKS)
[GMD/VAL-86-104] 06 p0757 N88-14644

Image understanding by Image-Seeking Adaptive Networks (ISAN)
[AD-A186214] 07 p0906 N88-15492

Computer control of a microgravity mammalian cell bioreactor 09 p1197 N88-17172

Expert system applications in spacecraft subsystem controllers 09 p1210 N88-17254

Beyond rules: The next generation of expert systems
09 p1210 N88-17256

Communication and control in an integrated manufacturing system 09 p1212 N88-17263

A comparison of the Cray 2 performance before and after the installation of memory pseudo-banking
[NASA-CR-177462] 09 p1215 N88-17287

Implementation of elementary functions in Ada
[CWI-NM-R8709] 09 p1218 N88-17303
Proceedings of the Workshop on Future Directions in Computer Architecture and Software
[AD-A184949] 10 p1373 N88-18191
Hardware implementation for special functions. An application for combat simulation
10 p1374 N88-18197
A comparative study of heuristic algorithms for task assignment in distributed computing systems
10 p1376 N88-18211
A paradigm for concurrency control performance evaluation 10 p1377 N88-18220
A strategy for failure prediction
10 p1380 N88-18243
Parallelism at the microlevel: Cooperative microcontrollers with real time considerations
10 p1381 N88-18246
Design for a TPL compiler system: A system for retargeting high level language programs
10 p1381 N88-18248
A measurement-based study of concurrency in a multiprocessor
[DE88-003536] 10 p1383 N88-18260
Measurement and effects of transport delays in a state-of-the-art F-16C flight simulator
[AD-A187367] 11 p1441 N88-18599
Modules of nanosecond logic electronics system with computer control
[DE88-700190] 11 p1479 N88-18826
KR: An efficient knowledge representation system
[AD-A187705] 11 p1529 N88-19129
Efficient instruction level simulation of computers
[AD-A187821] 11 p1529 N88-19130
Performance measurements of distributed simulation strategies
[AD-A187824] 11 p1529 N88-19133
The Livermore FORTRAN Kernels: A computer test of the numerical performance range — benchmark tests
[UCRL-53745] 11 p1531 N88-19144
NFEARS (Nonlinear Finite Element Adaptive Research Solver): A nonlinear adaptive finite element solver. Part 2: User's manual
[AD-A189009] 12 p1684 N88-20070
A report on the study of algorithms to enhance vector computer performance for the discretized one-dimensional time-dependent heat conduction equation: EPIC research, phase 1
[DE88-005642] 13 p1820 N88-20880
Performance analysis of slotted ring protocols in High Speed Local Area Networks (HSLANS)
[INF-87-31] 14 p1955 N88-21652
Parallel processes in the knowledge based system HYDRA
[REPT-87-38] 14 p1960 N88-21689
Methodology for software reliability prediction, volume 1
[AD-A190018] 15 p2110 N88-22571
Methodology for software reliability prediction, volume 3
[AD-A190019] 15 p2110 N88-22572
CX-LOG system conversion (user's manual and user interface)
[AD-A190273] 15 p2111 N88-22577
The Colored Stochastic Petri Net (CS-PN) software: Application to the validation and the performance evaluation of distributed systems
[ENST-87D005] 15 p2113 N88-22589
Implementation and performance analysis of parallel assignment algorithms on a hypercube computer
[AD-A190678] 15 p2115 N88-22600
Toward a mathematical formalism of performance, task difficulty, and activation 16 p2239 N88-23372
Fundamentals of microprocessor-based design: A tutorial, second edition
[DE88-006761] 16 p2244 N88-23406
Beyond Ada: Generating Ada code from equational specifications
[AD-A191866] 18 p2557 N88-25176
Solving bidiagonal systems of linear equations on the CDC CYBER 205
[CWI-NM-R8725] 18 p2558 N88-25187
Gaussian techniques on shared-memory multiprocessors
[DE88-010584] 19 p2716 N88-26126
GRAPHICS MANAGER (GFXMGR): An interactive graphics software program for the Advanced Electronics Design (AED) graphics controller, Model 767
[DE88-010370] 19 p2717 N88-26131
A multiprocess operating system for 16 bit microcomputers or porting Unix (trademark) to a NS32016 with enhancements 20 p2836 N88-26822
Aircraft refueling demonstrator using a microbot alpha 2 robot 21 p2926 N88-27367
Constructing a highly-available location service for a distributed environment
[AD-A192723] 21 p3001 N88-27801
Modeling and approximate performance analysis of multiuser computer systems
[ETN-88-92137] 21 p3002 N88-27806
The SAS System by forms: Putting statistical power into the hands of an end-user
[DE88-010512] 21 p3010 N88-27857
DAISY-DAMP: A distributed AI system for the dynamic allocation and management of power
23 p3254 N88-29373
SCARES: A Spacecraft Control Anomaly Resolution Expert System 23 p3256 N88-29381
Archetyping: A software generation and management methodology 23 p3256 N88-29382
Benchmarking expert system tools
23 p3259 N88-29399
A space station onboard scheduling assistant
23 p3259 N88-29402
Intelligent interface design and evaluation
23 p3260 N88-29405
Design consideration in constructing high performance embedded Knowledge-Based Systems (KBS)
23 p3261 N88-29415
A flexible search strategy for production systems
23 p3262 N88-29420
A new computational capability for ramjet projectiles
[AD-A196061] 24 p3327 N88-29812
Telescience testbed pilot program
[NASA-CR-183207] 24 p3412 N88-30309

COMPUTER SYSTEMS PROGRAMS
NT INPUT/OUTPUT ROUTINES
NT OPERATING SYSTEMS (COMPUTERS)
NT SUBROUTINE LIBRARIES (COMPUTERS)
PRMIXn: A computer program for thermophysical properties of real gases and gas mixtures
[GKSS-86/E/59] 01 p0020 N88-10125
The associative memory ME7
[ESA-TT-1033] 01 p0079 N88-10506
An evaluation of WPS-Plus word processing software for the IBM PC and compatibles
[DE87-011972] 01 p0081 N88-10518
Maximum likelihood estimates of parameters in linear systems with process and measurement noise
[DFVLR-FB-87-20] 01 p0083 N88-10532
A data analysis package for RDF-determination fromEXELFS-spectra
[USIP-87-07] 01 p0104 N88-10681
A severe weather forecast software package
02 p0206 N88-11294
The VAXONLINE software system at Fermilab
[DE87-013565] 02 p0220 N88-11387
Computational methods and software for differential equations and their applications
[DE87-014601] 02 p0226 N88-11424
A requirements specification for a software design support system
[NASA-CR-182333] 05 p0637 N88-13896
Software enhancements and modifications to Program FDTD executable on the Cray X-MP computer
[DE88-001877] 07 p0904 N88-15476
Feasibility of software built-in test for SDI (Strategic Defense Initiative) applications
[AD-A185750] 07 p0917 N88-15572
Thermal structural control modelling techniques --- spacecraft
[FOK-TR-R-86-030] 08 p0962 N88-15828
Computerized evaluation of interferograms of the Michelson Interferometer for Passive Atmospheric Sounding (MIPAS) Laboratory Model (LM)
08 p1019 N88-16177
Calculation of the flow through a single-sided sudden expansion with the Computer Program for Parabolic and Elliptic Flows (COPPEF) computer program
[VTH-LR-523] 09 p1163 N88-16973
FABSTRAN: A computer program for frame and beam static and transient response analysis (nonlinear)
[ARE-TR-86205] 09 p1182 N88-17079
Development of a comprehensive software engineering environment 09 p1203 N88-17211
Software for integrated manufacturing systems, part 1
09 p1211 N88-17261
Software for integrated manufacturing systems, part 2
09 p1211 N88-17262
Evaluating software testing methods to reduce testing duplication in US Army communications equipment acquisition
[AD-A186961] 09 p1216 N88-17292
FORTRAN 77 guidelines for the software projects RASP and ANDECS
[DFVLR-MITT-87-09] 09 p1218 N88-17301
Transient sound radiation from infinite thin plate
[ARE-TM(UHA)-87508] 09 p1243 N88-17449
An empirical analysis of the Lilith instruction set
10 p1373 N88-18193
Experimenting with parallel programing in logic
10 p1380 N88-18240
Real time artificial intelligence architecture
10 p1380 N88-18242
Experience with Omega: Implementation of a prototype programming environment, part 6
[AD-A187080] 10 p1385 N88-18270
Factors causing unexpected variations in Ada benchmarks
[AD-A187231] 10 p1388 N88-18291
Deriving abstractions from a software object network
[AD-A187472] 10 p1389 N88-18294
An Ethernet local area network controller with supporting operating system software
[DE88-003534] 10 p1392 N88-18304
Feasibility study of generating plans and strategies for software testing by knowledge based system
[AD-A187834] 11 p1529 N88-19134
SIMSAT: Simulation package for flexible systems. Beams in space
[TW-278] 13 p1730 N88-20348
Probabilistic analysis of crack containing structures with the PARIS code
[KFK-4286] 14 p1924 N88-21465
DASM: A tool for Decomposition and Analysis of Sequential Machines
[EUT-87-E-170] 14 p1956 N88-21660
Activities report of the Computer Science Department
[ETN-88-91980] 14 p1958 N88-21672
Three-dimensional mesh-generation and plotting routines for use with a boundary element program (BIE3D)
[AD-A188079] 14 p1958 N88-21675
Software structuring principles for VLSI CAD
[AD-A190366] 15 p2112 N88-22570
Parafrase restructuring of FORTRAN code for parallel processing 16 p2221 N88-23258
The radiometric processing of SLAR measuring values using the PARES program
[BCRS-86-04] 16 p2227 N88-23301
Results of the testing of the segmentation program on RESEDA
[BCRS-87-01] 16 p2228 N88-23304
Introduction to the VMS (DEC) operating system
[ENST-87D006] 16 p2245 N88-23409
IPC for modular software requires a third party connect
[AD-A189199] 16 p2246 N88-23414
Portability of software. The use of software in us hardware mixture
[MBB/LWD-11/S/PUB/253] 16 p2246 N88-23416
Digital monoplotting, part 1
[B8735122-PT-1] 17 p2369 N88-24106
Digital monoplotting, part 2
[B8735122-PT-2] 17 p2369 N88-24107
Automated analysis of crack growth rate for obtaining da/dN versus delta K relation
[FFA-TN-1987-70] 18 p2527 N88-24996
Nebula support software
[AD-A192281] 20 p2837 N88-26833
Capitalizing on experience with intelligence gateway software
[AD-A193362] 21 p3028 N88-27971
COMPASS ground based engine monitoring program for general application --- Condition Monitoring and Performance Analysis Software System (COMPASS)
[PNR90420] 22 p3044 N88-28064
Software modifications to total data reporting accessory for metabolic measurement cart
[AD-A193641] 22 p3132 N88-28623
An evaluation of Interactive Laboratory System software. ILS-PC/DOS: A digital signal processing software package
[AD-A193838] 22 p3138 N88-28657
Artificial intelligence software acquisition program, volume 2
[AD-A194239] 22 p3141 N88-28680
Project management software
22 p3161 N88-28821
Plasma torch design codes package
[SNIAS-881-430-115] 23 p3266 N88-29569
N-version software demonstration for digital flight controls
[NASA-CR-181483] 24 p3328 N88-29815
Development of a general software package for the analysis and synthesis of planar antenna arrays for space applications
[S-247-02] 24 p3359 N88-30000
Improvements of DCAP 1, phase 2-3/A
[D2-RP-AI-106] 24 p3414 N88-30325

COMPUTER SYSTEMS SIMULATION
The roll back chip: Hardware support for distributed simulation using time warp
[AD-A187823] 11 p1529 N88-19132

Development of training implying man-machine interface: From the aircraft to the spacecraft
19 p2700 N88-26052

COMPUTER TECHNIQUES
NT COMPUTER AIDED DESIGN
NT COMPUTER AIDED MANUFACTURING
NT COMPUTER AIDED MAPPING
NT COMPUTER AIDED TOMOGRAPHY
NT COMPUTER ANIMATION
NT COMPUTER ASSISTED INSTRUCTION

A parallel model of the kinetic depth effect using local computations
[AD-A181945] 01 p0083 N88-10536

Transactions of the 4th Army Conference on Applied Mathematics and Computing
[AD-A183544] 01 p0085 N88-10547

Problems in integrating geographic data
[DE87-012880] 01 p0106 N88-10689

Space lab system analysis
[NASA-CR-179207] 02 p0136 N88-10869

Proceedings of Conference on Vibrodiagnostics discussed 02 p0158 N88-10990

REDUCE-aided study of a problem in Hermitian matrix theory
[DE87-014331] 02 p0229 N88-11445

A review of computer-assisted photo interpretation research at USAETL (US Army Engineer Topographic Laboratories)
[AD-A184034] 03 p0346 N88-12186

Computer-controlled testing of visual-spatial ability
[AD-A183971] 03 p0357 N88-12249

JPRS report: Science and technology. China
[JPRS-CST-87-032] 03 p0376 N88-12365

Band 2 VHF antenna for home construction
[BBC-RD-1987/13] 04 p0432 N88-12677

Statistical inference: Computer oriented algorithmic approach
[DE87-013874] 04 p0478 N88-12948

Automatic telescope operations
04 p0519 N88-13190

Stress intensity factors for cracking metal structures under rapid thermal loading, phase 1
[AD-A184112] 05 p0591 N88-13606

Computer aided modeling and fatigue failure forecast under stochastic loading 05 p0607 N88-13720

Development of a data analysis system for the detection of lower level atmospheric turbulence with an acoustic sounder
[AD-A184972] 05 p0624 N88-13821

Efficient computation of periodic Green's functions with application to grating structures
[AD-A184853] 05 p0640 N88-13912

Computer-aided study of a class of Riemannian space-times
[DE87-703367] 05 p0645 N88-13950

Relational data handling system for scientists
[PB87-223426] 05 p0658 N88-14038

An automated supernova search and the design strategy
[DE88-001827] 05 p0660 N88-14051

Computer calculations of PIN diode limiter characteristics
[AD-A185563] 06 p0697 N88-14277

Stress effects and the optimum format of a scrolling seven-line VDT text window
[AD-A185559] 06 p0758 N88-14651

Virtual image processor: A prototype implementation
[AD-A185560] 06 p0758 N88-14652

Interaction of different modules in depth perception: Stereo and shading
[AD-A185607] 06 p0759 N88-14655

USSR report: Cybernetics, computers and automation technology
[JPRS-UCC-86-014] 06 p0761 N88-14669

Gene inference engine rule writer's guide
[AD-A185709] 06 p0762 N88-14675

An inexpensive real-time interactive three dimensional flight simulation system
[AD-A184868] 07 p0821 N88-14989

Inadequacy of conventional dynamic recovery mechanisms in the presence of temporary failures
[AD-A186311] 07 p0866 N88-15251

Data acquisition, reduction and analysis of shock and vibration testing using a super microcomputer
[AD-A186123] 07 p0867 N88-15260

Model-based building verification in aerial photographs
[AD-A186010] 07 p0870 N88-15278

Reliability modelling for fault-tolerant parallel processor
[AD-A185867] 07 p0900 N88-15451

Computer-aided analysis for the Mechanics of Granular Materials (MGM) experiment, part 2
07 p0926 N88-15626

Flow field measurements using hotwire anemometry
[AD-A187029] 09 p1160 N88-16951

Ultrasonic inspection of advanced CFRP structures by computer-controlled, pulse-echo technique
[ETN-88-91665] 09 p1177 N88-17051

Mathematical structures for speech recognition
[AD-A187063] 09 p1217 N88-17295

Application of ac-impedance method on determination of corrosion rate of metals
[DE88-750307] 10 p1300 N88-17771

Methods of eliciting information from experts
[AD-A187468] 10 p1372 N88-18189

Deriving abstractions from a software object network
[AD-A187472] 10 p1389 N88-18294

Contour-to-grid interpolation with nonlinear finite elements: A feasibility study
[AD-A188108] 11 p1503 N88-18980

Terrain Analyst Work Station (TAWS) demonstrations
[AD-A188139] 11 p1504 N88-18981

A spectral method for computing complete synthetic seismograms
[AD-A187663] 11 p1510 N88-19024

Computer Applications in Geotechnical Engineering (CAGE) and Geotechnical aspects of the Computer-Aided Structural Engineering (G-CASE) projects. User's guide. UTEXAS2 slope-stability package. Volume 1: User's manual
[AD-A187674] 11 p1511 N88-19025

Theory and practice of fault tolerance in distributed systems
[AD-A187559] 11 p1540 N88-19204

The optimum solution to instrument quantization effects 12 p1577 N88-19434

Automatic knowledge acquisition for aerial image interpretation
[AD-A188616] 12 p1638 N88-19810

The formal specification of computer systems
[AD-A188947] 12 p1675 N88-20013

Automatic restructuring of FORTRAN programs for parallel execution
[DE85-003585] 12 p1676 N88-20018

Modification, implementation, and evaluation of a remote terminal emulator as a software validation and stress testing tool
[AD-A188833] 12 p1678 N88-20034

Development of a dependency theory toolbox for database design
[AD-A188872] 12 p1707 N88-20216

A simplified computer code for reduction to burning rates of closed bomb pressure-time data (MINICB)
[AD-A189112] 13 p1736 N88-20380

A study of satellite emission computed tomography
[AD-A189567] 13 p1797 N88-20745

Advanced human factors engineering tool technologies
[AD-A189390] 13 p1812 N88-20825

Computer aided surface representation
[DE88-005408] 13 p1817 N88-20854

Quality enhancement with machine intelligence
[DE88-005639] 13 p1824 N88-20901

Exhaustive and pseudo-exhaustive testing
[AD-A190140] 15 p2111 N88-22574

Argus reference manual
[AD-A190382] 15 p2111 N88-22578

Simulation of fault tolerance in a hypercube arrangement of discrete processors
[AD-A189682] 15 p2114 N88-22594

A zonal approach for the solution of coupled Euler and potential solutions of flows with complex geometries
[AD-A189752] 15 p2114 N88-22595

MultiScheme: A parallel processing system based on MIT (Massachusetts Institute of Technology) scheme
[AD-A190383] 15 p2114 N88-22597

Data base design and implementation
[AD-A190414] 15 p2149 N88-22827

Computer tomography and hybrid optical/digital methods for aerodynamic measurements
[AD-A190909] 16 p2157 N88-22872

A computer model investigation of a half square log-periodic array
[AD-A190955] 16 p2190 N88-23062

Lewis Structures Technology, 1988. Volume 1: Structural Dynamics
[NASA-CP-3003-VOL-1] 16 p2217 N88-23226

Parallel computer methods for eigenvalue extraction
16 p2218 N88-23233

Parafrase restructuring of FORTRAN code for parallel processing 16 p2221 N88-23258

Extending problem solver capabilities through case-based inference
[AD-A191332] 16 p2243 N88-23401

Axiomatic specificatin of database domain statics
[PB88-176284] 16 p2250 N88-23444

Approximate agreement
[AD-A191030] 16 p2251 N88-23455

Fast Algorithm Simulation and Test (FAST) facility
[AD-A191183] 16 p2252 N88-23457

Sensitivity analysis and multidisciplinary optimization for aircraft design: Recent advances and results
[NASA-TM-100630] 17 p2302 N88-23766

Effectiveness evaluation of fault-tolerant multiprocessor systems
[AD-A191688] 18 p2554 N88-25158

A multiprocessor data flow accelerator module
[DE88-007587] 18 p2554 N88-25161

Feature extraction using the Hough transform
[AD-A190679] 18 p2555 N88-25165

Optical symbolic processor for expert system execution
[AD-A192005] 18 p2575 N88-25296

Computer aided remote control: A general concept for intervention in the nuclear, underwater, and space domains 19 p2699 N88-26046

Computer-aided research
[DE88-007771] 19 p2714 N88-26114

Fault diagnosis in distributed computer networks
[AD-A192406] 19 p2718 N88-26140

Application of Moment Iteration Method (MIM) to electromagnetic field computation
[PB88-194139] 20 p2789 N88-26546

Graphical communication and symbolism in a computerized cartography and map compilation system
[PB88-124672] 20 p2818 N88-26720

Inference and discovery in an exploratory laboratory
[AD-A192231] 20 p2832 N88-26801

Managing microcomputer applications: A primer and guide to good practice
[AD-A192992] 20 p2835 N88-26817

Computer-aided writing
[AD-A192516] 20 p2838 N88-26837

United States Air Force Graduate Student Summer Support Program, volume 2
[AD-A191122] 21 p2924 N88-27355

CEEG dynamic brain mapping: A new method to evaluate brain function in different psychological and drug conditions 21 p2977 N88-27685

Fourth generation neurocognitive pattern analysis system 21 p2977 N88-27686

A statistical procedure for the evaluation of presence/non-presence of stimulus-related EEG activity
21 p2978 N88-27689

Assessing and enhancing human performance: Utility of a workstation network
[AD-A192840] 21 p2991 N88-27743

Issues in computer-assisted interpretation of graphs and quantitative information
[PB88-116280] 21 p2998 N88-27783

A review of parallel methods for solving sets of linear equations and their application within optimisation algorithms
[AD-A193137] 21 p3006 N88-27830

Research for reducing the labor intensive nature of high-resolution terrain analysis feature extraction
[AD-A192661] 22 p3089 N88-28345

Computer-aided decision making
[AD-A194210] 22 p3137 N88-28651

An evaluation of Interactive Laboratory System software, ILS-PC/DOS: A digital signal processing software package
[AD-A193838] 22 p3138 N88-28657

A virtual statistical mechanical neural computer
[AD-A193962] 22 p3139 N88-28660

LO-CO-GRAF (low cost graphics): Generating maps to support command and control/crisis management using small computers
[AD-A193964] 22 p3139 N88-28661

Natural object categorization
[AD-A194103] 22 p3139 N88-28662

A computer-aided approach to nonlinear control systhesis
[NASA-CR-179391] 22 p3140 N88-28673

Rendering of surfaces from volume data
[AD-A193649] 22 p3143 N88-28689

Computer-controlled measurements of nonlinear standing waves
[AD-A193840] 22 p3147 N88-28717

Direct visualization of surfaces from computed tomography data
[AD-A193646] 22 p3153 N88-28758

Automatic landing by computer vision
[ETN-88-92991] 23 p3175 N88-28905

LRS-2: A specialized knowledge system for launch resource scheduling
[AD-A194625] 23 p3182 N88-28941

Analysis of edge detection techniques for radiographic image measurement
[AD-A193650] 23 p3186 N88-28961

Approximate evaluation of semi-Markov chain reliability models
[AD-A194669] 23 p3223 N88-29185

Analysis of the effect of faulty spares on the performance of diagnostic algorithms in reliable systems
[AD-A193526] 23 p3223 N88-29186

Alterations in upper extremity motor function in soldiers during acute high altitude exposure
[AD-A192676] 23 p3238 N88-29272
Failure modes and effects analysis automation
23 p3254 N88-29370
A static scheduler for the computer aided prototyping system: An implementation guide
[AD-A194340] 24 p3414 N88-30322

COMPUTER VISION
Evaluation of vision systems for teleoperated land vehicles
[DE87-013066] 03 p0330 N88-12100
End of year report for parallel vision algorithm design and implementation
[AD-A184327] 03 p0366 N88-12301
Low-level vision on warp and the apply programming model
[AD-A184330] 03 p0369 N88-12320
On the recognition of curved objects
[AD-A184441] 04 p0478 N88-12945
Implementation and performance of a complex vision system on a systolic array machine
[AD-A184331] 04 p0482 N88-12971
Dealing with unanticipated events in autonomous navigation
[DE88-000590] 05 p0590 N88-13602
Some vision algorithms 06 p0795 N88-14871
Time-domain robotic vision application
06 p0798 N88-14886
A demonstration of autonomous navigation and machine vision using the HERMIES-2B robot
[DE88-002298] 07 p0862 N88-15228
Parallel algorithms for computer vision on the connection machine
[AD-A185842] 07 p0901 N88-15456
Proceedings of Image Understanding Workshop, volume 1
[AD-A186103] 07 p0902 N88-15463
Proceedings of Image Understanding Workshop, volume 2
[AD-A186104] 07 p0902 N88-15464
Image understanding by Image-Seeking Adaptive Networks (ISAN)
[AD-A186214] 07 p0906 N88-15492
Vision algorithms and psychophysics
[AD-A186773] 09 p1200 N88-17193
Development of Moire machine vision
09 p1212 N88-17264
Implementation of a robotic flexible assembly system
09 p1212 N88-17265
Vision technology/algorithms for space robotics applications 09 p1212 N88-17267
Telerobotic truss assembly 09 p1213 N88-17272
Multiple-object motion estimation by maximal matching of 3-D point and line features 09 p1220 N88-17322
An overview of vision-based navigation for autonomous land vehicles 1986
[AD-A188186] 10 p1276 N88-17640
Visual integration and detection of discontinuities: The key role of intensity edges
[AD-A188012] 11 p1520 N88-19076
Object recognition on a systolic array
[AD-A187726] 11 p1534 N88-19164
Three-dimensional information from stereovision process 12 p1593 N88-19540
A texture analysis approach to computer vision for identification of roads in aerial photographs
[AD-A189340] 12 p1639 N88-19815
Retinotopic mapping of the human visual system with magnetoencephalography
[AD-A188557] 13 p1810 N88-20811
On relaxation algorithms based on Markov random fields
[AD-A189043] 13 p1814 N88-20840
Mathematic modeling of visual perception problems
[INPE-4355-PRE/1186] 13 p1823 N88-20897
Aspects and applications of primary processing of visual information
[INPE-4290-PRE/1161] 13 p1841 N88-21015
On the geometric interpretation of image contours
[RR-647-I-IMAG-57-LIFIA] 15 p2109 N88-22563
Concurrent algorithms for a mobile robot vision system
[DE88-005850] 15 p2117 N88-22614
Recognizing and locating partially occluded planar objects for assembly routines
[LAAS-87-360] 16 p2247 N88-23422
Conversational Analysis of Color Images (CAICOU): An interactive development system for the analyses of color images
[RR-641-I-IMAG-39-LIFIA] 17 p2342 N88-23964
Linguistic definition of generic models in computer vision
[RSRE-MEMO-4110] 17 p2386 N88-24182
Orbital navigation, docking and obstacle avoidance as a form of three dimensional model-based image understanding 17 p2388 N88-24194
A concurrent on-board vision system for a mobile robot
[DE88-007475] 19 p2676 N88-25914
Intermediate level computer vision processing algorithm development for the content addressable array parallel processor
[AD-A192086] 19 p2714 N88-26111
Sensor fusion for robot navigation
[DE88-008383] 20 p2809 N88-26663
Research into the architecture of CAD based robot vision systems
[AD-A193330] 21 p2997 N88-27776
Neural network research: A personal perspective
[AD-A192717] 21 p3003 N88-27808
Automatic landing by computer vision
[ETN-88-92991] 23 p3175 N88-28905
Optimization-driven machine-oriented motion measurement 23 p3245 N88-29312
Second Conference on Artificial Intelligence for Space Applications
[NASA-CP-3007] 23 p3251 N88-29351
Machine vision for real time orbital operations
23 p3253 N88-29367
Two dimensional convolute integers for machine vision and image recognition 23 p3254 N88-29369
A generic expert system for materials processing in space 23 p3255 N88-29376
Using primal sketch primitives as the basis for the Hough transform
[INPE-4564-PRE/1305] 24 p3412 N88-30310
An automated computerized vision technique for determination of three-dimensional object geometry
24 p3419 N88-30346

COMPUTERIZED CONTROL
U NUMERICAL CONTROL

COMPUTERIZED DESIGN
U COMPUTER AIDED DESIGN

COMPUTERIZED SIMULATION
NT ANALOG SIMULATION
NT DIGITAL SIMULATION
Current experimental and theoretical understanding of detonation waves in heterogeneous solid explosives
[DE87-012177] 01 p0032 N88-10201
Simulations using the pseudo-current algorithm
[DE87-012403] 01 p0040 N88-10255
Cloud climatology derived from the AFGWC (Air Force Global Weather Central) 3D-nephanalysis for January and July 1979
[AD-A183686] 01 p0070 N88-10446
Adaptive line of sight algorithms
[DE87-014275] 01 p0081 N88-10523
DETOUR: A deformed mesh/contour plot program
[DE87-013119] 01 p0082 N88-10525
Workshop on AI (Artificial Intelligence) and Simulation (2nd) held in Seattle, Washington on 14 July 1987
[AD-A183736] 01 p0084 N88-10542
Dynamical simulation of structural multiplicity in grain boundaries
[DE87-012746] 01 p0103 N88-10676
Application of new conformal solution of theories
[PB87-214557] 01 p0105 N88-10684
RE-1000 free-piston Stirling engine hydraulic output system description
[NASA-TM-100185] 01 p0108 N88-10700
Computer modeling of metal forming
[DE87-013804] 02 p0157 N88-10984
On adaptive signal processing of RF signals
[DE87-014182] 02 p0161 N88-11007
Computer simulation of thermal modeling of primary lithium cells 02 p0163 N88-11022
Results of a wind turbine/sealed lead-acid battery experiment
[DE87-012720] 02 p0166 N88-11044
Computations of hypervelocity impact using the CTH shock wave physics code
[DE87-013067] 02 p0169 N88-11062
Modeling shockwave deformation via molecular dynamics
[DE87-013157] 02 p0169 N88-11063
Computer modeling of two-phase flow
[CFDU/87/5] 02 p0171 N88-11078
Numerical simulation of Tollmien-Schlichting waves by use of a modified vortex particle-in-cell method
[IC-AERO-85-02] 02 p0171 N88-11079
Time-resolved absorption measurements on OMEGA
[DE87-014465] 02 p0179 N88-11112
Numerical simulation of laser filamentation experiments
[ETN-87-90959] 02 p0179 N88-11116
Production of NO by galactic cosmic rays and lightning
[DE87-014613] 02 p0197 N88-11230
Numerical simulation of Tokamaks: Ideal MHD equilibrium and stability
[DE87-013452] 02 p0218 N88-1137
Study into a data relay satellite mission analysis tool
[ESA-CR(P)-2422] 02 p0220 N88-1138
Projection-space iterative interpolation for limited-angle tomography in parallel- and fan-beam geometry, part 1
[DE87-013865] 02 p0221 N88-1139
On the relational modeling of discrete PDE problems
[DE87-013336] 02 p0224 N88-1140
Computer models for kinetic equations of magnetically confined plasmas
[DE87-011571] 02 p0236 N88-1148
A relativistic Monte Carlo binary collision model for use in plasma particle simulation codes
[DE87-013287] 02 p0237 N88-1148
Thin film microstructures: Simulation and theory
[DE87-014732] 02 p0246 N88-1155
Computer simulations of knock-on processes in bcc Ta crystal
[DE87-752980] 02 p0246 N88-1155
Improvements to the adaptive maneuvering logic program
[NASA-CR-3985] 03 p0262 N88-1164
Fin gaps and body slots of guided projectiles: Effects, data correlation and modeling
[AD-A184440] 03 p0270 N88-1169
Modeling of environmentally-induced effects within satellites. Part 1: NASCAP modeling of satellites
03 p0273 N88-1172
Charging calculations for the HIPPARCOS satellite
03 p0274 N88-1172
Electrodynamic tether system study
[NASA-CR-172024] 03 p0275 N88-1173
The structure and reactivity of heterogeneous surfaces and study of the geometry of surface complexes
[DE88-000156] 03 p0279 N88-1175
Numerical simulation of turbulent premixed combustion and decay of turbulent swirling flow
[DE87-014253] 03 p0284 N88-1178
An antenna array processing system for multiple source bearing estimation 03 p0305 N88-1192
Numerical simulation of the interaction of vortex rings in viscous fluid 03 p0318 N88-1200
Numerical study of the entrance flow and its transition in a circular pipe (2) 03 p0318 N88-1201
Numerical simulation of internal combustion engine flows: Development and users guide for MAGIC radial-azimuthal version
[DE87-014453] 03 p0332 N88-1209
On the control of a compliant robot arm
03 p0332 N88-1209
Teleoperator and robotics system analysis
[NASA-CR-179220] 03 p0334 N88-1210
A quasi-physical model for converting hourly global horizontal to direct normal insolation
[DE87-012273] 03 p0349 N88-1220
Radar measurement methods for the observation of convective clouds, and comparison of measurements and numerical simulation
[ESA-TT-1049] 03 p0352 N88-1222
The development of low level coastal flow fields when solar radiation is blocked by smoke
[DE87-014348] 03 p0354 N88-1223
Mass balances for a biological life support system simulation model 03 p0361 N88-1227
A simulation study of a speed control system for autonomous on-road operation of automotive vehicles
[AD-A184030] 03 p0362 N88-1227
Mapping a battlefield simulation onto message-passing parallel architectures
[NASA-CR-178396] 03 p0363 N88-1228
ERIC: An object-oriented simulation language
[AD-A184757] 03 p0364 N88-1229
Token execution strategies for distributed algorithms: Simulation studies
[AD-A184792] 03 p0365 N88-1229
The structure-mapping engine: Algorithm and examples
[AD-A184042] 03 p0368 N88-1231
Microcomputer control of a hydraulically actuated piston
[AD-A184130] 03 p0368 N88-1231
Monte Carlo simulation of modulated phases
[NASA-TM-89654] 03 p0369 N88-1232
Computer simulations of fragmentation
[DE87-900995] 03 p0375 N88-1235
Dynamics of atoms in low-symmetry systems
[AD-A184318] 03 p0375 N88-1236
Mathematical models of plasma discharge control in a tokamak
[DE87-702891] 03 p0378 N88-1237
Simulation of the layer-growth dynamics in silver films: Dynamics of adatom clusters and vacancy clusters on Ag(100)
[DE87-014784] 03 p0380 N88-1238

Competition Analysis Model (CAM). Volume 2: Computer manual
[AD-A184017] 03 p0384 N88-12411

NAVSIM 2: A computer program for simulating aided-inertial navigation for aircraft
[NASA-CR-177438] 04 p0398 N88-12478

Simulation of an enhanced TCAS 2 system in operation
[NASA-CR-181545] 04 p0398 N88-12479

An inexpensive real-time interactive three-dimensional flight simulation system
[AD-A184340] 04 p0402 N88-12499

Numerical simulation system
04 p0404 N88-12511

Analytical investigation of the dynamics of tethered constellations in Earth orbit (phase 2)
[NASA-CR-179218] 04 p0408 N88-12533

Simulation studies for surfaces and materials strength
[NASA-CR-181535] 04 p0412 N88-12557

The Pierce diode with an external circuit. Part 1: Simulations in the linear regime
[DE88-000413] 04 p0440 N88-12731

PRAAGE: An interactive IBM-PC code for unreliability/aging analysis
[DE87-012124] 04 p0453 N88-12803

A portable hypercube simulator
[DE87-013369] 04 p0478 N88-12947

A network definition and solution of simulation problems
[DE88-000675] 04 p0481 N88-12962

Development of the non-equilibrium reactive chemical transport code CHMTRNS
[DE88-000682] 04 p0481 N88-12964

Computer-aided X-ray image system design and evaluation
[DE88-000697] 04 p0481 N88-12965

GOLD: Integration of model-based control systems with artificial intelligence and workstations
[DE88-000506] 04 p0483 N88-12976

GOLD: Integration of model-based control systems with artificial intelligence and workstations
[DE88-000706] 04 p0483 N88-12977

Monocrystal sputtering by the computer simulation code ACOCT
[IPPJ-848] 04 p0493 N88-13035

Theory and simulations of Zone 2 microstructures in thin films
[DE87-014752] 04 p0499 N88-13071

Subjective probability, combination of expert opinion and probabilistic approaches to information retrieval
04 p0501 N88-13085

Practical and modern simulation by systematic connection of the LU-ADI code and the solution adaptive grid program 05 p0536 N88-13260

Programming techniques for high-speed processing of large scale numerical simulation on supercomputers
05 p0537 N88-13269

Rarefied gas numerical wind tunnel. 2: Two-dimensional and axially symmetric bodies 05 p0538 N88-13273

Numerical simulation of splash of droplet at unit gravity 05 p0538 N88-13275

A perspective of computational fluid dynamics
05 p0538 N88-13279

Navier-Stokes simulation of transonic transportation aircraft configurations. 1: Flow-field simulation over wing-fuselage combinations 05 p0540 N88-13288

Numerical simulation of transonic aircraft in comparison to wind tunnel test 05 p0540 N88-13289

Computation of transonic flows with nacelle simulation
[SNIAS-872-111-117] 05 p0542 N88-13300

Correction of inertial navigation system drift errors for an autonomous land vehicle using optical radar terrain data
[AD-A184973] 05 p0544 N88-13311

The role of experimental investigation and computational fluid dynamics during fighter aircraft design
05 p0546 N88-13326

A numerical study of the effects of curvature and convergence on dilution jet mixing
[NASA-TM-89878] 05 p0549 N88-13347

Computer code simulations of explosions in flow networks and comparison with experiments
[DE88-001946] 05 p0573 N88-13491

Noise modelling in the time domain with the aid of Spice
[PB87-221941] 05 p0573 N88-13492

Numerical and analytical study of the equivalent permittivity or permeability of nonhomogeneous materials. Application to the experimental electromagnetic characterization of composites
[SNIAS-872-430-104] 05 p0575 N88-13509

Dynamics of propellant feedline systems
[AD-A184985] 05 p0580 N88-13537

Physical analyses and numerical simulation of coherent turbulent structures in mixed layers, jets, and wakes
[ETN-88-91183] 05 p0581 N88-13548

Low thrust viscous nozzle flow fields prediction
[NASA-CR-182334] 05 p0582 N88-13551

Development of response models for the Earth Radiation Budget Experiment (ERBE) sensors. Part 1: Dynamic models and computer simulations for the ERBE nonscanner, scanner and solar monitor sensors
[NASA-CR-178292] 05 p0584 N88-13557

Collision-free motion of two robot arms in a common workspace
[CSE-87-00002] 05 p0589 N88-13596

Trajectory control of robot manipulators with closed-kinematic chain mechanism
[NASA-TM-89305] 05 p0591 N88-13605

Applications of fatigue analyses: Transportation
05 p0608 N88-13733

Free Lagrange reconnection algorithms for hydrocodes using a quadrilateral mesh
[DE88-001580] 05 p0611 N88-13752

An adaptive lattice algorithm for spectral line estimation
[AD-A184970] 05 p0634 N88-13876

SUSIE reference manual
[DE88-001462] 05 p0636 N88-13893

Optimal control of large space structures via generalized inverse matrix
[NASA-CR-182336] 05 p0639 N88-13907

Modeling and generating input processes
[DE87-013162] 05 p0645 N88-13948

Molecular dynamics studies of aromatic hydrocarbon liquids
[DE88-001473] 05 p0648 N88-13973

Computer modeling of complete IC fabrication process
[AD-A184807] 05 p0654 N88-14012

Range imagery algorithms for the detection of obstacles by autonomous vehicles
[AD-A185421] 05 p0659 N88-14045

Advanced simulation and analysis of a geopotential research mission
[NASA-CR-182355] 06 p0670 N88-14108

JPRS report: Science and technology. Japan
[JPRS-JST-87-029] 06 p0675 N88-14130

Numerical simulation of flight body circumference flow
06 p0676 N88-14137

Development of transonic speed cascade design method using Euler code and inverse solution
06 p0676 N88-14139

Surface gouging by hypervelocity sliding contact between metallic materials
[DE88-001937] 06 p0682 N88-14178

Advanced numerical modeling of microwave penetration and coupling for complex structures
[DE88-001873] 06 p0690 N88-14231

Documentation of computer programs for optimization and simulation of multicarrier SAW-based demodulator
[PB87-134532] 06 p0693 N88-14252

Model development for induction heating
[DE88-002376] 06 p0699 N88-14269

Computer simulation of the L/sub 3/-edge densitometer
[DE88-001944] 06 p0705 N88-14324

Numerical simulation of flows in axial and radial turbomachines using Euler solvers
06 p0713 N88-14372

Some investigations of molecular beam epitaxial growth of 3-5 semiconductor films via Monte-Carlo computer simulations, carrier tunnelling and spectroscopic ellipsometry
[AD-A185520] 06 p0789 N88-14839

Atmospheric entry heating of cosmic dust
06 p0794 N88-14865

Dynamics formulations for the real-time simulation of constrained motion 06 p0795 N88-14872

Viscous vortex flows 07 p0810 N88-14934

An orbit simulation study of a geopotential research mission including satellite-to-satellite tracking and disturbance compensation systems
[NASA-CR-182353] 07 p0823 N88-14997

Impact of solids on composite materials
[NASA-CR-182395] 07 p0827 N88-15015

Computer simulation of impurities and interfaces in body centered cubic metals
[PB88-108162] 07 p0832 N88-15047

Computer simulation of pencil glide in B.C.C. metals
[DE88-001802] 07 p0834 N88-15062

Channel access protocols for multihop packet radio networks
[AD-A186074] 07 p0842 N88-15106

An additional study and implementation of tone calibrated technique of modulation
[NASA-CR-182377] 07 p0844 N88-15117

High resolution simulation of turbulent flow in a channel
[AD-A186022] 07 p0848 N88-15150

Numerical calculation of appendage, flat plate junction flow
[AD-A186371] 07 p0850 N88-15156

Multitasked embedded multigrid for three-dimensional flow simulation
[NASA-CR-182398] 07 p0852 N88-15173

Numerical methods for fluid flow problems
[DE88-000156] 07 p0854 N88-15190

Computer simulations of ballistic experiments
[DE87-005835] 07 p0862 N88-15226

Analyses of the mass formula dependence of spallation product distribution
[DE88-750297] 07 p0864 N88-15243

Discrete reliability growth models using failure discounting
[AD-A186360] 07 p0866 N88-15252

Computing support for basic research in perception and cognition
[AD-A186192] 07 p0897 N88-15437

Massively parallel implementations of theories for apparent motion
[AD-A185841] 07 p0901 N88-15455

Computer aided design for Petri Nets
[AD-A186109] 07 p0902 N88-15465

Problems of organization of mass processes of simulation, acquisition and processing of experimental data at computers
[DE88-700547] 07 p0905 N88-15483

Improved input representation for enhancement of neural network performance
[DE88-001830] 07 p0907 N88-15496

Monte Carlo simulation of triangulated random surfaces in grand canonical ensemble
[DE88-700378] 07 p0941 N88-15718

Computers in theoretical physics
[DE88-700516] 07 p0941 N88-15720

A dynamic simulation and feedback control scheme for the U.S. Marine Corps' Airborne Remotely Operated Device (AROD)
[AD-A186587] 08 p0953 N88-15784

The NASA aircraft icing research program
08 p0957 N88-15803

Non-steady group combustion of a cloud of char particles
[DE87-010773] 08 p0966 N88-15849

Use of a general control simulation program to evaluate HVAC control stability
[DE88-000476] 08 p0975 N88-15896

A simultaneous M-ary channel hypothesis test with least-mean-square signal amplitude estimation
[AD-A186526] 08 p0978 N88-15913

Integration of Navier-Stokes equations in finite volume formulation 08 p0984 N88-15954

Finite Element Calculation Methods and Their Application to Turbomachinery Flows, volume 1
[VKI-LS-1987-05-VOL-1] 08 p0985 N88-15960

Introduction to the Modeling of Turbulence
[VKI-LS-81-06] 08 p0986 N88-15972

Examples of turbulence-model applications
08 p0987 N88-15975

Direct and large eddy simulation of turbulence. Summary of the state of art 1987 08 p0987 N88-15977

Turbulence modeling for compressible flows
08 p0987 N88-15978

Computer program for the calculation of the profile-vortices interactions (two dimensional inviscid incompressible flow with point singularities)
[ISL-R-124/86] 08 p0987 N88-15982

Qualitative and temporal reasoning in engine behavior analysis 08 p1056 N88-16383

Development of a task-level robot programming and simulation system 08 p1058 N88-16387

Automatic mathematical modeling for space application 08 p1060 N88-16402

LISP based simulation generators for modeling complex space processes 08 p1061 N88-16403

Knowledge-based simulation
08 p1061 N88-16404

Case-based reasoning for space applications: Utilization of prior experience in knowledge-based systems
08 p1065 N88-16432

Development of a computer model for missile simulation, or simulation of a kinetic coverage area for a target detection missile
[FOA-C-20666-2.5] 08 p1067 N88-16449

Development of a computer model for missile simulation, or simulation of a kinetic coverage area for a collimation guided missile
[FOA-C-20667-2.5] 08 p1067 N88-16450

User's guide to DIANE: A microcomputer program for modeling battery performance in electric vehicles
[DE88-003713] 08 p1068 N88-16456

FOR3D: A computer model for solving the LSS (Lee-Saad-Schultz) three-dimensional, wide angle wave equation
[AD-A186649] 08 p1090 N88-16511

Depth of origin of sputtered atoms: Experimental and theoretical study of Cu/Ru(0001)
[DE88-002648] 08 p1092 N88-16520

An integrated approach to rotorcraft human factors research
09 p1110 N88-16653

Contribution to the design of flexible manufacturing systems. Modeling, simulation, and evaluation of parameters
[ISAL-IDI1-87-04] 09 p1151 N88-16894

Optimizing HF antenna systems on the Dolphin and Sea Hawk helicopters
[AD-A186552] 09 p1152 N88-16901

Mode media interactions in an FEL (Free Electron Laser)
[DE88-003155] 09 p1172 N88-17029

Control system simulation for a single-link flexible arm
[AD-A187037] 09 p1174 N88-17035

An interactive-graphics method for dynamic system modelling, applying consistency rules
09 p1181 N88-17072

A comparison of different module configurations for multibandgap solar cells
[DE88-002718] 09 p1187 N88-17113

SWAN: An expert system with natural language interface for tactical air capability assessment
09 p1210 N88-17253

Development of a facility using robotics for testing automation of inertial instruments
09 p1213 N88-17271

The use of computer graphic simulation in the development of robotic systems
09 p1214 N88-17275

Acceleration techniques for decoupling algorithms in semiconductor simulation
[DE88-003593] 09 p1221 N88-17323

Plasma theory and simulation
[AD-A187100] 09 p1249 N88-17486

An evaluation of project scheduling techniques in a dynamic environment
[AD-A187057] 09 p1260 N88-17554

Radar returns from ground clutter in vicinity of airports
10 p1274 N88-17624

Wind shear radar simulation 10 p1274 N88-17625

Simulator investigation of wind shear recovery techniques 10 p1275 N88-17630

Numerical simulation of diffuser/combustor dome interaction 10 p1281 N88-17663

Simulation test beds for the space station electrical power system
[NASA-TM-100786] 10 p1290 N88-17715

ESL batteries and multi-segment applications --- ESA Simulation Language (ESL)
[CS-1029/00-QFIN4] 10 p1322 N88-17901

Multidimensional modeling of convective heat transfer with application to IC engines
[DE88-003398] 10 p1330 N88-17948

Emittance studies at the Los Alamos National Laboratory Free-Electron Laser (FEL)
[DE88-003146] 10 p1334 N88-17975

Instrumentation and quantitative methods of evaluation
[DE87-013639] 10 p1342 N88-18017

Simulation and modeling of whistler mode wave growth through cyclotron resonance with energetic electrons in the magnetosphere 10 p1353 N88-18089

Numerical simulations of the California current: Filament formation as related to baroclinic instability
[AD-A187573] 10 p1358 N88-18115

Hardware implementation for special functions: An application for combat simulation
10 p1374 N88-18197

Parallel discrete event simulation: A shared memory approach
[NASA-CR-182521] 10 p1395 N88-18312

Microscopic modeling of sound waves in granular material
[DE88-000348] 10 p1405 N88-18375

The numerical simulation of accelerator components
[DE87-011597] 10 p1412 N88-18423

Benchmarks of neutral beam injection codes for stellarators
[DE88-003786] 10 p1412 N88-18428

Plasma theory and simulation
[DE88-003620] 10 p1414 N88-18437

Simulation and processing of high resolution images of defects and interfaces in superconducting YBa2Cu3O7
[DE88-003856] 10 p1420 N88-18480

Cosmic strings: A problem or a solution
[DE88-003410] 10 p1429 N88-18535

La Recherche Aerospatiale, bimonthly bulletin, number 1987-2, 237/March-April
[ESA-TT-1074] 11 p1433 N88-18550

A computer simulation study of an expert system for walking machine motion planning
[AD-A187907] 11 p1438 N88-18577

Simulation of infrared spectra
[AD-A187881] 11 p1453 N88-18658

The coaxial colinear antenna: Theoretical and experimental models 11 p1475 N88-18803

The Pierce diode with an external circuit. 2: Non-uniform equilibria
[AD-A188027] 11 p1478 N88-18818

Computational studies of wave-shaping in a blast simulator by perforated plates in the driver
[AD-A188200] 11 p1483 N88-18850

Experimental results of a high-gain microwave FEL operating at 140 GHz
[DE88-004358] 11 p1492 N88-18907

Further development of a finite element model of orthogonal metal cutting
[DE88-004048] 11 p1494 N88-18921

The digital landmass simulation production overview
[AD-A187978] 11 p1503 N88-18978

Test results of a 40-kW Stirling engine and comparison with the NASA Lewis computer code predictions
[NASA-TM-87050] 11 p1508 N88-19013

A worked example of an application of the SAINT simulation program
[AD-A188198] 11 p1524 N88-19097

Mathematical modeling of two-state classification technology transfer summary and user's guide
[DE88-003849] 11 p1526 N88-19110

Efficient instruction level simulation of computers
[AD-A187821] 11 p1529 N88-19130

Optimal performance of distributed simulation programs
[AD-A187822] 11 p1529 N88-19131

Performance measurements of distributed simulation strategies
[AD-A187824] 11 p1529 N88-19133

Algorithmic alternatives
[DE88-003905] 11 p1531 N88-19149

Concepts and nomenclature in the world modeling system (a lesson in applied metaphysics)
[AD-A188246] 11 p1534 N88-19166

A computer graphics simulation of the endgame in aircraft combat survivability
[AD-A187826] 11 p1541 N88-19214

Computer modeling for optical waveguide sensors
[AD-A187702] 11 p1549 N88-19263

Design of an aeroelastic composite wing wind tunnel model
[AD-A188855] 12 p1582 N88-19466

Columbus Simulation Facility (CSF)
12 p1590 N88-19522

Orbital analysis of a STS (Space Transportation System) external tank in low earth orbit
[AD-A188829] 12 p1593 N88-19542

The use of hardware-in-the-loop techniques in the development of a modern air-to-surface missile system
12 p1597 N88-19562

Computer aided fast turnaround laboratory for research in VLSI (Very Large Scale Integration)
[AD-A189451] 12 p1624 N88-19715

Compressible friction coefficients in a simulated heat pipe
[AD-A188818] 12 p1627 N88-19735

A simulation of void lining during ductile fracture
[AD-A188404] 12 p1635 N88-19792

HELIOS modelling of point-focusing solar concentrators
[DE88-004933] 12 p1640 N88-19820

Comparison of simulation modeling and satellite techniques for monitoring ecological processes
[NASA-CR-182592] 12 p1641 N88-19825

Modification, implementation, and evaluation of a remote terminal emulator as a software validation and stress testing tool
[AD-A188833] 12 p1678 N88-20034

A numerical analysis of the dynamics of PRIZ operation
[AD-A188853] 12 p1678 N88-20035

Primal-dual parallel solution of very large sparse linear programs
[AD-A188500] 12 p1680 N88-20045

The automated symbolic derivation of state equations for dynamic systems
[DE88-005222] 12 p1683 N88-20060

ADAM (Acquisition Deployment and Maneuvering): The space game
[AD-A189512] 12 p1685 N88-20078

Simulation of nuclear collisions at high energies in the frames of quark-gluon string model
[DE88-700914] 12 p1690 N88-2011[illegible]

Improved zero dimensional model of a reversed field pinch fusion device
[DE88-005212] 12 p1693 N88-20127

X-ray source model for Z-pinch aluminum plasmas
[AD-A189509] 12 p1696 N88-20148

Systems analysis and simulation techniques: Essential tools for balanced complex weapon system designs in terms of performance and cost
12 p1702 N88-20187

Mars Lander/Rover vehicle development: An advanced space design project for USRA and NASA/OAST
[NASA-CR-182562] 12 p1709 N88-20226

AVSCOM'S modifications to Teledyne Systems Company's air-to-air fire control system simulation model
[AD-A189136] 13 p1722 N88-20294

Trajectory code studies, 1987
[DE88-006218] 13 p1728 N88-20335

SIMSAT: Simulation package for flexible systems. Beams in space
[TW-278] 13 p1730 N88-20346

Bipropellant combustion in a liquid rocket combustion chamber 13 p1733 N88-20359

Mixing of viscous fluids: Behavior of microstructures and chaos
[DE88-006287] 13 p1766 N88-20566

Multigrid solution of the Euler equations
13 p1769 N88-20582

Particle-dynamics calculations of gravity flow of inelastic frictional spheres
[DE88-005224] 13 p1770 N88-20596

Dynamics of high-speed mechanisms with elastic members 13 p1779 N88-20643

Human problem solving in dynamic environments: Understanding and supporting operators in large-scale, complex systems
[AD-A189539] 13 p1812 N88-20826

Simulation of measuring points for three dimensional measurements
[WPB-0115] 13 p1821 N88-20883

A fault injection experiment using the AIRLAB Diagnostic Emulation Facility
[NASA-CR-178390] 13 p1823 N88-20895

SEAT: A strategic engagement analysis tool
[DE88-000498] 13 p1830 N88-20941

Physics at large transverse momenta
[DE88-005758] 13 p1836 N88-20986

Numerical simulations of multiphoton processes in many electron atoms
[DE88-003293] 13 p1837 N88-20990

Activities report of the Toulouse Research Center
[ETN-88-91988] 13 p1850 N88-21077

Resonant Alfven wave instabilities driven by streaming fast particles 13 p1855 N88-21104

Determination of canopy loads for a light aircraft by wind tunnel testing and computer modelling
[BU-353] 14 p1869 N88-21167

Hygrothermomechanical fiber composite fatigue: Computational simulation
[NASA-TM-100840] 14 p1884 N88-21257

Activities report of the Energetics Department
[ETN-88-91981] 14 p1888 N88-21281

Numerical simulation of turbulent premixed combustion and decay of turbulent swirling flow
[DE88-006588] 14 p1888 N88-21284

Millimeter-wave pulse distortion by a single adsorption line simulating the terrestrial atmosphere
[PB88-161237] 14 p1906 N88-21388

Materials dependence of deformation texture development in various deformation modes
[DE88-004312] 14 p1922 N88-21457

Oceanographic export system development, year 1
[AD-A189134] 14 p1950 N88-21623

Activities report of the Computer Science Department
[ETN-88-91980] 14 p1958 N88-21672

Comprehensive model for laser instability in a CO2 laser with gaseous saturable absorber
14 p1979 N88-21808

Velocity and concentration fields over a crystal growing in a water solution: Experimental study and numerical simulation 14 p1987 N88-21856

Development and evaluation of an airplane fuel tank ullage composition model. Volume 2: Experimental determination of airplane fuel tank ullage compositions
[AD-A190408] 15 p2017 N88-22025

Linear state space modeling of a turbofan engine
[AD-A190110] 15 p2019 N88-22035

Moving-bank multiple model adaptive estimation applied to flexible spacestructure control
[AD-A190761] 15 p2026 N88-22071

Status of electric vehicle simulation programs at the INEL: Summer 1987
[DE88-006745] 15 p2058 N88-22271

Basic characteristics of heat-exchanger-type steam reformer heated by high-temperature helium gas (2): Analysis by simulation model (2)
[DE87-702962] 15 p2061 N88-22251

Finite element simulation of perforation of aluminum plates
[DE88-002092] 15 p2073 N88-22362

Computational simulation methods for composite fracture mechanics 15 p2079 N88-22396

Performance evaluation of molten salt thermal storage systems
[DE87-014645] 15 p2091 N88-22461

Advanced geothermal technologies
[DE88-004307] 15 p2091 N88-22463

Anthropomorphic phantom radiation dosimetry at the NATO standard reference point at Aberdeen Proving Ground
[AD-A190508] 15 p2103 N88-22528

An intelligent simulation model generator
[REPT-87-053] 15 p2109 N88-22562

A UNIX-based interactive VHDL (hardware description language) simulator
[AD-A189749] 15 p2109 N88-22565

Memory efficient evaluations of nonlinear stochastic equations and C3 applications
[AD-A189872] 15 p2110 N88-22569

SEARCH: An interactive computer program for optimizing two-variable, unconstrained experiments or simulation
[AD-A190593] 15 p2112 N88-22583

The modeling, simulation and comparison of interconnection networks for parallel processing
[AD-A190571] 15 p2115 N88-22599

Rapid prototyping of simulations in artificial intelligence environments
[DE88-004295] 15 p2117 N88-22612

Discrete event simulation in the artificial intelligence environment
[DE88-004296] 15 p2117 N88-22613

Properties of some Bayesian scoring procedures for computerized adaptive tests
[AD-A189925] 15 p2124 N88-22660

PLASMOR: A laser-plasma simulation code, part 2
[DE88-701289] 15 p2135 N88-22736

Transport simulations of ohmic ignition experiment: IGNITEX
[DE88-006055] 15 p2138 N88-22757

Interface formation and precursory dynamics
[AD-A190741] 15 p2144 N88-22794

Infrared simulation model Sensor Atmosphere Target (SENSAT)-2A
[DFVLR-FB-88-01] 16 p2165 N88-22910

Railgun rail gouging by hypervelocity sliding contact
[DE88-006866] 16 p2166 N88-22916

An integrated and modular digital modeling approach for the space station electrical power system development
[NASA-TM-100904] 16 p2170 N88-22935

A computer model investigation of a half square log-periodic array
[AD-A190955] 16 p2190 N88-23062

WAVFLD: A program to compute ionospheric height gain functions and field strengths at VLF
[AD-A191159] 16 p2191 N88-23066

Analysis of non-premixed turbulent reacting flows
16 p2196 N88-23100

Test code for the assessment and improvement of Reynolds stress models 16 p2197 N88-23105

Reynolds stress models of homogeneous turbulence
16 p2197 N88-23106

Evaluation of a theory for pressure-strain rate
16 p2198 N88-23108

Shear-layer structures in near-wall turbulence
16 p2198 N88-23110

The simulation of coherent structures in a laminar boundary layer 16 p2198 N88-23111

Fast algorithms for Euler and Navier-Stokes simulations
[AD-A190897] 16 p2208 N88-23175

Path following robot
[AD-A190960] 16 p2215 N88-23217

Automatic control of robot motion
[AD-A191012] 16 p2215 N88-23218

Computer simulation of a motor pump unit to aid in interpreting vibration data
[DE88-004481] 16 p2223 N88-23270

Algorithms and intuition
[NASA-CR-182900] 16 p2252 N88-23459

Piecewise linear approach for timing simulation of VLSI (Very-Large-Scale-Integrated) circuits on serial and parallel computers
[AD-A191328] 16 p2252 N88-23462

Simulation of FELIN logics: Polynomials roots simultaneous computation algorithms
[ETN-88-92182] 16 p2253 N88-23464

Domain decomposition in parallel reservoir simulation
[REPT-87-63] 16 p2254 N88-23469

Advanced turboprop aircraft flyover noise: Annoyance to counter-rotating-propeller configurations with an equal number of blades on each rotor, preliminary results
[NASA-TM-100612] 16 p2265 N88-23547

Numerical simulation for particle acceleration and trapping by an electromagnetic wave
16 p2277 N88-23626

Simulation code for ICF including radiative energy transfer 16 p2277 N88-23627

Some aspects of the unified model of non-ideal high-parameter plasmas: Electron EOS and conduction coefficients 16 p2277 N88-23632

Stability requirement FOT ignition and high gain implosion -- 2-D simulation for high neutron yield experiment -- 16 p2278 N88-23633

Two-dimensional focusing of self-magnetically insulated plasma focus diode 16 p2278 N88-23639

Coherent functional development: Key to successful future system integration 17 p2307 N88-23803

Numerical method for unsteady viscous-inviscid interaction to calculate buffeting
[ONERA-RSF-02/3617-AY-008-A]
17 p2338 N88-23949

Simulation: A simulation system in Ada
[FOA-A-20043-2.7] 17 p2385 N88-24176

Dialog design: General requirements and analysis of an Ada system --- user interface design
[FOA-C-20691-2.7] 17 p2385 N88-24177

A generic multibody simulation
[NASA-CR-182949] 17 p2388 N88-24198

Parallel discrete-event simulation of FCFS stochastic queueing networks
[NASA-CR-181669] 17 p2389 N88-24203

Parametric analysis of power requirements for space-based radar 17 p2399 N88-24260

ATHENA heat pipe transient model
17 p2412 N88-24344

Detailed transient model of a liquid-metal heat pipe
17 p2412 N88-24345

SP-100 control system modeling
17 p2414 N88-24356

ATHENA simulation of the 300 kW SP-100
17 p2414 N88-24357

EETAP (End-to-End Transient Analysis Program) for space nuclear power system simulation
17 p2418 N88-24381

A decade of computer simulations for space shuttle aerodynamics
[NASA-TM-100990] 18 p2459 N88-24603

Simulations of a missile with liquid payload under launch conditions
[AD-A191479] 18 p2463 N88-24625

Computational design of low aspect ratio wing-winglet configurations for transonic wind-tunnel tests
[NASA-CR-183021] 18 p2464 N88-24630

Analytic and numerical modeling of heat and material transport in electrical hypervelocity guns
[AD-A192178] 18 p2469 N88-24655

Use of a two-stage light-gas gun as an injector for electromagnetic railguns
[DE88-007200] 18 p2469 N88-24657

Simulations of the electrostatic charging of ESA communications satellites
[ESA-STM-239] 18 p2472 N88-24670

Computer simulation of turbulent combustion in reciprocating engines
[CFDU/87/11] 18 p2482 N88-24725

Calculation of assemblies bonded with quasi-elastic adhesives
[REPT-47-632/F] 18 p2493 N88-24793

Numerical simulations of the flat-plate laminar boundary layer in subsonic and supersonic flow
[PDR/CFDU/IC/36] 18 p2511 N88-24895

Numerical simulation of nonlinear structural dynamics of large scale unsteady flow
[ETN-88-92156] 18 p2513 N88-24908

An investigation of a distributed clock for local area networks with ring topology 18 p2516 N88-24924

Finite element analysis of an underground structure
[AD-A191747] 18 p2527 N88-24991

Yaw dynamics of horizontal axis wind turbines
[DE88-001137] 18 p2537 N88-25055

Report on project WIND: Preliminary experiments with the UK Meteorological Office mesoscale model, September 1987
[AD-A191621] 18 p2544 N88-25099

Analysis of lightning field changes during active thunderstorms in Florida 18 p2545 N88-25103

LispSEI: The programmer's manual
[AD-A191632] 18 p2556 N88-25172

A graphical, intelligent interface for discrete event simulations
[DE88-000522] 18 p2557 N88-25181

Computer simulation of uphill diffusion in ternary ionic system
[NASA-TT-20194] 18 p2573 N88-25285

Accelerator research studies
[DE88-007124] 18 p2574 N88-25290

Determination of doping profiles in silicon from resistivity measurements via the four-point probe in combination with layer strippings via anodic oxidation
18 p2583 N88-25347

Numerical simulation of compressible homogeneous turbulence: Effects of fluid compressibility
[PB88-127154] 19 p2597 N88-25433

An assessment of the state of the art in predicting the failure of ceramics
[DE88-008998] 19 p2621 N88-25551

Numerical grid generation and flow simulation in SSME thrust chamber 19 p2626 N88-25577

Proceedings of the 5th NAL Symposium on Aircraft Computational Aerodynamics
[NAL-SP-8] 19 p2635 N88-25630

On the NAL numerical simulator system
19 p2635 N88-25631

Numerical simulations of aerodynamic contribution of flows about a space-plane-type configuration
19 p2635 N88-25632

Aerodynamic simulation for complete ASKA aircraft configuration 19 p2637 N88-25641

Numerical simulation of viscous flows over transonic aircraft configurations 19 p2637 N88-25642

A numerical analysis of flow characteristics in laser propulsion system 19 p2637 N88-25645

Numerical simulation of the shock tube flows by TVD scheme 19 p2638 N88-25648

Trellis-coded - MPSK modulation techniques for MSAT-X(sup)1 19 p2648 N88-25721

Performance of the ICAO standard core service modulation and coding techniques
19 p2648 N88-25723

Picosecond measurements of gain-switching in a semiconductor laser driven by ultrashort electrical pulses
19 p2658 N88-25800

Non-stationary transport in MODFET's and heterojunction devices 19 p2659 N88-25804

Investigation of Rossby-number similarity in the neutral boundary layer using large-eddy simulation
[DE88-008910] 19 p2666 N88-25851

Thin-membrane Lamb-mode acoustic oscillators for chemical detection 19 p2673 N88-25895

An intelligent processing environment for real-time simulation
[NASA-CR-183056] 19 p2715 N88-26119

Hybrid simulations
[DE88-009125] 19 p2715 N88-26123

Logic and fault simulation on the Mach1000 hardware accelerator
[DE88-009794] 19 p2717 N88-26130

Adaptive residual mode filter control of distributed parameter systems for large space structure applications
19 p2719 N88-26143

Computer modeling of time dependent SBS (Stimulated Brillouin Scattering) in two and three dimensions
[DE88-008922] 19 p2720 N88-26150

Gone with the solar wind: A study of protons accelerated by interplanetary shocks 19 p2743 N88-26283

The role of aviation technology in the Caribbean Basin
[NASA-CR-183069] 20 p2745 N88-26289

Computer simulation of a single pilot flying a modern high performance helicopter
[NASA-TM-100182] 20 p2761 N88-26376

Computer simulation of multiple pilots flying a modern high performance helicopter
[NASA-TM-100183] 20 p2761 N88-26377

A simulation of post boost vehicle deployment of multiple reentry vehicles
[DE88-009537] 20 p2764 N88-26391

Computation equipment for damage simulation in laminated composites
[AD-A193013] 20 p2768 N88-26412

Rare Gas Halide (RGH) kinetics
[AD-A192352] 20 p2770 N88-26425

Grain boundaries
[DE88-009889] 20 p2773 N88-26446

Fundamental studies of elastomers
[DE88-009679] 20 p2778 N88-26471

Statistical mechanics of polymer systems
[DE88-011172] 20 p2778 N88-26477

Vortex filament simulation for the crosslinking rings
20 p2782 N88-26501

MAXWELL3: A 3D finite element electromagnetic modeling code
[DE88-010602] 20 p2790 N88-26551

Freely expanding detonation products: Scaling of rate processes
[DE88-007827] 20 p2799 N88-26606

Axisymmetric liquid sloshing under low-g conditions. Numerical simulation method (reference manual)
[NLR-TR-86057-U] 20 p2802 N88-26627

Fluid flow modeling in casting processes and its implications
[DE88-010009] 20 p2810 N88-26671

Analytical and experimental investigation of ringless piston concept
[AD-A192835] 20 p2810 N88-26673

Microstructural effects in static and dynamic numerical experiments
[DE88-004289] 20 p2813 N88-26690

Circulation statistics from seasonal and perpetual January and July simulations with the NCAR (National Center for Atmospheric Research) Community Climate Model (CCM1):R15
[PB88-192620] 20 p2823 N88-26748
Synoptic patterns related to tropical cyclone recurvature
[AD-A192338] 20 p2827 N88-26771
Automated system for mathematical processing of the data from a hybrid spectrometer
[DE87-702995] 20 p2836 N88-26820
Proceedings of the 2nd US-Japan Workshop on Advanced Plasma Modeling, volume 3
[IPPJ-867] 20 p2855 N88-26957
A Vlasov ion zero mass electron model for plasma simulations 20 p2855 N88-26958
Modeling of subtle kinetic processes in plasma simulation 20 p2856 N88-26959
Drift wave vortices and anomalous transport
[DE88-009562] 20 p2859 N88-26982
MACH2: A two-dimensional magnetohydrodynamic simulation code for complex experimental configurations
[AD-A192285] 20 p2860 N88-26988
Cosmological helium production simplified
[DE88-009576] 20 p2865 N88-27130
A feasibility study in path planning using optimization techniques
[AD-A193030] 21 p2894 N88-27177
Simulation of moisture diffusion of fiber reinforced components of aircraft for general air transportation
[IFL-IB-87-05] 21 p2907 N88-27253
Computer simulation of elastic properties of grain boundary materials
[DE88-011965] 21 p2916 N88-27305
SARLAC: A relativistic electron beam code
[AD-A193134] 21 p2932 N88-27411
Calculations of high-frequency parameters of disc-loaded waveguides
[DE88-702178] 21 p2933 N88-27417
STAR: Sandia Timing Analyzer Routine
[DE88-012412] 21 p2940 N88-27463
Implicit finite-difference simulation of an internal flow on a hypercube
[AD-A192474] 21 p2942 N88-27471
Simulation and analysis of wave propagation through random media 21 p2947 N88-27503
Numerical simulation and stability analysis of the absolutely and convectively unstable wake
[DFVLR-FB-88-09] 21 p2949 N88-27518
Initial electron distributions for free-electron lasers generated by injector and accelerator simulations
[DE88-007022] 21 p2953 N88-27540
Development of a hybrid simulator for robotic manipulators
[AD-A193119] 21 p2956 N88-27557
Control of free-flying space robot manipulator systems
[NASA-CR-183017] 21 p2956 N88-27562
Experimental validation of a zero-dimensional computer model for spark-ignition engines
[DE88-009034] 21 p2957 N88-27565
Solar cell modeling and simulation
[AD-A193249] 21 p2966 N88-27620
Approximate analytical formulas for electron density and collision frequency in the natural and nuclear-disturbed ionosphere and inner magnetosphere
[AD-A193129] 21 p2972 N88-27654
Large-eddy simulations of concentration fluctuations
[DE88-009480] 21 p2973 N88-27660
Update on the meso-microscale meteorological hierarchy
[DE88-009133] 21 p2975 N88-27670
Three-dimensional wind simulation
[DE88-009793] 21 p2975 N88-27671
Computer simulation procedure for designing airborne aerometric monitoring programs
[DE88-011896] 21 p2975 N88-27674
The VITE model: A neutral command circuit for a generating arm and articulator trajectories
[AD-A192715] 21 p2987 N88-27734
Demodulation processes in auditory perception
[AD-A193421] 21 p2988 N88-27740
Assessing and enhancing human performance: Utility of a workstation network
[AD-A192840] 21 p2991 N88-27743
Block Oriented Simulation System (BOSS)
[NASA-CR-182947] 21 p2995 N88-27760
Simulation methodology
[AD-A192548] 21 p2995 N88-27764
Bisimulation can't be traced
[AD-A192725] 21 p2996 N88-27766
Simulation of real time problem solving
[AD-A193436] 21 p2997 N88-27778
Verification of flight software written in C using ACSL
[DE88-008100] 21 p2998 N88-27779
Dose-enhancement effects in TaSi/Al- and Al-gate MOS devices
[DE88-005483] 21 p3020 N88-27926
Dynamical evolution of cosmic strings
[DE88-011724] 21 p3030 N88-27969
A computer model for the flow of a molten polymer in a narrow cavity
[NPL-DMA(A)-157] 22 p3058 N88-28146
Two-dimensional flow through a turbine cascade
[PDR/CFDU/IC/34] 22 p3076 N88-28264
High performance solutions of the Stokes problem using mini-elements, self-adaptive grids, and multigrid methods: Applications
[ECL-87-15] 22 p3077 N88-28266
Development and application of a finite element method to compute strongly heated turbulent flows
[ECL-88-02] 22 p3077 N88-28267
Variable-compression-ratio pistons for high power output diesel engines 22 p3084 N88-28316
Aspects of the 30-60 day oscillation in a GCM simulation 22 p3121 N88-28545
Simulation studies of the influence of sea-surface temperature anomalies on the Sahelian circulation and rainfall 22 p3122 N88-28553
Estimating reliability with discrete growth models
[AD-A193845] 22 p3143 N88-28692
Customizing Space Nuclear Power System Analysis Model (SNPSAM): Introducing a secondary coolant loop
[AD-A194620] 22 p3151 N88-28750
A new model for the simulation of interfaces at high temperature
[DE88-009926] 22 p3155 N88-28772
Computer simulation of electromigration in thin films
[AD-A194526] 22 p3157 N88-28782
The influence of numerical boundary conditions on transonic flow
[DFVLR-FB-88-06] 23 p3172 N88-28890
Automatic classification of digitally modulated signals
[AD-A194623] 23 p3203 N88-29064
Vortex dynamics of coherent and chaotic structures (including algorithms for computer simulations and diagnosis)
[AD-A193580] 23 p3212 N88-29117
Free electron lasers with small period wigglers
[DE88-011627] 23 p3218 N88-29156
Analysis of the hopfield neural networks and their application to pattern recognition
[AD-A193827] 23 p3239 N88-29279
Three-dimensional elliptic grid generation for an F-16
23 p3246 N88-29315
Feasibility study of a microprocessor controlled actuator test mechanism
[AD-A194654] 23 p3249 N88-29337
An algorithm for determining the location of points in computer simulations
[AD-A193713] 23 p3250 N88-29343
OMV docking simulator 23 p3255 N88-29379
The use of computer graphic simulation in the development of robotic systems
23 p3257 N88-29388
AI and simulation: What can they learn from each other 23 p3257 N88-29391
Acoustic pressure distribution on the bottom of a wedge-shaped ocean
[AD-A193961] 23 p3278 N88-29518
Stability experimental results of cable-in-conduit superconductor for fusion
[DE88-753424] 23 p3290 N88-29589
The interaction of Io with the plasma torus
23 p3306 N88-29704
Numerical methods: Euler time dependent solver
24 p3318 N88-29760
A fiber optic collective flight control system for helicopters
[AD-A195406] 24 p3328 N88-29818
Minimum-complexity helicopter simulation math model
[NASA-CR-177476] 24 p3328 N88-29819
Experiments and modeling of multi-component fuel behavior in combustion
[AD-A195011] 24 p3343 N88-29896
Numerical field model simulation of full scale fire tests in a closed spherical/cylindrical vessel
[AD-A195067] 24 p3359 N88-29998
Track performance considerations for monopulse radars
[AD-A196232] 24 p3360 N88-30007
The focal plane reception pattern calculation for a paraboloidal antenna with a nearby fence
[NASA-TM-100691] 24 p3365 N88-30039
The 1988 Goddard Conference on Space Applications of Artificial Intelligence
[NASA-CP-3009] 24 p3415 N88-30330
Automatic mathematical modeling for real time simulation system 24 p3420 N88-30356
A simulation engine: Combining an expert system with a simulation language 24 p3421 N88-30358
Adaptive control in positioning a rigid-flexible robot arm
[AD-A195194] 24 p3422 N88-30367
Knowledge based simulation: An artificial intelligence approach to system modeling and automating the simulation life cycle
[AD-A195838] 24 p3423 N88-30372
Design and performance analysis of a relational replicated database system
[AD-A196290] 24 p3437 N88-30456
The origin of the moon: Further studies of the giant impact 24 p3440 N88-30474

COMPUTERS
NT AIRBORNE/SPACEBORNE COMPUTERS
NT ANALOG COMPUTERS
NT CDC CYBER 205 COMPUTER
NT CRAY COMPUTERS
NT DIGITAL COMPUTERS
NT EMBEDDED COMPUTER SYSTEMS
NT HEWLETT-PACKARD COMPUTERS
NT HYBRID COMPUTERS
NT HYPERCUBE MULTIPROCESSORS
NT IBM COMPUTERS
NT MICROCOMPUTERS
NT MIMD (COMPUTERS)
NT MINICOMPUTERS
NT OPTICAL COMPUTERS
NT PARALLEL COMPUTERS
NT PERSONAL COMPUTERS
NT SEQUENTIAL COMPUTERS
NT SIMD (COMPUTERS)
NT SUPERCOMPUTERS
NT VAX COMPUTERS
Gender and cognitive style differences at the human-computer interface
[IPL-DITC-90/87] 01 p0077 N88-10493
Evaluating computers and their performance: Perspectives, pitfalls, and paths
[DE87-014264] 02 p0218 N88-11375
Los Alamos National Laboratory computer benchmarking 1986
[LA-10898-MS] 03 p0363 N88-12265
The development of ODE methods: A symbiosis between hardware and numerical analysis
[DE87-014925] 03 p0370 N88-12325
On computing environments in data analysis
[DE88-000078] 04 p0480 N88-12961
Prospectus for the development of a linear algebra library for high-performance computers
[DE88-003715] 08 p1068 N88-16457
Development and experimentation of an eye/brain/task testbed 09 p1205 N88-17219
A visual programming environment for the Navier-Stokes computer
[NASA-CR-181615] 10 p1390 N88-18299
Relaxing the brightness constancy assumption in computing optical flow
[AD-A187437] 10 p1410 N88-18410
Specialized instrumentation for computational fluid dynamics research
[AD-A188160] 11 p1482 N88-18849
JPRS report. Science and technology: Europe and Latin America
[JPRS-ELS-87-054] 12 p1573 N88-19406
Some questions of using coding theory and analytical calculation methods on computers
[DE88-700905] 12 p1676 N88-20021
JPRS report. Science and technology: Europe and Latin America
[JPRS-ELS-87-055] 12 p1686 N88-20086
Online aiding for human-computer interfaces
[AD-A189239] 13 p1815 N88-20842
JPRS report: Science and technology. Japan
[JPRS-JST-88-001] 15 p2051 N88-22218
JPRS report: Science and technology. Japan
[JPRS-JST-87-029] 15 p2052 N88-22228
Complex sound processing: An interdisciplinary approach
[AD-A189782] 15 p2102 N88-22523
Extension of computer based algorithms by operator analysis
[NASA-CR-182798] 15 p2111 N88-22575
Design of the Detector 2: A CMOS gate array for the study of concurrent error detection techniques
[AD-A191247] 16 p2193 N88-23079
A new block solver for large, full, unsymmetric, complex systems of linear algebraic equations
[AD-A190590] 16 p2256 N88-23483
Computer and model changes at National Meteorological Center (NWC) 18 p2547 N88-25116
Technical communication in the computer industry: An information-development process to track, measure and ensure quality 23 p3297 N88-29635
Heavy ion and proton tests for subsystem upset
[AD-A195267] 24 p3434 N88-30442

CONCATENATED CODES
The design plan of a VLSI single chip (255, 223) Reed-Solomon decoder 04 p0435 N88-12697
Error control techniques for satellite and space communications
[NASA-CR-181581] 05 p0576 N88-13516
A concatenated coded modulation scheme for error control
[NASA-CR-182639] 12 p1621 N88-19697
CONCAVITY
Analytical investigation of reflection of a regular or mach reflection over a secondary wedge
[AD-A185690] 06 p0703 N88-14316
The heat transfer and fluid dynamics of concave surface curvature
[AD-A193064] 21 p2943 N88-27479
CONCENTRATION (COMPOSITION)
NT ATMOSPHERIC MOISTURE
NT CARBON DIOXIDE CONCENTRATION
NT METEOROID CONCENTRATION
NT MOISTURE CONTENT
High ionic conductivity in PEO PPG block polymer and salt solutions
[AD-A183502] 01 p0026 N88-10168
Inerting and atmospheres 04 p0406 N88-12524
Investigation of the nature and concentration of vapor and mist during the cleaning of aircraft
[PML-1985-29] 05 p0623 N88-13817
Hydrochemical structure of Gulf Stream frontal zone waters 06 p0727 N88-14476
Realization of an instrument to measure temperature and concentration gradients in fluids --- microgravity
[CISE-3128] 09 p1168 N88-17003
An infra-red investigation of HAN (Hydroxylammonium Nitrate)-based liquid propellants
[AD-A187226] 10 p1307 N88-17815
Determination of the equilibrium concentration of characteristic defects by the measurement of thermal expansion using neutron scattering and laser interferometry
[ETN-88-91489] 11 p1490 N88-18890
Hydrogen embrittlement of gun steel
[AD-A188972] 13 p1740 N88-20407
An experimental method for species concentration measurements in a welding arc using laser-induced fluorescence
[DE88-005638] 13 p1778 N88-20636
Research on influence of individual sea water components on spectral brightness coefficient of outgoing radiation 13 p1785 N88-20682
The effect of H2S concentration and pH on the cracking resistance of AISI 410 stainless steel in 5 percent brine
[NPL-DMA(A)-149] 14 p1890 N88-21294
Ultrasonic oxygen sensor
[AD-A189723] 15 p2105 N88-22537
Selective detection in gas chromatography
[AD-A191499] 18 p2481 N88-24718
Preferential surface adsorption in miscible blends of polystyrene and poly(vinyl methyl ether)
[AD-A191451] 18 p2490 N88-24769
Workshop on Atmospheric OH
[BPT-7/87] 18 p2538 N88-25063
Measurement of atmospheric OH with laser differential optical absorption spectroscopy (LDOAS)
18 p2539 N88-25068
Tropospheric OH measurements by long path absorption with rapid spectral concordance
18 p2539 N88-25069
Determination of tropospheric H concentrations by a double-pulsed UV laser method
18 p2539 N88-25070
Development of continuous wave laser frequency modulation of OH in tropospheric concentrations range
18 p2540 N88-25073
Evaluation of the toxicity of products from the thermal degradation of materials
[ETN-88-91995] 18 p2549 N88-25130
Characterization of yttrium aluminum garnet/YAG/using 14 MeV neutron activation
[AD-A191925] 18 p2582 N88-25342
Pyrolyzed organic polymer nitrogen dioxide sensor
19 p2669 N88-25868
Retrieval of temperature and concentration profiles from a limited number of absorption measurements
21 p2947 N88-27501
National ambient Volatile Organic Compounds (VOCs) data base update, documentation
[PB88-195631] 21 p2971 N88-27646
Nonseismic, surface geophysical and geochemical prospecting technology
[PB88-196613] 23 p3227 N88-29207
CONCENTRATORS
Focusing solar energy collector
02 p0159 N88-10996
Fundamentals and techniques of nonimaging optics research
[DE87-014544] 02 p0236 N88-11488
Mechanically stacked multijunction solar cells: An update on Sandia programs
[DE87-014641] 03 p0347 N88-12190
Crystalline cell research status and direction
[DE87-014214] 03 p0382 N88-12402
Solar converging method 04 p0403 N88-12504
Radiation performance of AlGaAs concentrator cells and expected performance of cascade structures
[NASA-TM-100145] 04 p0465 N88-12878
Development of mechanically stacked tandem concentrator cells
[DE88-001926] 06 p0730 N88-14490
Performance of highly concentrating mirror collectors and collector systems
[DFVLR-FB-87-29] 09 p1186 N88-17107
Solar concentrator advanced development program, task 1
[NASA-CR-179489] 10 p1350 N88-18068
Side-by-side comparisons of evacuated compound parabolic concentrator and flat plate solar collector systems at temperatures of 90 to 100°C
[DE88-004717] 10 p1351 N88-18073
Performance and cost benefits associated with nonimaging secondary concentrators used in point-focus dish solar thermal applications
[DE88-001104] 13 p1792 N88-20718
Point-focus concentrator reflector assembly, phase 1
[DE88-003616] 13 p1792 N88-20720
Space station solar concentrator materials research
[NASA-TM-100862] 14 p1882 N88-21250
Recent advances in photovoltaic concentrator technology
[DE88-003948] 15 p2091 N88-22462
Thermal distortion analysis of the space station solar dynamic concentrator
[NASA-TM-100868] 19 p2606 N88-25475
Influence of refractive index and solar concentration on optical power absorption in slabs
[NASA-TM-4056] 19 p2726 N88-26190
Photovoltaic concentrator technology: Recent results
[DE88-009588] 20 p2819 N88-26726
Performance sensitivities for point-focus dish systems with secondary concentrators
[DE88-001152] 21 p2968 N88-27629
Photovoltaic Energy. Electricity from Sunlight: A current awareness bulletin
[DE88-008289] 21 p2969 N88-27634
CONCENTRIC CYLINDERS
Study of temperature and stress fields of two sliding cylinders
[ETN-88-92134] 20 p2815 N88-26704
CONCENTRIC SPHERES
Finitely many delta-interactions with supports on concentric spheres
[DE88-701834] 20 p2880 N88-27101
Radiative heat transfer to chemically reacting flow between concentric rotating spheres
[DE88-702538] 22 p3118 N88-28525
CONCENTRICITY
Fitting a circle to radially suppressed data
[NPL-DITC-103/87] 17 p2392 N88-24223
CONCORDE AIRCRAFT
Supersonic transport/hypersonic transport (SST/HST) development
[REPT-881-111-101] 21 p2896 N88-27192
CONCRETE STRUCTURES
The Shock and Vibration Bulletin. Part 4: Structural Dynamics and Modal Test and Analysis
[AD-A186751] 09 p1179 N88-17062
Analysis of reinforced concrete structures under the effects of localized detonations
09 p1179 N88-17064
Reinforced cocnrete arches under blast and shock environments 09 p1180 N88-17065
Reliability of structures with stiffness and strength degradation 09 p1180 N88-17068
CONCRETES
Reinforced flexural elements for TEMP-STRESS Program
[DE87-012961] 01 p0061 N88-10391
The ability of modified pavement quality concrete to resist ground erosion caused by VTOL aircraft
[BAE-ARG-238] 03 p0267 N88-11683
Open-graded bases for airfield pavements
[AD-A184461] 04 p0402 N88-12500
A laboratory study of asphalt concrete mix designs for high-contact pressure aircraft traffic
[AD-A185753] 06 p0670 N88-14106
Comparative study of nondestructive pavement testing, MacDill Air Force Base, Florida
[AD-A186082] 07 p0822 N88-14993
Investigation of the inter-relationship between base pavement stiffness and asphalt overlay compaction
[DOT/FAA/ES-88/1] 14 p1869 N88-21170
Design of overlays for rigid airport pavements
[DOT/FAA/PM-87/19] 18 p2468 N88-24652
A simple unified method for predicting the deflections of reinforced concrete structures
19 p2679 N88-25930
An assessment of modelling techniques for the finite element analysis of reinforced concrete plate and shell structures
[AD-A192263] 20 p2814 N88-26697
CONCURRENT PROCESSING
Strategies for concurrent processing of complex algorithms in data driven architectures
[NASA-CR-181435] 01 p0082 N88-10527
Petri nets as a support to symbolic execution of concurrent Ada programs
[REPT-87-007] 01 p0082 N88-10529
Local concurrent error detection and correction in data structures using virtual backpointers
[NASA-CR-181432] 01 p0106 N88-10692
Delft parallel processor 84/16
[PB87-226254] 03 p0366 N88-12305
Comparing barrier algorithms
[NASA-CR-178377] 04 p0476 N88-12934
Methods for design and evaluation of integrated hardware/software systems for concurrent computation
[NASA-CR-181522] 04 p0479 N88-12953
Indirect solution of static problems using concurrent vector processing computers
[DE87-012105] 05 p0636 N88-13889
Structuring data for concurrent vectorized processing in a transient dynamics finite element program
[DE87-013082] 05 p0636 N88-13890
Fault-tolerant computer architecture based on INMOS transputer processor 06 p0797 N88-14880
AFL-1: A programming language for massively concurrent computers
[AD-A186422] 07 p0906 N88-15489
SISAL: Initial MIMD performance results
10 p1375 N88-18208
A paradigm for concurrency control performance evaluation 10 p1377 N88-18220
Concurrency control and reliability in replicated database systems 10 p1377 N88-18221
Strategies for concurrent processing of complex algorithms 10 p1379 N88-18235
Resilient procedures: A structured replication approach 10 p1381 N88-18245
A digital logic simulator with concurrent programming considerations
[AD-A188823] 12 p1678 N88-20032
Support for concurrent computing environments
[AD-A188498] 12 p1680 N88-20043
The effects of two Carlucci initiatives concurrency and streamlining, on the test and evaluation phase of system acquisitions 12 p1704 N88-20198
The physical structure of concurrent problems and concurrent computers
[DE88-005812] 13 p1814 N88-20835
On proving register atomicity
[CWI-CS-R8707] 13 p1818 N88-20862
A proof rule process creation
[CWI-CS-R8710] 13 p1822 N88-20891
Merge and termination in process algebra
[CWI-CS-R8716] 13 p1826 N88-20918
Abstraction and empty process in process algebra
[CWI-CS-R8721] 13 p1826 N88-20919
Atomic multireader register --- computer storage
[CWI-CS-R8722] 14 p1954 N88-21648
Verification of an algorithm for log-time sorting by square comparison
[CWI-CS-R8729] 14 p1956 N88-21656
On the design of some systolic algorithms
[CS-8705] 14 p1957 N88-21666
The software repeater (an exercise in Z specification)
[RSRE-MEMO-4090] 14 p1958 N88-21677
Strategies for concurrent processing of complex algorithms in data driven architectures
[NASA-CR-181657] 16 p2193 N88-23083
Correctness proofs for systolic algorithms: A palindrome recognizer
[CWI-CS-R8747] 16 p2248 N88-23434
A very simple construction for atomic multiwriter register
[CWI-CS-R8751] 16 p2249 N88-23436
Concurrency efficiency user's manual
[AD-A190884] 16 p2251 N88-23450
Systolic algorithm for matrix-vector multiplication
[PB88-165394] 16 p2256 N88-23484
Readiness and failures in the algebra of communicating processes
[CWI-CS-R8748] 16 p2258 N88-23499

Design, implementation and evaluation of an operating system for a network of transputers
[AD-A186593] 18 p2559 N88-25193
Modeling and optimum time performance for concurrent processing
[NASA-CR-4167] 20 p2797 N88-26595
Contractions in comparing concurrency semantics
[CWI-CS-R8755] 20 p2840 N88-26850
Markov chain computations to a solution of the mutual-exclusion problem in concurrency
[REPT-87-89] 20 p2847 N88-26896
Computer system for the primary fly-by-wire control of civil transport aircraft (experimental system)
[FBW-TB-2086/88] 21 p2898 N88-27204
Model for dynamically structured communicating systems
[PB88-105283] 21 p2931 N88-27402
Bisimulation can't be traced
[AD-A192725] 21 p2996 N88-27766
Image processing using a parallel architecture
[AD-A192833] 21 p3002 N88-27803
Queueing network models for parallel processing of task systems: An operational approach
[NASA-CR-183174] 22 p3141 N88-28677
Using Petri nets for real-time development environments
[REPT-88-005] 22 p3141 N88-28679
The concurrent common Lisp development environment 23 p3263 N88-29422
Performance analysis of k-ary n-cube interconnection networks
[AD-A195542] 24 p3361 N88-30010
Performance prediction of concurrent systems
[NASA-CR-183175] 24 p3412 N88-30312

CONDENSATES
Rayleigh scattering measurements of a freejet with homogeneous condensation 03 p0319 N88-12020
An investigation of the infrared emission spectra of carbon condensates 14 p1886 N88-21272
Method of evaporation
[NASA-CASE-NPO-15609-2] 17 p2318 N88-23846

CONDENSATION
Experimental and theoretical study of condensation in multicomponent mixtures
[DE88-002715] 07 p0830 N88-15033
Vapor condensation on a turbulent liquid interface
08 p0962 N88-15939

CONDENSED MATTER PHYSICS
Shock-induced cooling in dense fluids
[DE87-014343] 02 p0170 N88-11067
Physics of condensed matter at extreme conditions
[DE88-006232] 13 p1832 N88-20958
Research in the theory of condensed matter and elementary particles
[DE88-010180] 22 p3151 N88-28749
Nonlinear optical processes in molecular systems
[AD-A193871] 23 p3282 N88-29546

CONDENSER RADIATORS
U CONDENSERS (LIQUEFIERS)
U HEAT RADIATORS

CONDENSERS
Dynamic isotope power system critical component verification 17 p2425 N88-24421
Vapor Compression Distillation Subsystem (VCDS) component enhancement, testing and expert fault diagnostics development, volume 1
[NASA-CR-172072] 22 p3134 N88-28634
Study of toluene rotary fluid management device and shear flow condenser performance for a space-based organic Rankine power system
[NASA-CR-180885] 24 p3338 N88-29872

CONDENSERS (LIQUEFIERS)
Design of a condenser-boiler for a binary mercury-organic Rankine cycle solar dynamic space power system
[AD-A184188] 03 p0348 N88-12198
Proceedings of the 1987 International Symposium on Condensing Heat Exchangers
[DE88-005230] 13 p1766 N88-20564
Experimental demonstrations of organic Rankine cycle waste heat rejection systems 17 p2432 N88-24469
Tower evaporator
[NASA-CASE-NPO-15609-2] 18 p2497 N88-24815

CONDENSING
NT FILM CONDENSATION
Statistical mechanical theory of condensed explosives
[DE87-009137] 01 p0031 N88-10197
An investigation of the behavior of outgassed molecules in thermal vacuums 02 p0133 N88-10836
Experimental and theoretical study of condensation in multicomponent vapors
[DE87-013663] 02 p0145 N88-10907
Turbine airfoil deposition models and their hot corrosion implications 02 p0189 N88-11178
Mesoscale very short-range numerical prediction with dynamical initialization including condensation heating
02 p0213 N88-11341
Experimental and theoretical study of condensation in multicomponent mixtures
[DE88-000897] 04 p0413 N88-12563
Inertial confinement fusion reactor cavity analysis
[DE88-000788] 04 p0492 N88-13028
Advanced condensing heat exchangers
[DE88-001485] 06 p0699 N88-14288
Equation of state of condensed materials physical principles and applications
[NASA-TT-20007] 08 p0968 N88-15855
Some problems of the theory of bubble growth and condensation in bubble chambers
[NASA-TT-20232] 13 p1771 N88-20593
Dependence of structure of stabilized ZrO2 coatings on condensation rate 16 p2180 N88-22990
Static dielectric breakdown strength of condensed heterogeneous high explosives
[AD-A191035] 16 p2183 N88-23014
Proceedings of the Cooling, Condensation, and Storage of Hydrogen Cluster Ions Workshop
[AD-A189857] 16 p2266 N88-23555
Associative two-body condensation in laser-cooled sodium and hydrogen 16 p2267 N88-23559
Key problems and hydrogen atom formation
16 p2269 N88-23573
The cluster ion approach to the condensation and storage of antihydrogen 16 p2269 N88-23575
Analysis of containerless condensation of polyatomic hydrogen ions, with emphasis on H3(+,-) association channels and a future workshop to study related topics
16 p2269 N88-23576
Small molecule and small cluster ion formation in a low-density containerless mixture of electrons, protons and hydrogen atoms 16 p2269 N88-23577
Transient analysis of heat pipe vapor dynamics
17 p2412 N88-24341
Analysis and interpretation of low gravity boiling experiments in the KC-135 17 p2432 N88-24466
Storage of thermal energy by means of an absorption cycle
[PB88-190814] 21 p2966 N88-27619
Finite-rate water condensation in combustion-heated wind tunnels
[NASA-TP-2833] 22 p3046 N88-28075
Electronic states of the Xe(sub n)HCl systems in gas and condensed phases
[AD-A193881] 23 p3192 N88-28997

CONDITIONED RESPONSES
U CONDITIONING (LEARNING)

CONDITIONING (LEARNING)
Short- and long-term effects of nonlethal levels of fast high-energy helium ions on retention of developed and formation of new behavioral patterns in rats
10 p1362 N88-18140
Two attentional models of classical conditioning: Variations in CS effectiveness revisited
[AD-A187697] 11 p1522 N88-19088
A neuronal model of classical conditioning
[AD-A188378] 12 p1670 N88-19999
Learning by experimentation
[AD-A188912] 12 p1681 N88-20053
Behavior, physiology and energy deposition in rats chronically exposed to 2450 MHz radiation
[PB88-171418] 16 p2237 N88-23363

CONDITIONS
NT ADIABATIC CONDITIONS
NT FLIGHT CONDITIONS
NT KUTTA-JOUKOWSKI CONDITION
NT LIPSCHITZ CONDITION
NT NONEQUILIBRIUM CONDITIONS
NT RUNWAY CONDITIONS

CONDUCTANCE
U RESISTANCE

CONDUCTING MEDIA
U CONDUCTORS

CONDUCTION BANDS
Silicon-germanium heterostructures
13 p1844 N88-21034
Recent data on Si:As impurity band conduction multiplexed arrays
[AD-A191752] 18 p2582 N88-25340
Investigation of electronic band structure of semiconductors by photoemission
[ETN-88-92370] 21 p3025 N88-27957

CONDUCTION ELECTRONS
Gaining control over rare earth valence fluctuations
[DE87-010116] 01 p0103 N88-10671
Point defect structure of Cr2O3
[AD-A187620] 11 p1556 N88-19317

CONDUCTIVE HEAT TRANSFER
Analytical treatment of the melting and solidification of latent heat store materials in finned tube geometries
[IKE-5-223] 03 p0314 N88-11985
Microgravity nucleation and particle coagulation experiments support
[NASA-CR-181540] 04 p0423 N88-12618
Microgravity nucleation and particle coagulation experiments support
[NASA-CR-181541] 04 p0423 N88-12619
The unsteady ground heat flow at the contact surface between a glacier run and the subsoil
08 p1014 N88-16147
A semianalytical solution of the heat conduction equation for several boundary conditions
08 p1014 N88-16148
Determination of the heat conduction coefficient of the soil from the advance of the diurnal temperature wave
08 p1015 N88-16151
Symbolic, algebraic, and numeric solutions to heat conduction problems using Green's functions
09 p1165 N88-16987
Numerical solutions of two moving boundary problems by both finite difference and finite element methods with applications
[DE88-002867] 09 p1230 N88-17374
Approximate solutions of heat conduction in a medium with variable properties
[AD-A186933] 10 p1326 N88-17925
Electron heat transport in TFR with Electron Cyclotron Resonance Heating (ECRH) 12 p1694 N88-20135
A report on the study of algorithms to enhance vector computer performance for the discretized one-dimensional time-dependent heat conduction equation: EPIC research, phase 1
[DE88-005642] 13 p1820 N88-20880
Efficiency of fusion during periodic-pulse laser-beam welding 14 p1897 N88-21324
A small concentration expansion for the effective heat conductivity of a random disperse two-component material, an assessment of Batchelor's renormalization method
[REPT-87-71] 16 p2207 N88-23166
Three-dimensional curved shell and solid-shell transition finite elements with temperature and temperature gradients as primary variables for steady state heat conduction
17 p2349 N88-23997
Mathematical modelling of the heat and water vapour transport in the human respiratory tract
17 p2382 N88-24160
Microgravity thaw experiment (MITEX)
17 p2427 N88-24439
Ammonia boiling in long tubes. Heat transfer and charge loss in vertical and horizontal tubes
[NASA-TT-20313] 19 p2667 N88-25858
Moment approach to neoclassical flows, currents and transport in auxiliary heated tokamaks
[DE88-008024] 21 p3016 N88-27901
Steady conduction of heat in prolate spheroidal systems
[LRT-WE-9-FB-16(1987)] 22 p3077 N88-28272
Heat transport in a parabolic tube of circular cross-section
[LRT-WE-9-FB-2(1988)] 22 p3078 N88-28274
Applications of an exponential finite difference technique
[NASA-TM-100939] 22 p3084 N88-28312
An analysis of heat transfer after loss of primary coolant in the SP-100 reactor system
[AD-A194619] 23 p3281 N88-29539

CONDUCTIVITY
Electronic conduction in molten sodium chloride
[DE87-010063] 02 p0144 N88-10901
DC conductivity studies in Li5AlO4 at intermediate temperatures and its possible application for the electrolysis of water
[AD-A185489] 06 p0697 N88-14276
Electromagnetic scattering from and natural resonances of the circular strip 13 p1759 N88-20523
The protonic Beta double prime aluminas: Preparation, stability, conductivity and structure
[DE88-008442] 20 p2768 N88-26415
Theoretical aspects of electron transport in modulated structures 20 p2865 N88-27016
Hydrogen concentration cells as converters of heat into electricity
[DE88-009662] 23 p3229 N88-29216

CONDUCTIVITY METERS
NT ELECTRICAL CONDUCTIVITY METERS

CONDUCTORS
NT BUS CONDUCTORS
NT ELECTRIC CONDUCTORS
NT ELECTRIC WIRE
NT ELECTROLYTES
NT HIGH TEMPERATURE SUPERCONDUCTORS
NT ION EXCHANGE MEMBRANE ELECTROLYTES
NT MOLTEN SALT ELECTROLYTES
NT NONAQUEOUS ELECTROLYTES
NT PHOTOCONDUCTORS
NT SOLID ELECTROLYTES
NT SUPERCONDUCTORS

Novel conductive polymers
[EP-PATENT-0-182-548-A2] 01 p0026 N88-10163

Experiments: Test range facilities, part 2
03 p0305 N88-11921

Electromagnetic scattering by a thick strip on a half-space
[PB87-227096] 03 p0306 N88-11928

The dc conductivity studies of an hydroxide ion conductor at intermediate temperatures
[AD-A186044] 07 p0847 N88-15142

Processing, fabrication, applications and limitations of inherently conducting polymers
[DE88-003210] 08 p0973 N88-15883

Lithium fast-ion conductors: Polymer based materials
[AD-A187879] 11 p1461 N88-18712

The effects of various conductor components on Nb3Sn filament prestrain in cable-in-conduit conductors
[DE88-003956] 11 p1479 N88-18824

Measurement of the properties of lossy materials inside a finite conducting cylinder
[NASA-CR-182664] 13 p1832 N88-20962

Characterization of proton conducting polymer blends
19 p2669 N88-25867

Conductor loss in superconducting power transmission cables
[DE88-011414] 23 p3290 N88-29586

CONES

NT ABLATIVE NOSE CONES
NT CONICAL BODIES
NT NOSE CONES
NT ROCKET NOSE CONES
NT SLENDER CONES

Hydroburst test of a carbon-carbon involute exit cone
[NASA-TP-2556] 06 p0671 N88-14112

Calculation of symmetric and asymmetric vortex seperation on cones and tangent ogives based on discrete vortex models
[NASA-CR-4122] 08 p0950 N88-15768

CONFERENCES

International Conference on the Aerodynamics at Low Reynolds Numbers between 10(4) and 10(6)
[ONRL-7-023-C] 01 p0002 N88-10010

Spacecraft 2000
[NASA-CP-2473] 01 p0015 N88-10084

Ceramic-Ceramic Composites Meeting in Belgium
[ONRL-7-020-R] 01 p0019 N88-10118

Remote Sensing-Arid Lands Workshop, Page, Arizona, June 10-12, 1986
[DE87-012368] 01 p0064 N88-10412

Remote sensing of environmental pollution
[DFVLR-MITT-87-04] 01 p0067 N88-10428

Transactions of the 4th Army Conference on Applied Mathematics and Computing
[AD-A183544] 01 p0085 N88-10547

ESA Workshop on Optical Interferometry in Space
[ESA-SP-273] 01 p0094 N88-10613

STIP Symposium on Physical Interpretation of Solar/Interplanetary and Cometary Intervals
[NASA-CR-181201] 01 p0110 N88-10709

Overview of STIP intervals 15-19
01 p0110 N88-10710

Solar events and their influence on the interplanetary medium 01 p0115 N88-10734

Knowledge Based Concepts and Artificial Intelligence: Applications to Guidance and Control
[AGARD-LS-155] 02 p0128 N88-10806

Fourteenth Space Simulation Conference: Testing for a Permanent Presence in Space
[NASA-CP-2446] 02 p0132 N88-10829

Space Construction
[NASA-CP-2490] 02 p0138 N88-10870

The 1986 Goddard Space Flight Center Battery Workshop
[NASA-CP-2486] 02 p0163 N88-11021

Turbine Engine Hot Section Technology, 1985
[NASA-CP-2405] 02 p0184 N88-11140

Proceedings of the Solar Thermal Technology Conference
[DE87-014441] 02 p0195 N88-11220

Siting and Geotechnical Program Focus and Directions. Report upon the deliberations of a workshop held at the Illinois Institute of Technology, Chicago, Illinois on August 4-5, 1986
[PB87-206272] 02 p0198 N88-11238

Mesoscale Analysis and Forecasting. Incorporating Nowcasting
[ESA-SP-282] 02 p0199 N88-11239

Tutorial and hands-on demonstration of a fluent interpreter for CARE 3
[NASA-TM-4011] 02 p0220 N88-11383

Proceedings of the Workshop on Opportunities for Atomic Physics Using Slow, Highly-Charged Ions
[DE87-013991] 02 p0231 N88-11457

Rotorcraft Design for Operations
[AGARD-CP-423] 03 p0262 N88-11649

Space Environment Technology --- conference
[ISBN-2-85428-170-5] 03 p0271 N88-11702

International Conference on Microstructology held in Gainesville, Florida on 7-9 May 1986
[AD-A184604] 03 p0290 N88-11822

Technical evaluation report on the Fluid Dynamics Panel Symposium on aerodynamic and related hydrodynamic studies using water facilities
[AGARD-AR-225] 03 p0312 N88-11968

Commercial Opportunities for Remote Sensing with Polar Platforms
[ESA-SP-269] 03 p0339 N88-12131

SPOT 1: First In-Flight Results --- conferences
[ISBN-2-85428-177-2] 03 p0340 N88-12143

The Conference on the Dynamics of Molecular Collisions held in Oglebay Park, Wheeling, West Virginia on 12-17 July 1987
[AD-A184690] 03 p0374 N88-12354

Spacecraft Fire Safety
[NASA-CP-2476] 04 p0406 N88-12520

Proceedings of the Fifth Symposium on Energy Engineering Sciences: Instrumentation, Diagnostics, and Material Behavior
[DE88-001479] 04 p0429 N88-12660

Proceedings: SDIO/DARPA Workshop on Laser Propulsion. Volume 3: Viewgraphs
[DE88-000964] 04 p0450 N88-12790

Proceedings of the Eleventh DOE Solar Photochemistry Research Conference
[DE88-000678] 04 p0466 N88-12883

Research papers and publications (1981-1987): Workload research program
[NASA-TM-100016] 04 p0474 N88-12924

Proceedings of the Japan-US Workshop P-92 on Plasma Material Interaction/High Heat Flux Data Needs for the Next Step Ignition and Steady State Devices
[DE87-013568] 04 p0494 N88-13042

Fifth Cambridge Workshop on Cool Stars, Stellar Systems and the Sun 04 p0502 N88-13092

Aerodynamics of Hypersonic Lifting Vehicles
[AGARD-CP-428] 05 p0529 N88-13219

Proceedings of the 4th NAL Symposium on Aircraft Computational Aerodynamics
[NAL-SP-7] 05 p0535 N88-13253

Special Course on Fundamentals of Fighter Aircraft Design
[AGARD-R-740] 05 p0544 N88-13315

Workshop on Avionics Corrosion Control
[AGARD-R-733] 05 p0547 N88-13331

Static Aeroelastic Effects on High Performance Aircraft
[AGARD-CP-403] 05 p0550 N88-13348

The 58th Shock and Vibration Symposium, volume 1
[NASA-CP-2488-VOL-1] 05 p0592 N88-13609

Fatigue 87, volume 1
[AD-A184045] 05 p0597 N88-13645

Scientific and Operational Requirements for TOMS Data
[NASA-CP-2497] 05 p0615 N88-13774

Proceedings of the 17th International Conference on Phenomena in Ionized Gases held in Budapest, Hungary, July 8-12, 1985. Invited papers
[DE87-703562] 05 p0651 N88-13987

Calendar of selected aeronautical and space meetings
[AGARD-CAL-87/1] 05 p0657 N88-14033

Calendar of selected aeronautical and space meetings
[AGARD-CAL-88/1] 05 p0658 N88-14037

Guidance for conference rapporteurs
[NASA-CR-182338] 05 p0659 N88-14042

Summary of discussions at the Ninth Meeting of the Sandia Cooperative Group on the Aerothermochemistry of Turbulent Combustion
[DE88-002281] 06 p0690 N88-14165

Proceedings of the 2nd Regional Electromagnetic Workshop at Argonne National Laboratory
[DE87-004633] 06 p0690 N88-14230

Report of the 3rd Finnish EISCAT Workshop --- European Incoherent Scatter Radar (EISCAT)
[REPT-111] 06 p0691 N88-14233

Eddy Current Seminar, 24-26 March 1986
[PB87-124988] 06 p0696 N88-14269

International workshop on two-phase flow fundamentals
[DE88-001478] 06 p0699 N88-14287

Introduction to Computational Fluid Dynamics
[VKI-LS-1987-02] 06 p0701 N88-14300

Airborne Visible/Infrared Imaging Spectrometer (AVIRIS): A description of the sensor, ground data processing facility, laboratory calibration, and first results
[NASA-CR-182365] 06 p0705 N88-14325

Small High Pressure Ratio Turbines --- conference
[VKI-LS-1987-07] 06 p0712 N88-14364

Fatigue 87, volume 2
[AD-A184046] 06 p0715 N88-14381

Strategic Defense Initiative Organization/DARPA (Defense Advanced Research Projects Agency) workshop on laser propulsion. Volume 1: Executive summary
[DE87-003254] 06 p0768 N88-14722

Research in elementary particle physics
[DE88-002130] 06 p0777 N88-14771

Langley Symposium on Aerodynamics, volume 1
[NASA-CP-2397] 07 p0809 N88-14926

Wind shear detection. Forward-looking sensor technology
[NASA-CP-10004] 07 p0817 N88-14970

Round table on the future of satellite communications and broadcasting in Europe
[ESA-STR-221] 07 p0843 N88-15112

Flow in Centrifugal Compressors --- conference
[VKI-LS-1987-01] 07 p0850 N88-15160

The results of the 1984/1985 Round-Robin Calibration of Reference Solar Cells for the Summit Working Group on Technology, Growth and Employment
[DE88-900215] 07 p0874 N88-15303

Highlights of the 70th Flight Mechanics Panel Symposium on Flight Vehicle Development Time and Cost Reduction
[AD-A185831] 07 p0901 N88-15454

Proceedings of Image Understanding Workshop, volume 1
[AD-A186103] 07 p0902 N88-15463

Proceedings of Image Understanding Workshop, volume 2
[AD-A186104] 07 p0902 N88-15464

Proceedings of the Second International Symposium on Methodologies for Intelligent Systems. Colloquia program
[DE88-001490] 07 p0907 N88-15498

Recent developments in the numerical solution of differential/algebraic systems
[DE88-001885] 07 p0912 N88-15535

Finnish-Soviet Symposium on Radio Astronomy (1st) held at Otaniemi on August 26-27, 1985
[PB87-140661] 07 p0944 N88-15736

Influence of Environmental Factors on Aircraft Wing Performance
[VKI-LS-1987-03] 08 p0951 N88-15771

Aeropropulsion '87. Session 4: Instrumentation and Controls Research
[NASA-CP-10003-SESS-4] 08 p0955 N88-15794

Aeropropulsion '87. Session 5: Subsonic Propulsion Technology
[NASA-CP-10003-SESS-5] 08 p0956 N88-15800

Aeropropulsion '87. Session 6: High-Speed Propulsion Technology
[NASA-CP-10003-SESS-6] 08 p0957 N88-15807

Cryogenic Fluid Management Technology Workshop. Volume 1: Presentation material and discussion
[NASA-CP-10001] 08 p0980 N88-15924

Computational Fluid Dynamics
[VKI-LS-1987-04] 08 p0984 N88-15951

Finite Element Calculation Methods and Their Application to Turbomachinery Flows, volume 1
[VKI-LS-1987-05-VOL-1] 08 p0985 N88-15960

Introduction to the Modeling of Turbulence
[VKI-LS-81-06] 08 p0986 N88-15972

Solid mechanics research for quantitative non-destructive evaluation
[AD-A186599] 08 p0993 N88-16010

The Shock and Vibration Bulletin. Part 3: Isolation and damping, vibration test criteria, and vibration analysis and test
[AD-A186750] 08 p0997 N88-16040

Proceedings of the 8th ESA Symposium on European Rocket and Balloon Programs and Related Research
[ESA-SP-270] 08 p1024 N88-16201

Ocean Colour Workshop --- conference
[ESA-SP-1083] 08 p1042 N88-16292

USSR Space Life Sciences Digest, issue 14
[NASA-CR-3922(16)] 08 p1045 N88-16317

Proceedings of the DOD Workload Assessment Workshop on Workload Assessment Techniques and Tools held in Dayton, Ohio on 27-28 September 1986
[AD-A185550] 08 p1052 N88-16352

Third Conference on Artificial Intelligence for Space Applications, part 1
[NASA-CP-2492-Pt-1] 08 p1055 N88-16360

Proceedings of the 21st ESLAB Symposium on Small Scale Processes in the Chromosphere/Corona, Interplanetary Medium and Planetary Magnetospheres
[ESA-SP-275] 08 p1094 N88-16582

NASA/Army Rotorcraft Technology. Volume 1: Aerodynamics, and Dynamics and Aeroelasticity
[NASA-CP-2495-VOL-1] 09 p1105 N88-16625

NASA/Army Rotorcraft Technology. Volume 2: Materials and Structures, Propulsion and Drive Systems, Flight Dynamics and Control, and Acoustics
[NASA-CP-2495-VOL-2] 09 p1106 N88-16632

Unispace 82 09 p1128 N88-16766

Proceedings of the ESA Workshop on Co-Orbiting Platform Elements (COPE)
[ESA-SP-1093] 09 p1129 N88-16777

The Shock and Vibration Bulletin. Part 2: Instrumentation, shock analysis, and shock testing
[AD-A186749] 09 p1178 N88-17053

The Shock and Vibration Bulletin. Part 4: Structural Dynamics and Modal Test and Analysis
[AD-A186751] 09 p1179 N88-17062

Space Bioreactor Science Workshop
[NASA-CP-2485] 09 p1196 N88-17168

First Annual Workshop on Space Operations Automation and Robotics (SOAR 87)
[NASA-CP-2491] 09 p1203 N88-17206

Scientific Colloquium in Honor of Prof. Dr. Rer. Nat. Hermann L. Jordan
[DFVLR-MITT-87-11] 09 p1240 N88-17432

Proceedings of the International Workshop on Engineering Design of Next Step Reversed Field Pinch Devices
[DE88-001915] 09 p1251 N88-17494

Airborne Wind Shear Detection and Warning Systems. First Combined Manufacturers' and Technologists' Conference
[NASA-CP-10006] 10 p1273 N88-17616

Advanced Technology for Aero Gas Turbine Components
[AGARD-CP-421] 10 p1279 N88-17647

High resolution electron and ion microscopy
[AERE-R-12502] 10 p1297 N88-17754

Second All-Union Conference on Physiology of Extreme States and Individual Protection of Man
10 p1363 N88-18147

Minutes of the meeting of the Indo-US Subcommission on Science and Technology (8th) held at Washington, D.C. on September 22-24, 1986
[PB88-130156] 10 p1423 N88-18503

International Conference on Industrial and Applied Mathematics
[AD-A188251] 11 p1483 N88-18851

The 58th Shock and Vibration Symposium, volume 2
[NASA-CP-2488-VOL-2] 11 p1499 N88-18948

8th Wind Energy Symposium
[DE88-770028] 11 p1507 N88-19004

Proceedings of the 12th Symposium of Japan Solar Energy Society
[DE88-770029] 11 p1507 N88-19005

Proceedings of the 1987 High-Efficiency Photovoltaic Subcontractors' Review Meeting
[DE88-003354] 11 p1508 N88-19011

Alternative Energy in the Midwest: Research and Applications. Conference Proceedings, Rosemont, Illinois, March 19-20, 1987
[PB88-142278] 11 p1509 N88-19015

Proceedings of the 19th DOE/NRC Airborne Waste Management and Air Cleaning Conference
[NUREG/CP-0086-VOL-1] 11 p1509 N88-19018

Proceedings of the 19th DOE/NRC Airborne Waste Management and Air Cleaning Conference
[NUREG/CP-0086-VOL-2] 11 p1509 N88-19019

Cumulative reports and publications through December 31, 1987
[NASA-CR-181624] 11 p1524 N88-19099

Multigrid methods: Special topics and applications --- conference
[GMD-120] 11 p1537 N88-19187

Sixteenth AINSE Plasma Physics Conference. Conference handbook
[DE88-700825] 11 p1552 N88-19290

Proceedings of US-Japan Heliotron-Stellarator Workshop, volume 3
[DE88-004788] 11 p1554 N88-19299

Proceedings of US-Japan Heliotron-Stellarator Workshop, volume 2
[DE88-004789] 11 p1554 N88-19300

Proceedings of the Polycrystalline Thin Film Program Meeting
[DE87-001169] 11 p1557 N88-19321

Proceedings of the First International Symposium on Physical and Technical Problems of Superconductivity Application in Power Generation
[DE88-700818] 11 p1559 N88-19332

Whither many-body theory. A summary of the Oulu Conference
[DE88-003095] 11 p1563 N88-19358

Thirteenth Biennial Guidance Test Symposium, volume 1
[AD-A185782] 12 p1576 N88-19427

Workshop on Design Loads for Advanced Fighters
[AGARD-R-746] 12 p1579 N88-19449

Proceedings of the 1st European In-Orbit Operations Technology Symposium
[ESA-SP-272] 12 p1585 N88-19484

Advances in Air-Launched Weapon Guidance and Control
[AGARD-CP-431] 12 p1596 N88-19553

Progress toward a cosmic dust collection facility on space station
[NASA-CR-182427] 12 p1598 N88-19566

Terrestrial Propagation Characteristics in Modern Systems of Communications, Surveillance, Guidance and Control
[AGARD-CP-407] 12 p1614 N88-19653

Proceedings of the Forest-Atmosphere Interaction Workshop
[CONF-8510250] 12 p1641 N88-19824

Proceedings of an ESA-NASA Workshop on a Joint Solid Earth Program
[NASA-CR-182642] 12 p1644 N88-19844

Proceedings of the 3rd European Symposium on Life Sciences Research in Space
[ESA-SP-271] 12 p1652 N88-19893

FOM contributions to the 14th European Conference on Controlled Fusion and Plasma Physics
[REPT-87-174] 12 p1693 N88-20129

Martian geomorphology and its relation to subsurface volatiles
[NASA-CR-182428] 12 p1711 N88-20237

Gordon Conference on Intermetallic Compounds held at Tilton, New Hampshire on 20-24 July 1987
[AD-A188502] 13 p1745 N88-20435

IAEA Specialists' Meeting on Graphite Component Structural Design
[DE88-780006] 13 p1746 N88-20439

Proceedings of the 1987 International Symposium on Condensing Heat Exchangers
[DE88-005230] 13 p1766 N88-20564

Cryogenic Fluid Management Technology Workshop. Volume 2: Roundtable Discussion of Technology Requirements
[NASA-CP-10009] 13 p1772 N88-20599

Sixteenth NASTRAN (trademark) Users' Colloquium
[NASA-CP-2505] 13 p1780 N88-20652

Dynamics of the Oceanic Surface Mixed Layer
[AD-A188348] 13 p1804 N88-20785

Regional Conference on the Analysis of the Unbalanced Mixed Model
[AD-A188747] 13 p1830 N88-20943

ONR Far East Scientific Bulletin, volume 12, number 3, July-September 1987
[AD-A188554] 13 p1851 N88-21081

Proceedings of the 3rd European Space Mechanisms and Tribology Symposium
[ESA-SP-279] 14 p1874 N88-21191

Towards a tribology information system: The results of a Planning Workshop held at the National Bureau of Standards, July-August 1985
[PB88-168604] 14 p1918 N88-21448

Climatology and space observations
[ISBN-2-85-428179-9] 14 p1935 N88-21536

CARE 3 User's Workshop
[NASA-CP-10011] 14 p1954 N88-21646

United States - Japan Seminar on Quantum Mechanical Aspects of Quantum Electronics
[AD-A186938] 14 p1974 N88-21781

Proceedings of the Seminar on Hydrodynamics and Crystal Growth
[ETN-88-92025] 14 p1987 N88-21853

Proceedings of the International Symposium on the Diversity and Similarity of Comets
[ESA-SP-278] 14 p1994 N88-21884

Summary of the 1987 Gordon Research Conference on Corrosion
[AD-A189737] 15 p2041 N88-22161

Lewis Structures Technology, 1988. Volume 3: Structural Integrity Fatigue and Fracture Wind Turbines HOST
[NASA-CP-3003-VOL-3] 15 p2081 N88-22408

Proceedings of the Lightning Threat Warning Workshop
[DE88-006607] 15 p2098 N88-22499

Ocean general circulation models: Report on proceedings of a meeting of ocean and climate modelers
[DE88-005530] 15 p2099 N88-22504

NASA scientific and technical publications: A catalog of Special Publications, Reference Publications, Conference Publications, and Technical Papers, 1987
[NASA-SP-7063(02)] 15 p2149 N88-22830

Studying Turbulence Using Numerical Simulation Databases. Proceedings of the 1987 Summer Program
[NASA-CR-182692] 16 p2194 N88-23086

A review of the NATO special group of experts on Naval hydromechanics and related problems
16 p2205 N88-23157

Lewis Structures Technology, 1988. Volume 1: Structural Dynamics
[NASA-CP-3003-VOL-1] 16 p2217 N88-23226

Contributions to geodesy, photogrammetry and cartography. Series 1, number 46 --- conference
[ISSN-0469-4244] 16 p2225 N88-23279

Proceedings of Symposium on Physics of Targ
Implosion and Pulsed Power Techniques
[IPPJ-859] 16 p2276 N88-23619

DOE (Department of Energy) national laboratories and the semiconductor industry: Continuing the joint planning
[PB88-170295] 16 p2281 N88-23657

Laminar Flow Aircraft Certification
[NASA-CP-2413] 17 p2296 N88-23737

The Design, Development and Testing of Complex Avionics Systems
[AGARD-CP-417] 17 p2302 N88-23767

Structural Ceramics
[NASA-CP-2427] 17 p2323 N88-23872

Noncontact Temperature Measurement
[NASA-CP-2503] 17 p2327 N88-23895

Latin American Symposium on Remote Sensing. 4th Brazilian Remote Sensing Symposium and 6th SELPER Plenary Meeting, volume 1 17 p2352 N88-24013

Space Station Human Factors Research Review. Volume 1: EVA Research and Development
[NASA-CP-2426-VOL-1] 17 p2379 N88-24145

Third Conference on Artificial Intelligence for Space Applications, part 2
[NASA-CP-2492-PT-2] 17 p2387 N88-24188

Transactions of the Fifth Symposium on Space Nuclear Power Systems
[DE88-006165] 17 p2417 N88-24374

Summary report on the Japan-US Workshop on the Assessment of Spectroscopic Data for Temperature and Density Measurements --- plasma diagnostics
[IPPJ-861] 17 p2439 N88-24512

Proceedings of the American Society for Composites
[AD-A189861] 18 p2477 N88-24693

High resolution radar techniques: Five contributions to MILINF 86
[PB88-172721] 18 p2498 N88-24821

Optics: Perspectives for Measurement Techniques and Signal Processing for Flight Guidance --- conference
[DFVLR-MITT-87-21] 18 p2516 N88-24928

Proceedings of the 1987 Biomass Thermochemical Conversion Contractors' Review Meeting
[DE88-006730] 18 p2535 N88-25041

Workshop on Atmospheric OH
[BPT-7/87] 18 p2538 N88-25063

The Effect of the Ionosphere on Communication, Navigation and Surveillance Systems Based on Ionospheric Effects Symposium held on 5-7 May 1987 in Springfield, Virginia
[AD-A191855] 18 p2541 N88-25081

Dynamics Explorer-2 measurements during an isolated auroral substorm
[AD-A191202] 18 p2543 N88-25091

Infinite dimensional dynamical systems and their finite dimensional analogues
[AD-A192041] 18 p2563 N88-25216

A Study of Space Station Contamination Effects --- conference
[NASA-CP-3002] 18 p2590 N88-25390

Zero/zero rotorcraft certification issues. Volume 1: Executive summary
[NASA-CR-177483-VOL-1] 19 p2602 N88-25453

Zero/zero rotorcraft certification issues. Volume 2: Plenary session presentations
[NASA-CR-177483-VOL-2] 19 p2602 N88-25454

Zero/zero rotorcraft certification issues. Volume 3: Working group results
[NASA-CR-177483-VOL-3] 19 p2602 N88-25455

The 24th JANNAF Combustion Meeting, volume 2
[AD-A190164] 19 p2622 N88-25554

The 24th JANNAF Combustion Meeting, volume 1
[AD-A190163] 19 p2627 N88-25585

Solid rocket motor performance: A workshop report
19 p2631 N88-25607

Proceedings of the 5th NAL Symposium on Aircraft Computational Aerodynamics
[NAL-SP-8] 19 p2635 N88-25630

Proceedings of the Mobile Satellite Conference
[NASA-CR-182964] 19 p2643 N88-25680

Organization of a Topical Meeting on Picosecond Electronics and Optoelectronics
[AD-A187138] 19 p2655 N88-25765

National Meeting on Remote Sensing Applied to Municipal Planning 19 p2681 N88-25939

Proceedings of the Colloquium on Space and Sea
[ESA-SP-280] 19 p2695 N88-26016

Electromechanical Research Symposium, August 20-21, 1987
[PB88-148457] 19 p2713 N88-26109

Report on the Second Catalog Interoperability Workshop
[NASA-TM-100701] 19 p2718 N88-26135

Workshop report and presentations from the Semiconductor Research Corporation-DOE Semiconductor Task Force Workshop
[DE88-007690] 19 p2733 N88-26232

Flight Mechanics Panel Symposium on Rotorcraft Design for Operations: Technical evaluation report
[AGARD-AR-243] 20 p2758 N88-26362
System identification in vehicle dynamics
[DFVLR-MITT-87-22] 20 p2785 N88-26518
Proceedings of the Array Signal Processing Symposium: Treaty Verification Program
[DE88-008346] 20 p2790 N88-26548
Proceedings of the 2nd US-Japan Workshop on Advanced Plasma Modeling, volume 3
[IPPJ-867] 20 p2855 N88-26957
Third International Conference on Superlattices, Microstructures and Microdevices
[AD-A191416] 20 p2861 N88-26995
Integrated Technology Rotor Methodology Assessment Workshop
[NASA-CP-10007] 21 p2889 N88-27148
Very High Speed Integrated Circuits (VHSIC)
[AD-A193225] 21 p2937 N88-27442
Aerodynamics of Hypersonic Lifting Vehicles: Fluid Dynamics Panel AGARD Symposium
[AGARD-AR-246] 21 p2943 N88-27480
Finite element methodology for integrated flow-thermal-structural analysis
[NASA-CR-183144] 21 p2964 N88-27606
Photovoltaic Energy. Electricity from Sunlight: A current awareness bulletin
[DE88-008289] 21 p2969 N88-27634
Electric and Magnetic Activity of the Central Nervous System: Research and Clinical Applications in Aerospace Medicine
[AGARD-CP-432] 21 p2977 N88-27663
Proceedings of the 14th Symposium on Aircraft Integrated Monitoring Systems
[DFVLR-MITT-88-04] 22 p3033 N88-28001
SPOT 1 Image Utilization, Assessment, Results
[ISBN-2-85-428188-8] 22 p3089 N88-28346
Proceedings of the Twelfth Annual Climate Diagnostics Workshop
[PB88-191747] 22 p3119 N88-28534
Management of large space projects --- conference
[ISBN-2-85-428192-6] 22 p3159 N88-28803
Visual Effects in the High Performance Aircraft Cockpit
[AGARD-LS-156] 23 p3241 N88-29291
MEVTV Workshop on Nature and Composition of Surface Units on Mars
[NASA-CR-183075] 23 p3300 N88-29654
The NASA Electric Propulsion Program
[NASA-TM-101324] 24 p3336 N88-29859
Performance Prediction for Coatings. Proceedings of a Workshop
[AD-A188973] 24 p3354 N88-29966
The 1988 Goddard Conference on Space Applications of Artificial Intelligence
[NASA-CP-3009] 24 p3415 N88-30330
Barriers to Information Transfer and Approaches Toward Their Reduction
[AGARD-CP-430] 24 p3437 N88-30458
Information technology to facilitate group interaction
24 p3438 N88-30463
NASA MEVTV Program Working Group Meeting: Volcanism on Mars
[NASA-CR-183074] 24 p3442 N88-30487
Workshop on the Origins of Solar Systems
[NASA-CR-183025] 24 p3451 N88-30536
CONFIDENCE
Error modeling and confidence interval estimation for inductively coupled plasma calibration curves
[AD-A186711] 09 p1250 N88-17488
A method to adjust climatological time series for discontinuous inhomogeneities
22 p3124 N88-28570
CONFIDENCE LIMITS
An APL workspace for conducting nonparametric statistical inference
[AD-A184971] 05 p0634 N88-13877
Determining differences in rates corresponding to a given significance level
[AD-A185004] 05 p0644 N88-13940
Robust prediction and interpolation for vector stationary processes, 2d enriched version
[AD-A185875] 07 p0865 N88-15247
A comparison of the effects of group dynamics on individuals assigned to integral and non-integral aircrews
[AD-A186467] 08 p1051 N88-16345
Measuring the dependence between two point processes through confidence intervals for the second order distribution
[AD-A186735] 08 p1074 N88-16481
Regional Conference on the Analysis of the Unbalanced Mixed Model
[AD-A188747] 13 p1830 N88-20943
Large quantile estimation under extreme-value conditions
[CWI-MS-R8711] 14 p1966 N88-21730
Mathematics clinic probabilistic position-fixing
[NASA-CR-182753] 15 p2125 N88-22672
Burn-in with mixed populations
[AD-A194651] 22 p3085 N88-28321
Exact lower confidence limits for the reliability of k of n systems for zero failures and nonconservativeness of the maximus method
[AD-A194299] 23 p3274 N88-29485
CONFIGURATION INTERACTION
Applications and limitations of deuterium labeling methods to neutron scattering studies of polymers
[DE87-012936] 02 p0151 N88-10945
The H5(+) potential energy hypersurface: Characterization of ten distinct energetically low-lying stationary points 16 p2267 N88-23561
Quantum Monte Carlo study of the MIES associated with H2(X 1 sigma g +) and H2(B 1 sigma u +)
16 p2268 N88-23564
On the bond distance in methane
[NASA-CR-181436] 22 p3150 N88-28741
An unsteady helicopter rotor: Fuselage interaction analysis
[NASA-CR-4178] 23 p3171 N88-28880
CONFIGURATION MANAGEMENT
AGARD standard aeroelastic configurations for dynamic response. Candidate configuration I.-wing 445.6
[NASA-TM-100492] 02 p0192 N88-11202
A study of the Department of Defense configuration management policies and procedures as applied to the FA-18 Strike/Fighter program
[AD-A18-872] 05 p0657 N88-14034
Chicago's O'Hare Runway Configuration Management System (RCMS). Volume 1: Description of the operational software
[AD-A185886] 07 p0821 N88-14990
Chicago's O'Hare Runway Configuration Management System (RCMS). Volume 2: Users guide
[AD-A186222] 08 p0953 N88-15783
Configuration management issues and objectives for a real-time research flight test support facility
[NASA-TM-100437] 13 p1813 N88-20832
Vibration isolation system for the Stratospheric Observatory For Infrared Astronomy (SOFIA)
14 p1926 N88-21483
Reconfigurable work station for a video display unit and keyboard
[NASA-CASE-MFS-26009-1-SB]
17 p2382 N88-24163
Configuration control in compiler construction
[AD-A193916] 22 p3135 N88-28639
System configuration management --- space systems
22 p3160 N88-28813
Management of large space projects. Case study: The Hermes program 22 p3162 N88-28830
Intelligent resource management for local area networks: Approach and evolution
23 p3256 N88-29385
Dynamically reconfigurable distributed database systems
[AD-A194716] 23 p3297 N88-29636
CONFIGURATIONS
Automatically reconfigurable computer architecture
10 p1375 N88-18204
CONFINEMENT
Relative merits of size, field, and current on ignited Tokamak performance: A comparison of CITs and Super-JETs
[DE88-000038] 02 p0241 N88-11521
Feasibility of alpha particle measurement in a magnetically confined plasma by CO2 laser Thomson scattering
[DE88-000039] 02 p0241 N88-11522
Human adaptation to isolated and confined environments
[NASA-CR-181502] 03 p0357 N88-12248
Confinement of energy in tokamak-10 plasma during electron-cyclotron-resonance heating
06 p0773 N88-14750
Long duration confinement of aquatic organisms in weightlessness (aquaspace) 07 p0887 N88-15380
Proceedings of the Energy Independence Conference: Fusion Energy and Plasma Physics
[DE88-700657] 09 p1253 N88-17507
Experimental investigation of two-dimensional confined jet thrust vector control
[AD-A189845] 15 p2027 N88-22077
Heating and confinement studies of electron cyclotron resonance heated plasmas in Heliotron E
[DE88-752312] 15 p2136 N88-22746
A study of runaway electron confinement in the ASDEX tokamak
[DE88-007327] 18 p2579 N88-25319
Physiological effects on man of long duration confinement in a carbon dioxide enriched environment
19 p2695 N88-26017
CONFIRMATION
U PROVING
CONFLUENCE
U CONVERGENCE
CONFORMAL MAPPING
The geometry of the Karnaugh map --- Boolean expressions
[ETN-87-90961] 02 p0227 N88-11432
Application of new conformal solution theories
[PB87-211934] 02 p0247 N88-11558
Superconformal invariance and superstring in background fields
[DE87-703097] 02 p0247 N88-11561
Shuttle computational grid generation
06 p0794 N88-14863
Centerplane source distribution for slender bodies
10 p1328 N88-17940
A numerical procedure for conformal mapping of the exterior of a circle onto the exterior of a wing profile with a spoiler
[ISL-R-110/86] 11 p1536 N88-19180
Conformal geometry, Hotine's conjecture, and differential geodesy
[AD-A189265] 13 p1790 N88-20709
What do multistep methods approximate
[PB88-148838] 13 p1828 N88-20932
Action-angle maps and scattering theory for some finite-dimensional integrable systems. The pure solution case
[CWI-PM-R8704] 13 p1831 N88-20955
Linear programming along the trajectory of the problem
[REPT-87-41] 14 p1956 N88-21662
Hyperbolicity and invariant measures for general C sq interval maps satisfying the Misiurewicz condition
[REPT-87-46] 14 p1966 N88-21733
Absolutely continuous invariant measures for C sq unimodal maps satisfying the Collet-Eckmann conditions
[REPT-87-55] 14 p1966 N88-21735
Nonlinear conformal transformations and Clifford algebras
[PB87-225942] 19 p2719 N88-26147
Image force expression for the dislocation near a crack
[DE88-701894] 20 p2814 N88-26692
Geometry of superconformal manifolds, part 1
[DE88-702405] 21 p3011 N88-27863
Geometry of superconformal manifolds, part 2
[DE88-702406] 21 p3011 N88-27864
A fast algorithm for the numerical evaluation of conformal mappings
[AD-A193903] 22 p3138 N88-28658
Distortion estimates for negative Schwarzian maps
[AD-A193172] 23 p3228 N88-29209
CONFORMAL TRANSFORMATIONS
U CONFORMAL MAPPING
CONFUSION
Resources, confusions and compatibility in dual axis tracking: Displays, controls and dynamics
[AD-A185871] 07 p0896 N88-15440
CONGESTION
Communications using channels formed by meteor bursts
[AD-A192088] 18 p2501 N88-24834
CONGRESSIONAL REPORTS
Budget reimbursements: The National Aeronautics and Space Administration's reimbursable work
[PB87-207296] 01 p0107 N88-10696
Results of the development motor 8 test firing
[GPO-78-692] 03 p0278 N88-11751
Global environmental change research
[S-HRG-100-301] 03 p0348 N88-12199
National Aeronautics and Space Administration Authorization Act, 1988
[PUB-LAW-100-147] 03 p0385 N88-12422
Department of Housing and Urban Development, and Certain Independent Agencies Appropriations, 1988, Part 2
[S-HRG-100-106-PT-2] 03 p0385 N88-12423
Department of Housing and Urban Development-Independent Agencies Appropriations for fiscal year 1988, Thursday, 9 April 1987: National Aeronautics and Space Administration
03 p0386 N88-12424
Department of Housing and Urban Development-Independent Agencies Appropriations for fiscal year 1988, Friday, 10 April 1987: National Aeronautics and Space Administration
03 p0386 N88-12425
National Aeronautics and Space Administration space station proposal, fiscal year 1988
[S-HRG-100-328] 05 p0659 N88-14043
The 1988 NASA (National Aeronautics and Space Administration) authorization
[GPO-80-245] 05 p0659 N88-14044

The 1988 National Aeronautics and Space Administration (NASA) authorization
[GPO-76-600] 06 p0792 N88-14854
Report to Congress on the Automotive Technology Development Program
[DE88-003742] 07 p0864 N88-15242
Advancing automation and robotics technology for the space station and for the US economy: Submitted to the United States Congress May 15, 1987
[NASA-TM-89811] 08 p0959 N88-15817
Advancing automation and robotics technology for the space station and for the US economy: Submitted to the United States Congress October 1, 1986
[NASA-TM-89190] 08 p0960 N88-15818
Department of Housing and Urban Development independent agencies appropriations for 1989. Part 7: National Aeronautics and Space Administration
[GPO-85-166] 16 p2286 N88-23689
Department of Defense Statement on the Technology Base to the Subcommittee on Defense Industry and Technology of the Committee on Armed Services, United States Senate, 100th Congress, second session
[AD-A191839] 18 p2588 N88-25376
Department of Defense statement on defense agency research and development to the Subcommittee on Defense of the Committee on Appropriations, United States House of Representatives, 100th Congress, second session
[AD-A191840] 18 p2588 N88-25377
Department of Defense Statement on the Balanced Technology Initiative to the Committee on Armed Services, United States Senate, 100th Congress, second session
[AD-A191841] 18 p2588 N88-25378
The FY 1989 Department of Defense statement on the Science and Technology Program to 100th Congress, second session
[AD-A191843] 18 p2588 N88-25380
Report to Congress on the effectiveness of the Civil Aviation Security Program
[AD-A195282] 24 p3322 N88-29784

CONICAL BODIES
NT SLENDER CONES
Conical wing with maximum lift-to-drag ratio in supersonic gas flow 04 p0425 N88-12633
Dynamic stability of hypersonic conical lifting vehicles according to Newton-Busemann theory
05 p0534 N88-13247
Interferometric data for a shock-wave/boundary-layer interaction
[NASA-TM-88227] 05 p0543 N88-13306
Development, construction and testing of a novel internal combustion engine with conical rotating slide valve
[DE88-900071] 05 p0589 N88-13593
Control of vortical separation on conical bodies
10 p1267 N88-17580
Fluid motion in a spinning, coning cylinder via spatial eigenfunction expansion
[AD-A190758] 15 p2066 N88-22319
Almond test body --- for microwave anechoic chambers
[NASA-CASE-LAR-13747-1] 18 p2502 N88-24845
Numerical calculations of the response of a spinning spheroidal payload to coning motion
[AD-A195890] 24 p3368 N88-30059

CONICAL FLARE
U CONES

CONICAL FLOW
Numerical calculations of the response of a spinning spheroidal payload to coning motion
[AD-A195890] 24 p3368 N88-30059

CONICAL SCANNING
Realization of a conical four-part antenna for the scanning of interference fields
[REPT-13-86] 01 p0034 N88-10216

CONICAL SHELLS
Effective treatment of membrane and shear locking phenomena in curved shear-deformable axisymmetric shell element 04 p0428 N88-12652
Analysis and testing of predamaged shell structures
04 p0428 N88-12653
Coupled FE and HIE method for exterior acoustics of axisymmetric shells --- finite element (FE) Helmholtz integral equation (HIE)
[ARE-TM(UHA)-87506] 09 p1243 N88-17448
Numerical and experimental research on propagation of elastic stress waves in conical shell under axial impulsive loading 15 p2053 N88-22238
Nonlinear liquid motion in conical containers
[LRT-WE-9-FB-10(1987)] 22 p3077 N88-28270

CONICS
NT ELLIPSES
NT PARABOLAS
On line search termination criteria for and convergence of conic algorithms for minimization
[DE88-002844] 09 p1227 N88-17351
Conic algorithms for unconstrained minimization with special consideration of problems with large sparse Hessians: A summary of research performed
[DE88-002549] 13 p1816 N88-20850
Algorithms with conic termination for nonlinear optimization
[DE88-005893] 13 p1816 N88-20851

CONIFERS
The use of airborne imaging spectrometer data to determine experimentally induced variation in coniferous canopy chemistry 05 p0612 N88-13761
Measuring near infrared spectral reflectance changes from water stressed conifer stands with AIS-2
05 p0613 N88-13765
Variations in spectral reflectance signature in healthy stands of pine and spruce
[FOA-C-30468-3.1] 22 p3116 N88-28512

CONJUGATE GRADIENT METHOD
S-step iterative methods for symmetric linear systems
[DE87-010819] 01 p0086 N88-10559
Implementation of preconditioned s-step conjugate gradient methods on a multiprocessor system with memory hierarchy
[DE87-014401] 02 p0222 N88-11400
Iterative solution of a nonlinear system arising in phase change problems
[DE87-014672] 02 p0226 N88-11426
Solution of geometrically nonlinear problem for reinforced shell of revolution having arbitrary shape
04 p0426 N88-12637
Indirect solution of static problems using concurrent vector processing computers
[DE87-012105] 05 p0636 N88-13889
Solution of non-symmetric linear systems by biconjugate gradients or conjugate gradients squared
[PB87-226387] 06 p0763 N88-14679
Upper bounds on the expected value of a convex function using gradient and conjugate function information
[AD-A186246] 07 p0910 N88-15517
Numerical experiments with a parallel conjugate gradient method
[DE88-002178] 08 p1066 N88-16445
Conjugate gradient spectral iterative technique
[PB88-126917] 10 p1398 N88-18337
Polynomial preconditioning for conjugate gradient methods
[DE88-005214] 10 p1399 N88-18342
Preconditioned conjugate gradient algorithms and software for solving large sparse linear systems
[DE88-002180] 13 p1816 N88-20849
Iterative finite element solver on transputer networks
16 p2218 N88-23235
A practical termination criterion for the conjugate gradient method
[REPT-87-62] 16 p2259 N88-23506
A taxonomy for conjugate gradient methods
[DE88-008574] 21 p3004 N88-27817

CONJUGATION
NT PHASE CONJUGATION
Optical bistable behavior of a planar quasi-waveguide interferometer made with a conjugated organic polymer film
[AD-A194349] 22 p3152 N88-28756

CONNECTICUT
The Windsor Locks, Connecticut tornado of 3 October 1979: An analysis of an intermittant severe weather event 02 p0208 N88-11305

CONNECTIONS
U JOINTS (JUNCTIONS)

CONNECTIVE TISSUE
NT BONE MARROW
NT COLLAGENS

CONNECTORS
NT ELECTRIC CONNECTORS
Development of an intermodule connector for serviceable spacecraft 14 p1877 N88-21212
Fabrication and electrical characterization of multilevel aluminum interconnects used to achieve silicon-hybrid wafer-scale integration
[AD-A190519] 15 p2060 N88-22282
Toggle release
[NASA-CASE-MSC-21354-1] 18 p2523 N88-24969
Developing a connector selection DBMS (database management system) using NIAM (Nijssen's Information Analysis Methodology)
[DE88-008110] 21 p3028 N88-27972
Connectionist models and artificial intelligence
[RR-684-I-IMAG-66-LIFIA] 22 p3142 N88-28684
Collet lock joint for space station truss
[NASA-CASE-MSC-21207-1] 23 p3222 N88-29180

CONNECTORS (ELECTRIC)
U ELECTRIC CONNECTORS

CONOIDS
U CONICAL BODIES

CONSCIOUSNESS
F-16 control stick response during +Gz-induced loss of consciousness
[AD-A184107] 04 p0400 N88-12491
Fighter design for human load limits
12 p1580 N88-19451
Physiological monitoring methodology in the USAFSAM centrifuge 21 p2924 N88-27356

CONSERVATION
NT ENERGY CONSERVATION
Conservatism implications of shock test tailoring for multiple design environments 05 p0592 N88-13611
Effects of fire on composition, biomass, and nutrients in oak scrub vegetation on John F. Kennedy Space Center, Florida
[NASA-TM-100305] 08 p1020 N88-16182
Period-doubling universality in multidimensional dissipative and conservative systems
[PB88-148812] 13 p1832 N88-20961
Application of remote sensing in the conservation of natural areas: Ribeira Valley 19 p2683 N88-25949

CONSERVATION EQUATIONS
Conservation and transport properties of turbulence with large density variations
[LA-10911-MS] 03 p0321 N88-12032
Breakdown of the conservative potential equation
07 p0809 N88-14929
A new boundary integral equation formulation for elastodynamic and elastostatic crack analysis
[AD-A192967] 20 p2815 N88-26702
Adaptive finite element methods for shells
[AD-A193221] 21 p2960 N88-27585
Shock waves in unsteady flows
[NASA-TT-20329] 23 p3214 N88-29134
Experimental and analytical study of two-phase flow in zero gravity
[AD-A195223] 24 p3358 N88-29993

CONSERVATION LAWS
Some aspects of high resolution numerical methods for hyperbolic systems of conservation laws, with applications to gas dynamics
[DMS-86-7] 03 p0321 N88-12031
New notions about space-time and gravitation
[DE87-703259] 03 p0383 N88-12408
High resolution finite volume methods on arbitrary grids via wave propagation
[NASA-CR-178397] 04 p0484 N88-12979
Nonlinear hyperbolic conservation laws
[AD-A184963] 05 p0580 N88-13538
A multistage time-stepping scheme for the thin-layer Navier-Stokes equations 07 p0810 N88-14932
Analysis of the spectral vanishing viscosity method for periodic conservation laws
[NASA-CR-181613] 09 p1231 N88-17378
A study of numerical methods for hyperbolic conservation laws with stiff source terms
[NASA-TM-100075] 10 p1399 N88-18343
Total Variation Diminishing (TVD) schemes of uniform accuracy
[NASA-TM-100552] 11 p1436 N88-18586
Plasma rotation in a tokamak
[DE88-700855] 12 p1693 N88-20128
Lie groups in prolongation theory
[B8721781] 14 p1907 N88-21743
Super Virasoro algebra and solvable supersymmetric quantum field theories
[DE88-752299] 15 p2127 N88-22661
Simulation of axisymmetric flow with H2O2 reactions
19 p2638 N88-25651
On the propagating speed in difference approximations for conservation laws 19 p2639 N88-25658
Semi-discrete approximations to nonlinear systems of conservation laws; consistency and L(infinity)-stability imply convergence
[NASA-CR-181683] 19 p2721 N88-26157
Numerical solution of weak forms of conservation laws on optimal unstructured triangular grids
20 p2797 N88-26597
Piecewise-parabolic methods for systems of hyperbolic conservation laws in multiprocessing environments
[DE88-010202] 23 p3248 N88-29329
An analysis of finite-difference and finite-volume formulations of conservation laws
[NASA-CR-177416] 24 p3370 N88-30071
Nonequilibrium flow computations. 1: An analysis of numerical formulations of conservation laws
[NASA-CR-177489] 24 p3425 N88-30384

CONSISTENCY
Consistency question in the renormalization group analysis of deep inelastic scattering
[DE87-703372] 04 p0487 N88-12999
Strong consistency of M-estimates for the linear model
[AD-A185487] 06 p0764 N88-14696

Strong consistency of estimation of number of regression variables when the errors are independent and their expectations are not equal to each other
[AD-A186025] 07 p0909 N88-15507
Strong consistency of maximum likelihood parameter estimation of superimposed exponential signals in noise
[AD-A186384] 07 p0911 N88-15526
On the direction of arrival estimation
[AD-A186031] 07 p0914 N88-15546
Consistent linearization of the element-independent corotational formulation for the structural analysis of general shells
[NASA-CR-178418] 09 p1181 N88-17078
Consistency of rule-based expert systems
[CWI-CS-R8736] 13 p1831 N88-20950
On a consistent estimate of the index of an extreme value distribution
[CWI-MS-R8710] 14 p1966 N88-21729
Derivation of consistent surface fixed fields for use in a global NWP model
[AD-A190131] 15 p2093 N88-22475
Constant amplitude fatigue life data for notched and unnotched annealed Ti-6Al-4V sheet
[AD-A193420] 21 p2913 N88-27287

CONSOLES
NT REMOTE CONSOLES
Western aeronautical test range real-time graphics software package MAGIC
[NASA-TM-100425] 13 p1757 N88-20506

CONSOLIDATION
Effects of combining vertical and horizontal information into a primary flight display
[NASA-TP-2783] 04 p0399 N88-12487
Characterization of an explosively consolidated rapidly solidified Fe-16Ni-9Cr-5Mo-2Cu alloy powder
[DE88-006733] 15 p2041 N88-22162
Superconductor consolidation
[DE88-010938] 21 p3024 N88-27949

CONSTANT SPEED PROPELLERS
U VARIABLE PITCH PROPELLERS

CONSTANTS
NT GRAVITATIONAL CONSTANT
NT HUBBLE CONSTANT
NT SOLAR CONSTANT
NT TIME CONSTANT
Evaluation and prediction of Henry's law constants and aqueous solubilities for solvents and hydrocarbon fuel components. Volume 1: Technical discussion
[AD-A188571] 12 p1613 N88-19643
Measurement of rate constants of elementary gas reactions of importance to upper atmosphere and combustion systems
[AD-A189432] 13 p1737 N88-20386
Involution-dependent constants and the cancellation of divergences in the 1-loop open string amplitude
[DE88-006537] 15 p2146 N88-22811
A simulation analysis of errors in the measurement of standard electrochemical rate constants from phase-selective impedance data
[AD-A192739] 20 p2770 N88-26426
Parameter identification of material constants in a composite shell structure
[DE88-008115] 22 p3086 N88-28326
Can we calculate the fundamental dimensionless constants of physics
[DE88-702641] 23 p3295 N88-29625

CONSTELLATIONS
NT AURIGA CONSTELLATION
NT CORONA BOREALIS CONSTELLATION
NT CYGNUS CONSTELLATION
NT LYRA CONSTELLATION
NT SCORPIUS CONSTELLATION

CONSTITUTION
Science, technology and the Constitution: Background paper
[PB88-142534] 12 p1708 N88-20222

CONSTITUTIONAL DIAGRAMS
U PHASE DIAGRAMS

CONSTITUTIVE EQUATIONS
Constitutive modeling of superalloy single crystals with verification testing 02 p0188 N88-11169
Deviatoric constitutive relationship for anisotropic materials
[AD-A184332] 03 p0295 N88-11854
Nonlinear thermoviscoelastic analysis of metallic plane curved beams 03 p0336 N88-12119
Application of viscoplastic constitutive equations in finite element programs
[KFK-4254] 03 p0370 N88-12329
A direct method to obtain constitutive model constants from cylinder impact test results
04 p0427 N88-12647
On a numerical method to solve contact problems --- forming processes
[B8711403] 05 p0642 N88-13930
A critical review of the development of several viscoplastic constitutive theories
[AD-A185652] 07 p0867 N88-15262
The paradoxical asymptotic status of massless springs
[AD-A185625] 07 p0928 N88-15637
Structure of a viscoplastic theory
[NASA-TM-100794] 11 p1501 N88-18968
Nonlinear Constitutive Relations for High Temperature Applications, 1986
[NASA-CP-10010] 14 p1928 N88-21498
A viscoplastic constitutive theory for metal matrix composites at high temperature
14 p1929 N88-21500
Development of a unified constitutive model for an isotropic nickel base superalloy Rene 80
14 p1929 N88-21501
An internal variable constitutive model for the large deformation of metals at high temperatures
14 p1929 N88-21503
Constitutive modeling and thermoviscoplasticity
14 p1930 N88-21506
A theory of viscoplasticity accounting for internal damage 14 p1930 N88-21508
A constitutive model with damage for high temperature superalloys 14 p1930 N88-21510
Evaluation of structural analysis methods for life prediction 14 p1930 N88-21511
Data requirements to model creep in 9Cr-1Mo-V steel
14 p1931 N88-21512
Controlled-strain rate tests at very low strain rates of 2618 aluminum at 200 C 14 p1931 N88-21513
An experimental comparison of several current viscoplastic constitutive models at elevated temperature
14 p1931 N88-21516
An automated procedure for material parameter evaluation for viscoplastic constitutive models
14 p1932 N88-21520
A constitutive material model for nonlinear finite element structural analysis using an iterative matrix approach
14 p1932 N88-21521
Unified constitutive models for high-temperature structural applications 14 p1932 N88-21523
Constitutive response of Rene 80 under thermal mechanical loads 14 p1932 N88-21524
A constitutive model for an overlay coating
14 p1933 N88-21525
Life assessment of combustor liner using unified constitutive models 15 p2077 N88-22384
Biaxial experiments supporting the development of constitutive theories for advanced high-temperature materials 15 p2078 N88-22386
Unified constitutive model development for metal matrix composites at high temperature
15 p2078 N88-22387
Unified constitutive model for single crystal deformation behavior with applications 15 p2078 N88-22388
Finite element (MARC) solution technologies for viscoplastic analyses 15 p2078 N88-22389
Models in nonlinear thermomechanics. Finite element models and constitutive models for large deformation elastoplasticity
[ETN-88-92240] 16 p2222 N88-23262
An endochronic rate-sensitive constitutive equation for metals, application to generalized creep and large deformations
[AD-A194167] 22 p3055 N88-28125
Constitutive modeling for isotropic materials
[NASA-CR-182132] 24 p3327 N88-29811
Anisotropic constitutive modeling for nickel-base single crystal superalloys
[NASA-CR-182157] 24 p3353 N88-29961
Stability of stick-slip phenomenon by using constitutive friction laws of Dietrich and Ruina
[ILR-MITT-197] 24 p3379 N88-30127

CONSTRAINTS
NT METEOROLOGICAL PARAMETERS
Integration of dynamic, aerodynamic and structural optimization of helicopter rotor blades
[NASA-CR-181441] 01 p0002 N88-10012
Altitude Control Working Group report
01 p0016 N88-10099
Study of closed loop control singularity in dynamic systems with a constraint on the final state
[LAAS-87-190] 02 p0223 N88-11405
Numerical solution of bound constrained problems
[DE88-000653] 03 p0371 N88-12334
An exact penalization viewpoint of constrained optimization
[DE88-001477] 04 p0486 N88-12995
Performance-limiting factors in MPD thrusters
[AD-A185605] 06 p0674 N88-14128
High pressure ratio turbine design constraints
[TRR-0279] 06 p0712 N88-14365
Parallel algorithms for unconstrained and constrained nonlinear optimization
[PB87-230454] 06 p0756 N88-14634
Collider constraints in the choices for wavelength and gradient scaling
[PB87-123691] 06 p0779 N88-14783
Dynamics formulations for the real-time simulation of constrained motion 06 p0795 N88-14872
Feasibility studies of optical processing of image bandwidth compression schemes
[AD-A186073] 07 p0932 N88-15660
Processing, fabrication, applications and limitations of inherently conducting polymers
[DE88-003210] 08 p0973 N88-15683
Computation of the tensile and bending restraint intensities of welded specimens by finite element method
[PB87-143798] 08 p0995 N88-16024
Limitation of spacecraft orbit near colinear libration center of limited elliptical three body problem
08 p1003 N88-16075
Resolution limitations and optimization of the ITT F4157 streak tube focus for fast (10 ps) operation
[DE88-003727] 09 p1169 N88-17007
Trimodal interpretation of constraints for planning
09 p1209 N88-17248
A posteriori error estimates in computational fluid mechanics 11 p1486 N88-18869
A tool for the analysis of quasi-Newton methods with application to unconstrained minimization
[DE88-005783] 11 p1532 N88-19153
Minimum weight design of rectangular and tapered helicopter rotor blades with frequency constraints
[NASA-TM-100561] 12 p1582 N88-19465
A representation for serial robotic tasks
12 p1681 N88-20048
Describing constraints on a digital circuit's behavior
[AD-A189200] 13 p1761 N88-20531
Practical constraints on sources for pulsed beam lithographies
[DE88-006594] 13 p1776 N88-20623
Active cooling design for scramjet engines using optimization methods
[NASA-TM-100581] 13 p1783 N88-20669
Constrained nonlinear programming
[DE88-005695] 13 p1817 N88-20860
Measurement of the elastic-plastic surface flaw back surface topology and its relation to constraint
[DE88-006765] 15 p2087 N88-22437
Minimum weight design of rotorcraft blades with multiple frequency and stress constraints
[NASA-TM-100569] 16 p2161 N88-22892
Discrete generalized networks: Application to integer constrained flow problems
[AD-A190823] 16 p2190 N88-23060
A constraint algorithm for maintaining rigid bonds in molecular dynamics simulations of large molecules
[AD-A191663] 18 p2572 N88-25277
Mechanisms for particle acceleration: Possibilities and constraints
[PB88-102538] 19 p2725 N88-26184
N = 2 supergravity in superspace: Solution to the constraints
[DE88-702135] 19 p2741 N88-26272
Range of a constrained random walk
[PB88-126867] 20 p2847 N88-26897
Cooperating knowledge-based systems
[NASA-CR-183109] 23 p3247 N88-29327
On recognizing ignorance 23 p3254 N88-29372
Constraints on the origin of fractured terrane, Northern Martian plains 23 p3304 N88-29684
Origin of northern lowland plains: Constraints from boundary morphology 23 p3305 N88-29687
The bounded rationality constraint: Experimental and analytical results
[AD-A195897] 24 p3413 N88-30318

CONSTRICTIONS
Design of a sound neck in connection with the model-support system of a transonic wind tunnel test section
[ILR-MITT-186(1987)] 14 p1869 N88-21171

CONSTRUCTION
Construction and characterization of amorphous-silicon test structures
[DE87-013595] 01 p0029 N88-10182
Mission Peculiar Equipment Support Structure: A platform for space construction
02 p0139 N88-10874
Marshall Space Flight Center's role in EASE/ACCESS mission management 02 p0139 N88-10875
Results of the ACCESS experiment
02 p0140 N88-10880
Development, construction and testing of a novel internal combustion engine with conical rotating slide valve
[DE88-900071] 05 p0589 N88-13593
Controlled ecological life support systems: Development of a plant growth module 05 p0630 N88-13854

Investigation of design concepts for large space structures to support military applications
[AD-A186098] 07 p0824 N88-15000
Fabrication techniques used in the construction of a high resolution X-ray framing camera
[DE88-002653] 07 p0856 N88-15200
Mechanical design and construction of a 200 mA, 100 keV, dc, negative ion accelerator
[DE88-003855] 11 p1548 N88-19257
State-of-the-art technologies for construction in space: A review
[AD-A186412] 12 p1585 N88-19483
The space station assembly phase: Flight telerobotic servicer feasibility, volume 1
[NASA-CR-182669] 13 p1731 N88-20351
Campaign graphs
[DE88-005336] 13 p1831 N88-20952
Materials qualification in oceanology and the offshore industry 19 p2700 N88-26050
Construction of gallium arsenide solar concentrator for space use
[AD-A194858] 23 p3230 N88-29222
Structure and dynamics of solutions of lithium salts relevant to battery construction
[AD-A195399] 24 p3366 N88-30044
CONSTRUCTION IN SPACE
U ORBITAL ASSEMBLY
CONSTRUCTION MATERIALS
Development of highly porous calcium silicate hydrate materials with extremely low thermal conductivity
[BMFT-FB-T-86-164] 02 p0150 N88-10941
Investigations on the crack growth retardation behavior and fatigue life prediction in structural materials
[PB87-143756] 07 p0827 N88-15016
Characterization of current steels. The 35 NCD 16 alloy in 30 mm diam laminated bars made by Aubert and Duval
[CEAT-41/N/76] 07 p0832 N88-15046
Space environmental effects on polymeric materials
[NASA-CR-182418] 07 p0838 N88-15082
Metals and Ceramics Division
[DE88-008955] 19 p2618 N88-25530
CONSULTING
Towards automated consulting: Design feedback from the performance of online documentation
[DE87-012243] 04 p0501 N88-13082
CONSUMABLES (SPACECREW SUPPLIES)
NT SPACE RATIONS
Orbital Spacecraft Consumables Resupply System (OSCRS): Monopropellant application to space station and OMV automatic refueling impacts of an ELV launch, volume 4
[NASA-CR-172029] 03 p0276 N88-11741
The determination of nutritional requirements for Safe Haven Food Supply System (emergency/survival foods)
06 p0792 N88-14856
Space and sea: Is there a place for ionization?
19 p2699 N88-26043
CONSUMERS
Spinoff, 1987
[NASA-TM-89652] 02 p0250 N88-11577
CONSUMPTION
NT ENERGY CONSUMPTION
NT FUEL CONSUMPTION
NT OXYGEN CONSUMPTION
CONTACT LENSES
A field study on soft contact lens wear in USAF military transport aircraft
[AD-A195962] 24 p3407 N88-30265
CONTACT LOADS
NT ROLLING CONTACT LOADS
On a numerical method to solve contact problems --- forming processes
[B8711403] 05 p0642 N88-13930
Analysis of load-bearing capacity of nitrided layer
[PB87-144176] 08 p0968 N88-15857
Reliability based analysis of contact problems
[NASA-CR-182117] 11 p1503 N88-18975
Spur gears: Optimal geometry, methods for generation and Tooth Contact Analysis (TCA) program
[NASA-CR-4135] 16 p2215 N88-23216
Design and evaluation of high contact ratio gearing
[NASA-CR-174958] 22 p3085 N88-28319
CONTACT RESISTANCE
Comparison of methods for the calculation of thermal contact resistance of the first Brazilian satellite
[NASA-TT-20180] 14 p1880 N88-21239
Friction, wear and electrical contact resistance of precious metal alloys
[DE88-011244] 21 p2938 N88-27450
CONTACTORS
Hollow cathode plasma coupling study, 1986
[NASA-CR-171985] 03 p0309 N88-11949
Advanced electric propulsion and space plasma contactor research
[NASA-CR-180862] 06 p0674 N88-14126
Plasma contactors for use with electodynamic tethers for power generation
[NASA-CR-182424] 08 p1087 N88-16547
Space plasma contactor research, 1987
[NASA-CR-182148] 16 p2280 N88-23649
CONTACTS (ELECTRIC)
U ELECTRIC CONTACTS
CONTACTS (GEOLOGY)
The unsteady ground heat flow at the contact surface between a glacier run and the subsoil
08 p1014 N88-16147
CONTAINERLESS MELTS
Preliminary study of a containerless processing facility for Columbus, executive summary
[ESA-ITT/AO/1-1834/85F] 01 p0032 N88-10203
Center for the Space Processing of Engineering Materials 07 p0838 N88-15083
Non-proprietary research projects of the Center for the Space Processing of Engineering Materials
[AR-2] 10 p1426 N88-18516
Containerless glass melting 15 p2051 N88-22222
Prospects for antiproton production and propulsion
16 p2267 N88-23556
Large hydrogen cluster ions 16 p2267 N88-23558
Infrared spectroscopy of H3(+)
16 p2268 N88-23565
Key problems and hydrogen atom formation
16 p2269 N88-23573
The cluster ion approach to the condensation and storage of antihydrogen 16 p2269 N88-23575
Analysis of containerless condensation of polyatomic hydrogen ions, with emphasis on H3(+,-) association channels and a futuro workshop to study related topics
16 p2269 N88-23576
Small molecule and small cluster ion formation in a low-density containerless mixture of electrons, protons and hydrogen atoms 16 p2269 N88-23577
Program for the feasibility of developing a high pressure acoustic levitator
[NASA-CR-182154] 20 p2782 N88-26498
CONTAINERS
Buckling and breakdown problems in structural mechanics. Failure of prestressed double-walled containers or rings
[MBB-UR-E-956/87] 13 p1783 N88-20671
Durability of compound cylinder under static internal-pressure repeat load of long duration
16 p2180 N88-22991
Sample decomposition in sealed teflon vessels
[NASA-TT-20189] 18 p2494 N88-24798
CONTAINMENT
Completely magnetically contained electrothermal thrusters
[AD-A185674] 06 p0674 N88-14129
The application of high-rate biaxial testing to the design of containment vessels for radioisotope heat sources
17 p2426 N88-24428
CONTAMINANTS
NT RADIOACTIVE CONTAMINANTS
NT TRACE CONTAMINANTS
Contamination control of the space shuttle Orbiter crew compartment 02 p0133 N88-10834
Influence of surfactants on damping of gravity-capillary waves. 1: Frequency dependence
04 p0459 N88-12843
Photoacoustic infrared laser spectroscopy for analyzing gaseous contaminants
[ETN-88-90805] 07 p0831 N88-15041
Pollution from motor vehicles and aircraft at Stapleton International Airport (abbreviated report), revision 2
[AD-A185916] 07 p0875 N88-15307
Estimation of aerial deposition and foliar uptake of xenobiotics: Assessment of current models
[DE88-000993] 09 p1188 N88-17117
Sampling intervals
[AD-A189445] 12 p1573 N88-19408
Reverse osmosis treatment to remove inorganic contaminants from drinking water
[PB88-147780] 12 p1605 N88-19598
Chemical cleaning of metal surfaces in vacuum systems by exposure to reactive gases
[AD-A188588] 12 p1608 N88-19616
Production and turnover of suspended organic detritus in the coastal water of the southeastern continental shelf
[DE88-005118] 14 p1951 N88-21631
A Study of Space Station Contamination Effects --- conference
[NASA-CP-3002] 18 p2590 N88-25390
Neutral environment for space station
18 p2590 N88-25391
Space station neutral external environment
18 p2590 N88-25392
Contaminant ions and waves in the space station environment 18 p2590 N88-25393
Space station particulate contamination environment
18 p2591 N88-25397
The particulate environment surrounding the space station: Estimates from the PACS data
18 p2591 N88-25398
Effects of meteoroids and space debris on the particulate environment for space station 18 p2591 N88-25399
Contamination of optical surfaces --- Space Station
18 p2592 N88-25400
Surface interactions relevant to space station contamination problems 18 p2592 N88-25401
Contamination of the space station environment by vented chemicals 18 p2592 N88-25403
Composite, meso-gamma scale diagnostic modeling
[DE88-008189] 19 p2689 N88-25983
Pollutant formation in heterogeneous mixtures of fuel drops and air
[DOE/CE-50052/H1] 19 p2689 N88-25986
Overview of the PRECP (processing of emissions by clouds and precipitation) Program
[DE88-008205] 20 p2822 N88-26741
Analysis of debris from accelerated life test of the Hughes five-year Vuilleumier cryocooler
[AD-A193101] 21 p2931 N88-27400
Blue-green laser diode research program
[AD-A191980] 23 p3218 N88-29153
Development of computer-controlled thermogravimetric instrumentation for measurement of environmental and high temperature volatilization and desorption of contaminants from polymeric materials
[AD-A195934] 24 p3343 N88-29900
CONTAMINATION
NT FUEL CONTAMINATION
NT SPACECRAFT CONTAMINATION
Use of a 35mm camera for remote surface cleanliness verification 02 p0133 N88-10835
An investigation of the behavior of outgassed molecules in thermal vacuums 02 p0133 N88-10836
Redistribution of particulates in shuttle bay during launch 02 p0133 N88-10837
Shear stress cleaning for surface departiculation
02 p0134 N88-10838
Space station contamination considerations
02 p0137 N88-10859
A life test of a 22-Newton (5-lbf) hydrazine rocket
[NASA-TM-100232] 03 p0278 N88-11750
Insect contamination protection for laminar flow surfaces 07 p0814 N88-14954
On copper peroxide
[NASA-TT-20263] 15 p2037 N88-22135
Reclamation of water contaminated with fuel system icing inhibitor. Phase 1: Literature review and information compilation
[DE88-006575] 16 p2183 N88-23013
A zoomable and adaptable hidden fine-mesh approach to solving advection-dispersion equations
[DE88-006174] 21 p3004 N88-27816
Experimental evaluation of resistojet thruster plume shields
[NASA-TM-101363] 24 p3338 N88-29868
Contamination and distortion of steady flow field induced by discrete frequency disturbances in aircraft gas engines
[AD-A195440] 24 p3370 N88-30069
CONTENT
NT BONE MINERAL CONTENT
CONTEXT
A review of hypertext in a NASA project management context 06 p0793 N88-14859
CONTEXT FREE LANGUAGES
Formal grammars and Markov models
[RSRE-MEMO-4051] 09 p1219 N88-17311
CONTINENTAL DRIFT
Crustal dynamics project data analysis, 1987. Volume 2: Mobile VLBI geodetic results, 1982-1986
[NASA-TM-100689-VOL-2] 08 p1035 N88-16280
Constraints on continental accretion from sedimentation 24 p3392 N88-30202
Metamorphic P-T paths and Precambrian crustal growth in East Antarctica 24 p3395 N88-30216
CONTINENTAL MARGINS
U CONTINENTAL SHELVES
CONTINENTAL SHELVES
Marine minerals: Exploring our new ocean frontier
[PB87-217725] 02 p0216 N88-11364
RRS DISCOVERY Cruise 161, 15 August (227)-19 September (262) 1986. Portuguese Ocean-continent boundary, plate boundaries west of Iberia and seismic structure of sediments off Madeira
[PB87-222006] 06 p0747 N88-14596
Sea resonance vibrational source of seismic waves
08 p1010 N88-16126
Continental shelf processes affecting the oceanography of the South Atlantic Bight
[DE88-004102] 09 p1196 N88-17156

Trace element geochemistry of the South Atlantic Bight
[DE88-003515] 10 p1356 N88-18108

Coordination: Southeast continental shelf studies
[DE88-003580] 10 p1357 N88-18110

Mesoscale coastal ocean dynamics
11 p1517 N88-19060

Synthesis of finite displacements and displacements in continental margins
[NASA-CR-182616] 12 p1642 N88-19832

Research on the physical oceanography of the Gulf Stream
[AD-A188512] 12 p1649 N88-19877

Circulation and exchange processes on the South Atlantic Bight Continental Shelf
[DE88-003330] 13 p1804 N88-20781

Production and turnover of suspended organic detritus in the coastal water of the southeastern continental shelf
[DE88-005118] 14 p1951 N88-21631

Simulation analysis of moored fluorometer time series from the Mid-Atlantic Bight
[DE88-006066] 15 p2099 N88-22505

A computerized investigation using the method of images to predict the sound field in a fluid wedge overlying a slow fluid half-space
[AD-A190013] 15 p2130 N88-22704

Influence of the Yukon River on the Bering Sea
[NASA-CR-182802] 17 p2376 N88-24126

Effects of a temperature-dependent rheology on large scale continental extension
[NASA-CR-183117] 20 p2825 N88-26759

Prediction of continental shelf sediment transport using a theoretical model of the wave-current boundary layer
[AD-A192272] 20 p2829 N88-26783

Stability of a coastal upwelling front over topography
[AD-A192354] 20 p2829 N88-26784

Mid to late proterozoic magmatism within Northeastern North America and its implications for the growth of the continental crust 24 p3397 N88-30229

CONTINENTS

NT AFRICA
NT ASIA
NT AUSTRALIA
NT EUROPE
NT NORTH AMERICA
NT SOUTH AMERICA

New method of estimating continentality of climate on global scale 06 p0725 N88-14460

Geomechanical model of seismofocal zone of active continental margin 08 p1011 N88-16128

Numerical studies of propagation of Lg waves across ocean continent boundaries using the Representation Theorem (RT) 10 p1353 N88-18085

Geophysical study of the structure and processes of the continental convergence zones: Alpine-Himalayan Belt
[NASA-CR-182647] 12 p1644 N88-19842

Continental surface processes and water cycle
14 p1937 N88-21555

Workshop on the Growth of Continental Crust
[NASA-CR-183073] 24 p3392 N88-30201

Constraints on continental accretion from sedimentation 24 p3392 N88-30202

Recycling of lower continental crust through foundering of cumulates from contaminated mafic intrusions
24 p3393 N88-30204

Growth of continental crust: Clues from Nd isotopes and Nb-Th relationships in mantle-derived magmas
24 p3393 N88-30205

An illustration of the complexity of continent formation
24 p3393 N88-30207

The Kerala Khondalite Belt (KKB) of Southern India: An ensialic mobile belt 24 p3393 N88-30208

Genesis of archean granitoids in the Pilbara block and implications for crustal growth 24 p3394 N88-30210

Does subduction zone magmatism produce average continental crust 24 p3394 N88-30214

Decoupled Rb-Sr and Sm-Nd isotopic evolution of the continental crust 24 p3395 N88-30216

The growth of continents and some consequences since 1.5 Ga 24 p3395 N88-30220

Thermal models pertaining to continental growth
24 p3397 N88-30230

Growth of the lower continental crust
24 p3398 N88-30236

Continental crustal formation and recycling: Evidence from oceanic basalts 24 p3398 N88-30238

Physical processes in the growth of the continental crust 24 p3398 N88-30240

Continental growth through time by underplating of subducted oceanic crust: Evidence from kimberlites in South Africa and SW Pacific 24 p3399 N88-30244

The growth of the continental crust: Constraints from radiogenic isotope geochemistry
24 p3399 N88-30245

Mineralization through geologic time: Evolution of continental crust 24 p3400 N88-30250

Growth of the continental crust: A planetary-mantle perspective 24 p3400 N88-30251

The effect of thicker oceanic crust in the Archaean on the growth of continental crust through time
24 p3401 N88-30254

CONTINUITY

On the relations between increasing functions associated with two-parameter continuous martingales
[AD-A185572] 06 p0765 N88-14699

Finite element method with continuous mass elements
[PB87-143384] 08 p0995 N88-16019

Continuity of symmetric stable processes
[AD-A190324] 15 p2125 N88-22667

CONTINUITY (MATHEMATICS)

The periodic Lyapunov equations
[REPT-86-007] 01 p0087 N88-10567

Estimation of gravity vector components from Bell gravity gradiometer and auxiliary data under consideration of topography and associated analytical upward continuation aspects
[AD-A188146] 10 p1355 N88-18099

Computation and characteristics of pulsatile multi-bifurcation flow 18 p2483 N88-24729

CONTINUITY EQUATION

Efficient numerical techniques for complex fluid flows
02 p0185 N88-11151

The p-version of the finite element method for elliptic equations of order 2l
[AD-A136334] 07 p0911 N88-15523

Experimental and analytical studies of compressible vortices 19 p2665 N88-25848

CONTINUOUS FLOW ELECTROPHORESIS

U ELECTROPHORESIS

CONTINUOUS RADIATION

NT MODULATED CONTINUOUS RADIATION

Application of lattice filtering techniques to CW measured time domain data
[AD-A184351] 04 p0431 N88-12671

Phenomena at a focus in a laser system
[AD-A185442] 05 p0588 N88-13585

Performance of a small, graphite electrode, multistage depressed collector with a 500-W, continuous wave, 4.8- to 9.6-GHz traveling wave tube
[NASA-TP-2788] 07 p0848 N88-15146

Evaluation of CWMS (Continuous-Wave Measurement System) single-wire dipole antenna
[DE88-003979] 09 p1155 N88-16920

CEBAF design overview and project status
[CEBAF-PR-88-001] 09 p1246 N88-17470

A technique for low level, wide range CW microwave power meter calibrations
[DE88-004147] 10 p1333 N88-17966

Nucleon resonances and nuclei: Experimental aspects
[CEBAF-PR-87-025] 11 p1545 N88-19233

The injector for the CEBAF CW superconducting linac
[CEBAF-PR-87-011] 11 p1546 N88-19241

Perturbation effects in the CEBAF beam transport system
[CEBAF-PR-87-010] 11 p1546 N88-19242

Investigation of multiple particle final states at CEBAF (Continuous Electron Beam Accelerator Facility)
[CEBAF-PR-87-026] 11 p1547 N88-19250

RF steering in the CEBAF CW superconducting linac
[CEBAF-PR-87-013] 11 p1547 N88-19251

The CEBAF project and its few-body research program
[CEBAF-PR-87-014] 11 p1547 N88-19253

Application of radio frequency superconductivity to recirculating linacs
[CEBAF-PR-88-002] 12 p1690 N88-20107

The continuous electron beam accelerator facility
[CEBAF-PR-87-017] 13 p1838 N88-20996

Discussion of two-mode two-photon CW laser oscillation 16 p2187 N88-23042

Effects of translational and rotational nonequilibrium on CW (Continuous Wave) chemical laser performance
[AD-A191425] 16 p2214 N88-23210

The loss parameters for very short bunches
[CEBAF-PR-88-005] 18 p2574 N88-25291

Effects of pulsed and CW (Continuous Wave) 2450 MHz radiation on transformation and chromosomes of human lymphocytes in vitro
[AD-A193104] 21 p2987 N88-27736

Analysis of free electron laser performance utilizing the National Bureau of Standards CW microtron
[AD-A194217] 23 p3219 N88-29160

Static and dynamic behavior of a quasi one-dimensional Heisenberg antiferromagnet in the long-range ordered state. A nuclear magnetic resonance study performed with a He3-He4 dilution refrigerator
[B8705564] 23 p3281 N88-29533

Aeronomic problems of the molecular oxygen photodissociation. Part 3: Solar spectral irradiances in the region of the O2 Herzberg continuum, Schumann-Runge bands and continuum
[AERONOMICA-ACTA-A-332-1988]
24 p3343 N88-29897

Aeronomic problems of molecular oxygen photodissociation. Part 4: The various parameters for the Herzberg continuum
[AERONOMICA-ACTA-A-333-1988]
24 p3352 N88-29955

CONTINUOUS WAVE LASERS

High intensity 5 eV O-atom exposure facility for material degradation studies 02 p0135 N88-10847

Silicon oxidation photoassisted with a continuous wave CO2 laser beam and contribution to the study of silica layers obtained
[LAAS-87-158] 02 p0179 N88-11115

Computer simulation of cw HF chemical laser unstable resonator performance
[AD-A185059] 05 p0587 N88-13581

An experimental study of CW HF chemical laser amplifier performance and zero power gain
[AD-A185241] 05 p0588 N88-13584

USSR report: Physics and mathematics
[JPRS-UPM-87-006] 06 p0708 N88-14344

Repetitively pulsed and continuous wave CO2 lasers pumped by a pulsed self-sustained discharge for thermal processing 06 p0709 N88-14346

Production-process CO2 laser with amplified pulse-repetition operation 06 p0771 N88-14739

Frequency locking of two lasers
[FOA-C-30456-3.1] 08 p0992 N88-16000

Remote measurement of aerosol stream velocity with continuous-wave CO2-laser 08 p1079 N88-16506

Mirrors for high-power continuous-wave Ar-lasers
09 p1235 N88-17404

Instabilities and chaos in a multimode, standing-wave, CW dye laser
[DE88-005028] 10 p1337 N88-17993

Studies of fluorine combustion
[AD-A187646] 11 p1452 N88-18656

Characteristics of welds joining parts of high-strength pipe steels and produced by beam of continuous-wave CO2-laser 14 p1897 N88-21325

Laser-heterodyne interferometry with streak camera detection
[DE88-003292] 14 p1914 N88-21437

Effects of translational and rotational nonequilibrium on CW (Continuous Wave) chemical laser performance
[AD-A191425] 16 p2214 N88-23210

Distributed feedback lasers
[NASA-CR-4154] 18 p2520 N88-24948

Strained layer and lattice matched transverse junction stripe quantum well lasers for continuous room temperature operation 20 p2863 N88-27004

CONTINUOUS WAVE RADAR

Method and apparatus for measuring distance
[NASA-CASE-MSC-20912-1] 20 p2793 N88-26568

CONTINUOUS WAVES

U CONTINUOUS RADIATION

CONTINUUM FLOW

Energy efficient continuous flow ash lockhopper
[NASA-CASE-NPO-16985-1-CU]
18 p2497 N88-24814

Studies of error in temperature measurement with thermistors in the range between continual and free-molecule flows
[NASA-TT-20302] 19 p2674 N88-25900

CONTINUUM MECHANICS

Relativistic stochastic mechanics
[PREPRINT-543] 06 p0790 N88-14842

A critical review of the development of several viscoplastic constitutive theories
[AD-A185652] 07 p0867 N88-15262

Conference on Maximum Principles and Eigenvalue Problems in Partial Differential Equations
[AD-A187870] 11 p1536 N88-19175

A continuum damage model for viscoelastic materials
[AD-A189426] 12 p1637 N88-19800

Stability and uniqueness in nonlinear continuum mechanics
[AD-A189616] 12 p1699 N88-20172

Problems in nonlinear continuum dynamics
[AD-A190538] 15 p2128 N88-22691

Small-scale cleavage test of polymer products
[PB88-165360] 16 p2181 N88-23001

On microphysical principles of thermofluid dynamics
[ETN-88-92095] 20 p2801 N88-26620

An anisotropic continuum damage model for creep-dominated, multiaxial loading histories
21 p2964 N88-27606

Some stability criteria in fluid and solid mechanics
21 p3027 N88-27966

A transversely isotropic thermoelastic theory
[NASA-TM-101302] 22 p3087 N88-28332

The construction of the thermoelasticity equations on the basis of contemporary notions of nonlinear continua mechanics
[NASA-TT-20307] 23 p3296 N88-29631
Theory of filtering and control with application to control of large space structures
[AD-A195500] 24 p3335 N88-29851
Damage initiation in the short beam shear test of composite materials using stiffness reduction
[AD-A194880] 24 p3340 N88-29883

CONTINUUM MODELING
Continuum modeling of large lattice structures: Status and projections
[NASA-TP-2767] 06 p0672 N88-14115
A continuum damage model for viscoelastic materials
[AD-A189426] 12 p1637 N88-19800
Continuum modeling and dynamic analysis of large truss structures 17 p2349 N88-23995
An anisotropic continuum damage model for creep-dominated, multiaxial loading histories
21 p2964 N88-27608

CONTINUUMS
Radio continuum emission from the ionized stellar winds of the cool supergiants in zeta Aurigae-like systems
04 p0514 N88-13160
Automatic continuum analysis of reflectance spectra
05 p0614 N88-13770
Continuum theories for fluid-particle flows: Some aspects of lift forces and turbulence
[DE88-007038] 18 p2511 N88-24898
Investigation of the higher-order elements in the SAMSON2 code
[AD-A193638] 23 p3271 N88-29465

CONTOUR SENSORS
Contour interactive extraction using image numerical treatment
[ISL-R-114/86] 15 p2113 N88-22587

CONTOURS
Detection of critical points: The first step to automatic line generalization 05 p0619 N88-13803
The aerodynamic design of hypersonic contoured axisymmetric nozzles including real gas effects
[VKI-TM-43] 06 p0665 N88-14076
Fast, colour displays of digital terrain elevation data
[AD-A185596] 06 p0729 N88-14485
The information metric for univariate linear elliptic models
[AD-A186385] 07 p0911 N88-15527
Contour-to-grid interpolation with nonlinear finite elements: A feasibility study
[AD-A188108] 11 p1503 N88-18960
On the geometric interpretation of image contours
[RR-647-I-IMAG-57-LIFIA] 15 p2100 N88-22563
Test results at transonic speeds on a contoured over-the-wing propfan model
[NASA-TM-88206] 23 p3177 N88-28918
Implementation of the NCAR (National Centre for Atmospheric Research) graphics package at ARL (Aeronautical Research Laboratory)
[AD-A195163] 24 p3391 N88-30193
A digital terrain model system for a microcomputer
[INPE-4610-PRE/1333] 24 p3413 N88-30316

CONTRACT MANAGEMENT
A comparison of the basket method and the stratified random sampling for contract change order negotiations
[AD-A184170] 04 p0500 N88-13080
The appropriate use of contract types in development contracts (a systems approach with emphasis on the European space sector)
[ESA-STR-222] 08 p1092 N88-16573
Streamlining invitation for bids
[AD-A188941] 12 p1705 N88-20206
Human organization --- space projects
22 p3160 N88-28808
Contracts 22 p3160 N88-28810

CONTRACT NEGOTIATION
A comparison of the basket method and the stratified random sampling for contract change order negotiations
[AD-A184170] 04 p0500 N88-13080
NASA (National Aeronautics and Space Administration) procurement. The 1973 space shuttle solid rocket motor contractor selection
[PB88-135264] 11 p1447 N88-18623
The impact of independent research and development regulations on companies not required to negotiate advanced independent research and development agreements
[AD-A190007] 15 p2147 N88-22818

CONTRACTION
On the relations between cyclic contraction ratio, flow stress, and deformation mechanisms in bainitic CrMoV steels
[VTT-36] 01 p0025 N88-10158
Cardiac contractility in weightlessness according to spatial ballistocardiography 07 p0890 N88-15393
On hypercontractivity of alpha-stable random variables, 0 less than alpha less than 2
[AD-A186425] 07 p0915 N88-15559
Contraction design for small low-speed wind tunnels
[NASA-CR-182747] 15 p2021 N88-22045

CONTRACTORS
A method for assessing the software engineering capability of contractors: Preliminary version
[AD-A187230] 10 p1388 N88-18290
A comparison of projection methods in the forecasting of overhead costs for seven government aerospace contractors
[AD-A187572] 10 p1425 N88-18514

CONTRACTS
NT INSURANCE (CONTRACTS)
A comparison of the basket method and the stratified random sampling for contract change order negotiations
[AD-A184170] 04 p0500 N88-13080
The appropriate use of contract types in development contracts (a systems approach with emphasis on the European space sector)
[ESA-STR-222] 08 p1092 N88-16573
Selling to NASA
[NASA-TM-89724] 12 p1705 N88-20208
Defense Small Business Innovation Research Program (SBIR). Volume 3: Air Force abstracts of phase 1 awards, 1987 17 p2448 N88-24548
Contracts 22 p3160 N88-28810

CONTRAROTATING PROPELLERS
Noise of a model high speed counterrotation propeller at simulated takeoff/approach conditions (F7/A7)
[NASA-TM-100206] 01 p0091 N88-10592
Summary of low-speed wind tunnel results of several high-speed counterrotation propeller configurations
[NASA-TM-100945] 18 p2458 N88-24597

CONTRAST
NT IMAGE CONTRAST
Contrast between the chemical, structural and electronic properties of thin films of Cu and Ni on the Ru(0001) surface
[DE88-002360] 07 p0938 N88-15698
Visual contrast sensitivity functions obtained from untrained observers using tracking and staircase procedures
[AD-A187715] 11 p1522 N88-19089
Brightness contrast and character height of five flat panel computer displays
[AD-A187743] 11 p1524 N88-19096
Auger electron spectroscopy of contrast-forming layers on metals
[NASA-TT-20182] 16 p2178 N88-22980

CONTROL
Conceptual issues in measuring the behavior of a distributed real-time process-control computer system
[DE87-009748] 05 p0638 N88-13898
Conceptual issues in measuring the behavior of a distributed real-time process-control computer system
[DE87-014251] 05 p0638 N88-13899
Controlling XeCl-laser by means of external signal with less than 2 W/cm (sup)2 intensity
14 p1972 N88-21768
Pulse duration control of XeCl*-laser by means of plasma shutter 14 p1973 N88-21774

CONTROL BOARDS
Quantifying some information processing aspects of the pilot's instrument crosscheck
[AD-A186114] 07 p0898 N88-15443
Design of a velocity and position control laboratory servo system
[AD-A186596] 08 p0990 N88-15997

CONTROL DEVICES
U CONTROL EQUIPMENT

CONTROL EQUIPMENT
NT CONTROL STICKS
NT CRYOSTATS
NT PRESSURE REGULATORS
NT SPEED REGULATORS
NT TELEOPERATORS
Optimal control of windpowered plants
[FOA-C-20610-2.7] 08 p1022 N88-16188
Ergonomics of car controls for disabled people, phase 1. Part 1: Chapters 1-7. Part 2: Appendices. Part 3: References
[ISBN-0-947767-82-7] 09 p1202 N88-17204
The KATE shell: An implementation of model-based control, monitor and diagnosis 09 p1210 N88-17255
A fiber-optic link for pressure control of ion sources
[DE88-001782] 09 p1248 N88-17484
Symmetries in nonlinear control systems and their applications 11 p1496 N88-18929
Western aeronautical test range real-time graphics software package MAGIC
[NASA-TM-100425] 13 p1757 N88-20506
Full electronic control system for diesel engine
16 p2185 N88-23025
An integrated on-chip pressure sensor for accurate control applications 19 p2671 N88-25880

CONTROL MOMENT GYROSCOPES
Equal-modulus vector programmed frequency control of minimally redundant structure of powered single-degree-of-freedom gyroscopes for spacecraft attitude control system 02 p0159 N88-10994
Gyrostabilizer system of Kvant module
08 p1006 N88-16099
SIRTF nod maneuvers
[NASA-TM-101007] 22 p3048 N88-28085
An approach to CMG steering using feedback linearization
[NASA-CR-183172] 24 p3422 N88-30369

CONTROL PANELS
U CONTROL BOARDS

CONTROL RODS
SP-100 system modeling: SNPSAM update
17 p2417 N88-24372

CONTROL SIMULATION
A simulation study of a speed control system for autonomous on-road operation of automotive vehicles
[AD-A184030] 03 p0362 N88-12279
Thermal structural control modelling techniques --- spacecraft
[FOK-TR-R-86-030] 08 p0962 N88-15828
Use of a general control simulation program to evaluate HVAC control stability
[DE88-000476] 08 p0975 N88-15896
Control variate selection for multiresponse simulation
[AD-A186637] 08 p1069 N88-16463
Flight test technique, illustrated by Advanced Technologies Testing Aircraft System (ATTAS)
09 p1240 N88-17433
Preliminary design of the ORION attitude control system
[AD-A187179] 10 p1292 N88-17729
Perception and control of simulated self motion
[AD-A187444] 10 p1372 N88-18188
A comparative survey of mathematical models for dynamic simulation of in-orbit manipulation operations
12 p1592 N88-19533
Dynamics modeling, simulation, and control of a spacecraft/manipulator system
12 p1592 N88-19534
Design of a spherical air bearing simulator for tests of the attitude control system of artificial satellites
[INPE-4284-PRE/1155] 12 p1595 N88-19551
Active vibration control of a cantilevered beam with three elastic coordinates
[AD-A188824] 12 p1636 N88-19797
Integrated autopilot/autothrottle based on a total energy control concept: Design and evaluation of additional autopilot modes
[NASA-CR-4131] 13 p1724 N88-20308
F-16 simulator for man-in-the-loop testing of aircraft control systems (SIMTACS)
[AD-A189675] 14 p1870 N88-21178
A packet-switched wide-area communication network simulator
[FUB-3-1986] 14 p1905 N88-21381
Multiple model parameter adaptive control for in-flight simulation
[AD-A190568] 15 p2021 N88-22044
Models describing muscle behavior and control
[LR-522] 16 p2238 N88-23368
The biomorphic model of the human operator controlling a single or a double integrator
[LR-505] 16 p2243 N88-23402
A queueing network model for analyzing a class of branch and bound algorithms on a master-slave architecture
[CWI-OS-R8717] 16 p2249 N88-23441
A software design tool for the analysis of robot dynamics properties
[NLR-MP-86064-U] 17 p2385 N88-24171
Four-axis side-arm flight control simulator investigation
[AD-A196026] 24 p3409 N88-30294

CONTROL STABILITY
Extensions of the small mu test for robust stability
[OUEL-1666/87-REV] 02 p0223 N88-11406
Survey on large scale system control methods
[NASA-CR-181556] 05 p0554 N88-13374
Equivalence of input-output stability and exponential stability for infinite dimensional systems
[TW-276] 05 p0638 N88-13903
Use of a general control simulation program to evaluate HVAC control stability
[DE88-000476] 08 p0975 N88-15896
A direct approach to almost disturbance and almost input-output decoupling
[MEMO-641] 08 p1072 N88-16471
Microscopic control of metallization stability
[AD-A187553] 10 p1421 N88-18487
Control test and validation for a large diameter high stability centrifuge 12 p1577 N88-19437

Modelling and control of an annular momentum control device
[NASA-CR-4138] 13 p1754 N88-20491
Mode priming in an overmoded gyrotron oscillator
[AD-A189151] 13 p1772 N88-20602
Systolic determination of absolute stability in feedback control systems
[OUEL-1704/87] 14 p1962 N88-21705
Boundary stabilization of the reaction-diffusion equation with unilateral conditions
[RR-315] 14 p1964 N88-21720
Servo-actuator control for sampled-data feedback disturbance rejection --- helicopters
[ESA-TT-1002] 16 p2163 N88-22903
Feedback decoupling and stabilization for linear systems with multiple exogenous variables
[ETN-88-92245] 16 p2255 N88-23474
Control law parameterization for an aeroelastic wind-tunnel model equipped with an active roll control system and comparison with experiment
[NASA-TM-100593] 17 p2308 N88-23807

CONTROL STICKS
Steering mechanism --- vehicles
[EP-PATENT-0-181-700-A1] 01 p0053 N88-10338
F-16 control stick response during +Gz-induced loss of consciousness
[AD-A184107] 04 p0400 N88-12491

CONTROL SURFACES
NT AILERONS
NT FLAPS (CONTROL SURFACES)
NT GUIDE VANES
NT JET FLAPS
NT JET VANES
NT LEADING EDGE FLAPS
NT RUDDERS
NT SPOILERS
NT TABS (CONTROL SURFACES)
NT TRAILING EDGE FLAPS
NT UPPER SURFACE BLOWN FLAPS
NT VORTEX FLAPS
NT WING FLAPS
Experimental aerothermodynamic research of hypersonic aircraft
[NASA-CR-181533] 04 p0399 N88-12483
Effectiveness of various control surfaces in quasi-steady and unsteady conditions
[AGARD-R-735] 10 p1284 N88-17682
Design of an aeroelastic composite wing wind tunnel model
[AD-A188855] 12 p1582 N88-19466
Multivariable control law design for the AFTI/F-16 with a failed control surface using a parameter-adaptive controller
[AD-A189848] 15 p2020 N88-22040
Stability and control methodology for conceptual aircraft design. Volume 1: Methodology manual
[AD-A191314] 16 p2164 N88-22906
Steady and unsteady transonic pressure measurements on a clipped delta wing for pitching and control-surface oscillations
[NASA-TP-2594] 23 p3173 N88-28895

CONTROL SYSTEMS
U CONTROL

CONTROL SYSTEMS DESIGN
The method of rigid armature flux orientation for the field-oriented control of highly dynamic drives with synchronous machines
[ETN-87-90405] 01 p0042 N88-10269
The design of a turboshaft speed governor using modern control techniques
[NASA-CR-175046] 01 p0053 N88-10339
Augmenting the control of a flexible manipulator with passive mechanical damping 01 p0055 N88-10350
Improvements to the precision pan and tilt head
[RSRE-MEMO-3996] 01 p0057 N88-10365
Adaptive control of hydraulic devices
[FB-1/85] 01 p0084 N88-10543
Digital algorithms for the control and dynamic decoupling of industrial robot axes
[ETN-87-90441] 01 p0084 N88-10546
Fiber optic engineering sensor system. Preliminary program management plan, phase 3 revision
[AD-A183663] 01 p0093 N88-10608
A survey of aircraft integrated control technology
[AR-004-561] 02 p0126 N88-10794
A preliminary investigation into the feasibility of implementing a direct sideforce control system on the Astra Hawk by means of an active control surface --- aircraft control
[ETN-87-90924] 02 p0126 N88-10795
Fault tolerant considerations and methods for guidance and control systems
[AGARD-AG-289] 02 p0126 N88-10796
Flight test of a resident backup software system
02 p0128 N88-10805
Investigation of control law for active flutter suppression
[NASA-TT-20126] 02 p0130 N88-10818
A treatment of jw-axis model-matching transformation zeros in the optimal H squared and H infinity control designs
[OUEL-1673/87] 02 p0223 N88-11407
Control and stabilization mechanisms of submunitions
[DFVLR-IB-111-86/9] 03 p0259 N88-11630
Theoretical and experimental study of flow-control devices for inlets of indraft wind tunnels
03 p0268 N88-11684
Control design challenges of large space systems and spacecraft control laboratory experiment (SCOLE)
[NASA-CR-178392] 03 p0275 N88-11735
Wavefront error sensing
[NASA-CR-181504] 03 p0321 N88-12030
A scientific workstation operator-interface for accelerator control
[DE87-014689] 03 p0362 N88-12278
Space station resistojet system requirements and interface definition study
[NASA-CR-180832] 04 p0409 N88-12541
US Naval Air Force avionic and electrical system corrosion prevention and control maintenance
05 p0547 N88-13334
Development of an interface for an ultrareliable fault-tolerant control system and an electronic servo-control unit
[NASA-TM-88236] 05 p0553 N88-13367
Survey on large scale system control methods
[NASA-CR-181556] 05 p0554 N88-13374
Design of low order controllers for robust disturbance rejection in large space structures
[AD-A185202] 05 p0555 N88-13376
Plant Growth Module (PGM) conceptual design
05 p0631 N88-13855
Behavioral Architecture Robot Control System (BARCS): A new way of building robots
[REPT-87-036] 05 p0638 N88-13902
Balanced realizations: Canonical form, parametrization, model reduction
[PB87-123360] 06 p0757 N88-14642
Knowledge acquisition for a simple expert controller
[NASA-TT-20118] 06 p0761 N88-14672
An autopilot design for the United States Marine Corps' airborne remotely operated device
[AD-A186379] 07 p0820 N88-14983
Advanced helicopter cockpit and control configurations for helicopter combat missions
[NASA-TM-100017] 07 p0821 N88-14988
Faraday cup characterization of electron beam welding parameters
[DE88-001896] 07 p0[illegible] N88-15241
Scientific research in the field of measurement and control technology
[SMBT-322] 07 p0907 N88-15493
A weighting sequence approach to the analysis and design of multivariable control systems
[AD-A186086] 07 p0917 N88-15570
Aeropropulsion '87. Session 2: Aeropropulsion Structures Research
[NASA-CP-10003-SESS-2] 08 p0954 N88-15785
Aeropropulsion '87. Session 4: Instrumentation and Controls Research
[NASA-CP-10003-SESS-4] 08 p0955 N88-15794
Directions in propulsion control
08 p0956 N88-15799
Supersonic STOVL propulsion technology program: An overview 08 p0957 N88-15808
Design of a velocity and position control laboratory servo system
[AD-A186506] 08 p0990 N88-15997
Clips as a knowledge based language
08 p1055 N88-16365
An innovative workstation 08 p1063 N88-16421
Neural networks as a possible architecture for the distributed control of space systems
08 p1064 N88-16431
Aircraft flight test trajectory control
[NASA-CR-179428] 09 p1120 N88-16707
Multisurface control mechanism for a deployable antenna: Far Infrared and Submillimeter Space Telescope (FIRST) technology study
[RP-FA-D003] 09 p1135 N88-16807
Design of a gas mass flow control system for the gas inlet installation of a solid fuel combustion chamber
[VTH-LR-471] 09 p1141 N88-16839
A control system for maintaining high stability in gas pressure
[DE88-003712] 09 p1175 N88-17042
Adaptive proximate time-optimal servomechanisms
09 p1175 N88-17043
A formal approach to validation and verification for knowledge-based control systems
09 p1207 N88-17233
Crew interface with a telerobotic control station
09 p1213 N88-17273
A method for designing robust multivariable feedback systems
[NASA-CR-182459] 09 p1225 N88-17341
Navigation planning using quadtrees
[DE88-003706] 09 p1225 N88-17343
Applications of nonlinear systems theory to control design
[NASA-CR-182485] 09 p1231 N88-17377
The impact of circulation control on rotary aircraft controls systems 10 p1271 N88-17601
Sensitivity of active vibration control to structural changes and model reduction 10 p1284 N88-17683
An application of eigenspace methods to symmetric flutter suppression
[NASA-CR-181618] 10 p1284 N88-17684
Light Electronic Control System (LECOS): A proposal for a interconnected error-tolerant, optoelectronic control system
[MBB-UT-004/87] 10 p1311 N88-17836
Active control technology with adaptive control concept in the aircraft construction
[MBB/LKE-294/S/PUB/295] 10 p1313 N88-17845
Local bifurcation control
[AD-A187435] 10 p1324 N88-17915
Joint services electronics program
[AD-A187587] 10 p1325 N88-17920
NASA/NBS (National Aeronautics and Space Administration/National Bureau of Standards) standard reference model for Telerobot Control System Architecture (NASREM)
[PB88-124773] 10 p1336 N88-17999
Study on a rotor speed control system for a horizontal axis windmill
[NAL-TR-931] 10 p1349 N88-18062
Parallels between control PDE's (Partial Differential Equations) and systems of ODE's (Ordinary Differential Equations)
[NASA-CR-182487] 10 p1396 N88-18331
On observer problems for systems governed by partial differential equations
[AD-A187430] 10 p1400 N88-18351
Further developments in exact state reconstruction in deterministic digital control systems
[NASA-TP-2812] 11 p1468 N88-18751
Optical links in the angle-data assembly of the 70-meter antennas 11 p1474 N88-18792
Optically controlled phased-array antenna technology for space communication systems
[NASA-TM-100852] 11 p1476 N88-18809
Construction of control systems with diversified redundancy for electrical machines
[BIA-5/86] 11 p1481 N88-18842
Time varying controller design for robot manipulator control
[AD-A188094] 11 p1494 N88-18915
Motion planning and control of robot manipulators via application of a computer graphics animated display
11 p1496 N88-18932
Design for performance enhancement in feedback control systems with multiple saturating nonlinearities
[NASA-CR-182614] 11 p1535 N88-19168
Control test and validation for a large diameter high stability centrifuge 12 p1577 N88-19437
Interaction between structural considerations and system design in advanced flight controls
12 p1580 N88-19458
Presentation of flight control design and handling quality commonality by separate surface stability augmentation for the family of commuter airplanes
[NASA-CR-182567] 12 p1583 N88-19471
Output aiming control
[AD-A188463] 12 p1583 N88-19473
On a knowledge based assisted system for highly autonomous control of experiment-manipulators in the Man-Tended Free Flyer 12 p1588 N88-19505
A knowledge-based approach for sensory-controlled assembly operations 12 p1588 N88-19506
Intelligent on board control for field emission electric propulsion system 12 p1589 N88-19513
Promising concepts for ground-to-orbit experiment teleoperation --- Columbus 12 p1590 N88-19518
Ground based supervisory and programming system for automatic experiment execution in orbit
12 p1590 N88-19519
Design of a spherical air bearing simulator for tests of the attitude control system of artificial satellites
[INPE-4284-PRE/1155] 12 p1595 N88-19551
Table with aerostatic bearings for simulation in one degree of freedom attitude control systems of artificial satellites
[INPE-4272-PRE/1144] 12 p1595 N88-19552
Advances in Air-Launched Weapon Guidance and Control
[AGARD-CP-431] 12 p1596 N88-19553

Automatic flight control system for modern helicopters
12 p1597 N88-19556

Speed control of a missile with throttleable ducted rocket propulsion 12 p1597 N88-19561

The use of hardware-in-the-loop-techniques in the development of a modern air-to-surface missile system
12 p1597 N88-19562

Reaction wheel control through digital technique using reference models
[INPE-4220-PRE/1100] 12 p1599 N88-19570

Analysis of the sensitivity of the attitude control system of an artificial satellite
[INPE-4285-PRE/1157] 12 p1599 N88-19573

Cold gas jet system for satellite attitude control-modeling and simulation
[INPE-4279-PRE/1150] 12 p1601 N88-19583

An analysis of DREO's (Defence Research Establishment Ottawa) analog rebalance loops for the CSG-2 (Canadian Strapdown Gyroscope) tuned-rotor gyroscope
[AD-A188577] 12 p1629 N88-19749

Low cost mobile robot
[AD-A188507] 12 p1633 N88-19778

Design of feedback control systems for stable plants with saturating actuators
[NASA-CR-182613] 12 p1681 N88-20050

Control augmented structural synthesis
[NASA-CR-4132] 13 p1721 N88-20290

Integrated autopilot/autothrottle based on a total energy control concept: Design and evaluation of additional autopilot modes
[NASA-CR-4131] 13 p1724 N88-20308

Computer-aided transformation of descriptive mode of mathematical models of a control system
13 p1756 N88-20503

Numerical methods in the resolution of control electrovalve model
[INPE-4154-RPE/540] 13 p1764 N88-20554

Control of structure in turbulent flows: Bifurcating and blooming jets
[AD-A189607] 13 p1766 N88-20562

Feasibility demonstration of a sensor for high-quality two-phase flow --- Space Station
[NLR-TR-87009-U] 13 p1767 N88-20569

Control strategies and hardware used in solar thermal applications
[DE88-004631] 13 p1794 N88-20731

Robust decentralized control of large flexible structures
[DE88-005416] 13 p1824 N88-20902

Using trace theory to model discrete events
[CS-8708] 13 p1824 N88-20904

Performance improvements of an F-15 airplane with an integrated engine-flight control system
[NASA-TM-100431] 14 p1867 N88-21159

Towards a practical microgravity environment --- isolation mount 14 p1878 N88-21223

Development and qualification of the OLYMPUS antenna pointing mechanism 14 p1879 N88-21227

A joint actuator design for a robotic manipulator
14 p1879 N88-21232

Modelling of a hydraulic motor and servo-valve to produce a desired system response using analogue and digital compensation techniques
[ETN-88-92079] 14 p1899 N88-21337

Development of a total electric vehicle drive system
[DE88-900367] 14 p1917 N88-21446

Development of a magnetically suspended, tetrahedron-shaped antenna pointing system
14 p1926 N88-21478

Practical considerations for structural control: System uncertainty, system time delay and truncation of small control forces
[PB88-163738] 14 p1933 N88-21526

Improving the man-machine interface to robotic systems
[NPL-DITC-100/87] 14 p1953 N88-21641

A new approach to almost decoupling problems for linear and nonlinear systems
[MEMO-660] 14 p1962 N88-21700

polynomial approach to the H sub infinity control design method
[MEMO-662] 14 p1962 N88-21701

A state-space approach to super-optimal H sup infinity control problems
[OUEL-1690/87] 14 p1962 N88-21702

Systolic determination of absolute stability in feedback control systems
[OUEL-1704/87] 14 p1962 N88-21705

Linear state space modeling of a turbofan engine
[AD-A190110] 15 p2019 N88-22035

Design of an integrated control system for flutter margin augmentation and gust load alleviation, tested on a dynamic windtunnel model
[PB88-149685] 15 p2020 N88-22038

Application of eigenstructure assignment techniques in the design of a longitudinal flight control system
[AD-A189644] 15 p2020 N88-22039

Telerobotic operation of conventional robot manipulators
[DE88-005718] 15 p2073 N88-22363

Representation, analysis and design of multirate discrete-time control systems
[AD-A190499] 15 p2116 N88-22608

Optical switching and control techniques using nonlinear optical wave mixing
[AD-A190467] 15 p2134 N88-22730

Development of a mobile research flight test support capability
[NASA-TM-100428] 16 p2159 N88-22883

Basic design of a flight director system for NAL STOL research aircraft
[DE88-751806] 16 p2162 N88-22897

Analysis and design of gain scheduled control systems
[NASA-CR-182867] 16 p2163 N88-22904

An investigation of the ability to recover from transients following failures for single-pilot rotorcraft
[NASA-TM-100078] 16 p2164 N88-22905

Microgravity robotics technology program
[NASA-TM-100898] 16 p2215 N88-23219

Integrated multidisciplinary analysis tool IMAT users' guide
[NASA-TM-100605] 16 p2223 N88-23273

Distributed matchmaking
[CWI-CS-R8750] 16 p2254 N88-23467

Contribution to the adaptive dynamic control of a robot manipulator
[LAAS-87-350] 16 p2255 N88-23475

Identification of control structures --- expert systems
[REPT-87-66] 16 p2255 N88-23479

Investigation of air transportation technology at Princeton University, 1986 17 p2294 N88-23724

Control law parameterization for an aeroelastic wind-tunnel model equipped with an active roll control system and comparison with experiment
[NASA-TM-100593] 17 p2308 N88-23807

Soviet spacecraft engineering research
[FASAC-TAR-3090] 17 p2311 N88-23823

Impact of control errors on the volume/weight demand of the Ventilation and Dryer (VAD) concept --- EURECA Botany Facility
[TN-RB524-006/87] 17 p2377 N88-24132

An algorithm for super-optimal H sup inf design: The 2-block case
[OUEL-1711/87] 17 p2391 N88-24210

A state-space approach to discrete-time super-optimal H sup inf control problems
[OUEL-1712/87] 17 p2391 N88-24211

Precise computer controlled positioning of robot end effectors using force sensors
[NASA-CR-182887] 17 p2391 N88-24213

The calculation of casually constrained optima in the active control of sound
[ISVR TR-147] 17 p2395 N88-24237

Safety constraints and considerations in the development of nuclear powered propulsion
17 p2401 N88-24276

Two-phase fluid management for a Rankine cycle isotope power system 17 p2405 N88-24303

Interaction of the control system with core nuclear design for fast spectrum space power reactors
17 p2405 N88-24304

Reactor instrumentation and control design and performance simulation for SP-100
17 p2406 N88-24306

An adaptive load-following control system for a space nuclear power system 17 p2406 N88-24307

SP-100 control system modeling
17 p2414 N88-24356

Automatic reactor control system for transient operation 17 p2436 N88-24493

An optimal disturbance rejection control system for multimegawatt space nuclear power systems
17 p2436 N88-24495

SP-100 ground engineering systems test facility control systems 17 p2436 N88-24496

Analysis and design of detection filters within closed-loop systems 18 p2525 N88-24980

Vibration protection of inelastic structures by means of active and passive control 18 p2528 N88-25001

The efficacy of using human myoelectric signals to control the limbs of robots in space
[NASA-CR-182901] 18 p2553 N88-25155

Electronic controller for reciprocating rotary crystallizer
[NASA-TM-101140] 18 p2584 N88-25354

Sensors for process control requirements for design and test 19 p2671 N88-25877

Analysis of the electrical harmonic characteristics of a slip recovery variable speed generating system for wind turbine applications
[DE88-001140] 19 p2687 N88-25972

ELIT: An autonomous underwater observation robot
19 p2699 N88-26048

Automation tools for demonstration of goal directed and self-repairing flight control systems
[NASA-CR-179433] 19 p2715 N88-26121

Stable discrete-time adaptive control
19 p2719 N88-26142

Adaptive residual mode filter control of distributed parameter systems for large space structure applications
19 p2719 N88-26143

Model reduction methods for control design
[NASA-CR-179434] 19 p2719 N88-26144

Computer simulation of multiple pilots flying a modern high performance helicopter
[NASA-TM-100183] 20 p2761 N88-26377

A reusable rocket engine intelligen control
[NASA-TM-100963] 20 p2766 N88-26401

Nonlinear identification of an aircraft for the direct calculation of an anticipatory control
20 p2787 N88-26535

Design of a controller to reduce residual vibration in the positioning control of flexible robotic manipulators
20 p2808 N88-26658

An introduction to robot joint control methods
[NLR-TR-86080-U] 20 p2811 N88-26677

Expert system application education project
[NASA-CR-183089] 20 p2843 N88-26867

Numerical optimization, system theoretic and software tools for the integrated design of flexible structures and their control systems
[AD-A192927] 21 p2895 N88-27183

Thermal-sensation control: A new method of controlling cooled/heated environments 21 p2930 N88-27394

A conceptual design study of a hovering system controller for an autonomous underwater vehicle
[AD-A193423] 21 p2930 N88-27399

The robust tracking control of nonlinear systems with uncertain dynamics 21 p2999 N88-27788

A PRELUDE (analysis and design of control systems-preliminary utilities depository): A data-based interactive system of control software, user's guide
[DFVLR-MITT-88-12] 21 p3000 N88-27795

More on exact state reconstruction in deterministic digital control systems
[NASA-TP-2847] 22 p3063 N88-28177

Strawman Optical Reception Development Antenna (SORDA) 22 p3065 N88-28187

DSS 13 microprocessor antenna controller
22 p3066 N88-28192

A computer-aided approach to nonlinear control synthesis
[NASA-CR-179391] 22 p3140 N88-28673

Design of multirate control systems via parameter optimization
[REPT-87-013] 22 p3142 N88-28686

Robust design of cascade control
[REPT-88-006] 22 p3142 N88-28687

Study of standard generic approach for spacecraft (S/C) autonomy and automation (phase 3). Book A: Autonomy concept description
[ESA-CR(P)-2555-VOL-1] 23 p3185 N88-28955

Study of standard generic approach for spacecraft (S/C) autonomy and automation (phase 3). Book B: Autonomy concept application example
[ESA-CR(P)-2555-VOL-2] 23 p3185 N88-28956

Study of standard generic approach for spacecraft (S/C) autonomy and automation (phase 3). Book C: Autonomy concept summary
[ESA-CR(P)-2555-VOL-3] 23 p3185 N88-28957

Study on design and control of torque-controlled manipulators
[NASA-TT-20197] 23 p3223 N88-29183

Distributed cooperating processes in a mobile robot control system 23 p3256 N88-29386

Concepts for robot motion primitives required for space station teleoperations 23 p3257 N88-29387

Generic supervisor: A knowledge-based tool for control of space station on-board systems
23 p3257 N88-29389

Programming model for distributed intelligent systems
23 p3257 N88-29390

Blackboard architectures and their relationship to autonomous space systems 23 p3261 N88-29414

Real-time space system control with expert systems
23 p3262 N88-29419

Computer-Aided-Control Engineering (CACE) primitives for robust and adaptive control systems, phase 1
[AD-A192446] 23 p3265 N88-29439

Space structure (dynamics and control) theme development
[NASA-TM-100597] 24 p3335 N88-29850

Aircraft battery state of charge and charge control system
[AD-A194979] 24 p3367 N88-30052

ARC length control for plasma welding
[NASA-CASE-MSC-20900-1] 24 p3380 N88-30131

Robust design of distributed controllers for large flexible space structures
[NASA-CR-183202] 24 p3380 N88-30134

The design of an intelligent multidisk control module for VME bus based systems
[AD-A195587] 24 p3411 N88-30303

A shared-world conceptual model for integrating space station life sciences telescience operations
24 p3416 N88-30333

Artificial intelligence in a mission operations and satellite test environment 24 p3416 N88-30334

Automated space vehicle control for rendezvous proximity operations 24 p3416 N88-30335

Automated satellite control in Ada
24 p3416 N88-30336

Low level image processing techniques using the pipeline image processing engine in the flight telerobotic servicer 24 p3418 N88-30346

CONTROL THEORY

The associative memory ME7
[ESA-TT-1033] 01 p0079 N88-10506

A survey of aircraft integrated control technology
[AR-004-561] 02 p0126 N88-10794

A treatment of jw-axis model-matching transformation zeros in the optimal H squared and H infinity control designs
[OUEL-1673/87] 02 p0223 N88-11407

On the control of a compliant robot arm
03 p0332 N88-12095

Identification of linear structural models
03 p0337 N88-12121

Analytical investigation of the dynamics of tethered constellations in Earth orbit (phase 2)
[NASA-CR-179218] 04 p0408 N88-12533

Natural control of flexible space structures
04 p0408 N88-12534

A modern control theory based algorithm for control of the NASA/JPL 70-meter antenna axis servos
04 p0436 N88-12706

Survey on large scale system control methods
[NASA-CR-181556] 05 p0554 N88-13374

Error control techniques for satellite and space communications
[NASA-CR-181581] 05 p0576 N88-13516

Trajectory control of robot manipulators with closed-kinematic chain mechanism
[NASA-TM-89305] 05 p0591 N88-13605

Control of an unstable launcher in atmospheric flight using minimax optimal control laws
[SNIAS-872-422-107] 05 p0638 N88-13901

Equivalence of input-output stability and exponential stability for infinite dimensional systems
[TW-276] 05 p0638 N88-13903

On linear periodic controllers
[DE87-011174] 05 p0639 N88-13904

Balanced realizations: Canonical form, parametrization, model reduction
[PB87-123360] 06 p0757 N88-14642

Heuristic control of the Utah/MIT dextrous robot hand
06 p0793 N88-14858

Scientific research in the field of measurement and control technology
[SMBT-322] 07 p0907 N88-15493

Simplified self-tuning control algorithms
[OUEL-1657/86] 07 p0907 N88-15494

Optimal observers for ARMA models
[OUEL-1659/86] 07 p0907 N88-15495

Characterization of all controlled invariant sub-spaces for spectral systems
[PB88-106636] 07 p0912 N88-15532

Directions in propulsion control
08 p0956 N88-15799

Design of a velocity and position control laboratory servo system
[AD-A186596] 08 p0990 N88-15997

A modal control based limiting performance formulation for shock excited systems 08 p0998 N88-16046

A direct approach to almost disturbance and almost input-output decoupling
[MEMO-641] 08 p1072 N88-16471

Some aspects of control for semilinear distributed parameter systems
[INPE-4147-PRE/1054] 08 p1075 N88-16484

Helicopter mathematical models and control law development for handling qualities research
09 p1108 N88-16642

Analytical interactive approach for phenomena involving structures, thermal and control aspects. Volume 1: Theory --- spacecraft structures
[ESA-CR(P)-2503-VOL-1] 09 p1134 N88-16803

Analytical interactive approach for phenomena involving structures, thermal, and control aspects. Volume 2: Toward the solution --- spacecraft structures
[ESA-CR(P)-2503-VOL-2] 09 p1134 N88-16804

Analytical interactive approach for phenomena involving structures, thermal, and control aspects. Volume 3: Executive summary --- spacecraft structures
[ESA-CR(P)-2503-VOL-3] 09 p1134 N88-16805

Adaptive proximate time-optimal servomechanisms
09 p1175 N88-17043

Feedback stabilization of distributed systems
[AD-A187111] 09 p1222 N88-17328

Regulation of nonlinear and generalized linear systems
[AD-A186706] 09 p1224 N88-17338

Boundary stabilization of thin elastic plates
[AD-A187123] 10 p1343 N88-18025

Nonlinear filtering and large deviations: A PDE-Control theoretic approach
[AD-A187436] 10 p1396 N88-18321

Boundary value problems for differential and functional differential equations
[AD-A187378] 10 p1400 N88-18349

Viscosity methods in optimal control of distributed systems
[AD-A188086] 10 p1401 N88-18357

Time varying controller design for robot manipulator control
[AD-A188094] 11 p1494 N88-18919

Kinematic and dynamic analyses of the Stanford/JPL robot hand
[DE88-004637] 11 p1495 N88-18923

Analysis and synthesis of two degrees of freedom control systems 11 p1495 N88-18928

Optimal control theory of load-following and parameter-tracking of nonlinear systems: An application of Pontryagin Maximum Principle to reactor dynamics
[DE88-004770] 11 p1532 N88-19152

Nonlinear input-output systems
[NASA-CR-182464] 11 p1535 N88-19171

Output aiming control
[AD-A188463] 12 p1583 N88-19473

Safe and fuel minimum reference trajectories for closed loop controlled approaches --- space stations
12 p1585 N88-19488

Computational aspects of robotic experiment manipulation in a microgravity environment
12 p1589 N88-19512

Dynamics modeling, simulation, and control of a spacecraft/manipulator system
12 p1592 N88-19534

Attitude control of an artificial satellite through the extension of the linear quadratic regulator theory
[INPE-4407-TDL/304] 12 p1600 N88-19577

Integrated autopilot/autothrottle based on a total energy control concept: Design and evaluation of additional autopilot modes
[NASA-CR-4131] 13 p1724 N88-20306

Using trace theory to model discrete events
[CS-8708] 13 p1824 N88-20904

An efficient gradient projection optimization scheme for a seven-degree-of-freedom redundant robot with spherical wrist
[DE88-005440] 14 p1919 N88-21453

A new approach to almost decoupling problems for linear and nonlinear systems
[MEMO-660] 14 p1962 N88-21700

A polynomial approach to the H sub infinity control design method
[MEMO-662] 14 p1962 N88-21701

A complexity transform for NP-complete problems
[OUEL-1708/87] 14 p1962 N88-21703

Bilinear systems in the frequency domain and an application to optimal control
[RR-320] 14 p1962 N88-21704

Parametric methods of analysing linear and nonlinear systems
[RR-315] 14 p1967 N88-21741

Model selection for the multiple model adaptive algorithm for in-flight simulation
[AD-A189715] 15 p2016 N88-22022

Multivariable control law design for the AFTI/F-16 with a failed control surface using a parameter-adaptive controller
[AD-A189848] 15 p2020 N88-22040

Wave propagation and dynamics of lattice structures
[AD-A190037] 15 p2025 N88-22066

Telerobotic operation of conventional robot manipulators
[DE88-005718] 15 p2073 N88-22363

Instrumentation for scientific computing in neural networks, information science, artificial intelligence and applied mathematics
[AD-A189981] 15 p2106 N88-22549

Insertions using geometric analysis and hybrid force-position control: Method and analysis
[DE87-013652] 15 p2117 N88-22611

Information capacity of Gaussian channels
[AD-A190316] 15 p2127 N88-22686

Feedback decoupling and stabilization for linear systems with multiple exogenous variables
[ETN-88-92245] 16 p2255 N88-23474

Identification of control structures --- expert systems
[REPT-87-66] 16 p2255 N88-23479

Derivative arrays, geometric control theory and realizations of linear descriptor systems
[AD-A190682] 16 p2260 N88-23513

Error control techniques for satellite and space communications
[NASA-CR-182886] 17 p2332 N88-23922

Generalized predictive control of multivariable systems
[OUEL-1640/86] 17 p2391 N88-24209

Experimental evaluation of the MIT-SNL period-generated minimum time control laws for the rapid adjustment of reactor power 17 p2436 N88-24494

Attitude control laws for gas-jet spacecraft
18 p2467 N88-24643

Estimation and control of distributed models for certain elastic systems arising in large space structures
[AD-A192120] 18 p2472 N88-24666

A feedback linearization approach to spacecraft control using momentum exchange devices
[NASA-CR-172057] 18 p2472 N88-24668

Dynamics of a flexible orbiting platform with MRMS
[ISSN-0285-6808] 18 p2473 N88-24673

Automatic feedback control of a rigid body for finite displacements 18 p2473 N88-24674

The coordination of multiple robotic manipulators
[AD-A190869] 18 p2522 N88-24963

Real-time implementation of a kinematic optimization scheme for seven-degree-of-freedom redundant robots with spherical wrists
[DE88-006785] 18 p2524 N88-24974

Mixed min-max optimization problem with restrictions
18 p2565 N88-25232

Structural properties of multivariable linear systems
[PB88-181375] 19 p2717 N88-26134

Stable discrete-time adaptive control
19 p2719 N88-26142

An introduction to robot joint control methods
[NLR-TR-86080-U] 20 p2811 N88-26677

The analysis and control of robotic manipulators operating at or near kinematically singular configurations
22 p3064 N88-28315

On the pseudo-linearization problem for nonlinear systems
[AD-A194021] 22 p3142 N88-28683

Gravitation control 22 p3158 N88-28795

Convex duality approach to the optimal control of diffusions
[AD-A194535] 23 p3266 N88-29442

Canonical forms in the control of DPS
[AD-A194671] 23 p3270 N88-29461

Minimizing escape probabilities: A large deviations approach
[AD-A194534] 23 p3275 N88-29496

Feedback stabilization of du/dt = Au + bf in Hilbert space when the normalization function is less than or equal to r
[AD-A193510] 23 p3277 N88-29506

Theory of filtering and control with application to control of large space structures
[AD-A195500] 24 p3335 N88-29851

K(sup th)-order extended linearization
[AD-A194786] 24 p3421 N88-30363

Analytical methods in stochastic control and nonlinear filtering
[AD-A194272] 24 p3426 N88-30388

CONTROL UNITS (COMPUTERS)

A timing evaluator for C programs generated by the model system
[AD-A191204] 17 p2385 N88-24174

Design and testing of a luminance and chrominance stabilization system for a computer-controlled color display
[AD-A191922] 18 p2554 N88-25159

An investigation of performance improvement in knowledge-based control systems
21 p2926 N88-27382

CONTROL VALVES

Dynamic modelling of an electromechanical valve using frequency response data
[AD-A187908] 11 p1494 N88-18918

Electromagnetic modeling of a control valve
[INPE-4140-PRE/1046] 12 p1622 N88-19700

Development of a motorized cryovalve for the control of superfluid liquid helium 14 p1925 N88-21477

A pyrotechnical opening valve
[SNIAS-MU/TYS-NT-2-06(0)] 16 p2167 N88-22922

Characterization of accelerating pipe flow
[AD-A193065] 21 p2943 N88-27481

CONTROLLABILITY

Investigation of pilot behavior in a training program for assessing handling qualities using a ground simulator
[ESA-TT-999] 03 p0357 N88-12247

Control of a flexible one-link manipulator
[AD-A185035] 05 p0590 N88-13598

Impact of flying qualities on mission effectiveness for helicopter air combat, volume 1
[NASA-CR-166558] 06 p0669 N88-14100

NASA/Army Rotorcraft Technology. Volume 2: Materials and Structures, Propulsion and Drive Systems, Flight Dynamics and Control, and Acoustics
[NASA-CP-2495-VOL-2] 09 p1106 N88-16632

Helicopter mathematical models and control law development for handling qualities research
09 p1108 N88-16642

Rotorcraft handing-qualities design criteria development 09 p1109 N88-16645

The impact of vertical axis characteristics on helicopter handling qualities
[AD-A188964] 12 p1583 N88-19474

Electron beam sensitive devices for controllability
[RR-658-I] 14 p1908 N88-21403

The effects of torque response and time delay on rotorcraft vertical axis handling qualities
[AD-A189873] 15 p2017 N88-22023

Preliminary airworthiness evaluation of the UH-60A with Advanced Digital Optical Control System (ADOCS)
[AD-A190674] 15 p2018 N88-22030

An investigation of the ability to recover from transients following failures for single-pilot rotorcraft
[NASA-TM-100078] 16 p2164 N88-22905

Advances in Flying Qualities
[AGARD-LS-157] 24 p3314 N88-29735

Advances in flying qualities: Concepts and criteria for a mission oriented flying qualities specification
24 p3314 N88-29739

A second look at MIL prime flying qualities requirements 24 p3314 N88-29740

The optimal control pilot model and applications
24 p3315 N88-29741

The role of simulation in flying qualities and flight control system related development 24 p3315 N88-29742

An analysis of lateral-directional handling qualities and Eigenstructure of high performance aircraft
[AD-A194874] 24 p3326 N88-29814

Minimum-complexity helicopter simulation math model
[NASA-CR-177476] 24 p3326 N88-29819

CONTROLLED ATMOSPHERES

NT CABIN ATMOSPHERES
NT HELIUM-OXYGEN ATMOSPHERES
NT INERT ATMOSPHERE
NT SPACECRAFT CABIN ATMOSPHERES

Fire-related medical science 04 p0406 N88-12525

Performance characteristics of magnesium-sodium nitrate flares in oxygen-nitrogen atmospheres
[AD-A185274] 05 p0570 N88-13476

Fibrous glass aerosols: A literature review
[AD-A188420] 12 p1672 N88-20006

Advancements in oxygen generation and humidity control by water vapor electrolysis
[NASA-CR-172073] 22 p3134 N88-28633

CONTROLLED FUSION

Massachusetts Institute of Technology Plasma Fusion Center: 1986-1987 Report to the President
[DE87-013518] 01 p0101 N88-10661

New directions in Vlasov plasma turbulence and anomalous transport
[DE87-014425] 02 p0238 N88-11500

Applications of neutral beam and rf technologies
[DE87-014936] 03 p0379 N88-12382

Advanced fusion power: A preliminary assessment
[AD-A185903] 07 p0933 N88-15664

Studies on parametric instabilities in high-frequency wave heating of fusion plasmas
[PH-156] 07 p0933 N88-15667

SOAR: Space orbiting advanced fusion power reactor
[AD-A189234] 13 p1732 N88-20356

Helium-3 fusion fuel resources for space power
17 p2410 N88-24330

CONTROLLED STABILITY

U CONTROL

CONTROLLERS

NT SERVOMECHANISMS
NT SERVOMOTORS

Space station propulsion technology: Space station propulsion system test bed test plan
[NASA-CR-179201] 01 p0017 N88-10104

Test of the Hipparcos payload in the Liege vacuum facility focal 02 p0135 N88-10850

A digital control system for high level acoustic noise generation 02 p0138 N88-10865

Minimisation of helicopter vibration through active control of structural response 03 p0264 N88-11662

On the control of a compliant robot arm
03 p0332 N88-12095

Local-optimal control in systems with delay
04 p0424 N88-12627

A modern control theory based algorithm for control of the NASA/JPL 70-meter antenna axis servos
04 p0436 N88-12706

On linear periodic controllers
[DE87-011174] 05 p0639 N88-13904

Intelligent controllers
[DE88-001862] 07 p0904 N88-15475

Evaluation of high-voltage, high-power, solid-state remote power controllers for amps
07 p0924 N88-15612

Space station propulsion technology
[NASA-CR-179260] 08 p0964 N88-15835

Pulse width modulator controller design for a brushless DC motor position servo
[AD-A186618] 08 p0980 N88-15921

Telerobotic controller development
08 p1056 N88-16370

Software simulation of time delay in teleoperation
08 p1056 N88-16371

Task path planning, scheduling and learning for free-ranging robot systems 08 p1058 N88-16386

A framework for real-time distributed expert systems: On-orbit spacecraft fault diagnosis, monitoring and control 08 p1066 N88-16440

Prototype space station automation system delivered and demonstrated at NASA 08 p1066 N88-16442

A control system for maintaining high stability in gas pressure
[DE88-003712] 09 p1175 N88-17042

Computer control of a microgravity mammalian cell bioreactor 09 p1197 N88-17172

Development and experimentation of an eye/brain/task testbed 09 p1205 N88-17219

Expert system applications in spacecraft subsystem controllers 09 p1210 N88-17254

TDAS: The Thermal Expert System (TEXSYS) data acquisition system 09 p1211 N88-17258

A method for designing robust multivariable feedback systems
[NASA-CR-182459] 09 p1225 N88-17341

Pumping systems and flow interfaces for rapid response electronic reheat controls 10 p1282 N88-17665

Possibilities for on-line surge suppression by fast guide vane adjustment in axial compressors
10 p1283 N88-17674

Optically controlled devices and ultrafast laser sources for signal processing
[AD-A187417] 10 p1338 N88-17995

An Ethernet local area network controller with supporting operating system software
[DE88-003534] 10 p1392 N88-18304

The implementation of artificial intelligence in control systems
[DE88-003497] 10 p1396 N88-18318

The representation of knowledge within model-based control systems
[DE88-004863] 10 p1396 N88-18319

The Telecommunications and Data Acquisition Report
[NASA-CR-182545] 11 p1471 N88-18774

New mode switching algorithm for the JPL 70-meter antenna servo controller 11 p1474 N88-18791

The design and implementation of the Technical Facilities Controller (TFC) for the Goldstone deep space communications complex 11 p1474 N88-18794

SETI data controllers 11 p1474 N88-18795

Research on output feedback control
[NASA-CR-182543] 11 p1534 N88-19167

Multi-axis control of telemanipulators
12 p1593 N88-19539

Advances in Air-Launched Weapon Guidance and Control
[AGARD-CP-431] 12 p1596 N88-19553

Speed control of a missile with throttleable ducted rocket propulsion 12 p1597 N88-19561

Practical system for the use of alcohol in diesel engines
[PB88-147863] 12 p1612 N88-19638

NAVLAB: An autonomous navigation testbed
[AD-A189049] 13 p1720 N88-20283

Control of structure in turbulent flows: Bifurcating and blooming jets
[AD-A189607] 13 p1766 N88-20562

Force distribution and trajectory control for closed kinematic chains with applications to walking machines
13 p1779 N88-20642

Industrial electric motors and controllers
[PB88-139589] 14 p1907 N88-21394

Multivariable control law design for the AFTI/F-16 with a failed control surface using a parameter-adaptive controller
[AD-A189848] 15 p2020 N88-22040

Microgravity mechanisms and robotics program
16 p2219 N88-23237

The TMS32010 evaluation module controller --- signal processor
[EUT-86-E-162] 16 p2245 N88-23407

Reconfigurable work station for a video display unit and keyboard
[NASA-CASE-MFS-26009-1-SB]
17 p2382 N88-24163

Connecting remote systems for demonstration of automation technologies 17 p2387 N88-24191

Genetic algorithms for adaptive real-time control in space systems 17 p2388 N88-24196

A universal computer control system for motors
[NASA-CASE-NPO-17134-1-CU]
18 p2506 N88-24864

Electronic controller for reciprocating rotary crystallizer
[NASA-TM-101140] 18 p2584 N88-25354

Adaptive residual mode filter control of distributed parameter systems for large space structure applications
19 p2719 N88-26143

L(sub infinity symbol)-approximations of complex functions and robust controllers for large flexible space structures
[PB88-186226] 20 p2764 N88-26390

COSPAS/SARSAT 406-MHz emergency beacon digital controller
[NASA-TM-100859] 20 p2792 N88-26566

Design of a controller to reduce residual vibration in the positioning control of flexible robotic manipulators
20 p2808 N88-26658

SP-100 Ground Engineering Systems: Test facility control systems
[DE88-009195] 21 p3015 N88-27895

The feasibility of the disturbance accommodating controller for precision antenna pointing
22 p3064 N88-28182

DSS 13 microprocessor antenna controller
22 p3066 N88-28192

Motion planning with obstacles and dynamic constraints 23 p3222 N88-29175

Nanosequencer digital logic controller
[NASA-CASE-NPO-16116-2] 23 p3245 N88-29310

Artificial intelligence applied to process signal analysis
23 p3252 N88-29359

Identification and control of time-varying flexible structures: An artificial intelligence approach
23 p3265 N88-29437

Robust design of distributed controllers for large flexible space structures
[NASA-CR-183202] 24 p3380 N88-30134

An intelligent training system for space shuttle flight controllers 24 p3415 N88-30331

CONVAIR MILITARY AIRCRAFT

U MILITARY AIRCRAFT

CONVECTION

NT FORCED CONVECTION
NT FREE CONVECTION
NT MARANGONI CONVECTION
NT RAYLEIGH-BENARD CONVECTION

Phase dynamics: A review and a perspective
[DE87-013173] 01 p0048 N88-10306

Statistical relationships between the mesoscale organization of convection and the large-scale wind profiles during GATE --- GARP Atlantic Tropical Experiment (GATE) 02 p0208 N88-11302

Convective cross section analysis
[PB87-204566] 02 p0216 N88-11361

Thermally driven convective cells and tokamak edge turbulence
[DE87-014424] 02 p0238 N88-11499

The duskside plasmapause/ring current interface: Convection and plasma wave observations
[MPE-PREPRINT-93] 02 p0243 N88-11533

A heat transfer model for a heated helium airship
[AD-A183786] 03 p0259 N88-11629

The diffusion-convection vortex method for solving two-dimensional incompressible Navier-Stokes equation
03 p0317 N88-12001

Banded ion morphology 04 p0468 N88-12892

Relations between chromospheric and coronal structure: flux-flux correlations and convective zone properties
04 p0510 N88-13138

Global convection patterns in the high latitude
[AD-A185794] 06 p0743 N88-14571

Stabilized Galerkin method for convection-diffusion problems
[PB87-234965] 06 p0764 N88-14694

Comments on the theory of absolute and convective instabilities
[PB87-124624] 06 p0783 N88-14806

Solar Dynamics and G-modes
[NASA-CR-180737] 06 p0805 N88-14911

The use of the direct measurement of solar radiation for the determination of Pasquill Stability Parameter
[AD-A186084] 07 p0946 N88-15750

Influence of the friction coefficients, the power and the flowrate on the two-phase flow instabilities in natural circulation
[DE88-700036] 08 p0983 N88-15946
Some stability results for the hopscotch difference method when applied to convection-diffusion equations
[CWI-NM-R8711] 08 p1072 N88-16465
Interaction of the cold conveyor belt with polar jet streaks
[AD-A186774] 09 p1192 N88-17145
Convective wind fields as investigated with doppler lidar
[PB88-115472] 09 p1193 N88-17151
Influence of convection on microstructure
[NASA-CR-182489] 10 p1302 N88-17784
Periodic natural convection in a rectangular enclosure of low aspect ratio 10 p1329 N88-17941
A multigrid preconditioner applied to a two-dimensional convection-diffusion problem
[DE88-004765] 10 p1397 N88-18329
Radial mixing in turbomachines
[AD-A188028] 11 p1482 N88-18847
Travelling waves and chaos in double-diffusive convection 11 p1484 N88-18857
The Hamiltonian structure of nonlinear elasticity: The convective representation of solids, rods, and plates
[AD-A187200] 11 p1498 N88-18943
MCT crystal growth
[NASA-CR-179297] 11 p1557 N88-19318
Dynamical modeling of marine boundary layer convection 13 p1797 N88-20750
Fingering flow patterns of thermosolutal convection in rectangular enclosures
[NASA-TM-100854] 14 p1911 N88-21417
Taiwan area mesoscale experiment: P-3 aircraft operations summary
[PB88-169073] 18 p2544 N88-25096
Dendritic growth in the presence of convection
18 p2580 N88-25328
Dynamics explorer data analysis
[NASA-CR-181428] 19 p2691 N88-25996
Satellite observed Mesoscale Convective System (MCS) propagation characteristics and a 3-12 hour heavy precipitation forecast index
[PB88-180161] 19 p2692 N88-26004
Cosmions and stars
[DE88-010886] 20 p2887 N88-27145
Time-dependent thermal convection of Earth mantle and double diffusive convection in magma chambers
[MITT-52] 21 p2974 N88-27663
Application of rectangular co-ordinates to the problem of laminar combined convection in a straight horizontal tube whose circumference is heated nonuniformly
[PDR/CFDU/IC/33] 22 p3076 N88-28263
The influence of conductivities consistent with field-aligned currents on high-latitude convection patterns
[TRITA-EPP-88-02] 22 p3119 N88-28533
The patterns of tropical convection during the 1986-87 ENSO 22 p3120 N88-28537
The dynamics and thermodynamics of a 30-60 day oscillation 22 p3121 N88-28543
Aspects of the 30-60 day oscillation in a GCM simulation 22 p3121 N88-28545
An observational study of interaction between large scale tropical cumulus convection and the equatorial circulation anomalies 22 p3124 N88-28564
Natural convection immersion cooling of an array of simulated chips in an enclosure filled with dielectric liquid
[AD-A193594] 23 p3207 N88-29088
Ionospheric convection and structure using ground-based digital ionosondes
[AD-A194246] 23 p3233 N88-29237
Influence of the convection on evaporation and combustion of a fuel droplet 24 p3351 N88-29948

CONVECTION CLOUDS
NT ARC CLOUDS
NT CUMULUS CLOUDS
Forecasting and nowcasting cumulus convection with soundings released from a storm-intercept vehicle
02 p0202 N88-11262
Detailed analysis of a mesoscale convective complex situation in the Carpathian Basin (Europe)
02 p0207 N88-11296
Effects of the large scale motion and horizontal inhomogeneity of the moist static instability on development of the mesoscale convective systems in the midlatitudes 02 p0207 N88-11297
Radar measurement methods for the observation of convective clouds, and comparison of measurements and numerical simulation
[ESA-TT-1049] 03 p0352 N88-12223
Study of isolated convective clouds in the lower Alps in summer 1984, using radar and a simple Weinstein numerical model
[ESA-TT-1061] 03 p0353 N88-12224
Cloud physics studies in SCPP (Sierra Cooperative Pilot Project) from 1977-87
[PB88-136924] 11 p1516 N88-19054
Stratospheric electric field and conductivity measurements over electrified convective clouds in the South American region, revised
[INPE-4046-PRE/1012-REV-3]
15 p2095 N88-22483
A study on electric fields and conductivity associated with electrified clouds in the region of South America
[INPE-4487-TDL/325] 15 p2096 N88-22486
Ice formation on aircraft
[ETN-88-92154] 18 p2545 N88-25104
Parametric methodologies of cloud vertical transport for acid deposition models
[PB88-191374] 20 p2825 N88-26762
Dynamic interaction of convective cumulus with large-scale environment
[MITT-55] 20 p2827 N88-26773

CONVECTION CURRENTS
Convective scale interaction: Arc cloud lines and the development and evolution of deep convection
[NASA-CR-181469] 02 p0215 N88-11357
Environmental and convective influence on tropical cyclone development versus non-development
[AD-A185231] 05 p0627 N88-13835
Analysis of quasi-geostrophic forcing during the AIMCS (Airborne Investigations of Mesoscale Convective System) Project. Volume 1: Discussion
[PB88-133095] 12 p1646 N88-19860
Numerical simulation of generation of mesoscale convective systems in large-scale environment
14 p1900 N88-21344
Open cell associated with warm advection
17 p2351 N88-24010

CONVECTIVE FLOW
NT RAYLEIGH-BENARD CONVECTION
Magnetic field twist driven by remote convective motions: Characteristics and twist rates 01 p0113 N88-10724
Preparative electrophoresis for space
[NASA-TP-2777] 02 p0156 N88-10977
Continuous flow electrophoresis system experiments on shuttle flights STS-6 and STS-7
[NASA-TP-2778] 02 p0156 N88-10978
On the role of convective motion during dendrite growth: Experiments under variable gravity, revised
[NASA-CR-179213] 02 p0156 N88-10979
Detailed analysis of a mesoscale convective complex situation in the Carpathian Basin (Europe)
02 p0207 N88-11296
Effects of the large scale motion and horizontal inhomogeneity of the moist static instability on development of the mesoscale convective systems in the midlatitudes 02 p0207 N88-11297
Convective scale interaction: Arc cloud lines and the development and evolution of deep convection
[NASA-CR-181469] 02 p0215 N88-11357
Conjugated heat transfer from a radiating fluid in a rectangular channel 03 p0317 N88-12003
High latitude F-region drift studies
[AD-A184466] 04 p0467 N88-12889
SHARP simulation of discontinuities in highly convective steady flow
[NASA-TM-100240] 05 p0642 N88-13931
Observations of a midlatitude squall line boundary layer wake
[AD-A185609] 06 p0746 N88-14589
The numerical and analytical study of bifurcation and multicellular flow instability due to natural convection between narrow horizontal isothermal cylindrical annuli at high Rayleigh numbers
[AD-A186113] 07 p0849 N88-15151
Assessment of VAS-derived products created by a simultaneous algorithm on a convectively active day
[AD A186158] 08 p1054 N88-16359
A payload for investigating the influence of convection on GaAs crystal growth 10 p1288 N88-17702
Disk pumping test
[AD-A187199] 11 p1440 N88-18591
Suspension of small metallic plates: A versatile sensor
[PB88-130901] 11 p1487 N88-18874
High Rayleigh number convection in rectangular enclosures with differentially heated vertical walls and aspect ratios between zero and unity
[NASA-TM-100277] 12 p1628 N88-19739
Velocity and concentration fields over a crystal growing in a water solution: Experimental study and numerical simulation 14 p1987 N88-21856
Transport processes during directional solidification and crystal growth: Scaling and experimental study
14 p1988 N88-21857
Convection effects on stability at the solidification front 14 p1988 N88-21860
Acoustic convective system
[NASA-CASE-NPO-17278-1-CU]
18 p2498 N88-24818
Dendritic growth in the presence of convection
18 p2580 N88-25328
Experimental and analytical studies of compressible vortices 19 p2665 N88-25848
Stationary, wave type, and chaos type convection in spherical symmetry geometries
[ETN-88-92358] 20 p2801 N88-26625

CONVECTIVE HEAT TRANSFER
Multidimensional modeling of convective heat transfer with application to IC engines
[DE87-011046] 01 p0055 N88-10353
Recent progress in magma energy extraction
[DE87-013083] 01 p0066 N88-10424
Radiative and free-convective heat transfer from a finite horizontal plate inside an enclosure
02 p0133 N88-10833
An approximate solution to the problem of heating massive bodies by both radiation and convection
[BLL-M-37315-(5828.4)] 02 p0170 N88-11068
The effect of heat transfer on the dispersion of cold dense gases
[OUEL-1688/87] 02 p0171 N88-11076
Heat transfer in the tip region of a rotor blade simulator 02 p0186 N88-11159
Finite element analysis of three-dimensional steady and unsteady temperature fields (computation of temperature distribution of turbine blade with composite cooling)
03 p0300 N88-11887
Multidimensional modeling of convective heat transfer with application to I.C. engines
[DE87-014983] 03 p0322 N88-12036
Measurement of local convective heat transfer coefficients from a smooth and roughened NACA-0012 airfoil: Flight test data
[NASA-TM-100284] 05 p0582 N88-13552
Cooling electronic equipment at simulated high altitude in hypobaric chambers
[AD-A185196] 05 p0584 N88-13560
Thin film and gradient-driven instability mechanisms
[PB88-101522] 07 p0853 N88-15182
Rational considerations for modelling human thermoregulation during cold water immersion
[AD-A186226] 08 p1048 N88-16329
Determination of the effect of walking on the forced convective heat transfer coefficient using an articulated mannikin
[AD-A186452] 08 p1049 N88-16335
Experimental study of local natural convection heat transfer in inclined and rotating enclosures
09 p1165 N88-16986
Interferometric study of natural convection heat transfer from a vertical flat plate with transverse roughness elements 10 p1327 N88-17935
Multidimensional modeling of convective heat transfer with application to IC engines
[DE88-003398] 10 p1330 N88-17948
Mixed turbulent convective heat transfer in vertical ducts 11 p1485 N88-18865
Convective heat transfer and its effect on inertial measurement units 12 p1578 N88-19442
Characteristics of the thermal environment
[AD-A188359] 12 p1641 N88-19827
Structures and fluxes in a deep convecting mixed layer 13 p1804 N88-20786
The mixed layer of the western equatorial Pacific Ocean
[HIG-1861] 13 p1805 N88-20789
Similarity theories and microturbulence in the atmospheric mixed layer 13 p1806 N88-20802
Heat transfer modeling of jet vane Thrust Vector Control (TVC) systems
[AD-A190106] 15 p2019 N88-22034
Heat transfer from a negatively buoyant wall jet
[NBS/GCR-88/541] 15 p2050 N88-22208
Thermal instability and heat transfer characteristics in water/ice systems
[AD-A189627] 15 p2062 N88-22297
Experimental measurements of heat transfer from an iced surface during artificial and natural cloud icing conditions
[AIAA-PAPER-86-1352] 17 p2293 N88-23718
Review of convectively cooled structures for hypersonic flight
[NASA-TM-87740] 17 p2310 N88-23817
Single phase liquid immersion cooling of discrete heat sources in a vertical channel
[AD-A191224] 17 p2337 N88-23944
Acoustic convective system
[NASA-CASE-NPO-17278-1-CU]
18 p2498 N88-24818

Thermal management of integrated microsensors
19 p2670 N88-25875
Multidimensional modeling of convective heat transfer with application to I.C. engines
[DE88-007446] 19 p2736 N88-26257
An arranging method on L/D of two-phase closed thermosyphons 20 p2783 N88-26508
Forced-convective boiling in small diameter tube
20 p2783 N88-26510
The heat transfer and fluid dynamics of concave surface curvature
[AD-A193064] 21 p2943 N88-27479
Application of rectangular co-ordinates to the problem of laminar combined convection in a straight horizontal tube whose circumference is heated nonuniformly
[PDR/CFDU/IC/33] 22 p3076 N88-28263
Estimation of transient heat transfer coefficients in multidimensional problems by using inverse heat transfer methods 23 p3210 N88-29108
Impact of ETO propellants on the aerothermodynamic analyses of propulsion components
[NASA-TM-101303] 24 p3374 N88-30094

CONVERGENCE

An exponential example for Terlaky's pivoting rule for the criss-cross simplex method
[REPT-87-18] 01 p0080 N88-10512
Semidiscrete Galerkin method for semilinear evolution equations with a differential operator of third order
[BONNER-MATHE-SCHR-181]
01 p0087 N88-10570
The use of advanced data sets in the short-range forecasting of the development of a tornadic thunderstorm along a mesoscale convergence zone
02 p0200 N88-11250
The spatially nonuniform convergence of the numerical solution of flows
[NASA-TM-100037] 02 p0226 N88-11429
Compactness of quasi-conforming element spaces, convergence of quasi-conforming element method
03 p0301 N88-11896
Concepts for radically increasing the numerical convergence rate of the Euler equations
[NASA-CR-177456] 04 p0395 N88-12463
Parallel superconvergent multigrid
[DE87-013153] 04 p0480 N88-12960
A numerical study of the effects of curvature and convergence on dilution jet mixing
[NASA-TM-89878] 05 p0549 N88-13347
A note on the use of symmetric line Gauss-Seidel for the steady upwind differenced Euler equations
[AD-A185223] 05 p0580 N88-13540
Characteristics of a separating confluent boundary layer and the downstream wake
[NASA-TM-100046] 06 p0704 N88-14323
Stochastic approximation and large deviations: General results for w.p.l. Convergence
[AD-A185818] 06 p0768 N88-14721
On the convergence of the p-version of the boundary element Galerkin method
[AD-A186198] 07 p0910 N88-15514
Weak convergence of sums of moving averages in the alpha-stable domain of attraction
[AD-A186430] 07 p0912 N88-15529
On rate of convergence of equivariation linear prediction estimates of the number of signals and frequencies of multiple sinusoids
[AD-A186034] 07 p0914 N88-15549
On the characterization of certain point processes
[AD-A186427] 07 p0916 N88-15560
Strong representation of weak convergence
[AD-A186433] 07 p0916 N88-15563
Target size and luminance effects on accommodation and vergence
[AD-A185861] 08 p1051 N88-16343
Strong convergence and convergence rates of approximating solutions for algebraic Riccati equations in Hilbert spaces
[AD-A186190] 08 p1072 N88-16464
Method of iterative coupling between periodic aerodynamic and dynamic fields
[PB87-169934] 09 p1113 N88-16669
On line search termination criteria for and convergence of conic algorithms for minimization
[DE88-002844] 09 p1227 N88-17351
A multigrid preconditioner applied to a two-dimensional convection-diffusion problem
[DE88-004765] 10 p1397 N88-18329
The convergence rate for the strong law of large numbers: General lattice distributions
[AD-A187580] 10 p1402 N88-18362
Probability bounds for M-Skorohod oscillations
[AD-A187981] 10 p1404 N88-18371
Geophysical study of the structure and processes of the continental convergence zones: Alpine-Himalayan Belt
[NASA-CR-182647] 12 p1644 N88-19842
Convolution metrics and rates of convergence in the CLT (Central Limit Theorem)
[AD-A189341] 12 p1686 N88-20084
A convergence theorem in process algebra
[CWI-CS-R8733] 13 p1827 N88-20920
Convergence of Runge-Kutta methods on classes of stiff initial value problems
[CWI-NM-R8717] 13 p1827 N88-20924
Some maximum norm estimates for the finite element method applied to nonlinear two dimensional boundary value problems
[ETN-88-91505] 14 p1964 N88-21715
The global convergence of partitioned BFGS on problems with convex decompositions and Lipschitzian gradients
[DE88-006249] 14 p1968 N88-21744
Development and application of the p-version of the finite element method
[AD-A190036] 15 p2120 N88-22633
Trust regions and projected gradients
[DE88-005829] 15 p2122 N88-22646
Detection of the number, locations and magnitudes of jumps
[AD-A190328] 15 p2125 N88-22671
Convergence qualification of partition algorithms in global optimization
[REPT-87-61] 16 p2259 N88-23505
Unique normal forms for lambda calculus with surjective pairing
[PB88-173539] 16 p2260 N88-23508
Accuracy versus convergence rates for a three dimensional multistage Euler code
[NASA-CR-181665] 16 p2261 N88-23519
Inference for a nonlinear semimartingale regression model
[AD-A190857] 16 p2262 N88-23527
Almost sure L(gamma)-norm convergence for data-based histogram density estimates
[AD-A189944] 17 p2393 N88-24228
Study of the convergence of a finite difference scheme for acoustic propagation in the atmosphere in a parabolic approximation. Statistical calculation of the sound field in the presence of kinematic turbulence
[ONERA-RS-8/3641-PY-160-P]
17 p2394 N88-24235
An empirical model of the effects of curvature and convergence on dilution jet mixing
[NASA-TM-100896] 18 p2466 N88-24640
Gram-Schmidt implementation of a linearly constrained adaptive array
[AD-A191651] 18 p2560 N88-25198
A concurrent neural network algorithm for the traveling salesman problem
[DE88-006981] 18 p2562 N88-25208
Stability and convergence of the Peaceman-Rachford ADI method for initial-boundary value problems
[CWI-NM-R8724] 18 p2566 N88-25243
Optimal discrete-time LQR problems for parabolic systems with unbounded input: Approximation and convergence
[NASA-CR-181673] 18 p2567 N88-25247
On the use of convergent beam electron diffraction for identification of antiphase boundaries in GaAs grown on Si
[DE88-008220] 18 p2585 N88-25362
Some supraconvergent schemes for hyperbolic equations on irregular grids
[DE88-009113] 19 p2720 N88-26151
Semi-discrete approximations to nonlinear systems of conservation laws; consistency and L(infinity)-stability imply convergence
[NASA-CR-181683] 19 p2721 N88-26157
Application of Moment Iteration Method (MIM) to electromagnetic field computation
[PB88-194139] 20 p2769 N88-26546
Conditions for finite convergence of algorithms for nonlinear programs and variational inequalities
[AD-A192355] 20 p2838 N88-26834
Stability and convergence in the numerical solution of stiff initial value problems
[B8881480] 23 p3272 N88-29474
Convergence acceleration for vector sequences and applications to computational fluid dynamics
[NASA-TM-101327] 24 p3424 N88-30377
Convergence of Galerkin approximations for operator Riccati equations: A nonlinear evolution equation approach
[NASA-CR-181706] 24 p3425 N88-30386

CONVERGENT NOZZLES

Static performance of nonaxisymmetric nozzles with yaw thrust-vectoring vanes
[NASA-TP-2813] 14 p1861 N88-21118
Effect of flow convergence on turbulence level in stream 14 p1973 N88-21773
Application of laser diffraction techniques to particle sizing in solid propellant rocket motors
[AD-A193841] 22 p3049 N88-28086

CONVERGENT-DIVERGENT NOZZLES

Static performance of an axisymmetric nozzle with post-exit vanes for multiaxis thrust vectoring
[NASA-TP-2800] 13 p1719 N88-20280
Static performance of nonaxisymmetric nozzles with yaw thrust-vectoring vanes
[NASA-TP-2813] 14 p1861 N88-21118
Nozzle fabrication technique
[NASA-CASE-MSC-21299-1] 18 p2475 N88-24684
Techniques utilized in the simulated altitude testing of a 2D-CD vectoring and reversing nozzle
[NASA-TM-100872] 19 p2604 N88-25464
Implicit finite-difference simulation of an internal flow in a nozzle: An example of a physical application on a hypercube
[AD-A192475] 21 p2942 N88-27472

CONVERSION

Ethanol as a fuel of a lorry. Use experience from a diesel engine modified to an otto engine
[DE88-752870] 21 p2958 N88-27569
Software engineering for the EBR-2 data acquisition system conversion
[DE88-009950] 22 p3136 N88-28647

CONVERTAPLANES

U V/STOL AIRCRAFT

CONVERTERS

Rust converters
[AD-A188767] 14 p1891 N88-21299

CONVERTIBLE FAN-SHAFT ENGINES

Test stand performance of a convertible engine for advanced V/STOL and rotorcraft propulsion
[NASA-TM-100211] 03 p0266 N88-11679
The convertible engine: A dual-mode propulsion system 09 p1108 N88-16639

CONVEXITY

Analytical investigation of reflection of a regular or mach reflection over a secondary wedge
[AD-A185690] 06 p0703 N88-14316
An O(n3L) interior point algorithm for convex quadratic programming
[AD-A186001] 07 p0909 N88-15504
Bounding the expectation of convex functions with limited distribution information
[AD-A186147] 07 p0910 N88-15512
Upper bounds on the expected value of a convex function using gradient and conjugate function information
[AD-A186246] 07 p0910 N88-15517
Sublinear upper bounds for stochastic programs with recourse, revision
[AD-A186436] 07 p0916 N88-15564
Multigrid methods in convex optimization
11 p1538 N88-19190
A primal-dual algorithm for the computation of the minimum of a convex function on the intersection of convex functions, and its application in data analysis
[RR-638-M] 18 p2563 N88-25217
Linear programming in R sup 3 and the skeleton and largest incircle of a convex polygon
[PB88-124664] 20 p2846 N88-26692

CONVOLUTION INTEGRALS

On the concept of resolution ellipse in aperture synthesis matched deconvolution with error analysis --- astronomical interferometry 01 p0095 N88-10621
Optimal application of Morrison's iterative noise removal for deconvolution. Appendices
[NASA-CR-182477] 09 p1231 N88-17376
Small degree solutions for the polynomial Bezout equation
[AD-A187630] 10 p1401 N88-18355
Convolution metrics and rates of convergence in the CLT (Central Limit Theorem)
[AD-A189341] 12 p1686 N88-20084
The algebraic structure of convolutional codes
[AD-A190280] 15 p2120 N88-22636
Near optimal blind deconvolution
[REPT-87-016] 15 p2123 N88-22655
Real time pipelined system for forming the sum of products in the processing of video data
[NASA-CASE-NPO-16462-1-CU]
17 p2384 N88-24169
A deconvolution technique using least-squares model-fitting and its application to optical pulse measurement
[NPL-DES-87] 22 p3144 N88-28694
Two dimensional convolute integers for machine vision and image recognition 23 p3254 N88-29369

CONVOLUTIONS (MATHEMATICS)

U CONVOLUTION INTEGRALS

COOL STARS

NT CARBON STARS
NT FLARE STARS
NT K STARS

NT M STARS
NT MIRA VARIABLES
NT S STARS
The M-type stars
[NASA-SP-492] 02 p0252 N88-11592
Basic properties and variability
02 p0252 N88-11593
Spectroscopy and nonthermal processes
02 p0252 N88-11594
Circumstellar shells, the formation of grains, and radiation transfer 02 p0252 N88-11596
Mass loss 02 p0253 N88-11597
Circumstellar chemistry 02 p0253 N88-11598
Fifth Cambridge Workshop on Cool Stars, Stellar Systems and the Sun 04 p0502 N88-13092
The photospheric magnetic fields of cool stars: Recent results of survey and time-variability programs
04 p0503 N88-13094
Flux tube dynamics and solar/stellar redshift measurements 04 p0503 N88-13095
Nonthermal phenomena in stellar coronae: Evidence from radio observations 04 p0503 N88-13096
Observational constraints and evidence for saturation
04 p0503 N88-13097
Heating of stellar chromospheres and coronae: Evidence for non-magnetic basal heating
04 p0503 N88-13098
Automatic photometric monitoring of [illegible] stars
04 p0504 N88-13103
Evidence for expanding magnetic loops in coronae of cool stars 04 p0510 N88-13134
Empirical relations between photospheric magnetic fields and atmospheric radiative losses for cool dwarf stars 04 p0511 N88-13145
Radio continuum emission from the ionized stellar winds of the cool supergiants in zeta Aurigae-like systems
04 p0514 N88-13160
IRAS and cool stellar mass loss
04 p0515 N88-13166
The Wilson-Bappu relationship: A barometric effect
04 p0516 N88-13170
IUE observations of the hybrid K3 II star Iota Aurigae and constraints on the outer atmospheric structure
04 p0516 N88-13171
Synthetic spectra for the N-type carbon star TX Psc
04 p0516 N88-13173

COOLANT LOSS
U LOSS OF COOLANT

COOLANTS
Quantitative determination of a hydrogen impurity in a sodium coolant by hydride thermal dissociation
[NASA-TT-20239] 13 p1740 N88-20402
Thermal-hydraulic considerations for particle bed reactors 17 p2400 N88-24266
The effect of operating temperature on open, multimegawatt space power systems
17 p2414 N88-24352
Fabrication of a niobium 1 percent zirconium containment for SP-100 primary lithium system materials mass transfer studies 17 p2417 N88-24373
Reactor core coolability with reduced power levels
17 p2425 N88-24425
Customizing Space Nuclear Power System Analysis Model (SNPSAM): Introducing a secondary coolant loop
[AD-A194620] 22 p3151 N88-28750

COOLERS
Cryogenics program overview
08 p0981 N88-15926
Ames Research Center cryogenics program
08 p0981 N88-15927
The Goddard Space Flight Center mechanical cooler program 08 p0983 N88-15944

COOLING
NT ABSORPTION COOLING
NT AIR COOLING
NT CRYOGENIC COOLING
NT EVAPORATIVE COOLING
NT FILM COOLING
NT GAS COOLING
NT LIQUID COOLING
NT MAGNETIC COOLING
NT PLASMA COOLING
NT QUENCHING (COOLING)
NT RADIANT COOLING
NT REGENERATIVE COOLING
NT SPACE COOLING (BUILDINGS)
NT SUPERCOOLING
NT SURFACE COOLING
NT SWEAT COOLING
NT THERMOELECTRIC COOLING
The dissociation of dense liquid nitrogen and shock cooling
[DE87-013490] 01 p0022 N88-10136
Applications of heat pipes to cool PWBS and hybrid microcircuits 02 p0136 N88-10858
Operating experiences and test results of six cold helium compressors
[DE87-012115] 02 p0157 N88-10982
Shock-induced cooling in dense fluids
[DE87-014343] 02 p0170 N88-11067
Heat transfer in the tip region of a rotor blade simulator 02 p0186 N88-11159
Coolant passage heat transfer with rotation
02 p0186 N88-11160
Heat transfer with very high free stream turbulence
02 p0186 N88-11161
Local heat/mass transfer and pressure drop in a two-pass rib-roughened channel for turbine airfoil cooling
[NASA-CR-179635] 03 p0322 N88-12039
Completely magnetically contained electrothermal thrusters
[AD-A185674] 06 p0674 N88-14129
Undercooling and nucleation in iron nickel alloys
[AD-A185500] 06 p0683 N88-14184
Investigation of the auto-tempering of low-carbon martensite
[PB87-143970] 07 p0833 N88-15053
Thermal stress analysis of a cooled monochromator crystal
[DE88-002116] 07 p0937 N88-15636
Rapid hypothermia subsequent to oral nicotinic acid and immersion in warm (30C) water
[AD-A186458] 08 p1050 N88-16339
Description of tests run in the T2 cryogenic wind tunnel
[PB87-170296] 09 p1113 N88-16672
Mesospheric dynamics and chemistry from SME data
[NASA-CR-182465] 09 p1191 N88-17139
The role of hydration on peripheral response to cold
[AD-A186448] 09 p1199 N88-17186
Mechanistic model for void distribution in flashing flow
[DE88-002948] 10 p1326 N88-17928
Disk pumping test
[AD-A187199] 11 p1440 N88-18591
Microstructural characterization of HSLA-100 GMA-weldments
[AD-A187782] 11 p1457 N88-18683
Microstructural characterization of the heat affected zone of HSLA (High Strength Low Alloy)-100 steel GMA (Gas Metal Arc)-weldment
[AD-A187825] 11 p1457 N88-18686
Theory of laser cooling and spectroscopy of harmonically trapped single atoms
[AD-A189576] 13 p1775 N88-20617
The cooling of electronic equipment in fighter aircraft
[MBB/LKE-312/S/PUB/258] 14 p186[illegible] N88-21147
On the theory of the conversion of metallic mixed phases. 5: Fluctuations and nucleation in sub-cooled phases
[NASA-TT-20249] 14 p1890 N88-21296
Laser cooling of neon metastable states
14 p1975 N88-21785
Structural analyses of engine wall cooling concepts and materials 15 p2081 N88-22405
Status, trends in research on internal combustion engines 16 p2185 N88-23027
Long duration coherent Lyman-alpha sources
16 p2268 N88-23571
Hydrogen turbines for space power systems: A simplified axial flow gas turbine model 17 p2419 N88-24385
Possible creep studies of lithium with a compact device 17 p2422 N88-24404
Reactor core coolability with reduced power levels
17 p2425 N88-24425
The effect of operating temperature and turbine blade cooling on Brayton cycle space power systems
17 p2435 N88-24489
Space power radiation cooled dc transmission line analysis 17 p2438 N88-24506
Fraction eutectic measurements in slowly cooled Pb - 15 wt percent Sn alloys
[NASA-CR-180830] 19 p2618 N88-25531
Heat pump augmented radiator for low-temperature space applications
[DE88-008369] 20 p2765 N88-26393
Thermal-sensation control: A new method of controlling cooled/heated environments 21 p2930 N88-27394
Some evidence for a Northern Hemispheric extratropic trigger mechanism of ENSO events
22 p3123 N88-28558
High temperature electric arc furnace
[NASA-CASE-MFS-28281-1] 23 p3181 N88-28938
Surface Tension Confined Liquid Cryogen Cooler (STCLCC)
[NASA-CASE-GSC-13112-1] 23 p3201 N88-29050
Thermocouple for heating and cooling of memory metal actuators
[NASA-CASE-NPO-17068-1-CU]
23 p3217 N88-29151
Spontaneous force optical traps
[AD-A196103] 24 p3377 N88-30114

COOLING FINS
Advanced radiator concepts utilizing honeycomb panel heat pipes
[NASA-CR-172017] 04 p0443 N88-12747

COOLING FLOWS (ASTROPHYSICS)
Finnish-Soviet Symposium on Radio Astronomy (1st) held at Otaniemi on August 26-27, 1985
[PB87-140661] 07 p0944 N88-15736

COOLING SYSTEMS
Understanding passive cooling systems
[PB87-210464] 02 p0194 N88-11211
The effect of maximum-allowable payload temperature on the mass of a multimegawatt space-based platform
[DE88-001921] 05 p0555 N88-13381
Self operating absorption cooling system using solar energy: Small power experimental plant
[DE88-900194] 07 p0874 N88-15299
An adiabatic demagnetization cooled bolometer system for millimeter continuum astronomy
07 p0943 N88-15735
Aircraft engine hot section technology: An overview of the HOST Project 08 p0957 N88-15804
Comparison of a thermoelectric cooling system and a groundwater heat pump
[DE88-001753] 08 p0984 N88-15950
Experimental study of secondary flow in the presence of two jet arrays on the wall of a turbine blade
[ECL-87-11] 08 p0987 N88-15981
Advanced techniques employed in blade cooling research 10 p1281 N88-17659
Active cooling design for scramjet engines using optimization methods
[NASA-TM-100581] 13 p1783 N88-20669
Development of an engineering model dynamic cooler --- spacecraft payloads
[F+W-TF-B-1885] 14 p1895 N88-21311
Superconducting magnet technique for ASTROMAG on the space station
[DE88-004560] 15 p2025 N88-22063
Liquid droplet radiator development
17 p2424 N88-24415
The effect of maximum allowable payload temperature on the mass of a multimegawatt space based platform
17 p2424 N88-24416
MACRAD: A mass analysis code for radiators
17 p2424 N88-24418
Heat pump-augmented systems for spacecraft thermal management 17 p2424 N88-24419
Dynamic isotope power system critical component verification 17 p2425 N88-24421
An experimental setup for the study of polarized He3 and dilute He3-He4 mixtures
[B8705589] 23 p3193 N88-29001
An analysis of heat transfer after loss of primary coolant in the SP-100 reactor system
[AD-A194619] 23 p3281 N88-29539

COOPERATION
Technology transfer from US Federal laboratories: Report of a roundtable
[PB88-144803] 12 p1709 N88-20228

COORDINATE SYSTEMS
U COORDINATES

COORDINATE TRANSFORMATIONS
Analytical treatment of the spatial trilateration problem (4, 6, 0, 0)
[SER-A-104] 01 p0085 N88-10548
A study on local level inertial surveying systems. Error model for the stationary system
[B8736714] 16 p2229 N88-23312
A description of the reference frames and the coordinate transformations used in AMEER (Aero-Mechanical Equations Evaluations Routines)
[DE88-007960] 19 p2720 N88-26153

COORDINATES
NT CARTESIAN COORDINATES
NT COMPUTATIONAL GRIDS
NT GEODETIC COORDINATES
NT HYPERBOLIC COORDINATES
NT LAGRANGE COORDINATES
NT SPHERICAL COORDINATES
Asymptotics of the effective potentials and wave functions of a three-body problem in suitable coordinates
[DE87-703323] 03 p0370 N88-12326
Separable orthogonal coordinates and particle creation for an accelerating observer
[DE87-703358] 05 p0657 N88-14029
Example of correlation between space and spin coordinates
[DE87-703366] 05 p0657 N88-14030
The Wilson-Fowler spline in a global IGES (Initial Graphics Exchange Specification) coordinate frame
[DE88-001942] 06 p0757 N88-14640
Evaluation of magnetic coordinates in finite-beta, asymmetric plasmas
[DE88-003665] 10 p1412 N88-18424

Reference position vector 12 p1577 N88-19432

Coordinate-momentum probability operator for point particles in a stationary electromagnetic field
[DE88-701165] 16 p2188 N88-23044

Full-wave calculations in flux coordinates for toroidal geometry
[DE88-010131] 20 p2860 N88-26985

Three-dimensional adaptive grid generation for body-fitted coordinate system
[NASA-CR-182192] 21 p2950 N88-27520

DATATRAN: Datum transformation software
[AD-A195723] 24 p3387 N88-30175

COORDINATION

Hydrogen Energy Coordinating Committee: Summary of DOE hydrogen programs for FY 1987
[DE88-003960] 10 p1306 N88-17811

The coordination cluster theory for metallic solutions
[DE88-005934] 13 p1738 N88-20389

Coordination in decision-making organizations
[AD-A191952] 19 p2739 N88-26261

Soluble metal chelate polymers of coordination numbers six, seven and eight
[AD-A192485] 21 p2917 N88-27314

Cockpit and cabin crew coordination
[AD-A192445] 21 p2993 N88-27752

COORDINATION POLYMERS

Soluble metal chelate polymers of coordination numbers six, seven and eight
[AD-A185094] 05 p0568 N88-13459

COPILOTS

U AIRCRAFT PILOTS

COPLANARITY

Modeling of some coplanar waveguide discontinuities
[NASA-TM-100808] 10 p1318 N88-17880

Confirmation of slow-waves in a crosstie overlay coplanar waveguide and its application to band-reject gratings and reflectors
[AD-A194981] 24 p3361 N88-30011

COPOLYMERIZATION

Conducting hybrid polymeric systems
[DE88-000527] 04 p0421 N88-12611

Polyether-polyester graft copolymer
[NASA-CASE-LAR-13447-1] 11 p1463 N88-18725

NMR analysis of a fluorocarbon copolymer
[DE88-002364] 15 p2043 N88-22170

Interactions in miscible polymer blends
[AD-A193824] 22 p3058 N88-28144

COPOLYMERS

NT VINYL COPOLYMERS

Novel polymers and copolymers and production of poly(acetylene)
[EP-PATENT-0-173-473-A2] 01 p0026 N88-10161

High ionic conductivity in PEO.PPG block polymer and salt solutions
[AD-A183502] 01 p0026 N88-10168

Polymer chain segment orientation during stress relaxation
[DE87-013392] 01 p0027 N88-10174

Applications and limitations of deuterium labeling methods to neutron scattering studies of polymers
[DE87-012936] 02 p0151 N88-10945

Urea-polyurethane and polydimethylsiloxane mixtures. Morphology control using a block copolymer
[ISAL-ID11-07-05] 02 p0153 N88-10959

Synthesis and characterization of block copolymers
[AD-A184405] 03 p0295 N88-11855

Synthesis and characterization of block copolymers
[AD-A184406] 03 p0296 N88-11856

Polymer composition --- cable insulation
[EP-PATENT-0-199-444-A1] 04 p0418 N88-12594

Synthesis, NMR characterization and electrical properties of siloxane-based polymer electrolytes
[AD-A184184] 04 p0418 N88-12596

Conductive polymers via reactive oligomer
[AD-A184270] 04 p0419 N88-12597

Advances in inherently conducting polymers
[DE88-000501] 04 p0421 N88-12610

Conducting hybrid polymeric systems
[DE88-000527] 04 p0421 N88-12611

Effect of sidechain length and crosslinking on ionic conductivity in polyphosphazene solid electrolytes
[AD-A184419] 04 p0497 N88-13058

Flexibilized copolyimide adhesives
[NASA-TM-89303] 05 p0570 N88-13474

Group contribution analysis of the damping behavior of homopolymers, statistical copolymers and interpenetrating polymer networks based on acrylic, vinyl and styrenic mers
[AD-A185904] 07 p0836 N88-15070

The morphology of emulsion polymerized latex particles
[DE88-002672] 08 p0972 N88-15879

Synthesis of high molecular weight peptide polymers and copolymers containing L-dopa residues
[AD-A186482] 08 p0973 N88-15887

Lithium/polymer electrolyte interfacial instability
[AD-A187164] 09 p1147 N88-16874

Study of molecular mobility of noncrystalline polymer alloys of different compatibility using mechanical spectrometry
[ISAL-87-0032] 09 p1149 N88-16883

Synthesis and structure property studies of toughened epoxy resins via functionalized polysiloxanes
[AD-A187984] 11 p1462 N88-18715

Synthesis and structure property studies of toughened epoxy resins via functionalized polysiloxanes. Friction and wear studies
[AD-A188258] 11 p1462 N88-18718

Polyether-polyester graft copolymer
[NASA-CASE-LAR-13447-1] 11 p1463 N88-18725

Statistical-mechanical study of polyvinylidene fluoride
[AD-A188310] 12 p1609 N88-19624

A new polymer-based hydrogen getter
[DE88-004538] 13 p1751 N88-20467

Ceramic materials from preceramic organometallic copolymers
[DE88-006067] 14 p1892 N88-21301

NMR analysis of a fluorocarbon copolymer
[DE88-002364] 15 p2043 N88-22170

Singlet oxygen behavior in solid polymer matrices
[DE88-005171] 15 p2043 N88-22171

Donor acceptor polymerization chemistry as a vehicle to low energy cure matrix resins
[AD-A190119] 15 p2044 N88-22179

Distribution of chain ends inside the polybutadiene microspheres of SB diblock copolymers
[AD-A191257] 16 p2182 N88-23007

High strength/high modulus aromatic heterocyclic ABA block copolymers
[AD-A191666] 18 p2491 N88-24774

Diffusion of homopolymers into nonequilibrium diblock copolymer structures
[DE88-005306] 18 p2494 N88-24794

Improved structural polymer alloys and composites
[AD-A192092] 19 p2619 N88-25538

Interaction of vinylidene fluoride: Tetrafluoroethylene copolymer with ammonia
[NASA-TT-20292] 19 p2620 N88-25542

Synthesis of model polymers and related structures in support of vinyl monomer grafting studies
[DE88-010245] 20 p2778 N88-26476

Initial adhesive screening of novel polyamide-imides and their copolymers
[NASA-TM-100641] 20 p2779 N88-26481

Ionic conductive polymers based on crosslinked elastic siloxane-ethylene oxide copolymers
[DE88-011243] 21 p2917 N88-27311

Spatial organization of homopolymer chains inside spherical polybutadiene domains of SB diblock copolymers
[AD-A193390] 21 p2918 N88-27321

Interactions in miscible polymer blends
[AD-A193824] 22 p3058 N88-28144

Dissolution rates of polymers and copolymers based on methyl, ethyl and butyl methacrylate
[AD-A194713] 23 p3197 N88-29027

Transport of organic vapors in multiphase polymer system
[AD-A194097] 23 p3198 N88-29033

Polyazidoesters as energetic polymers and copolymer components with fluoro derivatives
[AD-A194236] 23 p3199 N88-29039

COPPER

Relation between shock strength and strain-rate plasticity at maximum deviatoric stress
[DE87-011736] 01 p0061 N88-10390

Elastic moduli of copper under compression
[DE87-013137] 02 p0147 N88-10922

The water permeability of multi-layer coatings
[BLL-M-37252-(5828.4)] 02 p0148 N88-10927

Bond character at a silicon/copper surface
[AD-A184167] 03 p0295 N88-11851

Diffusion bonding depleted uranium to copper
[RFP-3783-REV] 03 p0333 N88-12098

The effect of organic inhibitors on the atmospheric corrosion and solderability of copper
[DE88-000261] 04 p0414 N88-12565

Studies on high-speed electroforming
[DE88-001395] 04 p0429 N88-12656

Data base on the high heat flux behaviour of metals and carbon materials for plasma facing components. Experiments at the 10 MW neutral beam injection test stand of the IPP Nagoya
[IPPJ-AM-53] 04 p0492 N88-13031

Jet initiation of PBX 9502
[DE88-000493] 05 p0571 N88-13481

The initiation and growth of small fatigue cracks in copper at room and cryogenic temperatures
05 p0600 N88-13668

Fatigue crack growth and fracture of copper-bismuth bicrystals 06 p0715 N88-14385

Orientation effects in copper single crystals fatigued at elevated temperatures 06 p0720 N88-14423

The influence of phosphorus on the solid state reaction between copper and silicon or germanium
[ETN-88-91361] 06 p0789 N88-1483

Model Cu/ZnO catalysts for methanol synthesis: The role of surface structure
[DE88-002354] 07 p0830 N88-15007

Microstructural observations of the Sn-Pb solder/Cu system and thermal fatigue of the solder joint
[DE88-001392] 07 p0832 N88-15046

Contrast between the chemical, structural and electronic properties of thin films of Cu and Ni on the Ru(0001) surface
[DE88-002360] 07 p0938 N88-1569

Localization of Cu 3d levels in the high Tc superconductor YBa2Cu3O approximately 7 by Cu2p X-ray photoelectron spectroscopy
[NOTA-INTERNA-887] 07 p0939 N88-15710

Electroformation: Principle electrochemical process of electrodeposition and electroformation of copper
[INPE-4374-NTE/274] 08 p0969 N88-15863

Copper electroforming from acid sulfate baths. Preliminary studies
[INPE-4375-RPE/554] 08 p0969 N88-15864

Investigation on diffusion reaction brazing of aluminium
[PB87-143368] 08 p0992 N88-16001

Magnetic investigations of superconductive polycrystalline (RE)1Ba2Cu3O(7-x) compounds (RE = Y, Gd, Ho, Dy)
[DE88-002537] 08 p1090 N88-16558

Coulomb interactions and effective strong coupling Hamiltonians in Cu-O superconductors
[DE88-002942] 08 p1090 N88-16561

Development of methods for low temperature diffusion bonding
[AD-A186875] 09 p1174 N88-17033

Free energy calculation via MD (molecular dynamics): Methodology and application to bicrystals
[DE88-002902] 09 p1256 N88-17532

Growth and electronic properties of strained metal overlayers
[DE87-010956] 10 p1417 N88-18463

The effects of various conductor components on Nb3Sn filament prestrain in cable-in-conduit conductors
[DE88-003956] 11 p1479 N88-18824

Atom probe microanalysis of superconducting YBa2Cu3O(sub 7-x)
[DE88-003203] 11 p1557 N88-19322

A direct correlation of strength with impact velocity
[AD-A189251] 13 p1741 N88-20409

A viscoplastic theory applied to copper
[NASA-TM-100831] 14 p1928 N88-21497

Thermal expansion behavior of randomly oriented short carbon fiber reinforced copper composites
[NASA-TT-20175] 15 p2031 N88-22099

Reciprocating sliding wear characteristics of copper-carbon fiber composites
[NASA-TT-20176] 15 p2031 N88-22100

Application of copper-carbon fiber composites to power semiconductor devices
[NASA-TT-20171] 15 p2031 N88-22101

Use of long-distance pair potentials in calculations of defect characteristics in metals
[DE88-701039] 15 p2037 N88-22138

Laser enhanced adhesion of copper films to sapphire substrates
[DE88-006802] 15 p2038 N88-22144

Vapor phase deposition and growth of polyimide films on copper
[AD-A189969] 15 p2044 N88-22178

RF properties of superconducting Pb electroplated onto Cu
[DE88-005918] 15 p2139 N88-22765

Magnetic anomalies in the rare earth oxide superconductors GdBa2Cu3O(7-x) and YbBa2Cu3O(7-x)
[AD-A190713] 15 p2144 N88-22793

Thermal conductivity, electrical conductivity and specific heat of copper-carbon fiber composite
[NASA-TT-20172] 16 p2172 N88-22948

High temperature superconductivity
[AD-A190259] 16 p2281 N88-23655

Effects of 67.5 MeV electron irradiation on Y-Ba-Cu-O and Gd-Ba-Cu-O high-temperature superconductors
[AD-A191271] 16 p2283 N88-23669

On quench sensitivity of Cu-Cr alloys
[NASA-TT-20174] 18 p2489 N88-24785

Fabrication of a flexible conductor by vapor deposition
[DE88-007500] 19 p2661 N88-25826

Anomalous RF magnetoresistance in copper at 4 K
[DE88-010232] 19 p2722 N88-26182

The T-T-T curve in Cu-Cr alloy
[NASA-TT-20167] 20 p2774 N88-26453

Oxygen vacancy ordering and superconductivity in YBa2Cu3O(sub 7-x)
[DE88-010005] 20 p2877 N88-27083
Pure metallic bridge and point-contact tunneling into single- and polycrystal YBa2Cu3O(sub 7-y)
[DE88-010030] 20 p2876 N88-27084
Electron irradiation effects in YBa2Cu3O7-Delta single crystals
[DE88-010050] 20 p2878 N88-27085
Growth and characterization of CuGaS2, CuAlS2 and CuGa0.9Al0.1S2 single crystals
[AD-A192963] 21 p3021 N88-27930
Relation between strength, creep and relaxation behavior in Cu and Al at room temperature
[ETN-88-92962] 23 p3195 N88-29015
Magnetic phase transitions in 90-K superconductors Ho1Ba2Cu3O(7-delta) and Gd1Ba2Cu3O(7-delta) observed by ZF-muon(+)SR
[DE88-752611] 23 p3290 N88-29588
Theoretical investigation of image states of the hydrogen covered Cu (100)
[DE88-702662] 23 p3292 N88-29604
An electrochemical impedance spectroscopy study of reactions at the metal/coating interface
24 p3355 N88-29975

COPPER ALLOYS
NT BRASSES
NT BRONZES
High velocity erosion of metal interfaces
[DE87-013937] 01 p0025 N88-10155
Effects of state recovery on creep buckling induced by thermomechanical loading 03 p0336 N88-12116
A comparison of high damping shape memory alloys with Cu-Mn-based and Fe-Cr-based alloys
[AD-A184110] 04 p0414 N88-12566
Phase diagram and thermochemical properties of the Al-Cu system
[ETN-88-91015] 05 p0566 N88-13447
Effectiveness of electrodeposited coatings in reducing atmospheric corrosion of copper substrates
[DE87-012651] 05 p0566 N88-13448
Fatigue crack growth behavior in hydrogen gas environment 06 p0716 N88-14391
The effects of low doses of 14 MeV neutrons on the tensile properties of three binary copper alloys
[DE88-003400] 11 p1458 N88-18691
Joining of dissimilar materials with the pulsed Nd-YAG laser
[DE88-003757] 11 p1458 N88-18693
Crystallization and glass formation in electron and laser beam irradiated Cu-Zr alloys
[DE88-003390] 11 p1464 N88-18729
Preparation and characterization of Cu2Zn1-xMnxGeS4
[AD-A188113] 11 p1556 N88-19315
Superconducting transition temperature of Cu-Nb microcomposites 14 p1973 N88-21775
Characterization of an explosively consolidated rapidly solidified Fe-16Ni-9Cr-5Mo-2Cu alloy powder
[DE88-006733] 15 p2041 N88-22162
Effects of cold working on precipitation in age hardenable alloys: On the copper alloys
[NASA-TT-20164] 16 p2177 N88-22973
Interface characterization of Cu-Cu and Cu-Ag-Cu low temperature solid state bonds
[AD-A191015] 16 p2283 N88-23667
Strain hardening at large strains in aluminum alloys
[DE88-007415] 18 p2484 N88-24737
Characterization of the 2219 Cegedur alloy. Data acquisition of the fracture mechanics --- aircraft construction materials
[REPT-48-442/F] 18 p2487 N88-24751
Aluminum alloy
[NASA-CASE-LAR-13924-1-CU]
18 p2487 N88-24753
The precipitation processes of Cu-Zr-Cr alloys
[NASA-TT-20168] 18 p2488 N88-24758
High temperature embrittleness of Cu-Cr alloy
[NASA-TT-20184] 18 p2488 N88-24759
Critical cooling rates on solution treatment of Cu-Cr and Cu-Be alloys
[NASA-TT-20163] 18 p2488 N88-24760
On the reversion phenomena of Cu-3 percent Ti alloys
[NASA-TT-20170] 18 p2488 N88-24762
On the abnormal phenomena observed in the electrical resistivity measurement during the decomposition process of saturated Cu-Fe alloys
[NASA-TT-20183] 18 p2507 N88-24869
Inelastic ion-surface collisions
[AFGL-TR-87-0206] 19 p2724 N88-26174
Formation of metastable structures and amorphous phases in Cu-W alloys using the triod sputtering technique
[DE88-009051] 21 p2915 N88-27298
Structural relationship between icosahedral and Frank-Kasper phases of Al-Li-Cu
[AD-A193768] 23 p3195 N88-29011

COPPER CHLORIDES
Efficient narrow linewidth waveguide dye laser pumped by CuCl laser 16 p2187 N88-23038

COPPER COMPOUNDS
NT COPPER CHLORIDES
NT COPPER OXIDES
NT COPPER SELENIDES
NT COPPER SULFIDES
Structural relationships in high temperature superconductors
[DE88-002924] 09 p1257 N88-17534
An investigation of metal complexes of some 2-substituted and 2,6-disubstituted pyridine N-oxides
11 p1460 N88-18701
Decomposition of hypochlorite in the presence of copper in a homogeneous medium
[NASA-TT-20199] 13 p1740 N88-20403
Copper peroxide
[NASA-TT-20245] 14 p1888 N88-21282
Improvements to Raney copper zinc methanol synthesis catalysts 17 p2318 N88-23844
The catalytic reactivity of thin film crystal surfaces
[DE88-006387] 19 p2732 N88-26228
Compilation of NRL publications on high temperature superconductivity
[AD-A189137] 21 p3019 N88-27921

COPPER OXIDES
Atomic-level studies of superconducting YBa2Cu3O sub 7-x
[DE88-002522] 06 p0788 N88-14831
Fabrication of YBa2Cu3O7 superconducting ceramics
[DE88-003012] 07 p0938 N88-15701
Theory of the tetragonal-to-orthorhombic structural phase transition in La2CuO4
[AD-A187141] 09 p1254 N88-17514
Bulk superconductivity in La2CuO4
[DE88-002509] 09 p1254 N88-17516
Superconductivity in La/sub 1.85-x/Nd/sub x/Sr/sub .15/CuO
[DE88-003014] 09 p1258 N88-17540
High temperature superconductivity research at Argonne National Laboratory
[DE88-003055] 09 p1258 N88-17541
Copper oxidation states, vacancy ordering and their effect on high temperature superconductivity
[DE88-003079] 09 p1258 N88-17542
Single-crystal structural study of La2Cu/sub 0.95/Li/sub 0.05/O4
[DE88-003482] 11 p1554 N88-19302
Potassium cuprate (3)
[NASA-TT-20246] 13 p1739 N88-20401
Characterization and fundamental studies on CuO sorbent materials to determine attrition mechanisms on substrate gamma alumina
[DE88-003674] 13 p1749 N88-20456
Large momentum pairing in one-dimensional systems
[AD-A189228] 13 p1835 N88-20981
The relationship of the chemical bonding topology of high critical temperature copper oxide superconductors to that of the chevrel phases and the ternary lanthanide rhodium borides
[AD-A189255] 13 p1845 N88-21042
On copper peroxide
[NASA-TT-20263] 15 p2037 N88-22135
Superconductivity and the tailoring of lattice parameters of the compound YBa2Cu3O(sub x)
[DE88-005904] 15 p2140 N88-22769
Thermochemistry and high temperature thermodynamic properties of rare earth-alkaline earth-copper oxide superconductors
[DE88-005976] 15 p2140 N88-22770
High temperature superconductors in the La(sub 1+x)Ba(sub 2-x)Cu O(sub y system
[DE88-006367] 15 p2145 N88-22802
Synthesis and characterization of high-T(sub c) screen-printed Y-Ba-Cu-O films on alumina
[NASA-TM-100860] 15 p2146 N88-22805
Comparison between muon spin rotation and neutron scattering studies on the 3-dimensional magnetic ordering of La2CuO(4-y) 17 p2396 N88-24244
Vacancy ordering in the basal plane of YBa2Cu3O(sub)z
[DE88-004572] 18 p2583 N88-25348
Paramagnetic spins in oxygen-loaded ceramic La2CuO4/sub 4+delta/
[DE88-007114] 19 p2619 N88-25539
Search for new high-temperature superconducting copper oxides
[DE88-009922] 19 p2735 N88-26245
All-electron local density theory of electronic structure and superconductivity in YBa2Cu3O7 and YBa2Cu3O6
[DE88-009944] 19 p2735 N88-26246
Phase transformations and thermodynamic behavior of the YBa2Cu3O(sub)x system via EMF measurements
[DE88-010054] 20 p2878 N88-27086
Superconducting properties of LaBa2Cu3O(sub x) and YBa2Cu3O(sub y)
[DE88-012038] 21 p3024 N88-27952
Preparation and characterization of isotopic oxygen-enriched yttrium barium copper oxide
[DE88-010939] 22 p3154 N88-28766
Possible mechanism for high-temperature superconductivity in the BaSr-La(Y)-CuO systems
[DE88-702060] 23 p3288 N88-29576
La2CuO(sub 4 + delta): A superconducting superoxide
[DE88-010325] 23 p3288 N88-29578
Theory of superconductivity in oxides
[AD-A195647] 24 p3433 N88-30432

COPPER SELENIDES
Device physics related to the granular nature of CuInSe2 solar cells
[DE88-001159] 21 p2967 N88-27622

COPPER SULFIDES
Physico-chemical studies on copper sulfide behavior in the CdS-Cu2S solar cell
[ETN-88-91068] 09 p1187 N88-17109
Electrically conducting polymer-copper sulphide composite films, preparation by treatment of polymer-copper (2) acetate composites with hydrogen sulfide
[NASA-TT-20204] 10 p1305 N88-17803
Investigation of the subsequent treatment and the stability of CuxS-CdS thin-film solar cells
[ETN-88-91488] 11 p1507 N88-19006
Activities of As, Sb, Bi and Pb in copper mattes and their effects on impurity elimination
[TKK-V-A10(1988)] 15 p2041 N88-22165

CORAL HEADS
U CORAL REEFS

CORAL REEFS
Mesoscale coastal ocean dynamics
11 p1517 N88-19060

CORDITE
U DOUBLE BASE PROPELLANTS

CORE FLOW
Flame driving of longitudinal instabilities in liquid fueled dump combustors
[AD-A183536] 01 p0006 N88-10033
High Rayleigh number convection in rectangular enclosures with differentially heated vertical walls and aspect ratios between zero and unity
[NASA-TM-100277] 12 p1628 N88-19739
Theoretical model and numerical solution for compressible viscous vortex cores
15 p2054 N88-22243
Physiological responses to acute exercise-heat stress
[AD-A192606] 21 p2986 N88-27732

CORE SAMPLING
Recommendations for a US ice coring program
[PB88-115043] 09 p1185 N88-17102
Data-base of Antarctic pre-Pleistocene sediment cores
[PB88-124151] 10 p1354 N88-18094
The comet rendezvous asteroid flyby mission
14 p2005 N88-21956
Retrieving samples from comet nuclei
14 p2006 N88-21959

CORES
NT EARTH CORE
NT HONEYCOMB CORES
NT REACTOR CORES
NT STELLAR CORES
Properties of Nb3Sn superconductor wires with composite cores
[KFK-4263] 02 p0246 N88-11557
Composite ceramic superconducting filaments for superconducting cable
[AD-A187833] 11 p1556 N88-19312
Low power consumption current transducer
[NASA-CASE-NPO-16888-1-CU]
17 p2335 N88-23937
High resolution detection of solute segregation to the cores of dislocations in grain boundaries
[DE88-009168] 20 p2877 N88-27078

CORIOLIS EFFECT
Effects of Coriolis acceleration on the vibrations of spinning structures 18 p2522 N88-24966
Activity-rotation relations for lower main sequence stars 23 p3298 N88-29640

CORN
Estimating scattered and absorbed radiation in plant canopies by remote sensing
[NASA-CR-181390] 02 p0193 N88-11205
Cytomorphology and ultrastructure of corn root meristem in weightlessness 12 p1651 N88-19891
Remote sensing techniques in the estimation of the area cultivated with beans, corn, and castor beans in the Irece County (Bahia State) 17 p2358 N88-24045

Spectral behavior of crops through analysis of LANDSAT-TM data 17 p2358 N88-24047
Evaluation of TM false color composites for crop discrimination 17 p2367 N88-24096

CORNEA
A field study on soft contact lens wear in USAF military transport aircraft
[AD-A195962] 24 p3407 N88-30285

CORNER FLOW
Experimental evaluation of turning vane designs for high-speed and coupled fan-drive corners of 0.1-scale model of NASA Lewis Research Center's proposed altitude wind tunnel
[NASA-TP-2661] 10 p1285 N88-17686
Laser velocimeter measurements in a wing-fuselage type juncture
[NASA-TM-100588] 15 p2014 N88-22012

CORNERS
Corner compensation structures for (110) oriented silicon
[DE88-003300] 10 p1417 N88-18455
Semilinear elliptic problems on domains with corners
[REPT-87-83] 20 p2846 N88-26888
Numerical treatment of the pressure singularity at a re-entrant corner
[AD-A193357] 21 p2944 N88-27488

CORONA BOREALIS CONSTELLATION
A large X-ray flare on Sigma 2 coronae borealis observed with exosat 04 p0508 N88-13121

CORONA DISCHARGES
U ELECTRIC CORONA

CORONAGRAPHS
Development of high stability fiber optic spectrophotometric systems for study of solar/stellar magnetic activity
[AD-A189327] 13 p1852 N88-21088

CORONAL HOLES
STIP Symposium on Physical Interpretation of Solar/Interplanetary and Cometary Intervals
[NASA-CR-181201] 01 p0110 N88-10709
Meterwave observations of a coronal hole
01 p0114 N88-10730
Study of the mechanism for solar wind formation
01 p0118 N88-10756

CORONAL LOOPS
Diagnostics of solar coronal loops at interferometric angular resolution 01 p0098 N88-10642
Active region flows 02 p0255 N88-11611
Pressure structure of solar coronal loops
02 p0256 N88-11618
A numerical study of the thermal stability of solar loops 02 p0256 N88-11619
Solar transition region and coronal response to heating rate perturbations 02 p0256 N88-11620
Loop interaction in the visible emission corona: Morphological details 02 p0256 N88-11622
Evidence for expanding magnetic loops in coronae of cool stars 04 p0510 N88-13134
Magnetic reconnection and solar flare loops
08 p1094 N88-16583
Flux tubes and loops in the solar chromosphere and corona 08 p1095 N88-16591
The effects of viscosity on resistive ballooning modes in line-tied coronal magnetic fields
08 p1097 N88-16599

CORONARY ARTERY DISEASE
Relationships between coronary heart disease risk factors and serum ionized calcium in Kennedy Space Center Cohort
[NASA-TM-100979] 10 p1368 N88-18177

CORONARY CIRCULATION
Response of coronary blood flow to step changes in plasma protein concentration in the isolated rat heart
12 p1651 N88-19892
Cardiac and peripheral circulation assessment by ultrasound on 3 astronauts during two 7-day space flights (1982 Salyut-7 - 1985 STS 51G)
12 p1656 N88-19921

CORONAS
NT CORONAL HOLES
NT CORONAL LOOPS
NT ELECTRIC CORONA
NT SOLAR CORONA
NT STELLAR CORONAS
LLE review
[DE87-014468] 02 p0178 N88-11110
Study of ionization equilibrium of high temperature and low density plasma
[DE87-703070] 02 p0238 N88-11502
Coronal magnetic fields produced by photospheric shear
[NASA-CR-181514] 03 p0390 N88-12447
Chromospheric and coronal heating in a bias-free sample of K dwarfs 04 p0518 N88-13184
Transverse flow deflections associated with fast coronal mass ejecta in interplanetary space
[DE88-003180] 09 p1263 N88-17566
Extended atmospheres of outer planet satellites and comets
[NASA-CR-181449] 10 p1430 N88-18540
The properties of solar coronal active regions deduced from X-ray line spectra
[AD-A193026] 20 p2886 N88-27141

COROTATION
Consistent linearization of the element-independent corotational formulation for the structural analysis of general shells
[NASA-CR-178418] 09 p1181 N88-17078
Prediction of the pressure distribution for radial inflow between co-rotating discs
[PNR90464] 22 p3076 N88-28261

CORPUSCLES (BLOOD)
U BLOOD CELLS

CORPUSCULAR RADIATION
NT BETA PARTICLES
NT ELECTRON BEAMS
NT ELECTRON PRECIPITATION
NT ENERGETIC PARTICLES
NT PRIMARY COSMIC RAYS
NT RADIATION BELTS
NT RELATIVISTIC ELECTRON BEAMS
NT SOLAR COSMIC RAYS
NT SOLAR ELECTRONS
NT SOLAR NEUTRONS
NT SOLAR PROTONS
Corpuscular plasma diagnostics complex on a tokamak with a strong field
[DE88-701576] 16 p2279 N88-23646

CORRECTION
NT ATMOSPHERIC CORRECTION
NT OPTICAL CORRECTION PROCEDURE
Wall interference tests of a CAST 10-2/DOA 2 airfoil in an adaptive-wall test section
[NASA-TM-4015] 02 p0122 N88-10772
Correction of inertial navigation system drift errors for an autonomous land vehicle using optical radar terrain data
[AD-A184973] 05 p0544 N88-13311
Photochemical ozone overburden correction
05 p0615 N88-13778
Correction method for Barker-coded modulation
06 p0691 N88-14240
Improved understanding of the loss-of-symmetry phenomenon in the conventional Kalman filter
[NASA-TM-100041] 06 p0766 N88-14709
Realization of active high pass filters for group velocity correction
[MPE-IN-REPT-47] 08 p0979 N88-15918
Intrinsic corrections to optical guiding in a free-electron laser: Beam Research Program
[DE88-002667] 09 p1172 N88-17026
Optimal correction problem of a multidimensional stochastic system
[AD-A186727] 09 p1228 N88-17353
Application of the multigrid technique to the pressure-correction equation for the SIMPLE algorithm --- Semi-Implicit Method for Pressure Linked Equations (SIMPLE) 11 p1539 N88-19196
Orbit correction requirements for a natural resources satellite
[INPE-4286-PRE/1158] 12 p1594 N88-19548
Holographically correcting synthetic aperture aberrations
[AD-A189510] 12 p1692 N88-20123
Orbit correction strategy for an Earth observation satellite
[INPE-4287-PRE/1159] 13 p1727 N88-20331
A numerical simulation of side force effects by aerodynamic flight trajectory correction
[ISL-CO-211/87] 21 p2896 N88-27191

CORRELATION
NT ANGULAR CORRELATION
NT AUTOCORRELATION
NT CORRELATION COEFFICIENTS
NT CORRELATION DETECTION
NT CROSS CORRELATION
NT DATA CORRELATION
NT SPECTRAL CORRELATION
NT STATISTICAL CORRELATION
Correlation of velocity and velocity-density turbulence in the exhaust of an atmospheric burner
02 p0185 N88-11147
The correlation between microstructure and thermomechanical properties of two-phase materials and porous sintered materials
[KFK-4205] 03 p0292 N88-11835
Interfacing distributed operating systems
[AD-A184489] 03 p0386 N88-12306
Using a new characterization of turbulent wind for accurate correlation of wind turbine response with wind speed
[DE88-001453] 04 p0466 N88-12681
Illustrative examples of principal component analysis using SYSTAT/FACTOR
[AD-A184920] 05 p0644 N88-13939
Example of correlation between space and spin coordinates
[DE87-703366] 05 p0657 N88-14030
Thermoelectric power in disordered electronic systems near the Anderson transition
[PREPRINT-547] 06 p0731 N88-14494
Correlation effects on double electron capture in highly-charged, low-energy ion-atom collisions
[DE87-013179] 07 p0930 N88-15651
High T/sub c/ superconductor as a strongly correlated state
[DE88-003194] 08 p1091 N88-16569
Strong consistency of certain information theoretic criteria for model selection in calibration, discriminant analysis and canonical correlation analysis
[AD-A186584] 09 p1232 N88-17385
Correlated processes in atomic collisions
[DE88-003508] 10 p1406 N88-18383
The correlation between methodological and low-level angle-of-arrival measurements 12 p1617 N88-19668
Correlations between photons in resonance fluorescence emitted by an atom near a metal surface
[AD-A188365] 12 p1689 N88-20102
A direct correlation of strength with impact velocity
[AD-A189251] 13 p1741 N88-20409
Estimation-correlation, modeling, and identification in adaptive array processors
[AD-A189130] 13 p1757 N88-20512
Periodically correlated processes and their stationary dilations
[NASA-CR-182904] 16 p2263 N88-23530
Sub-Saharan rainfall anomalies and global sea-surface temperature relationships for the recent fifteen year (1970-1984) period 22 p3122 N88-28552
Interannual variability of 850 mb temperatures during the Northern Hemisphere winter
22 p3123 N88-28562
The relationship between polar sea ice and the position of the near equatorial convergence zone
22 p3123 N88-28563
Computing partial correlations from the data matrix
[AD-A193904] 22 p3138 N88-28659
Extremal two-correlations of two-valued stationary one-dependent processes
[REPT-88-01] 22 p3145 N88-28704
Correlations between wettability and structure in monolayers of alkanethiols adsorbed on gold
[AD-A194348] 23 p3191 N88-28991
Application of optical correlation techniques to particle imaging velocimetry
[NASA-TM-101306] 23 p3218 N88-29152
Mathematical correlation between variations in solar radiation parameters. Part 1: Daily sums of global radiation and midday global radiation
[DE88-702742] 23 p3236 N88-29253
Performance of DS/SSMA communications in impulsive channels. Part 1: Correlation receivers
[AD-A195712] 24 p3362 N88-30021

CORRELATION COEFFICIENTS
Variances and higher order correlation coefficients: Continued
[RR-655-M] 18 p2563 N88-25219
Variations in the atmosphere associated with the 11-year solar cycle 22 p3122 N88-28557
Correlation method and sensors adapted to the environment 22 p3149 N88-28732

CORRELATION DETECTION
Corrections for the pseudorapidity gap correlation method --- particle correlations
[USIP-87-12] 09 p1245 N88-17463
Broadband correlation analysis
[AD-A188732] 13 p1814 N88-20839

CORRELATION FUNCTIONS
U CORRELATION

CORRELATORS
NT IMAGE CORRELATORS
Reception of pseudo noise-modulated signals using digital correlators for satellite navigation tasks
[ETN-87-90426] 01 p0037 N88-10234
A simplified, general-purpose deep-space ranging correlator design 11 p1473 N88-18786
Digital correlator for the portable channel prober measurement instrument
[AD-A189065] 14 p1904 N88-21377
Optical correlation using the magneto-optic device
[AD-A192342] 20 p2854 N88-26950
An optical 2-dimensional correlator for pattern recognition in embedded computing
[DE88-007198] 21 p2998 N88-27780

A fiber optic synchronous detector using sample-and-hold circuits
[DE88-010973] 21 p3016 N88-27899

Evaluation of multi-focus holographic lenses
[AD-A196167] 24 p3377 N88-30110

CORROSION

NT CAVITATION CORROSION
NT ELECTROCHEMICAL CORROSION
NT FRETTING CORROSION
NT FUEL CORROSION
NT HOT CORROSION
NT INTERGRANULAR CORROSION
NT RUSTING
NT SCALE (CORROSION)
NT STRESS CORROSION
NT STRESS CORROSION CRACKING

The corrosion of iron rotating hemispheres in 1 M sulfuric acid: An electrochemical impedance study
[DE87-014679] 02 p0148 N88-10925

Computer simulation of thermal modeling of primary lithium cells 02 p0163 N88-11022

Wear of iron and nickel in corrosive liquid environments
[NASA-TM-100246] 03 p0289 N88-11817

The effect of organic inhibitors on the atmospheric corrosion and solderability of copper
[DE88-000261] 04 p0414 N88-12565

Corrosion strength of niobium and its alloys
[DE87-703693] 04 p0416 N88-12578

Corrosion of ferritic steels by molten lithium: Influence of competing thermal gradient mass transfer and surface product reactions
[DE88-000334] 04 p0417 N88-12585

Ceramic technology for advanced heat engines project
[DE88-001520] 04 p0420 N88-12605

The role of inclusions in corrosion fatigue crack initiation in Q1N 05 p0604 N88-13699

Modeling the effect of sulfur on the threshold environmental cracking rate of steels in high temperature water 05 p0604 N88-13703

Monitoring corrosion and process physical-chemical parameters in electric power plants
[CISE-3708] 06 p0682 N88-14182

The factors which govern the acceleration of corrosion fatigue crack growth rate of a ferritic stainless steel
06 p0717 N88-14402

Fatigue thresholds of C-Mn steels in saline environments 06 p0717 N88-14403

Study of the vapor-liquid equilibria used in the fabrication process of hydrogen by thermochemistry
[DE88-900239] 07 p0830 N88-15035

Low frequency eddy current detection and evaluation of corrosion in aircraft skins
[ETN-88-91664] 09 p1144 N88-16859

Materials processing in space: An introduction to the G-480 payload 10 p1287 N88-17695

Application of ac-impedance method on determination of corrosion rate of metals
[DE88-750307] 10 p1300 N88-17771

Environment assisted degradation mechanisms in aluminum-lithium alloys
[NASA-CR-182482] 10 p1301 N88-17782

A review of pitting corrosion in high temperature aqueous solutions
[DE88-003547] 10 p1302 N88-17787

Corrosion behavior of sputter-deposited aluminum-based alloys exposed to chloride solutions
[AD-A187262] 10 p1303 N88-17794

Investigation of materials for inert electrodes in aluminum electrodeposition cells
[DE88-003380] 10 p1323 N88-17906

Fundamental studies of corrosion of nonoxide structural ceramics
[PB88-141536] 11 p1461 N88-18709

Corrosion, passivity and breakdown of alloys used in high energy density batteries
[DE88-004891] 13 p1743 N88-20422

Improve the lifetime of the hollow fiber sodium sulfur cell
[DE88-004861] 13 p1751 N88-20469

A five year weathering experiment with solar collectors
[DE88-900369] 13 p1796 N88-20740

JPRS report: Science and technology. USSR: Materials science
[JPRS-UMS-87-009] 14 p1884 N88-21261

Rust converters
[AD-A188767] 14 p1891 N88-21299

Durability testing of an iridium-plated storable rocket engine injector
[AD-A190707] 15 p2027 N88-22078

Galvanic corrosion initiatives
[AD-A190658] 15 p2040 N88-22155

Effect of P implantation on the corrosion behavior of Fe-Cr alloys
[DE88-005732] 15 p2040 N88-22158

Summary of the 1987 Gordon Research Conference on Corrosion
[AD-A189737] 15 p2041 N88-22161

User's manual for EULER3DS
[AD-A191048] 16 p2208 N88-23177

Microscopic control of semiconductor interface reactivity
[AD-A191193] 16 p2283 N88-23668

Corrosion and fatigue properties of FeCrB/Si metallic glass wires in aqueous environments
17 p2320 N88-23855

Structural Ceramics
[NASA-CP-2427] 17 p2323 N88-23872

Review of alkali metal and refractory alloy compatibility for Rankine cycle applications 17 p2428 N88-24447

Predictive corrosion modeling, volume 1
[AD-A191229] 18 p2485 N88-24739

Environmental integrity of coating/metal interface
[AD-A192184] 18 p2492 N88-24786

Corrosion in aircraft structures. Part 1: Text
[LR-527-PT-1] 20 p2775 N88-26458

Corrosion in aircraft structures. Part 2: Figures
[LR-527-PT-2] 20 p2775 N88-26459

Determination of Tafel constants in nonlinear polarization curves
[AD-A192335] 21 p2912 N88-27282

A critical review of IR drops and electrode potentials within pits, crevices and cracks
[AD-A192481] 21 p2935 N88-27431

Significance of the local electrode potential within pits, crevices and cracks
[AD-A192482] 21 p2935 N88-27432

Corrosion fatigue of small cracks: Mechanics and chemistry
[DE88-012121] 21 p2964 N88-27605

Proceedings of the 1987 Tri-Service Conference on Corrosion, volume 1
[AD-A191295] 22 p3053 N88-28114

Corrosion problems associated with computer disk packs 22 p3054 N88-28121

Electronic failure analysis-corrosion of avionics
22 p3054 N88-28122

Low cost corrosion sensors 22 p3054 N88-28123

A review of solid particle erosion of engineering materials
[DE88-010065] 22 p3054 N88-28124

Study of the erosion corrosion of alloys and coatings
[AD-A194337] 22 p3055 N88-28128

Erosion of metals exposed to hot, dense gases
[AD-A193708] 22 p3056 N88-28131

Some effects of nitrates on the tensile properties of Al 7075-T7351
[AD-A195118] 24 p3354 N88-29965

Performance Prediction for Coatings. Proceedings of a Workshop
[AD-A188973] 24 p3354 N88-29966

Degradation of protective coatings on steel in corrosive environments 24 p3354 N88-29969

Evaluation of organic coating deterioration and substrate corrosion in seawater using electrochemical impedance measurements 24 p3355 N88-29976

Alternative immersion accelerated testing of coating systems for Naval shoreline facilities
24 p3355 N88-29977

Zinc filled coatings 24 p3355 N88-29978

CORROSION PREVENTION

Workshop on Avionics Corrosion Control
[AGARD-R-733] 05 p0547 N88-13331

Avionic corrosion 05 p0547 N88-13332

Corrosion of electronic components
05 p0547 N88-13333

US Naval Air Force avionic and electrical system corrosion prevention and control maintenance
05 p0547 N88-13334

Corrosion in avionics and associated equipment; cause, effect and prevention 05 p0547 N88-13335

Avionics and corrosion 05 p0547 N88-13336

Simulated service test behavior of various internal and external coatings applied on CF6-50 first stage turbine blades
[NLR-MP-86018-U] 05 p0549 N88-13343

Ion plating for corrosion control
[AD-A185061] 05 p0565 N88-13442

Paints required for aeronautical construction
[SNIAS-872-551-102] 05 p0569 N88-13470

Multipurpose corrosion inhibitors for aerospace materials in Naval environments
[AD-A186726] 09 p1143 N88-16853

Corrosion-wear process under rolling-sliding motion
[AD-A189603] 13 p1778 N88-20835

Controlling stress corrosion cracking in mechanism components of ground support equipment
14 p1926 N88-21480

Development of a high-temperature resistant (700 F), corrosion-preventive organic coating
[AD-A191407] 16 p2182 N88-23009

Proceedings of the 1987 Tri-Service Conference on Corrosion, Volume 2
[AD-A189660] 17 p2319 N88-23847

Corrosion and corrosion inhibition of metals/alloys in methyphosphonic difluoride 17 p2319 N88-23850

Development of microencapsulated DNBM quaternary ammonium inhibitors for paints
17 p2319 N88-23851

Inadequacies of EMI-seal material: A corrosion study
17 p2319 N88-23852

Surface conditioning products as tools for corrosion removal and corrosion prevention
17 p2320 N88-23856

The effect of titanium reinforcement on the life of positive grids in lead-acid batteries 17 p2320 N88-23857

Recent advances in metallic/ceramic coatings for corrosion control in military applications
17 p2320 N88-23858

Carboxylate formation at the interface between a polyimide coating and cobalt 17 p2320 N88-23859

Agenda for advancing electrochemical science and technology 17 p2321 N88-23861

Vanadic hot corrosion of gas turbine blade coating materials 17 p2321 N88-23864

AC impedance analysis of corrosion fatigue in naval aircraft alloys
[AD-A190822] 17 p2322 N88-23865

The influence of cathodic protection on erosion-corrosion of metals and model alloys
[AD-A191613] 18 p2485 N88-24742

An investigation of ceramic coatings for protection of SiC from high-temperature corrosion
[DE88-007873] 18 p2493 N88-24790

Polyacrylic acid electrolyte-modified zinc phosphate conversion coatings for corrosion protection of steel
[DE88-004878] 19 p2617 N88-25527

Guide to the control of high temperature corrosion and protection of gas turbine materials
[PB88-107412] 20 p2760 N88-26370

Corrosion prevention in gas turbines
[NLR-MP-87029-U] 20 p2760 N88-26373

Development of protective coatings for ceramic tubular components
[PB88-197165] 20 p2776 N88-26463

Unified methods of accelerated laboratory tests of the preparations for temporary protection of cars
[NASA-TT-20298] 21 p2921 N88-27336

Proceedings of the 1987 Tri-Service Conference on Corrosion, volume 1
[AD-A191295] 22 p3053 N88-28114

Corrosion and stress corrosion of metals in decontamination solutions 22 p3054 N88-28118

Avionic and electrical system corrosion prevention and control maintenance 22 p3054 N88-28119

Shielding effectiveness of metallic joints versus corrosion prevention 22 p3054 N88-28120

Design guidelines for prevention of corrosion in combat and tactical vehicles
[AD-A194172] 22 p3055 N88-28126

Corrosion control through a better understanding of the metallic substrate/organic coating/interface
[AD-A193981] 22 p3056 N88-28132

Degradation of protective coatings on steel in corrosive environments 24 p3354 N88-29969

Reduced time frame for predicting coating performance 24 p3356 N88-29979

CORROSION RESISTANCE

NT OXIDATION RESISTANCE

Optimizing the application of high temperature corrosion resistant aluminum-silicon-base coatings
[BLL-M-37222-(5826.4)] 01 p0018 N88-10112

Polyitaconic acid macromolecule primer for adhesive bonding and corrosion control of aluminum
[DE87-013306] 01 p0027 N88-10173

Determination of the fatigue strength of mechanically, thermally and corrosively loaded multilayer materials
[ETN-87-90375] 01 p0058 N88-10372

JPRS report: Science and technology. USSR: Materials science
[JPRS-UMS-87-006] 03 p0285 N88-11791

Corrosion resistance of silver-plated carbon-aluminum composite 03 p0285 N88-11793

Corrosion-electrochemical and mechanical properties of composite graphite-carbide metal materials based on titanium and its alloys 03 p0285 N88-11794

Corrosion-resistant amorphous metallic coatings: Engineering development
[NASA-CR-181487] 03 p0287 N88-11802

Ion plating: Fundamental processing studies and synthesis of high performance coatings
[AD-A184766] 03 p0303 N88-11906

Double-effect absorption heat pump, phase 3
[PB87-232195] 03 p0317 N88-12005

Corrosion behavior of P/M mechanically alloyed IN-9052.1: An electro-chemical investigation
[AD-A184191] 04 p0414 N88-12567

Work-in-progress presented at the Army Symposium on Solid Mechanics, 1986: Lightening of the Force
[AD-A184791] 04 p0427 N88-12644

Composite materials applications program at the US Army Ballistic Research Laboratory: Work in progress
04 p0428 N88-12651

Corrosion control by composite material substitution with application to the M-939 5-ton truck
04 p0428 N88-12654

Corrosion susceptibility study of candidate pin materials for ALTC (Active Lithium/Thionyl Chloride) batteries
[DE88-001449] 04 p0440 N88-12734

Reliability of Li/SO2 cells for long-life applications
[DE88-001360] 04 p0440 N88-12735

An examination of coating failure on wing pivot fittings of f111 aircraft
[AD-A185028] 05 p0546 N88-13328

Corrosion resistance of sintered alloy steels
[BLL-M-37363-(5828.4)] 05 p0564 N88-13438

Effectiveness of electrodeposited coatings in reducing atmospheric corrosion of copper substrates
[DE87-013651] 05 p0586 N88-13448

Resistance of canopy materials against chemicals
[PML-1985-22] 05 p0589 N88-13466

Coupling effects between the ferrite and austenite phases during corrosion fatigue of a ferrite/austenite duplex stainless steel 05 p0605 N88-13706

The effect of ion implantation on the corrosion behavior of a high-density sintered tungsten alloy
[AD-A185713] 06 p0683 N88-14185

Study on characteristics of SCC propagation da/dt for welded joint
[PB87-143640] 07 p0869 N88-15270

Modification of properties of metals by high-power ion beams 08 p1079 N88-16507

Corrosion behavior of high density tungsten alloys
[AD-A187108] 09 p1143 N88-16852

Effect of low-temperature aging on the mechanical properties of cast stainless steels
[DE88-002872] 10 p1300 N88-17774

Studies of the initiation of pitting corrosion on stainless steels
[AERE-M-3615] 10 p1301 N88-17778

Corrosion performance of high damping alloys in 3.5 percent sodium chloride environment
[AD-A188048] 11 p1457 N88-18687

Corrosion resistance of electrodeposited amorphous Ni-Cr-P alloys
[DE88-005116] 11 p1459 N88-18695

Protecting old oil tanks made of steel against internal corrosion using organic coatings
[DE88-751089] 11 p1459 N88-18698

Institute for Materials Science and Engineering, Metallurgy: Technical activities 1987
[PB88-157722] 11 p1460 N88-18702

The intergranular segregation of boron in substoichiometric Ni3Al
[DE88-004783] 11 p1462 N88-18720

Anodic behavior of Ni-P and Ni-Cr-P metallic glasses
[DE88-005334] 11 p1463 N88-18722

Characteristics and use of lubricating greases
[DE88-751103] 11 p1463 N88-18723

The effects of thin polymeric surface films in reducing fretting corrosion and wear
[AD-A188633] 12 p1611 N88-19634

Hydrogen embrittlement of gun steel
[AD-A188972] 13 p1740 N88-20407

A fundamental understanding of the effect of alloying elements on the corrosion resistance of rapidly solidified Mg alloys
[AD-A189385] 13 p1741 N88-20413

Optimization of binary pigment coatings
[AD-A189103] 13 p1748 N88-20450

Controlling stress corrosion cracking in mechanism components of ground support equipment
14 p1926 N88-21480

Corrosion and electrochemical behavior of binary magnesium alloys
[AD-A190524] 15 p2040 N88-22154

The corrosion resistance of an aluminum alloy coated with polysilazane derived ceramics
[AD-A190703] 15 p2046 N88-22189

Corrosion of electroless nickel-coated steel
[AD-A191045] 16 p2179 N88-22985

Proceedings of the 1987 Tri-Service Conference on Corrosion, Volume 2
[AD-A189660] 17 p2319 N88-23847

Polyitaconic acid macromolecule primer for adhesive bonding and corrosion control of aluminum
17 p2319 N88-23849

Stress corrosion cracking properties of Al-Li alloys
17 p2320 N88-23853

Corrosion of tungsten alloys in marine environments
17 p2320 N88-23854

Ion beam alloying of aluminum for corrosion resistance 17 p2321 N88-23860

Improving knowledge of the corrosion behavior of aluminum alloys of the 7XXX series
[REPT-48-451/F] 18 p2486 N88-24750

Characterization of 7090 and 7091 profiles made with Cegedur powder --- powder metallurgy, aircraft construction materials
[REPT-48-441/F] 18 p2487 N88-24752

Optimization of mechanical/corrosion properties of TI-CODE 12 plate and sheet. Part 2: Thermomechanical processing effects
[DE88-007493] 19 p2616 N88-25517

Electrodeposition of amorphous Ni-Cr-P alloys
[DE88-006866] 19 p2616 N88-25521

Guide to the control of high temperature corrosion and protection of gas turbine materials
[PB88-107412] 20 p2760 N88-26370

Nickel aluminides: A new family of nickel + aluminum alloys featuring simple composition, low density, excellent oxidation resistance and high yield strength that increases with temperature
[DE88-010692] 20 p2776 N88-26461

Performance Prediction for Coatings. Proceedings of a Workshop
[AD-A188973] 24 p3354 N88-29966

Electrochemical evaluation of the long term corrosion resistance of polymer coated steel
24 p3355 N88-29974

Zinc filled coatings 24 p3355 N88-29978

Reduced time frame for predicting coating performance 24 p3356 N88-29979

CORROSION TESTS
NT SALT SPRAY TESTS

Crevice corrosion of stainless steels and related alloys. Part 2: Summary of experimental test data for input to mathematical model
[BR99671-PT-2] 03 p0289 N88-11816

Corrosion and deterioration testing in humid tropic environments
[AD-A186917] 10 p1302 N88-17783

Improving knowledge of the corrosion behavior of aluminum alloys of the 7XXX series
[REPT-48-451/F] 18 p2486 N88-24750

Reduced time frame for predicting coating performance 24 p3356 N88-29979

CORRUGATED PLATES

Stiffened titanium panels
[NASA-CASE-LAR-13814-1] 18 p2497 N88-24816

CORRUGATING

Characteristics of long size thermosyphons made of corrugated tube 20 p2784 N88-26511

Variational analysis of dielectrically loaded multidepth corrugated waveguides
[PB88-193602] 20 p2793 N88-26573

CORTICOSTEROIDS
NT ALDOSTERONE

Influence of general vertical vibration on relationships between mediators in various segments of brain
06 p0751 N88-14613

Evaluation of the endogenous glucocorticoid hypothesis of denervation atrophy
[NASA-CR-182848] 17 p2381 N88-24157

CORUNDUM
U ALUMINUM OXIDES

COS-B SATELLITE

COS-B in-orbit study
[ESA-CR(P)-2420] 01 p0017 N88-10102

COSINE SERIES

Method of assessing changes in biorhythmological structure of human physiological functions
19 p2706 N88-26088

COSMIC BACKGROUND EXPLORER SATELLITE

Surface scattering characteristics and the measurement of particulate contamination 02 p0137 N88-10862

Space Infrared Telescope Facility (SIRTF) design and thermal analysis 08 p0982 N88-15934

DIRBE External Calibrator (DEC)
[NASA-CR-180761] 12 p1631 N88-19760

COSMIC DUST
NT INTERPLANETARY DUST
NT ZODIACAL DUST

Composition, structure and chemistry of interstellar dust
[NASA-TM-88350] 02 p0253 N88-11603

Monte Carlo modeling and meteor showers
06 p0740 N88-14549

Atmospheric entry heating of cosmic dust
06 p0794 N88-14865

Exobiology and life science 07 p0883 N88-15358

Progress toward a cosmic dust collection facility on space station
[NASA-CR-182427] 12 p1598 N88-19566

A mass spectrometer evolved gas analysis experiment for in-situ analysis of cometary dust volatiles
13 p1854 N88-21097

CCD-observations of gas and dust jets in the coma of Comet Halley 14 p1998 N88-21912

Profiles of the major gas emissions and distribution of dust particles in the inner coma (0 to 10,000 km) of Comet Halley 14 p1999 N88-21919

Dust coma morphology of Comet Halley during the Giotto encounter 14 p2000 N88-21921

New properties of cometary dust
14 p2001 N88-21926

Anisotropic emission from comets: Fans versus jets. 1: Concept and modeling 14 p2001 N88-21927

Anisotropic emission from comets: Fans versus jets. 2: Periodic Comet Tempel 2 14 p2001 N88-21928

Comet P/Halley's near-nucleus jet activity
14 p2001 N88-21929

Dust photometry in the near nucleus region of Comet Halley from VEGA-2 observations
14 p2001 N88-21930

Dynamics of charged submicron grains in Halley's coma 14 p2001 N88-21931

Composition of cometary dust particles --- Halley
14 p2001 N88-21932

Isotopic composition of Halley dust
14 p2002 N88-21933

P/Halley dust coma: Grains or rocks?
14 p2002 N88-21936

The origin of low mass particles within and beyond the dust coma envelopes of Comet Halley
14 p2002 N88-21938

Optical and hydrodynamic implications of Comet Halley dust size distribution 14 p2003 N88-21939

Similarity and diversity of the polarization of comets
14 p2003 N88-21940

The dust around the nucleus of Comet Halley
14 p2003 N88-21942

Variation of grain properties at the dust outbursts --- Halley's comet 14 p2003 N88-21943

The evolution of the mass distribution of cometary particles 14 p2004 N88-21946

The dust tail of Comet Halley
14 p2008 N88-21974

Dust tail streamers and Halley's nucleus rotation
14 p2008 N88-21979

A spectroscopic study of absorption and emission features of interstellar dust components
[B8681462] 16 p2289 N88-23706

Stars, gas and dust in the Andromeda galaxy
[B8679680] 16 p2289 N88-23708

Optical and infrared observations of high latitude dust clouds --- interstellar matter
[B8621135] 16 p2289 N88-23709

Modeling of a cometary dust coma
[ETN-88-92980] 23 p3300 N88-29651

COSMIC GAMMA RAY BURSTS
U GAMMA RAY BURSTS

COSMIC GASES
NT INTERPLANETARY GAS
NT INTERSTELLAR GAS
NT NEUTRAL GASES

COSMIC PLASMA

Cosmology in the plasma universe
[TRITA-EPP-87-07] 05 p0660 N88-14053

Cosmic electric currents and the generalized Bennett pinch
[TRITA-EPP-87-14] 22 p3154 N88-28764

COSMIC RADIATION
U COSMIC RAYS

COSMIC RADIO WAVES
U EXTRATERRESTRIAL RADIO WAVES

COSMIC RAY SHOWERS

Cosmic-ray nuclear event with an anomalously strong concentration of energy and particles in the central region
[DE87-703376] 04 p0526 N88-13213

A combined cosmic ray muon spectrometer and high energy air shower array
[DE88-003057] 09 p1264 N88-17574

COSMIC RAYS
NT COSMIC RAY SHOWERS
NT GALACTIC COSMIC RAYS
NT GAMMA RAY BURSTS
NT PRIMARY COSMIC RAYS
NT SOLAR COSMIC RAYS

Summary and conclusions of the 6th Moriond workshop --- standard electroweak model
[USIP-87-11] 01 p0092 N88-10602

Solar modulation of the cosmic radiation in the heliosphere 01 p0112 N88-10720

Solar-geophysical data number 513, May 1987. Part 1: (Prompt reports). Data for April, March 1987 and late data
[PB87-204939] 01 p0119 N88-10760

Research in particles and fields
[NASA-CR-180412] 01 p0119 N88-10763

Particle injection and cosmic ray acceleration at collisionless parallel shocks
[DE88-000507] 04 p0430 N88-12665

Activities report in interplanetary space physics
[IFSI-86-5] 05 p0659 N88-14047

Budget and programs for 1986 research
[IFSI-86-16] 05 p0660 N88-14048

Cosmic ray NM-64 neutron monitor data 14, Rome, Italy, January - December 1985
[IFSI-87-8] 05 p0661 N88-14060

Astromag: A particle spectrometer for the Space Station
[PREPRINT-557] 06 p0707 N88-14336

Solar-geophysical activity reports for STIP (Study of Travelling Interplanetary Phenomena) interval 15, 12-21 February 1984 ground level event and STIP interval 16, 20 April-4 May 1984 Forbush decrease
[PB88-101274] 06 p0802 N88-14906

Rome Neutron Monitor (NM) - 64 data for 5 solar particle ground-level events
[IFSI-86-7] 06 p0806 N88-14918

A compilation of Sudden Storm Commencements (SSCs), associated interplanetary disturbances, and cosmic ray variations
[IFSI-86-11] 06 p0807 N88-14923

Xiphophorus: A system to recognize radiation-induced mutations and to study the effects of zero-gravity environment on embryo development
07 p0885 N88-15372

Application of correlation method of reception of direct and reflected cosmic radiation to study of plasmaspheres of planet and distribution of radiation brightness
08 p1004 N88-16085

Life sciences experiments on stratospheric balloons and sounding rockets 08 p1033 N88-16262

A research program in neutrino physics, cosmic rays and elementary particles
[DE88-003507] 09 p1264 N88-17575

Radiation problems in manned space flight with a view to the Space Station 12 p1658 N88-19934

Effects of cosmic heavy ion radiation and space microgravity on plant systems 12 p1658 N88-19936

HNC: A detector to study ultraheavy cosmic rays
12 p1713 N88-20252

A low-frequency measurement of the spectrum of the cosmic microwave background radiation
13 p1858 N88-21112

High energy cosmic muons and the calibration of the L3 electromagnetic calorimeter
[NOTA-INTERNA-895] 14 p2011 N88-21999

Hydrodynamical models of supernova SN 1987 A in the LMC
[DE88-701123] 15 p2151 N88-22837

A map of the cosmic background radiaton at 3 millimeters
[INPE-4529-PRE/1279] 15 p2152 N88-22850

Solar-geophysical data number 520, December 1987. Part 1: (Prompt reports). Data for November 1987, October 1987 and late data
[PB88-164199] 16 p2290 N88-23712

Observations of cosmic rays in the outer heliosphere
[NASA-CR-182942] 18 p2596 N88-25425

Products from cosmic-ray interactions in extraterrestrial matter: What they tell us about radiation backgrounds in space
[DE88-009143] 19 p2743 N88-26288

Effects of cosmic rays on single event upsets
[NASA-CR-183053] 20 p2793 N88-26569

Observation of a point source in Cygnus constellation with the underground detector at Frejus (France)
[PITHA-87/02] 20 p2884 N88-27122

Time-dependent mass loss from hot stars with and without radiative driving
[DE88-008899] 20 p2884 N88-27128

Studies of HZE particle interactions and transport for space radiation protection purposes
[NASA-TM-101159] 20 p2886 N88-27142

Research in particle and gamma-ray astrophysics
[NASA-CR-183111] 20 p2887 N88-27146

Are Centauros diffractive
[DE88-008767] 21 p3032 N88-27996

Embryogenesis and organogenesis of Carausius morosus under spaceflight conditions
22 p3061 N88-28167

On the nucleonics component of cosmic radiation, in the atmosphere
[DE88-702493] 22 p3166 N88-28854

Research in particle and gamma-ray astrophysics
[NASA-CR-183126] 24 p3455 N88-30566

The Single Event Upset (SEU) test facility on the Harwell tandem generator for cosmic ray simulation
[AERE-R-12896] 24 p3459 N88-30580

COSMIC X RAYS

Center for X-Ray Optics, 1986
[DE88-000715] 04 p0449 N88-12783

COSMOCHEMISTRY

Reports and contributions of the Max-Planck Institute of Chemistry (Otto Hahn Institute)
[REPT-1/87] 11 p1570 N88-19398

Advances in geochemistry and cosmochemistry: Trace element microdistributions with the synchrotron X-ray fluorescence microprobe
[DE88-006355] 15 p2032 N88-22108

Workshop on the Origins of Solar Systems
[NASA-CR-183025] 24 p3451 N88-30536

Nebular processes recorded in chondritic meteorites
24 p3451 N88-30541

Cosmochemical trends of volatile elements in the solar system 24 p3451 N88-30542

COSMOGONY

U COSMOLOGY

COSMOLOGY

NT BIG BANG COSMOLOGY

NT MISSING MASS (ASTROPHYSICS)

Spontaneous symmetry breaking in N = 3 supergravity
[DE87-702753] 01 p0109 N88-10705

New class of spherically symmetric interior solution with cosmological constant
[DE87-703095] 02 p0226 N88-11422

On the cosmological constant in the heterotic string theory
[DE87-703099] 02 p0247 N88-11562

On the degree of generality of inflationary solutions in cosmological models with a scalar field
[DE87-703079] 02 p0251 N88-11586

Crucial cosmological observations
[DE87-703081] 02 p0251 N88-11587

Geometrization of Planck length in composite gravity and supergravity
[DE87-703085] 02 p0251 N88-11588

Magnitude-redshift relation in a perturbed Friedmann universe
[DE87-753020] 02 p0252 N88-11590

Torsion as a source of expansion in a Bianchi type I universe in the self-consistent Einstein-Cartan theory of a perfect fluid with spin density
[AD-A184200] 03 p0322 N88-12037

Number count-redshift relation in universe models with nonzero cosmological constant
[DE87-703043] 03 p0388 N88-12435

Cosmology with decaying vacuum energy
[DE88-000698] 03 p0389 N88-12443

Homogeneous space-time of Goedel type in higher-derivate gravity
[DE87-703690] 04 p0500 N88-13077

Cosmological applications of singular hypersurfaces in general relativity 04 p0521 N88-13202

Galaxy formation by gravitational collapse in a universe dominated by cold dark matter 04 p0521 N88-13205

Model of earlier stage of universe's evolution
06 p0775 N88-14758

Evolution of perturbations in expanding universe
06 p0775 N88-14759

Gravitational interaction of massless fields with higher spins (s greater than 2) 06 p0775 N88-14760

Number count-redshift relation in a perturbed Friedmann universe
[DE88-750302] 07 p0945 N88-15743

Evolution from pure states into mixed states in de Sitter space
[DE88-750316] 07 p0945 N88-15745

Qualitative methods in nonhomogeneous cosmology
[DE88-700620] 10 p1417 N88-18458

Quark matter in astrophysics and cosmology
[DE88-003406] 10 p1429 N88-18534

Cosmic strings: A problem or a solution
[DE88-003410] 10 p1429 N88-18535

Velocity reversal and the arrows of time
[DE88-004237] 10 p1429 N88-18536

Notes on a class of homogeneous space-times
[DE88-700136] 11 p1562 N88-19353

Experimental analysis of absolute space-time Lorentz theories
[DE88-700140] 11 p1563 N88-19355

Seventy years of the general theory of relativity
[DE88-700784] 11 p1563 N88-19356

Can the causal pathologies of Goedel-type universes be avoided in higher-derivative gravity
[DE88-700185] 11 p1568 N88-19387

Reports and contributions of the Max-Planck Institute of Chemistry (Otto Hahn Institute)
[REPT-1/87] 11 p1570 N88-19398

Modified theory of gravity
[DE88-700835] 12 p1642 N88-19830

On (p,n) systematics and the cosmological connection
[DE88-005031] 12 p1712 N88-20245

Rotation of universe --- metagalaxies
14 p1974 N88-21780

Finite width corrections to the Nambu action for the Nielsen-Olesen string
[DE88-006996] 15 p2147 N88-22812

Density perturbations in a rotating universe
[DE87-703036] 15 p2151 N88-22840

String driven inflation
[DE88-006994] 15 p2151 N88-22841

Cosmology for high energy physicists
[DE88-005705] 15 p2151 N88-22842

Particle cosmology comes of age
[DE88-006998] 15 p2151 N88-22844

Stable, heavy, neutral particles in the sun and in toponium decay 17 p2452 N88-24568

Light propagation through gravitationally perturbed Friedmann universes 18 p2577 N88-25307

Inevitable inflation in Einstein-Cartan theory with improved energy-momentum tensor with spin
[NASA-TM-101146] 18 p2586 N88-25365

The geometry of the Virasoro group for physicists
[DE88-007374] 18 p2586 N88-25366

Cosmic wavefunction with induced gravity
[DE88-701873] 20 p2884 N88-27129

Cosmological helium production simplified
[DE88-009578] 20 p2885 N88-27130

Cosmions and stars
[DE88-010886] 20 p2887 N88-27145

Cosmological parameters and evolution of the galaxy luminosity function
[NASA-CR-183081] 21 p3030 N88-27986

Dynamical evolution of cosmic strings
[DE88-011724] 21 p3030 N88-27989

Newtonian and Einsteinian gravitation
22 p3158 N88-28791

Cosmological applications 22 p3158 N88-28794

Evolution of heavy-element abundances in the galactic halo and disk
[DE88-011736] 22 p3164 N88-28845

Cosmology in an N-dimensional vector space
[DE88-702550] 23 p3277 N88-29507

Clustering of galaxies and clusters of galaxies in a decaying-particle cosmological model with a massive decay product
[DE88-753434] 23 p3298 N88-29642

Systematic properties of clusters of galaxies in different cosmological scenarios 23 p3299 N88-29646

Activities in astrophysics
[INPE-4582-PRE/1316] 24 p3456 N88-30570

COSMONAUTS

Present stage of space medicine
10 p1364 N88-18151

Results of long-term electrocardiographic monitoring of cosmonauts 10 p1364 N88-18152

Hypnosis: Possible applications for cosmonauts
12 p1665 N88-19984

History of manned spaceflight
[CNES-NT-121] 21 p3032 N88-28000

COSMOS SATELLITES

NT INTERCOSMOS SATELLITES

Analysis of the orbit of Cosmos 1335 (1982-07A) at 3:12 resonance
[RAE-TR-87041] 14 p1872 N88-21185

Determining near-water wind speed using radar data from Cosmos-1500 artificial earth satellite
24 p3449 N88-30524

COSPAS

COSPAS/SARSAT 406-MHz emergency beacon digital controller
[NASA-TM-100859] 20 p2792 N88-26566

KOSPAS-SARSAT satellites used for ocean current study 24 p3450 N88-30534

COST ANALYSIS

Comparison of costs and benefits for dc and ac transmission
[DE87-008774] 02 p0167 N88-11052

Models for conducting economic analysis of alternative fuel vehicles
[AD-A184028] 03 p0334 N88-12103

Competition Analysis Model (CAM). Volume 2: Computer manual
[AD-A184017] 03 p0384 N88-12411

CNET (Chief of Naval Education and Training) Program Automated Tracking System (CPATS): A comprehensive study
[AD-A184694] 03 p0385 N88-12418

Hypersonic aerodynamics: Applications for HOTOL
05 p0535 N88-13252

A study of the Department of Defense configuration management policies and procedures as applied to the FA-18 Strike/Fighter program
[AD-A184872] 05 p0657 N88-14034

The 1988 NASA (National Aeronautics and Space Administration) authorization
[GPO-80-245] 05 p0659 N88-14044

Ceramic technology for advanced heat engines
[PB87-232997] 06 p0683 N88-14188

Life-cycle cost analysis of residential heat pumps and alternative HVAC (Heating, Ventilating and Air-Conditioning) systems
[DE88-003701] 07 p0839 N88-15090

The Shock and Vibration Bulletin. Part 1: Welcome, Keynote Address, Invited Papers, Nondevelopment Items Workshop and Pyrotechnic Shock Workshop
[AD-A186748] 08 p0997 N88-16034

Guidelines for qualifying non-development equipment to shock and vibration 08 p0997 N88-16036
Commonality analysis as a knowledge acquisition problem 08 p1062 N88-16413
A problem of machine repair with a variable number of heterogeneous servers
[INPE-4245-PRE/1118] 08 p1074 N88-16482
A model for estimating depot maintenance costs for Air Force fighter and attack aircraft
[AD-A187097] 09 p1105 N88-16624
A cost and benefit analysis of hydraulic fluid systems for the next generation of tactical aircraft
[AD-A186911] 09 p1116 N88-16690
Turbine engine monitoring systems: Can they benefit component improvement program management?
[AD-A186992] 09 p1120 N88-16706
Communications satellite systems operations with the space station. Volume 3: Supplementary technical report
[NASA-CR-180875] 09 p1133 N88-16794
Cape Blanco wind farm feasibility study
[DE88-003748] 10 p1348 N88-18059
Cape Blanco wind farm feasibility study
[DE88-003749] 10 p1349 N88-18060
Robustness in cost performance models
[AD-A187163] 11 p1566 N88-19374
Flight Vehicle Development Time and Cost Reduction
[AGARD-CP-424] 12 p1700 N88-20173
Picking winners: Parametric cost estimating and project management 12 p1700 N88-20176
Parametric study of the total cost of aircraft modernization in terms of development and equipment series costs 12 p1700 N88-20177
The increased time and cost of development: Causes and (some) remedies 12 p1701 N88-20178
Reasons for increasing development cost of rotary wing aircraft and ideas to reverse the trend
12 p1701 N88-20179
What can be done to face growing development costs
12 p1701 N88-20181
Schedule and cost control of development
12 p1704 N88-20196
Task allocation for efficient performance of a decentralized organization
[AD-A188699] 12 p1705 N88-20204
A cost analysis for the implementation of commonality in the family of commuter airplanes, revised
[NASA-CR-182569] 12 p1706 N88-20221
Expected value analysis for an unmanned expendable launch vehicle payload escape system
[AD-A189494] 13 p1728 N88-20337
Turnaround operations analysis for OTV. Volume 3: Technology development plan
[NASA-CR-179318] 13 p1729 N88-20342
Performance and cost benefits associated with nonimaging secondary concentrators used in point-focus dish solar thermal applications
[DE88-001104] 13 p1792 N88-20718
Advanced avionics system analysis. Modular avionics cost benefit study formulation
[AD-A189019] 14 p1867 N88-21158
Requirements and cost considerations for a Combined Space Nuclear Reactor Test Facility
[DE88-006763] 15 p2132 N88-22719
A method for estimating and controlling the cost of extending technology
[AD-A190717] 15 p2150 N88-22831
Status of CAD/CAM in medium-sized industries described 16 p2184 N88-23022
The multi-disciplinary design study: A life cycle cost algorithm
[NASA-CR-4156] 17 p2385 N88-24172
Requirements and cost considerations for a combined space nuclear reactor test facility
17 p2401 N88-24277
System capacity and economic modeling computer tool for satellite mobile communications systems
19 p2644 N88-25686
Engine component retirement for cause. Volume 1: Executive summary
[AD-A192730] 20 p2760 N88-26371
Finding minimum-cost circulations by successive approximation
[AD-A192724] 21 p3005 N88-27824
Approximations and optimal control for the pathwise average cost per unit time and discounted problems for wideband noise driven systems
[AD-A192712] 21 p3008 N88-27847
Sources and nature of cost analysis data base reference manual
[AD-A193099] 21 p3028 N88-27976
Price estimates and analysis
22 p3161 N88-28818
Aircraft avionics and missile system installation cost study. Volume 1: Technical report and appendices A through E
[AD-A194605] 23 p3178 N88-28923
A plan for time-phased incorporation of automation and robotics on the US space station
23 p3255 N88-29377
Finding minimum-cost circulations by canceling negative cycles
[AD-A194027] 23 p3271 N88-29468
Finding minimum-cost circulations by successive approximation
[AD-A194028] 23 p3272 N88-29469
New developments in capital cost estimating
[DE88-005392] 23 p3297 N88-29638
Aircraft airframe cost estimating relationships: Study approach and conclusions
[R-3255-AF] 24 p3324 N88-29795
The cost and performance implications of reliability improvements in the F-16A/B
[AD-A195096] 24 p3324 N88-29796
Aircraft avionics and missile system installation cost study. Volume 2: Appendices F and G
[AD-A195372] 24 p3325 N88-29801
Centaur operations at the space station: Cost and transportation analysis
[NASA-CR-182128] 24 p3332 N88-29835
Space systems cost study
[AD-A196024] 24 p3439 N88-30469

COST EFFECTIVENESS
Gallium arsenide and multibandgap solar cell research
[DE87-012260] 02 p0194 N88-11215
Nowcasting for the national economy needs
02 p0199 N88-11241
Automotive Stirling engine: Mod 2 design report
[NASA-CR-175106] 02 p0250 N88-11578
Experiments in fault tolerant software reliability
[NASA-CR-181554] 05 p0632 N88-13863
Concept definition study for recovery of tumbling satellites. Volume 2: Supporting research and technology report
[NASA-CR-179229] 06 p0672 N88-14117
Ceramic technology for advanced heat engines
[PB87 232997] 06 p0683 N88-14186
Methods for reducing computational costs of typical finite element unsteady hydrodynamic models
[AD-A185499] 06 p0702 N88-14312
Strategic Defense Initiative Organization/DARPA (Defense Advanced Research Projects Agency) workshop on laser propulsion. Volume 1: Executive summary
[DE87-003254] 06 p0768 N88-14722
Collider constraints in the choices for wavelength and gradient scaling
[PB87-123691] 06 p0779 N88-14783
Risk analysis methodology survey
07 p0922 N88-15604
A cost and benefit analysis of hydraulic fluid systems for the next generation of tactical aircraft
[AD-A186911] 09 p1116 N88-16690
Evaluation of bituminous materials used in pavement recycling projects at Tyndall, MacDill, and Hurlburt Air Force Bases
[AD-A188068] 10 p1317 N88-17871
Analysis of the performance of an air-water heat pump: Regulation of intrinsic performances
[DE88-900241] 10 p1349 N88-18061
Applications of lower cost computers to dimensional gaging
[BDX-613-3606] 11 p1525 N88-19108
Cost-effective orbit transfer modes for satellite retrieval and servicing — Space Station
12 p1586 N88-19489
Cost effective development of a national test bed
[NASA-TM-100321] 12 p1601 N88-19585
High shear rate rheometry of low-viscosity liquids
[AD-A188447] 12 p1627 N88-19733
Reducing rotary wing aircraft development time/cost through the use of simulation 12 p1702 N88-20186
Systems analysis and simulation techniques: Essential tools for balanced complex weapon system designs in terms of performance and cost
12 p1702 N88-20187
Minimizing development flight test time and cost in the US Air Force 12 p1703 N88-20192
EDF's studies and first choices regarding the design of electrical equipment
[NASA-TT-20222] 13 p1764 N88-20553
Advances in personal computers for scientific applications
[DE88-009824] 19 p2713 N88-26107
The intelligent QAR and its cost effective role in new generation AIMS — quick access recorder (QAR); aircraft integrated monitoring systems (AIMS)
22 p3035 N88-28020
Report to congress on the strategic defense system architecture
[AD-A195476] 24 p3426 N88-30393

COST ESTIMATES
Cost savings possible with Air Force conversion to JP-8 as its primary fuel
[AD-A183784] 01 p0030 N88-10192
Space station: National Aeronautics and Space Administration's 1987 cost estimate
[PB87-220760] 02 p0140 N88-10883
Determination of life cycle costs in astronautics
[MBB-UR-E-910/86-PUB] 02 p0249 N88-11572
Carbon Dioxide observational platform System (CO-OPS) Feasibility Study
[NASA-CR-179225] 06 p0671 N88-14113
Feasibility study of a carbon dioxide observational platform system. Volume 2: Programmatics
[NASA-CR-180404] 06 p0672 N88-14114
Highlights of the 70th Flight Mechanics Panel Symposium on Flight Vehicle Development Time and Cost Reduction
[AD-A185831] 07 p0901 N88-15454
Iterative-deepening heuristic search for optimal and semi-optimal resource allocation
08 p1062 N88-16410
A model for estimating depot maintenance costs for Air Force fighter and attack aircraft
[AD-A187097] 09 p1105 N88-16624
A comparison of projection methods in the forecasting of overhead costs for seven government aerospace contractors
[AD-A187572] 10 p1425 N88-18514
Analysis of learning curve fitting techniques
[AD-A187680] 11 p1535 N88-19173
Robustness in cost performance models
[AD-A187163] 11 p1566 N88-19374
Turnaround operations analysis for OTV. Volume 2: Detailed technical report
[NASA-CR-179317] 13 p1729 N88-20341
Turnaround operations analysis for OTV. Volume 4: WBS and dictionary and cost methodology
[NASA-CR-179319] 13 p1729 N88-20343
A method for estimating and controlling the cost of extending technology
[AD-A190717] 15 p2150 N88-22831
A comparative study of project estimating tools
[DE88-009059] 19 p2740 N88-26266
Knowledge-based cost estimating vs traditional software cost models
[DE88-009707] 20 p2883 N88-27116
Price estimates and analysis
22 p3161 N88-28818
Aircraft avionics and missile system installation cost study. Volume 1: Technical report and appendices A through E
[AD-A194605] 23 p3178 N88-28923
New developments in capital cost estimating
[DE88-005392] 23 p3297 N88-29638
Aircraft avionics and missile system installation cost study. Volume 2: Appendices F and G
[AD-A195372] 24 p3325 N88-29801

COST REDUCTION
Cost savings possible with Air Force conversion to JP-8 as its primary fuel
[AD-A183784] 01 p0030 N88-10192
Development of an innovative, low-cost solar collector
[PB87-206819] 02 p0194 N88-11210
Making space nickel/hydrogen batteries lighter and less expensive
[DE88-000168] 05 p0578 N88-13530
Methods for reducing computational costs of typical finite element unsteady hydrodynamic models
[AD-A185499] 06 p0702 N88-14312
Highlights of the 70th Flight Mechanics Panel Symposium on Flight Vehicle Development Time and Cost Reduction
[AD-A185831] 07 p0901 N88-15454
Guidelines for qualifying non-development equipment to shock and vibration 08 p0997 N88-16036
The ILV: A new commercial expendable launch vehicle — Industrial Launch Vehicle (ILV)
08 p1035 N88-16275
Commonality analysis as a knowledge acquisition problem 08 p1062 N88-16413
Small gas turbine engine technology
09 p1107 N88-16638
Software for integrated manufacturing systems, part 1
09 p1211 N88-17261
Software for integrated manufacturing systems, part 2
09 p1211 N88-17262
Apollo Lightcraft project
[NASA-CR-182575] 11 p1445 N88-18615
Commonality in the design and production of the H-423 (F3) and H-770 (F-15) RLG inertial navigation systems
12 p1577 N88-19431
Changes in USAF structural loads requirements
12 p1580 N88-19452

Concentrating photovoltaic collectors: Fabrication design
[PB88-148051] 12 p1640 N88-19821
The formal specification of computer systems
[AD-A188947] 12 p1675 N88-20013
Flight Vehicle Development Time and Cost Reduction
[AGARD-CP-424] 12 p1700 N88-20173
Risk reduction cost avoidance for full scale development begins with concept formulation
12 p1700 N88-20174
Development savings through parametric modeling of program costs 12 p1700 N88-20175
What can be done to face growing development costs
12 p1701 N88-20181
Development cost reduction using integrated CAE-CAD-CAM techniques 12 p1701 N88-20182
Organization of helicopter development activities with a view toward reduction of costs and cycles
12 p1704 N88-20200
Direct nuclear propulsion for Earth-to-orbit vehicles
17 p2400 N88-24271
Space systems cost study
[AD-A196024] 24 p3439 N88-30469

COSTS
NT AIRCRAFT PRODUCTION COSTS
NT LIFE CYCLE COSTS
NT LOW COST
NT OPERATING COSTS
Design study for asteroidal exploitation
03 p0389 N88-12445
A comparison of the basket method and the stratified random sampling for contract change order negotiations
[AD-A184170] 04 p0500 N88-13080
A plan for collecting ada software development cost, schedule and environment data
[AD-A185905] 07 p0902 N88-15460
A comparison of fitting techniques for the cumulative average learning curves with historical lot cost data
[AD-A187127] 09 p1227 N88-17349
Sigma system: Overview, prospects
15 p2052 N88-22230
Microvax networked computer system
[AD-A190308] 15 p2114 N88-22596
A method for estimating and controlling the cost of extending technology
[AD-A190717] 15 p2150 N88-22831
Timing regulations to prevent stratospheric-ozone depletion
[R-3495-JMO/RC] 19 p2690 N88-25987
Costs — space projects 22 p3160 N88-28816
Artificial intelligence costs, benefits, risks for selected spacecraft ground system automation scenarios
24 p3416 N88-30332
Information technology to facilitate group interaction
24 p3438 N88-30463

COTTON
Research on cotton plants grown in space
08 p1006 N88-16098
Identification of farming systems in the cotton area of West Burkina Faso from SPOT-1 data
22 p3097 N88-28389

COUCHES
Ergonomy and interior furnishing of the cabins of deep diving manned submarines: The Nautile example — couch 19 p2697 N88-26032

COUETTE FLOW
The aspect ratio dependence of the attractor dimension in Taylor-Couette flow
[AD-A196297] 24 p3369 N88-30065

COULOMB COLLISIONS
Effect of collisional broadening on the polarizability of a two-dimensional electron gas
[DE87-013928] 02 p0237 N88-11497
Application of a two fluid theoretical plasma transport model on current Tokamak reactor designs
[DE87-013511] 03 p0377 N88-12373
Coulomb interactions and effective strong coupling Hamiltonians in Cu-O superconductors
[DE88-002942] 08 p1090 N88-16561
Determination of molecular-ion structures through the use of accelerated beams
[DE88-002980] 09 p1246 N88-17467
QED description of relativistic Coulomb excitation in heavy ion collisions
[DE88-700834] 12 p1689 N88-20100

COULOMB POTENTIAL
Effect of collisional broadening on the polarizability of a two-dimensional electron gas
[DE87-013928] 02 p0237 N88-11497
Superfluidity of a two dimensional Boson Coulomb gas
[DE88-009827] 19 p2735 N88-26244

COUNTER ROTATION
Noise of a model high speed counterrotation propeller at simulated takeoff/approach conditions (F7/A7)
[NASA-TM-100206] 01 p0091 N88-10592
Turbines with counterrotating runners for aircraft power plants 02 p0158 N88-10092
Noise of a model counterrotation propeller with reduced aft rotor diameter at simulated takeoff/approach conditions (F7/A3)
[NASA-TM-100254] 05 p0647 N88-13961
Secondary flow measurements with L2F-technique in centrifugal compressors 10 p1283 N88-17676
Porous wind tunnel corrections for counterrotation propeller testing
[NASA-TM-100873] 15 p2015 N88-22019
The 2-D and 3-D time marching transonic potential flow method for propfans 16 p2220 N88-23245
Numerical solutions of the Euler equations for the flow field around counter-rotating propellers
19 p2636 N88-25638

COUNTERFLOW
Innovative, counterflow gas/fine solids, direct contact heat exchanger
[DE88-004744] 13 p1770 N88-20585
Superfluid turbulence in counterflowing helium II
19 p2665 N88-25849

COUNTERMEASURES
NT ANTIRADAR COATINGS
NT ELECTRONIC COUNTERMEASURES
NT JAMMING
NT OPTICAL COUNTERMEASURES
Application of the analysis phase of the instructional system development to the MK-105 magnetic minesweeping mission of the MH-53E helicopter
[AD-A186282] 07 p0822 N88-14994
Laser countermeasure impacts and penalties
[DE88-006871] 18 p2520 N88-24947
MIDIR (Mid-infrared) laser, phase 1
[AD-A193935] 23 p3220 N88-29166

COUNTERS
NT CERENKOV COUNTERS
NT ELECTRON COUNTERS
NT NEUTRON COUNTERS
NT NEUTRON SPECTROMETERS
NT PARTICLE TELESCOPES
NT PROPORTIONAL COUNTERS
NT RADIATION COUNTERS
NT SCINTILLATION COUNTERS
NT SPARK CHAMBERS
Design, fabricate, calibrate, test and deliver two satellite electron flux detectors
[AD-A190799] 16 p2169 N88-22930
The design and performance of a real-time self excited vocoder 19 p2653 N88-25753
Robust vector quantization for noisy channels
19 p2653 N88-25754
Analysis and improvement of the vector quantization in SELP (Stochastically Excited Linear Prediction)
19 p2653 N88-25756

COUNTING
A Prohorov bound for a Poisson process and a Bernoulli process
[CWI-MS-R8701] 09 p1232 N88-17388
Random truncation models and Markov processes
[CWI-MS-R8702] 09 p1232 N88-17389
Performance of a photon counting microchannel plate intensifier with wedge and strip image readout
[DE88-003831] 10 p1334 N88-17970
Product-integrals and counting processes
[CWI-MS-R8707] 14 p1965 N88-21727
Inference for a nonlinear semimartingale regression model
[AD-A190857] 16 p2262 N88-23527
Coincidence counting corrections under conditions used by A. DeVolpi
[NPL-RS(EXT)-90] 17 p2393 N88-24224

COUNTING CIRCUITS
NT SCALERS

COUPLED MODES
The Coupled Cluster Single and Double excitation (CCSD) method in quantum chemistry: An efficient formulation of the theory and application to closed shell molecular systems
[DE88-000475] 07 p0930 N88-15650
Hydromagnetic cavity eigenmodes in a non-uniform plasma 08 p1098 N88-16610
Studies of spectral line ratio fluctuations using inductively Coupled Plasma (ICP) light
[IRF-PREPRINT-100] 18 p2578 N88-25311
Coupled even-parity superconducting states: Square lattice
[AD-A193432] 21 p3022 N88-27938
Modal synthesis by use of substructures with fixed or free coupling points
[ILR-MITT-191] 22 p3069 N88-28341
Band pass with cavity resonators by use of three oscillation types
[ETN-88-92984] [illegible] p3209 N88-29096
Role of ordinary to extraordinary mode wave coupling in ionospheric heating experiments
[AD-A195335] 24 p3362 N88-30017

COUPLERS
NT COUPLING CIRCUITS
NT DIPLEXERS
Integrated fiber-optic coupler
[AD-A184494] 03 p0377 N88-12369
Eigenmode analysis of parallel waveguide couplers
[PB87-132122] 06 p0693 N88-14254
Coupled high power waveguide laser research
[AD-A189800] 15 p2071 N88-22345
Current-drive on the Versator-2 tokamak with a slotted-waveguide fast-wave coupler
[DE88-006261] 15 p2136 N88-22743
Study and implementation of ultrahigh frequency coupling devices using the fin line technology — millimeter waves
[ETN-88-92307] 20 p2796 N88-26588
Theoretical and experimental study of a mode-converting coupler for application to a harmonic gyrotron amplifier
[AD-A193760] 22 p3081 N88-28294

COUPLES
A substructure method for dynamic simulation of flexible mechanical systems with geometric nonlinearities
09 p1176 N88-17044

COUPLING
NT ELECTROMAGNETIC COUPLING
NT MAGNETOSPHERE-IONOSPHERE COUPLING
NT MICROWAVE COUPLING
NT OPTICAL COUPLING
NT SPIN-SPIN COUPLING
NT THERMODYNAMIC COUPLING
Optimum size of staged flux compression generators
[DE87-011741] 01 p0038 N88-10244
Modeling of environmentally-induced transients within satellites. Part 2: Discharge coupling transients
03 p0273 N88-11722
Ion-matrix coupling in polymer electrolytes from relaxation time studies
[AD-A184632] 03 p0293 N88-11841
Bonding and coupling of C sub 1 fragments on metal surfaces
[AD-A184186] 03 p0295 N88-11852
Modeling of proximity coupling between superconducting filaments in superconducting dipole magnets
[DE87-014684] 03 p0382 N88-12402
Coupled elastic rotor/body vibrations with inplane degrees of freedom 05 p0595 N88-13643
Non-minimal interaction of gravity with other physical fields: An overview
[DE87-703362] 05 p0624 N88-13819
Determination of the neutral current chiral coupling constants u sublsq, u subrsq, d sublsq and d subrsq from an (anti)neutrino-deuterium experiment
[B8715857] 06 p0779 N88-14780
Coulomb interactions and effective strong coupling Hamiltonians in Cu-O superconductors
[DE88-002942] 08 p1090 N88-16561
Coupling of microscopic and macroscopic processes in the Earth's magnetotail 08 p1095 N88-16566
Method of iterative coupling between periodic aerodynamic and dynamic fields
[PB87-169934] 09 p1113 N88-16669
Development of a coupled expert system for the spacecraft attitude control problem
09 p1205 N88-17223
Coupling finite element and spectral methods: First results
[NASA-CR-181606] 09 p1231 N88-17379
Renormalization group analysis of the temperature dependent coupling constant in massless theory
[DE88-751059] 09 p1259 N88-17552
Experimental evaluation of turning vane designs for high-speed and coupled fan-drive corners of 0.1-scale model of NASA Lewis Research Center's proposed altitude wind tunnel
[NASA-TP-2681] 10 p1285 N88-17686
Dynamics of coupled electron-nucleon motion in a laser field
[DE88-005063] 10 p1337 N88-17994
The dynamics of two coupled rigid bodies
[AD-A187592] 10 p1341 N88-18012
Piezoelectric laminates for torsional and bending modal control: Theory and experiment
10 p1343 N88-18029
The dynamics of coupled planar rigid bodies. Part 1: Reduction, equilibria and stability
[AD-A187467] 10 p1345 N88-18042
Application of a multigrid method to a buoyancy-induced flow problem
[DE88-003961] 10 p1397 N88-18326
A superelement component dynamic synthesis method 11 p1500 N88-18956

Efficient parallel architecture for highly coupled real-time linear system applications
[NASA-CR-182649] 12 p1675 N88-20015
Interaction of particulate and transformation toughening
[AD-A189321] 13 p1741 N88-20412
Comparison of methods for the calculation of thermal contact resistance of the first Brazilian satellite
[NASA-TT-20180] 14 p1880 N88-21239
Inductive spurious coupling of a dc-SQUID to resonant input circuit
[NOTA-INTERNA-894] 14 p1908 N88-21401
Equatorial dynamics and ocean-atmosphere coupling
14 p1938 N88-21565
Stabilization and control problems in structural dynamics
[AD-A190197] 15 p2073 N88-22361
Coupled bending-torsion steady-state response of pretwisted, nonuniform rotating beams using a transfer-matrix method
[NASA-TM-100596] 15 p2086 N88-22435
Control of combustion and acoustically coupled fluid dynamic instabilities 17 p2318 N88-23843
Magnetic drive coupling
[NASA-CASE-MSC-21171-1] 17 p2344 N88-23973
Optical pressure sealing couping (light joint)
[NASA-CASE-MFS-29348-1] 18 p2576 N88-25303
Velocity coupling 19 p2629 N88-25596
Analysis of plasma coupling with the prototype DIII-D ICRF antenna
[DE88-008085] 19 p2729 N88-26204
N=2 supergravity in superspace: different versions and matter couplings
[DE88-702137] 19 p2741 N88-26274
Coupling of a spark source mass spectrograph and a ND-YAG laser
[DE88-012116] 21 p2951 N88-27530
HPM (High-Power Microwave) coupling into realistic targets
[DE88-011788] 23 p3207 N88-29084
COUPLING CIRCUITS
Low frequency IF transformer designs having variable coupling
[RAE-TM-RAD-NAV-291] 01 p0043 N88-10272
Research relative to an advanced rod control system for quadrupole mass spectrometry applications
[NASA-CR-181458] 02 p0167 N88-11050
COUPLING COEFFICIENTS
A microwave FEL (Free Electron Laser) code using waveguide modes
[DE88-000225] 03 p0330 N88-12084
COUPLINGS
Ammonia transfer across rotating joints in space
14 p1927 N88-21492
Development of a rotary fluid transfer coupling and support mechanism for space station
14 p1928 N88-21493
Multi-metallic galvanic corrosion
[AD-A195995] 24 p3353 N88-29963
COURSES
U PATHS
COVARIANCE
Breakdown points of affine equivariant estimators of multivariate location and covariance matrices
[REPT-87-14] 01 p0088 N88-10574
Identification of multivariate outliers and leverage points by means of robust covariance matrices
[REPT-87-15] 01 p0088 N88-10575
Covariant Lorentz anomalies in higher dimensional space
[DE87-753021] 02 p0230 N88-11448
A heteroscedastic hierarchical model
[AD-A184256] 03 p0372 N88-12340
Illustrative examples of principal component analysis using BMDP/4M
[AD-A185179] 05 p0635 N88-13881
Illustrative examples of principal component analysis using SYSTAT/FACTOR
[AD-A184920] 05 p0644 N88-13939
Development of a technique for estimating noise covariances using multiple observers
[NASA-TM-4020] 06 p0669 N88-14098
On the asymptotic joint distributions of the eigenvalues of random matrices which arise under components of covariance model
[AD-A186387] 07 p0915 N88-15556
Operator foundation of functional integral in non-Abelian gauge theory
[DE88-700508] 07 p0941 N88-15719
Control variate selection for multiresponse simulation
[AD-A186637] 08 p1069 N88-16463
The linear dependency structure of covariance nonstationary time series
[AD-A186548] 09 p1232 N88-17383
Five-diagonal weighting scheme for geodetic profiles
[AD-A188033] 10 p1347 N88-18054
Covariance analysis and post-processing of gravity compensation effects for aided multi-state navigation systems
[PAPER-87-13] 12 p1577 N88-19430
Computer programs for calculating group cross-section covariances from uncertainty parameters in the ENDF/B-V format: UNC 32/33 — neutron physics
[ECN-202] 13 p1837 N88-20995
Mathematics clinic probabilistic position-fixing
[NASA-CR-182753] 15 p2125 N88-22672
State covariance assignment of discrete systems: Development and applications 17 p2393 N88-24225
Annotated computer output for split plot design: SAS GLM
[AD-A190800] 18 p2555 N88-25167
Optimal a priori covariance selection for the solution of ill-conditioned nonlinear inverse problems
18 p2564 N88-25222
Computing partial correlations from the data matrix
[AD-A193904] 22 p3138 N88-28659
The covariance of scalar fields scattered by pressure-release randomly rough surfaces
[AD-A192489] 22 p3146 N88-28714
COVERINGS
An experimental investigation of rocket ramjet nozzle assembly base pressures
[AD-A189714] 15 p2027 N88-22076
Solar cell cover glasses for satellites
15 p2052 N88-22225
Hatch cover
[NASA-CASE-MSC-21356-1] 18 p2472 N88-24671
COVES
U BAYS (TOPOGRAPHIC FEATURES)
COWELL METHOD
U NUMERICAL INTEGRATION
COWLINGS
Thermostructural analysis of simulated cowl lips
15 p2080 N88-22403
CRAB NEBULA
Gamma-ray imaging observations of the Crab and Cygnus regions 10 p1427 N88-18522
The application of imaging to the atmospheric Cerenkov technique: Observations of the Crab nebula
20 p2884 N88-27126
Application of two-dimensional imaging to very high energy gamma ray astronomy
[DE88-010120] 21 p3030 N88-27983
CRACK ARREST
Summary of HSST wide-plate crack-arrest tests and analyses
[DE88-002601] 08 p1000 N88-16061
Crack arrest fracture toughness of armor steels
[AD-A187711] 11 p1456 N88-18681
Applications of elastic-viscoplastic constitutive models in dynamic analyses of crack run-arrest events
14 p1930 N88-21507
Analysis of crack arrest toughness
[AD-A193340] 21 p2913 N88-27286
CRACK CLOSURE
Fatigue 87, volume 1
[AD-A184045] 05 p0597 N88-13645
Closure behavior under constant effective stress intensity loading conditions 05 p0598 N88-13656
The influence of the topography of fracture surfaces on crack closure 05 p0598 N88-13657
Significance of fatigue crack closure under spectrum loading 05 p0599 N88-13662
Fatigue crack propagation of short and long cracks: Phys. basis, prediction methods and engineering significance 05 p0599 N88-13664
The growth behavior of small fatigue cracks, the effect of microstructure and crack closure
05 p0600 N88-13673
An experimental study of closure behavior of naturally initiated small cracks 05 p0601 N88-13676
Behavior of long and short fatigue cracks in a powder metallurgy superalloy at room and at high temperature
05 p0601 N88-13677
Closure and propagation behavior of short fatigue cracks at different R-ratios 05 p0601 N88-13679
A unified model for fatigue crack initiation, short crack growth, long crack propagation, and closure effects
05 p0601 N88-13680
Observations on the effect of overloads on fatigue crack growth 05 p0602 N88-13684
Crack growth in contrasting titanium alloys under the conjoint action of high and low cycle fatigue
05 p0602 N88-13686
Near threshold growth of defects in engineering materials 05 p0603 N88-13691
Effects of MN dispersoids on near threshold fatigue crack growth in 2134 type alloys
05 p0603 N88-13692
Fatigue 87, volume 3
[AD-A184047] 05 p0604 N88-13700
Occurance and growth of fatigue cracks in corrosion environment 05 p0604 N88-13704
Fracture kinetics of corrosion fatigue
05 p0605 N88-13708
Constraint effects in fatigue crack growth
05 p0606 N88-13719
An optical interferometry technique to evaluate closure along a crack front 05 p0607 N88-13726
Fatigue 87, volume 2
[AD-A184046] 06 p0715 N88-14381
Notch-geometry effect on propagation threshold of short fatigue cracks in notched components
06 p0716 N88-14393
Influence of crack closure on fatigue crack propagation and threshold 06 p0716 N88-14394
The relationship between microstructural size and fatigue threshold in iron and steel
06 p0716 N88-14396
Effect of compressive portion of loading cycles on the near threshold fatigue closure behavior
06 p0717 N88-14398
Absolute fatigue thresholds in metallic materials
06 p0717 N88-14399
A model for ultra-low fatigue crack growth
06 p0717 N88-14404
Influence of stress ratio R on fatigue threshold delta K(th) for 40Cr steel 06 p0718 N88-14405
The effects of loading history on fatigue crack growth threshold 06 p0718 N88-14406
Threshold and crack-growth tests on pre-cracked specimens produced in cyclic compression
06 p0718 N88-14412
The effect of prestraining on fatigue crack growth in nickel-base alloys 06 p0719 N88-14415
Crack closure phenomena in modes 1 and 2 interactions 06 p0719 N88-14417
Effect of temperature exposure on fatigue crack propagation 06 p0720 N88-14421
Analysis of crack closure under plane strain conditions
[NASA-CR-182369] 06 p0722 N88-14439
Random loading fatigue crack growth: Crack closure considerations 06 p0797 N88-14881
Investigations on the crack growth retardation behavior and fatigue life prediction in structural materials
[PB87-143756] 07 p0827 N88-15016
Comparative investigations of indirect crack length measurement under fatigue loading in a corrosive environment
[GKSS-86/E/64] 11 p1502 N88-18972
The fatigue behavior of ferritic and austenitic steels at elevated temperatures
[DE88-006304] 13 p1744 N88-20431
Cyclic crack growth emanating at a round notch considering viscoplasticity
[AD-A189577] 13 p1781 N88-20655
Bimodular behavior and crack closure in compression in a brittle material
[AD-A191267] 16 p2224 N88-23275
Three-dimensional aspects of fatigue crack closure
[AD-A192296] 21 p2960 N88-27581
CRACK FORMATION
U CRACK INITIATION
CRACK GEOMETRY
Fatigue crack growth 05 p0608 N88-13734
Development and calibration of Direct Current Potential Difference (DCPD) crack length measurement equipment
[VTT-RR-480] 09 p1182 N88-17083
Scattering of impulsive acoustic waves by a semi-infinite crack in the plane interface of a half-space and a layer
[PB88-126396] 10 p1405 N88-18377
Comparative investigations of indirect crack length measurement under fatigue loading in a corrosive environment
[GKSS-86/E/64] 11 p1502 N88-18972
Sensitivity to crack initiation in thick assemblies. Test report 48-444
[REPT-48-444] 20 p2758 N88-26365
Wide range stress intensity factor expression for an edge-cracked round bar bend specimen
[AD-A196285] 24 p3382 N88-30147
CRACK INITIATION
Evaluation of cracking in aluminum cylinders
[PB87-201398] 01 p0024 N88-10149
A quantitative statistical model for cleavage fracture initiation in carbide strengthened steels
[ETN-87-90735] 01 p0025 N88-10157
Crack initiation life estimations for notched specimens with residual stresses based on local strains
[FF-17/1986] 01 p0060 N88-10385
Fracture mechanical analysis of the initiation and propagation of matrix and surface cracks in thermally loaded fiber composite models
[ETN-87-90439] 01 p0062 N88-10400
The effect of temperature on fatigue crack initiation from aluminosilicate inclusions
[PNR90377] 02 p0154 N88-10962

Crack behavior in ceramic materials under static, slowly increasing, and cyclic loading conditions
[KFK-4209] 02 p0154 N88-10964
An acoustic emission digital data acquisition workstation
[DE87-012425] 02 p0191 N88-11191
Some new fatigue tests in high temperature water and liquid sodium environment
[DE87-753019] 02 p0192 N88-11197
Fracture mechanism of fine grain graphite under high heat fluxes
[IPPJ-842] 02 p0242 N88-11527
Resistance of welded joints in high temperature Hastelloy N-type nickel alloy to hot crack formation
03 p0286 N88-11798
Flaw imaging and ultrasonic techniques for characterizing sintered silicon carbide
[NASA-TM-100177] 03 p0334 N88-12106
Application of fracture mechanics theory in the reliability analysis of structural ceramics in multiaxial loading
03 p0335 N88-12113
Crack initiation and propagation due to cyclic thermal gradients --- aircraft turbine blades
[ESA-TT-1023] 03 p0336 N88-12114
Spread of plastic deformation in notched and cracked plates 03 p0337 N88-12122
Computational methods and results for dynamic fracture 03 p0337 N88-12123
A probabilistic model of brittle crack formation
[AD-A184423] 03 p0338 N88-12129
Creep life prediction based on stochastic model of microstructurally short crack growth
[NASA-TM-100245] 04 p0456 N88-12825
Data base on the high heat flux behaviour of metals and carbon materials for plasma facing components. Experiments at the 10 MW neutral beam injection test stand of the IPP Nagoya
[IPPJ-AM-53] 04 p0492 N88-13031
Fatigue 87, volume 1
[AD-A184045] 05 p0597 N88-13645
Cyclic deformation and crack initiation
05 p0597 N88-13646
Effect of grain orientation on the origination and the initial growth of fatigue cracks in pure iron
05 p0597 N88-13647
The mechanics of fatigue-crack nucleation in a low-alloy steel under fretting conditions 05 p0597 N88-13649
Surface deformation and fatigue crack initiation of alpha-iron 05 p0598 N88-13651
The effect of ion beam mixed Ni-Al surface layers on PSB extrusion morphology in fatigued nickel
05 p0598 N88-13652
The orientations of dipolar walls produced by cyclic deformation 05 p0598 N88-13655
Growth of short fatigue cracks in a squeeze formed aluminum alloy 05 p0598 N88-13658
The effect of alpha platelet morphology and beta-grain size on the initiation and growth of short fatigue cracks in Ti65S 05 p0600 N88-13667
The initiation and growth of small fatigue cracks in copper at room and cryogenic temperatures
05 p0600 N88-13668
Behavior of short cracks in a 2024 aluminum alloy sheet tested at several stress ratios 05 p0600 N88-13669
The influence of microstructure and residual stresses on the initiation and propagation of short surface cracks on AlMgSi1 05 p0601 N88-13674
Threshold stress for fatigue crack initiation from a small crack 05 p0601 N88-13675
A unified model for fatigue crack initiation, short crack growth, long crack propagation, and closure effects
05 p0601 N88-13680
Fatigue of 30CrMnSiNi2A notched specimens under spectrum loading 05 p0602 N88-13689
The initiation and growth of fatigue cracks in carburised 9Cr1Mo steel 05 p0603 N88-13696
The role of inclusions in corrosion fatigue crack initiation in Q1N 05 p0604 N88-13699
Fatigue 87, volume 3
[AD-A184047] 05 p0604 N88-13700
A study of corrosion fatigue crack initiation, growth and the threshold condition under variable amplitude loading
05 p0604 N88-13701
The effect of environment on low cycle fatigue properties in HSLA steel 05 p0605 N88-13705
Coupling effects between the ferrite and austenite phases during corrosion fatigue of a ferrite/austenite duplex stainless steel 05 p0605 N88-13706
Fatigue crack propagation in Al-Zn-Mg bicrystals and its dependence on the environment
05 p0605 N88-13707
Crack initiation studies in hydrogen embrittled spring steel strip 05 p0605 N88-13710
Telemetric laser extensometry technique for monitoring deflections in small cracks 05 p0607 N88-13724
An overview of fatigue 05 p0608 N88-13729
Deformation mechanisms and crack initiation in fatigue 05 p0608 N88-13730
Fatigue 87, volume 2
[AD-A184046] 06 p0715 N88-14381
Threshold behaviour of semi-elliptic hydrogen-induced and fatigue-induced cracks 06 p0717 N88-14397
Threshold stress intensity for stable crack growth in high strength steel at ambient temperature and below
06 p0718 N88-14407
Role of interstitials and precipitates in initiation and propagation of L.C.F. cracks in austenitic stainless steels
06 p0718 N88-14411
Micromechanics of fatigue crack initiation under axial and torsional loadings 06 p0719 N88-14413
Study of the characteristic curve of hardening and softening during low-cycle fatigue process
06 p0719 N88-14414
Fatigue oxidation interaction in low cycle fatigue
06 p0719 N88-14420
The effect of temperature on fatigue crack initiation from aluminosilicate inclusions 06 p0720 N88-14427
Summary of comparison between experimental and analytical (including empirical) results for initiation of crack growth for surface cracks
[DE88-001604] 06 p0721 N88-14433
Fatigue life prediction modeling for turbine hot section materials
[NASA-TM-100291] 06 p0724 N88-14453
Determination of the critical crack length a (sub IC) in turbine discs
[PB87-144812] 07 p0820 N88-14986
Propagation of fatigue crack in the medium-carbon steel containing both martensite and ferrite
[PB87-143962] 07 p0869 N88-15273
Methods of improving compacting quality of intricately shaped powder components
[BLL-M-37412-(5828.4)] 08 p0968 N88-15859
Fracture-resistant characteristics of medium-strength plates with regard to the initiation, stable and unstable propagation of surface cracks
[PB87-144804] 08 p0996 N88-16025
To determine the stress distribution in the vicinity of GRP end pads where the specimen is held and loaded (CFC coupon specimens) --- glass reinforced plastic (GRP) carbon fiber composite (CFC)
[BAE-WST-R-RES-CFC-12023]
09 p1182 N88-17080
Further tests to determine the stress distribution in the vicinity of GRP end pads where the specimen is held and loaded (CFC coupon specimens) --- glass reinforced plastic (GRP) carbon fiber composite (CFC)
[BAE-WST-R-RES-CFC-12023-ADD-1]
09 p1182 N88-17081
La Recherche Aerospatiale, bimonthly bulletin, number 1987-2, 237/March-April
[ESA-TT-1074] 11 p1433 N88-18550
Influence of hydrogen on crack formation tendency in heat-affected zone with stress concentrator
14 p1887 N88-21276
The effect of H2S concentration and pH on the cracking resistance of AISI 410 stainless steel in 5 percent brine
[NPL-DMA(A)-149] 14 p1890 N88-21294
Evaluation of structural analysis methods for life prediction 14 p1930 N88-21511
Computational simulation methods for composite fracture mechanics 15 p2079 N88-22396
In situ fatigue loading stage inside scanning electron microscope 15 p2083 N88-22419
Grain boundary oxidation and low-cycle fatigue at elevated temperatures 15 p2083 N88-22420
Fatigue damage mapping 15 p2084 N88-22423
Life prediction modeling based on strainrange partitioning 15 p2084 N88-22425
Life prediction modeling based on cyclic damage accumulation 15 p2085 N88-22426
Fatigue damage modeling for coated single crystal superalloys 15 p2085 N88-22427
The analysis of fatigue crack growth mechanism and oxidation and fatigue life at elevated temperatures
[NASA-CR-182129] 16 p2179 N88-22987
Investigation of the effect of minimum loads and compression of load spectra on the prediction capacities of the ONERA crack model --- wings
[ONERA-RTS-33/7169-RY-064-R]
18 p2527 N88-24994
Cyclic fatigue damage characteristics observed for simple loadings extended to multiaxial life prediction
[NASA-CR-182126] 18 p2531 N88-25016
Dimensional analysis and experimental observation of the coupling phenomena between combustion and fracture of damaged propellant samples
19 p2630 N88-25603
Characterization of fatigue crack initiation and propagation in Ti-6Al-4V with electrical potential drop technique
[NASA-TM-100877] 19 p2681 N88-25937
Failure analysis of Chloride Silent Power, Ltd. PB cells
[DE88-010567] 21 p2938 N88-27448
AGARD engine disc cooperative test programme
[AGARD-R-766] 23 p3179 N88-28926
Development of creep fracture modelling in ceramics
[PB88-202825] 23 p3196 N88-29021
The use of a surface acoustic wave technique to study the growth behavior of small cracks in a high strength steel alloy 23 p3225 N88-29193
Thermal stress analysis in PMR-15 carbon fibre laminates
[ETN-88-93123] 24 p3341 N88-29886

CRACK OPENING DISPLACEMENT
Experimental investigation of ductile fracture by white light moire interferometry 22 p3087 N88-28329
Ultrasonic method and apparatus for determining crack opening load
[NASA-CASE-LAR-13889-1] 24 p3385 N88-30160

CRACK PROPAGATION
Evaluation of cracking in aluminum cylinders
[PB87-201398] 01 p0024 N88-10149
Behavior of graphites under intense heat loads
[DE87-012128] 01 p0028 N88-10179
Crack propagation behavior of the materials StE 460 and AlMg 4.5Mn
[FD-1/1986] 01 p0058 N88-10373
Modelling of crack-tip deformation and transient electrochemical processes in relation to corrosion fatigue of steels cathodically protected in marine environments
[NPL-DMA(A)-145] 01 p0059 N88-10379
Criteria for determination of significant load cycles in variable amplitude load sequences
[NLR-MP-86013-U] 01 p0060 N88-10386
Fatigue crack propagation of low-alloy steel in a vacuum environment
[DE87-013770] 01 p0061 N88-10393
Fracture mechanical analysis of the initiation and propagation of matrix and surface cracks in thermally loaded fiber composite models
[ETN-87-90439] 01 p0062 N88-10400
Mechanism of mechanical fatigue of fused silica
[DE87-014199] 02 p0152 N88-10950
Crack behavior in ceramic materials under static, slowly increasing, and cyclic loading conditions
[KFK-4209] 02 p0154 N88-10964
Elevated temperature crack growth
02 p0188 N88-11174
Applications of dislocation theory to crack growth problems 02 p0190 N88-11188
A numerical method for the treatment of kinked cracks in finite bodies 02 p0190 N88-11189
An acoustic emission digital data acquisition workstation
[DE87-012425] 02 p0191 N88-11191
Investigation on ductile fracture behavior of 3-inch diameter Type 304 stainless steel pipe with a circumferential through-wall crack
[DE87-753016] 02 p0191 N88-11196
Some new fatigue tests in high temperature water and liquid sodium environment
[DE87-753019] 02 p0192 N88-11197
Fracture mechanism of fine grain graphite under high heat fluxes
[IPPJ-842] 02 p0242 N88-11527
Resistance of welded joints in high temperature Hastelloy N-type nickel alloy to hot crack formation
03 p0286 N88-11798
Microstructural effects on the fatigue behavior of Fe-C-X alloys
[DE88-000155] 03 p0288 N88-11809
Investigation of creep crack growth in heat resistant tube steels
[ETN-87-90606] 03 p0288 N88-11813
Indentation damage in ceramics
[AD-A184686] 03 p0294 N88-11844
Crack initiation and propagation due to cyclic thermal gradients --- aircraft turbine blades
[ESA-TT-1023] 03 p0336 N88-12114
Kinetics of crack growth: Thermal/mechanical interaction 03 p0337 N88-12124
A probabilistic model of brittle crack formation
[AD-A184423] 03 p0338 N88-12129
Mechanical behavior of a controlled rolled high-strength low alloy steel plate, microalloyed with Nb and V
[DE87-703507] 04 p0415 N88-12571
Effects of stress-relieving on the mechanical properties and the structure of specimens of high-temperature fine-grained structural steels heat-treated to simulate welding
[BLL-CE-TRANS-8256-(9022.09)]
04 p0417 N88-12586
Development of advanced fiber reinforced ceramics
[DE88-000779] 04 p0420 N88-12604
Plastic strain localization between voids in shear deformation fields 04 p0427 N88-12648

Method for the ultrasonic inspection of the soundness of the metal in weld joints in two-ply pipes
[BLL-CE-TRANS-8265-(9022.09)] 04 p0453 N88-12805
Creep life prediction based on stochastic model of microstructurally short crack growth
[NASA-TM-100245] 04 p0456 N88-12825
Micromechanisms of fatigue crack growth and fracture toughness in metal matrix composites
[AD-A185200] 05 p0558 N88-13392
Environmentally assisted cracking: Overview of evidence for an adsorption-induced localised-slip process
[AD-A185175] 05 p0565 N88-13443
Stress intensity factors for cracking metal structures under rapid thermal loading, phase 1
[AD-A184112] 05 p0591 N88-13606
Fatigue 87, volume 1
[AD-A184045] 05 p0597 N88-13645
Effect of grain orientation on the origination and the initial growth of fatigue cracks in pure iron
05 p0597 N88-13647
The growth of persistent slip bands
05 p0597 N88-13648
Closure behavior under constant effective stress intensity loading conditions 05 p0598 N88-13656
Growth of short fatigue cracks in a squeeze formed aluminum alloy 05 p0598 N88-13658
Influence of microstructure and aging condition on the fatigue crack propagation in age hardened aluminium alloys 05 p0599 N88-13659
Fatigue crack growth behavior of A356-T6 cast aluminum alloy 05 p0599 N88-13660
Striations and the fatigue growth mechanism in a micro-alloyed steel 05 p0599 N88-13661
Near-threshold short crack growth behavior in Nimonic 105 05 p0599 N88-13663
Fatigue crack propagation of short and long cracks: Phys. basis, prediction methods and engineering significance 05 p0599 N88-13664
Low cycle fatigue life predictions of a 1CrMoV steel in terms of a J-controlled short crack growth model
05 p0599 N88-13665
The statistics of the shape of small fatigue cracks
05 p0599 N88-13666
The effect of alpha platelet morphology and beta-grain size on the initiation and growth of short fatigue cracks in Ti65S 05 p0600 N88-13667
Behavior of short cracks in a 2024 aluminum alloy sheet tested at several stress ratios 05 p0600 N88-13669
On the role of crack tip shielding in influencing the behavior of long and small fatigue cracks in aluminum-lithium alloy 2090 05 p0600 N88-13671
The influence of slip mechanism on fatigue of Mg and Mg-2.3Li 05 p0600 N88-13672
The growth behavior of small fatigue cracks: the effect of microstructure and crack closure
05 p0600 N88-13673
The influence of microstructure and residual stresses on the initiation and propagation of short surface cracks on AlMgSi1 05 p0601 N88-13674
Threshold stress for fatigue crack initiation from a small crack 05 p0601 N88-13675
Behavior of long and short fatigue cracks in a powder metallurgy superalloy at room and at high temperature
05 p0601 N88-13677
Propagation of small fatigue cracks in 2024-T3 aluminum alloy 05 p0601 N88-13678
Closure and propagation behavior of short fatigue cracks at different R-ratios 05 p0601 N88-13679
A unified model for fatigue crack initiation, short crack growth, long crack propagation, and closure effects
05 p0601 N88-13680
Fatigue crack retardation in aluminium alloys
05 p0602 N88-13681
Fatigue crack growth under random overloads
05 p0602 N88-13682
A dislocation model for fatigue crack propagation under variable amplitude loading 05 p0602 N88-13683
Observations on the effect of overloads on fatigue crack growth 05 p0602 N88-13684
A study of fatigue crack growth life under random stresses 05 p0602 N88-13685
Crack growth in contrasting titanium alloys under the conjoint action of high and low cycle fatigue
05 p0602 N88-13686
Variable amplitude fatigue crack growth in aluminum alloys 2090-T8E41 and 7075-T651
05 p0602 N88-13687
Crack growth prediction in 3D structures under aeronautical-type spectrum loadings
05 p0602 N88-13688
Near-threshold growth of defects in engineering materials 05 p0603 N88-13691
Effects of MN dispersoids on near threshold fatigue crack growth in 2134 type alloys
05 p0603 N88-13692
Crack propagation properties of sintered steel
05 p0604 N88-13698
The role of inclusions in corrosion fatigue crack initiation in Q1N 05 p0604 N88-13699
Fatigue 87, volume 3
[AD-A184047] 05 p0604 N88-13700
A study of corrosion fatigue crack initiation, growth and the threshold condition under variable amplitude loading
05 p0604 N88-13701
The influence of crack conditions on hydrogen uptake by steels 05 p0604 N88-13702
Modeling the effect of sulfur on the threshold environmental cracking rate of steels in high temperature water 05 p0604 N88-13703
Occurance and growth of fatigue cracks in corrosion environment 05 p0604 N88-13704
Coupling effects between the ferrite and austenite phases during corrosion fatigue of a ferrite/austenite duplex stainless steel 05 p0605 N88-13706
Fatigue crack propagation in Al-Zn-Mg bicrystals and its dependence on the environment
05 p0605 N88-13707
the influence of temper embrittlement on fatigue crack growth in hydrogen 05 p0605 N88-13709
Crack initiation studies in hydrogen embrittled spring steel strip 05 p0605 N88-13710
Fatigue mechanisms in ARALL, a fatigue resistant hybrid aluminum aramid composite material
05 p0605 N88-13711
The effect of heat treatment on fatigue crack growth in polycarbonate 05 p0606 N88-13714
Effect of test temperature and frequency on fatigue crack propagation in PVC 05 p0606 N88-13715
Environmental fracture toughness and static fatigue crack propagation of silica glass
05 p0606 N88-13716
Fatigue crack growth: Statistical considerations
05 p0606 N88-13718
Constraint effects in fatigue crack growth
05 p0606 N88-13719
A comparison of plastic work energy and external input for fatigue crack propagation 05 p0607 N88-13722
On the geometrical description of fatigue crack surfaces 05 p0607 N88-13727
An overview of fatigue 05 p0608 N88-13729
Environmentally assisted fatigue crack growth
05 p0608 N88-13731
Fatigue crack growth 05 p0608 N88-13734
The Shock and Vibration Digest, Volume 19, No. 12
05 p0610 N88-13746
Experimental studies on acoustic emission monitoring of crack propagation in offshore structures: A literature survey 05 p0610 N88-13748
Acoustic emissions at an open crack
[DE88-001504] 05 p0611 N88-13751
Fractographic study of fiber composites
06 p0677 N88-14146
The effect of texture on the crack growth resistance of alumina
[NASA-TM-100250] 06 p0686 N88-14206
Fatigue 87, volume 2
[AD-A184046] 06 p0715 N88-14381
Fatigue damage maps 06 p0715 N88-14382
An investigation of fatigue crack growth in a ductile material at high growth rates 06 p0715 N88-14383
Fatigue crack growth and fracture of copper-bismuth bicrystals 06 p0715 N88-14385
Influence of cleavage on fatigue propagation rates in a low carbon steel 06 p0716 N88-14389
Effect of metal surface properties on the fatigue crack growth behavior 06 p0716 N88-14390
Fatigue crack growth behavior in hydrogen gas environment 06 p0716 N88-14391
Near-threshold fatigue 06 p0716 N88-14392
Notch-geometry effect on propagation threshold of short fatigue cracks in notched components
06 p0716 N88-14393
Influence of crack closure on fatigue crack propagation and threshold 06 p0716 N88-14394
An explanation of the fractography of near-threshold fatigue in FCC metals 06 p0716 N88-14395
Threshold behaviour of semi-elliptic hydrogen-induced and fatigue-induced cracks 06 p0717 N88-14397
Effect of compressive portion of loading cycles on the near threshold fatigue closure behavior
06 p0717 N88-14398
Absolute fatigue thresholds in metallic materials
06 p0717 N88-14399
Thermometrical investigations on the near threshold fatigue crack propagation behavior
06 p0717 N88-14400
A re-evaluation of fatigue threshold test methods
06 p0717 N88-14401
The factors which govern the acceleration of corrosion fatigue crack growth rate of a ferritic stainless steel
06 p0717 N88-14402
Fatigue thresholds of C.Mn steels in saline environments 06 p0717 N88-14403
A model for ultra-low fatigue crack growth
06 p0717 N88-14404
The effects of loading history on fatigue crack growth threshold 06 p0718 N88-14406
Threshold stress intensity for stable crack growth in high strength steel at ambient temperature and below
06 p0718 N88-14407
The effect of shear lips on fatigue crack growth in Al-2024 sheet material 06 p0718 N88-14408
Near-threshold fatigue crack growth behavior at cryogenic temperature 06 p0718 N88-14409
The effect of non-metallic inclusions on fatigue and fatigue thresholds of 25Mn-5Cr-1Ni steel
06 p0718 N88-14410
Role of interstitials and precipitates in initiation and propagation of L.C.F. cracks in austenitic stainless steels
06 p0718 N88-14411
Threshold and crack-growth tests on pre-cracked specimens produced in cyclic compression
06 p0718 N88-14412
The effect of prestraining on fatigue crack growth in nickel-base alloys 06 p0719 N88-14415
Mixed mode fatigue crack growth using the Brasilian disc 06 p0719 N88-14416
Crack closure phenomena in modes 1 and 2 interactions 06 p0719 N88-14417
Effect of temperature exposure on fatigue crack propagation 06 p0720 N88-14421
Elevated temperature fatigue crack propagation
06 p0720 N88-14424
The effect of temperature on fatigue crack initiation from aluminosilicate inclusions 06 p0720 N88-14427
An analysis of temperature effect on LCF crack growth rates in superalloy GH36 06 p0721 N88-14431
Summary of comparison between experimental and analytical (including empirical) results for initiation of crack growth for surface cracks
[DE88-001604] 06 p0721 N88-14433
Analysis of crack closure under plane strain conditions
[NASA-CR-182369] 06 p0722 N88-14439
Study of the evolution of short cracks in fatigue analysis --- aircraft construction materials
[DCQ/L-46-555] 06 p0722 N88-14442
Fatigue life prediction modeling for turbine hot section materials
[NASA-TM-100291] 06 p0724 N88-14453
Transients in elevated temperature crack growth
[DE87-013189] 06 p0724 N88-14454
Development of crack under periodically pulsed laser radiation 06 p0774 N88-14754
Random loading fatigue crack growth: Crack closure considerations 06 p0797 N88-14881
Fracture study of windshield glass panes
06 p0799 N88-14891
Investigations on the crack growth retardation behavior and fatigue life prediction in structural materials
[PB87-143756] 07 p0827 N88-15016
Performance of low upper-shelf material under pressurized-thermal-shock loading (PTSE-2)
[DE88-002297] 07 p0832 N88-15049
Effect of overload ratios on fatigue crack growth behavior in Ti-6Al-4V alloy
[PB87-147062] 07 p0833 N88-15055
J-estimation procedure based on moire interferometry data
[AD-A185965] 07 p0867 N88-15258
Analysis of stable crack growth with isotropic and kinematic hardening
[PB87-144911] 07 p0868 N88-15266
Study on fracture behaviour of a joint with a crack in transverse hard layer: Effect of hard layer width on COD
[PB87-143855] 07 p0868 N88-15267
Study on characteristics of SCC propagation da/dt for welded joint
[PB87-143640] 07 p0869 N88-15270
Propagation of fatigue crack in the medium-carbon steel containg both martensite and ferrite
[PB87-143962] 07 p0869 N88-15273
Elastic-plastic fracture investigation on stable crack growth for plane stress
[PB87-144820] 08 p0995 N88-16022
Fracture-resistant characteristics of medium-strength plates with regard to the initiation, stable and unstable propagation of surface cracks
[PB87-144804] 08 p0996 N88-16025
Summary of HSST wide-plate crack-arrest tests and analyses
[DE88-002601] 08 p1000 N88-16061
Micromechanisms of fatigue crack growth and fracture toughness in metal matrix composites
[AD-A186941] 09 p1137 N88-16816

Finite element analysis of damaged cross-ply composite laminates
[CCMS-87-10] 09 p1139 N88-16829

Multipurpose corrosion inhibitors for aerospace materials in Naval environments
[AD-A186728] 09 p1143 N88-16853

Reliability of structures with stiffness and strength degradation 09 p1160 N88-17068

Experimental determination of crack growth rates in cyclic stress applications, for improving the forecasted computed durability in operation
[FF-14/1986] 09 p1182 N88-17085

Finite element analysis for the calculation of calibration curves of fracture mechanics specimen for semicircular surface cracks with several starting depths, for the crack depth measurement following the dc potential method
[GKSS-87/E/19] 09 p1183 N88-17086

Fracture mechanics characterization of crack growth under creep and fatigue conditions
[W-2/87] 09 p1183 N88-17087

Detection of hydrogen-assisted-cracking in U-0.8Ti alloy weldments by acoustic emission monitoring
[DE88-003221] 09 p1184 N88-17093

Analytical and experimental characterization of damage processes in composite laminates
[AD-A187221] 10 p1296 N88-17746

Mechanisms of intergranular attack and stress corrosion cracking of alloy 600 by high-temperature caustic solutions containing impurities
[DE87-012820] 10 p1300 N88-17773

Some aspects of the mechanics and mechanisms of dynamic brittle fracture 10 p1343 N88-18028

Theoretical analysis of adhesive fracture and crack-damage interactions 10 p1343 N88-18030

Fatigue crack growth due to random loading
[DE88-004641] 10 p1345 N88-18038

Brittle to ductile transition to cleavage fracture
[DE88-004074] 10 p1420 N88-18481

Effects of sulfur content on the plain strain fracture toughness of inertia welds in 4340 steel
[AD-A188192] 11 p1458 N88-18689

Effects of thermal and thermo-mechanical treatments on the mechanical properties of centrifugally cast alloy 718
[AD-A188195] 11 p1458 N88-18690

Fracture mechanisms and strengthening of slab lasers
[DE88-004002] 11 p1493 N88-18914

The stress field surrounding the tip of a crack propagating in a finite body 11 p1500 N88-18962

Numerical fracture mechanics using finite element method 11 p1501 N88-18966

Comparative investigations of indirect crack length measurement under fatigue loading in a corrosive environment
[GKSS-86/E/64] 11 p1502 N88-18972

Determination of the elastic-plastic fracture toughness parameters under special consideration of the activities of the European Group on Fracture (EGF)
[GKSS-87/E/30] 11 p1502 N88-18973

Study of the effects of metallurgical factors on the growth of fatigue microcracks
[AD-A188475] 12 p1608 N88-19615

Elevated temperature crack growth studies of advanced titanium aluminides
[AD-A189025] 12 p1608 N88-19618

Thermal-mechanical fatigue testing of a titanium-aluminide alloy
[AD-A189555] 12 p1609 N88-19620

Advanced durability analysis. Volume 1: Analytical methods
[AD-A188341] 12 p1635 N88-19789

On the energy release rate for dynamic transient anti-plane shear crack propagation in a general linear viscoelastic body
[AD-A188385] 12 p1635 N88-19791

Crack distribution and growth rates for critical fastener holes in Mirage wing RH79
[AD-A189080] 13 p1722 N88-20293

Composites strengthening
[AD-A189258] 13 p1734 N88-20364

High-temperature metal matrix composites
[AD-A189516] 13 p1734 N88-20367

Fracture characteristics of carbon and aramid unidirectional composites in interlaminar shear and open hole tensile tests
[NLR-TR-86083-U] 13 p1735 N88-20371

Materials Research Laboratory at Brown University
[AD-A186006] 13 p1739 N88-20396

Hydrogen induced cracks in armor steel weldments fabricated with austenitic filler alloys
[AD-A188733] 13 p1740 N88-20406

The effect of microstructure on the fatigue crack growth resistance of nickel base superalloys
[AD-A189526] 13 p1741 N88-20414

Threshold fatigue crack growth in Ti-6Al-2Sn-4Zr-6Mo
[AD-A189560] 13 p1741 N88-20415

Stress corrosion cracking and metal-induced embrittlement. Comparative studies of local chemistries
[DE88-003235] 13 p1742 N88-20419

Non-destructive evaluation techniques applied to the study of fatigue microcrack growth in steel alloys
[DE88-004090] 13 p1742 N88-20420

Fracture mechanics and creep crack growth of 1 percent Cr 1/2 percent Mo steel with and without prior exposure to creep conditions
[NLR-TR-86051-U] 13 p1743 N88-20426

PNL-1 improved ceramic composites through controlled fiber matrix interaction
[DE88-005680] 13 p1750 N88-20462

Laser ignition of nitramine composite propellants and crack propagation and branching in burning solid propellants
[AD-A189260] 13 p1753 N88-20483

A study of the dynamics of high temperature brittle intergranular fracture by acoustic emission
[AERE-R-12479] 13 p1780 N88-20650

Cyclic crack growth emanating at a round notch considering viscoplasticity
[AD-A189577] 13 p1781 N88-20655

Theory and experiments of fracture in cyclic compression: Single phase ceramics, transforming ceramics and ceramic composites
[DE88-005792] 13 p1781 N88-20659

Fracture criteria for discontinuously reinforced metal matrix composites
[NASA-CR-182665] 13 p1782 N88-20662

Crack resistance of multilayer ceramic-based composite material 14 p1885 N88-21265

Monolithic nature of transversely reinforced composites 14 p1885 N88-21267

JPRS report: Science and technology. USSR: Materials science
[JPRS-UMS-87-007] 14 p1895 N88-21312

Some structural aspects of crack propagation in heat-resistant steels under cyclic thermal and mechanical load 14 p1896 N88-21317

Growth of fatigue cracks in nickel alloys at high temperatures 14 p1896 N88-21318

Investigation of the behavior of fast propagating cracks using numerical simulation calculations
[W-6/87] 14 p1934 N88-21532

Fracture toughness testing of a ceramic matrix composite
[AD-A189846] 15 p2029 N88-22089

Fractography of composite delamination
[NASA-CR-182757] 15 p2030 N88-22096

The effective fracture toughness of aluminum at rapid heating rates
[AD-A189745] 15 p2038 N88-22146

Stress corrosion of ceramic materials
[AD-A190501] 15 p2045 N88-22187

Crack opening and extension in inert solid propellant. An experimental study
[AD-A189808] 15 p2048 N88-22201

Environmentally assisted crack growth in structural alloys: Perspectives and new directions
[AD-A190137] 15 p2076 N88-22377

The growth of corner cracks under the conjoint action of high and low cycle fatigue
[AD-A190510] 15 p2076 N88-22379

Mode 2 fracture mechanics 15 p2083 N88-22418

In situ fatigue loading stage inside scanning electron microscope 15 p2083 N88-22419

Grain boundary oxidation and low-cycle fatigue at elevated temperatures 15 p2083 N88-22420

Elevated temperature crack growth
15 p2084 N88-22421

Fatigue damage mapping 15 p2084 N88-22423

A simplified key-curve approach for J-R-curve testing of CT specimens
[VTT-RR-503] 15 p2088 N88-22444

Ultrasonic Time-Of-Flight Diffraction (TOFD) measurements of crack depths in an acceleration reservoir of a high velocity research gun
[DE88-006644] 16 p2164 N88-22907

Fatigue crack growth behavior of a single crystal alloy as observed through an in situ fatigue loading stage
[NASA-TM-100863] 16 p2179 N88-22986

The analysis of fatigue crack growth mechanism and oxidation and fatigue life at elevated temperatures
[NASA-CR-182129] 16 p2179 N88-22987

Fatigue crack growth under full-scale cyclic plasticity
[DFVLR-FB-87-48] 16 p2222 N88-23263

Crack retardation under load spectra. Experimental study and numerical simulation using the simplified K constant model --- light alloys, aircraft construction materials
[ONERA-RT-30/7169-RY-054-R]
16 p2222 N88-23266

Environment effects on crack propagation with tensile stress
[GKSS-87/E/46] 16 p2223 N88-23267

Study of mechanisms of time-dependent crack growth at elevated temperature
[DE88-006918] 16 p2223 N88-23271

On governing equations for crack layer propagation
[NASA-CR-182120] 16 p2223 N88-23272

Heating at a propagating crack tip in a viscoplastic material
[AD-A190952] 16 p2224 N88-23274

AC impedance analysis of corrosion fatigue in naval aircraft alloys
[AD-A190822] 17 p2322 N88-23865

Fracture mechanics 17 p2324 N88-23877

Effect of test sample geometry on the fatigue crack growth of X10NiCrAlTi 32 20 and NiCr22 Co 12Mo
[JUEL-SPEZ-399] 17 p2348 N88-23990

Analysis of crack-tip fields in a viscoplastic material
17 p2349 N88-23996

Composite repair of cracked aluminum alloy aircraft structure
[AD-A190514] 18 p2455 N88-24573

Mixed-mode fracture of uniaxial fiber reinforced composites
[AD-A191629] 18 p2478 N88-24700

Predictive corrosion modeling, volume 1
[AD-A191229] 18 p2485 N88-24739

Role of cracks in the creep of structural polycrystalline ceramics
[AD-A191485] 18 p2490 N88-24770

Environmental effects on slow crack growth in silicon nitride
[DE88-007206] 18 p2494 N88-24795

Fracture mechanics analysis for short cracks
[AD-A192002] 18 p2527 N88-24992

Some stress intensity factor equations
[FFA-TN-1987-07] 18 p2527 N88-24995

Automated analysis of crack growth rate for obtaining da/dN versus delta K relation
[FFA-TN-1987-70] 18 p2527 N88-24996

Resolved shear stress intensity coefficient and fatigue crack growth in large crystals
[NASA-CR-182137] 18 p2528 N88-24997

Self-consistent model for the brittle response of solids
18 p2528 N88-24999

Fatigue crack growth due to random loading
18 p2531 N88-25017

An assessment of the state of the art in predicting the failure of ceramics
[DE88-008998] 19 p2621 N88-25551

Dimensional analysis and experimental observation of the coupling phenomena between combustion and fracture of damaged propellant samples
19 p2630 N88-25603

Study of probabilistic fatigue crack growth and associated scatter under constant-and-variable amplitude loading spectrum
[AD-A192027] 19 p2679 N88-25929

Material void opening computation using particle method
[DE88-010950] 19 p2680 N88-25936

Characterization of fatigue crack initiation and propagation in Ti-6Al-4V with electrical potential drop technique
[NASA-TM-100877] 19 p2681 N88-25937

Accelerated fatigue crack growth behavior of PWA 1480 single crystal alloy and its dependence on the deformation mode
[NASA-TM-100943] 20 p2772 N88-26436

Study of the influence of metallurgical factors on fatigue and fracture of aerospace structural materials
[AD-A192909] 20 p2774 N88-26452

Irreversible deformations during fracture in polymers
[W-7/86] 20 p2780 N88-26485

Fatigue crack growth under far-field cyclic compression
[DE88-011215] 20 p2813 N88-26689

Automated measurement of crack length and load line displacement at elevated temperature
[AGARD-R-751] 20 p2814 N88-26695

A new boundary integral equation formulation for elastodynamic and elastostatic crack analysis
[AD-A192967] 20 p2815 N88-26702

Prediction of fatigue growth
[NLR-MP-87052-U] 20 p2816 N88-26707

Analysis of crack arrest toughness
[AD-A193340] 21 p2913 N88-27286

Three-dimensional aspects of fatigue crack closure
[AD-A192296] 21 p2960 N88-27581

Diffusion models of crack growth due to random overloads
[DE88-008811] 21 p2962 N88-27595

Corrosion fatigue of small cracks: Mechanics and chemistry
[DE88-012121] 21 p2964 N88-27605

Computation of failure probability of fatigue loaded cracked structures
[ETN-88-92360] 21 p2964 N88-27607

Analyses and correlations of environment assisted fatigue crack propagation for attachment lugs
22 p3053 N88-28116

Study of fatigue cracks in aluminum alloys. Influence of microstructure
[REPT-48-553] 22 p3056 N88-28134

Experimental investigation of ductile fracture by white light moire interferometry 22 p3087 N88-28329

Empirical fatigue crack growth data for a tension loaded threaded fastener
[AD-A194112] 22 p3088 N88-28334

Load interaction effects on compression fatigue crack growth in ductile solids
[FFA-TN-1988-12] 22 p3089 N88-28342

AGARD engine disc cooperative test programme
[AGARD-R-766] 23 p3179 N88-28926

Stress intensity factors for cracked metallic structures under rapid thermal loading
[AD-A191219] 23 p3193 N88-29004

Stress corrosion of ceramic materials
[AD-A191979] 23 p3195 N88-29016

Development of creep fracture modelling in ceramics
[PB88-202825] 23 p3196 N88-29021

The use of a surface acoustic wave technique to study the growth behavior of small cracks in a high strength steel alloy 23 p3225 N88-29193

Results on the influence of crack tip plasticity during dynamic crack growth
[AD-A193460] 23 p3225 N88-29194

Elastic-plastic analysis of part-through crack propagation in piping and pressure vessels
[DE88-701619] 23 p3225 N88-29198

Critical conditions for failure in materials subjected to high rates of loading
[AD-A194697] 23 p3226 N88-29201

J-integral measurement using moire interferometry
[AD-A193751] 23 p3226 N88-29202

Fatigue crack growth characteristics of ARALL (trademark)-1
[AD-A196185] 24 p3341 N88-29889

Stress intensity factors for cracked metallic structures under rapid thermal loading
[AES-8609709F-1] 24 p3353 N88-29962

Modeling of micromechanisms of fatigue and fracture in hybrid materials
[AD-A195604] 24 p3382 N88-30142

Automated early fatigue damage sensing system
[AD-A195717] 24 p3382 N88-30143

Fatigue crack propagation: Probabilistic modeling and statistical analysis
[AD-A195885] 24 p3384 N88-30155

The development of acoustic emission for structural integrity monitoring of aircraft
[AD-A196264] 24 p3427 N88-30398

CRACK TIPS

Modelling of crack-tip deformation and transient electrochemical processes in relation to corrosion fatigue of steels cathodically protected in marine environments
[NPL-DMA(A)-145] 01 p0059 N88-10379

Computational methods and results for dynamic fracture 03 p0337 N88-12123

A study of the crack tip parameters that govern environmentally assisted cracking by use of the rising displacement test 04 p0427 N88-12649

On the role of crack tip shielding in influencing the behavior of long and small fatigue cracks in aluminum-lithium alloy 2090 05 p0600 N88-13671

A unified model for fatigue crack initiation, short crack growth, long crack propagation, and closure effects
05 p0601 N88-13680

A dislocation model for fatigue crack propagation under variable amplitude loading 05 p0602 N88-13683

Observations on the effect of overloads on fatigue crack growth 05 p0602 N88-13684

Modeling the effect of sulfur on the threshold environmental cracking rate of steels in high temperature water 05 p0604 N88-13703

Effect of test temperature and frequency on fatigue crack propagation in PVC 05 p0606 N88-13715

Constraint effects in fatigue crack growth
05 p0606 N88-13719

Embrittling effect of the plastic zone
05 p0607 N88-13721

Telemetric laser extensometry technique for monitoring deflections in small cracks 05 p0607 N88-13724

An optical interferometry technique to evaluate closure along a crack front 05 p0607 N88-13726

Thermometrical investigations on the near threshold fatigue crack propagation behavior
06 p0717 N88-14400

Threshold stress intensity for stable crack growth in high strength steel at ambient temperature and below
06 p0718 N88-14407

Analysis of stable crack growth with isotropic and kinematic hardening
[PB87-144911] 07 p0868 N88-15266

Study on fracture behaviour of a joint with a crack in transverse hard layer: Effect of hard layer width on COD
[PB87-143855] 07 p0868 N88-15267

Stress strain fields at crack tip and stress intensity factors in Reissner's plate
[PB87-144945] 08 p0994 N88-16014

Numerical-experimental investigation of singularity at a crack in nonlinear rubber elasticity
11 p1500 N88-18961

Investigation of the components of the energy-momentum tensor in the neighborhood of crack tips under special materials and loading conditions
[W-4/87] 14 p1934 N88-21531

Heating at a propagating crack tip in a viscoplastic material
[AD-A190952] 16 p2224 N88-23274

Analysis of crack-tip fields in a viscoplastic material
17 p2349 N88-23996

Determination of the toughness of a brittle material using strain gages
[ETN-88-92540] 18 p2527 N88-24993

Plastic yielding at crack tips
[AD-A192549] 21 p2960 N88-27582

Results on the influence of crack tip plasticity during dynamic crack growth
[AD-A193460] 23 p3225 N88-29194

CRACKING (CHEMICAL ENGINEERING)

NT HYDROCRACKING
NT PYROLYSIS

A review of methanol vehicles and air quality impacts
[DE88-002646] 08 p1023 N88-16194

Thermal cracking and variable properties effects on free boundary layer diffusion flames
[NBS/GCR-88/542] 12 p1614 N88-19652

Turbine fuels from tar sands bitumen and heavy oil. Volume 2, phase 3: Process design specifications for a turbine fuel refinery charging San Ardo heavy crude oil
[AD-A190120] 16 p2183 N88-23011

CRACKING (FRACTURING)

NT STRESS CORROSION CRACKING

A study of the crack tip parameters that govern environmentally assisted cracking by use of the rising displacement test 04 p0427 N88-12649

Fracture kinetics of corrosion fatigue
05 p0605 N88-13708

On the geometrical description of fatigue crack surfaces 05 p0607 N88-13727

Effect of rare earth elements on the hydrogen-induced cracking in high strength low alloy steel
[PB87-143806] 07 p0833 N88-15052

Nonlinear line-spring model for surface crack analysis with particular reference to work hardening materials
[PB87-144838] 08 p0994 N88-16016

Analysis of composite laminates with matrix cracks
[CCMS-88-03] 11 p1451 N88-18645

Metallurgical analysis of fractured F-27 aircraft landing gear
[DE88-005885] 11 p1460 N88-18705

Reliability based analysis of contact problems
[NASA-CR-182117] 11 p1503 N88-18975

Advanced durability analysis. Volume 1: Analytical methods
[AD-A188341] 12 p1635 N88-19789

Fracture toughness testing of a ceramic matrix composite
[AD-A189846] 15 p2029 N88-22089

An investigation of the failure response of laminates under biaxial stress
[AD-A190039] 15 p2029 N88-22090

Stress-intensity factors for small surface and corner cracks in plates
[NASA-TM-100599] 15 p2088 N88-22445

A finite-element alternating method for two-dimensional Mode-1 crack configurations
[NASA-TM-100616] 16 p2224 N88-23276

Analysis and developments of failure concepts in fracture mechanics based on research results in the field of component safety topics: J-integral concept; crack resistance curves; dynamic criterion
[V-19/86] 18 p2530 N88-25009

Higher frequency ambient noise in the arctic ocean
[AD-A192203] 18 p2547 N88-25122

Automated measurement of crack length and load line displacement at elevated temperature
[AGARD-R-751] 20 p2814 N88-26695

Influence of microstructure and microdamage processes on fracture at high loading rates
[AD-A192957] 21 p2960 N88-27583

Environmental cracking of a superferritic stainless steel under slow strain rate conditions
22 p3053 N88-28117

AGARD (Advisory Group for Aerospace Research and Development) engine disc material cooperative test (supplementary program)
[AD-A193678] 23 p3179 N88-28925

AGARD engine disc cooperative test programme
[AGARD-R-766] 23 p3179 N88-28926

Stress intensity factors for cracked metallic structures under rapid thermal loading
[AD-A191219] 23 p3193 N88-29004

Critical conditions for failure in materials subjected to high rates of loading
[AD-A194697] 23 p3226 N88-29201

An improved boundary force method for analyzing cracked anisotropic materials
[NASA-TM-101495] 24 p3340 N88-29879

CRACKS

NT CRACK TIPS
NT MICROCRACKS
NT SHORT CRACKS
NT SURFACE CRACKS

The application of group radiators for the determination of tension crack corrosion
[BAM-06264] 01 p0022 N88-10141

Fatigue and thermal fatigue of Pb-Sn solder joints
[DE87-012881] 01 p0024 N88-10150

Stationary reconstruction method. Development, test and comparison in ultrasonic testing
[REPT-860125-TW] • 01 p0057 N88-10368

Mechanism of mechanical fatigue of fused silica
[DE87-014199] 02 p0152 N88-10950

Crevice corrosion of stainless steels and related alloys. Part 2: Summary of experimental test data for input to mathematical model
[BR99871-PT-2] 03 p0289 N88-11816

Welding and weldability of ductile intermetallic alloys
[DE87-014061] 04 p0416 N88-12582

Development of an acoustic emission monitor and monitoring techniques for long-term monitoring of U-0.8Ti electron-beam weldments for postweld cracking
[DE88-000819] 04 p0453 N88-12804

An adaptive subdivision method with crack prevention for rendering beta-spline objects
[AD-A184249] 04 p0477 N88-12940

Fatigue 87, volume 1
[AD-A184045] 05 p0597 N88-13645

Cyclic deformation and crack initiation
05 p0597 N88-13646

Effect of grain orientation on the origination and the initial growth of fatigue cracks in pure iron
05 p0597 N88-13647

The mechanics of fatigue-crack nucleation in a low-alloy steel under fretting conditions 05 p0597 N88-13649

Growth of short fatigue cracks in a squeeze formed aluminum alloy 05 p0598 N88-13658

Fatigue crack growth behavior of A356-T6 cast aluminum alloy 05 p0599 N88-13660

Near-threshold short crack growth behavior in Nimonic 105 05 p0599 N88-13663

Fatigue crack propagation of short and long cracks: Phys. basis, prediction methods and engineering significance 05 p0593 N88-13664

Low cycle fatigue life predictions of a 1CrMoV steel in terms of a J-controlled short crack growth model
05 p0599 N88-13665

The statistics of the shape of small fatigue cracks
05 p0599 N88-13666

The effect of alpha platelet morphology and beta-grain size on the initiation and growth of short fatigue cracks in Ti65S 05 p0600 N88-13667

The initiation and growth of small fatigue cracks in copper at room and cryogenic temperatures
05 p0600 N88-13668

Behavior of short cracks in a 2024 aluminum alloy sheet tested at several stress ratios 05 p0600 N88-13669

On the role of crack tip shielding in influencing the behavior of long and small fatigue cracks in aluminum-lithium alloy 2090 05 p0600 N88-13671

The influence of slip mechanism on fatigue of Mg and Mg-2.3Li 05 p0600 N88-13672

Threshold stress for fatigue crack initiation from a small crack 05 p0601 N88-13675

An experimental study of closure behavior of naturally initiated small cracks 05 p0601 N88-13676

Behavior of long and short fatigue cracks in a powder metallurgy superalloy at room and at high temperature
05 p0601 N88-13677

Closure and propagation behavior of short fatigue cracks at different R-ratios 05 p0601 N88-13679

A unified model for fatigue crack initiation, short crack growth, long crack propagation, and closure effects
05 p0601 N88-13680

Fatigue crack retardation in aluminium alloys
05 p0602 N88-13681

Fatigue crack growth under random overloads
05 p0602 N88-13682

A dislocation model for fatigue crack propagation under variable amplitude loading 05 p0602 N88-13683

Variable amplitude fatigue crack growth in aluminum alloys 2090-T8E41 and 7075-T651
05 p0602 N88-13687

Near-threshold growth of defects in engineering materials 05 p0603 N88-13691
Effects of MN dispersoids on near threshold fatigue crack growth in 2134 type alloys 05 p0603 N88-13692
The initiation and growth of fatigue cracks in carburised 9Cr1Mo steel 05 p0603 N88-13696
The role of inclusions in corrosion fatigue crack initiation in Q1N 05 p0604 N88-13699
Acoustic emissions at an open crack
[DE88-001504] 05 p0611 N88-13751
Fractographic study of fiber composites 06 p0677 N88-14146
Electron microscopy studies of tensile cyclic fatigue-tested silicon nitride ceramics
[DE88-001438] 06 p0685 N88-14196
Fatigue 87, volume 2
[AD-A184046] 06 p0715 N88-14381
Fatigue damage maps 06 p0715 N88-14382
An investigation of fatigue crack growth in a ductile material at high growth rates 06 p0715 N88-14383
On cleavage in fatigue for rail steels 06 p0716 N88-14388
Fatigue crack growth behavior in hydrogen gas environment 06 p0716 N88-14391
Notch-geometry effect on propagation threshold of short fatigue cracks in notched components 06 p0716 N88-14393
Influence of crack closure on fatigue crack propagation and threshold 06 p0716 N88-14394
An explanation of the fractography of near-threshold fatigue in FCC metals 06 p0716 N88-14395
Threshold behaviour of semi-elliptic hydrogen-induced and fatigue-induced cracks 06 p0717 N88-14397
Effect of compressive portion of loading cycles on the near threshold fatigue closure behavior 06 p0717 N88-14398
Influence of stress ratio R on fatigue threshold delta K(th) for 40Cr steel 06 p0718 N88-14405
Threshold stress intensity for stable crack growth in high strength steel at ambient temperature and below 06 p0718 N88-14407
Near-threshold fatigue crack growth behavior at cryogenic temperature 06 p0718 N88-14409
Role of interstitials and precipitates in initiation and propagation of L.C.F. cracks in austenitic stainless steels 06 p0718 N88-14411
Micromechanics of fatigue crack initiation under axial and torsional loadings 06 p0719 N88-14413
Study of the characteristic curve of hardening and softening during low-cycle fatigue process 06 p0719 N88-14414
The effect of prestraining on fatigue crack growth in nickel-base alloys 06 p0719 N88-14415
Mixed mode fatigue crack growth using the Brasilian disc 06 p0719 N88-14416
Elevated temperature fatigue crack propagation 06 p0720 N88-14424
Creep-fatigue cracking in high temperature turbine rotors 06 p0720 N88-14426
The effect of temperature on fatigue crack initiation from aluminosilicate inclusions 06 p0720 N88-14427
Sulfur-induced ductility-dip cracking in weld metal of low-carbon steel
[PB87-143814] 07 p0833 N88-15051
On the convergence of the p-version of the boundary element Galerkin method
[AD-A186198] 07 p0910 N88-15514
Fully plastic analysis of mixed mode plane-strain crack problems
[PB87-144929] 08 p0994 N88-16015
Crack opening displacement test in tension
[PB87-143848] 08 p0996 N88-16026
Mode 3 problems of doubly-periodic rhombic and rectangular array of equal cracks in an infinite plate
[PB87-144846] 08 p0996 N88-16031
Boundary elements combined with singular fields for three-dimensional cracked solids
[RAE-TR-87038] 09 p1183 N88-17088
Stress intensity and crack displacement for small edge cracks
[NASA-TP-2801] 09 p1184 N88-17095
Analytical and experimental characterization of damage processes in composite laminates
[AD-A187221] 10 p1296 N88-17746
A detailed microstructural examination of the cause of HAZ cracking in type 316 steel
[AERE-R-12428] 10 p1301 N88-17777
Durability and damage tolerance of aluminum castings
[AD-A186444] 10 p1341 N88-18013
Theoretical analysis of adhesive fracture and crack-damage interactions 10 p1343 N88-18030
Fatigue crack growth due to random loading
[DE88-004641] 10 p1345 N88-18038
Brittle to ductile transition to cleavage fracture
[DE88-004074] 10 p1420 N88-18481
On delamination of (+ or --theta sub m/90 sub n/2) sub s laminates subject to tensile loading
[AD-A188095] 11 p1447 N88-18626
Backscatter from flaws in fiber-reinforced composites 11 p1450 N88-18639
Joining of dissimilar materials with the pulsed Nd-YAG laser
[DE88-003757] 11 p1458 N88-18693
Thermal fatigue of stainless steel
[DE88-004146] 11 p1458 N88-18694
Reference standards for nondestructive tests
[AD-A187766] 11 p1497 N88-18936
Three-dimensional scattering of impulsive acoustic waves by a semi-infinite crack in the plane interface of a half space and a layer
[PB88-146998] 12 p1687 N88-20089
Crack distribution and growth rates for critical fastener holes in Mirage wing RH79
[AD-A189080] 13 p1722 N88-20293
Material instabilities in solids
[AD-A189525] 13 p1738 N88-20388
Hydrogen induced cracks in armor steel weldments fabricated with austenitic filler alloys
[AD-A188733] 13 p1740 N88-20406
Threshold fatigue crack growth in Ti-6Al-2Sn-4Zr-6Mo
[AD-A189560] 13 p1741 N88-20415
Nondestructive evaluation of carbon-carbon coatings
[AD-A189524] 13 p1748 N88-20453
Ductile failure
[AD-A189429] 13 p1781 N88-20654
Influence of hydrogen on crack formation tendency in heat-affected zone with stress concentrator 14 p1887 N88-21276
Cracking tendencies of restrained welds in high strength low alloy steels under hyperbaric conditions
[AD-A190255] 15 p2039 N88-22150
Ultrasonic characterization of ceramic joints
[DE88-005844] 15 p2043 N88-22173
An evaluation of nondestructive methods for ceramic heat exchanger applications
[DE88-006731] 15 p2068 N88-22328
Detection sensitivity in thick assemblies --- eddy currents, light alloys, aircraft construction materials
[REPT-48-912/F] 16 p2216 N88-23221
Nondestructive Evaluation (NDE) of structural ceramics by photoacoustic microscopy 17 p2325 N88-23884
SiC fiber reinforced reaction-bonded Si3N4 composites 17 p2326 N88-23892
Weldability of general purpose heat source iridium capsules 17 p2426 N88-24429
A method for the numerical solution of random Cauchy singular integral equation 18 p2565 N88-25234
Fracture physics of delamination of composite materials
[AD-A192021] 19 p2609 N88-25482
Study of probabilistic fatigue crack growth and associated scatter under constant-and-variable amplitude loading spectrum
[AD-A192027] 19 p2679 N88-25929
A simple unified method for predicting the deflections of reinforced concrete structures 19 p2679 N88-25930
Helium induced degradation in the weldability of an austenitic stainless steel
[DE88-009062] 20 p2773 N88-26443
Image force expression for the dislocation near a crack
[DE88-701894] 20 p2814 N88-26692
Time-domain boundary element analysis of dynamic near-tip fields for impact-loaded collinear cracks
[AD-A192930] 20 p2815 N88-26700
A new boundary integral equation formulation for elastodynamic and elastostatic crack analysis
[AD-A192967] 20 p2815 N88-26702
Application of controlled interfacial pore structures to kinetic studies in alumina
[DE88-010884] 21 p2919 N88-27326
Significance of the local electrode potential within pits, crevices and cracks
[AD-A192482] 21 p2935 N88-27432
Plastic yielding at crack tips
[AD-A192549] 21 p2960 N88-27582
Thermo-mechanical cracking in coated media with a cavity by a moving asperity friction
[AD-A193311] 21 p2961 N88-27586
Analysis of stiffness reduction, failure and stress concentration in fiber composite laminates
[AD-A193519] 22 p3050 N88-28096
The mechanical behavior of surface modified ceramics
[DE88-010564] 23 p3196 N88-29022
Obtaining stress intensity factors on cracks, by means of fitting techniques on numerical results calculated with the finite element method 24 p3384 N88-30153

CRAFT
U VEHICLES

CRANES
NT GANTRY CRANES
Renewed interest in airships for industry use discussed 04 p0424 N88-12628
Design and implementation of the ESL compact range underhung bridge crane
[NASA-CR-182396] 07 p0862 N88-15231
Oscillation damped movement of suspended objects
[DE88-005715] 15 p2086 N88-22433
Space spider crane
[NASA-CASE-LAR-13411-1-SB] 17 p2312 N88-23828
Required operational capacity for a 7-1/2 ton capacity, Air Mobile Crane (AMC)
[AD-A192023] 19 p2601 N88-25451

CRANKED WINGS
U SWEPT WINGS

CRANKS
U ECCENTRICS

CRASH LANDING
NT DITCHING (LANDING)
An analytical method for ditching analysis of an airborne vehicle
[NASA-CR-4120] 07 p0816 N88-14968
Aircraft accident report: Northwest Airlines, Inc., McDonnell Douglas DC-9-82, N312RC, Detroit Metropolitan Wayne County Airport, Romulus, Michigan, August 16, 1987
[PB88-910406] 19 p2601 N88-25449

CRASHES
NT CRASH LANDING
NT DITCHING (LANDING)
Full-scale transport controlled impact demonstration program
[NASA-TM-89642] 01 p0004 N88-10021
KRASH parametric sensitivity study: Transport category airplanes
[AD-A189962] 15 p2017 N88-22024
Improved procedure for impact probability computation of aircraft crash based on Ballanz model
[JUEL-SPEZ-425] 21 p2894 N88-27176
Crash simulation calculations and component idealization for an airframe. Computer code KRASH 79
[ETN-88-92971] 23 p3174 N88-28899
Centralized class A flight mishap investigation
[AD-A194397] 24 p3322 N88-29786

CRASHWORTHINESS
Steering mechanism --- vehicles
[EP-PATENT-0-181-700-A1] 01 p0053 N88-10338
Helicopter crashworthiness research program 09 p1107 N88-16635
Peak Acceleration Device (PAD)
[AD-A191639] 18 p2461 N88-24611
Fuel containment concepts: Transport category airplanes
[AD-A189818] 18 p2494 N88-24799
Crash simulation calculations and component idealization for an airframe. Computer code KRASH 79
[ETN-88-92971] 23 p3174 N88-28899

CRATERING
NT PROJECTILE CRATERING
A new look at the use of linear methods to predict aircraft dynamic response to taxi over bomb damaged and repaired airfields 09 p1180 N88-17069
Analysis of impact crater arrangement on the Venutian surface (from photographic materials of the Venera 15 and -16 spacecraft)
[NASA-TT-20211] 11 p1571 N88-19401
Martian geomorphology and its relation to subsurface volatiles
[NASA-CR-182428] 12 p1711 N88-20237
Early cratering rates and the nature of the Martian cratered uplands 23 p3306 N88-29694
Early intense cratering: Effects on growth of earth's crust 24 p3395 N88-30219

CRATERS
NT LUNAR CRATERS
NT METEORITE CRATERS
Bilateral symmetry elements of the Zhamanshin impact crater
[NASA-TT-20288] 15 p2096 N88-22490
Sub-kilometer rampart craters in the equatorial region of Mars: Possible implications for the state and distribution of regolith H2O 23 p3302 N88-29666
Topography of large craters on Mars: Implications for the highlands resurfacing history 23 p3306 N88-29691
Variation in the thickness of ejecta cover on Mars with increasing crater density 23 p3307 N88-29701

CRATONS
Archean crustal evolution of the northern North China Craton 24 p3398 N88-30235
Evolution of the Dharwar Craton: A terrain of early Archean crustal stability, long term orogenic cycles and large scale palaeobiological activity 24 p3399 N88-30241

Crustal underplating in the North American Craton: Evidence from the Petrogenesis of anorthositic rocks in the Middle Proterozoic Midcontinent Rift System
24 p3400 N88-30252

CRAY COMPUTERS
Software enhancements and modifications to Program FDTD executable on the Cray X-MP computer
[DE88-001877] 07 p0904 N88-15476
A comparison of the Cray-2 performance before and after the installation of memory pseudo-banking
[NASA-CR-177462] 09 p1215 N88-17287
A performance comparison of the Cray-2 and the Cray X-MP
[NASA-CR-177461] 09 p1216 N88-17288
Multitasking and microtasking experience on the NA S Cray-2 and ACF Cray X-MP
[NASA-CR-177464] 09 p1221 N88-17325
Vector performance of register-to-register vector computers
[DE88-004013] 10 p1364 N88-18265
Dynamic run-time graphics
[DE87-006997] 13 p1820 N88-20879
Vectorization of the odd-even hopscotch scheme and the alternating direction implicit scheme for the two-dimensional Burgers' equations
[CWI-NM-R8720] 16 p2249 N88-23440
The performance of the NEC SX-2 and Cray X-MP supercomputers
[DE88-009177] 20 p2635 N88-268i3
Supermap for Cray FORTRAN: A user's guide
[NASA-CR-177410] 24 p3412 N88-30308

CRAZING
U SURFACE CRACKS

CREATION
U CREATIVITY

CREATIVITY
Separable orthogonal coordinates and particle creation for an accelerating observer
[DE87-703358] 05 p0657 N88-14029
Innovation and creativity: A critical linkage
[DE88-003309] 10 p1426 N88-18515
Computer aided fast turnaround laboratory for research in VLSI (Very Large Scale Integration)
[AD-A189451] • 12 p1624 N88-19715
Idea processing for creativity and management
[DE88-006110] 19 p2714 N88-26113

CREEP ANALYSIS
A creep measurement of unidirectional epoxy-fiberglass rod
[DE87-014812] 04 p0411 N88-12553
Propagation of creep waves around rough cylindrical surface 09 p1234 N88-17400
Verification of the ADINA finite element code for creep analysis: Problems from the open literature
[DE88-011826] 21 p2962 N88-27594

CREEP BUCKLING
Effects of state recovery on creep buckling induced by thermomechanical loading 03 p0336 N88-12116
Effects of state recovery on creep buckling under variable loading 14 p1933 N88-21527
Interaction of creep and fatigue damage in gas turbine blade material
[PNR90440] 22 p3088 N88-28335

CREEP DIAGRAMS
Investigations of creep cavitation in Type 304 stainless steel
[DE87-014196] 03 p0287 N88-11803

CREEP PROPERTIES
NT SHEAR CREEP
Creep fatigue life prediction for engine hot section materials (isotropic): Third year progress review
02 p0188 N88-11173
Investigations of creep cavitation in Type 304 stainless steel
[DE87-014196] 03 p0287 N88-11803
Investigation of creep crack growth in heat resistant tube steels
[ETN-87-90606] 03 p0288 N88-11813
Effect of helium on irradiation creep in an austenitic stainless steel
[DE87-013754] 03 p0290 N88-11824
Modified 14Cr-16Ni stainless steels with improved creep resistance at 700 C due to tailored precipitate microstructures
[DE87-014788] 03 p0290 N88-11825
Computerized system for studies on creep of irradiated materials in the BR-10 reactor. Control system for electric motor
[DE87-702888] 03 p0310 N88-11952
Comparison of measured temperatures, thermal stresses and creep residues with predictions on a built-up titanium structure
[NASA-TM-88814] 03 p0337 N88-12125
Some stochastic aspects of intergranular creep cavitation
[DE88-000065] 04 p0416 N88-12581
Influence of creep on the precipitate structure under conditions of long-term creep. 4: Experiments on 10 CrMo 9 10 steel
[BLL-CE-TRANS-8256-(9022.09)]
04 p0417 N88-12589
Creep life prediction based on stochastic model of microstructurally short crack growth
[NASA-TM-100245] 04 p0456 N88-12825
Study of the influence of mechanical - thermal treatments on the creep behavior of a niobium stainless steel
[DE87-703506] 05 p0563 N88-13431
Cu-2 mechanical properties and microstructural stability of advanced steam cycle materials
[DE88-001519] 05 p0566 N88-13452
Thermo-mechanical behavior of high temperature fiber composites 06 p0678 N88-14149
Creep-fatigue cracking in high temperature turbine rotors 06 p0720 N88-14426
Dependence of strainrange partitioned fatigue life at elevated temperature on monotonic stress-strain properties 06 p0721 N88-14428
Axial creep-fatigue damage assessment in type 316 SS material 06 p0721 N88-14430
Transients in elevated temperature crack growth
[DE87-013189] 06 p0724 N88-14454
Creep test of Hastelloy X for use as the components of OGL-1 in helium environment
[DE88-750289] 07 p0834 N88-15059
Aeropropulsion '87. Session 1: Aeropropulsion Materials Research
[NASA-CP-10003-SESS-1] 09 p1118 N88-16697
Creep and fatigue research efforts on advanced materials 09 p1119 N88-16701
Effects of a regenerating heat treatment on the creep behavior and the lifetime during creep test loading
[ETN-88-91063] 09 p1144 N88-16855
The role of composition and microstructure gradients on weld metal properties and behavior
[DE88-004956] 10 p1303 N88-17791
Relationship between fatigue life in the creep-fatigue region and stress-strain response
[NASA-TM-100796] 10 p1345 N88-18040
Effects of thermal and thermo-mechanical treatments on the mechanical properties of centrifugally cast alloy 718
[AD-A188195] 11 p1458 N88-18690
Creep behavior of tungsten/niobium and tungsten/niobium-1 percent zirconium composites
[NASA-TM-100804] 11 p1460 N88-18707
Structure of a viscoplastic theory
[NASA-TM-100794] 11 p1501 N88-18968
Elevated temperature crack growth studies of advanced titanium aluminides
[AD-A189025] 12 p1608 N88-19618
High-temperature metal matrix composites
[AD-A189516] 13 p1734 N88-20367
Creep behavior of consolidated rapidly solidified Type 304 stainless steel powder containing helium
[DE88-005536] 13 p1743 N88-20424
Fracture mechanics and creep crack growth of 1 percent Cr 1/2 percent Mo steel with and without prior exposure to creep conditions
[NLR-TR-86051-U] 13 p1743 N88-20426
The fatigue behavior of ferritic and austenitic steels at elevated temperatures
[DE88-006304] 13 p1744 N88-20431
Processing, physical metallurgy and creep of NiAl + Ta and NiAl + Nb alloys
[NASA-CR-182113] 14 p1890 N88-21295
Some implications for cyclic plastic and viscoplastic equations based on nonproportional loading experiments
14 p1931 N88-21515
A unified creep-plasticity model suitable for thermo-mechanical loading 14 p1932 N88-21518
Effect of strain rate on high-temperature low-cycle fatigue behavior of Hastelloy X and Hastelloy XR
[DE88-752302] 15 p2037 N88-22140
Study of mechanisms of time-dependent crack growth at elevated temperature
[DE88-006918] 16 p2223 N88-23271
Creep behavior of tungsten/niobium and tungsten/niobium-1 percent zirconium composites
17 p2425 N88-24427
Role of cracks in the creep of structural polycrystalline ceramics
[AD-A191485] 18 p2490 N88-24770
Damage by creep fatigue: Influence of the visco-elasticity of the matrix
[PB88-124706] 18 p2528 N88-24998
Compression creep of filamentary composites
[NASA-CR-182550] 20 p2798 N88-26601
Effect of the matrix on the creep-behavior of carbon-carbon composite
[AD-A193211] 21 p2905 N88-27235
Controlling phase formation and stability to improve the high temperature creep resistance of austenitic stainless steels
[DE88-011401] 21 p2914 N88-27290
Creep behavior for Hastelloy-XR
[DE88-753428] 21 p2914 N88-27295
Verification of the ADINA finite element code for creep analysis: Problems from the open literature
[DE88-011826] 21 p2962 N88-27594
An anisotropic continuum damage model for creep-dominated, multiaxial loading histories
21 p2964 N88-27608
An endochronic rate-sensitive constitutive equation for metals, application to generalized creep and large deformations
[AD-A194167] 22 p3055 N88-28125
The high temperature creep deformation of Si3N4-6Y2O3-2Al2O3
[NASA-CR-183204] 23 p3190 N88-28981
Development of creep fracture modelling in ceramics
[PB88-202825] 23 p3196 N88-29021

CREEP RESISTANCE
U CREEP STRENGTH •

CREEP RUPTURE STRENGTH
Comparative tests of high temperature creep-rupture behavior of the austenitic CrNi steel DIN W.NR.1.4970 in argon and steam
[KFK-4261] 01 p0063 N88-10402
Stress rupture behavior of silicon carbide coated, low modulus carbon/carbon composites
[NASA-CR-180863] 06 p0678 N88-14150
Long-term aging of cast stainless steels: Mechanisms and resulting properties
[DE88-002888] 09 p1145 N88-16864
Aging degradation of cast stainless steels: Effects on mechanical properties
[DE88-003053] 09 p1145 N88-16866
Fracture mechanics characterization of crack growth under creep and fatigue conditions
[W-2/87] 09 p1183 N88-17087
Creep rupture analysis of a beam resting on high temperature foundation 14 p1930 N88-21509

CREEP STRENGTH
Development of creep resistant austenitic stainless steels for advanced steam cycle superheater application
[DE87-012929] 01 p0023 N88-10147
Modified 14Cr-16Ni stainless steels with improved creep resistance at 700 C due to tailored precipitate microstructures
[DE87-014788] 03 p0290 N88-11825
Effect of the matrix on the creep-behavior of carbon-carbon composite
[AD-A193211] 21 p2905 N88-27235

CREEP TESTS
Creep-fatigue behavior of NiCoCrAlY coated PWA 1480 02 p0189 N88-11176
A loading system for creep testing under constant compressive stress
[NASA-TT-20119] 06 p0722 N88-14441
Creep test of Hastelloy X for use as the components of OGL-1 in helium environment
[DE88-750289] 07 p0834 N88-15059
Effects of a regenerating heat treatment on the creep behavior and the lifetime during creep test loading
[ETN-88-91063] 09 p1144 N88-16855
Creep rupture analysis of a beam resting on high temperature foundation 14 p1930 N88-21509
Data requirements to model creep in 9Cr-1Mo-V steel
14 p1931 N88-21512
Controlled-strain rate tests at very low strain rates of 2618 aluminum at 200 C 14 p1931 N88-21513
Automated measurement of crack length and load line displacement at elevated temperature
[AGARD-R-751] 20 p2814 N88-26695
Automated measurement of crack length and load line displacement at elevated temperature
[NLR-MP-87049-U] 20 p2816 N88-26706
Prediction of long-term creep in polypropylene from short-term tests
[NPL-DMA(A)-156] 22 p3088 N88-28337

CRESTATRONS
U TRAVELING WAVE TUBES

CRESTS
U WAVES

CREVASSES
NT GLACIERS

CREVICES
U CRACKS

CREW PROCEDURES (INFLIGHT)
Parameter-adaptive model-following for in-flight simulation
[AD-A190567] 18 p2467 N88-24645

CREW PROCEDURES (PREFLIGHT)
Checklist interruption and resumption: A linguistic study
[NASA-CR-177460] 20 p2756 N88-26348

CREW STATIONS
U CREW WORKSTATIONS
CREW WORKSTATIONS
Personnel occupied woven envelope robot power [NASA-CR-182367] 07 p0856 N88-15196
Development of a C3 generic workstation: System overview 16 p2242 N88-23396
C3 generic workstation: Performance metrics and applications 16 p2242 N88-23397
Crewstation Information and Development System (CIDS) 17 p2304 N88-23781
Space station architectural elements model study [NASA-CR-4027] 18 p2464 N88-24632
CREWS
NT FLIGHT CREWS
NT SPACECREWS
Man rating the b-1B molecular sieve oxygen generation system [AD-A186275] 07 p0899 N88-15447
Portable, ambient air microclimate cooling in simulated desert and tropic conditions [AD-A186457] 08 p1050 N88-16338
Team problem solving: Effects of communication and function overlap [AD-A187010] 09 p1152 N88-16898
Checklist interruption and resumption: A linguistic study [NASA-CR-177460] 20 p2756 N88-26348
Human factors report on information management requirements for next-generation manned bombers [AD-A195870] 24 p3409 N88-30296
CRIMPING
U FOLDING
CRITERIA
NT STRUCTURAL DESIGN CRITERIA
Multiaxial fatigue failure criterion: A new approach 06 p0719 N88-14418
TECOM's research efforts in the dynamic environments 08 p0999 N88-16048
Strong consistency of certain information theoretic criteria for model selection in calibration, discriminant analysis and canonical correlation analysis [AD-A186584] 09 p1232 N88-17385
A practical termination criterion for the conjugate gradient method [REPT-87-62] 16 p2259 N88-23506
Systems for the 21st century 17 p2302 N88-23769
Accuracy criteria for evaluating supersonic aerodynamic coefficient predictions 24 p3317 N88-29756
CRITICAL EXPERIMENTS
Fast critical experiment data for space reactors [DE87-007005] 01 p0093 N88-10605
CRITICAL FLOW
Development of an equation of state for computation of supercompressibility factors, critical flow factors and other properties for wet, sour natural gases, synthetic gases and admixtures [PB88-202676] 20 p2798 N88-26602
Introduction and critical flow phenomena 23 p3169 N88-28870
Boundary layer development and transition 23 p3169 N88-28871
CRITICAL LOADING
Determination of the critical crack length a (sub IC) in turbine discs [PB87-144812] 07 p0820 N88-14986
CRITICAL MACH NUMBER
U CRITICAL VELOCITY
U MACH NUMBER
CRITICAL MASS
Particle bed reactor scaling relationships 17 p2400 N88-24267
CRITICAL POINT
Detection of critical points: The first step to automatic line generalization 05 p0619 N88-13803
Phase equilibria and density calculations in the critical region: A phenomenological correction for a classical equation of state [PB88-185335] 19 p2723 N88-26167
Critical point wetting drop tower experiment [NASA-CR-183062] 20 p2798 N88-26603
Investigation on refrigerant R12 critical boiling point in narrow flow pipes considered as model fluid [ETN-88-92374] 20 p2802 N88-26626
Nontrivial critical points for asymptotically quadratic function [DE88-101851] 20 p2845 N88-26881
Thermal conductivity of pure fluids in a large region around the critical point [ETN-88-92135] 20 p2881 N88-27103
Fluid physics double rack --- Spacelab [SD-TN-AI-012] 24 p3358 N88-29992
CRITICAL REYNOLDS NUMBER
U CRITICAL VELOCITY
U REYNOLDS NUMBER
CRITICAL SPEED
U CRITICAL VELOCITY
CRITICAL STRESS
U CRITICAL LOADING
CRITICAL TEMPERATURE
Welding and weldability of ductile intermetallic alloys [DE87-014061] 04 p0416 N88-12582
Magnetic field dependence of the specific heat of some high-T/sub c/ superconductors [DE87-014078] 04 p0497 N88-13063
Investigation of critical heating in narrow flow channels with R12 refrigerant as model fluid [GKSS-87/E/25] 09 p1163 N88-16972
Stability limits in the monoclinic-tetragonal transformations of zirconia [DE88-005924] 14 p1986 N88-21849
Dependence of high critical temperature of ceramic superconductors on the nominal Cu(sup 3 +)Cu(sup 2 +) ratio [DE88-702734] 23 p3293 N88-29611
CRITICAL VELOCITY
Critical Ionization Velocity (CIV) interaction: Some unsolved questions [TRITA-EPP-87-12] 09 p1250 N88-17491
On the role of the ionization frequency to gyrofrequency ratio in the critical ionization velocity interaction [TRITA-EPP-86-10] 10 p1410 N88-18414
Open channel flow near the resonance speed 18 p2514 N88-24918
A critical speed study for aircraft bias ply tires [AD-A193616] 22 p3084 N88-28313
CROP GROWTH
Estimating scattered and absorbed radiation in plant canopies by remote sensing [NASA-CR-181390] 02 p0193 N88-11205
Wheat production in controlled environments [UAES-PAPER-3324] 03 p0361 N88-12270
Controlled Ecological Life Support System: Design, Development, and Use of a Ground-Based Plant Growth Module [NASA-CP-2479] 05 p0630 N88-13852
CELSS Program Meeting 05 p0630 N88-13853
Controlled ecological life support systems: Development of a plant growth module 05 p0630 N88-13854
Plant Growth Module (PGM) conceptual design 05 p0631 N88-13855
Modeling the growth dynamics of four candidate crops for Controlled Ecological Life Support Systems (CELSS) 06 p0799 N88-14889
Report on phase 1 of the project estimate development of a model for yield estimation of sugar cane based on LANDSAT and agromet data [INPE-4466-RPE/560] 12 p1638 N88-19807
Assessment of crop loss from air pollutants: Meteorology-atmospheric chemistry and long range transport [PB88-146857] 15 p2089 N88-22448
Estimation of an area cultivated with wheat from LANDSAT data through a two-phase sampling method 17 p2357 N88-24041
Remote sensing techniques in the estimation of the area cultivated with beans, corn, and castor beans in the Irece County (Bahia State) 17 p2358 N88-24045
CANASATE: Sugar cane mapping by satellite 17 p2358 N88-24046
Identification of areas cultivated with soybeans in the cerrados regions, through digital processingof satellite images: A methodological approach 17 p2358 N88-24048
Comparative variations of spectral signatures in a cultivated area of the Paris Basin (27 May, 26 June, 1 July 1986) 22 p3095 N88-28382
LANDSAT TM and agrometeorological data for wheat yield estimation at the farm level [INPE-4591-PRE/1321] 24 p3388 N88-30180
CROP IDENTIFICATION
SPOT data for crop discrimination in southern Brazil 03 p0343 N88-12169
A procedure for automatic classification of crop areas [INPE-4467-PRE/1240] 13 p1790 N88-20708
A comparison of supervised maximum likelihood and decision tree classification for crop cover estimation from multitemporal LANDSAT MSS data 17 p2352 N88-24014
Spectral behavior of crops through analysis of LANDSAT-TM data 17 p2358 N88-24047
Identification of areas cultivated with soybeans in the cerrados regions, through digital processingof satellite images: A methodological approach 17 p2358 N88-24048
Separability of cultivation through digital analysis of SPOT and TM data [INPE-4541-PRE/1287] 19 p2685 N88-25963
Comparative study of crop and soil mapping using multitemporal and multispectral SPOT and LANDSAT data 22 p3091 N88-28354
Changes in species composition of heathland, monitored by means of remote sensing and field mapping: The results of the HEISPOT project 22 p3092 N88-28360
Evaluation of automatic texture analysis for increased crop identification accuracy with SPOT data 22 p3094 N88-28373
Digital and visual analysis of SPOT and TM data for crop discrimination in southern Brazil 22 p3096 N88-28385
Identification of farming systems in the cotton area of West Burkina Faso from SPOT-1 data 22 p3097 N88-28389
Using SPOT HRV data to update the distribution of the paddy field in Taiwan 22 p3097 N88-28393
CROP INVENTORIES
Crop forecasting in Brazil: A short history of productivity models [INPE-4150-PRE/1056] 12 p1637 N88-19801
A procedure for automatic classification of crop areas [INPE-4467-PRE/1240] 13 p1790 N88-20708
Methodological developments on crop inventories using SPOT and ground surveys 22 p3094 N88-28371
Evaluation of annual crop surfaces and territorial inventory in the Paris basin by combining classic statistical inquiries and SPOT data (Preliminary Evaluation Program for SPOT 127) 22 p3094 N88-28372
Attempt to inventory vines using oblique SPOT images 22 p3095 N88-28380
Evaluation of SPOT data for crop inventory and monitoring in Sudanian Africa: Example of Bane area (Burkina Faso) 22 p3096 N88-28388
Monitoring Tunisia's steppes with SPOT 22 p3097 N88-28390
CROP INVENTORIES BY REMOTE SENSING
U AGRISTARS PROJECT
CROP VIGOR
Estimating scattered and absorbed radiation in plant canopies by remote sensing [NASA-CR-181390] 02 p0193 N88-11205
Application of multitemporal SPOT data for crop monitoring: Effects of frost and drought 03 p0344 N88-12171
Species biology and potential for controlling four exotic plants (Ammophila arenaria, Carpobrotus edulis, Cortaderia jubata and Gasoul crystallinum) on Vandenberg Air Force Base, California [NASA-TM-100980] 10 p1363 N88-18148
Crop forecasting in Brazil: A short history of productivity models [INPE-4150-PRE/1056] 12 p1637 N88-19801
Changes in species composition of heathland, monitored by means of remote sensing and field mapping: The results of the HEISPOT project 22 p3092 N88-28360
CROPLANDS
U FARMLANDS
CROPS
Application of remote sensing to agricultural field trials [ISBN-90-6754-089-7] 06 p0729 N88-14483
CROSS CORRELATION
Cross-correlation of uniform cyclic difference set sequences [AD-A184879] 05 p0640 N88-13913
Stability, reliability and cross-mode correlations of tests in a recommended 8-minute performance assessment battery [NASA-CR-172039] 08 p1052 N88-16351
Detecting squeezed states by cross-correlation 14 p1978 N88-21806
A diagnostic technique used to obtain cross range radiation centers from antenna patterns [NASA-CR-182903] 16 p2192 N88-23071
Self similarity of two point correlations in wall bounded turbulent flows 16 p2195 N88-23089
The display of multivariate information: The effects of auto- and cross-correlation, reliability and heterogeneity [AD-A191070] 16 p2243 N88-23398
Development of advanced flow simulation system by water flow model: New method of velocity measurement using cross-correlation [DE88-753120] 20 p2799 N88-26608
Dependence of medium range forecast errors upon the large-scale initial state 22 p3126 N88-28585
CROSS FAULTS
U GEOLOGICAL FAULTS
CROSS FLOW
Comparison of different kinds of compact cross flow heat exchangers [DFVLR-FB-86-63] 01 p0046 N88-10305
A 15 cm aperture LED scintillometer for C(n) squared and crosswind measurements [KNMI-WR-87-3] 01 p0070 N88-10448
Laminar flow over a spinning projectile at an angle of attack 02 p0121 N88-10766
Aerothermal modeling program, phase 2 02 p0185 N88-11149

Dilution jet mixing program, phase 3
02 p0185 N88-11153

On the mixing of a row of jets with a confined crossflow 02 p0185 N88-11154

Theoretical analysis of primary instabilities in three dimensional boundary layer flows
[ESA-TT-1063] 03 p0315 N88-11992

Theory of one and two-pass cross-flow heat exchanger
[PB87-225157] 04 p0441 N88-12736

Comparative studies in the near-field of turbulent transports of heated and unheated jets normal to a cross stream 04 p0444 N88-12756

Computational design of natural laminar flow wings for transonic transport application 07 p0813 N88-14948

Numerical calculation of appendage, flat plate junction flow
[AD-A186371] 07 p0850 N88-15158

Cross flow in the Alps and flat foehn during the experiment MERKUR --- mesoscale experiment
08 p1013 N88-16142

A jet in a crossflow
[NASA-CR-182469] 09 p1113 N88-16674

Simulations of thermally induced winds and cross flow situations
[MITT-57] 09 p1193 N88-17148

Control of vortical separation on conical bodies
10 p1267 N88-17580

Leeside crossflow modeling in Euler space-marching computations
[NASA-TM-89710] 10 p1325 N88-17924

Investigation of non-symmetric jets in cross flow
10 p1327 N88-17932

Time-resolved heat transfer measurements and analysis in the wage region of a cylinder in crossflow
10 p1328 N88-17939

Experimental research on center of pressure of slender body with two pointed ends 14 p1864 N88-21137

Comparison of different kinds of compact crossflow heat exchangers
[ESA-TT-1076] 16 p2207 N88-23169

Crossflow vorticity sensor
[NASA-CASE-LAR-13436-1-CU]
17 p2300 N88-23759

The calculation of transonic flow over the shuttle orbiter using slender body theory 18 p2460 N88-24606

Cross stream differencing for integral boundary layer equations
[AD-A191744] 18 p2509 N88-24886

Measurement of burning rates of NOSOL-363 propellants under cross-flow and strand burner conditions using real-time X-ray radiography
19 p2623 N88-25560

Three-dimensional viscous flow computations of a circular jet in subsonic and supersonic cross flow
[NASA-CR-182153] 20 p2800 N88-26616

Cross flow induced vibrations in tube bundle by displaced and misaligned tube configurations
[ETN-88-92132] 20 p2801 N88-26621

A numerical study of turbulent plane jets in still and flowing environments employing two-equation k-epsilon model 23 p3211 N88-29109

CROSS SECTIONS

Convective cross section analysis
[PB87-204566] 02 p0216 N88-11361

Use of boundary-layer method for problem of sound propagation through channel with variable cross-section containing stream of fluid 09 p1233 N88-17396

Computer program for parameterization of nucleus-nucleus electromagnetic dissociation cross sections
[NASA-TM-4038] 16 p2270 N88-23584

Total photoionization cross sections of atomic oxygen from threshold to 44.3A
[NASA-CR-182992] 17 p2397 N88-24252

The role of integral experiments and nuclear cross section evaluations in space nuclear reactor design
17 p2404 N88-24293

Density diagnostics by hydrogen line intensity ratios: Excitation cross section between excited states
17 p2441 N88-24522

Distorted-wave-method calculation of electron-impact excitation of atomic ions 17 p2443 N88-24532

Nonlinear interaction between overall and local buckling of stiffened panels with symmetric cross-sections
[PB88-104054] 21 p2960 N88-27580

CROSSED FIELDS

Vortex dynamics and transport to the wall in a crossed-field plasma sheath
[DE87-013286] 01 p0100 N88-10657

Crossed molecular beam studies of substitution and exchange reactions
[DE88-006322] 14 p1980 N88-21814

Vortex formation and particle transport in a cross-field plasma sheath
[DE88-008931] 23 p3284 N88-29553

Vortex formation and particle transport in a cross-field plasma sheath
[AD-A194838] 24 p3432 N88-30425

CROSSINGS

HOC spectral analysis of an almost periodic random sequence in noise
[AD-A185528] 06 p0765 N88-14697

Higher order crossings
[AD-A190489] 15 p2121 N88-22641

CROSSLINKING

NT VULCANIZING

Effect of sidechain length and crosslinking on ionic conductivity in polyphosphazene solid electrolytes
[AD-A184419] 04 p0497 N88-13058

Development of microencapsulation techniques
[AD-A185019] 05 p0567 N88-13457

Interface effects on the mechanical properties of ceramic composites
[AD-A185899] 07 p0826 N88-15009

Polyether-polyester graft copolymer
[NASA-CASE-LAR-13447-1] 11 p1463 N88-18725

Study of crosslinking and nonelastic mechanical properties of epoxy and PSP networks --- epoxy resins; polystyrylpyridine resins (psp)
[ETN-88-92740] 21 p2921 N88-27337

The radiation sensitivity of select metal chelate polymers: Mechanistic changes at higher energies
[AD-A193467] 23 p3196 N88-29019

CROSSOVERS

Geosat crossover analysis in the tropical Pacific. Part 1: Constrained sinusoidal crossover adjustment
[NASA-CR-182391] 07 p0871 N88-15285

An efficient algorithm for computing the crossovers in satellite altimetry
[NASA-CR-182389] 07 p0871 N88-15286

CROSSTALK

Crosstalk in braided shield coaxial cables
01 p0035 N88-10224

The design and testing of an analog optical communication link capable of the simultaneous transmission of four frequency division multiplexed audio signals
[AD-A184695] 03 p0307 N88-11936

Crosstalk analysis of a broadband data communications system
[DE88-003652] 09 p1156 N88-16927

CRUCIBLES

Model development for induction heating
[DE88-002376] 06 p0699 N88-14289

A study of surface tension driven segregation in monotectic alloy systems
[NASA-CR-182894] 16 p2178 N88-22983

CRUCIFORM WINGS

Wind tunnel investigation of wing and control panel loads at transonic and supersonic speeds on some schematic cruciform missile configurations
[FFA-TN-1986-43-SUPPL-1] 22 p3039 N88-28044

CRUDE OIL

Aviation turbine fuels from tar sands bitumen and heavy oils. Part 2: Laboratory sample production
[AD-A185744] 06 p0687 N88-14211

Aviation turbine fuels from tar sands bitumen and heavy oils. Part 3: Laboratory sample production
[AD-A189278] 13 p1753 N88-20484

Turbine fuels from tar sands bitumen and heavy oil. Volume 2, phase 3: Process design specifications for a turbine fuel refinery charging San Ardo heavy crude oil
[AD-A190120] 16 p2183 N88-23011

CRUISE MISSILES

NT TOMAHAWK MISSILES

Performance optimization of a cruise missile using dynamic-stall induced lift augmentation
[AD-A190497] 15 p2017 N88-22027

CRUISING FLIGHT

Techniques for performance optimisation in cruise and manoeuverability 05 p0545 N88-13321

Propulsion challenges and opportunities for high-speed transport aircraft 08 p0958 N88-15809

The initial calculation of range and mission fuel during conceptual design --- aircraft design
[LR-525] 16 p2161 N88-22889

Inflow measurement made with a laser velocimeter on a helicopter model in forward flight. Volume 5: Tapered planform blades at an advance ratio of 0.23
[NASA-TM-100545] 17 p2299 N88-23755

Inflow measurements made with a laser velocimeter on a helicopter model in forward flight. Volume 1: Rectangular planform blades at an advance ration of 0.15
[NASA-TM-100541] 18 p2460 N88-24607

Periodic solutions in aircraft cruise-dash optimization
18 p2464 N88-24631

CRUSTAL DYNAMICS

U EARTH CRUST

U GEODYNAMICS

CRUSTAL FRACTURES

An algorithmic approach to crustal deformation analysis
[NASA-CR-181497] 03 p0349 N88-12203

An algorithmic approach to crustal deformation analysis 04 p0468 N88-12891

The analysis of recent crustal movements in static and kinematic models
[SER-B-279] 09 p1191 N88-17136

Study of fractures as subsidiary research of ground water in the Sergipe state: An approach through remote sensing data
[INPE-4319-TDL/286] 12 p1639 N88-19813

Correlation of data on strain accumulation adjacent to the San Andreas Fault with available models
[NASA-CR-180757] 13 p1796 N88-20742

Drilling investigation of a young magmatic intrusion beneath the Inyo Domes, Long Valley, California: Structural and textural studies
[DE88-006613] 18 p2541 N88-25078

CRUSTS

NT EARTH CRUST

NT LUNAR CRUST

NT PLANETARY CRUSTS

Crustal models of the evolving comet nucleus
14 p2005 N88-21953

CRYOGENIC COOLING

Measurement and analysis of cryogenic sapphire dielectric resonators and DROs
04 p0433 N88-12686

Low-noise cryogenic transmission line
04 p0434 N88-12688

A 2.3-GHz cryogenically cooled HEMT amplifier for DSS 13 04 p0434 N88-12689

Evaluation of a cryogenic refrigerator for cooling focal plane instrumentation --- satellite instruments
[BAE-TP-8095-VOL-1] 05 p0572 N88-13485

Evaluation of a cryogenic refrigerator for cooling focal plane instrumentation. Appendix B: Accommodation study --- satellite instruments
[BAE-TP-8095-VOL-2] 05 p0572 N88-13486

Oxygen chemisorption cryogenic refrigerator
[NASA-CASE-NPO-16734-1-CU]
06 p0689 N88-14223

Advanced fabrication techniques for hydrogen-cooled engine structures
[NASA-CR-3949] 06 p0723 N88-14447

Photoinduced low-temperature changes in optical losses in fiber optics based on chalcogenide glasses
06 p0770 N88-14731

Tests of cold helium compressors at Fermilab
[DE88-002837] 07 p0862 N88-15230

Cryogenic Fluid Management Technology Workshop. Volume 1: Presentation material and discussion
[NASA-CP-10001] 08 p0980 N88-15924

Cryogenics program overview
08 p0981 N88-15926

Ames Research Center cryogenics program
08 p0981 N88-15927

The Goddard Space Flight Center mechanical cooler program 08 p0983 N88-15944

Air Force cryocooler development for spacecraft
08 p0983 N88-15945

An infrared grating spectrometer for GIRL
[ETN-88-91071] 09 p1167 N88-16997

Study of helium transfer technology for STICCR: Fluid management
[NASA-CR-177463] 10 p1291 N88-17720

Low-noise cryogenically cooled broad-band microwave preamplifiers
[DE88-004561] 10 p1324 N88-17912

Cryocooler systems demonstration
[AD-A188025] 11 p1467 N88-18745

Development of an electronically-scanned pressure module for operation at cryogenic temperatures
[NASA-CR-181610] 12 p1629 N88-19746

Cyropreservation of isolated rat hepathocytes for future use in Spacelab experiments: Preliminary results
12 p1660 N88-19950

Workshop on Technology Development Issues for the Large Deployable Reflector (LDR)
[NASA-CP-2407] 12 p1710 N88-20235

Development of a motorized cryovalve for the control of superfluid liquid helium 14 p1925 N88-21477

Review of convectively cooled structures for hypersonic flight
[NASA-TM-87740] 17 p2310 N88-23817

Krypton based adsorption type cryogenic refrigerator
[NASA-CASE-NPO-17334-1-CU]
17 p2331 N88-23917

Cryogenic regenerator including saran-carbon heat conduction matrix
[NASA-CASE-NPO-17291-1-CU]
17 p2337 N88-23946

Analysis of debris from accelerated life test of the Hughes five-year Vuilleumier cryocooler
[AD-A193101] 21 p2931 N88-27400
CryoSQUID: A SQUID-based magnetic field sensor
[AD-A194237] 23 p3239 N88-29275
Static and dynamic behavior of a quasi one-dimensional Heisenberg antiferromagnet in the long-range ordered state. A nuclear magnetic resonance study performed with a He3-He4 dilution refrigerator
[B8705564] 23 p3281 N88-29533
Development of a unit cell for a Ge:Ga detector array
[NASA-CR-177445] 24 p3375 N88-30100
CRYOGENIC EQUIPMENT
Cryogenic cell -- neutron borehole logging
[GB-PATENT-2-139-745-A] 01 p0048 N88-10308
Operating experiences and test results of six cold helium compressors
[DE87-012115] 02 p0157 N88-10982
Materials studies for magnetic fusion energy applications at low temperatures-X
[PB87-232575] 03 p0381 N88-12395
A cold ejector for closed-cycle helium refrigerators
04 p0434 N88-12690
Evaluation of a cryogenic refrigerator for cooling focal plane instrumentation --- satellite instruments
[BAE-TP-8095-VOL-1] 05 p0572 N88-13485
Evaluation of a cryogenic refrigerator for cooling focal plane instrumentation. Appendix B: Accommodation study --- satellite instruments
[BAE-TP-8095-VOL-2] 05 p0572 N88-13486
Capacitive resonant transducer for the Frascati gravitational antenna
[IFSI-86-9] 05 p0578 N88-13528
AF cryogenic and fluid management spacecraft technology program 08 p0981 N88-15925
Cryogenics program overview
08 p0981 N88-15926
Ames Research Center cryogenics program
08 p0981 N88-15927
Orbital transfer vehicle studies overview
08 p0981 N88-15931
Large capacity cryopropellant orbital storage facility
08 p0981 N88-15932
Space Infrared Telescope Facility (SIRTF) design and thermal analysis 08 p0982 N88-15934
The Goddard Space Flight Center mechanical cooler program 08 p0983 N88-15944
Air Force cryocooler development for spacecraft
08 p0983 N88-15945
Development of a multiplexer module for use in a spaceborne cryogenic environment based on GaAs MESFET technology
[RPT/CRY/62463/BOP] 11 p1559 N88-19335
Development of a cryogenic stepping drive for ISO/LWS 14 p1878 N88-21220
Cryogenic mechanism for ISO camera
14 p1878 N88-21221
Materials testing at cryogenic temperatures
[BU-359] 14 p1923 N88-21462
Electromagnetic dampers for cryogenic applications
16 p2218 N88-23231
Extension of the vegetation mission to thermal infrared spectral bands
[CNES-T-86/224-CT/DRT/TIT/IO]
16 p2227 N88-23299
Low temperature storage container for transporting perishables to space station
[NASA-CASE-MFS-28248-1] 18 p2498 N88-24817
Study of a magnetic refrigerator for space applications for temperatures under 20 K
[NASA-TT-20283] 19 p2641 N88-25668
Cyrogenic test facilities for an optical cryomechanism qualification
[REPT-881-440-116] 21 p2901 N88-27219
Analysis of debris from accelerated life test of the Hughes five-year Vuilleumier cryocooler
[AD-A193101] 21 p2931 N88-27400
Surface Tension Confined Liquid Cryogen Cooler (STCLCC)
[NASA-CASE-GSC-13112-1] 23 p3201 N88-29050
CRYOGENIC FLUID STORAGE
Cryogenic Fluid Management Technology Workshop. Volume 1: Presentation material and discussion
[NASA-CP-10001] 08 p0980 N88-15924
AF cryogenic and fluid management spacecraft technology program 08 p0981 N88-15925
Cryogenics program overview
08 p0981 N88-15926
LeRC cryogenic fluid management program overview
08 p0981 N88-15928
Large capacity cryopropellant orbital storage facility
08 p0981 N88-15932
Space environmental considerations for a long-term cryogenic storage vessel 08 p0981 N88-15933
Thermal analysis for the Cryogenic Fluid Management Flight Experiment (CFMFE) 08 p0982 N88-15935
Development of on-orbit fluid gaging techniques
08 p0982 N88-15936
Technology requirements for an orbiting fuel depot: A necessary element of a space infrastructure
[NASA-TM-101370] 24 p3334 N88-29845
CRYOGENIC FLUIDS
NT FERMI LIQUIDS
NT LIQUID HELIUM
NT LIQUID HELIUM 2
NT LIQUID HYDROGEN
NT LIQUID NITROGEN
NT LIQUID OXYGEN
Cryogenic Fluid Management Technology Workshop. Volume 1: Presentation material and discussion
[NASA-CP-10001] 08 p0980 N88-15924
AF cryogenic and fluid management spacecraft technology program 08 p0981 N88-15925
Cryogenics program overview
08 p0981 N88-15926
Ames Research Center cryogenics program
08 p0981 N88-15927
Cryogenic fluid management program flight concept definition 08 p0981 N88-15929
SAMSS: An in-progress review of the Spacecraft Assembly, Maintenance, and Servicing Study
08 p0981 N88-15930
Orbital transfer vehicle studies overview
08 p0981 N88-15931
Space Infrared Telescope Facility (SIRTF) design and thermal analysis 08 p0982 N88-15934
Thermal analysis for the Cryogenic Fluid Management Flight Experiment (CFMFE) 08 p0982 N88-15935
Vapor condensation on a turbulent liquid interface
08 p0982 N88-15939
Computer-aided design analysis of 57-mm, angular-contact, cryogenic turbopump bearings
[NASA-TP-2816] 11 p1496 N88-18933
Cryogenic Fluid Management Technology Workshop. Volume 2: Roundtable Discussion of Technology Requirements
[NASA-CP-10009] 13 p1772 N88-20599
Nucleate pool boiling. High gravity to reduced gravity; liquid metals to cryogens 17 p2431 N88-24464
CRYOGENIC ROCKET PROPELLANTS
Cryogenic Fluid Management Technology Workshop. Volume 1: Presentation material and discussion
[NASA-CP-10001] 08 p0980 N88-15924
The HM-7 engine of Ariane's third stage
09 p1126 N88-16753
STS propellant scavenging systems study. Part 2, volume 1: Executive summary and study results
[NASA-CR-179275] 10 p1290 N88-17716
STS propellant scavenging systems study. Part 2, volume 2: Cost and WBS/dictionary
[NASA-CR-179276] 10 p1290 N88-17717
Noncryogenic propellants for a nuclear orbit transfer vehicle 17 p2428 N88-24444
Breadboard RL10-2B low-thrust operating mode (second iteration) test report
[NASA-CR-182160] 24 p3338 N88-29867
CRYOGENIC TEMPERATURE
Study on the cryogenic toughness of stainless steel weld metals
[PB87-143830] 07 p0834 N88-15057
Long-time tunneling in amorphous metals at helium temperatures
[DE88-701150] 16 p2281 N88-23654
Hot carrier effects in CMOS field effect transistors at cryogenic temperatures 19 p2662 N88-25829
Low noise cryogenic dielectric resonator oscillator
[NASA-CASE-NPO-17157-1-CU]
20 p2797 N88-26596
Cryogenic free jets
[DFVLR-FB-88-16] 21 p2900 N88-27210
CRYOGENIC WIND TUNNELS
Wall interference tests of a CAST 10-2/DOA 2 airfoil in an adaptive-wall test section
[NASA-TM-4015] 02 p0122 N88-10772
Description of tests run in the T2 cryogenic wind tunnel
[PB87-170296] 09 p1113 N88-16672
Pressure distributions from high Reynolds number transonic tests of an NACA 0012 airfoil in the Langley 0.3-meter transonic cryogenic tunnel
[NASA-TM-100526] 11 p1435 N88-18565
High Reynolds number transonic tests on a NACA 0012 airfoil in the Langley 0.3-meter transonic cryogenic tunnel
[NASA-TM-100527] 11 p1436 N88-18571
Preliminary experiments on surface flow visualization in the cryogenic wind tunnel by use of condensing or freezing gases
[NASA-CR-181634] 11 p1442 N88-18602
Aerodynamic performance and pressure distributions for a NASA SC(2)-0714 airfoil tested in the Langley 0.3-meter transonic cryogenic tunnel
[NASA-TM-4044] 18 p2456 N88-24580
Design study. Manipulator systems for model handling in European transonic wind tunnels
[ETN-88-91944] 18 p2468 N88-24651
Method of forming a multiple layer dielectric and a hot film sensor therewith
[NASA-CASE-LAR-13678-1] 18 p2584 N88-25355
Wall interference assessment/correction of data from tests of a CAST 10-2/DOA 2 airfoil in the Langley 0.3-m transonic cryogenic tunnel 20 p2751 N88-26331
Technology for pressure-instrumented thin airfoil models
[NASA-CR-4173] 23 p3180 N88-28933
CRYOGENICS
Thermal Control Working Group report
01 p0016 N88-10094
Characteristics and performance of the ESTEC large space simulator cryogenic system
02 p0135 N88-10849
Tensile behavior of superplastic Al-Cu-Li-Zr alloy 2090 at cryogenic temperatures
[DE87-014084] 02 p0147 N88-10923
Spectroscopic and retrieval studies in support of SCRIBE (Stratospheric Cryogenic Interferometer Balloon Experiment)
[AD-A184037] 03 p0351 N88-12216
Dramatically improved radiation hardness for CMOS silicon gate integrated circuits even down to cryogenic temperatures
[AD-A184672] 03 p0381 N88-12398
Design concepts for the ASTROMAG cryogenic system
[NASA-CR-181505] 04 p0497 N88-13060
Fatigue strength of alloy A286 at cryogenic temperature 05 p0603 N88-13695
Near-threshold fatigue crack growth behavior at cryogenic temperature 06 p0718 N88-14409
Cryogenic Fluid Management Technology Workshop. Volume 1: Presentation material and discussion
[NASA-CP-10001] 08 p0980 N88-15924
AF cryogenic and fluid management spacecraft technology program 08 p0981 N88-15925
Cryogenics program overview
08 p0981 N88-15926
Ames Research Center cryogenics program
08 p0981 N88-15927
LeRC cryogenic fluid management program overview
08 p0981 N88-15928
Cryogenic fluid management program flight concept definition 08 p0981 N88-15929
Large capacity cryopropellant orbital storage facility
08 p0981 N88-15932
Thermal analysis for the Cryogenic Fluid Management Flight Experiment (CFMFE) 08 p0982 N88-15935
Cryogenic acoustic microscopy
[AD-A187274] 10 p1299 N88-17767
Study on the dynamics of executive electromechanism with thyristor commutator for cryogenic systems
[DE87-703209] 12 p1622 N88-19702
A method of calculating nonstationary heat flow in hydrogasodynamic processes in closed cryogenic systems
[DE88-700884] 12 p1626 N88-19727
Development of a constitutive equation for HSLA (High-Strength Low-Alloy)-100 at cryogenic temperatures
[AD-A189243] 13 p1740 N88-2040[illegible]
Advanced components for spaceborne infrared astronomy
[NASA-CR-177470] 13 p1772 N88-20601
Materials testing at cryogenic temperatures
[BU-359] 14 p1923 N88-21462
Thin superconducting film characterization by surface acoustic waves
[AD-A190417] 15 p2143 N88-22791
Gigawatt, closed cycle, vapor core-MHD space power system conceptual design study
17 p2433 N88-24473
Thermodynamic modeling of the no-vent fill methodology for transferring cryogens in low gravity
[NASA-TM-100932] 18 p2476 N88-24686
Electrodynamic driver for the space thermoacoustic refrigerator (STAR)
[AD-A192337] 20 p2785 N88-26517
Development of external cooling cryo-resistive cable systems. Part 2: Insulation characteristics on 66 kV rated cryo-resistive testing cable
[DE88-770191] 20 p2793 N88-26571
A 2.3-GHz low-noise cryo-FET amplifier
22 p3066 N88-28195
LLE (Laboratory for Laser Energetics) review
[DE88-008065] 23 p3219 N88-29158

CRYOPUMPING
The Jeffcott equations in nonlinear rotordynamics
07 p0928 N88-15636
CRYOSORPTION
U SORPTION
CRYOSTATS
Components for cryostat --- spaceborne
[MBB/ISO-TN-CD00.003-REV-A]
01 p0032 N88-10207
Development activities for a 21-T superconducting magnet and cryostat
[DE88-004370] 11 p1558 N88-19327
Development of a motorized cryovalve for the control of superfluid liquid helium 14 p1925 N88-21477
CRYPTOGRAPHY
Components and cycles of a random function
[DE87-014155] 02 p0228 N88-11437
Minimum disclosure proofs of knowledge
[CWI-PM-R8710] 20 p2840 N88-26854
CRYSTAL DEFECTS
NT CRYSTAL DISLOCATIONS
NT EDGE DISLOCATIONS
NT POINT DEFECTS
NT SCREW DISLOCATIONS
NT VACANCIES (CRYSTAL DEFECTS)
Theory of defects in non-metallic solids
[DE87-014068] 02 p0152 N88-10949
Hydrogen annealing of P(sub) b and E prime defect centers in oxidized silicon wafers
[DE87-014293] 02 p0152 N88-10951
Defect characterization in quartz and related materials
[AD-A184754] 03 p0294 N88-11846
Impedance of passive lithium anodes in SOCl2 solutions under low-field polarization
[DE88-000922] 04 p0439 N88-12728
Structural characterization of ion implanted beta-SiC thin films
[DE87-014567] 05 p0656 N88-14027
Effect of optical inhomogeneities on space coherence of radiation emitted by laser with unstable resonator
06 p0771 N88-14738
The role of hydrogen in radiation-induced defect formation in polysilicon gate MOS devices
[DE87-012374] 06 p0785 N88-14814
X-ray measurements of phason distortion in ion-implanted Al-Mn
[DE87-014566] 07 p0937 N88-15694
Formation and passivation of new paramagnetic defects associated with thermal oxides on silicon
[DE88-002720] 07 p0938 N88-15699
Density of states of electrons bound to impurities in quantum wells of GaAlAs/GaAs
[INPE-4257-PRE/1130] 08 p1089 N88-16557
High-temperature charge-density studies of CeO/sub 2-x/ using X-ray and neutron diffraction techniques
[DE88-002988] 09 p1257 N88-17536
Control of solid-excitation-based photochemical dry etching of semiconductors by ion-bombardment-induced damage
[DE88-003214] 09 p1257 N88-17537
Models for ionic transport in glass
[DE88-002860] 10 p1304 N88-17799
Positron-annihilation 2D-ACAR studies of disordered and defected alloys
[DE88-003118] 10 p1416 N88-18454
Solving complex and disordered surface structures with electron diffraction
[DE88-003863] 10 p1418 N88-18467
Grazing incidence X-ray scattering study of defect structures in MBE GaAs/Si using synchrotron radiation
[DE88-004556] 10 p1420 N88-18483
Determination of the equilibrium concentration of characteristic defects by the measurement of thermal expansion using neutron scattering and laser interferometry
[ETN-88-91489] 11 p1490 N88-18890
Atomistic studies of the structure and properties of grain boundaries with substitutional impurities
[DE88-004161] 11 p1545 N88-19237
Structural characterization of undoped and doped GaAs: A comparative study of four techniques
[DE88-004552] 11 p1555 N88-19304
Spatial distribution of carbon and native defects in large-diameter bulk grown GaAs
[DE88-003870] 11 p1562 N88-19348
Hydrodynamic simulation of forced convection in the Czochralski process
[INPE-4471-TDL/323] 12 p1697 N88-20158
Experimental and theoretical methods for investigating helium effects in rapidly solidified metals
[DE88-005542] 13 p1743 N88-20425
A calorimetric determination of the enthalpy of formation and a description of the defect structure of the ordered beta-phase /Ni, Cu/ /1-x/ Al/x/
[NASA-TT-20157] 13 p1745 N88-20434
Fingering flow patterns of thermosolutal convection in rectangular enclosures
[NASA-TM-100854] 14 p1911 N88-21417
Materials dependence of deformation texture development in various deformation modes
[DE88-004312] 14 p1922 N88-21457
Experimental studies of elastic properties of crystals by Brillouin scattering
[DE88-005923] 14 p1986 N88-21848
Absolute pressure derivatives of deep level defects in 3-5 semiconductors
[DE88-006318] 15 p2140 N88-22772
The structure of the boron-hydrogen complex in silicon
[DE88-005433] 15 p2144 N88-22795
Annihilation momentum density of positrons trapped at vacancy-type defects in metals and alloys
[DE88-005936] 15 p2144 N88-22797
Development program for 1.93-micron lasers
[NASA-CR-4148] 16 p2212 N88-23198
Improved silicon carbide for advanced heat engines
17 p2324 N88-23879
Strength optimization of alpha-SiC by improved processing 17 p2324 N88-23880
Improved processing of Si3N4
17 p2325 N88-23882
Defects in cubic silicon carbide on silicon
17 p2408 N88-24317
On the use of convergent beam electron diffraction for identification of antiphase boundaries in GaAs grown on Si
[DE88-008220] 19 p2565 N88-25362
Defects in high-mobility semiconductor systems
[AD-A191618] 19 p2732 N88-26224
Aharonov-Bohm effects in disordered metals
20 p2864 N88-27006
EXAFS studies of the microstructure of semiconductor alloys, defects and semiconductor-metal interfaces
20 p2868 N88-27031
Aperiodic superlattices: Structured randomness
20 p2873 N88-27055
Fermi level dependent native defect formation: Consequences for metal-semiconductor and semiconductor-semiconductor interfaces
[DE88-008247] 20 p2875 N88-27066
Electron irradiation effects in YBa2Cu3O7-Delta single crystals
[DE88-010050] 20 p2878 N88-27085
Defect characterization of the redox behavior and stability of conducting oxides
[DE88-010799] 20 p2878 N88-27086
Migration and stability of HgCdTe lattice defects
[AD-A193293] 21 p3021 N88-27935
Probing the electronic and defect structure of perovskite superconductors
[DE88-008349] 21 p3022 N88-27939
Deep level defects in semiconductors: Stress and pressure studies
[DE88-010855] 21 p3024 N88-27948
Local environment approach for deep-level defects in semiconductors: Application to the vacancy in silicon
[DE88-702017] 23 p3287 N88-29573
An HVEM study of displacement cascade damage in Nb3Sn at 13 K
[DE88-009997] 23 p3289 N88-29584
Rapid thermal annealing of silicon layers amorphized by ion implantation
[DE88-702307] 23 p3290 N88-29591
Chemical kinetics of hydrogen and P(sub b) centers
[DE88-010528] 23 p3291 N88-29594
Localized excitations in one-dimensional molecular crystal with structural defect
[DE88-702691] 23 p3293 N88-29607
Streaking images that appear only in the plane of diffraction in undoped GaAs single crystals: Diffraction imaging (topography) by monochromatic synchrotron radiation
[NASA-CR-183267] 24 p3433 N88-30437
CRYSTAL DISLOCATIONS
NT EDGE DISLOCATIONS
NT SCREW DISLOCATIONS
Study of the microscopic mechanisms of cyclic deformation. Development of a new approach: The case of aluminum
[ISAL-87-0003] 02 p0149 N88-10936
Need for composites, new materials discussed
02 p0160 N88-11001
Raman scattering spectrum along a bevel etched GaAs on Si, TEM (Transmission Electron Microscope) study and GaAs P-I-N photodetector on Si
[DE88-000210] 04 p0498 N88-13066
Orientation effects in copper single crystals fatigued at elevated temperatures 06 p0720 N88-14423
Computer simulation of impurities and interfaces in body centered cubic metals
[PB88-108162] 07 p0832 N88-15047
Evolution of radiation-induced voids and dislocations at low temperature
[DE88-700350] 07 p0939 N88-15704
Some present limitations on the lattice imaging of grain boundaries
[DE87-014665] 09 p1256 N88-17530
Silicon and indium doping of GaAs: Measurements of the effect of doping on mechanical behavior and relation with dislocation formation
[DE88-003862] 11 p1554 N88-19303
Image force expression for the dislocation near a crack
[DE88-701894] 20 p2814 N88-26692
On the possibility of the soliton description of acoustic emission during plastic deformation of crystals
[DE88-701878] 20 p2876 N88-27075
Diffusion and solubility of some interstitial impurities in deformed metals
[DE88-701859] 21 p2914 N88-27296
The influence of solute segregation on the dislocation structure of small and large angle (001) twist boundaries in Fe-Sb alloys
[DE88-009166] 22 p3155 N88-28770
CRYSTAL GROWTH
NT CZOCHRALSKI METHOD
NT DIRECTIONAL SOLIDIFICATION (CRYSTALS)
NT EPITAXY
NT LIQUID PHASE EPITAXY
NT MOLECULAR BEAM EPITAXY
NT VAPOR PHASE EPITAXY
Prephase A study of a crystallization laboratory for Columbus, executive summary
[ESA-ITT/AO/1-1866/85F] 01 p0032 N88-10206
Direct formation of thin films and epitaxial overlayers at low temperatures using a low-energy (10-500 eV) ion beam deposition system
[DE87-012291] 01 p0103 N88-10675
Grain boundary phase equilibria in metallic systems
[DE87-014123] 01 p0104 N88-10679
Experimental and theoretical study of condensation in multicomponent vapors
[DE87-013663] 02 p0145 N88-10907
On the role of convective motion during dendrite growth. Experiments under variable gravity, revised
[NASA-CR-179213] 02 p0156 N88-10979
A finite element model for induction heating of a metal crucible
[DE87-014246] 02 p0246 N88-11551
The structure and reactivity of heterogeneous surfaces and study of the geometry of surface complexes
[DE88-000158] 03 p0279 N88-11754
International Conference on Microstructology held in Gainesville, Florida on 7-9 May 1986
[AD-A184604] 03 p0290 N88-11822
Consortium for Materials Development in Space. Technical section
[NASA-CR-181508] 03 p0296 N88-11859
Physical vapor transport crystal growth
03 p0296 N88-11860
Mass spectroscopic facility 03 p0296 N88-11861
Highly Non-Linear Optical (NLO) organic crystals
03 p0297 N88-11865
Highly Non-Linear Optical (NLO) organic crystals and films. Electrooptical organic materials
03 p0297 N88-11866
Numerical analysis of Marangoni convection in Bridgman method 03 p0319 N88-12014
Deformation mechanisms of thermostructural materials
[AD-A184070] 03 p0338 N88-12128
Simulation of the layer-growth dynamics in silver films: Dynamics of adatom clusters and vacancy clusters on Ag(100)
[DE87-014764] 03 p0380 N88-12390
Phase equilibrium and crystal growth studies on AgGaSe2 and related nonlinear optical materials
[AD-A184768] 03 p0382 N88-12400
Investigation of hexagonal ferrite film growth techniques for millimeter-wave systems applications
[AD-A184335] 03 p0383 N88-12406
Evaluation of the Mellen EDG furnace for growth of large diameter GaAs single crystals in a horizontal configuration
[DE88-000463] 04 p0498 N88-13068
United States - Japan Workshop on Dielectric and Piezoelectric Ceramics (3rd) held in Toyama, Japan on November 9-12, 1986
[AD-A185113] 05 p0568 N88-13460
MBE growth of InAsSb strained layer superlattices
[DE88-000365] 05 p0654 N88-14011
Molecular beam epitaxial growth and characterization of 3-5 compound semiconductor single and multiple interface structures
[AD-A185400] 05 p0656 N88-14021
Novel heterojunction devices
[DE87-013716] 05 p0656 N88-14026

Growth of solid solution single crystals
[NASA-TP-2787] 06 p0688 N88-14212
Heteroepitaxial growth of 3-5 semiconductor compounds by metal-organic chemical vapor deposition for device applications
[NASA-CR-182346] 06 p0788 N88-14832
Method for investigating the formation of crystals in a transparent material
[NASA-CASE-MFS-26008-1-CU]
06 p0788 N88-14835
Some investigations of molecular beam epitaxial growth of 3-5 semiconductor films via Monte-Carlo computer simulations, carrier tunnelling and spectroscopic ellipsometry
[AD-A185520] 06 p0789 N88-14839
Cellular solidification in a monotectic system
[NASA-TM-100317] 07 p0829 N88-15027
Allowable gravity levels for Spacelab, Columbus and EURECA --- materials science
[BF-R-66.525-2] 07 p0838 N88-15084
Resolution of holograms produced by the fluid experiment system and the holography ground system
07 p0923 N88-15609
A numerical study of transient heat and mass transfer in crystal growth 07 p0925 N88-15619
High-temperature electronics
08 p0956 N88-15797
A laboratory study of tin whisker growth
[ESA-STR-223] 08 p1089 N88-16553
Visible InGaAsP/GaAsP lasers produced by epitaxial growth from liquid phase 09 p1237 N88-17416
Superlattice photodetectors
[AD-A186956] 09 p1253 N88-17511
Molecular beam epitaxy for research on quantum well structures
[AD-A186791] 09 p1255 N88-17522
Electrochemical growth of linear conducting crystals in microgravity 10 p1287 N88-17698
Protein-crystal growth experiment (planned)
10 p1287 N88-17700
A payload for investigating the influence of convection on GaAs crystal growth 10 p1288 N88-17702
An advanced microcomputer design for processing of semiconductor materials 10 p1288 N88-17703
Application of Hoffman modulation contrast microscopy coupled with three-wavelength two-beam interferometry to the in situ direct observation of the growth process of a crystal in microgravity 10 p1288 N88-17704
Project Explorer takes its second step: GAS-608 in engineering development 10 p1288 N88-17707
Formation of optical waveguides by ion implantation
[DE88-003894] 10 p1409 N88-18407
High temperature processing of superconducting Y1Ba2Cu3O6.9
[DE88-003002] 10 p1416 N88-18449
Growth and electronic properties of strained metal overlayers
[DE87-010956] 10 p1417 N88-18463
Stability diagrams for epitaxial strained layers
[DE88-003935] 10 p1418 N88-18470
Nucleation and growth of calcium carbonate crystals on surface-modified polyethylene and polystyrene
[DE88-005126] 11 p1465 N88-18733
Development of a planar heterojunction bipolar transistor for very high speed logic
[AD-A188137] 11 p1478 N88-18820
Growth and characteristics of materials for tunable lasers in the near infrared spectral region
[NASA-CR-182501] 11 p1491 N88-18901
Proceedings of the 1987 High-Efficiency Photovoltaic Subcontractors' Review Meeting
[DE88-003354] 11 p1508 N88-19011
Optical waveguide formation by ion implantation of Ti or Ag
[DE88-004595] 11 p1551 N88-19278
MCT crystal growth
[NASA-CR-179297] 11 p1557 N88-19318
Growth of Cr,Nd:Gd3Sc2Al3O12 (Cr,Nd:GSAG) crystals by the Heat Exchanger Method (HEM)(trademark)
[DE88-004041] 11 p1558 N88-19326
Feasibility studies of the growth of 3-5 compounds of boron by MOCVD
[NASA-CR-181622] 11 p1561 N88-19343
Analysis of low gravity tolerance of model experiments for space station: Preliminary results for directional solidification
[NASA-CR-182657] 12 p1614 N88-19648
High Rayleigh number convection in rectangular enclosures with differentially heated vertical walls and aspect ratios between zero and unity
[NASA-TM-100277] 12 p1628 N88-19739
Mass transport and chemical demixing of Y-Ba-Cu-O compounds during sintering in temperature gradients
[DE88-004887] 12 p1696 N88-20151
Stability and uniqueness in nonlinear continuum mechanics
[AD-A189616] 12 p1699 N88-20172
Research on mercury cadmium telluride
[AD-A189155] 13 p1845 N88-21039
Initial stages of silicon growth on the (100) surface of silicon by localized laser CVD
[DE88-005420] 13 p1848 N88-21059
Proceedings of the Seminar on Hydrodynamics and Crystal Growth
[ETN-88-92025] 14 p1987 N88-21853
Numerical simulations of buoyancy driven flows in cylinders and cavities for vapor crystal growth
14 p1987 N88-21854
Velocity and concentration fields over a crystal growing in a water solution. Experimental study and numerical simulation 14 p1987 N88-21856
Transport processes during directional solidification and crystal growth: Scaling and experimental study
14 p1988 N88-21857
Selective growth velocity in needle crystals
14 p1988 N88-21858
Convection effects on stability at the solidification front 14 p1988 N88-21860
Grain growth behavior of extrusion consolidated centrifugally atomized Type 304 stainless steel powder
[DE88-006788] 15 p2038 N88-22143
Fundamental studies on high temperature deformation recrystallization, and grain growth of two-phase materials
[AD-A189725] 15 p2038 N88-22145
JPPS report: Science and technology. Japan
[JPRS-JST-88-002] 15 p2050 N88-22210
Single crystal growth by laser CVD
15 p2050 N88-22213
Pb(1-x)Sn(x)Te crystal growth in space
15 p2051 N88-22223
Atomic beam study of crystalline order and precipitation in nickel based alloys
[ETN-88-91994] 16 p2177 N88-22975
JPRS report: Science and technology. USSR: Materials science
[JPRS-UMS-88-006] 16 p2179 N88-22988
New method of grafting crystals
16 p2180 N88-22992
Tunable optical sources/growth and characterization of nonlinear optical materials
[AD-A190874] 16 p2274 N88-23608
Non-contact temperature measurement requirements for electronic materials processing
17 p2328 N88-23898
Method and apparatus for growing crystals
[NASA-CASE-MFS-28137-1] 17 p2446 N88-24544
Liquid encapsulated float zone process and apparatus
[NASA-CASE-MFS-28144-1] 17 p2446 N88-24545
Optical monitoring of protein crystal growth
[NASA-CR-182869] 18 p2484 N88-24738
Preparation for microgravity: The role of the microgravity materials science laboratory
[NASA-TM-100906] 18 p2497 N88-24811
Joint services electronics program research in electronics
[AD-A192206] 18 p2504 N88-24857
Dendritic growth in the presence of convection
18 p2580 N88-25328
Two puzzling aspects of protein crystal growth
18 p2580 N88-25329
The morphological stability of continuous intergranular phases: Thermodynamic considerations
[DE88-006328] 18 p2584 N88-25350
Electronic controller for reciprocating rotary crystallizer
[NASA-TM-101140] 18 p2584 N88-25354
Hanging drop crystal growth apparatus and method
[NASA-CASE-MFS-28206-1-SB]
18 p2585 N88-25356
Crystal growth apparatus
[NASA-CASE-MFS-28182-1] 18 p2585 N88-25357
Epitaxial iron films
[AD-A191815] 19 p2732 N88-26225
The structure and properties of grain boundaries in B2 ordered alloys
[DE88-009890] 20 p2773 N88-26447
Preparation of oxide superconductors
[DE88-009136] 20 p2875 N88-27063
Analysis of grain refinement and superplasticity in aluminum-magnesium alloys
[AD-A193029] 21 p2912 N88-27283
Processing and additive effects of ZrO2 on microstructure and dielectric porperties of BaTiO3 ceramics
[AD-A193126] 21 p2917 N88-27316
Growth and characterization of CuGaS2, CuAlS2 and CuGa0.9Al0.1S2 single crystals
[AD-A192963] 21 p3021 N88-27930
Phase equilibrium and crystal growth studies on AgGaSe2 and related nonlinear optical materials
[AD-A193763] 22 p3157 N88-28783
High temperature electric arc furnace
[NASA-CASE-MFS-28281-1] 23 p3181 N88-28938
New method for preparation of (Cd, Hg)Te thin films
[DE88-702727] 23 p3293 N88-29608
Growth and characterization of materials for tunable lasers in the near infrared spectral region
[NASA-CR-183132] 24 p3377 N88-30113
Growth of GaAs crystals by the Heat Exchanger Method for microwave device applications
[AD-A196028] 24 p3433 N88-30435

CRYSTAL LATTICES
NT BODY CENTERED CUBIC LATTICES
NT CUBIC LATTICES
NT FACE CENTERED CUBIC LATTICES
NT SUPERLATTICES
LLE review
[DE87-014468] 02 p0178 N88-11110
Surface chemistry of transition metal carbides: A theoretical analysis
[AD-A184237] 03 p0291 N88-11829
Modeling of irradiation-induced amorphization in a titanate ceramic
[DE87-014751] 03 p0292 N88-11833
New theory for competing interactions and microstructures in partially-ordered (liquid-crystalline) phases
[DE87-014739] 03 p0380 N88-12389
A study of mechanisms of hydrogen diffusion in separation devices
[DE88-000328] 04 p0416 N88-12584
Radiation induced collapse of the crystalline structure
[DE87-014407] 04 p0498 N88-13064
Raman scattering spectrum along a bevel etched GaAs on Si, TEM (Transmission Electron Microscope) study and GaAs P-I-N photodetector on Si
[DE88-000210] 04 p0498 N88-13066
MBE growth of InAsSb strained-layer superlattices
[DE88-000365] 05 p0654 N88-14011
The pseudopotential density functional method applied to semiconducting crystals
[ETN-88-91362] 05 p0656 N88-14024
Novel heterojunction devices
[DE87-013716] 05 p0656 N88-14026
Basic energy sciences research in the Metals and Ceramics Division of Oak Ridge National Laboratory
[DE87-013538] 06 p0681 N88-14171
Structural investigations of some metallic glasses
[ECN-198] 06 p0686 N88-14203
X-ray structure analyses and molecular mechanics analyses of dense energetic materials
[AD-A185462] 06 p0779 N88-14781
Silicon microscale mechanisms from (110) oriented wafers
[DE88-002096] 06 p0787 N88-14825
Structural relaxation in strained-layer heterostructures
[DE88-002326] 07 p0868 N88-15264
Phonon dispersion for several surfaces with ordered overlayers: A lattice dynamical study
07 p0876 N88-15315
Embedded cluster models for electronic structure and energetics of complex oxides
[DE88-003097] 07 p0938 N88-15702
Structural properties of high-T/sub c/ oxide super conductors
[DE88-002974] 08 p1090 N88-16563
Thermodynamic and conductivity studies of nonstoichiometric cerium dioxide by Coulometric titration: A simultaneous measurement
[DE88-003054] 08 p1091 N88-16566
Heavy Fermions and coherence in Kondo lattices. Specific heat of low energy excitation in Cer systems
[ETN-88-91080] 09 p1255 N88-17525
High-temperature charge-density studies of CeO/sub 2-x/ using X-ray and neutron diffraction techniques
[DE88-002988] 09 p1257 N88-17536
Molecular dynamics study of high-temperature grain-boundary stability in a (100) sigma = 29 bicrystal model
[DE88-002955] 09 p1258 N88-17546
Crystalline sulfur dioxide: Crystal field splittings, absolute band intensities and complex refractive indices derived from infrared spectra
[NASA-CR-182502] 09 p1258 N88-17547
Fabrication, phase transformation studies and characterization of SiC-AlN-Al2OC ceramics
[DE88-004053] 10 p1306 N88-17807
Study of quantum mechanical effects in deep submicron, grating-gate field effect transistors
[AD-A188283] 10 p1325 N88-17923
Optical characterization of GaAs/sub 1-x/Sb/sub x/ and GaAs/sub 1-x/Sb/sub x/GaAs strained layer superlattices
[DE88-003393] 10 p1418 N88-18464
Simple renormalization group method for calculating thermal equations of states
[DE88-700143] 11 p1454 N88-18668

National Center for Small-Angle Scattering Research: Reports on measurements carried out by users of the facilities of the NCSASR, December 1, 1985-September 30, 1987
[DE88-003754] 11 p1462 N88-18719

Algorithmic alternatives
[DE88-003905] 11 p1531 N88-19149

Atomistic simulation of low-energy beam deposition
[DE88-004344] 11 p1544 N88-19228

Single-crystal structural study of La2Cu/sub 0.95/Li/sub 0.05/O4
[DE88-003482] 11 p1554 N88-19302

Scanning tunneling microscopy of silver, gold, and aluminium monomers and small clusters on graphite
[DE88-003871] 11 p1562 N88-19349

Temperature dependence of Kr precipitation in Ni
[DE88-005953] 13 p1744 N88-20429

Lattice relaxation of the DX centers in Ga/sub 1-x/Al/sub x/As and of the pressure-induced deep donors in GaAs
[DE88-005452] 13 p1848 N88-21061

Effect of Mg impurity on local vibrations of U-centers in LiF lattice 14 p1969 N88-21753

Breathing mode lattice relaxation associated with carrier emission and capture by deep electronic levels in silicon
[DE88-003844] 14 p1985 N88-21842

Grain boundaries
[DE88-006628] 14 p1987 N88-21852

High energy cosmic muons and the calibration of the L3 electromagnetic calorimeter
[NOTA-INTERNA-895] 14 p2011 N88-21999

Absolute pressure derivatives of deep level defects in 3-5 semiconductors
[DE88-006318] 15 p2140 N88-22772

First-principles calculations of quasiparticle energies at surfaces and interfaces: Semiconductor surface-state spectra and band offsets
[DE88-006340] 15 p2141 N88-22773

Fundamental properties and devices applications of Ge(x)Si(1-x)/Si superlattices
[AD-A190129] 15 p2143 N88-22787

The structure of the boron-hydrogen complex in silicon
[DE88-005433] 15 p2144 N88-22795

MBE of HgCdTe
[AD-A191423] 16 p2283 N88-23671

Structural studies on La/sub 2/CuO/sub 4+delta/
[DE88-006828] 18 p2581 N88-25330

Abnormal diffusion of vacancies in metals
[DE88-701880] 20 p2773 N88-26441

Lattice strain in heteroepitaxial films
20 p2868 N88-27032

Lattice theory of fracture of solids with layered structure
[DE88-701867] 20 p2876 N88-27073

Derivation of space groups in mm2, 222 and mmm crystal classes
[DE88-701881] 20 p2876 N88-27076

Contribution to the study of order effects in the Ising model framework: Ground states and phase diagrams
[ONERA-NT-1987] 20 p2880 N88-27095

Picosecond transient reflectivity of unpinned gallium arsenide (100) surfaces
[AD-A193242] 21 p3021 N88-27933

Topics in quasicrystallography
21 p3023 N88-27947

Deep level defects in semiconductors: Stress and pressure studies
[DE88-010855] 21 p3024 N88-27948

Theory of surface melting and non-melting
[DE88-702652] 22 p3157 N88-28785

Soliton and polaron dynamics in conducting polymers
[DE88-702539] 23 p3198 N88-29035

CRYSTAL OPTICS

Gamma-ray optics of multi-beam Borrmann modes with possible applications to nuclear lasing
04 p0449 N88-12784

Use of lasers with F sub A(II)-color center KCl:Li crystals in the intraresonator laser spectroscopy method
06 p0769 N88-14729

Observation of instabilities in time during dynamic self-diffraction of light in anisotropic nonhomogeneous medium 06 p0769 N88-14730

High-efficiency GaAs semiconductor laser with longitudinal excitation by scanning electron beam
09 p1238 N88-17421

Note on the double crystal method of measuring heat transfer coefficient
[OUEL-1710/87] 17 p2338 N88-23950

Liquid crystal optics for laser systems
[DE88-008475] 20 p2854 N88-26948

CRYSTAL OSCILLATORS

NT PIEZOELECTRIC CRYSTALS

Surface wave accelerometer
[ETN-88-92000] 16 p2210 N88-23192

Quartz crystal resonators and oscillators for frequency control and timing applications
[AD-A193310] 21 p2937 N88-27443

Specifications and performance of ultrastable oscillators in the DORIS orbitography and positioning system
[ETN-88-92761] 24 p3331 N88-29831

CRYSTAL RECTIFIERS

Pierce diode with external circuit. Part 3: Chaotic behavior
[AD-A194837] 24 p3365 N88-30041

CRYSTAL STRUCTURE

Electronic structure of crystalline NaSn
[DE87-702583] 01 p0102 N88-10669

Structure of rapidly solidified Ni-Ti
[DE87-012252] 02 p0147 N88-10921

Field ion microscope studies of surface reconstructions
[DE87-014644] 02 p0147 N88-10924

Theory of defects in non-metallic solids
[DE87-014068] 02 p0152 N88-10949

Need for composites, new materials discussed
02 p0160 N88-11001

Production of metallic monocrystals described
03 p0286 N88-11796

Modelling and theories of alloy phase behavior
[DE87-014399] 03 p0287 N88-11804

International Conference on Microstructology held in Gainesville, Florida on 7-9 May 1986
[AD-A184604] 03 p0290 N88-11822

Surface chemistry of transition metal carbides: A theoretical analysis
[AD-A184237] 03 p0291 N88-11829

Indentation damage in ceramics
[AD-A184686] 03 p0294 N88-11844

Monte Carlo simulation of modulated phases
[NASA-TM-89654] 03 p0369 N88-12323

Shock-induced chemical synthesis of phases similar to the high temperature superconductor oxides
[DE87-013725] 03 p0380 N88-12387

Equilibria, lattices and chaotic dynamics of point vortices 04 p0444 N88-12758

Properties of refractory metals processed by enhanced sintering treatments
[AD-A184944] 05 p0565 N88-13440

Study of boundary structures
[AD-A184806] 05 p0655 N88-14013

Diffraction by glasses with a layer structure
[DE88-003059] 07 p0837 N88-15078

Change of europium crystallographic symmetry at helicoidal magnetic ordering
[DE88-700559] 07 p0939 N88-15707

Wave functions for bound states of relativistic electrons in a crystal at electron movement along crystallographic planes
[DE88-700563] 07 p0939 N88-15708

Interface characteristics and the mechanical properties of metal matrix composites
[AD-A186441] 08 p0966 N88-15845

JPRS report: Science and technology. USSR. Physics and mathematics
[JPRS-UPM-87-010] 08 p1075 N88-16485

Metal-oxide superconductor BaPbsub1-xBisubxO3: Unusual properties and new applications
08 p1077 N88-16494

New branch of solid-state physics
08 p1079 N88-16508

Experimental aspects of high-T/sub c/ superconductors
[DE88-003019] 08 p1080 N88-16564

Neutron- and X-ray-small angle scattering with Fe-base metallic glasses
[DE88-002538] 09 p1147 N88-16876

Physical properties of summer sea ice in the Fram Strait, June-July 1984
[AD-A186937] 09 p1194 N88-17156

Superconductivity and crystal structure of high-pressure phases in V-Ru-H system 09 p1239 N88-17426

Some present limitations on the lattice imaging of grain boundaries
[DE87-014665] 09 p1256 N88-17530

Corner compensation structures for (110) oriented silicon
[DE88-003300] 10 p1417 N88-18455

Growth and electronic properties of strained metal overlayers
[DE87-010956] 10 p1417 N88-18463

Solving complex and disordered surface structures with electron diffraction
[DE88-003863] 10 p1418 N88-18467

Order-disorder transition of Au and Pt (110) surfaces: The significance of relaxations and vibrations
[DE88-004651] 10 p1419 N88-18473

Perturbed angular correlations in zirconia ceramics
[DE88-004117] 11 p1464 N88-18731

The first gallium-arsenic compound containing a single Ga3As unit: Isolation and crystal structure of ((thf)Br2Ga)3As (thf = tetrahydrofuran)
[AD-A187457] 11 p1555 N88-19309

A procedure for estimating the crystal densities of organic explosives
[AD-A189023] 12 p1613 N88-19646

Fast protonic conducting solid electrolytes
[AD-A188524] 12 p1698 N88-20160

CdZnTe as a wide-band-gap absorber for a tandem, thin-film solar cell
[DE88-001114] 13 p1793 N88-20724

Modeling growth of interdendritic silicon ribbons
14 p1897 N88-21322

Ordered structures in YBa2Cu3O/sub 7-y/, La2Cu3O/sub 7-y/, La/sub 2-x/Sr/sub x/CuO/sub 4-par delta/ and related perovskites
[DE88-006461] 14 p1987 N88-21851

Grain boundaries
[DE88-006628] 14 p1987 N88-21852

Investigation and synthesis of high temperature and increased stiffness RSP aluminum alloys
[AD-A190407] 15 p2039 N88-22151

Superconductivity and the tailoring of lattice parameters of the compound YBa2Cu3O(sub x)
[DE88-005904] 15 p2140 N88-22769

Atomic beam study of crystalline order and precipitation in nickel based alloys
[ETN-88-91994] 16 p2177 N88-22975

New method of grafting crystals
16 p2180 N88-22992

High-strength ceramic based on tetragonal ZrO2 with Al2O3 admixture 16 p2180 N88-22996

Initial stages of molecular beam heteroepitaxial growth in GaAs-(Ca,Sr)F2 and GaAs/Si systems
[LAAS-87-355] 16 p2281 N88-23658

Disclination structures in carbon and graphite
[AD-A191056] 17 p2322 N88-23868

The structural analysis of some crystalline and semi-crystalline substances using X-ray and neutron diffraction 17 p2445 N88-24540

Fundamental studies of beta phase decomposition modes in titanium alloys
[AD-A191495] 18 p2485 N88-24740

Superplasticity: A fundamental investigation on deformation mechanism and cavitation phenomena
[AD-A191548] 18 p2485 N88-24741

Liquid carbon
[AD-A191707] 18 p2491 N88-24776

Raman characterization of AsF5-intercalated vapor grown graphite fibers
[AD-A191709] 18 p2491 N88-24778

Structural studies on La/sub 2/CuO/sub 4+delta/
[DE88-006828] 18 p2581 N88-25330

Magnetic superlattices
[AD-A191450] 18 p2581 N88-25334

Phase stability and alloy design of ordered intermetallics
[DE88-007479] 20 p2772 N88-26435

Strained layer and lattice matched transverse junction stripe quantum well lasers for continuous room temperature operation 20 p2863 N88-27004

Metallic superlattices 20 p2864 N88-27012

Growth of high quality CoSi2/Si superstructures on Si(111) 20 p2869 N88-27034

Characterization of structural and magnetic order of Er/Y superlattices 20 p2873 N88-27056

Raman and absorption spectrophotometric studies of selected lanthanide, californium-doped lanthanide, and actinide trihalides in the solid state
[DE88-008234] 20 p2874 N88-27061

Lattice theory of fracture of solids with layered structure
[DE88-701867] 20 p2876 N88-27073

Derivation of space groups in mm2, 222 and mmm crystal classes
[DE88-701881] 20 p2876 N88-27076

Electronic and geometric structure of silver and palladium on aluminum (111) in monoatomic surface layers
[ETN-88-92120] 20 p2879 N88-27093

Epitaxy and properties of two dimensional GaInAs semiconductor structures
[ETN-88-92357] 20 p2879 N88-27094

Contribution to the study of order effects in the Ising model framework: Ground states and phase diagrams
[ONERA-NT-1987] 20 p2880 N88-27095

Thermomechanical processing of Al alloy 2090 for grain refinement and superplasticity
[AD-A192333] 21 p2912 N88-27281

Analysis of grain refinement and superplasticity in aluminum-magnesium alloys
[AD-A193029] 21 p2912 N88-27283

Polarization selective Raman microspectroscopy
21 p2930 N88-27397

Meaning of energy diagrams used to describe hetero-structures
[DE88-702219] 21 p3023 N88-27943
Prediction of deep levels and equilibrium concentrations of defects in semiconductors 21 p3023 N88-27945
X-ray studies of strain, interface and impurities in semiconductors
[DE88-012460] 21 p3025 N88-27954
Characterization of crystalline silicon by electrochemical and Raman spectroscopy at the frontier semiconductor/electrolyte
[ETN-88-92354] 21 p3025 N88-27956
Raman spectroscopy on simple molecular systems at very high density
[DE88-010947] 23 p3191 N88-28987
Structural relationship between icosahedral and Frank-Kasper phases of Al-Li-Cu
[AD-A193768] 23 p3195 N88-29011
Influence of local volume forces on surface relaxation of pure metals and alloys: Applications to Ni, Al, Ni3Al
[DE88-702718] 23 p3195 N88-29014
Band electronic structures and crystal packing forces
[DE88-010247] 23 p3289 N88-29585
Preparation and testing of Nb-Zr and Nb-ZrO2 single crystals for deformation studies
[DE88-702798] 23 p3293 N88-29613
Crystal structures of ordered carbon metal alloys
[AD-A195597] 24 p3353 N88-29959
Discovery of a low temperature form of TAGN (Triaminoguanidinium Nitrate)
[AD-A196059] 24 p3357 N88-29989
Crystal structure and density of helium to 232 kbar
24 p3441 N88-30481

CRYSTAL SURFACES
The effect of additives on the reactivity of palladium surfaces for the chemisorption and hydrogenation of carbon monoxide: A surface science and catalytic study
[DE87-014685] 02 p0145 N88-10909
Materials preparation and longevity in hyperthermal atomic oxygen 03 p0297 N88-11862
The structure of adsorbed sulfur and carbon on molybdenum and rhenium single crystal surfaces, and their influence on carbon monoxide and hydrocarbon chemisorption
[DE88-001393] 04 p0499 N88-13073
Surface deformation and fatigue crack initiation of alpha-iron 05 p0598 N88-13651
Laser pulse width dependent surface ripples on silicon
[PB88-127311] 10 p1336 N88-17982
A scientific basis for an alternate cathode architecture
[AD-A191498] 18 p2481 N88-24717
The catalytic reactivity of thin film crystal surfaces
[DE88-006387] 19 p2732 N88-26228
Theory of surface melting and non-melting
[DE88-702652] 22 p3157 N88-28785
Attenuated total reflectance FT-IR spectroscopy to measure interfacial reaction kinetics at silica surfaces
[AD-A196330] 24 p3344 N88-29908

CRYSTALLINITY
EXELFS (Extended Electron Energy Loss Fine Structure) of amorphous and crystalline SiC
[DE87-013551] 02 p0151 N88-10948
Modeling of irradiation induced amorphization in a titanate ceramic
[DE87-014751] 03 p0292 N88-11833
Gamma-ray optics of multi-beam Borrmann modes with possible applications to nuclear lasing
04 p0449 N88-12784
Radiation induced collapse of the crystalline structure
[DE87-014407] 04 p0498 N88-13064
Microstructure of amorphous and crystalline zirconium alloys rapidly solidified
[DE87-703700] 05 p0564 N88-13432
Helium atom surface scattering apparatus for studies of crystalline surface dynamics
[DE88-002104] 06 p0787 N88-14826
Crystalline sulfur dioxide: Crystal field splittings, absolute band intensities and complex refractive indices derived from infrared spectra
[NASA-CR-182502] 09 p1258 N88-17547
Crystalline photovoltaic cell technology: Present and future
[DE88-004684] 13 p1795 N88-20734
Analysis of explosives 1: Computer programs for processing of X-ray powder deffraction data
[PB88-156898] 14 p1894 N88-21309
Blends of crystallizable polybutadienes
[AD-A194536] 23 p3197 N88-29026
Preliminary analysis of recent 2.2-4.2 micrometers telescopic observations of Elysium, Mars: Implications for crystallinity and hydration state of surface materials
23 p3306 N88-29692
A method for the quantitative determination of crystalline phases by X-ray
[NASA-TT-20324] 24 p3434 N88-30444

CRYSTALLITES
Characterization of catalysts with metal-support effects and of the species adsorbed on their surfaces
[DE87-014636] 04 p0414 N88-12564
Gigantic optical nonlinearity in low dimensional systems 14 p1975 N88-21786
Enhanced excitonic optical nonlinearity and exciton dynamics in semiconductor microstructures
14 p1977 N88-21795
The crystallization of tough thermoplastic resins in the presence of carbon fibers
[NASA-CR-182984] 20 p2776 N88-26464

CRYSTALLIZATION
NT DIRECTIONAL SOLIDIFICATION (CRYSTALS)
NT MELT SPINNING
NT RECRYSTALLIZATION
Stability relationship for water droplet crystallization with the NASA Lewis icing spray
[NASA-TM-100220] 02 p0125 N88-10790
Study of the micromechanical behavior of a SiO2-Al2O3-Li2O glass ceramic and its relation to the microstructure
[ISAL-ITC1-87-01] 02 p0153 N88-10960
Ultra-fine grained alloy material
[AD-A184500] 03 p0290 N88-11820
Joining of silicon carbide reinforced ceramics
[DE87-014881] 03 p0294 N88-11847
Continued research on direct contact heat exchangers: Effects of crystallization
[DE87-014931] 03 p0322 N88-12035
Investigations of crystallization velocity and boron diffusion in glassy iron-boron alloys and of activity coefficients of boron in crystalline iron-boron alloys
[ETN-87-90613] 03 p0381 N88-12393
Studies on some Ge-Se-Te glasses
[PD-MT-8721] 04 p0420 N88-12607
T.E.M. study of boehmite gels and of their transformation into alpha-alumina
[SNIAS-872-430-121] 05 p0656 N88-14023
Undercooling and nucleation in iron nickel alloys
[AD-A185500] 06 p0683 N88-14184
Processing and interfacial analysis of glass-ceramic to metal seals
[DE88-002999] 08 p0971 N88-15873
Protein-crystal growth experiment (planned)
10 p1287 N88-17700
Crystallization and glass formation in electron and laser beam irradiated Cu-Zr alloys
[DE88-003390] 11 p1464 N88-18729
In situ ultrahigh vacuum friction measurement and wear track analysis of ion implanted 304 stainless steel
[DE88-004537] 11 p1494 N88-18922
Formation of buried nitride layers in (110) silicon
[DE88-003255] 11 p1557 N88-19323
Zone crystallization experiments in mirror heating facilities
[BMFT-FB-W-86-023] 16 p2184 N88-23016
Effect of size of precipitates on recrystallization temperatures in Cu-Cr, Cu-Zr, and Cu-Zr-Cr alloys
[NASA-TT-20166] 18 p2489 N88-24763
NASA research Program: The roles of fluid motion and other transport phenomena in the morphology of materials
[NASA-CR-182801] 18 p2580 N88-25327
Electronic controller for reciprocating rotary crystallizer
[NASA-TM-101140] 18 p2584 N88-25354
The crystallization of tough thermoplastic resins in the presence of carbon fibers
[NASA-CR-182984] 20 p2776 N88-26464
Crystallization of aluminum hydroxide in the aluminum-air battery: Literature review, crystallizer design and results of integrated system tests
[DE88-010510] 20 p2797 N88-26594
Microchemical analysis of polycrystalline Ni3Al and other ordered alloys using the field-ion microscope atom probe
[DE88-011519] 21 p2914 N88-27294
Formation of metastable structures and amorphous phases in Cu-W alloys using the triod sputtering technique
[DE88-009051] 21 p2915 N88-27298
Homogeneity of glasses: Experiment WL-IHF-05 in D1 mission --- Spacelab
[ETN-88-92339] 21 p2924 N88-27353
Experiments in microgravity environment: Protein crystallization
[REPT-881-430-101] 21 p2924 N88-27354
Laser crystallized silicon films on alumina ceramic substrates and application to thin film c-Si solar cells
[PB88-131966] 22 p3116 N88-28515
Influence of the interface on the crystallization of amorphous Ge in Pb/Ge multilayers
[DE88-010072] 22 p3156 N88-28776
Origin of SNC kaersutitic amphibole: Experimental data 23 p3306 N88-29693

CRYSTALLOGRAPHY
Constitutive modeling for single crystal superalloys
02 p0187 N88-11168
International Conference on Microstructology held in Gainesville, Florida on 7-9 May 1986
[AD-A184604] 03 p0290 N88-11822
Effect of grain orientation on the origination and the initial growth of fatigue cracks in pure iron
05 p0597 N88-13647
The growth of persistent slip bands
05 p0597 N88-13648
The orientations of dipolar walls produced by cyclic deformation 05 p0598 N88-13655
The influence of slip mechanism on fatigue of Mg and Mg-2.3Li 05 p0600 N88-13672
An explanation of the fractography of near-threshold fatigue in FCC metals 06 p0716 N88-14395
Orientation effects in copper single crystals fatigued at elevated temperatures 06 p0720 N88-14423
A continuous oxidizer regression model for the combustion of composite solid propellants
[AD-A186742] 08 p0974 N88-15894
NBS/Sandia/ICDD electron diffraction database
[DE88-004635] 11 p1454 N88-18665
Stress corrosion cracking and metal-induced embrittlement: Comparative studies of local chemistries
[DE88-003235] 13 p1742 N88-20419
Recent progress in structure determination by LEED (Low-Energy Electron Diffraction) measure the properties of the deep donors (DX-cent)
[DE88-003851] 13 p1846 N88-21048
Interface characterization of Cu-Cu and Cu-Ag-Cu low temperature solid state bonds
[AD-A191015] 16 p2283 N88-23667
Influence of carbon fiber surface treatment
[ETN-88-92536] 18 p2492 N88-24787
Dendritic growth in the presence of convection
18 p2580 N88-25328
Topics in quasicrystallography
21 p3023 N88-27947
Characterization of crystalline silicon by electrochemical and Raman spectroscopy at the frontier semiconductor/electrolyte
[ETN-88-92354] 21 p3025 N88-27956
Muon-spin rotation experiment (micro + SR) on aluminum and indium after low temperature electron irradiation
[ETN-88-92985] 23 p3294 N88-29617
Crystal fractionation in the SNC meteorites: Implications for surface units on Mars 23 p3307 N88-29698

CRYSTALS
NT BICRYSTALS
NT BRAVAIS CRYSTALS
NT CRYSTAL OSCILLATORS
NT CRYSTALLITES
NT DENDRITIC CRYSTALS
NT DOPED CRYSTALS
NT LIQUID CRYSTALS
NT METAL CRYSTALS
NT MICROCRYSTALS
NT MIXED CRYSTALS
NT PIEZOELECTRIC CRYSTALS
NT POLYCRYSTALS
NT QUARTZ CRYSTALS
NT SINGLE CRYSTALS
NT WHISKERS (CRYSTALS)
Interaction between defects and the formation of dissipative structures in irradiated impure crystals
[DE87-703125] 02 p0246 N88-11552
Highly Non-Linear Optical (NLO) organic crystals
03 p0297 N88-11865
Highly Non-Linear Optical (NLO) organic crystals and films: Electrooptical organic materials
03 p0297 N88-11866
Theory of atomic additivity in molecular hyperpolizabilities 03 p0297 N88-11867
Large-aperture high-efficiency frequency doubling using tandem KDP crystals 03 p0301 N88-11894
Evaluation system for crystal streak cameras
[DE88-000238] 03 p0324 N88-12048
Interatomic Auger rates for the sodium fluoride crystal
[DE87-013012] 03 p0382 N88-12401
Crystalline cell research status and direction
[DE87-014214] 03 p0382 N88-12402
Research and development on high strength ceramic heaters discussed 04 p0404 N88-12508
Far infrared Fourier transform spectroscopy of semiconductors
[DE88-000188] 04 p0499 N88-13072
Cyclic deformation of an extruded AlMgSi alloy
05 p0598 N88-13654
Structure of layered crystals studied by high energy ion beams
[DE88-001675] 06 p0786 N88-14822
Diamond turning of silicon for optics applications
[DE88-002501] 07 p0840 N88-15095

Intracavity spectrum analyzer with NaF:F2(+):F3(-) crystal laser for long-wave IR wave band
07 p0919 N88-15584

Thermal stress analysis of a cooled monochromator crystal
[DE88-002116] 07 p0937 N88-15696

Gamma radiation at the 970 MeV plane positron channeling in diamond crystals
[DE88-700557] 07 p0939 N88-15705

Effect of irradiation on the diffusion evolution of void ensemble in crystals
[DE88-700558] 07 p0939 N88-15706

Wave functions for bound states of relativistic electrons in a crystal at electron movement along crystallographic planes
[DE88-700563] 07 p0939 N88-15708

Tunable Al2O3:Ti3+-laser with optical pumping
09 p1237 N88-17415

Recent progress in the dynamic applications of piezoelectric crystals 10 p1417 N88-18460

The structure and properties of twin boundaries in superconducting YBa2Cu3O7
[DE88-003864] 10 p1418 N88-18468

UHV (Ultra-High Vacuum) double crystal monochromator design
[DE88-003904] 11 p1456 N88-18676

Nucleation and growth of calcium carbonate crystals on surface-modified polyethylene and polystyrene
[DE88-005126] 11 p1465 N88-18733

Growth and characteristics of materials for tunable lasers in the near infrared spectral region
[NASA-CR-182501] 11 p1491 N88-18901

Investigation of defect and electronic interactions associated with GaAs device processing
[AD-A188021] 11 p1556 N88-19313

Raman scattering in mixed crystal semiconductors
12 p1696 N88-20149

Parametric study of acceleration-induced stresses and frequency changes in doubly-rotated crystal resonators
[AD-A189261] 13 p1761 N88-20532

Thermionic Technology Program. A: Insulator test and evaluation
[DE88-004707] 13 p1795 N88-20735

Multiple scattering of polarized light in cirrus clouds
13 p1801 N88-20768

Nonlinear refractive index measurements of glasses and crystals
[DE88-005673] 13 p1840 N88-21009

Effect of Mg impurity on local vibrations of U-centers in LiF lattice 14 p1969 N88-21753

Nucleation in super-saturated products
[NASA-TT-20275] 15 p2037 N88-22134

On rotating sphere-on-a-plate experiments and the questions of whether high angle grain boundaries melt below bulk melting temperatures
[DE88-006627] 15 p2038 N88-22142

High-performance polymeric materials
[AD-A190708] 15 p2046 N88-22190

Does the pipe diffusion of self-interstitials in crystals under stresses exist
[DE88-701027] 15 p2139 N88-22762

Optical characterization of microcrystals
[DE88-006622] 15 p2141 N88-22775

Tunable optical sources/growth and characterization of nonlinear optical materials
[AD-A190874] 16 p2274 N88-23608

Investigation of non-linear optical behavior of semiconductors for optical switching, volume 1
[AD-A191297] 16 p2274 N88-23611

Effects of irradiation on thermal coalescence of pores in real crystals
[DE88-701683] 16 p2282 N88-23663

Dynamic range compression/expansion of light beams by photorefractive crystals
[NASA-CASE-NPO-17140-1-CU]
17 p2438 N88-24508

Joint services electronics program
[AD-A190239] 18 p2503 N88-24848

NASA research Program: The roles of fluid motion and other transport phenomena in the morphology of materials
[NASA-CR-182801] 18 p2580 N88-25327

Structure and refinement of ordered aromatic heterocyclic polymers by diffraction methods: Application of results to electro-optic phenomena
[AD-A191859] 19 p2619 N88-25537

Time-resolved doubly bent crystal X-ray spectrometer
[DE88-007899] 20 p2805 N88-26637

Phase equilibrium and crystal growth studies on AgGaSe2 and related nonlinear optical materials
[AD-A193763] 22 p3157 N88-28783

Theory of surface melting and non-melting
[DE88-702652] 22 p3157 N88-28785

Short pulse X-ray diffraction studies of shocked and annealed crystals using the JANUS research laser
[DE88-011329] 23 p3288 N88-29570

Research on crystal and film ferroelectric materials for optoelectronic applications
[AD-A193512] 23 p3291 N88-29597

Absorption spectra and energy levels of Gd(3+), Nd(3+) and Cr(3+) in the garnet Gd3Sc2Ga3O12
[AD-A193634] 23 p3292 N88-29599

General equations for the motions of ice crystals and water drops in gravitational and electric fields
[NASA-CR-183229] 24 p3370 N88-30070

CTD
U CHARGE TRANSFER DEVICES

CUBANE

Theoretical investigations of nitrocubane decomposition
[AD-A194556] 23 p3200 N88-29047

CUBES (MATHEMATICS)

Twisted cube
[PB87-162814] 09 p1220 N88-17316

Procedure for converting a Wilson-Fowler spline to a cubic B-spline with double knots
[DE88-008971] 20 p2844 N88-26878

CUBIC EQUATIONS

Evaluation of closed cubic failure criterion for graphite/epoxy laminates
[NASA-CR-182375] 06 p0679 N88-14158

CUBIC LATTICES
NT BODY CENTERED CUBIC LATTICES
NT FACE CENTERED CUBIC LATTICES

Compilation of temperature factors of cubic elements
[PB88-108170] 21 p2908 N88-27260

Theoretical predictions of precipitate shapes in cubic alloys
[DE88-010856] 21 p2914 N88-27291

CUES

Handling qualities criterion for very low visibility rotorcraft 03 p0263 N88-11654

Effect of motion cues during complex curved approach and landing tasks: A piloted simulation study
[NASA-TP-2773] 04 p0398 N88-12480

The role of adaptive supplemental visual cuing in flight simulation
[AD-A185932] 07 p0822 N88-14992

Visual attention effects on discrimination of line orientation and line arrangement
[AD-A187013] 09 p1200 N88-17190

Visual integration and detection of discontinuities: The key role of intensity edges
[AD-A188012] 11 p1520 N88-19076

Analysis procedures and subjective flight results of a simulator validation and cue fidelity experiment
[NASA-TM-88270] 18 p2465 N88-24634

Eye and head response to an attention cue in a dual task paradigm
[AD-A191052] 18 p2551 N88-25143

CUESTAS
U RIDGES

CULTIVATION

Biomass recycle as a means to improve the energy efficiency of CELSS algal culture systems
03 p0358 N88-12254

Trickle water and feeding system in plant culture and light-dark cycle effects on plant growth
03 p0361 N88-12273

Controlled ecological life support systems: Development of a plant growth module 05 p0630 N88-13854

CULTURE (SOCIAL SCIENCES)

Maps for tourists. A systematic approach to tourist cartography 16 p2227 N88-23296

Linguistic and cultural barriers to the transfer of information 24 p3437 N88-30459

CULTURE TECHNIQUES

Superoxide dismutase assays
[AD-A183972] 03 p0356 N88-12242

Space Bioreactor Science Workshop
[NASA-CP-2485] 09 p1196 N88-17168

Suspension cell culture in microgravity and development of a space bioreactor 09 p1196 N88-17169

Space bioreactor: Design/process flow
09 p1197 N88-17170

Bioreactor design concepts 09 p1197 N88-17171

Shear and mixing effects on cells in agitated microcarrier tissue culture reactors 09 p1197 N88-17173

Fed-batch control based upon the measurement of intracellular NADH 09 p1197 N88-17175

Nutrient requirements and other factors involved in the culture of human kidney cells on microcarrier beads
09 p1197 N88-17176

Plant cell technologies in space: Background, strategies and prospects 09 p1198 N88-17177

Design concepts for bioreactors in space
09 p1198 N88-17179

Cell culture experiments planned for the space bioreactor 09 p1198 N88-17180

Research on a solar biotechnology based on the culture of photosynthetic cells
[DE88-900129] 10 p1359 N88-18120

Growth and differentiation of cells in organotypical rat embryo cerebellar culture developing in weightlessness
19 p2703 N88-26076

Effects of pulsed and CW (Continuous Wave) 2450 MHz radiation on transformation and chromosomes of human lymphocytes in vitro
[AD-A193104] 21 p2987 N88-27736

CUMULATIVE DAMAGE

Cumulative fatigue and life prediction of fibre composites. Part 1: Literature reviews
[BR101013] 02 p0142 N88-10893

Cumulative fatigue and life prediction of fibre composites. Part 2: Experimental techniques and results
[BR101014] 02 p0142 N88-10894

Ensuring the service life of designs (experience in aircraft construction) 02 p0157 N88-10986

Damage considerations in sizing aircraft cells. Life predictions
[SNIAS-872-111-116] 05 p0546 N88-13330

Colloquium on damage mechanics of graphite/expoxy laminates during fatigue
[DFVLR-MITT-87-08] 11 p1448 N88-18630

Damage mechanics of fiber reinforced plastics: A general view 11 p1448 N88-18631

Influence of different parameters on damage development — carbon fiber reinforced plastics
11 p1448 N88-18632

Initiation and propagation of damage in notched unidirectional and multidirectional CFRE resin laminates
11 p1449 N88-18633

Damage initiation and growth in sateen laminates under static and cyclic loading 11 p1449 N88-18634

Damage mechanisms of CFRP riveted joints
11 p1449 N88-18636

Damage mechanisms and fatigue life prediction of graphite/epoxy laminates 11 p1449 N88-18637

Fatigue damage development of various CFRP-laminates
[NASA-TT-20247] 16 p2172 N88-22945

Study of mechanisms of time-dependent crack growth at elevated temperature
[DE88-006918] 16 p2223 N88-23271

Interaction of creep and fatigue damage in gas turbine blade material
[PNR90440] 22 p3088 N88-28335

CUMULUS CLOUDS

Cumulus and thunderstorm initiation by mountains
02 p0207 N88-11301

Study of isolated convective clouds in the lower Alps in summer 1984, using radar and a simple Weinstein numerical model
[ESA-TT-1061] 03 p0353 N88-12224

Dynamic interaction of convective cumulus with large-scale environment
[MITT-55] 20 p2827 N88-26773

An observational study of interaction between large scale tropical cumulus convection and the equatorial circulation anomalies 22 p3124 N88-28564

CURIE TEMPERATURE

Spin disorder resistivity and bare Curie temperature in the ferromagnetic superconductor ErRh4B4
[DE88-003016] 10 p1415 N88-18445

CURING

The water absorption of model epoxy resin networks cured with aromatic diamines
[BR100722] 01 p0027 N88-10169

Addition polyimide composition
[EP-PATENT-0-167-304-A1] 01 p0053 N88-10337

Cure and properties of thermosetting polymers
[AD-A184669] 03 p0293 N88-11843

Effects of cure pressure on resin flow, voids, and mechanical properties
[AD-A184267] 03 p0295 N88-11853

Radiation curing: Comparison of heat, UV, and radiation curing
[OEFZS-4393] 06 p0689 N88-14224

Effect of post-cure heat-treatment on static and fatigue behaviour of XAS-914C carbon fibre composite
[AD-A186943] 10 p1294 N88-17735

High-temperature thermosets derived from the Diels-Alder polymerization of bisbenzocyclobutenes and bimaleimides
[AD-A188800] 13 p1747 N88-20449

Effect of moisture level in PBXW-109(E) (plastic-bonded explosive) mixes on the aging of the cured explosive
[AD-A190200] 15 p2048 N88-22202

Correlation between dielectric and structural properties during epoxy cure
[AD-A190696] 16 p2181 N88-22997

Cellular thermosetting fluoropolymers and process for making them
[NASA-CASE-GSC-13008-1] 17 p2326 N88-23894

Current and future molecular structures of aerospace organic matrix resins 18 p2477 N88-24695

The 700 F properties of autoclave cured PMR-2 composites
[NASA-TM-100923] 18 p2480 N88-24712
A compatible encapsulant for explosives
[DE88-007212] 18 p2495 N88-24806
Determination of the glass transition temperature of cured composite materials
[DT-87/62-R] 21 p2906 N88-27246
Determination of lumped-mass thermal properties associated with autoclave curing of graphite/epoxy composites 21 p2925 N88-27364
A fundamental study of P/M processed elevated temperature aluminum alloys
[AD-A192958] 23 p3194 N88-29005

CURL (VECTORS)
NT VORTICITY

CURRENT AMPLIFIERS
NT PHOTOMULTIPLIER TUBES

CURRENT CONVERTERS (AC TO DC)
Mathematical model for the dc-ac inverter for the Space Shuttle 06 p0793 N88-14860

CURRENT DENSITY
Simulations using the pseudo-current algorithm
[DE87-012403] 01 p0040 N88-10255
Abrikosov vortex motion and elementary pinning force in a SNS Josephson junction
[DE87-013607] 01 p0105 N88-10683
Use of polarimetry to measure the current profile in MTX
[DE87-013835] 02 p0237 N88-11495
Short-pulse high-current-density photoemission in high electric fields
[DE87-014909] 03 p0310 N88-11951
Magnetic fluctuation behaviour of current termination in reversed field pinch
[IPPJ-849] 04 p0492 N88-13034
Reversed field pinch plasmas with various boundary conditions
[DE88-000832] 05 p0653 N88-14004
Study of vibration relaxation in active medium of CO2-laser using phase-absorption method
07 p0919 N88-15582
Possibility of calculation of magnetic surface function gradient and related quantities
[DE88-700561] 07 p0936 N88-15686
Shape of the plasma boundary in TBR
[INPE-4388-PRE/1208] 08 p1086 N88-16540
Application of high temperature ceramic superconductors (CSC) to commercial tokamak reactors
[DE88-003973] 09 p1257 N88-17538
Application of ac-impedance method on determination of corrosion rate of metals
[DE88-750307] 10 p1300 N88-17771
Investigation of materials for inert electrodes in aluminum electrodeposition cells
[DE88-003380] 10 p1323 N88-17906
High-current density, high-brightness electron beams from large-area lanthanum hexaboride cathodes
[AD-A187700] 11 p1477 N88-18813
A novel class of positive electrodes for rechargeable batteries
[DE88-004559] 13 p1763 N88-20545
Simplified physical approach of the control by eddy current
[DE88-701076] 13 p1764 N88-20552
Stratospheric electric field and conductivity measurements over electrified convective clouds in the South American region, revised
[INPE-4046-PRE/1012-REV-3]
15 p2095 N88-22483
High-T(sub c) superconducting wire fabrication and testing
[DE88-005989] 15 p2144 N88-22798
High temperature superconductors in the La(sub 1+x)Ba(sub 2-x)Cu O(sub y system
[DE88-006367] 15 p2145 N88-22802
Electron current effect on stability of plasma channel
16 p2276 N88-23625
Carrier transport in semiconductor magnetic sensors under nonuniform fields 19 p2672 N88-25888
Poloidal field measurements using laser enhanced attenuation of an energetic lithium beam
[DE88-008360] 20 p2856 N88-26963
Linear thyratron
[AD-A194111] 23 p3208 N88-29094
Currents induced in a human being for electromagnetic fields to 10 kHz-50 MHz
[AD-A191977] 23 p3238 N88-29268

CURRENT DISTRIBUTION
Efficiency aspects of short, low velocity railguns
[AR-004-847] 04 p0405 N88-12517
Mathematical model for the dc-ac inverter for the Space Shuttle 06 p0793 N88-14860
The coaxial colinear antenna: Theoretical and experimental models 11 p1475 N88-18803

CURRENT SHEETS
Equilibrium and tearing stability of thin current layers in magnetic arcades 01 p0118 N88-10754
Observations of small scale structures using data from the wave experiment on the AMPTE-UKS spacecraft
08 p1099 N88-16612
On the potential role of concentrated field-aligned currents in solar physics 08 p1099 N88-16614
Observation of enhanced electric field in an RF-plugged sheet plasma in the RFC-XX-M open-ended machine
[IPPJ-857] 09 p1252 N88-17503
A study of the magnetic field annihilation process in the magnetosphere and some geotechnical applications
[DE88-004165] 10 p1355 N88-18096

CURRENTS (OCEANOGRAPHY)
U WATER CURRENTS

CURTAINS
Gain evaluation for an idealized curtain array antenna
[PB87-210290] 02 p0161 N88-11006

CURTISS-WRIGHT MILITARY AIRCRAFT
U MILITARY AIRCRAFT

CURVATURE
Fronts propagating with curvature dependent speed: Algorithms based on Hamilton-Jacobi formulations
[NASA-CR-178382] 01 p0077 N88-10495
A numerical study of the effects of curvature and convergence on dilution jet mixing
[NASA-TM-89878] 05 p0549 N88-13347
Vision algorithms and psychophysics
[AD-A186773] 09 p1200 N88-17193
The deposition rate dependence of plasma polymerization on the radius of curvature of the substrate
[DE88-003811] 10 p1412 N88-18429
Terrain classification from digital elevation data using slope and curvature information
[AD-A188940] 12 p1639 N88-19812
Complete minimal surfaces in R^3 of low total curvature
[DE88-006425] 15 p2118 N88-22619
Surface curvature and pressure gradient effects on turbulent flow: An assessment based on numerical solution of the Reynolds equations 17 p2338 N88-23954
Cylindrical surface profile and diameter measuring tool and method
[NASA-CASE-MFS-28287-1] 17 p2341 N88-23959
An empirical model of the effects of curvature and convergence on dilution jet mixing
[NASA-TM-100896] 18 p2466 N88-24640
Aerodynamics of lifting bodies with combined transverse and longitudinal curvature 19 p2598 N88-25436
Synoptic patterns related to tropical cyclone recurvature
[AD-A192338] 20 p2827 N88-26771
Applications of differential geometry to the shape analysis of gray-value images 21 p2924 N88-27358
A novel method to correct radiation pattern distortion of conformal antennas
[AD-A193675] 23 p3204 N88-29066
A technique for measuring area under a curve
[AD-A193559] 23 p3271 N88-29463

CURVE FITTING
A comparison of fitting techniques for the cumulative average learning curves with historical lot cost data
[AD-A187127] 09 p1227 N88-17349
Fitting a generalized parabola to data
[NPL-DITC-96/87] 09 p1229 N88-17364
Strategies for knot placement in least squares data fitting by splines
[NPL-DITC-101/87] 09 p1229 N88-17366
Using frequency-domain methods to identify XV-15 aeroelastic modes
[NASA-TM-100033] 10 p1277 N88-17646
Analysis of learning curve fitting techniques
[AD-A187680] 11 p1535 N88-19173
Position finding and tolerances
[AD-A187685] 11 p1540 N88-19205
Motion sickness: Quantitative, algorithmic malaise indication in real time
[AD-A189674] 15 p2101 N88-22518
Fitting a circle to radially suppressed data
[NPL-DITC-103/87] 17 p2392 N88-24223
Simplified curve fits for the transport properties of equilibrium air
[NASA-CR-178411] 18 p2513 N88-24911
Fitting an ellipse to data
[NPL-DITC-95/87] 22 p3143 N88-28693

CURVED BEAMS
Nonlinear thermoviscoelastic analysis of metallic plane curved beams 03 p0336 N88-12119
Delamination stresses in semicircular laminated composite bars
[NASA-TM-4026] 13 p1735 N88-20375
Non-isothermal elastoviscoplastic analysis of planar curved beams 14 p1933 N88-21526

CURVED PANELS
Vibration and buckling of geometrically imperfect laminated cylindrical shells 04 p0456 N88-12822
A study of damage tolerance in curved composite panels
[AD-A190617] 15 p2029 N88-22092

CURVED SURFACES
U CONTOURS
U SHAPES
U SURFACES

CURVES
Innovative design of composite structures: Further studies in the use of a curvilinear fiber format to improve structural efficiency
[NASA-CR-182576] 11 p1450 N88-18641
Method and models for R-curve instability calculations
[NASA-TM-100935] 16 p2224 N88-23278
Peturbational analysis of the curved anisotropic optical fiber for the birefringence due to the geometry
[PB88-171848] 19 p2726 N88-26189
The T-T-T curve in Cu-Cr alloy
[NASA-TT-20167] 20 p2774 N88-26453
The triangle: A multiprocessor architecture for fast curve and surface generation
[AD-A195882] 24 p3414 N88-30324

CURVES (GEOMETRY)
NT CATENARIES
NT S CURVES
Response of helical structures to high speed pulses or when can a helix be called an inductor
[DE87-014347] 01 p0090 N88-10587
Transversely anisotropic curved optical fibres: Variational analysis of a nonstandard Eigenproblem
[PB88-112966] 08 p1083 N88-16528
Numerical arc segmentation algorithm for a radio conference-NASARC, version 2.0: User's manual
[NASA-TM-100161] 09 p1156 N88-16928
Computation of the zeta-function of an algebraic curve with the differentials of the first kind
[PB88-127527] 10 p1399 N88-18339
Open or closed curves by regularized B-splines
[RR-652-M] 18 p2563 N88-25218
Calculating the self-intersections of Bezier curves
[AD-A192371] 19 p2721 N88-26156

CURVILINEAR COORDINATES
U SPHERICAL COORDINATES

CUT-OUTS
U OPENINGS

CUTANEOUS PERCEPTION
U TOUCH

CUTTERS
NT DRILLS
XCUT: A rule-based expert system for the automated process planning of machined parts
[DE87-011638] 05 p0639 N88-13905
Tribological studies on high speed steel cutting tools
[DE88-002550] 07 p0864 N88-15246
Characterization of coating wear phenomena in nitride and carbide coated tool inserts
[DE88-011196] 20 p2779 N88-26478

CUTTING
NT LASER CUTTING
NT METAL CUTTING
NT MILLING (MACHINING)
NT SHEARING
NT SPARK MACHINING
Diamond turning of silicon for optics applications
[DE88-002501] 07 p0840 N88-15095
A fast bottom-up algorithm for computing the cut sets of noncoherent fault trees
[DE88-003741] 09 p1220 N88-17320
Drilling metal matrix composites
[AD-A190480] 15 p2029 N88-22091
Contribution to the study of modern materials for cutting tools
[ISAL-IDI1-87-17] 16 p2185 N88-23029
High power axial flow CO2 laser
[ETN-88-91951] 18 p2521 N88-24959
Characterization of coating wear phenomena in nitride and carbide coated tool inserts
[DE88-011196] 20 p2779 N88-26478
Ductile-brittle transition of cutting behavior in diamond turning of single crystal Si
[DE88-008890] 20 p2809 N88-26664
Microcircuit trace cutting with focused ion beams
[AD-A196030] 24 p3367 N88-30050

CW RADAR
U CONTINUOUS WAVE RADAR

CYANIDE EMISSION
U CN EMISSION

CYANIDES
NT ACETONITRILE
NT CYANOGEN

CYANO COMPOUNDS
NT ISOCYANATES

Application of photosynthetic N(2)-fixing cyanobacteria to the CELSS program 03 p0358 N88-12257
The photochemistry of some possible cometary CN parent species 14 p1997 N88-21905
The evolution of CN emission in Halley's comet with heliocentric distance 14 p2006 N88-21961
First detection of HCN J = 9 to 8 (797 GHz) line emission: Very high densities in the Orion core
[MPE-PREPRINT-110] 22 p3165 N88-28847

CYANOGEN
Simultaneous, cospatial imaging of the Sun in cyanogen and singly-ionized calcium 04 p0507 N88-13114
Laser studies of the dynamics of free radical reactions
[DE88-004431] 10 p1337 N88-17989

CYANOPHYTA
U BLUE GREEN ALGAE

CYBERNETICS
USSR report: Cybernetics, computers and automation technology
[JPRS-UCC-86-014] 06 p0761 N88-14669
Spire based speaker-independent continuous speech recognition using mixed feature sets
[AD-A188834] 12 p1620 N88-19688
Novel nonlinear signal processing principles
[AD-A191644] 19 p2707 N88-26097

CYCLES
NT ACTIVITY CYCLES (BIOLOGY)
NT BRAYTON CYCLE
NT CARBON CYCLE
NT HYDROLOGICAL CYCLE
NT RANKINE CYCLE
NT SOLAR CYCLES
NT STIRLING CYCLE
NT STRESS CYCLES
NT SUNSPOT CYCLE
NT THERMODYNAMIC CYCLES
NT WORK-REST CYCLE
The impact of varves on solar physics
[NASA-CR-181519] 03 p0390 N88-12448
Cross-correlation of uniform cyclic difference set sequences
[AD-A184879] 05 p0640 N88-13913
Thermal mechanical low cycle fatigue of 25CDV4-10 steel 06 p0721 N88-14429
The 35-day cycle of Hercules X-1
[MPE-204] 11 p1571 N88-19405
Global mixed-layer natural and anthropogenic fluxes
13 p1807 N88-20803
The influence of uncompensated solution resistance on the determination and standard electrochemical rate constants using cyclic voltammetry and some comparisons with AC voltammetry
[AD-A192825] 20 p2770 N88-26427
Two families of graphs satisfying the cycle basis interpolation property
[PB88-127808] 20 p2846 N88-26890
Algorithm for generating the minimal cycle basis of a graph
[PB88-126610] 20 p2846 N88-26891
Modeling discrete bathtub and upside down bathtub mean residual life functions
[AD-A192000] 22 p3085 N88-28320
Time periodic control of a multi blade helicopter
[AD-A194435] 23 p3180 N88-28931
Finding minimum-cost circulations by canceling negative cycles
[AD-A194027] 23 p3271 N88-29468
The OFP (Operational Flight Program) update cycle needs you
[AD-A194910] 24 p3325 N88-29798

CYCLIC ACCELERATORS
NT BETATRONS
NT STORAGE RINGS (PARTICLE ACCELERATORS)
NT SYNCHROTRONS
Bevalac external beamline optics
[LBL-23240] 19 p2727 N88-26194
Rf cavity primer for cyclic proton accelerators
[DE88-010655] 20 p2853 N88-26938

CYCLIC COMPOUNDS
NT ADENOSINE TRIPHOSPHATE
NT ADENOSINES
NT ANTHRACENE
NT ATROPINE
NT AZOLES
NT AZULENE
NT BENZENE
NT CAFFEINE
NT CARBAZOLES
NT CYCLIC HYDROCARBONS
NT CYCLOBUTANE
NT CYCLOHEXANE
NT ERGOTAMINE
NT FURANS
NT HETEROCYCLIC COMPOUNDS
NT HMX
NT MORPHINE
NT NAPHTHALENE
NT NAPHTHENES
NT NICOTINIC ACID
NT PHTHALOCYANIN
NT PYRIDINES
NT PYRROLES
NT RDX
NT THYMINE
NT URACIL
NT XANTHINES
Thermoplastic elastomers as LOVA (Low Vulnerability Ammunition) binders
[AD-A184350] 04 p0419 N88-12599
Synthesis of energetic materials
[AD-A189115] 13 p1753 N88-20482
Aromatic cyclotriphosphazenes
[NASA-CASE-ARC-11428-3] 18 p2477 N88-24692
Structural study of the TGMDA-DDS system --- epoxy system
[ONERA-RT-4/3346-M] 18 p2493 N88-24792

CYCLIC HYDROCARBONS
NT ANTHRACENE
NT BENZENE
NT CYCLOBUTANE
NT CYCLOHEXANE
NT NAPHTHALENE
NT NAPHTHENES
High-temperature thermosets derived from the Diels-Alder polymerization of bisbenzocyclobutenes and bimaleimides
[AD-A188800] 13 p1747 N88-20449

CYCLIC LOADS
The effect of fretting corrosion on the fatigue strength of steel and cast iron under sinusoidal and random loading
[LBF-FB-177] 01 p0023 N88-10142
The fatigue properties of aerospace steels under constant amplitude and flight-by-flight simulated loading
[BAE-MSM-R-GEN-0566] 01 p0059 N88-10377
Criteria for determination of significant load cycles in variable amplitude load sequences
[NLR-MP-86013-U] 01 p0060 N88-10386
Influence of thermocyclic treatment on mobility of grain boundaries
[BLL-M-37329-(5828.4)] 02 p0149 N88-10933
Constitutive modeling for isotropic materials
02 p0188 N88-11171
The influence of load cycle reconstitution on fatigue behaviour
[ARL-STRUC-R-424] 02 p0192 N88-11198
A low-power arcjet cyclic lifetest
[NASA-TM-100233] 03 p0278 N88-11748
Crack initiation and propagation due to cyclic thermal gradients --- aircraft turbine blades
[ESA-TT-1023] 03 p0336 N88-12114
Composite materials applications program at the US Army Ballistic Research Laboratory: Work in progress
04 p0428 N88-12651
X-ray analysis of polycrystalline aluminum subjected to fatigue cycling
[NAL-TM-MT-8706] 05 p0564 N88-13434
Application of finite element methods with cyclic elasto-plastic strain analysis to low cycle fatigue analysis of engine components
[AR-004-512] 05 p0596 N88-13642
Fatigue 87, volume 3
[AD-A184047] 05 p0604 N88-13700
A study of corrosion fatigue crack initiation, growth and the threshold condition under variable amplitude loading
05 p0604 N88-13701
The effect of environment on low cycle fatigue properties in HSLA steel 05 p0605 N88-13705
Fatigue crack propagation in Al-Zn-Mg bicrystals and its dependence on the environment
05 p0605 N88-13707
Low cycle fatigue behaviour of notched specimens of nickel based superalloy single crystal
05 p0605 N88-13712
Computer aided modeling and fatigue failure forecast under stochastic loading 05 p0607 N88-13720
Embrittling effect of the plastic zone
05 p0607 N88-13721
X-ray fatigue failure prediction based on plasticity response to microcracks 05 p0607 N88-13725
Electron microscopy studies of tensile cyclic fatigue-tested silicon nitride ceramics
[DE88-001438] 06 p0685 N88-14196
Investigation of instability, dynamic forces, and effect of dynamic loading on strength of cages for the bearings in the high pressure oxygen turbopumps for the space shuttle main engine
[NASA-CR-178970] 06 p0714 N88-14378
On the relations between cyclic contraction ratio flowstress and deformation mechanisms in bainitic CrMoV steels
[DE87-753043] 08 p0968 N88-15856
Experimental determination of crack growth rates in cyclic stress applications, for improving the forecasted computed durability in operation
[FF-14/1986] 09 p1182 N88-17085
Elastoplastic response of unidirectional graphite/aluminum under combined tension-compression cyclic loading
[CCMS-88-01] 11 p1451 N88-18647
Lead-acid load-leveling battery testing at Argonne National Laboratory
[DE88-002853] 11 p1480 N88-18637
Evaluation of advanced lead-acid batteries developed for load-leveling applications
[DE88-002871] 11 p1481 N88-18638
The cyclic stress-strain behavior of a single crystal nickel-base superalloy
[NASA-TM-100269] 12 p1607 N88-19610
Cyclic crack growth emanating at a round notch considering viscoplasticity
[AD-A189577] 13 p1761 N88-20655
Cyclic uniaxial and biaxial hardening of type 304 stainless steel modeled by the viscoplasticity theory based on overstress 14 p1931 N88-21514
Some implications for cyclic plastic and viscoplastic equations based on nonproportional loading experiments
14 p1931 N88-21515
The growth of corner cracks under the conjoint action of high and low cycle fatigue
[AD-A190510] 15 p2076 N88-22379
High-temperature combustor liner tests in structural component response test facility
15 p2077 N88-22383
Life assessment of combustor liner using unified constitutive models 15 p2077 N88-22384
Development of a flexible and economic helicopter engine monitoring system
[PB88-165147] 16 p2160 N88-22887
Fatigue crack growth under full-scale cyclic plasticity
[DFVLR-FB-87-48] 16 p2222 N88-23263
A cyclic ground test of an ion auxiliary propulsion system: Description and operational considerations
[NASA-TM-100870] 17 p2313 N88-23829
Investigation of the long term effects of aging on carbon epoxy composites exposed naturally to the weather under cyclic loads. (Results of sampling after 2.5 years) Test report M1-641300
[CEAT-39/M/79-C-M1-641300]
17 p2316 N88-23834
An extended life and performance test of a low-power arcjet
[NASA-TM-100942] 18 p2476 N88-24687
Cyclic fatigue damage characteristics observed for simple loadings extended to multiaxial life prediction
[NASA-CR-182126] 18 p2531 N88-25016
Energy dissipation in a rolling aircraft tire
[NASA-CR-182978] 19 p2676 N88-25913
Fatigue crack growth under far-field cyclic compression
[DE88-011215] 20 p2813 N88-26689
Damage in a perforated graphite-epoxy plate under monotonic, cyclic biaxial loading
[ONERA-NT-1987-5] 20 p2816 N88-26708
Load interaction effects on compression fatigue crack growth in ductile solids
[FFA-TN-1988-12] 22 p3089 N88-28342
An investigation of constitutive models for predicting viscoplastic response during cyclic loading
[AD-A194875] 24 p3385 N88-30163

CYCLING
U CYCLES

CYCLOBUTANE
Research in energetic compounds
[AD-A192953] 20 p2781 N88-26494

CYCLOGENESIS
Australian East Coast cyclones 3: Case study of the storm of August 1986 02 p0204 N88-11276
Cumulus and thunderstorm initiation by mountains
02 p0207 N88-11301
The Windsor Locks, Connecticut tornado of 3 October 1979: An analysis of an intermittant severe weather event 02 p0208 N88-11305
Magnetospheric storms 03 p0272 N88-11711
Environmental and convective influence on tropical cyclone development versus non-development
[AD-A185231] 05 p0627 N88-13835
Simulation of a lee cyclogenesis using a numerical model 08 p1016 N88-16162
Interplanetary Magnetic Field (IMF) influence on the magnetic configuration and particle fluxes at geostationary orbit and on the substorm onset
08 p1031 N88-16247
A possible role for ionospheric ions in triggering a geomagnetic substorm onset 08 p1096 N88-16594
The structure and dynamics of monsoon depressions
10 p1355 N88-18102

Analysis of quasi-geostrophic forcing during the AIMCS (Airborne Investigations of Mesoscale Convective System) Project. Volume 1: Discussion
[PB88-133095] 12 p1646 N88-19860

A paper on horizontal deformation in the frontogenesis in south Brazil
[INPE-4469-TDL/322] 12 p1647 N88-19867

Tropical cyclones, 1987: Central North Pacific
[PB88-188081] 18 p2547 N88-25119

CYCLOHEXANE

Cross section of resonant Raman scattering of light by polyenes 07 p0920 N88-15591

CYCLONES

NT HURRICANES
NT TYPHOONS

Tropical cyclone center locations from enhanced infrared satellite imagery
[PB87-213450] 01 p0071 N88-10455

Summary of 1987 Atlantic tropical cyclone activity and verification of author's seasonal forecast
02 p0215 N88-11356

Tropical cyclone intensity prediction based on empirical orthogonal function representation of wind and shear fields
[AD-A184699] 03 p0353 N88-12229

Annual tropical cyclone report, 1986
[AD-A184082] 04 p0470 N88-12903

Lower-stratospheric/upper-tropospheric exchange processes associated with tropical cyclones as observed by TOMS 05 p0616 N88-13782

Opportunities for tropical cyclone motion research in the Northwest Pacific region
[AD-A185068] 05 p0627 N88-13834

Estimation of rainfall rates in tropical cyclones by passive microwave radiometry 06 p0744 N88-14577

The effect of latitude on the development of tropical cyclones
[AD-A185670] 06 p0746 N88-14590

Interim review of the possibilities and opportunities for the ONR tropical cyclone motion research initiative
[AD-A185679] 06 p0746 N88-14532

Thunderstorms with snow: A comprehensive, empirical study of their occurrence, development and structure
[AD-A185929] 07 p0879 N88-15329

Recent Colorado State University tropical cyclone research of interest to forecasters
[AD-A185996] 07 p0879 N88-15332

Typhoon structural evolution
[AD-A186090] 07 p0879 N88-15333

Numerical investigation of orographically enhanced instability
[AD-A186841] 09 p1189 N88-17125

The role of vortex structure in tropical cyclone motion
[AD-A190961] 16 p2235 N88-23351

Mariners weather log, volume 32, number 1, Winter 1988
[PB88-173869] 18 p2544 N88-25097

Suggested hurricane operational scenario for GOES I-M
[NASA-TM-89729] 19 p2692 N88-26002

Tropical cyclone report
[AD-A191883] 19 p2693 N88-26009

Passive microwave measurements of water vapor fields and rain for locating fronts in cyclonic storms
[AD-A195632] 24 p3404 N88-30267

CYCLONES (EQUIPMENT)

U CENTRIFUGES

CYCLOTETRAMETHYLENE TETRANITRAMINE

U HMX

CYCLOTRIMETHYLENE TRINITRAMINE

U RDX

CYCLOTRON FREQUENCY

Elements of plasma physics 03 p0271 N88-11703

Fundamental cyclotron frequency generation from a cusptron oscillator
[AD-A188187] 10 p1321 N88-17898

Microwave generation from a cusptron oscillator with a six-vane circuit
[AD-A188377] 12 p1619 N88-19680

The effects of a dc electric field on the current driven ion cyclotron instability
[AD-A188877] 12 p1695 N88-20142

Observations of electron cyclotron harmonic emissions associated with field-aligned electron beams
[SD-TR-87-33] 19 p2724 N88-26173

CYCLOTRON RADIATION

NT ION CYCLOTRON RADIATION

Nonthermal phenomena in stellar coronae: Evidence from radio observations 04 p0503 N88-13096

Higher harmonic generation in the induced resonance electron cyclotron maser
[AD-A186236] 07 p0858 N88-15210

Experimental evaluation for efficiency of excitation slow plasma and cyclotron waves in collective accelerators
[DE88-700566] 07 p0936 N88-15687

Absorption of cyclotron radiation in skin layer in Araks experiment 08 p1003 N88-16076

Conceptual design of a radio-frequency driven compact tokamak
[INPE-4364-PRE/1190] 08 p1085 N88-16535

Absorption of electron cyclotron radiation in tokamak plasmas with a superthermal tail in the electron velocity distribution
[INPE-4391-PRE/1211] 08 p1086 N88-16541

Advanced studies of integrable systems
[AD-A186792] 09 p1151 N88-16895

Microwave generation from a cusptron oscillator with a six-vane circuit
[AD-A188377] 12 p1619 N88-19680

Measurements of optically thin electron cyclotron emission from relativistic electrons
[DE88-004713] 12 p1688 N88-20096

Heating and confinement studies of electron cyclotron resonance heated plasmas in Heliotron E
[DE88-752312] 15 p2136 N88-22746

Kinetic modulational instability of electron cyclotron waves in plasmas
[DE88-701893] 20 p2859 N88-26978

EXO033319-2554.2: A 55-MG eclipsing AM Herculis binary
[MPE-PREPRINT-114] 22 p3163 N88-28838

CYCLOTRON RESONANCE

Nonthermal phenomena in stellar coronae: Evidence from radio observations 04 p0503 N88-13096

Anomalies in electromagnetic absorption of circularly polarized ultrasonic waves by tungsten within Doppler-shifted cyclotron resonance range
06 p0775 N88-14756

Development of FTMS methods for the detection of trace chemical species and development of FTMS methods for the analysis of various chemical species
[AD-A185857] 07 p0828 N88-15023

Current generation and induced conductivity of a plasma under common action of constant electric field and lower-hybrid or ECR waves
[DE88-700345] 07 p0935 N88-15680

The effect of asymmetric current-supporting electron velocity distributions on second harmonic electron cyclotron resonance heating: A ray-tracing treatment for the compass tokamak
[INPE-4389-PRE/1209] 08 p1087 N88-16549

Simulation and modeling of whistler mode wave growth through cyclotron resonance with energetic electrons in the magnetosphere 10 p1353 N88-18089

Application of ECR ion source beams in atomic physics
[DE88-003767] 10 p1406 N88-18384

ATF experimental plans
[DE88-004177] 10 p1414 N88-18439

Mode priming in an overmoded gyrotron oscillator
[AD-A189151] 13 p1772 N88-20602

Heating and confinement studies of electron cyclotron resonance heated plasmas in Heliotron E
[DE88-752312] 15 p2136 N88-22746

Status of RF superconductivity at Argonne National Laboratory
[DE88-005913] 15 p2144 N88-22796

Parallel gradient effects on ICRH (Ion Cyclotron Resonance Heating) in tokamaks
[DE88-009038] 19 p2730 N88-26216

Kinetic modulational instability of electron cyclotron waves in plasmas
[DE88-701893] 20 p2859 N88-26978

Ion kinetics in silane plasmas
[AD-A196202] 24 p3431 N88-30423

CYCLOTRON RESONANCE DEVICES

Optimization of mode converters for generating the fundamental TE(06) gyrotron output at 140 GHz
[IPF-87-1] 01 p0043 N88-10273

Mode purity measurements on gyrotrons for plasma heating at the stellarator W 7-AS
[IFF-87-3] 01 p0101 N88-10660

High peak power ka-band gyrotron oscillator experiment
[AD-A185424] 05 p0585 N88-13563

Theoretical and experimental investigation of electron beam acceleration and sub-millimeter wave generation in cyclotron resonant cavities
[AD-A184806] 05 p0649 N88-13975

Initial operation of a high-power whispering-gallery-mode gyrotron
[DE88-002500] 07 p0857 N88-15207

Higher harmonic generation in the induced resonance electron cyclotron maser
[AD-A186236] 07 p0858 N88-15210

Gyrotron development at the Instituto de Pesquisas Espaciais
[INPE-4240-PRE/1115] 08 p0990 N88-15992

Recent results of plasma research activities at the Instituto de Pesquisas Espaciais
[INPE-4383-PRE/1203] 08 p1085 N88-16538

First and second harmonic ECRH experience at gyrotron frequencies at LLNL
[DE88-003998] 10 p1413 N88-18430

High peak power Ka-band gyrotron oscillator experiments with slotted and unslotted cavities
[AD-A188109] 11 p1478 N88-18819

Trip electrical circuit of the gyrotron
[INPE-4336-NTE/273] 12 p1622 N88-19701

Time-dependent Slow-Time-Scale theory of free-running and phase-locked gyrotron oscillators
[AD-A188910] 12 p1629 N88-19752

Measurement technique for characterization of the gyrotron
[INPE-4322-RPE/550] 12 p1630 N88-19758

Mode priming in an overmoded gyrotron oscillator
[AD-A189151] 13 p1772 N88-20602

Synthesis method applied to the design of an electron gun for a gyrotron
[INPE-4357-TDL/298] 13 p1773 N88-20607

Calculation of the efficiency of a resonant cyclotronic electron maser (gyrotrons)
[INPE-4[illegible]87-PRE/1207] 14 p1915 N88-21444

Theoretical and experimental study of a mode-converting coupler for application to a harmonic gyrotron amplifier
[AD-A193760] 22 p3081 N88-28294

Wide band gyrotron traveling wave amplifier analysis
[AD-A194269] 23 p3216 N88-29139

The study of hydromagnetic waves and RF heating using the TORTUS tokamak, the development of diagnostic techniques based on submillimeter lasers and the gyrotron, and gas discharge 24 p3431 N88-30419

CYCLOTRONS

NT MICROTRONS

CYGNUS CONSTELLATION

Gamma-ray imaging observations of the Crab and Cygnus regions 10 p1427 N88-18522

Colliding stellar winds in the eclipsing Wolf-Rayet binary V444 Cygni
[NASA-CR-182937] 17 p2451 N88-24563

Gamma rays from Cygnus X-1: Modeling and nonthermal pair production
[DE88-006830] 18 p2596 N88-25426

Observation of a point source in Cygnus constellation with the underground detector at Frejus (France)
[PITHA-87/02] 20 p2884 N88-27122

CYLINDERS

Hot piston ring/cylinder liner materials: Selection and evaluation
[NASA-TM-100276] 08 p0971 N88-15872

Cast iron-base alloy for cylinder/regenerator housing
[NASA-CR-182116] 12 p1608 N88-19613

An interferometric investigation of the diffraction of planar shock waves over a half-diamond cylinder in air
[UTIAS-322] 13 p1768 N88-20575

Measurement of the properties of lossy materials inside a finite conducting cylinder
[NASA-CR-182664] 13 p1832 N88-20962

CYLINDRICAL AFTERBODIES

U AFTERBODIES
U CYLINDRICAL BODIES

CYLINDRICAL BODIES

NT ROTATING CYLINDERS

Possibilities for the modeling of dynamically loaded cylindrical structural parts in the wind tunnel
[KU-SFB-210/T/24] 01 p0001 N88-10005

Evaluation of cracking in aluminum cylinders
[PB87-201398] 01 p0024 N88-10149

Design and analysis of a broadband TM(sub 01) mode generator in cylindrical waveguide
[DE87-011308] 01 p0038 N88-10243

Cooling effect of a single evaporating droplet on a hot semi-infinite metal body
[PB87-201802] 01 p0046 N88-10294

The wear process during the RUNNING-IN of steel in lubricated sliding
[NAL-TR-922T] 02 p0181 N88-11130

Flow visualization on an ogive-nosed circular cylinder body at high incidence using the laser light sheet method
[ESA-TT-1066] 03 p0315 N88-11993

Scaling of size/time/temperature associated with dilatation and distortion in uniaxial specimens
03 p0336 N88-12117

Breaking wave forces on vertical cylinders
[RR-CE71] 03 p0338 N88-12126

Analytic model of an imploding Z pinch plasma colliding inelastically with a thin-shelled cylindrical target
[DE88-000051] 03 p0378 N88-12379

Driving mechanism of unsteady separation shock motion in hypersonic interactive flow 05 p0530 N88-13226

Three-dimensional flow past a two-dimensional body
05 p0539 N88-13280

Computational study of three-dimensional wake structures
[REPT-2] 05 p0539 N88-13281

Computation of flow around 2-D circular cylinder 05 p0539 N88-13284

Interferometric data for a shock-wave/boundary-layer interaction [NASA-TM-88227] 05 p0543 N88-13306

An analytical study of the effects of transverse shear deformation and anisotropy on buckling loads of laminated cylinders [NASA-TM-100508] 05 p0557 N88-13387

The simulation of the viscous flow around a cylinder by the random vortex method 05 p0579 N88-13534

Fiber-optic accelerometer investigation [AD-A185359] 05 p0584 N88-13561

Alignment and assembly tool for very large diameter cylinders [NASA-CASE-MFS-28001-2] 06 p0711 N88-14360

The numerical and analytical study of bifurcation and multicellular flow instability due to natural convection between narrow horizontal isothermal cylindrical annuli at high Rayleigh numbers [AD-A186113] 07 p0849 N88-15151

A project to experimentally and theoretically examine fluid interfacial wave phenomena in a rotating cylindrical geometry: Current results and future plans [DE88-003738] 09 p1165 N88-16984

Propagation of creep waves around rough cylindrical surface 09 p1234 N88-17400

An analytical study of the effects of transverse shear deformation and anisotropy on natural vibration frequencies of laminated cylinders [NASA-TM-100554] 10 p1295 N88-17739

The numerical and analytical study of bifurcation and multicellular flow instability due to natural convection between narrow horizontal isothermal cylindrical annuli at high Rayleigh numbers 10 p1328 N88-17937

Fluctuations and massive separation in three-dimensional shock-wave/boundary-layer interactions [NASA-TM-89224] 11 p1434 N88-18559

A study of damage tolerance in curved composite panels [AD-A190617] 15 p2029 N88-22092

Bodies in unsteady flow [AD-A190416] 15 p2064 N88-22308

Experimental determination of the coefficients of the hydraulic resistance of apertures in the rotary disks [AD-A190627] 15 p2066 N88-22317

Buckling of blast loaded cylinder [AD-A190124] 15 p2076 N88-22376

Thermal stress in high temperature cylindrical fasteners [NASA-TM-100611] 15 p2087 N88-22438

Multiple scattering from nonspherical targets [AD-A189939] 15 p2133 N88-22723

Experimental investigation of the hypersonic flow over a six finned configuration [AD-A190870] 16 p2157 N88-22871

Electromagnetic scattering from nonlinear anisotropic cylinders 17 p2333 N88-23930

Cylindrical surface profile and diameter measuring tool and method [NASA-CASE-MFS-28287-1] 17 p2341 N88-23959

Experimental investigation of simplest inhomogeneities in cylindrical slit line [DE88-702388] 21 p2933 N88-27418

Determination of the local heat-transfer characteristics on glaze ice accretions on a cylinder and a NACA 0012 airfoil 21 p2946 N88-27500

The three-dimensional stress field around a cylindrical inclusion in a plate of arbitrary thickness 21 p2963 N88-27602

Marangoni convection in finite cylindrical liquid bridges [LRT-WE-9-FB-5(1988)] 22 p3078 N88-28277

AGARD (Advisory Group for Aerospace Research and Development) engine disc material cooperative test (supplementary program) [AD-A193678] 23 p3179 N88-28925

Additional fracture and strength test results for A723 steel and 38644 titanium [AD-A196329] 24 p3353 N88-29960

The aspect ratio dependence of the attractor dimension in Taylor-Couette flow [AD-A196297] 24 p3369 N88-30065

CYLINDRICAL CHAMBERS

Overview of free-piston Stirling engine technology for space power application [NASA-TM-88886] 03 p0386 N88-12427

CYLINDRICAL PLASMAS

Effect of plasma rotation in tokamak on stabilizing action of electrically conducting wall 06 p0773 N88-14748

Experimental study of scattered waves and cylindrical antenna sheaths in a microwave driven plasma 11 p1553 N88-19293

Numerical research of dispersion properties of plasma cylindrical waveguides located in magnetic field [DE87-703009] 16 p2275 N88-23615

CYLINDRICAL SHELLS

Rational reinforcement of cylindrical shells with variable stiffness frames subjected to external pressure 04 p0426 N88-12638

A direct method to obtain constitutive model constants from cylinder impact test results 04 p0427 N88-12647

Analysis and testing of predamaged shell structures 04 p0428 N88-12653

Vibration and buckling of geometrically imperfect laminated cylindrical shells 04 p0456 N88-12822

Experimental studies on the tripping behavior of narrow T-stiffened flat plates subjected to hydrostatic pressure and underwater shock 05 p0592 N88-13613

Experimental investigation of damping characteristics of bolted structural connections for plates and shells [AD-A186075] 07 p0867 N88-15259

Influence of radiation and thermal conduction on temperature distribution in the thin wall of a hollow cylinder [INPE-4428-TDL/308] 12 p1626 N88-19730

Monolithic nature of transversely reinforced composites 14 p1885 N88-21267

Forced motion of initially stressed shells and plates 18 p2529 N88-25005

A study of fluid-structure problems 21 p2941 N88-27468

Nonlinear oscillations of a nonviscous cylindrical liquid system in weightlessness condition [LRT-WE-9-FB-14(1987)] 22 p3063 N88-28175

Nonlinear vibrations of imperfect thin walled cylindrical shells [ETN-88-92904] 23 p3227 N88-29205

Stresses in cylindrical shells with tangential nozzles submitted to external loads and internal pressure [CRIF-MT-172] 24 p3382 N88-30146

Large displacement and rotational formulation for laminated cylindrical shells including parabolic transverse shear [AD-A194871] 24 p3384 N88-30158

Behaviour and hysteresis losses of irreversible type-2 superconducting cylindrical shell [DE88-702708] 24 p3433 N88-30434

CYLINDROIDS

U CYLINDRICAL BODIES

CYTOCHROMES

Cytochrome electron transfer and biomolecular electronics [AD-A195482] 24 p3406 N88-30277

CYTOGENESIS

NT CELL DIVISION
NT DIFFERENTIATION (BIOLOGY)
NT HEMATOPOIESIS
NT MITOSIS

Review of cytoskeleton research in cell differentiation and development [AD-A185832] 07 p0882 N88-15353

Investigation of genetic structures of rat germ cells following flight aboard Cosmos-1514 biosatellite during their prenatal development 10 p1364 N88-18155

CYTOLOGY

Electron cytochemical detection of Ca(2)+-ATPase in protonema of moss funaria hygrometrica (Hedw.) under hypogravitation 06 p0749 N88-14602

Third Soviet-French Symposium on Space Cytology 07 p0893 N88-15411

Changes in hemostasis system of animals under conditions of granulocytopoiesis inhibition under effect of decreased barometric pressure 12 p1651 N88-19890

Cytomorphology and ultrastructure of corn root meristem in weightlessness 12 p1651 N88-19891

Electrical and chemical sensors for biological cell research 19 p2669 N88-25866

The effect of microgravity on mammalian cell polarization at the ultrastructural level --- Spacelab D1 mission 22 p3061 N88-28164

CYTOPLASM

Review of cytoskeleton research in cell differentiation and development [AD-A185832] 07 p0882 N88-15353

CZECHOSLOVAKIA

Proceedings of the First International Symposium on Physical and Technical Problems of Superconductivity Application in Power Generation [DE88-700818] 11 p1559 N88-19332

CZOCHRALSKI METHOD

Digital control of the Czochralski growth of Gallium arsenide-controller software reference manual [AD-A187210] 11 p1528 N88-19127

Autonomous Liquid Encapsulated Czochralski (LEC) growth of single crystal GaAs by intelligent digital control [AD-A187211] 11 p1555 N88-19305

Hydrodynamic simulation of forced convection in the Czochralski process [INPE-4471-TDL/323] 12 p1697 N88-20158

Modeling growth of interdendritic silicon ribbons 14 p1897 N88-21322

Stress corrosion of ceramic materials [AD-A190501] 15 p2045 N88-22187

Autonomous control system for Czochralski growth of LEC GaAs [AD-A189726] 15 p2141 N88-22779

Real time thermal imaging of high temperature semiconductor melts 17 p2330 N88-23914

Digital control of the czochralski growth of gallium arsenide. System reference manual. Valid for Czochralski growth controller software version 2.4 [AD-A191997] 19 p2732 N88-26227

D

D LAYER

U D REGION

D REGION

Future developments of auroral D-region research using the EISCAT VHF incoherent scatter radar 08 p1035 N88-16278

On formulating a simple D-region model [AD-A195841] 24 p3392 N88-30197

Photochemistry of ionospheric D-region with injection of nitrogen oxides 24 p3444 N88-30499

DAEMO (DATA ANALYSIS)

U DATA PROCESSING
U DATA REDUCTION
U DATA TRANSMISSION

DAMA

U DEMAND ASSIGNMENT MULTIPLE ACCESS

DAMAGE

NT CUMULATIVE DAMAGE
NT EARTHQUAKE DAMAGE
NT FIRE DAMAGE
NT FROST DAMAGE
NT IMPACT DAMAGE
NT LASER DAMAGE
NT METEORITIC DAMAGE
NT RADIATION DAMAGE
NT RAIN IMPACT DAMAGE
NT STORM DAMAGE

Space station integrated wall design and penetration damage control [NASA-CR-179169] 01 p0013 N88-10070

Structural reliability and damage tolerance of ceramic composites for high-temperature applications [PB87-208310] 01 p0019 N88-10119

Contribution to the study of composite materials and their damage [NASA-TT-20107] 02 p0143 N88-10897

Airworthiness of long-life jet transport structures 03 p0265 N88-11674

Indentation damage in ceramics [AD-A184686] 03 p0294 N88-11844

Analysis and testing of predamaged shell structures 04 p0428 N88-12653

Data base on the high heat flux behaviour of metals and carbon materials for plasma facing components. Experiments at the 10 MW neutral beam injection test stand of the IPP Nagoya [IPPJ-AM-53] 04 p0492 N88-13031

Fiber composite structural durability and damage tolerance. Simplified predictive methods [NASA-TM-100179] 05 p0560 N88-13409

Raman microprobe characterization of dielectric films following high-energy pulsed laser irradiation [DE88-000559] 05 p0588 N88-13587

Fretting wear and fretting fatigue damage 05 p0603 N88-13697

Study of damage in carbon fiber-epoxy composite materials. Utilization to assess broken specimens [DCQ/L-45-650/F] 06 p0678 N88-14152

Characterization of mechanical damage mechanisms in ceramic composite materials [AD-A185549] 06 p0686 N88-14205

Fatigue damage maps 06 p0715 N88-14382

Transients in elevated temperature crack growth [DE87-013189] 06 p0724 N88-14454

Ion mixing and surface modification in metal-semiconductor systems [DE88-001702] 06 p0786 N88-14823

Natural frequencies and structural integrity assessment of large space structures [AD-A186139] 07 p0824 N88-15001

Finite element analysis of damaged cross-ply composite laminates [CCMS-87-10] 09 p1139 N88-16829

Reliability of structures with stiffness and strength degradation 09 p1180 N88-17068

Analytical and experimental characterization of damage processes in composite laminates [AD-A187221] 10 p1296 N88-17746

Relationship between fatigue life in the creep-fatigue region and stress-strain response
[NASA-TM-100796] 10 p1345 N88-18040

Modeling of the non-auditory response to blast overpressure
[AD-A187397] 10 p1369 N88-18184

Atomistic simulation of low-energy beam deposition
[DE88-004344] 11 p1544 N88-19228

A continuum damage model for viscoelastic materials
[AD-A189426] 12 p1637 N88-19800

Abrasion resistant porous silica antireflective coatings
[DE88-006230] 14 p1894 N88-21308

Structural consequences of railgun augmentation
[DE88-007036] 15 p2023 N88-22058

A study of damage tolerance in curved composite panels
[AD-A190617] 15 p2029 N88-22092

Buckling of blast loaded cylinder
[AD-[illegible]30124] 15 p2076 N88-22376

Evolution of hardening and damage during viscoplastic deformation
[AD-A190714] 15 p2077 N88-22381

Rainfall rates and drop-size distributions for environmental testing
[AD-A191342] 16 p2236 N88-23354

Damage by creep fatigue: Influence of the visco-elasticity of the matrix
[PB88-124706] 18 p2528 N88-24998

Optical damage in epoxy polymers by millisecond light pulses
[DE88-008675] 19 p2620 N88-25547

Modulation efficiency limited high frequency performance of the MODFET 19 p2657 N88-25786

Laser induced surface emission of neutral species and its relationship to optical surface damage processes
[DE88-008035] 19 p2726 N88-26192

Stiffness degradation of composite laminates
20 p2767 N88-26405

Computation equipment for damage simulation in laminated composites
[AD-A193013] 20 p2768 N88-26412

The influence of foreign particles on bearing metals
[NASA-TT-20155] 20 p2775 N88-26454

Irreversible deformations during fracture in polymers
[W-7/86] 20 p2780 N88-26485

Mobile robot survival
[DE88-009108] 20 p2809 N88-26665

Damage in a perforated graphite-epoxy plate under monotonic cyclic biaxial loading
[ONERA-NT-1987-5] 20 p2816 N88-26708

Vibrational impacts of hush house operation
[DE88-006983] 21 p2899 N88-27207

Fiber-optics used to record high-speed photographs inside a pressurized tank during lethality testing
[DE88-011283] 21 p2951 N88-27529

Critical issues and directions for fracture mechanics and structural integrity
[AD-A193050] 21 p2960 N88-27584

The relationship between observed fatigue damage and life estimation models
[NASA-CR-182191] 21 p2965 N88-27611

Analysis of stiffness reduction, failure and stress concentration in fiber composite laminates
[AD-A193519] 22 p3050 N88-28096

Procedures for identification and handling of Printed Circuit Boards (PCBs)
[AD-A191177] 23 p3206 N88-29078

Photorefractive damage mechanism in electro-optic materials
[AD-A194560] 23 p3282 N88-29543

Damage initiation in the short beam shear test of composite materials using stiffness reduction
[AD-A194880] 24 p3340 N88-29883

Automated early fatigue damage sensing system
[AD-A195717] 24 p3382 N88-30143

An investigation of constitutive models for predicting viscoplastic response during cyclic loading
[AD-A194875] 24 p3385 N88-30163

DAMAGE ASSESSMENT

Calculation of the damage of highly loaded gas turbine disks under real flight conditions
[ETN-87-90416] 01 p0007 N88-10036

New fatigue damage analysis of complex engineering components based on Finite Element Methods (FEM)
[DFVLR-FB-87-15] 01 p0062 N88-10401

Investigation of large scale impact of air pollution components on forest ecosystems in Bavaria, West Germany
[DFVLR-FB-87-17] 01 p0068 N88-10434

Development of a method for forest damage inventory using multispectral scanner data
[KFK-PEF-25] 03 p0345 N88-12182

Failure control techniques for the SSME
[NASA-CR-179224] 04 p0409 N88-12537

Low-cost teleoperator-controlled vehicle for damage assessment and dose measurement
[DE88-000713] 04 p0451 N88-12794

Contribution of acoustic analysis to assess damage in fluid storage tanks under high pressure --- composite materials, filament winding
[SNIAS-872-430-119] 05 p0559 N88-13407

Overview of Austrian Airborne Imaging Spectrometer (AIS) programme and first results
05 p0612 N88-13762

Review of fatigue and fracture research at NASA Langley Research Center 09 p1106 N88-16633

Optimized approach to damage tolerance --- spacecraft
[FOK-FSS-R-87-024] 09 p1134 N88-16806

Sublaminate damage mechanisms in composite structures
[AD-A186807] 09 p1137 N88-16815

Mechanical properties of carbon fiber reinforced thermoplastic matrix composites
[NAL-TR-934] 09 p1139 N88-16827

A chemical precursor to optical damage: Studies by laser ionization mass spectrometry
[DE88-004321] 10 p1409 N88-18408

Profilometer for bomb-damage-repaired airfield pavements and measurement of pavement upheaval. Report 1: Technology evaluation
[AD-A187985] 11 p1442 N88-18601

Sub-scaling of projectile/target system damaged by hypervelocity
[AD-A188683] 12 p1634 N88-19779

Activities report of the Structures Department
[ETN-88-91986] 13 p1783 N88-20672

A theory of viscoplasticity accounting for internal damage 14 p1930 N88-21508

Creep rupture analysis of a beam resting on high temperature foundation 14 p1930 N88-21509

A constitutive model with damage for high temperature superalloys 14 p1930 N88-21510

Damage models for delamination and transverse fracture
[AD-A189652] 15 p2029 N88-22088

Oxide optical coatings prepared by metal-organic vapor deposition
[DE88-006809] 15 p2043 N88-22175

Impact damage in composite laminates
15 p2080 N88-22402

Life prediction modeling based on cyclic damage accumulation 15 p2085 N88-22426

Towards a damage tolerance philosophy for composite materials and structures
[NASA-TM-100548] 16 p2173 N88-22949

Tornado tracks in Southwestern Brazil, Eastern Paraguay, and Northwestern Argentina
17 p2362 N88-24071

Dimensional analysis and experimental observation of the coupling phenomena between combustion and fracture of damaged propellant samples
19 p2630 N88-25603

Characterization of fatigue crack initiation and propagation in Ti-6Al-4V with electrical potential drop technique
[NASA-TM-100877] 19 p2681 N88-25937

Principles of a nondestructive evaluation process for damage location, damage profile, and damage extension in welded joints by radiometric measurements
[MPA-86-02] 20 p2812 N88-26683

T55-L-714 engine development and qualification. Engine M11 low cycle fatigue test report. (0213-005-87)
[AD-A192765] 21 p2897 N88-27197

T55-I-714 engine development and qualification. Engine M11 low cycle fatigue test report. (0213-005-87), volume 2, part 1
[AD-A192766] 21 p2897 N88-27198

Techniques for characterizing damage zones in composite materials 21 p2905 N88-27240

Design and implementation of contact ultrasonic sensors to assess internal damage
[I-177/87] 21 p2906 N88-27247

An anisotropic continuum damage model for creep-dominated, multiaxial loading histories
21 p2964 N88-27608

Assessment of cochlear damage after microwave irradiation
[AD-A193237] 21 p2987 N88-27737

Study of the forests on the banks of the Gambia and criteria for detecting mortality 22 p3091 N88-28356

Contribution to the mapping of forests in an intensively divided area, with the help of SPOT image data
22 p3107 N88-28453

Evaluation of the contribution of SPOT in the framework of the mineral exploration program of the Aitutaki Atoll (Cook Islands). Preliminary study of the impact of the passage of Hurricane Sally 22 p3109 N88-28463

A comprehensive study on damage tolerance properties of notched composite laminates
[AD-A192952] 23 p3186 N88-28968

DAMAGE THRESHOLD

U YIELD POINT

DAMPERS

Rotational evolution of dynamically symmetric gyrostat with internal friction 24 p3446 N88-30509

DAMPING

NT ELASTIC DAMPING
NT LANDAU DAMPING
NT VIBRATION DAMPING
NT VISCOELASTIC DAMPING
NT VISCOUS DAMPING

Investigation of control law for active flutter suppression
[NASA-TT-20126] 02 p0130 N88-10818

Damping characteristics of a composite-reinforced stainless-steel tube
[DE87-012455] 02 p0191 N88-11192

A comparison of high damping shape memory alloys with Cu-Mn-based and Fe-Cr-based alloys
[AD-A184110] 04 p0414 N88-12566

Damping characteristics of a composite-reinforced stainless steel plate
[DE88-000303] 04 p0457 N88-12828

Influence of surfactants on damping of gravity-capillary waves. 1: Frequency dependence
04 p0459 N88-12843

An analysis of sound absorbing linings for the interior of the NASA Ames 80 x 120-foot wind tunnel
[NASA-CR-177396] 04 p0488 N88-13006

Non-linear shipboard shock analysis of the Tomahawk missile shock isolation system 05 p0592 N88-13614

Improvement of modal scaling factors using mass additive technique 05 p0593 N88-13620

Group contribution analysis of the damping behavior of homopolymers, statistical copolymers and interpenetrating polymer networks based on acrylic, vinyl and styrenic mers
[AD-A185904] 07 p0836 N88-15070

Coherent states for the damped harmonic oscillator
[AD-A186111] 07 p0922 N88-15599

On free decay damping tests
08 p0997 N88-16041

A modal control based limiting performance formulation for shock excited systems 08 p0998 N88-16046

Active control technology with adaptive control concept in the aircraft construction
[MBB/LKE-294/S/PUB/295] 10 p1313 N88-17845

Characterization of damped structural connections for multi-component systems
[NASA-TM-100801] 11 p1502 N88-18974

The impact of vertical axis characteristics on helicopter handling qualities
[AD-A188964] 12 p1583 N88-19474

Practical considerations for structural control: System uncertainty, system time delay and truncation of small control forces
[PB88-163738] 14 p1933 N88-21528

Oscillation damped movement of suspended objects
[DE88-005715] 15 p2086 N88-22433

Electromagnetic dampers for cryogenic applications
15 p2218 N88-23231

Characterization of structural connections for multicomponent systems 16 p2220 N88-23251

Driving of axial acoustic fields by side-wall stabilized premixed flames 19 p2629 N88-25592

Statistical evaluation of light water reactor piping damping data for use in PRA (Probabilistic Risk Assessment) analyses
[DE88-007708] 19 p2661 N88-25828

The importance of steady and dynamic inflow on the stability of rotor-body systems 21 p2890 N88-27156

Comparison of experimental rotor damping data-reduction techniques 21 p2891 N88-27159

Experimental determination of aerodynamic damping in a three-stage transonic axial-flow compressor
[NASA-TM-100953] 21 p2897 N88-27200

Damping characteristics of metal matrix composites
[AD-A193144] 21 p2904 N88-27233

Development of a nitrile rubber for dynamic damping
[AD-A194060] 22 p3058 N88-28145

Power flow analysis of two coupled plates with arbitrary characteristics
[NASA-CR-183165] 22 p3075 N88-28251

Waves and instabilities in an electron-positron plasma in an ultra-strong magnetic field
23 p3283 N88-29551

Analytical and experimental studies of beam waveguide absorbers for structural damping
[AD-A195085] 24 p3382 N88-30144

DAMPING FACTOR

U DAMPING

DAMPING IN PITCH
U DAMPING
U PITCH (INCLINATION)
DAMPING IN ROLL
U DAMPING
U ROLL
DAMPING IN YAW
U DAMPING
U YAW
DAMPING TESTS
Analytical and experimental studies of beam waveguide absorbers for structural damping
[AD-A195085] 24 p3382 N88-30144
DAMPNESS
U MOISTURE CONTENT
DANGER
U HAZARDS
DARK ADAPTATION
Effect of intermittent hypercapnia on visual analyzer function 07 p0896 N88-15431
Night Vision: Current Research and Future Directions, symposium proceedings
[PB88-132006] 11 p1550 N88-19274
Mechanisms of early light and dark adaptations
12 p1663 N88-19972
DARK MATTER
Might dark matter not be concentric with luminous matter
[DE87-703094] 02 p0252 N88-11589
Galaxy formation by gravitational collapse in a universe dominated by cold dark matter 04 p0521 N88-13205
Infrared constraints on the nature of dark matter
13 p1855 N88-21102
The comet flux and the 15 Myr galactic cycle
14 p1995 N88-21889
Stable, heavy, neutral particles in the sun and in toponium decay 17 p2452 N88-24568
Non-linear scale invariance in a cold-dark-matter universe
[DE88-011725] 23 p3299 N88-29644
Gravitational redshift of self-gravitating systems of dark matter in the universe
[DE88-702688] 23 p3300 N88-29650
DARKENING
NT LIMB DARKENING
DARKNESS
Trickle water and feeding system in plant culture and light-dark cycle effects on plant growth
03 p0361 N88-12273
The accommodative status in the dark of US Navy fighter pilots
[AD-A188188] 10 p1370 N88-18186
DART TURBOPROP ENGINES
U TURBOPROP ENGINES
DASSAULT AIRCRAFT
NT MIRAGE AIRCRAFT
Acceleration of prototype development and reduction of cost by multidisciplinary integration
12 p1704 N88-20199
DATA ACQUISITION
Space station propulsion technology: Space station propulsion system test bed test plan
[NASA-CR-179201] 01 p0017 N88-10104
Outgassing data for selecting spacecraft materials
[NASA-RP-1124] 01 p0019 N88-10117
Estimation from satellite imagery of summertime rainfall over varied space and time scales
[PB87-203246] 01 p0071 N88-10454
Input devices for tasks using interactive video
[NPL-DITC-87/87] 01 p0080 N88-10510
A CAMAC system controlled by an IBM AT computer for time-resolved spectroscopy
[DE87-010111] 01 p0080 N88-10514
EAGLES: An interactive environment for scientific computing
[DE87-013564] 01 p0084 N88-10541
Direct detection of optical radiation through a sampling orifice for inductively coupled plasma atomic emission spectroscopy
[DE87-013609] 01 p0101 N88-10662
The status of the international Halley watch
01 p0116 N88-10744
Nickel hydrogen low Earth orbit test program update and status 02 p0164 N88-11028
Further development of the dynamic gas temperature measurement system 02 p0184 N88-11141
An acoustic emission digital data acquisition workstation
[DE87-012425] 02 p0191 N88-11191
An isentropic coordinate model used in a mesoscale data assimilation system 02 p0212 N88-11333
The future of data in mesoscale numerical models
02 p0214 N88-11344
The challenge of using mesoscale data in mesoscale numerical models 02 p0214 N88-11346
Implementing and managing change: A guide for assessing information technology
[DE88-000035] 02 p0249 N88-11571
GEOSAT altimeter geophysical data record user handbook
[PB87-213336] 03 p0276 N88-11743
SPOT: A tool for agricultural statistics
03 p0344 N88-12170
A Workshop on Desert Processes, September 24-28, 1984: Report on the conference
[AD-A184599] 03 p0345 N88-12184
Calendar year 1985 solar and weather data for Austin, Texas
[PB87-220174] 03 p0352 N88-12219
The MicroVAX-based data acquisition system for D0
[DE87-014475] 03 p0366 N88-12303
Automated microwave dielectric constant measurement
[AD-A184182] 04 p0431 N88-12667
The Telecommunications and Data Acquisition Report
[NASA-CR-181546] 04 p0432 N88-12679
Traveling-wave maser closed-cycle refrigerator data acquisition and display system 04 p0437 N88-12708
Tau ranging revisited 04 p0437 N88-12710
Computerized certification of digital ultrasonic instrumentation
[DE88-000820] 04 p0488 N88-13008
Automatic photometric monitoring of cool stars
04 p0504 N88-13103
High frequency data acquisition system for space shuttle main engine testing 05 p0595 N88-13630
The Portable Instant Display and Analysis Spectrometer (PIDAS) 05 p0611 N88-13756
Plant Growth Module (PGM) conceptual design
05 p0631 N88-13855
Software design for an airborne gravity measurement system
[AD-A185000] 05 p0634 N88-13876
Boeing 727 MLS (Microwave Landing System) terminal instrument procedures (TERPS) approach data collection and processing, data report
[AD-A185523] 06 p0667 N88-14090
Area detectors for X-ray spectroscopy
[DE88-001429] 06 p0679 N88-14163
Description of data handling system installed December 11, 1986 --- EISCAT 06 p0692 N88-14242
AVIRIS onboard data handling and control
06 p0706 N88-14332
Application of remote sensing to agricultural field trials
[ISBN-90-6754-089-7] 06 p0729 N88-14483
The archiving of meteor research information
06 p0732 N88-14505
Tropical hydrology
[WMO-655] 06 p0745 N88-14584
Acquisition of gust statistics from Aircraft integrated Data Systems (AIDS) recorded data
[NLR-MP-86048-U-ISS-2] 06 p0745 N88-14586
Facilities for research and weather observations on the 213 m tower at Cabauw (Netherlands) and at remote locations
[KNMI-WR-87-5] 06 p0746 N88-14587
Wave and wind data sources, environmental conditions committee report, International Ship and Offshore Structures Congress
[PB87-234902] 06 p0746 N88-14588
Data acquisition, reduction and analysis of shock and vibration testing using a super microcomputer
[AD-A186123] 07 p0867 N88-15260
Data on existing wind energy converters in Denmark
[DE88-900199] 07 p0874 N88-15300
Collecting of new data on existing wind energy converters
[DE88-900221] 07 p0875 N88-15305
Biotechnology in western Europe
[PB88-105887] 07 p0883 N88-15360
A learning model as a basis for investigations of the effects of gravity on the learning processes and memory formulation 07 p0886 N88-15374
Problems of organization of mass processes of simulation, acquisition and processing of experimental data at computers
[DE88-700547] 07 p0905 N88-15483
SSME environment database development
[NASA-CR-179245] 08 p0964 N88-15836
Laboratory vibration test schedules development beyond MIL-STD-810D 08 p0999 N88-16050
Alouette-ISIS program summary
[NASA-CR-180747] 08 p1023 N88-16195
High-speed assembly language (80386/80387) programming for laser spectra scan control and data acquisition providing improved resolution water vapor spectroscopy
[NASA-CR-4117] 08 p1053 N88-16355
Interactive knowledge acquisition tools
08 p1060 N88-16401
Flow field measurements using hotwire anemometry
[AD-A187029] 09 p1160 N88-16951
Data acquisition and analysis system for the Sandia 34-meter Vertical Axis Wind Turbine
[DE88-002417] 09 p1187 N88-17112
Design knowledge capture for the space station
09 p1208 N88-17239
TDAS: The Thermal Expert System (TEXSYS) data acquisition system 09 p1211 N88-17258
Management Information and Downloader Interface System (MIDIS)
[AD-A186978] 09 p1261 N88-17557
A reliable data collection/control system
10 p1289 N88-17706
Speech recognition: Acoustic-phonetic knowledge acquisition and representation
[AD-A187293] 10 p1320 N88-17893
Evaluation of surface energy and radiation balance systems on the Konza Prairie
[NASA-CR-182534] 10 p1355 N88-18097
Developments in National Weather Service meteorological data collection programs as related to EPA (Environmetal Protection Agency) air pollution models
[PB88-130240] 10 p1356 N88-18104
Minimum Energy Routing through Interactive Techniques (MERIT) modeling
[NASA-CR-182535] 10 p1356 N88-18105
Methods of eliciting information from experts
[AD-A187468] 10 p1372 N88-18189
MICRO system for control, acquisition and processing of experimental data
[DE88-700724] 10 p1386 N88-18278
SETI data controllers 11 p1474 N88-18795
Overview of multi-input frequency domain modal testing methods with an emphasis on sine testing
11 p1499 N88-18949
Data acquisition and processing for surface plate calibration
[AD-A187264] 11 p1564 N88-19366
The global positioning system as an aid to the testing of inertial navigation units (volume 1, addendum 1)
[AD-A185783] 12 p1578 N88-19443
Automatic data acquisition system utilizing microcomputers: Automatic Meteorological Stations (AMS)
[INPE-4215-PRE/1096] 12 p1646 N88-19859
Homogenizing surface and satellite observations of cloud: Aspects of bias in surface data
[AD-A188523] 12 p1648 N88-19869
A knowledge acquisition tool for the intelligent processing of materials
[AD-A188952] 12 p1679 N88-20036
Pion absorption in nuclei: The pion(+ or -),proton reactions
[LA-10997-T] 12 p1688 N88-20098
RIAR automated research and management systems
[DE88-700934] 12 p1706 N88-20209
An analysis of physiological data related to motion sickness for use in a real-time motion sickness indicator
[AD-A189589] 13 p1810 N88-20812
Solar cell experiment on the first satellite of the Brazilian complete space mission
[INPE-4248-PRE/1121] 14 p1860 N88-21238
A data acquisition system for atmospheric tracer studies
[DE88-006211] 14 p1391 N88-21869
Enhancement of data acquisition and numerical computation capabilities for unsteady fluid dynamics
[AD-A190115] 15 p2063 N88-22302
Calibration and processing of AVHRR data for temperature estimation
[INPE-4493-PRE/1257] 15 p2095 N88-22485
A multivariate variational objective analysis-assimilation method. Part 2: Case study results with and without satellite data
[NASA-CR-182653] 15 p2097 N88-22492
Real-time environmental Arctic monitoring (R-TEAM)
[AD-A189948] 15 p2099 N88-22508
Complex sound processing: An interdisciplinary approach
[AD-A189782] 15 p2102 N88-22523
Fast analog-to-digital converter
[DE88-701488] 15 p2106 N88-22543
Application of static memory for data acquisition and transmission into a computer
[DE88-701491] 15 p2106 N88-22544
A compact high resolution piezoresistive digital tactile sensor
[DE88-000430] 16 p2210 N88-23188
Low-cost optical data acquisition system for blade vibration measurement 16 p2219 N88-23240
Accurate positioning of long, flexible ARM's (Articulated Robotic Manipulator) 16 p2219 N88-23243
Seasonal variation for structural strength value
[PB88-169248] 16 p2222 N88-23260

Overground Excess Sound Attenuation (ESA). Volume 1: Experimental study for flat grassy terrains
[AD-A191289] 16 p2265 N88-23549
The Engineer Studies Center guide to research and data collection
[AD-A189971] 16 p2285 N88-23680
Investigation of air transportation technology at Ohio University, 1986 17 p2293 N88-23719
Modeling of functional specifications for onboard software: Experience with the Rafale avionics system
17 p2303 N88-23777
Presentation of the METEOSAT system and the roles of EUMETSAT within the meteorological community
17 p2357 N88-24039
ERS-1 data products and services and their value for tropical countries 17 p2357 N88-24040
Processing of HRPT data from the NOAA series satellites 17 p2359 N88-24053
Cessna 172 MLS (Microwave Landing System) terminal instrument procedures (TERPS) approach data collection and processing data report
[AD-A191241] 18 p2461 N88-24613
Adaptive data acquisition multiplexing system and method
[NASA-CASE-MSC-21170-1] 18 p2471 N88-24662
Taiwan area mesoscale experiment: P-3 aircraft operations summary
[PB88-169073] 18 p2544 N88-25098
Knowledge acquisition tool implementation
[AD-A190415] 18 p2555 N88-25164
SAMS: The synchronization and monitoring system for ATF (Advanced Toroidal Facility) data acquisition provides unified data access for ATF data acquisition
[DE88-007268] 18 p2589 N88-25386
The JPL MSAT mobile laboratory and the pilot field experiments 19 p2646 N88-25708
Ultrasonic and video computerized data acquisition for automated welding
[DE88-006741] 19 p2677 N88-25918
Monitoring of divers/astronauts during missions
19 p2698 N88-26036
RAGS (Realtime Acquisition and Graphics System): An off-the-shelf hardware and system software small data acquisition computer
[DE88-008399] 19 p2716 N88-26128
Meteorological satellite product support and research for project GALE
[NASA-CR-180989] 19 p2727 N88-26193
Measurement of HO2 and other trace gases in the stratosphere using a high resolution far-infrared spectrometer at 28 KM
[NASA-CR-180400] 20 p2821 N88-26737
Computer controlled data acquisition system for the NASA 1986 Rocket Triggered Lightning Program
[DE88-008335] 20 p2826 N88-26766
An expeditious technique for keyboard input of information to FORTRAN computer programs
[DE88-009617] 20 p2840 N88-26855
An overview of the development of a linear broadband analog fiber-optic link
[DE88-008668] 20 p2854 N88-26945
An integrated, multi-vendor distributed data acquisition system
[DE88-008900] 20 p2882 N88-27113
FTMP data acquisition environment
[NASA-TM-100636] 21 p2938 N88-27447
Army space systems for terrestrial applications
[AD-A192735] 21 p2965 N88-27613
The Hanford meteorological data collection system and data base
[DE88-008632] 21 p2975 N88-27672
Synopsis of a computer program designed to interface a personal computer with the fast data acquisition system of a time-of-flight mass spectrometer
[NASA-CR-177474] 21 p3001 N88-27798
SERI standard broadband format: A solar and meteorological data archival format
[DE88-001145] 21 p3028 N88-27975
Test and calibration system for monitoring the Advanced Technologies Testing Aircraft System (ATTAS) data acquisition system 22 p3037 N88-28029
Mark IV-85 mission support planning and future mission set 22 p3067 N88-28202
Research for reducing the labor intensive nature of high-resolution terrain analysis feature extraction
[AD-A192661] 22 p3089 N88-28345
SPOT data acquisition and distribution
22 p3115 N88-28505
Software engineering for the EBR-2 data acquisition system conversion
[DE88-009950] 22 p3136 N88-28647
Computer-controlled measurements of nonlinear standing waves
[AD-A193840] 22 p3147 N88-28717
Space shuttle phase B wind tunnel model and test information. Volume 2: Orbiter configuration
[NASA-CR-178415-VOL-2-PT-1]
23 p3171 N88-28881
Knowledge acquisition and rapid protyping of an expert system: Dealing with real world problems
23 p3258 N88-29394
Acquisition of gust statistics from AIDS-recorded data
24 p3313 N88-29733
MIZEX (marginal ice zone experiment) 1987 SAR (Synthetic Aperture Radar) data summary
[AD-A195560] 24 p3364 N88-30035
Laser sensing for identification and control of distributed parameter systems
[AD-A195886] 24 p3379 N88-30124
Microwave remote sensing at INPE (Institute for Space Research) Brazil: Concepts and future prospects of soil moisture studies
[INPE-4569-PRE/1310] 24 p3388 N88-30178
China's acquisition and use of foreign aviation technology
[AD-A194827] 24 p3440 N88-30471

DATA ADAPTIVE EVALUATOR/MONITOR
U DATA PROCESSING
U DATA REDUCTION
U DATA TRANSMISSION

DATA ANALYSIS
U DATA PROCESSING
U DATA REDUCTION

DATA BASE MANAGEMENT SYSTEMS
Object-oriented data base management for robot programming
[ETN-87-90367] 01 p0105 N88-10687
High performance clause indexing
[DE87-011399] 01 p0106 N88-10688
A new compression method with fast searching on large databases
[DE87-010986] 01 p0106 N88-10691
File management using balanced trees
[ENST-87D001] 01 p0106 N88-10693
The microcomputer as an engineering management tool
[DE87-014882] 02 p0219 N88-11378
Summaries of the FY 1987 applied mathematical sciences research program
[DE87-014447] 02 p0225 N88-11416
Design and development of a database for spectral data and analysis results
[DE87-011323] 02 p0247 N88-11564
Definitions as database records
[DE87-014057] 02 p0248 N88-11570
Comparison of pascal and the dBASE 3 PLUS language in programming an inventory management system
[AD-A184027] 03 p0365 N88-12300
Electronic Records Administration at the Savannah River Plant
[DE87-014842] 03 p0384 N88-12415
IDMS application documentation made easy
[DE88-000199] 03 p0384 N88-12416
User's guide to NCAR (National Center for Atmospheric Research) CCM1
[PB87-224366] 04 p0469 N88-12899
Managing distributed derived data: A preliminary proposal
[DE88-000714] 04 p0481 N88-12966
A data translation method for heterogeneous database systems 04 p0501 N88-13081
Towards automated consulting: Design feedback from the performance of online documentation
[DE87-012243] 04 p0501 N88-13082
Relational data handling system for scientists
[PB87-223426] 05 p0658 N88-14038
Scientific data manipulation in a relational database system
[PB87-124400] 06 p0791 N88-14850
Computer aided design for Petri Nets
[AD-A186109] 07 p0902 N88-15465
GENLPLOT: An interactive program for display and analysis of data, user's manual
[DE88-002292] 07 p0905 N88-15485
Enhancement of computer system for applications software branch 07 p0923 N88-15610
Expert system development for commonality analysis in space programs 07 p0928 N88-15635
Interface between astrophysical datasets and distributed database management systems (DAVID)
[NASA-CR-182394] 07 p0942 N88-15731
SSME environment database development
[NASA-CR-179245] 08 p0964 N88-15836
Third Conference on Artificial Intelligence for Space Applications, part 1
[NASA-CP-2492-Pt-1] 08 p1055 N88-16360
Conceptual information processing: A robust approach to KBS-DBMS integration 08 p1063 N88-16422
Foundation: Transforming data bases into knowledge bases 08 p1063 N88-16423
Proposal of a methodology for the conceptual design of the Distributed Data Base
[INPE-4315-TDL/282] 08 p1093 N88-16576
Critical issues in NASA information systems
[NASA-CR-182380] 08 p1093 N88-16577
Design and implementation of a data base system for Digital Land Mass System (DLMS) data
[FEL-IR-1987-19] 09 p1185 N88-17101
Nested transactions, conflict-based locking, and dynamic atomicity
[AD-A187033] 09 p1217 N88-17294
Management of complex information in support of evolving autonomous expert systems
[AD-A186680] 09 p1224 N88-17337
Application of a database system for inventory management of classified material
[AD-A186986] 09 p1261 N88-17558
KBGIS-II: A knowledge-based geographic information system
[NASA-CR-182492] 09 p1261 N88-17559
Computer-Aided Design Information System (CADIS): User's manual
[DE88-004365] 10 p1424 N88-18509
Cockpit data management
[NASA-CR-178407] 11 p1438 N88-18579
Cockpit data management
[NASA-CR-178407-SUPPL] 11 p1438 N88-18580
Ceramic technology for advanced heat engines program data base
[DE88-003922] 11 p1464 N88-18730
The design and implementation of pedagogical software for the multi-backend/multi-lingual database system
[AD-A188106] 11 p1530 N88-19135
The design of the POSTGRES storage system
[AD-A187244] 11 p1564 N88-19365
UNIVERS product, phase 1
[AD-A187405] 11 p1564 N88-19367
Supporting valid time: An historical algebra
[AD-A187740] 11 p1565 N88-19368
Accessing hierarchical databases via SQL transactions in a multi-model database system
[AD-A187878] 11 p1565 N88-19369
Regenerative life support system research
[NASA-CR-182606] 12 p1671 N88-20006
Towards a solution to the proper integration of a logic programming system and a large knowledge based management system
[AD-A188949] 12 p1705 N88-20207
The TempIS Project: Performance analysis of temporal queries
[AD-A188354] 12 p1706 N88-20213
The TEMPIS project: Current status
[AD-A188963] 12 p1707 N88-20220
Martian Clouds Data Workshop
[NASA-CR-182431] 12 p1711 N88-20238
HISPLT: A history graphics post processor for wave propagation codes
[DE88-005507] 13 p1817 N88-20857
CSQPLT: A graphics post processor for multidimensional wave propagation codes
[DE88-005508] 13 p1817 N88-20858
Using design axioms and topology to model database semantics
[CWI-CS-R8711] 13 p1818 N88-20863
Distributed transaction processing and the Camelot system
[AD-A188614] 13 p1821 N88-20885
Reference model for DBMS (database management system) user facility
[PB88-169446] 13 p1851 N88-21080
Laboratory Information Management System (LIMS): A case study
[NASA-TM-100835] 14 p1961 N88-21697
Common database interface for heterogeneous software engineering tools
[AD-A189628] 14 p1991 N88-21870
Design of an algorithm to translate nested relational algebra queries to GENESIS trace manager commands
[AD-A190502] 15 p2112 N88-22581
A graphics editor for structured analysis with a data dictionary
[AD-A190618] 15 p2112 N88-22584
Modeling a parallel architecture for image processing
[RR-646-I] 15 p2114 N88-22593
Application of new technologies to DTIC document processing
[AD-A189778] 15 p2148 N88-22823
Data base design and implementation
[AD-A190414] 15 p2149 N88-22827
Georelational data model
[INPE-4490-PRE/1254] 15 p2149 N88-22829
Axiomatic specificatin of database domain statics
[PB88-176284] 16 p2250 N88-23444

Data management and language enhancement for generalized set theory computer language for operation of large relational databases
[NASA-CR-182868] 16 p2250 N88-23446

PPDS compas-primer
[DE88-701589] 16 p2266 N88-23554

Reference nuclear data for space applications
[DE88-007041] 16 p2270 N88-23583

Data base management in CAD/CAM systems. Requirements for CAD/CAM data bases, actual market offer, advice for an efficient data base management, development tendencies
[MBB/LWD-11/S/PUB/254] 16 p2285 N88-23683

Automated database design technology and tools
[NASA-CR-182875] 16 p2286 N88-23687

Crewstation Information and Development System (CIDS) 17 p2304 N88-23781

EnviroNET: An interactive space-environment information resource
[NASA-TM-101137] 17 p2309 N88-23812

Reports on cartography and geodesy. Series 1, no. 99
[ETN-88-92387] 18 p2533 N88-25025

West German Geodetic Working Group: Official topographic-cartographic information system (ATKIS), content description 18 p2533 N88-25026

West German Geodetic Working Group: Official topographic-cartographic information system (ATKIS), technical conception 18 p2533 N88-25027

Creation of digital topographic models with the ALK-GIAP. The DLM 25 as an example
18 p2534 N88-25031

Topographic data processing for environmental planning 18 p2534 N88-25032

State of development of ALK (October 1986)
18 p2534 N88-25035

Geometric rectangular data file (GERD): An aid to the rapid access to position data 18 p2534 N88-25037

Photovoltaic Advanced Research and Development Project, solar radiation research
[DE88-001143] 18 p2537 N88-25056

The human genome: Computational challenges
[DE88-006465] 18 p2549 N88-25131

The ATF (Advanced Toroidal Facility) Data M Management System
[DE88-007265] 18 p2589 N88-25385

Computer-aided research
[DE88-007771] 19 p2714 N88-26114

Report on the Second Catalog Interoperability Workshop
[NASA-TM-100701] 19 p2718 N88-26135

MVS (Multiple Virtual Storage) batch computing and data management at ANL
[DE88-007342] 19 p2718 N88-26137

Real time data base management
[AD-A191758] 19 p2739 N88-26265

Issues and recommendations associated with distributed computation and data management systems for the space sciences
[NASA-CR-183026] 20 p2881 N88-27108

Computer science and technology: Knowledge-based system for physical database design
[PB88-193289] 20 p2882 N88-27109

Towards knowledge bases-semantics, rules and object-oriented programming
[PR86-108154] 20 p2882 N88-27110

Space shuttle phase B wind tunnel model and test information. Volume 2: Orbiter configuration
[NASA-CR-178415-VOL-2-PT-2]
21 p2893 N88-27172

Database design and management in engineering optimization
[AD-A193325] 21 p3003 N88-27813

Developing a connector selection DBMS (database management system) using NIAM (Nijssen's Information Analysis Methodology)
[DE88-008110] 21 p3028 N88-27972

Pattern information processing and multimedia database system: Current research on multimedia information system
[PB88-131917] 21 p3028 N88-27973

Sources and nature of cost analysis data base reference manual
[AD-A193099] 21 p3028 N88-27976

Space shuttle phase B wind tunnel model and test information. Volume 2: Orbiter configuration
[NASA-CR-178415-VOL-2-PT-1]
23 p3171 N88-28881

Regional environmental studies using national data bases and GIS (Geographic Information System)
[DE88-008368] 23 p3230 N88-29225

A relational data-knowledge base system and its potential in developing a distributed data-knowledge system 23 p3251 N88-29353

Analyst-centered models for systems design, analysis, and development 23 p3253 N88-29364

Avionic expert systems 23 p3253 N88-29365

Intelligent resource management for local area networks: Approach and evolution
23 p3256 N88-29385

The emergence of multi-user expert systems
23 p3260 N88-29406

Central user and browse service --- ERS-1 ground segment
[CU-PG-MDA-SY-0005] 23 p3297 N88-29637

Catalog of open clusters and associated interstellar matter
[NASA-RP-1202] 23 p3300 N88-29652

Space shuttle phase B wind tunnel model and test information. Volume 3: Launch configuration
[NASA-CR-178416-VOL-3-PT-2]
24 p3315 N88-29744

Space shuttle phase B wind tunnel model and test information. Volume 1: Booster configuration
[NASA-CR-178414-VOL-1-PT-1]
24 p3315 N88-29745

Space shuttle phase B wind tunnel model and test information. Volume 1: Booster configuration
[NASA-CR-178414-VOL-1-PT-2]
24 p3320 N88-29770

An operations manual for the digital data system
[NASA-CR-181638] 24 p3415 N88-30329

The second generation intelligent user interface for the crustal dynamics data information system
24 p3419 N88-30352

The P-3 Scheduling Support System (P-3 S3)
[AD-A194824] 24 p3436 N88-30450

Integrating images, applications, and communications networks, volume 5
[AD-A195854] 24 p3436 N88-30452

DATA BASES

Standard reference data publications, 1985-1986
[PB87-210241] 01 p0021 N88-10128

Digital Name Data Base Antarctic as a component of a landscape data base of the Antarctic
01 p0065 N88-10419

Nickel hydrogen low Earth orbit test program update and status 02 p0164 N88-11028

Using bibliographic databases in technology transfer
[NASA-CR-181403] 02 p0222 N88-11399

Design and development of a database for spectral data and analysis results
[DE87-011323] 02 p0247 N88-11564

Maintaining state constraints in relational databases: A proof theoretic basis
[DE87-014329] 02 p0248 N88-11569

Energy Data Base: Subject Thesaurus
[DE87-008007] 03 p0384 N88-12414

Advanced techniques for the storage and use of very large, heterogeneous spatial databases. The representation of geographic knowledge: Toward a universal framework --- relations (mathematics)
[NASA-CR-181517] 03 p0385 N88-12421

Statistical distribution of solar radiation (hourly sums): Cumulative frequency curves preparation of a European data set and direction for use
[PB87-107454] 04 p0467 N88-12886

Cloud cover determination in polar regions from satellite imagery
[NASA-CR-181544] 04 p0471 N88-12908

A tight upper bound for the speed-up of parallel best-first branch-and-bound algorithms
[AD-A184246] 04 p0477 N88-12939

Data base on the high heat flux behaviour of metals and carbon materials for plasma facing components: Experiments at the 10 MW neutral beam injection test stand of the IPP Nagoya
[IPPJ-AM-53] 04 p0492 N88-13031

The RAE experimental data-base for missiles at high Mach number and its use in assessing CFD methods
05 p0534 N88-13250

A rudimentary database for three-dimensional objects using structural representation
[CSE-87-00004] 05 p0590 N88-13597

Improvement of modal scaling factors using mass additive technique 05 p0593 N88-13620

Space shuttle main engine vibration data base
05 p0595 N88-13631

Role of technical information in innovation
[PB87-235388] 05 p0658 N88-14039

Boeing 727 MLS (Microwave Landing System) terminal instrument procedures (TERPS) approach data collection and processing, data report
[AD-A185523] 06 p0667 N88-14090

Octree data structures and creation by stacking
[PB87-234795] 06 p0758 N88-14650

Using user models and automatic expertise acquisition in data base interactions
[PB87-234357] 06 p0791 N88-14848

Geographic application of the relational data base system Cantor
[PB87-120945] 06 p0791 N88-14851

Communications for the DTroll distributed database system
[AD-A185579] 06 p0791 N88-14853

A review of hypertext in a NASA project management context 06 p0793 N88-14859

Overview of the Langley viscous drag reduction program 07 p0812 N88-14946

FAA air traffic control operations concepts. Volume 2: ACF/ACCC (Area Control Facility/Area Control Computer Complex) terminal and en route controllers
[AD-A185980] 07 p0818 N88-14974

FAA air traffic control operations concepts. Volume 3: ISSS (Initial Sector Suite System) en route controllers
[AD-A185981] 07 p0818 N88-14975

FAA air traffic control operations concepts. Volume 4: TAAS (Terminal Advanced Automation System) terminal controllers
[AD-A185982] 07 p0818 N88-14976

FAA air traffic control operations concepts. Volume 5: ATCT/TCCC (Airport Traffic Control Tower/Tower Control Computer Complex) tower controllers
[AD-A185983] 07 p0818 N88-14977

An approach to validation and verification of the communications load model with supporting user's guide
[AD-A185926] 07 p0840 N88-15098

Research study for materials/properties test results database
[NASA-CR-178923] 07 p0861 N88-15222

Determination of network attributes from a high resolution terrain data base
[AD-A186078] 07 p0870 N88-15279

Explicit construction and analysis of some efficient empirical production functions in data envelopment analysis
[AD-A185907] 07 p0908 N88-15502

Thermodynamic values from computer summation of group additivity data
[AD-A186131] 07 p0940 N88-15711

DoD Gateway Information System (DGIS): Common command language mapping
[AD-A185951] 07 p0942 N88-15726

Self-adaptive data bases
[AD-A186414] 07 p0942 N88-15729

Catalog of infrared observations. Part 1: Data
[NASA-RP-1196-PT-1-ED-2] 07 p0944 N88-15738

SSME environment database development
[NASA-CR-179245] 08 p0964 N88-15836

TECOM's research efforts in the dynamic environments 08 p0999 N88-16048

Methodology for testing and validating knowledge bases 08 p1055 N88-16364

HSTDEK: Developing a methodology for construction of large-scale, multi-use knowledge bases
08 p1057 N88-16377

Space shuttle main engine anomaly data and inductive knowledge based systems: Automated corporate expertise 08 p1060 N88-16398

Conceptual information processing: A robust approach to KBS-DBMS integration 08 p1063 N88-16422

Foundation: Transforming data bases into knowledge bases 08 p1063 N88-16423

A data structure and algorithm for fault diagnosis
08 p1065 N88-16432

The crustal dynamics intelligent user interface anthology
[NASA-TM-100693] 08 p1067 N88-16448

Rotorcraft handling-qualities design criteria development 09 p1109 N88-16645

Global digital data sets of soil type, soil texture, surface slope and other properties: Documentation of archived data tape
[NASA-TM-100685] 09 p1185 N88-17097

User's guide to a data base of current environmental monitoring projects in the US-Canadian transboundary region
[DE88-002476] 09 p1188 N88-17119

An efficient representation of spatial information for expert reasoning in robotic vehicles
09 p1214 N88-17278

Metal hydrides
[DE88-005083] 10 p1299 N88-17766

Extension of nuclear structure data base searches for gamma-ray laser candidates
[DE88-004288] 10 p1336 N88-17985

Data-base of Antarctic pre-Pleistocene sediment cores
[PB88-124151] 10 p1354 N88-18094

A paradigm for concurrency control performance evaluation 10 p1377 N88-18220

Concurrency control and reliability in replicated database systems 10 p1377 N88-18221

Utilization of the JANAF (Joint Army Navy Air Force) database for chemical thermodynamic calculations
[DE88-004571] 10 p1423 N88-18501

Space shuttle phase B wind tunnel test database
[NASA-CR-4121] 11 p1444 N88-18611

NBS/Sandia/ICDD electron diffraction database
[DE88-004635] 11 p1454 N88-18665
The metallurgical database of Aladin: An alloy design system
[AD-A187724] 11 p1457 N88-18682
Overview of multi-input frequency domain modal testing methods with an emphasis on sine testing
11 p1499 N88-18949
The design and implementation of pedagogical software for the multi-backend/multi-lingual database system
[AD-A188106] 11 p1530 N88-19135
TYPICAL: A knowledge representation system for automated discovery and inference
[AD-A187483] 11 p1533 N88-19160
The design of the POSTGRES storage system
[AD-A187244] 11 p1564 N88-19365
Allocation of database files across parallel stores for efficient processing of partial-match queries
[AD-A188196] 11 p1565 N88-19371
Mono- and bistatic radar coverage diagrams including diffractive wave propagation 12 p1616 N88-19660
Historical electromagnetic propagation condition database description
[AD-A189157] 12 p1621 N88-19695
Department of Defense World Geodetic System 1984: Its definition and relationships with local geodetic systems
[AD-A188815] 12 p1639 N88-19811
Terrain classification from digital elevation data using slope and curvature information
[AD-A188940] 12 p1639 N88-19812
Worldwide distributions of shipboard surface meteorological observations for EM propagation analysis
[AD-A188771] 12 p1648 N88-19871
Application of ARIADNE: A data bank-based information system for human physiology research --- Spacelab Anthrorack 12 p1662 N88-19962
An evaluation of historical algebras
[AD-A188350] 12 p1684 N88-20067
A directory of databases available through SearchMAESTRO
[AD-A188813] 12 p1706 N88-20214
Design methodology for allocating data in a distributed database
[AD-A188826] 12 p1706 N88-20215
Development of a dependency theory toolbox for database design
[AD-A188872] 12 p1707 N88-20216
Database of average-power damage thresholds at 1064 nm
[DE88-004352] 13 p1776 N88-20626
An analysis of physiological data related to motion sickness for use in a real-time motion sickness indicator
[AD-A189589] 13 p1810 N88-20812
Knowledge retrieval as specialized inference
[AD-A189042] 13 p1823 N88-20899
Towards a tribology information system: The results of a Planning Workshop held at the National Bureau of Standards, July-August 1985
[PB88-168604] 14 p1918 N88-21448
Perfect knowledge and beyond --- chess endgames
[REPT-87-37] 14 p1967 N88-21738
Common database interface for heterogeneous software engineering tools
[AD-A189628] 14 p1991 N88-21870
LGM-30B stage 2 disected motor test report
[AD-A190771] 15 p2027 N88-22079
An expert system for discrete component digital circuit design
[AD-A189680] 15 p2059 N88-22274
Analysis of head response to torso acceleration. Volume 2: Description of data retrieval, analysis and display software
[PB88-156765] 15 p2104 N88-22536
A UNIX-based interactive VHDL (hardware description language) simulator
[AD-A189749] 15 p2109 N88-22565
ONTIC: A knowledge representation system for mathematics
[AD-A190553] 15 p2121 N88-22643
Sources of digital spatial data for geographic information systems
[AD-A189788] 15 p2148 N88-22824
Space communication link propagation data for selected cities within the multiple beam and steerable antenna coverage areas of the advanced communications technology satellite
[NASA-TM-100861] 16 p2191 N88-23070
Axiomatic specificatin of database domain statics
[PB88-176264] 16 p2250 N88-23444
Editfont an interactive font editing system
[AD-A191007] 16 p2251 N88-23453
A description of an automated database comparison program
[NASA-TM-100609] 16 p2253 N88-23463
Leave-K-Out diagnostics for time series
[AD-A191343] 16 p2261 N88-23518
Overground Excess Sound Attenuation (ESA). Volume 1: Experimental study for flat grassy terrains
[AD-A191289] 16 p2265 N88-23549
Reference nuclear data for space applications
[DE88-007041] 16 p2270 N88-23583
Data base management in CAD/CAM systems. Requirements for CAD/CAM data bases, actual market offer, advice for an efficient data base management, development tendencies
[MBB/LWD-11/S/PUB/254] 16 p2285 N88-23683
A likelihood based grouping method for multidimensional observations. An interactive method used on large transportation data bases
[REPT-87-74] 16 p2286 N88-23685
BRYNTRN: A baryon transport computer code, computation procedures and data base
[NASA-TM-4037] 16 p2290 N88-23714
Operation and performance of an integrated helicopter communication system 17 p2305 N88-23787
The SAGE geographic analysis system
17 p2361 N88-24063
Implantation of a geo-cartographical information system through microcomputers 17 p2361 N88-24064
An irradiation performance data base for nitride fuels
17 p2427 N88-24438
Cessna 172 MLS (Microwave Landing System) terminal instrument procedures (TERPS) approach data collection and processing data report
[AD-A191241] 18 p2461 N88-24613
Evaluation of NMC (National Meteorological Center) global analyses: 1979-1987
[PB88-178157] 18 p2544 N88-25096
Identification and acoustic characterization of seamounts
[AD-A192204] 18 p2548 N88-25123
EPL (Equational Programing Language) system design: Intermediate processing steps
[AD-A191203] 18 p2556 N88-25169
Phase diagrams in materials science and the use of the computer in their calculation
[PB88-155262] 18 p2586 N88-25364
Defense Technical Information Center cataloging guidelines
[AD-A192200] 18 p2589 N88-25382
Design of partially replicated distributed database systems: An integrated methodology
18 p2589 N88-25383
ECMWF (European Centre for Medium Range Weather Forecasts) global analyses 1979-1986: Circulation statistics and data evaluation
[PB88-178165] 19 p2692 N88-26001
The CERSAT archiving and processing center --- ERS-1 19 p2701 N88-26059
Accurate, productive aerodynamic simulation on patched mesh systems
[AD-A192040] 19 p2714 N88-26110
Meteorological satellite product support and research for project GALE
[NASA-CR-180989] 19 p2727 N88-26193
Analysis and synthesis of decision-making organizations
[AD-A191948] 19 p2738 N88-26258
SIMS: Single Interface to Multiple Systems
[AD-A192264] 20 p2837 N88-26832
Nucleon-nucleus interaction data base: Total nuclear and absorption cross sections
[NASA-TM-4053] 20 p2852 N88-26935
Automatic line network extraction from aerial imagery of urban areas through knowledge based image analysis
[AD-A193067] 21 p2965 N88-27615
National air toxics information clearinghouse: NATICH data base users guide for data viewing, February 1988
[PB88-197470] 21 p2970 N88-27645
Space shuttle natural environment analysis
[NASA-CR-179337] 21 p2976 N88-27676
A PRELUDE (analysis and design of control systems preliminary utilities depository). A data-based interactive system of control software, user's guide
[DFVLR-MITT-88-12] 21 p3000 N88-27795
Basic database operations on the butterfly parallel processor: Experiment results
[AD-A193199] 21 p3002 N88-27804
Capitalizing on experience with intelligence gateway software
[AD-A193362] 21 p3028 N88-27971
SPOT: A data capture and data updating tool for the French National Geographic Institute's (IGN's) cartographic data base 22 p3114 N88-28497
On the modes of growing-season precipitation over central North America 22 p3124 N88-28567
The effects of changes in observation and data assimilation systems on CAC climate data sets
22 p3124 N88-28568
Evaluation of global data sets for climate studies
22 p3124 N88-28569
A method to adjust climatological time series for discontinuous inhomogeneities
22 p3124 N88-28570
Global-scale temperature changes to August 1987 and a comparison of satellite and conventional data
22 p3125 N88-28572
Optimization techniques for relational database systems 22 p3137 N88-28650
Computing partial correlations from the data matrix
[AD-A193904] 22 p3138 N88-28659
ALGRES: A system for the specification and prototyping of complex databases
[REPT-87-018] 22 p3140 N88-28668
A comparison of typical meteorological year solar radiation information with the SOLMET data base
[DE88-009242] 23 p3234 N88-29247
Level 1 Ada/SQL (Structured Query Language) database language interface user's guide
[AD-A194480] 23 p3249 N88-29335
A fast parametric maximum flow algorithm, revision
[AD-A194026] 23 p3250 N88-29345
A relational data-knowledge base system and its potential in developing a distributed data-knowledge system 23 p3251 N88-29353
Hologram representation of design data in an expert system knowledge base 23 p3251 N88-29354
An expert system for reliability modeling
23 p3252 N88-29355
A knowledge-based decision support system for payload scheduling 23 p3252 N88-29358
An approach to combining heuristic and qualitative reasoning in an expert system 23 p3253 N88-29362
Avionic expert systems 23 p3253 N88-29365
Knowledge elicitation for an operator assistant system in process control tasks 23 p3253 N88-29366
Failure modes and effects analysis automation
23 p3254 N88-29370
Knowledge based programming environments: A perspective 23 p3258 N88-29393
A methodology for multiple rule system integration and resolution within a singular knowledge base
23 p3261 N88-29413
A survey of the current experimental database for lower hybrid current-drive and heating
[DE88-009830] 23 p3283 N88-29552
Central user and browse service --- ERS-1 ground segment
[CU-PG-MDA-SY-0005] 23 p3297 N88-29637
More than a solar cycle of synoptic solar and coronal data: A video presentation
[NASA-CR-181459] 23 p3308 N88-29708
The advice taker/inquirer: A system for high-level acquisition of expert knowledge
24 p3421 N88-30359
Partitioned storage for temporal databases
[AD-A195093] 24 p3436 N88-30451
Technical opinions regarding knowledge-based integrated information systems engineering, volume 8
[AD-A195857] 24 p3436 N88-30454
Design and performance analysis of a relational replicated database system
[AD-A196290] 24 p3437 N88-30456

DATA BUSSES
U CHANNELS (DATA TRANSMISSION)

DATA COMPACTION
U DATA COMPRESSION

DATA COMPRESSION
Study, design, and evaluation of data reduction by encoding or information extraction. Part 1: Data generation analysis --- multispectral satellite imagery
[NLR-TR-85094-L-PT-1] 01 p0078 N88-10501
Study, design and evaluation of data reduction by encoding or information extraction. Part 2: Operational considerations --- multispectral satellite imagery
[NLR-TR-85094-L-PT-2] 01 p0079 N88-10502
Study, design and evaluation of data reduction by encoding or information extraction. Part 3: Algorithm design --- multispectral satellite imagery
[NLR-TR-85094-L-PT-3] 01 p0079 N88-10503
Study, design and evaluation of data reduction by encoding or information extraction. Part 4: Performance demonstration --- multispectral satellite imagery
[NLR-TR-85094-L-PT-4] 01 p0079 N88-10504
Study, design and evaluation of data reduction by encoding or information extraction. Part 5: Algorithm implementation aspects --- multispectral satellite imagery
[NLR-TR-85094-L-PT-5] 01 p0079 N88-10505
Study on data compression systems for operational remote sensing --- meteosat imagery
[NLR-TR-86029-L] 05 p0620 N88-13808
Study of synthetic aperture radar data compression and encoding. Part 3: Performance evaluation of speckle suppression and data compression algorithms
[NLR-TR-85065-L-PT-3] 06 p0692 N88-14248

Study of synthetic aperture radar data compression and encoding. Part 4: Algorithm implementation aspects
[NLR-TR-85085-L-PT-4] 06 p0692 N88-14249
Study of synthetic aperture radar data compression and encoding. Part 1: SAR image data analysis
[NLR-TR-85085-L-PT-1] 07 p0843 N88-15115
Study of synthetic aperture radar data compression and encoding. Part 2: SAR image speckle suppression and data compression algorithms
[NLR-TR-85085-L-PT-2] 07 p0843 N88-15116
Feasibility studies of optical processing of image bandwidth compression schemes
[AD-A186073] 07 p0932 N88-15660
A hybrid transform/DPCM encoder for data compression
[DE88-003725] 09 p1154 N88-16919
A hybrid transform/DPCM encoder for data compression
[DE87-014852] 13 p1758 N88-20518
A study of data compactation using numerical methods
[INPE-4317-TDL/284] 13 p1828 N88-20929
Performance of data compression codes in channels with errors
[AD-A189667] 15 p2055 N88-22253
Efficient and fast data compression codes for discrete sources with memory
[ETN-88-92233] 16 p2246 N88-23420
Narrative compression coding for a channel with errors
[AD-A191577] 19 p2642 N88-25673
Optical interconnections for digital image coding
21 p2928 N88-27381
Compression and decompression of imaging sensor signals (CADISS): A multiprocessor system for image compression/decompression on board scientific satellites
[NLR-TR-87076-L] 24 p3414 N88-30323

DATA CONVERSION ROUTINES
NT SUBROUTINES
Design and implementation of a data base system for Digital Land Mass System (DLMS) data
[FEL-IR-1987-19] 09 p1185 N88-17101

DATA CONVERTERS
NT ANALOG TO DIGITAL CONVERTERS
NT DIGITAL TO ANALOG CONVERTERS
Data on existing wind energy converters in Denmark
[DE88-900199] 07 p0874 N88-15300
Collecting of new data on existing wind energy converters
[DE88-900221] 07 p0875 N88-15305

DATA CORRELATION
High temperature low cycle fatigue behavior and creep-fatigue interation of MA 6000 ODS alloy
06 p0720 N88-14425
Method for joint adjustment of satellite and surface geodetic networks 08 p1007 N88-16105
Unidimensional Rasch model and multidimensional data: An analytic approach
[PB88-105861] 10 p1372 N88-18187
Loran-C monitor correlation over a 92-mile baseline in Ohio 17 p2293 N88-23720
Study of data distributions and functions for the development of thermodynamic equations of state
[PB88-196365] 18 p2587 N88-25370

DATA FLOW ANALYSIS
Advanced Information Processing System (AIPS) proof-of-concept system functional design I/O network system services
[NASA-CR-181488] 03 p0384 N88-12413
Massive fine-grain parallelism in array computation: A data flow solution 10 p1382 N88-18254
Automated data flow diagram verification
10 p1382 N88-18255
Data flow graph optimization in IF1
[DE88-004396] 11 p1532 N88-19151
Verification of a systolic algorithm for string comparison
[CWI-CS-R8734] 13 p1819 N88-20873
A fully abstract semantics for data flow nets
[CWI-CS-R8724] 13 p1822 N88-20893
An extension of the MS pivoting rule to capacitated network flow problems
[REPT-87-33] 14 p1963 N88-21711
Strategies for concurrent processing of complex algorithms in data driven architectures
[NASA-CR-181657] 16 p2193 N88-23083
Adapting high-level language programs for parallel processing using data flow 16 p2218 N88-23234
Mentat: An object-oriented macro data flow system
[NASA-TM-101165] 17 p2388 N88-24199
Statistical properties of real time events in an ATC (Air Traffic Control) system
[PB88-118781] 20 p2756 N88-26353
Finding minimum-cost circulations by canceling negative cycles
[AD-A192727] 21 p3005 N88-27825
Modularity in the PASCAL model compiler
[NPL-DITC-111/88] 22 p3139 N88-28664
Faster algorithms for the shortest path problem
[AD-A194031] 23 p3250 N88-29347
Improved time bounds for the maximum flow problem
[AD-A194034] 23 p3272 N88-29471

DATA HANDLING SYSTEMS
U DATA SYSTEMS

DATA INTEGRATION
Adaptive segmentation evaluation
[AD-A190965] 16 p2274 N88-23609
Remote sensing and data integration. Practical solutions for resource managers 17 p2356 N88-24034

DATA LINKS
Coherent infrared detection, volume B --- CO2 laser intersatellite data link
[ESA-CR(P)-2392-VOL-1] 01 p0034 N88-10218
Coherent infrared detection, volume D --- CO2 laser intersatellite data link
[ESA-CR(P)-2392-VOL-2] 01 p0034 N88-10219
Interoperability and integration of data relay satellite systems 03 p0339 N88-12134
The atmosphere of Mars and optical communications
04 p0434 N88-12692
Test and evaluation of the transputer in a multi-transputer system
[AD-A184969] 05 p0631 N88-13859
Land mobile satellite transmission measurements at 869 MHz. A comparison of error probabilities for various message block durations and fade margins as a function of vegetation shadowing
[NASA-CR-179929] 06 p0693 N88-14255
Media independent interface
[NASA-CR-172033] 08 p1066 N88-16446
Media independent interface. Interface control document
[NASA-CR-172032] 08 p1067 N88-16447
The European space physics analysis network
08 p1099 N88-16613
Horizontal estimation and information fusion in multitarget and multisensor environments
[AD-A186935] 09 p1224 N88-17336
Code division multiple access applied to fiber optic data transmission
[AD-A186873] 09 p1247 N88-17477
Information transfer in the National Airspace System
10 p1275 N88-17634
Design and implementation of a fiber optic RS232 link
[AD-A187319] 10 p1409 N88-18409
Cockpit data management
[NASA-CR-178407-SUPPL] 11 p1438 N88-18580
Development of VLSI optical data link
[AD-A187883] 11 p1549 N88-19265
Development of VLSI optical data link
[AD-A187884] 11 p1549 N88-19266
A pointing mechanism for intersatellite link system
14 p1874 N88-21194
Spatial distribution of traffic in a cellular mobile data network
[EUT-87-E-168] 14 p1904 N88-21378
Degradation of downlink distance measurement indexes by the addition of a third tone --- tone ranging
[CNES-CT/DRT/TIT/TR-122-T]
15 p2058 N88-22268
Connecting remote systems for demonstration of automation technologies 17 p2387 N88-24191
Development and validation of transmission measurements techniques of image contrast, utilizing existing IR imagers
[AD-A191471] 18 p2541 N88-25079
NASA's mobile satellite development program
19 p2643 N88-25682
Mobile satellite service for Canada
19 p2643 N88-25683
Development of the network architecture of the Canadian MSAT system 19 p2646 N88-25702
An operational open-end file transfer protocol for mobile satellite communications 19 p2651 N88-25738
Model for dynamically structured communicating systems
[PB88-105283] 21 p2931 N88-27402
Long haul underwater fiber optic link
[AD-A194487] 23 p3282 N88-29542
Optical multiple access intersatellite links
[BAE-TP-8502] 24 p3361 N88-30013
The LTPP communication processor --- Columbus and Hermes
[CL/CP/SES/FR/004] 24 p3415 N88-30328

DATA MANAGEMENT
Personal computers: A powerful tool for project management
[DE87-013381] 02 p0219 N88-11377
Confidentiality of data --- Columbus Polar Platforms
03 p0339 N88-12136
Performance evaluation of artificial intelligence systems
[AD-A184054] 03 p0368 N88-12316
Relational data handling system for scientists
[PB87-223426] 05 p0658 N88-14038
Report of the first session of the International Working Group on Data Management for the Global Precipitation Climatology project
[WCP-132] 06 p0745 N88-14582
Data processing of the JPA instrument. Part 1: Data management
[IFSI-86-15-PT-1] 06 p0757 N88-14645
Self-adaptive data bases
[AD-A186414] 07 p0942 N88-15729
Knowledge-based monitoring of the pointing control system on the Hubble space telescope
08 p1057 N88-16378
A multiprocessing architecture for real-time monitoring
08 p1059 N88-16390
Commonality analysis as a knowledge acquisition problem 08 p1062 N88-16413
Media independent interface
[NASA-CR-172033] 08 p1066 N88-16446
The crustal dynamics intelligent user interface anthology
[NASA-TM-100693] 08 p1067 N88-16448
Telemetry applications handbook
[AD-A186825] 09 p1132 N88-16789
MPAD MCC workstation system: ADDAM and EEVE
09 p1203 N88-17209
Beyond rules: The next generation of expert systems
09 p1210 N88-17256
Nested transactions, conflict-based locking, and dynamic atomicity
[AD-A187033] 09 p1217 N88-17294
Using SIR (Scientific Information Retrival) system for data management during a field program
[DE88-001555] 10 p1424 N88-18508
Rocketdyne automated dynamics data analysis and management system 11 p1499 N88-18954
National Severe Storms Laboratory, fiscal year 1987
[PB88-140106] 12 p1647 N88-19863
JEDA (Joint Environmental Data Analysis) Center report on tropical Pacific subsurface thermal data management, 1986
[PB88-140090] 12 p1649 N88-19875
Editing master oceanographic observation data set 4
[AD-A188405] 12 p1649 N88-19876
National Informatics Centre: Profile of services
[PB88-134135] 12 p1706 N88-20211
GADL: A gate array description language
[EUT-87-E-165] 14 p1907 N88-21396
Higher levels of a silicon compiler
[EUT-86-E-163] 14 p1955 N88-21650
Generating layouts for random logic: Cell generation schemes
[EUT-86-E-164] 14 p1956 N88-21658
Technology mapping from Boolean expressions to standard cells
[EUT-87-E-174] 14 p1963 N88-21709
An optimal CMOS structure for the design of a cell library
[EUT-87-E-166] 14 p1985 N88-21841
Sigma system: Overview, prospects
15 p2052 N88-22230
Synthetic-aperture radars viewed as interferometers with matched filter processing of the collected data
[AD-A190608] 15 p2057 N88-22262
Proposals for the pre-operational use of data from the European Remote Sensing Satellite ERS-1
[BCRS-86-02] 16 p2227 N88-23300
WMO Region 2/Region 5 Training Seminar on Climate Data Management and User Services
[WCP-133] 16 p2234 N88-23344
A timestamp ordering mechanism with dynamic selection of rollback objects 16 p2257 N88-23489
Adaptive segmentation evaluation
[AD-A190965] 16 p2274 N88-23609
Data management strategies in the industrial environment
[NLR-MP-87002-U] 16 p2286 N88-23684
Test philosophy of the EH101 integrated avionic
17 p2303 N88-23775
Implantation of a geo-cartographical information system through microcomputers 17 p2361 N88-24064
Image management research
17 p2380 N88-24150
The ATF (Advanced Toroidal Facility) Data M Management System
[DE88-007265] 18 p2589 N88-25365
The CERSAT archiving and processing center --- ERS-1 19 p2701 N88-26059
Real time data base management
[AD-A191758] 19 p2739 N88-26265

The role of working memory in language comprehension
[AD-A192721] 20 p2833 N88-26805
A PRELUDE (analysis and design of control systems-preliminary utilities depository). A data-based interactive system of control software, user's guide
[DFVLR-MITT-88-12] 21 p3000 N88-27795
The Sundstrand B747-400 data management unit
22 p3035 N88-28021
Investigation of the use of High Order Languages (HOLs) for on-board software
[CRI/FR/HOL-C/1/87] 23 p3251 N88-29349
Automated cataloging and characterization of space-derived data 24 p3420 N88-30354
A design for a ground-based data management system 24 p3420 N88-30355
Knowledge-Based Integrated Information Systems Development Methodologies Plan. Knowledge-Based Integrated Information Systems Engineering (KBIISE) report, volume 2
[AD-A195851] 24 p3436 N88-30455

DATA PROCESSING
NT ASSOCIATIVE PROCESSING (COMPUTERS)
NT BATCH PROCESSING
NT CENSORED DATA (MATHEMATICS)
NT CEPSTRAL ANALYSIS
NT CONCURRENT PROCESSING
NT DATA CORRELATION
NT DATA REDUCTION
NT DATA RETRIEVAL
NT DATA SMOOTHING
NT DATA STORAGE
NT DATA TRANSFER (COMPUTERS)
NT DISTRIBUTED PROCESSING
NT MULTIPROCESSING (COMPUTERS)
NT ONBOARD DATA PROCESSING
NT OPTICAL DATA PROCESSING
NT PARALLEL PROCESSING (COMPUTERS)
NT PIPELINING (COMPUTERS)
NT SCENE ANALYSIS
NT SIGNAL ANALYSIS
NT SIGNAL PROCESSING
NT VOICE DATA PROCESSING
TIROS-N/NOAA A-J space environment monitor subsystem
[PB87-203998] 01 p0015 N88-10083
Manual for GetData version 3.1: A FORTRAN utility program for time history data
[NASA-TM-88288] 01 p0081 N88-10520
EAGLES: An interactive environment for scientific computing
[DE87-013564] 01 p0084 N88-10541
Horizontal shape matching applied to VAS data --- Visible and Infrared Spin Scan Radiometer Atmospheric Sounder (VAS) 02 p0201 N88-11254
A mini system for nowcasting
02 p0204 N88-11278
The Pacific Weather Center Satellite Facility: An overview 02 p0205 N88-11286
Comments on the challenge of using mesoscale data in mesoscale numerical models
02 p0214 N88-11348
Personal computers: A powerful tool for project management
[DE87-013381] 02 p0219 N88-11377
Knowledge acquisition issues encountered during the development of an estimating expert system
[DE87-013320] 02 p0248 N88-11568
An algorithmic approach to crustal deformation analysis
[NASA-CR-181497] 03 p0349 N88-12203
Antithesis: A study in clause combining and discourse structure
[AD-A184789] 03 p0368 N88-12313
Experimental and theoretical study of condensation in multicomponent mixtures
[DE88-000897] 04 p0413 N88-12563
Interferometry theory for the block 2 processor
[NASA-CR-181551] 04 p0440 N88-12730
Complex for ocean study from space and hydroacoustic stations 04 p0458 N88-12836
A data analysis environment for HP (Hewlett-Packard) 1000 computers
[DE87-010511] 04 p0477 N88-12936
On computing environments in data analysis
[DE88-000078] 04 p0480 N88-12961
A computer code to process and plot laser altimetry data interactively on a microcomputer
[NASA-TM-100687] 05 p0554 N88-13371
The analysis of nonstationary vibration data
05 p0592 N88-13610
A new method to real-normalize measured complex modes 05 p0593 N88-13618
TOMS: The Antarctic ozone hole and ozone trends
05 p0615 N88-13775
Application of TOMS data to weather analysis models
05 p0617 N88-13787
TOMS ozone data compared at mesoscale resolution to tropopause heights from the AVE radiosonde network and to VAS radiances over the south-central United States 05 p0617 N88-13790
Development of a data analysis system for the detection of lower level atmospheric turbulence with an acoustic sounder
[AD-A184972] 05 p0624 N88-13821
Hanford Meteorological Station computer codes. Volume 5: The TOWER computer code
[DE88-001610] 05 p0628 N88-13843
File usage analysis and resource usage prediction: A measurement-based study
[NASA-CR-181553] 05 p0633 N88-13867
Predictability of process resource usage: A measurement-based study of UNIX
[NASA-CR-181562] 05 p0633 N88-13869
Performability modeling based on real data: A casestudy
[NASA-CR-181563] 05 p0633 N88-13870
Conceptual issues in measuring the behavior of a distributed real-time process-control computer system
[DE87-014251] 05 p0638 N88-13899
Status, outlook of optical technology in information equipment field 06 p0689 N88-14222
EISCAT research in Finland in 1986
06 p0691 N88-14234
Data analysis at the Oulu (Finland) EISCAT laboratory
06 p0691 N88-14241
Computer simulation of the L/sub 3/-edge densitometer
[DE88-001944] 06 p0705 N88-14324
AVIRIS onboard data handling and control
06 p0706 N88-14332
AVIRIS ground data-processing system
06 p0707 N88-14333
Regional weather satellite data processing center opens in Tashkent 06 p0725 N88-14457
Effective methods of gravimetric and magnetometric data processing 06 p0728 N88-14479
Geographic application of the relational data base system Cantor
[PB87-120945] 06 p0791 N88-14851
Digital processing of flight test data without using anti-aliasing filters, using a helicopter as an example
[DFVLR-MITT-87-12] 07 p0819 N88-14981
Data acquisition, reduction and analysis of shock and vibration testing using a super microcomputer
[AD-A186123] 07 p0867 N88-15260
SEQUAL (seasonal Equatorial Atlantic) meteorological data from Moorings S2, S5 and S6 (March 1983 - March 1985)
[PB88-108048] 07 p0880 N88-15337
Moored current meter data from the Canary Basin near 32 deg N, 24 W (84-1986), volume 40
[PB88-108105] 07 p0882 N88-15351
Quantifying some information processing aspects of the pilot's instrument crosscheck
[AD-A186114] 07 p0898 N88-15443
Multichannel scaling analyzer
[DE88-700541] 07 p0905 N88-15481
Algorithm and program for recognition of compactly positioned vertices of events for the HPD minimum guidance system
[DE88-700542] 07 p0905 N88-15482
Problems of organization of mass processes of simulation, acquisition and processing of experimental data at computers
[DE88-700547] 07 p0905 N88-15483
Strategies of data analysis
[AD-A186033] 07 p0914 N88-15548
NASA (National Aeronautics and Space Administration) ADP (Automated Data Processing) system: Information on the automated mission and the payload tracking system
[PB88-104989] 07 p0942 N88-15730
High Resolution Picture Transmission (HRPT) data processing from NOAA series satellites
[INPE-4372-PRE/1195] 08 p0963 N88-15831
SSME environment database development
[NASA-CR-179245] 08 p0964 N88-15836
Summary record of presentations to the Federal Telecommunication Standards Committee/Fiber optics task group
[PB88-110853] 08 p0978 N88-15911
Laboratory vibration test schedules development beyond MIL-STD-810D 08 p0999 N88-16050
Method for joint adjustment of satellite and surface geodetic networks 08 p1007 N88-16105
Processes in the quiet and disturbed equatorial-low latitude ionosphere: Sundial campaign, 1984
[INPE-4152-PRE/1057] 08 p1036 N88-16282
A knowledge-based system for monitoring the electrical power system of the Hubble Space Telescope
08 p1058 N88-16380
Spacelab Data Processing Facility (SLDPF) quality assurance expert systems development
08 p1059 N88-16394
Media independent interface
[NASA-CR-172033] 08 p1066 N88-16446
New directions for multivariate statistical computation and data analysis
[AD-A186523] 08 p1074 N88-16480
TOPP: A post-processor for TOPAZ, the one dimensional pipe flow analysis code
[DE88-003711] 09 p1164 N88-16981
Application of satellite data in variational analysis for global cyclonic systems
[NASA-CR-182468] 09 p1193 N88-17152
Comparison of alphanumeric data entry methods for advanced helicopter cockpits
[AD-A186934] 09 p1201 N88-17201
The effectiveness of caches and data prefetch buffers in large-scale shared memory multiprocessors
[DE88-003594] 09 p1223 N88-17334
Code division multiple access applied to fiber optic data transmission
[AD-A186873] 09 p1247 N88-17477
Data reduction and analysis of HELIOS plasma wave data
[NASA-CR-182466] 09 p1264 N88-17572
Wide band data transmission system using optical fibers
[DE88-004555] 10 p1319 N88-17889
Minimum Energy Routing through Interactive Techniques (MERIT) modeling
[NASA-CR-182535] 10 p1356 N88-18105
A VLSI implementable block oriented data driven multiprocessor 10 p1381 N88-18249
Data prefetching in shared memory multiprocessors
[DE88-003576] 10 p1394 N88-18314
Fixed and adaptive interframe image prediction for remote piloting application
[AD-A187987] 11 p1471 N88-18771
Effect of experimental variables on flash thermal diffusivity data analysis
[DE88-003631] 11 p1487 N88-18877
Rocketdyne automated dynamics data analysis and management system 11 p1499 N88-18954
Multisource context classification methods in remote sensing 11 p1504 N88-18985
Interfacing of a microcomputer with a simultaneous atomic-emission spectrometer
[PB88-139571] 11 p1526 N88-19109
Spaceborne gravity gradiometry characterizing the data type 12 p1644 N88-19847
Quality control of upper air conventional data (TEMP and PILOT)
[INPE-4223-RPE/546] 12 p1647 N88-19862
Design of the primary pre-TRMM and TRMM ground truth site
[NASA-CR-182609] 12 p1647 N88-19865
Some questions of using coding theory and analytical calculation methods on computers
[DE88-700905] 12 p1676 N88-20021
Procedure for initial data input and checkup in the system for film data mathematical processing
[DE88-700926] 12 p1676 N88-20022
Experimental analysis of algorithms
[AD-A188528] 12 p1677 N88-20028
Experience with Berkeley UNIX interprocess communications
[AD-A188353] 12 p1680 N88-20041
The use of least squares in undetermined problems
[DE88-004473] 12 p1682 N88-20059
Pion absorption in nuclei: The pion(+ or -),proton reactions
[LA-10997-T] 12 p1688 N88-20098
Investigation of low energy space plasma
[NASA-CR-182611] 12 p1694 N88-20138
RIAR automated research and management systems
[DE88-700934] 12 p1706 N88-2020
The Joint NASA/Goddard-University of Maryland Research Program in Charged Particle and High Energy Photon Detector Technology
[NASA-CR-182612] 12 p1712 N88-20247
A comparison of two chord keyboard coding systems for alphanumeric data entry
[AD-A189230] 13 p1813 N88-20834
Distributed transaction processing and the Camelot system
[AD-A188614] 13 p1821 N88-20885
Optimal and conventional space-time processing in flow noise
[AD-A189104] 13 p1833 N88-20965
Aspects and applications of primary processing of visual information
[INPE-4290-PRE/1161] 13 p1841 N88-21015
The German processing and archiving facility for ERS-1
[ESA-CR(P)-2531] 13 p1851 N88-21082

Data processing method for high angle of attack testing with rolling angle 14 p1864 N88-21134

Lasers: Invention to application
[PB88-161583] 14 p1914 N88-21436

From satellite altimetry to ocean topography, a survey of data processing techniques
[ETN-88-91841] 14 p1939 N88-21575

DASM: A tool for Decomposition and Analysis of Sequential Machines
[EUT-87-E-170] 14 p1956 N88-21660

Data analysis of an observation of the quasar 3C 273 in the high-energy X-ray range, and the significance for astrophysical models
[ETN-88-91493] 14 p1993 N88-21878

Real-time flight test data distribution and display
[NASA-TM-100424] 15 p2022 N88-22050

Baseline observing system experiments using the AFGL global data assimilation system
[AD-A188861] 15 p2024 N88-22062

Basic research on flame radiation
[PB88-168372] 15 p2032 N88-22105

Fast analog-to-digital converter
[DE88-701488] 15 p2106 N88-22543

Digital processing of flight data of a helicopter without using anti-aliasing filters
[ESA-TT-1094] 16 p2161 N88-22890

Multiple address facility for packet radio: An investigation of performance/complexity trade off
[AD-A191043] 16 p2190 N88-23064

Computer-assisted symbolization by raster data processing --- mapping 16 p2225 N88-23284

Near-real-time TOMS, telecommunications and meteorological support for the 1987 Airborne Antarctic Ozone Experiment
[NASA-CR-4133] 16 p2233 N88-23338

Axiomatic specificatin of database domain statics
[PB88-176284] 16 p2250 N88-23444

Parallelism in a Prolog knowledge base machine
[ETN-88-92187] 16 p2255 N88-23477

New generation knowledge processing, volume 3'
[AD-A190167] 16 p2285 N88-23682

VISSR line number monitoring system
17 p2351 N88-24008

Some problems with regard to the TOVS processing detected by using NOAA-HRPT data check program
17 p2351 N88-24009

Latin American Symposium on Remote Sensing. 4th Brazilian Remote Sensing Symposium and 6th SELPER Plenary Meeting, volume 1 17 p2352 N88-24013

Presentation of the METEOSAT system and the roles of EUMETSAT within the meteorological community
17 p2357 N88-24039

Identification of areas cultivated with soybeans in the cerrados regions, through digital processingof satellite images: A methodological approach
17 p2358 N88-24048

Digital processing of infrared and visible images from the GOES satellite and its integration with meteorological radar data 17 p2360 N88-24057

Thematic mapping utilizing data from the Thematic Mapper sensor of the LANDSAT satellite
17 p2361 N88-24060

Parallel binary and parallel coded decimal time code formats
[AD-A190126] 17 p2384 N88-24170

Unified interchange format for computer data (standard file format)
[ESA-STR-225] 17 p2386 N88-24183

Western Pacific Omega validation: Project description
[AD-A191753] 18 p2462 N88-24617

Automated test device for FASR (Fixed Array Surveillance Radar) beam steering componentry
[AD-A191650] 18 p2500 N88-24829

Information and stochastic systems
[AD-A192167] 18 p2501 N88-24838

Optical computer and optical methods for data processing 18 p2518 N88-24939

Vectorization of raster algorithms for elevation data processing 18 p2534 N88-25036

Development and validation of transmission measurements techniques of image contrast, utilizing existing IR imagers
[AD-A191471] 18 p2541 N88-25079

Evaluation of NMC (National Meteorological Center) global analyses: 1979-1987
[PB88-178157] 18 p2544 N88-25096

Visual information processing in the perception of features and objects
[AD-A192026] 18 p2552 N88-25148

LispSEI: The programmer's manual
[AD-A191632] 18 p2556 N88-25172

IGUANA: Interactive graphics utility for automated NEC analysis
[AD-A191760] 18 p2556 N88-25174

PAFEC level 6.2 application program
[AD-A191037] 18 p2562 N88-25209

Phase diagrams in materials science and the use of the computer in their calculation
[PB88-155262] 18 p2586 N88-25364

Defense Technical Information Center cataloging guidelines
[AD-A192200] 18 p2589 N88-25382

The ATF (Advanced Toroidal Facility) Data M Management System
[DE88-007265] 18 p2589 N88-25385

SAMS: The synchronization and monitoring system for ATF (Advanced Toroidal Facility) data acquisition provides unified data access for ATF data acquisition
[DE88-007268] 18 p2589 N88-25386

Diagnostic studies of the HxOy-NzOy-O3 photochemical system using data from NASA GTE field expeditions
[NASA-CR-183038] 19 p2689 N88-25984

ECMWF (European Centre for Medium Range Weather Forecasts) global analyses 1979-1986: Circulation statistics and data evaluation
[PB88-178165] 19 p2692 N88-26001

The CERSAT archiving and processing center --- ERS-1 19 p2701 N88-26059

Idea processing for creativity and management
[DE88-006110] 19 p2714 N88-26113

An intelligent processing environment for real-time simulation
[NASA-CR-183056] 19 p2715 N88-26119

Checkout system software for INPE satellites
[INPE-4554-PRE/1297] 19 p2715 N88-26120

Meteorological satellite product support and research for project GALE
[NASA-CR-180989] 19 p2727 N88-26193

Treatment of systematic errors in the processing of wide angle sonar sensor data for robotic navigation
[DE88-008961] 20 p2756 N88-26352

Statistical properties of real time events in an ATC (Air Traffic Control) system
[PB88-118781] 20 p2756 N88-26353

Laser ranging data analysis
[NASA-CR-183115] 20 p2792 N88-26567

Automated system for mathematical processing of the data from a hybrid spectrometer
[DE87-702995] 20 p2836 N88-26820

Narrative domain implementation
[AD-A192265] 20 p2843 N88-26868

Knowledge-based cost estimating vs traditional software cost models
[DE88-009707] 20 p2883 N88-27116

Supercomputer for parallel data analysis
[DE88-702148] 21 p2995 N88-27759

A programmable systolic array for factorial analysis. Part 2: The symmetric eigenvalue problem
[AD-A192396] 21 p2995 N88-27762

Issues in computer-assisted interpretation of graphs and quantitative information
[PB88-116280] 21 p2998 N88-27783

Basic database operations on the butterfly parallel processor: Experiment results
[AD-A193199] 21 p3002 N88-27804

Analysis of lower hybrid current drive and rampup experiments on the JT-60 tokamak
[DE88-753136] 21 p3018 N88-27915

Pattern information processing and multimedia database system: Current research on multimedia information system
[PB88-131917] 21 p3028 N88-27973

Non-Gaussian models for surface clutter
22 p3068 N88-28212

Atlantic SST variability and high latitude climate fluctuations 22 p3122 N88-28551

The effects of changes in observation and data assimilation systems on CAC climate data sets
22 p3124 N88-28568

Evaluation of global data sets for climate studies
22 p3124 N88-28569

Software modifications to total data reporting accessory for metabolic measurement cart
[AD-A193641] 22 p3132 N88-28623

Research on wide area workstations
[AD-A192529] 22 p3136 N88-28643

Proof-of-principle high speed electronic imaging system, phase 2
[AD-A193798] 23 p3181 N88-28937

Hierarchical organization for large, dynamic radio networks
[AD-A193942] 23 p3204 N88-29067

Distortions in processed signals and their application in electronic design. Part 3: An automated generator of communication jamming signals
[DE88-702733] 23 p3205 N88-29072

Waveform analysis on the IBM PC
[AD-A194249] 23 p3248 N88-29330

ADP (Automated Data Processing) requirements definition and documentation through user-developed prototypes
[AD-A194407] 23 p3248 N88-29332

Expert system technology as a data processing tool
23 p3263 N88-29427

Advanced information processing system: Input/output network management software
[NASA-CR-181678] 23 p3264 N88-29431

On the design and optimization of distributed signal detection and parameter estimation systems
[AD-A193934] 23 p3266 N88-29446

Automatic prober for the dc characterisation of gallium arsenide devices. Part 2: The data sorting and display facility
[AD-A195408] 24 p3377 N88-30111

Method for combined image interpolation-restoration through a fir filter design technique
[INPE-4561-PRE/1302] 24 p3413 N88-30315

Spacelab data processing facility (SLDPF) Quality Assurance (QA)/Data Accounting (DA) expert systems: Transition from prototypes to operational systems
24 p3420 N88-30353

Automated cataloging and characterization of space-derived data 24 p3420 N88-30354

DATA PROCESSING EQUIPMENT
NT AIRBORNE/SPACEBORNE COMPUTERS
NT ANALOG COMPUTERS
NT CDC CYBER 205 COMPUTER
NT COMPUTERS
NT CRAY COMPUTERS
NT DATA PROCESSING TERMINALS
NT DIGITAL COMPUTERS
NT EMBEDDED COMPUTER SYSTEMS
NT HEWLETT-PACKARD COMPUTERS
NT HYBRID COMPUTERS
NT HYPERCUBE MULTIPROCESSORS
NT IBM COMPUTERS
NT MICROCOMPUTERS
NT MICROPROCESSORS
NT MIMD (COMPUTERS)
NT MINICOMPUTERS
NT OPTICAL COMPUTERS
NT PARALLEL COMPUTERS
NT PERIPHERAL EQUIPMENT (COMPUTERS)
NT PERSONAL COMPUTERS
NT PRINTERS (DATA PROCESSING)
NT REMOTE CONSOLES
NT SEQUENTIAL COMPUTERS
NT SIMD (COMPUTERS)
NT SUPERCOMPUTERS
NT VAX COMPUTERS

Concepts and techniques for support of real time distributed operating systems
[AD-A184491] 03 p0367 N88-12307

A comparison of two chord keyboard coding systems for alphanumeric data entry
[AD-A189230] 13 p1813 N88-20834

A methodolgy, based on analytical modeling, for the design of parallel and distributed architectures for relational database query processors
[AD-A189844] 15 p2149 N88-22825

Measurement data processing system based on personal computer: For scramjet combustion test
[DE88-751807] 16 p2174 N88-22959

Real time pipelined system for forming the sum of products in the processing of video data
[NASA-CASE-NPO-16462-1-CU]
17 p2384 N88-24169

DATA PROCESSING TERMINALS

Health hazards of video display terminals: A comprehensive, annotated bibliography on a critical issue of workplace health and safety with sources for obtaining items and list of terminal suppliers
[RSI-IAS-4] 03 p0355 N88-12240

Performance and preference with various VDT (Video Display Terminal) phosphors
[AD-A184085] 04 p0475 N88-12925

Presentation of map information on a color display
[FOA-C-20687-2.7] 17 p2368 N88-24103

Adaptive data acquisition multiplexing system and method
[NASA-CASE-MSC-21170-1] 18 p2471 N88-24662

Frequency addressable beams for land mobile communications 19 p2652 N88-25744

DATA PROCESSORS
U DATA PROCESSING EQUIPMENT

DATA READOUT SYSTEMS
U DATA SYSTEMS
U DISPLAY DEVICES

DATA RECORDERS

Maintenance support for military aircraft by intelligent on-board maintenance data panel
22 p3034 N88-28012

The intelligent QAR and its cost effective role in new generation AIMS --- quick access recorder (QAR); aircraft integrated monitoring systems (AIMS)
22 p3035 N88-28020

Development of a maintenance data bus monitor and recorder 22 p3036 N88-29022

DATA RECORDING

Detective quantum efficiency and design of a parallel data recording system for EXELFS-measurements --- electron microscopy
[USIP-87-06] 01 p0050 N88-10318

The management of software in airborne recording systems 22 p3035 N88-28019

DATA REDUCTION

NT DATA SMOOTHING

Study, design, and evaluation of data reduction by encoding or information extraction. Part 1: Data generation analysis --- multispectral satellite imagery
[NLR-TR-85094-L-PT-1] 01 p0078 N88-10501

Study, design and evaluation of data reduction by encoding or information extraction. Part 2: Operational considerations --- multispectral satellite imagery
[NLR-TR-85094-L-PT-2] 01 p0079 N88-10502

Study, design and evaluation of data reduction by encoding or information extraction. Part 3: Algorithm design --- multispectral satellite imagery
[NLR-TR-85094-L-PT-3] 01 p0079 N88-10503

Study, design and evaluation of data reduction by encoding or information extraction. Part 4: Performance demonstration --- multispectral satellite imagery
[NLR-TR-85094-L-PT-4] 01 p0079 N88-10504

Study, design and evaluation of data reduction by encoding or information extraction. Part 5: Algorithm implementation aspects --- multispectral satellite imagery
[NLR-TR-85094-L-PT-5] 01 p0079 N88-10505

Short reference year
[PB87-107470] 03 p0352 N88-12221

The Macintosh computer as a tool for rapid data analysis and for producing camera ready viewgraphs/publications
[DE87-014350] 03 p0362 N88-12280

A digital low pass filter for the reduction of large quantities of data
[ESA-TT-1058] 03 p0363 N88-12281

Analysis of photopole data reduction models
05 p0593 N88-13616

The Portable Instant Display and Analysis Spectrometer (PIDAS) 05 p0611 N88-13756

AIS-2 radiometry and a comparison of methods for the recovery of ground reflectance
05 p0611 N88-13757

Software design for an airborne gravity measurement system
[AD-A185000] 05 p0634 N88-13878

Data analysis at the Oulu (Finland) EISCAT laboratory
06 p0691 N88-14241

The archiving of meteor research information
06 p0732 N88-14505

A computer decision-making process for the elimination of noise from data
[AD-A185746] 06 p0759 N88-14659

Data acquisition and analysis system for the Sandia 34-meter Vertical Axis Wind Turbine
[DE88-002417] 09 p1187 N88-17112

Data reduction and analysis of HELIOS plasma wave data
[NASA-CR-182466] 09 p1264 N88-17572

Multi-processor reduction machines
10 p1382 N88-18253

An improved data reduction procedure for accelerometer centrifuge data 12 p1577 N88-19436

A view of unconstrained optimization
[AD-A188327] 12 p1684 N88-20066

Data traffic reduction schemes for sparse Cholesky factorizations
[NASA-CR-181626] 13 p1813 N88-20831

Data analysis of an observation of the quasar 3C 273 in the high-energy X-ray range, and the significance for astrophysical models
[ETN-88-91493] 14 p1993 N88-21878

A multivariate variational objective analysis-assimilation method. Part 2: Case study results with and without satellite data
[NASA-CR-182653] 15 p2097 N88-22492

Data volume reduction for imaging radar polarimetry
[NASA-CASE-NPO-17184-1-CU]
20 p2788 N88-26541

Comparison of experimental rotor damping data-reduction techniques 21 p2891 N88-27159

Calibration and data reduction techniques for the AFGL infrared array spectrometer 21 p2927 N88-27374

Development of a hot-wire measurement technique for moderate intensity three-dimensional flows
22 p3080 N88-28289

Autonomous image data reduction by analysis and interpretation 24 p3418 N88-30347

DATA RETRIEVAL

The microcomputer as an engineering management tool
[DE87-014882] 02 p0219 N88-11378

Using bibliographic databases in technology transfer
[NASA-CR-181403] 02 p0222 N88-11399

Description of data handling system installed December 11, 1986 --- EISCAT 06 p0692 N88-14242

SSME environment database development
[NASA-CR-179245] 08 p0964 N88-15836

Retrieval of three-dimensional wind and temperature fields from single-Doppler radar data
12 p1646 N88-19858

Basic research on flame radiation
[PB88-168372] 15 p2032 N88-22105

Analysis of head response to torso acceleration. Volume 2: Description of data retrieval, analysis and display software
[PB88-156765] 15 p2104 N88-22536

Retrieval of temperature and concentration profiles from a limited number of absorption measurements
21 p2947 N88-27501

DATA SAMPLING

Using a parallel computer system for statistical resampling methods
[REPT-87-47] 14 p1960 N88-21690

Digital processing of flight data of a helicopter without using anti-aliasing filters
[ESA-TT-1094] 16 p2161 N88-22890

Servo-actuator control for sampled-data feedback disturbance rejection --- helicopters
[ESA-TT-1002] 16 p2163 N88-22903

Application of sampling techniques to near-field far-field transformation
[ESA-CR(P)-2546] 24 p3359 N88-30002

DATA SIMULATION

Use of simulated satellite radiances from a mesoscale numerical model to understand kinematic and dynamic processes 02 p0202 N88-11261

Simulation of mesoscale satellite sounder data from a mesoscale numerical model 02 p0214 N88-11345

Windfield simulations from a hierarchy of nested meso- and micrometeorological models
02 p0215 N88-11351

High resolution satellite imagery simulation --- treaty verification
[FOA-C-30462-3.3.9.3] 05 p0620 N88-13810

Inversion of simulated satellite signals
08 p1017 N88-16168

Improved resolution atmospheric density measurements based on simulations 08 p1027 N88-16221

Simulation of measuring points for three dimensional measurements
[WPB-0115] 13 p1821 N88-20883

Simulation: A simulation system in Ada
[FOA-A-20043-2.7] 17 p2385 N88-24176

DATA SMOOTHING

Algorithms and hardware for efficient image smoothing
[TR-149] 03 p0365 N88-12296

Improvements in profiler wind estimates using smoothed data in the spectrum finder algorithm
[PB88-102181] 07 p0881 N88-15342

Multigrid methods in convex optimization
11 p1538 N88-19190

Stabilization of explicit difference schemes by smoothing techniques
[CWI-NM-R8714] 13 p1827 N88-20923

Weighted averaging method for image smoothing reported 14 p1901 N88-21352

Smoothing technique to resolve X-ray spectra in laser nuclear fusion 15 p2053 N88-22235

Residual smoothing for accelerating the Alternating Direction Implicit (ADI) iteration method for elliptic difference equations
[CWI-NM-R8721] 16 p2259 N88-23500

A fast and efficient procedure for generalized cross-validation with large data sets. Application to image reconstruction
[RR-669-M] 18 p2563 N88-25220

DATA STORAGE

Measurements in the functional mock up test of the NAL QSTOL aircraft control system
[NAL-TR-928] 02 p0126 N88-10793

Design and implementation of a debugger for an abstract machine
[AD-A184691] 03 p0363 N88-12283

UNIX benchmark system
[AD-A184492] 03 p0367 N88-12308

Competition Analysis Model (CAM). Volume 2: Computer manual
[AD-A184017] 03 p0384 N88-12411

Advanced techniques for the storage and use of very large, heterogeneous spatial databases. The representation of geographic knowledge: Toward a universal framework --- relations (mathematics)
[NASA-CR-181517] 03 p0385 N88-12421

Complex for ocean study from space and hydroacoustic stations 04 p0458 N88-12836

A rudimentary database for three-dimensional objects using structural representation
[CSE-87-00004] 05 p0590 N88-13597

Storing and retrieving data in a parallel distributed memory system
[AD-A185177] 05 p0637 N88-13897

Status, outlook of optical technology in information equipment field 06 p0689 N88-14222

The archiving of meteor research information
06 p0732 N88-14505

Octree data structures and creation by stacking
[PB87-234795] 06 p0758 N88-14650

A review of hypertext in a NASA project management context 06 p0793 N88-14859

SSME environment database development
[NASA-CR-179245] 08 p0964 N88-15836

Similarity networks as a knowledge representation for space applications 08 p1062 N88-16411

Data prefetching in shared memory multiprocessors
[DE88-003576] 10 p1394 N88-18314

The design of the POSTGRES storage system
[AD-A187244] 11 p1564 N88-19365

Allocation of database files across parallel stores for efficient processing of partial-match queries
[AD-A188196] 11 p1565 N88-19371

RIAR automated research and management systems
[DE88-700934] 12 p1706 N88-20209

Holographic disk for data storage
14 p1972 N88-21771

A data acquisition system for atmospheric tracer studies
[DE88-006211] 14 p1991 N88-21869

Method and device for the detection and identification of a helicopter
[NASA-TT-20251] 15 p2129 N88-22698

The flying characteristics of the membrane slider bearing 18 p2522 N88-24965

The CERSAT archiving and processing center --- ERS-1 19 p2701 N88-26059

Use of optical disk technology at the Air Command and Staff College
[AD-A192424] 21 p3027 N88-27969

Space shuttle phase B wind tunnel model and test information. Volume 2: Orbiter configuration
[NASA-CR-178415-VOL-2-PT-1]
23 p3171 N88-28881

Laser sensing for identification and control of distributed parameter systems
[AD-A195886] 24 p3379 N88-30124

Partitioned storage for temporal databases
[AD-A195093] 24 p3436 N88-30451

DATA STRUCTURES

Local concurrent error detection and correction in data structures using virtual backpointers
[NASA-CR-181432] 01 p0106 N88-10692

Advanced techniques for the storage and use of very large, heterogeneous spatial databases. The representation of geographic knowledge: Toward a universal framework --- relations (mathematics)
[NASA-CR-181517] 03 p0385 N88-12421

Octree data structures and creation by stacking
[PB87-234795] 06 p0758 N88-14650

A data structure and algorithm for fault diagnosis
08 p1065 N88-16432

Unidimensional Rasch model and multidimensional data: An analytic approach
[PB88-105861] 10 p1372 N88-18187

Portable (and disposable) interpreters
10 p1380 N88-18237

The effects of data structure on total time on test plots
[AD-A187628] 10 p1389 N88-18296

Dynamic processor self-scheduling for general parallel nested loops
[DE88-003572] 10 p1393 N88-18311

TYPICAL: A knowledge representation system for automated discovery and inference
[AD-A187483] 11 p1533 N88-19160

Development in data structures in PHOCUS for digital mapping 18 p2534 N88-25034

EPL (Equational Programing Language) system design: Intermediate processing steps
[AD-A191203] 18 p2556 N88-25169

Algorithms and data structures for an expanded family of matroid intersection problems
[AD-A191482] 18 p2562 N88-25213

Design of high performance microcomputers for numerical data processing
[ETN-88-92371] 20 p2835 N88-26818

An introduction to the nested sequence of tuples data model and algebra
[REPT-87-049] 22 p3145 N88-28702

Lisp Object State Saver (LOSS): A facility used to save partial schedules of the Hubble Space Telescope
24 p3421 N88-30360

DATA SYSTEMS

NT AIR DATA SYSTEMS

Interfacing distributed operating systems
[AD-A184489] 03 p0366 N88-12306

Description of data handling system installed December 11, 1986 --- EISCAT 06 p0692 N88-14242

The crustal dynamics intelligent user interface anthology
[NASA-TM-100693] 08 p1067 N88-16448

MPAD MCC workstation system: ADDAM and EEVE
09 p1203 N88-17209

Modular CAMAC system, 2
[DE88-700237] 11 p1525 N88-19106

Baseline observing system experiments using the AFGL global data assimilation system
[AD-A188861] 15 p2024 N88-22062

Proposals for the pre-operational use of data from the European Remote Sensing Satellite ERS-1
[BCRS-86-02] 16 p2227 N88-23300

DATA TRANSFER (COMPUTERS)

Measurement of fault-tolerant parallel processors
[PB87-208328] 01 p0084 N88-10539

Analysis of counting errors in the phase/Doppler particle analyzer
[NASA-TM-100231] 03 p0323 N88-12043

Guidelines for exchanging computerized information
[DE88-004736] 10 p1425 N88-18510

Interconnection of high-speed local area networks
17 p2390 N88-24205

Theory of numerical information environment and its applications 19 p2640 N88-25666

An operational open-end file transfer protocol for mobile satellite communications 19 p2651 N88-25738

The high speed local area network
19 p2717 N88-26133

DATA TRANSMISSION

NT ALOHA SYSTEM
NT AUTOMATIC PICTURE TRANSMISSION
NT CODE DIVISION MULTIPLE ACCESS
NT FREQUENCY DIVISION MULTIPLE ACCESS
NT MULTIPLE ACCESS
NT PACKET TRANSMISSION
NT SINGLE CHANNEL PER CARRIER TRANSMISSION

Telemetry, Tracking, and Control Working Group report 01 p0016 N88-10096

Data Management Working Group report
01 p0016 N88-10097

Digital receiver structures and methods for the determination of the scanning frequency in modems for fast data transmission via telephone channels
[ETN-87-90429] 01 p0037 N88-10235

Study on the suitability of a European data relay satellite to support a system of remote sensing satellites
[ESA-CR(P)-2400] 01 p0063 N88-10406

Rapid toxicity detection in water quality control utilizing automated multispecies biomonitoring for permanent space stations 02 p0135 N88-10848

An examination of the Advanced Communications Technology Satellite (ACTS) and its application to the Defense Data Network (DDN)
[AD-A184003] 03 p0276 N88-11742

Lewis Information Network (LINK): Background and overview
[NASA-TM-100162] 03 p0305 N88-11925

Design of source coders and joint source/channel coders for noisy channels
[NASA-CR-181547] 04 p0432 N88-12678

An exact analysis and performance of framed ALOHA with capture
[AD-A185006] 05 p0574 N88-13500

Test and evaluation of the transputer in a multi-transputer system
[AD-A184969] 05 p0631 N88-13859

Soliton mode of propagation of light pulses through single-mode optical fibers and problems of its experimental realization 07 p0920 N88-15592

Development and study of fibre-optic link lines on the basis of the KEM-8-4PD, KEM-8-4PR quantum-electronic modules
[DE88-700372] 07 p0932 N88-15663

Requirements and options for communications services in support of the Systems Autonomy Demonstration Project 08 p1057 N88-16374

A hybrid transform/DPCM encoder for data compression
[DE88-003725] 09 p1154 N88-16919

Experimental Radio Data System (RDS): A survey of reception reliability in the UK
[BBC-RD-1987/17] 09 p1155 N88-16922

Crosstalk analysis of a broadband data communications system
[DE88-003652] 09 p1156 N88-16927

Code division multiple access applied to fiber optic data transmission
[AD-A186873] 09 p1247 N88-17477

Information transfer in the National Airspace System
10 p1275 N88-17634

Signal processing for an optical wide band data transmission system
[DE88-003854] 10 p1319 N88-17888

Wide band data transmission system using optical fibers
[DE88-004555] 10 p1319 N88-17889

Personal computers and All-in-1: Document transfer and translation
[DE88-003760] 10 p1384 N88-18264

Failure-resistant Fibre-Optical Communication Line (FOCL)
[DE88-700470] 10 p1408 N88-18400

Guidelines for exchanging computerized information
[DE88-004736] 10 p1425 N88-18510

AITI Test Report 87-002: Pratt and Whitney technical order transfer tests
[DE88-004045] 11 p1564 N88-19363

AITI Report 87-003: Honeywell technical order transfer tests
[DE88-004046] 11 p1564 N88-19364

Terrestrial Propagation Characteristics in Modern Systems of Communications, Surveillance, Guidance and Control
[AGARD-CP-407] 12 p1614 N88-19653

Envelope and phase statistics for non-Gaussian noise and resulting error probabilities for digital communications systems 12 p1617 N88-19672

A concatenated coded modulation scheme for error control
[NASA-CR-182639] 12 p1621 N88-19697

A hybrid transform/DPCM encoder for data compression
[DE87-014852] 13 p1758 N88-20518

Datacast: The transmission system
[BBC-RD-1988/1] 14 p1905 N88-21385

Application of static memory for data acquisition and transmission into a computer
[DE88-701491] 15 p2106 N88-22544

Multiple address facility for packet radio: An investigation of performance/complexity trade off
[AD-A191043] 16 p2190 N88-23064

A PC-based receiver-decoder for remote sensor monitoring
[DE88-004733] 16 p2192 N88-23075

Investigation of air transportation technology at Ohio University, 1986 17 p2293 N88-23719

Connecting remote systems for demonstration of automation technologies 17 p2387 N88-24191

Automated test device for FASR (Fixed Array Surveillance Radar) beam steering componentry
[AD-A191650] 18 p2500 N88-24829

Land mobile satellite demonstration system
19 p2646 N88-25706

A framework for implementing data services in multi-service mobile satellite systems
19 p2650 N88-25733

Robust vector quantization for noisy channels
19 p2653 N88-25754

The performance of Eurocom error correction schemes for data communications
[FEL-1987-56] 20 p2792 N88-26563

An integrated circuit for error protection in modern data communication systems conforming to Eurocom specifications
[FEL-1987-48] 20 p2796 N88-26593

A high speed serial link interface for SANDAC-V
[DE88-007694] 20 p2842 N88-26861

Use of fiber optic equipment for security
[DE88-007898] 20 p2853 N88-26943

A VLSI single-chip (225,223) Reed-Solomon encoder with interleaver
[NASA-CASE-NPO-17280-1-CU]
21 p2902 N88-27220

Multichannel data transmission through a fiber optic cable
[AD-A193842] 22 p3070 N88-28221

Use of a coherent square wave reference to demodulate BPSK (Binary Phase Shift Keying) carriers and a visual indicator of the quality of received QPSK (Quadrature Phase Shift Keying) carriers
[AD-A193528] 23 p3204 N88-29065

Hierarchical organization for large, dynamic radio networks
[AD-A193942] 23 p3204 N88-29067

Distortions in processed signals and their application in electronic design. Part 1: Basic and general formulations
[DE88-702731] 23 p3204 N88-29070

An OKQPSK modem incorporating numerically controlled carrier synthesis
[DE88-009536] 23 p3244 N88-29304

Design of a self-timed VLSI multicomputer communication controller
[AD-A194567] 24 p3361 N88-30014

Integrating images, applications, and communications networks, volume 5
[AD-A195854] 24 p3436 N88-30452

DATING

U CHRONOLOGY
U TIME MEASUREMENT

DAYGLOW

Theoretical and observational problems with Holes in the far UV dayglow
[AD-A188190] 10 p1355 N88-18100

DAYTIME

The lengthening and shortening of the day
[KNMI-TR-91] 05 p0628 N88-13839

Peculiarities of daytime ionosphere of Venus during years of low and high solar activity
08 p1005 N88-16091

Task listing: Visually assisted and visually dependent tasks for fighter aircraft
[AD-A191041] 16 p2244 N88-23404

Atmospheric angular momentum and length of day
[AD-A194505] 23 p3233 N88-29238

DBS (SATELLITES)

U DIRECT BROADCAST SATELLITES

DC (CURRENT)

U DIRECT CURRENT

DC 9 AIRCRAFT

Aircraft accident report: Northwest Airlines, Inc., McDonnell Douglas DC-9-82, N312RC, Detroit Metropolitan Wayne County Airport, Romulus, Michigan, August 16, 1987
[PB88-910406] 19 p2601 N88-25449

DE LAVAL NOZZLES

U CONVERGENT-DIVERGENT NOZZLES

DEACCLIMATIZATION

U ACCLIMATIZATION

DEACTIVATION

Deactivation of alumina based catalysts
11 p1455 N88-18673

DEAD RECKONING

Advanced dead reckoning navigation for mobile robots
03 p0262 N88-11646

Simple 2-D navigation for wheeled vehicles
[DE88-007115] 20 p2756 N88-26351

DEADWEIGHT

U STATIC LOADS

DEBRIS

NT SPACE DEBRIS

Far infrared circumstellar debris shells of red supergiant stars 04 p0515 N88-13165

Fretting wear and fretting fatigue damage
05 p0603 N88-13697

Analysis of debris from accelerated life test of the Hughes five-year Vuilleumier cryocooler
[AD-A193101] 21 p2931 N88-27400

DEBUGGING

U CHECKOUT

DEBYE TEMPERATURE

U SPECIFIC HEAT

DECAMETRIC WAVES

A Jupiter Data Analysis Program (JDAP) research grant on wave accessibility and attributes
[NASA-CR-182348] 06 p0804 N88-14908

Ray tracing of Jovian low frequency radiation
[NASA-CR-179262] 08 p1101 N88-16620

DECAY

NT ALPHA DECAY
NT NEUTRON DECAY
NT NEUTRON EMISSION
NT PLASMA DECAY
NT RADIOACTIVE DECAY
NT SPACECRAFT GLOW
NT WEAK ENERGY INTERACTIONS
NT WEAK INTERACTIONS (FIELD THEORY)

Numerical simulation of turbulent premixed combustion and decay of turbulent swirling flow
[DE87-014253] 03 p0284 N88-11787

On charm decays: Present status and future goals
[DE87-013586] 03 p0375 N88-12356

Dynamical analysis of molecular decay at spherical surfaces
[AD-A184908] 05 p0647 N88-13964

Surface and interface electronic structure
[DE88-003363] 09 p1258 N88-17545

An experimental measurement of metal multilayer X-ray reflectivity degradation due to intense X-ray flux
[LA-10989-T] 11 p1547 N88-19255

Orbital analysis of a STS (Space Transportation System) external tank in low earth orbit
[AD-A188829] 12 p1593 N88-19542

Numerical simulation of turbulent premixed combustion and decay of turbulent swirling flow
[DE88-006588] 14 p1886 N88-21284

Study of energy levels and decay mechanisms for singlet Rydberg states of molecular nitrogen
[AD-A192505] 21 p3014 N88-27886

An exponential decay estimate for the stationary perturbation of Poiseuille flow [AD-A193480] 23 p3210 N88-29105
The influence of delay effects on the decay of liquid jets [MPIS-14/1987] 23 p3214 N88-29130

DECAY RATES
Influences of the astrophysical environment on nuclear decay rates [DE88-001461] 04 p0522 N88-13208
On free decay damping tests 08 p0997 N88-16041
Note on boundary stabilization of wave equations [AD-A187113] 09 p1227 N88-17348
An exponential decay estimate for the stationary perturbation of Poiseuille flow [AD-A193480] 23 p3210 N88-29105

DECELERATION
NT SPIN REDUCTION
Control and stabilization mechanisms of submunitions [DFVLR-IB-111-86/9] 03 p0259 N88-11630
X-ray pulsars: Accretion flow deceleration 03 p0390 N88-12451
Atmospheric entry heating of cosmic dust 06 p0794 N88-14865
Liquid ventilation: New data and possible use in space medicine 12 p1654 N88-19908
An experimental investigation of decelerating flow about two-dimensional cambered plates [DE88-006598] 13 p1766 N88-20567
Soft-ground aircraft arresting systems [AD-A190838] 16 p2165 N88-22912
New concepts for atmospheric braking deceleration in planetary atmosphere entry [SNIAS-CAS-DECE-P003-DPAA] 16 p2168 N88-22923

DECELERATORS
U BRAKES (FOR ARRESTING MOTION)

DECEPTION
The Soviet Stealth fighter: Check or checkmate [AD-A195200] 24 p3323 N88-29791

DECIMETER WAVES
Observations of the brightness temperature distribution of the quiet solar corona at decametric wavelengths 01 p0114 N88-10729

DECISION ELEMENTS
U LOGICAL ELEMENTS

DECISION MAKING
Optimization of a controlled two-server maintenance system [INPE-4202-PRE/1083] 01 p0107 N88-10694
Application of knowledge-based techniques to aircraft trajectory generation and control 02 p0129 N88-10811
Knowledge acquisition issues encountered during the development of an estimating expert system [DE87-013320] 02 p0248 N88-11568
Interfacing distributed operating systems [AD-A184489] 03 p0366 N88-12306
Performance evaluation of artificial intelligence systems [AD-A184054] 03 p0368 N88-12316
The pros and cons of using a CAI package on a central computer as opposed to a microprocessor: What's your CAI MO, mainframe or micro [DE87-011123] 04 p0475 N88-12929
Material design of high-purpose glass discussed 06 p0675 N88-14133
An empirical investigation of load indices for load balancing applications [AD-A185763] 06 p0724 N88-14451
A computer decision-making process for the elimination of noise from data [AD-A185746] 06 p0759 N88-14659
Artificial intelligence systems 06 p0761 N88-14670
Using concept mapping to define problems and identify key kernels during the development of a decision support system [AD-A185636] 06 p0762 N88-14674
Tools and technologies for expert systems: A human factors perspective 06 p0797 N88-14882
Human performance data needed for training device design decisions [AD-A185988] 07 p0898 N88-15441
A software planning and development methodology with resource allocation capability [AD-A186088] 07 p0902 N88-15462
Computer aided design for Petri Nets [AD-A186109] 07 p0902 N88-15465
Proceedings of the Second International Symposium on Methodologies for Intelligent Systems. Colloquia program [DE88-001490] 07 p0907 N88-15498
Contributions to selection and ranking theory with special reference to logistic populations [AD-A185629] 07 p0917 N88-15568
Air Force Human Resources Laboratory technical reports and technical papers [AD-A186830] 09 p1201 N88-17200
A situation-response model for intelligent pilot aiding 09 p1208 N88-17241
A human performance modelling approach to intelligent decision support systems 09 p1208 N88-17242
Autonomous control procedures for shuttle rendezvous proximity operations 09 p1208 N88-17244
Artificial Intelligence (AI), Operations Research (OR), and Decision Support Systems (DSS): A conceptual framework 09 p1209 N88-17245
Advanced decision aiding techniques applicable to space 09 p1209 N88-17250
Real-time artificial intelligence issues in the development of the adaptive tactical navigator 09 p1211 N88-17260
Management of complex information in support of evolving autonomous expert systems [AD-A186680] 09 p1224 N88-17337
Critical issues for establishment of a permanently-occupied lunar base [AD-A187128] 09 p1263 N88-17567
Windshear training aid. Volume 1: Overview, pilot guide, training program [PB88-127196] 10 p1276 N88-17637
Real time artificial intelligence architecture 10 p1380 N8[illegible]
Development of a graphics based two-attribute [illegible] assessment program with application to mission planning [AD-A187276] 10 p1388 N88-18292
A two-stage isolated-word recognition system using discriminant analysis [AD-A187425] 10 p1402 N88-18360
Modeling incorrect responses to multiple-choice items with multilinear formula score theory [AD-A187887] 11 p1522 N88-19090
Effects of stress on judgement and decision making in dynamic tasks [AD-A188203] 11 p1523 N88-19092
When decision aids fail [AD-A187531] 11 p1523 N88-19095
Evaluating expert system tools: A framework and methodology-workshops [AD-A187190] 11 p1533 N88-19159
De Finetti's approach to group decision making [AD-A188074] 11 p1536 N88-19177
Computer aided tactics for air combat 12 p1597 N88-19559
Brain activity during tactical decision-making. Part 2: Probe-evoked potentials and workload [AD-A188688] 12 p1667 N88-19994
Physics for robots [AD-A189056] 12 p1682 N88-20054
Design methodology for allocating data in a distributed database [AD-A188226] 12 p1706 N88-20215
The design of aircraft using the decision support problem technique [NASA-CR-4134] 13 p1721 N88-20291
Expected value analysis for an unmanned expendable launch vehicle payload escape system [AD-A189494] 13 p1728 N88-20337
A personalized and prescriptive decision aid for choice from a database of options [AD-A188726] 13 p1811 N88-20820
SEAT: A strategic engagement analysis tool [DE88-000498] 13 p1830 N88-20944
Expert systems for decision support in military aircraft mission preparation [NLR-MP-87013-U] 13 p1830 N88-20946
Application of expert systems in project management decision aiding [NASA-CR-180762] 13 p1850 N88-21074
Applicability of nonlinear programming in decision support systems: Realization of user-friendly software [REPT-87-42] 14 p1957 N88-21663
Selective mechanisms in auditory and bimodal signal processing [AD-A190529] 15 p2103 N88-22530
Conflict resolution in cooperative systems [AD-A190351] 15 p2104 N88-22535
C3 generic workstation: Performance metrics and applications 16 p2242 N88-23397
Bayesian solutions to a 2 x 2 decision matrix using interval scaled payoffs with an application to foreign policy decisions [AD-A190863] 16 p2260 N88-23511
A change in system design emphasis: From machine to man 17 p2304 N88-23782
A proposal of adaptation of a knowledge-based scene analysis model to some remote sensing problems 17 p2354 N88-24026
Remote sensing and data integration: Practical solutions for resource managers 17 p2356 N88-24034
A proposal of adaptation of a knowledge-based scene analysis model to some remote sensing problems 17 p2362 N88-24068
Timesharing performance as an indicator of pilot mental workload [NASA-CR-182807] 18 p2552 N88-25150
Representation and decision mechanisms in artificial intelligence [AD-A191083] 18 p2560 N88-25197
A perspective of PC-based probabilistic risk assessment [DE88-006715] 18 p2568 N88-25251
Selection and effects of channels in distributed communication and decision making tasks: A theoretical review and a proposed research paradigm [AD-A191807] 18 p2587 N88-25375
Modeling and evaluation of variable structure organizations [AD-A191947] 18 p2588 N88-25381
High-speed optical logic using GaAs 19 p2656 N88-25773
Algorithmic generation of feasible system architectures [AD-A191722] 19 p2713 N88-26106
Analysis and synthesis of decision-making organizations [AD-A191948] 19 p2738 N88-26258
Decision aiding and coordination in decision-making organizations [AD-A191950] 19 p2738 N88-26259
Modeling and evaluation of expert systems in decisionmaking organizations [AD-A191951] 19 p2739 N88-26260
Coordination in decision-making organizations [AD-A191952] 19 p2739 N88-26261
A semantic approach to fairness [CWI-CS-R8759] 20 p2840 N88-26853
Expert system application education project [NASA-CR-183089] 20 p2843 N88-26867
The integration of decision support problems into feature modeling based design 21 p2927 N88-27372
Linear programming for Air Force decision aiding 21 p2928 N88-27378
Future SDI (Strategic Defense Initiative) decision making [AD-A192794] 21 p3010 N88-27860
Rules, schema and decision making [AD-A193389] 21 p3027 N88-27967
Computer aided decision making [AD-A194210] 22 p3137 N88-28651
Linear goal programming as a military decision aid [AD-A194276] 22 p3137 N88-28652
A virtual statistical mechanical neural computer [AD-A193962] 22 p3139 N88-28660
LO-CO-GRAF (low cost graphics): Generating maps to support command and control/crisis management using small computers [AD-A193964] 22 p3139 N88-28661
Decision making aids: Methods and risks 22 p3161 N88-28820
Project management software 22 p3161 N88-28821
LRS-2: A specialized knowledge system for launch resource scheduling [AD-A194625] 23 p3182 N88-28941
Method for Veterbi decoding of large constraint length convolutional codes [NASA-CASE-NPO-17310-1-CU] 23 p3183 N88-28946
Motion planning for legged locomotion systems on uneven terrain 23 p3221 N88-29170
Evaluation of atmospheric effects for operational tactical decision aid [AD-A194205] 23 p3232 N88-29236
A knowledge-based decision support system for payload scheduling 23 p3252 N88-29358
An approach to combining heuristic and qualitative reasoning in an expert system 23 p3253 N88-29362
On the design and optimization of distributed signal detection and parameter estimation systems [AD-A193934] 23 p3266 N88-29446
SDI (Strategic Defense Initiative): A policy analysis [AD-A194240] 23 p3275 N88-29493
Distributed knowledge base systems for diagnosis and information retrieval [AD-A193107] 23 p3296 N88-29633
Reduced flexibility in processing Titan 4 space launch vehicles at Cape Canaveral Air Force Station [AD-A194908] 24 p3332 N88-29834

A detection theory analysis of visual display performance
[AD-A196291] 24 p3409 N88-30292
The bounded rationality constraint: Experimental and analytical results
[AD-A195897] 24 p3413 N88-30318
The advice taker/inquirer: A system for high-level acquisition of expert knowledge
24 p3421 N88-30359
Verification and validation of rulebased systems for Hubble Space Telescope ground support
24 p3421 N88-30361
Venture theory: A model of decision weights
[AD-A194809] 24 p3426 N88-30391
Looking beyond the strategic defense initiative
[AD-A195079] 24 p3427 N88-30394
Strategic, organizational and standardization aspects of integrated information systems, volume 6
[AD-A195855] 24 p3437 N88-30457
Technical change needs organizational change
24 p3438 N88-30466

DECISION THEORY
NT STATISTICAL DECISION THEORY
Modeling of human judgement in multicriteria analysis using pairwise comparison
[REPT-87-01] 01 p0076 N88-10484
Using concept mapping to define problems and identify key kernels during the development of a decision support system
[AD-A185636] 06 p0762 N88-14674
Deriving descriptions of the mind
[AD-A186647] 08 p1052 N88-16349
Modeling incorrect responses to multiple-choice items with multilinear formula score theory
[AD-A187887] 11 p1522 N88-19090
Task allocation for efficient performance of a decentralized organization
[AD-A188699] 12 p1705 N88-20204
Expert system techniques and decision support system: A case study (Dec. 1985 - Jun. 1986)
[ETN-88-91347] 13 p1821 N88-20884
Problem solving in a natural task as a function of experience
[AD-A191180] 16 p2243 N88-23399
A comparison of supervised maximum likelihood and decision tree classification for crop cover estimation from multitemporal LANDSAT MSS data
17 p2352 N88-24014
An extension of the Hopfield-Tank model for solution of the multiple traveling salesmen problem
[DE88-008377] 19 p2715 N88-26122
Combining expert opinions: An optimization framework
[REPT-87-84] 20 p2846 N88-26895
Uncertainty analysis in automatic robot programming
[RR-695-I-IMAG-68-LIFIA] 22 p3142 N88-28685

DECODERS
NT VITERBI DECODERS
NOSTRADAMUS programmable translator user's manual and programmer's manual
[DE87-013414] 01 p0083 N88-10533
More on the decoder error probability for Reed-Solomon codes 04 p0435 N88-12699
On the VLSI design of a pipeline Reed-Solomon decoder using systolic arrays 04 p0436 N88-12700
Packet telecommand. System performance assessment study --- onboard data handling
[FTÇ/TNOT/0015/SAAB] 07 p0843 N88-15113
Further results on finite-state codes
11 p1472 N88-18782
Speech coding at 4800 bps for mobile satellite communications 19 p2652 N88-25749
Development of an 8000 bps voice codec for AvSat
19 p2653 N88-25755

DECODING
A method resolving an ambiguity of measured distances by means of NAVSTAR GPS signals
01 p0065 N88 10417
Weighted decoding of block codes and some topics on decoding complexity
[ENST-87E005] 02 p0221 N88-11394
A lower bound for the decoder error probability of the linear MDS code 11 p1472 N88-18780
A concatenated coded modulation scheme for error control
[NASA-CR-182639] 12 p1621 N88-19697
Performance of single and multiple system AM stereo decoder receivers
[PB88-168307] 15 p2057 N88-22265
Soft decoding of recorded HF data
[FOA-C-30473-3.3] 15 p2058 N88-22269
Parallel memory addressing using coincident optical pulses
[AD-A189767] 15 p2106 N88-22547
A PC-based receiver-decoder for remote sensor monitoring
[DE88-004733] 16 p2192 N88-23075
Method for Veterbi decoding of large constraint length convolutional codes
[NASA-CASE-NPO-17310-1-CU]
23 p3183 N88-28946

DECOMPOSITION
NT AMMONOLYSIS
NT CRACKING (CHEMICAL ENGINEERING)
NT HYDROCRACKING
NT PHOTODECOMPOSITION
NT PHOTODISSOCIATION
NT PHOTOLYSIS
NT PROPELLANT DECOMPOSITION
NT PYROLYSIS
NT RADIOLYSIS
NT THERMAL DECOMPOSITION
Prediction and spectral decomposition of wide sense stationary processes on Z squared
[ENST-87C001] 01 p0087 N88-10564
A surface science investigation of potential intermediates, catalysts, and promoters in the synthesis of higher alcohols by metals
[DE87-014188] 02 p0144 N88-10906
Using MINOS (Modular In-core Nonlinear Optimization System) as a subroutine for decomposition
[DE87-013086] 02 p0221 N88-11390
Free radical detection and reactions in the decomposition of energetic materials
[AD-A184677] 03 p0296 N88-11858
Performance analysis of advanced spacecraft TPS
[NASA-CR-181532] 04 p0399 N88-12484
Application of Vandermonde decomposition to directional and modal analysis of broadband transients
[AD-A185007] 05 p0646 N88-13956
DC conductivity studies in Li5AlO4 at intermediate temperatures and its possible application for the electrolysis of water
[AD-A185489] 06 p0697 N88-14276
Hydroxide ion conductors as possible electrolytes in intermediate temperature fuel cells
[AD-A185508] 06 p0731 N88-14495
High temperature solar electrothermal processing-3. Zinc from zinc oxide at 1200-1675K using a non-consumable anode
[AD-A186600] 09 p1141 N88-16836
Determination of the melting and decomposition points of different materials in an oxygen stream
[INFORME-I-158/86] 09 p1142 N88-16844
Analysis of the decomposition of transparent polymer materials (blocks) under the action of laser beams in free generation mode
[AD-A187090] 09 p1147 N88-16873
DSC (Differential Scanning Calorimeter) stability test for liquid propellants: A preliminary report
[AD-A187115] 09 p1150 N88-16888
A three-dimensional dual potential procedure for rotational flows 10 p1329 N88-17942
A multiprocessor scheme for the singular value decomposition
[DE88-003591] 10 p1388 N88-18288
Fast Poisson solver on irregular regions by boundary integral-based domain decomposition methods
[DE88-003583] 10 p1399 N88-18340
Domain decomposition preconditioners for the spectral collocation method
[NASA-CR-181620] 10 p1400 N88-18345
High temperature processing of superconducting Y1Ba2Cu3O6.9
[DE88-003002] 10 p1416 N88-18449
Ceramic decomposition under irradiation
[DE88-004327] 11 p1464 N88-18732
Parallel pseudospectral domain decomposition techniques
[NASA-CR-181629] 11 p1524 N88-19101
Decomposition of hypochlorite in the presence of copper in a homogeneous medium
[NASA-TT-20199] 13 p1740 N88-20403
Molecular dynamics of laser ablation of a polymer coating
[DE88-004337] 13 p1750 N88-20466
DASM: A tool for Decomposition and Analysis of Sequential Machines
[EUT-87-E-170] 14 p1956 N88-21660
Structural decomposition of multiple time scale Markov processes
[AD-A189739] 15 p2123 N88-22657
Surface enhanced Raman scattering applied to surface chemical kinetics
[AD-A191275] 16 p2176 N88-22969
A low dimensional dynamical system for the wall layer
16 p2194 N88-23088
Fundamental studies of beta phase decomposition modes in titanium alloys
[AD-A191495] 18 p2485 N88-24740
Sample decomposition in sealed teflon vessels
[NASA-TT-20189] 18 p2494 N88-24798
Liquid phase decomposition in slurry fuels
19 p2624 N88-25564
Chemical kinetics modeling of HMX combustion
19 p2633 N88-25617
A domain decomposition method for boundary layer problems
[DE88-008917] 19 p2666 N88-25852
Two domain decomposition techniques for Stokes problems
[DE88-008724] 19 p2720 N88-26149
Manufacturing of a barium titanate with high dielectric coefficient by decomposition of precipitates of double oxalates
[ISAL-IDI1-83-02] 21 p2911 N88-27278
Coherent structures in the axisymmetric turbulent jet mixing layer 21 p2947 N88-27504
A study on Lebesgue decomposition of measures induced by stable processes
[AD-A192893] 21 p3009 N88-27850
Decomposition of energetic materials on the drop-weight impact machine
[DE88-009154] 22 p3059 N88-28152
Experiments and modeling of multi-component fuel behavior in combustion
[AD-A195011] 24 p3343 N88-29896
Decomposition of hydrazine by high frequency glow electrical discharges
[NASA-TT-20240] 24 p3344 N88-29906

DECOMPRESSION
U PRESSURE REDUCTION

DECOMPRESSION SICKNESS
Contribution of ultrasonic Doppler detection of circulating bubbles to human interventions under the sea and in space 19 p2697 N88-26029
Decompression procedures and accidents in space and sea 19 p2698 N88-26035
Reducing risks inherent in operating underwater craft: The contribution of classification, the example of the SAGA highly autonomous support submarine
19 p2699 N88-26042
Analysis of clinical symptoms of human decompression sickness during altitude chamber studies
19 p2703 N88-26074

DECONTAMINATION
Corrosion and stress corrosion of metals in decontamination solutions 22 p3054 N88-28118

DECOUPLING
Digital algorithms for the control and dynamic decoupling of industrial robot axes
[ETN-87-90441] 01 p0084 N88-10546
Decoupling and stabilization of speed and height in F4 Phantom aircraft using output feedback
[ETN-87-90926] 02 p0125 N88-10787
Ion-matrix coupling in polymer electrolytes from relaxation time studies
[AD-A184632] 03 p0293 N88-11841
The consequences of intergrain Josephson coupling in ceramic high-temperature superconductors
[DE87-013713] 06 p0785 N88-14816
Decoupling identities and predictable transformations in exchangeability
[AD-A186013] 07 p0913 N88-15540
A direct approach to almost disturbance and almost input-output decoupling
[MEMO-641] 08 p1072 N88-16471
Acceleration techniques for decoupling algorithms in semiconductor simulation
[DE88-003593] 09 p1221 N88-17323
A new approach to almost decoupling problems for linear and nonlinear systems
[MEMO-660] 14 p1962 N88-21700
Feedback decoupling and stabilization for linear systems with multiple exogenous variables
[ETN-88-92245] 16 p2255 N88-23474
Continuous decoupling transformations for linear boundary value problems
[ETN-88-92248] 16 p2258 N88-23493

DECREMENTING
U REDUCTION

DEEP SPACE
NT INTERPLANETARY SPACE
NT INTERSTELLAR SPACE

DEEP SPACE NETWORK
The Telecommunications and Data Acquisition Report
[NASA-CR-181546] 04 p0432 N88-12679
Low-noise cryogenic transmission line
04 p0434 N88-12688
A 2.3-GHz cryogenically cooled HEMT amplifier for DSS 13 04 p0434 N88-12689
Frequency doubling conversion efficiencies for deep space optical communications 04 p0434 N88-12691
The 8.4-GHz low-noise maser pump source assembly
04 p0436 N88-12705
A modern control theory based algorithm for control of the NASA/JPL 70-meter antenna axis servos
04 p0436 N88-12706

Power density measurements in the near field of the DSS 13 26-meter antenna 04 p0437 N88-12711
Deep space target location with Hubble Space Telescope (HST) and Hipparcos data
[NASA-CR-182520] 10 p1427 N88-18524
The Telecommunications and Data Acquisition Report
[NASA-CR-182545] 11 p1471 N88-18774
The JPL trapped mercury ion frequency standard
11 p1471 N88-18776
An optimal structure for a 34-meter millimeter-wave center-fed BWG antenna: The Cross-Box concept
11 p1472 N88-18778
A 2.3-GHz maser at Usuda, Japan, for TDRSS-orbiting VLBI experiment 11 p1472 N88-18779
A simplified, general-purpose deep-space ranging correlator design 11 p1473 N88-18786
A noise-adding radiometer for the Parkes antenna
11 p1473 N88-18788
X-band system performance of the very large array
11 p1473 N88-18789
DSS 14 64-meter antenna S- and X-band efficiency and system noise temperature calibrations, September 1987
11 p1473 N88-18790
Optical links in the angle-data assembly of the 70-meter antennas 11 p1474 N88-18792
The design and implementation of the Technical Facilities Controller (TFC) for the Goldstone deep space communications complex 11 p1474 N88-18794
Simulated performance of an order statistic threshold strategy for detection of narrowband signals
11 p1474 N88-18796
The Deep Space Network
[NASA-CR-182700] 13 p1759 N88-20524
The Telecommunications and Data Acquisition Report
[NASA-CR-183131] 22 p3063 N88-28178
The limits of direct satellite tracking with the Global Positioning System (GPS) 22 p3064 N88-28179
X-band resonant ring operation at 450 kW
22 p3064 N88-28181
Digital carrier demodulation for the DSN Advanced Receiver 22 p3064 N88-28183
Telemetry SNR improvement using the DSN Advanced Receiver with results for Pioneer 10
22 p3064 N88-28184
Advanced Receiver tracking of Voyager 2 near solar conjunction 22 p3065 N88-28185
Strawman Optical Reception Development Antenna (SORDA) 22 p3065 N88-28187
DSN very long baseline interferometry system Mark IV-88 22 p3067 N88-28199
Mark IV-85 mission support planning and future mission set 22 p3067 N88-28202
Determination of the Venus flyby orbits of the Soviet Vega probes using VLBI techniques
22 p3067 N88-28203
Mars earth-based radar: 1986 results and 1988-1990 opportunities 23 p3306 N88-29697
The Deep Space Network: An instrument for radio astronomy research
[NASA-CR-183219] 24 p3453 N88-30554

DEEP WATER
Deep water mass circulation in the Alboran Basin Measurements - January to April 1982: ALBORAN 2
[AD-A189205] 13 p1803 N88-20777

DEFECTS
NT CRYSTAL DEFECTS
NT CRYSTAL DISLOCATIONS
NT EDGE DISLOCATIONS
NT INCLUSIONS
NT POINT DEFECTS
NT SCREW DISLOCATIONS
NT SPEECH DEFECTS
NT SURFACE DEFECTS
NT VACANCIES (CRYSTAL DEFECTS)
Theory of defects in non-metallic solids
[DE87-014068] 02 p0152 N88-10949
Detection of defects on structures
[EP-PATENT-0-210-794-A2] 04 p0453 N88-12807
Vibration and buckling of geometrically imperfect laminated cylindrical shells 04 p0456 N88-12822
Flaw effects: Behavior in operation of delamination in a crossed multilayer composite specimen
[DCQ/L-47-363/F] 06 p0678 N88-14153
Study on automatic detection and identification of defects in weld by microcomputer
[PB87-143897] 07 p0863 N88-15237
Methods of improving compacting quality of intricately shaped powder components
[BLL-M-37412-(5828.4)] 08 p0968 N88-15859
Nondestructive control: Modeling of electromagnetic phenomena, defect characterization, and sensor optimization
[ECL-86-14] 08 p0993 N88-16008
Acoustic emission measurements of PWR weld materials with inserted defects
[AERE-R-12386] 10 p1341 N88-18016
Flaw identification from forced vibration testing
[DE88-002641] 10 p1342 N88-18018
The influence of small defects on tensile specimen ductility and symmetry of deformation
[AD-A187983] 10 p1346 N88-18044
Grain boundaries, planar defects and superconducting properties of YBa2Cu3O7
[DE88-003477] 10 p1419 N88-18475
Simulation and processing of high resolution images of defects and interfaces in superconducting YBa2Cu3O7
[DE88-003856] 10 p1420 N88-18480
Fracture toughness of steel weldments containing lack of penetration defects 11 p1501 N88-18965
Investigation of defect and electronic interactions associated with GaAs device processing
[AD-A188021] 11 p1556 N88-19313
Study of defects in metals by positron annihilation
[DE88-701042] 13 p1745 N88-20432
Gordon Conference on Intermetallic Compounds held at Tilton, New Hampshire on 20-24 July 1987
[AD-A188502] 13 p1745 N88-20435
A defect investigation of Thunderflash MK N5 (Navy)
[MRL-TN-522] 13 p1754 N88-20488
Implementation and evaluation of a combined test-error correction procedure for memories with defects
[EUT-87-E-169] 14 p1955 N88-21651
Use of long-distance pair potentials in calculations of defect characteristics in metals
[DE88-701039] 15 p2037 N88-22138
Nondestructive evaluation of sintered ceramics
15 p2083 N88-22416
Processing defects and strength of alumina substrates
[W-10/87] 15 p2087 N88-22441
The use of rule induction to assist in the diagnosis of avionic circuit board defects
[ETN-88-92077] 16 p2162 N88-22899
Nondestructive evaluation of large scale composite components
[AD-A190998] 16 p2173 N88-22954
Micro-Raman analysis of dielectric optical thin films
[AD-A191228] 17 p2445 N88-24537
Harmfulness of defects: Behaviour in service of a delamination in a composite containing many differently oriented layers
[PB88-124714] 18 p2479 N88-24705
Application of magnification xeroradiography to advanced ceramics
[DE88-009965] 20 p2778 N88-26473
Microfocus X-ray techniques for flaw location
[DE88-008636] 20 p2812 N88-26680
Defects and disorder in amorphous and damaged silicon
[AD-A192277] 20 p2879 N88-27089
Defects in high-mobility semiconductor systems
[AD-A192298] 20 p2879 N88-27090
NDE performance in predicting failure strength of spherical composite specimens with implanted flaws
[DE88-008223] 21 p2959 N88-27575
Critical issues and directions for fracture mechanics and structural integrity
[AD-A193050] 21 p2960 N88-27584
Probing the electronic and defect structure of perovskite superconductors
[DE88-008349] 21 p3022 N88-27939
Direct and inverse diffraction problems for QNDE (Quantitative Non-Destructive Evaluation) applications
[AD-A194721] 22 p3085 N88-28322
Phase equilibrium and crystal growth studies on AgGaSe2 and related nonlinear optical materials
[AD-A193763] 22 p3157 N88-28783
The effect of oriented defects on long-range ordering of hydrocarbon films: Azulene on Pt(111)
[AD-A196089] 24 p3344 N88-29904
Predicting the durability of adhesives and coatings by remote detection of hidden defects and coating-thickness irregularities: A theoretical and numerical study
24 p3355 N88-29972

DEFENSE COMMUNICATIONS SATELLITE SYSTEM
NT FLEET SATELLITE COMMUNICATION SYSTEM

DEFENSE INDUSTRY
The military techniques of tomorrow. A contribution to active peace assurance
[MBB-UA-1049/87] 10 p1315 N88-17860
The effects of two Carlucci initiatives concurrency and streamlining, on the test and evaluation phase of system acquisitions 12 p1704 N88-20198
JPRS report: Science and technology. Japan
[JPRS-JST-88-001] 15 p2051 N88-22218
JPRS report: Science and technology. Japan
[JPRS-JST-87-029] 15 p2052 N88-22228
Department of Defense Statement on the Technology Base to the Subcommittee on Defense Industry and Technology of the Committee on Armed Services, United States Senate, 100th Congress, second session
[AD-A191839] 18 p2588 N88-25376

DEFENSE METEOROLOGICAL SATELLITE PROGRAM
U DMSP SATELLITES

DEFENSE PROGRAM
Source header list. Volume 2: L through Z
[AD-A184001] 03 p0385 N88-12419
Information analysis centers in the department of defense, revision
[AD-A184002] 03 p0385 N88-12420
Source header list. Volume 1: A through K
[AD-A184000] 04 p0501 N88-13086
University research initiative research program summaries
[AD-A184876] 05 p0658 N88-14035
Source hierarchy list. Volume 3: P through Z
[AD-A185902] 07 p0942 N88-15724
Concurrency control and reliability in replicated database systems 10 p1377 N88-18221
Streamlining invitation for bids
[AD-A188941] 12 p1705 N88-20206
A directory of databases available through SearchMAESTRO
[AD-A188813] 12 p1706 N88-20214
Free electron lasers in strategic defense
[DE88-007024] 17 p2394 N88-24231
Department of Defense statement on the X-ray Lithography Program to the Research and Development Subcommittee of the House Armed Services Committee of 100th Congress, second session
[AD-A191854] 18 p2582 N88-25341
Department of Defense Statement on the Technology Base to the Subcommittee on Defense Industry and Technology of the Committee on Armed Services, United States Senate, 100th Congress, second session
[AD-A191839] 18 p2588 N88-25376
Department of Defense statement on defense agency research and development to the Subcommittee on Defense of the Committee on Appropriations, United States House of Representatives, 100th Congress, second session
[AD-A191840] 18 p2588 N88-25377
Department of Defense Statement on the Balanced Technology Initiative to the Committee on Armed Services, United States Senate, 100th Congress, second session
[AD-A191841] 18 p2588 N88-25378
The Department of Defense report on the merit review process for competitive selection of university research projects and an analysis of the potential for expanding the geographic distribution of research for the Committees on Appropriations, United States Congress
[AD-A191842] 18 p2588 N88-25379
The FY 1989 Department of Defense statement on the Science and Technology Program to 100th Congress, second session
[AD-A191843] 18 p2588 N88-25380
The Army's role in space: Support for the battlefield commander
[RAND-P-7396] 19 p2721 N88-26159
The Oak Ridge National Laboratory strategic defense initiative shield optimization program
[DE88-008946] 19 p2721 N88-26160
An agenda for the strategic defense initiative
[RAND-P-7404] 20 p2847 N88-26898
The Oak Ridge National Laboratory strategic defense initiative shield optimization program: Executive summary
[DE88-008016] 20 p2847 N88-26899
Monitoring space weaponry: Detection and verification issues
[DE88-008726] 20 p2847 N88-26900
SDI: Myth or reality
[DE88-009121] 20 p2847 N88-26901
SDI and/or arms control
[RAND-P-7357] 20 p2848 N88-26903
Overview of the SDI (Strategic Defense Initiative) Program in short wavelength chemical lasers
[DE88-007912] 21 p3010 N88-27861
Stress/fatigue and the ARNG (Army National Guard) aviator
[AD-A194184] 22 p3132 N88-28621
SDI (Strategic Defense Initiative): A policy analysis
[AD-A194240] 23 p3275 N88-29493
SDI (Strategic Defense Initiative). Where do we go from here
[AD-A194544] 23 p3275 N88-29497
SSTS (Space Surveillance and Tracking System): The importance of early test and evaluation organizational participation
[AD-A193745] 23 p3276 N88-29499

DEFLAGRATION
Flame acceleration and transition to detonation in channels
[DE87-014193] 03 p0284 N88-11786
Steady tonation and flagration waves in reactive continua
[RARDE-2/73] 03 p0315 N88-11989

On the possibility of high velocity deflagration front propagation by radiative energy transfer
[AD-A189022] 12 p1613 N88-19645
Deformation, fracture and explosive properties of reactive materials
[AD-A193080] 21 p2923 N88-27348

DEFLATING
U INFLATABLE STRUCTURES
U PRESSURE REDUCTION

DEFLECTION
Telemetric laser extensometry technique for monitoring deflections in small cracks 05 p0607 N88-13724
Mechanisms in thermal mechanical forming of plates
[AD-A187797] 11 p1486 N88-18744
Computer aided deflection measurement of an aircraft wing
[AD-A187778] 12 p1581 N88-19461
Data processing method for high angle of attack testing with rolling angle 14 p1864 N88-21134
Further study of relation of von Karman equation for elastic large deflection problem and Schrodinger equation for quantum eigenvalues problem
14 p1899 N88-21341
Cubic spline solution of symmetric buckling problems of clamped shallow spherical shells
15 p2053 N88-22239
Deflection of a circular liquid jet on a flat plate perpendicular to the flow direction
[NASA-TT-20279] 16 p2207 N88-23173
Fast acting optical beam detection and deflection system
[AD-A192161] 18 p2521 N88-24954
Plate response analysis using shock tube
[AD-A190828] 18 p2526 N88-24987
Simulation of diaphragm-type IC pressure sensors
19 p2672 N88-25887
A simple unified method for predicting the deflections of reinforced concrete structures
19 p2679 N88-25930
Optical measurement of propeller blade deflections
[NASA-TP-2841] 22 p3079 N88-28286
Optical measurement of unducted fan blade deflections
[NASA-TM-100966] 23 p3216 N88-29142
Free vibration of rectangular plates with a small initial curvature
[NASA-CR-179370] 24 p3383 N88-30148

DEFLECTORS
The Shock and Vibration Bulletin. Part 4: Structural Dynamics and Modal Test and Analysis
[AD-A186751] 09 p1179 N88-17062
Qualification by analysis of IUS plume deflectors
09 p1179 N88-17063
Multimode-waveguide laser beam deflector
[DE88-006222] 13 p1776 N88-20622

DEFORESTATION
Monitoring Moneragala (Sri Lanka) with SPOT imagery
22 p3099 N88-28405
Study of deforestation in the Vosges (France) by remote sensing 22 p3107 N88-28452

DEFORMATION
NT AXIAL STRAIN
NT ELASTIC BENDING
NT ELASTIC BUCKLING
NT ELASTIC DEFORMATION
NT PLASTIC DEFORMATION
NT STATIC DEFORMATION
NT TENSILE DEFORMATION
NT WAVE FRONT DEFORMATION
On the association of erupting magnetic fields with eruptive prominences and coronal mass ejections
01 p0113 N88-10727
Modeling shockwave deformation via molecular dynamics
[DE87-013157] 02 p0169 N88-11063
Buckling of viscoelastic columns
02 p0190 N88-11187
Investigation of the deformation behavior of ferritic two-phase Fe-Ni-Al alloys with high concentrations of the intermetallic (Fe, Ni)Al phase at high temperatures
[ETN-87-90605] 03 p0288 N88-11812
Deformation mechanisms of thermostructural materials
[AD-A184070] 03 p0338 N88-12128
An algorithmic approach to crustal deformation analysis
[NASA-CR-181497] 03 p0349 N88-12203
Finite deformations of shell with rigid inclusion
04 p0426 N88-12639
Fatigue failure of thin porous strips
04 p0426 N88-12640
Explicit and implicit soil modelling for dynamic soil-structure interaction problems
04 p0428 N88-12650
Effective treatment of membrane and shear locking phenomena in curved shear-deformable axisymmetric shell element 04 p0428 N88-12652
A refined nonlinear analysis of laminated composite plates and shells
[AD-A184436] 04 p0454 N88-12811
An algorithmic approach to crustal deformation analysis 04 p0468 N88-12891
Measurement of model deformation in wind tunnels
05 p0551 N88-13358
An analytical study of the effects of transverse shear deformation and anisotropy on buckling loads of laminated cylinders
[NASA-TM-100508] 05 p0557 N88-13387
Cyclic deformation and crack initiation
05 p0597 N88-13646
The orientations of dipolar walls produced by cyclic deformation 05 p0598 N88-13655
Striations and the fatigue growth mechanism in a micro-alloyed steel 05 p0599 N88-13661
The influence of slip mechanism on fatigue of Mg and Mg-2.3Li 05 p0600 N88-13672
Fatigue 87, volume 3
[AD-A184047] 05 p0604 N88-13700
Deformation mechanisms and crack initiation in fatigue 05 p0608 N88-13730
Deformation, fatigue and fracture behavior of two cast anisotropic supetalloys 05 p0608 N88-13732
Viscoelastic properties of EA951 adhesive: A source of creep deformations of a strongback
[DE88-001581] 06 p0685 N88-14197
The evaluation of a deformable diffraction grating for a stigmatic EUV spectroheliometer
[NASA-CR-182371] 06 p0707 N88-14337
Fatigue 87, volume 2
[AD-A184046] 06 p0715 N88-14381
Cyclic deformation behaviour of cast irons with various graphite shapes in the temperature range 20 C less than or = T less than or = 500 C 06 p0715 N88-14384
Transients in elevated temperature crack growth
[DE87-013189] 06 p0724 N88-14454
Composite reliability enhancement via preloading
[AD-A185938] 07 p0826 N88-15010
Deformation effects on microwave reflectivity
[AD-A185684] 07 p0844 N88-15120
Deformation induced cracking in steel girder bridges and retrofit guidelines
[PB88-102710] 07 p0868 N88-15265
The aerophotogrammetric determination of Earth surface deformations
[SER-C-321] 07 p0872 N88-15288
Assessment of anomalous gravitational field of elastic Earth 07 p0921 N88-15594
Study on the mechanical stresses in the elements of the model of a toroidal magnet of a tokamak with strong field
[DE88-700343] 07 p0935 N88-15679
Steady-state deformation of some lithium ceramics
[DE88-003116] 08 p0972 N88-15882
A review of research in rotor loads
09 p1106 N88-16629
Investigation of the deformation behavior of the intermetallic phase (Fe,Ni)Al at high temperatures
[ETN-88-91062] 09 p1143 N88-16854
Successful mixed formulation for axisymmetric shell analysis employing discontinuous stress fields of the same order as the displacement field
[DE88-700021] 09 p1178 N88-17052
An analytical study of the effects of transverse shear deformation and anisotropy on natural vibration frequencies of laminated cylinders
[NASA-TM-100554] 10 p1295 N88-17739
Micro-mechanisms of deformation in SiC/Al composites
[AD-A188282] 10 p1296 N88-17749
Boundary integral analysis of flow and deformation of long bubbles in capillaries
[DE88-002110] 10 p1326 N88-17927
Acoustic emission-microstructural relations in ferritic steels. Part 3: The effect of inclusion content
[AERE-R-12041] 10 p1341 N88-18015
The analysis of deformations and strains in composites by moire interferometry
[AD-A187482] 10 p1345 N88-18043
Continuous deformation algorithm on the product space of unit simplices, revised version
[PB88-114210] 10 p1387 N88-18281
Stability diagrams for epitaxial strained layers
[DE88-003935] 10 p1418 N88-18470
Approximate method for predicting the permanent set in a beam in vacuo and in water subject to a shock wave 11 p1500 N88-18957
Deformations in VLBI antennas
[NASA-TM-100696] 11 p1502 N88-18970
Vibrations of shells containing fluid
12 p1635 N88-19787
Geophysical study of the structure and processes of the continental convergence zones: Alpine-Himalayan Belt
[NASA-CR-182647] 12 p1644 N88-19842
A paper on horizontal deformation in the frontogenesis in south Brazil
[INPE-4469-TDL/322] 12 p1647 N88-19867
Processing, structure and properties of heavily deformed in situ composites
[AD-A189611] 13 p1742 N88-20416
Use of the LLNL 40 kV electric gun to study the shock response of 21-6-9 stainless steel
[DE87-014550] 13 p1742 N88-20418
Grain refinement during primary breakdown of alloy 718
[DE88-005193] 13 p1743 N88-20423
Gordon Conference on Intermetallic Compounds held at Tilton, New Hampshire on 20-24 July 1987
[AD-A188502] 13 p1745 N88-20435
Geodetic measurement of deformation east of the San Andreas fault in Central California
[NASA-CR-182709] 13 p1798 N88-20754
Mechanical properties of sea ice and sea ice deformation in the near-shore zone
[PB88-147889] 13 p1804 N88-20782
Materials dependence of deformation texture development in various deformation modes
[DE88-004312] 14 p1922 N88-21457
Pressure induced ageing of polymers
14 p1929 N88-21504
A unified creep-plasticity model suitable for thermo-mechanical loading 14 p1932 N88-21518
Fundamental studies on high temperature deformation recrystallization, and grain growth of two-phase materials
[AD-A189725] 15 p2038 N88-22145
The buckling and vibration of composite plates using the Levy method considering shear deformation and rotary inertia
[AD-A189743] 15 p2076 N88-22374
Evolution of hardening and damage during viscoplastic deformation
[AD-A190714] 15 p2077 N88-22381
Unified constitutive model for single crystal deformation behavior with applications 15 p2078 N88-22388
Fundamental properties and devices applications of Ge(x)Si(1-x)/Si superlattices
[AD-A190129] 15 p2143 N88-22787
Deformation of rapidly solidified dispersion strengthened titanium alloys
[AD-A190793] 16 p2179 N88-22984
Disclination structures in carbon and graphite
[AD-A191056] 17 p2322 N88-23868
Superplasticity: A fundamental investigation on deformation mechanism and cavitation phenomena
[AD-A191548] 18 p2485 N88-24741
Role of cracks in the creep of structural polycrystalline ceramics
[AD-A191485] 18 p2490 N88-24770
Influence of strain rate on the substructure evolution and yield behavior of Ti-6Al-4V
[DE88-006457] 19 p2616 N88-25520
Accelerated fatigue crack growth behavior of PWA 1480 single crystal alloy and its dependence on the deformation mode
[NASA-TM-100943] 20 p2772 N88-26436
Irreversible deformations during fracture in polymers
[W-7/86] 20 p2780 N88-26485
Spatial dynamics of deformable multibody systems with variable kinematic structure 20 p2813 N88-26687
Diffusion and solubility of some interstitial impurities in deformed metals
[DE88-701859] 21 p2914 N88-27296
Slew-induced deformations in a space-based electromagnetic rail gun 21 p2929 N88-27385
Development of a biaxial test system for thin-walled metal tubes using tensile-compressive axial load and internal-external pressure
[DE88-011279] 21 p2962 N88-27592
DYNA3D (Nonlinear Dynamic Analysis of Structures in Three Dimensions) user's manual
[DE88-012242] 21 p2963 N88-27604
Theory of acoustoplasticity and ultrasonic measurements of residual stresses
22 p3087 N88-28328
The high temperature creep deformation of Si3N4-6Y2O3-2Al2O3
[NASA-CR-183204] 23 p3190 N88-28981
Static and dynamic metal-metal friction at plastic stress levels
[DE88-011281] 23 p3222 N88-29176
Intraplate deformation, stress in the lithosphere and the driving mechanism for plate motions
[NASA-CR-183121] 23 p3231 N88-29231
Preparation and testing of Nb-Zr and Nb-ZrO2 single crystals for deformation studies
[DE88-702798] 23 p3293 N88-29613

DEGENERATION

Regularity properties of a doubly degenerate equation in hydrology
[REPT-87-07] 01 p0064 N88-10409

Squeezed state in degenerate parametric amplification discussed by H. Takahasi in 1963
14 p1976 N88-21790

Squeezed states of light 14 p1976 N88-21791

Quantum statistics of parametric oscillators above threshold 14 p1979 N88-21811

Signal processing with degenerate four-wave mixing
[AD-A191496] 18 p2499 N88-24825

Regularity of solutions for nonlinear degenerate elliptic boundary value problems
[DE88-702646] 22 p3146 N88-28710

DEGRADATION

NT BIODEGRADATION
NT THERMAL DEGRADATION
NT WAVE DEGRADATION

Mechanisms of polymer degradation using an oxygen plasma generator
[NASA-TM-100681] 01 p0018 N88-10110

Mathematical modelling of solar ultraviolet radiation induced optical degradation in anodized aluminum
02 p0135 N88-10846

High intensity 5 eV O-atom exposure facility for material degradation studies 02 p0135 N88-10847

Models of degradation of stratified composite structures
[ONERA-RT-13/3542-RY-061-R]
02 p0142 N88-10892

Degradation mechanisms of materials for large space systems in low Earth orbit
[NASA-CR-181472] 02 p0143 N88-10896

Prevention of radiation induced degradations and of electrostatic perturbations on the Arabsat spacecraft in flight results 03 p0275 N88-11734

Surface catalytic degradation study of two linear perfluoropolyalkylethers at 345 C
[NASA-TP-2774] 04 p0410 N88-12543

Micromechanics of the degradation of composite materials
[SNIAS-872-430-113] 05 p0559 N88-13405

Development of a data analysis system for the detection of lower level atmospheric turbulence with an acoustic sounder
[AD-A184972] 05 p0624 N88-13821

Mechanistic studies of polymeric samples exposed aboard STS 8
[NASA-CR-182364] 06 p0686 N88-14202

Feasibility studies of optical processing of image bandwidth compression schemes
[AD-A186073] 07 p0932 N88-15660

Improved perfluoroalkylether fluid development
[NASA-CR-180872] 08 p0967 N88-15851

Space environmental effects on polymeric materials
[NASA-CR-182454] 09 p1148 N88-16879

Radiant power degradation of silicon-doped gallium arsenide and gallium aluminum arsenide infrared light-emitting diodes
[AD-A186726] 09 p1157 N88-16935

Time dependent degradation of energetic electrons in gaseous and condensed media
[DE88-002912] 09 p1246 N88-17465

Operation of gas turbine engines in dust-laden environments 10 p1280 N88-17654

Environment assisted degradation mechanisms in aluminum-lithium alloys
[NASA-CR-182482] 10 p1301 N88-17782

An experimental measurement of metal multilayer X-ray reflectivity degradation due to intense X-ray flux
[LA-10989-T] 11 p1547 N88-19255

Carbon residue studies of polyphenyl ethers and ester-based lubricants using a microcarbon residue tester
[AD-A188585] 12 p1611 N88-19632

MOSFET performance degradation due to hot carriers
13 p1848 N88-21063

The performance of perfluoropolyalkylether oils under boundary lubrication conditions
[AD-A191057] 17 p2323 N88-23869

Shape stability in composites
18 p2479 N88-24706

Predictive corrosion modeling, volume 1
[AD-A191229] 18 p2485 N88-24739

Environment assisted degradation mechanisms in advanced light metals
[NASA-CR-182907] 18 p2486 N88-24746

Evaluation of the toxicity of products from the thermal degradation of materials
[ETN-88-91995] 18 p2549 N88-25130

Molecular characterization of structure and bonding in thin film materials
[DE88-006811] 18 p2584 N88-25351

Temperature-dependent tensile and shear response of graphite/aluminum
[NASA-CR-182914] 19 p2609 N88-25484

Modeling and experimental measurements of solid propellant flame structure 19 p2631 N88-25605

Predicting optical degradation of a laser beam through a turbulent shear layer 21 p2927 N88-27376

Degradation of fiber composites during storage
[FOA-C-20702-2.6] 22 p3051 N88-28102

The behavior of a Costas loop in the presence of space telemetry signals 22 p3067 N88-28198

Long-term behavior of energy production systems with the example of HELIOS and SYMPHONIE
[ETN-88-92988] 23 p3230 N88-29223

Photoacoustic Fourier transform infrared spectroscopy: An early detection technique for coatings degradation
24 p3354 N88-29968

Degradation of protective coatings on steel in corrosive environments 24 p3354 N88-29969

Prediction of degradation of polymeric coating materials 24 p3354 N88-29970

A reliability-based program for predicting the service life of organic coating systems 24 p3355 N88-29971

DEGREES OF FREEDOM

Traction-drive seven degrees-of-freedom telerobot arm: A concept for manipulation in space
[DE87-010895] 01 p0054 N88-10346

Coupled elastic rotor/body vibrations with inplane degrees of freedom 05 p0596 N88-13643

Analysis and synthesis of two degrees of freedom control systems 11 p1495 N88-18928

An efficient gradient projection optimization scheme for a seven-degree-of-freedom redundant robot with spherical wrist
[DE88-005440] 14 p1919 N88-21453

Distributions of quadratic forms
[AD-A190224] 15 p2124 N88-22663

The VITE model: A neutral command circuit for a generating arm and articulator trajectories
[AD-A192715] 21 p2987 N88-27734

Bifurcations of periodic solutions of non-integrable Hamiltonians with two degrees of freedom: Numerical and analytical results
[DE88-702747] 23 p3272 N88-29473

DEHUMIDIFICATION

Experimental studies of heat and mass exchange in parallel-passage rotary desiccant dehumidifiers for solar cooling applications
[DE88-001119] 10 p1350 N88-18069

DEHYDRATION

Evidence for human adaptive response to dehydration: Increase of circulating protein mass
[AD-A186225] 08 p1048 N88 16328

The role of hydration on peripheral response to cold
[AD-A186448] 09 p1199 N88-17186

Medical problems related to altitude in: Human performance physiology and environmental medicine at terrestrial extremes, chapter 14
[AD-A188340] 12 p1666 N88-19989

Variability in intake and dehydration in young men during a simulated desert walk
[AD-A192654] 22 p3131 N88-28613

DEICERS

Calibration of the ARL (Aeronautical Research Laboratories) rain and icing facility
[AD-A186776] 09 p1121 N88-16710

JUH-1H redesigned pneumatic boot deicing system flight test evaluation
[AD-A194918] 24 p3322 N88-29785

DEICING

Theoretical analysis of the electrical aspects of the basic electro-impulse problem in aircraft de-icing applications
[NASA-CR-180845] 05 p0543 N88-13310

Effects of aircraft deicing/antiicing fluids on airfoil characteristics 08 p0952 N88-15776

The NASA aircraft icing research program
08 p0957 N88-15803

DEICING SYSTEMS

U DEICERS

DEIMOS

Power requirements for mining and microwave processing of extraterrestrial resources
17 p2420 N88-24389

DEKATRONS

U COUNTERS

DELAMINATING

A stochastic delamination growth model for fatigue loaded laminated composite materials
02 p0141 N88-10888

Free-edge delamination: Laminate width and loading conditions effects
[NASA-TM-100238] 04 p0411 N88-12551

Higher order theory analysis of a modified free-edge delamination specimen 04 p0455 N88-12820

Strain-energy-release rate analysis of the end-notched flexure specimen using the finite-element method
[NASA-TM-100494] 05 p0608 N88-13735

Flaw effects: Behavior in operation of delamination in a crossed multilayer composite specimen
[DCQ/L-47-363/F] 06 p0678 N88-14153

Measurement of mechanical parameters to define damage criteria in delamination of crossed stratified layers
[DCQ/L-47-361/F] 06 p0678 N88-14154

Delamination durability of composite materials for rotorcraft 09 p1107 N88-16634

A fiber-resin micromechanics analysis of the delamination front in a DCB specimen
[NASA-TM-100540] 10 p1294 N88-17737

Cost 501 Project UK10 part 3: Thermal fatigue damage of Fecralloy steel-sprayed and co-extruded tubing
[AERE-R-12230] 10 p1343 N88-18026

On delamination of (+ or - theta sub m/90 sub n/2) sub s laminates subject to tensile loading
[AD-A188095] 11 p1447 N88-18626

Damage mechanics of fiber reinforced plastics: A general view 11 p1448 N88-18631

Ply-level failure analysis of a graphite/epoxy laminate under bearing-bypass loading
[NASA-TM-100578] 13 p1735 N88-20372

Delamination stresses in semicircular laminated composite bars
[NASA-TM-4026] 13 p1735 N88-20375

Detection of bondline delaminations in multilayer structures with lossy components
[NASA-CR-182716] 14 p1883 N88-21256

Damage models for delamination and transverse fracture
[AD-A189652] 15 p2029 N88-22088

Fractography of composite delamination
[NASA-CR-182757] 15 p2030 N88-22096

Postbuckling delamination of a stiffened composite panel using finite element methods
[NASA-CR-182803] 15 p2030 N88-22098

Delamination analysis in crossed layer composites
[REPT-48-447/F] 16 p2171 N88-22942

Characterization of Mode 1 and Mode 2 delamination growth and thresholds in graphite/peek composites
[NASA-TM-100577] 16 p2172 N88-22947

Mechanics of instability-related delimination growth
[NASA-TM-100622] 17 p2349 N88-23998

Thermographic detection of buried debonds
[AD-A192115] 18 p2475 N88-24680

Detecting delaminations in CFRP specimens using X-ray techniques
[FFA-TN-1988-04] 18 p2479 N88-24704

Harmfulness of defects: Behaviour in service of a delamination in a composite containing many differently oriented layers
[PB88-124714] 18 p2479 N88-24705

Local delamination buckling in layered structures
18 p2480 N88-24711

Fracture physics of delamination of composite materials
[AD-A192021] 19 p2609 N88-25482

Instability-related delamination growth of embedded and edge delaminations 20 p2767 N88-26406

Three-dimensional analysis of a postbuckled embedded delamination
[NASA-TP-2823] 20 p2812 N88-26684

Failure analysis of laminated composite angles
21 p2959 N88-27578

Fracture behavior in multidimensional fiber-reinforced composites 22 p3051 N88-28099

DELAWARE

Seasonal cycling of sulfur and iron in porewaters of a Delaware salt marsh
[NASA-CR-182385] 07 p0876 N88-15311

DELAWARE BAY (US)

YABLED cruises part 2: Data from YABLED-17 through YABLED-26, January-October 1985
[PB88-163597] 14 p1950 N88-21627

DELAWARE RIVER BASIN (US)

YABLED cruises part 2: Data from YABLED-17 through YABLED-26, January-October 1985
[PB88-163597] 14 p1950 N88-21627

DELAY

On oscillation of a kind of integro-differential equation with delay
[DE87-703059] 02 p0225 N88-11417

Design of efficient FIR filters with minimal delay
[PB87-100434] 04 p0438 N88-12717

A finite element analysis of adhesively bonded composite joints including geometric nonlinearity, nonlinear viscoelasticity moisture diffusion and delayed failure
[AD-A187455] 10 p1296 N88-17747

A pyrotechnic delay ignition system for a submarine launched marine signal
[MRL-R-1079] 13 p1754 N88-20487

Time characteristics of ultrashort light pulses from dye lasers with distributed feedback
14 p1970 N88-21759
Investigation of combustion in large vortices
[AD-A190406] 15 p2035 N88-22121
Estimation of time- and state-dependent delays and other parameters in functional differential equations
[NASA-CR-181663] 17 p2383 N88-24164
The influence of delay effects on the decay of liquid jets
[MPIS-14/1987] 23 p3214 N88-29130

DELAY CIRCUITS
On adaptive signal processing of RF signals
[DE87-014192] 02 p0161 N88-11007
Measured noise performance of a direct-sequence spread-spectrum system and a comparison of single vice dual-channel delay-lock loops
[AD-A186288] 07 p0843 N88-15110
Modules of nanosecond logic electronics system with computer control
[DE88-700190] 11 p1479 N88-18828

DELIVERY
NT PAYLOAD DELIVERY (STS)
NT WEAPONS DELIVERY
Developmental airdrop testing techniques and devices
[AGARD-AG-300-VOL-6] 04 p0398 N88-12481

DELPHI METHOD (FORECASTING)
Critical issues for establishment of a permanently-occupied lunar base
[AD-A187128] 09 p1263 N88-17567

DELTA DART AIRCRAFT
U F-106 AIRCRAFT

DELTA FUNCTION
Finitely many delta-interactions with supports on concentric spheres
[DE88-701834] 20 p2880 N88-27101

DELTA MODULATION
Method for set-up for researching signal curve development
[NASA-TT-20235] 13 p1760 N88-20526

DELTA WINGS
An experimental investigation of dynamic ground effect
[NASA-CR-4105] 04 p0394 N88-12458
Computation of flow past conical hypersonic wings using a second order Godunov method
05 p0533 N88-13241
Vortex formation over delta, double-delta and wave rider configurations at supersonic speeds
05 p0533 N88-13243
Study of the effect of mass transfer on a transonic boundary layer. Application to flow relaminarization
[ETN-88-91169] 05 p0541 N88-13296
Delta wing in incompressible flow. Experimental study in F2
[ONERA-RT-36/1147-AN-249-G]
05 p0541 N88-13298
Examples of static aeroelastic effects on present combat aircraft projects 05 p0550 N88-13349
Supersonic aerodynamics of delta wings
[NASA-TP-2771] 10 p1273 N88-17615
Design loads for Swedish military aircraft in a twenty years' perspective 12 p1580 N88-19456
Research on flow control
[AD-A189014] 12 p1627 N88-19736
Tests on the AFWAL 65 deg delta wing at NLR: A study of vortex flow development between Mach = 0.4 and 4
[NLR-MP-86058-U] 13 p1717 N88-20266
The international vortex flow experiment: A test case for compressible Euler codes
[NLR-MP-86076-U] 13 p1717 N88-20267
Computational technique for compressible vortex flows using the integral equation solution
[NASA-CR-182695] 13 p1718 N88-20271
Vortex flow over a delta wing with apex flaps using laser flow visualisation
[BU-356] 14 p1862 N88-21121
Experimental investigation of the transonic flow at the leeward side of a delta wing at high incidence
[LR-518] 16 p2156 N88-22861
Investigation on the movement of vortex burst position with dynamically changing angle of attack for a schematic deltawing in a watertunnel with correlation to similar studies in windtunnel 16 p2204 N88-23152
Numerical study of delta wing leading edge blowing
[NASA-CR-183101] 20 p2752 N88-26335
Flow around a delta wing with or without a canard control surface (phi BA = 60 deg). Part 1: Hydrodynamic visualization in permanent regime
[ONERA-RT-10/2891-AN-101-A-PT-1]
21 p2892 N88-27170
An experimental study of the effect of pitch rate on delta wing aerodynamics and stability
[NASA-CR-183159] 21 p2893 N88-27173
Optimal control of the wing rock phenomenon
21 p2927 N88-27373
Delta wing configurations 23 p3167 N88-28860
Steady and unsteady transonic pressure measurements on a clipped delta wing for pitching and control-surface oscillations
[NASA-TP-2594] 23 p3173 N88-28895

DELTAS
SDVS (State Delta Verification System): Program verification system development fiscal year 1986
[AD-A184338] 03 p0366 N88-12302
Expectations for water level deviations at the delta works: Zierikzee (Netherlands), November 1981-February 1986
[KNMI-TR-93] 05 p0628 N88-13840
Turbidity patterns in the delta waters of southwest Netherlands on Thematic Mapper (TM) and multispectral scanner (MSS) satellite images
[BCRS-86-06] 16 p2227 N88-23303
Study of the Arachon (France) underwater delta using Thematic Mapper data 19 p2702 N88-26064

DEMAGNETIZATION
An adiabatic demagnetization cooled bolometer system for millimeter continuum astronomy
07 p0943 N88-15735
Statistical analysis of feasibility of non-destructive inspection of mechanical properties of hot worked pipes of alloy steels
[BLL-M-37598-(5828.4)] 14 p1922 N88-21455

DEMAND ASSIGNMENT MULTIPLE ACCESS
L-band and SHF multiple access schemes for the MSAT system 19 p2650 N88-25734
Integrated voice/data protocols for satellite channels
19 p2651 N88-25739

DEMINERALIZING
NT BONE DEMINERALIZATION

DEMODULATION
An additional study and implementation of tone calibrated technique of modulation
[NASA-CR-182377] 07 p0844 N88-15117
The ratio detector: A method of amplitude insensitive frequency demodulation
[RAE-TR-87008] 09 p1153 N88-16910
Trellis-coded MPSK modulation techniques for MSAT-X(sup)1 19 p2648 N88-25721
Demodulation processes in auditory perception
[AD-A193421] 21 p2988 N88-27740
Observational/numerical study of the upper ocean response to hurricanes
[AD-A193592] 22 p3128 N88-28598

DEMODULATORS
NT MODEMS
NT PHASE DEMODULATORS
Documentation of computer programs for optimization and simulation of multicarrier SAW-based demodulator
[PB87-134532] 06 p0693 N88-14252
Multicarrier demodulator design, volume 1 --- communication satellites
[ESA-CR(P)-2468-VOL-1] 09 p1158 N88-16941
Multicarrier demodulator design. Volume 2: Executive summary --- communication satellites
[ESA-CR(P)-2468-VOL-2] 09 p1158 N88-16942
A Differential Phase Shift Keying (DPSK) modulator for a frequency hopping short wave system
[FOA-C-30460-3.3] 18 p2501 N88-24840
Digital carrier demodulation for the DSN Advanced Receiver 22 p3064 N88-28183

DEMOGRAPHY
Problems in integrating geographic data
[DE87-012880] 01 p0106 N88-10689
Contributions to selection and ranking theory with special reference to logistic populations
[AD-A185629] 07 p0917 N88-15568
Ion content and infrared absorption of moist atmospheric air
[AD-A188839] 12 p1643 N88-19838
Survival analysis using additive risk models
[AD-A189053] 13 p1825 N88-20906
Behavioral, psychological and demographic predictors of physical fitness
[AD-A192697] 21 p2986 N88-27733
Utilization of remote sensing for the observation of urban populations. Ongoing research in Quito (Ecuador)
22 p3098 N88-28399

DEMONSTRATION
U PROVING

DENATURATION (BIOPOLYMERS)
U BIOPOLYMER DENATURATION

DENDRITIC CRYSTALS
On the role of convective motion during dendrite growth. Experiments under variable gravity, revised
[NASA-CR-179213] 02 p0156 N88-10979
Modeling growth of interdendritic silicon ribbons
14 p1897 N88-21322
Dendritic growth in the presence of convection
18 p2580 N88-25328
Survey of the literature on fractals with possible applications to phase change processes
[DE88-012240] 21 p2911 N88-27277

DENDRITIC DRAINAGE
U DRAINAGE PATTERNS

DENSE PLASMAS
NT PLASMA FOCUS
NT STRONGLY COUPLED PLASMAS
Variable collision frequency effects on hose and sausage instabilities in relativistic electron beams
[AD-A184206] 04 p0490 N88-13021
Photoionization of atoms and ions: Application of time-dependent response method within the density functional theory
[AD-A185686] 07 p0930 N88-15649
Absorption of electron cyclotron waves by superthermal electron velocity distributions in tokamak plasmas
[INPE-4385-PRE/1205] 08 p1086 N88-16539
New mode conversion process and overdense plasma heating in the electron cyclotron range of frequencies
[IPPJ-854] 10 p1411 N88-18420
Consistency between current ramp-up/recharging scenario by non-inductive current drive and dense and cold divertor plasma. Conceptual design study of FY86 FER
[DE88-751438] 14 p1984 N88-21833
Application of particle simulations to the NRL laser experiment
[AD-A191641] 18 p2520 N88-24953
The influence of ionization within a plasma opening switch
[AD-A193147] 21 p3017 N88-27306

DENSIFICATION
Cast iron freezing mechanisms
03 p0298 N88-11870
Sintering and densification of particulate composites: Inclusion size and clustering
[DE88-002230] 06 p0685 N88-14199

DENSIMETERS
Gamma-ray densitometry: Nondestructive analysis of density evolution during ceramic powder processing
[DE88-006671] 15 p2047 N88-22198

DENSITOMETERS
NT MICRODENSITOMETERS
Computer simulation of the L/sub 3/-edge densitometer
[DE88-001944] 06 p0705 N88-14324

DENSITY (MASS/VOLUME)
NT ATMOSPHERIC DENSITY
NT SPACE DENSITY
Relationships governing change in density in liquid ferrous alloys
[BLL-M-37305-(5828.4)] 02 p0149 N88-10935
Correlation of velocity and velocity-density turbulence in the exhaust of an atmospheric burner
02 p0185 N88-11147
Conservation and transport properties of turbulence with large density variations
[LA-10911-MS] 03 p0321 N88-12032
Studies on some Ge-Se-Te glasses
[PD-MT-8721] 04 p0420 N88-12607
Hydrogen and deuterium in the local interstellar medium 04 p0521 N88-13204
Evolution of spectral densities in weakly inhomogeneous plasmas
[PB87-137402] 06 p0784 N88-14811
Experimental and theoretical studies of dense fluid mixtures
[DE88-002710] 07 p0831 N88-15039
Assessment of anomalous gravitational field of elastic Earth 07 p0921 N88-15594
Void formation in solidification
[DE88-003895] 11 p1452 N88-18650
Injection compression for short fiber reinforced plastics
[SNIAS-881-430-118] 21 p2922 N88-27344
A theoretical determination of the density at a traveling source that emitts particles
[ISAS RN-351] 21 p3013 N88-27883
Diamond like carbon coatings: Categorization by atomic number density
[NASA-CR-174895] 22 p3059 N88-28151

DENSITY (NUMBER/VOLUME)
NT CARRIER DENSITY (SOLID STATE)
NT ELECTRON DENSITY (CONCENTRATION)
NT ELECTRON DENSITY PROFILES
NT ELECTRON DISTRIBUTION
NT ION DENSITY (CONCENTRATION)
NT IONOSPHERIC ELECTRON DENSITY
NT IONOSPHERIC ION DENSITY
NT MAGNETOSPHERIC ELECTRON DENSITY
NT MAGNETOSPHERIC ION DENSITY
NT METEOROID CONCENTRATION
NT PARTICLE DENSITY (CONCENTRATION)

NT PLASMA DENSITY
NT PROTON DENSITY (CONCENTRATION)
NT SPACE DENSITY

Simulations using the pseudo-current algorithm
[DE87-012403] 01 p0040 N88-10255

Rayleigh scattering measurements of a freejet with homogeneous condensation 03 p0319 N88-12020

Refueling and density control in the ZT-40M reversed field pinch
[DE88-000504] 04 p0493 N88-13040

X-rays, color, and the Vaughan-Preston gap
04 p0510 N88-13135

Sliding charge density waves and related problems
[AD-A186720] 09 p1157 N88-16934

Large ionic species in sooting acetylene and benzene flames 24 p3348 N88-29932

DENSITY (RATE/AREA)
U FLUX DENSITY

DENSITY DISTRIBUTION

The pseudopotential density functional method applied to semiconducting crystals
[ETN-88-91362] 05 p0656 N88-14024

Maximum likelihood principle and model selection when the true model is unspecified
[AD-A186027] 07 p0914 N88-15544

Effects of uniform target density on random search
[AD-A186468] 08 p1073 N88-16473

To relate measurements of gravity and geoid anomalies over the oceans to near surface density distributions
[AD-A192168] 18 p2547 N88-25120

Experimental and analytical studies of compressible vortices 19 p2665 N88-25848

Turbulence modelling of flows with non-uniform density 22 p3075 N88-28256

DENSITY MEASUREMENT

Time-resolved temperature and density measurements in ionizing, uniformly irradiated UV-laser-produced plasmas
[DE87-014649] 02 p0238 N88-11504

A composite grating for moire interferometry
[AD-A186330] 07 p0832 N88-15044

Velocity and density measurements in a turbulent nonpremixed flame with comparison to numerical model predictions
[DE87-014695] 08 p0967 N88-15854

Improved resolution atmospheric density measurements based on simulations 08 p1027 N88-16221

Small scale plasma density structures observed by the Viking double probe instrument --- Swedish satellite
08 p1098 N88-16604

Development of an engineering model atmosphere for Mars
[NASA-CR-182462] 09 p1263 N88-17568

Assessment of intercompartment fluid shifts by blood densitometry in astronauts 12 p1661 N88-19958

Study of photochromic materials for use in optical signal processing
[AD-A189068] 13 p1839 N88-21006

Investigation of the inter-relationship between base pavement stiffness and asphalt overlay compaction
[DOT/FAA/ES-88/1] 14 p1869 N88-21170

Estimates of masses, volumes and densities of short-period comet nuclei 14 p2004 N88-21950

Density measurements on solids and liquids
[PB88-164934] 15 p2036 N88-22129

Gamma-ray densitometry: Nondestructive analysis of density evolution during ceramic powder processing
[DE88-006671] 15 p2047 N88-22198

A method of atmospheric density measurements during space shuttle entry using ultraviolet-laser Rayleigh scattering
[NASA-TM-100056] 15 p2069 N88-22337

Annihilation momentum density of positrons trapped at vacancy-type defects in metals and alloys
[DE88-005936] 15 p2144 N88-22797

Summary report on the Japan-US Workshop on the Assessment of Spectroscopic Data for Temperature and Density Measurements --- plasma diagnostics
[IPPJ-861] 17 p2439 N88-24512

Measurements of Z(sub eff) profile with a visible bremsstrahlung continuum detector array
17 p2443 N88-24529

A rapid electrochemical technique for determining the current efficiency for cadmium plating
[AD-A193679] 22 p3056 N88-28130

Wave structures in thermospheric density from satellite electrostatic triaxial accelerometer measurements
[AD-A194134] 23 p3233 N88-29240

DENSITY WAVE MODEL

Dynamical and photometric studies of Saturn's rings
12 p1711 N88-20241

Electrostatic whistler mode conversion at plasma resonance
[AD-A192951] 20 p2860 N88-26989

DEOXYRIBONUCLEIC ACID

DNA damage and repair in human skin in situ
[DE87-014288] 03 p0356 N88-12241

Biopolymers: Protein and nucleic acids
[AD-A185837] 07 p0835 N88-15066

Spleen lymphocyte nucleic acids in pregnant rats flown in space and their offspring 07 p0892 N88-15403

Optimization of the southern electrophoretic transfer method
[DE88-004527] 10 p1299 N88-17765

Effect of weightlessness on replicative function of rat hepatocyte DNA 10 p1360 N88-18129

Ultraviolet (180 to 300 nm) action spectra for inactivation and DNA photoproduct formation of Bacillus subtilis spores under ultrahigh vacuum 12 p1657 N88-19931

Calculation of far infrared absorption in B poly(dA) poly(dT)
[AD-A193128] 21 p2918 N88-27318

Storing bits on a DNA polymer chain
[AD-A195701] 24 p3356 N88-29981

DEPENDENCE
NT SPATIAL DEPENDENCIES
NT TEMPERATURE DEPENDENCE
NT TIME DEPENDENCE

Dependence effects in unique signal transmission
[DE88-010331] 21 p2933 N88-27419

DEPENDENCY
U DEPENDENCE

DEPLETION
NT OZONE DEPLETION

Diffusion bonding depleted uranium to copper
[RFP-3783-REV] 03 p0333 N88-12098

Research studies on extreme ultraviolet and soft X-ray lasers
[AD-A189163] 12 p1633 N88-19773

The timing and mechanism of depletion in Lewisian granulites 24 p3394 N88-30209

DEPLOYMENT

Automation strategy and results for an airbase command and control information system
[NLR-MP-86031-U] 01 p0035 N88-10223

Why mechanisms are critical to spacecraft performance 09 p1125 N88-16737

Space station structures development
[NASA-CR-179261] 09 p1133 N88-16792

The impact of deployment rates on the effectiveness of strategic defenses
[AD-A186907] 09 p1233 N88-17393

Automatic in-orbit payload deployment mechanisms, logistic operations and transport vehicle design compatibilities 12 p1586 N88-19493

Workshop on Technology Development Issues for the Large Deployable Reflector (LDR)
[NASA-CP-2407] 12 p1710 N88-20235

The evaluation and selection of a 5th ground antenna site for the global positioning system
[AD-A189495] 13 p1720 N88-20286

A 60-meter erectable assembly concept for a control of flexible structures flight experiment
[NASA-TM-100497] 14 p1873 N88-21190

Payload deployment system --- STS
14 p1875 N88-21199

The development status of the strongback array --- spacecraft structure 14 p1875 N88-21201

DARM: A new deployment and retraction mechanism which does not need electric power
14 p1876 N88-21206

Deployment, hold down and release mechanisms for Wind Scatterometer Antenna (WSA) --- ERS-1 wind scatterometer antenna (WSA) 14 p1876 N88-21207

Design of a linear actuator and breadboard test result --- far IR telescope 14 p1877 N88-21217

The EURECA antenna deployment and retraction mechanisms 14 p1878 N88-21225

Thermally stable deployable structure
14 p1925 N88-21472

Motion synchronization of a mechanism to deploy and restow a truss beam 14 p1925 N88-21474

A spin and deployment mechanism
14 p1926 N88-21479

Real-time environmental Arctic monitoring (R-TEAM)
[AD-A189948] 15 p2099 N88-22508

Tethered diagnostic package for use from the space station
[DE88-006264] 16 p2167 N88-22921

Payload deployment method and system
[NASA-CASE-MSC-21330-1] 18 p2470 N88-24660

A simulation of post boost vehicle deployment of multiple reentry vehicles
[DE88-009537] 20 p2764 N88-26391

Remotely Operated Vehicle (ROV) reliability study, phase 1
[AD-A194367] 23 p3222 N88-29177

Antisatellite weapons and satellite deployment strategies
[AD-A195014] 24 p3427 N88-30396

DEPOLARIZATION

Investigation of lidar backscatter including depolarization and higher scattering orders
[ETN-87-90431] 01 p0052 N88-10334

Airborne lidar studies of Arctic polar stratospheric clouds 01 p0069 N88-10443

Scattering and depolarization by random rough terrain and vegetation covered terrain-unified full wave approach 12 p1615 N88-19657

Theory of Muon method for study of solid and liquid hydrogen 14 p1972 N88-21770

DEPOLARIZERS
U DEPOLARIZATION

DEPOSITION
NT ANODIZING
NT ELECTRODEPOSITION
NT ELECTROLESS DEPOSITION
NT ELECTROPLATING
NT VACUUM DEPOSITION
NT VAPOR DEPOSITION

Low temperature deposition by laser induced breakdown in the vapor phase
[DE87-007509] 01 p0024 N88-10151

Use of sol-gels in the application of ceramic oxide thin films
[DE87-013610] 01 p0028 N88-10176

The dependence of the normalized ice accretion thickness on cloud-physical parameters
[DFVLR-FB-87-08] 01 p0072 N88-10464

Direct formation of thin films and epitaxial overlayers at low temperatures using a low-energy (10-500 eV) ion beam deposition system
[DE87-012291] 01 p0103 N88-10675

Multilayer monochromators for neutron spectrometers
[DE87-014291] 02 p0175 N88-11093

Turbine airfoil deposition models and their hot corrosion implications 02 p0189 N88-11178

CuInSe2 solar cell research by sputter deposition
[DE87-001184] 02 p0195 N88-11219

Compilation and analysis of air quality data in support of acid deposition research
[DE87-014428] 02 p0196 N88-11226

Thin film microstructures: Simulation and theory
[DE87-014732] 02 p0246 N88-11553

Tribological properties of rf-sputtered MoS2 coatings
[DE88-000266] 04 p0452 N88-12802

A review of parameterizations of microphysical processes in clouds for application in models of regional atmospheric deposition
[DE88-000451] 04 p0471 N88-12909

Far-infrared spectra of lithium deposited on a gold electrode: Interpretation using a cluster model
[AD-A184231] 04 p0495 N88-13050

Computation of rime ice accretion on airfoils
[FFA-TN-1987-08] 05 p0542 N88-13301

Effects of hydrolysis on metallo-organic solution deposition of PZT films
[ATR-86(8443)-1] 06 p0679 N88-14160

The tribological properties of MoS2 coatings in vacuum, low relative humidity and high relative humidity environments
[DE88-001611] 06 p0711 N88-14356

On 1064 nm and 350 nm laser damage thresholds of high index oxide films deposited from organic solutions and sols
[DE88-001636] 07 p0859 N88-15217

Astrophysics and the solar nebula
07 p0883 N88-15355

Nb3Al formation in sputter-deposited Nb/Al mutli-layer samples
[DE88-003192] 08 p0970 N88-15868

Spray deposition: A fundamental study of droplet impingement, spreading and consolidation
[AD-A186627] 08 p0970 N88-15869

Submerged arc flux welding with CaF2-CaO SiO2 fluxes. Possible electrochemical effects on weld metal
[DE88-003107] 08 p0992 N88-16004

Simulation of global wet and dry deposition of nitric acid in a three-dimensional chemistry-transport model
[DE87-009847] 09 p1188 N88-17116

Estimation of aerial deposition and foliar uptake of xenobiotics: Assessment of current models
[DE88-000993] 09 p1188 N88-17117

Surface acoustic wave deposition sensor
[DE87-006527] 09 p1243 N88-17452

Corrosion behavior of sputter-deposited aluminum-based alloys exposed to chloride solutions
[AD-A187262] 10 p1303 N88-17794

Adhesion of vapour phase deposited ultra-thin polyimide films on polycrystalline silver
[AD-A187930] 10 p1306 N88-17810

The soft/hard wet anodization of aluminum oxide and its use in a thin film multilayered capacitor
[AD-A187575] 10 p1325 N88-17919

Apparatus for the study of silicon film deposition and silicon etching
[AD-A187616] 10 p1334 N88-17972
The deposition rate dependence of plasma polymerization on the radius of curvature of the substrate
[DE88-003811] 10 p1412 N88-18429
Growth and electronic properties of strained metal overlayers
[DE87-010956] 10 p1417 N88-18463
Atomistic simulation of low-energy beam deposition
[DE88-004344] 11 p1544 N88-19228
The influence of processing variables on physical properties of sol-gel derived TiO2 films
[DE88-005155] 11 p1559 N88-19331
Scanning tunneling microscopy of silver, gold, and aluminium monomers and small clusters on graphite
[DE88-003871] 11 p1562 N88-19349
Polymeric materials for electro-optic testing
[AD-A188382] 12 p1610 N88-19627
Thin-film diffusion barriers for metal-semiconductor contacts
[AD-A188712] 13 p1844 N88-21035
Photon-controlled growth of multilayered structures
[DE88-005061] 13 p1847 N88-21054
A novel method for sputter-deposition of high T(sub c) superconductor films via a computer-controlled mass analyzed ion beam
[DE88-006001] 13 p1848 N88-21064
An experimental and theoretical study of the ice accretion process during artificial and natural icing conditions
[NASA-CR-182119] 14 p1865 N88-21143
Spatial and temporal distribution of precipitation chemistry across Maryland in 1984, volume 1
[PB88-148929] 14 p1943 N88-21595
Laser photodeposition and etching study
[AD-A190535] 15 p2040 N88-22153
Thin film research diagnostics instrumentation
[AD-A191240] 16 p2213 N88-23207
Standardized ice accretion thickness as a function of cloud physics parameters
[ESA-TT-1080] 16 p2234 N88-23346
Electrophoretic coatings. Part 1: Sandia applications
[DE88-008666] 20 p2776 N88-26465
The effects of Hertzian stress and test ambient on the friction coefficient of MsS2 coatings
[DE88-008118] 20 p2777 N88-26467
Overview of the PRECP (processing of emissions by clouds and precipitation) Program
[DE88-008205] 20 p2822 N88-26741
Carbon deposition model for oxygen-hydrocarbon combustion, volume 1
[NASA-CR-179375] 21 p2908 N88-27254
Carbon deposition model for oxygen-hydrocarbon combustion, volume 2
[NASA-CR-179376] 21 p2908 N88-27255
Amorphous silicon solar cells using a metal substrate
[PB88-131941] 21 p2968 N88-27628
Foliar nitrate reductase: A marker for assimilation of atmospheric nitrogen oxides
[DE88-010453] 21 p2971 N88-27648
Atomic layer epitaxy of ZnS and ZnSe
[AD-A192307] 21 p3020 N88-27928
Erosion/redeposition modeling and calculations for carbon
[DE88-010382] 22 p3057 N88-28139
Atmospheric deposition of nitrate to the ocean surface
23 p3231 N88-29227
New method for preparation of (Cd, Hg)Te thin films
[DE88-702727] 23 p3293 N88-29608
Cluster beam studies
[AD-A195182] 24 p3434 N88-30443

DEPOSITS
Raman scattering as a diagnostic technique for cathode characterization
[AD-A184434] 04 p0439 N88-12726
Development of a laboratory test for multiport injector deposits: Approaches 1 and 2
[AD-A190697] 15 p2048 N88-22203
Development of a laboratory test for multiport fuel injector deposits - evaluation of the Jet Fuel Thermal Oxidation Test apparatus (JFTOT)
[AD-A191313] 16 p2183 N88-23015
Constraints on the origin of fractured terrane, Northern Martian plains 23 p3304 N88-29684
Early cratering rates and the nature of the Martian cratered uplands 23 p3306 N88-29694
Ridged and gullied terrains in the Martian uplands
23 p3307 N88-29700

DEPRESSIONS (TOPOGRAPHY)
U STRUCTURAL BASINS

DEPRESSURIZATION
U PRESSURE REDUCTION

DEPRIVATION
NT SLEEP DEPRIVATION

DEPTH
Transform fault earthquakes in the North Atlantic: Source mechanisms and depth of faulting
03 p0350 N88-12208
Master plots for predicting the case-depth in laser surface treatments
[PB87-221875] 05 p0586 N88-13574
The effect of microstructure on the surface crack length: Crack depth relationship for short cracks
05 p0600 N88-13670
CTD observations in the coastal transition zone off northern California, 16-25 February 1987
[AD-A187283] 10 p1357 N88-18111
Airborne electromagnetic sounding of sea ice thickness and sub-ice bathymetry
[AD-A188939] 12 p1649 N88-19879
Physical, chemical and CTD (Conductivity/Temperature/Depth) data from the Marathon 2 expedition
[AD-A189930] 15 p2099 N88-22507
Television monitor field shifter and an opto-electronic method for obtaining a stereo image of optimal depth resolution and reduced depth distrotion on a single screen
[NASA-CASE-NPO-17249-1-CU]
17 p2332 N88-23924
Construction of approximations to acoustic Green's functions for nonhomogeneous oceans using transmutation
[PB88-185384] 18 p2548 N88-25126
Variational analysis of dielectrically loaded multidepth corrugated waveguides
[PB88-193602] 20 p2793 N88-26573
MIZPAC (marginal ice zone Pacific) 84-86 CTD (Conductivity, Temperature, Depth) data report
[AD-A192478] 21 p2976 N88-27679
Signal processing software for ground penetrating radar, user's manual
[AD-A194286] 23 p3203 N88-29059
Improvements in techniques of microwave thermography
[AD-A193620] 23 p3239 N88-29276
Kalman filter-based algorithms for estimating depth from image sequences
[AD-A195818] 24 p3424 N88-30380

DEPTH MEASUREMENT
Estimation of marine boundary layer depth and relative humidity with multispectral satellite measurements
[AD-A184881] 05 p0620 N88-13804
Penetration depth measurements of YBa2Cu3O/sub 7-delta/ at 4 MHz
[DE88-003493] 10 p1420 N88-18478
Improvements in end point detection --- semiconductor fabrication
[RSRE-MEMO-4035/A] 14 p1899 N88-21336
In-flight measurement of ice growth on an airfoil using an array of ultrasonic transducers
[AIAA-PAPER-87-0178] 17 p2293 N88-23717
Mining volume measurement system
[NASA-CASE-LAR-13519-1] 17 p2342 N88-23963
Contribution of spaceborne high resolution radiometers to mapping of precoastal depths
19 p2701 N88-26063

DEPTH PERCEPTION
U SPACE PERCEPTION

DERIVATION
Studies on syntheses of amine-carboxyboranes (boron analogues of amino acids) and derivatives
[AD-A184838] 05 p0557 N88-13386
Deriving descriptions of the mind
[AD-A186647] 08 p1052 N88-16349
Norm inequalities for derivatives and differences
[DE88-002920] 09 p1230 N88-17371
Derivation of consistent surface fixed fields for use in a global NWP model
[AD-A190131] 15 p2093 N88-22475
Absolute pressure derivatives of deep level defects in 3-5 semiconductors
[DE88-006318] 15 p2140 N88-22772
Microstructure of thin intercalated benezene derived graphite fibers
[AD-A191724] 19 p2618 N88-25534

DESCENT
NT PARACHUTE DESCENT
Study of descent of probes with high lift-drag ratio into the atmosphere of Jupiter 08 p1006 N88-16101

DESCENT TRAJECTORIES
NT REENTRY TRAJECTORIES
The Valec fireball and predicted meteorite fall
06 p0739 N88-14547
Investigation of the validity of the non-rotating planet assumption for three-dimensional earth atmospheric entry
[AD-A194877] 24 p3331 N88-29829

DESCRIPTIONS
Linguistic definition of generic models in computer vision
[RSRE-MEMO-4110] 17 p2386 N88-24182

DESCRIPTIVE GEOMETRY
Workshop on the Integration of Finite Element Modeling with Geometric Modeling
[NASA-CR-182515] 11 p1526 N88-19111
Finite element meshing of ANSYS (trademark) solid models 11 p1526 N88-19115
Solid/FEM integration at SNLA
[SAND-87-0882A] 11 p1526 N88-19116
Octree based automatic meshing from CSG models
11 p1527 N88-19117
Geometrical and topological issues in octree based automatic meshing 11 p1527 N88-19118
A hierarchical structure for automatic meshing and adaptive FEM analysis 11 p1527 N88-19119
Geometric versus finite element modeling current and future trends at Northrop 11 p1528 N88-19125
Definition and display of pro[illegible]ed sweep-objects --- computer graphics
[REPT-87-45] 14 p1957 N88-21665

DESERTIFICATION
Desertification in the Sahelian and Sudanian Zones of West Africa
[PB87-217063] 03 p0345 N88-12183
Environmental processes and spectral reflectance characteristics associated with soil erosion in desert fringe regions
[NASA-CR-182332] 05 p0620 N88-13811
Sensitivity of general circulation models to surface processes 14 p1937 N88-21556
Evaluation of the grassy biomass in the Sahelian zone in the South Tamesna region (Niger): Prospects and limits of use of SPOT data 22 p3092 N88-28359
Preliminary comparative analysis of LANDSAT and SPOT data for the study of the sanding phenomenon: Zaafrane region (Algeria) 22 p3099 N88-28402

DESERTS
NT SAHARA DESERT (AFRICA)
Enhancement of surface-atmosphere fluxes by desert-fringe vegetation through reduction of surface albedo and of soil heat flux
[NASA-CR-181442] 02 p0197 N88-11231
Desertification in the Sahelian and Sudanian Zones of West Africa
[PB87-217063] 03 p0345 N88-12183
A Workshop on Desert Processes, September 24-28, 1984: Report on the conference
[AD-A184599] 03 p0345 N88-12184
Environmental processes and spectral reflectance characteristics associated with soil erosion in desert fringe regions
[NASA-CR-182332] 05 p0620 N88-13811
Daily dynamics of some physiological indicators of man under desert condition 06 p0750 N88-14605
Summary of along-track data from the Earth radiation budget satellite for several major desert regions
[NASA-RP-1197] 13 p1802 N88-20772

DESICCANTS
Mass transfer mechanisms for water adsorbed on silica gel
[DE88-005993] 15 p2032 N88-22107

DESICCATION
U DRYING

DESIGN ANALYSIS
A feasibility study of a hypersonic real-gas facility
[NASA-CR-180423] 01 p0008 N88-10043
Space station integrated wall design and penetration damage control
[NASA-CR-179169] 01 p0013 N88-10070
Redesign of solid rocket booster/external tank attachment ring for the space transportation system
[NASA-TM-100476] 01 p0017 N88-10101
Design and analysis of a broadband TM(sub 01) mode generator in cylindrical waveguide
[DE87-011308] 01 p0038 N88-10243
V-band IMPATT power amplifier
[NASA-CR-180711] 01 p0042 N88-10267
Assessment of the COFSI/MAST I project
[NASA-CR-181366] 01 p0053 N88-10340
Study of free-piston Stirling engine driven linear alternators
[NASA-CR-181425] 01 p0055 N88-10355
Monitored background radiometer
02 p0133 N88-10831
Vacuum pumps and systems: A review of current practice 02 p0134 N88-10839
Contribution to the development of smart design techniques for VLSI integrated circuits --- CMOS
[LAAS-87-181] 02 p0221 N88-11395
A neutron detector based on microchannel plates
[DE87-014703] 02 p0232 N88-11466
Saturn: A large area X-ray simulation accelerator
[DE87-012021] 02 p0233 N88-11472

A conceptual design of Final Focus Systems for linear colliders
[DE87-012840] 02 p0234 N88-11475

Rotorcraft Design for Operations
[AGARD-CP-423] 03 p0262 N88-11649

The influence of operational requirements on LHX concept formulation 03 p0262 N88-11650

Design requirements for future commercial operations
03 p0262 N88-11651

Combined calculation of deformation and stress for the body and sabot of an APFSDS
03 p0302 N88-11899

Physical design of parameters of Nd YAG disk laser
03 p0302 N88-11904

Conceptual design of a high-resolution pion (0) spectrometer
[DE87-014757] 03 p0324 N88-12047

Conservatism implications of shock test tailoring for multiple design environments
[DE87-013927] 03 p0338 N88-12127

The design and preliminary calibration of a boundary-layer flow channel
[NASA-CR-178399] 04 p0394 N88-12457

Structural analysis of a bolted joint concept for the space shuttle's solid rocket motor casing
[NASA-TM-89092] 04 p0407 N88-12531

Optimization techniques applied to passive measures for in-orbit spacecraft survivability
[NASA-CR-179216] 04 p0408 N88-12532

New feedback design methodologies for large space structures A multi-criterion optimization approach
04 p0408 N88-12535

Multicast gateway design considerations
[PB87-219960] 04 p0430 N88-12663

On the VLSI design of a pipeline Reed-Solomon decoder using systolic arrays 04 p0436 N88-12700

A procedural method for the efficient implementation of full-custom VLSI designs 04 p0436 N88-12701

On dynamic loads in parallel shaft transmissions. 1: Modelling and analysis
[NASA-TM-100180] 04 p0451 N88-12797

On dynamic loads in parallel shaft transmissions. 2: Parameter study
[NASA-TM-100181] 04 p0452 N88-12798

Nonlinear axial stiffness characteristics of axisymmetric bolted joints 04 p0452 N88-12799

Design and development of absorption heat pumps
[DE88-900082] 04 p0466 N88-12885

An expert system for materials design
[DE88-000191] 04 p0483 N88-12974

Design concepts for the ASTROMAG cryogenic system
[NASA-CR-181505] 04 p0497 N88-13060

Thermodynamic properties for natural gas binaries
[PB87-226833] 04 p0500 N88-13074

Aerodynamics of Hypersonic Lifting Vehicles
[AGARD-CP-428] 05 p0529 N88-13219

Lifting bodies: An attractive aerodynamic configuration choice for hypervelocity vehicles
05 p0534 N88-13248

Design of wings and wing/body configurations for transonic and supersonic speeds
05 p0545 N88-13318

Aeroelastic analysis of modern transport aircraft --- European Airbus
[SNIAS-872-111-102] 05 p0546 N88-13329

Design and assembly sequence analysis of option 3 for CETF reference space station
[NASA-TM-100503] 05 p0553 N88-13369

Evaluation of device figure of merit in microwave switching circuit design
[AD-A184896] 05 p0577 N88-13520

A complete linearized theory for the analysis and design of two-dimensional hydrofoils near a free surface
[UTIAS-TN-264] 05 p0579 N88-13531

Conservatism implications of shock test tailoring for multiple design environments 05 p0592 N88-13611

Near-threshold growth of defects in engineering materials 05 p0603 N88-13691

Utilization of dynamic characteristics of materials to optimize military explosive charges. Application to antiship devices
[SNIAS-872-320-101] 05 p0610 N88-13743

STAEBL/general composites with hygrothermal effects (STAEBL/GENCOM)
[NASA-TM-100266] 05 p0611 N88-13754

High speed propeller performance and noise predictions at takeoff/landing conditions
[NASA-TM-100267] 05 p0646 N88-13960

Photon counting image sensor development for astronomical applications
[NASA-CR-181507] 05 p0660 N88-14049

Ducted propeller design and analysis
[DE88-001925] 06 p0664 N88-14069

Nonlinear aerodynamic wing design
[NASA-CR-3950] 06 p0665 N88-14079

Large-Scale Advanced Prop-Fan (LAP) blade design
[NASA-CR-174790] 06 p0668 N88-14097

Design verification and fabrication of active control systems for the DAST ARW-2 high aspect ratio wing, part 1
[NASA-CR-177959-PT-1] 06 p0669 N88-14101

Design verification and fabrication of active control systems for the DAST ARW-2 high aspect ratio wing. Part 2: Appendices
[NASA-CR-177959-PT-2] 06 p0669 N88-14102

Small High Pressure Ratio Turbines --- conference
[VKI-LS-1987-07] 06 p0712 N88-14364

High pressure ratio turbine design constraints
[TRR-0279] 06 p0712 N88-14365

Mainline performance prediction for radial inflow turbines 06 p0712 N88-14366

Conclusions from a research program on mixed flow gas generator turbines 06 p0713 N88-14368

Highlights from a research program on a very highly loaded axial gas generator turbine
06 p0713 N88-14369

Aerodynamic design of first stage turbines for small aero engines 06 p0713 N88-14370

Design, fabrication and delivery of a miniature Cassegrainian concentrator solar array system
[NASA-CR-179237] 06 p0730 N88-14493

Controlled Ecological Life Support Systems (CELSS) conceptual design option study
[NASA-CR-177421] 06 p0754 N88-14625

Using concept mapping to define problems and identify key kernels during the development of a decision support system
[AD-A185636] 06 p0762 N88-14674

Overview of the TIBER 2 (Thermal Ignition/Burn Experimental Reactor) design
[DE88-001892] 06 p0783 N88-14804

Maximum entropy/optimal projection design synthesis for decentralized control of large space structures
[AD-A186359] 07 p0824 N88-15003

Space station onboard propulsion system: Technology study
[NASA-CR-179233] 07 p0825 N88-15006

Simplified procedures for designing composite bolted joints
[NASA-TM-100281] 07 p0828 N88-15020

Flow in Centrifugal Compressors --- conference
[VKI-LS-1987-01] 07 p0850 N88-15160

Centrifugal compressors 07 p0850 N88-15162

The technology of centrifugal compressors: A design approach and new goals for research
07 p0850 N88-15163

Identification and avoidance of instabilities in high performance turbomachinery 07 p0850 N88-15164

Flow in labyrinth seals and its influence on rotor stability of turbocompressors 07 p0851 N88-15168

Human performance data needed for training device design decisions
[AD-A185988] 07 p0898 N88-15441

On two methods of identifying influential sets of observations
[AD-A186270] 07 p0910 N88-15518

The development of test methodology for testing glassy materials 07 p0927 N88-15633

Development of direct-inverse 3-D methods for applied aerodynamic design and analysis
[NASA-CR-182436] 08 p0950 N88-15767

Aeropropulsion '87. Session 2: Aeropropulsion Structures Research
[NASA-CP-10003-SESS-2] 08 p0954 N88-15785

Aeropropulsion structures 08 p0954 N88-15786

Determining structural performance
08 p0954 N88-15787

Life prediction technologies for aeronautical propulsion systems 08 p0954 N88-15788

Integrated analysis and applications
08 p0954 N88-15789

Aircraft engine hot section technology: An overview of the HOST Project 08 p0957 N88-15804

Analysis, design, construction and testing of a reaction wheel model for space applications
[INPE-4358-TDL/299] 08 p0963 N88-15834

Servicer system demonstration plan and capability development
[NASA-CR-179246] 08 p0975 N88-15895

Liquid spring design methodology for shock isolation system applications 08 p0998 N88-16043

Design and test of a spacecraft instrument shock isolator 08 p0998 N88-16044

Review of fatigue and fracture research at NASA Langley Research Center 09 p1106 N88-16633

A note on the aerodynamic design of thin parallel-sided aerofoil sections
[ARL-AERO-TM-388] 09 p1114 N88-16677

Columbus feasibility studies. Volume 1: Requirements and system concept
[ETN-88-91073] 09 p1134 N88-16799

Design procedures for fiber composite box beams
[NASA-TM-100296] 09 p1139 N88-16828

Study on a double reflector compact range --- satellite antennas
[S-201-05] 09 p1153 N88-16908

The WAFTER: A versatile wear and friction tester
[MRL-TN-519] 09 p1169 N88-17012

Design feasibility report on investigation of magnetic bearings for the ocean colour monitor radiometer scanner
[BAE-TP-7849] 09 p1174 N88-17036

An integration test for accelerometer evaluation
09 p1178 N88-17054

Study of large solar arrays (SOLA), phase 2A
[BAE-SS/1109] 09 p1186 N88-17106

A comparison of different module configurations for multibandgap solar cells
[DE88-002718] 09 p1187 N88-17113

Bioreactor design concepts 09 p1197 N88-17171

Design of a neural network simulator on a transputer array 09 p1205 N88-17221

Interchange of electronic design through VHDL and EIS 09 p1205 N88-17222

The IDEAL (Integrated Design and Engineering Analysis Languages) modeling methodology: Capabilities and Applications 09 p1206 N88-17227

Interfacing slave designs to Fastbus: Practical experience
[DE88-002807] 09 p1215 N88-17286

CEBAF design overview and project status
[CEBAF-PR-88-001] 09 p1246 N88-17470

Two-phase reduced gravity experiments for a space reactor design
[DE86-015530] 09 p1247 N88-17475

Study of Large Solar Arrays (SOLA). Phase 2A. Amplifying information to final report (SS/1109)
[BAE-SS/1110] 09 p1248 N88-17480

The TITAN Reversed-Field Pinch Reactor: Design-point determination and parametric studies
[DE88-001824] 09 p1251 N88-17498

A transonic-small-disturbance wing design methodology
[NASA-TP-2806] 10 p1273 N88-17614

An integrated aero/mechanical performance approach to high technology turbine design
10 p1280 N88-17657

Design and test of a high blade speed, high work capacity transonic turbine 10 p1281 N88-17658

Design and development of an advanced F100 compressor 10 p1283 N88-17678

Design and testing of a front stage for an advanced high pressure compressor 10 p1283 N88-17679

The design of trellis codes for fading channels
[NASA-CR-182523] 10 p1320 N88-17891

Solid-state voltage standard performance and design guidelines
[PB88-123757] 10 p1322 N88-17905

A computational study of thrust augmenting ejectors based on a viscous-inviscid approach
10 p1326 N88-17929

Three-dimensional incompressible flowfield analysis for establishing rotor designs which optimize power extraction 10 p1329 N88-17943

Optimal design and parameter identification of flexible rotor-bearing systems 10 p1339 N88-18002

Design sensitivity analysis of nonlinear structural systems and numerical implementation with established finite element codes 10 p1344 N88-18032

Optimum design of geodesically stiffened composite plates
[NASA-CR-182499] 10 p1344 N88-18035

Design and implementation of a fiber optic RS232 link
[AD-A187319] 10 p1409 N88-18409

A collaborative program of research in engineering sciences
[DE88-003383] 10 p1423 N88-18504

A performance index approach to aerodynamic design with the use of analysis codes only
[NASA-TP-2805] 11 p1433 N88-18552

The aerodynamic design optimisation of a forward swept wing fighter aircraft
[CAR-87-18] 11 p1433 N88-18553

Modification of integrated partial payload lifting assembly
[NASA-CR-182573] 11 p1443 N88-18607

Orbiter transfer vehicle concept definition and system analysis study. Volume 4: Space station accommodations. Revision 1
[NASA-CR-179293] 11 p1444 N88-18609

Orbital transfer vehicle concept definition and system analysis study. Volume 4, Appendix A: Space station accommodations. Revision 1
[NASA-CR-179294] 11 p1444 N88-18610

An optimal structure for a 34-meter millimeter-wave center-fed BWG antenna: The Cross-Box concept
11 p1472 N88-18778

STA-2A NDT testing
[NASA-CR-179301] 11 p1497 N88-18937

Application of advanced computational technology to propulsion CFD
[NASA-TM-100843] 11 p1525 N88-19102

Aerodynamic characteristics of wings designed with a combined-theory method to cruise at a Mach number of 4.5
[NASA-TP-2799] 12 p1575 N88-19420

Evaluation of a miniature horizontal pendulum tilt transducer 12 p1577 N88-19435

Presentation of structural component designs for the family of commuter airplanes
[NASA-CR-182568] 12 p1581 N88-19463

A class 2 weight assessment for the implementation of commonality and preliminary structural designs for the family of commuter airplanes
[NASA-CR-182565] 12 p1581 N88-19464

Rotorcraft flight-propulsion control integration: An eclectic design concept
[NASA-TP-2815] 12 p1584 N88-19475

Conceptualization and design of a variable-gravity research facility
[NASA-CR-182574] 12 p1595 N88-19550

Structural shape optimization in multidisciplinary system synthesis
[NASA-TM-100538] 12 p1614 N88-19650

VSLI design generators
[AD-A188706] 12 p1623 N88-19707

Concentrating photovoltaic collectors: Fabrication design
[PB88-148051] 12 p1640 N88-19821

Regenerative life support system research
[NASA-CR-182606] 12 p1671 N88-20006

Development savings through parametric modeling of program costs 12 p1700 N88-20175

The Joint NASA/Goddard-University of Maryland Research Program in Charged Particle and High Energy Photon Detector Technology
[NASA-CR-182612] 12 p1712 N88-20247

The design and use of a temperature-compensated hot-film anemometer system for boundary-layer flow transition detection on supersonic aircraft
[NASA-TM-100421] 13 p1723 N88-20304

Turnaround operations analysis for OTV. Volume 1: Executive summary
[NASA-CR-179316] 13 p1729 N88-20340

Turnaround operations analysis for OTV. Volume 2: Detailed technical report
[NASA-CR-179317] 13 p1729 N88-20341

Synthesis method applied to the design of an electron gun for a gyrotron
[INPE-4357-TDL/298] 13 p1773 N88-20607

On the sensitivity of complex, internally coupled systems
[NASA-TM-100537] 13 p1813 N88-20829

A new algorithm for general multiobjective optimization
[NASA-TM-100536] 13 p1813 N88-20830

Potential off-normal events and associated radiological source terms for the compact ignition tokamak: Fusion Safety Program
[DE88-004112] 13 p1842 N88-21024

Optimal filament shells loaded with internal pressure in a centrifugal force field 14 p1885 N88-21266

Design, optimization and construction of a dc-SQUID with complete flux transformer circuits
[PB88-160742] 14 p1907 N88-21399

Performance of elastomeric bearings
[PB88-159470] 14 p1918 N88-21450

Advanced transmission studies
[NASA-TM-100867] 14 p1919 N88-21454

Computational aspects of sensitivity calculations in transient structural analysis
[NASA-TM-100589] 14 p1924 N88-21467

Aero/structural tailoring of engine blades (AERO/STAEBL)
[NASA-CR-180805] 14 p1959 N88-21682

Comparison of entropy generation and conventional design methods for heat exchangers
[AD-A190256] 15 p2064 N88-22306

FLOSIN: A fluid loop analyzer for SINDA
15 p2066 N88-22321

Constellation sizing for modest directed energy platforms
[DE88-007033] 15 p2070 N88-22343

Improvements to tilt rotor performance through passive blade twist control
[NASA-TM-100583] 15 p2086 N88-22434

Water facilities in retrospect and prospect: An illuminating tool for vehicle design
16 p2200 N88-23126

Aerodynamic and thermal modeling of electromagnetic brakes. Evaluation of convective exchange coefficients and friction losses in the rough wall channels
[ISAL-ITC1-87-02] 16 p2215 N88-23214

Mixed finite element formulation applied to shape optimization 16 p2221 N88-23252

Design of high yield microprocessors
[ETN-88-92184] 16 p2245 N88-23410

Silicon compilers: Application to the compilation of the control area
[ETN-88-92186] 16 p2247 N88-23425

Full potential methods for analysis/design of complex aerospace configurations
[NASA-CR-3982] 17 p2296 N88-23736

Sensitivity analysis and multidisciplinary optimization for aircraft design: Recent advances and results
[NASA-TM-100630] 17 p2302 N88-23766

A structured approach to weapon system design
17 p2303 N88-23773

A change in system design emphasis: From machine to man 17 p2304 N88-23782

Interfacing and integrating hardware and software design systems 17 p2306 N88-23796

A design analysis for an automated robotic workpiece manipulator 17 p2344 N88-23975

Assessment of nuclear reactor concepts for low power space applications 17 p2423 N88-24409

The Curie point radiator 17 p2424 N88-24420

Computational design of low aspect ratio wing-winglet configurations fór transonic wind-tunnel tests
[NASA-CR-183021] 18 p2464 N88-24630

Design study. Manipulator systems for model handling in European transonic wind tunnels
[ETN-88-91944] 18 p2468 N88-24651

A design study of onboard navigation and guidance during aerocapture at Mars
[NASA-CR-172053] 18 p2469 N88-24654

Designing to safe power limits in hybrid circuits
[DE88-005533] 18 p2506 N88-24865

Optimization of reserve lithium thionyl chloride battery electrochemical design parameters
[DE88-007109] 18 p2506 N88-24868

Aurora status and plans
[DE88-006476] 18 p2521 N88-24955

Applications of fault tree analysis to the design process
[DE88-007048] 18 p2525 N88-24982

Limits of design feasibility of multiwing wind turbines with individual articulated wing structure
[ILR-MITT-180] 18 p2537 N88-25052

Systems analysis of INTOR-like designs
[DE88-004422] 18 p2578 N88-25316

Design studies of low aspect-ratio torsatrons
[DE88-007562] 18 p2579 N88-25320

Space station architectural elements and issues definition study
[NASA-CR-3941] 18 p2587 N88-25371

Two-dimensional viscous flow computations of hypersonic scramjet nozzle flowfields at design and off-design conditions
[NASA-CR-182150] 19 p2603 N88-25459

Advanced heat receiver conceptual design study
[NASA-CR-180901] 19 p2688 N88-25977

Mechanisms for particle acceleration: Possibilities and constraints
[PB88-102538] 19 p2725 N88-26184

Some operational aspects of a rotating advanced-technology space station for the year 2025
[NASA-CR-181617] 20 p2765 N88-26397

Radar cross section studies/compact range research
[NASA-CR-183124] 20 p2792 N88-26565

The Oak Ridge Heat Pump Design Model: Mark 3 version program documentationon
[DE88-007863] 20 p2799 N88-26607

Improvement of head-up display standards. Volume 1: Head-up display design guide, appendix
[AD-A192973] 20 p2834 N88-26809

Programs for preliminary design of composite materials which were developed by the design group of Aerospatiale Aquitaine
[REPT-881-430-112] 21 p2907 N88-27251

Estimation of power-energy plots for secondary batteries
[DE88-011922] 21 p2940 N88-27460

Optimization of planetary gears
[ETN-88-92375] 21 p2958 N88-27573

Modal testing in the design evaluation of wind turbines
[DE88-010374] 21 p2968 N88-27632

Magnetic heat pumps
[DE88-012058] 21 p2969 N88-27639

Computer simulation procedure for designing airborne aerometric monitoring programs
[DE88-011896] 21 p2975 N88-27674

Development of direct-inverse 3-D methods for applied transonic aerodynamic wing design and analysis
[NASA-CR-183127] 22 p3037 N88-28033

Dual adaptive control: Design principles and applications
[NASA-CR-177485] 22 p3038 N88-28038

Advanced computational methods for turbomachinery blade design
[PNR90438] 22 p3044 N88-28065

Holographic interferometry for flow visualization studies in high speed fans
[PNR90459] 22 p3045 N88-28072

Structural Tailoring of Advanced Turboprops (STAT)
[NASA-CR-180861] 22 p3045 N88-28074

Design analysis in polymeric materials
[NPL-DMA(A)-159] 22 p3058 N88-28147

Coupled inviscid - boundary layer methods for turbomachinery blading design
[PNR90437] 22 p3076 N88-28280

Modeling, designing and simulating a pointing control system for balloon-borne solar experiments
[NASA-TM-100337] 22 p3082 N88-28300

Design and evaluation of high contact ratio gearing
[NASA-CR-174958] 22 p3085 N88-28319

Reliable onboard computing for critical space systems
[RR-670-I] 22 p3135 N88-28641

A contribution to the quantitative analysis of the influence of design parameters on the optimal design of passenger aircraft
[ETN-88-92979] 23 p3176 N88-28912

SRB/SLEEC (Solid Rocket Booster/Shingle Lap Extendible Exit Cone) feasibility study, volume 1
[NASA-CR-178973] 23 p3187 N88-28964

LLE (Laboratory for Laser Energetics) review
[DE88-008065] 23 p3219 N88-29158

Leaf spring
[GB-PATENT-2-192-689-A] 23 p3222 N88-29179

Digital filter design techniques
[AD-A194484] 23 p3274 N88-29486

Euler analysis of a swirl recovery vane design for use with an advanced single-rotation propfan
[NASA-TM-101357] 24 p3320 N88-29771

Spacecraft mass estimation, relationships and engine data: Task 1.1 of the lunar base systems study
[NASA-CR-172061] 24 p3332 N88-29836

Design criteria for extraction with chemical reaction and liquid membrane permeation
[NASA-TT-20352] 24 p3343 N88-29899

Circuit design criteria for stable lateral inhibition neural networks
[AD-A195066] 24 p3366 N88-30046

Advanced planar array development for space station
[NASA-CR-179373] 24 p3389 N88-30181

Design and performance analysis of a relational replicated database system
[AD-A196290] 24 p3437 N88-30456

DESIGN OF EXPERIMENTS
U EXPERIMENT DESIGN

DESIGN TO COST

Operational groups at the Aerospatiale Aircraft Division
[SNIAS-872-111-107] 05 p0658 N88-14036

The space station assembly phase: Flight telerobotic servicer feasibility, volume 1
[NASA-CR-182689] 13 p1731 N88-20351

DESORPTION

Study of field adsorption using pulsed-laser field ion microscopy
[DE88-000310] 03 p0330 N88-12085

Ro-vibrational laser spectroscopy of ESD neutrals from chemisorbed species
[DE87-013011] 04 p0447 N88-12770

Photon stimulated desorption from oxidized Al(110)
[DE88-002209] 06 p0787 N88-14828

Particle desorption from nonconducting surfaces by high energy heavy ions
[ETN-88-91088] 09 p1245 N88-17461

Laser-induced desorption determinations of surface diffusion on Rh(111)
[DE88-005159] 11 p1454 N88-18667

Laser measurements of state-resolved Ga and in atom sticking and desorption on metal and semiconductor surfaces
[AD-A187644] 11 p1555 N88-19310

Electron stimulated desorption and coherent electron scattering
[AD-A189091] 13 p1835 N88-20978

Image charge, coherent scattering, and symmetry effects in electron stimulated desorption: O(-) from O sub 2 condensed on metals
[AD-A189093] 13 p1835 N88-20979

The magnitude of secondary electron contributions in photon stimulated desorption
[AD-A189094] 13 p1835 N88-20980

Hydrogen pumping and release by graphite under high flux plasma bombardment
[DE88-005880] 13 p1842 N88-21021

Implications of the trapping-desorption and direct inelastic scattering channels on Dicke-narrowed lineshapes
[AD-A191410] 16 p2270 N88-23581

A mass spectrometer for the analysis of thermally labile compounds 19 p2668 N88-25859
Isothermal measurement and thermal desorption using SAW devices 19 p2671 N88-25881
Development of computer-controlled thermogravimetric instrumentation for measurement of environmental and high temperature volatilization and desorption of contaminants from polymeric materials
[AD-A195934] 24 p3343 N88-29900

DESPINNING
U SPIN REDUCTION

DESTRUCTION
Destruction test of small scaled solid propellant motors
[ISAS-R-620] 03 p0278 N88-11752
Formation and destruction of nitrous oxide in lean, premixed combustion
[DE88-001390] 05 p0562 N88-13423

DESTRUCTIVE TESTS
NT BURST TESTS

DESULFURIZING
Compact regenerable sulfur scrubber for phosphoric acid fuel cells
[AD-A191356] 16 p2230 N88-23318

DESYNCHRONIZATION (BIOLOGY)
Desynchronization of heart rate and breathing frequency after transmeridional flight across three time zones
12 p1663 N88-19968
Risk of hypertension and functional cerebral laterality in oil expedition works in far north
12 p1665 N88-19980
Biological rhythms, sleep, and wakefulness in prolonged confinement 19 p2696 N88-26022

DESYNCHRONIZED SLEEP
U RAPID EYE MOVEMENT STATE

DETECTION
NT AIRCRAFT DETECTION
NT CHANGE DETECTION
NT CORRELATION DETECTION
NT MISSILE DETECTION
NT RADAR DETECTION
NT REMOTE SENSING
NT SIGNAL DETECTION
NT TARGET RECOGNITION
NT ULTRASONIC FLAW DETECTION
Detection of CO2-induced climate change
[DE87-013127] 01 p0071 N88-10457
Optimal detection of sensor failures in flight control systems using deterministic observers
02 p0128 N88-10803
Incipient fault detection study for advanced spacecraft systems
[NASA-CR-172014] 02 p0183 N88-11138
Detection of vapors of flammable liquids in air by atmospheric sampling mass spectrometry/mass spectrometry
[DE88-000030] 02 p0196 N88-11227
Evaluation of one-sided nuclear magnetic resonance for remote detection of explosives
[AD-A184490] 03 p0296 N88-11857
Free radical detection and reactions in the decomposition of energetic materials
[AD-A184677] 03 p0296 N88-11858
Techniques for fire detection
04 p0406 N88-12521
Incipient failure detection of space shuttle main engine turbopump bearings using vibration envelope detection
05 p0595 N88-13629
Development of FTMS methods for the detection of trace chemical species and development of FTMS methods for the analysis of various chemical species
[AD-A185857] 07 p0828 N88-15023
A comparison of film-based tomography and computed tomography for advanced ceramic materials
[DE88-003114] 07 p0837 N88-15079
Study on automatic detection and identification of defects in weld by microcomputer
[PB87-143897] 07 p0863 N88-15237
Inadequacy of conventional dynamic recovery mechanisms in the presence of temporary failures
[AD-A186311] 07 p0866 N88-15251
Model-based building verification in aerial photographs
[AD-A186010] 07 p0870 N88-15278
NORSAR detection processing system
[AD-A185968] 07 p0877 N88-15318
Object detection in images from outdoor scenes using evidential reasoning
[FOA-C-30461-3.3] 08 p1020 N88-16183
A data structure and algorithm for fault diagnosis
08 p1065 N88-16432
Effects of uniform target density on random search
[AD-A186468] 08 p1073 N88-16473
Low frequency eddy current detection and evaluation of corrosion in aircraft skins
[ETN-88-91664] 09 p1144 N88-16859
Fundamental aspects of the physics of remote sensing
[ESA-TT-1045] 09 p1185 N88-17100
Pattern-recognition softwares detecting the onset of failures in complex systems
[DE88-002861] 09 p1220 N88-17318
Strong consistency of certain information theoretic criteria for model selection in calibration, discriminant analysis and canonical correlation analysis
[AD-A186584] 09 p1232 N88-17385
Airborne Wind Shear Detection and Warning Systems: First Combined Manufacturers' and Technologists' Conference
[NASA-CP-10006] 10 p1273 N88-17616
Windshear detection effect of static air temperature bias 10 p1274 N88-17621
Lidar windshear detection and avoidance: Performance and technical assessment 10 p1274 N88-17626
The advanced low-level windshear alert system operational demonstration results, Summer, 1987, Denver Stapleton International Airport 10 p1275 N88-17633
NMR (Nuclear Magnetic Resonance) imaging for detecting binder/plasticizers in green-state structural ceramics
[DE88-003111] 10 p1304 N88-17800
Detection of signals in non-Gaussian correlated noise derived from Cauchy processes
[AD-A187488] 10 p1320 N88-17894
Trace analysis by MS/MS on a double focussing mass spectrometer
[AD-A187954] 10 p1334 N88-17973
Tactile sensing and inverse problems
[AD-A187464] 10 p1340 N88-18011
Piezoelectric laminates for torsional and bending model control: Theory and experiment
10 p1343 N88-18029
Rapid underway sediment classification by electrical methods
[AD-A187477] 10 p1357 N88-18114
CARS measurements of combustion. 2: Gas species concentration measurements
[NAL-TR-940] 11 p1453 N88-18663
Diagnostics for research in atomization and turbulent two-phase flows
[AD-A187338] 11 p1482 N88-18843
Visual integration and detection of discontinuities: The key role of intensity edges
[AD-A188012] 11 p1520 N88-19076
Simultaneous estimation and detection of bias shifts for inertial navigation systems 12 p1576 N88-19429
Homogenizing surface and satellite observations of cloud. Aspects of bias in surface data
[AD-A188523] 12 p1648 N88-19869
Analysis, estimation, and control for perturbed and singular systems and for systems subject to discrete events
[AD-A188496] 12 p1677 N88-20026
Detecting serial correlation in the error structure of a cross-lagged panel model
[AD-A189070] 12 p1685 N88-20077
Specification for an infrared satellite surveillance system for the detection of aircraft
[AD-A189592] 13 p1797 N88-20746
Reduced tolerance imaging 2, volume 2
[AD-A189604] 13 p1829 N88-20939
Searches for forces weaker than gravity
[DE88-003579] 13 p1832 N88-20959
Optimal and conventional space-time processing in flow noise
[AD-A189104] 13 p1833 N88-20965
Physics at large transverse momenta
[DE88-005758] 13 p1836 N88-20986
Enzyme-based fiber optic sensors
[DE88-005674] 13 p1840 N88-21013
Detection of bondline delaminations in multilayer structures with lossy components
[NASA-CR-182716] 14 p1883 N88-21256
Laser pulse detection with infrared range semiconductor detectors
[DE88-700857] 14 p1914 N88-21432
Spectrographic detection of nitrogen impurity in helium
[DE88-752301] 15 p2033 N88-22111
Optimum signal processing in distributed sensor systems
[AD-A189443] 15 p2055 N88-22250
A multiple model adaptive tracking algorithm against airborne targets
[AD-A190619] 15 p2057 N88-22263
Detecting the gas bubbles in a liquid metal coolant by means of magnetic flowmeters
[DE88-701427] 15 p2062 N88-22294
Infrared differential absorption lidar for vapor detection
[AD-A190600] 15 p2098 N88-22497
Proceedings of the Lightning Threat Warning Workshop
[DE88-006607] 15 p2098 N88-22499
An evaluation of the effects of high visual taskload on the separate behaviors involved in complex monitoring performance
[AD-A190641] 15 p2105 N88-22538
Finding texture boundaries in images
[AD-A190554] 15 p2117 N88-22609
Mechanisms mediating the perception of complex acoustic patterns
[AD-A190112] 15 p2130 N88-22705
Expanded envelope concepts for aircraft control-element failure detection and identification
[NASA-CR-181664] 16 p2160 N88-22886
Universal detection of ions by replacement-ion chromatography employing an anion-replacement method and an ultraviolet-visible spectrophotometric detector
[AD-A191326] 16 p2176 N88-22971
Thomson scattering for determining electron concentrations and temperatures in an inductively coupled plasma. 2: Description and evaluation of a multichannel instrument
[AD-A191324] 16 p2280 N88-23652
Shape detection in remote sensing through graph isomorphism 17 p2354 N88-24028
TES: A modular systems approach to expert system development for real-time space applications
17 p2388 N88-24197
Dynamic range compression/expansion of light beams by photorefractive crystals
[NASA-CASE-NPO-17140-1-CU]
17 p2438 N88-24508
User's guide to the Fault Inferring Nonlinear Detection System (FINDS) computer program
[NASA-CR-178410] 18 p2462 N88-24619
Fast acting optical beam detection and deflection system
[AD-A192161] 18 p2521 N88-24954
Analysis and design of detection filters within closed-loop systems 18 p2525 N88-24980
Lightning detection and locating systems
18 p2546 N88-25112
Effectiveness evaluation of fault-tolerant multiprocessor systems
[AD-A191688] 18 p2554 N88-25158
Quench detection by fluid dynamic means in cable-in-conduit superconductors
[DE88-007269] 18 p2585 N88-25359
Trellis-coded CPM for satellite-based mobile communications 19 p2648 N88-25718
Interleaver design for trellis-coded differential 8-PSK modulation with non-coherent detection
19 p2648 N88-25719
Evaluation of engineering leak before break assessment methods by piping tests
[PB88-126982] 20 p2788 N88-26538
Laser spectoscopy of plasmas
[AD-A193009] 20 p2861 N88-26991
High resolution detection of solute segregation to the cores of dislocations in grain boundaries
[DE88-009168] 20 p2877 N88-27078
Detection of absorption lines in the spectra of X-ray bursts from X1608-52
[ISAS-RN-360] 20 p2887 N88-27143
The P delta V fundamental gas leak calibration system qualification report
[DE88-008964] 21 p2951 N88-27526
The detection and interpretation of long-term changes in ozone from space
[NASA-TM-101135] 21 p2971 N88-27650
Array detectors for plasma spectrochemistry
[AD-A194220] 22 p3052 N88-28105
Low cost corrosion sensors 22 p3054 N88-28123
Recent advances in optical spectroscopy using high performance array detectors
[AD-A194219] 22 p3152 N88-28753
Analysis of edge detection techniques for radiographic image measurement
[AD-A193650] 23 p3186 N88-28961
Infrared detection using Rydberg atoms
[AD-A194308] 23 p3191 N88-28990
Basic research in electronics (JSEP) Joint Services Electronics Program
[AD-A193072] 23 p3206 N88-29079
Airborne radar technology for windshear detection
[NASA-CR-183203] 23 p3236 N88-29257
An investigation of acoustic cavitation produced by pulsed ultrasound
[AD-A193523] 23 p3278 N88-29516
Neutrino detection primer
[AD-A193805] 23 p3280 N88-29529
Noncontact photo-thermal sensing
[AD-A195450] 24 p3344 N88-29905
Performance Prediction for Coatings. Proceedings of a Workshop
[AD-A188973] 24 p3354 N88-29966
Ultrasonic detection of diffusion and adhesion loss
24 p3354 N88-29967

Photoacoustic Fourier transform infrared spectroscopy. An early detection technique for coatings degradation
24 p3354 N88-29968

Predicting the durability of adhesives and coatings by remote detection of hidden defects and coating-thickness irregularities: A theoretical and numerical study
24 p3355 N88-29972

Electrical detection of coating deterioration
24 p3355 N88-29973

Experimental aspects of using time-averaged holographic interferometry to detect barely visible impact damage in a graphite/epoxy composite plate
[AD-A194418] 24 p3375 N88-30097

Laser sensing for identification and control of distributed parameter systems
[AD-A195886] 24 p3379 N88-30124

In situ fault detection by the hybrid ray mode method
[AD-A195226] 24 p3381 N88-30137

Automated early fatigue damage sensing system
[AD-A195717] 24 p3382 N88-30143

DETECTORS

Spectrometric test of a linear array sensor
[NASA-TM-100676] 01 p0064 N88-10414

An account of a flare related shock event recorded by the energetic particle detector EPONA of the Giotto spacecraft during September 1985 (STIP interval 18)
01 p0118 N88-10757

Semiconductor detector performance for low-energy X-rays
[DE87-014132] 02 p0244 N88-11542

Detecting squeezed states by cross-correlation
14 p1978 N88-21806

Miniature respiratory sensor
[AD-A193430] 23 p3243 N88-29300

DETERIORATION

Space environmental effects on polymeric materials
[NASA-CR-182454] 09 p1148 N88-16879

Corrosion and deterioration testing in humid tropic environments
[AD-A186917] 10 p1302 N88-17783

Electrical detection of coating deterioration
24 p3355 N88-29973

Evaluation of organic coating deterioration and substrate corrosion in seawater using electrochemical impedance measurements 24 p3355 N88-29976

DETERMINANTS

Optimal detection of sensor failures in flight control systems using deterministic observers
02 p0128 N88-10803

Deterministic uncertainty analysis
[DE88-006139] 13 p1829 N88-20942

DETERMINATION

U MEASUREMENT

DETONABLE GAS MIXTURES

Photochemical ignition studies. 3: Ignition by efficient and resonant multiphoton photochemical formation of microplasmas
[AD-A184644] 03 p0283 N88-11780

Measurement of detonation temperature of hydrogen-oxygen mixture by CARS (Coherent Anti-Stokes Raman Spectroscopy)
[NASA-TT-20227] 13 p1739 N88-20398

DETONATION

A study of diverging detonation in high-explosive systems
[DE87-006070] 01 p0031 N88-10194

Real time analysis of detonation products
[DE87-007453] 01 p0031 N88-10195

Shock measurements on explosives in the supra compressive region
[DE87-008423] 01 p0031 N88-10196

Statistical mechanical theory of condensed explosives
[DE87-009137] 01 p0031 N88-10197

Optically time-resolved detonation break out
[DE87-010340] 01 p0031 N88-10199

Experimental measurements and numerical simulations of metal spallation by detonating solid explosives
[DE87-013227] 01 p0054 N88-10347

The use of fiber optics in the determination of temperature and extent of reaction in detonating explosives
[DE87-012632] 01 p0094 N88-10612

Visible emission from granular explosives during shock initiation
[DE87-012361] 02 p0155 N88-10970

The equation of state of PETN detonation products
[DE87-013796] 02 p0155 N88-10971

Spectroscopic studies of shocked and detonating explosives
[DE87-014216] 02 p0155 N88-10972

Flame acceleration and transition to detonation in channels
[DE87-014193] 03 p0284 N88-11786

A transient model for thermal detonation
[IKE-2-75] 03 p0314 N88-11984

Steady tonation and flagration waves in reactive continua
[RARDE-2/73] 03 p0315 N88-11989

Particle transport in microdetonations --- inertial confinement fusion pellets
[OEFZS-4402] 09 p1164 N88-16976

Blast waves generated by planar detonations
[DE88-002219] 09 p1164 N88-16979

Analysis of reinforced concrete structures under the effects of localized detonations
09 p1179 N88-17064

A lecture on detonation-shock dynamics
[DE88-004313] 11 p1487 N88-18879

Measurement of detonation temperature of hydrogen-oxygen mixture by CARS (Coherent Anti-Stokes Raman Spectroscopy)
[NASA-TT-20227] 13 p1739 N88-20398

Theoretical investigation of the wave shaping process in a section of ladder fracture tape
[MRL-R-1081] 13 p1771 N88-20595

Timing control system
[NASA-CASE-NPO-16882-1-CU]
18 p2506 N88-24863

A concept for an electro-optic explosive device
[DE88-009696] 21 p2923 N88-27349

Semiconductor. bridge (SCB) igniter studies. 1: Comparison of SCB and hot-wire pyrotechnic actuators
[DE88-008802] 23 p3200 N88-29046

DETONATION WAVES

Current experimental and theoretical understanding of detonation waves in heterogeneous solid explosives
[DE87-012177] 01 p0032 N88-10201

Effect of dissipation on propagation of spherical detonation shock wave 02 p0159 N88-10998

Thrust and specific impulse of repetitively-pulsed-laser propulsion rocket 03 p0318 N88-12012

Blast waves generated by planar detonations
[DE88-002219] 09 p1164 N88-16979

Flame propagation in the approximation of straight-line trajectories of burning products
[DE88-700675] 10 p1297 N88-17756

Diffusion description of flame propagation due to the translational motion of burning reaction products
[DE88-700676] 10 p1297 N88-17757

Combustion theory and related questions
[AD-A189160] 13 p1737 N88-20382

Detonation velocity of the hydrazinum nitrate-hydrazine water system
[NASA-TT-20213] 13 p1770 N88-20590

Numerical modeling of divergent detonation wave
14 p1903 N88-21373

Shock initiation studies on heterogeneous explosives
[DE88-008681] 21 p2923 N88-27351

DETONATORS

Langlie Test Method Program for use with the HP-41CV/X calculator
[DE88-001935] 06 p0687 N88-14210

An electro-optic explosive igniter
[DE88-004728] 11 p1466 N88-18738

A concept for an electro-optic explosive device
[DE88-009696] 21 p2923 N88-27349

DEUTERIUM

Applications and limitations of deuterium labeling methods to neutron scattering studies of polymers
[DE87-012936] 02 p0151 N88-10945

Refueling and density control in the ZT-40M reversed field pinch
[DE88-000504] 04 p0493 N88-13040

Hydrogen and deuterium in the local interstellar medium 04 p0521 N88-13204

Magneto-Inertia Confinement Approach (MICA) to fusion in dynamic Z-pinch formed from a frozen deuterium-tritium tube
[IPPJ-856] 09 p1252 N88-17504

Helium-3 fusion fuel resources for space power
17 p2410 N88-24330

Effect of hydrogen, deuterium and oxygen on the anelastic properties of refractory alloys
[DE88-007349] 18 p2484 N88-24736

Deuterium isotope effects in the combustion of formulated nitramine propellants
19 p2632 N88-25611

Factors which affect operation of a plasma focus in various gases
[DE88-701882] 20 p2858 N88-26975

DEUTERIUM COMPOUNDS

Energy transfer studies with lasers
[DE88-004864] 10 p1337 N88-17991

DEUTERIUM PLASMA

SOAR: Space orbiting advanced fusion power reactor
[AD-A189234] 13 p1732 N88-20356

DEUTERON IRRADIATION

Experimental set-up for measurements of Compton scattering cross section on light nuclei
[DE88-700161] 12 p1688 N88-20097

Study of defects in metals by positron annihilation
[DE88-701042] 13 p1745 N88-20432

DEUTERONS

Experimental studies of electromagnetic properties of few body systems
[DE87-014610] 02 p0161 N88-11008

Ion energy diagnostics for voltage determinations in plasma-erosion-opening-switch experiments
[DE88-004822] 11 p1479 N88-18827

DEVELOPERS (PHOTOGRAPHY)

U PHOTOGRAPHIC DEVELOPERS

DEVELOPING NATIONS

Unispace 82 09 p1128 N88-16766

Centre for International Co-Operation and Approriate Technology (CICAT)
[PB88-165501] 18 p2590 N88-25389

Use of SPOT data in preliminary steps of road project studies especially suited for developing countries
22 p3098 N88-28396

DEVIATION

The deviation of light rays passing through a curved windscreen --- aircraft
[BAE-MSC.115] 01 p0093 N88-10610

Stochastic approximation and large deviations: General results for w.p.l. Convergence
[AD-A185818] 06 p0768 N88-14721

Nonlinear filtering and large deviations: A PDE-Control theoretic approach
[AD-A187436] 10 p1396 N88-18321

Asymptotic expansions for large deviation probabilities in the strong law of large numbers
[AD-A187432] 10 p1402 N88-18361

Deviation equation as an equation of motion
[DE88-702134] 19 p2722 N88-26161

DEVITRIFICATION

U CRYSTALLIZATION

DEW POINT

Use of time changes of surface data parameters in short range forecasting 02 p0206 N88-11291

DEWAR SYSTEMS

U CRYOGENIC EQUIPMENT

DEWETTING

U DRYING

DIABETES MELLITUS

Design considerations for the development of an implantable sensor for the continuous measurement of glucose in the diabetic patient 17 p2382 N88-24159

DIAGNOSIS

Proceedings of Conference on Vibrodiagnostics discussed 02 p0158 N88-10990

Programmable 10 MHz optical fiducial system for hydrodiagnostic cameras
[DE87-013223] 02 p0175 N88-11091

In-flight diagnosis: Analysis of spurious events --- spacecraft 03 p0274 N88-11724

The development of diagnostic fuses
[SAND-86-0395] 03 p0311 N88-11963

Diagnostics aid for mass spectrometer trouble-shooting
[DE88-000350] 03 p0324 N88-12049

Computer-controlled testing of visual-spatial ability
[AD-A183971] 03 p0357 N88-12249

The characterization of diagnostic tasks for engineering systems
[DE88-000093] 04 p0483 N88-12973

Diagnostic reasoning in digital systems
[NASA-CR-181564] 05 p0633 N88-13871

Human physical fields 06 p0750 N88-14609

Diagnostic emulation: Implementation and user's guide
[NASA-CR-178391] 06 p0756 N88-14638

A solid phase enzyme-linked immunosorbent assay for the antigenic detection of Legionella pneumophila (serogroup 1): A compliment for the space station diagnostic capability 06 p0795 N88-14868

Development of a prototype H-46 helicopter diagnostic expert system
[AD-A186077] 07 p0809 N88-14924

Modal analyses of the Kernville diagnostic canister
[DE88-003268] 07 p0870 N88-15277

Development of methods for the study of space motion sickness 07 p0892 N88-15408

Diagnostic value of some load tests in evaluation of nonspecific electrocardiographic changes
07 p0895 N88-15426

An interactive visual interface for Fastbus diagnostics
[DE88-002569] 07 p0900 N88-15453

Innovating systems and techniques for the diagnosis of materials and industrial plants
[CISE-3856] 08 p0976 N88-15901

On line instrument systems for monitoring steam turbogenerators
[CISE-3860] 08 p0990 N88-15995

Prognosis using spectral embedding --- weather forecasting 08 p1016 N88-16157

An easy-to-use diagnostic system development shell
08 p1055 N88-16366

An inference engine for embedded diagnostic systems
08 p1056 N88-16367
Qualitative and temporal reasoning in engine behavior analysis
08 p1058 N88-16383
EUREX D: An expert system for failure diagnosis and recovery in the TCS of the European retrievable carrier EURECA
08 p1058 N88-16385
A data structure and algorithm for fault diagnosis
08 p1065 N88-16432
Integrated diagnostics 09 p1111 N88-16655
Knowledge based jet engine diagnostics
09 p1203 N88-17210
Diagnosis: Reasoning from first principles and experiential knowledge 09 p1207 N88-17236
Diagnostics for research in atomization and turbulent two-phase flows
[AD-A187338] 11 p1482 N88-18843
Three-dimensional computer graphics brain-mapping project
[AD-A187202] 11 p1528 N88-19126
Expert systems: Their impact on performance and cognitive strategies in diagnostic inference
[AD-A188518] 12 p1677 N88-20027
Progress in diagnostic techniques for SC cavities
[CEBAF-PR-88-003] 13 p1772 N88-20600
Clinical measurements using fiber optic sensors
[DE88-005624] 15 p2134 N88-22731
Thin film research diagnostics instrumentation
[AD-A191240] 16 p2213 N88-23207
Leave-K-Out diagnostics for time series
[AD-A191343] 16 p2261 N88-23518
Optical diagnostics for a high power, rf-inductively coupled plasma
[DE88-007822] 18 p2579 N88-25322
Fracture physics of delamination of composite materials
[AD-A192021] 19 p2609 N88-25482
Asynchronous optical sampling for laser-based combustion diagnostics in high pressure flames
[AD-A192920] 20 p2770 N88-26428
Laser diagnostics applied to advanced combustion systems
[DE88-753119] 20 p2806 N88-26649
Laser probes and numerical modeling as process diagnostics in chemical vapor deposition
[DE88-011622] 21 p2911 N88-27275
Vortex dynamics of coherent and chaotic structures (including algorithms for computer simulations and diagnosis)
[AD-A193580] 23 p3212 N88-29117
Improvements in techniques of microwave thermography
[AD-A193620] 23 p3239 N88-29276
Distributed knowledge base systems for diagnosis and information retrieval
[AD-A193107] 23 p3296 N88-29633
Optical measurements of soot and temperature profiles in premixed propane-oxygen flames
[NASA-TM-101343] 24 p3358 N88-29997
Stress related failures causing open metallization
[AD-A195061] 24 p3383 N88-30150

DIAGRAMS
NT BENDING DIAGRAMS
NT BLOCK DIAGRAMS
NT CIRCUIT DIAGRAMS
NT COLOR-MAGNITUDE DIAGRAM
NT CREEP DIAGRAMS
NT FEYNMAN DIAGRAMS
NT HERTZSPRUNG-RUSSELL DIAGRAM
NT PHASE DIAGRAMS
NT S-N DIAGRAMS
NT STRESS-STRAIN DIAGRAMS
Integrated 3-parameter diagram for determining thermodynamic properties of fluids
03 p0298 N88-11874
CUEMAP: A tool for generating hierarchical charts and dataflow diagrams
[DE88-004778] 10 p1387 N88-18284
PLOT3D (version-5): A computer code for drawing three dimensional graphs, maps and histograms, in single or multiple colours, for mono or stereoscopic viewing
[DE88-701410] 15 p2108 N88-22558
Characterization of lubricants in terms of transition diagram data
[AD-A194264] 23 p3197 N88 29025

DIAMAGNETISM
The thermal conductivity of dirty type 2 superconductors
[B8681488] 23 p3294 N88-29615

DIAMETERS
The angular diameter of alpha Scorpii in the near-infrared Ca II triplet 04 p0514 N88-13162
Explosive absorption of laser beam of finite diameter
07 p0921 N88-15597
Cylindrical surface profile and diameter measuring tool and method
[NASA-CASE-MFS-28287-1] 17 p2341 N88-23959
Hole diameters in plates impacted by projectiles
21 p2929 N88-27386
Effect of fiber diameter on the reliability of composites - automated laser diffraction implementation
[AD-A193524] 23 p3188 N88-28972

DIAMINES
NT GUANIDINES
The water absorption of model epoxy resin networks cured with aromatic diamines
[BR100722] 01 p0027 N88-10169

DIAMOND WINGS
U LOW ASPECT RATIO WINGS
U SWEPT WINGS

DIAMONDS
Theory of the carbon phase diagram at high pressures and temperatures
[DE87-012245] 01 p0028 N88-10180
Diamond turning of silicon for optics applications
[DE88-002501] 07 p0840 N88-15095
Gamma radiation at the 970 MeV plane positron channeling in diamond crystals
[DE88-700557] 07 p0939 N88-15705
Drilling metal matrix composites
[AD-A190480] 15 p2029 N88-22091
Diamond like carbon coatings: Categorization by atomic number density
[NASA-CR-174895] 22 p3059 N88-28151
The diamond as a new electronic material
[NASA-TT-20354] 23 p3209 N88-29098
Diamond film by hot filament CVD method
[NASA-TT-20335] 23 p3294 N88-29618

DIAPHRAGMS (MECHANICS)
Diffraction effects during materials treatment with laser beams
[ETN-87-90614] 03 p0328 N88-12075
Low gravity liquid motions in spacecraft
08 p0982 N88-15941
Test of a prototype gate with fast opening equipping the shock tube 0 2 40 m at CEG
[PB87-227864] 1[illegible] p2604 N88-25465
Simulation of diaphragm-type IC pressure sensors
19 p2672 N88-25887

DIATOMIC GASES
Evaluation and compilation of thermodynamic properties of high temperature chemical species
[AD-A187509] 11 p1452 N88-18654

DIATOMIC MOLECULES
On the signal strength dependency on pressure in laser sub-Doppler saturation spectroscopy with special attention to gaseous diatonic molecules
[USIP-87-13] 09 p1171 N88-17023
Theory of the dissociation dynamics of small molecules on metal surfaces: Finite temperature studies
[DE88-006495] 15 p2132 N88-22716
A constraint algorithm for maintaining rigid bonds in molecular dynamics simulations of large molecules
[AD-A191653] 18 p2572 N88-25277
Nuclear magnetic ordering and paramagnetic relaxation of diatomic molecules in Ca (OH)2
[B8681469] 23 p3281 N88-29532

DIATOMS (UNICELLULAR PLANTS)
U ALGAE

DICARBOXYLIC ACIDS
Synthesis and characterization of 1,2-cyclobutenedicarboxamides: Thermally generated polymers and Diels-Alder adducts
[AD-A188591] 12 p1641 N88-19633

DICHLORIDES
A theoretical model of the washout of trace gases by raindrops in the atmosphere 17 p2375 N88-24125

DICHROISM
Near-infrared dichroism of a mesogenic transition metal complex and its solubility in nematic hosts
[DE87-014471] 03 p0287 N88-11805

DICHROMATES
U CHROMATES

DICKE RADIOMETERS
Implications of the trapping-desorption and direct inelastic scattering channels on Dicke-narrowed lineshapes
[AD-A191410] 16 p2270 N88-23581

DICKE TYPE RADIOMETERS
U DICKE RADIOMETERS

DICTIONARIES
Energy Data Base: Subject Thesaurus
[DE87-008007] 03 p0384 N88-12414
IDMS application documentation made easy
[DE88-000199] 03 p0384 N88-12416
A graphics editor for structured analysis with a data dictionary
[AD-A190618] 15 p2112 N88-22584
NASA combined file postings statistics based on NASA thesaurus, Jan. 1968 - July 1988
[NASA-CR-182985] 18 p2589 N88-25384
A glossary for carbon dioxide and climate
[DE88-007885] 19 p2689 N88-25982

DIELECTRIC CONSTANT
U PERMITTIVITY

DIELECTRIC MATERIALS
U DIELECTRICS

DIELECTRIC POLARIZATION
Effect of collisional broadening on the polarizability of a two-dimensional electron gas
[DE87-013928] 02 p0237 N88-11497
Spontaneous decay and atomic fluorescence near a metal surface of an absorbing dielectric
[AD-A187508] 13 p1835 N88-20975
Field-aligned structure of the storm time Pc 5 wave of November 14-15, 1979
[AD-A193022] 21 p2972 N88-27653

DIELECTRIC PROPERTIES
NT PERMITTIVITY
Voltammetric investigation of porous silicon for integrated circuit applications
[DE87-009287] 02 p0166 N88-11042
Dielectric response of ionic conductors
[DE87-013552] 02 p0166 N88-11045
Coupling and absorption phenomena in semiconductor-clad dielectric optical waveguides
[DE87-013446] 03 p0307 N88-11939
United States - Japan Workshop on Dielectric and Piezoelectric Ceramics (3rd) held in Toyama, Japan on November 9-12, 1986
[AD-A185113] 05 p0568 N88-13460
Numerical and analytical study of the equivalent permittivity or permeability of nonhomogeneous materials. Application to the experimental electromagnetic characterization of composites
[SNIAS-872-430-104] 05 p0575 N88-13509
Ionic transport and electrical relaxation in glass
[DE88-000887] 05 p0657 N88-14028
Vibrational properties of disordered solids: Far infrared studies: Performance report
[DE88-001474] 06 p0786 N88-14821
Power and charge dissipation from an electrodynamic tether 06 p0795 N88-14869
Dielectric behavior of electromagnetic (EM) windows materials irradiated by a CW CO2 high-power laser --- hypersonic/reentry vehicles
[ISL-CO-239/86] 09 p1154 N88-16913
RELIC: A reliability simulator for integrated circuits
[AD-A187493] 11 p1477 N88-18811
Microwave dielectric spectrum of rocks
[NASA-TM-89719] 12 p1642 N88-19831
Microwave and structural properties of saline ice
[AD-A189307] 13 p1803 N88-20779
Increasing the rate at which ceramic castings undergo preliminary heat-treatment in an ultra-high frequency magnetic field 14 p1886 N88-21275
Microwave dispersion and absorption in tissues: Molecular mechanisms
[AD-A190118] 15 p2100 N88-22512
Correlation between dielectric and structural properties during epoxy cure
[AD-A190696] 16 p2181 N88-22997
Static dielectric breakdown strength of condensed heterogeneous high explosives
[AD-A191035] 16 p2183 N88-23014
Deep dielectric charging effects due to high energy electrons in earth's outer magnetosphere
[AD-A192154] 18 p2541 N88-25083
Theoretical basis for an experimental test with regard to the origin of VHF (Very High Frequency) radiation from natural lightning
[DE88-007535] 18 p2544 N88-25102
Development of external cooling cryo-resistive cable systems. Part 2: Insulation characteristics on 66 kV rated cryo-resistive testing cable
[DE88-770191] 20 p2793 N88-26571
Variational analysis of dielectrically loaded multidepth corrugated waveguides
[PB88-193602] 20 p2793 N88-26573
Low noise cryogenic dielectric resonator oscillator
[NASA-CASE-NPO-17157-1-CU]
20 p2797 N88-26596
Modeling of subtle kinetic processes in plasma simulation 20 p2856 N88-26959
Manufacturing of a barium titanate with high dielectric coefficient by decomposition of precipitates of double oxalates
[ISAL-IDI1-88-02] 21 p2911 N88-27278
Processing and additive effects of ZrO2 on microstructure and dielectric porperties of BaTiO3 ceramics
[AD-A193126] 21 p2917 N88-27316
Surface-wave model uncertainty assessment
[AD-A193094] 21 p2932 N88-27408

DIELECTRICS

Effects on the resonant frequencies caused by loading a spherical cavity with a dielectric sphere
[AD-A193864] 23 p3277 N88-29511

DIELECTRICS
NT RADOME MATERIALS
Energy transformation in molecular electronic systems
[DE87-013916] 03 p0282 N88-11771
Automated microwave dielectric constant measurement
[AD-A184182] 04 p0431 N88-12667
Measurement and analysis of cryogenic sapphire dielectric resonators and DROs
04 p0433 N88-12686
Raman microprobe characterization of dielectric films following high-energy pulsed laser irradiation
[DE88-000559] 05 p0588 N88-13587
Extinction by dielectric particles at optical and infrared wavelength
[AD-A184818] 05 p0650 N88-13981
Dependence of acoustical characteristics of laser-induced breakdown in dielectric materials on shape of inelastic region 06 p0774 N88-14753
Assessment of electroceramics research in Europe and the Middle East
[AD-A186377] 07 p0836 N88-15074
Deformation effects on microwave reflectivity
[AD-A185684] 07 p0844 N88-15120
Materials for acceleration by surface electromagnetic waves
[DE88-700312] 07 p0846 N88-15133
Failure modes of laminate structures
[DE88-002579] 08 p0996 N88-16033
Plane wave diffraction by a thin dielectric wedge
[RSRE-MEMO-4045] 09 p1153 N88-16912
Guided-wave approaches to spectrally selective energy absorption
[NASA-CR-182532] 10 p1320 N88-17892
Voltammetric investigation of porous silicon for integrated circuit applications
[DE88-004024] 11 p1456 N88-18677
Research on high-specific-heat dielectrics
[AD-A187248] 11 p1461 N88-18710
Layered-capacitor method for dielectric bridge measurements. Algorithms for inversion and parameter fitting: Documentation, verification, data analysis
[PB88-131479] 11 p1505 N88-18989
Transport properties of conductive polymers
[AD-A188411] 12 p1610 N88-19628
Transformation coefficient in wave-field acceleration scheme
[DE88-700158] 13 p1757 N88-20507
Vapor-mist for lightweight high voltage space insulation systems
[DE87-011704] 13 p1762 N88-20538
Causes of damage in multilayer dielectric coatings exposed to high average power visible laser radiation
[DE88-005363] 13 p1775 N88-20619
Spontaneous decay and atomic fluorescence near a metal surface of an absorbing dielectric
[AD-A187508] 13 p1835 N88-20975
Spacecraft dielectric surface charging property determination
[NASA-CR-180879] 14 p1881 N88-21243
Method for characterizing end-plate surface resistance of dielectric resonator 14 p1903 N88-21371
On the theory of electromagnetic scattering from a raindrop splash
[AD-A188720] 14 p1906 N88-21393
Infrared reflection-absorption spectroscopy of hyperfine layers on surfaces of semiconductors and dielectrics
14 p1969 N88-21755
Exact image theory for the problem, of dielectric/magnetic slab
[NASA-CR-182865] 16 p2189 N88-23055
Optimization of metal-dielectric laser mirrors of TiO2/SiO2 and silver
[ESA-TT-1068] 16 p2212 N88-23199
Low gravity thermal management using dielectrophoretic forces 17 p2432 N88-24470
Micro-Raman analysis of dielectric optical thin films
[AD-A191228] 17 p2445 N88-24537
Arcing and rf signal generation during target irradiation by a high-energy, pulsed neutral particle beam
[DE88-007169] 18 p2471 N88-24664
Born-type reconstruction of material parameters of an inhomogeneous, lossy dielectric slab from reflected-field data
[PB88-188958] 18 p2569 N88-25261
Molecular characterization of structure and bonding in thin film materials
[DE88-006811] 18 p2584 N88-25351
Method of forming a multiple layer dielectric and a hot film sensor therewith
[NASA-CASE-LAR-13678-1] 18 p2584 N88-25355
Research and development programs on advanced structural ceramics in Korea 19 p2633 N88-25620
Characteristics of shielded microstrip lines on GaAs-Si at millimeter-wave frequencies 19 p2657 N88-25787
Dielectric compound parabolic concentrating solar collector with frustrated total internal reflection absorber
[DE88-009986] 19 p2688 N88-25976
Visible tunable source
[DE88-006442] 20 p2854 N88-26944
Processing and additive effects of ZrO2 on microstructure and dielectric porperties of BaTiO3 ceramics
[AD-A193126] 21 p2917 N88-27316
Preparation and properties of high Q microwave dielectrics in the (CA, SR, BA) zirconate system
[AD-A193127] 21 p2918 N88-27317
Effects of surface tension and contact angle on sensible heating and boiling incipience in dielectric falling films
[DE88-007057] 21 p2945 N88-27492
Measurement of the thermal conductivity of dielectric thin solid films with a thermal comparator
[DE88-008468] 21 p3016 N88-27898
On the self-consistent equation for the microscopic local electric field in dielectric systems
[PREPRINT-589] 22 p3074 N88-28247
Stress corrosion of ceramic materials
[AD-A191979] 23 p3195 N88-29016
Basic research in electronics (JSEP) Joint Services Electronics Program
[AD-A193072] 23 p3206 N88-29079
Natural convection immersion cooling of an array of simulated chips in an enclosure filled with dielectric liquid
[AD-A193594] 23 p3207 N88-29088
Effects on the resonant frequencies caused by loading a spherical cavity with a dielectric sphere
[AD-A193864] 23 p3277 N88-29511
Research on crystal and film ferroelectric materials for optoelectronic applications
[AD-A193512] 23 p3291 N88-29597
Polymer-ceramic composites
[AD-A195789] 24 p3356 N88-29983
Transient interaction of electromagnetic pulses in dielectrics and microwave biophysics
[AD-A195687] 24 p3360 N88-30008
Dielectric millimeter waveguides: A feasibility study for a novel dielectric millimeter waveguide
[AD-A195104] 24 p3366 N88-30042

DIELECTRONIC SATELLITE LINES
U RESONANCE LINES

DIELS-ALDER REACTIONS
Study of improved methods for predicting chemical equilibria
[DE87-014647] 02 p0145 N88-10908
High-temperature thermosets derived from the Diels-Alder polymerization of bisbenzocyclobutenes and bimaleimides
[AD-A188800] 13 p1747 N88-20449

DIENCEPHALON
NT HYPOTHALAMUS
NT THALAMUS

DIENES
NT BUTADIENE
NT POLYBUTADIENE

DIES
Studies on estimation of nickel in zinc base die casting by D.C. polarography
[PD-MT-8729] 04 p0417 N88-12588

DIESEL ENGINES
Piston ring friction and vehicle fuel economy
[DE87-014536] 02 p0181 N88-11127
Use of natural gas diesel engines in mechanical pulp production: A preliminary study
[DE87-753065] 02 p0181 N88-11129
Adiabatic diesel engine component development: Reference engine for on-highway applications
[NASA-CR-179531] 03 p0386 N88-12428
Ceramic technology for advanced heat engines project
[DE88-001529] 04 p0420 N88-12605
Report to Congress on the Automotive Technology Development Program
[DE88-003742] 07 p0864 N88-15242
The effects of fuel composition on ignition delay in homogeneous charge and direct injection compression ignition engines
[DE88-003691] 09 p1143 N88-16849
Effect of translucence of engineering ceramics on heat transfer in diesel engines
[DE88-003732] 10 p1305 N88-17904
Experimental study of thermal loading at the wall of an industrial Diesel motor
[ISAL-IDI1-87-10] 10 p1339 N88-18000
Liquid sprays and flow studies in the direct-injection diesel engine under motored conditions
[NASA-TM-100135] 11 p1440 N88-18594
Prototype thin-film thermocouple/heat-flux sensor for a ceramic-insulated diesel engine
[NASA-TM-100798] 11 p1490 N88-18892
Concept and analysis of a direct-injection alcohol layer charge motor
[ETN-88-91482] 11 p1495 N88-18925
Practical system for the use of alcohol in diesel engines
[PB88-147863] 12 p1612 N88-19638
Engine testing for synfuel operation
[DE88-006044] 13 p1779 N88-20645
Cetane scale evaluation and possible modification
[AD-A189730] 15 p2048 N88-22200
JPRS report: Science and technology. Japan
[JPRS-JST-87-026] 16 p2184 N88-23018
Full electronic control system for diesel engine
16 p2185 N88-23025
Status, trends in research on internal combustion engines 16 p2185 N88-23027
Servojet retrofit
[AD-A191075] 18 p2522 N88-24964
Direct gas injection with glow plug ignition
[PB88-187323] 19 p2676 N88-25911
An investigation of high pressure/late cycle injection of CNG (Compressed Natural Gas) as a fuel for rail applications
[DE88-009000] 19 p2677 N88-25917
Pulsed spray structure and atomisation techniques
[AD-A192280] 20 p2800 N88-26614
Documentation of the Benson Diesel Engine Simulation Program
[NASA-TM-100940] 21 p2898 N88-27201
Ceramic technology for advanced heat engines project
[DE88-008945] 21 p2919 N88-27323
The 210-HP diesel engine endurance and performance testing with fire resistant diesel fuel
[AD-A193153] 21 p2956 N88-27558
Basic mechanisms of diesel lubrication correlation of bench and engine tests
[AD-A193360] 21 p2956 N88-27561
Ethanol as a fuel of a lorry. Use experience from a diesel engine modified to an otto engine
[DE88-752870] 21 p2958 N88-27569
Diesel combustion fundamentals, phase 1, volume 1
[AD-A193831] 22 p3052 N88-28107
Modeling of spray combustion in direct injection diesel engine
[AD-A193787] 22 p3084 N88-28314
Variable-compression-ratio pistons for high power output diesel engines 22 p3084 N88-28316

DIESEL FUELS
Formation of sediments in fuels containing added sulphonic acids --- marine diesel fuels
[RAE-TM-NAV-ENG-1163] 09 p1150 N88-16891
Concept and analysis of a direct-injection alcohol layer charge motor
[ETN-88-91482] 11 p1495 N88-18925
Analysis of model fuels and their compatibility with selected elastomers, part 1
[AD-A188361] 12 p1612 N88-19639
Flammability characteristics of distillate fuels
[AD-A188497] 12 p1612 N88-19642
Engine testing for synfuel operation
[DE88-006044] 13 p1779 N88-20645
Cetane scale evaluation and possible modification
[AD-A189730] 15 p2048 N88-22200
An investigation of high pressure/late cycle injection of CNG (Compressed Natural Gas) as a fuel for rail applications
[DE88-009000] 19 p2677 N88-25917
Effects of ceramic surfaces on autoignition in a constant volume combustion apparatus
[AD-A193055] 21 p2909 N88-27266
A study relating to the fog oil replacement program
[AD-A192536] 21 p2923 N88-27347
The 210-HP diesel engine endurance and performance testing with fire resistant diesel fuel
[AD-A193153] 21 p2956 N88-27558
Diesel combustion fundamentals, phase 1, volume 1
[AD-A193831] 22 p3052 N88-28107

DIETS
Operation Everest 2: Nutrition and body composition
[AD-A186449] 08 p1049 N88-16333
Manipulation of muscle glycogen concentrations using high and low carbohydrate diets and exercise
[AD-A187732] 11 p1519 N88-19069
Dietary factors related to physical fitness
[AD-A190272] 15 p2103 N88-22527

DIFFERENCE EQUATIONS
Cross-correlation of uniform cyclic difference set sequences
[AD-A184879] 05 p0640 N88-13913

fully redundant double difference algorithm for ining minimum variance estimates from GPS ervations 06 p0667 N88-14089
SA-CR-182363]
nalysis of smoothing matrices for the preconditioning elliptic difference equations 09 p1228 N88-17357
VI-NM-R8705]
Predicting oscillatory finite difference solutions to the at equation: A comparative study of the coefficient and atrix methods 13 p1825 N88-20911
D-A189591]
Accuracy versus convergence rates for a three mensional multistage Euler code 16 p2261 N88-23519
NASA-CR-181665]
Numerical solutions to stochastic difference equations 18 p2564 N88-25229
A comparative study of Chebyshev acceleration and esidue smoothing in the solution of nonlinear elliptic difference equations 18 p2569 N88-25259
CWI-NM-R8723]
Effects of numerical dissipation on finite-volume solutions of compressible flow problems 21 p2944 N88-27485
[AD-A193173]
Interferometric tomography of continuous fields with incomplete projections 22 p3081 N88-28295
[NASA-CR-183181]

IFFERENCES
GPS vertical axis performance enhancement for helicopter precision landing approach 04 p0397 N88-12477
[NASA-CR-177443]
On the norm equivalence of singularly perturbed elliptic difference operators 13 p1826 N88-20913
[DE88-006353]

DIFFERENTIAL ALGEBRA
U MATRICES (MATHEMATICS)

DIFFERENTIAL ANALYZERS
Digital method for correction of the phase error in the discrete generation of periodic signals in real time 12 p1618 N88-19676
[INPE-4327-RPE/552]

DIFFERENTIAL EQUATIONS
NT BIHARMONIC EQUATIONS
NT BURGER EQUATION
NT CAUCHY-RIEMANN EQUATIONS
NT COSINE SERIES
NT ELLIPTIC DIFFERENTIAL EQUATIONS
NT EULER-CAUCHY EQUATIONS
NT FOKKER-PLANCK EQUATION
NT GAUSS EQUATION
NT HELMHOLTZ VORTICITY EQUATION
NT HYPERBOLIC DIFFERENTIAL EQUATIONS
NT PARABOLIC DIFFERENTIAL EQUATIONS
NT PARTIAL DIFFERENTIAL EQUATIONS
NT POISSON EQUATION
NT RICCATI EQUATION
NT VLASOV EQUATIONS
NT VORTICITY EQUATIONS
The reliability of numerical solutions of ordinary differential equations, obtained by implicit calculation schemes 01 p0085 N88-10549
[PTB-W-30]
Parallel computation of a domain decomposition method 01 p0086 N88-10560
[DE87-011444]
Implementation and evaluation of several continuously imbedded methods of Sarafyan 02 p0221 N88-11393
[DE88-000025]
On oscillation of a kind of integro-differential equation with delay 02 p0225 N88-11417
[DE87-703059]
Oscillatory and nonoscillatory properties of first order differential equations with piecewise constant deviating arguments 02 p0225 N88-11418
[DE87-703061]
Finite-dimensional matrix representation of the differential operator, determinental form and zeros of special functions 02 p0225 N88-11421
[DE87-703091]
The method of lines for time dependent free boundary problems 02 p0226 N88-11423
[DE87-013929]
Computational methods and software for differential equations and their applications 02 p0226 N88-11424
[DE87-014601]
Parallel methods for ordinary differential equations 02 p0226 N88-11425
[DE87-014667]
A collection of test problems for ordinary differential equation solvers which have provisions for rootfinding 02 p0226 N88-11428
[DE88-000045]
Numerical modeling: Finite methods 03 p0304 N88-11918
Operator multiple-tasking study for remotely operated platforms 03 p0362 N88-12276
[AD-A184487]
The development of ODE methods: A symbiosis between hardware and numerical analysis 03 p0370 N88-12325
[DE87-014925]
Implementation of the Runge-Kutta-Fehlberg method for solution of ordinary differential equations on a parallel processor 03 p0370 N88-12331
[AD-A184660]
Applications of a theory of ferromagnetic hysteresis 03 p0373 N88-12348
[DE87-014725]
Oscillation theory for linear second-order differential systems 04 p0484 N88-12983
[DE87-011393]
The shifted Adams method for ordinary differential equations 04 p0486 N88-12994
[DE88-000810]
A note on the use of symmetric line Gauss-Seidel for the steady upwind differenced Euler equations 05 p0580 N88-13540
[AD-A185223]
The numerical and analytic of implicit differential equations and their application to control and circuit problems 05 p0641 N88-13922
[AD-A185404]
Development of an unsteady wake theory appropriate for aeroelastic analyses of rotors in hover and forward flight 06 p0664 N88-14075
[NASA-CR-182357]
Steady waves in a nonlinear theory of viscoelasticity 06 p0723 N88-14448
[AD-A185548]
Development of symbolic computation methods for nonlinear dynamics 06 p0758 N88-14653
[AD-A185562]
Pseudodifferential operators on the circle and finite differences 06 p0763 N88-14681
[PB87-222352]
Local and global techniques for the tracking of periodic solutions of parameter-dependent functional differential equations 06 p0766 N88-14704
[AD-A185756]
Characteristic trajectories of generalized Lanchester equations 06 p0766 N88-14705
[AD-A185762]
Shadow systems and attractors in reaction-diffusion equations 06 p0766 N88-14706
[AD-A185804]
There exists a C sup infinity symbol Kupka-Smale diffeomorphism of S sup 2 with neither sinks nor sources 06 p0769 N88-14725
[PB87-225967]
Modeling the growth dynamics of four candidate crops for Controlled Ecological Life Support Systems (CELSS) 06 p0799 N88-14889
Theoretical investigations of chaotic dynamics 07 p0867 N88-15261
[AD-A186404]
Recent developments in the numerical solution of differential/algebraic systems 07 p0912 N88-15535
[DE88-001885]
Boundary value problems for ordinary differential equations with multiple turning points 09 p1228 N88 17354
[CWI-AM-R8701]
Diagonally implicit Runge-Kutta-Nystrom methods for oscillatory problems 09 p1228 N88-17356
[CWI-NM-R8704]
A note on a diagonally implicit Runge-Kutta-Nystrom method 09 p1228 N88-17358
[CWI-NM-R8706]
Stability results for theta methods applied to a class of stiff differential-algebraic equations 09 p1228 N88-17360
[CWI-NM-R8708]
Perturbation theory for dual semigroups 2: Time-dependent perturbations in the sun-reflexive case 09 p1230 N88-17369
[PB88-113097]
Core spline method for solution of quantum-mechanical systems of differential equations for bound states 09 p1259 N88-17551
[DE88-700492]
Parallels between control PDE's (Partial Differential Equations) and systems of ODE's (Ordinary Differential Equations) 10 p1398 N88-18331
[NASA-CR-182487]
Straightening and the Stanley decomposition for the (2;n)-nilpotent vectorfield 10 p1398 N88-18336
[PB88-126685]
Boundary value problems for differential and functional differential equations 10 p1400 N88 18349
[AD-A187378]
Generalized equations for emittance and field energy of high-current beams in periodic focusing 10 p1404 N88-18372
[DE88-004448]
Performance and optimization of direct implicit time integration schemes for use in electrostatic particle simulation codes 10 p1406 N88-18381
[DE88-003254]
A cause of divergence in the Kalman gain equation 12 p1578 N88-19438
What do multistep methods approximate 13 p1828 N88-20932
[PB88-148838]
Analytic solutions to dynamic equations of plasma armature railguns 15 p2023 N88-22057
[DE88-006842]
Fluid motion in a spinning, coning cylinder via spatial eigenfunction expansion 15 p2066 N88-22319
[AD-A190758]
Evolution of hardening and damage during viscoplastic deformation 15 p2077 N88-22381
[AD-A190714]
Logarithmically connected, repetitive computer networks and numerical applications 15 p2114 N88-22592
[DE88-006632]
A zonal approach for the solution of coupled Euler and potential solutions of flows with complex geometries 15 p2114 N88-22595
[AD-A189752]
Numerical solution of nonlinear algebraic equations in stiff ODE solving 15 p2118 N88-22622
[DE88-006634]
Numerical methods for singularly perturbed differential equations with applications 15 p2119 N88-22628
[AD-A189786]
Normed Bellman equation with degenerate diffusion coefficients and its application to differential equations 15 p2120 N88-22637
[AD-A190319]
Formal solution of differential linear systems in the proximity of a singularity 16 p2258 N88-23495
[ETN-88-92190]
Estimation of time- and state-dependent delays and other parameters in functional differential equations 17 p2383 N88-24164
[NASA-CR-181663]
Minimal parameter solution of the orthogonal matrix differential equation 17 p2383 N88-24165
[NASA-TM-4043]
Existence of periodic solutions in n-dimensional retarded functional differential equations 17 p2392 N88-24221
[RR-325]
Computational sciences 18 p2564 N88-25226
[AD-A190826]
Approximate solution of random differential equation 18 p2565 N88-25233
Solution of Faddeev-Yakubovsky differential equations by the finite-dimensional approximation method for four spinless particles in the 1 + 3 scattering problem 19 p2719 N88-26145
[DE87-702983]
Propagation of inernio-acoustic gravity waves in a rotating and radiating opaque atmosphere 20 p2823 N88-26750
[DE88-701866]
A practical shifted Adams algorithm 20 p2837 N88-26830
[DE88-008573]
Canonical construction of differential operators intertwining representations of real semisimple Lie groups 20 p2845 N88-26882
[DE88-701852]
Theory of pseudo-differential operators over C* algebras 20 p2845 N88-26883
[DE88-701860]
A full but elementary treatment of systems of homogeneous ordinary linear differential equations with constant coefficients 20 p2845 N88-26887
[REPT-87-82]
A Wong-Zakai type theorem for certain discontinuous semimartingales 21 p3005 N88-27822
[AD-A192713]
KRYSI, an ODE solver combining a semi-implicit Runge-Kutta method and a preconditioned Krylov method 21 p3008 N88-27841
[DE88-012245]
Rational Newton algorithms to compute formal solutions of linear differential equations in an irregular singular point 22 p3140 N88-28670
[RR-704-M]
Second order differential equations in the complex domain 22 p3144 N88-28695
[RR-674-M]
Convex duality approach to the optimal control of diffusions 23 p3266 N88-29442
[AD-A194535]
On the distribution equations 23 p3270 N88-29454
[DE88-702217]
Minimizing escape probabilities: A large deviations approach 23 p3275 N88-29496
[AD-A194534]
Mathematical theory and calculations of magnetic hysteresis curves 23 p3277 N88-29510
[DE88-011055]
Resonance excitation of linear and non-linear spiral density waves in a gaseous disk 23 p3299 N88-29643
Automatic qualitative analysis of ordinary differential equations using piecewise linear approximations 24 p3424 N88-30379
[AD-A196310]

DIFFERENTIAL GEOMETRY
NT LIE GROUPS
NT RIEMANN MANIFOLD
NT TENSOR ANALYSIS
On Hotelling's approach to testing for a nonlinear parameter in regression 17 p2393 N88-24229
[AD-A191189]

Applications of differential geometry to the shape analysis of gray-value images 21 p2924 N88-27358
Critical values of functionals on Banach surfaces
[DE88-702735] 23 p3272 N88-29472

DIFFERENTIAL INTERFEROMETRY
A review of some flow visualization experiments carried out at the Institut Franco-Allemand de Recherches (ISL) shock tubes
[ISL-CO-243/86] 09 p1163 N88-16974

DIFFERENTIAL OPERATORS
U DIFFERENTIAL EQUATIONS
U OPERATORS (MATHEMATICS)

DIFFERENTIAL PULSE CODE MODULATION
A hybrid transform/DPCM encoder for data compression
[DE88-003725] 09 p1154 N88-16919

DIFFERENTIAL THERMAL ANALYSIS
U THERMAL ANALYSIS

DIFFERENTIATION (BIOLOGY)
Xiphophorus: A system to recognize radiation-induced mutations and to study the effects of zero-gravity environment on embryo development
07 p0885 N88-15372
Questions on the evolution of the development program of the vertebrate inner ear under long term zero-g conditions 07 p0886 N88-15379
Differentiation of hemopoietic stem cells during adaptation to high altitude 07 p0893 N88-15410
Embryonic development of guppy in weightlessness
10 p1360 N88-18127
Growth and differentiation of cells in organotypical rat embryo cerebellar culture developing in weightlessness
19 p2703 N88-26076
Growth and differentiation of Bacillus subtilis under microgravity conditions 22 p3060 N88-28158

DIFFRACTION
NT ELECTRON DIFFRACTION
NT FRESNEL DIFFRACTION
NT NEUTRON DIFFRACTION
NT PULSE DIFFRACTION
NT WAVE DIFFRACTION
NT X RAY DIFFRACTION
The deviation of light rays passing through a curved windscreen --- aircraft
[BAE-MSC.115] 01 p0093 N88-10610
Use of a 35mm camera for remote surface cleanliness verification 02 p0133 N88-10835
Uniform geometrical theory of diffraction
03 p0303 N88-11911
A theoretical study of enhanced Smith-Purcell radiation from a bigrating
[AD-A184530] 03 p0329 N88-12080
Interior impedance wedge diffraction with surface waves
[NASA-CR-182405] 07 p0854 N88-15186
Nonlinear and diffraction effects in sound beams with random transverse structure 09 p1235 N88-17402
Geophysical diffraction tomography for imaging isolated subsurface inclusions
[DE88-003918] 11 p1505 N88-18990
Three-dimensional scattering of impulsive acoustic waves by a semi-infinite crack in the plane interface of a half space and a layer
[PB88-146998] 12 p1687 N88-20089
An interferometric investigation of the diffraction of planar shock waves over a half-diamond cylinder in air
[UTIAS-322] 13 p1768 N88-20575
Space infrared telescope facility wide field and diffraction limited array camera (IRAC)
[NASA-CR-182704] 13 p1853 N88-21092
Research on certain aspects of laser diffraction particle sizing relevant to autonomous self-diagnosing instrumentation
[AD-A190220] 15 p2071 N88-22348
A hardware/software system for implementing geophysical diffraction tomography
[DE88-006411] 15 p2094 N88-22480
Ultrasonic Time-Of-Flight Diffraction (TOFD) measurements of crack depths in an acceleration reservoir of a high velocity research gun
[DE88-006644] 16 p2164 N88-22907
Joint services electronics program
[AD-A191749] 18 p2504 N88-24853
Structure and refinement of ordered aromatic heterocyclic polymers by diffraction methods: Application of results to electro-optic phenomena
[AD-A191859] 19 p2619 N88-25537
Scattering patterns of dihedral corner reflectors with impedance surface impedances
[NASA-CR-183078] 20 p2789 N88-26545
Acoustic diffraction by an absorbing finite strip in a moving fluid
[PB88-191382] 20 p2849 N88-26912
The evaluation of a deformable diffraction grating for a stigmatic EUV spectroheliometer
[NASA-CR-183064] 20 p2853 N88-26941
Are Centauros diffractive
[DE88-008767] 21 p3032 N88-27996
Application of laser diffraction techniques to particle sizing in solid propellant rocket motors
[AD-A193841] 22 p3049 N88-28089
Comparison of edge diffraction theories
[AD-A193880] 22 p3070 N88-28223
Direct and inverse diffraction problems for QNDE (Quantitative Non-Destructive Evaluation) applications
[AD-A194721] 22 p3085 N88-28322
Approximate and numerical methods in acousto-optics. Part 1: Normal incidence of the light
[AD-A194294] 22 p3152 N88-28755
Effect of fiber diameter on the reliability of composites - automated laser diffraction implementation
[AD-A193524] 23 p3188 N88-28972
Qualitative characteristics of open waveguide resonator spectra
[DE88-702387] 23 p3202 N88-29056
Evaluation of multi-focus holographic lenses
[AD-A196167] 24 p3377 N88-30110
Diffraction imaging (topography) with monochromatic synchrotron radiation
[NASA-CR-183264] 24 p3433 N88-30431
Streaking images that appear only in the plane of diffraction in undoped GaAs single crystals: Diffraction imaging (topography) by monochromatic synchrotron radiation
[NASA-CR-183267] 24 p3433 N88-30437

DIFFRACTION GRATINGS
U GRATINGS (SPECTRA)

DIFFRACTION LIMITED CAMERAS
Inverse scattering analysis of diffraction limited SAR
[FOA-C-30459-3.2] 05 p0576 N88-13512

DIFFRACTION PATHS
Sound propagation over uneven ground and irregular topography
[NASA-CR-182956] 20 p2849 N88-26911

DIFFRACTION PATTERNS
Photodiode matrix for the analysis of two-beam interferences
[PTB-OPT-23] 01 p0048 N88-10310
Performances of an Actively Stabilized Stellar Interferometer (ASSI): Faint magnitudes, low fringe contrast measurements and operationality
01 p0097 N88-10641
Phase-locked semiconductor quantum well laser arrays
[AD-A185155] 05 p0588 N88-13583
New description of Lau effect based on theory of raster image forming process 06 p0772 N88-14744
Research on acoustical scattering, diffraction catastrophes, optics of bubbles, photoacoustics, and acoustical phase conjugation
[AD-A185785] 06 p0776 N88-14761
Diffraction by glasses with a layer structure
[DE88-003059] 07 p0837 N88-15078
The magic of carrier patterns in moire interferometry
[AD-A187582] 10 p1296 N88-17748
Measuring accuracy of 3-dimensional bodies by the GOMER-1 device
[DE87-703230] 12 p1628 N88-19744
Nonlinear optical principles and the photorefractive effect applied to optical phase conjugation
[AD-A188856] 12 p1691 N88-20119
A review on holography, its principles and applications
[ISL-CO-242/86] 15 p2069 N88-22336
Complex space monofilar approximation of diffraction currents on a conducting half plane
[NASA-CR-182883] 16 p2273 N88-23605
Multiple scattering effects in drop sizing of dense fuel sprays by laser diffraction 24 p3346 N88-29917

DIFFRACTION PROPAGATION
An improved spherical earth diffraction algorithm for SEKE
[AD-A195847] 24 p3360 N88-30005

DIFFRACTION RADIATION
Diffraction transition radiation from periodic electron bunches
[AD-A193593] 23 p3280 N88-29528

DIFFRACTION TELESCOPES
U SPECTROSCOPIC TELESCOPES

DIFFRACTOMETERS
Realization of an instrument to measure temperature and concentration gradients in fluids --- microgravity
[CISE-3128] 09 p1168 N88-17003

DIFFUSE RADIATION
Optical spectroscopy of IRAS sources with infrared emission bands. 1: IRAS 21282 + 5050 and the diffuse interstellar bands
[NASA-CR-181387] 01 p0094 N88-10611
Magnetic diffuse scattering
[DE87-013539] 04 p0489 N88-13014
Calibration of the EGRET gamma ray telescope with a back-scattered laser beam 06 p0800 N88-14895
DIRBE External Calibrator (DEC)
[NASA-CR-180761] 12 p1631 N88-19760
Investigation of the diffuse ultraviolet background with DE data
[NASA-CR-182863] 19 p2741 N88-26271

DIFFUSERS
Combustor-diffuser interaction program
02 p0185 N88-11152
Numerical prediction of turbulent flows in dump diffusers 05 p0537 N88-13265
Numerical simulation of axisymmetric turbulent flow in combustors and diffusors
[NASA-CR-4115] 10 p1268 N88-17582
The advantage of variable geometry for turbine engines at low power 10 p1280 N88-17653
Numerical simulation of diffuser/combustor dome interaction 10 p1281 N88-17663

DIFFUSION
NT AMBIPOLAR DIFFUSION
NT ATMOSPHERIC DIFFUSION
NT GASEOUS DIFFUSION
NT IONIC DIFFUSION
NT MAGNETIC DIFFUSION
NT MOLECULAR DIFFUSION
NT PARTICLE DIFFUSION
NT PLASMA DIFFUSION
NT SELF DIFFUSION (SOLID STATE)
NT SPECIES DIFFUSION
NT SURFACE DIFFUSION
NT THERMAL DIFFUSION
NT TURBULENT DIFFUSION
New concepts for high current self-sustained diffuse discharge closing switches
[DE87-011678] 01 p0040 N88-10252
A microstructural lattice model for strain oriented problems. A combined Monte Carlo finite element technique
[NASA-TM-100215] 02 p0150 N88-10939
Thermophysical Properties Measurement Facility (TPMF) --- Columbus space station
[ESA-CR(P)-2417] 02 p0157 N88-10981
Differencing the diffusion equation on a mesh of triangles and quadrilaterals
[DE87-011550] 02 p0224 N88-11408
An adaptive pseudo-spectral method for reaction diffusion problems
[NASA-CR-178394] 02 p0224 N88-11414
Review of diffusion barrier technology for application in SP-100 fuel pins
[DE88-000021] 02 p0234 N88-11480
The diffusion-convection vortex method for solving two-dimensional incompressible Navier-Stokes equation
03 p0317 N88-12001
Thermal analysis of electromagnetic launcher rails
[DE88-000166] 04 p0405 N88-12514
A study of mechanisms of hydrogen diffusion in separation devices
[DE88-000328] 04 p0416 N88-12584
Thermophoresis of spherical aerosol particle at arbitrary Knudsen numbers 04 p0461 N88-12850
Automated design of controlled diffusion blades
[NASA-TM-100251] 05 p0542 N88-13304
Numerical methods for reaction-diffusion problems with non-differentiable kinetics
[AD-A185405] 05 p0641 N88-13923
Freidlin-Wentzell type estimates and the law of the iterated logarithm for a class of stochastic processes related to symmetric statistics
[AD-A185366] 05 p0644 N88-13944
On the correlation free forms for nonlinear stochastic systems
[DE87-011169] 05 p0645 N88-13947
An evaluation of a translator for finite element data to resistor/capacitor data for the heat diffusion equation
[DE87-013926] 06 p0698 N88-14285
Stabilized Galerkin method for convection-diffusion problems
[PB87-234985] 06 p0764 N88-14694
Diffusion first passage times: Approximations and related differential equations
[AD-A185592] 06 p0765 N88-14700
Shadow systems and attractors in reaction-diffusion equations
[AD-A185804] 06 p0766 N88-14706
A new method of boundary parameter estimation for a two-dimensional diffusion system under noisy observations
[NASA-CR-178405] 06 p0767 N88-14714
Sound pressure distribution in front of a serrated boundary: Standing wave suppression and diffusion
07 p0928 N88-15639
Some stability results for the hopscotch difference method when applied to convection-diffusion equations
[CWI-NM-R8711] 08 p1072 N88-16465
Oxygen diffusion in high T/sub c/-superconductors
[DE88-002965] 08 p1090 N88-16562

Oscillations of solar models with internal element diffusion
[DE88-003156] 09 p1264 N88-17573
Ytterbium monolayer diffusion barriers at Hg(1-x)Cd(x)Te/Al junctions
[AD-A188013] 10 p1299 N88-17768
Diffusion studies in amorphous NiZr alloys
[DE88-003009] 10 p1301 N88-17781
A multigrid preconditioner applied to a two-dimensional convection-diffusion problem
[DE88-004765] 10 p1397 N88-18329
High temperature processing of superconducting Y1Ba2Cu3O6.9
[DE88-003002] 10 p1416 N88-18449
Improved magnetization for YBa2Cu3O/sub 7 delta annealed in oxygen above 1000 C
[DE88-003934] 10 p1418 N88-18469
Fundamental studies of corrosion of nonoxide structural ceramics
[PB88-141536] 11 p1461 N88-18709
The intergranular segregation of boron in substoichiometric Ni3Al
[DE88-004783] 11 p1462 N88-18720
Subroutines for solving the equation of diffusion in media with anisotropic properties
[DE88-700743] 11 p1536 N88-19179
Path integration on the upper half-plane
[DE88-751050] 12 p1682 N88-20057
Vertical turbulent transfer of matter in thin ocean surface layer during daytime heating 13 p1787 N88-20693
Thin-film diffusion barriers for metal-semiconductor contacts
[AD-A188712] 13 p1844 N88-21035
Modeling scalar flux and the energy and dissipation equations 16 p2196 N88-23096
Analysis of non-premixed turbulent reacting flows
16 p2196 N88-23100
Research in nonlinear partial differential equations and bifurcation theory
[AD-A190986] 16 p2260 N88-23514
Nonlinear wave and diffusion equations
[AD-A191421] 16 p2265 N88-23544
Microscopic control of semiconductor interface reactivity
[AD-A191193] 16 p2283 N88-23668
Theory of neutron moisture probes and interpretation of measurements in complex soil and water systems
17 p2342 N88-23965
A review of diffusion barrier technology for application in SP-100 fuel pins 17 p2410 N88-24328
Chemical compatibility between silicon carbide and a nickel aluminide
[DE88-006188] 18 p2479 N88-24708
Diffusion of homopolymers into nonequilibrum diblock copolymer structures
[DE88-005306] 18 p2494 N88-24794
Application of computational fluid dynamics to design of compressor cascade 19 p2639 N88-25655
Five-point form of the nodal diffusion method and comparison with finite-difference
[DE88-004141] 19 p2720 N88-26154
Theory of oxygen content, atomic ordering and oxygen diffusion in 1,2,3 superconducting oxides as a function of temperature and oxygen pressure
[DE88-007961] 19 p2735 N88-26248
Abnormal diffusion of vacancies in metals
[DE88-701880] 20 p2773 N88-26441
Comparison theorems and their use in the analysis of some nonlinear diffusion problems
[DE88-010032] 20 p2845 N88-26884
Neoclassical diffusion due to trapping/detrapping orbits in stellarators
[DE88-008566] 20 p2857 N88-26968
Simulation of moisture diffusion of fiber reinforced components of aircraft for general air transportation
[IFL-IB-87-05] 21 p2907 N88-27253
Diffusion and solubility of some interstitial impurities in deformed metals
[DE88-701859] 21 p2914 N88-27296
The diffusion of vorticity from a plane boundary
[AD-A192706] 21 p2942 N88-27474
Diffusion models of crack growth due to random overloads
[DE88-008811] 21 p2962 N88-27595
Large-eddy simulations of concentration fluctuations
[DE88-009480] 21 p2973 N88-27660
Project wind, phase 4 (smoke test). Meadow Brook Valley, Red Bluff, California
[AD-A194742] 22 p3128 N88-28596
On the nucleonics component of cosmic radiation, in the atmosphere
[DE88-702493] 22 p3166 N88-28854
Evaluation of a diffusion/trapping model for hydrogen ingress in high-strength alloys
[AD-A194301] 23 p3194 N88-29008
Transport of organic vapors in multiphase polymer system
[AD-A194097] 23 p3198 N88-29033
Convex duality approach to the optimal control of diffusions
[AD-A194535] 23 p3266 N88-29442
Polynomial definition of discrete field points of map of diffusion equation, part 1
[AD-A193697] 23 p3271 N88-29467
Minimizing escape probabilities. A large deviations approach
[AD-A194534] 23 p3275 N88-29496
Ultrasonic detection of diffusion and adhesion loss
24 p3354 N88-29967
Analytical methods in stochastic control and nonlinear filtering
[AD-A194272] 24 p3426 N88-30388

DIFFUSION BONDING
U DIFFUSION WELDING

DIFFUSION COEFFICIENT
Influence of a magnetic field on the diffusion of small particles in a turbulent flow
[DE87-702677] 01 p0046 N88-10291
Mass transport by diffusion 03 p0297 N88-11864
Optimal correction problem of a multidimensional stochastic system
[AD-A186727] 09 p1228 N88-17353
A finite element analysis of adhesively bonded composite joints including geometric nonlinearity, nonlinear viscoelasticity moisture diffusion and delayed failure
[AD-A187455] 10 p1296 N88-17747
Normed Bellman equation with degenerate diffusion coefficients and its application to differential equations
[AD-A190319] 15 p2120 N88-22637
Development of a model procedure for the determination of volume diffusion lengths by transient measurements on monocrystal silicon solar cells
[ETN-88-92119] 20 p2821 N88-26733

DIFFUSION EFFECT
U DIFFUSION

DIFFUSION ELECTRODES
Advanced materials for solid oxide fuel cells
[DE88-002338] 10 p1350 N88-18071
The kinetics of contact noise in NaBeta alumina
[AD-A190651] 15 p2130 N88-22707

DIFFUSION FLAMES
Combustion in turbulent jets and buoyant flames
[PB87-232674] 03 p0263 N88-11779
Extinguishing diffusion flames with dry powder and halon at low Froude numbers
[PB87-111365] 06 p0679 N88-14159
Mixing and combustion of pulsed gas jets
[PB88-112834] 06 p0680 N88-14169
Mixing and combustion of pulsed gas jets
[PB88-108014] 06 p0680 N88-14170
Carbon monoxide and turbulence-chemistry interactions. Blowoff and extinction of turbulent diffusion flames
[AD-A186276] 07 p0828 N88-15025
Diffusion description of flame propagation due to the translational motion of burning reaction products
[DE88-700676] 10 p1297 N88-17757
Fuels combustion research
[AD-A187688] 11 p1453 N88-18657
Studies on homogeneous and heterogeneous reactive flows 11 p1484 N88-18861
Thermal cracking and variable properties effects on free boundary layer diffusion flames
[NBS/GCR-88/541] 12 p1614 N88-19652
Turbulence and flame propagation
[PB87-228912] 19 p2612 N88-25499
Combustion rate limits of hydrogen plus hydrocarbon fuel. Air diffusion flames from an opposed jet burner technique 19 p2624 N88-25567
Heterogeneous diffusion flame stabilization
[AD-A193014] 20 p2771 N88-26429
The structure and stability of nonpremixed gas jet flames 21 p2908 N88-27257
A study of the interaction of diffusion flames with a vortex pair flowfield 21 p2908 N88-27258
Experimental research of combustion systems
21 p2927 N88-27371
Radiation from soot-containing flames
24 p3347 N88-29927
Flamelet chemistry modelling of soot formation for radiation 24 p3348 N88-29928
The influence of pressure on soot formation
24 p3349 N88-29934
Three-dimensional combustor predictors. A comparison of equilibrium and laminar flamelet chemistry models
24 p3350 N88-29940

DIFFUSION LENGTH
Multigroup flux-limited asymptotic diffusion Fokker-Planck equation
[DE88-700958] 15 p2118 N88-22615

DIFFUSION THEORY
Dynamical friction
[DE88-002194] 06 p0711 N88-14358
Effect of irradiation on the diffusion evolution of void ensemble in crystals
[DE88-700558] 07 p0939 N88-15706
COMESH: A corner mesh finite difference code to solve multigroup diffusion equations in multidimensions
[DE88-701248] 15 p2108 N88-22555
Multigroup flux-limited asymptotic diffusion Fokker-Planck equation
[DE88-700958] 15 p2118 N88-22615

DIFFUSION WELDING
Stress state of welded joints of dissimilar materials obtained by diffusion welding 03 p0286 N88-11799
The mechanical properties of solid state diffusion bonds between Ti-6Al-4V and 304L stainless steel
[BAS-TR-113-1987] 03 p0332 N88-12093
Diffusion bonding depleted uranium to copper
[RFP-3783-REV] 03 p0333 N88-12098
Investigation on diffusion reaction brazing of aluminium
[PB87-143368] 08 p0992 N88-16001
Development of methods for low temperature diffusion bonding
[AD-A186875] 09 p1174 N88-17033
Diffusion welding of aluminomagnesium alloys to ceramics 14 p1898 N88-21333
Joints in fiber-reinforced aluminum alloys
[NASA-TT-20160] 15 p2031 N88-22104
Interface characterization of Cu-Cu and Cu-Ag-Cu low temperature solid state bonds
[AD-A191015] 16 p2283 N88-23667
An investigation into the metallurgical aspects of joining rapidly-solidified aluminum alloys
[AD-A194677] 23 p3194 N88-29009

DIFFUSIVITY
IR laser excitation in molecules: Chaos and diffusive energy growth
[DE87-013147] 02 p0178 N88-11105
Investigation of structure-permeability relationships of silicone polymer membranes
[PB87-230181] 03 p0293 N88-11839
Mass transport phenomena between bubbles and dissolved gases in liquids under reduced gravity conditions
[NASA-TM-100273] 11 p1455 N88-18672
Modeling of turbulent transport as a volume process
16 p2196 N88-23099
UV-Laser reactions of molecular adsorbates
[AD-A190796] 16 p2212 N88-23201
Calculation of oxidation rates for iron in CO-CO2
[DE88-007313] 18 p2487 N88-24757

DIFLUORIDES
NT CALCIUM FLUORIDES

DIFLUORO COMPOUNDS
NT POLYTETRAFLUOROETHYLENE
NT TEFLON (TRADEMARK)
Corrosion and corrosion inhibition of metals/alloys in methyphosphonic difluoride 17 p2319 N88-23850

DIGESTIVE SYSTEM
NT GASTROINTESTINAL SYSTEM
NT INTESTINES
NT STOMACH

DIGITAL CIRCUITS
U DIGITAL ELECTRONICS
U LOGIC CIRCUITS

DIGITAL COMMAND SYSTEMS
Low cost telemetry and telecommand system for remote measurement of magnitude character
[INPE-4273-PRE/1145] 12 p1598 N88-19564

DIGITAL COMMUNICATION
U PULSE COMMUNICATION

DIGITAL COMPUTERS
NT CDC CYBER 205 COMPUTER
NT HEWLETT-PACKARD COMPUTERS
NT MICROCOMPUTERS
NT MIMD (COMPUTERS)
NT MINICOMPUTERS
NT PARALLEL COMPUTERS
NT PERSONAL COMPUTERS
NT SEQUENTIAL COMPUTERS
NT SIMD (COMPUTERS)
NT VAX COMPUTERS
Reliability modeling of fault-tolerant computer based systems 02 p0127 N88-10801
Technology upgrade of a silicon compiler
[AD-A184873] 05 p0655 N88-14016
Microprocessor emulating the intermediate code for FORTRAN compiler
[DE88-700540] 07 p0900 N88-15452
The formal specification of computer systems
[AD-A188947] 12 p1675 N88-20013
Evaluation of chemical and atmospheric sciences research
[AD-A188468] 12 p1687 N88-20091

Interfacing and integrating hardware and software design systems
17 p2306 N88-23796

Specification for IBM/IBM compatible 3480 tape cartridge
[NASA-TM-100702] 17 p2384 N88-24168

Architecture for optical digital computers
[AD-A195477] 24 p3430 N88-30416

DIGITAL DATA

An acoustic emission digital data acquisition workstation
[DE87-012425] 02 p0191 N88-11191

Directory of geomagnetic observatories with high-resolution digital results, 1987
[PB87-221156] 03 p0348 N88-12201

High frequency data acquisition system for space shuttle main engine testing
05 p0595 N88-13630

Space shuttle main engine vibration data base
05 p0595 N88-13631

Fast, colour displays of digital terrain elevation data
[AD-A185596] 06 p0729 N88-14485

Digital signal processing algorithms for automatic voice recognition
06 p0793 N88-14862

Digital processing of flight test data without using anti-aliasing filters, using a helicopter as an example
[DFVLR-MITT-87-12] 07 p0819 N88-14981

Determination of network attributes from a high resolution terrain data base
[AD-A186078] 07 p0870 N88-15279

Textural features for image classification in remote sensing
[INPE-4169-PRE/1066] 08 p1020 N88-16181

Critical issues in NASA information systems
[NASA-CR-182380] 08 p1093 N88-16577

Information transfer in the National Airspace System
10 p1275 N88-17634

Space shuttle phase B wind tunnel test database
[NASA-CR-4121] 11 p1444 N88-18611

Fixed and adaptive interframe image prediction for remote piloting application
[AD-A187987] 11 p1471 N88-18771

The digital landmass simulation production overview
[AD-A187978] 11 p1503 N88-18978

Digital data dubbing capability
[AD-A188252] 11 p1525 N88-19105

The US Army Electronic Map Data (EMD) initiative
[AD-A188209] 11 p1565 N88-19372

Envelope and phase statistics for non-Gaussian noise and resulting error probabilities for digital communications systems
12 p1617 N88-19672

Digital method for correction of the phase error in the discrete generation of periodic signals in real time
[INPE-4327-RPE/552] 12 p1618 N88-19676

An application of digital cartography updating middle and small scale thematic maps using orbital data
[INPE-4460-TDL/317] 12 p1637 N88-19805

Report on phase 1 of the project estimate development of a model for yield estimation of sugar cane based on LANDSAT and agromet data
[INPE-4466-RPE/560] 12 p1638 N88-19807

Digital Topographic Support System (DTSS)
[AD-A188304] 12 p1638 N88-19808

Terrain classification from digital elevation data using slope and curvature information
[AD-A188940] 12 p1639 N88-19812

Development of a digital terrain modeling system for microcomputers
[INPE-4406-TDL/303] 12 p1639 N88-19816

Some questions of using coding theory and analytical calculation methods on computers
[DE88-700905] 12 p1676 N88-20021

Interpolation algorithms for digital terrain models
[INPE-4373-PRE/1196] 13 p1820 N88-20877

Proposal for a parallel system with image processing applications
[INPE-4293-PRE/1164] 14 p1961 N88-21696

Direct bit detection receiver noise performance analysis for 32-PSK and 64-PSK modulated signals
[AD-A190009] 15 p2056 N88-22256

Calibration and processing of AVHRR data for temperature estimation
[INPE-4493-PRE/1257] 15 p2095 N88-22485

NASA and the challenge of ISDN: The role of satellites in an ISDN world
[NASA-CR-182749] 15 p2126 N88-22676

Textural features for image classification in remote sensing
17 p2354 N88-24027

Thematic mapping utilizing data from the Thematic Mapper sensor of the LANDSAT satellite
17 p2361 N88-24060

Geometric image correction: An approach for the registration of LANDSAT-TM digital images supported by topographical maps of medium and great scales
17 p2361 N88-24061

Visualization of digital terrain models
17 p2364 N88-24081

Application of its transformation in color enhancement of LANDSAT imagery
17 p2365 N88-24082

Preliminary study on the application of digital processing of TM-LANDSAT data in the mapping of apple orchards in Fraiburgo (SC)
17 p2367 N88-24093

Reports on cartography and geodesy. Series 1, no. 99
[ETN-88-92387] 18 p2533 N88-25025

Digital maps for an electronic traffic guide
18 p2534 N88-25033

Development in data structures in PHOCUS for digital mapping
18 p2534 N88-25034

Space shuttle phase B wind tunnel model and test information. Volume 2: Orbiter configuration
[NASA-CR-178415-VOL-2-PT-2]
21 p2893 N88-27172

Optical interconnections for digital image coding
21 p2928 N88-27381

Analysis of remotely sensed imagery using digital morphology
[AD-A192738] 21 p2965 N88-27614

Relief effect correction on LANDSAT imagery for forest applications using digital terrain models
[INPE-4611-PRE/1334] 24 p3388 N88-30179

Method for combined image interpolation-restoration through a fir filter design technique
[INPE-4561-PRE/1302] 24 p3413 N88-30315

An operations manual for the digital data system
[NASA-CR-181688] 24 p3415 N88-30329

DIGITAL ELECTRONICS

NT LOGIC CIRCUITS

Establishment of complete minimum test sets for digital circuits with safety engineering significance
[ETN-88-90599] 05 p0578 N88-13526

Avionics systems integration technology
09 p1110 N88-16654

Describing constraints on a digital circuit's behavior
[AD-A189200] 13 p1761 N88-20531

Analytical sensor redundancy assessment
[NASA-CR-182892] 16 p2163 N88-22901

DIGITAL FILTERS

NT FIR FILTERS

Ultra-low power digital filter
[AD-A184485] 03 p0310 N88-11959

Integrated circuit design
[AD-A184486] 03 p0311 N88-11960

A digital low pass filter for the reduction of large quantities of data
[ESA-TT-1058] 03 p0363 N88-12281

Design of digital filters for electronic instrumentation
[PB87-100418] 04 p0438 N88-12716

Implementation of an FIR band pass filter using a bit-slice processor
[AD-A184895] 05 p0634 N88-13875

Digital processing of flight test data without using anti-aliasing filters, using a helicopter as an example
[DFVLR-MITT-87-12] 07 p0819 N88-14981

Description, analysis and simulation of a new realization of digital filters
[AD-A187763] 11 p1477 N88-18814

Computation of LMS (Least-Mean-Square) and matched digital filters for optical clutter suppression
[AD-A188885] 12 p1687 N88-20093

Intergrated circuit design, phase 2
[AD-A189060] 13 p1760 N88-20530

Utilization of space color transformation, linear contrast and filtration for enhancement of colored digital images
[INPE-4310-PRE/1176] 14 p1983 N88-21831

Digital processing of flight data of a helicopter without using anti-aliasing filters
[ESA-TT-1094] 16 p2161 N88-22890

Digital filter unit for selection of spectrometric information
[DE87-702990] 16 p2246 N88-23415

Modeling, filtering and control of stochastic processes --- communication networks
[ENST-87E021] 17 p2333 N88-23925

Spatial filtering on digital images
17 p2354 N88-24025

A numerically efficient digital matched filter for periodic and windowed periodic radar waveforms
[AD-A193132] 21 p2932 N88-27410

A method of improving remote reproduction of a sound field by one-third-octave analysis and digital filtering
[RAE-TM-FS(F)-679] 22 p3147 N88-28722

Computer aided filter design
[AD-A193959] 23 p3208 N88-29093

Digital filter design techniques
[AD-A194484] 23 p3274 N88-29486

DIGITAL NAVIGATION

Digital fiber optic displacement sensors
18 p2518 N88-24937

Accuracy of satellite data navigation
[AD-A195877] 24 p3322 N88-29787

DIGITAL RADAR SYSTEMS

The Newcastle meteor radar
06 p0741 N88-14556

Moving Target Indicator (MTI) interface for simple radar
[FOA-C-30463-3.2] 09 p1154 N88-16914

DIGITAL SIMULATION

The importance sampling and its application to radar simulation
01 p0012 N88-10065

Model adaptation and imbalance compensation in rotors with active magnetic bearings
[ETN-87-90440] 01 p0056 N88-10361

Monte Carlo calculations for the simulation of channeling experiments on irradiated aluminum alloys. Calculation of angle-dependent efficiency curves
[HMI-B-433] 01 p0092 N88-10597

Numerical simulation of unsteady separated flows
[AD-A184132] 04 p0442 N88-12741

Computer modeling aids studies of precipitation formation
04 p0458 N88-12832

Numerical simulation of the Reversed Field Pinch
[AD-A184353] 04 p0491 N88-13023

Numerical simulation of the hypersonic flow around lifting vehicles
05 p0532 N88-13234

The polar ionosphere and interplanetary field
[AD-A185386] 05 p0624 N88-13822

An extension to the multilevel logic simulator for microcomputers
[AD-A185032] 05 p0634 N88-13879

Analysis, design, construction and testing of a reaction wheel model for space applications
[INPE-4358-TDL/299] 08 p0963 N88-15834

Simulation of a typical flow in a broad valley
08 p1015 N88-16154

Simulation of a lee cyclogenesis using a numerical model
08 p1016 N88-16162

Numerical simulation of the flow about New Zealand
08 p1017 N88-16163

Numerical modeling of radiation fog
08 p1017 N88-16166

Inversion of simulated satellite signals
08 p1017 N88-16168

Numerical simulation of the interaction of pressure waves with laminar and turbulent boundary layers
[DFVLR-FB-87-18] 09 p1161 N88-16960

Numerical simulation of thermally generated mountain-foreland circulation
[DFVLR-FB-87-30] 09 p1190 N88-17132

Simulations of thermally induced winds and cross flow situations
[MITT-57] 09 p1193 N88-17148

Coronal heating by means of helical magnetohydrodynamic turbulence
[AD-A187084] 10 p1410 N88-18413

A digital logic simulator with concurrent programming considerations
[AD-A188823] 12 p1678 N88-20032

Simulation of electron cyclotron heating in TFR
12 p1693 N88-20130

Modelling of a hydraulic motor and servo-valve to produce a desired system response using analogue and digital compensation techniques
[ETN-88-92079] 14 p1899 N88-21337

Numerical simulation of medium scale disturbance on meiyu front
14 p1900 N88-21346

investigation of the behavior of fast propagating cracks using numerical simulation calculations
[W-6/87] 14 p1934 N88-21532

Numerical treatment of Navier-Stokes equations
[REPT-87-22] 16 p2206 N88-23162

Simulation and computer aided engineering (the necessity of an integrated approach)
[NLR-MP-86050-U] 17 p2386 N88-24178

CFD benefits, goals, stepping-stones and techniques: Proposals for the scientific programme of the European Reserch Centre on flow, turbulence and combustion --- computational fluid dynamics
[CFDU/88/1] 18 p2510 N88-24894

Direct numerical simulations of the PDF's (Probability Density Functions) of a passive scalar in a forced mixing layer
[AD-A192134] 18 p2568 N88-25256

Direct simulations of chemically reacting turbulent mixing layers, part 2
[NASA-CR-180853] 19 p2667 N88-25857

Noise and chaos in driven Josephson junctions
19 p2734 N88-26238

A high fidelity real-time simulation of a small turboshaft engine
[NASA-TM-100991] 20 p2761 N88-26378

A simulation analysis of errors in the measurement of standard electrochemical rate constants from phase-selective impedance data
[AD-A192739] 20 p2770 N88-26426

The influence of uncompensated solution resistance on the determination and standard electrochemical rate constants using cyclic voltammetry and some comparisons with AC voltammetry
[AD-A192825] 20 p2770 N88-26427

Simulation models for the dynamics of tracked vehicle systems: State-of-the-art and open problems
20 p2785 N88-26522

Parameter identification of the passenger simulation model MADYMO: Methods and experience
20 p2788 N88-26536

Robust digital model following controller for helicopters
[DFVLR-FB-88-07] 21 p2898 N88-27203

Simulation of attitude and maneuvers for the Brazilian spin-stabilized satellite
[INPE-4271-PRE/1143] 22 p3046 N88-28079

Digital terrain modelling with SPOT data and geological applications 22 p3110 N88-28474

Automatic production of orthophoto using SPOT images 22 p3112 N88-28487

Automatic creation of digital terrain models from SPOT image pairs 22 p3113 N88-28490

A method for determining absolute velocities from hydrographic data: The numerical code
[AD-A193997] 22 p3129 N88-28603

Description of a tool for the simulation of imagery systems 22 p3147 N88-28724

Acoustic-seismic helicopter detection
22 p3149 N88-28734

Crash simulation calculations and component idealization for an airframe. Computer code KRASH 79
[ETN-88-92971] 23 p3174 N88-28899

Coupling expert systems and simulation
23 p3252 N88-29360

Modeling of a cometary dust coma
[ETN-88-92980] 23 p3300 N88-29651

Numerical simulation of unsteady incompressible flow in a partially-filled rotating cylinder
[AD-A196001] 24 p3371 N88-30073

Numerical simulation of the interaction of pressure waves with laminar and turbulent boundary layers
[ESA-TT-1089] 24 p3371 N88-30075

Numerical simulation of unsteady incompressible viscous flows in generalized coordinate systems
[NASA-TM-101016] 24 p3373 N88-30085

A digital simulation technique for the Dryden atmospheric model
[NASA-TT-20342] 24 p3404 N88-30266

DIGITAL SYSTEMS
NT DIGITAL NAVIGATION
NT DIGITAL RADAR SYSTEMS

Digital system bus integrity
[NASA-CR-181446] 01 p0006 N88-10030

ELF/VLF/LF propagation and system design
[AD-A183261] 01 p0033 N88-10212

A compact digital communications system. Part 3: Generalising the phase locked loop
[RSRE-MEMO-4027-PT-3] 01 p0035 N88-10222

Implementation of a digital optical matrix-vector multiplier using a holographic look-up table and residue arithmetic
[NASA-CR-180431] 01 p0078 N88-10496

Reliability modeling of fault-tolerant computer based systems 02 p0127 N88-10801

A digital control system for high level acoustic noise generation 02 p0138 N88-10865

A digital audio link to the Channel Islands in the UHF television band: Preliminary experimental results
[BBC-RD-1987/9] 02 p0161 N88-11011

A review of computer-assisted photo interpretation research at USAETL (US Army Engineer Topographic Laboratories)
[AD-A184034] 03 p0346 N88-12186

SBNR (Signed Binary Number Representations) digital signal processor architecture
[AD-A184603] 03 p0364 N88-12290

Microcomputer control of a hydraulically actuated piston
[AD-A184130] 03 p0368 N88-12317

Digital-flight-control-system software written in automated-engineering-design language: A user's guide of verification and validation tools
[NASA-TM-88313] 04 p0401 N88-12494

Diagnostic reasoning in digital systems
[NASA-CR-181564] 05 p0633 N88-13871

Error propagation in a digital avionic mini processor
[NASA-CR-181565] 05 p0633 N88-13872

Two digital X-ray imaging systems for applications in X-ray diffraction
[PB87-123683] 06 p0669 N88-14103

An analysis of simplified feed architectures for MMIC (Monolithic Microwave Integrated Circuit) T/R (Transmit/Receive) module arrays
[AD-A185474] 06 p0697 N88-14275

Diagnostic emulation: Implementation and user's guide
[NASA-CR-178391] 06 p0756 N88-14638

Estimating the distribution of fault latency in a digital processor
[NASA-TM-100521] 06 p0760 N88-14666

A Multipurpose Adaptive Controller (MAC) for real time digital regulation
[REPT-87-028] 06 p0762 N88-14673

Online monitoring of laserpulses using the GPIB-interface of a Tektronix 2430 Digital Storage Oscilloscope
[DE88-002836] 07 p0856 N88-15201

Proceedings of Image Understanding Workshop, volume 1
[AD-A186103] 07 p0902 N88-15463

Advanced gyros in spacecraft control. Digital capture loops for dry tuned gyros
[LITEF-120046] 08 p0962 N88-15827

Digital control of high frequency pulse-width modulated inverters
[ETN-87-90711] 09 p1157 N88-16936

Spectral density estimates of coarsely quantized random vibration data 09 p1178 N88-17055

Regulation of nonlinear and generalized linear systems
[AD-A183706] 09 p1224 N88-17338

Transport delay compensation for computer-generated imagery systems
[NASA-TM-100084] 10 p1277 N88-17645

Formal multilevel hierarchical verification of synchronous MOS VLSI circuits
[AD-A187532] 10 p1324 N88-17918

Orthogonal patterns in binary neural networks
[NASA-TM-100060] 10 p1396 N88-18320

Subpicosecond optical digital computation using phase conjugate parametric generators
[AD-A188279] 10 p1410 N88-18411

Further developments in exact state reconstruction in deterministic digital control systems
[NASA-TP-2812] 11 p1468 N88-18751

Terrain Analyst Work Station (TAWS) demonstrations
[AD-A188139] 11 p1504 N88-18981

The Quick Response Multicolor Printer (QRMP) system
[AD-A188140] 11 p1504 N88-18982

Digital data dubbing capability
[AD-A188252] 11 p1525 N88-19105

Autonomous Liquid Encapsulated Czochralski (LEC) growth of single crystal GaAs by intelligent digital control
[AD-A187211] 11 p1555 N88-19305

Digital bit error rate estimator for telemetry links
[INPE-4351-TDL/295] 12 p1598 N88-19563

Radio and radar holes and multipath zones: The global and local influences on atmospheric refractive structure and resulting adverse radio and radar performance
12 p1617 N88-19667

Space-diversity effects on line-of-sight propagation paths 12 p1617 N88-19670

The 6 GHz propagation measurements over a 51 km path in the UK 12 p1617 N88-19673

Evaluating the performance of the LPC (Linear Predictive Coding) 2.4 kbps (kilobits per second) processor with bit errors using a sentence verification task
[AD-A188573] 12 p1620 N88-19686

A methodology for hardware verification based on logic simulation
[AD-A188553] 12 p1622 N88-19704

A digital circuit design environment
[AD-A188831] 12 p1623 N88-19709

VLSI implementations for digital signal processing
[AD-A189612] 12 p1624 N88-19719

Soft maps for US Army electronic map background applications
[AD-A188427] 12 p1638 N88-19809

Architecture specification for PAVE PILLAR avionics
[AD-A188722] 13 p1723 N88-20303

Operational viewpoint of the X-29A digital flight control system
[NASA-TM-100434] 14 p1866 N88-21152

Digital correlator for the portable channel prober measurement instrument
[AD-A189065] 14 p1904 N88-21377

DataViews: A personalizable, interactive, data display system for the decisionmaker
[AD-A186509] 14 p1991 N88-21868

Preliminary airworthiness evaluation of the UH-60A with Advanced Digital Optical Control System (ADOCS)
[AD-A190674] 15 p2018 N88-22030

Subharmonic aliasing and its effects on the AFTI/F-16 digital flight control system
[AD-A190614] 15 p2020 N88-22042

A fully abstract semantics for event-based simulation
[AD-A190560] 15 p2060 N88-22283

Exhaustive and pseudo-exhaustive testing
[AD-A190140] 15 p2111 N88-22574

Design and implementation of VLSI prime factor algorithm processor
[AD-A190483] 15 p2112 N88-22580

Representation, analysis and design of multirate discrete-time control systems
[AD-A190499] 15 p2116 N88-22608

Two papers on a symbolic analyzer for MOS (Metal-Oxide Semiconductors) circuits
[AD-A188617] 15 p2139 N88-22761

Sources of digital spatial data for geographic information systems
[AD-A189788] 15 p2148 N88-22824

Computer tomography and hybrid optical/digital methods for aerodynamic measurements
[AD-A190909] 16 p2157 N88-22872

Automated test device for FASR (Fixed Array Surveillance Radar) beam steering componentry
[AD-A191650] 18 p2500 N88-24829

Some unsolved problems in modelling self-timed circuits using Petri Nets, series B, number 2
[PB88-181466] 18 p2507 N88-24872

Digital television routing systems. A survey of optical and electrical techniques
[BBC-RD-1988/3] 19 p2654 N88-25763

Digital control of the czochralski growth of gallium arsenide. System reference manual. Valid for Czochralski growth controller software version 2.4
[AD-A191997] 19 p2732 N88-26227

Digital communication transmitter and receiver test procedures
[AD A191218] 20 p2788 N88-26540

COSPAS/SARSAT 406-MHz emergency beacon digital controller
[NASA-TM-100859] 20 p2792 N88-26566

Development of a hybrid simulator for robotic manipulators
[AD-A193119] 21 p2956 N88-27557

More on exact state reconstruction in deterministic digital control systems
[NASA-TP-2847] 22 p3063 N88-28177

Use of a coherent square wave reference to demodulate BPSK (Binary Phase Shift Keying) carriers and a visual indicator of the quality of received QPSK (Quadrature Phase Shift Keying) carriers
[AD-A193528] 23 p3204 N88-29065

Distortions in processed signals and their application in electronic design. Part 1: Basic and general formulations
[DE88-702731] 23 p3204 N88-29070

Digital phase-lock loop having an estimator and predictor of error
[NASA-CASE-NPO-17196-1-CU]
23 p3205 N88-29076

Ionospheric convection and structure using ground-based digital ionosondes
[AD-A194246] 23 p3233 N88-29237

Object discrimination via bulk temperature/velocity filtering, phase 1
[AD-A194533] 23 p3274 N88-29487

N-version software demonstration for digital flight controls
[NASA-CR-181483] 24 p3328 N88-29815

Performance of DS/SSMA communications in impulsive channels. Part 1: Correlation receivers
[AD-A195712] 24 p3362 N88-30021

Estimation of short-wavelength gravity on a dense grid using digital terrain elevation data
[AD-A196325] 24 p3391 N88-30196

Binary star measurements using digital speckle interferometer of 6-m telescope
24 p3448 N88-30521

DIGITAL TECHNIQUES

Digital receiver structures and methods for the determination of the scanning frequency in modems for fast data transmission via telephone channels
[ETN-87-90429] 01 p0037 N88-10235

A digital audio link to the Channel Islands in the UHF television band: Protection of television signals from digitally modulated interference
[BBC-RD-1987/7] 02 p0161 N88-11010

Development of standard cells in NMOS technology for the design of digital integrated circuits
[FI-62-TB-6] 03 p0310 N88-11953

Input/output technologies: An overview of image scanning, storage, and display
[DE87-014837] 04 p0476 N88-12933

Measured characteristics of 800/900 MHz mobile radio channels with high-angle propagation through moderately dense foliage
[CRC-1398] 05 p0573 N88-13493

Modem for digital phase modulation. Results and summary
[PB87-149233] 07 p0845 N88-15129

Evaluation of the flooding areas of the Sao Goncalo Canal through LANDSAT 5 thematic mapper images
[INPE-4118-PRE/1039] 08 p1020 N88-16185

Digital image processing: A summary of main techniques
[INPE-4404-PRE/1220] 08 p1068 N88-16454

Digital image processing
[INPE-4131-TDL/264] 08 p1083 N88-16527

Techniques of flow visualization
[AGARD-AG-302] 09 p1164 N88-16977
Digital imaging techniques for single- and multi-phase reacting flowfields 10 p1327 N88-17933
A microspectrofluorometer system based on real time digital techniques
[REPT-86-014] 11 p1490 N88-18891
Reaction wheel control through digital technique using reference models
[INPE-4220-PRE/1100] 12 p1599 N88-19570
Digital enhancement of flow field images
[NASA-TP-2770] 13 p1813 N88-20833
On-board processing for mobile satellite communications
[ESA-CR(P)-2519] 14 p1905 N88-21382
Classification of small image areas by digital correlation for the connection of different images in photogrammetry and long-range reconnaissance
[ETN-88-91506] 14 p1940 N88-21578
Comparative utilization of analog and digital processes in the treatment of MSS-LANDSAT data for studying the national parks of Brazil
[INPE-4011-TDL/240] 15 p2090 N88-22456
Development of a digital sun sensor for a spin-stabilized satellite
[INPE-4508-TDL/327] 16 p2169 N88-22929
Computer assisted generalization of buildings for digital landscape models by classification methods
16 p2226 N88-23294
Digital avionics design and reliability analyzer
[NASA-CR-181641] 16 p2254 N88-23472
Visual enhancement of digital color imagery utilizing transformation in color coordinates (IHS transformation)
[INPE-4482-PRE/1248] 16 p2273 N88-23606
Method of digital surface photometry of galaxies and its application to the edge-on galaxy NGC 5907
16 p2287 N88-23695
Clinical applications of computerized thermography
17 p2330 N88-23915
Digital processing of infrared and visible images from the GOES satellite and its integration with meteorological radar data 17 p2360 N88-24057
Temporal analysis of the changes in Parque Estadual de Jacupiranga vegetation through digital treatment of LANDSAT imagery 17 p2367 N88-24094
Evaluation of TM false color composites for crop discrimination 17 p2367 N88-24096
A digitally implemented phase-locked loop detection scheme for analysis of the phase and power stability of a calibration tone 22 p3066 N88-28196
Avionics system design for high energy fields: A guide for the designer and airworthiness specialist
[NASA-CR-181590] 23 p3178 N88-28919
Nanosequencer digital logic controller
[NASA-CASE-NPO-16116-2] 23 p3245 N88-29310
Evaluation of LANDSAT-TM data for geomorphological mapping
[INPE-4593-PRE/1324] 24 p3386 N88-30168
Use of digital images as a mineral prospecting tool in the tin province of Goias, Brazil
[INPE-4537-PRE/1284] 24 p3387 N88-30173
LANDSAT-TM data to map flooded areas
[INPE-4594-PRE/1324] 24 p3387 N88-30177

DIGITAL TELEVISION
Accommodating the residue of processed or computed digital video signals within the 8 bit CCIR recommendation 601
[BBC-RD-1987/12] 04 p0432 N88-12676
Digital video bit-rate reduction: DPCM for sub-Nyquist PAL
[BBC-RD-1987/16] 05 p0573 N88-13494
Television motion measurement for DATV and other applications
[BBC-RD-1987/11] 05 p0573 N88-13496
Limiting of YUV digital video signals
[BBC-RD-1987/22] 09 p1155 N88-16924

DIGITAL TO ANALOG CONVERTERS
Digital to analog and analog to digital conversion using pulse duration modulation
[ETN-87-90415] 01 p0078 N88-10499
Life sciences flight experiments microcomputer
06 p0792 N88-14857
Description, analysis and simulation of a new realization of digital filters
[AD-A187763] 11 p1477 N88-18814

DIGITAL TRANSDUCERS
Vital signs rate meter
[AD-A187015] 09 p1198 N88-17183
Photo-optical converter of angular displacements in digital servomechanisms
[DE87-703206] 14 p1961 N88-21698

DIGITIZERS
U ANALOG TO DIGITAL CONVERTERS

DIGITS
NT BINARY DIGITS
Experiments in isolated digit recognition using the multilayer perception
[RSRE-MEMO-4073] 17 p2333 N88-23927

DIHEDRAL ANGLE
Scattering patterns of dihedral corner reflectors with impedance surface impedances
[NASA-CR-183078] 20 p2789 N88-26545

DIHEDRAL EFFECT
U LATERAL STABILITY

DIKES (GEOLOGY)
U ROCK INTRUSIONS

DILATATION
U STRETCHING

DILATOMETERS
U EXTENSOMETERS

DILUTION
NT GEOMETRIC DILUTION OF PRECISION
Dilution jet mixing program, phase 3
02 p0185 N88-11153
Influence of bond dilution on the free surface and interface Potts ferromagnetism
[DE87-703360] 04 p0497 N88-13061
A numerical study of the effects of curvature and convergence on dilution jet mixing
[NASA-TM-89878] 05 p0549 N88-13347
An empirical model of the effects of curvature and convergence on dilution jet mixing
[NASA-TM-100896] 18 p2466 N88-24640
DARPA-URI consortium meetings on submicron heterostructures of diluted magnetic semiconductors
[AD-A193499] 23 p3206 N88-29081

DIMENSIONAL ANALYSIS
Dimensional analysis of nonlinear oscillations in brain, heart and muscle
[DE87-014749] 06 p0751 N88-14614
Display and processing of multidimensional signals with the aid of fractal image sequences
[ETN-88-92131] 20 p2806 N88-26642

DIMENSIONAL MEASUREMENT
The determination of exhaust cloud dimensions from films of space shuttle launches
[NASA-CR-4103] 06 p0732 N88-14500
Development and calibration of Direct Current Potential Difference (DCPD) crack length measurement equipment
[VTT-RR-480] 09 p1182 N88-17083
Effect of fiber diameter on the reliability of composites - automated laser diffraction implementation
[AD-A193524] 23 p3188 N88-28972

DIMENSIONAL STABILITY
NT SHELL STABILITY
NT STRUCTURAL STABILITY
Carbon-fiber reinforced plastics
04 p0403 N88-12506
New equilibrium forms of free surface of confined magnetic fluid 06 p0770 N88-14734
Cost 501 Project UK10 part 3: Thermal fatigue damage of Fecralloy steel-sprayed and co-extruded tubing
[AERE-R-12230] 10 p1343 N88-18026
Contribution to the study of materials behavior in space environment
[SNIAS-881-430-104] 23 p3189 N88-28977

DIMENSIONLESS NUMBERS
NT FROUDE NUMBER
NT HIGH REYNOLDS NUMBER
NT LOW REYNOLDS NUMBER
NT MACH NUMBER
NT NUSSELT NUMBER
NT PECLET NUMBER
NT PRANDTL NUMBER
NT RAYLEIGH NUMBER
NT REYNOLDS NUMBER
NT RICHARDSON NUMBER
Can we calculate the fundamental dimensionless constants of physics
[DE88-702641] 23 p3295 N88-29625

DIMENSIONS
NT DEPTH
NT DIAMETERS
NT DIFFUSION LENGTH
NT FILM THICKNESS
NT FRACTALS
NT HEIGHT
NT LENGTH
NT RADII
NT SCALE HEIGHT
NT TARGET THICKNESS
Multidimensional modeling of convective heat transfer with application to IC engines
[DE87-011046] 01 p0055 N88-10353
EVA reference manual
[DE87-014073] 01 p0082 N88-10526
An interactive optimization procedure for the computer aided dimensioning of integrated circuits
[ETN-87-90414] 01 p0082 N88-10531
Two dimensional imaging observations of meter-decameter bursts associated with the February 1986 flare activity 01 p0113 N88-10723
Theory of the one- and two-dimensional electron gas
[DE87-012864] 02 p0244 N88-11540
A two-dimensional finite difference program for thermal analysis of rocket thrust chambers
[NASA-TM-100191] 04 p0409 N88-12539
INS3D: An incompressible Navier-Stokes code in generalized three-dimensional coordinates
[NASA-TM-100012] 04 p0485 N88-12991
BASIC desk-top computer program for the three-dimensional static configuration of an extensible flexible cable in a uniform stream
[AD-A184852] 05 p0609 N88-13737
Evolution of mean square magnetic vector potential in compressible, two-dimensional, magnetofluid turbulence
[AD-A184985] 05 p0651 N88-13990
Comparison of 2D memory SEU transport simulation with experiments
[ATR-86(8139)-2-REV-A] 05 p0656 N88-14025
The inverse back scattering problem for the Schroedinger equation in two space dimensions
[AD-A185603] 06 p0765 N88-14701
A new method of boundary parameter estimation for a two-dimensional diffusion system under noisy observations
[NASA-CR-178405] 06 p0767 N88-14714
An inexpensive real-time interactive three dimensional flight simulation system
[AD-A184868] 07 p0821 N88-14989
The KIVA-2 computer program for transient multidimensional chemically reactive flows with sprays
[DE88-000502] 07 p0854 N88-15191
Three dimensional display of meteorological scientific data
[DE88-000776] 07 p0880 N88-15339
Dimensions of ignition zones in blow-outs of combustible gases from rectangular and circular ports
07 p0918 N88-15577
Adaptive finite element methods for parabolic systems in one- and two-space dimensions
[AD-A186534] 08 p1073 N88-16475
Zero-dimensional model of a reversed field pinch fusion reactor
[DE88-005213] 10 p1414 N88-18442
GERA computer code for calculation of two-dimensional electromagnetic fields in resonators and electron-optical systems by the finite element method
[DE88-700678] 11 p1480 N88-18831
Applications of lower cost computers to dimensional gaging
[BDX-613-3606] 11 p1525 N88-19108
Motion in a random gyrotropic environment in D dimensions
[PB87-170650] 12 p1685 N88-20079
Strings in four dimensions
[DE88-006435] 14 p1990 N88-21864
Finite dimensionality in the complex Ginzburg-Landau equation
[DE88-006480] 16 p2263 N88-23534
The two-dimensional one component plasma in a doubly periodic background: Exact results
[AD-A191260] 16 p2280 N88-23650
Three-dimensional models of conventional and vertical junction laser-photovoltaic energy converters
[NASA-TM-4039] 17 p2370 N88-24111
Solving time-dependent two-dimensional eddy current problems
[NASA-TM-100875] 18 p2566 N88-25239
Computer modeling of time dependent SBS (Stimulated Brillouin Scattering) in two and three dimensions
[DE88-008922] 19 p2720 N88-26150
The MAFIA approach to solving Maxwell's equations in three dimensions
[DE88-007826] 19 p2720 N88-26155
Analysis of gas turbine test cell number 1, Lemoore Naval Air Station, California
[AD-A192870] 20 p2762 N88-26380
Vertical viewing ECE diagnostic for the D3-D tokamak
[DE88-010586] 20 p2860 N88-26987
Global gauge anomaly of classical groups in even dimension
[DE88-008572] 22 p3158 N88-28797
Comparison of 2-D Fourier and spatial techniques for removing noise in real-time X-ray radiography
[AD-A193700] 23 p3187 N88-28962
Bifurcations of periodic solutions of non-integrable Hamiltonians with two degrees of freedom: Numerical and analytical results
[DE88-702747] 23 p3272 N88-29473
Cosmology in an N-dimensional vector space
[DE88-702550] 23 p3277 N88-29507

Robust finite-dimensional LQG (Linear Quadric Gaussian)-based controllers for a class of distributed parameter systems
[AD-A194872] 24 p3425 N88-30382

DIMERIZATION

Synthesis and characterization of 1,2-cyclobutenedicarboxamides: Thermally generated polymers and Diels-Alder adducts
[AD-A188591] 12 p1611 N88-19633

DIMERS

Van der Waals clusters of aromatic molecules studied using supersonic molecular jet spectroscopy
[AD-A186087] 07 p0929 N88-15644

Energy-related atomic and molecular structure and scattering studies
[DE88-004246] 10 p1406 N88-18386

Chemical activation of molecules by metals: Experimental studies of electron distributions and bonding
[DE88-004465] 10 p1407 N88-18393

Comparison of low temperature photoluminescence of bulk MBE (Molecular Beam Epitaxy) grown AlGaAs and GaAs using a graphite generated dimer versus a standard tetramer arsenic group-V source
[DE88-004939] 11 p1558 N88-19329

Scanning tunneling microscopy of silver, gold, and aluminium monomers and small clusters on graphite
[DE88-003871] 11 p1562 N88-19349

Electrochemistry in near-critical and supercritical fluids. 5: The dimerization of quinoline and acridine radical anions and dianions in ammonia from -70 C to 150 C
[AD-A190858] 16 p2175 N88-22967

DIMINUTION

U REDUCTION

DINING PHILOSOPHERS PROBLEM

A nonmythical generalization of Dekker's algorithm and its ramifications --- mutually exclusive processes
[CS-8702] 01 p0080 N88-10513

DIODES

NT AVALANCHE DIODES
NT CRYSTAL RECTIFIERS
NT GERMANIUM DIODES
NT GUNN DIODES
NT JUNCTION DIODES
NT LIGHT EMITTING DIODES
NT MIM DIODES
NT PHOTODIODES
NT PLASMA DIODES
NT SCHOTTKY DIODES
NT SEMICONDUCTOR DIODES
NT THERMIONIC DIODES
NT TUNNEL DIODES

Diode pumped solid-state laser oscillators for spectroscopic applications
[NASA-CR-180576] 01 p0052 N88-10331

High energy efficient solid state laser sources
[NASA-CR-181362] 01 p0052 N88-10332

Generating soft X-ray spectra using the SPEED pentaxial diode
[DE87-013591] 01 p0098 N88-10647

Trajectory versus PIC methods in diode design
[DE87-012135] 02 p0166 N88-11043

Quantum well laser diodes: Modeling and realization of GaAs/GaAlAs
[LAAS-87-165] 02 p0179 N88-11116

Ultrafast photoconductor detector-laser-diode ransmitter
DE87-013803] 03 p0329 N88-12082

Fast autotuning of a hydrogen maser by cavity Q nodulation 04 p0436 N88-12707

The Pierce diode with an external circuit. Part 1: Simulations in the linear regime
DE88-000413] 04 p0440 N88-12731

Computer calculations of PIN diode limiter haracteristics
AD-A185563] 06 p0697 N88-14277

Evaluation of a satellite laser ranging technique using seudonoise code modulated laser diodes
NASA-CR-182347] 06 p0708 N88-14343

Magnetically insulated ion diode with a gas-breakdown lasma anode
NPE-4382-PRE/1202] 08 p1085 N88-16537

Radiant power degradation of silicon-doped gallium rsenide and gallium aluminum arsenide infrared ght-emitting diodes
AD-A186726] 09 p1157 N88-16935

Solid state research
AD-A185987] 09 p1253 N88-17508

Evaluation of a temperature remote sensing technique
AD-A187885] 10 p1347 N88-18053

The Pierce diode with an external circuit. 2: Non-uniform quilibria
D-A188027] 11 p1478 N88-18818

Diode pumped fiber laser
D-A187694] 11 p1491 N88-18902

The qualitative determination of high injection effects in flux-loaded P-I-N diodes using the recombination radiation measuring method
[ETN-88-91475] 11 p1560 N88-19336

Study of the vibrational modes of subsurface oxygen on Al (111) using diode laser infrared reflection-absorption spectroscopy
[AD-A188322] 12 p1632 N88-19769

High power, high efficiency, 2D laser diode arrays for pumping solid state lasers
[DE88-004042] 13 p1777 N88-20632

Surface-emitting two-dimensional laser diode arrays constructed on zig-zag heat sink surface
[DE88-005215] 14 p1915 N88-21439

Development of Electromagnetic PIC code for LIB diode 16 p2276 N88-23622

Two-dimensional focusing of self-magnetically insulated plasma focus diode 16 p2278 N88-23639

Research on anode plasma behavior of flashover pulsed ion sources 16 p2279 N88-23640

Study on the flashover ion diode with cryogenic anode 16 p2279 N88-23642

High pressure operation of beam diodes for generating relativistic electron beams 16 p2279 N88-23643

MSAT-X electronically steered phased array antenna system 19 p2647 N88-25712

Energy variations in optical pulses from gain-switched AlGaAs diode lasers 19 p2658 N88-25796

Microwave and millimeter-wave resonant tunneling diodes 19 p2659 N88-25809

Quantum transport calculation of resonant-tunneling response time 19 p2659 N88-25810

Silicon pulse sharpening diodes-switching kilovolts in 10's of picoseconds 19 p2661 N88-25824

Electrical study of metal/group 3-5 semiconductor interfaces: Comparison with the atomic-level studies 20 p2874 N88-27059

Silicon-on-insulator pin diodes
[AD-A193359] 21 p2937 N88-27445

Techniques and instrumentation for transient characterization of metal-insulator-semiconductor diodes. Applications to metal-insulator InP system
[ECL-87-17] 21 p3025 N88-27959

The 1985-86 measurements with the tunable diode laser absorption spectrometer
[PB88-214002] 23 p3231 N88-29226

On 3-5 heterojunction structures and high speed devices
[AD-A195464] 24 p3433 N88-30438

DIOXIDES

NT CARBON DIOXIDE
NT HYDROGEN PEROXIDE
NT QUARTZ
NT SILICON DIOXIDE
NT SULFUR DIOXIDES

Hydrogen retention and release from uranium dioxide
[DE88-002042] 07 p0829 N88-15030

A dense and strong ceramic material made from zirconium dioxide 14 p1886 N88-21274

Low temperature film growth of the oxides of zinc, aluminum and vanadium (and related systems, oxides of gold and germanium, nitrides of aluminum and tungsten) by reactive sputter deposition
[AD-A193497] 23 p3191 N88-28986

DIPHOSPHATES

Use of diphosphonates to correct disorders in calcium metabolism and mineral composition of bone tissue with 60-day hypokinesia in rats
[NASA-TT-20220] 13 p1809 N88-20807

DIPLEXERS

A polarization diversity meteorological radar system
[AD-A189291] 13 p1758 N88-20515

DIPOLE ANTENNAS

NBS (National Bureau of Standards) calibration procedures for horizontal dipole antennas (25 to 1000 MHz)
[PB87-210233] 03 p0305 N88-11922

The use of coaxial transmission line elements in log-periodic dipole arrays
[AD-A184864] 05 p0574 N88-13499

Evaluation of CWMS (Continuous-Wave Measurement System) single-wire dipole antenna
[DE88-003979] 09 p1155 N88-16920

Improved backfire antenna using circular dipole 11 p1468 N88-18757

An improved method for calculating power density in the Fresnel region of circular parabolic reflector antennas
[AD-A190569] 15 p2060 N88-22284

DIPOLE MOMENTS

NT ELECTRIC MOMENTS
NT MAGNETIC MOMENTS

The polarization field for pulsed Raman transitions
[DE87-013118] 01 p0035 N88-10227

Theoretical atomic and molecular photophysics
[DE87-014249] 02 p0231 N88-11458

Core-core and core-valence correlation
[NASA-CR-182552] 11 p1544 N88-19226

Cooperative effects and intrinsic optical bistability in collections of atoms
[AD-A193993] 23 p3280 N88-29530

Passage of relativistic magnetic dipole moments through magnetic fields
[DE88-702640] 23 p3295 N88-29624

DIPOLES

Dipole component of relict radiation determined from Relikt experiment data 08 p1002 N88-16070

Mushroom-shaped currents (eddy dipoles) under rotation and stratification conditions 13 p1784 N88-20678

DIPPING

The effect on initial bond strength and durability of a Phosphoric Acid Dip (PAD) following chromic acid anodising of aluminum
[ARE-TM(UMM)-87402] 10 p1300 N88-17772

Studies on hot-dip zinc-aluminum coated sheet steels
[ETN-88-92217] 15 p2042 N88-22166

DIRAC EQUATION

Polarization of electrons in an electromagnetic wave field in the presence of magnetic field
[DE88-700169] 13 p1757 N88-20509

DIRECT BROADCAST SATELLITES

Study of reconfigurable payloads for direct broadcast satellites, summary
[DBS87-0004] 09 p1135 N88-16808

An outdoor unit for Direct Broadcast Satellite (DBS) digital sound reception
[BMFT-FB-W-86-016] 16 p2189 N88-23050

Organization of the TDF1/TDF2 program 22 p3161 N88-28827

DIRECT CURRENT

Comparison of costs and benefits for dc and ac transmission
[DE87-008774] 02 p0167 N88-11052

Analysis of nickel sulphamate bath using charging current compensated D.C. polarography
[NAL-TM-MT-8705] 05 p0564 N88-13433

Digital control of a direct current converter for a hybrid vehicle
[LAAS-87-266] 05 p0578 N88-13527

DC conductivity studies in Li5AlO4 at intermediate temperatures and its possible application for the electrolysis of water
[AD-A185489] 06 p0697 N88-14276

The dc conductivity studies of an hydroxide ion conductor at intermediate temperatures
[AD-A186044] 07 p0847 N88-15142

The effect of propane on atomic spectrometric signals in the direct current plasma
[DE88-002457] 07 p0934 N88-15676

Pulse width modulator controller design for a brushless DC motor position servo
[AD-A186618] 08 p0980 N88-15921

Sliding charge density waves and related problems
[AD-A186720] 09 p1157 N88-16934

Development and calibration of Direct Current Potential Difference (DCPD) crack length measurement equipment
[VTT-RR-480] 09 p1182 N88-17083

Rapid underway sediment classification by electrical methods
[AD-A187477] 10 p1357 N88-18114

Photoconductor switch and circuit analysis
[AD-A188168] 11 p1478 N88-18821

Automatic prober for the dc characterization of gallium arsenide devices. Part 1: The measurement facility
[AD-A187583] 11 p1560 N88-19337

Inductive spurious coupling of a dc-SQUID to resonant input circuit
[NOTA-INTERNA-894] 14 p1908 N88-21401

Electrical dc conductivity of pitch
[AD-A191266] 16 p2182 N88-23008

The LDCM actuator for vibration suppression
[NASA-CR-182898] 17 p2335 N88-23940

Arcjet power supply and start circuit
[NASA-CASE-LEW-14374-1] 23 p3181 N88-28939

The dc power control for a liquid-fed resistojet
[NASA-TM-101326] 24 p3338 N88-29869

Numerical simulation of the function of scientific instrumentation for measuring the speed of electron devices
[AD-A194969] 24 p3376 N88-30103

Automatic prober for the dc characterisation of gallium arsenide devices. Part 2: The data sorting and display facility
[AD-A195408] 24 p3377 N88-30111

DIRECT POWER GENERATORS

NT ALKALINE BATTERIES
NT ELECTROSTATIC GENERATORS
NT FUEL CELLS
NT HYDROGEN OXYGEN FUEL CELLS
NT MAGNETOHYDRODYNAMIC GENERATORS
NT METAL AIR BATTERIES

NT NICKEL ZINC BATTERIES
NT PHOSPHORIC ACID FUEL CELLS
NT PHOTOELECTRIC GENERATORS
NT PHOTOVOLTAIC CELLS
NT PRIMARY BATTERIES
NT RADIOISOTOPE BATTERIES
NT REGENERATIVE FUEL CELLS
NT SNAP 19
NT SODIUM SULFUR BATTERIES
NT SOLAR CELLS
NT THERMAL BATTERIES
NT THERMIONIC CONVERTERS
NT THERMOELECTRIC GENERATORS
NT VERTICAL JUNCTION SOLAR CELLS
NT ZINC-OXYGEN BATTERIES
Data on existing wind energy converters in Denmark
[DE88-900199] 07 p0874 N88-15300
Collecting of new data on existing wind energy converters
[DE88-900221] 07 p0875 N88-15305
Direct nuclear propulsion for Earth-to-orbit vehicles
17 p2400 N88-24271
Ultra high temperature direct propulsion
17 p2401 N88-24275
Safety constraints and considerations in the development of nuclear powered propulsion
17 p2401 N88-24276
Nuclear propulsion: Past, present and future
17 p2427 N88-24441
Gas core reactors for direct nuclear propulsion
17 p2428 N88-24442
Long-term behavior of energy production systems with the example of HELIOS and SYMPHONIE
[ETN-88-92988] 23 p3230 N88-29223

DIRECTION FINDING
Monitoring of harmful interference to the HF (High Frequency) broadcasting service. 3: Results of the June 1986 coordinated monitoring period
[PB87-210274] 01 p0036 N88-10229
Bearing detection in the presence of two sources of varying coherence using the complex cepstrum
[NASA-CR-181605] 09 p1243 N88-17451
Method for determining artillery position
[NASA-TT-20238] 13 p1834 N88-20973
Method for determining artillery position
[NASA-TT-20237] 13 p1834 N88-20974
Method for determining artillery position
[NASA-TT-20236] 14 p1979 N88-21813
Acoustic direction finding of flying helicopters
22 p3148 N88-28728
Examples of the application of acoustics for the detection and classification of targets 22 p3148 N88-28729
A fiber optic beamforming processor for wideband direction finding
[AD-A194962] 24 p3428 N88-30404
Ultra-wideband direction finding using a fiber optic beamforming processor
[AD-A194861] 24 p3430 N88-30413

DIRECTIONAL ANTENNAS
NT DIPOLE ANTENNAS
NT HELICAL ANTENNAS
NT LOG PERIODIC ANTENNAS
NT LOOP ANTENNAS
NT PARABOLIC ANTENNAS
NT REFLECTOR ANTENNAS
NT SLOT ANTENNAS
NT STEERABLE ANTENNAS
NT TWO REFLECTOR ANTENNAS
Study of advanced satellite concept using a multifeed reconfigurable antenna
[ESA-CR(P)-2406-VOL-1] 01 p0013 N88-10073
Study of advanced satellite concept using a multifeed reconfigurable antenna. Detailed report on mission definition, coverage analysis and performance requirements, antenna geometry
[ITS-TR-014.C/85] 01 p0013 N88-10074
Study of advanced satellite concept using a multifeed reconfigurable antenna. Detailed report on Polarization Sensitive Reflector (PSR) and offset parabolic antennas, Appendix 1
[ESA-CR(P)-2406-VOL-3] 01 p0013 N88-10075
Study of advanced satellite concept using a multifeed reconfigurable antenna. Appendix 3 : Feeding network, final performance analysis, study of reconfiguration possibilities
[ITS-TR-032/85] 01 p0014 N88-10076
Shape optimization of linear antennas
[ETN-87-90413] 01 p0036 N88-10233
Adaptive detection in non-stationary interference, part 3
[AD-A185622] 07 p0844 N88-15118
Performance of linear vertical antenna in refractive multimode waveguide 08 p1076 N88-16489
Investigation of design considerations for Telemetry, Tracking and Command (TT and C) antenna system on Naval Postgraduate School Orion mini-satellite
[AD-A187130] 10 p1291 N88-17718
The characteristics of two broadband (2 MHz to 10 MHz) switched vee antennas
[AD-A187874] 11 p1471 N88-18770
Sidelobe level of an adaptive array using the SMI (Sampled Matrix Inversion) algorithm
[AD-A193131] 21 p2932 N88-27409

DIRECTIONAL CONTROL
NT THRUST VECTOR CONTROL
Effect of rotation on the lateral stability of a free-flying column subjected to an axial thrust with directional control
[AD-A188690] 13 p1728 N88-20338
Compliant robotic structures, part 3
[AD-A192426] 21 p2955 N88-27556

DIRECTIONAL SOLIDIFICATION (CRYSTALS)
Contributions to the investigation of mechanical behavior of gamma/gamma NbC Cotac composites at medium and at high temperature
[ESA-TT-1031] 03 p0280 N88-11760
Development of a shell system for DS moulds at RR precision casting facility --- directional solidification (DS)
[PNR90400] 09 p1151 N88-16893
Influence of convection on microstructure
[NASA-CR-182489] 10 p1302 N88-17784
Study of the production of some superconducting and magnetic materials by solidification in the drop tube and drop tower
[NASA-CR-182494] 11 p1461 N88-18708
MCT crystal growth
[NASA-CR-179297] 11 p1557 N88-19318
Analysis of low gravity tolerance of model experiments for space station: Preliminary results for directional solidification
[NASA-CR-182657] 12 p1614 N88-19648
Transport processes during directional solidification and crystal growth: Scaling and experimental study
14 p1988 N88-21857
Convection effects on stability at the solidification front 14 p1988 N88-21860
SSME single-crystal turbine blade dynamics
16 p2221 N88-23257

DIRECTIONAL STABILITY
NT GYROSCOPIC STABILITY
Effects of the installation and operation of jet-exhaust yaw vanes on the longitudinal and lateral-directional characteristics of the F-14 airplane
[NASA-TP-2769] 04 p0393 N88-12455
A comparison between theory and experiment for the yaw moment induced by a loose internal part
[AD-A187053] 09 p1131 N88-16787
Calculation of aerodynamic characteristics of airplane configurations at high angles of attack
[NASA-CR-4182] 23 p3172 N88-28891

DIRECTIVITY
The wavenumber. An alternative to the directional coupler for multimode analysis in oversized waveguides
[IPF-87-2] 01 p0037 N88-10237
Study on a unidirectional ring laser gyro. Part 1: Proposition of the principle and studies on the components
[NAL-TR-933] 09 p1169 N88-17010
Special relativity theory (one-dimensional case) without the postulate on the equality of directions
[DE88-701368] 16 p2284 N88-23674
An analysis of the efficiency and directivity of the sound generated by a moving laser source
[AD-A192220] 20 p2849 N88-26914

DIRECTORIES
Middle Atmosphere Program: Handbook for MAP, volume 24
[NASA-CR-181451] 01 p0069 N88-10444
Directory of geomagnetic observatories with high-resolution digital results, 1987
[PB87-221156] 03 p0348 N88-12201
Director of R and D institutions (Government of India)
[PB88-127162] 10 p1285 N88-17685
A directory of databases available through SearchMAESTRO
[AD-A188813] 12 p1706 N88-20214
Federal Council on Science, Engineering and Technology: Committee on Computer Research and Applications, Subcommittee on Science and Engineering Computing: The US Supercomputer Industry
[DE88-011262] 21 p2994 N88-27756
Design and performance analysis of a relational replicated database system
[AD-A196290] 24 p3437 N88-30456

DIRICHLET PROBLEM
IMPSOR: A fully vectorized FORTRAN code for three dimensional moving boundary problems with Dirichlet or Neumann boundary conditions
[DE87-014964] 02 p0226 N88-11427
Parameter estimation for the Dirichlet-Multinomial Distribution (DMD) using supplementary beta-binomial data
[AD-A186335] 07 p0911 N88-15524
Nontrivial critical points for asymptotically quadratic function
[DE88-101851] 20 p2845 N88-26881
Semilinear elliptic problems on domains with corners
[REPT-87-83] 20 p2846 N88-26888
Dirichlet prior in Bayesian estimation of item response curves
[AD-A195311] 24 p3426 N88-30392

DIRIGIBLES
U AIRSHIPS

DISCHARGE COEFFICIENT
Measurement of the electron density and the attachment rate coefficient in silane/helium discharges
[AD-A184268] 04 p0496 N88-13051

DISCHARGE TUBES
U GAS DISCHARGE TUBES

DISCHARGERS
NT STATIC DISCHARGERS

DISCONNECT DEVICES
Toggle release
[NASA-CASE-MSC-21354-1] 18 p2523 N88-24969

DISCONNECTORS
U DISCONNECT DEVICES

DISCONTINUITY
Interactions of oblique interplanetary discontinuities and their manifestations during STIP intervals 15-19
01 p0119 N88-10759
A numerical method for the treatment of kinked cracks in finite bodies 02 p0190 N88-11189
SHARP simulation of discontinuities in highly convective steady flow
[NASA-TM-100240] 05 p0642 N88-13931
Modeling of some coplanar waveguide discontinuities
[NASA-TM-100808] 10 p1318 N88-17880
The relation of solar wind structure to hydromagnetic discontinuities
[DE88-004304] 10 p1431 N88-18546
Visual integration and detection of discontinuities: The key role of intensity edges
[AD-A188012] 11 p1520 N88-19076
Detection of the number, locations and magnitudes of jumps
[AD-A190328] 15 p2125 N88-22671
Discontinuous inverse Sturm-Liouville problems with symmetric potentials
[DE88-009803] 19 p2720 N88-26152
A Wong-Zakai type theorem for certain discontinuous semimartingales
[AD-A192713] 21 p3005 N88-27822

DISCOVERING
U EXPLORATION

DISCOVERY (ORBITER)
Lateral and longitudinal stability and control parameters for the space shuttle discovery as determined from flight test data
[NASA-TM-100555] 13 p1724 N88-20309

DISCRETE FUNCTIONS
Analytical treatment of the spatial trilateration problem (4, 6, 0, 0)
[SER-A-104] 01 p0085 N88-10548
The periodic Lyapunov equations
[REPT-86-007] , 01 p0087 N88-10567
Nonlinear techniques for detection and filtering of discrete-time signals 02 p0160 N88-11004
Stability of semidiscrete approximations for hyperbolic initial-boundary-value problems: An eigenvalue analysis
[NASA-TM-88328] 02 p0227 N88-11434
Solution of the two-dimensional Euler equations on unstructured triangular meshes
04 p0396 N88-12469
Tactile sensing and inverse problems
[AD-A187464] 10 p1340 N88-18011
Ideal shrinking and expansion of discrete sequences
[NASA-TM-88202] 11 p1524 N88-19100
Boltzmann-Fokker-Planck calculations using standard discrete-ordinates codes
[DE88-005393] 11 p1537 N88-19185
Using trace theory to model discrete events
[CS-8708] 13 p1824 N88-20904
Representation, analysis and design of multirate discrete-time control systems
[AD-A190499] 15 p2116 N88-22608
Parallel discrete-event simulation of FCFS stochastic queueing networks
[NASA-CR-181669] 17 p2389 N88-24203
Optimal discrete-time LQR problems for parabolic systems with unbounded input: Approximation and convergence
[NASA-CR-181673] 18 p2567 N88-25247
Modeling discrete bathtub and upside down bathtub mean residual life functions
[AD-A192000] 22 p3085 N88-28320

Stability of semidiscrete approximations for hyperbolic initial-boundary-value problems: Stationary modes
[NASA-TM-100994] 23 p3270 N88-29455
Polynomial definition of discrete field points of map of diffusion equation, part 1
[AD-A193697] 23 p3271 N88-29467

DISCRIMINANT ANALYSIS (STATISTICS)
Feature selection applied to radar target identification
[AD-A183880] 01 p0034 N88-10215
The importance of the lower level windshear profile in tornado/non-tornado discrimination
02 p0208 N88-11304
Strong consistency of certain information theoretic criteria for model selection in calibration, discriminant analysis and canonical correlation analysis
[AD-A186584] 09 p1232 N88-17385
Nonparametric discriminant analysis applied to the extraction and selection of radar target signature features
[AD-A191849] 18 p2501 N88-24833

DISCRIMINANT FUNCTIONS
U DISCRIMINANT ANALYSIS (STATISTICS)

DISCRIMINATION
NT BRIGHTNESS DISCRIMINATION
NT TACTILE DISCRIMINATION
NT VISUAL DISCRIMINATION
Automated satellite cloud analysis: A multispectral approach to the problem of snow/cloud discrimination
[AD-A185672] 06 p0746 N88-14591
Environmental gradient analysis, ordination, and classification in environmental impact assessments
[AD-A187294] 11 p1509 N88-19016
Auditory pattern memory: Mechanisms of tonal sequence discrimination by human observers
[AD-A190337] 15 p2104 N88-22534
A method for discrimination of radar targets using complex natural resonances
[AD-A191848] 18 p2500 N88-24832
Object discrimination via bulk temperature/velocity filtering, phase 1
[AD-A194533] 23 p3274 N88-29487
Discrimination studies using short-period P waves at upper mantle distances
[AD-A195468] 24 p3401 N88-30257

DISCRIMINATORS
NT FREQUENCY DISCRIMINATORS
A two-stage isolated-word recognition system using discriminant analysis
[AD-A187425] 10 p1402 N88-18360
Rules, schema and decision making
[AD-A193389] 21 p3027 N88-27967

DISEASES
NT ANEMIAS
NT ASTHMA
NT BACTERIAL DISEASES
NT BONE DEMINERALIZATION
NT CANCER
NT CORONARY ARTERY DISEASE
NT DIABETES MELLITUS
NT EPILEPSY
NT FIBROSIS
NT FUNGAL DISEASES
NT HEART DISEASES
NT INFECTIOUS DISEASES
NT MYOCARDIAL INFARCTION
NT NEOPLASMS
NT OCCUPATIONAL DISEASES
NT OSTEOPOROSIS
NT PARASITIC DISEASES
NT RADIATION SICKNESS
NT TACHYCARDIA
Physiological and immunological aspects of human adaptation to temperature elevation in a closed environment 07 p0895 N88-15424
Forecasting complications of cardiovascular disease in flight personnel 10 p1361 N88-18136
Central serous chorioretinopathy in USAF aviators: A review
[AD-A195697] 24 p3407 N88-30280

DISHES
U PARABOLIC REFLECTORS

DISILICIDES
Study on iron disilicide thermoelectric generator
[AD-A193082] 22 p3116 N88-28517

DISK GALAXIES
Infrared constraints on the nature of dark matter
13 p1855 N88-21102
The stability of disk galaxies and constraints on their mass-luminosity ratio
[SER-C-PREPUBL-FASC-27] 24 p3455 N88-30565

DISKS
Kinetic theory for plane flows of rough, inelastic, circular disks 21 p2946 N88-27499

DISKS (SHAPES)
NT ACTUATOR DISKS
NT INTERVERTEBRAL DISKS
NT ROTATING DISKS
Physical design of parameters of Nd:YAG disk laser
03 p0302 N88-11904
Mixed mode fatigue crack growth using the Brasilian disc 06 p0719 N88-14416
Development of composite polymer-glass edge claddings for Nova laser disks
[DE88-002389] 07 p0860 N88-15220
Disk pumping test
[AD-A187199] 11 p1440 N88-18591
AGARD (Advisory Group for Aerospace Research and Development) engine disc material cooperative test (supplementary program)
[AD-A193678] 23 p3179 N88-28925

DISLOCATIONS (MATERIALS)
NT CRYSTAL DISLOCATIONS
NT EDGE DISLOCATIONS
NT SCREW DISLOCATIONS
Applications of dislocation theory to crack growth problems 02 p0190 N88-11188
A dislocation model for fatigue crack propagation under variable amplitude loading 05 p0602 N88-13683
Dislocation free zone model of fracture under reverse loading
[DE88-002676] 07 p0869 N88-15276
An investigation of the influence of dislocation substructures on the deformation behavior of AK, DQ steel sheets
[DE88-006337] 14 p1889 N88-21289

DISORDERS
Instanton in supersymmetric theory with static disorder
[DE88-700357] 07 p0940 N88-15716
Raman scattering in mixed crystal semiconductors
12 p1696 N88-20149
Defects and disorder in amorphous and damaged silicon
[AD-A192277] 20 p2879 N88-27089
Normative developmental equations for the EEG and their sensitivity to neurological and psychiatric disorders
21 p2977 N88-27687

DISORIENTATION
NT DESYNCHRONIZATION (BIOLOGY)
NT DISORDERS
NT JET LAG

DISPENSERS
Aerodynamic aspects of the configurational systems layout of a dispenser
[MBB-UA-1047/87] 10 p1315 N88-17863
Deployable booms and antennas on AMPTE-IRM
14 p1874 N88-21198
Preliminary airworthiness evaluation of the UH-60A equipped with the XM-139 VOLCANO mine dispensing system
[AD-A190604] 15 p2018 N88-22029
A scientific basis for an alternate cathode architecture
[AD-A191498] 18 p2481 N88-24717
Method of dispensing reagent chemicals in space
[NASA-CASE-LAR-13607-1-CU]
23 p3200 N88-29048

DISPERSING
The effect of heat transfer on the dispersion of cold dense gases
[OUEL-1688/87] 02 p0171 N88-11076
Aircraft engine exhaust plume dynamics
[AD-A184238] 04 p0400 N88-12488
Activities at government research laboratories reported 04 p0403 N88-12503
Compatability of dispersion-strengthened platinum with resistojet propellants
[NASA-TP-2765] 04 p0409 N88-12538
Full scale and wind tunnel surface pressure measurements on the T.R.R.L. spray dispersion programme vehicles
[REPT-8623] 09 p1114 N88-16676
Design and characteristics of a liquid aerosol generator
[AD-A186942] 09 p1174 N88-17034
Dispersive hole transport in SiO2
[AD-A187077] 09 p1254 N88-17513
Soft X-ray beamsplitters and highly dispersive multilayer mirrors for use as soft X-ray laser cavity components
[DE88-004003] 11 p1549 N88-19270
Dense-spray structure and phenomena. Part 1: Turbulence/dispersed-phase interactions
[AD-A190606] 15 p2065 N88-22315
Microwave dispersion and absorption in tissues: Molecular mechanisms
[AD-A190118] 15 p2100 N88-22512
The optical properties of aerosols
[AD-A191420] 16 p2176 N88-22972
Examination of methods for pollen storage and dispersal
[TN-RB524-097/86] 17 p2378 N88-24134
Acoustic wave dispersion in a viscous, compressible, liquid-filled cylindrical elastic tube
19 p2722 N88-26164
Prediction of regional pollutant dispersion using a nested-grid, three-dimensional numerical model
21 p2971 N88-27649
Measuring dispersion effects of factors in factorial experiments
[AD-A193216] 21 p3006 N88-27831
Project wind, phase 4 (smoke test), Meadow Brook Valley, Red Bluff, California
[AD-A194742] 22 p3128 N88-28596
Particle size measurements in sooting combustion systems 24 p3348 N88-29931

DISPERSION
Development on thin wall tubes of dispersion type
[DE87-703384] 05 p0571 N88-13483
Dynamical properties of aluminium from experimental dispersion relations
[DE88-700240] 11 p1459 N88-18697
NOAA (National Oceanic and Atmospheric Administration) Meteorology Division support to the Environmental Protection Agency
[PB88-179866] 19 p2689 N88-25980
A zoomable and adaptable hidden fine-mesh approach to solving advection-dispersion equations
[DE88-006174] 21 p3004 N88-27816

DISPERSION PRECIPITATION HARDENING
U PRECIPITATION HARDENING

DISPERSIONS
NT AEROSOLS
NT COLLOIDS
NT EMULSIONS
NT FOG
NT LIQUID-GAS MIXTURES
NT SMOKE
High explosive moulding powders from RDX and aqueous polyurethane dispersions
[AD-A185026] 05 p0568 N88-13458
High temperature low cycle fatigue of oxide dispersion strengthened and single crystal nickel base superalloys
06 p0720 N88-14422
High temperature low cycle fatigue behavior and creep-fatigue interation of MA 6000 ODS alloy
06 p0720 N88-14425
A survey of denser-than-air atmospheric dispersion models
[DE88-006626] 15 p2092 N88-22467
Preparation and characterization of ceramic materials based on Al2O3 reinforced with a ZrO2 dispersion
[ISAL-87-0041] 21 p2922 N88-27340
Theoretical and experimental investigations on the structure of stationary shock waves in gas particle dispersions
[ETN-88-92983] 23 p3213 N88-29122

DISPLACEMENT
NT CRACK OPENING DISPLACEMENT
A numerical method for the treatment of kinked cracks in finite bodies 02 p0190 N88-11189
A study of the crack tip parameters that govern environmentally assisted cracking by use of the rising displacement test 04 p0427 N88-12649
The dynamics of solar magnetic flux tubes subjected to resonant foot point shaking 04 p0507 N88-13118
Hypersonic laminar boundary layer: Parametric study for the representation of real gas effects
05 p0532 N88-13236
Telemetric laser extensometry technique for monitoring deflections in small cracks 05 p0607 N88-13724
Stresses and displacements in two, three and four layered structures submitted to flexible or rigid loads
[AD-A185707] 06 p0723 N88-14450
Generalized displacement method in the finite element analysis of incompressible material
[PB87-143434] 08 p0995 N88-16018
Calculated sputtering and atomic displacement cross-sections for applications to medium voltage analytical electron microscopy
[DE88-002904] 09 p1168 N88-17006
A summary of experimental results on square plates and stiffened panels subjected to air-blast loading
09 p1178 N88-17057
Stress intensity and crack displacement for small edge cracks
[NASA-TP-2801] 09 p1184 N88-17095
Dynamic analysis of plane frames by microcomputer
11 p1531 N88-19143
Synthesis of finite displacements and displacements in continental margins
[NASA-CR-182616] 12 p1642 N88-19832
The effects of humidity on the profile of photographic plates
[NPL-DMOM-88] 14 p1913 N88-21429
Photo-optical converter of angular displacements in digital servomechanisms
[DE87-703208] 14 p1961 N88-21698

An efficient Mindlin finite strip plate element based on assumed strain distribution 15 p2081 N88-22407

Automatic feedback control of a rigid body for finite displacements 18 p2473 N88-24674

Large displacement and rotational formulation for laminated cylindrical shells including parabolic transverse shear
[AD-A194871] 24 p3384 N88-30158

DISPLACEMENT MEASUREMENT

Device for measuring hole elongation in a bolted joint
[NASA-CASE-LAR-13453-1] 06 p0712 N88-14361

A composite grating for moire interferometry
[AD-A186330] 07 p0832 N88-15044

A quantitative method for evaluating sensor layouts
09 p1178 N88-17056

Experimental and analytical investigation on a proposed embedded fiber optic displacement sensor
[AD-A189030] 12 p1630 N88-19756

Digital fiber optic displacement sensors
18 p2518 N88-24937

A review of non-contacting displacement measurement techniques used to monitor the movement of rotor blades in gas turbine aero engines
[PNR90457] 22 p3045 N88-28071

Optical measurement of propeller blade deflections
[NASA-TP-2841] 22 p3079 N88-28286

J-integral measurement using moire interferometry
[AD-A193751] 23 p3226 N88-29202

A technique for measuring area under a curve
[AD-A193559] 23 p3271 N88-29463

DISPLAY DEVICES
NT HEAD-UP DISPLAYS
NT HELMET MOUNTED DISPLAYS
NT PLASMA DISPLAY DEVICES
NT POSITION INDICATORS
NT TACHOMETERS

Color display programming for aviation
[DFVLR-MITT-87-03] 01 p0006 N88-10031

Input devices for tasks using interactive video
[NPL-DITC-87/87] 01 p0080 N88-10510

Fiber optic engineering sensor system. Preliminary program management plan, phase 3 revision
[AD-A183663] 01 p0093 N88-10608

The impact of new computer technology on accelerator control
[DE87-014021] 02 p0219 N88-11376

MBB simulation facilities applied for rotorcraft research 03 p0263 N88-11655

The flight evaluation of an advanced engine display and monitoring system 03 p0264 N88-11659

Helicopter (performance) management
03 p0264 N88-11666

Integrated voice and visual systems research topics
[NASA-CR-177417] 03 p0356 N88-12246

Computer-controlled testing of visual-spatial ability
[AD-A183971] 03 p0357 N88-12249

A scientific workstation operator-interface for accelerator control
[DE87-014689] 03 p0362 N88-12278

Effects of combining vertical and horizontal information into a primary flight display
[NASA-TP-2783] 04 p0399 N88-12487

Traveling-wave maser closed-cycle refrigerator data acquisition and display system 04 p0437 N88-12708

Input/output technologies: An overview of image scanning, storage, and display
[DE87-014837] 04 p0476 N88-12933

An interactive computer graphics network monitor for a tactical communications network
[AD-A184131] 04 p0477 N88-12938

Displaying three-dimensional data
[AD-A185347] 05 p0580 N88-13541

The Portable Instant Display and Analysis Spectrometer (PIDAS) 05 p0611 N88-13756

The use of color in electronic maps. Part 1: Generation and analysis of color on the Gould/DeAnza image processing system
[IZF-1986-32] 05 p0635 N88-13882

Fast, colour displays of digital terrain elevation data
[AD-A185596] 06 p0729 N88-14485

Use of colour on electronic data displays (second study)
[PB87-126744] 06 p0754 N88-14627

A general solution to the silhouette problem
[NASA-TP-2695] 06 p0755 N88-14629

Stress effects and the optimum format of a scrolling seven-line VDT text window
[AD-A185559] 06 p0758 N88-14651

FAA air traffic control operations concepts. Volume 1: ATC background and analysis methodology
[AD-A185979] 07 p0818 N88-14973

An inexpensive real-time interactive three dimensional flight simulation system
[AD-A184868] 07 p0821 N88-14989

The role of adaptive supplemental visual cuing in flight simulation
[AD-A185932] 07 p0822 N88-14992

Three dimensional display of meteorological scientific data
[DE88-000776] 07 p0880 N88-15339

Creating title blocks for vehicle animations
[AD-A185620] 07 p0904 N88-15473

Through-transmission/pulse-echo ultrasonic equipment evaluation
[AD-A186340] 07 p0929 N88-15641

Electro-optical studies of semiconductor compounds for electroluminescent and laser devices
[PH-155] 07 p0937 N88-15693

Comparison of alphanumeric data entry methods for advanced helicopter cockpits
[AD-A186934] 09 p1201 N88-17201

An intelligent tutor for the space domain
09 p1204 N88-17217

The advanced low-level windshear alert system operational demonstration results, Summer, 1987, Denver Stapleton International Airport 10 p1275 N88-17633

Information transfer in the National Airspace System
10 p1275 N88-17634

Helicopter external vision requirements and visual display characteristics: A report/bibliography, revision A
[AD-A187075] 10 p1276 N88-17641

Electrochromic cells with lutetium diphthalocyanine and semisolid polymer electrolytes
[AD-A188031] 10 p1352 N88-18078

Generation of specific chromaticities on CRT monitors
[AD-A187739] 11 p1440 N88-18590

Report on desktop publishing
[AD-A187698] 11 p1528 N88-19128

A comparison of keyboard designs for cockpit applications
[AD-A187775] 12 p1581 N88-19460

Soft maps for US Army electronic map background applications
[AD-A188427] 12 p1638 N88-19809

Brain activity during tactical decision-making. Part 2: Probe-evoked potentials and workload
[AD-A188688] 12 p1667 N88-19994

Human efficiency for visual detection of targets on CRT displays using a two-level multiple channel time history format
[AD-A188419] 12 p1670 N88-20001

OMV man/system simulation integration: A preliminary analysis and recommendation
[NASA-CR-182602] 12 p1671 N88-20005

Visual display representation of multidimensional systems: The effect of information correlation and display integrality
[AD-A188655] 12 p1672 N88-20010

CODAC (Cockpit Oriented Display of Aircraft Configurations) version 1.4 user's guide
[NASA-CR-181650] 13 p1718 N88-20273

Development of an interactive real-time graphics system for the display of vehicle space positioning
[NASA-TM-100429] 13 p1730 N88-20344

Restoration techniques for redisplay of LANDSAT-5 satellite imagery
[INPE-4189-PRE/1076] 13 p1791 N88-20712

Multi-crew pictorial format display evaluation
[AD-A189349] 13 p1812 N88-20824

Solid-state electrochemical processes in dye films
[AD-A188756] 13 p1844 N88-21036

The PC/AT compatible computer as a mission control center display processor at Ames-Dryden Flight Research Facility
[NASA-TM-100426] 14 p1955 N88-21654

DataViews: A personalizable, interactive, data display system for the decisionmaker
[AD-A188509] 14 p1991 N88-21868

Effects of update and refresh rates on flight simulation visual displays
[NASA-TM-100415] 15 p2018 N88-22033

Geometric modeling of flight information for graphical cockpit display
[AD-A190484] 15 p2021 N88-22043

Real-time flight test data distribution and display
[NASA-TM-100424] 15 p2022 N88-22050

Basic research on flame radiation
[PB88-168372] 15 p2032 N88-22105

A 3-D solid rendering of NDT data
[DE88-006199] 15 p2076 N88-22373

Auditory pattern memory: Mechanisms of tonal sequence discrimination by human observers
[AD-A190337] 15 p2104 N88-22534

A graphics editor for structured analysis with a data dictionary
[AD-A190618] 15 p2112 N88-22584

Two-dimensional graphics tools for a transputer based display board
[NASA-TM-100820] 15 p2113 N88-22591

Basic design studies for the realization of liquid crystal display systems in aircraft
[VA-87-001] 16 p2163 N88-22900

Crewstation Information and Development System (CIDS) 17 p2304 N88-23781

Presentation of map information on a color display
[FOA-C-20687-2.7] 17 p2368 N88-24103

Virtual interface environment
17 p2381 N88-24153

Denver ARTCC evaluation of PROFS (Prototype Regional Observations and Forecast System) mesoscale weather products 18 p2547 N88-25117

Eye and head response to an attention cue in a dual task paradigm
[AD-A191052] 18 p2551 N88-25143

Design and testing of a luminance and chrominance stabilization system for a computer-controlled color display
[AD-A191922] 18 p2554 N88-25159

IGUANA: Interactive graphics utility for automated NEC analysis
[AD-A191760] 18 p2556 N88-25174

Considerations involved in the display of finite element results using animation
[DE88-007581] 18 p2559 N88-25189

On-line measurement of heat of combustion
[NASA-CR-183076] 19 p2738 N88-26255

XDATAP
[DE88-007161] 20 p2837 N88-26827

Editfont: An interactive font editing system
[AD-A192373] 20 p2838 N88-26836

An evaluation of flight path formats head-up and head-down
[NASA-CR-4176] 21 p2897 N88-27196

The effect of input device on user performance with a menu-based natural language interface
[AD-A193095] 21 p2996 N88-27772

Improvement of head-up display standards. Volume 4: Head-up display dynamics flight tests
[AD-A193617] 22 p3042 N88-28060

System status display evaluation
[NASA-CR-4181] 22 p3042 N88-28061

Stereo and eye movement
[AD-A193588] 22 p3142 N88-28681

Rendering of surfaces from volume data
[AD-A193649] 22 p3143 N88-28689

Future visual environment and concerns
23 p3242 N88-29299

Use of color CRTs (Cathode Ray Tubes) in aircraft cockpit: A literature search, revision B
[AD-A195062] 24 p3324 N88-29797

A detection theory analysis of visual display performance
[AD-A196291] 24 p3409 N88-30292

DISPLAY SYSTEMS
U DISPLAY DEVICES

DISPOSAL
NT HAZARDOUS MATERIAL DISPOSAL (IN SPACE)
NT WASTE DISPOSAL

Real time AI expert system for robotic applications
08 p1061 N88-16408

Nuclear-powered space debris sweeper
17 p2418 N88-24380

DISRUPTING

Modeling of thermal effects on TIBER 2 (Thermal Ignition/Burn Experimental Reactor) divertor during plasma disruptions
[DE88-001893] 06 p0783 N88-14805

Vaporization studies of plasma interactive materials in simulated plasma disruption events
[DE88-010100] 19 p2731 N88-26222

DISSIPATION
NT ENERGY DISSIPATION
NT OHMIC DISSIPATION

FLIP (Fluid-Implicit-Particle): A low-dissipation, particle-in-cell method for fluid flow
[DE87-014745] 03 p0313 N88-11981

A dissipation principle and its consequences for structured shock waves in thermoelastic materials
[DE87-013723] 04 p0454 N88-12813

Canonical transformations and exact invariants for dissipative systems
[DE87-703663] 04 p0485 N88-12985

Reynolds-stress and dissipation rate budgets in a turbulent channel flow
[NASA-TM-89451] 07 p0852 N88-15174

Period-doubling universality in multidimensional dissipative and conservative systems
[PB88-148812] 13 p1832 N88-20961

A physically consistent model for artificial dissipation in transonic potential flow computations
[NASA-TM-100846] 15 p2122 N88-22652

On 3-5 transistors for MM-wave applications
[AD-A191580] 19 p2661 N88-25625

Determination of multiaxial flow surfaces at elevated temperatures using the concept of dissipation potential
[ORNL/TM-10787] 24 p3383 N88-30149

DISSIPATORS
U DISSIPATION

DISSOCIATION
NT AUTOIONIZATION
NT GAS DISSOCIATION
NT PHOTODISSOCIATION
NT RADIOLYSIS
NT THERMAL DISSOCIATION

Nitrogen at high pressure
[DE87-013797] 01 p0021 N88-10130

Nitrogen at very high pressure
[DE87-013800] 01 p0021 N88-10131

Chemical equilibrium calculations for the high pressure and temperature dissociation of liquid nitrogen
[DE87-013788] 01 p0021 N88-10135

The dissociation of dense liquid nitrogen and shock cooling
[DE87-013490] 01 p0022 N88-10136

Computational fluid dynamics and aerothermodynamics
[NASA-CR-182490] 09 p1166 N88-16989

Atomic data for hydrogens in collisions with electrons: Addenda
[IPPJ-AM-55-ADD] 09 p1252 N88-17502

Excimer laser photolysis studies of T-V (Translation-to-Vibration) energy transfer
[AD-A189613] 13 p1837 N88-20989

NNEPEQ: Chemical equilibrium version of the Navy/NASA Engine Program
[NASA-TM-100851] 14 p1868 N88-21161

Theory of the dissociation dynamics of small molecules on metal surfaces: Finite temperature studies
[DE88-006495] 15 p2132 N88-22716

The H5(+) potential energy hypersurface: Characterization of ten distinct energetically low-lying stationary points 16 p2267 N88-23561

Theoretical calculations of XeF ground state kinetics
[AD-A191398] 16 p2270 N88-23580

Computer program for parameterization of nucleus-nucleus electromagnetic dissociation cross sections
[NASA-TM-4038] 16 p2270 N88-23584

Molecular sources of ionospheric holes
[AD-A191857] 18 p2541 N88-25082

Half collision studies of inelastic energy transfer processes
[DE88-008096] 19 p2724 N88-26178

High resolution spectroscopy of dissociating molecules
[DE88-007959] 20 p2851 N88-26924

Theory of the dissociation dynamics of small molecules on metal surfaces: Finite temperature studies
[DE88-007763] 21 p3013 N88-27882

Modification of YBa2Cu3O(7-x) ceramics by adsorbed water and other gases
[DE88-011518] 22 p3057 N88-28140

Measurements of XeF (Xenon Fluoride) ground state dissociation and vibrational equilibration
[AD-A194611] 23 p3280 N88-29527

Nonequilibrium flow of a dissociating gas in a horizontal channel with axial temperature variation
[DE88-702536] 24 p3373 N88-30089

Ion kinetics in silane plasmas
[AD-A196202] 24 p3431 N88-30423

DISSOLUTION
U DISSOLVING

DISSOLVED GASES

Mass transport phenomena between bubbles and dissolved gases in liquids under reduced gravity conditions
[NASA-TM-100273] 11 p1455 N88-18672

DISSOLVING

De-alloying
[DE87-012488] 01 p0022 N88-10139

Irreversible dissolution of solid solutions: A kinetic and stoichiometric model
[DE88-009194] 19 p2614 N88-25513

Dissolution rates of polymers and copolymers based on methyl, ethyl and butyl methacrylate
[AD-A194713] 23 p3197 N88-29027

DISSYMMETRY
U ASYMMETRY

DISTANCE
NT DIFFUSION LENGTH
NT RADAR RANGE
NT RADIO RANGE
NT RANGE AND RANGE RATE TRACKING

Research in geodesy based upon radio interferometric observations of GPS (Global Positioning System) satellites
[AD-A184040] 03 p0346 N88-12187

A computational examination of orthogonal distance regression
[AD-A184374] 03 p0371 N88-12337

Results of one way transit time measuring in navigation experiment NAVEX
[DFVLR-MITT-87-17] 14 p1865 N88-21145

The Monte Generoso-Zimmerwald (Switzerland) baseline from satellite laser ranging data using various analysis techniques
[LR-533] 14 p1940 N88-21576

The distance to the center of the galaxy: H2O maser proper motions in Sgr B2(N)
[MPE-PREPRINT-104] 16 p2288 N88-23702

Modeling the primary events of photosynthesis using chlorophyll containing fixed distance donor-acceptor molecules
[DE88-010033] 20 p2831 N88-26793

DISTANCE MEASURING EQUIPMENT
NT ALTIMETERS
NT LASER ALTIMETERS
NT LASER RANGE FINDERS
NT RADIO ALTIMETERS
NT RANGE FINDERS

Contributions to geodesy, photogrammetry, and cartography. Series 2, number 45
[ISSN-0469-4244] 01 p0065 N88-10416

A method resolving an amibiguity of measured distances by means of NAVSTAR GPS signals
01 p0065 N88-10417

Degradation of downlink distance measurement indexes by the addition of a third tone --- tone ranging
[CNES-CT/DRT/TIT/TR-122-T]
15 p2058 N88-22268

Method and apparatus for measuring distance
[NASA-CASE-MSC-20912-1] 20 p2793 N88-26568

DISTANCE PERCEPTION
U SPACE PERCEPTION

DISTILLATION

Flammability characteristics of distillate fuels
[AD-A188497] 12 p1612 N88-19642

Feasibility of producing jet fuel from GPGP (Great Plains Gasification Plant) by-products
[DE88-010233] 20 p2781 N88-26492

Vapor Compression Distillation Subsystem (VCDS) component enhancement, testing and expert fault diagnostics development, volume 2
[NASA-CR-172076] 21 p2994 N88-27755

Vapor Compression Distillation Subsystem (VCDS) component enhancement, testing and expert fault diagnostics development, volume 1
[NASA-CR-172072] 22 p3134 N88-28634

DISTILLATION EQUIPMENT

Vapor compression distiller and membrane technology for water revitalization 03 p0359 N88-12262

DISTORTION
NT FLOW DISTORTION
NT SIGNAL DISTORTION
NT SURFACE DISTORTION

USSR report: Physics and mathematics
[JPRS-UPM-87-006] 06 p0708 N88-14344

Compensation of small-scale phase distortions by means of a Fourier phase corrector
06 p0708 N88-14345

Distortional buckling formulae for thin-walled channel columns
[PB87-124012] 06 p0722 N88-14437

X-ray measurements of phason distortion in ion-implanted Al-Mn
[DE87-014566] 07 p0937 N88-15694

Flat-field response and geometric distortion measurements of optical streak cameras
[DE88-002394] 09 p1168 N88-17005

Reduction of residual stresses and distortion in girth welded pipes
[AD-A187728] 11 p1494 N88-18920

Effect of spatial inlet temperature and pressure distortion on turbofan engine stability
[NASA-TM-100850] 14 p1868 N88-21162

Millimeter-wave pulse distortion by a single adsorption line simulating the terrestrial atmosphere
[PB88-161237] 14 p1906 N88-21388

Ultrasonic beam distortion in transversely isotropic media
[DE88-005937] 15 p2129 N88-22699

Analytical approximation of a distorted reflector surface defined by a discrete set of points
[NASA-TM-101323] 21 p2934 N88-27424

A Navier-Stokes study of cascade flow fields including inlet distortion and rotating stall
[AD-A193109] 21 p2943 N88-27483

Effects of pulsed and CW (Continuous Wave) 2450 MHz radiation on transformation and chromosomes of human lymphocytes in vitro
[AD-A193104] 21 p2987 N88-27736

Distortion functions
[DE88-752634] 21 p3015 N88-27896

Distortion effects in isoparametric elements, an analytic approach
[PNR90454] 22 p3145 N88-28703

Aerodynamics of seeing on large transport aircraft
[NASA-CR-183122] 23 p3174 N88-28896

A novel method to correct radiation pattern distortion of conformal antennas
[AD-A193675] 23 p3204 N88-29066

Distortions in processed signals and their application in electronic design. Part 1: Basic and general formulations
[DE88-702731] 23 p3204 N88-29070

Distortions in processed signals and their application in electronic design. Part 2: A new variable signal generator
[DE88-702732] 23 p3205 N88-29071

Distortion estimates for negative Schwarzian maps
[AD-A193172] 23 p3228 N88-29209

Theory of filtering and control with application to control of large space structures
[AD-A195500] 24 p3335 N88-29851

Contamination and distortion of steady flow field induced by discrete frequency disturbances in aircraft gas engines
[AD-A195440] 24 p3370 N88-30069

DISTRIBUTED AMPLIFIERS

Enhanced performance ultrabroadoand distributed amplifiers 19 p2656 N88-25775

DISTRIBUTED FEEDBACK LASERS

Distributed feedback effects in lasers and high gain laser instabilities in optically pumped CH3F
03 p0329 N88-12079

Time characteristics of ultrashort light pulses from dye lasers with distributed feedback
14 p1970 N88-21759

Characteristics of distributed feedback lasers discussed 16 p2185 N88-23028

Distributed feedback lasers
[NASA-CR-4154] 18 p2520 N88-24948

DISTRIBUTED PARAMETER SYSTEMS

Structural frequency functions for an impulsive, distributed forcing function
[DE87-013811] 03 p0333 N88-12101

A new method of boundary parameter estimation for a two-dimensional diffusion system under noisy observations
[NASA-CR-178405] 06 p0767 N88-14714

A unified framework for approximation in inverse problems for distributed parameter systems
[NASA-CR-181621] 10 p1400 N88-18346

Calculation of the distributed loads on the blades of individual multiblade propellers in axial flow using linear and nonlinear lifting surface theories
[NASA-TT-20173] 13 p1719 N88-20278

Feedback control of distributed parameter systems with applications to large space structures
[AD-A190536] 15 p2025 N88-22068

Instrumentation to provide an active control capability for distributed parameter systems
[AD-A190043] 15 p2076 N88-22375

Boundary shape identification problems in two-dimensional domains related to thermal testing of materials
[NASA-CR-181654] 15 p2105 N88-22541

The Colored Stochastic Petri Net (CS-PN) software: Application to the validation and the performance evaluation of distributed systems
[ENST-87D005] 15 p2113 N88-22589

Approximation methods for the identification and control of distributed parameter systems
[AD-A190201] 15 p2124 N88-22662

An approximation theory for the identification of nonlinear distributed parameter systems
[NASA-CR-181658] 16 p2260 N88-23510

Galerkin approximation for inverse problems for nonautonomous nonlinear distributed systems
[NASA-CR-181676] 18 p2567 N88-25246

Finite-dimensional approximation for optimal fixed-order compensation of distributed parameter systems
[NASA-CR-181674] 20 p2843 N88-26873

Connectionist models and artificial intelligence
[RR-684-I-IMAG-66-LIFIA] 22 p3142 N88-28684

Laser sensing for identification and control of distributed parameter systems
[AD-A195886] 24 p3379 N88-30124

Robust finite-dimensional LQG (Linear Quadric Gaussian)-based controllers for a class of distributed parameter systems
[AD-A194872] 24 p3425 N88-30382

DISTRIBUTED PROCESSING

A nonmythical generalization of Dekker's algorithm and its ramifications --- mutually exclusive processes
[CS-8702] 01 p0080 N88-10513

Methodology of performance evaluation of real time distributed systems
[ENST-87D003] 02 p0228 N88-11440

Token execution strategies for distributed algorithms: Simulation studies
[AD-A184792] 03 p0365 N88-12294

Layering central authentication on the interactive services of an existing homogeneous distributed system
[DE87-011544] 03 p0366 N88-12304

Interfacing distributed operating systems
[AD-A184489] 03 p0366 N88-12306

Concepts and techniques for support of real time distributed operating systems
[AD-A184491] 03 p0367 N88-12307

Managing distributed derived data: A preliminary proposal
[DE88-000714] 04 p0481 N88-12966

Storing and retrieving data in a parallel distributed memory system
[AD-A185177] 05 p0637 N88-13897

Conceptual issues in measuring the behavior of a distributed real-time process-control computer system
[DE87-009748] 05 p0638 N88-13898

Conceptual issues in measuring the behavior of a distributed real-time process-control computer system
[DE87-014251] 05 p0638 N88-13899

Connecting RPC (Remote Procedure Call)-based distributed systems using wide-area networks
[PB87-234423] 05 p0658 N88-14041

An empirical investigation of load indices for load balancing applications
[AD-A185763] 06 p0724 N88-14451

Objects architecture: A comprehensive design approach for real-time, distributed, fault-tolerant, reactive operating systems
[AD-A185476] 06 p0755 N88-14631

Distribution of records on a ring of processors
[PB87-235784] 06 p0758 N88-14649

Distributed infimum approximation
[PB87-234969] 06 p0764 N88-14695

Communications for the DTroll distributed database system
[AD-A185579] 06 p0791 N88-14853

Study of communication options in a distributed data handling system and survey of advanced man machine communications schemes. Work package 1: Interprocess communication
[ESA-CR(P)-2447] 07 p0843 N88-15114

Annotated bibliography on reliable system design
[PB88-109848] 07 p0866 N88-15254

UNITY: A framework for study of parallel programming problem-solving
[AD-A185616] 07 p0906 N88-15490

Interface between astrophysical datasets and distributed database management systems (DAVID)
[NASA-CR-182394] 07 p0942 N88-15731

Reliability issues in distributed operating systems
[PB88-100870] 08 p0993 N88-16009

A distributed architecture for intelligent monitoring and anomaly diagnosis of the Hubble Space Telescope
08 p1057 N88-16379

A knowledge-based system for monitoring the electrical power system of the Hubble Space Telescope
08 p1058 N88-16380

Problem solving as intelligent retrieval from distributed knowledge sources 08 p1059 N88-16392

Application of parallel distributed processing to space based systems 08 p1059 N88-16393

Neural network based speech synthesizer: A preliminary report 08 p1064 N88-16429

A framework for real-time distributed expert systems: On-orbit spacecraft fault diagnosis, monitoring and control 08 p1066 N88-16440

Prototype space station automation system delivered and demonstrated at NASA 08 p1066 N88-16442

Proposal of a methodology for the conceptual design of the Distributed Data Base
[INPE-4315-TDL/282] 08 p1093 N88-16576

Analysis of tasks for dynamic man/machine load balancing in advanced helicopters
[DE88-003735] 09 p1117 N88-16696

Replication and reconfiguration in a distributed mail repository
[AD-A186967] 09 p1151 N88-16897

First Annual Workshop on Space Operations Automation and Robotics (SOAR 87)
[NASA-CP-2491] 09 p1203 N88-17206

Development of a comprehensive software engineering environment 09 p1203 N88-17211

Task allocation in a distributed computing system
09 p1206 N88-17230

Software for integrated manufacturing systems, part 1
09 p1211 N88-17261

Software for integrated manufacturing systems, part 2
09 p1211 N88-17262

The implementation and use of Ada on distributed systems with high reliability requirements
[NASA-CR-182481] 09 p1221 N88-17326

Clouds: A support architecture for fault tolerant, distributed systems 10 p1375 N88-18206

A distributed system architecture based on macro dataflow model 10 p1376 N88-18210

A comparative study of heurstic algorithms for task assignment in distributed computing systems
10 p1376 N88-18211

Distributed control of large parallel computers
10 p1376 N88-18215

The design of load balancing strategies for distributed systems 10 p1376 N88-18216

Experiments with parallel program execution on a network of workstations 10 p1377 N88-18217

Distributed query processing: Present status and future direction 10 p1377 N88-18219

Concurrency control and reliability in replicated database systems 10 p1377 N88-18221

An anlysis of the reliability of tree-structured interconnection networks 10 p1378 N88-18228

On the number of task assignments in distributed computing systems 10 p1378 N88-18230

Reuse: A Reliable Unified Service Environment for distributed systems 10 p1379 N88-18231

Resilient procedures: A structured replication approach 10 p1381 N88-18245

Features of a TeraFlop supercomputer
[DE88-003540] 10 p1384 N88-18263

Optimal performance of distributed simulation programs
[AD-A187822] 11 p1529 N88-19131

The roll back chip: Hardware support for distributed simulation using time warp
[AD-A187823] 11 p1529 N88-19132

Performance measurements of distributed simulation strategies
[AD-A187824] 11 p1529 N88-19133

Distributed computation of graphics primitives on a transputer network
[NASA-TM-100814] 11 p1531 N88-19147

A shared memory algorithm and proof for the alternative construct in CSP (Communicating Sequential Processes)
[AD-A187820] 11 p1533 N88-19156

Implementing dynamic arrays: A challenge for high-performance machines
[AD-A188142] 11 p1533 N88-19157

Theory and practice of fault tolerance in distributed systems
[AD-A187559] 11 p1540 N88-19204

Uncertain knowledge in distributed systems
[AD-A189017] 12 p1685 N88-20076

Design methodology for allocating data in a distributed database
[AD-A188826] 12 p1706 N88-20215

Two normal form theorems for Communicating Sequential Processes (CSP) program
[CWI-CS-R8735] 13 p1819 N88-20874

Distributed transaction processing and the Camelot system
[AD-A188614] 13 p1821 N88-20885

On the design of parallel numerical methods in message passing and shared memory environments
[DE88-003566] 13 p1822 N88-20888

An amoeba replicated service organisation --- Amoeba operating system
[CWI-CS-R8723] 13 p1822 N88-20892

GADL: A gate array description language
[EUT-87-E-165] 14 p1907 N88-21396

Higher levels of a silicon compiler
[EUT-86-E-163] 14 p1955 N88-21650

Generating layouts for random logic: Cell generation schemes
[EUT-86-E-164] 14 p1956 N88-21658

ESKISS: A program for optimal state assignment
[EUT-87-E-167] 14 p1956 N88-21659

Distributed operating systems: An overview
[INF-87-29] 14 p1960 N88-21688

Conception of a knowledge-based system for designing distributed systems
[DFVLR-MITT-87-16] 14 p1961 N88-21694

Technology mapping from Boolean expressions to standard cells
[EUT-87-E-174] 14 p1963 N88-21709

An optimal CMOS structure for the design of a cell library
[EUT-87-E-166] 14 p1985 N88-21841

Argus reference manual
[AD-A190382] 15 p2111 N88-22578

The Colored Stochastic Petri Net (CS-PN) software: Application to the validation and the performance evaluation of distributed systems
[ENST-87D005] 15 p2113 N88-22589

A methodolgy, based on analytical modeling, for the design of parallel and distributed architectures for relational database query processors
[AD-A189844] 15 p2149 N88-22825

Distributed matchmaking
[CWI-CS-R8750] 16 p2254 N88-23467

A timestamp ordering mechanism with dynamic selection of rollback objects 16 p2257 N88-23489

TALOS: A distributed architecture for intelligent monitoring and anomaly diagnosis of the Hubble Space Telescope 17 p2388 N88-24193

Low authority control of large space structures using a constrained threshold control formulation
18 p2472 N88-24667

Design, implementation and evaluation of an operating system for a network of transputers
[AD-A186593] 18 p2559 N88-25193

Design of partially replicated distributed database systems: An integrated methodology
18 p2589 N88-25383

Distributed mathematics in a heterogeneous environment
[DE88-009128] 19 p2716 N88-26124

The high speed local area network
19 p2717 N88-26133

Fault diagnosis in distributed computer networks
[AD-A192406] 19 p2718 N88-26140

Research in computer science 1985/6
[PB88-113840] 20 p2835 N88-26815

Correctness criteria for process migration
[NASA-CR-182939] 20 p2836 N88-26823

Distributed fault tolerant embeddings of binary trees in hypercubes
[AD-A192929] 20 p2839 N88-26840

Issues and recommendations associated with distributed computation and data management systems for the space sciences
[NASA-CR-183026] 20 p2881 N88-27108

An integrated, multi-vendor distributed data acquisition system
[DE88-008900] 20 p2882 N88-27113

Computational fluid dynamics on parallel processors
[AD-A192397] 21 p2941 N88-27469

Distributed algorithms for probabilistic solution of computational vision problems
[AD-A193150] 21 p2997 N88-27773

A menu-driven menu editor and associated menu system
[DE88-008026] 21 p2998 N88-27781

Constructing a highly-available location service for a distributed environment
[AD-A192723] 21 p3001 N88-27801

Intelligent test integration system
23 p3254 N88-29371

Distributed cooperating processes in a mobile robot control system 23 p3256 N88-29386

AI and simulation: What can they learn from each other 23 p3257 N88-29391

An expert system for a distributed real-time trainer
23 p3261 N88-29411

Large-grain pipelining on distributed-memory multiprocessors
[DE88-009974] 23 p3264 N88-29432

On the design and optimization of distributed signal detection and parameter estimation systems
[AD-A193934] 23 p3266 N88-29446

Dynamically reconfigurable distributed database systems
[AD-A194716] 23 p3297 N88-29636

Performance analysis of FDDI
[NASA-CR-183206] 24 p3413 N88-30321

Parallel and distributed computation for fault-tolerant object recognition 24 p3419 N88-30350

Knowledge-based integrated information systems engineering: Highlights and bibliography. Knowledge-Based Integrated Information Systems Engineering (KBIISE) Project, volume 1
[AD-A195850] 24 p3435 N88-30449

DISTRIBUTION (PROPERTY)
NT ANGULAR DISTRIBUTION
NT ANTENNA RADIATION PATTERNS
NT BOLTZMANN DISTRIBUTION
NT BRIGHTNESS DISTRIBUTION
NT CHARGE DISTRIBUTION
NT CURRENT DISTRIBUTION
NT DIFFRACTION PATTERNS
NT ELECTRON DENSITY PROFILES
NT ELECTRON DISTRIBUTION
NT ENERGY DISTRIBUTION
NT FLOW DISTRIBUTION
NT FORCE DISTRIBUTION
NT FREQUENCY DISTRIBUTION
NT HOLE DISTRIBUTION (ELECTRONICS)
NT HOLE DISTRIBUTION (MECHANICS)
NT INTERFERENCE LIFT
NT ION DISTRIBUTION
NT LOAD DISTRIBUTION (FORCES)
NT MASS DISTRIBUTION
NT MOMENT DISTRIBUTION
NT PRESSURE DISTRIBUTION

NT RADIAL DISTRIBUTION
NT RADIATION DISTRIBUTION
NT SIDELOBES
NT SPATIAL DISTRIBUTION
NT SPECTRAL ENERGY DISTRIBUTION
NT STAR DISTRIBUTION
NT STRAIN DISTRIBUTION
NT STRESS CONCENTRATION
NT STRESS DISTRIBUTION
NT TEMPERATURE DISTRIBUTION
NT VELOCITY DISTRIBUTION
NT VERTICAL DISTRIBUTION

Measurement of agglomerate strength distributions in agglomerated powders
[DE87-013605] 01 p0090 N88-10591

A 10 W transverse flow excimer laser
03 p0302 N88-11901

Macroscopic distribution of fiber finish
[DCO/L-48-283/F] 07 p0827 N88-15013

Advanced communication systems: A report on fiber optic technology and its possible applications in the gas industry
[PB88-112792] 07 p0845 N88-15125

On the extreme points of the set of all 2xn bivariate positive quadrant dependent distributions with fixed marginals and some applications
[AD-A186316] 07 p0911 N88-15521

Some new approaches to multivariate probability distributions
[AD-A186038] 07 p0914 N88-15551

An analytic model for ionization distributions produced in nanometer sites by protons
[DE88-003943] 10 p1406 N88-18385

Stratospheric trace gas distributions from fair infrared thermal emission spectroscopy
13 p1797 N88-20749

The Earth radiation budget and its spatial and temporal variations 14 p1936 N88-21548

Assessment of crop loss from air pollutants: Meteorology-atmospheric chemistry and long range transport
[PB88-146857] 15 p2089 N88-22448

Rocket-borne low energy ion measurements in space
18 p2593 N88-25412

Measurements of vacuum arc ion charge state distributions
[DE88-008249] 23 p3284 N88-29558

DISTRIBUTION FUNCTIONS

Measures of diversity based on fuzzy multinomial distributions
[DE87-010617] 02 p0228 N88-11439

Enhanced noise and Raman scattering in plasma
[DE87-014466] 02 p0238 N88-11501

Monte Carlo analysis of neoclassical transport for a compact helical system
[IPPJ-850] 04 p0492 N88-13033

Extrema of skewed stable processes
[AD-A185422] 05 p0642 N88-13925

Further studies in estimation of life distribution characteristics from censored data
[AD-A184862] 05 p0643 N88-13937

Restoration of particle pitch angle distribution functions by a maximum entropy algorithm
[ATR-86(7098)-3] 05 p0648 N88-13969

Slowing down tail enhanced, neoclassical and classical alpha particle fluxes in tokamak reactors
[DE88-001930] 06 p0783 N88-14806

Electron acceleration by wave processes in the earth's ionosphere
[AD-A186110] 07 p0877 N88-15320

Bounding the expectation of convex functions with limited distribution information
[AD-A186147] 07 p0910 N88-15512

A smooth nonparametric quantile estimator from right-censored data
[AD-A186180] 07 p0915 N88-15552

Electron temperature measurements in an argon/cesium plasma diode
[AD-A188835] 12 p1695 N88-20141

Peetre's Theorem and generalized functions
[MEMO-661] 14 p1967 N88-21742

Distributions of quadratic forms
[AD-A190224] 15 p2124 N88-22663

Estimation of convolution tails
[AD-A190323] 15 p2125 N88-22666

A model of intrazonal trip distribution considering centrality index 16 p2257 N88-23486

Symmetrized nearest neighbor regression estimates
[AD-A191998] 18 p2568 N88-25254

Ion thermal conductivity and ion distribution function in the banana regime
[IPPJ-865] 19 p2729 N88-26208

A modal approach to Arctic noise modelling with implied vertical coherence
[AD-A192966] 20 p2850 N88-2[illegible]916

Moment approach to neoclassical flows, currents and transport in auxiliary heated tokamaks
[DE88-008024] 21 p3016 N88-27901

Analysis of lower hybrid current drive and rampup experiments on the JT-60 tokamak
[DE88-753136] 21 p3018 N88-27915

Equilibrium distribution functions for limited plasma-molecular systems
[DE88-702412] 21 p3018 N88-27916

Comparison of the bidirectional reflectance distribution function of various surfaces
[NASA-TM-101317] 22 p3153 N88-28760

On the nucleonics component of cosmic radiation, in the atmosphere
[DE88-702493] 22 p3166 N88-28854

Wigner distribution function: Relation to short-term spectral estimation, smoothing and performance in noise
[AD-A193865] 23 p3275 N88-29492

Sequential approach to Colombeau's theory of generalized functions
[DE88-701869] 23 p3276 N88-29503

Moment invariants for particle beams
[DE88-011052] 23 p3281 N88-29537

DISTRIBUTION MOMENTS
NT MEAN
NT ORTHOGONALITY
NT STANDARD DEVIATION

Variances and higher order correlation coefficients: Continued
[RR-655-M] 18 p2563 N88-25219

DISTRIBUTORS

Harmonic considerations for electrical distribution feeders
[DE88-007849] 18 p2505 N88-24860

DISTURBANCE THEORY
U PERTURBATION THEORY

DISTURBANCES

A finite-amplitude analysis of the buoyant instability of a highly viscous film over a less viscous half-space
13 p1769 N88-20581

DISULFIDES

Lithium/disulfide battery R and D
[DE88-003032] 11 p1481 N88-18839

DITCHING (LANDING)

An analytical method for ditching analysis of an airborne vehicle
[NASA-CR-4120] 07 p0816 N88-14968

DITHIOLS
U THIOLS

DIURNAL RHYTHMS
U CIRCADIAN RHYTHMS

DIURNAL VARIATIONS

Asymmetry and variations of solar limb darkening along the diameter defined by diurnal motion in April 1981
04 p0506 N88-13111

An analytical soil thermodynamic model for the diurnal variation of ground surface temperature
[AD-A185388] 05 p0625 N88-13823

The lengthening and shortening of the day
[KNMI-TR-91] 05 p0628 N88-13839

Variations of the semi-diurnal tidal wind in the meteor region with periods of about 27 and 13.5 days
06 p0734 N88-14516

Tidal activity in the meteor zone over Budrio, Italy
06 p0734 N88-14517

Density variations of meteor flux along the Earth's orbit 06 p0739 N88-14545

Area of reduced electron concentration in terrestrial plasmasphere 08 p1003 N88-16078

Determination of the heat conduction coefficient of the soil from the advance of the diurnal temperature wave
08 p1015 N88-16151

Solar tides in the upper equatorial thermosphere: A comparison between AE-E data and the NCAR thermospheric general circulation model
[AD-A186160] 08 p1023 N88-16196

The influence of atmospheric thermal tides on diurnal variations in chemical constituents in the mesosphere
11 p1512 N88-19035

Radiation balance components above the tropical evergreen Amazon forests (3rd campaign of data collection)
[INPE-4195-PRE/1079] 11 p1513 N88-19039

Computer simulation of tropospheric chemistry
[JUEL-2144] 13 p1798 N88-20756

Diurnal variations in optical depth at Mars: Observations and interpretations
[NASA-TM-100057] 18 p2595 N88-25420

Interpretation of the northward B sub z (NBZ) Birkeland current system and polar cap convection patterns in terms of the impulsive penetration model
[AERONOMICA-ACTA-A-321-1987]
18 p2595 N88-25422

Urbanization: Its detection and effect in the United States climate record 22 p3125 N88-28571

Comparison of morning with afternoon nitrogen elimination in resting subjects breathing 100 percent oxygen
[AD-A196191] 24 p3407 N88-30282

DIVERGENCE

A study of diverging detonation in high-explosive systems
[DE87-006070] 01 p0031 N88-10194

The application of divergence equation in the analysis of heavy rainfall 02 p0207 N88-11299

Particle velocity and stress gage measurements in spherical diverging flow
[DE87-007333] 03 p0321 N88-12033

Wing divergence of trimmed aircraft
05 p0550 N88-13354

Periodically pulsed excimer master oscillator-regenerative amplifier laser set
06 p0772 N88-14741

Particle-gas temperature differentials resulting from time-dependent radiative-conductive heat flux divergences in the tenuous dust-laden atmosphere of mars
[AD-A185888] 07 p0945 N88-15747

A cause of divergence in the Kalman gain equation
12 p1578 N88-19438

Effect of electron beam divergence on the gain of free electron lasers 14 p1902 N88-21358

Involution-dependent constants and the cancellation of divergences in the 1-loop open string amplitude
[DE88-006537] 15 p2146 N88-22811

Current flight test experience related to structural divergence of forward-swept wings
[NASA-TM-100445] 18 p2464 N88-24633

Utilization of a single clear-air Doppler radar beam to measure vertical divergence
[AD-A195543] 24 p3405 N88-30271

DIVERTERS

Simulation an experiment on plasma instability investigation in a tokamak with a divertor
[DE88-700352] 07 p0935 N88-15683

Two-dimensional analysis for a scrapeoff and divertor regions with an MHD model: Conceptual design study of FY86 FER
[DE88-751069] 09 p1251 N88-17497

Design of divertor plate and measurements of double-null open divertor plasma in the JFT-2M tokamak
[DE88-753130] 21 p3016 N88-27914

DIVIDING (MATHEMATICS)

Spectral representation of infinitely divisible processes
[AD-A186210] 07 p0910 N88-15515

DIVING (UNDERWATER)

Challenges of physiological monitoring in a Navy operational setting 16 p2239 N88-23374

Subsea approach to work systems development
17 p2379 N88-24146

Proceedings of the Colloquium on Space and Sea
[ESA-SP-280] 19 p2695 N88-26016

Experience in occupational medicine, derived from 16 operational deep saturation trials: 5 dives in GUSI from 150 to 600 m 19 p2695 N88-26018

Life in a hyperbaric environment: A new O2-H2 breathing mixture for industrial diving 19 p2695 N88-26019

Technical challenges in the development of a European space suit system and comparison with underwater suits
19 p2696 N88-26024

The relationship between preflight underwater training and space motion sickness 19 p2696 N88-26025

Similarities between diving operations and space missions 19 p2697 N88-26027

Contribution of ultrasonic Doppler detection of circulating bubbles to human interventions under the sea and in space 19 p2697 N88-26029

Different techniques for intervening under the sea: Possible links with space applications
19 p2697 N88-26030

The SAGA highly autonomous assistance submarine
19 p2698 N88-26034

Decompression procedures and accidents in space and sea 19 p2698 N88-26035

Monitoring of divers/astronauts during missions
19 p2698 N88-26036

Safety aspects in design and operation practice of GKSS underwater simulation plant GUSI
19 p2698 N88-26037

Reducing risks inherent in operating underwater craft: The contribution of classification, the example of the SAGA highly autonomous support submarine
19 p2699 N88-26042

Space and sea: Is there a place for ionization?
19 p2699 N88-26043

ELIT: An autonomous underwater observation robot
19 p2699 N88-26048

Study of human factors engineering criteria for Extra Vehicular Activity (EVA) systems, volume 2
[STF23-F87025-VOL-2] 24 p3409 N88-30293

DIVISION

Theory of dividing vortons 03 p0318 N88-12009

best copy available

DMSP SATELLITES
Instantaneous pictures of the high-latitude electrodynamics using Viking and DMSP/F7 observations --- Swedish satellite
08 p1025 N88-16209
An assessment of the application of in situ ion-density data from DMSP to modeling of transionospheric scintillation
[AD-A188919] 12 p1643 N88-19840
DMSP-SSM/1 NASA algorithm validation using primarily LANDSAT and secondarily DMSP and/or AVHRR visible and thermal infrared satellite imagery
[NASA-CR-182979] 18 p2532 N88-25024
Investigations of magnetosphere-ionosphere coupling relevant to operational systems
[AD-A195972] 24 p3391 N88-30195
Passive microwave measurements of water vapor fields and rain for locating fronts in cyclonic storms
[AD-A195632] 24 p3404 N88-30267
DNA
U DEOXYRIBONUCLEIC ACID
DO-28 AIRCRAFT
Flight test preparation and measuring data validation for parameter identification 20 p2786 N88-26529
DOCKING
U SPACECRAFT DOCKING
DOCUMENT STORAGE
After ten years of metafiles: Where does the Computer Graphics Metafile fit
[DE88-001840] 07 p0904 N88-15474
Common database interface for heterogeneous software engineering tools
[AD-A189628] 14 p1991 N88-21870
Narrative compression coding for a channel with errors
[AD-A191577] 19 p2642 N88-25673
DOCUMENTATION
Documentation as a management strategy for reaching goals in high-risk research-oriented projects
[DE87-012394] 01 p0105 N88-10685
Guidance for conference rapporteurs
[NASA-CR-182338] 05 p0659 N88-14042
Alouette-ISIS program summary
[NASA-CR-180747] 08 p1023 N88-16195
A hypertext writing environment and its cognitive basis
[AD-A188179] 10 p1389 N88-18298
Documentation for computer code NACL
[LBL-21859] 11 p1531 N88-19145
NASA scientific and technical publications: A catalog of Special Publications, Reference Publications, Conference Publications, and Technical Papers, 1987
[NASA-SP-7063(02)] 15 p2149 N88-22830
The -mdoc macro package: A software tool to support computer documentation standards
[DE88-000500] 18 p2559 N88-25188
Documentation of the Benson Diesel Engine Simulation Program
[NASA-TM-100940] 21 p2898 N88-27201
Engineering data compendium. Human perception and performance. User's guide
[LC-87-19560] 21 p2993 N88-27749
Engineering data compendium. Human perception and performance, volume 1
[LC-87-19560] 22 p3134 N88-28630
Engineering data compendium. Human perception and performance, volume 2
[LC-87-19560] 22 p3134 N88-28631
Engineering data compendium. Human perception and performance, volume 3
[LC-87-19560] 22 p3134 N88-28632
Bibliography of Lewis Research Center technical publications announced in 1987
[NASA-TM-100910] 22 p3162 N88-28832
Technical communication in the computer industry: An information-development process to track, measure and ensure quality 23 p3297 N88-29635
DOCUMENTS
NT ABSTRACTS
NT ASTRONOMICAL CATALOGS
NT BIBLIOGRAPHIES
NT CATALOGS (PUBLICATIONS)
NT ENGINEERING DRAWINGS
NT HANDBOOKS
NT MANUALS
NT PAPERS
NT PERIODICALS
NT PRESIDENTIAL REPORTS
NT RECORDS
NT SUPPLEMENTS
NT TEXTBOOKS
NT TEXTS
NT THESES
NT USER MANUALS (COMPUTER PROGRAMS)
A summary of the Naval Postgraduate School research program
[AD-A186362] 07 p0942 N88-15727
Index of USA-CERL publications for October 1984 - June 1987
[AD-A186375] 07 p0942 N88-15728
FY87 scientific and technical reports, articles, papers, and presentations
[NASA-TM-100318] 08 p1093 N88-16578
Preliminary analysis of an integrated logistics system for OSSA payloads. Volume 3: OSSA integrated logistics support planning document 12 p1584 N88-19480
Streamlining invitation for bids
[AD-A188941] 12 p1705 N88-20206
Application of new technologies to DTIC document processing
[AD-A189778] 15 p2148 N88-22823
Publications on acoustics research at the Langley Research Center during 1980-1986
[NASA-TM-100590] 21 p3013 N88-27881
Development of graded reference radiographs for aluminum welds, phase 1
[AD-A195594] 24 p3381 N88-30140
DOGS
Combined effect of ionizing radiation and altered gas atmosphere on central nervous system
10 p1367 N88-18168
DOMAINS
Modeling XV-15 tilt-rotor aircraft dynamics by frequency and time-domain identification techniques
03 p0263 N88-11657
Weak convergence of sums of moving averages in the alpha-stable domain of attraction
[AD-A186430] 07 p0912 N88-15529
Computational analysis of propagation properties of integrated-optical waveguides using a domain integral equation
[PB87-163358] 09 p1154 N88-16917
Time domain wave propagation in multilayered integrated circuits
[AD-A187462] 10 p1324 N88-17916
Fast Poisson solver on irregular regions by boundary integral-based domain decomposition methods
[DE88-003583] 10 p1399 N88-18340
Domain decomposition preconditioners for the spectral collocation method
[NASA-CR-181620] 10 p1400 N88-18345
Parallel pseudospectral domain decomposition techniques
[NASA-CR-181629] 11 p1524 N88-19101
Boundary shape identification problems in two-dimensional domains related to thermal testing of materials
[NASA-CR-181654] 15 p2105 N88-22541
A domain decomposition method for boundary layer problems
[DE88-008917] 19 p2666 N88-25852
Two domain decomposition techniques for Stokes problems
[DE88-008724] 19 p2720 N88-26149
A microcomputer based frequency-domain processor for laser Doppler anemometry
[NASA-TM-100998] 20 p2803 N88-26634
Spatial organization of homopolymer chains inside spherical polybutadiene domains of SB diblock copolymers
[AD-A193390] 21 p2918 N88-27321
Multiple solutions and bifurcation for a class of nonlinear Sturm-Liouville eigenvalue problems on an unbounded domain
[AD-A195954] 24 p3426 N88-30389
DOMES (GEOLOGY)
Diapirs of the Mediterranean ridge: The tectonic regime of an incipient accreted terrane
24 p3396 N88-30224
DOMES (STRUCTURAL FORMS)
Airborne tracking sunphotometer apparatus and system
[NASA-CASE-ARC-11622-1] 06 p0730 N88-14492
DONOR MATERIALS
Excimer laser-assisted deposition of GaAs, AlAs and (Al,Ga)As from Lewis acid-base adducts
[AD-A184588] 03 p0329 N88-12081
Modeling the primary events of photosynthesis using chlorophyll containing fixed distance donor-acceptor molecules
[DE88-010033] 20 p2831 N88-26793
DOORS
Some highlights on ROSAT mechanisms
14 p1874 N88-21195
DOPED CRYSTALS
Structural characterization of ion implanted beta-SiC thin films
[DE87-014567] 05 p0656 N88-14027
Investigation of silicon surface passivation by silicon nitride film deposition
[NASA-CR-182350] 06 p0729 N88-14487
Use of lasers with F sub A(II)-color center KCl:Li crystals in the intraresonator laser spectroscopy method
06 p0769 N88-14729
Structural characterization of undoped and doped GaAs: A comparative study of four techniques
[DE88-004552] 11 p1555 N88-1930
Growth of Cr,Nd:Gd3Sc2Al3O12 (Cr,Nd:GSAG) crystals by the Heat Exchanger Method (HEM)(trademark)
[DE88-004041] 11 p1558 N88-1932
Optical absorption in doped CdxHg1-xTe
[AD-A187434] 11 p1560 N88-1933
Pressure-dependent DLTS (Deep Level Transient Spectroscopy) experiments on Si-doped AlGaAs
[DE88-003842] 13 p1846 N88-21047
Singlet oxygen behavior in solid polymer matrices
[DE88-005171] 15 p2043 N88-22171
Superconductivity and the tailoring of lattice parameters of the compound YBa2Cu3O(sub x)
[DE88-005904] 15 p2140 N88-2276
Electrical and optical properties of Hg/sub 1-x/Cd/sub x/Te doped layers grown by Liquid Phase Epitaxy (LPE)
[DE88-701023] 16 p2281 N88-2385
Improved GaP doped SiGe thermoelectric material
17 p2437 N88-24503
Determination of doping profiles in silicon from resistivity measurements via the four-point probe in combination with layer strippings via anodic oxidation
18 p2583 N88-25347
Electron tunneling in junctions doped with semiconductors and metals 19 p2734 N88-26236
Superlattice doping interfaces
20 p2866 N88-27019
Blue-green laser diode research program
[AD-A191980] 23 p3218 N88-29153
Solid-state laser research report: Energy transfer in non-uniform codoped crystals
[AD-A194358] 23 p3219 N88-29161
Development of a unit cell for a Ge:Ga detector array
[NASA-CR-177445] 24 p3375 N88-30100
Growth and characterization of materials for tunable lasers in the near infrared spectral region
[NASA-CR-183132] 24 p3377 N88-30113
DOPES
Blue-green laser diode research program
[AD-A183517] 01 p0051 N88-10323
Investigation of two laser beam coupling and amplification in Ce-doped SBN single crystals
03 p0327 N88-12069
Numerical calculations of dopant diffusion involving flashlamp heating of silicon 21 p2929 N88-27384
DOPING (ADDITIVES)
U ADDITIVES
DOPPLER EFFECT
The sequential evaluation of Doppler satellite observations
[REPT-141] 01 p0010 N88-10057
Analysis of counting errors in the phase/Doppler particle analyzer
[NASA-TM-100231] 03 p0323 N88-12043
Flux tube dynamics and solar/stellar redshift measurements 04 p0503 N88-130
Doppler snapshots 04 p0508 N88-13125
Anomalies in electromagnetic absorption of circularly polarized ultrasonic waves by tungsten within Doppler-shifted cyclotron resonance range
06 p0775 N88-14756
Experimental research of electron beam instability on the Doppler anomalous effect
[DE88-700565] 07 p0932 N88-15658
A generalized description of the anomalous Doppler resonance and the stabilizing role of ion dynamics
[INPE-4384-PRE/1204] 08 p1081 N88-16512
Comparison of UNL laser imaging and sizing system and a phase/Doppler system for analyzing sprays from a NASA nozzle
[NASA-CR-182437] 09 p1161 N88-16956
Product kinetic and internal energy distributions via velocity-aligned Doppler spectroscopy
[DE88-003510] 10 p1298 N88-17764
Position, scale, and rotation invariant target recognition using range imagery
[AD-A188828] 12 p1633 N88-19772
Observations of the upper ocean using a multi-beam Doppler sonar
[AD-A188896] 12 p1649 N88-19878
A polarization diversity meteorological radar system
[AD-A189291] 13 p1758 N88-20515
Observations of waves and Langmuir circulation with Doppler sonars 13 p1805 N88-20790
Determination of beam orientation of optical diagnostics of excited 200-MeV hydrogen atoms resulting from photodetachment of H(-)ions
[AD-A189076] 14 p1981 N88-21823
Laser Doppler anemometry
[NASA-TM-100072] 16 p2210 N88-23167

Considerations pertinent to the Doppler effect for space reactors 17 p2399 N88-24264
De[illegible] Doppler radar imaging
[AD-A[illegible]1509] 18 p2499 N88-24826
Feature extraction using the Hough transform
[AD-A190679] 18 p2555 N88-25165
Doppler distortion of solar Fraunhofer lines in zodiacal light by reflection from interplanetary dust
19 p2740 N88-26270
Developing diagnostic methods for plasma-particle interaction
[DE88-007726] 20 p2858 N88-26973
Laser spectoscopy of plasmas
[AD-A193009] 20 p2861 N88-26991
Radar information from the partial derivatives of the echo signal phase from a point scatterer
[AD-A193402] 21 p2933 N88-27415
Is the 3C273 quasar Mach nearer
[DE88-702235] 21 p3030 N88-27988
The behavior of a Costas loop in the presence of space telemetry signals 22 p3067 N88-28198
Particle sizing in combustion systems, using scattered laser light
[AD-A196231] 24 p3352 N88-29953
Doppler-corrected differential detection system
[NASA-CASE-NPO-16987-1-CU]
24 p3359 N88-30001

DOPPLER RADAR
NT MULTISTATIC RADAR
New nowcasting opportunities using modern meteorological radar 02 p0199 N88-11245
Nowcasting microbursts using Doppler radar in a forecaster-computer environment
02 p0200 N88-11246
Use of a 5 cm Doppler radar to detect and forecast severe thunderstorms in a real time forecast operation
02 p0200 N88-11247
Thunderstorm nowcasting using Doppler radar and soundings 02 p0200 N88-11248
A real-time system for automatic single-Doppler wind field analysis 02 p0200 N88-11249
Diagnosing short term changes in temperature and moisture profiles from single Doppler radar
02 p0200 N88-11251
Delay-Doppler radar imaging
[AD-A184165] 03 p0308 N88-11943
Study of an airborne Doppler radar: Project Asterix
[BLL-MO-TRANS-1667-(9022.552)]
04 p0432 N88-12675
Media calibrations of the Doppler signal for a gravitational wave experiment --- interplanetary medium
[IFS-46-13] 05 p0625 N88-13825
Meteor observation by the Kyoto meteor radar
06 p0733 N88-14507
Meteor detection on ST (MST) radars
06 p0740 N88-14554
The Cyclone meteor radar system for routine wind measurements in the lower thermosphere
06 p0741 N88-14555
Radar observations of changes in precipitation size spectra associated with lightning
06 p0744 N88-14576
Wind shear detection. Forward-looking sensor technology
[NASA-CP-10004] 07 p0817 N88-14970
Waveform for short-dwell-time meteorological Doppler radars
[PB88-102199] 07 p0845 N88-15126
Problems and possible solutions involved in hard target calibration of coherent Doppler lidar
07 p0922 N88-15602
Development of a Doppler wind lidar system for atmospheric wind measurements
08 p1027 N88-16217
Remote measurement of aerosol stream velocity with continuous-wave CO2-laser 08 p1079 N88-16506
Meteorological radar and its usage in the Navy
[AD-A186650] 09 p1152 N88-16902
Backscattering signal analysis concerning a three-dimensional object configuration on the basis of object motion
[ESA-TT-1044] 09 p1154 N88-16915
Airborne Wind Shear Detection and Warning Systems: First Combined Manufacturers' and Technologists' Conference
[NASA-CP-10006] 10 p1273 N88-17616
Airborne Doppler radar technology for wind shear detection 10 p1274 N88-17622
Crew interface with windshear systems
10 p1275 N88-17631
Status of FAA terminal Doppler weather radar programs 10 p1275 N88-17632
The advanced low-level windshear alert system operational demonstration results, Summer, 1987, Denver Stapleton International Airport 10 p1275 N88-17633
New monostatic balanced Doppler velocimeter using a polarization preserving fiber
[PB88-130869] 11 p1480 N88-18895
Ground clutter processing for wind measurements with airport surveillance radars
[AD-A187708] 11 p1514 N88-19044
Retrieval of three-dimensional wind and temperature fields from single-Doppler radar data
12 p1646 N88-19858
Remote sensing of meteorological parameters with the aid of a clear-air Doppler radar
[PB88-142518] 12 p1647 N88-19864
Development and testing of the gust front algorithm
[AD-A189722] 14 p1949 N88-21622
A very wide frequency band pulsed/IF radar system
[NASA-CR-182889] 16 p2190 N88-23059
TDWR (Terminal Doppler Weather Radar) clutter residue map generation and usage
[AD-A191148] 16 p2235 N88-23352
Doppler radar with multiphase modulation of transmitted and reflected signal
[NASA-CASE-MSC-18808-1] 17 p2332 N88-23923
Observation of stratiform rain with 94 GHz and s-b and Doppler radar
[AD-A192013] 18 p2544 N88-25100
Aircraft/lidar turbulence comparison
18 p2546 N88-25111
The Federal Aviation Administration/Massachusetts Institute of Technology (FAA/MIT) Lincoln Laboratory Doppler weather radar program
18 p2547 N88-25118
TDWR (Terminal Doppler Weather Radar) PRF (Pulse Repetition Frequency) selection criteria
[AD-A193089] 21 p2932 N88-27407
Definition of long ocean wave slope for radar applications
[AD-A193198] 21 p2933 N88-27412
Application of acoustic-Doppler current profiler and expendable bathythermograph measurements to the study of the velocity structure and transport of the Gulf Stream
[NASA-CR-183188] 22 p3129 N88-28605
Application of the Hilbert transform to Doppler radar signals from a hypervelocity gun
[AD-A193690] 22 p3148 N88-28716
Airborne radar technology for windshear detection
[NASA-CR-183203] 23 p3236 N88-29257
The NAE atmospheric research aircraft
24 p3313 N88-29730
Doppler radar analysis of coastal marine atmospheric boundary layer structure during a cold air outbreak
[AD-A196023] 24 p3403 N88-30261
Utilization of a single clear-air Doppler radar beam to measure vertical divergence
[AD-A195543] 24 p3405 N88-30271

DORNIER AIRCRAFT
NT DO-28 AIRCRAFT

DORNIER DO-28 AIRCRAFT
U DO-28 AIRCRAFT

DOSAGE
NT RADIATION DOSAGE
Dexamethasone as prophylaxis for acute mountain sickness. Effect of dose level
[AD-A185848] 08 p1047 N88-16325
Low doses of atropine sulfate impair retention of a well-learned spatial task
[AD-A194065] 23 p3237 N88-29266
Heavy ion and proton tests for subsystem upset
[AD-A195267] 24 p3434 N88-30442

DOSE
U DOSAGE

DOSIMETERS
NT THRESHOLD DETECTORS (DOSIMETERS)
Low altitude flux and dose measurements during two solar flare events 01 p0111 N88-10713
Fabricate, calibrate and test a dosimeter for integration into the CRRES (Combined Release and Radiation Effects Satellite) satellite
[AD-A185439] 05 p0585 N88-13564
NBS (National Bureau of Standards) measurement services: Fricke dosimetry in high-energy electron beams
[PB88-110374] 06 p0781 N88-14795
An analytic model for ionization distributions produced in nanometer sites by protons
[DE88-003943] 10 p1406 N88-18385
Characterization of space radiation environment in terms of the energy deposition in functionally important volumes
[DE88-005627] 15 p2100 N88-22513
Anthropomorphic phantom radiation dosimetry at the NATO standard reference point at Aberdeen Proving Ground
[AD-A190508] 15 p2103 N88-22526
Dosimetric mapping inside Biorack --- Spacelab D1 mission 22 p3082 N88-28169
A study of the National Physics Laboratory microdosimetry research programme in collaboration with the University of Leeds (United Kingdom)
[NPL-RS(EXT)-93] 23 p3217 N88-29148

DOSIMETRY
U DOSIMETERS

DOUBLE BASE PROPELLANTS
NT DOUBLE BASE ROCKET PROPELLANTS
Nonlinear mechanisms of solid propellant combustion instability 19 p2628 N88-25588

DOUBLE BASE ROCKET PROPELLANTS
Ignition studies in a two-stage closed vessel using various igniter materials
[ISL-CO-231/86] 09 p1142 N88-16843
Combustion of a double base fuel in the presence of inert gases
[INPE-4516-RPE/564] 16 p2170 N88-22936

DOUBLE STARS
NT BINARY STARS
NT CATACLYSMIC VARIABLES
NT DWARF NOVAE
NT ECLIPSING BINARY STARS
NT NEMESIS (STAR)
Observation of a point source in Cygnus constellation with the underground detector at Frejus (France)
[PITHA-87/02] 20 p2864 N88-27122

DOUGLAS AIRCRAFT
NT DC 9 AIRCRAFT

DOUGLAS DC-9 AIRCRAFT
U DC 9 AIRCRAFT

DOUGLAS MILITARY AIRCRAFT
U MILITARY AIRCRAFT

DOVAP
U DOPPLER EFFECT

DOWNLINKING
Rapid toxicity detection in water quality control utilizing automated multispecies biomonitoring for permanent space stations 02 p0135 N88-10848
Analysis of the ICE combiner for multiple antenna arraying 04 p0436 N88-12704
MARCE data evaluation 10 p1286 N88-17693
X-band system performance of the very large array
11 p1473 N88-18789
Project SKYLITE: A design exploration
[AD-A187906] 11 p1511 N88-19030
INPE position paper on the CCSDS standardized method of link budget computation
[INPE-4533-NTE/279] 15 p2148 N88-22820
Satellite communications experiment for the Ontario air ambulance service 19 p2646 N88-25705
A VLSI single-chip (225,223) Reed-Solomon encoder with interleaver
[NASA-CASE-NPO-17280-1-CU]
21 p2902 N88-27220
A statistical rain attenuation prediction model with application to the advanced communication technology satellite project. 1: Theoretical development and application to yearly predictions for selected cities in the United States
[NASA-CR-179498] 23 p3205 N88-29077

DOWNWASH
Reduction of tilt rotor download using circulation control 10 p1271 N88-17605
A simple, analytic 3-dimensional downburst model based on boundary layer stagnation flow
[NASA-TM-100632] 22 p3042 N88-28058

DPCM (MODULATION)
U DIFFERENTIAL PULSE CODE MODULATION

DRAFTING (DRAWING)
Development of a line-drawing algorithm
[CS-8701] 01 p0082 N88-10530

DRAG
NT AERODYNAMIC DRAG
NT FRICTION DRAG
NT INTERFERENCE DRAG
NT PRESSURE DRAG
NT SATELLITE DRAG
NT SUPERSONIC DRAG
NT VISCOUS DRAG
Boundary effects on the drag of an oscillating sphere: Applications to the magnetic sphere rheometer. Attenuation and dispersion of acoustic waves in nematic liquid crystals 04 p0488 N88-13007
The drag of slender axisymmetric cones in rarefied hypersonic flow 05 p0531 N88-13229
Aerodynamic and propeller performance characteristics of a propfan-powered, semispan model
[NASA-TM-86705] 06 p0667 N88-14092
Propulsion challenges and opportunities for high-speed transport aircraft 08 p0958 N88-15809
Influence of base modifications on in-flight base drag in the presence of jet exhaust for Mach numbers from 0.7 to 1.5
[NASA-TP-2802] 11 p1488 N88-18881

Experimental investigation of hypersonic aerodynamics
[NASA-CR-182973] 18 p2458 N88-24591
Continuum theories for fluid-particle flows: Some aspects of lift forces and turbulence
[DE88-007038] 18 p2511 N88-24898
Drag measurements on a laminar flow body of revolution in Langley's 13 inch magnetic suspension and balance system
[NASA-CR-182909] 19 p2597 N88-25432
Ludwig Prandtl collected treatises on applied mechanics, hydro- and aerodynamics, part 2. IV interfaces and resistance
[NASA-TT-20315] 20 p2752 N88-26338
Why plasma armature railguns don't work (and what can be done about it)
[DE88-007900] 20 p2763 N88-26384
Experimental investigation of turbulent flow in smooth and longitudinal grooved tubes
[NASA-TM-77480] 20 p2800 N88-26615
Infrared detectors based on the photon drag effect and intersubband absorption by a two-dimensional electron gas 20 p2867 N88-27024

DRAG BALANCE
U AERODYNAMIC BALANCE
U LIFT DRAG RATIO

DRAG CHUTES
Discrete vortex analysis of unsteady flow about two-dimensional cambered plates
[DE88-006597] 14 p1909 N88-21407
Unsteady flow about cambered plates
[AD-A191226] 17 p2337 N88-239[illegible]5

DRAG COEFFICIENTS
An experimental evaluation of advanced rotorcraft airfoils in the NASA Ames eleven-foot transonic wind tunnel
[NASA-CR-166587] 03 p0261 N88-11640
The effect of sting interference at low speeds on the drag coefficient of an ellipsoidal body using a magnetic suspension and balance system
[NASA-CR-181611] 13 p1718 N88-20274

DRAG DEVICES
NT DRAG CHUTES
NT LEADING EDGE FLAPS
NT SPOILERS
NT TRAILING EDGE FLAPS
NT VORTEX FLAPS
NT WING FLAPS

DRAG EFFECT
U DRAG

DRAG MEASUREMENT
Flow field measurements using hotwire anemometry
[AD-A187029] 09 p1160 N88-16951
Precision measurement of the Fresnel drag coefficient using a ring laser
[AD-A196025] 24 p3366 N88-30043
Experimental determination of drag modifications due to elastic compliant surfaces using quantitative visual techniques
[AD-A194785] 24 p3372 N88-30082

DRAG REDUCTION
Transonic analysis and design of axisymmetric bodies in nonuniform flow
[NASA-CR-4101] 01 p0003 N88-10013
Investigations on a transonic airfoil with a 30 mm wide perforation/cavity arrangement
[ESA-TT-1072] 03 p0260 N88-11634
Navier-Stokes analysis of laminar flow control of a two-dimensional airfoil 05 p0540 N88-13286
Wakes of two dimensional bluff bodies in subsonic flow. Influence of a separating plate and of a pulsed injection of momentum
[IMFL-4200-86/75] 05 p0541 N88-13297
Combined riblet and lebu drag reduction system
[NASA-CASE-LAR-13286-1] 06 p0664 N88-14071
Turbulence, turbulence control, and drag reduction
[AD-A185643] 06 p0665 N88-14080
Flight and wind-tunnel measurements showing base drag reduction provided by a trailing disk for high Reynolds number turbulent flow for subsonic and transonic Mach numbers
[NASA-TP-2638] 06 p0701 N88-14299
Wall turbulence control 07 p0812 N88-14943
Overview of the Langley viscous drag reduction program 07 p0812 N88-14946
Natural laminar flow nacelle for transport aircraft
07 p0813 N88-14949
Flight research on natural laminar flow
07 p0813 N88-14950
Design and experimental evaluation of a swept supercritical Laminar Flow Control (LFC) airfoil
07 p0813 N88-14951
Riblets for aircraft skin-friction reduction
07 p0814 N88-14955
Airfoil large eddy breakup devices for turbulent drag reduction 07 p0814 N88-14956
Viscous drag reduction of horizontal plates
[VKI-TN-159] 07 p0851 N88-15171
Full scale and wind tunnel surface pressure measurements on the T.R.R.L. spray dispersion programme vehicles
[REPT-8623] 09 p1114 N88-16676
An application of active surface heating for augmenting lift and reducing drag of an airfoil
[NASA-TM-100563] 11 p1436 N88-18570
Structure of shear flow turbulence and its control
[AD-A187909] 11 p1482 N88-18846
Changes in the turbulent boundary layer structure associated with net drag reduction by outer layer manipulators
[NASA-CR-178152] 11 p1483 N88-18853
Flight tests of external modifications used to reduce blunt base drag
[NASA-TM-100433] 13 p1719 N88-20279
Investigation into the effects of flap end modifications on the performance of a wing with a single slotted flap
[BU-357] 14 p1866 N88-21148
Control of laminar flow around of the wing in free-air conditions
[AD-A187479] 15 p2013 N88-22004
Enhanced viscous flow drag reduction using acoustic excitation
[NASA-CR-182734] 15 p2062 N88-22295
Study of a system for reducing base drag by controlling vortices
[REPT-87/43] 17 p2295 N88-23730
An assessment of the drag reduction properties of riblets and the penalties of off-design conditions
[RAE-TM-AERO-2113] 17 p2295 N88-23731
High-flaps for natural laminar flow airfoils
17 p2296 N88-23739
Wind tunnel testing of low-drag airfoils
17 p2297 N88-23741
Flight experiences with laminar flow
17 p2297 N88-23744
Operational considerations for laminar flow aircraft
17 p2298 N88-23748
Injection of drag reducing additives into turbulent water flows
[AD-A192072] 18 p2509 N88-24888
Manipulation of the structure of a turbulent boundary layer 18 p2512 N88-24901
Aerodynamic analysis of natural laminar flow airfoil
19 p2634 N88-25624
Drag reduction of turbulent boundary layers by means [illegible]ved surfaces
[E[illegible]92618] 20 p2802 N88-26630
Investigations on drag reduction in turbulent pipe flows by addition of ionic and nonionic high polymers
[ETN-88-92380] 21 p2949 N88-27515
VSAERO analysis of tip planforms for the free-tip rotor
[NASA-CR-177487] 22 p3038 N88-28036
A new method of calculating the boundary layer characteristics downstream of manipulators. Part 1: Boundary layer integral parameters
[PNR90455] 22 p3078 N88-28279
A new method of calculating the boundary layer characteristics downstream of manipulators. Part 2: Skin friction and net drag reduction
[PNR90456] 22 p3078 N88-28280
A preliminary investigation of drag reduction and mechanism for a blunt body of revolution with slanted base
[NASA-TT-20349] 24 p3317 N88-29753
Compression pylon
[NASA-CASE-LAR-13777-1] 24 p3323 N88-29789
Development and design of windtunnel and test facility for RPV (Remote Piloted Vehicle) enhancement devices
[AD-A194842] 24 p3329 N88-29822
The viscous flow on surfaces with streamline riblets
[ESA-TT-1091] 24 p3370 N88-30067

DRAGULATORS
U BRAKES (FOR ARRESTING MOTION)

DRAINAGE
Open-graded bases for airfield pavements
[AD-A184461] 04 p0402 N88-12500
Partial likelihood analysis of time series models with application to rainfall-runoff data
[AD-A191157] 16 p2261 N88-23516
Characteristics of drainage determinations in aerial photographs and relief determination on different scales planialtimetric charts for three soils in the state of Sao Paulo 17 p2367 N88-24095
Criteria for planimetric and altimetric correction of maps restituted from aerial photographs in 1:100,000 scale
17 p2367 N88-24097
Use of remote sensing in the study of superficial formation certifying the development of integrated economy-ca[illegible] example: Rio Claro (SP) region
19 p2683 N88-25950

DRAINAGE PATTERNS
Hydrologic models for land-atmosphere retrospective studies of the use of LANDSAT and AVHRR data
[NASA-CR-182862] 20 p2818 N88-26716

DRAINING
U DRAINAGE

DRAWINGS
NT ENGINEERING DRAWINGS
PLOT3D (version-5): A computer code for drawing three dimensional graphs, maps and histograms, in single or multiple colours, for mono or stereoscopic viewing
[DE88-701410] 15 p2108 N88-22558

DREDGING
Use of SPOT HRV data in the US Army Corps of Engineers dredging program 22 p3109 N88-28466

DRIFT
Theoretical investigations of drift waves in a magnetic quadrupole 18 p2578 N88-25312

DRIFT (INSTRUMENTATION)
Testing of a gravimeter LCR G 785
[B8735061] 20 p2806 N88-26643

DRIFT RATE
Sea ice kinematics: Space and time scales
[AD-A191162] 17 p2376 N88-24128

DRILLING
Design and test of high performance composite tubes for use in deep water drilling and production systems
[SNIAS-872-430-107] 05 p0572 N88-13487
High performance composite tubes for offshore applications
[SNIAS-872-430-116] 05 p0572 N88-13488
Geological evolution and analysis of confirmed or suspected gas hydrate localities. Volume 9: Formation and stability of gas hydrates of the Middle America Trench
[DE88-001007] 10 p1347 N88-19050
Drilling metal matrix composites
[AD-A190480] 15 p2029 N88-22091

DRILLS
Investigation into the operation of the new special drills for drilling holes in thin components made of composite materials --- aircraft components
[LR-519] 16 p2215 N88-23215
Frequency Analysis of Acoustic Emission - Application to machining and welding
[DE88-701478] 18 p2570 N88-25262

DRINKING
Reverse osmosis treatment to remove inorganic contaminants from drinking water
[PB88-147780] 12 p1605 N88-19598
Variability in intake and dehydration in young men during a simulated desert walk
[AD-A192654] 22 p3131 N88-28613

DROGUE PARACHUTES
U DRAG CHUTES

DROGUES
U TOWED BODIES

DRONE AIRCRAFT
Towards the unmanned cockpit
02 p0129 N88-10812

DRONE HELICOPTERS
U DRONE AIRCRAFT
U HELICOPTERS

DRONE VEHICLES
NT DRONE AIRCRAFT
An efficient representation of spatial information for expert reasoning in robotic vehicles
09 p1214 N88-17278

DROP SIZE
Stability relationship for water droplet crystallization with the NASA Lewis icing spray
[NASA-TM-100220] 02 p0125 N88-10790
Drop formation from an orifice in an electric field
[DE87-014405] 03 p0322 N88-12034
Analysis of counting errors in the phase/Doppler particle analyzer
[NASA-TM-100231] 03 p0323 N88-12043
Anthropogenic effects on the droplet formation process, and ion concentrations in droplets --- clouds
08 p1018 N88-16175
Digital imaging techniques for single- and multi-phase reacting flowfields 10 p1327 N88-17933
Three-dimensional trajectory analyses of two drop sizing instruments: PMS OAP and PMS FSSP
[NASA-CR-4113] 11 p1437 N88-18574
Diagnostics for research in atomization and turbulent two-phase flows
[AD-A187338] 11 p1482 N88-18843
A propagation campaign in a marine environment utilizing a digital system at 36 GHz 12 p1618 N88-19675
Droplet size characteristics and energy input requirements of emulsions formed using high-intensity-pulsed electric fields
[DE88-005912] 15 p2128 N88-22682
Rainfall rates and drop-size distributions for environmental testing
[AD-A191342] 16 p2236 N88-23354

A theoretical model of the washout of trace gases by raindrops in the atmosphere 17 p2375 N88-24125

Small-droplet spray measurements with a scattered-light scanner
[NASA-TM-100973] 20 p2806 N88-26645

Experimental research of combustion systems
21 p2927 N88-27371

Cloud simulation warm cloud experiments: Droplet growth and aerosol scavenging
[AD-A192944] 21 p2974 N88-27666

Holographic determination of droplet size distributions
[DFVLR-MITT-88-05] 22 p3074 N88-28250

Alternative fuel spray behavior
24 p3345 N88-29912

Simulation study of spraying, streaming and vaporization phenomena associated with fuel injection
24 p3345 N88-29914

Multiple scattering effects in drop sizing of dense fuel sprays by laser diffraction 24 p3346 N88-29917

Influence of operating conditions on the atomization and distribution of fuel by air blast atomizers
24 p3346 N88-29918

DROP TESTS

Study of aeropropulsion laboratory pressure drop rig and recommended test procedure
[AD-A184333] 03 p0322 N88-12038

Decomposition of energetic materials on the drop-weight impact machine
[DE88-009154] 22 p3059 N88-28152

Calibration of quartz load cells: An in-situ procedure for instrumented falling weight impact machines
[NPL-DMA(A)-155] 22 p3081 N88-28297

DROP TOWERS

Study of the production of some superconducting and magnetic materials by solidification in the drop tube and drop tower
[NASA-CR-182494] 11 p1461 N88-18708

Critical point wetting drop tower experiment
[NASA-CR-183062] 20 p2798 N88-26603

DROP TUBES
U DROP TOWERS

DROP WEIGHT TESTS
U DROP TESTS

DROPS (LIQUIDS)
NT RAINDROPS

Cooling effect of a single evaporating droplet on a hot semi-infinite metal body
[PB87-201802] 01 p0046 N88-10294

Stability relationship for water droplet crystallization with the NASA Lewis icing spray
[NASA-TM-100220] 02 p0125 N88-10790

Ignition and flame propagation in sprays
[AD-A184679] 03 p0283 N88-11781

A method for remote sensing of precipitable water vapor and liquid in the atmosphere using a 22-ghz radiometer
[AD-A184204] 03 p0354 N88-12232

Experimental evidence for modifying the current physical model for ice accretion on aircraft surfaces
[NASA-TM-87184] 04 p0397 N88-12473

The TAB method for numerical calculation of spray droplet breakup
[DE87-011756] 04 p0442 N88-12743

Energy balance in laser-irradiated vaporizing droplets
[DE88-000525] 04 p0449 N88-12782

Numerical simulation of splash of droplet at unit gravity 05 p0538 N88-13275

Operating envelopes of particle sizing instrumentation used for icing research
[NASA-CR-180870] 05 p0586 N88-13573

A study of the interaction of laser light with liquid propellant drops
[AD-A185117] 05 p0587 N88-13582

Extinction by dielectric particles at optical and infrared wavelength
[AD-A184818] 05 p0650 N88-13981

Undercooling and nucleation in iron nickel alloys
[AD-A185500] 06 p0683 N88-14184

Atmospheric science 07 p0883 N88-15357

Spray deposition: A fundamental study of droplet impingement, spreading and consolidation
[AD-A186627] 08 p0970 N88-15869

Investigation of real-time two-dimensional visualization of fuel spray liquid/vapor distribution via exciplex fluorescence
[AD-A188208] 10 p1307 N88-17816

Transient cooling of a hot surface by droplets evaporation, March 1986 - March 1987
[PB88-153341] 10 p1330 N88-17950

Droplet formation for liquid monopropellant jets
[AD-A187172] 10 p1331 N88-17956

Turbulence interactions in single- and multi-phase turbulent mixing and combustion processes
[AD-A187505] 10 p1332 N88-17960

Three-dimensional trajectory analyses of two drop sizing instruments: PMS OAP and PMS FSSP
[NASA-CR-4113] 11 p1437 N88-18574

Electrohydrodynamic migration of charged droplets in an insulating fluid
[NASA-TM-100849] 14 p1912 N88-21424

Laser induced ignition of propellants
[AD-A191100] 16 p2168 N88-22927

Rainfall rates and drop-size distributions for environmental testing
[AD-A191342] 16 p2236 N88-23354

Method of evaporation
[NASA-CASE-NPO-15609-2] 17 p2318 N88-23846

Liquid droplet radiator development
17 p2424 N88-24415

The liquid droplet radiator in space: A parametric approach 17 p2427 N88-24437

Tower evaporator
[NASA-CASE-NPO-15609-2] 18 p2497 N88-24815

The behavior of drop-containing turbulent eddies
[AD-A191669] 18 p2509 N88-24883

Simple high speed camera with CCD-sensor
[MPIS-8/1987] 18 p2518 N88-24940

Hanging drop crystal growth apparatus and method
[NASA-CASE-MFS-28206-1-SB]
18 p2585 N88-25356

Crystal growth apparatus
[NASA-CASE-MFS-28182-1] 18 p2585 N88-25357

Droplet formation for liquid monopropellant jets
19 p2623 N88-25557

Fuel droplet vaporization and temperature distributions of axisymmetric unsteady sprays
19 p2626 N88-25579

Small-droplet spray measurements with a scattered-light scanner
[NASA-TM-100973] 20 p2806 N88-26645

Numerical simulation of fuel droplet interactions and breakup
[AD-A192431] 21 p2941 N88-27470

Combustion studies of acoustically suspended liquid droplets
[AD-A193892] 23 p3192 N88-28998

High energy and high intensity laser effects on aerosols: Changes in droplet morphology, surrounding temperature and vapor concentration
[AD-A193625] 23 p3220 N88-29164

Influence of the convection on evaporation and combustion of a fuel droplet 24 p3351 N88-29948

General equations for the motions of ice crystals and water drops in gravitational and electric fields
[NASA-CR-183229] 24 p3370 N88-30070

DROSOPHILA

Drosophila geotaxis as a tool for the study of aging
10 p1288 N88-17706

Effects of short spaceflights on Drosophila melanogaster embryogenesis and life span 22 p3061 N88-28166

DROUGHT

Enhancement of surface-atmosphere fluxes by desert-fringe vegetation through reduction of surface albedo and of soil heat flux
[NASA-CR-181442] 02 p0197 N88-12231

Application of multitemporal SPOT data for crop monitoring: Effects of frost and drought
03 p0344 N88-12171

Drought: solar activity link established by Leningrad geophysicists 04 p0458 N88-12835

A drought watch system
[WCP-134] 16 p2234 N88-23345

Using space photography of the Earth in the classroom: Drought in Africa
[NASA-CR-182948] 19 p2685 N88-25960

DROUGHT CONDITIONS
U DROUGHT

DROWSINESS
U SLEEP

DRUG THERAPY
U CHEMOTHERAPY

DRUGS
NT ADRENERGICS
NT ANTIBIOTICS
NT ANTICONVULSANTS
NT ATROPINE
NT CAFFEINE
NT EPINEPHRINE
NT ERGOTAMINE
NT HEMOSTATICS
NT MORPHINE
NT NOREPINEPHRINE
NT PSYCHOTROPIC DRUGS
NT SEDATIVES
NT SEROTONIN
NT STIMULANTS
NT TRANQUILIZERS

Effect of pyrocetam on mouse resistance to hypoxic hypoxia 2-3 months after exposure to X-radiation
07 p0895 N88-15425

Dexamethasone as prophylaxis for acute mountain sickness: Effect of dose level
[AD-A185848] 08 p1047 N88-16325

Efficiency of human workers and means to increase it
12 p1666 N88-19986

A cardiostimulant protein from the Australian Red Waratah Sea anemone, Actinia tenebrosa
18 p2550 N88-25138

Measurement and classification of the mode of action of antidepressant drugs 21 p2983 N88-27714

Measurement of electrical activity in the CNS with cortical evoked potentials and EEG: Efficacy profiles of drugs using factor analysis 21 p2983 N88-27715

An approach to studying the effects of psychostimulants on cerebral electrical activity in the non-human primate
21 p2983 N88-27716

Emetic mechanism in acute radiation sickness
[AD-A194102] 23 p3238 N88-29267

DRUMLINS
U GLACIAL DRIFT

DRUMS (CONTAINERS)

Containment of a silicone fluid free surface in reduced gravity using barrier coatings
[NASA-TM-101314] 24 p3371 N88-30072

DRY CELLS
NT NICKEL ZINC BATTERIES

DRY FRICTION

Dry adhesive friction of elastomers: A study of the fundamental mechanical aspects
[ETN-88-92903] 23 p3198 N88-29036

DRY HEAT

Geothermal energy technology issues, R and D (Research and Development) and cooperative arrangements
[PB88-193107] 21 p2967 N88-27626

DRYING
NT DEHUMIDIFICATION
NT DEHYDRATION

Effect of the band-gap characteristics on laser-induced dry etching of semiconductors
[DE88-001853] 07 p0937 N88-15695

The mechanical behavior of particle filled thermoplastics
[ETN-88-92234] 16 p2181 N88-22999

Impact of control errors on the volume/weight demand of the Ventilation and Dryer (VAD) concept --- EURECA Botany Facility
[TN-RB524-006/87] 17 p2377 N88-24132

Prospects for hot dry rock in the future
[DE88-010909] 20 p2820 N88-26730

Ellipsometric imaging of drying sol-gel films
[DE88-011785] 21 p2921 N88-27335

DTA (ANALYSIS)
U THERMAL ANALYSIS

DTMB-111 GROUND EFFECT MACHINE
U GROUND EFFECT MACHINES

DTMB-430 GROUND EFFECT MACHINE
U GROUND EFFECT MACHINES

DUAL MODE PROPULSION
U HYBRID PROPULSION

DUALITY PRINCIPLE

An extension of the MS pivoting rule to capacitated network flow problems
[REPT-87-33] 14 p1963 N88-21711

DUALITY THEOREM

Position finding and tolerances
[AD-A187685] 11 p1540 N88-19205

Action-angle maps and scattering theory for some finite-dimensional integrable systems. The pure solution case
[CWI-PM-R8704] 13 p1831 N88-20955

Lagrangian of the self-duality equation and d = 10, N = 2b supergravity
[DE88-701554] 24 p3455 N88-30563

DUCTED FANS

Velocity scaled aeroelastic testing of an unducted fan
[GTL-191] 05 p0548 N88-13337

A dynamic simulation and feedback control scheme for the U.S. Marine Corps' Airborne Remotely Operated Device (AROD)
[AD-A186597] 08 p0953 N88-15784

Aerodynamic performance of a scale-model, counter-rotating unducted fan 10 p1282 N88-17666

Airborne remote operated device
[DE88-010324] 21 p2895 N88-27188

DUCTED FLOW

Flow field measurements in a 90 degree turning duct
02 p0186 N88-11157

Mixed turbulent convective heat transfer in vertical ducts 11 p1485 N88-18865

A survey of oscillating flow in Stirling engine heat exchangers
[NASA-CR-182108] 15 p2067 N88-22322

An investigation of ducted propellers in axisymmetric shear flow 16 p2202 N88-23136

Surface curvature and pressure gradient effects on turbulent flow: An assessment based on numerical solution of the Reynolds equations 17 p2338 N88-23954

Antenna heights for the optimum utilization of the oceanic evaporation duct. Part 3: Results from the Mediterranean measurements, volume 2
[AD-A192311] 20 p2791 N88-26554
Antenna heights for the optimum utilization of the oceanic evaporation duct. Part 1: Results from the Pacific measurements. Part 2: Results from the Key West measurements, volume 1
[AD-A192358] 20 p2791 N88-26555
DUCTED PROPELLERS
U SHROUDED PROPELLERS
DUCTED ROCKET ENGINES
Speed control of a missile with throttleable ducted rocket propulsion 12 p1597 N88-19561
An experimental investigation of rocket ramjet nozzle assembly base pressures
[AD-A189714] 15 p2027 N88-22076
DUCTILITY
Investigation on ductile fracture behavior of 3-inch diameter Type 304 stainless steel pipe with a circumferential through-wall crack
[DE87-753016] 02 p0191 N88-11196
Ultra-fine grained alloy material
[AD-A184500] 03 p0290 N88-11820
Modified 14Cr-16Ni stainless steels with improved creep resistance at 700 C due to tailored precipitate microstructures
[DE87-014788] 03 p0290 N88-11825
Welding and weldability of ductile intermetallic alloys
[DE87-014061] 04 p0416 N88-12582
Investigation by differential scanning calorimetry of microstructure in a superplastic Al-Mg-Zr alloy
[AD-A184902] 05 p0564 N88-13439
An investigation of fatigue crack growth in a ductile material at high growth rates 06 p0715 N88-14383
Sulfur-induced ductility-dip cracking in weld metal of low-carbon steel
[PB87-143814] 07 p0833 N88-15051
J-estimation procedure based on moire interferometry data
[AD-A185965] 07 p0867 N88-15258
The relationship of tensile specimen size and geometry effects to unique constitutive parameters for ductile materials
[AD-A186020] 08 p0994 N88-16012
The influence of small defects on tensile specimen ductility and symmetry of deformation
[AD-A187983] 10 p1346 N88-18044
Brittle to ductile transition to cleavage fracture
[DE88-004074] 10 p1420 N88-18481
Effects of sulfur content on the plain strain fracture toughness of inertia welds in 4340 steel
[AD-A188192] 11 p1458 N88-18689
A simulation of void lining during ductile fracture
[AD-A188404] 12 p1635 N88-19792
Material instabilities in solids
[AD-A189525] 13 p1738 N88-20388
Development of a constitutive equation for HSLA (High-Strength Low-Alloy)-100 at cryogenic temperatures
[AD-A189243] 13 p1740 N88-20408
Ductile failure
[AD-A189429] 13 p1781 N88-20654
The effect of strain rate on the strength and ductility of SiCw/2124 Al composite
[CUEL-1692/87] 14 p1924 N88-21466
The effective fracture toughness of aluminum at rapid heating rates
[AD-A189745] 15 p2038 N88-22146
The variation of torsional ductility of high purity aluminum with temperature and strain rate
[DE88-005618] 18 p2487 N88-24755
Theoretical and experimental damping values of piping systems at high ductilities
[DE88-006717] 18 p2526 N88-24986
Extended ductility of Al and alpha-Fe alloys through dynamic recovery mechanisms
[DE88-008679] 19 p2616 N88-25522
Optimizing superplastic response in lithium containing aluminum-magnesium alloys
[AD-A192217] 20 p2774 N88-26451
Ductile-brittle transition of cutting behavior in diamond turning of single crystal Si
[DE88-008890] 20 p2809 N88-26664
Microchemical analysis of polycrystalline Ni3Al and other ordered alloys using the field-ion microscope atom probe
[DE88-011519] 21 p2914 N88-27294
Plastic yielding at crack tips
[AD-A192549] 21 p2960 N88-27582
Experimental investigation of ductile fracture by white light moire interferometry 22 p3087 N88-28329
Load interaction effects on compression fatigue crack growth in ductile solids
[FFA-TN-1988-12] 22 p3089 N88-28342
Modeling of micromechanisms of fatigue and fracture in hybrid materials
[AD-A195604] 24 p3382 N88-30142
DUCTS
NT ACOUSTIC DUCTS
NT AIR DUCTS
NT ANNULAR DUCTS
Ducted propeller design and analysis
[DE88-001925] 06 p0664 N88-14069
Aeropropulsion '87. Session 3: Internal Fluid Mechanics Research
[NASA-CP-10003-SESS-3] 08 p0954 N88-15790
Inlets, ducts and nozzles 08 p0955 N88-15791
An estimate of the noise shielding on the fuselage resulting from installing a short duct around an advanced propeller
[NASA-TM-100262] 10 p1405 N88-18379
Unsteady heat transfer in turbine blade ducts: Focus on combustor sources
[NASA-TM-100815] 11 p1486 N88-18870
Electromagnetic propagation in PEC and absorbing curved S-ducts
[NASA-TM-100833] 12 p1621 N88-19698
Flow/acoustic interaction in duct inflow
[AD-A189264] 13 p1833 N88-20967
Numerical and experimental investigation of multiple shock wave/turbulent boundary layer interactions in a rectangular duct
[AD-A190772] 15 p2066 N88-22320
ALEX results: A comparison of measurements from a round and a rectangular duct with 3-D code predictions
[DE88-005947] 15 p2135 N88-22741
Numerical analysis of duct flow using three-dimensional parabolized Navier-Stokes equation
19 p2638 N88-25652
MHD (magnetohydrodynamic) thermal hydraulic analysis of three-dimensional liquid metal flows in fusion blanket ducts
[DE88-009929] 19 p2731 N88-26219
Steady and unsteady internal flow computations via the solution of the compressible Navier Stokes equations for low Mach numbers 23 p3209 N88-29100
Optical measurement of unducted fan blade deflections
[NASA-TM-100966] 23 p3216 N88-29142
DUMMIES
Determination of the effect of walking on the forced convective heat transfer coefficient using an articulated mannikin
[AD-A186452] 08 p1049 N88-16335
User's guide: Lower neck transducer for the Hybrid 3 dummy
[PB88-133319] 12 p1628 N88-19743
Evaluation tests of lower neck transducer for the Hybrid 3 Dummy
[PB88-133327] 12 p1628 N88-19745
Anthropomorphic phantom radiation dosimetry at the NATO standard reference point at Aberdeen Proving Ground
[AD-A190508] 15 p2103 N88-22528
DUMMY LOADS
U IMPEDANCE
U OUTPUT
DUMP COMBUSTORS
Flame driving of longitudinal instabilities in liquid fueled dump combustors
[AD-A183536] 01 p0006 N88-10033
DUNES
Environmental processes and spectral reflectance characteristics associated with soil erosion in desert fringe regions
[NASA-CR-182332] 05 p0620 N88-13811
Dune fields in central Western Argentina
17 p2366 N88-24086
A bibliography of dunes: Earth, Mars, and Venus
[NASA-CR-4149] 20 p2885 N88-27134
Discrimination of sand transport rates and environmental consequences in central Egypt from SPOT data
22 p3093 N88-28366
Preliminary comparative analysis of LANDSAT and SPOT data for the study of the sanding phenomenon: Zaafrane region (Algeria) 22 p3099 N88-28402
DUNGEYS WIND SHEAR MECHANISM
U WIND SHEAR
DUPLICATING
U REPRODUCTION (COPYING)
DURABILITY
Durability (lifetime) predictions adhesively bonded structures
[AD-A184069] 03 p0335 N88-12110
Work-in-progress presented at the Army Symposium on Solid Mechanics, 1986: Lightening of the Force
[AD-A184791] 04 p0427 N88-12644
Durability of powdered aluminum structures
04 p0429 N88-12655
High polymer sensor materials discussed
06 p0676 N88-14140
Experimental determination of crack growth rates in cyclic stress applications, for improving the forecasted computed durability in operation
[FF-14/1986] 09 p1182 N88-17085
The effect on initial bond strength and durability of a Phosphoric Acid Dip (PAD) following chromic acid anodising of aluminum
[ARE-TM(UMM)-87402] 10 p1300 N88-17772
Advanced durability analysis. Volume 1: Analytical methods
[AD-A188341] 12 p1635 N88-19789
Durability testing of an iridium-plated storable rocket engine injector
[AD-A190707] 15 p2027 N88-22078
Computational structural mechanics for engine structures 15 p2080 N88-22399
Durability of continuous fiber reinforced metal matrix composites
[AD-A193868] 22 p3050 N88-28097
Predicting the durability of adhesives and coatings by remote detection of hidden defects and coating-thickness irregularities: A theoretical and numerical study
24 p3355 N88-29972
DURATION
U TIME
DUST
NT COSMIC DUST
NT INTERPLANETARY DUST
NT TERRESTRIAL DUST BELT
NT ZODIACAL DUST
Stratospheric particles: Synchrotron X-ray fluorescence determination of trace element contents
[DE87-012482] 02 p0198 N88-11234
Circumstellar shells, the formation of grains, and radiation transfer 02 p0252 N88-11596
Physics and chemistry 07 p0883 N88-15359
Particle-gas temperature differentials resulting from time-dependent radiative-conductive heat flux divergences in the tenuous dust-laden atmosphere of mars
[AD-A185888] 07 p0945 N88-15747
Aerosols in Martian Atmosphere and Natural Dust Observation (AMANDO). Proposal for the Mars orbiter balloon and rover to study the Martian atmosphere, its thermal content, and its interaction with the soil
[IFSI-87-9] 08 p1100 N88-16619
Christiansen effect in infrared spectra of soil-derived atmospheric dusts
[AD-A187071] 09 p1248 N88-17479
Operation of gas turbine engines in dust-laden environments 10 p1280 N88-17654
Simulation of the plasma interaction with thin dust clouds 11 p1552 N88-19291
How dirty is Mars' North Polar cap, and why isn't it black 23 p3303 N88-29677
The surface composition of Mars from earthbased observations 23 p3306 N88-29696
AGN (OIII) emission line profiles: Dependencies on galaxy inclination and Balmer decrement
[INPE-4596-PRE/1324] 24 p3459 N88-30577
DUST COLLECTORS
Characteristics of pressure loss during filtration using a porous ceramic filter
[DE88-752547] 20 p2798 N88-26804
DWARF NOVAE
SW UMa and V426 Oph: EXOSAT surprises
19 p2740 N88-26269
Regular orbital variations in the ultraviolet resonance lines of YZ Cnc
[MPE-PREPRINT-117] 22 p3165 N88-28850
The ultrashort period dwarf nova SW Ursae Majoris
24 p3453 N88-30553
DWARF STARS
NT DWARF NOVAE
NT FLARE STARS
NT RED DWARF STARS
The atmospheres of M dwarfs: Observations
02 p0253 N88-11601
M dwarfs: Theoretical work 02 p0253 N88-11602
The photospheric magnetic fields of cool stars: Recent results of survey and time-variability programs
04 p0503 N88-13094
Angular momentum evolution of young stars
04 p0504 N88-13099
Post-zero-age main sequence rotation
04 p0504 N88-13100
Atmospheres of stars in the limits of thin and thick convection zones: The M dwarfs
04 p0505 N88-13104
Differential B and V light curves of the bright BY Draconis star HD80715 04 p0509 N88-13130
Broadband linear polarization and chromospheric CaII H and K line emission in late-type main sequence stars
04 p0511 N88-13140
The onset of chromospheric activity among the A- and F- type stars 04 p0511 N88-13144

Empirical relations between photospheric magnetic fields and atmospheric radiative losses for cool dwarf stars 04 p0511 N88-13145

VLA observations of the X-ray bright Hyades M-dwarfs 04 p0512 N88-13147

MHD energy fluxes for late type dwarfs 04 p0512 N88-13148

A search for very low mass (brown dwarf) stars as wide binaries using a seven element infrared camera-photometer 04 p0512 N88-13150

Chromospheric and coronal heating in a bias-free sample of K dwarfs 04 p0518 N88-13184

Measurements of stellar magnetic fields: Empirical constraints on dynamo and rotational evolution theories 04 p0518 N88-13185

M dwarfs from the Einstein medium sensitivity survey 04 p0519 N88-13188

Duplicity in the solar neighborhood. Part 3: New spectroscopic elements for nine solar-type binary stars [SER-C-PREPUBL-FASC-18-PT-3] 18 p2592 N88-25405

Molecular hydrogen in galaxies 23 p3299 N88-29645

Duplicity in the solar neighborhood. Part 4: Spectroscopic orbits for four dwarf M stars [SER-C-PREPUBL-FASC-21] 24 p3454 N88-30561

DYADICS

Statistical analysis of dyadic stationary processes [AD-A193057] 21 p3009 N88-27853

DYE LASERS

Status, development of laser devices in China 03 p0303 N88-11907

Laser induced fluorescent study of relativistic electron beams [AD-A184456] 04 p0447 N88-12774

All-optical beam control by forced Rayleigh scattering [AD-A184315] 04 p0490 N88-13018

Laser action from syn-(methyl,methyl) bimane [AD-A186314] 07 p0858 N88-15211

Time characteristics of travelling wave lasing with two-photon picosecond optical pumping 07 p0918 N88-15578

Study of kinetics of intracavity absorption in pulsed dye lasers 07 p0919 N88-15585

Characteristics of LKI-501 tunable dye laser with dyes in solid matrix 07 p0920 N88-15587

Dye laser for holographic interferometry 07 p0920 N88-15588

Energy disposal in ion-molecule reactions [AD-A186772] 09 p1171 N88-17019

Dye lasers pumped by radiation from high-power semiconductor lasers 09 p1237 N88-17417

Photoionization dynamics of excited molecular states [DE88-002982] 09 p1246 N88-17468

Product kinetic and internal energy distributions via velocity-aligned Doppler spectroscopy [DE88-003510] 10 p1298 N88-17764

Modern pulsed wavemeters [DE88-003875] 10 p1335 N88-17978

Nonlinear optics with broad-band lasers [DE88-005026] 10 p1337 N88-17992

Instabilities and chaos in a multimode, standing-wave, CW dye laser [DE88-005028] 10 p1337 N88-17993

Studies of fluorine combustion [AD-A187646] 11 p1452 N88-18656

Diode pumped fiber laser [AD-A187694] 11 p1491 N88-18902

Quenched-laser operation of a Littman dye oscillator [DE88-004020] 11 p1493 N88-18915

Resonantly-enhanced, four-photon ionization of krypton at laser intensities exceeding 10(12) W/sq cm [DE88-005038] 11 p1544 N88-19229

Discharge excitation of dye vapors [AD-A188428] 12 p1632 N88-19770

Resonance energy transfer between carbon monoxide and oxygen molecules using dye laser intracavity absorption spectroscopy [AD-A188488] 12 p1689 N88-20104

Instrumentation for collisional energy transfer studies [AD-A188495] 12 p1689 N88-20105

Doubly periodic output from a dye laser pumped by a free-running argon laser [DE88-005027] 13 p1778 N88-20633

XeCl laser-pumped nanosecond dye lasers 14 p1902 N88-21359

A picosecond tunable ultrashort cavity dye laser 14 p1902 N88-21361

Theoretical study of colliding pulse mode-locking in dye lasers 14 p1903 N88-21366

Time characteristics of ultrashort light pulses from dye lasers with distributed feedback 14 p1970 N88-21759

Solid hosts for dye laser rods. Part 1: Criteria for choosing a host material [DE88-006478] 15 p2072 N88-22355

Efficient narrow linewidth waveguide dye laser pumped by CuCl laser 16 p2187 N88-23038

XUV source for ultra-high resolution photoionization spectroscopy [DE88-007531] 19 p2614 N88-25510

A plasma ultraviolet source for short wavelength lasers [AD-A192844] 21 p2952 N88-27537

DYES

Saturable absorbers for colliding pulse-locked Nd:YAG lasers 03 p0302 N88-11902

Characteristics of LKI-501 tunable dye laser with dyes in solid matrix 07 p0920 N88-15587

Nonlinear optical waveguides containing a transition metal-based dye molecule [DE88-003257] 11 p1550 N88-19275

Evidence for laser emission from the TICT exciplex of coumarin dyes [DE88-702544] 23 p3220 N88-29167

DYNAMIC CHARACTERISTICS

NT AERODYNAMIC DRAG
NT AERODYNAMIC STABILITY
NT AIRCRAFT STABILITY
NT BOUNDARY LAYER STABILITY
NT COMBUSTION STABILITY
NT CONTROL STABILITY
NT DIRECTIONAL STABILITY
NT DRAG
NT DYNAMIC PRESSURE
NT DYNAMIC STABILITY
NT FLAME STABILITY
NT FLOW CHARACTERISTICS
NT FLOW DISTRIBUTION
NT FLOW STABILITY
NT FLOW VELOCITY
NT FREQUENCY STABILITY
NT FRICTION DRAG
NT GYROSCOPIC STABILITY
NT INTERFERENCE DRAG
NT INTERFERENCE LIFT
NT JET LIFT
NT LATERAL STABILITY
NT LIFT
NT LONGITUDINAL STABILITY
NT LOW SPEED STABILITY
NT MAGNETOHYDRODYNAMIC STABILITY
NT MOTION STABILITY
NT PRESSURE DRAG
NT ROTARY STABILITY
NT SATELLITE DRAG
NT SOLAR WIND VELOCITY
NT SPACECRAFT STABILITY
NT SUPERSONIC DRAG
NT TRANSIENT RESPONSE
NT VISCOUS DRAG
NT ZERO LIFT

Determination of the dynamic parameters of annular clearances with turbulent flow and incompressible media [ETN-87-90434] 01 p0047 N88-10303

Contribution to the dynamical analysis of rheolinear nonconservative, gyroscopic systems using finite element methods [ETN-87-90410] 01 p0050 N88-10320

Exact solution of the inverse problem for a six-link manipulator with a mechanical offset [DE87-702646] 01 p0054 N88-10349

Structure-dependent matrix representation of manipulator kinematics and its inverse solution [DE87-752966] 02 p0229 N88-11447

Dynamic image interpretation for autonomous vehicle navigation [AD-A184043] 03 p0262 N88-11647

The structure and reactivity of heterogeneous surfaces and study of the geometry of surface complexes [DE88-000158] 03 p0279 N88-11754

Hovering helicopter flight dynamics: A study of vertical motion [AR 004-526] 04 p0399 N88-12485

Dynamics of cables and chains 05 p0610 N88-13747

Molecular dynamics studies of aromatic hydrocarbon liquids [DE88-001473] 05 p0643 N88-13973

Dynamic processes in field-reversed-configuration compact toroids [DE87-014756] 05 p0652 N88-13998

Studies of the structural dynamic behavior of satellite antenna system [AD-A185526] 06 p0673 N88-14121

Gas diffusion studies in steady and nonsteady cavities [AD-A185795] 06 p0704 N88-14318

On the pairing process in an excited, plane, turbulent mixing layer [AD-A186355] 07 p0850 N88-15157

Blade vibration due to different flow excitation 07 p0851 N88-15166

Data acquisition, reduction and analysis of shock and vibration testing using a super microcomputer [AD-A186123] 07 p0867 N88-15260

State-of-the-art for assessing earthquake hazards in the United States. Report 26: Parameters for specifying magnitude-related earthquake ground motions [AD-A185997] 07 p0877 N88-15319

Global bifurcation of periodic solutions with symmetry [AD-A185881] 07 p0908 N88-15501

Critical analysis of the dynamic behavior laws for metallic materials -- ballistics [ISL-NB-401/86] 08 p0969 N88-15862

Method of iterative coupling between periodic aerodynamic and dynamic fields [PB87-169934] 09 p1113 N88-16669

Predicting dynamic separation characteristics of general configurations [AD-A186689] 09 p1116 N88-16691

Experimental and theoretical study on cavitation inception and bubbly flow dynamics. Part 1: Design, development and operation of a cavitation susceptibility meter. Part 2: Linearized dynamics of bubbly and cavitating flows with bubble dynamics effects [AD-A187133] 09 p1160 N88-16952

Dynamic analysis of multimesh-gear helicopter transmissions [NASA-TP-2789] 09 p1176 N88-17045

Frequency response functions of a nonlinear system 09 p1180 N88-17070

Optimal correction problem of a multidimensional stochastic system [AD-A186727] 09 p1228 N88-17353

An evaluation of project scheduling techniques in a dynamic environment [AD-A187057] 09 p1260 N88-17554

Mechanisms of wear in single- and two-phase materials [DE88-003846] 10 p1305 N88-17806

The dynamics of two coupled rigid bodies [AD-A187592] 10 p1341 N88-18012

The dynamics of coupled planar rigid bodies. Part 1: Reduction, equilibria and stability [AD-A187467] 10 p1345 N88-18042

Collaborative studies of polar cap ionospheric dynamics [AD-A187888] 10 p1355 N88-18098

Energy transfers for multilayer hydrodynamic ocean models: General formulation and specific examples [AD-A187604] 10 p1358 N88-18116

Dynamic observers as asymptotic limits of recursive filters: Special cases [AD-A187578] 10 p1397 N88-18324

Growth and electronic properties of strained metal overlayers [DE87-010956] 10 p1417 N88-18463

State-of-the-art for assessing earthquake hazards in the US. Parameters for specifying intensity-related earthquake ground motions [AD-A188230] 11 p1512 N88-19032

Implementing dynamic arrays: A challenge for high-performance machines [AD-A188142] 11 p1533 N88-19157

Picosecond laser studies of excited state processes [AD-A189606] 12 p1607 N88-19607

Dynamics of small and large scale irregularities at sub-auroral latitudes [AD-A189052] 12 p1645 N88-19853

A numerical analysis of the dynamics of PRIZ operation [AD-A188853] 12 p1678 N88-20035

A study of methods to predict and measure the transmission of sound through the walls of light aircraft [NASA-CR-182656] 12 p1687 N88-20090

Dynamics of high-speed mechanisms with elastic members 13 p1779 N88-20643

Large-scale ocean dynamics 14 p1938 N88-21562

The effects of torque response and time delay on rotorcraft vertical axis handling qualities [AD-A189873] 15 p2017 N88-22023

KRASH parametric sensitivity study: Transport category airplanes [AD-A189962] 15 p2017 N88-22024

Nonlinear analysis and optimal design of dynamic mechanical systems for spacecraft application [AD-A190644] 15 p2026 N88-22070

Molecular dynamics of materials possessing high energy content [AD-A190034] 15 p2034 N88-22118

Unsteady flow field measurements using LDV (Laser Doppler Velocimetry) [AD-A189907] 15 p2063 N88-22298

The CRREL (Cold Regions Research and Engineering Laboratory) Hopkinson bar apparatus [AD-A190599] 15 p2077 N88-22380

Railgun rail gouging by hypervelocity sliding contact
[DE88-006866] 16 p2166 N88-22916

The nonlinear dynamics of a spacecraft coupled to the vibration of a contained fluid
[DE88-007035] 16 p2168 N88-22925

North Carolina Biomolecular Engineering and Materials Applications Center (NC-BEMAC)
[AD-A190923] 16 p2237 N88-23364

Dynamic characteristics of a vibrating beam with periodic variation in bending stiffness
[NASA-TP-2697] 17 p2348 N88-23988

Time-frequency representations for speech signals
[AD-A188661] 18 p2499 N88-24819

A dynamic analysis of piezoelectric strained elements
[AD-A191478] 18 p2503 N88-24851

Infinite dimensional dynamical systems and their finite dimensional analogues
[AD-A192041] 18 p2563 N88-25216

A constraint algorithm for maintaining rigid bonds in molecular dynamics simulations of large molecules
[AD-A191663] 18 p2572 N88-25277

Theoretical studies of dynamics combustion
[DE88-007565] 19 p2611 N88-25495

The MUF (Maximum Usable Frequency) (3000) as an indicator for F-region variations
[AD-A191655] 19 p2690 N88-25991

Half collision studies of inelastic energy transfer processes
[DE88-008096] 19 p2724 N88-26178

Decision aiding and coordination in decision-making organizations
[AD-A191950] 19 p2736 N88-26259

On the dynamic behavior of balloon during its launch; application of panel method and extension to unsteady problem
[ISAS-RN-622] 20 p2751 N88-26330

Numerical simulation of fuel droplet interactions and breakup
[AD-A192431] 21 p2941 N88-27470

Coupled experimental and theoretical investigations of instability, chaos and turbulence in an axisymmetric jet flow
[AD-A192943] 21 p2942 N88-27476

An analysis of horizontal temperature gradients and heat content in the mixed layer and the surface forcing during PATCHEX
[AD-A192330] 21 p2976 N88-27678

Research in applied mathematics
[AD-A192385] 21 p3004 N88-27820

Literal dynamic modeling
[REPT-881-440-114] 22 p3048 N88-28083

The dynamic behavior of a turbulent boundary layer subjected to a shock-induced separation
[AD-A194164] 22 p3075 N88-28252

Reaction dynamics on semiconductor surfaces
[AD-A194305] 22 p3156 N88-28781

Spallation and dynamic fracture as an effect of laser induced shock-waves
[AD-A193513] 23 p3188 N88-28971

A multiple-scales partial solution of the pulse-forced Rayleigh-Plesset equation of cavitation bubble dynamics
[AD-A193733] 23 p3212 N88-29118

Interactions between synoptic and planetary scales of motion
[AD-A192328] 23 p3234 N88-29246

Transformations of short-term visual memory
[AD-A193873] 23 p3241 N88-29290

The acoustic field scattered from some approximate pressure release materials
[AD-A194766] 23 p3278 N88-29515

A dynamic analysis of piezoelectric strained elements
[AD-A196079] 24 p3432 N88-30430

DYNAMIC CONTROL

The method of rigid armature flux orientation for the field-oriented control of highly dynamic drives with synchronous machines
[ETN-87-90405] 01 p0042 N88-10269

Photochemical ozone overburden correction
05 p0615 N88-13778

Investigation, development, and application of optimal output feedback theory. Volume 3: The relationship between dynamic compensators and observers and Kalman filters
[NASA-CR-4107] 05 p0638 N88-13900

Turbulence, turbulence control, and drag reduction
[AD-A185643] 06 p0665 N88-14080

Development of symbolic computation methods for nonlinear dynamics
[AD-A185562] 06 p0758 N88-14653

An autopilot design for the United States Marine Corps' airborne remotely operated device
[AD-A186379] 07 p0820 N88-14983

Roles of knowledge in motor learning
[AD-A186420] 07 p0897 N88-15438

Resources, confusions and compatibility in dual axis tracking: Displays, controls and dynamics
[AD-A185871] 07 p0898 N88-15440

A dynamic simulation and feedback control scheme for the U.S. Marine Corps' Airborne Remotely Operated Device (AROD)
[AD-A186597] 08 p0953 N88-15784

Control system simulation for a single-link flexible arm
[AD-A187037] 09 p1174 N88-17035

Viscosity methods in optimal control of distributed systems
[AD-A188086] 10 p1401 N88-18357

A wind tunnel model with dynamic control
[BU-352] 13 p1724 N88-20310

Modelling and control of an annular momentum control device
[NASA-CR-4138] 13 p1754 N88-20491

The dynamic control of robotic manipulators in space
[NASA-CR-182710] 13 p1779 N88-20646

Linear state space modeling of a turbofan engine
[AD-A190110] 15 p2019 N88-22035

Feedback control of distributed parameter systems with applications to large space structures
[AD-A190536] 15 p2025 N88-22068

Effect of friction and control parameters on the tracking accuracy of a target seeker
[AD-A190010] 15 p2056 N88-22257

Problems in nonlinear continuum dynamics
[AD-A190538] 15 p2126 N88-22691

Vibration control of large structures
[AD-A191358] 16 p2168 N88-22928

Automatic control of robot motion
[AD-A191012] 16 p2215 N88-23218

Contribution to the adaptive dynamic control of a robot manipulator
[LAAS-87-350] 16 p2255 N88-23475

Dynamics and control of turbulent shear flows
[AD-A191527] 18 p2508 N88-24879

A method for reducing the coning of a spinning vehicle
[DE88-010971] 21 p2896 N88-27189

Development of a hybrid simulator for robotic manipulators
[AD-A193119] 21 p2956 N88-27557

Vibration control of large structures
[AD-A193317] 21 p2961 N88-27587

Hierarchical organization for large, dynamic radio networks
[AD-A193942] 23 p3204 N88-29067

Anti-aliasing filters for dynamics and control experiments
[AD-A193758] 23 p3226 N88-29203

Topics in adaptive control and inference
[AD-A194718] 23 p3266 N88-29443

Dynamics of articulated aerospace structures
[AD-A195685] 24 p3324 N88-29794

DYNAMIC LOADS

NT AERODYNAMIC LOADS
NT BLAST LOADS
NT CONTACT LOADS
NT CYCLIC LOADS
NT GUST LOADS
NT IMPACT LOADS
NT LANDING LOADS
NT ROLLING CONTACT LOADS
NT SHOCK LOADS
NT TRANSIENT LOADS
NT VIBRATORY LOADS
NT WING LOADING

Possibilities for the modeling of dynamically loaded cylindrical structural parts in the wind tunnel
[KU-SFB-210/T/24] 01 p0001 N88-10005

Determination of the fatigue strength of mechanically, thermally and corrosively loaded multilayer materials
[ETN-87-90375] 01 p0058 N88-10372

Effect of viscosity on a vertical cylinder due to surface waves
[ETN-87-90960] 02 p0171 N88-11075

Diffraction moire: The dynamic regime
[DE87-014883] 03 p0335 N88-12111

Breaking wave forces on vertical cylinders
[RR-CE71] 03 p0338 N88-12126

Dynamic response of a 330 KW horizontal axis wind turbine generator
[DE87-014867] 03 p0347 N88-12195

Free-edge delamination: Laminate width and loading conditions effects
[NASA-TM-100238] 04 p0411 N88-12551

Static standing and dynamic walking of a practical biped robot
[DE88-001367] 04 p0451 N88-12795

On dynamic loads in parallel shaft transmissions. 1: Modelling and analysis
[NASA-TM-100180] 04 p0451 N88-12797

On dynamic loads in parallel shaft transmissions. 2: Parameter study
[NASA-TM-100181] 04 p0452 N88-12798

Input turbulence features at a megawatt-size wind turbine, Medicine Bow, Wyoming
[DE88-000098] 04 p0464 N88-12873

Measurements and calculations of aerodynamic torques for a vertical-axis wind turbine
[DE88-001783] 04 p0465 N88-12876

Experimental studies on the tripping behavior of narrow T-stiffened flat plates subjected to hydrostatic pressure and underwater shock 05 p0592 N88-13613

BASIC desk-top computer program for the three-dimensional static configuration of an extensible flexible cable in a uniform stream
[AD-A184852] 05 p0609 N88-13737

RADSPHERE: A computer program for calculating the steady-state, axially symmetric, forced response and radiation field of a submerged spherical shell
[AD-A185025] 05 p0609 N88-13738

Accurate rotor loads prediction using the FLAP (Force and Loads Analysis Program) dynamics code
[DE88-001109] 05 p0623 N88-13815

Structuring data for concurrent vectorized processing in a transient dynamics finite element program
[DE87-013082] 05 p0636 N88-13880

Mean and peak wind load reduction on heliostats
[DE87-012281] 07 p0873 N88-15298

Pressure and mass velocity measurements in solids subjected to dynamic loadings 07 p0921 N88-15595

Study on the mechanical stresses in the elements of the model of a toroidal magnet of a tokamak with strong field
[DE88-700343] 07 p0935 N88-15679

SAHAYOG: A testbed for load sharing under failure
[AD-A186615] 08 p1069 N88-16480

Analysis of tasks for dynamic man/machine load balancing in advanced helicopters
[DE88-003735] 09 p1117 N88-16696

Strength and toughness of a brittle material
[VTT-RR-479] 09 p1183 N88-17089

VAWT (Vertical-Axis Wind Turbine) stochastic loads produced by atmospheric turbulence
[DE88-001355] 09 p1187 N88-17110

The use of multigrid techniques in the solution of the Elrod algorithm for a dynamically loaded journal bearing
[NASA-CR-180873] 10 p1331 N88-17954

Preliminary results from the dynamic response testing of the Westinghouse 600-kW wind turbine
[DE88-001123] 10 p1350 N88-18070

Analysis of wind turbines on offshore support structures excited by random wind and random waves
[DE88-004772] 10 p1351 N88-18074

Determination of the ultimate loads for corrugated-steel, barrel-type shell structures
[AD-A187716] 11 p1498 N88-18944

Computer aided deflection measurement of an aircraft wing
[AD-A187778] 12 p1581 N88-19461

Changes in the status of the human tibia during antiorthostatic hypokinesia
[NASA-TT-20221] 13 p1810 N88-20813

Pressure measurements of impinging jet with asymmetric nozzle
[NASA-CR-182759] 15 p2014 N88-22011

Development of a computer code CRACK for elastic and elastoplastic fracture mechanics analysis of 2-D structures by finite element technique
[DE88-701231] 15 p207[illegible] N88-22370

FLAP (Force and Loads Analysis Program) code development and validation
[DE88-001131] 15 p2075 N88-22371

The CRREL (Cold Regions Research and Engineering Laboratory) Hopkinson bar apparatus
[AD-A190599] 15 p2077 N88-22380

Behaviour of fibre-reinforced composites under dynamic loading
[AD-A191310] 16 p2174 N88-22955

Dynamic shear band development in plane strain
[AD-A190915] 18 p2526 N88-24988

Finite element analysis of an underground structure
[AD-A191747] 18 p2527 N88-24991

Dynamic response of plates to moving loads: Structural impedance and finite element methods
18 p2528 N88-25000

The solution of the Elrod algorithm for a dynamically loaded journal bearing using multigrid techniques
[NASA-TM-100941] 19 p2666 N88-25854

Diffusion models of crack growth due to random overloads
[DE88-008811] 21 p2962 N88-27585

Modal testing in the design evaluation of wind turbines
[DE88-010374] 21 p2968 N88-27632

Static and dynamic metal-metal friction at plastic stress levels
[DE88-011281] 23 p3222 N88-29176

Influence of peak pressure on the substructure evolution and shock wave profiles of Ti-6Al-4V
[DE88-006458] 23 p3225 N88-29197

An investigation of acoustic cavitation produced by pulsed ultrasound
[AD-A193523] 23 p3278 N88-29516

Ultrasonic method and apparatus for determining crack opening load
[NASA-CASE-LAR-13889-1] 24 p3385 N88-30160

DYNAMIC MODELS

Use of simulated satellite radiances from a mesoscale numerical model to understand kinematic and dynamic processes 02 p0202 N88-11261

Mesoscale very short-range numerical prediction with dynamical initialization including condensation heating
02 p0213 N88-11341

A simplified approach to the dynamics of charged particles in the magnetosphere
03 p0273 N88-11718

A statistical rain attenuation prediction model with application to the advanced communication technology satellite project. Part 2: Theoretical development of a dynamic model and application to rain fade durations and tolerable control delays for fade countermeasures
[NASA-TM-100242] 03 p0308 N88-11945

Development of response models for the Earth Radiation Budget Experiment (ERBE) sensors. Part 1: Dynamic models and computer simulations for the ERBE nonscanner, scanner and solar monitor sensors
[NASA-CR-178292] 05 p0584 N88-13557

The tail lobe ion spectrometer: Theory and observations
[IFSI-86-12] 05 p0585 N88-13569

The kinetics and dynamics of iodine monofluoride formation in gas-phase collisions
[AD-A185715] 06 p0709 N88-14352

Characteristic trajectories of generalized Lanchester equations
[AD-A185762] 06 p0786 N88-14705

The global balance of dynamic vorticity in relation to heat sources and sinks 07 p0876 N88-15316

Roles of knowledge in motor learning
[AD-A186420] 07 p0897 N88-15438

Three-dimensional unsteady flow elicited by finite wings and complex configurations
[AD-A186464] 08 p0951 N88-15770

Attitude dynamics for satellites stabilized through spin
[INPE-4403-NTE/275] 08 p0963 N88-15833

Dynamic modeling of the middle atmosphere
08 p1028 N88-16227

A unified model for the WTS and the generation on Pi 2 pulsations --- Westward Traveling Surge (WTS)
08 p1096 N88-16593

A possible role for ionospheric ions in triggering a geomagnetic substorm onset 08 p1096 N88-16594

Dynamic tests of the Ariane launch vehicle
09 p1126 N88-16749

Dynamical characteristics of weak turbulence
[AD-A186724] 09 p1161 N88-16957

Dynamic modelling by finite element method of an elasto-acoustic beam with due consideration of flow and viscosity
[PB87-178166] 09 p1164 N88-16978

Control system simulation for a single-link flexible arm
[AD-A187037] 09 p1174 N88-17035

An interactive graphics method for dynamic system modeling, applying consistency rules
09 p1181 N88-17072

The analysis of recent crustal movements in static and kinematic models
[SER-B-279] 09 p1191 N88-17136

A model for stationary and dynamic impression of undercooled boiling in coupled thermohydraulic and neutron physics calculations of nuclear reactors
[IKE-6-171] 09 p1247 N88-17472

Strength and structure of Ga sub 1-xIn sub xAs alloys
[AD-A188092] 10 p1303 N88-17795

Microwave semiconductor research-materials, devices and circuits
[AD-A187121] 10 p1415 N88-18444

A superelement component dynamic synthesis method 11 p1500 N88-18956

Center for nonlinear dynamics of the brain
[AD-A187245] 11 p1518 N88-19068

Realtime pilot model parameter identification
[AD-A188873] 12 p1584 N88-19476

A comparative survey of mathematical models for dynamic simulation of in-orbit manipulation operations
12 p1592 N88-19533

Dynamics modeling, simulation, and control of a spacecraft/manipulator system
12 p1592 N88-19534

Visualization of the air flowing through a dynamic model of the vocal folds
[ISVR-TR-154] 14 p1952 N88-21634

Procedures for updating dynamic mathematical models
[EMSB-23/86] 14 p1964 N88-21716

Laser photodeposition and etching study
[AD-A190535] 15 p2040 N88-22153

The role of vortex structure in tropical cyclone motion
[AD-A190961] 16 p2235 N88-23351

The representational code of the internal model of dynamic systems: An individual differences and dual task approach
[AD-A190976] 16 p2244 N88-23403

Behavior of a two-layered beam under impact loading
[OUEL-1716/87] 17 p2349 N88-23993

Nonlinear flying quality parameters based on dynamic inversion
[AD-A192146] 18 p2464 N88-24627

A dynamic model of liquid propellant combustion
19 p2622 N88-25556

Modeling and evaluation of expert systems in decisionmaking organizations
[AD-A191951] 19 p2739 N88-26260

Coordination in decision-making organizations
[AD-A191952] 19 p2739 N88-26261

Dynamic modelling and estimation of the error due to asynchronism in a redundant asynchronous multiprocessor system
[NASA-CR-177427] 21 p2898 N88-27205

Control of free-flying space robot manipulator systems
[NASA-CP-183017] 21 p2956 N88-27562

On the dynamics of the metagalaxy
[TRITA-EPP-88-05] 22 p3166 N88-28852

Performance of GPS-aided INS during high-dynamic maneuvers
[AD-A194624] 23 p3175 N88-28903

Vortex dynamics of coherent and chaotic structures (including algorithms for computer simulations and diagnosis)
[AD-A193580] 23 p3212 N88-29117

Dynamics of interacting galaxies
23 p3299 N88-29647

Procedures for updating dynamic mathematical models, test phase --- spacecraft hardware
[MEBS-38/87] 24 p3335 N88-29852

MANIF --- spacecraft modeling program
[MANIP-217A] 24 p3335 N88-29855

Nonlinear dynamics of coupled oscillator arrays
[AD-A194888] 24 p3367 N88-30053

Modeling robot flexibility for endpoint force control
[AD-A195923] 24 p3380 N88-30132

Continental growth through time by underplating of subducted oceanic crust: Evidence from kimberlites in South Africa and SW Pacific 24 p3399 N88-30244

Dynamical systems and motion vision
[AD-A195932] 24 p3422 N88-30366

DYNAMIC PRESSURE

A 150,000 pounds per square inch dynamic pressure calibrator
[AD-A190653] 15 p2069 N88-22335

Synthesis of metastable superconductors by high dynamic pressure
[DE88-005620] 15 p2139 N88-22764

DYNAMIC PROGRAMMING

Investigation and implementation of an algorithm for computing optimal search paths
[AD-A185927] 07 p0902 N88-15461

On stochastic optimality of policies in first passage problems
[AD-A186293] 07 p0915 N88-15554

Optimal correction problem of a multidimensional stochastic system
[AD-A186727] 09 p1228 N88-17353

Spire based speaker-independent continuous speech recognition using mixed feature sets
[AD-A188834] 12 p1620 N88-19688

Application of dynamic programming to image registration
[ENST-87E022] 18 p2557 N88-25180

SIMS: Single Interface to Multiple Systems
[AD-A192284] 20 p2837 N88-26832

DYNAMIC PROPERTIES

U DYNAMIC CHARACTERISTICS

DYNAMIC RESPONSE

NT TRANSIENT RESPONSE

Investigation of interactions between limb-manipulator dynamics and effective vehicle roll control characteristics
[NASA-CR-3983] 01 p0007 N88-10039

Blade loss transient dynamics analysis, volume 1. Task 2: TETRA 2 theoretical development
[NASA-CR-179632] 02 p0125 N88-10791

Blade loss transient dynamics analysis, volume 2. Task 2: TETRA 2 user's manual
[NASA-CR-179633] 02 p0126 N88-10792

Effect of adhesive layers on impact damage and dynamic response in composite laminates
02 p0141 N88-10887

AGARD standard aeroelastic configurations for dynamic response. Candidate configuration I.-wing 445.6
[NASA-TM-100492] 02 p0192 N88-11202

Dynamic response of a 330 KW horizontal axis wind turbine generator
[DE87-014887] 03 p0347 N88-12195

An experimental investigation of dynamic ground effect
[NASA-CR-4105] 04 p0394 N88-12458

A method for the efficient calculation of elastic rotor blade dynamic response in forward flight
04 p0394 N88-12460

Aircraft dynamic response calculation based on discrete-continual model 04 p0424 N88-12624

A comparison of structural frequency response functions measured with forces from 500 to 250,000 lb
[DE88-000668] 04 p0457 N88-12829

Using a new characterization of turbulent wind for accurate correlation of wind turbine response with wind speed
[DE88-001453] 04 p0486 N88-12981

Aircraft dynamics: Aerodynamic aspects and wind tunnel techniques 05 p0545 N88-13320

Modal survey of the space shuttle solid rocket motor using multiple input methods 05 p0593 N88-13617

Dynamical analysis of molecular decay at spherical surfaces
[AD-A184908] 05 p0647 N88-13964

Analysis and test evaluation of the dynamic response and stability of three advanced turboprop models at low forward speed
[NASA-CR-175026] 06 p0668 N88-14096

Studies of the structural dynamic behavior of satellite antenna system
[AD-A185526] 06 p0673 N88-14121

Acquisition of gust statistics from Aircraft Integrated Data Systems (AIDS) recorded data
[NLR-MP-86049-U-ISS-2] 06 p0745 N88-14586

Rotor dynamic behavior of centrifugal pumps
08 p0975 N88-15898

Modal analysis using frequency response measurement data 08 p0976 N88-15899

Kinetic isolation tether experiment
[NASA-CR-182458] 09 p1135 N88-16810

The Shock and Vibration Bulletin. Part 2: Instrumentation, shock analysis, and shock testing
[AD-A186740] 09 p1178 N88-17053

Retarded potential technique applied for shock wave loading of doubly symmetric submerged structures
09 p1179 N88-17058

Mechanical impact: Theoretical simulation and correlation 09 p1179 N88-17060

Measurement, data analysis and prediction of pyrotechnic shock from pin-pullers and separation joints
09 p1179 N88-17061

A new look at the use of linear methods to predict aircraft dynamic response to taxi over bomb damaged and repaired airfields 09 p1180 N88-17069

Dynamic response of a geared train of rotors subjected to random support excitations 09 p1181 N88-17073

Monitoring interfacial dynamics by pulsed laser techniques
[DE88-003362] 10 p1335 N88-17976

Dynamic response of some structural elements fabricated from a non-linear elastic material
10 p1344 N88-18031

Qualification of frequency response functions using the rigid-body response
[DE88-000745] 10 p1344 N88-18033

Frequency response function estimation at level
[DE88-002644] 10 p1344 N88-18034

Vibration and flutter characteristics of the SR7L large-scale propfan
[NASA-TM-100272] 10 p1344 N88-18036

On the dynamic estimation of relative weights for observation and forecast in numerical weather prediction
[NASA-CR-182531] 10 p1356 N88-18106

Elastoplastic response of unidirectional graphite/aluminum under combined tension-compression cyclic loading
[CCMS-88-01] 11 p1451 N88-18647

Microwave response of an HEMT photoconductor
[NASA-TM-100819] 11 p1480 N88-18835

Prediction of the response and optimal control of stochastic parametrically and externally excited nonlinear systems 11 p1496 N88-18930

Dynamic substructuring for shock spectrum analysis using component mode synthesis
11 p1499 N88-18950

Dynamic analysis of plane frames by microcomputer
11 p1531 N88-19143

Response of coronary blood flow to step changes in plasma protein concentration in the isolated rat heart
12 p1651 N88-19892

Dynamics of high-speed mechanisms with elastic members 13 p1779 N88-20643

Application of the NARMAX method to nonlinear frequency response estimation [RR-319] 14 p1964 N88-21721
Shape sensitivity analysis of wing static aeroelastic characteristics [NASA-TP-2808] 15 p2018 N88-22031
Feedback control of distributed parameter systems with applications to large space structures [AD-A190536] 15 p2025 N88-22068
Galvanic corrosion initiatives [AD-A190658] 15 p2040 N88-22155
Influence of unsteady aerodynamic forces on dynamic response of variable sweep aircraft 15 p2054 N88-22245
The concept of an impact resonance diagram for characterizing the nonlinear response of impact vibration [DE88-005475] 15 p2086 N88-22432
Coupled bending-torsion steady-state response of pretwisted, nonuniform rotating beams using a transfer-matrix method [NASA-TM-100596] 15 p2086 N88-22435
The analysis of non-linear dynamic behavior (including snap-through) of postbuckled plates by simple analytical solution [NASA-TM-89165] 15 p2087 N88-22439
Vibration control of large structures [AD-A191358] 16 p2168 N88-22928
Dynamic fracture toughness evaluation by measurement of CTOD [WNS/ASD-88-02] 16 p2178 N88-22982
Investigation on the movement of vortex burst position with dynamically changing angle of attack for a schematic deltawing in a watertunnel with correlation to similar studies in windtunnel 16 p2204 N88-23152
Revised Impact Dynamic Design-Analysis Method (RIDDAM) [AD-A190479] 16 p2217 N88-23225
Stall flutter analysis of propfans 16 p2221 N88-23258
An adaptive load-following control system for a space nuclear power system 17 p2406 N88-24307
Research on aero-thermodynamic distortion induced structural dynamic response of multi-stage compressor blading [AD-A192169] 18 p2456 N88-24584
The flying characteristics of the membrane slider bearing 18 p2522 N88-24965
Theoretical and experimental damping values of piping systems at high ductilities [DE88-006717] 18 p2526 N88-24986
Dynamic response of plates to moving loads: Structural impedance and finite element methods 18 p2528 N88-25000
Vehicle dynamics: Identification in the frequency domain 20 p2785 N88-26523
Frequency domain identification of the dynamics of a scaled remotely-piloted helicopter 20 p2786 N88-26524
Multivariable identification of a flexible transport aircraft 20 p2786 N88-26525
Identification methods for transport dynamical investigations 20 p2787 N88-26531
Instrumentation for the measurement of penetrator dynamic response to permit force estimation [DE88-010808] 20 p2809 N88-26666
Experimental and theoretical study of the dynamic operational behavior of a three stage radial compressor [ETN-88-92129] 20 p2811 N88-26676
Contact force history and dynamic response due to the impact of a soft projectile [NASA-TM-100961] 20 p2811 N88-26679
AGARD standard aeroelastic configurations for dynamic response. 1: Wing 445.6 [AGARD-R-765] 21 p2896 N88-27193
The robust tracking control of nonlinear systems with uncertain dynamics 21 p2999 N88-27788
Self-energies and the interactions of particles with surfaces [DE88-010451] 21 p3014 N88-27885
Maximum dynamic responses using matched filter theory and random process theory [NASA-TM-100853] 22 p3042 N88-28059
The dynamic behavior of a turbulent boundary layer subjected to a shock-induced separation [AD-A194164] 22 p3075 N88-28252
Modal synthesis by use of substructures with fixed or free coupling points [ILR-MITT-181] 22 p3089 N88-28341
Experimental investigation of propfan aeroelastic response in off-axis flow with mistuning [NASA-TM-101320] 22 p3089 N88-28344
Structural dynamics of maneuvering aircraft [AD-A192376] 23 p3176 N88-28908
Nonlinear dynamic analysis and optimal control of shallow shells 23 p3224 N88-29191
Dynamic response of a 330-kW horizontal axis wind turbine generator [DE88-001136] 23 p3228 N88-29212
Dynamic analysis of computer and communications sytems: Semi-Markov approach 23 p3244 N88-29305
The Flight of Flexible Aircraft in Turbulence: State-of-the-Art in the Description and Modelling of Atmospheric Turbulence [AGARD-R-734] 24 p3312 N88-29725
Status review of atmosphere turbulence and aircraft response 24 p3312 N88-29726
Aircraft dynamics: Aerodynamic aspects and wind tunnel techniques 24 p3313 N88-29731
Acquisition of gust statistics from AIDS-recorded data 24 p3313 N88-29733
Analytical study of graphite-epoxy tube response to thermal loads [NASA-CR-183215] 24 p3341 N88-29884
Rotational evolution of dynamically symmetric gyrostat with internal friction 24 p3446 N88-30509

DYNAMIC STABILITY
NT AERODYNAMIC STABILITY
NT AIRCRAFT STABILITY
NT BOUNDARY LAYER STABILITY
NT COMBUSTION STABILITY
NT CONTROL STABILITY
NT DIRECTIONAL STABILITY
NT FLAME STABILITY
NT FLOW STABILITY
NT FREQUENCY STABILITY
NT GYROSCOPIC STABILITY
NT LATERAL STABILITY
NT LONGITUDINAL STABILITY
NT LOW SPEED STABILITY
NT MAGNETOHYDRODYNAMIC STABILITY
NT MOTION STABILITY
NT ROTARY STABILITY
NT SPACECRAFT STABILITY
Hypersonic static and dynamic stability of axisymmetric shapes: A comparison of prediction methods and experiment 05 p0534 N88-13246
Dynamic stability of hypersonic conical lifting vehicles according to Newton-Busemann theory 05 p0534 N88-13247
Dynamic behavior of dissymmetric rotor bearings modelled with a periodic coefficient large system 05 p0596 N88-13640
Analysis and test evaluation of the dynamic stability of three advanced turboprop models at zero forward speed [NASA-CR-175025] 06 p0666 N88-14095
Investigation of instability, dynamic forces, and effect of dynamic loading on strength of cages for the bearings in the high pressure oxygen turbopumps for the space shuttle main engine [NASA-CR-178970] 06 p0714 N88-14378
Effect of plasma rotation in tokamak on stabilizing action of electrically conducting wall 06 p0773 N88-14748
Parametric dependence in the equilibrium dynamics of rotating structures [AD-A187817] 11 p1498 N88-18945
On relaxation algorithms based on Markov random fields [AD-A189043] 13 p1814 N88-20840
Vibrations of structures with parametric uncertainties [AD-A190400] 15 p2076 N88-22378
An experimental study to determine the flow and the subsonic static and dynamic stability characteristics of aircraft operating at high angles-of-attack 16 p2201 N88-23129
Unstable behavior of lasers and other optical systems [AD-A190875] 16 p2213 N88-23204
Optimal rheological characteristics in dynamic stability of polymer flow through porous media [DE88-001225] 21 p2918 N88-27322
Application of the Single-Axis rate Table (SAT) of the DFVLR for the evaluation of stationary and dynamic gyro properties [DFVLR-MITT-88-09] 21 p2952 N88-27533
Dynamic stability of elastic rotor-bearing systems via Liapunov's direct method 21 p2958 N88-27571
Utilizing dynamic stability of orient parts [AD-A195730] 24 p3427 N88-30397

DYNAMIC STRUCTURAL ANALYSIS
Efficient placement of structural dynamics sensors on the space station [NASA-CR-172015] 01 p0017 N88-10103
A DMAP for updating dynamic mathematical models with measured data [NLR-MP-86027-U] 01 p0060 N88-10387
Recent advances in structural dynamics of large space structures [NASA-TM-100513] 02 p0138 N88-10867
Structural Assembly Demonstration Experiment (SADE) [NASA-CR-179205] 02 p0138 N88-10868
Concurrent algorithms for transient nonlinear FE analysis [NASA-CR-181455] 02 p0221 N88-11389
Frequency domain identification of structural dynamic systems with general damping matrices 03 p0337 N88-12120
Linearized aeroelastic analysis of a wind turbine with a two-bladed rotor [ETN-87-90600] 03 p0347 N88-12192
A comparison of structural frequency response functions measured with forces from 500 to 250,000 lb [DE88-000668] 04 p0457 N88-12829
Aircraft interior noise reduction by alternate resonance tuning [NASA-CR-181530] 04 p0488 N88-13005
Predictions of F-111 TACT aircraft buffet response and correlations of fluctuating pressures measured on aluminum and steel models and the aircraft [NASA-CR-4069] 05 p0529 N88-13218
The 58th Shock and Vibration Symposium, volume 1 [NASA-CP-2488-VOL-1] 05 p0582 N88-13609
Improvement of modal scaling factors using mass additive technique 05 p0593 N88-13620
Initial dynamic load estimates during configuration design 05 p0593 N88-13621
Viscous damped space structure for reduced jitter 05 p0594 N88-13623
A system identification technique based on the random decrement signatures. Part 1: Theory and simulation 05 p0594 N88-13625
A system identification technique based on the random decrement signatures. Part 2: Experimental results 05 p0594 N88-13626
An efficient frequency response solution for nonproportionally damped systems 05 p0595 N88-13634
Shape optimization of damping layers 05 p0595 N88-13635
Dynamic response of laminated composite plates using a three-dimensional hybrid-stress finite-element formulation 05 p0596 N88-13639
Dynamic behavior of dissymmetric rotor bearings modelled with a periodic coefficient large system 05 p0596 N88-13640
Utilization of dynamic characteristics of materials to optimize military explosive charges. Application to antiship devices [SNIAS-872-320-101] 05 p0610 N88-13743
Accurate rotor loads prediction using the FLAP (Force and Loads Analysis Program) dynamics code [DE88-001109] 05 p0623 N88-13815
Analysis and test evaluation of the dynamic response and stability of three advanced turboprop models at low forward speed [NASA-CR-175026] 06 p0668 N88-14096
Studies of the structural dynamic behavior of satellite antenna system [AD-A185526] 06 p0673 N88-14121
Studies on fluid-structural vibration using boundary element method [PB87-129508] 06 p0699 N88-14291
Distortional buckling formulae for thin-walled channel columns [PB87-124012] 06 p0722 N88-14437
Boundary element analysis for dynamic loading of a circular plate on an elastic medium [CI-86] 06 p0722 N88-14443
Fast algorithms for structural optimization and least squares [AD-A185766] 06 p0724 N88-14452
Determining structural performance 08 p0954 N88-15787
Modal analysis using frequency response measurement data 08 p0976 N88-15899
The nonlinear dynamic response of an elastic-plastic thin plate under impulse loading [AD-A182147] 08 p0994 N88-16013
Dynamic analysis of a structure with sliding base 08 p0998 N88-16045
A summary of recent NASA/Army contributions to rotorcraft vibrations and structural dynamics technology 09 p1105 N88-16629
Rotorcraft aeroelastic stability 09 p1106 N88-16631
Parametric and experimental analysis using a power flow approach [NASA-CR-182460] 09 p1116 N88-16693
A substructure method for dynamic simulation of flexible mechanical systems with geometric nonlinearities 09 p1176 N88-17044
The Shock and Vibration Bulletin. Part 2: Instrumentation, shock analysis, and shock testing [AD-A186749] 09 p1178 N88-17053
Retarded potential technique applied for shock wave loading of doubly symmetric submerged structures 09 p1179 N88-17059

Mechanical impact: Theoretical simulation and correlation 09 p1179 N88-17060

Dynamic stress at critical locations of a structure as a criterion for mathematical model modification
09 p1180 N88-17066

Reliability of structures with stiffness and strength degradation 09 p1180 N88-17068

Experimental identification of nonlinear structural models
[DE88-001795] 09 p1184 N88-17094

Dynamic response of some structural elements fabricated from a non-linear elastic material
10 p1344 N88-18031

Frequency response function estimation at level
[DE88-002644] 10 p1344 N88-18034

A component synthesis method using Lanczos vectors
[DE88-002263] 10 p1403 N88-18368

The 58th Shock and Vibration Symposium, volume 2
[NASA-CP-2488-VOL-2] 11 p1499 N88-18948

A superelement component dynamic synthesis method 11 p1500 N88-18956

Numerical fracture mechanics using finite element method 11 p1501 N88-18966

Characterization of damped structural connections for multi-component systems
[NASA-TM-100801] 11 p1502 N88-18974

Computer aided deflection measurement of an aircraft wing
[AD-A187778] 12 p1581 N88-19461

Preliminary investigation of stability of a fin-stiffened slender strut
[NASA-TM-4034] 12 p1599 N88-19568

A numerical study of automated dynamic relaxation for nonlinear static tensioned structures
[AD-A188372] 12 p1635 N88-19790

Control augmented structural synthesis
[NASA-CR-4132] 13 p1721 N88-20290

The Euler-Bernoulli beam equation with boundary energy dissipation
[AD-A189517] 13 p1765 N88-20560

A flight test investigation into flow separation and structural response for a transport aircraft at buffet onset
[RAE-TR-87006] 14 p1867 N88-21156

Some structural aspects of crack propagation in heat-resistant steels under cyclic thermal and mechanical load 14 p1896 N88-21317

Stress-strain behaviour of a bolt hole in carbon fibre composite plates
[BU-354] 14 p1923 N88-21460

The effect of strain rate on the strength and ductility of SiCw/2124 Al composite
[OUEL-1692/87] 14 p1924 N88-21466

Computational aspects of sensitivity calculations in transient structural analysis
[NASA-TM-100589] 14 p1924 N88-21467

Test facilities of the structural dynamics branch of NASA Lewis Research Center
[NASA-TM-100800] 14 p1934 N88-21534

Wave propagation and dynamics of lattice structures
[AD-A190037] 15 p2025 N88-22066

Wave propagation and dynamics of lattice structures
[AD-A190611] 15 p2025 N88-22069

Nonlinear analysis and optimal design of dynamic mechanical systems for spacecraft application
[AD-A190644] 15 p2026 N88-22070

Stabilization and control problems in structural dynamics
[AD-A190197] 15 p2073 N88-22361

FLAP (Force and Loads Analysis Program) code development and validation
[DE88-001131] 15 p2075 N88-22371

Lewis Structures Technology, 1988. Volume 2: Structural Mechanics
[NASA-CP-3003-VOL-2] 15 p2077 N88-22382

Lewis Structures Technology, 1988. Volume 3: Structural Integrity Fatigue and Fracture Wind Turbines HOST
[NASA-CP-3003-VOL-3] 15 p2081 N88-22408

Structural dynamics branch research and accomplishments for fiscal year 1987
[NASA-TM-100279] 15 p2088 N88-22446

On the computation of stationary deterministic behavior of nonlinear dynamic systems with applications to rotor-bearing structures
[ETN-88-92241] 16 p2214 N88-23213

Lewis Structures Technology, 1988. Volume 1: Structural Dynamics
[NASA-CP-3003-VOL-1] 16 p2217 N88-23226

Periodic response of nonlinear systems
16 p2217 N88-23228

Characterization of structural connections for multicomponent systems 16 p2220 N88-23251

Integrated multidisciplinary analysis tool IMAT users' guide
[NASA-TM-100605] 16 p2223 N88-23273

Unsteady pressure and structural response measurements of an elastic supercritical wing
[NASA-TM-100591] 17 p2299 N88-23756

Preliminary 2-D shell analysis of the space shuttle solid rocket boosters
[NASA-TM-100515] 17 p2346 N88-23989

Parameter identification methods for improving structural dynamic models
[NASA-TM-100812] 17 p2349 N88-23994

Continuum modeling and dynamic analysis of large truss structures 17 p2349 N88-23995

Application of integrated fluid-thermal-structural analysis methods
[NASA-TM-100625] 17 p2350 N88-24001

Parallel processors and nonlinear structural dynamics algorithms and software
[NASA-CR-182925] 17 p2387 N88-24187

Aircraft aeroelasticity and structural dynamics research at the NASA Langley Research Center: Some illustrative results
[NASA-TM-100627] 18 p2459 N88-24596

Current flight test experience related to structural divergence of forward-swept wings
[NASA-TM-100445] 18 p2464 N88-24633

Experimental study of active vibration control
[AD-A191454] 18 p2526 N88-24989

Dynamic response of plates to moving loads: Structural impedance and finite element methods
18 p2528 N88-25000

Reduced order modelling and analytical model modification for structural dynamics and control
18 p2529 N88-25006

Analysis and developments of failure concepts in fracture mechanics based on research results in the field of component safety topics: J-integral concept; crack resistance curves; dynamic criterion
[V-19/86] 18 p2530 N88-25009

Multishaker modal testing
[NASA-CR-179355] 18 p2530 N88-25010

SRM propellant and polymer materials structural test program
[NASA-TP-2821] 18 p2530 N88-25013

Single-mode projection filters for modal parameter identification for flexible structures
[NASA-CR-182680] 18 p2566 N88-25244

Design of a controller to reduce residual vibration in the positioning control of flexible robotic manipulators
20 p2808 N88-26658

Contact force history and dynamic response due to the impact of a soft projectile
[NASA-TM-100961] 20 p2811 N88-26679

A general-purpose approach to computer-aided dynamic analysis of a flexible helicopter
[NASA-TM-101002] 20 p2816 N88-26709

Vibration control of large structures
[AD-A193317] 21 p2961 N88-27587

DYNA3D (Nonlinear Dynamic Analysis of Structures in Three Dimensions) user's manual
[DE88-012242] 21 p2963 N88-27604

Power flow analysis of two coupled plates with arbitrary characteristics
[NASA-CR-183165] 22 p3075 N88-28251

A critical speed study for aircraft bias ply tires
[AD-A193616] 22 p3084 N88-28313

Structural dynamics of maneuvering aircraft
[AD-A192376] 23 p3176 N88-28908

Recursive mass matrix factorization and inversion: An operator approach to open- and closed-chain multibody dynamics
[NASA-CR-182516] 23 p3247 N88-29326

ASKA-acoustics: Theory and applications --- vibro acoustics
[FFA-TN-1988-13] 23 p3279 N88-29519

Space structure (dynamics and control) theme development
[NASA-TM-100597] 24 p3335 N88-29850

Geometric and material nonlinear analysis of structures comprising rectangular hollow sections
[CE-79] 24 p3382 N88-30141

DYNAMIC TESTS

Computer-controlled testing of visual-spatial ability
[AD-A183971] 03 p0357 N88-12249

Modal analyses of the Kernville diagnostic canister
[DE88-003268] 07 p0870 N88-15277

Dynamic testing: Seven years later
08 p0997 N88-16035

Dynamic tests of the Ariane launch vehicle
09 p1126 N88-16749

Comprehensive analysis of helicopters with bearingless rotors
[NASA-CR-182537] 10 p1390 N88-18300

Cost effective development of a national test bed
[NASA-TM-100321] 12 p1601 N88-19585

KRASH parametric sensitivity study: Transport category airplanes
[AD-A189962] 15 p2017 N88-22024

Hybrid procedure for dynamic measurements in transonic wind tunnels: Demonstrated by pitch oscillation
[DFVLR-FB-88-19] 21 p2900 N88-27211

Soviet dynamic fracture mechanics research
[FASAC-TAR-3140] 21 p2962 N88-27597

DYNAMICAL SYSTEMS

Dynamics of spacecraft control laboratory experiment (SCOLE) slew maneuvers
[NASA-CR-4098] 01 p0014 N88-10082

Vortex dynamics and transport to the wall in a crossed-field plasma sheath
[DE87-013286] 01 p0100 N88-10657

Dynamical simulation of structural multiplicity in grain boundaries
[DE87-012746] 01 p0103 N88-10676

Hot spots: Subnanometer femtosecond energy localization
[DE87-010276] 02 p0155 N88-10968

Modeling shockwave deformation via molecular dynamics
[DE87-013157] 02 p0169 N88-11063

Dimension densities for turbulent systems with spatially decaying correlation functions
[DE87-010119] 02 p0169 N88-11066

IR laser excitation in molecules: Chaos and diffusive energy growth
[DE87-013147] 02 p0175 N88-11105

Possible dynamical mechanisms for the Martian polar warming phenomenon
[NASA-CR-181454] 02 p0254 N88-11605

A deterministic approach to turbulence: Chaos in Rayleigh-Benard convection 03 p0313 N88-11975

Transition to turbulence via spatio-temporal intermittency 03 p0313 N88-11976

Point vortex dynamics: Recent results and open problems
[DE87-014759] 03 p0314 N88-11982

Dynamics and stability of bipedal locomotion robots
03 p0333 N88-12096

Measurements of vapor flux, liquid water contents, precipitation rates and riming in a Utah mountain cloud system
[PB87-224945] 04 p0469 N88-12900

Propagation of random initial conditions in time
04 p0486 N88-12993

Novel dynamical investigations of excitons and their structure in semiconductors
[DE87-014868] 04 p0499 N88-13070

Non-minimal interaction of gravity with other physical fields: An overview
[DE87-703362] 05 p0624 N88-13819

Approaches and possible improvements in the area of multibody dynamics modeling
[NASA-CR-179227] 06 p0663 N88-14067

Dynamical friction
[DE88-002194] 06 p0711 N88-14358

Darboux transformation and special solutions for the two-dimensional Toda lattice
[PREPRINT-562] 06 p0764 N88-14692

Group quantization of constrained systems
[PREPRINT-564] 06 p0790 N88-14844

Anomalous scaling laws in multifractal objects
[NOTA-INTERNA-883] 07 p0916 N88-15565

The Jeffcott equations in nonlinear rotordynamics
07 p0928 N88-15636

Attitude determination of artificial satellites through joint application of static and dynamic optimal estimation techniques
[INPE-4415-TDL/306] 08 p0963 N88-15832

Dynamic finite element with diagonalized consistent mass matrix and elastic-plastic impact calculation
[PB87-143376] 08 p0995 N88-16020

The entropy of the Lorentz model
08 p1015 N88-16153

Lie algebraic method in filtering and identification
[CWI-PM-R8606] 08 p1072 N88-16467

An interactive-graphics method for dynamic system modelling, applying consistency rules
09 p1181 N88-17072

Magneto-Inertia Confinement Approach (MICA) to fusion in dynamic Z-pinch formed from a frozen deuterium-tritium tube
[IPPJ-856] 09 p1252 N88-17504

An analysis of the motion and effects of hairpin vortices
[AD-A187261] 10 p1331 N88-17958

Dynamical properties of aluminum from experimental dispersion relations
[DE88-700240] 11 p1450 N88-18697

Optimal control theory of load-following and parameter-tracking of nonlinear systems: An application of Pontryagin Maximum Principle to reactor dynamics
[DE88-004770] 11 p1532 N88-19152

Photohydrodynamical processes near compact objects
11 p1569 N88-19390

Motion simulation for in-orbit operations
12 p1589 N88-19514
Analysis of a rotating advanced-technology space station for the year 2025
[NASA-CR-178345] 12 p1600 N88-19580
The automated symbolic derivation of state equations for dynamic systems
[DE88-005222] 12 p1683 N88-20060
Transient dynamics of fibre reinforced composite plates
[IIT-B/CE/RR/87-1] 13 p1734 N88-20370
Unfoldings of quasi-periodic tori
[ZW-8706] 13 p1828 N88-20928
Period-doubling universality in multidimensional dissipative and conservative systems
[PB88-148812] 13 p1832 N88-20961
Optical studies of dynamical processes in disordered system
[DE88-005965] 13 p1837 N88-20993
Laser spectroscopy and dynamics of combustion intermediates
[DE88-006541] 15 p2033 N88-22110
On new solvable many-body dynamical systems with velocity dependent forces
[PREPRINT-581] 15 p2127 N88-22683
A low dimensional dynamical system for the wall layer
16 p2194 N88-23086
Coherent structures and dynamical systems
16 p2199 N88-23119
On the computation of stationary deterministic behavior of nonlinear dynamic systems with applications to rotor-bearing structures
[ETN-88-92241] 16 p2214 N88-23213
Dynamic range compression/expansion of light beams by photorefractive crystals
[NASA-CASE-NPO-17140-1-CU]
17 p2438 N88-24508
Reliability of stochastically forced systems (extended version)
[CWI-AM-R8801] 18 p2526 N88-24985
Infinite dimensional dynamical systems and their finite dimensional analogues
[AD-A192041] 18 p2563 N88-25216
Dynamical properties of a collapsing spherical cavity
19 p2623 N88-25562
Stability of dynamical systems supported by rubber springs 19 p2680 N88-25932
System identification in vehicle dynamics
[DFVLR-MITT-87-22] 20 p2785 N88-26518
Parameter estimation of dynamical systems
20 p2785 N88-26519
Simulation models for the dynamics of tracked vehicle systems: State-of-the-art and open problems
20 p2785 N88-26522
Dynamical evolution of cosmic strings
[DE88-011724] 21 p3030 N88-27989
An analytical investigation of geared system dynamics containing spur and helical gears
22 p3085 N88-28317
General analytic solution of certain functional equations of addition type
[PREPRINT-583] 22 p3144 N88-28699
Analytical investigation of the dynamics of tethered constellations in earth orbit
[NASA-CR-179371] 23 p3184 N88-28950
Method of forming dynamic membrane on stainless steel support
[NASA-CASE-MSC-18172-3] 23 p3201 N88-29052
Coupling expert systems and simulation
23 p3252 N88-29360
Unfoldings of quasi-periodic tori
[B8811118] 23 p3278 N88-29513
Can we calculate the fundamental dimensionless constants of physics
[DE88-702641] 23 p3295 N88-29625
Studies on pressure responses of gas bubbles contributions of condensed droplets in bubbles generated by a uniform nucleation
[NASA-TT-20343] 24 p3370 N88-30068
Prediction and measurement of human pilot dynamic characteristics in a manned rotorcraft simulation
[NASA-CR-183246] 24 p3410 N88-30297
Dynamical systems and motion vision
[AD-A195932] 24 p3422 N88-30366
Intramolecular dynamics: A study of molecules at high levels of vibrational excitation
[AD-A195265] 24 p3428 N88-30400
Ring current role in dynamics of fluctuating electron and ion fluxes in low latitude magnetosphere
24 p3447 N88-30514

DYNAMICS
Dynamics of propellant feedline systems
[AD-A184865] 06 p0580 N88-13537
Recursive forward dynamics for multiple robot arms moving a common task object
[NASA-CR-182526] 10 p1340 N88-18008
Improved description of base dynamics in the modeling of bipolar transistors
[PB88-181516] 19 p2732 N88-26229
Structural dynamics of high-latitude magnetosphere determined from solar electron data
24 p3444 N88-30500

DYNAMICS EXPLORER SATELLITES
NT DYNAMICS EXPLORER 1 SATELLITE

DYNAMICS EXPLORER 1 SATELLITE
Dynamics explorer data analysis
[NASA-CR-181428] 19 p2691 N88-25996
Investigation of the diffuse ultraviolet background with DE data
[NASA-CR-182863] 19 p2741 N88-26271

DYNAMO THEORY
Atmospheres of stars in the limits of thin and thick convection zones: The M dwarfs
04 p0506 N88-13104

DYNAMOMETERS
Design verification tests for an axial gap permanent magnet compressor motor
[DE87-014380] 02 p0167 N88-11049

DYNAMOS
U ROTATING GENERATORS

DYSPROSIUM
Epitaxial growth and new phase of single crystal Dy by molecular beam epitaxy
[DE88-002850] 09 p1256 N88-17531

E

E GLASS
NT S GLASS
Cumulative fatigue and life prediction of fibre composites. Part 2: Experimental techniques and results
[BR101014] 02 p0142 N88-10804
Effects of processing variables on the behavior of E-glass/913 and XAS carbon fibre/913 laminates subjected to hot/wet environmental conditions
[BR101940] 09 p1138 N88-16820

E LAYERS
U E REGION

E REGION
NT SPORADIC E LAYER
The new CP3 06 p0691 N88-14237
Meteor matter interaction with the Earth's atmosphere and the ionospheric E-region structure
06 p0738 N88-14537
The rocket and scatter experiment ROSE: Presentation of the scientific payload 08 p1034 N88-16269
Spectrophotometric remote sensing of the diffuse aurora
[AD-A188599] 12 p1643 N88-19837
Rocket measurements of ionospheric electron temperature over Natal
[INPE-4485-PRE/1250] 15 p2096 N88-22469
Studies of ionosphere/magnetosphere dynamics using SABRE and HILAT
[AD-A190947] 16 p2232 N88-23333
Low frequency electrostatic turbulence in the polar cap E-region
[DRI-3-88] 18 p2540 N88-25077

EAR
NT COCHLEA
NT MIDDLE EAR
NT OTOLITH ORGANS
NT SEMICIRCULAR CANALS
NT VESTIBULES
Questions on the evolution of the development program of the vertebrate inner ear under long term zero-g conditions 07 p0866 N88-15379
Assessment of cochlear damage after microwave irradiation
[AD-A193237] 21 p2987 N88-27737

EARLY STARS
NT A STARS
NT B STARS
NT HOT STARS
NT O STARS
NT WHITE DWARF STARS
NT WOLF-RAYET STARS
Magnetic fields on K and M stars
04 p0510 N88-13137
The Einstein survey of the young stars in the Orion Nebula 04 p0518 N88-13182
Galactic interstellar abundance surveys with IUE and IRAS 04 p0522 N88-13206

EARLY WARNING SYSTEMS
Icing detector with early warning capability
[AOA-4.1.0055] 03 p0325 N88-12050
Radio and radar holes and multipath zones: The global and local influences on atmospheric refractive structure and resulting adverse radio and radar performance
12 p1617 N88-19667

SPOT imagery for landslide cartography in mountainous areas. Example of the French Maritime Alps
22 p3105 N88-2844

EARTH (PLANET)
Steady distortion of shape of geoid and normal gravity field under influence of tidal potential
04 p0459 N88-1283
A Jupiter Data Analysis Program (JDAP) research grant on wave accessibility and attributes
[NASA-CR-182348] 06 p0804 N88-1480
Assessment of anomalous gravitational field of elastic Earth 07 p0921 N88-1559
Planet X probe: A fresh new look at an old familiar place 10 p1287 N88-1788
A program for the calculation of radio-wave transmission loss over the spherical earth and over obstacles
12 p1616 N88-1968
Evaluation of a model of the Earth's gravity field
[EPSHOM-003/87] 17 p2373 N88-24116
Research in particle and gamma-ray astrophysics
[NASA-CR-183111] 20 p2887 N88-27146
Spectral analysis of the Elatina varve series
[NASA-CR-183085] 24 p3402 N88-30280
Exotic minerals in 3,500 million year old rocks: Evidence for large meteorite impacts 24 p3440 N88-30475
LSU scientists discover evidence of large meteorite impacts on the early earth 24 p3441 N88-30480

EARTH ALBEDO
The role of anisotropy in the long range reconnaissance of the albedo of land surfaces 08 p1017 N88-16169
Nimbus 7 Solar Backscatter Ultraviolet (SBUV) spectral scan solar irradiance and Earth radiance product user's guide
[NASA-RP-1199] 09 p1184 N88-17098

EARTH ATMOSPHERE
NT D REGION
NT E REGION
NT EARTH IONOSPHERE
NT F REGION
NT F 2 REGION
NT FREE ATMOSPHERE
NT LOWER ATMOSPHERE
NT LOWER IONOSPHERE
NT MESOPAUSE
NT MESOSPHERE
NT MIDDLE ATMOSPHERE
NT MIDLATITUDE ATMOSPHERE
NT OZONOSPHERE
NT PRIMITIVE EARTH ATMOSPHERE
NT SPORADIC E LAYER
NT STRATOPAUSE
NT STRATOSPHERE
NT THERMOSPHERE
NT TROPOPAUSE
NT TROPOSPHERE
NT UPPER ATMOSPHERE
NT UPPER IONOSPHERE
A study of carbon monoxide distribution determinations for a global transport model
[NASA-CR-181423] 01 p0067 N88-10432
The effects of minor trace gases on the transfer of thermal infrared radiation through the Earth's atmosphere 04 p0468 N88-12893
National Center for Atmospheric Research
[PB87-228391] 04 p0470 N88-12901
A review of parameterizations of microphysical processes in clouds for application in models of regional atmospheric deposition
[DE88-000451] 04 p0471 N88-12909
Anti-Stokes generation of 226 nm light
[DE88-001612] 05 p0589 N88-13590
Ozone formation due to interaction of meteoroids with Earth's atmosphere 06 p0738 N88-14536
The global climate system: Autumn 1984 to spring 1986
[CSM-R84/86] 06 p0745 N88-14580
Nonuniformity of electromagnetic field at Lambda = 10.6 micron wavelength inside atmospheric aerosol particles
06 p0772 N88-14743
A long term radiological risk model for plutonium-fueled and fission reactor space nuclear system
[DE87-010466] 06 p0779 N88-14782
Microsecond beam propagation in air
[DE88-002221] 07 p0845 N88-15127
Chapter 2: Threshold for Raman conversion of FEL laser pulses in the atmosphere
[DE88-002470] 07 p0859 N88-15215
MAXIE 1 (Magnetospheric Atmospheric X-ray Imaging Experiment) Program
[AD-A185876] 07 p0877 N88-15317
Atmospheric heating from optical absorption by aerosols
[DE88-002654] 07 p0878 N88-15327
Estimation of broadband planetary albedo from operational narrowband satellite measurements
[PB88-107644] 07 p0945 N88-15748

A raytrace method for a laterally heterogeneous environment
[AD-A186525] 08 p0978 N88-15912
Vertical atmospheric sounding
[INPE-4370-PRE/1195] 08 p1006 N88-16283
Induced turbulence in aerosol-loaded atmospheres, Jun. 1987
[DE87-014724] 09 p1192 N88-17141
Parameterization of radiative transfer in the Earth's atmosphere with specific applications to clouds
10 p1353 N88-18097
Theoretical and observational problems with Halos in the far UV dayglow
[AD-A188190] 10 p1355 N88-18100
Remote sensing of atmospheric optical thickness and sea-water attenuation when submerged: Wavelength selection and anticipated errors
[AD-A187609] 11 p1548 N88-19262
Review of recent developments in evaporation ducting assessment 12 p1616 N88-19664
High resolution infrared absorption spectra of various trace gases present in the upper atmosphere of the Earth
[NASA-CR-182590] 12 p1642 N88-19829
The effects of atmospheric and thermohaline variability on the validation of the GEOSAT altimeter oceanographic signal between Scotland and Iceland
[AD-A189324] 12 p1650 N88-19882
Investigations of high resolution imaging through the Earth's atmosphere using speckle interferometry
[AD-A189295] 12 p1692 N88-20121
An automated ozone photometer
[NASA-TM-100064] 14 p1908 N88-21404
Introduction to the dynamics of the ocean and the atmosphere 14 p1935 N88-21537
Observational and theoretical studies of greenhouse climate effects
[DE88-006237] 14 p1948 N88-21621
Ozone in the atmosphere 18 p2539 N88-25064
Brunt-Doppler ducting of buoyancy waves in a temperature- and wind-stratified atmosphere
18 p2542 N88-25086
Linear and nonlinear acoustic wave propagation in the atmosphere
[NASA-CR-4157] 18 p2571 N88-25268
High spatial frequency thermal blooming instability: A linear stability analysis
[DE88-010711] 20 p2807 N88-26655
The seasonal exchange of carbon dioxide between the atmosphere and the terrestrial biosphere: Extrapolation from site-specific models to regional models
[DE88-007870] 20 p2822 N88-26740
Our climate in danger
[DE88-701824] 20 p2822 N88-26743
The NASA Marshall engineering thermosphere model
[NASA-CR-179359] 20 p2825 N88-26760
The application of imaging to the atmospheric Cerenkov technique: Observations of the Crab nebula
20 p2884 N88-27126
Multifilter spectrometer (FEB) for microwave atmospheric sounder
[AD-A192312] 21 p2935 N88-27426
Activities report of the Institute for Extraterrestrial Physics
[MPE-206] 21 p3029 N88-27981
On the nucleonics component of cosmic radiation in the atmosphere
[DE88-702493] 22 p3166 N88-28854
Atmospheric angular momentum and length of day
[AD-A194505] 23 p3233 N88-29238
Basic causes of amplitude modulation in climatic/weather parameters
[DE88-702743] 23 p3236 N88-29254
Hadrons produced in atmospheric interactions
[DE88-702492] 23 p3309 N88-29712
Implementation of the NCAR (National Centre for Atmospheric Research) graphics package at ARL (Aeronautical Research Laboratory)
[AD-A195163] 24 p3391 N88-30193
Did the greenhouse effect kill the dinosaurs
24 p3442 N88-30484

EARTH AXIS
Axial anisotropy of the intensity of the cosmic ray nuclear component
[IFSI-87-7] 05 p0662 N88-14061

EARTH CORE
Seismic body waves and the earth's inner core
[DE88-007395] 19 p2691 N88-25994
An illustration of the complexity of continent formation
24 p3393 N88-30207

EARTH CRUST
A new approach to modeling and interpreting electromagnetic sounding data
[DE88-000460] 04 p0438 N88-12715
An algorithmic approach to crustal deformation analysis 04 p0468 N88-12891
Effective methods of gravimetric and magnetometric data processing 06 p0728 N88-14479
New data on structure of earth's crust and seismicity of basins in Atlantic and Indian Oceans
08 p1010 N88-16123
Crustal dynamics project data analysis, 1987. Volume 1: Fixed station VLBI geodetic results, 1979-1986
[NASA-TM-100682] 08 p1035 N88-16279
Crustal dynamics project data analysis, 1987. Volume 2: Mobile VLBI geodetic results, 1982-1986
[NASA-TM-100689-VOL-2] 08 p1035 N88-16280
The analysis of recent crustal movements in static and kinematic models
[SER-B-279] 09 p1191 N88-17136
Materials of the World Data Center B. Deep Seismic Sounding (DSS): Pacific data 09 p1196 N88-17167
Numerical studies of propagation of Lg waves across ocean continent boundaries using the Representation Theorem (RT) 10 p1353 N88-17085
Analysis of gases in the earth's crust
[PB88-141619] 10 p1354 N88-18093
Crustal Dynamics Project: Catalogue of site information
[NASA-RP-1198] 11 p1513 N88-19037
Isotopic and chemical studies of early crustal metasedimentary rocks
[NASA-CR-182711] 14 p1944 N88-21601
The interpretation of crustal dynamics data in terms of plate interactions and active tectonics of the Anatolian Plate and surrounding regions in the Middle East
[NASA-CR-183024] 18 p2543 N88-25092
Influence of scattering on seismic waves: Physical mechanisms contributing to attenuation in the crust
[AD-A191699] 19 p2690 N88-25992
Seismic reflection experiments imaging the physical nature of crustal structures in southern California
23 p3232 N88-29235
Relationships among earth's gravity field, magnetic field, crustal structure and the magnetic character of crustal rocks
[AD-A195539] 24 p3392 N88-30198
Workshop on the Growth of Continental Crust
[NASA-CR-183073] 24 p3392 N88-30201
Constraints on continental accretion from sedimentation 24 p3392 N88-30202
Nd isotopes and crustal growth rate
24 p3392 N88-30203
Recycling of lower continental crust through foundering of cumulates from contaminated mafic intrusions
24 p3393 N88-30204
Growth of continental crust: Clues from Nd isotopes and Nb-Th relationships in mantle-derived magmas
24 p3393 N88-30205
Pluton emplacement and magmatic arc construction: A model from the Patagonian batholith
24 p3393 N88-30206
The Kerala Khondalite Belt (KKB) of Southern India: An ensialic mobile belt 24 p3393 N88-30209
Genesis of archean granitoids in the Pilbara block and implications for crustal growth 24 p3394 N88-30210
Role of zircon in tracing crustal growth and recycling
24 p3394 N88-30211
Construction of mass-age curves for the continental crust: An empirical model and an example from the western US 24 p3394 N88-30213
Does subduction zone magmatism produce average continental crust 24 p3394 N88-30214
Pb isotope constraints on the extent of crustal recycling into a steady state mantle 24 p3394 N88-30215
Decoupled Rb-Sr and Sm-Nd isotopic evolution of the continental crust 24 p3395 N88-30216
Metamorphic P-T paths and Precambrian crustal growth in East Antarctica 24 p3395 N88-30218
Early intense cratering: Effects on growth of earth's crust 24 p3395 N88-30219
The growth of continents and some consequences since 1.5 Ga 24 p3395 N88-30220
The early archaean crustal history of West Greenland as recorded by detrital zircons 24 p3395 N88-30221
Deep seismic reflection profiling and continental growth curves 24 p3396 N88-30222
Growth of early archaean crust in the ancient Gneiss complex of Swaziland and adjacent Barberton Greenstone Belt, Southern Africa 24 p3396 N88-30223
Evidence for crustal recycling during the Archean: The parental magmas of the stillwater complex
24 p3396 N88-30226
Changing styles of crustal growth in Southern Africa: Constraints from geochemical and Sr-Nd isotope studies in Archanan to Pan African terrains
24 p3396 N88-30227
Structure of Southwestern Michipicoten Greenstone Belt, Ontario: Evidence for Archean accretion
24 p3397 N88-30228
Mid to late proterozoic magmatism within Northeastern North America and its iplications for the growth of the continental crust 24 p3397 N88-30229
Thermal models pertaining to continental growth
24 p3397 N88-30230
Ridge-trench collision in Archean and Post-Archean crustal growth: Evidence from southern Chile
24 p3397 N88-30233
Reappraisal of the geology of Kangimut Sammisoq, Ameralik Fjord, Southern West Greenland: Crustal structure and interpretation of isotopic data
24 p3398 N88-30234
Archean crustal evolution of the northern North China Craton 24 p3398 N88-30235
Growth of the lower continental crust
24 p3398 N88-30236
The complexity, depth, and rapidity of processes that formed the lunar crust 24 p3398 N88-30237
Continental crustal formation and recycling: Evidence from oceanic basalts 24 p3398 N88-30238
Geochronological and lead-isotope evidences for rapid crust formation in middle-proterozoic time: The Labrador example 24 p3398 N88-30239
Physical processes in the growth of the continental crust 24 p3398 N88-30240
Trace element differences between Archean, Proterozoic and Phanerozoic crustal components: Implications for crustal growth processes
24 p3399 N88-30243
The growth of the continental crust: Constraints from radiogenic isotope geochemistry
24 p3399 N88-30245
Crustal growth in the Archean: The geochemical evidence 24 p3400 N88-30246
Solid earth as a recycling systems and the lateral growth of Precambrian North America 24 p3400 N88-30249
Mineralization through geologic time: Evolution of continental crust 24 p3400 N88-30250
Growth of the continental crust: A planetary-mantle perspective 24 p3400 N88-30251
Crustal underplating in the North American Craton: Evidence from the Petrogenesis of anorthositic rocks in the Middle Proterozoic Midcontinent Rift System
24 p3400 N88-30252
Late-Archaean crustal growth in the Lewisian Complex of Northwest Scotland: Diachroneity in magmatic accretion and implications for models of crustal growth
24 p3401 N88-30253
The effect of thicker oceanic crust in the Archaean on the growth of continental crust through time
24 p3401 N88-30254
Volcanic contribution to crustal growth in the Central Andes: A new estimate and a discussion of uncertainties
24 p3401 N88-30255
The second generation intelligent user interface for the crustal dynamics data information system
24 p3419 N88-30352
Non-atmospheric noble gases from CO(sub 2) well ga
24 p3441 N88-30476
Lava thicknesses: Implications for rheological and crustal development 24 p3443 N88-30490

EARTH ENVIRONMENT
Global environmental change research
[S-HRG-100-301] 03 p0348 N88-12199

EARTH FIGURE
U GEODESY

EARTH GRAVITATION
Estimability of potential coefficients from orbit perturbations — satellite geodesy
[REPT-88.1] 01 p0064 N88-10406
On the theory of the Michelson-Morley experiment in the Earth's gravitational field
[DE87-703077] 02 p0198 N88-11233
Study of a satellite-to-satellite tracking gravity mission
[ESA-CR(P)-2419] 02 p0198 N88-11237
Steady distortion of shape of geoid and normal gravity field under influence of tidal potential
04 p0459 N88-12839
Analysis and synthesis of the Earth's gravity field variable in space and time using vector surface spherical functions
[SER-C-325] 07 p0878 N88-15326
Assessment of anomalous gravitational field of elastic Earth 07 p0921 N88-15534
Department of Defense World Geodetic System 1984: Its definition and relationships with local geodetic systems
[AD-A188815] 12 p1639 N88-19811
Terrestrial gravity data and comparisons with satellite data 12 p1644 N88-19848
Gradiometer accommodation on board a drag-free satellite 12 p1645 N88-19850
Gradiometer mission spectral analysis and simulation studies: Past and future 12 p1645 N88-19851

Comparisons of global topographic/isostatic models to the Earth's observed gravity field
[NASA-CR-182696] 13 p1798 N88-20752

Program for the feasibility of developing a high pressure acoustic levitator
[NASA-CR-182154] 20 p2782 N88-26498

EARTH IONOSPHERE
NT D REGION
NT E REGION
NT F REGION
NT F 2 REGION
NT LOWER IONOSPHERE
NT SPORADIC E LAYER
NT UPPER IONOSPHERE

The combined release and radiation effects satellite, a joint NASA/DOD program 02 p0135 N88-10851

Ionospheric total electron content estimation for single-frequency global positioning system receivers
02 p0161 N88-11005

Ionosphere and plasmasphere
03 p0272 N88-11709

Satellite environment: Polar orbits
03 p0272 N88-11713

JPRS report: Science and technology. China
[JPRS-CST-87-031] 03 p0299 N88-11880

Height profile inversion of ionospheric movement from observed parameters of HF radio echoes
03 p0299 N88-11884

Method estimating integral mean value of enhancement factor and path latitude for whistlers below magnetic latitude 10 deg 03 p0300 N88-11885

Activities report of the Ionospheric Observatory
[UIO-SR-87-01] 05 p0625 N88-13827

Polar Geophysical Institute's studies of magnetosphere, ionosphere 06 p0728 N88-14480

Global convection patterns in the high latitude
[AD-A185794] 06 p0743 N88-14571

Solar-geophysical activity reports for STIP (Study of Travelling Interplanetary Phenomena) interval 15, 12-21 February 1984 ground level event and STIP interval 16, 20 April-4 May 1984 Forbush decrease
[PB88-101274] 06 p0802 N88-14906

EISCAT (European incoherent scatter radar) electron density studies
[AD-A185998] 07 p0841 N88-15099

TRACKER: A 3-D radio ray tracing code
[DE88-003267] 07 p0847 N88-15137

Holography of the ionosphere at HIPAS
[AD-A186237] 07 p0877 N88-15322

Satellite monitoring of earthquake precursor effects in magnetosphere 08 p1007 N88-16103

Diagnostic concept of the resonance cone technique and its application in ground and space experiments
08 p1027 N88-16222

Developments in instrumental techniques for observations of magnetospheric and ionospheric shaped charge releases 08 p1031 N88-16248

CAESAR investigations --- Coordinated Auroral Experiment using Scatter And Rockets (CAESAR)
08 p1031 N88-16249

Collaborative studies of polar cap ionospheric dynamics
[AD-A187888] 10 p1355 N88-18098

Temporal evolution of ionospheric electric field driven by field-aligned current 11 p1469 N88-18761

USU (Utah State University) Center of Excellence in Theory and Analysis of the Geo-Plasma Environment
[AD-A187687] 11 p1511 N88-19026

Propagation in longitudinally varying ducts, with emphasis on guiding to antiguiding transitions
12 p1615 N88-19658

An assessment of the application of in situ ion-density data from DMSP to modeling of transionospheric scintillation
[AD-A188919] 12 p1643 N88-19840

Dynamics of small and large scale irregularities at sub-auroral latitudes
[AD-A189052] 12 p1645 N88-19853

WAVFLD: A program to compute ionospheric height gain functions and field strengths at VLF
[AD-A191159] 16 p2191 N88-23066

Ionospheric research in Antarctica
[INPE-4521-PRE/1273] 16 p2232 N88-23331

Centrifugal acceleration of ions in the polar magnetosphere
[NASA-TM-101148] 17 p2374 N88-24120

The Effect of the Ionosphere on Communication, Navigation and Surveillance Systems Based on Ionospheric Effects Symposium held on 5-7 May 1987 in Springfield, Virginia
[AD-A1[illegible]1855] 18 p2541 N88-25081

Rocket-borne low energy ion measurements in space
18 p2593 N88-25412

Dynamics explorer data analysis
[NASA-CR-181428] 19 p2691 N88-25996

High latitude ionospheric radio studies
[AD-A192270] 20 p2824 N88-26753

Rocket measurements within a polar cap arc ionospheric modelling
[AD-A192381] 20 p2824 N88-26754

On the dynamics of the auroral ionosphere during the breakup of a substorm
[AD-A193368] 21 p2972 N88-27657

Optimized observation periods required to achieve geodetic accuracies using the global positioning system
[AD-A193844] 22 p3041 N88-28052

A model of the ionosphere in the altitude interval 50 to 4000 km. Part 1: Atomic ions (H(+), He(+), N(+), O(+))
[DFVLR-FB-88-11-PT-1] 23 p3233 N88-29241

A model of the ionosphere in the altitude interval 50 to 4000 km. Part 2: Molecular ions (N2(+), NO(+), O2(+)) and electron density
[DFVLR-FB-88-12-PT-2] 23 p3234 N88-29242

The effect of equatorial ionospheric irregularities on the performance of a south-looking OTH-B (Over-The-Horizon-Backscatter) radar
[AD-A195090] 24 p3362 N88-30018

On formulating a simple D-region model
[AD-A195841] 24 p3392 N88-30197

Model representation of electron concentration distribution in outer middle-latitude ionosphere using data from Intercosmos-19 artificial earth satellite
24 p3447 N88-30513

EARTH LIMB

Description of data on the Nimbus 7 LIMS map archive tape: Water vapor and nitrogen dioxide
[NASA-TP-2761] 06 p0744 N88-14572

EARTH MAGNETOSPHERE
NT GEOMAGNETIC TAIL
NT MAGNETOPAUSE

Current-driven lower hybrid waves at the inner edge of the ring current --- magnetosphere
[MPE-PREPRINT-94] 02 p0243 N88-11534

Morphology of the Earth's environment
03 p0272 N88-11706

Hot plasmas in the Earth's magnetosphere
03 p0272 N88-11710

A simplified approach to the dynamics of charged particles in the magnetosphere
03 p0273 N88-11718

Slow-mode shocks in the earth's magnetosphere
[DE88-000483] 04 p0468 N88-12895

Conditions for geomagnetically trapping sub-micron lunar ejecta between L = 1.2 and L = 3.1
04 p0521 N88-13203

Activities report of the Ionospheric Observatory
[UIO-SR-87-01] 05 p0625 N88-13827

Laboratory and near-earth space plasma as a key to the plasma universe
[TRITA-EPP-87-09] 05 p0652 N88-13996

Polar Geophysical Institute's studies of magnetosphere, ionosphere 06 p0728 N88-14480

Curvature driven drift mirror instability in the magnetosphere
[IFSI-86-14] 06 p0742 N88-14568

MAXIE 1 (Magnetospheric Atmospheric X-ray Imaging Experiment) Program
[AD-A185878] 07 p0877 N88-15317

Satellite monitoring of earthquake precursor effects in magnetosphere 08 p1007 N88-16103

Developments in instrumental techniques for observations of magnetospheric and ionospheric shaped charge releases 08 p1031 N88-16248

CAESAR investigations --- Coordinated Auroral Experiment using Scatter And Rockets (CAESAR)
08 p1031 N88-16249

Proceedings of the 21st ESLAB Symposium on Small Scale Processes in the Chromosphere/Corona, Interplanetary Medium and Planetary Magnetospheres
[ESA-SP-275] 08 p1094 N88-16582

Microphysics of the auroral acceleration region of other regions of the magnetosphere 08 p1096 N88-16592

Numerical simulation of solar wind and magnetospheric phenomena 08 p1097 N88-16600

Ion flows in magnetospheric flux transfer events
08 p1098 N88-16607

Simulation and modeling of whistler mode wave growth through cyclotron resonance with energetic electrons in the magnetosphere 10 p1353 N88-18089

A study of the magnetic field annihilation process in the magnetosphere and some geotechnical applications
[DE88-004165] 10 p1355 N88-18096

USU (Utah State University) Center of Excellence in Theory and Analysis of the Geo-Plasma Environment
[AD-A187687] 11 p1511 N88-19026

Energetic particle drift motions in the outer dayside magnetosphere
[DE88-005097] 11 p1512 N88-19034

Electric fields in Earth orbital space: Magnetospheric structural dynamic response to external variables
[AD-A188592] 12 p1643 N88-1963

Observation of a hydromagnetic wave in the earth's magnetosphere
[AD-A188942] 12 p1644 N88-1964

Studies of ionosphere/magnetosphere dynamics using SABRE and HILAT
[AD-A190947] 16 p2232 N88-23333

A plasma wave instrument on the AMPTE/IRM (Active Magnetospheric Particle Tracing Explorers/Ion Release Module) spacecraft
[AD-A191216] 16 p2233 N88-23336

Centrifugal acceleration of ions in the polar magnetosphere
[NASA-TM-101148] 17 p2374 N88-24120

Spacecraft requirements for predictions of geomagnetic activity (a tutorial)
[AD-A191943] 19 p2685 N88-25959

Outer zone electron precipitation produced by a VLF transmitter
[AD-A191944] 19 p2691 N88-25993

MAXIE-1 (Magnetospheric Atmospheric X-ray Imaging Experiment)
[AD-A192846] 21 p2902 N88-27221

Field-aligned structure of the storm time Pc 5 wave of November 14-15, 1979
[AD-A193022] 21 p2972 N88-27653

The low-latitude auroral boundary: Steady-state and time-dependent representations
[AD-A193200] 21 p2972 N88-27654

Solar flares and magnetospheric particles: Investigations based upon the ONR-602 and ONR-604 experiments
[AD-A193396] 21 p3031 N88-27994

Structural dynamics of high-latitude magnetosphere determined from solar electron data
24 p3444 N88-30500

Ring current role in dynamics of fluctuating electron and ion fluxes in low-latitude magnetosphere
24 p3447 N88-30514

Plasma of earth's magnetosphere ring currents: Model compared with results of AMPTE/CCE experiment
24 p3447 N88-30515

EARTH MANTLE

Upper mantle heterogeneity and composition of primary ocean island magmas 08 p1009 N88-16120

Ocean floor magmatism and problems of lithosphere formation 08 p1009 N88-16121

Study of asthenosphere: Project ELAS
08 p1013 N88-16138

The determination of gravity and topography from seismic velocities, accounting for dynamic behavior of the Earth's mantle
[ETN-88-92420] 17 p2374 N88-24117

Carbon analysis in natural olivine crystals of deep origin
[NASA-TT-20311] 19 p2734 N88-26239

Time-dependent thermal convection of Earth mantle and double diffusive convection in magma chambers
[MITT-52] 21 p2974 N88-27663

Workshop on the Growth of Continental Crust
[NASA-CR-183073] 24 p3392 N88-30201

Recycling of lower continental crust through foundering of cumulates from contaminated mafic intrusions
24 p3393 N88-30204

An illustration of the complexity of continent formation
24 p3393 N88-30207

Pb isotope constaints on the extent of crustal recycling into a steady state mantle 24 p3394 N88-30215

The petrogenesis of oceanic kimberlites and included mantle megacrysts: The Malaitan alnoite
24 p3397 N88-302[illegible]

Growth of the continental crust: A planetary-mantle perspective 24 p3400 N88-30251

Discrimination studies using short-period P waves at upper mantle distances
[AD-A195468] 24 p3401 N88-30257

Non-atmospheric noble gases from CO(sub 2) well ga
24 p3441 N88-30476

EARTH MOVEMENTS
NT EARTHQUAKES
NT LANDSLIDES

The analysis of recent crustal movements in static and kinematic models
[SER-B-279] 09 p1191 N88-17130

State-of-the-art for assessing earthquake hazards in the US. Parameters for specifying intensity-related earthquake ground motions
[AD-A188230] 11 p1512 N88-19032

Description of ground motion data processing codes, volume 2
[DE88-007137] 15 p2095 N88-22481

Influence of scattering on seismic waves: Physical mechanisms contributing to attenuation in the crust
[AD-A191699] 19 p2690 N88-259[illegible]

Stochastic geologic effects on near-field ground motions in alluvium
[AD-A192315] 21 p2972 N88-27652

EARTH OBSERVATIONS (FROM SPACE)
NT SATELLITE OBSERVATION
NT SPOT (FRENCH SATELLITE)

Study of a payload for Columbus Polar Platform Earth observation demonstration mission, executive summary
[ESA-CR(P)-2412] 01 p0014 N88-10079

Payload configurations and serviceability --- Columbus Polar Platforms 03 p0339 N88-12133

Legal protection of the Polar Platform's users
03 p0339 N88-12135

Market potential for commercial remote sensing
03 p0339 N88-12137

MBB-ERNO view of remote sensing commercialization
03 p0340 N88-12140

Latitude coverage of observations of the middle atmosphere by solar absorption spectrometry from a heliosynchronous orbit
[AERONOMICA-ACTA-A-316-1987]
06 p0742 N88-14566

From pattern to process: The strategy of the Earth Observing System. Volume 2: EOS Science Steering Committee report
[NASA-TM-89702] 07 p0871 N88-15283

Academic course Space Methods for Studying Modern Landscapes of Continents 08 p1012 N88-16133

The Cryogenic Infrared Spectrometer and Telescope for the Atmosphere (CRISTA) experiment on Astro-SPAS
08 p1034 N88-16270

Status and prospects of the Joint Research Commitee (JRC) work on the application of ocean colour monitoring from space 08 p1043 N88-16299

Canadian activities and goals in remote sensing of ocean colour and fluorescence from space
08 p1043 N88-16300

Federal Republic of Germany's interests, activities and goals in remote sensing of ocean colour/fluorescence from space 08 p1043 N88-16302

French activities in ocean colour observations
08 p1043 N88-16303

The use of chlorophyll fluorescence measurements from space for separating constituents of sea water
08 p1043 N88-16307

Unispace 82 09 p1128 N88-16766

Proceedings of the ESA Workshop on Co-Orbiting Platform Elements (COPE)
[ESA-SP-1083] 09 p1129 N88-16777

An overview of the current Earth observation programs (Europe, USA, and Japan) 09 p1129 N88-16778

Polar platform element of Space Station: Mission objectives, European priorities, candidate instrumentation and selection procedure 09 p1129 N88-16779

Tethers: An outline of a new concept for Earth observation 09 p1129 N88-16781

Microgravity payloads and missions for Space Station: Some issues affecting compatibility with other payloads
09 p1129 N88-16783

Report of the Workshop on Space Systems Possibilities for a Global Energy and Water Cycle Experiment
[WCP-137] 09 p1193 N88-17147

Planet X probe: A fresh new look at an old familiar place 10 p1287 N88-17699

Space-based remote sensing of the Earth: A report to the Congress
[NASA-TM-89709] 10 p1346 N88-18046

NASA's geodynamics program
12 p1644 N88-19845

Space projects for the 90's relevant to climatology
14 p1935 N88-21539

The International Satellite Land-Surface Climatology Project (ISLSCP) 14 p1937 N88-21558

Measurement of the water content of soil from space and application to the regional water balance
14 p1938 N88-21561

Study of the dynamic topography of oceans by means of satellite altimetry 14 p1938 N88-21567

International cooperation in remote sensing: The ESA experience 17 p2356 N88-24038

The role of space borne imaging radars in environmental monitoring: Some shuttle imaging radar results in Asia
[NASA-TM-101178] 18 p2502 N88-24844

Overview of space missions and techniques for ocean monitoring 19 p2700 N88-26053

The Army's role in space: Support for the battlefield commander
[RAND-P-7396] 19 p2721 N88-26159

The detection and interpretation of long-term changes in ozone from space
[NASA-TM-101135] 21 p2971 N88-27650

Determining earth's rotation from laser observations of Lageos artificial earth satellite (during period of main merit campaign) 24 p3449 N88-30528

Obligue metallogenic zones recognized by interpreting space photographs of southern Tien Shan
24 p3450 N88-30529

EARTH OBSERVING SYSTEM (EOS)

Radiometric calibration of the Earth observing system's imaging sensors
[NASA-CR-181542] 04 p0463 N88-12865

HIRIS (High Resolution Imaging Spectrometer: Science opportunities for the 1990s. Earth observing system. Volume 2C. Instrument panel report
[NASA-TM-89703] 07 p0871 N88-15282

From pattern to process: The strategy of the Earth Observing System. Volume 2: EOS Science Steering Committee report
[NASA-TM-89702] 07 p0871 N88-15283

SAR (Synthetic Aperture Radar). Earth observing system. Volume 2F. Instrument panel report
[NASA-TM-89701] 07 p0871 N88-15284

EARTH ORBITAL ENVIRONMENTS

Effect of NASA advanced designs on thermal behavior of Ni-H2 cells
[NASA-TM-100197] 01 p0021 N88-10132

Partial analysis of experiment LDEF A-0114
[NASA-CR-179236] 06 p0780 N88-14787

Investigation of the feasibility of an analytical method of accounting for the effects of atmospheric drag on satellite motion 07 p0923 N88-15608

A Study of Space Station Contamination Effects --- conference
[NASA-CP-3002] 18 p2590 N88-25390

Neutral environment for space station
18 p2590 N88-25391

Space station neutral external environment
18 p2590 N88-25392

Contaminant ions and waves in the space station environment 18 p2590 N88-25393

Space station induced electromagnetic effects
18 p2591 N88-25394

Space station contamination study: Assessment of contaminant spectral brightness
18 p2591 N88-25395

Calculation of space station infrared irradiance from atmosphere-induced emissions
18 p2591 N88-25396

Space station particulate contamination environment
18 p2591 N88-25397

The particulate environment surrounding the space station: Estimates from the PACS data
18 p2591 N88-25398

Effects of meteoroids and space debris on the particulate environment for space station 18 p2591 N88-25399

Contamination of optical surfaces --- Space Station
18 p2592 N88-25400

Surface interactions relevant to space station contamination problems 18 p2592 N88-25401

Laboratory experiments of relevance to the space station environment 18 p2592 N88-25402

Contamination of the space station environment by vented chemicals 18 p2592 N88-25403

Application of superconducting technology to earth-to-orbit electromagnetic launch systems
[DE88-010022] 20 p2763 N88-26386

Relationship between characteristics of low-energy electrons and geomagnetic disturbance in geostationary orbit 24 p3444 N88-30501

EARTH ORBITING SPACE STATIONS
U SPACE STATIONS

EARTH ORBITS
NT GEOSYNCHRONOUS ORBITS

The combined release and radiation effects satellite, a joint NASA/DOD program 02 p0135 N88-10851

Nickel hydrogen low Earth orbit test program update and status 02 p0164 N88-11028

Spacecraft surface exposure to atomic oxygen in low Earth orbit 03 p0273 N88-11715

Low Earth orbit environmental effects on the space station photovoltaic power generation systems
[NASA-TM-100230] 03 p0387 N88-12429

Precise near-earth navigation with GPS: A survey of techniques 04 p0433 N88-12682

Simulation and analysis of a geopotential research mission
[NASA-CR-182354] 06 p0670 N88-14109

Investigation of design concepts for large space structures to support military applications
[AD-A186098] 07 p0824 N88-15000

Single-burn transfer to nominally periodic orbit in the vicinity of point L2 of Earth-Sun system and related problems 08 p1006 N88-16100

Verification of a micro-thrusting model to maintain satellites in low orbit
[AD-A186874] 09 p1133 N88-16793

A lunar transportation system
[NASA-CR-182561] 11 p1567 N88-19379

State-of-the-art technologies for construction in space: A review
[AD-A188412] 12 p1585 N88-19483

Orbital analysis of a STS (Space Transportation System) external tank in low earth orbit
[AD-A188829] 12 p1593 N88-19542

NAVARES: A prototype expert system for NAVSTAR anomaly resolution
[AD-A189491] 12 p1600 N88-19579

Survey of the Air Force P78-2 (SCATHA) satellite plasma wave data during electron gun operations
[AD-A191014] 16 p2168 N88-22926

The prediction of satellite lifetimes
[RAE-TR-87030] 17 p2310 N88-23818

Advanced nuclear rocket engine mission analysis
[DE88-006797] 18 p2475 N88-24681

A standard library for modeling satellite orbits on a microcomputer
[AD-A195759] 24 p3331 N88-29830

Particle trajectories and potentials in a plane sheath moving in a magnetoplasma
[AD-A196228] 24 p3390 N88-30190

EARTH PLANETARY STRUCTURE

Department of Defense World Geodetic System 1984: Its definition and relationships with local geodetic systems
[AD-A188815] 12 p1639 N88-19811

Ultrasonic physical modeling of seismic wave propagation from graben-like structures
[AD-A189066] 13 p1796 N88-20744

DOD 1985 world magnetic model: Charts and grid values
[AD-A191484] 18 p2541 N88-25080

Deep seismic reflection profiling and continental growth curves 24 p3396 N88-30222

EARTH RADIATION
U TERRESTRIAL RADIATION

EARTH RADIATION BUDGET

Atlas of wide-field-of-view outgoing longwave radiation derived from Nimbus 7 Earth radiation budget data set - November 1978 to October 1985
[NASA-RP-1186] 01 p0070 N88-10451

Earth Radiation Budget Satellite (ERBS) orbiting profiles and Ni-Cd use 02 p0165 N88-11034

An Earth radiation budget climate model
[NASA-CR-182368] 06 p0744 N88-14578

High-spatial-resolution TOVS observations for the FIRE/SRB Wisconsin experiment region from October 14 through November 2, 1986
[NASA-TM-100522] 06 p0747 N88-14593

EARTH RADIATION BUDGET EXPERIMENT

Development of response models for the Earth Radiation Budget Experiment (ERBE) sensors. Part 2: Analysis of the ERBE integrating sphere ground calibration
[NASA-CR-178293] 01 p0049 N88-10316

Development of response models for the Earth Radiation Budget Experiment (ERBE) sensors. Part 4: Preliminary nonscanner models and count conversion algorithms
[NASA-CR-178295] 01 p0050 N88-10317

Atlas of wide-field-of-view outgoing longwave radiation derived from Nimbus 7 Earth radiation budget data set - November 1978 to October 1985
[NASA-RP-1186] 01 p0070 N88-10451

Development of response models for the Earth Radiation Budget Experiment (ERBE) sensors. Part 3: ERBE scanner measurement accuracy analysis due to reduced housekeeping data
[NASA-CR-178294] 05 p0583 N88-13553

Development of response models for the Earth Radiation Budget Experiment (ERBE) sensors. Part 1: Dynamic models and computer simulations for the ERBE nonscanner, scanner and solar monitor sensors
[NASA-CR-178292] 05 p0584 N88-13557

Report of the Joint Scientific Commitee Ad Hoc Working Group on Radiative Flux Measurements --- Earth radiation budget
[WCP-136] 06 p0742 N88-14567

Operational aspects of a spacecraft planning/scheduling expert system
08 p1062 N88-16415

Summary of along-track data from the Earth radiation budget satellite for several major desert regions
[NASA-RP-1197] 13 p1802 N88-20772

The Earth radiation budget and its spatial and temporal variations 14 p1936 N88-21548

EARTH RESOURCES
NT AQUIFERS
NT COAL
NT CRUDE OIL
NT FORESTS
NT FOSSIL FUELS
NT GEOTHERMAL RESOURCES
NT GLACIERS
NT ICEBERGS
NT LAND ICE
NT MARINE RESOURCES

NT NATURAL GAS
NT OIL FIELDS
NT RAIN FORESTS
NT TAR SANDS
NT UNDERWATER RESOURCES
NT WATER RESOURCES

Study of Earth from space and strengthening of economy 01 p0010 N88-10055

Space photographs of the Onega-Ladoga isthmus and prediction of useful minerals 08 p1008 N88-16108

Use of space photographs for geomorphological studies in southwestern Tajikistan 08 p1008 N88-16109

Critical issues in NASA information systems
[NASA-CR-182380] 08 p1093 N88-16577

Fine attitude measurement system study. Volume 1: Executive summary
[BAE-TP-7831-VOL-1] 09 p1133 N88-16795

Fine attitude measurement system study, volume 2
[BAE-TP-7831-VOL-2] 09 p1133 N88-16796

Fine attitude measurement system study. Volume 3: Appendices
[BAE-TP-7831-VOL-3] 09 p1133 N88-16797

System-wide medium-term environment programme for the period 1990-1995. Strategies of the United Nations system for the environment
[UNEP/GCSS.I/2] 12 p1641 N88-19826

The use of four-photon Raman spectroscopy for the remote sensing of natural objects
[NASA-TT-20257] 13 p1791 N88-20716

Earth resources: A continuing bibliography with indexes (issue 57)
[NASA-SP-7041(57)] 16 p2229 N88-23314

A proposal for a project entitled assessment of forest resources in Uruguay submitted to the United Nations Industrial Development Organization (UNIDO)
17 p2352 N88-24016

The application of satellites in connection with the environment
[ETN-88-92474] 18 p2532 N88-25020

Survey for least bell's vireo in riparian habitat on Vandenberg Air Force Base, Santa Barbara County, California
[NASA-TM-100984] 20 p2822 N88-26744

EARTH RESOURCES EXPERIMENT PACKAGE
U EREP

EARTH RESOURCES PROGRAM

Earth resources: A continuing bibliography with indexes (issue 55)
[NASA-SP-7041(55)] 01 p0065 N88-10415

Earth resources: A continuing bibliography with indexes (supplement 56)
[NASA-SP-7041(56)] 10 p1347 N88-18051

EARTH RESOURCES TECHNOLOGY SATELLITES
U LANDSAT SATELLITES

EARTH ROTATION

Crustal dynamics project data analysis, 1987. Volume 1: Fixed station VLBI geodetic results, 1979-1986
[NASA-TM-100682] 08 p1035 N88-16279

On error equations for determining Earth rotation parameters with VLBI network 13 p1756 N88-20500

Determination of Earth rotation by the combination of data from different space geodetic systems
[NASA-CR-181388] 13 p1791 N88-20713

Basic research for the geodynamics program
[NASA-CR-183149] 21 p2973 N88-27662

Intraseasonal variability in atmospheric surface pressure and relationship to polar motion
22 p3120 N88-28540

Investigation of the validity of the non-rotating planet assumption for three-dimensional earth atmospheric entry
[AD-A194877] 24 p3331 N88-29829

Determining earth's rotation from laser observations of Lageos artificial earth satellite (during period of main ment campaign) 24 p3449 N88-30528

EARTH SHAPE
U GEODESY

EARTH SURFACE

Unified Sun and sky illumination for shadows under trees
[DE87-014232] 01 p0083 N88-10535

The aerophotogrammetric determination of Earth surface deformations
[SER-C-321] 07 p0872 N88-15288

Space applications in geography
08 p1007 N88-16104

Multistep component analysis of correlations
08 p1009 N88-16115

Electromagnetic induction in spherical earth containing oceans and continents in electrical contact with underlying section: Theory, method, example
08 p1011 N88-16127

Vertical atmospheric sounding
[INPE-4370-PRE/1195] 08 p1036 N88-16283

Earth penetrator strain gage applications
[DE88-002260] 09 p1166 N88-16993

General determination of Earth surface type and cloud amount using multispectral AVHRR data
[NOAA-TR-NESDIS-39] 11 p1506 N88-18997

Terrestrial Propagation Characteristics in Modern Systems of Communications, Surveillance, Guidance and Control
[AGARD-CP-407] 12 p1614 N88-19653

Estimating the solar irradiance of an intermountain region using GOES (Geostationary Operational Environmental Satellite) satellite data: A test of two statistical models
[AD-A188414] 12 p1642 N88-19834

Resolution of the magnetotelluric method for determining local inhomogeneities in the sedimentary cover 13 p1789 N88-20701

Remote sensing of earth terrain
[NASA-CR-182677] 13 p1790 N88-20711

Measurement from satellites of land surface parameters and fluxes in the thermal infrared bands: Problems and methods 14 p1937 N88-21557

The International Satellite Land-Surface Climatology Project (ISLSCP) 14 p1937 N88-21558

A low cost automatic Earth observation satellite tracking ground receiving station 17 p2309 N88-23815

The Shuttle Imaging Radar B (SIR-B) experiment report
[NASA-CR-182923] 17 p2334 N88-23932

Comparison of the solar radiation estimation method by satellites 17 p2360 N88-24055

A bibliography of dunes: Earth, Mars, and Venus
[NASA-CR-4149] 20 p2885 N88-27134

Metric applications of SPOT's lateral stereoscopy
22 p3111 N88-28480

Interactions between air and ground sound at the Earth surface 22 p3149 N88-28733

Estimation of short-wavelength gravity on a dense grid using digital terrain elevation data
[AD-A196325] 24 p3391 N88-30196

EARTH TIDES

Steady distortion of shape of geoid and normal gravity field under influence of tidal potential
04 p0459 N88-12839

Observations of Earth tides by the German Geodetic Research Institute, division 1, in the period 1979-1985 at the Berchtesgaden and Wettzell stations
[SER-B-280] 07 p0872 N88-15291

Effectiveness of oceanographic method in earthquake prediction 08 p1010 N88-16124

EARTH-MOON SYSTEM

Relative motion near the triangular libration points in the Earth-Moon system 01 p0097 N88-10636

The dust ring of the Earth
[RAE-TRANS-2163] 22 p3119 N88-28530

EARTHNET

National Point Of Contact (NPOC)-SPOT inquiry 1986
[NLR-MP-86055-U] 05 p0620 N88-13807

International cooperation in remote sensing: The ESA experience 17 p2356 N88-24038

EARTHQUAKE DAMAGE

SPOT for earthquake hazard zoning in southern Italy, a provisional report 03 p0342 N88-12161

State-of-the-art for assessing earthquake hazards in the US. Parameters for specifying intensity-related earthquake ground motions
[AD-A188230] 11 p1512 N88-19032

EARTHQUAKE RESISTANT STRUCTURES

Practical considerations for structural control: System uncertainty, system time delay and truncation of small control forces
[PB88-163738] 14 p1933 N88-21528

EARTHQUAKES

Historical catalog of Southern Great Basin earthquakes, 1868-1978
[DE87-014340] 02 p0196 N88-11232

Siting and Geotechnical Program Focus and Directions. Report upon the deliberations of a workshop held at the Illinois Institute of Technology, Chicago, Illinois on August 4-5, 1986
[PB87-206272] 02 p0198 N88-11238

SPOT for earthquake hazard zoning in southern Italy, a provisional report 03 p0342 N88-12161

Earthquake source mechanisms and transform fault tectonics in the Gulf of California
03 p0349 N88-12206

Interseismic deformation for normal fault earthquakes
03 p0349 N88-12207

Transform fault earthquakes in the North Atlantic: Source mechanisms and depth of faulting
03 p0350 N88-12208

Hypocenters (1977-1984) around the Richton Dome and the Melvin, Alabama, 1978 earthquake
[DE87-014336] 03 p0351 N88-12214

RRS DISCOVERY Cruise 161, 15 August (227)-19 September (262) 1986. Portuguese Ocean-continent boundary, plate boundaries west of Iberia and seismic structure of sediments off Madeira
[PB87-222006] 06 p0747 N88-14596

State-of-the-art for assessing earthquake hazards in the United States. Report 26: Parameters for specifying magnitude-related earthquake ground motions
[AD-A185997] 07 p0877 N88-15318

Satellite monitoring of earthquake precursor effects in magnetosphere 08 p1007 N88-16103

Effectiveness of oceanographic method in earthquake prediction 08 p1010 N88-16124

Comprehensive method for defining seismogenic zones 08 p1011 N88-16129

Correlation between seismic activity and variations of microseismic oscillations 08 p1011 N88-16131

Naval weapons center active fault map series
[AD-A188425] 12 p1643 N88-19835

Correlation of data on strain accumulation adjacent to the San Andreas Fault with available models
[NASA-CR-180757] 13 p1796 N88-20742

Tectonics and three-dimensional structure of spreading centers: Microearthquake studies and tomographic inversions
[PB88-163290] 14 p1945 N88-21602

Earthquakes from peninsular India: Data from the Gauribidanur seismic array
[DE88-701232] 15 p2093 N88-22471

Characteristics of seismic sources of some Asian earthquakes and Soviet underground explosions from Gauribidanur array records
[DE88-701233] 15 p2093 N88-22472

Specific features of emanation, temperature and hydrodynamic fields in the epicentral zone of tectonic earthquake
[DE88-701140] 17 p2373 N88-24114

SPOT for earthquake hazard zoning in southern Italy
22 p3093 N88-28365

EBERT SPECTROMETERS

An infrared grating spectrometer for GIRL
[ETN-88-91071] 09 p1167 N88-16997

EBR-2 REACTOR
U EXPERIMENTAL BREEDER REACTOR 2

EBULLITION
U BOILING

ECCENTRIC ORBITS

An evaluation of semianalytical satellite theory against long arcs of real data for highly eccentric orbits
[AD-A185825] 08 p0960 N88-15819

ECCENTRICITY

Relative motion of two satellites in close-elliptical orbits
[AD-A188851] 12 p1594 N88-19543

Orbit determination of 1965-09A for analysis of the eccentricity at 15th-order resonance
[RAE-TR-87059] 22 p3047 N88-28081

ECCENTRICS

Pin joints, gears, springs, cranks and other novel micromechanical structures
[DE88-002504] 07 p0864 N88-15245

ECHELON FAULTS
U GEOLOGICAL FAULTS

ECHO SOUNDING

Detection of targets in the presence of clutter using target echo modulations caused by rotating structures
[REPT-12-86] 01 p0036 N88-10231

Utilization of dense packed planar acoustic echosounders to identify turbulence structure in the lowest levels of the atmosphere
[AD-A191006] 16 p2233 N88-23335

ECHOCARDIOGRAPHY

Cardiovascular adaptation to zero-g during a long term flight (237 days) on board the Salyut 7 Soviet space station (1984) 12 p1655 N88-19920

Variation of carotid flow under load, studied by the Doppler echo method --- acceleration tolerance
[REPT-1149] 23 p3240 N88-29282

ECHOES
NT CLUTTER
NT RADAR ECHOES
NT RADIO ECHOES
NT SIGNAL REFLECTION
NT VENUS RADAR ECHOES

Radar information from the partial derivatives of the echo signal phase from a point scatterer
[AD-A193402] 21 p2933 N88-27415

ECLIPSES
NT SOLAR ECLIPSES

Was the eclipse comet of 1893 a disconnected coronal transient? 01 p0115 N88-10733

Calculation of eclipses for elliptical orbits
[INPE-4412-NTE/277] 12 p1594 N88-19545

Colliding stellar winds in the eclipsing Wolf-Rayet binary V444 Cygni
[NASA-CR-182937] 17 p2451 N88-24563

ECLIPSING BINARY STARS
NT DWARF NOVAE

The hard X-ray eclipse in the intermediate polar EX Hydrae
[MPE-PREPRINT-95] 02 p0251 N88-11582

Contemporaneous B,V,R,I photometry and H alpha spectroscopy of YY Gem 04 p0513 N88-13155

Light curve behaviour in the near IR of the CG Cyg system 04 p0513 N88-13156

A flash spectrum of Cl I, C I, N I, and Ni II absorption in 31 Cygni: A direct observation of the reversing layer 04 p0513 N88-13158

New results from high angular resolution observations of alpha Ori 04 p0514 N88-13161

Stromgren photometry of RSCVn and HD108102 04 p0519 N88-13187

BE Ursae Majoris: A detached binary with a unique reprocessing spectrum [NASA-CR-182419] 08 p1083 N88-16526

EXO033319-2554.2: A 55-MG eclipsing AM Herculis binary [MPE-PREPRINT-114] 22 p3163 N88-28838

ECLOGITE

Crustal evolution and the eclogite to granulite phase transition in xenoliths from the West African Craton 24 p3395 N88-30217

ECOLOGICAL SYSTEMS

U ECOLOGY

ECOLOGY

NT COASTAL ECOLOGY

China report: Science and technology [JPRS-CST-87-015] 03 p0298 N88-11873

Compilation of 1986 annual reports of the Navy ELF (Extremely Low Frequency) communications system ecological monitoring program, volume 1 [AD-A184561] 03 p0306 N88-11930

Compilation of 1986 annual reports of the Navy ELF (Extremely Low Frequency) communications system ecological monitoring program, volume 2 [AD-A184562] 03 p0306 N88-11931

New book on space ecology reviewed 07 p0897 N88-15434

Detection of soil erosion with Thematic Mapper (TM) satellite data within Pinyon-Juniper woodlands [NASA-CR-182476] 09 p1185 N88-17103

Comparison of simulation modeling and satellite techniques for monitoring ecological processes [NASA-CR-182592] 12 p1641 N88-19825

Characteristics of the thermal environment [AD-A188359] 12 p1641 N88-19827

Changes in the Antarctic atmosphere due to the reduction of stratospheric ozone [ETN-88-92565] 18 p2540 N88-25074

Ecological risk factors related to environmental uses of genetically engineered organisms [DE88-006674] 18 p2549 N88-25132

Extremely Low Frequency (ELF) communications system ecological monitoring program: Summary of 1986 progress [AD-A192014] 19 p2642 N88-25676

ECONOMETRICS

Explicit construction and analysis of some efficient empirical production functions in data envelopment analysis [AD-A185907] 07 p0908 N88-15502

Estimation and testing in truncated and nontruncated linear median-regression models [AD-A186317] 07 p0911 N88-15522

ECONOMIC ANALYSIS

New technologies and intellectual property: An economic analysis [N-2601-NSF] 01 p0107 N88-10695

Models for conducting economic analysis of alternative fuel vehicles [AD-A184028] 03 p0334 N88-12103

Application of Organic Rankine Cycles (ORCs) to decentralized power generation, preliminary study [DE87-753331] 03 p0347 N88-12197

A large-scale perspective on ecosystems 03 p0360 N88-12265

Economics of fusion reactors [DE88-000580] 05 p0653 N88-14002

Mathematical-cartographic modeling of economic utilization of Atlantic Ocean 06 p0726 N88-14460

Summary of the report of the Senior Committee on Environmental, Safety and Economic Aspects of Magnetic Fusion Energy [DE88-003270] 07 p0937 N88-15692

An extended Cobb-Douglas form for use in production economics [AD-A186372] 07 p0943 N88-15733

Definition and economic evaluation of Space Solar Power Systems (SSPS), part 1 [ILR-MITT-184-1(1987)] 08 p1022 N88-16189

Definition and economic evaluation of Space Solar Power Systems (SSPS), part 2 [ILR-MITT-184-2(1987)] 08 p1022 N88-16190

Exponential lower bounds for finding Brouwer fixed points [DE88-002864] 10 p1425 N88-18513

An economic analysis of a multi-commodity fruit and vegetable irradiator [DE88-003425] 11 p1524 N88-19098

Status of emerging technologies: An economic/technological assessment to the year 2000 [PB88-155775] 11 p1567 N88-19381

Robotics applications in the testing of inertial sensors 12 p1577 N88-19433

An assessment methodology for thermal energy storage evaluation [DE88-004642] 13 p1794 N88-20732

European Progress on Space (EPOS): Participation in the creation of long term European space programs [ILR-MITT-189] 14 p1871 N88-21180

Northern lights: The economic and practical potential of imported power from Canada [DE88-006026] 15 p2093 N88-22473

Production costs of hydrocarbon fuels from biomass [DE88-006667] 18 p2495 N88-24804

Technical and economic evaluation of emerging biomass pyrolysis processes for gasoline production 18 p2536 N88-25048

System capacity and economic modeling computer tool for satellite mobile communications systems 19 p2644 N88-25686

Mutually exclusive alternatives by clustering [DE88-007707] 20 p2882 N88-27115

PAX ECONOPACK economic analysis package users manual [AD-A192949] 20 p2883 N88-27117

A comparative economic evaluation of industrial heat pumps. Part 2: Addendum [DE88-011701] 22 p3117 N88-28519

Absorption heat pumps [DE88-752820] 23 p3229 N88-29218

Possibilities of economical improvements for Moon based rocket propulsion using lunar propellants [ILR-MITT-196] 24 p3338 N88-29871

ECONOMIC DEVELOPMENT

Messerschmitt-Boelkow-Blohm: A company with a tradition 10 p1316 N88-17866

Spin off businesses as mechanisms for transferring technologies [DE88-005640] 13 p1852 N88-21085

ECONOMIC FACTORS

Problems in integrating geographic data [DE87-012880] 01 p0106 N88-10689

Nowcasting for the national economy needs 02 p0199 N88-11241

GSSR powder metallurgy research, production expanding 03 p0286 N88-11797

Commercial perspective of an imaging spectrometer development program 03 p0340 N88-12138

Summary of the report of the Senior Committee on Environmental, Safety and Economic Aspects of Magnetic Fusion Energy [DE88-003270] 07 p0937 N88-15692

Technical-economical evaluation of a novel propfan concept in comparison with the turbofan for the nineties [ETN-88-91022] 11 p1441 N88-18596

Review of commercial spacecraft: Recovery and repair experiences: Implications for future spacecraft designs and operations 12 p1531 N88-19528

Activities report of Lufthansa [ISSN-0176-5086] 16 p2155 N88-22855

Corrosion in aircraft structures. Part 1: Text [LR-527-PT-1] 20 p2775 N88-26458

Corrosion in aircraft structures. Part 2: Figures [LR-527-PT-2] 20 p2775 N88-26459

Trends in civil aircraft propulsion [PNR90441] 22 p3044 N88-28067

Real-time space system control with expert systems 23 p3262 N88-29419

ECONOMIC IMPACT

Understanding and accepting fusion as an alternative energy source [DE88-004356] 10 p1413 N88-18432

Understanding CO2 and climate [PB88-167655] 16 p2234 N88-23341

Evaluation of a flood period (June, 1984) in the southern region of Laguna dos Patos, through remote sensing data, meteorological and oceanographic 17 p2365 N88-24083

Acid rain: Delays and management changes in the Federal research program [GAO/RCED-87-89] 19 p2690 N88-25988

Economic impact of space flight activities in West Germany: Influence of allocations of Bundesministerium fuer Forschung und Technologie [ETN-88-92108] 21 p2901 N88-27215

ECONOMICS

Study of Earth from space and strengthening of economy 01 p0010 N88-10055

A role for national laboratories in enhancing economic competitiveness. The example of high-temperature superconductors: CNSS papers, No. 1 [DE87-013633] 03 p0379 N88-12386

Technology transfer to China [PB87-223418] 04 p0502 N88-13087

The role of basic research in society [DE88-000459] 04 p0502 N88-13090

Economics of fusion reactors [DE88-000580] 05 p0653 N88-14002

Impressions, observations and comments on science and technology in Japan [PB87-235743] 06 p0799 N88-14893

On the role of complete reducibility in general competitive equilibrium models [DE88-005693] 13 p1851 N88-21083

Advances in applied superconductivity: A preliminary evaluation of goals and impacts [DE88-006441] 14 p1986 N88-21844

Technology transfer to China. Volume 2: Working papers, part 1 [PB88-158704] 14 p1992 N88-21872

Review of power requirements for satellite remote sensing systems 17 p2419 N88-24387

Remote sensing applied to the monitoring of mineral extraction in the proximity of urban areas: Pros and cons 19 p2684 N88-25954

A basis of settlement: Economic foundations of permanent pioneer communities [DE88-010907] 20 p2762 N88-26382

Political and economic barriers to information transfer 24 p3437 N88-30460

Formulation and solution of economic equilibrium problems [AD-A196034] 24 p3439 N88-30470

ECONOMY

Japanese industrial research on lean combustion: A case study. International Research Monitoring Program [DE87-013839] 02 p0144 N88-10904

Advancing automation and robotics technology for the space station and for the US economy: Submitted to the United States Congress October 1, 1987 [NASA-TM-100777] 08 p0959 N88-15816

Advancing automation and robotics technology for the space station and for the US economy. Submitted to the United States Congress October 1, 1986 [NASA-TM-89190] 08 p0960 N88-15818

The impact of hemp production on the development of the municipalities of Araras, Leme, Santa Cruz da Conceicao and Pirassununga 19 p2683 N88-25948

Use of remote sensing in the study of superficial formation certifying the development of integrated economy-case example: Rio Claro (SP) region 19 p2683 N88-25950

ECOSYSTEMS

Spatial characterization of acid rain stress in Canadian Shield Lakes [NASA-CR-181136] 01 p0067 N88-10430

Spatial characterization of acid rain stress in Canadian Shield Lakes [NASA-CR-180577] 01 p0067 N88-10431

Investigation of large scale impact of air pollution components on forest ecosystems in Bavaria, West Germany [DFVLR-FB-87-17] 01 p0068 N88-10434

Compilation of 1986 annual reports of the Navy ELF (Extremely Low Frequency) communications system ecological monitoring program, volume 2 [AD-A184562] 03 p0306 N88-11931

Compilation of 1986 annual reports of the Navy ELF (Extremely Low Frequency) communications system ecological monitoring program, volume 3 [AD-A184563] 03 p0306 N88-11932

A modular BLSS simulation model 03 p0359 N88-12260

A large-scale perspective on ecosystems 03 p0360 N88-12265

Disturbance and recovery of Arctic Alaskan tundra terrain: A review of recent investigations [AD-A184442] 04 p0467 N88-12607

Semi-arid ecosystem development as a function of resource processing and allocation [DE88-000890] 07 p0875 N88-15308

ELF (Extremely Low Frequency) communications system ecological monitoring program: Electromagnetic field measurements and engineering support, 1986 [AD-A188057] 11 p1509 N88-19017

Comparison of simulation modeling and satellite techniques for monitoring ecological processes [NASA-CR-182592] 12 p1641 N88-19825

The use of SLAR and SIRA imagenes for the classification of forest typen in tropical rain forests 17 p2356 N88-24036

Structure and dynamics of vegetation in the middle semi-arid tropics. Ouixaba's Caatinga (PE): Terrain analysis of MSS/LANDSAT data 17 p2358 N88-24049

Interpretation of MSS/LANDSAT data for evaluation of physical distribution of mangroves in Cananeia-Iguape (SP) 17 p2363 N88-24072

Application of remote sensing in the conservation of natural areas: Ribeira Valley 19 p2683 N88-25949

Spatial and spectral registration of Javanese landscape units with SPOT 22 p3092 N88-28362

Investigation of the large-scale impact of air pollution components on forest ecosystems in Bavaria
[ESA-TT-1087] 24 p3390 N88-30187

ECS
U EUROPEAN COMMUNICATIONS SATELLITE

EDDIES
U VORTICES

EDDY CURRENTS

Eddy current density in wedge-shaped conducting cylinders with inhomogeneous conductivity
[ETN-87-90404] 01 p0042 N88-10268

Pulsed eddy-current inspection of thin-walled stainless steel tubing
[DE88-001492] 04 p0457 N88-12830

Proceedings of the 2nd Regional Electromagnetic Workshop at Argonne National Laboratory
[DE87-004633] 06 p0690 N88-14230

Eddy Current Seminar, 24-26 March 1986
[PB87-124988] 06 p0696 N88-14269

A pulsed eddy current method for examining thin-walled stainless steel tubing
[DE88-002294] 07 p0866 N88-15255

Nondestructive control: Modeling of electromagnetic phenomena, defect characterization, and sensor optimization
[ECL-86-14] 08 p0993 N88-16008

Low frequency eddy current detection and evaluation of corrosion in aircraft skins
[ETN-88-91664] 09 p1144 N88-16859

Simplified physical approach of the control by eddy current
[DE88-701076] 13 p1764 N88-20552

Eddy current losses induced by rotation of magnetisation
[BLL-M-37634-(5828.4)] 14 p1890 N88-21298

Eddy current nondestructive inspection of graphite epoxy using ferrite cup core probes
[AD-A1[illegible]823] 15 p2074 N88-22365

Aerodynamic and thermal modeling of electromagnetic brakes. Evaluation of convective exchange coefficients and friction losses in the rough wall channels
[ISAL-ITC1-87-02] 16 p2215 N88-23214

Detection sensitivity in thick assemblies --- eddy currents, light alloys, aircraft construction materials
[REPT-48-912/F] 16 p2216 N88-23221

Solving time-dependent two-dimensional eddy current problems
[NASA-TM-100875] 18 p2566 N88-25239

Investigation of Rossby-number similarity in the neutral boundary layer using large-eddy simulation
[DF88-008910] 19 p2666 N88-25851

Sensitivity to crack initiation in thick assemblies. Test report 48-444
[REPT-48-444] 20 p2758 N88-26365

The calculation of time dependent eddy currents in tokamaks
[REPT-206] 23 p3286 N88-29568

EDDY DIFFUSION
U TURBULENT DIFFUSION

EDDY VISCOSITY

Evaluation of a research circulation control airfoil using Navier-Stokes methods 10 p1269 N88-17591

Determining Langmuir circulation parameters on basis of similarity theory 13 p1785 N88-20680

On the zonal momentum balance at the equator
13 p1805 N88-20788

Interaction of a strong vortex with decaying turbulence
[DE88-007102] 14 p1911 N88-21420

EDGE DISLOCATIONS

The growth of persistent slip bands
05 p0597 N88-13648

The effects of thin anodic films on the cyclic microstrain/macrostrain behavior of tungsten
05 p0597 N88-13650

Cyclic deformation of an extruded AlMgSi alloy
05 p0598 N88-13654

The orientations of dipolar walls produced by cyclic deformation 05 p0598 N88-13655

EDGE LOADING

An integral equation analysis of inelastic shells
03 p0336 N88-12118

FEB (Multifilter Electronics Box) lifting device analysis, revision A
[AD-A192313] 21 p2935 N88-27427

Failure analysis of quasi-isotropic composite laminates with free edges under off-axis loading
22 p3049 N88-28092

EDGES
NT LEADING EDGES
NT SHARP LEADING EDGES
NT TRAILING EDGES

Heavy-particle collisions in the plasma edge
[DE87-012928] 02 p0237 N88-11493

Recognizing rigid objects by aligning them with an image
[AD-A184253] 03 p0368 N88-12318

Helicity dissipation in the plasma edge
[DE87-014762] 03 p0378 N88-12376

Free-edge delamination: Laminate width and loading conditions effects
[NASA-TM-100238] 04 p0411 N88-12551

Local likelihood method in the problems related to change points
[AD-A185604] 06 p0768 N88-14718

Statistical investigations of the behavior of a product correlator and an edge detector in critical situations
[MBB-UA-1034/87] 06 p0781 N88-14793

Edge plasmas and plasma/wall interactions in an ignition-class reversed field pinch
[DE88-001825] 06 p0782 N88-14799

L2,3 XANES of the high T sub c superconductor YBa2Cu3O7 with variable oxygen content
[NOTA-INTERNA-888] 06 p0788 N88-14837

A composite grating for moire interferometry
[AD-A186330] 07 p0832 N88-15044

Development of composite polymer-glass edge claddings for Nova laser disks
[DE88-002389] 07 p0860 N88-15220

Proceedings of Image Understanding Workshop, volume 1
[AD-A186103] 07 p0902 N88-15463

Stress intensity and crack displacement for small edge cracks
[NASA-TP-2801] 09 p1184 N88-17095

Visual integration and detection of discontinuities: The key role of intensity edges
[AD-A188012] 11 p1520 N88-19076

Generalised threshold selection for edge detection
[RAE-TR-87035] 14 p1941 N88-21581

Finding texture boundaries in images
[AD-A190554] 15 p2117 N88-22609

The theory of flotation
[NASA-TT-20276] 16 p2207 N88-23172

Measurements of edge turbulence with Langmuir probes in currentless Heliotron E plasmas
[DE88-752313] 16 p2275 N88-23617

Curvature of blended rolled edge reflectors at the shadow boundary contour
[NASA-CR-182974] 18 p2576 N88-25300

Instability-related delamination growth of embedded and edge delaminations 20 p2767 N88-26406

Comparison of edge diffraction theories
[AD-A193880] 22 p3070 N88-28223

Analysis of edge detection techniques for radiographic image measurement
[AD-A193650] 23 p3186 N88-28961

A linear-time algorithm for finding a minimum spanning pseudoforest
[AD-A194029] 23 p3250 N88-29346

Improved time bounds for the maximum flow problem
[AD-A194034] 23 p3272 N88-29471

EDITING

Personal computers and All-In-1: Document transfer and translation
[DE88-003760] 10 p1384 N88-18264

Editing master oceanographic observation data set 4
[AD-A188405] 12 p1649 N88-19876

Editfont an interactive font editing system
[AD-A191007] 16 p2251 N88-23453

Editfont: An interactive font editing system
[AD-A192373] 20 p2838 N88-26836

Script editor: An editor for the specification phase in the development of computer based learning
[REPT-87-68] 20 p2839 N88-26846

EDITING ROUTINES (COMPUTERS)

A hypertext writing environment and its cognitive basis
[AD-A188179] 10 p1389 N88-18298

Editfont an interactive font editing system
[AD-A191007] 16 p2251 N88-23453

Editfont: An interactive font editing system
[AD-A192373] 20 p2838 N88-26836

EDUCATION
NT ASTRONAUT TRAINING
NT FLIGHT TRAINING
NT MAINTENANCE TRAINING
NT PILOT TRAINING
NT SPACE FLIGHT TRAINING

An object-oriented architecture for intelligent tutoring systems
[AD-A184790] 03 p0368 N88-12314

CNET (Chief of Naval Education and Training) Program Automated Tracking System (CPATS): A comprehensive study
[AD-A184694] 03 p0385 N88-12418

The pros and cons of using a CAI package on a central computer as opposed to a microprocessor: What's your CAI MO, mainframe or micro
[DE87-011123] 04 p0475 N88-12929

Special Course on Fundamentals of Fighter Aircraft Design
[AGARD-R-740] 05 p0544 N88-13315

Calendar of selected aeronautical and space meetings
[AGARD-CAL-87/1] 05 p0657 N88-14033

Learning to program methodically. 3: The newly designed course of the elementary programming
[PB87-119871] 06 p0757 N88-14643

A study of the minority college programs at the NASA Johnson Space Center 06 p0798 N88-14887

Activities report of the Technical University of Twente
[ETN-88-90620] 06 p0799 N88-14892

Field evaluation of interactive simulation for maintenance training: SH-3 helicopter electro-mechanical bladefold system
[AD-A185923] 07 p0821 N88-14991

Application of the analysis phase of the instructional system development to the MK-105 magnetic minesweeping mission of the MH-53E helicopter
[AD-A186282] 07 p0822 N88-14994

Compilation and development of K-6 aerospace materials for implementation in NASA spacelink electronic information system 07 p0922 N88-15805

A summary of the Naval Postgraduate School research program
[AD-A186362] 07 p0942 N88-15727

Academic course Space Methods for Studying Modern Landscapes of Continents 08 p1012 N88-16133

Overlearning and positive thinking alleviate negative effects of stress on performance
[FOA-C-50051-5.3] 08 p1051 N88-16344

The use and generation of illustrative examples in computer-based instructional systems
08 p1060 N88-16400

ESA Bulletin No. 25
[ISSN-0376-4265] 09 p1128 N88-16767

Training in satellite ground system operations
09 p1129 N88-16775

The desktop interface in intelligent tutoring systems
09 p1205 N88-17225

Computer assisted instruction: Two decades in perspective
[AD-A186813] 09 p1216 N88-17289

Training guidelines in non-destructive testing techniques
[DE88-700613] 10 p1342 N88-18019

Interdisciplinary research in mathematics, science and technology education
[PB88-131446] 10 p1398 N88-18333

The design and implementation of pedagogical software for the multi-backend/multi-lingual database system
[AD-A188106] 11 p1530 N88-19135

Report of the participation in the International Training Course: Remote Sensing in Village Forestry
[INPE-4476-NTE/278] 12 p1637 N88-19802

Aircrew training devices: Utility and utilization of advanced instructional features, phase 4
[AD-A188418] 12 p1670 N88-20000

Field dependence-independence and its relationship to flight training performance
[AD-A188888] 12 p1670 N88-20003

Northeast Artificial Intelligence Consortium (NAIC) administrative matters and ancillary functions, volume 1
[AD-A189466] 12 p1682 N88-20055

Text organization and comprehensibility in technical writing
[AD-A188913] 12 p1707 N88-20217

Down-to-Earth approach for final projects in Karlsruhe (Federal Republic of Germany)
16 p2226 N88-23292

Elementary and middle school science improvement project
[NASA-CR-179328] 16 p2285 N88-23679

Technique to obtain the agricultural ownership limits by satellite imagery, to approve control, and to accompany agricultural activity 19 p2682 N88-25943

Using space photography of the Earth in the classroom: Drought in Africa
[NASA-CR-182948] 19 p2685 N88-25960

Selection and training of subjects to live and work in hostile and unusual environments
19 p2696 N88-26026

Communication training for aircrews: A review of theoretical and pragmatic aspects of training program design
[NASA-CR-177459] 20 p2756 N88-26349

Inference and discovery in an exploratory laboratory
[AD-A192231] 20 p2832 N88-26801

United States Air Force Graduate Student Summer Support Program, volume 2
[AD-A191122] 21 p2924 N88-27355
Can CNV amplitude predict ability to accomplish a demanding task? 21 p2980 N88-27700
Space imagery as a teaching aid in secondary education 22 p3114 N88-28500
Training of the Group for the Development of Aerospace Remote sensing 22 p3114 N88-28501
Effects of psychophysical lifting training on maximal repetitive lifting capacity
[AD-A192605] 23 p3238 N88-29271
Future air-to-air training for the RF-4
[AD-A194363] 23 p3240 N88-29284
Proposed improvements to the USAF flight screening program
[AD-A194506] 23 p3240 N88-29285
Commentary on Harold Hotelling's articles on the teaching of statistics
[AD-A194215] 23 p3273 N88-29484
Integration of LANTIRN (Low Altitude Navigation and Targeting Infrared for Night) into operational fighter training
[AD-A194906] 24 p3325 N88-29799

EEG (ELECTROENCEPHALOGRAMS)
U ELECTROENCEPHALOGRAPHY

EFFECTIVENESS
NT COST EFFECTIVENESS
NT SYSTEM EFFECTIVENESS
Effectiveness of electrodeposited coatings in reducing atmospheric corrosion of copper substrates
[DE87-013651] 05 p0566 N88-13448
Impact of flying qualities on mission effectiveness for helicopter air combat, volume 1
[NASA-CR-166568] 06 p0669 N88-14100
The effectiveness of caches and data prefetch buffers in large-scale shared memory multiprocessors
[DE88-003594] 09 p1223 N88-17334
Ion beam modification of film stress and the effectiveness of thin film encapsulants on GaAs
[DE88-004458] 11 p1558 N88-19328
Film cooling effectiveness on a flat plate in high free-stream turbulence using a single row of 30 deg slant-hole injectors
[AD-A190500] 15 p2147 N88-22816
Effectiveness evaluation of fault-tolerant multiprocessor systems
[AD-A191686] 18 p2554 N88-25158
Report to Congress on the effectiveness of the Civil Aviation Security Program
[AD-A195282] 24 p3322 N88-29784

EFFECTORS
U CONTROL EQUIPMENT

EFFERENT NERVOUS SYSTEMS
A survey of artificial neural systems
[AD-A184759] 03 p0368 N88-12312
Motor control in man and monkey
11 p1518 N88-19065

EFFICIENCY
NT CHARGE EFFICIENCY
NT COMBUSTION EFFICIENCY
NT COMPRESSOR EFFICIENCY
NT ENERGY CONVERSION EFFICIENCY
NT NOZZLE EFFICIENCY
NT POWER EFFICIENCY
NT PROPELLER EFFICIENCY
NT PROPULSIVE EFFICIENCY
NT THERMODYNAMIC EFFICIENCY
NT TRANSMISSION EFFICIENCY
High energy efficient solid state laser sources
[NASA-CR-181362] 01 p0052 N88-10332
Impact of turbulence modeling on numerical accuracy and efficiency of compressible flow simulations
[NASA-TM-88333] 02 p0173 N88-11088
Semiconductor detector performance for low-energy X-rays
[DE87-014132] 02 p0244 N88-11542
Efficiency analysis of airborne Electronic CounterMeasures (ECM) systems
[AD-A184606] 03 p0306 N88-11934
High power ion thruster performance
[NASA-TM-100127] 04 p0409 N88-12542
MHD energy fluxes for late type dwarfs
04 p0512 N88-13148
An empirical investigation of load indices for load balancing applications
[AD-A185763] 06 p0724 N88-14451
An efficient algorithm for computing the crossovers in satellite altimetry
[NASA-CR-182389] 07 p0871 N88-15286
Advanced propeller research
08 p0957 N88-15806
Knowledge representation by connection matrices: A method for the on-board implementation of large expert systems 08 p1065 N88-16434
Frequency-sampling design of two-dimensional FIR digital filters with nonuniform samples
[AD-A187773] 11 p1477 N88-18815
Limiting efficiency of a thermionic diode
[DE88-700598] 11 p1479 N88-18830
Growth of Cr,Nd:Gd3Sc2Al3O12 (Cr,Nd:GSAG) crystals by the Heat Exchanger Method (HEM)(trademark)
[DE88-004041] 11 p1558 N88-19326
Efficiency of human workers and means to increase it
12 p1666 N88-19986
Minimizing development flight test time and cost in the US Air Force 12 p1703 N88-20192
Engineering management for validation prototype phase 12 p1703 N88-20195
High power, high efficiency, 2D laser diode arrays for pumping solid state lasers
[DE88-004042] 13 p1777 N88-20632
Demonstration of efficient full aperture Type 1/Type 2 third harmonic conversion on Nova
[DE88-003834] 14 p1914 N88-21438
Polysilicon-contacted p+ emitters for silicon solar cell applications
[DE88-005106] 14 p1942 N88-21586
Supercomputer programming environments
[AD-A190887] 16 p2251 N88-23452
Study of light transmission methods from scintillators to optical fiber with wave length shifter
[DE88-701587] 18 p2574 N88-25292
Advanced energy system program
[PB88-183025] 19 p2686 N88-25965
An efficient computational tool for ramjet combustor research
[DE88-010034] 20 p2760 N88-26369
Heat pump augmented radiators for spacecraft thermal management
[DE88-007890] 20 p2764 N88-26392
A matroid algorithm and its application to the efficient solution of two optimization problems on graphs, revision
[AD-A192709] 20 p2838 N88-26838
Efficiency optimization for FEL oscillators
[AD-A192541] 21 p2952 N88-27536
A rapid electrochemical technique for determining the current efficiency for cadmium plating
[AD-A193679] 22 p3056 N88-28130
Solar energy absorption efficiency of an ellipsoidal receiver-reactor with specularly reflecting walls
[AD-A193726] 22 p3117 N88-28520
Recent advances in high-power microwave amplifiers
[DE88-007820] 23 p3206 N88-29083
An efficient patched grid Navier-Stokes solution for multiple bodies, phase 1
[AD-A194166] 23 p3211 N88-29110
Experimental and analytical study of two-phase flow in zero gravity
[AD-A195223] 24 p3358 N88-29993
A standard architecture for controlling robots
[AD-A195929] 24 p3423 N88-30371

EFFLUENTS
Real-time evaluation and prediction of coastal dispersion near the SW tip of Africa --- effluents
02 p0210 N88-11318
Comparison of open and closed multimegawatt space power systems 17 p2414 N88-24353

EFFORT
Attention, effort, and fatigue: Neuropsychological perspectives 16 p2241 N88-23387

EFFUSIVES
NT LAVA
Low pressure gas flow analysis through an effusive inlet using mass spectrometry
[NASA-CR-182712] 14 p1910 N88-21413
Progress in determining the thickness and distribution of volcanic materials on Mars 23 p3302 N88-29670
Volcano evolution on Mars 23 p3305 N88-29686

EGGS
Effects of heavy ions on egg-developing systems
12 p1658 N88-19935

EGYPT
Discrimination of sand transport rates and environmental consequences in central Egypt from SPOT data
22 p3093 N88-28366
Evaluation of SPOT imagery contribution to petroleum exploration: The Suez Rift (Egypt)
22 p3102 N88-28425

EIGENFUNCTIONS
U EIGENVECTORS

EIGENSTATES
U EIGENVECTORS

EIGENVALUES
The polarization field for pulsed Raman transitions
[DE87-013118] 01 p0035 N88-10227
On the maximum of solutions for a semilinear elliptic problem
[REPT-87-08] 01 p0086 N88-10554
Stability of semidiscrete approximations for hyperbolic initial-boundary-value problems: An eigenvalue analysis
[NASA-TM-88328] 02 p0227 N88-11434
Stability of spheroidal spheromak plasma by use of force-free approximation
[IPPJ-846] 02 p0241 N88-11523
Investigation, development and application of optimal output feedback theory. Vol 4: Measures of eigenvalue/eigenvector sensitivity to system parameters and unmodeled dynamics
[NASA-CR-4108] 04 p0482 N88-12969
Ballooning modes or Fourier modes in a toroidal plasma?
[AD-A184299] 04 p0491 N88-13022
Eigenvalue projection theory for linear operator equations of electromagnetics
[AD-A185434] 05 p0575 N88-13504
Simultaneous structural and control optimization via linear quadratic regulator eigenstructure assignment
05 p0594 N88-13622
Eigenvalues and eigenvectors of field tensors and associated energy tensors
[DE88-001951] 06 p0763 N88-14682
Diffusion first passage times: Approximations and related differential equations
[AD-A185592] 06 p0765 N88-14700
The effect of response scaling on the detection of singularities in multiresponse estimation
[AD-A185964] 07 p0908 N88-15503
On the asymptotic joint distributions of the eigenvalues of random matrices which arise under components of covariance model
[AD-A186387] 07 p0915 N88-15558
Transversely anisotropic curved optical fibres: Variational analysis of a nonstandard Eigenproblem
[PB88-112966] 08 p1083 N88-16528
An efficient method for computing leading Eigenvalues and Eigenvectors of large asymmetric matrices
09 p1159 N88-16949
Developments related to scattering eigen elements in Schroedinger operators for particles with spin
[ETN-88-91077] 09 p1229 N88-17361
On an overdetermined Neumann problem
[AD-A187451] 10 p1401 N88-18352
Eigenvalue problems
[AD-A188069] 10 p1401 N88-18356
An O(N squared) method for computing the eigensystem of N by N symmetric tridiagonal matrices by the divide and conquer approach
[NASA-CR-181647] 11 p1537 N88-19184
An application of dimensionless Eigenvalues to underwater acoustic ducts
[AD-A188167] 11 p1542 N88-19219
Design graphs for the first two bending Eigenvibration forms of rotating beams consisting of two beam points
[IW-86006R] 13 p1783 N88-20670
Numerical solution of ill posed problems in partial differential equations
[AD-A189383] 13 p1825 N88-20909
Further study of relation of von Karman equation for elastic large deflection problem and Schrodinger equation for quantum eigenvalues problem
14 p1899 N88-21341
A parallel algorithm for computing the singular value decomposition of a matrix
[DE88-007059] 14 p1958 N88-21673
Application of eigenstructure assignment techniques in the design of a longitudinal flight control system
[AD-A189644] 15 p2020 N88-22039
Fluid motion in a spinning, coning cylinder via spatial eigenfunction expansion
[AD-A190758] 15 p2066 N88-22319
Parallel computer methods for eigenvalue extraction
16 p2218 N88-23233
Reduced order models for nonlinear aerodynamics
16 p2220 N88-23248
Theoretical investigations of drift waves in a magnetic quadrupole 18 p2578 N88-25312
Eigenmatrix representations of radiance distributions in layered natural waters with wind-roughened surfaces
[PB88-188701] 20 p2828 N88-26780
Computing small singular values of bidiagonal matrices with guaranteed high relative accuracy. LAPACK working note number 3
[DE88-008465] 20 p2837 N88-26823
Eigenmodes of a random walk on a 2-D lattice torus with one trap
[DE88-007830] 20 p2844 N88-26874
Superconducting rf and beam-cavity interactions
[DE88-008598] 20 p2852 N88-26936
Computation of the eigenvalues for perturbations of Poiseuille flow using a two-point boundary value method
[AD-A193479] 23 p3210 N88-29104
Solving the symmetric tridiagonal eigenvalue problem on the hypercube
[AD-A193905] 23 p3250 N88-29344

Numerical calculations of the response of a spinning spheroidal payload to coning motion
[AD-A195890] 24 p3368 N88-30059
Regularity and numerical solution of eigenvalue problems with piecewise analytic data
[AD-A194993] 24 p3425 N88-30387
Multiple solutions and bifurcation for a class of nonlinear Sturm-Liouville eigenvalue problems on an unbounded domain
[AD-A195954] 24 p3426 N88-30389

EIGENVECTORS
Graph partitioning by eigenvectors
[AD-A184430] 03 p0372 N88-12338
New feedback design methodologies for large space structures: A multi-criterion optimization approach
04 p0408 N88-12535
Investigation, development and application of optimal output feedback theory. Vol. 4: Measures of eigenvalue/eigenvector sensitivity to system parameters and unmodeled dynamics
[NASA-CR-4108] 04 p0482 N88-12969
Eigenvectors of distance-regular graphs
[AD-A185375] 05 p0641 N88-13919
Eigenmode analysis of parallel waveguide couplers
[PB87-132122] 06 p0693 N88-14254
Eigenvalues and eigenvectors of field tensors and associated energy tensors
[DE88-001951] 06 p0763 N88-14682
Eigenvectors of graphs
[AD-A185538] 06 p0765 N88-14698
An efficient method for computing leading Eigenvalues and Eigenvectors of large asymmetric matrices
09 p1159 N88-16949
An application of eigenspace methods to symmetric flutter suppression
[NASA-CR-181618] 10 p1284 N88-17684
Eigenvalue problems
[AD-A188069] 10 p1401 N88-18356
A component synthesis method using Lanczos vectors
[DE88-002263] 10 p1403 N88-18368
An O(N squared) method for computing the eigensystem of N by N symmetric tridiagonal matrices by the divide and conquer approach
[NASA-CR-181647] 11 p1537 N88-19184
Application of eigenstructure assignment techniques in the design of a longitudinal flight control system
[AD-A189644] 15 p2020 N88-22039
Fluid motion in a spinning, coning cylinder via spatial eigenfunction expansion
[AD-A190758] 15 p2066 N88-22319
Reduced order models for nonlinear aerodynamics
16 p2220 N88-23248
Discontinuous inverse Sturm-Liouville problems with symmetric potentials
[DE88-009803] 19 p2720 N88-26152
Observational/numerical study of the upper ocean response to hurricanes
[AD-A193592] 22 p3128 N88-28598

EIKONAL EQUATION
Eikonal solutions to optical model coupled-channel equations
[NASA-TP-2830] 24 p3428 N88-30402

EINSTEIN EQUATIONS
Torsion as a source of expansion in a Bianchi type I universe in the self-consistent Einstein-Cartan theory of a perfect fluid with spin density
[AD-A184200] 03 p0322 N88-12037
Cosmological applications of singular hypersurfaces in general relativity 04 p0521 N88-13202
Ambiguity in determining the effective action for string-corrected Einstein gravity
[PB87-166153] 09 p1259 N88-17550
Raychaudhuri equation in the self-consistent Einstein-Cartan theory with spin-density
[NASA-TM-101145] 17 p2447 N88-24546
Inflation in Einstein-Cartan theory with energy-momentum tensor with spin
[NASA-TM-101164] 17 p2447 N88-24547
Inevitable inflation in Einstein-Cartan theory with improved energy-momentum tensor with spin
[NASA-TM-101146] 18 p2586 N88-25365
N = 2 supergravity in superspace: different versions and matter couplings
[DE88-702137] 19 p2741 N88-26274
Towards a finite quantum gravity
[DE88-701497] 23 p3294 N88-29619

EINSTEIN OBSERVATORY
U HEAO 2

EISCAT RADAR SYSTEM (EUROPE)
Report of the 3rd Finnish EISCAT Workshop --- European Incoherent Scatter Radar (EISCAT)
[REPT-111] 06 p0691 N88-14233
EISCAT research in Finland in 1986
06 p0691 N88-14234
Finnish contributions to EISCAT science in 1986
06 p0691 N88-14235
CP-1-H analysis tests 06 p0691 N88-14236
The new CP3 06 p0691 N88-14237
The solution of large linear inverse problems
06 p0691 N88-14238
Incoherent radar spectra 06 p0691 N88-14239
Correction method for Barker-coded modulation
06 p0691 N88-14240
Data analysis at the Oulu (Finland) EISCAT laboratory
06 p0691 N88-14241
Description of data handling system installed December 11, 1986 --- EISCAT 06 p0692 N88-14242
EISCAT research programs for 1987
06 p0692 N88-14244
EISCAT (European incoherent scatter radar) electron density studies
[AD-A185998] 07 p0841 N88-15099
First results from the Viking associated Aureld-VIP rocket and EISCAT campaign --- auroras; Swedish satellite
08 p1026 N88-16211
CAESAR investigations --- Coordinated Auroral Experiment using Scatter And Rockets (CAESAR)
08 p1031 N88-16249
EISCAT measurements of ion velocities during Coordinated Auroral Experiment using Scatter And Rockets (CAESAR) campaign 08 p1031 N88-16251
Future developments of auroral D-region research using the EISCAT VHF incoherent scatter radar
08 p1035 N88-16278
Coordinated Auroral Experiments using Scatter And Rocket investigations (CAESAR investigations)
[MPAE-W-47-87-13] 15 p2096 N88-22487

EJECTA
Conditions for geomagnetically trapping sub-micron lunar ejecta between L = 1.2 and L = 3.1
04 p0521 N88-13203
Magnetic field draping about coronal mass ejecta
[DE88-001805] 05 p0661 N88-14057
Dynamics of meteor streams
06 p0732 N88-14503
Bilateral symmetry elements of the Zhamanshin impact crater
[NASA-TT-20286] 15 p2096 N88-22490
Effects of meteoroids and space debris on the particulate environment for space station 18 p2591 N88-25399
Variation in the thickness of ejecta cover on Mars with increasing crater density 23 p3307 N88-29701

EJECTION
NT STELLAR MASS EJECTION
Design of a gas mass flow control system for the gas inlet installation of a solid fuel combustion chamber
[VTH-LR-471] 09 p1141 N88-16839
Ejection mechanisms in the sublayer of a turbulent channel 16 p2195 N88-23090
Ejection situations in the U-2/TR-1: An analysis of emotions and events
[AD-A192872] 21 p2893 N88-27175

EJECTORS
A cold ejector for closed-cycle helium refrigerators
04 p0434 N88-12690
A computational study of thrust augmenting ejectors based on a viscous-inviscid approach
10 p1326 N88-17929
CRRES chemical release mechanisms
14 p1874 N88-21192
A spin and deployment mechanism
14 p1926 N88-21479
Numerical and experimental investigation of multiple shock wave/turbulent boundary layer interactions in a rectangular duct
[AD-A190772] 15 p2066 N88-22320

EL NINO
On the interannual variability of South American climate and the Southern Oscillation 04 p0470 N88-12905
Equatorial dynamics and ocean-atmosphere coupling
14 p1938 N88-21565
The patterns of tropical convection during the 1986-87 ENSO 22 p3120 N88-28537
Prolonged periods of above-normal temperatures in Canada, 1986/87 22 p3120 N88-28538
Zonal wind observations at Christmas Island (2 deg N, 157 deg W) during the 1986-1987 El-Nino
22 p3120 N88-28539
Climatology of various synoptic systems over the tropical North Pacific 22 p3121 N88-28542
Modes of interannual climate variability and Sahel rainfall anomalies 22 p3121 N88-28547
Tropospheric biennial variability and its relationship to the southern oscillation 22 p3121 N88-28549
ENSO, sea-surface temperatures and African rainfall
22 p3122 N88-28550
Sub-Saharan rainfall anomalies and global sea-surface temperature relationships for the recent fifteen year (1970-1984) period 22 p3122 N88-28552
Simulation studies of the influence of sea-surface temperature anomalies on the Sahelian circulation and rainfall 22 p3122 N88-28553
On the energy source of 1982-83 ENSO episode simulated by the NCAR community climate model
22 p3122 N88-28556
Some evidence for a Northern Hemispheric extratropic trigger mechanism of ENSO events
22 p3123 N88-28558
The impact of the El Nino event on the ECMWF model performance 22 p3125 N88-28576

ELASTIC ANISOTROPY
Wave propagation in laminated composite plates
[AD-A188999] 12 p1604 N88-19594
A hybrid-stress finite element approach for stress and vibration analysis in linear anisotropic elasticity
[NASA-CR-179311] 12 p1634 N88-19784

ELASTIC BARS
Unstable elastic materials and the visco-elastic response of bars in tension
[AD-A187969] 11 p1498 N88-18946

ELASTIC BENDING
The Hamiltonian structure of nonlinear elasticity: The convective representation of solids, rods, and plates
[AD-A187200] 11 p1498 N88-18943
The surface crack problem in an orthotropic plate under bending and tension
[NASA-CR-178281] 18 p2531 N88-25014
Compliant robotic structures, part 3
[AD-A192426] 21 p2955 N88-27556

ELASTIC BODIES
Scattering of longitudinal wave normally incident on discal cavity in elastic body 08 p1077 N88-16492
The Hamiltonian structure of nonlinear elasticity: The convective representation of solids, rods, and plates
[AD-A187200] 11 p1498 N88-18943
The quasi-static contact problem with friction for three dimensional elastic bodies
[REPT-87-51] 14 p1918 N88-21447
Dynamic stability of elastic rotor-bearing systems via Liapunov's direct method 21 p2958 N88-27571
Dynamics of articulated aerospace structures
[AD-A195685] 24 p3324 N88-29794

ELASTIC BUCKLING
Vibration and buckling of geometrically imperfect laminated cylindrical shells 04 p0456 N88-12822
Local delamination buckling in layered structures
18 p2480 N88-24711

ELASTIC COLLISIONS
U ELASTIC SCATTERING

ELASTIC CONSTANTS
U ELASTIC PROPERTIES

ELASTIC CYLINDERS
Study of temperature and stress fields of two sliding cylinders
[ETN-88-92134] 20 p2815 N88-26704
The acoustic field scattered from some approximate pressure release materials
[AD-A194768] 23 p3278 N88-29515

ELASTIC DAMPING
NT VISCOELASTIC DAMPING
Theoretical and experimental damping values of piping systems at high ductilities
[DE88-006717] 18 p2526 N88-24986

ELASTIC DEFORMATION
NT ELASTIC BENDING
NT ELASTIC BUCKLING
An integral equation analysis of inelastic shells
03 p0336 N88-12118
A critical review of the development of several viscoplastic constitutive theories
[AD-A185652] 07 p0867 N88-15262
On the relations between cyclic contraction ratio flowstress and deformation mechanisms in bainitic CrMoV steels
[DE87-753043] 08 p0968 N88-15856
The relationship of tensile specimen size and geometry effects to unique constitutive parameters for ductile materials
[AD-A186020] 08 p0994 N88-16012
A substructure method for dynamic simulation of flexible mechanical systems with geometric nonlinearities
09 p1176 N88-17044
Stress intensity and crack displacement for small edge cracks
[NASA-TP-2801] 09 p1184 N88-17095
A large strain thermomechanical forming model for elastic-viscoplastic behavior in metals
10 p1301 N88-17780
Institute for Materials Science and Engineering, Fracture and Deformation Division: Technical activities, 1987
[PB88-153622] 10 p1345 N88-18039
Unstable elastic materials and the visco-elastic response of bars in tension
[AD-A187969] 11 p1498 N88-18946
On the dissipative response due to discontinuous strains in bars of unstable elastic material
[AD-A188114] 11 p1498 N88-18947

Equilibrium shocks in plane deformations of incompressible elastic materials
[AD-A188696] 12 p1636 N88-19796
Body tensor formalism in finite deformation elasticity and application to the torsion of a circular cylinder
13 p1780 N88-20651
An analysis of large deformation axisymmetric inelastic problems by finite element and boundary element methods 13 p1782 N88-20664
Unified constitutive models for high-temperature structural applications 14 p1932 N88-21523
A constitutive model for an overlay coating
14 p1933 N88-21525
Non-isothermal elastoviscoplastic analysis of planar curved beams 14 p1933 N88-21526
Phenomenological modelling of rate-dependent plasticity for high strain rate problems
[DE88-006647] 15 p2087 N88-22440
Critical issues and directions for fracture mechanics and structural integrity
[AD-A193050] 21 p2960 N88-27584
An endochronic rate-sensitive constitutive equation for metals, application to generalized creep and large deformations
[AD-A194167] 22 p3055 N88-28125
Dynamics of articulated aerospace structures
[AD-A195685] 24 p3324 N88-29794

ELASTIC MEDIA
Refraction of shear wave into nonlinearly elastic or elastoplastic half-space 02 p0159 N88-10999
Boundary element analysis for dynamic loading of a circular plate on an elastic medium
[CI-86] 06 p0722 N88-14443
Functional and mechanical analysis of continuous media-application to the study of elastic composites with periodic structure: Homogenization
[NASA-TT-20188] 18 p2480 N88-24710
A numerical treatment of the fluid/elastic interface under range-dependent environments
[AD-A192476] 21 p3005 N88-27821

ELASTIC MODULUS
U MODULUS OF ELASTICITY

ELASTIC PLATES
An exact theory of elastic plates
[ETN-87-90675] 01 p0062 N88-10396
Correction to a single higher order theory of elastic plates
[ETN-87-90676] 01 p0062 N88-10397
Boundary stabilization of thin elastic plates
[AD-A187123] 10 p1343 N88-18025
Acoustic radiation from line- and point-loaded plates: Uniformly asymptotic solutions
[AD-A189367] 13 p1834 N88-20969
Kinematic support using elastic elements
14 p1926 N88-21481
Estimation and control of distributed models for certain elastic systems arising in large space structures
[AD-A192120] 18 p2472 N88-24666
Tripping of stiffened plates using a refined beam theory
[AD-A193989] 22 p3087 N88-28333
Elastic wave dispersion in laminated composite plate
[AD-A192289] 23 p3188 N88-28967

ELASTIC PROPERTIES
NT AEROELASTICITY
NT ANELASTICITY
NT ELASTOPLASTICITY
NT HYDROELASTICITY
NT MAGNETOSTRICTION
NT MODULUS OF ELASTICITY
NT PHOTOELASTICITY
NT PROPORTIONAL LIMIT
NT THERMOELASTICITY
NT THERMOVISCOELASTICITY
NT VISCOELASTICITY
Contribution to the numerical calculation of fracture-mechanical quantities for elastic and elastic-plastic material behavior, especially for mixed loads
[ETN-87-90435] 01 p0062 N88-10399
Perfine: Personal finite elements on a microcomputer
[ETN-87-90678] 01 p0082 N88-10528
Energy changes in transforming solids
[DE87-011257] 02 p0191 N88-11194
Ultrasonic characterization of the nonlinear elastic properties of unidirectional graphite/epoxy composites
[NASA-CR-4100] 03 p0281 N88-11767
A method for the efficient calculation of elastic rotor blade dynamic response in forward flight
04 p0394 N88-12460
Carbon-fiber reinforced plastics
04 p0403 N88-12506
Natural control of flexible space structures
04 p0408 N88-12534
Model for ultrasonic attenuation and elastic constant in chromium and its alloys
[DE87-703478] 04 p0415 N88-12570
Nonlinear acoustics
[AD-A184271] 04 p0488 N88-13004
Soliton twin boundaries of the cubic-tetragonal martensitic transformations in ferroelastic materials
[DE87-014741] 04 p0495 N88-13047
Coupled elastic rotor/body vibrations with inplane degrees of freedom 05 p0596 N88-13643
Two low-order mixed methods for the elasticity problem
[PB87-225272] 05 p0610 N88-13749
A simulation study of the flight dynamics of elastic aircraft. Volume 1: Experiment, results and analysis
[NASA-CR-4102] 06 p0669 N88-14099
The effective elastic properties of low-density foams
[DE87-014629] 06 p0684 N88-14194
Thermometrical investigations on the near threshold fatigue crack propagation behavior
06 p0717 N88-14400
Fastening high resistance bolts in real assemblies
[CRIF-MT-171] 07 p0861 N88-15221
Assessment of anomalous gravitational field of elastic Earth 07 p0921 N88-15594
Interrelation and measurement of formability, strengthening, and thermomechanical processing under metalworking conditions
[DE88-002485] 08 p0967 N88-15850
Ultrasonic characterization of layered composite systems 10 p1404 N88-18374
Probabilistic and reliability design procedures for flexible airfield pavements: Elastic layered method
[AD-A187533] 11 p1442 N88-18600
Mechanical response of unidirectional boron/aluminum under combined loading
[NASA-CR-182595] 12 p1604 N88-19591
High shear rate rheometry of low-viscosity liquids
[AD-A188447] 12 p1627 N88-19733
The elastic analysis of a thin toroidal shell
[AD-A187801] 12 p1635 N88-19785
Wave curves for simple isotropic elastic solids
[AD-A188865] 12 p1636 N88-19798
Stress analysis in elastic solids with many cracks
[AD-A189015] 12 p1636 N88-19799
The Euler-Bernoulli beam equation with boundary energy dissipation
[AD-A189517] 13 p1765 N88-20560
Dynamics of high-speed mechanisms with elastic members 13 p1779 N88-20643
Mathematical models of sound waves in fluids
[AD-A189270] 13 p1834 N88-20968
Guidelines for estimation and characterization of the thermo-mechanical properties of new optical materials
[DE88-004359] 13 p1840 N88-21010
Woven frameworks for three-dimensional reinforcement 14 p1884 N88-21262
Further study of relation of von Karman equation for elastic large deflection problem and Schrodinger equation for quantum eigenvalues problem
14 p1899 N88-21341
Investigation of the components of the energy-momentum tensor in the neighborhood of crack tips under special materials and loading conditions
[W-4/87] 14 p1934 N88-21531
The elastic properties of monoclinic ZrO2
[DE88-005920] 14 p1986 N88-21847
Experimental studies of elastic properties of crystals by Brillouin scattering
[DE88-005923] 14 p1986 N88-21848
Brillouin scattering and transmission electron microscopy studies of radiation-induced elastic softening, disordering and amorphization of intermetallic compounds
[DE88-005927] 14 p1987 N88-21850
High-performance polymeric materials
[AD-A190708] 15 p2046 N88-22190
A three-dimensional model for the elastic properties of a foam
[DE88-006197] 15 p2046 N88-22192
A new method of measuring multigrade oil shear elasticity and viscosity at high shear rates
[AD-A190145] 15 p2064 N88-22304
The CRREL (Cold Regions Research and Engineering Laboratory) Hopkinson bar apparatus
[AD-A190599] 15 p2077 N88-22380
Measurement of the elastic-plastic surface flaw back surface topology and its relation to constraint
[DE88-006765] 15 p2087 N88-22437
Parallel computer methods for eigenvalue extraction
16 p2218 N88-23233
Energy transfer processes in free radicals: A collaborative experimental and theoretical investigation
[AD-A191264] 16 p2269 N88-23578
Mixed-mode fracture of uniaxial fiber reinforced composites
[AD-A191629] 18 p2478 N88-24700
Vibration protection of inelastic structures by means of active and passive control 18 p2528 N88-25001
Vibrations of rotating thick or thin rings
18 p2529 N88-25003
Time-domain boundary element analysis of dynamic near-tip fields for impact-loaded collinear cracks
[AD-A192930] 20 p2815 N88-26700
Off-boundary approach to the boundary element method
[AD-A192931] 20 p2815 N88-26701
Characterization of elastic-plastic properties of AS4/APC-2 thermoplastic composite
[NASA-CR-183145] 21 p2906 N88-27242
An IETS (Inelastic Electron Tunneling Spectroscopy) study of surface reactions applicable to adhesion
[AD-A192274] 21 p2909 N88-27261
Computer simulation of elastic properties of grain boundary materials
[DE88-011965] 21 p2916 N88-27305
Ionic conductive polymers based on crosslinked elastic siloxane-ethylene oxide copolymers
[DE88-011243] 21 p2917 N88-27311
Three-dimensional aspects of fatigue crack closure
[AD-A192296] 21 p2960 N88-27581
Effects of applied stress and temperature on the nonlinear elastic properties of graphite fibers
[AD-A194469] 22 p3050 N88-28093
A critical speed study for aircraft bias ply tires
[AD-A193616] 22 p3084 N88-28313
Elastic behavior of a rubber layer bonded between two rigid spheres
[AD-A193698] 23 p3198 N88-29030
Metal halide optical glasses
[AD-A193794] 23 p3198 N88-29032
Experimental determination of drag modifications due to elastic compliant surfaces using quantitative visual techniques
[AD-A194785] 24 p3372 N88-30082
A dynamic analysis of piezoelectric strained elements
[AD-A196079] 24 p3432 N88-30430

ELASTIC SCATTERING
The elastic scattering of intermediate energy protons from (40)Ca and (208)Pb 01 p0092 N88-10599
Experimental studies of electromagnetic properties of few body systems
[DE87-014610] 02 p0161 N88-11008
On the spin structure of the elastic ppbar scattering amplitude
[NOTA-INTERNA-892] 06 p0778 N88-14772
A research program in neutrino physics, cosmic rays and elementary particles
[DE88-003507] 09 p1264 N88-17575
Pion elastic and inelastic scattering near N = 28
[LA-10968-T] 11 p1544 N88-19232
Medium high energy physics at Syracuse University
[DE88-003670] 11 p1545 N88-19235
Nuclear structure studies by the scattering of medium-energy electrons
[DE88-003803] 11 p1545 N88-19236
Intermediate energy neutrino physics
[DE88-005378] 13 p1836 N88-20984
Nuclear structure studies at intermediate energies
[DE88-006683] 18 p2571 N88-25271
Theoretical atomic and molecular physics
[DE88-007122] 19 p2724 N88-26175
Comparison of exclusive reactions at large momentum transfer
[DE88-007544] 20 p2851 N88-26922
Are Centauros diffractive
[DE88-008767] 21 p3032 N88-27996
Dispersion effects in elastic electron scattering from C12
[B8805297] 23 p3281 N88-29536
Eikonal solutions to optical model coupled-channel equations
[NASA-TP-2830] 24 p3428 N88-30402

ELASTIC SHELLS
RADSPHERE: A computer program for calculating the steady-state, axially symmetric, forced response and radiation field of a submerged spherical shell
[AD-A185025] 05 p0609 N88-13738
The elastic analysis of a thin toroidal shell
[AD-A187801] 12 p1635 N88-19785
The acoustic field scattered from some approximate pressure release materials
[AD-A194768] 23 p3278 N88-29515

ELASTIC STABILITY
U DAMPING

ELASTIC STRENGTH
U PROPORTIONAL LIMIT

ELASTIC WAVES
NT AERODYNAMIC NOISE
NT AIRCRAFT NOISE
NT BAROCLINIC WAVES
NT BLADE SLAP NOISE
NT CAPILLARY WAVES
NT COMPRESSION WAVES
NT DETONATION WAVES
NT ELECTROSTATIC WAVES
NT ENGINE NOISE
NT GRAVITY WAVES
NT ION ACOUSTIC WAVES
NT IONIC WAVES
NT JET AIRCRAFT NOISE
NT LAMB WAVES
NT MAGNETOACOUSTIC WAVES
NT MAGNETOHYDRODYNAMIC WAVES
NT NOISE (SOUND)
NT OBLIQUE SHOCK WAVES
NT P WAVES
NT PHONON BEAMS
NT PHONONS
NT PLASMA WAVES
NT POLARIZED ELASTIC WAVES
NT RAYLEIGH WAVES
NT RIPPLES
NT S WAVES
NT SEISMIC WAVES
NT SHOCK WAVES
NT SONIC BOOMS
NT SOUND WAVES
NT STRESS WAVES
NT THERMAL NOISE
NT TOLLMEIN-SCHLICHTING WAVES
NT ULTRASONIC RADIATION

Density flows at the mountain edge
08 p1016 N88-16156

Scattering of longitudinal wave normally incident on discal cavity in elastic body 08 p1077 N88-16492

Numerical simulation of the interaction of pressure waves with laminar and turbulent boundary layers
[DFVLR-FB-87-18] 09 p1161 N88-16960

A spectral method for computing complete synthetic seismograms
[AD-A187663] 11 p1510 N88-19024

Three-dimensional scattering of impulsive acoustic waves by a semi-infinite crack in the plane interface of a half space and a layer
[PB88-146998] 12 p1687 N88-20089

Phase velocity and attenuation of plane elastic waves in a particle-reinforced composite medium
[AD-A189414] 13 p1734 N88-20366

Initial condition effect on pressure waves in an axisymmetric jet
[NASA-TM-100915] 16 p2209 N88-23184

Remote sensing of acoustic properties of shallow water sediments: A review
[AD-A192107] 18 p2570 N88-25267

Numerical simulation of the interaction of pressure waves with laminar and turbulent boundary layers
[ESA-TT-1089] 24 p3371 N88-30075

Determination of the specific area of liquid gas and the velocity of weak pressure waves in aqueous foams
[NASA-TT-20347] 24 p3373 N88-30087

ELASTICITY
U ELASTIC PROPERTIES

ELASTICIZERS
U PLASTICIZERS

ELASTODYNAMICS
NT ELASTIC DAMPING
NT ELASTOHYDRODYNAMICS
NT VISCOELASTIC DAMPING

Elastodynamic ray theory and asymptotic methods for direct and inverse scattering problems
03 p0335 N88-12108

The acoustic-electric field analysis of multilayered surface acoustic wave devices
[ETN-88-91592] 09 p1242 N88-17446

Transient analysis of a plate on an elastic foundation under a moving load 19 p2680 N88-25933

Determination of the residual stresses in welded structures using the elastoplastodynamic method
[ETN-88-92745] 22 p3087 N88-28330

ELASTOHYDRODYNAMICS

Film thicknesses in circular elastohydrodynamic contacts
[PB87-123725] 06 p0710 N88-14354

The numerical solution of the elastohydrodynamically lubricated line and point contact problem, using multigrid techniques
[ISBN-90-9001583-3] 06 p0714 N88-14377

ELASTOMERS
NT VULCANIZED ELASTOMERS

Rheological behaviors of an elastomeric membrane
[DE87-013105] 01 p0061 N88-10392

Rheological and aging characterization of elastomers
[DE87-009598] 02 p0151 N88-10944

Urea-polyurethane and polydimethylsiloxane mixtures. Morphology control using a block copolymer
[ISAL-IDI1-87-05] 02 p0153 N88-10959

Buckling of viscoelastic columns
02 p0190 N88-11187

Thermoplastic elastomer compositions --- cable jackets
[EP-PATENT-0-204-453-A1] 04 p0418 N88-12593

Thermoplastic elastomers as LOVA (Low Vulnerability Ammunition) binders
[AD-A184350] 04 p0419 N88-12599

Process for the production of a thermoplastic elastomer composition
[EP-PATENT-0-202-782-A2] 05 p0569 N88-13465

Coaxial cable connector
[NASA-CASE-NPO-16764-1-CU]
06 p0696 N88-14270

Thermoplastic elastomers as LOVA binders
[AD-A185864] 07 p0835 N88-15067

Thermoplastic elastomers as LOVA binders
[AD-A185865] 07 p0835 N88-15068

Structure-property relationships in thermoplastic elastomers 4. Dynamic mechanical relaxations in poly(dioxolane), poly(butyltrioxocane) and poly(propylene oxide) polyurethanes
[AD-A186278] 07 p0836 N88-15073

Factors affecting the sticking of insects on modified aircraft wings
[NASA-CR-182451] 09 p1148 N88-16878

Morphology control and reinforcing mechanisms using an elastomer in an epoxy network based on diamine menthane
[ISAL-IDI1-87-09] 09 p1148 N88-16881

Thermoplastic elastomers as LOVA binders
[AD-A186563] 10 p1304 N88-17797

Cavitation in model elastomeric composites
[AD-A187401] 11 p1447 N88-18625

The effects of thin polymeric surface films in reducing fretting corrosion and wear
[AD-A188633] 12 p1611 N88-19634

Analysis of model fuels and their compatibility with selected elastomers, part 1
[AD-A188361] 12 p1612 N88-19639

Investigation of constrained-layer technique using exact elasticity theory
[AD-A188664] 12 p1636 N88-19795

Performance of elastomeric bearings
[PB88-159470] 14 p1918 N88-21450

High-performance polymeric materials
[AD-A190708] 15 p2046 N88-22190

Armoured vehicle track elastomers: Research and development at MRL
[MRL-GD-0012] 19 p2620 N88-25541

Fundamental studies of elastomers
[DE88-009679] 20 p2778 N88-26471

Development of a nitrile rubber for dynamic damping
[AD-A194060] 22 p3058 N88-28145

Dry adhesive friction of elastomers: A study of the fundamental mechanical aspects
[ETN-88-92903] 23 p3198 N88-29036

ELASTOPLASTICITY

Estimation multiaxial elastic-plastic notch stresses and strains in combined loading
[FB-2/1986] 01 p0060 N88-10382

The use of Hencky's equations for the estimation of multiaxial elastic-plastic notch stresses and strains
[FB-3/1986] 01 p0060 N88-10383

Contribution to the numerical calculation of fracture-mechanical quantities for elastic and elastic-plastic material behavior, especially for mixed loads
[ETN-87-90435] 01 p0062 N88-10399

A numerical and analytical investigation of Rayleigh-Taylor instability in a solid tungsten plate
[DE87-013593] 01 p0087 N88-10562

Refraction of shear wave into nonlinearly elastic or elastoplastic half-space 02 p0159 N88-10999

Spread of plastic deformation in notched and cracked plates 03 p0337 N88-12122

Computation of bonded assemblies: Elastoplastic adhesives, first part
[SNIAS-NT-18926/AQET] 05 p0569 N88-13467

Application of finite element methods with cyclic elasto-plastic strain analysis to low cycle fatigue analysis of engine components
[AR-004-512] 05 p0596 N88-13642

Behavior of a steel cylinder under the influence of a local load in the elastic and elasto-plastic area
[PB87-154787] 07 p0869 N88-15272

The nonlinear dynamic response of an elastic-plastic thin plate under impulse loading
[AD-A182147] 08 p0994 N88-16013

Dynamic finite element with diagonalized consistent mass matrix and elastic-plastic impact calculation
[PB87-143376] 08 p0995 N88-16020

Elastic-plastic fracture investigation on stable crack growth for plane stress
[PB87-144820] 08 p0995 N88-16022

The J-integral concept for elastic-plastic material behavior
[W-5/87] 08 p1000 N88-16059

Matrix-fiber stress transfer in composite materials: Elasto-plastic model with an interphase layer
[PB88-136635] 11 p1450 N88-18643

Elastoplastic response of unidirectional graphite/aluminum under combined tension-compression cyclic loading
[CCMS-88-01] 11 p1451 N88-18647

An analysis of large deformation axisymmetric inelastic problems by finite element and boundary element methods 13 p1782 N88-20664

Non-isothermal elastoviscoplastic analysis of planar curved beams 14 p1933 N88-21526

Development of a computer code CRACK for elastic and elastoplastic fracture mechanics analysis of 2-D structures by finite element technique
[DE88-701231] 15 p2075 N88-22370

Numerical analysis of critical penetration velocity for jet perpendicular penetration 16 p2186 N88-23037

Models in nonlinear thermomechanics: Finite element models and constitutive models for large deformation elastoplasticity
[ETN-88-92240] 16 p2222 N88-23262

Crack retardation under load spectra: Experimental study and numerical simulation using the simplified K constant model --- light alloys, aircraft construction materials
[ONERA-RT-30/7169-RY-054-R]
16 p2222 N88-23266

Theoretical and experimental damping values of piping systems at high ductilities
[DE88-006717] 18 p2526 N88-24986

A comparison of analytical techniques for modeling the Rayleigh-Taylor response of elastic-plastic solids
[DE88-010372] 21 p2962 N88-27596

Determination of the residual stresses in welded structures using the elastoplastodynamic method
[ETN-88-92745] 22 p3087 N88-28330

Results on the influence of crack tip plasticity during dynamic crack growth
[AD-A193460] 23 p3225 N88-29194

ELASTOSTATICS

The quasi-static contact problem with friction for three dimensional elastic bodies
[REPT-87-51] 14 p1918 N88-21447

A new boundary integral equation formulation for elastodynamic and elastostatic crack analysis
[AD-A192967] 20 p2815 N88-26702

ELECTRETS

Thin film electret boundary layer transition detector: A feasibility study
[AD-A185675] 07 p0856 N88-15199

Observations on electrostatic effects in a filter test system
[AD-A188797] 13 p1736 N88-20378

ELECTRIC AIRCRAFT
U FLY BY WIRE CONTROL

ELECTRIC APPLIANCES
U ELECTRIC EQUIPMENT

ELECTRIC ARCS

Recovery of vacuum gaps after arcing
[DE87-013852] 01 p0039 N88-10250

Experimental study and modeling of the physical mechanisms of the gliding spark
[ESA-TT-1029] 01 p0070 N88-10447

Current-filamentation instability in railgun arcs
[AD-A184618] 03 p0269 N88-11693

An investigation of unipolar arcing at atmospheric pressure in aluminum 2024 and aluminum coated glass slides
[AD-A184903] 05 p0577 N88-13521

Theoretical model of the cathode spot on a unipolar arc
[AD-A190109] 15 p2059 N88-22277

Welding torch gas cup extension
[NASA-CASE-MFS-29252-1] 17 p2345 N88-23980

Arc-textured metal surfaces for high thermal emittance space radiators
[NASA-TM-100894] 18 p2487 N88-24754

Extinction behavior of low voltage switching arc under consideration of cathodic coatings and dynamic arc column
[ETN-88-92384] 20 p2796 N88-26591

Physical-chemical reactions at welding arc/molten pool interfaces
[DE88-007717] 20 p2808 N88-26662

Measurements of vacuum arc ion charge state distributions
[DE88-008249] 23 p3284 N88-29558

ELECTRIC AUTOMOBILES
Metal-air battery assessment
[DE88-011361] 21 p2940 N88-27459

ELECTRIC BATTERIES
NT ALKALINE BATTERIES
NT LEAD ACID BATTERIES
NT LITHIUM SULFUR BATTERIES
NT METAL AIR BATTERIES
NT NICKEL CADMIUM BATTERIES
NT NICKEL HYDROGEN BATTERIES
NT NICKEL IRON BATTERIES
NT NICKEL ZINC BATTERIES
NT PRIMARY BATTERIES
NT REDOX CELLS
NT SODIUM SULFUR BATTERIES
NT STORAGE BATTERIES
NT THERMAL BATTERIES
NT ZINC-BROMIDE BATTERIES
NT ZINC-OXYGEN BATTERIES
Ionically conductive polymers: Application to solid state batteries
[AD-A183733] 01 p0037 N88-10239
Zinc-redox battery: A technology update
[DE87-010737] 01 p0040 N88-10256
Evaluation of LiCl- LiBr- KBr electrolyte for Li- alloy/metal disulfide cells
[DE87-011356] 01 p0041 N88-10258
Overcharge protection in Li-alloy/metal disulfide cells
[DE87-011364] 01 p0041 N88-10260
Lithium/iron sulfide batteries: Development and demonstration
[DE87-014222] 01 p0042 N88-10265
Highlights of the Chemical Technology Division's research activities
[DE88-000233] 03 p0282 N88-11773
Applications of multivalent ionic conductors to polymeric electrolyte batteries
[AD-A184252] 04 p0439 N88-12722
Corrosion susceptibility study of candidate pin materials for ALTC (Active Lithium/Thionyl Chloride) batteries
[DE88-001449] 04 p0440 N88-12734
Reliability of Li/SO2 cells for long-life applications
[DE88-001360] 04 p0440 N88-12735
A hydrogen/nickel oxide battery for remote applications
[DE87-009048] 04 p0464 N88-12872
High energy density rechargeable batteries for aerospace power requirements
[AD-A184883] 05 p0577 N88-13519
An investigation of the rechargability of certain modified forms of MnO2
[AD-A185919] 07 p0847 N88-15140
User's guide to DIANE: A microcomputer program for modeling battery performance in electric vehicles
[DE88-003713] 08 p1068 N88-16456
The European space battery test center
09 p1125 N88-16738
The railgun and its power source
[MRL-R-1058] 09 p1130 N88-16786
Laboratory evaluation and analysis of advanced lead-acid load-leveling batteries
[DE88-002851] 10 p1349 N88-18064
Fuel cell/battery hybrid vehicle assessment
[DE88-005087] 10 p1427 N88-18520
Lithium/disulfide battery R and D
[DE88-003032] 11 p1481 N88-18839
Improving battery reliability by using regression trees
[DE88-004539] 11 p1481 N88-18841
Performance test results for the Eaton dc development power train in an electric test bed vehicle
[DE88-005458] 12 p1622 N88-19699
An electrochemical and spectroscopic study of electrode systems
[AD-A189274] 13 p1737 N88-20384
Corrosion, passivity and breakdown of alloys used in high energy density batteries
[DE88-004891] 13 p1743 N88-20422
Polymeric electrolytes for ambient temperature lithium batteries
[DE88-004896] 13 p1763 N88-20547
Mission directed goals for electric vehicle battery research and development: The Task Force on electric vehicle battery goals
[DE88-005601] 13 p1763 N88-20548
Testing and development of electric vehicle batteries for EPRI Electric Transportation Program
[DE88-005894] 13 p1764 N88-20551
GTE battery management system: State of charge indicator evaluation
[DE88-006800] 15 p2058 N88-22272
Nickel hydroxide active material densities
[AD-A191411] 16 p2230 N88-23319
Energy storage for nuclear burst power systems
17 p2426 N88-24431
An overview of advanced battery development at Sandia National Laboratories
[DE88-006823] 18 p2506 N88-24867
Optimization of reserve lithium thionyl chloride battery electrochemical design parameters
[DE88-007109] 18 p2506 N88-24868
All inorganic ambient temperature rechargeable lithium battery
[DE88-008425] 19 p2662 N88-25834
Advanced photovoltaic power system technology for lunar base applications
[NASA-TM-100965] 20 p2766 N88-26402
Loss evaluation of self-commutated power conditioner for battery energy storage system
[DE88-752075] 20 p2794 N88-26575
Exploratory battery technology development and testing report for 1986
[DE[illegible]870] 20 p2794 N88-26578
Modeling and thermal management of advanced batteries
[DE88-010023] 20 p2794 N88-26580
Molten salt electrolytes for high-temperature lithium cells
[DE88-010058] 20 p2794 N88-26581
Computer controlled procedures for traction battery power performance tests
[ETN-88-92352] 20 p2796 N88-26589
High power pulse energy system concept
[AD-A192440] 21 p2935 N88-27429
Preparation and development of advanced battery catalysts
[AD-A193206] 21 p2937 N88-27441
Estimation of power-energy plots for secondary batteries
[DE88-011922] 21 p2940 N88-27460
Advanced calcium-thionyl chloride high-power battery
[AD-A194401] 22 p3072 N88-28238
Optimization and scale-up performance of polymer electrolyte batteries
[AD-A193987] 22 p3073 N88-28243
The overcharge behavior of polymer electrolyte cells
[AD-A193984] 22 p3117 N88-28522
Structure and dynamics of solutions of lithium salts relevant to battery construction
[AD-A195399] 24 p3366 N88-30044
Aircraft battery state of charge and charge control system
[AD-A194979] 24 p3367 N88-30052

ELECTRIC BRIDGES
Balancing strain gauge bridges
[GB-PATENT-2-129-567-A] 01 p0048 N88-10307
Comparative evaluation of resistive and inductive techniques for measuring temperature of superconducting transition
[DE88-700603] 10 p1417 N88-18457
Layered-capacitor method for dielectric bridge measurements: Algorithms for inversion and parameter fitting. Documentation, verification, data analysis
[PB88-131479] 11 p1505 N88-18989
Development of an optical feedback based high accuracy beam transmissometer
[AD-A189396] 12 p1692 N88-20122
Giant Josephson signal in wide superconducting films
14 p1973 N88-21777
Pure metallic bridge and point-contact tunneling into single- and polycrystal YBa2Cu3O(sub 7-y)
[DE88-010030] 20 p2878 N88-27084

ELECTRIC CHARGE
NT ELECTRIC DIPOLES
NT ELECTROSTATIC CHARGE
NT ION CHARGE
NT SPACE CHARGE
Simulations using the pseudo-current algorithm
[DE87-012403] 01 p0040 N88-10255
Theory of the one- and two-dimensional electron gas
[DE87-012864] 02 p0244 N88-11540
A theoretical analysis of the deactivation of metal surfaces upon carburization
[AD-A184556] 03 p0290 N88-11821
Analysis of nickel sulphamate bath using charging current compensated D.C. polarography
[NAL-TM-MT-8705] 05 p0564 N88-13433
An investigation of the rechargability of certain modified forms of MnO2
[AD-A185919] 07 p0847 N88-15140
Sliding charge density waves and related problems
[AD-A186720] 09 p1157 N88-16934
High-temperature charge-density studies of CeO/sub 2-x/ using X-ray and neutron diffraction techniques
[DE88-002988] 09 p1257 N88-17536
Survey of the Air Force P78-2 (SCATHA) satellite plasma wave data during electron gun operations
[AD-A191014] 16 p2168 N88-22926
Finite element simulation of the atmosphere's electromagnetic response to charge perturbations associated with lightning 17 p2375 N88-24124
The theory of random alloys
[DE88-006408] 18 p2487 N88-24756
Development of test methods for the electrostatic properties of nonhomogeneous fabrics, phase 2
[AD-A190853] 18 p2489 N88-24767
Electronic and ionic transport in polymers
[AD-A191642] 18 p2490 N88-24772
A severe spacecraft charging event on SCATHA in September 1982
[AD-A193007] 20 p2765 N88-26396
Results from life test in progress on eagle-picher nickel cadmium cells
[AD-A192816] 21 p2936 N88-27434
Discrete variational methods and their application to electronic structures
[DE88-702215] 21 p3[illegible] N88-27888
Model for bimetallic interfaces, part 2
[DE88-702672] 22 p3157 N88-28787

ELECTRIC CHOPPERS
Low-current behavior and current chopping of vacuum arcs
[ISBN-90-9001649-X] 05 p0578 N88-13529

ELECTRIC CIRCUITS
U CIRCUITS

ELECTRIC COILS
NT MAGNET COILS
NT MAGNETIC COILS
Departmental report on program EMTP-machine windings surge transients. Travelling wave method
[PB87-123733] 04 p0438 N88-12719

ELECTRIC CONDUCTORS
Eddy current density in wedge-shaped conducting cylinders with inhomogeneous conductivity
[ETN-87-90404] 01 p0042 N88-10268
Dielectric response of ionic conductors
[DE87-013552] 02 p0166 N88-11045
Advances in inherently conducting polymers
[DE88-000501] 04 p0421 N88-12610
Departmental report on program EMTP-machine windings surge transients. Travelling wave method
[PB87-123733] 04 p0438 N88-12719
Molecular and supramolecular orientation in conducting polymers
[DE88-000533] 05 p0569 N88-13472
Hydroxide ion conductors as possible electrolytes in intermediate temperature fuel cells
[AD-A185508] 06 p0731 N88-14495
Failure modes of laminate structures
[DE88-002579] 08 p0996 N88-16033
Electronic and ionic transport in polymers
[AD-A187253] 11 p1452 N88-18651
The effects of various conductor components on Nb3Sn filament prestrain in cable-in-conduit conductors
[DE88-003956] 11 p1479 N88-18824
Contrasting conductance/viscosity relations in liquid states of vitreous and polymer solid electrolytes
[AD-A189378] 13 p1748 N88-20452
Electron emission from conductors subjected to intense, short-pulse electric fields
[DE88-005412] 13 p1836 N88-20985
Strategies in the topological approach to electromagnetic interference control
[AD-A189874] 15 p2056 N88-22255
Fast ion conducting glasses
[AD-A191412] 16 p2183 N88-23010
Fabrication of a flexible conductor by vapor deposition
[DE88-007500] 19 p2661 N88-25826
Determination of quantum corrections for electrical conductivity mechanism of three dimensional, perturbed copper coatings. Weak localization and electron-electron interaction
[ETN-88-92378] 21 p2941 N88-27466

ELECTRIC CONNECTORS
Design principles and practices for implementation of MIL-STD-1760 in aircraft and stores
[AD-A183724] 01 p0005 N88-10027
Coaxial cable connector
[NASA-CASE-NPO-16764-1-CU]
06 p0696 N88-14270
Measurement of shielding effectiveness of different cable and shielding configurations by mode-stirred techniques
[PB88-155791] 10 p1319 N88-17885
Separable electrical connectors for space. A tribological and electrical assessment 14 p1879 N88-21231
Development of a slip-ring system for energy transfer in space conditions. Space flight qualification and extended life tests
[BMFT-FB-W-86-019] 16 p2169 N88-22932
Investigation of non-linear optical behavior of semiconductors for optical switching, volume 1
[AD-A191297] 16 p2274 N88-23611

Studies of optical matrix multiplication and reconfigurable optical interconnect concepts
[AD-A191635] 18 p2575 N88-25295
Circuit design criteria for stable lateral inhibition neural networks
[AD-A195066] 24 p3386 N88-30046

ELECTRIC CONTACTS
Toward pulsed power uses for photoconductive semiconductor switches: Closing switches
[DE87-012020] 01 p0041 N88-10262
Ohmic contacting schemes to gallium arsenide devices
[DE87-014627] 02 p0244 N88-11544
Influence of arsenic superficial enrichment on the ohmicity of the n-GaAs:In/Au contact
[ECL-87-09] 08 p1089 N88-16554
Development of a planar heterojunction bipolar transistor for very high speed logic
[AD-A188137] 11 p1478 N88-18820
The physics of very small structures
[AD-A187672] 11 p1556 N88-19311
Corrosion-wear process under rolling-sliding motion
[AD-A189603] 13 p1778 N88-20635
Stable, high-efficiency, CuInSe2-based, polycrystalline, thin-film tandem solar cells
[DE88-001116] 13 p1793 N88-20726
Thin-film diffusion barriers for metal-semiconductor contacts
[AD-A188712] 13 p1844 N88-21035
Polysilicon-contacted p+ emitters for silicon solar cell applications
[DE88-005106] 14 p1942 N88-21586
The kinetics of contact noise in NaBeta alumina
[AD-A190651] 15 p2130 N88-22707
The influence of current stressing on the structure of Ag contacts to GaAs
[DE88-005988] 15 p2140 N88-22771
Effects of 67.5 MeV electron irradiation on Y-Ba-Cu-O and Gd-Ba-Cu-O high-temperature superconductors
[AD-A191271] 16 p2283 N88-23669
Friction, wear and electrical contact resistance of precious metal alloys
[DE88-011244] 21 p2938 N88-27450

ELECTRIC CONTROL
Electrical flight commands in transport aircraft
[SNIAS-872-111-108] 05 p0551 N88-13361

ELECTRIC CORONA
The effects of corona on current surges induced on conducting lines by EMP: A comparison of experiment data with results of analytic corona models
[DE87-014970] 03 p0305 N88-11924
Personal overview of solar wind 6
[DE88-003147] 10 p1430 N88-18543
Molecular collision processes in gases and at surfaces
[AD-A189518] 13 p1836 N88-20982
The growth potential of corona discharges from aircraft flying in precipitation
[AD-A190507] 15 p2094 N88-22478
Theoretical basis for an experimental test with regard to the origin of VHF (Very High Frequency) radiation from natural lightning
[DE88-007535] 18 p2544 N88-25102

ELECTRIC CURRENT
NT ALTERNATING CURRENT
NT ARC DISCHARGES
NT AURORAL ELECTROJETS
NT BEAM CURRENTS
NT DIRECT CURRENT
NT EDDY CURRENTS
NT ELECTRIC ARCS
NT ELECTRIC CORONA
NT ELECTRIC DISCHARGES
NT ELECTRIC SPARKS
NT EQUATORIAL ELECTROJET
NT EXTERNAL SURFACE CURRENTS
NT FLASHOVER
NT GAS DISCHARGES
NT GLOW DISCHARGES
NT HIGH CURRENT
NT IONOSPHERIC CURRENTS
NT LIGHTNING
NT LINE CURRENT
NT LOW CURRENTS
NT PLASMA CURRENTS
NT RING CURRENTS
NT THRESHOLD CURRENTS
A tutorial on Rogowski coil theory and operation
[DE88-000[illegible]6] 02 p0230 N88-11449
MHD (magnetohydrodynamics) channel development
[DE87-014126] 02 p0237 N88-11[illegible]
Rotation of magnetized particle in electrically conducting viscous medium 06 p0770 N88-14733
Mathematical model for the dc-ac inverter for the Space Shuttle 06 p0793 N88-14860

Simulation an experiment on plasma instability investigation in a tokamak with a divertor
[DE88-700352] 07 p0935 N88-15683
The effects of a geomagnetic storm on thermospheric circulation
[AD-A186638] 09 p1190 N88-17128
Temporal evolution of ionospheric electric field driven by field-aligned current 11 p1469 N88-18761
Bloch oscillations in small Josephson junctions: Their manifestation in switching effects
14 p1969 N88-21756
Optical sensors for the measurement of electric current and voltage
[PB88-172945] 16 p2193 N88-23077
Monte Carlo analysis of lateral collection diode arrays
[RSRE-MEMO-4080] 17 p2335 N88-23938
Photocurrent modeling of modern microcircuit PN junctions
[DE88-007037] 19 p2662 N88-25832
Fast parametrization procedure for solar cells
[PB88-186416] 19 p2686 N88-25966
Computer programs for high-current beam transport in accelerators
[AD-A192356] 20 p2838 N88-26835
A rapid electrochemical technique for determining the current efficiency for cadmium plating
[AD-A193679] 22 p3056 N88-28130
Current induced by high-altitude electromagnetic pulse (HEMP) on wire above ground
[FOA-C-30485-4.2] 22 p3072 N88-28235

ELECTRIC DIPOLES
Power flow in terms of Poynting vector for Extremely Low Frequency (ELF) dipole sources in seawater
[ARE-TM(UTM)-87102] 01 p0035 N88-10221
Electromagnetic interaction between an electric discharge and cabling inside a satellite
03 p0274 N88-11725
Theory of atomic additivity in molecular hyperpolizabilities 03 p0297 N88-11867
Electromagnetic scattering from and natural resonances of the circular strip 13 p1759 N88-20523
On the self-consistent equation for the microscopic local electric field in dielectric systems
[PREPRINT-589] 22 p3074 N88-28247

ELECTRIC DISCHARGES
NT ARC DISCHARGES
NT ELECTRIC ARCS
NT ELECTRIC CORONA
NT ELECTRIC SPARKS
NT FLASHOVER
NT GAS DISCHARGES
NT GLOW DISCHARGES
NT LIGHTNING
Characterization of surface discharge switches and high performance applications
[DE87-011763] 01 p0041 N88-10261
Segmented hollow cathode discharges for copper ion lasers
[ETN-87-90403] 01 p0052 N88-10333
International Ultraviolet Explorer (IUE) spacecraft battery performance update 02 p0164 N88-11033
Discharge phenomena --- spacecraft
03 p0274 N88-11723
Electromagnetic interaction between an electric discharge and cabling inside a satellite
03 p0274 N88-11725
Electromagnetic effects of a discharge on circuitry --- spacecraft 03 p0274 N88-11726
Irradiation testing 03 p0274 N88-11727
MARECS-A case 03 p0274 N88-11729
Electromagnetic compatibility (EMC) phenomena and prevention of the effects --- spacecraft
03 p0274 N88-11731
Discharge prevention of geosynchronous orbit conductive thermal control materials and grounding systems 03 p0274 N88-11732
Electrostatic discharges in geostationary orbit: The case of Telecom 1 03 p0275 N88-11733
Prevention of radiation induced degradations and of electrostatic perturbations on the Arabsat spacecraft in flight results 03 p0275 N88-11734
Mathematical models of plasma discharge control in a tokamak
[DE87-702891] 03 p0378 N88-12377
Nitrogen energy transfer study
[AD-A184457] 04 p0464 N88-12869
Electromagnetics and electrothermal approach to evaluate failures in microelectronic devices caused by electrostatic discharges: Stochastical aspects of the device reliability
[AD-A184906] 05 p0577 N88-13522
Atmospheric electricity
[NASA-CR-179239] 06 p0744 N88-14575
State parameters of pulse-discharge plasma in xenon-filled closed tube 06 p0773 N88-14747

Power and charge dissipation from an electrodynamic tether 06 p0795 N88-14869
A numerical thermal model of the rapid solidification parameters in the capacitor discharge welding process
[DE88-002206] 07 p0864 N88-15244
Atmospheric science 07 p0883 N88-15357
Investigation of self-discharge characteristics of spacecraft nickel-cadmium cells at elevated temperatures
[AD-A186497] 08 p0979 N88-15919
Wire-cut electrical discharge machinability of ceramics
[AD-A186989] 09 p1146 N88-16870
Air gap testing using Trailing Wire Antenna (TWA) waveform
[AD-A187639] 11 p1477 N88-18812
Partial discharges and the electrical aging of cross linked polyethene (XLPE) cable insulation
[EUT-86-E-160] 14 p1892 N88-21300
The growth potential of corona discharges from aircraft flying in precipitation
[AD-A190507] 15 p2094 N88-22478
Kinetics of electrons and molecules at plasma-beam discharge in molecular gases
[DE88-701196] 16 p2275 N88-23616
Electrostatic discharge test apparatus
[NASA-CASE-MSC-21094-1] 18 p2518 N88-24941
Deep dielectric charging effects due to high energy electrons in earth's outer magnetosphere
[AD-A192154] 18 p2541 N88-25083
Theoretical basis for an experimental test with regard to the origin of VHF (Very High Frequency) radiation from natural lightning
[DE88-007535] 18 p2544 N88-25102
Plasma neutralizer work at BNL (Brookhaven National Laboratory)
[DE88-007046] 18 p2579 N88-25317
Spacecraft requirements for predictions of geomagnetic activity (a tutorial)
[AD-A191943] 19 p2685 N88-25959
A severe spacecraft-charging event on SCATHA in September 1982
[AD-A193007] 20 p2765 N88-26396
Electron-impact-ionization and electron-attachment cross sections of radicals important in transient gaseous discharges
[AD-A192248] 20 p2770 N88-26424
A bibliography and author index for electrical discharges in vacuum (1897-1986)
[DE88-008744] 20 p2794 N88-26579
Failure analysis of Chloride Silent Power, Ltd. PB cells
[DE88-010567] 21 p2936 N88-27446
Production of intensive electron beam impulsions by setup of pseudoglare discharges
[ISL-CO-210/87] 21 p3019 N88-27920
Surface properties in electric discharge machining
[NASA-TT-20243] 23 p3223 N88-29182
In-house capacitor technology program
[AD-A194804] 24 p3367 N88-30049
Transverse CO2 laser two-dimensional gain distributions
[AD-A196240] 24 p3378 N88-30119

ELECTRIC ENERGY STORAGE
Technology Base Research Project for electrochemical energy storage
[DE88-000649] 04 p0464 N88-12868
On the potential role of concentrated field-aligned currents in solar physics 08 p1099 N88-16614
Assessment of energy storage concepts for use in sprint power 17 p2407 N88-24312
Development of inductive storage pulsed power generators
[AD-A193878] 22 p3117 N88-28521

ELECTRIC EQUIPMENT
US Naval Air Force avionic and electrical system corrosion prevention and control maintenance
05 p0547 N88-13334
Avionic and electrical system corrosion prevention and control maintenance 22 p3054 N88-28119

ELECTRIC EQUIPMENT TESTS
The European space battery test center
09 p1125 N88-16738
EDF's studies and first choices regarding the design of electrical equipment
[NASA-TT-20222] 13 p1764 N88-20553

ELECTRIC FIELD STRENGTH
Electrodynamics of midnight sector of auroral oval in period of slight disturbance 08 p1003 N88-16077
Magnetic control of low pressure discharges
[AD-A186794] 10 p1322 N88-17900
Development of a ground-conductivity map for the area of the Federal Republic of Germany from measured field-strength contours 12 p1615 N88-19656
Mono- and bistatic radar coverage diagrams including diffractive wave propagation 12 p1616 N88-19660

Measurement technique for characterization of the gyrotron
[INPE-4322-RPE/550] 12 p1630 N88-19758

ELECTRIC FIELDS

The polarization field for pulsed Raman transitions
[DE87-013118] 01 p0035 N88-10227

Studies on temporal field emission from stainless steel surfaces
[DE87-014237] 02 p0147 N88-10919

Progress in stellarator/heliotron research, 1981-1986: Executive summary
[DE88-000017] 02 p0241 N88-11519

Short-pulse high-current-density photoemission in high electric fields
[DE87-014909] 03 p0310 N88-11951

Drop formation from an orifice in an electric field
[DE87-014405] 03 p0322 N88-12034

Effect of electrostatic field on behaviour of peripheric plasma at high-frequency heating
[DE87-703328] 03 p0378 N88-12378

The effect of object potentials on the wake of a flowing plasma
[AD-A184038] 03 p0379 N88-12385

Thermal analysis of electromagnetic launcher rails
[DE88-000166] 04 p0405 N88-12514

An electric field meter based upon a new principle: A dummy displacement electrode. Application to aerospace vehicles
[SNIAS-872-422-106] 05 p0585 N88-13567

Electric field measurements on Viking: First results
[TRITA-EPP-87-04] 05 p0625 N88-13826

Research for electric energy systems
[DE88-001733] 06 p0695 N88-14265

Finite-element method for three-dimensional electric and electromagnetic field problems
[PB87-138731] 06 p0696 N88-14274

Materials for acceleration by surface electromagnetic waves
[DE88-700312] 07 p0846 N88-15133

Dynamics Explorer guest investigator
[NASA-CR-181494] 07 p0878 N88-15325

Lightning spectra in the near infrared
[DE88-002218] 07 p0880 N88-15341

Current generation and induced conductivity of a plasma under common action of constant electric field and lower-hybrid or ECR waves
[DE88-700345] 07 p0935 N88-15680

Embedded cluster models for electronic structure and energetics of complex oxides
[DE88-003097] 07 p0938 N88-15702

First results of balloon-borne X-ray and electric field observations near the footprint of the Viking satellite
08 p1026 N88-16215

Acceleration of auroral particles by magnetic field-aligned electric fields 08 p1031 N88-16246

Low frequency electrostatic waves observed on board the Coordinated Auroral Experiment using Scatter And Rockets (CAESAR) 2 payload 08 p1032 N88-16253

Processes in the quiet and disturbed equatorial-low latitude ionosphere: Sundial campaign, 1984
[INPE-4152-PRE/1057] 08 p1036 N88-16282

Nonlinear diffusion in the presence of a time-dependent external electric field
[INPE-4378-PRE/1198] 08 p1085 N88-16533

Preliminary results from the dc electric field experiment on Viking — Swedish satellite
[TRITA-EPP-87-03] 09 p1190 N88-17130

Acceleration of auroral particles by magnetic field-aligned electric fields
[TRITA-EPP-87-08] 09 p1190 N88-17131

The acoustic-electric field analysis of multilayered surface acoustic wave devices
[ETN-88-91592] 09 p1242 N88-17446

Observation of enhanced electric field in an RF-plugged sheet plasma in the RFC-XX-M open-ended machine
[IPPJ-857] 09 p1252 N88-17503

Effect of external electrostatic field on catecholamine secretion by rat adrenals 10 p1366 N88-18166

Light absorption by an atom moving inside a spherical box
[AD-A187241] 10 p1407 N88-18395

Temporal evolution of ionospheric electric field driven by field-aligned current 11 p1469 N88-18761

Return stroke velocities and currents using a solid state silicon detector system 11 p1515 N88-19050

Electric fields in Earth orbital space. Magnetospheric structural dynamic response to external variables
[AD-A188592] 12 p1643 N88-19836

Waves and static electric fields in the auroral acceleration region 12 p1646 N88-19856

The effects of a dc electric field on the current driven ion cyclotron instability
[AD-A188877] 12 p1695 N88-20142

Atmospheric electrical modeling in support of the NASA F-106 storm hazards project
[NASA-CR-181639] 13 p1799 N88-20758

Upward propagating electric fields from thunderstorms and VLF transmitters 13 p1801 N88-20767

Double layer polarization of nonconducting spheroidal particles and its application to Kerr effect
[ISSN-0208-5658] 13 p1832 N88-20960

Comparison of analytic and full guiding center behavior at a trapped-passing interface in stellarators
[DE88-004174] 13 p1842 N88-21025

Arcs in cesium seeded noble gases resulting from a magnetically induced electric field
[EUT-87-E-177] 13 p1843 N88-21028

Competing interactions in metallic superlattices
[DE88-005344] 13 p1847 N88-21057

Particle simulation research by plasma parametric heating caused by strong laser
14 p1903 N88-21368

Statistical analysis of feasibility of non-destructive inspection of mechanical properties of hot worked pipes of alloy steels
[BLL-M-37598-(5828.4)] 14 p1922 N88-21455

Optical properties of quantum well structures with electric field: Life time free switching of luminescence intensity and virtual charge-induced ultrafast optical nonlinearity 14 p1976 N88-21794

Physical processes in the vicinity of the cometopause interpreted on the basis of plasma, magnetic field and plasma wave data measured on board VEGA-2 spacecraft — Halley's comet 14 p1996 N88-21894

Correlation between magnetic and electric field fluctuations observed during flyby near Halley's comet
14 p1996 N88-21897

Stratospheric electric field and conductivity measurements over electrified convective clouds in the South American region, revised
[INPE-4046-PRE/1012-REV-3]
15 p2095 N88-22483

A study on electric fields and conductivity associated with electrified clouds in the region of South America
[INPE-4487-TDL/325] 15 p2096 N88-22486

On the acceleration of electrons and positive ions in the same direction along magnetic field lines by parallel electric fields
[IRF-PREPRINT-103] 15 p2096 N88-22488

Experimental comparison of lightning simulation techniques to CV-580 airborne lightning strike measurements
[AD-A190576] 15 p2098 N88-22496

Droplet size characteristics and energy input requirements of emulsions formed using high-intensity-pulsed electric fields
[DE88-005912] 15 p2128 N88-22692

Parametric instabilities of inhomogeneous plasma near the lower-hybrid resonance
[DE88-701201] 15 p2137 N88-22748

High power, high frequency radiation from beam-plasma interactions
[AD-A190207] 15 p2137 N88-22752

Classical non-Abelian solutions for nonstandard Lagrangians
[DE88-701305] 16 p2263 N88-23532

Low gravity thermal management using dielectrophoretic forces 17 p2432 N88-24470

Cascade fluorescences from laser-excited lithium atom for plasma diagnostics 17 p2442 N88-24526

Electromagnetic penetration into a conducting circular cylinder through a narrow slot, TE case
[AD-A191602] 18 p2500 N88-24828

Electric field measurement by S-520-9 sounding rocket using the time of flight technique of lithium ion beam
[ISAS-RN-367] 18 p2543 N88-25095

Space station induced electromagnetic effects
18 p2591 N88-25394

Dynamics explorer data analysis
[NASA-CR-181428] 19 p2691 N88-25996

Calculation of the line shapes of radiators immersed in plasma 19 p2729 N88-26210

Degradation of beam brightness by field emission from a cathode shroud
[DE88-008345] 20 p2794 N88-26576

High spatial frequency thermal blooming instability: A linear stability analysis
[DE88-010711] 20 p2807 N88-26655

Interaction of biological systems with static and ELF electric and magnetic fields
[DE88-007951] 20 p2831 N88-26792

Sources of polarized ions and atoms
[DE88-010910] 20 p2852 N88-26931

Field-enhanced lithium ion sources for PBFA 2
[DE88-007195] 20 p2856 N88-26960

Ultrafast optical nonlinearity in quantum well structures with electric field 20 p2863 N88-27003

Electric and Magnetic Activity of the Central Nervous System: Research and Clinical Applications in Aerospace Medicine
[AGARD-CP-432] 21 p2977 N88-27683

Electric and magnetic brain activity related to cognitive performance 21 p2979 N88-27692

Staggered-grid finite element solution technique for the Maxwell's equations in the time domain
[DE88-011731] 21 p3007 N88-27838

On plasma stability under anisotropic random electric field influence
[DE88-702422] 21 p3019 N88-27918

Measurement of macroscopic electric fields in solar plasma structures
[AD-A193291] 21 p3031 N88-27993

TE/TM (Transverse Electric/Transverse Magnetic) height profile measurements of transpolar VLF (Very Low Frequency) signals
[AD-A194503] 22 p3069 N88-28216

The far field from a hybrid electromagnetic pulse (HPD) simulator
[FOA-C-30480-4.2] 22 p3071 N88-28231

On the self-consistent equation for the microscopic local electric field in dielectric systems
[PREPRINT-589] 22 p3074 N88-28247

Physiological effects of extremely low frequency electric and magnetic fields
[DE88-752814] 22 p3132 N88-28620

A study of electronic transport and breakdown in SiO2
[AD-A194258] 22 p3156 N88-28780

Kinetic theory for electrostatic waves due to transverse velocity shears
[AD-A193404] 23 p3284 N88-29557

Ion gun generated electromagnetic interference on the SCATHA satellite
[AD-A195179] 24 p3335 N88-29853

Wave propagation and remote sensing
24 p3364 N88-30029

General equations for the motions of ice crystals and water drops in gravitational and electric fields
[NASA-CR-183229] 24 p3370 N88-30070

ELECTRIC FILTERS

NT BANDSTOP FILTERS
NT DIGITAL FILTERS
NT FIR FILTERS
NT MICROWAVE FILTERS
NT RADAR FILTERS
NT RADIO FILTERS
NT TRACKING FILTERS
NT WAVEGUIDE FILTERS

On adaptive signal processing of RF signals
[DE87-014192] 02 p0161 N88-11007

Documentation of computer programs for optimization and simulation of multicarrier SAW-based demodulator
[PB87-134532] 06 p0693 N88-14252

A contribution to the realization of active filters for high frequency applications
[ETN-88-90611] 06 p0696 N88-14272

ELECTRIC FUSES

Experimental and mathematical investigation of response characteristics and aging phenomena in safety fuse elements
[ETN-88-91478] 11 p1480 N88-18832

ELECTRIC GENERATORS

NT AC GENERATORS
NT ALKALINE BATTERIES
NT DIRECT POWER GENERATORS
NT DYNAMOMETERS
NT ELECTROSTATIC GENERATORS
NT FUEL CELLS
NT HYDROGEN OXYGEN FUEL CELLS
NT MAGNETOHYDRODYNAMIC GENERATORS
NT METAL AIR BATTERIES
NT NICKEL ZINC BATTERIES
NT PHOSPHORIC ACID FUEL CELLS
NT PHOTOELECTRIC GENERATORS
NT PHOTOVOLTAIC CELLS
NT PRIMARY BATTERIES
NT RADIOISOTOPE BATTERIES
NT REGENERATIVE FUEL CELLS
NT ROTATING GENERATORS
NT SNAP 19
NT SODIUM SULFUR BATTERIES
NT SOLAR CELLS
NT SOLAR DYNAMIC POWER SYSTEMS
NT SOLAR GENERATORS
NT THERMAL BATTERIES
NT THERMIONIC CONVERTERS
NT THERMOELECTRIC GENERATORS
NT TURBOGENERATORS
NT VERTICAL JUNCTION SOLAR CELLS
NT ZINC-OXYGEN BATTERIES

Evaluation of stand-alone inverters for remote applications
[DE87-010957] 01 p0040 N88-10257

Solar energy: European research and development
[PB87-107645] 04 p0463 N88-12866

Design description report for a photovoltaic power system for a remote satellite earth terminal
[NASA-CR-179586] 04 p0465 N88-12875

Laser production and heating of plasma for MHD application
[NASA-TP-2798] 10 p1415 N88-18443
Advances in applied superconductivity: A preliminary evaluation of goals and impacts
[DE88-006441] 14 p1986 N88-21844
Superconductivity in power engineering
[DE88-701414] 15 p2141 N88-22776
Analysis of the electrical harmonic characteristics of a slip recovery variable speed generating system for wind turbine applications
[DE88-001140] 19 p2687 N88-25972
Analysis of the electrical characteristics of a Westinghouse variable speed generating system for wind turbine applications
[DE88-001139] 20 p2818 N88-26721
Comparative analysis of the space power architecture studies
[NASA-TM-100977] 22 p3049 N88-28090

ELECTRIC IGNITION
Measuring technical and mathematical investigation of multiple reignition at the switching of a motor using vacuum circuit breakers
[ETN-87-90406] 01 p0042 N88-10270
Electrical ignition of HAN-based liquid propellants
[AD-A191349] 18 p2495 N88-24801

ELECTRIC IMPULSES
U ELECTRIC PULSES

ELECTRIC MOMENTS
Neutrino electrodynamics and possible effects for solar neutrinos
[DE88-701647] 23 p3308 N88-29705

ELECTRIC MOTOR VEHICLES
DOT fuel-cell-powered bus feasibility study
[DE87-012705] 01 p0107 N88-10699
Performance monitoring and analysis of electric van fleet vehicles
[DE88-900066] 04 p0502 N88-13091
Digital control of a direct current converter for a hybrid vehicle
[LAAS-87-266] 05 p0578 N88-13527
Research and development of advanced lead-acid batteries for electric vehicle propulsion
[DE87-014661] 07 p0873 N88-15297
User's guide to DIANE: A microcomputer program for modeling battery performance in electric vehicles
[DE88-003713] 08 p1068 N88-16456
Fuel cell/battery hybrid vehicle assessment
[DE88-005087] 10 p1427 N88-18520
Electric vehicle demonstration project
[DE88-004076] 11 p1566 N88-19376
Performance test results for the Eaton dc development power train in an electric test bed vehicle
[DE88-005458] 12 p1622 N88-19699
Mission directed goals for electric vehicle battery research and development: The Task Force on electric vehicle battery goals
[DE88-005601] 13 p1763 N88-20548
Testing and development of electric vehicle batteries for EPRI Electric Transportation Program
[DE88-005894] 13 p1764 N88-20551
Development of a total electric vehicle drive system
[DE88-900367] 14 p1917 N88-21446
Status of electric vehicle simulation programs at the INEL: Summer 1987
[DE88-006745] 15 p2058 N88-22271
A microcomputer-based control and simulation of an advanced IPM (Interior Permanent Magnet) synchronous machine drive system for electric vehicle propulsion
[DE88-006735] 18 p2505 N88-24859
Test results of the Electric Vehicle Field-Laboratory Correspondence Program, phase 1 report
[DE88-007706] 19 p2661 N88-25827
Computer controlled procedures for traction battery power performance tests
[ETN-88-92352] 20 p2796 N88-26589
Voltage directive drive with claw pole motor and control without rotor position indicator
[ETN-88-93120] 24 p3366 N88-30047

ELECTRIC MOTORS
NT ASYNCHRONOUS MOTORS
NT INDUCTION MOTORS
NT STEPPING MOTORS
NT SYNCHRONOUS MOTORS
NT TORQUE MOTORS
Computerized system for studies on creep of irradiated materials in the BR-10 reactor: Control system for electric motor
[DE87-702888] 03 p0310 N88-11952
The use of alloy 117 as a liquid metal current collector
[AD-A185740] 06 p0698 N88-14281
Pulse width modulator controller design for a brushless DC motor position servo
[AD-A186618] 08 p0980 N88-15921
Electro-mechanical vibratory system
11 p1500 N88-18958
Performance test results for the Eaton dc development power train in an electric test bed vehicle
[DE88-005458] 12 p1622 N88-19699
Development of a total electric vehicle drive system
[DE88-900367] 14 p1917 N88-21446
High output paraffin actuators: Utilization in aerospace mechanisms 14 p1924 N88-21470
Computer simulation of a motor pump unit to aid in interpreting vibration data
[DE88-004481] 16 p2223 N88-23270
The LDCM actuator for vibration suppression
[NASA-CR-182898] 17 p2335 N88-23940
A microcomputer-based control and simulation of an advanced IPM (Interior Permanent Magnet) synchronous machine drive system for electric vehicle propulsion
[DE88-006735] 18 p2505 N88-24859
Contribution to speed regulation of small motors with phase-locked loops
[ETN-88-92373] 20 p2796 N88-26590
Voltage directive drive with claw pole motor and control without rotor position indicator
[ETN-88-93120] 24 p3366 N88-30047

ELECTRIC NETWORKS
Design principles and practices for implementation of MIL-STD-1760 in aircraft and stores
[AD-A183724] 01 p0005 N88-10027
Development of methods for the analysis of the frequency and voltage statics of electricity users and electrical networks
[ETN-87-90412] 01 p0043 N88-10271
Performance optimization of electronic networks in the frequency domain
[PB87-123873] 04 p0438 N88-12720
Photoconductor switch and circuit analysis
[AD-A188166] 11 p1478 N88-18821
ECP (Electrical Circuitry Program): A proposed program for electrical circuitry analysis
[AD-A190494] 15 p2060 N88-22280
Some equivalent circuit models for AC impedance analysis of pyrite/solution interface
[DE88-010574] 21 p2939 N88-27452
On broadband matching of multiport electrical networks with applications
[AD-A194224] 23 p3207 N88-29086

ELECTRIC POTENTIAL
NT BIOELECTRIC POTENTIAL
NT COULOMB POTENTIAL
NT LOW VOLTAGE
NT QUANTUM WELLS
NT THRESHOLD VOLTAGE
On the interaction of a planar metal surface with a charge and with a molecule
[DE87-703083] 02 p0147 N88-10920
Departmental report on program EMTP-machine windings surge transients: Travelling wave method
[PB87-123733] 04 p0438 N88-12719
Conditions for geomagnetically trapping sub-micron lunar ejecta between L = 1.2 and L = 3.1
04 p0521 N88-13203
High energy density rechargeable batteries for aerospace power requirements
[AD-A184883] 05 p0577 N88-13519
Rotation of magnetized particle in electrically conducting viscous medium 06 p0770 N88-14733
Calculated sputtering and atomic displacement cross-sections for applications to medium voltage analytical electron microscopy
[DE88-002904] 09 p1168 N88-17006
Development and calibration of Direct Current Potential Difference (DCPD) crack length measurement equipment
[VTT-RR-480] 09 p1182 N88-17083
Nonlinear dynamic maximum power theorem
[AD-A187491] 11 p1477 N88-18810
Hercules: A power analyzer for MOS VLSI circuits
[AD-A188702] 12 p1623 N88-19706
Analysis of pre-flight modulator voltage calibration data for the Voyager plasma science experiment
[NASA-CR-182577] 12 p1710 N88-20236
Bloch oscillations in small Josephson junctions: Their manifestation in switching effects
14 p1969 N88-21756
Modeling the effects of heavy charged particles on MOSFETs (Metal-Oxide-Semiconductor Field Effect Transistors)
[AD-A190575] 15 p2143 N88-22792
Optical sensors for the measurement of electric current and voltage
[PB88-172945] 16 p2193 N88-23077
An electrostatic potential comparator
[AD-A192051] 18 p2557 N88-25177
Generation, and forming of ultrashort high voltage pulses 19 p2657 N88-25782
Carrier transport in semiconductor magnetic sensors under nonuniform fields 19 p2672 N88-25868
Characterization of fatigue crack initiation and propagation in Ti-6Al-4V with electrical potential drop technique
[NASA-TM-100877] 19 p2681 N88-25807
Fast parametrization procedure for solar cells
[PB88-186416] 19 p2686 N88-25966
Voltages induced by lightning on electric power distribution lines: Field data and analysis results for the period July 1984-1986
[DE88-007841] 19 p2693 N88-26006
Discontinuous inverse Sturm-Liouville problems with symmetric potentials
[DE88-009803] 19 p2720 N88-26152
Transport study on Si/Si(1-x)Ge(x) superlattices selectively doped by secondary implantation of Sb
20 p2867 N88-27027
A planar IC compatible transferred electron device for millimeter-wave operation
[AD-A192692] 21 p2936 N88-27433
Results from life test in progress on eagle-picher nickel cadmium cells
[AD-A192816] 21 p2936 N88-27434
Studies of the intact human brain: Implications for performance 21 p2977 N88-27684
Dissecting the visual and auditory pathways by means of the two-input technique 21 p2978 N88-27690
Event-related brain potentials as indices of mental workload and attentional allocation
21 p2979 N88-27696
Using ERPS to study human information processing
21 p2980 N88-27698
Withstand voltage of slightly polluted insulator chains in humid weather conditions
[DE88-752818] 22 p3072 N88-28237
Development of inductive storage pulsed power generators
[AD-A193878] 22 p3117 N88-28521

ELECTRIC POWER CONVERSION
U ELECTRIC GENERATORS

ELECTRIC POWER PLANTS
NT FUEL CELL POWER PLANTS
NT NUCLEAR POWER PLANTS
NT SOLAR THERMAL ELECTRIC POWER PLANTS
USSR report: Engineering and equipment
[JPRS-UEQ-87-008] 04 p0423 N88-12621
Solar energy: European research and development
[PB87-107645] 04 p0463 N88-12866
Cu-2 mechanical properties and microstructural stability of advanced steam cycle materials
[DE88-001519] 05 p0566 N88-13452
Monitoring corrosion and process physical-chemical parameters in electric power plants
[CISE-3708] 06 p0682 N88-14182
Innovating systems and techniques for the diagnosis of materials and industrial plants
[CISE-3856] 08 p0976 N88-15901
On line instrument systems for monitoring steam turbogenerators
[CISE-3860] 08 p0990 N88-15995
The role of repowering in America's power generation future
[DOE/FE-0096] 10 p1351 N88-18076
An analysis of gas-steam total power recovery energy system 20 p2784 N88-26512

ELECTRIC POWER SUPPLIES
NT AIRCRAFT POWER SUPPLIES
NT SOLAR DYNAMIC POWER SYSTEMS
NT SPACE STATION POWER SUPPLIES
NT SPACECRAFT POWER SUPPLIES
Evaluation of stand-alone inverters for remote applications
[DE87-010957] 01 p0040 N88-10257
The fundamentals of photovoltaic system electrical design
[DE87-009061] 02 p0194 N88-11214
Operation of multistage power supplies for electron beam welding installations 03 p0286 N88-11800
Recent progress in space photovoltaic systems
[NASA-TM-100208] 03 p0311 N88-11966
A 40-kW fuel cell field test summary utilities activities report
[PB88-112800] 06 p0731 N88-14496
Evaluation of high-voltage, high-power, solid-state remote power controllers for amps
07 p0924 N88-15612
Microprocessor control and networking for the amps breadboard 07 p0924 N88-15615
Plasma contactors for use with electodynamic tethers for power generation
[NASA-CR-182424] 08 p1087 N88-16547
Test results on dual resonant power supply with flat top and flat bottom current
[DE87-007506] 09 p1157 N88-16933
Project Explorer takes its second step: GAS-608 in engineering development 10 p1288 N88-17707

A methodology to assess the effects of high altitude electromagnetic pulse (HEMP) on electric power systems
[DE88-000338] 11 p1476 N88-18808
High frequency power distribution system
[NASA-CR-175071] 17 p2335 N88-23939
Arc lamp power supply using a voltage multiplier
[NASA-CASE-LAR-13202-1] 17 p2335 N88-23942
Magnet shielding analysis for SOAR: A space fusion reactor 17 p2400 N88-24269
Magnetically switched power supply system for lasers
[NASA-CASE-NPO-16402-2] 18 p2505 N88-24862
Photovoltaic energy systems
[DE88-007504] 19 p2687 N88-25968
Advanced photovoltaic power system technology for lunar base applications
[NASA-TM-100965] 20 p2766 N88-26402

ELECTRIC POWER TRANSMISSION
Comparison of costs and benefits for dc and ac transmission
[DE87-008774] 02 p0167 N88-11052
The ac power system testbed
[NASA-CR-175068] 03 p0309 N88-11948
Safety research of insulating materials of cable for nuclear power generating station
[NASA-TT-20202] 13 p1752 N88-20477
Power transmission studies for tethered SP-100
[NASA-TM-100864] 14 p1883 N88-21251
Northern lights: The economic and practical potential of imported power from Canada
[DE88-006026] 15 p2093 N88-22473
Optical sensors for the measurement of electric current and voltage
[PB88-172945] 16 p2193 N88-23077
Harmonic considerations for electrical distribution feeders
[DE88-007849] 18 p2505 N88-24860
Technologies applicable to space tethers
[NASA-CR-183055] 19 p2606 N88-25471
Voltages induced by lightning on electric power distribution lines: Field data and analysis results for the period July 1984-1986
[DE88-007841] 19 p2693 N88-26006

ELECTRIC PROPULSION
NT ELECTROMAGNETIC PROPULSION
NT ELECTROSTATIC PROPULSION
NT ION PROPULSION
NT LASER PROPULSION
NT PLASMA PROPULSION
Auxiliary propulsion system flight package
[NASA-CR-180828] 02 p0141 N88-10886
A low-power arcjet cyclic lifetest
[NASA-TM-100233] 03 p0278 N88-11748
Post-test analyses of aqueous batteries developed for electric propulsion
[DE88-000655] 03 p0311 N88-11965
High power ion thruster performance
[NASA-TM-100127] 04 p0409 N88-12542
Advanced electric propulsion and space plasma contactor research
[NASA-CR-180862] 06 p0674 N88-14126
Performance-limiting factors in MPD thrusters
[AD-A185605] 06 p0674 N88-14128
Completely magnetically contained electrothermal thrusters
[AD-A185674] 06 p0674 N88-14129
ESA Bulletin No. 10
[ETN-87-90514] 09 p1123 N88-16728
Electric propulsion: A controversial must for long-lived applications satellites 09 p1124 N88-16735
A comparative study of various electric propulsion systems and their impact on a nominal ship design
[AD-A187800] 11 p1477 N88-18816
Physical fluid mechanics in MPD thrusters
[AD-A190309] 15 p2138 N88-22754
Megawatt level electric propulsion perspectives 17 p2404 N88-24294
High power ion thruster performance 17 p2404 N88-24295
Electric propulsion options for the SP-100 reference mission 17 p2404 N88-24296
Status of high power electric propulsion technology 17 p2428 N88-24443
Performance and long duration test of a 30 kw thermal arcjet engine
[AD-A190962] 18 p2474 N88-24677
Performance of a hydrogen pulsed electrothermal thruster. Strategic defense initiative organization innovative science and technology. SBIR, phase 1
[AD-A191999] 18 p2475 N88-24679
The NASA Electric Propulsion Program
[NASA-TM-101324] 24 p3336 N88-29859
Performance and lifetime assessment of MPD arc thruster technology
[NASA-TM-101293] 24 p3336 N88-29860
The dc power control for a liquid-fed resistojet
[NASA-TM-101326] 24 p3338 N88-29869
Successful completion of a cyclic ground test of a mercury ion auxiliary propulsion system
[NASA-TM-101351] 24 p3339 N88-29873

ELECTRIC PULSES
NBS (National Bureau of Standards) wideband sampling wattmeter
[PB87-210324] 03 p0323 N88-12041
On M-ARY sequential hypotheses testing for the classification of radar signals
[AD-A184094] 04 p0430 N88-12666
State parameters of pulse-discharge plasma in xenon-filled closed tube 06 p0773 N88-14747
Pulsed power sources based on MHD generators (a state-of-art review)
[DE88-700296] 07 p0935 N88-15677
Optimum transformer design for a pulsed power system
[DE88-006054] 13 p1760 N88-20525
Harmonic and rectangular pulse reproduction through current transformers
[EUT-86-E-159] 14 p1907 N88-21395

ELECTRIC REACTORS
NT SATURABLE REACTORS

ELECTRIC ROCKET ENGINES
NT ARC JET ENGINES
NT ELECTROSTATIC ENGINES
NT ELECTROTHERMAL ENGINES
NT ION ENGINES
NT MERCURY ION ENGINES
NT PLASMA ENGINES
NT RESISTOJET ENGINES
Nuclear electric power for multimegawatt orbit transfer vehicles 17 p2399 N88-24261

ELECTRIC SPARKS
Experimental study and modeling of the physical mechanisms of the gliding spark
[ESA-TT-1029] 01 p0070 N88-10447

ELECTRIC STIMULI
Facilitory effects of voluntary movements on vestibulomotor reaction 12 p1664 N88-19976

ELECTRIC SWITCHES
NT VACUUM ARC SWITCHES
Characterization of PEOS (Plasma Erosion Opening Switch) plasma parameters and conduction phase properties
[AD-A189024] 12 p1624 N88-19714

ELECTRIC WELDING
NT ARC WELDING
NT ELECTRON BEAM WELDING
NT GAS TUNGSTEN ARC WELDING
NT PLASMA ARC WELDING

ELECTRIC WIRE
Properties of Nb3Sn superconductor wires with composite cores
[KFK-4263] 02 p0246 N88-11557
Electromagnetic interaction between an electric discharge and cabling inside a satellite 03 p0274 N88-11725
A design philosophy for grounding and inter-unit wiring
[EMCR-20/85] 03 p0310 N88-11954
Discussions in support of the design-philosophy for grounding and inter-unit wiring
[EMCR-21/85] 03 p0310 N88-11955
Assessment of existing specifications against the design-philosophy for grounding and inter-unit wiring (EMCR 20/85)
[EMCR-22/85] 03 p0310 N88-11956
Alternatives to the techniques implicit in the design philosophy, and the penalties in performance associated with them --- grounding and wiring
[EMCR-31/85] 03 p0310 N88-11957
Powder metallurgical preparation of A15 superconductors
[ETN-88-91072] 09 p1144 N88-16858
Nature of gigantic resistance fluctuations in metal-oxide-semiconductor wires
[DE88-002905] 09 p1256 N88-17533
Evaluation of flammability for cable-like polymers
[NASA-TT-20225] 13 p1752 N88-20476
On the use of thermal degradation data to predict cable ignition performance
[DE88-002276] 19 p2621 N88-25549

ELECTRIC WIRING
U ELECTRIC WIRE
U WIRING

ELECTRICAL BREAKDOWN
U ELECTRICAL FAULTS

ELECTRICAL CONDUCTIVITY
U ELECTRICAL RESISTIVITY

ELECTRICAL CONDUCTIVITY METERS
Definition and use of sensors for measuring electrical conductivity in thunderclouds
[ESA-TT-1047] 03 p0352 N88-12222

ELECTRICAL ENGINEERING
Electrical heating method --- pipelines, metal tanks
[GB-PATENT-2-137-059-A] 01 p0043 N88-10274
Center for Electronics and Electrical Engineering Technical Progress Bulletin covering center programs, October to December 1986 with 1987 CEEE events calendar
[PB87-226890] 02 p0168 N88-11058
Center for Electronics and Electrical Engineering technical publication announcements covering center programs, July to September 1986 with 1987 CEEE events calendar
[PB87-223442] 02 p0168 N88-11059
Center for Electronics and Electrical Engineering Technical Progress Bulletin covering center programs, January to March 1987 with 1987 CEEE events calendar
[PB87-224648] 03 p0309 N88-11946
Electronics engineering thrust area report, FY86
[DE87-014616] 03 p0309 N88-11950
A design-philosophy for grounding and inter-unit wiring
[EMCR-20/85] 03 p0310 N88-11954
National Science Foundation
[PB87-228375] 03 p0384 N88-12410
Bulletin of the Yamagata University (Engineering), Volume 20, No. 1, January 1988
[ISSN-0085-834X] 07 p0839 N88-15091
Helsinki University of Technology Communications Laboratory
[PB88-112974] 10 p1318 N88-17881
Construction of control systems with diversified redundancy for electrical machines
[BIA-5/86] 11 p1481 N88-18842
MacCAD (Macintosh Computer Aided Design), computer aided design tool for system analysis
[AD-A189241] 13 p1815 N88-20843
Center for Electronics and Electrical Engineering technical publication announcements covering Center programs, July to September 1987
[PB88-196530] 20 p2793 N88-26572
Analytical determination of critical crack size in solar cells
[NASA-CR-183128] 20 p2821 N88-26736
Statistical analysis of the LMS (Last Mean Squares) and modified stochastic gradient
[AD-A195497] 24 p3424 N88-30376

ELECTRICAL FAULTS
NT SHORT CIRCUITS
In-flight diagnosis: Analysis of spurious events --- spacecraft 03 p0274 N88-11724
Low-current behavior and current chopping of vacuum arcs
[ISBN-90-9001649-X] 05 p0578 N88-13529
RELIC: A reliability simulator for integrated circuits
[AD-A187493] 11 p1477 N88-18811
Air gap testing using Trailing Wire Antenna (TWA) waveform
[AD-A187639] 11 p1477 N88-18812
Application of knowledge based systems to the maintenance of inertial system electronics 12 p1578 N88-19441

ELECTRICAL GROUNDING
A design-philosophy for grounding and inter-unit wiring
[EMCR-20/85] 03 p0310 N88-11954
Discussions in support of the design-philosophy for grounding and inter-unit wiring
[EMCR-21/85] 03 p0310 N88-11955
Assessment of existing specifications against the design-philosophy for grounding and inter-unit wiring (EMCR 20/85)
[EMCR-22/85] 03 p0310 N88-11956
Alternatives to the techniques implicit in the design philosophy, and the penalties in performance associated with them --- grounding and wiring
[EMCR-31/85] 03 p0310 N88-11957
Human engineering laboratory grounding analysis (HELGA)-2
[AD-A185367] 05 p0578 N88-13524

ELECTRICAL IMPEDANCE
NT CONTACT RESISTANCE
NT ELECTRICAL RESISTANCE
NT SKIN RESISTANCE
NT TRANSCONDUCTANCE
Surface topography and electrical response of metal-electrolyte interface
[DE87-013553] 02 p0166 N88-11046
Study of the distribution of a multi-electrode circular system sensitivity for the reconstruction of bioelectrical impedance images
[ISAL-IDI1-87-01] 02 p0217 N88-11368
Time domain electromagnetic waves in multilayered media
[AD-A185055] 05 p0574 N88-13502
Analytical solution of the equations for a coaxial plasma gun operating in the snowplow mode. 1: Weak coupling limit
[AD-A185370] 05 p0652 N88-13994

Application of ac-impedance method on determination of corrosion rate of metals
[DE88-750307] 10 p1300 N88-17771
Operators manual for a computer controlled impedance measurement system
[AD-A187513] 10 p1324 N88-17917
Characterization of proton conducting polymer blends
19 p2669 N88-25867
Electrical detection of coating deterioration
24 p3355 N88-29973
Electrochemical evaluation of the long term corrosion resistance of polymer coated steel
24 p3355 N88-29974
An electrochemical impedance spectroscopy study of reactions at the metal/coating interface
24 p3355 N88-29975
Evaluation of organic coating deterioration and substrate corrosion in seawater using electrochemical impedance measurements 24 p3355 N88-29976
Review of Radio Science, 1984-1986
24 p3363 N88-30023
Electromagnetic metrology 24 p3363 N88-30024

ELECTRICAL INSULATION
The influence of microvoids on the electrical strength of glass fiber reinforced epoxy resins
[ETN-87-90443] 01 p0030 N88-10189
Design and testing of electrical insulation for superconducting coils
[DE87-012256] 01 p0039 N88-10246
Discharge prevention of geosynchronous orbit conductive thermal control materials and grounding systems 03 p0274 N88-11732
Polymer composition --- cable insulation
[EP-PATENT-0-199-444-A1] 04 p0418 N88-12594
Coaxial cable connector
[NASA-CASE-NPO-16764-1-CU]
06 p0696 N88-14270
Particle desorption from nonconducting surfaces by high energy heavy ions
[ETN-88-91088] 09 p1245 N88-17461
Application of high temperature ceramic superconductors (CSC) to commercial tokamak reactors
[DE88-003973] 09 p1257 N88-17538
Measurement of shielding effectiveness of different cable and shielding configurations by mode-stirred techniques
[PB88-155791] 10 p1319 N88-17885
Evaluation of flammability for cable-like polymers
[NASA-TT-20225] 13 p1752 N88-20476
Vapor-mist for lightweight high voltage space insulation systems
[DE87-011704] 13 p1762 N88-20538
Power transmission studies for tethered SP-100
[NASA-TM-100864] 14 p1883 N88-21251
Partial discharges and the electrical aging of cross linked polyethene (XLPE) cable insulation
[EUT-86-E-160] 14 p1892 N88-21300
Irradiation test results on thermionic fuel element sheath insulators 17 p2402 N88-24280
Research and development of electrical insulators for thermionic applications 17 p2429 N88-24449
Ceramic electrical insulator development for thermoelectric SACE power system
17 p2430 N88-24459
Development of external cooling cryo-resistive cable systems. Part 2: Insulation characteristics on 66 kV rated cryo-resistive testing cable
[DE88-770191] 20 p2793 N88-26571
A model for insulated wires in the method of moments code NEC (Numerical Electromagnetics Code)
[DE88-008920] 20 p2794 N88-26577
Withstand voltage of slightly polluted insulator chains in humid weather conditions
[DE88-752818] 22 p3072 N88-28237
System suitable for observing surface plasmon in a semi-infinite semiconductor superlattice
[DE88-702686] 23 p3293 N88-29606

ELECTRICAL LEADS
U ELECTRIC CONDUCTORS

ELECTRICAL MEASUREMENT
NT POLAROGRAPHY
Optical power line voltage and current measurement systems. Volume 1: Limits to the precision of electro-optic and magneto-optic sensors
[DE87-014558] 02 p0175 N88-11092
Analysis of free cutting brass by A.C. polarography
[PD-MT-8728] 04 p0417 N88-12587
Electromagnetic tests
[SNIAS-872-430-103] 05 p0575 N88-13508
An electric field meter based upon a new principle: A dummy displacement electrode. Application to aerospace vehicles
[SNIAS-872-422-106] 05 p0585 N88-13567
Electric field measurements on Viking: First results
[TRITA-EPP-87-04] 05 p0625 N88-13826
High frequency periodic time domain waveform measurement system
[PB87-225256] 06 p0695 N88-14264
Development and calibration of Direct Current Potential Difference (DCPD) crack length measurement equipment
[VTT-RR-480] 09 p1182 N88-17083
Preliminary results from the dc electric field experiment on Viking --- Swedish satellite
[TRITA-EPP-87-03] 09 p1190 N88-17130
Automatic prober for the dc characterization of gallium arsenide devices. Part 1: The measurement facility
[AD-A187583] 11 p1560 N88-19337
Planning, construction, and commissioning of a vacuum apparatus with a cold surface for the measurement of transistor functions at 20 K
[JUEL-SPEZ-397] 12 p1622 N88-19703
Separable electrical connectors for space: A tribological and electrical assessment 14 p1879 N88-21231
Calculating depletion region carrier concentrations with capacitance-voltage measurements and etching
[AD-A189630] 15 p2141 N88-22777
Electrochemistry in near-critical and supercritical fluids. 5: The dimerization of quinoline and acridine radical anions and dianions in ammonia from -70 C to 150 C
[AD-A190858] 16 p2175 N88-22967
Optical sensors for the measurement of electric current and voltage
[PB88-172945] 16 p2193 N88-23077
Electrochemistry in near-critical and supercritical fluids. 6: The electrochemistry of ferrocene and phenazine in acetonitrile between 25C and 300C
[AD-A192171] 18 p2482 N88-24723
Recent advances in capacitance type of blade tip clearance measurements
[NASA-TM-101291] 19 p2603 N88-25460
Voltages induced by lightning on electric power distribution lines: Field data and analysis results for the period July 1984-1986
[DE88-007841] 19 p2693 N88-26006
The influence of uncompensated solution resistance on the determination and standard electrochemical rate constants using cyclic voltammetry and some comparisons with AC voltammetry
[AD-A192825] 20 p2770 N88-26427
A rapid electrochemical technique for determining the current efficiency for cadmium plating
[AD-A193679] 22 p3056 N88-28130
Results of the use of an automated electrical measuring instrument calibration system
[SNIAS-881-430-107] 23 p3217 N88-29146
Electrical detection of coating deterioration
24 p3355 N88-29973
Electrochemical evaluation of the long term corrosion resistance of polymer coated steel
24 p3355 N88-29974
Evaluation of organic coating deterioration and substrate corrosion in seawater using electrochemical impedance measurements 24 p3355 N88-29976

ELECTRICAL PROPERTIES
NT CAPACITANCE
NT CAPACITANCE-VOLTAGE CHARACTERISTICS
NT CARRIER MOBILITY
NT CHARGE DISTRIBUTION
NT CONTACT RESISTANCE
NT DIELECTRIC PROPERTIES
NT ELECTRIC MOMENTS
NT ELECTRICAL IMPEDANCE
NT ELECTRICAL RESISTANCE
NT ELECTRICAL RESISTIVITY
NT ELECTRON MOBILITY
NT ELECTROSTRICTION
NT FERROELECTRICITY
NT HOLE MOBILITY
NT INDUCTANCE
NT KONDO EFFECT
NT MAGNETORESISTIVITY
NT PERMITTIVITY
NT PHOTOCONDUCTIVITY
NT PHOTOVOLTAIC EFFECT
NT PIEZOELECTRICITY
NT PLASMA CONDUCTIVITY
NT PROXIMITY EFFECT (ELECTRICITY)
NT PYROELECTRICITY
NT SKIN RESISTANCE
NT SUPERCONDUCTIVITY
NT TRANSCONDUCTANCE
Electrical behavior of layers implanted with low energy pions in Si
[INPE-4199-PRE/1051] 01 p0102 N88-10670
The preparation of thin films for photovoltaic conversion by novel MOCVD techniques
[DE87-001185] 02 p0194 N88-11212
Electrical properties of high T/sub c/ superconductors under high pressures
[DE87-012818] 02 p0245 N88-11546
Vacuum ultraviolet electronic properties of liquids
[DE88-000165] 03 p0282 N88-11772
Research and development on high strength ceramic heaters discussed 04 p0404 N88-12508
Synthesis, NMR characterization and electrical properties of siloxane-based polymer electrolytes
[AD-A184184] 04 p0418 N88-12596
A study of charged particles/radiation damage to VLSI device materials
[NASA-CR-172036] 05 p0577 N88-13518
Material design of high performance glasses discussed 06 p0688 N88-14216
Picosecond cable calibrator: Beam Research Program
[DE88-002375] 06 p0695 N88-14266
Investigation of silicon surface passivation by silicon nitride film deposition
[NASA-CR-182350] 06 p0729 N88-14487
Contrast between the chemical, structural and electronic properties of thin films of Cu and Ni on the Ru(0001) surface
[DE88-002360] 07 p0938 N88-15698
Rapid underway sediment classification by electrical methods
[AD-A187477] 10 p1357 N88-18114
Electrical properties of medium field chem-prep varistors
[DE88-006147] 13 p1762 N88-20540
Scale-up of a batch-type chemical powder preparation process for high field varistor fabrication
[DE88-006601] 13 p1762 N88-20541
Measurement of the properties of lossy materials inside a finite conducting cylinder
[NASA-CR-182664] 13 p1832 N88-20962
A general 2D electrical model for diagonally connected MHD generators
[DE88-004283] 14 p1984 N88-21835
Electrical circuit modeling of reversed field pinches
[DE88-005942] 15 p2136 N88-22745
Preparation of large area NbN/AlN/NbN Josephson junctions
[DE88-006074] 15 p2145 N88-22799
Laser induced ignition of propellants
[AD-A191100] 16 p2168 N88-22927
Electrical dc conductivity of pitch
[AD-A191266] 16 p2182 N88-23008
The inspection of electronic metallurgical bonds
[AD-A192197] 18 p2486 N88-24745
Progress and challenges in HEMT LSI technology
19 p2656 N88-25779
The structure and properties of RF reactive sputtered IrO2 films 19 p2672 N88-25884
Electrodynamic driver for the space thermoacoustic refrigerator (STAR)
[AD-A192337] 20 p2785 N88-26517
Analysis of the electrical characteristics of a Westinghouse variable speed generating system for wind turbine applications
[DE88-001139] 20 p2818 N88-26721
Pressure-dependent measurement on n + GaAs (Si, Sn): The effect of deep donor (DX) states on the electrical properties and presistent photoconductivity effects
20 p2866 N88-27020
Electrical properties of p-type and n-type ZnSe-ZnTe strained-layer superlattices 20 p2868 N88-27029
MBE growth of HgTe/CdTe superlattices on Si(100) substrates 20 p2869 N88-27033
On a-Si:H/a-SiN(x):H superlattices: Confinement or contamination 20 p2870 N88-27040
Influence of interfaces on electronic and magnetic properties of MnSe/ZnSe superlattices near monolayer limit 20 p2872 N88-27050
Electrical study of metal/group 3-5 semiconductor interfaces: Comparison with the atomic-level studies
20 p2874 N88-27059
Investigations on the MBE (Molecular Beam Epitaxy) growth and properties of Al(sub y)Ga(sub y)In(sub 1-x-y)AsInP and InGaAs-InAlAs superlattices
[DE88-009105] 21 p3022 N88-27941
Electrical properties of metal-oxide-silicon structures with sol-gel oxides
[DE88-011791] 22 p3156 N88-28779
Cytochrome electron transfer and biomolecular electronics
[AD-A195482] 24 p3406 N88-30277
A dynamic analysis of piezoelectric strained elements
[AD-A196079] 24 p3432 N88-30430

ELECTRICAL RESISTANCE
NT CONTACT RESISTANCE
NT SKIN RESISTANCE
NT TRANSCONDUCTANCE
The development of a high temperature static strain gage system 02 p0184 N88-11142
On the stressing of annealed NITINOL: The electrical resistance and calorimetric effects
[AD-A184465] 04 p0414 N88-12569

Studies of alumina additions in zirconia - magnesia [DE87-703500] 04 p0419 N88-12602
Extraction of MOS VLSI (Very-Large-Scale-Integrated) circuit models including critical interconnect parasitics [AD-A185847] 08 p0979 N88-15914
Comparative evaluation of resistive and inductive techniques for measuring temperature of superconducting transition [DE88-700603] 10 p1417 N88-18457
Method for characterizing end-plate surface resistance of dielectric resonator 14 p1903 N88-21371
Effects of cold working on precipitation in age hardenable alloys: On the copper alloys [NASA-TT-20164] 16 p2177 N88-22973
Liquid carbon [AD-A191707] 18 p2491 N88-24776
Observation of metallic conductivity in liquid carbon [AD-A191723] 19 p2618 N88-25533
The influence of uncompensated solution resistance on the determination and standard electrochemical rate constants using cyclic voltammetry and some comparisons with AC voltammetry [AD-A192825] 20 p2770 N88-26427
A critical review of IR drops and electrode potentials within pits, crevices and cracks [AD-A192481] 21 p2935 N88-27431
Friction, wear and electrical contact resistance of precious metal alloys [DE88-011244] 21 p2938 N88-27450
Conductivity mechanism and operating behavior of electrically conductive adhesives on the example of a power transistor [ETN-88-92355] 21 p2940 N88-27464
Shielding effectiveness of metallic joints versus corrosion prevention 22 p3054 N88-28120
Superconducting properties of oxygen deficient YBa2Cu3O(sub 7-delta) [DE88-009969] 22 p3155 N88-28774
Electrical properties of materials for elevated temperature resistance strain gage application [NASA-CR-182214] 24 p3376 N88-30106

ELECTRICAL RESISTIVITY
NT KONDO EFFECT
NT MAGNETORESISTIVITY
NT PHOTOCONDUCTIVITY
NT PLASMA CONDUCTIVITY
NT SUPERCONDUCTIVITY
Eddy current density in wedge-shaped conducting cylinders with inhomogeneous conductivity [ETN-87-90404] 01 p0042 N88-10268
Electrical behavior of layers implanted with low energy pions in Si [INPE-4199-PRE/1051] 01 p0102 N88-10670
Electrical conductivity and equation of state measurements on planetary fluids at high pressures and temperatures [DE87-013787] 01 p0110 N88-10708
Continuous flow electrophoresis system experiments on shuttle flights STS-6 and STS-7 [NASA-TP-2778] 02 p0156 N88-10978
Frozen-field, rigid-beam, uniform-conductivity-channel tracking force calculation [DE87-012510] 02 p0190 N88-11190
Transport analysis of OH and NBI heated discharges in JT-60 [DE87-752985] 02 p0239 N88-11511
External surface charging mechanisms --- spacecraft 03 p0273 N88-11719
A quantum theoretical study of polyimides [NASA-CR-181495] 03 p0292 N88-11831
Wittig synthesis of conductive segmented block polymer compositions [AD-A184018] 03 p0295 N88-11850
Research and development on high strength ceramic heaters discussed 04 p0404 N88-12508
Ultimate velocities for induction launchers [DE87-012360] 04 p0404 N88-12513
Studies on some Ge-Se-Te glasses [PD-MT-8721] 04 p0420 N88-12607
Proton abstraction as a route to conductive polymers [AD-A184019] 04 p0421 N88-12612
Resistivity of EuBa2(Cu/sub 1-y/Zn/sub y/)3O/sub x/ as a ffunction of temperature, magnetic field, pressure and Zn concentration [DE87-014740] 04 p0499 N88-13069
Human engineering laboratory grounding analysis (HELGA)-2 [AD-A165367] 05 p0578 N88-13524
Superconducting material development 06 p0688 N88-14217
Conductivity studies on hydroxide ion conductors in the Li-Al-O-H system at intermediate temperatures [AD-A185714] 06 p0697 N88-14279
Phase behavior in the Li-Al-O-H system at intermediate temperatures [AD-A185732] 06 p0697 N88-14280
Rotation of magnetized particle in electrically conducting viscous medium 06 p0770 N88-14733
Effect of plasma rotation in tokamak on stabilizing action of electrically conducting wall 06 p0773 N88-14748
Interface characteristics and the mechanical properties of metal matrix composites [AD-A186441] 08 p0966 N88-15845
Study of asthenosphere: Project ELAS 08 p1013 N88-16138
Influence of arsenic superficial enrichment on the ohmicity of the n-GaAs In/Au contact [ECL-87-09] 08 p1089 N88-16554
Interpretation of the temperature dependence of conductivity in superconducting oxides [DE88-003028] 08 p1091 N88-16565
Thermodynamic and conductivity studies of nonstoichiometric cerium dioxide by Coulometric titration. A simultaneous measurement [DE88-003054] 08 p1091 N88-16566
High temperature solar electrothermal processing-3. Zinc from zinc oxide at 1200-1675K using a non-consumable anode [AD-A186600] 09 p1141 N88-16836
Evaluation of the magnetic induction conductivity method for detecting frazil ice deposits [AD-A186940] 09 p1194 N88-17157
Structural relationships in high temperature superconcuctors [DE88-002924] 09 p1257 N88-17534
Effect of the subgap conductance on the metastable states in a Josephson tunnel junction [DE88-003102] 09 p1258 N88-17543
Electrically conducting polymer-copper sulphide composite films, preparation by treatment of polymer-copper (2) acetate composites with hydrogen sulfide [NASA-TT-20204]. 10 p1305 N88-17803
Design of a charge sensitive preamplifier on high resistivity silicon [DE88-003491] 10 p1323 N88-17907
Rapid underway sediment classification by electrical methods [AD-A187477] 10 p1357 N88-18114
Realistic conductivity geometry model of the human head for interpretation of neuromagnetic data [PB88-112230] 10 p1369 N88-18179
The physics of metallic superlattices. An experimental point of view [DE88-003080] 10 p1416 N88-18452
Determination of distributed resistance of base of bipolar transistors measuring noise spectral densities [DE88-700197] 11 p1479 N88-18829
Limiting efficiency of a thermionic diode [DE88-700598] 11 p1479 N88-18830
Morphological studies of conductive polymers [AD-A188456] 12 p1610 N88-19629
Development of a ground-conductivity map for the area of the Federal Republic of Germany from measured field-strength contours 12 p1615 N88-19656
Characterization of PEOS (Plasma Erosion Opening Switch) plasma parameters and conduction phase properties [AD-A189024] 12 p1624 N88-19714
Changes in blood conductivity during immersion 12 p1663 N88-19969
Fast protonic conducting solid electrolytes [AD-A188524] 12 p1698 N88-20160
Simplified physical approach of the control by eddy current [DE88-701076] 13 p1764 N88-20552
New method of examining micrononhomogeneity of local centers in high-resistivity semiconductor materials under scanning electron microscope 14 p1969 N88-21754
Electrical resistivities of some compound forming liquid metal alloys [PB88-145172] 15 p2037 N88-22137
Research on stable processible conducting polymers for electronic applications [AD-A190246] 15 p2044 N88-22180
Temperature-dependent conductivity of oxygen-depleted YBCO ceramics [AD-A190340] 15 p2044 N88-22182
Analysis of anomalous resistivity during the conduction phase of the plasma erosion opening switch [DE88-006382] 15 p2061 N88-22286
Stratospheric electric field and conductivity measurements over electrified convective clouds in the South American region, revised [INPE-4046-PRE/1012-REV-3] 15 p2095 N88-22483
A study on electric fields and conductivity associated with electrified clouds in the region of South America [INPE-4487-TDL/325] 15 p2096 N88-22486
Physical, chemical and CTD (Conductivity/Temperature/Depth) data from the Marathon 2 expedition [AD-A189930] 15 p2099 N88-22507
Thermal conductivity, electrical conductivity and specific heat of copper-carbon fiber composite [NASA-TT-20172] 16 p2172 N88-22948
Electrical dc conductivity of pitch [AD-A191266] 16 p2182 N88-23008
Electrical anisotropy of layered semiconductor ZrSe2 16 p2257 N88-23488
Some aspects of the unified model of non-ideal high-parameter plasmas: Electron EOS and conduction coefficients 16 p2277 N88-23632
Optimisation of the thermoelectric figure of merit of modified silicon germanium alloys [AD-A191347] 16 p2283 N88-23670
Electrical resistivity as quantum chaos [DE88-007026] 16 p2284 N88-23675
Apparatus for the measurement of resistivity of glasses and ceramics 17 p2431 N88-24460
The precipitation processes of Cu-Zr-Cr alloys [NASA-TT-20168] 18 p2488 N88-24758
On the reversion phenomena of Cu-3 percent Ti alloys [NASA-TT-20170] 18 p2488 N88-24762
Size effects in the electrical resistivity of benzene-derived carbon fibers [AD-A191708] 18 p2491 N88-24777
Raman characterization of AsF5-intercalated vapor grown graphite fibers [AD-A191709] 18 p2491 N88-24778
Electrical conduction in thin film carbons [AD-A191726] 18 p2491 N88-24780
On the abnormal phenomena observed in the electrical resistivity measurement during the decomposition process of saturated Cu-Fe alloys [NASA-TT-20183] 18 p2507 N88-24869
Sulfur-tolerant anode materials [DE88-011034] 18 p2537 N88-25054
Determination of doping profiles in silicon from resistivity measurements via the four-point probe in combination with layer strippings via anodic oxidation 18 p2583 N88-25347
Stress modeling of microdiaphragm pressure sensors 19 p2670 N88-25873
Surface acoustic wave gas sensor based on film conductivity changes 19 p2673 N88-25894
Theory on conductivity measurement technique for Langmuir probes in the stratosphere [INPE-4514-PRE/1268] 19 p2692 N88-25999
Search for new high-temperature superconducting copper oxides [DE88-009922] 19 p2735 N88-26245
Electrical resistivity of carbon-carbon composites [AD-A193006] 20 p2768 N88-26410
Precipitation study by electrical resistivity measurement in Ni-Al alloys [DE88-701877] 20 p2773 N88-26440
Visible tunable source [DE88-006442] 20 p2854 N88-26944
Defect characterization of the redox behavior and stability of conducting oxides [DE88-010799] 20 p2878 N88-27088
On the electrical properties of carbon/carbon composites densified by chemical deposit in vapor phase [SNIAS-881-430-117] 21 p2907 N88-27252
Thermal cycling tests on surface-mount assemblies [DE88-007695] 21 p2939 N88-27453
Conductivity mechanism and operating behavior of electrically conductive adhesives on the example of a power transistor [ETN-88-92355] 21 p2940 N88-27464
Determination of quantum corrections for electrical conductivity mechanism of three dimensional, perturbed copper coatings. Weak localization and electron-electron interaction [ETN-88-92378] 21 p2941 N88-27466
MIZPAC (marginal ice zone Pacific) 84-86 CTD (Conductivity, Temperature, Depth) data report [AD-A192478] 21 p2976 N88-27679
A resistive-film based force transducer for the study of exercise [AD-A192601] 21 p2986 N88-27730
High temperature electric arc furnace [NASA-CASE-MFS-28281-1] 23 p3181 N88-28938
Polymeric electrolytes [AD-A193766] 23 p3198 N88-29031
Soliton and polaron dynamics in conducting polymers [DE88-702539] 23 p3198 N88-29035
The 1983 direct strike lightning data, part 1 [NASA-TM-86426-PT-1] 23 p3237 N88-29259
The 1983 direct strike lightning data, part 2 [NASA-TM-86426-PT-2] 23 p3237 N88-29260
The 1983 direct strike lightning data, part 3 [NASA-TM-86426-PT-3] 23 p3237 N88-29261

Thermostimulated conductivity in amorphous semiconductors with non-exponential density of localized states
[DE88-702737] 23 p3293 N88-29612

Electrical conductivity of GaAs layers implanted on semi-insulator nondoped substrates
[CERT-422000/RF] 23 p3294 N88-29614

Temperature dependence of conductivity and of Hall coefficients for noble metal films
[ETN-88-92981] 23 p3294 N88-29616

ELECTRICITY

NT ALTERNATING CURRENT
NT ATMOSPHERIC ELECTRICITY
NT AURORAL ELECTROJETS
NT EQUATORIAL ELECTROJET
NT GEOELECTRICITY
NT IONOSPHERIC CURRENTS
NT STATIC ELECTRICITY

Use of natural gas diesel engines in mechanical pulp production: A preliminary study
[DE87-753065] 02 p0181 N88-11129

Northern lights: The economic and practical potential of imported power from Canada
[DE88-006026] 15 p2093 N88-22473

A qualitative approach to electricity
[AD-A189854] 15 p2128 N88-22693

Inference and discovery in an exploratory laboratory
[AD-A192231] 20 p2832 N88-26801

Plasma technology: Preliminary studies 2
[DE88-752815] 22 p3154 N88-28763

ELECTRIFICATION

Utilization of LANDSAT-TM imagery in the hydroenergetic inventory of the Paraiba de Sul River Basin 17 p2364 N88-24077

ELECTRO-OPTICAL EFFECT

X-ray diffraction imaging (topography) of electroopticcrystals by synchrotron radiation
[NASA-CR-183266] 24 p3432 N88-30427

ELECTRO-OPTICAL PHOTOGRAPHY

Progress toward a crystal streak camera using tungsten bronze crystals for the electrooptic material
[DE87-013110] 03 p0323 N88-12044

PLZT (Lead-Lathanium-Zirconium-Titanium) electro-optic photographic system
[AD-A193473] 23 p3215 N88-29137

ELECTRO-OPTICAL SWITCHING

U OPTICAL SWITCHING

ELECTRO-OPTICS

Masking effects of fine and coarse grain pictorial noise
[IZF-1985-21] 01 p0076 N88-10485

An optoelectronic alignment telescope for straightness measurements
[ETN-87-90383] 01 p0093 N88-10609

Programmable 10 MHz optical fiducial system for hydrodiagnostic cameras
[DE87-013223] 02 p0175 N88-11091

Consortium for Materials Development in Space Technical section
[NASA-CR-181508] 03 p0296 N88-11859

Highly Non-Linear Optical (NLO) organic crystals and films. Electrooptical organic materials
03 p0297 N88-11866

Limits to the precision of electro-optic and magneto-optic sensors
[PB87-212536] 03 p0323 N88-12040

A high-speed, eight-frame image intensified electro-optic camera with 200-800mm zoom objective capability
[DE88-000229] 03 p0326 N88-12059

Development of optical modulators for measurements of solar magnetic fields
[NASA-TM-100315] 04 p0490 N88-13016

Optoelectronic measurement methods for ballistic experiments
[PB87-110706] 05 p0583 N88-13554

Status, outlook of optical technology in information equipment field 06 p0689 N88-14222

Multilayer holographic functional element in analog-digital converter 07 p0921 N88-15593

Electro-optical studies of semiconductor compounds for electroluminescent and laser devices
[PH-155] 07 p0937 N88-15693

Fiber optics for controls 08 p0956 N88-15798

Gyrotron development at the Instituto de Pesquisas Espaciais
[INPE-4240-PRE/1115] 08 p0990 N88-15992

Management Information and Downloader Interface System (MIDIS)
[AD-A186978] 09 p1261 N88-17557

Optically controlled devices and ultrafast laser sources for signal processing
[AD-A187417] 10 p1338 N88-17995

Multidimensional system analysis of electro-optic sensors with sampled deterministic output
[AD-A187083] 10 p1408 N88-18399

An electro-optic explosive igniter
[DE88-004728] 11 p1466 N88-18738

Automated radar target recognition based on models of neural nets 11 p1476 N88-18804

AFGL (Air Force Geophysics Laboratory) fiscal year 1988 Air Force technical objectives document
[AD-A187701] 11 p1503 N88-18977

Polymeric materials for electro-optic testing
[AD-A188382] 12 p1610 N88-19627

A numerical analysis of the dynamics of PRIZ operation
[AD-A188853] 12 p1678 N88-20035

Nonlinear optical principles and the photorefractive effect applied to optical phase conjugation
[AD-A188856] 12 p1691 N88-20119

Summary and conclusions on electrooptical streak camera project
[DE88-006616] 15 p2069 N88-22334

Collective rotation of molecules driven by the angular momentum of light in a nematic film
[FUB-6-1986] 15 p2131 N88-22714

Gas source MBE (Molecular Beam Epitaxy)
[AD-A189763] 15 p2142 N88-22782

Research on materials and components for opto-electronic signal processing and computing
[AD-A190130] 15 p2143 N88-22788

Applications research studies of microtubules
[AD-A190855] 16 p2182 N88-23005

High-speed electron beam lithography devices discussed 16 p2185 N88-23023

Instrumentation for ultrafast electronics
[AD-A191379] 16 p2193 N88-23080

Fast Algorithm Simulation and Test (FAST) facility
[AD-A191183] 16 p2252 N88-23457

Fiber waveguide sensors for intelligent materials
[NASA-CR-183028] 17 p2343 N88-23968

Topological stereochemistry
[AD-A191867] 18 p2477 N88-24691

Silicon-sapphire waveguides
[AD-A191754] 18 p2504 N88-24854

Investigations in electro-optical multistability for signal processing 18 p2518 N88-24938

Structure and refinement of ordered aromatic heterocyclic polymers by diffraction methods: Application of results to electro-optic phenomena
[AD-A191859] 19 p2619 N88-25537

Organization of a Topical Meeting on Picosecond Electronics and Optoelectronics
[AD-A187136] 19 p2655 N88-25765

A non-contact picosecond prober for integrated circuit testing 19 p2655 N88-25766

Picosecond sampling of integrated circuits
19 p2655 N88-25767

Electro-optic sampling of high-speed, InP-based integrated circuits 19 p2655 N88-25769

Photoconductive generation of sub-picosecond electrical pulses and their measurement applications
19 p2656 N88-25778

Picosecond switching in Josephson tunnel junctions
19 p2657 N88-25780

Fast GaAs photoconductive detectors with high sensitivity integrated in coplanar systems onto GaAs substrates 19 p2658 N88-25790

Picosecond optoelectronic switches using composite electronic materials 19 p2658 N88-25792

A technique for wing suppressed IR sampling
19 p2658 N88-25794

Energy variations in optical pulses from gain-switched AlGaAs diode lasers 19 p2658 N88-25796

Picosecond optical autocorrelation experiments on fast photodetectors 19 p2659 N88-25802

High-speed phenomena in GaAs multiple-quantum-wells 19 p2660 N88-25812

Characteristics and application of wideband guided-wave devices 19 p2660 N88-25817

A new optoelectronic CW microwave source
19 p2660 N88-25818

Optical modulation above 20 GHz using a waveguide electrooptic switch 19 p2660 N88-25819

Picosecond response of an optically controlled millimeter wave phase shifter 19 p2660 N88-25820

Electron device probing in the femtosecond time scale
19 p2660 N88-25821

Picosecond optoelectronic study of a thin film transmission line structure 19 p2661 N88-25823

Integrated optoelectronic circuits utilizing InGaAsP grown by molecular beam epitaxy (erbium doping of MBE GaAs)
[AD-A192269] 20 p2795 N88-26584

The evaluation of a deformable diffraction grating for a stigmatic EUV spectroheliometer
[NASA-CR-183064] 20 p2853 N88-26941

Electro-optical studies of Al(x)Ga(1-x)As/GaAs coupled quantum wells 20 p2862 N88-26999

Novel quantum well optical devices
20 p2868 N88-27028

A concept for an electro-optic explosive device
[DE88-009696] 21 p2923 N88-27349

Picosecond optoelectronic sampling of electrical waveforms produced by an optically excited field effect transistor
[AD-A192384] 21 p2935 N88-27428

Solar cell modeling and simulation
[AD-A193249] 21 p2966 N88-27620

Molecular beam epitaxy of GaP films on Si substrates
[PB88-131974] 21 p3020 N88-27923

Strawman Optical Reception Development Antenna (SORDA) 22 p3065 N88-28187

A high frequency GaAlAs travelling wave electro-optic modulator at 0.82 micrometers
[NASA-TM-100970] 22 p3073 N88-28240

Recent advances in optical spectroscopy using high performance array detectors
[AD-A194219] 22 p3152 N88-28753

MIDIR (Mid-Infrared) laser, phase 1
[AD-A193935] 23 p3220 N88-29166

Photorefractive damage mechanism in electro-optic materials
[AD-A194560] 23 p3282 N88-29543

Quasi-liquid crystalline materials with special electro-optic properties
[AD-A194579] 23 p3282 N88-29544

Center for opto-electronic systems research instrumentation grant
[AD-A193711] 23 p3282 N88-29545

Studies on strained (In,Ga)As/GaAs semiconductors and optical devices 23 p3287 N88-29575

Research on crystal and film ferroelectric materials for optoelectronic applications
[AD-A193512] 23 p3291 N88-29597

Electronic and optical devices and applications
24 p3363 N88-30027

Mode locking of semiconductor laser with external cavity
[AD-A196018] 24 p3378 N88-30117

Report on an overseas visit to USA relating to the thermoelastic measurement of stresses, 16-21 August 1987
[AD-A195313] 24 p3385 N88-30161

A fiber optic beamforming processor for wideband direction finding
[AD-A194862] 24 p3428 N88-30404

Center for opto-electronic systems research
[AD-A195159] 24 p3429 N88-30411

Ultra wideband direction finding using a fiber optic beamforming processor
[AD A194861] 24 p3430 N88-30413

Common modules: A success story
[AD-A195937] 24 p3430 N88-30415

Power MISFETs on OnP
[AD-A195242] 24 p3433 N88-30436

ELECTROACOUSTIC TRANSDUCERS

NT HYDROPHONES
NT MICROPHONES

Noncontact temperature measurements of hot steel bodies using an electromagnetic acoustic transducer (EMAT)
[DE88-000560] 04 p0446 N88-12765

ELECTROCARDIOGRAMS

U ELECTROCARDIOGRAPHY

ELECTROCARDIOGRAPHY

Vital signs rate meter
[AD-A187015] 09 p1198 N88-17183

Results of long-term electrocardiographic monitoring of cosmonauts 10 p1364 N88-18152

ELECTROCATALYSTS

Metal containing polymers as fuel cell catalysts
[AD-A184605] 03 p0347 N88-12194

Internal reforming development for solid oxide fuel cells
[DE87-006518] 04 p0464 N88-12871

Electrochemical hydrogen concentrator for phosphoric acid fuel cells
[AD-A191355] 16 p2229 N88-23317

Compact regenerable sulfur scrubber for phosphoric acid fuel cells
[AD-A191356] 16 p2230 N88-23318

In situ spectroscopic studies of transition metal macrocycles as catalysts for the electrochemical reduction of oxygen
[PB88-203195] 20 p2769 N88-26416

Electrocatalysts for oxygen electrodes
[DE88-008397] 20 p2819 N88-26724

Electrocatalytic reduction of oxygen on modified oxide surfaces
[NASA-TM-101333] 24 p3352 N88-29952

ELECTROCHEMICAL CELLS

NT ALKALINE BATTERIES
NT ELECTRIC BATTERIES
NT FUEL CELLS
NT HYDROGEN OXYGEN FUEL CELLS
NT LEAD ACID BATTERIES

NT LITHIUM SULFUR BATTERIES
NT METAL AIR BATTERIES
NT NICKEL CADMIUM BATTERIES
NT NICKEL HYDROGEN BATTERIES
NT NICKEL IRON BATTERIES
NT NICKEL ZINC BATTERIES
NT PHOSPHORIC ACID FUEL CELLS
NT PRIMARY BATTERIES
NT REDOX CELLS
NT REGENERATIVE FUEL CELLS
NT SODIUM SULFUR BATTERIES
NT STORAGE BATTERIES
NT THERMAL BATTERIES
NT ZINC-BROMIDE BATTERIES
NT ZINC-OXYGEN BATTERIES

Effect of NASA advanced designs on thermal behavior of Ni-H2 cells
[NASA-TM-100197] 01 p0021 N88-10132

New materials for electrochemical cells
[AD-A183659] 01 p0037 N88-10238

Zinc-redox battery A technology update
[DE87-010737] 01 p0040 N88-10256

The 250AH/90A active lithium-thionyl chloride cell for Centaur-G application 02 p0163 N88-11023

ECC (Electrochemical Concentration Cell) ozonesonde observations at South Pole, Antarctica during 1986
[PB87-207502] 02 p0197 N88-11228

Reliability of Li/SO2 cells for long-life applications
[DE88-001360] 04 p0440 N88-12735

Technology Base Research Project for electrochemical energy storage
[DE88-000649] 04 p0464 N88-12868

Re-usable thin-layer spectroelectrochemical cell for non-aqueous solvent systems
[AD-A186951] 09 p1248 N88-17478

Electrochemical hydrogen concentrator for phosphoric acid fuel cells
[AD-A191355] 16 p2229 N88-23317

Thermal and power availability transient responses for the Argonne monolithic solid oxide fuel cell
17 p2419 N88-24384

Optimization of reserve lithium thionyl chloride battery electrochemical design parameters
[DE88-007109] 18 p2506 N88-24868

Photovoltaic cells with n-silicon and conductive polymers
[ETN-88-92133] 20 p2821 N88-26734

Preparation and development of advanced battery catalysts
[AD-A193208] 21 p2937 N88-27441

The overcharge behavior of polymer electrolyte cells
[AD-A193984] 22 p3117 N88-28522

ELECTROCHEMICAL CORROSION

Modelling of crack-tip deformation and transient electrochemical processes in relation to corrosion fatigue of steels cathodically protected in marine environments
[NPL-DMA(A)-145] 01 p0059 N88-10379

Crevice corrosion of stainless steels and related alloys. Part 2: Summary of experimental test data for input to mathematical model
[BR99871-PT-2] 03 p0289 N88-11816

Corrosion behavior of P/M mechanically alloyed IN-9052 1: An electro-chemical investigation
[AD-A184191] 04 p0414 N88-12567

Corrosion behavior of high density tungsten alloys
[AD-A187108] 09 p1143 N88-16852

Corrosion performance of high damping alloys in 3.5 percent sodium chloride environment
[AD-A188048] 11 p1457 N88-18687

Corrosion-wear process under rolling-sliding motion
[AD-A189603] 13 p1778 N88-20635

Corrosion and electrochemical behavior of binary magnesium alloys
[AD-A190624] 15 p2040 N88-22154

Galvanic corrosion initiatives
[AD-A190658] 15 p2040 N88-22155

High temperature oxidation and electrochemical studies related to hot corrosion
[AD-A190699] 15 p2040 N88-22156

Corrosion Research Center, University of Minnesota
[DE88-006681] 15 p2041 N88-22160

Corrosion and corrosion inhibition of metals/alloys in methylphosphonic difluoride 17 p2319 N88-23850

Preventing aircraft corrosion by predictive corrosion modeling 17 p2321 N88-23863

AC impedance analysis of corrosion fatigue in naval aircraft alloys
[AD-A190822] 17 p2322 N88-23865

The influence of cathodic protection on erosion-corrosion of metals and model alloys
[AD-A191613] 18 p2485 N88-24742

Effect of double layer structure on the determination of corrosion rates from polarization measurements
[DE88-010097] 20 p2774 N88-26448

Corrosion of aluminum alloys by IRFNA
[AD-A194319] 22 p3055 N88-28127

Laser and electrochemical studies of metallizations in electronic devices
[AD-A193786] 23 p3208 N88-29090

Multi-metallic galvanic corrosion
[AD-A195995] 24 p3353 N88-29963

ELECTROCHEMICAL OXIDATION

The photophysics and chemistry of PAH (Polycyclic Aromatic Hydrocarbons) compounds
[DE87-014455] 02 p0153 N88-10954

Reduction of CO2 to methanol and methane by photo and dark reactions on semiconductor and metal electrodes
[PB87-226825] 02 p0156 N88-10975

Voltammetric investigation of porous silicon for integrated circuit applications
[DE87-009287] 02 p0166 N88-11042

Submerged arc flux welding with CaF2-CaO-SiO2 fluxes: Possible electrochemical effects on weld metal
[DE88-003107] 08 p0992 N88-16004

Electrosorptive detection based on double-layer capacitance for selective anion monitoring in ion chromatography. Part 1: Mercury electrodes
[AD-A188780] 12 p1606 N88-19603

Characterization of redox states of nickel hydroxide film electrodes by in-situ Raman spectroscopy
[AD-A189288] 13 p1741 N88-20411

High temperature oxidation and electrochemical studies related to hot corrosion
[AD-A190699] 15 p2040 N88-22156

Electrochemical hydrogen concentrator for phosphoric acid fuel cells
[AD-A191355] 16 p2229 N88-23317

AC impedance analysis of corrosion fatigue in naval aircraft alloys
[AD-A190822] 17 p2322 N88-23865

Electrochemistry in near-critical and supercritical fluids. 6: The electrochemistry of ferrocene and phenazine in acetonitrile between 25C and 300C
[AD-A192171] 18 p2482 N88-24723

Studies in support of oxidation-resistant composite materials
[AD-A193320] 21 p2905 N88-27238

ELECTROCHEMISTRY
NT ELECTROLYSIS
NT PHOTOELECTROCHEMISTRY

De-alloying
[DE87-012488] 01 p0022 N88-10139

Evaluation of LiCl-LiBr-KBr electrolyte for Li-alloy/metal disulfide cells
[DE87-011356] 01 p0041 N88-10258

Overcharge protection in Li-alloy/metal disulfide cells
[DE87-011364] 01 p0041 N88-10260

The corrosion of iron rotating hemispheres in 1 M sulfuric acid: An electrochemical impedance study
[DE87-014679] 02 p0148 N88-10925

The 1986 Goddard Space Flight Center Battery Workshop
[NASA-CP-2486] 02 p0163 N88-11021

Computer simulation of thermal modeling of primary lithium cells 02 p0163 N88-11022

Fault tree safety analysis of a large Li/SOCl(sub)2 spacecraft battery 02 p0163 N88-11025

Chemical analysis of charged Li/SO(sub)2 cells
02 p0163 N88-11026

Advances in nickel hydrogen technology at Yardney Battery Division 02 p0164 N88-11029

Photocatalytic electrochemistry at a biological-membrane metal-colloid interface
[DE87-009122] 02 p0166 N88-11041

Stress corrosion cracking of high-strength steels in aqueous environments 03 p0289 N88-11818

Thin films for geothermal sensing
[DE88-000154] 03 p0326 N88-12061

Metal containing polymers as fuel cell catalysts
[AD-A184605] 03 p0347 N88-12194

Metal intercalation characteristics of n-HfS2 photoelectrodes in non-aqueous electrolytes
[AD-A184381] 03 p0383 N88-12407

Advances in inherently conducting polymers
[DE88-000501] 04 p0421 N88-12610

Chemically modified microelectrode arrays. New kinds of electronic devices
[AD-A184389] 04 p0439 N88-12724

The effect of ion implantation on the corrosion behavior of a high-density sintered tungsten alloy
[AD-A185713] 06 p0683 N88-14185

Conductivity studies on hydroxide ion conductors in the Li-Al-O-H system at intermediate temperatures
[AD-A185714] 06 p0697 N88-14279

Phase behavior in the Li-Al-O-H system at intermediate temperatures
[AD-A185732] 06 p0697 N88-14280

Electrochemical characteristics of acid electrolytes for fuel cells
[PB88-104641] 06 p0731 N88-14497

Fundamental studies of surfaces processes and trace analysis using solid electrodes
[AD-A186156] 07 p0828 N88-15024

Surface chemistry of chemically sensitive field effect transistors
[AD-A185917] 07 p0847 N88-15139

The dc conductivity studies of an hydroxide ion conductor at intermediate temperatures
[AD-A186044] 07 p0847 N88-15142

Electrochemical processing of solid waste
[NASA-CR-182413] 08 p0967 N88-15852

Electroformation. Principle electrochemical process of electrodeposition and electroformation of copper
[INPE-4374-NTE/274] 08 p0969 N88-15863

Electrochemical carbon dioxide concentrator subsystem development
[NASA-CR-177411] 08 p1053 N88-16353

Factors governing light driven electron and proton translocation in proteins across membranes
[DE88-002716] 08 p1082 N88-16519

Re-usable thin-layer spectroelectrochemical cell for non-aqueous solvent systems
[AD-A186951] 09 p1248 N88-17478

Electrochemical growth of linear conducting crystals in microgravity 10 p1287 N88-17638

Studies in finite time thermodynamics
[DE88-004531] 10 p1423 N88 18500

Electronic and ionic transport in polymers
[AD-A187253] 11 p1452 N88-18651

Electrochemical and optical investigations on ion-implanted TiO2 samples
[ETN-88-91485] 11 p1455 N88-18670

Voltammetric investigation of porous silicon for integrated circuit applications
[DE88-004024] 11 p1456 N88-18677

Solar-assisted hydrogen generation by photoelectrocatalysis
[PB88-160932] 12 p1605 N88-19597

Some applications of surface Raman and infrared spectroscopies to mechanistic electrochemistry involved adsorbed species
[AD-A188777] 12 p1606 N88-19602

An electrochemical and spectroscopic study of electrode systems
[AD-A189274] 13 p1737 N88-20384

A fundamental understanding of the effect of alloying elements on the corrosion resistance of rapidly solidified Mg alloys
[AD-A189385] 13 p1741 N88-20413

Thermionic Technology Program: A: Insulator test and evaluation
[DE88-004707] 13 p1795 N88-20735

Solid-state electrochemical processes in dye films
[AD-A188756] 13 p1844 N88-21036

Electronic and ionic transport in polymers
[AD-A190434] 15 p2045 N88-22185

Electrochemistry in near-critical and supercritical fluids. 5: The dimerization of quinoline and acridine radical anions and dianions in ammonia from -70 C to 150 C
[AD-A190858] 16 p2175 N88-22967

Water tunnel measurements by an electrochemical method 16 p2203 N88-23146

North Carolina Biomolecular Engineering and Materials Applications Center (NC-BEMAC)
[AD-A190923] 16 p2237 N88-23364

Agenda for advancing electrochemical science and technology 17 p2321 N88-23861

Electrochemistry in liquid crystals
[AD-A191554] 18 p2481 N88-24719

Electrochemistry in near-critical and supercritical fluids. 6: The electrochemistry of ferrocene and phenazine in acetonitrile between 25C and 300C
[AD-A192171] 18 p2482 N88-24723

In situ spectroscopic studies of transition metal macrocycles as catalysts for the electrochemical reduction of oxygen
[PB88-203195] 20 p2769 N88-26416

A simulation analysis of errors in the measurement of standard electrochemical rate constants from phase-selective impedance data
[AD-A192739] 20 p2770 N88-26426

The influence of uncompensated solution resistance on the determination and standard electrochemical rate constants using cyclic voltammetry and some comparisons with AC voltammetry
[AD-A192825] 20 p2770 N88-26427

High power pulse energy system concept
[AD-A192440] 21 p2935 N88-27429

Corrosion fatigue of small cracks: Mechanics and chemistry
[DE88-012121] 21 p2964 N88-27605

Advanced EMU electrochemically regenerable CO2 and moisture absorber module breadboard
[NASA-CR-172054] 21 p2993 N88-27754

A rapid electrochemical technique for determining the current efficiency for cadmium plating
[AD-A193679] 22 p3056 N88-28130
Advanced calcium-thionyl chloride high-power battery
[AD-A194401] 22 p3072 N88-28238
Studies of photochemically and electrochemically driven electron transport in zeolites
[DE88-008644] 22 p3155 N88-28769
Phenomena of the ionic transport in the stress corrosion of metals
[DE88-702502] 23 p3195 N88-29013
Polymeric electrolytes
[AD-A193766] 23 p3198 N88-29031
Electrochemical and optical studies of model photosynthetic systems
[DE88-009291] 23 p3237 N88-29264
Potential induced structural transformations of the Au(100) and Au(111) surfaces
[DE88-005446] 23 p3287 N88-29571
An electrochemical impedance spectroscopy study of reactions at the metal/coating interface
24 p3355 N88-29975
Evaluation of organic coating deterioration and substrate corrosion in seawater using electrochemical impedance measurements 24 p3355 N88-29976
Cytochrome electron transfer and biomolecular electronics
[AD-A195482] 24 p3406 N88-30277

ELECTROCHROMISM
Electrochromic thin films
[DE88-751099] 11 p1559 N88-19334
The structure and properties of RF reactive sputtered IrO2 films 19 p2672 N88-25884

ELECTROCONDUCTIVITY
U ELECTRICAL RESISTIVITY

ELECTRODE MATERIALS
Interfacial effects in thin Li/PEO cells at room temperature
[AD-A186974] 09 p1157 N88-16931
Re-usable thin-layer spectroelectrochemical cell for non-aqueous solvent systems
[AD-A186951] 09 p1248 N88-17478

ELECTRODEPOSITION
NT ELECTROPLATING
Surface coatings and catalyst production by electrodeposition 03 p0297 N88-11863
Mass transport by diffusion 03 p0297 N88-11864
Studies on high-speed electroforming
[DE88-001395] 04 p0429 N88-12656
Effectiveness of electrodeposited coatings in reducing atmospheric corrosion of copper substrates
[DE87-013651] 05 p0566 N88-13448
Electroformation: Principle electrochemical process of electrodeposition and electroformation of copper
[INPE-4374-NTE/274] 08 p0969 N88-15863
Materials processing in space: An introduction to the G-480 payload 10 p1287 N88-17695
Ion chromatography in the manufacture of multilayer circuit boards
[DE88-002428] 10 p1322 N88-17902
Investigation of materials for inert electrodes in aluminum electrodeposition cells
[DE88-003380] 10 p1323 N88-17906
Corrosion resistance of electrodeposited amorphous Ni-Cr-P alloys
[DE88-005116] 11 p1459 N88-18695
Institute for Materials Science and Engineering. Metallurgy: Technical activities 1987
[PB88-157722] 11 p1460 N88-18702
Technology base research on zinc/air battery systems
[DE88-004893] 13 p1763 N88-20546
Electrodeposition of amorphous Ni-Cr-P alloys
[DE88-006868] 19 p2616 N88-25521

ELECTRODES
NT ANODES
NT CATHODES
NT CELL ANODES
NT CELL CATHODES
NT DIFFUSION ELECTRODES
NT HOLLOW CATHODES
NT ION SELECTIVE ELECTRODES
NT PHOTOCATHODES
NT PLASMA ELECTRODES
NT SOLID ELECTRODES
NT THERMIONIC CATHODES
NT TUBE CATHODES
Overcharge protection in Li-alloy/metal disulfide cells
[DE87-011364] 01 p0041 N88-10260
The corrosion of iron rotating hemispheres in 1 M sulfuric acid: An electrochemical impedance study
[DE87-014679] 02 p0148 N88-10925
Reduction of CO2 to methanol and methane by photo and dark reactions on semiconductor and metal electrodes
[PB87-226825] 02 p0156 N88-10975
Surface topography and electrical response of metal-electrolyte interface
[DE87-013553] 02 p0166 N88-11046
Performance of high power S-band klystrons focused with permanent magnet
[DE87-753024] 02 p0167 N88-11053
DSA RuO2/TiO2 electrode modeled by ion implantation: An in situ characterization by photoacoustic and photocurrent spectroscopy
[DE87-009129] 02 p0245 N88-11545
Post-test analyses of aqueous batteries developed for electric propulsion
[DE88-000655] 03 p0311 N88-11965
Effects of pressure fluctuations on nickel electrodes
[AD-A184293] 03 p0311 N88-11967
Metal intercalation characteristics of n-HfS2 photoelectrodes in non-aqueous electrolytes
[AD-A184381] 03 p0383 N88-12407
Chemically modified microelectrode arrays. New kinds of electronic devices
[AD-A184389] 04 p0439 N88-12724
Far-infrared spectra of lithium deposited on a gold electrode: Interpretation using a cluster model
[AD-A184231] 04 p0495 N88-13050
An electric field meter based upon a new principle: A dummy displacement electrode. Application to aerospace vehicles
[SNIAS-872-422-106] 05 p0585 N88-13567
Behavior and structure of metal vapor arc plasma between molten electrodes
[DE88-001854] 06 p0782 N88-14801
Performance of a small, graphite electrode, multistage depressed collector with a 500-W, continuous wave, 4.8- to 9.6-GHz traveling wave tube
[NASA-TP-2788] 07 p0848 N88-15146
Research and development of advanced lead-acid batteries for electric vehicle propulsion
[DE87-014661] 07 p0873 N88-15297
High temperature solar electrothermal processing-3. Zinc from zinc oxide at 1200-1675K using a non-consumable anode
[AD-A186600] 09 p1141 N88-16836
The 5-GHz operation of the ITT and RCA streak tubes with a 7.5-ns time window
[DE88-003342] 09 p1169 N88-17008
Materials development for JPL oxygen plant
[DE88-003067] 10 p1297 N88-17752
Magnetic control of low pressure discharges
[AD-A186794] 10 p1322 N88-17900
Investigation of materials for inert electrodes in aluminum electrodeposition cells
[DE88-003380] 10 p1323 N88-17906
Determination of optimum electrolyte composition for molten carbonate fuel cells literature review
[DE88-001015] 10 p1348 N88-18058
Reactions of some thiol collectors at noble-metal and pyrite electrodes
[PB88-138318] 11 p1455 N88-18674
Photochemical energy storage: Studies of inorganic photoassistance agents
[DE88-002596] 11 p1508 N88-19010
In-situ vibrational spectroscopy of specifically adsorbed azide on silver electrodes
[AD-A188511] 12 p1605 N88-19600
Electrosorptive detection based on double-layer capacitance for selective anion monitoring in ion chromatography. Part 1: Mercury electrodes
[AD-A188780] 12 p1606 N88-19603
An electrochemical and spectroscopic study of electrode systems
[AD-A189274] 13 p1737 N88-20384
Aluminum-air battery development
[DE88-006618] 13 p1762 N88-20543
Electron emission from conductors subjected to intense, short-pulse electric fields
[DE88-005412] 13 p1836 N88-20985
Application of copper-carbon fiber composites to power semiconductor devices
[NASA-TT-20171] 15 p2031 N88-22101
Growth and deformation mechanisms of refractory alloy hybrid materials
[AD-A190492] 15 p2039 N88-22152
Evaporation characteristics of elements during vacuum arc remelting of alloy A-286 15 p2055 N88-22248
Laser induced ignition of propellants
[AD-A191100] 16 p2168 N88-22927
Effects of cadmium electrode properties on nickel-cadmium cell performance
[AD-A191394] 16 p2193 N88-23081
Nickel hydroxide active material densities
[AD-A191411] 16 p2230 N88-23319
AMTEC electrode development
17 p2409 N88-24324
High power density electrodes for AMTEC
17 p2437 N88-24501
Electrochemistry in liquid crystals
[AD-A191554] 18 p2481 N88-24719
Optical investigations of the thermal boundary layer in arc plasmas 18 p2578 N88-25313
Electrode films of porous agarose: The effects of physical structure on electron transport processes
[DE88-007366] 19 p2611 N88-25493
Employment of porous polytetrafluoroethylene Membrane with a hydrophilic and hydrophobic stratal structure for construction of an enzyme electrode
[NASA-TT-20296] 19 p2620 N88-25543
Performance of lightweight nickel electrodes
[NASA-TM-100958] 20 p2771 N88-26430
Nickel hydrogen cell positive-electrode studies: Cobalt segregation in reducing environments
[AD-A193025] 20 p2796 N88-26587
Electrocatalysts for oxygen electrodes
[DE88-008397] 20 p2819 N88-26724
A critical review of IR drops and electrode potentials within pits, crevices and cracks
[AD-A192481] 21 p2935 N88-27431
The kinetics of charge-transfer reactions on passive lithium electrodes
[DE88-009256] 21 p2939 N88-27454
Metal-air battery assessment
[DE88-011361] 21 p2940 N88-27459
Post-test observations on CSPL (Chloride Silent Power Limited) cells
[DE88-011975] 21 p2940 N88-27461
Monolithic fuel cells
[DE88-012004] 21 p2969 N88-27636
Corrosion of aluminium alloys by IRFNA
[AD-A194319] 22 p3055 N88-28127
Liquid metal thermal-electric converter electrode development
[DE88-009252] 23 p3230 N88-29221
An electrochemical impedance spectroscopy study of reactions at the metal/coating interface
24 p3355 N88-29975

ELECTRODYNAMICS
NT ELECTROHYDRODYNAMICS
NT ELECTROMECHANICS
NT QUANTUM ELECTRODYNAMICS
Continuous flow electrophoresis system experiments on shuttle flights STS-6 and STS-7
[NASA-TP-2778] 02 p0156 N88-10978
Electrodynamic tether system study
[NASA-CR-172024] 03 p0275 N88-11737
Hollow cathode plasma coupling study, 1986
[NASA-CR-171985] 03 p0309 N88-11949
Theoretical analysis of the electrical aspects of the basic electro-impulse problem in aircraft de-icing applications
[NASA-CR-180845] 05 p0543 N88-13310
Colloidal stability of oxidized silicon particles in ethanolic and aqueous media
[DE87-014783] 05 p0562 N88-13421
Tethers in space handbook
[NASA-CR-181371] 06 p0673 N88-14123
Performance-limiting factors in MPD thrusters
[AD-A185605] 06 p0674 N88-14128
Power and charge dissipation from an electrodynamic tether 06 p0795 N88-14869
New techniques for rocket and balloon-borne instrumentation for investigations of the structure, dynamics and electrodynamics of the middle atmosphere 08 p1027 N88-16220
Electrodynamics of the high latitude middle atmosphere 08 p1028 N88-16225
Polar cusp electrodynamics 08 p1030 N88-16242
Processes in the quiet and disturbed equatorial-low latitude ionosphere: Sundial campaign, 1984
[INPE-4152-PRE/1057] 08 p1036 N88-16282
Plasma contactors for use with electodynamic tethers for power generation
[NASA-CR-182424] 08 p1087 N88-16547
Comparative evaluation of resistive and inductive techniques for measuring temperature of superconducting transition
[DE88-700603] 10 p1417 N88-18457
Phase transitions in two-dimensional superconducting arrays in a transverse magnetic field
[INPE-4457-RPE/559] 12 p1697 N88-20157
Theoretical investigation of EM wave generation and radiation in the ULF, ELF and VLF bands by the electrodynamic orbiting tether
[NASA-CR-182720] 13 p1760 N88-20529
Chronometrically invariant formulation of electrodynamics equation
[DE88-701030] 13 p1849 N88-21071
Galilei relativity principle in classical electrodynamics
[DE87-703203] 14 p1904 N88-21376
A general 2D electrical model for diagonally connected MHD generators
[DE88-004283] 14 p1984 N88-21835
Dynamics of charged submicron grains in Halley's coma 14 p2001 N88-21931

Space plasma contactor research, 1987
[NASA-CR-182148] 16 p2280 N88-23649
Electrodynamic driver for the space thermoacoustic refrigerator (STAR)
[AD-A192337] 20 p2785 N88-26517
Snapshots of high-latitude electrodynamics using Viking and DMSP/F7 observations
[TRITA-EPP-88-01] 23 p3234 N88-29244
Neutrino electrodynamics and possible effects for solar neutrinos
[DE88-701647] 23 p3308 N88-29705

ELECTRODYNAMOMETERS
U DYNAMOMETERS

ELECTROENCEPHALOGRAM
U ELECTROENCEPHALOGRAPHY

ELECTROENCEPHALOGRAPHY
Change in functional activity of cortical brain structures and their blood supply in alert rabbits in response to rocking 04 p0473 N88-12916
Dimensional analysis of nonlinear oscillations in brain, heart and muscle
[DE87-014749] 06 p0751 N88-14614
Measurement and modification of sensorimotor system function during visual-motor performance
[AD-A186351] 07 p0889 N88-15387
An innovative workstation 08 p1063 N88-16421
Development and experimentation of an [illegible]o/brain/task testbed 09 p12[illegible] N88-17219
The linear dependency structure of covariance nonstationary time series
[AD-A186548] 09 p1232 N88-17383
Realistic conductivity geometry model of the human head for interpretation of neuromagnetic data
[PB88-112230] 10 p1369 N88-18179
Electromagnetic metrics of mental workload
[AD-A188205] 11 p1523 N88-19093
Brain activity during tactical decision-making. Part 2: Probe-evoked potentials and workload
[AD-A188686] 12 p1667 N88-19994
Neurocognitive predictions of performance
[AD-A188323] 12 p1669 N88-19998
Retinotopic mapping of the human visual system with magnetoencephalography
[AD-A189557] 13 p1810 N88-20811
Identification of visual evoked response parameters sensitive to pilot mental state
[NASA-CR-4140] 13 p1811 N88-20822
Steady-state evoked potentials possibilities for mental-state estimation 16 p2240 N88-23380
Electroencephalographic changes during equilibrium test in the presence of rhythmic photic interference
19 p2703 N88-26075
Effect of different modes of voluntary control of breathing on human electroencephalogram with exposure to acute hypoxic hypoxia 19 p2707 N88-26093
Physiological monitoring methodology in the USAFSAM centrifuge 21 p2924 N88-27356
Normative developmental equations for the EEG and their sensitivity to neurological and psychiatric disorders
21 p2977 N88-27687
The application of non-stationary data analysis techniques in the identification of changes in the electroencephalogram associated with the onset of drowsiness 21 p2978 N88-27688
A statistical procedure for the evaluation of presence/non-presence of stimulus-related EEG activity
21 p2978 N88-27689
The effect of endogenous alpha on hemispheric asymmetries and the relationship of frontal theta to sustained attention 21 p2980 N88-27701
Evoked potential analysis of impact acceleration experiments 21 p2981 N88-27708
EEG indices of G-induced Loss Of Consciousness (G-LOC) 21 p2982 N88-27709
Electroencephalographic correlates of pilot performance: Simulation and in-flight studies
21 p2982 N88-27711
Measurement of electrical activity in the CNS with cortical evoked potentials and EEG: Efficacy profiles of drugs using factor analysis 21 p2983 N88-27715
An approach to studying the effects of psychostimulants on cerebral electrical activity in the non-human primate
21 p2983 N88-27716
Correlation between EEG abnormal activity and aircraft accidents: A long term observation
21 p2984 N88-27719
Detection of latent epilepsy in aircrew candidates
21 p2984 N88-27720
New method for the study of spontaneous brain activity
[AD-A193813] 22 p3132 N88-28624
Methods and instrumentation for biomagnetism
[AD-A193811] 23 p3239 N88-29278

ELECTROEROSION
U SPARK MACHINING

ELECTROEXPLOSIVE DEVICES
U INITIATORS (EXPLOSIVES)

ELECTROFORMING
Studies on high-speed electroforming
[DE88-001395] 04 p0429 N88-12656
Electroformation: Principle electrochemical process of electrodeposition and electroformation of copper
[INPE-4374-NTE/274] 08 p0969 N88-15863
Copper electroforming from acid sulfate baths: Preliminary studies
[INPE-4375-RPE/554] 08 p0969 N88-15864

ELECTROGENERATORS
U ELECTRIC GENERATORS

ELECTROHYDRAULIC CONTROL
U ELECTRIC CONTROL
U HYDRAULIC CONTROL

ELECTROHYDRODYNAMICS
Preparative electrophoresis for space
[NASA-TP-2777] 02 p0156 N88-10977
Instantaneous pictures of the high-latitude electrodynamics using Viking and DMSP/F7 observations --- Swedish satellite
08 p1025 N88-16209
Electrohydrodynamic migration of charged droplets in an insulating fluid
[NASA-TM-100849] 14 p1912 N88-21424

ELECTROJETS
NT AURORAL ELECTROJETS
NT EQUATORIAL ELECTROJET

ELECTROKINETICS
Preparative electrophoresis for space
[NASA-TP-2777] 02 p0156 N88-10977
Mathematical models of continuous flow electrophoresis: Electrophoresis technology
[NASA-CR-179241] 07 p0828 N88-15021
The electrokinetic behavior of calcium oxalate monohydrate in macromolecular solutions
[NASA-TM-101144] 18 p2493 N88-24791

ELECTROLESS DEPOSITION
Acoustic wave electroless deposition monitor
[DE88-004023] 11 p1489 N88-18887
Corrosion of electroless nickel-coated steel
[AD-A191045] 16 p2179 N88-22985

ELECTROLUMINESCENCE
Electro-optical studies of semiconductor compounds for electroluminescent and laser devices
[PH-155] 07 p0937 N88-15693
Study for the determination of general and specific properties of wide energy-band gap HgCdTe in the 1 to 2 micrometer wavelength range
[AD-A191091] 17 p2334 N88-23934

ELECTROLUMINESCENT LAMPS
U ELECTROLUMINESCENCE
U LUMINAIRES

ELECTROLYSIS
Phase purity of NiCo2O4, a catalyst candidate for electrolysis of water
[NASA-TM-100239] 05 p0556 N88-13385
DC conductivity studies in Li5AlO4 at intermediate temperatures and its possible application for the electrolysis of water
[AD-A185489] 06 p0697 N88-14276
Electrochemical processing of solid waste
[NASA-CR-182413] 08 p0967 N88-15852
Cavitation inception
[AD-A189220] 13 p1765 N88-20557

ELECTROLYTE METABOLISM
Biorhythmic aspects of intercontinental Antarctic adaptation 08 p1046 N88-16321
Fluid volume changes in astronauts: How they fit our understanding of physiology 12 p1655 N88-19919
The influence of space flight on water-salt homeostasis in man and animals 12 p1659 N88-19943
Physiology of prolonged bed rest
[NASA-TM-101010] 22 p3130 N88-28607

ELECTROLYTES
NT ION EXCHANGE MEMBRANE ELECTROLYTES
NT MOLTEN SALT ELECTROLYTES
NT NONAQUEOUS ELECTROLYTES
NT SOLID ELECTROLYTES
Adhesion properties of polyelectrolyte-chemisorbed zinc phosphate conversion coatings
[DE87-012489] 01 p0029 N88-10186
Evaluation of LiCl-LiBr-KBr electrolyte for Li-alloy/metal disulfide cells
[DE87-011356] 01 p0041 N88-10258
Overcharge protection in Li-alloy/metal disulfide cells
[DE87-011364] 01 p0041 N88-10260
Synthesis of novel acid electrolytes for phosphoric acid fuel cells
[PB87-221305] 01 p0066 N88-10426
Surface topography and electrical response of metal-electrolyte interface
[DE87-013553] 02 p0166 N88-11046
Ion-matrix coupling in polymer electrolytes from relaxation time studies
[AD-A184632] 03 p0293 N88-11841
Metal intercalation characteristics of n-HfS2 photoelectrodes in non-aqueous electrolytes
[AD-A184381] 03 p0383 N88-12407
Applications of multivalent ionic conductors to polymeric electrolyte batteries
[AD-A184252] 04 p0439 N88-12722
Colloidal stability of oxidized silicon particles in ethanolic and aqueous media
[DE87-014783] 05 p0562 N88-13421
Analysis of nickel sulphamate bath using charging current compensated D.C. polarography
[NAL-TM-MT-8705] 05 p0564 N88-13433
Ionic transport and electrical relaxation in glass
[DE88-000887] 05 p0657 N88-14028
Geochemistry of freezing brines, low-temperature properties of sodium chloride
[AD-A185751] 06 p0680 N88-14168
Conductivity studies on hydroxide ion conductors in the Li-Al-O-H system at intermediate temperatures
[AD-A185714] 06 p0697 N88-14279
Hydroxide ion conductors as possible electrolytes in intermediate temperature fuel cells
[AD-A185508] 06 p0731 N88-14495
Electrochemical characteristics of acid electrolytes for fuel cells
[PB88-104641] 06 p0731 N88-14497
The dc conductivity studies of an hydroxide ion conductor at intermediate temperatures
[AD-A186044] 07 p0847 N88-15142
Excess thermodynamic properties of aqueous electrolytes to high temperatures and pressures
[DE88-001768] 07 p0940 N88-15712
High temperature solar electrothermal processing-3. Zinc from zinc oxide at 1200-1675K using a non-consumable anode
[AD-A186600] 09 p1141 N88-16836
Some investigations of electrical discharges at the surfaces of solid cathodes immersed in aqueous electrolyte solutions
[PB87-168209] 09 p1159 N88-16946
Materials development for JPL oxygen plant
[DE88-003067] 10 p1297 N88-17752
Models for ionic transport in glass
[DE88-002860] 10 p1304 N88-17799
Electrochromic cells with lutetium diphthalocyanine and semisolid polymer electrolytes
[AD-A188031] 10 p1352 N88-18078
In-situ vibrational spectroscopy of specifically adsorbed azide on silver electrodes
[AD-A188511] 12 p1605 N88-19600
Human adaptation to various hypercapnic conditions in relation to salivary electrolyte dynamics and renal function 12 p1664 N88-19977
Contrasting conductance/viscosity relations in liquid states of vitreous and polymer solid electrolytes
[AD-A189378] 13 p1748 N88-20452
Polymeric electrolytes for ambient temperature lithium batteries
[DE88-004896] 13 p1763 N88-20547
Double layer polarization of nonconducting spheroidal particles and its application to Kerr effect
[ISSN-0208-5658] 13 p1832 N88-20960
Prediction of high-temperature thermodynamic properties of mixed electrolyte solutions including solubility equilibria, vapor pressure depression and boiling point elevation
[DE88-006344] 13 p1849 N88-21069
Prediction of thermodynamic properties, including solubility equilibria and vapor pressures, for mixed aqueous electrolytes to high temperatures
[DE88-006317] 14 p1990 N88-21863
Fast ion conducting glasses
[AD-A191412] 16 p2183 N88-23010
Characterization of crystalline silicon by electrochemical and Raman spectroscopy at the frontier semiconductor/electrolyte
[ETN-88-92354] 21 p3025 N88-27956
Advanced calcium-thionyl chloride high-power battery
[AD-A194401] 22 p3072 N88-28238
Optimization and scale-up performance of polymer electrolyte batteries
[AD-A193987] 22 p3073 N88-28243
Performance of polymer electrolyte cells at +25 to +100 C
[AD-A193988] 22 p3073 N88-28244
Hormonal regulation of fluid and electrolytes: Effects of heat exposure and exercise in the heat
[AD-A192655] 22 p3131 N88-28614
Potential induced structural transformations of the Au(100) and Au(111) surfaces
[DE88-005446] 23 p3287 N88-29571

High power storage system based on thin film solid ionics
[AD-A193623] 23 p3291 N88-29596
Multi-metallic galvanic corrosion
[AD-A195995] 24 p3353 N88-29963
Structure and dynamics of solutions of lithium salts relevant to battery construction
[AD-A195399] 24 p3366 N88-30044

ELECTROLYTIC CELLS
New materials for electrochemical cells
[AD-A183659] 01 p0037 N88-10238
Ionically conductive polymers: Application to solid state batteries
[AD-A183733] 01 p0037 N88-10239
Evaluation of LiCl- LiBr- KBr electrolyte for Li- alloy/metal disulfide cells
[DE87-011356] 01 p0041 N88-10258
The corrosion of iron rotating hemispheres in 1 M sulfuric acid: An electrochemical impedance study
[DE87-014679] 02 p0148 N88-10925
Effects of pressure fluctuations on nickel electrodes
[AD-A184293] 03 p0311 N88-11967
Survey state of the art: Electrical load management techniques and equipment
[AD-A184083] 05 p0577 N88-13517
An investigation of the rechargability of certain modified forms of MnO2
[AD-A185919] 07 p0847 N88-15140
Investigation of self-discharge characteristics of spacecraft nickel-cadmium cells at elevated temperatures
[AD-A186497] 08 p0979 N88-15919
Investigation of materials for inert electrodes in aluminum electrodeposition cells
[DE88-003380] 10 p1323 N88-17906
Determination of optimum electrolyte composition for molten carbonate fuel cells literature review
[DE88-001015] 10 p1348 N88-18058
Recent advances in solid polymer electrolyte fuel cell technology
[DE88-005380] 15 p2092 N88-22464
Oxygen reduction in fuel cell electrolytes
[DE88-008240] 20 p2819 N88-26723
Preparation and development of advanced battery catalysts
[AD-A193208] 21 p2937 N88-27441
Estimation of power-energy plots for secondary batteries
[DE88-011922] 21 p2940 N88-27460
Optimization and scale-up performance of polymer electrolyte batteries
[AD-A193987] 22 p3073 N88-28243
Performance of polymer electrolyte cells at +25 to +100 C
[AD-A193988] 22 p3073 N88-28244
The overcharge behavior of polymer electrolyte cells
[AD-A193984] 22 p3117 N88-28522
Morphological changes in polymer electrolyte cells
[AD-A195821] 24 p3368 N88-30054

ELECTROMAGNETIC ABSORPTION
NT GAMMA RAY ABSORPTION
NT INFRARED ABSORPTION
NT MULTIPHOTON ABSORPTION
NT PHOTOABSORPTION
NT ULTRAVIOLET ABSORPTION
NT X RAY ABSORPTION
Pure dephasing of a vibrational adbond
[AD-A185222] 05 p0609 N88-13740
Anomalies in electromagnetic absorption of circularly polarized ultrasonic waves by tungsten within Doppler shifted cyclotron resonance range
06 p0775 N88-14756
Characteristics of thermooptical sound excitation in metals 08 p1076 N88-16486
Absorption of electron cyclotron radiation in tokamak plasmas with a superthermal tail in the electron velocity distribution
[INPE-4391-PRE/1211] 08 p1086 N88-16541
Linear theory of generation of longitudinal sound waves in semiconductors upon interband absorption of optical radiation 09 p1234 N88-17397
Numerical simulation of the propagation and absorption due to air breakdown of long microwave pulses
[DE88-005227] 11 p1475 N88-18798
Photochemistry at structured surfaces: A classical electromagnetic approach
[AD-A189519] 13 p1737 N88-20387
Anisotropy of light absorption by color centers in waveguides produced on photochromic glasses by diffusion 14 p1896 N88-21320
Microwave dispersion and absorption in tissues. Molecular mechanisms
[AD-A190118] 15 p2100 N88-22512
Research on materials and components for opto-electronic signal processing and computing
[AD-A190130] 15 p2143 N88-22788
Light scattering of intracellular gas vacuoles: Anomalous behavior of forward and perpendicular light scattering of a cyanobacterium due to intracellular gas vacuoles
[BCRS-87-08] 16 p2228 N88-23308
Research investigation directed toward extending the useful range of the electromagnetic spectrum, appendix
[AD-A190199] 17 p2332 N88-23921
Influence of refractive index and solar concentration on optical power absorption in slabs
[NASA-TM-4056] 19 p2726 N88-26190
Diode laser ignition of high explosives and pyrotechnics
[DE88-008771] 21 p2923 N88-27352
Bioeffects of electromagnetic waves
24 p3364 N88-30032

ELECTROMAGNETIC ACCELERATION
Multi-stage plasma thruster
[AD-A183635] 01 p0017 N88-10105

ELECTROMAGNETIC COMPATIBILITY
Electromagnetic compatibility (EMC) phenomena and prevention of the effects --- spacecraft
03 p0274 N88-11731
A design-philosophy for grounding and inter-unit wiring
[EMCR-20/85] 03 p0310 N88-11954
Discussions in support of the design-philosophy for grounding and inter-unit wiring
[EMCR-21/85] 03 p0310 N88-11955
Measurements in an electromagnetic test laboratory
[SNIAS-872-430-102] 05 p0575 N88-13507
Model of space platform electromagnetic (EMC) configuration
[ESA-CR(P)-2500] 09 p1135 N88-16809
Recommended test specification for the electromagnetic compatibility of aircraft equipment
[RAE-TM-FS(F)-510] 14 p1867 N88-21155
Radio frequency compatibility between IRS and SPOT 3: Preliminary study
[CNES-86/CT/DRT/TIT/TR/011]
14 p1905 N88-21383
Strategies in the topological approach to electromagnetic interference control
[AD-A189874] 15 p2056 N88-22255
Electromagnetic compatability: An introduction to the theory of interference and shielding, 3rd revised edition
[PB88-165410] 15 p2057 N88-22264
The electromagnetic threat to future avionic systems
17 p2305 N88-23790
Aircraft field degradation and electromagnetic compatibility
[PB88-183975] 19 p2602 N88-25456
Study and temporal simulation of the electromagnetic susceptibility of interconnected systems
[ECL-87-19] 22 p3071 N88-28228
Electromagnetic compatibility. View of the near future
[SNIAS-881-422-104] 22 p3071 N88-28229

ELECTROMAGNETIC CONTROL
U ELECTROMAGNETS
U REMOTE CONTROL

ELECTROMAGNETIC COUPLING
NT MICROWAVE COUPLING
NT OPTICAL COUPLING
An excitation-term modification for a certain class of electromagnetic aperture-coupling problems
[DE88-000260] 04 p0437 N88-12713
Advanced numerical modeling of microwave penetration and coupling for complex structures
[DE88-001873] 06 p0690 N88-14231

ELECTROMAGNETIC DEDUCTION
U MAGNETIC INDUCTION

ELECTROMAGNETIC FIELDS
NT FAR FIELDS
NT NEAR FIELDS
Numerical predictions of EML system performance
[DE87-011727] 01 p0011 N88-10061
Theory of atoms in strong, pulsed electromagnetic fields. 2: A free electron and a harmonically bound electron
[DE87-012571] 01 p0035 N88-10225
Anechoic Chamber test of the Electromagnetic Measurement System ground test unit
[DE87-012998] 01 p0035 N88-10226
Simulations using the pseudo-current algorithm
[DE87-012403] 01 p0040 N88-10255
Different ways of looking at the electromagnetic vacuum
[DE87-013150] 01 p0089 N88-10584
Research in particles and fields
[NASA-CR-180412] 01 p0119 N88-10763
Quantum-mechanical aspects of classically chaotic driven systems
[DE87-013152] 02 p0178 N88-11106
Electromagnetic effects of a discharge on circuitry --- spacecraft 03 p0274 N88-11726
Numerical modeling: Integral equation method
03 p0304 N88-11919
A microwave FEL (Free Electron Laser) code using waveguide modes
[DE88-000225] 03 p0330 N88-12084
A new approach to modeling and interpreting electromagnetic sounding data
[DE88-000460] 04 p0438 N88-12715
Proceedings of the 2nd Regional Electromagnetic Workshop at Argonne National Laboratory
[DE87-004633] 06 p0690 N88-14230
Advanced numerical modeling of microwave penetration and coupling for complex structures
[DE88-001873] 06 p0690 N88-14231
Spectral- and spatial-domain filtering and sampling approach to the numerical solution of electromagnetic scattering problems
[PB88-106711] 06 p0694 N88-14261
Finite-element method for three-dimensional electric and electromagnetic field problems
[PB87-138731] 06 p0696 N88-14274
Human physical fields *06 p0750 N88-14608
Eigenvalues and eigenvectors of field tensors and associated energy tensors
[DE88-001951] 06 p0763 N88-14682
Nonuniformity of electromagnetic field at Lambda = 10.6 micron wavelength inside atmospheric aerosol particles
06 p0772 N88-14743
Electromagnetic fields backscattered from an s-shaped inlet cavity with an absorber coating on its inner walls
[NASA-CR-182401] 07 p0845 N88-15130
Interaction of intense electromagnetic fields with SF/sub 6/ molecules and clusters in supersonic expansion
[DE88-700310] 07 p0846 N88-15132
Treatment of small wire loops in the method of moments code NEC (Numerical Electromagnetics Code)
[DE88-002995] 07 p0846 N88-15136
Experimental investigation of a three-stage railgun incorporating puff-switching
[MRL-R-1056] 09 p1130 N88-16785
Exact image principle in electromagnetic field computation
[EL-57] 09 p1153 N88-16907
Evaluation of CWMS (Continuous-Wave Measurement System) single-wire dipole antenna
[DE88-003979] 09 p1155 N88-16920
A qualitative study of wake fields for very short bunches
[DE88-002565] 09 p1164 N88-16980
Space-time processing of field produced by moving source 09 p1234 N88-17389
Properties of superconducting tunnel structures in microwave radiation field 09 p1239 N88-17424
Time-domain reciprocity theorems for electromagnetic fields in dispersive media
[PB88-126925] 10 p1319 N88-17886
Forces on neutral atoms due to electromagnetic fields
[AD-A187461] 10 p1408 N88-18396
The stability of free-electron lasers against filamentation
[DE88-004712] 10 p1414 N88-18435
A dynamic analysis of the parallel-plate EMP (electromagnetic pulse) simulator using a wire mesh approximation and the numerical electromagnetics code
[AD-A187535] 11 p1470 N88-18767
GERA computer code for calculation of two-dimensional electromagnetic fields in resonators and electron-optical systems by the finite element method
[DE88-700678] 11 p1480 N88-18831
ELF (Extremely Low Frequency) communications system ecological monitoring program: Electromagnetic field measurements and engineering support, 1986
[AD-A188057] 11 p1509 N88-19017
Critical phenomena and electromagnetic effects in biological membranes
[AD-A188156] 11 p1518 N88-19064
Validation of GEMACS (General Electromagnetic Model for the Analysis of Complex Systems) for modeling lightning-induced electromagnetic fields
[AD-A188822] 12 p1620 N88-19667
Observation of a hydromagnetic wave in the earth's magnetosphere
[AD-A188942] 12 p1644 N88-19841
Negative-energy quanta
[DE88-700904] 12 p1689 N88-20101
Structural integrity of metallic armature rail guns
[AD-A188735] 13 p1728 N88-20333
Photochemistry at structured surfaces: A classical electromagnetic approach
[AD-A189519] 13 p1737 N88-20387
Transformation coefficient in wave-field acceleration scheme
[DE88-700158] 13 p1757 N88-20507
Optimum transformer design for a pulsed power system
[DE88-006054] 13 p1760 N88-20525

Resolution of the magnetotelluric method for determining local inhomogeneities in the sedimentary cover 13 p1789 N88-20701
Reduced tolerance imaging 2, volume 2 [AD-A189604] 13 p1829 N88-20939
Numerical simulations of multiphoton processes in many electron atoms [DE88-003293] 13 p1837 N88-20990
Topics in curved and flat space electromagnetism 13 p1854 N88-21100
Exact image method for Gaussian beam problems involving a planar interface [NASA-CR-182702] 14 p1905 N88-21380
A qualitative approach to electricity [AD-A189854] 15 p2128 N88-22693
Coordinate-momentum probability operator for point particles in a stationary electromagnetic field [DE88-701165] 16 p2188 N88-23044
Exact image theory for the problem of dielectric/magnetic slab [NASA-CR-182865] 16 p2189 N88-23055
Finite elements for the computation of three-dimensional electromagnetic fields in inhomogeneous media (revised) [PB88-173471] 16 p2190 N88-23057
A computer model investigation of a half square log-periodic array [AD-A190955] 16 p2190 N88-23062
Pulsed power simulation problems in magic [AD-A191110] 16 p2191 N88-23065
KOMPOT Program complex for the calculation of spatial magnetostatic fields of electromagnetic systems [DE88-701691] 16 p2192 N88-23072
Development of Electromagnetic PIC code for LIB diode 16 p2276 N88-23622
Finite element simulation of the atmosphere's electromagnetic response to charge perturbations associated with lightning 17 p2375 N88-24124
Electromagnetic penetration into a conducting circular cylinder through a narrow slot, TE case [AD-A191602] 18 p2500 N88-24828
Electromagnetic field penetration into structures [AD-A192127] 18 p2501 N88-24836
Space station induced electromagnetic effects 18 p2591 N88-25394
Gravitation and polarization properties of electromagnetic field [DE88-702166] 19 p2654 N88-25761
Application of Moment Iteration Method (MIM) to electromagnetic field computation [PB88-194139] 20 p2789 N88-26546
A maximum entropy solution for the underdetermined electromagnetic field within a volume [DE88-007020] 20 p2790 N88-26550
MAXWELL3: A 3D finite element electromagnetic modeling code [DE88-010602] 20 p2790 N88-26551
Research in electromagnetic shielding theory. Part1. Shielding by rectangular enclosures [AD-A192881] 20 p2791 N88-26557
Computer programs for high-current beam transport in accelerators [AD-A192356] 20 p2838 N88-26835
Research in particle and gamma-ray astrophysics [NASA-CR-183111] 20 p2887 N88-27146
SSVCO feed characteristics [DE88-011322] 22 p3068 N88-28208
Activities report of the Electromagnetic Environment Division [FOA-C-30484-3.2/3.3/4.1/4.2] 22 p3071 N88-28233
Open bosonic string in background electromagnetic field [DE88-702140] 23 p3201 N88-29053
Development of a multiport-hybrid-mode exciter for use in antennas for polarimetric field measurements [REPT-12-87] 23 p3205 N88-29075
The 1983 direct strike lightning data, part 1 [NASA-TM-86426-PT-1] 23 p3237 N88-29259
The 1983 direct strike lightning data, part 2 [NASA-TM-86426-PT-2] 23 p3237 N88-29260
The 1983 direct strike lightning data, part 3 [NASA-TM-86426-PT-3] 23 p3237 N88-29261
Currents induced in a human being for electromagnetic fields to 10 kHz-50 MHz [AD-A191977] 23 p3238 N88-29268
Passage of relativistic magnetic dipole moments through magnetic fields [DE88-702640] 23 p3295 N88-29624
Neutrino electrodynamics and possible effects for solar neutrinos [DE88-701647] 23 p3308 N88-29705
Electromagnetic metrology 24 p3363 N88-30024
Bioeffects of electromagnetic waves 24 p3364 N88-30032
Research in particle and gamma-ray astrophysics [NASA-CR-183126] 24 p3455 N88-30566

ELECTROMAGNETIC INTERACTIONS
NT LASER PLASMA INTERACTIONS
NT PLASMA-ELECTROMAGNETIC INTERACTION
Electromagnetic interaction between an electric discharge and cabling inside a satellite 03 p0274 N88-11725
Numerical modeling: Finite methods 03 p0304 N88-11918
Rotation of magnetized particle in electrically conducting viscous medium 06 p0770 N88-14733
Parametric and resonance interaction of ultrashort light pulses in nonlinear multilevel medium 06 p0773 N88-14746
Statistical model of interaction of electromagnetic waves with natural objects being sensed 08 p1008 N88-16112
Particle acceleration to high energies and amplification of coherent radiation by electromagnetic interactions in plasmas [DE88-701020] 15 p2135 N88-22737
Space-charge-wave solid state microwave amplifier [AD-A193792] 23 p3208 N88-29091

ELECTROMAGNETIC INTERFERENCE
NT CHIRP
NT CROSSTALK
NT ELECTROMAGNETIC NOISE
NT IONOSPHERIC NOISE
NT JAMMING
NT RADIO FREQUENCY INTERFERENCE
NT SHOT NOISE
NT THERMAL NOISE
NT WHISTLERS
NT WHITE NOISE
Crosstalk in braided shield coaxial cables 01 p0035 N88-10224
Ionospheric total electron content estimation for single-frequency global positioning system receivers 02 p0161 N88-11005
Electromagnetic effects of a discharge on circuitry --- spacecraft 03 p0274 N88-11726
Irradiation testing 03 p0274 N88-11727
MARECS-A case 03 p0274 N88-11729
Experimental and analytic studies of the triggered lightning environment of the F106B [NASA-CR-4104] 04 p0469 N88-12897
Two-signal cross modulation effects, half-IF effects and interference criteria in land mobile sharing with UHF (Ultra High Frequency) television [PB87-228037] 05 p0576 N88-13514
Receiver susceptibility measurements relating to interference between UHF (Ultra High Frequency) television and land mobile radio services [PB87-228029] 06 p0690 N88-14228
Radio frequency electromagnetic interference fields. A study in Swedish industry [FOA-E-30007-3.3] 06 p0692 N88-14247
New description of Lau effect based on theory of raster image forming process 06 p0772 N88-14744
Shielding effectiveness against electromagnetic interference [DE88-003664] 07 p0846 N88-15131
Space-time processing of field produced by moving source 09 p1234 N88-17399
Measurement of shielding effectiveness of different cable and shielding configurations by mode-stirred techniques [PB88-155791] 10 p1319 N88-17885
Satellite interference analysis and simulation using personal computers [NASA-CR-182522] 10 p1319 N88-17890
A dynamic analysis of the parallel-plate EMP (electromagnetic pulse) simulator using a wire mesh approximation and the numerical electromagnetics code [AD-A187535] 11 p1470 N88-18767
Envelope and phase statistics for non-Gaussian noise and resulting error probabilities for digital communications systems 12 p1617 N88-19672
Influence of hydrometeorological factors on visibility of objects detected by radar 13 p1790 N88-20707
Strategies in the topological approach to electromagnetic interference control [AD-A189874] 15 p2056 N88-22255
Electromagnetic compatability: An introduction to the theory of interference and shielding, 3rd revised edition [PB88-165410] 15 p2057 N88-22264
The electromagnetic threat to future avionic systems 17 p2305 N88-23790
Inadequacies of EMI-seal material: A corrosion study 17 p2319 N88-23852
Adaptive interference techniques for mobile antennas 19 p2647 N88-25714
Modulation and coding for fast fading mobile satellite communication channels 19 p2648 N88-25722
Random quantum interference in microdevices 20 p2866 N88-27021
Quantum interference and transport in microstructures 20 p2866 N88-27022
Study and temporal simulation of the electromagnetic susceptibility of interconnected systems [ECL-87-19] 22 p3071 N88-28228
Electromagnetic compatibility. View of the near future [SNIAS-881-422-104] 22 p3071 N88-28229
Electromagnetic interference to radar and radio link systems caused by large scale wind turbines [FOA-C-30486-3.2] 22 p3071 N88-28234
Ion gun generated electromagnetic interference on the SCATHA satellite [AD-A195179] 24 p3335 N88-29853

ELECTROMAGNETIC MEASUREMENT
Anechoic Chamber test of the Electromagnetic Measurement System ground test unit [DE87-012998] 01 p0035 N88-10226
Measurements in an electromagnetic test laboratory [SNIAS-872-430-102] 05 p0575 N88-13507
Electromagnetic tests [SNIAS-872-430-103] 05 p0575 N88-13508
Numerical and analytical study of the equivalent permittivity or permeability of nonhomogeneous materials. Application to the experimental electromagnetic characterization of composites [SNIAS-872-430-104] 05 p0575 N88-13509
Microwave and structural properties of saline ice [AD-A189307] 13 p1803 N88-20779
Wind measurements by electromagnetic probes [NASA-TM-4066] 23 p3236 N88-29256
The 1983 direct strike lightning data, part 1 [NASA-TM-86426-PT-1] 23 p3237 N88-29259
The 1983 direct strike lightning data, part 2 [NASA-TM-86426-PT-2] 23 p3237 N88-29260
The 1983 direct strike lightning data, part 3 [NASA-TM-86426-PT-3] 23 p3237 N88-29261

ELECTROMAGNETIC NOISE
NT IONOSPHERIC NOISE
NT SHOT NOISE
NT THERMAL NOISE
NT WHISTLERS
NT WHITE NOISE
Surface effects and low frequency noises in GaAs field effect transistors [LAAS-87-179] 02 p0168 N88-11055
Signal to noise ratios --- SPOT images 03 p0341 N88-12150
On a circular correlation technique for filtering randomly noisy data [AD-A184317] 04 p0431 N88-12669
Area of reduced electron concentration in terrestrial plasmasphere 08 p1003 N88-16078
Calculation of noise in spatial speckle-field holograms under conditions of saturated photoresponse 09 p1235 N88-17403
Studies of nonlinear and chaotic phenomena in solid state systems [DE88-002330] 09 p1254 N88-17515
Contact and current noise in beta alumina and Nasicon ceramics [AD-A189168] 12 p1611 N88-19635
Envelope and phase statistics for non-Gaussian noise and resulting error probabilities for digital communications systems 12 p1617 N88-19672
Evaluation of chemical and atmospheric sciences research [AD-A188468] 12 p1687 N88-20091
Fluxons and order in long Josephson junctions [AD-A190879] 16 p2282 N88-23665
Research investigation directed toward extending the useful range of the electromagnetic spectrum [AD-A190198] 17 p2332 N88-23920
Research investigation directed toward extending the useful range of the electromagnetic spectrum, appendix [AD-A190199] 17 p2332 N88-23921
A Differential Phase Shift Keying (DFSK) modulator for a frequency hopping short wave system [FOA-C-30460-3.3] 18 p2501 N88-24840
Extending the impulse response in order to reduce errors due to impulse noise and signal fading 19 p2649 N88-25730
Noise in piezoresistive and capacitive sensors 19 p2670 N88-25874
Analytical description of noise in phase-conjugate resonators [PB88-171947] 19 p2726 N88-26188
Study and temporal simulation of the electromagnetic susceptibility of interconnected systems [ECL-87-19] 22 p3071 N88-28228
SQUID (superconducting quantum interference device) arrays for simultaneous magnetic measurements: Calibration and source localization performance [AD-A193815] 23 p3216 N88-29143
Electromagnetic noise and interference 24 p3363 N88-30028

ELECTROMAGNETIC PROPAGATION
U ELECTROMAGNETIC WAVE TRANSMISSION
ELECTROMAGNETIC PROPERTIES
NT ABSORPTIVITY
NT BIDIRECTIONAL REFLECTANCE
NT BIREFRINGENCE
NT BRIGHTNESS
NT BRIGHTNESS DISTRIBUTION
NT COLOR
NT DICHROISM
NT FARADAY EFFECT
NT INDUCTANCE
NT KERR ELECTROOPTICAL EFFECT
NT KERR MAGNETOOPTICAL EFFECT
NT LUMINOSITY
NT MAGNETORESISTIVITY
NT OPACITY
NT OPTICAL BISTABILITY
NT OPTICAL PROPERTIES
NT OPTICAL REFLECTION
NT PHOSPHORESCENCE
NT PHOTOCONDUCTIVITY
NT PHOTOELASTICITY
NT PROXIMITY EFFECT (ELECTRICITY)
NT RADIANCE
NT REFLECTANCE
NT REFRACTIVITY
NT SKY BRIGHTNESS
NT SPECTRAL REFLECTANCE
NT STELLAR LUMINOSITY
NT STIGMATISM
NT TRANSLUCENCE
NT TRANSMISSIVITY
NT TRANSMITTANCE
NT TRANSPARENCE
NT TURBIDITY
NT WATER COLOR
Analysis of the electromagnetic performance characteristics of stripline transformers
[DE87-012515] 01 p0042 N88-10264
Experimental studies of electromagnetic properties of few body systems
[DE87-014610] 02 p0161 N88-11008
Modulation of an intense beam by an external microwave source: Theory and simulation
[AD-A185683] 07 p0848 N88-15145
Electron paramagnetic resonance studies of Mn(2+) in 2-6 semiconductor alloys 11 p1560 N88-19340
Electromagnetic modeling of a control valve
[INPE-4140-PRE/1048] 12 p1622 N88-19700
Research in remote sensing of vegetation
[NASA-CR-182663] 12 p1639 N88-19817
Joint services electronics program
[AD-A189262] 13 p1761 N88-20533
Topics in curved and flat space electromagnetism
13 p1854 N88-21100
Properties of superconductors with strong electron-phonon interaction 14 p1974 N88-21779
Preparation and properties of high Q microwave dielectrics in the (CA, SR, BA) zirconate system
[AD-A193127] 21 p2918 N88-27317
ELECTHOMAGNETIC PROPULSION
NT MASS DRIVERS (PAYLOAD DELIVERY)
Analysis of a series of electromagnetic launcher firings
[AR-005-131] 04 p0405 N88-12516
Electromagnetic powered vehicles (EMPV) for Mars exploration 17 p2419 N88-24388
Power and energy requirements for electromagnetic launchers 17 p2420 N88-24391
Fabrication issues and technology development for HELEOS (Hypervelocity Electromagnetic Launcher for Equation Of State)
[DE88-007419] 18 p2470 N88-24658
Application of superconducting technology to earth-to-orbit electromagnetic launch systems
[NASA-TM-101134] 20 p2763 N88-26385
ELECTROMAGNETIC PULSES
Theory of atoms in strong, pulsed electromagnetic fields. 2: A free electron and a harmonically bound electron
[DE87-012571] 01 p0035 N88-10225
Optical damage in polymers by millisecond light pulses
[DE87-013106] 02 p0151 N88-10943
Method for single-shot measurement of picosecond laser pulse-lengths without electronic time dispersion
[DE87-013171] 02 p0178 N88-11107
Singularity expansion method: Target Resonances
03 p0303 N88-11912
The effects of corona on current surges induced on conducting lines by EMP: A comparison of experiment data with results of analytic corona models
[DE87-014970] 03 p0305 N88-11924
The development of diagnostic fuses
[SAND-86-0395] 03 p0311 N88-11963
Ultimate velocities for induction launchers
[DE87-012360] 04 p0404 N88-12513
Nitrogen energy transfer study
[AD-A184457] 04 p0464 N88-12869
All-optical beam control by forced Rayleigh scattering
[AD-A184315] 04 p0490 N88-13018
Theoretical analysis of the electrical aspects of the basic electro-impulse problem in aircraft de-icing applications
[NASA-CR-180845] 05 p0543 N88-13310
Solitons in stimulated Raman scattering: Generation and control of ultrashort optical pulses
[AD-A185141] 05 p0650 N88-13983
A paper about electromagnetic pulse and principles of EMP protection
[FOA-C-30455-4.2] 06 p0692 N88-14246
Ferromagnetic mitigation of electromagnetic pulse effects
[AD-A185685] 06 p0694 N88-14258
Parametric and resonance interaction of ultrashort light pulses in nonlinear multilevel medium
06 p0773 N88-14746
High repetition rate electron beam RF-acceleration and sub-millimeter wave generation via a free electron laser
[AD-A186066] 07 p0858 N88-15209
A dynamic analysis of the parallel-plate EMP (electromagnetic pulse) simulator using a wire mesh approximation and the numerical electromagnetics code
[AD-A187535] 11 p1470 N88-18767
Numerical simulation of the propagation and absorption due to air breakdown of long microwave pulses
[DE88-005227] 11 p1475 N88-18798
A methodology to assess the effects of high altitude electromagnetic pulse (HEMP) on electric power systems
[DE88-000338] 11 p1475 N88-18808
Photoconductor switch and circuit analysis
[AD-A188168] 11 p1478 N88-18821
Electrophoretically deposited styrene-acrylate coatings for suppression of internal electromagnetic pulse effects
[DE88-003820] 12 p1609 N88-19621
Two-dimensional electron fluid computer calculations of nanosecond pulse, low pressure microwave air breakdown in a rectangular waveguide and their verification by experimental measurement
[DE88-004407] 12 p1618 N88-19678
Electron emission from conductors subjected to intense, short-pulse electric fields
[DE88-005412] 13 p1836 N88-20965
Equipment test methods for externally produced electromagnetic transients
[RAE-TM-FS(F)-457] 14 p1865 N88-21140
Space-time structure of ultrashort light pulses formed during stimulated backscattering of laser beam
14 p1972 N88-21767
EMR (Electromagnetic Radiation) test facilities evaluation of reverberating chamber located at RADC (Rome Air Development Center), Griffiss AFB (Air Force Base), Rome, New York
[PB88-178827] 15 p2022 N88-22048
Investigations of test methodology for the stress loading facility
[PB88-166095] 15 p2022 N88-22049
Parallel memory addressing using coincident optical pulses
[AD-A189767] 15 p2106 N88-22547
Investigation of ultrashort traveling-wave amplified spontaneous emission 16 p2187 N88-23040
The electromagnetic threat to future avionic systems
17 p2305 N88-23790
Arcing and rf signal generation during target irradiation by a high-energy, pulsed neutral particle beam
[DE88-007169] 18 p2471 N88-24664
Optical damage in epoxy polymers by millisecond light pulses
[DE88-008675] 19 p2620 N88-25547
High bandwidth optoelectronic signal link for use in an EMP (electromagnetic pulse) plus radiation environment
[DE88-009254] 20 p2790 N88-26549
The use of commercial off-the-shelf equipment and its impact on C3 (Command, Control and Communications EMP (electromagnetic pulse, survivability
[AD-A192614] 20 p2791 N88-26556
Research in electromagnetic shielding theory. Part 2: EMP (electromagnetic pulse) simulation using small loops
[AD-A192882] 20 p2791 N88-26558
Picosecond optoelectronic sampling of electrical waveforms produced by an optically excited field effect transistor
[AD-A192384] 21 p2935 N88-27428
A GaAs solid state device model for high power applications
[DE88-011320] 21 p2939 N88-27457
Direct measurement of solids: High temperature sensing. Experimental development and testing of high temperature pulsed EMATs
[DE88-009859] 21 p2954 N88-27546
Wave equations for pulse propagation
[DE88-011760] 21 p2954 N88-27548
Electromagnetic characterization and acceptance test of the electromagnetic pulse (EMP) simulator SPERANS
[FOA-C-30476-4.2] 22 p3071 N88-28230
The far field from a hybrid electromagnetic pulse (HPD) simulator
[FOA-C-30480-4.2] 22 p3071 N88-28231
Current induced by high-altitude electromagnetic pulse (HEMP) on wire above ground
[FOA-C-30485-4.2] 22 p3072 N88-28235
An interface for the connection of the SCP2160A pulse analyser to a Hewlett-Packard desk-top computer
[RSRE-MEMO-4030] 22 p3073 N88-28245
Effects of charge distribution within a particle beam on the sub-Cerenkov radiation
[AD-A193992] 22 p3150 N88-28742
Waveform analysis on the IBM PC
[AD-A194249] 23 p3248 N88-29330
EMPTAC (Electromagnetic Pulse Test Aircraft) user's guide
[AD-A195072] 24 p3360 N88-30036
Transient interaction of electromagnetic pulses in dielectrics and microwave biophysics
[AD-A195687] 24 p3360 N88-30008
Electromagnetic noise and interference
24 p3363 N88-30028
ELECTROMAGNETIC PUMPS
Optimization of SP-100 thermoelectric electromagnetic pump 17 p2418 N88-24382
ELECTROMAGNETIC RADIATION
NT AIRGLOW
NT BLACK BODY RADIATION
NT BREMSSTRAHLUNG
NT CENTIMETER WAVES
NT CERENKOV RADIATION
NT CN EMISSION
NT COHERENT ELECTROMAGNETIC RADIATION
NT COHERENT LIGHT
NT COSMIC X RAYS
NT CYCLOTRON RADIATION
NT DAYGLOW
NT DECAMETRIC WAVES
NT DECIMETER WAVES
NT DIFFRACTION RADIATION
NT ELECTROMAGNETIC PULSES
NT ELECTROMAGNETIC SURFACE WAVES
NT EXTRATERRESTRIAL RADIO WAVES
NT EXTREME ULTRAVIOLET RADIATION
NT FAR INFRARED RADIATION
NT FAR ULTRAVIOLET RADIATION
NT GALACTIC RADIO WAVES
NT GAMMA RAY BURSTS
NT GAMMA RAYS
NT GEOCORONAL EMISSIONS
NT H WAVES
NT HYDROXYL EMISSION
NT INFRARED RADIATION
NT ION CYCLOTRON RADIATION
NT KILOMETRIC WAVES
NT LASER BEAMS
NT LIGHT (VISIBLE RADIATION)
NT LIGHT BEAMS
NT LONG WAVE RADIATION
NT LYMAN ALPHA RADIATION
NT MICROWAVE EMISSION
NT MICROWAVES
NT MILLIMETER WAVES
NT MODULATED CONTINUOUS RADIATION
NT MONOCHROMATIC RADIATION
NT NEAR INFRARED RADIATION
NT NEAR ULTRAVIOLET RADIATION
NT NIGHTGLOW
NT NONEQUILIBRIUM RADIATION
NT NONTHERMAL RADIATION
NT PHONON BEAMS
NT PHOTON BEAMS
NT PLANETARY RADIATION
NT PLASMONS
NT POLARIZED ELECTROMAGNETIC RADIATION
NT POLARIZED LIGHT
NT RADIO BURSTS
NT RADIO EMISSION
NT RADIO WAVES
NT SHORT WAVE RADIATION
NT SKY RADIATION
NT SOLAR RADIO BURSTS
NT SOLAR RADIO EMISSION
NT SOLAR X-RAYS
NT SUBMILLIMETER WAVES
NT SUNLIGHT
NT SYNCHROTRON RADIATION
NT TERRESTRIAL RADIATION
NT THERMAL RADIATION
NT TROPOSPHERIC RADIATION
NT TYPE 3 BURSTS

NT ULTRAVIOLET RADIATION
NT WHISTLERS
NT X RAYS
NT ZODIACAL LIGHT

Compilation of 1986 annual reports of the Navy ELF (Extremely Low Frequency) communications system ecological monitoring program, volume 1
[AD-A184561] 03 p0306 N88-11930

Compilation of 1986 annual reports of the Navy ELF (Extremely Low Frequency) communications system ecological monitoring program, volume 2
[AD-A184562] 03 p0306 N88-11931

Compilation of 1986 annual reports of the Navy ELF (Extremely Low Frequency) communications system ecological monitoring program, volume 3
[AD-A184563] 03 p0306 N88-11932

Scaling the electromagnetically driven explosive shock simulator 05 p0592 N88-13612

Cerenkov radiation field analysis due to a passing electron beam
[AD-A184870] 05 p0649 N88-13976

On the wave excitation in the turbulent meteor trace
06 p0737 N88-14530

Power and charge dissipation from an electrodynamic tether 06 p0795 N88-14869

Interaction of intense electromagnetic fields with SF/sub 6/ molecules and clusters in supersonic expansion
[DE88-700310] 07 p0846 N88-15132

Materials for acceleration by surface electromagnetic waves
[DE88-700312] 07 p0846 N88-15133

Plane longitudinal waves in solutions of Maxwell equations
[DE88-700347] 07 p0846 N88-15135

Propagation of radiation along a constricting optical waveguide 07 p0920 N88-15590

Satellite monitoring of earthquake precursor effects in magnetosphere 08 p1007 N88-16103

Statistical model of interaction of electromagnetic waves with natural objects being sensed
08 p1008 N88-16112

Instability of strong-absorption domain in semiconductor 08 p1077 N88-16495

Interaction of acoustic and electromagnetic waves involved in anomalous skin effect
08 p1079 N88-16503

Advanced studies of integrable systems
[AD-A186792] 09 p1151 N88-16895

Transient electromagnetic scattering from heterogeneous lossy spheres
[AD-A186669] 09 p1152 N88-16903

Plane wave diffraction by a thin dielectric wedge
[RSRE-MEMO-4045] 09 p1153 N88-16912

Direct scattering of electromagnetic waves by one- and two-dimensional objects and its use for inverse profiling
[PB88-126909] 10 p1319 N88-17887

Velocity reversal and the arrows of time
[DE88-004237] 10 p1429 N88-18536

Backscattering from three dimensional conducting bodies
[AD-A187570] 11 p1470 N88-18766

ELF (Extremely Low Frequency) communications system ecological monitoring program. Electromagnetic field measurements and engineering support, 1986
[AD-A188057] 11 p1509 N88-19017

Experimental aspects of hypernuclear physics at CEBAF
[CEBAF-R-86-013] 11 p1546 N88-19245

Electromagnetic propagation in PEC and absorbing curved S-ducts
[NASA-TM-100833] 12 p1621 N88-19698

Airborne electromagnetic sounding of sea ice thickness and sub-ice bathymetry
[AD-A188939] 12 p1649 N88-19879

Time-domain system for identification of the natural resonant frequencies of aircraft relevant to electromagnetic compatibility testing
[PB88-164520] 13 p1759 N88-20519

Theoretical investigation of EM wave generation and radiation in the ULF, ELF and VLF bands by the electrodynamic orbiting tether
[NASA-CR-182720] 13 p1760 N88-20529

Three-wave parametric resonance in plasma of relativistic electron flux 14 p1972 N88-21772

AGARD Highlights 88/1 14 p2012 N88-22001

Strategies in the topological approach to electromagnetic interference control
[AD-A189874] 15 p2056 N88-22255

Electromagnetic sensor arrays for nondestructive evaluation and robot control
[AD-A190210] 15 p2056 N88-22260

Theoretical studies of the heating of toroidal plasmas with radiofrequency electromagnetic radiation
[DE88-006913] 15 p2137 N88-22749

IREPS (Integrated Refractive Effects Prediction System) 3.0, user's manual
[AD-A190398] 16 p2188 N88-23045

Theoretical and numerical solution of the forward-scattering problem in a circularly cylindrical configuration
[PB88-173489] 16 p2189 N88-23056

Numerical simulation for particle acceleration and trapping by an electromagnetic wave
16 p2277 N88-23626

Electromagnetic penetration into a conducting circular cylinder through a narrow slot, TE case
[AD-A191602] 18 p2500 N88-24828

Electromagnetic field penetration into structures
[AD-A192127] 18 p2501 N88-24836

Joint services electronics program
[AD-A191749] 18 p2504 N88-24853

Theoretical basis for an experimental test with regard to the origin of VHF (Very High Frequency) radiation from natural lightning
[DE88-007535] 18 p2544 N88-25102

Extremely Low Frequancy (ELF) communications program. Non-ionizing electromagnetic radiation literature evaluation and assessment, 1986-1987 literature review
[AD-A192024] 19 p2642 N88-25677

Method and apparatus for measuring distance
[NASA-CASE-MSC-20912-1] 20 p2793 N88-26568

Comparative analysis of passive communications satellites employing the SHF and HF spectrum for use in a strategic role
[AD-A194682] 24 p3362 N88-30019

Review of Radio Science, 1984-1986
24 p3363 N88-30023

Bioeffects of electromagnetic waves
24 p3364 N88-30032

Time-domain far-field scattering of plane electromagnetic waves by a penetrable object in the Born approximation
[PB87-176129] 24 p3365 N88-30040

Vanderbilt free electron laser project in biomedical and materials research
[AD-A195961] 24 p3378 N88-30121

ELECTROMAGNETIC SCATTERING
NT HALOS
NT LIGHT SCATTERING
NT MICROWAVE SCATTERING
NT MIE SCATTERING
NT RAMAN SPECTRA
NT RAYLEIGH SCATTERING
NT THOMSON SCATTERING
NT X RAY SCATTERING

Input signal shaping: K-pulse
03 p0304 N88-11917

Experiments: Test range facilities, part 1
03 p0304 N88-11920

Electromagnetic scattering by a thick strip on a half-space
[PB87-227096] 03 p0306 N88-11928

A comparative analysis of equatorial and auroral-zone phase scintillation data
[AD-A184509] 03 p0350 N88-12212

New main reflector, subreflector and dual chamber concepts for compact range applications
[NASA-CR-181506] 04 p0402 N88-12498

A study of scattering from E-plane circuit elements
[AD-A184473] 04 p0431 N88-12673

Efficient computation of periodic Green's functions with application to grating structures
[AD-A184853] 05 p0640 N88-13912

Spectral- and spatial-domain filtering and sampling approach to the numerical solution of electromagnetic scattering problems
[PB88-106711] 06 p0694 N88-14261

Study of extended least-square iterative techniques in electromagnetic scattering by penetrable objects
[PB88-105879] 06 p0694 N88-14262

Electromagnetic scattering problem in the wave-vector-time domain
[PB88-106083] 06 p0694 N88-14263

EISCAT (European incoherent scatter radar) electron density studies
[AD-A185998] 07 p0841 N88-15099

Absorption, scattering, and thermal radiation by conductive fibers
[AD-A186105] 07 p0842 N88-15106

Interior impedance wedge diffraction with surface waves
[NASA-CR-182405] 07 p0854 N88-15186

The application of vector diffraction to the scalar anomalous diffraction approximation of Van de Hulst
[AD-A185930] 07 p0929 N88-15643

Transient electromagnetic scattering from heterogeneous lossy spheres
[AD-A186669] 09 p1152 N88-16903

Calculation of the spatial-temporal deformation of laser pulses in multiple scattering
[MBB-Z-111/87] 10 p1311 N88-17837

Direct scattering of electromagnetic waves by one- and two-dimensional objects and its use for inverse profiling
[PB88-126909] 10 p1319 N88-17887

Three-dimensional transient electromagnetic modeling for exploration geophysics 10 p1346 N88-18047

A dynamic analysis of the parallel-plate EMP (electromagnetic pulse) simulator using a wire mesh approximation and the numerical electromagnetics code
[AD-A187535] 11 p1470 N88-18767

The application of the hybrid iterative method to scattering by perfectly conducting bodies of revolution
11 p1475 N88-18802

Experimental study of scattered waves and cylindrical antenna sheaths in a microwave driven plasma
11 p1553 N88-19293

An efficient numerical algorithm for solving scattering and inverse scattering problems of electromagnetic waves
[AD-A188479] 12 p1619 N88-19684

Electromagnetic scattering from and natural resonances of the circular strip 13 p1759 N88-20523

Electromagnetic shadowing by an exponentially distributed rough surface
[AD-A189677] 14 p1906 N88-21391

Electromagnetic scattering by an exponentially distributed rough surface with the introduction of a rough surface generation technique
[AD-A189678] 14 p1906 N88-21392

On the theory of electromagnetic scattering from a raindrop splash
[AD-A188720] 14 p1906 N88-21393

Polarimetric ISAR imaging using either measured or calculated transient signatures
[AD-A190077] 15 p2056 N88-22259

Models for electromagnetic scattering from the sea at extremely low grazing angles
[AD-A190472] 15 p2057 N88-22261

Efficiency of some computational techniques for electromagnetic scattering problems
[PB88-148895] 16 p2187 N88-23043

Computer program for parameterization of nucleus-nucleus electromagnetic dissociation cross sections
[NASA-TM-4038] 16 p2270 N88-23584

Electromagnetic scattering from nonlinear anisotropic cylinders 17 p2333 N88-23930

Born-type reconstruction of material parameters of an inhomogeneous, lossy dielectric slab from reflected-field data
[PB88-188958] 18 p2569 N88-25261

Curvature of blended rolled edge reflectors at the shadow boundary contour
[NASA-CR-182974] 18 p2576 N88-25300

New hybrid method for solving time-domain integral equations (one-dimensional scattering problems)
[PB88-186192] 20 p2789 N88-26547

Stochastic modeling of EM scattering from foliage
[AD-A192258] 20 p2790 N88-26553

Comparison of edge diffraction theories
[AD-A193880] 22 p3070 N88-28223

Diffraction by a simple deep phase object --- integrated circuit measurement
[RSRE-MEMO-4039] 22 p3070 N88-28224

Review of Radio Science, 1984-1986
24 p3363 N88-30023

Fields and waves 24 p3363 N88-30025

Time-domain far-field scattering of plane electromagnetic waves by a penetrable object in the Born approximation
[PB87-176129] 24 p3365 N88-30040

ELECTROMAGNETIC SHIELDING

Crosstalk in braided shield coaxial cables
01 p0035 N88-10224

Shielding effectiveness against electromagnetic interference
[DE88-003664] 07 p0846 N88-15131

Measurement of shielding effectiveness of different cable and shielding configurations by mode-stirred techniques
[PB88-155791] 10 p1319 N88-17885

Strategies in the topological approach to electromagnetic interference control
[AD-A189874] 15 p2056 N88-22255

Electromagnetic compatability: An introduction to the theory of interference and shielding. 3rd revised edition
[PB88-165410] 15 p2057 N88-22264

Electromagnetic field penetration into structures
[AD-A192127] 18 p2501 N88-24836

Research in electromagnetic shielding theory. Part 1: Shielding by rectangular enclosures
[AD-A192881] 20 p2791 N88-26557

Research in electromagnetic shielding theory. Part 2: EMP (electromagnetic pulse) simulation using small loops
[AD-A192882] 20 p2791 N88-26558
Shielding effectiveness of metallic joints versus corrosion prevention 22 p3054 N88-28120
Electromagnetic noise and interference
24 p3363 N88-30028

ELECTROMAGNETIC SPECTRA
NT BALMER SERIES
NT ELECTRONIC SPECTRA
NT FRAUNHOFER LINES
NT GAMMA RAY SPECTRA
NT H ALPHA LINE
NT H BETA LINE
NT H LINES
NT INFRARED SPECTRA
NT K LINES
NT LINE SPECTRA
NT LYMAN SPECTRA
NT MICROWAVE SPECTRA
NT RADIO SPECTRA
NT RAMAN SPECTRA
NT RYDBERG SERIES
NT SOLAR SPECTRA
NT STELLAR SPECTRA
NT ULTRAVIOLET SPECTRA
NT VIBRATIONAL SPECTRA
NT VISIBLE SPECTRUM
NT X RAY SPECTRA
Extreme ultraviolet beam-foil spectroscopy of highly ionized neon and argon
[AD-A185197] 05 p0561 N88-13418
Research investigation directed toward extending the useful range of the electromagnetic spectrum
[AD-A190198] 17 p2332 N88-23920
Research investigation directed toward extending the useful range of the electromagnetic spectrum, appendix
[AD-A190199] 17 p2332 N88-23921
The electromagnetic spectrum: The information mine
[AD-A194316] 22 p3069 N88-28215

ELECTROMAGNETIC SURFACE WAVES
Interior impedance wedge diffraction with surface waves
[NASA-CR-182405] 07 p0854 N88-15186

ELECTROMAGNETIC WAVE FILTERS
NT BANDPASS FILTERS
NT BANDSTOP FILTERS
NT DIGITAL FILTERS
NT ELECTRIC FILTERS
NT FIR FILTERS
NT MATCHED FILTERS
NT MICROWAVE FILTERS
NT OPTICAL FILTERS
NT RADAR FILTERS
NT RADIO FILTERS
NT TRACKING FILTERS
NT WAVEGUIDE FILTERS
A notch filter instrument for measuring ELF (Extremely Low Frequency) MSK (Minimum Shift Keying) signals
[AD-A193324] 21 p2933 N88-27414

ELECTROMAGNETIC WAVE TRANSMISSION
NT HALOS
NT IONOSPHERIC PROPAGATION
NT LIGHT SCATTERING
NT LIGHT TRANSMISSION
NT MICROWAVE ATTENUATION
NT MICROWAVE TRANSMISSION
NT MULTIPATH TRANSMISSION
NT RADAR TRANSMISSION
NT RADIO TRANSMISSION
NT SCATTER PROPAGATION
NT SHORT WAVE RADIO TRANSMISSION
NT SPREAD SPECTRUM TRANSMISSION
NT TELEVISION TRANSMISSION
NT TRANSEQUATORIAL PROPAGATION
ELF/VLF/LF propagation and system design
[AD-A183261] 01 p0033 N88-10212
Open accelerating structures
[DE87-010540] 01 p0092 N88-10603
A computer code to calculate line by line atmospheric transmission spectra on a microcomputer
[NASA-TM-100686] 05 p0554 N88-13372
An investigation of millimeter wave propagation in the atmosphere: Measurement program
[AD-A184837] 05 p0574 N88-13498
Time domain electromagnetic waves in multilayered media
[AD-A185055] 05 p0574 N88-13502
Analysis of electromagnetic wave propagation in slightly inhomogeneous hollow waveguides
[DFVLR-FB-87-23] 09 p1152 N88-16904
Studies on nonlinear mechanisms of excimer laser propagation in fused silica fibers
[AD-A186822] 09 p1156 N88-16929
Active and passive remote sensing of ice
[AD-A186685] 09 p1195 N88-17162
An evaluation of the impact of variable temporal and spatial data resolution upon IREPS (Integrated Refractive Effects Prediction System)
[AD-A187764] 11 p1470 N88-18769
Integral equations with modified fundamental solutions for exterior boundary value problems from electromagnetic wave theory
[ETN-88-91483] 11 p1475 N88-18800
USU (Utah State University) Center of Excellence in Theory and Analysis of the Geo-Plasma Environment
[AD-A187687] 11 p1511 N88-19026
Historical electromagnetic propagation condition database description
[AD-A189157] 12 p1621 N88-19695
Electric fields in Earth orbital space. Magnetospheric structural dynamic response to external variables
[AD-A188592] 12 p1643 N88-19836
Worldwide distributions of shipboard surface meteorological observations for EM propagation analysis
[AD-A188771] 12 p1648 N88-19871
High speed transcendental elementary function architecture in support of the Vector Wave Equation (VWE)
[AD-A189746] 15 p2119 N88-22627
Parametric instabilities of inhomogeneous plasma near the lower-hybrid resonance
[DE88-701201] 15 p2137 N88-22748
Beam waves in random inhomogeneous media
[DE88-701631] 16 p2190 N88-23058
Pulsed power simulation problems in magic
[AD-A191110] 16 p2191 N88-23065
WAVFLD: A program to compute ionospheric height gain functions and field strengths at VLF
[AD-A191159] 16 p2191 N88-23066
Validate algorithms for the determination of rainfall rates from SSM/I microwave satellite imagery
[AD-A191337] 16 p2236 N88-23353
Development of 20 GHz monolithic transmit modules
[NASA-CR-182134] 17 p2445 N88-24539
Propagation of neutralized ion beams
[AD-A191599] 18 p2574 N88-25289
Theoretical plasma physics research of active space experiments
[AD-A192075] 18 p2577 N88-25309
New hybrid method for solving time-domain integral equations (one-dimensional scattering problems)
[PB88-186192] 20 p2789 N88-26547
On the self-trapping of an electromagnetic wave in magnetized plasma
[DE88-701872] 20 p2858 N88-26974
Airborne measurement of low frequency atmospheric noise ALFAN 1
[AD-A193056] 21 p2931 N88-27405
SARLAC: A relativistic electron beam code
[AD-A193134] 21 p2932 N88-27411
Staggered-grid finite element solution technique for the Maxwell's equations in the time domain
[DE88-011731] 21 p3007 N88-27838
Propagation of charged particle beams in the atmosphere
[AD-A193185] 21 p3014 N88-27887
Electromagnetic wave incoherent reflection by a half-space of weakly-ionized plasma with an absorbing boundary
[DE88-702413] 21 p3019 N88-27917
The spatial and temporal variability of the arctic atmospheric boundary layer and its effect on electromagnetic (EM) propagation
[AD-A193958] 23 p3204 N88-29068
Currents induced in a human being for electromagnetic fields to 10 kHz-50 MHz
[AD-A191977] 23 p3238 N88-29268
Nonlinear optical phase conjugation techniques to reduce the physical size of lasers
[AD-A196170] 24 p3379 N88-30122
Consideration of plasma opening switches from a wave propagation perspective
[AD-A195681] 24 p3431 N88-30421

ELECTROMAGNETIC WAVES
U ELECTROMAGNETIC RADIATION

ELECTROMAGNETICS
U ELECTROMAGNETISM

ELECTROMAGNETISM
NT MAGNETOSTATICS
Response of helical structures to high speed pulses or when can a helix be called an inductor
[DE87-014347] 01 p0090 N88-10587
Process support compressor motor electromagnetic design summary
[DE87-014359] 02 p0167 N88-11048
Eigenvalue projection theory for linear operator equations of electromagnetics
[AD-A185434] 05 p0575 N88-13504
Nature and the nonlinear evolution of electrostatic waves associated with the AMPTE (Active Magnetosphere Particle Tracer Explorers) solar wind releases
[AD-A185471] 06 p0806 N88-14020
Properties of a magnetic dipole
[AD-A186128] 07 p0922 N88-15600
Primordial nucleosynthesis during the keV era
[DE88-002233] 08 p1104 N88-16623
Exact image principle in electromagnetic field computation
[EL-57] 09 p1153 N88-16907
Investigation of iterative and spectral Galerkin techniques for solving electromagnetic boundary value problems 09 p1155 N88-16925
Cold gas jet system for satellite attitude control-modeling and simulation
[INPE-4279-PRE/1150] 12 p1601 N88-19583
Influence of magnetic material on the transient of a controle electrovalve
[INPE-4418-PRE/1223] 12 p1624 N88-19713
Electric fields in Earth orbital space. Magnetospheric structural dynamic response to external variables
[AD-A188592] 12 p1643 N88-19836
Topics in curved and flat space electromagnetism
13 p1854 N88-21100
Electromagnetic shadowing by an exponentially distributed rough surface
[AD-A189677] 14 p1906 N88-21391
Launchability of base-driven electromagnetic projectiles
[AD-A189635] 15 p2023 N88-22055
Electromagnetic dampers for cryogenic applications
16 p2218 N88-23231
Electromagnetic manipulation of atomic hydrogen
16 p2268 N88-23568
Electromagnetic damping and vibration isolation of space structures
[AD-A191492] 18 p2471 N88-24665
A model for insulated wires in the method of moments code NEC (Numerical Electromagnetics Code)
[DE88-008920] 20 p2794 N88-26577
Gravitation electromagnetic theory
22 p3158 N88-28790
Gravitation and electromagnetism
22 p3158 N88-28792
Electromagnetic theory of the gravitation
22 p3158 N88-28793
Cosmological applications 22 p3158 N88-28794
Electromagnetic metrology 24 p3363 N88-30024
X- and gamma-ray background observations in Antarctic
[INPE-4583-PRE/1317] 24 p3459 N88-30578

ELECTROMAGNETS
NT SUPERCONDUCTING MAGNETS
Exact solutions to the governing dynamic equations of plasma armature electromagnetic railguns
[DE87-014442] 01 p0011 N88-10063
Different ways of looking at the electromagnetic vacuum
[DE87-013150] 01 p0089 N88-10584
Process support compressor motor electromagnetic design summary
[DE87-014359] 02 p0167 N88-11048
Performance evaluation of a half-wave resonant slot antenna over perfect ground using NEC (Numerical Electromagnetic Code)
[AD-A184004] 03 p0308 N88-11942
An excitation-term modification for a certain class of electromagnetic aperture-coupling problems
[DE88-000260] 04 p0437 N88-12713
A long electromagnetic wiggler for the paladin free-electron laser experiments
[DE88-000970] 05 p0588 N88-13589
Development of a strong electromagnet wiggler
[DE88-000971] 05 p0645 N88-13952
Development of a laced electromagnetic wiggler
[DE88-000972] 05 p0646 N88-13953
Proceedings of the 2nd Regional Electromagnetic Workshop at Argonne National Laboratory
[DE87-004633] 06 p0690 N88-14230
Test results on dual resonant power supply with flat top and flat bottom current
[DE87-007506] 09 p1157 N88-16933

ELECTROMECHANICAL DEVICES
Operator multiple-tasking study for remotely operated platforms
[AD-A184487] 03 p0362 N88-12276
Corrosion behavior of high density tungsten alloys
[AD-A187108] 09 p1143 N88-16952
Dynamic modelling of an electromechanical valve using frequency response data
[AD-A187908] 11 p1494 N88-18918
Dynamics of high-speed mechanisms with elastic members 13 p1779 N88-20643
The 15-meter diameter hoop/column antenna surface control actuator system 14 p1924 N88-21489

Aerodynamic and thermal modeling of electromagnetic brakes. Evaluation of convective exchange coefficients and friction losses in the rough wall channels
[ISAL-ITC1-87-02] 16 p2215 N88-23214
Nickel hydroxide active material densities
[AD-A191411] 10 p2230 N88-23319

ELECTROMECHANICS
A feasibility study of a hypersonic real-gas facility
[NASA-CR-180423] 01 p0008 N88-10043
On the glitches in the force transmitted by an electrodynamic exciter to a structure
05 p0594 N88-13624
Electromechanical timing measurement technique
[DE88-005098] 11 p1489 N88-18889
Dynamic modelling of an electromechanical valve using frequency response data
[AD-A187908] 11 p1494 N88-18918
Electromechanical Research Symposium, August 20-21, 1987
[PB88-148457] 19 p2713 N88-26109

ELECTROMIGRATION
Computer simulation of electromigration in thin films
[AD-A194526] 22 p3157 N88-28782

ELECTROMOTIVE FORCES
NT PONDEROMOTIVE FORCES
Effects of cold working on precipitation in age hardenable alloys: On the copper alloys
[NASA-TT-20164] 16 p2177 N88-22973

ELECTRON ACCELERATION
Simulation of tokamak runaway-electron events. Study of the response of materials by use of an electron linear accelerator
[IPPJ-841] 02 p0242 N88-11528
Nonthermal phenomena in stellar coronae: Evidence from radio observations 04 p0503 N88-13096
Electron acceleration by wave processes in the earth's ionosphere
[AD-A186110] 07 p0877 N88-15320
Wave acceleration of auroral electrons
08 p1031 N88-16245
Electron acceleration by laser fields in a gas
[DE88-003337] 08 p1082 N88-16523
Collective acceleration of electrons and ions in a high relativistic electron beam
[DE88-005261] 13 p1838 N88-20998
Relationship between characteristics of low-energy electrons and geomagnetic disturbance in geostationary orbit 24 p3444 N88-30501

ELECTRON ACCELERATORS
NT BETATRONS
Phase control of the microwave radiation in free electron laser two-beam accelerator
[DE88-001460] 07 p0859 N88-15219
Energy distribution of Cerenkov radiation for finite frequency intervals
[AD-A186901] 09 p1244 N88-17454
A ring model of the lasertron
[DE88-004656] 10 p1323 N88-17908
Nucleon resonances and nuclei: Experimental aspects
[CEBAF-PR-87-025] 11 p1545 N88-19233
RF steering in the CEBAF CW superconducting linac
[CEBAF-PR-87-013] 11 p1547 N88-19251
The CEBAF project and its few-body research program
[CEBAF-PR-87-014] 11 p1547 N88-19253
Two dimensional simulations of multipass beam breakup
[CEBAF-PR-87-008] 11 p1547 N88-19254
Application of radio frequency superconductivity to recirculating linacs
[CEBAF-PR-88-002] 12 p1690 N88-20107
On (e,e'N) reactions
[CEBAF-PR-87-028] 12 p1690 N88-20109
Trajectory code studies, 1987
[DE88-006218] 13 p1728 N88-20335
The continuous electron beam accelerator facility
[CEBAF-PR-87-017] 13 p1836 N88-20996
Design of electron beam accelerator for microwave application
[DE88-005252] 13 p1838 N88-20999
The loss parameters for very short bunches
[CEBAF-PR-88-005] 18 p2574 N88-25291

ELECTRON AFFINITY
K-CO on transition metals: A local ionic interaction
[AD-A184342] 04 p0496 N88-13056

ELECTRON ATTACHMENT
Ion and electron interactions of atmospheric importance
[AD-A192255] 20 p2824 N88-26751

ELECTRON BEAM WELDING
Operation of multistage power supplies for electron beam welding installations 03 p0286 N88-11800
Development of an acoustic emission monitor and monitoring techniques for long-term monitoring of U-0.8Ti electron-beam weldments for postweld cracking
[DE88-000819] 04 p0453 N88-12804
Faraday cup characterization of electron beam welding parameters
[DE88-001896] 07 p0864 N88-15241
Detection of hydrogen-assisted-cracking in U-0.8Ti alloy weldments by acoustic emission monitoring
[DE88-003221] 09 p1184 N88-17093
Microstructural characterization and properties of 3Cr-1.5Mo-0.1V thick section electron beam welds
[DE88-004330] 18 p2486 N88-24747
An investigation into the metallurgical aspects of joining rapidly-solidified aluminum alloys
[AD-A194677] 23 p3194 N88-29009

ELECTRON BEAMS
NT RELATIVISTIC ELECTRON BEAMS
Effects of electron and proton irradiations on n/p and p/n GaAs cells grown by MOCVD
[NASA-TM-100199] 01 p0042 N88-10266
Electron beam requirements for soft X-ray/XUV free-electron lasers
[DE87-011750] 01 p0051 N88-10325
Linear emittance damper with megagauss fields
[DE87-013562] 01 p0093 N88-10606
Electron beam irradiation effects on carbon fiber reinforced PEEK composite
[DE87-753001] 02 p0142 N88-10890
Studies on temporal field emission from stainless steel surfaces
[DE87-014237] 02 p0147 N88-10919
Hydrogen annealing of P(sub) b and E prime defect centers in oxidized silicon wafers
[DE87-014293] 02 p0152 N88-10951
Trajectory versus PIC methods in diode design
[DE87-012135] 02 p0166 N88-11043
On the collective variables description of a high gain free electron laser
[DE87-013315] 02 p0178 N88-11108
Enhanced noise and Raman scattering in plasma
[DE87-014466] 02 p0238 N88-11501
Fusion reactivity enhancement due to ion tail formation by beam and ion cyclotron heating
[DE87-753018] 02 p0240 N88-11518
Effects of injection of free electron lasers on axial velocity spread of beams 03 p0299 N88-11878
Excimer laser cell with longitudinal electron-beam excitation 03 p0302 N88-11903
A theoretical study of enhanced Smith-Purcell radiation from a bigrating
[AD-A184530] 03 p0329 N88-12080
The lasertron RF generator for FEL (Free-Electron Laser) applications
[DE88-000515] 04 p0448 N88-12776
Development of an acoustic emission monitor and monitoring techniques for long-term monitoring of U-0.8Ti electron-beam weldments for postweld cracking
[DE88-000819] 04 p0453 N88-12804
Use of electron beam instruments to determine fluctuations in vertical refraction partial angle
04 p0461 N88-12853
Narrow linewidth gain measurements in a KrF excimer amplifier pumped longitudinally by a high-power electron beam
[DE88-001365] 05 p0586 N88-13575
Theoretical and experimental investigation of electron beam acceleration and sub-millimeter wave generation in cyclotron resonant cavities
[AD-A184806] 05 p0649 N88-13975
Cerenkov radiation field analyses due to a passing electron beam
[AD-A184870] 05 p0649 N88-13976
Optimization of field emission electron beam sources for high-power lasers
[PB87-218814] 06 p0708 N88-14341
NBS (National Bureau of Standards) measurement services: Fricke dosimetry in high-energy electron beams
[PB88-110374] 06 p0781 N88-14795
Stabilized X-ray generator power supply
[DE88-700297] 07 p0830 N88-15034
Cage mode propagation experiments
[AD-A186019] 07 p0841 N88-15100
Microsecond beam propagation in air
[DE88-002221] 07 p0845 N88-15127
High repetition rate electron beam RF-acceleration and sub-millimeter wave generation via a free electron laser
[AD-A186086] 07 p0858 N88-15209
Generation of light pulses in semiconductor laser upon excitation by several electron beams
07 p0920 N88-15589
Experimental research of electron beam instability on the Doppler anomalous effect
[DE88-700565] 07 p0932 N88-15658
Experimental evaluation for efficiency of excitation slow plasma and cyclotron waves in collective accelerators
[DE88-700566] 07 p0936 N88-15687
Gyrotron development at the Instituto de Pesquisas Espaciais
[INPE-4240-PRE/1115] 08 p0990 N88-15992
MAIMIK: A high current electron beam experiment on a sounding rocket from Andoya rocket range (Norway)
08 p1030 N88-16243
Electron acceleration by laser fields in a gas
[DE88-003337] 08 p1082 N88-16523
Resolution limitations and optimization of the ITT F4157 streak tube focus for fast (10 ps) operation
[DE88-003727] 09 p1169 N88-17007
Intrinsic corrections to optical guiding in a free electron laser: Beam Research Program
[DE88-002667] 09 p1172 N88-17026
Mode media interactions in an FEL (Free Electron Laser)
[DE88-003155] 09 p1172 N88-17029
High-efficiency GaAs semiconductor laser with longitudinal excitation by scanning electron beam
09 p1238 N88-17421
Periodic-pulse semiconductor laser with electron-beam pumping 09 p1238 N88-17422
CEBAF design overview and project status
[CEBAF-PR-88-001] 09 p1246 N88-17470
Intense electron beams
[DE88-002456] 09 p1247 N88-17474
A ring model of the lasertron
[DE88-004656] 10 p1323 N88-17908
Preliminary injector, accelerator, and beamline design for rf-linac-driven XUV free-electron lasers
[DE88-003185] 10 p1336 N88-17983
Betatron oscillations in a free electron laser
[DE88-004859] 10 p1337 N88-17990
Tapered wiggler analysis of high gain free electron laser oscillators
[AD-A187997] 10 p1338 N88-17997
The stability of free-electron lasers against filamentation
[DE88-004712] 10 p1414 N88-18435
Effects of X irradiation and high field electron injection on the electrical properties of rapid thermal oxides
[DE88-002642] 10 p1417 N88-18461
Operation of electron-beam controlled CO2 laser at 6 atmospheres 11 p1468 N88-18758
Microwave radiation from rotating, annular electron beams 11 p1475 N88-18801
High-current density, high-brightness electron beams from large-area lanthanum hexaboride cathodes
[AD-A187700] 11 p1477 N88-18813
The injector for the CEBAF CW superconducting linac
[CEBAF-PR-87-011] 11 p1546 N88-19241
Perturbation effects in the CEBAF beam transport system
[CEBAF-PR-87-010] 11 p1546 N88-19242
High energy polarized electron beams
[CEBAF-R-87-002] 11 p1546 N88-19244
Investigation of multiple particle final states at CEBAF (Continuous Electron Beam Accelerator Facility)
[CEBAF-PR-87-026] 11 p1547 N88-19250
Two dimensional simulations of multipass beam breakup
[CEBAF-PR-87-008] 11 p1547 N88-19254
An analysis of whistler-mode radiation from the Spacelab-2 electron beam, revision
[AD-A188228] 11 p1552 N88-19267
Generalised scattering model for the quantum modulation of electrons 11 p1563 N88-19357
Application of radio frequency superconductivity to recirculating linacs
[CEBAF-PR-88-002] 12 p1690 N88-20107
Optics of the CEBAF CW superconducting accelerator
[CEBAF-PR-87-012] 12 p1690 N88-20110
Electronic properties of semiconductor inversion layers in sub-micron structures
[AD-A188635] 12 p1698 N88-20161
Mode priming in an overmoded gyrotron oscillator
[AD-A189151] 13 p1772 N88-20602
Development of electrostatic-accelerator free-electron lasers
[AD-A189507] 13 p1774 N88-20614
The continuous electron beam accelerator facility
[CEBAF-PR-87-017] 13 p1838 N88-20996
Rapid e-beam heating for measuring thermodynamics of metastable materials
[DE88-003565] 13 p1849 N88-21066
Effect of electron beam divergence on the gain of free electron lasers 14 p1902 N88-21356
Electron beam sensitive devices for controllability
[RR-658-I] 14 p1908 N88-21403
New method of examining micrononhomogeneity of local centers in high-resistivity semiconductor materials under scanning electron microscope 14 p1969 N88-21754
Kinetics of slow electrons in excimer laser with electron-beam pumping 14 p1970 N88-21760
Emission characteristics of XeCl-laser excited by electron beam of microsecond duration
14 p1970 N88-21762

Growth and deformation mechanisms of refractory alloy hybrid materials
[AD-A190492] 15 p2039 N88-22152
Directed-energy electron-beam processing of a hypoeutectic Cr90Ta10 alloy
[DE88-005621] 15 p2040 N88-22157
Discharge excitation of the XeF C to A transition
[DE88-006448] 15 p2070 N88-22339
Numerical modeling specific energy charcteristics of excimer KrF lasers with electron beam excitation
[DE88-701525] 15 p2070 N88-22344
Nonlinear effects in plasma wake field acceleration
[DE88-700972] 15 p2134 N88-22734
High power, high frequency radiation from beam-plasma interactions
[AD-A190207] 15 p2137 N88-22752
Survey of the Air Force P78-2 (SCATHA) satellite plasma wave data during electron gun operations
[AD-A191014] 15 p2168 N88-22926
JPRS report: Science and technology. USSR: Materials science
[JPRS-UMS-88-006] 16 p2179 N88-22988
High-speed electron beam lithography devices discussed 16 p2185 N88-23023
Beam waves in random inhomogeneous media
[DE88-701631] 16 p2190 N88-23058
Kinetics of electrons and molecules at plasma-beam discharge in molecular gases
[DE88-701196] 16 p2275 N88-23616
Isotope separation using tuned laser and electron beam
[NASA-CASE-NPO-16907-1-CU] 18 p2483 N88-24732
Microstructural characterization and properties of 3Cr-1.5Mo-O.1V thick section electron beam welds
[DE88-004330] 18 p2486 N88-24747
Integral equation for the laser field: Multimode description of a free-electron laser oscillator
[DE88-007050] 18 p2521 N88-24956
Null steering applications of polynomials with unimodular coefficients
[AD-A191067] 18 p2562 N88-25211
Trochoidal analysis of scattered electrons in a merged electron-ion beam
[NASA-CASE-NPO-16789-1-CU] 18 p2573 N88-25281
Accelerator research studies
[DE88-007124] 18 p2574 N88-25290
The loss parameters for very short bunches
[CEBAF-PR-88-005] 18 p2574 N88-25291
Observations of electron cyclotron harmonic emissions associated with field-aligned electron beams
[SD-TR-87-33] 19 p2724 N88-26173
REFLEX: An energy deposition code that models the effects of electron reflection during electron beam heating tests
[DE88-009789] 19 p2726 N88-26186
Accelerator research studies
[DE88-008236] 19 p2726 N88-26187
Vaporization studies of plasma interactive materials in simulated plasma disruption events
[DE88-010100] 19 p2731 N88-26222
Electron-impact-ionization and electron-attachment cross sections of radicals important in transient gaseous discharges
[AD-A192248] 20 p2770 N88-26424
The free-electron laser: Theoretical innovations and gas-loaded experiment 20 p2806 N88-26646
Results from the SLAC lasertron
[DE88-007816] 20 p2806 N88-26647
Inelastic mean free paths of electrons and positrons in matter
[DE88-008086] 20 p2851 N88-26929
Visible tunable source
[DE88-006442] 20 p2854 N88-26944
Excitonic properties of GaAs-AlGaAs nanostructures
20 p2867 N88-27023
High-speed, precision processing using an electron beam 21 p2929 N88-27391
Equipment for an advanced electron beam lithography system
[AD-A192956] 21 p2936 N88-27435
Optical guiding in the separable beam limit
[AD-A192452] 21 p2952 N88-27534
Production of intensive electron beam impulsions by setup of pseudoglare discharges
[ISL-CO-210/87] 21 p3019 N88-27920
Guided radiation beams in free electron lasers
[AD-A194525] 22 p3082 N88-28305
Development of inductive storage pulsed power generators
[AD-A193878] 22 p3117 N88-28521
Effects of charge distribution within a particle beam on the sub-Cerenkov radiation
[AD-A193992] 22 p3150 N88-28742
The NBS/NRL (National Bureau of Standards/Naval Research Laboratory) free electron laser facility
[AD-A194214] 23 p3219 N88-29159
Diffraction transition radiation from periodic electron bunches
[AD-A193593] 23 p3280 N88-29528
Plasmoid propagation
[AD-A192378] 23 p3284 N88-29555
Microcircuit trace cutting with focused ion beams
[AD-A196030] 24 p3367 N88-30050
Reactive plasticizers in negative E-beam resists
[AD-A195161] 24 p3368 N88-30056
Influence of plasma parameters on VLF radiation in near-rocket region 24 p3448 N88-30518

ELECTRON BOMBARDMENT
The design and development of mercury vaporisers for use with electron-bombardment ion engines
[RAE-TR-70042] 01 p0018 N88-10108
The effect of oriented defects on long-range ordering of hydrocarbon films: Azulene on Pt(111)
[AD-A196089] 24 p3344 N88-29904

ELECTRON BUNCHING
A crude scaling law for lasertrons
[DE88-003880] 09 p1173 N88-17032
Multipass beam breakup in recirculating linacs
[CEBAF-PR-87-007] 12 p1690 N88-20111
Calculation of the efficiency of a resonant cyclotronic electron maser (gyrotrons)
[INPE-4387-PRE/1207] 14 p1915 N88-21444
Results from the SLAC lasertron
[DE88-007816] 20 p2806 N88-26647
Diffraction transition radiation from periodic electron bunches
[AD-A193593] 23 p3280 N88-29528

ELECTRON CAPTURE
Electron capture from solids by positrons
[DE87-011355] 02 p0232 N88-11463
Final (n,l) state-resolved electron capture by multiply charged ions from neutral atoms
[IPPJ-AM-54] 04 p0492 N88-13030
Correlation effects on double electron capture in highly-charged, low-energy ion-atom collisions
[DE87-013179] 07 p0930 N88-15651
Correlation effects on double electron capture in highly-charged, low-energy ion-atom collisions
[DE87-013179] 07 p0930 N88-15651
Total and partial cross sections for electron capture for C(q+) (q = 6-2) and O(q+) (q = 8-2) ions in collisions with H, H2 and He atoms
[IPPJ-AM-56] 09 p1252 N88-17501
Application of ECR ion source beams in atomic physics
[DE88-003767] 10 p1406 N88-18384
A neutral-beam diagnostic for fast confined alpha particles in a burning plasma: Applicatoin on CIT (Compact Ignition Tokamak)
[DE88-004890] 11 p1554 N88-19301
Breathing mode lattice relaxation associated with carrier emission and capture by deep electronic levels in silicon
[DE88-003844] 14 p1985 N88-21842
Selective detection in gas chromatography
[AD-A191499] 18 p2481 N88-24718

ELECTRON COLLISIONS
U ELECTRON SCATTERING

ELECTRON COMPOUNDS
U INTERMETALLICS

ELECTRON COUNTERS
Multichannel electron counter with high space resolution
[DE88-700564] 07 p0857 N88-15204
Design, fabricate, calibrate, test and deliver two satellite electron flux detectors
[AD-A190799] 16 p2169 N88-22930

ELECTRON CYCLOTRON HEATING
ATF (Advanced Toroidal Facility) ECH (Electron Cyclotron Heating) waveguide component development and testing
[DE88-001432] 06 p0782 N88-14797
Activities report of the Institute of Plasma Physics
[ETN-88-91020] 07 p0933 N88-15668
A ray-tracing study of electron cyclotron resonance heating in tokamak plasmas with a superthermal electron tail
[INPE-4381-PRE/1201] 08 p1085 N88-16536
Absorption of electron cyclotron waves by superthermal electron velocity distributions in tokamak plasmas
[INPE-4385-PRE/1205] 08 p1086 N88-16539
Absorption of electron cyclotron radiation in tokamak plasmas with a superthermal tail in the electron velocity distribution
[INPE-4391-PRE/1211] 08 p1086 N88-16541
The effect of asymmetric current-supporting electron velocity distributions on second harmonic electron cyclotron resonance heating: A ray-tracing treatment for the compass tokamak
[INPE-4389-PRE/1209] 08 p1087 N88-16549
New mode conversion process and overdense plasma heating in the electron cyclotron range of frequencies
[IPPJ-854] 10 p1411 N88-18420
First and second harmonic ECRH experience at gyrotron frequencies at LLNL
[DE88-003998] 10 p1413 N88-18430
Trip electrical circuit of the gyrotron
[INPE-4336-NTE/273] 12 p1622 N88-19701
Measurements of optically thin electron cyclotron emission from relativistic electrons
[DE88-004713] 12 p1688 N88-20096
Simulation of electron cyclotron heating in TFR
12 p1693 N88-20130
Electron heat transport in TFR with Electron Cyclotron Resonance Heating (ECRH) 12 p1694 N88-20135
A high field launch for electron cyclotron heating using an external window
[DE88-005350] 13 p1836 N88-21000
Preparing the Alcator C bolometer system for use on MTX (Microwave Tokamak Experiment)
[DE88-006724] 15 p2134 N88-22733
ECRH current drive in tokamak plasmas
[IPPJ-864] 19 p2729 N88-26209
A mode-transforming polarization-rotatable launcher for the ATF (Advanced Toroidal Facility) fusion experiment
[DE88-005070] 19 p2730 N88-26213
A survey of the current experimental database for lower hybrid current-drive and heating
[DE88-009830] 23 p3283 N88-29552
Initial operation and edge plasma studies in ATF (Advanced Toroidal Facility)
[DE88-011400] 23 p3285 N88-29562

ELECTRON DENSITY (CONCENTRATION)
NT CARRIER DENSITY (SOLID STATE)
NT ELECTRON DENSITY PROFILES
NT IONOSPHERIC ELECTRON DENSITY
NT MAGNETOSPHERIC ELECTRON DENSITY
Fast wave injection into high temperature tokamak plasmas in the lower-hybrid-density regime of JIPP T-IIU
[ISSN-0469-4732] 01 p0099 N88-10649
Electron capture from solids by positrons
[DE87-014355] 02 p0232 N88-11463
Enhanced noise and Raman scattering in plasma
[DE87-014466] 02 p0238 N88-11501
Enhanced Thomson scattering from laser plasmas
[DE87-014463] 02 p0238 N88-11503
Loop interaction in the visible emission corona: Morphological details 02 p0256 N88-11622
The effect of object potentials on the wake of a flowing plasma
[AD-A184038] 03 p0379 N88-12385
Equilibrium calculations of ionization in tracer flames
[PB87-104154] 04 p0412 N88-12555
J = O Task Force
[DE88-001326] 04 p0450 N88-12788
Measurement of the electron density and the attachment rate coefficient in silane/helium discharges
[AD-A184268] 04 p0496 N88-13051
EISCAT (European incoherent scatter radar) electron density studies
[AD-A185998] 07 p0841 N88-15099
Interaction between a module cluster and a plasma in a magnetic field
[PB87-148276] 07 p0934 N88-15675
The effect of propane on atomic spectrometric signals in the direct current plasma
[DE88-002457] 07 p0934 N88-15676
Relativistic plasma concentration measuring by Bremsstrahlung
[DE88-700560] 07 p0936 N88-15685
Embedded cluster models for electronic structure and energetics of complex oxides
[DE88-003097] 07 p0938 N88-15702
Absorption of electron cyclotron waves by superthermal electron velocity distributions in tokamak plasmas
[INPE-4385-PRE/1205] 08 p1086 N88-16539
Double layer formed by beam driven ion-acoustic turbulence
[INPE-4292-PRE/1163] 08 p1086 N88-16543
Experimental investigation of double layers formed by ion-acoustic turbulence
[INPE-4296-PRE/1167] 08 p1086 N88-16544
Diagonal and off-diagonal disorder in doped quantum wells
[INPE-4255-PRE/1128] 08 p1089 N88-16556
Minimum necessary intensity of source of preionization for stabilization of a self-sustaining laser discharge with mean power raised by electron beam or X-rays
[PB87-178158] 09 p1171 N88-17024
F-layer polar cap arcs
[AD-A186592] 09 p1190 N88-17127
Chemical activation of molecules by metals: Experimental studies of electron distributions and bonding
[DE88-004465] 10 p1407 N88-18383

Specific heat of novel thin-film material systems
10 p1415 N88-18446

Positron-annihilation 2D-ACAR studies of disordered and defected alloys
[DE88-003118] 10 p1416 N88-18454

Penetration depth measurements of YBa2Cu3O/sub 7-delta/ at 4 MHz
[DE88-003493] 10 p1420 N88-18478

Two-dimensional electron fluid computer calculations of nanosecond pulse, low pressure microwave air breakdown in a rectangular waveguide and their verification by experimental measurement
[DE88-004407] 12 p1618 N88-19678

Measurements of optically thin electron cyclotron emission from relativistic electrons
[DE88-004713] 12 p1688 N88-20096

Large scale plasma irregularities observed in the nighttime ionosphere over Natal using a rocket-borne Langmuir probe
[INPE-4422-PRE/1226] 12 p1694 N88-20139

Upward propagating electric fields from thunderstorms and VLF transmitters 13 p1801 N88-20767

Thomson scattering for determining electron concentrations and temperatures in an inductively coupled plasma. 1: Assessment of the technique for a low-flow, low-power plasma
[AD-A191323] 16 p2280 N88-23651

Thomson scattering for determining electron concentrations and temperatures in an inductively coupled plasma. 2: Description and evaluation of a multichannel instrument
[AD-A191324] 16 p2280 N88-23652

Narrow-band photographic observations of the HII Region S296 in Canis Major 16 p2288 N88-23696

Density diagnostics by hydrogen line intensity ratios: Excitation cross section between excited states
17 p2441 N88-24522

Spectral diagnostics for temperature and density measurements on ATF 17 p2442 N88-24525

Cascade fluorescences from laser-excited lithium atom for plasma diagnostics 17 p2442 N88-24526

The theory of random alloys
[DE88-006408] 18 p2487 N88-24756

A two-wavelength infrared interferometer/polarimeter system for CIT (Compact Ignition Tokamak)
[DE88-007681] 18 p2579 N88-25321

Superthermal electron processes in the upper atmosphere of Uranus: Aurora and electroglow
[NASA-TM-101150] 18 p2594 N88-25417

Simultaneously time- and space-resolved spectroscopic characterization of laser-produced plasmas
[DE88-008038] 19 p2728 N88-26202

All-electron local density theory of electronic structure and superconductivity in YBa2Cu3O7 and YBa2Cu3O6
[DE88-009944] 19 p2735 N88-26246

Megagauss field variation along axis of wire target in laser produced plasma
[DE88-701895] 20 p2859 N88-26979

Ultraviolet-visible spectroscopy of laser-produced aluminum plasmas
[AD-A193004] 20 p2860 N88-26990

Far-infrared studies of doped AlGaAs/GaAs multiple-quantum-well structures
20 p2862 N88-26998

Optical guiding in the separable beam limit
[AD-A192452] 21 p2952 N88-27534

Approximate analytical formulae for electron density and collision frequency in the natural and nuclear-disturbed ionosphere and inner magnetosphere
[AD-A193129] 21 p2972 N88-27654

A study of tunneling phenomena in gallium arsenide aluminum gallium arsenide heterostructures
21 p3023 N88-27946

Linear thyratron
[AD-A194111] 23 p3208 N88-29094

On formulating a simple D-region model
[AD-A195841] 24 p3392 N88-30197

Model representation of electron concentration distribution in outer middle-latitude ionosphere using data from Intercosmos-19 artificial earth satellite
24 p3447 N88-30513

ELECTRON DENSITY PROFILES

Height profile inversion of ionospheric movement from observed parameters of HF radio echoes
03 p0299 N88-11884

Investigations on an RF plasma related to plasma etching
[ETN-88-91366] 06 p0784 N88-14809

Electron acceleration by wave processes in the earth's ionosphere
[AD-A186110] 07 p0877 N88-15320

Comparison of simultaneous MST radar and electron density probe measurements in the polar mesosphere --- Mesospheric, Stratospheric, Tropospheric (MST)
08 p1028 N88-16226

Electron density profile reconstruction by maximum entropy method with multichannel HCN laser interferometer system on SPAC 7
[IPPJ-858] 11 p1553 N88-19295

Arcs in cesium seeded noble gases resulting from a magnetically induced electric field
[EUT-87-E-177] 13 p1843 N88-21028

Support for FY87 midlatitude electron-density calibration campaign
[AD-A190174] 15 p2094 N88-22476

ELECTRON DETECTORS
U ELECTRON COUNTERS

ELECTRON DIFFRACTION

Surface modification by metal deposition and laser irradiation 01 p0023 N88-10148

Energy-selected electron diffraction experiments using the rocking-crystal method in the raster microscope for the investigation of localization effects in single crystals
[ETN-87-90409] 01 p0104 N88-10682

Extending the range of Low Energy Electron Diffraction (LEED) surface structure determination: Co-adsorbed molecules, incommensurate overlayers and alloy surface order studied by new video and electron counting LEED techniques
[DE88-001401] 06 p0786 N88-14820

Solving complex and disordered surface structures with electron diffraction
[DE88-003863] 10 p1418 N88-18467

NBS/Sandia/ICDD electron diffraction database
[DE88-004635] 11 p1454 N88-18665

Recent progress in structure determination by LEED (Low-Energy Electron Diffraction) measure the properties of the deep donors (DX-cent)
[DE88-003851] 13 p1846 N88-21048

Electron diffraction evidence for the ordering of excess nickel atoms by relation to stoichiometry in nickel-rich beta'-NiAl formation of a nickel-aluminum (Ni2Al) superlattices
[NASA-TT-20177] 14 p1890 N88-21297

Fundamental properties and devices applications of Ge(x)Si(1-x)/Si superlattices
[AD-A190129] 15 p2143 N88-22787

On the use of convergent beam electron diffraction for identification of antiphase boundaries in GaAs grown on Si
[DE88-008220] 18 p2585 N88-25362

Diffraction transition radiation from periodic electron bunches
[AD-A193593] 23 p3280 N88-29528

The effect of oriented defects on long-range ordering of hydrocarbon films: Azulene on Pt(111)
[AD-A196089] 24 p3344 N88-29904

ELECTRON DISTRIBUTION
NT ELECTRON DENSITY PROFILES

Self-consistent modification of a fast tail distribution by resonant fields in nonuniform plasmas
[AD-A183790] 01 p0090 N88-10650

The single particle and collective descriptions of the anomalous Doppler resonance and the role of ion dynamics
[INPE-4390-PRE/1210] 08 p0976 N88-15904

Interaction of acoustic and electromagnetic waves involved in anomalous skin effect
08 p1079 N88-16503

The structure of the sideband spectrum in free electron lasers
[AD-A186952] 09 p1170 N88-17015

A moment approach to modeling negative ion sources
[AD-A188858] 12 p1691 N88-20114

Electron temperature measurements in an argon/cesium plasma diode
[AD-A188835] 12 p1695 N88-20141

Hot electron diagnostics using X-ray imaging on GAMMA10 17 p2443 N88-24530

Application of particle simulations to the NRL laser experiment
[AD-A191641] 18 p2520 N88-24953

Observations of electron cyclotron harmonic emissions associated with field-aligned electron beams
[SD-TR-87-33] 19 p2724 N88-26173

On the conjugacy of the aurora: High and low latitudes
[AD-A193008] 20 p2824 N88-26755

Initial electron distributions for free-electron lasers generated by injector and accelerator simulations
[DE88-007022] 21 p2953 N88-27540

ELECTRON EMISSION
NT FIELD EMISSION
NT PHOTOELECTRIC EMISSION
NT SECONDARY EMISSION

Electron emission from conductors subjected to intense, short-pulse electric fields
[DE88-005412] 13 p1836 N88-20985

JPRS report: Science and technology. China
[JPRS-CST-87-041] 14 p1902 N88-21365

Breathing mode lattice relaxation associated with carrier emission and capture by deep electronic levels in silicon
[DE88-003844] 14 p1985 N88-21842

Theoretical model of the cathode spot on a unipolar arc
[AD-A190109] 15 p2059 N88-22277

Question on the measurement of the metal work function in an electron spectrometer by the secondary-electron emission threshold method
[NASA-TT-20190] 16 p2178 N88-22979

Degradation of beam brightness by field emission from a cathode shroud
[DE88-008345] 20 p2794 N88-26576

Effects of secondary electron emission on the collector and source sheaths of a finite ion temperature plasma
[DE88-008930] 20 p2858 N88-26971

Hot electron emission in semiconductors
[AD-A194101] 23 p3292 N88-29601

ELECTRON ENERGY
NT ELECTRON STATES

The optimum illumination conditions for EXELFS studies in a CTEM
[USIP-87-08] 01 p0092 N88-10600

A data analysis package for RDF-determination fromEXELFS-spectra
[USIP-87-07] 01 p0104 N88-10681

EXELFS (Extended Electron Energy Loss Fine Structure) of amorphous and crystalline SiC
[DE87-013551] 02 p0151 N88-10948

Analysis of energy confinement of sideaway discharges
[DE87-753008] 02 p0240 N88-11515

Application of a two fluid theoretical plasma transport model on current Tokamak reactor designs
[DE87-013511] 03 p0377 N88-12373

The effect of object potentials on the wake of a flowing plasma
[AD-A184038] 03 p0379 N88-12385

Methods and first results of plasma non-isothermal parameters measurements in meteor trails
06 p0737 N88-14531

Absorption of cyclotron radiation in skin layer in Araks experiment 08 p1003 N88-16076

Geometric structure, pseudoband gaps, and surface vibrational resonances on metal surfaces
[AD-A187001] 09 p1143 N88-16851

Magnetic control of low pressure discharges
[AD-A186794] 10 p1322 N88-17900

Kinetic studies following state-selective laser excitation
[DE88-004094] 10 p1335 N88-17981

Limiting efficiency of a thermionic diode
[DE88-700598] 11 p1479 N88-18830

Measurements of optically thin electron cyclotron emission from relativistic electrons
[DE88-004713] 12 p1688 N88-20096

Electron temperature measurements in an argon/cesium plasma diode
[AD-A188835] 12 p1695 N88-20141

To what extent is mass loading responsible for the Venus bowshock precursor?
[NASA-TM-89307] 12 p1711 N88-20239

Experimental studies of plasma heating due to the parametric decay of a large amplitude pump into lower hybrid waves 13 p1841 N88-21017

Arcs in cesium seeded noble gases resulting from a magnetically induced electric field
[EUT-87-E-177] 13 p1843 N88-21028

Calculation of the efficiency of a resonant cyclotronic electron maser (gyrotrons)
[INPE-4387-PRE/1207] 14 p1915 N88-21444

Rocket measurements of ionospheric electron temperature over Natal
[INPE-4485-PRE/1250] 15 p2096 N88-22489

Time-resolved spectroscopic measurement of anode plasma in magnetically-insulated diode
16 p2279 N88-23641

Thomson scattering for determining electron concentrations and temperatures in an inductively coupled plasma. 1: Assessment of the technique for a low-flow, low-power plasma
[AD-A191323] 16 p2280 N88-23651

Thomson scattering for determining electron concentrations and temperatures in an inductively coupled plasma. 2: Description and evaluation of a multichannel instrument
[AD-A191324] 16 p2280 N88-23652

Spectral diagnostics for temperature and density measurements on ATF 17 p2442 N88-24525

Hot electron diagnostics using X-ray imaging on GAMMA10 17 p2443 N88-24530

The Io sulfur torus in 1981
[NASA-TM-101130] 18 p2595 N88-25419

Outer zone electron precipitation produced by a VLF transmitter
[AD-A191944] 19 p2691 N88-25893

Properties of hydrogen/helium accretion plasmas
[DE88-006831] 19 p2728 N88-26197
Thermal inhibition by megagauss field due to variation of electron temperature in laser plasma
[DE88-701887] 20 p2859 N88-26977
Studying the physics and operation of multi-terminal near-micron and sub-micron length, hot electron semiconductor devices
[AD-A193380] 21 p2938 N88-27446
A study of tunneling phenomena in gallium arsenide-aluminum gallium arsenide heterostructures
21 p3023 N88-27946

ELECTRON FLUX
U ELECTRONS
U FLUX (RATE)

ELECTRON FLUX DENSITY
Field-aligned fluxes of energetic electrons related to the onset of magnetospheric substorms
08 p1096 N88-16595
Observations and analyses of summer whistlers at the Great Wall Station of Antarctica
11 p1469 N88-18759

ELECTRON GAS
Effect of collisional broadening on the polarizability of a two-dimensional electron gas
[DE87-013928] 02 p0237 N88-11497
Theory of the one- and two-dimensional electron gas
[DE87-012864] 02 p0244 N88-11540
Self-similar solutions of MHD equations of plasma filament in the case of complete degenerated ultrarelativistic electron gas
[DE88-700684] 10 p1412 N88-18426
Electrical resistivity as quantum chaos
[DE88-007026] 16 p2284 N88-23675

ELECTRON GUNS
Gyrotron development at the Instituto de Pesquisas Espaciais
[INPE-4240-PRE/1115] 08 p0990 N88-15992
Synthesis method applied to the design of an electron gun for a gyrotron
[INPE-4357-TDL/298] 13 p1773 N88-20007
Development of electrostatic-accelerator free-electron lasers
[AD-A189507] 13 p1774 N88-20614
Modulatable thin film field emission space gun
[AD-A189279] 13 p1845 N88-21043
Survey of the Air Force P78-2 (SCATHA) satellite plasma wave data during electron gun operations
[AD-A191014] 16 p2168 N88-22926

ELECTRON IMPACT
Simulation of tokamak runaway-electron events. Study of the response of materials by use of an electron linear accelerator
[IPPJ-841] 02 p0242 N88-11528
Atomic data for hydrogens in collisions with electrons. Addenda
[IPPJ-AM-55-ADD] 09 p1252 N88-17502
Contributions of autoionizing resonances to the electron collisional excitation rates for Be-like ions
[AD-A190924] 18 p2572 N88-25275
Development of the field-induced electron injection and impact ionization (F4I) technique for radiation hardness testing of MOS (Metal-Oxide-Semiconductor) gate insulators
[AD-A192114] 18 p2583 N88-25345
Electron impact ionization cross-section of some organic compounds
[DE88-702044] 23 p3280 N88-29525
Ion kinetics in silane plasmas
[AD-A196202] 24 p3431 N88-30423

ELECTRON INTENSITY
U ELECTRON FLUX DENSITY

ELECTRON INTERACTIONS
U ELECTRON SCATTERING

ELECTRON IONIZATION
U IONIZATION

ELECTRON IRRADIATION
Effects of 67.5 MeV electron irradiation on Y-Ba-Cu-O and Gd-Ba-Cu-O high-temperature superconductors
[AD-A191271] 16 p2283 N88-23669
Electron irradiation effects in YBa2Cu3O7-Delta single crystals
[DE88-010050] 20 p2878 N88-27085
Muon-spin rotation experiment (micro + SR) on aluminum and indium after low temperature electron irradiation
[ETN-88-92985] 23 p3294 N88-29617

ELECTRON MICROSCOPES
Electron sputtering in the analytical electron microscope. Calculations and experimental data
[DE87-011457] 01 p0049 N88-10312
Development of methods for low temperature diffusion bonding
[AD-A186875] 09 p1174 N88-17033
The measurement of chemical compositon with high spatial resolution using a dedicated scanning transmission electron microscope
[AERE-R-12317] 10 p1297 N88-17753
The contribution of electron microscopy of materials science to society
[DE88-006341] 15 p2028 N88-22082
In situ fatigue loading stage inside scanning electron microscope 15 p2083 N88-22419
Equipment for an advanced electron beam lithography system
[AD-A192956] 21 p2936 N88-27435

ELECTRON MICROSCOPY
Contribution to the study of the Ti-Al phase diagram by conventional and high resolution electron microscopy
[ESA-TT-1021] 01 p0023 N88-10143
Si - SiO2 interfaces. A High Resolution Transmission Electron Microscopy (HRTEM) study
[DE87-012255] 01 p0028 N88-10181
Detective quantum efficiency and design of a parallel data recording system for EXELFS-measurements -- electron microscopy
[USIP-87-06] 01 p0050 N88-10318
The optimum illumination conditions for EXELFS studies in a CTEM
[USIP-87-08] 01 p0092 N88-10600
Instrumental and operational aspects of an EXELFS system connected to JEOL 100C STEM
[USIP-87-09] 01 p0092 N88-10601
Energy-selected electron diffraction experiments using the rocking-crystal method in the raster microscope for the investigation of localization effects in single crystals
[ETN-87-90409] 01 p0104 N88-10682
Analytical electron microscopy characterization of boron in sintered alpha-SiC
[DE87-012532] 02 p0142 N88-10889
Study of the morphology of thermosetting matrices
[ONERA-RT-5/3346-M] 02 p0153 N88-10961
Solute segregation to phase interfaces and grain boundaries: Studies by analytical electron microscopy and profile deconvolution
[DE87-012129] 02 p0243 N88-11537
Modified 14Cr-16Ni stainless steels with improved creep resistance at 700 C due to tailored precipitate microstructures
[DE87-014788] 03 p0290 N88-11825
Fractographic study of fiber composites
06 p0677 N88-14146
Effect of temperature exposure on fatigue crack propagation 06 p0720 N88-14421
Atomic-level studies of superconducting YBa2Cu3O sub 7-x
[DE88-002522] 06 p0788 N88-14831
Study on the correlation of polystyrene (PS) film craze to its fracture behaviour by TEM (Transmission Electron Microscopy)
[PB87-143343] 08 p0970 N88-15870
Characterization of duplex stainless steel by TEM (Transmission Electron Microscopy), SANS (Small Angle Neutron Scattering) and APFIM (Atom-Probe Field Ion Microscopy) techniques
[DE88-002916] 09 p1145 N88-16865
Calculated sputtering and atomic displacement cross-sections for applications to medium voltage analytical electron microscopy
[DE88-002904] 09 p1168 N88-17006
Optimization of imaging energy filters for analytical electron microscopy
[ETN-88-91079] 09 p1248 N88-17483
High resolution electron and ion microscopy
[AERE-R-12502] 10 p1297 N88-17754
Transmission electron microscopy studies of titanium-containing braze/alumina seals
[DE88-005243] 10 p1303 N88-17792
Application of nondestructive testing techniques to materials testing
[AD-A187645] 10 p1342 N88-18021
Simulation and processing of high resolution images of defects and interfaces in superconducting YBa2Cu3O7
[DE88-003856] 10 p1420 N88-18480
Electron tunneling microscopy
[AD-A187426] 11 p1452 N88-18652
Structural characterization of undoped and doped GaAs. A comparative study of four techniques
[DE88-004552] 11 p1555 N88-19304
Electron microscopy study of morphology and composition of a ferrisilicate catalyst
[DE88-005754] 11 p1562 N88-19352
Examination of polysulfide sealants by scanning electron microscopy
[MRL-R-1096] 13 p1752 N88-20478
Improved methods for high resolution electron microscopy
[DE88-005731] 13 p1774 N88-20609
Electron beam sensitive devices for controllability
[RR-658-1] 14 p1908 N88-21403
New method of examining micrononhomogeneity of local centers in high-resistivity semiconductor materials under scanning electron microscope 14 p1969 N88-21754
Brillouin scattering and transmission electron microscopy studies of radiation-induced elastic softening, disordering and amorphization of intermetallic compounds
[DE88-005927] 14 p1987 N88-21850
Grain boundaries
[DE88-006628] 14 p1987 N88-21852
The contribution of electron microscopy of materials science to society
[DE88-006341] 15 p2028 N88-22082
An investigation of the crystalchemistry and thermochemistry of selected mineral systems
[AD-A189758] 15 p2142 N88-22781
Interface characterization of Cu-Cu and Cu-Ag-Cu low temperature solid state bonds
[AD-A191015] 16 p2283 N88-23667
SHaRE: Collaborative materials science research
[DE88-007175] 18 p2467 N88-24646
Electron microscopy of ceramic superconductors
[DE88-006446] 23 p3288 N88-29580
Degradation of protective coatings on steel in corrosive environments 24 p3354 N88-29969
Scanning electron microscopy study of adhesion in sea urchin blastulae
[NASA-CR-182136] 24 p3406 N88-30275

ELECTRON MOBILITY
Effect of collisional broadening on the polarizability of a two-dimensional electron gas
[DE87-013928] 02 p0237 N88-11497
Transport coefficients close to the mobility edge and nonlinear sigma model composite operators -- electron transport
[PREPRINT-541] 06 p0777 N88-14767
Thermodynamic and conductivity studies of nonstoichiometric cerium dioxide by Coulometric titration: A simultaneous measurement
[DE88-003054] 08 p1091 N88-16566
Defects in high mobility semiconductor systems
[AD-A191618] 19 p2732 N88-26224
Transport study on Si/Si(1-x)Ge(x) superlattices selectively doped by secondary implantation of Sb
20 p2867 N88-27027
A GaAs solid state device model for high power applications
[DE88-011320] 21 p2939 N88-27457

ELECTRON MULTIPLIERS
U PHOTOMULTIPLIER TUBES

ELECTRON OPTICS
Optimization of imaging energy filters for analytical electron microscopy
[ETN-88-91079] 09 p1248 N88-17483
GERA computer code for calculation of two-dimensional electromagnetic fields in resonators and electron-optical systems by the finite element method
[DE88-700678] 11 p1480 N88-18831
Advanced electron optics for vibrational spectroscopy
[AD-A188469] 12 p1629 N88-19747
The new UCSB (University of California, Santa Barbara) compact far-infrared FEL
[AD-A190864] 16 p2212 N88-23203

ELECTRON ORBITALS
Core-core and core-valence correlation
[NASA-CR-182552] 11 p1544 N88-19226
Theoretical studies of the potential surface for the F + H2 greater than HF + H reaction
[NASA-CR-182551] 11 p1557 N88-19319
Numerical simulations of multiphoton processes in many electron atoms
[DE88-003293] 13 p1837 N88-20990

ELECTRON OSCILLATIONS
Tapered wiggler analysis of high gain free electron laser oscillators
[AD-A187997] 10 p1338 N88-17997
Research on a two-stage free electron laser oscillator
[AD-A195991] 24 p3377 N88-30115

ELECTRON PARAMAGNETIC RESONANCE
Formation and passivation of new paramagnetic defects associated with thermal oxides on silicon
[DE88-002720] 07 p0938 N88-15699
Electron Spin Resonance (ESR) measurements on intermediate-valence Ce: compounds doped with paramagnetic ions: CeOs2 Gd ion and CePd3 Mn-ion
[ETN-88-91081] 09 p1256 N88-17526
Electron paramagnetic resonance studies of Mn(2+) in 2-6 semiconductor alloys 11 p1560 N88-19340
Excitations in magnetic low-dimensional systems. A spectroscopic study
[ETN-88-92230] 15 p2129 N88-22697
Structure and function of the manganese complex involved in photosynthetic oxygen evolution determined by X-ray adsorption spectroscopy and electron paramagnetic resonance spectroscopy
[DE88-010360] 21 p2985 N88-27725

Paramagnetic point defects in boron-implanted HgO.7CdO.3Te
[AD-A193276] 21 p3021 N88-27934
Photorefractive damage mechanism in electro-optic materials
[AD-A194560] 23 p3282 N88-29543
Chemical kinetics of hydrogen and P(sub b) centers
[DE88-010528] 23 p3291 N88-29594

ELECTRON PATHS
U ELECTRON TRAJECTORIES

ELECTRON PHONON INTERACTIONS
Properties of superconductors with strong electron-phonon interaction 14 p1974 N88-21779
Electron-Rayleigh wave interaction in thin film carbons
[AD-A191727] 18 p2492 N88-24781
Electron-phonon interactions in In(0.53)Ga(0.47)As and in In(0.53)Ga(0.47)As/InP quantum wells
20 p2869 N88-27037
Hot electrons in silicon dioxide: Ballistic to steady-state transport 20 p2871 N88-27042
The theory of electron-polar phonon scattering rates in semiconductor micro-structures
20 p2871 N88-27043
Anharmonic model for high-Tc superconductors
[DE88-702196] 21 p3020 N88-27924

ELECTRON PHOTON CASCADES
Energy cascading in the beat-wave accelerator
[DE87-014727] 03 p0377 N88-12374
Model-independent requirements to the source of positrons in the galactic centre
[DE88-700968] 14 p1992 N88-21874
Cascade fluorescences from laser-excited lithium atom for plasma diagnostics 17 p2442 N88-24526

ELECTRON PLASMA
Nonlinear, relativistic Langmuir waves in astrophysical magnetospheres
[NASA-CR-182422] 08 p1024 N88-16197
Self-similar solutions of MHD equations of plasma filament in the case of complete degenerated ultrarelativistic electron gas
[DE88-700684] 10 p1412 N88-18426
Electron heat transport in TFR with Electron Cyclotron Resonance Heating (ECRH) 12 p1694 N88-20135
Arcs in cesium seeded noble gases resulting from a magnetically induced electric field
[EUT-87-E-177] 13 p1843 N88-21028
The foreshock region upstream from the Comet Halley bow shock 14 p1995 N88-21893
Measurement of time evolution of plasma electron component parameters on the Ogra-4 device by the Thomson scattering method
[DE88-701575] 16 p2282 N88-23662
Nonlinear optical properties and subpicosecond dynamics of excitons and electron-hole plasmas in multiple quantum well structures
[AD-A191926] 19 p2727 N88-26196
Alternative analysis of CO2-laser-produced plasma waves
[DE88-006434] 19 p2730 N88-26215

ELECTRON PRECIPITATION
Configurations of the quiet polar cap and its response to a sudden increase of the energy input rate epsilon
[DMI-GEOPHYS-PAPERS-R-74]
03 p0350 N88-12210
Relativistic electron precipitations in a pulsating aurora
04 p0468 N88-12894
First results from the Viking associated Aureld-VIP rocket and EISCAT campaign --- auroras, Swedish satellite
08 p1026 N88-16211
Spectrophotometric remote sensing of the diffuse aurora
[AD-A188599] 12 p1643 N88-19837
Stimulated Emission of Energetic Particles (SEEP)
[AD-A188724] 13 p1853 N88-21094
The Jovian aurora: Electron or ion precipitation
[NASA-TM-101153] 17 p2452 N88-24566
Outer zone electron precipitation produced by a VLF transmitter
[AD-A191944] 19 p2691 N88-25993
Rocket measurements within a polar cap arc: Ionospheric modelling
[AD-A192381] 20 p2824 N88-26754
On the conjugacy of the aurora: High and low latitudes
[AD-A193008] 20 p2824 N88-26755
Investigation of the potential impact of new photonic materials on optical processing systems
21 p2924 N88-27359
The low-latitude auroral boundary: Steady-state and time-dependent representations
[AD-A193200] 21 p2972 N88-27656

ELECTRON PROBES
Quantitative electron probe microanalysis investigation of the oxidation of high temperature alloys at low oxygen partial pressures
[JUEL-2120] 03 p0288 N88-11811

ELECTRON PUMPING
Electron acceleration by wave processes in the earth's ionosphere
[AD-A186110] 07 p0877 N88-15320
Generation of light pulses in semiconductor laser upon excitation by several electron beams
07 p0920 N88-15589
Nuclear excitation via the motion of electrons in a strong laser field
[AD-A187166] 09 p1171 N88-17017
Semiconductor laser with electron-beam pumping and fiber-optic output waveguide 09 p1235 N88-17405
High-efficiency GaAs semiconductor laser with longitudinal excitation by scanning electron beam
09 p1238 N88-17421
Periodic-pulse semiconductor laser with electron-beam pumping 09 p1238 N88-17422
X-ray lasers: State of art and prospect
[ETN-88-92003] 14 p1914 N88-21434
Blue-green laser diode research program
[AD-A191980] 23 p3218 N88-29153
Proof of the feasibility of coherent and incoherent schemes for pumping a gamma-ray laser
[AD-A193856] 23 p3220 N88-29165

ELECTRON RADIATION
NT BETA PARTICLES
NT ELECTRON BEAMS
NT RELATIVISTIC ELECTRON BEAMS

ELECTRON RECOMBINATION
NT RADIATIVE RECOMBINATION

ELECTRON RING ACCELERATORS
U STORAGE RINGS (PARTICLE ACCELERATORS)

ELECTRON SCATTERING
Ab initio methods for electron-molecule collisions
[DE87-011728] 01 p0092 N88-10598
Electron interactions with nuclei
[DE87-014587] 02 p0232 N88-11460
Complex scattering dynamics and the integer quantum Hall effect
[DE87-011790] 02 p0243 N88-11536
Extending the range of Low Energy Electron Diffraction (LEED) surface structure determination: Co-adsorbed molecules, incommensurate overlayers and alloy surface order studied by new video and electron counting LEED techniques
[DE88-001401] 06 p0786 N88-14820
Electron scattering off palladium isotopes: An investigation of the equivalence of the anharmonic vibrator model and the interacting boson model
[B8671274] 07 p0931 N88-15654
Hyperspherical coordinate theory of two-electron processes: Future plans
[DE87-010653] 08 p1081 N88-16516
Group 2A metastable collision complexes: Spectroscopy and behavior in intense radiation fields
[AD-A186737] 08 p1082 N88-16524
Semiclassical theory of the nuclear response function. Quasielastic electron scattering
[ETN-88-91082] 09 p1245 N88-17459
Investigation of a new magnetic dipole mode in the heavy, deformed nuclei 154 Sm, 156 Gd, 158 Gd, 164 Dy, 168 Er, and 174 Yb with high resolution electron scattering
[ETN-88-91084] 09 p1245 N88-17460
A research program in neutrino physics, cosmic rays and elementary particles
[DE88-003507] 09 p1264 N88-17575
Correlated processes in atomic collisions
[DE88-003508] 10 p1406 N88-18383
Generalised scattering model for the quantum modulation of electrons 11 p1563 N88-19357
Photohydrodynamical processes near compact objects
11 p1569 N88-19390
Advanced electron optics for vibrational spectroscopy
[AD-A188469] 12 p1629 N88-19747
Experimental set-up for measurements of Compton scattering cross section on light nuclei
[DE88-700161] 12 p1688 N88-20097
Models of recombination lines in radio H2 regions
[INPE-4302-TDL/277] 12 p1710 N88-20232
Electron stimulated desorption and coherent electron scattering
[AD-A189091] 13 p1835 N88-20978
Renormalized Fermi liquid theory for disordered electron systems and the metal-insulator transition
[NOTA-INTERNA-900] 14 p1988 N88-21862
Effective electron interactions due to virtual charge and spin excitations in an extended Hubbard model for Cu-O superconductors
[DE88-005971] 15 p2139 N88-22766
An electron-scattering study of N-15
[ETN-88-92479] 16 p2266 N88-23552
Measurement of time evolution of plasma electron component parameters on the Ogra-4 device by the Thomson scattering method
[DE88-701575] 16 p2282 N88-23662
Distorted-wave-method calculation of electron-impact excitation of atomic ions 17 p2443 N88-24532
Trochoidal analysis of scattered electrons in a merged electron-ion beam
[NASA-CASE-NPO-16789-1-CU]
18 p2573 N88-25281
Ion and electron interactions of atmospheric importance
[AD-A192255] 20 p2824 N88-26751
Inelastic electron scattering and electron-hole excitations in iron and nickel
[DE88-011643] 21 p2915 N88-27303
Nonlinear dynamics of the electron self-field interaction
[DE88-010597] 21 p2934 N88-27420
Self energy corrections to the ab initio band structures: Chromium
[DE88-701825] 21 p3020 N88-27927
Effect of a laser field in the electron inelastic scattering into plasma fields
[DE88-702295] 23 p3218 N88-29157
On selection rules and inelastic electron scattering at intermediate energies
[DE88-701833] 23 p3280 N88-29526
Dispersion effects in elastic electron scattering from C12
[B8805297] 23 p3281 N88-29536

ELECTRON SOURCES
Higher harmonic generation in the induced resonance electron cyclotron maser
[AD-A186236] 07 p0858 N88-15210
The measurement of chemical compositon with high spatial resolution using a dedicated scanning transmission electron microscope
[AERE-R-12317] 10 p1297 N88-17753
X-ray source model for Z-pinch aluminum plasmas
[AD-A189509] 12 p1696 N88-20148
Program to research laser-driven thermionic electron sources for free electron lasers
[AD-A190473] 15 p2072 N88-22353
Optical guiding in the separable beam limit
[AD-A192452] 21 p2952 N88-27534

ELECTRON SPECTROSCOPY
Application of spin-sensitive electron spectroscopies to investigations of electronic and magnetic properties of solid surfaces and epitaxial systems
[DE87-014235] 02 p0245 N88-11550
Multichannel electron counter with high space resolution
[DE88-700564] 07 p0857 N88-15204
Near threshold behavior of photoelectron satellite intensities
[DE88-002231] 08 p1081 N88-16512
Studies of the electron spectrum with reference to the clean surfaces of iron, cobalt and nickel and their subsequent exposure to oxygen
11 p1459 N88-18700
An electron spectroscopic investigation of high-temperature superconducting oxides
[DE88-003807] 11 p1558 N88-19325
An interpretation of the ethylenic, carbidic, and graphite auger lineshapes of chemisorbed carbon species
[AD-A189092] 13 p1736 N88-20379
Question on the measurement of the metal work function in an electron spectrometer by the secondary-electron emission threshold method
[NASA-TT-20190] 16 p2178 N88-22979
Interface characterization of Cu-Cu and Cu-Ag-Cu low temperature solid state bonds
[AD-A191015] 16 p2283 N88-23667
Ballistic transport and hot electron spectroscopy in Tunneling Hot Electron Transfer Amplifier (THETA)
19 p2659 N88-25808
Resonant tunneling electron spectroscopy
19 p2660 N88-25811
An IETS (Inelastic Electron Tunneling Spectroscopy) study of surface reactions applicable to adhesion
[AD-A192274] 21 p2909 N88-27261
Application of Auger electron spectroscopy to the study of trace element effects on weldability
[DE88-010457] 21 p2915 N88-27301

ELECTRON SPIN RESONANCE
U ELECTRON PARAMAGNETIC RESONANCE

ELECTRON STATES
Nitrogen energy transfer study
[AD-A184457] 04 p0464 N88-12869
Effect of rapid solidification on short range order: A magnetic study
[AD-A185216] 05 p0565 N88-13444
Density of states of electrons bound to impurities in quantum wells of GaAlAs/GaAs
[INPE-4257-PRE/1130] 08 p1089 N88-16557
Energy disposal in ion-molecule reactions
[AD-A186772] 09 p1171 N88-17019

Electronic and chemical structure of 3-5/metal and Si/metal interfaces
[AD-A186579] 09 p1254 N88-17518
Clusters: Link between molecules and solids
[AD-A188170] 11 p1543 N88-19224
Investigation of multiple particle final states at CEBAF (Continuous Electron Beam Accelerator Facility)
[CEBAF-PR-87-026] 11 p1547 N88-19250
Photoenhanced attachment for optical control of diffuse discharges
[AD-A188989] 12 p1696 N88-20147
Overview of hydrogen clusters
16 p2267 N88-23557
Direct subpicosecond measurement of carrier mobility of photoexcited electrons in GaAs
19 p2659 N88-25803
Monte Carlo investigation of hot photoexcited electron relaxation in GaAs 19 p2659 N88-25805
Charge storage and switching phenomena in metal complexes
[AD-A193778] 23 p3192 N88-28996
Electronic states of the Xe(sub n)HCl systems in gas and condensed phases
[AD-A193881] 23 p3192 N88-28997
Theoretical investigation of image states of the hydrogen covered Cu (100)
[DE88-702662] 23 p3292 N88-29604

ELECTRON SWEEPING
U SWEEP FREQUENCY

ELECTRON TELESCOPES
U PARTICLE TELESCOPES

ELECTRON TEMPERATURE
U ELECTRON ENERGY

ELECTRON TRAJECTORIES
Trajectory versus PIC methods in diode design
[DE87-012135] 02 p0166 N88-11043

ELECTRON TRANSFER
Monte Carlo simulation of primitive atom-transfer reactions in solution
[AD-A183977] 03 p0375 N88-12360
Vectorial electron transfer on designed surfaces
[PB87-232229] 03 p0381 N88-12394
A strategy to determine the transition state of an electron transfer reaction
[AD-A183976] 03 p0382 N88-12404
K-CO on transition metals: A local ionic interaction
[AD-A184342] 04 p0496 N88-13056
The role of electronic structure calculation in mechanistic analysis of electron transfer reactions in the liquid phase
[DE87-014395] 05 p0647 N88-13963
Photoinduced charge separation by polymer-bound chromophores
[DE88-002101] 06 p0685 N88-14198
Artificial photosynthesis using chlorophyll based carotenoid-quinone triads
[DE88-001660] 07 p0884 N88-15362
Effects of energy, distance and orientation on electron transfer rates studied by pulse radiolysis in organic media
[DE88-002906] 08 p1082 N88-16521
Insights into the mechanisms of chemical reactions: Reaction paths for chemical reactions
[DE88-003041] 10 p1297 N88-17755
Energy transfer and photochemistry in biomimetic solar conversion
[PB88-130026] 10 p1348 N88-18057
Correlated processes in atomic collisions
[DE88-003508] 10 p1406 N88-18383
Electron transfer to iron(3) oxide colloids
[DE88-002885] 10 p1416 N88-18448
Mechanisms of photoinduced electron transfer
[DE88-004917] 13 p1836 N88-20983
Electrochemistry in near-critical and supercritical fluids. 5: The dimerization of quinoline and acridine radical anions and dianions in ammonia from -70 C to 150 C
[AD-A190858] 16 p2175 N88-22967
Spectroscopic data relevant to alpha particle diagnostics 17 p2442 N88-24527
Electrode films of porous agarose: The effects of physical structure on electron transport processes
[DE88-007366] 19 p2611 N88-25493
Ballistic transport and hot electron spectroscopy in Tunneling Hot Electron Transfer Amplifier (THETA)
19 p2659 N88-25808
Mechanisms of photochemical energy conversion by chlorophyll
[DE88-008763] 20 p2819 N88-26725
Ferromagnetic/semiconductor hybrid structures
20 p2865 N88-27013
Hot electrons in silicon dioxide: Ballistic to steady-state transport 20 p2871 N88-27042
Vertical electronic transport in novel semiconductor heterojunction structures 20 p2871 N88-27045
Factors governing light driven electron and proton translocation in proteins across membranes
[DE88-011120] 21 p2984 N88-27724
Studies of photochemically and electrochemically driven electron transport in zeolites
[DE88-008644] 22 p3155 N88-28769
Electrochemical and optical studies of model photosynthetic systems
[DE88-009291] 23 p3237 N88-29264
Cytochrome electron transfer and biomolecular electronics
[AD-A195482] 24 p3406 N88-30277

ELECTRON TRANSITIONS
Gaining control over rare earth valence fluctuations
[DE87-010116] 01 p0103 N88-10671
A strategy to determine the transition state of an electron transfer reaction
[AD-A183976] 03 p0382 N88-12404
XUV emission features from the Livermore soft X-ray laser experiments
[DE88-000420] 04 p0448 N88-12779
J = O Task Force
[DE88-001326] 04 p0450 N88-12788
Wavelengths of the 3p-3d transitions of the Co- and Fe-like ions: The effects of electron correlation
[DE88-000219] 04 p0498 N88-13067
Nitrogen scale-up
[AD-A185702] 06 p0709 N88-14351
Thermoelectric power in disordered electronic systems near the Anderson transition
[PREPRINT-547] 06 p0731 N88-14494
Experimental observation of photoresonance of electrons localized above surface of solid hydrogen
06 p0774 N88-14755
Electronic band structure and photoemission: A review and projection
[DE88-002236] 06 p0787 N88-14829
Electron scattering off palladium isotopes: An investigation of the equivalence of the anharmonic vibrator model and the interacting boson model
[B8671274] 07 p0931 N88-15654
Theoretical studies of atomic transitions
[DE88-004719] 10 p1407 N88-18389
Nuclear transitions induced by atomic excitations
[DE88-004311] 11 p1545 N88-19239
Correlations between photons in resonance fluorescence emitted by an atom near a metal surface
[AD-A188365] 12 p1689 N88-20102
Macroscopic quantum jumps in a single atom
14 p1975 N88-21784
Laser cooling of neon metastable states
14 p1975 N88-21785
Theoretical studies of solar-pumped lasers
[NASA-CR-182929] 17 p2344 N88-23971
Transition probabilities in OH A 2 sigma + - X 2 pi c: Bands with v prime = 0 and 1, v double prime = 0 to 4
[NASA-CR-182946] 18 p2584 N88-25353
Inner-shell X-ray line spectra of highly ionized titanium, chromium, iron and nickel and their appliation to laboratory plasmas
[PB87-225181] 19 p2730 N88-26212

ELECTRON TUBES
NT CATHODE RAY TUBES
NT COLD CATHODE TUBES
NT CYCLOTRON RESONANCE DEVICES
NT GAS DISCHARGE TUBES
NT IMAGE DISSECTOR TUBES
NT IMAGE TUBES
NT KLYSTRONS
NT MAGNETRONS
NT MICROWAVE TUBES
NT PHOTOMULTIPLIER TUBES
NT THERMIONIC DIODES
NT THYRATRONS
NT TRAVELING WAVE TUBES
NT VIDICONS

ELECTRON TUNNELING
Superconducting properties of metallic superlattices
[DE87-012725] 01 p0023 N88-10146
Vacuum ultraviolet electronic properties of liquids
[DE88-000165] 03 p0282 N88-11772
Monte Carlo simulation of primitive atom-transfer reactions in solution
[AD-A183977] 03 p0375 N88-12360
Studies of tunneling in metals under high pressure
06 p0775 N88-14757
Macroscopic quantum effects in a Josephson tunnel junction
[DE88-002239] 06 p0787 N88-14830
Some investigations of molecular beam epitaxial growth of 3-5 semiconductor films via Monte-Carlo computer simulations, carrier tunnelling and spectroscopic ellipsometry
[AD-A185520] 06 p0789 N88-14839
Experimental aspects of high-T/sub c/ superconductors
[DE88-003019] 08 p1090 N88-16564
Properties of superconducting tunnel structures in microwave radiation field 09 p1239 N88-17424
Electron tunneling microscopy
[AD-A187426] 11 p1452 N88-18652
Joint services electronics program
[AD-A188173] 11 p1478 N88-18822
The physics of very small structures
[AD-A187672] 11 p1556 N88-19311
Microelectronic applications of the conductor-thin insulator-semiconductor (CIS) structure
11 p1560 N88-19341
Dynamical aspects of carrier tunneling in semiconductor superlattices 14 p1977 N88-21799
Long-time tunneling in amorphous metals at helium temperatures
[DE88-701150] 16 p2281 N88-23654
Local density of states in double-barrier resonant tunneling structures
[AD-A190673] 16 p2281 N88-23656
A proposed Quantum Well Injection Transit Time device (QWITT) 1[illegible] p2657 N88-25785
Ballistic transport and hot electron spectroscopy in Tunneling Hot Electron Transfer Amplifier (THETA)
19 p2659 N88-25808
Microwave and millimeter-wave resonant tunneling diodes 19 p2659 N88-25809
Resonant tunneling electron spectroscopy
19 p2660 N88-25811
Electron device probing in the femtosecond time scale
19 p2660 N88-25821
Electron tunneling in junctions doped with semiconductors and metals 19 p2734 N88-26236
Third International Conference on Superlattices, Microstructures and Microdevices
[AD-A191416] 20 p2861 N88-26995
Theoretical aspects of electron transport in modulated structures 20 p2865 N88-27016
Resonant tunneling transistors and resonant tunneling hot electron spectroscopy 20 p2866 N88-27018
Pressure-dependent measurement on n + GaAs (Si, Sn): The effect of deep donor (DX) states on the electrical properties and presistent photoconductivity effects
20 p2866 N88-27020
Resonant tunneling in InGaAs-InP double-barrier structures and superlattices 20 p2871 N88-27047
Excellent negative differential resistance of InGaAs/InAlAs resonant tunneling barrier structures and applications to a new functional device, RHET
20 p2872 N88-27048
Pure metallic bridge and point-contact tunneling into single- and polycrystal YBa2Cu3O(sub 7-y)
[DE88-010030] 20 p2878 N88-27084
An IETS (Inelastic Electron Tunneling Spectroscopy) study of surface reactions applicable to adhesion
[AD-A192274] 21 p2909 N88-27261
Solar energy conversion through the interaction of plasmons with tunnel junctions. Part A: Solar cell analysis. Part B: Photoconductor analysis
[NASA-CR-183044] 21 p2967 N88-27621
A study of tunneling phenomena in gallium arsenide-aluminum gallium arsenide heterostructures
21 p3023 N88-27946
Tunnelling currents in reverse biased CMT photodiodes
[RSRE-MEMO-4137] 23 p3209 N88-29097

ELECTRON-HOLE DROPS
Free carrier nonlinear optics 14 p1977 N88-21796

ELECTRON-ION RECOMBINATION
NT RADIATIVE RECOMBINATION
Molecular sources of ionospheric holes
[AD-A191857] 18 p2541 N88-25082

ELECTRON-POSITRON ANNIHILATION
U POSITRON ANNIHILATION

ELECTRON-POSITRON PAIRS
Vector boson pair production in e(+)e(-) collisions
[PREPRINT-549] 06 p0778 N88-14774
Electronic factors for K-shell-electron conversion probability and electron-positron pair formation probability in electric monopole transitions
[DE87-753040] 08 p1089 N88-16551

ELECTRONIC AIRCRAFT
Testing of the engine compartment fire extinguishing system in the F/EF-111 aircraft
[AD-A188801] 12 p1576 N88-19423

ELECTRONIC AMPLIFIERS
U AMPLIFIERS

ELECTRONIC CONTROL
Engine/airframe response evaluation of the HH-60A helicopter equipped with the T700-GE-701 transient droop improvement electronic control unit
[AD-A184443] 04 p0401 N88-12492
Radio frequency electromagnetic interference fields: A study in Swedish industry
[FOA-E-30007-3.3] 06 p0692 N88-14247
Faraday cup characterization of electron beam welding parameters
[DE88-001896] 07 p0864 N88-15241

Pumping systems and flow interfaces for rapid response electronic reheat controls 10 p1282 N88-17665

Photo-optical converter of angular displacements in digital servomechanisms
[DE87-703208] 14 p1961 N88-21698

The design of an intelligent multidisk control module for VME bus based systems
[AD-A195587] 24 p3411 N88-30303

ELECTRONIC COUNTERMEASURES
NT ANTIRADAR COATINGS

A study of infrared missile seekers and the countermeasure techniques employed to defeat them
[ETN-87-90927] 02 p0131 N88-10822

Airborne bistatic radar applications
[ETN-87-90930] 02 p0163 N88-11020

JPRS report: Science and technology. China
[JPRS-CST-87-031] 03 p0299 N88-11880

Efficiency analysis of airborne Electronic CounterMeasures (ECM) systems
[AD-A184606] 03 p0306 N88-11934

A Gram-Schmidt space-time adaptive canceller using adaptive lattice filters
[AD-A189684] 14 p1959 N88-21684

High speed transcendental elementary function architecture in support of the Vector Wave Equation (VWE)
[AD-A189746] 15 p2119 N88-22627

Acta aeronautica et astronautica sinica (selected articles)
[AD-A191552] 18 p2455 N88-24575

Computation of ECM (Electronic Counter-Measures) war reserve materiel spare requirements
[AD-A193301] 21 p2897 N88-27195

Sidelobe level of an adaptive array using the SMI (Sampled Matrix Inversion) algorithm
[AD-A193131] 21 p2932 N88-27409

Distortions in processed signals and their application in electronic design. Part 3: An automated generator of communication jamming signals
[DE88-702733] 23 p3205 N88-29072

The surface evaporative duct height product: An evaluation
[AD-A195918] 24 p3392 N88-30199

ELECTRONIC EQUIPMENT
NT AVALANCHE DIODES
NT BIPOLAR TRANSISTORS
NT CHARGE COUPLED DEVICES
NT CHARGE TRANSFER DEVICES
NT CMOS
NT CRYSTAL RECTIFIERS
NT DIODES
NT ELECTRONIC FILTERS
NT ELECTRONIC MODULES
NT ELECTRONIC PACKAGING
NT ELECTRONIC TRANSDUCERS
NT FIELD EFFECT TRANSISTORS
NT GALLIUM ARSENIDE LASERS
NT GERMANIUM DIODES
NT GUNN DIODES
NT HETEROJUNCTION DEVICES
NT HIGH ELECTRON MOBILITY TRANSISTORS
NT JFET
NT JUNCTION DIODES
NT JUNCTION TRANSISTORS
NT LIGHT EMITTING DIODES
NT METAL OXIDE SEMICONDUCTORS
NT MIM (SEMICONDUCTORS)
NT MIM DIODES
NT MINIATURE ELECTRONIC EQUIPMENT
NT MIS (SEMICONDUCTORS)
NT MODFETS
NT MSM (SEMICONDUCTORS)
NT PHOTODIODES
NT PHOTOVOLTAIC CELLS
NT PLASMA DIODES
NT RUBY LASERS
NT SCHOTTKY DIODES
NT SEMICONDUCTOR DEVICES
NT SEMICONDUCTOR DIODES
NT SEMICONDUCTOR LASERS
NT SILICON TRANSISTORS
NT SIS (SEMICONDUCTORS)
NT SOI (SEMICONDUCTORS)
NT SOLAR CELLS
NT SOLID STATE DEVICES
NT SOLID STATE LASERS
NT SOS (SEMICONDUCTORS)
NT SPACECRAFT ELECTRONIC EQUIPMENT
NT THERMIONIC DIODES
NT THERMISTORS
NT THYRISTORS
NT TRANSFERRED ELECTRON DEVICES
NT TRANSISTOR AMPLIFIERS
NT TRANSISTORS
NT TUNNEL DIODES
NT VARISTORS
NT VERTICAL JUNCTION SOLAR CELLS
NT YAG LASERS

Center for Electronics and Electrical Engineering Technical Progress Bulletin covering center programs, October to December 1986 with 1987 CEEE events calendar
[PB87-226890] 02 p0168 N88-11058

Center for Electronics and Electrical Engineering technical publication announcements covering center programs, July to September 1986 with 1987 CEEE events calendar
[PB87-223442] 02 p0168 N88-11059

Application of electronic fuel injection to the optimum engine for methanol utilization
[PB87-201950] 02 p0180 N88-11120

A tutorial on Rogowski coil theory and operation
[DE88-000006] 02 p0230 N88-11449

Identifying areas of leading edge Japanese science and technology: Patent activity and citation analysis using US POC (Patent Office Classification) classification
[PB87-204095] 02 p0249 N88-11575

Estimating payload internal temperatures and radiator size for multimegawatt space platforms
[DE88-000244] 03 p0275 N88-11738

Center for Electronics and Electrical Engineering Technical Progress Bulletin covering center programs, January to March 1987 with 1987 CEEE events calendar
[PB87-224648] 03 p0309 N88-11946

Electronic system reliability and effectiveness
[AD-A184522] 03 p0311 N88-11961

Dramatically improved radiation hardness for CMOS silicon gate integrated circuits even down to cryogenic temperatures
[AD-A184672] 03 p0381 N88-12398

Design of digital filters for electronic instrumentation
[PB87-100418] 04 p0438 N88-12716

Alternating current circuit theory and pulsed NMR (Nuclear Magnetic Resonance)
[DE88-000641] 04 p0440 N88-12732

Corrosion of electronic components
05 p0547 N88-13333

Development of an interface for an ultrareliable fault-tolerant control system and an electronic servo-control unit
[NASA-TM-88236] 05 p0553 N88-13367

Electromagnetics and electrothermal approach to evaluate failures in microelectronic devices caused by electrostatic discharges. Stochastical aspects of the device reliability
[AD-A184906] 05 p0577 N88-13522

Fabricate, calibrate and test a dosimeter for integration into the CRRES (Combined Release and Radiation Effects Satellite) satellite
[AD-A185439] 05 p0585 N88-13564

Developments in electronics ceramics reported
06 p0684 N88-14192

Use of colour on electronic data displays (second study)
[PB87-126744] 06 p0754 N88-14627

Survey of electronic measurement needs below 10 MHz
[PB88-110366] 07 p0844 N88-15121

Supportability in aircraft systems through technology and acquisition strategy applications
[AD-A186465] 08 p0949 N88-15759

Validation of a stochastic model to determine failure rates for communication-electronic systems
[AD-A186536] 08 p0980 N88-15920

A study of the TCAS 2 collision avoidance system mounted on a Boeing 737 aircraft
[NASA-CR-182457] 09 p1116 N88-16687

Interchange of electronic design through VHDL and EIS 09 p1205 N88-17222

Joint services electronics program
[AD-A187587] 10 p1325 N88-17920

MBE growth, characterization and electronic device processing of HgCdTe, HgZnTe related heterojunctions and HgCdTe-CdTe superlattices
[AD-A187456] 10 p1421 N88-18486

A new fire protection concept for electronic equipment
[AD-A188884] 12 p1614 N88-19651

Development of an electronically-scanned pressure module for operation at cryogenic temperatures
[NASA-CR-181610] 12 p1629 N88-19746

Joint services electronics program
[AD-A189262] 13 p1761 N88-20533

The cooling of electronic equipment in fighter aircraft
[MBB/LKE-312/S/PUB/258] 14 p1866 N88-21147

A data acquisition system for atmospheric tracer studies
[DE88-006211] 14 p1991 N88-21869

Investigations of test methodology for the stress loading facility
[PB88-166095] 15 p2022 N88-22049

Experimental studies on electronic properties of HgTe/CdTe and Hg sub 1-x Cd sub x Te/CdTe heterostructures and superlattices
[AD-A189826] 15 p2142 N88-22783

Nondestructive evaluation of large scale composite components
[AD-A190998] 16 p2173 N88-22954

A PC-based receiver-decoder for remote sensor monitoring
[DE88-004733] 16 p2192 N88-23075

X-ray production in low energy proton stopping
[NASA-TM-100619] 16 p2270 N88-23582

Developing systems using state-of-the-art CAD/CAM technology 17 p2306 N88-23795

Single phase liquid immersion cooling of discrete heat sources in a vertical channel
[AD-A191224] 17 p2337 N88-23944

Joint services electronics program
[AD-A192076] 18 p2504 N88-24856

The inspection of metallurgical bounds in electronic systems
[AD-A192064] 18 p2582 N88-25343

Electronic controller for reciprocating rotary crystallizer
[NASA-TM-101140] 18 p2584 N88-25354

Aircraft field degradation and electromagnetic compatibility
[PB88-183975] 19 p2602 N88-25456

Research and development programs on advanced structural ceramics in Korea 19 p2633 N88-25620

Failure rate prediction of electronic components
[PB87-228953] 19 p2678 N88-25925

The Oak Ridge National Laboratory strategic defense initiative shield optimization program
[DE88-008946] 19 p2721 N88-26160

Decision aiding and coordination in decision-making organizations
[AD-A191950] 19 p2738 N88-26259

High bandwidth optoelectronic signal link for use in an EMP (electromagnetic pulse) plus radiation environment
[DE88-009254] 20 p2790 N88-26549

The Oak Ridge National Laboratory strategic defense initiative shield optimization program: Executive summary
[DE88-008016] 20 p2847 N88-26899

Superconducting electronic film structures
[AD-A192907] 20 p2879 N88-27091

Investigation of expert system design approaches for electronic design environments
21 p2926 N88-27365

A method for estimating the susceptibility of electronic systems to HPM (High Power Microwave)
[DE88-012246] 21 p2934 N88-27422

FEB (Multifilter Electronics Box) lifting device analysis, revision A
[AD-A192313] 21 p2935 N88-27427

Equipment for an advanced electron beam lithography system
[AD-A192956] 21 p2936 N88-27435

Electronic failure analysis-corrosion of avionics
22 p3054 N88-28122

Burn-in with mixed populations
[AD-A194651] 22 p3085 N88-28321

Avionics system design for high energy fields. A guide for the designer and airworthiness specialist
[NASA-CR-181590] 23 p3178 N88-28919

Laser and electrochemical studies of metallizations in electronic devices
[AD-A193786] 23 p3208 N88-29090

Center for opto-electronic systems research instrumentation grant
[AD-A193711] 23 p3282 N88-29545

Numerical simulation of the function of scientific instrumentation for measuring the speed of electron devices
[AD-A194969] 24 p3376 N88-30103

Electronic materials and devices prepared by molecular beam epitaxy
[AD-A195694] 24 p3433 N88-30433

ELECTRONIC EQUIPMENT TESTS

Instrument for radiation testing/screening electronic devices over an extended temperature range
[AD-A184245] 03 p0326 N88-12060

The Shock and Vibration Bulletin. Part 1: Welcome, Keynote Address, Invited Papers, Nondevelopment Items Workshop and Pyrotechnic Shock Workshop
[AD-A186748] 08 p0997 N88-16034

Designing electronics for pyrotechnic shock
08 p0997 N88-16038

The ESA centralized management system for satellite electronic test and checkout instrumentation
09 p1124 N88-16731

The response of a power MOSFET (N-channel) and a dielectric isolated operational amplifier to the combined environmental effects of high temperature and total dose gamma radiation 17 p2406 N88-24309

Aircraft field degradation and electromagnetic compatibility
[PB88-183975] 19 p2602 N88-25456

A non-contact picosecond prober for integrated circuit testing 19 p2655 N88-25766

Development of an airborne facility for advanced avionics research
[NLR-MP-87012-U] 20 p2760 N88-26368

RLE progress report, January 1 to December 31, 1987
[RLE-PR-130] 21 p3011 N88-27869

ELECTRONIC FILTERS

Advanced capacitor development
[AD-A189985] 15 p2059 N88-22276

ELECTRONIC LEVELS

U ELECTRON ENERGY
U ENERGY LEVELS

ELECTRONIC MAIL

Replication and reconfiguration in a distributed mail repository
[AD-A186967] 09 p1151 N88-16897

ELECTRONIC MODULES

New approach to telemetry development will significantly increase productivity of Joint Test Assembly (JTA) teams
[DE88-001676] 05 p0554 N88-13373

Application of knowledge based systems to the maintenance of inertial system electronics
12 p1578 N88-19441

ELECTRONIC PACKAGING

Applications of heat pipes to cool PWBS and hybrid microcircuits 02 p0136 N88-10858

Plasma and ion etching for failure analysis. Part 2. The etching of plastic encapsulant and other semiconductor device materials, using the Technics Giga Etch 100-E plasma etch system
[AERE-R-12212] 09 p1177 N88-17050

Advanced packaging for VLSI/VHSIC (Very Large Scale Integrated Circuits/Very High Speed Integrated Circuits) applications: Electrical, thermal and mechanical considerations, an IR and D report
[AD-A189666] 14 p1965 N88-21724

Hermetically sealable package for hybrid solid-state electronic devices and the like
[NASA-CASE-MSC-20181-1] 17 p2335 N88-23941

Application-specific packaging for custom micromechanical structures 19 p2671 N88-25879

ELECTRONIC PHOTOGRAPHY

U ELECTRO-OPTICAL PHOTOGRAPHY

ELECTRONIC SIGNAL MEASUREMENT

U SIGNAL MEASUREMENT

ELECTRONIC SPECTRA

Multichannel electron counter with high space resolution
[DE88-700564] 07 p0857 N88-15204

Contributions of autoionizing resonances to the electron collisional excitation rates for Be-like ions
[AD-A190924] 18 p2572 N88-25275

Basic research in electronics (JSEP) Joint Services Electronics Program
[AD-A193072] 23 p3206 N88-29079

ELECTRONIC STRUCTURE

U ATOMIC STRUCTURE

ELECTRONIC SWITCHES

U SWITCHING CIRCUITS

ELECTRONIC TRANSDUCERS

Definition and use of sensors for measuring electrical conductivity in thunderclouds
[ESA-TT-1047] 03 p0352 N88-12222

ELECTRONIC WARFARE

Radar ECCM's new area: Anti-STEALTH and anti-ARM 03 p0299 N88-11881

Brain activity during tactical decision-making. Part 2: Probe-evoked potentials and workload
[AD-A188688] 12 p1667 N88-19994

The integration of artificial intelligence techniques to improve the effectiveness of electronic countermeasure strategies in a tactical environment
[AD-A189483] 12 p1682 N88-20056

Bragg-cell receiver study
[NASA-CR-182684] 13 p1761 N88-20535

The electromagnetic threat to future avionic systems
17 p2305 N88-23790

ELECTRONICS

Detective quantum efficiency and design of a parallel data recording system for EXELFS-measurements — electron microscopy
[USIP-87-06] 01 p0050 N88-10318

Center for Electronics and Electrical Engineering technical publication announcements covering Center programs, July to September 1987
[PB88-196530] 20 p2793 N88-26572

ELECTRONS

NT CONDUCTION ELECTRONS
NT FREE ELECTRONS
NT HIGH ENERGY ELECTRONS
NT HOT ELECTRONS
NT PHOTOELECTRONS
NT POLARONS
NT RELATIVISTIC ELECTRON BEAMS
NT SOLAR ELECTRONS

Theory of atoms in strong, pulsed electromagnetic fields. 2: A free electron and a harmonically bound electron
[DE87-012571] 01 p0035 N88-10225

Ab initio methods for electron-molecule collisions
[DE87-011728] 01 p0092 N88-10598

Low altitude flux and dose measurements during two solar flare events 01 p0111 N88-10713

Electronic conduction in molten sodium chloride
[DE87-010063] 02 p0144 N88-10901

Confinement time of electrons and H(-)/D(-) ions in the Uramoto type sheet plasma
[IPPJ-852] 04 p0492 N88-13032

Prompt simultaneous acceleration of protons and electrons to relativistic energies by shock waves in solar flares
[IPPJ-851] 04 p0493 N88-13037

Tetrahedral carbon and interstitial electrons in Li cluster: CLi4 and (LiCH3)4
[AD-A184277] 04 p0496 N88-13055

Experimental observation of photoresonance of electrons localized above surface of solid hydrogen
06 p0774 N88-14755

Improving the method of calculating electronic properties of narrow bandgap semiconductors
07 p0926 N88-15627

Study of tau pairs and search for new particles
[B8680488] 07 p0931 N88-15655

Field-aligned fluxes of energetic electrons related to the onset of magnetospheric substorms
08 p 096 N88-16595

Introductory review: Physics of electron slowing-down processes
[DE88-002918] 09 p1246 N88-17466

Dynamics of coupled electron-nucleon motion in a laser field
[DE88-005063] 10 p1337 N88-17994

Suppression of X-rays generated by runaway electrons in ATF
[DE88-004179] 10 p1414 N88-18440

Electron transfer to iron(3) oxide colloids
[DE88-002885] 10 p1416 N88-18448

The electronic structure of YBa2Cu3O/sub 7-delta/ above and below T/sub c/
[DE88-003495] 10 p1420 N88-18479

Calculations of rate constants for the three-body recombination of H2 in the presence of H2
[NASA-CR-182548] 11 p1454 N88-18664

Nuclear structure studies by the scattering of medium-energy electrons
[DE88-003803] 11 p1545 N88-19236

High pressure electronic transport in semiconductors
[AD-A187428] 11 p1555 N88-19308

Gas phase reactions of electrons, negative ions and free-radicals with transition metal complexes
11 p1560 N88-19339

Measurements of optically thin electron cyclotron emission from relativistic electrons
[DE88-004713] 12 p1688 N88-20096

Polarization of electrons in an electromagnetic wave field in the presence of magnetic field
[DE88-700169] 13 p1757 N88-20509

Image charge, coherent scattering, and symmetry effects in electron stimulated desorption: O(-) from O sub 2 condensed on metals
[AD-A189093] 13 p1835 N88-20979

The magnitude of secondary electron contributions in photon stimulated desorption
[AD-A189094] 13 p1835 N88-20980

Topics in curved and flat space electromagnetism
13 p1854 N88-21100

Kinetics of slow electrons in excimer laser with electron-beam pumping 14 p1970 N88-21760

Three-wave parametric resonance in plasma of relativistic electron flux 14 p1972 N88-21772

Ground-state correlations in C12 and the mechanism of the (e,e'p) reaction
[B8729349] 14 p1980 N88-21816

Developments in ceramic superconducting materials
15 p2052 N88-22229

On the acceleration of electrons and positive ions in the same direction along magnetic field lines by parallel electric fields
[IRF-PREPRINT-103] 15 p2096 N88-22488

Improvement of plasma confinement due to electron Landau damping in tokamaks
[DE88-752339] 15 p2136 N88-22747

Effective electron interactions due to virtual charge and spin excitations in an extended Hubbard model for Cu-O superconductors
[DE88-005971] 15 p2139 N88-22766

Survey of the Air Force P78-2 (SCATHA) satellite plasma wave data during electron gun operations
[AD-A191014] 16 p2168 N88-22926

Small molecule and small cluster ion formation in a low-density containerless mixture of electrons, protons and hydrogen atoms 16 p2269 N88-23577

Electron current effect on stability of plasma channel
16 p2276 N88-23625

Ion generator and ion application system
[NASA-CASE-MFS-28122-1] 17 p2397 N88-24253

Contributions of autoionizing resonances to the electron collisional excitation rates for Be-like ions
[AD-A190924] 18 p2572 N88-25275

A study of runaway electron confinement in the ASDEX tokamak
[DE88-007327] 18 p2579 N88-25319

Physical properties of f electron systems
[DE88-006886] 18 p2581 N88-25331

Contaminant ions and waves in the space station environment 18 p2590 N88-25393

Electronic structure of Zintl phase compounds by nonlinear optimization
[DE88-009998] 19 p2613 N88-25508

Modulation efficiency limited high frequency performance of the MODFET 19 p2657 N88-25786

Primer on coupling collective electronic oscillations to nuclei
[LA-10878] 19 p2723 N88-26170

Experiments on insulation of relativistic electron flows in oblique and tapered magnetic fields
[DE88-007199] 19 p2724 N88-26176

Electron-positron physics at 1 TeV
[DE88-009019] 19 p2725 N88-26180

Electron-acoustic waves in a beam-plasma system
[DE88-702053] 19 p2729 N88-26207

Infrared detectors based on the photon drag effect and intersubband absorption by a two-dimensional electron gas 20 p2867 N88-27024

A 10 microns photoexcited avalanche gain due to electron impact ionization from GaAs quantum well superlattices 20 p2867 N88-27026

Monte Carlo simulations of femtosecond relaxation of photoexcited electrons in AlGaAs/GaAs quantum wells
20 p2869 N88-27036

Direct measurement of ultrafast electron-hole plasma expansion at high density at an asymmetric GaAs quantum well 20 p2871 N88-27044

Superconductivity of heavy-electron uranium compounds
[DE88-007901] 20 p2875 N88-27065

Nonlinear dynamics of the electron self-field interaction
[DE88-010597] 21 p2934 N88-27420

Theory and simulation of relaxed plasmoids
[AD-A192884] 21 p3032 N88-27997

Large area nuclear particle detectors using ET materials
[NASA-CR-180777] 23 p3215 N88-29136

Particle trajectories and potentials in a plane sheath moving in a magnetoplasma
[AD-A196228] 24 p3390 N88-30190

Ring current role in dynamics of fluctuating electron and ion fluxes in low-latitude magnetosphere
24 p3447 N88-30514

ELECTROPHORESIS

Preparative electrophoresis for space
[NASA-TP-2777] 02 p0156 N88-10977

Continuous flow electrophoresis system experiments on shuttle flights STS-6 and STS-7
[NASA-TP-2778] 02 p0156 N88-10978

Mathematical models of continuous flow electrophoresis: Electrophoresis technology
[NASA-CR-179241] 07 p0826 N88-15021

Use of hydrophilic polymer coatings for control of electroosmosis and protein adsorption
07 p0925 N88-15620

A comparison of algorithms for the analysis of images generated by two-dimensional electrophoresis
[DE88-003730] 09 p1220 N88-17319

GAS 450: A space payload for the People Central Coast Student Experimenters 10 p1289 N88-17709

Optimization of the southern electrophoretic transfer method
[DE88-004527] 10 p1299 N88-17765

Electrophoretically deposited styrene-acrylate coatings for suppression of internal electromagnetic pulse effects
[DE88-003820] 12 p1609 N88-19621

Moving wall, continuous flow electrophoresis apparatus
[NASA-CASE-MFS-28142-1] 17 p2318 N88-23845

Electrophoretic coatings. Part 1: Sandia applications
[DE88-008666] 20 p2776 N88-26465

ELECTROPHOTOMETERS

A new technique for rocket and space-borne investigations of time-dependant auroral morphology
08 p1030 N88-16241

Five channel auroral photometer
[REPT-112] 24 p3375 N88-30101

ELECTROPHOTOMETRY
Surface photometric investigations for spiral galaxies of large dimension structures in edge-on gemetry
[ETN-88-92126] 21 p3030 N88-27985

ELECTROPHYSICS
NT ELECTRO-OPTICS
NT MOLECULAR ELECTRONICS
Air Force ultrafast optical electronics center
[AD-A191491] 17 p2438 N88-24507
Joint services electronics program
[AD-A190239] 18 p2503 N88-24848
Joint services electronics program
[AD-A192076] 18 p2504 N88-24856

ELECTROPHYSIOLOGY
Biophysical and biochemical mechanisms in synaptic transmitter release
[AD-A187059] 09 p1199 N88-17184
Brain potentials and personality: A new look at stress susceptibility
[AD-A186931] 09 p1199 N88-17189
Center for nonlinear dynamics of the brain
[AD-A187245] 11 p1518 N88-19068
Studies of model ion channels in defect-free multibilayers of phospholipids
[AD-A188740] 16 p2238 N88-23365
Challenges of physiological monitoring in a Navy operational setting 16 p2239 N88-23374
Electric and Magnetic Activity of the Central Nervous System: Research and Clinical Applications in Aerospace Medicine
[AGARD-CP-432] 21 p2977 N88-27683
Normative developmental equations for the EEG and their sensitivity to neurological and psychiatric disorders
21 p2977 N88-27687
The application of non-stationary data analysis techniques in the identification of changes in the electroencephalogram associated with the onset of drowsiness 21 p2978 N88-27688
A statistical procedure for the evaluation of presence/non-presence of stimulus-related EEG activity
21 p2978 N88-27689
Electric and magnetic brain activity related to cognitive performance 21 p2979 N88-27692
Cognitive task demands as reflected in physiological measures 21 p2980 N88-27699
The effect of endogenous alpha on hemispheric asymmetries and the relationship of frontal theta to sustained attention 21 p2980 N88-27701
Psychophysiological measures of drowsiness as estimators of mental fatigue and performance degradation during sleep deprivation 21 p2980 N88-27702
Fighter pilot performance during airborne and simulator missions: Physiological comparisons
21 p2981 N88-27704
Event-related and steady potential changes in the brain related to workload during tracking
21 p2981 N88-27705
The neuroelectric selection of Naval aviation personnel: An evaluation 21 p2981 N88-27707
An approach to studying the effects of psychostimulants on cerebral electrical activity in the non-human primate
21 p2983 N88-27716
Relation between VEP and visual function in lesions of the optic nerve and visual pathway
21 p2983 N88-27718
The auditory evoked response in military pilots
21 p2984 N88-27721

ELECTROPLATING
Synergism of electroplating and vacuum processes
[DE87-013496] 01 p0033 N88-10211
Composite ceramic superconducting filaments for superconducting cable
[AD-A187833] 11 p1556 N88-19312
RF properties of superconducting Pb electroplated onto Cu
[DE88-005918] 15 p2139 N88-22765

ELECTRORETINOGRAPHY
Microesotropia patients performa well as military jet pilots 21 p2925 N88-27363

ELECTROSEISMIC EFFECT
U ELECTRIC CURRENT
U SEISMIC WAVES

ELECTROSTATIC CHARGE
The physics of charge separation preceding lightning strokes in thunderclouds
[NASA-CR-178371] 01 p0071 N88-10452
Introduction to the problem of environmentally induced discharges 03 p0273 N88-11717
Charging calculations for the HIPPARCOS satellite
03 p0274 N88-11728
Effect of electrostatic field on behaviour of peripheric plasma at high-frequency heating
[DE87-703328] 03 p0378 N88-12378
Conditions for geomagnetically trapping sub-micron lunar ejecta between L = 1.2 and L = 3.1
04 p0521 N88-13203
Study of electrostatic modulation of fuel sprays to enhance combustion performance in an aviation gas turbine
[AD-A184967] 05 p0548 N88-13341
Electromagnetics and electrothermal approach to evaluate failures in microelectronic devices caused by electrostatic discharges: Stochastical aspects of the device reliability
[AD-A184906] 05 p0577 N88-13522
Lightning discharge protection rod
[NASA-CASE-LAR-13470-1] 06 p0666 N88-14083
Simulations of the electrostatic charging of ESA communications satellites
[ESA-STM-239] 18 p2472 N88-24670
Reference filters for electrostatic charging tendency measurements of fuels
[AD-A191717] 18 p2495 N88-24803
An electrostatic potential comparator
[AD-A192051] 18 p2557 N88-25177
Procedures for identification and handling of Printed Circuit Boards (PCBs)
[AD-A191177] 23 p3206 N88-29078

ELECTROSTATIC ENGINES
Advanced electric propulsion research
[NASA-CR-182130] 16 p2170 N88-22937

ELECTROSTATIC EROSION
U SPARK MACHINING

ELECTROSTATIC FIELDS
U ELECTRIC FIELDS

ELECTROSTATIC GENERATORS
Proposal for construction of an Energetic Particle Injector (EPI)
[INPE-4242-RPE/548] 12 p1690 N88-20112

ELECTROSTATIC PLASMA
U PLASMAS (PHYSICS)

ELECTROSTATIC PROBES
Comparison of simultaneous MST radar and electron density probe measurements in the polar mesosphere --- Mesospheric, Stratospheric, Tropospheric (MST)
08 p1028 N88-16226
Asymmetric double Langmuir probe for fast and automatic measurements of plasma temperature
[DE88-004773] 10 p1414 N88-18436
An experimental investigation of an arcjet thruster exhaust using Langmuir probes
[NASA-TM-100258] 14 p1883 N88-21253
Measurements of edge turbulence with Langmuir probes in currentless Heliotron E plasmas
[DE88-752313] 16 p2275 N88-23617
Rocket-borne low energy ion measurements in space
18 p2593 N88-25412
Theory on conductivity measurement technique for Langmuir probes in the stratosphere
[INPE-4514-PRE/1268] 19 p2692 N88-25999
Calibration technique and study on metrological characteristics of a high-voltage inverse square-law function generator
[DE88-702101] 22 p3072 N88-28236

ELECTROSTATIC PROPULSION
NT ION PROPULSION
Advanced electric propulsion and space plasma contactor research
[NASA-CR-180862] 06 p0674 N88-14126

ELECTROSTATIC WAVES
Nature and the nonlinear evolution of electrostatic waves associated with the AMPTE (Active Magnetosphere Particle Tracer Explorers) solar wind releases
[AD-A185471] 06 p0806 N88-14920
Electrostatic VLF emission determined from rocket and satellite experiments 08 p1002 N88-16068
Low frequency electrostatic waves observed on board the Coordinated Auroral Experiment using Scatter And Rockets (CAESAR) 2 payload 08 p1032 N88-16253
Theoretical investigations of drift waves in a magnetic quadrupole 18 p2578 N88-25312
Electrostatic whistler mode conversion at plasma resonance
[AD-A192951] 20 p2860 N88-26989
Kinetic theory for electrostatic waves due to transverse velocity shears
[AD-A193404] 23 p3284 N88-29557

ELECTROSTATICS
Physics and device design of vacuum integrated circuits 01 p0039 N88-10251
Electromagnetic compatibility (EMC) phenomena and prevention of the effects --- spacecraft
03 p0274 N88-11731
Electrostatic discharges in geostationary orbit: The case of Telecom 1 03 p0275 N88-11733
Prevention of radiation induced degradations and of electrostatic perturbations on the Arabsat spacecraft: in flight results 03 p0275 N88-11734
Some new ideas in liquid detectors
[DE88-000732] 04 p0446 N88-12768
Analysis of geophysical data bases and models for spacecraft interactions
[AD-A184809] 05 p0555 N88-13375
Plasma theory and simulation
[AD-A187100] 09 p1249 N88-17486
Dynamical aspects of electrostatic double layers
[TRITA-EPP-87-13] 09 p1250 N88-17492
Mechanical design and construction of a 200 mA, 100 keV, dc, negative ion accelerator
[DE88-003855] 11 p1548 N88-19257
GRADIO three-axis electrostatic accelerometers
12 p1645 N88-19849
Waves and static electric fields in the auroral acceleration region 12 p1646 N88-19856
Nonlinear optical principles and the photorefractive effect applied to optical phase conjugation
[AD-A188856] 12 p1691 N88-20119
The effects of a dc electric field on the current driven ion cyclotron instability
[AD-A188877] 12 p1695 N88-20142
Observations on electrostatic effects in a filter test system
[AD-A188797] 13 p1736 N88-20378
Development of electrostatic accelerator free-electron lasers
[AD-A189507] 13 p1774 N88-20614
Chaotic diffusion across magnetic field in a model of electrostatic turbulent plasma
[PREPRINT-566] 14 p1985 N88-21839
A qualitative approach to electricity
[AD-A189854] 15 p2128 N88-22693
The new UCSB (University of California, Santa Barbara) compact far-infrared FEL
[AD-A190864] 16 p2212 N88-23203
A new fiber-optic-based ion sensor
[AD-A191322] 16 p2274 N88-23612
Development of test methods for the electrostatic properties of nonhomogeneous fabrics, phase 2
[AD-A190853] 18 p2489 N88-24767
Demixing of aqueous polymer two-phase systems in low gravity
[NASA-TM-101141] 18 p2496 N88-24809
Electrostatic discharge test apparatus
[NASA-CASE-MSC-21094-1] 18 p2518 N88-24941
Low frequency electrostatic turbulence in the polar cap E-region
[DRI-3-88] 18 p2540 N88-25077
A severe spacecraft-charging event on SCATHA in September 1982
[AD-A193007] 20 p2765 N88-26396
Meaning of energy diagrams used to describe hetero-structures
[DE88-702219] 21 p3023 N88-27943
Wave structures in thermospheric density from satellite electrostatic triaxial accelerometer measurements
[AD-A194134] 23 p3233 N88-29240

ELECTROSTRICTION
Piezoelectric and electrostrictive materials for transducer applications, volume 1
[AD-A194957] 24 p3374 N88-30096
Piezoelectric and electrostrictive materials for transducer applications, volume 2
[AD-A194956] 24 p3376 N88-30104
Piezoelectric and electrostrictive materials for transducer applications, volume 3
[AD-A194949] 24 p3377 N88-30112

ELECTROTHERMAL ENGINES
NT ARC JET ENGINES
NT PLASMA ENGINES
NT RESISTOJET ENGINES
Characterization of the arc/spark excitation sources used in the spectrometric oil analysis program
[AD-A187131] 10 p1297 N88-17758
Development and qualification of an Augmented Electro-Thermal Hydrazine Thruster (AEHT) with 0.1 to 0.2 N vacuum thrust
[BMFT-FB-W-86-012] 16 p2169 N88-22931
Performance of a hydrogen pulsed electrothermal thruster: Strategic defense initiative organization innovative science and technology. SBIR, phase 1
[AD-A191999] 18 p2475 N88-24679

ELEMENT ABUNDANCE
U ABUNDANCE

ELEMENTARY EXCITATIONS
NT EXCITONS
NT MAGNONS
NT PHONON BEAMS
NT PHONONS
NT PLASMONS
NT POLARONS
First-principles calculations of quasiparticle energies at surfaces and interfaces: Semiconductor surface-state spectra and band offsets
[DE88-006340] 15 p2141 N88-22773

Electronic structure, elementary excitations, optical and transport properties of semiconductor superlattices
[AD-A190795] 18 p2581 N88-25333

ELEMENTARY PARTICLE INTERACTIONS
NT ELECTRON CAPTURE
NT HIGH ENERGY INTERACTIONS
NT NUCLEAR CAPTURE
NT NUCLEON-NUCLEON INTERACTIONS
NT STRONG INTERACTIONS (FIELD THEORY)
NT WEAK ENERGY INTERACTIONS
NT WEAK INTERACTIONS (FIELD THEORY)
Experimental studies of elementary particle interactions at high energies
[DE88-000804] 05 p0648 N88-13971
Corrections for the pseudorapidity gap correlation method --- particle correlations
[USIP-87-12] 09 p1245 N88-17463
Topics in gauge theories and the unification of elementary particle interactions
[DE88-008112] 19 p2738 N88-26256
Nucleon-nucleus interaction data base: Total nuclear and absorption cross sections
[NASA-TM-4053] 20 p2852 N88-26935
Activities report of the Werner-Heisenberg Institute of Physics
[ETN-88-92946] 21 p3015 N88-27893
Production of pi(0) mesons and charged hadrons in nu bar neon and nu neon charges current interactions
[MPI-PAE/EXP.EL.188] 22 p3150 N88-28743

ELEMENTARY PARTICLES
NT ALPHA PARTICLES
NT ANTINEUTRINOS
NT ANTINUCLEONS
NT ANTIPARTICLES
NT ANTIPROTONS
NT BARYONS
NT BETA PARTICLES
NT BOSONS
NT CONDUCTION ELECTRONS
NT DEUTERONS
NT ELECTRON-POSITRON PAIRS
NT ELECTRONS
NT FAST NEUTRONS
NT FERMIONS
NT FREE ELECTRONS
NT GLUONS
NT GRAVITONS
NT HADRONS
NT HIGH ENERGY ELECTRONS
NT HOT ELECTRONS
NT KAONS
NT LEPTONS
NT MESON RESONANCE
NT MESONS
NT MUONS
NT NEUTRINOS
NT NEUTRONS
NT NUCLEONS
NT PARTONS
NT PHOTOELECTRONS
NT PHOTONS
NT PIONS
NT POLARONS
NT POSITRONS
NT PROTONS
NT QUARKS
NT SOLAR ELECTRONS
NT SOLAR NEUTRINOS
NT SOLAR NEUTRONS
NT SOLAR PROTONS
NT THERMAL NEUTRONS
Current experiments in elementary particle physics
[DE87-013961] 02 p0231 N88-11456
Research program in elementary particle theory
[DE88-000159] 02 p0233 N88-11468
Research in elementary particle physics
[DE88-002130] 06 p0777 N88-14771
A simplified model of elementary particles
[NOTA-INTERNA-890] 07 p0930 N88-15647
Experimental elementary particle physics at the University of Pittsburgh
[DE88-003542] 11 p1545 N88-19234
Theory of elementary particle studies in weak iteration and grand unification and studies in accelerator design
[DE88-004261] 11 p1545 N88-19238
Research in high energy elementary particle physics
[DE88-006065] 13 p1837 N88-20994
Research in the theory of condensed matter and elementary particles
[DE88-010180] 22 p3151 N88-28749

ELEVATION
Terrain classification from digital elevation data using slope and curvature information
[AD-A188940] 12 p1639 N88-19812
Interpolation algorithms for digital terrain models
[INPE-4373-PRE/1196] 13 p1820 N88-20877
Prediction of high-temperature thermodynamic properties of mixed electrolyte solutions including solubility equilibria, vapor pressure depression and boiling point elevation
[DE88-006344] 13 p1849 N88-21069
Mapping from LANDSAT and SPOT satellite imagery
17 p2352 N88-24018
Vectorization of raster algorithms for elevation data processing 18 p2534 N88-25036
The use of SPOT data for mapping and DEM production --- digital elevation model (DEM)
22 p3110 N88-28475
Automatic extraction of high resolution elevation data from SPOT stereo images 22 p3113 N88-28489
Estimation of short-wavelength gravity on a dense grid using digital terrain elevation data
[AD-A196325] 24 p3391 N88-30196

ELEVATION ANGLE
Results on the low elevation angle propagation experiment, part 1
[TUD-R-328] 06 p0693 N88-14250

ELEVATIONS (DRAWINGS)
U DRAWINGS

ELEVATORS (LIFTS)
Analytical investigation of the dynamics of tethered constellations in Earth orbit (phase 2)
[NASA-CR-179218] 04 p0408 N88-12533
A device and methodology for measuring repetitive lifting VO2max (oxygen consumption rate)
[AD-A185195] 05 p0630 N88-13850
Tether Elevator Crawler Systems (TECS)
07 p0927 N88-15631
Orbiter processing facility service platform failure and redesign 14 p1928 N88-21494

ELIMINATION
Elimination of subboundaries in 0.5-micron-thick Si-on-insulation films produced by ZMR
[AD-A184590] 03 p0381 N88-12396
Eliminating columns in the simplex method for linear programming
[DE88-004191] 10 p1386 N88-18277
Elimination of quantifiers of linear variables and corresponding transfer principles
[DE88-005692] 13 p1826 N88-20912
Comparison of morning with afternoon nitrogen elimination in resting subjects breathing 100 percent oxygen
[AD-A196191] 24 p3407 N88-30282

ELLIPSES
Spectral methods: Analysis and applications to flow problems
[AD-A186265] 07 p0850 N88-15156
The information metric for univariate linear elliptic models
[AD-A186385] 07 p0911 N88-15527
Wind tunnel tests of elliptical missile body configurations at Mach numbers 0.4 to 5.0
[AD-A193525] 22 p3038 N88-28040
Fitting an ellipse to data
[NPL-DITC-95/87] 22 p3143 N88-28693

ELLIPSOIDS
The effect of sting interference at low speeds on the drag coefficient of an ellipsoidal body using a magnetic suspension and balance system
[NASA-CR-181611] 13 p1718 N88-20274
Periodic orbits around a satellite modelled as a triaxial ellipsoid
[AD-A190592] 15 p2022 N88-22051
Solar energy absorption efficiency of an ellipsoidal receiver-reactor with specularly reflecting walls
[AD-A193726] 22 p3117 N88-28520
A calculation of the turbulent boundary layer on a slender ellipsoid at low incidence
[FFA-TN-1988-02] 23 p3213 N88-29126

ELLIPSOMETERS
Some investigations of molecular beam epitaxial growth of 3-5 semiconductor films via Monte-Carlo computer simulations, carrier tunnelling and spectroscopic ellipsometry
[AD-A185520] 06 p0789 N88-14839
Thin film research diagnostics instrumentation
[AD-A191240] 16 p2213 N88-23207
Ellipsometric imaging of drying sol-gel films
[DE88-011785] 21 p2921 N88-27335

ELLIPTIC DIFFERENTIAL EQUATIONS
Finite elements for 2D elliptic equations with moving nodes
[DE87-013501] 02 p0224 N88-11410
Research and development of finite elements and iterative algorithms for elliptic partial differential equations
[DE88-001381] 05 p0643 N88-13934
The p-version of the finite element method for elliptic equations of order 2l
[AD-A186334] 07 p0911 N88-15523
A parallel block cyclic reduction algorithm for the fast solution of elliptic equations
[DE88-003595] 09 p1221 N88-17324
Analysis of smoothing matrices for the preconditioning of elliptic difference equations
[CWI-NM-R8705] 09 p1228 N88-17357
Recent progress in the p and h-p version on the finite element method
[AD-A187254] 10 p1400 N88-18347
The h-p version of the finite element method for problems with nonhomogeneous essential boundary condition
[AD-A187356] 10 p1400 N88-18348
Generation of surface grids through elliptic partial differential equations for aircraft and missile configurations
[AD-A186631] 11 p1535 N88-19169
The inverse power method for semilinear elliptic equations
[DE88-006427] 15 p2118 N88-22620
Residual smoothing for accelerating the Alternating Direction Implicit (ADI) iteration method for elliptic difference equations
[CWI-NM-R8721] 16 p2259 N88-23500
Multigrid methods for elliptic Partial Differential Equations (PDEs)
[CWI-NM-R8722] 18 p2566 N88-25242
A comparative study of Chebyshev acceleration and residue smoothing in the solution of nonlinear elliptic difference equations
[CWI-NM-R8723] 18 p2569 N88-25259
Unified multilevel adaptive finite element methods for elliptic problems
[DE88-011938] 21 p3007 N88-27840
Composite grid generation for aircraft configurations with the EAGLE code 23 p3246 N88-29321
Nonlinear elliptic problems with critical exponent in shrinking annuli
[W-02/87] 23 p3273 N88-29477
Elliptic equations with nearly critical growth
[W-16-87] 23 p3273 N88-29478
Generation of surface grids through elliptic partial differential equations for aircraft and missile configurations
[AD-A195639] 24 p3424 N88-30378

ELLIPTIC FUNCTIONS
On the maximum of solutions for a semilinear elliptic problem
[REPT-87-08] 01 p0086 N88-10554
A comparison of adaptive refinement techniques for elliptic problems
[DE88-000805] 04 p0485 N88-12987
General solution of certain functional equations
[PREPRINT-554] 06 p0764 N88-14689
Mode 3 problems of doubly-periodic rhombic and rectangular array of equal cracks in an infinite plate
[PB87-144846] 08 p0996 N88-16031
On the norm equivalence of singularly perturbed elliptic difference operators
[DE88-006353] 13 p1826 N88-20913
Computation of a complete elliptic integral of the first kind using q-expansion 16 p2257 N88-23490
Semilinear elliptic problems on domains with corners
[REPT-87-83] 20 p2846 N88-26888
Three-dimensional elliptic grid generation technique with application to turbomachinery cascades
[NASA-TM-101330] 24 p3372 N88-30078

ELLIPTIC INTEGRALS
U ELLIPTIC FUNCTIONS

ELLIPTICAL CYLINDERS
An experimental investigation of appendage-flat plate junction flow. Volume 2: Elliptical nose appendage data base
[AD-A184974] 05 p0580 N88-13539
Numerical simulation of the shock tube flows by TVD scheme 19 p2638 N88-25648

ELLIPTICAL GALAXIES
Stochasticity in elliptical galaxies
[SER-C-PREPUBL-FASC-20] 17 p2450 N88-24556

ELLIPTICAL ORBITS
NT TRANSFER ORBITS
Limitation of spacecraft orbit near colinear libration center of limited elliptical three body problem
08 p1003 N88-16075
Periodic orbits of limited elliptical three body problem
08 p1004 N88-16081
Relative motion of two satellites in close-elliptical orbits
[AD-A188851] 12 p1594 N88-19543
Calculation of eclipses for elliptical orbits
[INPE-4412-NTE/277] 12 p1594 N88-19545

ELLIPTICAL POLARIZATION
Observation of instabilities in time during dynamic self-diffraction of light in anisotropic nonhomogeneous medium 06 p0769 N88-14730

ELLIPTICITY

Dependence of acoustical characteristics of laser-induced breakdown in dielectric materials on shape of inelastic region 06 p0774 N88-14753

Wind tunnel studies of circulation control elliptical airfoils 10 p1270 N88-17598

ELONGATION

Development of a polyimide matrix for filament winding with improved extensibility and fracture toughness for permanent use at 200 C
[BMFT-FB-T-86-118] 01 p0030 N88-10190

The effect of strain rate on the yield behavior of iron-base LRO alloys at elevated temperatures
[DE87-014893] 03 p0288 N88-11808

BASIC desk-top computer program for the three-dimensional static configuration of an extensible flexible cable in a uniform stream
[AD-A184852] 05 p0609 N88-13737

Effects of sulfur content on the plain strain fracture toughness of inertia welds in 4340 steel
[AD-A188192] 11 p1458 N88-18689

Determination of the modulus of elasticity of structural silicone sealants
[PB88-157458] 14 p1893 N88-21307

Superplasticity: A fundamental investigation on deformation mechanism and cavitation phenomena
[AD-A191548] 18 p2485 N88-24741

Phenomena of the ionic transport in the stress corrosion of metals
[DE88-702502] 23 p3195 N88-29013

EMANATION

U EMISSION

EMBEDDED COMPUTER SYSTEMS

NT AIRBORNE/SPACEBORNE COMPUTERS

An embedded multiprocessor computer for proof-of-principle testing of exploratory systems concepts
[DE87-012735] 02 p0218 N88-11372

Praxis: The programming language. An advanced overview
[DE87-014319] 02 p0220 N88-11388

The implementation and use of Ada on distributed systems with high reliability requirements
[NASA-CR-182481] 09 p1221 N88-17326

Factors causing unexpected variations in Ada benchmarks
[AD-A187231] 10 p1388 N88-18291

Implementing embedded artificial intelligence rules within algorithmic programming languages
[NASA-CR-178393] 14 p1959 N88-21686

A high speed serial link interface for SANDAC-V
[DE88-007694] 20 p2842 N88-26861

MINIAC: A small embedded computer
[DE88-008142] 21 p2994 N88-27757

An optical 2-dimensional correlator for pattern recognition in embedded computing
[DE88-007198] 21 p2998 N88-27780

Design consideration in constructing high performance embedded Knowledge-Based Systems (KBS)
23 p3261 N88-29415

EMBEDDING

Embedding topological median algebras in products of dendrons
[PB88-100888] 06 p0767 N88-14713

Study of the embedded atom method of atomistic calculations for metals and alloys
[DE88-002798] 07 p0835 N88-15065

Embedded cluster models for electronic structure and energetics of complex oxides
[DE88-003097] 07 p0938 N88-15702

Prognosis using spectral embedding -- weather forecasting 08 p1016 N88-16157

Experimental and analytical investigation on a proposed embedded fiber optic displacement sensor
[AD-A189030] 12 p1630 N88-19756

Effects of toroidal forces in current loops embedded in a background plasma
[AD-A188878] 12 p1695 N88-20143

Graph labelings
[AD-A189649] 14 p1964 N88-21722

Embedded minimal sufaces with an infinite number of ends
[DE88-006429] 15 p2126 N88-22680

Instability-related delamination growth of embedded and edge delaminations 20 p2767 N88-26406

Distributed fault tolerant embeddings of binary trees in hypercubes
[AD-A192929] 20 p2839 N88-26840

Laboratory feasibility study of a composite embedded fiber optic sensor for measurement of structural vibrations
[AD-A194270] 22 p3152 N88-28754

Archetyping: A software generation and management methodology 23 p3256 N88-29382

A parametric study of embedded cantilever retaining walls: The results of a finite element study
[RR-CE83] 24 p3383 N88-30152

EMBOLISMS

NT AEROEMBOLISM

EMBRITTLEMENT

Tensile properties of extrusion consolidated Type 304 SS rapidly solidified powders
[DE87-014875] 05 p0566 N88-13450

Experimental method for investigating helium effects in irradiated vanadium
[DE88-002891] 08 p0969 N88-15865

Kinetics and mechanism of thermal aging embrittlement of duplex stainless steels
[DE88-002987] 08 p0969 N88-15866

Long-term-aging embrittlement of cast duplex stainless steels: Mechanism and kinetics
[DE88-002929] 09 p1145 N88-16861

Influence of post-anneal cooling treatments on suppression of cryogenic intergranular fracture in experimental Ni-free high-Mn austenitic steels
[DE88-002766] 09 p1145 N88-16863

Long-term aging of cast stainless steels: Mechanisms and resulting properties
[DE88-002888] 09 p1145 N88-16864

Aging degradation of cast stainless steels: Effects on mechanical properties
[DE88-003053] 09 p1145 N88-16866

Neutron- and X-ray-small angle scattering with Fe-base metallic glasses
[DE88-002538] 09 p1147 N88-16876

Effect of low-temperature aging on the mechanical properties of cast stainless steels
[DE88-002872] 10 p1300 N88-17774

Weldability of tritium-charged 304L stainless steel
[DP-1740] 12 p1607 N88-19611

Stress corrosion cracking and metal-induced embrittlement: Comparative studies of local chemistries
[DE88-003235] 13 p1742 N88-20419

Creep behavior of consolidated rapidly solidified Type 304 stainless steel powder containing helium
[DE88-005536] 13 p1743 N88-20424

A study of the dynamics of high temperature brittle intergranular fracture by acoustic emission
[AERE-R-12479] 13 p1780 N88-20650

The role of oxygen on the mechanical behavior of molybdenum alloys 17 p2401 N88-24278

High temperature embrittleness of Cu-Cr alloy
[NASA-TT-20184] 18 p2488 N88-24759

Method and apparatus for non-destructive testing of temper embrittlement in steels
[NASA-CASE-LAR-13817-1] 23 p3195 N88-29012

EMBRYOLOGY

Embryonic development of guppy in weightlessness
10 p1360 N88-18127

Effects of heavy ions on egg-developing systems
12 p1658 N88-19935

Embryonic development of the newt Cynops pyrrhogaster in very weak magnetic fields
[ISAS-RN-357] 19 p2702 N88-26068

Effects of short spaceflights on Drosophila melanogaster embryogenesis and life span 22 p3061 N88-28166

Embryogenesis and organogenesis of Carausius morosus under spaceflight conditions
22 p3061 N88-28167

The role of gravity in the establishment of the dorso/ventral axis in the amphibian embryo --- Spacelab D1 mission 22 p3062 N88-28168

EMBRYOS

Changes in the morphological and molecular biological processes during early embryo development in amphibians under micro-g conditions 07 p0885 N88-15371

Xiphophorus: A system to recognize radiation-induced mutations and to study the effects of zero-gravity environment on embryo development
07 p0885 N88-15372

Semi-microdroplet assay for cell adhesion molecules
[NASA-CR-183139] 24 p3406 N88-30274

Immunofluorescence localization of dissociation supernatant and extracellular matrix components in Lytechinus pictus sectioned embryos
[NASA-CR-183137] 24 p3406 N88-30276

EMERGENCIES

The determination of nutritional requirements for Safe Haven Food Supply System (emergency/survival foods)
06 p0792 N88-14856

Sudden in-flight incapacitation in general aviation
[AD-A187044] 09 p1115 N88-16682

Safety study: Commercial emergency medical service helicopter operation
[PB88-917001] 12 p1575 N88-19422

IEMIS (Integrated Emergency Management Information System) floodplain mapping based on a LIDAR derived data set
[AD-A193071] 21 p2966 N88-27616

Cockpit and cabin crew coordination
[AD-A192445] 21 p2993 N88-27752

Application of SPOT imagery for oil spill contingency planning 22 p3108 N88-28460

EMERGENCY LOCATOR TRANSMITTERS

COSPAS/SARSAT 406-MHz emergency beacon digital controller
[NASA-TM-100859] 20 p2792 N88-26566

EMISSION

NT ACOUSTIC EMISSION
NT BIOLUMINESCENCE
NT CHEMILUMINESCENCE
NT CN EMISSION
NT ELECTROLUMINESCENCE
NT ELECTRON EMISSION
NT EXHAUST EMISSION
NT FIELD EMISSION
NT FLUORESCENCE
NT HYDROXYL EMISSION
NT ION EMISSION
NT LASER INDUCED FLUORESCENCE
NT LIGHT EMISSION
NT LUMINESCENCE
NT MICROWAVE EMISSION
NT NEUTRON EMISSION
NT OPTICAL RESONANCE
NT PARTICLE EMISSION
NT PHOSPHORESCENCE
NT PHOTOELECTRIC EMISSION
NT PHOTOIONIZATION
NT PHOTOLUMINESCENCE
NT RADIO BURSTS
NT RADIO EMISSION
NT RESONANCE FLUORESCENCE
NT SECONDARY EMISSION
NT SOLAR RADIO BURSTS
NT SOLAR RADIO EMISSION
NT SPACECRAFT GLOW
NT SPECTRAL EMISSION
NT SPONTANEOUS EMISSION
NT STIMULATED EMISSION
NT THERMAL EMISSION
NT THERMIONIC EMISSION
NT TYPE 3 BURSTS
NT WATER MASERS
NT X RAY FLUORESCENCE

Quantum electrodynamics based on self-energy: Spontaneous emission in cavities
[DE87-703071] 02 p0232 N88-11461

Studies of the processing of single words using positron tomographic measures of cerebral blood flow change
[AD-A184058] 03 p0356 N88-12244

Emerging environmental constraints on the use of gasoline and diesel fuel and tradeoffs associated with the use of alternative fuels
[DE87-011504] 04 p0422 N88-12614

Impacts of world development on selected characteristics of the atmosphere: An integrative approach. Volume 1: Main report
[DE88-001495] 07 p0875 N88-15309

Impacts of world development on selected characteristics of the atmosphere: An integrative approach. Volume 2: Appendices
[DE88-001496] 07 p0875 N88-15310

Emission angles for soft X-ray coherent transition radiation
[AD-A186851] 09 p1151 N88-16896

Emission of gamma rays from various materials pulsed with 14-MeV neutrons
[DE88-003837] 11 p1544 N88-19227

A study of satellite emission computed tomography
[AD-A189567] 13 p1797 N88-20745

Effects of translational and rotational nonequilibrium on CW (Continuous Wave) chemical laser performance
[AD-A191425] 16 p2214 N88-23210

Timing regulations to prevent stratospheric-ozone depletion
[R-3495-JMO/RC] 19 p2690 N88-25987

Laser induced surface emission of neutral species and its relationship to optical surface damage processes
[DE88-008035] 19 p2726 N88-26192

Review of methods for remote sensing of atmospheric emissions from stationary sources
[PB88-190483] 20 p2821 N88-26739

Radiative heat transfer and selective emission in planar slab coatings on hot emissive substrates
[AD-A193133] 21 p2918 N88-27319

Filling of the atmospheric transmission window due to emission from very high rotational levels of NO and O3
[AD-A194670] 23 p3233 N88-29239

EMISSION SPECTRA

Optical spectroscopy of IRAS sources with infrared emission bands. 1: IRAS 21282+5050 and the diffuse interstellar bands
[NASA-CR-181387] 01 p0094 N88-10611

Photolytic processes for measurement of combustion heats of formation and reaction rates
[DE87-014047] 02 p0144 N88-10905
Visible emission from granular explosives during shock initiation
[DE87-012361] 02 p0155 N88-10970
Design study for measurement of neutral hydrogen atom density by laser induced fluorescence method
[DE87-752964] 02 p0179 N88-11114
X-ray emission from high-Z spherical laser plasmas: Implications for plasma dynamics
[DE87-014722] 02 p0239 N88-11506
Design and development of a database for spectral data and analysis results
[DE87-011323] 02 p0247 N88-11564
Spectroscopy and nonthermal processes
02 p0252 N88-11594
Spectroscopic and retrieval studies in support of SCRIBE (Stratospheric Cryogenic Interferometer Balloon Experiment)
[AD-A184037] 03 p0351 N88-12216
Investigations of extragalactic hydroxyl
03 p0389 N88-12441
Excess emission in the wings of the Hydrogen Balmer lines during a flare on the late-type dMe star YZ CMi
04 p0511 N88-13146
Emission features in IRAS LRS spectra of MS, S and CS stars 04 p0514 N88-13163
The Wilson-Bappu relationship: A barometric effect
04 p0516 N88-13170
JHK photometry of CN-rich field giants
04 p0516 N88-13175
Water masers associated with 2 carbon stars: EU Andromedae and V778 Cygni 04 p0517 N88-13176
Chromospheric variability mechanisms affecting pre-main sequence stars 04 p0517 N88-13180
The Einstein survey of the young stars in the Orion Nebula 04 p0518 N88-13182
M dwarfs from the Einstein medium sensitivity survey
04 p0519 N88-13188
A helium flare on the active G5 dwarf Kappa Ceti
04 p0519 N88-13189
Atomic beam studies of the interaction of hydrogen with transition metal surfaces
[DE88-000208] 05 p0648 N88-13970
Satellite observations of extreme ultraviolet radiation
[AD-A185043] 05 p0661 N88-14059
Characterization of Er,Cr:YSGG
[AD-A185885] 07 p0932 N88-15659
Gamma radiation at the 970 MeV plane positron channeling in diamond crystals
[DE88-700557] 07 p0939 N88-15705
Low-power photolytically pumped lasers
[DE88-002448] 08 p0991 N88-15998
VLBI research on OH-maser IN W33
08 p1001 N88-16064
Holes in OI 130 nm emission fields of upper atmosphere during day 08 p1004 N88-16082
Long range reconnaissance of trace gases: A special aspect of emission spectroscopy
08 p1018 N88-16172
Stimulated Raman scattering of picosecond light pulses in long dispersive medium 08 p1078 N88-16498
Soft X-ray absorption and emission spectra and the electronic structure of the Ba2YCu3O/sub 7-x/ superconductor
[DE88-002609] 08 p1090 N88-16559
Theoretical studies of mass loss and shock phenomena in cool star envelopes
[NASA-CR-182433] 08 p1099 N88-16616
The structure of the sideband spectrum in free electron lasers
[AD-A186952] 09 p1170 N88-17015
Excimer plasma displays
[AD-A186731] 09 p1250 N88-17489
The development of emission tomography for the nuclear industry
[AERE-R-12319] 10 p1341 N88-18014
Simulation of infrared spectra
[AD-A187881] 11 p1453 N88-18658
Theory of two-photon emission from atomic inner shells
[AD-A187742] 11 p1543 N88-19223
Presentations to the SuperHILAC Program Advisory Committee
[DE88-003853] 11 p1547 N88-19256
Spectroscopic studies of a laser-produced carbon plasma in the near and extreme ultraviolet
11 p1553 N88-19292
Stratospheric trace gas distributions from far infrared thermal emission spectroscopy
13 p1797 N88-20749
IUE program SUGSD: Variability time scale of H Ly-alpha from Uranus
[NASA-CR-182706] 13 p1856 N88-21107
The astrophysics of nebulae and active galactic nuclear emission-line regions: New methods and applications
13 p1858 N88-21111
An investigation of the infrared emission spectra of carbon condensates 14 p1886 N88-21272
Techniques for studying fast reactions in liquids
[DE88-005917] 14 p1888 N88-21285
Spatial distribution of O(supra 1D) from Comet Halley
14 p1999 N88-21913
Objective-prism spectra of the Comets Honda (1968 e), Hartley-Good (1985 I) and Halley
14 p2000 N88-21924
The evolution of CN emission in Halley's comet with heliocentric distance 14 p2006 N88-21961
On the interpretation of the CH cometary spectrum
14 p2007 N88-21969
Alkali metal diffuse band lasers
[AD-A190244] 15 p2071 N88-22350
Sequential excitation preparation of molecular energy levels with special structural and chemical properties
[AD-A190041] 15 p2132 N88-22718
Tokamak studies of density sensitive line ratios
17 p2441 N88-24521
IUE evidence on the nature of the innermost broad-line region in Seyfert 1 galaxies 17 p2450 N88-24552
Molecular sources of ionospheric holes
[AD-A191857] 18 p2541 N88-25082
Optical diagnostics for a high power, rf-inductively coupled plasma
[DE88-007822] 18 p2579 N88-25322
Ultraviolet-visible spectroscopy of laser-produced aluminum plasmas
[AD-A193004] 20 p2860 N88-26990
Analysis of emission features in IRAS LRS spectra
21 p2928 N88-27380
Spectral line shapes from highly ionized sodium plasmas
[AD-A193401] 21 p3017 N88-27907
Array detectors for plasma spectrochemistry
[AD-A194220] 22 p3052 N88-28105
Modification of YBa2Cu3O(7-x) ceramics by adsorbed water and other gases
[DE88-011518] 22 p3057 N88-28140
The electromagnetic spectrum: The information mine
[AD-A194316] 22 p3069 N88-28215
High spatial resolution observations of neutral atomic carbon in the molecular clouds M17 and W51
[MPE-PREPRINT-109] 22 p3164 N88-28846
First detection of HCN J = 9 to 8 (797 GHz) line emission: Very high densities in the Orion core
[MPE-PREPRINT-110] 22 p3165 N88-28847
EMISSIVITY
Lidar-radiometric method for determining liquid-water content of cirrus clouds 04 p0461 N88-12854
Determination of cloud base height and emissivity from downwelling angular radiances
[AD-A185985] 07 p0879 N88-15331
An analysis of whistler-mode radiation from the Spacelab-2 electron beam, revision
[AD-A188228] 11 p1552 N88-19287
Multilayer thermal insulation tests
[INPE-4475-PRE/1243] 12 p1626 N88-19729
Measurement of emissivity of industrial surfaces using a simple method
[NASA-TT-20165] 15 p2036 N88-22130
The thermal radiative properties of metals at high temperature
[DE88-006625] 15 p2038 N88-22141
Direct emissivity measurements on liquids and corrections to multi-color pyrometers
17 p2329 N88-23906
Laser pyrometry 17 p2330 N88-23910
Anomalous emissivity from periodic micro-machined silicon surfaces 19 p2670 N88-25872
A probabilistic model of the apparent radiance of a rough sea
[AD-A193867] 22 p3129 N88-28602
Soot and radiation in a gas turbine combustor
[AD-A191991] 23 p3179 N88-28924
EMISSOGRAPHS
U RECORDING INSTRUMENTS
EMITTANCE
Linear emittance damper with megagauss fields
[DE87-013562] 01 p0093 N88-10606
Emittance studies at the Los Alamos National Laboratory Free-Electron Laser (FEL)
[DE88-003146] 10 p1334 N88-17975
Generalized equations for emittance and field energy of high-current beams in periodic focusing
[DE88-004448] 10 p1404 N88-18372
The new UCSB (University of California, Santa Barbara) compact far-infrared FEL
[AD-A190864] 16 p2212 N88-23203
Enhanced emittance of oxidized 304 stainless steel
17 p2423 N88-24408
EMITTERS
NT THERMIONIC CATHODES
NT THERMIONIC EMITTERS
New application of transition metal carbides detailed
06 p0675 N88-14132
Optimal selection of global positioning system set to minimize emitter location errors
[AD-A189559] 12 p1579 N88-19447
Large-aperture sparse array antenna systems of moderate bandwidth for multiple emitter location
[AD-A188409] 12 p1619 N88-19683
Bragg-cell receiver study
[NASA-CR-182684] 13 p1761 N88-20535
Passive DF: A tutorial, part 1
[NASA-CR-182669] 13 p1815 N88-20846
Modulatable thin film field emission space gun
[AD-A189279] 13 p1845 N88-21043
Polysilicon-contacted p+ emitters for silicon solar cell applications
[DE88-005106] 14 p1942 N88-21586
Mathematics clinic probabilistic position-fixing
[NASA-CR-182753] 15 p2125 N88-22672
EMOTIONAL FACTORS
Ejection situations in the U-2/TR-1: An analysis of emotions and events
[AD-A192872] 21 p2893 N88-27175
EMPENNAGE
U TAIL ASSEMBLIES
EMPTYING
Gastric emptying during walking and running: Effects of varied exercise intensity
[AD-A194025] 23 p3240 N88-29281
EMULSIONS
Reactions of porphyrins in surfactant assemblies, microemulsions and in solutions
[AD-A184797] 05 p0560 N88-13412
Analysis of relativistic nucleus-nucleus interactions in emulsion chambers 07 p0926 N88-15624
The morphology of emulsion polymerized latex particles
[DE88-002672] 08 p0972 N88-15879
National Center for Small-Angle Scattering Research: Reports on measurements carried out by users of the facilities of the NCSASR, December 1, 1985-September 30, 1987
[DE88-003754] 11 p1462 N88-18719
Droplet size characteristics and energy input requirements of emulsions formed using high-intensity-pulsed electric fields
[DE88-005912] 15 p2128 N88-22692
ENAMELS
Contribution to the development of coated fiber ceramic insolation material
[ETN-88-92361] 21 p2906 N88-27243
ENCAPSULATED MICROCIRCUITS
Chemical multisensors with selective encapsulation of ion-selective membranes 19 p2670 N88-25869
ENCAPSULATING
Development of microencapsulation techniques
[AD-A185019] 05 p0567 N88-13457
Development of encapsulated lithium hydride thermal energy storage for space power systems
[DE88-004762] 11 p1507 N88-19001
Ion beam modification of film stress and the effectiveness of thin film encapsulants on GaAs
[DE88-004458] 11 p1558 N88-19328
Development of microencapsulated DNBM quaternary ammonium inhibitors for paints
17 p2319 N88-23851
The application of high-rate biaxial testing to the design of containment vessels for radioisotope heat sources
17 p2426 N88-24428
Liquid encapsulated float zone process and apparatus
[NASA-CASE-MFS-28144-1] 17 p2446 N88-24545
A compatible encapsulant for explosives
[DE88-007212] 18 p2495 N88-24806
Primerless RTV silicones
[BDX-613-3807] 24 p3356 N88-29980
ENCKE COMET
On orbits and association of meteor streams with Comets P/Halley and P/Encke
14 p2003 N88-21945
A model of the nongravitational motion of Comet P/Encke 14 p2010 N88-21993
ENCLOSURES
The use of Kevlar on aero-engine fan containment casings
[PNR90410] 02 p0182 N88-11134
Plant Growth Module (PGM) conceptual design
05 p0631 N88-13855
Some performance comparisons for a fluid dynamics code
[PB88-113709] 07 p0852 N88-15175
Thermosolutal convection in high-aspect-ratio enclosures
[NASA-TM-100803] 11 p1486 N88-18871

Fingering flow patterns of thermosolutal convection in rectangular enclosures
[NASA-TM-100854] 14 p1911 N88-21417

Research in electromagnetic shielding theory Part1 Shielding by rectangular enclosures
[AD-A192881] 20 p2791 N88-26557

ENCODERS
U CODERS

ENCODING
U CODING

END EFFECTORS

The ESA/Fokker service end-effector subsystem: A robotic/man-compatible servicing approach
12 p1587 N88-19502

System and concept design of the SSRMS latching end effector --- Space Station 14 p1875 N88-21204

Precise computer controlled positioning of robot end effectors using force sensors
[NASA-CR-182887] 17 p2391 N88-24213

END MORAINES
U GLACIAL DRIFT

END PLATES

Method for characterizing end-plate surface resistance of dielectric resonator 14 p1903 N88-21371

END-TO-END DATA SYSTEMS

Solid Earth mission end-to-end data system study
[C04825.08/FR] 17 p2309 N88-23811

ENDANGERED SPECIES

Survey for least bell's vireo in riparian habitat on Vandenberg Air Force Base, Santa Barbara County, California
[NASA-TM-100984] 20 p2822 N88-26744

ENDOCRINE GLANDS
NT ADRENAL GLAND
NT HYPOTHALAMUS
NT PITUITARY GLAND
NT TESTES

ENDOCRINE SECRETIONS
NT ALDOSTERONE
NT CORTICOSTEROIDS
NT HORMONES
NT PITUITARY HORMONES

ENDOCRINE SYSTEMS

Interplanetary travel: Is gravity needed to close the loop
[NASA-TM-101013] 22 p3132 N88-28622

ENDOCRINOLOGY

Investigations of the reproductive physiology of the rainbow trout (Salmo gairdneri Richardson)
07 p0885 N88-15370

Endocrine responses to resistance exercise
[AD-A188681] 12 p1667 N88-19993

Hormonal regulation of fluid and electrolytes: Effects of heat exposure and exercise in the heat
[AD-A192655] 22 p3131 N88-28614

ENDOSCOPES

Ultrafast holography using optical fibers
[ISL-R-101/86] 02 p0176 N88-11096

ENDOTHELIUM

Interactions of cultured human endothelial cells with polymeric surfaces
[PB88-112255] 10 p1369 N88-18178

ENDOTHERMIC REACTIONS

Investigation by differential scanning calorimetry of microstructure in a superplastic Al-Mg-Zr alloy
[AD-A184902] 05 p0564 N88-13439

ENERGETIC PARTICLES
NT ARGON PLASMA
NT BETA PARTICLES
NT BOUNDARY LAYER PLASMAS
NT CESIUM PLASMA
NT COLD PLASMAS
NT COLLISIONAL PLASMAS
NT COLLISIONLESS PLASMAS
NT CONDUCTION ELECTRONS
NT COSMIC PLASMA
NT CYLINDRICAL PLASMAS
NT DENSE PLASMAS
NT DEUTERIUM PLASMA
NT ELECTRON PLASMA
NT ELECTRONS
NT EVEN-EVEN NUCLEI
NT HEAVY NUCLEI
NT HELIUM PLASMA
NT HIGH ENERGY ELECTRONS
NT HIGH TEMPERATURE PLASMAS
NT HOT ELECTRONS
NT HYDROGEN PLASMA
NT HYPERNUCLEI
NT LASER PLASMAS
NT METALLIC PLASMAS
NT NITROGEN PLASMA
NT NONEQUILIBRIUM PLASMAS
NT NONUNIFORM PLASMAS
NT NUCLEI (NUCLEAR PHYSICS)
NT ODD-ODD NUCLEI
NT OXYGEN PLASMA
NT PLASMA FOCUS
NT PLASMAS (PHYSICS)
NT RELATIVISTIC PLASMAS
NT ROTATING PLASMAS
NT SEMICONDUCTOR PLASMAS
NT SOLAR WIND
NT SPACE PLASMAS
NT SPHERICAL PLASMAS
NT STELLAR WINDS
NT STRONGLY COUPLED PLASMAS
NT THERMAL PLASMAS
NT TOROIDAL PLASMAS

The elastic scattering of intermediate energy protons from (40)Ca and (208)Pb 01 p0092 N88-10599

Solar energetic particles events observed by Prognoz-10 Intercosmos (May-October 1985)
01 p0111 N88-10716

An account of a flare related shock event recorded by the energetic particle detector EPONA of the Giotto spacecraft during September 1985 (STIP interval 18)
01 p0118 N88-10757

Particle desorption from nonconducting surfaces by high energy heavy ions
[ETN-88-91088] 09 p1245 N88-17461

Time dependent degradation of energetic electrons in gaseous and condensed media
[DE88-002912] 09 p1246 N88-17465

Research in experimental nuclear physics
[DE88-004100] 10 p1408 N88-18397

Energetic particle drift motions in the outer dayside magnetosphere
[DE88-005097] 11 p1512 N88-19034

Proposal for construction of an Energetic Particle Injector (EPI)
[INPE-4242-RPE/548] 12 p1690 N88-20112

Stimulated Emission of Energetic Particles (SEEP)
[AD-A188724] 13 p1853 N88-21094

Observation of energetic particles (E greater than 30 keV) by the Giotto experiment EPA in the magnetic cavity of Comet Halley 14 p1997 N88-21903

Nuclear and ionic charge distribution experiment on ISEE-1 and ISEE-3
[NASA-CR-180776] 23 p3183 N88-28947

ENERGY

Inflation in Einstein-Cartan theory with energy-momentum tensor with spin
[NASA-TM-101164] 17 p2447 N88-24547

Difficulties with interpretation of underground muons from Cygnus X-3
[DE88-701645] 23 p3309 N88-29710

ENERGY ABSORPTION
NT ELECTROMAGNETIC ABSORPTION
NT GAMMA RAY ABSORPTION
NT INFRARED ABSORPTION
NT MODERATION (ENERGY ABSORPTION)
NT MOLECULAR ABSORPTION
NT MULTIPHOTON ABSORPTION
NT PHOTOABSORPTION
NT RADIATION ABSORPTION
NT THERMAL ABSORPTION
NT THERMALIZATION (ENERGY ABSORPTION)
NT ULTRAVIOLET ABSORPTION
NT X RAY ABSORPTION

Vibration-absorbing characteristics of metal-polymer shells 02 p0158 N88-10991

Time-resolved absorption measurements on OMEGA
[DE87-014465] 02 p0173 N88-11112

Toward detecting California shrubland canopy chemistry with AIS data 05 p0613 N88-13764

Fractographic study of fiber composites
06 p0677 N88-14146

Helicopter crashworthiness research program
09 p1107 N88-16635

Thermal energy storage by means of an absorption cycle
[ETN-88-91614] 09 p1186 N88-17108

Note on boundary stabilization of wave equations
[AD-A187113] 09 p1227 N88-17348

Guided wave approaches to spectrally selective energy absorption
[NASA-CR-182532] 10 p1320 N88-17892

Transmitting boundary for finite-difference calculations with finite modeling of an infinite medium
[AD-A191441] 18 p2570 N88-25264

REFLEX: An energy deposition code that models the effects of electron reflection during electron beam heating tests
[DE88-009789] 19 p2726 N88-26186

ENERGY ABSORPTION FILMS

Investigation of the subsequent treatment and the stability of CuxS-CdS thin-film solar cells
[ETN-88-91488] 11 p1507 N88-19006

ENERGY BANDS
NT BLOCH BAND
NT CONDUCTION BANDS

Banded ion morphology 04 p0468 N88-12892

Population inversion in gapless semiconductors as result of interband pumping 06 p0770 N88-14732

Tailorable infrared sensing device with strain layer superlattice structure
[NASA-CASE-NPO-16607-1-CU]
06 p0788 N88-14836

Self energy corrections to the ab initio band structures: Chromium
[DE88-701825] 21 p3020 N88-27927

Investigation of electronic band structure of semiconductors by photoemission
[ETN-88-92370] 21 p3025 N88-27957

Multiphoton transitions in semiconductors in the non-perturbative approach
[DE88-702664] 22 p3157 N88-28786

ENERGY BUDGETS
NT ATMOSPHERIC HEAT BUDGET
NT EARTH RADIATION BUDGET
NT HEAT BUDGET

Energy balance in laser-irradiated vaporizing droplets
[DE88-000525] 04 p0449 N88-12782

Reynolds-stress and dissipation rate budgets in a turbulent channel flow
[NASA-TM-89451] 07 p0852 N88-15174

Use of the thermodynamic evaporation formula of Hoffmann in energy balance models for flowing water
08 p1013 N88-16143

Energy balance and discharge of an Alpine glacier, illustrated by Mount Vernagtferner in the Oetzal Alps, Tyrol 08 p1014 N88-16145

Low authority control of large space structures using a constrained threshold control formulation
18 p2472 N88-24667

ENERGY CONSERVATION

Cost savings possible with Air Force conversion to JP-8 as its primary fuel
[AD-A183784] 01 p0030 N88-10192

Automotive Stirling engine: Mod 2 design report
[NASA-CR-175106] 02 p0250 N88-11578

Oxygen enriched combustion system performance study
[DE88-001500] 05 p0562 N88-13424

Riblets for aircraft skin-friction reduction
07 p0814 N88-14955

Feedback stabilization of distributed systems
[AD-A187111] 09 p1222 N88-17328

Mathematical modeling of two-state classification technology transfer summary and user's guide
[DE88-003849] 11 p1526 N88-19110

Systems approach to energy quality and efficiency
[PB88-139506] 12 p1640 N88-19823

Large-Scale Advanced Prop-Fan (LAP)
[NASA-CR-182112] 13 p1723 N88-20306

Overview of the DOE-ECUT Tribology Program
[DE88-002878] 13 p1778 N88-20637

Applicability of aerospace thermal insulation technologies to the civilian sector
[DE88-003717] 13 p1852 N88-21086

Overview of 1987 moonlight project
15 p2052 N88-22231

Wave energy flow conservation for propagation in inhomogeneous Vlasov-Maxwell equilibria
[DE88-006705] 15 p2055 N88-22251

NASA advanced turboprop research and concept validation program
[NASA-TM-100891] 16 p2163 N88-22902

Three axis attitude control system
[NASA-CASE-GSC-12970-1] 17 p2308 N88-23808

NASA/industry advanced turboprop technology program
[NASA-TM-100929] 18 p2466 N88-24641

Reduction in mill air compressor power requirements through installation of a variable frequency speed control
[DE88-008493] 23 p3221 N88-29171

ENERGY CONSUMPTION

Use of natural gas diesel engines in mechanical pulp production: A preliminary study
[DE87-753065] 02 p0181 N88-11129

Optimized ground coupled heat pump mechanical package
[DE87-014899] 04 p0441 N88-12738

Life-cycle cost analysis of residential heat pumps and alternative HVAC (Heating, Ventilating and Air-Conditioning) systems
[DE88-003701] 07 p0839 N88-15090

Short Reference Years: Short weather data sets for faster simulations of solar energy systems and energy consumption in buildings
[DE88-900198] 07 p0881 N88-15343

Regulation of energy metabolism during parachute jumps 07 p0896 N88-15428

Hercules: A power analyzer for MOS VLSI circuits
[AD-A188702] 12 p1623 N88-19706

Droplet size characteristics and energy input requirements of emulsions formed using high-intensity-pulsed electric fields
[DE88-005912] 15 p2128 N88-22692

Sunshine project for FY 1987 outlined
16 p2184 N88-23021

Tactical Rubidium Frequency Standard (TRFS)
[AD-A191049] 16 p2193 N88-23078

Costs and benefits of AC propulsion
[PB88-173380] 16 p2287 N88-23691

ENERGY CONVERSION
NT BIOMASS ENERGY PRODUCTION
NT GEOTHERMAL ENERGY CONVERSION
NT OCEAN THERMAL ENERGY CONVERSION
NT PHOTOTHERMAL CONVERSION
NT PHOTOVOLTAIC CONVERSION
NT SOLAR ENERGY CONVERSION
NT WATERWAVE ENERGY CONVERSION

Fifty years in synthetic fuels information: Have we lost a strategic national resource
[DE87-010902] 02 p0155 N88-10973

Satellite techniques of solar resource assessment for focusing and non-focusing solar collector systems
[DE88-001657] 07 p0874 N88-15298

Advanced energy conversion concept for beamed-energy propulsion
[AD-A187336] 10 p1324 N88-17914

Point-focus concentrator reflector assembly, phase 1
[DE88-003616] 13 p1792 N88-20720

Multi-hundred kilowatt roll ring assembly evaluation results
[NASA-TM-100865] 14 p1904 N88-21375

Rotating-hoop, pulsed-energy converter
17 p2426 N88-24433

A multimegawatt space power source radiator design
17 p2427 N88-24436

Energy conversion system optimization study for multimegawatt space nuclear power application
17 p2436 N88-24492

Mechanisms of photochemical energy conversion by chlorophyll
[DE88-008763] 20 p2819 N88-26725

Comparative analysis of the space power architecture studies
[NASA-TM-100977] 22 p3049 N88-28090

Hydrogen concentration cells as converters of heat into electricity
[DE88-009662] 23 p3229 N88-29216

ENERGY CONVERSION EFFICIENCY

High-efficiency silicon solar cells: Numerical modeling, transient measurements, efficiency goals, and v-shaped grooves
[DE87-012842] 01 p0066 N88-10423

Recent progress in magma energy extraction
[DE87-013083] 01 p0066 N88-10424

Focusing solar energy collector
02 p0159 N88-10996

The fundamentals of photovoltaic system electrical design
[DE87-009061] 02 p0194 N88-11214

Gallium arsenide and multibandgap solar cell research
[DE87-012260] 02 p0194 N88-11215

Tapping the earth's geothermal resources: Hydrothermal today, magma tomorrow
[DE87-014718] 02 p0196 N88-11223

Electricity from photovoltaic solar cells. Flat-Plate Solar Array Project of the US Department of Energy's National Photovoltaics Program: 10 years of progress
[NASA-TM-89653] 03 p0346 N88-12188

Performance analysis of solar thermal power systems
[DE88-000563] 04 p0465 N88-12874

International Energy Agency (IEA) Small Solar Power Systems (SSPS) sodium cavity and external receiver performance comparison
[DE88-001310] 04 p0465 N88-12879

An overview of the DOE/SANDIA/USDA vertical axis wind turbine Test Bed Project
[DE88-000604] 05 p0622 N88-13812

The high performance solar array GSR3
[SNIAS-872-422-108] 05 p0622 N88-13814

Development of mechanically stacked tandem concentrator cells
[DE88-001926] 06 p0730 N88-14490

Actual performance and economic feasibility of residential solar water heaters
[INPE-4399-RPE/555] 08 p1023 N88-16191

Variable band gap materials for thermophotovoltaic generators
[AD-A188858] 09 p1186 N88-17104

A comparison of different module configurations for multibandgap solar cells
[DE88-002718] 09 p1187 N88-17113

The application of liquid-metal MHD (magnetohydrodynamics) to renewable energy sources
[DE88-003083] 09 p1251 N88-17495

A ring model of the lasertron
[DE88-004656] 10 p1323 N88-17908

Laser production and heating of plasma for MHD application
[NASA-TP-2798] 10 p1415 N88-18443

Coherent VUV source at 130 nm: Theory and modeling
[DE88-003874] 11 p1549 N88-19269

Wind energy resource survey of New Zealand: National resource assessment
[PB88-139365] 12 p1640 N88-19822

Research on multibandgap solar cells
[DE87-012261] 13 p1792 N88-20721

Stable, high-efficiency, CuInSe2-based, polycrystalline, thin-film tandem solar cells
[DE88-001116] 13 p1793 N88-20726

Crystalline photovoltaic cell technology: Present and future
[DE88-004684] 13 p1795 N88-20734

Overview of recent activities in the Heat Cycle Research Program
[DE88-005544] 13 p1795 N88-20738

Thin-film cadmium telluride solar cells
[DE88-001107] 13 p1846 N88-21050

Recent advances in photovoltaic concentrator technology
[DE88-003948] 15 p2091 N88-22462

Comparison of electrically driven lasers for space power transmission
[NASA-TM-4045] 16 p2212 N88-23197

Three-dimensional models of conventional and vertical junction laser-photovoltaic energy converters
[NASA-TM-4039] 17 p2370 N88-24111

Overview of NASA Lewis Research Center free-piston Stirling engine technology activities applicable to space power systems 17 p2398 N88-24255

Benefits of 20 kHz PMAD in a nuclear space station
17 p2398 N88-24256

Acoustical gas core reactor with MHD power generation for burst power in a bimodal system
17 p2403 N88-24290

A liquid metal MHD concept for multimegawatt space power application 17 p2413 N88-24348

Parametric analyses of the TE SP-100 system performance 17 p2415 N88-24358

The closed Brayton cycle: An energy conversion system for near-term military space missions
17 p2435 N88-24488

Progress in InP solar cell research
[NASA-TM-100914] 18 p2507 N88-24870

An investigation of high pressure/late cycle injection of CNG (Compressed Natural Gas) as a fuel for rail applications
[DE88-009000] 19 p2677 N88-25917

Integrated solar reforming for thermochemical energy transport
[DE88-005010] 19 p2686 N88-25967

Study of Staebler-Wronsky degradation effect in a Si:H based P-I-N solar cells
[NASA-CR-182564] 19 p2687 N88-25970

Dielectric compound parabolic concentrating solar collector with frustrated total internal reflection absorber
[DE88-009986] 19 p2688 N88-25976

Photovoltaic concentrator technology: Recent results
[DE88-009588] 20 p2819 N88-26726

Estimation of power-energy plots for secondary batteries
[DE88-011922] 21 p2940 N88-27460

Solar energy conversion through the interaction of plasmons with tunnel junctions. Part A: Solar cell analysis. Part B: Photoconductor analysis
[NASA-CR-183044] 21 p2967 N88-27621

Experimental fabrication of thin film single crystalline solar cells
[PB88-131958] 22 p3116 N88-28516

An examination of wake effects and power production for a group of large wind turbines
[DE88-009906] 22 p3117 N88-28518

Energy conversion measurements in laser-sustained argon plasmas for application to rocket propulsion
[AD-A194931] 24 p3337 N88-29861

ENERGY CONVERTERS
U DIRECT POWER GENERATORS

ENERGY DENSITY
U FLUX DENSITY

ENERGY DISSIPATION

A data analysis package for RDF-determination fromEXELFS-spectra
[USIP-87-07] 01 p0104 N88-10681

Navier-Stokes cascade analysis with a stiff Kappa-Epsilon turbulence solver
[NASA-TM-100218] 02 p0123 N88-10778

EXELFS (Extended Electron Energy Loss Fine Structure) of amorphous and crystalline SiC
[DE87-013551] 02 p0151 N88-10948

Focusing solar energy collector
02 p0159 N88-10996

Potential formation in the plasma confinement region of a radio-frequency plugged linear device
[IPPJ-843] 02 p0242 N88-11526

XeCl excimer laser with magnetic compressor
03 p0299 N88-118

Physical design of parameters of Nd:YAG disk laser
03 p0302 N88-11904

On helicity fluctuations and the energy cascade in turbulence
[NASA-CR-178403] 03 p0321 N88-12028

Resistor cooling in a vacuum
[DE88-000696] 04 p0440 N88-12733

Heating of stellar chromospheres and coronae: Evidence for non-magnetic basal heating
04 p0503 N88-13098

Chromospheric and coronal heating in a bias-free sample of K dwarfs 04 p0518 N88-13184

Power and charge dissipation from an electrodynamic tether 06 p0795 N88-14869

Ionization losses in BGO
[NOTA-INTERNA-889] 07 p0856 N88-15198

Study of vibration relaxation in active medium of CO2-laser using phase-absorption method
07 p0919 N88-15582

Effect of peel angle on peel force
[AD-A186117] 08 p0972 N88-15878

Stellar energy loss and anomalous contributions to the (photon photon) (neutrino antineutrino) interaction
[DE88-700618] 10 p1428 N88-18529

Experimental study of scattered waves and cylindrical antenna sheaths in a microwave driven plasma
11 p1553 N88-19293

The Euler-Bernoulli beam equation with boundary energy dissipation
[AD-A189517] 13 p1765 N88-20560

On the zonal momentum balance at the equator
13 p1805 N88-20788

Thermal modeling of solar central receiver cavities
[DE88-004940] 14 p1943 N88-21594

Modeling scalar flux and the energy and dissipation equations 16 p2196 N88-23096

A general form for the dissipation length scale in turbulent shear flows 16 p2197 N88-23104

On the magnetic structure and energy balance of EUV-emitting plasma in the quiet Sun
17 p2452 N88-24567

Electromagnetic damping and vibration isolation of space structures
[AD-A191492] 18 p2471 N88-24665

Extrema principles of entrophy production and energy dissipation in fluid mechanics
[NASA-TM-100992] 18 p2519 N88-24946

Energy dissipation in a rolling aircraft tire
[NASA-CR-182978] 19 p2676 N88-25913

Propagation of charged particle beams in the atmosphere
[AD-A193185] 21 p3014 N88-27887

Customizing Space Nuclear Power System Analysis Model (SNPSAM): Introducing a secondary coolant loop
[AD-A194620] 22 p3151 N88-28750

Mathematical theory and calculations of magnetic hysteresis curves
[DE88-011055] 23 p3277 N88-29510

ENERGY DISTRIBUTION
NT SPECTRAL ENERGY DISTRIBUTION

Measurement of parallel ion energy distribution function in PISCES plasma
[DE88-000108] 03 p0378 N88-12380

The closest solar analogs in the bright star catalogue
04 p0506 N88-13110

Statistical properties of small high-velocity events in the solar transition region 04 p0506 N88-13112

Lagrangian procedures for higher order field equations
[DE87-703365] 05 p0640 N88-13911

Calibration of the EGRET gamma ray telescope with a back-scattered laser beam 06 p0800 N88-14895

A survey study of energy distribution in component stars of Algol-type binary systems 06 p0801 N88-14901

Energy distribution of Cerenkov radiation for finite frequency intervals
[AD-A186901] 09 p1244 N88-17454

Product kinetic and internal energy distributions via velocity-aligned Doppler spectroscopy
[DE88-003510] 10 p1298 N88-17764

Procedure for detection and identification of a helicopter
[NASA-TT-20234] 13 p1722 N88-20297

Kinetics of slow electrons in excimer laser with electron-beam pumping 14 p1970 N88-21760

Femtosecond studies in hot carrier relaxation in GaAs and AlGaAs 14 p1977 N88-21801

Angular resolved energy analysis of (69)Ga + ions from a gallium liquid metal ion source
[AERE-R-12649] 15 p2139 N88-22760

An evaluation of energy-independent heavy ion transport coefficient approximations
[NASA-TM-101158] 17 p2397 N88-24251
Evaluation of surface energy and radiation balance systems for FIFE
[NASA-CR-183118] 20 p2828 N88-26778
Energy distribution and transfer in flowing hydrogen microwave plasmas 21 p3019 N88-27919

ENERGY EFFICIENCY TRANSPORT PROGRAM
U ACEE PROGRAM

ENERGY EXCHANGE
U ENERGY TRANSFER

ENERGY GAPS (SOLID STATE)
Wide bandgap passivation layers on silicon
[DE87-014307] 02 p0244 N88-11543
Improving the method of calculating electronic properties of narrow bandgap semiconductors
07 p0926 N88-15627
Effect of the band-gap characteristics on laser-induced dry etching of semiconductors
[DE88-001853] 07 p0937 N88-15695
Experimental aspects of high-T/sub c/ superconductors
[DE88-003019] 08 p1090 N88-16564
Interpretation of the temperature dependence of conductivity in superconducting oxides
[DE88-003028] 08 p1091 N88-16565
Variable band gap materials for thermophotovoltaic generators
[AD-A186858] 09 p1186 N88-17104
Raman scattering in mixed crystal semiconductors
12 p1696 N88-20149
Research on multibandgap solar cells
[DE87-012261] 13 p1792 N88-20721
Study for the determination of general and specific properties of wide energy-band gap HgHdTe in the 1-2 micrometer wavelength range
[AD-A189177] 13 p1845 N88-21041
Developments in ceramic superconducting materials
15 p2052 N88-22229
Meaning of energy diagrams used to describe hetero-structures
[DE88-702219] 21 p3023 N88-27943
Techniques and instrumentation for transient characterization of metal-insulator-semiconductor diodes. Applications to metal-insulator InP system
[ECL-87-17] 21 p3025 N88-27959
Theoretical investigation of image states of the hydrogen covered Cu (100)
[DE88-702662] 23 p3292 N88-29604

ENERGY LEVELS
NT ATOMIC ENERGY LEVELS
NT ELECTRON STATES
NT GROUND STATE
NT MOLECULAR ENERGY LEVELS
Accurate ab initio calculations which demonstrate a 3 Pi u ground state for Al2
[NASA-TM-89302] 01 p0102 N88-10666
Electronic structure of crystalline NaSn
[DE87-702583] 01 p0102 N88-10669
Studies on surface chemical states of some metals and ceramics bombarded with energetic light-ions
[DE87-752975] 02 p0145 N88-10910
J = O Task Force
[DE88-001326] 04 p0450 N88-12788
Characterization of Er,Cr:YSGG
[AD-A185885] 07 p0932 N88-15659
Wave functions for bound states of relativistic electrons in a crystal at electron movement along crystallographic planes
[DE88-700563] 07 p0939 N88-15708
Low-power photolytically pumped lasers
[DE88-002448] 08 p0991 N88-15998
New branch of solid-state physics
08 p1079 N88-16508
Near threshold behavior of photoelectron satellite intensities
[DE88-002231] 08 p1081 N88-16512
Design, construction and operation of a small RFP for turbulent plasma studies
[INPE-4241-PRE/1116] 08 p1087 N88-16545
Properties of nuclei and elementary particles at low and intermediate energies
[DE88-001913] 09 p1244 N88-17456
Frequency response function estimation at level
[DE88-002644] 10 p1344 N88-18034
Charge exchange in low energy (keV) and hyperthermal energy (10-100 eV) ion scattering
[AD-A187643] 11 p1543 N88-19222
Spectral line-broadening codes for hydrogen-, helium- and lithium-like ions in plasmas
[DE88-005238] 11 p1552 N88-19289
A neutral-beam diagnostic for fast confined alpha particles in a burning plasma. Applicatoin on CIT (Compact Ignition Tokamak)
[DE88-004890] 11 p1554 N88-19301
A moment approach to modeling negative ion sources
[AD-A188858] 12 p1691 N88-20114
An experimental method for species concentration measurements in a welding arc using laser-induced fluorescence
[DE88-005638] 13 p1778 N88-20636
Quantum Monte Carlo study of the MIES associated with H2 (X 1 sigma sub g (+)) and H2 (B 1 sigma sub u (+))
[AD-A189063] 13 p1835 N88-20977
Image charge, coherent scattering, and symmetry effects in electron stimulated desorption: O(-) from O sub 2 condensed on metals
[AD-A189093] 13 p1835 N88-20979
Discharge excitation of the XeF C to A transition
[DE88-006448] 15 p2070 N88-22339
Fermi level stabilization in semiconductors: Implications for implant activation efficiency
[DE88-006332] 15 p2145 N88-22801
On 1/n-expansion and wave functions
[DE88-701639] 16 p2260 N88-23509
Optical properties of heterostructures and superlattices
[AD-A191542] 18 p2581 N88-25335
Accuracy of analytic energy level formulas applied to hadronic spectroscopy of heavy mesons
[NASA-TM-4042] 19 p2725 N88-26185
Energy levels and magneto-electric effects in some quasi uni-dimensional semiconductor heterostructures
20 p2864 N88-27009
Superconducting electronic film structures
[AD-A192907] 20 p2879 N88-27091
Filling of the atmospheric transmission window due to emission from very high rotational levels of NO and O3
[AD-A194670] 23 p3233 N88-29239
Electronic states in tunneling semiconductor superlattices
[DE88-011571] 23 p3290 N88-29587
Absorption spectra and energy levels of Gd(3+), Nd(3+) and Cr(3+) in the garnet Gd3Sc2Ga3O12
[AD-A193634] 23 p3292 N88-29599
Relativistic theory of the Lamb shift based on self energy
[DE88-702658] 23 p3295 N88-29626

ENERGY LOSSES
U ENERGY DISSIPATION

ENERGY METHODS
NT BERNSTEIN ENERGY PRINCIPLE
NT STRAIN ENERGY METHODS
A work station for EXELFS data acquisition and analysis
[USIP-87-10] 01 p0078 N88-10498
The optimum illumination conditions for EXELFS studies in a CTEM
[USIP-87-08] 01 p0092 N88-10600
Instrumental and operational aspects of an EXELFS system connected to JEOL 100C STEM
[USIP-87-09] 01 p0092 N88-10601
A data analysis package for RDF-determination fromEXELFS-spectra
[USIP-87-07] 01 p0104 N88-10681
Fully plastic analysis of mixed mode plane-strain crack problems
[PB87-144929] 08 p0994 N88-16015

ENERGY OF FORMATION
Use of long-distance pair potentials in calculations of defect characteristics in metals
[DE88-701039] 15 p2037 N88-22138

ENERGY POLICY
Fifty years in synthetic fuels information: Have we lost a strategic national resource
[DE87-010902] 02 p0155 N88-10973
Numerical and experimental investigation of the unsteady temperature distribution in solar central receivers
[ESA-TT-1050] 03 p0347 N88-12193
Energy Data Base: Subject Thesaurus
[DE87-008007] 03 p0384 N88-12414
Emerging environmental constraints on the use of gasoline and diesel fuel and tradeoffs associated with the use of alternative fuels
[DE87-011504] 04 p0422 N88-12614
Fuel cells --- military applications
[PML-1986-43] 05 p0622 N88-13813
Satellite power systems under consideration by the United Nations 09 p1128 N88-16773
The role of repowering in America's power generation future
[DOE/FE-0096] 10 p1351 N88-18076
Understanding and accepting fusion as an alternative energy source
[DE88-004356] 10 p1413 N88-18432
Technical highlights of the Alternative Fuels Utilization Program
[DE88-005064] 15 p2049 N88-22205
Solar dynamic power systems
[ETN-88-92969] 23 p3230 N88-29224

ENERGY REQUIREMENTS
A large X-ray flare on Sigma 2 coronae borealis observed with exosat 04 p0508 N88-13121
Power systems for production, construction, life support and operations in space
[NASA-TM-100838] 14 p1883 N88-21254
Droplet size characteristics and energy input requirements of emulsions formed using high-intensity-pulsed electric fields
[DE88-005912] 15 p2128 N88-22692

ENERGY SOURCES
A proposal for a project entitled assessment of forest resources in Uruguay submitted to the United Nations Industrial Development Organization (UNIDO)
17 p2352 N88-24016

ENERGY SPECTRA
NT ELECTRONIC SPECTRA
NT NEUTRON SPECTRA
Relativisitic heavy ion collisions
[DE87-014292] 02 p0232 N88-11462
Heavy element compositions and energy spectra of galactic and solar cosmic rays 03 p0272 N88-11714
A multiple-time-scale turbulence model based on variable partitioning of turbulent kinetic energy spectrum
[NASA-CR-179222] 04 p0444 N88-12754
Spectral evolution equation for the sideband instability in a free-electron laser oscillator
[DE88-000510] 04 p0447 N88-12771
Simultaneous, cospatial imaging of the Sun in cyanogen and singly-ionized calcium 04 p0507 N88-13114
Multiply charged particles in primary cosmic rays with energy less than or equal to 2 TeV
07 p0921 N88-15596
Fully turbulent internal flow excitation of pipe systems
08 p1000 N88-16056
Observations of gamma bursts from GBS 0526-66
08 p1001 N88-16065
Interpretation of equatorial current meter data as internal waves
[PB88-108113] 08 p1044 N88-16309
New branch of solid-state physics
08 p1079 N88-16508
Near threshold behavior of photoelectron satellite intensities
[DE88-002231] 08 p1081 N88-16512
Investigation of the quantitative determination of two dimensional sea surface wave spectra from shipborne radar measurements
[GKSS-87/E/10] 09 p1195 N88-17163
Properties of nuclei and elementary particles at low and intermediate energies
[DE88-001913] 09 p1244 N88-17456
Vibration spectra of oxygen and vanadium atoms in vanadium-oxygen disordered interstitial alloys
[DE87-703166] 13 p1740 N88-20404
Study of spectra of sea waves on horizontally nonuniform current in rip zone 13 p1788 N88-20699
Energy spectra of pick-up ions recorded during the encounter of Giotto with Comet Halley
14 p1997 N88-21901
Spectral measurements in a disturbed boundary layer over snow
[AD-A190217] 15 p2097 N88-22494
Computing X-ray effects in optics
[DE88-006722] 15 p2134 N88-22732
Time-frequency representations for speech signals
[AD-A188661] 18 p2498 N88-24819
Accuracy of analytic energy level formulas applied to hadronic spectroscopy of heavy mesons
[NASA-TM-4042] 19 p2725 N88-26185
Meaning of energy diagrams used to describe hetero-structures
[DE88-702219] 21 p3023 N88-27943
Cascade model of gamma-ray bursts: Power-law and annihilation-line components
[NASA-TM-101176] 21 p3032 N88-27998
Nuclear and ionic charge distribution experiment on ISEE-1 and ISEE-3
[NASA-CR-180776] 23 p3183 N88-28947

ENERGY STORAGE
NT ELECTRIC ENERGY STORAGE
NT HEAT STORAGE
Electrical Power Working Group report
01 p0016 N88-10095
Ionically conductive polymers: Application to solid state batteries
[AD-A183733] 01 p0037 N88-10239
Apparatus for storing kinetic energy
[EP-PATENT-0-181-736-A1] 01 p0066 N88-10422
Results of a wind turbine/sealed lead-acid battery experiment
[DE87-012720] 02 p0166 N88-11044
Electrodynamic tether system study
[NASA-CR-172024] 03 p0275 N88-11737

Heats of mixing for thermal energy storage systems. Phase 1: Selection of suitable liquid-liquid mixtures
[DE87-014971] 03 p0347 N88-12196

A study of the optimal transition temperatue of PCM (Phase Change Material) wallboard for solar energy storage
[DE88-001522] 04 p0466 N88-12882

Extended abstracts: Eighth Battery and Electrochemical Contractors' Conference
[DE88-000960] 06 p0730 N88-14489

Solar assisted absorption or motor driven heat pump with earth seasonal storage, part 1
[DE88-900191] 09 p1187 N88-17114

Value-assessment of energy storage concepts in burst power systems
[DE87-013756] 09 p1187 N88-17115

Development of encapsulated lithium hydride thermal energy storage for space power systems
[DE88-004762] 11 p1507 N88-19001

Photochemical energy storage: Studies of inorganic photoassistance agents
[DE88-002596] 11 p1508 N88-19010

Proof of the feasibility of coherent and incoherent schemes for pumping a gamma-ray laser
[AD-A189238] 13 p1774 N88-20613

Power systems for production, construction, life support and operations in space
[NASA-TM-100838] 14 p1883 N88-21254

Energy storage and transport by reversible chemical reactions
[DE88-900370] 14 p1942 N88-21587

Overview of 1987 moonlight project
15 p2052 N88-22231

Performance evaluation of molten salt thermal storage systems
[DE87-014645] 15 p2091 N88-22461

Value of energy storage in pulsed space power systems
[AD-A191311] 16 p2170 N88-22938

Nickel hydroxide active material densities
[AD-A191411] 16 p2230 N88-23319

The cluster ion approach to the condensation and storage of antihydrogen 16 p2269 N88-23575

Aerospace energy systems laboratory: Requirements and design approach
[NASA-TM-100423] 17 p2390 N88-24206

Energy storage evaluation for burst power applications
17 p2426 N88-24430

Energy storage for nuclear burst power systems
17 p2426 N88-24431

Value assessment of energy storage concepts in burst power systems 17 p2426 N88-24432

Rotating-hoop, pulsed-energy converter
17 p2426 N88-24433

Candidate advanced energy storage concepts for multimegawatt burst power systems
17 p2426 N88-24434

High power density alkaline fuel cell technology for MMW space burst power 17 p2429 N88-24451

Polymer fuel cell as an energy storage component for space power applications 17 p2429 N88-24452

Solar assisted absorption or motor driven heat pump with earth seasonal storage. Part 2: Tables and figures
[DE88-900226] 19 p2686 N88-25964

Effect of LEO cycling at shallow depths of discharge on MANTECH IPV nickel-hydrogen cells
[NASA-TM-101300] 19 p2688 N88-25978

Loss evaluation of self-commutated power conditioner for battery energy storage system
[DE88-752075] 20 p2794 N88-26575

Recent developments in nickel hydrogen technology
[DE88-011246] 21 p2939 N88-27456

Storage of thermal energy by means of an absorption cycle
[PB88-190814] 21 p2966 N88-27619

Thermal energy storage
[DE88-010753] 21 p2967 N88-27625

Energy storage considerations for a robotic Mars surface sampler
[NASA-TM-100969] 22 p3166 N88-28853

Transient thermal analysis of three fast-charging latent heat storage configurations for a space-based power system
[DE88-009714] 23 p3186 N88-28960

Charge storage and switching phenomena in metal complexes
[AD-A193778] 23 p3192 N88-28996

Proof of the feasibility of coherent and incoherent schemes for pumping a gamma-ray laser
[AD-A193856] 23 p3220 N88-29165

High power storage system based on thin film solid ionics
[AD-A193623] 23 p3291 N88-29598

Regenerative fuel cell energy storage system for a low earth orbit space station
[NASA-CR-174802] 24 p3389 N88-30184

ENERGY STORAGE DEVICES
U ENERGY STORAGE

ENERGY TECHNOLOGY
NT GEOTHERMAL TECHNOLOGY

Solar thermal technology
[DE87-001171] 02 p0195 N88-11218

Spinoff, 1987
[NASA-TM-89652] 02 p0250 N88-11577

JPRS report: Science and technology. China
[JPRS-CST-87-031] 03 p0299 N88-11880

The Black College satellite telecommunications network planning in support of energy-related collaborative research
[DE88-000182] 03 p0307 N88-11940

Proceedings of the Fifth Symposium on Energy Engineering Sciences: Instrumentation, Diagnostics, and Material Behavior
[DE88-001479] 04 p0429 N88-12660

Basic energy sciences research in the Metals and Ceramics Division of Oak Ridge National Laboratory
[DE87-013538] 06 p0681 N88-14171

Research needs for hydrocarbon fuels
[DE87-014555] 06 p0687 N88-14209

Satellite power systems under consideration by the United Nations 09 p1128 N88-16773

Thermal energy storage by means of an absorption cycle
[ETN-88-91614] 09 p1186 N88-17108

Side-by-side comparisons of evacuated compound parabolic concentrator and flat plate solar collector systems at temperatures of 90 to 100°C
[DE88-004717] 10 p1351 N88-18073

Understanding and accepting fusion as an alternative energy source
[DE88-004356] 10 p1413 N88-18432

Minutes of the meeting of the Indo-US Subcommission on Science and Technology (8th) held at Washington, D.C. on September 22-24, 1986
[PB88-130158] 10 p1423 N88-18503

Proceedings of the 12th Symposium of Japan Solar Energy Society
[DE88-770029] 11 p1507 N88-19005

Alternative Energy in the Midwest: Research and Applications. Conference Proceedings, Rosemont, Illinois, March 19-20, 1987
[PB88-142278] 11 p1509 N88-19015

Starpower: The US and the international quest for fusion energy
[PB88-128731] 11 p1551 N88-19283

Systems approach to energy quality and efficiency
[PB88-139506] 12 p1640 N88-19823

Federal Ocean Energy Technology
[DE87-012279] 13 p1792 N88-20722

Power from the sun: Principles of high temperature solar thermal technology
[DE87-001104] 13 p1795 N88-20736

Technology '87: Research and Development Laboratory Technology Transfer Program
[DE88-003142] 13 p1852 N88-21084

JPRS report: Science and technology. Japan
[JPRS-JST-87-029] 15 p2052 N88-22228

Overview of 1987 moonlight project
15 p2052 N88-22231

JPRS report: Science and technology. Japan
[JPRS-JST-87-026] 16 p2184 N88-23018

Sunshine project for FY 1987 outlined
16 p2184 N88-23021

Advanced energy system program
[PB88-183025] 19 p2686 N88-25965

Fuel cell systems program plan: Fiscal year 1988
[DE88-011080] 20 p2820 N88-26731

ENERGY TRANSFER

Laser probes of natural gas ignition chemistry
[PB87-209599] 01 p0021 N88-10129

Acceleration to hypervelocities using minimum energy concepts
[DE87-011796] 01 p0089 N88-10583

An interactive computer program for materials analysis by means of ion scattering
[MRL-R-1040] 01 p0091 N88-10596

A microstructural lattice model for strain oriented problems: A combined Monte Carlo finite element technique
[NASA-TM-100215] 02 p0150 N88-10939

Migration and transfer of triplet energy in selected polymer systems
[DE87-014432] 02 p0152 N88-10953

Hot spots: Subnanometer femtosecond energy localization
[DE87-010276] 02 p0155 N88-10968

Energy transformation in molecular electronic systems
[DE87-013916] 03 p0282 N88-11771

Kinetics of crack growth: Thermal/mechanical interaction 03 p0337 N88-12124

Application of solar technology to fuel production chemical processing, and thermochemical energy transport: Status and future
[DE87-014172] 03 p0346 N88-12189

Configurations of the quiet polar cap and its response to a sudden increase of the energy input rate epsilon
[DMI-GEOPHYS-PAPERS-R-74]
03 p0350 N88-12210

The Conference on the Dynamics of Molecular Collisions held in Oglebay Park, Wheeling, West Virginia on 12-17 July 1987
[AD-A184690] 03 p0374 N88-12354

Theory of heat and moisture exchange between finely disperse storm-generated spray and turbulent air flow
04 p0461 N88-12851

Nitrogen energy transfer study
[AD-A184457] 04 p0464 N88-12869

Variable collision frequency effects on hose and sausage instabilities in relativistic electron beams
[AD-A184206] 04 p0490 N88-13021

Intramolecular energy transfer reactions as a method for metal complex assisted production of hydrogen
[DE88-001621] 05 p0562 N88-13425

Energy dependence of ion-induced sputtering yields of monatomic solids in the low energy region
[IPPJ-AM-52] 05 p0651 N88-13988

Photoinduced charge separation by polymer-bound chromophores
[DE88-002101] 06 p0685 N88-14198

Nitrogen scale-up
[AD-A185702] 06 p0709 N88-14351

Solar cosmic ray propagation in high-velocity solar wind stream 08 p1002 N88-16073

The role of anabatic winds in the heating of valleys
08 p1014 N88-16144

FTE like variations in the geomagnetic field at ground based conjugate stations in the cusp regions
[INPE-4345-PRE/1182] 08 p1024 N88-16199

Effects of energy, distance and orientation on electron transfer rates studied by pulse radiolysis in organic media
[DE88-002906] 08 p1082 N88-16521

Group 2A metastable collision complexes: Spectroscopy and behavior in intense radiation fields
[AD-A186737] 08 p1082 N88-16524

Energy transmission using coherent, quasimonochromatic light beams
09 p1241 N88-17436

Energy distribution of Cerenkov radiation for finite frequency intervals
[AD-A186901] 09 p1244 N88-17454

A dynamical system/coherent structure approach to the fully developed turbulent wall layer
10 p1267 N88-17578

Kinetic studies following state-selective laser excitation
[DE88-004094] 10 p1335 N88-17981

Energy transfer studies with lasers
[DE88-004864] 10 p1337 N88-17991

Research on fluid dynamic energy separation
[DE88-002776] 10 p1339 N88-18001

Energy transfer and photochemistry in biomimetic solar conversion
[PB88-130026] 10 p1348 N88-18057

Energy transfers for multilayer hydrodynamic ocean models: General formulation and specific examples
[AD-A187604] 10 p1358 N88-18116

Spectroscopic studies of energy transfer in photosynthetic reaction centers of higher plants
[DE88-003850] 10 p1359 N88-18121

State-to-state dynamics of molecular energy transfer
[DE88-003282] 10 p1406 N88-18382

Coronal heating by means of helical magnetohydrodynamic turbulence
[AD-A187084] 10 p1410 N88-18413

Photophysics and photochemistry of poly(di-n hexylsilane) in room temperature solution
[AD-A187890] 11 p1462 N88-18714

Nonlinear dynamic maximum power theorem
[AD-A187491] 11 p1477 N88-18810

Transient radiative energy transfer in incompressible laminar flows
[NASA-CR-182605] 11 p1488 N88-18883

On the possibility of high velocity deflagration front propagation by radiative energy transfer
[AD-A189022] 12 p1613 N88-19645

Millimeter and submillimeter wave research: Spectroscopy, energy transfer, and techniques
[AD-A188952] 12 p1620 N88-19691

On the energy release rate for dynamic transient anti-plane shear crack propagation in a general linear viscoelastic body
[AD-A188385] 12 p1635 N88-19791

Resonance energy transfer between carbon monoxide and oxygen molecules using dye laser intracavity absorption spectroscopy
[AD-A188488] 12 p1689 N88-20104

Instrumentation for collisional energy transfer studies
[AD-A188495] 12 p1689 N88-20105

To what extent is mass loading responsible for the Venus bowshock precursor?
[NASA-TM-89307] 12 p1711 N88-20239

Solar flares and magnetic topology
[AD-A188692] 12 p1712 N88-20244

Molecular dynamics of laser ablation of a polymer coating
[DE88-004337] 13 p1750 N88-20466

Turbulent transfer of momentum and heat in boundary layer of fluid beyond an obstacle. 1: Hydrodynamic characteristics 13 p1787 N88-20690

Power spectral density analysis of wind-shear turbulence for related flight simulations
[NASA-CR-182721] 13 p1802 N88-20773

Energy and momentum fluxes through the sea surface
13 p1806 N88-20798

Excimer laser photolysis studies of T-V (Translation-to-Vibration) energy transfer
[AD-A189613] 13 p1837 N88-20989

Observations on energy transport in tokamaks: A new formula for turbulent transport
[DE88-005309] 13 p1841 N88-21019

Physical process for maintenance of mean meridional and zonal circulation of atmosphere in middle latitudes, volume 2 14 p1900 N88-21345

Calculation of the efficiency of a resonant cyclotronic electron maser (gyrotrons)
[INPE-4387-PRE/1207] 14 p1915 N88-21444

Energy storage and transport by reversible chemical reactions
[DE88-900370] 14 p1942 N88-21587

Electronic energy transfer processes in the alkali/alkaline earth metal vapors
[AD-A190035] 15 p2034 N88-22119

Molecular reaction and energy transfer rate estimation for chemical-laser analysis
[AD-A190664] 15 p2035 N88-22126

Reactions of N2(A sup 3 sigma sup + sub u) candidates for short wavelength lasers
[DE88-007018] 15 p2070 N88-22342

Characterization of space radiation environment in terms of the energy deposition in functionally important volumes
[DE88-005627] 15 p2100 N88-22513

The adhesive bonding of thermoplastic composites
[AD-A190994] 16 p2173 N88-22953

Study of one-dimensional spectral dynamic equations of the Reynolds stresses in homogeneous anisotropic turbulence: Application to split-spectrum modeling
16 p2196 N88-23095

Local structure of intercomponent energy transfer in homogeneous turbulent shear flow
16 p2197 N88-23103

The decay of isotropic turbulence in a rapidly rotating frame 16 p2197 N88-23107

Energy transfer processes in free radicals: A collaborative experimental and theoretical investigation
[AD-A191264] 16 p2269 N88-23578

Proceedings of Symposium on Physics of Target Implosion and Pulsed Power Techniques
[IPPJ-859] 16 p2276 N88-23619

Simulation code for ICF including radiative energy transfer 16 p2277 N88-23627

Bimolecular reactions and energy-transfer processes of highly vibrationally excited molecules related to energetic materials
[AD-A189013] 18 p2571 N88-25270

Energy-transfer properties and mechanisms
[DE88-007107] 18 p2571 N88-25272

Spectroscopy and energy transfer kinetics of the interhalogens
[AD-A192103] 18 p2583 N88-25344

Transition probabilities in OH A 2 sigma + - X 2 pi i: Bands with v prime' = 0 and 1, v double prime = 0 to 4
[NASA-CR-182946] 18 p2584 N88-25353

Numerical investigation of acoustic energy exchange through flow turning 19 p2629 N88-25593

Numerical simulation studies of laminar-turbulent transition in the plan channel 19 p2665 N88-25850

Pressure drop and heat transfer in turbulent non-Newtonian pipe flow of advanced energy transmission fluids
[DE88-010021] 19 p2666 N88-25853

Integrated solar reforming for thermochemical energy transport
[DE88-005010] 19 p2686 N88-25967

Half collision studies of inelastic energy transfer processes
[DE88-008096] 19 p2724 N88-26178

Electrodynamic driver for the space thermoacoustic refrigerator (STAR)
[AD-A192337] 20 p2785 N88-26517

Effects of cosmic rays on single event upsets
[NASA-CR-183053] 20 p2793 N88-26569

Energy migration, motion and order in synthetic polymers
[AD-A193334] 21 p2918 N88-27320

Energy distribution and transfer in flowing hydrogen microwave plasmas 21 p3019 N88-27919

Chemically-produced N2(A) to NO(X) energy transfer in a supersonic flow
[AD-A192501] 22 p3082 N88-28302

On the energy source of 1982-83 ENSO episode simulated by the NCAR community climate model
22 p3122 N88-28556

The active layer of the upper Atlantic Ocean
22 p3124 N88-28566

Solid-state laser research report: Energy transfer in non-uniform codoped crystals
[AD-A194358] 23 p3219 N88-29161

Preliminary studies of NF3 + H2 production of N2(A3 sigma(+)u) in a supersonic flow
[AD-A194479] 23 p3219 N88-29162

N2(A3epsilon u+) by reaction of N2F4 + H2 in a supersonic flow
[AD-A194493] 23 p3219 N88-29163

Vanderbilt free electron laser project in biomedical and materials research
[AD-A195961] 24 p3378 N88-30121

Energy budget and ground temperatures in hot regions
[AD-A196298] 24 p3404 N88-30268

ENGINE AIRFRAME INTEGRATION

Transonic analysis and design of axisymmetric bodies in nonuniform flow
[NASA-CR-4101] 01 p0003 N88-10013

ENGINE ANALYZERS

Proceedings of the 14th Symposium on Aircraft Integrated Monitoring Systems
[DFVLR-MITT-88-04] 22 p3033 N88-28001

Use of penetrating radiations for the dynamic examination of aero gas turbines
[PNR90470] 22 p3045 N88-26073

ENGINE CONTROL

NT ROCKET ENGINE CONTROL
NT TURBOJET ENGINE CONTROL

A heat transfer model for a heated helium airship
[AD-A183786] 03 p0259 N88-11629

The flight evaluation of an advanced engine display and monitoring system 03 p0264 N88-11659

Engine/airframe response evaluation of the HH-60A helicopter equipped with the T700-GE-701 transient droop improvement electronic control unit
[AD-A184443] 04 p0401 N88-12492

Pumping systems and flow interfaces for rapid response electronic reheat controls 10 p1282 N88-17665

Possibilities for on-line surge suppression by fast guide vane adjustment in axial compressors
10 p1283 N88-17674

ENGINE DESIGN

NT ROCKET ENGINE DESIGN

The design and development of mercury vaporisers for use with electron-bombardment ion engines
[RAE-TR-70042] 01 p0018 N88-10108

First article test noise survey of the A/F32T-9 large turbo fan engine enclosed noise suppressor system, Sky Harbor IAP (International Airport), Phoenix, Arizona
[AD-A183799] 01 p0090 N88-10588

The wide chord fan blade: A Rolls Royce first
[PNR90416] 02 p0125 N88-10789

Turbines with counterrotating runners for aircraft power plants 02 p0158 N88-10992

Transmission efficiency in advanced aerospace powerplant
[PNR90391] 02 p0182 N88-11133

Computer aided engineering/manufacturing at Rolls-Royce
[PNR90595] 02 p0222 N88-11397

Advanced natural gas fueled engine development. Part 1: Design and analyses
[PB87-224804] 03 p0331 N88-12087

Advanced natural gas fueled engine development. Part 2: Materials investigation
[PB87-223160] 03 p0331 N88-12088

The structure-mapping engine: Algorithm and examples
[AD-A184042] 03 p0368 N88-12315

Adiabatic diesel engine component development: Reference engine for on-highway applications
[NASA-CR-179531] 03 p0386 N88-12428

Automated design of controlled diffusion blades
[NASA-TM-100251] 05 p0542 N88-13304

Development of an integrated BEM approach for hot fluid structure interaction
[NASA-CR-181577] 05 p0556 N88-13384

Ceramic technology for advanced heat engines
[PB87-232997] 06 p0683 N88-14188

Development, features of roller rocker arm reported
06 p0689 N88-14219

Small High Pressure Ratio Turbines --- conference
[VKI-LS-1987-07] 06 p0712 N88-14364

Hot piston ring tests
[NASA-TM-100256] 06 p0729 N88-14486

Aeropropulsion '87. Session 5: Subsonic Propulsion Technology
[NASA-CP-10003-SESS-5] 08 p0956 N88-15800

Small engine technology programs
08 p0956 N88-15801

Aircraft engine hot section technology: An overview of the HOST Project 08 p0957 N88-15804

Advanced propeller research
08 p0957 N88-15806

Propulsion challenges and opportunities for high-speed transport aircraft 08 p0958 N88-15809

NASA/Army Rotorcraft Technology. Volume 2: Materials and Structures, Propulsion and Drive Systems, Flight Dynamics and Control, and Acoustics
[NASA-CP-2495-VOL-2] 09 p1106 N88-16632

Technology developments for a compound cycle engine 09 p1107 N88-16637

Small gas turbine engine technology
09 p1107 N88-16638

The convertible engine: A dual-mode propulsion system 09 p1108 N88-16639

Aeropropulsion '87. Session 1: Aeropropulsion Materials Research
[NASA-CP-10003-SESS-1] 09 p1118 N88-16697

Impact and promise of NASA aeropropulsion technology 09 p1118 N88-16698

High temperature polymer matrix composites
09 p1119 N88-16700

Ceramics for engines 09 p1119 N88-16704

An investigation into the feasibility of using a dual-combustion mode ramjet in a high Mach number tactical missile
[AD-A186906] 09 p1119 N88-16705

Advanced Technology for Aero Gas Turbine Components
[AGARD-CP-421] 10 p1279 N88-17647

The coming revolution in turbine engine technology
10 p1279 N88-17648

An examination of the impact of potential advances in component technology for future military engines
10 p1279 N88-17650

Specification of an engine and its components starting from a consideration of aircraft missions
10 p1279 N88-17651

Experimental evaluation of a translating nozzle sidewall radial turbine 10 p1280 N88-17656

An integrated aero/mechanical performance approach to high technology turbine design
10 p1280 N88-17657

Design and testing of a small radial turbine for auxiliary power units 10 p1281 N88-17661

Design and aerodynamic performance of a small mixed-flow gas generator turbine
10 p1281 N88-17662

Development of a plenum chamber burner system for an advanced VTOL engine 10 p1281 N88-17664

Analysis of possible transmission arrangements applicable for driving single or twin counterrotating fans on propfan engines 10 p1282 N88-17670

Advanced propfan analysis for the family of commuter airplanes
[NASA-CR-182566] 12 p1582 N88-19468

Optimizing powerplant design and development cycles
12 p1701 N88-20183

Activities report of the Energetics Department
[ETN-88-91981] 14 p1888 N88-21281

Visualisation of the flow at the tip of a high speed axial flow turbine rotor: An assessment of flow visualisation techniques and the requirement of the experimental turbine
[AD-A189929] 15 p2063 N88-22301

Continuous fiber ceramic matrix composites for heat engine components 15 p2082 N88-22411

Full electronic control system for diesel engine
16 p2185 N88-23025

Status, trends in research on internal combustion engines 16 p2185 N88-23027

Status and prognosis for alternative engine materials
[NASA-TM-100903] 18 p2486 N88-24749

Design, manufacture and spin test of high contact ratio helicopter transmission utilizing Self-Aligning Bearingless Planetary (SABP)
[NASA-CR-4155] 18 p2524 N88-24975

Development of a generic combustion stability code for liquid propellant rocket engines
19 p2626 N88-25576

Numerical grid generation and flow simulation in SSME thrust chamber 19 p2626 N88-25577

Boundary layer simulator (BLIMPJ) improvement
19 p2627 N88-25582
Motor test data comparisons with laboratory data and stability predictions 19 p2629 N88-25594
A multiple chamber volume-filling model for prediction of transient solid rocket motor ballistic performance
19 p2633 N88-25618
Analysis of flow through pump of large rocket engine
19 p2637 N88-25646
Extensive verification of blade-to-blade flow code based on Denton scheme 19 p2638 N88-25654
Application of computational fluid dynamics to design of compressor cascade 19 p2639 N88-25655
Permanent magnet excitation of axial flow synchronous machines with high rotation moment
[ETN-88-92385] 20 p2796 N88-26592
Analytical and experimental investigation of ringless piston concept
[AD-A192835] 20 p2810 N88-26673
The design and fabrication of a Stirling engine heat exchanger module with an integral heat pipe
[NASA-TM-101296] 20 p2820 N88-26732
Documentation of the Benson Diesel Engine Simulation Program
[NASA-TM-100940] 21 p2898 N88-27201
Analytical and experimental investigation of ringless piston concept
[AD-A193213] 21 p2956 N88-27559
The design and testing of aero engines to minimise hazard from birds
[PNR90436] 22 p3040 N88-28049
Trends in civil aircraft propulsion
[PNR90441] 22 p3044 N88-28067
Variable-compression-ratio pistons for high power output diesel engines 22 p3084 N88-28316
V2500 engine collaboration
[PNR90423] 24 p3326 N88-29803
Developing the Rolls-Royce Tay
[PNR90447] 24 p3327 N88-29809
Combustion and fuels in gas turbine engines
[AGARD-CP-422] 24 p3345 N88-29910
Voltage directive drive with claw pole motor and control without rotor position indicator
[ETN-88-93120] 24 p3366 N88-30047
Impact of ETO propellants on the aerothermodynamic analyses of propulsion components
[NASA-TM-101303] 24 p3374 N88-30094

ENGINE FAILURE
A natural low frequency oscillation in the wake of an airfoil near stalling conditions
[NASA-TM-100213] 02 p0123 N88-10779
Blade excitation criteria developed for aero derived engines in Arctic Alaska
[PNR90368] 02 p0182 N88-11131
Incipient failure detection of space shuttle main engine turbopump bearings using vibration envelope detection
05 p0595 N88-13629
Preliminary airworthiness evaluation of a UH-1 equipped with a terrain mapping receiver antenna
[AD-A186274] 07 p0819 N88-14980
RB-ARD: A proof of concept rule-based abort
08 p1065 N88-16435
Verification of obstacle accountability areas using a simple mathematical model. Part 1: Description of general model and application for a specific case --- engine failure at takeoff
[NLR-TR-85069-U] 09 p1115 N88-16683
Army maintenance: Actions to reduce the likelihood of helicopter gear failures
[PB88-135256] 11 p1433 N88-18551
Flight simulator experiments concerning take-off visibility minima
[NLR-TR-86050-U] 13 p1719 N88-20281

ENGINE INLETS
Boundary layer profile investigations downstream of an aero-engine intake anti-icing air exhaust slot
[PNR90378] 02 p0171 N88-11080
Numerical and experimental investigation of multiple shock wave/turbulent boundary layer interactions in a rectangular duct
[AD-A190772] 15 p2066 N88-22320
The calculation of the flow through a two-dimensional faired diffuser
[PNR90433] 22 p3076 N88-28259
Experimental and analytical evaluation of the effects of simulated engine inlets on the blade vibratory stresses of the SR-3 model prop-fan
[NASA-CR-174959] 23 p3179 N88-28927

ENGINE MONITORING INSTRUMENTS
Engine condition monitoring civil requirements: A British Airways view 22 p3033 N88-28002
From turboprop aircraft to multi-engined jet aircraft Aircraft Integrated Monitoring Systems (AIMS)
22 p3033 N88-28005
German Air Force requirements for the on-board life monitoring system (OLMOS) on Tornado
22 p3033 N88-28007
Onboard Life Monitoring System (OLMOS), hardware equipment onboard and on ground
22 p3034 N88-28009
Onboard Life Monitoring System (OLMOS): Engine life cycle calculation and trending 22 p3034 N88-28010
V2500 Condition Monitoring and Performance Analysis Software System (COMPASS): Overview of system --- aircraft engine
[PNR90418] 22 p3139 N88-28666
Development and installation of an instrumentation package for GE F404 investigative testing
[AD-A196265] 24 p3376 N88-30107

ENGINE NOISE
Advanced turboprop wing installation effects measured by unsteady blade pressure and noise
[NASA-TM-100200] 01 p0002 N88-10008
First article test noise survey of the A/F32T-9 large turbo fan engine enclosed noise suppressor system, Sky Harbor IAP (International Airport), Phoenix, Arizona
[AD-A183799] 01 p0090 N88-10588
Noise emission of civil and military aero-engines. Sources of generation and measures for attenuation
[ETN-87-91021] 01 p0091 N88-10595
Measured and calculated acoustic attenuation rates of tuned resonator arrays for two surface impedance distribution models with flow
[NASA-TP-2766] 09 p1241 N88-17440
Annoyance caused by advanced turboprop aircraft flyover noise: Single-rotating propeller configuration
[NASA-TP-2782] 09 p1242 N88-17441
Noise assessment of unsuppressed TF-34-GE-100A engine at Warfield ANG, Baltimore, Maryland
[AD-A189966] 15 p2129 N88-22702
First article noise survey of the A/F32T-9 large turbo fan engine enclosed noise suppressor system: far-field noise, Ellsworth AFB, South Dakota
[AD-A191938] 19 p2602 N88-25457

ENGINE PARTS
Development of a statistically proven injection molding method for reaction bonded silicon nitride, sintering reaction bonded silicon nitride, and sintered silicon nitride
[ETN-87-90575] 02 p0160 N88-11002
Investment foundry melting stock: Rolls Royce requirements and demands in terms of quality and the relationship to end product performance
[PNR90397] 02 p0160 N88-11003
Stirling engine research at national and university laboratories in Japan
[DE87-014622] 02 p0180 N88-11123
High temperature stress-strain analysis
02 p0188 N88-11170
Adiabatic diesel engine component development: Reference engine for on-highway applications
[NASA-CR-179531] 03 p0386 N88-12428
Composite mechanics for engine structures
[NASA-TM-100176] 04 p0411 N88-12552
Application of finite element methods with cyclic elasto-plastic strain analysis to low cycle fatigue analysis of engine components
[AR-004-512] 05 p0596 N88-13642
An analysis of temperature effect on LCF crack growth rates in superalloy GH36 06 p0721 N88-14431
Aeropropulsion '87. Session 1: Aeropropulsion Materials Research
[NASA-CP-10003-SESS-1] 09 p1118 N88-16697
Ceramics for engines 09 p1119 N88-16704
Turbine engine monitoring systems: Can they benefit component improvement program management?
[AD-A186992] 09 p1120 N88-16706
Development of a shell system for DS moulds at RR precision casting facility --- directional solidification (DS)
[PNR90400] 09 p1151 N88-16893
A comparison of measurements from the A/E35U-3 and PWMA (Portable Wear Metal Analyzer) spectrometers
[AD-A186855] 09 p1177 N88-17047
An examination of the impact of potential advances in component technology for future military engines
10 p1279 N88-17650
Specification of an engine and its components starting from a consideration of aircraft missions
10 p1279 N88-17651
Free-piston Stirling engine diaphragm-coupled heat-actuated heat pump component technology program, phase 1C
[DE88-003654] 10 p1330 N88-17949
Ceramic bearings for use in gas turbine engines
[NASA-TM-100288] 10 p1340 N88-18007
An evaluation of effectiveness of PTFE (polytetrafluoroethylene) type friction reducers on reducing friction and wear
[AD-A187440] 10 p1340 N88-18010
Effects of thermal and thermo-mechanical treatments on the mechanical properties of centrifugally cast alloy 718
[AD-A188195] 11 p1458 N88-18690
Structural analysis methods development for turbine hot section components
[NASA-TM-100298] 11 p1501 N88-18967
Sampling intervals
[AD-A189445] 12 p1573 N88-19408
Advanced Gas Turbine (AGT) Technology Development Project, ceramic component developments
[NASA-CR-180871] 12 p1709 N88-20229
Aircraft corrosion problems and research in the Netherlands
[NLR-MP-86066-U] 13 p1744 N88-20427
Small engine components test facility turbine testing cell
[NASA-TM-100887] 15 p2019 N88-22037
Specialty three-dimensional finite element analysis codes 15 p2079 N88-22393
Computational structural mechanics for engine structures 15 p2080 N88-22399
Thermal-structural analyses of Space Shuttle Main Engine (SSME) hot section components
15 p2081 N88-22404
Evaluation of ceramic thermal barrier coatings for gas turbine engine components
[ETN-88-91947] 16 p2181 N88-22998
Molten salt corrosion of SiC and Si3N4
17 p2325 N88-23885
Thermal cyclic durability testing of ceramic materials for turbine engines 17 p2325 N88-23886
Fractographic and microstructural evaluation of 3500-hour durability specimens
17 p2325 N88-23887
Thermal stress minimized, two component, turbine shroud seal
[NASA-CASE-LEW-14212-1] 17 p2345 N88-23978
Composite piston
[NASA-CASE-LAR-13435-1] 17 p2346 N88-23981
Status and prognosis for alternative engine materials
[NASA-TM-100903] 18 p2486 N88-24749
Component improvement of free-piston Stirling engine key technology for space power
[NASA-TM-100950] 19 p2607 N88-25476
Guide to the control of high temperature corrosion and protection of gas turbine materials
[PB88-107412] 20 p2760 N88-26370
Engine component retirement for cause. Volume 1: Executive summary
[AD-A192730] 20 p2760 N88-26371
The outlook for ceramics in heat engines, 1990-2010: Results of a worldwide Delphi survey
[DE88-010075] 20 p2778 N88-26475
Ceramic Technology for Advanced Heat Engines Program data base
[DE88-008954] 20 p2780 N88-26489
T55-I-714 engine development and qualification: Engine M11 low cycle fatigue test report. (0213-005-87), volume 2, part 1
[AD-A192766] 21 p2897 N88-27198
Ceramic technology for advanced heat engines project
[DE88-008945] 21 p2919 N88-27323
Studies of dynamic contact of ceramics and alloys for advanced heat engines
[DE88-008996] 21 p2919 N88-27324
JTDE 1 XTE34 materials research and development report
[AD-A194268] 22 p3044 N88-28063
V2500 engine collaboration
[PNR90423] 24 p3326 N88-29803
Determination of the hydroperoxide potential of jet fuels
[AD-A195975] 24 p3357 N88-29991
An investigation of constitutive models for predicting viscoplastic response during cyclic loading
[AD-A194875] 24 p3385 N88-30163

ENGINE TESTS
NT COLD FLOW TESTS
NT STATIC FIRING
Diagnosis of flow channel in aircraft gas-turbine engines on basis of vibration spectrum characteristics
02 p0159 N88-10993
The use of holographic interferometry for turbomachinery fan evaluation during rotating tests
[PNR90390] 02 p0176 N88-11098
Marine gas turbines - engine health monitoring, new approaches
[PNR90369] 02 p0182 N88-11132
Test stand performance of a convertible engine for advanced V/STOL and rotorcraft propulsion
[NASA-TM-100211] 03 p0266 N88-11679
SPRE 1 free-piston Stirling engine testing at NASA Lewis Research Center
[NASA-TM-100241] 03 p0277 N88-11747

A life test of a 22-Newton (5-lbf) hydrazine rocket
[NASA-TM-100232] 03 p0278 N88-11750

Performance and combustion characteristics of direct-injection stratified-charge rotary engines
[NASA-TM-100134] 04 p0400 N88-12490

Incipient failure detection of space shuttle main engine turbopump bearings using vibration envelope detection
05 p0595 N88-13629

High frequency data acquisition system for space shuttle main engine testing 05 p0595 N88-13630

Hot piston ring tests
[NASA-TM-100256] 06 p0729 N88-14486

Efficiency testing of a helicopter transmission planetary reduction stage
[NASA-TP-2795] 07 p0861 N88-15224

Pattern recognition techniques for failure trend detection in SSME ground tests 07 p0924 N88-15614

Propulsion estimation techniques
07 p0927 N88-15632

Space station propulsion technology
[NASA-CR-179260] 08 p0964 N88-15835

SSME environment database development
[NASA-CR-179245] 08 p0964 N88-15836

Hot piston ring/cylinder liner materials Selection and evaluation
[NASA-TM-100276] 08 p0971 N88-15872

Space shuttle main engine anomaly data and inductive knowledge based systems Automated corporate expertise 08 p1060 N88-16398

ESA Bulletin No 15 Ariane the European launcher for the 1980's
[ESA-BULLETIN-NO-15] 09 p1125 N88-16741

Design and testing of a small radial turbine for auxiliary power units 10 p1281 N88-17661

Design and development of an advanced F100 compressor 10 p1283 N88-17678

Rocketdyne automated dynamics data analysis and management system 11 p1499 N88-18954

Test results of a 40-kW Stirling engine and comparison with the NASA Lewis computer code predictions
[NASA-TM-87050] 11 p1508 N88-19013

Engine testing for synfuel operation
[DE88-006044] 13 p1779 N88-20645

Performance improvements of an F-15 airplane with an integrated engine-flight control system
[NASA-TM-100431] 14 p1867 N88-21159

NNEPEQ Chemical equilibrium version of the Navy/NASA Engine Program
[NASA-TM-100851] 14 p1868 N88-21161

China constructing high-altitude test cell
14 p1901 N88-21351

Small engine components test facility turbine testing cell
[NASA-TM-100887] 15 p2019 N88-22037

LGM-30B stage 2 disected motor test report
[AD-A190771] 15 p2027 N88-22079

High-temperature combustor liner tests in structural component response test facility
15 p2077 N88-22383

Description of an oscillating flow pressure drop test rig
[NASA-TM-100905] 16 p2170 N88-22933

The 1988 overview of free-piston Stirling technology for space power at the NASA Lewis Research Center
[NASA-TM-100795] 16 p2170 N88-22934

SSME technology test bed fast shutdown assessment
[NASA-CR-179354] 17 p2314 N88-23831

Liquid metal testing at ETEC for the SP-100 program
17 p2428 N88-24446

Aircraft emissions characterization TF41-A2, TF30-P103 and TF30-P109 engines
[AD-A192053] 18 p2466 N88-24638

Aircraft accident report Air New Orleans DBA continental express flight 962 British Aerospace 3101 (Jetstream 31) N331CY New Orleans International Airport, Kenner, Louisiana, May 26 1987
[PB88-910408] 19 p2601 N88-25450

Techniques utilized in the simulated altitude testing of a 2D-CD vectoring and reversing nozzle
[NASA-TM-100872] 19 p2604 N88-25464

An investigation of high pressure/late cycle injection of CNG (Compressed Natural Gas) as a fuel for rail applications
[DE88-009000] 19 p2677 N88-25917

Environmental monitoring of a titan 34D 5 1/2 segment solid rocket motor static firing
[AD-A192975] 20 p2766 N88-26400

Ceramic Technology for Advanced Heat Engines Program data base
[DE88-008954] 20 p2780 N88-26489

T55-L-714 engine development and qualification Engine M11 low cycle fatigue test report (0213-005-87)
[AD-A192765] 21 p2897 N88-27197

T55-I-714 engine development and qualification Engine M11 low cycle fatigue test report (0213-005-87), volume 2, part 1
[AD-A192766] 21 p2897 N88-27198

Documentation of the Benson Diesel Engine Simulation Program
[NASA-TM-100940] 21 p2898 N88-27201

Ceramic technology for advanced heat engines project
[DE88-008945] 21 p2919 N88-27323

The 210-HP diesel engine endurance and performance testing with fire resistant diesel fuel
[AD-A193153] 21 p2956 N88-27558

Analytical and experimental investigation of ringless piston concept
[AD-A193213] 21 p2956 N88-27559

Basic mechanisms of diesel lubrication correlation of bench and engine tests
[AD-A193360] 21 p2956 N88-27561

Phase 1 results from the Stirling-powered vehicle project
[NASA-TM-100978] 21 p3029 N88-27980

JTDE 1 XTE34 materials research and development report
[AD-A194268] 22 p3044 N88-28063

Orbital transfer vehicle 3000 LBF thrust chamber assembly hot fire test program
[NASA-CR-182145] 24 p3336 N88-29858

Fuel property effects on the US Navy's TF30 engine
24 p3345 N88-29911

Comparison of the performance of a reverse flow annular combustion chamber under low and high pressure conditions 24 p3347 N88-29923

Fuel effects on flame radiation and hot-section durability 24 p3347 N88-29925

Testing of a variable-stroke Stirling engine
[NASA-TM-100899] 24 p3440 N88-30472

ENGINEERING

A review of the knowledge engineering process
02 p0129 N88-10814

ENGINEERING DEVELOPMENT

U PRODUCT DEVELOPMENT

ENGINEERING DRAWINGS

Build install and demonstrate a variable stroke pump control and windmill system
[DE87-014656] 03 p0347 N88-12191

DOE data exchange format specification, mechanical products/drafting Version 1.2.2 CADCAM-045
[DE88-001923] 07 p0904 N88-15477

Free-piston Stirling engine diaphragm-coupled heat-actuated heat pump component technology program, phase 1C
[DE88-003654] 10 p1330 N88-17949

Engineering drawings and changes Storing and controlling by the tens of terrabytes
[DE88-007605] 18 p2589 N88-25387

ENGINEERING MANAGEMENT

The microcomputer as an engineering management tool
[DE87-014882] 02 p0219 N88-11378

Image processing for optical engineering applications
[PB87-210035] 03 p0376 N88-12364

Proceedings of the Fifth Symposium on Energy Engineering Sciences Instrumentation, Diagnostics, and Material Behavior
[DE88-001479] 04 p0429 N88-12660

The characterization of diagnostic tasks for engineering systems
[DE88-000093] 04 p0483 N88-12973

Summaries of FY 1987 engineering research
[DE88-002572] 07 p0840 N88-15096

Physics rationale for the engineering specifications for ZTH
[DE88-000938] 07 p0936 N88-15690

Research in progress at the Institute for Computer Applications in Science and Engineering
[NASA-CR-181607] 08 p1053 N88-16354

Interchange of electronic design through VHDL and EIS 09 p1205 N88-17222

The IDEAL (Integrated Design and Engineering Analysis Languages) modeling methodology Capabilities and Applications 09 p1206 N88-17227

Non-proprietary research projects of the Center for the Space Processing of Engineering Materials
[AR-2] 10 p1426 N88-18516

Engineering thrust areas, 1988
[DE88-005103] 11 p1468 N88-18753

Description of MSFC engineering photographic analysis
[NASA-TM-4035] 11 p1491 N88-18900

Picking winners Parametric cost estimating and project management 12 p1700 N88-20176

Reasons for increasing development cost of rotary wing aircraft and ideas to reverse the trend
12 p1701 N88-20179

Engineering management for validation prototype phase 12 p1703 N88-20195

Schedule and cost control of development
12 p1704 N88-20196

A perspective of PC-based probabilistic risk assessment
[DE88-006715] 18 p2568 N88-25251

Pyrotechnic system failures Causes and prevention
[NASA-TM-100633] 20 p2765 N88-26394

The NASA Marshall engineering thermosphere model
[NASA-CR-179359] 20 p2825 N88-26760

Numerical methods for incompressible viscous flows with engineering applications
[NASA-CR-183143] 21 p2948 N88-27508

Engineering data compendium Human perception and performance User's guide
[LC-87-19560] 21 p2993 N88-27749

TRANSL A PATRAN translator subroutine library
[DE88-010976] 21 p2998 N88-27784

Engineering data compendium Human perception and performance, volume 1
[LC-87-19560] 22 p3134 N88-28630

Engineering data compendium Human perception and performance, volume 2
[LC-87-19560] 22 p3134 N88-28631

Engineering data compendium Human perception and performance, volume 3
[LC-87-19560] 22 p3134 N88-28632

An improvement in the numerical integration procedure used in the NASA Marshall engineering thermosphere model
[NASA-CR-179389] 24 p3392 N88-30200

ENGINES

NT AIR BREATHING ENGINES
NT APOGEE BOOST MOTORS
NT ARC JET ENGINES
NT BOOSTER ROCKET ENGINES
NT CONVERTIBLE FAN-SHAFT ENGINES
NT DIESEL ENGINES
NT DUCTED ROCKET ENGINES
NT ELECTRIC ROCKET ENGINES
NT ELECTROSTATIC ENGINES
NT ELECTROTHERMAL ENGINES
NT FREE-PISTON ENGINES
NT GAS TURBINE ENGINES
NT HELICOPTER ENGINES
NT HYDRAZINE ENGINES
NT HYDROGEN ENGINES
NT HYDROGEN OXYGEN ENGINES
NT INTERNAL COMBUSTION ENGINES
NT ION ENGINES
NT J-57 ENGINE
NT JET ENGINES
NT LIQUID AIR CYCLE ENGINES
NT LIQUID PROPELLANT ROCKET ENGINES
NT MERCURY ION ENGINES
NT NOZZLELESS ROCKET ENGINES
NT NUCLEAR ENGINE FOR ROCKET VEHICLES
NT NUCLEAR ROCKET ENGINES
NT PISTON ENGINES
NT PLASMA ENGINES
NT RAMJET ENGINES
NT RESISTOJET ENGINES
NT REUSABLE ROCKET ENGINES
NT ROCKET ENGINES
NT ROTARY ENGINES
NT SOLID PROPELLANT ROCKET ENGINES
NT SPACE SHUTTLE BOOSTERS
NT SPACE SHUTTLE MAIN ENGINE
NT STIRLING ENGINES
NT SUPERSONIC COMBUSTION RAMJET ENGINES
NT TF-30 ENGINE
NT TF-34 ENGINE
NT TURBINE ENGINES
NT TURBOFAN ENGINES
NT TURBOJET ENGINES
NT TURBOPROP ENGINES
NT UPPER STAGE ROCKET ENGINES
NT WANKEL ENGINES

Structural reliability and damage tolerance of ceramic composites for high-temperature applications
[PB87-208310] 01 p0019 N88-10119

Heat engine regenerators Research status and needs
[DE87-013581] 01 p0054 N88-10348

Analysis of wear metals in engine oils using the atomic absorption spectrophotometric method
[NAL-TM-MT-8704] 05 p0564 N88-13435

Fuel nitrogen conversion in a supercharged spark ignition engine
[DE88-003739] 08 p0974 N88-15893

Ceramic technology for advanced heat engines program data base
[DE88-003922] 11 p1464 N88-18730

Design features of small Brayton cycles for autonomous underwater vehicles
[AD-A187799] 11 p1506 N88-18999

Advanced components for spaceborne infrared astronomy
[NASA-CR-177470] 13 p1772 N88-20601

Some design considerations for ceramic components in heat engine applications 17 p2323 N88-23875

Nondestructive evaluation of structural ceramics
17 p2324 N88-23876

Improved silicon carbide for advanced heat engines
17 p2324 N88-23879

Improved silicon nitride for advanced heat engines
17 p2324 N88-23881

Experimental validation of a zero-dimensional computer model for spark-ignition engines
[DE88-009034] 21 p2957 N88-27565

A lubrication study of engine bearings
21 p2958 N88-27574

Empirical flutter prediction method
[AD-A195699] 24 p3327 N88-29810

ENGLAND

Experimental Radio Data System (RDS): A survey of reception reliability in the UK
[BBC-RD-1987/17] 09 p1155 N88-16922

ENGLISH LANGUAGE

Language modelling for automatic speech recognition: A review
[RSRE-MEMO-4038] 01 p0084 N88-10544

Conversion of productions in OPS5 to their equivalent English
[ORNL/TM-10246] 24 p3411 N88-30306

ENHANCEMENT

U AUGMENTATION

ENLARGING

U EXPANSION

ENRICHMENT

NT ISOTOPIC ENRICHMENT

ENSTROPHY

U VORTICITY

ENTHALPY

NT GIBBS FREE ENERGY
NT HEAT OF FORMATION
NT HEAT OF FUSION
NT LATENT HEAT

Theory of interstitial solutions
[BLL-M-37314-(5828.4)] 02 p0233 N88-11469

An automated flow calorimeter for heat capacity and enthalpy measurements at elevated temperatures and pressures
[DE88-002357] 07 p0857 N88-15206

Thermodynamic values from computer summation of group additivity data
[AD-A186131] 07 p0940 N88-15711

Cohesive energies of transition metal silicides and phosphides — Knudsen effusion
[AD-A186691] 09 p1254 N88-17519

A calorimetric determination of the enthalpy of formation and a description of the defect structure of the ordered beta-phase /Ni, Cu/ /1-x/ Al/x/
[NASA-TT-20157] 13 p1745 N88-20434

Radiative processes affecting ocean mixed-layer heat content and their monitoring from satellite
13 p1806 N88-20800

The thermodynamic properties of organic oxygen compounds
[DE88-001208] 13 p1849 N88-21065

Evaluation of direct methane conversion to higher hydrocarbons and oxygenates
[DE88-003812] 15 p2049 N88-22204

Research in nonlinear partial differential equations and bifurcation theory
[AD-A190986] 16 p2260 N88-23514

The thermodynamic properties of quinoline and isoquinoline
[DE88-001218] 18 p2484 N88-24735

Calculation of the specific and volumetric enthalpies of Ge-Si alloys
[DE88-008949] 21 p3026 N88-27965

ENTIRE FUNCTIONS

Lax representation and complete integrability for the periodic relativistic Toda lattice
[PREPRINT-594] 22 p3146 N88-28711

ENTRAINMENT

A study of chaos and mixing in Rayleigh-Taylor and Richtmyer-Meshkov unstable interfaces
[AD-A184751] 03 p0320 N88-12026

Turbulent mixing in a rotating, stratified fluid
04 p0445 N88-12759

Wall turbulence control 07 p0812 N88-14943

Foam generation and air entrainment near a free surface
[AD-A185986] 07 p0848 N88-15149

An experimental investigation of straight and curved annular wall jets
[NASA-CR-182546] 11 p1434 N88-18557

Structures and fluxes in a deep convecting mixed layer 13 p1804 N88-20786

Subduction 13 p1806 N88-20796

Gravity currents with heat transfer effects
[PB88-180047] 16 p2205 N88-23158

Gas diffusion studies in steady and nonsteady cavities
18 p2512 N88-24902

Direct numerical simulations of the PDF's (Probability Density Functions) of a passive scalar in a forced mixing layer
[AD-A192134] 18 p2568 N88-25256

ENTROPY

Cosmology with decaying vacuum energy
[DE88-000698] 03 p0389 N88-12443

A dissipation principle and its consequences for structured shock waves in thermoelastic materials
[DE87-013723] 04 p0454 N88-12813

Maximum entropy/optimal projection design synthesis for decentralized control of large space structures
[AD-A186359] 07 p0824 N88-15003

Thermodynamic values from computer summation of group additivity data
[AD-A186131] 07 p0940 N88-15711

The entropy of the Lorentz model
08 p1015 N88-16153

A study of the free energy of the Lenz-Ising model using the cluster variation method of Morita
[AD-A186023] 08 p1073 N88-16476

Outlier resistant predictive source encoding for a Gaussian stationary nominal source
[AD-A186725] 09 p1232 N88-17387

The approach to equilibrium in a quark-gluon plasma
[DE88-002117] 09 p1251 N88-17499

Studies in finite time thermodynamics
[DE88-004531] 10 p1423 N88-18500

Unsteady transonic small-disturbance theory including entropy and vorticity effects
[NASA-TM-100568] 12 p1575 N88-19418

Linear and nonlinear acoustics with nonuniform entropy in combustion chambers 12 p1607 N88-19609

The thermodynamic properties of organic oxygen compounds
[DE88-001208] 13 p1849 N88-21065

Research in nonlinear partial differential equations and bifurcation theory
[AD-A190986] 16 p2260 N88-23514

Extrema principles of entrophy production and energy dissipation in fluid mechanics
[NASA-TM-100992] 18 p2519 N88-24946

Improved potential flow computational methods with Euler corrections for airfoil and wing/body design
[AD-A192303] 20 p2752 N88-26334

Investigations on the entropy of cloudy air
[ESA-TT-1060] 23 p3234 N88-29245

Monotone recurrence relations, their Birkhoff orbits and topological entropy
[AD-A193481] 23 p3276 N88-29504

ENTROPY (STATISTICS)

NT MAXIMUM ENTROPY METHOD

Adaptive time series analysis using predictive inference and entropy
[AD-A191858] 18 p2560 N88-25199

ENVIRONMENT EFFECTS

Investigation of large scale impact of air pollution components on forest ecosystems in Bavaria, West Germany
[DFVLR-FB-87-17] 01 p0068 N88-10434

Testimony to the US Senate on the greenhouse effect
[DE87-013995] 01 p0071 N88-10458

Global environmental change research
[S-HRG-100-301] 03 p0348 N88-12199

Emerging environmental constraints on the use of gasoline and diesel fuel and tradeoffs associated with the use of alternative fuels
[DE87-011504] 04 p0422 N88-12614

Disturbance and recovery of Arctic Alaskan tundra terrain: A review of recent investigations
[AD-A184442] 04 p0467 N88-12887

Impacts of world development on selected characteristics of the atmosphere: An integrative approach. Volume 1: Main report
[DE88-001495] 07 p0875 N88-15309

Impacts of world development on selected characteristics of the atmosphere: An integrative approach. Volume 2: Appendices
[DE88-001496] 07 p0875 N88-15310

Summary of the report of the Senior Committee on Environmental, Safety and Economic Aspects of Magnetic Fusion Energy
[DE88-003270] 07 p0937 N88-15692

Effects of fire on composition, biomass, and nutrients in oak scrub vegetation on John F. Kennedy Space Center, Florida
[NASA-TM-100305] 08 p1020 N88-16182

Trends in research and development in the Netherlands. The influence of national science policy between 1973 and 1986
[B8701588] 08 p1094 N88-16580

Cape Blanco wind farm feasibility study
[DE88-003748] 10 p1348 N88-18059

Cape Blanco wind farm feasibility study
[DE88-003749] 10 p1349 N88-18060

Review of selenium thermodynamic data
[DE88-006194] 13 p1849 N88-21088

Assessment of crop loss from air pollutants. Meteorology-atmospheric chemistry and long range transport
[PB88-146857] 15 p2089 N88-22446

Detection, monitoring and analysis of some environmental effects of fires in the Amazon region through utilization of NOAA and LANDSAT satellite imagery and aircraft data
[INPE-4503-TDL/326] 16 p2230 N88-23322

Environmental projects. Volume 6: Environmental assessment: New 34-meter antenna at Venus site
[NASA-CR-182922] 17 p2332 N88-23919

Detection of biomass burning and smoke plumes in the Amazon region through NOAA satellite imagery
17 p2365 N88-24085

Environmental effects on slow crack growth in silicon nitride
[DE88-007206] 18 p2494 N88-24795

Changes in the Antarctic atmosphere due to the reduction of stratospheric ozone
[ETN-88-92565] 18 p2540 N88-25074

Monitoring biological impacts of space shuttle launches from Vandenberg Air Force Base: Establishment of baseline conditions
[NASA-TM-100982] 18 p2549 N88-25133

Photointerpretation with instrumentation for evaluation of environmental impact: Mata Atlantica in Cubatao
19 p2683 N88-25946

Study of evolution of vegetal cover and slide scars in the Cubatao municipality-Sao Paulo
19 p2683 N88-25947

Application of remote sensing in the conservation of natural areas: Ribeira Valley 19 p2683 N88-25949

Remote sensing applied to the monitoring of mineral extraction in the proximity of urban areas: Pros and cons
19 p2684 N88-25954

Health and environmental consequences of the Chernobyl nuclear power plant accident
[DOE/ER-0332] 19 p2689 N88-25985

Acid rain: Delays and management changes in the Federal research program
[GAO/RCED-87-89] 19 p2690 N88-25988

Discrimination of sand transport rates and environmental consequences in central Egypt from SPOT data
22 p3093 N88-28366

Regional environmental studies using national data bases and GIS (Geographic Information System)
[DE88-008368] 23 p3230 N88-29225

Investigation of the large-scale impact of air pollution components on forest ecosystems in Bavaria
[ESA-TT-1087] 24 p3390 N88-30187

ENVIRONMENT MANAGEMENT

Activities report in aeronautics and astronautics
[ETN-88-91332] 13 p1859 N88-21115

The suitability of SPOT imagery for monitoring landscape patterns 22 p3094 N88-28376

ENVIRONMENT MODELS

Conception and discussion of a model describing ice formation on various obstacles
[ONERA-NT-1986-6] 01 p0072 N88-10460

Effects of enviromentally imposed roughness on airfoil performance 08 p0952 N88-15778

Evaluation of regional-scale air quality models: Chairmen reports from four workshops
[DE88-001397] 10 p1352 N88-18080

Tactical Rubidium Frequency Standard (TRFS)
[AD-A191049] 16 p2193 N88-23078

Coordination in decision-making organizations
[AD-A191952] 19 p2739 N88-26261

Weathering of sulfides on Mars
23 p3301 N88-29662

ENVIRONMENT POLLUTION

NT AIR POLLUTION
NT GLOBAL AIR POLLUTION
NT INDOOR AIR POLLUTION
NT OIL POLLUTION
NT WATER POLLUTION

Remote sensing of environmental pollution
[DFVLR-MITT-87-04] 01 p0067 N88-10428

Space station contamination considerations
02 p0137 N88-10859

First flight of the ATMOS instrument during the Spacelab 3 Mission, April 29 through May 6, 1985
[NASA-CR-182360] 06 p0728 N88-14482

Environmental projects. Volume 4: Asbestos survey
[NASA-CR-182527] 10 p1353 N88-18083

System-wide medium-term environment programme for the period 1990-1995: Strategies of the United Nations system for the environment
[UNEP/GCSS.I/2] 12 p1641 N88-19826

Evaluation of existing total human exposure models
[PB88-146840] 15 p2101 N88-22517

JPRS report Science and technology China
[JPRS-CST-88-001] 16 p2186 N88-23036

Acid Precipitation A current awareness bulletin
[DE88-007987] 20 p2821 N88-26738

ENVIRONMENT PROTECTION

System-wide medium-term environment programme for the period 1990-1995 Strategies of the United Nations system for the environment
[UNEP/GCSS.I/2] 12 p1641 N88-19826

Perspectives in microclimate cooling involving protective clothing in hot environments
[AD-A188370] 12 p1671 N88-20007

Environmental projects Volume 5 part 1 Study of subsurface contamination Part 2 Guide to implement environmental compliance programs
[NASA-CR-182691] 13 p1796 N88-20741

NOAA (National Oceanic and Atmospheric Administration) Meteorology Division support to the Environmental Protection Agency
[PB88-179866] 19 p2689 N88-25980

Vegetation studies on Vandenberg Air Force Base California
[NASA-TM-100985] 20 p2831 N88-26795

ENVIRONMENT SIMULATION
NT ALTITUDE SIMULATION
NT NEUTRAL BUOYANCY SIMULATION
NT SPACE ENVIRONMENT SIMULATION
NT WEIGHTLESSNESS SIMULATION

Portable, ambient air microclimate cooling in simulated desert and tropic conditions
[AD-A186457] 08 p1050 N88-16338

ENVIRONMENT SIMULATORS
NT SOLAR SIMULATORS
NT SPACE SIMULATORS

ENVIRONMENTAL CHAMBERS
U TEST CHAMBERS

ENVIRONMENTAL CHEMISTRY
NT AEROTHERMOCHEMISTRY
NT ATMOSPHERIC CHEMISTRY
NT BIOGEOCHEMISTRY
NT GEOCHEMISTRY
NT MARINE CHEMISTRY

Environment assisted degradation mechanisms in aluminum-lithium alloys
[NASA-CR-182482] 10 p1301 N88-17782

Workshop on Atmospheric OH
[BPT-7/87] 18 p2538 N88-25063

ENVIRONMENTAL CONTROL

Development of a graphical display on the DMS test bed 06 p0794 N88-14864

Man rating the b-1B molecular sieve oxygen generation system
[AD-A186275] 07 p0899 N88-15447

Space station accommodations for life sciences research facilities Phase 1 Conceptual design and programmatics studies for Missions SAAX0307, SAAX0302 and the transition from SAAX0307 to SAAX0302 Volume 2 Study results
[NASA-CR-179244] 08 p0962 N88-15829

Prototype space station automation system delivered and demonstrated at NASA 08 p1066 N88-16442

Computer control of a microgravity mammalian cell bioreactor 09 p1197 N88-17172

Fed-batch control based upon the measurement of intracellular NADH 09 p1197 N88-17175

ARGES An expert system for fault diagnosis within space-based ECLS systems 23 p3255 N88-29380

Development of computer-controlled thermogravimetric instrumentation for measurement of environmental and high temperature volatilization and desorption of contaminants from polymeric materials
[AD-A195934] 24 p3343 N88-29900

ENVIRONMENTAL LABORATORIES

MBA payload testing by Compact Antenna Test Range (CATR)
[ESA-CR(P)-2473] 08 p0977 N88-15906

A test facility for the in-vacuo assessment of dry lubricants and small mechanisms at cryogenic temperatures 14 p1878 N88-21224

ENVIRONMENTAL MONITORING

TIROS-N/NOAA A-J space environment monitor subsystem
[PB87-203998] 01 p0015 N88-10083

Remote sensing of environmental pollution
[DFVLR-MITT-87-04] 01 p0067 N88-10428

Airborne lidar experiments at the Savannah River Plant
[NASA-TM-4007] 02 p0194 N88-11209

NOAA's (National Oceanic and Atmospheric Administration's) Northeast Monitoring Program (NEMP) A report on progress of the first five years (1979-84) and a plan for the future
[PB87-210100] 02 p0196 N88-11225

Applicability of SPOT for forest inventory, mapping and change monitoring 03 p0344 N88-12174

Contribution of SPOT data to the physiographic study of coastal environment La Pointe d'Arcay and l'Anse de l'Aiguillon (France) 03 p0344 N88-12176

Global environmental change research
[S-HRG-100-301] 03 p0348 N88-12199

Evaluation of the sensidyne toxic gas sensor for HF (Hydrogen Fluoride) vapor
[DE88-000647] 04 p0446 N88-12767

On-site meteorological program guidance for regulatory modeling applications
[PB87-227542] 06 p0731 N88-14498

Integrated Global Background Monitoring Network
[DE88-001503] 06 p0731 N88-14499

Current issues in atmospheric change
[NASA-CR-182406] 08 p1039 N88-16287

Fatigue and damage tolerance design data for carbon fibre composites
[BAE-MSM-R-GEN-0454] 09 p1138 N88-16818

User's guide to a data base of current environmental monitoring projects in the US-Canadian transboundary region
[DE88-002476] 09 p1188 N88-17119

Computer control of a microgravity mammalian cell bioreactor 09 p1197 N88-17172

Fed-batch control based upon the measurement of intracellular NADH 09 p1197 N88-17175

Meteorological and aerosol measurements from the NOAA WP-3D aircraft during WATOX-86, January 4-9, 1986
[PB88-120860] 10 p1352 N88-18079

Environmental projects Volume 4 Asbestos survey
[NASA-CR-182527] 10 p1353 N88-18083

ELF (Extremely Low Frequency) communications system ecological monitoring program Electromagnetic field measurements and engineering support, 1986
[AD-A188057] 11 p1509 N88-19017

System-wide medium-term environment programme for the period 1990-1995 Strategies of the United Nations system for the environment
[UNEP/GCSS.I/2] 12 p1641 N88-19826

Aerosol lidar for environment protection and meteorology
[DFVLR-FB-87-43] 14 p1982 N88-21828

Real-time environmental Arctic monitoring (R-TEAM)
[AD-A189948] 15 p2099 N88-22508

Geochemistry of the middle and lower atmosphere Environmental impact through the deterioration of the ozone layer
[INPE-4477-PRE/1241] 16 p2230 N88-23321

Study of reservoir water quality utilizing remote sensing techniques Methodological concepts 17 p2364 N88-24076

The role of space borne imaging radars in environmental monitoring Some shuttle imaging radar results in Asia
[NASA-TM-101178] 18 p2502 N88-24844

The application of satellites in connection with the environment
[ETN-88-92474] 18 p2532 N88-25020

Monitoring biological impacts of space shuttle launches from Vandenberg Air Force Base Establishment of baseline conditions
[NASA-TM-100982] 18 p2549 N88-25133

Evaluation of the ion trap mass spectrometer for potential application in the space station
[DE88-008940] 19 p2674 N88-25902

Environmental monitoring of a titan 34D 5 1/2 segment solid rocket motor static firing
[AD-A192975] 20 p2766 N88-26400

The role of space borne imaging radars in environmental monitoring Some shuttle imaging radar results in Asia
[NASA-TM-101175] 20 p2789 N88-26544

Advanced life support control/monitor instrumentation concepts for flight application
[NASA-CR-177378] 20 p2833 N88-26807

Initial testing of the tunable diode laser absorption spectrometer for measuring HNO3 in diesel engine exhaust, stage 2
[PB88-193073] 21 p2970 N88-27641

Computer simulation procedure for designing airborne aerometric monitoring programs
[DE88-011896] 21 p2975 N88-27674

An evaluation of SPOT imagery for wetland monitoring 22 p3091 N88-28353

Review of the studies of geography and environment and studies on spectral characteristics of SPOT HRV data 22 p3091 N88-28358

Spatial and spectral registration of Javanese landscape units with SPOT 22 p3092 N88-28362

Following the seasonal evolution of a natural environment in a humid tropical region Preliminary Evaluation of SPOT (PEPS) number 186 Bangui Central Africa 22 p3093 N88-28368

An evaluation of the applicability of SPOT stereoscopic imagery to the Canada Land Use Monitoring Program (CLUMP) 22 p3099 N88-28403

Monitoring Moneragala (Sri Lanka) with SPOT imagery 22 p3099 N88-28405

Assessment of SPOT satellite based system in humid tropical vegetation identification classification and monitoring 22 p3100 N88-28408

ENVIRONMENTAL QUALITY
NT AIR QUALITY
NT WATER QUALITY

User's guide to a data base of current environmental monitoring projects in the US-Canadian transboundary region
[DE88-002476] 09 p1188 N88-17119

ENVIRONMENTAL SURVEYS

Compilation of 1986 annual reports of the Navy ELF (Extremely Low Frequency) communications system ecological monitoring program, volume 1
[AD-A184561] 03 p0306 N88-11930

Compilation of 1986 annual reports of the Navy ELF (Extremely Low Frequency) communications system ecological monitoring program, volume 2
[AD-A184562] 03 p0306 N88-11931

Compilation of 1986 annual reports of the Navy ELF (Extremely Low Frequency) communications system ecological monitoring program, volume 3
[AD-A184563] 03 p0306 N88-11932

Environmental gradient analysis, ordination, and classification in environmental impact assessments
[AD-A187294] 11 p1509 N88-19016

Toxic effects of man-made mineral fibers with particular reference to ceramic fibers
[AD-A187949] 11 p1519 N88-19072

Environmental projects Volume 6 Environmental assessment New 34-meter antenna at Venus site
[NASA-CR-182922] 17 p2332 N88-23919

Extremely Low Frequency (ELF) communications system ecological monitoring program Summary of 1986 progress
[AD-A192014] 19 p2642 N88-25676

ENVIRONMENTAL TEMPERATURE
U AMBIENT TEMPERATURE

ENVIRONMENTAL TESTS
NT COLD WEATHER TESTS
NT CORROSION TESTS
NT HIGH TEMPERATURE TESTS
NT LOW TEMPERATURE TESTS
NT NEUTRAL BUOYANCY SIMULATION
NT SALT SPRAY TESTS
NT UNDERWATER TESTS

Partial analysis of experiment LDEF A-0114
[NASA-CR-179236] 06 p0780 N88-14787

Major spacecraft hardware testing in Europe 09 p1125 N88-16740

Effects of processing variables on the behavior of E-glass/913 and XAS carbon fibre/913 laminates subjected to hot/wet environmental conditions
[BR101940] 09 p1138 N88-16820

Cavitation inception
[AD-A189220] 13 p1765 N88-20557

Environment test laboratory
[ETN-88-91885] 14 p1869 N88-21166

Effect of loading conditions on environment-sensitive fracture
[BR102697] 14 p1934 N88-21533

Hybrid PV HgCdTe IR detectors technology reliability and failure program Environmental stress testing plan
[AD-A191165] 16 p2211 N88-23195

Laser cladding of Ni, Nb and Mg alloys for improved environmental resistance at high temperature
[AD-A191274] 16 p2213 N88-23208

Materials qualification in oceanology and the offshore industry 19 p2700 N88-26050

Flight testing under extreme environmental conditions
[AGARD-AG-300-VOL-8] 21 p2951 N88-27525

Qualification test levels for units to be derived from mechanical test data analysis — ESA
[REPT-87-158-EI/ET/AG] 24 p3381 N88-30139

ENVIRONMENTS
NT AEROSPACE ENVIRONMENTS
NT CHROMOSPHERE
NT EARTH ENVIRONMENT
NT EARTH MAGNETOSPHERE
NT EARTH ORBITAL ENVIRONMENTS
NT FRICTIONLESS ENVIRONMENTS
NT GEOMAGNETIC TAIL
NT HIGH ALTITUDE ENVIRONMENTS
NT HIGH GRAVITY ENVIRONMENTS
NT HIGH TEMPERATURE ENVIRONMENTS
NT ICE ENVIRONMENTS
NT INNER RADIATION BELT
NT INTERPLANETARY SPACE
NT INTERSTELLAR SPACE
NT JUPITER ATMOSPHERE
NT LOW TEMPERATURE ENVIRONMENTS
NT MAGNETOPAUSE
NT MARINE ENVIRONMENTS
NT MARS ATMOSPHERE

NT MARS ENVIRONMENT
NT MIDLATITUDE ATMOSPHERE
NT NEPTUNE ATMOSPHERE
NT PLANETARY ATMOSPHERES
NT PLANETARY ENVIRONMENTS
NT PLANETARY IONOSPHERES
NT ROTATING ENVIRONMENTS
NT SATELLITE ATMOSPHERES
NT SATURN ATMOSPHERE
NT SOLAR ATMOSPHERE
NT SPACECRAFT ENVIRONMENTS
NT STELLAR ATMOSPHERES
NT THERMAL ENVIRONMENTS
NT URANUS ATMOSPHERE
NT VENUS ATMOSPHERE
NT VENUS CLOUDS

The impact of environmental factors on the performance of millimeter wave seekers in smart munitions
[DE87-014277] 03 p0270 N88-11697

Wear of iron and nickel in corrosive liquid environments
[NASA-TM-100246] 03 p0289 N88-11817

On computing environments in data analysis
[DE88-000076] 04 p0480 N88-12961

User interface for a partially incompatible system software environment with non-ADP users
[DE88-001518] 04 p0482 N88-12968

Avionics and corrosion 05 p0547 N88-13336

Interim review of the possibilities and opportunities for the ONR tropical cyclone motion research initiative
[AD-A185679] 06 p0746 N88-14592

A hypertext writing environment and its cognitive basis
[AD-A188179] 10 p1389 N88-18298

Motion in a random gyrotropic environment in D dimensions
[PB87-170650] 12 p1685 N88-20079

Effects of natural environment on first generation solid rocket booster thermal protection system materials
[NASA-TM-100329] 17 p2373 N88-24113

The Environment for Application Software Integration and Execution (EASIE) version 1.0. Volume 4: System installation and maintenance guide
[NASA-TM-100576] 17 p2386 N88-24185

Relating design and environmental variables to reliability 17 p2418 N88-24383

An intelligent processing environment for real-time simulation
[NASA-CR-183056] 19 p2715 N88-26119

Distributed mathematics in a heterogeneous environment
[DE88-009128] 19 p2716 N88-26124

Thermal conductivity of selected foams and systems from 100 to 300 K
[PB88-201553] 20 p2777 N88-26466

Nutrient requirements for high stress environments
[AD-A194595] 23 p3243 N88-29301

Multi-metallic galvanic corrosion
[AD-A195995] 24 p3353 N88-29963

Analysis of environmental parameters from the Panama City tower radar experiment
[AD-A194994] 24 p3404 N88-30264

ENZYME ACTIVITY
NT FERMENTATION

A solid phase enzyme-linked immunosorbent assay for the antigenic detection of Legionella pneumophila (serogroup 1): A compliment for the space station diagnostic capability 06 p0795 N88-14868

Myosin Ca sup (2+), Mg sup (2+)-adenosine triphosphatase activity in ray myocardium following 30-day expose to 1.1 and 2.0 G 10 p1362 N88-18141

Oxidative enzyme activity in healthy subjects and individuals with neurocirculatory dystonia during graded exercise 10 p1367 N88-18170

Dexamethasone regulates glutamine synthetase expression in rat skeletal muscles
[NASA-CR-182935] 18 p2549 N88-25129

Methods of quantifying and enhancing reactive oxygen species production 21 p2924 N88-27357

ENZYMES
NT CARBONIC ANHYDRASE
NT CATALASE
NT CHOLINESTERASE
NT CYTOCHROMES

Electron cytochemical detection of Ca(2)+-ATPase in protonema of moss funaria hygrometrica (H e d w.) under hypogravitation 06 p0749 N88-14602

Spectroscopic studies of energy transfer in photosynthetic reaction centers of higher plants
[DE88-003850] 10 p1359 N88-18121

Enzyme-based fiber optic sensors
[DE88-005674] 13 p1840 N88-21013

North Carolina Biomolecular Engineering and Materials Applications Center (NC-BEMAC)
[AD-A190923] 16 p2237 N88-23364

Employment of porous polytetrafluoroethylene Membrane with a hydrophilic and hydrophobic stratal structure for construction of an enzyme electrode
[NASA-TT-20296] 19 p2620 N88-25543

The design of methane activation catalysis
[DE88-002265] 23 p3199 N88-29043

ENZYMOLOGY

Superoxide dismutase assays
[AD-A183972] 03 p0356 N88-12242

EOS
U LANDSAT SATELLITES

EPHEMERIDES

Dynamic positioning at sea using the global positioning system
[AD-A184453] 04 p0397 N88-12476

Integrated systems with applications to the multi-phases of the ephemerides, physics and methematics of the upper atmosphere
[AD-A185748] 06 p0743 N88-14570

Optimized observation periods required to achieve geodetic accuracies using the global positioning system
[AD-A193844] 22 p3041 N88-28052

EPHEMERIS TIME

IMP 7 (Explorer 47) trajectory, September 26, 1972 to September 25, 1978
[NASA-CR-182697] 14 p1871 N88-21183

EPIDEMIOLOGY

Illustrations of a density-equalizing map projection technique
[DE87-013992] 02 p0339 N88-12130

JPRS report: Science and technology. USSR: Life sciences
[JPRS-ULS-87-012] 03 p0355 N88-12238

JPRS report: Science and technology. USSR: Life sciences
[JPRS-ULS-87-009] 04 p0473 N88-12915

Toxic effects of man-made mineral fibers with particular reference to ceramic fibers
[AD-A187949] 11 p1519 N88-19072

USSR report: Life sciences. Biomedical and behavioral sciences
[JPRS-UBB-87-010] 12 p1651 N88-19889

EPILEPSY

Detection of latent epilepsy in aircrew candidates
21 p2984 N88-27720

EPINEPHRINE
NT NOREPINEPHRINE

Individual functional typology of sympathoadrenal system as indicator of physiological status in adverse environments 12 p1665 N88-19979

A program for the study of skeletal muscle catabolism following physical trauma
[AD-A189771] 15 p2102 N88-22521

Distinctive features in blood clotting and fibrinolytic properties under effect of epinephrine in presence of hypoxia and hypercapnia 19 p2705 N88-26082

EPITAXY
NT LIQUID PHASE EPITAXY
NT MOLECULAR BEAM EPITAXY
NT VAPOR PHASE EPITAXY

Structure of rapidly solidified Ni-Ti
[DE87-012252] 02 p0147 N88-10921

Novel heterojunction devices
[DE87-013716] 05 p0656 N88-14026

Heteroepitaxial growth of 3-5 semiconductor compounds by metal-organic chemical vapor deposition for device applications
[NASA-CR-182346] 06 p0788 N88-14832

The role of thermodynamic phase diagrams and lattice matching in superlattice growth
[DE88-003113] 08 p1091 N88-16568

Visible InGaAsP/GaAsP lasers produced by epitaxial growth from liquid phase 09 p1237 N88-17416

Formation of optical waveguides by ion implantation
[DE88-003894] 10 p1409 N88-18407

Deposition of device quality epitaxial layers of gallium nitride and indium nitride for electronic applications
[AD-A188001] 11 p1453 N88-18661

Development of VLSI optical data link
[AD-A187883] 11 p1549 N88-19265

Development of VLSI optical data link
[AD-A187884] 11 p1549 N88-19266

Laser evaporation studies
[AD-A189815] 15 p2071 N88-22346

Fundamental properties and devices applications of Ge(x)Si(1-x)/Si superlattices
[AD-A190129] 15 p2143 N88-22787

Equilibrium stability of strained epitaxial layers on a rigid substrate
[INPE-4254-PRE/1127] 15 p2145 N88-22804

Limited reaction processing for semiconductor device fabrication
[AD-A190913] 16 p2283 N88-23666

Growth of high quality CoSi2/Si superstructures on Si(111) 20 p2869 N88-27034

Epitaxy and properties of two dimensional GaInAs semiconductor structures
[ETN-88-92357] 20 p2879 N88-27094

Superconducting thin films, composites and junctions
[AD-A193123] 21 p2937 N88-27440

Atomic layer epitaxy of ZnS and ZnSe
[AD-A192307] 21 p3020 N88-27928

Blue-green laser diode research program
[AD-A191980] 23 p3218 N88-29153

Laser induced chemical vapor epitaxial growth of gallium arsenide films
[AD-A194254] 23 p3291 N88-29595

EPOCHS
U TIME MEASUREMENT

EPOXIDES
U EPOXY COMPOUNDS

EPOXY COMPOUNDS
NT PROPYLENE OXIDE

An interdisciplinary approach to predictive modeling of structural adhesive bonding: Factors affecting the durability of titanium/epoxy bonds
[AD-A189503] 12 p1611 N88-19636

Thermoviscoelastic characterization and predictions of Kevlar/epoxy composite laminates
[NASA-CR-182878] 16 p2172 N88-22946

Structural study of impregnating resins of TGMDA/DDS type
[ETN-88-92167] 20 p2780 N88-26488

Degradation of fiber composites during storage
[FOA-C-20702-2.6] 22 p3051 N88-28102

Electrical detection of coating deterioration
24 p3355 N88-29973

EPOXY MATRIX COMPOSITES
NT BORON-EPOXY COMPOSITES

Study of the morphology of thermosetting matrices
[ONERA-RT-5/3346-M] 02 p0153 N88-10961

Cure and properties of thermosetting polymers
[AD-A184669] 03 p0293 N88-11843

A creep measurement of unidirectional epoxy-fiberglass rod
[DE87-014812] 04 p0411 N88-12553

In-situ characterization of the interface of glass reinforced composites
[AD-A185136] 05 p0557 N88-13391

Utilization of microwave measuring systems for nondestructive control of composite materials
[SNIAS-872-430-109] 05 p0559 N88-13402

Study of damage in carbon fiber-epoxy composite materials. Utilization to assess broken specimens
[DCQ/L-45-650/F] 06 p0678 N88-14152

Flaw effects: Behavior in operation of delamination in a crossed multilayer composite specimen
[DCQ/L-47-363/F] 06 p0678 N88-14153

Measurement of mechanical parameters to define damage criteria in delamination of crossed stratified layers
[DCQ/L-47-361/F] 06 p0678 N88-14154

Experimental and theoretical investigation of mechanically fastened composites
[AD-A185896] 07 p0826 N88-15008

Interfacial shear strength of pitch and high strain pan fibers in an epoxy matrix
[AD-A185966] 07 p0826 N88-15011

Improving the interlaminar shear strength of carbon fiber-epoxy composites through carbon fiber bromination
[NASA-TM-100248] 07 p0827 N88-15018

Study of selection criteria for adhesives used in aircraft structure bonding
[ETN-88-91619] 08 p0971 N88-15875

Fatigue and damage tolerance design data for carbon fibre composites
[BAE-MSM-R-GEN-0454] 09 p1138 N88-16818

Effect of post-cure heat-treatment on static and fatigue behaviour of XAS-914C carbon fibre composite
[AD-A186943] 10 p1294 N88-17735

Damage mechanisms of CFRP riveted joints
11 p1449 N88-18636

Matrix-fiber stress transfer in composite materials: Elasto-plastic model with an interphase layer
[PB88-136635] 11 p1450 N88-18643

An experimental and numerical study of notch sensitivity of ARALL laminates
[CCMS-88-04] 11 p1450 N88-18644

Oxidation and protection of fiberglass-epoxy composite masts for photovoltaic arrays in the low Earth orbital environment
[NASA-TM-100839] 11 p1465 N88-18734

The place for thermoplastic composites in structural components
[AD-A189149] 12 p1604 N88-19596

Fracture characteristics of carbon and aramid unidirectional composites in interlaminar shear and open hole tensile tests
[NLR-TR-86083-U] 13 p1735 N88-20371

Environmental effects on the post-impact compressive strength of CFC
[RAE-TM-MAT-STR-1088] 14 p1884 N88-21258

An investigation of the mechanical properties of improved carbon fibre composite materials
[RAE-TR-86021] 14 p1884 N88-21259

The percolation approach as a basis for experimental research on the mechanical properties of composite materials 14 p1886 N88-21271

Elementary characterization of Fibredux 913 CTS 5 34 percent preimpregnated carbon-epoxy from Ciba Geigy
[M-484300] 16 p2171 N88-22941

Investigation of the long term effects of aging on carbon epoxy composites exposed naturally to the weather under cyclic loads. (Results of sampling after 2.5 years). Test report M1-641300
[CEAT-39/M/79-C-M1-641300] 17 p2316 N88-23834

Elementary characterization of preimpregnated carbon epoxy T400H/DA0506 from STRUCTIL. Test report Mf 577100
[CEAT-047426] 18 p2478 N88-24703

Determination of the glass transition temperature of cured composite materials
[DT-87/62-R] 21 p2906 N88-27246

EPOXY RESINS

The water absorption of model epoxy resin networks cured with aromatic diamines
[BR100722] 01 p0027 N88-10169

The influence of microvoids on the electrical strength of glass fiber reinforced epoxy resins
[ETN-87-90443] 01 p0030 N88-10189

Shear strength of the ASDEX upgrade Toroidal Field (TF) coil insulation. Rupture, fatigue and creep behavior — tokamak
[IPP-1/230] 01 p0059 N88-10376

Optical damage in polymers by millisecond light pulses
[DE87-013106] 02 p0151 N88-10943

The effect of thermal shock on carbon fiber epoxy composites
[FOA-C-20675-2.6] 08 p0965 N88-15841

Structural study of the impregnating resins of the type TGMDA/DDS --- expoxy resins
[ETN-88-91616] 08 p0965 N88-15842

Morphology control and reinforcing mechanisms using an elastomer in an epoxy network based on diamine menthane
[ISAL-IDI1-87-09] 09 p1148 N88-16881

Analytical and experimental characterization of damage processes in composite laminates
[AD-A187221] 10 p1296 N88-17746

Initiation and propagation of damage in notched unidirectional and multidirectional CFRE resin laminates 11 p1449 N88-18633

Synthesis and structure property studies of toughened epoxy resins via functionalized polysiloxanes
[AD-A187984] 11 p1462 N88-18715

Synthesis and structure property studies of toughened epoxy resins via functionalized polysiloxanes. Friction and wear studies
[AD-A188258] 11 p1462 N88-18718

Environmental effects on the post-impact compressive strength of CFC
[RAE-TM-MAT-STR-1088] 14 p1884 N88-21258

Eddy current nondestructive inspection of graphite epoxy using ferrite cup core probes
[AD-A189823] 15 p2074 N88-22365

The adhesive bonding of thermoplastic composites
[AD-A190994] 16 p2173 N88-22953

Behaviour of fibre-reinforced composites under dynamic loading
[AD-A191310] 16 p2174 N88-22955

Correlation between dielectric and structural properties during epoxy cure
[AD-A190696] 16 p2181 N88-22997

Interfacial shear phenomena in graphite epoxy composites under impact loading using dynamic moire interferometry
[DE88-006773] 18 p2479 N88-24709

High strength/sigh modulus aromatic heterocyclic ABA block copolymers
[AD-A191666] 18 p2491 N88-24774

The influence of the chemical nature of resins on their reticulation kinetics and the consequences for their nonelastic mechanical properties
[ETN-88-92539] 18 p2493 N88-24786

Structural study of the TGMDA-DDS system --- epoxy system
[ONERA-RT-4/3346-M] 18 p2493 N88-24792

Research work completed at the Naval Surface Warfare Center Solid State Group of the Radiation Division
[AD-A191627] 18 p2582 N88-25339

Properties of two composite materials made of toughened epoxy resin and high-strain graphite fiber
[NASA-TP-2826] 19 p2609 N88-25480

Optical damage in epoxy polymers by millisecond light pulses
[DE88-008675] 19 p2620 N88-25547

High temperature resins for injection. High temperature pre-impregnated
[RC-648676] 20 p2780 N88-26486

Polymerization of epoxy matrix composites using pulsed microwaves
[CERT-3/1324-MO] 20 p2780 N88-26487

Structural study of impregnating resins of TGMDA/DDS type
[ETN-88-92167] 20 p2780 N88-26488

Relation between the mechanical characteristics of carbon-resin composites and their impact strength
[REPT-48-284/F] 21 p2907 N88-27249

Simulation of moisture diffusion of fiber reinforced components of aircraft for general air transportation
[IFL-IB-87-05] 21 p2907 N88-27253

Rubber-modified epoxies: Interfacial tension and morphology
[AD-A192464] 21 p2917 N88-27313

Study of crosslinking and nonelastic mechanical properties of epoxy and PSP networks --- epoxy resins, polystyrylpyridine resins (psp)
[ETN-88-92740] 21 p2921 N88-27337

Optical emission behavior and radiation resistance of epoxy resins
[DE88-752629] 23 p3196 N88-29023

Alternative immersion accelerated testing of coating systems for Naval shoreline facilities 24 p3355 N88-29977

Experimental aspects of using time-averaged holographic interferometry to detect barely visible impact damage in a graphite/epoxy composite plate
[AD-A194418] 24 p3375 N88-30097

EQUATIONS

On error equations for determining Earth rotation parameters with VLBI network 13 p1756 N88-20500

EQUATIONS OF MOTION

NT EULER EQUATIONS OF MOTION
NT HELMHOLTZ VORTICITY EQUATION
NT HYDRODYNAMIC EQUATIONS
NT KINEMATIC EQUATIONS
NT KINETIC EQUATIONS
NT NAVIER-STOKES EQUATION
NT REYNOLDS EQUATION

Research on one-dimensional two-phase flow. Theory on hydrodynamic balance in two fluid model and its application
[DE87-702615] 01 p0045 N88-10290

Nonlinear fluid equations for a low collisionality toroidal plasma
[DE87-013006] 01 p0100 N88-10655

Decoupling and stabilization of speed and height in F4 Phantom aircraft using output feedback
[ETN-87-90926] 02 p0125 N88-10787

Modeling shockwave deformation via molecular dynamics
[DE87-013157] 02 p0169 N88-11063

On the collective variables description of a high gain free electron laser
[DE87-013315] 02 p0178 N88-11108

Improvements to the adaptive maneuvering logic program
[NASA-CR-3985] 03 p0262 N88-11648

The evolution of HOBO
[DE87-014742] 03 p0313 N88-11980

Theory of dividing vortons 03 p0318 N88-12009

Effect of void gas lying between fluid slugs in nutation dampers 03 p0319 N88-12015

Linearized aeroelastic analysis of a wind turbine with a two-bladed rotor
[ETN-87-90600] 03 p0347 N88-12192

A method for the efficient calculation of elastic rotor blade dynamic response in forward flight 04 p0394 N88-12460

Natural control of flexible space structures 04 p0408 N88-12534

Aircraft dynamic response calculation based on discrete-continual model 04 p0424 N88-12624

Local optimal control in systems with delay 04 p0424 N88-12627

Analytical studies of axially symmetric motion of an incompressible viscous fluid between two concentric rotating spheres 04 p0444 N88-12757

Non-linear maximum likelihood estimation of stability derivatives from range data
[NAL-TM-SE-8608] 05 p0552 N88-13365

Dynamics of propellant feedline systems
[AD-A184865] 05 p0580 N88-13537

Tutorial on elementary bifurcation theory
[DE87-014849] 05 p0642 N88-13932

Analytical solution of the equations for a coaxial plasma gun operating in the snowplow mode. 1: Weak coupling limit
[AD-A185370] 05 p0652 N88-13994

Dynamics formulations for the real-time simulation of constrained motion 06 p0795 N88-14872

Post-Newtonian equations of motion in an expanding universe
[DE88-750303] 07 p0945 N88-15744

Viscous flows, part 2 08 p0986 N88-15968

Gyrotron development at the Instituto de Pesquisas Espaciais
[INPE-4240-PRE/1115] 08 p0990 N88-15992

A modal control based limiting performance formulation for shock excited systems 08 p0998 N88-16046

The effects of rotor unbalance on the vertical response of a soft-mounted block 08 p1000 N88-16057

Relativistic electromagnetic waves in an electron-ion plasma
[NASA-CR-182421] 08 p1085 N88-16532

Mechanical impact: Theoretical simulation and correlation 09 p1179 N88-17060

Maneuverable reentry vehicle trajectory footprints. Calculation and properties
[DE88-004726] 10 p1292 N88-17726

Generalized equations for emittance and field energy of high-current beams in periodic focusing
[DE88-004448] 10 p1404 N88-18372

Experimental set-up and mathematical modeling of H-shaped beam type structure
[AD-A187196] 11 p1466 N88-18743

On exterior variational calculus
[DE88-700861] 12 p1683 N88-20062

Quantization of quadratic friction revisited
[DE88-700839] 12 p1686 N88-20081

Contribution to theory of quasigeostrophic motions of finite amplitude in viscous stratified ocean 13 p1788 N88-20695

Experimental and theoretical studies of coherent and nonthermal processes in semiconductors probed by femtosecond laser techniques 14 p1977 N88-21800

A model of the nongravitational motion of Comet P/Encke 14 p2010 N88-21993

A three dimensional non-singular modelling of rigid manipulators
[AD-A189707] 15 p2116 N88-22604

Singular Lagrangians: Classical dynamics and quantization. Lectures for young scientists
[DE88-701158] 15 p2146 N88-22806

A numerical model of unsteady, subsonic aeroelastic behavior
[NASA-TM-101126] 16 p2156 N88-22862

The nonlinear dynamics of a spacecraft coupled to the vibration of a contained fluid
[DE88-007035] 16 p2168 N88-22925

Coherent structures --- in turbulent flows 16 p2199 N88-23121

Solution of the compressible Navier-Stokes equations of motion by Chebyshev polynomials for laminar shock-boundary layer flow
[AD-A191033] 16 p2208 N88-23176

Application of Navier-Stokes analysis to stall flutter 16 p2220 N88-23249

Classical non-Abelian solutions for nonstandard Lagrangians
[DE88-701305] 16 p2263 N88-23532

Analysis for fuel implosion in ICF target and pellet gain 16 p2276 N88-23620

Integrability of fermionic string in superfluid Hamiltonian approach
[DE88-701662] 16 p2284 N88-23678

Nonlinear programming extensions to rational function approximation methods for unsteady aerodynamic forces
[NASA-TP-2776] 18 p2463 N88-24623

Particle-laden weakly swirling free jets: Measurements and predictions
[NASA-TM-100920] 18 p2466 N88-24639

Effects of Coriolis acceleration on the vibrations of spinning structures 18 p2522 N88-24966

Vibrations of rotating thick or thin rings 18 p2529 N88-25003

Forced motion of initially stressed shells and plates 18 p2529 N88-25005

A constraint algorithm for maintaining rigid bonds in molecular dynamics simulations of large molecules
[AD-A191683] 18 p2572 N88-25277

Color charge motion in non-Abelian fields
[DE88-701306] 19 p2642 N88-25672

LLNL Granular Solids Flow Project
[DE88-008023] 19 p2664 N88-25844

Stability of dynamical systems supported by rubber springs 19 p2680 N88-25932

A description of the reference frames and the coordinate transformations used in AMEER (Aero-Mechanical Equations Evaluations Routines)
[DE88-007960] 19 p2720 N88-26153

Deviation equation as an equation of motion
[DE88-702134] 19 p2722 N88-26161

Random vibration analysis of rattling structures
[DE88-007196] 20 p2813 N88-26691

Neoclassical diffusion due to trapping/detrapping orbits in stellarators
[DE88-008566] 20 p2857 N88-26968

Effects of static equilibrium and higher-order nonlinearities on rotor blade stability in hover
21 p2890 N88-27157

In-flight motor torque estimates for the second-stage Strypi 9 launch vehicle
[DE88-010833] 21 p2902 N88-27222

Lax representation and complete integrability for the periodic relativistic Toda lattice
[PREPRINT-594] 22 p3146 N88-28711

Open bosonic string in background electromagnetic field
[DE88-702140] 23 p3201 N88-29053

The acoustic field scattered from some approximate pressure release materials
[AD-A194768] 23 p3278 N88-29515

General equations for the motions of ice crystals and water drops in gravitational and electric fields
[NASA-CR-183229] 24 p3370 N88-30070

Nonlinear stress-strain and inelastic rebound with exponential stiffness
[AD-A195667] 24 p3384 N88-30159

Canonical variables and canonical integrals for motion in near-circular orbits 24 p3446 N88-30512

Lagrangian of the self-duality equation and d = 10, N = 2b supergravity
[DE88-701554] 24 p3455 N88-30563

EQUATIONS OF STATE

Nitrogen at high pressure
[DE87-013797] 01 p0021 N88-10130

Application of new conformal solution of theories
[PB87-214557] 01 p0105 N88-10684

Electrical conductivity and equation of state measurements on planetary fluids at high pressures and temperatures
[DE87-013787] 01 p0110 N88-10708

The equation of state of PETN detonation products
[DE87-013796] 02 p0155 N88-10971

Material behaviour at high rates of strain
[OUEL-1684/87] 02 p0192 N88-11200

The LLNL 150-mm equation-of-state gun system
[DE88-000423] 04 p0405 N88-12519

Studies of pressure-velocity coupling schemes for analysis of incompressible and compressible flows
[NASA-CR-181526] 04 p0443 N88-12748

Core bounce supernovae
[DE87-014910] 04 p0520 N88-13197

Utilization of FEP energetics
[NASA-CR-182373] 06 p0714 N88-14379

Experimental and theoretical studies of dense fluid mixtures
[DE88-002710] 07 p0831 N88-15039

Equation of state of condensed materials physical principles and applications
[NASA-TT-20007] 08 p0968 N88-15855

Zero temperature quark matter equation of state
[DE88-003408] 10 p1422 N88-18496

Simple renormalization group method for calculating thermal equations of states
[DE88-700143] 11 p1454 N88-18668

Further developments in exact state reconstruction in deterministic digital control systems
[NASA-TP-2812] 11 p1468 N88-18751

The automated symbolic derivation of state equations for dynamic systems
[DE88-005222] 12 p1683 N88-20060

The automated symbolic derivation of state equations for dynamic systems
[DE88-000968] 13 p1830 N88-20945

Quark core stars, quark stars and strange stars
[DE88-006991] 17 p2450 N88-24555

Use of a two-stage light-gas gun as an injector for electromagnetic railguns
[DE88-007200] 18 p2469 N88-24657

Fabrication issues and technology development for HELEOS (Hypervelocity Electromagnetic Launcher for Equation Of State)
[DE88-007419] 18 p2470 N88-24658

The high pressure sound velocity and equation of state of aqueous solutions of hydroxylammonium nitrate and triethanolammonium nitrate
[AD-A191740] 18 p2570 N88-25266

Nuclear and astrophysical evidence on the equation of state
[DE88-007397] 18 p2572 N88-25279

Study of data distributions and functions for the development of thermodynamic equations of state
[PB88-196365] 18 p2587 N88-25370

Phase equilibria and density calculations in the critical region: A phenomenological correction for a classical equation of state
[PB88-185335] 19 p2723 N88-26167

Equation of state of solid neon from X-ray diffraction measurements to 110 GPa
[DE88-008723] 19 p2734 N88-26241

Development of an equation of state for computation of supercompressibility factors, critical flow factors and other properties for wet, sour natural gases, synthetic gases and admixtures
[PB88-202676] 20 p2798 N88-26602

Freely expanding detonation products: Scaling of rate processes
[DE88-007827] 20 p2799 N88-26606

Nonlinear equation of state effects and the momentum-dilution trade-off in a turbulent buoyant jet
[DE88-701839] 20 p2799 N88-26610

An analysis of the efficiency and directivity of the sound generated by a moving laser source
[AD-A192220] 20 p2849 N88-26914

Shock wave compression and metallization of simple molecules
[DE88-008031] 20 p2851 N88-26925

On linear relationship between shock velocity and particle velocity
[DE88-701827] 20 p2880 N88-27099

State variable approach to deformation phenomena in Face Centered Cubic (FCC) metals
[VTT-44] 24 p3354 N88-29964

EQUATORIAL ATMOSPHERE

Atmosphere dynamics in the equatorial meteor zone
06 p0733 N88-14508

Characteristics of atmospheric disturbances with a quasi-two day period 06 p0734 N88-14515

Longitudinal variations of equatorial ionosphere determined from Intercosmos-19 artificial Earth satellite data 08 p1003 N88-16074

Solar tides in the upper equatorial thermosphere: A comparison between AE-E data and the NCAR thermospheric general circulation model
[AD-A186160] 08 p1023 N88-16196

Study of passages of cross-equatorial current during southern monsoon 14 p1900 N88-21347

In-situ plasma bubble observations associated with equatorial spread-F over Natal
[INPE-4488-PRE/1252] 15 p2095 N88-22482

One equatorial anomaly in nighttime ionospheric F region 24 p3447 N88-30517

EQUATORIAL ELECTROJET

Project CONDOR: Middle atmosphere wind structure obtained with lightweight inflatable spheres near the equatorial electrojet 08 p1028 N88-16230

EQUATORIAL ORBITS

NT STATIONARY ORBITS

EQUATORIAL REGIONS

CTD/02 measurements during 1984 and 1985 as part of the Equatorial Pacific Ocean Climate Studies (EPOCS)
[PB88-102082] 06 p0748 N88-14600

Processes in the quiet and disturbed equatorial low latitude ionosphere: Sundial campaign 1984
[INPE-4152-PRE/1057] 08 p1036 N88-16282

Interpretation of equatorial current meter data as internal waves
[PB88-108113] 08 p1044 N88-16309

An analysis of longitude variations in the equatorial spectrum of Saturn 10 p1430 N88-18539

Equatorial turbulence: Mixed layer and thermocline
13 p1804 N88-20787

On the zonal momentum balance at the equator
13 p1805 N88-20788

Mixed-layer shear related to wind stress in the central equatorial Pacific 13 p1805 N88-20793

Equatorial dynamics and ocean-atmosphere coupling
14 p1938 N88-21565

CTD/O2 data collected in 1985 and 1986 for EPOCS (Equatorial Pacific Ocean Climate Studies)
[PB88-160775] 14 p1951 N88-21629

A study of the dynamics of the Intertropical Convergence Zone (ITCZ) in a symmetric atmosphere-ocean model
[NASA-TM-86220] 19 p2693 N88-26005

The relationship between polar sea ice and the position of the near equatorial convergence zone
22 p3123 N88-28563

EQUATORS

Tropic heat MR (Meteorological Recorder) meteorological data (April 1984 - June 1985)
[PB88-161286] 14 p1948 N88-21620

EQUILIBRIUM

Grain boundary phase equilibria in metallic systems
[DE87-014123] 01 p0104 N88-10679

Equilibrium and tearing stability of thin current layers in magnetic arcades 01 p0118 N88-10754

Study of ionization equilibrium of high temperature and low density plasma
[DE87-703070] 02 p0238 N88-11502

Application of prediction of equilibrium to servo-controlled calorimetry measurements
[DE87-013745] 03 p0324 N88-12046

Phase equilibrium and crystal growth studies on AgGaSe2 and related nonlinear optical materials
[AD-A184768] 03 p0382 N88-12400

Theoretical studies of multicomponent mixtures: Phase equilibrium and transport
[DE88-002717] 07 p0831 N88-15040

Equilibrium retention in the nozzle of oxygen hydrogen propulsion systems 07 p0924 N88-15816

Free-boundary equilibrium problem for helically symmetric plasmas
[DE88-700101] 07 p0934 N88-15674

General equilibrium characteristics of a dual-lift helicopter system
[NASA-TP-2615] 12 p1573 N88-19407

Domain perturbation method in the static equilibrium of masses in rotation
[INPE-4217-PRE/1098] 12 p1686 N88-20085

Wave energy flow conservation for propagation in inhomogeneous Vlasov-Maxwell equilibria
[DE88-006705] 15 p2055 N88-22251

Equilibrium stability of strained epitaxial layers on a rigid substrate
[INPE-4254-PRE/1127] 15 p2145 N88-22804

On the prediction of equilibrium states in homogeneous turbulence
[NASA-CR-181659] 16 p2207 N88-23174

The two-dimensional one component plasma in a doubly periodic background: Exact results
[AD-A191260] 16 p2280 N88-23650

Equilibrium distribution functions for limited plasma-molecular systems
[DE88-702412] 21 p3018 N88-27916

The VPE-hydride technique with alloy source: Equilibrium analysis
[AD-A194036] 22 p3157 N88-28784

EQUILIBRIUM DIAGRAMS

U PHASE DIAGRAMS

EQUILIBRIUM EQUATIONS

Flap-lag-torsion aeroelastic stability of a circulation control rotor in forward flight 10 p1271 N88-17600

The dynamics of coupled planar rigid bodies. Part 1: Reduction, equilibria and stability
[AD-A187467] 10 p1345 N88-1804

Error questions in the computation of solution manifolds of parametrized equations
[AD-A188648] 12 p1684 N88-2006

Effects of translational and rotational nonequilibrium on CW (Continuous Wave) chemical laser performance
[AD-A191425] 16 p2214 N88-2321

A thermal equilibrium model for multi-megawatt space platforms 17 p2410 N88-2433

On the Nash point equilibria in the calculus of variations
[AD-A194959] 24 p3424 N88-30381

Formulation and solution of economic equilibrium problems
[AD-A196034] 24 p3439 N88-30470

EQUILIBRIUM FLOW

Continuation finite element analysis of viscoelastic fluids 04 p0445 N88-12761

Simplified curve fits for the transport properties of equilibrium air
[NASA-CR-178411] 18 p2513 N88-24911

EQUILIBRIUM METHODS

A parametric study of embedded cantilever retaining walls: The results of a finite element study
[RR-CE83] 24 p3383 N88-30152

EQUIPMENT SPECIFICATIONS

A program to study antiprotons in the cosmic rays: Arizona collaboration
[NASA-CR-180702] 01 p0120 N88-10764

Photon counting image sensor development for astronomical applications
[NASA-CR-181507] 05 p0660 N88-14049

Servicer system demonstration plan and capability development
[NASA-CR-179246] 08 p0975 N88-15895

Electric design rules related to latch-up and radiation — simulation
[FOA-E-30006-3.1] 08 p0979 N88-15917

Supercritical fluid extraction-gas chromatography of Volatile Organic Compounds (VOC) from tenax devices
[PB88-124300] 10 p1298 N88-1775

An attempt to measure the diffuse brightness of the sky at submillimeter wavelengths
12 p1710 N88-20233

The Joint NASA/Goddard-University of Maryland Research Program in Charged Particle and High Energy Photon Detector Technology
[NASA-CR-182612] 12 p1712 N88-20247

Considerations in GaAs standard cell design
[DE88-003310] 14 p1985 N88-2184

UARS spacecraft recorder
[NASA-CR-180768] 15 p2068 N88-2233

In situ fatigue loading stage inside scanning electron microscope 15 p2083 N88-2241

Research sensors 15 p2085 N88-22430
Preliminary study of a coherent radar
[BCRS-86-03] 16 p2189 N88-23051
Processing of HRPT data from the NOAA series satellites 17 p2359 N88-24053
High power density electrodes for AMTEC
17 p2437 N88-24501
Tower evaporator
[NASA-CASE-NPO-15609-2] 18 p2497 N88-24815
Electrostatic discharge test apparatus
[NASA-CASE-MSC-21094-1] 18 p2518 N88-24941
Mars rover/sample return mission requirements affecting space station
[NASA-CR-172048] 18 p2594 N88-25414
An 8.4-GHz dual maser front end for Parkes reimplementation 22 p3066 N88-28197
Baseband assembly analog-to-digital converter board
22 p3067 N88-28201
An electronically tuned, stable 8415-MHz dielectric resonator FET oscillator for space applications
22 p3068 N88-28205
Description of a tool for the simulation of imagery systems 22 p3147 N88-28724
Elemental composition of the Martian surface
23 p3302 N88-29665
Gamma-ray/neutron spectroscopy from the Mars observer 23 p3302 N88-29671
Very high energy cosmic gamma rays from radio and X-ray pulsars 23 p3309 N88-29711

EQUIVALENCE
Topological equivalence of certain function spaces 2
[PB88-100904] 06 p0767 N88-14712
Symmetry and equivalence restrictions in electronic structure calculations
[NASA-TM-89252] 11 p1557 N88-19320
On the norm equivalence of singularly perturbed elliptic difference operators
[DE88-006357] 13 p1826 N88-20913
Constructive version of the approximation induction principle
[PB88-165477] 15 p2122 N88-22647
On matrix pencil equivalents of a general polynomial matrix
[MATH-REPT-207] 23 p3273 N88-29479

EQUIVALENT CIRCUITS
A study of scattering from E-plane circuit elements
[AD-A184473] 04 p0431 N88-12673
Equivalent circuit consideration on the rotation of resonant modes of double resonant vibrators
07 p0839 N88-15092
Analyses by equivalent mechanical circuits of bending vibration bars with load-impedance at one end
07 p0840 N88-15093
An investigation of the equivalent circuit and carrier lifetimes of Si/SiGe heterostructure p-n diodes for frequencies between 0.5 and 18.5 MHz
[FOA-C-30469-3.2] 09 p1256 N88-17529
On the choice of a element low-noise preamplifier on bipolar transistors
[DE88-700639] 10 p1322 N88-17904
Some equivalent circuit models for AC impedance analysis of pyrite/solution interface
[DE88-010574] 21 p2939 N88-27452

ERBE
U EARTH RADIATION BUDGET EXPERIMENT

ERBIUM
Characterization of Er,Cr YSGG
[AD-A185885] 07 p0932 N88-15659
The YAlO(sub 3):Er laser
[PB88-130877] 11 p1493 N88-18911
Integrated optoelectronic circuits utilizing InGaAsP grown by molecular beam epitaxy (erbium doping of MBE GaAs)
[AD-A192269] 20 p2795 N88-26584
Characterization of structural and magnetic order of Er/Y superlattices 20 p2873 N88-27056

ERECTION
U CONSTRUCTION

EREP
Earth resources: A continuing bibliography with indexes (issue 55)
[NASA-SP-7041(55)] 01 p0065 N88-10415

ERGODIC PROCESS
Nonlinear relaxation and ergodicity breakdown in random anisotropy spin glasses
[PREPRINT-565] 06 p0764 N88-14693

ERGOMETERS
A new isodynamically-braked arm ergometer including the demonstration of a prototype
12 p1661 N88-19957

ERGONOMICS
U HUMAN FACTORS ENGINEERING

ERGOTAMINE
Does dihydroergotamine used in therapeutical doses influence the physical and psychomotor performance of young pilots or other traffic drivers subjected to hypotonia?
[ETN-88-92136] 20 p2832 N88-26799

EROSION
NT SOIL EROSION
High velocity erosion of metal interfaces
[DE87-013937] 01 p0025 N88-10155
The ability of modified pavement quality concrete to resist ground erosion caused by VTOL aircraft
[BAE-ARG-238] 03 p0267 N88-11683
Spacecraft surface exposure to atomic oxygen in low Earth orbit 03 p0273 N88-11715
Materials preparation and longevity in hyperthermal atomic oxygen 03 p0297 N88-11862
Pipe and bend erosion by pneumatic transport of solids at high temperature
[DE88-001345] 04 p0429 N88-12658
Data base on the high heat flux behaviour of metals and carbon materials for plasma facing components: Experiments at the 10 MW neutral beam injection test stand of the IPP Nagoya
[IPPJ-AM-53] 04 p0492 N88-13031
PISCES: Plasma-surface interactions and materials research
[DE88-001323] 04 p0494 N88-13044
Studies in Aeolian geology
[NASA-CR-182328] 05 p0625 N88-13828
Modern concept concerning transport of bottom sediments in abyssal regions of world ocean
06 p0728 N88-14478
Gas erosion of impeller housing in the operation of a high-temperature, high-pressure helium circulator
[DE88-002607] 09 p1175 N88-17041
Detection of soil erosion with Thematic Mapper (TM) satellite data within Pinyon Juniper woodlands
[NASA-CR-182476] 09 p1185 N88-17103
Operation of gas turbine engines in dust-laden environments 10 p1280 N88-17654
Effects of ion implantation on cavitation erosion of a cobalt based metal/carbide alloy
[AD-A187239] 10 p1303 N88-17793
Mechanisms of wear in single- and two-phase materials
[DE88-003646] 10 p1305 N88-17806
High performance Solid Rocket Motor (SRM) submerged nozzle/combustion cavity flowfield assessment
[NASA-CR-179307] 11 p1446 N88-18622
Characterization of PEOS (Plasma Erosion Opening Switch) plasma parameters and conduction phase properties
[AD-A189024] 12 p1624 N88-19714
Erosion in dual-phase microstructures
[DE88-004507] 13 p1743 N88-20421
Reduction of erosion in elbows due to flow modifications, phase 1
[DE88-001028] 13 p1769 N88-20584
Hydrogen pumping and release by graphite under high flux plasma bombardment
[DE88-005880] 13 p1842 N88-21021
Durability testing of an iridium-plated storable rocket engine injector
[AD-A190707] 15 p2027 N88-22078
Investigation of laser diagnostics of PACVD processes for depositing hard face coatings
[DE88-007083] 15 p2043 N88-22176
Analysis of anomalous resistivity during the conduction phase of the plasma erosion opening switch
[DE88-006382] 15 p2061 N88-22286
Analytic and numerical modeling of heat and material transport in electrical hypervelocity guns
[AD-A192178] 18 p2469 N88-24655
Internal erosion rates of a 10-kW xenon ion thruster
[NASA-TM-100954] 18 p2476 N88-24688
The influence of cathodic protection on erosion-corrosion of metals and model alloys
[AD-A191613] 18 p2485 N88-24742
A 3 MW wood fired gas turbine at Red Boiling Springs, Tennessee 18 p2536 N88-25051
Solid rocket motor performance: A workshop report
19 p2631 N88-25607
Study of evolution of vegetal cover and slide scars in the Cubatao municipality-Sao Paulo
19 p2683 N88-25947
Oxidation-erosion of metals and alloys: Models, verification, and prediction
[DE88-010016] 21 p2915 N88-27300
A review of solid particle erosion of engineering materials
[DE88-010065] 22 p3054 N88-28124
Study of the erosion corrosion of alloys and coatings
[AD-A194337] 22 p3055 N88-28128
Erosion of metals exposed to hot, dense gases
[AD-A193708] 22 p3056 N88-28131
Erosion/redeposition modeling and calculations for carbon
[DE88-010382] 22 p3057 N88-28139
Analysis of edge detection techniques for radiographic image measurement
[AD-A193650] 23 p3186 N88-28961
Spectral characteristics and the extent of paleosols of the Palouse formation
[NASA-CR-180947] 23 p3228 N88-29210
Distribution and timing of thick transient air-fall deposits in Electris: implications for the nature of the upland plains 23 p3303 N88-29674

EROSIVE BURNING
A study of flame spreading and combustion phenomena of stick propellants
[AD-A193598] 22 p3052 N88-28106

ERROR ANALYSIS
Error estimates for finite element approximations of parabolic variational equations
[BONNER-MATHE-SCHR-179]
01 p0087 N88-10569
Semidiscrete Galerkin method for semilinear evolution equations with a differential operator of third order
[BONNER-MATHE-SCHR-181]
01 p0087 N88-10570
On the concept of resolution ellipse in aperture synthesis matched deconvolution with error analysis --- astronomical interferometry 01 p0095 N88-10621
Some approaches to the design of high integrity software 02 p0127 N88-10799
A general approach to error propagation
[DE87-014287] 02 p0224 N88-11412
A critical assessment of wind tunnel results for the NACA 0012 airfoil
[NASA-TM-100019] 03 p0260 N88-11636
Analysis of undulator field errors for XUV FELs (Extreme Ultraviolet Free Electron Laser)
[DE87-014734] 03 p0328 N88-12073
Detector normalization --- SPOT remote sensors
03 p0341 N88-12151
Kinds of bootstraps and kinds of jackknives, discussed in terms of a year of weather-related data
[AD-A184495] 03 p0353 N88-12227
Accommodating the residue of processed or computed digital video signals within the 8 bit CCIR recommendation 601
[BBC-RD-1987/12] 04 p0432 N88-12676
More on the decoder error probability for Reed-Solomon codes 04 p0435 N88-12699
Kinematic formulation of finite elements for plate bending 04 p0455 N88-12821
Correction of inertial navigation system drift errors for an autonomous land vehicle using optical radar terrain data
[AD-A184973] 05 p0544 N88-13311
Error control techniques for satellite and space communications
[NASA-CR-181581] 05 p0576 N88-13516
Assessment of the reliability of a correction procedure for WGT (Wet Globe Thermometer) (Botsball) measurements of heat stress
[AD-A185193] 05 p0584 N88-13559
Operating envelopes of particle sizing instrumentation used for icing research
[NASA-CR-180870] 05 p0586 N88-13573
Experiments in fault tolerant software reliability
[NASA-CR-181554] 05 p0632 N88-13863
Reliability of voting in fault-tolerant software systems for small output spaces
[TR-87-16] 05 p0632 N88-13864
Effectiveness of back-to-back testing
[TR-87-08] 05 p0632 N88-13865
Diagnostic reasoning in digital systems
[NASA-CR-181564] 05 p0633 N88-13871
Error propagation in a digital avionic mini processor
[NASA-CR-181565] 05 p0633 N88-13872
Flightpath reconstruction and systematic radar error estimation from multiradar range-azimuth measurements
[NLR-MP-85064-U] 06 p0693 N88-14251
How to estimate the total number of errors in a software system
[PB87-132130] 06 p0758 N88-14647
Estimating the distribution of fault latency in a digital processor
[NASA-TM-100521] 06 p0760 N88-14666
Round-off error propagation in four generally applicable, recursive, least-squares-estimation schemes
[NASA-TM-100055] 06 p0766 N88-14708
Improved understanding of the loss-of-symmetry phenomenon in the conventional Kalman filter
[NASA-TM-100041] 06 p0766 N88-14709
Error assessments of widely-used orbit error approximations in satellite altimetry
[NASA-CR-182390] 07 p0823 N88-14998

Estimating system reliability: Monte Carlo methods, sensitivity and errors in input parameters
[AD-A186182] 07 p0865 N88-15248
How errors in component reliability affect system reliability
[AD-A186264] 07 p0865 N88-15249
Geosat crossover analysis in the tropical Pacific. Part 1: Constrained sinusoidal crossover adjustment
[NASA-CR-182391] 07 p0871 N88-15285
Determination of cloud base height and emissivity from downwelling angular radiances
[AD-A185985] 07 p0879 N88-15331
Tracking procedure for non-normally distributed measurement errors
[AD-A186287] 07 p0903 N88-15468
Necessary and sufficient conditions for the convergence of integrated and mean-integrated r-th order error of histogram density estimates
[AD-A186037] 07 p0914 N88-15550
Investigation of candidate data structures and search algorithms to support a knowledge based fault diagnosis system 07 p0923 N88-15606
Zeroshift of piezoelectric accelerometers in pyroshock measurements 08 p0997 N88-16039
Limiting accuracy of scatterometer determination of wind speed over ocean from satellite
08 p1007 N88-16107
Assessment of VAS-derived products created by a simultaneous algorithm on a convectively active day
[AD-A186158] 08 p1054 N88-16359
Error analysis for geotechnical engineering
[AD-A186795] 09 p1189 N88-17124
Advances in reliable numerical computation: A summary --- conference
[NPL-DITC-102/87] 09 p1229 N88-17367
Designing variable-length codes with good error-recovery properties
[BBC-RD-1987/19] 10 p1317 N88-17876
Seventy-meter antenna performance predictions: GTD analysis compared with traditional ray-tracing methods
11 p1474 N88-18793
Improvement in robot positioning accuracy by a kinematic identification model 11 p1496 N88-18931
Error detection and recovery for robot motion planning with uncertainty
[AD-A187746] 11 p1534 N88-19165
Accurate efficient evaluation of Bessel transform: Programs and error analysis
[AD-A187718] 11 p1536 N88-19174
Position finding and tolerances
[AD-A187685] 11 p1540 N88-19205
Digital bit error rate estimator for telemetry links
[INPE-4351-TDL/295] 12 p1598 N88-19563
Design of the primary pre-TRMM and TRMM ground truth site
[NASA-CR-182609] 12 p1647 N88-19865
The effects of atmospheric and thermohaline variability on the validation of the GEOSAT altimeter oceanographic signal between Scotland and Iceland
[AD-A189324] 12 p1650 N88-19882
An experiment in software reliability: Additional analyses using data from automated replications
[NASA-CR-178395] 12 p1676 N88-20017
Procedure for initial data input and checkup in the system for film data mathematical processing
[DE88-700926] 12 p1676 N88-20022
Error questions in the computation of solution manifolds of parametrized equations
[AD-A188648] 12 p1684 N88-20068
Detecting serial correlation in the error structure of a cross-lagged panel model
[AD-A189070] 12 p1685 N88-20077
Formulation of a general technique for predicting pneumatic attenuation errors in airborne pressure sensing devices
[NASA-TM-100430] 13 p1723 N88-20302
Generalized expression for radio navigation parameter error 13 p1787 N88-20691
On a bound of the modeling errors of black-box transfer function estimates
[EUT-87-E-173] 14 p1963 N88-21708
Aircraft accident report: North Star Aviation, Inc., PA-32 RT-300, N39614 and Alameda Aero Club Cessna 172, N75584, Oakland, California, March 31, 1987
[PB87-910412] 15 p2016 N88-22021
Methodology for software reliability prediction, volume 1
[AD-A190018] 15 p2110 N88-22571
Methodology for software reliability prediction, volume 3
[AD-A190019] 15 p2110 N88-22572
A posterior error estimation in a finite element method for parabolic partial differential equations
[AD-A190296] 15 p2120 N88-22636
Analysis and testing of the SURE program
[NASA-TP-2817] 15 p2123 N88-22653
A study on local level inertial surveying systems: Error model for the stationary system
[B8736714] 16 p2229 N88-23312
Note on the double crystal method of measuring heat transfer coefficient
[OUEL-1710/87] 17 p2338 N88-23950
Adjusting a finite element model using vibration type experimental data: Concept and error detection
[ONERA-RT-7/3313-RY-060-R]
17 p2392 N88-24220
A recursive prediction error parameter estimator for nonlinear models
[RR-326] 17 p2392 N88-24222
Determination of doping profiles in silicon from resistivity measurements via the four-point probe in combination with layer strippings via anodic oxidation
18 p2583 N88-25347
Studies of error in temperature measurement with thermistors in the range between continual and free-molecule flows
[NASA-TT-20302] 19 p2674 N88-25900
A simulation analysis of errors in the measurement of standard electrochemical rate constants from phase-selective impedance data
[AD-A192739] 20 p2770 N88-26426
Coherent RF error statistics
[AD-A193002] 20 p2792 N88-26560
A control program for global radiation measurements
[KNMI-TR-100] 20 p2824 N88-26757
Dynamic modelling and estimation of the error due to asynchronism in a redundant asynchronous multiprocessor system
[NASA-CR-177427] 21 p2898 N88-27205
Studies on system performance of SPOT (space and ground segments) 22 p3112 N88-28485
A bulk model for the unstable planetary boundary layer over the sea: A sensitivity investigation
[DM-51] 22 p3129 N88-28600
Stereo and eye movement
[AD-A193588] 22 p3142 N88-28681
Fine resolution errors in secondary surveillance radar altitude reporting
[RSRE-87019] 23 p3175 N88-28906
Digital phase-lock loop having an estimator and predictor of error
[NASA-CASE-NPO-17196-1-CU]
23 p3205 N88-29076
NBS (National Bureau of Standards) measurement services: The NBS photodetector spectral response calibration transfer program
[PB88-201595] 24 p3376 N88-30109
Performance prediction of concurrent systems
[NASA-CR-183175] 24 p3412 N88-30312
Achieving real-time performance in FIESTA
24 p3418 N88-30344

ERROR BAND
U ACCURACY

ERROR CORRECTING CODES
Local concurrent error detection and correction in data structures using virtual backpointers
[NASA-CR-181432] 01 p0106 N88-10692
A simplified procedure for correcting both errors and erasures of a Reed-Solomon code using the Euclidean algorithm 04 p0435 N88-12698
More on the decoder error probability for Reed-Solomon codes 04 p0435 N88-12699
Further results on finite-state codes
11 p1472 N88-18782
Implementation and evaluation of a combined test-error correction procedure for memories with defects
[EUT-87-E-169] 14 p1955 N88-21651
FORTRAN 77 error handling of the RASP library
[DFVLR-MITT-87-14] 14 p1957 N88-21669
Error reduction in two-dimensional pulse-area modulation, with application to computer-generated transparencies --- optical field synthesis
[EUT-87-E-172] 14 p1982 N88-21825
A general approach for automating source code verification
[AD-A191461] 18 p2556 N88-25170
Long haul communications in the HF spectrum utilizing high speed modems
[AD-A194683] 24 p3360 N88-30003

ERROR CORRECTING DEVICES
Multimedia sensory systems for the solution of the error recovery problem --- robots
[REPT-87-010] 01 p0084 N88-10545
Design of source coders and joint source/channel coders for noisy channels
[NASA-CR-181547] 04 p0432 N88-12678
Implementation of encoders and decoders for Reed-Solomon codes
[PB88-126628] 10 p1387 N88-18286
A control technique for improved robot performance
17 p2391 N88-24212
The performance of Eurocom error correction schemes for data communications
[FEL-1987-56] 20 p2792 N88-26563
An integrated circuit for error protection in modern data communication systems conforming to Eurocom specifications
[FEL-1987-48] 20 p2796 N88-26593

ERROR DETECTION CODES
Local concurrent error detection and correction in data structures using virtual backpointers
[NASA-CR-181432] 01 p0106 N88-10692
A lower bound for the decoder error probability of the linear MDS code 11 p1472 N88-18780
Frame synchronization performance and analysis
11 p1473 N88-18787
Error detection and recovery for robot motion planning with uncertainty
[AD-A187746] 1[illegible] p1534 N88-19165
Shorts in self-checking circuits
[RR-657-I] 14 p1908 N88-21402
Random access memory testing: Theory and practice. The gains of fault modeling
[EUT-86-E-161] 14 p1955 N88-21649
Implementation and evaluation of a combined test-error correction procedure for memories with defects
[EUT-87-E-169] 14 p1955 N88-21651
Self-checking logic arrays
[RR-656-I] 15 p2106 N88-22545
Design of the Detector 2: A CMOS gate array for the study of concurrent error detection techniques
[AD-A191247] 16 p2193 N88-23079
Automatically generated acceptance test: A software reliability experiment
[NASA-CR-181667] 17 p2347 N88-23984
Knowledge-based fault diagnosis on future space vehicles 23 p3254 N88-29374

ERROR FUNCTIONS
A prediction-error estimation algorithm for nonlinear output-affine systems
[RR-314] 14 p1959 N88-21679

ERROR SIGNALS
Solution of the Lloyd-Max quantizer parameters by the method of successive substitution
[AD-A187829] 11 p1540 N88-19207
Long haul communications in the HF spectrum utilizing high speed modems
[AD-A194683] 24 p3360 N88-30003

ERRORS
NT INSTRUMENT ERRORS
NT PHASE ERROR
NT PILOT ERROR
NT POSITION ERRORS
NT ROOT-MEAN-SQUARE ERRORS
NT TRUNCATION ERRORS
Measurement of fault-tolerant parallel processors
[PB87-208328] 01 p0084 N88-10539
Optical alignment of Centaur's inertial guidance system
[NASA-TM-88844] 04 p0405 N88-12515
Calibration of a laser-pumped, thermographic phosphor remote thermometry system
[DE88-000452] 04 p0449 N88-12781
Radial orbit error reduction and sea surface topography determination using satellite altimetry
04 p0462 N88-12861
GOLD: Integration of model-based control systems with artificial intelligence and workstations
[DE88-000706] 04 p0483 N88-12977
Determination of total ozone from HIRS2/MSU sounding data 05 p0619 N88-13799
AVHRR/HIRS (Advanced Very High Resolution Radiometer/High Resolution Infra-Red Sounder) operational method for satellite based sea surface temperature determination
[PB88-107594] 06 p0708 N88-14340
Space station software reliability analysis based on failures observed during testing at the multisystem integration facility 06 p0798 N88-14884
Packet error probabilities in frequency-hopped spread spectrum packet radio networks: Markov frequency hopping patterns considered
[AD-A186071] 07 p0841 N88-15104
Inadequacy of conventional dynamic recovery mechanisms in the presence of temporary failures
[AD-A186311] 07 p0866 N88-15251
Annotated bibliography on reliable system design
[PB88-109848] 07 p0866 N88-15254
Roles of knowledge in motor learning
[AD-A186420] 07 p0897 N88-15438
Strong consistency of estimation of number of regression variables when the errors are independent and their expectations are not equal to each other
[AD-A186025] 07 p0909 N88-15507
Statistical measures of clipped random signals
08 p1000 N88-16055

Investigation of vibration problems with heterodyne holographic interferometer 08 p1000 N88-16058

Exploring hypotheses in attitude control fault diagnosis 08 p1058 N88-16384

Comparison of direct and heterodyne detection optical intersatellite communication links 09 p1169 N88-17013

Calculating measurement imprecision and uncertainty [DE88-003981] 09 p1233 N88-17391

Error modeling and confidence interval estimation for inductively coupled plasma calibration curves [AD-A186711] 09 p1250 N88-17488

Emittance studies at the Los Alamos National Laboratory Free-Electron Laser (FEL) [DE88-003146] 10 p1334 N88-17975

Systematic errors of the FSU global spectral model 10 p1356 N88-18103

Source and event selection for radio-planetary frame tie measurements using the Phobos Landers 11 p1471 N88-18775

Using ridge regression in systematic pointing error corrections 11 p1472 N88-18777

A lower bound for the decoder error probability of the linear MDS code 11 p1472 N88-18780

A comparison of VLSI architectures for time and transform domain decoding of Reed-Solomon codes 11 p1472 N88-18783

A posteriori error estimates in computational fluid mechanics 11 p1486 N88-18869

Core-core and core-valence correlation [NASA-CR-182552] 11 p1544 N88-19226

Covariance analysis and post-processing of gravity compensation effects for aided multi-state navigation systems [PAPER-87-13] 12 p1577 N88-19430

On error equations for determining Earth rotation parameters with VLBI network 13 p1756 N88-20500

Two dimensional uncorrelated bias in fix algorithms [NASA-CR-182683] 13 p1815 N88-20847

A low-frequency measurement of the spectrum of the cosmic microwave background radiation 13 p1858 N88-21112

Investigation of the misfueling of reciprocating piston aircraft engines [NASA-TP-2803] 14 p1865 N88-21144

The Spring 1985 high precision baseline test of the JPL GPS-based geodetic system [NASA-CR-182686] 14 p1940 N88-21577

Merit of Hadamard transform active absorption spectrometer described 15 p2053 N88-22232

An expert system for discrete component digital circuit design [AD-A189680] 15 p2059 N88-22274

COBOL Analysis System (CAS) users manual [PB88-171442] 16 p2250 N88-23445

Error control techniques for satellite and space communications [NASA-CR-182886] 17 p2332 N88-23922

Theory of neutron moisture probes and interpretation of measurements in complex soil and water systems 17 p2342 N88-23965

The modeling of error budget analysis and tolerance specifications for BRESEX multiband linear array CCD camera 17 p2355 N88-24029

Digital processing of infrared and visible images from the GOES satellite and its integration with meteorological radar data 17 p2360 N88-24057

Geometric image correction: An approach for the registration of LANDSAT-TM digital images supported by topographical maps of medium and great scales 17 p2361 N88-24061

Study of methods of post-processing applied to a problem of standard classification 17 p2362 N88-24067

Fault diagnosis in orbital refueling operations 17 p2381 N88-24154

Coincidence counting corrections under conditions used by A. DeVolpi [NPL-RS(EXT)-90] 17 p2393 N88-24224

Angular position measurements at high temperatures and high radiation environments 17 p2434 N88-24479

Reducing sensitivity to errors in free electron laser amplifiers [DE88-007017] 18 p2522 N88-24960

Effectiveness evaluation of fault-tolerant multiprocessor systems [AD-A191688] 18 p2554 N88-25158

Robust vector quantization for noisy channels 19 p2653 N88-25754

Some supraconvergent schemes for hyperbolic equations on irregular grids [DE88-009113] 19 p2720 N88-26151

A VLSI single-chip (225,223) Reed-Solomon encoder with interleaver [NASA-CASE-NPO-17280-1-CU] 21 p2902 N88-27220

A unified approach to estimation in linear models with fixed and mixed effects [AD-A193060] 21 p3006 N88-27829

The feasibility of the disturbance accommodating controller for precision antenna pointing 22 p3064 N88-28182

The effects of changes in observation and data assimilation systems on CAC climate data sets 22 p3124 N88-28568

Analysis of the dynamic extended range forecast experiment 22 p3126 N88-28581

Correction of systematic errors in NMC medium range forecasts 22 p3126 N88-28584

Dependence of medium range forecast errors upon the large-scale initial state 22 p3126 N88-28585

Theoretical and practical limits of predictability of the NMC medium-range model 22 p3127 N88-28586

The predictability of low frequency patterns in the NMC MRF 22 p3127 N88-28587

On Wiener-Masani's algorithm for finding the generating function of multivariate stochastic processes [NASA-CR 182905] 23 p3273 N88-29481

In situ fault detection by the hybrid ray mode method [AD-A195226] 24 p3381 N88-30137

ERS-1 (ESA SATELLITE)

The German processing and archiving facility for ERS-1 [ESA-CR(P)-2531] 13 p1851 N88-21082

Seasat orbit determination experiments in preparation for the ERS-1 altimetry mission [ETN-88-91842] 14 p1871 N88-21182

Deployment, hold down and release mechanisms for Wind Scatterometer Antenna (WSA) --- ERS-1 wind scatterometer antenna (WSA) 14 p1876 N88-21207

Proposals for the pre-operational use of data from the European Remote Sensing Satellite ERS-1 [BCRS-86-02] 16 p2227 N88-23300

Preparation of the operational phase of the European Remote Sensing Satellite ERS-1 [BCRS-87-06] 16 p2228 N88-23307

Study of the plan for a national data center for the European Remote Sensing Satellite ERS-1 [BCRS-87-11] 16 p2228 N88-23309

ERS-1 data products and services and their value for tropical countries 17 p2357 N88-24040

The CERSAT archiving and processing center --- ERS-1 19 p2701 N88-26059

Ocean satellite data and the needs of designers and operators of marine units 19 p2701 N88-26061

Central user and browse service --- ERS-1 ground segment [CU-PG-MDA-SY-0005] 23 p3297 N88-29637

ERS-1: A satellite with an oceanographic mission [NLR-MP-86072-U] 24 p3333 N88-29838

Development of procedures for performing end-to-end tests on the ERS-1 radar altimeter and AMI using a compact antenna test range --- Active Microwave Instrument (AMI) [ESA-CR(P)-2558] 24 p3363 N88-30022

A study of the feasibility of using sea and wind information from the ERS-1 satellite. Part 1: Wind scatterometer data [NASA-CR-182833] 24 p3386 N88-30167

A study of the feasibility of using sea and wind information from the ERS-1 satellite. Part 2: Use of scatterometer and altimeter data in wave modeling and assimilation [ESA-CR(P)-2604-PT-2] 24 p3387 N88-30176

ERTS

U LANDSAT SATELLITES

ERYTHROCYTES

Hypoxic hypoxia as a stimulus of erythropoiesis in vivo and in vitro 07 p0885 N88-15373

Polycythemia and hydration status: Effects on blood volume and thermoregulation during exercise-heat stress [AD-A185946] 07 p0888 N88-15383

Differentiation of hemopoietic stem cells during adaptation to high altitude 07 p0893 N88-15410

Life sciences experiments on stratospheric balloons and sounding rockets 08 p1033 N88-16262

Hemolysis in runners as evidenced by low serum haptoglobin: Implications for preflight monitoring of astronauts [NASA TM-100304] 11 p1518 N88-19067

Human erykthrocyte metabolism in the presence of hyperoxygenation during antiorthostatic hypokinesia 19 p2706 N88-26092

ESA

U EUROPEAN SPACE AGENCY

ESA SATELLITES

NT COS-B SATELLITE
NT ERS-1 (ESA SATELLITE)
NT EUROPEAN COMMUNICATIONS SATELLITE
NT EXOSAT SATELLITE
NT GEOS SATELLITES (ESA)
NT HIPPARCOS SATELLITE
NT INFRARED SPACE OBSERVATORY (ISO)
NT L-SAT
NT MARECS MARITIME SATELLITES
NT METEOSAT SATELLITE

Report on the scientific satellites of the European Space Agency [ESA-SP-1090] 01 p0014 N88-10081

The TV-SAT/TDF/TELE-X pyrotechnical system [CNES-87/CT/DRT/TVE/IL/358] 08 p0974 N88-15891

Coordinated use of European test facilities 09 p1123 N88-16726

Control and stabilization of ESA satellites 09 p1124 N88-16734

Projects under development 09 p1126 N88-16750

ESA Bulletin No. 24 [ISSN-0376-4265] 09 p1127 N88-16755

Report presented by the European Space Agency to the 22nd COSPAR meeting [ESA-SP-1014] 09 p1129 N88-16776

Assessment of optical communications systems for Data Relay Satellite. Volume 1: Executive summary [ESA-CR(P)-2488-VOL-1] 18 p2502 N88-24841

Assessment of optical communications systems for the Data Relay Satellite [ESA-CR(P)-2488-VOL-2] 18 p2502 N88-24842

Study of a safe attitude for the Infrared Space Observatory (ISO) during perigee pass [SNIAS-881-440-113] 23 p3185 N88-28954

PSDE/SAT 2: Preliminary spacecraft configuration study, executive summary [ESA-CR(P)-2618] 24 p3333 N88-29840

The high-throughput X-ray spectroscopy mission: The mission-science report [ESA-SP-1097] 24 p3453 N88-30557

ESA SPACECRAFT

NT COLUMBUS SPACE STATION
NT COS-B SATELLITE
NT ERS-1 (ESA SATELLITE)
NT ESA SATELLITES
NT EUROPEAN COMMUNICATIONS SATELLITE
NT EXOSAT SATELLITE
NT GEOS SATELLITES (ESA)
NT GIOTTO MISSION
NT HIPPARCOS SATELLITE
NT INFRARED SPACE OBSERVATORY (ISO)
NT L-SAT
NT MARECS MARITIME SATELLITES
NT METEOSAT SATELLITE

Study on conceptual design of spacecraft using Computer Aided Engineering (CAE) [SNIAS-920-CA/TS] 24 p3333 N88-29841

ESAKI DIODES

U TUNNEL DIODES

ESCAPE CAPSULES

Hypervelocity Technology (HVT) crew escape 09 p1214 N88-17280

ESCAPE SYSTEMS

Hypervelocity Technology (HVT) crew escape 09 p1214 N88-17280

Expected value analysis for an unmanned expendable launch vehicle payload escape system [AD-A189494] 13 p1728 N88-20337

ESCHERICHIA

Study of certain biological characteristics of bacteria during the French-Soviet CYTOS-2 space experiment 04 p0473 N88-12917

The effects of microgravity on genetic recombination in Escherichia coli --- Spacelab D1 mission 22 p3060 N88-28157

ESKERS

U GLACIAL DRIFT

ESRO

U EUROPEAN SPACE AGENCY

ESRO SATELLITES

U ESA SATELLITES

ESTERS

NT ACRYLATES
NT CARBAMATES (TRADENAME)
NT CARBOXYLATES
NT ISOCYANATES
NT LACTATES
NT PETN
NT POLYCARBONATES
NT POLYESTERS
NT SULFONATES
NT URETHANES

Polyvinyl esters of omega-H-perfluoroacids and polyvinyl alcohol obtained from them [AD-A184633] 03 p0279 N88-11755

Carbon residue studies of polyphenyl ethers and ester-based lubricants using a microcarbon residue tester
[AD-A188585] 12 p1611 N88-19632

Dual mechanism bifunctional polymers. Design, synthesis and application of a new category of metal ion complexing agents
[DE88-008233] 20 p2777 N88-26468

Polyazidoesters as energetic polymers and copolymer components with fluoro derivatives
[AD-A194236] 23 p3199 N88-29039

ESTIMATES
NT COST ESTIMATES

Estimates of satellite EHF communication outages due to attenuation by rain
[AD-A183969] 03 p0307 N88-11941

Exploiting auxiliary information about items in the estimation of Rasch item difficulty parameters
[AD-A184383] 03 p0372 N88-12341

Studies on estimation of nickel in zinc base die casting by D.C. polarography
[PD-MT-8729] 04 p0417 N88-12588

Model-based motion estimation and its application to restoration and interpolation of motion pictures
[AD-A185054] 05 p0584 N88-13558

Estimation of marine boundary layer depth and relative humidity with multispectral satellite measurements
[AD-A184881] 05 p0620 N88-13804

An adaptive lattice algorithm for spectral line estimation
[AD-A184970] 05 p0634 N88-13876

Further studies in estimation of life distribution characteristics from censored data
[AD-A184862] 05 p0643 N88-13937

Freidlin-Wentzell type estimates and the law of the iterated logarithm for a class of stochastic processes related to symmetric statistics
[AD-A185366] 05 p0644 N88-13944

New method of estimating continentality of climate on global scale 06 p0725 N88-14460

Round-off error propagation in four generally applicable, recursive, least-squares-estimation schemes
[NASA-TM-100055] 06 p0766 N88-14708

A new method of boundary parameter estimation for a two-dimensional diffusion system under noisy observations
[NASA-CR-178405] 06 p0767 N88-14714

Testing and interval estimation in a change-point model allowing at most one change
[AD-A185525] 06 p0767 N88-14716

On estimating the basin-scale ocean circulation from satellite altimetry. Part 1: Straightforward spherical harmonic expansion
[NASA-CR-182387] 07 p0882 N88-15352

Strong consistency of estimation of number of regression variables when the errors are independent and their expectations are not equal to each other
[AD-A186025] 07 p0909 N88-15507

Detecting and interval estimation about a slope change point
[AD-A186030] 07 p0909 N88-15509

A new method of estimation in a moving average model of order one
[AD-A186039] 07 p0909 N88-15510

Estimation and testing in truncated and nontruncated linear median-regression models
[AD-A186317] 07 p0911 N88-15522

Parameter estimation for the Dirichlet-Multinomial Distribution (DMD) using supplementary beta-binomial data
[AD-A186335] 07 p0911 N88-15524

On simultaneous estimation of the number of signals and frequencies under a model with multiple sinusoids
[AD-A186026] 07 p0913 N88-15543

Nonparametric estimation of the generalized variance
[AD-A186029] 07 p0914 N88-15545

On the direction of arrival estimation
[AD-A186031] 07 p0914 N88-15546

On rate of convergence of equivariation linear prediction estimates of the number of signals and frequencies of multiple sinusoids
[AD-A186034] 07 p0914 N88-15549

Necessary and sufficient conditions for the convergence of integrated and mean-integrated r-th order error of histogram density estimates
[AD-A186037] 07 p0914 N88-15550

Attitude determination of artificial satellites through joint application of static and dynamic optimal estimation techniques
[INPE-4415-TDL/306] 08 p0963 N88-15832

Estimation and comparison of changes in the presence of information right censoring by modeling the censoring process
[AD-A186320] 08 p1074 N88-16478

New model to estimate the perforation power of kinetic energy projectiles
[PB87-166757] 09 p1175 N88-17040

Sea surface current estimates off central California as derived from enhanced AVHRR (Advanced Very High Resolution Radiometer) infrared images
[AD-A186867] 09 p1194 N88-17155

Horizontal estimation and information fusion in multitarget and multisensor environments
[AD-A186935] 09 p1224 N88-17336

A note on computing robust regression estimates via iteratively reweighted least squares
[AD-A186709] 09 p1227 N88-17352

Frequency response function estimation at level
[DE88-002644] 10 p1344 N88-18034

On the dynamic estimation of relative weights for observation and forecast in numerical weather prediction
[NASA-CR-182531] 10 p1356 N88-18106

Well-posedness and spectral estimation for infinite dimensional systems
[AD-A187621] 10 p1401 N88-18354

Spacecraft telecommunications system mass estimates 11 p1473 N88-18784

A posteriori error estimates in computational fluid mechanics 11 p1486 N88-18869

Optimal recursive maximum likelihood estimation
[AD-A187980] 11 p1536 N88-19176

Simultaneous estimation and detection of bias shifts for inertial navigation systems 12 p1576 N88-19429

Preliminary analysis of an integrated logistics system for OSSA payloads. Volume 1: Executive summary
12 p1584 N88-19478

Digital bit error rate estimator for telemetry links
[INPE-4351-TDL/295] 12 p1598 N88-19563

Lower bounds on acceleration estimation accuracy
[AD-A188383] 12 p1619 N88-19681

Cramer-Rao bounds on the accuracy of location and velocity estimations using CCD optical sensors
[AD-A188481] 12 p1629 N88-19748

Estimation of the probability of a long time to the first entrance to a state in a semi-Markov model
[AD-A188960] 12 p1685 N88-20074

Picking winners: Parametric cost estimating and project management 12 p1700 N88-20176

Estimation-correlation, modeling, and identification in adaptive array processors
[AD-A189130] 13 p1757 N88-20512

Detection and angle estimation of coherent plane waves 13 p1759 N88-20522

Energy and momentum fluxes through the sea surface
13 p1806 N88-20798

Bias reduction when there is no unbiased estimate
[AD-A189407] 13 p1829 N88-20937

Regional Conference on the Analysis of the Unbalanced Mixed Model
[AD-A188747] 13 p1830 N88-20943

Temperature estimates for a free flowing railgun plasma
[MRL-R-1054] 13 p1843 N88-21032

Moving-bank multiple model adaptive estimation applied to flexible spacestructure control
[AD-A190761] 15 p2026 N88-22071

Boundary shape identification problems in two-dimensional domains related to thermal testing of materials
[NASA-CR-181654] 15 p2105 N88-22541

Consistent estimates of autoregressive parameters for autoregressive moving average models
[RR-663-I] 15 p2109 N88-22564

Estimation of convolution tails
[AD-A190323] 15 p2125 N88-22666

Analysis of a range estimator which uses MLS angle measurements
[NASA-CR-182896] 16 p2160 N88-22884

Multichannel 2-D power spectral estimation and applications
[AD-A191273] 16 p2191 N88-23068

Stochastic estimation of conditional eddies in turbulent channel flow 16 p2194 N88-23087

Studies in reliability and inference
[AD-A191389] 16 p2217 N88-23223

Parameter estimation for boundary value problems by integral equations of the second kind
[NASA-CR-181660] 17 p2332 N88-23918

Comparison of the solar radiation estimation method by satellites 17 p2360 N88-24055

Digital processing of infrared and visible images from the GOES satellite and its integration with meteorological radar data 17 p2360 N88-24057

Improved estimators in simultaneous estimation of scale parameters
[AD-A191108] 17 p2392 N88-24216

Performance estimates for operations conducted while wearing individual protective equipment. User manual
[AD-A191871] 18 p2553 N88-25154

Symmetrized nearest neighbor regression estimates
[AD-A191998] 18 p2568 N88-25254

Preliminary estimates of radiation exposures for manned interplanetary missions from anomalously large solar flare events
[NASA-TM-100620] 18 p2596 N88-25427

Estimation of balloon position from wind data
[DE88-008968] 19 p2597 N88-25434

Instrumentation for the measurement of penetrator dynamic response to permit force estimation
[DE88-010608] 20 p2809 N88-26666

Hydrologic models for land-atmosphere retrospective studies of the use of LANDSAT and AVHRR data
[NASA-CR-182861] 20 p2817 N88-26712

Dynamic modelling and estimation of the error due to asynchronism in a redundant asynchronous multiprocessor system
[NASA-CR-177427] 21 p2898 N88-27205

Estimation of power-energy plots for secondary batteries
[DE88-011922] 21 p2940 N88-27460

A unified approach to estimation in linear models with fixed and mixed effects
[AD-A193060] 21 p3006 N88-27829

On the estimation of a variance ratio
[AD-A193190] 21 p3009 N88-27854

Use of LANDSAT images of vegetation cover to estimate effective hydraulic properties of soils
[NASA-CR-183185] 22 p3116 N88-28514

Estimation forces acting on an underwater vehicle with G.P.S. (Global Positioning System) and Kalman filtering
[AD-A194339] 23 p3175 N88-28901

Progress in determining the thickness and distribution of volcanic materials on Mars 23 p3302 N88-29670

Spacecraft mass estimation, relationships and engine data. Task 1.1 of the lunar base systems study
[NASA-CR-172061] 24 p3332 N88-29836

Monte-Carlo estimation of the influence of plant architecture parameters on spectral brightness
24 p3450 N88-30533

ESTIMATING
NT ORBITAL POSITION ESTIMATION
NT PARAMETER IDENTIFICATION
NT SYSTEM IDENTIFICATION

Estimating scattered and absorbed radiation in plant canopies by remote sensing
[NASA-CR-181390] 02 p0193 N88-11205

The maximum likelihood estimator method of image reconstruction: Its fundamental characteristics and their origin
[DE88-000462] 05 p0636 N88-13892

Development of a technique for estimating noise covariances using multiple observers
[NASA-TM-4020] 06 p0669 N88-14096

Estimating the distribution of fault latency in a digital processor
[NASA-TM-100521] 06 p0760 N88-14666

Recursive m-estimators of location and scale for dependent sequences
[AD-A186292] 07 p0903 N88-15469

A modified kernel quantile estimator under censoring
[AD-A186364] 07 p0911 N88-15525

Estimation of multivariate binary density using orthonormal functions
[AD-A186386] 07 p0912 N88-15528

A smooth nonparametric quantile estimator from right-censored data
[AD-A186180] 07 p0915 N88-15552

Short data length effects in an asymptotically efficient ARMA (AutoRegressive Moving Average) spectral estimator
[AD-A186561] 08 p1068 N88-16458

A model for estimating depot maintenance costs for Air Force fighter and attack aircraft
[AD-A187097] 09 p1105 N88-16624

A generalized quantile estimator under censoring
[AD-A188280] 10 p1402 N88-18364

Fixed and adaptive interframe image prediction for remote piloting application
[AD-A187987] 11 p1471 N88-18771

Calibration of the solar radiation estimation method by satellites
[INPE-4349-PRE/1185] 12 p1646 N88-19861

Tidal estimation in the Pacific with application to SEASAT altimetry
[NASA-TM-100694] 13 p1803 N88-20780

Empirical and hierarchical Bayes competitors of preliminary test estimators in two sample problems
[AD-A190327] 15 p2125 N88-22670

Mental-State Estimation, 1987
[NASA-CP-2504] 16 p2239 N88-23370

Improved estimators in simultaneous estimation of scale parameters
[AD-A191108] 17 p2392 N88-24216

RSMASS: A simple model for estimating reactor/shield masses 17 p2414 N88-24355

Asymptotic theory for weighted least squares estimators in Aalen's additive risk model
[AD-A191085] 18 p2562 N88-25210
Estimating reliability with discrete growth models
[AD-A193845] 22 p3143 N88-28692
Digital phase-lock loop having an estimator and predictor of error
[NASA-CASE-NPO-17196-1-CU]
23 p3205 N88-29076
Estimation of transient heat transfer coefficients in multidimensional problems by using inverse heat transfer methods 23 p3210 N88-29108
A minitab macro for the Kaplan-Meier product limit estimator and the Tarone-Ware class of tests
[AD-A194298] 23 p3248 N88-29331
On the design and optimization of distributed signal detection and parameter estimation systems
[AD-A193934] 23 p3266 N88-29446
Two biased estimation techniques in linear regression: Application to aircraft
[NASA-TM-100649] 23 p3274 N88-29489

ESTUARIES
The effect of wind and currents on gas exchange in an estuarine system
[NASA-CR-181424] 01 p0073 N88-10468
YABLED cruises part 2. Data from YABLED-17 through YABLED-26, January-October 1985
[PB88-163597] 14 p1950 N88-21627
SPOT investigations of estuaries and coastal zones: An overview 22 p3107 N88-28455
The monitoring of sediment transport, water circulation and mixing in estuaries and coastal waters
22 p3108 N88-28457
Evaluation of SPOT data for remote sensing of physical and biological properties of estuaries and coastal zones
22 p3108 N88-28458
Contributions of SPOT imagery to the study of the littoral environments of Saloum (Senegal)
22 p3109 N88-28467

ETALONS
Fabry-Perot etalons as prefilters for astronomical far infrared Fourier transform spectroscopy
[MPE-205] 16 p2273 N88-23603
High-speed optical logic using GaAs
19 p2656 N88-25773

ETCHING
Metallography of maraging 350 steel
[DE87-013746] 04 p0418 N88-12591
Partial analysis of experiment LDEF A-0114
[NASA-CR-179236] 06 p0780 N88-14787
Investigations on an RF plasma related to plasma etching
[ETN-88-91366] 06 p0784 N88-14809
Effect of the band-gap characteristics on laser-induced dry etching of semiconductors
[DE88-001853] 07 p0937 N88-15695
Plasma and ion etching for failure analysis. Part 2: The etching of plastic encapsulant and other semiconductor device materials, using the Technics Giga Etch 100-E plasma etch system
[AERE-R-12212] 09 p1177 N88-17050
Control of solid-excitation-based photochemical dry etching of semiconductors by ion-bombardment-induced damage
[DE88-003214] 09 p1257 N88-17537
The mechanism of anisotropic silicon etching and its relevance for micromachinings
[MBB-UA-1013/86] 10 p1311 N88-17838
Apparatus for the study of silicon film deposition and silicon etching
[AD-A187616] 10 p1334 N88-17972
SiO2 film stress distribution during thermal oxidation of Si
[AD-A189552] 12 p1612 N88-19637
Metal contacts to cadmium telluride (CdTe)
[AD-A188306] 12 p1698 N88-20159
Laser photodeposition and etching study
[AD-A190535] 15 p2040 N88-22153
Calculating depletion region carrier concentrations with capacitance-voltage measurements and etching
[AD-A189630] 15 p2141 N88-22777
Microelectronics the next fifteen years
17 p2305 N88-23792
Excitonic properties of GaAs-AlGaAs nanostructures
20 p2867 N88-27023
Equipment for building and testing superconductive flux flow electronic devices
[AD-A192959] 21 p2936 N88-27436

ETHANE
Optical determination of the virial coefficients of the gases C2H4, C2H6 and SF6
[ETN-87-90610] 03 p0282 N88-11776
Catalytic combustion of methane
[PB88-123112] 07 p0829 N88-15028
Gas hydrate model development and validation
[DE88-001004] 10 p1298 N88-17762
Temperature dependence of ultraviolet absorption cross sections of chlorofluoroethanes
[AERONOMICA-ACTA-A-325-1987]
18 p2482 N88-24726

ETHANE NITRILE
U ACETONITRILE

ETHANOL
U ETHYL ALCOHOL

ETHERS
Surface catalytic degradation study of two linear perfluoropolyalkylethers at 345 C
[NASA-TP-2774] 04 p0410 N88-12543
Improved perfluoroalkylether fluid development
[NASA-CR-180872] 08 p0967 N88-15851
Space environmental effects on polymeric materials
[NASA-CR-182454] 09 p1148 N88-16879
Carbon residue studies of polyphenyl ethers and ester-based lubricants using a microcarbon residue tester
[AD-A188585] 12 p1611 N88-19632
The performance of perfluoropolyalkylether oils under boundary lubrication conditions
[AD-A191057] 17 p2323 N88-23869
Preferential surface adsorption in miscible blends of polystyrene and poly(vinyl methyl ether)
[AD-A191451] 18 p2490 N88-24769

ETHYL ALCOHOL
Practical system for the use of alcohol in diesel engines
[PB88-147863] 12 p1612 N88-19638
Ethanol as a fuel of a lorry. Use experience from a diesel engine modified to an otto engine
[DE88-752870] 21 p2958 N88-27569

ETHYL COMPOUNDS
Dissolution rates of polymers and copolymers based on methyl, ethyl and butyl methacrylate
[AD-A194713] 23 p3197 N88-29027

ETHYLENE
NT VINYLIDENE
Ionic conductive polymers based on crosslinked elastic siloxane-ethylene oxide copolymers
[DE88-011243] 21 p2917 N88-27311

ETHYLENE COMPOUNDS
NT CHLOROETHYLENE
Organic metal (ET)4Hg3Br8A quasi-two-dimensional superconductor 14 p1974 N88-21778

ETIOLOGY
Trace-element metabolism in man and animals in the presence of hypoxic states of diverse etiology
07 p0889 N88-15390

ETTINGSHAUSEN COOLERS
U THERMOELECTRIC COOLING

EUCLIDEAN GEOMETRY
NT ANALYTIC GEOMETRY
NT ANGLE OF ATTACK
NT ANGLES (GEOMETRY)
NT BRAGG ANGLE
NT CARTESIAN COORDINATES
NT CATENARIES
NT CIRCLES (GEOMETRY)
NT CIRCUMFERENCES
NT CONICS
NT CUBES (MATHEMATICS)
NT DESCRIPTIVE GEOMETRY
NT DIHEDRAL ANGLE
NT ELEVATION ANGLE
NT ELLIPSES
NT FIXED POINTS (MATHEMATICS)
NT GEODESIC LINES
NT ICOSAHEDRONS
NT INFLECTION POINTS
NT LEADING EDGE SWEEP
NT LINES (GEOMETRY)
NT OBLATE SPHEROIDS
NT PARABOLAS
NT POINTS (MATHEMATICS)
NT POLYGONS
NT POLYHEDRONS
NT PROJECTIVE GEOMETRY
NT PROLATE SPHEROIDS
NT PYRAMIDS
NT QUADRANTS
NT RADII
NT RECTANGLES
NT RHOMBOIDS
NT S CURVES
NT SWEEP ANGLE
NT SWEEPBACK
NT TANGENTS
NT TORUSES
NT TRIANGLES
Complete minimal surfaces in R^3 of low total curvature
[DE88-006425] 15 p2118 N88-22619
Mathematical morphology for structures without translation symmetry
[CWI-AM-R8803] 18 p2566 N88-25241

EUCLIDEAN SPACE
U EUCLIDEAN GEOMETRY

EUKARYOTES
Biorack experiments in Spacelab D-1 and TML-1: Further developments in gravitational biology
12 p1661 N88-19953
The evolution of glutathione metabolism in phototrophic microorganisms
[NASA-CR-182902] 19 p2695 N88-26015

EULER EQUATIONS OF MOTION
Numerical solution of Euler equations for compressible fluids by the finite element method, volume 3
[ETN-87-90650] 02 p0170 N88-11070
Computation of transonic separated wing flows using an Euler/Navier-Stokes zonal approach
[NASA-TM-88311] 02 p0173 N88-11089
Numerical calculation of two dimensional fluid flow with strong shocks
[KFK-4191] 03 p0314 N88-11986
Application of Runge Kutta time marching scheme for the computation of transonic flows in turbomachines
[NASA-TM-86997] 04 p0394 N88-12461
Concepts for radically increasing the numerical convergence rate of the Euler equations
[NASA-CR-177456] 04 p0395 N88-12463
Solution of the two-dimensional Euler equations on unstructured triangular meshes
04 p0396 N88-12462
A free-Lagrange method for 2-D compressible flows
[DE88-000216] 04 p0442 N88-12745
Numerical analysis of flow through scramjet engine inlets 05 p0532 N88-13233
A 3-D Euler solution for hypersonic Mach numbers
05 p0533 N88-13240
The off-design performance of hypersonic waveriders
05 p0533 N88-13244
Time-marching finite-difference methods for the three-dimensional Euler equations of contravariant velocity components 05 p0539 N88-13285
A Cartesian finite-volume method for the Euler equations 05 p0579 N88-13532
Solution procedure for the Navier-Stokes equations applied to rotors 05 p0579 N88-13533
A note on the use of symmetric line Gauss-Seidel for the steady upwind differenced Euler equations
[AD-A185223] 05 p0580 N88-13540
SHARP simulation of discontinuities in highly convective steady flow
[NASA-TM-100240] 05 p0642 N88-13931
Development of transonic speed cascade design method using Euler code and inverse solution
06 p0676 N88-14139
Euler solution of multiblade rotor flow
[NASA-TM-100014] 06 p0704 N88-14322
Numerical simulation of flows in axial and radial turbomachines using Euler solvers
06 p0713 N88-14372
Computational fluid dynamics overview
07 p0809 N88-14927
Upwind relaxation algorithms for Euler/Navier-Stokes equations 07 p0810 N88-14931
Viscous vortex flows 07 p0810 N88-14934
Multitasked embedded multigrid for three-dimensional flow simulation
[NASA-CR-182398] 07 p0852 N88-15173
An explicit method for the solution of the Euler equations, applied to unsteady two dimensional flows
[ETN-88-90807] 07 p0855 N88-15194
Advanced propeller research
08 p0957 N88-15806
Upwind formulations for the Euler equations
08 p0984 N88-15952
A survey of upwind principles for the multidimensional Euler equations 08 p0984 N88-15953
Characteristic flux averaging approach to the solution of Euler's equations 08 p0984 N88-15955
Inviscid flows, part 2 08 p0985 N88-15966
Viscous flows, part 1 08 p0986 N88-15967
Radial compressor design using an Euler solver
10 p1283 N88-17675
Three dimensional Euler solutions for hypersonic Mach numbers
[MBB-UR-944/87] 10 p1315 N88-17859
Finite element methods of analysis for high speed viscous flows
[NASA-CR-182529] 11 p1483 N88-18852
Compact high order schemes for the Euler equations
[NASA-CR-181625] 11 p1530 N88-19138
A generalisation of Hall's scheme for solving the Euler equations for two-dimensional flows
11 p1537 N88-19188
Solution of the Euler equations: Explicit schemes acceleration by a multigrid method
11 p1538 N88-19192
Unstructured multigrid methods
11 p1538 N88-19193

Applications of a multigrid finite volume method with Runge-Kutta time integrations for solving the Euler and Navier-Stokes equations 11 p1539 N88-19201
An L-U implicit multigrid algorithm to solve the Euler equations for transonic flow in rotating turbomachinery passages 13 p1718 N88-20270
Solution of two-dimensional Euler equations. Experience with a finite volume code
[DFVLR-FB-87-41] 13 p1767 N88-20572
Multigrid solution of the Euler equations
13 p1769 N88-20582
A symmetric set of Euler angles and oblique orientation space sections
[DE88-005317] 13 p1847 N88-21056
An explicit method for the solution of the Euler equations applied to unsteady two-dimensional flows
[MBB/LKE-121/S/PUB/257] 14 p1910 N88-21411
Choice of implicit and explicit operators for the upwind differencing method
[NASA-TM-100857] 14 p1964 N88-21718
On the prediction of highly vortical flows using an Euler equation model, part 2
[AD-A190245] 15 p2064 N88-22305
High-resolution shock-capturing schemes for inviscid and viscous hypersonic flows
[NASA-TM-100097] 15 p2122 N88-22651
Accuracy versus convergence rates for a three dimensional multistage Euler code
[NASA-CR-181665] 16 p2261 N88-23519
Incompressible Euler solution on a multiblock grid around a car configuration
[FFA-TN-1987-65] 18 p2457 N88-24586
Applications of the Navier-Stokes equations to wings and complex configurations using a zonal approach
[NASA-TM-100080] 18 p2459 N88-24602
Accurate multigrid solution of the Euler equations on unstructured and adaptive meshes
[NASA-CR-181679] 18 p2460 N88-24608
Composite reduced Navier-Stokes procedures for flow problems with strong pressure interactions
[AD-A191127] 18 p2508 N88-24875
Numerical simulations of flow around shuttle orbiter
19 p2635 N88-25633
Numerical solutions of the Euler equations for the flow field around counter-rotating propellers
19 p2636 N88-25638
Numerical simulation of supersonic free-jets
19 p2636 N88-25639
Numerical calculation of three dimensional flow by TVD scheme 19 p2638 N88-25649
An implicit, high order accurate, upwind scheme for unsteady Euler equations 19 p2639 N88-25657
On the stationary solutions of three-dimensional Euler equations by the TVD difference schemes
19 p2639 N88-25660
Improved potential flow computational methods with Euler corrections for airfoil and wing/body design
[AD-A192303] 20 p2752 N88-26334
A diagonally inverted LU implicit multigrid scheme
[NASA-TM-100911] 20 p2753 N88-26340
Vortex methods for separated flows
[NASA-TM-100068] 20 p2753 N88-26342
Euler equation computations for the flow over a hovering helicopter rotor
[NASA-CR-177493] 22 p3038 N88-28037
The influence of numerical boundary conditions on transonic flow
[DFVLR-FB-88-06] 23 p3172 N88-28890
Accurate solutions, parameter studies and comparisons for the Euler and potential flow equations
[NASA-TM-100664] 23 p3173 N88-28892
Generation of multiple block grids for arbitrary 3D geometries 23 p3246 N88-29317
Mesh generation for industrial application of Euler and Navier Stokes solvers 23 p3247 N88-29323
A streamwise upwind algorithm for the Euler and Navier-Stokes equations applied to transonic flows
[NASA-TM-101019] 24 p3316 N88-29751
Space marching Euler solvers
24 p3318 N88-29759
Numerical methods: Euler time dependent solver
24 p3318 N88-29760
Euler analysis of a swirl recovery vane design for use with an advanced single-rotation propfan
[NASA-TM-101357] 24 p3320 N88-29771

EULER-CAUCHY EQUATIONS
On the distribution equations
[DE88-702217] 23 p3270 N88-29454

EULER-LAGRANGE EQUATION
A free-Lagrange method for 2-D compressible flows
[DE88-000216] 04 p0442 N88-12745
Three-dimensional, free-Lagrange hydrodynamics
[DE88-000494] 04 p0443 N88-12749
Free Lagrange reconnection algorithms for hydrocodes using a quadrilateral mesh
[DE88-001580] 05 p0611 N88-13752
Perturbative coherence in field theory
[DE88-700366] 07 p0941 N88-15717
The dynamics of an oscillating four-bar linkage
09 p1181 N88-17074
A Lagrangian model of dry thermals
[DM-50] 09 p1193 N88-17150
An adaptive grid technique for solution of the Euler equations 13 p1768 N88-20579
Introduction to classical mechanics of systems with constraints, part 1
[DE88-701055] 13 p1832 N88-20957
Introduction to classical mechanics of systems with constraints, part 2
[DE88-701056] 13 p1849 N88-21072
A semigroup for Lagrangian 1D isentropic flow
[DE88-006464] 18 p2513 N88-24912
Fuel droplet vaporization and temperature distributions of axisymmetric unsteady sprays
19 p2626 N88-25579

EURECA (ESA)
Allowable gravity-levels for Spacelab, Columbus and EURECA — materials science
[BF-R-66 525-2] 07 p0838 N88-15084
External payload servicing: Operational requirements and technology 12 p1593 N88-19541
Exobiology and botany facilities for EURECA
12 p1652 N88-19898
Microgravity User Support Center (MUSC) for EURECA, Spacelab and Columbus missions
12 p1660 N88-19947
Latching mechanisms for IOC — EURECA
14 p1875 N88-21205
The EURECA antenna deployment and retraction mechanisms 14 p1878 N88-21225
Botany Facility pre-phase C/D. Core payload for EURECA, volume 2
[BF-RP-ER-015-VOL-2] 17 p2377 N88-24130
Life Support Subsystem (LSS). Concept for the Botany Facility — EURECA
[TN-RB524-107/86] 17 p2377 N88-24131
Impact of control errors on the volume/weight demand of the Ventilation and Dryer (VAD) concept — EURECA Botany Facility
[TN-RB524-006/87] 17 p2377 N88-24132
Summary of the activities performed during the Botany Facility (BF) predevelopment phase for the Life Support S/S (LSS)
[TB-RB524-002/87] 17 p2378 N88-24133
Examination of methods for pollen storage and dispersal
[TN-RB524-097/86] 17 p2378 N88-24134
Botany Facility. Thermal Control (TC) subsystem test report on experiment container of laboratory model and breadboard centrifuge
[BF-TN-ER-061/86] 17 p2378 N88-24135
Botany Facility: Test report on breadboard tests for the determination of the heat transfer at the glass disk and of the temperature distribution in the fluorescent tube
[BF-TN-ER-053] 17 p2378 N88-24136
Botany Facility: Breadboarding results of the illumination system
[SIRA-A/7373/WP110/MAC003]
17 p2378 N88-24137
Botany Facility: Magnetic fluid seal considerations for the centrifuge
[SIRA-A/7373/WP110/MAC004]
17 p2378 N88-24138
Botany Facility: Considerations and analyses of the balancing system philosophy proposed for the BF centrifuge
[SIRA-A/7373/WP110/PWF001]
17 p2378 N88-24139
Botany Facility: The problems of plant fixation
[SIRA-A/7373/WP220/RJS/001]
17 p2379 N88-24140
Botany Facility: Problems of water supply, plant nutrients and soil in the Botany Facility
[SIRA-A/7373/WP220/RJS/003]
17 p2379 N88-24141
Supply and distribution of plant nutrients in the Botany Facility
[SIRA-A/7373/WP220/RJS/004]
17 p2379 N88-24142
EURECA Botany Facility. Technical note: Removal of phytotoxins
[SIRA-A/7373/WP220/RJS/005]
17 p2379 N88-24143
Botany Facility pre-phase C/D. Core payload for EURECA, volume 1
[BF-RP-ER-015-VOL-1] 17 p2379 N88-24144
Operational facilities of EURECA A1 mission
[ETN-88-91939] 18 p2496 N88-24810
Study of standard generic approach for spacecraft (S/C) autonomy and automation (phase 3). Book B: Autonomy concept application example
[ESA-CR(P)-2555-VOL-2] 23 p3185 N88-28956

EUROPE
COST-73 and its application in very short rang
forecasting 02 p0199 N88-1124
Foreign language identification. First step in the translation process
[DE87-011065] 02 p0248 N88-1156
Composite materials in western Europe
[PB87-102943] 03 p0279 N88-1175
Short reference year
[PB87-107470] 03 p0352 N88-1222
Solar energy. European research and developmen
[PB87-107645] 04 p0463 N88-128
European industrial consortia for space projects: Thei
origins, development and possible evolution
09 p1128 N88-1676
An investigation of terrain related variables for predicting the multipath fade depth distribution on terrestria
microwave lines 12 p1515 N88-1965
Ozone sonde and Dobson spectrometer data obtained during the MAP/GLOBUS 1983 campaign over Western Europe
[BPT-5/87] 13 p1802 N88-2077
European transonic wind tunnel project. Assistance to the design group
[ONERA-RSF-11/0694-GY-010-G]
21 p2900 N88-2720
Studies concerning the European transonic wind tunnel
[ONERA-RSF-10/0694-GY-010-G]
21 p2900 N88-2720
Application of SPOT to agricultural information systems in temperate regions 22 p3093 N88-2836

EUROPEAN AIRBUS
NT A-300 AIRCRAFT
NT A-320 AIRCRAFT
Assessment of software quality for the AIRBUS A310 automatic pilot 02 p0128 N88-1080
Aeroelastic analysis of modern transport aircraft — European Airbus
[SNIAS-872-111-102] 05 p0546 N88-1332
Testing of a schematic transport plane model in several European windtunnels
[PB87-170270] 09 p1113 N88-1667
Airbus, the successful European cooperation
[MBB-UT-005/87] 10 p1313 N88-1784
Automatic riveting machine for spherically-formed airframe structures
[ETN-88-91024] 11 p1495 N88-1892
Airbus 1987: Success in Europe
[ETN-88-92099] 20 p2758 N88-2636
Variable wing camber control systems for the future Airbus program
[MBB-UT-104/88] 23 p3180 N88-2893

EUROPEAN COMMUNICATIONS SATELLITE
Alternative force structuring strategies for militar
satellite communication systems
[AD-A189492] 13 p1758 N88-2051
Study of the assembly, integration and verification programs of telecommunication satellites applicable to other satellite programs
[MATRA-100/CC/MLG/031/87]
24 p3334 N88-2984

EUROPEAN INCOHERENT SCATTER RADAR
U EISCAT RADAR SYSTEM (EUROPE)

EUROPEAN LARGE TELECOMM SATELLITE
U L-SAT

EUROPEAN RETRIEVABLE CARRIER
U EURECA (ESA)

EUROPEAN SPACE AGENCY
Battery development and testing at ESA
02 p0164 N88-1102
Generic specifications for hybrid microcircuits
[ESA-PSS-01-608-ISSUE-2] 06 p0696 N88-1427
Overview of ESA's activities in ocean colour remote sensing 08 p1042 N88-1629
The appropriate use of contract types in developmen
contracts (a systems approach with emphasis on the European space sector)
[ESA-STR-222] 08 p1092 N88-1657
Studies for future scientific projects
09 p1123 N88-1672
A policy for international relations
09 p1123 N88-1672
ESA Bulletin No. 10
[ETN-87-90514] 09 p1123 N88-1672
Specialist support for projects: Activities, methods and infrastructure 09 p1124 N88-1672
The objectives and methods of the technologica
research program 09 p1124 N88-1673
The ESA centralized management system for satellite
electronic test and checkout instrumentation
09 p1124 N88-1673
ESTEC's product assurance activities
09 p1125 N88-1673
Projects under development 09 p1126 N88-1675

ESA Bulletin No. 24 |ISSN-0376-4265| 09 p1127 N88-16755

Programs under development and operations 09 p1127 N88-16762

The new approach to the definition of the ESA technological research program 09 p1127 N88-16763

Promotion of European components for ESA projects 09 p1128 N88-16764

ESA Bulletin No. 25 |ISSN-0376-4265| 09 p1128 N88-16767

Entry into force of the ESA convention 09 p1128 N88-16768

Parallel-processing computer systems and their possible applications in the agency 09 p1128 N88-16774

Report presented by the European Space Agency to the 22nd COSPAR meeting |ESA-SP-1014| 09 p1129 N88-16776

PCM telemetry standard |ESA-PSS-46(TTC.A.02)ISSUE-1| 09 p1132 N88-16790

Study for history of technology developments in European space projects |REPT-8518-1| 10 p1286 N88-17690

Spacelab: An international success story |NASA-SP-487| 11 p1566 N88-19375

The European Space Agency's role in life sciences and research in space 12 p1652 N88-19894

Life sciences in the framework of the ESA microgravity program and future flight opportunities 12 p1652 N88-19895

The preparation, assembly and mounting of RF coaxial cables |ESA-PSS-01-718-ISSUE-1| 13 p1756 N88-20504

Design method for Ada programs |ESA-CR(P)-2528| 14 p1958 N88-21671

Preparing for the new programs. The ESA technological research and development program 1988-1990 |ESA-SP-1095| 17 p2309 N88-23814

International cooperation in remote sensing. The ESA experience 17 p2356 N88-24038

The technical reporting and approval procedure for materials and processes |ESA-PSS-01-700-ISSUE-1| 22 p3162 N88-28833

Material and process selection and quality control for ESA space systems and associated equipment |ESA-PSS-01-70-ISSUE-3| 23 p3224 N88-29190

Focus 86: A summary of the 1986 annual report of the activities of the European Space Agency |ESA-BR-34| 23 p3309 N88-29713

Candidate functions for advanced technology implementation in the Columbus mission planning environment 24 p3417 N88-30340

With an eye to the future. ESA general studies program 1988 |ESA-SP-1100| 24 p3435 N88-30447

ESA report to the 27th COSPAR meeting |ESA-SP-1098| 24 p3453 N88-30556

EUROPEAN SPACE PROGRAMS

Columbus preparatory program. Payload element study on a technology demonstration mission, executive summary |CS-RP-AI-016| 01 p0014 N88-10080

Report on the scientific satellites of the European Space Agency |ESA-SP-1090| 01 p0014 N88-10081

Preliminary study of a biotechnology research facility for microgravity, executive summary |MATRA-EPT/AS/VT209/246/NT| 01 p0032 N88-10204

Preliminary study of a gravitational biology facility for Columbus, executive summary |MATRA-EPT/AS/VT209/255/NT| 01 p0032 N88-10205

Components for cryostat --- spaceborne |MBB/ISO-TN-CD00.003-REV-A| 01 p0032 N88-10207

Robotic sensors and actuators for a service manipulator system. Volume 1: Executive summary |MATRA-EPT/DT/VT187/120| 01 p0053 N88-10341

Robotic sensors and actuators for a service manipulator system. Volume 2: Service Manipulator System (SMS) handbook |MATRA-EPT/DT/VT187/227| 01 p0053 N88-10342

Robotic sensors and actuators for a service manipulator system. Volume 3, phase A report and program plan |MATRA-EPT/DT/VT187/228| 01 p0054 N88-10343

Study on the suitability of a European data relay satellite to support a system of remote sensing satellites |ESA-CR(P)-2400| 01 p0063 N88-10406

Aquarack: Aims and Possible Research Projects |DFVLR-MITT-87-01| 01 p0073 N88-10469

Life support systems for biological experiments under weightlessness in the German and European space programs 01 p0074 N88-10477

ESA Workshop on Optical Interferometry in Space |ESA-SP-273| 01 p0094 N88-10613

Space station based interferometry 01 p0096 N88-10626

ESA technological research activities on lightweight mirrors --- spaceborne interferometry 01 p0096 N88-10629

Aerospace research at the National Aerospace Laboratory (NLR) |ETN-87-90821| 01 p0107 N88-10697

Mechanical design of the ac bracket package for the RETE experiment |IFSI-87-4| 05 p0555 N88-13379

Budget and programs for 1986 research |IFSI-86-16| 05 p0660 N88-14048

Generic specifications for hybrid microcircuits |ESA-PSS-01-608-ISSUE-2| 06 p0696 N88-14273

Activities report in aircraft design and astronautics |ETN-88-90618| 07 p0809 N88-14925

Round table on the future of satellite communications and broadcasting in Europe |ESA-STR-221| 07 p0843 N88-15112

Study of a Radio Relay Link (RRL). Cassini mission. Data package for final presentation |ESA-CR(P)-2472| 07 p0847 N88-15138

The role of the DFVLR project management life sciences in the space program of the Federal Republic of Germany 07 p0884 N88-15364

German space policy on the threshold of the century. Analysis and proposals for the future |ETN-88-90573| 07 p0943 N88-15734

The TV-SAT/TDF/TELE-X pyrotechnical system |CNES-87/CT/DRT/TVE/IL/358| 08 p0974 N88-15891

The German scientific balloon and sounding rocket program 08 p1024 N88-16202

The Norwegian scientific balloon and sounding rocket program 1987-1990 08 p1025 N88-16204

Swiss scientific balloon and sounding rocket experiments 1985-1987 08 p1025 N88-16206

Flight results of the ESA experiment modules in Materials Science Experiment Rocket (MASER) 1 08 p1033 N88-16261

Europe's position concerning ocean colour activities 08 p1042 N88-16293

Overview of ESA's activities in ocean colour remote sensing 08 p1042 N88-16294

Federal Republic of Germany's interests, activities and goals in remote sensing of ocean colour/fluorescence from space 08 p1043 N88-16302

The European space physics analysis network 08 p1099 N88-16613

ESA Bulletin No. 8 |ETN-87-90513| 09 p1122 N88-16718

Studies for future scientific projects 09 p1123 N88-16720

The 2.4 m Space Telescope and ESA participation in the program 09 p1123 N88-16721

European developments in antenna technology 09 p1123 N88-16725

Coordinated use of European test facilities 09 p1123 N88-16726

ESA Bulletin No. 10 |ETN-87-90514| 09 p1123 N88-16728

Specialist support for projects. Activities, methods and infrastructure 09 p1124 N88-16729

The objectives and methods of the technological research program 09 p1124 N88-16730

Heat pipes for space use 09 p1124 N88-16736

The European space battery test center 09 p1125 N88-16738

ESTEC's product assurance activities 09 p1125 N88-16739

Major spacecraft hardware testing in Europe 09 p1125 N88-16740

ESA Bulletin No. 15: Ariane, the European launcher for the 1980's |ESA-BULLETIN-NO-15| 09 p1125 N88-16741

Projects under development 09 p1126 N88-16750

ESA Bulletin No. 24 |ISSN-0376-4265| 09 p1127 N88-16755

The Meteosat operational program 09 p1127 N88-16759

Programs under development and operations 09 p1127 N88-16762

The new approach to the definition of the ESA technological research program 09 p1127 N88-16763

European industrial consortia for space projects. Their origins, development and possible evolution 09 p1128 N88-16765

ESA Bulletin No. 25 |ISSN-0376-4265| 09 p1128 N88-16767

Parallel-processing computer systems and their possible applications in the agency 09 p1128 N88-16774

Report presented by the European Space Agency to the 22nd COSPAR meeting |ESA-SP-1014| 09 p1129 N88-16776

Proceedings of the ESA Workshop on Co-Orbiting Platform Elements (COPE) |ESA-SP-1093| 09 p1129 N88-16777

An overview of the current Earth observation programs (Europe, USA, and Japan) 09 p1129 N88-16778

The Columbus program, an overview 09 p1130 N88-16784

Coorbiting Platform Utilization Study (CPLUS), executive summary --- Columbus |SN-WP-4000-DOC-6609/85/F| 09 p1133 N88-16798

Study on long term evolution towards European manned space flight. Volume 1: Executive summary |MBB-RA3-004/87-VOL-1| 10 p1286 N88-17689

Study for history of technology developments in European space projects |REPT-8518-1| 10 p1286 N88-17690

AZUR, the first German research satellite 625-A, 1964-1969 10 p1310 N88-17827

Trends in the development of space transportation systems |MBB-UR-911/86| 10 p1315 N88-17857

JPRS report: Science and Technology. Europe and Latin America |JPRS-ELS-88-002| 10 p1316 N88-17870

Columbus feasibility studies. Volume 4: Integration, test, and operations |ETN-88-90576| 11 p1445 N88-18614

Assembly and servicing of a European Space Station 12 p1586 N88-19492

Utilization of SMS and EVA for the servicing of European Space Station 12 p1587 N88-19500

The ESA/Fokker service end-effector subsystem. A robotic/man-compatible servicing approach 12 p1587 N88-19502

Robotic intelligence issues for space manipulator monitoring, control programming 12 p1588 N88-19504

Robotics servicing experiment --- European space programs 12 p1591 N88-19529

Definition of the EUROSIM simulation subsystem 12 p1592 N88-19532

Man-tended options for European space robotics 12 p1593 N88-19538

The European Space Agency's role in life sciences and research in space 12 p1652 N88-19894

Life sciences in the framework of the ESA microgravity program and future flight opportunities 12 p1652 N88-19895

Life science techonology --- space applications 12 p1653 N88-19900

European activities in exobiological research in space 12 p1657 N88-19929

European Progress on Space (EPOS). Participation in the creation of long term European space programs |ILR-MITT-189| 14 p1871 N88-21180

Investigation of European remote sensing user needs in accessing MOS-1 payload |ESA-CR(P)-2535| 14 p1940 N88-21580

Securing the timescale of the NAVEX-reference clock and rate determinations by time comparisons with the help of the Global Positioning System (GPS) --- Spacelab D1 mission |DFVLR-MITT-87-20| 16 p2159 N88-22879

Navigation experiment NAVEX. The reading differences between all ground station measuring clocks during each Spacelab pass of the D1 mission |DFVLR-MITT-87-23| 16 p2159 N88-22880

New concepts for atmospheric braking deceleration in planetary atmosphere entry |SNIAS-CAS-DECE-P003-DPAA| 16 p2168 N88-22923

Preparation of the operational phase of the European Remote Sensing Satellite ERS-1 |BCRS-87-06| 16 p2228 N88-23307

Study of the plan for a national data center for the European Remote Sensing Satellite ERS-1 |BCRS-87-11| 16 p2228 N88-23309

Preparing for the new programs. The ESA technological research and development program 1988-1990 |ESA-SP-1095| 17 p2309 N88-23814

Colombus feasibility studies, executive summary |ETN-88-92334| 17 p2311 N88-23820

Insert design handbook |ESA-PSS-03-1202-ISSUE-1| 17 p2311 N88-23822

International cooperation in remote sensing. The ESA experience 17 p2356 N88-24038

The high-throughput X-ray spectroscopy mission E6889478 MN513835 --- ESA program |ESA-SP-1092| 17 p2450 N88-24554

Economic impact of space flight activities in West Germany: Influence of allocations of Bundesministerium fuer Forschung und Technologie
[ETN-88-92106] 21 p2901 N88-27215

Cyrogenic test facilities for an optical cryomechanism qualification
[REPT-881-440-116] 21 p2901 N88-27219

Study on NAVSAT system evaluation, phase 2. Part 1: Study results
[NLR-TR-87061-L-PT-1] 22 p3041 N88-28054

Reaching for the skies: The Ariane family story and beyond. An introduction to Europe's successful series of space transportation systems
[ESA-BR-42] 22 p3046 N88-28078

Study of biological effects and radiation protection to future European manned space flights
[DGT-33061] 23 p3281 N88-29535

Focus 86: A summary of the 1986 annual report of the activities of the European Space Agency
[ESA-BR-34] 23 p3309 N88-29713

Study on long-term evolution towards European manned spaceflight. Volume 1: Executive summary
[ERNO-OX1-002/88-VOL-1] 24 p3330 N88-29827

ERS-1: A satellite with an oceanographic mission
[NLR-MP-86072-U] 24 p3333 N88-29838

Study of the assembly, integration and verification programs of telecommunication satellites applicable to other satellite programs
[MATRA-100/CC/MLG/031/87]
24 p3334 N88-29847

Interim Flight Opportunity (IFO). Volume 1: Executive summary --- space platform
[SE/LS/AP-36-818/CN-VOL-1]
24 p3334 N88-29849

Qualification test levels for units to be derived from mechanical test data analysis --- ESA
[REPT-87-158-EI/ET/AG] 24 p3381 N88-30139

Study on industrial organization for European Ground Support Equipment (EGSE) to support European space programs. Volume 1: Technical reports
[SD-RP-AI-009-VOL-1] 24 p3435 N88-30446

With an eye to the future: ESA general studies program 1988
[ESA-SP-1100] 24 p3435 N88-30447

Study on industrial organization for European Ground Support Equipment (EGSE) to support European space programs. Volume 2: Technical reports
[SD-RP-AI-009-VOL-2] 24 p3435 N88-30448

ESA report to the 27th COSPAR meeting
[ESA-SP-1098] 24 p3453 N88-30556

The high-throughput X-ray spectroscopy mission: The mission-science report
[ESA-SP-1097] 24 p3453 N88-30557

EUROPEAN SPACE RESEARCH ORGANIZATION
U EUROPEAN SPACE AGENCY

EUROPEAN SPACE RESEARCH ORGANIZATION SAT
U ESA SATELLITES

EUROPIUM

Change of europium crystallographic symmetry at helicoidal magnetic ordering
[DE88-700559] 07 p0939 N88-15707

EUROPIUM COMPOUNDS

Resistivity of EuBa2(Cu/sub 1-y/Zn/sub y/)3O/sub x/ as a ffunction of temperature, magnetic field, pressure and Zn concentration
[DE87-014740] 04 p0499 N88-13069

Growth of Pb/sub 1-x/Eu/sub x/Te epitaxial layers by the liquid phase epitaxy technique
[DE88-701022] 15 p2139 N88-22763

EUTECTIC ALLOYS

Directed-energy electron-beam processing of a hypoeutectic Cr90Ta10 alloy
[DE88-005621] 15 p2040 N88-22157

Fraction eutectic measurements in slowly cooled Pb - 15 wt percent Sn alloys
[NASA-CR-180830] 19 p2618 N88-25531

EUTECTIC COMPOSITES

Influence of convection on microstructure
[NASA-CR-182489] 10 p1302 N88-17784

EUTECTIC DIAGRAMS
U PHASE DIAGRAMS

EUTECTICS
NT EUTECTIC ALLOYS

Low-pressure eutectic bonding of depleted uranium to copper
[DE87-014625] 02 p0181 N88-11128

Ultra-fine grained alloy material
[AD-A184500] 03 p0290 N88-11820

Laser cladding of Ni, Nb and Mg alloys for improved environmental resistance at high temperature
[AD-A191274] 16 p2213 N88-23208

EVACUATING (TRANSPORTATION)

Smoke hoods: Net safety benefit analysis --- aircraft accidents
[CAA-PAPER-87017] 23 p3174 N88-28898

EVALUATION
NT TRAINING EVALUATION

Hardware fault insertion and instrumentation system: Mechanization and validation
[NASA-CR-181445] 01 p0076 N88-10497

An evaluation of WPS-Plus word processing software for the IBM PC and compatibles
[DE87-011972] 01 p0081 N88-10518

Assessment of software quality for the AIRBUS A310 automatic pilot 02 p0128 N88-10804

Experiments of the selection of a method evaluating the fire resistance of some materials based on macromolecular compounds
[NASA-TT-20129] 02 p0154 N88-10966

An evaluation of the LLC-460 solar collector
[DE88-000052] 02 p0196 N88-11224

Evaluating computers and their performance: Perspectives, pitfalls, and paths
[DE87-014264] 02 p0218 N88-11375

Hypocenters (1977-1984) around the Richton Dome and the Melvin, Alabama, 1978 earthquake
[DE87-014336] 03 p0351 N88-12214

Los Alamos National Laboratory computer benchmarking 1986
[LA-10898-MS] 03 p0363 N88-12285

An evaluation plan of bus architectures and protocols using the NASA Ames intelligent redundant actuation system
[NASA-CR-177458] 04 p0398 N88-12482

Non-linearity in measurement systems: Evaluation method and application to microwave radiometers
04 p0433 N88-12684

Standard fatigue test specimens for fastener evaluation
[AGARD-AG-304] 04 p0455 N88-12818

Methods for design and evaluation of integrated hardware/software systems for concurrent computation
[NASA-CR-181522] 04 p0479 N88-12953

Evaluation of device figure of merit in microwave switching circuit design
[AD-A184896] 05 p0577 N88-13520

Test and evaluation of the transputer in a multi-transputer system
[AD-A184969] 05 p0631 N88-13859

Analysis and test evaluation of the dynamic stability of three advanced turboprop models at zero forward speed
[NASA-CR-175025] 06 p0668 N88-14095

Analysis and test evaluation of the dynamic response and stability of three advanced turboprop models at low forward speed
[NASA-CR-175026] 06 p0668 N88-14096

The evaluation of a deformable diffraction grating for a stigmatic EUV spectroheliometer
[NASA-CR-182371] 06 p0707 N88-14337

Experiences in teleoperation of land vehicles
[DE88-001695] 06 p0711 N88-14357

Evaluation method of the brittle fracture strength in structurally stress-concentrated regions
[PB87-129490] 06 p0721 N88-14435

Controlled Ecological Life Support Systems (CELSS) physiochemical waste management systems evaluation
[NASA-CR-177422] 06 p0754 N88-14626

Software-implemented fault insertion: An FTMP example
[NASA-CR-178423] 06 p0761 N88-14668

Evaluation of high-voltage, high-power, solid-state remote power controllers for amps
07 p0924 N88-15612

A study to evaluate STS heads-up ascent trajectory performance employing a minimum-Hamiltonian optimization strategy
[NASA-TP-2793] 08 p0960 N88-15820

Calculation evaluation of the boundary conditions of autoinflammation of propulsive charges
[PB87-139044] 08 p0974 N88-15890

Actual performance and economic feasibility of residential solar water heaters
[INPE-4399-RPE/555] 08 p1023 N88-16191

Using output to evaluate and refine rules in rule-based expert systems 08 p1055 N88-16362

Evaluating software testing methods to reduce testing duplication in US Army communications equipment acquisition
[AD-A186961] 09 p1216 N88-17292

Corrosion and deterioration testing in humid tropic environments
[AD-A186917] 10 p1302 N88-17783

Evaluation of bituminous materials used in pavement recycling projects at Tyndall, MacDill, and Hurlburt Air Force Bases
[AD-A188068] 10 p1317 N88-17871

Laboratory evaluation and analysis of advanced lead-acid load-leveling batteries
[DE88-002851] 10 p1349 N88-18064

Supercomputer performance: The theory, practice, and results
[DE88-004697] 10 p1384 N88-18286

A method for assessing the software engineering capability of contractors. Preliminary version
[AD-A187230] 10 p1388 N88-18290

Quantitative non-destructive evaluation of porous composite materials based on ultrasonic wave propagation
[NASA-CR-182544] 11 p1447 N88-18627

Lead-acid load-leveling battery testing at Argonne National Laboratory
[DE88-002853] 11 p1480 N88-18837

Evaluation of advanced lead acid batteries developed for load-leveling applications
[DE88-002871] 11 p1481 N88-18838

The judgement and evaluation of long-term investments demonstrated by means of a civil aircraft program
12 p1701 N88-20180

The effects of two Carlucci initiatives concurrency and streamlining, on the test and evaluation phase of system acquisitions 12 p1704 N88-20198

Combustion theory and related questions
[AD-A189160] 13 p1737 N88-20382

Method to evaluate image-recovery algorithms based on task performance
[DE88-005382] 13 p1816 N88-20853

Development and evaluation of instrumentation and methods for multi-element analysis
[AD-A189345] 13 p1841 N88-21018

Multi-hundred kilowatt roll ring assembly evaluation results
[NASA-TM-100865] 14 p1904 N88-21375

A graph separator theorem and its application to Gaussian elimination to optimize Boolean expressions for parallel evaluation
[AD-A188527] 14 p1962 N88-21706

EMR (Electromagnetic Radiation) test facilities evaluation of reverberating chamber located at RADC (Rome Air Development Center), Griffiss AFB (Air Force Base), Rome, New York
[PB88-178827] 15 p2022 N88-22048

Today's photovoltaic systems: An evaluation of their performance
[DE88-006926] 15 p2090 N88-22457

Prediction of physical fitness: Estimated percent body fat using body circumferences versus weight-height measures
[AD-A190233] 15 p2103 N88-22526

Instrumentation for ultrafast electronics
[AD-A191379] 16 p2193 N88-23080

Evaluation of the endogenous glucocorticoid hypothesis of denervation atrophy
[NASA-CR-182848] 17 p2381 N88-24157

Evaluation of the communications impact of a low power arcjet thruster
[NASA-TM-100926] 18 p2475 N88-24682

Evaluating evaporation with satellite thermal data
[AD-A192042] 18 p2531 N88-25019

Effectiveness evaluation of fault-tolerant multiprocessor systems
[AD-A191688] 18 p2554 N88-25158

Multi-sensor integration on the NCUBE hypercube computer
[DE88-007472] 18 p2554 N88-25162

Evaluation of vertical monopole antennas with elevated radials
[DE88-008339] 19 p2654 N88-25760

Performance evaluation for multiprocessors programmed using monitors
[DE88-010056] 19 p2718 N88-26138

Engineering research centers and their evaluation
[PB88-180054] 19 p2739 N88-26262

Procedures for peer review assessments
[DE88-007749] 19 p2739 N88-26263

Evaluation of engineering leak before break assessment methods by piping tests
[PB88-126982] 20 p2788 N88-26538

Loss evaluation of self-commutated power conditioner for battery energy storage system
[DE88-752075] 20 p2794 N88-26575

Australian structures response evaluation: Ground shock and air blast measurements for site investigation survey
[MRL-TN-526] 20 p2813 N88-26685

An evaluation of flight path formats head-up and head-down
[NASA-CR-4176] 21 p2897 N88-27196

Evaluation of fracture models through pressurized-thermal-shock testing
[DE88-011834] 21 p2963 N88-27603

Performance evaluation of large-area glass-mirror heliostats
[DE88-011883] 21 p2969 N88-27636

System status display evaluation
[NASA-CR-4181] 22 p3042 N88-28061

Development of sensors for ceramic components in advanced propulsion systems. Survey and evaluation of measurement techniques for temperature, strain and heat flux for ceramic components in advanced propulsion systems
[NASA-CR-182111] 22 p3081 N88-28299

Design and evaluation of high contact ratio gearing
[NASA-CR-174958] 22 p3085 N88-28319

Reliability assessment of Surface Mount Technology (SMT)
[AD-A193759] 23 p3208 N88-29089

Present state of knowledge of the upper atmosphere 1988. An assessment report
[NASA-RP-1208] 23 p3232 N88-29233

SSTS (Space Surveillance and Tracking System): The importance of early test and evaluation organizational participation
[AD-A193745] 23 p3276 N88-29499

Quality measures and assurance for AI (Artificial Intelligence) software
[NASA-CR-4187] 24 p3411 N88-30304

EVANESCENCE

Monolithic integration on a GaAs substrate of a quarter ring laser and an optical guide coupled by an evanescent wave
[ETN-88-92308] 17 p2344 N88-23969

EVAPORATION

NT EVAPOTRANSPIRATION
NT TRANSPIRATION

Preparation and properties of evaporated CdTe films
[DE87-012270] 02 p0195 N88-11216

Production of atom flows at materials evaporation by laser radiation
[DE87-703327] 03 p0328 N88-12074

Ceramics thin film 04 p0403 N88-12505

Effects of rainfall on the seasonal thermocline
[AD-A184432] 04 p0472 N88-12912

Use of the thermodynamic evaporation formula of Hoffmann in energy balance models for flowing water
08 p1013 N88-16143

Laval nozzle flow of a binary, retrograde mixture
[MPIS-1/1987] 11 p1488 N88-18862

Review of recent developments in evaporation ducting assessment 12 p1616 N88-19664

Model catalyst studies of SMSI (Strong Metal/Support Interactions) and the role of D-electrons in chemisorption and catalysis
[DE88-004518] 13 p1738 N88-20393

The thermodynamic properties of organic oxygen compounds
[DE88-001208] 13 p1849 N88-21065

Superfine grain development by laser
15 p2050 N88-22215

Hard ceramic film by laser PVD
15 p2051 N88-22216

Evaporation characteristics of elements during vacuum arc remelting of alloy A-286 15 p2055 N88-22248

Laser evaporation studies
[AD-A189815] 15 p2071 N88-22346

Method of evaporation
[NASA-CASE-NPO-15609-2] 17 p2318 N88-23846

Transient analysis of heat pipe vapor dynamics
17 p2412 N88-24341

Heating and evaporation of turbulent liquid films. Measurement of film thickness and the onset of nucleate boiling
[DE88-006388] 18 p2512 N88-24905

Evaluating evaporation with satellite thermal data
[AD-A192042] 18 p2531 N88-25019

Report on project WIND: Preliminary experiments with the UK Meteorological Office mesoscale model, September 1987
[AD-A191621] 18 p2544 N88-25099

Liquid phase decomposition in slurry fuels
19 p2624 N88-25564

Antenna heights for the optimum utilization of the oceanic evaporation duct. Part 3: Results from the Mediterranean measurements, volume 2
[AD-A192311] 20 p2791 N88-26554

Antenna heights for the optimum utilization of the oceanic evaporation duct. Part 1: Results from the Pacific measurements. Part 2: Results from the Key West measurements, volume 1
[AD-A192358] 20 p2791 N88-26555

Schottky-barrier formation on a covalent semiconductor without Fermi-level pinning: The Metal-MoS2(0001) interface
[AD-A193044] 21 p3021 N88-27931

Influence of the convection on evaporation and combustion of a fuel droplet 24 p3351 N88-29948

EVAPORATION RATE

Development of computer-controlled thermogravimetric instrumentation for measurement of environmental and high temperature volatilization and desorption of contaminants from polymeric materials
[AD-A195934] 24 p3343 N88-29900

EVAPORATIVE COOLING

NT FILM COOLING
NT SWEAT COOLING

Cooling effect of a single evaporating droplet on a hot semi-infinite metal body
[PB87-201802] 01 p0046 N88-10294

The role of low-level cooling in a conceptual model of the Australian summertime cool change: Implications for very-short-range forecasting 02 p0204 N88-11275

Advanced radiator concepts utilizing honeycomb panel heat pipes
[NASA-CR-172017] 04 p0443 N88-12747

Transient cooling of a hot surface by droplets evaporation. March 1986 - March 1987
[PB88-153341] 10 p1330 N88-17950

EVAPORATORS

Tower evaporator
[NASA-CASE-NPO-15609-2] 18 p2497 N88-24815

An experimental investigation of transient characteristics in a gravity-assisted heat pipe 20 p2783 N88-26506

Forced-convective boiling in small diameter tube
20 p2783 N88-26510

EVAPOTRANSPIRATION

Estimating regional evapotranspiration from remotely sensed data by surface energy balance models
[NASA-CR-181400] 01 p0064 N88-10411

Remote Sensing And Lands Workshop, Page, Arizona, June 10-12, 1986
[DE87-012368] 01 p0064 N88-10412

EVASIVE ACTIONS

The isotropic rocket: A surveillance evasion game
[REPT-87-21] 05 p0645 N88-13949

EVECTION

U ORBIT PERTURBATION

EVEN-EVEN NUCLEI

Influence of pairing correlations on the probability and dynamics of tunneling through the barrier in fission and fusion of complex nuclei
[DE88-701500] 23 p3286 N88-29570

EVOKED RESPONSE (PSYCHOPHYSIOLOGY)

Visual evoked responses to sinusoidal gratings presented in central and right visual fields, 1
[DE87-014731] 04 p0473 N88-12919

Brain activity during tactical decision-making. Part 2: Probe-evoked potentials and workload
[AD-A188688] 12 p1667 N88-19994

Identification of visual evoked response parameters sensitive to pilot mental state
[NASA-CR-4140] 13 p1811 N88-20822

Pupil measures of alertness and mental load
16 p2239 N88-23378

Probe-evoked event-related potential techniques for evaluating aspects of attention and information processing 16 p2240 N88-23379

Steady-state evoked potentials possibilities for mental-state estimation 16 p2240 N88-23380

Primary task event-related potentials related to different aspects of information processing
16 p2240 N88-23382

The N2-P3 complex of the evoked potential and human performance 16 p2241 N88-23388

Eye and head response to an attention cue in a dual task paradigm
[AD-A191052] 18 p2551 N88-25143

Contra- and ipsilateral auditory stimuli produce different activation patterns at the human auditory cortex: A neuromagnetic study
[PB88-181490] 19 p2708 N88-26098

Auditory evoked magnetic fields in man
[PB88-193446] 20 p2831 N88-26796

A statistical procedure for the evaluation of presence/non-presence of stimulus-related EEG activity
21 p2978 N88-27689

Dissecting the visual and auditory pathways by means of the two-input technique 21 p2978 N88-27690

Squid instrumentation for neuromagnetic study of complex brain activity 21 p2978 N88-27691

Neuromagnetic evidence of place mechanisms for frequency and intensity coding in the human auditory cortex 21 p2979 N88-27693

Neurophysiological precursors of accurate visuomotor performance 21 p2981 N88-27706

The effect of mild hypoxia on the vestibular evoked response 21 p2982 N88-27713

Measurement of electrical activity in the CNS with cortical evoked potentials and EEG: Efficacy profiles of drugs using factor analysis 21 p2983 N88-27715

The auditory evoked response in military pilots
21 p2984 N88-27721

Human auditory and visual continuous evoked potentials 23 p3238 N88-29269

EVOLUTION

Rotational evolution of dynamically symmetric gyrostat with internal friction 24 p3446 N88-30509

Evolution of thermal structure of Benguela upswelling system according to satellite and shipboard data
24 p3449 N88-30525

EVOLUTION (DEVELOPMENT)

NT BIOLOGICAL EVOLUTION
NT CHEMICAL EVOLUTION
NT GALACTIC EVOLUTION
NT LUNAR EVOLUTION
NT PLANETARY EVOLUTION
NT STAR FORMATION
NT STELLAR EVOLUTION
NT STELLAR MASS ACCRETION

Semidiscrete Galerkin method for semilinear evolution equations with a differential operator of third order
[BONNER-MATHE-SCHR-181]
01 p0087 N88-10570

High explosive simulations of supernovae and the supernova shell fragmentation model of solar system formation
[DE87-014708] 02 p0251 N88-11584

Cosmological applications of singular hypersurfaces in general relativity 04 p0521 N88-13202

The evolution of local mechanical properties of Al 2219-T851 during fatigue 05 p0598 N88-13653

Model of earlier stage of universe's evolution
06 p0775 N88-14758

Evolution of perturbations in expanding universe
06 p0775 N88-14759

The origin of the spicule skeleton of fresh water sponges (Spongillides) 07 p0885 N88-15368

Limb regeneration in amphibians, a suitable model for investigations of the effects of weightlessness as regards evolution and modifications 07 p0885 N88-15369

Evolution from pure states into mixed states in de Sitter space
[DE88-750316] 07 p0945 N88-15745

Morphological manifestations of primate adaptation to orthograde statics and walking erect
10 p1366 N88-18162

Five New South Wales barrier lagoons: Their macrobenthic fauna and seagrass communities
11 p1517 N88-19059

Cometary evolution: Clues from chondritic interplanetary dust particles 14 p2002 N88-21934

Crustal models of the evolving comet nucleus
14 p2005 N88-21953

Diversity of comets, synergic temperature effects and the stability of organic compounds in icy nuclei
14 p2005 N88-21955

The structure of the Halley meteor stream and the orbital history of the comet 14 p2008 N88-21975

The mass loss rates of periodic comets
14 p2010 N88-21991

Aerial photography as an instrument of municipal and regional planning: Metropolitan area of Sao Paulo (SP)
19 p2684 N88-25957

Embryonic development of the newt Cynops pyrrhogaster in very weak magnetic fields
[ISAS-RN-357] 19 p2702 N88-26068

Cometary nucleus as aggregate of planetesimals
[ISAS-RN-364] 19 p2741 N88-26275

Evolution of hairpin vortices in a shear flow
[NASA-TM-100858] 20 p2845 N88-26885

Dynamical evolution of cosmic strings
[DE88-011724] 21 p3030 N88-27989

Intercrater plains deposits and the origin of Martian valleys 23 p3301 N88-29661

Volcano evolution on Mars 23 p3305 N88-29686

Mid to late proterozoic magmatism within Northeastern North America and its iplications for the growth of the continental crust 24 p3397 N88-30229

Thermal models pertaining to continental growth
24 p3397 N88-30230

Ridge-trench collision in Archean and Post-Archean crustal growth: Evidence from southern Chile
24 p3397 N88-30233

Archean crustal evolution of the northern North China Craton 24 p3398 N88-30235

Growth of the lower continental crust
24 p3398 N88-30236

The complexity, depth, and rapidity of processes that formed the lunar crust 24 p3398 N88-30237

Geochronological and lead-isotope evidences for rapid crust formation in middle-proterozoic time: The Labrador example 24 p3398 N88-30239

Physical processes in the growth of the continental crust 24 p3398 N88-30240

Evolution of the Dharwar Craton: A terrain of early Archean crustal stability, long term orogenic cycles and large scale palaeobiological activity
24 p3399 N88-30241

Lithospheric evolution of the Northern Arabian Shield: Chemical and isotopic evidence from basalts, xenoliths and granites 24 p3399 N88-30242

Trace element differences between Archean, Proterozoic and Phanerozoic crustal components: Implications for crustal growth processes
24 p3399 N88-30243

Continental growth through time by underplating of subducted oceanic crust: Evidence from kimberlites in South Africa and SW Pacific 24 p3399 N88-30244

Growth of planetary crusts 24 p3400 N88-30247

Mineralization through geologic time: Evolution of continental crust 24 p3400 N88-30250

Volcanic contribution to crustal growth in the Central Andes: A new estimate and a discussion of uncertainties
24 p3401 N88-30255

A compilation of information and data on the Manson impact structure
[NASA-CR-183169] 24 p3401 N88-30258

Noble gases, C,N, and Si isotopes in interstellar SiC form the Murchison carbonaceous chondrite
24 p3442 N88-30483

Observations of star formation
24 p3451 N88-30538

Nebular processes recorded in chondritic meteorites
24 p3451 N88-30541

EVOLUTION (LIBERATION)
NT GAS EVOLUTION

EXACTNESS
U PRECISION

EXCHANGING
NT CHARGE EXCHANGE
NT GAS EXCHANGE
NT ION EXCHANGING
NT RESONANCE CHARGE EXCHANGE

Lower-stratospheric/upper-tropospheric exchange processes associated with tropical cyclones as observed by TOMS 05 p0616 N88-13782

EXCIMER LASERS

XeCl excimer laser with magnetic compressor
03 p0299 N88-11879

JPRS report: Science and technology. China
[JPRS-CST-87-031] 03 p0299 N88-11880

JPRS report: Science and technology. China
[JPRS-CST-87-034] 03 p0301 N88-11897

A 10 W transverse flow excimer laser
03 p0302 N88-11901

Excimer laser cell with longitudinal electron-beam excitation 03 p0302 N88-11903

JPRS Report: Science and Technology. China
[JPRS-CST-87-033] 03 p0326 N88-12062

Operational performance of repetitive KrF, XeCl excimer lasers 03 p0327 N88-12068

Gas flow effects in pulse avalanche discharge XeCl excimer lasers 03 p0328 N88-12070

Narrow linewidth gain measurements in a KrF excimer amplifier pumped longitudinally by a high-power electron beam
[DE88-001365] 05 p0586 N88-13575

Photocurrent generation from basic metals, utilizing a short pulsed ArF excimer laser
[AD-A184928] 05 p0587 N88-13579

Anti-Stokes generation of 226 nm light
[DE88-001612] 05 p0589 N88-13590

Chemical analysis for excimer laser systems
[DE88-001941] 05 p0589 N88-13591

Laser development, evolution of applied technologies described 06 p0689 N88-14221

Periodically pulsed excimer master oscillator-regenerative amplifier laser set
06 p0772 N88-14741

Studies on nonlinear mechanisms of excimer laser propagation in fused silica fibers
[AD-A186822] 09 p1156 N88-16929

Where directed energy stands in strategic defense
[DE88-005092] 10 p1403 N88-18365

Practical constraints on sources for pulsed beam lithographies
[DE88-006594] 13 p1776 N88-20623

XeF excimer laser pumped by high-intensity relativistic electron beam 14 p1901 N88-21355

Folded long-pulse XeCl excimer laser described
14 p1901 N88-21357

Kinetics of slow electrons in excimer laser with electron-beam pumping 14 p1970 N88-21760

Effects of emission energy transient in periodic-pulse XeCl excimer laser of approximately 400 W average power 14 p1971 N88-21763

Laser processing-status, perspectives
15 p2050 N88-22211

Numerical modelling specific energy charctenstics of excimer KrF lasers with electron beam excitation
[DE88-701525] 15 p2070 N88-22344

Alkali metal diffuse band lasers
[AD-A190244] 15 p2071 N88-22350

Thin film research diagnostics instrumentation
[AD-A191240] 16 p2213 N88-23207

Theoretical calculations of XeF ground state kinetics
[AD-A191398] 16 p2270 N88-23580

Realization of an XeCl laser producing 100W on average
[ETN-88-92541] 17 p2344 N88-23970

Aurora status and plans
[DE88-006476] 18 p2521 N88-24955

Use of magnetic materials in excimer laser circuits
[DE88-006449] 19 p2674 N88-25903

Systematics of excimer laser ablation: Thin film preparation of high T(sub c) material
[DE88-010569] 19 p2675 N88-25909

Laser and electrochemical studies of metallizations in electronic devices
[AD-A193786] 23 p3208 N88-29090

EXCIMERS

Excimer laser-assisted deposition of GaAs, AlAs and (Al,Ga)As from Lewis acid-base adducts
[AD-A184588] 03 p0329 N88-12081

Energy disposal in ion-molecule reactions
[AD-A186772] 09 p1171 N88-17019

Excimer plasma displays
[AD-A186731] 09 p1250 N88-17489

EXCITATION
NT ACOUSTIC EXCITATION
NT ATOMIC EXCITATIONS
NT HARMONIC EXCITATION
NT MOLECULAR EXCITATION
NT SELF EXCITATION
NT WAVE EXCITATION

KR + laser excitation of NH2 in atmospheric pressure flames
[AD-A183421] 01 p0050 N88-10322

IR laser excitation in molecules: Chaos and diffusive energy growth
[DE87-013147] 02 p0178 N88-11105

Excimer laser cell with longitudinal electron-beam excitation 03 p0302 N88-11903

Excitation of natural oscillations of a boundary layer by an external acoustic field 04 p0425 N88-12634

An excitation-term modification for a certain class of electromagnetic aperture-coupling problems
[DE88-000260] 04 p0437 N88-12713

Alternating current circuit theory and pulsed NMR (Nuclear Magnetic Resonance)
[DE88-000641] 04 p0440 N88-12732

J = O Task Force
[DE88-001326] 04 p0450 N88-12788

Thermomechanical cracking in coated media due to high speed asperity excitation
[AD-A184176] 04 p0454 N88-12809

Mechanical shock test specification using nonstationary random excitation models
[DE87-013650] 04 p0454 N88-12812

Vibration and parametric excitation in rotating asymmetric circular plates 04 p0456 N88-12823

Implementation of a new shock testing procedure using nonstationary random excitation
[DE87-014643] 04 p0456 N88-12827

Nitrogen energy transfer study
[AD-A184457] 04 p0464 N88-12869

On the glitches in the force transmitted by an electrodynamic exciter to a structure
05 p0594 N88-13624

Blade excitation due to unsteady flow phenomena
07 p0851 N88-15167

The Coupled Cluster Single and Double excitation (CCSD) method in quantum chemistry: An efficient formulation of the theory and application to closed shell molecular systems
[DE88-000475] 07 p0930 N88-15650

The effect of propane on atomic spectrometric signals in the direct current plasma
[DE88-002457] 07 p0934 N88-15676

Fully turbulent internal flow excitation of pipe systems
08 p1000 N88-16056

Nuclear excitation via the motion of electrons in a strong laser field
[AD-A187166] 09 p1171 N88-17017

Photoionization dynamics of excited molecular states
[DE88-002982] 09 p1246 N88-17468

Atomic data for hydrogens in collisions with electrons: Addenda
[IPPJ-AM-55-ADD] 09 p1252 N88-17502

Memory effects on infrared adsorbate spectra
[AD-A186976] 09 p1253 N88-17512

Frequency response function estimation at level
[DE88-002644] 10 p1344 N88-18034

Correlated processes in atomic collisions
[DE88-003508] 10 p1406 N88-18383

Electronic structure, charge transfer excitations and high temperature superconductivity
[DE88-003096] 10 p1416 N88-18453

Experimental aspects of hypernuclear physics at CEBAF
[CEBAF-R-86-013] 11 p1546 N88-19245

Presentations to the SuperHILAC Program Advisory Committee
[DE88-003853] 11 p1547 N88-19256

Picosecond laser studies of excited state processes
[AD-A189606] 12 p1607 N88-19607

Reactions of N2(A(3)(SIGMA)/sub u/(+)) and candidates for short wavelength lasers
[DE88-005366] 12 p1632 N88-19767

Discharge excitation of dye vapors
[AD-A188428] 12 p1632 N88-19770

QED description of relativistic Coulomb excitation in heavy ion collisions
[DE88-700834] 12 p1689 N88-20100

Seasonal variations and excitation mechanisms of the equatorially trapped waves 13 p1798 N88-20751

Image charge, coherent scattering, and symmetry effects in electron stimulated desorption: O(-) from O sub 2 condensed on metals
[AD-A189093] 13 p1835 N88-20979

The magnitude of secondary electron contributions in photon stimulated desorption
[AD-A189094] 13 p1835 N88-20980

Electronic energy transfer processes in the alkali/alkaline earth metal vapors
[AD-A190035] 15 p2034 N88-22119

Discharge excitation of the XeF C to A transition
[DE88-006448] 15 p2070 N88-22339

Numerical modelling specific energy charctenstics of excimer KrF lasers with electron beam excitation
[DE88-701525] 15 p2070 N88-22344

Effect of vibrational excitation on rate parameters of atmospheric reactions
[AD-A190464] 15 p2094 N88-22477

Sequential excitation preparation of molecular energy levels with special structural and chemical properties
[AD-A190041] 15 p2132 N88-22718

Effective electron interactions due to virtual charge and spin excitations in an extended Hubbard model for Cu-O superconductors
[DE88-005971] 15 p2139 N88-22766

First-principles calculations of quasiparticle energies at surfaces and interfaces: Semiconductor surface-state spectra and band offsets
[DE88-006340] 15 p2141 N88-22773

The effect of internal relaxation on optoacoustic conversion in liquids
[AD-A191307] 16 p2176 N88-22970

Saturation and the limit of jet mixing enhancement by single frequency plane wave excitation: Experiment and theory
[NASA-TM-100882] 17 p2295 N88-23732

Search for bound states of the eta-meson in light nuclei 17 p2397 N88-24248

Robust adaptive regulation without persistent excitation
[NASA-TM-100571] 18 p2561 N88-25204

Trochoidal analysis of scattered electrons in a merged electron-ion beam
[NASA-CASE-NPO-16789-1-CU]
18 p2573 N88-25281

Optical properties of heterostructures and superlattices
[AD-A191542] 18 p2581 N88-25335

Direct subpicosecond measurement of carrier mobility of photoexcited electrons in GaAs
19 p2659 N88-25803

Longitudinally localized optical carrier injection for femtosecond transport studies 19 p2659 N88-25806

Dynamics of below-gap photoexcitation in GaAs quantum wells 19 p2660 N88-25815

Enhancement of volume H(-) production by vibrationally pre-exciting the hydrogen molecules
[DE88-010783] 20 p2853 N88-26937

Magnetic excitations in transition metal systems
[DE88-011022] 21 p2912 N88-27279

Inelastic electron scattering and electron-hole excitations in iron and nickel
[DE88-011843] 21 p2915 N88-27303

Picosecond optoelectronic sampling of electrical waveforms produced by an optically excited field effect transistor
[AD-A192384] 21 p2935 N88-27428

Nonlinear stochastic interaction in aeroelastic structures
[AD-A193427] 21 p2961 N88-27589

Evidence for laser emission from the TICT exciplex of coumarin dyes
[DE88-702544] 23 p3220 N88-29167

Investigation of non-classical effects in two-photon interference processes 23 p3282 N88-29541

Localized excitations in one-dimensional molecular crystal with structural defect
[DE88-702691] 23 p3293 N88-29607

Localized excitations in one-dimensional molecular crystal with structural defect
[DE88-702691] 23 p3293 N88-29607

EXCITED STATES
U EXCITATION

EXCITONS
A physico-chemical study of some areas of fundamental significance to biophysics
[DE87-013457] 02 p0217 N88-11365
Novel dynamical investigations of excitons and their structure in semiconductors
[DE87-014868] 04 p0499 N88-13070
Enhanced excitonic optical nonlinearity and exciton dynamics in semiconductor microstructures
14 p1977 N88-21795
Dynamical aspects of carrier tunneling in semiconductor superlattices 14 p1977 N88-21799
Experimental and theoretical studies of coherent and nonthermal processes in semiconductors probed by femtosecond laser techniques 14 p1977 N88-21800
Exciton relaxation phenomena in a disordered system
14 p1978 N88-21802
Nonlinear optical properties and subpicosecond dynamics of excitons and electron-hole plasmas in multiple quantum well structures
[AD-A191926] 19 p2727 N88-26196
Excitonic properties of GaAs-AlGaAs nanostructures
20 p2867 N88-27023
Laser spectroscopy of quantum well and superlattice structures
[AD-A193336] 21 p3022 N88-27937

EXCLUSION
Markov chain computations to a solution of the mutual-exclusion problem in concurrency
[REPT-87-89] 20 p2847 N88-26896

EXCRETION
Biorhythmic aspects of intercontinental Antarctic adaptation 08 p1046 N88-16321

EXECUTIVE AIRCRAFT
U GENERAL AVIATION AIRCRAFT
U PASSENGER AIRCRAFT

EXECUTIVE SYSTEMS (COMPUTERS)
U OPERATING SYSTEMS (COMPUTERS)

EXERCISE
U PHYSICAL EXERCISE

EXERCISE PHYSIOLOGY
Oxygen transport during exercise at extreme simulated altitude: Operation Everest 2
[AD-A185720] 06 p0752 N88-14620
Influence of a 6 hr head-out water immersion on different tests of endurance performance capacity
12 p1653 N88-19903
P-31 Magnetic Resonance Spectroscopy (MRS) of limb muscles during bedrest with exercise countermeasures
12 p1656 N88-19925
Effects of anti-g suit inflation on renin and aldosterone response physical exercise 12 p1659 N88-19944
A new isodynamically-braked arm ergometer including the demonstration of a prototype
12 p1661 N88-19957
Fish as a tool for testing fitness in space
12 p1662 N88-19963
Endocrine responses to resistance exercise
[AD-A188681] 12 p1667 N88-19993
Hormonal regulation of fluid and electrolytes: Effects of heat exposure and exercise in the heat
[AD-A192655] 22 p3131 N88-28614
Effects of air polution on human exercise performance
[AD-A192660] 22 p3131 N88-28617
Gastric emptying during walking and running: Effects of varied exercise intensity
[AD-A194025] 23 p3240 N88-29281

EXERTION
U PHYSICAL WORK

EXHAUST EMISSION
Adiabatic diesel engine component development: Reference engine for on-highway applications
[NASA-CR-179531] 03 p0386 N88-12428
Summary and analysis of comments on the recommended practice for the measurement of refueling emissions
[PB88-101530] 07 p0876 N88-15313
Aircraft emissions characterization: TF41-A2, TF30-P103 and TF30-P109 engines
[AD-A192053] 18 p2466 N88-24638
A 3 MW wood fired gas turbine at Red Boiling Springs, Tennessee 18 p2536 N88-25051
Motor vehicles as sources of compounds important to tropospheric and stratospheric ozone
[PB88-195219] 18 p2540 N88-25076
Initial testing of the tunable diode laser absorption spectrometer for measuring HNO3 in diesel engine exhaust, stage 2
[PB88-193073] 21 p2970 N88-27641

EXHAUST FLOW SIMULATION
Investigation of the effect of laterally ejected gas jets on flows
[ISL-R-107/86] 05 p0581 N88-13545
Split-coefficient matrix solution and experimental study of axisymmetric underexpanded exhaust plumes
15 p2054 N88-22242

EXHAUST GASES
Boundary layer profile investigations downstream of an aero-engine intake anti-icing air exhaust slot
[PNR90378] 02 p0171 N88-11080
The determination of exhaust cloud dimensions from films of space shuttle launches
[NASA-CR-4103] 06 p0732 N88-14500
Hydrogen chloride measurements in launch-vehicle exhaust clouds
[DE87-011552] 08 p0964 N88-15837
Exhaust-gas pressure and temperature survey of F404-GE-400 turbofan engine
[NASA-TM-88273] 13 p1724 N88-20307
An experimental investigation of an arcjet thruster exhaust using Langmuir probes
[NASA-TM-100258] 14 p1883 N88-21253
Investigation of aeroacoustic mechanisms by remote thermal imaging
[DE88-002612] 15 p2021 N88-22046
An experimental investigation of rocket ramjet nozzle assembly base pressures
[AD-A189714] 15 p2027 N88-22076
Split coefficient matrix solution and experimental study of axisymmetric underexpanded exhaust plumes
15 p2054 N88-22242
Aircraft emissions characterization: TF41-A2, TF30-P103 and TF30-P109 engines
[AD-A192053] 18 p2466 N88-24638
Techniques utilized in the simulated altitude testing of a 2D-CD vectoring and reversing nozzle
[NASA-TM-100872] 19 p2604 N88-25464

EXHAUST JETS
U EXHAUST GASES

EXHAUST NOZZLES
NT CONVERGENT-DIVERGENT NOZZLES
Hydroburst test of a carbon-carbon involute exit cone
[NASA-TP-2556] 06 p0671 N88-14112
An experimental and numerical investigation of swirling flows in a rectangular nozzle 06 p0700 N88-14295
Advanced Technology for Aero Gas Turbine Components
[AGARD-CP-421] 10 p1279 N88-17647
Experimental evaluation of a translating nozzle sidewall radial turbine 10 p1280 N88-17656
A computational study of thrust augmenting ejectors based on a viscous-inviscid approach
10 p1326 N88-17929
Exhaust-gas pressure and temperature survey of F404-GE-400 turbofan engine
[NASA-TM-88273] 13 p1724 N88-20307
Variable Mach number wall jets for control/propulsion on hypervelocity projectiles/interceptors: Tests with an existing model
[AD-A192845] 21 p2892 N88-27167
Application of laser diffraction techniques to particle sizing in solid propellant rocket motors
[AD-A193841] 22 p3049 N88-28089
Numerical simulation of nozzle flows
[AD-A195144] 24 p3369 N88-30064

EXHAUST SYSTEMS
Adiabatic diesel engine component development: Reference engine for on-highway applications
[NASA-CR-179531] 03 p0386 N88-12428

EXHAUSTION
Metabolic and cardiorespiratory parameters during three consecutive days of exhaustive running
[AD-A192598] 21 p2985 N88-27728

EXISTENCE THEOREMS
Existence and stability of transition layers
[AD-A185806] 06 p0766 N88-14707
On a class of similarity solutions of the equation u sub t = (absolute value of u sup m-1 u sub x) sub x with m greater than -1
[REPT-87-54] 14 p1963 N88-21713

EXITS (DOORS)
U DOORS

EXOBIOLOGY
Preliminary study of a gravitational biology facility for Columbus: executive summary
[MATRA-EPT/AS/VT209/255/NT]
01 p0032 N88-10205
Aquarack: Aims and Possible Research Projects
[DFVLR-MITT-87-01] 01 p0073 N88-10469
The Aquarack as a potential instrument for basic research work in space biology: Inventory and scientific dispositions 01 p0073 N88-10470
Life support systems for biological experiments under weightlessness in the German and European space programs 01 p0074 N88-10477
Aerospace medicine and biology: A continuing bibliography with indexes
[NASA-SP-7011(303)] 02 p0217 N88-11367
Environmental life support system technology study --- space flight
[ESA-CR(P)-2432] 02 p0218 N88-11371
Aerospace medicine and biology: A continuing bibliography with indexes
[NASA-SP-7011(304)] 04 p0474 N88-12922
Aerospace medicine and biology: A continuing bibliography with indexes (supplement 305)
[NASA-SP-7011(305)] 06 p0752 N88-14616
Exobiology and life science 07 p0883 N88-15358
Proceedings and program draft in Gravitational Biology in the Federal Republic of Germany --- Effects of Weightlessness on the Human Organism
[ESA-TT-988] 07 p0884 N88-15363
Some remarks on gravitational biology
07 p0884 N88-15366
JPRS report: Science and technology. USSR: Space Biology and Aerospace Medicine, volume 21, no. 3, May - June 1987
[JPRS-USB-88-001] 07 p0889 N88-15389
JPRS report: Science and technology. USSR: Space Biology and Aerospace Medicine, volume 21, no. 4, July - August 1987
[JPRS-USB-88-002] 07 p0893 N88-15412
Bibliography of space biology and medicine
07 p0897 N88-15435
JPRS report: Science and technology. USSR: Space
[JPRS-USP-87-006] 08 p1001 N88-16063
Space biology and medicine 08 p1006 N88-16096
Life sciences experiments on stratospheric balloons and sounding rockets 08 p1033 N88-16262
The D-1 Biorack results: A base for further space biological investigations 08 p1033 N88-16263
Contribution of stratospheric balloon flights in space biology 08 p1033 N88-16266
USSR Space Life Sciences Digest, issue 14
[NASA-CR-3922(16)] 08 p1045 N88-16317
Aerospace medicine and biology: A continuing bibliography with indexes (supplement 307)
[NASA-SP-7011(307)] 08 p1049 N88-16332
Publications of the exobiology program for 1986: A special bibliography
[NASA-TM-4029] 09 p1203 N88-17205
Present stage of space medicine
10 p1364 N88-18151
NASA Workshop on Biological Adaptation
[NASA-TM-89468] 10 p1368 N88-18174
USSR Space Life Sciences Digest, issue 15
[NASA-CR-3922([illegible])] 10 p1368 N88-18175
Aerospace medicine and biology: A cumulative index to a continuing bibliography (supplement 306)
[NASA-SP-7011(306)] 10 p1369 N88-18180
Aerospace medicine and biology: A continuing bibliography with indexes (supplement 308)
[NASA-SP-7011(308)] 10 p1369 N88-18183
Genetic research in space
[NASA-TT-20216] 11 p1518 N88-19066
The ESA facility Biorack 12 p1652 N88-19897
Exobiology and botany facilities for EURECA
12 p1652 N88-19898
BIOTEX, a project for biotechnological basic experiments under microgravity --- Spacelab
12 p1652 N88-19899
Life science techonology --- space applications
12 p1653 N88-19900
Plant biology in space 12 p1654 N88-19910
Plant cell cultures in space biology studies
12 p1654 N88-19913
The use of plant protoplasts in biotechnological space research 12 p1655 N88-19914
Ecological algal system in microgravity conditions: Preliminary results 12 p1655 N88-19915
Closed system physiology: Role of oxygen in the development of wheat 12 p1655 N88-19916
Aspects of bioregenerative life support systems
12 p1655 N88-19917
European activities in exobiological research in space
12 p1657 N88-19929
Survival under space vacuum: Biochemical aspects
12 p1657 N88-19930
Ultraviolet (180 to 300 nm) action spectra for inactivation and DNA photoproduct formation of Bacillus subtilis spores under ultrahigh vacuum 12 p1657 N88-19931
Survival and mutation induction of dehydrated yeast cells after UV exposure 12 p1657 N88-19932
Cellular effects of heavy ions: Experimental results and theoretical approaches --- space radiation
12 p1658 N88-19933
Effects of heavy ions on egg-developing systems
12 p1658 N88-19935
Medilab: A project of a medical laboratory in space
12 p1660 N88-19946
Cell cultures in space: From basic research to biotechnology 2 12 p1660 N88-19948

Cyropreservation of isolated rat hepathocytes for future use in Spacelab experiments: Preliminary results
12 p1660 N88-19950

Organs and tissues regeneration in amphibia under the space flight conditions 12 p1660 N88-19951

Antibiotic activity in space, results and hypothesis
12 p1660 N88-19952

Biorack experiments in Spacelab D-1 and TML-1: Further developments in gravitational biology
12 p1661 N88-19953

Why life science in space? The next step to go beyond 12 p1661 N88-19954

Aerospace medicine and biology: A continuing bibliography with indexes (supplement 309)
|NASA-SP-7011(309)| 13 p1810 N88-20814

USSR Space Life Sciences Digest, issue 16
|NASA-CR-3922(19)| 15 p2101 N88-22515

Aerospace medicine and biology: A continuing bibliography with indexes (supplement 310)
|NASA-SP-7011(310)| 16 p2238 N88-23369

Botany Facility pre-phase C/D. Core payload for EURECA, volume 1
|BF-RP-ER-015-VOL-1| 17 p2379 N88-24144

USSR Space Life Sciences Digest, Issue 17
|NASA-CR-3922(20)| 17 p2381 N88-24155

Aerospace medicine and biology. A continuing bibliography with indexes (supplement 311)
|NASA-SP-7011(311)| 17 p2382 N88-24161

Aerospace medicine and biology. A continuing bibliography with indexes (supplement 312)
|NASA-SP-7011(312)| 18 p2551 N88-25141

JPRS report: Science and technology. USSR: Space Biology and Aerospace Medicine, volume 22, no. 1, January - February 1988
|JPRS-USB-88-005| 19 p2702 N88-26069

Macaca rhesus tolerance to + Gz accelerations
19 p2704 N88-26080

USSR space life sciences digest, issue 18
|NASA-CR-3922(21)| 19 p2707 N88-26096

Aerospace medicine and biology: A continuing bibliography with indexes (supplement 313)
|NASA-SP-7011(313)| 20 p2832 N88-26800

Aerospace Medicine and Biology: A continuing bibliography with indexes (supplement 314)
|NASA-SP-7011(314)| 21 p2988 N88-27742

Biorack on Spacelab D1: An overview of the first flight of Biorack, an ESA facility for life sciences research in microgravity
|ESA-SP-1091| 22 p3059 N88-28154

A brief overview of the results of the experiments using the ESA Biorack Facility on the German Spacelab D1 mission 22 p3060 N88-28155

The Biorack facility and its performance during the D1 Spacelab mission 22 p3060 N88-28156

The effects of microgravity on genetic recombination in Escherichia coli --- Spacelab D1 mission
22 p3060 N88-28157

Growth and differentiation of Bacillus subtilis under microgravity conditions 22 p3060 N88-28158

The Antibio experiment --- Spacelab D1 mission
22 p3060 N88-28159

Contraction behavior and protoplasmic streaming in the slime mold Physarum polycephalum (Physarum kinetics) --- Spacelab D1 mission 22 p3060 N88-28160

The Paramecium experiment --- Spacelab D1 mission
22 p3060 N88-28161

The biological clock of Chlamydomonas reinhardii in space 22 p3061 N88-28162

Effect of microgravity on lymphocyte activation --- Spacelab D1 mission 22 p3061 N88-28163

The effect of microgravity on mammalian cell polarization at the ultrastructural level --- Spacelab D1 mission
22 p3061 N88-28164

Graviperception of lentil seedling roots grown in space
22 p3061 N88-28165

Effects of short spaceflights on Drosophila melanogaster embryogenesis and life span 22 p3061 N88-28166

Embryogenesis and organogenesis of Carausius morosus under spaceflight conditions
22 p3061 N88-28167

The role of gravity in the establishment of the dorso/ventral axis in the amphibian embryo --- Spacelab D1 mission 22 p3062 N88-28168

Dosimetric mapping inside Biorack --- Spacelab D1 mission 22 p3062 N88-28169

Biorack thermal performance during the D1 mission --- Spacelab 22 p3062 N88-28170

Biosample: Preservation, handling and observation system synthesis and breadboarding --- Spacelab
|ESA-CR(P)-2609| 24 p3336 N88-29857

Aerospace medicine and biology: A continuing bibliography with indexes (supplement 315)
|NASA-SP-7011(315)| 24 p3407 N88-30281

EXOSAT SATELLITE

The X-ray orbital lightcurves of AR Lac and TY Pyx
04 p0509 N88-13123

Evidence for expanding magnetic loops in coronae of cool stars 04 p0510 N88-13134

Exosat results on the dMe flare Star Wolf 630AB and on VB 8 04 p0512 N88-13151

Investigation of nuclei of active galaxies as well as sources in the Large Magellanic Cloud using the X-ray astronomy satellite EXOSAT
|ETN-88-91494| 11 p1570 N88-19399

The 35-day cycle of Hercules X-1
|MPE-204| 11 p1571 N88-19405

EXOSAT observations of active galaxies in the medium-energy X-ray domain
|ETN-88-91499| 14 p1993 N88-21879

SW UMa and V426 Oph: EXOSAT surprises
19 p2740 N88-26269

EXOSAT observations of Hercules X-1
|MPE-PREPRINT-119| 22 p3164 N88-28841

EXOTHERMIC REACTIONS

Hot-spot reaction in unsustained shocks
|DE87-011781| 01 p0044 N88-10277

The carbon dioxide chaperon efficiency for the reaction H + O2 + M yields HO2 + M from ignition delay times behind reflected shock waves
|NASA-TM-100125| 07 p0830 N88-15036

EXPANDABLE STRUCTURES

NT BALLOONS
NT GAS BAGS
NT HIGH ALTITUDE BALLOONS
NT INFLATABLE STRUCTURES
NT JIMSPHERE BALLOONS

Assessment of the COFSI/MAST I project
|NASA-CR-181366| 01 p0053 N88-10340

EXPANSION

NT GAS EXPANSION
NT SERIES EXPANSION
NT THERMAL EXPANSION

The expansion of magnetic clouds
01 p0115 N88-10737

Singularity expansion method: Target Resonances
03 p0303 N88-11912

Cosmology with decaying vacuum energy
|DE88-000698| 03 p0389 N88-12443

Pulse-mode expansions and refractive indices in plane-wave propagation
|DE88-001328| 04 p0437 N88-12714

Qualification of expansion and joint welding procedures of tube-to-tubesheet joints for heat exchangers in nuclear power plants
|DE87-703526| 05 p0589 N88-13592

Bubble expansion and collapse studies
|DE88-002377| 06 p0699 N88-14290

A directed method for locating the focus of expansion
|AD-A185840| 07 p0906 N88-15491

Harmonic expansion for the magnetic field of the helical solenoid
|DE88-700100| 07 p0928 N88-15638

Post-Newtonian equations of motion in an expanding universe
|DE88-750303| 07 p0945 N88-15744

Evolution from pure states into mixed states in de Sitter space
|DE88-750316| 07 p0945 N88-15745

Calculation of the flow through a single-sided sudden expansion with the Computer Program for Parabolic and Elliptic Flows (COPPEF) computer program
|VTH-LR-523| 09 p1163 N88-16973

Asymptotic expansions for large deviation probabilities in the strong law of large numbers
|AD-A187432| 10 p1402 N88-18361

Piston-driven, unsteady separation at a sudden expansion in a tube: Flow visualization and Laser Doppler Anemometer (LDA) measurements
|ETN-88-92104| 15 p2068 N88-22329

String driven inflation
|DE88-006994| 15 p2151 N88-22841

Cosmology for high energy physicists
|DE88-005705| 15 p2151 N88-22842

Self-similar expansions in ion beam fusion
16 p2278 N88-23635

Dynamic range compression/expansion of light beams by photorefractive crystals
|NASA-CASE-NPO-17140-1-CU|
17 p2438 N88-24508

Turbulent heat transfer and fluid flow measurements downstream of abrupt expansions and in a cavity of a circular tube at a uniform wall temperature
18 p2515 N88-24920

The Department of Defense report on the merit review process for competitive selection of university research projects and an analysis of the potential for expanding the geographic distribution of research for the Committees on Appropriations, United States Congress
|AD-A191842| 18 p2588 N88-25379

Non equilibrium expansion of a radiating gas in a channel of varying section
|DE88-702063| 19 p2665 N88-25845

An interferometric measurement technique for railgun structures
|AD-A192851| 21 p2901 N88-27217

Perturbation expansions generated by an approximate propagator
|DE88-702435| 21 p3011 N88-27866

Velocity measurements downstream of a sudden expansion using the Laser Doppler Velocimeters (LDV) technique. Part 1: Method of measurement and experimental facility
|FOA-C-20700-2.1-PT-1| 22 p3076 N88-28262

Performance of the Los Alamos expanding telescope
|DE88-010924| 22 p3151 N88-28751

Qualification of expansion and welding procedures of tube-to-tubesheet joints for heat exchangers in nuclear power plants
|DE88-701621| 23 p3221 N88-29174

Cosmology in an N-dimensional vector space
|DE88-702550| 23 p3277 N88-29507

EXPANSION WAVES

U ELASTIC WAVES

EXPECTANCY HYPOTHESIS

Object detection in images from outdoor scenes using evidential reasoning
|FOA-C-30461-3.3| 08 p1020 N88-16183

EXPECTATION

Expectations for water level deviations at the delta works: Zierikzee (Netherlands), November 1981-February 1986
|KNMI-TR-93| 05 p0628 N88-13840

Strong consistency of estimation of number of regression variables when the errors are independent and their expectations are not equal to each other
|AD-A186025| 07 p0909 N88-15507

On the expectation of the product of four matrix-valued Gaussian random variables
|EUT-87-E-178| 13 p1828 N88-20927

EXPEDITIONS

Huurre expedition to the North Pole in 1984
|PB87-220935| 04 p0462 N88-12858

Varifront 3 expedition data report (USNS DE STEIGUER CRUISE 1202-82). Bioluminescence, hydrographic, nutrient, and satellite data from the Gulf of California (November-December 1981)
|AD-A185011| 05 p0620 N88-13805

Risk of hypertension and functional cerebral laterality in oil expedition works in far north
12 p1665 N88-19980

Physical, chemical and CTD (Conductivity/Temperature/Depth) data from the Marathon 2 expedition
|AD-A189930| 15 p2099 N88-22507

EXPENDABLE STAGES (SPACECRAFT)

Communications satellite systems operations with the space station. Volume 3: Supplementary technical report
|NASA-CR-180875| 09 p1133 N88-16794

Assessment of mixed fleet potential for space station launch and assembly
|NASA-TM-100550| 11 p1443 N88-18608

EXPERIENCE

Diagnosis: Reasoning from first principles and experiential knowledge 09 p1207 N88-17236

EXPERIMENT DESIGN

NT FACTORIAL DESIGN

Preliminary study of a containerless processing facility for Columbus, executive summary
|ESA-ITT/AO/1-1834/85F| 01 p0032 N88-10203

Investigations of the survey of the reproductive biology of Xiphophorus in an Aquarack
01 p0074 N88-10471

Control design challenges of large space systems and spacecraft control laboratory experiment (SCOLE)
|NASA-CR-178392| 03 p0275 N88-11735

Access to microgravity: A technical description of the NAE T-33 microgravity facility
|NAE-AN-47| 04 p0405 N88-12518

Experimental use of artificial intelligence for (future) ATC systems
|PB87-106449| 04 p0482 N88-12970

Controlled Ecological Life Support System: Design, Development, and Use of a Ground-Based Plant Growth Module
|NASA-CP-2479| 05 p0630 N88-13852

CELSS Program Meeting 05 p0630 N88-13853

Controlled ecological life support systems: Development of a plant growth module 05 p0630 N88-13854

CP-1-H analysis tests 06 p0691 N88-14236

The standard theory group: Summary and conclusions
|PREPRINT-551| 06 p0778 N88-14776

A possible accelerator experiment to solve the solar neutrino puzzle
|PREPRINT-556| 06 p0778 N88-14778

Overview of the TIBER 2 (Thermal Ignition/Burn Experimental Reactor) design
|DE88-001892| 06 p0783 N88-14804

Allowable gravity-levels for Spacelab, Columbus and EURECA --- materials science
[BF-R-66 525-2] 07 p0838 N88-15084

Optimal repeated measurements designs for comparing test treatments with a control
[AD-A185999] 07 p0917 N88-15569

Tether Elevator Crawler Systems (TECS)
07 p0927 N88-15631

The ESA Anthrorack project: Integrated research in human physiology 08 p1033 N88-16265

Basic physics program for a low energy antiproton source in North America
[DE88-003148] 08 p1082 N88-16522

Microphysics of the auroral acceleration region of other regions of the magnetosphere 08 p1096 N88-16592

Microgravity payloads and missions for Space Station: Some issues affecting compatibility with other payloads
09 p1129 N88-16783

The challenge of G-376 10 p1288 N88-17705

The NORSTAR Program: Space shuttle to space station 10 p1289 N88-17710

Annotated computer output for split plot design: GENSTAT ANOVA
[AD-A187120] 10 p1385 N88-18271

Experimental aspects of hypernuclear physics at CEBAF
[CEBAF-R-86-013] 11 p1546 N88-19245

Promising concepts for ground-to-orbit experiment teleoperation --- Columbus 12 p1590 N88-19518

Ground based supervisory and programming system for automatic experiment execution in orbit
12 p1590 N88-19519

Life sciences research in space: The requirement for animal models 12 p1654 N88-19909

Implications of shiftwork in space for human physiology experiments 12 p1659 N88-19942

Some reflections on the standardization of bed-rest procedures for weightlessness simulation (cardiovascular and endocrine apsects) 12 p1662 N88-19961

Animal research on the Space Station
12 p1662 N88-19964

Interfacial adhesion: Theory and experiment
[NASA-TM-100830] 13 p1742 N88-20417

Three-dimensional shear layer experiments and their use as test cases for calculation methods
[NLR-MP-86036-U] 13 p1767 N88-20570

Experimental verification of a finite-difference time-domain thin slot algorithm
[DE88-005572] 13 p1817 N88-20859

Equipment test methods for externally produced electromagnetic transients
[RAE-TM-FS(F)-457] 14 p1865 N88-21140

Recommended test specification for the electromagnetic compatibility of aircraft equipment
[RAE-TM-FS(F)-510] 14 p1867 N88-21155

Efficient monotone sequential design
[CWI-MS-R8705] 14 p1962 N88-21707

Simulation of cometary nuclei
14 p2005 N88-21954

Short experiment study of four-wire helical antennas (half turn half wave)
[CNES-CT/DRT/TIT/AN-249-T]
15 p2058 N88-22266

Experimental design and structural optimization
[PB88-169255] 15 p2087 N88-22436

Experimental study on the influence of wind on acoustic pressure sensors
[ISL-R-121/86] 15 p2131 N88-22712

The German Front Experiment 1987: Experimental design
[DFVLR-MITT-87-24] 16 p2234 N88-23343

The WOCE Core Project Planning Meeting on the Gyre Dynamics Experiment --- ocean dynamics
[WCP-139] 16 p2236 N88-23358

Experimental design and structural optimization
[ETN-88-92232] 16 p2257 N88-23492

Analysis of means in some nonstandard situations
[ETN-88-92247] 16 p2262 N88-23522

Operational facilities of EURECA A1 mission
[ETN-88-91939] 18 p2496 N88-24810

Study of flow tracer behavior models and experimental validation with multiple exposure holographic velocimetry
[IMFL-87/30] 20 p2801 N88-26622

Simulation of the neutronic characteristics of large fast neutron reactors
[ETN-88-92305] 20 p2853 N88-26940

Fluid physics double rack --- Spacelab
[SD-TN-AI-012] 24 p3358 N88-29992

Accommodation concept for fluid physics facilities, volume 2 --- Spacelab
[SG-TN-AI-027-VOL-2] 24 p3358 N88-29994

EXPERIMENTAL AIRCRAFT

U RESEARCH AIRCRAFT

EXPERIMENTAL BREEDER REACTOR 2

Pattern-recognition software detecting the onset of failures in complex systems
[DE88-002861] 09 p1220 N88-17318

EXPERIMENTATION

NT PHYSICS AND CHEMISTRY EXPERIMENT IN SPACE

Dynamics of spacecraft control laboratory experiment (SCOLE) slew maneuvers
[NASA-CR-4098] 01 p0014 N88-10082

A plethysmograph for measuring pulmonary ventilation in small animals
[AD-A184978] 05 p0629 N88-13846

Experimental Radio Data System (RDS): A survey of reception reliability in the UK
[BBC-RD-1987/17] 09 p1155 N88-16922

On-orbit technology experiment facility definition
[NASA-TM-100614] 17 p2311 N88-23824

Modeling, designing and simulating a pointing control system for balloon-borne solar experiments
[NASA-TM-100337] 22 p3082 N88-28300

EXPERT SYSTEMS

Data Model of Objects and Relations (DAMOR): A data model for knowledge representation
[REPT-87-05] 01 p0085 N88-10553

Knowledge Based Concepts and Artificial Intelligence Applications to Guidance and Control
[AGARD-LS-155] 02 p0128 N88-10806

Overview of AGARD Lecture Series No. 155: Knowledge-based concepts and artificial intelligence applications to guidance and control
02 p0128 N88-10807

AI expert system technology issues for guidance and control applications 02 p0128 N88-10808

DEDALE: An expert system for analog circuit maintenance 02 p0128 N88-10809

An expert system for aircraft conflict resolution in dense airspaces 02 p0129 N88-10810

Towards the unmanned cockpit
02 p0129 N88-10812

Generating diagnostic knowledge from a structural and functional description 02 p0129 N88-10813

A review of the knowledge engineering process
02 p0129 N88-10814

A rule-based system for arrival sequencing and scheduling in air traffic control 02 p0129 N88-10815

How to use PROLOG for expert system programming
02 p0129 N88-10816

Real-time expert systems: A status report
02 p0129 N88-10817

Mesoscale thunderstorm forecasting using RAOB data, surface mesonet observations, and an expert system
02 p0206 N88-11293

Contribution to the development of smart design techniques for VLSI integrated circuits --- CMOS
[LAAS-87-181] 02 p0221 N88-11395

Semantic network processing systems --- artificial intelligence
[OUEL-1677/87] 02 p0223 N88-11401

Synthesizing controllers for uncertain systems by a quantitative pole-placement
[PB87-195590] 02 p0223 N88-11403

On the relational modeling of discrete PDE problems
[DE87-013336] 02 p0224 N88-11409

RANDOM NUMBER: A syntax-directed package to produce random numbers in user-specified, univariate distributions. User's guide
[DE87-014278] 02 p0228 N88-11436

Knowledge acquisition issues encountered during the development of an estimating expert system
[DE87-013320] 02 p0248 N88-11568

JPRS report: Science and technology. China
[JPRS-CST-87-026] 03 p0269 N88-11688

Diagnostics aid for mass spectrometer trouble-shooting
[DE88-000350] 03 p0324 N88-12049

The user's guide to the BACK system --- knowledge representation
[KIT-42] 03 p0367 N88-12310

A prototype expert system for separation science
[DE87-013542] 03 p0371 N88-12333

Potential applications of expert systems and operations research to space station logistics functions
[NASA-CR-180473] 03 p0372 N88-12342

An evaluation plan of bus architectures and protocols using the NASA Ames intelligent redundant actuation system
[NASA-CR-177458] 04 p0398 N88-12482

Expert robots in nuclear plants
[DE87-014839] 04 p0452 N88-12800

Experimental use of artificial intelligence for (future) ATC systems
[PB87-106449] 04 p0482 N88-12970

The characterization of diagnostic tasks for engineering systems
[DE88-000093] 04 p0483 N88-12973

An expert system for materials design
[DE88-000191] 04 p0483 N88-12974

GOLD: Integration of model-based control systems with artificial intelligence and workstations
[DE88-000506] 04 p0483 N88-12976

GOLD: Integration of model-based control systems with artificial intelligence and workstations
[DE88-000706] 04 p0483 N88-12977

Intelligent signal analysis and recognition
[NASA-CR-181531] 04 p0501 N88-13084

ZEUS: A knowledge-based expert system that assists in predicting visibility at airbases
[AD-A184197] 05 p0626 N88-13829

A single-station weather forecasting expert system
[AD-A184889] 05 p0627 N88-13832

XCUT: A rule based expert system for the automated process planning of machined parts
[DE87-011638] 05 p0639 N88-13905

Using hierarchically structured problem-solving knowledge in a rule-based process planning system
[DE87-011639] 05 p0639 N88-13906

Computer architectures for artificial intelligence
[PB87-123824] 06 p0761 N88-14671

Knowledge acquisition for a simple expert controller
[NASA-TT-20118] 06 p0761 N88-14672

Using user models and automatic expertise acquisition in data base interactions
[PB87-234357] 06 p0791 N88-14848

National Aeronautics and Space Administration (NASA)/American Society for Engineering Education (ASEE) Summer Faculty Fellowship Program, 1987, Volume 2
[NASA-CR-172009-VOL-2] 06 p0796 N88-14874

A general architecture for intelligent training systems
06 p0796 N88-14875

Dynamics, control and sensor issues pertinent to robotic hands for the EVA retriever system
06 p0796 N88-14876

Tools and technologies for expert systems: A human factors perspective 06 p0797 N88-14882

Development of a prototype H-46 helicopter diagnostic expert system
[AD-A186077] 07 p0809 N88-14924

Expert system study for spacecraft management
[TL-2699-ISS-1] 07 p0824 N88-15004

Intelligent controllers
[DE88-001862] 07 p0904 N88-15475

Integration of symbolic and algorithmic hardware and software for the automation of space station subsystems
[NASA-TM-89705] 07 p0907 N88-15497

Proceedings of the Second International Symposium on Methodologies for Intelligent Systems: Colloquia program
[DE88-001490] 07 p0907 N88-15498

Investigation of candidate data structures and search algorithms to support a knowledge based fault diagnosis system 07 p0923 N88-15606

Microprocessor control and networking for the amps breadboard 07 p0924 N88-15615

Expert system technology 07 p0926 N88-15628

Expert system development for commonality analysis in space programs 07 p0928 N88-15635

A knowledge-based object recognition system for applications in the space station
[NASA-CR-182411] 08 p0989 N88-15991

Cirrus: An automated protocol analysis tool
[AD-A186646] 08 p1052 N88-16348

Third Conference on Artificial Intelligence for Space Applications, part 1
[NASA-CP-2492-Pt-1] 08 p1055 N88-16360

Verification issues for rule-based expert systems
08 p1055 N88-16361

Using output to evaluate and refine rules in rule-based expert systems 08 p1055 N88-16362

Temporal and contextual knowledge in model-based expert systems 08 p1055 N88-16363

An easy-to-use diagnostic system development shell
08 p1055 N88-16366

An inference engine for embedded diagnostic systems
08 p1056 N88-16367

CLIPS: An expert system tool for delivery and training
08 p1056 N88-16368

Integration of symbolic and algorithmic hardware and software for the automation of space station subsystems
08 p1056 N88-16373

HSTDEK: Developing a methodology for construction of large-scale, multi-use knowledge bases
08 p1057 N88-16377

Knowledge-based monitoring of the pointing control system on the Hubble space telescope
08 p1057 N88-16378

A distributed architecture for intelligent monitoring and anomaly diagnosis of the Hubble Space Telescope
08 p1057 N88-16379

A knowledge-based system for monitoring the electrical power system of the Hubble Space Telescope 08 p1058 N88-16380

Artificial intelligence and space power systems automation 08 p1058 N88-16381

Embedded expert system for space shuttle main engine maintenance 08 p1058 N88-16382

Exploring hypotheses in attitude control fault diagnosis 08 p1058 N88-16384

EUREX D: An expert system for failure diagnosis and recovery in the TCS of the European retrievable carrier EURECA 08 p1058 N88-16385

Expert systems relations in space applications 08 p1059 N88-16391

Problem solving as intelligent retrieval from distributed knowledge sources 08 p1059 N88-16392

Application of parallel distributed processing to space based systems 08 p1059 N88-16393

Spacelab Data Processing Facility (SLDPF) quality assurance expert systems development 08 p1059 N88-16394

ESSAA: Embedded system safety analysis assistant 08 p1060 N88-16396

Intelligent process development of foam molding for the Thermal Protection System (TPS) of the space shuttle external tank 08 p1060 N88-16397

Space shuttle main engine anomaly data and inductive knowledge based systems: Automated corporate expertise 08 p1060 N88-16398

An expert system to analyze high frequency dependent data for the space shuttle main engine turbopumps 08 p1060 N88-16399

Interactive knowledge acquisition tools 08 p1060 N88-16401

Real time AI expert system for robotic applications 08 p1061 N88-16408

Commonality analysis as a knowledge acquisition problem 08 p1062 N88-16413

Qualitative models for planning: A gentle introduction 08 p1062 N88-16414

Operational aspects of a spacecraft planning/scheduling expert system 08 p1062 N88-16415

Planning activities in space 08 p1063 N88-16417

Interfacing the expert: Characteristics and requirements for the user interface in expert systems 08 p1063 N88-16419

Conceptual information processing: A robust approach to KBS-DBMS integration 08 p1063 N88-16422

The intelligent user interface for NASA's advanced information management systems 08 p1063 N88-16424

Scheduling spacecraft operations 08 p1064 N88-16426

The resource envelope as a basis for space station management system scheduling 08 p1064 N88-16427

Prototype resupply scheduler 08 p1064 N88-16428

Case-based reasoning for space applications: Utilization of prior experience in knowledge-based systems 08 p1065 N88-16433

Knowledge representation by connection matrices: A method for the on-board implementation of large expert systems 08 p1065 N88-16434

RB-ARD: A proof of concept rule-based abort 08 p1065 N88-16435

A learning apprentice for software parts composition 08 p1065 N88-16436

Automatic program generation from specifications using Prolog 08 p1065 N88-16437

On acquisition of programming knowledge 08 p1065 N88-16438

A framework for real-time distributed expert systems: On-orbit spacecraft fault diagnosis, monitoring and control 08 p1066 N88-16440

TES: A modular systems approach to expert system development for real time space applications 08 p1066 N88-16441

Prototype space station automation system delivered and demonstrated at NASA 08 p1066 N88-16442

Applications of expert systems for satellite autonomy 08 p1066 N88-16443

The crustal dynamics intelligent user interface anthology [NASA-TM-100693] 08 p1067 N88-16448

Dynamic function allocation in fighter cockpits [AD-A185397] 09 p1201 N88-17199

First Annual Workshop on Space Operations Automation and Robotics (SOAR 87) [NASA-CP-2491] 09 p1203 N88-17206

Space shuttle onboard navigation console expert/trainer system 09 p1203 N88-17208

MPAD MCC workstation system: ADDAM and EEVE 09 p1203 N88-17209

Knowledge based jet engine diagnostics 09 p1203 N88-17210

Simplifying the construction of domain-specific automatic programming systems: The NASA automated software development workstation project 09 p1204 N88-17212

The knowledge-based software assistant 09 p1204 N88-17213

An intelligent training system for payload-assist module deploys 09 p1204 N88-17214

Development of a coupled expert system for the spacecraft attitude control problem 09 p1205 N88-17223

The desktop interface in intelligent tutoring systems 09 p1205 N88-17225

Approaches to the verification of rule-based expert systems 09 p1206 N88-17232

A formal approach to validation and verification for knowledge-based control systems 09 p1207 N88-17233

Expert system verification concerns in an operations environment 09 p1207 N88-17234

Building validation tools for knowledge-based systems 09 p1207 N88-17235

Diagnosis: Reasoning from first principles and experiential knowledge 09 p1207 N88-17236

Verifying shuttle onboard software using expert systems 09 p1207 N88-17237

Design knowledge capture for the space station 09 p1208 N88-17239

CONFIG: Qualitative simulation tool for analyzing behavior of engineering devices 09 p1208 N88-17240

The empirical accuracy of uncertain inference models 09 p1208 N88-17243

Robotic planner expert system (RPLANES) 09 p1209 N88-17246

Expert mission planning and replanning scheduling system for NASA KSC payload operations 09 p1209 N88-17247

Trimodal interpretation of constraints for planning 09 p1209 N88-17248

Advanced decision aiding techniques applicable to space 09 p1209 N88-17250

Automatic routing module 09 p1210 N88-17251

SWAN: An expert system with natural language interface for tactical air capability assessment 09 p1210 N88-17253

Expert system applications in spacecraft subsystem controllers 09 p1210 N88-17254

The KATE shell: An implementation of model-based control, monitor and diagnosis 09 p1210 N88-17255

Beyond rules: The next generation of expert systems 09 p1210 N88-17256

TDAS: The Thermal Expert System (TEXSYS) data acquisition system 09 p1211 N88-17258

Implementing clips on a parallel computer 09 p1211 N88-17259

An efficient representation of spatial information for expert reasoning in robotic vehicles 09 p1214 N88-17278

A type-oriented approach to knowledged-based systems [MA-47] 09 p1222 N88-17329

Management of complex information in support of evolving autonomous expert systems [AD-A186680] 09 p1224 N88-17337

An expert system to support the verification/validation of flight-critical software [MBB-UT-102/87] 10 p1314 N88-17852

Methods of eliciting information from experts [AD-A187468] 10 p1372 N88-18189

Archetyping: A knowledge-based reuse paradigm 10 p1376 N88-18214

Optical symbolic processor for expert system execution [AD-A187494] 10 p1385 N88-18268

A computer simulation study of an expert system for walking machine motion planning [AD-A187907] 11 p1438 N88-18577

The metallurgical database of Aladin: An alloy de sign system [AD-A187724] 11 p1457 N88-18682

Rocketdyne automated dynamics data analysis and management system 11 p1499 N88-18954

Optical symbolic processor for expert system execution [AD-A187882] 11 p1525 N88-19103

Feasibility study of generating plans and strategies for software testing by knowledge based system [AD-A187834] 11 p1529 N88-19134

Evaluating expert system tools: A framework and methodology-workshops [AD-A187190] 11 p1533 N88-19159

Application of knowledge based systems to the maintenance of inertial system electronics 12 p1578 N88-19441

Robotic intelligence issues for space manipulator monitoring, control programming 12 p1588 N88-19504

On a knowledge based assisted system for highly autonomous control of experiment-manipulators in the Man-Tended Free Flyer 12 p1588 N88-19505

A knowledge-based approach for sensory controlled assembly operations 12 p1588 N88-19506

Treatment of unforeseen situations by online knowledge-based diagnostic systems --- spacecraft maintenance 12 p1589 N88-19511

NAVARES: A prototype expert system for NAVSTAR anomaly resolution [AD-A189491] 12 p1600 N88-19579

Regenerative life support system research [NASA-CR-182606] 12 p1671 N88-20006

Expert systems: Their impact on performance and cognitive strategies in diagnostic inference [AD-A188518] 12 p1677 N88-20027

Knowledge-based system analysis and control [AD-A188163] 12 p1681 N88-20049

Physics for robots [AD-A189056] 12 p1682 N88-20054

Northeast Artificial Intelligence Consortium (NAIC) administrative matters and ancillary functions, volume 1 [AD-A189466] 12 p1682 N88-20055

The concept of intelligent integrated interactive CAD systems [CWI-CS-R8717] 13 p1818 N88-20865

Organization of design knowledge in an intelligent CAD environment [CWI-CS-R8720] 13 p1819 N88-20868

An integrated data description language for coding design knowledge [CWI-CS-R8731] 13 p1819 N88-20871

An implementation of the OPS5 language for computers compatible with IBM-PC [INPE-4291-PRE/1162] 13 p1821 N88-20882

Expert system techniques and decision support system: A case study (Dec. 1985 - Jun. 1986) [ETN-88-91347] 13 p1821 N88-20884

The use of an automated flight test management system in the development of a rapid-prototyping flight research facility [NASA-TM-100435] 13 p1823 N88-20896

SEAT: A strategic engagement analysis tool [DE88-000498] 13 p1830 N88-20944

Expert systems for decision support in military aircraft mission preparation [NLR-MP-87013-U] 13 p1830 N88-20946

Consistency of rule-based expert systems [CWI-CS-R8736] 13 p1831 N88-20950

Application of expert systems in project management decision aiding [NASA-CR-180762] 13 p1850 N88-21074

A menu-driven knowledge retrieval system accessing ASCII data [DE88-001742] 13 p1851 N88-21079

Oceanographic export system development, year 1 [AD-A189134] 14 p1950 N88-21623

Implementing embedded artificial intelligence rules within algorithmic programming languages [NASA-CR-178393] 14 p1959 N88-21686

Parallel processes in the knowledge based system HYDRA [REPT-87-38] 14 p1960 N88-21689

Conception of a knowledge-based system for designing distributed systems [DFVLR-MITT-87-16] 14 p1961 N88-21694

Representing knowledge in two distinct descriptions: Extensional vs. intensional [CWI-CS-R8728] 14 p1961 N88-21699

Kalman filter residual expert system [AD-A190520] 15 p2020 N88-22041

Characteristics of LSI-wiring expert system discussed 15 p2052 N88-22226

An expert system for discrete component digital circuit design [AD-A189680] 15 p2059 N88-22274

Inference engine for expert systems [INPE-4465-TDL/321] 15 p2113 N88-22590

Design and implementation of a parallel computer for expert system applications [DE88-005288] 15 p2115 N88-22601

Memory-based expert systems [AD-A190203] 15 p2116 N88-22606

Rapid prototyping of simulations in artificial intelligence environments [DE88-004295] 15 p2117 N88-22612

Rapid prototyping of complex avionics system architectures [ETN-88-92275] 16 p2162 N88-22898

The use of rule induction to assist in the diagnosis of avionic circuit board defects
[ETN-88-92077] 16 p2162 N88-22899
Design as a formal, knowledge engineered activity
[CWI-CS-R8744] 16 p2248 N88-23431
Knowledge engineering in design
[CWI-CS-R8745] 16 p2248 N88-23432
STRUTEX: A prototype knowledge-based system for initially configuring a structure to support point loads in two dimensions
[NASA-TM-100613] 16 p2250 N88-23448
Intelligent systems interconnection: What should come after open systems interconnection?
[CWI-CS-R8742] 16 p2253 N88-23465
Automatic control of an industrial process and computer aided process control by means of an expert system
[LAAS-88-004] 16 p2255 N88-23476
Identification of control structures --- expert systems
[REPT-87-65] 16 p2255 N88-23479
Architecture and role of the Sensor Subsystem in future aircraft weapon systems 17 p2302 N88-23770
Rapid prototyping of complex avionic system architectures 17 p2302 N88-23771
Psychosensory cockpit ergonomics, advantages of intelligent information systems 17 p2304 N88-23784
A proposal of adaptation of a knowledge-based scene analysis model to some remote sensing problems
17 p2354 N88-24026
A proposal of adaptation of a knowledge-based scene analysis model to some remote sensing problems
17 p2362 N88-24068
Fault diagnosis in orbital refueling operations
17 p2381 N88-24154
Third Conference on Artificial Intelligence for Space Applications, part 2
[NASA-CP-2492-PT-2] 17 p2387 N88-24188
Integration of symbolic and algorithmic hardware and software for the automation of space station subsystems
17 p2387 N88-24190
Connecting remote systems for demonstration of automation technologies 17 p2387 N88-24191
Knowledge based system verification and validation as related to automation of space station subsystems: Rationale for a knowledge based system lifecycle
17 p2387 N88-24192
TALOS: A distributed architecture for intelligent monitoring and anomaly diagnosis of the Hubble Space Telescope 17 p2388 N88-24193
Genetic algorithms for adaptive real-time control in space systems 17 p2388 N88-24195
TES: A modular systems approach to expert system development for real-time space applications
17 p2388 N88-24197
Expert systems approach to modeling systems with the ATHENA thermal-hydraulics code
17 p2416 N88-24365
Knowledge based systems in nondestructive evaluation
[DE88-006653] 18 p2525 N88-24981
Timesharing performance as an indicator of pilot mental workload
[NASA-CR-182807] 18 p2552 N88-25150
Application of flight systems methodologies to the validation of knowledge-based systems
[NASA-TM-100442] 18 p2561 N88-25207
Optical symbolic processor for expert system execution
[AD-A192005] 18 p2575 N88-25296
Ultrasonic and video computerized data acquisition for automated welding
[DE88-006741] 19 p2677 N88-25918
BOLETIM: An expert system for weather forecasting
[INPE-4538-TDL/329] 19 p2693 N88-26011
Automation tools for demonstration of goal directed and self-repairing flight control systems
[NASA-CR-179433] 19 p2715 N88-26121
An expert system model using predicate transition nets
[AD-A191953] 19 p2718 N88-26141
Modeling and evaluation of expert systems in decisionmaking organizations
[AD-A191951] 19 p2739 N88-26260
A comparative study of project estimating tools
[DE88-009059] 19 p2740 N88-26266
Intelligent guidance and control for wind shear encounter
[NASA-CR-183060] 20 p2755 N88-26347
A reusable rocket engine intelligen control
[NASA-TM-100963] 20 p2766 N88-26401
Preliminary study within a project for the development of intelligent assistance to piloting: Formal description of combat pilot expertise and implementation of an interactive system to represent operations
[CERMA-87-31] 20 p2833 N88-26806
Delfi-3 as a development environment for expert systems
[REPT-8767] 20 p2839 N88-26845
A network approach to the certainty factor model --- expert systems
[CWI-CS-R8757] 20 p2840 N88-26852
Expert system application education project
[NASA-CR-183089] 20 p2843 N88-26867
NEXT: An expert system development tool to support engineering design
[NLR-MP-86070-U] 20 p2843 N88-26871
Combining expert opinions: An optimization framework
[REPT-87-84] 20 p2846 N88-26895
Computer science and technology: Knowledge-based system for physical database design
[PB88-193289] 20 p2882 N88-27109
Knowledge representation in geographic information systems
[ETN-88-92470] 20 p2882 N88-27112
EXSAT: Expert system to configure telecommunication satellites
[SNIAS-881-440-101] 21 p2902 N88-27223
United States Air Force Graduate Student Summer Support Program, volume 2
[AD-A191122] 21 p2924 N88-27355
Investigation of expert system design approaches for electronic design environments
21 p2926 N88-27365
An investigation of performance improvement in knowledge-based control systems
21 p2928 N88-27382
Computer-Aided Engineering (CAE) for engineering design 21 p2929 N88-27390
The MELCOM PSI 2 AI workstation
21 p2930 N88-27395
Motor-response learning at a process control panel by an autonomous robot
[DE88-005055] 21 p2955 N88-27554
Vapor Compression Distillation Subsystem (VCDS) component enhancement, testing and expert fault diagnostics development, volume 2
[NASA-CR-172076] 21 p2994 N88-27755
Implementation of an OPS5 derivative on the Novix RISC processor
[DE88-011392] 21 p2994 N88-27758
Block Oriented Simulation System (BOSS)
[NASA-CR-182947] 21 p2995 N88-27760
Benefits of an object approach in a computer aided design environment
[SNIAS-881-440-102] 21 p3000 N88-27791
Intelligent Mobile Autonomous System (IMAS)
[AD-A193181] 21 p3003 N88-27811
Introduction to artificial intelligence and expert systems
[SNIAS-881-320-101] 21 p3004 N88-27814
Expert system contribution to logistics improvement
[SNIAS-881-320-102] 21 p3004 N88-27815
Faultfinder: A diagnostic expert system with graceful degradation for onboard aircraft applications
22 p3035 N88-28018
Heat exchanger demonstration expert system
22 p3066 N88-28193
From the extraction of linear networks towards following of them on SPOT images with the help of a knowledge-based interpretation system
22 p3113 N88-28494
Rule-based circuit optimization for CMOS VLSI
22 p3137 N88-28649
Cooperating knowledge-based systems
[NASA-CR-183109] 23 p3247 N88-29327
Second Conference on Artificial Intelligence for Space Applications
[NASA-CP-3007] 23 p3251 N88-29351
Space station as a vital focus for advancing the technologies of automation and robotics
[IAF-86-62] 23 p3251 N88-29352
A relational data-knowledge base system and its potential in developing a distributed data-knowledge system 23 p3251 N88-29353
Hologram representation of design data in an expert system knowledge base 23 p3251 N88-29354
An expert system for reliability modeling
23 p3252 N88-29355
A software engineering approach to expert system design and verification 23 p3252 N88-29356
Issues on the use of meta-knowledge in expert systems 23 p3252 N88-29357
A knowledge-based decision support system for payload scheduling 23 p3252 N88-29358
Coupling expert systems and simulation
23 p3252 N88-29360
Optimization of low gravity materials processing experiments using expert systems
23 p3252 N88-29361
An approach to combining heuristic and qualitative reasoning in an expert system 23 p3253 N88-29362
Expertise and reasoning with possibility: An explanation of modal logic and expert systems
23 p3253 N88-29363
Analyst-centered models for systems design, analysis, and development 23 p3253 N88-29364
Avionic expert systems 23 p3253 N88-29365
Knowledge elicitation for an operator assistant system in process control tasks 23 p3253 N88-29366
Machine vision for real time orbital operations
23 p3253 N88-29367
Automatic object recognition
23 p3254 N88-29368
Two dimensional convolute integers for machine vision and image recognition 23 p3254 N88-29369
On recognizing ignorance 23 p3254 N88-29372
Expert systems for MSFC power systems
23 p3255 N88-29375
A generic expert system for materials processing in space 23 p3255 N88-29376
ARGES: An expert system for fault diagnosis within space-based ECLS systems 23 p3255 N88-29380
SCARES: A Spacecraft Control Anomaly Resolution Expert System 23 p3256 N88-29381
A scheduling and resource management system for space applications 23 p3256 N88-29383
An expert systems application to space base data processing 23 p3256 N88-29384
Generic supervisor: A knowledge-based tool for control of space station on-board systems
23 p3257 N88-29389
Knowledge based programming environments: A perspective 23 p3258 N88-29393
Knowledge acquisition and rapid protyping of an expert system: Dealing with real world problems
23 p3258 N88-29394
Automated generation of spacecraft activity plans
23 p3258 N88-29396
Intelligent interfaces for expert systems
23 p3258 N88-29397
Requirements for a tool to aid in the development of expert systems for space station applications
23 p3258 N88-29398
Benchmarking expert system tools
23 p3259 N88-29399
Two implementations of the Expert System for the Flight Analysis System (ESFAS) project
23 p3259 N88-29400
Life-span knowledge engineering for space operations
23 p3259 N88-29401
NOA: A Network Operator Assistant for scheduling Tracking and Data Relay Satellite System (TDRSS)
23 p3259 N88-29403
Experiment scheduling for Spacelab missions
23 p3259 N88-29404
The emergence of multi-user expert systems
23 p3260 N88-29406
An expert system for a distributed real-time trainer
23 p3261 N88-29411
Utilization of artificial intelligence techniques for the Space Station power system 23 p3261 N88-29412
A methodology for multiple rule system integration and resolution within a singular knowledge base
23 p3261 N88-29413
Design consideration in constructing high performance embedded Knowledge-Based Systems (KBS)
23 p3261 N88-29415
Validation of expert systems 23 p3262 N88-29416
Mathematical algorithms for approximate reasoning
23 p3262 N88-29418
Real-time space system control with expert systems
23 p3262 N88-29419
A flexible search strategy for production systems
23 p3262 N88-29420
Semantic based man-machine interface for real-time communication 23 p3262 N88-29421
Automated software development workstation
23 p3263 N88-29423
An expert system for natural language processing
23 p3263 N88-29426
Expert system technology as a data processing tool
23 p3263 N88-29427
Next-generation space manipulator
23 p3263 N88-29428
Parallel real-time expert systems
[AD-A193673] 23 p3264 N88-29434
Contribution of expert systems to avionics advance: Application on AS30 laser weapon system
[SNIAS-881-320-103] 23 p3267 N88-29449
Active explanation reduction: An approach to the multiple explanations problem
[AD-A194127] 23 p3276 N88-29501
Threat expert system technology advisor
[NASA-CR-177479] 24 p3328 N88-29816
The 1988 Goddard Conference on Space Applications of Artificial Intelligence
[NASA-CP-3009] 24 p3415 N88-30330

An intelligent training system for space shuttle flight controllers 24 p3415 N88-30331
Artificial intelligence costs, benefits, risks for selected spacecraft ground system automation scenarios 24 p3416 N88-30332
Artificial intelligence in a mission operations and satellite test environment 24 p3416 N88-30334
Automated space vehicle control for rendezvous proximity operations 24 p3416 N88-30335
Automated satellite control in Ada 24 p3416 N88-30336
Knowledge based tools for Hubble Space Telescope planning and scheduling: Constraints and strategies 24 p3417 N88-30338
The proposal entry processor: Telescience applications for Hubble Space Telescope science operations 24 p3417 N88-30339
Candidate functions for advanced technology implementation in the Columbus mission planning environment 24 p3417 N88-30340
A rule-based systems approach to spacecraft communications configuration optimization 24 p3417 N88-30341
MOORE: A prototype expert system for diagnosing spacecraft problems 24 p3418 N88-30343
Achieving real-time performance in FIESTA 24 p3418 N88-30344
Mission telemetry system monitor: A real-time knowledge-based system 24 p3418 N88-30345
Low level image processing techniques using the pipeline image processing engine in the flight telerobotic servicer 24 p3418 N88-30346
An interactive testbed for development of expert tools for pattern recognition 24 p3419 N88-30349
The second generation intelligent user interface for the crustal dynamics data information system 24 p3419 N88-30352
Spacelab data processing facility (SLDPF) Quality Assurance (QA)/Data Accounting (DA) expert systems: Transition from prototypes to operational systems 24 p3420 N88-30353
Automated cataloging and characterization of space-derived data 24 p3420 N88-30354
A design for a ground-based data management system 24 p3420 N88-30355
Automatic mathematical modeling for real time simulation system 24 p3420 N88-30356
A simulation engine: Combining an expert system with a simulation language 24 p3421 N88-30358
The advice taker/inquirer: A system for high-level acquisition of expert knowledge 24 p3421 N88-30359
Verification and validation of rulebased systems for Hubble Space Telescope ground support 24 p3421 N88-30361
The need for a comprehensive expert system development methodology 24 p3421 N88-30362
Knowledge-based integrated information systems engineering: Highlights and bibliography. Knowledge-Based Integrated Information Systems Engineering (KBIISE) Project, volume 1 [AD-A195850] 24 p3435 N88-30449
Technical opinions regarding knowledge-based integrated information systems engineering, volume 8 [AD-A195857] 24 p3436 N88-30454
Knowledge-Based Integrated Information Systems Development Methodologies Plan. Knowledge-Based Integrated Information Systems Engineering (KBIISE) report, volume 2 [AD-A195851] 24 p3436 N88-30455
Information retrieval systems evolve-advances for easier and more successful use 24 p3438 N88-30462

EXPLODING CONDUCTOR CIRCUITS
U CIRCUITS

EXPLORATION
NT MINERAL EXPLORATION
NT OIL EXPLORATION
NT SPACE EXPLORATION
Remote acoustic sounding of ferromanganese nodules 06 p0727 N88-14471
Research on visual information processing with special reference to oculomotor behavior in the areas of exploration, recognition and search [AD-A186598] 08 p1051 N88-16346
Analysis of gases in the earth's crust [PB88-141619] 10 p1354 N88-18093

EXPLORER SATELLITES
NT COSMIC BACKGROUND EXPLORER SATELLITE
NT DYNAMICS EXPLORER 1 SATELLITE
NT EXPLORER 47 SATELLITE
NT EXPLORER 51 SATELLITE
NT EXPLORER 54 SATELLITE
NT EXPLORER 55 SATELLITE
NT INTERNATIONAL SUN EARTH EXPLORER 3
NT INTERNATIONAL SUN EARTH EXPLORERS
NT SOLAR MESOSPHERE EXPLORER
Alouette-ISIS program summary [NASA-CR-180747] 08 p1023 N88-16195
Into the thermosphere: The atmosphere explorers [NASA-SP-490] 10 p1353 N88-18084

EXPLORER 47 SATELLITE
IMP 7 (Explorer 47) trajectory, September 26, 1972 to September 25, 1978 [NASA-CR-182697] 14 p1871 N88-21183

EXPLORER 51 SATELLITE
Into the thermosphere: The atmosphere explorers [NASA-SP-490] 10 p1353 N88-18084

EXPLORER 54 SATELLITE
Into the thermosphere: The atmosphere explorers [NASA-SP-490] 10 p1353 N88-18084

EXPLORER 55 SATELLITE
Into the thermosphere: The atmosphere explorers [NASA-SP-490] 10 p1353 N88-18084

EXPLOSION SUPPRESSION
Correlation of air pressure drop and flame arrestor characteristics for explosion suppression materials [AD-A184960] 05 p0548 N88-13340

EXPLOSIONS
NT AERIAL EXPLOSIONS
NT CHEMICAL EXPLOSIONS
NT GAS EXPLOSIONS
NT NUCLEAR EXPLOSIONS
NT UNDERGROUND EXPLOSIONS
NT UNDERWATER EXPLOSIONS
Chemical analysis of charged Li/SO(sub)2 cells 02 p0163 N88-11026
High explosive simulations of supernovae and the supernova shell fragmentation model of solar system formation [DE87-014708] 02 p0251 N88-11584
General-Purpose Heat Source Safety Verification Test Program: Edge-on flyer plate tests [DE87-006309] 03 p0376 N88-12362
Aircraft fire safety research 04 p0406 N88-12526
Scaling the electromagnetically driven explosive shock simulator 05 p0592 N88-13612
On the simulation of ballistic shock loads 05 p0593 N88-13615
Langlie Test Method Program for use with the HP-41CV/X calculator [DE88-001935] 06 p0687 N88-14210
Analysis and interpretation of satellite fragmentation data 06 p0798 N88-14885
Explosive absorption of laser beam of finite diameter 07 p0921 N88-15597
Blast waves generated by planar detonations [DE88-002219] 09 p1164 N88-16979
Reinforced cocnrete arches under blast and shock environments 09 p1180 N88-17065
NF85: A three-dimensional, air-dynamics computer code for analyzing explosions in structures [DE88-005085] 10 p1331 N88-17953
Modeling of the non-auditory response to blast overpressure [AD-A187397] 10 p1369 N88-18184
Supernova mechanisms: Before and after SN1987a [DE88-003489] 10 p1429 N88-18533
Theoretical investigation of the wave shaping process in a section of ladder fracture tape [MRL-R-1081] 13 p1771 N88-20595
Nuclear and astrophysical evidence on the equation of state [DE88-007397] 18 p2572 N88-25279
Development of an experimental system for studying fast transient ignition phenomena [DE88-011917] 21 p2911 N88-27276
Stochastic geologic effects on near-field ground motions in alluvium [AD-A192315] 21 p2972 N88-27652
Initiation of explosive molten aluminum-water interactions at wet or underwater surfaces [DE88-004686] 23 p3194 N88-29006

EXPLOSIVE DEVICES
NT BOMBS (ORDNANCE)
NT BOOSTERS (EXPLOSIVES)
NT DETONATORS
NT INITIATORS (EXPLOSIVES)
NT PRIMERS (EXPLOSIVES)
NT SHAPED CHARGES
NT TORPEDOES
Influence of shock wave and gas pressure on the behavior of a pyrotechnical device [SNIAS-872-430-111] 05 p0570 N88-13477
Measurement, data analysis and prediction of pyrotechnic shock from pin-pullers and separation joints 09 p1179 N88-17061
Investigation of Super*Zip separation joint [NASA-TM-4031] 15 p2026 N88-22072
Toggle release [NASA-CASE-MSC-21354-1] 18 p2523 N88-24969

EXPLOSIVE FORMING
Characterization of an explosively consolidated rapidly solidified Fe-16Ni-9Cr-5Mo-2Cu alloy powder [DE88-006733] 15 p2041 N88-22162
Superconductor consolidation [DE88-010938] 21 p3024 N88-27949

EXPLOSIVE WELDING
Tool and process for miniature explosive joining of tubes [NASA-CASE-LAR-13662-1] 06 p0711 N88-14359
Evaluation of explosive bonding for patching aluminum with aluminum [AD-A193303] 21 p2913 N88-27285

EXPLOSIVES
NT HMX
NT RDX
NT TETRYL
NT TRINITROTOLUENE
A study of diverging detonation in high-explosive systems [DE87-006070] 01 p0031 N88-10194
Shock measurements on explosives in the supra compressive region [DE87-008423] 01 p0031 N88-10196
Statistical mechanical theory of condensed explosives [DE87-009137] 01 p0031 N88-10197
Optically time-resolved detonation break out [DE87-010340] 01 p0031 N88-10199
Microstructural effects in shock initiation of granular explosives [DE87-011282] 01 p0031 N88-10200
Current experimental and theoretical understanding of detonation waves in heterogeneous solid explosives [DE87-012177] 01 p0032 N88-10201
The use of fiber optics in the determination of temperature and extent of reaction in detonating explosives [DE87-012632] 01 p0094 N88-10612
Pyrotechnic component development at Sandia National Laboratory [DE87-006899] 02 p0154 N88-10967
Hot spots: Subnanometer femtosecond energy localization [DE87-010276] 02 p0155 N88-10968
Visible emission from granular explosives during shock initiation [DE87-012361] 02 p0155 N88-10970
Spectroscopic studies of shocked and detonating explosives [DE87-014216] 02 p0155 N88-10972
High explosive simulations of supernovae and the supernova shell fragmentation model of solar system formation [DE87-014708] 02 p0251 N88-11584
Evaluation of one-sided nuclear magnetic resonance for remote detection of explosives [AD-A184490] 03 p0296 N88-11857
The LLNL 150-mm equation-of-state gun system [DE88-000423] 04 p0405 N88-12519
DOE explosives safety manual [DE88-000831] 04 p0422 N88-12616
High explosive moulding powders from RDX and aqueous polyurethane dispersions [AD-A185026] 05 p0568 N88-13458
Compatibility of explosives: A data base system [PB87-234464] 06 p0687 N88-14208
Calculation evaluation of the boundary conditions of autoinflammation of propulsive charges [PB87-139044] 08 p0974 N88-15890
Organic coatings to improve the storageability and safety of pyrotechnic compositions [AD-A187158] 09 p1150 N88-16889
Mechanism of and particle size effects on shock sensitivity of heterogeneous pressed explosives: Preliminary assessment of binderless RDX in fuze trains [MRL-R-1077] 09 p1150 N88-16892
EXPLO: Explosives thermal analysis computer code [DE88-001938] 10 p1307 N88-17814
An electro-optic explosive igniter [DE88-004728] 11 p1466 N88-18738
Novel analytical X-ray Non-Destructive Evaluation (NDE) tool for quality control of energetic materials [AD-A187737] 11 p1497 N88-18935
A procedure for estimating the crystal densities of organic explosives [AD-A189023] 12 p1613 N88-19646
Ignition and high speed photography of energetic materials with a copper vapor laser [DE88-004831] 12 p1631 N88-19765
Anomalous shock sensitivity/density relationship for RDX-polyethylene wax and related formulations from MRL Small Scale Gap Test (SSGT) measurements [MRL-R-1099] 13 p1739 N88-20399
A comparative assessment of US and UK explosives qualified as replacements for tetryl [MRL-R-1094] 13 p1754 N88-20486

Some properties of Australian produced explosive composition H-6 [MRL-TN-525] 13 p1754 N88-20490

Analysis of explosives. 1: Computer programs for processing of X-ray powder deffraction data [PB88-156898] 14 p1894 N88-21309

Effect of moisture level in PBXW-109(E) (plastic-bonded explosive) mixes on the aging of the cured explosive [AD-A190200] 15 p2048 N88-22202

Static dielectric breakdown strength of condensed heterogeneous high explosives [AD-A191035] 16 p2183 N88-23014

Thermal decomposition studies of explosives for component applications [DE88-007201] 18 p2495 N88-24805

A compatible encapsulant for explosives [DE88-007212] 18 p2495 N88-24806

An extinguisher to quench propellant fires [AD-A190785] 18 p2497 N88-24813

The viscosity of molten TNT [MRL-R-1100] 19 p2622 N88-25553

Research in energetic compounds [AD-A192953] 20 p2781 N88-26494

Deformation, fracture and explosive properties of reactive materials [AD-A193080] 21 p2923 N88-27348

A concept for an electro-optic explosive device [DE88-009696] 21 p2923 N88-27349

Relative flow rates of explosive powders [DE88-010767] 21 p2923 N88-27350

Stochastic geologic effects on near-field ground motions in alluvium [AD-A192315] 21 p2972 N88-27652

Decomposition of energetic materials on the drop-weight impact machine [DE88-009154] 22 p3059 N88-28152

Response of SMA (Shielded Metal Arc) and narrow gap HY80 weldments to explosive shock loading [AD-A195994] 24 p3385 N88-30162

EXPONENTIAL FUNCTIONS

NT LOGARITHMS

The matrix exponential in transient structural analysis 05 p0593 N88-13619

Strong consistency of maximum likelihood parameter estimation of superimposed exponential signals in noise [AD-A186384] 07 p0911 N88-15526

Exponential lower bounds for finding Brouwer fixed points [DE88-002864] 10 p1425 N88-18513

Electromagnetic shadowing by an exponentially distributed rough surface [AD-A189677] 14 p1906 N88-21391

High speed transcendental elementary function architecture in support of the Vector Wave Equation (VWE) [AD-A189746] 15 p2119 N88-22627

A note on phase-type, almost phase type, generalized hyperexponential and Coxian distribution, revision [AD-A191236] 16 p2261 N88-23517

Portable implementation of a generic exponential function in Ada [DE88-007693] 19 p2715 N88-26117

Applications of an exponential finite difference technique [NASA-TM-100939] 22 p3084 N88-28312

EXPONENTS

Nonlinear elliptic problems with critical exponent in shrinking annuli [W-02/87] 23 p3273 N88-29477

EXPORTS

U INTERNATIONAL TRADE

EXPOSURE

High intensity 5 eV O-atom exposure facility for material degradation studies 02 p0135 N88-10847

Effects of solvent exposures on poly(etheretherketone) (PEEK) and PEEK-fiberglass composites [MLM-3405] 03 p0281 N88-11766

Materials preparation and longevity in hyperthermal atomic oxygen 03 p0297 N88-11862

Investigation of the exposure to harmful compounds in the workshop of nondestructive materials testing at Gilze-Rijen (Netherlands) [PML-1985-42] 05 p0623 N88-13816

Effects of aviation fluids on fiber composite material [FOA-C-20674-2.6] 08 p0965 N88-15840

Corrosion and deterioration testing in humid tropic environments [AD-A186917] 10 p1302 N88-17783

Los Alamos optical materials reliability, maintainability, and exposure testing program [DE88-001953] 10 p1409 N88-18404

Chemical cleaning of metal surfaces in vacuum systems by exposure to reactive gases [AD-A188586] 12 p1608 N88-19616

Medical problems related to altitude in: Human performance physiology and environmental medicine at terrestrial extremes. chapter 14 [AD-A188340] 12 p1666 N88-19989

Evaluation of existing total human exposure models [PB88-146840] 15 p2101 N88-22517

Assessment of cochlear damage after microwave irradiation [AD-A193237] 21 p2987 N88-27737

Alternative immersion accelerated testing of coating systems for Naval shoreline facilities 24 p3355 N88-29977

Reduced time frame for predicting coating performance 24 p3356 N88-29979

EXPRESSIONS (MATHEMATICS)

U FORMULAS (MATHEMATICS)

EXTARS

U X RAY STARS

EXTENDED DURATION SPACE FLIGHT

U LONG DURATION SPACE FLIGHT

EXTENSIONS

Personnel occupied woven envelope robot power [NASA-CR-182367] 07 p0856 N88-15196

A note on extended quasi-likelihood [AD-A186318] 07 p0915 N88-15555

EXTENSOMETERS

Strain gages in engineering geodesy [SER-C-320] 01 p0048 N88-10309

Optimization of dilatometer test procedures [DE87-014998] 04 p0447 N88-12769

Small-diameter wire tensile testing [DE88-000835] 04 p0455 N88-12815

Computer grading of extensometers (BS 3846) [NPL-DMA(A)-152] 15 p2108 N88-22560

EXTERNAL COMBUSTION ENGINES

NT STIRLING ENGINES

EXTERNAL STORE SEPARATION

Store separation of nuclear weapons [DE87-010778] 02 p0124 N88-10785

Airframe/store compatibility 05 p0545 N88-13323

Airplane load drop and missile firing: Experimental methods for predicting trajectories [PB87-170494] 09 p1117 N88-16695

Store separation and missile firing from aircraft: Experimental methods for trajectory projection [NASA-TT-20214] 11 p1439 N88-18589

The present status and the future of missile aerodynamics [NASA-TM-100063] 24 p3320 N88-29773

EXTERNAL STORES

Design principles and practices for implementation of MIL-STD-1760 in aircraft and stores [AD-A183724] 01 p0005 N88-10027

Method to predict external store carriage characteristics at transonic speeds [NASA-CR-4170] 22 p3037 N88-28034

Preliminary airworthiness evaluation of the UH-60A/ESSS (External Stores Support System) with HELLFIRE launcher installed [AD-A196187] 24 p3323 N88-29793

EXTERNAL SURFACE CURRENTS

Complex space monofilar approximation of diffraction currents on a conducting half plane [NASA-CR-182883] 16 p2273 N88-23605

EXTERNAL TANKS

Redesign of solid rocket booster/external tank attachment ring for the space transportation system [NASA-TM-100476] 01 p0017 N88-10101

Structural analysis of the space shuttle solid rocket booster/external tank attach ring [NASA-TM-100510] 11 p1446 N88-18618

Orbital analysis of a STS (Space Transportation System) external tank in low earth orbit [AD-A188829] 12 p1593 N88-19542

Modification and development of the external tank hydrogen vent umbilical system for the space shuttle vehicle 14 p1928 N88-21496

External tank gamma ray imaging telescope study. Final review, phase 2 [NASA-CR-179320] 15 p2150 N88-22834

The effects of RCS jet firing on the isolated Orbiter and mated coast phases of the glide return to launch site maneuver at Mach number 6 (IA302B) [NASA-CR-180223] 20 p2766 N88-26403

EXTERNALLY BLOWN FLAPS

NT UPPER SURFACE BLOWN FLAPS

EXTINCTION

NT INTERSTELLAR EXTINCTION

Measurements of iridium and the meteoric impact hypothesis at cretaceous end [DE87-703765] 04 p0521 N88-13200

Carbon monoxide and turbulence-chemistry interactions: Blowoff and extinction of turbulent diffusion flames [AD-A186276] 07 p0828 N88-15025

Optical characterization of tropospheric aerosols [AD-A187839] 11 p1511 N88-19029

SAGE 1 and SAM 2 measurements of 1 micron aerosol extinction in the free troposphere [NASA-CR-182945] 17 p2374 N88-24121

Dynamics of propellant ignition 19 p2628 N88-25590

Extinction behavior of low voltage switching arc under consideration of cathodic coatings and dynamic arc column [ETN-88-92384] 20 p2796 N88-26591

Evaluation of atmospheric effects for operational tactical decision aid [AD-A194205] 23 p3232 N88-29236

Optical measurements of soot in premixed flames [NASA-TM-101305] 24 p3373 N88-30090

A compilation of information and data on the Manson impact structure [NASA-CR-183169] 24 p3401 N88-30258

Intermediate polars observed in Brazil in the last eight years [INPE-4567-PRE/1308] 24 p3454 N88-30559

EXTINGUISHERS

U FIRE EXTINGUISHERS

EXTINGUISHING

Spacecraft fire detection and extinguishment: A bibliography [NASA-CR-180880] 11 p1444 N88-18612

An extinguisher to quench propellant fires [AD-A190785] 18 p2497 N88-24813

Extinguishing agent for magnesium fire, phases 5 and 6 [AD-A192436] 21 p2930 N88-27398

Ignition and extinguishing of a Solid Fuel Ramjet (SOFRAM) [FOA-C-20713-2.1] 24 p3337 N88-29865

EXTRACTION

NT GEOTHERMAL ENERGY EXTRACTION

NT ION EXTRACTION

Low extractable wipers for cleaning space flight hardware 02 p0137 N88-10863

Increasing the rate at which ceramic castings undergo preliminary heat-treatment in an ultra-high frequency magnetic field 14 p1886 N88-21275

Automatic line network extraction from aerial imagery of urban areas through knowledge based image analysis [AD-A193067] 21 p2965 N88-27615

Uses of lunar sulfur [DE88-009119] 21 p3031 N88-27990

Design criteria for extraction with chemical reaction and liquid membrane permeation [NASA-TT-20352] 24 p3343 N88-29899

EXTRAGALACTIC LIGHT

U EXTRATERRESTRIAL RADIATION

U LIGHT (VISIBLE RADIATION)

EXTRAGALACTIC MEDIA

U INTERGALACTIC MEDIA

EXTRAGALACTIC RADIO SOURCES

NT RADIO GALAXIES

NT RADIO JETS (ASTRONOMY)

Neutron stars observations as astrophysical probes 06 p0800 N88-14896

VLBI research on OH-maser IN W33 08 p1001 N88-16064

Relativistic jet models for the BL Lacertae object Mrk 421 during three epochs of observation [NASA-TM-89727] 13 p1853 N88-21090

EXTRAPOLATION

Operational experiment in very short range forecast of precipitation 02 p0204 N88-11280

Extrapolation of extremum values of the wind velocity 08 p1015 N88-16150

Report of Atmospheric-Canopy Exchange Panel [DE88-004478] 14 p1944 N88-21597

Comparison of results based on a deterministic versus a statistical uncertainty analysis [DE88-010751] 21 p3010 N88-27858

Application of sampling techniques to near-field far-field transformation [ESA-CR(P)-2546] 24 p3359 N88-30002

Convergence acceleration for vector sequences and applications to computational fluid dynamics [NASA-TM-101327] 24 p3424 N88-30377

EXTRATERRESTRIAL ENVIRONMENTS

NT CHROMOSPHERE

NT EARTH ORBITAL ENVIRONMENTS

NT INTERPLANETARY SPACE

NT INTERSTELLAR SPACE

NT JUPITER ATMOSPHERE

NT MARS ATMOSPHERE

NT MARS ENVIRONMENT

NT NEPTUNE ATMOSPHERE

NT PLANETARY ATMOSPHERES

NT PLANETARY ENVIRONMENTS

NT PLANETARY IONOSPHERES

NT SATELLITE ATMOSPHERES

NT SATURN ATMOSPHERE
NT SOLAR ATMOSPHERE
NT STELLAR ATMOSPHERES
NT URANUS ATMOSPHERE
NT VENUS ATMOSPHERE
NT VENUS CLOUDS

EXTRATERRESTRIAL INTELLIGENCE
The Telecommunications and Data Acquisition Report
[NASA-CR-181546] 04 p0432 N88-12679
Intelligent signal analysis and recognition
[NASA-CR-181531] 04 p0501 N88-13084

EXTRATERRESTRIAL LIFE
Publications of the exobiology program for 1986: A special bibliography
[NASA-TM-4029] 09 p1203 N88-17205
European activities in exobiological research in space
12 p1657 N88-19929

EXTRATERRESTRIAL MATTER
NT COSMIC PLASMA
NT DARK MATTER
NT INTERPLANETARY GAS
NT INTERSTELLAR GAS
NT INTERSTELLAR MATTER
NT NEUTRAL GASES
Products from cosmic-ray interactions in extraterrestrial matter: What they tell us about radiation backgrounds in space
[DE88-009143] 19 p2743 N88-26288

EXTRATERRESTRIAL RADIATION
NT EXTRATERRESTRIAL RADIO WAVES
NT GALACTIC COSMIC RAYS
NT GALACTIC RADIATION
NT GALACTIC RADIO WAVES
NT GAMMA RAY BURSTS
NT INTERSTELLAR RADIATION
NT PLANETARY RADIATION
NT PRIMARY COSMIC RAYS
NT RADIO BURSTS
NT SOLAR COSMIC RAYS
NT SOLAR ELECTRONS
NT SOLAR NEUTRINOS
NT SOLAR NEUTRONS
NT SOLAR PROTONS
NT SOLAR RADIATION
NT SOLAR RADIO BURSTS
NT SOLAR RADIO EMISSION
NT SOLAR WIND
NT SOLAR X-RAYS
NT STELLAR RADIATION
NT STELLAR WINDS
NT SUNLIGHT
NT TYPE 3 BURSTS
NT ZODIACAL LIGHT
Irradiations. Accumulated doses. Heavy ions --- space environment 03 p0272 N88-11708
Fabricate, calibrate and test a dosimeter for integration into the CRRES (Combined Release and Radiation Effects Satellite) satellite
[AD-A185439] 05 p0585 N88-13564
Characterization of space radiation environment in terms of the energy deposition in functionally important volumes
[DE88-005627] 15 p2100 N88-22513
Space nuclear reactor shielding optimization studies
17 p2408 N88-24320
From general relativity to the theory of superstrings
18 p2587 N88-25369

EXTRATERRESTRIAL RADIO WAVES
NT GALACTIC RADIO WAVES
NT RADIO BURSTS
NT SOLAR RADIO BURSTS
NT SOLAR RADIO EMISSION
NT TYPE 3 BURSTS
Analysis of deep sky sources found by the infrared astronomy satellite
[AD-A189605] 13 p1853 N88-21089
New CCIR report on SETI 22 p3067 N88-28204

EXTRATERRESTRIAL ROVING VEHICLES
U ROVING VEHICLES

EXTRAVEHICULAR ACTIVITY
Structural Assembly Demonstration Experiment (SADE)
[NASA-CR-179205] 02 p0138 N88-10868
Space Construction
[NASA-CP-2490] 02 p0138 N88-10870
Experimental assembly of structures in EVA: Hardware morphology and development issues
02 p0139 N88-10872
Access flight hardware design and development
02 p0139 N88-10873
Mission Peculiar Equipment Support Structure: A platform for space construction
02 p0139 N88-10874
Marshall Space Flight Center's role in EASE/ACCESS mission management 02 p0139 N88-10875
A monograph of the National Space Transportation System Office (NSTSO) integration activities conducted at the NASA Lyndon B. Johnson Space Center for the EASE/ACCESS payload flown on STS 61-B
02 p0139 N88-10876
Research and development at the Marshall Space Flight Center Neutral Buoyancy Simulator
02 p0139 N88-10878
A synopsis of the EVA training conducted on EASE/ACCESS for STS-61-B 02 p0140 N88-10879
Results of the ACCESS experiment
02 p0140 N88-10880
EASE (Experimental Assembly of Structures in EVA) overview of selected results 02 p0140 N88-10881
Space suit extravehicular hazards protection development
[NASA-TM-100458] 04 p0475 N88-12927
Automatic antenna switching design for Extra Vehicular Activity (EVA) communication system
06 p0797 N88-14883
Goal driven kinematic simulation of flexible arm robot for space station missions 08 p1059 N88-16388
NASA Office of Space Flight (OSF) in-orbit servicing program 12 p1587 N88-19498
In-orbit and laboratory exchange of ORUs designed/not designed for servicing 12 p1587 N88-19499
Utilization of SMS and EVA for the servicing of European Space Station 12 p1587 N88-19500
EVA, the technological challenge
12 p1592 N88-19535
The space station assembly phase: Flight telerobotic servicer feasibility. Volume 2: Methodology and case study
[NASA-CR-182690] 13 p1731 N88-20352
An evaluation of the methods for rescuing EVA (Extravehicular Activities) crewmembers and recovering equipment detached and adrift from the space station
[AD-A189683] 14 p1871 N88-21181
Design, development and evaluation of Stanford/Ames EVA prehensors
[NASA-CR-182688] 15 p2105 N88-22540
An investigation of conformable antennas for the astronaut backpack communication system
[NASA-CR-182908] 17 p2333 N88-23929
Space Station Human Factors Research Review. Volume 1: EVA Research and Development
[NASA-CP-2426-VOL-1] 17 p2379 N88-24145
Advanced EVA system design requirements study
17 p2380 N88-24147
Nuclear electric power for multimegawatt orbit transfer vehicles 17 p2399 N88-24261
Space cabin atmosphere and extracurricular sortie --- embolisms 19 p2696 N88-26023
The US space programme spacewalk/extravehicular activity experience: Past, present and future
19 p2697 N88-26031
Decompression procedures and accidents in space and sea 19 p2698 N88-26035
Safety of extravehicular space activities
19 p2698 N88-26038
Marintek's ocean basin, a training facility for extravehicular activity? 19 p2698 N88-26041
Man versus machine: The role of astronauts in extravehicular activity 19 p2699 N88-26045
Maintenance and supply options
[NASA-CR-172062] 24 p3332 N88-29837
Study of human factors engineering criteria for extravehicular activity (EVA) systems, volume 1
[STF23-F87025-VOL-1] 24 p3410 N88-30298

EXTRAVEHICULAR MOBILITY UNITS
Advanced EMU electrochemically regenerable CO2 and moisture absorber module breadboard
[NASA-CR-172054] 21 p2993 N88-27754

EXTREMA
U RANGE (EXTREMES)

EXTREME ULTRAVIOLET RADIATION
Electron beam requirements for soft X-ray/XUV free-electron lasers
[DE87-011750] 01 p0051 N88-10325
What's needed in the UV and EUV
02 p0255 N88-11612
Analysis of undulator field errors for XUV FELs (Extreme Ultraviolet Free Electron Laser)
[DE87-014734] 03 p0328 N88-12073
XUV emission features from the Livermore soft X-ray laser experiments
[DE88-000420] 04 p0448 N88-12779
Extreme ultraviolet beam-foil spectroscopy of highly ionized neon and argon
[AD-A185197] 05 p0561 N88-13418
Satellite observations of extreme ultraviolet radiation
[AD-A185043] 05 p0661 N88-14059
The evaluation of a deformable diffraction grating for a stigmatic EUV spectroheliometer
[NASA-CR-182371] 06 p0707 N88-14337
The EUV line flux variations and activity in Alpha Orionis 08 p1032 N88-16256
Preliminary injector, accelerator, and beamline design for rf-linac-driven XUV free-electron lasers
[DE88-003185] 10 p1336 N88-17983
Spectroscopic studies of a laser-produced carbon plasma in the near and extreme ultraviolet
11 p1553 N88-19292
Projected performance of RF-linac-driven free-electron lasers in the VUV and soft X-ray regions
[DE88-004294] 13 p1776 N88-20625
XUV source for ultra-high resolution photoionization spectroscopy
[DE88-007531] 19 p2614 N88-25510
Progress toward a soft X-ray FEL
[DE88-007669] 19 p2675 N88-25905
Development of a free-electron laser user facility for the extreme ultraviolet
[DE88-007892] 21 p2953 N88-27541

EXTREMELY HIGH FREQUENCIES
An investigation on Faraday rotators and quarter-wave plates of a 35 GHz radar signature system
[DFVLR-FB-87-14] 01 p0037 N88-10236
V-band IMPATT power amplifier
[NASA-CR-180711] 01 p0042 N88-10267
Optimization of mode converters for generating the fundamental TE(06) gyrotron output at 140 GHz
[IPF-87-1] 01 p0043 N88-10273
Estimates of satellite EHF communication outages due to attenuation by rain
[AD-A183969] 03 p0307 N88-11941
High peak power ka-band gyrotron oscillator experiment
[AD-A185424] 05 p0585 N88-13563
Technology developments to meet tomorrow's need for higher satellite frequencies 09 p1124 N88-16732
High peak power Ka-band gyrotron oscillator experiments with slotted and unslotted cavities
[AD-A188109] 11 p1478 N88-18819
An EHF telecommunication system engineering model
12 p1618 N88-19674
Research on Faraday rotators and quarter-wave plates of a 35-GHz radar signature system
[ESA-TT-1081] 16 p2189 N88-23052
Experimental radio frequency link for Ka-band communications applications
[NASA-TM-100824] 18 p2470 N88-24659
An evaluation of two millimeter wave propagation models for horizontal atmospheric attenuation at 70-115 GHZ
[AD-A192699] 21 p2931 N88-27403
The 44/20 GHz ground terminal
[AD-A194002] 23 p3204 N88-29069

EXTREMELY LOW FREQUENCIES
ELF/VLF/LF propagation and system design
[AD-A183261] 01 p0033 N88-10212
Power flow in terms of Poynting vector for Extremely Low Frequency (ELF) dipole sources in seawater
[ARE-TM(UTM)-87102] 01 p0035 N88-10221
Compilation of 1986 annual reports of the Navy ELF (Extremely Low Frequency) communications system ecological monitoring program, volume 1
[AD-A184561] 03 p0306 N88-11930
Compilation of 1986 annual reports of the Navy ELF (Extremely Low Frequency) communications system ecological monitoring program, volume 2
[AD-A184562] 03 p0306 N88-11931
Compilation of 1986 annual reports of the Navy ELF (Extremely Low Frequency) communications system ecological monitoring program, volume 3
[AD-A184563] 03 p0306 N88-11932
Applicability of extremely low frequency global resonances for study of Venusian storm activity
08 p1005 N88-16093
ELF (Extremely Low Frequency) communications system ecological monitoring program: Electromagnetic field measurements and engineering support, 1986
[AD-A188057] 11 p1509 N88-19017
WAVFLD: A program to compute ionospheric height gain functions and field strengths at VLF
[AD-A191159] 16 p2191 N88-23066
Extremely Low Frequency (ELF) communications system ecological monitoring program: Summary of 1986 progress
[AD-A192014] 19 p2642 N88-25676
Extremely Low Frequency (ELF) communications program: Non-ionizing electromagnetic radiation literature evaluation and assessment, 1986-1987 literature review
[AD-A192024] 19 p2642 N88-25677
Interaction of biological systems with static and ELF electric and magnetic fields
[DE88-007951] 20 p2831 N88-26792
Experimental proof of quasilongitudinal propagation of low-frequency waves in middle latitudes in upper ionosphere 24 p3447 N88-30516

EXTREMELY LOW RADIO FREQUENCIES
Ultra-low frequency vibration data acquisition concerns in operating flight simulators
[DE88-004795] 10 p1285 N88-17687
EXTREMUM VALUES
NT LIMITS (MATHEMATICS)
NT MAXIMA
NT MINIMA
Extrapolation of extremum values of the wind velocity
08 p1015 N88-16150
On a consistent estimate of the index of an extreme value distribution
[CWI-MS-R8710] 14 p1966 N88-21729
Approximations in extreme value theory
[AD-A189817] 15 p2124 N88-22659
Extreme value for dependent sequences via the Stein-Chen method of poisson approximation
[AD-A190325] 15 p2125 N88-22668
EXTRUDING
NT PULTRUSION
Slip casting and extruding shapes of rhenium with metal oxide additives. Part 2: Development of grain stabilized rhenium parts for resistojets
[NASA-CR-180851] 03 p0278 N88-11749
Activities at government research laboratories reported 04 p0403 N88-12503
Continuation finite element analysis of viscoelastic fluids 04 p0445 N88-12761
Tensile properties of extrusion consolidated Type 304 SS rapidly solidified powders
[DE87-014875] 05 p0566 N88-13450
Development on thin wall tubes of dispersion type
[DE87-703384] 05 p0571 N88-13483
Cyclic deformation of an extruded AlMgSi alloy
05 p0598 N88-13654
Fabrication of YBa2Cu3O7 superconducting ceramics
[DE88-003012] 07 p0938 N88-15701
Cost 501 Project UK10 part 3. Thermal fatigue damage of Fecralloy steel-sprayed and co-extruded tubing
[AERE-R-12230] 10 p1343 N88-18026
Processing, physical metallurgy and creep of NiAl + Ta and NiAl + Nb alloys
[NASA-CR-182113] 14 p1890 N88-21295
Grain growth behavior of extrusion consolidated centrifugally atomized Type 304 stainless steel powder
[DE88-006788] 15 p2038 N88-22143
Mechanical testing and microscopic analysis of structure of extruded powder aluminum
[DE88-007193] 19 p2617 N88-25528
Volcanic contribution to crustal growth in the Central Andes: A new estimate and a discussion of uncertainties
24 p3401 N88-30255
EYE (ANATOMY)
NT CORNEA
NT FOVEA
NT OCULOMOTOR NERVES
NT PUPILS
NT RETINA
Motion and space sickness 04 p0404 N88-12510
Vision of details in space and time
[B8711402] 06 p0753 N88-14624
Effect of intermittent hypercapnia on visual analyzer function 07 p0896 N88-15431
Considerations concerning the basic bandwidth reduction of high definition television systems (HDTV) component signals, based on psychophysiological properties of the eye
[IRT-B-83/87] 09 p1153 N88-16909
A-scan ultrasound measurement of ocular changes during accommodation
[AD-A186818] 09 p1198 N88-17181
Development and experimentation of an eye/brain/task testbed 09 p1205 N88-17219
Multiaperture optical system research
[AD-A188211] 11 p1549 N88-19267
Protection against laser damage to human body reviewed 15 p2053 N88-22237
Laboratory equipment update
[AD-A189781] 15 p2102 N88-22522
Future visual environment and concerns
23 p3242 N88-29299
Central serous chorioretinopathy in USAF aviators: A review
[AD-A195697] 24 p3407 N88-30280
EYE MOVEMENTS
NT NYSTAGMUS
NT SACCADIC EYE MOVEMENTS
NT VESTIBULAR NYSTAGMUS
Quantifying some information processing aspects of the pilot's instrument crosscheck
[AD-A186114] 07 p0898 N88-15443
Research on visual information processing with special reference to oculomotor behavior in the areas of exploration, recognition and search
[AD-A186598] 08 p1051 N88-16346
An innovative workstation 08 p1063 N88-16421
Refinement of eye-point-of-regard measurement with helicopter pilots in a flight experiment
[ESA-TT-1073] 09 p1200 N88-17195
Development and experimentation of an eye/brain/task testbed 09 p1205 N88-17219
Neck receptor stimulation in 0 and 1 g
12 p1658 N88-19938
Studies of the vestibulo-ocular reflex on STS 4, 5 and 6
[NASA-TM-100461] 12 p1666 N88-19987
Eye and head response to an attention cue in a dual task paradigm
[AD-A191052] 18 p2551 N88-25143
A human factors evaluation of the Advanced Visual Technology System (AVTS) eye tracking oculometer
21 p2925 N88-27361
Fighter pilot performance during airborne and simulator missions: Physiological comparisons
21 p2981 N88-27704
Stereo and eye movement
[AD-A193588] 22 p3142 N88-28681
Eye movements and spatial pattern vision
[AD-A195496] 24 p3408 N88-30290
EYE PROTECTION
Aerosol lidar for environment protection and meteorology
[DFVLR-FB-87-43] 14 p1982 N88-21828

F

F CENTERS
U COLOR CENTERS
F DISPLAYS
U F REGION
F LAYER
U F REGION
F REGION
NT F 2 REGION
A comparative analysis of equatorial and auroral-zone phase scintillation data
[AD-A184509] 03 p0350 N88-12212
High latitude F-region drift studies
[AD-A184466] 04 p0467 N88-12889
The polar ionosphere and interplanetary field
[AD-A185386] 05 p0624 N88-13822
CP-1-H analysis tests 06 p0691 N88-14236
EISCAT (European incoherent scatter radar) electron density studies
[AD-A185998] 07 p0841 N88-15099
Dynamics Explorer guest investigator
[NASA-CR-181494] 07 p0878 N88-15325
Multispectral optical observations of ionospheric F-region storm effects at low latitude
[INPE-4231-PRE/1105] 08 p1024 N88-16198
MAIMIK: A high current electron beam experiment on a sounding rocket from Andoya rocket range (Norway)
08 p1030 N88-16243
Effect of neutral wind on the latitudinal variation of nighttime F-layer vertical movements
08 p1030 N88-16244
F-layer polar cap arcs
[AD-A186592] 09 p1190 N88-17127
High altitude chemical release systems for project BIME (Brazilian Ionospheric Modification Experiments) project IMS (Ionospheric Modification Studies) project PIIE (Polar Ionospheric Irregularities Experiment) project polar arcs
[AD-A188299] 12 p1642 N88-19833
Dynamics of small and large scale irregularities at sub-auroral latitudes
[AD-A189052] 12 p1645 N88-19853
Model of Jovian F region ionosphere
[NASA-CR-182587] 13 p1855 N88-21105
In-situ plasma bubble observations associated with equatorial spread-F over Natal
[INPE-4488-PRE/1252] 15 p2095 N88-22482
Rocket measurements of ionospheric electron temperature over Natal
[INPE-4485-PRE/1250] 15 p2096 N88-22489
The MUF (Maximum Usable Frequency) (3000) as an indicator for F-region variations
[AD-A191655] 19 p2690 N88-25991
Investigation of the Sun-aligned F-region walls and related phenomena in the auroral latitude range
[AFGL-TR-87-0248] 19 p2692 N88-26000
Design, development, fabrication and launch support for a high altitude release of neodymium vapor
[AD-A194196] 22 p3118 N88-28527
Ionospheric convection and structure using ground-based digital ionosondes
[AD-A194246] 23 p3233 N88-29237
One equatorial anomaly in nighttime ionospheric F region 24 p3447 N88-30517
F STARS
The onset of chromospheric activity among the A- and F- type stars 04 p0511 N88-13144
An analysis of the photospheric line profiles in F, G, and K supergiants 04 p0513 N88-13157
F 2 REGION
Longitudinal variations of equatorial ionosphere determined from Intercosmos-19 artificial Earth satellite data 08 p1003 N88-16074
F-80 AIRCRAFT
U T-33 AIRCRAFT
F-4 AIRCRAFT
Robust control system design
02 p0127 N88-10800
F-110 AIRCRAFT
U F-4 AIRCRAFT
F-14 AIRCRAFT
Effects of the installation and operation of jet-exhaust yaw vanes on the longitudinal and lateral-directional characteristics of the F-14 airplane
[NASA-TP-2769] 04 p0393 N88-12455
Computational design of natural laminar flow wings for transonic transport application 07 p0813 N88-14948
Techniques used in the F-14 variable-sweep transition flight experiment
[NASA-TM-100444] 24 p3374 N88-30093
F-15 AIRCRAFT
Fighter design for human load limits
12 p1580 N88-19451
Performance improvements of an F-15 airplane with an integrated engine-flight control system
[NASA-TM-100431] 14 p1867 N88-21159
Augmentor performance of an F100 engine model derivative engine in an F-15 airplane
[NASA-TM-86745] 17 p2307 N88-23805
F-16 AIRCRAFT
Fighter design for human load limits
12 p1580 N88-19451
The integration of artificial intelligence techniques to improve the effectiveness of electronic countermeasure strategies in a tactical environment
[AD-A189483] 12 p1682 N88-20056
F-16 simulator for man-in-the-loop testing of aircraft control systems (SIMTACS)
[AD-A189675] 14 p1870 N88-21178
Multivariable control law design for the AFTI/F-16 with a failed control surface using a parameter-adaptive controller
[AD-A189848] 15 p2020 N88-22040
Subharmonic aliasing and its effects on the AFTI/F-16 digital flight control system
[AD-A190614] 15 p2020 N88-22042
Three-dimensional elliptic grid generation for an F-16
23 p3246 N88-29315
The cost and performance implications of reliability improvements in the F-16A/B
[AD-A195096] 24 p3324 N88-29796
LANTIRN simulator training in the F-16C
[AD-A195201] 24 p3330 N88-29826
F-18 AIRCRAFT
A study of the Department of Defense configuration management policies and procedures as applied to the FA-18 Strike/Fighter program
[AD-A184872] 05 p0657 N88-14034
Surface flow visualization of separated flows on the forebody of an F-18 aircraft and wind-tunnel model
[NASA-TM-100436] 14 p1863 N88-21127
F-27 AIRCRAFT
Metallurgical analysis of fractured F-27 aircraft landing gear
[DE88-005885] 11 p1460 N88-18705
F-106 AIRCRAFT
An experimental investigation of dynamic ground effect
[NASA-CR-4105] 04 p0394 N88-12458
Experimental and analytic studies of the triggered lightning environment of the F106B
[NASA-CR-4104] 04 p0469 N88-12897
Vortex dynamics 07 p0812 N88-14945
Atmospheric electrical modeling in support of the NASA F-106 storm hazards project
[NASA-CR-181639] 13 p1799 N88-20758
Sensitivity of F-106B leading-edge-vortex images to flight and vapor-screen parameters
[NASA-TP-2818] 17 p2300 N88-23760
Investigations into the triggered lightning response of the F106B thunderstorm research aircraft
[NASA-CR-3902] 23 p3236 N88-29258
F-111 AIRCRAFT
Predictions of F-111 TACT aircraft buffet response and correlations of fluctuating pressures measured on aluminum and steel models and the aircraft
[NASA-CR-4069] 05 p0529 N88-13218
FAB (PROGRAMMING LANGUAGE)
U FORTRAN
FABRICATION
NT SPACE MANUFACTURING

Fabrication of standardized piezoelectric polymer shock gauges by the Bauer method
[DE87-012738] 01 p0049 N88-10315

Optimization of SIS mixer elements
[NASA-CR-180710] 01 p0104 N88-10680

Multilayer monochromators for neutron spectrometers
[DE87-014291] 02 p0175 N88-11093

Preparation and properties of evaporated CdTe films
[DE87-012270] 02 p0195 N88-11216

Review of diffusion barrier technology for application in SP-100 fuel pins
[DE88-000021] 02 p0234 N88-11480

Investigation of the fabrication parameters of laser mirrors with hard oxide interference coatings
[ESA-TT-1064] 03 p0329 N88-12077

Mechanically stacked multijunction solar cells: An update on Sandia programs
[DE87-014641] 03 p0347 N88-12190

Development of advanced fiber reinforced ceramics
[DE88-000779] 04 p0420 N88-12604

Raman scattering spectrum along a bevel etched GaAs on Si, TEM (Transmission Electron Microscope) study and GaAs P-I-N photodetector on Si
[DE88-000210] 04 p0498 N88-13066

Performance monitoring and analysis of electric van fleet vehicles
[DE88-900066] 04 p0502 N88-13091

Fabrication of composites by chemical vapor deposition
[DE87-014565] 05 p0559 N88-13408

The production of ultrasmall and superfine holographic diffraction gratings using synchrotron radiation and lithographic techniques
[AD-A185395] 05 p0585 N88-13562

Fabricate, calibrate and test a dosimeter for integration into the CRRES (Combined Release and Radiation Effects Satellite) satellite
[AD-A185439] 05 p0585 N88-13564

Computer modeling of complete IC fabrication process
[AD-A184807] 05 p0654 N88-14012

Design verification and fabrication of active control systems for the DAST ARW-2 high aspect ratio wing, part 1
[NASA-CR-177959-PT-1] 06 p0669 N88-14101

Design verification and fabrication of active control systems for the DAST ARW-2 high aspect ratio wing. Part 2: Appendices
[NASA-CR-177959-PT-2] 06 p0669 N88-14102

Investigation of silicon surface passivation by silicon nitride film deposition
[NASA-CR-182350] 06 p0729 N88-14487

Development of mechanically stacked tandem concentrator cells
[DE88-001926] 06 p0730 N88-14490

Study of the vapor-liquid equilibria used in the fabrication process of hydrogen by thermochemistry
[DE88-900239] 07 p0830 N88-15035

Development of a low noise 10 K J-T refrigeration system
[AD-A186004] 07 p0838 N88-15085

Fabrication techniques used in the construction of a high resolution X-ray framing camera
[DE88-002653] 07 p0856 N88-15200

Pin joints, gears, springs, cranks and other novel micromechanical structures
[DE88-002504] 07 p0864 N88-15245

Fabrication of YBa2Cu3O7 superconducting ceramics
[DE88-003012] 07 p0938 N88-15701

High-temperature electronics
08 p0956 N88-15797

Processing, fabrication, applications and limitations of inherently conducting polymers
[DE88-003210] 08 p0973 N88-15883

Effects of fabrication on the fatigue capacity of welded steel structures
[PB87-144226] 08 p0995 N88-16021

Fabrication and packaging of discontinuous MIM (Metal-Insulator-Metal) film arrays for efficient MM wave and IR detection and mixing
[AD-A186809] 09 p1146 N88-16869

Nanoelectronics
[AD-A186969] 09 p1156 N88-16930

GaAs varactor diode MMIC fabrication technology --- monolithic microwave integrated circuit (MMIC)
[RSRE-MEMO-4022] 09 p1158 N88-16943

Interdisciplinary research in applied mathematics
[AD-A186793] 09 p1226 N88-17344

CEBAF design overview and project status
[CEBAF-PR-88-001] 09 p1246 N88-17470

Fabrication, phase transformation studies and characterization of SiC-AiN-Al2OC ceramics
[DE88-004053] 10 p1306 N88-17807

An integrated pressure sensor for in-vivo use
10 p1333 N88-17965

On systolic architectures for interpolation and integration 10 p1382 N88-18250

Fabrication and evaluation of transmissive multilayer optics for 8 keV X-rays
[DE88-003999] 10 p1409 N88-18402

The effect of magnetic impurities and barriers on the magnetization and critical current of fine filament NbTi composites
[DE88-004443] 10 p1419 N88-18472

Design and fabrication of advanced hybrid circuits for high energy physics
[DE88-004392] 11 p1479 N88-18825

Measurements as a process
[DE88-005275] 11 p1497 N88-18938

Radiation effects on gallium arsenide integrated optical devices
[DE88-004107] 11 p1551 N88-19277

Atomic monolayer metallic superlattices
[DE88-005348] 12 p1607 N88-19612

Development of a CCD characterization system
[INPE-4361-TDL/301] 12 p1623 N88-19712

Concentrating photovoltaic collectors: Fabrication design
[PB88-148051] 12 p1640 N88-19821

Use of reinforced inorganic cement materials for spark wire and drift chamber wire frames
[NASA-CR-180759] 13 p1746 N88-20438

A new process for synthesis of silicon nitride powders for advanced ceramics
[AD-A189354] 13 p1748 N88-20451

Scale-up of a batch-type chemical powder preparation process for high field varistor fabrication
[DE88-006601] 13 p1762 N88-20541

Low threshold ridge waveguide single quantum well lasers 13 p1777 N88-20631

Research on high-efficiency, stacked, multijunction, amorphous silicon alloy thin-film solar cells
[DE88-001108] 13 p1793 N88-20723

Research on single-crystal CdTe solar cells
[DE88-001115] 13 p1793 N88-20725

Stable, high-efficiency, CuInSe2-based, polycrystalline, thin-film tandem solar cells
[DE88-001116] 13 p1793 N88-20726

Design of the Sandia-Israel 20-kW reflux heat-pipe solar receiver/reactor
[DE88-001312] 13 p1794 N88-20729

Molybdenum-base cermet fuel development
[DE88-005529] 13 p1839 N88-21003

Focused ion beam fabrication of graded channel FET's in GaAs and Si
[AD-A189166] 13 p1845 N88-21040

Thin-film cadmium telluride solar cells
[DE88-001107] 13 p1846 N88-21050

Solar cell experiment on the first satellite of the Brazilian complete space mission
[INPE-4248-PRE/1121] 14 p1880 N88-21238

Surface-emitting two-dimensional laser diode arrays constructed on zig-zag heat sink surface
[DE88-005215] 14 p1915 N88-21439

Polysilicon-contacted p+ emitters for silicon solar cell applications
[DE88-005106] 14 p1942 N88-21586

Fabrication and characterization of semiconductor lasers of Pb(1-x)Sn(x)Te
[INPE-4253-PRE/1126] 15 p2072 N88-22357

Synthesis of metastable superconductors by high dynamic pressure
[DE88-005620] 15 p2139 N88-22764

Beam assisted fabrication of 3-5/Si monolithic devices
[AD-A189979] 15 p2142 N88-22785

High-T(sub c) superconducting wire fabrication and testing
[DE88-005989] 15 p2144 N88-22798

Preparation of large area NbN/AlN/NbN Josephson junctions
[DE88-006074] 15 p2145 N88-22799

Design, fabricate, calibrate, test and deliver two satellite electron flux detectors
[AD-A190799] 16 p2169 N88-22930

Limited reaction processing for semiconductor device fabrication
[AD-A190913] 16 p2283 N88-23666

Study for the determination of general and specific properties of wide energy-band gap HgCdTe in the 1 to 2 micrometer wavelength range
[AD-A191091] 17 p2334 N88-23934

Miniature traveling wave tube and method of making
[NASA-CASE-LEW-14520-1] 17 p2335 N88-23936

Fabrication of SP-100 fuel barrier structures by chemical vapor deposition 17 p2416 N88-24371

Molybdenum-base cermet fuel development
17 p2434 N88-24481

Nozzle fabrication technique
[NASA-CASE-MSC-21299-1] 18 p2475 N88-24684

Sol/gel processing techniques for glass matrix composites
[AD-A191748] 18 p2478 N88-24701

Strong fibers
[DE88-007798] 19 p2610 N88-25486

Fabrication of a flexible conductor by vapor deposition
[DE88-007500] 19 p2661 N88-25826

Thermionic integrated circuit program
[DE88-010119] 19 p2662 N88-25833

Interface modification in Nicalon (trademark)/SiC composites
[DE88-009708] 20 p2767 N88-26409

Fabrication technology
[DE88-010598] 20 p2855 N88-26955

Epitaxy and properties of two dimensional GaInAs semiconductor structures
[ETN-88-92357] 20 p2879 N88-27094

Focused ion beam fabrication of graded channel FETs in GaAs and Si
[AD-A193098] 21 p2936 N88-27439

Experimental fabrication of thin film single crystalline solar cells
[PB88-131958] 21 p2967 N88-27627

Amorphous silicon solar cells using a metal substrate
[PB88-131941] 21 p2968 N88-27628

Optical evaluation of prototype stretched-membrane mirror modules for solar central receivers
[DE88-011884] 21 p2969 N88-27637

Ceramic fabrication technology for high-T(sub)c materials
[DE88-012060] 21 p3024 N88-27953

Development of 30 micrometers extrinsic silicon multiplexed infrared deterctor array
[NASA-CR-177446] 22 p3082 N88-28301

Experimental fabrication of thin film single crystalline solar cells
[PB88-131958] 22 p3116 N88-28516

Fabrication of bulk superconducting ceramics
[DE88-009956] 22 p3155 N88-28773

Method for Veterbi decoding of large constraint length convolutional codes
[NASA-CASE-NPO-17310-1-CU]
23 p3183 N88-28946

A fundamental study of P/M processed elevated temperature aluminum alloys
[AD-A192958] 23 p3194 N88-29005

Advanced processing and properties of high performance alloys
[AD-A193767] 23 p3194 N88-29010

Preparation of superconducting YBa2Cu3O(sub 7-x) films by magnetron sputtering
[DE88-009977] 23 p3289 N88-29583

Tolerances for phase locking of semiconductor laser arrays
[AD-A195974] 24 p3378 N88-30120

Ion exchange processes for fabrication of integrated optical waveguide structures into glass substrates
[VTT-46] 24 p3429 N88-30405

Cluster beam studies
[AD-A195182] 24 p3434 N88-30443

FABRICS

NT PARACHUTE FABRICS

Low extractable wipers for cleaning space flight hardware 02 p0137 N88-10863

A hybrid fibreglass-CFRP cloth for new furnishings --- aircraft cabins
[SNIAS-872-111-109] 05 p0558 N88-13396

Flammability test on aircraft seats equipped with fire barrier fabrics for the Porcher company
[CEAT-M5-525200] 06 p0666 N88-14084

Method of obtaining of fire resistant polyacrylonitrile fiber or cloth from it
[AD-A185941] 07 p0836 N88-15071

Composite materials for rail transit systems
[NASA-CR-178401] 10 p1294 N88-17738

Tribological properties of alumina-boria-silicate fabric from 25 to 850 C
[NASA-TM-100806] 11 p1464 N88-18726

Fabric space radiators
[DE88-005569] 14 p1880 N88-21237

A reflux tube fabric radiator 17 p2421 N88-24394

Fabric radiators 17 p2427 N88-24435

Development of materials for fabric radiators
17 p2429 N88-24448

Investigation of leaks in fiberglass-reinforced pressure vessels by direct observation of hollow fibers in glass cloth
[DE88-006936] 19 p2609 N88-25485

Stressed fabric abrasion test procedure for urethane coated fabric fuel tanks
[AD-A196327] 24 p3356 N88-29982

FABRY-PEROT INTERFEROMETERS

Experimental measurements and numerical simulations of metal spallation by detonating solid explosives
[DE87-013227] 01 p0054 N88-10347

Program to development an optical transistor and switch
[AD-A185666] 06 p0697 N88-14278

Modern pulsed wavemeters
[DE88-003875] 10 p1335 N88-17978
Study of the ionic and neutral species in the coma of Comet Halley with an image intensifier camera
14 p2006 N88-21962
FABRY-PEROT LASERS
U LASERS
FABRY-PEROT SPECTROMETERS
A new liquid helium-cooled Fabry-Perot spectrometer used in a far infrared astronomical balloon experiment
08 p1028 N88-16224
Velocity resolved far-infrared spectroscopy of galactic sources 13 p1854 N88-21099
Fabry-Perot etalons as prefilters for astronomical far infrared Fourier transform spectroscopy
[MPE-205] 16 p2273 N88-23603
FACE CENTERED CUBIC LATTICES
State variable approach to deformation phenomena in Face Centered Cubic (FCC) metals
[VTT-44] 24 p3354 N88-29964
FACETS
U FLAT SURFACES
FACILITIES
Lewis materials research and technology: An overview
09 p1119 N88-16699
FACSIMILE COMMUNICATION
NT AUTOMATIC PICTURE TRANSMISSION
Document transfer by a digital satellite link
[NLR-MP-86071-U] 20 p2792 N88-26564
FACSIMILE TRANSMISSION
U FACSIMILE COMMUNICATION
FACTOR ANALYSIS
Assessment of fatigue in aviation crews
[AD-A184129] 03 p0356 N88-12245
Application of Vandermonde decomposition to directional and modal analysis of broadband transients
[AD-A185007] 05 p0646 N88-13956
On the work needed to factor a symmetric positive definite matrix
[AD-A185781] 06 p0759 N88-14660
Use of principal component method for analysis of multidimensional quantitative data in biomedical investigations 19 p2706 N88-26089
A programmable systolic array for factorial analysis. Part 2: The symmetric eigenvalue problem
[AD-A192396] 21 p2995 N88-27762
Recursive mass matrix factorization and inversion: An operator approach to open- and closed-chain multibody dynamics
[NASA-CR-182516] 23 p3247 N88-29328
Advancement of latent trait theory
[AD-A194302] 24 p3408 N88-30289
FACTORIAL DESIGN
Statistical selection procedures
[AD-A185868] 07 p0913 N88-15538
SEARCH: An interactive computer program for optimizing two-variable, unconstrained experiments or simulation
[AD-A190593] 15 p2112 N88-22583
Contribution to the automatic generation of floor plan placing --- integrated circuit design
[ETN-88-92193] 16 p2247 N88-23426
A programmable systolic array for factorial analysis. Part 2: The symmetric eigenvalue problem
[AD-A192396] 21 p2995 N88-27762
Measuring dispersion effects of factors in factorial experiments
[AD-A193216] 21 p3006 N88-27831
FACTORIES
U INDUSTRIAL PLANTS
FACTORIZATION
Numerical computation of transonic potential flow about 3-dimensional inlets
[NAL-TR-924] 02 p0122 N88-10770
Concurrent algorithms for transient nonlinear FE analysis
[NASA-CR-181455] 02 p0221 N88-11389
QR factorization of a dense matrix on a shared-memory multiprocessor
[DE88-001506] 04 p0480 N88-12956
Two classes of preconditioners computed using block matrix factorization techniques
[DE88-001313] 04 p0485 N88-12988
Analysis of a parallel solution method for tridiagonal systems
[PB87-230538] 06 p0762 N88-14678
Parallel LU-factorization algorithms for dense matrices
[DE88-002179] 07 p0904 N88-15478
A Schur-complement method for sparse quadratic programming
[DE88-002520] 07 p0904 N88-15479
A parallel algorithm for the general LU-factorization
[DE88-002177] 08 p1066 N88-16444
Navier-Stokes simulation of wind-tunnel flow using LU-ADI factorization algorithm
[NASA-TM-100042] 10 p1268 N88-17584
A multiprocessor scheme for the singular value decomposition
[DE88-003591] 10 p1388 N88-18288
Compact high order schemes for the Euler equations
[NASA-CR-181625] 11 p1530 N88-19138
QR factorization of a dense matrix on a hypercube multiprocessor
[DE88-009187] 19 p2716 N88-26129
Factorization of large integers on a massively parallel computer
[DE88-011625] 21 p2999 N88-27786
Second order differential equations in the complex domain
[RR-674-M] 22 p3144 N88-28695
FACULAE
Solar-geophysical data number 513, May 1987. Part 2: (Comprehensive reports). Data for November 1986 and miscellanea
[PB87-204974] 01 p0119 N88-10761
Spectral images and multi-component models of the chromospheres of AR Lacertae
11 p1568 N88-19384
FADDEEV EQUATIONS
Solution of Faddeev-Yakubovsky differential equations by the finite-dimensional approximation method for four spinless particles in the 1 + 3 scattering problem
[DE87-702983] 19 p2719 N88-26145
A systolic array for efficient execution of the Faddeev algorithm
[DE88-011330] 22 p3135 N88-28635
FADING
NT SIGNAL FADING
A statistical rain attenuation prediction model with application to the advanced communication technology satellite project. Part 2: Theoretical development of a dynamic model and application to rain fade durations and tolerable control delays for fade countermeasures
[NASA-TM-100242] 03 p0308 N88-11945
Spread spectrum mobile radio communications
[AD-A187487] 11 p1470 N88-18765
Identification of microwave line-of-sight multipath components 12 p1616 N88-19665
Refractive index, meteorology and fading in line-of-sight transmission paths 12 p1616 N88-19666
Radio and radar holes and multipath zones: The global and local influences on atmospheric refractive structure and resulting adverse radio and radar performance
12 p1617 N88-19667
MM-wave propagation and application in military communication systems 12 p1617 N88-19669
Space-diversity effects on line-of-sight propagation paths 12 p1617 N88-19670
The 6 GHz propagation measurements over a 51 km path in the UK 12 p1617 N88-19673
FAHRENHEIT TEMPERATURE SCALE
U TEMPERATURE SCALES
FAIL-SAFE SYSTEMS
Towards a damage tolerance philosophy for composite materials and structures
[NASA-TM-100548] 16 p2173 N88-22949
FAILURE
NT ENGINE FAILURE
NT STRUCTURAL FAILURE
NT SYSTEM FAILURES
Fatigue failure of thin porous strips
04 p0426 N88-12640
Programmable Logic Arrays (PLA's) design for testability
[PB87-102935] 04 p0438 N88-12718
An examination of coating failure on wing pivot fittings of f111 aircraft
[AD-A185028] 05 p0546 N88-13328
Electromagnetics and electrothermal approach to evaluate failures in microelectronic devices caused by electrostatic discharges: Stochastical aspects of the device reliability
[AD-A184906] 05 p0577 N88-13522
Computer aided modeling and fatigue failure forecast under stochastic loading 05 p0607 N88-13720
Deformation mechanisms and crack initiation in fatigue 05 p0608 N88-13730
A data structure and algorithm for fault diagnosis
08 p1065 N88-16432
Maximum likelihood estimates for the discrete application of the AMSAA growth model
[AD-A186921] 09 p1177 N88-17048
A finite element analysis of adhesively bonded composite joints including geometric nonlinearity, nonlinear viscoelasticity moisture diffusion and delayed failure
[AD-A187455] 10 p1296 N88-17747
Latent failures and coverage in fault-tolerant systems. A VLSI CMOS circuit design technique to aid test generation
[AD-A187615] 10 p1325 N88-17921
Estimating system and component reliabilities under partial information on cause of failure
[AD-A189107] 13 p1780 N88-20653
Multivariable control law design for the AFTI/F-16 with a failed control surface using a parameter-adaptive controller
[AD-A189848] 15 p2020 N88-22040
An investigation of the failure response of laminates under biaxial stress
[AD-A190039] 15 p2029 N88-22090
Galvanic corrosion initiatives
[AD-A190058] 15 p2040 N88-22155
Hybrid PV HgCdTe IR detectors technology reliability and failure program. Environmental stress testing plan
[AD-A191165] 16 p2211 N88-23195
Aircraft accident report: Midair collision of SkyWest Airlines Swearingen METRO 2, N163SW, and Mooney M20, N6485U, Kearns, Utah, January 15, 1987
[PB88-910404] 20 p2755 N88-26346
Probabilistic anisotropic failure criteria for composite materials
[AD-A193046] 21 p2904 N88-27232
NDE performance in predicting failure strength of spherical composite specimens with implanted flaws
[DE88-008223] 21 p2959 N88-27575
Influence of microstructure and microdamage processes on fracture at high loading rates
[AD-A192957] 21 p2960 N88-27583
Analysis of stiffness reduction, failure and stress concentration in fiber composite laminates
[AD-A193519] 22 p3050 N88-28006
Approximate evaluation of semi-Markov chain reliability models
[AD-A194669] 23 p3223 N88-29185
Plastic flow and failure modeling under high strain rate loading
[AD-A194223] 23 p3226 N88-29199
Critical conditions for failure in materials subjected to high rates of loading
[AD-A194697] 23 p3226 N88-29201
Systolic array fault tolerance performance analysis
[AD-A193521] 23 p3244 N88-29306
Exact lower confidence limits for the reliability of k of n systems for zero failures and nonconservativeness of the maximus method
[AD-A194299] 23 p3274 N88-29485
Criteria for matrix dominated failure
[AD-A196263] 24 p3341 N88-29887
Multi-metallic galvanic corrosion
[AD-A195995] 24 p3353 N88-29963
Electrochemical evaluation of the long term corrosion resistance of polymer coated steel
24 p3355 N88-29974
Automated early fatigue damage sensing system
[AD-A195717] 24 p3382 N88-30143
Stress related failures causing open metallization
[AD-A195061] 24 p3383 N88-30150
Heavy ion and proton tests for subsystem upset
[AD-A195267] 24 p3434 N88-30442
FAILURE ANALYSIS
Compendium of post-failure analysis techniques for composite materials
[AD-A183783] 01 p0018 N88-10113
Endurance testing of a natural gas-fueled rotary engine
[PB87-215703] 01 p0055 N88-10356
Optimal detection of sensor failures in flight control systems using deterministic observers
02 p0128 N88-10803
The 1986 Goddard Space Flight Center Battery Workshop
[NASA-CP-2486] 02 p0163 N88-11021
Fault tree safety analysis of a large Li/SOCl(sub)2 spacecraft battery 02 p0163 N88-11025
Failure analysis of a 3.5 inch, 50 ampere-hour nickel-hydrogen cell 02 p0164 N88-11030
Blade excitation criteria developed for aero derived engines in Arctic Alaska
[PNR90368] 02 p0182 N88-11[illegible]
Joining of silicon carbide reinforced ceramics
[DE87-014881] 03 p0294 N88-11847
Scaling of size/time/temperature associated with dilatation and distortion in uniaxial specimens
03 p0336 N88-12117
Kinetics of crack growth: Thermal/mechanical interaction 03 p0337 N88-12124
Electricity from photovoltaic solar cells. Flat-Plate Solar Array Project of the US Department of Energy's National Photovoltaics Program: 10 years of progress
[NASA-TM-89653] 03 p0346 N88-12185
Analysis of 7- X 10-foot high speed wind tunnel shaft loads in support of fan blade failure investigation
[NASA-TM-100504] 04 p0402 N88-12496
Failure analysis of composite structure materials
[AD-A184468] 04 p0410 N88-12548

Corrosion of electronic components
05 p0547 N88-13333

Applications of fatigue analyses: Transportation
05 p0608 N88-13733

Evaluation of closed cubic failure criterion for graphite/epoxy laminates
[NASA-CR-182375] 06 p0679 N88-14158

On the influence of false plots on tracking relaibility: Simulations and preliminary analyses
[FOA-C-30443-3.2] 06 p0692 N88-14245

A software reliability model with variable fault exposure coefficient
[REPT-87-029] 06 p0757 N88-14646

Estimating the distribution of fault latency in a digital processor
[NASA-TM-100521] 06 p0760 N88-14666

Space station software reliability analysis based on failures observed during testing at the multisystem integration facility 06 p0798 N88-14884

Impact of solids on composite materials
[NASA-CR-182395] 07 p0827 N88-15015

Verification of FANTASTIC integrated code
07 p0924 N88-15613

Pattern recognition techniques for failure trend detection in SSME ground tests 07 p0924 N88-15614

Delamination durability of composite materials for rotorcraft 09 p1107 N88-16634

Mechanical properties of carbon fiber reinforced thermoplastic matrix composites
[NAL-TR-934] 09 p1139 N88-16827

Residual stiffness and strength of Kevlar/epoxy laminated impulsively loaded to 7.9 ktaps
[DE88-003724] 09 p1149 N88-16886

Plasma and ion etching for failure analysis. Part 2. The etching of plastic encapsulant and other semiconductor device materials, using the Technics Giga Etch 100-E plasma etch system
[AERE-R-12212] 09 p1177 N88-17050

The failure and fracture analysis of adhesive bonds
[ETN-87-90713] 09 p1181 N88-17077

CONFIG: Qualitative simulation tool for analyzing behavior of engineering devices
09 p1208 N88-17240

The implementation and use of Ada on distributed systems with high reliability requirements
[NASA-CR-182481] 09 p1221 N88-17326

Studies of the initiation of pitting corrosion on stainless steels
[AERE-M-3615] 10 p1301 N88-17778

Institute for Materials Science and Engineering, Fracture and Deformation Division: Technical activities, 1987
[PB88-153622] 10 p1345 N88-18039

A strategy for failure prediction
10 p1380 N88-18243

Finite element analysis of adhesively bonded composite joints including geometric nonlinearity, nonlinear viscoelasticity, moisture diffusion and delayed failure
[PB88-147822] 11 p1451 N88-18648

Study of the mechanical behavior of a 2-D carbon-carbon composite
[NASA-CR-182594] 11 p1451 N88-18649

A nonlinear computational model for the strength and failure of composite plates and shells
11 p1501 N88-18964

Treatment of unforeseen situations by online knowledge-based diagnostic systems --- spacecraft maintenance 12 p1589 N88-19511

Mechanical response of unidirectional boron/aluminum under combined loading
[NASA-CR-182595] 12 p1604 N88-19591

On the energy release rate for dynamic transient anti-plane shear crack propagation in a general linear viscoelastic body
[AD-A188385] 12 p1635 N88-19791

Ply-level failure analysis of a graphite/epoxy laminate under bearing-bypass loading
[NASA-TM-100578] 13 p1735 N88-20372

Improve the lifetime of the hollow fiber sodium sulfur cell
[DE88-004881] 13 p1751 N88-20469

Fracture criteria for discontinuously reinforced metal matrix composites
[NASA-CR-182665] 13 p1782 N88-20662

Strength and failure analysis of composite laminate containing a circular hole with reinforcement
[AD-A189629] 14 p1884 N88-21260

Failure mechanism of He-Ne lasers
14 p1902 N88-21362

Shorts in self-checking circuits
[RR-657-I] 14 p1908 N88-21402

Probabilistic analysis of crack containing structures with the PARIS code
[KFK-4286] 14 p1924 N88-21465

On the danger of redundancies in some aerospace mechanisms 14 p1925 N88-21475

Orbiter processing facility service platform failure and redesign 14 p1928 N88-21494

Random access memory testing: Theory and practice. The gains of fault modeling
[EUT-86-E-161] 14 p1955 N88-21649

The 1988 failure rate screening data for fusion reliability and risk analysis
[DE88-006798] 14 p1984 N88-21837

Investigation of Super*Zip separation joint
[NASA-TM-4031] 15 p2026 N88-22072

Modeling failures of intermittently used machines
[AD-A190298] 15 p2074 N88-22367

Buckling of blast loaded cylinder
[AD-A190124] 15 p2076 N88-22376

Experiments investigating advanced materials under thermomechanical loading 15 p2077 N88-22385

Monolithic ceramic analysis using the SCARE program
15 p2081 N88-22409

Fracture technology for brittle materials
15 p2083 N88-22417

The use of rule induction to assist in the diagnosis of avionic circuit board defects
[ETN-88-92077] 16 p2162 N88-22899

An investigation of the ability to recover from transients following failures for single-pilot rotorcraft
[NASA-TM-100078] 16 p2164 N88-22905

Characterization of Mode 1 and Mode 2 delamination growth and thresholds in graphite/peek composites
[NASA-TM-100577] 16 p2172 N88-22947

Readiness and failures in the algebra of communicating processes
[CWI-CS-R8748] 16 p2258 N88-23499

Fault tree analysis and synthesis
[ETN-88-92236] 16 p2261 N88-23521

Local buckling and crippling of composite stiffener sections
[NASA-TM-101133] 17 p2317 N88-23840

User's guide to the Fault Inferring Nonlinear Detection System (FINDS) computer program
[NASA-CR-178410] 18 p2462 N88-24619

Internal erosion rates of a 10-kW xenon ion thruster
[NASA-TM-100954] 18 p2476 N88-24688

Environment assisted degradation mechanisms in advanced light metals
[NASA-CR-182907] 18 p2486 N88-24746

Analysis and design of detection filters within closed-loop systems 18 p2525 N88-24980

An assessment of the state of the art in predicting the failure of ceramics
[[illegible]88-008998] 19 p2621 N88-25551

Dimensional analysis and experimental observation of the coupling phenomena between combustion and fracture of damaged propellant samples
19 p2630 N88-25603

Failure rate prediction of electronic components
[PB87-228953] 19 p2678 N88-25925

Determining system maintainability as a probability
[DE88-007722] 19 p2679 N88-25927

Pyrotechnic system failures: Causes and prevention
[NASA-TM-100633] 20 p2765 N88-26394

Diagnosing faults in autonomous robot plan execution
[NASA-CR-182480] 20 p2841 N88-26859

Failure analysis of Chloride Silent Power, Ltd. PB cells
[DE88-010567] 21 p2938 N88-27448

Sodium/sulfur cell evaluation results
[DE88-011488] 21 p2938 N88-27451

Failure analysis of laminated composite angles
21 p2959 N88-27578

Computation of failure probability of fatigue loaded cracked structures
[ETN-88-92360] 21 p2964 N88-27607

Vapor Compression Distillation Subsystem (VCDS) component enhancement, testing and expert fault diagnostics development, volume 2
[NASA-CR-172076] 21 p2994 N88-27755

Failure analysis of quasi-isotropic composite laminates with free edges under off-axis loading
22 p3049 N88-28092

Fracture behavior in multidimensional fiber-reinforced composites 22 p3051 N88-28099

Proceedings of the 1987 Tri-Service Conference on Corrosion, volume 1
[AD-A191295] 22 p3053 N88-28114

An expert system for reliability modeling
23 p3252 N88-29355

Failure modes and effects analysis automation
23 p3254 N88-29370

ARGES: An expert system for fault diagnosis within space-based ECLS systems 23 p3255 N88-29380

Utilization of artificial intelligence techniques for the Space Station power system 23 p3261 N88-29412

A nonlinear filtering process diagnostic system for the Space Station 23 p3262 N88-29417

Intelligent fault diagnosis and failure management of flight control actuation systems
[NASA-CR-177481] 24 p3323 N88-29790

Failure analysis for gas turbines
[NLR-MP-87037-U] 24 p3326 N88-29808

Rupture of carbon fiber reinforced plastics (T300-914) composite materials: Influence of initial first ply failures on the fatigue behavior
[SNIAS-881-422-103] 24 p3342 N88-29892

FAILURE MODES

Joints in carbon fibre reinforced composites
[BR99969] 01 p0019 N88-10114

Fracture mode research of boron aluminum composite materials by Acoustic Emission (AE)
[NAL-TR-927] 02 p0142 N88-10891

Behavior of bolted joints in composite laminates
06 p0677 N88-14148

Causes and distribution of failures in semiconductor lasers (a review) 07 p0919 N88-15581

FMEAssist: A knowledge-based approach to Failure Modes and Effects Analysis 08 p1060 N88-16395

ESSAA: Embedded system safety analysis assistant
08 p1060 N88-16396

Mode 2 fracture mechanics 15 p2083 N88-22418

Some design considerations for ceramic components in heat engine applications 17 p2323 N88-23875

Evaluation of UN fuel pin failure modes and motion of fuel during severe accidents for reactors in space
17 p2425 N88-24424

Fatigue failure of regenerator screens in a high frequency Stirling engine 17 p2436 N88-24491

Analysis of notched metal matrix composites under tension loading
[NASA-TM-100629] 18 p2480 N88-24713

Applications of fault tree analysis to the design process
[DE88-007048] 18 p2525 N88-24982

Loading rate sensitivity of open hole composites in compression
[NASA-TM-100634] 19 p2610 N88-25490

Failure analysis of laminated composite angles
21 p2959 N88-27578

Micromechanics of composite laminate compression failures
[NASA-CR-183179] 22 p3050 N88-28098

Thin film-residual stress assessment
[AD-A193205] 23 p3196 N88-29018

A study of the floating roller peel test for adhesives
[AD-A194114] 23 p3198 N88-29034

Visual related accidents/incidents
23 p3242 N88-29293

Failure modes and effects analysis automation
23 p3254 N88-29370

FAINT OBJECT CAMERA

A search for very low mass (brown dwarf) stars as wide binaries using a seven element infrared camera-photometer 04 p0512 N88-13150

FAINT OBJECTS

Survival analysis, or what to do with upper limits in astronomical surveys
[NASA-CR-182936] 17 p2449 N88-24551

Ultraviolet spectra of two magnetic white dwarfs and ultraviolet spectra of subluminous objects found in the Kiso Schmidt survey
[NASA-CR-183051] 18 p2593 N88-25408

Observations of faint field galaxies
[NASA-CR-183251] 24 p3453 N88-30555

FAIRCHILD MILITARY AIRCRAFT

U MILITARY AIRCRAFT

FAIRINGS

Effect of a model support strut on measurement of aerodynamic longitudinal and lateral coefficients
[PB87-170288] 09 p1113 N88-16670

Ariane 4, long version. Pressure distribution measurements on two models of different scale of the Ariane 4 nose fairings in the transonic tunnel of F+W Emmen (Switzerland) with varying tunnel configurations. Comparison with measurements taken at Modane (France) and with calculations after the Euler method
[F+W-TF-1878] 09 p1122 N88-16716

The Ariane fairing and its separation systems
09 p1126 N88-16754

FALLING SPHERES

Improved resolution atmospheric density measurements based on simulations 08 p1027 N88-16221

Project CONDOR: Middle atmosphere wind structure obtained with lightweight inflatable spheres near the equatorial electrojet 08 p1028 N88-16230

FALLOUT

Health and environmental consequences of the Chernobyl nuclear power plant accident
[DOE/ER-0332] 19 p2689 N88-25985

Acute radiation syndrones and their management
[DE88-009839] 20 p2831 N88-26797

FALSE ALARMS

Response of wind shear warning systems to turbulence with implication of nuisance alerts
10 p1274 N88-17618

Windshear warning aerospatiale approach
10 p1274 N88-17620
Airworthiness considerations
10 p1276 N88-17636
On adaptive cell-averaging CFAR (Constant False-Alarm Rate) radar signal detection
[AD-A196286] 24 p3360 N88-30009
Evaluation of LISBON TAR SSR radar
[EEC/NOTE-5/87] 24 p3362 N88-30015

FAN BLADES
First article test noise survey of the A/F32T-9 large turbo fan engine enclosed noise suppressor system, Sky Harbor IAP (International Airport), Phoenix, Arizona
[AD-A183799] 01 p0090 N88-10586
The wide chord fan blade: A Rolls Royce first
[PNR90416] 02 p0125 N88-10789
The use of holographic interferometry for turbomachinery fan evaluation during rotating tests
[PNR90390] 02 p0176 N88-11098
The use of Kevlar on aero-engine fan containment casings
[PNR90410] 02 p0182 N88-11134
Analysis of 7- X 10-foot high speed wind tunnel shaft loads in support of fan blade failure investigation
[NASA-TM-100504] 04 p0402 N88-12496
Aerodynamic performance of a scale-model, counter-rotating unducted fan 10 p1282 N88-17666
The composite blade structural analyzer (COBSTRAN)
15 p2078 N88-22390
Structural tailoring of advanced turboprops
15 p2080 N88-22400
Detailed on-blade measurements on a transonic fan in unstalled supersonic flutter
[PNR90424] 22 p3039 N88-28043
An experimental investigation of two 15 percent-scale wind tunnel fan-blade designs
[NASA-TM-88256] 22 p3046 N88-28076
Optical measurement of unducted fan blade deflections
[NASA-TM-100966] 23 p3216 N88-29142

FANLIFT DEVICES
U LIFT FANS

FANS
Supersonic throughflow fans for high-speed aircraft
08 p0958 N88-15810

FAR FIELDS
Helicopter main-rotor speed effects on far-field acoustic levels
[NASA-TM-100512] 02 p0230 N88-11451
High power phased array and tailored gain semiconductor lasers 03 p0329 N88-12078
Far field of steady waves produced by local perturbation sources in stream of stratified fluid
06 p0771 N88-14736
Overestimation of on-axis power density by the Fraunhofer (far-field) approximation
[AD-A186399] 07 p0843 N88-15111
Study on a double reflector compact range --- satellite antennas
[S-201-05] 09 p1153 N88-16908
State-of-the-art for assessing earthquake hazards in the US. Parameters for specifying intensity-related earthquake ground motions
[AD-A188230] 11 p1512 N88-19032
Determination of characteristic radiation properties of a torus antenna: Integral equation method
[DFVLR-FB-87-46] 16 p2188 N88-23049
Transmitting boundary for finite-difference calculations with finite modeling of an infinite medium
[AD-A191441] 18 p2570 N88-25264
First article noise survey of the A/F32T-9 large turbo fan engine enclosed noise suppressor system, far-field noise, Ellsworth AFB, South Dakota
[AD-A191938] 19 p2602 N88-25457
Fatigue crack growth under far-field cyclic compression
[DE88-011215] 20 p2813 N88-26689
The far field from a hybrid electromagnetic pulse (HPD) simulator
[FOA-C-30480-4.2] 22 p3071 N88-28231
Development and demonstration of an on-board mission planner for helicopters
[NASA-CR-177482] 24 p3328 N88-29817
Application of sampling techniques to near-field far-field transformation
[ESA-CR(P)-2546] 24 p3359 N88-30002

FAR INFRARED RADIATION
Precise measurement of refractive index and absorption coefficient of near millimeter wave and far infrared materials
[AD-A184538] 03 p0293 N88-11840
Absorption of far IR-radiation by H2O-N2 complexes under atmospheric conditions 04 p0462 N88-12855
Far-infrared spectra of lithium deposited on a gold electrode: Interpretation using a cluster model
[AD-A184231] 04 p0495 N88-13050
Far infrared Fourier transform spectroscopy of semiconductors
[DE88-000188] 04 p0499 N88-13072
Far infrared circumstellar debris shells of red supergiant stars 04 p0515 N88-13165
Justification and prospects of observations of interstellar, far-infrared emission lines, using a small-sized balloon-borne telescope 08 p1032 N88-16254
Fast switching of far infrared radiation by refractive index change in semiconductors using photoionization
[ETN-88-91490] 11 p1551 N88-19279
Development of electrostatic-accelerator free-electron lasers
[AD-A189507] 13 p1774 N88-20614
Stratospheric trace gas distributions from fair infrared thermal emission spectroscopy
13 p1797 N88-20749
Velocity resolved far-infrared spectroscopy of galactic sources 13 p1854 N88-21099
Far-infrared (120-300 micron) observations of the Carina Nebula 14 p1993 N88-21876
Theoretical studies of Resonance Enhanced Stimulated Raman Scattering (RESRS) of frequency-doubled Alexandrite laser wavelength in cesium vapor
[NASA-CR-182870] 15 p2036 N88-22133
Experimental studies on electronic properties of HgTe/CdTe and Hg sub 1-z Cd sub x Te/CdTe heterostructures and superlattices
[AD-A189826] 15 p2142 N88-22783
Fabry-Perot etalons as prefilters for astronomical far infrared Fourier transform spectroscopy
[MPE-205] 16 p2273 N88-23603
Balloon-borne three-meter telescope for far-infrared and submillimeter astronomy
[NASA-CR-182924] 17 p2449 N88-24550
Infrared and far-infrared laser development for plasma diagnostics at Oak Ridge National Laboratory
[DE88-007262] 19 p2674 N88-25904
Far- and mid-infrared properties of metal-insulator composite materials
[AD-A193227] 21 p2905 N88-27236
Calculation of far infrared absorption in B poly(dA).poly(dT)
[AD-A193128] 21 p2918 N88-27318
IR (infrared) sky radiance distributions in the marine boundary layer
[AD-A193683] 22 p3119 N88-28531
Far infrared supplement: Catalog of infrared observations, second edition
[NASA-RP-1205] 24 p3452 N88-30545

FAR ULTRAVIOLET RADIATION
NT LYMAN ALPHA RADIATION
Vacuum ultraviolet electronic properties of liquids
[DE88-000165] 03 p0282 N88-11772
A comprehensive exploration of late-type stars in the far-ultraviolet 04 p0520 N88-13194
Theoretical and observational problems with Holes in the far UV dayglow
[AD-A188190] 10 p1355 N88-18100
Survival and mutation induction of dehydrated yeast cells after UV exposure 12 p1657 N88-19932
Wavelength scaling of lithium-like recombination scheme for X-UV gain production --- X-ray lasers
[ETN-88-92002] 13 p1778 N88-20634

FARADAY EFFECT
An investigation on Faraday rotators and quarter-wave plates of a 35 GHz radar signature system
[DFVLR-FB-87-14] 01 p0037 N88-10236
Laser induced fluorescent study of relativistic electron beams
[AD-A184456] 04 p0447 N88-12774
Research on Faraday rotators and quarter-wave plates of a 35-GHz radar signature system
[ESA-TT-1081] 16 p2189 N88-23052
Studies for the definition of a Faraday converter for space nuclear systems 17 p2411 N88-24339
Thermal and mechanical analysis of the Faraday shield for the compact ignition tokamak
[DE88-007855] 20 p2856 N88-26962

FARADAY ROTATION
U FARADAY EFFECT

FARM CROPS
NT COFFEE
NT CORN
NT COTTON
NT FRUITS
NT GRAINS (FOOD)
NT LEGUMINOUS PLANTS
NT POTATOES
NT RICE
NT SOYBEANS
NT SUGAR CANE
NT WHEAT
Low-temperature thermochemical conversion of high moisture biomass feedstocks 18 p2536 N88-25047

FARMLANDS
Evaluation of SPOT imagery for monitoring irrigated lands 22 p3090 N88-28352

FAST FOURIER TRANSFORMATIONS
Synthetic-aperture radars viewed as interferometers with matched filter processing of the collected data
[AD-A190608] 15 p2057 N88-22262
Design and implementation of VLSI prime factor algorithm processor
[AD-A190483] 15 p2112 N88-22580
Spatial filtering on digital images
17 p2354 N88-24025
Simulation and analysis of wave propagation through random media 21 p2947 N88-27503
Detection of acceleration (+Gz) induced blackout by matched-filtering of visual evoked potentials
21 p2982 N88-27710
Waveform analysis on the IBM PC
[AD-A194249] 23 p3248 N88-29330

FAST NEUTRONS
Superconductivity of pseudobinary compounds A15 (V-Cr)3Si, (V-MO)3Si, Mo3(Si-Re) bombarded with fast neutrons 03 p0285 N88-11792
Neutron radiation tolerance of Au-activated silicon
17 p2408 N88-24316
Simulation of the neutronic characteristics of large fast neutron reactors
[ETN-88-92305] 20 p2853 N88-26940

FAST NUCLEAR REACTORS
NT EXPERIMENTAL BREEDER REACTOR 2
NT LIQUID METAL FAST BREEDER REACTORS
The results of application studies for space nuclear power 17 p2398 N88-24259
BIFOLD: A dual-mode nuclear space power system
17 p2404 N88-24292
Interaction of the control system with core nuclear design for fast spectrum space power reactors
17 p2405 N88-24304
A dynamic model for the aft accumulator in the TE SP-100 system 17 p2414 N88-24354
Parametric analyses of the TE SP-100 system performance 17 p2415 N88-24358
Simulation of the neutronic characteristics of large fast neutron reactors
[ETN-88-92305] 20 p2853 N88-26940
Heat and mass transfer in a transport channel
[DE88-701968] 21 p2945 N88-27490

FASTENERS
NT BOLTS
NT LOCKS (FASTENERS)
NT PINS
NT RIVETS
NT SCREWS
Standard fatigue test specimens for fastener evaluation
[AGARD-AG-304] 04 p0455 N88-12818
Experimental and theoretical investigation of mechanically fastened composites
[AD-A185896] 07 p0826 N88-15008
Fastening high resistance bolts in real assemblies
[CRIF-MT-171] 07 p0861 N88-15221
The Shock and Vibration Digest, volume 20, no. 3
12 p1635 N88-19786
Crack distribution and growth rates for critical fastener holes in Mirage wing RH79
[AD-A189080] 13 p1722 N88-20293
Thermal stress in high temperature cylindrical fasteners
[NASA-TM-100611] 15 p2087 N88-22438
Toggle release
[NASA-CASE-MSC-21354-1] 18 p2523 N88-24969
Standard fatigue specimens for fastener evaluation --- aircraft components
[FFA-TN-1987-68] 24 p3384 N88-30157

FATIGUE (BIOLOGY)
NT FLIGHT FATIGUE
NT MUSCULAR FATIGUE
Assessment of fatigue in aviation crews
[AD-A184129] 03 p0356 N88-12245
Assessment of physical activity intensity by heart rate during sleep limited military operations
[AD-A185913] 07 p0888 N88-15382
Computer response time measurements of mood, fatigue and symptom scale items: Implications for scale response time uses
[AD-A186093] 07 p0888 N88-15384
The use of heart rate in the prescription and evaluation of exercise programs
[AD-A186454] 08 p1049 N88-16336
Carbamates, atropine, and diazepam: Effects on performance in the running rat
[AD-A188009] 11 p1517 N88-19062
Causes and prevention of occupational Repetition Strain Injuries (RSI) 11 p1521 N88-19083

Individual functional typology of sympathoadrenal system as indicator of physiological status in adverse environments 12 p1665 N88-19979

Challenges of physiological monitoring in a Navy operational setting 16 p2239 N88-23374

Attention, effort, and fatigue: Neuropsychological perspectives 16 p2241 N88-23387

Neurophysiological predictors of quality of performance 16 p2242 N88-23391

Method for observing changes in functional state of human operator 20 p2830 N88-26789

Psychophysiological measures of drowsiness as estimators of mental fatigue and performance degradation during sleep deprivation 21 p2980 N88-27702

Neurophysiological patterns of operational fatigue: Preliminary results 21 p2981 N88-27703

Plasma volume expansion in rats: Effects on thermoregulation and exercise
[AD-A192656] 22 p3130 N88-28606

The impact of hyperthermia and hypohydration on circulation, strength, endurance and health
[AD-A192657] 22 p3131 N88-28615

Stress/fatigue and the ARNG (Army National Guard) aviator
[AD-A194184] 22 p3132 N88-28621

FATIGUE (MATERIALS)
NT ACOUSTIC FATIGUE
NT BENDING FATIGUE
NT METAL FATIGUE
NT STRUCTURAL STRAIN
NT THERMAL FATIGUE

Low cycle fatigue on isotropic fine-grained graphite
[DE87-702627] 01 p0028 N88-10177

Determination of the fatigue strength of mechanically, thermally and corrosively loaded multilayer materials
[ETN-87-90375] 01 p0058 N88-10372

New fatigue damage analysis of complex engineering components based on Finite Element Methods (FEM)
[DFVLR-FB-87-15] 01 p0062 N88-10401

Mechanism of mechanical fatigue of fused silica
[DE87-014199] 02 p0152 N88-10950

Creep-fatigue behavior of NiCoCrAlY coated PWA 1480 02 p0189 N88-11176

Lewis' enhanced laboratory for research into the fatigue and constitutive behavior of high temperature materials
02 p0189 N88-11177

The influence of load cycle reconstitution on fatigue behaviour
[ARL-STRUC-R-424] 02 p0192 N88-11198

Prediction of fatigue cracking and rupture of large structures
[ONERA-RT-31/7169-RY-055-R]
02 p0192 N88-11199

Review of investigations of aeronautical fatigue in the Federal Republic of Germany
[LBF-S-178] 02 p0192 N88-11201

Operational load measurements on service helicopters
03 p0263 N88-11658

Laminated ferrous composites based on ultrahigh carbon (UHC) steels
[AD-A184617] 03 p0280 N88-11764

Deformation mechanisms of thermostructural materials
[AD-A184070] 03 p0338 N88-12128

Mechanical behavior of a controlled rolled high-strength low alloy steeel plate, microalloyed with Nb and V
[DE87-703507] 04 p0415 N88-12571

Work-in-progress presented at the Army Symposium on Solid Mechanics, 1986: Lightening of the Force
[AD-A184791] 04 p0427 N88-12644

Micromechanisms of fatigue crack growth and fracture toughness in metal matrix composites
[AD-A185200] 05 p0558 N88-13392

X-ray analysis of polycrystalline aluminium subjected to fatigue cycling
[NAL-TM-MT-8706] 05 p0564 N88-13434

Fatigue 87, volume 3
[AD-A184047] 05 p0604 N88-13700

Fracture kinetics of corrosion fatigue
05 p0605 N88-13708

Fatigue crack growth: Statistical considerations
05 p0606 N88-13718

Telemetric laser extensometry technique for monitoring deflections in small cracks 05 p0607 N88-13724

An optical interferometry technique to evaluate closure along a crack front 05 p0607 N88-13726

On the geometrical description of fatigue crack surfaces 05 p0607 N88-13727

An overview of fatigue 05 p0608 N88-13729

Deformation mechanisms and crack initiation in fatigue 05 p0608 N88-13730

Experimental studies on acoustic emission monitoring of crack propagation in offshore structures: A literature survey 05 p0610 N88-13748

Study of the evolution of short cracks in fatigue analysis --- aircraft construction materials
[DCQ/L-46-555] 06 p0722 N88-14442

Random loading fatigue crack growth: Crack closure considerations 06 p0797 N88-14881

Contribution to modeling flexion fatigue damage in unidirectional composite materials
[ECL-87-12] 08 p0965 N88-15843

The Shock and Vibration Bulletin. Part 3: Isolation and damping, vibration test criteria, and vibration analysis and test
[AD-A186750] 08 p0997 N88-16040

The development of laboratory vibration test schedules: Philosophies and techniques 08 p0999 N88-16049

Fatigue effects of a swept sine test
08 p0999 N88-16054

Aeropropulsion '87. Session 1: Aeropropulsion Materials Research
[NASA-CP-10003-SESS-1] 09 p1118 N88-16697

Micromechanisms of fatigue crack growth and fracture toughness in metal matrix composites
[AD-A186941] 09 p1137 N88-16816

Fatigue behaviour of hybrid composites
[BR102236] 09 p1138 N88-16819

Mechanical properties of carbon fiber reinforced thermoplastic matrix composites
[NAL-TR-934] 09 p1139 N88-16827

Multipurpose corrosion inhibitors for aerospace materials in Naval environments
[AD-A186728] 09 p1143 N88-16853

Development of methods for low temperature diffusion bonding
[AD-A186875] 09 p1174 N88-17033

Fracture mechanics characterization of crack growth under creep and fatigue conditions
[W-2/87] 09 p1183 N88-17087

Effect of post-cure heat-treatment on static and fatigue behaviour of XAS-914C carbon fibre composite
[AD-A186943] 10 p1294 N88-17735

Influence of different parameters on damage development --- carbon fiber reinforced plastics
11 p1448 N88-18632

Effects of thermal and thermo-mechanical treatments on the mechanical properties of centrifugally cast alloy 718
[AD-A188195] 11 p1458 N88-18690

Status of the special-purpose airfoil families
[DE88-001124] 11 p1506 N88-18998

Elevated temperature crack growth studies of advanced titanium aluminides
[AD-A189025] 12 p1608 N88-19618

The Shock and Vibration Digest, volume 20, no. 3
12 p1635 N88-19786

Crack distribution and growth rates for critical fastener holes in Mirage wing RH79
[AD-A189080] 13 p1722 N88-20293

High-temperature metal matrix composites
[AD-A189516] 13 p1734 N88-20367

The effect of microstructure on the fatigue crack growth resistance of nickel base superalloys
[AD-A189526] 13 p1741 N88-20414

Threshold fatigue crack growth in Ti-6Al-2Sn-4Zr-6Mo
[AD-A189560] 13 p1741 N88-20415

Environmentally assisted crack growth in structural alloys: Perspectives and new directions
[AD-A190137] 15 p2076 N88-22377

Lewis Structures Technology, 1988. Volume 2: Structural Mechanics
[NASA-CP-3003-VOL-2] 15 p2077 N88-22382

Mode 2 fracture mechanics 15 p2083 N88-22418

In situ fatigue loading stage inside scanning electron microscope 15 p2083 N88-22419

Grain boundary oxidation and low-cycle fatigue at elevated temperatures 15 p2083 N88-22420

Cumulative fatigue damage models
15 p2084 N88-22422

Fatigue damage mapping 15 p2084 N88-22423

Spectrum fatigue testing for materials characterization
[VTT-RR-502] 15 p2088 N88-22443

Fatique crack growth behavior of a single crystal alloy as observed through an in situ fatigue loading stage
[NASA-TM-100863] 16 p2179 N88-22986

Proceedings of the 1987 Tri-Service Conference on Corrosion, Volume 2
[AD-A189660] 17 p2319 N88-23847

Corrosion and fatique properties of FeCrB/Si metallic glass wires in aqueous environments
17 p2320 N88-23855

Effect of test sample geometry on the fatigue crack growth of X10NiCrAlTi 32 20 and NiCr22 Co 12Mo
[JUEL-SPEZ-399] 17 p2348 N88-23990

Fatigue failure of regenerator screens in a high frequency Stirling engine 17 p2436 N88-24491

Design of overlays for rigid airport pavements
[DOT/FAA/PM-87/19] 18 p2468 N88-24652

Predictive corrosion modeling, volume 1
[AD-A191229] 18 p2485 N88-24739

Resolved shear stress intensity coefficient and fatigue crack growth in large crystals
[NASA-CR-182137] 18 p2528 N88-24997

Fatigue crack growth due to random loading
18 p2531 N88-25017

Fatigue testing and damage development in continuous fiber reinforced metal matrix composites
[NASA-TM-100628] 19 p2610 N88-25489

Research on fractography of heat-resistant alloys
19 p2634 N88-25625

Study of probabilistic fatigue crack growth and associated scatter under constant-and-variable amplitude loading spectrum
[AD-A192027] 19 p2679 N88-25929

Study of the influence of metallurgical factors on fatigue and fracture of aerospace structural materials
[AD-A192909] 20 p2774 N88-26452

Fatigue of lithium-aluminum alloys: An example of localization of the plastic deformation
[ETN-88-92309] 20 p2775 N88-26456

Significance of the local electrode potential within pits, crevices and cracks
[AD-A192482] 21 p2935 N88-27432

Three-dimensional aspects of fatigue crack closure
[AD-A192296] 21 p2960 N88-27581

Applications of fatigue analyses: Aircraft engines
[PNR90439] 22 p3044 N88-28066

Empirical fatigue crack growth data for a tension loaded threaded fastener
[AD-A194112] 22 p3088 N88-28334

Interaction of creep and fatigue damage in gas turbine blade material
[PNR90440] 22 p3088 N88-28335

The use of a surface acoustic wave technique to study the growth behavior of small cracks in a high strength steel alloy 23 p3225 N88-29193

Fatigue crack growth characteristics of ARALL (trademark)-1
[AD-A196185] 24 p3341 N88-29889

Modeling of micromechanisms of fatigue and fracture in hybrid materials
[AD-A195604] 24 p3382 N88-30142

Automated early fatigue damage sensing system
[AD-A195717] 24 p3382 N88-30143

Fatigue crack propagation: Probabilistic modeling and statistical analysis
[AD-A195885] 24 p3384 N88-30155

An investigation of constitutive models for predicting viscoplastic response during cyclic loading
[AD-A194875] 24 p3385 N88-30163

The development of acoustic emission for structural integrity monitoring of aircraft
[AD-A196264] 24 p3427 N88-30398

FATIGUE DIAGRAMS
U S-N DIAGRAMS

FATIGUE LIFE

The effect of fretting corrosion on the fatigue strength of steel and cast iron under sinusoidal and random loading
[LBF-FB-177] 01 p0023 N88-10142

Determination of the fatigue strength of mechanically, thermally and corrosively loaded multilayer materials
[ETN-87-90375] 01 p0058 N88-10372

The effect of size and surface on the lifetime prediction of StE 460 notched bars
[FD-6/1986] 01 p0058 N88-10374

The fatigue properties of aerospace steels under constant amplitude and flight-by-flight simulated loading
[BAE-MSM-R-GEN-0566] 01 p0059 N88-10377

Fatigue life evaluation according to local strain concept
[FF-14/1985] 01 p0059 N88-10381

Estimation multiaxial elastic-plastic notch stresses and strains in combined loading
[FB-2/1986] 01 p0060 N88-10382

Stress-strain analysis and life predictions of a notched shaft under multiaxial loading
[FB-5/1986] 01 p0060 N88-10384

Crack initiation life estimations for notched specimens with residual stresses based on local strains
[FF-17/1986] 01 p0060 N88-10385

Criteria for determination of significant load cycles in variable amplitude load sequences
[NLR-MP-86013-U] 01 p0060 N88-10386

Cumulative fatigue and life prediction of fibre composites. Part 1: Literature reviews
[BR101013] 02 p0142 N88-10893

Cumulative fatigue and life prediction of fibre composites. Part 2: Experimental techniques and results
[BR101014] 02 p0142 N88-10894

Blade excitation criteria developed for aero derived engines in Arctic Alaska
[PNR90368] 02 p0182 N88-11131

Marine gas turbines - engine health monitoring, new approaches
[PNR90369] 02 p0182 N88-11132

Creep fatigue life prediction for engine hot section materials (isotropic): Third year progress review 02 p0188 N88-11173

The influence of load cycle reconstitution on fatigue behaviour [ARL-STRUC-R-424] 02 p0192 N88-11198

Review of investigations of aeronautical fatigue in the Federal Republic of Germany [LBF-S-178] 02 p0192 N88-11201

Operational load measurements on service helicopters 03 p0263 N88-11658

Durability of powdered aluminum structures 04 p0429 N88-12655

Input turbulence features at a megawatt-size wind turbine, Medicine Bow, Wyoming [DE88-000098] 04 p0464 N88-12873

Damage considerations in sizing aircraft cells. Life predictions [SNIAS-872-111-116] 05 p0546 N88-13330

Welded joint fatigue of a AISI 304 L type stainless steel [DE87-703530] 05 p0592 N88-13607

A study of fatigue crack growth life under random stresses 05 p0602 N88-13685

The how and why of variable amplitude testing 05 p0603 N88-13690

Tensile mean stress effects on uniaxial fatigue behavior of 1045 HR steel 05 p0603 N88-13694

Fretting wear and fretting fatigue damage 05 p0603 N88-13697

A study of corrosion fatigue crack initiation, growth and the threshold condition under variable amplitude loading 05 p0604 N88-13701

Low cycle fatigue behaviour of notched specimens of nickel based superalloy single crystal 05 p0605 N88-13712

Fatigue characteristics of ion treated surfaces 05 p0606 N88-13713

The effect of heat treatment on fatigue crack growth in polycarbonate 05 p0606 N88-13714

Effect of test temperature and frequency on fatigue crack propagation in PVC 05 p0606 N88-13715

Environmental fracture toughness and static fatigue crack propagation of silica glass 05 p0606 N88-13716

Effect of interface on mechanical properties of graphite/201 aluminum composites 05 p0606 N88-13717

Constraint effects in fatigue crack growth 05 p0606 N88-13719

Computer aided modeling and fatigue failure forecast under stochastic loading 05 p0607 N88-13720

A comparison of plastic work energy and external input for fatigue crack propagation 05 p0607 N88-13722

Fatigue under nonnormal random stresses using Monte Carlo method 05 p0607 N88-13723

X-ray fatigue failure prediction based on plasticity response to microcracks 05 p0607 N88-13725

Development of research on fatigue of spot-weld in automobile structures in Japan 05 p0608 N88-13728

Accurate rotor loads prediction using the FLAP (Force and Loads Analysis Program) dynamics code [DE88-001109] 05 p0623 N88-13815

Temperature dependent mechanical properties of an alumina fiber reinforced aluminum composite 06 p0677 N88-14147

Fatigue 87, volume 2 [AD-A184046] 06 p0715 N88-14381

Effect of hold time on fatigue of lead rich PbSn solder 06 p0715 N88-14387

Near-threshold fatigue 06 p0716 N88-14392

Fatigue oxidation interaction in low cycle fatigue 06 p0719 N88-14420

High temperature low cycle fatigue of oxide dispersion strengthened and single crystal nickel base superalloys 06 p0720 N88-14422

High temperature low cycle fatigue behavior and creep-fatigue interation of MA 6000 ODS alloy 06 p0720 N88-14425

Creep-fatigue cracking in high temperature turbine rotors 06 p0720 N88-14426

Dependence of strainrange partitioned fatigue life at elevated temperature on monotonic stress-strain properties 06 p0721 N88-14428

Fatigue life prediction modeling for turbine hot section materials [NASA-TM-100291] 06 p0724 N88-14453

Investigations on the crack growth retardation behavior and fatigue life prediction in structural materials [PB87-143756] 07 p0827 N88-15016

Developing an accelerated endurance test for greases: A status report [AD-A185963] 07 p0836 N88-15072

Life prediction of thermomechanical fatigue using total strain version of strainrange partitioning (SRP): A proposal [NASA-TP-2779] 07 p0867 N88-15263

Life prediction technologies for aeronautical propulsion systems 08 p0954 N88-15788

Analysis of load-bearing capacity of nitrided layer [PB87-144176] 08 p0968 N88-15857

Experimental investigation on the bending fatigue performance of gas carbonitrided and carburized gears [PB87-147997] 08 p0992 N88-16003

Effects of fabrication on the fatigue capacity of welded steel structures [PB87-144226] 08 p0995 N88-16021

Effects of a regenerating heat treatment on the creep behavior and the lifetime during creep test loading [ETN-88-91063] 09 p1144 N88-16855

VAWT (Vertical-Axis Wind Turbine) stochastic loads produced by atmospheric turbulence [DE88-001355] 09 p1187 N88-17110

Relationship between fatigue life in the creep-fatigue region and stress-strain response [NASA-TM-100796] 10 p1345 N88-18040

Statistical evaluation of experimental results from fatigue strength tests on CFRP composite materials 11 p1449 N88-18635

Damage mechanisms and fatigue life prediction of graphite/epoxy laminates 11 p1449 N88-18637

Advanced durability analysis. Volume 1: Analytical methods [AD-A188341] 12 p1635 N88-19789

Dynamic tensile cyclic fatigue of Si3N4 [DE88-003919] 13 p1781 N88-20658

Fatigue load measurements and evaluation of the 25m Horizontal Axis Wind Turbine (HAWT) at Petten, The Netherlands [NLR-MP-86054-U] 13 p1782 N88-20660

European approaches in standard spectrum development --- aircraft load spectra [NLR-MP-87007-U] 13 p1782 N88-20661

Hygrothermomechanical fiber composite fatigue: Computational simulation [NASA-TM-100840] 14 p1884 N88-21257

Effect of protective coatings on high-temperature fatigue of heat-resistant alloys 14 p1895 N88-21314

A constitutive model for an overlay coating 14 p1933 N88-21525

Life assessment of combustor liner using unified constitutive models 15 p2077 N88-22384

Computational structural mechanics for engine structures 15 p2080 N88-22399

Large-scale wind turbine structures 15 p2085 N88-22429

Random Process Simulation for stochastic fatigue analysis [NASA-TM-100464] 15 p2123 N88-22654

Fatigue damage development of various CFRP-laminates [NASA-TT-20247] 16 p2172 N88-22945

The analysis of fatigue crack growth mechanism and oxidation and fatigue life at elevated temperatures [NASA-CR-182129] 16 p2179 N88-22987

Durability of compound cylinder under static internal-pressure repeat load of long duration 16 p2180 N88-22991

Computerized life and reliability modelling for turboprop transmissions [NASA-TM-100918] 16 p2215 N88-23220

Application of the ONERA model to the life estimation under fatigue cracking of a Al-Li alloy. Parameter identification and test-experiment comparison under FALSTAFF loading [ONERA-RT-32/7169-RY-063-R] 16 p2222 N88-23264

Damage by creep fatigue: Influence of the visco-elasticity of the matrix [PB88-124706] 18 p2528 N88-24998

Cyclic fatigue damage characteristics observed for simple loadings extended to multiaxial life prediction [NASA-CR-182126] 18 p2531 N88-25016

Surface fatigue life of CBN and vitreous ground carburized and hardened AISI 9310 spur gears [NASA-TM-100960] 19 p2677 N88-25916

Investigation of rolling contact fatigue of ball bearings [NASA-TT-20196] 19 p2678 N88-25922

Prediction of fatigue life of notched specimens under aircraft loading and importance of the relative method in the case of local strain approach, part 2 [TAE-595-PT-2] 19 p2680 N88-25934

Engine component retirement for cause. Volume 1: Executive summary [AD-A192730] 20 p2760 N88-26371

Stiffness degradation of composite laminates 20 p2767 N88-26405

Accelerated fatigue crack growth behavior of PWA 1480 single crystal alloy and its dependence on the deformation mode [NASA-TM-100943] 20 p2772 N88-26436

Fatigue crack growth under far-field cyclic compression [DE88-011215] 20 p2813 N88-26689

Prediction of fatigue growth [NLR-MP-87052-U] 20 p2816 N88-26707

Constant amplitude fatigue life data for notched and unnotched annealed Ti-6Al-4V sheet [AD-A193420] 21 p2913 N88-27287

Optimal design of viscoelastic structures 21 p2959 N88-27579

The relationship between observed fatigue damage and life estimation models [NASA-CR-182191] 21 p2965 N88-27611

Onboard Life Monitoring System (OLMOS): Engine life cycle calculation and trending 22 p3034 N88-28010

Tornado: Airframe fatigue life monitoring 22 p3034 N88-28011

Applications of fatigue analyses: Aircraft engines [PNR90439] 22 p3044 N88-28066

Analyses and correlations of environment assisted fatigue crack propagation for attachment lugs 22 p3053 N88-28116

The effect of coatings on fatigue in aerospace materials --- gas turbine engines [PNR90460] 22 p3059 N88-28150

Human acclimatization and physical performance at high altitude [AD-A192651] 22 p3130 N88-28611

AGARD (Advisory Group for Aerospace Research and Development) engine disc material cooperative test (supplementary program) [AD-A193678] 23 p3179 N88-28925

Spray automated balancing of rotors: Methods and materials [NASA-CR-182151] 24 p3330 N88-29825

Rupture of carbon fiber reinforced plastics (T300-914) composite materials: Influence of initial first ply failures on the fatigue behavior [SNIAS-881-422-103] 24 p3342 N88-29892

FATIGUE TESTS

Study of the microscopic mechanisms of cyclic deformation. Development of a new approach: The case of aluminum [ISAL-87-0003] 02 p0149 N88-10936

Creep fatigue life prediction for engine hot section materials (isotropic): Third year progress review 02 p0188 N88-11173

Creep-fatigue behavior of NiCoCrAlY coated PWA 1480 02 p0189 N88-11176

Some new fatigue tests in high temperature water and liquid sodium environment [DE87-753019] 02 p0192 N88-11197

Review of investigations of aeronautical fatigue in the Federal Republic of Germany [LBF-S-178] 02 p0192 N88-11201

JPRS report: Science and technology. China [JPRS-CST-87-025] 03 p0300 N88-11888

Standard fatigue test specimens for fastener evaluation [AGARD-AG-304] 04 p0455 N88-12818

Application of finite element methods with cyclic elasto-plastic strain analysis to low cycle fatigue analysis of engine components [AR-004-512] 05 p0596 N88-13642

Fatigue 87, volume 1 [AD-A184045] 05 p0597 N88-13645

The mechanics of fatigue-crack nucleation in a low-alloy steel under fretting conditions 05 p0597 N88-13649

Fatigue crack growth behavior of A356-T6 cast aluminum alloy 05 p0599 N88-13660

Variable amplitude fatigue crack growth in aluminum alloys 2090-T8E41 and 7075-T651 05 p0602 N88-13687

Fatigue of 30CrMnSiNi2A notched specimens under spectrum loading 05 p0602 N88-13689

The how and why of variable amplitude testing 05 p0603 N88-13690

Fatigue strength of alloy A286 at cryogenic temperature 05 p0603 N88-13695

The role of inclusions in corrosion fatigue crack initiation in Q1N 05 p0604 N88-13699

Crack initiation studies in hydrogen embrittled spring steel strip 05 p0605 N88-13710

Applications of fatigue analyses: Transportation 05 p0608 N88-13733

Fatigue crack growth 05 p0608 N88-13734

Cyclic fatigue of ceramics at high temperatures [PB87-127700] 06 p0685 N88-14200

Fatigue 87, volume 2 [AD-A184046] 06 p0715 N88-14381

An investigation of fatigue crack growth in a ductile material at high growth rates 06 p0715 N88-14383

Cyclic deformation behaviour of cast irons with various graphite shapes in the temperature range 20 C less than or = T less than or = 500 C 06 p0715 N88-14384

Effect of hold time on fatigue of lead rich PbSn solder
06 p0715 N88-14387

Absolute fatigue thresholds in metallic materials
06 p0717 N88-14399

A re-evaluation of fatigue threshold test methods
06 p0717 N88-14401

Fatigue thresholds of C.Mn steels in saline environments 06 p0717 N88-14403

Mixed mode fatigue crack growth using the Brasilian disc 06 p0719 N88-14416

Crack closure phenomena in modes 1 and 2 interactions 06 p0719 N88-14417

Study of the evolution of short cracks in fatigue analysis --- aircraft construction materials
[DCO/L-46-555] 06 p0722 N88-14442

Characterization of current steels. The 35 NCD 16 alloy in 30 mm diam laminated bars made by Aubert and Duval
[CEAT-41/N/76] 07 p0832 N88-15046

Static and dynamic determination of aluminum oxide toughness
[PB87-146999] 07 p0869 N88-15275

Fatigue and damage tolerance design data for carbon fibre composites
[BAE-MSM-R-GEN-0454] 09 p1138 N88-16818

Colloquium on damage mechanics of graphite/expoxy laminates during fatigue
[DFVLR-MITT-87-08] 11 p1448 N88-18630

Statistical evaluation of experimental results from fatigue strength tests on CFRP composite materials
11 p1449 N88-18635

Comparative investigations of indirect crack length measurement under fatigue loading in a corrosive environment
[GKSS-86/E/64] 11 p1502 N88-18972

Determination of the elastic-plastic fracture toughness parameters under special consideration of the activities of the European Group on Fracture (EGF)
[GKSS-87/E/30] 11 p1502 N88-18973

Effects of moisture, elevated temperature, and fatigue loading on the behavior of graphite/epoxy buffer strip panels with center cracks
[NASA-TM-100558] 12 p1603 N88-19590

The cyclic stress-strain behavior of a single crystal nickel-base superalloy
[NASA-TM-100269] 12 p1607 N88-19610

Thermal-mechanical fatigue testing of a titanium-aluminide alloy
[AD-A189555] 12 p1609 N88-19620

Thermal-mechanical fatigue testing of a titanium-aluminide alloy
[AD-A189555] 12 p1609 N88-19620

Crack distribution and growth rates for critical fastener holes in Mirage wing RH79
[AD-A189080] 13 p1722 N88-20293

Dynamic tensile cyclic fatigue of Si3N4
[DE88-003919] 13 p1781 N88-20658

An investigation of the mechanical properties of improved carbon fibre composite materials
[RAE-TR-86021] 14 p1884 N88-21259

Effect of protective coatings on high-temperature fatigue of heat-resistant alloys 14 p1895 N88-21314

Growth of fatigue cracks in nickel alloys at high temperatures 14 p1896 N88-21318

Bithermal fatigue of a nickel-base superalloy single crystal
[NASA-TM-100885] 15 p2042 N88-22168

Spectrum fatigue testing for materials characterization
[VTT-RR-502] 15 p2088 N88-22443

Test procedures and standards for mechanical property measurements on metal matrix composites
[NPL-DMA(A)-153] 16 p2172 N88-22944

Application of the ONERA model to the life estimation under fatigue cracking of a Al-Li alloy. Parameter identification and test-experiment comparison under FALSTAFF loading
[ONERA-RT-32/7169-RY-063-R]
16 p2222 N88-23264

Detecting delaminations in CFRP specimens using X-ray techniques
[FFA-TN-1988-04] 18 p2479 N88-24704

Predictive corrosion modeling, volume 1
[AD-A191229] 18 p2485 N88-24739

Fatigue testing and damage development in continuous fiber reinforced metal matrix composites
[NASA-TM-100628] 19 p2610 N88-25489

Apparatus for pressure welding of titanium structures with a controlled rate of deformation
[RAE-TRANS-2161] 19 p2677 N88-25915

Automated measurement of crack length and load line displacement at elevated temperature
[AGARD-R-751] 20 p2814 N88-26695

T55-L-714 engine development and qualification. Engine M11 low cycle fatigue test report. (0213-005-87)
[AD-A192765] 21 p2897 N88-27197

T55-L-714 engine development and qualification. Engine M11 low cycle fatigue test report. (0213-005-87), volume 2, part 1
[AD-A192766] 21 p2897 N88-27198

Study of fatigue cracks in aluminum alloys. Influence of microstructure
[REPT-48-553] 22 p3056 N88-28134

AGARD engine disc cooperative test programme
[AGARD-R-766] 23 p3179 N88-28926

Damage initiation in the short beam shear test of composite materials using stiffness reduction
[AD-A194880] 24 p3340 N88-29883

Standard fatigue specimens for fastener evaluation --- aircraft components
[FFA-TN-1987-68] 24 p3384 N88-30157

The development of acoustic emission for structural integrity monitoring of aircraft
[AD-A196264] 24 p3427 N88-30398

FATTY ACIDS

NT ACETIC ACID

FAULT MECHANICS

U FRACTURE MECHANICS

FAULT TOLERANCE

Hardware fault insertion and instrumentation system: Mechanization and validation
[NASA-CR-181445] 01 p0078 N88-10497

Measurement of fault-tolerant parallel processors
[PB87-208328] 01 p0084 N88-10539

Fault tolerant considerations and methods for guidance and control systems
[AGARD-AG-289] 02 p0126 N88-10796

Computing systems dependability and fault tolerance: Basic concepts and terminology
02 p0127 N88-10797

Some approaches to the design of high integrity software 02 p0127 N88-10799

Robust control system design
02 p0127 N88-10800

Reliability modeling of fault-tolerant computer based systems 02 p0127 N88-10801

ISAURE: Integration of security and fault tolerance in the REALITE 2000 system 02 p0127 N88-10802

Flight test of a resident backup software system
02 p0128 N88-10805

Software reliability models for fault-tolerant avionics computers and related topics
[NASA-CR-181440] 02 p0220 N88-11382

Development of an interface for an ultrareliable fault-tolerant control system and an electronic servo-control unit
[NASA-TM-88236] 05 p0553 N88-13367

Study of fault tolerant techniques for satellite data handling
[FTT/REP/0001/SAAB] 05 p0632 N88-13860

Experiments in fault tolerant software reliability
[NASA-CR-181554] 05 p0632 N88-13863

Reliability of voting in fault-tolerant software systems for small output spaces
[TR-87-16] 05 p0632 N88-13864

Effectiveness of back-to-back testing
[TR-87-08] 05 p0632 N88-13865

RSDIMU acceptance testing system: Overview of acceptance software and procedures
05 p0632 N88-13866

Objects architecture: A comprehensive design approach for real-time, distributed, fault-tolerant, reactive operating systems
[AD-A185476] 06 p0755 N88-14631

Diagnostic emulation: Implementation and user's guide
[NASA-CR-178391] 06 p0756 N88-14638

Estimating the distribution of fault latency in a digital processor
[NASA-TM-100521] 06 p0760 N88-14666

Software-implemented fault insertion: An FTMP example
[NASA-CR-178423] 06 p0761 N88-14668

National Aeronautics and Space Administration (NASA)/American Society for Engineering Education (ASEE) Summer Faculty Fellowship Program, 1987, Volume 2
[NASA-CR-172009-VOL-2] 06 p0796 N88-14874

Fault-tolerant computer architecture based on INMOS transputer processor 06 p0797 N88-14880

Inadequacy of conventional dynamic recovery mechanisms in the presence of temporary failures
[AD-A186311] 07 p0866 N88-15251

Annotated bibliography on reliable system design
[PB88-109848] 07 p0866 N88-15254

Reliability modelling for fault-tolerant parallel processor
[AD-A185867] 07 p0900 N88-15451

Investigation of candidate data structures and searc algorithms to support a knowledge based fault diagnos system 07 p0923 N88-1560

EUREX D: An expert system for failure diagnosis an recovery in the TCS of the European retrievable carr EURECA 08 p1058 N88-1638

Integrated diagnostics 09 p1111 N88-1665

SURE reliability analysis: Program and mathematic
[NASA-TP-2764] 09 p1231 N88-1738

Examples of nonconservatism in the CARE 3 progra
[NASA-TM-100524] 09 p1233 N88-1739

Latent failures and coverage in fault-tolerant systems: A VLSI CMOS circuit design technique to aid tes generation
[AD-A187615] 10 p1325 N88-17921

Navigation recovery block design description
[NASA-CR-182473] 10 p1342 N88-18022

Clouds: A support architecture for fault tolerant, distributed systems 10 p1375 N88-18206

Resilient procedures: A structured replication approach 10 p1381 N88-18245

Automated radar target recognition based on models of neural nets 11 p1476 N88-18804

Theory and practice of fault tolerance in distributed systems
[AD-A187559] 11 p1540 N88-19204

Evaluation of network communication multiprocessor fault tolerance
[INPE-4305-PRE/1171] 12 p1674 N88-20011

An experiment in software reliability: Additional analyses using data from automated replications
[NASA-CR-178395] 12 p1676 N88-20017

A survey of provably correct fault-tolerant clock synchronization techniques
[NASA-TM-100553] 13 p1823 N88-20894

A fault injection experiment using the AIRLAB Diagnostic Emulation Facility
[NASA-CR-178390] 13 p1823 N88-20895

CARE 3 User's Workshop
[NASA-CP-10011] 14 p1954 N88-21646

Methodology for software reliability prediction, volume 1
[AD-A190018] 15 p2110 N88-22571

Methodology for software reliability prediction, volume 3
[AD-A190019] 15 p2110 N88-22572

Exhaustive and pseudo-exhaustive testing
[AD-A190140] 15 p2111 N88-22574

Argus reference manual
[AD-A190382] 15 p2111 N88-22578

Simulation of fault tolerance in a hypercube arrangement of discrete processors
[AD-A189682] 15 p2114 N88-22594

Analysis and testing of the SURE program
[NASA-TP-2817] 15 p2123 N88-22653

A fault tolerant supervision system
[INPE-4419-TDL/307] 15 p2148 N88-22819

Approximate agreement
[AD-A191030] 16 p2251 N88-23455

The PAWS and STEM reliability analysis programs
[NASA-TM-100572] 16 p2262 N88-23526

Rule-based fault-tolerant flight control
17 p2294 N88-23725

Development of a generic architecture
17 p2303 N88-23774

Toggle release
[NASA-CASE-MSC-21354-1] 18 p2523 N88-24969

Analysis and design of detection filters within closed-loop systems 18 p25[illegible]5 N88-24980

Effectiveness evaluation of fault-tolerant multiprocessor systems
[AD-A191688] 18 p2554 N88-25158

Semi-Markov adjunction to the Computer-Aided Markov Evaluator (CAME)
[NASA-CR-181645] 19 p2678 N88-25924

Distributed fault tolerant embeddings of binary trees in hypercubes
[AD-A192929] 20 p2839 N88-26840

Diagnosing faults in autonomous robot plan execution
[NASA-CR-182480] 20 p2841 N88-26859

An evaluation methodology for dependable multiprocessors
[AD-A192799] 20 p2842 N88-26863

FTMP data acquisition environment
[NASA-TM-100636] 21 p2938 N88-27447

Faultfinder: A diagnostic expert system with graceful degradation for onboard aircraft applications
22 p3035 N88-28018

Reliable onboard computing for critical space systems
[RR-670-I] 22 p3135 N88-28641

Approximate evaluation of semi-Markov chain reliability models
[AD-A194669] 23 p3223 N88-29185

Analysis of the effect of faulty spares on the performance of diagnostic algorithms in reliable systems
[AD-A193526] 23 p3223 N88-29186

Systolic array fault tolerance performance analysis
[AD-A193521] 23 p3244 N88-29306
Knowledge-based fault diagnosis on future space vehicles 23 p3254 N88-29374
ARGES: An expert system for fault diagnosis within space-based ECLS systems 23 p3255 N88-29380
SCARES: A Spacecraft Control Anomaly Resolution Expert System 23 p3256 N88-29381
Knowledge acquisition and rapid protyping of an expert system: Dealing with real world problems
23 p3258 N88-29394
Reasoning about fault diagnosis for the space station common module thermal control system
23 p3258 N88-29395
A methodology for multiple rule system integration and resolution within a singular knowledge base
23 p3261 N88-29413
Semantic based man-machine interface for real-time communication 23 p3262 N88-29421
MOORE: A prototype expert system for diagnosing spacecraft problems 24 p3418 N88-30343
Achieving real-time performance in FIESTA
24 p3418 N88-30344
Parallel and distributed computation for fault-tolerant object recognition 24 p3419 N88-30350

FAULT TREES

Fault tree safety analysis of a large Li/SOCl(sub)2 spacecraft battery 02 p0163 N88-11025
Diagnostic reasoning in digital systems
[NASA-CR-181564] 05 p0633 N88-13871
Conceptual issues in measuring the behavior of a distributed real-time process-control computer system
[DE87-009748] 05 p0638 N88-13898
Fault tree reliability analysis of the Naval Postgraduate School mini-satellite (ORION)
[AD-A186283] 07 p0866 N88-15250
A fast bottom-up algorithm for computing the cut sets of noncoherent fault trees
[DE88-003741] 09 p1220 N88-17320
Fault tree analysis and synthesis
[ETN-88-92236] 16 p2261 N88-23521
Applications of fault tree analysis to the design process
[DE88-007048] 18 p2525 N88-24982
Logic and fault simulation on the Mach1000 hardware accelerator
[DE88-009794] 19 p2717 N88-26130

FAUNA

U ANIMALS

FCC LATTICES

U FACE CENTERED CUBIC LATTICES

FDMA

U FREQUENCY DIVISION MULTIPLE ACCESS

FEASIBILITY

Laser gyro attitude control system feasibility
[AD-A189368] 13 p1720 N88-20285
Feasibility report: Operation of light air cushion vehicle at McMurdo Sound, Antarctica
[AD-A189057] 13 p1755 N88-20494

FEASIBILITY ANALYSIS

Preliminary study of a containerless processing facility for Columbus, executive summary
[ESA-ITT/AO/1-1834/85F] 01 p0032 N88-10203
The 250AH/90A active lithium-thionyl chloride cell for Centaur-G application 02 p0163 N88-11023
Evaluation of a scale-model experiment to investigate long-range acoustic propagation
[NASA-TP-2748] 02 p0230 N88-11450
Feasibility of alpha particle measurement in a magnetically confined plasma by CO2 laser Thomson scattering
[DE88-000039] 02 p0241 N88-11522
The Black College satellite telecommunications network planning in support of energy-related collaborative research
[DE88-000182] 03 p0307 N88-11940
Repulsive force support system feasibility study
[NASA-CR-178400] 04 p0402 N88-12497
Light funnel concentrator panel for solar power
[NASA-CR-179223] 04 p0464 N88-12870
The VISTA spacecraft: Advantages of ICF (Inertial Confinement Fusion) for interplanetary fusions propulsion applications
[NASA-CR-181549] 04 p0491 N88-13024
Ground vehicle convoying
[DE88-000360] 04 p0502 N88-13088
Performance monitoring and analysis of electric van fleet vehicles
[DE88-900066] 04 p0502 N88-13091
Study of the feasiblity of a satellite communication system for road transportation home office to vehicle communication. Volume 1: Conceptual analysis
[SC/87-E/6-VOL-1] 05 p0575 N88-13505
Study of the feasibility of a satellite communication system for road transportation home office to vehicle communication. Volume 2: Market study
[SC/87-E/6-VOL-2] 05 p0575 N88-13506
The gamma-ray laser project
[AD-A184824] 05 p0587 N88-13578
Stress intensity factors for cracking metal structures under rapid thermal loading, phase 1
[AD-A184112] 05 p0591 N88-13606
Feasibility study for gas-grain simulation facility
[NASA-CR-177468] 05 p0646 N88-13954
Feasibility study of a carbon dioxide observational platform system. Volume 2: Programmatics
[NASA-CR-180404] 06 p0672 N88-14114
Diamond turning of silicon for optics applications
[DE88-002501] 07 p0840 N88-15095
Holography of the ionosphere at HIPAS
[AD-A186237] 07 p0877 N88-15322
Measurement and modification of sensorimotor system function during visual-motor performance
[AD-A186351] 07 p0889 N88-15387
The feasibility of using TAE as the UIL for the space station and for other internal NASA tasks and projects
07 p0925 N88-15618
Columbus feasibility studies. Volume 1: Requirements and system concept
[ETN-88-91073] 09 p1134 N88-16799
Study of large solar arrays (SOLA), phase 2A
[BAE-SS/1109] 09 p1186 N88-17106
A proposal for a feasibility study on the design of software interfaces in large systems
[NPL-DITC-89/87] 09 p1222 N88-17330
Feasibility of chemical lasers based on chain reaction involving hydrogen fluorination with thermal branching mechanism 09 p1238 N88-17420
Study of Large Solar Arrays (SOLA). Phase 2A: Amplifying information to final report (SS/1109)
[BAE-SS/1110] 09 p1248 N88-17480
Rendezvous and docking verification and demonstration in orbit, executive summary
[MBB-303-16/86] 10 p1291 N88-17719
Cape Blanco wind farm feasibility study
[DE88-003748] 10 p1348 N88-18059
Cape Blanco wind farm feasibility study
[DE88-003749] 10 p1349 N88-18060
Rapid underway sediment classification by electrical methods
[AD-A187477] 10 p1357 N88-18114
Computer architecture for research in meteorology and atmospheric chemistry
[PB88-145313] 11 p1510 N88-19020
An economic analysis of a multi-commodity fruit and vegetable irradiator
[DE88-003425] 11 p1524 N88-19098
Feasibility study of generating plans and strategies for software testing by knowledge based system
[AD-A187834] 11 p1529 N88-19134
Feasibility studies of the growth of 3-5 compounds of boron by MOCVD
[NASA-CR-181622] 11 p1561 N88-19343
The status of R and D for superconducting power transmission systems
[DE88-003499] 11 p1561 N88-19346
Mars Lander/Rover vehicle development: An advanced space design project for USRA and NASA/OAST
[NASA-CR-182570] 11 p1567 N88-19380
A technique for capture analysis of low thrust missions in a planetary system
[AD-A188934] 12 p1594 N88-19544
A new fire protection concept for electronic equipment
[AD-A188884] 12 p1614 N88-19651
An investigation of classical dynamic scaling techniques applied to an oleo-pneumatic landing gear strut
[AD-A187664] 13 p1721 N88-20292
Proof of the feasibility of coherent and incoherent schemes for pumping a gamma-ray laser
[AD-A189238] 13 p1774 N88-20613
Federal Ocean Energy Technology
[DE87-012279] 13 p1792 N88-20722
An assessment methodology for thermal energy storage evaluation
[DE88-004642] 13 p1794 N88-20732
Conservative finite volume solutions of a linear hyperbolic transport equation in two and three dimensions using multiple grids
[NASA-CR-182715] 13 p1828 N88-20934
Molybdenum-base cermet fuel development
[DE88-005529] 13 p1839 N88-21003
Modulatable thin film field emission space gun
[AD-A189279] 13 p1845 N88-21043
Statistical analysis of feasibility of non-destructive inspection of mechanical properties of hot worked pipes of alloy steels
[BLL-M-37598-(5828.4)] 14 p1922 N88-21455
Preliminary market analysis for large zeolite crystals
[NASA-CR-182882] 15 p2049 N88-22207
Superconductivity in power engineering
[DE88-701414] 15 p2141 N88-22776
Time-domain frequency-selective optical memories: A study of the basic mechanisms and potential systems
[AD-A190854] 16 p2274 N88-23607
MBE of HgCdTe
[AD-A191423] 16 p2283 N88-23671
Colombus feasibility studies, executive summary
[ETN-88-92334] 17 p2311 N88-23820
Automatically generated acceptance test: A software reliability experiment
[NASA-CR-181667] 17 p2347 N88-23984
Assessment of nuclear reactor concepts for low power space applications 17 p2423 N88-24409
Heat pump-augmented systems for spacecraft thermal management 17 p2424 N88-24419
Molybdenum-base cermet fuel development
17 p2434 N88-24481
TRICE design, evaluation and feasibility tests
17 p2437 N88-24498
Search and rescue satellite system (SERES), phase A0
[ETN-88-92335] 18 p2472 N88-24669
The efficacy of using human myoelectric signals to control the limbs of robots in space
[NASA-CR-182901] 18 p2553 N88-25155
Technical feasibility study of applying auto-control methods to plating process solutions
[DE88-008014] 19 p2641 N88-25670
Inertial fusion in the nineties
[DE88-007913] 19 p2730 N88-26214
Feasibility of producing jet fuel from GPGP (Great Plains Gasification Plant) by-products
[DE88-010233] 20 p2781 N88-26492
Program for the feasibility of developing a high pressure acoustic levitator
[NASA-CR-182154] 20 p2782 N88-26498
SDI: Myth or reality
[DE88-009121] 20 p2847 N88-26901
Study of comet nucleus gamma-ray spectrometer penetration system
[NASA-CR-177393] 20 p2883 N88-27120
Theoretical-numerical study of feasibility of use of winglets on low aspect ration wings at subsonic and transonic Mach numbers at reduce drag
[NASA-CR-4174] 21 p2892 N88-27168
Supersonic transport/hypersonic transport (SST/HST) development
[REPT-881-111-101] 21 p2896 N88-27192
Experimental investigation of simplest inhomogeneities in cylindrical slit line
[DE88-702388] 21 p2933 N88-27418
Application of Dynamic Extended Range Forecasting (DERF) to the monthly forecast problem
22 p3125 N88-28578
Laboratory feasibility study of a composite embedded fiber optic sensor for measurement of structural vibrations
[AD-A194270] 22 p3152 N88-28754
Performance and technical tolerance --- space projects 22 p3160 N88-28812
SRB/SLEEC (Solid Rocket Booster/Shingle Lap Extendible Exit Cone) feasibility study, volume 1
[NASA-CR-178973] 23 p3187 N88-28964
Space-charge-wave solid state microwave amplifier
[AD-A193792] 23 p3208 N88-29091
Large area nuclear particle detectors using ET materials
[NASA-CR-180777] 23 p3215 N88-29136
Advanced development waste processing unit for combat vehicles, phase 2
[AD-A193793] 23 p3243 N88-29302
Feasibility study of a microprocessor controlled actuator test mechanism
[AD-A194654] 23 p3249 N88-29337
Lattice-matched HgZnTe epitaxy development
[AD-A193677] 23 p3292 N88-29600
New developments in capital cost estimating
[DE88-005392] 23 p3297 N88-29638
JUH-1H redesigned pneumatic boot deicing system flight test evaluation
[AD-A194918] 24 p3322 N88-29785
Dielectric millimeter waveguides: A feasibility study for a novel dielectric millimeter waveguide
[AD-A195104] 24 p3366 N88-30042

FEATURE EXTRACTION

U PATTERN RECOGNITION

FEDERAL BUDGETS

National Aeronautics and Space Administration Authorization Act, 1988
[PUB-LAW-100-147] 03 p0385 N88-12422
Department of Housing and Urban Development, and Certain Independent Agencies Appropriations, 1988, Part 2
[S-HRG-100-106-PT-2] 03 p0385 N88-12423

Department of Housing and Urban Development-Independent Agencies Appropriations for fiscal year 1988, Thursday, 9 April 1987: National Aeronautics and Space Administration
03 p0386 N88-12424

Department of Housing and Urban Development-Independent Agencies Appropriations for fiscal year 1988, Friday, 10 April 1987: National Aeronautics and Space Administration
03 p0386 N88-12425

The 1988 NASA (National Aeronautics and Space Administration) authorization
[GPO-80-245] 05 p0659 N88-14044

The 1988 National Aeronautics and Space Administration (NASA) authorization
[GPO-76-600] 06 p0792 N88-14854

Department of Housing and Urban Development independent agencies appropriations for 1989. Part 7: National Aeronautics and Space Administration
[GPO-85-166] 16 p2286 N88-23689

The Department of Defense report on the merit review process for competitive selection of university research projects and an analysis of the potential for expanding the geographic distribution of research for the Committees on Appropriations, United States Congress
[AD-A191842] 18 p2588 N88-25379

Competition: Issued on establishing and using Federally funded research and development centers
[PB88-178884] 23 p3296 N88-29632

FEDERAL REPUBLIC OF GERMANY

U WEST GERMANY

FEED SYSTEMS

Trickle water and feeding system in plant culture and light-dark cycle effects on plant growth
03 p0361 N88-12273

Dynamics of propellant feedline systems
[AD-A184865] 05 p0580 N88-13537

Gas feed system for the T-15 tokamak discharge chamber
[DE88-700351] 07 p0935 N88-15682

An advanced extruder-feeder biomass liquefaction reactor system 18 p2535 N88-25042

FEEDBACK

NT BIOFEEDBACK
NT NONLINEAR FEEDBACK
NT SENSORY FEEDBACK

New feedback design methodologies for large space structures: A multi-criterion optimization approach
04 p0408 N88-12535

Investigation, development and application of optimal output feedback theory. Vol. 4: Measures of eigenvalue/eigenvector sensitivity to system parameters and unmodeled dynamics
[NASA-CR-4108] 04 p0482 N88-12969

Sojourn times in the M/G/1 queue with deterministic feedback
[CWI-OS-R8708] 08 p1074 N88-16479

The linear dependency structure of covariance nonstationary time series
[AD-A186548] 09 p1232 N88-17383

Local bifurcation control
[AD-A187435] 10 p1324 N88-17915

Summary of Payload Integration Plan (PIP) for Starlab-1 flight experiment, enclosure 3
[NASA-TM-89713] 11 p1522 N88-19086

A comparison of keyboard designs for cockpit applications
[AD-A187775] 12 p1581 N88-19460

Development of an optical feedback based high accuracy beam transmissometer
[AD-A189396] 12 p1692 N88-20122

Robust decentralized control of large flexible structures
[DE88-005416] 13 p1824 N88-20902

Ultrahigh coherent semiconductor lasers and their applications to Rb atomic clock
14 p1976 N88-21789

Generation of number-phase minimum uncertainty states 14 p1978 N88-21803

Conditions for information capacity of the discrete-time Gaussian channel to be increased by feedback
[AD-A190317] 15 p2127 N88-22687

Optimizing feedback utilization in motor skill training
[AD-A191559] 18 p2552 N88-25146

A random access algorithm for environments with capture and limited feedback capabilities
[AD-A192233] 20 p2790 N88-26552

Force servo control of a commercial gantry robot
[DE88-006649] 20 p2808 N88-26660

Mode locking of semiconductor laser with external cavity
[AD-A196018] 24 p3378 N88-30117

FEEDBACK CONTROL

NT CASCADE CONTROL

The design of a turboshaft speed governor using modern control techniques
[NASA-CR-175046] 01 p0053 N88-10339

Study of closed loop control singularity in dynamic systems with a constraint on the final state
[LAAS-87-180] 02 p0223 N88-11405

Extensions of the small mu test for robust stability
[OUEL-1666/87-REV] 02 p0223 N88-11406

An autonomous, closed-loop pointing system for use with satellite optics
[DE87-012011] 02 p0235 N88-11483

Active control of helicopter vibration using multiloop self-adaptive control 03 p0264 N88-11660

A modern control theory based algorithm for control of the NASA/JPL 70-meter antenna axis servos
04 p0436 N88-12706

Fast autotuning of a hydrogen maser by cavity Q modulation 04 p0436 N88-12707

Design of low order controllers for robust disturbance rejection in large space structures
[AD-A185202] 05 p0555 N88-13376

Simultaneous structural and control optimization via linear quadratic regulator eigenstructure assignment
05 p0594 N88-13622

On linear periodic controllers
[DE87-011174] 05 p0639 N88-13904

Super-short yttrium aluminate pulse generator with controlled resonator Q-factor 06 p0772 N88-14740

Active control of flexural vibrations in beams
06 p0794 N88-14866

An autopilot design for the United States Marine Corps' airborne remotely operated device
[AD-A186379] 07 p0820 N88-14983

MIG welding with pulsed wire feed
[PB87-143582] 07 p0863 N88-15234

Pulsed plasma arc welding process with double closed-loop adaptive penetration control system
[PB87-143780] 07 p0863 N88-15236

A weighting sequence approach to the analysis and design of multivariable control systems
[AD-A186086] 07 p0917 N88-15570

A dynamic simulation and feedback control scheme for the U.S. Marine Corps' Airborne Remotely Operated Device (AROD)
[AD-A186597] 08 p0953 N88-15784

Identification and feedback control of machine tool vibrations
[PB88-109715] 08 p0976 N88-15902

Design of a velocity and position control laboratory servo system
[AD-A186596] 08 p0990 N88-15997

Large-angle slewing maneuvers for flexible spacecraft
[NASA-CR-4123] 08 p1000 N88-16060

A direct approach to almost disturbance and almost input-output decoupling
[MEMO-641] 08 p1072 N88-16471

A method for designing robust multivariable feedback systems
[NASA-CR-182459] 09 p1225 N88-17341

A methodology for the synthesis of robust feedback systems
[NASA-CR-182455] 09 p1225 N88-17342

A fiber-optic link for pressure control of ion sources
[DE88-001782] 09 p1248 N88-17484

Robust controller design for flexible structures
[AD-A187217] 10 p1340 N88-18009

Piezoelectric laminates for torsional and bending model control: Theory and experiment
10 p1343 N88-18029

Time delays and boundary feedback stabilization in one-dimensional viscoelasticity, appendices A through H
[AD-A187534] 10 p1401 N88-18353

Research on output feedback control
[NASA-CR-182543] 11 p1534 N88-19167

Design for performance enhancement in feedback control systems with multiple saturating nonlinearities
[NASA-CR-182614] 11 p1535 N88-19168

Active feedback interaction with a shear layer
[AD-A188525] 12 p1573 N88-19410

Speed control of a missile with throttleable ducted rocket propulsion 12 p1597 N88-19561

The use of hardware-in-the-loop-techniques in the development of a modern air-to-surface missile system
12 p1597 N88-19562

An analysis of DREO's (Defence Research Establishment Ottawa) analog rebalance loops for the CSG-2 (Canadian Strapdown Gyroscope) tuned-rotor gyroscope
[AD-A188577] 12 p1629 N88-19749

Active vibration control of a cantilevered beam with three elastic coordinates
[AD-A188824] 12 p1636 N88-19797

Design of feedback control systems for stable plants with saturating actuators
[NASA-CR-182613] 12 p1681 N88-20050

Gas consumption estimation of an attitude control system of an artificial satellite (utilizing DRF) in limit cycle phase
[INPE-4338-RPE/553] 13 p1731 N88-20350

Sojourn times in feedback queues
[CWI-OS-R8710] 13 p1830 N88-20947

A feedback double path compensating control structure for the attitude control of a flexible spacecraft
[INPE-4464-PRE/1239] 14 p1880 N88-21240

Implementation of a visual servoing system for evaluation of robotic refueling applications
[AD-A189676] 14 p1954 N88-21645

A new approach to almost decoupling problems for linear and nonlinear systems
[MEMO-660] 14 p1962 N88-21700

A complexity transform for NP-complete problems
[OUEL-1708/87] 14 p1962 N88-21703

Systolic determination of absolute stability in feedback control systems
[OUEL-1704/87] 14 p1962 N88-21705

Open questions in closed-loop photodetection
14 p1979 N88-21812

Application of eigenstructure assignment techniques in the design of a longitudinal flight control system
[AD-A189644] 15 p2020 N88-22039

Multivariable control law design for the AFTI/F-16 with a failed control surface using a parameter-adaptive controller
[AD-A189848] 15 p2020 N88-22040

Feedback control of distributed parameter systems with applications to large space structures
[AD-A190536] 15 p2025 N88-22068

Approximation methods for the identification and control of distributed parameter systems
[AD-A190201] 15 p2124 N88-22662

Servo-actuator control for sampled-data feedback disturbance rejection --- helicopters
[ESA-TT-1002] 16 p2163 N88-22903

Analysis and design of gain scheduled control systems
[NASA-CR-182867] 16 p2163 N88-22904

Models describing muscle behavior and control
[LR-522] 16 p2238 N88-23368

Feedback decoupling and stabilization for linear systems with multiple exogenous variables
[ETN-88-92245] 16 p2255 N88-23474

Investigation of air transportation technology at Princeton University, 1986 17 p2294 N88-23724

Control of combustion and acoustically coupled fluid dynamic instabilities 17 p2318 N88-23843

Precise computer controlled positioning of robot end effectors using force sensors
[NASA-CR-182887] 17 p2391 N88-24213

Experimental evaluation of the MIT-SNL period-generated minimum time control laws for the rapid adjustment of reactor power 17 p2436 N88-24494

An optimal disturbance rejection control system for multimegawatt space nuclear power systems
17 p2436 N88-24495

Automatic feedback control of a rigid body for finite displacements 18 p2473 N88-24674

Analysis and design of detection filters within closed-loop systems 18 p2525 N88-24980

Multishaker modal testing
[NASA-CR-179355] 18 p2530 N88-25010

Design and testing of a luminance and chrominance stabilization system for a computer-controlled color display
[AD-A191922] 18 p2554 N88-25159

Frequency Analysis of Acoustic Emission - Application to machining and welding
[DE88-701478] 18 p2570 N88-25262

F-14 modeling study
[NASA-CR-4164] 19 p2603 N88-25462

Control of combustion instabilities in ramjet motors
19 p2625 N88-25574

Joint angle sensors for closed-loop control
19 p2673 N88-25891

Automatic calibration of space based manipulators and mechanisms
[NASA-CR-182804] 19 p2676 N88-25912

RRSAS (Robotic Radiation Survey and Analysis System) Project: A real time sensor driven robotic system
[DE88-006825] 20 p2808 N88-26661

Vibration control of large structures
[AD-A193317] 21 p2961 N88-27587

Feedback control of a hyperbolic partial-differential equation with viscoelastic damping
[AD-A192896] 21 p3003 N88-27810

Time periodic control of a multi-blade helicopter
[AD-A194435] 23 p3180 N88-28931

Robust control of multivariable and large scale systems
[AD-A194250] 23 p3266 N88-29441

Pilot modeling 24 p3314 N88-29736

Pilot modeling applications 24 p3314 N88-29737

An analysis of lateral-directional handling qualities and Eigenstructure of high performance aircraft
[AD-A194874] 24 p3328 N88-29814
Track performance considerations for monopulse radars
[AD-A196232] 24 p3360 N88-30007
K(sup th)-order extended linearization
[AD-A194786] 24 p3421 N88-30363
An approach to CMG steering using feedback linearization
[NASA-CR-183172] 24 p3422 N88-30369

FEEDERS
Harmonic considerations for electrical distribution feeders
[DE88-007849] 18 p2505 N88-24860

FEEDFORWARD CONTROL
A linear quadratic Gaussian with loop transfer recovery proximity operations autopilot for spacecraft
[NASA-CR-172028] 02 p0227 N88-11433
Investigation, development, and application of optimal output feedback theory. Volume 3: The relationship between dynamic compensators and observers and Kalman filters
[NASA-CR-4107] 05 p0638 N88-13900

FEEDING (SUPPLYING)
Utilizing dynamic stability of orient parts
[AD-A195730] 24 p3427 N88-30397

FEELINGS
U SENSORY FEEDBACK

FEMALES
Temperature regulation at rest and exercise during the human menstrual cycle
[AD-A186461] 08 p1050 N88-16341
Meta-analysis of leadership differences between males and females and the effect on performance
[AD-A187769] 11 p1564 N88-19361
Human factor in engineering work
12 p1663 N88-19970
Fit evaluation of female body armor
[AD-A188721] 14 p1953 N88-21638

FERMENTATION
Fed-batch control based upon the measurement of intracellular NADH 09 p1197 N88-17175
Design concepts for bioreactors in space
09 p1198 N88-17179

FERMI LIQUIDS
Renormalized Fermi liquid theory for disordered electron systems and the metal-insulator transition
[NOTA-INTERNA-900] 14 p1988 N88-21862

FERMI SURFACES
High T/sub c/ superconductor as a strongly correlated state
[DE88-003194] 08 p1091 N88-16569
Fermi level stabilization in semiconductors: Implications for implant activation efficiency
[DE88-006332] 15 p2145 N88-22801
Fermi level dependent native defect formation: Consequences for metal-semiconductor and semiconductor-semiconductor interfaces
[DE88-008247] 20 p2875 N88-27066

FERMIONS
NT ANTINEUTRINOS
NT BARYONS
NT CONDUCTION ELECTRONS
NT FAST NEUTRONS
NT LEPTONS
NT MESON RESONANCE
NT MUONS
NT NEUTRINOS
NT NEUTRONS
NT PROTONS
NT SOLAR NEUTRINOS
NT SOLAR NEUTRONS
NT SOLAR PROTONS
NT THERMAL NEUTRONS
Scalar densities and baryon mass differences in lattice QCD with Wilson fermions
[PREPRINT-544] 06 p0778 N88-14773
Phenomenological model of superconductivity of heavy fermions in U(sub 1-x)ThsubxBesub13
09 p1238 N88-17423
Magnetic properties of heavy fermion superconductors
[ETN-88-91078] 09 p1255 N88-17524
Heavy Fermions and coherence in Kondo lattices: Specific heat of low energy excitation in Cer systems
[ETN-88-91080] 09 p1255 N88-17525
Symmetry problems in particle physics
[DE88-004927] 12 p1688 N88-20099
Chiral symmetry breaking in finite quantum electrodynamics
[DE88-700860] 12 p1699 N88-20169
Mixing coefficients of the lattice weak Hamiltonian with dimension five operators
[PREPRINT-576] 14 p1968 N88-21749
Integrability of fermionic string in superfluid Hamiltonian approach
[DE88-701662] 16 p2284 N88-23678
Introduction to covariant formulation of superstring (field) theory
[DE87-703038] 18 p2586 N88-25363
Geometry of superconformal manifolds, part 1
[DE88-702405] 21 p3011 N88-27863
An overview of lattice QCD
[DE88-010867] 21 p3026 N88-27963
Gravitational redshift of self-gravitating systems of dark matter in the universe
[DE88-702688] 23 p3300 N88-29650

FERRIC IONS
Determination of aquo-complexes of chromium and iron in chromium plating and polishing solutions by ion chromatography
[AD-A190168] 15 p2039 N88-22148

FERRIMAGNETS
Theoretical and experimental investigations on a linear, permanently excited stepping motor
[ETN-88-91061] 09 p1158 N88-16939
The operational behavior of microprocessor-controlled and pulsed inverter-fed synchronous machines with permanent magnet excitation
[ETN-88-91479] 11 p1480 N88-18833

FERRITES
Static magnetization and microwave loss in shock-modified ferrites
[DE87-012362] 02 p0146 N88-10916
Loss measurement of 3-port ferrite switches in the 90 GHz range
[ESA-TT-1054] 03 p0310 N88-11958
Investigation of hexagonal ferrite film growth techniques for millimeter-wave systems applications
[AD-A184335] 03 p0383 N88-12406
The initiation and growth of fatigue cracks in carburised 9Cr1Mo steel 05 p0603 N88-13696
Propagation of fatigue crack in the medium-carbon steel containg both martensite and ferrite
[PB87-143962] 07 p0869 N88-15273
New technique for enhancing helium production in ferritic materials
[DE88-003048] 09 p1142 N88-16847
Eddy current nondestructive inspection of graphite epoxy using ferrite cup core probes
[AD-A189823] 15 p2074 N88-22365

FERRITIC STAINLESS STEELS
Laminated ferrous composites based on ultrahigh carbon (UHC) steels
[AD-A184617] 03 p0280 N88-11764
Reduced-activation ferritic steels: A comparison with Cr-Mo steels
[DE88-000332] 03 p0290 N88-11826
Impact behavior of 9-Cr and 12-Cr ferritic steels after low-temperature irradiation
[DE88-000333] 03 p0291 N88-11827
Mechanical properties of an acicular ferrite steel microalloyed to niobium and vanadium
[DE87-703547] 04 p0415 N88-12574
Swelling behavior of ferritic/martensitic steels
[DE88-001757] 06 p0682 N88-14177
Fracture-mechanical, statistics and fractographic investigations on the steel 20 MnMoNi 55 in the ductile-brittle transition domain
[ETN-88-91064] 09 p1144 N88-16856
Cost 501 Project U.K.10. Part 4: The oxidation of fecralloy steel co-extruded onto strong steel substrates
[AERE-R-12432-PT-4] 11 p1456 N88-18679
The fatigue behavior of ferritic and austenitic steels at elevated temperatures
[DE88-006304] 13 p1744 N88-20431
Low-chromium reduced-activation ferritic steels
[DE88-009060] 19 p2617 N88-25524
Environmental cracking of a superferritic stainless steel under slow strain rate conditions
22 p3053 N88-28117

FERROALLOYS
U IRON ALLOYS

FERROCENES
Investigation of fuel additive effects on sooting flames
[AD-A186403] 07 p0829 N88-15026

FERROELECTRICITY
Improper ferroelectricity: A theoretical and experimental study
[AD-A184614] 03 p0381 N88-12397
Assessment of electroceramics research in Europe and the Middle East
[AD-A186377] 07 p0836 N88-15074
Radiation hardness evaluation of thin film ferroelectric capacitors
[DE88-001357] 07 p0848 N88-15147
Physics and chemistry 07 p0883 N88-15359
Ferroelectric properties and impact behavior of the PVF2 polymer and the VF2/C2F3H polarized copolymers --- vinylidene polyfluorides
[ISL-CO-245/86] 08 p0971 N88-15876
Piezoelectric laminates for torsional and bending model control: Theory and experiment
10 p1343 N88-18029
Statistical-mechanical study of polyvinylidene fluoride
[AD-A188310] 12 p1609 N88-19624
Effect of uniaxial compression on physical and mechanical properties of ferroelectric ceramic material
16 p2180 N88-22993
Topological stereochemistry
[AD-A191867] 18 p2477 N88-24691
Research on crystal and film ferroelectric materials for optoelectronic applications
[AD-A193512] 23 p3291 N88-29597

FERROMAGNETIC MATERIALS
Applications of a theory of ferromagnetic hysteresis
[DE87-014725] 03 p0373 N88-12348
Influence of bond dilution on the free surface and interface Potts ferromagnetism
[DE87-703360] 04 p0497 N88-13061
Spin disorder resistivity and bare Curie temperature in the ferromagnetic superconductor ErRh4B4
[DE88-003016] 10 p1415 N88-18445
Excitations in magnetic low-dimensional systems: A spectroscopic study
[ETN-88-92230] 15 p2129 N88-22697
The Curie point radiator 17 p2424 N88-24420

FERROMAGNETISM
Influence of bond dilution on the free surface and interface Potts ferromagnetism
[DE87-703360] 04 p0497 N88-13061
Magnetic rare earth superlattices
[DE88-003483] 10 p1418 N88-18465
Simplified physical approach of the control by eddy current
[DE88-701076] 13 p1764 N88-20552
Algorithm for accounting the conditions in infinity for two-dimensional magnetostatics problems
[DE88-701673] 16 p2264 N88-23541
The Potts model in a random field
19 p2721 N88-26158
Ferromagnetic/semiconductor hybrid structures
20 p2865 N88-27013
Properties of synthetic magnetic superlattices
20 p2865 N88-27014
Observation of ferromagnetism in ultrathin f.c.c. films by spin polarised neutron reflection
20 p2865 N88-27015
Contribution to the study of order effects in the Ising model framework: Ground states and phase diagrams
[ONERA-NT-1987] 20 p2880 N88-27095

FERROUS METALS
JPRS report: Science and technology. USSR: Materials science
[JPRS-UMS-87-006] 03 p0285 N88-11791
GSSR powder metallurgy research, production expanding 03 p0286 N88-11797
Concentration coefficients of elements in ferromanganese nodules relative to ocean sediments
06 p0726 N88-14464
Remote acoustic sounding of ferromanganese nodules
06 p0727 N88-14471
Ferromanganese nodules of Antarctic sector in Pacific Ocean 06 p0727 N88-14472

FET (TRANSISTORS)
U FIELD EFFECT TRANSISTORS

FETUSES
Mother-fetus system as object for investigation of mechanisms of physiological effect of weightlessness
07 p0891 N88-15402
Spleen lymphocyte nucleic acids in pregnant rats flown in space and their offspring 07 p0892 N88-15403
Brain morphogenesis in rats developing in weightlessness 07 p0894 N88-15415

FEYNMAN DIAGRAMS
Chiral symmetry in the path-integral approach
[DE88-700833] 12 p1699 N88-20168
Calculations in perturbative string field theory
[DE88-011616] 22 p3158 N88-28798

FFT
U FAST FOURIER TRANSFORMATIONS

FIBER COMPOSITES
NT CARBON FIBER REINFORCED PLASTICS
NT GLASS FIBER REINFORCED PLASTICS
Ceramic-Ceramic Composites Meeting in Belgium
[ONRL-7-020-R] 01 p0019 N88-10118
Pressure effects on the thermal stability of SiC fibers
[NASA-TM-100146] 01 p0019 N88-10120
Behavior of graphites under intense heat loads
[DE87-012128] 01 p0028 N88-10179
Fiber-reinforced composite hot gas filters
[DE87-012257] 01 p0033 N88-10208

Fracture mechanical analysis of the initiation and propagation of matrix and surface cracks in thermally loaded fiber composite models
[ETN-87-90439] 01 p0062 N88-10400

Electron beam irradiation effects on carbon fiber reinforced PEEK composite
[DE87-753001] 02 p0142 N88-10890

Cumulative fatigue and life prediction of fibre composites. Part 1: Literature reviews
[BR101013] 02 p0142 N88-10893

Cumulative fatigue and life prediction of fibre composites. Part 2: Experimental techniques and results
[BR101014] 02 p0142 N88-10894

Need for composites, new materials discussed
02 p0160 N88-11001

The ability of modified pavement quality concrete to resist ground erosion caused by VTOL aircraft
[BAE-ARG-238] 03 p0267 N88-11683

Processing and properties of SiC/Nicalon composites
[DE87-013885] 03 p0279 N88-11757

Transply crack density detection by acousto-ultrasonics
[NASA-TM-100224] 03 p0279 N88-11758

Contributions to the investigation of mechanical behavior of gamma/gamma NbC Cotac composites at medium and at high temperature
[ESA-TT-1031] 03 p0280 N88-11760

Plasticity of fibrous composites
[AD-A184637] 03 p0280 N88-11765

Ultrasonic characterization of the nonlinear elastic properties of unidirectional graphite/epoxy composites
[NASA-CR-4100] 03 p0281 N88-11767

Development and application of composites
03 p0286 N88-11795

Carbon fiber reinforced glass matrix composites for space based applications
[AD-A184355] 04 p0410 N88-12546

Molecular composites: Processing, post-treatment and mechanics
[AD-A184458] 04 p0410 N88-12547

Interfacial strength development in thermoplastic resins and fiber-reinforced thermoplastic composites
[NASA-CR-181525] 04 p0411 N88-12549

Development of advanced fiber reinforced ceramics
[DE88-000779] 04 p0420 N88-12604

Optimal ribbing of long plate made of composite material 04 p0426 N88-12641

In-situ characterization of the interface of glass reinforced composites
[AD-A185136] 05 p0557 N88-13391

Fiber composite structural durability and damage tolerance: Simplified predictive methods
[NASA-TM-100179] 05 p0560 N88-13409

Study of ceramic-fiber/ceramic sol-gel based matrix composites
[SNIAS-872-430-120] 05 p0569 N88-13469

Design and test of high performance composite tubes for use in deep water drilling and production systems
[SNIAS-872-430-107] 05 p0572 N88-13487

Fatigue mechanisms in ARALL, a fatigue resistant hybrid aluminum aramid composite material
05 p0605 N88-13711

Temperature dependent mechanical properties of an alumina fiber reinforced aluminum composite
06 p0677 N88-14147

Thermo-mechanical behavior of high temperature fiber composites 06 p0678 N88-14149

Advanced organic composite materials for aircraft structures: Future program
[NASA-CR-181467] 06 p0678 N88-14155

Bending properties of aluminum base composite with CVD-fiber
[PB87-130878] 06 p0678 N88-14156

Characterization of mechanical damage mechanisms in ceramic composite materials
[AD-A185549] 06 p0686 N88-14205

Interface effects on the mechanical properties of ceramic composites
[AD-A185899] 07 p0826 N88-15009

Bibliography of textbooks on fibre reinforced plastics (212 books)
[PB87-146080] 07 p0827 N88-15017

Numerical solution methods for viscoelastic orthotropic materials
[NASA-CR-182381] 08 p0971 N88-15874

Effect of an optimized fiber orientation on transonic flutter characteristics of a high-aspect-ratio composite wing
[NAL-TR-930] 09 p1120 N88-16709

Fatigue behaviour of hybrid composites
[BR102236] 09 p1138 N88-16819

Design procedures for fiber composite box beams
[NASA-TM-100296] 09 p1139 N88-16828

Effect of post-cure heat-treatment on static and fatigue behaviour of XAS-914C carbon fibre composite
[AD-A186943] 10 p1294 N88-17735

Fabrication and materials evaluation of high performance aligned ceramic fibre reinforced glass matrix composite
[AERE-R-12517] 10 p1294 N88-17736

A fiber-resin micromechanics analysis of the delamination front in a DCB specimen
[NASA-TM-100540] 10 p1294 N88-17737

Mechanics of composite materials: Past, present and future
[NASA-TM-100793] 10 p1295 N88-17744

Finite element substructuring methods for composite mechanics
[NASA-TM-100297] 10 p1296 N88-17745

Friction and wear of monolithic and fiber reinforced silicon-ceramics sliding against IN-718 alloy at 25 to 800 C in atmospheric air at ambient pressure
[NASA-TM-100294] 10 p1304 N88-17796

Testing of a tail rotor system in a fiber composite type of construction
[MBB-UD-472/86] 10 p1314 N88-17854

Cavitation in model elastomeric composites
[AD-A187401] 11 p1447 N88-18625

Damage mechanics of fiber reinforced plastics: A general view 11 p1448 N88-18631

Backscatter from flaws in fiber-reinforced composites
11 p1450 N88-18639

Innovative design of composite structures: Further studies in the use of a curvilinear fiber format to improve structural efficiency
[NASA-CR-182576] 11 p1450 N88-18641

Matrix-fiber stress transfer in composite materials: Elasto-plastic model with an interphase layer
[PB88-136635] 11 p1450 N88-18643

Radiation and temperature effects on the time-dependent response of T300/934 graphite/epoxy
[NASA-CR-182603] 11 p1451 N88-18646

Oxidation and protection of fiberglass-epoxy composite masts for photovoltaic arrays in the low Earth orbital environment
[NASA-TM-100839] 11 p1465 N88-18734

Ultrasonic-velocity studies of composite and heterogeneous materials
[AD-A189000] 12 p1604 N88-19595

The place for thermoplastic composites in structural components
[AD-A189149] 12 p1604 N88-19596

Structural materials: The changing scene
12 p1703 N88-20190

Viscoelastic behavior of a polyetheretherketone (PEEK) composite
[AD-A189545] 13 p1734 N88-20368

Transient dynamics of fibre reinforced composite plates
[IIT-B/CE/RR/87-1] 13 p1734 N88-20370

Interfacial chemistry-structure and fracture of ceramic composites
[DE88-005516] 13 p1750 N88-20461

Hygrothermomechanical fiber composite fatigue: Computational simulation
[NASA-TM-100840] 14 p1884 N88-21257

Monolithic nature of transversely reinforced composites 14 p1885 N88-21267

Interface structure and properties of alumina/glass ceramic composites
[DE88-006219] 14 p1892 N88-21302

Superconducting transition temperature of Cu-Nb microcomposites 14 p1973 N88-21775

Structure and surface characterizations of high strength carbon fibers
[AD-A189642] 15 p2029 N88-22087

Damage models for delamination and transverse fracture
[AD-A189652] 15 p2029 N88-22088

Fracture toughness testing of a ceramic matrix composite
[AD-A189846] 15 p2029 N88-22089

An investigation of the failure response of laminates under biaxial stress
[AD-A190039] 15 p2029 N88-22090

Interfacial structure-property relationships at the fiber-matrix interphase in advanced composites
[AD-A190649] 15 p2030 N88-22093

Thermal expansion behavior of randomly oriented short carbon fiber reinforced copper composites
[NASA-TT-20175] 15 p2031 N88-22099

Reciprocating sliding wear characteristics of copper-carbon fiber composites
[NASA-TT-20176] 15 p2031 N88-22100

Fiber-reinforced plastic composites. Possibilities and limitations of applications as machine-construction materials
[NASA-TT-20159] 15 p2031 N88-22102

Processing, microstructure, and mechanical properties of silicon carbide particulate reinforced aluminum alloys
[AD-A188981] 15 p2037 N88-22136

The composite blade structural analyzer (COBSTRAN)
15 p2078 N88-22390

Whisker-reinforced ceramic composites for heat engine components 15 p2082 N88-22410

Nondestructive evaluation by acousto-ultrasonics
15 p2082 N88-22412

Design studies of primary aircraft structures in ARALL laminates
[LR-520] 16 p2160 N88-22888

A study of failure characteristics in thermoplastic composite material
[AD-A190613] 16 p2171 N88-22940

Behaviour of fibre-reinforced composites under dynamic loading
[AD-A191310] 16 p2174 N88-22955

Acousto-ultrasonic input-output characterization of unidirectional fiber composite plate by SV waves
[NASA-CR-4152] 16 p2217 N88-23224

Ceramics for turbine engines
17 p2323 N88-23873

Ceramic matrix composites 17 p2325 N88-23888

Polymer precursors for ceramic composites
17 p2326 N88-23890

SiC fiber reinforced reaction-bonded Si_3N_4 composites 17 p2326 N88-23892

Input-output characterization of fiber composites by SH waves
[NASA-CR-4153] 17 p2347 N88-23986

Creep behavior of tungsten/niobium and tungsten/niobium-1 percent zirconium composites
17 p2425 N88-24427

Carbon matrix composites prospective roles for biotechnology 18 p2477 N88-24694

Mixed-mode fracture of uniaxial fiber reinforced composites
[AD-A191629] 18 p2478 N88-24700

Sol/gel processing techniques for glass matrix composites
[AD-A191748] 18 p2478 N88-24701

Interaction of ultrasonic waves with composite plates
[AD-A191879] 18 p2478 N88-24702

Analysis of notched metal matrix composites under tension loading
[NASA-TM-100629] 18 p2480 N88-24713

Multiple scattering of waves in discrete random media
[AD-A191068] 18 p2499 N88-24823

Fatigue testing and damage development in continuous fiber reinforced metal matrix composites
[NASA-TM-100628] 19 p2610 N88-25489

Loading rate sensitivity of open hole composites in compression
[NASA-TM-100634] 19 p2610 N88-25490

Acousto-ultrasonic input-output characterization of unidirectional fiber composite plate by P waves
[NASA-CR-4162] 19 p2678 N88-25923

Structural optimization of fiber composite turbomachine blades
[ETN-88-92351] 20 p2760 N88-26372

The two isotropic asymptotes of fiber composites
[AD-A192305] 21 p2904 N88-27231

Effects of electron beam irradiation on mechanical properties at low and high temperature of fiber reinforced composites using PEEK as matrix material
[DE88-753134] 21 p2905 N88-27239

Fabrication of SiC fiber reinforced glass matrix by extrusion process and investigation of its mechanical properties
[ETN-88-92367] 21 p2906 N88-27244

Programs for preliminary design of composite materials which were developed by the design group of Aerospatiale Aquitaine
[REPT-881-430-112] 21 p2907 N88-27251

Simulation of moisture diffusion of fiber reinforced components of aircraft for general air transportation
[IFL-IB-87-05] 21 p2907 N88-27253

As-received microstructure of a SiC/Ti-15-3 composite
[NASA-TM-100938] 22 p3050 N88-28095

Analysis of stiffness reduction, failure and stress concentration in fiber composite laminates
[AD-A193519] 22 p3050 N88-28096

Durability of continuous fiber reinforced metal matrix composites
[AD-A193868] 22 p3050 N88-28097

Fracture behavior in multidimensional fiber-reinforced composites 22 p3051 N88-28099

Wave propagation and vibration of fibre reinforced laminates
[AD-A194144] 22 p3051 N88-28101

Elastic wave dispersion in laminated composite plate
[AD-A192289] 23 p3188 N88-28967

The effects of moisture loss and elevated temperature upon the material damping of fibre reinforced polymer matrix composites
[UTIAS-324] 23 p3188 N88-28970

Effect of fiber diameter on the reliability of composites - automated laser diffraction implementation
[AD-A193524] 23 p3188 N88-28972

An investigation of some basic properties of hybrid composite materials
[AD-A194136] 23 p3189 N88-28975

Investigation of a SiC/Ti-24Al-11Nb composite
[NASA-TM-100956] 23 p3190 N88-28980

A test for interfacial effects and stress transfer in ceramic matrix composites
[NASA-CR-182873] 24 p3340 N88-29880

A study of the critical factors controlling the synthesis of ceramic matrix composites from preceramic polymers
[AD-A195405] 24 p3340 N88-29881

FIBER OPTICS

Test equipment with fiber optic data bus and laser gyro strapdown system LTN-90 for the helicopter BO-105
[ESA-TT-1038] 01 p0005 N88-10025

Data Management Working Group report
01 p0016 N88-10097

Mid infrared LHS system packaging using flexible waveguides
[NASA-CR-181192] 01 p0093 N88-10607

Fiber optic engineering sensor system. Preliminary program management plan, phase 3 revision
[AD-A183663] 01 p0093 N88-10608

The use of fiber optics in the determination of temperature and extent of reaction in detonating explosives
[DE87-012632] 01 p0094 N88-10612

Fiber-linked telescope arrays on the ground and in space 01 p0095 N88-10626

Optical fiber interferometric sensor to measure temperature in gas flow
[ENST-87E006] 02 p0170 N88-11071

Ultrafast holography using optical fibers
[ISL-R-101/86] 02 p0176 N88-11096

Effects of radiation damage in optical fibers: A tutorial
[PB87-210308] 02 p0235 N88-11482

Radiation-induced transient attenuation of optical fibers at 800 and 1300 nm
[DE87-013165] 02 p0235 N88-11485

The design and construction of a thermally controlled single mode fiber switch
[ETN-87-90929] 02 p0236 N88-11491

The design and testing of an analog optical communication link capable of the simultaneous transmission of four frequency division multiplexed audio signals
[AD-A184695] 03 p0307 N88-11936

Integrated fiber-optic coupler
[AD-A184494] 03 p0377 N88-12369

An inexpensive real-time interactive three-dimensional flight simulation system
[AD-A184340] 04 p0402 N88-12499

Spectroscopic monitoring of RS CVn stars at Kitt Peak using the Penn State fiber optic echelle
04 p0509 N88-13127

In-situ characterization of the interface of glass reinforced composites
[AD-A185136] 05 p0557 N88-13391

Fiber-optic accelerometer investigation
[AD-A185359] 05 p0584 N88-13561

Streak camera dynamic range optimization
[DE88-001632] 05 p0586 N88-13571

Optical probe
[EP-PATENT-0-210-869-A1] 05 p0650 N88-13984

JPRS report: Science and technology. Japan
[JPRS-JST-87-027] 06 p0688 N88-14213

Developments in optical sensor technologies described 06 p0689 N88-14220

Program description of FIBRAM: A radiation attenuation model for optical fibers
[PB87-230686] 06 p0690 N88-14229

AVIRIS foreoptics, fiber optics and on-board calibrator
06 p0706 N88-14328

Photoinduced low-temperature changes in optical losses in fiber optics based on chalcogenide glasses
06 p0770 N88-14731

Fiber optic video link
[FOA-C-30444-3.1] 06 p0780 N88-14789

Fiber optic single mode sensors
[FOA-C-30453-3.1] 06 p0780 N88-14790

An inexpensive real-time interactive three dimensional flight simulation system
[AD-A184868] 07 p0821 N88-14989

Advanced communication systems: A report on fiber optic technology and its possible applications in the gas industry
[PB88-112792] 07 p0845 N88-15125

Soliton mode of propagation of light pulses through single-mode optical fibers and problems of its experimental realization 07 p0920 N88-15592

Fiber optics refractometer for absorption machines
[DE88-002296] 07 p0932 N88-15662

Development and study of fibre-optic link lines on the basis of the KEM-8-4PD, KEM-8-4PR quantum-electronic modules
[DE88-700372] 07 p0932 N88-15663

Aeropropulsion '87. Session 4: Instrumentation and Controls Research
[NASA-CP-10003-SESS-4] 08 p0955 N88-15794

Optical measurement systems
08 p0955 N88-15796

Fiber optics for controls 08 p0956 N88-15798

Summary record of presentations to the Federal Telecommunication Standards Committee/Fiber optics task group
[PB88-110853] 08 p0978 N88-15911

Stimulated Raman scattering of picosecond light pulses in long dispersive medium 08 p1078 N88-16498

Pressure and tension dependence of phase shift of polarization modes in birefringent single-mode fiber-optic waveguide 08 p1078 N88-16501

Parametric interaction of optical modes in fiber-optic light guide 09 p1235 N88-17406

Multichannel anisotropic single-mode fiber optics for transducers 09 p1240 N88-17429

Code division multiple access applied to fiber optic data transmission
[AD-A186873] 09 p1247 N88-17477

Failure-resistant Fibre-Optical Communication Line (FOCL)
[DE88-700470] 10 p1408 N88-18400

Design and implementation of a fiber optic RS232 link
[AD-A187319] 10 p1409 N88-18409

A conceptual design of an inertial navigation system for an autonomous submersible testbed vehicle
[AD-A188038] 11 p1438 N88-18578

Joint services electronics program
[AD-A188173] 11 p1478 N88-18822

Optically coupled tactile sensor array for robotics
11 p1550 N88-19273

A prototype fibre optic gyroscope for missile guidance applications 12 p1596 N88-19554

A fiber optic gyro strapdown reference system for guided weapons 12 p1597 N88-19560

Development of a high speed InGaAs/InP Schottky barrier photodetector for millimeter-wave fiber optical links
[AD-A188594] 12 p1629 N88-19750

Experimental and analytical investigation on a proposed embedded fiber optic displacement sensor
[AD-A189030] 12 p1630 N88-19756

Development of fiber optic systems for recording and transmitting holographic information
[AD-A189406] 13 p1773 N88-20603

Remote fiber fluorimetry techniques for pressure measurements
[DE88-004486] 13 p1773 N88-20604

Enzyme-based fiber optic sensors
[DE88-005674] 13 p1840 N88-21013

Development of high stability fiber optic spectrophotometric systems for study of solar/stellar magnetic activity
[AD-A189327] 13 p1852 N88-21088

Berry's phase in fiber optics 14 p1977 N88-21797

Amplification of signals in fiber optics using the stimulated Raman effect
[AD-A190281] 15 p2133 N88-22727

A 104-km unrepeatered bidirectional fiber optic demonstration link
[AD-A190282] 15 p2134 N88-22728

Clinical measurements using fiber optic sensors
[DE88-005624] 15 p2134 N88-22731

Tethered diagnostic package for use from the space station
[DE88-006264] 16 p2167 N88-22921

A new fiber-optic-based ion sensor
[AD-A191322] 16 p2274 N88-23612

A new fiber-optic-based phase-resolved phosphorescence spectrometer
[AD-A191325] 16 p2275 N88-23613

The role of fiberoptics in remote temperature measurement 17 p2329 N88-23909

Fiber waveguide sensors for intelligent materials
[NASA-CR-183028] 17 p2343 N88-23968

Optics: Perspectives for Measurement Techniques and Signal Processing for Flight Guidance --- conference
[DFVLR-MITT-87-21] 18 p2516 N88-24928

Navigation using the Teldix fiber-optic gyroscope
18 p2517 N88-24933

Digital fiber optic displacement sensors
18 p2518 N88-24937

Activities report of the Division of Optical Technology
[FOA-C-30477-3] 18 p2576 N88-25299

Optical pressure sealing couping (light joint)
[NASA-CASE-MFS-29348-1] 18 p2576 N88-25303

Low-loss, high-isolation, fiber-optic isolator
[NASA-CASE-NPO-17207-1-CU]
18 p2576 N88-25304

Overview of NASA research in fiber optics for aircraft controls
[NASA-TM-100919] 19 p2603 N88-25458

High speed opto-isolator for radar applications
19 p2658 N88-25795

MESFET compatible IMSM detectors
19 p2659 N88-25801

Radar and EW applications of multi-gigahertz optical components and systems 19 p2660 N88-25816

Characteristics and application of wideband guided-wave devices 19 p2660 N88-25817

Fiber optic sensors 19 p2670 N88-25870

Active phase compensation system for fiber optic holography
[NASA-TM-101295] 20 p2805 N88-26641

Fiber optic sensors with internal referencing
[NASA-TM-100893] 20 p2806 N88-26644

Use of fiber optic equipment for security
[DE88-007898] 20 p2853 N88-26943

An overview of the development of a linear broadband analog fiber-optic link
[DE88-008668] 20 p2854 N88-26945

A concept for an electro-optic explosive device
[DE88-009696] 21 p2923 N88-27349

Fiber-optics used to record high-speed photographs inside a pressurized tank during lethality testing
[DE88-011283] 21 p2951 N88-27529

A fiber optic synchronous detector using sample-and-hold circuits
[DE88-010973] 21 p3016 N88-27899

Modulated-splitting-ratio fiber-optic temperature sensor
[NASA-TM-101332] 22 p3042 N88-28062

Multichannel data transmission through a fiber optic cable
[AD-A193842] 22 p3070 N88-28221

Fiber optic sensing systems using high frequency resonant sensing heads with intensity sensors
[NASA-TM-101318] 22 p3080 N88-28293

Laboratory feasibility study of a composite embedded fiber optic sensor for measurement of structural vibrations
[AD-A194270] 22 p3152 N88-28754

Long haul underwater fiber optic link
[AD-A194487] 23 p3282 N88-29542

A fiber optic collective flight control system for helicopters
[AD-A195406] 24 p3328 N88-29818

Performance analysis of FDDI
[NASA-CR-183206] 24 p3413 N88-30321

A fiber optic beamforming processor for wideband direction finding
[AD-A194862] 24 p3428 N88-30404

Ultra-wideband direction finding using a fiber optic beamforming processor
[AD-A194861] 24 p3430 N88-30413

FIBER ORIENTATION

Ultrasonic characterization of the nonlinear elastic properties of unidirectional graphite/epoxy composites
[NASA-CR-4100] 03 p0281 N88-11767

Generalized coupled-mode equations, applications to fiber couplers 03 p0298 N88-11875

Determination of the fiber ratio in carbon fiber/resin composites by means of image analysis
[SNIAS-872-422-101] 05 p0558 N88-13398

Advanced organic composite materials for aircraft structures: Future program
[NASA-CR-181467] 06 p0678 N88-14155

Contribution to modeling flexion fatigue damage in unidirectional composite materials
[ECL-87-12] 08 p0965 N88-15843

Experimental study on the effect of fiber orientation on flutter characteristics of high-aspect-ratio transport wing
[NAL-TR-936] 09 p1120 N88-16708

Effect of an optimized fiber orientation on transonic flutter characteristics of a high-aspect-ratio composite wing
[NAL-TR-930] 09 p1120 N88-16709

A study of the mechanical behavior of a 2-D carbon-carbon composite 11 p1449 N88-18638

Innovative design of composite structures: Further studies in the use of a curvilinear fiber format to improve structural efficiency
[NASA-CR-182576] 11 p1450 N88-18641

Reinforcing of thermoplastic polycarbonate and polysulfone with carbon fibers: Production and characteristics of UD-compound objects
[NASA-TT-20158] 13 p1735 N88-20374

A viscoplastic constitutive theory for metal matrix composites at high temperature
14 p1929 N83-21500

Thermal expansion behavior of randomly oriented short carbon fiber reinforced copper composites
[NASA-TT-20175] 15 p2031 N88-22099

Reciprocating sliding wear characteristics of copper-carbon fiber composites
[NASA-TT-20176] 15 p2031 N88-22100

Fatigue damage development of various CFRP-laminates
[NASA-TT-20247] 16 p2172 N88-22945
Rupture of carbon fiber reinforced plastics (T300-914) composite materials: Influence of initial first ply failures on the fatigue behavior
[SNIAS-881-422-103] 24 p3342 N88-29892

FIBER REINFORCED COMPOSITES
Fiber-reinforced composite hot-gas filters
[DE87-012257] 01 p0033 N88-10208
Carbon fiber reinforced glass matrix composites for space based applications
[AD-A184355] 04 p0410 N88-12546
Molecular composites: Processing, post-treatment and mechanics
[AD-A184458] 04 p0410 N88-12547

FIBER STRENGTH
Pressure effects on the thermal stability of SiC fibers
[NASA-TM-100146] 01 p0019 N88-10120
Carbon-fiber reinforced aluminum
04 p0403 N88-12507
Lifetime of pristine optical fibers
[ETN-88-92246] 16 p2273 N88-23602
Strong fibers
[DE88-007798] 19 p2610 N88-25486
Relation between the mechanical characteristics of carbon-resin composites and their impact strength
[REPT-48-284/F] 21 p2907 N88-27249
A test for interfacial effects and stress transfer in ceramic matrix composites
[NASA-CR-182873] 24 p3340 N88-29880
Rupture of carbon fiber reinforced plastics (T300-914) composite materials: Influence of initial first ply failures on the fatigue behavior
[SNIAS-881-422-103] 24 p3342 N88-29892

FIBERGLASS
U GLASS FIBERS

FIBERS
NT BORON FIBERS
NT CARBON FIBERS
NT CERAMIC FIBERS
NT GLASS FIBERS
NT HAIR
NT METAL FIBERS
NT NYLON (TRADEMARK)
NT OPTICAL FIBERS
NT REINFORCING FIBERS
NT SYNTHETIC FIBERS
Ceramic composites by chemical vapor infiltration
[DE87-009128] 01 p0029 N88-10185
The friction and wear of TPS fibers
[NASA-CR-181496] 03 p0291 N88-11830
Method of obtaining of fire resistant polyacrylonitrile fiber or cloth from it
[AD-A185941] 07 p0836 N88-15071
Absorption, scattering, and thermal radiation by conductive fibers
[AD-A186105] 07 p0842 N88-15106
Comparison of ultrasonic flaw detection analysis for spherical composite test specimens using two data acquisition techniques
[DE88-005002] 12 p1634 N88-19782
The influence of the fiber-matrix bond on the mechanical behavior of NICALON/SiC composites
[DE88-006155] 13 p1734 N88-20369
Recommendations on developing polycrystalline alumina fiber 13 p1756 N88-20502
Polymer precursors for SiC ceramic materials
17 p2326 N88-23889
Raman characterization of AsF5-intercalated vapor grown graphite fibers
[AD-A191709] 18 p2491 N88-24778
Stress measurements in graphite fibers by laser raman spectroscopy
[AD-A191710] 18 p2491 N88-24779
Interface modification in Nicalon (trademark)/SiC composites
[DE88-009708] 20 p2767 N88-26409
A micromechanics model of the stiffness and strength of laminates with fiber waviness
[NASA-CR-181670] 20 p2768 N88-26413
Laboratory feasibility study of a composite embedded fiber optic sensor for measurement of structural vibrations
[AD-A194270] 22 p3152 N88-28754

FIBERS (MATHEMATICS)
Division algebras and sphere fibrations
[ETN-87-90677] 01 p0087 N88-10566

FIBONACCI NUMBERS
On color polynomials of Fibonacci graphs
[AD-A184133] 04 p0486 N88-12996
Relaxed heaps: An alternative to fibonacci heaps
[AD-A194030] 23 p3272 N88-29470

FIBRINOGEN
Distinctive features in blood clotting and fibrinolytic properties under effect of epinephrine in presence of hypoxia and hypercapnia 19 p2705 N88-26082

FIBROSIS
Toxic effects of man-made mineral fibers with particular reference to ceramic fibers
[AD-A187949] 11 p1519 N88-19072
Hierarchical structure in polymeric solids and its influence on properties
[AD-A194720] 23 p3197 N88-29029

FIBROUS MATERIALS
U FIBERS

FIDELITY
U ACCURACY

FIDUCIARIES
Programmable 10 MHz optical fiducial system for hydrodiagnostic cameras
[DE87-013223] 02 p0175 N88-11091

FIELD EFFECT TRANSISTORS
NT JFET
NT MODFETS
Phase 2 development of a 12 GHz MMIC FET amplifier
[IM-I86-1010] 01 p0038 N88-10240
Surface effects and low frequency noises in GaAs field effect transistors
[LAAS-87-179] 02 p0168 N88-11055
A study of charged particles/radiation damage to VLSI device materials
[NASA-CR-172036] 05 p0577 N88-13518
A GaAs MESFET balanced mixer with very low intermodulation
[AD-A184848] 05 p0655 N88-14015
Surface chemistry of chemically sensitive field effect transistors
[AD-A185917] 07 p0847 N88-15139
A report on the effects of neutron irradiation of GaAs semiconductors
[AD-A186816] 09 p1253 N88-17510
Nature of gigantic resistance fluctuations in metal-oxide-semiconductor wires
[DE88-002905] 09 p1256 N88-17533
Design of a charge sensitive preamplifier on high resistivity silicon
[DE88-003491] 10 p1323 N88-17907
Study of quantum mechanical effects in deep submicron, grating-gate field effect transistors
[AD-A188283] 10 p1325 N88-17923
Development of a multiplexer module for use in a spaceborne cryogenic environment based on GaAs MESFET technology
[RPT/CRY/62463/BOP] 11 p1559 N88-19335
Microelectronic applications of the conductor-thin insulator-semiconductor (CIS) structure
11 p1560 N88-19341
Radiation response of thin oxides grown by rapid thermal oxidation and rapid thermal annealing techniques
[DE88-003632] 11 p1561 N88-19347
Planning, construction, and commissioning of a vacuum apparatus with a cold surface for the measurement of transistor functions at 20 K
[JUEL-SPEZ-397] 12 p1622 N88-19703
Response characteristics of dual MOSFET gamma-ray sensors produced by Mitel Corporation
[AD-A189026] 12 p1630 N88-19755
Characterization of enhanced Schottky-barrier InGaAs/Al(1-x)As strained channel modulation-doped field-effect transistors
[AD-A188820] 12 p1698 N88-20162
Fundamental studies and device development in beta silicon carbide
[AD-A189540] 12 p1699 N88-20165
Focused ion beam fabrication of graded channel FET's in GaAs and Si
[AD-A189166] 13 p1845 N88-21040
Energy loss rates for light holes in InGaAs/GaAs strained layer single quantum wells
[DE88-005744] 13 p1848 N88-21062
MOSFET performance degradation due to hot carriers
13 p1848 N88-21063
Examination of temperature effects on gate-to-drain avalanche breakdown in GaAs MESFETs (Metal-Semiconductor Field Effect Transistors) by measuring light emission under RF drive
[AD-A189634] 15 p2141 N88-22778
Modeling the effects of heavy charged particles on MOSFETs (Metal-Oxide-Semiconductor Field Effect Transistors)
[AD-A190575] 15 p2143 N88-22792
The response of a power MOSFET (N-channel) and a dielectric isolated operational amplifier to the combined environmental effects of high temperature and total dose gamma radiation 17 p2406 N88-24309
Modeling of radiation dose dependence of MOSFETs
17 p2416 N88-24370
The response of selected semiconductor technolog to the combined environmental effects of high temperat and total dose gamma radiation
17 p2431 N88-2446
Development of 20 GHz monolithic transmit module
[NASA-CR-182134] 17 p2445 N88-2453
A monolithic reduced-size Ku-Band SPOT (Single-Po Double Throw) FET switch
[DE88-006273] 18 p2505 N88-2485
Planar fully ion-implanted high power InP MISFET
[AD-A191589] 18 p2582 N88-2533
Multigigahertz logic based on InP-MISFET's exhibitin extremely high transconductance
19 p2656 N88-2577
An optically strobed sample and hold circuit
19 p2656 N88-2577
Enhanced performance ultrabroadband distribute amplifiers 19 p2656 N88-2577
MESFET compatible IMSM detectors
19 p2659 N88-2580
Hot carrier effects in CMOS field effect transistors a cryogenic temperatures 19 p2662 N88-2582
Electrical and chemical sensors for biological ce research 19 p2669 N88-2586
Chemical multisensors with selective encapsulation o ion-selective membranes 19 p2670 N88-2586
Miniature radiation dosimeter for in vivo radiation measurements 19 p2672 N88-2588
Effect of process conditions on aluminum oxide thin film used in pH ISFET 19 p2673 N88-25892
Microwave amplifiers
[AD-A192974] 20 p2795 N88-26585
Transport in GaAs heterojunction ring structures
20 p2864 N88-27011
Resonant tunneling transistors and resonant tunneling hot electron spectroscopy 20 p2866 N88-27018
Random quantum interference in microdevices
20 p2866 N88-27021
Picosecond optoelectronic sampling of electrical waveforms produced by an optically excited field effect transistor
[AD-A192384] 21 p2935 N88-27428
Focused ion beam fabrication of graded channel FETs in GaAs and Si
[AD-A193098] 21 p2936 N88-27439
Techniques and instrumentation for transient characterization of metal-insulator-semiconductor diodes. Applications to metal-insulator InP system
[ECL-87-17] 21 p3025 N88-27959
A 2.3-GHz low-noise cryo-FET amplifier
22 p3066 N88-28195
An electronically tuned, stable 8415-MHz dielectric resonator FET oscillator for space applications
22 p3068 N88-28205
Large-signal modeling of gallium arsenide field-effect transistors 22 p3073 N88-28242
Functional study of the Si/SiO2 structures. Application to the implementation of an integrated ion sensor
[ECL-87-16] 22 p3073 N88-28246
Development and experimental verification of a two-dimensional numerical model of piezoelectrically induced threshold voltage shifts in GaAs MESFETs
[AD-A193462] 23 p3206 N88-29080
Optoelectronic gain control of a microwave single stage GaAs MESFET amplifier
[NASA-CR-182201] 24 p3368 N88-30055
Power MISFETs on OnP
[AD-A195242] 24 p3433 N88-30436
Joint services electronics program
[AD-A195731] 24 p3434 N88-30439

FIELD EMISSION
Different ways of looking at the electromagnetic vacuum
[DE87-013150] 01 p0089 N88-10584
Studies on temporal field emission from stainless steel surfaces
[DE87-014237] 02 p0147 N88-10919
Conditions for geomagnetically trapping sub-micron lunar ejecta between L = 1.2 and L = 3.1
04 p0521 N88-13203
New application of transition metal carbides detailed
06 p0675 N88-14132
Optimization of field emission electron beam sources for high-power lasers
[PB87-218814] 06 p0708 N88-14341
The acoustic-electric field analysis of multilayered surface acoustic wave devices
[ETN-88-91592] 09 p1242 N88-17446
Intelligent on board control for field emission electric propulsion system 12 p1589 N88-19513
A study of the interaction of light with sub-micron metallic surfaces
[DE88-003138] 13 p1776 N88-20624
Modulatable thin film field emission space gun
[AD-A189279] 13 p1845 N88-21043

Degradation of beam brightness by field emission from a cathode shroud
[DE88-008345] 20 p2794 N88-26576

Development of liquid metal field-emission sources for use in fast repetitive opening switches
[AD-A192230] 20 p2795 N88-26583

Progress in diagnostic techniques for SC (superconducting) cavities
[DE88-008600] 20 p2876 N88-27077

FIELD OF VIEW

Two dimensional path planning with obstacles and shadows
[AD-A184075] 04 p0397 N88-12474

A system overview of the Airborne Visible/Infrared Imaging Spectrometer (AVIRIS)
06 p0705 N88-14326

Space infrared telescope facility wide field and diffraction limited array camera (IRAC)
[NASA-CR-182704] 13 p1853 N88-21092

Flight simulator: Field of view utilized in performing tactical maneuvers
[AD-A192412] 20 p2762 N88-26379

Assessments of maneuverability with the TeleOperated Vehicle (TOV)
[AD-A191584] 21 p2993 N88-27751

Visual sensitivities under reduced oxygen
[AD-A195628] 24 p3406 N88-30279

FIELD STRENGTH

NT ELECTRIC FIELD STRENGTH
NT MAGNETIC FLUX

Monocrystalline silicon gradiometer for gravity experiments in space
[NASA-CR-181452] 01 p0050 N88-10321

Magnetic flux tubes as sources of wave generation
04 p0505 N88-13108

Measurements of stellar magnetic fields: Empirical constraints on dynamo and rotational evolution theories
04 p0518 N88-13185

Observations and analysis of the photospheric magnetic fields on dwarf G, K and M stars
04 p0520 N88-13196

Nonuniformity of electromagnetic field at Lambda = 10 6 micron wavelength inside atmospheric aerosol particles
06 p0772 N88-14743

Local properties of index-alpha stable fields
[AD-A186432] 07 p0912 N88-15530

Evaluation of CWMS (Continuous-Wave Measurement System) single-wire dipole antenna
[DE88-003979] 09 p1155 N88-16920

Some measurements of height gain at V.H.F.
12 p1617 N88-19671

Magnet strength fluctuations in the SSC (Superconducting Super Collider) lattice. Part 2: Frequency modulation
[DE88-006491] 15 p2141 N88-22774

Classical non-Abelian solutions for nonstandard Lagrangians
[DE88-701305] 16 p2263 N88-23532

Optical sensing of magnetic fields
19 p2670 N88-25871

Measurement of macroscopic electric fields in solar plasma structures
[AD-A193291] 21 3031 N88-27993

FIELD THEORY (ALGEBRA)

NT CUBIC EQUATIONS
NT QUADRATIC EQUATIONS

Prediction and spectral decomposition of wide sense stationary processes on Z squared
[ENST-87C001] 01 p0087 N88-10564

Integrable quantum systems and classical Lie algebras
[DE88-700872] 12 p1683 N88-20063

On the equivalence of four-dimensional self-duality equations to continual analog of the main chiral field problem
[DE88-700871] 12 p1686 N88-20083

String theory and algebraic geometry of moduli spaces
[CWI-PM-R8705] 13 p1849 N88-21070

Exact image theory for the problem of dielectric/magnetic slab
[NASA-CR-182865] 16 p2189 N88-23055

An introduction to poloidal and toroidal fields
[MITT-54] 17 p2394 N88-24232

General relativity invariance and string field theory
[DE88-702045] 19 p2737 N88-26252

Algebraic and arithmetic geometry in string theory
[CWI-PM-R8708] 20 p2848 N88-26904

Theory of Laplacian fractals: Diffusion limited aggregation and dielectric breakdown model
[PREPRINT-590] 22 p3144 N88-28701

FIELD THEORY (PHYSICS)

NT GRAND UNIFIED THEORY
NT INSTANTONS
NT QUANTUM CHROMODYNAMICS
NT STRONG INTERACTIONS (FIELD THEORY)
NT UNIFIED FIELD THEORY
NT WEAK INTERACTIONS (FIELD THEORY)

Anomalies in gauge theories
[DE87-014087] 02 p0229 N88-11444

Regular effective action of gauge field theory and quantum gravity
[DE87-703076] 02 p0247 N88-11560

On the degree of generality of inflationary solutions in cosmological models with a scalar field
[DE87-703079] 02 p0251 N88-11586

New notions about space-time and gravitation
[DE87-703259] 03 p0383 N88-12408

Gravity from symmetry breakdown of a gauge affine theory
[DE88-001671] 04 p0500 N88-13079

Non-minimal interaction of gravity with other physical fields: An overview
[DE87-703362] 05 p0624 N88-13819

Lagrangian procedures for higher order field equations
[DE87-703365] 05 p0640 N88-13911

Introduction to string field theory
[DE87-014583] 05 p0657 N88-14032

Gravitational interaction of massless fields with higher spins (s greater than 2) 06 p0775 N88-14760

Nonsymmetric metrics in nonlinear field theory
[DE88-700509] 07 p0913 N88-15537

Existence of absolutely closed universe
08 p1080 N88-16509

Activities report in nuclear physics
[ETN-88-91609] 09 p1245 N88-17458

Research in theoretical physics
[DE88-003201] 09 p1259 N88-17548

Single nucleon coincidence cross sections in a relativistic mean field theory
[CEBAF-PR-87-016] 11 p1546 N88-19243

On exterior variational calculus
[DE88-700861] 12 p1683 N88-20062

Topics in string theory: Task D
[DE88-004532] 12 p1699 N88-20167

Super Virasoro algebra and solvable supersymmetric quantum field theories
[DE88-752299] 15 p2127 N88-22681

To the field theory with a fundamental mass
[DE88-701159] 15 p2146 N88-22807

Secondary gauge conditions in field theory
[DE88-701499] 15 p2147 N88-22814

On a generalization of renormalization group equations to quantum field theories of an arbitrary type
[DE88-701143] 16 p2263 N88-23531

Computational quantum field theory
[DE88-700918] 16 p2284 N88-23672

Introduction to covariant formulation of superstring (field) theory
[DE87-703038] 18 p2586 N88-25363

Combining relativity and quantum mechanics: Schroedinger's interpretation of psi
[DE88-701899] 20 p2880 N88-27102

Superalgebras with Grassmann algebra-valued structure constants from superfields
[DE88-702239] 21 p3011 N88-27862

Closed string fields as parameters of extra gauge symmetry of open string field theory
[DE88-702046] 21 p3026 N88-27960

The Hilbert space of the closed bosonic string
[USIP-88-04] 22 p3151 N88-28747

Research in the theory of condensed matter and elementary particles
[DE88-010180] 22 p3151 N88-28749

Calculations in perturbative string field theory
[DE88-011616] 22 p3158 N88-28798

On the quantization of constrained generalized dynamics
[DE88-702223] 23 p3277 N88-29505

On neutrino fields in Einstein-Cartan theory
[MATH-REPT-208] 23 p3295 N88-29629

Introduction to string theory
[DE88-702706] 24 p3435 N88-30445

FIGHTER AIRCRAFT

NT F-4 AIRCRAFT
NT F-14 AIRCRAFT
NT F-15 AIRCRAFT
NT F-16 AIRCRAFT
NT F-18 AIRCRAFT
NT F-27 AIRCRAFT
NT F-106 AIRCRAFT
NT F-111 AIRCRAFT
NT HARRIER AIRCRAFT
NT MIG AIRCRAFT
NT MIRAGE AIRCRAFT

HiMAT flight program: Test results and program assessment overview
[NASA-TM-86725] 01 p0005 N88-10026

Comparison of wind tunnel and flight test afterbody and nozzle pressures for a twin-jet fighter aircraft at transonic speeds
[NASA-TP-2588] 02 p0121 N88-10765

Application of knowledge-based techniques to aircraft trajectory generation and control
02 p0129 N88-10811

The influence of load cycle reconstitution on fatigue behaviour
[ARL-STRUC-R-424] 02 p0192 N88-11198

Soviet aviation technology's state of the art SU-27 fighter
[AD-A184121] 03 p0259 N88-11628

Improvements to the adaptive maneuvering logic program
[NASA-CR-3985] 03 p0262 N88-11648

Flight propulsion control integration for V/STOL aircraft
[NASA-TM-100226] 03 p0267 N88-11680

Special Course on Fundamentals of Fighter Aircraft Design
[AGARD-R-740] 05 p0544 N88-13315

Fundamentals of fighter aircraft design
05 p0544 N88-13316

Mission requirements and aircraft sizing
05 p0545 N88-13317

Design of wings and wing/body configurations for transonic and supersonic speeds
05 p0545 N88-13318

Aircraft dynamics: Aerodynamic aspects and wind tunnel techniques 05 p0545 N88-13320

Techniques for performance optimisation in cruise and manoeuverability 05 p0545 N88-13321

Fundamentals of fighter aircraft design: Engine intake and afterbody 05 p0545 N88-13322

Airframe/store compatibility 05 p0545 N88-13323

Aeroelasticity and optimization in fighter aircraft design
05 p0546 N88-13324

Materials for fighter aircraft 05 p0546 N88-13325

Requirements and recommendations for the development of theoretical codes and experimental facilities in the near future 05 p0546 N88-13327

Examples of static aeroelastic effects on present combat aircraft projects 05 p0550 N88-13349

Trends in aeroelastic analysis of combat aircraft
05 p0550 N88-13350

A study of the Department of Defense configuration management policies and procedures as applied to the FA-18 Strike/Fighter program
[AD-A184872] 05 p0657 N88-14034

NASA supersonic STOVL propulsion technology program
[NASA-TM-100227] 06 p0668 N88-14093

Highlights of the 70th Flight Mechanics Panel Symposium on Flight Vehicle Development Time and Cost Reduction
[AD-A185831] 07 p0901 N88-15454

A model for estimating depot maintenance costs for Air Force fighter and attack aircraft
[AD-A187097] 09 p1105 N88-16624

A cost and benefit analysis of hydraulic fluid systems for the next generation of tactical aircraft
[AD-A186911] 09 p1116 N88-16690

Dynamic function allocation in fighter cockpits
[AD-A185397] 09 p1201 N88-17199

Neural network based architectures for aerospace applications 09 p1204 N88-17218

An examination of the impact of potential advances in component technology for future military engines
10 p1279 N88-17650

Research and development. Technical-scientific publications (1956-1987): Retrospective view and prospects. Jubilee edition on the occasion of the 75th birthday of Dipl.-Engr. Dr.-Engr. E. H. Ludwig Boelkow
[ISSN-0931-9751] 10 p1309 N88-17819

Future fighter maneuverability for air combat
[MBB/LKE-1/S/PUB/120] 10 p1312 N88-17843

Flight testing of fighter aircraft
[MBB/LKE-62/S/PUB/292] 10 p1312 N88-17844

The aerodynamic design optimisation of a forward swept wing fighter aircraft
[CAR-87-18] 11 p1433 N88-18553

Testing of the engine compartment fire extinguishing system in the F/EF-111 aircraft
[AD-A188801] 12 p1576 N88-19423

Workshop on Design Loads for Advanced Fighters
[AGARD-R-746] 12 p1579 N88-19449

Changes in USAF structural loads requirements
12 p1580 N88-19452

The relationship between operational flight manoeuvre parameters and design parameters
12 p1580 N88-19454

Design loads for Swedish military aircraft in a twenty years' perspective 12 p1580 N88-19456

Determination of design loads for modern combat aircraft 12 p1580 N88-19457

Manned simulation: Helpful means to determine and improve structural load criteria 12 p1581 N88-19459

Computer aided tactics for air combat
12 p1597 N88-19559

Avionics acquisition, trends and future approaches 12 p1702 N88-20184
Use of demonstration/validation prototypes: Impact on total development costs and times 12 p1703 N88-20194
Crack distribution and growth rates for critical fastener holes in Mirage wing RH79 [AD-A189080] 13 p1722 N88-20293
Viscoelastic behavior of a polyetheretherketone (PEEK) composite [AD-A189545] 13 p1734 N88-20368
The cooling of electronic equipment in fighter aircraft [MBB/LKE-312/S/PUB/258] 14 p1866 N88-21147
Model selection for the multiple model adaptive algorithm for in-flight simulation [AD-A189715] 15 p2016 N88-22022
Multivariable control law design for the AFTI/F-16 with a failed control surface using a parameter-adaptive controller [AD-A189848] 15 p2020 N88-22040
Kalman filter residual expert system [AD-A190520] 15 p2020 N88-22041
Flow visualization study of vortex manipulation on fighter configurations at high angles of attack 16 p2201 N88-23130
Task listing: Visually assisted and visually dependent tasks for fighter aircraft [AD-A191041] 16 p2244 N88-23404
PAN AIR analysis of the NASA/MCAIR 279-3: An advanced supersonic V/STOL fighter/attack aircraft [NASA-TM-86838] 17 p2298 N88-23750
Pilot report: AFTI (Advanced Fighter Technology Integration) F-111 [AD-A192937] 21 p2895 N88-27184
A cockpit natural language study: Vocabulary and grammar analyses [AD-A193289] 21 p2993 N88-27753
The impact of increased aircraft reliability on maintenance facility design [AD-A194395] 22 p3042 N88-28057
Combat aircraft 23 p3169 N88-28868
Inflight rearming [AD-A193564] 23 p3176 N88-28909
Multiple-Purpose Subsonic Naval Aircraft (MPSNA): Multiple Application Propfan Study (MAPS) [NASA-CR-175104] 23 p3177 N88-28917
Computers in weapons systems: A look at the F-15 [AD-A194498] 23 p3178 N88-28920
General operational and training visual concerns 23 p3242 N88-29295
Grid generation on and about a cranked-wing fighter aircraft configuration 23 p3246 N88-29318
Grid generation for an advanced fighter aircraft 23 p3246 N88-29319
Algebraic grid generation for fighter type aircraft 23 p3246 N88-29320
Aircraft dynamics: Aerodynamic aspects and wind tunnel techniques 24 p3313 N88-29731
The Soviet Stealth fighter: Check or checkmate [AD-A195200] 24 p3323 N88-29791
The cost and performance implications of reliability improvements in the F-16A/B [AD-A195096] 24 p3324 N88-29796
Integration of LANTIRN (Low Altitude Navigation and Targeting Infrared for Night) into operational fighter training [AD-A194906] 24 p3325 N88-29799

FIGURE OF MERIT
Evaluation of device figure of merit in microwave switching circuit design [AD-A184896] 05 p0577 N88-13520
High-resolution Real-Time Radiography (RTR) system design [AD-A187107] 09 p1166 N88-16992
Optimisation of the thermoelectric figure of merit of modified silicon germanium alloys [AD-A191347] 16 p2283 N88-23670
Preparation of improved PbSnTe thermoelectric alloys and evaluation of their figure of merit [AD-A191346] 17 p2445 N88-24538

FILAMENT WINDING
Development of a polyimide matrix for filament winding with improved extensibility and fracture toughness for permanent use at 200 C [BMFT-FB-T-86-118] 01 p0030 N88-10190
Composite bearing materials containing solid lubricant in filamentary form, stages 3 and 4 [IRD-87/2] 01 p0054 N88-10344
Core material --- honeycombs [EP-PATENT-0-196-926-A2] 05 p0558 N88-13393
The structures of large wound propulsion shells --- carbon fiber composites filament winding [SNIAS-872-430-118] 05 p0559 N88-13406
Comparison of ultrasonic flaw detection analysis for spherical composite test specimens using two data acquisition techniques [DE88-005002] 12 p1634 N88-19782
Woven frameworks for three-dimensional reinforcement 14 p1884 N88-21262
Optimal filament shells loaded with internal pressure in a centrifugal force field 14 p1885 N88-21266
Design of booster wound structures --- spacecraft structures [SNIAS-881-430-102] 21 p2905 N88-27228
Reinforced plastics: Winding and weaving technologies for space products [SNIAS-881-430-103] 21 p2922 N88-27341
NDE performance in predicting failure strength of spherical composite specimens with implanted flaws [DE88-008223] 21 p2959 N88-27575

FILAMENT WOUND CONSTRUCTION
U FILAMENT WINDING

FILAMENTS
Modeling of proximity coupling between superconducting filaments in superconducting dipole magnets [DE87-014684] 03 p0382 N88-12403
Solar-geophysical data number 514, June 1987. Part 2: (Comprehensive reports). Data for December 1986 [PB87-217279] 03 p0390 N88-12450
Mechanism of change of vortex structure orientation in type-2 superconductors 09 p1239 N88-17425
Solar-geophysical data number 519, November 1987. Part 2: (Comprehensive reports). Data for May 1987 and miscellanea [PB88-158910] 14 p2011 N88-21997
Diamond film by hot filament CVD method [NASA-TT-20335] 23 p3294 N88-29618

FILAMENTS (SOLAR PHYSICS)
U SOLAR PROMINENCES

FILE MAINTENANCE (COMPUTERS)
File usage analysis and resource usage prediction: A measurement-based study [NASA-CR-181553] 05 p0633 N88-13867
Usage analysis of user files in UNIX [NASA-CR-181561] 05 p0633 N88-13868
Relational data handling system for scientists [PB87-223426] 05 p0658 N88-14038
Ada user library [FOA-C-20657-2.7] 16 p2246 N88-23418
Unified interchange format for computer data (standard file format) [ESA-STR-225] 17 p2386 N88-24183
The SMITE object oriented backing store [RSRE-MEMO-4147] 23 p3244 N88-29308

FILLERS
Microstructural characterization of HSLA-100 GMA-weldments [AD-A187782] 11 p1457 N88-18683
Plasma joining of metal matrix composites [AD-A188559] 12 p1604 N88-19593
Hydrogen induced cracks in armor steel weldments fabricated with austenitic filler alloys [AD-A186733] 13 p1740 N88-20406
Ultrasonic characterization of ceramic joints [DE88-005844] 15 p2043 N88-22173
The mechanical behavior of particle filled thermoplastics [ETN-88-92234] 16 p2181 N88-22999

FILLETS
Methods of improving compacting quality of intricately shaped powder components [BLL-M-37412-(5828.4)] 08 p0968 N88-15859

FILM BOILING
Effects of surface tension and contact angle on sensible heating and boiling incipience in dielectric falling films [DE88-007057] 21 p2945 N88-27492

FILM CONDENSATION
Dilution refrigerator with non-valve adsorption system of sup 3/He circulation [DE88-700974] 15 p2050 N88-22209

FILM COOLING
Film cooling heat transfer on a turbine airfoil 02 p0186 N88-11156
Finite element analysis of three-dimensional steady and unsteady temperature fields (computation of temperature distribution of turbine blade with composite cooling) 03 p0300 N88-11887
National Aerospace Laboratory experiment 04 p0404 N88-12509
Film cooling effectiveness on a flat plate in high free-stream turbulence using a single row of 30 deg slant-hole injectors [AD-A190500] 15 p2147 N88-22816
Investigation of annular flow at high evaporation rates in view of liquid film cooling [DFVLR-FB-88-08] 21 p2949 N88-27517
Studies of gas turbine heat transfer airfoil surface and end-wall cooling effects [AD-A195165] 24 p3326 N88-29805
The thermal behavior of film cooled turbulent boundary layers as affected by longitudinal vortices [AD-A195155] 24 p3374 N88-30095

FILM THICKNESS
Characterization of the dimensions of colloidal calcium carbonate dispersions in toluene with neutron small-angle scattering [ECN-197] 06 p0680 N88-14167
Film thicknesses in circular elastohydrodynamic contacts [PB87-123725] 06 p0710 N88-14354
Effect of the gate oxide thickness on the speed of MOS integrated circuits [PB88-155783] 10 p1323 N88-17910
Specific heat of novel thin-film material systems 10 p1415 N88-18446
Basic mechanisms of diesel lubrication correlation of bench and engine tests [AD-A193360] 21 p2956 N88-27561

FILTERING
U FILTRATION

FILTERS
Least squares linear lags and limited memory filters [NASA-CR-178381] 03 p0372 N88-12339
Single-mode projection filters for modal parameter identification for flexible structures [NASA-CR-182680] 18 p2566 N88-25244

FILTRATION
NT SPATIAL FILTERING
Fiber-reinforced composite hot-gas filters [DE87-012257] 01 p0033 N88-10208
Reduction of temperature rise in high-speed photography [NASA-TM-100222] 02 p0176 N88-11100
Vapor compression distiller and membrane technology for water revitalization 03 p0359 N88-12262
Plume mechanics and aerosol growth processes [AD-A184467] 04 p0442 N88-12742
Proceedings of the 19th DOE/NRC Airborne Waste Management and Air Cleaning Conference [NUREG/CP-0086-VOL-1] 11 p1509 N88-19018
Proceedings of the 19th DOE/NRC Airborne Waste Management and Air Cleaning Conference [NUREG/CP-0086-VOL-2] 11 p1509 N88-19019
WKBJ method and strained coordinates for high frequency inertial wave filtering [INPE-4214-PRE/1095] 11 p1537 N88-19186
Observations on electrostatic effects in a filter test system [AD-A188797] 13 p1736 N88-20378
Reference filters for electrostatic charging tendency measurements of fuels [AD-A191717] 18 p2495 N88-24803
Characteristics of pressure loss during filtration using a porous ceramic filter [DE88-752547] 20 p2798 N88-26604

FINANCE
National Aeronautics and Space Administration Authorization Act, 1988 [PUB-LAW-100-147] 03 p0385 N88-12422
Department of Housing and Urban Development, and Certain Independent Agencies Appropriations, 1988, Part 2 [S-HRG-100-106-PT-2] 03 p0385 N88-12423
Means of financing --- space projects 22 p3161 N88-28823

FINANCIAL MANAGEMENT
Financial reporting: NASA (National Aeronautics and Space Administration) can improve compliance with GAO (General Accounting Office) standards and treasury requirements [PB88-172523] 18 p2587 N88-25373
Costs --- space projects 22 p3160 N88-28816
Value engineering --- space projects 22 p3160 N88-28817
Price estimates and analysis 22 p3161 N88-28818
Value analysis 22 p3161 N88-28819
Management of large space projects. Financial means. Part 1: Financing of constructors 22 p3161 N88-28822
Means of financing --- space projects 22 p3161 N88-28823
The role and the place of insurance of large space projects 22 p3161 N88-28826

FINE STRUCTURE
A work station for EXELFS data acquisition and analysis [USIP-87-10] 01 p0078 N88-10498
The optimum illumination conditions for EXELFS studies in a CTEM [USIP-87-08] 01 p0092 N88-10600

Instrumental and operational aspects of an EXELFS system connected to JEOL 100C STEM
[USIP-87-09] 01 p0092 N88-10601
Solar interferometry with a 4-aperture nonredundant and stabilized network 01 p0097 N88-10639
A data analysis package for RDF-determination fromEXELFS-spectra
[USIP-87-07] 01 p0104 N88-10681
EXELFS (Extended Electron Energy Loss Fine Structure) of amorphous and crystalline SiC
[DE87-013551] 02 p0151 N88-10948
Theoretical modeling of the fine structures in sunspots 02 p0256 N88-11617
Main results of atmospheric fine structure parameter observation in the lower thermosphere
06 p0735 N88-14518
Statistical fine structure in inhomogeneously broadened absorption lines in solids
[AD-A190341] 16 p2174 N88-22957
Statistical fine structure in the inhomogeneously broadened electronic origin of pentacene in p-terphenyl
[AD-A191211] 16 p2176 N88-22968
Functional and mechanical analysis of continuous media-application to the study of elastic composites with periodic structure: Homogenization
[NASA-TT-20188] 18 p2480 N88-24710
EXAFS studies of the microstructure of semiconductor alloys, defects and semiconductor-metal interfaces
20 p2868 N88-27031
Structural studies of (Ga,In)(As,P) alloys and (InAs) sub m (GaAs) sub n strained-layer superlattices by fluorescence-detected EXAFS 20 p2872 N88-27051
Can we calculate the fundamental dimensionless constants of physics
[DE88-702641] 23 p3295 N88-29625

FINENESS RATIO
Planform effects on the supersonic aerodynamics of multibody configurations
[NASA-TP-2762] 04 p0393 N88-12454

FINES
Study of mean free path effects on growth of ultrafine metallic aerosols
[AD-A190206] 15 p2039 N88-22149
Fine grain development by laser CVD
15 p2050 N88-22214
Superfine grain development by laser
15 p2050 N88-22215

FINGERS
Tactile sensing and inverse problems
[AD-A187464] 10 p1340 N88-18011

FINISHES
NT ENAMELS
NT GLAZES
Macroscopic distribution of fiber finish
[DCQ/L-48-283/F] 07 p0827 N88-15013

FINITE DIFFERENCE THEORY
Description of NCAR (National Center for Atmospheric Research) Community Climate Model (CCM1)
[PB87-203782] 01 p0072 N88-10462
A numerical and analytical investigation of Rayleigh-Taylor instability in a solid tungsten plate
[DE87-013593] 01 p0087 N88-10562
Finite difference solution of a generic differential equation
[PB87-205878] 01 p0087 N88-10568
FDM-FEM zonal method for viscous flow computations over multiple-bodies
[NAL-TR-925T] 02 p0170 N88-11069
Comparison between numerical solutions and measurements for a high speed turbine blade
[PNR90402] 02 p0172 N88-11082
Improved numerical methods for turbulent viscous recirculating flows 02 p0185 N88-11148
Differencing the diffusion equation on a mesh of triangles and quadrilaterals
[DE87-011550] 02 p0224 N88-11408
QUICKSILVER: A 3D, electromagnetic, PIC code
[DE87-013013] 02 p0245 N88-11547
Efficient numerical approaches for predicting supersonic flows with viscous/inviscid interaction
03 p0260 N88-11637
Numerical modeling: Finite methods
03 p0304 N88-11918
Numerical and experimental investigation of the unsteady temperature distribution in solar central receivers
[ESA-TT-1050] 03 p0347 N88-12193
Application of the finite difference method to the solution of mixed partial differential equations for the case of transonic flow
[ETN-87-90760] 03 p0370 N88-12327
A two-dimensional finite difference program for thermal analysis of rocket thrust chambers
[NASA-TM-100191] 04 p0409 N88-12539
Calculation of three-dimensional stationary turbulent boundary layer on root section of wing ignoring compressibility 04 p0424 N88-12630
Generating meshes for finite-difference analysis using a solid modeler
[DE88-001458] 04 p0439 N88-12729
Time-marching finite-difference methods for the three-dimensional Euler equations of contravariant velocity components 05 p0539 N88-13285
Steady waves in a nonlinear theory of viscoelasticity
[AD-A185548] 06 p0723 N88-14448
Numerical simulation of a controlled boundary layer
07 p0810 N88-14933
The numerical and analytical study of bifurcation and multicellular flow instability due to natural convection between narrow horizontal isothermal cylindrical annuli at high Rayleigh numbers
[AD-A186113] 07 p0849 N88-15151
Stability analysis of finite difference schemes for hyperbolic systems, and problems in applied and computational linear algebra
[AD-A185824] 07 p0908 N88-15499
Unsteady transonic algorithm improvements for realistic aircraft applications
[NASA-TM-100516] 08 p0949 N88-15760
The simulation of three-dimensional viscous supersonic flow past blunt bodies with a hybrid implicit/explicit finite difference method
[DFVLR-FB-87-32] 08 p0950 N88-15765
Computational Fluid Dynamics
[VKI-LS-1987-04] 08 p0984 N88-15951
A survey of upwind principles for the multidimensional Euler equations 08 p0984 N88-15953
Integration of Navier-Stokes equations in finite volume formulation 08 p0984 N88-15954
Adaptive finite difference methods in fluid dynamics
08 p0985 N88-15958
A study of finite difference and finite element vertical discretization schemes for baroclinic prediction equations
[AD-A186617] 08 p1040 N88-16291
FOR3D: A computer model for solving the LSS (Lee-Saad-Schultz) three-dimensional, wide angle wave equation
[AD-A186649] 08 p1080 N88-16511
Numerical calculation of turbulent recirculating flows
[TUM-LSM-84/29] 09 p1161 N88-16959
A quasi-three-dimensional calculation procedure for the prediction of flow and heat transfer in heat exchanger passages 09 p1165 N88-16985
Numerical solutions of two moving boundary problems by both finite difference and finite element methods with applications
[DE88-002867] 09 p1230 N88-17374
Navier-Stokes computations for circulation control airfoils 10 p1269 N88-17592
EXPLO: Explosives thermal analysis computer code
[DE88-001938] 10 p1307 N88-17814
A three-dimensional dual potential procedure for rotational flows 10 p1329 N88-17942
Application of a multigrid method to a buoyancy-induced flow problem
[DE88-003961] 10 p1397 N88-18326
Total Variation Diminishing (TVD) schemes of uniform accuracy
[NASA-TM-100552] 11 p1436 N88-18566
Accurate boundary conditions for exterior problems in gas dynamics
[NASA-TM-100807] 11 p1537 N88-19182
An adaptive grid finite difference method for time-dependent Magnetohydrodynamic (MHD) flows and its astrogeophysical applications
11 p1553 N88-19294
Experimental verification of a finite-difference time-domain thin slot algorithm
[DE88-005572] 13 p1817 N88-20859
Predicting oscillatory finite difference solutions to the heat equation: A comparative study of the coefficient and matrix methods
[AD-A189591] 13 p1825 N88-20911
A Lagrangian moving grid scheme for one-dimensional evolutionary partial differential equations
[CWI-NM-R8713] 13 p1827 N88-20922
Monolithic nature of transversely reinforced composites 14 p1885 N88-21267
Investigation of the behavior of fast propagating cracks using numerical simulation calculations
[W-6/87] 14 p1934 N88-21532
COMESH: A corner mesh finite difference code to solve multigroup diffusion equations in multidimensions
[DE88-701248] 15 p2108 N88-22555
Efficient, high resolution computations of projectile and missile flow fields
[AD-A191086] 16 p2158 N88-22873
Reduced order models for nonlinear aerodynamics
16 p2220 N88-23248
The good, the bad and the ugly: Comparing high-speed computer systems
[DE88-007498] 16 p2245 N88-23412
Study of the convergence of a finite difference scheme for acoustic propagation in the atmosphere in a parabolic approximation. Statistical calculation of the sound field in the presence of kinematic turbulence
[ONERA-RS-8/3641-PY-160-P]
17 p2394 N88-24235
Fundamental limits to the velocity of solid armatures in railguns 18 p2469 N88-24656
Cross stream differencing for integral boundary layer equations
[AD-A191744] 18 p2509 N88-24886
Adaptive local grid refinement in computational fluid mechanics
[AD-A192215] 18 p2510 N88-24890
Adaptive grid refinement for numerical weather prediction
[AD-A192172] 18 p2544 N88-25101
Transmitting boundary for finite-difference calculations with finite modeling of an infinite medium
[AD-A191441] 18 p2570 N88-25264
Modelling of thermal plasma systems
18 p2578 N88-25314
A multiple chamber volume-filling model for prediction of transient solid rocket motor ballistic performance
19 p2633 N88-25618
An implicit, high order accurate, upwind scheme for unsteady Euler equations 19 p2639 N88-25657
On the propagating speed in difference approximations for conservation laws 19 p2639 N88-25658
Some supraconvergent schemes for hyperbolic equations on irregular grids
[DE88-009113] 19 p2720 N88-26151
Five-point form of the nodal diffusion method and comparison with finite-difference
[DE88-004141] 19 p2720 N88-26154
Semi-discrete approximations to nonlinear systems of conservation laws; consistency and L(infinity)-stability imply convergence
[NASA-CR-181683] 19 p2721 N88-26157
Axisymmetric liquid sloshing under low-g conditions. Numerical simulation method (reference manual)
[NLR-TR-86057-U] 20 p2802 N88-26627
Implicit finite-difference simulation of an internal flow on a hypercube
[AD-A192474] 21 p2942 N88-27471
Implicit finite-difference simulation of an internal flow in a nozzle: An example of a physical application on a hypercube
[AD-A192475] 21 p2942 N88-27472
User's manual for C-HEMP: A two-dimensional wave propagation code. Volume 1: Description and derivations of the code
[AD-A193197] 21 p2944 N88-27466
Numerical predictions for the flow induced by an enclosed rotating disc
[PNR90463] 22 p3078 N88-28281
Applications of an exponential finite difference technique
[NASA-TM-100939] 22 p3084 N88-28312
Transient thermal analysis of three fast-charging latent heat storage configurations for a space-based power system
[DE88-009714] 23 p3186 N88-28960
Space marching Euler solvers
24 p3318 N88-29759
Three-dimensional gas turbine combustor modelling
24 p3349 N88-29937
On the application of finite-difference techniques for the computation of the flow field in gas turbine combustors with complex geometries 24 p3349 N88-29938
Numerical field model simulation of full scale fire tests in a closed spherical/cylindrical vessel
[AD-A195067] 24 p3359 N88-29998
An analysis of finite-difference and finite-volume formulations of conservation laws
[NASA-CR-177416] 24 p3370 N88-30071
Finite-difference simulations of Rayleigh-wave scattering by shallow heterogeneity
[AD-A194961] 24 p3402 N88-30259

FINITE ELEMENT METHOD
Contribution to the dynamical analysis of rheolinear nonconservative, gyroscopic systems using finite element methods
[ETN-87-90410] 01 p0050 N88-10320
Stress-strain behavior of components subject to residual stresses taking the example of an orifice plate
[FF-10/1986] 01 p0059 N88-10375
A DMAP for updating dynamic mathematical models with measured data
[NLR-MP-86027-U] 01 p0060 N88-10387
Thermal stress analysis of space shuttle orbiter subjected to reentry aerodynamic heating
[NASA-TM-88286] 01 p0061 N88-10389

best copy available

Reinforced flexural elements for TEMP-STRESS Program
[DE87-012961] 01 p0061 N88-10391

A mixed finite element method for the computation of stress in a composite with loaded holes
[ONERA-RT-34/4242-RY-054-R]
01 p0062 N88-10395

Correction to a single higher order theory of elastic plates
[ETN-87-90676] 01 p0062 N88-10397

Contribution to the numerical calculation of fracture-mechanical quantities for elastic and elastic-plastic material behavior, especially for mixed loads
[ETN-87-90435] 01 p0062 N88-10399

New fatigue demage analysis of complex engineering components based on Finite Element Methods (FEM)
[DFVLR-FB-87-15] 01 p0062 N88-10401

DETOUR: A deformed mesh/contour plot program
[DE87-013119] 01 p0082 N88-10525

Perfine: Personal finite elements on a microcomputer
[ETN-87-90678] 01 p0082 N88-10528

Error estimates for finite element approximations of parabolic variational equations
[BONNER-MATHE-SCHR-179]
01 p0087 N88-10569

A microstructural lattice model for strain oriented problems: A combined Monte Carlo finite element technique
[NASA-TM-100215] 02 p0150 N88-10939

FDM-FEM zonal method for viscous flow computations over multiple-bodies
[NAL-TR-925T] 02 p0170 N88-11069

Numerical solution of Euler equations for compressible fluids by the finite element method, volume 3
[ETN-87-90650] 02 p0170 N88-11070

Implementation of finite element quality assurance in a commercial industrial organisation
[PNR90393] 02 p0183 N88-11137

Reliability of finite element methods in North America
[AGARD-R-748] 02 p0184 N88-11139

Component specific modeling
02 p0187 N88-11166

Constitutive modeling for single crystal superalloys
02 p0187 N88-11168

Constitutive modeling for isotropic materials
02 p0188 N88-11171

Constitutive modeling for isotropic materials
02 p0188 N88-11172

Thermal expansion mismatch and oxidation in thermal barrier coatings 02 p0189 N88-11182

A numerical method for the treatment of kinked cracks in finite bodies 02 p0190 N88-11189

Concurrent algorithms for transient nonlinear FE analysis
[NASA-CR-181455] 02 p0221 N88-11389

Finite elements for 2D elliptic equations with moving nodes
[DE87-013501] 02 p0224 N88-11410

A finite element model for induction heating of a metal crucible
[DE87-014246] 02 p0246 N88-11551

Stability of mechanical joints in launching vehicles: Local and global stationary values of energy density
03 p0270 N88-11696

Theoretical investigation of stress concentrations in damaged carbon fibre reinforced plastic plate structures. Volume 1: Main text
[BR99872-VOL-1] 03 p0280 N88-11761

Theoretical investigation of stress concentrations in damaged carbon fibre reinforced plastic plate structures. Volume 2: Tables, figures and plates
[BR99873-VOL-2] 03 p0280 N88-11762

Three-dimensional finite element based, interative approach for analysis of laminated composites
03 p0280 N88-11763

Finite element analysis of three-dimensional steady and unsteady temperature fields (computation of temperature distribution of turbine blade with composite cooling)
03 p0300 N88-11887

Generalized hybrid variational principle, corresponding finite element model 03 p0301 N88-11895

Compactness of quasi-conforming element spaces, convergence of quasi-conforming element method
03 p0301 N88-11896

Numerical modeling. Finite methods
03 p0304 N88-11918

Calculation of the three dimensional flow in the impeller of hydraulic turbomachines using a finite element method
[ETN-87-90612] 03 p0315 N88-11988

Application of viscoplastic constitutive equations in finite element programs
[KFK-4254] 03 p0370 N88-12329

Total linearisation method for solving viscous free boundary flow problems by the finite element method
[PB87-222337] 04 p0441 N88-12737

NACHOS 2: A finite element computer program for incompressible flow problems. Part 2: User's manual
[DE86-001451] 04 p0443 N88-12750

TOPAZ: The transient one-dimensional pipe flow analyzer: An update on code improvements and increased capabilities
[DE88-001781] 04 p0443 N88-12751

Continuation finite element analysis of viscoelastic fluids 04 p0445 N88-12761

Nonlinear axial stiffness characteristics of axisymmetric bolted joints 04 p0452 N88-12799

A refined nonlinear analysis of laminated composite plates and shells
[AD-A184436] 04 p0454 N88-12811

Kinematic formulation of finite elements for plate bending 04 p0455 N88-12821

Large change-of-curvature effects in quadratic finite elements for CAD of membrane structures
04 p0480 N88-12958

A comparison of adaptive refinement techniques for elliptic problems
[DE88-000805] 04 p0485 N88-12987

The finite element method for electronic structure
[DE88-001708] 04 p0485 N88-12989

A finite element procedure for interference-fit and cold-working problems with limited yielding
[AR-004-517] 04 p0485 N88-12992

Trends in aeroelastic analysis of combat aircraft
05 p0550 N88-13350

Finite-element grid improvement by minimization of stiffness matrix trace
[NASA-TM-100255] 05 p0591 N88-13604

Finite element model for the stress and flexibility analysis of curved pipes
[DE87-703632] 05 p0592 N88-13606

Non-linear shipboard shock analysis of the Tomahawk missile shock isolation system 05 p0592 N88-13614

Modal survey of the space shuttle solid rocket motor using multiple input methods 05 p0593 N88-13617

Initial dynamic load estimates during configuration design 05 p0593 N88-13621

Exact finite element method analysis of viscoelastic tapered structures to transient loads
05 p0595 N88-13632

An efficient frequency response solution for nonproportionally damped systems
05 p0595 N88-13634

Shape optimization of damping layers
05 p0595 N88-13635

Dynamic response of laminated composite plates using a three-dimensional hybrid-stress finite-element formulation 05 p0596 N88-13639

Significance of foundation-soil separation in dynamic soil-structure interaction 05 p0596 N88-13641

Application of finite element methods with cyclic elasto-plastic strain analysis to low cycle fatigue analysis of engine components
[AR-004-512] 05 p0596 N88-13642

Strain-energy-release rate analysis of the end-notched flexure specimen using the finite-element method
[NASA-TM-100494] 05 p0608 N88-13735

An element of a multilayer shell for the computation of composite structures
[ONERA-RT-14/3542-RY-051-R]
05 p0610 N88-13742

Thermal finite-element analysis of space shuttle main engine turbine blade
[NASA-TM-100117] 05 p0610 N88-13745

Two low-order mixed methods for the elasticity problem
[PB87-225272] 05 p0610 N88-13749

Structuring data for concurrent vectorized processing in a transient dynamics finite element program
[DE87-013082] 05 p0636 N88-13890

Research and development of finite elements and iterative algorithms for elliptic partial differential equations
[DE88-001381] 05 p0643 N88-13934

Finite-element method for three-dimensional electric and electromagnetic field problems
[PB87-138731] 06 p0696 N88-14274

An evaluation of a translator for finite element data to resistor/capacitor data for the heat diffusion equation
[DE87-013926] 06 p0698 N88-14285

Extensions of the control volume based finite element method for fluid flow problems 06 p0700 N88-14296

Introduction to Computational Fluid Dynamics
[VKI-LS-1987-02] 06 p0701 N88-14300
Introduction 06 p0701 N88-14301
Finite element techniques 06 p0701 N88-14303

A zonal approach for the solution of coupled Euler and potential solutions of flows with complex geometries
[AD-A185465] 06 p0702 N88-14310

Methods for reducing computational costs of typical finite element unsteady hydrodynamic models
[AD-A185499] 06 p0702 N88-14312

Calculations of the turbulent wake behind a slender self-propelled double-body and comparisons with experiment
[AD-A185661] 06 p0703 N88-14314

Geometrically nonlinear analysis of stiffened panels
06 p0722 N88-14440

A periodic small-cluster approach to many-body problems
[DE88-002235] 06 p0763 N88-14663

Stabilized Galerkin method for convection-diffusion problems
[PB87-234985] 06 p0764 N88-14694

Impact of solids on composite materials
[NASA-CR-182395] 07 p0827 N88-15015

SRB combustion dynamics analysis computer program (CDA-1)
[NASA-CR-182404] 07 p0830 N88-15032

User manual for ATILA, a finite-element code for modeling piezoelectric transducers
[AD-A185948] 07 p0847 N88-15141

Hybrid FEM (Finite Element Method) approach to stress distribution in the vicinity of a notch in non-homogeneous materials
[PB87-143392] 07 p0868 N88-15298

The p-version of the finite element method for elliptic equations of order 2l
[AD-A186334] 07 p0911 N88-15523

Nacelle-wing interactions (studies 1986) development of a finite element code in a multi-domain version
[ONERA-RTS-10/3417-AY-308A]
08 p0950 N88-15764

Finite element methods for compressible flows
08 p0964 N88-15956

Finite Element Calculation Methods and Their Application to Turbomachinery Flows, volume 1
[VKI-LS-1987-05-VOL-1] 08 p0985 N88-15960
Finite element fundamentals, part 1
08 p0985 N88-15961
Finite element fundamentals, part 2
08 p0985 N88-15962
Finite element method computer implementation
08 p0985 N88-15963
Inviscid flows, part 1. Formulation of inviscid rotational flow problems by velocity potential and stream function methods. Applications to turbomachines
08 p0985 N88-15964

Finite Element Calculation Methods and Their Application to Turbomachinery, volume 2
[VKI-LS-1987-05-VOL-2] 08 p0985 N88-15965
Inviscid flows, part 2 08 p0985 N88-15966
Viscous flows, part 1 08 p0986 N88-15967
Viscous flows, part 2 08 p0986 N88-15968
Viscous flows. Part 3: Formulation of the Navier-Stokes equations by stream function vorticity methods
08 p0986 N88-15969
Mesh generation 08 p0986 N88-15971

Scanning finite element calculation method
[PB87-143442] 08 p0995 N88-16017

Generalized displacement method in the finite element analysis of incompressible material
[PB87-143434] 08 p0995 N88-16018

Finite element method with continuous mass elements
[PB87-143384] 08 p0995 N88-16019

Dynamic finite element with diagonalized consistent mass matrix and elastic-plastic impact calculation
[PB87-143376] 08 p0995 N88-16020

Computation of the tensile and bending restraint intensities of welded specimens by finite element method
[PB87-143798] 08 p0995 N88-16024

Mixed method of finite strip and finite element
[PB87-143467] 08 p0996 N88-16027

A study of finite difference and finite element vertical discretization schemes for baroclinic prediction equations
[AD-A186617] 08 p1040 N88-16291

Adaptive finite element methods for parabolic systems in one- and two-space dimensions
[AD-A186534] 08 p1073 N88-16475

Finite element analysis of damaged cross-ply composite laminates
[CCMS-87-10] 09 p1139 N88-16829

Dynamic modelling by finite element method of an elasto-acoustic beam with due consideration of flow and viscosity
[PB87-178166] 09 p1164 N88-16978

Qualification by analysis of IUS plume deflectors
09 p1179 N88-17063

Optimized structure design using reanalysis techniques 09 p1180 N88-17067

Dynamic response of a geared train of rotors subjected to random support excitations 09 p1181 N88-17073

Self-adaptive analysis of three-dimensional structures using a p-version of finite element method
[FFA-TN-1987-31] 09 p1182 N88-17084

Finite element analysis for the calculation of calibration curves of fracture mechanics specimen for semicircular surface cracks with several starting depths, for the crack depth measurement following the dc potential method
[GKSS-87/E/19] 09 p1183 N88-17086

A comparison of the predicted and measured gravitational stresses in VAWT (Vertical Axis Wind Turbine) blades
[DE88-002113] 09 p1187 N88-17111

An automatic finite element mesh generator
[AD-A188039] 09 p1216 N88-17291

A raster scan algorithm for generating visible parametric surfaces
[DE88-003222] 09 p1220 N88-17321

Finite element mesh generation and isoparametric elements
[NPL-DITC-97/87] 09 p1229 N88-17365

Numerical solutions of two moving boundary problems by both finite difference and finite element methods with applications
[DE88-002867] 09 p1230 N88-17374

Coupling finite element and spectral methods: First results
[NASA-CR-181606] 09 p1231 N88-17379

Measured and calculated acoustic attenuation rates of tuned resonator arrays for two surface impedance distribution models with flow
[NASA-TP-2766] 09 p1241 N88-17440

Coupled FE and HIE method for exterior acoustics of axisymmetric shells --- finite element (FE) Helmholtz integral equation (HIE)
[ARE-TM(UHA)-87506] 09 p1243 N88-17448

Finite element substructuring methods for composite mechanics
[NASA-TM-100297] 10 p1296 N88-17745

A finite element analysis of adhesively bonded composite joints including geometric nonlinearity, nonlinear viscoelasticity moisture diffusion and delayed failure
[AD-A187455] 10 p1296 N88-17747

A large strain thermomechanical forming model for elastic-viscoplastic behavior in metals
10 p1301 N88-17780

Zonal solutions for viscous flow problems. Finite approximations in fluid mechanics
[MBB/LKE-122/S/PUB/226] 10 p1313 N88-17846

Boundary integral analysis of flow and deformation of long bubbles in capillaries
[DE88-002110] 10 p1326 N88-17927

Design sensitivity analysis of nonlinear structural systems and numerical implementation with established finite element codes 10 p1344 N88-18032

Vibration and flutter characteristics of the SR7L large-scale propfan
[NASA-TM-100272] 10 p1344 N88-18036

Benchmark computation and finite element performance evaluation for a rhombic plate bending problem
[AD-A187402] 10 p1345 N88-18041

Recent progress in the p and h-p version on the finite element method
[AD-A187254] 10 p1400 N88-18347

The h-p version of the finite element method for problems with nonhomogeneous essential boundary condition
[AD-A187356] 10 p1400 N88-18348

Eigenvalue problems
[AD-A188060] 10 p1401 N88-18356

On delamination of (+ or - theta sub m/90 sub n/2) sub s laminates subject to tensile loading
[AD-A188095] 11 p1447 N88-18626

Finite element analysis of adhesively bonded composite joints including geometric nonlinearity, nonlinear viscoelasticity, moisture diffusion and delayed failure
[PB88-147822] 11 p1451 N88-18648

Study of the mechanical behavior of a 2-D carbon-carbon composite
[NASA-CR-182594] 11 p1451 N88-18649

Experimental set-up and mathematical modeling of H-shaped beam type structure
[AD-A187196] 11 p1466 N88-18743

GERA computer code for calculation of two-dimensional electromagnetic fields in resonators and electron-optical systems by the finite element method
[DE88-700678] 11 p1480 N88-18831

Finite element methods of analysis for high speed viscous flows
[NASA-CR-182529] 11 p1483 N88-18852

A velocity-pressure integrated, mixed interpolation, Galerkin finite element method for high Reynolds number laminar flows
[NASA-CR-179264] 11 p1486 N88-18868

Further development of a finite element model of orthogonal metal cutting
[DE88-004048] 11 p1494 N88-18921

The 58th Shock and Vibration Symposium, volume 2
[NASA-CP-2488-VOL-2] 11 p1499 N88-18948

Dynamic substructuring for shock spectrum analysis using component mode synthesis
11 p1499 N88-18950

Approximate method for predicting the permanent set in a beam in vacuo and in water subject to a shock wave 11 p1500 N88-18957

Numerical fracture mechanics using finite element method 11 p1501 N88-18966

Effect of element size on the solution accuracies of finite-element heat transfer and thermal stress analyses of space shuttle orbiter
[NASA-TM-88292] 11 p1502 N88-18971

Contour-to-grid interpolation with nonlinear finite elements: A feasibility study
[AD-A188108] 11 p1503 N88-18980

Workshop on the Integration of Finite Element Modeling with Geometric Modeling
[NASA-CR-182515] 11 p1526 N88-19111

Integration of finite element modeling with solid modeling through a dynamic interface 11 p1526 N88-19112

Approaches to the automatic generation and control of finite element meshes 11 p1526 N88-19113

Integration of geometric modeling and advanced finite element preprocessing 11 p1526 N88-19114

Finite element meshing of ANSYS (trademark) solid models 11 p1526 N88-19115

Solid/FEM integration at SNLA
[SAND-87-0882A] 11 p1526 N88-19116

Octree based automatic meshing from CSG models
11 p1527 N88-19117

Geometrical and topological issues in octree based automatic meshing 11 p1527 N88-19118

A hierarchical structure for automatic meshing and adaptive FEM analysis 11 p1527 N88-19119

Toward automatic finite element analysis
11 p1527 N88-19120

Finite octree meshing through topologically driven geometric operators 11 p1527 N88-19121

Design modeling for shape optimization
11 p1527 N88-19122

Shape optimization of three-dimensional stamped and solid automotive components
[GMR-5168] 11 p1528 N88-19123

Postprocessing techniques for 3D non-linear structures 11 p1528 N88-19124

Geometric versus finite element modeling current and future trends at Northrop 11 p1528 N88-19125

Multigrid methods: Special topics and applications --- conference
[GMD-120] 11 p1537 N88-19187

A generalisation of Hall's scheme for solving the Euler equations for two-dimensional flows
11 p1537 N88-19188

A multigrid solver for two-dimensional transonic full potential flow calculations 11 p1538 N88-19189

Multigrid methods in convex optimization
11 p1538 N88-19190

Implementation of multigrid in SOLA algorithm --- fluid flow 11 p1538 N88-19191

Solution of the Euler equations: Explicit schemes acceleration by a multigrid method
11 p1538 N88-19192

Unstructured multigrid methods
11 p1538 N88-19193

Discretizations for multigrid methods
11 p1539 N88-19198

Reliability analyses of a surface mounted package using finite element simulation
[AD-A189488] 12 p1624 N88-19717

Sub-scaling of projectile/target system damaged by hypervelocity
[AD-A188683] 12 p1634 N88-19779

A hybrid-stress finite element approach for stress and vibration analysis in linear anisotropic elasticity
[NASA-CR-179311] 12 p1634 N88-19784

Vibrations of shells containing fluid
12 p1635 N88-19787

On analysis of viscoelastic structures
[AD-A188445] 12 p1636 N88-19793

A technique for local refinement of the stress field by finite element method
[INPE-4219-PRE/1099] 12 p1683 N88-20061

Further refinement and applications of the mixed computational algorithm for plane elastic contact problems
[AD-A188308] 12 p1683 N88-20065

NFEARS (Nonlinear Finite Element Adaptive Research Solver): A nonlinear adaptive finite element solver. Part 2: User's manual
[AD-A189009] 12 p1684 N88-20070

Study of inhomogeneously filled cylindrical resonant cavities by the finite integration technique
[PB88-133707] 12 p1697 N88-20156

Finite element calculations for aerodynamic coefficients of a 3-dimensional body in subsonic flow using Green's function method
[NASA-TT-20208] 13 p1718 N88-20272

Effect of rotation on the lateral stability of a free-flying column subjected to an axial thrust with directional control
[AD-A188690] 13 p1728 N88-20338

Nondestructive evaluation of carbon-carbon coatings
[AD-A189524] 13 p1748 N88-20453

Dynamics of high-speed mechanisms with elastic members 13 p1779 N88-20643

Finite element methods for quasi-prismatic bodies with application to gears 13 p1779 N88-20644

A preliminary investigation of finite-element modeling for composite rotor blades
[NASA-TM-100559] 13 p1781 N88-20656

Theory and experiments of fracture in cyclic compression: Single phase ceramics, transforming ceramics and ceramic composites
[DE88-005792] 13 p1781 N88-20659

Finite element methodology for nonlinear free and harmonic forced vibrations of beam and plate structures
13 p1782 N88-20663

An analysis of large deformation axisymmetric inelastic problems by finite element and boundary element methods 13 p1782 N88-20664

Correlation of data on strain accumulation adjacent to the San Andreas Fault with available models
[NASA-CR-180757] 13 p1796 N88-20742

The use of a barotropic finite element model for the study of circulation on the continental shelf of the southeast coast of Brazil
[INPE-4401-PRE/1218] 13 p1802 N88-20774

Finite State Tables for general computer programming applications
[DE88-006254] 13 p1820 N88-20881

A knowledge system for automatic finite element mesh generation: AMEKS
[DE87-014894] 13 p1826 N88-20914

Local refinement of stress field by finite element method
[INPE-4321-TDL/288] 13 p1828 N88-20930

Modeling of laser ultrasound generation in a weld pool
[DE88-005546] 13 p1834 N88-20971

JPRS report: Science and technology. China
[JPRS-CST-87-042] 14 p1899 N88-21338

Finite element explicit algorithm for solving temporal temperature fields 14 p1899 N88-21339

Analysis of induction motors based on the numerical solution of the magnetic field and circuit equations
[EL-59] 14 p1907 N88-21398

Evaluation of structural analysis methods for life prediction 14 p1930 N88-21511

On the global/local time incrementing for viscoplastic analysis 14 p1932 N88-21519

A constitutive material model for nonlinear finite element structural analysis using an iterative matrix approach
14 p1932 N88-21521

Nonlinear structural analysis of a turbine airfoil using the Walker viscoplastic material model for B1900 + Hf
14 p1932 N88-21522

On 3-D inelastic analysis methods for hot section components. Volume 1: Special finite element models
[NASA-CR-180893] 14 p1934 N88-21535

Some maximum norm estimates for the finite element method applied to nonlinear two dimensional boundary value problems
[ETN-88-91505] 14 p1964 N88-21715

A general 2D electrical model for diagonally connected MHD generators
[DE88-004283] 14 p1984 N88-21835

Moving-bank multiple model adaptive estimation applied to flexible spacestructure control
[AD-A190761] 15 p2026 N88-22071

Postbuckling delamination of a stiffened composite panel using finite element methods
[NASA-CR-182803] 15 p2030 N88-22096

Finite element simulation of perforation of aluminum plates
[DE88-002092] 15 p2073 N88-22362

Development of a computer code CRACK for elastic and elastoplastic fracture mechanics analysis of 2-D structures by finite element technique
[DE88-701231] 15 p2075 N88-22370

Elasto-plastic analysis using a stress-based finite element method and an endochronic theory of plasticity
[DE88-003001] 15 p2075 N88-22372

Finite element (MARC) solution technologies for viscoplastic analyses 15 p2078 N88-22389

Three-dimensional inelastic approximate analysis code (MOMM) 15 p2079 N88-22392

Specialty three-dimensional finite element analysis codes 15 p2079 N88-22393

MHOST: An efficient finite element program for inelastic analysis of solids and structures
15 p2079 N88-22394

Fatigue damage modeling for coated single crystal superalloys 15 p2085 N88-22427

Development and application of the p-version of the finite element method
[AD-A190036] 15 p2120 N88-22633

A posterior error estimation in a finite element method for parabolic partial differential equations
[AD-A190296] 15 p2120 N88-22636

Homogenization study of matrix behavior in a composite material
[ONERA-RT-1/7256-RY-060-R]
16 p2172 N88-22943

Dynamic fracture toughness evaluation by measurement of CTOD
[WNS/ASD-88-02] 16 p2178 N88-22982

Finite elements for the computation of three-dimensional electromagnetic fields in inhomogeneous media (revised)
[PB88-173471] 16 p2190 N88-23057

Parallel computer methods for eigenvalue extraction
16 p2218 N88-23233

Iterative finite element solver on transputer networks
16 p2218 N88-23235

Mixed finite element formulation applied to shape optimization 16 p2221 N88-23252

Models in nonlinear thermomechanics. Finite element models and constitutive models for large deformation elastoplasticity
[ETN-88-92240] 16 p2222 N88-23262

A nonlinear computation for composite structures
[ONERA-RT-15/3542-RY-062-R]
16 p2222 N88-23265

A finite-element alternating method for two-dimensional Mode-1 crack configurations
[NASA-TM-100616] 16 p2224 N88-23276

Experimental design and structural optimization
[ETN-88-92232] 16 p2257 N88-23492

Three-dimensional curved shell and solid-shell transition finite elements with temperature and temperature gradients as primary variables for steady state heat conduction
17 p2349 N88-23997

The Shock and Vibration Digest, volume 20, no. 4
17 p2391 N88-24214

State-of-the-art in true space-time finite element method 17 p2391 N88-24215

Adjusting a finite element model using vibration type experimental data. Concept and error detection
[ONERA-RT-7/3313-RY-060-R]
17 p2392 N88-24220

Simulations of a missile with liquid payload under launch conditions
[AD-A191479] 18 p2463 N88-24625

Fundamental limits to the velocity of solid armatures in railguns 18 p2469 N88-24656

Mixed-mode fracture of uniaxial fiber reinforced composites
[AD-A191629] 18 p2478 N88-24700

Adaptive local grid refinement in computational fluid mechanics
[AD-A192215] 18 p2510 N88-24890

A variational finite element method for three-dimensional, steady, compressible, viscous flows
18 p2512 N88-24904

Improving the performance of a finite element method using vector analysis on CRAY 1
[ETN-88-92153] 18 p2513 N88-24907

Finite element solution of 3-D turbulent Navier-Stokes equations for propeller-driven slender bodies
18 p2515 N88-24919

Finite element analysis of an underground structure
[AD-A191747] 18 p2527 N88-24991

Fracture mechanics analysis for short cracks
[AD-A192002] 18 p2527 N88-24992

Dynamic response of plates to moving loads: Structural impedance and finite element methods
18 p2528 N88-25000

The stress analysis of ceramic, polymeric, and metallic composite systems by the finite element method
18 p2529 N88-25004

Reduced order modelling and analytical model modification for structural dynamics and control
18 p2529 N88-25006

Considerations involved in the display of finite element results using animation
[DE88-007581] 18 p2559 N88-25189

Algorithms and software for solving finite element equations on serial and parallel architectures
[NASA-CR-183027] 18 p2559 N88-25191

PAFEC level 6.2 application program
[AD-A191037] 18 p2562 N88-25209

NFEARS: A nonlinear adaptive finite element solver, part 1
[AD-A191823] 18 p2563 N88-25215

Probabilistic finite element methods
18 p2564 N88-25223

New mixed finite element methods
18 p2567 N88-25248

Fuel droplet vaporization and temperature distributions of axisymmetric unsteady sprays
19 p2626 N88-25579

Finite element analysis of incompressible viscous flow around multi-element aerofoils 19 p2635 N88-25634

Improved method for stress and compatibility analysis of multicomponent rotating systems
[NASA-TM-100884] 19 p2680 N88-25935

Semi-discrete approximations to nonlinear systems of conservation laws; consistency and L(infinity)-stability imply convergence
[NASA-CR-181683] 19 p2721 N88-26157

Stability of spheromak against current driven modes: Effects of flux hole on stability
[IPPJ-868] 19 p2730 N88-26211

Finite element approximation to a model problem of transonic flow
[DE88-701835] 20 p2752 N88-26333

A finite element analysis for the hydroforming of aluminum
[DE88-008050] 20 p2784 N88-26516

MAXWELL3: A 3D finite element electromagnetic modeling code
[DE88-010602] 20 p2790 N88-26551

Velocity-pressure integrated versus penalty finite element methods for high Reynolds number flows
[NASA-CR-179357] 20 p2803 N88-26635

Finite element welding computations using general purpose nonlinear analysis codes
[DE88-005398] 20 p2806 N88-26659

Three-dimensional analysis of a postbuckled embedded delamination
[NASA-TP-2823] 20 p2812 N88-26684

An assessment of modelling techniques for the finite element analysis of reinforced concrete plate and shell structures
[AD-A192263] 20 p2814 N88-26697

Thermo-viscoelastic analysis of composite materials, volume 1
[NASA-CR-183048-VOL-1] 21 p2904 N88-27230

An h-p adaptive finite element method for steady compressible flow 21 p2941 N88-27467

A study of fluid-structure problems
21 p2941 N88-27468

St[illegible] function-vorticity finite elements and the resol[illegible] Navier-Stokes equations
[DE88-702[illegible] 21 p2945 N88-27494

Optimal design of viscoelastic structures
21 p2959 N88-27579

Adaptive finite element methods for shells
[AD-A193221] 21 p2960 N88-27585

Verification of the ADINA finite element code for creep analysis: Problems from the open literature
[DE88-011826] 21 p2962 N88-27594

DYNA3D (Nonlinear Dynamic Analysis of Structures in Three Dimensions) user's manual
[DE88-012242] 21 p2963 N88-27604

Finite element methodology for integrated flow-thermal-structural analysis
[NASA-CR-183144] 21 p2964 N88-27606

Staggered-grid finite element solution technique for the Maxwell's equations in the time domain
[DE88-011731] 21 p3007 N88-27838

Unified multilevel adaptive finite element methods for elliptic problems
[DE88-011938] 21 p3007 N88-27840

Finite element method for plate structures with inclined angles
[ILR-MITT-182] 21 p3008 N88-27842

Coupled inviscid - boundary layer methods for turbomachinery blading design
[PNR90437] 22 p3076 N88-28260

High performance solutions of the Stokes problem using mini-elements, self-adaptive grids, and multigrid methods: Applications
[ECL-87-15] 22 p3077 N88-28266

Development and application of a finite element method to compute strongly heated turbulent flows
[ECL-88-02] 22 p3077 N88-28267

Two-dimensional sequential and concurrent finite element analysis of unstiffened and stiffened aluminum and composite panels with hole
[NASA-CR-183083] 22 p30[illegible]6 N88-28325

Mixed finite element methods to compute stress in a load composite specimen with holes. Numerical results
[ONERA-RT-37/4242-RY-062-R]
22 p3088 N88-28336

Parametric identification of mechanical structures
[ETN-88-92881] 22 p3088 N88-28339

Refining finite element models. Numerical application to a lattice structure. Study of a macroelement of Timoshenko beam type
[ONERA-RT-8/3313-RY-070-R]
22 p3144 N88-28696

Distortion effects in isoparametric elements, an analytic approach
[PNR90454] 22 p3145 N88-28703

Finite Element Composite Analysis Program (FECAP) for a microcomputer
[NASA-TM-100670] 23 p3190 N88-28982

Development and experimental verification of a two-dimensional numerical model of piezoelectrically induced threshold voltage shifts in GaAs MESFETs
[AD-A193462] 23 p3206 N88-29080

Static and dynamic metal-metal friction at plastic stress levels
[DE88-011281] 23 p3222 N88-29176

Elastic-plastic analysis of part-through crack propagation in piping and pressure vessels
[DE88-701619] 23 p3225 N88-29198

An adaptive overlapping local grid refinement method for two-dimensional parabolic systems
[AD-A193560] 23 p3271 N88-29464

Investigation of the higher-order elements in the SAMSON2 code
[AD-A193638] 23 p3271 N88-29465

Finite element analysis of steady and transiently moving/rolling nonlinear viscoelastic structure. Part 1: Theory
[NASA-CR-179886] 23 p3273 N88-29480

Analysis of the transmission of sound into the passenger compartment of a propeller aircraft using the finite element method
[FFA-TN-1988-15] 23 p3279 N88-29520

Damage initiation in the short beam shear test of composite materials using stiffness reduction
[AD-A194880] 24 p3340 N88-29883

Numerical modelling of premixed flames in gaseous media 24 p3350 N88-29944

Geometric and material nonlinear analysis of structures comprising rectangular hollow sections
[CE-79] 24 p3382 N88-30141

A parametric study of embedded cantilever retaining walls: The results of a finite element study
[RR-CE83] 24 p3383 N88-30152

Obtaining stress intensity factors on cracks, by means of fitting techniques on numerical results calculated with the finite element method 24 p3384 N88-30153

FINITE IMPULSE RESPONSE FILTERS

U FIR FILTERS

FINITE VOLUME METHOD

Computational fluid dynamics in the United Kingdom
[RAE-TM-AERO-2098] 02 p0171 N88-11073

High resolution finite volume methods on arbitrary grids via wave propagation
[NASA-CR-178397] 04 p0484 N88-12979

Solution of some 3-D viscous and inviscid supersonic flow problems by finite-volume space-marching schemes
05 p0532 N88-13235

The role of computation fluid dynamics in aeronautical engineering (4). The development and applications of implicit TVD finite volume code
05 p0536 N88-13259

Compressible Euler solution on a multiblock grid around a wing-fuselage configuration
[FFA-TN-1987-46] 05 p0542 N88-13303

A Cartesian finite-volume method for the Euler equations 05 p0579 N88-13532

Euler solution of multiblade rotor flow
[NASA-TM-100014] 06 p0704 N88-14322

Finite-volume scheme for transonic potential flow about airfoils and bodies in an arbitrarily shaped channel
07 p0809 N88-14928

A multistage time-stepping scheme for the thin-layer Navier-Stokes equations 07 p0810 N88-14932

Computational Fluid Dynamics
[VKI-LS-1987-04] 08 p0984 N88-15951

Integration of Navier-Stokes equations in finite volume formulation 08 p0984 N88-15954

Numerical implementation and performance of Reynolds stress closures in finite volume computations of recirculating and strongly swirling flows
08 p0987 N88-15976

Solution of the three-dimensional Navier-Stokes equations for transonic flow using a multigrid method
10 p1267 N88-17579

Radial compressor design using an Euler solver
10 p1283 N88-17675

Applications of a multigrid finite volume method with Runge-Kutta time integrations for solving the Euler and Navier-Stokes equations 11 p1539 N88-19201

The construction of a three-dimensional finite volume grid generator for a wing in a wind tunnel with application to Navier-Stokes flow solvers
[FFA-TN-1987-58] 13 p1719 N88-20277

Solution of two-dimensional Euler equations: Experience with a finite volume code
[DFVLR-FB-87-41] 13 p1767 N88-20572

Conservative finite volume solutions of a linear hyperbolic transport equation in two and three dimensions using multiple grids
[NASA-CR-182715] 13 p1828 N88-20934

Mixed direct-inverse problem of transonic cascade
15 p2054 N88-22244

Zero-lift drag predictions in supersonic flow for complex configurations 15 p2054 N88-22246

The 2-D and 3-D time marching transonic potential flow method for propfans 16 p2220 N88-23245

The role of computational fluid dynamics in aeronautical engineering (5). Improvements and applications of implicit TVD finite volume code 19 p2638 N88-25653

On the accuracy of upwind biased finite volume method 19 p2639 N88-25656

Navier-Stokes simulation of shock-tube flows over a wedge-type step by finite volume method
[ISAS-RN-628] 20 p2797 N88-26599

Preliminary design and analysis of procedures for the numerical generation of 3D block-structured grids
[NLR-TR-86102-U] 20 p2802 N88-26628

Effects of numerical dissipation on finite-volume solutions of compressible flow problems
[AD-A193173] 21 p2944 N88-27485

Investigation of viscous/inviscid interaction in transonic flow over airfoils with suction
[NASA-CR-183112] 21 p2945 N88-27490

Runge-Kutta finite-volume simulation of laminar transonic flow over the ONERA M6 wing using the Navier-Stokes equations
[FFA-TN-1987-06] 22 p3039 N88-28045

On the application of finite-difference techniques for the computation of the flow field in gas turbine combustors with complex geometries 24 p3349 N88-29938

An analysis of finite-difference and finite-volume formulations of conservation laws
[NASA-CR-177416] 24 p3370 N88-30071

Numerical simulation of unsteady incompressible viscous flows in generalized coordinate systems
[NASA-TM-101016] 24 p3373 N88-30085

FINITE-STATE MACHINES
U TURING MACHINES

FINLAND

Huurre expedition to the North Pole in 1984
[PB87-220935] 04 p0462 N88-12858

Report of the 3rd Finnish EISCAT Workshop --- European-Incoherent Scatter Radar (EISCAT)
[REPT-111] 06 p0691 N88-14233

EISCAT research in Finland in 1986
06 p0691 N88-14234

EISCAT research programs for 1987
06 p0692 N88-14244

Helsinki University of Technology Communications Laboratory
[PB88-112974] 10 p1318 N88-17881

Research field of fire technology in Finland
[DE88-751094] 11 p1467 N88-18747

Last spring frosts and first autumn frosts in Finland
[FMI-6] 19 p2693 N88-26008

On the global radiation incident variously orientated surfaces on the South Coast of Finland
[FMI-5] 20 p2823 N88-26746

FINNED BODIES

Analytical treatment of the melting and solidification of latent heat store materials in finned tube geometries
[IKE-5-223] 03 p0314 N88-11985

Performance evaluation of plate-fin heat exchangers
[AD-A187798] 11 p1482 N88-18845

FINS
NT COOLING FINS

Fin gaps and body slots of guided projectiles: Effects, data correlation and modeling
[AD-A184440] 03 p0270 N88-11698

The effects of sweep and bluntness on a glancing shock wave turbulent boundary layer interaction
05 p0531 N88-13227

The use of aeroelastic wind tunnel models to prove structural design 05 p0551 N88-13255

Indirect measurement of local condensing heat-transfer coefficient around horizontal finned tubes
[AD-A186929] 09 p1160 N88-16950

Measurement of forces and moments on, and velocity about a body of revolution with an attached fin at angles of attack
[AD-A187796] 11 p1433 N88-18554

Preliminary investigation of stability of a fin-stiffened slender strut
[NASA-TM-4034] 12 p1590 N88-19566

Fish as a tool for testing fitness in space
12 p1662 N88-19963

Experimental investigation of the hypersonic flow over a six finned configuration
[AD-A190870] 16 p2157 N88-22871

Study and implementation of ultrahigh frequency coupling devices using the fin line technology --- millimeter waves
[ETN-88-92307] 20 p2796 N88-26588

The use of fins to reduce the pressure drop in a rotating cavity with a radial flow
[PNR90465] 22 p3079 N88-28282

Feasibility study of a microprocessor controlled actuator test mechanism
[AD-A194654] 23 p3249 N88-29337

FIR FILTERS

Design of efficient FIR filters with minimal delay
[PB87-100434] 04 p0438 N88-12717

Implementation of an FIR band pass filter using a bit-slice processor
[AD-A184895] 05 p0634 N88-13875

Frequency-sampling design of two-dimensional FIR digital filters with nonuniform samples
[AD-A187773] 11 p1477 N88-18815

Digital filter design techniques
[AD-A194484] 23 p3274 N88-29486

FIRE CONTROL

Helicopter fire control: Advantages of an automatic target tracker 03 p0264 N88-11667

AVSCOM'S modifications to Teledyne Systems Company's air-to-air fire control system simulation model
[AD-A189136] 13 p1722 N88-20294

Method and device for the detection and identification of a helicopter
[NASA-TT-20251] 15 p2129 N88-22696

FIRE DAMAGE

Effects of fire on composition, biomass, and nutrients in oak scrub vegetation on John F. Kennedy Space Center, Florida
[NASA-TM-100305] 08 p1020 N88-16182

Evaluation of a burned area and the vegetation regeneration affected by the burning in the Parque Nacional de Brazilia through TM/LANDSAT data
17 p2363 N88-24073

FIRE EXTINGUISHERS

Spacecraft Fire Safety
[NASA-CP-2476] 04 p0406 N88-12520

Fire extinguishment and inhibition in spacecraft environments 04 p0406 N88-12523

Inerting and atmospheres 04 p0406 N88-12524

Aircraft fire safety research 04 p0406 N88-12526

Space station internal environmental and safety concerns 04 p0407 N88-12527

Extinguishing diffusion flames with dry powder and halon at low Froude numbers
[PB87-111365] 06 p0679 N88-14159

Testing of the engine compartment fire extinguishing system in the F/EF-111 aircraft
[AD-A188801] 12 p1576 N88-19423

An extinguisher to quench propellant fires
[AD-A190785] 18 p2497 N88-24813

Next-generation fire extinguishing agent. Phase 1: Suppression concepts
[AD-A192279] 19 p2614 N88-25514

Extinguishing agent for magnesium fire, phases 5 and 6
[AD-A192436] 21 p2930 N88-27398

FIRE FIGHTING

Test results and predictions for the response of near-ceiling sprinkler links in a full-scale compartment fire
[NBSIR-87/3633] 01 p0033 N88-10209

Research field of fire technology in Finland
[DE88-751094] 11 p1467 N88-18747

FIRE PREVENTION

Comparison of fire resistance of metallic and nonmetallic structures
[SNIAS-872-551-101] 05 p0572 N88-13489

Spacecraft fire detection and extinguishment: A bibliography
[NASA-CR-180880] 11 p1444 N88-18612

Procedures for quantitative sensitivity and performance validation studies of a deterministic fire safety model
[NBS/GCR-88/544] 11 p1469 N88-18762

A new fire protection concept for electronic equipment
[AD-A188884] 12 p1614 N88-19651

Spacecraft fire-safety experiments for space station: Technology development mission
[NASA-CR-182114] 13 p1731 N88-20353

Flame retardants
[NASA-TT-20250] 13 p1739 N88-20400

A systems analysis of fire suppression alternatives for the US space station
[AD-A189847] 15 p2025 N88-22064

Study of benefits of passenger protective breathing equipment from analysis of past accidents
[DOT/FAA/CT-88/03] 18 p2461 N88-24610

Aircraft accident report: Air New Orleans, DBA continental express flight 962 British Aerospace 3101 (Jetstream 31), N331CY, New Orleans International Airport, Kenner, Louisiana, May 26, 1987
[PB88-910408] 19 p2601 N88-25450

Fire retardant coatings for military equipment: A review
[MRL-R-1104] 19 p2619 N88-25540

Flame retardation treatment of synthetic rubbers and synthetic resins
[NASA-TT-20265] 19 p2620 N88-25544

FIRE RESISTANCE
U FLAMMABILITY

FIRE RETARDANTS
U FLAME RETARDANTS

FIREPROOFING

Comparison of fire resistance of metallic and nonmetallic structures
[SNIAS-872-551-101] 05 p0572 N88-13489

FIRES
NT FOREST FIRES

Measurements of gas velocities and temperatures in a large open pool fire
[DE87-005853] 03 p0261 N88-11641

Measurements in large JP-4 pool fires
[DE87-013445] 03 p0284 N88-11783

Spacecraft Fire Safety
[NASA-CP-2476] 04 p0406 N88-12520

Techniques for fire detection
04 p0406 N88-12521

Fire-related standards and testing
04 p0406 N88-12522

Fire extinguishment and inhibition in spacecraft environments 04 p0406 N88-12523

Inerting and atmospheres 04 p0406 N88-12524

Fire-related medical science 04 p0406 N88-12525

Aircraft fire safety research 04 p0406 N88-12526

Space station internal environmental and safety concerns 04 p0407 N88-12527

Microgravity combustion fundamentals
04 p0407 N88-12528

Spacecraft material flammability testing and configurations 04 p0407 N88-12529

Catalog of compartment fire model algorithms and associated computer subroutines
[PB88-110861] 07 p0839 N88-15087

Effects of additives on fire properties of polyethylene
[AD-A187064] 09 p1146 N88-16871

Testing of the engine compartment fire extinguishing system in the F/EF-111 aircraft
[AD-A188801] 12 p1576 N88-19423

Flammability characteristics of distillate fuels
[AD-A188497] 12 p1612 N88-19642

A new fire protection concept for electronic equipment
[AD-A188884] 12 p1614 N88-19651

Numerical simulation of near-surface environments and particulate clouds generated by large-area fires
[AD-A188375] 12 p1641 N88-19828

Heat transfer from a negatively buoyant wall jet
[NBS/GCR-88/541] 15 p2050 N88-22208

Detection, monitoring and analysis of some environmental effects of fires in the Amazon region through utilization of NOAA and LANDSAT satellite imagery and aircraft data
[INPE-4503-TDL/326] 16 p2230 N88-23322

Detection of biomass burning and smoke plumes in the Amazon region through NOAA satellite imagery
17 p2365 N88-24085

An extinguisher to quench propellant fires
[AD-A190785] 18 p2497 N88-24813

Current fire safety design aspects of commuter aircraft
[DOT/FAA/CT-87/32] 19 p2600 N88-25448

Experimental and theoretical analysis of the radiative transfer within a sooty pool fire
[DE88-007099] 20 p2769 N88-26419

Extinguishing agent for magnesium fire, phases 5 and 6
[AD-A192436] 21 p2930 N88-27398

The 210-HP diesel engine endurance and performance testing with fire resistant diesel fuel
[AD-A193153] 21 p2956 N88-27558

Numerical field model simulation of full scale fire tests in a closed spherical/cylindrical vessel
[AD-A195067] 24 p3359 N88-29998

FIREWORKS
U PYROTECHNICS

FIRING (IGNITING)
NT ROCKET FIRING
NT STATIC FIRING
NT TEST FIRING

A nondissipative Pyrotechnic Arming and Firing Unit (PAFU)
[CRA/REPO/8019] 02 p0155 N88-10974

FIRMWARE

High bit rate serial input multipliers
[REPT-87-012] 11 p1530 N88-19140

A serial input pipelined multiplier
[REPT-87-030] 11 p1530 N88-19141
On serial-input multipliers for two-complement numbers
[REPT-86-035] 11 p1536 N88-19181
FISH
U FISHES
FISHERIES
Two decades of achievement in the ocean, 1968-1988
[PB88-167077] 16 p2236 N88-23356
Contribution of space to marine activities
19 p2700 N88-26057
FISHES
Investigations of the survey of the reproductive biology of Xiphophorus in an Aquarack
01 p0074 N88-10471
Xiphophorus as an experimental system for genetic and biological development studies under microgravity conditions 01 p0074 N88-10472
Long term investigations of the growth, metabolism, and reproduction of fish under conditions close to weightlessness 01 p0074 N88-10473
Compilation of 1986 annual reports of the Navy ELF (Extremely Low Frequency) communications system ecological monitoring program, volume 3
[AD-A184563] 03 p0306 N88-11932
Irradiation preservation of seafood: Literature review
[DE88-001691] 05 p0631 N88-13858
Investigations of the reproductive physiology of the rainbow trout (Salmo gairdneri Richardson)
07 p0885 N88-15370
Function-dependent plasticity in the nervous system
07 p0886 N88-15377
Embryonic development of guppy in weightlessness
10 p1360 N88-18127
Fish as a tool for testing fitness in space
12 p1662 N88-19963
FISHTAILING
U YAW
FISSION
New nuclear structure calculations and the astrophysical r-process
[DE88-000979] 08 p1082 N88-16518
FISSION ELECTRIC CELLS
Noncryogenic propellants for a nuclear orbit transfer vehicle 17 p2428 N88-24444
FISSION PRODUCTS
Analysis of a nuclear orbital transfer vehicle reentry accident 17 p2425 N88-24426
FISSURES (GEOLOGY)
The aerophotogrammetric determination of Earth surface deformations
[SER-C-321] 07 p0872 N88-15288
Experimental and theoretical constraints on the origin of mid-ocean ridge geothermal fluids
13 p1804 N88-20784
FITNESS
NT PHYSICAL FITNESS
Three-dimensional adaptive grid generation for body-fitted coordinate system
[NASA-CR-182192] 21 p2950 N88-27520
FITTING
Evaluation of the US Army fitting program for the integrated helmet unit of the integrated helmet and display sighting system
[AD-A191616] 18 p2465 N88-24635
FITTINGS
An examination of coating failure on wing pivot fittings of f111 aircraft
[AD-A185028] 05 p0546 N88-13326
User's manual for EULER3DS
[AD-A191048] 16 p2208 N88-23177
Expandable pallet for space station interface attachments
[NASA-CASE-MSC-21117-1] 23 p3185 N88-28958
FITZGERALD-LORENTZ CONTRACTION
U LORENTZ CONTRACTION
FIX
U FIXING
FIXED POINTS (MATHEMATICS)
Numerical resolution of the equations of three-dimensional stable compressible transonic flows
[PB87-168415] 08 p1113 N88-16673
Exponential lower bounds for finding Brouwer fixed points
[DE88-002864] 10 p1425 N88-18513
Solving reflexive domain equations in a category of complete metric spaces
[CWI-CS-R8709] 13 p1832 N88-20956
FIXED WINGS
Boeing 727 MLS (Microwave Landing System) terminal instrument procedures (TERPS) approach data collection and processing, data report
[AD-A185523] 06 p0667 N88-14090
Analysis of a fixed-pitch X-wing rotor employing lower surface blowing 10 p1271 N88-17602
Fixed wing CCW aerodynamics with and without supplementary thrust deflection
10 p1272 N88-17607
Aircraft aeroelasticity and structural dynamics research at the [illegible] Langley Research Center: Some illustrative results
[NASA-TM-100627] 18 p2459 N88-24598
Analysis of a fixed-pitch X-wing rotor employing lower surface blowing
[AD-A167379] 24 p3321 N88-29779
FIXED-WING AIRCRAFT
U AIRCRAFT CONFIGURATIONS
U FIXED WINGS
FIXING
Botany Facility: The problems of plant fixation
[SIRA-A/7373/WP220/HJS/001]
17 p2379 N88-24140
FLAME FRONTS
U FLAME PROPAGATION
FLAME HOLDERS
Ignition and flameholding in supersonic flow by injection of dissociated hydrogen 05 p0560 N88-13410
Flame stabilization in a reheat combustor
24 p3346 N88-29921
FLAME INTERACTION
U CHEMICAL REACTIONS
U FLAME PROPAGATION
FLAME IONIZATION
Combustion of hydrogen and hydrocarbons in fluorine
[AD-A188018] 11 p1453 N88-18662
Kinetic mechanisms for ionization and afterburning suppression
[AD-A189219] 13 p1737 N88-20383
Selective detection in gas chromatography
[AD-A191499] 18 p2481 N88-24718
FLAME PROBES
Studies of fluorine combustion
[AD-A187646] 11 p1452 N88-18656
FLAME PROPAGATION
Turbulent Bunsen burner flames
[ETN-87-90433] 01 p0021 N88-10134
Fronts propagating with curvature dependent speed: Algorithms based on Hamilton-Jacobi formulations
[NASA-CR-178382] 01 p0077 N88-10495
Measurement of solid propellant combustion velocity by means of microwaves
[CERT-1/1316-MO] 03 p0283 N88-11778
Ignition and flame propagation in sprays
[AD-A184679] 03 p0283 N88-11781
Fire-related standards and testing
04 p0406 N88-12522
Space station internal environmental and safety concerns 04 p0407 N88-12527
Microgravity combustion fundamentals
04 p0407 N88-12528
The effect of microgravity on flame spread over a thin fuel
[NASA-TM-100195] 08 p0967 N88-15853
Heat transfer from impinging flame jets
[ETN-88-91610] 09 p1162 N88-16964
Flame propagation in the approximation of straight-line trajectories of burning products
[DE88-700675] 10 p1297 N88-17756
Diffusion description of flame propagation due to the translational motion of burning reaction products
[DE88-700676] 10 p1297 N88-17757
Studies on homogeneous and heterogeneous reactive flows 11 p1484 N88-18861
Linear and nonlinear acoustics with nonuniform entropy in combustion chambers 12 p1607 N88-19609
Flammability characteristics of distillate fuels
[AD-A188497] 12 p1612 N88-19642
Evaluation of flammability for cable-like polymers
[NASA-TT-20225] 13 p1752 N88-20476
Problems appearing at interface balances --- flames
14 p1987 N88-21855
On the structure, propagation, extinction and stability of laminar premixed flames in dissociation equilibrium
18 p2483 N88-24728
Turbulence and flame propagation
[PB87-228912] 19 p2612 N88-25499
Flame spread mechanisms over PMMA surfaces
[NASA-TT-20284] 19 p2612 N88-25500
Effect of thickness on downward flame spread over paper
[NASA-TT-20282] 19 p2612 N88-25501
Combustion rate limits of hydrogen plus hydrocarbon fuel: Air diffusion flames from an opposed jet burner technique 19 p2624 N88-25567
Mach 2 combustion characteristics of hydrogen/hydrocarbon fuel mixtures
19 p2625 N88-25568
Recent advances in photochemical techniques for ignition and combustion enhancement
19 p2625 N88-25570
Minimum ignition energy measurements using laser induced spark initiation 19 p2632 N88-25610
Ignition and flame spread of PMMA
[NASA-TT-20290] 20 p2771 N88-26431
Premixed turbulent flame propagation
[AD-A192955] 21 p2909 N88-27265
Summary of discussions at the Tenth Meeting of the Sandia Cooperative Group on the Aerothermochemistry of Turbulent Combustion
[DE88-008467] 21 p2910 N88-27269
Theoretical study and numerical simulation of flame fronts
[PB88-122932] 22 p3051 N88-28104
A study of flame spreading and combustion phenomena of stick propellants
[AD-A193598] 22 p3052 N88-28106
Interactions between coherent structures and premixed flame fronts
[ETN-88-92885] 22 p3053 N88-28111
Combustion dynamics and thermal structure of a planar spray flame 23 p3190 N88-28985
Numerical modelling of premixed flames in gaseous media 24 p3350 N88-29944
Gaseous premixed flames in non-uniform flows
24 p3351 N88-29945
Flamespreading processes in obliquely loaded stick propellant beds
[AD-A195081] 24 p3352 N88-29956
FLAME QUENCHING
U EXTINGUISHING
U QUENCHING (COOLING)
FLAME RETARDANTS
Thermoplastic elastomer compositions --- cable jackets
[EP-PATENT-0-204-453-A1] 04 p0418 N88-12593
Flame retardant phenolic foams
[EP-PATENT-0-223-489-A2] 05 p0568 N88-13464
Method of obtaining of fire resistant polyacrylonitrile fiber or cloth from it
[AD-A185941] 07 p0836 N88-15071
Effects of additives on fire properties of polyethylene
[AD-A187064] 09 p1146 N88-16871
Fire tests on loose-fill insulation materials
[DE88-751182] 11 p1467 N88-18748
Kinetic mechanisms for ionization and afterburning suppression
[AD-A189219] 13 p1737 N88-20383
Flame retardants
[NASA-TT-20250] 13 p1739 N88-20400
Differential technology in plastics industries differentiation in combination technology nonflammability technology
[NASA-TT-20256] 18 p2494 N88-24797
Fire retardant coatings for military equipment: A review
[MRL-R-1104] 19 p2619 N88-25540
Flame retardation treatment of synthetic rubbers and synthetic resins
[NASA-TT-20285] 19 p2620 N88-25544
The 210-HP diesel engine endurance and performance testing with fire resistant diesel fuel
[AD-A193153] 21 p2956 N88-27558
FLAME SPECTROSCOPY
Single-laboratory evaluation of SW-846 methods 7090/7091 determination of beryllium by flame and furnace atomic absorption spectrophotometry
[PB88-171434] 16 p2175 N88-22963
La Recherche Aerospatiale, bimonthly bulletin, number 1987-3, 238/May-June
[ESA-TT-1075] 16 p2206 N88-23161
FLAME SPRAYING
Combustion dynamics and thermal structure of a planar spray flame 23 p3190 N88-28985
FLAME STABILITY
Flame driving of longitudinal instabilities in liquid fueled dump combustors
[AD-A183536] 01 p0006 N88-10033
Combustion related shear-flow dynamics in elliptic supersonic jets 05 p0531 N88-13232
Mixing and combustion of pulsed gas jets
[PB88-112834] 06 p0680 N88-14169
Bistable cellular flames
[DE88-003074] 09 p1142 N88-16846
Basic instability mechanisms in chemically reacting subsonic and supersonic flows
[AD-A190101] 15 p2034 N88-22120
The structure and stability of spherically expanding flames 17 p2318 N88-23842
On the structure, propagation, extinction and stability of laminar premixed flames in dissociation equilibrium
18 p2483 N88-24728
Development of a computerized analysis for solid propellant combustion instability with turbulence
[NASA-CR-182351] 19 p2611 N88-25497
Flame stabilization in a reheat combustor
24 p3346 N88-29921

Modeling the stability of a turbulent premixed flame, downstream from a step by a Lagrangian method
24 p3350 N88-29943

FLAME TEMPERATURE
The development of a user friendly thermodynamic code for the personal computer 19 p2623 N88-25559
Soot and radiation in a gas turbine combustor
[AD-A191991] 23 p3179 N88-28924

FLAMEOUT
On the structure, propagation, extinction and stability of laminar premixed flames in dissociation equilibrium
18 p2483 N88-24728

FLAMES
NT DIFFUSION FLAMES
NT PREMIXED FLAMES
KR+ laser excitation of NH2 in atmospheric pressure flames
[AD-A183421] 01 p0050 N88-10322
Flame acceleration and transition to detonation in channels
[DE87-014193] 03 p0284 N88-11786
Development of many-body methods for flame chemistry and large molecule applications
[AD-A184451] 03 p0284 N88-11789
Equilibrium calculations of ionization in tracer flames
[PB87-104154] 04 p0412 N88-12555
Correlation of air pressure drop and flame arrestor characteristics for explosion suppression materials
[AD-A184960] 05 p0548 N88-13340
Formation and destruction of nitrous oxide in lean, premixed combustion
[DE88-001390] 05 p0562 N88-13423
Summary of discussions at the Ninth Meeting of the Sandia Cooperative Group on the Aerothermochemistry of Turbulent Combustion
[DE88-002281] 06 p0680 N88-14165
Velocity and density measurements in a turbulent nonpremixed flame with comparison to numerical model predictions
[DE87-014695] 08 p0967 N88-15854
Removal of out-of-plane distortion in mild steel panels using flame heating, volume 1
[AD-A187802] 11 p1457 N88-18684
Removal of out-of-plane distortion in mild steel panels using flame heating, volume 2
[AD-A187803] 11 p1457 N88-18685
On the possibility of high velocity deflagration front propagation by radiative energy transfer
[AD-A189022] 12 p1613 N88-19645
Laser ignition of nitramine composite propellants and crack propagation and branching in burning solid propellants
[AD-A189260] 13 p1753 N88-20483
Measurement of species concentrations in flames by laser-induced fluorescence
[DE88-007096] 14 p1889 N88-21286
Application of laser-induced fluorescence in an atmospheric-pressure boron-seeded flame
[AD-A189631] 14 p1889 N88-21287
Problems appearing at interface balances --- flames
14 p1987 N88-21855
Numerical simulation of turbulent flames using vortex methods
[AD-A189813] 15 p2034 N88-22116
Application of Rayleigh scattering to turbulent flow with heat transfer and combustion
[AD-A191565] 18 p2481 N88-24720
Measurement of the radiative properties of gas and oil flames
[NASA-TT-20299] 19 p2612 N88-25502
Modeling and experimental measurements of solid propellant flame structure 19 p2631 N88-25605
Ultraviolet imaging of hydrogen flames
[DE88-009152] 20 p2769 N88-26422
Asynchronous optical sampling for laser-based combustion diagnostics in high pressure flames
[AD-A192920] 20 p2770 N88-26428
Study of the local behavior of a flame
[ETN-88-92300] 20 p2771 N88-26433
Reducing adhesion and agglomeration within a cloud of combustible particles
[NASA-TM-100902] 20 p2788 N88-26539
Summary of discussions at the Tenth Meeting of the Sandia Cooperative Group on the Aerothermochemistry of Turbulent Combustion
[DE88-008467] 21 p2910 N88-27269
A study of flame spreading and combustion phenomena of stick propellants
[AD-A193598] 22 p3052 N88-28106
Interactions between coherent structures and premixed flame fronts
[ETN-88-92885] 22 p3053 N88-28111

FLAMMABILITY
Experiments of the selection of a method evaluating the fire resistance of some materials based on macromolecular compounds
[NASA-TT-20129] 02 p0154 N88-10966
Detection of vapors of flammable liquids in air by atmospheric sampling mass spectrometry/mass spectrometry
[DE88-000030] 02 p0196 N88-11227
Flammability limits in cocurrent smoldering combustion
[DE87-014102] 03 p0284 N88-11785
Fabrication and testing of fire resistant graphite composite panels
[NASA-CR-177397] 04 p0397 N88-12472
Spacecraft Fire Safety
[NASA-CP-2476] 04 p0406 N88-12520
Fire-related standards and testing
04 p0406 N88-12522
Spacecraft material flammability testing and configurations 04 p0407 N88-12529
An experimental investigation of the ignition and flammability limits of various hydrocarbon fuels in a two-dimensional solid fuel ramjet
[AD-A184968] 05 p0549 N88-13342
Flammability test on aircraft seats equipped with fire barrier fabrics for the Porcher company
[CEAT-M5-525200] 06 p0666 N88-14084
Flammability, smoke and toxicity test on fire barrier fabric from the Porcher company --- Airbus aircraft
[ETN-88-91168] 06 p0666 N88-14085
Correlation between flammability and heat of combustion of polymers
[NASA-TT-20116] 08 p0973 N88-15884
Review of thermal properties of graphite composite materials
[NASA-TM-100049] 09 p1139 N88-16825
Flammability characteristics of distillate fuels
[AD-A188497] 12 p1612 N88-19642
Evaluation of flammability for cable-like polymers
[NASA-TT-20225] 13 p1752 N88-20476
Burning characteristics and flammability of PVC cables in groups
[NASA-TT-20226] 14 p1893 N88-21303
Ignition and flammability characteristics of solid fuel ramjets 19 p2626 N88-25575
Reducing adhesion and agglomeration within a cloud of combustible particles
[NASA-TM-100902] 20 p2788 N88-26539
Determination of relative flammability of materials by pyrolysis and gas-chromatographic light hydrocarbon analysis
[DE88-012449] 24 p3343 N88-29898

FLAMMABLE GASES
NT GASEOUS FUELS
NT LIQUEFIED NATURAL GAS

FLANGES
Crack distribution and growth rates for critical fastener holes in Mirage wing RH79
[AD-A189080] 13 p1722 N88-20293
GTAW characterization for weld penetration on 304L stainless steel
[DE88-010611] 20 p2810 N88-26672
FEB structural analysis, revision H
[AD-A192302] 20 p2814 N88-26698

FLAP CONTROL
U AIRCRAFT CONTROL
U FLAPS (CONTROL SURFACES)

FLAPPING
Propulsive performance of a lifting flapping wing
17 p2295 N88-23733

FLAPPING HINGES
Impacts of rotor hub design criteria on the operational capabilities of rotorcraft systems
03 p0264 N88-11663
Flap-lag equations of motion of rigid, articulated rotor blades with three hinge sequences
[NASA-TM-100023] 04 p0401 N88-12495

FLAPS (CONTROL SURFACES)
NT JET FLAPS
NT LEADING EDGE FLAPS
NT TRAILING EDGE FLAPS
NT UPPER SURFACE BLOWN FLAPS
NT VORTEX FLAPS
NT WING FLAPS
Flap-lag equations of motion of rigid, articulated rotor blades with three hinge sequences
[NASA-TM-100023] 04 p0401 N88-12495
Design and control of repairs of carbon fiber lift augmentation flaps in the ATR42 aircraft
[SNIAS-872-111-112] 05 p0529 N88-13217
Validation elements of the computation methods and measurement techniques for high lift aerodynamic systems
[SNIAS-872-111-101] 05 p0541 N88-13299
An experimental investigation of the aerodynamics of a NACA 64A010 airfoil-flap combination with and without flap oscillations. Part 1: Steady-state characteristics
[NASA-TM-88217] 05 p0542 N88-13305
Flaps-up takoff performance of the OV-1D aircraft with YT53-L-704 engine installed
[AD-A185960] 07 p0819 N88-14979
An experimental investigation of the flap-lag-torsion aeroelastic stability of a small-scale hingeless helicopter rotor in hover
[NASA-TP-2546] 13 p1715 N88-20257
Operational considerations for laminar flow aircraft
17 p2298 N88-23748
Characteristics of merging shear layers and turbulent wakes of a multi-element airfoil
[NASA-TM-100053] 18 p2511 N88-24900
The identification of the direct lift control flap system of the research aircraft ATTAS
20 p2786 N88-26527
Variable wing camber control systems for the future Airbus program
[MBB-UT-104/88] 23 p3180 N88-28932

FLARE STARS
A spectral survey of 26 G9-M6 flare stars in the solar neighborhood 04 p0512 N88-13149
Exosat results on the dMe flare Star Wolf 630AB and on VB 8 04 p0512 N88-13151
IUE/Optical/VLA flares on AD Leo
04 p0512 N88-13152
Microwave observations of red dwarf flare stars
04 p0513 N88-13153
A VLA survey of dMe flare stars
04 p0513 N88-13154
Flares: Solar and stellar
[PB87-124962] 06 p0806 N88-14917

FLASH BLINDNESS
A comparison of visual evoked potential and behavioral measures of flashblindness in humans
[AD-A189757] 15 p2101 N88-22519

FLASH LAMPS
Laser induced ignition of propellants
[AD-A191099] 16 p2213 N88-23206

FLASH POINT
Flash threshold of shocked aluminum silicofluoride
[DE88-003978] 10 p1339 N88-18005

FLASH TUBES
U FLASH LAMPS

FLASHING (VAPORIZING)
Mechanistic model for void distribution in flashing flow
[DE88-002948] 10 p1326 N88-17928

FLASHOVER
Gases released by surface flashover of insulators
[DE87-013851] 01 p0039 N88-10249
Withstand voltage of slightly polluted insulator chains in humid weather conditions
[DE88-752818] 22 p3072 N88-28237

FLAT COAXIAL TRANSMISSION LINES
U MICROSTRIP TRANSMISSION LINES

FLAT PLATES
A note on the instability of a vortex sheet leaving a semi-infinite plate
[DFVLR-FB-87-16] 01 p0004 N88-10019
Radiative and free-convective heat transfer from a finite horizontal plate inside an enclosure
02 p0133 N88-10833
Heat transfer with very high free stream turbulence
02 p0186 N88-11161
Kinematic formulation of finite elements for plate bending 04 p0455 N88-12821
A Cartesian finite-volume method for the Euler equations 05 p0579 N88-13532
An experimental investigation of appendage-flat plate junction flow. Volume 2: Elliptical nose appendage data base
[AD-A184974] 05 p0580 N88-13539
Experimental studies on the tripping behavior of narrow T-stiffened flat plates subjected to hydrostatic pressure and underwater shock 05 p0592 N88-13613
Analysis of photopole data reduction models
05 p0593 N88-13616
Dynamic response of laminated composite plates using a three-dimensional hybrid-stress finite-element formulation 05 p0596 N88-13639
Dual cylindrical wave Laser-Doppler method for measurement of skin friction in fluid flow
06 p0700 N88-14297
Numerical calculation of appendage, flat plate junction flow
[AD-A186371] 07 p0850 N88-15158
Investigation of large-scale structures in the near wake of a parallel flat plate
[DFVLR-FB-87-31] 09 p1162 N88-16967
Interferometric study of natural convection heat transfer from a vertical flat plate with transverse roughness elements 10 p1327 N88-17935

Side-by-side comparisons of evacuated compound parabolic concentrator and flat plate solar collector systems at temperatures of 90 to 100°C
[DE88-004717] 10 p1351 N88-18073
Effects of waves on the boundary layer of a surface-piercing flat plate: Experiment and theory
[AD-A188356] 12 p1626 N88-19731
Modification of parabolic dish antenna pattern using two symmetrically placed circular flat plates
[AD-A189543] 13 p1758 N88-20517
Investigation of heat transfer to a flat plate in a shock tube
[AD-A189538] 13 p1766 N88-20561
Film cooling effectiveness on a flat plate in high free-stream turbulence using a single row of 30 deg slant-hole injectors
[AD-A190500] 15 p2147 N88-22816
Test code for the assessment and improvement of Reynolds stress models 16 p2197 N88-23105
Deflection of a circular liquid jet on a flat plate perpendicular to the flow direction
[NASA-TT-20279] 16 p2207 N88-23173
Two-equation low-Reynolds-number turbulence modeling of transitional boundary layer flows characteristic of gas turbine blades
[NASA-CR-4145] 16 p2209 N88-23185
Numerical simulations of the flat-plate laminar boundary layer in subsonic and supersonic flow
[PDR/CFDU/IC/36] 18 p2511 N88-24895
Forced motion of initially stressed shells and plates
18 p2529 N88-25005
Active control of 2-D instability waves on an axisymmetric body
[AD-A191578] 19 p2663 N88-25835
Drag reduction of turbulent boundary layers by means of grooved surfaces
[ETN-88-92618] 20 p2802 N88-26630
Comparison of edge diffraction theories
[AD-A193860] 22 p3070 N88-28223
Modal synthesis by use of substructures with fixed or free coupling points
[ILR-MITT-191] 22 p3089 N88-28341
Stability and drag reduction in a boundary layer with microbubbles
[AD-A191975] 23 p3209 N88-29099
Studies of gas turbine heat transfer airfoil surface and end-wall cooling effects
[AD-A195165] 24 p3326 N88-29805
Investigation of large-scale structures in the near wake of a parallel flat plate
[ESA-TT-1100] 24 p3372 N88-30080

FLAT SURFACES
Film thicknesses in circular elastohydrodynamic contacts
[PB87-123725] 06 p0710 N88-14354
Solid modelling with faceted primitives
[ETN-88-91593] 09 p1218 N88-17305

FLAVOR (PARTICLE PHYSICS)
Quark core stars, quark stars and strange stars
[DE88-006991] 17 p2450 N88-24555
Experimental elementary particle physics
[DE88-007510] 18 p2572 N88-25274
A method for the analysis of heavy flavor decays
[NOTA-INTERNA-909] 22 p3150 N88-28744

FLAW DETECTION
U NONDESTRUCTIVE TESTS

FLAWS
U DEFECTS

FLEET SATELLITE COMMUNICATION SYSTEM
Thermal testing by internal IR heating of the FEP module 02 p0136 N88-10654

FLEETSATCOM
U FLEET SATELLITE COMMUNICATION SYSTEM

FLEXIBILITY
Processing and properties of SiC/Nicalon composites
[DE87-013885] 03 p0279 N88-11757
On the control of a compliant robot arm
03 p0332 N88-12095
A swept wing panel in a low speed flexible walled test section
[NASA-CR-4106] 05 p0540 N88-13292
Flexibilized copolyimide adhesives
[NASA-TM-89303] 05 p0570 N88-13474
Control of a flexible one-link manipulator
[AD-A185035] 05 p0590 N88-13598
Finite element model for the stress and flexibility analysis of curved pipes
[DE87-703632] 05 p0592 N88-13608
Stability analysis of a rigid body with a flexible attachment using the energy-casimir method
[AD-A185646] 06 p0723 N88-14449
Solid modelling for the manipulative robot arm (power) and adaptive vision control for space station missions
08 p1061 N88-16409
Implementation of a robotic flexible assembly system
09 p1212 N88-17265
Probabilistic and reliability design procedures for flexible airfield pavements: Elastic layered method
[AD-A187533] 11 p1442 N88-18600
Adaptive control of a manipulator with a flexible link
[NASA-CR-181637] 11 p1476 N88-18807
Free boundary problems arising in the control of a flexible robot arm
[AD-A189124] 12 p1634 N88-19781
PNL-1 improved ceramic composites through controlled fiber matrix interaction
[DE88-005680] 13 p1750 N88-20462
A 60-meter erectable assembly concept for a control of flexible structures flight experiment
[NASA-TM-100497] 14 p1873 N88-21190
Ultrasonic characterization of ceramic joints
[DE88-005844] 15 p2043 N88-22173
Vibration and control of flexible rotor supported by magnetic bearings
[NASA-TM-100888] 17 p2345 N88-23977
Single-mode projection filters for modal parameter identification for flexible structures
[NASA-CR-182680] 18 p2566 N88-25244
Empty test section streamlining of the transonic self-streamlining wind tunnel fitted with new walls
[NASA-CR-181680] 19 p2598 N88-25442
Reduced flexibility in processing Titan 4 space launch vehicles at Cape Canaveral Air Force Station
[AD-A194908] 24 p3332 N88-29834
Modeling robot flexibility for endpoint force control
[AD-A195923] 24 p3380 N88-30132

FLEXIBLE BODIES
NT FLEXIBLE SPACECRAFT
Wall interference tests of a CAST 10-2/DOA 2 airfoil in an adaptive-wall test section
[NASA-TM-4015] 02 p0122 N88-10772
Recent advances in structural dynamics of large space structures
[NASA-TM-100513] 02 p0138 N88-10867
Identification of linear structural models
03 p0337 N88-12121
Finite deformations of shell with rigid inclusion
04 p0426 N88-12639
A simulation study of the flight dynamics of elastic aircraft. Volume 1: Experiment, results and analysis
[NASA-CR-4102] 06 p0669 N88-14099
Studies of the structural dynamic behavior of satellite antenna system
[AD-A185526] 06 p0673 N88-14121
A simulation study of the flight dynamics of elastic aircraft. Volume 2: Data
[NASA-CR-4102-VOL-2] 08 p0959 N88-15813
Control system simulation for a single-link flexible arm
[AD-A187037] 09 p1174 N88-17035
A substructure method for dynamic simulation of flexible mechanical systems with geometric nonlinearities
09 p1176 N88-17044
Robust controller design for flexible structures
[AD-A187217] 10 p1340 N88-18009
Experimental set-up and mathematical modeling of H-shaped beam type structure
[AD-A187196] 11 p1466 N88-18743
Structure of shear flow turbulence and its control
[AD-A187909] 11 p1482 N88-18846
A superelement component dynamic synthesis method 11 p1500 N88-18956
Predictive wall adjustment strategy for two-dimensional flexible walled adaptive wind tunnel: A detailed description of the first one-step method
[NASA-CR-181635] 12 p1573 N88-19409
Moveable thermal joints for deployable or steerable spacecraft radiator systems
[NLR-MP-87016-U] 13 p1730 N88-20347
Dynamic modelling of flexible rotor shafts mounted on hydrodynamic bearings 13 p1779 N88-20641
Optimal control and identification of space structures
[AD-A190033] 15 p2025 N88-22065
Approximation methods for the identification and control of distributed parameter systems
[AD-A190201] 15 p2124 N88-22662
Analysis of rotating flexible blades using MSC/NASTRAN 16 p2222 N88-23259
Nonlinear programming extensions to rational function approximation methods for unsteady aerodynamic forces
[NASA-TP-2776] 18 p2463 N88-24623
Experimental study of active vibration control
[AD-A191454] 18 p2526 N88-24989
Large planar maneuvers for articulated flexible manipulators
[NASA-CR-183079] 19 p2711 N88-26104
Experiments in adaptive control of a very flexible one link manipulator 20 p2842 N88-26865
Identification and control of time-varying flexible structures: An artificial intelligence approach
23 p3265 N88-29437
Current and proposed gust criteria and analysis methods: An FAA overview 24 p3311 N88-29718
Measured and predicted responses of the Nord 260 aircraft to the low altitude atmospheric turbulence
24 p3312 N88-29723
Dynamics of articulated aerospace structures
[AD-A195685] 24 p3324 N88-29794
Robust design of distributed controllers for large flexible space structures
[NASA-CR-183202] 24 p3380 N88-30134

FLEXIBLE SPACECRAFT
Structures and Materials Working Group report
01 p0016 N88-10093
Attitude Control Working Group report
01 p0016 N88-10099
Pinhole occulter experiment
[NASA-CR-179206] 02 p0235 N88-11481
Control design challenges of large space systems and spacecraft control laboratory experiment (SCOLE)
[NASA-CR-178392] 03 p0275 N88-11735
Natural control of flexible space structures
04 p0408 N88-12534
Simultaneous structural and control optimization via linear quadratic regulator eigenstructure assignment
05 p0594 N88-13622
Personnel occupied woven envelope robot power
[NASA-CR-182367] 07 p0856 N88-15196
Large-angle slewing maneuvers for flexible spacecraft
[NASA-CR-4123] 08 p1000 N88-16060
Emulating a flexible space structure: Modeling
[NASA-TM-100320] 09 p1135 N88-16812
SIMSAT: Simulation package for flexible systems. Beams in space
[TW-278] 13 p1730 N88-20348
Robust decentralized control of large flexible structures
[DE88-005416] 13 p1824 N88-20902
A feedback double path compensating control structure for the attitude control of a flexible spacecraft
[INPE-4464-PRE/1239] 14 p1880 N88-21240
Maximum likelihood parameter identification of flexible spacecraft
[LR-508] 16 p2168 N88-22924
L(sub infinity symbol)-approximations of complex functions and robust controllers for large flexible space structures
[PB88-186226] 20 p2764 N88-26390
Numerical optimization, system theoretic and software tools for the integrated design of flexible structures and their control systems
[AD-A192927] 21 p2895 N88-27183

FLEXING
Strain-energy-release rate analysis of the end-notched flexure specimen using the finite-element method
[NASA-TM-100494] 05 p0608 N88-13735
Cyclic fatigue of ceramics at high temperatures
[PB87-127700] 06 p0685 N88-14200
Active control of flexural vibrations in beams
06 p0794 N88-14866
An engineering study of hybrid adaptation of wind tunnel walls for three-dimensional testing
[NASA-CR-178374] 07 p0814 N88-14957
Contribution to modeling flexion fatigue damage in unidirectional composite materials
[ECL-87-12] 08 p0965 N88-15843
Mechanical properties of carbon fiber reinforced thermoplastic matrix composites
[NAL-TR-934] 09 p1139 N88-16827

FLEXURE
U FLEXING

FLICKER
Universal power spectra for wave turbulence: Applications to wind waves, flicker noise, solar wind spectrum and classical second sound
10 p1318 N88-17879

FLIGHT ALTITUDE
Decoupling and stabilization of speed and height in F4 Phantom aircraft using output feedback
[ETN-87-90926] 02 p0125 N88-10787

FLIGHT CHARACTERISTICS
NT FLIGHT ENVELOPES
Rotorcraft Design for Operations
[AGARD-CP-423] 03 p0262 N88-11649
Mission-oriented flying qualities criteria for helicopter design via in-flight simulation 03 p0263 N88-11652
Investigation of vertical axis handling qualities for helicopter hover and NOE flight
03 p0263 N88-11653
Handling qualities criterion for very low visibility rotorcraft 03 p0263 N88-11654
MBB simulation facilities applied for rotorcraft research 03 p0263 N88-11655
Impacts of rotor hub design criteria on the operational capabilities of rotorcraft systems
03 p0264 N88-11663
Development and application of computational aerothermodynamics flowfield computer codes
[NASA-CR-181534] 04 p0395 N88-12465

Hovering helicopter flight dynamics: A study of vertical motion
[AR-004-526] 04 p0399 N88-12485
Model helicopter rotor rig and associated strain gauge balance for performance studies
[NAL-TM-AE-8704] 05 p0552 N88-13364
A simulation study of the flight dynamics of elastic aircraft. Volume 1: Experiment, results and analysis
[NASA-CR-4102] 06 p0669 N88-14099
Impact of flying qualities on mission effectiveness for helicopter air combat, volume 1
[NASA-CR-166568] 06 p0669 N88-14100
Handling qualities of a wide-body transport airplane utilizing Pitch Active Control Systems (PACS) for relaxed static stability application
[NASA-TP-2482] 07 p0821 N88-14987
A simulation study of the flight dynamics of elastic aircraft. Volume 2: Data
[NASA-CR-4102-VOL-2] 08 p0950 N88-15813
Lateral stability and control derivatives extracted from space shuttle Challenger flight data
[NASA-TM-100520] 09 p1132 N88-16788
Workshop on Design Loads for Advanced Fighters
[AGARD-R-746] 12 p1579 N88-19449
Manned simulation: Helpful means to determine and improve structural load criteria 12 p1581 N88-19459
Bifurcations in unsteady aerodynamics-implications for testing
[NASA-TM-100083] 15 p2015 N88-22014
Airworthiness and flight characteristics test of a ski assembly for the UH-60A Black Hawk helicopter
[AD-A191414] 16 p2162 N88-22895
Certification aspects of airplanes which may operate with significant natural laminar flow 17 p2298 N88-23749
Airbus 1987: Success in Europe
[ETN-88-92099] 20 p2758 N88-26364
Contribution to the numerical solution of airplane spin motion
[ETN-88-92368] 21 p2896 N88-27190
A numerical simulation of side force effects by aerodynamic flight trajectory correction
[ISL-CO-211/87] 21 p2896 N88-27191
Japan Air Line's Aircraft Integrated Monitoring System (AIMS) activities 22 p3034 N88-28014
Advances in Flying Qualities
[AGARD-LS-157] 24 p3314 N88-29735
Advances in flying qualities: Concepts and criteria for a mission oriented flying qualities specification
24 p3314 N88-29739
A second look at MIL prime flying qualities requirements 24 p3314 N88-29740
The role of simulation in flying qualities and flight control system related development 24 p3315 N88-29742

FLIGHT CLOTHING
Validation of mathematical model predictions of immersion survival times
[IAM-652] 14 p1952 N88-21635
Further development of a mathematical model for the specification of immersion clothing insulation
[IAM-653] 14 p1954 N88-21644

FLIGHT COMPUTERS
U AIRBORNE/SPACEBORNE COMPUTERS

FLIGHT CONDITIONS
Calculation of the damage of highly loaded gas turbine disks under real flight conditions
[ETN-87-90416] 01 p0007 N88-10036

FLIGHT CONTROL
NT ANNULAR SUSPENSION AND POINTING SYSTEM
NT AUTOMATIC FLIGHT CONTROL
NT AUTOMATIC LANDING CONTROL
NT FLY BY WIRE CONTROL
NT POINTING CONTROL SYSTEMS
NT THRUST VECTOR CONTROL
Digital system bus integrity
[NASA-CR-181446] 01 p0006 N88-10030
A survey of aircraft integrated control technology
[AR-004-561] 02 p0126 N88-10794
Robust control system design
02 p0127 N88-10800
Optimal detection of sensor failures in flight control systems using deterministic observers
02 p0128 N88-10803
Flight test of a resident backup software system
02 p0128 N88-10805
The flight evaluation of an advanced engine display and monitoring system 03 p0264 N88-11659
Flight propulsion control integration for V/STOL aircraft
[NASA-TM-100226] 03 p0267 N88-11680
An evaluation plan of bus architectures and protocols using the NASA Ames intelligent redundant actuation system
[NASA-CR-177458] 04 p0398 N88-12482
Digital-flight-control-system software written in automated-engineering-design language: A user's guide of verification and validation tools
[NASA-TM-88313] 04 p0401 N88-12494
Applications of the hybrid automated reliability predictor
[NASA-TP-2760] 04 p0475 N88-12928
Nonlinear lift control at high speed and high angle of attack using vortex flow technology
05 p0545 N88-13319
Integrated control and display research for transition and vertical flight on the NASA V/STOL Research Aircraft (VSRA)
[NASA-TM-100029] 05 p0551 N88-13359
Electrical flight commands in transport aircraft
[SNIAS-872-111-108] 05 p0551 N88-13361
Reduced order optimal command applied to longitudinal automatic pilots
[SNIAS-872-111-114] 05 p0552 N88-13362
Control of an unstable launcher in atmospheric flight using minimax optimal control laws
[SNIAS-872-422-107] 05 p0638 N88-13901
Advanced helicopter cockpit and control configurations for helicopter combat missions
[NASA-TM-100017] 07 p0821 N88-14988
Guidance of high-altitude sounding rockets using the S19 and Spinning Rocket Attitude Control (SPINRAC) systems 08 p1034 N88-16273
NASA/Army Rotorcraft Technology. Volume 1: Aerodynamics, and Dynamics and Aeroelasticity
[NASA-CP-2495-VOL-1] 09 p1105 N88-16625
Helicopter mathematical models and control law development for handling qualities research
09 p1108 N88-16642
Rotorcraft flight-propulsion control integration
09 p1108 N88-16643
Rotorcraft technology at Boeing Vertol: Recent advances 09 p1111 N88-16658
A piloted simulation investigating handling qualities and performance requirements of a single-pilot helicopter in air combat employing a helmet-driven turreted gun
[AD-A186878] 09 p1116 N88-16689
Lateral stability and control derivatives extracted from space shuttle Challenger flight data
[NASA-TM-100520] 09 p1132 N88-16788
MPAD MCC workstation system: ADDAM and EEVE
09 p1203 N88-17209
User interface devices for mission control
09 p1205 N88-17224
Flight test technique, illustrated by Advanced Technologies Testing Aircraft System (ATTAS)
09 p1240 N88-17433
Light Electronic Control System (LECOS): A proposal for a interconnected error-tolerant, optoelectronic control system
[MBB-UT-004/87] 10 p1311 N88-17836
Trends in the distribution of tasks between commercial pilots and flight control systems
[MBB-UT-008/87] 10 p1314 N88-17851
The development of manoeuvre load criteria for agile aircraft 12 p1579 N88-19450
Interaction between structural considerations and system design in advanced flight controls
12 p1580 N88-19458
Manned simulation: Helpful means to determine and improve structural load criteria 12 p1581 N88-19459
Presentation of flight control design and handling quality commonality by separate surface stability augmentation for the family of commuter airplanes
[NASA-CR-182567] 12 p1583 N88-19471
The impact of vertical axis characteristics on helicopter handling qualities
[AD-A188964] 12 p1583 N88-19474
User perceptions of side-arm flight control in rotary-wing aircraft
[AD-A188519] 12 p1672 N88-20009
A fault injection experiment using the AIRLAB Diagnostic Emulation Facility
[NASA-CR-178390] 13 p1823 N88-20895
Operational viewpoint of the X-29A digital flight control system
[NASA-TM-100434] 14 p1866 N88-21152
Performance improvements of an F-15 airplane with an integrated engine-flight control system
[NASA-TM-100431] 14 p1867 N88-21159
F-16 simulator for man-in-the-loop testing of aircraft control systems (SIMTACS)
[AD-A189675] 14 p1870 N88-21178
The PC/AT compatible computer as a mission control center display processor at Ames-Dryden Flight Research Facility
[NASA-TM-100426] 14 p1955 N88-21654
Examination of the effects of using Ada (trade name) in flight control software
[AD-A189670] 14 p1959 N88-21683
Application of eigenstructure assignment techniques in the design of a longitudinal flight control system
[AD-A189644] 15 p2020 N88-22039
Multivariable control law design for the AFTI/F-16 with a failed control surface using a parameter-adaptive controller
[AD-A189848] 15 p2020 N88-22040
Kalman filter residual expert system
[AD-A190520] 15 p2020 N88-22041
Subharmonic aliasing and its effects on the AFTI/F-16 digital flight control system
[AD-A190614] 15 p2020 N88-22042
Multiple model parameter adaptive control for in-flight simulation
[AD-A190568] 15 p2021 N88-22044
Basic design of a flight director system for NAL STOL research aircraft
[DE88-751806] 16 p2162 N88-22897
Analytical sensor redundancy assessment
[NASA-CR-182892] 16 p2163 N88-22901
Stability and control methodology for conceptual aircraft design. Volume 1: Methodology manual
[AD-A191314] 16 p2164 N88-22906
Integrated avionics reliability 17 p2294 N88-23723
Investigation of air transportation technology at Princeton University, 1986 17 p2294 N88-23724
Rule-based fault-tolerant flight control
17 p2294 N88-23725
A comparison of integrated and separate systems for flight control and navigation 17 p2303 N88-23779
Software engineering for the British Aerospace Experimental Aircraft Programme (EAP)
17 p2306 N88-23798
Development of an airborne facility for advanced avionics research 17 p2307 N88-23801
Parameter-adaptive model-following for in-flight simulation
[AD-A190567] 18 p2467 N88-24645
Simultaneous multiple control force exertion capabilities of males and females versus helicopter control force design limits
[AD-A191653] 18 p2553 N88-25153
Model reduction methods for control design
[NASA-CR-179434] 19 p2719 N88-26144
Control of flight through microburst wind shear using deterministic trajectory optimization
20 p2761 N88-26375
Computer simulation of a single pilot flying a modern high-performance helicopter
[NASA-TM-100182] 20 p2761 N88-26376
Theoretical and experimental investigations of a vortex drag behind a wing profile with spoiler
[ISL-PU-309/87] 21 p2892 N88-27169
Investigations of aircraft control with jet spoilers
[ISL-R-112/87] 21 p2898 N88-27202
Robust digital model following controller for helicopters
[DFVLR-FB-88-07] 21 p2898 N88-27203
Improvement of head-up display standards. Volume 4: Head-up display dynamics flight tests
[AD-A193617] 22 p3042 N88-28060
System status display evaluation
[NASA-CR-4181] 22 p3042 N88-28061
Improvement of head-up display standards. Volume 2: Evaluation of head-up displays to enhance unusual attitude recovery
[AD-A194601] 23 p3178 N88-28921
Improvement of head-up display standards. Volume 5: Head up display ILS (Instrument Landing System) accuracy flight tests
[AD-A194602] 23 p3178 N88-28922
Time periodic control of a multi-blade helicopter
[AD-A194435] 23 p3180 N88-28931
Avionic expert systems 23 p3253 N88-29365
Motion planning for a free-flying robot
23 p3255 N88-29378
Advances in Flying Qualities
[AGARD-LS-157] 24 p3314 N88-29735
Low-speed longitudinal flying qualities of modern transport aircraft 24 p3314 N88-29738
Advances in flying qualities: Concepts and criteria for a mission oriented flying qualities specification
24 p3314 N88-29739
The role of simulation in flying qualities and flight control system related development 24 p3315 N88-29742
Intelligent fault diagnosis and failure management of flight control actuation systems
[NASA-CR-177481] 24 p3323 N88-29790
A multiprocessor avionics system for an unmanned research vehicle
[AD-A194806] 24 p3325 N88-29800
An analysis of lateral-directional handling qualities and Eigenstructure of high performance aircraft
[AD-A194874] 24 p3328 N88-29814

N-version software demonstration for digital flight controls
[NASA-CR-181483] 24 p3328 N88-29815
A fiber optic collective flight control system for helicopters
[AD-A195406] 24 p3328 N88-29818
Controlled degradation of resolution of high-quality flight simulator images for training effectiveness evaluation
[AD-A196189] 24 p3330 N88-29823
Four-axis side-arm flight control simulator investigation
[AD-A196026] 24 p3409 N88-30294
Improvement of head-up display standards. Volume 3: An evaluation of head-up display safety
[AD-A195787] 24 p3410 N88-30300
Space station proximity operations windows: Human factors design guidelines
[NASA-TM-88233] 24 p3410 N88-30301
An intelligent training system for space shuttle flight controllers 24 p3415 N88-30331

FLIGHT CREWS
NT SPACECREWS
An aerodynamic performance evaluation of the NASA/Ames Research Center advanced concepts flight simulator
[NASA-TM-89659] 03 p0268 N88-11685
Assessment of fatigue in aviation crews
[AD-A184129] 03 p0356 N88-12245
A comparison of the effects of group dynamics on individuals assigned to integral and non-integral aircrews
[AD-A186467] 08 p1051 N88-16345
Ultra-low frequency vibration data acquisition concerns in operating flight simulators
[DE88-004795] 10 p1285 N88-17687
Forecasting complications of cardiovascular disease in flight personnel 10 p1361 N88-18136
Cockpit data management
[NASA-CR-178407] 11 p1438 N88-18579
First encounters of the close kind: The formation process of airline flight crews
[AD-A187977] 11 p1523 N88-19091
Field dependence-independence and its relationship to flight training performance
[AD-A188888] 12 p1670 N88-20003
Multi-crew pictorial format display evaluation
[AD-A189349] 13 p1812 N88-20824
Proceedings of the Workshop on the Assessment of Crew Workload Measurements Methods, Techniques and Procedures. Volume 1: Preliminary Selection of Measures
[AD-A189004] 13 p1812 N88-20827
Development of a C3 generic workstation: System overview 16 p2242 N88-23396
Communication training for aircrews: A review of theoretical and pragmatic aspects of training program design
[NASA-CR-177459] 20 p2756 N88-26349
Detection of latent epilepsy in aircrew candidates
21 p2984 N88-27720
Cockpit and cabin crew coordination
[AD-A192445] 21 p2993 N88-27752
Future air-to-air training for the RF-4
[AD-A194383] 23 p3240 N88-29284
A field study on soft contact lens wear in USAF military transport aircraft
[AD-A195962] 24 p3407 N88-30285

FLIGHT ENVELOPES
Full-envelope aerodynamic modeling of the Harrier aircraft
[NASA-TM-88376] 05 p0552 N88-13363
Australian aerodynamic design codes for aerial tow bodies
[AD-A189048] 13 p1715 N88-20258
Multiple model parameter adaptive control for in-flight simulation
[AD-A190568] 15 p2021 N88-22044
Flight testing a V/STOL aircraft to identify a full-envelope aerodynamic model
[NASA-TM-100996] 17 p2301 N88-23762
Current flight test experience related to structural divergence of forward-swept wings
[NASA-TM-100445] 18 p2464 N88-24633

FLIGHT FATIGUE
Measurement and modification of sensorimotor system function during visual-motor performance
[AD-A186351] 07 p0889 N88-15387

FLIGHT HAZARDS
NT METEOROID HAZARDS
Aircraft accidents
[JB-84] 01 p0004 N88-10020
Contributions to the modeling of wind shear for danger studies
[ETN-87-90442] 01 p0072 N88-10463
The dependence of the normalized ice accretion thickness on cloud-physical parameters
[DFVLR-FB-87-08] 01 p0072 N88-10464
Meteorological systems support to critical shuttle requirements on the Eastern Test Range --- STS
02 p0205 N88-11281
Influence of Environmental Factors on Aircraft Wing Performance
[VKI-LS-1987-03] 08 p0951 N88-15771
Characterization of meteorological phenomena influencing aircraft operations 08 p0951 N88-15772
The influence of wind shear, downdraft, and turbulence in aircraft performance 08 p0952 N88-15773
The potential influence of rain on airfoil performance
08 p0952 N88-15774
Effects of wing simulated ground frost on aircraft performance 08 p0952 N88-15775
Low altitude windshear threat to commercial aircraft
08 p0952 N88-15777
Analysis of bird strikes to UK registered aircraft 1985 (civil aircraft over 5700 kg maximum weight
[CAA-PAPER-87012] 09 p1115 N88-16684
Lapwings and birdstrikes. The biology of the lapwing Vanellus vanellus in relation to the birdstrike hazard it presents
[CAA-PAPER-87015] 14 p1865 N88-21142
Bibliography of icing on aircraft (status 1987)
[DFVLR-MITT-87-18] 16 p2158 N88-22876
Standardized ice accretion thickness as a function of cloud physics parameters
[ESA-TT-1080] 16 p2234 N88-23346
Ice formation on aircraft
[ETN-88-92154] 18 p2545 N88-25104
Flight-management strategies for escape from microburst encounters
[NASA-TM-4057] 19 p2603 N88-25461
New ice detection system 22 p3037 N88-28030
Contributions to the modeling of wind shear for danger studies
[NASA-TT-20293] 23 p3174 N88-28900

FLIGHT INSTRUMENTS
NT ATTITUDE INDICATORS
NT AUTOMATIC PILOTS
NT FLIGHT TEST INSTRUMENTS
NT HORIZON SCANNERS
NT RADIO ALTIMETERS
Geometric modeling of flight information for graphical cockpit display
[AD-A190484] 15 p2021 N88-22043
Basic design studies for the realization of liquid crystal display systems in aircraft
[VA-87-001] 16 p2163 N88-22900
The pneumatic wind shear sensor: A tool for meteorological investigations and flight management
22 p3036 N88-28024
New ice detection system 22 p3037 N88-28030
The NAE atmospheric research aircraft
24 p3313 N88-29730
Improvement of head-up display standards. Volume 3: An evaluation of head-up display safety
[AD-A195787] 24 p3410 N88-30300

FLIGHT MANAGEMENT SYSTEMS
Optimal detection of sensor failures in flight control systems using deterministic observers
02 p0128 N88-10803
Application of flight systems methodologies to the validation of knowledge-based systems
[NASA-TM-100442] 18 p2561 N88-25207
Development of an airborne facility for advanced avionics research
[NLR-MP-87012-U] 20 p2760 N88-26368

FLIGHT MECHANICS
Maximum likelihood estimates of parameters in linear systems with process and measurement noise
[DFVLR-FB-87-20] 01 p0083 N88-10532
Revision of the information standards for flight mechanics
[DFVLR-MITT-87-06] 03 p0265 N88-11675
The Proceedings of the Symposium on Mechanics for Space Flight
[ISAS-SP-5] 03 p0317 N88-12006
Aerodynamics of Hypersonic Lifting Vehicles
[AGARD-CP-428] 05 p0529 N88-13219
Calendar of selected aeronautical and space meetings
[AGARD-CAL-87/1] 05 p0657 N88-14033
Highlights of the 70th Flight Mechanics Panel Symposium on Flight Vehicle Development Time and Cost Reduction
[AD-A185831] 07 p0901 N88-15454
An overview of key technology thrusts at Bell Helicopter Textron 09 p1111 N88-16657
Special flight mechanical features of the bearingless helicopter rotor
[MBB-FM-315/O] 10 p1309 N88-17825
Intelligent interfaces for expert systems
23 p3258 N88-29397

FLIGHT OPERATIONS
NT CREW PROCEDURES (INFLIGHT)
Report of safety survey: Human integration of approach charts
[DOT/FAA/PM-87/15] 01 p0076 N88-10488
A linear quadratic Gaussian with loop transfer recovery proximity operations autopilot for spacecraft
[NASA-CR-172028] 02 p0227 N88-11433
Eighth Session of the Commission for Aeronautical Meteorology (abridged)
[WMO-673] 06 p0745 N88-14585
Moisture plotting of carbon fiber composite in flight operations
[MBB-UT-119/87] 09 p1138 N88-16823
Selected aspects of triazolam in relation to aviator performance in naval flight operations
[AD-A189322] 12 p1667 N88-19996

FLIGHT OPTIMIZATION
Optimal thrust vector control of coplanar orbital evasive maneuvers
[AD-A189544] 13 p1730 N88-20346
Periodic solutions in aircraft cruise-dash optimization
18 p2464 N88-24631
The OFP (Operational Flight Program) update cycle needs you
[AD-A194910] 24 p3325 N88-29798

FLIGHT PATHS
Approach trajectory planning system for maximum concealment
[NASA-TM-88258] 02 p0227 N88-11435
The Avionics Flight Evaluation System (AFES) of the DFVLR
[ESA-TT-1037] 03 p0266 N88-11677
Flightpath reconstruction and systematic radar error estimation from multiradar range-azimuth measurements
[NLR-MP-85064-U] 06 p0693 N88-14251
Verification of obstacle accountability areas using a simple mathematical model. Part 1: Description of general model and application for a specific case --- engine failure at takeoff
[NLR-TR-85069-U] 09 p1115 N88-16683
Automatic routing module 09 p1210 N88-17251
The estimation of target trajectory parameters from Closest Point of Approach (CPA) time measurements in a field of acoustic sensors
[FB-3-87] 11 p1439 N88-18586
Development of an interactive real-time graphics system for the display of vehicle space positioning
[NASA-TM-100429] 13 p1730 N88-20344
Method for determining artillery position
[NASA-TT-20237] 13 p1834 N88-20974
Modification of the BLUEMAX 2 terrain following model to incorporate radar detection
[AD-A190594] 15 p2017 N88-22028
Geometric modeling of flight information for graphical cockpit display
[AD-A190484] 15 p2021 N88-22043
Flight penetration of wind shear: Control strategies
17 p2294 N88-23727
Method for prediction and determination of takeoff performance for vectored thrust vehicles
[AD-A191809] 18 p2463 N88-24626
Periodic solutions in aircraft cruise-dash optimization
18 p2464 N88-24631
Geographical information for design purposes
[NLR-MP-87014-U] 20 p2818 N88-26719
An evaluation of flight path formats head-up and head-down
[NASA-CR-4176] 21 p2897 N88-27196

FLIGHT PERFORMANCE
U FLIGHT CHARACTERISTICS

FLIGHT RECORDERS
Development of a multipurpose smart recorder for general aviation aircraft
[NASA-CR-168353] 18 p2465 N88-24637
Maintenance support for military aircraft by intelligent on-board maintenance data panel
22 p3034 N88-28012
The management of software in airborne recording systems 22 p3035 N88-28019
The intelligent QAR and its cost effective role in new generation AIMS --- quick access recorder (QAR); aircraft integrated monitoring systems (AIMS)
22 p3035 N88-28020
Development of a maintenance data bus monitor and recorder 22 p3036 N88-28022
The role played by FDRs in understanding the windshear phenomenon 22 p3036 N88-28023

FLIGHT RULES
NT INSTRUMENT FLIGHT RULES
NT VISUAL FLIGHT RULES
Air traffic control
[FAA-ORDER-7110.65E] 12 p1576 N88-19426

FLIGHT SAFETY
Report of safety survey: Human integration of approach charts
[DOT/FAA/PM-87/15] 01 p0076 N88-10488

UK airmiss statistics
[CAP-530] 03 p0261 N88-11642
Report of the helicopter human factors working group --- accident prevention
[CAA-PAPER-87007] 03 p0361 N88-12274
Airline safety: A comparative analysis
[AD-A185358] 05 p0543 N88-13306
The influence of wind shear, downdraft, and turbulence in aircraft performance 08 p0952 N88-15773
Instrumentation utilisation for risk control in safety operations --- balloons and rockets
08 p1030 N88-16240
Annual review of aircraft accident data: US air carrier operations calendar year 1985
[PB88-135843] 10 p1276 N88-17638
AEV local verification for aviation, precipitation and temperature programs: AV, REL, TEM (September 1987 revision)
[PB88-115662] 10 p1355 N88-18101
Medical and psychological problems of assuring flight safety under present conditions
10 p1359 N88-18123
Proceedings of a Workshop on Innovative Solutions for Safety in Air Transportation
[ILR-MITT-178(1987)] 11 p1437 N88-18573
Activities report in air traffic control
[ETN-88-91092] 11 p1438 N88-18581
Safe rendezvous approach to a space station by impulsive transfers and continuous thrust arcs
12 p1585 N88-19486
Proceedings of the Workshop on the Assessment of Crew Workload Measurements Methods, Techniques and Procedures. Volume 1: Preliminary Selection of Measures
[AD-A189004] 13 p1812 N88-20827
UK airmiss statistics
[REPT-3/87] 14 p1865 N88-21141
UK airmiss statistics
[CAA-1/87] 17 p2300 N88-23761
Meteorological and Environmental Inputs to Aviation Systems
[NASA-CP-2498] 18 p2545 N88-25105
General-aviation's view of progress in the aviation weather system 18 p2546 N88-25110
Aircraft field degradation and electromagnetic compatibility
[PB88-183975] 19 p2602 N88-25456
Flight-management strategies for escape from microburst encounters
[NASA-TM-4057] 19 p2603 N88-25461
System identification in vehicle dynamics
[DFVLR-MITT-87-22] 20 p2785 N88-26518
The exploitation of Aircraft Integrated Monitoring System (AIMS) data in height-keeping studies for aircraft operating above FL 290 22 p3036 N88-28026
UK airmisses involving commercial air transport
[CAA-1/88] 23 p3176 N88-28907

FLIGHT SIMULATION
The fatigue properties of aerospace steels under constant amplitude and flight-by-flight simulated loading
[BAE-MSM-R-GEN-0566] 01 p0059 N88-10377
Contributions to the modeling of wind shear for danger studies
[ETN-87-90442] 01 p0072 N88-10463
Global positioning satellite-based automatic landing system and wind estimated feedback for the AH-64 helicopter 02 p0124 N88-10784
Improvements to the adaptive maneuvering logic program
[NASA-CR-3985] 03 p0262 N88-11648
Rotorcraft Design for Operations
[AGARD-CP-423] 03 p0262 N88-11649
Investigation of vertical axis handling qualities for helicopter hover and NOE flight
03 p0263 N88-11653
An inexpensive real-time interactive three-dimensional flight simulation system
[AD-A184340] 04 p0402 N88-12499
CGI delay compensation
[NASA-TM-86703] 04 p0476 N88-12932
Shock tunnels for real gas hypersonics
05 p0530 N88-13223
Overlooked potential of systems with Markovian coefficients
[NLR-MP-86049-U] 05 p0552 N88-13366
Noise of a model counterrotation propeller with reduced aft rotor diameter at simulated takeoff/approach conditions (F7/A3)
[NASA-TM-100254] 05 p0647 N88-13961
Experimental design of a piloted helicopter off-axis-tracking simulation using a helmet mounted display
[AD-A186226] 07 p0820 N88-14982
Handling qualities of a wide-body transport airplane utilizing Pitch Active Control Systems (PACS) for relaxed static stability application
[NASA-TP-2482] 07 p0821 N88-14987
An inexpensive real-time interactive three dimensional flight simulation system
[AD-A184868] 07 p0821 N88-14989
The role of adaptive supplemental visual cuing in flight simulation
[AD-A185932] 07 p0822 N88-14992
A simulation study of the flight dynamics of elastic aircraft. Volume 2: Data
[NASA-CR-4102-VOL-2] 08 p0959 N88-15813
Numerical analysis of motion of solid bodies in atmosphere 08 p1079 N88-16505
Rotorcraft handling-qualities design criteria development 09 p1109 N88-16645
Status of NASA/Army rotorcraft research and development piloted flight simulation
09 p1110 N88-16651
Helicopters as test carriers for avionics systems (HETAS)
[DFVLR-IB-112-85/18] 09 p1116 N88-16692
Upgrading of NASA-Ames high-energy hypersonic facilities: A Study
[NASA-CR-182475] 09 p1122 N88-16717
Frequency-response identification of XV-15 tilt-rotor aircraft dynamics 10 p1277 N88-17643
Transport delay compensation for computer-generated imagery systems
[NASA-TM-100084] 10 p1277 N88-17645
Realtime pilot model parameter identification
[AD-A188873] 12 p1584 N88-19476
Standardized environmental fatigue sequence for the evaluation of composite components in combat aircraft (ENSTAFF = ENvironmental falSTAFF)
[LBF-FB-179] 13 p1722 N88-20300
Power spectral density analysis of wind-shear turbulence for related flight simulations
[NASA-CR-182721] 13 p1802 N88-20773
Determination of canopy loads for a light aircraft by wind tunnel testing and computer modelling
[BU-353] 14 p1869 N88-21167
China constructing high-altitude test cell
14 p1901 N88-21351
Masking of motion cues by random motion: Comparison of human performance with a signal detection model
[UTIAS-313] 14 p1953 N88-21639
Model selection for the multiple model adaptive algorithm for in-flight simulation
[AD-A189715] 15 p2016 N88-22022
Effects of update and refresh rates on flight simulation visual displays
[NASA-TM-100415] 15 p2018 N88-22033
Application of eigenstructure assignment techniques in the design of a longitudinal flight control system
[AD-A189644] 15 p2020 N88-22039
Multiple model parameter adaptive control for in flight simulation
[AD-A190568] 15 p2021 N88-22044
Probe-evoked event-related potential techniques for evaluating aspects of attention and information processing 16 p2240 N88-23379
Wind tunnel investigation of wing and control panel loads at transonic and supersonic speeds on some schematic cruciform missile configurations
[FFA-TN-1986-43] 18 p2457 N88-24585
Parameter-adaptive model-following for in-flight simulation
[AD-A190567] 18 p2467 N88-24645
Simulator evaluation of lineup visual landing aids for night carrier landing
[AD-A191212] 18 p2468 N88-24648
F-14 modeling study
[NASA-CR-4164] 19 p2603 N88-25462
Research on piloting under conditions of breakdown in flight
[PB87-217980] 19 p2710 N88-26102
On the dynamic behavior of balloon during its launch, application of panel method and extension to unsteady problem
[ISAS-RN-622] 20 p2751 N88-26330
A high fidelity real-time simulation of a small turboshaft engine
[NASA-TM-100991] 20 p2761 N88-26378
Robust digital model following controller for helicopters
[DFVLR-FB-88-07] 21 p2896 N88-27203
System status display evaluation
[NASA-CR-4181] 22 p3042 N88-28061
Complex configurations 23 p3167 N88-28861
Contributions to the modeling of wind shear for danger studies
[NASA-TT-20293] 23 p3174 N88-28900
The role of simulation in flying qualities and flight control system related development 24 p3315 N88-29742
Minimum-complexity helicopter simulation math model
[NASA-CR-177476] 24 p3328 N88-29819
A digital simulation technique for the Dryden atmospheric model
[NASA-TT-20342] 24 p3404 N88-30266
Prediction and measurement of human pilot dynamic characteristics in a manned rotorcraft simulation
[NASA-CR-183246] 24 p3410 N88-30297

FLIGHT SIMULATORS
NT COCKPIT SIMULATORS
A research on pilot performance in the case of aircraft malfunction
[ETN-87-90652] 02 p0217 N88-11369
A research on pilot performance in a flight incident situation
[ETN-87-90653] 02 p0217 N88-11370
Mission-oriented flying qualities criteria for helicopter design via in-flight simulation 03 p0263 N88-11652
MBB simulation facilities applied for rotorcraft research 03 p0263 N88-11655
Research simulators for helicopters
03 p0263 N88-11656
An aerodynamic performance evaluation of the NASA/Ames Research Center advanced concepts flight simulator
[NASA-TM-89659] 03 p0268 N88-11685
An inexpensive real-time interactive three-dimensional flight simulation system
[AD-A184340] 04 p0402 N88-12499
The role of adaptive supplemental visual cuing in flight simulation
[AD-A185932] 07 p0822 N88-14992
Application of the analysis phase of the instructional system development to the MK-105 magnetic minesweeping mission of the MH-53E helicopter
[AD-A186282] 07 p0822 N88-14994
Scientific Colloquium in Honor of Prof. Dr. Rer. Nat. Hermann L. Jordan
[DFVLR-MITT-87-11] 09 p1240 N88-17432
Flight test technique, illustrated by Advanced Technologies Testing Aircraft System (ATTAS)
09 p1240 N88-17433
Investigation of the influence of wind shear on the aerodynamic characteristics of aircraft using a vortex-lattice method 10 p1274 N88-17619
Ultra-low frequency vibration data acquisition concerns in operating flight simulators
[DE88-004795] 10 p1285 N88-17687
Measurement and effects of transport delays in a state-of-the-art F-16C flight simulator
[AD-A187367] 11 p1441 N88-18599
Aircrew training devices: Utility and utilization of advanced instructional features, phase 4
[AD-A188418] 12 p1670 N88-20000
F-16 simulator for man-in-the-loop testing of aircraft control systems (SIMTACS)
[AD-A189675] 14 p1870 N88-21178
First flight simulator test of the head-up display for NAL QSTOL experimental aircraft (ASUKA)
[DE88-751804] 16 p2162 N88-22896
A look toward the future of complex avionics systems development using the USAF Test Pilot School's avionics systems test training aircraft 17 p2306 N88-23797
Digital monoplotting, part 1
[B8735122-PT-1] 17 p2365 N88-24106
Digital monoplotting, part 2
[B8735122-PT-2] 17 p2369 N88-24107
Analysis procedures and subjective flight results of a simulator validation and cue fidelity experiment
[NASA-TM-88270] 18 p2465 N88-24634
An OOD (Object-Oriented Design) paradigm for flight simulators
[AD-A191097] 18 p2467 N88-24647
F-14 modeling study
[NASA-CR-4164] 19 p2603 N88-25462
Flight simulator: Field of view utilized in performing tactical maneuvers
[AD-A192412] 20 p2762 N88-26379
An evaluation of flight path formats head-up and head-down
[NASA-CR-4176] 21 p2897 N88-27196
Simulator sickness in the AH-64 Apache combat mission simulator
[AD-A193419] 21 p2988 N88-27739
System status display evaluation
[NASA-CR-4181] 22 p3042 N88-28061
OMV docking simulator 23 p3255 N88-29379
Controlled degradation of resolution of high-quality flight simulator images for training effectiveness evaluation
[AD-A196189] 24 p3330 N88-29823
LANTIRN simulator training in the F-16C
[AD-A195201] 24 p3330 N88-29826

FLIGHT STABILITY TESTS
Preliminary airworthiness evaluation of the UH-60A equipped with the XM-139 VOLCANO mine dispensing system
[AD-A190604] 15 p2018 N88-22029

FLIGHT STRESS (BIOLOGY)
NT SPACE FLIGHT STRESS
Brain activity during tactical decision-making. Part 2: Probe-evoked potentials and workload
[AD-A188680] 12 p1667 N88-19994

FLIGHT TECHNICAL ERROR
U PILOT ERROR

FLIGHT TEST INSTRUMENTS
Test equipment with fiber optic data bus and laser gyro strapdown system LTN-90 for the helicopter BO-105
[ESA-TT-1036] 01 p0005 N88-10025
Effect of installation and calibration errors of sensors on system identification results of an aircraft
[ESA-TT-1059] 03 p0266 N88-11676
Boeing 727 MLS (Microwave Landing System) terminal instrument procedures (TERPS) approach data collection and processing, data report
[AD-A185523] 06 p0667 N88-14090
Refinement of eye-point-of-regard measurement with helicopter pilots in a flight experiment
[ESA-TT-1073] 09 p1200 N88-17195
Flight test technique, illustrated by Advanced Technologies Testing Aircraft System (ATTAS)
09 p1240 N88-17433
Trajectory measurement of the Fokker 100 aircraft during autoland testing
[NLR-MP-86010-U] 20 p2758 N88-26366
Development of an airborne facility for advanced avionics research
[NLR-MP-87012-U] 20 p2760 N88-26368
Interface techniques and systems for standard aircraft data buses 22 p3036 N88-28028
Test and calibration system for monitoring the Advanced Technologies Testing Aircraft System (ATTAS) data acquisition system 22 p3037 N88-28029

FLIGHT TESTS
NT FLIGHT STABILITY TESTS
NT SPACE TRANSPORTATION SYSTEM 4 FLIGHT
HiMAT flight program: Test results and program assessment overview
[NASA-TM-86725] 01 p0005 N88-10026
Comparison of wind tunnel and flight test afterbody and nozzle pressures for a twin-jet fighter aircraft at transonic speeds
[NASA-TP-2588] 02 p0121 N88-10765
Flight research at NASA Ames Research Center: A test pilot's perspective
[NASA-TM-100025] 02 p0125 N88-10788
Flight test of a resident backup software system
02 p0128 N88-10805
Auxiliary propulsion system flight package
[NASA-CR-180828] 02 p0141 N88-10886
The 1986 Goddard Space Flight Center Battery Workshop
[NASA-CP-2486] 02 p0163 N88-11021
BRASILSAT A2: Ground and in-orbit anomalies
02 p0164 N88-11032
Handling qualities criterion for very low visibility rotorcraft 03 p0263 N88-11654
The Avionics Flight Evaluation System (AFES) of the DFVLR
[ESA-TT-1037] 03 p0266 N88-11677
Comparison of flight-measured and calculated temperatures on the space shuttle orbiter
[NASA-TM-88278] 03 p0321 N88-12029
Developmental airdrop testing techniques and devices
[AGARD-AG-300-VOL-6] 04 p0398 N88-12481
Human respiratory responses during high performance flight
[AGARD-AG-312] 04 p0474 N88-12923
Full-envelope aerodynamic modeling of the Harrier aircraft
[NASA-TM-88376] 05 p0552 N88-13363
Visible boundary layer transition points through flight tests 06 p0675 N88-14136
An investigation of the effects of the propeller slipstream on a wing boundary layer 06 p0700 N88-14293
Flight and wind-tunnel measurements showing base drag reduction provided by a trailing disk for high Reynolds number turbulent flow for subsonic and transonic Mach numbers
[NASA-TP-2638] 06 p0701 N88-14299
First results from the Airborne Visible/Infrared Imaging Spectrometer (AVIRIS) 06 p0707 N88-14335
Laminar flow integration: Flight tests status and plans
07 p0813 N88-14952
Digital processing of flight test data without using anti-aliasing filters, using a helicopter as an example
[DFVLR-MITT-87-12] 07 p0819 N88-14981
Overview of NASA PTA propfan flight test program
08 p0957 N88-15805
Analysis of shock and vibration environments for cargo on C9B transport aircraft 08 p0999 N88-16051
Comprehensive inflight vibration and acoustic testing
08 p0999 N88-16052
NASA/Army Rotorcraft Technology. Volume 3: Systems Integration, Research Aircraft, and Industry
[NASA-CP-2495-VOL-3] 09 p1110 N88-16650
Rotorcraft flight research with emphasis on rotor systems 09 p1111 N88-16656
McDonnell Douglas Helicopter Company independent research and development: Preparing for the future
09 p1111 N88-16660
A flight-test methodology for identification of an aerodynamic model for a V/STOL aircraft
[NASA-TM-100087] 09 p1117 N88-16694
Aircraft flight test trajectory control
[NASA-CR-179428] 09 p1120 N88-16707
ASSESS-2: An aircraft simulation of Spacelab
09 p1123 N88-16723
Flight test technique, illustrated by Advanced Technologies Testing Aircraft System (ATTAS)
09 p1240 N88-17433
Recommendations for ground effects research for V/STOL and STOL aircraft and associated equipment for large scale testing
[NASA-CR-177429] 10 p1268 N88-17585
A potential flight evaluation of an upper-surface-blowing/circulation-control-wing concept
10 p1272 N88-17609
X-29A forward-swept-wing flight research program status
[NASA-TM-100413] 10 p1277 N88-17644
Flight testing of fighter aircraft
[MBB/LKE-62/S/PUB/292] 10 p1312 N88-17844
Effect of transition aerodynamics on aeroassist flight experiment trajectories
[NASA-TM-100546] 11 p1446 N88-18620
Influence of base modifications on in-flight base drag in the presence of jet exhaust for Mach numbers from 0.7 to 1.5
[NASA-TP-2802] 11 p1486 N88-18881
Analysis of in-flight acoustic data for a twin-engined turboprop airplane
[NASA-CR-178389] 11 p1543 N88-19220
Calculated unsteady aerodynamics of wings
[AD-A189608] 12 p1574 N88-19415
A perspective on 15 years of proof-of-concept aircraft development and flight research at Ames-Moffett by the Rotorcraft and Powered-Lift Flight Projects Division, 1970-1985
[NASA-RP-1187] 12 p1582 N88-19467
Minimizing development flight test time and cost in the US Air Force 12 p1703 N88-20192
Improved flight test productivity using advanced on line data systems 12 p1703 N88-20193
A review of technologies applicable to low-speed flight of high-performance aircraft investigated in the Langley 14- x 22-foot subsonic tunnel
[NASA-TP-2796] 13 p1717 N88-20264
Flight tests of external modifications used to reduce blunt base drag
[NASA-TM-100433] 13 p1719 N88-20279
A correlation study of X-29A aircraft and associated analytical development
[NASA-CR-183103] 13 p1722 N88-20296
Aircraft flight flutter testing at the NASA Ames-Dryden Flight Research Facility
[NASA-TM-100417] 13 p1723 N88-20301
The design and use of a temperature-compensated hot-film anemometer system for boundary-layer flow transition detection on supersonic aircraft
[NASA-TM-100421] 13 p1723 N88-20304
Lateral and longitudinal stability and control parameters for the space shuttle discovery as determined from flight test data
[NASA-TM-100555] 13 p1724 N88-20309
Western aeronautical test range real-time graphics software package MAGIC
[NASA-TM-100425] 13 p1757 N88-20506
Preliminary in-flight boundary layer transition measurements on a 45 deg swept wing at Mach Numbers between 0.9 and 1.8
[NASA-TM-100412] 13 p1772 N88-20598
Atmospheric electrical modeling in support of the NASA F-106 storm hazards project
[NASA-CR-181639] 13 p1799 N88-20758
Configuration management issues and objectives for a real-time research flight test support facility
[NASA-TM-100437] 13 p1813 N88-20832
The use of an automated flight test management system in the development of a rapid-prototyping flight research facility
[NASA-TM-100436] 13 p1823 N88-20896
Predictive monitoring research: Summary of the PREMON system
[NASA-CR-182687] 13 p1824 N88-20905
An experimental and theoretical study of the ice accretion process during artificial and natural icing conditions
[NASA-CR-182119] 14 p1865 N88-21143
Development and flight test of an experimental maneuver autopilot for a highly maneuverable aircraft
[NASA-TP-2618] 14 p1867 N88-21153
A flight test investigation into flow separation and structural response for a transport aircraft at buffet onset
[RAE-TR-87006] 14 p1867 N88-21156
Development of an integrated set of research facilities for the support of research flight test
[NASA-TM-100427] 14 p1869 N88-21169
The NASA integrated test facility and its impact on flight research
[NASA-TM-100418] 14 p1870 N88-21177
Psychophysical load of glider pilots on long-duration flights
[DFVLR-FB-87-38] 14 p1953 N88-21642
The PC/AT compatible computer as a mission control center display processor at Ames-Dryden Flight Research Facility
[NASA-TM-100426] 14 p1955 N88-21654
Bifurcations in unsteady aerodynamics-implications for testing
[NASA-TM-100083] 15 p2015 N88-22014
Real-time flight test data distribution and display
[NASA-TM-100424] 15 p2022 N88-22050
The growth potential of corona discharges from aircraft flying in precipitation
[AD-A190507] 15 p2094 N88-22476
Oil flow patterns on a series of capsule-type re-entry vehicles at hypersonic speeds
[DE88-751805] 16 p2155 N88-22858
Development of a mobile research flight test support capability
[NASA-TM-100429] 16 p2159 N88-22883
Digital processing of flight data of a helicopter without using anti-aliasing filters
[ESA-TT-1094] 16 p2161 N88-22890
Airworthiness and flight characteristics test of a ski assembly for the UH-60A Black Hawk helicopter
[AD-A191414] 16 p2162 N88-22895
Experimental investigation of Hover flowfields in water at the McDonnell Douglas Research Laboratories
16 p2202 N88-23135
Boundary layer flow visualization for flight testing
17 p2297 N88-23742
Flight experiences with laminar flow
17 p2297 N88-23744
Operational considerations for laminar flow aircraft
17 p2298 N88-23748
Flight testing a V/STOL aircraft to identify a full-envelope aerodynamic model
[NASA-TM-100996] 17 p2301 N88-23762
The integration, characterisation and trialling of a modern complex airborne radar 17 p2305 N88-23791
Rotorcraft TCAS (traffic alert and collision avoidance system) evaluation: Group 3 results
[AD-A191719] 18 p2461 N88-24614
Western Pacific Omega validation: Project description
[AD-A191753] 18 p2462 N88-24617
Method for prediction and determination of takeoff performance for vectored thrust vehicles
[AD-A191809] 18 p2463 N88-24626
Current flight test experience related to structural divergence of forward-swept wings
[NASA-TM-100445] 18 p2461 N88-24633
Analysis procedures and subjective flight results of a simulator validation and cue fidelity experiment
[NASA-TM-88270] 18 p2465 N88-24634
Flight research and testing
[NASA-TM-100439] 20 p2758 N88-26361
Flight test preparation and measuring data validation for parameter identification 20 p2786 N88-26529
Utilization of identification methods in the time and frequency domain for the determination of the XV-15 (tilt-rotor) dynamics for lateral motion in hover flight
20 p2787 N88-26532
Application of complementary parameter identification techniques to flight test data of a transport aircraft
20 p2787 N88-26533
A comparison of theory and flight test of the BO 105/BMR in hover and forward flight
21 p2890 N88-27155
Pilot report: AFTI (Advanced Fighter Technology Integration) F-111
[AD-A192937] 21 p2895 N88-27194
Air-to-air radar flight testing
[AGARD-AG-300-VOL-7] 21 p2932 N88-27406
Flight testing under extreme environmental conditions
[AGARD-AG-300-VOL-8] 21 p2951 N88-27525
Hypersonic flight testing
[DE88-001655] 21 p3015 N88-27884

Improvement of head-up display standards. Volume 4: Head-up display dynamics flight tests
[AD-A193617] 22 p3042 N88-28060

Proof-of-principle high speed electronic imaging system, phase 2
[AD-A193798] 23 p3181 N88-28937

Two biased estimation techniques in linear regression: Application to aircraft
[NASA-TM-100649] 23 p3274 N88-29489

Flight test equipment for the on-board measurement of wind turbulence 24 p3311 N88-29719

Angle of attack and sideslip estimation using an inertial reference platform
[AD-A194876] 24 p3319 N88-29769

Preliminary airworthiness evaluation of the UH-60A/ESSS (External Stores Support System) with HELLFIRE launcher installed
[AD-A196187] 24 p3323 N88-29793

A multiprocessor avionics system for an unmanned research vehicle
[AD-A194806] 24 p3325 N88-29800

An analysis of lateral-directional handling qualities and Eigenstructure of high performance aircraft
[AD-A194874] 24 p3328 N88-29814

Space structure (dynamics and control) theme development
[NASA-TM-100597] 24 p3335 N88-29850

Techniques used in the F-14 variable-sweep transition flight experiment
[NASA-TM-100444] 24 p3374 N88-30093

FLIGHT TIME

General aviation activity and avionics survey: 1986 data
[AD-A189986] 15 p2013 N88-22003

FLIGHT TRAINING

NT SPACE FLIGHT TRAINING

An aerodynamic performance evaluation of the NASA/Ames Research Center advanced concepts flight simulator
[NASA-TM-89659] 03 p0268 N88-11685

The role of adaptive supplemental visual cuing in flight simulation
[AD-A185832] 07 p0822 N88-14992

Field dependence-independence and its relationship to flight training performance
[AD-A188888] 12 p1670 N88-20003

An enumeration of research to determine the optimal design and use of Army flight training simulators
[AD-A191242] 18 p2468 N88-24649

Flight simulator: Field of view utilized in performing tactical maneuvers
[AD-A192412] 20 p2762 N88-26379

Proposal for a new aggressor aircraft
[AD-A194311] 22 p3041 N88-28056

Future air-to-air training for the RF-4
[AD-A194363] 23 p3240 N88-29284

Proposed improvements to the USAF flight screening program
[AD-A194506] 23 p3240 N88-29285

Integration of LANTIRN (Low Altitude Navigation and Targeting Infrared for Night) into operational fighter training
[AD-A194906] 24 p3325 N88-29799

FLIGHT VEHICLES

Flight vehicle system identification: Status and prospects 20 p2785 N88-26520

FLIR DETECTORS

Wind shear detection. Forward-looking sensor technology
[NASA-CP-10004] 07 p0817 N88-14970

Passive autonomous infrared sensor technology
[AD-A188698] 13 p1839 N88-21005

A multiple model adaptive tracking algorithm against airborne targets
[AD-A190619] 15 p2057 N88-22263

IR (infrared) sky radiance distributions in the marine boundary layer
[AD-A193683] 22 p3119 N88-28531

FLOAT ZONES

Liquid encapsulated float zone process and apparatus
[NASA-CASE-MFS-28144-1] 17 p2446 N88-24545

Marangoni convection in finite cylindrical liquid bridges
[LRT-WE-9-FB-5(1988)] 22 p3078 N88-28277

FLOATING

Flotation processes
[PB88-180302] 18 p2540 N88-25075

FLOATING POINT ARITHMETIC

The warp computer: Architecture, implementation, and performance
[AD-A184329] 03 p0363 N88-12286

Implementation and performance of a complex vision system on a systolic array machine
[AD-A184331] 04 p0482 N88-12971

A comparison of the Cray-2 performance before and after the installation of memory pseudo-banking
[NASA-CR-177482] 09 p1215 N88-17287

The Livermore FORTRAN Kernels: A computer test of the numerical performance range — benchmark tests
[UCRL-53745] 11 p1531 N88-19144

Scientific computing environments
[AD-A191239] 17 p2385 N88-24175

MIPS: The good, the bad and the useful
[NASA-CR-182893] 17 p2386 N88-24184

FLOATS

Moored current meter data from the Canary Basin near 32 deg N, 24 W (84-1986), volume 40
[PB88-108105] 07 p0882 N88-15351

FLOOD CONTROL

Flood monitoring using SPOT
03 p0342 N88-12162

Review of the potential of satellite remote sensing for marine flood protection
[IOS-237] 07 p0870 N88-15280

FLOOD PLAINS

Flood monitoring using SPOT
03 p0342 N88-12162

A comparative thematic mapping analysis of SPOT data: The Vientiane Plain (Laos) 03 p0343 N88-12163

Geomorphologic sector maps of Niquizanga-Mayares, province of San Juan, Argentina
17 p2368 N88-24098

Oxidation and reduction rates for organic carbon in the Amazon mainstream tributary and floodplain, inferred from distributions of dissolved gases
[NASA CR-182943] 18 p2538 N88-25062

IEMIS (Integrated Emergency Management Information System) floodplain mapping based on a LIDAR derived data set
[AD-A193071] 21 p2966 N88-27616

A comparative thematic mapping analysis of SPOT data: The Vientiane Plain (Lao PDR)
22 p3096 N88-28366

FLOOD PREDICTIONS

Flood monitoring using SPOT
03 p0342 N88-12162

NWS (National Weather Service) watch/warning verification flash flood, winter storm and high wind, January 1980 - June 1986
[PB87-223053] 04 p0469 N88-12698

Review of the potential of satellite remote sensing for marine flood protection
[IOS-237] 07 p0870 N88-15280

Large quantile estimation under extreme-value conditions
[CWI-MS-R8711] 14 p1966 N88-21730

FLOODS

Flood monitoring using SPOT
03 p0342 N88-12162

Hurricane Elena storm surge data
[AD-A184573] 03 p0353 N88-12228

Evaluation of the flooding areas of the Sao Goncalo Canal through LANDSAT 5 thematic mapper images
[INPE-4118-PRE/1039] 08 p1020 N88-16185

Project CODEAMA/FUNCATE (test-area of Barreirinha-AM): Field report
[INPE-4500-RPE/563] 15 p2080 N88-22455

Taiwan area mesoscale experiment: Daily operations summary
[PB88-169081] 16 p2235 N88-23348

Evaluation of the floodable area of the canal of Sao Goncalo through TM-LANDSAT 5 imagery
17 p2364 N88-24076

Evaluation of a flood period (June, 1984) in the southern region of Laguna dos Patos, through remote sensing data, meteorological and oceanographic
17 p2365 N88-24080

Mapping of plant associations and the variation of surface water in the Pantanal Mato-Grossense National Park, through remote sensing techniques
17 p2366 N88-24092

The impact of disorganized occupation of urban sub-basins: Sub-basin of the Cabucu River, metropolitan area of Sao Paulo (SP) 19 p2682 N88-25945

IEMIS (Integrated Emergency Management Information System) floodplain mapping based on a LIDAR derived data set
[AD-A193071] 21 p2966 N88-27616

LANDSAT-TM data to map flooded areas
[INPE-4584-PRE/1324] 24 p3387 N88-30177

Constraints on continental accretion from sedimentation 24 p3382 N88-30202

FLORA

U PLANTS (BOTANY)

FLORIDA

Nearshore wave transformation study of sites near Port Canaveral Inlet, Florida
[AD-A186985] 09 p1195 N88-17159

Design of the primary pre-TRMM and TRMM ground truth site
[NASA-CR-182609] 12 p1647 N88-19865

Pre-convective environmental conditions indicative of non-tornadic severe thunderstorm winds over Southeast Florida
[AD-A188679] 12 p1648 N88-19870

Distribution of summertime lightning as a function of low-level wind flow in central Florida
[PB88-160759] 14 p1948 N88-21619

Current velocity and hydrographic observations in the Straits of Florida, the Caribbean Sea and offshore of the Antillean Archipelago: Subtropical Atlantic Climate Studies (STACS) 1986
[PB88-160767] 14 p1951 N88-21626

Critical nuclear launch issues: A perspective from the State of Florida 17 p2423 N88-24412

FLOTATION

The theory of flotation
[NASA-TT-20278] 16 p2207 N88-23172

Flotation processes
[PB88-180302] 18 p2540 N88-25075

FLOTATION SYSTEMS

U FLOATS

FLOW CHAMBERS

Moving wall, continuous flow electrophoresis apparatus
[NASA-CASE-MFS-28142-1] 17 p2318 N88-23845

FLOW CHARACTERISTICS

NT BOUNDARY LAYER STABILITY
NT FLAME STABILITY
NT FLOW DISTRIBUTION
NT FLOW STABILITY
NT FLOW VELOCITY
NT MAGNETOHYDRODYNAMIC STABILITY

Direct Absorption Receiver flow experiments
[DE87-014655] 02 p0196 N88-11221

Experimental investigation of the subsonic high-altitude operation of the NASA Lewis 10- by 10-foot supersonic wind tunnel
[NASA-TM-100214] 08 p0959 N88-15814

The bimodality of large scale averaged flow parameters — statistical weather forecasting
08 p1016 N88-16159

Numerical simulation of diffuser/combustor dome interaction 10 p1281 N88-17683

Problems in fluid dynamics
[NASA-CR-182678] 14 p1909 N88-21410

Flow quality of NAL two-dimensional transonic wind tunnel. Part 1: Mach number distributions, flow angularities and preliminary study of side wall boundary layer suction
[NASA-TT-20209] 16 p2165 N88-22911

Forced response unsteady aerodynamics in a multistage compressor 18 p2512 N88-24903

A numerical analysis of flow characteristics in laser propulsion system 19 p2637 N88-25645

Flow characteristics of a model annular combustor
24 p3347 N88-29924

FLOW CHARTS

The circular serial autocorrelation computer program
[AD-A184795] 03 p0365 N88-12295

Formalizing reusable software components in the programmer's apprentice
[AD-A185843] 07 p0801 N88-15457

FLOW COEFFICIENTS

NT DISCHARGE COEFFICIENT

Measurement of rate constants of elementary gas reactions of importance to upper atmosphere and combustion systems
[AD-A189432] 13 p1737 N88-20386

FLOW DEFLECTION

Transverse flow deflections associated with fast coronal mass ejecta in interplanetary space
[DE88-003180] 09 p1263 N88-17586

Computation of flow around NACA0012 airfoil at high angle of attack 19 p2636 N88-25640

FLOW DISTORTION

Moving wall, continuous flow electrophoresis apparatus
[NASA-CASE-MFS-28142-1] 17 p2318 N88-23845

Cross flow induced vibrations in tube bundle by displaced and misaligned tube configurations
[ETN-88-92132] 20 p2801 N88-26621

Numerical simulation of fuel droplet interactions and breakup
[AD-A192431] 21 p2941 N88-27470

FLOW DISTRIBUTION

Rayleigh-Benard convection in a Hele-Shaw cell: A numerical study
[KFK-4212] 01 p0044 N88-10280

Numerical computation of transonic potential flow about 3-dimensional inlets
[NAL-TR-924] 02 p0122 N88-10770

Wall interference tests of a CAST 10-2/DOA 2 airfoil in an adaptive-wall test section
[NASA-TM-4015] 02 p0122 N88-10772

The phenomenology of Karman vortex streets via sound in oscillatory flow
[MPIS-MITT-84-1987] 02 p0122 N88-10775

Navier-Stokes cascade analysis with a stiff Kappa-Epsilon turbulence solver
[NASA-TM-100218] 02 p0123 N88-10778

A natural low frequency oscillation in the wake of an airfoil near stalling conditions
[NASA-TM-100213] 02 p0123 N88-10779

FDM-FEM zonal method for viscous flow computations over multiple-bodies
[NAL-TR-925T] 02 p0170 N88-11069

Computer modeling of two-phase flow
[CFDU/87/5] 02 p0171 N88-11078

Large scale structures in turbulent pipe flow
[MPIS-MITT-83-1987] 02 p0172 N88-11085

The four spot time-of-flight laser anemometer
02 p0184 N88-11145

Fuel-injector/air-swirl characterization
02 p0185 N88-11150

Combustor-diffuser interaction program
02 p0185 N88-11152

Heat transfer in a real engine environment
02 p0186 N88-11155

Flow field measurements in a 90 degree turning duct
02 p0186 N88-11157

Heat transfer with very high free stream turbulence
02 p0186 N88-11161

Flow in a model turbine stator
02 p0187 N88-11163

A preliminary demonstration of the use of boundary-layer models of flow in complex terrain for high resolution surface wind forecasting 02 p0212 N88-11330

The spatially nonuniform convergence of the numerical solution of flows
[NASA-TM-100037] 02 p0226 N88-11429

Active region flows 02 p0255 N88-11611

The physics and mathematical description of the Achilles heel of stationary wind turbine aerodynamics. The tip flow
[R-812-D] 03 p0260 N88-11635

Efficient numerical approaches for predicting supersonic flows with viscous/inviscid interaction
03 p0260 N88-11637

Theoretical and experimental study of flow-control devices for inlets of indraft wind tunnels
03 p0268 N88-11684

Wake shield 03 p0298 N88-11871

Homogeneous turbulence two-point closures and applications to one-point closures
03 p0312 N88-11973

Calculation of the three dimensional flow in the impeller of hydraulic turbomachines using a finite element method
[ETN-87-90612] 03 p0315 N88-11988

Measurement of gas flow velocities near obstacles. Analysis and optimization of an optical barrier velocimeter. Associated signal processing
[ESA-TT-1056] 03 p0315 N88-11991

Laser Doppler measurements in a turbulent free jet
[ESA-TT-1067] 03 p0315 N88-11994

Mechanical and flow excited vibrations of elastic plates and cylindrical shells in dense fluids
03 p0316 N88-11996

Application of an upwind algorithm to the parabolized Navier-Stokes equations 03 p0316 N88-12000

An experimental investigation of quasi-conical shock wave/turbulent boundary layer interactions
03 p0317 N88-12004

Thrust and specific impulse of repetitively-pulsed-laser propulsion rocket 03 p0318 N88-12012

Numerical simulation and visualization of a flowfield by interaction of two parallel two-dimensional freejets
03 p0320 N88-12021

Visualization of the flow field around a generic destroyer model in a simulated turbulent atmospheric boundary layer
[AD-A184658] 03 p0320 N88-12023

Calibration of a five hole probe and testing of an evaluation method for flow field measurements
[ESA-TT-1051] 03 p0325 N88-12051

Properties of the atmospheric boundary layer above a subtropical oceanic front
[AD-A184006] 03 p0351 N88-12215

The development of low level coastal flow fields when solar radiation is blocked by smoke
[DE87-014348] 03 p0354 N88-12230

Application of the finite difference method to the solution of mixed partial differential equations for the case of transonic flow
[ETN-87-91760] 03 p0370 N88-12327

An experimental investigation of noise generation and noise reduction in a pipe flow downstream of a discontinuous area enlargement
[ESA-TT-1027] 03 p0374 N88-12351

Development and application of computational aerothermodynamics flowfield computer codes
[NASA-CR-181534] 04 p0395 N88-12465

Three-dimensional unsteady flow elicited by finite wings and complex configurations 04 p0395 N88-12468

A study of two-phase flow in a reduced gravity environment
[NASA-CR-172035] 04 p0422 N88-12617

Ideal-viscoplastic extrusion model with application to deforming pistons in light-gas guns
[UTIAS-TN-266] 04 p0429 N88-12657

Equilibria, lattices and chaotic dynamics of point vortices 04 p0444 N88-12758

Optimization of explicit time-stepping algorithms and Stream-Function-Coordinate (SFC) concept for fluid dynamics problems 04 p0445 N88-12762

Experimental investigations on blunt bodies and corner configurations in hypersonic flow
05 p0530 N88-13225

Driving mechanism of unsteady separation shock motion in hypersonic interactive flow 05 p0530 N88-13226

Numerical simulation of the hypersonic flow around lifting vehicles 05 p0532 N88-13234

Solution of some 3-D viscous and inviscid supersonic flow problems by finite-volume space-marching schemes
05 p0532 N88-13235

Numerical experiments with hypersonic flows beneath a cone-delta-wing combination 05 p0532 N88-13238

A 3-D Euler solution for hypersonic Mach numbers
05 p0533 N88-13240

Computation of flow past conical hypersonic wings using a second order Godunov method
05 p0533 N88-13241

Aerothermodynamics research at NASA Ames
05 p0533 N88-13242

Vortex formation over delta, double-delta and wave rider configurations at supersonic speeds
05 p0533 N88-13243

Numerical optimization of conical flow waveriders including detailed viscous effects
05 p0533 N88-13245

An analysis of the compressible-viscous flow field around a 3D-oscillating wing 05 p0535 N88-13254

Computation of dynamic stall of NACA0012 airfoil by block pentadiagonal matrix scheme
05 p0535 N88-13255

Numerical calculations of the flowfield around propellers 05 p0536 N88-13261

Navier-Stokes simulation of transonic transportation aircraft configurations. 1: Flow field simulation over wing-fuselage combinations 05 p0540 N88-13288

Computation of transonic flows with nacelle simulation
[SNIAS-872-111-117] 05 p0542 N88-13300

Compressible Euler solution on a multiblock grid around a wing fuselage configuration
[FFA-TN-1987-46] 05 p0542 N88-13303

Vortex interaction with a leading-edge of finite thickness
[NASA-CR-182341] 05 p0543 N88-13307

Unsteady aerodynamics of an oscillating cascade in a compressible flow field
[NASA-TM-100219] 05 p0549 N88-13346

A numerical study of the effects of curvature and convergence on dilution jet mixing
[NASA-TM-89878] 05 p0549 N88-13347

The simulation of the viscous flow around a cylinder by the random vortex method 05 p0579 N88-13534

An experimental investigation of appendage-flat plate junction flow. Volume 2: Elliptical nose appendage data base
[AD-A184974] 05 p0580 N88-13539

Conditional second order closure for turbulent shear flows
[AD-A185369] 05 p0581 N88-13542

Low thrust viscous nozzle flow fields prediction
[NASA-CR-182334] 05 p0582 N88-13551

Transonic Navier-Stokes computations of strake-generated vortex interactions for a fighter-like configuration 06 p0664 N88-14073

Numerical study of chemically reacting flows using an LU scheme
[NASA-CR-180882] 06 p0668 N88-14094

Numerical simulation of flight body circumference flow
06 p0676 N88-14137

Research on internal fluid mechanism between turbine blades 06 p0676 N88-14138

Computation of turbulent flow of air through smooth and rough pipes using a two-equation turbulence model
06 p0700 N88-14298

A zonal approach for the solution of coupled Euler and potential solutions of flows with complex geometries
[AD-A185465] 06 p0702 N88-14310

Computational methods for complex flowfields
[AD-A185793] 06 p0703 N88-14317

Gasdynamic effects in linear MHD generators
[ETN-88-91372] 06 p0784 N88-14810

A theory for the core flow of leading-edge vortices
07 p0810 N88-14935

Wind tunnel wall interference
07 p0811 N88-14938

Preliminary calibration and test results from the National Transonic Facility 07 p0811 N88-14941

Separated flow 07 p0812 N88-14944

Computational design of natural laminar flow wings for transonic transport application 07 p0813 N88-14948

Turbulence in hypersonic flow
[AD-A185624] 07 p0815 N88-14961

Mathematical models of continuous flow electrophoresis. Electrophoresis technology
[NASA-CR-179241] 07 p0828 N88-15021

On the pairing process in an excited, plane, turbulent mixing layer
[AD-A186355] 07 p0850 N88-15157

Flow in volutes and the influence on the flow in centrifugal compressors 07 p0851 N88-15169

An investigation into flow regimes for two-phase helium flow
[DE88-002834] 07 p0853 N88-15181

Blood redistribution in man with lower body negative pressure 07 p0891 N88-15397

Laser thermal propulsion
[AD-A186407] 07 p0933 N88-15666

An experimental mapping of the flow field behind a glaze ice shape on a NACA 0012 airfoil
[NASA-CR-180847] 08 p0950 N88-15766

Theoretical and experimental studies of the transonic flow field and associated boundary conditions near a longitudinally-slotted wind-tunnel wall
[NASA-CR-181169] 08 p0959 N88-15815

Mean velocities and Reynolds stresses in the juncture flow and in the shear layer downstream of an appendage
[AD-A185819] 08 p0980 N88-15923

Numerical simulation of turbulent spots in channel and boundary layer flows 08 p0983 N88-15948

Active control of jet flowfields
[AD-A186736] 08 p0989 N88-15989

Experimental investigation of shock-induced disturbances on transonic airfoils
[DFVLR-FB-87-28] 09 p1112 N88-16666

Full scale and wind tunnel surface pressure measurements on the T.R.R.L. spray dispersion programme vehicles
[REPT-8623] 09 p1114 N88-16676

CFD validation experiments for internal flows
[NASA-TM-100797] 09 p1114 N88-16679

Flow field measurements using hotwire anemometry
[AD-A187029] 09 p1160 N88-16951

Investigation of large-scale structures in the near wake of a parallel flat plate
[DFVLR-FB-87-31] 09 p1162 N88-16967

Two-phase flow forms and pressure drop in horizontal T tube joints with vertical branch
[GKSS-87/E/12] 09 p1163 N88-16969

Techniques of flow visualization
[AGARD-AG-302] 09 p1164 N88-16977

Investigations of a circulation control airfoil flowfield using an advanced laser velocimeter
10 p1269 N88-17589

Evaluation of a research circulation control airfoil using Navier-Stokes methods 10 p1269 N88-17591

On the effect of leading edge blowing on circulation control airfoil aerodynamics 10 p1270 N88-17595

Pressure distributions and oil-flow patterns for a swept circulation-control wing 10 p1270 N88-17596

The impact of circulation control on rotary aircraft controls systems 10 p1271 N88-17601

Investigation of dynamic stall using LDV (Laser Doppler Velocimetry). Mean flow studies
[AD-A187629] 10 p1272 N88-17611

Numerical methods for propeller aerodynamics and acoustics at DFVLR 10 p1282 N88-17668

Investigation of dihedral effects in compressor cascades 10 p1282 N88-17672

Parametric study of choke flutter with a linear theory
10 p1283 N88-17673

Secondary flow measurements with L2F-technique in centrifugal compressors 10 p1283 N88-17676

Zonal solutions for viscous flow problems. Finite approximations in fluid mechanics
[MBB/LKE-122/S/PUB/226] 10 p1313 N88-17846

Mechanistic model for void distribution in flashing flow
[DE88-002948] 10 p1326 N88-17928

A computational study of thrust augmenting ejectors based on a viscous-inviscid approach
10 p1326 N88-17929

Investigation of non-symmetric jets in cross flow
10 p1327 N88-17932

The numerical and analytical study of bifurcation and multicellular flow instability due to natural convection between narrow horizontal isothermal cylindrical annuli at high Rayleigh numbers 10 p1328 N88-17937

Three-dimensional incompressible flowfield analysis for establishing rotor designs which optimize power extraction
10 p1329 N88-17943

Experimental research on swept shock wave/boundary layer interactions
[AD-A187250] 10 p1331 N88-17957

Flow patterns induced by vortices
[NAL-TR-932] 10 p1332 N88-17963

Relaxing the brightness constancy assumption in computing optical flow
[AD-A187437] 10 p1410 N88-18410

Liquid sprays and flow studies in the direct-injection diesel engine under motored conditions
[NASA-TM-100135] 11 p1440 N88-18594

High performance Solid Rocket Motor (SRM) submerged nozzle/combustion cavity flowfield assessment
[NASA-CR-179307] 11 p1446 N88-18622

A code development system for computational fluid dynamics
[AD-A188050] 11 p1482 N88-18848

Three-dimensional flow fields past reentry vehicles
11 p1484 N88-18858

Mixed turbulent convective heat transfer in vertical ducts
11 p1485 N88-18865

Two and three dimensional elliptic flows
11 p1485 N88-18866

A discretization of the integral equation for the time dependent linearized subsonic potential flow over a wing
[AD-A188534] 12 p1574 N88-19411

Three-dimensional incompressible Navier-Stokes computations of internal flows
[NASA-TM-100076] 12 p1576 N88-19425

A new parabolized Navier-Stokes code for chemically reacting flow fields
12 p1625 N88-19721

Calculation of flow about posts and powerhead model
[NASA-CR-179305] 12 p1625 N88-19722

Accelerating the computation of steady state solutions for non-equilibrium, chemically reacting flow fields
12 p1625 N88-19724

On the Kutta condition for flows around lifting airfoils and wings
[DFVLR-FB-87-40] 13 p1717 N88-20268

Air-jet spoiler
[BU-364] 13 p1722 N88-20299

Numerical model of the time independent mean flow in a rotating rocket motor
13 p1733 N88-20360

Coherent structure-reflective turbulent viscous flow modeling
[AD-A188339] 13 p1765 N88-20556

Graphics and flow visualization of computer generated flow fields
[NASA-CR-182679] 13 p1767 N88-20573

Reduction of erosion in elbows due to flow modifications, phase 1
[DE88-001028] 13 p1769 N88-20584

Measurement and analysis of the noise radiated by low Mach numbers centrifugal blowers
[AD-A189226] 13 p1833 N88-20966

Data processing method for high angle of attack testing with rolling angle
14 p1864 N88-21134

Research on flow around bluff bodies, flow induced vibrations
14 p1864 N88-21135

The 30 x 30 inch wind tunnel
[IC-AERO-87-01] 14 p1869 N88-21168

Experimental and numerical study of liquid distribution in dispersive-annular flow
[DE88-700844] 14 p1909 N88-21406

Solutions for direct and indirect problems in free surface flows
[REPT-87-35] 14 p1909 N88-21409

Mean flow structure in the near wake of a turbulent junction vortex
[PB88-150115] 14 p1910 N88-21416

High Reynolds number, low Mach number, steady flow field calculations over a NACA 0012 airfoil using Navier-Stokes and interactive boundary layer theory
[AD-A189871] 15 p2013 N88-22005

Transonic Navier-Stokes computations of strake-generated vortex interactions for a fighter-like configuration
[NASA-TM-100009] 15 p2014 N88-22010

Contraction design for small low-speed wind tunnels
[NASA-CR-182747] 15 p2021 N88-22045

Turbulent reacting flows and supersonic combustion
[AD-A189690] 15 p2034 N88-22115

An investigation of flow structure, mixing and chemical reaction in combusting turbulent flows
[AD-A189980] 15 p2034 N88-22117

Unsteady flow field measurements using LDV (Laser Doppler Velocimetry)
[AD-A189907] 15 p2063 N88-22298

On the prediction of highly vortical flows using an Euler equation model, part 2
[AD-A190245] 15 p2064 N88-22305

Interaction of a two-dimensional bluff body and incompressible jet and annulus flows
[AD-A190503] 15 p2064 N88-22310

Cavitation inception in rectangular two-dimensional slots
[AD-A190677] 15 p2066 N88-22318

Changes in the California current system observed off northern California during July-August 1986
[AD-A190027] 15 p2100 N88-22510

MPD (magnetoplasmadynamic) thrust chamber flow dynamics
[AD-A189940] 15 p2137 N88-22751

Oil flow patterns on a series of capsule-type re-entry vehicles at hypersonic speeds
[DE88-751805] 16 p2155 N88-22858

Experimental investigation of the transonic flow at the leeward side of a delta wing at high incidence
[LR-518] 16 p2156 N88-22861

Propulsion and airframe aerodynamic interactions of supersonic V/STOL configurations. Volume 1: Wind tunnel test pressure data report
[NASA-CR-177343-VOL-1] 16 p2157 N88-22866

Propulsion and airframe aerodynamic interactions of supersonic V/STOL configurations. Volume 2: Wind tunnel test force and moment data report
[NASA-CR-177343-VOL-2] 16 p2157 N88-22867

Propulsion and airframe aerodynamic interactions of supersonic V/STOL configurations. Volume 4: Summary
[NASA-CR-177343-VOL-4] 16 p2157 N88-22868

Experimental investigation of the hypersonic flow over a six finned configuration
[AD-A190870] 16 p2157 N88-22871

Computer tomography and hybrid optical/digital methods for aerodynamic measurements
[AD-A190909] 16 p2157 N88-22872

Efficient, high resolution computations of projectile and missile flow fields
[AD-A191086] 16 p2158 N88-22873

Description of an oscillating flow pressure drop test rig
[NASA-TM-100905] 16 p2170 N88-22933

Vortex breakdown and control experiments in the Ames-Dryden water tunnel 16 p2200 N88-23127

Short duration flow establishment on a profile in a Water-Ludwieg-Tunnel 16 p2201 N88-23134

Experimental investigation of Hover flowfields in water at the McDonnell Douglas Research Laboratories
16 p2202 N88-23135

Matched index laser anemometry systems for flow studies in complex geometries 16 p2203 N88-23145

A comparative study of vortex flows in wind and water tunnels 16 p2204 N88-23151

The role of vortex structure in tropical cyclone motion
[AD-A190961] 16 p2235 N88-23351

A numerical study of the hot gas environment around a STOVL aircraft in ground proximity
[NASA-TM-100895] 17 p2295 N88-23729

Unsteady flow about cambered plates
[AD-A191226] 17 p2337 N88-23945

Indentification of shallow groundwater regions in semi-arid Brazil by remote sensing methods
17 p2355 N88-24030

Theoretical and experimental investigation of swirl flow phase separators for microgravity applications
17 p2411 N88-24335

A compressible vapor flux model for transient heat pipe analysis 17 p2412 N88-24343

ATHENA simulation of the 300 kW SP-100
17 p2414 N88-24357

Theoretical prediction of single phase turbulent flow distribution in particulate bed reactors
17 p2419 N88-24386

Microgravity two-phase fluid flow pattern modeling
17 p2432 N88-24467

Experiment investigation on longitudinal characteristics of the forward swept wing
[AD-A191553] 18 p2456 N88-24582

Supplements to the study of the wake of a Mirage G8 model at F2 -- wind tunnel
[CERT-RT-OA-20/5025-AYD] 18 p2458 N88-24596

A decade of computer simulations for space shuttle aerodynamics
[NASA-TM-100990] 18 p2459 N88-24603

Solid rocket motor aft field joint flow field analysis
[NASA-CR-179266] 18 p2474 N88-24675

Research study: Space shuttle main engine plume flowfield model
[NASA-CR-179336] 18 p2474 N88-24676

Analysis of molecular mixing and chemical reaction in mixing layer
[AD-A191600] 18 p2482 N88-24721

Computation and characteristics of pulsatile multi-bifurcation flow 18 p2483 N88-24729

Joint services electronics program
[AD-A191749] 18 p2504 N88-24853

Transient particle deposition in a boundary layer of impulsive flow over a flat plate
[AD-A191537] 18 p2508 N88-24880

Theoretical investigation of 3-D shock wave-turbulent boundary layer interactions, part 6
[AD-A191546] 18 p2509 N88-24882

Axisymmetric viscid-inviscid interaction by a frozen vorticity approximation
[AD-A191743] 18 p2509 N88-24885

Fast algorithm development for large-eddy simulation of circular-jet turbulence
[AD-A192044] 18 p2509 N88-24887

Two dimensional hyperbolic grid generation
[VKI-TN-162] 18 p2511 N88-24897

Characteristics of merging shear layers and turbulent wakes of a multi-element airfoil
[NASA-TM-100053] 18 p2511 N88-24900

A single streamwise vortical structure and its instability in shear flows 18 p2515 N88-24921

Application of advanced grid generation techniques for flow field computations about complex configurations
[NASA-CR-183049] 18 p2515 N88-24922

Two-dimensional viscous flow computations of hypersonic scramjet nozzle flowfields at design and off-design conditions
[NASA-CR-182150] 19 p2603 N88-25459

The viscosity of molten TNT
[MRL-R-1100] 19 p2622 N88-25553

Numerical investigation of acoustic energy exchange through flow turning 19 p2629 N88-25593

Proceedings of the 5th NAL Symposium on Aircraft Computational Aerodynamics
[NAL-SP-8] 19 p2635 N88-25630

Navier-Stokes analysis of transonic transport aircraft empennage 19 p2636 N88-25637

Numerical calculation of three dimensional flow by TVD scheme 19 p2638 N88-25649

The modified-fluid-in-cell method to which adaptive mesh and multigrid were applied
19 p2640 N88-25664

Study of the structure of turbulence in accelerating transitional boundary layers
[AD-A191698] 19 p2663 N88-25837

Analysis and synthesis of decision-making organizations
[AD-A191948] 19 p2738 N88-26258

Decision aiding and coordination in decision-making organizations
[AD-A191950] 19 p2738 N88-26259

Heterogeneous diffusion flame stabilization
[AD-A193014] 20 p2771 N88-26429

The Proceedings of the Symposium on Mechanics for Space Flight 1987
[ISAS-SP-6] 20 p2782 N88-26499

Numerical analysis of reconnection of vortex rings
20 p2782 N88-26500

Vortex filament simulation for the crosslinking rings
20 p2782 N88-26501

Crosslinking of two vortex rings side by side
20 p2782 N88-26502

Forced-convective boiling in small diameter tube
20 p2783 N88-26510

Wind tunnel study of atmospheric diffusion in unstable stratified boundary layer. Part 2: Characteristic scale and diffusion
[DE88-753109] 20 p2823 N88-26749

Flow around a delta wing with or without a canard control surface (phi BA 60 deg). Part 1: Hydrodynamic visualization in permanent regime
[ONERA-RT-10/2891-AN-101-A-PT-1]
21 p2892 N88-27170

Prediction of the aeroelastic behavior of tuned blades. Application to aircraft engines
[ISAL-87-0046] 21 p2897 N88-27199

Gaseous tracer techniques for pore structure characterization of granular materials
[DE88-011542] 21 p2911 N88-27274

Design of a mechanism to control wind tunnel turbulence 21 p2926 N88-27370

A Navier-Stokes study of cascade flow fields including inlet distortion and rotating stall
[AD-A193109] 21 p2943 N88-27483

Cavitation inception in a turbulent shear flow
[DE88-011486] 21 p2946 N88-27497

Turbulent flow field visualization with integral interferometric imaging and computed tomography
21 p2950 N88-27521

Study of three dimensional transonic flow separations
[AD-A193018] 22 p3037 N88-28032

Euler equation computations for the flow over a hovering helicopter rotor
[NASA-CR-177493] 22 p3038 N88-28037

Mass transport in flow of sources
[LRT-WE-9-FB-4(1987)] 22 p3077 N88-28268

Mass transport in a parabolic conduit
[LRT-WE-9-FB-1(1988)] 22 p3077 N88-28273

Experimental tools: The tunnel and the model 23 p3168 N88-28864

Computational tools for simulation methodologies 23 p3168 N88-28865

Transport-type configurations 23 p3169 N88-28867

Combat aircraft 23 p3169 N88-28868

Missiles, fuselages and similar bodies 23 p3169 N88-28869

Introduction and critical flow phenomena 23 p3169 N88-28870

Vortex flows 23 p3170 N88-28875

Noise generation and boundary layer effects in vortex-airfoil interaction and methods of digital hologram analysis for these flow fields [AD-A194191] 23 p3171 N88-28883

Unsteady flow past an NACA 0012 airfoil at high angles of attack [AD-A194650] 23 p3172 N88-28886

Aerodynamics of seeing on large transport aircraft [NASA-CR-183122] 23 p3174 N88-28896

Flow visualization by laser sheet [AD-A194481] 23 p3211 N88-29111

Coupling between radiation and gas dynamics [AD-A194593] 23 p3211 N88-29113

Navier-Stokes calculations of transonic flows past cavities [NASA-CR-180484] 23 p3212 N88-29116

High effectiveness contour matching contact heat exchanger [NASA-CASE-MSC-20840-1] 23 p3214 N88-29132

Study of experimental technique of oil flow with emphasis on quantitative determination of the flow position parameters on the surface [NASA-TT-20341] 23 p3215 N88-29135

Application of optical correlation techniques to particle imaging velocimetry [NASA-TM-101306] 23 p3218 N88-29152

Preliminary studies of NF3 + H2 production of N2(A3 sigma(+)u) in a supersonic flow [AD-A194479] 23 p3219 N88-29162

Three-dimensional elliptic grid generation for an F-16 23 p3246 N88-29315

Component adaptive grid generation for aircraft configurations 23 p3246 N88-29316

Generation of multiple block grids for arbitrary 3D geometries 23 p3246 N88-29317

Grid generation for an advanced fighter aircraft 23 p3246 N88-29319

Algebraic grid generation for fighter type aircraft 23 p3246 N88-29320

Analytical surfaces and grids 23 p3247 N88-29322

Grid generation around transport aircraft configurations using a multi-block structured computational domain 23 p3247 N88-29325

Lava flow-field morphology: A case study from Mount Etna, Sicily 23 p3303 N88-29676

Numerical solutions of unsteady inviscid transonic turbine cascade flows [AD-A196111] 24 p3316 N88-29748

A streamwise upwind algorithm for the Euler and Navier-Stokes equations applied to transonic flows [NASA-TM-101019] 24 p3316 N88-29751

Space marching Euler solvers 24 p3318 N88-29759

Prediction of base-flows 24 p3319 N88-29765

The computation of flow past an oblique wing using the thin-layer Navier-Stokes equations [NASA-TM-88317] 24 p3320 N88-29774

Computational methods for the problems of the tip vortex [NASA-CR-181438] 24 p3320 N88-29775

A new computational capability for ramjet projectiles [AD-A196061] 24 p3327 N88-29812

An experimental study of an adaptive-wall wind tunnel [NASA-CR-183152] 24 p3329 N88-29821

Alternative fuel spray behavior 24 p3345 N88-29912

Flow characteristics of a model annular combustor 24 p3347 N88-29924

Flamelet chemistry modeling of soot formation for radiation 24 p3348 N88-29928

On the application of finite-difference techniques for the computation of the flow field in gas turbine combustors with complex geometries 24 p3349 N88-29938

Analysis of the flow through double swirl airblast atomizers 24 p3351 N88-29949

Volumetric measurement of vorticity vectors by optical probe [AD-A195997] 24 p3369 N88-30061

User's manual for three dimensional boundary layer (BL3-D) code [NASA-CR-174899] 24 p3369 N88-30063

Assessment of a 3-D boundary layer analysis to predict heat transfer and flow field in a turbine passage [NASA-CR-174894] 24 p3370 N88-30066

Contamination and distortion of steady flow field induced by discrete frequency disturbances in aircraft gas engines [AD-A195440] 24 p3370 N88-30069

Numerical simulation of unsteady incompressible flow in a partially-filled rotating cylinder [AD-A196001] 24 p3371 N88-30073

Investigation of large-scale structures in the near wake of a parallel flat plate [ESA-TT-1100] 24 p3372 N88-30080

Experimental and numerical investigation of the effect of distributed suction on oblique shock wave/turbulent boundary layer interaction [NASA-TM-101334] 24 p3372 N88-30084

Studies of unsteady axial-compressor functioning 24 p3380 N88-30129

Determination of multiaxial flow surfaces at elevated temperatures using the concept of dissipation potential [ORNL/TM-10787] 24 p3383 N88-30149

Vibrational power flow analysis of rods and beams [NASA-CR-183166] 24 p3383 N88-30151

Knowledge-based flow field zoning [NASA-TM-101023] 24 p3412 N88-30314

FLOW EQUATIONS

NT BOUNDARY LAYER EQUATIONS
NT HELMHOLTZ VORTICITY EQUATION
NT NAVIER-STOKES EQUATION
NT REYNOLDS EQUATION
NT VON KARMAN EQUATION
NT VORTICITY EQUATIONS

An inviscid model of planar, separated flows of finite extent [RAE-TR-86070] 01 p0044 N88-10279

Use of a thermodynamic analog for pneumatic transport in horizontal pipes [AD-A184076] 04 p0441 N88-12740

Computation of transonic flows with nacelle simulation [SNIAS-872-111-117] 05 p0542 N88-13300

Research on internal fluid mechanism between turbine blades 06 p0676 N88-14138

Introduction to Computational Fluid Dynamics [VKI-LS-1987-02] 06 p0701 N88-14300

Wind tunnel wall interference 07 p0811 N88-14938

Centrifugal compressors 07 p0850 N88-15162

Flow in volutes and the influence on the flow in centrifugal compressors 07 p0851 N88-15169

Upwind formulations for the Euler equations 08 p0984 N88-15952

Integration of Navier-Stokes equations in finite volume formulation 08 p0984 N88-15954

Characteristic flux averaging approach to the solution of Euler's equations 08 p0984 N88-15955

Time accurate techniques using characteristic flux averaging with application to unsteady aerodynamics 08 p0985 N88-15957

Finite element fundamentals, part 1 08 p0985 N88-15961

Finite element fundamentals, part 2 08 p0985 N88-15962

Inviscid flows, part 2 08 p0985 N88-15966

Viscous flows, part 2 08 p0986 N88-15968

Review of the equations of fluid mechanics and heat transfer 08 p0986 N88-15970

Numerical resolution of the equations of three-dimensional stable compressible transonic flows [PB87-168415] 09 p1113 N86-16673

Implementation of multigrid in SOLA algorithm --- fluid flow 11 p1538 N88-19191

Solution of the Euler equations: Explicit schemes acceleration by a multigrid method 11 p1538 N88-19192

Unstructured multigrid methods 11 p1538 N88-19193

On the Kutta condition for flows around lifting airfoils and wings [DFVLR-FB-87-40] 13 p1717 N88-20268

Transonic flow field analysis for real fuselage configurations 14 p1864 N88-21133

Coherent structures --- in turbulent flows 16 p2199 N88-23121

Modeling of cavitation phenomena in homogeneous flow in transitory regimes in pipes [ISAL-IDI1-87-15] 17 p2337 N88-23948

Analysis of molecular mixing and chemical reaction in mixing layer [AD-A191600] 18 p2482 N88-24721

Transient particle deposition in a boundary layer of impulsive flow over a flat plate [AD-A191537] 18 p2508 N88-24880

Numerical simulation of nonlinear structural dynamics of large scale unsteady flow [ETN-88-92156] 18 p2513 N88-24908

Accurate solutions, parameter studies and comparisons for the Euler and potential flow equations [NASA-TM-100664] 23 p3173 N88-28892

European research program on viscous flows [DFVLR-AVA-IB-227-87-A-15] 23 p3214 N88-29129

Mathematical problems of nonlinear wave propagation and of waves in heterogeneous media [AD-A195970] 24 p3368 N88-30057

FLOW FIELDS

U FLOW DISTRIBUTION

FLOW GEOMETRY

Instability of steady flow with constant vorticity in vessels with elliptical cross section 02 p0159 N88-10997

Laser thermal propulsion [AD-A186407] 07 p0933 N88-15666

Transonic flow field analysis for real fuselage configurations 14 p1864 N88-21133

Three dimensional spectral energy measurement on turbulence subjected to a high degree of plane deformation [ETN-88-92537] 18 p2511 N88-24896

Active control of 2-D instability waves on an axisymmetric body [AD-A191578] 19 p2663 N88-25835

Direct-solution techniques for viscous flows and their control [AD-A194775] 23 p3211 N88-29114

FLOW MEASUREMENT

Experimental investigation in a wind tunnel of the stability and vorticity of the vortex breakdown phenomenon above delta wings, using the ultrasonic laser method [DFVLR-FB-87-06] 01 p0003 N88-10017

Turbulent Bunsen burner flames [ETN-87-90433] 01 p0021 N88-10134

Measurement techniques in low-speed turbulent flows: A report on EUROMECH 202 [NLR-MP-86038-U] 01 p0045 N88-10283

Nonintrusive ultrasonic flow measurement techniques and their applications to BTU metering [DE87-011390] 01 p0045 N88-10286

Optical flow diagnostic measurements in turbomachinery [PNR90396] 02 p0172 N88-11081

Comparison between numerical solutions and measurements for a high speed turbine blade [PNR90402] 02 p0172 N88-11082

Large scale structures in turbulent pipe flow [MPIS-MITT-83-1987] 02 p0172 N88-11085

The four spot time-of-flight laser anemometer 02 p0184 N88-11145

Observations of wind waves on a reservoir [IOS-234] 02 p0193 N88-11206

The air flow on hills from models and experiments [BMFT-FB-T-86-175] 02 p0198 N88-11236

A calculation method for the propulsive jet and its aerodynamic interaction with an afterbody [ESA-TT-1039] 03 p0259 N88-11632

Investigations on a transonic airfoil with a 30 mm wide perforation/cavity arrangement [ESA-TT-1072] 03 p0260 N88-11634

Laser Doppler measurements in a turbulent free jet [ESA-TT-1067] 03 p0315 N88-11994

Calibration of a five hole probe and testing of an evaluation method for flow field measurements [ESA-TT-1051] 03 p0325 N88-12051

Interferometric data for a shock-wave/boundary-layer interaction [NASA-TM-88227] 05 p0543 N88-13306

Determination of a flow velocity field using four-exposure laser holography [IMFL-3114-85/32] 05 p0585 N88-13565

Dual mode laser velocimeter [NASA-CASE-ARC-11634-1] 06 p0709 N88-14350

Measurements in centrifugal compressors 07 p0850 N88-15161

An automated flow calorimeter for heat capacity and enthalpy measurements at elevated temperatures and pressures [DE88-002357] 07 p0857 N88-15206

Moored current meter data from the Canary Basin near 32 deg N, 24 W (84-1986), volume 40 [PB88-108105] 07 p0882 N88-15351

Transonic wind tunnel calibration 1986: Force measurements on three ONERA-C5 models and three half sphere cylinder calibration bodies in the F + W transonic test section [F + W-FO-1854] 09 p1122 N88-16714

Influence of the wall boundary layer on force measurements on half models in the transonic wind tunnel [F + W-TF-1876] 09 p1122 N88-16715

Investigation of large-scale structures in the near wake of a parallel flat plate [DFVLR-FB-87-31] 09 p1162 N88-15967

Turbine flow meter with optical fiber pick-up [NAL-TR-923] 09 p1169 N88-17009

Boundary-layer and wake measurements on a swept, circulation-control wing 10 p1270 N88-17597
Turbulence interactions in single- and multi-phase turbulent mixing and combustion processes
[AD-A187505] 10 p1332 N88-17960
Laser Doppler velocimetry primer
[NASA-CR-177386] 12 p1631 N88-19761
Tests on the AFWAL 65 deg delta wing at NLR: A study of vortex flow development between Mach = 0.4 and 4
[NLR-MP-86058-U] 13 p1717 N88-20266
Verification of the momemtum theory for rotors using measurements on a model helicopter
[R-840-S] 13 p1718 N88-20275
Comparison between computed and measured swirl and turbulence in reciprocating engines
[PDR/CFDU/IC/32] 13 p1779 N88-20647
Deep water mass circulation in the Alboran Basin. Measurements - January to April 1982: ALBORAN 2
[AD-A189205] 13 p1803 N88-20777
Measurements on a helicopter rotor
[R-764-S] 14 p1861 N88-21119
Correlation and spectral density measurements by LDA --- flow measurement
[ISL-CO-244/86] 14 p1910 N88-21412
Low pressure gas flow analysis through an effusive inlet using mass spectrometry
[NASA-CR-182712] 14 p1910 N88-21413
Boundary-layer and wake measurements on a swept, circulation-control wing
[NASA-TM-89426] 15 p2014 N88-22013
Inflow measurement made with a laser velocimeter on a helicopter model in forward flight. Volume 3: Rectangular planform blades at an advance ratio of 0.30
[NASA-TM-100543] 15 p2015 N88-22015
Piston-driven, unsteady separation at a sudden expansion in a tube: Flow visualization and Laser Doppler Anemometer (LDA) measurements
[ETN-88-92104] 15 p2068 N88-22329
Computer tomography and hybrid optical/digital methods for aerodynamic measurements
[AD-A190909] 16 p2157 N88-22872
Flow measurements in a water tunnel using a holocinematographic velocimeter
16 p2203 N88-23141
Matched index laser anemometry systems for flow studies in complex geometries 16 p2203 N88-23145
Flow velocity measurements by image processing of optically modulated traces 16 p2203 N88-23147
A non-invasive experimental technique for the measurement of unsteady velocity and vorticity fields
16 p2204 N88-23148
The development of a microanemometer: New possibilities for measuring very low air velocities
[ETN-88-92244] 16 p2210 N88-23191
Crossflow vorticity sensor
[NASA-CASE-LAR-13436-1-CU]
17 p2300 N88-23759
Supplements to the study of the wake of a Mirage G8 model at F2 --- wind tunnel
[CERT-RT-OA-20/5025-AYD] 18 p2458 N88-24596
Inflow measurements made with a laser velocimeter on a helicopter model in forward flight. Volume 1: Rectangular planform blades at an advance ration of 0.15
[NASA-TM-100541] 18 p2460 N88-24607
Method of forming a multiple layer dielectric and a hot film sensor therewith
[NASA-CASE-LAR-13678-1] 18 p2584 N88-25355
Study of flow tracer behavior models and experimental validation with multiple exposure holographic velocimetry
[IMFL-87/30] 20 p2801 N88-26622
Velocity measurements and flow visualization in turbulent three-dimensional supersonic flows using oxygen flow tagging
[AD-A192551] 21 p2892 N88-27165
Investigation of the quasi-steady approach used in transient two-phase flow analysis
[DE88-004303] 21 p2944 N88-27489
Laser-Doppler measurements of turbulence structures in free streams behind flat and rotation symmetrical profiles
[ETN-88-92336] 21 p2948 N88-27510
Use of penetrating radiations for the dynamic examination of aero gas turbines
[PNR90470] 22 p3045 N88-28073
Velocity measurements downstream of a sudden expansion using the Laser Doppler Velocimeters (LDV) technique. Part 1: Method of measurement and experimental facility
[FOA-C-20700-2.1-PT-1] 22 p3076 N88-28262
Calibration of a triple wire probe for turbulence measurements
[AD-A193956] 22 p3081 N88-28296
Project wind, phase 4 (smoke test), Meadow Brook Valley, Red Bluff, California
[AD-A194742] 22 p3128 N88-28596
Reynolds number effects and the wind tunnel environment 23 p3168 N88-28862
Construction of a laser Doppler anemometer and its use for the testing of a novel probe for the measurement of the variations of the lateral component of the vortex vector
[MPIS-13/1987] 23 p3217 N88-29147
Volumetric measurement of vorticity vectors by optical probe
[AD-A195997] 24 p3369 N88-30061
Investigation of large-scale structures in the near wake of a parallel flat plate
[ESA-TT-1100] 24 p3372 N88-30080
Laser Doppler Velocimeter (LDV) and pressure measurements of gas particle flows in bends
[VKI-TN-163] 24 p3372 N88-30083
Positron emission tomography: A new technique for observing fluid behavior in engineering systems
[PNR90471] 24 p3374 N88-30091

FLOW PATTERNS
U FLOW DISTRIBUTION

FLOW RATE
U FLOW VELOCITY

FLOW REGULATORS
Combined riblet and lebu drag reduction system
[NASA-CASE-LAR-13286-1] 06 p0664 N88-14071
Moving wall continuous flow electronphoresis apparatus
[NASA-CASE-MFS-28142-1] 17 p2318 N88-23845
Energy efficient continuous flow ash lockhopper
[NASA-CASE-NPO-16985-1-CU]
18 p2497 N88-24814
The use of fins to reduce the pressure drop in a rotating cavity with a radial flow
[PNR90465] 22 p3079 N88-28282

FLOW RESISTANCE
NT AERODYNAMIC DRAG
NT FRICTION DRAG
NT SUPERSONIC DRAG
NT VISCOUS DRAG
The axisymmetric sealing gap with variable viscosity: A variable hydraulic resistance
[ETN-87-90604] 03 p0314 N88-11987

FLOW SEPARATION
U BOUNDARY LAYER SEPARATION
U SEPARATED FLOW

FLOW STABILITY
NT BOUNDARY LAYER STABILITY
NT FLAME STABILITY
NT MAGNETOHYDRODYNAMIC STABILITY
Experimental investigation in a wind tunnel of the stability and vorticity of the vortex breakdown phenomenon above delta wings, using the ultrasonic laser method
[DFVLR-FB-87-06] 01 p0003 N88-10017
A note on the instability of a vortex sheet leaving a semi-infinite plate
[DFVLR-FB-87-16] 01 p0004 N88-10019
Instability of steady flow with constant vorticity in vessels with elliptical cross-section 02 p0159 N88-10997
Computer modeling of two-phase flow
[CFDU/87/5] 02 p0171 N88-11078
Nonequilibrium fluctuations and transport in sheared fluids 03 p0316 N88-11999
Numerical study of the entrance flow and its transition in a circular pipe (2) 03 p0318 N88-12011
A study of chaos and mixing in Rayleigh-Taylor and Richtmyer-Meshkov unstable interfaces
[AD-A184751] 03 p0320 N88-12026
On the instability of thin circular shear layers
04 p0395 N88-12467
The use of alloy 117 as a liquid metal current collector
[AD-A185740] 06 p0698 N88-14281
Numerical simulation of a controlled boundary layer
07 p0810 N88-14933
Mathematical models of continuous flow electrophoresis: Electrophoresis technology
[NASA-CR-179241] 07 p0828 N88-15021
The numerical and analytical study of bifurcation and multicellular flow instability due to natural convection between narrow horizontal isothermal cylindrical annuli at high Rayleigh numbers
[AD-A186113] 07 p0849 N88-15151
On the parabolized Navier Stokes equations without sublayer assumptions
[AD-A186127] 07 p0849 N88-15152
Chemical reactions in turbulent mixing flows
[AD-A186141] 07 p0849 N88-15153
Effects of turbulence on stationary and non-stationary processes in C-systems
[AD-A186215] 07 p0849 N88-15154
Identification and avoidance of instabilities in high performance turbomachinery 07 p0850 N88-15164
Thin film and gradient-driven instability mechanisms
[PB88-101522] 07 p0853 N88-15182
The effect of asymmetric heating on flow stability and heat transfer for flow in a vertical tube
[DE88-003242] 07 p0855 N88-15193
Influence of the friction coefficients, the power and the flowrate on the two-phase flow instabilities in natural circulation
[DE88-700036] 08 p0983 N88-15946
Flight results of the ESA experiment modules in Materials Science Experiment Rocket (MASER) 1
08 p1033 N88-16261
Numerical resolution of the equations of three-dimensional stable compressible transonic flows
[PB87-168415] 09 p1113 N88-16673
Control of vortical separation on conical bodies
10 p1267 N88-17580
Possibilities for on-line surge suppression by fast guide vane adjustment in axial compressors
10 p1283 N88-17674
Instability and transition in curved channel flow
10 p1328 N88-17938
Droplet formation for liquid monopropellant jets
[AD-A187172] 10 p1331 N88-17956
On the stability of the supersonic boundary layer
11 p1435 N88-18561
Measurement of rate constants of elementary gas reactions of importance to upper atmosphere and combustion systems
[AD-A189432] 13 p1737 N88-20386
Development of disturbances in swept wing flows
[NASA-CR-182675] 13 p1768 N88-20574
Effect of spatial inlet temperature and pressure distortion on turbofan engine stability
[NASA-TM-100850] 14 p1868 N88-21162
Problems in fluid dynamics
[NASA-CR-182678] 14 p1909 N88-21410
Hydrodynamical regimes in molten metals under a horizontal temperature gradient
14 p1988 N88-21859
The sensitivity of boundary layer instability growth rates to compliant wall properties
[AD-A190433] 15 p2064 N88-22309
Generation and coalescence of bubbles and stability of foams under microgravity conditions
[BMFT-FB-W-86-020] 16 p2184 N88-23017
Self similarity of two point correlations in wall bounded turbulent flows 16 p2195 N88-23089
Inflectional instabilities in the wall region of bounded turbulent shear flows 16 p2199 N88-23114
Coherent structures and modeling: Some background comments 16 p2199 N88-23120
Control of combustion and acoustically coupled fluid dynamic instabilities 17 p2318 N88-23843
Numerical simulation of nonlinear structural dynamics of large scale unsteady flow
[ETN-88-92156] 18 p2513 N88-24908
A single streamwise vortical structure and its instability in shear flows 18 p2515 N88-24921
Low frequency pressure oscillations in a model ramjet combustor 19 p2625 N88-25571
Numerical simulation of transition to turbulence in plane Poiseuille flow by a spectral method
19 p2640 N88-25661
Fluid dynamics of high performance turbomachines
[AD-A192073] 19 p2664 N88-25840
Analysis and modeling of complex non stationary flows
[PB88-127188] 19 p2664 N88-25842
Cross flow induced vibrations in tube bundle by displaced and misaligned tube configurations
[ETN-88-92132] 20 p2801 N88-26621
Stationary, wave type, and chaos type convection in spherical symmetry geometries
[ETN-88-92358] 20 p2801 N88-26625
Numerical simulation and stability analysis of the absolutely and convectively unstable wake
[DFVLR-FB-88-09] 21 p2949 N88-27518
The Kelvin-Helmholtz instability in a stratified shear flow
[CFD/88/2] 22 p3076 N88-28265
Stability of parallel inviscid shear flow with mean spanwise variation
[FFA-TN-1987-57] 22 p3079 N88-28285
Boundary layer development and transition
23 p3169 N88-28871
Transition at hypersonic speeds
[NASA-CR-178315] 24 p3368 N88-30058

FLOW THEORY
NT MIXING LENGTH FLOW THEORY
Research on one-dimensional two-phase flow: Theory on hydrodynamic balance in two fluid model and its application
[DE87-702615] 01 p0045 N88-10290
Numerical calculation of the turbulent flow about a cubic body
[ETN-87-90418] 01 p0047 N88-10302

A flow function method for the axisymmetric calculation of the transonic turbomachine flow taking into account the flow differences in circumferential direction
[ETN-87-90428] 01 p0056 N88-10359

Theoretical investigations of three turbine cascades using a two dimensional time marching procedure
[DFVLR-FB-87-02] 01 p0057 N88-10362

Calculation of stationary and low frequency unsteady flows in a steam turbine end stage
[MITT-23] 01 p0057 N88-10364

Shearing flow over Stokes wave. Part one: General theory
[ETN-87-90957] 02 p0171 N88-11074

The physics and mathematical description of the Achilles heel of stationary wind turbine aerodynamics: The tip flow
[R-812-D] 03 p0260 N88-11635

Linear and nonlinear theories of flow through an actuator disk --- windpowered pumps
[R-803-A] 03 p0316 N88-11995

Steady shearing in a viscoplastic solid
[AD-A184341] 04 p0454 N88-12810

Implicit time dependent methods for inviscid and viscous compressible flows 06 p0701 N88-14304

Viscous drag reduction of horizontal plates
[VKI-TN-159] 07 p0851 N88-15171

An efficient method for computing leading Eigenvalues and Eigenvectors of large asymmetric matrices
09 p1159 N88-16949

Numerical calculation of turbulent recirculating flows
[TUM-LSM-84/29] 09 p1161 N88-16959

Numerical and physical aspects of large eddy simulation of turbulent flows
[ETN-88-91611] 09 p1162 N88-16965

Activities report of the Aerodynamics Department
[ETN-88-91979] 14 p1862 N88-21123

Theoretical investigations of three turbine cascades using a 2-D time marching procedure
[ESA-TT-1077] 16 p2207 N88-23170

FLOW VELOCITY
NT SOLAR WIND VELOCITY

The four spot time-of-flight laser anemometer
02 p0184 N88-11145

Correlation of velocity and velocity-density turbulence in the exhaust of an atmospheric burner
02 p0185 N88-11147

Measurements of gas velocities and temperatures in a large open pool fire
[DE87-005853] 03 p0261 N88-11641

A 10 W transverse flow excimer laser
03 p0302 N88-11901

Numerical study of the entrance flow and its transition in a circular pipe (2) 03 p0318 N88-12011

Geometric analysis of ensemble of solutions in two-phase flow and complete resolution of problem of choking
[DE88-001687] 04 p0445 N88-12764

Variations of the vertical and horizontal velocities of the small-scale structures and the physical problems related to overshoot layers 04 p0507 N88-13115

Ducted propeller design and analysis
[DE88-001925] 06 p0664 N88-14069

Review of nucleation and incipient boiling under pool and forced convection conditions
08 p0982 N88-15938

Investigation of vibration problems with heterodyne holographic interferometer 08 p1000 N88-16058

Experimental and theoretical study on cavitation inception and bubbly flow dynamics. Part 1: Design, development and operation of a cavitation susceptibility meter. Part 2: Linearized dynamics of bubbly and cavitating flows with bubble dynamics effects
[AD-A187133] 09 p1160 N88-16952

An analysis of the closure conditions for two-fluid models of two-phase flow
[DE88-003355] 09 p1164 N88-16982

Turbine flow meter with optical fiber pick-up
[NAL-TR-923] 09 p1169 N88-17009

O2-I laser (Oxygen-iodine) mixing studies using LIF (Laser Induced Fluorescence)
[AD-A186667] 09 p1171 N88-17018

Parametric study of choke flutter with a linear theory
10 p1283 N88-17673

Possibilities for on-line surge suppression by fast guide vane adjustment in axial compressors
10 p1283 N88-17674

Development and application of oxygen flow tagging for velocity measurements and flow visualization in turbulent three-dimensional supersonic flows
[AD-A187982] 10 p1289 N88-17714

Laser velocimeter measurements of solids in multiphase flow
[DE88-000196] 11 p1487 N88-18876

Laser fluorescence velocimeter
[AD-A189010] 12 p1630 N88-19753

Laser Doppler velocimetry primer
[NASA-CR-177386] 12 p1631 N88-19761

Perspectives in microclimate cooling involving protective clothing in hot environments
[AD-A188370] 12 p1671 N88-20007

Boundary effects on the drag of a cylinder in axial motion at low Reynolds number 13 p1768 N88-20578

Turbulent transfer of momentum and heat in boundary layer of fluid beyond an obstacle. 1: Hydrodynamic characteristics 13 p1787 N88-20690

Contribution to theory of quasigeostrophic motions of finite amplitude in viscous stratified ocean
13 p1788 N88-20695

Correlation and spectral density measurements by LDA --- flow measurement
[ISL-CO-244/86] 14 p1910 N88-21412

An investigation of flow structure, mixing and chemical reaction in combusting turbulent flows
[AD-A189980] 15 p2034 N88-22117

Calorimetric technique for measuring liquid helium flow rate
[DE88-701308] 16 p2200 N88-23123

Flow velocity measurements by image processing of optically modulated traces 16 p2203 N88-23147

The development of a microanemometer: New possibilities for measuring very low air velocities
[ETN-88-92244] 16 p2210 N88-23191

Evaluation of a flood period (June, 1984) in the southern region of Laguna dos Patos, through remote sensing data, meteorological and oceanographic
17 p2365 N88-24083

Reference filters for electrostatic charging tendency measurements of fuels
[AD-A191717] 18 p2435 N88-24803

Correlations of velocity and temperature fluctuations in the stagnation-point flow of circular cylinder in turbulent flow
[NASA-TM-100930] 19 p2597 N88-25435

Velocity coupling 19 p2629 N88-25596

The propagation of pressure perturbations in bubbly air/water flows 19 p2664 N88-25843

Development of advanced flow simulation system by water flow model. New method of velocity measurement using cross-correlation
[DE88-753120] 20 p2799 N88-26608

Cryogenic free jets
[DFVLR-FB-88-16] 21 p2900 N88-27210

Optimal rheological characteristics in dynamic stability of polymer flow through porous media
[DE88-001225] 21 p2918 N88-27322

Relative flow rates of explosive powders
[DE88-010767] 21 p2923 N88-27350

Heat and mass transfer in a transport channel
[DE88-701968] 21 p2945 N88-27493

Energy distribution and transfer in flowing hydrogen microwave plasmas 21 p3019 N88-27919

Velocity measurements downstream of a sudden expansion using the Laser Doppler Velocimeters (LDV) technique. Part 1: Method of measurement and experimental facility
[FOA-C-20700-2.1-PT-1] 22 p3076 N88-28262

NF (a 1 delta) production in a supersonic flow using N2F4 + H2 in a BCL-16 nozzle
[AD-A194478] 22 p3082 N88-28304

Delta wing configurations 23 p3167 N88-28860

Unsteady water channel
[AD-A194231] 23 p3171 N88-28884

A study of the effect of random input motion on low Reynolds number flows
[AD-A195559] 24 p3316 N88-29747

Flow characteristics of a model annular combustor
24 p3347 N88-29924

FLOW VISUALIZATION
NT NUMERICAL FLOW VISUALIZATION

Dispersion in the wake of aircraft. An investigation of the effects of a ground plane on trailing vortices. Literature survey
[IC-AERO-REP-86-04] 01 p0003 N88-10014

Optical flow diagnostic measurements in turbomachinery
[PNR90396] 02 p0172 N88-11081

Improving coherent visualization by means of film optical filtering --- projectile visualization
[ISL-R-116/86] 02 p0176 N88-11097

Flow visualization on an ogive-nosed circular cylinder body at high incidence using the laser light sheet method
[ESA-TT-1066] 03 p0315 N88-11993

The diffusion-convection vortex method for solving two-dimensional incompressible Navier-Stokes equation
03 p0317 N88-12001

An experimental investigation of quasi-conical shock wave/turbulent boundary layer interactions
03 p0317 N88-12004

Numerical simulation and visualization of a flowfield by interaction of two parallel two-dimensional freejets
03 p0320 N88-12021

Visualization of the flow field around a generic destroyer model in a simulated turbulent atmospheric boundary layer
[AD-A184658] 03 p0320 N88-12023

Structural characteristics of dean vortices in a curved channel
[AD-A184724] 03 p0320 N88-12024

Development of flow visualization techniques for use in the Hot Gas Laboratory
[BAE-ARG 233] 03 p0325 N88-12052

Experimental aerothermodynamic research of hypersonic aircraft
[NASA-CR-181533] 04 p0399 N88-12483

Observations on the hydrodynamic flow visualization at ONERA
[PD-FM-8718] 04 p0444 N88-12753

Experimental investigations on blunt bodies and corner configurations in hypersonic flow
05 p0530 N88-13225

An ultra-high-speed cinematographic method for the study of wakes in hypersonic ballistic ranges
05 p0531 N88-13228

Flow visualization in computational fluid dynamics
05 p0538 N88-13277

Visualization of an aircraft accident based on digital flight data recorder information 05 p0538 N88-13278

Transient development of stratification in a partially divided enclosure
[DE87-011742] 05 p0572 N88-13490

Vortical Flows Research Program of the Fluid Dynamics Research Branch
[NASA-TM-88332] 05 p0582 N88-13549

Flow diagnostics and visualization in wind tunnels and flight 07 p0811 N88-14940

A flow visualization study of the leading edge separation bubble on a NACA 0012 airfoil with simulated glaze ice
[NASA-CR-180846] 07 p0816 N88-14966

An experimental investigation of the chopping of helicopter main rotor tip vortices by the tail rotor. Part 2: High speed photographic study
[NASA-CR-177457] 09 p1114 N88-16678

Velocity interferometry in shock tubes and shock tunnels
[ISL-CO-203/87] 09 p1122 N88-16713

Unsteady behavior of three-dimensional vortices relevant to turbulent boundary layers
[AD-A186767] 09 p1161 N88-16958

A review of some flow visualization experiments carried out at the Institut Franco-Allemand de Recherches (ISL) shock tubes
[ISL-CO-243/86] 09 p1163 N88-16974

Techniques of flow visualization
[AGARD-AG-302] 09 p1164 N88-16977

Development and application of oxygen flow tagging for velocity measurements and flow visualization in turbulent three-dimensional supersonic flows
[AD-A187982] 10 p1289 N88-17714

Experimental research on swept shock wave/boundary layer interactions
[AD-A187250] 10 p1331 N88-17957

Preliminary experiments on surface flow visualization in the cryogenic wind tunnel by use of condensing or freezing gases
[NASA-CR-181634] 11 p1442 N88-18602

Production by pyrolysis of diffusion particles for velocimetry in shock tubes
[ISL-R-119/86] 11 p1455 N88-18671

Hydrodynamic simulation of forced convection in the Czochralski process
[INPE-4471-TDL/323] 12 p1697 N88-20158

An experimental investigation of decelerating flow about two-dimensional cambered plates
[DE88-006598] 13 p1766 N88-20567

Graphics and flow visualization of computer generated flow fields
[NASA-CR-182679] 13 p1767 N88-20573

Digital enhancement of flow [illegible] images
[NASA-TP-2770] [illegible] p1813 N88-20833

Vortex flow over a delta wing with apex flaps using laser flow visualisation
[BU-356] 14 p1862 N88-21121

Surface flow visualization of separated flows on the forebody of an F-18 aircraft and wind-tunnel model
[NASA-TM-100436] 14 p1863 N88-21127

Investigation into the effects of flap end modifications on the performance of a wing with a single slotted flap
[BU-357] 14 p1866 N88-21148

Main features of the 0.43m x 0.43m wind tunnel
[AXM-132] 14 p1870 N88-21175

Visualization of the air flowing through a dynamic model of the vocal folds
[ISVR-TR-154] 14 p1952 N88-21634

Unsteady flow field measurements using LDV (Laser Doppler Velocimetry)
[AD-A189907] 15 p2063 N88-22298
Visualization of flows in turbomachinery
[AD-A189927] 15 p2063 N88-22299
Visualisation of the flow at the tip of a high speed axial flow turbine rotor
[AD-A189928] 15 p2063 N88-22300
Visualisation of the flow at the tip of a high speed axial flow turbine rotor: An assessment of flow visualisation techniques and the requirement of the experimental turbine
[AD-A189929] 15 p2063 N88-22301
Dense-spray structure and phenomena. Part 2: Pressure-atomized sprays
[AD-A190312] 15 p2064 N88-22307
Interaction of a two-dimensional bluff body and incompressible jet and annulus flows
[AD-A190503] 15 p2064 N88-22310
Chemically reacting turbulent flow
[AD-A190522] 15 p2065 N88-22311
Numerical and experimental investigation of multiple shock wave/turbulent boundary layer interactions in a rectangular duct
[AD-A190772] 15 p2066 N88-22320
Piston-driven, unsteady separation at a sudden expansion in a tube: Flow visualization and Laser Doppler Anemometer (LDA) measurements
[ETN-88-92104] 15 p2068 N88-22329
Oil flow patterns on a series of capsule-type re-entry vehicles at hypersonic speeds
[DE88-751805] 16 p2155 N88-22858
Structure of turbulent shear flows
16 p2198 N88-23113
Water facilities in retrospect and prospect: An illuminating tool for vehicle design
16 p2200 N88-23126
Qualification of a water tunnel for force measurements on aeronautical models 16 p2200 N88-23128
Flow visualization study of vortex manipulation on fighter configurations at high angles of attack
16 p2201 N88-23130
Description of a water tank facility: Study of a missile at high incidence 16 p2201 N88-23133
Experimental investigation of Hover flowfields in water at the McDonnell Douglas Research Laboratories
16 p2202 N88-23135
Water flow visualisation of a ramrocket combustion chamber 16 p2202 N88-23138
The ONERA water tunnels test possibilities for flow visualization in aeronautical and Naval domains
16 p2202 N88-23139
The use of a water towing tank for aerodynamic testing and methods for quantitative evaluation of photographs
16 p2202 N88-23140
Flow measurements in a water tunnel using a holocinematographic velocimeter
16 p2203 N88-23141
Three-dimensional flow visualization using laser-sheet scanning 16 p2203 N88-23143
Flow velocity measurements by image processing of optically modulated traces 16 p2203 N88-23147
A non-invasive experimental technique for the measurement of unsteady velocity and vorticity fields
16 p2204 N88-23148
Some visualization studies on turbulent boundary layers using multiwire hydrogen bubble generation
16 p2204 N88-23153
Structure of unsteady flows at leading- and trailing-edges: Flow visualization and its interpretation
16 p2205 N88-23154
La Recherche Aerospatiale, bimonthly bulletin, number 1987-3, 238/May-June
[ESA-TT-1075] 16 p2206 N88-23161
Study of a system for reducing base drag by controlling vortices
[REPT-87/43] 17 p2295 N88-23730
Boundary layer flow visualization for flight testing
17 p2297 N88-23742
Acoustically excited heated jets. 1: Internal excitation
[NASA-CR-4129-PT-1] 17 p2298 N88-23751
Acoustically excited heated jets. 2: In search of a better understanding
[NASA-CR-4129-PT-2] 17 p2299 N88-23752
Acoustically excited heated jets. 3: Mean flow data
[NASA-CR-4129-PT-3] 17 p2299 N88-23753
Single phase liquid immersion cooling of discrete heat sources in a vertical channel
[AD-A191224] 17 p2337 N88-23944
Dual wavelength holographic interferometry system
[NASA-CASE-MFS-28242-1] 17 p2341 N88-23960
Unsteady flow around a profile subjected to pulsed motions
[ETN-88-92151] 18 p2458 N88-24594
Quantitative use of exciplex-based vapor/liquid visualization systems, users' manual
[AD-A191649] 19 p2610 N88-25491
A review of particle sizing methods in rocket propulsion 19 p2630 N88-25597
Solid rocket motor performance: A workshop report
19 p2631 N88-25607
A twin-mirrored galvanometer laser light sheet generator
[NASA-TM-100587] 19 p2674 N88-25901
The determination of the topological structure of skin friction lines on a rectangular wing-body combination
[NASA-CR-4168] 20 p2753 N88-26343
Development of advanced flow simulation system by water flow model. New method of velocity measurement using cross-correlation
[DE88-753120] 20 p2799 N88-26608
Study of flow tracer behavior models and experimental validation with multiple exposure holographic velocimetry
[IMFL-87/30] 20 p2801 N88-26622
Velocity measurements and flow visualization in turbulent three-dimensional supersonic flows using oxygen flow tagging
[AD-A192551] 21 p2892 N88-27165
Flow around a delta wing with or without a canard control surface (phi BA = 60 deg). Part 1: Hydrodynamic visualization in permanent regime
[ONERA-RT-10/2891-AN-101-A-PT-1]
21 p2892 N88-27170
The structure and stability of nonpremixed gas jet flames 21 p2908 N88-27257
Experimental research of combustion systems
21 p2927 N88-27371
Liquid crystals for unsteady surface shear stress visualization
[DE88-010570] 21 p2951 N88-27527
Holographic interferometry for flow visualization studies in high speed fans
[PNR90459] 22 p3045 N88-28072
Use of penetrating radiations for the dynamic examination of aero gas turbines
[PNR90470] 22 p3045 N88-28073
Holographic flow visualization
[PNR90466] 22 p3079 N88-28283
Calibration of a triple wire probe for turbulence measurements
[AD-A193956] 22 p3081 N88-28296
Noise generation and boundary layer effects in vortex-airfoil interaction and methods of digital hologram analysis for these flow fields
[AD-A194191] 23 p3171 N88-28883
Three-dimensional vortex interactions
[AD-A194066] 23 p3172 N88-28889
Flow visualization on a small scale
[AD-A194728] 23 p3181 N88-28935
Flow visualization by laser sheet
[AD-A194481] 23 p3211 N88-29111
Application of Particle Image Displacement Velocimetry (PIDV) to complex flows: Velocity field measurements in front of a heavy gas cloud
[VKI-TN-166] 23 p3213 N88-29125
Study of experimental technique of oil flow with emphasis on quantitative determination of the flow position parameters on the surface
[NASA-TT-20341] 23 p3215 N88-29135
A study of the effect of random input motion on low Reynolds number flows
[AD-A195559] 24 p3316 N88-29747
Positron emission tomography: A new technique for observing fluid behavior in engineering systems
[PNR90471] 24 p3374 N88-30091
Use of holography in vibration and flutter study of fans
[PNR90458] 24 p3375 N88-30098
FLOWMETERS
NT HOT-WIRE FLOWMETERS
Nonintrusive ultrasonic flow measurement techniques and their applications to BTU metering
[DE87-011390] 01 p0045 N88-10286
An automated flow calorimeter for heat capacity and enthalpy measurements at elevated temperatures and pressures
[DE88-002357] 07 p0857 N88-15206
Low-g propellant gaging 08 p0982 N88-15937
Detecting the gas bubbles in a liquid metal coolant by means of magnetic flowmeters
[DE86-701427] 15 p2062 N88-22294
Calorimetric technique for measuring liquid helium flow rate
[DE88-701308] 16 p2200 N88-23123
Crossflow vorticity sensor
[NASA-CASE-LAR-13436-1-CU]
17 p2300 N88-23759
A monolithic gas flow sensor with polyimide as thermal insulator 19 p2669 N88-25864
FLTSATCOM
U FLEET SATELLITE COMMUNICATION SYSTEM
FLUCTUATION
U VARIATIONS
FLUCTUATION THEORY
Measurements of the free stream fluctuations above a turbulent boundary layer
[NASA-TM-100036] 06 p0704 N88-14321
FLUENCE
Microstructural change of Al on H implantation
[IPPJ-847] 04 p0493 N88-13036
Experimental method for investigating helium effects in irradiated vanadium
[DE88-002891] 08 p0969 N88-15865
FLUID AMPLIFICATION
U FLUID AMPLIFIERS
FLUID AMPLIFIERS
Microminiature fluidic amplifier
19 p2669 N88-25865
FLUID BOUNDARIES
NT LIQUID-LIQUID INTERFACES
NT LIQUID-SOLID INTERFACES
NT LIQUID-VAPOR INTERFACES
Fluid motion in a spinning, coning cylinder via spatial eigenfunction expansion
[AD-A190758] 15 p2066 N88-22319
A numerical treatment of the fluid/elastic interface under range-dependent environments
[AD-A192476] 21 p3005 N88-27821
FLUID DYNAMICS
NT AERODYNAMICS
NT AEROTHERMODYNAMICS
NT COMPUTATIONAL FLUID DYNAMICS
NT ELASTOHYDRODYNAMICS
NT ELECTROHYDRODYNAMICS
NT GAS DYNAMICS
NT HYDRODYNAMICS
NT INTERACTIONAL AERODYNAMICS
NT MAGNETOHYDRODYNAMICS
NT RAREFIED GAS DYNAMICS
NT ROTOR AERODYNAMICS
NT SUPERSONICS
NT UNSTEADY AERODYNAMICS
NT VORTEX SHEDDING
The structure of separated flow regions occurring near the leading edge of airfoils including transition
[NASA-CR-181434] 01 p0002 N88-10011
Plasma properties
[DE87-013662] 01 p0101 N88-10663
Aerospace research at the National Aerospace Laboratory (NLR)
[ETN-87-90821] 01 p0107 N88-10697
Vortex/boundary-layer interactions: Data report, volume 2
[NASA-CR-181463] 02 p0122 N88-10769
Efficient numerical techniques for complex fluid flows
02 p0185 N88-11151
Technical evaluation report on the Fluid Dynamics Panel Symposium on aerodynamic and related hydrodynamic studies using water facilities
[AGARD-AR-225] 03 p0312 N88-11968
Special Course on Modern Theoretical and Experimental Approaches to Turbulent Flow Structure and its Modelling
[AGARD-R-755] 03 p0312 N88-11970
Homogeneous turbulence two-point closures and applications to one-point closures
03 p0312 N88-11973
Dynamics and routes to chaos from quasiperiodicity
03 p0312 N88-11974
A deterministic approach to turbulence: Chaos in Rayleigh-Benard convection 03 p0313 N88-11975
Transition to turbulence via spatio-temporal intermittency 03 p0313 N88-11976
Determination of fractal dimension, connection of space and temporal chaos and application to experimental results 03 p0313 N88-11977
A study of chaos and mixing in Rayleigh-Taylor and Richtmyer-Meshkov unstable interfaces
[AD-A184751] 03 p0320 N88-12026
Dynamics of reverse flows at pump inlet
04 p0425 N88-12636
European hypersonic wind tunnels
05 p0530 N88-13221
Combustion related shear-flow dynamics in elliptic supersonic jets 05 p0531 N88-13232
Application of modified loss and deviation correlations to transonic axial compressors
[AGARD-R-745] 05 p0549 N88-13344
Static aeroelastic effects on the flutter of a supercritical wing 05 p0550 N88-13353
Displaying three-dimensional data
[AD-A185347] 05 p0580 N88-13541
A system of three-dimensional complex variables
[NASA-TM-88318] 05 p0645 N88-13951
Calendar of selected aeronautical and space meetings
[AGARD-CAL-87/1] 05 p0657 N88-14033

Studies of supersonic turbulence and hot-wire response using Laser-Induced Fluorescence (LIF)
06 p0664 N88-14072

Post stall behavior in axial-flow compressors
[AD-A185712] 06 p0665 N88-14081

Utilization of FEP energetics
[NASA-CR-182373] 06 p0714 N88-14379

JPRS report: Science and technology. USSR: Physics and mathematics
[JPRS-UPM-87-008] 06 p0769 N88-14727

Some performance comparisons for a fluid dynamics code
[PB88-113709] 07 p0852 N88-15175

Rayleigh-Taylor instability in compressible fluids
[DE88-002473] 07 p0852 N88-15179

USSR report: Physics and mathematics
[JPRS-UPM-87-002] 07 p0918 N88-15575

Resolution of holograms produced by the fluid experiment system and the holography ground system
07 p0923 N88-15609

Acta Aerodynamica Sinica (selected articles)
[AD-A185723] 08 p0949 N88-15757

Computational prediction of propellant reorientation
08 p0982 N88-15940

Experimental and theoretical study on cavitation inception and bubbly flow dynamics. Part 1: Design, development and operation of a cavitation susceptibility meter. Part 2: Linearized dynamics of bubbly and cavitating flows with bubble dynamics effects
[AD-A187133] 09 p1160 N88-16952

O2-I laser (Oxygen-iodine) mixing studies using LIF (Laser Induced Fluorescence)
[AD-A186667] 09 p1171 N88-17018

Experimental research on swept shock wave/boundary layer interactions
[AD-A187250] 10 p1331 N88-17957

Research on fluid dynamic energy separation
[DE88-002776] 10 p1339 N88-18001

On the start up of supersonic underexpanded jets --- Mach disks 11 p1435 N88-18563

Suspension of small metallic plates: A versatile sensor
[PB88-130901] 11 p1487 N88-18874

Structures and fluxes in a deep convecting mixed layer 13 p1804 N88-20786

Hamiltonian description of the interaction of surface waves with mixed-layer currents
13 p1806 N88-20799

Development of an optical diagnostic instrument. Part 2: Instrument development --- space laboratories
[NLR-TR-87079-L-PT-2] 13 p1841 N88-21016

Enhancement of data acquisition and numerical computation capabilities for unsteady fluid dynamics
[AD-A190115] 15 p2063 N88-22302

Effect of freestream turbulence on a two dimensional cascade, with different surface roughness, at high Reynolds number
[AD-A190615] 15 p2065 N88-22316

Review and assessment of the HOST turbine heat transfer program 15 p2086 N88-22431

A physically consistent model for artificial dissipation in transonic potential flow computations
[NASA-TM-100846] 15 p2122 N88-22652

MPD (magnetoplasmadynamic) thrust chamber flow dynamics
[AD-A189940] 15 p2137 N88-22751

Tip vortices of isolated wings and helicopter rotor blades
[AD-A191336] 16 p2158 N88-22874

Aerodynamic and Related Hydrodynamic Studies Using Water Facilities
[AGARD-CP-413] 16 p2200 N88-23125

Qualification of a water tunnel for force measurements on aeronautical models 16 p2200 N88-23128

The use of a water towing tank for aerodynamic testing and methods for quantitative evaluation of photographs
16 p2202 N88-23140

Coronal fluid-dynamics in laser fusion
16 p2278 N88-23634

Control of combustion and acoustically coupled fluid dynamic instabilities 17 p2318 N88-23843

Noncontact temperature measurements in the microgravity fluids and transport phenomena discipline
17 p2328 N88-23901

Fluid dynamics of spherical cavity reactors
17 p2403 N88-24291

Dynamics and control of turbulent shear flows
[AD-A191527] 18 p2508 N88-24879

Nonlinear waves
[AD-A192148] 18 p2510 N88-24889

Gas diffusion studies in steady and nonsteady cavities
18 p2512 N88-24902

Correlations of velocity and temperature fluctuations in the stagnation-point flow of circular cylinder in turbulent flow
[NASA-TM-100930] 19 p2597 N88-25435

Fluid dynamics of high performance turbomachines
[AD-A192073] 19 p2664 N88-25840

Boundary layer development as a function of chamber pressure in the NASA Lewis 1030:1 area ratio rocket nozzle
[NASA-TM-100917] 19 p2664 N88-25841

Scaling laws for homogeneous turbulent shear flows in a rotating frame
[NASA-CR-181672] 19 p2665 N88-25847

Stationary, wave type, and chaos type convection in spherical symmetry geometries
[ETN-88-92358] 20 p2801 N88-26625

Computer science research, 1987: Computation Directorate
[DE88-008637] 20 p2834 N88-26812

Fluid dynamical model of ultrarelativistic heavy ion collisions
[DE88-007905] 20 p2850 N88-26921

The heat transfer and fluid dynamics of concave surface curvature
[AD-A193064] 21 p2943 N88-27479

Flow dynamics stimulated by hairpin-like vortices in initially laminar boundary layers
[AD-A194253] 22 p3075 N88-28254

Accommodation concept for fluid physics facilities, volume 2 --- Spacelab
[SG-TN-AI-027-VOL-2] 24 p3358 N88-29994

Assessment of a 3-D boundary layer analysis to predict heat transfer and flow field in a turbine passage
[NASA-CR-174894] 24 p3370 N88-30066

FLUID FILLED SHELLS

NT LIQUID FILLED SHELLS

Calculation of the eigenvibrations of axisymmetric fluid configurations with a singularity method, taking into account surface tension effects under reduced gravity
[ETN-87-90438] 01 p0048 N88-10304

Coupled FE and HIE method for exterior acoustics of axisymmetric shells --- finite element (FE) Helmholtz integral equation (HIE)
[ARE-TM(UHA)-87506] 09 p1243 N88-17448

The Shock and Vibration Digest, volume 20, no. 3
12 p1635 N88-19786

Vibrations of shells containing fluid
12 p1635 N88-19787

The nonlinear dynamics of a spacecraft coupled to the vibration of a contained fluid
[DE88-007035] 16 p2168 N88-22925

Quantitative particle characterization by scattered ultrasound 20 p2848 N88-26908

FLUID FILMS

NT SQUEEZE FILMS

Studies of thin surface films aim at seeing deep ocean processes 04 p0460 N88-12847

Literature review of solid lubrication mechanisms
[AD-A185010] 05 p0567 N88-13456

Research on acoustical scattering, diffraction catastrophes, optics of bubbles, photoacoustics, and acoustical phase conjugation
[AD-A185785] 06 p0776 N88-14761

Calculation on film preparation and film motion of a swirl atomizer
[DFVLR-FB-87-25] 09 p1162 N88-16962

Standardization of lubricity test
[AD-A187776] 11 p1465 N88-18736

Lubricating properties of molybdenum disulfide. Part 3: Performance of molybdenum disulfide-containing oils in fluid lubrication
[NASA-TT-20156] 13 p1752 N88-20480

Heating and evaporation of turbulent liquid films: Measurement of film thickness and the onset of nucleate boiling
[DE88-006388] 18 p2512 N88-24905

The use of liquid films for spacecraft survivability to laser radiation
[AD-A192954] 20 p2765 N88-26395

FLUID FILTERS

NT AIR FILTERS

Fiber-reinforced composite hot-gas filters
[DE87-012257] 01 p0033 N88-10208

Reference filters for electrostatic charging tendency measurements of fuels
[AD-A191717] 18 p2495 N88-24803

FLUID FLOW

NT AIR CURRENTS
NT AIR FLOW
NT AIR JETS
NT ANNULAR FLOW
NT AXIAL FLOW
NT AXISYMMETRIC FLOW
NT BAROTROPIC FLOW
NT BASE FLOW
NT BELTRAMI FLOW
NT BLASIUS FLOW
NT BLOOD FLOW
NT BOUNDARY LAYER FLOW
NT BOUNDARY LAYER SEPARATION
NT CAPILLARY FLOW
NT CASCADE FLOW
NT CAVITATION FLOW
NT CHANNEL FLOW
NT COAXIAL FLOW
NT COMBUSTIBLE FLOW
NT COMPRESSIBLE FLOW
NT CONICAL FLOW
NT CONTINUUM FLOW
NT CONVECTIVE FLOW
NT COOLING FLOWS (ASTROPHYSICS)
NT CORE FLOW
NT CORNER FLOW
NT COUETTE FLOW
NT COUNTERFLOW
NT CRITICAL FLOW
NT CROSS FLOW
NT DUCTED FLOW
NT EQUILIBRIUM FLOW
NT FREE FLOW
NT FREE MOLECULAR FLOW
NT FUEL FLOW
NT GAS FLOW
NT HELICAL FLOW
NT HYPERSONIC FLOW
NT HYPERVELOCITY FLOW
NT INCOMPRESSIBLE FLOW
NT INLET FLOW
NT INVISCID FLOW
NT ISOTHERMAL FLOW
NT JET FLOW
NT JET MIXING FLOW
NT JET STREAMS (METEOROLOGY)
NT LAMINAR FLOW
NT LIQUID FLOW
NT MAGNETOHYDRODYNAMIC FLOW
NT MASS FLOW
NT MERIDIONAL FLOW
NT MOLECULAR FLOW
NT MULTIPHASE FLOW
NT NONEQUILIBRIUM FLOW
NT NONNEWTONIAN FLOW
NT NONUNIFORM FLOW
NT NOZZLE FLOW
NT ONE DIMENSIONAL FLOW
NT OPEN CHANNEL FLOW
NT OSCILLATING FLOW
NT PARALLEL FLOW
NT PIPE FLOW
NT PLASTIC FLOW
NT POTENTIAL FLOW
NT PROPELLANT TRANSFER
NT RADIAL FLOW
NT RAYLEIGH-BENARD CONVECTION
NT REATTACHED FLOW
NT RECIRCULATIVE FLUID FLOW
NT REVERSED FLOW
NT SECONDARY FLOW
NT SEPARATED FLOW
NT SHEAR FLOW
NT SINGLE-PHASE FLOW
NT SLIP FLOW
NT SMALL PERTURBATION FLOW
NT SOLIDS FLOW
NT STAGNATION FLOW
NT STEADY FLOW
NT STEAM FLOW
NT STOKES FLOW
NT STRATIFIED FLOW
NT SUBSONIC FLOW
NT SUPERCRITICAL FLOW
NT SUPERSONIC FLOW
NT SUPERSONIC JET FLOW
NT THREE DIMENSIONAL FLOW
NT TRANSITION FLOW
NT TRANSONIC FLOW
NT TURBULENT FLOW
NT TWO DIMENSIONAL FLOW
NT TWO PHASE FLOW
NT UNIFORM FLOW
NT UNSTEADY FLOW
NT VERTICAL AIR CURRENTS
NT VISCOUS FLOW
NT WALL FLOW
NT WATER FLOW
NT WEDGE FLOW

Performance of rotary regenerative heat exchanger: A numerical simulation 01 p0046 N88-10292

Experimental and theoretical studies of vertical annular liquid jets
[DE87-013907] 01 p0047 N88-10299

Nonlinear fluid equations for a low collisionality toroida
plasma
[DE87-013006] 01 p0100 N88-10655

Analytical modeling of helicopter static and dynamic induced velocity in GRASP
[NASA-TM-100026] 02 p0123 N88-10777

Heat transfer in the tip region of a rotor blade simulator 02 p0186 N88-11159

Direct Absorption Receiver flow experiments
[DE87-014655] 02 p0196 N88-11221

Fundamentals of turbulence for turbulence modeling and simulation 03 p0312 N88-11971

The evolution of HOBO
[DE87-014742] 03 p0313 N88-11980

FLIP (Fluid-Implicit-Particle): A low-dissipation, particle-in-cell method for fluid flow
[DE87-014745] 03 p0313 N88-11981

Structural characteristics of dean vortices in a curved channel
[AD-A184724] 03 p0320 N88-12024

Theory of one and two-pass cross-flow heat exchanger
[PB87-225157] 04 p0441 N88-12736

Studies of pressure-velocity coupling schemes for analysis of incompressible and compressible flows
[NASA-CR-181526] 04 p0443 N88-12748

Three-dimensional, free-Lagrange hydrodynamics
[DE88-000494] 04 p0443 N88-12749

The modelling of orientation in planar polymer welding flows
[AD-A184404] 04 p0451 N88-12793

A spatial marching technique for the inviscid blunt body problem 05 p0533 N88-13239

A perspective of computational fluid dynamics
05 p0538 N88-13279

Development of an integrated BEM approach for hot fluid structure interaction
[NASA-CR-181577] 05 p0556 N88-13384

Three-dimensional dynamic labyrinth seal analysis
[AD-A185353] 05 p0590 N88-13599

Fluid mass and thermal loading effects on the modal characteristics of space shuttle main engine liquid oxygen inlet splitter vanes 05 p0594 N88-13628

Turbulence, turbulence control, and drag reduction
[AD-A185643] 06 p0665 N88-14080

Description and analysis of a cascade control of fluid flow
[PB87-112686] 06 p0698 N88-14282

Model development for induction heating
[DE88-002376] 06 p0699 N88-14289

Extensions of the control volume based finite element method for fluid flow problems 06 p0700 N88-14296

Dual cylindrical wave Laser-Doppler method for measurement of skin friction in fluid flow
06 p0700 N88-14297

A study of rotor broadband noise mechanisms and helicopter tail rotor noise 06 p0777 N88-14766

The numerical and analytical study of bifurcation and multicellular flow instability due to natural convection between narrow horizontal isothermal cylindrical annuli at high Rayleigh numbers
[AD-A186113] 07 p0849 N88-15151

Numerical methods for fluid flow problems
[DE88-000156] 07 p0854 N88-15190

An automated flow calorimeter for heat capacity and enthalpy measurements at elevated temperatures and pressures
[DE88-002357] 07 p0857 N88-15206

Turbomachinery 08 p0955 N88-15792

Chemical reacting flows 08 p0955 N88-15793

Fluid mechanical issues in polymer processing
[DE88-002767] 08 p0972 N88-15880

Zero-G thermodynamic vent system for shuttle/Centaur 08 p0983 N88-15943

Comparative performance of the conjugate gradient and SOR (Successive Over Relaxation) methods for computational thermal hydraulics
[DE88-002553] 08 p0988 N88-15986

Response of a sequential damper to shock inputs
08 p0998 N88-16042

Study of pattern formation at liquid interfaces
[DE88-001399] 09 p1160 N88-16954

Techniques of flow visualization
[AGARD-AG-302] 09 p1164 N88-16977

TOPP: A post-processor for TOPAZ, the one dimensional pipe flow analysis code
[DE88-003711] 09 p1164 N88-16981

A project to experimentally and theoretically examine fluid interfacial wave phenomena in a rotating cylindrical geometry: Current results and future plans
[DE88-003738] 09 p1165 N88-16984

Use of boundary-layer method for problem of sound propagation through channel with variable cross-section containing stream of fluid 09 p1233 N88-17396

Two-dimensional analysis for a scrapeoff and divertor regions with an MHD model. Conceptual design study of FY86 FER
[DE88-751069] 09 p1251 N88-17497

Overview of heat transfer and fluid flow problem areas encountered in Stirling engine modeling
[NASA-TM-100131] 09 p1262 N88-17561

Pumping systems and flow interfaces for rapid response electronic reheat controls 10 p1282 N88-17665

One-dimensional leakage-flow vibration instabilities
[DE88-002875] 10 p1330 N83-17947

Application of a multigrid method to a buoyancy-induced flow problem
[DE88-003961] 10 p1397 N88-18326

Experimental investigation of low gravity two-phase flow behavior
[DE88-003779] 11 p1466 N88-18741

Experiments on the flow of viscoelastic fluids between eccentric rotating cylinders 12 p1625 N88-19723

Rotational flow of rarefied gas between two coaxial cylinders with slip conditions
[INPE-4277-PRE/1149] 12 p1627 N88-19738

Fluidization mechanisms in slurry flows
[DE88-005191] 13 p1766 N88-20563

Velocity and concentration measurements in flowing suspensions by nuclear magnetic resonance
[DE88-006225] 13 p1770 N88-20589

Subduction 13 p1806 N88-20796

Hamiltonian description of the interaction of surface waves with mixed-layer currents
13 p1806 N88-20799

Development of a rotary fluid transfer coupling and support mechanism for space station
14 p1928 N88-21493

Mixing: Stretching, breakup and chaos
[DE88-006699] 15 p2067 N88-22327

Deflection of a circular liquid jet on a flat plate perpendicular to the flow direction
[NASA-TT-20279] 16 p2207 N88-23173

Modal forced response of propfans in yawed flow
16 p2221 N88-23253

Numerical modelling of flows using phoenics
17 p2339 N88-23955

Dual wavelength holographic interferometry system
[NASA-CASE-MFS-28242-1] 17 p2341 N88-23960

Pressure measuring probe
[NASA-CASE-LAR-13853-1] 17 p2341 N88-23961

Simulations of a missile with liquid payload under launch conditions
[AD-A191479] 18 p2463 N88-24625

Adaptive local grid refinement in computational fluid mechanics
[AD-A192215] 18 p2510 N88-24890

A semigroup for Lagrangian 1D isentropic flow
[DE88-006464] 18 p2513 N88-24912

NASA research Program: The roles of fluid motion and other transport phenomena in the morphology of materials
[NASA-CR-182801] 18 p2580 N88-25327

Applications of some new ideas on irreversible processes to particular fluids
[AD-A191610] 19 p2663 N88-25836

The propagation of pressure perturbations in bubbly air/water flows 19 p2664 N88-25843

Multigrid computation of practical fluid flows and heat transfer
[DE88-010064] 20 p2799 N88-26609

Use of direct solvers for multidimensional fluid flow computations
[DE88-010063] 20 p2799 N88-26611

Fluid flow modeling in casting processes and its implications
[DE88-010009] 20 p2810 N88-26671

Acoustic diffraction by an absorbing finite strip in a moving fluid
[PB88-191382] 20 p2849 N88-26912

Optimal rheological characteristics in dynamic stability of polymer flow through porous media
[DE88-001225] 21 p2918 N88-27322

Characterization of accelerating pipe flow
[AD-A193065] 21 p2943 N88-27481

Effects of numerical dissipation on finite-volume solutions of compressible flow problems
[AD-A193173] 21 p2944 N88-27485

Numerical treatment of the pressure singularity at a re-entrant corner
[AD-A193357] 21 p2944 N88-27488

Stream function-vorticity finite elements and the resolution of the Navier-Stokes equations
[DE88-702318] 21 p2945 N88-27494

Superfluid Helium On-Orbit Transfer (SHOOT) operations
[NASA-TM-101009] 22 p3048 N88-28084

Solidification with natural circulation
[DE88-011197] 22 p3074 N88-28248

Study of experimental technique of oil flow with emphasis on quantitative determination of the flow position parameters on the surface
[NASA-TT-20341] 23 p3215 N88-29135

Mapping of volcanic units at Alba Patera, Mars
23 p3301 N88-29663

Lava flow-field morphology: A case study from Mount Etna, Sicily 23 p3303 N88-29676

Preliminary investigation of flow modeling during solid propellant processing
[AD-A196168] 24 p3357 N88-29987

Experimental and analytical study of two-phase flow in zero gravity
[AD-A195223] 24 p3358 N88-29993

The use of upwind schemes at high Reynolds number: A cautionary note
[AD-A196227] 24 p3371 N88-30074

Approximation of viscoelastic stresses from Newtonian turbulent kinematics
[AD-A194317] 24 p3371 N88-30077

Simulations of lava flows on Mars
24 p3443 N88-30495

Small-scale volcanic landforms indicative of distributary tube systems 24 p3444 N88-30496

Volcanic styles at Alba Patera, Mars: Implications of lava flow morphology to the volcanic history
24 p3444 N88-30497

FLUID INJECTION
NT GAS INJECTION
NT WATER INJECTION

Insect contamination protection for laminar flow surfaces 07 p0814 N88-14954

Numerical simulation of ignition of hydrogen jet in hot air 19 p2637 N88-25647

FLUID JET AMPLIFIERS
U FLUID AMPLIFIERS

FLUID JETS
NT AIR JETS
NT FREE JETS
NT GAS JETS
NT HYDRAULIC JETS

JPRS report: Science and technology. China
[JPRS-CST-87-034] 03 p0301 N88-11897

Analysis of compressible flow on high-velocity jet penetration 03 p0302 N88-11898

Droplet formation for liquid monopropellant jets
[AD-A187172] 10 p1331 N88-17956

Effect of mass-velocity on liquid jet atomization in Mach 1 gasflow
[NASA-TM-100813] 16 p2211 N88-23194

Supercritical fluid chromatography/supersonic jet spectroscopy
[DE88-007935] 19 p2614 N88-25511

Droplet formation for liquid monopropellant jets
19 p2623 N88-25557

Liquid Engine Jet Atomization Workshop report
19 p2627 N88-25584

Small-droplet spray measurements with a scattered-light scanner
[NASA-TM-100973] 20 p2806 N88-26645

The influence of delay effects on the decay of liquid jets
[MPIS-14/1987] 23 p3214 N88-29130

FLUID MANAGEMENT

Components for cryostat --- spaceborne
[MBB/ISO-TN-CD00.003-REV-A]
01 p0032 N88-10207

Space station integrated propulsion and fluid system study: Fluid systems configuration databook
[NASA-CR-179215] 03 p0278 N88-11753

Space station resistojet system requirements and interface definition study
[NASA-CR-180832] 04 p0409 N88-12541

AF cryogenic and fluid management spacecraft technology program 08 p0981 N88-15925

Cryogenics program overview
08 p0981 N88-15926

Ames Research Center cryogenics program
08 p0981 N88-15927

LeRC cryogenic fluid management program overview
08 p0981 N88-15928

Cryogenic fluid management program flight concept definition 08 p0981 N88-15929

Orbital transfer vehicle studies overview
08 p0981 N88-15931

Large capacity cryopropellant orbital storage facility
08 p0981 N88-15932

Thermal analysis for the Cryogenic Fluid Management Flight Experiment (CFMFE) 08 p0982 N88-15935

Zero-G thermodynamic vent system for shuttle/Centaur 08 p0983 N88-15943

Study of helium transfer technology for STICCR: Fluid management
[NASA-CR-177463] 10 p1291 N88-17720

Cryogenic Fluid Management Technology Workshop. Volume 2: Roundtable Discussion of Technology Requirements
[NASA-CP-10009] 13 p1772 N88-20599

Vibration characteristics of pumped fluid systems (VCPFS) --- microgravity payloads
[ESA-CR(P)-2499] 14 p1895 N88-21310

Development of a motorized cryovalve for the control of superfluid liquid helium 14 p1925 N88-21477

FLOSIN: A fluid loop analyzer for SINDA
15 p2066 N88-22321

Two-phase fluid management for a Rankine cycle isotope power system 17 p2405 N88-24303

Turbomachinery in space 17 p2408 N88-24321

Superfluid Helium On-Orbit Transfer (SHOOT) operatons
[NASA-TM-101009] 22 p3048 N88-28084

Study of toluene rotary fluid management device and shear flow condenser performance for a space-based organic Rankine power system
[NASA-CR-180885] 24 p3338 N88-29872

FLUID MECHANICS

NT AERODYNAMICS
NT AEROTHERMODYNAMICS
NT COMPUTATIONAL FLUID DYNAMICS
NT ELASTOHYDRODYNAMICS
NT ELECTROHYDRODYNAMICS
NT FLUID DYNAMICS
NT GAS DYNAMICS
NT HYDRODYNAMICS
NT HYDROMECHANICS
NT HYDROSTATICS
NT INTERACTIONAL AERODYNAMICS
NT MAGNETOHYDRODYNAMICS
NT PNEUMATICS
NT RAREFIED GAS DYNAMICS
NT ROTOR AERODYNAMICS
NT SUPERSONICS
NT UNSTEADY AERODYNAMICS
NT VORTEX SHEDDING

Rayleigh-Taylor instability in compressible fluids
[DE87-013494] 01 p0047 N88-10297

Mean flow structure of a turbulent junction vortex
[PB87-206231] 01 p0047 N88-10301

Steady state theta pinch concept for slow formation of FRC
[ISSN-0469-4732] 01 p0098 N88-10648

USSR Report: Engineering and Equipment
[JPRS-UEQ-87-007] 02 p0157 N88-10985

A preliminary study of a fluid science laboratory for space station (Columbus). Part 4: Executive summary
[NLR-TR-87023-L-PT-4] 02 p0170 N88-11072

Personal Computer (PC) based image processing applied to fluid mechanics
[NASA-TM-100024] 02 p0172 N88-11087

Point vortex dynamics: Recent results and open problems
[DE87-014759] 03 p0314 N88-11982

The Proceedings of the Symposium on Mechanics for Space Flight
[ISAS-SP-5] 03 p0317 N88-12006

Some experiences with the viscous-inviscid interaction approach
[NASA-TM-100015] 04 p0395 N88-12466

Low gravity fluid-thermal experiments
[DE88-000553] 04 p0423 N88-12620

Proceedings of the Fifth Symposium on Energy Engineering Sciences: Instrumentation, Diagnostics, and Material Behavior
[DE88-001479] 04 p0429 N88-12660

NACHOS 2: A finite element computer program for incompressible flow problems. Part 2: User's manual
[DE88-001451] 04 p0443 N88-12750

A spatial marching technique for the inviscid blunt body problem 05 p0533 N88-13239

Experimental study of the fluid mechanics of unsteady turbulent boundary layers
[AD-A184856] 05 p0580 N88-13536

Numerical analysis, computing and fundamental studies in fluid mechanics
[DE88-001912] 05 p0582 N88-13550

Damping analysis of flexural waves in fluid-loaded single and constrained plates
[AD-A185116] 05 p0609 N88-13739

Research on internal fluid mechanism between turbine blades 06 p0676 N88-14138

Internal fluid mechanics research on supercomputers for aerospace propulsion systems
[NASA-TM-100289] 07 p0854 N88-15188

Aeropropulsion '87. Session 3: Internal Fluid Mechanics Research
[NASA-CP-10003-SESS-3] 08 p0954 N88-15790

Inlets, ducts and nozzles 08 p0955 N88-15791

Chemical reacting flows 08 p0955 N88-15793

Aeropropulsion '87. Session 4: Instrumentation and Controls Research
[NASA-CP-10003-SESS-4] 08 p0955 N88-15794

Aeropropulsion '87. Session 5: Subsonic Propulsion Technology
[NASA-CP-10003-SESS-5] 08 p0956 N88-15800

Aeropropulsion '87. Session 6: High-Speed Propulsion Technology
[NASA-CP-10003-SESS-6] 08 p0957 N88-15807

Fluid mechanical issues in polymer processing
[DE88-002767] 08 p0972 N88-15880

Review of the equations of fluid mechanics and heat transfer 08 p0986 N88-15970

Active control of jet flowfields
[AD-A186736] 08 p0989 N88-15989

An efficient method for computing leading Eigenvalues and Eigenvectors of large asymmetric matrices
09 p1159 N88-16949

Techniques of flow visualization
[AGARD-AG-302] 09 p1164 N88-16977

Investigation of surface tension driven convection as a feasibility study for a micro-gravity experiment
[NASA-CR-182504] 11 p1466 N88-18739

International Conference on Industrial and Applied Mathematics
[AD-A188251] 11 p1483 N88-18851

Studies on homogeneous and heterogeneous reactive flows 11 p1484 N88-18861

Numerical analysis, computing and fundamental studies in fluid mechanics
[DE88-005343] 12 p1625 N88-19725

A review of approaches to the study of turbulence modification by means of non-Newtonian additives
[AD-A188799] 12 p1627 N88-19734

Research on flow control
[AD-A189014] 12 p1627 N88-19736

Fluidization mechanisms in slurry flows
[DE88-005191] 13 p1766 N88-20563

Fluid-thermal-structural study of aerodynamically heated leading edges
[NASA-TM-100579] 13 p1783 N88-20666

On the structure of pulsed plasma jets
13 p1843 N88-21030

Mixing: Stretching, breakup and chaos
[DE88-006699] 15 p2067 N88-22327

Physical fluid mechanics in MPD thrusters
[AD-A190309] 15 p2138 N88-22754

Research and technology
[NASA-TM-100172] 15 p2153 N88-22851

The nonlinear dynamics of a spacecraft coupled to the vibration of a contained fluid
[DE88-007035] 16 p2168 N88-22925

Fundamental aspects of the structure of supersonic turbulent boundary layers
[AD-A191494] 18 p2456 N88-24581

Internal fluid dynamics within a nonspinning partially liquid-filled shell due to burster rupture
[AD-A191055] 18 p2507 N88-24874

Heating and evaporation of turbulent liquid films: Measurement of film thickness and the onset of nucleate boiling
[DE88-006388] 18 p2512 N88-24905

Extrema principles of entrophy production and energy dissipation in fluid mechanics
[NASA-TM-100992] 18 p2519 N88-24946

A Navier-Stokes solver for cascade flows
[NASA-CR-181682] 19 p2666 N88-25856

Laser probes and numerical modeling as process diagnostics in chemical vapor deposition
[DE88-011622] 21 p2911 N88-27275

Some stability criteria in fluid and solid mechanics
21 p3027 N88-27966

A study of the vortex sheet method for solving the Prandtl boundary layer equations
[DE88-011346] 22 p3074 N88-28249

Three-dimensional vortex interactions
[AD-A194066] 23 p3172 N88-28889

A limiting viscosity approach to the Riemann problem for materials exhibiting change of phase
[AD-A193477] 23 p3210 N88-29103

Development of the Simplified Compressor Model (SCM) for performance analysis of gaseous diffusion compressors
[DE88-009066] 23 p3221 N88-29173

Fluid physics double rack --- Spacelab
[SD-TN-AI-012] 24 p3358 N88-29992

FLUID POWER

Microcomputer control of a hydraulically actuated piston
[AD-A184130] 03 p0368 N88-12317

Laser thermal propulsion
[AD-A186407] 07 p0933 N88-15666

Advanced energy conversion concept for beamed-energy propulsion
[AD-A187336] 10 p1324 N88-17914

FLUID PRESSURE

Physics of immiscible flow in porous media
[PB88-131008] 11 p1487 N88-18873

FLUID TRANSMISSION LINES

Ammonia transfer across rotating joints in space
14 p1927 N88-21492

FLUID TRANSPIRATION

U TRANSPIRATION

FLUID-SOLID INTERACTIONS

NT GAS-SOLID INTERACTIONS

Experimental study of three-dimensional turbulent jet-solid boundary interaction 01 p0046 N88-10293

Time-dependent hypersonic viscous interactions
[AD-A185764] 06 p0665 N88-14082

Studies on fluid-structural vibration using boundary element method
[PB87-129508] 06 p0699 N88-14291

Validation of the Underwater Shock Analysis (USA) program. Part 1: Theoretical considerations --- ship design
[REPT-5073713-86-01] 06 p0702 N88-14308

Abrasion and impact resistant coatings
[DE88-003562] 13 p1750 N88-20464

FLUIDIC CIRCUITS

Microminiature fluidic amplifier
19 p2669 N88-25865

FLUIDICS

Dynamics and control of turbulent shear flows
[AD-A191527] 18 p2508 N88-24879

Pulsatile fluidic pump performance at elevated temperatures
[DE88-008046] 19 p2677 N88-25919

FLUIDS

China report: Science and technology
[JPRS-CST-87-015] 03 p0298 N88-11873

Integrated 3-parameter diagram for determining thermodynamic properties of fluids
03 p0298 N88-11874

Theory of neutron scattering experiments on momentum distributions in quantum fluids
[DE87-01369] 05 p0648 N88-13968

New equilibrium forms of free surface of confined magnetic fluid 06 p0770 N88-14734

Experimental and theoretical constraints on the origin of mid-ocean ridge geothermal fluids
13 p1804 N88-20784

Fluids, gels and glasses under extreme conditions of pressure and temperature
[AD-A190655] 15 p2035 N88-22125

FLUORESCENCE

NT LASER INDUCED FLUORESCENCE
NT PHOSPHORESCENCE
NT RESONANCE FLUORESCENCE
NT X RAY FLUORESCENCE

KR - laser excitation of NH2 in atmospheric pressure flames
[AD-A183421] 01 p0050 N88-10322

Photolytic processes for measurement of combustion heats of formation and reaction rates
[DE87-014047] 02 p0144 N88-10905

Theoretical atomic and molecular photophysics
[DE87-014249] 02 p0231 N88-11458

OH(A-X) fluorescence from photodissociative excitation of HO2 at 157.5 nm
[NASA-CR-181580] 05 p0563 N88-13429

Artificial photosynthesis using chlorophyll based carotenoid-quinone triads
[DE88-001660] 07 p0884 N88-15362

The use of chlorophyll fluorescence measurements from space for separating constituents of sea water
08 p1043 N88-16307

Fed-batch control based upon the measurement of intracellular NADH 09 p1197 N88-17175

Excimer plasma displays
[AD-A186731] 09 p1250 N88-17489

Investigation of real-time two-dimensional visualization of fuel spray liquid/vapor distribution via exciplex fluorescence
[AD-A188268] 10 p1307 N88-17816

Multicomponent analysis using synchronous-excitation phase-resolved fluorescence spectroscopy
[AD-A188883] 12 p1606 N88-19604

Discharge excitation of dye vapors
[AD-A188428] 12 p1632 N88-19770

Nondestructive evaluation of carbon-carbon coatings
[AD-A189524] 13 p1748 N88-20453

Remote fiber fluorimetry techniques for pressure measurements
[DE88-004486] 13 p1773 N88-20604

Laser fluorescence spectroscopy of zinc neutrals originating from laser-irradiated and ion-bombarded zinc sulfide and zinc surfaces
[DE88-006033] 13 p1776 N88-20620

Noncontact thermometry via laser pumped, thermographic phosphors: Characterization of systematic errors and industrial applications
[DE88-005599] 13 p1777 N88-20628

Spontaneous decay and atomic fluorescence near a metal surface of an absorbing dielectric
[AD-A187508] 13 p1835 N88-20975

What has been done and what will be done by subnatural linewidth spectroscopy 14 p1978 N88-21807

Polarization of molecular fluorescence bands in comets: Recent observations and interpretation
14 p1998 N88-21907
Light scattering of intracellular gas vacuoles: Anomalous behavior of forward and perpendicular light scattering of a cyanobacterium due to intracellular gas vacuoles
[BCRS-87-08] 16 p2228 N88-23308
A new fiber-optic-based ion sensor
[AD-A191322] 16 p2274 N88-23612
Cascade fluorescences from laser-excited lithium atom for plasma diagnostics 17 p2442 N88-24526
Flux density measurements of neutral iron in TEXTOR with laser induced fluorescence
17 p2442 N88-24528
Optical diagnostics for a high power, rf-inductively coupled plasma
[DE88-007822] 18 p2579 N88-25322
Determination of low molecular weight thiols using monobromobimane fluorescent labeling and high-performance liquid chromatography
[NASA-CR-182932] 19 p2608 N88-25478
Laser fluorescence spectroscopy of zinc neutrals originating from laser-irradiated and ion-bombarded zinc sulfide and zinc surfaces
[DE88-008037] 20 p2769 N88-26418
Physical-chemical reactions at welding arc/molten pool interfaces
[DE88-007717] 20 p2808 N88-26662
Molecular fluorescence measurements with a charge-coupled device detector
[AD-A194221] 22 p3080 N88-28291
Program to increase the measurement capabilities of the AFGL (Air Force Geophysics Laboratory) fixed and mobile high altitude lidar systems
[AD-A194614] 23 p3203 N88-29063
Molecular fluorescence measurements with a charge-coupled device detector
[AD-A194437] 23 p3216 N88-29141
Autoionization for lower level detrapping in X-ray lasers
[AD-A195845] 24 p3379 N88-30123
Immunofluorescence localization of dissociation supernatant and extracellular matrix components in Lytechinus pictus sectioned embryos
[NASA-CR-183137] 24 p3406 N88-30276

FLUORESCENT EMISSION
U FLUORESCENCE

FLUORIDES
NT ALUMINUM FLUORIDES
NT CALCIUM FLUORIDES
NT CHLORINE FLUORIDES
NT HYDROFLUORIC ACID
NT LITHIUM FLUORIDES
NT NITROGEN FLUORIDES
NT POLYVINYL FLUORIDE
NT SODIUM FLUORIDES
NT SULFUR FLUORIDES
NT URANIUM FLUORIDES
The kinetics and dynamics of iodine monofluoride formation in gas-phase collisions
[AD-A185715] 06 p0709 N88-14352
SBIR-Long fluoride fiber
[AD-A188595] 13 p1754 N88-20492
NMR analysis of a fluorocarbon copolymer
[DE88-002364] 15 p2043 N88-22170
Interaction of vinylidene fluoride: Tetrafluoroethylene copolymer with ammonia
[NASA-TT-20292] 19 p2620 N88-25542
NF (a 1 delta) production in a supersonic flow using N2F4 + H2 in a BCL-16 nozzle
[AD-A194478] 22 p3082 N88-28304

FLUORINATION
Elementary fluorination of polymers
[ETN-88-90812] 07 p0836 N88-15075
Feasibility of chemical lasers based on chain reaction involving hydrogen fluorination with thermal branching mechanism 09 p 238 N88-17420
Polymerization of fluorinated diacetylenes
[AD-A188051] 11 p1462 N88-18716
A new approach to highly fluorinated lubricants
[AD-A190523] 15 p2045 N88-22188

FLUORINE
Studies of fluorine combustion
[AD-A187646] 11 p1452 N88-18656
Combustion of hydrogen and hydrocarbons in fluorine
[AD-A188018] 11 p1453 N88-18662
Numerical modelling specific energy charcteristics of excimer KrF lasers with electron beam excitation
[DE88-701525] 15 p2070 N88-22344

FLUORINE COMPOUNDS
NT ALUMINUM FLUORIDES
NT CALCIUM FLUORIDES
NT CHLORINE FLUORIDES
NT DIFLUORO COMPOUNDS
NT FLUORIDES
NT FLUORINE ORGANIC COMPOUNDS
NT FLUORO COMPOUNDS
NT FLUOROCARBONS
NT FLUOROHYDROCARBONS
NT FLUOROPOLYMERS
NT HYDROFLUORIC ACID
NT LITHIUM FLUORIDES
NT NITROGEN FLUORIDES
NT POLYTETRAFLUOROETHYLENE
NT POLYVINYL FLUORIDE
NT SODIUM FLUORIDES
NT SULFUR FLUORIDES
NT TEFLON (TRADEMARK)
NT URANIUM FLUORIDES
Photocurrent generation from basic metals, utilizing a short pulsed ArF excimer laser
[AD-A184928] 05 p0587 N88-13579
Study of the micromechanical properties of fluor glasses based on ZrF4
[ISAL-ITC1-87-03] 09 p1148 N88-16882
Theoretical calculations of XeF ground state kinetics
[AD-A191398] 16 p2270 N88-23580

FLUORINE ORGANIC COMPOUNDS
NT FLUOROCARBONS
NT FLUOROHYDROCARBONS
NT FLUOROPOLYMERS
NT POLYVINYL FLUORIDE
NT TEFLON (TRADEMARK)
Supersonic turbines for organic fluid Rankine cycles from 3 to 1300 kW 06 p0713 N88-14375
Improved perfluoroalkylether fluid development
[NASA-CR-180872] 08 p0967 N88-15851

FLUORO COMPOUNDS
NT DIFLUORO COMPOUNDS
NT FLUORINE ORGANIC COMPOUNDS
NT FLUOROCARBONS
NT FLUOROHYDROCARBONS
NT FLUOROPOLYMERS
NT POLYTETRAFLUOROETHYLENE
NT TEFLON (TRADEMARK)
Organic Rankine-cycle power systems working fluids study: Topical report No. 1: Fluorinol 85
[DE87-014604] 02 p0195 N88-11217
Flash threshold of shocked aluminum silicofluoride
[DE88-003978] 10 p1339 N88-18005
Polyazidoesters as energetic polymers and copolymer components with fluoro derivatives
[AD-A194236] 23 p3199 N88-29039

FLUOROCARBONS
Impact on ozone attainment of CFC (chlorofluorocarbon) controls used to prevent future depletion of stratospheric ozone
[PB88-195177] 19 p2690 N88-25989
Substituted 1,1,1-Triaryl-2,2,2-Trifluoroethanes and processes for their synthesis
[NASA-CASE-LEW-14345-1] 20 p2767 N88-26404

FLUOROHYDROCARBONS
NT POLYTETRAFLUOROETHYLENE
NT TEFLON (TRADEMARK)
Distributed feedback effects in lasers and high gain laser instabilities in optically pumped CH3F
03 p0329 N88-12079
Polymerization of fluorinated diacetylenes
[AD-A188051] 11 p1462 N88-18716
Thermal oxide growth on silicon: Intrinsic stress and silicon cleaning effects
[AD-A188790] 13 p1736 N88-20377
Natural convection immersion cooling of an array of simulated chips in an enclosure filled with dielectric liquid
[AD-A193594] 23 p3207 N88-29088

FLUOROPLASTICS
U FLUOROPOLYMERS

FLUOROPOLYMERS
NT POLYTETRAFLUOROETHYLENE
NT POLYVINYL FLUORIDE
NT TEFLON (TRADEMARK)
Ferroelectric properties and impact behavior of the PVF2 polymer and the VF2/C2F3H polarized copolymers -- vinylidene polyfluorides
[ISL-CO-245/86] 08 p0971 N88-15876
Cellular thermosetting fluoropolymers and process for making them
[NASA-CASE-GSC-13008-1] 17 p2326 N88-23894
Substituted 1,1,1-Triaryl-2,2,2-Trifluoroethanes and processes for their synthesis
[NASA-CASE-LEW-14345-1] 20 p2767 N88-26404
Polymer-ceramic composites
[AD-A193244] 21 p2905 N88-27237
Plasma treatment of polymers for improved adhesion
[DE88-011623] 21 p2921 N88-27334

FLUOROSCOPY
A microspectrofluorometer system based on real time digital techniques
[REPT-86-014] 11 p1490 N88-18891

FLUTING
U GROOVING

FLUTTER
NT SUPERSONIC FLUTTER
NT TRANSONIC FLUTTER
Flutter suppression and gust load alleviation. Part 1: Results of phase 1 to 3. Part 2: Description of the Garteur model
[MBB/LKE-292/S/PUB/191] 01 p0007 N88-10038
A natural low frequency oscillation in the wake of an airfoil near stalling conditions
[NASA-TM-100213] 02 p0123 N88-10779
Static aeroelastic effects on the flutter of a supercritical wing 05 p0550 N88-13353
Integration of a supersonic unsteady aerodynamic code into the NASA FASTEX system
[NASA-CR-182329] 06 p0663 N88-14068
Parametric study of choke flutter with a linear theory
10 p1283 N88-17673
The application of modern aeroelastic developments for future projects
[MBB-UT-007/87] 10 p1313 N88-17850
The effects of rotational flow, viscosity, thickness, and shape on transonic flutter dip phenomena
[NASA-TM-100811] 11 p1502 N88-18969
A semianalytical technique for sensitivity analysis of unsteady aerodynamic computations
[NASA-TM-100810] 11 p1503 N88-18976
Application of a flux vector splitting methodology towards the solution of unsteady transonic flows, with future emphasis on the blade flutter problem
[AD-A189500] 13 p1716 N88-20260
Design of an integrated control system for flutter margin augmentation and gust load alleviation, tested on a dynamic windtunnel model
[PB88-149885] 15 p2020 N88-22038
Development of aeroelastic analysis methods for turborotors and propfans, including mistuning
16 p2219 N88-23244
Application of Navier-Stokes analysis to stall flutter
16 p2220 N88-23249
Empirical flutter prediction method
[AD-A195699] 24 p3327 N88-29810

FLUTTER ANALYSIS
Investigation of control law for active flutter suppression
[NASA-TT-20126] 02 p0130 N88-10818
The Green's function method for fully unsteady aerodynamics around three-dimensional bodies and its application to flutter analysis
[UTIAS-298] 03 p0260 N88-11639
Velocity scaled aeroelastic testing of an unducted fan
[GTL-191] 05 p0548 N88-13337
Influence of the static deformation on a wing in the unsteady aerodynamic 05 p0551 N88-13357
Modern wing flutter analysis by computational fluid dynamics methods
[NASA-TM-100531] 07 p0816 N88-14965
Unsteady transonic algorithm improvements for realistic aircraft applications
[NASA-TM-100516] 08 p0949 N88-15760
Experimental study on the effect of fiber orientation on flutter characteristics of high-aspect-ratio transport wing
[NAL-TR-936] 09 p1120 N88-16708
Effect of an optimized fiber orientation on transonic flutter characteristics of a high-aspect-ratio composite wing
[NAL-TR-930] 09 p1120 N88-16709
An application of eigenspace methods to symmetric flutter suppression
[NASA-CR-181618] 10 p1284 N88-17684
La Recherche Aerospatiale, bimonthly bulletin, number 1987-2, 237/March-April
[ESA-TT-1074] 11 p1433 N88-18550
Modeling of limit cycle stall flutter oscillations
12 p1583 N88-19472
Aircraft flight flutter testing at the NASA Ames-Dryden Flight Research Facility
[NASA-TM-100417] 13 p1723 N88-20301
A computational procedure for automated flutter analysis 16 p2220 N88-23250
Vibration and flutter analysis of the SR-7L large-scale propfan 16 p2221 N88-23254
Supersonic axial-flow fan flutter
16 p2221 N88-23255
A characteristic method for calculating the generalized flat flutter aerodynamic forces
[NASA-TT-20300] 19 p2598 N88-25438
Parametric flutter studies of an arrow-wing configuration: Some early results
[NASA-TM-100608] 19 p2599 N88-25444
Detailed on-blade measurements on a transonic fan in unstalled supersonic flutter
[PNR90424] 22 p3039 N88-28043
A streamwise upwind algorithm for the Euler and Navier-Stokes equations applied to transonic flows
[NASA-TM-101019] 24 p3316 N88-29751

Application of unsteady aerodynamic methods for transonic aeroelastic analysis
[NASA-TM-100665] 24 p3317 N88-29754
Recent advances in transonic computational aeroelasticity
[NASA-TM-100663] 24 p3321 N88-29778
Use of holography in vibration and flutter study of fans
[PNR90458] 24 p3375 N88-30098

FLUX (RATE PER UNIT AREA)
U FLUX DENSITY

FLUX (RATE)
NT HEAT FLUX
NT MAGNETIC FLUX
NT SOLAR FLUX
Change in interplanetary shock acceleration preceding STIP Interval 17 01 p0112 N88-10719
Coronal mass ejections: The long-term variation of their occurrence rate and the solar wind mass flux
01 p0114 N88-10732
VLA observations of rapid 6 cm flux variations in alpha Ori 04 p0515 N88-13169
A comprehensive exploration of late-type stars in the far-ultraviolet 04 p0520 N88-13194
Gamma ray lines from novae
04 p0526 N88-13214
FTE like variations in the geomagnetic field at ground based conjugate stations in the cusp regions
[INPE-4345-PRE/1182] 08 p1024 N88-16199
Interplanetary Magnetic Field (IMF) influence on the magnetic configuration and particle fluxes at geostationary orbit and on the substorm onset
08 p1031 N88-16247
Johnson noise thermometer for high radiation and high temperature environments
[DE88-003770] 10 p1323 N88-17911
Turbulence interactions in single- and multi-phase turbulent mixing and combustion processes
[AD-A187505] 10 p1332 N88-17960
Energy and momentum fluxes through the sea surface
13 p1806 N88-20798
Radiative processes affecting ocean mixed-layer heat content and their monitoring from satellite
13 p1806 N88-20800
Three-wave parametric resonance in plasma of relativistic electron flux 14 p1972 N88-21772
Design, fabricate, calibrate, test and deliver two satellite electron flux detectors
[AD-A190799] 16 p2169 N88-22930
Johnson noise thermometer for high-radiation and high-temperature environments
17 p2434 N88-24480
Ring current role in dynamics of fluctuating electron and ion fluxes in low-latitude magnetosphere
24 p3447 N88-30514

FLUX DENSITY
NT CURRENT DENSITY
NT ELECTRON FLUX DENSITY
NT ILLUMINANCE
NT IRRADIANCE
NT LUMINANCE
NT LUMINOUS INTENSITY
NT NEUTRON FLUX DENSITY
NT PARTICLE FLUX DENSITY
NT RADIANCE
NT RADIANT FLUX DENSITY
NT SOLAR CONSTANT
NT SOLAR FLUX DENSITY
NT SOUND INTENSITY
An evaluation of the LEC-460 solar collector
[DE88-000052] 02 p0196 N88-11224
Kinetics of crack growth: Thermal/mechanical interaction 03 p0337 N88-12124
Power density measurements in the near field of the DSS 13 26-meter antenna 04 p0437 N88-12711
Measurements of vapor flux, liquid water contents, precipitation rates and riming in a Utah mountain cloud system
[PB87-224945] 04 p0469 N88-12900
Calibration of the Ca II K line-core density and the magnetic flux density in stars using solar data
04 p0507 N88-13116
VLA observations of the X-ray bright Hyades M-dwarfs
04 p0512 N88-13147
MHD energy fluxes for late type dwarfs
04 p0512 N88-13148
Density variations of meteor flux along the Earth's orbit 06 p0739 N88-14545
Some models of the Geminids meteor stream formation 06 p0740 N88-14551
Experimental study of thermal loading at the wall of an industrial Diesel motor
[ISAL-ID11-87-10] 10 p1339 N88-18000
Applications of energy density theory in cyclic plasticity
[AD-A186047] 10 p1342 N88-18023
An experimental measurement of metal multilayer X-ray reflectivity degradation due to intense X-ray flux
[LA-10989-T] 11 p1547 N88-19255
Corrosion, passivity and breakdown of alloys used in high energy density batteries
[DE88-004891] 13 p1743 N88-20422
Study on the burnout with variations of flow twisting over tube length
[DE87-703170] 14 p1909 N88-21405
The turbulent heat flux in low Mach number flows with large density variations
[DE88-006445] 14 p1911 N88-21419
Correlation between magnetic and electric field fluctuations observed during flyby near Halley's comet
14 p1996 N88-21897
Magnetic fusion energy plasma interactive and high heat flux components. Volume 5: Technical assessment of critical issues in the steady state operation of fusion confinement devices
[DE88-006920] 15 p2136 N88-22744
Local density of states in double-barrier resonant tunneling structures
[AD-A190673] 16 p2281 N88-23656
Flux density measurements of neutral iron in TEXTOR with laser induced fluorescence
17 p2442 N88-24528
Difficulties with interpretation of underground muons from Cygnus X-3
[DE88-701645] 23 p3309 N88-29710
Matching P.S.D.: Design loads
24 p3312 N88-29720
In-house capacitor technology program
[AD-A194804] 24 p3367 N88-30049
Vibrational power flow analysis of rods and beams
[NASA-CR-183166] 24 p3383 N88-30151

FLUX MAPPING
U FLUX DENSITY
U MAPPING

FLUX PINNING
Generation of flux tube waves in stellar convection zones. 1: Longitudinal tube waves
[NASA-TM-101152] 17 p2451 N88-24561

FLUX VECTOR SPLITTING
Numerical simulation of the hypersonic flow around lifting vehicles 05 p0532 N88-13234
A Cartesian finite-volume method for the Euler equations 05 p0579 N88-13532
Vectorization of a multigrid method for the compressible Navier-Stokes equations
[PB87-230496] 06 p0698 N88-14284
Application of a flux vector splitting methodology towards the solution of unsteady transonic flows, with future emphasis on the blade flutter problem
[AD-A189500] 13 p1716 N88-20260
Splitting of inviscid fluxes for real gases
[NASA-TM-100856] 14 p1964 N88-21717
Choice of implicit and explicit operators for the upwind differencing method
[NASA-TM-100857] 14 p1964 N88-21718

FLUXES
Optimum size of staged flux compression generators
[DE87-011741] 01 p0038 N88-10244
Investigation of the structure of coatings of self fluxing alloys fused by laser energy
[BLL-M-37301-(5828.4)] 02 p0148 N88-10930
Slowing down tail enhanced, neoclassical and classical alpha particle fluxes in tokamak reactors
[DE88-001930] 06 p0783 N88-14806
Submerged arc flux welding with CaF2-CaO-SiO2 fluxes: Possible electrochemical effects on weld metal
[DE88-003107] 08 p0992 N88-16004
Cleanliness tests with the Omega Meter: A comparative study for solder flux removal
[DE88-004634] 11 p1460 N88-18704
Evaluation of solder flux solvents in a vapor-degreasing application for hybrid microcircuits
[BDX-613-3638] 11 p1468 N88-18752

FLUXMETERS
U MAGNETIC MEASUREMENT
U MEASURING INSTRUMENTS

FLY BY WIRE CONTROL
Flight test of a resident backup software system
02 p0128 N88-10805
Recent Sikorsky R and D progress
09 p1111 N88-16659
Integrated Application of Active Controls (IAAC) technology to an advanced subsonic transport project: Program review
[NASA-CR-3880] 17 p2301 N88-23763
Computer system for the primary fly-by-wire control of civil transport aircraft (experimental system)
[FBW-TB-2086/88] 21 p2898 N88-27204

FLYBY MISSIONS
NT ASTEROID MISSIONS
NT GIOTTO MISSION
Final phase of Project Vega 01 p0009 N88-10053
Overview of plasma observations during the Halley flybys 01 p0116 N88-10743
The status of the international Halley watch
01 p0116 N88-10744
Correlation between magnetic and electric field fluctuations observed during flyby near Halley's comet
14 p1996 N88-21897
Halley's environments by the Japanese Suisei spacecraft 14 p1999 N88-21915
Determination of the Venus flyby orbits of the Soviet Vega probes using VLBI techniques
22 p3067 N88-28203

FLYING PERSONNEL
NT AIRCRAFT PILOTS
NT ASTRONAUTS
NT COSMONAUTS
NT FLIGHT CREWS
NT ORBITAL WORKERS
NT PILOTS (PERSONNEL)
NT SPACECREWS

FLYING PLATFORM STABILITY
U AERODYNAMIC STABILITY

FLYING QUALITIES
U FLIGHT CHARACTERISTICS

FLYING WING AIRCRAFT
U TAILLESS AIRCRAFT

FLYWHEELS
Apparatus for storing kinetic energy
[EP-PATENT-0-181-736-A1] 01 p0066 N88-10422
Value-assessment of energy storage concepts in burst power systems
[DE87-013756] 09 p1187 N88-17115
An advanced low-cost 2-axis active magnetic bearing flywheel --- satellite attitude control
14 p1877 N88-21213
Qualification of the OLYMPUS reaction wheel
14 p1878 N88-21226
Evolution of large momentum and reaction wheels
14 p1879 N88-21230
Three axis attitude control system
[NASA-CASE-GSC-12970-1] 17 p2308 N88-23808
Assessment of energy storage concepts for use in sprint power 17 p2407 N88-24312
Nuclear Rankine/flywheel MMW space power concept
17 p2413 N88-24349
Energy storage for nuclear burst power systems
17 p2426 N88-24431
Value assessment of energy storage concepts in burst power systems 17 p2426 N88-24432
Rotating-hoop, pulsed-energy converter
17 p2426 N88-24433
Candidate advanced energy storage concepts for multimegawatt burst power systems
17 p2426 N88-24434

FOAMING
Investigations of the stability of the cell opening of soft polyurethane foams
[ETN-88-91481] 11 p1463 N88-18724

FOAMS
A process for producing phenolic foams
[EP-PATENT-0-170-357-A1] 01 p0026 N88-10162
Study of aeropropulsion laboratory pressure drop rig and recommended test procedure
[AD-A184333] 03 p0322 N88-12038
Flame retardant phenolic foams
[EP-PATENT-0-223-489-A2] 05 p0568 N88-13464
The effective elastic properties of low-density foams
[DE87-014629] 06 p0684 N88-14194
Foam generation and air entrainment near a free surface
[AD-A185986] 07 p0848 N88-15149
An experimental investigation of the hydrodynamic and heat-transfer behavior of aqueous foam in laminar tube flow
[DE88-0049[illegible]4] 11 p1483 N88-18855
A study of methods to predict and measure the transmission of sound through the walls of light aircraft
[NASA-CR-182656] 12 p1687 N88-20090
A three-dimensional model for the elastic properties of a foam
[DE88-006197] 15 p2046 N88-22192
Soft-ground aircraft arresting systems
[AD-A190838] 16 p2165 N88-22912
Generation and coalescence of bubbles and stability of foams under microgravity conditions
[BMFT-FB-W-86-020] 16 p2184 N88-23017
Cellular thermosetting fluoropolymers and process for making them
[NASA-CASE-GSC-13008-1] 17 p2326 N88-23894
Determination of radiative properties of fiberglass and foam insulations
[DE88-007845] 21 p2920 N88-27331
Determination of the specific area of liquid gas and the velocity of weak pressure waves in aqueous foams
[NASA-TT-20347] 24 p3373 N88-30087

FOCAL PLANE ARRAYS
U FOCAL PLANE DEVICES

FOCAL PLANE DEVICES
Experiment control and data system for an infrared detector array with maximum sensitivity
[ETN-88-91497] 09 p1136 N88-16813
Integrated focal plane star sensor
[OG-RT/86-0156] 09 p1262 N88-17562
Mid infrared multichannel focal plane breadboard --- pushbroom sensors
[RT-87/014] 14 p1982 N88-21827
The application of an image intensifier to atmospheric Cerenkov gamma ray astronomy
[MPE-PREPRINT-115] 22 p3163 N88-28839
The focal plane reception pattern calculation for a paraboloidal antenna with a nearby fence
[NASA-TM-100691] 24 p3365 N88-30039
Imaging instrument of the vegetation payload (SPOT 4)
[SNIAS-881-440-107] 24 p3386 N88-30169

FOCI
NT PLASMA FOCUS

FOCUSING
NT SELF FOCUSING
A conceptual design of Final Focus Systems for linear colliders
[DE87-012840] 02 p0234 N88-11475
Resolution limitations and optimization of the LLNL streak camera focus
[DE88-001633] 05 p0586 N88-13572
Phenomena at a focus in a laser system
[AD-A185442] 05 p0588 N88-13585
Theory of induced spatial incoherence
[AD-A185005] 05 p0651 N88-13992
Dual mode laser velocimeter
[NASA-CASE-ARC-11634-1] 06 p0709 N88-14350
A directed method for locating the focus of expansion
[AD-A185840] 07 p0906 N88-15491
Study of combination type CO2 laser welding system
[PB87-143764] 08 p0992 N88-16002
Resolution limitations and optimization of the ITT F4157 streak tube focus for fast (10 ps) operation
[DE88-003727] 09 p1169 N88-17007
A-scan ultrasound measurement of ocular changes during accommodation
[AD-A186818] 09 p1198 N88-17181
Visual attention effects on discrimination of line orientation and line arrangement
[AD-A187013] 09 p1200 N88-17190
Trace analysis by MS/MS on a double focussing mass spectrometer
[AD-A187954] 10 p1334 N88-17973
Overview of applications of Laser-Induced Breakdown Spectroscopy (LIBS)
[DE88-004314] 10 p1336 N88-17987
Generalized equations for emittance and field energy of high-current beams in periodic focusing
[DE88-004448] 10 p1404 N88-18372
Geodetic measurement of deformation east of the San Andreas fault in Central California
[NASA-CR-182709] 13 p1798 N88-20754
Focused ion beam fabrication of graded channel FET's in GaAs and Si
[AD-A189166] 13 p1845 N88-21040
Manufacturing of ultrasonic focused probes
[VTT-RR-487] 15 p2074 N88-22368
Hybrid particle simulation for focusing of rotating and propagating LIB 16 p2276 N88-23624
A multi-frame ion pinhole camera for intense ion beam transport and focusing experiments
[DE88-007283] 18 p2516 N88-24926
Aurora status and plans
[DE88-006476] 18 p2521 N88-24955
Aurora status and plans
[DE88-006476] 18 p2521 N88-24955
Heavy ion fusion system assessment: Final focus and transport model
[LBL-23040] 19 p2725 N88-26183
Microfocus X-ray techniques for flaw location
[DE88-008636] 20 p2812 N88-26680
Signal processing software for ground penetrating radar, user's manual
[AD-A194286] 23 p3203 N88-29059
Image focusing in space and time
[AD-A195839] 24 p3429 N88-30410

FOETUSES
U FETUSES

FOG
A proposal of the nowcasting system for sea fog
02 p0202 N88-11264
Forecasting boundary layer clouds and fog: A review of operational numerical models
02 p0208 N88-11307
Two-dimensional numerical modeling of the life cycle of fog 02 p0209 N88-11311
Numerical modeling of radiation fog
08 p1017 N88-16166
Scattering of optical radiation by bursting water particles in fog 09 p1236 N88-17410
Fog, rain and aerosol attenuation in the atmosphere
[AD-A190867] 16 p2235 N88-23350
Rapid-scanning Fourier transform spectrometer for studies of propagation of near-millimeter-wave radiation through clear air and fog
[AD-A193752] 22 p3070 N88-28219
Flow visualization on a small scale
[AD-A194728] 23 p3181 N88-28935

FOIL BEARINGS
Foil gas bearing system endurance testing dynamic isotope power system 17 p2405 N88-24302

FOILS
Chromic acid anodizing of aluminum foil
[NASA-CR-178417] 07 p0837 N88-15077

FOILS (MATERIALS)
NT METAL FOILS
Multilayered foils as radiation entrance windows and spectral filters for image converters in the ultrasoft X-ray wavelength region
[MPE-PREPRINT-90] 02 p0176 N88-11099
RIIM two-pulse injector experiments
[DE88-000926] 05 p0653 N88-14005

FOKKER AIRCRAFT
NT F-27 AIRCRAFT

FOKKER BOND TESTERS
U ADHESION TESTS

FOKKER F 27 AIRCRAFT
U F-27 AIRCRAFT

FOKKER FRIENDSHIP AIRCRAFT
U F-27 AIRCRAFT

FOKKER-PLANCK EQUATION
Nonequilibrium fluctuations and transport in sheared fluids 03 p0316 N88-11999
Boltzmann-Fokker-Planck calculations using standard discrete-ordinates codes
[DE88-005393] 11 p1537 N88-19185
Propagator solutions of partial differential equations applied to plasma transport
[DE88-006432] 13 p1816 N88-20852
Memory efficient evaluations of nonlinear stochastic equations and C3 applications
[AD-A189872] 15 p2110 N88-22569
Multigroup flux-limited asymptotic diffusion Fokker-Planck equation
[DE88-700958] 15 p2118 N88-22615
Nonlinear stochastic interaction in aeroelastic structures
[AD-A193427] 21 p2961 N88-27589

FOLDING
Nonpreemptive run-time scheduling issues on a multitasked, multiprogrammed multiprocessor with dependencies, bidimensional tasks, folding and dynamic graphs
[DE88-003598] 09 p1223 N88-17335
Motion synchronization of a mechanism to deploy and restow a truss beam 14 p1925 N88-21474
Theoretical study of the folded waveguide
[DE88-007877] 19 p2654 N88-25759

FOLDING STRUCTURES
Multisurface control mechanism for a deployable antenna: Far Infrared and Submillimeter Space Telescope (FIRST) technology study
[RP-FA-D003] 09 p1135 N88-16807
Automatic in-orbit payload deployment mechanisms, logistic operations and transport vehicle design compatibilities 12 p1586 N88-19493
The CTM program of masts and the CTM engineering model --- spacecraft mechanism
14 p1874 N88-21196
The development status of the strongback array --- spacecraft structure 14 p1875 N88-21201
The X-beam as a deployable boom for the space station 14 p1925 N88-21473
Alternative module configurations for advanced solar arrays on low orbit and extended lifetime missions (AMOC 2)
[ESA-CR(P)-2581] 24 p3389 N88-30182

FOLIAGE
Stochastic modeling of EM scattering from foliage
[AD-A192258] 20 p2790 N88-26553
Foliar nitrate reductase: A marker for assimilation of atmospheric nitrogen oxides
[DE88-010453] 21 p2971 N88-27648

FOOD
Controlled Ecological Life Support System. Design, Development, and Use of a Ground-Based Plant Growth Module
[NASA-CP-2479] 05 p0630 N88-13852
Irradiation preservation of seafood: Literature review
[DE88-001691] 05 p0631 N88-13858

FOOD INTAKE
The determination of nutritional requirements for Safe Haven Food Supply System (emergency/survival foods)
06 p0792 N88-14856
Operation Everest 2: Nutrition and body composition
[AD-A186449] 08 p1049 N88-16333

FOOD PROCESSING
NT PRESERVING
Food irradiation seminar: Asia and the Pacific
[DE88-700432] 09 p1202 N88-17203
International cooperative effort to establish ASTM (American Society for Testing and Materials) standards for the measurement of radiation dose for food processing
[DE88-002702] 10 p1372 N88-18190
An economic analysis of a multi-commodity fruit and vegetable irradiator
[DE88-003425] 11 p1524 N88-19098

FOOD PRODUCTION (IN SPACE)
Food production and gas exchange system using blue-green alga (spirulina) for CELSS
03 p0358 N88-12253
Biomass recycle as a means to improve the energy efficiency of CELSS algal culture systems
03 p0358 N88-12254
Non-conventional approaches to food processing in CELSS. 1: Algal proteins: Characterization and process optimization 03 p0358 N88-12256
Sunlight supply and gas exchange systems in microalgal bioreactor 03 p0359 N88-12258
A review of recent activities in the NASA CELSS program 03 p0359 N88-12259
Mass balances for a biological life support system simulation model 03 p0361 N88-12272
Modeling the growth dynamics of four candidate crops for Controlled Ecological Life Support Systems (CELSS)
06 p0799 N88-14889
Regenerative life support system research
[NASA-CR-182606] 12 p1671 N88-20006

FOOTPRINTS
Maneuverable reentry vehicle trajectory footprints: Calculation and properties
[DE88-004726] 10 p1292 N88-17726

FORBIDDEN TRANSITIONS
Migration and transfer of triplet energy in selected polymer systems
[DE87-014432] 02 p0152 N88-10953
Theoretical studies of atomic transitions
[DE88-004719] 10 p1407 N88-18389
Macroscopic quantum jumps in a single atom
14 p1975 N88-21784
Forbidden transitions as ion-temperature sensitive lines 17 p2441 N88-24520

FORBUSH DECREASES
Overview of the MONSEE UAG report on STIP intervals No. 15 and 16. The 24-25 April 1984 Forbush decrease period 01 p0111 N88-10712

FORBUSH EFFECT
U FORBUSH DECREASES

FORCE
Repulsive force support system feasibility study
[NASA-CR-178400] 04 p0402 N88-12497

FORCE DISTRIBUTION
Lift distribution and velocity field measurements for a three-dimensional, steady blade/vortex interaction
[NASA-TM-100013] 07 p0815 N88-14962
Computer aided deflection measurement of an aircraft wing
[AD-A187778] 12 p1581 N88-19461
Force distribution and trajectory control for closed kinematic chains with applications to walking machines
13 p1779 N88-20642
Linear force device
[NASA-CASE-MSC-20549-2] 18 p2516 N88-24927

FORCE FIELDS
U FIELD THEORY (PHYSICS)

FORCE-FREE MAGNETIC FIELDS
Coronal magnetic fields produced by photospheric shear
[NASA-CR-181514] 03 p0390 N88-12447

FORCED CONVECTION
Effects of forced and free convections on structural temperatures of space shuttle orbiter during reentry flight
[NASA-TM-86800] 01 p0043 N88-10275
Dynamics and routes to chaos from quasiperiodicity
03 p0312 N88-11974
Regressed relations for forced convection heat transfer in a direct injection stratified charge rotary engine
[NASA-TM-100124] 05 p0549 N88-13345
Review of nucleation and incipient boiling under pool and forced convection conditions
08 p0982 N88-15938
Forced-convective boiling in small diameter tube
20 p2783 N88-26510

Stability experimental results of cable-in-conduit superconductor for fusion
[DE88-753424] 23 p3290 N88-29589
Impact of ETO propellants on the aerothermodynamic analyses of propulsion components
[NASA-TM-101303] 24 p3374 N88-30094

FORCED OSCILLATION
U FORCED VIBRATION

FORCED VIBRATION
Assessment of structural integrity from forced vibration testing
[DE87-014642] 02 p0191 N88-11195
Mechanical and flow excited vibrations of elastic plates and cylindrical shells in dense fluids
03 p0316 N88-11996
Structural frequency functions for an impulsive, distributed forcing function
[DE87-013811] 03 p0333 N88-12101
A review of two-phase flow-induced vibration
[DE88-001955] 09 p1160 N88-16955
Flaw identification from forced vibration testing
[DE88-002641] 10 p1342 N88-18018
Finite element methodology for nonlinear free and harmonic forced vibrations of beam and plate structures
13 p1782 N88-20663
The concept of an impact resonance diagram for characterizing the nonlinear response of impact vibration
[DE88-005475] 15 p2086 N88-22432
Forced response unsteady aerodynamics in a multistage compressor 18 p2512 N88-24903
Experimental and theoretical investigation of passive damping concepts for member forced and free vibration
[NASA-CR-183082] 20 p2814 N88-26693

FORCED VIBRATORY MOTION EQUATIONS
U EQUATIONS
U FORCED VIBRATION

FOREBODIES
NT ABLATIVE NOSE CONES
NT NOSE CONES
NT NOSES (FOREBODIES)
NT ROCKET NOSE CONES
Surface flow visualization of separated flows on the forebody of an F-18 aircraft and wind-tunnel model
[NASA-TM-100436] 14 p1863 N88-21127
Wind-tunnel investigation of actuated forebody strakes for yaw control at high angles of attack
17 p2299 N88-23754
Actuated forebody strakes
[NASA-CASE-LAR-13983-1] 18 p2464 N88-24628

FORECASTING
NT DELPHI METHOD (FORECASTING)
NT LONG RANGE WEATHER FORECASTING
NT NOWCASTING
NT NUMERICAL WEATHER FORECASTING
NT PERFORMANCE PREDICTION
NT PREDICTION ANALYSIS TECHNIQUES
NT STATISTICAL WEATHER FORECASTING
NT TECHNOLOGICAL FORECASTING
NT WEATHER FORECASTING
Testimony to the US Senate on the greenhouse effect
[DE87-013995] 01 p0071 N88-10458
Hanford Meteorological Station computer codes. Volume 2: The PROD computer code
[DE87-014807] 02 p0215 N88-11355
Forecast of current patterns for an eddy tracking experiment in the Norwegian coastal current
[PB87-224853] 06 p0747 N88-14595
Recent Colorado State University tropical cyclone research of interest to forecasters
[AD-A185996] 07 p0879 N88-15332
Forecasting complications of cardiovascular disease in flight personnel 10 p1361 N88-18136
A comparison of projection methods in the forecasting of overhead costs for seven government aerospace contractors
[AD-A187572] 10 p1425 N88-18514
Specific features of emanation, temperature and hydrodynamic fields in the epicentral zone of tectonic earthquake
[DE88-701140] 17 p2373 N88-24114
An investigation of Soviet capabilities in extended range arctic ice forecasting
[AD-A191082] 17 p2376 N88-24127
FAA aviation forecasts fiscal years 1988-1999
[AD-A191711] 18 p2455 N88-24576
Modelling and forecasting deep ocean and near surface mesoscale eddies: Hindcasting and forecasting with, and coupling a surface boundary layer model to, the Harvard quasigeostrophic model 19 p2694 N88-26013
Prospects for hot dry rock in the future
[DE88-010909] 20 p2820 N88-26730
An interagency working group on lightning threat warning
[DE88-009828] 20 p2826 N88-26767

FORECASTS
U FORECASTING

FOREIGN BODIES
The influence of foreign particles on bearing metals
[NASA-TT-20155] 20 p2775 N88-26454

FOREIGN POLICY
NT INTERNATIONAL COOPERATION
NT INTERNATIONAL RELATIONS
Technology transfer to China. Volume 2: Working papers, part 2
[PB88-158712] 14 p1992 N88-21873
Bayesian solutions to a 2 × 2 decision matrix using interval scaled payoffs with an application to foreign policy decisions
[AD-A190863] 16 p2260 N88-23511
Department of Defense Statement on the Balanced Technology Initiative to the Committee on Armed Services, United States Senate, 100th Congress, second session
[AD-A191841] 18 p2588 N88-25378

FOREIGN TRADE
U INTERNATIONAL TRADE

FORENSIC SCIENCES
U LAW (JURISPRUDENCE)

FOREST FIRES
Evaluation of a burned area and the vegetation regeneration affected by the burning in the Parque Nacional de Brazilia through TM/LANDSAT data
17 p2363 N88-24073
History of wildland fires on Vandenberg Air Force Base, California
[NASA-TM-100983] 18 p2549 N88-25134

FOREST MANAGEMENT
Use of SPOT panchromatic imagery to update forest maps of northern Quebec, Canada
03 p0344 N88-12172
Stand based forest inventory from SPOT IMAGE. First experiments 03 p0344 N88-12173
Applicability of SPOT for forest inventory, mapping and change monitoring 03 p0344 N88-12174
Effects of fire on composition, biomass, and nutrients in oak scrub vegetation on John F. Kennedy Space Center, Florida
[NASA-TM-100305] 08 p1020 N88-16182
Investigations on the application of space photographs (Spacelab metric camera) for routine inventories of extensively managed forest areas
[DFVLR-FB-87-22] 09 p1185 N88-17098
Report of the participation in the International Training Course: Remote Sensing in Village Forestry
[INPE-4476-NTE/278] 12 p1637 N88-19802
The radar scattering coefficient as a function of forest stand parameters and viewing angle. An empirical study of the Pinus sylvestris L. in the Kootwijk forest (The Netherlands), extended with observations in the Speulder and Sprielder forest (The Netherlands)
[ETN-88-91348] 13 p1760 N88-20527
Earth resources: A continuing bibliography with indexes (issue 57)
[NASA-SP-7041(57)] 16 p2229 N88-23314
Utilization of TM/LANDSAT images in the implanted forests mapping in the Mogi-Guacu Region (SP-Brazil)
17 p2357 N88-24042
Mobile satellite communications in the Forest Service
19 p2654 N88-25757
Satellite remote sensing for forest management. A review illustrated with research results on SPOT 1 data
22 p3106 N88-28443
An evaluation of the utility of SPOT and Thematic Mapper data for providing forest inventory information
22 p3106 N88-28444
SPOT-1 satellite imagery for forest inventory in Sweden 22 p3106 N88-28445
Forest management applications of SPOT data in Australia 22 p3106 N88-28447
SPOT multispectral data and maritime pine stands in southwest of France 22 p3106 N88-28448
Stand-based forestry inventory from SPOT image
22 p3106 N88-28449
Potential of SPOT imagery as a tool for forest mapping in Quebec 22 p3107 N88-28450
Assessment of large area forest disturbances caused by biotic and abiotic factors on the basis of SPOT images 22 p3107 N88-28451

FORESTS
NT RAIN FORESTS
Investigation of large scale impact of air pollution components on forest ecosystems in Bavaria, West Germany
[DFVLR-FB-87-17] 01 p0068 N88-10434
Correlation between aircraft MSS and LIDAR remotely sensed data on a forested wetland in South Carolina
[NASA-TM-89643] 02 p0193 N88-11204
Development of a method for forest damage inventory using multispectral scanner data
[KFK-PEF-25] 03 p0345 N88-12182
Proceedings of the Third Airborne Imaging Spectrometer Data Analysis Workshop
[NASA-CR-181552] 05 p0611 N88-13755
The use of airborne imaging spectrometer data to determine experimentally induced variation in coniferous canopy chemistry 05 p0612 N88-13761
Overview of Austrian Airborne Imaging Spectrometer (AIS) programme and first results
05 p0612 N88-13762
Improved canopy reflectance modeling and scene inference through improved understanding of scene pattern
[NASA-CR-182488] 10 p1347 N88-18049
Mapping of the mangroves of the Guanabarra Bay through the utilization of remote sensing techniques
[INPE-3942-TDL/229] 12 p1637 N88-19804
Proceedings of the Forest Atmosphere Interaction Workshop
[CONF-8510250] 12 p1641 N88-19824
Remote sensing of earth terrain
[NASA-CR-182677] 13 p1790 N88-20711
Report of Atmospheric-Canopy Exchange Panel
[DE88-004478] 14 p1944 N88-21597
Aerodynamic aspects of the Amazon Forest
[INPE-4445-TDL/313] 15 p2098 N88-22501
Detection, monitoring and analysis of some environmental effects of fires in the Amazon region through utilization of NOAA and LANDSAT satellite imagery and aircraft data
[INPE-4503-TDL/326] 16 p2230 N88-23322
Radar penetration in the Amazonian rain forest
17 p2352 N88-24015
A proposal for a project entitled assessment of forest resources in Uruguay submitted to the United Nations Industrial Development Organization (UNIDO)
17 p2352 N88-24016
Airborne and spaceborne radar images for geologic and environmental mapping in the Amazon rain forest, Brazil
17 p2353 N88-24021
The use of SLAR and SIRA imagenes for the classification of forest typen in tropical rain forests
17 p2356 N88-24036
Utilization of TM/LANDSAT images in the implanted forests mapping in the Mogi-Guacu Region (SP-Brazil)
17 p2357 N88-24042
Anomalies in the vegetation in the Alto Xingu - MT
17 p2357 N88-24043
Radar penetration in the Amazonian rain forest
17 p2358 N88-24044
Stereoscopic photographs, ground and aerial, of trees used in the arborization of Curitiba (PR)
17 p2366 N88-24091
Mapping of plant associations and the variation of surface water in the Pantanal Mato-Grossense National Park, through remote sensing techniques
17 p2366 N88-24092
Interpreting forest biome productivity and cover utilizing nested scales of image resolution and biogeographical analysis
[NASA-CR-183036] 20 p2817 N88-26711
Spatial and spectral registration of Javanese landscape units with SPOT 22 p3092 N88-28362
Forest mapping by visual interpretation of SPOT images 22 p3106 N88-28446
Contribution to the mapping of forests in an intensively divided area, with the help of SPOT image data
22 p3107 N88-28453
SPOT 1: Image utilization, assessment, results. A study of the Elburgon Forest area (Kenya) showing the spectral responses of different forest tree species
22 p3107 N88-28454
A linear-time algorithm for finding a minimum spanning pseudoforest
[AD-A194029] 23 p3250 N88-29346
Recent measurements of ozone in the Amazon forests
[INPE-4494-PRE/1258] 24 p3389 N88-30185
Investigation of the large scale impact of air pollution components on forest ecosystems in Bavaria
[ESA-TT-1087] 24 p3390 N88-30187
Some results from the Amazon Forest micrometeorological experiment
[INPE-4631-PRE/1346] 24 p3403 N88-30263

FORGING
Isothermal forging and its effect on the microstructure of powder route nickel alloy AP1
[RAE-TM-P-1094] 01 p0022 N88-10138
Status of titanium alloys R and D described
03 p0298 N88-11876
The effect of deformation rate on JBK-75 stainless steel forgings
[DE88-001696] 07 p0834 N88-15061
Brief evaluation of the alloy 17-4-PH (Z5 CNU 17-04). Semifinished product: 205 mm dia forged roller, test reports
[DF/NH-3616/84] 17 p2322 N88-23866

FORM
U SHAPES

FORM PERCEPTION
U SPACE PERCEPTION
FORMALDEHYDE
Evidence for first polymer in Comet Halley: Polyoxymethylene 14 p1997 N88-21906
FORMALISM
Extending Green's function formalism to general nonlinear equations
[DE87-013541] 02 p0224 N88-11411
Algebraic specification of process algebra, including two examples
[PB88-106729] 07 p0912 N88-15531
Prediction and analysis of basic gravitational microlensing phenomena 11 p1550 N88-19272
A comparative survey of mathematical models for dynamic simulation of in-orbit manipulation operations
12 p1592 N88-19533
Body tensor formalism in finite deformation elasticity and application to the torsion of a circular cylinder
13 p1780 N88-20651
Early reheating and cosmic strings
13 p1855 N88-21103
Hamiltonian formalism in the model of the relativistic string with rigidity
[DE88-701503] 15 p2147 N88-22815
Theoretical and numerical solution of the forward-scattering problem in a circularly cylindrical configuration
[PB88-173489] 16 p2189 N88-23056
Toward a mathematical formalism of performance, task difficulty, and activation 16 p2239 N88-23372
Spatial filtering on digital images
17 p2354 N88-24025
Stochasticity in a Q-machine plasma
18 p2578 N88-25315
FORMAT
UNIX benchmark system
[AD-A184492] 03 p0367 N88-12308
Stress effects and the optimum format of a scrolling seven-line VDT text window
[AD-A185559] 06 p0758 N88-14651
DOE data exchange format specification, mechanical products/drafting. Version 1.2.2. CADCAM-045
[DE88-001923] 07 p0904 N88-15477
Innovative design of composite structures. Further studies in the use of a curvilinear fiber format to improve structural efficiency
[NASA-CR-182576] 11 p1450 N88-18641
Output formatting in Apple-soft BASIC
[DE88-701413] 15 p2108 N88-22559
Parallel binary and parallel coded decimal time code formats
[AD-A190126] 17 p2384 N88-24170
Unified interchange format for computer data (standard file format)
[ESA-STR-225] 17 p2386 N88-24183
A five-layer Open Systems Interconnection (OSI) implementation 17 p2390 N88-24204
A detection theory analysis of visual display performance
[AD-A196291] 24 p3409 N88-30292
Partitioned storage for temporal databases
[AD-A195093] 24 p3436 N88-30451
FORMATION HEAT
U HEAT OF FORMATION
FORMING TECHNIQUES
NT CASTING
NT CENTRIFUGAL CASTING
NT COLD WORKING
NT ELECTROFORMING
NT EXPLOSIVE FORMING
NT EXTRUDING
NT FORGING
NT HOT WORKING
NT INJECTION MOLDING
NT INVESTMENT CASTING
NT PRESSING (FORMING)
NT PULTRUSION
NT ROLL FORMING
NT SLIP CASTING
NT STAMPING
Computer modeling of metal forming
[DE87-013804] 02 p0157 N88-10984
The formation of optical membrane reflector surfaces using uniform pressure loading
[DE87-012275] 03 p0376 N88-12367
Growth of short fatigue cracks in a squeeze formed aluminum alloy 05 p0598 N88-13658
TMA-microrheological testing of polymers (thermomechanical analysis)
[PB87-228805] 06 p0683 N88-14187
Composite ceramic superconducting filaments for superconducting cable
[AD-A187833] 11 p1556 N88-19312
Metals. Preliminary study for an Innovation-Oriented research Program (IOP)
[ETN-88-91317] 14 p1889 N88-21290
Innovation-Oriented research Program (IOP) metals. Annexes
[ETN-88-91318] 14 p1889 N88-21291
Simulation of thermo-mechanical forming processes: A mixed Eulerian-Langrangian finite element method
[PB88-155247] 14 p1933 N88-21530
FORMULAS
Orbit accuracy requirement of GPS for precise positioning and orbit determination within local area
13 p1756 N88-20499
FORMULAS (MATHEMATICS)
On the volume of a n-dimensional simplex
[REPT-87-16] 01 p0086 N88-10557
Incoherent radar spectra 06 p0691 N88-14230
Investigation of the higher-order elements in the SAMSON2 code
[AD-A193638] 23 p3271 N88-29465
FORMULATIONS
The effect of RDX particle size on the shock sensitivity of cast PBX formulations. 2: Bimodal compositions
[DE87-009581] 01 p0031 N88-10198
A procedure for estimating the crystal densities of organic explosives
[AD-A186023] 12 p1613 N88-19646
Investigation of the higher-order elements in the SAMSON2 code
[AD-A193638] 23 p3271 N88-29465
Large displacement and rotational formulation for laminated cylindrical shells including parabolic transverse shear
[AD-A194871] 24 p3384 N88-30158
Formulation and solution of economic equilibrium problems
[AD-A196034] 24 p3439 N88-30470
FORTRAN
Manual for GetData version 3.1: A FORTRAN utility program for time history data
[NASA-TM-88288] 01 p0081 N88-10520
EAGLES: An interactive environment for scientific computing
[DE87-013564] 01 p0084 N88-10541
IMPSOR: A fully vectorized FORTRAN code for three dimensional moving boundary problems with Dirichlet or Neumann boundary conditions
[DE87-014964] 02 p0226 N88-11427
BIMOND3: Monotone piecewise bicubic Hermite interpolation code
[DE87-014612] 02 p0229 N88-11442
Documentation of NCAR (National Centre for Atmospheric Research) CCM1 program modules
[PB87-213567] 03 p0352 N88-12220
FORTRAN compiler performance benchmarks for the IBM personal computer
[LA-10883-MS] 03 p0363 N88-12284
Los Alamos National Laboratory computer benchmarking 1986
[LA-10898-MS] 03 p0363 N88-12285
Generating meshes for finite-difference analysis using a solid modeler
[DE88-001458] 04 p0439 N88-12729
A review and analysis of Fortran 8x
[DE88-001320] 04 p0479 N88-12955
Mixing Microsoft C and Microsoft FORTRAN program modules on the IBM Personal Computer
[DE88-001947] 05 p0637 N88-13895
Microprocessor emulating the intermediate code for FORTRAN compiler
[DE88-700540] 07 p0900 N88-15452
FORTRAN 77 programming guidelines
[DFVLR-MITT-87-10] 07 p0905 N88-15487
FORTRAN 77 guidelines for the software projects RASP and ANDECS
[DFVLR-MITT-87-09] 09 p1218 N88-17301
Pattern-recognition software detecting the onset of failures in complex systems
[DE88-002861] 09 p1220 N88-17318
Debugging FORTRAN on a shared memory machine
[DE88-003589] 10 p1386 N88-18276
The Livermore FORTRAN Kernels: A computer test of the numerical performance range --- benchmark tests
[UCRL-53745] 11 p1531 N88-19144
Automatic restructuring of FORTRAN programs for parallel execution
[DE88-003585] 12 p1676 N88-20018
FORTRAN 77 error handling of the RASP library
[DFVLR-MITT-87-14] 14 p1957 N88-21669
User's manual for LINEAR, a FORTRAN program to derive linear aircraft models
[NASA-TP-2768] 14 p1967 N88-21740
Parafrase restructuring of FORTRAN code for parallel processing 16 p2221 N88-23258
A description of an automated database comparison program
[NASA-TM-100609] 16 p2253 N88-23461
CIMAG2: The computer program to generate color images
[AD-A191847] 18 p2557 N88-25175
Advances in personal computers for scientific applications
[DE88-009824] 19 p2713 N88-26107
The MAFIA approach to solving Maxwell's equations in three dimensions
[DE88-007826] 19 p2720 N88-26155
An interactive computer code for preliminary design of solid propellant rocket motors
[AD-A192869] 20 p2766 N88-26399
Directions for programming in FORTRAN 77
[NASA-TT-20317] 20 p2839 N88-26842
An expeditious technique for keyboard input of information to FORTRAN computer programs
[DE88-009617] 20 p2840 N88-26855
FORTRAN 77 implementation of abstract datatype models
[DFVLR-MITT-88-08] 21 p3000 N88-27794
A computer program package for introductory one-dimensional digital signal processing applications
[AD-A194656] 23 p3249 N88-29338
Supermap for Cray FORTRAN: A user's guide
[NASA-CR-177410] 24 p3412 N88-30308
FORWARD LOOKING INFRARED DETECTORS
U FLIR DETECTORS
FORWARD SCATTERING
Theoretical and numerical solution of the forward-scattering problem in a circularly cylindrical configuration
[PB88-173489] 15 p2189 N88-23056
Application of laser diffraction techniques to particle sizing in solid propellant rocket motors
[AD-A193841] 22 p3049 N88-28089
FOSSIL FUELS
NT COAL
NT CRUDE OIL
NT NATURAL GAS
Fluidization mechanisms in slurry flows
[DE88-005191] 13 p1766 N88-20563
FOSSIL METEORITE CRATERS
U FOSSILS
U METEORITE CRATERS
FOSSILS
Disclination structures in carbon and graphite
[AD-A191056] 17 p2322 N88-23868
FOUNDATIONS
NT PILE FOUNDATIONS
Open-graded bases for airfield pavements
[AD-A184461] 04 p0402 N88-12500
A passive vibration-cancelling isolation mount
05 p0595 N88-13636
Significance of foundation-soil separation in dynamic soil-structure interaction 05 p0596 N88-13641
Computer-Aided Structural Engineering (CASE) project: Development of design formulas for ribbed mat foundations on expansive soils
[AD-A194807] 24 p3412 N88-30307
FOURIER ANALYSIS
Ballooning modes or Fourier modes in a toroidal plasma?
[AD-A184299] 04 p0491 N88-13022
The k-grid Fourier analysis of multigrid-type iterative methods
[AD-A186315] 07 p0910 N88-15520
Computerized evaluation of interferograms of the Michelson Interferometer for Passive Atmospheric Sounding (MIPAS) Laboratory Model (LM)
08 p1019 N88-16177
Some applications of surface Raman and infrared spectroscopies to mechanistic electrochemistry involved adsorbed species
[AD-A188777] 12 p1606 N88-19602
FTIR (Fourier Transform Infrared) and FTNMR (Fourier Transform Nuclear Magnetic Resonance) study of organophosphorus surface reactions
[AD-A188337] 12 p1609 N88-19625
Non-oscillatory spectral Fourier methods for shock wave calculations
[NASA-CR-181675] 19 p2720 N88-26148
SARLAC: A relativistic electron beam code
[AD-A193134] 21 p2932 N88-27411
Comparison of 2-D Fourier and spatial techniques for removing noise in real-time X-ray radiography
[AD-A193700] 23 p3187 N88-28962
FOURIER TRANSFORMATION
NT FAST FOURIER TRANSFORMATIONS
Pyroelectric line scanner for remote IR imaging of vehicles
[DE87-012127] 02 p0235 N88-11484

Wavepacket propagation and current startup near the lower hybrid frequency in the torus
[IPPJ-840] 02 p0242 N88-11529
Precise measurement of refractive index and absorption coefficient of near millimeter wave and far infrared materials
[AD-A184538] 03 p0293 N88-11840
Homogeneous turbulence two-point closures and applications to one-point closures
03 p0312 N88-11973
Mutual admittance between slots in cylinders of arbitrary shape
[AD-A184254] 04 p0439 N88-12723
Far infrared Fourier transform spectroscopy of semiconductors
[DE88-000188] 04 p0499 N88-13072
Exploiting the IR: Solar and stellar spectroscopy in the IR 04 p0504 N88-13102
Vectorizing the FFTs on supercomputer SX system
05 p0537 N88-13270
Arrays for discrete Fourier transform
[REPT-87-019] 05 p0632 N88-13861
Development of FTMS methods for the detection of trace chemical species and development of FTMS methods for the analysis of various chemical species
[AD-A185857] 07 p0828 N88-15023
Prognosis using spectral embedding --- weather forecasting 08 p1016 N88-16157
Comparison of sensitivity and precision of holographic and speckle-interferometry methods with Fourier-plane recording 08 p1078 N88-16500
Optical Fourier transformation by lensless method with perforated mask and with modified Talbot interferometer for analysis of interferograms 09 p1236 N88-17408
An infra-red investigation of HAN (Hydroxylammonium Nitrate)-based liquid propellants
[AD-A187226] 10 p1307 N88-17815
Explicit approximations for strictly nonlinear oscillators with slowly varying parameters with applications to free electron lasers
[DE88-004116] 10 p1336 N88-17984
Accurate efficient evaluation of Bessel transform: Programs and error analysis
[AD-A187718] 11 p1536 N88-19174
Some applications of surface Raman and infrared spectroscopies to mechanistic electrochemistry involved adsorbed species
[AD-A188777] 12 p1606 N88-19602
FTIR (Fourier Transform Infrared) and FTNMR (Fourier Transform Nuclear Magnetic Resonance) study of organophosphorus surface reactions
[AD-A188337] 12 p1609 N88-19625
Optical signal processing using nonlinear optics
[AD-A188461] 12 p1691 N88-20117
Restoration techniques for redisplay of LANDSAT-5 satellite imagery
[INPE-4189-PRE/1076] 13 p1791 N88-20712
Numerical simulations of multiphoton processes in many electron atoms
[DE88-003293] 13 p1837 N88-20990
Finite elements for the computation of three-dimensional electromagnetic fields in inhomogeneous media (revised)
[PB88-173471] 16 p2190 N88-23057
Computer simulation of a motor pump unit to aid in interpreting vibration data
[DE88-004481] 16 p2223 N88-23270
Finite dimensionality in the complex Ginzburg-Landau equation
[DE88-006480] 16 p2263 N88-23534
Fabry-Perot etalons as prefilters for astronomical far infrared Fourier transform spectroscopy
[MPE-205] 16 p2273 N88-23603
Analysis of binarized Hartley phase-only filter performance with respect to stochastic noise
[DE88-007604] 18 p2519 N88-24945
Integral equation for the laser field: Multimode description of a free-electron laser oscillator
[DE88-007050] 18 p2521 N88-24956
Feature extraction using the Hough transform
[AD-A190679] 18 p2555 N88-25165
On frequency response for nonlinear systems
[RR-323] 18 p2563 N88-25221
Photon limited image processing in the space-time domain
[AD-A193142] 21 p2972 N88-27655
A wideband, high-resolution spectrum analyzer
22 p3066 N88-28194
Goldstone solar system radar performance analysis
22 p3068 N88-28206
Rapid-scanning Fourier transform spectrometer for studies of propagation of near-millimeter-wave radiation through clear air and fog
[AD-A193752] 22 p3070 N88-28219
Fourier transform of gravitational synchrotron radiation
[PREPRINT-588] 22 p3144 N88-28700
Application of the Hilbert transform to Doppler radar signals from a hypervelocity gun
[AD-A193690] 22 p3146 N88-28716
Photoacoustic Fourier transform infrared spectroscopy: An early detection technique for coatings degradation
24 p3354 N88-29968

FOURIER-BESSEL TRANSFORMATIONS
Solution of large order Fourier-Bessel equations
[ARE-TM(UHA)-88504] 23 p3272 N88-29475

FOVEA
Retinotopic mapping of the human visual system with magnetoencephalography
[AD-A189557] 13 p1810 N88-20811

FRACTALS
Processing of fractal functions by linear and nonlinear operators
[RAE-TR-85079] 01 p0088 N88-10571
Phase transition of multifractals
[DE87-014344] 03 p0383 N88-12409
Physics and chemistry 07 p0883 N88-15359
Anomalous scaling laws in multifractal objects
[NOTA-INTERNA-883] 07 p0916 N88-15565
Fractal images: Procedure and theory
[AD-A187014] 09 p1217 N88-17293
Interactive generation of fractal objects
[CWI-CS-R8706] 09 p1218 N88-17302
A fractal analysis of brittle fracture
[AD-A188334] 12 p1635 N88-19788
Image segmentation via fractal dimension
[AD-A188825] 12 p1678 N88-20033
Porosity and fractality of a cometary nucleus
14 p2004 N88-21951
Display and processing of multidimensional signals with the aid of fractal image sequences
[ETN-88-92131] 20 p2806 N88-26642
Survey of the literature on fractals with possible applications to phase change processes
[DE88-012240] 21 p2911 N88-27277
Fractal surface finish
[DE88-007972] 22 p3057 N88-28137
Theory of Laplacian fractals: Diffusion limited aggregation and dielectric breakdown model
[PREPRINT-590] 22 p3144 N88-28701

FRACTIONATION
NT CHEMICAL FRACTIONATION
NT HYDROCRACKING
High-density jet fuels from coal syncrudes, appendix 4
[DE88-003132] 10 p1307 N88-17813
Aviation turbine fuels from tar sands bitumen and heavy oils. Part 3: Laboratory sample production
[AD-A189278] 13 p1753 N88-20484
Impact-induced devolatilization and hydrogen isotopic fractionation of serpentine: Implications for planetary accretion
[NASA-CR-182877] 16 p2175 N88-22966
Turbine fuels from tar sands bitumen and heavy oil. Volume 2, phase 3: Process design specifications for a turbine fuel refinery charging San Ardo heavy crude oil
[AD-A190120] 16 p2183 N88-23011
Photochrome from green plants: Assay, purification and characterization
[DE88-007511] 19 p2702 N88-26067
Real-time measurements of the size fractionation of ambient black carbon aerosols at elevated humidities
[DE88-010870] 23 p3215 N88-29138
Crystal fractionation in the SNC meteorites: Implications for surface units on Mars 23 p3307 N88-29698

FRACTIONS
Mass flow rate influence on void fraction of two-phase helium flow
[DE88-702456] 21 p2945 N88-27495

FRACTOGRAPHY
Failure analysis of composite structure materials
[AD-A184468] 04 p0410 N88-12548
Fractographic study of fiber composites
06 p0677 N88-14146
Fatigue crack growth behavior in hydrogen gas environment 06 p0716 N88-14391
An explanation of the fractography of near-threshold fatigue in FCC metals 06 p0716 N88-14395
Fracture-mechanical, statistics and fractographic investigations on the steel 20 MnMoNi 55 in the ductile-brittle transition domain
[ETN-88-91064] 09 p1144 N88-16856
Nondestructive evaluation of structural ceramics by photoacoustic microscopy
[NASA-CR-180858] 09 p1146 N88-16868
Image correlation on an IBM-PC for characterization of advanced ceramics
[DE88-002829] 09 p1149 N88-16885
Some aspects of the mechanics and mechanisms of dynamic brittle fracture 10 p1343 N88-18028
The intergranular segregation of boron in substoichiometric Ni3Al
[DE88-004783] 11 p1462 N88-18720
Comparative investigations of indirect crack length measurement under fatigue loading in a corrosive environment
[GKSS-86/E/64] 11 p1502 N88-18972
Crack distribution and growth rates for critical fastener holes in Mirage wing RH79
[AD-A189080] 13 p1722 N88-20293
Fracture characteristics of carbon and aramid unidirectional composites in interlaminar shear and open hole tensile tests
[NLR-TR-86063-U] 13 p1735 N88-20371
A study of the dynamics of high temperature brittle intergranular fracture by acoustic emission
[AERE-R-12479] 13 p1780 N88-20650
Fractography of composite delamination
[NASA-CR-182757] 15 p2030 N88-22096
Characterization of sintered SiC by using NDE
15 p2082 N88-22413
Fractographic and microstructural evaluation of 3500-hour durability specimens
17 p2325 N88-23887
The postirradiation tensile properties and microstructure of several vanadium alloys
[DE88-007140] 19 p2615 N88-25515
Research on fractography of heat-resistant alloys
19 p2634 N88-25625

FRACTURE MECHANICS
A quantitative statistical model for cleavage fracture initiation in carbide strengthened steels
[ETN-87-90735] 01 p0025 N88-10157
Low cycle fatigue on isotropic fine-grained graphite
[DE87-702627] 01 p0028 N88-10177
Contribution to the numerical calculation of fracture-mechanical quantities for elastic and elastic-plastic material behavior, especially for mixed loads
[ETN-87-90435] 01 p0062 N88-10399
Fracture mechanical analysis of the initiation and propagation of matrix and surface cracks in thermally loaded fiber composite models
[ETN-87-90439] 01 p0062 N88-10400
New fatigue damage analysis of complex engineering components based on Finite Element Methods (FEM)
[DFVLR-FB-87-15] 01 p0062 N88-10401
Fracture mode research of boron aluminum composite materials by Acoustic Emission (AE)
[NAL-TR-927] 02 p0142 N88-10891
Elevated temperature crack growth
02 p0188 N88-11174
Composite structural materials
[NASA-CR-181416] 02 p0190 N88-11186
Applications of dislocation theory to crack growth problems 02 p0190 N88-11188
Energy changes in transforming solids
[DE87-011257] 02 p0191 N88-11194
Investigation on ductile fracture behavior of 3-inch diameter Type 304 stainless steel pipe with a circumferential through-wall crack
[DE87-753016] 02 p0191 N88-11196
Fracture mechanism of fine grain graphite under high heat fluxes
[IPPJ-842] 02 p0242 N88-11527
The Shock and Vibration Digest, Volume 19, No. 11
03 p0265 N88-11673
The Shock and Vibration Digest, Volume 19, No. 10
03 p0335 N88-12112
Application of fracture mechanics theory in the reliability analysis of structural ceramics in multiaxial loading
03 p0335 N88-12113
Investigation of reliability of strength values measured on CFRP test bars by statistical methods. Part 1: Probability distributions for strength analysis
[ESA-TT-1036] 03 p0336 N88-12115
Computational methods and results for dynamic fracture 03 p0337 N88-12123
Kinetics of crack growth: Thermal/mechanical interaction 03 p0337 N88-12124
Ceramic technology for advanced heat engines project
[DE88-001520] 04 p0420 N88-12605
Work-in-progress presented at the Army Symposium on Solid Mechanics, 1986: Lightening of the Force
[AD-A184791] 04 p0427 N88-12644
Method for the ultrasonic inspection of the soundness of the metal in weld joints in two-ply pipes
[BLL-CE-TRANS-8265-(9022.09)]
04 p0453 N88-12805
Environmentally assisted cracking: Overview of evidence for an adsorption-induced localised-slip process
[AD-A185175] 05 p0565 N88-13443
Stress intensity factors for cracking metal structures under rapid thermal loading, phase 1
[AD-A184112] 05 p0591 N88-13606
Near-threshold growth of defects in engineering materials 05 p0603 N88-13891

Interaction of microstructure and fatigue in tool steels
05 p0603 N88-13693

Environmental fracture toughness and static fatigue crack propagation of silica glass
05 p0606 N88-13716

Deformation, fatigue and fracture behavior of two cast anisotropic superalloys 05 p0608 N88-13732

Strain-energy-release rate analysis of the end-notched flexure specimen using the finite-element method
[NASA-TM-100494] 05 p0608 N88-13735

Fracture analysis of drawn composite dual-phase steel wire
[DE88-001396] 06 p0681 N88-14173

Fatigue 87, volume 2
[AD-A184046] 06 p0715 N88-14381

Fatigue life prediction modeling for turbine hot section materials
[NASA-TM-100291] 06 p0724 N88-14453

Random loading fatigue crack growth: Crack closure considerations 06 p0797 N88-14881

Fracture study of windshield glass panes
06 p0799 N88-14891

Determination of the critical crack length a (sub IC) in turbine discs
[PB87-144812] 07 p0820 N88-14986

J-estimation procedure based on moire interferometry data
[AD-A185965] 07 p0867 N88-15258

Study on fracture behaviour of a joint with a crack in transverse hard layer: Effect of hard layer width on COD
[PB87-143855] 07 p0868 N88-15267

Dislocation free zone model of fracture under reverse loading
[DE88-002676] 07 p0869 N88-15276

Interface characteristics and the mechanical properties of metal matrix composites
[AD-A186441] 08 p0966 N88-15845

Study on the correlation of polystyrene (PS) film craze to its fracture behaviour by TEM (Transmission Electron Microscopy)
[PB87-143343] 08 p0970 N88-15870

Effect of peel angle on peel force
[AD-A186117] 08 p0972 N88-15878

Solid mechanics research for quantitative non-destructive evaluation
[AD-A186599] 08 p0993 N88-16010

The relationship of tensile specimen size and geometry effects to unique constitutive parameters for ductile materials
[AD-A186020] 08 p0994 N88-16012

Elastic-plastic fracture investigation on stable crack growth for plane stress
[PB87-144820] 08 p0995 N88-16022

Study on the fracture behavior of 9 percent Ni steel welded joint
[PB87-143863] 08 p0995 N88-16023

The J-integral concept for elastic-plastic material behavior
[W-5/87] 08 p1000 N88-16059

Summary of HSST wide-plate crack-arrest tests and analyses
[DE88-002601] 08 p1000 N88-16061

NASA/Army Rotorcraft Technology. Volume 2: Materials and Structures, Propulsion and Drive Systems, Flight Dynamics and Control, and Acoustics
[NASA-CP-2495-VOL-2] 09 p1106 N88-16632

Review of fatigue and fracture research at NASA Langley Research Center 09 p1106 N88-16633

Delamination durability of composite materials for rotorcraft 09 p1107 N88-16634

Ceramics for engines 09 p1119 N88-16704

Study of the temperature dependence of the mechanical characteristics of the steels GX 5 CrNi 13 4 and GGG 40 in tensile and bending tests
[DE88-001469] 09 p1143 N88-16850

Fracture-mechanical, statistics and fractographic investigations on the steel 20 MnMoNi 55 in the ductile-brittle transition domain
[ETN-88-91064] 09 p1144 N88-16856

Influence of post-anneal cooling treatments on suppression of cryogenic intergranular fracture in experimental Ni-free high-Mn austenitic steels
[DE88-002766] 09 p1145 N88-16863

The failure and fracture analysis of adhesive bonds
[ETN-87-90713] 09 p1181 N88-17077

Finite element analysis for the calculation of calibration curves of fracture mechanics specimen for semicircular surface cracks with several starting depths, for the crack depth measurement following the dc potential method
[GKSS-87/E/19] 09 p1183 N88-17086

Fracture mechanics characterization of crack growth under creep and fatigue conditions
[W-2/87] 09 p1183 N88-17087

Boundary elements combined with singular fields for three-dimensional cracked solids
[RAE-TR-87038] 09 p1183 N88-17088

Applications of energy density theory in cyclic plasticity
[AD-A186947] 10 p1342 N88-18023

Some aspects of the mechanics and mechanisms of dynamic brittle fracture 10 p1343 N88-18028

Theoretical analysis of adhesive fracture and crack-damage interactions 10 p1343 N88-18030

Fatigue crack growth due to random loading
[DE88-004641] 10 p1345 N88-18038

Institute for Materials Science and Engineering, Fracture and Deformation Division: Technical activities, 1987
[PB88-153622] 10 p1345 N88-18039

Cavitation in model elastomeric composites
[AD-A187401] 11 p1447 N88-18625

Damage mechanics of fiber reinforced plastics: A general view 11 p1448 N88-18631

Study of the mechanical behavior of a 2-D carbon-carbon composite
[NASA-CR-182594] 11 p1451 N88-18649

Effects of sulfur content on the plain strain fracture toughness of inertia welds in 4340 steel
[AD-A188192] 11 p1458 N88-18689

Computer aided testing procedure for stress corrosion cracking investigations
[GKSS-86/E/63] 11 p1460 N88-18706

Synthesis and structure property studies of toughened epoxy resins via functionalized polysiloxanes
[AD-A187984] 11 p1462 N88-18715

Fracture mechanisms and strengthening of slab lasers
[DE88-004002] 11 p1493 N88-18914

Fracture characteristics of a viscoelastic polymer under constant load: Experiments and analysis
11 p1501 N88-18963

Numerical fracture mechanics using finite element method 11 p1501 N88-18966

Determination of the elastic-plastic fracture toughness parameters under special consideration of the activities of the European Group on Fracture (EGF)
[GKSS-87/E/30] 11 p1502 N88-18973

Study of the effects of metallurgical factors on the growth of fatigue microcracks
[AD-A188475] 12 p1608 N88-19615

A simulation of void lining during ductile fracture
[AD-A188404] 12 p1635 N88-19792

Further refinement and applications of the mixed computational algorithm for plane elastic contact problems
[AD-A188308] 12 p1683 N88-20065

High-temperature metal matrix composites
[AD-A189516] 13 p1734 N88-20367

Fracture characteristics of carbon and aramid unidirectional composites in interlaminar shear and open hole tensile tests
[NLR-TR-86083-U] 13 p1735 N88-20371

Materials Research Laboratory at Brown University
[AD-A188006] 13 p1739 N88-20396

Stress corrosion cracking and metal-induced embrittlement: Comparative studies of local chemistries
[DE88-003235] 13 p1742 N88-20419

Non-destructive evaluation techniques applied to the study of fatigue microcrack growth in steel alloys
[DE88-004090] 13 p1742 N88-20420

Fracture mechanics and creep crack growth of 1 percent Cr 1/2 percent Mo steel with and without prior exposure to creep conditions
[NLR-TR-86051-U] 13 p1743 N88-20426

Use of reinforced inorganic cement materials for spark wire and drift chamber wire frames
[NASA-CR-180759] 13 p1746 N88-20438

Fracture criterion of reactor graphite under multiaxial stresses 13 p1746 N88-20442

A study of the dynamics of high temperature brittle intergranular fracture by acoustic emission
[AERE-R-12479] 13 p1780 N88-20650

Theory and experiments of fracture in cyclic compression: Single phase ceramics, transforming ceramics and ceramic composites
[DE88-005792] 13 p1781 N88-20659

Fracture criteria for discontinuously reinforced metal matrix composites
[NASA-CR-182665] 13 p1782 N88-20662

ONR Far East Scientific Bulletin, volume 12, number 3, July-September 1987
[AD-A188554] 13 p1851 N88-21081

JPRS report: Science and technology. USSR: Materials science
[JPRS-UMS-87-009] 14 p1884 N88-21261

Crack resistance of multilayer ceramic-based composite material 14 p1885 N88-21265

The Nordic J-R curve round robin test program --- reactor steel
[VTT-RR-510] 14 p1923 N88-21459

Probabilistic analysis of crack containing structures with the PARIS code
[KFK-4286] 14 p1924 N88-21465

Investigation of the components of the energy-momentum tensor in the neighborhood of crack tips under special materials and loading conditions
[W-4/87] 14 p1934 N88-21531

Effect of loading conditions on environment-sensitive fracture
[BR102697] 14 p1934 N88-21533

Investigation of Super*Zip separation joint
[NASA-TM-4031] 15 p2026 N88-22072

Damage models for delamination and transverse fracture
[AD-A189652] 15 p2029 N88-22088

Fracture toughness testing of a ceramic matrix composite
[AD-A189846] 15 p2029 N88-22089

The effective fracture toughness of aluminum at rapid heating rates
[AD-A189745] 15 p2038 N88-22146

Stress corrosion of ceramic materials
[AD-A190501] 15 p2045 N88-22187

A test for interfacial effects and stress transfer in ceramic matrix composites
[NASA-CR-182758] 15 p2046 N88-22194

Crack opening and extension in inert solid propellant: An experimental study
[AD-A189808] 15 p2048 N88-22201

Environmentally assisted crack growth in structural alloys: Perspectives and new directions
[AD-A190137] 15 p2076 N88-22377

Lewis Structures Technology, 1988. Volume 2: Structural Mechanics
[NASA-CP-3003-VOL-2] 15 p2077 N88-22382

Computational simulation methods for composite fracture mechanics 15 p2079 N88-22396

Lewis Structures Technology, 1988. Volume 3: Structural integrity Fatigue and Fracture Wind Turbines HOST
[NASA-CP-3003-VOL-3] 15 p2081 N88-22408

Monolithic ceramic analysis using the SCARE program
15 p2081 N88-22409

Fracture technology for brittle materials
15 p2083 N88-22417

Mode 2 fracture mechanics 15 p2083 N88-22418

Elevated temperature crack growth
15 p2084 N88-22421

Large-scale wind turbine structures
15 p2085 N88-22429

Processing defects and strength of alumina substrates
[W-10/87] 15 p2087 N88-22441

A simplified key-curve approach for J-R-curve testing of CT specimens
[VTT-RR-503] 15 p2088 N88-22444

A study of failure characteristics in thermoplastic composite material
[AD-A190613] 16 p2171 N88-22940

Surface crack analysis applied to impact damage in a thick graphite-epoxy composite
[NASA-TM-100600] 16 p2173 N88-22950

A piecewise quadratic strength tensor theory for composites
[AD-A190929] 16 p2173 N88-22952

The adhesive bonding of thermoplastic composites
[AD-A190994] 16 p2173 N88-22953

Dynamic fracture toughness evaluation by measurement of CTOD
[WNS/ASD-88-02] 16 p2178 N88-22982

Fracture morphologies of carbon-black-loaded SBR (Styrene-Butadiene Rubber) subjected to low-cycle, high-stress fatigue
[DE88-006808] 16 p2181 N88-23002

Fatigue crack growth under full-scale cyclic plasticity
[DFVLR-FB-87-48] 16 p2222 N88-23263

Bimodular behavior and crack closure in compression in a brittle material
[AD-A191267] 16 p2224 N88-23275

Strain intensity factor approach for predicting the strength of continuously reinforced metal matrix composites
[NASA-TM-100617] 17 p2317 N88-23838

Structural Ceramics
[NASA-CP-2427] 17 p2323 N88-23872

Friction and wear of ceramics
17 p2323 N88-23874

Some design considerations for ceramic components in heat engine applications 17 p2323 N88-23875

Nondestructive evaluation of structural ceramics
17 p2324 N88-23876

Fracture mechanics 17 p2324 N88-23877

Structural ceramics research
17 p2324 N88-23878

Effect of test sample geometry on the fatigue crack growth of X10NiCrAlTi 32 20 and NiCr22 Co 12Mo
[JUEL-SPEZ-399] 17 p2348 N88-23990

Mechanics of instability-related delimination growth
[NASA-TM-100622] 17 p2349 N88-23998

Design of overlays for rigid airport pavements
[DOT/FAA/PM-87/19] 18 p2468 N88-24652

Mixed-mode fracture of uniaxial fiber reinforced composites
[AD-A191629] 18 p2478 N88-24700

Local delamination buckling in layered structures
18 p2480 N88-24711

Characterization of the 2219 Cegedur alloy. Data acquisition of the fracture mechanics --- aircraft construction materials
[REPT-48-442/F] 18 p2487 N88-24751

Isothermal and bithermal thermomechanical fatigue behavior of a NiCoCrAlY-coated single crystal superalloy
[NASA-TM-100907] 18 p2489 N88-24766

Fracture of solid state lasers
[DE88-007023] 18 p2522 N88-24961

Stress corrosion cracking of A723 steel pressure vessels: Two case studies
[AD-A191741] 18 p2527 N88-24990

Fracture mechanics analysis for short cracks
[AD-A192002] 18 p2527 N88-24992

Investigation of the effect of minimum loads and compression of load spectra on the prediction capacities of the ONERA crack model --- wings
[ONERA-RTS-33/7169-RY-064-R]
18 p2527 N88-24994

Self-consistent model for the brittle response of solids
18 p2528 N88-24999

Analysis and developments of failure concepts in fracture mechanics based on research results in the field of component safety topics: J-integral concept, crack resistance curves, dynamic criterion
[V-19/86] 18 p2530 N88-25009

An assessment of the state of the art in predicting the failure of ceramics
[DE88-008998] 19 p2621 N88-25551

Dimensional analysis and experimental observation of the coupling phenomena between combustion and fracture of damaged propellant samples
19 p2630 N88-25603

Research on fractography of heat-resistant alloys
19 p2634 N88-25625

A simple unified method for predicting the deflections of reinforced concrete structures
19 p2679 N88-25930

The effects of thin compressive films on indentation fracture toughness measurements
[AD-A192243] 20 p2779 N88-26480

Research on the kinetics of phase changes in solids
[AD-A192222] 20 p2814 N88-26696

Prediction of fatigue growth
[NLR-MP-87052-U] 20 p2816 N88-26707

Analytical determination of critical crack size in solar cells
[NASA-CR-183128] 20 p2821 N88-26736

An investigation of soft launch and instability breakup with a two-stage light gas gun
[DE88-010371] 21 p2901 N88-27218

Processing and properties of advanced aluminum alloys
[AD-A193224] 21 p2912 N88-27284

Analysis of crack arrest toughness
[AD-A193340] 21 p2913 N88-27286

Adhesion of hydrated silicate films
[DE88-011250] 21 p2920 N88-27333

Failure analysis of laminated composite angles
21 p2959 N88-27578

Plastic yielding at crack tips
[AD-A192549] 21 p2960 N88-27582

Influence of microstructure and microdamage processes on fracture at high loading rates
[AD-A192957] 21 p2960 N88-27583

Critical issues and directions for fracture mechanics and structural integrity
[AD-A193050] 21 p2960 N88-27584

Soviet dynamic fracture mechanics research
[FASAC-TAR-3140] 21 p2962 N88-27597

Corrosion fatigue of small cracks: Mechanics and chemistry
[DE88-012121] 21 p2964 N88-27605

Size effects in linear elastic fracture mechanics
21 p2964 N88-27609

Applications of fatigue analyses: Aircraft engines
[PNR90439] 22 p3044 N88-28066

Fracture behavior in multidimensional fiber-reinforced composites 22 p3051 N88-28099

Stress corrosion evaluation of powder metallurgy aluminum alloy 7091 with the breaking load test method
22 p3053 N88-28115

Experimental investigation of ductile fracture by white light moire interferometry 22 p3087 N88-28329

Empirical fatigue crack growth data for a tension loaded threaded fastener
[AD-A194112] 22 p3088 N88-28334

Wave and fracture phenomena in impacted ceramics
[AD-A192946] 23 p3196 N88-29020

The use of a surface acoustic wave technique to study the growth behavior of small cracks in a high strength steel alloy 23 p3225 N88-29193

Results on the influence of crack tip plasticity during dynamic crack growth
[AD-A193460] 23 p3225 N88-29194

Critical conditions for failure in materials subjected to high rates of loading
[AD-A194697] 23 p3226 N88-29201

A technique for measuring area under a curve
[AD-A193559] 23 p3271 N88-29463

Constraints on the origin of fractured terrane, Northern Martian plains 23 p3304 N88-29684

Additional fracture and strength test results for A723 steel and 38644 titanium
[AD-A196329] 24 p3353 N88-29960

Stress intensity factors for cracked metallic structures under rapid thermal loading
[AES-8609709F-1] 24 p3353 N88-29962

Modeling of micromechanisms of fatigue and fracture in hybrid materials
[AD-A195604] 24 p3382 N88-30142

Obtaining stress intensity factors on cracks, by means of fitting techniques on numerical results calculated with the finite element method 24 p3384 N88-30153

FRACTURE RESISTANCE
U FRACTURE STRENGTH

FRACTURE STRENGTH

Toughening of alpha-alumina: Preliminary results
[DE87-702776] 01 p0028 N88-10178

Development of a polyimide matrix for filament winding with improved extensibility and fracture toughness for permanent use at 200 C
[BMFT-FB-T-86-118] 01 p0030 N88-10190

Interfacial strength development in thermoplastic resins and fiber-reinforced thermoplastic composites
[NASA-CR-181525] 04 p0411 N88-12549

Plastic strain localization between voids in shear deformation fields 04 p0427 N88-12648

Micromechanisms of fatigue crack growth and fracture toughness in metal matrix composites
[AD-A185200] 05 p0558 N88-13392

Fatigue mechanisms in ARALL, a fatigue resistant hybrid aluminum aramid composite material
05 p0605 N88-13711

Environmental fracture toughness and static fatigue crack propagation of silica glass
05 p0606 N88-13716

Embrittling effect of the plastic zone
05 p0607 N88-13721

Fractographic and microstructural aspects of fracture toughness testing in irradiated 304 stainless steel
[DE88-000795] 06 p0681 N88-14172

Characterization of mechanical damage mechanisms in ceramic composite materials
[AD-A185549] 06 p0686 N88-14205

The effect of non-metallic inclusions on fatigue and fatigue thresholds of 25Mn-5Cr-1Ni steel
06 p0718 N88-14410

Evaluation method of the brittle fracture strength in structurally stress-concentrated regions
[PB87-129490] 06 p0721 N88-14435

Comparison of the strength of single and multiple bolted joints in CFRP
[PB87-123766] 06 p0722 N88-14438

Fatigue, fracture and strain hardening of high carbon hardened alloy steel
[AD-A186101] 07 p0831 N88-15043

Investigation of the auto-tempering of low-carbon martensite
[PB87-143970] 07 p0833 N88-15053

New mechanism of the high temperature (reversible) temper brittleness of alloy steels
[PB87-143954] 07 p0833 N88-15056

Study on the cryogenic toughness of stainless steel weld metals
[PB87-143830] 07 p0834 N88-15057

Static and dynamic determination of aluminum oxide toughness
[PB87-146999] 07 p0869 N88-15275

Improved silicon nitride for advanced heat engines
[NASA-CR-175006] 08 p0973 N88-15886

Fracture-resistant characteristics of medium-strength plates with regard to the initiation, stable and unstable propagation of surface cracks
[PB87-144804] 08 p0996 N88-16025

Micromechanisms of fatigue crack growth and fracture toughness in metal matrix composites
[AD-A186941] 09 p1137 N88-16816

Investigation of microstructural factors that cause low fracture toughness in silicon carbide whisker/Al alloy composites
[AD-A186443] 09 p1137 N88-16817

Microstructures and properties of SiC whisker-reinforced mullite composites
[DE88-002611] 09 p1139 N88-16826

Strength and toughness of a brittle material
[VTT-RR-479] 09 p1183 N88-17089

Finite element substructuring methods for composite mechanics
[NASA-TM-100297] 10 p1296 N88-17745

Some aspects of the mechanics and mechanisms of dynamic brittle fracture 10 p1343 N88-18028

Crack arrest fracture toughness of armor steels
[AD-A187711] 11 p1456 N88-18681

Reduction of residual stresses and distortion in girth welded pipes
[AD-A187728] 11 p1494 N88-18920

Fracture toughness of steel weldments containing lack of penetration defects 11 p1501 N88-18965

Determination of the elastic-plastic fracture toughness parameters under special consideration of the activities of the European Group on Fracture (EGF)
[GKSS-87/E/30] 11 p1502 N88-18973

Microdesigning of lightweight/high strength ceramic materials
[AD-A188526] 12 p1610 N88-19631

A fractal analysis of brittle fracture
[AD-A188334] 12 p1635 N88-19788

Composites strengthening
[AD-A189258] 13 p1734 N88-20364

Fracture criterion of reactor graphite under multiaxial stresses 13 p1746 N88-20442

Degradations of thermal shock resistance and the fracture toughness of reactor graphite subjected to neutron irradiation 13 p1747 N88-20445

Application of ISRM testing methods to fracture toughness testing of graphite 13 p1747 N88-20446

Notch sensitivity of graphite materials for VHTR
13 p1747 N88-20447

Guidelines for estimation and characterization of the thermo-mechanical properties of new optical materials
[DE88-004359] 13 p1840 N88-21010

Structure and strength of boron-aluminum composites
14 p1885 N88-21264

Study of strength characteristics of glass-reinforced plastic by acoustic emissions method
14 p1885 N88-21268

Fracture toughness characterization of SA508 and Sa533B RPB steels
[CISE-3908] 14 p1889 N88-21292

Interface structure and properties of alumina/glass ceramic composites
[DE88-006219] 14 p1892 N88-21302

Growth of fatigue cracks in nickel alloys at high temperatures 14 p1896 N88-21318

The Nordic J-R curve round robin test program --- reactor steel
[VTT-RR-510] 14 p1923 N88-21459

Thermally stable deployable structure
14 p1925 N88-21472

Fracture toughness testing of a ceramic matrix composite
[AD-A189846] 15 p2029 N88-22089

Interlaminar fracture toughness of thermoplastic composites
[NASA-TM-100532] 15 p2030 N88-22097

Postbuckling delamination of a stiffened composite panel using finite element methods
[NASA-CR-182803] 15 p2030 N88-22098

The effective fracture toughness of aluminum at rapid heating rates
[AD-A189745] 15 p2038 N88-22146

Fracture toughness of silicon nitride-silicon nitride joints bonded with oxynitride glass
[DE88-005548] 15 p2043 N88-22172

Strength and microstructure of ceramics
[AD-A190712] 15 p2046 N88-22191

Computational simulation methods for composite fracture mechanics 15 p2079 N88-22396

Processing defects and strength of alumina substrates
[W-10/87] 15 p2087 N88-22441

Increasing strength of graphite/epoxy bolted joints by introducing an adhesively bonded metallic insert
[FFA-TN-1987-45] 15 p2088 N88-22442

A piecewise quadratic strength tensor theory for composites
[AD-A190929] 16 p2173 N88-22952

Dynamic fracture toughness evaluation by measurement of CTOD
[WNS/ASD-88-02] 16 p2178 N88-22982

Strength and cracking resistance of ceramics. Report 3: SiC ceramics 16 p2180 N88-22994

Ceramic matrix composites 17 p2325 N88-23888

Polymer precursors for ceramic composites
17 p2326 N88-23890

High strength/high modulus aromatic heterocyclic ABA block copolymers
[AD-A191666] 18 p2491 N88-24774

Effect of Zr or Cr content on the fracture toughness of the high purity Al-Zn-Mg alloys
[NASA-TT-20294] 19 p2616 N88-25518

Research on fractography of heat-resistant alloys
19 p2634 N88-25625
The effects of thin compressive films on indentation fracture toughness measurements
[AD-A192243] 20 p2779 N88-26480
Fracture resistance of a TiB2 particle/SiC matrix composite at elevated temperature
[NASA-TM-100967] 20 p2779 N88-26482
Analysis of transverse strength of composites using percolation theory
[AD-A193204] 21 p2904 N88-27234
Fracture behavior in multidimensional fiber-reinforced composites 22 p3051 N88-28099
Advanced processing and properties of high performance alloys
[AD-A193767] 23 p3194 N88-29010
Additional fracture and strength test results for A723 steel and 38644 titanium
[AD-A196329] 24 p3353 N88-29960
Modeling of micromechanisms of fatigue and fracture in hybrid materials
[AD-A195604] 24 p3382 N88-30142

FRACTURE TOUGHNESS
U FRACTURE STRENGTH

FRACTURES (MATERIALS)
NT CRACK TIPS
NT CRACKS
NT MICROCRACKS
NT SHORT CRACKS
NT SURFACE CRACKS
Shear failure in round bar tensile tests of Al-Zn-Mg-Cu alloys
[PB87-143632] 07 p0869 N88-15271
Institute for Materials Science and Engineering, Fracture and Deformation Division: Technical activities, 1987
[PB88-153622] 10 p1345 N88-18039
The influence of small defects on tensile specimen ductility and symmetry of deformation
[AD-A187983] 10 p1346 N88-18044
A fractal analysis of brittle fracture
[AD-A188334] 12 p1635 N88-19788
Interfacial chemistry-structure and fracture of ceramic composites
[DE88-005516] 13 p1750 N88-20461
Mixed-mode fracture of uniaxial-fiber reinforced composites
[AD-A191629] 18 p2478 N88-24700
Fracture physics of delamination of composite materials
[AD-A192021] 19 p2609 N88-25482
Irreversible deformations during fracture in polymers
[W-7/86] 20 p2780 N88-26485
Principles of a nondestructive evaluation process for damage location, damage profile, and damage extension in welded joints by radiometric measurements
[MPA-86-02] 20 p2812 N88-26683
Deformation, fracture and explosive properties of reactive materials
[AD-A193080] 21 p2923 N88-27348
Development of creep fracture modelling in ceramics
[PB88-202825] 23 p3196 N88-29021
Hydrogen embrittlement of iron-nickel alloys
[AD-A195909] 24 p3353 N88-29958

FRACTURING
NT CRACKING (FRACTURING)
NT CRUSTAL FRACTURES
NT STRESS CORROSION CRACKING
Small-diameter wire tensile testing
[DE88-000835] 04 p0455 N88-12815
The influence of the topography of fracture surfaces on crack closure 05 p0598 N88-13657
Fracture analysis of drawn composite dual-phase steel wire
[DE88-001396] 06 p0681 N88-14173
Fatigue crack growth and fracture of copper-bismuth bicrystals 06 p0715 N88-14385
Acoustic emission-microstructural relations in ferritic steels. Part 3: The effect of inclusion content
[AERE-R-12041] 10 p1341 N88-18015
Some aspects of the mechanics and mechanisms of dynamic brittle fracture 10 p1343 N88-18028
Theoretical analysis of adhesive fracture and crack-damage interactions 10 p1343 N88-18030
A study of the mechanical behavior of a 2-D carbon-carbon composite 11 p1449 N88-18638
Fracture mechanisms and strengthening of slab lasers
[DE88-004302] 11 p1493 N88-18914
A study of the dynamics of high temperature brittle intergranular fracture by acoustic emission
[AERE-R-12479] 13 p1780 N88-20650
Crack resistance of multilayer ceramic-based composite material 14 p1885 N88-21265
Fracture of solid state lasers
[DE88-007023] 18 p2522 N88-24961
Lattice theory of fracture of solids with layered structure
[DE88-701867] 20 p2876 N88-27073
Influence of microstructure and microdamage processes on fracture at high loading rates
[AD-A192957] 21 p2960 N88-27583
Evaluation of fracture models through pressurized-thermal-shock testing
[DE88-011834] 21 p2963 N88-27603
Wave and fracture phenomena in impacted ceramics
[AD-A192946] 23 p3196 N88-29020

FRAGMENTATION
Computer simulations of fragmentation
[DE87-900985] 03 p0375 N88-12358
The mechanics of fatigue-crack nucleation in a low-alloy steel under fretting conditions 05 p0597 N88-13649
The role of fragmentation in interaction of meteoroids with the Earth's atmosphere 06 p0737 N88-14532
Analysis and interpretation of satellite fragmentation data 06 p0798 N88-14885
Small-scale structure in solar flare radio emission
08 p1097 N88-16598
Splinter generator
[MBB-UA-1048/87] 11 p1491 N88-18897
Fragmentation and flow in central collisions
[DE88-005386] 13 p1837 N88-20991
Milliwatt generator project
[DE88-011261] 20 p2853 N88-26939
Studies of HZE particle interactions and transport for space radiation protection purposes
[NASA-TM-101159] 20 p2886 N88-27142

FRAMES
NT AIRFRAMES
NT CHASSIS
FABSTRAN: A computer program for frame and beam static and transient response analysis (nonlinear)
[ARE-TR-86205] 09 p1182 N88-17079
Control augmented structural synthesis
[NASA-CR-4132] 13 p1721 N88-20290
Use of reinforced inorganic cement materials for spark wire and drift chamber wire frames
[NASA-CR-180759] 13 p1746 N88-20438

FRAMES (DATA PROCESSING)
A unified framework for approximation in inverse problems for distributed parameter systems
[NASA-CR-181621] 10 p1400 N88-18346
Frame synchronization performance and analysis
11 p1473 N88-18787

FRAMING CAMERAS
Fabrication techniques used in the construction of a high resolution X-ray framing camera
[DE88-002653] 07 p0856 N88-15200

FRANCE
ISAURE: integration of security and fault tolerance in the REALITE 2000 system 02 p0127 N88-10802
Operational activity and improvements in the services and facilities of the balloon launch centers in France
08 p1030 N88-16238
The use of simulation in the development of the Airbus 12 p1702 N88-20188
Acceleration of prototype development and reduction of cost by multidisciplinary integration
12 p1704 N88-20199
EDF's studies and first choices regarding the design of electrical equipment
[NASA-TT-20222] 13 p1764 N88-20553
Evaluation of annual crop surfaces and territorial inventory in the Paris basin by combining classic statistical inquiries and SPOT data (Preliminary Evaluation Program for SPOT 127) 22 p3094 N88-28372
Detailed geological mapping of the massif of Sainte Victoire (Provence, France) using SPOT imagery. Comparison with other multisource data. New tectonic interpretation of this region 22 p3105 N88-28442
Metrology in France: Industrial aspects and its status in the world
[SNIAS-881-430-109] 22 p3146 N88-28713

FRAUNHOFER LINES
Doppler distortion of solar Fraunhofer lines in zodiacal light by reflection from interplanetary dust
19 p2740 N88-26270

FRAUNHOFER REGION
U FAR FIELDS

FREDHOLM EQUATIONS
An approximation technique for solving a system of Fredholm integral equations for asymmetric detector response functions
[AD-A190577] 15 p2121 N88-22645
Numerical solution of linear integral equations with random forcing terms 18 p2565 N88-25237
Generalized Jordan chains and two bifurcation theorems of Krasnoselskii
[AD-A192353] 21 p3008 N88-27845

FREDHOLM OPERATORS
U FREDHOLM EQUATIONS
U OPERATORS (MATHEMATICS)

FREE ATMOSPHERE
SAGE 1 and SAM 2 measurements of 1 micron aerosol extinction in the free troposphere
[NASA-CR-182945] 17 p2374 N88-24121

FREE BOUNDARIES
The method of lines for time dependent free boundary problems
[DE87-013929] 02 p0226 N88-11423
Total linearisation method for solving viscous free boundary flow problems by the finite element method
[PB87-222337] 04 p0441 N88-12737
Computation of free boundaries
[PB87-226023] 06 p0763 N88-14680
Free-boundary equilibrium problem for helically symmetric plasmas
[DE88-700101] 07 p0934 N88-15674
Free boundary problems arising in the control of a flexible robot arm
[AD-A189124] 12 p1634 N88-19781
Some numerical methods for the computation of capillary free boundaries governed by the Navier-Stokes equations
[REPT-87-69] 16 p2206 N88-23167
Free boundary control of the Markov process
[AD-A192401] 21 p3008 N88-27846

FREE CONVECTION
NT RAYLEIGH-BENARD CONVECTION
Effects of forced and free convections on structural temperatures of space shuttle orbiter during reentry flight
[NASA-TM-86800] 01 p0043 N88-10275
Thin film and gradient-driven instability mechanisms
[PB88-101522] 07 p0853 N88-15182
A Lagrangian model of dry thermals
[DM-50] 09 p1193 N88-17150
Thermosolutal convection in high-aspect-ratio enclosures
[NASA-TM-100803] 11 p1486 N88-18871
Analysis of low gravity tolerance of model experiments for space station: Preliminary results for directional solidification
[NASA-CR-182657] 12 p1614 N88-19648
Thermal cracking and variable properties effects on free boundary layer diffusion flames
[NBS/GCR-88/542] 12 p1614 N88-19652
High Rayleigh number convection in rectangular enclosures with differentially heated vertical walls and aspect ratios between zero and unity
[NASA-TM-100277] 12 p1628 N88-19739
Experimental and analytical studies of compressible vortices 19 p2665 N88-25848

FREE ELECTRON LASERS
Visible free electron laser oscillator
[AD-A183871] 01 p0051 N88-10324
Electron beam requirements for soft X-ray/XUV free-electron lasers
[DE87-011750] 01 p0051 N88-10325
Induction linac-driven free-electron lasers: Status and future prospects
[DE87-012914] 01 p0051 N88-10329
Millimeter wave tokamak heating and current drive with a high power free electron laser
[DE87-011324] 01 p0099 N88-10651
Studies on temporal field emission from stainless steel surfaces
[DE87-014237] 02 p0147 N88-10919
Brightness and coherence of radiation from undulators and high-gain free electron lasers
[DE87-011093] 02 p0177 N88-11102
Sideband suppression by an intracavity optical filter in the Los Alamos free-electron laser oscillator
[DE87-011740] 02 p0177 N88-11103
A high-power RF linear accelerator for FELs (Free-Electron Lasers)
[DE87-011795] 02 p0177 N88-11104
On the collective variables description of a high gain free electron laser
[DE87-013315] 02 p0178 N88-11108
Development of a high-energy crowbar for the Los Alamos free-electron laser
[DE87-014748] 02 p0179 N88-11113
Effects of injection of free electron lasers on axial velocity spread of beams 03 p0299 N88-11878
Status, development of laser devices in China
03 p0303 N88-11907
Analysis of undulator field errors for XUV FELs (Extreme Ultraviolet Free Electron Laser)
[DE87-014734] 03 p0328 N88-12073
A microwave FEL (Free Electron Laser) code using waveguide modes
[DE88-000225] 03 p0330 N88-12084
Spectral evolution equation for the sideband instability in a free-electron laser oscillator
[DE88-000510] 04 p0447 N88-12771

The free electron laser sideband instability reconsidered
[AD-A184269] 04 p0447 N88-12773

High-power RF-pulsed modulators for the Los Alamos free-electron laser
[DE88-000514] 04 p0448 N88-12775

The lasertron RF generator for FEL (Free-Electron Laser) applications
[DE88-000515] 04 p0448 N88-12776

Analysis of sideband spectra from untapered undulator using analytical technique
[DE87-014763] 04 p0448 N88-12778

Output power enhancement of AC Raman free-electron laser
[DE88-000503] 04 p0449 N88-12786

The generation and suppression of synchrotron sidebands
[DE88-000532] 04 p0449 N88-12787

Comparison of sideband spectra obtained from analytical formula and from numerical simulation in free-electron laser
[DE88-000521] 04 p0450 N88-12789

A long electromagnetic wiggler for the paladin free-electron laser experiments
[DE88-000970] 05 p0588 N88-13589

Development of a strong electromagnet wiggler
[DE88-000971] 05 p0645 N88-13952

Development of a laced electromagnetic wiggler
[DE88-000972] 05 p0646 N88-13953

Laser development, evolution of applied technologies described 06 p0689 N88-14221

Strategic Defense Initiative Organization/DARPA (Defense Advanced Research Projects Agency) workshop on laser propulsion. Volume 1: Executive summary
[DE87-003254] 06 p0768 N88-14722

High repetition rate electron beam RF-acceleration and sub-millimeter wave generation via a free electron laser
[AD-A186066] 07 p0858 N88-15209

Chapter 2: Threshold for Raman conversion of FEL laser pulses in the atmosphere
[DE88-002470] 07 p0859 N88-15215

Phase control of the microwave radiation in free electron laser two-beam accelerator
[DE88-001460] 07 p0859 N88-15219

The structure of the sideband spectrum in free electron lasers
[AD-A186952] 09 p1170 N88-17015

Intrinsic corrections to optical guiding in a free-electron laser: Beam Research Program
[DE88-002667] 09 p1172 N88-17026

Mode media interactions in an FEL (Free Electron Laser)
[DE88-003155] 09 p1172 N88-17029

Intense electron beams
[DE88-002456] 09 p1247 N88-17474

Microwave system for the microwave Tokamak experiment (MTX)
[DE88-002391] 09 p1250 N88-17487

Conceptual designs of a 50 NM FEL (Free-Electron Laser) oscillator and a 20-40 NM SASE (Self-Amplified Spontaneous Emission) amplifier
[DE88-003150] 10 p1334 N88-17974

Emittance studies at the Los Alamos National Laboratory Free-Electron Laser (FEL)
[DE88-003146] 10 p1334 N88-17975

Physics modeling support contract
[DE88-004039] 10 p1335 N88-17980

Preliminary injector, accelerator, and beamline design for rf-linac-driven XUV free-electron lasers
[DE88-003185] 10 p1336 N88-17983

Explicit approximations for strictly nonlinear oscillators with slowly varying parameters with applications to free electron lasers
[DE88-004116] 10 p1336 N88-17984

Betatron oscillations in a free electron laser
[DE88-004859] 10 p1337 N88-17990

Tapered wiggler analysis of high gain free electron laser oscillators
[AD-A187997] 10 p1338 N88-17997

Where directed energy stands in strategic defense
[DE88-005092] 10 p1403 N88-18365

The stability of free-electron lasers against filamentation
[DE88-004712] 10 p1414 N88-18435

Microwave radiation from rotating, annular electron beams 11 p1475 N88-18801

Experimental results of a high-gain microwave FEL operating at 140 GHz
[DE88-004358] 11 p1492 N88-18907

Development of electrostatic-accelerator free-electron lasers
[AD-A189507] 13 p1774 N88-20614

Wiggler taper optimization for free-electron-laser amplifiers with moderate space-charge effects
[DE88-003758] 13 p1775 N88-20618

Projected performance of RF-linac-driven free-electron lasers in the VUV and soft X-ray regions
[DE88-004294] 13 p1776 N88-20625

Effect of electron beam divergence on the gain of free electron lasers 14 p1902 N88-21358

Research on variable-period wiggler type free electron lasers 14 p1902 N88-21360

Pulsed magnet fields for free-electron lasers
14 p1903 N88-21367

Extension of free-electron lasers into the extreme ultraviolet
[DE88-005373] 15 p2070 N88-22341

Program to research laser-driven thermionic electron sources for free electron lasers
[AD-A190473] 15 p2072 N88-22353

The new UCSB (University of California, Santa Barbara) compact far-infrared FEL
[AD-A190864] 16 p2212 N88-23203

Free electron lasers in strategic defense
[DE88-007024] 17 p2394 N88-24231

Integral equation for the laser field: Multimode description of a free-electron laser oscillator
[DE88-007050] 18 p2521 N88-24956

Reducing sensitivity to errors in free electron laser amplifiers
[DE88-007017] 18 p2522 N88-24960

Progress toward a soft X-ray FEL
[DE88-007669] 19 p2675 N88-25905

Generation of coherent soft X-rays using a single-pass free-electron laser amplifier
[DE88-009137] 19 p2675 N88-25907

Application of pulse compression and shaping to the FEL photoelectric injector
[DE88-007908] 19 p2675 N88-25910

The free-electron laser: Theoretical innovations and gas-loaded experiment 20 p2806 N88-26646

The propagation of irradiance moments of an aberrated, apodized FEL beam
[DE88-008972] 20 p2806 N88-26648

The chirped-pulse free-electron laser
[DE88-009289] 20 p2807 N88-26651

Novel magnetic materials research using free electron lasers
[DE88-009989] 20 p2807 N88-26652

Optical guiding in the separable beam limit
[AD-A192452] 21 p2952 N88-27534

Efficiency optimization for FEL oscillators
[AD-A192541] 21 p2952 N88-27536

Research opportunities below 300 nm at the NBS Free-Electron Laser Facility
[AD-A193100] 21 p2953 N88-27538

Initial electron distributions for free-electron lasers generated by injector and accelerator simulations
[DE88-007022] 21 p2953 N88-27540

Development of a free-electron laser user facility for the extreme ultraviolet
[DE88-007892] 21 p2953 N88-27541

Transverse resistive wall instability in a high-power, short-wavelength free-electron laser
[DE88-011730] 21 p2954 N88-27549

On the small signal gain of free electron lasers in the low-current regime
[DFVLR-FB-88-10] 21 p2955 N88-27552

Genetic effects of low level microwave radiation
[AD-A192687] 21 p2984 N88-27722

Guided radiation beams in free electron lasers
[AD-A194525] 22 p3082 N88-28305

Free electron lasers with small period wigglers
[DE88-011627] 23 p3218 N88-29156

The NBS/NRL (National Bureau of Standards/Naval Research Laboratory) free electron laser facility
[AD-A194214] 23 p3219 N88-29159

Analysis of free electron laser performance utilizing the National Bureau of Standards CW microtron
[AD-A194217] 23 p3219 N88-29160

Research on a two-stage free electron laser oscillator
[AD-A195991] 24 p3377 N88-30115

Bibliography of Soviet laser developments, number 88, March - April 1987
[AD-A195976] 24 p3378 N88-30116

Vanderbilt free electron laser project in biomedical and materials research
[AD-A195961] 24 p3378 N88-30121

Ultrafast processes and spectroscopy with free electron lasers
[AD-A195248] 24 p3379 N88-30126

FREE ELECTRONS

Inelastic mean free paths of electrons and positrons in matter
[DE88-008086] 20 p2851 N88-26929

FREE ENERGY

NT GIBBS FREE ENERGY

Soliton twin boundaries of the cubic-tetragonal martensitic transformations in ferroelastic materials
[DE87-014741] 04 p0495 N88-13047

A study of the free energy of the Lenz-Ising model using the cluster variation method of Morita
[AD-A186023] 08 p1073 N88-16476

Theory of the tetragonal-to-orthorhombic structural phase transition in La2CuO4
[AD-A187141] 09 p1254 N88-17514

Free energy calculation via MD (molecular dynamics): Methodology and application to bicrystals
[DE88-002902] 09 p1256 N88-17532

Surface free energy of laser-produced bond percolators
[PB88-130885] 11 p1493 N88-18913

On the theory of the conversion of metallic mixed phases. 5: Fluctuations and nucleation in sub-cooled phases
[NASA-TT-20249] 14 p1890 N88-21296

FREE FLIGHT

Non-linear maximum likelihood estimation of stability derivatives from range data
[NAL-TM-SE-8608] 05 p0552 N88-13365

Australian aerodynamic design codes for aerial low bodies
[AD-A189048] 13 p1715 N88-20256

Effect of rotation on the lateral stability of a free-flying column subjected to an axial thrust with directional control
[AD-A188690] 13 p1728 N88-20338

Proof-of-principle high speed electronic imaging system, phase 2
[AD-A193798] 23 p3181 N88-28937

Motion planning for a free-flying robot
23 p3255 N88-29378

FREE FLOW

NASA-VOF3D: A three-dimensional computer program for incompressible flows with free surfaces
[DE87-011849] 01 p0045 N88-10288

Measurement of airfoil heat transfer coefficients on a turbine stage 02 p0186 N88-11156

Effects of free stream turbulence, Reynolds number and incidence angle on axial turbine cascade performance
05 p0548 N88-13339

Measurements of the free stream fluctuations above a turbulent boundary layer
[NASA-TM-100036] 06 p0704 N88-14321

Transport and stability properties of free shear flows
13 p1768 N88-20577

Temperature estimates for a free flowing railgun plasma
[MRL-R-1054] 13 p1843 N88-21032

Instruments for use in experimental studies of complex turbulent shear flow: Three component LDVs
[AD-A190526] 15 p2065 N88-22312

Effect of freestream turbulence on a two dimensional cascade, with different surface roughness, at high Reynolds number
[AD-A190615] 15 p2065 N88-22316

Film cooling effectiveness on a flat plate in high free-stream turbulence using a single row of 30 deg slant-hole injectors
[AD-A190500] 15 p2147 N88-22816

Experimental study of bypass transition in a boundary layer
[NASA-TM-100913] 16 p2209 N88-23186

Stagnating turbulent reacting flows
[AD-A191449] 18 p2508 N88-24877

Study of the structure of turbulence in accelerating transitional boundary layers
[AD-A191698] 19 p2663 N88-25837

Experimental study of unsteady separating turbulent boundary layers
[AD-A192997] 21 p2943 N88-27477

Unsteady water channel
[AD-A194231] 23 p3171 N88-28884

Containment of a silicone fluid free surface in reduced gravity using barrier coatings
[NASA-TM-101314] 24 p3371 N88-30072

FREE JETS

Experimental study of three-dimensional turbulent jet-solid boundary interaction 01 p0046 N88-10293

Heat transfer with very high free stream turbulence
02 p0186 N88-11161

The vertical test section (VMK) of DFVLR in Cologne-Porz, Federal Republic of Germany (status 1986)
[ESA-TT-1053] 03 p0267 N88-11682

Laser Doppler measurements in a turbulent free jet
[ESA-TT-1067] 03 p0315 N88-11994

Rayleigh scattering measurements of a freejet with homogeneous condensation 03 p0319 N88-12020

Numerical simulation and visualization of a flowfield by interaction of two parallel two-dimensional freejets
03 p0320 N88-12021

Numerical analysis of flow characteristics of supersonic free-jets 05 p0538 N88-13274

Investigation of the effect of laterally ejected gas jets on flows
[ISL-R-107/86] 05 p0581 N88-13545

Molecular collision processes in gases and at surfaces
[AD-A189518] 13 p1836 N88-20982
Effect of initial tangential velocity distribution on the mean evolution of a swirling turbulent free jet
[NASA-TM-100934] 18 p2458 N88-24592
Particle-laden weakly swirling free jets: Measurements and predictions
[NASA-TM-100920] 18 p2466 N88-24639
Numerical simulation of supersonic free-jets
19 p2636 N88-25639
Cryogenic free jets
[DFVLR-FB-88-16] 21 p2900 N88-27210

FREE MOLECULAR FLOW
Analysis of free molecular effects on the attitude of satellites in geostationary transfer orbit. Part 1: Theoretical analysis
[DFVLR-IB-222-86-A/08] 01 p0014 N88-10077
Analysis of free molecular effects on the attitude of satellites in geostationary transfer orbit. Part 2: Force and torque measurement in free molecular wind tunnel tests
[DFVLR-IB-222-86-A/07] 01 p0014 N88-10078
Experiences using the Mark IV supersonic hypersonic arbitrary body program 05 p0534 N88-13249
Studies of error in temperature measurement with thermistors in the range between continual and free-molecule flows
[NASA-TT-20302] 19 p2674 N88-25900

FREE OSCILLATIONS
U FREE VIBRATION

FREE RADICALS
NT HYDROXYL RADICALS
Photolytic processes for measurement of combustion heats of formation and reaction rates
[DE87-014047] 02 p0144 N88-10905
Free radical detection and reactions in the decomposition of energetic materials
[AD-A184677] 03 p0296 N88-11858
Physiological and biochemical aspects of toxic effects of oxidants in man's environment (air, water)
07 p0890 N88-15391
Laser studies of the dynamics of free radical reactions
[DE88-004431] 10 p1337 N88-17989
Gas phase reactions of electrons, negative ions and free-radicals with transition metal complexes
11 p1560 N88-19339
Photolytic formation of free radicals and their effect on hydrocarbon pyrolysis chemistry in a concentrated solar environment
[DE88-004129] 13 p1794 N88-20730
Photodissociation lifetimes of CH and CD radicals in comets 14 p1998 N88-21908
Infrared absorption spectroscopy and chemical kinetics of free radicals
[DE88-006536] 15 p2033 N88-22112
Time-resolved studies of free radicals and laser-initiated chain reactions
[DE88-006569] 16 p2266 N88-23553
Energy transfer processes in free radicals: A collaborative experimental and theoretical investigation
[AD-A191264] 16 p2269 N88-23578

FREE STREAM EFFECTS
U FREE FLOW

FREE STREAMS
U FREE FLOW

FREE VIBRATION
Calculation of the eigenvibrations of axisymmetric fluid configurations with a singularity method, taking into account surface tension effects under reduced gravity
[ETN-87-90438] 01 p0048 N88-10304
Finite element methodology for nonlinear free and harmonic forced vibrations of beam and plate structures
13 p1782 N88-20663
Calculation of displacement, constraints and eigenmodes of rotating blades
[ETN-88-92296] 16 p2224 N88-23277
Experimental and theoretical investigation of passive damping concepts for member forced and free vibration
[NASA-CR-183082] 20 p2814 N88-26693
Free vibration of rectangular plates with a small initial curvature
[NASA-CR-179370] 24 p3383 N88-30148

FREE-PISTON ENGINES
Study of free-piston Stirling engine driven linear alternators
[NASA-CR-181425] 01 p0055 N88-10355
RE-1000 free-piston Stirling engine hydraulic output system description
[NASA-TM-100185] 01 p0108 N88-10700
SPRE 1 free-piston Stirling engine testing at NASA Lewis Research Center
[NASA-TM-100241] 03 p0277 N88-11747
Shock tunnels for real gas hypersonics
05 p0530 N88-13223
Description of an oscillating flow pressure drop testing
[NASA-TM-100905] 16 p2170 N88-22933
The 1988 overview of free-piston Stirling technology for space power at the NASA Lewis Research Center
[NASA-TM-100795] 16 p2170 N88-22934
Overview of NASA Lewis Research Center free-piston Stirling engine technology activities applicable to space power systems 17 p2398 N88-24255
Component improvement of free-piston Stirling engine key technology for space power
[NASA-TM-100950] 19 p2607 N88-25476

FREEZING
NT ZONE MELTING
Nowcasting rain/snow transitions and freezing rain
02 p0202 N88-11265
Experimental evidence for modifying the current physical model for ice accretion on aircraft surfaces
[NASA-TM-87184] 04 p0397 N88-12473
Geochemistry of freezing brines: low-temperature properties of sodium chloride
[AD-A185751] 06 p0680 N88-14168
Evaluation of the magnetic induction conductivity method for detecting frazil ice deposits
[AD-A186940] 09 p1194 N88-17157
Mesoscale monitoring of the soil freeze/thaw boundary from orbital microwave radiometry
[NASA-CR-182659] 12 p1645 N88-19855
Dendritic growth in the presence of convection
18 p2580 N88-25328
Component stress during freeze/thaw cycling
[DE88-011204] 21 p2938 N88-27449
Effect of thermal cycling on CSPL (Chloride Silent Power Ltd.) sodium/sulfur cells
[DE88-011205] 21 p2939 N88-27455

FREEZING POINTS
U MELTING POINTS

FREIGHT
U CARGO

FRENCH SATELLITES
NT SPOT (FRENCH SATELLITE)
The heat pipe network of TDF-1/TV-SAT: Review of the development af completion
[SNIAS-881-440-103] 23 p3213 N88-29127

FRENCH SPACE PROGRAMS
Development of the SPOT commercial service: Preliminary conclusions after six months of operations
03 p0340 N88-12144
SPOT Image Corporation: Early results
03 p0340 N88-12146
The new generation of SPOT satellites
03 p0345 N88-12178
The French balloon and sounding rocket space program 08 p1025 N88-16203
French activities in ocean colour observations
08 p1043 N88-16303
The Earthnet Heat Capacity Mapping Mission (HCMM) data-processing system at Lannion (France)
09 p1127 N88-16761
The French spaceborne oceanography program
19 p2701 N88-26058
Perspectives for the SPOT program
22 p3115 N88-28508
Closing of the Preliminary Evaluation Program for SPOT (PEPS): Assessment of the acquisition, production, and monitoring of PEPS 22 p3115 N88-28509
Organization of the TDF1/TDF2 program
22 p3161 N88-28827
Microwave remote sensing in the French industries
[ETN-88-93081] 24 p3387 N88-30171

FREON
Kinetics of homogeneous nucleation in superheated F-11 and F-21 liquid freons
[NASA-TT-20286] 19 p2613 N88-25503
Investigation on refrigerant R12 critical boiling point in narrow flow pipes considered as model fluid
[ETN-88-92374] 20 p2802 N88-26626

FREQUENCIES
NT ACOUSTIC FREQUENCIES
NT AUDIO FREQUENCIES
NT BEAT FREQUENCIES
NT BROADBAND
NT CARRIER FREQUENCIES
NT CYCLOTRON FREQUENCY
NT EXTREMELY HIGH FREQUENCIES
NT EXTREMELY LOW FREQUENCIES
NT EXTREMELY LOW RADIO FREQUENCIES
NT HIGH FREQUENCIES
NT INFRASONIC FREQUENCIES
NT INTERMEDIATE FREQUENCIES
NT IONIZATION FREQUENCIES
NT LOW FREQUENCIES
NT MAXIMUM USABLE FREQUENCY
NT MICROWAVE FREQUENCIES
NT PLASMA FREQUENCIES
NT RADIO FREQUENCIES
NT RESONANT FREQUENCIES
NT SUPERHIGH FREQUENCIES
NT SWEEP FREQUENCY
NT ULTRAHIGH FREQUENCIES
NT VERY HIGH FREQUENCIES
NT VERY LOW FREQUENCIES
Modeling XV-15 tilt-rotor aircraft dynamics by frequency and time-domain identification techniques
03 p0263 N88-11657
Structural frequency functions for an impulsive, distributed forcing function
[DE87-013811] 03 p0333 N88-12101
Lower bounds on bearing accuracy for closely spaced sources
[AD-A184258] 04 p0486 N88-12997
Program to development an optical transistor and switch
[AD-A185666] 06 p0697 N88-14278
On simultaneous estimation of the number of signals and frequencies under a model with multiple sinusoids
[AD-A186026] 07 p0913 N88-15543
On rate of convergence of equivariation linear prediction estimates of the number of signals and frequencies of multiple sinusoids
[AD-A186034] 07 p0914 N88-15549
Qualification of frequency response functions using the rigid-body response
[DE88-000745] 10 p1344 N88-18033
Frequency response function estimation at level
[DE88-002644] 10 p1344 N88-18034
Frequency-sampling design of two-dimensional FIR digital filters with nonuniform samples
[AD-A187773] 11 p1477 N88-18815
Minimum weight design of rectangular and tapered helicopter rotor blades with frequency constraints
[NASA-TM-100561] 12 p1582 N88-19465
Sensitivity reduction over a frequency band
[AD-A189123] 12 p1621 N88-19694
Wavenumber - frequency structure of turbulent flow in a channel from a direct simulation
[AD-A189079] 12 p1627 N88-19737
Theoretical investigation of EM wave generation and radiation in the ULF, ELF and VLF bands by the electrodynamic orbiting tether
[NASA-CR-182720] 13 p1760 N88-20529
Optimal and conventional space-time processing in flow noise
[AD-A189104] 13 p1833 N88-20965
NBS (National Bureau of Standards) measurement services. GOES (Geostationary Operational Environmental Satellite) time code dissemination: Description and operation
[PB88-168760] 14 p1880 N88-21235
Minimum weight design of rotorcraft blades with multiple frequency and stress constraints
[NASA-TM-100569] 16 p2161 N88-22892
Time-frequency representations for speech signals
[AD-A188661] 18 p2498 N88-24819
Exact tests for variance component models with unequal cell frequencies in the last stage
[AD-A191645] 18 p2568 N88-25253
Frequency Analysis of Acoustic Emission - Application to machining and welding
[DE88-701478] 18 p2570 N88-25262
A microcomputer based frequency-domain processor for laser Doppler anemometry
[NASA-TM-100998] 20 p2803 N88-26634
Investigation of the validity of Reynolds averaged turbulence models at the frequencies that occur in turbomachinery
[NASA-CR-182162] 22 p3048 N88-28087
Effect of phase errors in stepped-frequency radar systems
[AD-A194476] 23 p3203 N88-29061
Contamination and distortion of steady flow field induced by discrete frequency disturbances in aircraft gas engines
[AD-A195440] 24 p3370 N88-30069

FREQUENCY ANALYZERS
An expert system to analyze high frequency dependent data for the space shuttle main engine turbopumps
08 p1060 N88-16399

FREQUENCY ASSIGNMENT
Telemetry, Tracking, and Control Working Group report 01 p0016 N88-10096
HF (High Frequency) broadcasting planning model: A comparison of two versions
[PB87-210282] 01 p0036 N88-10230
High data rate modem simulation for the space station multiple-access communications system
06 p0795 N88-14870
Numerical arc segmentation algorithm for a radio conference-NASARC (version 2.0) technical manual
[NASA-TM-100160] 08 p0977 N88-15910

FREQUENCY BANDS
U FREQUENCIES

FREQUENCY CONTROL
NT AUTOMATIC FREQUENCY CONTROL

Optically tuned MM-wave IMPATT source
|AD-A185250| 05 p0577 N88-13523
Frequency locking of two lasers
|FOA-C-30456-3.1| 08 p0992 N88-16000
Fiber-coupled external-cavity semiconductor high power laser
|AD-A188454| 13 p1774 N88-20611
Investigation of boundary layer disturbances caused by periodic heating of a thin ribbon
|AD-A190572| 15 p2065 N88-22314
Interleaver design for trellis-coded differential 8-PSK modulation with non-coherent detection
19 p2648 N88-25719
Quartz crystal resonators and oscillators for frequency control and timing applications
|AD-A193310| 21 p2937 N88-27443
Three-dimensional vortex interactions
|AD-A194066| 23 p3172 N88-28889
Reduction in mill air compressor power requirements through instalation of a variable frequency speed control
|DE88-008493| 23 p3221 N88-29171

FREQUENCY CONVERSION
U FREQUENCY CONVERTERS

FREQUENCY CONVERTERS
NT FREQUENCY DIVIDERS
NT FREQUENCY MULTIPLIERS
NT FREQUENCY SYNTHESIZERS
NT UP-CONVERTERS
Non-linear materials (TAS)
|AD-A189197| 12 p1633 N88-19775
Electrostatic whistler mode conversion at plasma resonance
|AD-A192951| 20 p2860 N88-26989
Nonlinear materials for frequency conversion
|DE88-008343| 20 p2875 N88-27067

FREQUENCY DISCRIMINATORS
Acoustic emission frequency discrimination
|NASA-CASE-MSC-20467-1| 17 p2342 N88-23966

FREQUENCY DISTRIBUTION
Statistical distribution of solar radiation (hourly sums): Cumulative frequency curves preparation of a European data set and direction for use
|PB87-107454| 04 p0467 N88-12886
Analysis, suppression of land clutter characteristics reported 14 p1903 N88-21369
Wigner distribution function: Relation to short-term spectral estimation, smoothing and performance in noise
|AD-A193865| 23 p3275 N88-29492

FREQUENCY DIVIDERS
Interactive computer programme for the analysis of a two-way Wilkinson divider/combiner
|PB88-105424| 20 p2837 N88-26831

FREQUENCY DIVISION MULTIPLE ACCESS
Mobilestar field test program
19 p2646 N88-25707
Comparison of CDMA and FDMA for the MobileStar(sm) system 19 p2649 N88-25724
A study on the co- and adjacent channel protection requirements for mobile satellite ACSSB modulation
19 p2650 N88-25732
Rivista Tecnica Selenia, volume 10, no. 3, 1987
|ETN-88-92717| 22 p3068 N88-28210
The Frequency Division Multiple Access/Time Domain Multiplex (FDMA/TDM) system reviewed
22 p3069 N88-28214

FREQUENCY DIVISION MULTIPLEXING
The design and testing of an analog optical communication link capable of the simultaneous transmission of four frequency division multiplexed audio signals
|AD-A184695| 03 p0307 N88-11936

FREQUENCY HOPPING
Performance analysis of coded frequency-hopped spread-spectrum systems with unknown interference
|AD-A186069| 07 p0841 N88-15103
Coding for spread-spectrum communications networks
|AD-A185667| 07 p0844 N88-15119
The ratio detector: A method of amplitude insensitive frequency demodulation
|RAE-TR-87008| 09 p1153 N88-16910
Soft decoding of recorded HF data
|FOA-C-30473-3.3| 15 p2058 N88-22269
A Differential Phase Shift Keying (DPSK) modulator for a frequency hopping short wave system
|FOA-C-30460-3.3| 18 p2501 N88-24840

FREQUENCY MEASUREMENT
NO2 heterodyne frequency measurements with a tunable diode laser, a CO laser transfer oscillator and CO2 laser standards
|NASA-CR-182393| 06 p0710 N88-14353
Material parameter measurements at high temperatures
|NASA-CR-182707| 13 p1739 N88-20397
Apparatus for using a time interval counter to measure frequency stability
|NASA-CASE-NPO-17325-1-CU|
18 p2502 N88-24846
Airborne measurement of low frequency atmospheric noise ALFAN 1
|AD-A193056| 21 p2931 N88-27405
A notch filter instrument for measuring ELF (Extremely Low Frequency) MSK (Minimum Shift Keying) signals
|AD-A193324| 21 p2933 N88-27414

FREQUENCY MODULATION
NT FREQUENCY SHIFT KEYING
Large-aperture high-efficiency frequency doubling using tandem KDP crystals 03 p0301 N88-11894
Fast autotuning of a hydrogen maser by cavity Q modulation 04 p0436 N88-12707
Study of vibration relaxation in active medium of CO2-laser using phase-absorption method
07 p0919 N88-15582
Telemetry applications handbook
|AD-A186825| 09 p1132 N88-16789
The ratio detector: A method of amplitude insensitive frequency demodulation
|RAE-TR-87008| 09 p1153 N88-16910
Magnet strength fluctuations in the SSC (Superconducting Super Collider) lattice. Part 2: Frequency modulation
|DE88-006491| 15 p2141 N88-22774
Statistical fine structure in the inhomogeneously broadened electronic origin of pentacene in p-terphenyl
|AD-A191211| 16 p2176 N88-22968
A study on the co- and adjacent channel protection requirements for mobile satellite ACSSB modulation
19 p2650 N88-25732

FREQUENCY MULTIPLIERS
Powerful picosecond ultraviolet laser output at 354.7 nanometers 03 p0327 N88-12063
Frequency doubling conversion efficiencies for deep space optical communications 04 p0434 N88-12691
Optical frequency doubling in Ti:LiMbO3 waveguide resonators
|ETN-88-91486| 11 p1550 N88-19271

FREQUENCY RANGES
NT RADIO RANGE

FREQUENCY REGULATION
U FREQUENCY CONTROL

FREQUENCY RESPONSE
Further development of the dynamic gas temperature measurement system 02 p0184 N88-11141
An efficient frequency response solution for nonproportionally damped systems
05 p0595 N88-13634
Dynamic restructuring of pulsed CO2 laser frequency and multiple-peak generation in a cell with IR-absorbing gas in the resonator 07 p0919 N88-15580
Strategic placement of accelerometers to measure forces by the sum of weighted accelerations
|DE88-002262| 10 p1333 N88-17968
On frequency response for nonlinear systems
|RR-323| 18 p2563 N88-25221

FREQUENCY REUSE
Rearrangement procedures in regenerative multibeammobile communications satellites with frequency reuse 19 p2650 N88-25735

FREQUENCY SHIFT
Frequency chirping in pulse modulated gain and real index guided single quantum well lasers
19 p2658 N88-25798

FREQUENCY SHIFT KEYING
ELF/VLF/LF propagation and system design
|AD-A183261| 01 p0033 N88-10212
The 2 FSK/QPSK (Frequency Shift Keying/Quadrature Phase Shift Keying) transmitter and receiver: Design and performance
|AD-A190028| 15 p2056 N88-22258
An FSK (Frequency Shift Keying) telemetry module for vector measuring current meters
|AD-A192142| 18 p2470 N88-24661
A notch filter instrument for measuring ELF (Extremely Low Frequency) MSK (Minimum Shift Keying) signals
|AD-A193324| 21 p2933 N88-27414

FREQUENCY STABILITY
X-band uplink ground systems development: Part 2
04 p0436 N88-12703
On-orbit frequency stability analysis of the GPS NAVSTAR 8 rubidium clock and NAVSTARs 9 and 10 cesium clocks
|AD-A184984| 05 p0544 N88-13312
Study and construction of a compact hydrogen maser with a high-degree of frequency stability
|PB87-151122| 07 p0859 N88-15216
Investigation of boundary layer disturbances caused by periodic heating of a thin ribbon
|AD-A190572| 15 p2065 N88-22314
Apparatus for using a time interval counter to measure frequency stability
|NASA-CASE-NPO-17325-1-CU|
18 p2502 N88-24846
Laser CO2/TEA frequency-stabilized by phase conjugation 22 p3082 N88-28303
Three-dimensional vortex interactions
|AD-A194066| 23 p3172 N88-28889
The aspect ratio dependence of the attractor dimension in Taylor-Couette flow
|AD-A196297| 24 p3369 N88-30065

FREQUENCY STANDARDS
Study and construction of a compact hydrogen maser with a high-degree of frequency stability
|PB87-151122| 07 p0859 N88-15216
Atomic clocks research: An overview
|AD-A185567| 07 p0930 N88-15648
Recommendations for organising the calibration of pure-tone audiometers
|NPL-AC-112| •09 p1167 N88-16988
The JPL trapped mercury ion frequency standard
11 p1471 N88-18776
Tactical Rubidium Frequency Standard (TRFS)
|AD-A191049| 16 p2193 N88-23078
Tactical Rubidium Frequency Standard (TRFS), volume 2
|AD-A191190| 18 p2503 N88-24850
Tactical Rubidium Frequency Standard (TRFS), volume 1
|AD-A192981| 20 p2805 N88-26640
A three-dimensional model of the gas-cell atomic frequency standard
|AD-A193218| 21 p3011 N88-27868
Electromagnetic metrology 24 p3363 N88-30024

FREQUENCY SYNTHESIZERS
Mechanisms mediating perception of complex acoustic patterns
|AD-A189765| 15 p2102 N88-22520
Instrumentation for ultrafast electronics
|AD-A191379| 16 p2193 N88-23080

FREQUENCY TRANSLATION
U FREQUENCY CONVERTERS

FRESH WATER
Karst and submarine fresh water discharge in the Antalya area, southern Turkey 22 p3102 N88-28421

FRESNEL DIFFRACTION
Diffraction effects during materials treatment with laser beams
|ETN-87-90614| 03 p0328 N88-12075
Precision measurement of the Fresnel drag coefficient using a ring laser
|AD-A196025| 24 p3366 N88-30043

FRESNEL INTEGRALS
Overestimation of on-axis power density by the Fraunhofer (far-field) approximation
|AD-A186399| 07 p0843 N88-15111
Beam quality of stable and unstable resonators: A theoretical approach
|DFVLR-FB-87-35| 14 p1982 N88-21826

FRESNEL LENSES
Construction of gallium arsenide solar concentrator for space use
|AD-A194658| 23 p3230 N88-29222

FRESNEL REGION
An improved method for calculating power density in the Fresnel region of circular parabolic reflector antennas
|AD-A190569| 15 p2060 N88-22284

FRESNEL-KIRCHHOFF INTEGRALS
U FRESNEL INTEGRALS

FRETTING
The mechanics of fatigue-crack nucleation in a low-alloy steel under fretting conditions 05 p0597 N88-13640
Fretting wear and fretting fatigue damage
05 p0603 N88-13697

FRETTING CORROSION
The effect of fretting corrosion on the fatigue strength of steel and cast iron under sinusoidal and random loading
|LBF-FB-177| 01 p0023 N88-10142
The effects of thin polymeric surface films in reducing fretting corrosion and wear
|AD-A188633| 12 p1611 N88-19634

FRICTION
NT AERODYNAMIC DRAG
NT DRY FRICTION
NT FLOW RESISTANCE
NT FRICTION DRAG
NT SKIN FRICTION
NT SLIDING FRICTION
NT STATIC FRICTION
NT SUPERSONIC DRAG
NT VISCOUS DRAG

Research on one-dimensional two-phase flow. Theory on hydrodynamic balance in two fluid model and its application
|DE87-702615| 01 p0045 N88-10290
Piston ring friction and vehicle fuel economy
|DE87-014536| 02 p0181 N88-11127
The wear process during the RUNNING-IN of steel in lubricated sliding
|NAL-TR-922T| 02 p0181 N88-11130
The friction and wear of TPS fibers
|NASA-CR-181496| 03 p0291 N88-11830
Ignition and combustion of metals in oxygen
04 p0407 N88-12530
Canonical transformations and exact invariants for dissipative systems
|DE87-703663| 04 p0485 N88-12985
On a numerical method to solve contact problems --- forming processes
|B8711403| 05 p0642 N88-13930
Development, features of roller rocker arm reported
06 p0689 N88-14219
The tribological properties of MoS2 coatings in vacuum, low relative humidity and high relative humidity environments
|DE88-001611| 06 p0711 N88-14356
Dynamical friction
|DE88-002194| 06 p0711 N88-14358
Mechanisms of rolling contact spalling
|NASA-CR-179243| 06 p0714 N88-14380
Centaur G Prime modal test 09 p1181 N88-17075
Friction and wear of monolithic and fiber reinforced silicon-ceramics sliding against IN-718 alloy at 25 to 800 C in atmospheric air at ambient pressure
|NASA-TM-100294| 10 p1304 N88-17796
Adhesion, friction and micromechanical properties of ceramics
|NASA-TM-100782| 10 p1305 N88-17801
Tribology of ceramics: Report of the Committee on Tribology of Ceramics
|NASA-CR-182506| 10 p1305 N88-17802
One-dimensional leakage-flow vibration instabilities
|DE88-002875| 10 p1330 N88-17947
Aircraft and ground vehicle friction correlation test results obtained under winter runway conditions during joint FAA/NASA Runway Friction Program
|NASA-TM-100506| 11 p1438 N88-18582
Synthesis and structure property studies of toughened epoxy resins via functionalized polysiloxanes. Friction and wear studies
|AD-A188258| 11 p1462 N88-18716
Reaction wheel experimental model of artificial satellite attitude control: Construction, simulation, and tests
|INPE-4274-PRE/1146| 11 p1490 N88-18896
In situ ultrahigh vacuum friction measurement and wear track analysis of ion implanted 304 stainless steel
|DE88-004537| 11 p1494 N88-18922
Quantization of quadratic friction revisited
|DE88-700839| 12 p1686 N88-20081
Particle-dynamics calculations of gravity flow of inelastic, frictional spheres
|DE88-005224| 13 p1770 N88-20586
Structural clearances and internal friction: Simulation by Eigen distortions
|ISSN-0208-5658| 13 p1779 N88-20640
Advances in contact algorithms and their application to tires
|NASA-TP-2781| 14 p1922 N88-21456
Effect of friction and control parameters on the tracking accuracy of a target seeker
|AD-A190010| 15 p2056 N88-22257
Traction model development
|AD-A188450| 15 p2073 N88-22359
Friction and wear of ceramics
17 p2323 N88-23874
LLNL granular solids flow project
|DE88-007492| 18 p2513 N88-24906
LLNL Granular Solids Flow Project
|DE88-008023| 19 p2664 N88-25844
Entrance and exit region friction factor models for annular seal analysis
|NASA-CR-183084| 19 p2676 N88-25921
Friction, wear and electrical contact resistance of precious metal alloys
|DE88-011244| 21 p2938 N88-27450
Granular flow: Particle-dynamics simulations of steady flow
|DE88-011342| 21 p2948 N88-27506
Thermo-mechanical cracking in coated media with a cavity by a moving asperity friction
|AD-A193311| 21 p2961 N88-27586
Development of high temperature, high pressure rotating shaft seals
|DE88-001029| 23 p3221 N88-29172

RICTION COEFFICIENT
U COEFFICIENT OF FRICTION

FRICTION DRAG
NT AERODYNAMIC DRAG
NT SUPERSONIC DRAG
NT VISCOUS DRAG
Combined riblet and lebu drag reduction system
|NASA-CASE-LAR-13286-1| 06 p0664 N88-14071
Friction drag reduction (a speculative essay)
|INPE-4278-PRE/1150| 08 p0988 N88-15985
An assessment of the drag reduction properties of riblets and the penalties of off-design conditions
|RAE-TM-AERO-2113| 17 p2295 N88-23731

FRICTION FACTOR
Further refinement and applications of the mixed computational algorithm for plane elastic contact problems
|AD-A188308| 12 p1683 N88-20065
Drag reduction of turbulent boundary layers by means of grooved surfaces
|ETN-88-92618| 20 p2802 N88-26630
Investigations of rough surface effects on friction factors in turbulent pipe flow
|AD-A193774| 22 p3075 N88-28255

FRICTION LOSS COEFFICIENT
U FRICTION FACTOR

FRICTION MEASUREMENT
The WAFTER: A versatile wear and friction tester
|MRL-TN-519| 09 p1169 N88-17012
In situ ultrahigh vacuum friction measurement and wear track analysis of ion implanted 304 stainless steel
|DE86-004537| 11 p1494 N88-18922
Water tunnel measurements by an electrochemical method 16 p2203 N88-23146
Boundary layer measurements using hot-film sensors
17 p2297 N88-23743

FRICTION PRESSURE DROP
U SKIN FRICTION

FRICTION REDUCTION
Multipath gear-friction planetary transmissions
04 p0424 N88-12629
Riblets for aircraft skin-friction reduction
07 p0814 N88-14955
Airfoil large eddy breakup devices for turbulent drag reduction 07 p0814 N88-14956
Friction drag reduction (a speculative essay)
|INPE-4278-PRE/1150| 08 p0988 N88-15985
An evaluation of effectiveness of PTFE (polytetrafluoroethylene) type friction reducers on reducing friction and wear
|AD-A187440| 10 p1340 N88-18010
On the torque and wear behavior of selected thin film MOS2 lubricated gimbal bearings
14 p1926 N88-21485

FRICTION WELDING
Effects of sulfur content on the plain strain fracture toughness of inertia welds in 4340 steel
|AD-A188192| 11 p1458 N88-18689
Friction welding: Advanced method of producing end cutting tool 14 p1897 N88-21327
Characteristics of joint formation during friction welding of Ti alloys to Nb alloys 14 p1898 N88-21329
Optimum duration of steady-state stage in friction welding of metals without artificial braking
14 p1898 N88-21330
The effect of notch root radius on the determination of toughness in ultrahigh strength steel friction welds
|AD-A195952| 24 p3384 N88-30156

FRICTIONLESS ENVIRONMENTS
Variational and nonvariational theory of frictionless adhesive contact between bodies
|REPT-87-11| 01 p0054 N88-10345
Nonlinear liquid motion in conical containers
|LRT-WE-9-FB-10(1987)| 22 p3077 N88-28270

FRINGE PATTERNS
U DIFFRACTION PATTERNS

FRIT
Titanium powder frit made during the transformation alpha-beta
|ETN-88-91999| 16 p2177 N88-22976

FROGS
Synopsis of the Spacelab D-1 frog statolith experiment STATEX 12 p1659 N88-19940
Organs and tissues regeneration in amphibia under the space flight conditions 12 p1660 N88-19951

FRONTAL AREAS (METEOROLOGY)
U FRONTS (METEOROLOGY)

FRONTS (METEOROLOGY)
NT COLD FRONTS
Longer-duration post-frontal precipitation at Vancouver International Airport, 1953-1983
02 p0203 N88-11269
Observational analysis of the interaction between fronts and the orography in Taiwan during the late winter monsoon season 02 p0203 N88-11270
Conceptual models of Baiu front and Baiu frontal disturbances in multiscale characteristics --- East Asia
02 p0203 N88-11271
The numerical simulation of the mesoscale characteristics associated with Baiu front. Part 1: Structure, low-level jet and radiation characteristics
02 p0203 N88-11272
A one-dimensional model of thermally-driven coastal front evolution 02 p0204 N88-11274
Properties of the atmospheric boundary layer above a subtropical oceanic front
|AD-A184006| 03 p0351 N88-12215
Interactions between the Asian monsoons, the tropical Pacific and the southern hemisphere extratropics
04 p0470 N88-12907
BARS-1M meteorological complex carried on IL-18 airplane 06 p0725 N88-14458
North Pacific Ocean. Tradewind region east of Hawaii, R/V Thomas G Thompson: 25 September - 1 November 1972. STD data report
|AD-A186566| 08 p1044 N88-16311
North Pacific Ocean. Subarctic front central Pacific, R/V Thomas G. Thompson: 8 September - 9 October 1975. CTD data report
|AD-A186567| 08 p1044 N88-16312
North Pacific Ocean. Northwest Pacific Transition Zone, R/V Thomas G. Thompson: 19 March - 1 May 1971. STD data report
|AD-A186568| 08 p1044 N88-16313
North Pacific Ocean. Central Pacific Transition Zone, R/V Thomas G. Thompson: 25 March - 3 May 1968. STD data report
|AD-A186570| 09 p1195 N88-17160
A paper on horizontal deformation in the frontogenesis in south Brazil
|INPE-4469-TDL/322| 12 p1647 N88-19867
Numerical model of Rayleigh instability and spin-off eddies on fronts 13 p1788 N88-20696
The pressure drag and momentum flux during a cold frontal passage over the Alps 13 p1800 N88-20763
Mixed-layer fronts in the California current
13 p1805 N88-20794
Numerical simulation of medium scale disturbance on meiyu front 14 p1900 N88-21346
Development and testing of the gust front algorithm
|AD-A189722| 14 p1949 N88-21622
The effects of time-dependent winds and ocean eddies on ice motion in a marginal ice zone
|AD-A190105| 15 p2100 N88-22511
Observations of frontal instabilities on an upwelling filament
|AD-A191051| 17 p2375 N88-24122
Meteorological features during the marginal ice zone experiment from 20 March to 10 April 1987
|AD-A193960| 23 p3235 N88-29251

FROST
Measurements of vapor flux, liquid water contents, precipitation rates and riming in a Utah mountain cloud system
|PB87-224945| 04 p0469 N88-12900
Effects of wing simulated ground frost on aircraft performance 08 p0952 N88-15775
Last spring frosts and first autumn frosts in Finland
|FMI-6| 19 p2693 N88-26008

FROST DAMAGE
Application of multitemporal SPOT data for crop monitoring: Effects of frost and drought
03 p0344 N88-12171

FROUDE NUMBER
A complete linearized theory for the analysis and design of two-dimensional hydrofoils near a free surface
|UTIAS-TN-264| 05 p0579 N88-13531
Steady ship waves at low Froude numbers, part 2
|AD-A176805| 09 p1160 N88-16953
Centerplane source distribution for slender bodies
10 p1328 N88-17940

FROZEN FOODS
Low temperature storage container for transporting perishables to space station
|NASA-CASE-MFS-28248-1| 18 p2498 N88-24817

FRUITS
Preliminary study on the application of digital processing of TM-LANDSAT data in the mapping of apple orchards in Fraiburgo (SC) 17 p2367 N88-24093

FUEL CAPSULES
Weldability of general purpose heat source iridium capsules 17 p2426 N88-24429

FUEL CELL CATALYSTS
U ELECTROCATALYSTS

FUEL CELL POWER PLANTS
A 40-kW fuel cell field test summary utilities activities report
|PB88-112800| 06 p0731 N88-14496

FUEL CELLS
NT HYDROGEN OXYGEN FUEL CELLS
NT PHOSPHORIC ACID FUEL CELLS
NT REGENERATIVE FUEL CELLS
DOT fuel-cell-powered bus feasibility study
|DE87-012705| 01 p0107 N88-10699

Battery development and testing at ESA
02 p0164 N88-11027
Highlights of the Chemical Technology Division's research activities
[DE88-000233] 03 p0282 N88-11773
Metal containing polymers as fuel cell catalysts
[AD-A184605] 03 p0347 N88-12194
Internal reforming development for solid oxide fuel cells
[DE87-006518] 04 p0464 N88-12871
Phase purity of NiCo2O4, a catalyst candidate for electrolysis of water
[NASA-TM-100239] 05 p0556 N88-13385
High energy density rechargeable batteries for aerospace power requirements
[AD-A184883] 05 p0577 N88-13519
Fuel cells --- military applications
[PML-1986-43] 06 p0622 N88-13813
Extended abstracts: Eighth Battery and Electrochemical Contractors' Conference
[DE88-000960] 06 p0730 N88-14489
Hydroxide ion conductors as possible electrolytes in intermediate temperature fuel cells
[AD-A185506] 06 p0731 N88-14495
A 40-kW fuel cell field test summary utilities activities report
[PB88-112800] 06 p0731 N88-14496
Value-assessment of energy storage concepts in burst power systems
[DE87-013756] 09 p1187 N88-17115
Determination of optimum electrolyte composition for molten carbonate fuel cells literature review
[DE88-001015] 10 p1348 N88-18058
Advanced materials for solid oxide fuel cells
[DE88-002338] 10 p1350 N88-18071
Fuel cell/battery hybrid vehicle assessment
[DE88-005087] 10 p1427 N88-18520
Flammability characteristics of distillate fuels
[AD-A188497] 12 p1612 N88-19642
Recent advances in solid polymer electrolyte fuel cell technology
[DE88-005380] 15 p2092 N88-22464
Value of energy storage in pulsed space power systems
[AD-A191311] 16 p2170 N88-22938
Monolithic fuel cell based power source for sprint power generation 17 p2407 N88-24313
Thermal and power availability transient responses for the Argonne monolithic solid oxide fuel cell
17 p2419 N88-24384
Energy storage for nuclear burst power systems
17 p2426 N88-24431
Value assessment of energy storage concepts in burst power systems 17 p2426 N88-24432
Polymer fuel cell as an energy storage component for space power applications 17 p2429 N88-24452
Sulfur-tolerant anode materials
[DE88-001034] 18 p2537 N88-25054
Phosphoric acid electric utility fuel cell technology development
[DE88-010187] 20 p2795 N88-26582
Oxygen reduction in fuel cell electrolytes
[DE88-008240] 20 p2819 N88-26723
Electrocatalysts for oxygen electrodes
[DE88-008397] 20 p2819 N88-26724
Fuel cell systems program plan: Fiscal year 1988
[DE88-011080] 20 p2820 N88-26731
Monolithic fuel cells
[DE88-012004] 21 p2969 N88-27638
Development of planar geometry solid oxide fuel cell technology, phase 1
[PB88-210356] 23 p3229 N88-29215
Electrocatalytic reduction of oxygen on modified oxide surfaces
[NASA-TM-101333] 24 p3352 N88-29952
Fuel cells for space use
[FCP-TR-DOS-SY-026] 24 p3389 N88-30183

FUEL COMBUSTION
NT NUCLEAR FUEL BURNUP
SCRAM JET (Supersonic Combustion Ramjet) combustion experiments 04 p0404 N88-12512
Oxygen enriched combustion system performance study
[DE88-001500] 05 p0562 N88-13424
Characterizing particle combustion in a Rijke burner
[AD-A186157] 08 p0966 N88-15847
A holographic investigation of particulates in metallized solid fuel ramjet combustion
[AD-A186887] 09 p1140 N88-16831
The effects of fuel composition on ignition delay in homogeneous charge and direct injection compression ignition engines
[DE88-003691] 09 p1143 N88-16849
Studies of fluorine combustion
[AD-A187646] 11 p1452 N88-18656
Fuels combustion research
[AD-A187688] 11 p1453 N88-18657
Fuels combustion research
[AD-A189114] 13 p1736 N88-20381
Basic research on natural gas combustion phenomena
[PB88-168380] 14 p1887 N88-21278
Application of laser-induced fluorescence in an atmospheric-pressure boron-seeded flame
[AD-A189631] 14 p1889 N88-21287
AFRAPT (Air Force Research in Aero Propulsion Technology) trainee program
[AD-A190525] 15 p2035 N88-22123
Effect of mass-velocity on liquid jet atomization in Mach 1 gasflow
[NASA-TM-100813] 16 p2211 N88-23194
Coal particle behaviour in a counter-current combustor
[TAE-606] 19 p2612 N88-25498
Characteristic time correlations to liquid fuel ramjet combustion efficiency 19 p2624 N88-25566
Combustion rate limits of hydrogen plus hydrocarbon fuel: Air diffusion flames from an opposed jet burner technique 19 p2624 N88-25567
Dual Stokes cars measurements in supersonic combusting flow 19 p2625 N88-25569
Ignition and flammability characteristics of solid fuel ramjets 19 p2626 N88-25575
Pollutant formation in heterogeneous mixtures of fuel drops and air
[DOE/CE-50052/H1] 19 p2689 N88-25986
Laser diagnostics applied to advanced combustion systems
[DE88-753119] 20 p2806 N88-26649
Effects of ceramic surfaces on autoignition in a constant volume combustion apparatus
[AD-A193055] 21 p2909 N88-27266
The application of the two-fluid model of turbulence to the 3-D simulation of turbulent combustion in reciprocating engines
[PDR/CFDU/IC/37] 22 p3052 N88-28110
Modeling of spray combustion in direct injection diesel engine
[AD-A193787] 22 p3084 N88-28314
Combustion studies of acoustically suspended liquid droplets
[AD-A193892] 23 p3192 N88-28998
Experiments and modeling of multi-component fuel behavior in combustion
[AD-A195011] 24 p3343 N88-29896
Alternative fuel spray behavior
24 p3345 N88-29912
Atomization of alternative fuels
24 p3345 N88-29913
Turbulence effects on the droplet distribution behind airblast atomizers 24 p3346 N88-29915
Multiple scattering effects in drop sizing of dense fuel sprays by laser diffraction 24 p3346 N88-29917
Influence of operating conditions on the atomization and distribution of fuel by air blast atomizers
24 p3346 N88-29918
The characterizatin of combustion by fuel composition: Measurements in a small conventional combustor
24 p3346 N88-29920
Flame stabilization in a reheat combustor
24 p3346 N88-29921
High performance turbofan afterburner systems
24 p3347 N88-29922
Comparison of the performance of a reverse flow annular combustion chamber under low and high pressure conditions 24 p3347 N88-29923
Radiation transfer in gas turbine combustors
24 p3348 N88-29929
Gas turbine smoke measurement: A smoke generator for the assessment of current and future techniques
24 p3348 N88-29930
Rates of formation of soot from hydrocarbon flames and its destruction 24 p3349 N88-29933
Modeling the stability of a turbulent premixed flame, downstream from a step by a Lagrangian method
24 p3350 N88-29943
Gaseous premixed flames in non-uniform flows
24 p3351 N88-29945
Modeling and experimental study of a reactive flow confined with well injection 24 p3351 N88-29946
Influence of the convection on evaporation and combustion of a fuel droplet 24 p3351 N88-29948
A small annular combustor of high power density, wide operating range and low manufacturing cost
24 p3351 N88-29951

FUEL CONSERVATION
U FUEL CONSUMPTION

FUEL CONSUMPTION
Japanese industrial research on lean combustion: A case study: International Research Monitoring Program
[DE87-013839] 02 p0144 N88-10904
Automotive Stirling engine: Mod 2 design report
[NASA-CR-175106] 02 p0250 N88-11578
Development of strength in cements
[PB87-232971] 06 p0684 N88-14189
Small engine technology programs
08 p0956 N88-15801
X-wing potential for Navy applications
10 p1271 N88-17604
The advantage of variable geometry for turbine engines at low power 10 p1280 N88-17653
Minimum Energy Routing through Interactive Techniques (MERIT) modeling
[NASA-CR-182535] 10 p1356 N88-18105
Review of the state of the art and projected technology of low heat rejection engines
[PB88-131255] 11 p1496 N88-18934
High shear rate rheometry of low-viscosity liquids
[AD-A188447] 12 p1627 N88-19733
Large-Scale Advanced Prop-Fan (LAP)
[NASA-CR-182112] 13 p1723 N88-20306
Gas consumption estimation of an attitude control system of an artificial satellite (utilizing DRF) in limit cycle phase
[INPE-4338-RPE/553] 13 p1731 N88-20350
Status of alcohol fuels utilization technology for highway transportation: A 1986 perspective. Volume 2: Compression ignition engines
[DE88-006059] 13 p1753 N88-20485
The initial calculation of range and mission fuel during conceptual design --- aircraft design
[LR-525] 16 p2161 N88-22889
NASA advanced turboprop research and concept validation program
[NASA-TM-100891] 16 p2163 N88-22902
The effect of weathering on octane quality for winter-grade and summer-grade gasolines
[AD-A190640] 16 p2183 N88-23012
Sunshine project for FY 1987 outlined
16 p2184 N88-23021
NASA/industry advanced turboprop technology program
[NASA-TM-100929] 18 p2466 N88-24641
Computer simulation of turbulent combustion in reciprocating engines
[CFDU/87/11] 18 p2482 N88-24725

FUEL CONTAMINATION
Formation of sediments in fuels containing added sulphonic acids --- marine diesel fuels
[RAE-TM-NAV-ENG-1163] 09 p1150 N88-16891
Fuel containment concepts: Transport category airplanes
[AD-A189818] 18 p2494 N88-24799
Development of a test method to determine potential peroxide content in turbine fuels. Part 2
[AD-A192244] 23 p3199 N88-29042
Atomization of alternative fuels
24 p3345 N88-29913
Fuel effects on flame radiation and hot-section durability 24 p3347 N88-29925

FUEL CONTROL
Investigation of the need for in-use dispensing rate limits and fuel nozzle geometry standardization
[PB88-102611] 07 p0839 N88-15089
AF cryogenic and fluid management spacecraft technology program 08 p0981 N88-15925
Nozzle airflow influences on fuel patternation
24 p3346 N88-29916

FUEL CORROSION
Molten salt corrosion of SiC and Si3N4
17 p2325 N88-23885
Development of reliable fuel pins for space reactor applications 17 p2409 N88-24326

FUEL ELEMENTS (NUCLEAR REACTORS)
U NUCLEAR FUEL ELEMENTS

FUEL FLOW
NT PROPELLANT TRANSFER
SCRAM JET (Supersonic Combustion Ramjet) combustion experiments 04 p0404 N88-12512
Dynamics of propellant feedline systems
[AD-A184865] 05 p0580 N88-13537
Investigation of the flow and combustion behavior in a solid fuel combustion chamber, including the measuring program
[VTH-LR-460] 09 p1141 N88-16838
Arcjet thruster research and technology, phase 1
[NASA-CR-182107] 17 p2314 N88-23830

FUEL INJECTION
Application of electronic fuel injection to the optimum engine for methanol utilization
[PB87-201950] 02 p0180 N88-11120
Performance and combustion characteristics of direct-injection stratified-charge rotary engines
[NASA-TM-100134] 04 p0400 N88-12490
SCRAM JET (Supersonic Combustion Ramjet) combustion experiments 04 p0404 N88-12512
A three-barrel repeating pneumatic pellet injector for plasma fueling of the Joint European Torus
[DE88-000330] 04 p0491 N88-13026

Regressed relations for forced convection heat transfer in a direct injection stratified charge rotary engine
[NASA-TM-100124] 05 p0549 N88-13345

Ignition and flameholding in supersonic flow by injection of dissociated hydrogen 05 p0560 N88-13410

A study of the interaction of laser light with liquid propellant drops
[AD-A185117] 05 p0587 N88-13582

Fuel-injector/air-swirl characterization
[NASA-CR-180864] 07 p0820 N88-14985

Liquid sprays and flow studies in the direct-injection diesel engine under motored conditions
[NASA-TM-100135] 11 p1440 N88-18594

Concept and analysis of a direct-injection alcohol layer charge motor
[ETN-88-91482] 11 p1495 N88-18925

Practical system for the use of alcohol in diesel engines
[PB88-147863] 12 p1612 N88-19638

Development of a laboratory test for multiport fuel injector deposits - evaluation of the Jet Fuel Thermal Oxidation Test apparatus (JFTOT)
[AD-A191313] 16 p2183 N88-23015

Full electronic control system for diesel engine
16 p2185 N88-23025

Liquid Engine Jet Atomization Workshop report
19 p2627 N88-25584

Direct gas injection with glow plug ignition
[PB88-187323] 19 p2676 N88-25911

Pollutant formation in heterogeneous mixtures of fuel drops and air
[DOE/CE-50052/H1] 19 p2689 N88-25986

Heterogeneous diffusion flame stabilization
[AD-A193014] 20 p2771 N88-26429

Pulsed spray structure and atomisation techniques
[AD-A192280] 20 p2800 N88-26614

The 210-HP diesel engine endurance and performance testing with fire resistant diesel fuel
[AD-A193153] 21 p2956 N88-27558

Modeling of spray combustion in direct injection diesel engine
[AD-A193787] 22 p3084 N88-28314

The dc power control for a liquid-fed resistojet
[NASA-TM-101326] 24 p3338 N88-29869

Combustion and fuels in gas turbine engines
[AGARD-CP-422] 24 p3345 N88-29910

Simulation study of spraying, streaming and vaporization phenomena associated with fuel injection
24 p3345 N88-29914

Spray performance of a vaporizing fuel injector
24 p3346 N88-29919

Modeling and experimental study of a reactive flow confined with wall injection 24 p3351 N88-29946

FUEL PRODUCTION

Application of solar technology to fuel production chemical processing, and thermochemical energy transport: Status and future
[DE87-014172] 03 p0346 N88-12189

Design study for asteroidal exploitation
03 p0389 N88-12445

The 210-HP diesel engine endurance and performance testing with fire resistant diesel fuel
[AD-A193153] 21 p2956 N88-27558

FUEL PUMPS

Pumping systems and flow interfaces for rapid response electronic reheat controls 10 p1282 N88-17665

Two phase flow in a rotating screw tube (screw tube pump). Investigation of the function and efficiency of the screw tube pump
[MPIS-16/1987] 23 p3222 N88-29178

UEL SPRAYS

Fuel-injector/air-swirl characterization
02 p0185 N88-11150

Ignition and flame propagation in sprays
[AD-A184679] 03 p0283 N88-11781

SCRAM JET (Supersonic Combustion Ramjet) combustion experiments 04 p0404 N88-12512

Study of electrostatic modulation of fuel sprays to enhance combustion performance in an aviation gas turbine
[AD-A184967] 05 p0548 N88-13341

Investigation of real-time two-dimensional visualization of fuel spray liquid/vapor distribution via exciplex fluorescence
[AD-A188268] 10 p1307 N88-17816

Liquid sprays and flow studies in the direct-injection diesel engine under motored conditions
[NASA-TM-100135] 11 p1440 N88-18594

Quantitative use of exciplex-based vapor/liquid visualization systems, users' manual
[AD-A191649] 19 p2610 N88-25491

Effects of ceramic surfaces on autoignition in a constant volume combustion apparatus
[AD-A193055] 21 p2909 N88-27266

Modeling of spray combustion in direct injection diesel engine
[AD-A193787] 22 p3084 N88-28314

Alternative fuel spray behavior
24 p3345 N88-29912

Atomization of alternative fuels
24 p3345 N88-29913

Simulation study of spraying, streaming and vaporization phenomena associated with fuel injection
24 p3345 N88-29914

Turbulence effects on the droplet distribution behind airblast atomizers 24 p3346 N88-29915

Nozzle airflow influences on fuel patternation
24 p3346 N88-29916

Multiple scattering effects in drop sizing of dense fuel sprays by laser diffraction 24 p3346 N88-29917

Influence of operating conditions on the atomization and distribution of fuel by air blast atomizers
24 p3346 N88-29918

Spray performance of a vaporizing fuel injector
24 p3346 N88-29919

The characterizatin of combustion by fuel composition: Measurements in a small conventional combustor
24 p3346 N88-29920

The performance of a surrogate blend in simulating JP-4 in a spray-fueled combustor 24 p3347 N88-29926

FUEL SYSTEMS

NT AIRCRAFT FUEL SYSTEMS

Aircraft fire safety research 04 p0406 N88-12526

Safety implications of onboard refueling vapor recovery systems
[PB88-102603] 07 p0839 N88-15088

An irradiation performance data base for nitride fuels
17 p2427 N88-24438

Fuel containment concepts: Transport category airplanes
[AD-A189818] 18 p2494 N88-24799

Servojet retrofit -
[AD-A191075] 18 p2522 N88-24964

Mach 2 combustion characteristics of hydrogen/hydrocarbon fuel mixtures
19 p2625 N88-25568

FUEL TANKS

NT WING TANKS

An experimental comparison of two designs of mercury propellant tank for use with an electric propulsion engine
[RAE-TR-75109] 01 p0018 N88-10109

Measurements in large JP-4 pool fires
[DE87-013445] 03 p0284 N88-11783

Performance analysis of advanced spacecraft TPS
[NASA-CR-181532] 04 p0399 N88-12484

Orbital Spacecraft Consumables Resupply System (OSCRS). Volume 1: Executive summary
[NASA-CR-172010] 05 p0553 N88-13368

Development of on-orbit fluid gaging techniques
08 p0982 N88-15936

Development and evaluation of an airplane fuel tank ullage composition model. Volume 2: Experimental determination of airplane fuel tank ullage compositions
[AD-A190408] 15 p2017 N88-22025

Domain decomposition in parallel reservoir simulation
[REPT-87-63] 16 p2254 N88-23469

Fuel containment, lightning protection and damage tolerance in large composite primary aircraft structures
[NASA-CR-3875] 17 p2317 N88-23839

Stressed fabric abrasion test procedure for urethane coated fabric fuel tanks
[AD-A196327] 24 p3356 N88-29982

FUEL TESTS

J85-21 fuel nozzle atomization tests
[AD-A189394] 12 p1613 N88-19647

Development of a laboratory test for multiport fuel injector deposits - evaluation of the Jet Fuel Thermal Oxidation Test apparatus (JFTOT)
[AD-A191313] 16 p2183 N88-23015

Aircraft emissions characterization: TF41-A2, TF30-P103 and TF30-P109 engines
[AD-A192053] 18 p2466 N88-24638

Fuel property effects on the US Navy's TF30 engine
24 p3345 N88-29911

FUELING

U REFUELING

FUELS

NT AIRCRAFT FUELS
NT ANTIMISTING FUELS
NT AUTOMOBILE FUELS
NT CERAMIC NUCLEAR FUELS
NT CHEMICAL FUELS
NT COAL
NT CRUDE OIL
NT DIESEL FUELS
NT FOSSIL FUELS
NT GASEOUS FUELS
NT GASOHOL (FUEL)
NT GASOLINE
NT HYDROCARBON FUELS
NT HYDROGEN FUELS
NT JET ENGINE FUELS
NT JP-4 JET FUEL
NT JP-5 JET FUEL
NT JP-8 JET FUEL
NT KEROSENE
NT LIQUEFIED NATURAL GAS
NT LIQUID FUELS
NT MONOPROPELLANTS
NT NATURAL GAS
NT NUCLEAR FUELS
NT SPENT FUELS
NT SYNTHETIC FUELS

Compendium of significant events in the recent development of alcohol fuels in the United States
[DE87-013355] 01 p0032 N88-10202

Application of electronic fuel injection to the optimum engine for methanol utilization
[PB87-201950] 02 p0180 N88-11120

High pressure autoignition of natural gas/air mixtures and the problem of engine knock
[DE87-013799] 03 p0284 N88-11784

Investigation of fuel additive effects on sooting flames
[AD-A186403] 07 p0829 N88-15026

The effect of microgravity on flame spread over a thin fuel
[NASA-TM-100195] 08 p0967 N88-15853

Bistable cellular flames
[DE88-003074] 09 p1142 N88-16848

The chemistry of the hypochlorite neutralization of hydrazine fuels
[DE88-002971] 10 p1307 N88-17812

J85-21 fuel nozzle atomization tests
[AD-A189394] 12 p1613 N88-19647

Alternative fuels: Information on DOE's (Department of Energy's) methanol vehicle demonstration program
[PB88-118203] 13 p1753 N88-20481

Status of alcohol fuels utilization technology for highway transportation: A 1986 perspective. Volume 2: Compression ignition engines
[DE88-006059] 13 p1753 N88-20485

Molybdenum-base cermet fuel development
[DE88-005529] 13 p1839 N88-21003

Kinetics of combustion of finely divided solid fuel in granules
[BLL-M-37626-(5828.4)] 14 p1888 N88-21283

History of wildland fires on Vandenberg Air Force Base, California
[NASA-TM-100983] 18 p2549 N88-25134

Ethanol as a fuel of a lorry. Use experience from a diesel engine modified to an otto engine
[DE88-752870] 21 p2958 N88-27569

Soot and radiation in a gas turbine combustor
[AD-A191991] 23 p3179 N88-28924

FULL SCALE TESTS

Numerical field model simulation of full scale fire tests in a closed spherical/cylindrical vessel
[AD-A195067] 24 p3359 N88-29998

FUMES

Summary report of the history and events pertinent to the Civil Aeromedical Institute's evaluation of providing smoke/fume protective breathing equipment for airline passenger use
[AD-A184499] 03 p0261 N88-11645

FUMIGATION

Practical system for the use of alcohol in diesel engines
[PB88-147863] 12 p1612 N88-19638

FUNCTION GENERATORS

Normal form of a fully resonant Hamiltonian function
[PB88-100946] 06 p0767 N88-14711

Interactive generation of fractal objects
[CWI-CS-R8706] 09 p1218 N88-17302

High-voltage inverse-square function generator
[DE88-701109] 15 p2058 N88-22270

Calibration technique and study on metrological characteristics of a high-voltage inverse square-law function generator
[DE88-702101] 22 p3072 N88-28236

FUNCTION SPACE

NT BANACH SPACE
NT HILBERT SPACE

Isotropic probability measures in infinite dimensional spaces: Inverse problems/prior information/stochastic inversion
[NASA-CR-181555] 05 p0643 N88-13936

Topological equivalence of certain function spaces 2
[PB88-100904] 06 p0767 N88-14712

Linear spaces, absolute retracts and the compact extension property
[PB88-181110] 18 p2564 N88-25225

FUNCTIONAL ANALYSIS

NT BANACH SPACE
NT CONVOLUTION INTEGRALS
NT FOURIER TRANSFORMATION
NT FREDHOLM EQUATIONS

NT HARMONIC ANALYSIS
NT HILBERT SPACE
NT HILBERT TRANSFORMATION
NT INTEGRAL EQUATIONS
NT INTEGRAL TRANSFORMATIONS
NT J INTEGRAL
NT LAPLACE TRANSFORMATION
NT SINGULAR INTEGRAL EQUATIONS
NT VOLTERRA EQUATIONS
NT ZONAL HARMONICS
On the correlation free forms for nonlinear stochastic systems
[DE87-011169] 05 p0645 N88-13947
Local and global techniques for the tracking of periodic solutions of parameter-dependent functional differential equations
[AD-A185756] 06 p0766 N88-14704
Remark on the multiple Wiener integral
[AD-A186015] 07 p0913 N88-15541
Admissible and singular translates of stable processes
[AD-A186426] 07 p0917 N88-15571
Matrix functions in the stability of higher-order numerical schemes
[INPE-4245-PRE/1119] 08 p1073 N88-16472
Boundary value problems for differential and functional differential equations
[AD-A187378] 10 p1400 N88-18349
Well-posedness and spectral estimation for infinite dimensional systems
[AD-A187621] 10 p1401 N88-18354
On exterior variational calculus
[DE88-700861] 12 p1683 N88-20062
On the equivalence of four-dimensional self-duality equations to continual analog of the main chiral field problem
[DE88-700871] 12 p1686 N88-20083
Further extensions of the choquet-deny and deny theorems with applications in characterization theory
[AD-A193358] 21 p3006 N88-27834
Weak solution of the Langevin equation on a generalized functional space
[AD-A194290] 23 p3270 N88-29456
Robust finite-dimensional LQG (Linear Quadric Gaussian)-based controllers for a class of distributed parameter systems
[AD-A194872] 24 p3425 N88-30382

FUNCTIONAL DESIGN SPECIFICATIONS
Components for cryostat --- spaceborne
[MBB/ISO-TN-CD00.003-REV-A]
01 p0032 N88-10207
Access flight hardware design and development
02 p0139 N88-10873
An introduction to the GOES I-M imager and sounder instruments and the GVAR retransmission format
[NOAA-TR-NESDIS-33] 02 p0140 N88-10884
Research relative to an advanced rod control system for quadrupole mass spectrometry applications
[NASA-CR-181458] 02 p0167 N88-11050
Present status of the high resolution spectrometers
[CEBAF-PR-87-029] 02 p0234 N88-11478
Hard X-ray telescope HAPI-1 and its observation of Crab pulsar 03 p0269 N88-11692
Hollow cathode plasma coupling study, 1986
[NASA-CR-17198[illegible]] 03 p0309 N88-11949
Assessment of existing specifications against the design-philosophy for grounding and inter-unit wiring (EMCR 20/85)
[EMCR-22/85] 03 p0310 N88-11956
Alternatives to the techniques implicit in the design philosophy, and the penalties in performance associated with them --- grounding and wiring
[EMCR-31/85] 03 p0310 N88-11957
Study of an airborne Doppler radar: Project Asterix
[BLL-MO-TRANS-1667-(9022.552)]
04 p0432 N88-12675
Generic specifications for hybrid microcircuits
[ESA-PSS-01-608-ISSUE-2] 06 p0696 N88-14273
Research sensors 08 p0955 N88-15795
Optical measurement systems
08 p0955 N88-15796
Contribution to the design of flexible manufacturing systems: Modeling, simulation, and evaluation of parameters
[ISAL-IDI1-87-04] 09 p1151 N88-16894
Construction of airborne radars for remote sensing
[PB88-113063] 09 p1154 N88-16916
An approach to the hierarchical specification, design and verification of software
[RSRE-MEMO-4063] 09 p1223 N88-17332
Supercritical fluid extraction-gas chromatography of Volatile Organic Compounds (VOC) from tenax devices
[PB88-124300] 10 p1298 N88-17759
Algebra of Communicating Processes (ACP)tau: A universal axiom system for process specification
[CWI-CS-R8725] 13 p1819 N88-20869
Recommended test specification for the electromagnetic compatibility of aircraft equipment
[RAE-TM-FS(F)-510] 14 p1867 N88-21155
Towards a practical microgravity environment --- isolation mount 14 p1878 N88-21223
Further development of a mathematical model for the specification of immersion clothing insulation
[IAM-653] 14 p1954 N88-21644
Using Colored Stochastic Petri Net (CS-PN) software for protocol specification, validation, and evaluation
[ENST-87C004] 15 p2113 N88-22588
A pyrotechnical opening valve
[SNIAS-MU/TYS-NT-2-06(0)] 16 p2167 N88-22922
Development of a digital sun sensor for a spin-stabilized satellite
[INPE-4508-TDL/327] 16 p2169 N88-22929
Present, future of automotive hybrid IC applications discussed 16 p2185 N88-23024
A PC-based receiver-decoder for remote sensor monitoring
[DE88-004733] 16 p2192 N88-23075
Critical issues for SOAR: The space orbiting advanced fusion power reactor 17 p2433 N88-24474
Low cross-section Mo-Nb thermocouples for nuclear application: The state-of-the-art
17 p2433 N88-24477
Parachute for in-flight training on parachute ejection
[REPT-87-11] 18 p2458 N88-24593
Preparation for microgravity: The role of the microgravity materials science laboratory
[NASA-TM-100906] 18 p2497 N88-24811
Application-specific packaging for custom micromechanical structures 19 p2671 N88-25879
Software engineering guidelines for RASP and ANDECS: Requirements and architectural design
[DFVLR-MITT-88-07] 21 p3000 N88-27793
DSN very long baseline interferometry system Mark IV-88 22 p3067 N88-28199
Atmospheric Lidar Experiment In Space (ALEXIS)
[DFVLR-MITT-88-10] 22 p3118 N88-28526
Reliable onboard computing for critical space systems
[RR-670-I] 22 p3135 N88-28641
On eclecticism in specifications: A case study centered around Petri nets --- software engineering
[REPT-87-008] 22 p3140 N88-28671
Customizing Space Nuclear Power System Analysis Model (SNPSAM): Introducing a secondary coolant loop
[AD-A194620] 22 p3151 N88-28750
Performance and technical tolerance --- space projects 22 p3160 N88-28812
Formal specification of a secure document control system for SMITE
[RSRE-88002] 23 p3245 N88-29309
Specifications and performance of ultrastable oscillators in the DORIS orbitography and positioning system
[ETN-88-92761] 24 p3331 N88-29831
Qualification test levels for units to be derived from mechanical test data analysis --- ESA
[REPT-87-158-EI/ET/AG] 24 p3381 N88-30139
Study of human factors engineering criteria for extravehicular activity (EVA) systems, volume 1
[STF23-F87025-VOL-1] 24 p3410 N88-30298

FUNCTIONALS
A functional interpretation of the logistic equation
[REPT-87-037] 05 p0645 N88-13946
Evaluation of quantum mechanics path integrals by the approximations exact on a class of polynomial functionals
[DE88-702434] 21 p3011 N88-27865
On a class of functionals invariant under a Z(sup n) action
[AD-A193474] 23 p3269 N88-29451
Practical higher-order functional and logic programming based on lambda-calculus and set-abstraction
[AD-A193645] 23 p3271 N88-29466
Critical values of functionals on Banach surfaces
[DE88-702735] 23 p3272 N88-29472

FUNCTIONS (MATHEMATICS)
NT ABEL FUNCTION
NT ANALYTIC FUNCTIONS
NT ASYMPTOTES
NT BOOLEAN FUNCTIONS
NT CONFORMAL MAPPING
NT COORDINATE TRANSFORMATIONS
NT COSINE SERIES
NT DELTA FUNCTION
NT DISCRETE FUNCTIONS
NT DISCRIMINANT ANALYSIS (STATISTICS)
NT DISTRIBUTION FUNCTIONS
NT ELLIPTIC FUNCTIONS
NT ENTIRE FUNCTIONS
NT ERROR FUNCTIONS
NT EXPONENTIAL FUNCTIONS
NT FAST FOURIER TRANSFORMATIONS
NT FOURIER TRANSFORMATION
NT FOURIER-BESSEL TRANSFORMATIONS
NT FRESNEL INTEGRALS
NT GREEN'S FUNCTIONS
NT HAMILTONIAN FUNCTIONS
NT HANKEL FUNCTIONS
NT HYPERBOLIC FUNCTIONS
NT HYPERGEOMETRIC FUNCTIONS
NT KERNEL FUNCTIONS
NT LAGUERRE FUNCTIONS
NT LAPLACE TRANSFORMATION
NT LIAPUNOV FUNCTIONS
NT LINEAR TRANSFORMATIONS
NT LOGARITHMS
NT LORENTZ TRANSFORMATIONS
NT MAXWELL-BOLTZMANN DENSITY FUNCTION
NT MELLIN TRANSFORMS
NT MEROMORPHIC FUNCTIONS
NT MODULATION TRANSFER FUNCTION
NT MONOTONE FUNCTIONS
NT NORMAL DENSITY FUNCTIONS
NT OPTICAL TRANSFER FUNCTION
NT ORTHOGONAL FUNCTIONS
NT ORTHONORMAL FUNCTIONS
NT PENALTY FUNCTION
NT PERIODIC FUNCTIONS
NT POINT SPREAD FUNCTIONS
NT POISSON DENSITY FUNCTIONS
NT PROBABILITY DENSITY FUNCTIONS
NT PROBABILITY DISTRIBUTION FUNCTIONS
NT RAYLEIGH DISTRIBUTION
NT RECURSIVE FUNCTIONS
NT SPACE-TIME FUNCTIONS
NT SPHERICAL HARMONICS
NT SPLINE FUNCTIONS
NT STEP FUNCTIONS
NT STRESS FUNCTIONS
NT TANGENTS
NT TIME FUNCTIONS
NT TRANSCENDENTAL FUNCTIONS
NT TRANSFER FUNCTIONS
NT TRIGONOMETRIC FUNCTIONS
NT WALSH FUNCTION
NT WEIBULL DENSITY FUNCTIONS
NT WEIGHTING FUNCTIONS
Solution of nonlinear least-squares problems
[AD-A184010] 03 p0371 N88-12335
A computational examination of orthogonal distance regression
[AD-A184374] 03 p0371 N88-12337
Strong consistency of M-estimates for the linear model
[AD-A185487] 06 p0764 N88-14696
On the relations between increasing functions associated with two-parameter continuous martingales
[AD-A185572] 06 p0765 N88-14699
Upper bounds on the expected value of a convex function using gradient and conjugate function information
[AD-A186246] 07 p0910 N88-15517
Operator foundation of functional integral in non-Abelian gauge theory
[DE88-700508] 07 p0941 N88-15719
An extended Cobb-Douglas form for use in production economics
[AD-A186372] 07 p0943 N88-15733
Implementation of elementary functions in Ada
[CWI-NM-R8709] 09 p1218 N88-17303
Design and implementation of elementary functions in Ada
[CWI-NM-R8710] 09 p1218 N88-17304
An algebraic approach to a calculus of functional differences: Fixed differences and integrals
[AD-A187079] 09 p1227 N88-17346
Computation of the zeta-function of an algebraic curve with the differentials of the first kind
[PB88-127527] 10 p1399 N88-18339
A view of unconstrained optimization
[AD-A188327] 12 p1684 N88-20066
The inverse problem and the pseudo-empirical orthogonal function method of solution. Part 1: Theory. Part 2: Application
[AD-A188894] 12 p1684 N88-20069
Analiticity in fourth order wave equations
[DE88-700837] 12 p1686 N88-20080
Large momentum pairing in one-dimensional systems
[AD-A189228] 13 p1835 N88-20981
Random processes, turbulence and disordering fields
[AD-A191399] 16 p2209 N88-23181
Proposal for standard mathematical packages in Ada
[CWI-NM-R8718] 16 p2249 N88-23439
Estimation of time- and state-dependent delays and other parameters in functional differential equations
[NASA-CR-181663] 17 p2383 N88-24164
A simple explanation of the Stokes phenomenon
[AD-A193253] 21 p3006 N88-27832
An overview of lattice QCD
[DE88-010867] 21 p3026 N88-27963

An exponential decay estimate for the stationary perturbation of Poiseuille flow
[AD-A193480] 23 p3210 N88-29105
Multicriteria integer programming for problems involving linear and nonlinear utility functions
[AD-A194530] 23 p3249 N88-29336
Algorithms for nonlinear least-squares problems
[AD-A196071] 24 p3411 N88-30305

FUNGAL DISEASES
A solid phase enzyme-linked immunosorbent assay for the antigenic detection of Legionella pneumophila (serogroup 1): A compliment for the space station diagnostic capability 06 p0795 N88-14868

FUNGI
NT YEAST

FUNGICIDES
NT CAFFEINE
NT XANTHINES

FURAN RESINS
NT KEVLAR (TRADEMARK)
NT POLYAMIDE RESINS

FURANS
Novel conductive polymers
[EP-PATENT-0-182-548-A2] 01 p0026 N88-10163
The first gallium-arsenic compound containing a single Ga3As unit: Isolation and crystal structure of ((thf)Br2Ga)3As (thf = tetrahydrofuran)
[AD-A187457] 11 p1555 N88-19309

FURLABLE ANTENNAS
Aerospatiale unfurlable reflector and associated mechanisms 14 p1875 N88-21203

FURNACES
NT IMAGE FURNACES
NT SOLAR FURNACES
Metallurgy laboratory for Columbus, executive summary
[SNIAS-813-CA/TS] 02 p0157 N88-10980
Evaluation of the Mellen EDG furnace for growth of large diameter GaAs single crystals in a horizontal configuration
[DE88-000463] 04 p0498 N88-13068
Oxygen enriched combustion system performance study
[DE88-001500] 05 p0562 N88-13424
High-temperature photoelectron spectroscopy. An increased sensitivity spectrometer for studying vapor-phase species produced at furnace temperatures greater than 2000K
[AD-A186542] 09 p1140 N88-16835
Heat transfer from impinging flame jets
[ETN-88-91610] 09 p1162 N88-16964
Proceedings of the 1987 International Symposium on Condensing Heat Exchangers
[DE88-005230] 13 p1766 N88-20564
High temperature testing of C/C (Carbon/Carbon) composites
[AD-A193012] 20 p2768 N88-26411
Plasma technology: Preliminary studies 2
[DE88-752815] 22 p3154 N88-28703

FUSELAGE MOUNTING
U AIRCRAFT PRODUCTION

FUSELAGES
Controlling the dynamic environment during NOE flight 03 p0264 N88-11661
A 0.15-scale study of configuration effects on the aerodynamic interaction between main rotor and fuselage
[NASA-CR-166577] 04 p0395 N88-12462
Navier-Stokes simulation of transonic transportation aircraft configurations. 1: Flow-field simulation over wing-fuselage combinations 05 p0540 N88-13288
Compressible Euler solution on a multiblock grid around a wing-fuselage configuration
[FFA-TN-1987-46] 05 p0542 N88-13303
Coupled elastic rotor/body vibrations with inplane degrees of freedom 05 p0596 N88-13643
A study of the utilization of advanced composites in fuselage structures of commercial aircraft
[NASA-CR-172405] 06 p0679 N88-14157
Riblets for aircraft skin-friction reduction 07 p0814 N88-14955
Study on utilization of advanced composites in fuselage structures of large transports
[NASA-CR-172406] 07 p0827 N88-15014
Low frequency eddy current detection and evaluation of corrosion in aircraft skins
[ETN-88-91664] 09 p1144 N88-16859
General fuselage coordinates for the calculation of three-dimensional boundary layers
[MBB/LKE-122/S/PUB/244] 13 p1771 N88-20596
Transonic flow field analysis for real fuselage configurations 14 p1864 N88-21133
Experimental comparison of lightning simulation techniques to CV-580 airborne lightning strike measurements
[AD-A190576] 15 p2098 N88-22496
Multi-body aircraft with an all-movable center fuselage actively controlling fuselage pressure drag
[NASA-CASE-LAR-13511-1] 17 p2301 N88-23765
Helicopter anti-torque system using fuselage strakes
[NASA-CASE-LAR-13630-1] 17 p2308 N88-23809
Vibration testing of ACT fuselage 19 p2634 N88-25627
Research investigation of helicopter main rotor/tail rotor interaction noise
[NASA-CR-4143] 19 p2722 N88-26165
Missiles, fuselage and similar bodies 23 p3167 N88-28858
Missiles, fuselages and similar bodies 23 p3169 N88-28869
Test of an 0.8-scale model of the AH-64 Apache in the NASA Langley full-scale wind tunnel
[AD-A196129] 24 p3319 N88-29768

FUSES
The development of diagnostic fuses
[SAND-86-0395] 03 p0311 N88-11963
A comparative assessment of US and UK explosives qualified as replacements for tetryl
[MRL-R-1094] 13 p1754 N88-20486

FUSES (ORDNANCE)
Mechanism of and particle size effects on shock sensitivity of heterogeneous pressed explosives. Preliminary assessment of binderless RDX in fuze trains
[MRL-R-1077] 09 p1150 N88-16892
Recommended replacements for tetryl in Australian production fuzes and related ordnance
[MRL-R-1089] 13 p1754 N88-20489

FUSIFORM SHAPES
U CONES

FUSION (MELTING)
Analytical treatment of the melting and solidification of latent heat store materials in finned tube geometries
[IKE-5-223] 03 p0314 N88-11985

FUSION REACTORS
NT SPHEROMAKS
NT STELLARATORS
Plasma properties
[DE87-013662] 01 p0101 N88-10663
Fusion reactor physics and technology studies
[DE87-013691] 01 p0101 N88-10664
Technical evaluation of major candidate blanket systems for fusion power reactor
[DE87-752989] 02 p0239 N88-11512
Low activation ferritic alloys for nuclear fusion reactors
[DE87-010711] 03 p0286 N88-11801
Reduced-activation ferritic steels: A comparison with Cr-Mo steels
[DE88-000332] 03 p0290 N88-11826
The LPX (Long Pulse Experiment) facility
[DE87-010493] 03 p0311 N88-11964
Applications of neutral beam and rf technologies
[DE87-014936] 03 p0379 N88-12382
Inertial confinement fusion reactor cavity analysis
[DE88-000788] 04 p0492 N88-13028
Refueling and density control in the ZT-40M reversed field pinch
[DE88-000504] 04 p0493 N88-13040
PISCES: Plasma-surface interactions and materials research
[DE88-001323] 04 p0494 N88-13044
ICRF launcher studies
[DE88-001710] 04 p0495 N88-13046
Advanced concepts theory annual report 1986
[AD-A184986] 05 p0651 N88-13991
Dynamic processes in field-reversed-configuration compact toroids
[DE87-014756] 05 p0652 N88-13998
A short introduction to the status and motivation for reversed field pinch and compact toroid research
[DE88-000487] 05 p0652 N88-13999
A review of the experimental and theoretical status of the reversed-field pinch
[DE88-000529] 05 p0652 N88-14000
Economics of fusion reactors
[DE88-000580] 05 p0653 N88-14002
Subcommittee for MHD theory
[DE88-000596] 05 p0653 N88-14003
Transport scaling in the collisionless-detrapping regime in stellarators
[DE88-001511] 05 p0653 N88-14006
Microwave superheaters for fusion
[DE88-001656] 05 p0653 N88-14007
The TITAN oscillating-field current-drive system
[DE88-001823] 06 p0782 N88-14798
Edge plasmas and plasma/wall interactions in an ignition-class reversed field pinch
[DE88-001825] 06 p0782 N88-14799
The TITAN magnet configuration
[DE88-001826] 06 p0782 N88-14800
Reversed field pinch experiments: Summary of progress report
[DE88-002367] 07 p0934 N88-15673
Main physics features driving design concept and physics design constraints. Conceptual design study of FY86 FER
[DE88-750309] 07 p0936 N88-15689
Conceptual design study of Fusion Experimental Reactor (FY86 FER): Safety
[DE88-751071] 10 p1411 N88-18418
Diagnostics for ATF
[DE88-004175] 10 p1414 N88-18438
ATF experimental plans
[DE88-004177] 10 p1414 N88-18439
Zero-dimensional model of a reversed field pinch fusion reactor
[DE88-005213] 10 p1414 N88-18442
Low aspect ratio torsatrons
[DE88-004173] 11 p1552 N88-19284
Potential benefits of a broad magnetic fusion R and D program
[DE88-003288] 11 p1553 N88-19297
Summaries of FY86 research in the Applied Plasma Physics Fusion Theory Program
[DE88-004242] 11 p1554 N88-19298
Proceedings of US-Japan Heliotron-Stellarator Workshop, volume 3
[DE88-004788] 11 p1554 N88-19299
Proceedings of US-Japan Heliotron-Stellarator Workshop, volume 2
[DE88-004789] 11 p1554 N88-19300
Proceedings of US-Japan Heliotron-Stellarator Workshop, volume 4
[DE88-004787] 12 p1693 N88-20126
Improved zero dimensional model of a reversed field pinch fusion device
[DE88-005212] 12 p1693 N88-20127
Application of railgun principle to high-velocity hydrogen pellet injection for magnetic fusion reactor refueling
[DE88-005830] 13 p1728 N88-20334
The Magnetically Insulated Inertial Confinement Fusion (MICF): A novel approach
[DE88-005460] 13 p1842 N88-21026
Outlook for the fusion hybrid and tritium-breeding fusion reactors
[PB88-149281] 13 p1843 N88-21029
Analyses and experiments on the integrity and lifetime predictions of plasma-facing components in fusion reactors
[DE87-702957] 15 p2135 N88-22735
Magnet shielding analysis for SOAR: A space fusion reactor 17 p2400 N88-24269
A fusion based plasma propulsion system 17 p2401 N88-24274
SOAR: Space orbiting advanced fusion power reactor 17 p2416 N88-24366
Energy requirements for HE-3 mining operations on the Moon 17 p2420 N88-24390
Design studies of low aspect-ratio torsatrons
[DE88-007562] 18 p2579 N88-25320
Heavy ion fusion system assessment: Final focus and transport model
[LBL-23040] 19 p2725 N88-26183
The JET (Joint European Torus) multipellet launcher and fueling of JET plasmas by multipellet injection
[DE88-008367] 19 p2729 N88-26206
Inertial fusion in the nineties
[DE88-007913] 19 p2730 N88-26214
Pulsed power driver technologies for inertial confinement fusion power reactors
[DE88-009260] 19 p2731 N88-26221
Development of high current and high brightness negative hydrogen ion sources
[DE88-010882] 20 p2852 N88-26934
Optical imaging diagnostics for fusion plasmas
[DE88-997572] 21 p3018 N88-27910

FUSION WELDING
NT ARC WELDING
NT BRAZING
NT ELECTRON BEAM WELDING
NT GAS TUNGSTEN ARC WELDING
NT GAS WELDING
NT PLASMA ARC WELDING
Gas tungsten arc welding of Al-10Fe-5Ce
[AD-A184202] 03 p0334 N88-12104
Efficiency of fusion during periodic-pulse laser-beam welding 14 p1897 N88-21324

FUSION-FISSION HYBRID REACTORS
Development of fast breeder reactors in China 16 p2186 N88-23032

FUZZY SETS
Modeling of human judgement in multicriteria analysis using pairwise comparison
[REPT-87-01] 01 p0076 N88-10484
Foundations of O-theory 2: Measurements and relation to fuzzy set theory
[DE88-000013] 04 p0485 N88-12986
Multidimensional least squares fitting of fuzzy models
[AD-A185148] 05 p0640 N88-13916

Least squares for fuzzy vector data regression
[AD-A185156] 05 p0640 N88-13917
An application of fuzzy set theory to statistical hypothesis testing
[AD-A186705] 09 p1232 N88-17386
Measures of similarity between fuzzy concepts: A comparative analysis
[AD-A189430] 13 p1825 N88-20910
An expert system model using predicate transition nets
[AD-A191953] 19 p2718 N88-26141

FUZZY SYSTEMS
Measures of diversity based on fuzzy multinomial distributions
[DE87-010617] 02 p0228 N88-11439
Foundations of O-theory 2: Measurements and relation to fuzzy set theory
[DE88-000013] 04 p0485 N88-12986

F4H AIRCRAFT
U F-4 AIRCRAFT

G

G FORCE
U ACCELERATION (PHYSICS)

G STARS
NT SUN
The X-ray orbital lightcurves of AR Lac and TY Pyx
04 p0509 N88-13129
An analysis of the photospheric line profiles in F, G, and K supergiants 04 p0513 N88-13157
Sensitivity of the H alpha line to expansion, geometrical extent and temperature gradient in the G and K supergiant chromospheres 04 p0514 N88-13159
A helium flare on the active G5 dwarf Kappa Ceti
04 p0519 N88-13189
Observations and analysis of the photospheric magnetic fields on dwarf G, K and M stars
04 p0520 N88-13196

GADOLINIUM
Magnetic investigations of the one-dimensional Heisenberg magnet Gd2Cl3
[ETN-88-91083] 09 p1241 N88-17438
Magnetic phase transitions in 90-K superconductors Ho1Ba2Cu3O(7-delta) and Gd1Ba2Cu3O(7-delta) observed by ZF-muon(+)SR
[DE88-752611] 23 p3290 N88-29588
Absorption spectra and energy levels of Gd(3+), Nd(3+) and Cr(3+) in the garnet Gd3Sc2Ga3O12
[AD-A193834] 23 p3292 N88-29599

GAGES
U MEASURING INSTRUMENTS

GAIN (AMPLIFICATION)
U AMPLIFICATION

GALACTIC CLUSTERS
NT LOCAL GROUP (ASTRONOMY)
NT VIRGO GALACTIC CLUSTER
Finnish-Soviet Symposium on Radio Astronomy (1st) held at Otaniemi on August 26-27, 1985
[PB87-140661] 07 p0944 N88-15736
Galaxy evolution in dense clusters
13 p1855 N88-21101
Infrared constraints on the nature of dark matter
13 p1855 N88-21102
Multiple object redshift determinations in clusters of galaxies using OCTOPUS
[INPE-4528-PRE/1278] 15 p2150 N88-22835
New measurements of radial velocities in clusters of galaxies
[INPE-4527-PRE/1277] 15 p2152 N88-22845
Clustering of galaxes and clusters of galaxies in a decaying-particle cosmological model with a massive decay product
[DE88-753434] 23 p3298 N88-29642
Systematic properties of clusters of galaxies in different cosmological scenarios 23 p3299 N88-29646
Catalog of open clusters and associated interstellar matter
[NASA-RP-1202] 23 p3300 N88-29652

GALACTIC COSMIC RAYS
Production of NO by galactic cosmic rays and lightning
[DE87-014813] 02 p0197 N88-11230
Heavy element compositions and energy spectra of galactic and solar cosmic rays 03 p0272 N88-11714
Preliminary estimates of galactic cosmic ray exposures for manned interplanetary missions
[NASA-TM-100519] 05 p0661 N88-14058
Axial anisotropy of the intensity of the cosmic ray nuclear component
[IFSI-87-7] 05 p0662 N88-14061
A benchmark for galactic cosmic ray transport codes
[NASA-TM-101157] 17 p2453 N88-24571
The application of imaging to the atmospheric Cerenkov technique: Observations of the Crab nebula
20 p2884 N88-27126

GALACTIC EVOLUTION
Kinematics and galactic structure
[PREPRINT-18] 03 p0389 N88-12442
Cosmology with decaying vacuum energy
[DE88-000698] 03 p0389 N88-12443
New cosmological scenario
[DE87-703357] 04 p0520 N88-13198
Galaxy formation by gravitational collapse in a universe dominated by cold dark matter 04 p0521 N88-13205
Number count-redshift relation in a perturbed Friedmann universe
[DE88-750302] 07 p0945 N88-15743
Nonequilibrium ionization of pregalactic plasma and lessening of relic radiation anisotropy
08 p1002 N88-16071
Existence of absolutely closed universe
08 p1080 N88-16509
The origin of the diffuse X-ray background and the formation of galaxies and voids
10 p1428 N88-18527
Effects of galactic chemical evolution on thorium/neodymium cosmochronology
[DE88-003829] 11 p1570 N88-19397
Galaxy evolution in dense clusters
13 p1855 N88-21101
Cosmological parameters and evolution of the galaxy luminosity function
[NASA-CR-183081] 21 p3030 N88-27986
Evolution of heavy-element abundances in the galactic halo and disk
[DE88-011736] 22 p3164 N88-28845
Molecular hydrogen in galaxies
23 p3298 N88-29645
Starbursts and their dynamics
[NASA-CR-180227] 24 p3452 N88-30549
Observations of faint field galaxies
[NASA-CR-183251] 24 p3453 N88-30555
A deep redshift survey of field galaxies. Comments on the reality of the Butcher-Oemler effect
[NASA-CR-183255] 24 p3454 N88-30558

GALACTIC MASS
Molecular clouds at high galactic latitudes
11 p1569 N88-19392
Infrared constraints on the nature of dark matter
13 p1855 N88-21102
Global properties of star formation in spiral galaxies
14 p1994 N88-21883

GALACTIC NUCLEI
NT ACTIVE GALACTIC NUCLEI
Extragalactic VLBI objects: Candidates for optical interferometry? 01 p0094 N88-10616
Galactic nuclei and quasars at high angular resolution
01 p0098 N88-10644
Investigations of extragalactic hydroxyl
03 p0389 N88-12441
Investigation of nuclei of active galaxies as well as sources in the Large Magellanic Cloud using the X-ray astronomy satellite EXOSAT
[ETN-88-91494] 11 p1570 N88-19399
The astrophysics of nebulae and active galactic nuclear emission-line regions: New methods and applications
13 p1858 N88-21111
Model-independent requirements to the source of positrons in the galactic centre
[DE88-700968] 14 p1992 N88-21874
The galactic nucleus at mm-, sub-mm and far-infrared wavelengths
[MPE-PREPRINT-102] 16 p2288 N88-23700
The distance to the center of the galaxy: H2O maser proper motions in Sgr B2(N)
[MPE-PREPRINT-104] 16 p2288 N88-23702
Thermal-nonthermal relationships in active galactic nuclei
[B8681482] 16 p2289 N88-23707
IUE evidence on the nature of the innermost broad-line region in Seyfert 1 galaxies 17 p2450 N88-24552

GALACTIC RADIATION
NT GALACTIC COSMIC RAYS
NT GALACTIC RADIO WAVES
Investigations of extragalactic hydroxyl
03 p0389 N88-12441
Galactic interstellar abundance surveys with IUE and IRAS 04 p0522 N88-13206
Observations of the large scale anisotropy in the cosmic background radiation at 3 mm
[INPE-4425-PRE/1229] 12 p1712 N88-20249
Stars, gas and dust in the Andromeda galaxy
[B8679680] 16 p2289 N88-23708
Gamma radiation from center of the galaxy of the order of MeV values
[MPE-207] 21 p3032 N88-27999
Measurement of galactic radio emission at frequency 37 GHz from aboard spacecraft
24 p3448 N88-30520

GALACTIC RADIO WAVES
Measurement of galactic radio emission at frequency 37 GHz from aboard spacecraft
24 p3448 N88-30520

GALACTIC ROTATION
Might dark matter not be concentric with luminous matter
[DE87-703094] 02 p0252 N88-11589
Kinematics and dynamics of barred spiral galaxies
03 p0388 N88-12440
Dipole component of relict radiation determined from Relikt experiment data 08 p1002 N88-16070
The velocity field of the outer galaxy
[B8681472] 20 p2885 N88-27132
The kinematics of late-type supergiants
[SER-C-PREPUBL-FASC-28] 24 p3454 N88-30560
The dynamics of SBO galaxies. Part 1: The data
[SER-C-PREPUBL-FASC-22] 24 p3455 N88-30567

GALACTIC STRUCTURE
Kinematics and galactic structure
[PREPRINT-18] 03 p0389 N88-12442
Comments on H. Arp The persistent problem of spiral galaxies
[TRITA-EPP-87-05] 05 p0660 N88-14052
Prediction and analysis of basic gravitational microlensing phenomena 11 p1550 N88-19272
The comet flux and the 15 Myr galactic cycle
14 p1995 N88-21889
Differential spectral synthesis of the stellar populations in the bulges of spiral galaxies 17 p2451 N88-24558

GALAXIES
NT ACTIVE GALAXIES
NT ANDROMEDA GALAXY
NT BARRED GALAXIES
NT DISK GALAXIES
NT ELLIPTICAL GALAXIES
NT GALACTIC CLUSTERS
NT IRREGULAR GALAXIES
NT LOCAL GROUP (ASTRONOMY)
NT MAGELLANIC CLOUDS
NT MILKY WAY GALAXY
NT RADIO GALAXIES
NT SEYFERT GALAXIES
NT SPIRAL GALAXIES
NT STARBURST GALAXIES
NT VIRGO GALACTIC CLUSTER
Number count-redshift relation in universe models with nonzero cosmological constant
[DE87-703043] 03 p0388 N88-12435
The origin of the diffuse X-ray background and the formation of galaxies and voids
10 p1428 N88-18527
EXOSAT observations of active galaxies in the medium-energy X-ray domain
[ETN-88-91499] 14 p1993 N88-21879
Near-infrared observations of cepheids: The distance to M33 15 p2152 N88-22846
Method of digital surface photometry of galaxies and its application to the edge-on galaxy NGC 5907
16 p2287 N88-23695
Dynamics of interacting galaxies
23 p3299 N88-29647
Observations of faint field galaxies
[NASA-CR-183251] 24 p3453 N88-30555
A deep redshift survey of field galaxies. Comments on the reality of the Butcher-Oemler effect
[NASA-CR-183255] 24 p3454 N88-30558

GALAXY GROUPS
U GALACTIC CLUSTERS

GALERKIN METHOD
Semidiscrete Galerkin method for semilinear evolution equations with a differential operator of third order
[BONNER-MATHE-SCHR-181]
01 p0087 N88-10570
Numerical solution of Euler equations for compressible fluids by the finite element method, volume 3
[ETN-87-90650] 02 p0170 N88-11070
An adaptive pseudo-spectral method for reaction diffusion problems
[NASA-CR-178394] 02 p0224 N88-11414
An evaluation of a translator for finite element data to resistor/capacitor data for the heat diffusion equation
[DE87-013926] 06 p0698 N88-14285
Stabilized Galerkin method for convection-diffusion problems
[PB87-234985] 06 p0764 N88-14684
SRB combustion dynamics analysis computer program (CDA-1)
[NASA-CR-182404] 07 p0830 N88-15032
On the convergence of the p-version of the boundary element Galerkin method
[AD-A186198] 07 p0910 N88-15514

Radiative heat transfer solutions in plane-parallel participating media: Application to multilayer insulations for space vehicles
[INPE-4221-PRE/1101] 08 p0962 N88-15824

Investigation of iterative and spectral Galerkin techniques for solving electromagnetic boundary value problems 09 p1155 N88-16925

Successful mixed formulation for axisymmetric shell analysis employing discontinuous stress fields of the same order as the displacement field
[DE88-700021] 09 p1178 N88-17052

Shuttle rocket booster computational fluid dynamics
[NASA-CR-182518] 10 p1293 N88-17733

Dynamic response of some structural elements fabricated from a non-linear elastic material
10 p1344 N88-18031

Comprehensive analysis of helicopters with bearingless rotors
[NASA-CR-182537] 10 p1390 N88-18300

Finite element methods of analysis for high speed viscous flows
[NASA-CR-182529] 11 p1483 N88-18852

A velocity-pressure integrated, mixed interpolation, Galerkin finite element method for high Reynolds number laminar flows
[NASA-CR-179264] 11 p1486 N88-18868

A posterior error estimation in a finite element method for parabolic partial differential equations
[AD-A190296] 15 p2120 N88-22636

Numerical solution of linear integral equations with random forcing terms 18 p2565 N88-25237

Galerkin approximation for inverse problems for nonautonomous nonlinear distributed systems
[NASA-CR-181676] 18 p2567 N88-25246

New mixed finite element methods
18 p2567 N88-25248

Numerical simulation and stability analysis of the absolutely and convectively unstable wake
[DFVLR-FB-88-09] 21 p2949 N88-27518

Convergence of Galerkin approximations for operator Riccati equations: A nonlinear evolution equation approach
[NASA-CR-181706] 24 p3425 N88-30386

GALILEAN SATELLITES
NT IO

GALILEO MISSION
U GALILEO PROJECT

GALILEO PROBE
Galileo probe parachute test program: Wake properties of the Galileo probe at Mach numbers from 0.25 to 0.95
[NASA-RP-1130] 11 p1488 N88-18884

GALILEO PROJECT
A new code for Galileo 22 p3065 N88-28186

Mission telemetry system monitor: A real-time knowledge-based system 24 p3418 N88-30345

GALILEO SPACECRAFT
Experimental investigation of hypersonic aerodynamics
[NASA-CR-182973] 18 p2458 N88-24591

GALLIUM
IRAC test report. Gallium doped silicon band 2: Read noise and dark current
[NASA-TM-87813] 09 p1159 N88-16945

Angular resolved energy analysis of (69)Ga+ ions from a gallium liquid metal ion source
[AERE-R-12649] 15 p2139 N88-22760

Tunable optical sources/growth and characterization of nonlinear optical materials
[AD-A190874] 16 p2274 N88-23608

Nuclear magnetic resonance spectrometer
[AD-A192928] 21 p2950 N88-27523

Growth and characterization of CuGaS2, CuAlS2 and CuGa0.9Al0.1S2 single crystals
[AD-A192963] 21 p3021 N88-27930

Development of a unit cell for a Ge:Ga detector array
[NASA-CR-177445] 24 p3375 N88-30100

GALLIUM ARSENIDE LASERS
AlGaAs heterojunction lasers
[NASA-CR-4119] 09 p1171 N88-17020

Visible InGaAsP/GaAsP lasers produced by epitaxial growth from liquid phase 09 p1237 N88-17416

High-efficiency GaAs semiconductor laser with longitudinal excitation by scanning electron beam
09 p1238 N88-17421

New semiconductor laser structure for an optical communication system
[ETN-88-92353] 20 p2807 N88-26654

Diode laser ignition of high explosives and pyrotechnics
[DE88-008771] 21 p2923 N88-27352

GALLIUM ARSENIDES
NT ALUMINUM GALLIUM ARSENIDES

Effects of electron and proton irradiations on n/p and p/n GaAs cells grown by MOCVD
[NASA-TM-100199] 01 p0042 N88-10266

Study and realization of Schottky diodes for forthcoming integrated hyperfrequency devices
[LAAS-87-062] 02 p0167 N88-11054

Surface effects and low frequency noises in GaAs field effect transistors
[LAAS-87-179] 02 p0168 N88-11055

Quantum well laser diodes: Modeling and realization of GaAs/GaAlAs
[LAAS-87-165] 02 p0179 N88-11116

Gallium arsenide and multibandgap solar cell research
[DE87-012260] 02 p0194 N88-11215

Ohmic contacting schemes to gallium arsenide devices
[DE87-014627] 02 p0244 N88-11544

Photoluminescence studies of GaAs/AlAs superlattices
[DE87-013817] 02 p0245 N88-11548

Study and optimization of a technological process for the fabrication of heterojunction bipolar transistors. Applications to high speed devices
[LAAS-87-134] 02 p0246 N88-11555

Molecular beam heteroepitaxy: (Ca,Sr)F2-GaAs system
[LAAS-87-168] 02 p0246 N88-11556

Excimer laser-assisted deposition of GaAs, AlAs and (Al,Ga)As from Lewis acid-base adducts
[AD-A184588] 03 p0329 N88-12081

Performance of GaAs and silicon concentrator cells under 37 MeV proton irradiation
[NASA-TM-100144] 04 p0465 N88-12877

Radiation performance of AlGaAs concentrator cells and expected performance of cascade structures
[NASA-TM-100145] 04 p0465 N88-12878

Evaluation of the Mellen EDG furnace for growth of large diameter GaAs single crystals in a horizontal configuration
[DE88-000463] 04 p0498 N88-13068

Fundamental studies in the OM-CVD growth of Ga-In-As-Sb
[AD-A184822] 05 p0655 N88-14014

A GaAs MESFET balanced mixer with very low intermodulation
[AD-A184848] 05 p0655 N88-14015

Resonant level lifetime in GaAs/AlGaAs double-barrier structures
[AD-A185376] 05 p0655 N88-14020

Analytical investigations of bulk wave resonators in the piezoelectric thin film on gallium-arsenide configuration
[AD-A185716] 06 p0789 N88-14840

GaAs MMIC yield evaluation --- monolithic microwave integrated circuits (MMIC)
[ESA-CR(P)-2470] 08 p0979 N88-15916

Influence of arsenic superficial enrichment on the ohmicity of the n-GaAs:In/Au contact
[ECL-87-09] 08 p1089 N88-16554

Nanoelectronics
[AD-A186969] 09 p1156 N88-16930

Radiant power degradation of silicon-doped gallium arsenide and gallium aluminum arsenide infrared light-emitting diodes
[AD-A186726] 09 p1157 N88-16935

GaAs varactor diode MMIC fabrication technology --- monolithic microwave integrated circuit (MMIC)
[RSRE-MEMO-4022] 09 p1158 N88-16943

Forward-biased current annealing of radiation damaged gallium arsenide and silicon solar cells
[AD-A186904] 09 p1186 N88-17105

A report on the effects of neutron irradiation of GaAs semiconductors
[AD-A186816] 09 p1253 N88-17510

A payload for investigating the influence of convection on GaAs crystal growth 10 p1288 N88-17702

Strength and structure of Ga sub 1-xIn sub xAs alloys
[AD-A188092] 10 p1303 N88-17795

Wafer scale implementation of a GaAs systolic signal processor cell 10 p1381 N88-18247

Grazing incidence X-ray scattering study of defect structures in MBE GaAs/Si using synchrotron radiation
[DE88-004556] 10 p1420 N88-18483

Development of a planar heterojunction bipolar transistor for very high speed logic
[AD-A188137] 11 p1478 N88-18820

Positron annihilation spectroscopy of AlGaAs/GaAs interfaces in MOCVD-grown GaAs heterojunction solar cells
[DE88-003903] 11 p1508 N88-19012

Digital control of the Czochralski growth of Gallium arsenide-controller software reference manual
[AD-A187210] 11 p1528 N88-19127

Development of VLSI optical data link
[AD-A187883] 11 p1549 N88-19265

Development of VLSI optical data link
[AD-A187884] 11 p1549 N88-19266

Radiation effects on gallium arsenide integrated optical devices
[DE88-004107] 11 p1551 N88-19277

Silicon and indium doping of GaAs: Measurements of the effect of doping on mechanical behavior and relation with dislocation formation
[DE88-003862] 11 p1554 N88-19303

Structural characterization of undoped and doped GaAs: A comparative study of four techniques
[DE88-004552] 11 p1555 N88-19304

Autonomous Liquid Encapsulated Czochralski (LEC) growth of single crystal GaAs by intelligent digital control
[AD-A187211] 11 p1555 N88-19305

The first gallium-arsenic compound containing a single Ga3As unit: Isolation and crystal structure of ((thf)Br2Ga)3As (thf = tetrahydrofuran)
[AD-A187457] 11 p1555 N88-19309

Laser measurements of state-resolved Ga and In atom sticking and desorption on metal and semiconductor surfaces
[AD-A187644] 11 p1555 N88-19310

Investigation of defect and electronic interactions associated with GaAs device processing
[AD-A188021] 11 p1556 N88-19313

Ion beam modification of film stress and the effectiveness of thin film encapsulants on GaAs
[DE88-004458] 11 p1558 N88-19328

Comparison of low temperature photoluminescence of bulk MBE (Molecular Beam Epitaxy) grown AlGaAs and GaAs using a graphite generated dimer versus a standard tetramer arsenic group-V source
[DE88-004939] 11 p1558 N88-19329

Development of a multiplexer module for use in a spaceborne cryogenic environment based on GaAs MESFET technology
[RPT/CRY/62463/BOP] 11 p1559 N88-19335

Automatic prober for the dc characterization of gallium arsenide devices. Part 1: The measurement facility
[AD-A187583] 11 p1560 N88-19337

Spatial distribution of carbon and native defects in large-diameter bulk grown GaAs
[DE88-003870] 11 p1562 N88-19348

Emerging technologies program 3-5: Microelectronics Panel report
[AD-A189463] 12 p1624 N88-19716

Development of a high speed InGaAs/InP Schottky barrier photodetector for millimeter-wave fiber optical links
[AD-A188594] 12 p1629 N88-19750

Acoustic phonons, surface plasmons and surface acoustic plasmons in a superlattice and their nonreciprocal device applications
[AD-A188918] 12 p1698 N88-20163

Modeling and transport in semiconductor devices
[AD-A188760] 13 p1844 N88-21037

Research on mercury cadmium telluride
[AD-A189155] 13 p1845 N88-21039

Focused ion beam fabrication of graded channel FET's in GaAs and Si
[AD-A189166] 13 p1845 N88-21040

Optical study of germanium, germanium plus arsenic, and germanium plus gallium implants in gallium arsenide
[AD-A189600] 13 p1845 N88-21045

Electrical characteristics of MBE (Molecular Beam Epitaxy)-grown GaAs/sub 1-x/Sb/sub x on InP and correlation with film microstructure
[DE88-003841] 13 p1847 N88-21053

X-ray diffraction study of a thin GaAs film on Si(100)
[DE88-005290] 13 p1847 N88-21055

Lattice relaxation of the DX centers in Ga/sub 1-x/Al/sub x/As and of the pressure-induced deep donors in GaAs
[DE88-005452] 13 p1848 N88-21061

Energy loss rates for light holes in InGaAs/GaAs strained layer single quantum wells
[DE88-005744] 13 p1848 N88-21062

Atmospheric attenuation of near infrared radiation propagating through fog 14 p1899 N88-21342

First report on InGaAs hall device
14 p1903 N88-21372

Monolithic microwave integrated circuit technology for advanced space communication
[NASA-TM-100829] 14 p1906 N88-21389

New method of examining micrononhomogeneity of local centers in high-resistivity semiconductor materials under scanning electron microscope 14 p1969 N88-21754

Considerations in GaAs standard cell design
[DE88-003310] 14 p1985 N88-21840

In situ TEM observations of heavy ion damage in gallium arsenide
[DE88-005964] 14 p1986 N88-21843

Stress corrosion of ceramic materials
[AD-A190501] 15 p2045 N88-22187

The influence of current stressing on the structure of Ag contacts to GaAs
[DE88-005988] 15 p2140 N88-22771

Examination of temperature effects on gate-to-drain avalanche breakdown in GaAs MESFETs (Metal-Semiconductor Field Effect Transistors) by measuring light emission under RF drive
[AD-A189634] 15 p2141 N88-22778
Autonomous control system for Czochralski growth of LEC GaAs
[AD-A189726] 15 p2141 N88-22779
Design and evaluation of single-lobed far-field pattern laser arrays: AlGaAs/GaAs and InGaAsP/InP systems --- optical communication
[LAAS-88-023] 16 p2214 N88-23211
Local density of states in double-barrier resonant tunneling structures
[AD-A190673] 16 p2281 N88-23656
Initial stages of molecular beam heteroepitaxial growth in GaAs-(Ca,Sr)F2 and GaAs/Si systems
[LAAS-87-355] 16 p2281 N88-23658
Microscopic control of semiconductor interface reactivity
[AD-A191193] 16 p2283 N88-23668
Monolithic integration on a GaAs substrate of a quarter ring laser and an optical guide coupled by an evanescent wave
[ETN-88-92308] 17 p2344 N88-23969
Joint services electronics program research in electronics
[AD-A192206] 18 p2504 N88-24857
A monolithic reduced-size Ku-Band SPOT (Single-Pole Double Throw) FET switch
[DE88-006273] 18 p2505 N88-24858
Monolithic GaAs Ku-band one watt constant phase variable power amplifier
[DE88-006272] 18 p2506 N88-24866
Optical nonlinearities in GaAs/GaAlAs multiple quantum wells fabricated by metalorganic chemical vapor deposition for use in optical signal processing
[AD-A191558] 18 p2582 N88-25337
On the use of convergent beam electron diffraction for identification of antiphase boundaries in GaAs grown on Si
[DE88-008220] 18 p2585 N88-25362
InP/GaInAs/InP PIN photodiode with FWHM less than 18 ps 19 p2658 N88-25799
Monte Carlo investigation of hot photoexcited electron relaxation in GaAs 19 p2659 N88-25805
Picosecond carrier transport in GaAs quantum wells
19 p2660 N88-25813
Quantum-confined stark effect in InGaAs/InP quantum wells grown by metal-organic chemical vapor deposition
19 p2660 N88-25814
Dynamics of below-gap photoexcitation in GaAs quantum wells 19 p2660 N88-25815
Aging behavior of Au-based ohmic contacts to GaAs
[NASA-CR-182146] 19 p2662 N88-25831
Defects in high-mobility semiconductor systems
[AD-A191618] 19 p2732 N88-26224
Digital control of the czochralski growth of gallium arsenide. System reference manual. Valid for Czochralski growth controller software version 2.4
[AD-A191997] 19 p2732 N88-26227
X-ray response of GaAlAs/GaAs radiation hardened double: Heterostructure photodiode compared to Si PIN photodiodes
[DE88-007425] 19 p2733 N88-26231
Development of a GaAs solid state device model for high power applications
[DE88-009048] 19 p2734 N88-26242
Integrated optoelectronic circuits utilizing InGaAsP grown by molecular beam epitaxy (erbium doping of MBE GaAs)
[AD-A192269] 20 p2795 N88-26584
Transport in GaAs heterojunction ring structures
20 p2864 N88-27011
Pressure-dependent measurement on n + GaAs (Si, Sn): The effect of deep donor (DX) states on the electrical properties and presistent photoconductivity effects
20 p2866 N88-27020
Direct imaging of the columnar structure of GaAs quantum wells 20 p2868 N88-27030
Direct measurement of ultrafast electron-hole plasma expansion at high density at an asymmetric GaAs quantum well 20 p2871 N88-27044
Photoluminescence studies of InGaAlAs quaternary alloys
[DE88-007197] 20 p2874 N88-27062
Defects in high-mobility semiconductor systems
[AD-A192298] 20 p2879 N88-27090
Thermal conductivity of isotopically pure semiconductors, superlattices, semiconductor alloys and semiconductors as a function of temperature; control of the segregation coefficient in LEC crystal growth; and photo-Hall measurements of GaAs
21 p2927 N88-27375
Picosecond optoelectronic sampling of electrical waveforms produced by an optically excited field effect transistor
[AD-A192384] 21 p2935 N88-27428
Studying the physics and operation of multi-terminal near-micron and sub-micron length, hot electron semiconductor devices
[AD-A193380] 21 p2938 N88-27446
A GaAs solid state device model for high power applications
[DE88-011320] 21 p2939 N88-27457
Phase comparator for range imaging laser radar
[DE88-008109] 21 p2954 N88-27545
Photodiodes for optical communication in the near infrared
[ETN-88-92379] 21 p3016 N88-27900
Picosecond transient reflectivity of unpinned gallium arsenide (100) surfaces
[AD-A193242] 21 p3021 N88-27933
Investigations on the MBE (Molecular Beam Epitaxy) growth and properties of Al(sub y)Ga(sub y)In(sub 1-x-y)AsInP and InGaAs-InAlAs superlattices
[DE88-009105] 21 p3022 N88-27941
Large-signal modeling of gallium arsenide field-effect transistors 22 p3073 N88-28242
Development and experimental verification of a two-dimensional numerical model of piezoelectrically induced threshold voltage shifts in GaAs MESFETs
[AD-A193462] 23 p3206 N88-29080
Metal grid base heterojunction transistor operating at 60 and 94 GHz
[AD-A194763] 23 p3207 N88-29087
The diamond as a new electronic material
[NASA-TT-20354] 23 p3209 N88-29098
Construction of gallium arsenide solar concentrator for space use
[AD-A194658] 23 p[illegible] N88-29222
Studies on strained (In,Ga)As/GaAs semiconductors and optical devices 23 p3287 N88-29575
Laser induced chemical vapor epitaxial growth of gallium arsenide films
[AD-A194254] 23 p3291 N88-29595
Electrical conductivity of GaAs layers implanted on semi-insulator nondoped substrates
[CERT-422000/RF] 23 p3294 N88-29614
High frequency GaAlAs modulator and photodetector for phased array antenna applications
[NASA-TM-101328] 24 p3367 N88-30048
Optoelectronic gain control of a microwave single stage GaAs MESFET amplifier
[NASA-CR-182201] 24 p3368 N88-30055
Automatic prober for the dc characterisation of gallium arsenide devices. Part 2: The data sorting and display facility
[AD-A195408] 24 p3377 N88-30111
Growth of GaAs crystals by the Heat Exchanger Method for microwave device applications
[AD-A196028] 24 p3433 N88-30435
Streaking images that appear only in the plane of diffraction in undoped GaAs single crystals. Diffraction imaging (topography) by monochromatic synchrotron radiation
[NASA-CR-183267] 24 p3433 N88-30437
Joint services electronics program
[AD-A195731] 24 p3434 N88-30439

GALLIUM COMPOUNDS
NT ALUMINUM GALLIUM ARSENIDES
NT GALLIUM ARSENIDES
NT GALLIUM NITRIDES
NT GALLIUM PHOSPHIDES
Phase equilibrium and crystal growth studies on AgGaSe2 and related nonlinear optical materials
[AD-A184768] 03 p0382 N88-12400

GALLIUM NITRIDES
Deposition of device quality epitaxial layers of gallium nitride and indium nitride for electronic applications
[AD-A188001] 11 p1453 N88-18661

GALLIUM PHOSPHIDES
Effect of high-temperature annealing on the microstructure and thermoelectric properties of GaP doped SiGe
[NASA-TM-100164] 01 p0029 N88-10188
Preparation and characterization of members of the system (Zn,Se)1-xGaPx
[AD-A185073] 05 p0655 N88-14019
High-efficiency thin-film silicon-on-GaP solar cell for improved radiation resistance
[AD-A190268] 15 p2091 N88-22460
Improved GaP doped SiGe thermoelectric material
17 p2437 N88-24503
Improved properties of SiGe/GaP alloys
[NASA-CASE-NPO-17259-1-CU]
18 p2585 N88-25358
Molecular beam epitaxy of GaP films on Si substrates
[PB88-131974] 21 p3020 N88-27923
Vibration spectra induced by impurities in 3-5-compounds semiconductors
[DE88-702730] 23 p3293 N88-29610

GALVANIC CELLS
U ELECTROLYTIC CELLS

GALVANIZING
U ZINC COATINGS

GALVANOMAGNETIC EFFECTS
Integrated magnetic field sensor using high magnetotransistors
[ETN-88-92356] 21 p2941 N88-27465

GALVANOMAGNETISM
U GALVANOMAGNETIC EFFECTS

GALVANOMETERS
A twin-mirrored galvanometer laser light sheet generator
[NASA-TM-100587] 19 p2674 N88-25901

GAME THEORY
The isotropic rocket: A surveillance evasion game
[REPT-87-21] 05 p0645 N88-13949
Uncertain knowledge in distributed systems
[AD-A189017] 12 p1685 N88-20076
Perfect knowledge and beyond --- chess endgames
[REPT-87-37] 14 p1967 N88-21738
Interactive, networked moving platform simulators
[AD-A192374] 23 p3182 N88-28940
Stochastic game approach to guidance design
[AD-A194574] 23 p3276 N88-29498

GAMETOCYTES
NT EGGS

GAMMA RADIATION
U GAMMA RAYS

GAMMA RAY ABSORPTION
Gamma-ray optics of multi-beam Borrmann modes with possible applications to nuclear lasing
04 p0449 N88-12784

GAMMA RAY ASTRONOMY
Gamma ray lines from novae
04 p0526 N88-13214
A search for medium energy gamma ray pulsars
11 p1568 N88-19385
Very high energy gamma ray astrophysics
[DE88-005821] 13 p1854 N88-21095
Topics in curved and flat space electromagnetism
13 p1854 N88-21100
External tank gamma ray imaging telescope study. Final review, phase 2
[NASA-CR-179320] 15 p2150 N88-22834
Spectral modelling of the soft gamma ray repeater
[DE88-007027] 17 p2453 N88-24570
The application of imaging to the atmospheric Cerenkov technique: Observations of the Crab nebula
20 p2884 N88-27126
Application of two-dimensional imaging to very high energy gamma ray astronomy
[DE88-010120] 21 p3030 N88-27983
Gamma radiation from center of the galaxy of the order of MeV values
[MPE-207] 21 p3032 N88-27999
The application of an image intensifier to atmospheric Cerenkov gamma ray astronomy
[MPE-PREPRINT-115] 22 p3163 N88-28839
Very high energy cosmic gamma rays from radio and X-ray pulsars 23 p3309 N88-29711
Gamma radiation expected from supernova 1987A in large magellanic cloud 24 p3445 N88-30505

GAMMA RAY BURSTS
HEAO-1 observations of gamma-ray bursts
07 p0947 N88-15756
Observations of gamma bursts from GBS 0526-66
08 p1001 N88-16065
Spectral modelling of the soft gamma ray repeater
[DE88-007027] 17 p2453 N88-24570
Cascade model of gamma-ray bursts: Power-law and annihilation-line components
[NASA-TM-101176] 21 p3032 N88-27998
On the origin of gamma ray bursts
[MPE-PREPRINT-120] 22 p3166 N88-28855

GAMMA RAY LASERS
Gamma-ray optics of multi-beam Borrmann modes with possible applications to nuclear lasing
04 p0449 N88-12784
The gamma-ray laser project
[AD-A184824] 05 p0587 N88-13578
Extension of nuclear structure data base searches for gamma-ray laser candidates
[DE88-004288] 10 p1336 N88-17965
A nuclear structure study of the proposed gamma-ray laser candidate nucleus Re-186
[DE88-004299] 10 p1336 N88-17986
Shape isomers as candidates for the gamma ray laser storage state
[DE88-005228] 11 p1492 N88-18909

SDIO/IST ultrashort wavelength laser: Novel experimental schemes for observing the Mossbauer effect in long-lived nuclear levels
[AD-A190275] 15 p2072 N88-22351
SDIO/IST ultrashort wavelength laser. Mossbauer effect in gamma-ray lasers
[AD-A190306] 15 p2072 N88-22352
Primer on coupling collective electronic oscillations to nuclei
[LA-10878] 19 p2723 N88-26170
Proof of the feasibility of coherent and incoherent schemes for pumping a gamma-ray laser
[AD-A193856] 23 p3220 N88-29165

GAMMA RAY OBSERVATORY
Orbital Spacecraft Consumables Resupply System (OSCRS). Volume 2: Study results
[NASA-CR-172011] 03 p0268 N88-11687
Calibration of the EGRET gamma ray telescope with a back-scattered laser beam 06 p0800 N88-14895

GAMMA RAY SPECTRA
Gamma ray lines from novae
04 p0526 N88-13214
Gamma radiation at the 970 MeV plane positron channeling in diamond crystals
[DE88-700557] 07 p0939 N88-15705
Gamma-ray imaging observations of the Crab and Cygnus regions 10 p1427 N88-18522
Spectral modelling of the soft gamma ray repeater
[DE88-007027] 17 p2453 N88-24570
Characterization of yttrium aluminum garnet/YAG/using 14 MeV neutron activation
[AD-A191925] 18 p2582 N88-25342
VAXGAP: A code for the routine analysis of gamma-ray pulse-height spectra on a VAX computer
[DE88-011702] 22 p3137 N88-28648

GAMMA RAY SPECTROMETERS
Measurement of the gamma-ray response of some commercial silicon detectors
[AD-A187431] 11 p1543 N88-19221
Content of natural radioactive elements in Venusian rocks determined using data from Vega-1 and Vega-2 stations 13 p1726 N88-20323
The gamma-ray spectrometer experiment on the solar maximum mission satellite
[NASA-CR-182977] 17 p2452 N88-24569
Study of comet nucleus gamma-ray spectrometer penetration system
[NASA-CR-177393] 20 p2883 N88-27120
Gamma-ray/neutron spectroscopy from the Mars observer 23 p3302 N88-29671

GAMMA RAY TELESCOPES
Infra-red lamp panel study and assessment application to thermal vacuum testing of sigma telescope
02 p0132 N88-10830
Calibration of the EGRET gamma ray telescope with a back-scattered laser beam 06 p0800 N88-14895
Crystal diffraction lenses for imaging gamma-ray telescope
[DE88-003084] 08 p1083 N88-16529
Gamma-ray imaging observations of the Crab and Cygnus regions 10 p1427 N88-18522

GAMMA RAYS
NT GAMMA RAY BURSTS
Research in particles and fields
[NASA-CR-180412] 01 p0119 N88-10763
Program description of FIBRAM: A radiation attenuation model for optical fibers
[PB87-230686] 06 p0690 N88-14229
Shielding analysis of a small compact space nuclear reactor
[AD-A185566] 06 p0779 N88-14784
Combined effect of microwaves and ionizing radiation
07 p0893 N88-15413
Solar event of 27 April 1981 08 p1004 N88-16084
Gamma-ray and neutron spectroscopy of planetary surfaces and atmospheres
[DE88-004287] 10 p1430 N88-18541
Measurement of the gamma-ray response of some commercial silicon detectors
[AD-A187431] 11 p1543 N88-19221
Emission of gamma rays from various materials pulsed with 14-MeV neutrons
[DE88-003837] 11 p1544 N88-19227
Response characteristics of dual MOSFET gamma-ray sensors produced by Mitel Corporation
[AD-A189026] 12 p1630 N88-19755
The imaging of extra-galactic low-energy gamma-ray sources prospects, techniques, and instrumentation
[NASA-CR-182536] 12 p1713 N88-20251
Proof of the feasibility of coherent and incoherent schemes for pumping a gamma-ray laser
[AD-A189238] 13 p1774 N88-20613
Gamma-ray densitometry: Nondestructive analysis of density evolution during ceramic powder processing
[DE88-006671] 15 p2047 N88-22198
The response of a power MOSFET (N-channel) and a dielectric isolated operational amplifier to the combined environmental effects of high temperature and total dose gamma radiation 17 p2406 N88-24309
MMW shielding design and analysis
17 p2430 N88-24457
The response of selected semiconductor technologies to the combined environmental effects of high temperature and total dose gamma radiation
17 p2431 N88-24462
Utilization of the IR telescope gimbaling system as a stabilized pointing platform for balloon payloads. Volume 1: Technical results
[NASA-CR-179339] 18 p2522 N88-24962
Gamma rays from Cygnus X-1: Modeling and nonthermal pair production
[DE88-006830] 18 p2596 N88-25426
JFET/SOS (Junction Field-Effect Transistor/Silicon-on-Sapphire) devices: Gamma-radiation-induced effects
[AD-A193001] 20 p2795 N88-26586
Research in particle and gamma-ray astrophysics
[NASA-CR-183111] 20 p2867 N88-27146
Gamma radiation from center of the galaxy of the order of MeV values
[MPE-207] 21 p3032 N88-27999
The radiation sensitivity of select metal chelate polymers: Mechanistic changes at higher energies
[AD-A193467] 23 p3196 N88-29019
Phase modulation of recoilless gamma radiation in Mossbauer spectroscopy
[ETN-88-92648] 24 p3428 N88-30403
A coded mask telescope for observations of X and gamma ray sources in the southern sky
[INPE-4580-PRE/1314] 24 p3453 N88-30551
Research in particle and gamma-ray astrophysics
[NASA-CR-183126] 24 p3455 N88-30566
X- and gamma-ray background observations in Antarctic
[INPE-4583-PRE/1317] 24 p3459 N88-30578

GANTRIES
U GANTRY CRANES

GANTRY CRANES
Force servo control of a commercial gantry robot
[DE88-006649] 20 p2808 N88-26660

GAPS
NT ENERGY GAPS (SOLID STATE)
NT SPARK GAPS
Recovery of vacuum gaps after arcing
[DE87-013852] 01 p0039 N88-10250
Fin gaps and body slots of guided projectiles: Effects, data correlation and modeling
[AD-A184440] 03 p0270 N88-11698
The axisymmetric sealing gap with variable viscosity: A variable hydraulic resistance
[ETN-87-90604] 03 p0314 N88-11987
Geometric structure, pseudoband gaps, and surface vibrational resonances on metal surfaces
[AD-A187001] 09 p1143 N88-16851

GARNETS
NT YTTRIUM-ALUMINUM GARNET
Mode locking in Nd-laser by means of Gd-Sc-Ga-garnet shutter 09 p1237 N88-17412
Hydrodynamic simulation of forced convection in the Czochralski process
[INPE-4471-TDL/323] 12 p1697 N88-20158
High-efficiency Y-Sc-Ga:Cr (sup)3+,Tu (sup)3+,Ho (sup)3+ garnet laser (gl= 2.088 gmm at room temperature 14 p1971 N88-21766
Absorption spectra and energy levels of Gd(3+), Nd(3+) and Cr(3+) in the garnet Gd3Sc2Ga3O12
[AD-A193634] 23 p3292 N88-29599

GARP
U GLOBAL ATMOSPHERIC RESEARCH PROGRAM

GAS ANALYSIS
NT OZONOMETRY
Metal-sensing layer-semiconductor and metal-sensing layer-metal heterostructure gas sensors
[DE87-011293] 01 p0103 N88-10674
Developments in optical sensor technologies described 06 p0689 N88-14220
Analysis of gases in the earth's crust
[PB86-141619] 10 p1354 N88-18093
Method for sampling of methyl salicylate vapor in air using passivated stainless steel syringes and analysis by gas chromatography
[AD-A187838] 11 p1447 N88-18624
Breath-by-breath measurement of alveolar gas exchange 12 p1653 N88-19905
A mass spectrometer evolved gas analysis experiment for in-situ analysis of cometary dust volatiles
13 p1854 N88-21097
An automated ozone photometer
[NASA-TM-100064] 14 p1908 N88-21404
CCD-observations of gas and dust jets in the coma of Comet Halley 14 p1998 N88-21912
Profiles of the major gas emissions and distribution of dust particles in the inner coma (0 to 10,000 km) of Comet Halley 14 p1999 N88-21919
Gas coma of Comet Giacobini-Zinner: Emission from grains 14 p2000 N88-21923
Structure/property/reactivity relations among nitramine and other energetic materials
[AD-A190878] 16 p2481 N88-24716
Geological evolution and analysis of confirmed or suspected gas hydrate localities. Volume 2: Basin analysis, formation and stability of gas hydrates in the Black Sea
[DE88-001052] 18 p2532 N88-25023
Method and device for determining heats of combustion of gaseous hydrocarbons
[NASA-CASE-LAR-13528-1] 23 p3193 N88-29002
The behaviour of synthetic fuels in a small transparent combustor 24 p3351 N88-29950
Energy budget and ground temperatures in hot regions
[AD-A196298] 24 p3404 N88-30268

GAS ATOMIZATION
Laboratory scale inert gas atomizer for producing rapidly solidified powders
[DE88-006734] 16 p2497 N88-24812
Theoretical and experimental investigations on the structure of stationary shock waves in gas particle dispersions
[ETN-88-92983] 23 p3213 N88-29122

GAS BAGS
An experimental comparison of two designs of mercury propellant tank for use with an electric propulsion engine
[RAE-TR-75109] 01 p0018 N88-10109

GAS BEARINGS
Design of a spherical air bearing simulator for tests of the attitude control system of artificial satellites
[INPE-4284-PRE/1155] 12 p1595 N88-19551
Foil gas bearing system endurance testing dynamic isotope power system 17 p2405 N88-24302
Dynamic isotope power system critical component verification 17 p2425 N88-24421

GAS CHROMATOGRAPHY
Laser probes of propellant combustion chemistry
[AD-A184854] 05 p0561 N88-13415
Chemical analysis for excimer laser systems
[DE88-001941] 05 p0589 N88-13591
Application of inverse gas chromatography to fluidity studies
[DE88-002896] 10 p1296 N88-17750
Supercritical fluid extraction-gas chromatography of Volatile Organic Compounds (VOC) from tenax devices
[PB88-124300] 10 p1298 N88-17759
Method for sampling of methyl salicylate vapor in air using passivated stainless steel syringes and analysis by gas chromatography
[AD-A187838] 11 p1447 N88-18624
Chromatographic and related reactors
[AD-A188452] 12 p1605 N88-19599
Gas-chromatographic analysis of products of thermal reactions of aerosol in Venusian cloud layer on Vega-1 and Vega-2 automatic interplanetary stations
13 p1725 N88-20318
Fuels combustion research
[AD-A189114] 13 p1736 N88-20381
Chromatographic and mass spectrometric separation and analysis
[AD-A190113] 16 p2174 N88-22958
Selective detection in gas chromatography
[AD-A191499] 16 p2481 N88-24718
Thermal decomposition studies of explosives for component applications
[DE88-007201] 18 p2495 N88-24805
Fundamental studies of separation processes
[DE88-007487] 19 p2611 N88-25494
Determination of relative flammability of materials by pyrolysis and gas-chromatographic light hydrocarbon analysis
[DE88-012449] 24 p3343 N88-29898

GAS COMPOSITION
NT CARBON DIOXIDE CONCENTRATION
The composition of the gas in the loading inlet of the Space Shuttle Orbiter
[ETN-87-90430] 01 p0012 N88-10069
Diagnostics of atmospheric chemistry through ozone measurement
[INPE-4230-PRE/1105] 01 p0068 N88-10437
Role of testing total gas (O2 and CO2) tension of blood plasma in the study of human gas homeostasis
07 p0894 N88-15419
Requirements for temperature and species concentration measurements in microgravity combustion experiments 17 p2329 N88-23903
Laser Diagnostics for combustion temperature and species measurements 17 p2330 N88-23912

GAS COOLED REACTORS
NT HIGH TEMPERATURE GAS COOLED REACTORS
NT HIGH TEMPERATURE NUCLEAR REACTORS

Gas-cooled reactor for space power systems
[DE87-011549] 02 p0233 N88-11471
Gas-cooled reactor power systems for space
[DE88-005220] 11 p1545 N88-19240
IAEA Specialists' Meeting on Graphite Component Structural Design
[DE88-780006] 13 p1746 N88-20439
Basic characteristics of heat-exchanger-type steam reformer heated by high-temperature helium gas (2). Analysis by simulation model (2)
[DE87-702962] 15 p2061 N88-22291
A critique of NERVA based nuclear reactor design and performance for MMW space propulsion applications
17 p2404 N88-24297
Gas-cooled reactor power systems for space
17 p2413 N88-24350
Inherently safe space reactors
17 p2415 N88-24363
Multimegawatt nuclear power system for lunar base applications 17 p2416 N88-24367
Gas core reactors for direct nuclear propulsion
17 p2428 N88-24442
Transient analyses of multimegawatt space reactors
17 p2430 N88-24456
The NERVA derivative reactor and a systematic approach to multiple space power requirements
17 p2430 N88-24458
Burst power gas core reactor with MHD power generation 17 p2433 N88-24472

GAS COOLING
Strain rate effects in fast-gas-cooled uranium-titanium and uranium-niobium alloys
[OUEL-1683/87] 02 p0149 N88-10937
Thermal and mechanical analysis of the Faraday shield for the compact ignition tokamak
[DE88-007855] 20 p2856 N88-26962
Studies of gas turbine heat transfer airfoil surface and end-wall cooling effects
[AD-A195165] 24 p3326 N88-29805

GAS DETECTORS
ECC (Electrochemical Concentration Cell) ozonesonde observations at South Pole, Antarctica during 1986
[PB87-207502] 02 p0197 N88-11228
Combustion control with smart sensors
[DE87-013688] 03 p0281 N88-11768
Fundamental study on gas monitoring in CELSS
03 p0359 N88-12263
Plant Growth Module (PGM) conceptual design
05 p0631 N88-13855
High polymer sensor materials discussed
06 p0676 N88-14140
Computer modeling for optical waveguide sensors
[AD-A187702] 11 p1549 N88-19263
Ultrasonic oxygen sensor
[AD-A189723] 15 p2105 N88-22537
Alternate techniques for noble-gas detection
[DE88-009471] 19 p2613 N88-25507
Pyrolyzed organic polymer nitrogen dioxide sensor
19 p2669 N88-25868
Surface acoustic wave gas sensor based on film conductivity changes 19 p2673 N88-25894
Tin oxide microsensors on thin silicon membranes
19 p2673 N88-25897
Method for the isotopically selective detection of inert gases
[DE88-008370] 20 p2769 N88-26421

GAS DIFFUSION
U GASEOUS DIFFUSION

GAS DISCHARGE COUNTERS
U COUNTERS
U GAS DISCHARGE TUBES

GAS DISCHARGE TUBES
NT THYRATRONS
Gas feed system for the T-15 tokamak discharge chamber
[DE88-700351] 07 p0935 N88-15682

GAS DISCHARGES
Gas flow effects in pulse avalanche discharge XeCl excimer lasers 03 p0328 N88-12070
Measurement of the electron density and the attachment rate coefficient in silane/helium discharges
[AD-A184268] 04 p0496 N88-13051
Electron-impact-ionization and electron-attachment cross sections of radicals important in transient gaseous discharges
[AD-A192248] 20 p2770 N88-26424
Investigations on beam quality of high frequency excited CO2 high performance lasers
[ETN-88-92363] 21 p2954 N88-27550
The study of hydromagnetic waves and RF heating using the TORTUS tokamak, the development of diagnostic techniques based on submillimeter lasers and the gyrotron, and gas discharge 24 p3431 N88-30419

GAS DISSOCIATION
Initial results with the LLNL 2-D chemical-radiative-transport model of the troposphere and stratosphere
[DE88-004355] 11 p1512 N88-19033

GAS DYNAMICS
NT AERODYNAMICS
NT AEROTHERMODYNAMICS
NT INTERACTIONAL AERODYNAMICS
NT RAREFIED GAS DYNAMICS
NT ROTOR AERODYNAMICS
NT SUPERSONICS
NT UNSTEADY AERODYNAMICS
Fundamentals of numerical magnetohydrodynamics
[DE87-011769] 01 p0100 N88-10656
Dynamic effects of stellar winds and associated HII regions on the interstellar medium
[ETN-87-90421] 01 p0109 N88-10706
A simple self-breaking 2 MV gas switch
[DE87-014346] 02 p0166 N88-11047
The calculation of thermal rate constants for gas-phase and heterogeneous reactions in combustion processes
[AD-A184435] 03 p0284 N88-11788
Numerical simulation and visualization of a flowfield by interaction of two parallel two-dimensional freejets
03 p0320 N88-12021
Some aspects of high resolution numerical methods for hyperbolic systems of conservation laws, with applications to gas dynamics
[DMS-86-7] 03 p0321 N88-12031
Gas dynamic characteristics in past axial flow CO2 laser 03 p0327 N88-12067
Some asymptotic modes of transonic vortex flow
04 p0425 N88-12632
Model of solar-wind magnetosphere coupling
04 p0525 N88-13211
Dynamic stability of hypersonic conical lifting vehicles according to Newton-Busemann theory
05 p0534 N88-13247
Influence of shock wave and gas pressure on the behavior of a pyrotechnical device
[SNIAS-872-430-111] 05 p0570 N88-13477
Performance-limiting factors in MPD thrusters
[AD-A185605] 06 p0674 N88-14128
Gasdynamic effects in linear MHD generators
[ETN-88-91372] 06 p0784 N88-14810
Realization of the immediate objectives of the Aero-Gas Dynamics and Vibration Laboratory (LAGG) at the National Center for Research, Science and Technology (PUSPIPTEK) at Serpong, Java (Indonesia). Project TTA-79
[GG/QPR-10] 08 p1092 N88-16572
New techniques in computational aerodynamics
[AD-A186719] 09 p1112 N88-16664
High performance Solid Rocket Motor (SRM) submerged nozzle/combustion cavity flowfield assessment
[NASA-CR-179307] 11 p1446 N88-18622
Upper-thermospheric observations and neutral-gas dynamics at high latitudes during solar maximum
[AD-A188058] 11 p1512 N88-19031
Accurate boundary conditions for exterior problems in gas dynamics
[NASA-TM-100807] 11 p1537 N88-19182
Theoretical studies of the potential surface for the F + H2 greater than HF + H reaction
[NASA-CR-182551] 11 p1557 N88-19319
A modeling analysis program for the JPL table mountain Io sodium cloud data
[NASA-CR-182555] 11 p1570 N88-19400
A method of calculating nonstationary heat flow in hydrogasodynamic processes in closed cryogenic systems
[DE88-700664] 12 p1626 N88-19727
Heat pipe transient analysis: Vapor dynamics
[DE88-005132] 13 p1767 N88-20568
Problems in fluid dynamics
[NASA-CR-182678] 14 p1909 N88-21410
Random-choice based hybrid methods for one and two dimensional gas dynamics
[CAR-88-01] 14 p1910 N88-21415
A model of the anisotropic structure of the neutral gas coma of a comet 14 p1999 N88-21918
The role of hydrogen thermalization in shaping the Lyman-alpha coma --- comets 14 p2007 N88-21971
Investigation of combustion in large vortices
[AD-A190406] 15 p2035 N88-22121
Research sensors 15 p2085 N88-22430
Transient analysis of heat pipe vapor dynamics
17 p2412 N88-24341
Heat pipe transient analysis: Vapor dynamics
17 p2421 N88-24397
Entrance and exit region friction factor models for annular seal analysis
[NASA-CR-183084] 19 p2678 N88-25921
A shock-tube experiment on gases mixing processes associated with CO2/N2 mixing gasdynamic laser
[ISAS-RN-350] 20 p2797 N88-26598
Nozzle lip effects on gas expansion into the plume backflow region
[AD-A192806] 21 p2942 N88-27475
Investigations on beam quality of high frequency excited CO2 high performance lasers
[ETN-88-92363] 21 p2954 N88-27550
Coupling between radiation and gas dynamics
[AD-A194593] 23 p3211 N88-29113

GAS EVOLUTION
Different trapping mechanisms of gases by water ice and their relevance for comet nuclei
14 p2007 N88-21970

GAS EXCHANGE
Contribution of bubbles and waves to air-sea CO2 flux, with implications for remote sensing
[PB87-203980] 01 p0073 N88-10467
The effect of wind and currents on gas exchange in an estuarine system
[NASA-CR-181424] 01 p0073 N88-10468
Environmental life support system technology study --- space flight
[ESA-CR(P)-2432] 02 p0218 N88-11371
Controlled Ecological Life Support System: Regenerative Life Support Systems in Space
[NASA-CP-2480] 03 p0357 N88-12251
Food production and gas exchange system using blue-green alga (spirulina) for CELSS
03 p0358 N88-12253
Operation of an experimental algal gas exchanger for use in a CELSS 03 p0358 N88-12255
Sunlight supply and gas exchange systems in microalgal bioreactor 03 p0359 N88-12258
Preliminary experimental results of gas recycling subsystems except carbon dioxide concentration
03 p0359 N88-12261
Fundamental study on gas monitoring in CELSS
03 p0359 N88-12263
Influence of stratification in near-surface water layer on intensity of gas exchange between atmosphere and water 04 p0459 N88-12841
Influence of gas exchange between ocean and atmosphere on formation of atmospheric pressure field
06 p0726 N88-14467

GAS EXPANSION
A fluid simulation of the AMPTE lithium gas releases in the solar wind
[TRITA-EPP-87-06] 05 p0661 N88-14056
A study of single and binary ion plasma expansion into laboratory-generated plasma wakes
[NASA-CR-4125] 10 p1412 N88-18427
Molecular collision processes in gases and at surfaces
[AD-A189518] 13 p1836 N88-20982
Nozzle lip effects on gas expansion into the plume backflow region
[AD-A192806] 21 p2942 N88-27475

GAS EXPLOSIONS
A transient model for thermal detonation
[IKE-2-75] 03 p0314 N88-11984
Computer code simulations of explosions in flow networks and comparison with experiments
[DE88-001946] 05 p0573 N88-13491
Laser induced ignition of propellants
[AD-A191100] 16 p2168 N88-22927
Application of Particle Image Displacement Velocimetry (PIDV) to complex flows: Velocity field measurements in front of a heavy gas cloud
[VKI-TN-166] 23 p3213 N88-29125

GAS FLOW
NT AIR CURRENTS
NT AIR FLOW
NT CONTINUUM FLOW
NT COOLING FLOWS (ASTROPHYSICS)
NT EQUILIBRIUM FLOW
NT FREE MOLECULAR FLOW
NT JET STREAMS (METEOROLOGY)
NT MERIDIONAL FLOW
NT MOLECULAR FLOW
NT NONEQUILIBRIUM FLOW
NT PIPE FLOW
NT SLIP FLOW
NT TRANSITION FLOW
NT VERTICAL AIR CURRENTS
Blowdown of two-component gas mixtures in branching systems
[DE87-011392] 01 p0045 N88-10287
Vortex/boundary-layer interactions: Data report, volume 1
[NASA-CR-181462] 02 p0121 N88-10768
Optical fiber interferometric sensor to measure temperature in gas flow
[ENST-87E006] 02 p0170 N88-11071
Gas dynamic characteristics in past axial flow CO2 laser 03 p0327 N88-12067

Gas flow effects in pulse avalanche discharge XeCl excimer lasers 03 p0328 N88-12070
Conical wing with maximum lift-to-drag ratio in supersonic gas flow 04 p0425 N88-12633
On the numerical simulation of three-dimensional hypersonic flow 05 p0532 N88-13237
Rarefied gas numerical wind tunnel. 2: Two-dimensional and axially symmetric bodies 05 p0538 N88-13273
Experimental investigation of heterogeneous compressible shear layers 06 p0700 N88-14294
Gas diffusion studies in steady and nonsteady cavities
[AD-A185795] 06 p0704 N88-14318
Method of calculations for flow of ideal gas through plane and axisymmetric nozzles with broken-line contour
06 p0771 N88-14737
Programs for calculating transient Darcian flow through non-uniform materials
[DE88-001924] 07 p0852 N88-15177
SSME environment database development
[NASA-CR-179245] 08 p0964 N88-15836
A comparison of experimental and theoretical results for labyrinth gas seals with honeycomb stators
[NASA-CR-182441] 08 p0993 N88-16006
Gasflows in the transition region above sunspot
08 p1095 N88-16586
Design of a gas mass flow control system for the gas inlet installation of a solid fuel combustion chamber
[VTH-LR-471] 09 p1141 N88-16839
Modeling of pulsed gas flow lasers
[DFVLR-FB-87-19] 09 p1171 N88-17021
Development and application of oxygen flow tagging for velocity measurements and flow visualization in turbulent three-dimensional supersonic flows
[AD-A187962] 10 p1289 N88-17714
Self-pumped phase conjugation in a supersonically flowing medium
[AD-A188281] 10 p1338 N88-17996
The effect of combustion gas flow on the rotational dynamics of a spinning solid fuel rocket
13 p1732 N88-20358
Innovative, counterflow gas/fine solids, direct contact heat exchanger
[DE88-004744] 13 p1770 N88-20585
Low pressure gas flow analysis through an effusive inlet using mass spectrometry
[NASA-CR-182712] 14 p1910 N88-21413
Ammonia transfer across rotating joints in space
14 p1927 N88-21492
Effect of mass-velocity on liquid jet atomization in Mach 1 gasflow
[NASA-TM-100813] 16 p2211 N88-23194
Compressible flow in a pie-shaped cylinder rotating about the vertex 18 p2460 N88-24604
Measurement of the radiative properties of gas and oil flames
[NASA-TT-20299] 19 p2612 N88-25502
Rarefied gas numerical wind tunnel 3. Universal code for three dimensional bodies 19 p2637 N88-25644
Non equilibrium expansion of a radiating gas in a channel of varying section
[DE88-702063] 19 p2665 N88-25845
A monolithic gas flow sensor with polyimide as thermal insulator 19 p2669 N88-25864
Remote sensing and satellite applications to the needs of the gas and pipeline industry
[PB88-202668] 20 p2817 N88-26714
Some properties of ignition gases. Review of measuring results in the years 1981-1986)
[PB88-106968] 21 p2906 N88-27259
Gaseous tracer techniques for pore structure characterization of granular materials
[DE88-011542] 21 p2911 N88-27274
Computation of flow and diffusion process in gas centrifuges
[ETN-88-92366] 21 p2949 N88-27514
Low density real gas flows about hypersonic vehicles
[AD-A194251] 22 p3075 N88-28253
Nonequilibrium flow of a radiating gas in a vertical channel with axial temperature variation
[DE88-702535] 23 p3212 N88-29120
Modeling of pulsed gas flow lasers
[ESA-TT-1090] 23 p3220 N88-29169
Laser Doppler Velocimeter (LDV) and pressure measurements of gas particle flows in bends
[VKI-TN-163] 24 p3372 N88-30083
Nonequilibrium flow of a dissociating gas in a horizontal channel with axial temperature variation
[DE88-702536] 24 p3373 N88-30089
Transverse CO2 laser two-dimensional gain distributions
[AD-A196240] 24 p3378 N88-30119

GAS GENERATOR ENGINES
U ENGINES
U GAS GENERATORS

GAS GENERATORS
Vapor generation of fuels
[PB88-109897] 08 p0974 N88-15892
Experimental evaluation of a translating nozzle sidewall radial turbine 10 p1280 N88-17656
Design and aerodynamic performance of a small mixed-flow gas generator turbine
10 p1281 N88-17662
Speed control of a missile with throttleable ducted rocket propulsion 12 p1597 N88-19561
Preliminary analysis of helium generation and its effects on the SP-100 system performance
17 p2422 N88-24406

GAS GIANT PLANETS
NT JUPITER (PLANET)
NT NEPTUNE (PLANET)
NT URANUS (PLANET)
Numerical evidence that the motion of Pluto is chaotic
[AD-A195920] 24 p3455 N88-30568

GAS GUNS
NT LIGHT GAS GUNS
Ultrasonic Time-Of-Flight Diffraction (TOFD) measurements of crack depths in an acceleration reservoir of a high velocity research gun
[DE88-006644] 16 p2164 N88-22907
Use of a two-stage light-gas gun as an injector for electromagnetic railguns
[DE88-007200] 18 p2469 N88-24657

GAS HEATING
Finite element analysis of three-dimensional steady and unsteady temperature fields (computation of temperature distribution of turbine blade with composite cooling)
03 p0300 N88-11887
Microwave superheaters for fusion
[DE88-001656] 05 p0653 N88-14007
Assessment of opportunities for gas-fired sintering in the advanced ceramics and powdered metals industries
[PB88-197157] 19 p2620 N88-25545

GAS INJECTION
Direct gas injection with glow plug ignition
[PB88-187323] 19 p2676 N88-25911
Three-dimensional viscous flow computations of a circular jet in subsonic and supersonic cross flow
[NASA-CR-182153] 20 p2800 N88-26616

GAS IONIZATION
NT ATMOSPHERIC IONIZATION
NT AURORAL IONIZATION
NT FLAME IONIZATION
The study of excited oxygen molecule gas species production and quenching on thermal protection system materials
[NASA-CR-172027] 02 p0233 N88-11470
Critical Ionization Velocity (CIV) interaction: Some unsolved questions
[TRITA-EPP-87-12] 09 p1250 N88-17491
On the role of the ionization frequency to gyrofrequency ratio in the critical ionization velocity interaction
[TRITA-EPP-86-10] 10 p1410 N88-18414
High-order multiphoton ionization of the noble gases
[DE88-007489] 18 p2571 N88-25273

GAS JETS
Investigation of the effect of laterally ejected gas jets on flows
[ISL-R-107/86] 05 p0581 N88-13545
Mixing and combustion of pulsed gas jets
[PB88-112834] 06 p0680 N88-14169
Mixing and combustion of pulsed gas jets
[PB88-108014] 06 p0680 N88-14170
Dimensions of ignition zones in blow-outs of combustible gases from rectangular and circular ports
07 p0918 N88-15577
On the start up of supersonic underexpanded jets --- Mach disks 11 p1435 N88-18563
Cold gas jet system for satellite attitude control-modeling and simulation
[INPE-4279-PRE/1150] 12 p1601 N88-19583
Anisotropic emission from comets: Fans versus jets. 1: Concept and modeling 14 p2001 N88-21927
Noncondensing round turbulent gas jets in liquids
[AD-A191191] 16 p2206 N88-23179

GAS LASERS
NT CARBON DIOXIDE LASERS
NT CARBON MONOXIDE LASERS
NT EXCIMER LASERS
NT HCN LASERS
NT HELIUM-NEON LASERS
NT HF LASERS
NT KRYPTON FLUORIDE LASERS
NT NITROGEN LASERS
NT TEA LASERS
NT ULTRAVIOLET LASERS
NT XENON CHLORIDE LASERS
NT XENON FLUORIDE LASERS
Segmented hollow cathode discharges for copper ion lasers
[ETN-87-90403] 01 p0052 N88-10333
Status, development of laser devices in China
03 p0303 N88-11907
JPRS Report: Science and Technology. China
[JPRS-CST-87-033] 03 p0326 N88-12062
Laser development, evolution of applied technologies described 06 p0689 N88-14221
Neutronics conceptual design of a UF6-fueled gaseous laser system 17 p2422 N88-24405
High power axial flow CO2 laser
[ETN-88-91951] 18 p2521 N88-24959
A shock-tube experiment on gases mixing processes associated with CO2/N2 mixing gasdynamic laser
[ISAS-RN-350] 20 p2797 N88-26596
Model for pulse amplification by a gaseous laser amplifier
[DE88-011729] 20 p2808 N88-26657
MIDIR (Mid-Infrared) laser, phase 1
[AD-A193935] 23 p3220 N88-29166
Bibliography of Soviet laser developments, number 88, March - April 1987
[AD-A195978] 24 p3378 N88-30116

GAS LIQUEFACTION
U CONDENSING

GAS LUBRICANTS
Friction drag reduction (a speculative essay)
[INPE-4278-PRE/1150] 08 p0988 N88-15965

GAS LUBRICATED BEARINGS
U GAS BEARINGS

GAS MASERS
NT HYDROGEN MASERS

GAS MIXTURES
NT AIR
NT ALVEOLAR AIR
NT DETONABLE GAS MIXTURES
NT HIGH TEMPERATURE AIR
PRMIXn: A computer program for thermophysical properties of real gases and gas mixtures
[GKSS-86/E/59] 01 p0020 N88-10125
Blowdown of two-component gas mixtures in branching systems
[DE87-011392] 01 p0045 N88-10287
Detailed mechanism of benzene oxidation
[NASA-TM-100202] 03 p0282 N88-11775
Flame acceleration and transition to detonation in channels
[DE87-014193] 03 p0284 N88-11796
TOPAZ: The transient one-dimensional pipe flow analyzer: An update on code improvements and increased capabilities
[DE88-001781] 04 p0443 N88-12751
Development of a low noise 10 K J-T refrigeration system
[AD-A185258] 05 p0571 N88-13484
Chemical analysis for excimer laser systems
[DE88-001941] 05 p0589 N88-13591
Nonlinear reflection of sound wave in gas mixture
06 p0769 N88-14728
The carbon dioxide chaperon efficiency for the reaction H + O2 + M yields HO2 + M from ignition delay times behind reflected shock waves
[NASA-TM-100125] 07 p0830 N88-15036
Study of vibration relaxation in active medium of CO2-laser using phase-absorption method
07 p0919 N88-15582
Magnetic control of low pressure discharges
[AD-A186794] 10 p1322 N88-17900
Basic research on natural gas combustion phenomena
[PB88-168380] 14 p1887 N88-21278
Use of nonporous metals membranes for the seperation of hydrogen from gas mixtures
[BMFT-FB-T-86-206] 14 p1888 N88-21280
Ultrasonic oxygen sensor
[AD-A189723] 15 p2105 N88-22537
Trace gas measurements in the troposphere using tunable diode lasers 18 p2540 N88-25072
Antimisting kerosene: Low temperature degradation and blending
[NASA-CR-182725] 20 p2781 N88-26495
A shock-tube experiment on gases mixing processes associated with CO2/N2 mixing gasdynamic laser
[ISAS-RN-350] 20 p2797 N88-26596
An experimental setup for the study of polarized He3 and dilute He3-He4 mixtures
[B8705589] 23 p3193 N88-29001

GAS PHASES
U VAPOR PHASES

GAS PIPES
Technology survey for a robot which will investigate the condition of underground pipe
[PB87-209979] 01 p0055 N88-10351
Analysis and application of the constant tensile load test for polyethylene gas pipe materials
[DE88-002868] 10 p1345 N88-18037
Characteristics of welds joining parts of high-strength pipe steels and produced by beam of continuous-wave CO2-laser 14 p1897 N88-21325

Trailer shield assembly for a welding torch
[NASA-CASE-MFS-29260-1] 18 p2524 N88-24972

Remote sensing and satellite applications to the needs of the gas and pipeline industry
[PB88-202668] 20 p2817 N88-26714

GAS PRESSURE

Correlation of air pressure drop and flame arrestor characteristics for explosion suppression materials
[AD-A184960] 05 p0548 N88-13340

Gas diffusion studies in steady and nonsteady cavities
[AD-A185795] 06 p0704 N88-14318

On the signal strength dependency on pressure in laser sub-Doppler saturation spectroscopy with special attention to gaseous diatonic molecules
[USIP-87-13] 09 p1171 N88-17023

A control system for maintaining high stability in gas pressure
[DE88-003712] 09 p1175 N88-17042

On the start up of supersonic underexpanded jets --- Mach disks 11 p1435 N88-18563

Measurement of rate constants of elementary gas reactions of importance to upper atmosphere and combustion systems
[AD-A189432] 13 p1737 N88-20386

Gas diffusion studies in steady and nonsteady cavities 18 p2512 N88-24902

GAS RECOVERY

Food production and gas exchange system using blue-green alga (spirulina) for CELSS 03 p0358 N88-12253

An overview of Japanese CELSS research activities 03 p0360 N88-12267

An analysis of gas-steam total power recovery energy system 20 p2784 N88-26512

GAS SPECTROSCOPY

On the signal strength dependency on pressure in laser sub-Doppler saturation spectroscopy with special attention to gaseous diatonic molecules
[USIP-87-13] 09 p1171 N88-17023

GAS STREAMS

Spray deposition: A fundamental study of droplet impingement, spreading and consolidation
[AD-A186627] 08 p0970 N88-15869

GAS TEMPERATURE

Further development of the dynamic gas temperature measurement system 02 p0184 N88-11141

Measurements of gas velocities and temperatures in a large open pool fire
[DE87-005853] 03 p0261 N88-11641

Research sensors 08 p0955 N88-15795

Research sensors 15 p2085 N88-22430

Anomalies in the heat-capacity signatures of submonolayer adsorbates with attractive lateral interactions
[AD-A190736] 15 p2147 N88-22817

Nonequilibrium flow of a radiating gas in a vertical channel with axial temperature variation
[DE88-702535] 23 p3212 N88-29120

Nonequilibrium flow of a dissociating gas in a horizontal channel with axial temperature variation
[DE88-702536] 24 p3373 N88-30089

GAS TRANSPORT

Investigations of the dispersion of spontaneously released heavy gases
[WA-81] 01 p0066 N88-10427

TOPAZ: The transient one-dimensional pipe flow analyzer: An update on code improvements and increased capabilities
[DE88-001781] 04 p0443 N88-12751

Preliminary study of niobium alloy contamination by transport through helium 17 p2402 N88-24279

GAS TUNGSTEN ARC WELDING

Gas tungsten arc welding of Al-10Fe-5Ce
[AD-A184202] 03 p0334 N88-12104

An experimental method for species concentration measurements in a welding arc using laser-induced fluorescence
[DE88-005638] 13 p1778 N88-20636

Development of remote control welding system of large structures
[PB87-219853] 22 p3083 N88-28309

GAS TURBINE ENGINES

NT CONVERTIBLE FAN-SHAFT ENGINES
NT HYDROGEN ENGINES
NT J-57 ENGINE
NT JET ENGINES
NT RAMJET ENGINES
NT SUPERSONIC COMBUSTION RAMJET ENGINES
NT TF-30 ENGINE
NT TURBOFAN ENGINES
NT TURBOJET ENGINES
NT TURBOPROP ENGINES

Turbines with counterrotating runners for aircraft power plants 02 p0158 N88-10992

Diagnosis of flow channel in aircraft gas-turbine engines on basis of vibration spectrum characteristics 02 p0159 N88-10993

Development of a statistically proven injection molding method for reaction bonded silicon nitride, sintering reaction bonded silicon nitride, and sintered silicon nitride
[ETN-87-90575] 02 p0160 N88-11002

Investment foundry melting stock. Rolls Royce requirements and demands in terms of quality and the relationship to end product performance
[PNR90397] 02 p0160 N88-11003

Turbine Engine Hot Section Technology, 1985
[NASA-CP-2405] 02 p0184 N88-11140

The development of a high temperature static strain gage system 02 p0184 N88-11142

The Lewis Strain Gauge Laboratory: Status and plans 02 p0184 N88-11146

Fuel-injector/air-swirl characterization 02 p0185 N88-11150

Combustor-diffuser interaction program 02 p0185 N88-11152

Dilution jet mixing program, phase 3 02 p0185 N88-11153

On the mixing of a row of jets with a confined crossflow 02 p0185 N88-11154

Measurement of airfoil heat transfer coefficients on a turbine stage 02 p0186 N88-11158

Heat transfer in the tip region of a rotor blade simulator 02 p0186 N88-11159

Coolant passage heat transfer with rotation 02 p0186 N88-11160

Heat transfer with very high free stream turbulence 02 p0186 N88-11161

Prediction of turbine blade heat transfer 02 p0187 N88-11162

Flow in a model turbine stator 02 p0187 N88-11163

3D inelastic analysis methods for hot section components 02 p0187 N88-11164

3-D inelastic analysis methods for hot section components 02 p0187 N88-11165

Component specific modeling 02 p0187 N88-11166

Constitutive modeling of superalloy single crystals with verification testing 02 p0188 N88-11169

High temperature stress-strain analysis 02 p0188 N88-11170

Constitutive modeling for isotropic materials 02 p0188 N88-11171

Constitutive modeling for isotropic materials 02 p0188 N88-11172

Creep fatigue life prediction for engine hot section materials (isotropic): Third year progress review 02 p0188 N88-11173

Elevated temperature crack growth 02 p0188 N88-11174

Life prediction and constitutive models for engine hot section anisotropic materials program 02 p0188 N88-11175

Turbine airfoil deposition models and their hot corrosion implications 02 p0189 N88-11178

Experimental verification of vapor deposition rate theory in high velocity burner rigs 02 p0189 N88-11179

Effects of surface chemistry on hot corrosion life 02 p0189 N88-11180

Thermal expansion mismatch and oxidation in thermal barrier coatings 02 p0189 N88-11182

Thermal barrier coating life prediction model development 02 p0190 N88-11183

Composite mechanics for engine structures
[NASA-TM-100176] 04 p0411 N88-12552

A numerical study of the effects of curvature and convergence on dilution jet mixing
[NASA-TM-89878] 05 p0549 N88-13347

Turbine engine supportability study for Army Aviation Systems Command (AVSCOM)
[DE88-002339] 07 p0820 N88-14984

Fuel-injector/air-swirl characterization
[NASA-CR-180864] 07 p0820 N88-14985

Life modeling of thermal barrier coatings for aircraft gas turbine engines
[NASA-TM-100283] 07 p0834 N88-15060

Small gas turbine engine technology 09 p1107 N88-16638

Self-lubricating coatings for high-temperature applications 09 p1119 N88-16703

Advanced Technology for Aero Gas Turbine Components
[AGARD-CP-421] 10 p1279 N88-17647

The advantage of variable geometry for turbine engines at low power 10 p1280 N88-17653

A research program on the aerodynamics of a highly loaded turbine stage 10 p1280 N88-17655

Experimental evaluation of a translating nozzle sidewall radial turbine 10 p1280 N88-17656

An integrated aero/mechanical performance approach to high technology turbine design 10 p1280 N88-17657

Advanced techniques employed in blade cooling research 10 p1281 N88-17659

Design and aerodynamic performance of a small mixed-flow gas generator turbine 10 p1281 N88-17662

Possibilities for on-line surge suppression by fast guide vane adjustment in axial compressors 10 p1283 N88-17674

Ceramic bearings for use in gas turbine engines
[NASA-TM-100288] 10 p1340 N88-18007

Open-cycle centrifugal vapor-compression heat pump
[PB88-157391] 11 p1488 N88-18885

Error evaluation of some practical thermocouple probes for gas turbine combustor tests
[NAL-TR-938] 11 p1489 N88-18886

Effect of spatial inlet temperature and pressure distortion on turbofan engine stability
[NASA-TM-100850] 14 p1868 N88-21162

Review and assessment of the HOST turbine heat transfer program 15 p2086 N88-22431

Evaluation of ceramic thermal barrier coatings for gas turbine engine components
[ETN-88-91947] 16 p2181 N88-22998

Thermal stress minimized, two component, turbine shroud seal
[NASA-CASE-LEW-14212-1] 17 p2345 N88-23978

Corrosion prevention in gas turbines
[NLR-MP-87029-U] 20 p2760 N88-26373

COMPASS ground based engine monitoring program for general application --- Condition Monitoring and Performance Analysis Software System (COMPASS)
[PNR90420] 22 p3044 N88-28064

RB211 developments
[PNR90444] 22 p3045 N88-28069

A review of non-contacting displacement measurement techniques used to monitor the movement of rotor blades in gas turbine aero engines
[PNR90457] 22 p3045 N88-28071

The effect of coatings on fatigue in aerospace materials --- gas turbine engines
[PNR90460] 22 p3059 N88-28150

Managing and controlling change
[PNR90419] 22 p3159 N88-28801

V2500 engine collaboration
[PNR90423] 24 p3326 N88-29803

Constitutive modeling for isotropic materials
[NASA-CR-182132] 24 p3327 N88-29811

Spray automated balancing of rotors: Methods and materials
[NASA-CR-182151] 24 p3330 N88-29825

Radiation transfer in gas turbine combustors 24 p3348 N88-29929

Gas turbine smoke measurement: A smoke generator for the assessment of current and future techniques 24 p3348 N88-29930

Assessment of a 3-D boundary layer analysis to predict heat transfer and flow field in a turbine passage
[NASA-CR-174894] 24 p3370 N88-30066

GAS TURBINES

Optical sizing of soot in gas turbine combustors and exhaust augmentor tubes
[AD-A183785] 01 p0006 N88-10034

Calculation of the damage of highly loaded gas turbine disks under real flight conditions
[ETN-87-90416] 01 p0007 N88-10036

Comparison of different kinds of compact cross flow heat exchangers
[DFVLR-FB-86-63] 01 p0048 N88-10305

The influence of high free stream turbulence, intensive cooling and wake on the external heat transfer of convectively cooled gas turbine blades
[ETN-87-90432] 01 p0056 N88-10360

Development of a statistically proven injection molding method for reaction bonded silicon nitride, sintering reaction bonded silicon nitride, and sintered silicon nitride
[ETN-87-90575] 02 p0160 N88-11002

Blade excitation criteria developed for aero derived engines in Arctic Alaska
[PNR90368] 02 p0182 N88-11131

Marine gas turbines - engine health monitoring, new approaches
[PNR90369] 02 p0182 N88-11132

Combustion characteristics of gas turbine alternative fuels
[NASA-TM-100247] 05 p0548 N88-13338

Effects of free stream turbulence, Reynolds number and incidence angle on axial turbine cascade performance 05 p0548 N88-13339

Study of electrostatic modulation of fuel sprays to enhance combustion performance in an aviation gas turbine
[AD-A184967] 05 p0548 N88-1334

HOST turbine heat transfer program summary
[NASA-TM-100280] 06 p0704 N88-14320
Recent advances in high temperature instrumentation for hot section applications
[NASA-TM-100282] 06 p0707 N88-14339
Small High Pressure Ratio Turbines — conference
[VKI-LS-1987-07] 06 p0712 N88-14364
High pressure ratio turbine design constraints
[TRR-0279] 06 p0712 N88-14365
Mainline performance prediction for radial inflow turbines 06 p0712 N88-14366
Conclusions from a research program on mixed flow gas generator turbines 06 p0713 N88-14368
Highlights from a research program on a very highly loaded axial gas generator turbine
06 p0713 N88-14369
Aerodynamic design of first stage turbines for small aero engines 06 p0713 N88-14370
Aerodynamic testing of small turbines
06 p0713 N88-14371
Aerodynamic design and test performance of supersonic turbines for the Vulcain rocket engine
06 p0713 N88-14373
Report to Congress on the Automotive Technology Development Program
[DE88-003742] 07 p0864 N88-15242
Small engine technology programs
08 p0956 N88-15801
Aircraft engine hot section technology: An overview of the HOST Project 08 p0957 N88-15804
Turbine engine monitoring systems: Can they benefit component improvement program management?
[AD-A186992] 09 p1120 N88-16706
Turbine flow meter with optical fiber pick-up
[NAL-TR-923] 09 p1169 N88-17009
Wake interaction effects on the transition process on turbine blades
[AD-A188020] 10 p1332 N88-17962
Measurements of gas turbine combustor and engine augmentor tube sooting characteristics
[AD-A187831] 11 p1440 N88-18592
Gas cleaning at high temperatures and pressures for gas turbines
[DE88-751171] 11 p1440 N88-18593
Quality assurance of ceramic materials and gas turbine components
[IZFP-850303-TW] 11 p1465 N88-18735
Structural analysis methods development for turbine hot section components
[NASA-TM-100298] 11 p1501 N88-18967
Assessment, development and application of combustor aerothermal models
[NASA-TM-100290] 12 p1582 N88-19469
Hot corrosion in gas turbines: A new, unique and informative technique is EASE (Electronic Absorption Spectroscopy Experiments)
[AD-A188508] 12 p1583 N88-19470
Elevated temperature crack growth studies of advanced titanium aluminides
[AD-A189025] 12 p1608 N88-19618
Advanced Gas Turbine (AGT) Technology Development Project, ceramic component developments
[NASA-CR-180871] 12 p1709 N88-20229
Advanced Gas Turbine (AGT) technology development project
[NASA-CR-180891] 12 p1709 N88-20230
Research as part of the Air Force in aero propulsion technology (AFRAPT) program
[AD-A190336] 15 p2019 N88-22036
Small engine components test facility turbine testing cell
[NASA-TM-100887] 15 p2019 N88-22037
AFRAPT (Air Force Research in Aero Propulsion Technology) trainee program
[AD-A190525] 15 p2035 N88-22123
Experimental determination of the coefficients of the hydraulic resistance of apertures in the rotary disks
[AD-A190627] 15 p2066 N88-22317
Study on shaft seals for potassium turbine
[EL-891] 15 p2074 N88-22364
Comparison of different kinds of compact crossflow heat exchangers
[ESA-TT-1076] 16 p2207 N88-23169
Two-equation low-Reynolds-number turbulence modeling of transitional boundary layer flows characteristic of gas turbine blades
[NASA-CR-4145] 16 p2209 N88-23185
The effects of inlet turbulence and rotor/stator interactions on the aerodynamics and heat transfer of a large-scale rotating turbine model. Part 4: Aerodynamic data tabulation
[NASA-CR-179469] 17 p2339 N88-23956
Hydrogen turbines for space power systems: A simplified axial flow gas turbine model 17 p2419 N88-24385
Research on aero-thermodynamic distortion induced structural dynamic response of multi-stage compressor blading
[AD-A192169] 18 p2456 N88-24584
An empirical model of the effects of curvature and convergence on dilution jet mixing
[NASA-TM-100896] 18 p2466 N88-24640
Evaluation of manure as a feedstock for gas turbines
18 p2536 N88-25050
A 3 MW wood fired gas turbine at Red Boiling Springs, Tennessee 18 p2536 N88-25051
Hydrogen turbines for space power systems: A simplified axial flow gas turbine model
[DE88-009585] 19 p2677 N88-25920
Engine component retirement for cause. Volume 1: Executive summary
[AD-A192730] 20 p2760 N88-26371
Analysis of gas turbine test cell number 1, Lemoore Naval Air Station, California
[AD-A192870] 20 p2762 N88-26380
Use of penetrating radiations for the dynamic examination of aero gas turbines
[PNR90470] 22 p3045 N88-28073
Interaction of creep and fatigue damage in gas turbine blade material
[PNR90440] 22 p3088 N88-28335
AGARD (Advisory Group for Aerospace Research and Development) engine disc material cooperative test (supplementary program)
[AD-A193678] 23 p3179 N88-28925
Failure analysis for gas turbines
[NLR-MP-87037-U] 24 p3326 N88-29808
Gas turbine combustion modeling
24 p3349 N88-29936
Three-dimensional gas turbine combustor modelling
24 p3349 N88-29937
On the application of finite-difference techniques for the computation of the flow field in gas turbine combustors with complex geometries 24 p3349 N88-29938
Numerical modeling of combustion processes in gas turbines 24 p3350 N88-29939
Mocelling of CO oxidation in dilution jet flows
24 p3351 N88-29947
Determination of the hydroperoxide potential of jet fuels
[AD-A195975] 24 p3357 N88-29991
User's manual for three dimensional boundary layer (BL3-D) code
[NASA-CR-174899] 24 p3369 N88-30063
Contamination and distortion of steady flow field induced by discrete frequency disturbances in aircraft gas engines
[AD-A195440] 24 p3370 N88-30069

GAS VISCOSITY
Influence of viscosity on the structure of a magnetic neutral layer 08 p1098 N88-16605
Negative viscosity in global circulations
13 p1786 N88-20685

GAS WELDING
NT BRAZING
Weldability of a leaded carbon steel
[PB88-110341] 07 p0861 N88-15225

GAS-GAS INTERACTIONS
NT ASSOCIATION REACTIONS
Vortex/boundary-layer interactions. Data report, volume 1
[NASA-CR-181462] 02 p0121 N88-10768
Vortex/boundary-layer interactions. Data report, volume 2
[NASA-CR-181463] 02 p0122 N88-10769
Experimental study of interacting vortex rings
03 p0318 N88-12007
Experimental study of secondary flow in the presence of two jet arrays on the wall of a turbine blade
[ECL-87-11] 08 p0987 N88-15981
Transition metal cluster chemistry
[AD-A188731] 13 p1740 N88-20405
Numerical and experimental investigation of multiple shock wave/turbulent boundary layer interactions in a rectangular duct
[AD-A190772] 15 p2066 N88-22320
Coupling between radiation and gas dynamics
[AD-A134593] 23 p3211 N88-29113

GAS-LIQUID INTERACTIONS
NT AIR SEA ICE INTERACTIONS
NT AIR WATER INTERACTIONS
Bipropellant combustion in a liquid rocket combustion chamber 13 p1733 N88-20359
Advanced chemical heat pumps using liquid-vapor reactions
[DE88-006760] 16 p2205 N88-23159
Microgravity two-phase fluid flow pattern modeling
17 p2432 N88-24467

GAS-SOLID INTERACTIONS
Wake shield 03 p0298 N88-11871
Feasibility study for gas-grain simulation facility
[NASA-CR-177468] 05 p0646 N88-13954
Theoretical studies of kinetic mechanisms of negative ion formation in plasmas
[AD-A185735] 06 p0784 N88-14812
Different trapping mechanisms of gases by water ice and their relevance for comet nuclei
14 p2007 N88-21970
Microvax networked computer system
[AD-A190308] 15 p2114 N88-22596
An improved external recycle reactor for determining gas-solid reaction kinetics
[NASA-TM-101160] 19 p2611 N88-25492

GASDYNAMIC LASERS
Modeling of pulsed gas flow lasers
[DFVLR-FB-87-19] 09 p1171 N88-17021
Non equilibrium expansion of a radiating gas in a channel of varying section
[DE88-702063] 19 p2665 N88-25845
Modeling of pulsed gas flow lasers
[ESA-TT-1090] 23 p3220 N88-29169

GASEOUS CAVITATION
U CAVITATION FLOW
U GAS FLOW

GASEOUS DIFFUSION
Microgravity nucleation and particle coagulation experiments support
[NASA-CR-181540] 04 p0423 N88-12618
Microgravity nucleation and particle coagulation experiments support
[NASA-CR-181541] 04 p0423 N88-12619
Gas separation using solid electrolytes described
06 p0675 N88-14131
Gas diffusion studies in steady and nonsteady cavities
[AD-A185795] 06 p0704 N88-14318
Investigations of the influence of chemical reactions of the vertical flow of gaseous and particulate compounds
08 p1017 N88-16165
Measuring thin film properties using SAW (Surface Acoustic Wave) devices: Diffusivity and surface area
[DE88-002216] 13 p1834 N88-20970
Synthesis and analysis of novel polymers with potential for providing both high permselectivity and permeability in gas separation applications
[DE88-006533] 15 p2043 N88-22174
Mechanisms of gas permeation through polymer membranes: Renewal proposal for period December 1, 1986 - November 30, 1989
[DE88-007436] 18 p2494 N88-24796
Gas diffusion studies in steady and nonsteady cavities
18 p2512 N88-24902
Computation of flow and diffusion process in gas centrifuges
[ETN-88-92366] 21 p2949 N88-27514
Development of the Simplified Compressor Model (SCM) for performance analysis of gaseous diffusion compressors
[DE88-009066] 23 p3221 N88-29173

GASEOUS FISSION REACTORS
Acoustical gas core reactor with MHD power generation for burst power in a bimodal system
17 p2403 N88-24290

GASEOUS FUELS
NT NATURAL GAS
Feasibility of a complex compound heat pump
[PB88-113022] 07 p0853 N88-15183

GASES
NT AIR
NT ALVEOLAR AIR
NT AMMONIA
NT ARGON
NT ARGON ISOTOPES
NT CARBON DIOXIDE
NT CARBON MONOXIDE
NT COLD GAS
NT COMPRESSED GAS
NT DETONABLE GAS MIXTURES
NT DEUTERIUM
NT DIATOMIC GASES
NT DISSOLVED GASES
NT EXHAUST GASES
NT GAS MIXTURES
NT GAS STREAMS
NT GASEOUS FUELS
NT HELIUM
NT HELIUM ISOTOPES
NT HIGH PRESSURE OXYGEN
NT HIGH TEMPERATURE AIR
NT HIGH TEMPERATURE GASES
NT HYDROGEN
NT HYDROGEN ISOTOPES
NT IDEAL GAS
NT INTERPLANETARY GAS
NT INTERSTELLAR GAS
NT IONIZED GASES
NT KRYPTON

NT KRYPTON ISOTOPES
NT LIQUEFIED NATURAL GAS
NT LIQUID AMMONIA
NT LIQUID HELIUM
NT LIQUID HELIUM 2
NT LIQUID HYDROGEN
NT LIQUID NITROGEN
NT LIQUID OXYGEN
NT MOLECULAR GASES
NT MONATOMIC GASES
NT NATURAL GAS
NT NEON
NT NEUTRAL GASES
NT NITROGEN
NT NITROGEN ISOTOPES
NT OXYGEN
NT OXYGEN ISOTOPES
NT OZONE
NT RADON
NT RADON ISOTOPES
NT RARE GASES
NT RAREFIED GASES
NT REAL GASES
NT TRITIUM
NT XENON

Gases released by surface flashover of insulators
[DE87-013851] 01 p0039 N88-10249

Application of new conformal solution of theories
[PB87-214557] 01 p0105 N88-10684

Lattice gas hydrodynamics 03 p0313 N88-11978

Study of field adsorption using pulsed-laser field ion microscopy
[DE88-000310] 03 p0330 N88-12085

Porosity influence on the strength and elasticity of first-year sea ice
[AD-A184493] 03 p0354 N88-12233

The effect of environment on low cycle fatigue properties in HSLA steel 05 p0605 N88-13705

Gas separation using solid electrolytes described
06 p0675 N88-14131

First flight of the ATMOS instrument during the Spacelab 3 Mission, April 29 through May 6, 1985
[NASA-CR-182360] 06 p0728 N88-14482

European reacting flow research: A final assessment
[AD-A185833] 07 p0828 N88-15022

Dimensions of ignition zones in blow-outs of combustible gases from rectangular and circular ports
07 p0918 N88-15577

Gas feed system for the T-15 tokamak discharge chamber
[DE88-700351] 07 p0935 N88-15682

Operation Everest 2: Comparison of four instruments for measuring blood oxygen saturation
[AD-A186456] 08 p1049 N88-16337

Electron acceleration by laser fields in a gas
[DE88-003337] 08 p1082 N88-16523

Time dependent degradation of energetic electrons in gaseous and condensed media
[DE88-002912] 09 p1246 N88-17465

Atomic and molecular gas phase spectrometry
[AD-A187562] 11 p1452 N88-18655

Gas consumption estimation of an attitude control system of an artificial satellite (utilizing DRF) in limit cycle phase
[INPE-4336-RPE/553] 13 p1731 N88-20350

Stratospheric trace gas distributions from fair infrared thermal emission spectroscopy
13 p1797 N88-20749

Detecting the gas bubbles in a liquid metal coolant by means of magnetic flowmeters
[DE88-701427] 15 p2062 N88-22294

Gas source MBE (Molecular Beam Epitaxy)
[AD-A189763] 15 p2142 N88-22782

User's manual for EULER3DS
[AD-A191048] 16 p2208 N88-23177

Research in nonlinear partial differential equations and bifurcation theory
[AD-A190986] 16 p2260 N88-23514

Heating and evaporation of turbulent liquid films: Measurement of film thickness and the onset of nucleate boiling
[DE88-006388] 18 p2512 N88-24905

Factors which affect operation of a plasma focus in various gases
[DE88-701882] 20 p2858 N88-26975

Infrared detectors based on the photon drag effect and intersubband absorption by a two-dimensional electron gas 20 p2867 N88-27024

Experimental study of planetary gases with applications to planetary interior models
[NASA-CR-183096] 20 p2886 N88-27137

Sinterable ceramic powders from laser-heated gases
[AD-A194162] 23 p3197 N88-29024

The kinematics of Milky Way halo gas
23 p3299 N88-29648

Numerical modelling of premixed flames in gaseous media 24 p3350 N88-29944

GASIFICATION
NT COAL GASIFICATION

The applicability of the catalytic wet-oxidation to CELSS 03 p0360 N88-12264

Bench-scale studies on fluid-bed pyrolysis of wood using different contact gases 18 p2536 N88-25049

Feasibility of producing jet fuel from GPGP (Great Plains Gasification Plant) by-products
[DE88-010233] 20 p2781 N88-26492

GASOHOL (FUEL)

Compendium of significant events in the recent development of alcohol fuels in the United States
[DE87-013355] 01 p0032 N88-10202

Vapor generation of fuels
[PB88-109897] 08 p0974 N88-15892

GASOLINE

Safety implications of onboard refueling vapor recovery systems
[PB88-102603] 07 p0839 N88-15068

Summary and analysis of comments on the recommended practice for the measurement of refueling emissions
[PB88-101530] 07 p0876 N88-15313

Vapor generation of fuels
[PB88-109897] 08 p0974 N88-15892

The effect of weathering on octane quality for winter-grade and summer-grade gasolines
[AD-A190640] 16 p2183 N88-23012

Development of a laboratory test for multiport fuel injector deposits - evaluation of the Jet Fuel Thermal Oxidation Test apparatus (JFTOT)
[AD-A191313] 16 p2183 N88-23015

Upgrading pyrolysis vapors to aromatic gasoline with zeolite catalysis at atmospheric pressure
18 p2536 N88-25045

Research on hydrotreating catalysts to hydrodeoxygenate biocrude oils
18 p2536 N88-25046

Technical and economic evaluation of emerging biomass pyrolysis processes for gasoline production
.18 p2536 N88-25048

GASTROINTESTINAL SYSTEM
NT INTESTINES
NT STOMACH

Gastric emptying during walking and running: Effects of varied exercise intensity
[AD-A194025] 23 p3240 N88-29281

GATES (CIRCUITS)

Wide-area communication under Amoeba
[PB87-234431] 06 p0760 N88-14665

Impurity bands in quantum wells
[INPE-4250-PRE/1123] 08 p1089 N88-16552

Effect of the gate oxide thickness on the speed of MOS integrated circuits
[PB88-155783] 10 p1323 N88-17910

Study of quantum mechanical effects in deep submicron, grating-gate field effect transistors
[AD-A188283] 10 p1325 N88-17923

Parts-R-Us
[AD-A188621] 12 p1622 N88-19705

GM: A gate matrix layout generator
[EUT-87-E-179] 13 p1820 N88-20875

GADL: A gate array description language
[EUT-87-E-165] 14 p1907 N88-21396

Design of the Detector 2: A CMOS gate array for the study of concurrent error detection techniques
[AD-A191247] 16 p2193 N88-23079

Planar fully ion-implanted high power InP MISFETs
[AD-A191589] 18 p2582 N88-25338

Development of the field-induced electron injection and impact ionization (F4I) technique for radiation hardness testing of MOS (Metal-Oxide-Semiconductor) gate insulators
[AD-A192114] 18 p2583 N88-25345

The response of ultrathin palladium gate sensors to hydrogen and carbon monoxide
19 p2672 N88-25885

Picosecond optoelectronic sampling of electrical waveforms produced by an optically excited field effect transistor
[AD-A192384] 21 p2935 N88-27428

GATES (OPENINGS)

Test of a prototype gate with fast opening equipping the shock tube 0 2.40 m at CEG
[PB87-227884] 19 p2604 N88-25465

GAUGE INVARIANCE

Anomalies in gauge theories
[DE87-014087] 02 p0229 N88-11444

Inequivalent quantizations and fundamentally perfect spaces
[DE87-014225] 02 p0229 N88-11446

Magnitude-redshift relation in a perturbed Friedmann universe
[DE87-753020] 02 p0252 N88-11590

Comment on the Adler-Bardeen theorem and related problems
[DE88-751051] 10 p1403 N88-18367

Chiral symmetry breaking in finite quantum electrodynamics
[DE88-700860] 12 p1699 N88-20188

Recent developments in the path integral approach to anomalies
[DE87-703032] 15 p2118 N88-22616

Path integral, BRS symmetry, and string and membrane theories
[DE88-752300] 15 p2146 N88-22810

Quantization of axial electrodynamics
[DE88-701498] 15 p2147 N88-22813

General relativity invariance and string field theory
[DE88-702045] 19 p2737 N88-26252

Some remarks on geodesics in gauge groups and harmonic maps
[DE88-702665] 22 p3115 N88-28510

GAUGE THEORY

Anomalies in gauge theories
[DE87-014087] 02 p0229 N88-11444

Research program in elementary particle theory
[DE88-000159] 02 p0233 N88-11468

Finite size scaling and lattice gauge theory
[DE87-014139] 02 p0245 N88-11549

Regular effective action of gauge field theory and quantum gravity
[DE87-703076] 02 p0247 N88-11560

Geometrization of Planck length in composite gravity and supergravity
[DE87-703085] 02 p0251 N88-11588

A supersymmetric Lagrangian for Poincare gauge theories of gravity
[DE88-001670] 04 p0500 N88-13078

Gravity from symmetry breakdown of a gauge affine theory
[DE88-001671] 04 p0500 N88-13079

Operator foundation of functional integral in non-Abelian gauge thoory
[DE88-700508] 07 p0941 N88-15719

Secondary gauge conditions in field theory
[DE88-701499] 15 p2147 N88-22814

Rigid symmetries and BRST-invariance in gauge theories
[PB88-180948] 18 p2572 N88-25280

Introduction to lattice gauge theory
[DE88-006073] 18 p2584 N88-25349

Topics in gauge theories and the unification of elementary particle interactions
[DE88-008112] 19 p2738 N88-26256

Closed string fields as parameters of extra gauge symmetry of open string field theory
[DE88-702046] 21 p3026 N88-27980

Theoretical particle physics
[DE88-011499] 23 p3295 N88-29621

Lagrangian of the self-duality equation and d = 10, N = 2b supergravity
[DE88-701554] 24 p3455 N88-30563

GAUSS EQUATION

Local properties of index-alpha stable fields
[AD-A186432] 07 p0912 N88-15530

Application of artificial intelligence to impulsive orbital transfers 08 p1066 N88-16439

Gaussian techniques on shared memory multiprocessor computers
[DE88-005426] 13 p1817 N88-20855

Exact image method for Gaussian beam problems involving a planar interface
[NASA-CR-182702] 14 p1905 N88-21380

Limiting distributions of non-linear vector functions of stationary Gaussian processes
[AD-A194569] 23 p3274 N88-29488

GAUSS FUNCTION
U GAUSS EQUATION

GAUSS-MARKOV THEOREM

Computational behavior of Gauss-Newton methods
[DE87-014486] 02 p0224 N88-11413

Concentration inequalities for Gauss Markov estimators
[CWI-MS-R8706] 14 p1965 N88-21726

A unified approach to estimation in linear models with fixed and mixed effects
[AD-A193060] 21 p3006 N88-27829

GAUSSIAN DISTRIBUTIONS
U NORMAL DENSITY FUNCTIONS

GAUSSIAN ELIMINATION

A graph separator theorem and its application to Gaussian elimination to optimize Boolean expressions for parallel evaluation
[AD-A188527] 14 p1962 N88-21706

Gaussian techniques on shared-memory multiprocessors
[DE88-010594] 19 p2716 N88-26126

Reducing the parallel solution time of sparse circuit matrices using reordered Gaussian elimination and relaxation
[AD-A195152] 24 p3366 N88-30045

GAUSSIAN NOISE
U RANDOM NOISE

GAUSSMETERS
U MAGNETOMETERS

GC-130 AIRCRAFT
U C-130 AIRCRAFT

GCR (REACTORS)
U GAS COOLED REACTORS

GDOP
U GEOMETRIC DILUTION OF PRECISION

GEAR TEETH
A hydrodynamic analysis of fluid flow between meshing spur gear teeth
[AD-A187671] 11 p1482 N88-18644
Spur gears: Optimal geometry, methods for generation and Tooth Contact Analysis (TCA) program
[NASA-CR-4135] 16 p2215 N88-23216

GEARS
Assessment of the COFSI/MAST I project
[NASA-CR-181366] 01 p0053 N88-10340
Improving repairability of gears
02 p0158 N88-10989
Multipath gear-friction planetary transmissions
04 p0424 N88-12629
On dynamic loads in parallel shaft transmissions. 1: Modelling and analysis
[NASA-TM-100180] 04 p0451 N88-12797
On dynamic loads in parallel shaft transmissions. 2: Parameter study
[NASA-TM-100181] 04 p0452 N88-12798
Efficiency testing of a helicopter transmission planetary reduction stage
[NASA-TP-2795] 07 p0861 N88-15224
Pin joints, gears, springs, cranks and other novel micromechanical structures
[DE88-002504] 07 p0864 N88-15245
Rotorcraft transmission 08 p0956 N88-15802
Experimental investigation on the bending fatigue performance of gas carbonitrided and carburized gears
[PB87-147997] 08 p0992 N88-16003
Results of NASA/Army transmission research
09 p1108 N88-16640
Dynamic analysis of multimesh-gear helicopter transmissions
[NASA-TP-2789] 09 p1176 N88-17045
Dynamic response of a geared train of rotors subjected to random support excitations 09 p1181 N88-17073
Gear systems for advanced turboprops
10 p1282 N88-17667
Analysis of possible transmission arrangements applicable for driving single or twin counterrotating fans on propfan engines 10 p1282 N88-17670
Army maintenance: Actions to reduce the likelihood of helicopter gear failures
[PB88-135256] 11 p1433 N88-18551
Finite element methods for quasi-prismatic bodies with application to gears 13 p1779 N88-20644
The performance of thin solid films for satellite gears
14 p1876 N88-21209
Advanced transmission studies
[NASA-TM-100867] 14 p1919 N88-21454
Spur gears: Optimal geometry, methods for generation and Tooth Contact Analysis (TCA) program
[NASA-CR-4135] 16 p2215 N88-23216
Linear force device
[NASA-CASE-MSC-20549-2] 18 p2516 N88-24927
Design, manufacture and spin test of high contact ratio helicopter transmission utilizing Self-Aligning Bearingless Planetary (SABP)
[NASA-CR-4155] 18 p2524 N88-24975
Determination of settings of a tilted head-cutter for generation of hypoid and spiral bevel gears
[NASA-CR-182138] 18 p2524 N88-24976
Surface fatigue life of CBN and vitreous ground carburized and hardened AISI 9310 spur gears
[NASA-TM-100960] 19 p2677 N88-25916
A review of gear housing dynamics and acoustics literature
[NASA-CR-183110] 20 p2811 N88-26675
Optimization of planetary gears
[ETN-88-92375] 21 p2958 N88-27573
An analytical investigation of geared system dynamics containing spur and helical gears
22 p3085 N88-28317
Design and evaluation of high contact ratio gearing
[NASA-CR-174958] 22 p3085 N88-28319
High hot-hardness gear lubricant evaluations, phase 2
[AD-A192309] 23 p3196 N88-29017

GEL PERMEATION CHROMATOGRAPHY
U LIQUID CHROMATOGRAPHY

GELATION
Cure and properties of thermosetting polymers
[AD-A184669] 03 p0293 N88-11843
Molecular engineering of ceramics
[DE88-000174] 04 p0420 N88-12603
Glassy GeO2 obtained by the gel process
[NASA-TT-20125] 06 p0685 N88-14201
The numerical simulation of viscous flows with change of phase and chemical reaction
[DE88-003204] 15 p2062 N88-22292

GELLED PROPELLANTS
NT GELLED ROCKET PROPELLANTS
Characterization of aluminum/RP-1 gel propellant properties
[NASA-TM-100951] 18 p2496 N88-24808

GELLED ROCKET PROPELLANTS
Burning rate measurements of Non-Newtonian Liquid Propellant (NNLP) 19 p2623 N88-25561

GELS
NT DOUBLE BASE ROCKET PROPELLANTS
NT SILICA GEL
Use of sol-gels in the application of ceramic oxide thin films
[DE87-013610] 01 p0028 N88-10176
Molecular engineering of ceramics
[DE88-000174] 04 p0420 N88-12603
T.E.M. study of boehmite gels and of their transformation into alpha-alumina
[SNIAS-872-430-121] 05 p0656 N88-14023
Fluids, gels and glasses under extreme conditions of pressure and temperature
[AD-A190655] 15 p2035 N88-22125
Cellular thermosetting fluoropolymers and process for making them
[NASA-CASE-GSC-13008-1] 17 p2326 N88-23894
Electrode films of porous agarose: The effects of physical structure on electron transport processes
[DE88-007366] 19 p2611 N88-25493
Characterization of the surface area and porosity of sol-gel films using saw devices
[DE88-008794] 20 p2875 N88-27069
Preparation and properties of new inorganic glasses and gel-derived solids
[AD-A192922] 21 p2917 N88-27315
Method of dispensing reagent chemicals in space
[NASA-CASE-LAR-13607-1-CU]
23 p3200 N88-29048

GEMINID METEOROIDS
Some models of the Geminids meteor stream formation 06 p0740 N88-14551

GENERAL AVIATION AIRCRAFT
NT AGRICULTURAL AIRCRAFT
NT DO-28 AIRCRAFT
Wind-tunnel investigation of a full-scale general aviation airplane equipped with an advanced natural laminar flow wing
[NASA-TP-2772] 01 p0002 N88-10009
Aircraft accident reports, brief format, US civil and foreign aviation. Issue number 1: 1986 accidents
[PB87-916903] 02 p0123 N88-10781
Semiempirical method for prediction of aerodynamic forces and moments on a steadily spinning light airplane
[NASA-TM-4009] 04 p0393 N88-12456
Wind tunnel results for a high-speed, natural laminar-flow airfoil designed for general aviation aircraft
[NASA-TM-87602] 06 p0665 N88-14078
Aircraft accident reports: Brief format, US Civil and Foreign Aviation, Issue Number 4 of 1986 accidents
[PB87-916906] 06 p0666 N88-14086
Sudden in-flight incapacitation in general aviation
[AD-A187044] 09 p1115 N88-16682
Investigation of the misfueling of reciprocating piston aircraft engines
[NASA-TP-2803] 14 p1865 N88-21144
It's time to reinvent the general aviation airplane
17 p2294 N88-23726
High-flaps for natural laminar flow airfoils
17 p2296 N88-23739
Certification aspects of airplanes which may operate with significant natural laminar flow 17 p2298 N88-23749
Development of a multipurpose smart recorder for general aviation aircraft
[NASA-CR-168353] 18 p2465 N88-24637

GENERAL DYNAMICS AIRCRAFT
NT F-106 AIRCRAFT
NT F-111 AIRCRAFT

GENERAL DYNAMICS MILITARY AIRCRAFT
U MILITARY AIRCRAFT

GENERATORS
Optimum size of staged flux compression generators
[DE87-011741] 01 p0038 N88-10244
Cast iron-base alloy for cylinder/regenerator housing
[NASA-CR-182116] 12 p1608 N88-19613

GENETIC CODE
The human genome: Computational challenges
[DE88-006465] 18 p2549 N88-25131

GENETIC ENGINEERING
Biopolymers: Protein and nucleic acids
[AD-A185837] 07 p0835 N88-15066
Synthesis of high molecular weight peptide polymers and copolymers containing L-dope residues
[AD-A186462] 08 p0973 N88-15887
Potential use of the bioreactor to determine effects of microgravity and other environmental parameters on growth of hybridoma cells 09 p1198 N88-17178
The use of plant protoplasts in biotechnological space research 12 p1655 N88-19914
Biology and Medicine Division
[DE87-009280] 14 p1952 N88-21632
Saccharification of cellulose by combined fungal and bacterial preparations 17 p2316 N88-23833
The human genome: Computational challenges
[DE88-006465] 18 p2549 N88-25131
Ecological risk factors related to environmental uses of genetically engineered organisms
[DE88-006674] 18 p2549 N88-25132

GENETICS
JPRS report: Science and technology. USSR: Life sciences
[JPRS-ULS-87-009] 04 p0473 N88-12915
Review of cytoskeleton research in cell differentiation and development
[AD-A185832] 07 p0882 N88-15353
A theoretical concept for state changes and shape changes in weightlessness 07 p0884 N88-15365
Physiological and biochemical aspects of toxic effects of oxidants in man's environment (air, water)
07 p0890 N88-15391
Investigation of genetic structures of rat germ cells following flight aboard Cosmos-1514 biosatellite during their prenatal development 10 p1364 N88-18155
Genetic research in space
[NASA-TT-20216] 11 p1518 N88-19066
A Darwinian approach to artificial neural systems
[DE87-013184] 13 p1824 N88-20900
ECUT (Energy Conversion and Utilization Technologies) program: Biocatalysis Project
[NASA-CR-182917] 17 p2370 N88-24110
Genetic effects of low level microwave radiation
[AD-A192687] 21 p2984 N88-27722
The effects of microgravity on genetic recombination in Escherichia coli --- Spacelab D1 mission
22 p3060 N88-28157

GENITOURINARY SYSTEM
NT KIDNEYS
NT TESTES

GEO ENVIRONMENTS
U EARTH ORBITAL ENVIRONMENTS

GEOASTROPHYSICS
U ASTROPHYSICS
U GEOPHYSICS

GEOBOTANY
Overview of Austrian Airborne Imaging Spectrometer (AIS) programme and first results
05 p0612 N88-13762

GEOCHEMISTRY
NT BIOGEOCHEMISTRY
Development of an X-ray fluorescence microprobe at the National Synchrotron Light Source, Brookhaven National Laboratory: Early results: Comparison with data from other techniques
[NASA-CR-181468] 02 p0236 N88-11486
A mineral reconnaissance sampling manual for Costa Rica: Central American energy and resource project
[DE87-014997] 04 p0462 N88-12859
Summaries of physical research in the geosciences
[DE88-000833] 04 p0468 N88-12896
RRS DISCOVERY cruise 160, 30 June-25 July, 1986. Geochemical sampling over the Madeira and Porcupine Abyssal Plains
[PB87-222030] 04 p0471 N88-12910
Geochemistry of freezing brines, low-temperature properties of sodium chloride
[AD-A185751] 06 p0680 N88-14165
Research needs for hydrocarbon fuels
[DE87-014555] 06 p0687 N88-14209
Petrogenesis of basalts from the Archean Matachewan Dike Swarm Superior Province of Canada
06 p0796 N88-14875
Nature and origin of mineral coatings on volcanic rocks of the Black Mountain, Stonewall Mountain, and Kane Springs Wash volcanic centers, Southern Nevada
[NASA-CR-181437] 09 p1191 N88-17140
Earth materials research: Report of a Workshop on Physics and Chemistry of Earth Materials
[NASA-CR-182519] 10 p1298 N88-17761
Analysis of gases in the earth's crust
[PB88-141619] 10 p1354 N88-18093
Trace element geochemistry of the South Atlantic Bight
[DE88-003515] 10 p1356 N88-18108

Reports and contributions of the Max-Planck Institute of Chemistry (Otto Hahn Institute)
[REPT-1/87] 11 p1570 N88-19398
Advances in geochemistry and cosmochemistry: Trace element microdistributions with the synchrotron X-ray fluorescence microprobe
[DE88-006355] 15 p2032 N88-22108
Geochemistry of the middle and lower atmosphere: Environmental impact through the deterioration of the ozone layer
[INPE-4477-PRE/1241] 16 p2230 N88-23321
A sedimentological and mineralogical study of the Koogah Formation, New South Wales
18 p2542 N88-25087
SPOT images and geochemical mapping of lateritic covers in southern Mali 22 p3105 N88-28438
MEVTV Workshop on Nature and Composition of Surface Units on Mars
[NASA-CR-183075] 23 p3300 N88-29654
Mars: Spectral signatures seen and unseen
23 p3301 N88-29659
Aqueous alteration in S-N-C meteorites and implications for weathering products on Mars
23 p3303 N88-29673
Pb isotope constaints on the extent of crustal recycling into a steady state mantle 24 p3394 N88-30215
Crustal evolution and the eclogite to granulite phase transition in xenoliths from the West African Craton
24 p3395 N88-30217
Changing styles of crustal growth in Southern Africa: Constraints from geochemical and Sr-Nd isotope studies in Archaean to Pan African terrains
24 p3396 N88-30227
Continental crustal formation and recycling: Evidence from oceanic basalts 24 p3398 N88-30238
Evolution of the Dharwar Craton: A terrain of early Archean crustal stability, long term orogenic cycles and large scale palaeobiological activity
24 p3399 N88-30241
The growth of the continental crust: Constraints from radiogenic isotope geochemistry
24 p3399 N88-30245
Crustal growth in the Archean: The geochemical evidence 24 p3400 N88-30246
Crustal underplating in the North American Craton: Evidence from the Petrogenesis of anorthositic rocks in the Middle Proterozoic Midcontinent Rift System
24 p3400 N88-30252
Terrestrial versus giant planet formation
24 p3451 N88-30543

GEOCHRONOLOGY
Measurements of iridium and the meteoric impact hypothesis at cretaceous end
[DE87-703765] 04 p0521 N88-13200
Tectonics of sedimentary cover and basement of Labrador Sea 06 p0726 N88-14468
New data on the formation conditions and age of the Kamensk and Gusev astroblemes
[NASA-TT-20212] 11 p1513 N88-19040
Workshop on the Growth of Continental Crust
[NASA-CR-183073] 24 p3392 N88-30201
Role of zircon in tracing crustal growth and recycling
24 p3394 N88-30211
Construction of mass-age curves for the continental crust: An empirical model and an example from the western US 24 p3394 N88-30213
Pb isotope constaints on the extent of crustal recycling into a steady state mantle 24 p3394 N88-30215
Metamorphic P-T paths and Precambrian crustal growth in East Antarctica 24 p3395 N88-30218
The early archaean crustal history of West Greenland as recorded by detrital zircons 24 p3395 N88-30221
Growth of early archaean crust in the ancient Gneiss complex of Swaziland and adjacent Barberton Greenstone Belt, Southern Africa 24 p3396 N88-30223
Structure of Southwestern Michipicoten Greenstone Belt, Ontario: Evidence for Archean accretion
24 p3397 N88-30228
Geochronological and lead-isotope evidences for rapid crust formation in middle-proterozoic time: The Labrador example 24 p3398 N88-30239
The growth of the continental crust: Constraints from radiogenic isotope geochemistry
24 p3399 N88-30245
Mineralization through geologic time: Evolution of continental crust 24 p3400 N88-30250
Late-Archaean crustal growth in the Lewisian Complex of Northwest Scotland: Diachroneity in magmatic accretion and implications for models of crustal growth
24 p3401 N88-30253
The effect of thicker oceanic crust in the Archaean on the growth of continental crust through time
24 p3401 N88-30254
Spectral analysis of the Elatina varve series
[NASA-CR-183085] 24 p3402 N88-30260

GEOCORONAL EMISSIONS
Lyman alpha SMM/UVSP absolute calibration and geocoronal correction
[NASA-TM-100314] 03 p0389 N88-12446

GEODESIC LINES
The information metric for univariate linear elliptic models
[AD-A186385] 07 p0911 N88-15527
Some remarks on geodesics in gauge groups and harmonic maps
[DE88-702665] 22 p3115 N88-28510

GEODESY
NT CELESTIAL GEODESY
Strain gages in engineering geodesy
[SER-C-320] 01 p0048 N88-10309
Accuracy of GPS surveying technique and its possible application to the Wegener project --- Mediterranean tectonics
[REPT-85.3] 01 p0063 N88-10407
Study of a satellite-to-satellite tracking gravity mission
[ESA-CR(P)-2419] 02 p0198 N88-11237
Software design for an airborne gravity measurement system
[AD-A185000] 05 p0634 N88-13878
Five-diagonal weighting scheme for geoidal profiles
[AD-A188033] 10 p1347 N88-18054
A smart, mapping, charting and geodesy control generator, phase 1
[AD-A188184] 10 p1347 N88-18055
Estimation of gravity vector components from Bell gravity gradiometer and auxiliary data under consideration of topography and associated analytical upward continuation aspects
[AD-A188146] 10 p1355 N88-18099
Reports on cartography and geodesy. Series 1, report 98
[ISSN-0469-4236] 11 p1506 N88-18993
Geodetic positioning by employment of the GPS-NAVSTAR satellites applying the techniques of VLBI and sequential recursive optimal estimation
[INPE-4438-TDL/311] 12 p1594 N88-19547
Department of Defense World Geodetic System 1984: Its definition and relationships with local geodetic systems
[AD-A188815] 12 p1639 N88-19811
Conformal geometry, Hotine's conjecture, and differential geodesy
[AD-A189265] 13 p1790 N88-20709
Determination of Earth rotation by the combination of data from different space geodetic systems
[NASA-CR-181388] 13 p1791 N88-20713
The Spring 1985 high precision baseline test of the JPL GPS-based geodetic system
[NASA-CR-182686] 14 p1940 N88-21577
Estimation of geopotential from satellite-to-satellite range rate data: Numerical results
[NASA-CR-180771] 14 p1941 N88-21583
Validate algorithms for the determination of rainfall rates from SSM/I microwave satellite imagery
[AD-A191337] 16 p2236 N88-23353
Spectral analysis in the linear geodetic boundary value problem
[B8735056] 16 p2259 N88-23502
Criteria for planimetric and altimetric correction of maps restituted from aerial photographs in 1:100,000 scale
17 p2367 N88-24097
Geodesy by radio interferometry: Optimization of wet path delay algorithms using microwave radiometer data
[PB88-167739] 18 p2496 N88-24820
Research project Loran-C of the Geometric Service of the Ministry of Public Works
[B8735055] 20 p2757 N88-26356
Optimized observation periods required to achieve geodetic accuracies using the global positioning system
[AD-A193844] 22 p3041 N88-28052

GEODETIC ACCURACY
Research in geodesy based upon radio interferometric observations of GPS (Global Positioning System) satellites
[AD-A184040] 03 p0346 N88-12187
A demonstration of high precision GPS orbit determination for geodetic applications
04 p0432 N88-12680
Precision analysis of regular networks
[B8709808] 05 p0620 N88-13806
Determination of TRANET (tracking station coordinates for tracking network) and SMTP (Special Mission Tracking Program) tracking station coordinates for use in the WGS (World Geodetic System) 84
[AD-A185863] 07 p0817 N88-14972
Generalized expression for radio navigation parameter error 13 p1787 N88-20691
Research project Loran-C of the Geometric Service of the Ministry of Public Works
[B8735055] 20 p2757 N88-26356
Optimized observation periods required to achieve geodetic accuracies using the global positioning system
[AD-A193844] 22 p3041 N88-28052
Estimation of short-wavelength gravity on a dense grid using digital terrain elevation data
[AD-A196325] 24 p3391 N88-30196

GEODETIC COORDINATES
Control of the German main triangulation network by macrometer measurement 1983-1985 (KONMAC)
[SER-B-282] 01 p0063 N88-10404
Analytical treatment of the spatial trilateration problem (4, 6, 0, 0)
[SER-A-104] 01 p0085 N88-10548
Method for joint adjustment of satellite and surface geodetic networks 08 p1007 N88-16105
New possibilities for using gravity data in developing geodetic coordinate systems 08 p1009 N88-16116
Reports on cartography and geodesy. Series 1, report 98
[ISSN-0469-4236] 11 p1506 N88-18993
The significance of orientation unknowns in station and net adjustments 11 p1506 N88-18994
The orientation of global satellite networks
11 p1506 N88-18996

GEODETIC SATELLITES
NT GEOS 2 SATELLITE
NT GEOSAT SATELLITES
Control of the German main triangulation network by macrometer measurement 1983-1985 (KONMAC)
[SER-B-282] 01 p0063 N88-10404
Accuracy of GPS surveying technique and its possible application to the Wegener project --- Mediterranean tectonics
[REPT-85.3] 01 p0063 N88-10407
Determination of TRANET (tracking station coordinates for tracking network) and SMTP (Special Mission Tracking Program) tracking station coordinates for use in the WGS (World Geodetic System) 84
[AD-A185863] 07 p0817 N88-14972

GEODETIC SURVEYS
Control of the German main triangulation network by macrometer measurement 1983-1985 (KONMAC)
[SER-B-282] 01 p0063 N88-10404
Accuracy of GPS surveying technique and its possible application to the Wegener project --- Mediterranean tectonics
[REPT-85.3] 01 p0063 N88-10407
Research in geodesy based upon radio interferometric observations of GPS (Global Positioning System) satellites
[AD-A184040] 03 p0346 N88-12187
Considering refraction in leveling with laser plane
04 p0462 N88-12857
Precision analysis of regular networks
[B8709808] 05 p0620 N88-13806
Observations of Earth tides by the German Geodetic Research Institute, division 1, in the period 1979-1985 at the Berchtesgaden and Wettzell stations
[SER-B-280] 07 p0872 N88-15291
Crustal dynamics project data analysis, 1987. Volume 1: Fixed station VLBI geodetic results, 1979-1986
[NASA-TM-100682] 08 p1035 N88-16279
Crustal dynamics project data analysis, 1987. Volume 2: Mobile VLBI geodetic results, 1982-1986
[NASA-TM-100689-VOL-2] 08 p1035 N88-16280
Crustal Dynamics Project: Catalogue of site information
[NASA-RP-1198] 11 p1513 N88-19037
Geodetic measurement of deformation east of the San Andreas fault in Central California
[NASA-CR-182709] 13 p1798 N88-20754
Global Positioning System (GPS) exploitation by ODOT (Ohio Department of Transportation)
[PB88-172796] 16 p2159 N88-22862
Basic research for the geodynamics program
[NASA-CR-183149] 21 p2973 N88-27862
A comparison: Static and future kinematic GPS (Global Positioning System) surveys
[AD-A194666] 23 p3175 N88-28904
DATATRAN: Datum transformation software
[AD-A195723] 24 p3387 N88-30175
Estimation of short-wavelength gravity on a dense grid using digital terrain elevation data
[AD-A196325] 24 p3391 N88-30196
Analytical method for approximate geodetic referencing of scanner images of meteorological artificial earth satellites using control points 24 p3449 N88-30527

GEODYNAMICS
The interpretation of crustal dynamics data in terms of plate motions and regional deformation near plate boundaries
[NASA-CR-181475] 03 p0349 N88-12205
The Telecommunications and Data Acquisition Report
[NASA-CR-181546] 04 p0432 N88-12679

Crustal dynamics project data analysis, 1987. Volume 1: Fixed station VLBI geodetic results, 1979-1986
[NASA-TM-100682] 08 p1035 N88-16279
Crustal dynamics project data analysis, 1987. Volume 2: Mobile VLBI geodetic results, 1982-1986
[NASA-TM-100689-VOL-2] 08 p1035 N88-16280
Crustal Dynamics Project: Catalogue of site information
[NASA-RP-1198] 11 p1513 N88-19037
Proceedings of an ESA-NASA Workshop on a Joint Solid Earth Program
[NASA-CR-182642] 12 p1644 N88-19844
NASA's geodynamics program
12 p1644 N88-19845
Drilling investigation of a young magmatic intrusion beneath the Inyo Domes, Long Valley, California: Structural and textural studies
[DE88-006613] 18 p2541 N88-25078
The interpretation of crustal dynamics data in terms of plate interactions and active tectonics of the Anatolian Plate and surrounding regions in the Middle East
[NASA-CR-183024] 18 p2543 N88-25092
SPOT imagery preliminary contribution to cartography and geodynamics in the Benue trough (Nigeria)
22 p3103 N88-28429

GEOELECTRICITY
Electromagnetic induction in spherical earth containing oceans and continents in electrical contact with underlying section: Theory, method, example
08 p1011 N88-16127
Temporal evolution of ionospheric electric field driven by field-aligned current 11 p1469 N88-18761

GEOFRACTURES
U GEOLOGICAL FAULTS

GEOGRAPHIC INFORMATION SYSTEMS
Problems in integrating geographic data
[DE87-012880] 01 p0106 N88-10689
KBGIS-II: A knowledge-based geographic information system
[NASA-CR-182492] 09 p1261 N88-17559
Air Force geographic information and analysis system
[DE88-001420] 10 p1424 N88-18505
Development of a digital terrain modeling system for microcomputers
[INPE-4406-TDL/303] 12 p1639 N88-19816
An overview of the army GIS (Geographic Information Systems) Research Program
[AD-A189711] 14 p1992 N88-21871
Updating of the municipal official register of real estate through a geographical information system
[INPE-4459-PRE/1238] 15 p2090 N88-22453
Sources of digital spatial data for geographic information systems
[AD-A189788] 15 p2148 N88-22824
Georelational data model
[INPE-4490-PRE/1254] 15 p2149 N88-22829
Inventory of topographic mapping and standardization of geographic names as the basis of a Geographic Information System (GIS) 16 p2225 N88-23281
Remote sensing and data integration: Practical solutions for resource managers 17 p2356 N88-24034
Implantation of a geo-cartographical information system through microcomputers 17 p2361 N88-24064
Research on enhancing the utilization of digital multispectral data and geographic information systems in global habitability studies
[NASA-CR-182799] 17 p2368 N88-24101
Updating of municipal official register of real estate through the geographical information system
19 p2684 N88-25952
Hydrologic models for land-atmosphere retrospective studies of the use of LANDSAT and AVHRR data
[NASA-CR-182861] 20 p2817 N88-26712
Hydrologic models for land-atmosphere retrospective studies of the use of LANDSAT and AVHRR data
[NASA-CR-182862] 20 p2818 N88-26716
Geographical information for design purposes
[NLR-MP-87014-U] 20 p2818 N88-26719
Knowledge representation in geographic information systems
[ETN-88-92470] 20 p2882 N88-27112
Review of geographic processing techniques applicable to regional analysis
[DE88-010759] 21 p2970 N88-27643
An evaluation of the applicability of SPOT stereoscopic imagery to the Canada Land Use Monitoring Program (CLUMP) 22 p3099 N88-28403
Use of SPOT imagery in a geographic information system 22 p3114 N88-28498
SEP/VIPS 32 geographic information system. Processing and thematic analysis of images, maps, and associated data 22 p3114 N88-28499
Contribution of SPOT to geographic information systems 22 p3114 N88-28502
A digital terrain model system for a microcomputer
[INPE-4610-PRE/1333] 24 p3413 N88-30316

GEOGRAPHY
NT HYPSOGRAPHY
NT OROGRAPHY
Advanced techniques for the storage and use of very large, heterogeneous spatial databases. The representation of geographic knowledge: Toward a universal framework --- relations (mathematics)
[NASA-CR-181517] 03 p0385 N88-12421
Geographic application of the relational data base system Cantor
[PB87-120945] 06 p0791 N88-14851
Space applications in geography
08 p1007 N88-16104
The Systeme d'Analyse Geographique (SAGE) geographic analysis system 17 p2353 N88-24019
The SAGE geographic analysis system
17 p2361 N88-24063
The Department of Defense report on the merit review process for competitive selection of university research projects and an analysis of the potential for expanding the geographic distribution of research for the Committees on Appropriations, United States Congress
[AD-A191842] 18 p2588 N88-25379
The impact of disorganized occupation of urban sub-basins: Sub-basin of the Cabucu River, metropolitan area of Sao Paulo (SP) 19 p2682 N88-25945
Application of interactive graphic system (CAD/CAM) in the determination of process evolution in land use in the Ribeirao Preto municipality 19 p2684 N88-25956
Aerial photography as an instrument of municipal and regional planning: Metropolitan area of Sao Paulo (SP)
19 p2684 N88-25957
Remote sensing applied to integrated regional development programs 19 p2685 N88-25958

GEOIDS
Five-diagonal weighting scheme for geoidal profiles
[AD-A188033] 10 p1347 N88-18054
Department of Defense World Geodetic System 1984: Its definition and relationships with local geodetic systems
[AD-A188815] 12 p1639 N88-19811
Evaluation of a model of the Earth's gravity field
[EPSHOM-003/87] 17 p2373 N88-24116
The determination of gravity and topography from seismic velocities, accounting for dynamic behavior of the Earth's mantle
[ETN-88-92420] 17 p2374 N88-24117
To relate measurements of gravity and geoid anomalies over the oceans to near surface density distributions
[AD-A192168] 18 p2547 N88-25120

GEOLOGICAL FAULTS
NT AFRICAN RIFT SYSTEM
NT SAN ANDREAS FAULT
Gravity and fault structures, Long Valley Caldera, California
[DE87-014117] 02 p0197 N88-11229
Geological interpretation of a SPOT image over Kenya: The Gregory rift network of faults
03 p0343 N88-12164
The interpretation of crustal dynamics data in terms of plate motions and regional deformation near plate boundaries
[NASA-CR-181475] 03 p0349 N88-12205
Earthquake source mechanisms and transform fault tectonics in the Gulf of California
03 p0349 N88-12206
Interseismic deformation for normal fault earthquakes
03 p0349 N88-12207
Transform fault earthquakes in the North Atlantic: Source mechanisms and depth of faulting
03 p0350 N88-12208
State-of-the-art for assessing earthquake hazards in the United States. Report 26: Parameters for specifying magnitude-related earthquake ground motions
[AD-A185997] 07 p0877 N88-15319
Space photographs of the Onega-Ladoga isthmus and prediction of useful minerals 08 p1008 N88-16108
Use of space photographs for paleoseismogeological studies (on the example of Mongolian Altay)
08 p1008 N88-16110
Geomechanical model of seismofocal zone of active continental margin 08 p1011 N88-16128
State-of-the-art for assessing earthquake hazards in the US. Parameters for specifying intensity-related earthquake ground motions
[AD-A188230] 11 p1512 N88-19032
Naval weapons center active fault map series
[AD-A188425] 12 p1643 N88-19835
Ultrasonic physical modeling of seismic wave propagation from graben-like structures
[AD-A189066] 13 p1796 N88-20744
Study of fracturing for groundwater research in the Sergipe state with remote sensing products
17 p2359 N88-24052
Rate of slip on the Altin Dagh Fault (North Tibet, China) 22 p3102 N88-28420
Geologic applications of SPOT-1, TM, and NOAA-7 data: Finding and defining unmapped structural features
22 p3104 N88-28434
Mechanics of thrust fault formation
23 p3231 N88-29229
Diapirs of the Mediterranean ridge: The tectonic regime of an incipient accreted terrane
24 p3396 N88-30224
Faulting and its relation to volcanism: Mars western equatorial region 24 p3443 N88-30489

GEOLOGICAL SURVEYS
SPOT for earthquake hazard zoning in southern Italy, a provisional report 03 p0342 N88-12161
Application of SPOT-1 data to mineral exploration in Nevada 03 p0343 N88-12163
Geological interpretation of a SPOT image over Kenya: The Gregory rift network of faults
03 p0343 N88-12164
Evolution of remote sensing utilization in geological mapping and ore exploration: Example in Zimbabwe
03 p0343 N88-12165
Modern concept concerning transport of bottom sediments in abyssal regions of world ocean
06 p0728 N88-14478
Remote sensing in mineral exploration
[PB87-138558] 06 p0729 N88-14484
Space photographs of the Onega-Ladoga isthmus and prediction of useful minerals 08 p1008 N88-16108
International role of US geoscience
[NASA-CR-182407] 08 p1035 N88-16281
Solid Earth mission end-to-end data system study
[C04825.08/FR] 17 p2309 N88-23811
The use of SPOT images for water resources surveys in the Kasserine Basin (Tunisia)
22 p3090 N88-28349
Utilizing SPOT data for seismic shot-line mapping and environmental monitoring in oil and gas exploration
22 p3098 N88-28401
First results of international investigations of the applications of SPOT-1 data to geologic problems, mineral and energy exploration 22 p3101 N88-28419
Karst and submarine fresh water discharge in the Antalya area, southern Turkey 22 p3102 N88-28421
Results of the Geosat program to evaluate SPOT data for petroleum and mineral exploration
22 p3102 N88-28422
The application of SPOT data to the structural geology of western Nevada 22 p3102 N88-28423
Evaluation of SPOT imagery for discriminating vegetation communities associated with surficial and bedbrock geology and identifying anomalous and stressed vegetation associated with mineralization
22 p3103 N88-28426
Role of SPOT in geological application of remote sensing 22 p3103 N88-28428
SPOT imagery preliminary contribution to cartography and geodynamics in the Benue trough (Nigeria)
22 p3103 N88-28429
An evaluation of SPOT imagery for Earth science studies in the Antarctic. Preliminary Evaluation Program (PEPS) 289 for SPOT 22 p3103 N88-28430
Methodology for the use of SPOT imagery in petroleum exploration. Example of the Bas-Languedoc area (France) 22 p3104 N88-28432
Spectral and spatial attribute evaluation of SPOT data in geological mapping of precambrian terrains in semiarid environment of Brazil 22 p3104 N88-28436
Detailed geological mapping of the massif of Sainte Victoire (Provence, France) using SPOT imagery. Comparison with other multisource data. New tectonic interpretation of this region 22 p3105 N88-28442
Digital terrain modelling with SPOT data and geological applications 22 p3110 N88-28474
Radiometric analysis and potential of SPOT HRV imagery for applications in urban environments and geology 22 p3112 N88-28486

GEOLOGY
NT GEOCHRONOLOGY
NT GEOMORPHOLOGY
NT GLACIOLOGY
NT HYDROGEOLOGY
NT LITHOLOGY
NT MARS VOLCANOES
NT OROGRAPHY
NT PETROGRAPHY
NT PETROLOGY
NT PHOTOGEOLOGY
NT STRUCTURAL PROPERTIES (GEOLOGY)
NT SUBDUCTION (GEOLOGY)
NT TECTONICS
NT VOLCANOES
NT VOLCANOLOGY
NBS (National Bureau of Standards) research reports (April 1987)
[PB87-210258] 01 p0018 N88-10111

JPRS report: Science and technology. China
[JPRS-CST-87-032] 03 p0376 N88-12365
Summaries of physical research in the geosciences
[DE88-000833] 04 p0468 N88-12896
Research needs for hydrocarbon fuels
[DE87-014555] 06 p0687 N88-14209
The adaption and use of research codes for performance assessment
[DE88-000552] 06 p0756 N88-14639
Earth materials research: Report of a Workshop on Physics and Chemistry of Earth Materials
[NASA-CR-182519] 10 p1298 N88-17761
Geological evolution and analysis of confirmed or suspected gas hydrate localities. Volume 10: Basin analysis, formation and stability of gas hydrates of the Aleutian Trench and the Bering Sea
[DE88-001008] 10 p1346 N88-18048
New data on the formation conditions and age of the Kamensk and Gusev astroblemes
[NASA-TT-20212] 11 p1513 N88-19040
JPRS report: Science and technology. China
[JPRS-CST-88-003] 13 p1755 N88-20495
JPRS report: Science and technology. USSR: Earth sciences
[JPRS-UES-88-001] 13 p1784 N88-20674
Activities and objectives of the Polar Research Board
[DE88-004543] 13 p1797 N88-20747
JPRS report: Science and technology. China
[JPRS-CST-87-041] 14 p1902 N88-21365
Groundwater sapping valleys: Experimental studies, geological controls and implications to the interpretation of valley networks on Mars
[NASA-CR-182718] 15 p2152 N88-22847
A proposal of adaptation of a knowledge-based scene analysis model to some remote sensing problems
17 p2362 N88-24068
Geological evolution and analysis of confirmed or suspected gas hydrate localities. Volume 2: Basin analysis, formation and stability of gas hydrates in the Black Sea
[DE88-001052] 18 p2532 N88-25023
Territorial management program
19 p2682 N88-25942
Vegetation studies on Vandenberg Air Force Base, California
[NASA-TM-100985] 20 p2831 N88-26795
Mars: Near-infrared comparative spectroscopy during the 1986 opposition 23 p3301 N88-29658
Intercrater plains deposits and the origin of Martian valleys 23 p3301 N88-29661
Elemental composition of the Martian surface
23 p3302 N88-29665
Distribution and timing of thick transient air-fall deposits in Electris: Implications for the nature of the upland plains 23 p3303 N88-29674
Geology of six possible Martian landing sites
23 p3304 N88-29682
Documenting volcano-tectonic episodes in Mars' stratigraphic record 23 p3306 N88-29695
NASA MEVTV Program Working Group Meeting: Volcanism on Mars
[NASA-CR-183074] 24 p3442 N88-30487

GEOMAGNETIC ANOMALIES
U MAGNETIC ANOMALIES

GEOMAGNETIC CROTCHETS
U SUDDEN IONOSPHERIC DISTURBANCES

GEOMAGNETIC EFFECTS
U MAGNETIC EFFECTS

GEOMAGNETIC FIELD
U GEOMAGNETISM

GEOMAGNETIC MICROPULSATIONS
Monitoring of Pc3 pulsations in solar wind and at Earth by interplanetary magnetic field
08 p1002 N88-16069
Report on ground-based activity at Andoya (Norway) in relation to the Aureld-VIP high rocket and to the Viking satellite --- Swedish satellite 08 p1026 N88-16212
Field-aligned structure of the storm time Pc 5 wave of November 14-15, 1979
[AD-A193022] 21 p2972 N88-27653

GEOMAGNETIC PULSATIONS
NT GEOMAGNETIC MICROPULSATIONS
Auroral X-ray images during a pulsation event
08 p1026 N88-16214
The effects of a geomagnetic storm on thermospheric circulation
[AD-A186636] 09 p1190 N88-17128

GEOMAGNETIC STORMS
U MAGNETIC STORMS

GEOMAGNETIC TAIL
The tail lobe ion spectrometer: Theory and observations
[IFSI-86-12] 05 p0585 N88-13569
Coupling of microscopic and macroscopic processes in the Earth's magnetotail 08 p1095 N88-16588
Evidence of small-scale reconnection in the magnetosphere 08 p1097 N88-16601
Interpretation of the northward B sub z (NBZ) Birkeland current system and polar cap convection patterns in terms of the impulsive penetration model
[AERONOMICA-ACTA-A-321-1987]
18 p2595 N88-25422
Relationship between characteristics of low-energy electrons and geomagnetic disturbance in geostationary orbit 24 p3444 N88-30501

GEOMAGNETICALLY TRAPPED PARTICLES
U RADIATION BELTS

GEOMAGNETISM
Solar activity, magnetic clouds, and geomagnetic storms 01 p0115 N88-10735
Narsarsuaq (Greenland) Geophysical Observatory. Magnetic results, 1984
[ISBN-87-7478-281-9] 02 p0198 N88-11235
Solar-geophysical data number 514, June 1987. Part 1: (Prompt reports). Data for May 1987, April 1987 and late data
[PB87-217261] 02 p0257 N88-11626
Morphology of the Earth's environment
03 p0272 N88-11706
Radiation belts 03 p0272 N88-11707
Directory of geomagnetic observatories with high-resolution digital results, 1987
[PB87-221156] 03 p0348 N88-12201
Narssarssuaq Geophysical Observatory: Magnetic results, 1980-83. Instrumentation and formulas
[ISBN-87-7478-280-0] 03 p0350 N88-12209
Statistics of the geomagnetic secular variation for the past 5Ma
[NASA-CR-181558] 04 p0467 N88-12890
Tectonics and magmatism of Walvis Ridge and Discovery Rise (Atlantic Ocean)
06 p0726 N88-14463
Radar observations of high-latitude lower-thermospheric and upper-mesospheric winds and their response to geomagnetic activity 06 p0742 N88-14563
Solar-geophysical activity reports for STIP (Study of Travelling Interplanetary Phenomena) interval 15, 12-21 February 1984 ground level event and STIP interval 16, 20 April-4 May 1984 Forbush decrease
[PB88-101274] 06 p0802 N88-14906
A compilation of Sudden Storm Commencements (SSCs), associated interplanetary disturbances, and cosmic ray variations
[IFSI-86-11] 06 p0807 N88-14923
Flare doublet: Interplanetary and geomagnetic affects
08 p1001 N88-16066
FTE like variations in the geomagnetic field at ground based conjugate stations in the cusp regions
[INPE-4345-PRE/1182] 08 p1024 N88-16199
Criteria of interplanetary parameters causing intense magnetic storms (Dst less than -100nT)
[NASA-CR-182423] 08 p1024 N88-16200
Balloon measurement of magnetic field during substorms in auroral zone 08 p1026 N88-16213
Acceleration of auroral particles by magnetic field-aligned electric fields 08 p1031 N88-16246
A study of the magnetic field annihilation process in the magnetosphere and some geotechnical applications
[DE88-004165] 10 p1355 N88-18096
Energetic particle drift motions in the outer dayside magnetosphere
[DE88-005097] 11 p1512 N88-19034
Observation of a hydromagnetic wave in the earth's magnetosphere
[AD-A188942] 12 p1644 N88-19841
Proceedings of an ESA-NASA Workshop on a Joint Solid Earth Program
[NASA-CR-182642] 12 p1644 N88-19844
Spaceborne magnetometry 12 p1644 N88-19846
Magnetic results, 1985
[ISBN-8-77-478282-7] 14 p1944 N88-21600
Simultaneous observation of upward moving field aligned energetic electrons and ions on auroral zone field lines
[IRF-PREPRINT-102] 16 p2231 N88-23326
Solar-geophysical data number 520, December 1987. Part 1: (Prompt reports). Data for November 1987, October 1987 and late data
[PB88-164199] 16 p2290 N88-23712
DOD 1985 world magnetic model: Charts and grid values
[AD-A191484] 18 p2541 N88-25080
Spacecraft requirements for predictions of geomagnetic activity (a tutorial)
[AD-A191943] 19 p2685 N88-25959
Scaling laws for geomagnetic tail current sheet acceleration
[AD-A193379] 19 p2691 N88-25998

GEOMETRIC ACCURACY
Registration of SPOT images
03 p0341 N88-12155

GEOMETRIC DILUTION OF PRECISION
GPS vertical axis performance enhancement for helicopter precision landing approach
[NASA-CR-177443] 04 p0397 N88-12477
Automatic omega station and LOP (Line Of Position) selection
[AD-A193302] 21 p2894 N88-27179

GEOMETRIC RECTIFICATION (IMAGERY)
First assessment of processing and use of SPOT images by the Institut Geographique Nationale --- French National Geographic Institute 03 p0341 N88-12148
Some characteristics in synthetic aperture radar (SAR) raw data and SAR images
[FOA-C-30483-3.2] 22 p3071 N88-28232
The use of SPOT imagery on analytical photogrammetric instruments 22 p3110 N88-28471
A geometrical analysis of SPOT data
22 p3111 N88-28478

GEOMETRICAL ACOUSTICS
Elastodynamic ray theory and asymptotic methods for direct and inverse scattering problems
*03 p0335 N88-12108
Application of ray theory to propagation of low frequency noise from wind turbines
[NASA-CR-178367] 03 p0373 N88-12349
Correcting ray field failures caused by focusing in an inhomogeneous duct: A critical look at the Gaussian beam method 12 p1616 N88-19663
Propagation of acoustic disturbances in transonic flow fields of lifting wings
[DFVLR-FB-88-13] 21 p3013 N88-27880

GEOMETRICAL HYDROMAGNETICS
U MAGNETOHYDRODYNAMICS

GEOMETRICAL OPTICS
Intrinsic and extrinsic geometric quality --- SPOT images 03 p0341 N88-12154
A prototype ray tracer
[AD-A184863] 05 p0634 N88-13874
Backscattering from three dimensional conducting bodies
[AD-A187570] 11 p1470 N88-18768
Scattering and depolarization by random rough terrain and vegetation covered terrain-unified full wave approach 12 p1615 N88-19657
Semiclassical theory of injected lasers with arbitrary stable and unstable resonators
[AD-A189514] 13 p1775 N88-20615
Models for electromagnetic scattering from the sea at extremely low grazing angles
[AD-A190472] 15 p2057 N88-22261

GEOMETRICAL THEORY OF DIFFRACTION
Theoretical Aspects of Target Classification
[AGARD-LS-152] 03 p0303 N88-11909
Target strength: An overview of some recent theoretical developments 03 p0303 N88-11910
Uniform geometrical theory of diffraction
03 p0303 N88-11911
Backscattering from three dimensional conducting bodies
[AD-A187570] 11 p1470 N88-18768
Seventy-meter antenna performance predictions: GTD analysis compared with traditional ray-tracing methods
11 p1474 N88-18793
Models for electromagnetic scattering from the sea at extremely low grazing angles
[AD-A190472] 15 p2057 N88-22261
Fields and waves 24 p3363 N88-30025

GEOMETRODYNAMICS
U RELATIVITY

GEOMETRY
NT ANALYTIC GEOMETRY
NT ANGLE OF ATTACK
NT ANGLES (GEOMETRY)
NT BOSE GEOMETRY
NT BRAGG ANGLE
NT CARTESIAN COORDINATES
NT CATENARIES
NT CIRCLES (GEOMETRY)
NT CIRCUMFERENCES
NT COLLINEARITY
NT COMPUTATIONAL GEOMETRY
NT CONICS
NT COPLANARITY
NT CRACK GEOMETRY
NT CUBES (MATHEMATICS)
NT CURVATURE
NT CURVES (GEOMETRY)
NT DESCRIPTIVE GEOMETRY
NT DIFFERENTIAL GEOMETRY
NT DIHEDRAL ANGLE
NT ELEVATION ANGLE
NT ELLIPSES
NT EUCLIDEAN GEOMETRY
NT FIXED POINTS (MATHEMATICS)
NT FLOW GEOMETRY
NT FRACTALS

NT GEODESIC LINES
NT HILBERT SPACE
NT HOMOTOPY THEORY
NT ICOSAHEDRONS
NT INFLECTION POINTS
NT INVARIANT IMBEDDINGS
NT LEADING EDGE SWEEP
NT LIE GROUPS
NT LINES (GEOMETRY)
NT METRIC SPACE
NT NOZZLE GEOMETRY
NT OBLATE SPHEROIDS
NT PARABOLAS
NT POINTS (MATHEMATICS)
NT POLYGONS
NT POLYHEDRONS
NT PROJECTIVE GEOMETRY
NT PROLATE SPHEROIDS
NT PYRAMIDS
NT QUADRANTS
NT RADII
NT RECTANGLES
NT RHOMBOIDS
NT RIEMANN MANIFOLD
NT S CURVES
NT SPECIMEN GEOMETRY
NT SWEEP ANGLE
NT SWEEPBACK
NT TANGENTS
NT TENSOR ANALYSIS
NT TOPOLOGY
NT TORUSES
NT TRIANGLES
NT VECTOR ANALYSIS
NT VORTICITY

TIPS-1 user's manual: Cray-1 version [DE87-013297] 01 p0081 N88-10522

Aerodynamic design and performance of a bent-axis geometry vehicle [DE87-013726] 02 p0124 N88-10786

The structure and reactivity of heterogeneous surfaces and study of the geometry of surface complexes [DE88-000158] 03 p0279 N88-11754

Observations on the hydrodynamic flow visualization at ONERA [PD-FM-8718] 04 p0444 N88-12753

The linear characteristic method in XYZ geometry [DE87-011668] 04 p0484 N88-12984

Introduction to string field theory [DE87-014583] 05 p0657 N88-14032

A zonal approach for the solution of coupled Euler and potential solutions of flows with complex geometries [AD-A185465] 06 p0702 N88-14310

Eigenvectors of graphs [AD-A185538] 06 p0765 N88-14698

Application of a full potential method for analysis of complex aircraft geometries 07 p0809 N88-14930

Horn design equations for the NBS (National Bureau of Standards) horn-type noise standards [PB88-110226] 07 p0844 N88-15122

The information metric for univariate linear elliptic models [AD-A186385] 07 p0911 N88-15527

A multistage mesh generator for solving the average-passage equation system [NASA-CR-179539] 08 p0951 N88-15769

Mixed method of finite strip and finite element [PB87-143467] 08 p0996 N88-16027

Nonlinear evolution of the internal kink mode in toroidal geometry for shaped tokamak plasmas [DE88-003655] 08 p1087 N88-16550

A project to experimentally and theoretically examine fluid interfacial wave phenomena in a rotating cylindrical geometry: Current results and future plans [DE88-003738] 09 p1165 N88-16984

Flat-field response and geometric distortion measurements of optical streak cameras [DE88-002394] 09 p1168 N88-17005

A finite element analysis of adhesively bonded composite joints including geometric nonlinearity, nonlinear viscoelasticity moisture diffusion and delayed failure [AD-A187455] 10 p1296 N88-17747

Design sensitivity analysis of nonlinear structural systems and numerical implementation with established finite element codes 10 p1344 N88-18032

Computer aided geometric design [AD-A187324] 10 p1389 N88-18293

Optimal selection of global positioning system set to minimize emitter location errors [AD-A189559] 12 p1579 N88-19447

An interactive user-friendly approach to surface-fitting three-dimensional geometries [NASA-CR-4126] 12 p1682 N88-20058

Conformal geometry, Hotine's conjecture, and differential geodesy [AD-A189265] 13 p1790 N88-20709

Campaign graphs [DE88-005336] 13 p1831 N88-20952

Advanced probabilistic methods for quantifying the effects of various uncertainties in structural response 15 p2080 N88-22401

Boundary shape identification problems in two-dimensional domains related to thermal testing of materials [NASA-CR-181654] 15 p2105 N88-22541

The elliptic Sinh-Gordon equation and the construction of toroidal soap bubbles [DE88-006426] 15 p2113 N88-22585

Geometric methods and the gauge structure of Berry's phase [DE88-006538] 15 p2127 N88-22682

Matched index laser anemometry systems for flow studies in complex geometries 16 p2203 N88-23145

Spur gears: Optimal geometry, methods for generation and Tooth Contact Analysis (TCA) program [NASA-CR-4135] 16 p2215 N88-23216

Derivative arrays, geometric control theory and realizations of linear descriptor systems [AD-A190682] 16 p2260 N88-23513

Hybrid particle simulation for focusing of rotating and propagating LIB 16 p2276 N88-23624

The geometric workstation, a new approach for geometric corrections of remotely sensed data 17 p2352 N88-24017

Internal fluid dynamics within a nonspinning partially liquid-filled shell due to burster rupture [AD-A191055] 18 p2507 N88-24874

Modeling of geometric reasoning for robot programming [ETN-88-92290] 18 p2561 N88-25202

Optical investigations of the thermal boundary layer in arc plasmas 18 p2578 N88-25313

The geometry of the Virasoro group for physicists [DE88-007374] 18 p2586 N88-25366

Control of combustion instabilities in ramjet motors 19 p2625 N88-25574

Effect of burn-path tortuosity on the burn rate of composite propellants 19 p2630 N88-25602

How much do edges affect the ignition of a homogeneous reactive solid: Summary to date 19 p2631 N88-25608

Numerical simulations of aerodynamic contribution of flows about a space-plane-type configuration 19 p2635 N88-25632

Accurate, productive aerodynamic simulation on patched mesh systems [AD-A192040] 19 p2714 N88-26110

Voyager imaging photometry and radiative transfer modeling of the spoke-like features in Saturn's outer B-ring 19 p2742 N88-26278

Development of liquid metal field-emission sources for use in fast repetitive opening switches [AD-A192230] 20 p2795 N88-26583

Full-wave calculations in flux coordinates for toroidal geometry [DE88-010131] 20 p2860 N88-26965

Aharonov-Bohm effects in disordered metals 20 p2864 N88-27008

Design and development of courseware for goniometry [REPT-87-73] 20 p2881 N88-27106

The influence of weld metal properties, weld geometry and applied load on weld system performance [AD-A193403] 21 p2961 N88-27588

An investigation of techniques for determination of optimum/self-optimizing systems 21 p2963 N88-27600

Automatic line network extraction from aerial imagery of urban areas through knowledge based image analysis [AD-A193067] 21 p2965 N88-27615

Parallel solutions to geometric problems on the scan model of computation [AD-A192321] 21 p3004 N88-27819

Geometry of superconformal manifolds, part 1 [DE88-702405] 21 p3011 N88-27863

Geometry of superconformal manifolds, part 2 [DE88-702406] 21 p3011 N88-27864

Delta wing configurations 23 p3167 N88-28860

Ice detector [NASA-CASE-LAR-13776-1] 23 p3217 N88-29149

Cooperating knowledge-based systems [NASA-CR-183109] 23 p3247 N88-29327

Holomorphic geometry of interacting string [DE88-702714] 23 p3295 N88-29627

Numerical modelling of premixed flames in gaseous media 24 p3350 N88-29944

An automated computerized vision technique for determination of three-dimensional object geometry 24 p3419 N88-30348

GEOMORPHOLOGY

SPOT for earthquake hazard zoning in southern Italy, a provisional report 03 p0342 N88-12161

The impact of varves on solar physics [NASA-CR-181519] 03 p0390 N88-12448

Geophysical-geomorphological statistical regionalization of North Atlantic 06 p0726 N88-14466

Tectonics of sedimentary cover and basement of Labrador Sea 06 p0726 N88-14468

Use of space photographs for geomorphological studies in southwestern Tajikistan 08 p1008 N88-16109

Use of space photographs for paleoseismogeological studies (on the example of Mongolian Altay) 08 p1008 N88-16110

Geological evolution and analysis of confirmed or suspected gas hydrate localities. Volume 10: Basin analysis, formation and stability of gas hydrates of the Aleutian Trench and the Bering Sea [DE88-001008] 10 p1346 N88-18048

Geological evolution and analysis of confirmed or suspected gas hydrate localities. Volume 9: Formation and stability of gas hydrates of the Middle America Trench [DE88-001007] 10 p1347 N88-18050

Martian geomorphology and its relation to subsurface volatiles [NASA-CR-182428] 12 p1711 N88-20237

Project CODEAMA/FUNCATE (test-area of Barreirinha-AM): Field report [INPE-4500-RPE/563] 15 p2090 N88-22455

Bilateral symmetry elements of the Zhamanshin impact crater [NASA-TT-20288] 15 p2096 N88-22490

Airborne and spaceborne radar images for geologic and environmental mapping in the Amazon rain forest, Brazil 17 p2353 N88-24021

Subsurface morphology and geoarchaeology revealed by spaceborne and airborne radar 17 p2353 N88-24022

Utilization of LANDSAT-TM , for aiding in the localization of archeological sites in the state of Sao Paulo 17 p2362 N88-24069

The breaked anticlines, cuesta and crest homoclines, ortoclinal valleys, and other forms of relief outcrops delineated with the help of remote sensing imagery 17 p2366 N88-24089

Geomorphologic sector maps of Niquizanga-Mayares, province of San Juan, Argentina 17 p2368 N88-24098

Geological evolution and analysis of confirmed or suspected gas hydrate localities. Volume 2: Basin analysis, formation and stability of gas hydrates in the Black Sea [DE88-001052] 18 p2532 N88-25023

Use of remote sensing in the study of superficial formation certifying the development of integrated economy-case example: Rio Claro (SP) region 19 p2683 N88-25950

Remote sensing applied to integrated regional development programs 19 p2685 N88-25958

MEVTV Workshop on Nature and Composition of Surface Units on Mars [NASA-CR-183075] 23 p3300 N88-29654

The history of Martian volcanism determined from a revised relative chronology 23 p3301 N88-29657

Morphologic contrasts between Nirgal and Auqakuh Valles, Mars: Evidence of different crustal properties 23 p3304 N88-29681

Geology of six possible Martian landing sites 23 p3304 N88-29682

Stratigraphy of the Kasei Valles region, Mars 23 p3305 N88-29690

High resolution Viking Orbiter images: A useful data source for testing the viability of geomorphic processes attributed to Martian landforms 23 p3307 N88-29703

Evaluation of LANDSAT-TM data for geomorphological mapping [INPE-4593-PRE/1324] 24 p3386 N88-30168

Eruptive viscosity and volcano morphology 24 p3442 N88-30488

The Martian highland paterae: Evidence for explosive volcanism on Mars 24 p3443 N88-30492

Physical properties of surface materials on Martian volcanoes: Dust-covered lava and ash 24 p3443 N88-30493

Rifts of deeply eroded Hawaiian basaltic shields: A structural analog for large Martian volcanoes 24 p3443 N88-30494

Small-scale volcanic landforms indicative of distributary tube systems 24 p3444 N88-30496

GEON (TRADEMARK)

U POLYVINYL CHLORIDE

GEOPHYSICAL OBSERVATORIES

Narsarsuaq (Greenland) Geophysical Observatory. Magnetic results, 1984 [ISBN-87-7478-281-9] 02 p0198 N88-11235

Directory of geomagnetic observatories with high-resolution digital results, 1987
[PB87-221156] 03 p0348 N88-12201

Narssarssuaq Geophysical Observatory: Magnetic results, 1980-83. Instrumentation and formulas
[ISBN-87-7478-280-0] 03 p0350 N88-12209

Magnetic results, 1985
[ISBN-8-77-478282-7] 14 p1944 N88-21600

GEOPHYSICAL SATELLITES

NT COSMOS SATELLITES
NT INTERCOSMOS SATELLITES

Wave structures in thermospheric density from satellite electrostatic triaxial accelerometer measurements
[AD-A194134] 23 p3233 N88-29240

GEOPHYSICS

Mathematics applied to nuclear geophysics
[INPE-4234-PRE/1109] 01 p0086 N88-10561

Solar-geophysical data number 513, May 1987. Part 1: (Prompt reports). Data for April, March 1987 and late data
[PB87-204939] 01 p0119 N88-10760

Solar-geophysical data number 513, May 1987. Part 2: (Comprehensive reports). Data for November 1986 and miscellanea
[PB87-204974] 01 p0119 N88-10761

Institute of Geophysics and Planetary Physics at Lawrence Livermore National Laboratory
[DE87-014618] 02 p0251 N88-11583

Solar-geophysical data number 514, June 1987. Part 1: (Prompt reports). Data for May 1987, April 1987 and late data
[PB87-217261] 02 p0257 N88-11626

Publications and final reports on contracts and grants, 1986 (National Environmental Satellite, Data and Information Service)
[PB87-220810] 03 p0352 N88-12218

Solar-geophysical data number 514, June 1987. Part 2: (Comprehensive reports). Data for December 1986
[PB87-217279] 03 p0390 N88-12450

USSR report: Earth sciences
[JPRS-UES-86-006] 04 p0458 N88-12831

Summaries of physical research in the geosciences
[DE88-000833] 04 p0468 N88-12896

Isotropic probability measures in infinite dimensional spaces: Inverse problems/prior information/stochastic inversion
[NASA-CR-181555] 05 p0643 N88-13936

Research needs for hydrocarbon fuels
[DE87-014555] 06 p0687 N88-14209

USSR report: Earth sciences
[JPRS-UES-87-004] 06 p0725 N88-14455

Tectonics and magmatism of Walvis Ridge and Discovery Rise (Atlantic Ocean)
06 p0726 N88-14463

Geophysical-geomorphological statistical regionalization of North Atlantic
06 p0726 N88-14466

Effective methods of gravimetric and magnetometric data processing 06 p0728 N88-14479

Polar Geophysical Institute's studies of magnetosphere, ionosphere 06 p0728 N88-14480

Solar-geophysical data number 515, July 1987. Part 1: (Prompt reports). Data for June 1987, May 1987 and late data
[PB87-233177] 06 p0805 N88-14912

Solar-geophysical data number 515, July 1987. Part 2: (Comprehensive reports). Data for January 1987 and miscellanea
[PB87-233185] 06 p0805 N88-14913

Solar-geophysical data number 515, July 1987. Supplement (explanation of data reports)
[PB87-233169] 06 p0805 N88-14914

Solar-geophysical activity reports for STIP (Study of Travelling Interplanetary Phenomena) Interval 15, 12-21 February 1984 ground level event and STIP Interval 16, 20 April-4 May 1984 Forbush decrease
[PB87-232658] 06 p0805 N88-14915

USSR report: Earth sciences
[JPRS-UES-87-003] 08 p1009 N88-16119

Processes in the quiet and disturbed equatorial-low latitude ionosphere: Sundial campaign, 1984
[INPE-4152-PRE/1057] 08 p1036 N88-16282

Interplanetary and geophysical effects of a coronal transient 08 p1095 N88-16587

Earth materials research: Report of a Workshop on Physics and Chemistry of Earth Materials
[NASA-CR-182519] 10 p1298 N88-17761

Three-dimensional transient electromagnetic modeling for exploration geophysics 10 p1346 N88-18047

Solar-geophysical data number 517, September 1987. Part 1: (Prompt reports). Data for August, July 1987 and late data
[PB88-128426] 10 p1430 N88-18544

Solar-geophysical data number 517, September 1987. Part 2: (Comprehensive reports). Data for March 1987 and miscellanea
[PB88-128434] 10 p1431 N88-18545

AFGL (Air Force Geophysics Laboratory) fiscal year 1988 Air Force technical objectives document
[AD-A187701] 11 p1503 N88-18977

An adaptive grid finite difference method for time-dependent Magnetohydrodynamic (MHD) flows and its astrogeophysical applications
11 p1553 N88-19294

Geophysical study of the structure and processes of the continental convergence zones: Alpine-Himalayan Belt
[NASA-CR-182647] 12 p1644 N88-19842

Proceedings of an ESA-NASA Workshop on a Joint Solid Earth Program
[NASA-CR-182642] 12 p1644 N88-19844

Solar-geophysical data number 518, October 1987. Part 2: (Comprehensive reports). Data for April 1987
[PB88-138060] 12 p1711 N88-20242

Solar-geophysical data number 518, October 1987. Part 1: (Prompt reports). Data for September 1987, August 1987 and late data
[PB88-138078] 12 p1712 N88-20243

Interactive automated system for testing analog units of digital seismic stations 13 p1789 N88-20702

Inversion algorithms for geophysical problems
[AD-A189252] 13 p1815 N88-20845

Physics of condensed matter at extreme conditions
[DE88-006232] 13 p1832 N88-20958

ONR Far East Scientific Bulletin, volume 12, number 3, July-September 1987
[AD-A188554] 13 p1851 N88-21081

The Spring 1985 high precision baseline test of the JPL GPS-based geodetic system
[NASA-CR-182686] 14 p1940 N88-21577

Solar-geophysical data number 519, November 1987. Part 2: (Comprehensive reports). Data for May 1987 and miscellanea
[PB88-158910] 14 p2011 N88-21997

A hardware/software system for implementing geophysical diffraction tomography
[DE88-006411] 15 p2094 N88-22480

Bilateral symmetry elements of the Zhamanshin impact crater
[NASA-TT-20288] 15 p2096 N88-22490

Solar-geophysical data number 520, December 1987. Part 1: (Prompt reports). Data for November 1987, October 1987 and late data
[PB88-164199] 16 p2290 N88-23712

An integrated study of the Alto Paranaiba Kimberlite Province, Minas Gerais, Brazil: A possible tool for diamond exploration 17 p2355 N88-24031

Remote sensing of acoustic properties of shallow water sediments: A review
[AD-A192107] .18 p2570 N88-25267

Geophysical monitoring for climatic change, number 15
[PB88-180146] 19 p2692 N88-26003

Solar-geophysical data number 521, January 1988. Part 1: (Prompt reports). Data for December 1987, November 1987 and late data
[PB88-179213] 19 p2743 N88-26284

Solar-geophysical data number 521, January 1988. Part 2: (Comprehensive reports). Data for July 1987 and miscellanea
[PB88-179221] 19 p2743 N88-26285

Reports of planetary geology and geophysics program, 1987
[NASA-TM-4041] 20 p2885 N88-27133

Solar-geophysical data number 522, February 1988. Part 2: (Comprehensive reports). Data for August 1987 and miscellanea
[PB88-194741] 20 p2886 N88-27138

Solar-geophysical data number 522, February 1988. Part 1: (Prompt reports). Data for January 1988, December 1987 and late data
[PB88-194733] 20 p2886 N88-27139

Development of radiation and cloud parameterization programs for AFGL (Air Force Geophysics Laboratory) global models
[AD-A193369] 21 p2973 N88-27658

Program to increase the measurement capabilities of the AFGL (Air Force Geophysics Laboratory) fixed and mobile high altitude lidar systems
[AD-A194614] 23 p3203 N88-29063

Solar-geophysical data number 523, March 1988. Part 2: (Comprehensive reports). Data for September 1987 and miscellanea
[PB88-212774] 24 p3458 N88-30576

GEOPOTENTIAL

NT GEOPOTENTIAL HEIGHT

The contraction of satellite orbits under the influence of air drag. Part 8: Orbital lifetime in an oblate atmosphere, when perigee distance is perturbed by odd zonal harmonics in the geopotential
[RAE-TR-86069-PT-8] 01 p0010 N88-10058

A study of a satellite-to-satellite tracking configuration by application of linear perturbation theory
[REPT-86.3] 01 p0011 N88-10059

Estimability of potential coefficients from orbit perturbations --- satellite geodesy
[REPT-86.1] 01 p0064 N88-10408

Advanced simulation and analysis of a geopotential research mission
[NASA-CR-182355] 06 p0670 N88-14108

Simulation and analysis of a geopotential research mission
[NASA-CR-182354] 06 p0670 N88-14109

Estimation of geopotential from satellite-to-satellite range rate data: Numerical results
[NASA-CR-180771] 14 p1941 N88-21583

Modeling and estimation of a low degree geopotential model from terrestrial gravity data
[NASA-CR-182808] 16 p2232 N88-23330

GEOPOTENTIAL HEIGHT

Mean pressure distribution and geostrophic circulation in the meteor zone 06 p0734 N88-14513

New possibilities for using gravity data in developing geodetic coordinate systems 08 p1009 N88-16116

Persistence characteristics of 500 mb blocking and zonal flows in the mid-latitudes of the Northern and Southern Hemispheres 10 p1353 N88-18088

Monthly mean global climatology of temperature, wind, geopotential height, and pressure for 0 - 120 km
[NASA-TM-100697] 15 p2099 N88-22503

Global atmospheric circulation statistics, 1000-1 mb
[PB88-168240] 16 p2234 N88-23340

The relative utility of persistence and medium-range dynamical forecasts of monthly mean 700 mb heights
22 p3127 N88-28588

GEOPOTENTIAL RESEARCH MISSION

An orbit simulation study of a geopotential research mission including satellite-to-satellite tracking and disturbance compensation systems
[NASA-CR-182353] 07 p0823 N88-14997

GEOPRESSURE

Geothermal energy technology: Issues, R and D (Research and Development) and cooperative arrangements
[PB88-193107] 21 p2967 N88-27626

GEOS SATELLITES (ESA)

A European apogee boost motor for GEOS
09 p1123 N88-16719

GEOS SATELLITES (ESRO)

U GEOS SATELLITES (ESA)

GEOS 2 SATELLITE

Interplanetary Magnetic Field (IMF) influence on the magnetic configuration and particle fluxes at geostationary orbit and on the substorm onset
08 p1031 N88-16247

GEOS-B SATELLITE

U GEOS 2 SATELLITE

GEOSAT SATELLITES

GEOSAT altimeter geophysical data record user handbook
[PB87-213336] 03 p0276 N88-11743

Geosat crossover analysis in the tropical Pacific. Part 1: Constrained sinusoidal crossover adjustment
[NASA-CR-182391] 07 p0871 N88-15285

GEOSTATIONARY OPERATIONAL ENVIRON SATS

U GOES SATELLITES

GEOSTATIONARY PLATFORMS

U SYNCHRONOUS PLATFORMS

GEOSTATIONARY SATELLITES

U SYNCHRONOUS SATELLITES

GEOSTROPHIC WIND

An improved method of analyzing surface geostrophic winds and pressure 02 p0212 N88-11334

Mean pressure distribution and geostrophic circulation in the meteor zone 06 p0734 N88-14513

A study of the mechanism of internal gravity wave generation by quasigeostrophic meteorological motions
06 p0735 N88-14520

Longitudinal peculiarities of meridional circulation in lower thermosphere and mesosphere
06 p0736 N88-14525

Analysis of quasi-geostrophic forcing during the AIMCS (Airborne Investigations of Mesoscale Convective Systems) Project. Volume 2: Results for June 14 through July 16, 1984
[PB88-123807] 10 p1354 N88-18092

Analysis of quasi-geostrophic forcing during the AIMCS (Airborne Investigations of Mesoscale Convective System) Project. Volume 1: Discussion
[PB88-133095] 12 p1645 N88-19860

Contribution to theory of quasigeostrophic motions of finite amplitude in viscous stratified ocean
13 p1788 N88-20695
Physical process for maintenance of mean meridional and zonal circulation of atmosphere in middle latitudes, volume 2 14 p1900 N88-21345
Geostrophic flow in the central Bering Sea, Fall 1986 and Summer 1987
[PB88-174354] 16 p2237 N88-23360
Three-dimensional temperature fields in the atmosphere up to 50 km altitude
[ETN-88-92150] 18 p2542 N88-25089
Modelling and forecasting deep ocean and near surface mesoscale eddies: Hindcasting and forecasting with, and coupling a surface boundary layer model to, the Harvard quasigeostrophic model 19 p2694 N88-26013

GEOSYNCHRONOUS EARTH ORBITAL ENVIRONMENTS
U EARTH ORBITAL ENVIRONMENTS

GEOSYNCHRONOUS ORBITS
The geosynchronous plasma environment
03 p0273 N88-11716
External surface charging mechanisms --- spacecraft
03 p0273 N88-11719
An allotment planning concept and related computer software for planning the fixed satellite service at the 1988 space WARC
[NASA-TM-100244] 03 p0308 N88-11944
Planning for future operational sensors and other priorities
[PB87-220802] 03 p0325 N88-12056
Observation guidelines for a Total Ozone Mapping Spectrometer (TOMS) in geosynchronous orbit
05 p0619 N88-13801
A laser communication experiment utilizing the ACT satellite and an airborne laser transceiver
[NASA-TM-100792] 11 p1492 N88-18910
Study of the optimization of satellite system design for transfer orbit
[MBB-URV-135] 13 p1727 N88-20332
Spacecraft trajectories
[ISBN-2-35-428166-7] 15 p2023 N88-22054
Centaur operations at the space station
[NASA-CR-179593] 19 p2606 N88-25473
Relationship between characteristics of low-energy electrons and geomagnetic disturbance in geostationary orbit 24 p3444 N88-30501

GEOTECHNICAL ENGINEERING
Siting and Geotechnical Program Focus and Directions. Report upon the deliberations of a workshop held at the Illinois Institute of Technology, Chicago, Illinois on August 4-5, 1986
[PB87-206272] 02 p0198 N88-11238
Error analysis for geotechnical engineering
[AD-A186795] 09 p1189 N88-17124
A study of the magnetic field annihilation process in the magnetosphere and some geotechnical applications
[DE88-004165] 10 p1355 N88-18096
Computer Applications in Geotechnical Engineering (CAGE) and Geotechnical aspects of the Computer-Aided Structural Engineering (G-CASE) projects. User's guide. UTEXAS2 slope-stability package. Volume 1: User's manual
[AD-A187674] 11 p1511 N88-19025

GEOTEMPERATURE
Determining deep heat flow under complex geothermal conditions 08 p1011 N88-16130

GEOTHERMAL ANOMALIES
Metamorphic P-T paths and Precambrian crustal growth in East Antarctica 24 p3395 N88-30218

GEOTHERMAL ENERGY CONVERSION
Status of the Magma Energy Project
[DE88-002413] 13 p1792 N88-20719
Overview of recent activities in the Heat Cycle Research Program
[DE88-005544] 13 p1795 N88-20738

GEOTHERMAL ENERGY EXTRACTION
Recent progress in magma energy extraction
[DE87-013063] 01 p0066 N88-10424
Status of the Magma Energy Project
[DE88-002413] 13 p1792 N88-20719

GEOTHERMAL ENERGY UTILIZATION
Tapping the earth's geothermal resources: Hydrothermal today, magma tomorrow
[DE87-014718] 02 p0196 N88-11223
Application of Organic Rankine Cycles (ORCs) to decentralized power generation, preliminary study
[DE87-753331] 03 p0347 N88-12197
Advanced geothermal technologies
[DE88-004307] 15 p2091 N88-22463
Prospects for hot dry rock in the future
[DE88-010909] 20 p2820 N88-26730

GEOTHERMAL RESOURCES
Tapping the earth's geothermal resources: Hydrothermal today, magma tomorrow
[DE87-014718] 02 p0196 N88-11223
Overview of recent activities in the Heat Cycle Research Program
[DE88-005544] 13 p1795 N88-20738
Advanced geothermal technologies
[DE88-004307] 15 p2091 N88-22463
Prospects for hot dry rock in the future
[DE88-010909] 20 p2820 N88-26730
Unstable heat pipes
[DE88-010780] 23 p3229 N88-29217

GEOTHERMAL TECHNOLOGY
Thin films for geothermal sensing
[DE88-000154] 03 p0326 N88-12061
Advanced geothermal technologies
[DE88-004307] 15 p2091 N88-22463
Prospects for hot dry rock in the future
[DE88-010909] 20 p2820 N88-26730
Geothermal energy technology: Issues, R and D (Research and Development) and cooperative arrangements
[PB88-193107] 21 p2967 N88-27626

GEOTHERMOMETRY
U GEOTEMPERATURE

GEP TELESCOPES
U PARTICLE TELESCOPES

GERDIEN ARC HEATERS
U ARC HEATING
U HEATING EQUIPMENT

GERMAN INFRARED LABORATORY
An infrared grating spectrometer for GIRL
[ETN-88-91071] 09 p1167 N88-16997

GERMANIUM
Si - SiO2 interfaces: A High Resolution Transmission Electron Microscopy (HRTEM) study
[DE87-012255] 01 p0026 N88-10181
Effect of high-temperature annealing on the microstructure and thermoelectric properties of GaP doped SiGe
[NASA-TM-100164] 01 p0029 N88-10188
Thermal expansion of some Ge-Se-Te glasses
[PD-MT-8722] 04 p0420 N88-12606
Studies on some Ge-Se-Te glasses
[PD-MT-8721] 04 p0420 N88-12607
The influence of phosphorus on the solid state reaction between copper and silicon or germanium
[ETN-88-91361] 06 p0789 N88-14838
The migration of grain boundaries in ceramic materials with particular reference to the sintering process
[DE88-004085] 10 p1306 N88-17808
Preparation and characterization of Cu2Zn1-xMnxGeS4
[AD-A188113] 11 p1556 N88-19315
Development of Si/SiGe heterostructures
[AD-A189527] 13 p1845 N88-21044
Optical study of germanium, germanium plus arsenic, and germanium plus gallium implants in gallium arsenide
[AD-A189600] 13 p1845 N88-21045
Fundamental properties and devices applications of Ge(x)Si(1-x)/Si superlattices
[AD-A190129] 15 p2143 N88-22787
Interface formation and precursory dynamics
[AD-A190741] 15 p2144 N88-22794
Interaction of slow neutrons with Ge74 single crystals
[DE87-703010] 17 p2445 N88-24536
Defects in high-mobility semiconductor systems
[AD-A191618] 19 p2732 N88-26224
Influence of the interface on the crystallization of amorphous Ge in Pb/Ge multilayers
[DE88-010072] 22 p3156 N88-28776
Low temperature film growth of the oxides of zinc, aluminum and vanadium (and related systems, oxides of gold and germanium, nitrides of aluminum and tungsten) by reactive sputter deposition
[AD-A193497] 23 p3191 N88-28986
Development of a unit cell for a Ge:Ga detector array
[NASA-CR-177445] 24 p3375 N88-30100

GERMANIUM ALLOYS
Factors determining the morphology of precipitation in aluminum-germanium and aluminum-silicon alloys
[DE87-014682] 03 p0267 N88-11806
Stability diagrams for epitaxial strained layers
[DE88-003935] 10 p1418 N88-18470
Optimisation of the thermoelectric figure of merit of modified silicon germanium alloys
[AD-A191347] 16 p2283 N88-23670
Preparation of improved PbSnTe thermoelectric alloys and evaluation of their figure of merit
[AD-A191346] 17 p2445 N88-24538
Improved properties of SiGe/GaP alloys
[NASA-CASE-NPO-17259-1-CU]
18 p2585 N88-25358
Metastability in SiGe/Si strained-layer structures
[DE88-007603] 18 p2585 N88-25361
Hydrogenated amorphous silicon-germanium alloys
[DE88-001147] 19 p2620 N88-25546
Calculation of the specific and volumetric enthalpies of Ge-Si alloys
[DE88-008949] 21 p3026 N88-27965

GERMANIUM COMPOUNDS
Silicon-germanium heterostructures
13 p1844 N88-21034
Improved GaP doped SiGe thermoelectric material
17 p2437 N88-24503
Photorefractive damage mechanism in electro-optic materials
[AD-A194560] 23 p3282 N88-29543

GERMANIUM DIODES
An investigation of the equivalent circuit and carrier lifetimes of Si/SiGe heterostructure p-n diodes for frequencies between 0.5 and 18.5 MHz
[FOA-C-30469-3.2] 09 p1256 N88-17529

GERMANIUM RECTIFIERS
U GERMANIUM DIODES

GERMANY
History of aeroelasticity in Germany from the beginning to 1945
[ESA-TT-1082] 24 p3319 N88-29767

GET AWAY SPECIALS (STS)
Low frequency VLBI in space using GAS-Can satellites: Report on the May 1987 JPL Workshop
[NASA-CR-182362] 06 p0801 N88-14904
The 1987 Get Away Special Experimenter's Symposium
[NASA-CP-2500] 10 p1286 N88-17691
Microgravity research at the University of Mexico: Experiments in payload G-006 10 p1286 N88-17692
Materials processing in space: An introduction to the G-480 payload 10 p1287 N88-17695
Ten past and ten future GAS/MAUS-payloads
10 p1287 N88-17696
An update to the MITRE/WPI Space Shuttle Program GASCAN G-408 10 p1287 N88-17697
Electrochemical growth of linear conducting crystals in microgravity 10 p1287 N88-17698
Planet X probe: A fresh new look at an old familiar place 10 p1287 N88-17699
Protein-crystal growth experiment (planned)
10 p1287 N88-17700
The photons payload, G-494: A learning experience
10 p1288 N88-17701
A payload for investigating the influence of convection on GaAs crystal growth 10 p1288 N88-17702
An advanced microcomputer design for processing of semiconductor materials 10 p1288 N88-17703
Project Explorer takes its second step: GAS-608 in engineering development 10 p1288 N88-17707
GAS 450: A space payload for the People Central Coast Student Experimenters 10 p1289 N88-17709
The NORSTAR Program: Space shuttle to space station 10 p1289 N88-17710
Lightsats and their attraction to budget oriented Federal agencies 10 p1289 N88-17711
GAS eleven node thermal model (GEM)
10 p1289 N88-17712
Aerospace payload support systems
[AFGL-TR-87-0241] 24 p3334 N88-29843

GETTERS
A new polymer-based hydrogen getter
[DE88-004538] 13 p1751 N88-20467

GIACOBINI-ZINNER COMET
An overview of STIP interval 18: September 1985, the G-Z encounter 01 p0116 N88-10741
Comparative plasma tails of Venus and comets
01 p0116 N88-10742
The status of the international Halley watch
01 p0116 N88-10744
Large-scale interaction of the solar wind with comets Halley and Giacobini-Zinner 01 p0117 N88-10745
Solar wind-cometary interaction at the ionopause and associated phenomena 01 p0117 N88-10748
Space missions to Comets Halley and Giacobini-Zinner 03 p0272 N88-11712
Analysis of the ICE combiner for multiple antenna arraying 04 p0436 N88-12704
A comparison between wave observations performed in the environments of Comets Halley and Giacobini-Zinner 14 p1996 N88-21896
Narrow-band photometry of Comet P/Giacobini-Zinner at the time of ICE encounter 14 p1998 N88-21911
Gas coma of Comet Giacobini-Zinner: Emission from grains 14 p2000 N88-21923
Determination of the content of CO(+) and H2O(+) ions in the tail of Comet Giacobini-Zinner and Comet Halley 14 p2006 N88-21964

GIANT STARS
NT ASYMPTOTIC GIANT BRANCH STARS
NT CARBON STARS
NT RED GIANT STARS
Mass loss 02 p0253 N88-11587

A re-examination of the corona-wind dividing line: Diagnostics of non-coronal atmospheres
04 p0504 N88-13101

Atmospheres of stars in the limits of thick and thin convection zones: M giants 04 p0505 N88-13105

Carbon abundances and C12/C13 ratios in M giants
04 p0515 N88-13167

JHK photometry of CN-rich field giants
04 p0516 N88-13175

A comprehensive exploration of late-type stars in the far-ultraviolet 04 p0520 N88-13194

AGB (Asymptotic Giant Branch): Star evolution
[DE88-001829] 07 p0945 N88-15742

Spectroscopic determinations of surface gravities of giant stars, and ultraviolet observations of RR Lyrae and X Arietis 11 p1569 N88-19391

Review of the theoretical changes of surface chemistry during massive star evolution
[SER-C-PREPUBL-FASC-17] 18 p2593 N88-25411

Asymptotic giant branch stars in the Infrared Astronomical Satellite (IRAS) catalogs: Selection and analysis of the population characteristics
[MPE-PREPRINT-116] 22 p3163 N88-28840

GIBBS FREE ENERGY

Certain questions of thermodynamic theory of weak solutions 18 p2586 N88-25368

GIMBALS

Balloon-borne three-meter telescope for far-infrared and submillimeter astronomy
[NASA-CR-182310] 09 p1262 N88-17565

Experience with duplex bearings in narrow angle oscillating applications 14 p1926 N88-21484

On the torque and wear behavior of selected thin film MOS2 lubricated gimbal bearings
14 p1926 N88-21485

Two gimbal bearing case studies: Some lessons learned 14 p1927 N88-21487

Utilization of the IR telescope gimbaling system as a stabilized pointing platform for balloon payloads. Volume 1: Technical results
[NASA-CR-179339] 18 p2522 N88-24962

GIOTTO MISSION

Space missions to Comets Halley and Giacobini-Zinner 03 p0272 N88-11712

Data processing of the JPA instrument. Part 1: Data management
[IFSI-86-15-PT-1] 06 p0757 N88-14645

Giotto: A mission to Halley's Comet
09 p1127 N88-16756

Energy spectra of pick-up ions recorded during the encounter of Giotto with Comet Halley
14 p1997 N88-21901

Observation of energetic particles (E greater than 30 keV) by the Giotto experiment EPA in the magnetic cavity of Comet Halley 14 p1997 N88-21903

Evidence for first polymer in Comet Halley: Polyoxymethylene 14 p1997 N88-21906

The Giotto extended mission
14 p2005 N88-21957

Alternative cometary targets for the Giotto extended mission 14 p2010 N88-21990

GIRDERS

Deformation induced cracking in steel girder bridges and retrofit guidelines
[PB88-102710] 07 p0868 N88-15265

GLACIAL DRIFT

The unsteady ground heat flow at the contact surface between a glacier run and the subsoil
08 p1014 N88-16147

Large ice masses: Characteristics, behaviour and relation to climate 14 p1939 N88-21569

GLACIERS

Energy balance and discharge of an Alpine glacier, illustrated by Mount Vernagtferner in the Oetzal Alps, Tyrol 08 p1014 N88-16145

Vertical sounding of th air layer close to a glacier on Mount Vernagferner in the Oetzal Alps, Tyrol (experiment LUZIVER 1983) 08 p1015 N88-16152

Large ice masses: Characteristics, behaviour and relation to climate 14 p1939 N88-21569

Topography of an Antartic ice stream
22 p3092 N88-28361

GLACIOFLUVIAL DEPOSITS
U GLACIAL DRIFT

GLACIOLOGY

NASA Oceanic Processes Program
[NASA-TM-4025] 10 p1357 N88-18109

SPOT image exploitation for glacial mass balance fluctuation monitoring in the French Alps
22 p3090 N88-28350

Topography of an Antartic ice stream
22 p3092 N88-28361

GLANDS (ANATOMY)
NT ADRENAL GLAND
NT HYPOTHALAMUS
NT PITUITARY GLAND
NT TESTES

GLASS
NT BOROSILICATE GLASS
NT E GLASS
NT GLASS FIBERS
NT METALLIC GLASSES
NT S GLASS
NT SILICA GLASS
NT SPIN GLASS

Ion-implantation-induced stress in glasses: Variation of damage mode efficiency with changes in glass structure
[DE87-013523] 01 p0026 N88-10175

Mechanism of mechanical fatigue of fused silica
[DE87-014199] 02 p0152 N88-10950

Stress measurements in sol-gel films
[DE87-014467] 02 p0153 N88-10955

Study of the micromechanical behavior of a SiO2-Al2O3-Li2O glass ceramic and its relation to the microstructure
[ISAL-ITC1-87-01] 02 p0153 N88-10960

Preparation of oxide glasses from metal alkoxides by sol-gel method
[NASA-TT-20124] 02 p0154 N88-10965

Some speculations on the mechanisms of abrasive grinding and polishing
[DE87-014242] 02 p0181 N88-11126

Carbon fiber reinforced glass matrix composites for space based applications
[AD-A184355] 04 p0410 N88-12546

Thermal expansion of some Ge-Se-Te glasses
[PD-MT-8722] 04 p0420 N88-12606

Reliability of Li/SO2 cells for long-life applications
[DE88-001360] 04 p0440 N88-12735

Composite materials with glass matrix
[SGR/PR-4305/86-SV/JC] 05 p0558 N88-13394

Ionic transport and electrical relaxation in glass
[DE88-000887] 05 p0657 N88-14028

Material design of high-purpose glass discussed
06 p0675 N88-14133

Reactions and bonding between glasses and titanium
[DE88-000603] 06 p0685 N88-14195

Glassy GeO2 obtained by the gel process
[NASA-TT-20125] 06 p0685 N88-14201

Material design of high performance glasses discussed 06 p0688 N88-14216

Photoinduced low-temperature changes in optical losses in fiber optics based on chalcogenide glasses
06 p0770 N88-14731

Fracture study of windshield glass panes
06 p0799 N88-14891

Diffraction by glasses with a layer structure
[DE88-003059] 07 p0837 N88-15078

Development of composite polymer-glass edge claddings for Nova laser disks
[DE88-002389] 07 p0860 N88-15220

The development of test methodology for testing glassy materials 07 p0927 N88-15633

Processing and interfacial analysis of glass-ceramic to metal seals
[DE88-002999] 08 p0971 N88-15873

Review of nucleation and incipient boiling under pool and forced convection conditions
08 p0982 N88-15938

JPRS report: Science and technology. USSR: Physics and mathematics
[JPRS-UPM-87-010] 08 p1075 N88-16485

Study of the micromechanical properties of fluor glasses based on ZrF4
[ISAL-ITC1-87-03] 09 p1148 N88-16882

LFCM (Liquid-Fed Ceramic Melter) vitrification technology
[DE88-003441] 09 p1149 N88-16887

Models for ionic transport in glass
[DE88-002860] 10 p1304 N88-17799

Metal modification for improved glass-ceramic to metal seals: 1. Auger results on ion implantation and vapor deposition films
[DE88-005244] 10 p1339 N88-18006

Crystallization and glass formation in electron and laser beam irradiated Cu-Zr alloys
[DE88-003390] 11 p1464 N88-18729

Phosphorus oxynitride glass for laser applications
[DE88-005413] 12 p1632 N88-19768

Fast protonic conducting solid electrolytes
[AD-A188524] 12 p1698 N88-20160

Materials Research Laboratory at Brown University
[AD-A188006] 13 p1739 N88-20396

Processing of glass to aluminum (low melting metals) seals via an injection molding technique
[DE88-004689] 13 p1751 N88-20468

Nonlinear refractive index measurements of glasses and crystals
[DE88-005673] 13 p1840 N88-21009

Theoretical studies on the electronic structure and properties of complex ceramic crystals and glasses
[DE88-005837] 13 p1846 N88-21049

Interface structure and properties of alumina/glass ceramic composites
[DE88-006219] 14 p1892 N88-21302

Determination of the modulus of elasticity of structural silicone sealants
[PB88-157458] 14 p1893 N88-21307

Anisotropy of light absorption by color centers in waveguides produced on photochromic glasses by diffusion 14 p1896 N88-21320

Radiation absorption in neodymium glasses during passage of strong laser pulse 14 p1969 N88-21757

Fluids, gels and glasses under extreme conditions of pressure and temperature
[AD-A190655] 15 p2035 N88-22125

Fracture toughness of silicon nitride-silicon nitride joints bonded with oxynitride glass
[DE88-005548] 15 p2043 N88-22172

Containerless glass melting 15 p2051 N88-22222

Solar cell cover glasses for satellites
15 p2052 N88-22225

Magnetic anomalies in the rare earth oxide superconductors GdBa2Cu3O(7-x) and YbBa2Cu3O(7-x)
[AD-A190713] 15 p2144 N88-22793

Remarks on solid state amorphizing transformations
[DE88-006452] 15 p2145 N88-22803

Fast ion conducting glasses
[AD-A191412] 16 p2183 N88-23010

Investigation of non-linear optical behavior of semiconductors for optical switching, volume 1
[AD-A191297] 16 p2274 N88-23611

Noncontact temperature measurement in glass and other transparent materials 17 p2328 N88-23900

Apparatus for the measurement of resistivity of glasses and ceramics 17 p2431 N88-24460

Glass forming ranges of amorphous alloys
[DE88-007897] 20 p2772 N88-26438

Statistical mechanics of polymer systems
[DE88-011172] 20 p2778 N88-26477

Semiconductor microcrystallites in porous glass and their applications in optics 20 p2863 N88-27005

Fabrication of SiC fiber reinforced glass matrix by extrusion process and investigation of its mechanical properties
[ETN-88-92367] 21 p2906 N88-27244

Preparation and properties of new inorganic glasses and gel-derived solids
[AD-A192922] 21 p2917 N88-27315

Performance evaluation of large-area glass-mirror heliostats
[DE88-011883] 21 p2969 N88-27636

Metal halide optical glasses
[AD-A193794] 23 p3198 N88-29032

Ion exchange processes for fabrication of integrated optical waveguide structures into glass substrates
[VTT-46] 24 p3429 N88-30405

GLASS COATINGS

Short fiber reinforced thermoplastic composites for armor applications: Interfacial bonding
[DE8 -004007] 10 p1295 N88-17742

Improved glass-ceramic to metal seals in actuator and detonator applications with an aluminum-containing austenitic stainless steel
[DE88-004691] 13 p1749 N88-20458

SBIR-Long fluoride fiber
[AD-A188595] 13 p1754 N88-20492

The Time-Temperature-Transformation (TTT) diagram as a basis for relating the formation and properties of reactive coatings
[AD-A190872] 16 p2182 N88-23006

GLASS FIBER REINFORCED PLASTICS

The influence of microvoids on the electrical strength of glass fiber reinforced epoxy resins
[ETN-87-90443] 01 p0030 N88-10189

Interactive buckling effects in stiffened FRP panels
[ARE-TM(UMS)-87204] 01 p0059 N88-10378

Determination of through-plane shear moduli for glass-reinforced plastics
[PB87-106274] 04 p0418 N88-12592

In-situ characterization of the interface of glass reinforced composites
[AD-A185136] 05 p0557 N88-13391

Fractographic study of fiber composites
06 p0677 N88-14146

Experimental and theoretical investigation of mechanically fastened composites
[AD-A185896] 07 p0826 N88-15008

To determine the stress distribution in the vicinity of GRP end pads where the specimen is held and loaded (CFC coupon specimens) --- glass reinforced plastic (GRP) carbon fiber composite (CFC)
[BAE-WST-R-RES-CFC-12023] 09 p1182 N88-17080

Further tests to determine the stress distribution in the vicinity of GRP end pads where the specimen is held and loaded (CFC coupon specimens) --- glass reinforced plastic (GRP) carbon fiber composite (CFC)
[BAE-WST-R-RES-CFC-12023-ADD-1] 09 p1182 N88-17081

Studies of traverse impact damage in composite materials using a Hopkinson pressure-bar technique
[OUEL-1706/87] 14 p1883 N88-21255

Study of strength characteristics of glass-reinforced plastic by acoustic emissions method
14 p1885 N88-21268

Rocket motor case materials. An evaluation of new fibers for composites
[FOA-C-20696-2.1] 21 p2906 N88-27245

Development of a glass fiber wing following the construction regulation FAR Part 23
[ETN-88-92966] 23 p3189 N88-28979

GLASS FIBERS

Effects of solvent exposures on poly(etheretherketone) (PEEK) and PEEK-fiberglass composites
[MLM-3405] 03 p0281 N88-11766

Development and application of composites
03 p0286 N88-11795

A creep measurement of unidirectional epoxy-fiberglass rod
[DE87-014812] 04 p0411 N88-12553

A hybrid fibreglass-CFRP cloth for new furnishings --- aircraft cabins
[SNIAS-872-111-109] 05 p0558 N88-13396

High temperature adhesive
[PB87-109229] 06 p0683 N88-14186

Evaluation of the thermal effectiveness of urethane foam and fiberglass as insulation systems for tank cars
[PB88-100797] 06 p0686 N88-14207

Interfacial shear strength of pitch and high strain pan fibers in an epoxy matrix
[AD-A185966] 07 p0826 N88-15011

The strength of hybrid composites
[BR101991] 09 p1138 N88-16821

Fabrication and materials evaluation of high performance aligned ceramic fibre reinforced glass matrix composite
[AERE-R-12517] 10 p1294 N88-17736

Lunar fiberglass: Properties and process design
[NASA-CR-182580] 11 p1466 N88-18740

Mast material test program (MAMATEP)
[NASA-TM-100821] 12 p1604 N88-19592

Fibrous glass aerosols: A literature review
[AD-A188420] 12 p1672 N88-20008

Use of reinforced inorganic cement materials for spark wire and drift chamber wire frames
[NASA-CR-180759] 13 p1746 N88-20438

SBIR-Long fluoride fiber
[AD-A188595] 13 p1754 N88-20492

Dependence of formation of radiative color centers in optical glass fibers on technological factors
14 p1896 N88-21321

Corrosion and fatigue properties of FeCrB/Si metallic glass wires in aqueous environments
17 p2320 N88-23855

Sol/gel processing techniques for glass matrix composites
[AD-A191748] 18 p2478 N88-24701

Calculational model development for fibrous thermal insulation transient test procedures
[DE88-007843] 18 p2493 N88-24789

Novel fiber preforms: Rare earth doping
[AD-A191540] 18 p2575 N88-25294

Investigation of leaks in fiberglass-reinforced pressure vessels by direct observation of hollow fibers in glass cloth
[DE88-006936] 19 p2609 N88-25485

Excitation of single-mode glass fiber by partially coherent sources
[ETN-88-92121] 20 p2854 N88-26951

Effects of electron beam irradiation on mechanical properties at low and high temperature of fiber reinforced composites using PEEK as matrix material
[DE88-753134] 21 p2905 N88-27239

Contribution to the development of coated fiber ceramic insulation material
[ETN-88-92361] 21 p2906 N88-27243

Determination of radiative properties of fiberglass and foam insulations
[DE88-007845] 21 p2920 N88-27331

GLASS LASERS

Large-scale stimulated rotational Raman scattering experiments using the LLNL Nova laser
[DE87-012661] 01 p0051 N88-10328

Thermal stress in the edge cladding of Nova glass laser disks
[DE88-000425] 04 p0448 N88-12780

An investigation of unipolar arcing at atmospheric pressure in aluminum 2024 and aluminum coated glass slides
[AD-A184903] 05 p0577 N88-13521

JPRS report: Science and technology. USSR: Physics and mathematics
[JPRS-UPM-87-008] 06 p0769 N88-14727

Phosphorus oxynitride glass for laser applications
[DE88-005413] 12 p1632 N88-19766

Radiation absorption in neodymium glasses during passage of strong laser pulse 14 p1969 N88-21757

Development of high efficiency q-switched glass laser via sol-gel processing
[AD-A192301] 23 p3218 N88-29154

GLASS TRANSITION TEMPERATURE

Studies on some Ge-Se-Te glasses
[PD-MT-8721] 04 p0420 N88-12607

Correlations of norbornenyl crosslinked polyimide resin structures with resin thermo-oxidative stability, resin glass transition temperature and composite initial mechanical properties
[NASA-TM-100791] 09 p1147 N88-16877

Determination of the glass transition temperature of cured composite materials
[DT-87/62-R] 21 p2906 N88-27246

GLAUERT COEFFICIENT
U AERODYNAMIC FORCES
U MACH NUMBER

GLAZES

A flow visualization study of the leading edge separation bubble on a NACA 0012 airfoil with simulated glaze ice
[NASA-CR-180846] 07 p0816 N88-14966

An experimental mapping of the flow field behind a glaze ice shape on a NACA 0012 airfoil
[NASA-CR-180847] 08 p0950 N88-15766

Laser surface melting
[BMFT-FB-T-86-072] 14 p1914 N88-21435

GLIDE LANDINGS

The effects of RCS jet firing on the isolated Orbiter and mated coast phases of the glide return to launch site maneuver at Mach number 6 (IA302B)
[NASA-CR-180223] 20 p2766 N88-26403

GLIDERS

Investigations of the laminar-turbulent boundary layer transition for the improvement of the performance of powered glider aircraft profiles
[ETN-88-91094] 11 p1436 N88-18569

GLIDING

Computer simulation of pencil glide in B.C.C. metals
[DE88-001802] 07 p0834 N88-15062

GLOBAL AIR POLLUTION

Spatial characterization of acid rain stress in Canadian Shield Lakes
[NASA-CR-181136] 01 p0067 N88-10430

Spatial characterization of acid rain stress in Canadian Shield Lakes
[NASA-CR-180577] 01 p0067 N88-10431

Global environmental change research
[S-HRG-100-301] 03 p0348 N88-12199

GLOBAL ATMOSPHERIC RESEARCH PROGRAM

Statistical relationships between the mesoscale organization of convection and the large-scale wind profiles during GATE --- GARP Atlantic Tropical Experiment (GATE) 02 p0208 N88-11302

Seasonal variations and excitation mechanisms of the equatorially trapped waves 13 p1798 N88-20751

Diagnostic studies of the HxOy-NzOy-O3 photochemical system using data from NASA GTE field expeditions
[NASA-CR-183038] 19 p2689 N88-25984

GLOBAL POSITIONING SYSTEM

Accurate position measuring spacecraft package
[ESA-CR(P)-2398-VOL-1] 01 p0004 N88-10022

Accurate position measuring spacecraft package, executive summary
[ESA-CR(P)-2398-VOL-2] 01 p0004 N88-10023

Accuracy of GPS surveying technique and its possible application to the Wegener project --- Mediterranean tectonics
[REPT-85.3] 01 p0063 N88-10407

Contributions to geodesy, photogrammetry, and cartography. Series 2, number 45
[ISSN-0469-4244] 01 p0065 N88-10416

A method resolving an ambiguity of measured distances by means of NAVSTAR GPS signals
01 p0065 N88-10417

Global positioning satellite-based automatic landing system and wind estimated feedback for the AH-64 helicopter 02 p0124 N88-10784

Ionospheric total electron content estimation for single-frequency global positioning system receivers
02 p0161 N88-11005

Research in geodesy based upon radio interferometric observations of GPS (Global Positioning System) satellites
[AD-A184040] 03 p0346 N88-12187

Balloon track data analysis
[AD-A184750] 03 p0350 N88-12213

Dynamic positioning at sea using the global positioning system
[AD-A184453] 04 p0397 N88-12476

GPS vertical axis performance enhancement for helicopter precision landing approach
[NASA-CR-177443] 04 p0397 N88-12477

A demonstration of high precision GPS orbit determination for geodetic applications
04 p0432 N88-12680

Precise near-earth navigation with GPS: A survey of techniques 04 p0433 N88-12682

On-orbit frequency stability analysis of the GPS NAVSTAR 8 rubidium clock and NAVSTARs 9 and 10 cesium clocks
[AD-A184984] 05 p0544 N88-13312

Use of the global positioning system for trajectory determination of SRAM 2 missiles at the Eastern Test Range
[AD-A185266] 05 p0544 N88-13314

A fully redundant double difference algorithm for obtaining minimum variance estimates from GPS observations
[NASA-CR-182363] 06 p0667 N88-14089

Surveying with GPS in Australia
11 p1504 N88-18986

Application of the Global Positioning System (GPS) time receivers to the fundamental station Wettzell
11 p1506 N88-18995

The global positioning system as an aid to the testing of inertial navigation units (volume 1, addendum 1)
[AD-A185783] 12 p1578 N88-19443

Optimal selection of global positioning system set to minimize emitter location errors
[AD-A189559] 12 p1579 N88-19447

Geodetic positioning by employment of the GPS-NAVSTAR satellites applying the techniques of VLBI and sequential recursive optimal estimation
[INPE-4438-TDL/311] 12 p1594 N88-19547

NAVARES: A prototype expert system for NAVSTAR anomaly resolution
[AD-A189491] 12 p1600 N88-19579

The evaluation and selection of a 5th ground antenna site for the global positioning system
[AD-A189495] 13 p1720 N88-20286

An investigation of Doppler satellite positioning multi-station adjustment software
13 p1730 N88-20345

Orbit accuracy requirement of GPS for precise positioning and orbit determination within local area
13 p1756 N88-20499

Satellite acquisition: Global positioning system acquisition changes after Challenger's accident
[PB88-155536] 14 p1880 N88-21236

The Spring 1985 high precision baseline test of the JPL GPS-based geodetic system
[NASA-CR-182686] 14 p1940 N88-21577

Securing the timescale of the NAVEX-reference clock and rate determinations by time comparisons with the help of the Global Positioning System (GPS) --- Spacelab D1 mission
[DFVLR-MITT-87-20] 16 p2159 N88-22879

Global Positioning System (GPS) exploitation by ODOT (Ohio Department of Transportation)
[PB88-172796] 16 p2159 N88-22882

Investigation of air transportation technology at Ohio University, 1986 17 p2293 N88-23719

Integrated multisensor navigation systems
17 p2294 N88-23722

Development of an airborne facility for advanced avionics research 17 p2307 N88-23801

Adjustment in photogrammetry: Methods, programs and applications
[B8735130] 17 p2369 N88-24105

Inertial reference system with Global Positioning System (GPS) support 18 p2518 N88-24936

Miltipath measurements for land mobile satellite service using global positioning system signals
19 p2645 N88-25700

NAVSTAR global positioning system
[AD-A192609] 20 p2757 N88-2635

Position and velocity determination using a Globa Positioning System: An outline
[B8735052] 20 p2757 N88-26355

The Sercel TR5S Global Positioning System (GPS) receiver
[ETN-88-92473] 20 p2757 N88-26357

A positioning system based on NAVSAT
[NLR-MP-87016-U] 20 p2757 N88-26358

Spacecraft applications of advanced global positioning system technology
[NASA-CR-172063] 20 p2757 N88-26359

Spacecraft applications of advanced global positioning system technology
[NASA-CR-172055] 21 p2694 N88-27180

Optimized observation periods required to achieve geodetic accuracies using the global positioning system
[AD-A193844] 22 p3041 N88-28052

The limits of direct satellite tracking with the Global Positioning System (GPS) 22 p3064 N88-28179

Estimation forces acting on an underwater vehicle with G.P.S. (Global Positioning System) and Kalman filtering
[AD-A194339] 23 p3175 N88-28901

Performance of GPS-aided INS during high-dynamic maneuvers
[AD-A194624] 23 p3175 N88-28903

A comparison: Static and future kinematic GPS (Global Positioning System) surveys
[AD-A194666] 23 p3175 N88-28904

GLOBULAR CLUSTERS

The formation of single millisecond pulsars in globular clusters
[MPE-PREPRINT-97] 10 p1428 N88-18525

GLOBULINS

NT FIBRINOGEN

GLOSSARIES

U DICTIONARIES

GLOTTIS

Visualization of the air flowing through a dynamic model of the vocal folds
[ISVR-TR-154] 14 p1952 N88-21634

GLOVES

Constructing Gloved wings for aerodynamic studies
[NASA-TM-100440] 14 p1863 N88-21128

Design, development and evaluation of Stanford/Ames EVA prehensors
[NASA-CR-182688] 15 p2105 N88-22540

Four-axis side-arm flight control simulator investigation
[AD-A196026] 24 p3409 N88-30294

GLOW

U LUMINESCENCE

GLOW DISCHARGES

Magnetic control of low pressure discharges
[AD-A186794] 10 p1322 N88-17900

An experimental and theoretical investigation of optogalvanic effects
[AD-A189618] 12 p1625 N88-19720

Measurement of rate constants of elementary gas reactions of importance to upper atmosphere and combustion systems
[AD-A189432] 13 p1737 N88-20386

In-situ reactive of X-ray optics by glow discharge
[DE88-009840] 20 p2854 N88-26947

Direct determination of part-per-billion levels of volatile organics in water and soil samples using glow discharge mass spectrometry
[DE88-011389] 21 p2910 N88-27272

Low temperature film growth of the oxides of zinc, aluminum and vanadium (and related systems, oxides of gold and germanium, nitrides of aluminum and tungsten) by reactive sputter deposition
[AD-A193497] 23 p3191 N88-28986

Decomposition of hydrazine by high frequency glow electrical discharges
[NASA-TT-20240] 24 p3344 N88-29906

GLUCOSE

Observing effect of laser radiation of low-frequency Raman scattering of light 06 p0772 N88-14742

Saccharification of cellulose by combined fungal and bacterial preparations 17 p2316 N88-23833

Evaluation of the endogenous glucocorticoid hypothesis of denervation atrophy
[NASA-CR-182848] 17 p2381 N88-24157

Design considerations for the development of an implantable sensor for the continuous measurement of glucose in the diabetic patient 17 p2382 N88-24159

GLUCOSIDES

NT NUCLEOSIDES

GLUONS

The approach to equilibrium in a quark-gluon plasma
[DE88-002117] 09 p1251 N88-17499

Computational quantum field theory
[DE88-700918] 16 p2284 N88-23672

Tagging of gamma yields qq bar events and direct measurement of the gluon structure function at HERA
[NOTA-INTERNA-910] 22 p3151 N88-28745

GLUTAMIC ACID

Human blood glutamic acid level with exposure to high ambient concentrations of ammonia
10 p1351 N88-18134

GLUTAMINE

A program for the study of skeletal muscle catabolism following physical trauma
[AD-A189771] 15 p2102 N88-22521

Dexamethasone regulates glutamine synthetase expression in rat skeletal muscles
[NASA-CR-182935] 18 p2549 N88-25129

GLUTATHIONE

The evolution of glutathione metabolism in phototrophic microorganisms
[NASA-CR-182902] 19 p2695 N88-26015

GLYCERINS

U GLYCEROLS

GLYCEROLS

Transparent metal model study of the use of a cellular growth front to form aligned monotectic composite materials
[NASA-CR-182414] 08 p0969 N88-15861

Metabolic and cardiorespiratory parameters during three consecutive days of exhaustive running
[AD-A192598] 21 p2985 N88-27728

GLYCOGENS

Influence of skeletal muscle glycogen on passive rewarming after hypothermia
[AD-A186451] 08 p1049 N88-16334

Manipulation of muscle glycogen concentrations using high and low carbohydrate diets and exercise
[AD-A187732] 11 p1519 N88-19069

GLYCOLS

High ionic conductivity in PEO.PPG block polymer and salt solutions
[AD-A183502] 01 p0026 N88-10168

Physical properties of immiscible polymers
03 p0297 N88-11868

Effects of aircraft deicing/antiicing fluids on airfoil characteristics 08 p0952 N88-15776

Thermogravimetric analysis of polymeric materials for an intermediate temperature solid electrolyte
[DE88-004854] 10 p1306 N88-17809

GNEISS

The timing and mechanism of depletion in Lewisian granulites 24 p3394 N88-30209

Growth of early archaean crust in the ancient Gneiss complex of Swaziland and adjacent Barberton Greenstone Belt, Southern Africa 24 p3396 N88-30223

Reappraisal of the geology of Kangimut Sammisoq, Ameralik Fjord, Southern West Greenland: Crustal structure and interpretation of isotopic data
24 p3398 N88-30234

GOAL THEORY

Plans for discourse
[AD-A192242] 20 p2832 N88-26802

GOALS

Space Assembly, Maintenance, and Servicing Study (SAMSS) 01 p0015 N88-10089

Space technology to meet future needs
[NASA-CR-181473] 02 p0130 N88-10819

Spinoff
[NASA-TM-89651] 03 p0386 N88-12426

Lifting bodies: An attractive aerodynamic configuration choice for hypervelocity vehicles
05 p0534 N88-13248

Recent trends in superconductor development discussed 06 p0688 N88-14215

Supersonic STOVL propulsion technology program: An overview 08 p0957 N88-15808

Present stage of space medicine
10 p1364 N88-18151

Energy-related atomic and molecular structure and scattering studies
[DE88-004246] 10 p1406 N88-18386

Communication satellites: Guidelines for a strategic plan
[NASA-TM-89306] 12 p1599 N88-19569

Defending secrets, sharing data: New locks and keys for electronic information
[PB88-143185] 12 p1706 N88-20210

Johnson Space Center's strategic game plan: Charting a course to the year 2000 and beyond
[NASA-TM-89733] 13 p1850 N88-21076

Orbital transfer vehicle: Concept definition and system analysis study
[NASA-CR-179315] 15 p2024 N88-22060

NASA and the challenge of ISDN: The role of satellites in an ISDN world
[NASA-CR-182749] 15 p2126 N88-22676

Advanced development of double-injection, deep-impurity semiconductor switches
[NASA-CR-182118] 18 p2583 N88-25346

Computer-Aided Engineering (CAE) for engineering design 21 p2929 N88-27390

GODDARD EXPERIMENT PACKAGE TELESCOPE

U PARTICLE TELESCOPES

GOERTLER INSTABILITY

On the onset of three-dimensionality and time-dependence in the Goertler vortex problem
[NASA-CR-178404] 03 p0260 N88-11638

The strong nonlinear interaction of Tollmien-Schlichting waves and Taylor-Goertler vortices in curved channel flow
[NASA-CR-181697] 24 p3311 N88-29716

On the generation of mean flows by the interaction of Goertler vortices and Tollmien-Schlichting waves in curved channel flows
[NASA-CR-181690] 24 p3315 N88-29743

GOES SATELLITES

GOES observations for the FIRE/SRB Wisconsin experiment region from October 11 through November 2, 1986
[NASA-TM-100485] 01 p0071 N88-10453

An introduction to the GOES I-M imager and sounder instruments and the GVAR retransmission format
[NOAA-TR-NESDIS-33] 02 p0140 N88-10884

Improved geostationary satellite soundings for the mesoscale weather analysis/forecast operation
02 p0200 N88-11252

VAS products as indices of thunderstorms and severe local storm potential --- Visible and Infrared Spin Scan Radiometer Atmospheric Sounder (VAS)
02 p0201 N88-11253

Operational cloud-clearing techniques of VAS radiance data --- Visible and Infrared Spin Scan Radiometer Atmospheric Sounder (VAS) 02 p0201 N88-11256

Automated detection of severe thunderstorms using geosynchronous infrared data 02 p0201 N88-11257

The Pacific Weather Center Satellite Facility: An overview 02 p0205 N88-11286

Suggested severe local storm operational scenario for GOES I-M
[NASA-TM-100686] 11 p1515 N88-19052

NBS (National Bureau of Standards) measurement services. GOES (Geostationary Operational Environmental Satellite) time code dissemination: Description and operation
[PB88-168760] 14 p1880 N88-21235

Solar-geophysical data number 520, December 1987. Part 2: (Comprehensive reports). Data for June 1987 and miscellanea
[PB88-164207] 15 p2152 N88-22849

GOGGLES

Development, testing and evaluation of a night vision goggle compatible BO-105 for night low level operation
03 p0265 N88-11668

Advanced programming and control techniques for complex mechanical systems
[AD-A190238] 15 p2071 N88-22349

GOLD

Far-infrared spectra of lithium deposited on a gold electrode: Interpretation using a cluster model
[AD-A184231] 04 p0495 N88-13050

Some present limitations on the lattice imaging of grain boundaries
[DE87-014665] 09 p1256 N88-17530

Order-disorder transition of Au and Pt (110) surfaces. The significance of relaxations and vibrations
[DE88-004651] 10 p1419 N88-18473

Ion-beam mixing and amorphization in Au/Zr bilayers
[DE88-005999] 15 p2140 N88-22767

Femtosecond nonequilibrium electronic heat transport in thin gold films 19 p2653 N88-25807

Grain boundaries
[DE88-009689] 20 p2773 N88-26446

Low temperature film growth of the oxides of zinc, aluminum and vanadium (and related systems, oxides of gold and germanium, nitrides of aluminum and tungsten) by reactive sputter deposition
[AD-A193497] 23 p3191 N88-28986

Correlations between wettability and structure in monolayers of alkanethiols adsorbed on gold
[AD-A194348] 23 p3191 N88-28991

Potential induced structural transformations of the Au(100) and Au(111) surfaces
[DE88-005446] 23 p3287 N88-29571

GOLD ALLOYS

Aging behavior of Au-based ohmic contacts to GaAs
[NASA-CR-182146] 19 p2662 N88-25831

High resolution detection of solute segregation to the cores of dislocations in grain boundaries
[DE88-009168] 20 p2877 N88-27078

GONADS

NT TESTES

GONDOLAS

Balloon-borne three-meter telescope for far-infrared and submillimeter astronomy
[NASA-CR-182310] 09 p1262 N88-17565

Adaptive control of scientific balloon-borne gondola attitude 13 p1755 N88-20497

Balloon-borne three-meter telescope for far-infrared and submillimeter astronomy
[NASA-CR-182924] * 17 p2440 N88-24550

Utilization of the IR telescope gimbaling system as a stabilized pointing platform for balloon payloads. Volume 1: Technical results
[NASA-CR-179339] 18 p2522 N88-24962

GONIOMETERS
Joint angle sensors for closed-loop control
19 p2673 N88-25891

GOODNESS OF FIT
Asymptotic error bounds for power approximations to multinomial tests of fit
[MEMO-640] 08 p1072 N88-16470
The striae in the dust tails of great comets: A formal comparison of the goodness of fit by various theories, and a new proposal 14 p2002 N88-21937
An innovation approach to goodness of fit tests in R sup m
[CWI-MS-R8712] 16 p2259 N88-23501
Fitting a circle to radially suppressed data
[NPL-DITC-103/87] 17 p2392 N88-24223
Fitting an ellipse to data
[NPL-DITC-95/87] 22 p3143 N88-28693

GOVERNMENT PROCUREMENT
Supportability in aircraft systems through technology and acquisition strategy applications
[AD-A186465] 08 p0949 N88-15759
NASA (National Aeronautics and Space Administration) procurement: The 1973 space shuttle solid rocket motor contractor selection
[PB88-135264] 11 p1447 N88-18623
Streamlining invitation for bids
[AD-A188941] 12 p1705 N88-20206
MANPRINT handbook for RFP (Request For Proposal) development
[AD-A188321] 13 p1850 N88-21075
Microvax networked computer system
[AD-A190308] 15 p2114 N88-22596
Department of Defense Statement on the Technology Base to the Subcommittee on Defense Industry and Technology of the Committee on Armed Services, United States Senate, 100th Congress, second session
[AD-A191839] 18 p2588 N88-25376
The use of commercial off-the-shelf equipment and its impact on C3 (Command, Control and Communications EMP (electromagnetic pulse) survivability
[AD-A192614] 20 p2791 N88-26556
The cost and performance implications of reliability improvements in the F-16A/B
[AD-A195096] 24 p3324 N88-29796

GOVERNMENT/INDUSTRY RELATIONS
Structures and Materials Working Group report
01 p0016 N88-10093
The British Technology Group
[ONRL-7-022-R] 01 p0107 N88-10698
Summaries of FY 1987 engineering research
[DE88-002572] 07 p0840 N88-15096
Lightsats and their attraction to budget oriented Federal agencies 10 p1289 N88-17711
A study of technology transfer arrangements for national laboratories
[DE88-005423] 11 p1567 N88-19382
The effects of two Carlucci initiatives concurrency and streamlining, on the test and evaluation phase of system acquisitions 12 p1704 N88-20198
The influence of infrastructure on the costs and timescales of collaborative programmes
12 p1704 N88-20201
The impact of independent research and development regulations on companies not required to negotiate advanced independent research and development agreements
[AD-A190007] 15 p2147 N88-22818
Civil missions applications study
17 p2417 N88-24376
Class 2 design update for the family of commuter airplanes
[NASA-CR-182681] 18 p2464 N88-24629
The Department of Defense report on the merit review process for competitive selection of university research projects and an analysis of the potential for expanding he geographic distribution of research for the Committees on Appropriations, United States Congress
AD-A191842] 18 p2588 N88-25379
Workshop report and presentations from the emiconductor Research Corporation-DOE emiconductor Task Force Workshop
DE88-007690] 19 p2733 N88-26232
Economic impact of space flight activities in West ermany. Influence of allocations of Bundesministerium r Forschung und Technologie
TN-88-92106] 21 p2901 N88-27215
rgonne National Laboratory technology transfer report, 87
E88-010091] 23 p3298 N88-29639

GOVERNMENTS
Freedom of Information Act: Fee waiver practices at the FBI (Federal Bureau of Investigation)
[PB87-216727] 02 p0249 N88-11573
Center for Electronics and Electrical Engineering Technical Progress Bulletin covering center programs, January to March 1987 with 1987 CEEE events calender
[PB87-224648] 03 p0309 N88-11946
University research initiative research program summaries
[AD-A184876] 05 p0658 N88-14035
Role of the technical report in technological innovation
[PB87-232500] 05 p0658 N88-14040
Federal plan for meteorological services and supporting research, fiscal year 1988
[PB88-118716] 07 p0880 N88-15336
A study of federal technology transfer to the commercial sector
[AD-A187017] 09 p1262 N88-17560
Journal of Research of the National Bureau of Standards, volume 92, number 5, September-October 1987
[PB88-124409] 10 p1426 N88-18518
Journal of Research of the National Bureau of Standards, volume 92, number 6, November-December 1987
[PB88-138516] 10 p1426 N88-18519
National Informatics Centre: Profile of services
[PB88-134135] 12 p1706 N88-20211
Technology transfer from US Federal laboratories: Report of a roundtable
[PB88-144803] 12 p1709 N88-20228

GOVERNORS
U SPEED REGULATORS

GRABENS
U GEOLOGICAL FAULTS

GRADIENT INDEX OPTICS
Optical characterization of silica aerogel
[DE88-008916] 20 p2854 N88-26946

GRADIENTS
NT ELECTRON DENSITY PROFILES
NT POTENTIAL GRADIENTS
NT PRESSURE GRADIENTS
NT TEMPERATURE GRADIENTS
NT THERMOCLINES
Monocrystalline silicon gradiometer for gravity experiments in space
[NASA-CR-181452] 01 p0050 N88-10321
High gradient superconducting quadrupoles
[DE87-013590] 02 p0244 N88-11541
Conservation and transport properties of turbulence with large density variations
[LA-10911-MS] 03 p0321 N88-12032
Numerical solution of bound constrained problems
[DE88-000653] 03 p0371 N88-12334
An application of a gradient relaxation method to noisy infrared images
[AD-A184666] 03 p0377 N88-12371
Collider constraints in the choices for wavelength and gradient scaling
[PB87-123691] 06 p0779 N88-14783
Trust regions and projected gradients
[DE88-005829] 15 p2122 N88-22646
Probing the possibility of a (12)C/(13)C abundance gradient from observations of interstellar CH +
[DE88-008908] 20 p2884 N88-27125
The gradient method for interface tracking
[AD-A194477] 23 p3248 N88-29334

GRADUATION
U CALIBRATING

GRAFTING
New method of grafting crystals
16 p2180 N88-22992
Modification of polymers by photografting processes
17 p2323 N88-23871

GRAIN BOUNDARIES
Observations of localized grain boundary dislocations in series of (001) and (110) symmetrical tilt boundaries in aluminum
[DE87-014011] 01 p0025 N88-10156
A simulation study of interfaces in Ni, Al and Ni3Al with and without boron
[DE87-013156] 01 p0102 N88-10667
Grain boundary effects in processing high T/sub c/ superconductors
[DE87-009297] 01 p0103 N88-10673
Dynamical simulation of structural multiplicity in grain boundaries
[DE87-012746] 01 p0103 N88-10676
Understanding the transport properties of silicon grain boundaries and how they relate to I.C. applications of polysilicon
[DE87-013809] 01 p0104 N88-10677
Grain boundary phase equilibria in metallic systems
[DE87-014123] 01 p0104 N88-10679
Analytical electron microscopy characterization of boron in sintered alpha-SiC
[DE87-012532] 02 p0142 N88-10689
Influence of thermocyclic treatment on mobility of grain boundaries
[BLL-M-37329-(5828.4)] 02 p0149 N88-10933
Applications of dislocation theory to crack growth problems 02 p0190 N88-11186
Solute segregation to phase interfaces and grain boundaries: Studies by analytical electron microscopy and profile deconvolution
[DE87-012129] 02 p0243 N88-11537
On the search for experimentally observed grain boundary phase transitions
[DE87-012747] 02 p0244 N88-11539
Slip casting and extruding shapes of rhenium with metal oxide additives. Part 2: Development of grain stabilized rhenium parts for resistojets
[NASA-CR-180851] 03 p0278 N88-11749
Microstructural effects on the fatigue behavior of Fe-C-X alloys
[DE88-000155] 03 p0288 N88-11809
Ultra-fine grained alloy material
[AD-A184500] 03 p0290 N88-11820
International Conference on Microstructology held in Gainesville, Florida on 7-9 May 1986
[AD-A184604] 03 p0290 N88-11822
Microstructural characterization of irradiated PWR steels using the atom probe field-ion microscope
[DE88-000341] 03 p0291 N88-11828
Indentation damage in ceramics
[AD-A184686] 03 p0294 N88-11844
Some stochastic aspects of intergranular creep cavitation
[DE88-000065] 04 p0416 N88-12581
Welding and weldability of ductile intermetallic alloys
[DE87-014061] 04 p0416 N88-12582
Cyclic deformation and crack initiation
05 p0597 N88-13646
Effect of grain orientation on the origination and the initial growth of fatigue cracks in pure iron
05 p0597 N88-13647
Study of boundary structures
[AD-A184808] 05 p0655 N88-14013
Computer simulation of impurities and interfaces in body centered cubic metals
[PB88-108162] 07 p0832 N88-15047
Microstructural observations of the Sn-Pb solder/Cu system and thermal fatigue of the solder joint
[DE88-001392] 07 p0832 N88-15048
The influence of grain boundary chemistry and structure on the intergranular attack and intergranular stress corrosion cracking of austenitic alloys
[DE88-002436] 07 p0835 N88-15063
Grain boundary and surface diffusion in oxides
[DE88-002348] 07 p0938 N88-15697
Influence of post-anneal cooling treatments on suppression of cryogenic intergranular fracture in experimental Ni-free high-Mn austenitic steels
[DE88-002766] 09 p1145 N88-16863
Some present limitations on the lattice imaging of grain boundaries
[DE87-014665] 09 p1256 N88-17530
Molecular dynamics study of high-temperature grain-boundary stability in a (100) sigma = 29 bicrystal model
[DE88-002955] 09 p1258 N88-17546
The migration of grain boundaries in ceramic materials with particular reference to the sintering process
[DE88-004085] 10 p1306 N88-17808
Grain boundaries, planar defects and superconducting properties of YBa2Cu3O7
[DE88-003477] 10 p1419 N88-18475
Simulation and processing of high resolution images of defects and interfaces in superconducting YBa2Cu3O7
[DE88-003856] 10 p1420 N88-18480
Influence of grain boundary phosphorus segregation on hydrogen embrittlement in steel
[DE88-700176] 11 p1459 N88-18696
The intergranular segregation of boron in substoichiometric Ni3Al
[DE88-004783] 11 p1462 N88-18720
Atomistic studies of the structure and properties of grain boundaries with substitutional impurities
[DE88-004161] 11 p1545 N88-19237
Gordon Conference on Intermetallic Compounds held at Tilton, New Hampshire on 20-24 July 1987
[AD-A188502] 13 p1745 N88-20435
JPRS report: Science and technology. USSR: Materials science
[JPRS-UMS-87-007] 14 p1895 N88-21312
Dependence of hydrogen embrittlement of austenitic stainless steels on structural state of grain boundaries
14 p1896 N88-21316
Grain boundaries
[DE88-006628] 14 p1987 N88-21852

On rotating sphere-on-a-plate experiments and the questions of whether high angle grain boundaries melt below bulk melting temperatures
[DE88-006627] 15 p2038 N88-22142

Investigation and synthesis of high temperature and increased stiffness RSP aluminum alloys
[AD-A190407] 15 p2039 N88-22151

Strength and microstructure of ceramics
[AD-A190712] 15 p2046 N88-22191

Grain boundary oxidation and low-cycle fatigue at elevated temperatures 15 p2083 N88-22420

Interface formation and precursory dynamics
[AD-A190741] 15 p2144 N88-22794

SSME single-crystal turbine blade dynamics
16 p2221 N88-23257

Disclination structures in carbon and graphite
[AD-A191056] 17 p2322 N88-23868

The role of oxygen on the mechanical behavior of molybdenum alloys 17 p2401 N88-24278

The morphological stability of continuous intergranular phases: Thermodynamic considerations
[DE88-006328] 18 p2584 N88-25350

The postirradiation tensile properties and microstructure of several vanadium alloys
[DE88-007140] 19 p2615 N88-25515

Phase stability and alloy design of ordered intermetallics
[DE88-007479] 20 p2772 N88-26435

Grain boundary structure in Ni3Al
[DE88-009164] 20 p2773 N88-26444

The effects of gradients on boundary stability
[DE88-009592] 20 p2773 N88-26445

Grain boundaries
[DE88-009889] 20 p2773 N88-26446

The structure and properties of grain boundaries in B2 ordered alloys
[DE88-009890] 20 p2773 N88-26447

Effects of grain boundary composition on properties of YBa2Cu3O/sub 7-x/
[DE88-007679] 20 p2875 N88-27064

High resolution detection of solute segregation to the cores of dislocations in grain boundaries
[DE88-009168] 20 p2877 N88-27078

Analysis of grain refinement and superplasticity in aluminum-magnesium alloys
[AD-A193029] 21 p2912 N88-27283

Processing and properties of advanced aluminum alloys
[AD-A193224] 21 p2912 N88-27284

Microchemical analysis of polycrystalline Ni3Al and other ordered alloys using the field-ion microscope atom probe
[DE88-011519] 21 p2914 N88-27294

Computer simulation of elastic properties of grain boundary materials
[DE88-011965] 21 p2916 N88-27305

Study of feasibility and optimization conditions of laser treatments: Application of the local recrystallization of aluminum
[ISAL-87-0048] 21 p2916 N88-27309

The influence of solute segregation on the dislocation structure of small and large angle (001) twist boundaries in Fe-Sb alloys
[DE88-009166] 22 p3155 N88-28770

Atomistic simulation of silicon grain boundaries
[DE88-009925] 22 p3155 N88-28771

A new model for the simulation of interfaces at high temperature
[DE88-009926] 22 p3155 N88-28772

Transverse expansion of individual carbon and graphite filaments
[AD-A195073] 24 p3342 N88-29891

GRAIN SIZE

Development of ultrafine grains and related properties in Hadfield manganese steels
[DE87-011884] 01 p0024 N88-10154

Microstructural effects in shock initiation of granular explosives
[DE87-011282] 01 p0031 N88-10200

Precision metrology comparing ultrasonic and other techniques for the determination of steel thickness
[DE87-011051] 02 p0230 N88-11452

Structure and grain coarsening during the processing of engineering ceramics
[NASA-TM-100235] 03 p0293 N88-11838

Characterization of catalysts with metal-support effects and of the species adsorbed on their surfaces
[DE87-014836] 04 p0414 N88-12564

Influence of microstructure and aging condition on the fatigue crack propagation in age hardened aluminium alloys 05 p0599 N88-13659

The effect of alpha platelet morphology and beta-grain size on the initiation and growth of short fatigue cracks in Ti65S 05 p0600 N88-13667

Near-threshold fatigue 06 p0716 N88-14392

Microstructure and magnetic properties of cobalt-chromium alloys
[DE88-002762] 07 p0835 N88-15064

Acoustic backscattering from bottom sediment at normal incidence in the laboratory
[AD-A186905] 09 p1242 N88-17443

Processing of nanophase ceramics
[DE88-005985] 13 p1752 N88-20475

Grain growth behavior of extrusion consolidated centrifugally atomized Type 304 stainless steel powder
[DE88-006788] 15 p2038 N88-22143

JPRS report: Science and technology. Japan
[JPRS-JST-88-002] 15 p2050 N88-22210

Fine grain development by laser CVD
15 p2050 N88-22214

Superfine grain development by laser
15 p2050 N88-22215

Analysis of dust grain properties in two star forming regions through comparison of theoretical models to observations 17 p2451 N88-24559

The first synthesis of chem-prep varistor LAC (Lightning Arrestor Connector) granules
[DE88-008005] 21 p2936 N88-27438

GRAINS (FOOD)
NT CORN
NT RICE
NT WHEAT

Food Irradiation Newsletter, Vol. 11, No. 1
[DE88-700808] 12 p1671 N88-20004

GRAMMARS

Formal grammars and Markov models
[RSRE-MEMO-4051] 09 p1219 N88-17311

Semi-applicative programming
10 p1380 N88-18239

A parser generator for finitely ambiguous context-free grammars
[CWI-CS-R8712] 13 p1818 N88-20864

A cockpit natural language study: Vocabulary and grammar analyses
[AD-A193289] 21 p2993 N88-27753

Linguistic semantics for parallel computation
[PB88-105960] 21 p2995 N88-27761

GRAND UNIFIED THEORY
NT UNIFIED FIELD THEORY

Status of the electroweak theory
[DE88-002342] 10 p1422 N88-18494

Theory of elementary particle studies in weak iteration and grand unification and studies in accelerator design
[DE88-004261] 11 p1545 N88-19238

Diffraction theory in QCD and beyond
[DE88-005958] 13 p1837 N88-20992

Superstrings
[DE87-702982] 19 p2737 N88-26249

GRANITE

Evaluation of AIS-2 (1986) data over hydrothermally altered granitoid rocks of the Singatse Range (Yerington) Nevada and comparison with 1985 AIS-1 data
05 p0613 N88-13767

The timing and mechanism of depletion in Lewisian granulites 24 p3394 N88-30209

Genesis of archean granitoids in the Pilbara block and implications for crustal growth 24 p3394 N88-30210

Crustal evolution and the eclogite to granulite phase transition in xenoliths from the West African Craton
24 p3395 N88-30217

GRANTS

Materials sciences programs: Fiscal Year 1987
[DE88-000672] 04 p0429 N88-12659

GRANULAR MATERIALS

Visible emission from granular explosives during shock initiation
[DE87-012361] 02 p0155 N88-10970

Computer-aided analysis for the Mechanics of Granular Materials (MGM) experiment, part 2
07 p0926 N88-15626

Microscopic modeling of sound waves in granular material
[DE88-000348] 10 p1405 N88-18375

Kinetics of combustion of finely divided solid fuel in granules
[BLL-M-37626-(5828.4)] 14 p1888 N88-21283

Gas coma of Comet Giacobini-Zinner: Emission from grains 14 p2000 N88-21923

P/Halley dust coma: Grains or rocks?
14 p2002 N88-21936

Variation of grain properties at the dust outbursts — Halley's comet 14 p2003 N88-21943

Nature of Comet Halley's organic grains inferred from infrared spectra 14 p2007 N88-21973

Laboratory amorphous carbon: A possible analog of cometary dust 14 p2009 N88-21981

LLNL granular solids flow project
[DE88-007492] 18 p2513 N88-24906

LLNL Granular Solids Flow Project
[DE88-008023] 19 p2684 N88-25844

Granulation of pyrotechnic tracer composition R284T
[MRL-TN-528] 20 p2780 N88-26490

Gaseous tracer techniques for pore structure characterization of granular materials
[DE88-011542] 21 p2911 N88-27274

Granular flow: Particle-dynamics simulations of steady flow
[DE88-011342] 21 p2948 N88-27506

Device physics related to the granular nature of CuInSe2 solar cells
[DE88-001159] 21 p2967 N88-27622

GRAPH THEORY

Strategies for concurrent processing of complex algorithms in data driven architectures
[NASA-CR-181435] 01 p0082 N88-10527

Graph partitioning by eigenvectors
[AD-A184430] 03 p0372 N88-12338

A characterization of separating pairs and triplets in a graph
[AD-A184278] 04 p0477 N88-12941

On the number of minimum size separating vertex sets in a graph
[AD-A184279] 04 p0478 N88-12942

On color polynomials of Fibonacci graphs
[AD-A184133] 04 p0486 N88-12996

Eigenvectors of distance-regular graphs
[AD-A185375] 05 p0641 N88-13919

On the work needed to factor a symmetric positive definite matrix
[AD-A185781] 06 p0759 N88-14660

Eigenvectors of graphs
[AD-A185538] 06 p0765 N88-14698

The perfectly matchable subgraph polytope of an arbitrary graph
[AD-A185993] 07 p0913 N88-15539

Algorithms for transitive reduction of an acyclic graph
[PB87-162822] 09 p1220 N88-17317

Strategies for concurrent processing of complex algorithms 10 p1379 N88-18236

Implementing logical variables on a graph reduction architecture 10 p1382 N88-18252

The clique polytope of a graph
[MEMO-663] 14 p1963 N88-21710

Graph labelings
[AD-A189649] 14 p1964 N88-21722

Compact representation of the separating k-sets of a graph
[AD-A189650] 14 p1965 N88-21723

The total interval of a graph
[AD-A189648] 15 p2119 N88-22625

Structural decomposition of multiple time scale Markov processes
[AD-A189739] 15 p2123 N88-22657

Graphs related to Held's simple group
[CWI-PM-28707] 16 p2264 N88-23536

Edge-disjoint homotopic paths in straight-line planar graphs
[CWI-OS-R8716] 16 p2264 N88-23537

Decomposition of graphs on surfaces and a homotopic circulation theorem
[CWI-OS-R8719] 16 p2264 N88-23538

A mixed-integer linear programming problem which is efficiently solvable
[AD-A191028] 18 p2556 N88-25168

Research in enumeration and graph theory with applications to computer science
[AD-A191567] 18 p2556 N88-25171

Efficient parallel algorithm for the connected component problem and its implementation on the DPP84 (Delft Parallel Processor)
[PB87-225959] 19 p2715 N88-26118

Extensible networks. Part 1: Principles and constructions
[REPT-87-91-PT-1] 20 p2642 N88-26864

Two families of graphs satisfying the cycle basis interpolation property
[PB88-127808] 20 p2846 N88-26880

GRAPHIC ARTS
NT COMPUTER ANIMATION

Active control of jet flowfields
[AD-A186736] 08 p0989 N88-15980

Computer aided geometric design
[AD-A187324] 10 p1389 N88-18293

A digital circuit design environment
[AD-A188831] 12 p1623 N88-19709

MacCAD (Macintosh Computer Aided Design), computer aided design tool for system analysis
[AD-A189241] 13 p1815 N88-20843

Efficient, high resolution computations of projectile and missile flow fields
[AD-A191086] 16 p2158 N88-22873

Algorithms and intuition
[NASA-CR-182900] 16 p2252 N88-23459

The ISI (Information Sciences Institute) grapher manual
[AD-A192198] 18 p2561 N88-25200

Editfont: An interactive font editing system
[AD-A192373] 20 p2838 N88-26836

GRAPHITE

NT PYROLYTIC GRAPHITE

Oxidation of TSX graphite over the temperature range 450 to 1200°C
[DE87-012230] 01 p0020 N88-10127

Low cycle fatigue on isotropic fine-grained graphite
[DE87-702627] 01 p0028 N88-10177

Behavior of graphites under intense heat loads
[DE87-012128] 01 p0028 N88-10179

Comparison of high purity fine grain graphites from different suppliers with regard to physical, mechanical, and thermal properties — Joint European Torus wall protection
[JUEL-SPEZ-401] 02 p0154 N88-10963

Transply crack density detection by acousto-ultrasonics
[NASA-TM-100224] 03 p0279 N88-11758

Corrosion-electrochemical and mechanical properties of composite graphite-carbide metal materials based on titanium and its alloys 03 p0285 N88-11794

Fabrication and testing of fire resistant graphite composite panels
[NASA-CR-177397] 04 p0397 N88-12472

Data base on the high heat flux behaviour of metals and carbon materials for plasma facing components: Experiments at the 10 MW neutral beam injection test stand of the IPP Nagoya
[IPPJ-AM-53] 04 p0492 N88-13031

Proceedings of the Japan-US Workshop P-92 on Plasma Material Interaction/High Heat Flux Data Needs for the Next Step Ignition and Steady State Devices
[DE87-013568] 04 p0494 N88-13042

PISCES: Plasma-surface interactions and materials research
[DE88-001323] 04 p0494 N88-13044

Cyclic deformation behaviour of cast irons with various graphite shapes in the temperature range 20 C less than or = T less than or = 500 C 06 p0715 N88-14384

Effect of point defects on graphite lattice parameters
[DE88-700340] 07 p0827 N88-15019

Performance of a small, graphite electrode, multistage depressed collector with a 500-W, continuous wave, 4.8- to 9.6-GHz traveling wave tube
[NASA-TP-2788] 07 p0848 N88-15146

Review of thermal properties of graphite composite materials
[NASA-TM-100049] 09 p1139 N88-16825

Helium-ion-induced release of hydrogen from graphite
[DE88-002599] 09 p1142 N88-16846

Neutron and X-ray scattering studies of layered solids
09 p1246 N88-17469

Comparison of low temperature photoluminescence of bulk MBE (Molecular Beam Epitaxy) grown AlGaAs and GaAs using a graphite generated dimer versus a standard tetramer arsenic group-V source
[DE88-004939] 11 p1558 N88-19329

An interpretation of the ethylenic, carbidic, and graphite auger lineshapes of chemisorbed carbon species
[AD-A189092] 13 p1736 N88-20379

IAEA Specialists' Meeting on Graphite Component Structural Design
[DE88-780006] 13 p1746 N88-20439

The statistical characterization of tensile strengths for a nuclear-type graphite 13 p1746 N88-20440

Statistical considerations of graphite strength for assessing design allowable stresses
13 p1746 N88-20441

Fracture criterion of reactor graphite under multiaxial stresses 13 p1746 N88-20442

High temperature Young's modulus of IG-110 graphite
13 p1746 N88-20443

Effects of high temperature neutron irradiation on the physical, chemical and mechanical properties of fine-grained isotropic graphite 13 p1747 N88-20444

Degradations of thermal shock resistance and the fracture toughness of reactor graphite subjected to neutron irradiation 13 p1747 N88-20445

Application of ISRM testing methods to fracture toughness testing of graphite 13 p1747 N88-20446

Notch sensitivity of graphite materials for VHTR
13 p1747 N88-20447

Nondestructive testings of HTGR graphites
13 p1747 N88-20448

Recent progress in structure determination by LEED (Low-Energy Electron Diffraction) measure the properties of the deep donors (DX-cent)
[DE88-003651] 13 p1846 N88-21048

Microplasticity phenomena in graphite/magnesium metal matrix composites
[DE88-006772] 15 p2029 N88-22086

Characterization of Mode 1 and Mode 2 delamination growth and thresholds in graphite/peek composites
[NASA-TM-100577] 16 p2172 N88-22947

Disclination structures in carbon and graphite
[AD-A191056] 17 p2322 N88-23868

Interfacial shear phenomena in graphite epoxy composites under impact loading using dynamic moire interferometry
[DE88-006773] 18 p2479 N88-24709

Raman characterization of AsF5-intercalated vapor grown graphite fibers
[AD-A191709] 18 p2491 N88-24778

Stress measurements in graphite fibers by laser raman spectroscopy
[AD-A191710] 18 p2491 N88-24779

Electron-Rayleigh wave interaction in thin film carbons
[AD-A191727] 18 p2492 N88-24781

Photoconductivity in carbon fibers
[AD-A191728] 18 p2492 N88-24782

Effect of uniaxial stress on the Raman spectra of graphite fibers
[AD-A191730] 18 p2492 N88-24783

Microstructure of thin intercalated benezene derived graphite fibers
[AD-A191724] 19 p2618 N88-25534

Graphite as a picosecond laser activated opening switch 19 p2657 N88-25783

Effects of applied stress and temperature on the nonlinear elastic properties of graphite fibers
[AD-A194469] 22 p3050 N88-28093

Transverse expansion of individual carbon and graphite filaments
[AD-A195073] 24 p3342 N88-29891

GRAPHITE-EPOXY COMPOSITES

Effect of adhesive layers on impact damage and dynamic response in composite laminates
02 p0141 N88-10887

A stochastic delamination growth model for fatigue loaded laminated composite materials
02 p0141 N88-10888

The effect of bromination of carbon fibers on the coefficient of thermal expansion of graphite fiber-epoxy composites
[NASA-TM-100236] 02 p0143 N88-10899

Ultrasonic characterization of the nonlinear elastic properties of unidirectional graphite/epoxy composites
[NASA-CR-4100] 03 p0281 N88-11767

Study of zero CTE (Coefficients of Thermal Expansion) of graphite/epoxy composites
[DE87-013557] 04 p0412 N88-12554

Corrosion control by composite material substitution with application to the M-939 5-ton truck
04 p0428 N88-12654

Evaluation of closed cubic failure criterion for graphite/epoxy laminates
[NASA-CR-182375] 06 p0679 N88-14158

Study on utilization of advanced composites in fuselage structures of large transports
[NASA-CR-172406] 07 p0827 N88-15014

Investigation of low velocity impact damage on filamentary composite materials
07 p0923 N88-15607

Postbuckling of laminated anisotropic panels
[NASA-TM-100509] 08 p0994 N88-16011

A fiber-resin micromechanics analysis of the delamination front in a DCB specimen
[NASA-TM-100540] 10 p1294 N88-17737

Radiation and temperature effects on the time-dependent response of T300/934 graphite/epoxy
[NASA-CR-182603] 11 p1451 N88-18646

Effects of moisture, elevated temperature, and fatigue loading on the behavior of graphite/epoxy buffer strip panels with center cracks
[NASA-TM-100558] 12 p1603 N88-19590

Simulated impact damage in a thick graphite/epoxy laminate using spherical indenters
[NASA-TM-100539] 13 p1733 N88-20363

Ply-level failure analysis of a graphite/epoxy laminate under bearing-bypass loading
[NASA-TM-100578] 13 p1735 N88-20372

The buckling and vibration of composite plates using the Levy method considering shear deformation and rotary inertia
[AD-A189743] 15 p2076 N88-22374

Increasing strength of graphite/epoxy bolted joints by introducing an adhesively bonded metallic insert
[FFA-TN-1987-45] 15 p2088 N88-22442

Surface crack analysis applied to impact damage in a thick graphite-epoxy composite
[NASA-TM-100600] 16 p2173 N88-22950

Fuel containment, lightning protection and damage tolerance in large composite primary aircraft structures
[NASA-CR-3875] 17 p2317 N88-23839

Properties of two composite materials made of toughened epoxy resin and high-strain graphite fiber
[NASA-TP-2826] 19 p2609 N88-25480

Loading rate sensitivity of open hole composites in compression
[NASA-TM-100634] 19 p2610 N88-25490

Stiffness degradation of composite laminates
20 p2767 N88-26405

Compression creep of filamentary composites
[NASA-CR-182550] 20 p2798 N88-26601

Damage in a perforated graphite-epoxy plate under monotonic, cyclic biaxial loading
[ONERA-NT-1987-5] 20 p2816 N88-26708

Determination of lumped-mass thermal properties associated with autoclave curing of graphite/epoxy composites 21 p2925 N88-27364

Failure analysis of laminated composite angles
21 p2959 N88-27578

A comprehensive study on damage tolerance properties of notched composite laminates
[AD-A192952] 23 p3188 N88-28968

Analytical study of graphite-epoxy tube response to thermal loads
[NASA-CR-183215] 24 p3341 N88-29884

Experimental aspects of using time-averaged holographic interferometry to detect barely visible impact damage in a graphite/epoxy composite plate
[AD-A194418] 24 p3375 N88-30097

GRAPHITE-POLYIMIDE COMPOSITES

Effect of long-term thermal aging on coated Celion/LARC-160 composites
[NASA-TM-100495] 04 p0410 N88-12544

The 700 F properties of autoclave cured PMR-2 composites
[NASA-TM-100923] 18 p2480 N88-24712

A thermally modified polymer matrix composite material with structural integrity to 371 C
[NASA-TM-100922] 19 p2609 N88-25483

Loading rate sensitivity of open hole composites in compression
[NASA-TM-100634] 19 p2610 N88-25490

GRAPHITIZATION

Electronic and structural studies of carbon/carbon composites
[AD-A191729] 19 p2609 N88-25481

Anomalous temperature-dependent negative magnetoresistance in pregraphitic carbons
[AD-A191725] 19 p2619 N88-25535

Brominated graphite fibers and method of producing the same
[NASA-CASE-LEW-14698-1] 24 p3341 N88-29888

GRAPHS (CHARTS)

NT BOND GRAPHS

The ISI (Information Sciences Institute) grapher: A portable tool for displaying graphs pictorially
[AD-A184354] 04 p0478 N88-12944

Eigenvectors of graphs
[AD-A185538] 06 p0765 N88-14698

Nonpreemptive run-time scheduling issues on a multitasked, multiprogrammed multiprocessor with dependencies, bidimensional tasks, folding and dynamic graphs
[DE88-003598] 09 p1223 N88-17335

Design graphs for the first two bending Eigenvibration forms of rotating beams consisting of two beam points
[IW-86006R] 13 p1783 N88-20670

Campaign graphs
[DE88-005336] 13 p1831 N88-20952

Shape detection in remote sensing through graph isomorphism 17 p2354 N88-24028

A matroid algorithm and its application to the efficient solution of two optimization problems on graphs, revision
[AD-A192709] 20 p2838 N88-26838

Algorithm for generating the minimal cycle basis of a graph
[PB88-126610] 20 p2846 N88-26891

Issues in computer-assisted interpretation of graphs and quantitative information
[PB88-116280] 21 p2998 N88-27783

GRASSES

NT SEA GRASSES

Estimating scattered and absorbed radiation in plant canopies by remote sensing
[NASA-CR-181390] 02 p0193 N88-11205

GRASSLANDS

Estimating regional evapotranspiration from remotely sensed data by surface energy balance models
[NASA-CR-181400] 01 p0064 N88-10411

Evaluation of surface energy and radiation balance systems on the Konza Prairie
[NASA-CR-182534] 10 p1355 N88-18097

Measuring and modeling near surface reflected and emitted radiation fluxes at the FIFE site
[NASA-CR-182660] 12 p1640 N88-19818

Mapping of plant associations and the variation of surface water in the Pantanal Mato-Grossense National Park, through remote sensing techniques
17 p2366 N88-24092

Canopy reflectance modeling in a tropical wooded grassland
[NASA-CR-182981] 19 p2685 N88-25961

Use of SPOT satellite in agrohydrology: Detection of spring water excess in a grassland region
22 p3091 N88-28357
Evaluation of the grassy biomass in the Sahelian zone in the South Tamesna region (Niger): Prospects and limits of use of SPOT data 22 p3092 N88-28359
Changes in species composition of heathland, monitored by means of remote sensing and field mapping: The results of the HEISPOT project 22 p3092 N88-28360
Characterization, topology, and cartography of grasslands for the development of fodder resources. (Preliminary Evaluation Program for SPOT number 26)
22 p3095 N88-28377
Study of savannah formation in the Sudanian zone. Northwest sector of the La Comoe park, Ivory Coast
22 p3097 N88-28391

GRASSMANN ALGEBRA
U VECTOR SPACES

GRATINGS (SPECTRA)
Single-periodic multilayer grating laser Doppler vibrometer 03 p0327 N88-12066
Distributed feedback effects in lasers and high gain laser instabilities in optically pumped CH3F
03 p0329 N88-12079
A theoretical study of enhanced Smith-Purcell radiation from a bigrating
[AD-A184530] 03 p0329 N88-12080
Surface polariton resonances and reflectance on a bigrating
[AD-A184663] 03 p0377 N88-12370
All-optical beam control by forced Rayleigh scattering
[AD-A184315] 04 p0490 N88-13018
The production of ultrasmall and superfine holographic diffraction gratings using synchrotron radiation and lithographic techniques
[AD-A185395] 05 p0585 N88-13562
Efficient computation of periodic Green's functions with application to grating structures
[AD-A184853] 05 p0640 N88-13912
The evaluation of a deformable diffraction grating for a stigmatic EUV spectroheliometer
[NASA-CR-182371] 06 p0707 N88-14337
Use of spherical optics in high resolution soft X-ray grating monochromators
[PB87-125191] 06 p0780 N88-14788
A composite grating for moire interferometry
[AD-A186330] 07 p0832 N88-15044
Study of quantum mechanical effects in deep submicron, grating-gate field effect transistors
[AD-A188283] 10 p1325 N88-17923
Holographically correcting synthetic aperture aberrations
[AD-A189510] 12 p1692 N88-20123
Enhancement of second harmonic generation on silver gratings by resonant excitation of surface plasmon
[ETN-88-92304] 17 p2439 N88-24509
The evaluation of a deformable diffraction grating for a stigmatic EUV spectroheliometer
[NASA-CR-183064] 20 p2853 N88-26941
Precise rotational alignment of X-ray transmission diffraction gratings
[DE88-010599] 21 p2911 N88-27273
On the multiple grating spectrometer resolving power
[PREPRINT-585] 22 p3153 N88-28761
A theoretical and experimental investigation into the use of SAW weighting techniques in optical diffraction gratings
[RSRE-MEMO-4128] 23 p3283 N88-29549

GRAVIMETERS
Allowance for influence of gravity field nonuniformity
08 p1012 N88-16137
The superconducting gravimeter: Application, calibration, and further development
[SER-C-329] 09 p1167 N88-16998
Results of the International Comparison of Absolute Gravimeters (2nd) held in Sevres, France in June-July 1985
[AD-A189869] 15 p2093 N88-22474
Testing of a gravimeter LCR G 785
[B8735061] 20 p2806 N88-26643

GRAVIMETRY
Study of a satellite-to-satellite tracking gravity mission
[ESA-CR(P)-2419] 02 p0198 N88-11237
Solution of three-dimensional inverse problem of gravimetry in contact surfaces class by local corrections method 04 p0460 N88-12648
On deviations from Newton's law and the proposal for a Fifth Force
[DE87-703368] 04 p0487 N88-13001
Effective methods of gravimetric and magnetometric data processing 06 p0728 N88-14479
Results of the International Comparison of Absolute Gravimeters (2nd) held in Sevres, France in June-July 1985
[AD-A189869] 15 p2093 N88-22474
Satellite gradiometry
[B8735057] 16 p2229 N88-23313
Evaluation of a model of the Earth's gravity field
[EPSHOM-003/87] 17 p2373 N88-24116

GRAVIRECEPTORS
NT OTOLITH ORGANS
Morphology and development of the inner ear of Anurans 07 p0886 N88-15378
Gravisensing in lentil seedling roots grown in space (Spacelab D-1 mission) 12 p1654 N88-19911
How does Physarum polycephalum perceive and use gravity? 12 p1655 N88-19918
Synopsis of the Spacelab D-1 frog statolith experiment STATEX 12 p1659 N88-19940
Experiments concerning gravisensitivity of protozoa
12 p1660 N88-19949
Contraction behavior and protoplasmic streaming in the slime mold Physarum polycephalum (Physarum kinetics) --- Spacelab D1 mission 22 p3060 N88-28160
Graviperception of lentil seedling roots grown in space
22 p3061 N88-28165

GRAVITATION
NT ARTIFICIAL GRAVITY
NT EARTH GRAVITATION
NT GRAVITY ANOMALIES
NT LUNAR GRAVITATION
NT PLANETARY GRAVITATION
NT REDUCED GRAVITY
NT STELLAR GRAVITATION
Inequivalent quantizations and fundamentally perfect spaces
[DE87-014225] 02 p0229 N88-11446
Regular effective action of gauge field theory and quantum gravity
[DE87-703076] 02 p0247 N88-11560
Analytical average model of studies on orbital resonance 03 p0269 N88-11689
Torsion as a source of expansion in a Bianchi type I universe in the self-consistent Einstein-Cartan theory of a perfect fluid with spin density
[AD-A184200] 03 p0322 N88-12037
New notions about space-time and gravitation
[DE87-703259] 03 p0383 N88-12408
Gravitational accretion of hot dark matter
03 p0388 N88-12439
On deviations from Newton's law and the proposal for a Fifth Force
[DE87-703368] 04 p0487 N88-13001
Homogeneous space-time of Goedel type in higher-derivate gravity
[DE87-703690] 04 p0500 N88-13077
A supersymmetric Lagrangian for Poincare gauge theories of gravity
[DE88-001670] 04 p0500 N88-13078
Software design for an airborne gravity measurement system
[AD-A185000] 05 p0634 N88-13878
Relativistic theory of gravitation and new concepts about space-time 09 p1240 N88-17431
Ambiguity in determining the effective action for string-corrected Einstein gravity
[PB87-166153] 09 p1259 N88-17550
On higher derivative gravity
[DE88-700619] 10 p1354 N88-18090
Applications of Lie group methods to the equations of magnetohydrodynamics 10 p1411 N88-18422
Hamiltonian approach to relativistic theory of gravity and to general relativity theory
[DE88-700404] 10 p1422 N88-18492
Connection between general observers and Lanczos potential
[DE88-700139] 11 p1563 N88-19354
Covariance analysis and post-processing of gravity compensation effects for aided multi-state navigation systems
[PAPER-87-13] 12 p1577 N88-19430
Relativistic theory of gravitation and criticism of General Relativity Theory (GRT)
[DE88-701304] 16 p2284 N88-23673
Gravitation and polarization properties of electromagnetic field
[DE88-702166] 19 p2654 N88-25761
Quantum gravity and new forces
[DE88-007829] 19 p2737 N88-26250
Prediction of velocity and temperature profiles in thermally driven gravity currents applied to stratified thermal storage tanks
[DE88-004452] 21 p2946 N88-27496
Gravitation electromagnetic theory
22 p3158 N88-28790
Newtonian and Einsteinian gravitation
22 p3158 N88-28791
Gravitation and electromagnetism
22 p3158 N88-28792
Electromagnetic theory of the gravitation
22 p3158 N88-28793
Cosmological applications 22 p3158 N88-28794
Gravitation control 22 p3158 N88-28795
Gravitational propulsion 22 p3158 N88-28796
Towards a finite quantum gravity
[DE88-701497] 23 p3294 N88-29619

GRAVITATION THEORY
NT SUPERGRAVITY
Gravity from symmetry breakdown of a gauge affine theory
[DE88-001671] 04 p0500 N88-13079
Non-minimal interaction of gravity with other physical fields: An overview
[DE87-703362] 05 p0624 N88-13819
A theoretical model for neutrino masses and mixing
[PREPRINT-553] 06 p0776 N88-14777
Analysis and synthesis of the Earth's gravity field variable in space and time using vector surface spherical functions
[SER-C-325] 07 p0878 N88-15328
On higher derivative gravity
[DE88-700619] 10 p1354 N88-18090
Qualitative methods in nonhomogeneous cosmology
[DE88-700620] 10 p1417 N88-18458
Modified theory of gravity
[DE88-700835] 12 p1642 N88-19830
Einstein metrics and Brans-Dicke superfields
[DE88-006992] 15 p2146 N88-22809
String driven inflation
[DE88-006994] 15 p2151 N88-22841
Bogolyubov transformation in relativistic theory of gravitation
[DE88-701502] 16 p2232 N88-23329
Inevitable inflation in Einstein-Cartan theory with improved energy-momentum tensor with spin
[NASA-TM-101146] 18 p2586 N88-25365
From general relativity to the theory of superstrings
18 p2587 N88-25369

GRAVITATIONAL COLLAPSE
Core bounce supernovae
[DE87-014910] 04 p0520 N88-13197
Galaxy formation by gravitational collapse in a universe dominated by cold dark matter 04 p0521 N88-13205
Supernova mechanisms: Before and after SN1987a
[DE88-003489] 10 p1429 N88-18533
Hydrodynamical equations for spherical gravitational collapse in terms of a generalized theory of gravitation with higher derivatives
[DE87-703027] 15 p2151 N88-22838
Microwave spectroscopy and gravitational collapse
18 p2594 N88-25413

GRAVITATIONAL CONSTANT
New class of spherically symmetric interior solution with cosmological constant
[DE87-703095] 02 p0226 N88-11422
Crucial cosmological observations
[DE87-703081] 02 p0251 N88-11587
On deviations from Newton's law and the proposal for a Fifth Force
[DE87-703368] 04 p0487 N88-13001
Some considerations on measuring the Newtonian gravitational constant G in an orbiting laboratory
07 p0922 N88-15603
Cosmic wavefunction with induced gravity
[DE88-701873] 20 p2884 N88-27129

GRAVITATIONAL EFFECTS
NT GRAVITATIONAL LENSES
NT LAGRANGIAN EQUILIBRIUM POINTS
Preliminary study of a biotechnology research facility for microgravity, executive summary
[MATRA-EPT/AS/VT209/246/NT]
01 p0032 N88-10204
Preliminary study of a gravitational biology facility for Columbus, executive summary
[MATRA-EPT/AS/VT209/255/NT]
01 p0032 N88-10205
Estimability of potential coefficients from orbit perturbations --- satellite geodesy
[REPT-86.1] 01 p0064 N88-10408
Continuous flow electrophoresis system experiments on shuttle flights STS-6 and STS-7
[NASA-TP-2778] 02 p0156 N88-10978
On the role of convective motion during dendrite growth: Experiments under variable gravity, revised
[NASA-CR-179213] 02 p0156 N88-10979
Surface coatings and catalyst production by electrodeposition 03 p0297 N88-11863
Estimations of gravitational effects on thermal denaturation process in a biopolymer
03 p0316 N88-12013
A study of chaos and mixing in Rayleigh-Taylor and Richtmyer-Meshkov unstable interfaces
[AD-A184751] 03 p0320 N88-12026
Steady distortion of shape of geoid and normal gravity field under influence of tidal potential
04 p0459 N88-12839

Two-layer stratified flow analysis of gravity currents and turbidity currents in lakes, reservoirs and the ocean
04 p0463 N88-12864

Research and development of anti-G life support systems. Part 1: Development and evaluation of uniform-pressure anti-G suits
[AD-A185658] 06 p0754 N88-14628

Gravitational interaction of massless fields with higher spins (s greater than 2) 06 p0775 N88-14760

Allowable gravity-levels for Spacelab, Columbus and EURECA --- materials science
[BF-R-66.525-2] 07 p0838 N88-15084

Proceedings and program draft in Gravitational Biology in the Federal Republic of Germany --- Effects of Weightlessness on the Human Organism
[ESA-TT-988] 07 p0884 N88-15363

A theoretical concept for state changes and shape changes in weightlessness 07 p0884 N88-15365

Some remarks on gravitational biology
07 p0884 N88-15366

Investigations of Paramecium cells analyzed under microgravity conditions 07 p0884 N88-15367

The origin of the spicule skeleton of fresh water sponges (Spongillides) 07 p0885 N88-15368

Limb regeneration in amphibians, a suitable model for investigations of the effects of weightlessness as regards evolution and modifications 07 p0885 N88-15369

Investigations of the reproductive physiology of the rainbow trout (Salmo gairdneri Richardson)
07 p0885 N88-15370

Changes in the morphological and molecular biological processes during early embryo development in amphibians under micro-g conditions 07 p0885 N88-15371

A learning model as a basis for investigations of the effects of gravity on the learning processes and memory formulation 07 p0886 N88-15374

Morphology and development of the inner ear of Anurans 07 p0886 N88-15378

Human and animal hypovolemic reactions to increasing +Gz accelerations 07 p0890 N88-15395

JPRS report: Science and technology. USSR: Space Biology and Aerospace Medicine, volume 21, no. 4, July - August 1987
[JPRS-USB-88-002] 07 p0893 N88-15412

Experiments with rats flown aboard Cosmos-1667 biosatellite (main objectives, conditions and results)
07 p0893 N88-15414

JPRS report: Science and technology. USSR: Space
[JPRS-USP-87-006] 08 p1001 N88-16063

Magnetic field of planet Uranus: Predictions, measurements, interpretations 08 p1005 N88-16094

Preliminary Material Science Experiment Rocket (MASER) 1 results and the evolution of the MASER program 08 p1033 N88-16260

Flight results of the ESA experiment modules in Materials Science Experiment Rocket (MASER) 1
08 p1033 N88-16261

Life sciences experiments on stratospheric balloons and sounding rockets 08 p1033 N88-16262

The D-1 Biorack results: A base for further space biological investigations 08 p1033 N88-16263

Scientific objectives and functional requirements of life sciences in the Space Station 08 p1033 N88-16264

The ESA Anthrorack project: Integrated research in human physiology 08 p1033 N88-16265

Contribution of stratospheric balloon flights in space biology 08 p1033 N88-16266

White blood cells in space: An experiment for the first Spacelab mission 09 p1127 N88-16757

Looking for new gravitational forces with antiprotons
[DE88-003154] 09 p1192 N88-17142

Potential use of the bioreactor to determine effects of microgravity and other environmental parameters on growth of hybridoma cells 09 p1198 N88-17178

Research in theoretical physics
[DE88-003201] 09 p1259 N88-17546

Microgravity research at the University of Mexico: Experiments in payload G-006 10 p1286 N88-17692

Ten past and ten future GAS/MAUS-payloads
10 p1287 N88-17696

Drosophila geotaxis as a tool for the study of aging
10 p1288 N88-17706

Embryonic development of guppy in weightlessness
10 p1360 N88-18127

Myosin Ca sup (2+), Mg sup (2+)-adenosine triphosphatase activity in ray myocardium following 30-day expose to 1.1 and 2.0 G 10 p1362 N88-18141

Investigation of genetic structures of rat germ cells following flight aboard Cosmos-1514 biosatellite during their prenatal development 10 p1364 N88-18155

Two-dimensional static otolith model
10 p1367 N88-18167

Hemodynamic effects of beta-adrenergic blocking with obsidan in clinostatic and orthostatic positions
10 p1367 N88-18171

NASA Workshop on Biological Adaptation
[NASA-TM-89468] 10 p1368 N88-18174

Study of the production of some superconducting and magnetic materials by solidification in the drop tube and drop tower
[NASA-CR-182494] 11 p1461 N88-18708

Conceptualization and design of a variable-gravity research facility
[NASA-CR-182574] 12 p1595 N88-19550

Proceedings of the 3rd European Symposium on Life Sciences Research in Space
[ESA-SP-271] 12 p1652 N88-19893

The European Space Agency's role in life sciences and research in space 12 p1652 N88-19894

The ESA facility Biorack 12 p1652 N88-19897

The respiratory system under weightlessness
12 p1653 N88-19901

Plant biology in space 12 p1654 N88-19910

Cardiovascular adaptation to zero-g during a long term flight (237 days) on board the Salyut 7 Soviet space station (1984) 12 p1655 N88-19920

Effects of cosmic heavy ion radiation and space microgravity on plant systems 12 p1658 N88-19936

Experiments concerning gravisensitivity of protozoa
12 p1660 N88-19949

Antibiotic activity in space, results and hypothesis
12 p1660 N88-19952

Biorack experiments in Spacelab D-1 and TML-1: Further developments in gravitational biology
12 p1661 N88-19953

Why life science in space? The next step to go beyond 12 p1661 N88-19954

The suspended Japanese quail as an animal model for experiments related to microgravity
12 p1662 N88-19960

Domain perturbation method in the static equilibrium of masses in rotation
[INPE-4217-PRE/1098] 12 p1686 N88-20085

Mechanical design of a ultrahigh gravity UHV facility to launch and recover a low-speed projectile tested on board KC 135 14 p1877 N88-21216

Space experiment plan FMPT
15 p2051 N88-22220

Amorphous semiconductors made in space
15 p2051 N88-22221

Containerless glass melting 15 p2051 N88-22222

Generation and coalescence of bubbles and stability of foams under microgravity conditions
[BMFT-FB-W-86-020] 16 p2184 N88-23017

The determination of gravity and topography from seismic velocities, accounting for dynamic behavior of the Earth's mantle
[ETN-88-92420] 17 p2374 N88-24117

An experiment to investigate Rankine cycle two-phase microgravity issues 17 p2409 N88-24322

Nucleate pool boiling: High gravity to reduced gravity; liquid metals to cryogens 17 p2431 N88-24464

Flotation processes
[PB88-180302] 18 p2540 N88-25075

Cardiovascular effects of weightlessness and ground-based simulation
[NASA-TM-88314] 18 p2551 N88-25140

Fraction eutectic measurements in slowly cooled Pb - 15 wt percent Sn alloys
[NASA-CR-180830] 19 p2618 N88-25531

Noninvasive examination of bones during long-term hypokinesia 19 p2704 N88-26077

Industrial processes influenced by gravity
[NASA-CR-182140] 20 p2782 N88-26497

Thermostatistical estimations of vapor-state molecules affected by gravity in a heat pipe
20 p2783 N88-26505

An experimental investigation of transient characteristics in a gravity-assisted heat pipe 20 p2783 N88-26506

EEG indices of G-induced Loss Of Consciousness (G-LOC) 21 p2982 N88-27709

The auditory evoked response in military pilots
21 p2984 N88-27721

Biorack on Spacelab D1: An overview of the first flight of Biorack, an ESA facility for life sciences research in microgravity
[ESA-SP-1091] 22 p3059 N88-28154

A brief overview of the results of the experiments using the ESA Biorack Facility on the German Spacelab D1 mission 22 p3060 N88-28155

The Biorack facility and its performance during the D1 Spacelab mission 22 p3060 N88-28156

The effects of microgravity on genetic recombination in Escherichia coli --- Spacelab D1 mission
22 p3060 N88-28157

Growth and differentiation of Bacillus subtilis under microgravity conditions 22 p3060 N88-28158

The Antibio experiment --- Spacelab D1 mission
22 p3060 N88-28159

Contraction behavior and protoplasmic streaming in the slime mold Physarum polycephalum (Physarum kinetics) --- Spacelab D1 mission 22 p3060 N88-28160

The Paramecium experiment --- Spacelab D1 mission
22 p3060 N88-28161

The biological clock of Chlamydomonas reinhardii in space 22 p3061 N88-28162

Effect of microgravity on lymphocyte activation --- Spacelab D1 mission 22 p3061 N88-28163

The effect of microgravity on mammalian cell polarization at the ultrastructural level --- Spacelab D1 mission
22 p3061 N88-28164

Graviperception of lentil seedling roots grown in space
22 p3061 N88-28165

Effects of short spaceflights on Drosophila melanogaster embryogenesis and life span 22 p3061 N88-28166

Embryogenesis and organogenesis of Carausius morosus under spaceflight conditions
22 p3061 N88-28167

The role of gravity in the establishment of the dorso/ventral axis in the amphibian embryo --- Spacelab D1 mission 22 p3062 N88-28168

Interplanetary travel: Is gravity needed to close the loop
[NASA-TM-101013] 22 p3132 N88-28622

Gravitation electromagnetic theory
22 p3158 N88-28790

Newtonian and Einsteinian gravitation
22 p3158 N88-28791

Gravitation control 22 p3158 N88-28795

The origin of the moon: Further studies of the giant impact 24 p3440 N88-30474

GRAVITATIONAL FIELDS

Precise orbit computation, gravity model adjustment and altimeter data processing for the ERS-1 altimetry mission
[ESA-CR(P)-2436] 02 p0130 N88-10820

On the theory of the Michelson-Morley experiment in the Earth's gravitational field
[DE87-703077] 02 p0198 N88-11233

Study of a satellite-to-satellite tracking gravity mission
[ESA-CR(P)-2419] 02 p0198 N88-11237

Spherical harmonic expansion of the Levitus Sea surface topography
[NASA-CR-181448] 02 p0216 N88-11362

Covariant Lorentz anomalies in higher dimensional space
[DE87-753021] 02 p0230 N88-11448

GEOSAT altimeter geophysical data record user handbook
[PB87-213336] 03 p0276 N88-11743

East coast gravity validation study
[AD-A184292] 03 p0351 N88-12217

Non-minimal interaction of gravity with other physical fields: An overview
[DE87-703362] 05 p0624 N88-13819

Advanced simulation and analysis of a geopotential research mission
[NASA-CR-182355] 06 p0670 N88-14108

Analysis and synthesis of the Earth's gravity field variable in space and time using vector surface spherical functions
[SER-C-325] 07 p0878 N88-15328

Assessment of anomalous gravitational field of elastic Earth 07 p0921 N88-15594

Perturbations of the Sun's gravitational field due to solar oscillations
[DE88-002099] 07 p0946 N88-15751

Solar oscillations, gravitational multipole field of the Sun and the solar neutrino paradox
[DE88-002100] 07 p0946 N88-15752

New possibilities for using gravity data in developing geodetic coordinate systems 08 p1009 N88-16116

Qualitative methods in nonhomogeneous cosmology
[DE88-700620] 10 p1417 N88-18453

Hamiltonian approach to relativistic theory of gravity and to general relativity theory
[DE88-700404] 10 p1422 N88-18492

Seventy years of the general theory of relativity
[DE88-700784] 11 p1563 N88-19356

Comparisons of global topographic/isostatic models to the Earth's observed gravity field
[NASA-CR-182696] 13 p1798 N88-20752

Spin precession in stationary gravitational fields
[DE88-701107] 15 p2093 N88-22470

Hydrodynamical equations for spherical gravitational collapse in terms of a generalized theory of gravitation with higher derivatives
[DE87-703027] 15 p2151 N88-22838

Direct numerical simulation of buoyantly driven turbulence 16 p2196 N88-23097

Bogolyubov transformation in relativistic theory of gravitation
[DE88-701592] 16 p2232 N88-23329

Relativistic theory of gravitation and criticism of General Relativity Theory (GRT)
[DE86-701304] 16 p2284 N88-23673

Evaluation of a model of the Earth's gravity field
[EPSHOM-003/87] 17 p2373 N88-24116

Non-Newtonian gravity or gravity anomalies?
[NASA-TM-4030] 17 p2374 N88-24118

Gravitation and polarization properties of electromagnetic field
[DE88-702166] 19 p2654 N88-25761

Symmetry problem of energy-momentum tensor and the creation of gravitational field
[DE88-702442] 21 p3026 N88-27964

Gravitational redshift of self-gravitating systems of dark matter in the universe
[DE88-702688] 23 p3300 N88-29650

General equations for the motions of ice crystals and water drops in gravitational and electric fields
[NASA-CR-183229] 24 p3370 N88-30070

Estimation of short-wavelength gravity on a dense grid using digital terrain elevation data
[AD-A196325] 24 p3391 N88-30196

Relationships among earth's gravity field, magnetic field, crustal structure and the magnetic character of crustal rocks
[AD-A195539] 24 p3392 N88-30198

Gravity anomalies, plate tectonics and the lateral growth of Precambrian North America 24 p3400 N88-30248

Resonance effects accompanying motion with low thrust in earth-moon system 24 p3446 N88-30510

GRAVITATIONAL LENSES

Prediction and analysis of basic gravitational microlensing phenomena 11 p1550 N88-19272

Light propagation through gravitationally perturbed Friedmann universes 18 p2577 N88-25307

GRAVITATIONAL PHYSIOLOGY

Scientific objectives and functional requirements of life sciences in the Space Station 08 p1033 N88-16264

The ESA Anthrorack project: Integrated research in human physiology 08 p1033 N88-16265

ESA's facility for research in human physiology in space: Anthrorack 12 p1652 N88-19896

The respiratory system under weightlessness
12 p1653 N88-19901

Respiratory parameters aboard an aircraft performing parabolic flights 12 p1653 N88-19902

Influence of a 6 hr head-out water immersion on different tests of endurance performance capacity
12 p1653 N88-19903

Second-generation respiratory monitoring system for microgravity studies in man 12 p1653 N88-19906

Lung function in simulated microgravity
12 p1654 N88-19907

Fluid volume changes in astronauts: How they fit our understanding of physiology 12 p1655 N88-19919

Cardiovascular adaptation to zero-g during a long term flight (237 days) on board the Salyut 7 Soviet space station (1984) 12 p1655 N88-19920

Cardiac and peripheral circulation assessment by ultrasound on 3 astronauts during two 7-day space flights (1982 Salyut-7 - 1985 STS 51G)
12 p1656 N88-19921

Load and control of the cardiocirculatory system in weightlessness 12 p1656 N88-19922

Neuro-reflex mechanisms of circulation regulation in simulated microgravity 12 p1656 N88-19923

Physiological reactions upon controlled changes of blood distribution in humans 12 p1656 N88-19924

P-31 Magnetic Resonance Spectroscopy (MRS) of limb muscles during bedrest with exercise countermeasures
12 p1656 N88-19925

Disuse condition stimulates bone resorption in organ culture 12 p1656 N88-19926

An in vitro model system to study the effect of microgravity and loading conditions on the mineralization and resorption of skeletal tissues
12 p1657 N88-19927

Vestibular integrated function and microgravity
12 p1658 N88-19937

Neck receptor stimulation in 0 and 1 g
12 p1658 N88-19938

Synopsis of the Spacelab D-1 frog statolith experiment STATEX 12 p1659 N88-19940

The rate of adaptation to altered g in the human centrifuge: Implications for simulations of mass-discrimination in space flight
12 p1659 N88-19941

Effects of anti-g suit inflation on renin and aldosterone response physical exercise 12 p1659 N88-19944

Medilab: A project of a medical laboratory in space
12 p1660 N88-19946

Experiments concerning gravisensitivity of protozoa
12 p1660 N88-19949

Organs and tissues regeneration in amphibia under the space flight conditions 12 p1660 N88-19951

A new isodynamically-braked arm ergometer including the demonstration of a prototype
12 p1661 N88-19957

Assessment of intercompartment fluid shifts by blood densitometry in astronauts 12 p1661 N88-19958

Application of ARIADNE: A data bank-based information system for human physiology research --- Spacelab Anthrorack 12 p1662 N88-19962

Regulation of hemodynamics upon imitation of the transition to weightlessness (mathematical modeling)
13 p1810 N88-20817

Leg volume change under Lower Body Negative Pressure (LBNP) in dependence on stratification
[DFVLR-FB-87-47] 16 p2238 N88-23367

GRAVITATIONAL POTENTIAL

U GRAVITATIONAL FIELDS

GRAVITATIONAL RADIATION

U GRAVITATIONAL WAVES

GRAVITATIONAL WAVE ANTENNAS

Capacitive resonant transducer for the Frascati gravitational antenna
[IFSI-86-9] 05 p0578 N88-13528

Preliminary comparison of some coincidence methods for gravitational wave detectors
[NOTA-INTERNA-903] 14 p1945 N88-21604

GRAVITATIONAL WAVES

Media calibrations of the Doppler signal for a gravitational wave experiment --- interplanetary medium
[IFSI-86-13] 05 p0625 N88-13825

Activities report in interplanetary space physics
[IFSI-86-5] 05 p0659 N88-14047

Budget and programs for 1986 research
[IFSI-86-16] 05 p0660 N88-14048

Data recorded by the Rome room temperature gravitational wave antenna, during the supernova SN 1987 A in the Large Magellanic Cloud
[NOTA-INTERNA-879] 06 p0806 N88-14922

Dynamic modeling of the middle atmosphere
08 p1028 N88-16227

Observational evidence for saturation of gravity waves and the production of turbulence in the mesosphere
08 p1028 N88-16229

Equation of acoustic and gravitational waves in stratified moving medium 08 p1077 N88-16493

Equation of gravitational-gyroscopic waves: Angular potential and its applications 08 p1079 N88-16504

Preliminary comparison of some coincidence methods for gravitational wave detectors
[NOTA-INTERNA-903] 14 p1945 N88-21604

Light propagation through gravitationally perturbed Friedmann universes 18 p2577 N88-25307

Fourier transform of gravitational synchrotron radiation
[PREPRINT-588] 22 p3144 N88-26700

Acoustic-optical detector of gravitational waves based on high-quality crystals
[DE88-702459] 23 p3232 N88-29232

On the degenerate Ferrari-Ibanez solution for colliding plane gravitational waves
[MATH-REPT-209] 23 p3296 N88-29630

GRAVITONS

Comment on non-renormalization theorem in the four dimensional superstrings
[DE88-752551] 18 p2586 N88-25367

GRAVITROPISM

Gravisensing in lentil seedling roots grown in space (Spacelab D-1 mission) 12 p1654 N88-19911

GRAVITY

U GRAVITATION

GRAVITY ANOMALIES

Gravity and fault structures, Long Valley Caldera, California
[DE87-014117] 02 p0197 N88-11229

Study of a satellite-to-satellite tracking gravity mission
[ESA-CR(P)-2419] 02 p0198 N88-11237

Geophysical-geomorphological statistical regionalization of North Atlantic
06 p0726 N88-14466

Assessment of anomalous gravitational field of elastic Earth 07 p0921 N88-15594

A three-dimensional gravity model of the geologic structure of Long Valley caldera
[DE88-006331] 16 p2231 N88-23324

Modeling and estimation of a low degree geopotential model from terrestrial gravity data
[NASA-CR-182808] 16 p2232 N88-23330

Non-Newtonian gravity or gravity anomalies?
[NASA-TM-4030] 17 p2374 N88-24118

To relate measurements of gravity and geoid anomalies over the oceans to near surface density distributions
[AD-A192168] 18 p2547 N88-25120

Gravity anomalies, plate tectonics and the lateral growth of Precambrian North America 24 p3400 N88-30248

GRAVITY GRADIOMETERS

Monocrystalline silicon gradiometer for gravity experiments in space
[NASA-CR-181452] 01 p0050 N88-10321

Estimation of gravity vector components from Bell gravity gradiometer and auxiliary data under consideration of topography and associated analytical upward continuation aspects
[AD-A188146] 10 p1355 N88-18099

Spaceborne gravity gradiometry characterizing the data type 12 p1644 N88-19847

GRADIO three-axis electrostatic accelerometers
12 p1645 N88-19849

Gradiometer accommodation on board a drag-free satellite 12 p1645 N88-19850

Gradiometer mission spectral analysis and simulation studies: Past and future 12 p1645 N88-19851

Satellite gradiometry
[B8735057] 16 p2229 N88-23313

GRAVITY PROBE B

A 1987 progress report of manufacturing techniques for Gravity Probe B gyroscope rotors
[NASA-TM-100312] 02 p0176 N88-11101

GRAVITY WAVES

NT BAROCLINIC WAVES

Toward operational forecasting and detection of weather-producing gravity waves
02 p0208 N88-11303

Dispersion equation for plane capillary-gravity wave on free surface of viscous incompressible fluid
04 p0459 N88-12842

Influence of surfactants on damping of gravity-capillary waves. 1: Frequency dependence
04 p0459 N88-12843

Meteor observation by the Kyoto meteor radar
06 p0733 N88-14507

A study of the mechanism of internal gravity wave generation by quasigeostrophic meteorological motions
06 p0735 N88-14520

Study of internal gravity waves in the meteor zone
06 p0735 N88-14521

Numerical modeling of troposphere-induced gravity wave propagation 06 p0735 N88-14522

A statistical study of variations of internal gravity wave energy characteristics in meteor zone
06 p0735 N88-14523

Internal gravity waves in the meteor zone in the Tbilisi Region 06 p0736 N88-14528

Observations of inertial period waves and vertical velocities in the tropical middle atmosphere using the MST radar technique 06 p0742 N88-14562

An analysis of apparent-motion vectors in, and the structure of, A mid-latitude sporadic E layer using a 2.66 MHz radar
[AD-A186126] 07 p0877 N88-15321

Rayleigh lidar observations of gravity wave activity in the stratosphere and lower mesosphere
[NASA-CR-182384] 09 p1189 N88-17123

Universal power spectra for wave turbulence: Applications to wind waves, flicker noise, solar wind spectrum and classical second sound
10 p1318 N88-17879

Evolution of acoustic gravity wave packet in spatially and temporally varying wind 11 p1469 N88-18760

Seasonal variations and excitation mechanisms of the equatorially trapped waves 13 p1798 N88-20751

Observations of waves and Langmuir circulation with Doppler sonars 13 p1805 N88-20790

Propagation of acoustic gravity wave spectrum through vertical wind shear region 16 p2186 N88-23035

Gravity currents with heat transfer effects
[PB88-180047] 16 p2205 N88-23158

Propagation of linear gravity waves in a relativistic atmosphere
[DE88-702062] 19 p2691 N88-25995

Propagation of inernio-acoustic gravity waves in a rotating and radiating opaque atmosphere
[DE88-701866] 20 p2823 N88-26750

GRAVSAT SATELLITES

U GEOPOTENTIAL RESEARCH MISSION

GRAY SCALE

Weighted averaging method for image smoothing reported 14 p1901 N88-21352

Visualization of digital terrain models
17 p2364 N88-24081

Applications of differential geometry to the shape analysis of gray-value images 21 p2924 N88-27358

GRAZING

All-optical beam control by forced Rayleigh scattering
[AD-A184315] 04 p0490 N88-13018

Acoustic scattering from composite wind-wave surfaces 3: Forward scatter intensities and spatial coherence at low and high frequencies and small grazing angles for Bubble-free regimes
[AD-A185908] 07 p0881 N88-15345

Models for electromagnetic scattering from the sea at extremely low grazing angles
[AD-A190472] 15 p2057 N88-22261

Characterization, topology, and cartography of grasslands for the development of fodder resources. (Preliminary Evaluation Program for SPOT number 26) 22 p3095 N88-28377

GRAZING FLOW

Measured and calculated acoustic attenuation rates of tuned resonator arrays for two surface impedance distribution models with flow [NASA-TP-2766] 09 p1241 N88-17440

GRAZING INCIDENCE

Backscatter from a periodic rough surface at near grazing incidence [NASA-CR-182397] 07 p0845 N88-15128

Grazing incidence X-ray scattering study of defect structures in MBE GaAs/Si using synchrotron radiation [DE88-004556] 10 p1420 N88-18483

Design, construction and performance of the ROSAT high resolution X-ray mirror assembly [MPE-PREPRINT-101] 15 p2150 N88-22836

An experimental study of the coherent under-ice reflectivity of sound in the Greenland Sea Marginal Ice Zone 18 p2546 N88-25125

The XRD (X-Ray Diode) array, the grazing incidence spectrometer and the X-ray imaging camera on PBFA 2 [DE88-007282] 19 p2728 N88-26200

GRAZING LANDS

U GRASSLANDS

GREASES

Low extractable wipers for cleaning space flight hardware 02 p0137 N88-10863

Developing an accelerated endurance test for greases: A status report [AD-A185963] 07 p0836 N88-15072

Improved perfluoroalkylether fluid development [NASA-CR-180872] 08 p0967 N88-15851

Characteristics and use of lubricating greases [DE88-751103] 11 p1463 N88-18723

Evaluation of solder flux solvents in a vapor-degreasing application for hybrid microcircuits [BDX-613-3638] 11 p1466 N88-18752

GREAT BASIN (US)

Historical catalog of Southern Great Basin earthquakes, 1868-1978 [DE87-014340] 02 p0198 N88-11232

GREAT BRITAIN

U UNITED KINGDOM

GREEN THEOREM

U GREEN'S FUNCTIONS

GREEN'S FUNCTIONS

Extending Green's function formalism to general nonlinear equations [DE87-013541] 02 p0224 N88-11411

The Green's function method for fully unsteady aerodynamics around three-dimensional bodies and its application to flutter analysis [UTIAS-298] 03 p0260 N88-11639

Efficient computation of periodic Green's functions with application to grating structures [AD-A184853] 05 p0640 N88-13912

Method of two-time Green functions in molecular hydrodynamics of superfluid liquid 06 p0771 N88-14735

Green's function for a ball [AD-A186239] 07 p0910 N88-15516

Symbolic, algebraic, and numeric solutions to heat conduction problems using Green's functions 09 p1165 N88-16987

Comment on the Adler-Bardeen theorem and related problems [DE88-751051] 10 p1403 N88-18367

Investigation of a ray-mode representation of the Green's function in a rectangular cavity [PB88-131677] 11 p1469 N88-18763

Estimates of green tensors for certain boundary value problems [NASA-TT-20203] 11 p1535 N88-19172

Finite element calculations for aerodynamic coefficients of a 3-dimensional body in subsonic flow using Green's function method [NASA-TT-20206] 13 p1718 N88-20272

Monte Carlo modified method for Green function. Algorithm and computer code for calculations in equal mass many-body system [DE88-701114] 14 p1957 N88-21667

Construction of approximations to acoustic Green's functions for nonhomogeneous oceans using transmutation [PB88-185384] 18 p2548 N88-25126

Green's function approach to roughening transition of one-dimensional restricted solid on solid model [DE88-702723] 23 p3278 N88-29512

GREENHOUSE EFFECT

Testimony to the US Senate on the greenhouse effect [DE87-013995] 01 p0071 N88-10458

Global environmental change research [S-HRG-100-301] 03 p0348 N88-12199

The effects of minor trace gases on the transfer of thermal infrared radiation through the Earth's atmosphere 04 p0468 N88-12893

Carbon dioxide and climate 14 p1936 N88-21545

Observational and theoretical studies of greenhouse climate effects [DE88-006237] 14 p1948 N88-21621

A primer on greenhouse gases [DE88-007576] 19 p2689 N88-25981

Surface energy balance of three general circulation models: Current climate and response to increasing atmospheric CO2 [DE88-010967] 21 p2975 N88-27673

Atmospheric science issues in Congress 22 p3125 N88-28573

Episodic vs. epochal release of SO2 on Mars 23 p3305 N88-29688

Nineteenth Lunar and Planetary Science Conference. Press abstracts [NASA-CR-183037] 24 p3440 N88-30473

Did the greenhouse effect kill the dinosaurs 24 p3442 N88-30484

GREENLAND

Narsarsuaq (Greenland) Geophysical Observatory. Magnetic results, 1984 [ISBN-87-7478-281-9] 02 p0198 N88-11235

Narssarssuaq Geophysical Observatory: Magnetic results, 1980-83. Instrumentation and formulas [ISBN-87-7478-280-0] 03 p0350 N88-12209

The ice conditions in the Greenland waters, 1981 [ISBN-87-7478-276-2] 05 p0629 N88-13844

The Greenland Sea Project: The Arctemiz project 14 p1939 N88-21573

Meteorological features during the marginal ice zone experiment from 20 March to 10 April 1987 [AD-A193960] 23 p3235 N88-29251

GREGORIAN ANTENNAS

A new approach for shaping of dual-reflector antennas [NASA-CR-182581] 11 p1476 N88-18806

GRID GENERATION (MATHEMATICS)

Problem and solution formulations for the generation of 3D block-structured grids --- aircraft design [NLR-MP-86020-U] 01 p0005 N88-10028

Generation of body-fitted grids for two dimensional interior domains by the solution of a system of Poisson equations using multigrid techniques [GMD-246] 01 p0044 N88-10281

Generating meshes for finite-difference analysis using a solid modeler [DE88-001458] 04 p0439 N88-12729

Analytical method for generating computational grids about complete aircraft configurations 05 p0540 N88-13287

Shuttle computational grid generation 06 p0794 N88-14863

A multistage mesh generator for solving the average-passage equation system [NASA-CR-179539] 08 p0951 N88-15769

Adaptive finite difference methods in fluid dynamics 08 p0985 N88-15958

Mesh generation 08 p0986 N88-15971

An automatic finite element mesh generator [AD-A186939] 09 p1216 N88-17291

Finite element mesh generation and isoparametric elements [NPL-DITC-97/87] 09 p1229 N88-17365

Approaches to the automatic generation and control of finite element meshes 11 p1526 N88-19113

Generation of surface grids through elliptic partial differential equations for aircraft and missile configurations [AD-A186631] 11 p1535 N88-19169

The construction of a three-dimensional finite volume grid generator for a wing in a wind tunnel with application to Navier-Stokes flow solvers [FFA-TN-1987-58] 13 p1719 N88-20277

A knowledge system for automatic finite element mesh generation: AMEKS [DE87-014894] 13 p1826 N88-20914

Three-dimensional mesh-generation and plotting routines for use with a boundary element program (BIE3D) [AD-A188079] 14 p1958 N88-21675

Development of adaptive grid schemes based on Poisson grid generators [AD-A190953] 16 p2262 N88-23526

Two dimensional hyperbolic grid generation [VKI-TN-162] 18 p2511 N88-24897

Application of advanced grid generation techniques for flow field computations about complex configurations [NASA-CR-183049] 18 p2515 N88-24922

Numerical simulations of flow around shuttle orbiter 19 p2635 N88-25633

The role of computational fluid dynamics in aeronautical engineering (5). Improvements and applications of implicit TVD finite volume code 19 p2638 N88-25653

Grid generation of a helicopter rotary-wing 19 p2640 N88-25665

Finite element welding computations using general purpose nonlinear analysis codes [DE88-005398] 20 p2808 N88-26659

Three-dimensional adaptive grid generation for body-fitted coordinate system [NASA-CR-182192] 21 p2950 N88-27520

Three dimensional grid generation for complex configurations: Recent progress [AGARD-AG-309] 23 p3245 N88-29313

Lessons learned in the mesh generation for PN/S calculations 23 p3245 N88-29314

Three-dimensional elliptic grid generation for an F-16 23 p3246 N88-29315

Component adaptive grid generation for aircraft configurations 23 p3246 N88-29316

Generation of multiple block grids for arbitrary 3D geometries 23 p3246 N88-29317

Grid generation on and about a cranked-wing fighter aircraft configuration 23 p3246 N88-29318

Grid generation for an advanced fighter aircraft 23 p3246 N88-29319

Algebraic grid generation for fighter type aircraft 23 p3246 N88-29320

Composite grid generation for aircraft configurations with the EAGLE code 23 p3246 N88-29321

Analytical surfaces and grids 23 p3247 N88-29322

Mesh generation for industrial application of Euler and Navier Stokes solvers 23 p3247 N88-29323

Experience with three dimensional composite grids 23 p3247 N88-29324

Grid generation around transport aircraft configurations using a multi-block structured computational domain 23 p3247 N88-29325

Adaptive mesh generation for viscous flows using Delaunay triangulation [NASA-CR-181699] 24 p3316 N88-29749

Three-dimensional elliptic grid generation technique with application to turbomachinery cascades [NASA-TM-101330] 24 p3372 N88-30078

Knowledge-based flow field zoning [NASA-TM-101023] 24 p3412 N88-30314

GRIDS (MATHEMATICS)

U COMPUTATIONAL GRIDS

GRIGG-SKJELLERUP COMET

The Giotto extended mission 14 p2005 N88-21957

Alternative cometary targets for the Giotto extended mission 14 p2010 N88-21990

GRINDING

Surface fatigue life of CBN and vitreous ground carburized and hardened AISI 9310 spur gears [NASA-TM-100960] 19 p2677 N88-25916

GRINDING (MATERIAL REMOVAL)

Reaming experiments for the lethality test system [DE88-007902] 20 p2763 N88-26383

GRINDING MACHINES

Size-reduction and sorting behavior in sieve hammer mills [ETN-88-91480] 11 p1467 N88-18749

GROOVES

Heat transfer characteristics of arterial heat pipe with axial grooves 03 p0319 N88-12017

Riblets for aircraft skin-friction reduction 07 p0814 N88-14955

An assessment of the drag reduction properties of riblets and the penalties of off-design conditions [RAE-TM-AERO-2113] 17 p2295 N88-23731

Drag reduction of turbulent boundary layers by means of grooved surfaces [ETN-88-92618] 20 p2802 N88-26630

GROOVING

Surface gouging by hypervelocity sliding contact between metallic materials [DE88-001937] 06 p0682 N88-14178

Experimental investigation of turbulent flow in smooth and longitudinal grooved tubes [NASA-TM-77480] 20 p2800 N88-26615

GROUND BASED CONTROL

NT AIR TRAFFIC CONTROL

Teleoperation and control study --- orbital servicing [BAE-TP-8268] 01 p0076 N88-10489

Space shuttle onboard navigation console expert/trainer system 09 p1203 N88-17208

An intelligent training system for payload-assist module deploys 09 p1204 N88-17214

Promising concepts for ground-to-orbit experiment teleoperation --- Columbus 12 p1590 N88-19518

Ground based supervisory and programming system for automatic experiment execution in orbit 12 p1590 N88-19519

A teleoperated manipulator system concept for unmanned platforms --- Columbus 12 p1593 N88-19537

Optimization of the dilation characteristic on the control jurisdiction of an area control facility
[AD-A191720] 18 p2461 N88-24615

SP-100 Ground Engineering Systems: Test facility control systems
[DE88-009195] 21 p3015 N88-27895

GROUND CREWS

Training in satellite ground system operations
09 p1129 N88-16775

GROUND EFFECT (AERODYNAMICS)

Dispersion in the wake of aircraft: An investigation of the effects of a ground plane on trailing vortices. Literature survey
[IC-AERO-REP-86-04] 01 p0003 N88-10014

An experimental investigation of dynamic ground effect
[NASA-CR-4105] 04 p0394 N88-12458

Propulsion-induced effects caused by out-of-ground effects
[NASA-TM-100032] 06 p0666 N88-14088

Recommendations for ground effects research for V/STOL and STOL aircraft and associated equipment for large scale testing
[NASA-CR-177429] 10 p1268 N88-17585

Model-scale sound propagation experiment
[NASA-TM-100602] 15 p2130 N88-22709

A numerical study of the hot gas environment around a STOVL aircraft in ground proximity
[NASA-TM-100695] 17 p2295 N88-23729

Aerodynamics in ground effect and predicted landing ground roll of a fighter configuration with a secondary-nozzle thrust reverser
[NASA-TP-2834] 24 p3317 N88-29752

GROUND EFFECT (COMMUNICATIONS)

Discharge prevention of geosynchronous orbit conductive thermal control materials and grounding systems 03 p0274 N88-11732

An investigation of terrain related variables for predicting the multipath fade depth distribution on terrestrial microwave lines 12 p1615 N88-19654

A review of the role of surface reflection in multipath propagation over terrestrial microwave links
12 p1615 N88-19655

Development of a ground-conductivity map for the area of the Federal Republic of Germany from measured field-strength contours 12 p1615 N88-19656

Analysis, suppression of land clutter characteristics reported 14 p1903 N88-21369

Performance study of a unipole antenna with conventional and elevated radial wire ground screens
[AD-A193283] 21 p2933 N88-27413

GROUND EFFECT MACHINES

Feasibility report: Operation of light air cushion vehicle at McMurdo Sound, Antarctica
[AD-A189057] 13 p1755 N88-20494

GROUND HANDLING

EASE/ACCESS ground processing at Kennedy Space Center 02 p0139 N88-10877

Turnaround operations analysis for OTV. Volume 2: Detailed technical report
[NASA-CR-179317] 13 p1729 N88-20341

Turnaround operations analysis for OTV. Volume 3: Technology development plan
[NASA-CR-179318] 13 p1729 N88-20342

Turnaround operations analysis for OTV. Volume 4: WBS and dictionary and cost methodology
[NASA-CR-179319] 13 p1729 N88-20343

GROUND STATE

A mechanism for symmetry breaking in antiferromagnetic Heisenberg systems
[ETN-88-91320] 05 p0657 N88-14031

Ground-state correlations in C12 and the mechanism of the (e,e'p) reaction
[BA729349] 14 p1860 N88-21816

Overview of hydrogen clusters
16 p2267 N88-23557

Energy-transfer properties and mechanisms
[DE88-007107] 18 p2571 N88-25272

Ground state properties and electronic structure of high T sub c superconductors
[DE88-007485] 18 p2585 N88-25360

Contribution to the study of order effects in the Ising model framework: Ground states and phase diagrams
[ONERA-NT-1987] 20 p2880 N88-27095

The 2D Rydberg series in Al I
[NASA-TM-101189] 22 p3150 N88-28740

The ground state of the bosonic string
[USIP-88-01] 22 p3151 N88-28746

Measurements of XeF (Xenon Fluoride) ground state dissociation and vibrational equilibration
[AD-A194611] 23 p3260 N88-29527

GROUND STATIONS

NT INTEGRATED MISSION CONTROL CENTER
NT POLYSTATION DOPPLER TRACKING SYSTEM

Development of response models for the Earth Radiation Budget Experiment (ERBE) sensors. Part 2: Analysis of the ERBE integrating sphere ground calibration
[NASA-CR-178293] 01 p0049 N88-10316

The status of the international Halley watch
01 p0116 N88-10744

Results of the satellite and the Toulouse (France) receiving station operator --- SPOT
03 p0341 N88-12149

The Telecommunications and Data Acquisition Report
[NASA-CR-181546] 04 p0432 N88-12679

A hydrogen/nickel oxide battery for remote applications
[DE87-009048] 04 p0464 N88-12872

Design description report for a photovoltaic power system for a remote satellite earth terminal
[NASA-CR-179586] 04 p0465 N88-12875

Dobson-stations performance assessment using TOMS data 05 p0618 N88-13792

A single-station weather forecasting expert system
[AD-A184889] 05 p0627 N88-13832

Satellite ground-terminal user simulation
[NASA-TM-100234] 06 p0694 N88-14260

AVIRIS ground data-processing system
06 p0707 N88-14333

How ground-based observations contribute to rocket, balloon and space shuttle experiments: Experience from the past and outlook for the future
08 p1026 N88-16216

The Earthnet Heat Capacity Mapping Mission (HCMM) data-processing system at Lannion (France)
09 p1127 N88-16761

The design and implementation of the Technical Facilities Controller (TFC) for the Goldstone deep space communications complex 11 p1474 N88-18794

Application of the Global Positioning System (GPS) time receivers to the fundamental station Wettzell
11 p1506 N88-18995

Crustal Dynamics Project: Catalogue of site information
[NASA-RP-1198] 11 p1513 N88-19037

Multiple-beam ground station reflector antenna system: A preliminary study
[EUT-87-E-171] 14 p1904 N88-21379

An outdoor unit for Direct Broadcast Satellite (DBS) digital sound reception
[BMFT-FB-W-86-016] 16 p2189 N88-23050

A low cost automatic Earth observation satellite tracking ground receiving station 17 p2309 N88-23815

Service offerings and interfaces for the ACTS network of Earth stations
[NASA-TM-100809] 18 p2471 N88-24663

An 8.4-GHz dual maser front end for Parkes reimplementation 22 p3066 N88-28197

DSS 14 antenna calibrations for GSSR/VLA Saturn radar experiments 22 p3068 N88-28207

Business telecommunications using satellite microterminals: Gaining the competitive edge
[ESA-BR-49] 22 p3070 N88-28225

Determination of satcom access power levels within the ground segment
[RSRE-MEMO-4097] 22 p3070 N88-28226

GROUND SUPPORT EQUIPMENT

Research on Electrodynamic Tether Effects (RETE) experiment Electrical Ground Support Equipment (EGSE) --- tethered satellite
[IFSI-87-2] 05 p0555 N88-13378

RETE experiment Assembly, Integration, and Verification (AIV) activities
[IFSI-87-6] 05 p0555 N88-13380

Controlling stress corrosion cracking in mechanism components of ground support equipment
14 p1926 N88-21480

V2500 Condition Monitoring and Performance Analysis Software System (COMPASS): Overview of system --- aircraft engine
[PNR90418] 22 p3139 N88-28666

Artificial intelligence costs, benefits, risks for selected spacecraft ground system automation scenarios
24 p3416 N88-30332

Study on industrial organization for European Ground Support Equipment (EGSE) to support European space programs. Volume 1: Technical reports
[SD-RP-AI-009-VOL-1] 24 p3435 N88-30446

Study on industrial organization for European Ground Support Equipment (EGSE) to support European space programs. Volume 2: Technical reports
[SD-RP-AI-009-VOL-2] 24 p3435 N88-30448

GROUND SUPPORT SYSTEMS

EASE/ACCESS ground processing at Kennedy Space Center 02 p0139 N88-10877

Knowledge-based simulation
08 p1061 N88-16404

Columbus feasibility studies. Volume 4: Integration, test, and operations
[ETN-88-90576] 11 p1445 N88-18614

Microgravity User Support Center (MUSC) for EURECA, Spacelab and Columbus missions
12 p1660 N88-19947

The German processing and archiving facility for ERS-1
[ESA-CR(P)-2531] 13 p1851 N88-21082

Development of a mobile research flight test support capability
[NASA-TM-100428] 16 p2159 N88-22883

Reduced flexibility in processing Titan 4 space launch vehicles at Cape Canaveral Air Force Station
[AD-A194908] 24 p3332 N88-29834

Aerospace payload support systems
[AFGL-TR-87-0241] 24 p3334 N88-29843

Study on industrial organization for European Ground Support Equipment (EGSE) to support European space programs. Volume 1: Technical reports
[SD-RP-AI-009-VOL-1] 24 p3435 N88-30446

Study on industrial organization for European Ground Support Equipment (EGSE) to support European space programs. Volume 2: Technical reports
[SD-RP-AI-009-VOL-2] 24 p3435 N88-30448

GROUND TESTS

NT COLD FLOW TESTS
NT PRELAUNCH TESTS
NT STATIC FIRING

Ground shock profiles for an accidental explosion at the proposed Large Rocket Test Facility at Arnold Engineering Development Center
[DE88-002652] 07 p0853 N88-15180

Pattern recognition techniques for failure trend detection in SSME ground tests 07 p0924 N88-15614

A simulation study of the flight dynamics of elastic aircraft. Volume 2: Data
[NASA-CR-4102-VOL-2] 08 p0959 N88-15813

Coordinated use of European test facilities
09 p1123 N88-16726

The NASA integrated test facility and its impact on flight research
[NASA-TM-100418] 14 p1870 N88-21177

Description of ground motion data processing codes, volume 2
[DE88-007137] 15 p2095 N88-22481

A cyclic ground test of an ion auxiliary propulsion system: Description and operational considerations
[NASA-TM-100870] 17 p2313 N88-23829

Requirements and cost considerations for a combined space nuclear reactor test facility
17 p2401 N88-24277

Conceptual design of the SP-100 GES test site
17 p2402 N88-24284

Selection of a handling and maintenance option for the SP-100 ground engineering system test
17 p2402 N88-24285

SP-100 flight qualification testing assessment
17 p2424 N88-24414

SP-100 ground engineering systems test facility control systems 17 p2436 N88-24496

Australian structures response evaluation: Ground shock and air blast measurements for site investigation survey
[MRL-TN-526] 20 p2813 N88-26685

Successful completion of a cyclic ground test of a mercury ion auxiliary propulsion system
[NASA-TM-101351] 24 p3339 N88-29873

GROUND TRACKS

NT SATELLITE GROUND TRACKS

Radial track of moving objects determined by HF backscatter technique 14 p1901 N88-21354

GROUND TRUTH

From pattern to process: The strategy of the Earth Observing System: Volume 2: EOS Science Steering Committee report
[NASA-TM-89702] 07 p0871 N88-15283

Spectral measurements for correcting LANDSAT data for atmospheric effects 17 p2362 N88-24066

Evaluation of an estimation system for an irrigated area in a tropical region through TM-LANDSAT imagery
17 p2363 N88-24075

Evaluation of the mangrove area at the Piaui River (SE) through remote sensing 17 p2365 N88-24086

Stereoscopic photographs, ground and aerial, of trees used in the arborization of Curitiba (PR)
17 p2366 N88-24091

Integrating multispectral imagery and ground level hyperspectral signature data
[AD-A195976] 24 p3386 N88-30186

GROUND WATER

Water source heat pump: How to get home heating and cooling from your own back yard
[DE88-900180] 07 p0875 N88-15306

Boundary-integral-equation method for computing the three-dimensional flow of groundwater
[PB88-126891] 10 p1330 N88-17951

Reverse osmosis treatment to remove inorganic contaminants from drinking water
[PB88-147780] 12 p1605 N88-19598

Study of fractures as subsidiary research of ground water in the Sergipe state: An approach through remote sensing data
[INPE-4319-TDL/286] 12 p1639 N88-19813

Environmental projects. Volume 5, part 1: Study of subsurface contamination. Part 2: Guide to implement environmental compliance programs
[NASA-CR-182691] 13 p1796 N88-20741

Groundwater sapping valleys: Experimental studies, geological controls and implications to the interpretation of valley networks on Mars
[NASA-CR-182718] 15 p2152 N88-22847

A core hole into the hydrothermal system of the Long Valley caldera
[DE88-006335] 16 p2231 N88-23325

Indentification of shallow groundwater regions in semi-arid Brazil by remote sensing methods
17 p2355 N88-24030

Study of fracturing for groundwater research in the Sergipe state with remote sensing products
17 p2359 N88-24052

A zoomable and adaptable hidden fine-mesh approach to solving advection-dispersion equations
[DE88-006174] 21 p3004 N88-27816

Comparing different images for ground water survey based on lineament analysis 22 p3104 N88-28435

GROUND WAVE PROPAGATION

Surface-wave model uncertainty assessment
[AD-A193094] 21 p2932 N88-27408

GROUND WIND

Statistical very short-range forecasting via analogues
02 p0206 N88-11290

Short-term forecasting of lightning based on the surface wind field at Kennedy Space Center
02 p0208 N88-11306

Mesoscale surface field analysis from routine observations --- pressure, wind fields
02 p0209 N88-11315

High resolution determination of true surface winds at sea from wind and pressure data
02 p0210 N88-11316

A preliminary demonstration of the use of boundary-layer models of flow in complex terrain for high resolution surface wind forecasting 02 p0212 N88-11330

Cross flow in the Alps and flat foehn during the experiment MERKUR --- mesoscale experiment
08 p1013 N88-16142

Simulation of a typical flow in a broad valley
08 p1015 N88-16154

Moscow USSR. Limited surface observations climatic summary (LISOCS), parts A-F
[AD-A188080] 11 p1514 N88-19046

GROUND-TO-AIR MISSILES
U SURFACE TO AIR MISSILES

GROUP BEHAVIOR
U GROUP DYNAMICS

GROUP DYNAMICS

A comparison of the effects of group dynamics on individuals assigned to integral and non-integral aircrews
[AD-A186467] 08 p1051 N88-16345

Group adaptation and individual adjustment in antarctica: A summary of recent research
[AD-A186605] 08 p1051 N88-16347

First encounters of the close kind: The formation process of airline flight crews
[AD-A187977] 11 p1523 N88-19091

De Finetti's approach to group decision making
[AD-A188074] 11 p1536 N88-19177

The relationship between group process and performance 17 p2448 N88-24549

The human element in space: Lessons from Antarctica
[AD-A193440] 21 p2988 N88-27741

GROUP THEORY
NT AUTOMORPHISMS

Group analysis of equations arising in ocean acoustics
04 p0472 N88-12914

Group quantization of constrained systems
[PREPRINT-564] 06 p0790 N88-14844

Non-steady group combustion of a cloud of char particles
[DE87-010773] 08 p0966 N88-15849

The r-rank of the groups of exceptional Lie type
[CWI-PM-R8607] 08 p1072 N88-16468

A note on compactifications of products of semigroups
[CWI-PM-R8701] 08 p1072 N88-16469

Some aspects of control for semilinear distributed parameter systems
[INPE-4147-PRE/1054] 08 p1075 N88-16484

Perturbation theory for dual semigroups 2. Time-dependent perturbations in the sun-reflexive case
[PB88-113097] 09 p1230 N88-17369

Renormalization group analysis of the temperature dependent coupling constant in massless theory
[DE88-751059] 09 p1259 N88-17552

Mathematical foundations of signal processing. 2: The role of group theory
[AD-A188482] 12 p1620 N88-19685

Integrable quantum systems and classical Lie algebras
[DE88-700872] 12 p1683 N88-20063

SUSY anomaly in quantum-mechanical systems
[DE88-700890] 12 p1699 N88-20170

Group theoretic interpretations of Askey's scheme of hypergeometric orthogonal polynomials
[CWI-PM-R8703] 13 p1831 N88-20954

Lie groups in prolongation theory
[B8721781] 14 p1967 N88-21743

On generalized lie-like algebras
[PREPRINT-574] 14 p1968 N88-21748

Lumped model generation and evaluation: Sensitivity and Lie algebraic techniques with applications to combustion
[AD-A190402] 15 p2127 N88-22689

Perturbation theory for dual semigroups. Part 3: Nonlinear Lipschitz continuous perturbations in the Sun-reflexive case
[CWI-AM-R8706-PT-3] 16 p2263 N88-23535

Using Clifford algebras for the geometry of a tube domain (and its corresponding bounded domain) in the complexified Minkowski space of arbitrary dimension
[REPT-87-64] 16 p2264 N88-23540

Special relativity theory (one-dimensional case) without the postulate on the equality of directions
[DE88-701368] 16 p2284 N88-23674

Perturbation theory for dual semigroups. Part 4: The intertwining formula and the canonical pairing
[CWI-AM-R8802-PT-4] 18 p2569 N88-25258

Nontrivial critical points for asymptotically quadratic function
[DE88-101851] 20 p2845 N88-26881

Algebraic and arithmetic geometry in string theory
[CWI-PM-R8708] 20 p2848 N88-26904

Some remarks on geodesics in gauge groups and harmonic maps
[DE88-702665] 22 p3115 N88-28510

Global gauge anomaly of classical groups in even dimension
[DE89-008572] 22 p3158 N88-28797

Invariant ideals of multiplicity free algebraic group actions
[B8803517] 23 p3277 N88-29509

GROUP VELOCITY

Realization of active high pass filters for group velocity correction
[MPE-IN-REPT-47] 08 p0979 N88-15918

GROUP 7A COMPOUNDS
U HALOGEN COMPOUNDS

GROWTH
NT CROP GROWTH
NT CRYSTAL GROWTH
NT CZOCHRALSKI METHOD
NT DIRECTIONAL SOLIDIFICATION (CRYSTALS)
NT EPITAXY
NT LIQUID PHASE EPITAXY
NT MOLECULAR BEAM EPITAXY
NT VAPOR PHASE EPITAXY
NT VEGETATION GROWTH

Long term investigations of the growth, metabolism, and reproduction of fish under conditions close to weightlessness 01 p0074 N88-10473

A stochastic delamination growth model for fatigue loaded laminated composite materials
02 p0141 N88-10888

Molecular beam heteroepitaxy: (Ca,Sr)F2-GaAs system
[LAAS-87-168] 02 p0246 N88-11556

A functional interpretation of the logistic equation
[REPT-87-037] 05 p0645 N88-13946

Maximum likelihood estimates for the discrete application of the AMSAA growth model
[AD-A186921] 09 p1177 N88-17048

Synthesis and characterization of thin films
[AD-A187335] 10 p1421 N88-18485

Thermal oxide growth on silicon: Intrinsic stress and silicon cleaning effects
[AD-A188790] 13 p1736 N88-20377

Some problems of the theory of bubble growth and condensation in bubble chambers
[NASA-TT-20232] 13 p1771 N88-20593

Study of mean free path effects on growth of ultrafine metallic aerosols
[AD-A190206] 15 p2039 N88-22149

Vapor phase deposition and growth of polyimide films on copper
[AD-A189969] 15 p2044 N88-22178

The growth potential of corona discharges from aircraft flying in precipitation
[AD-A190507] 15 p2094 N88-22478

Mechanics of instability-related delimination growth
[NASA-TM-100622] 17 p2349 N88-23998

Biological patterns of growth in postnatal ontogenesis of lower primates 19 p2705 N88-26087

Growth and differentiation of Bacillus subtilis under microgravity conditions 22 p3060 N88-28158

The Paramecium experiment --- Spacelab D1 mission
22 p3060 N88-28161

Lattice-matched HgZnTe epitaxy development
[AD-A193677] 23 p3292 N88-29600

Growth of continental crust: Clues from Nd isotopes and Nb-Th relationships in mantle-derived magmas
24 p3393 N88-30205

GRUMMAN AIRCRAFT
NT F-14 AIRCRAFT
NT F-111 AIRCRAFT
NT OV-1 AIRCRAFT

GRUMMAN OV-1C AIRCRAFT
U OV-1 AIRCRAFT

GUANIDINES

The 1,2,3-triaminoguanidinium nitrate: An alternate explanation of the nitrate anion disorder
[AD-A188386] 12 p1612 N88-19640

Discovery of a low temperature form of TAGN (Triaminoguanidinium Nitrate)
[AD-A196059] 24 p3357 N88-29989

GUARDS (SHIELDS)

Trailer shield assembly for a welding torch
[NASA-CASE-MFS-29260-1] 18 p2524 N88-24972

GUIDANCE (MOTION)
NT AIRCRAFT GUIDANCE
NT COMMAND GUIDANCE
NT INERTIAL GUIDANCE
NT LASER GUIDANCE
NT MAP MATCHING GUIDANCE
NT MIDCOURSE GUIDANCE
NT RENDEZVOUS GUIDANCE
NT SPACECRAFT GUIDANCE
NT STRAPDOWN INERTIAL GUIDANCE
NT TERMINAL GUIDANCE

Fault tolerant considerations and methods for guidance and control systems
[AGARD-AG-289] 02 p0126 N88-10796

Guidance of high-altitude sounding rockets using the S19 and Spinning Rocket Altitude Control (SPINRAC) systems 08 p1034 N88-16273

Sounding rockets/microgravity products and service
08 p1035 N88-16277

Guidance and control of air-launched armaments: An aeroengineer's perspective 12 p1597 N88-19557

Terrestrial Propagation Characteristics in Modern Systems of Communications, Surveillance, Guidance and Control
[AGARD-CP-407] 12 p1614 N88-19653

Local free-space mapping and path guidance for mobile robots
[AD-A192970] 20 p2810 N88-26674

Approximations and implementations of nonlinear filtering schemes
[AD-A194685] 23 p3271 N88-29462

Stochastic game approach to guidance design
[AD-A194574] 23 p3276 N88-29498

GUIDANCE SENSORS

Fine attitude measurement system study. Volume 1: Executive summary
[BAE-TP-7831-VOL-1] 09 p1133 N88-16795

Fine attitude measurement system study, volume 2
[BAE-TP-7831-VOL-2] 09 p1133 N88-16796

Fine attitude measurement system study. Volume 3: Appendices
[BAE-TP-7831-VOL-3] 09 p1133 N88-16797

Advanced guidance algorithms for homing missiles with bearings-only measurements
[AD-A190435] 15 p2017 N88-22026

The optical accelerometer: A novel sensor for vertical flight guidance 18 p2518 N88-24935

GUIDE VANES
NT JET VANES

Test stand performance of a convertible engine for advanced V/STOL and rotorcraft propulsion
[NASA-TM-100211] 03 p0266 N88-11679

Possibilities for on-line surge suppression by fast guide vane adjustment in axial compressors
10 p1283 N88-17674

Experimental evaluation of turning vane designs for high-speed and coupled fan-drive corners of 0.1-scale model of NASA Lewis Research Center's proposed altitude wind tunnel
[NASA-TP-2681] 10 p1285 N88-17686

GULF OF ALASKA

North Pacific Ocean. Gulf of Alaska, R/V Thomas G. Thompson: 1 February - 8 March 1967. STD data report
[AD-A186569] 08 p1045 N88-16314

GULF OF CALIFORNIA (MEXICO)

The interpretation of crustal dynamics data in terms of plate motions and regional deformation near plate boundaries
[NASA-CR-181475] 03 p0349 N88-12205

Earthquake source mechanisms and transform fault tectonics in the Gulf of California
03 p0349 N88-12206

GULF OF MEXICO
Hurricane climatology for the Atlantic and Gulf coasts of the United States
[PB88-114657] 08 p1039 N88-16288

GULF STREAM
Study of evolution of Gulf Stream cyclinic eddy
06 p0727 N88-14473
Hydrochemical structure of Gulf Stream frontal zone waters 06 p0727 N88-14476
Estimates of ocean-atmosphere thermal interaction in Gulf Stream energy-active test range in winter of 1984
13 p1785 N88-20679
Phenomenological description of eddy registered in Gulf Stream 13 p1787 N88-20694
Studies toward observing and modelling large energetic ocean regions
[AD-A189267] 13 p1803 N88-20778
Application of acoustic-Doppler current profiler and expendable bathythermograph measurements to the study of the velocity structure and transport of the Gulf Stream
[NASA-CR-183188] 22 p3129 N88-28605

GULFS
NT GULF OF ALASKA
NT GULF OF CALIFORNIA (MEXICO)
NT GULF OF MEXICO

GUM VULCANIZATES
U VULCANIZED ELASTOMERS

GUMBEL THEORY
U RANGE (EXTREMES)

GUN LAUNCHERS
Effects of barrel joints on hypervelocity projectiles
[DE87-013447] 02 p0157 N88-10983
Reaming experiments for the lethality test system
[DE88-007902] 20 p2763 N88-26383

GUN PROPELLANTS
Thermoplastic elastomers as LOVA (Low Vulnerability Ammunition) binders
[AD-A184350] 04 p0419 N88-12599
High pressure strand burn rate tests of polyvinylnitrate/nitramine propellants
[AD-A184178] 04 p0422 N88-12615
Thermoplastic elastomers as LOVA binders
[AD-A185864] 07 p0835 N88-15067
Thermoplastic elastomers as LOVA binders
[AD-A185865] 07 p0835 N88-15068
Droplet formation for liquid monopropellant jets
[AD-A187172] 10 p1331 N88-17956
Continued studies on programmed-splitting stick propellant
[AD-A188987] 12 p1613 N88-19644
Electrical ignition of HAN-based liquid propellants
[AD-A191349] 18 p2495 N88-24801
Measurement of burning rates of NOSOL-363 propellants under cross-flow and strand burner conditions using real-time X-ray radiography
19 p2623 N88-25560
Burning rate measurements of Non-Newtonian Liquid Propellant (NNLP) 19 p2623 N88-25561
Gas phase combustion chemistry of nitramine propellants
[AD-A195082] 24 p3344 N88-29902
Flamespreading processes in obliquely loaded stick propellant beds
[AD-A195081] 24 p3352 N88-29956

GUN TURRETS
A piloted simulation investigating handling qualities and performance requirements of a single-pilot helicopter in air combat employing a helmet-driven turreted gun
[AD-A186878] 09 p1116 N88-16689

GUNFIRE
Analysis of a series of electromagnetic launcher firings
[AR-005-131] 04 p0405 N88-12516
Efficiency aspects of short, low velocity railguns
[AR-004-847] 04 p0405 N88-12517

GUNN DIODES
NT TRANSFERRED ELECTRON DEVICES
Focused ion beam fabrication of graded channel FETs in GaAs and Si
[AD-A193098] 21 p2936 N88-27439

GUNPOWDER
U GUN PROPELLANTS

GUNS (ORDNANCE)
NT ARTILLERY
The LLNL 150-mm equation-of-state gun system
[DE88-000423] 04 p0405 N88-12519
A piloted simulation investigating handling qualities and performance requirements of a single-pilot helicopter in air combat employing a helmet-driven turreted gun
[AD-A186878] 09 p1116 N88-16689
Hydrogen embrittlement of gun steel
[AD-A188972] 13 p1740 N88-20407
Preliminary measurements of heat flux in a subsonic gun simulator
[AD-A191090] 16 p2208 N88-23178
An interferometric measurement technique for railgun structures
[AD-A192851] 21 p2901 N88-27217
Combustion diagnostics of propellant with new grain geometries
[AD-A194944] 24 p3342 N88-29895

GUST ALLEVIATORS
Design of an integrated control system for flutter margin augmentation and gust load alleviation, tested on a dynamic windtunnel model
[PB88-149865] 15 p2020 N88-22038
The Flight of Flexible Aircraft in Turbulence: State-of-the-Art in the Description and Modelling of Atmospheric Turbulence
[AGARD-R-734-ADD] 24 p3311 N88-29717
A review of measured gust responses in the light of modern analysis methods 24 p3312 N88-29724
Measurement and analysis of low altitude atmospheric turbulence obtained using a specially instrumented Gnat aircraft 24 p3313 N88-29728

GUST LOADS
Flutter suppression and gust load alleviation. Part 1: Results of phase 1 to 3. Part 2: Description of the Garteur model
[MBB/LKE-292/S/PUB/181] 01 p0007 N88-10038
Acquisition of gust statistics from Aircraft Integrated Data Systems (AIDS) recorded data
[NLR-MP-86048-U-ISS-2] 06 p0745 N88-14586
Turbulence structure during high wind
08 p1014 N88-16149
Extrapolation of extremum values of the wind velocity
08 p1015 N88-16150
Maximum dynamic responses using matched filter theory and random process theory
[NASA-TM-100653] 22 p3042 N88-28059
Current and proposed gust criteria and analysis methods: An FAA overview 24 p3311 N88-29718
Comparison of the influence of different gust models on structural design 24 p3312 N88-29722
A review of measured gust responses in the light of modern analysis methods 24 p3312 N88-29724
The Flight of Flexible Aircraft in Turbulence: State-of-the-Art in the Description and Modelling of Atmospheric Turbulence
[AGARD-R-734] 24 p3312 N88-29725
An interim comparison of operational CG records in turbulence on small and large civil aircraft
24 p3313 N88-29729
Acquisition of gust statistics from AIDS-recorded data
24 p3313 N88-29733
Extreme gusts distribution 24 p3314 N88-29734

GUSTS
Analyses and assessments of span wise gust gradient data from NASA B-57B aircraft
[NASA-CR-178288] 01 p0002 N88-10007
Status of FAA terminal Doppler weather radar programs 10 p1275 N88-17632
Development and testing of the gust front algorithm
[AD-A189722] 14 p1949 N88-21622
Matching P.S.D.: Design loads
24 p3312 N88-29720
A summary of methods for establishing airframe design loads from continuous gust design criteria
24 p3312 N88-29721
An interim comparison of operational CG records in turbulence on small and large civil aircraft
24 p3313 N88-29729
Re-assessment of gust statistics using CAADRP data
24 p3313 N88-29732

GUT
U GRAND UNIFIED THEORY

GUY WIRES
The effect of mass, wind angle and erection technique on the aeroelastic behaviour of a cable-stayed bridge model
[NAE-AN-46] 04 p0455 N88-12819

GYMNASTICS
U PHYSICAL EXERCISE

GYRATION
NT COROTATION
NT COUNTER ROTATION
NT EARTH ROTATION
NT MOLECULAR ROTATION
NT MUON SPIN ROTATION
NT PRECESSION
NT QUENCHING (ATOMIC PHYSICS)
NT REVOLVING
NT ROTATION
NT SATELLITE ROTATION
NT SOLAR ROTATION
NT STELLAR ROTATION

GYRATORS
NT MICROWAVE FILTERS

GYRES
Current velocity and hydrographic observations in the Straits of Florida, the Caribbean Sea and offshore of the Antillean Archipelago: Subtropical Atlantic climate studies (STACS) 1984 and 1985
[PB88-149299] 12 p1649 N88-19874
The WOCE Core Project Planning Meeting on the Gyre Dynamics Experiment --- ocean dynamics
[WCP-139] 16 p2236 N88-23359

GYROFREQUENCY
On the role of the ionization frequency to gyrofrequency ratio in the critical ionization velocity interaction
[TRITA-EPP-86-10] 10 p1410 N88-18414

GYROMAGNETISM
NT GYROFREQUENCY

GYROPLANES
U HELICOPTERS

GYROS
U GYROSCOPES

GYROSCOPE FLUIDS
Equation of gravitational-gyroscopic waves: Angular potential and its applications 08 p1079 N88-16504

GYROSCOPES
NT ATTITUDE GYROS
NT CONTROL MOMENT GYROSCOPES
NT GYROSTABILIZERS
NT LASER GYROSCOPES
NT OPTICAL GYROSCOPES
NT TUNING FORK GYROSCOPES
Contribution to the dynamical analysis of rheolinear nonconservative, gyroscopic systems using finite element methods
[ETN-87-90410] 01 p0050 N88-10320
A 1987 progress report of manufacturing techniques for Gravity Probe B gyroscope rotors
[NASA-TM-100312] 02 p0176 N88-11101
A conceptual design of an inertial navigation system for an autonomous submersible testbed vehicle
[AD-A188038] 11 p1438 N88-18578
Thirteenth Biennial Guidance Test Symposium, volume 1
[AD-A185782] 12 p1576 N88-19427
Robotics applications in the testing of inertial sensors
12 p1577 N88-19433
The optimum solution to instrument quantization effects 12 p1577 N88-19434
Rate and dynamic tests on the Canadian Strapdown Gyroscope (CSG-2) 12 p1578 N88-19439
The German Honeywell ring laser gyro: Development and test results 12 p1578 N88-19440
Advances in Air-Launched Weapon Guidance and Control
[AGARD-CP-431] 12 p1596 N88-19553
A prototype fibre optic gyroscope for missile guidance applications 12 p1596 N88-19554
A fiber optic gyro strapdown reference system for guided weapons 12 p1597 N88-19560
Laser gyro attitude control system feasibility
[AD-A189368] 13 p1720 N88-20285
Application of the Single-Axis rate Table (SAT) of the DFVLR for the evaluation of stationary and dynamic gyro properties
[DFVLR-MITT-88-09] 21 p2952 N88-27533
The anatomy of the gyroscope
[AGARD-AG-313] 22 p3079 N88-28287

GYROSCOPIC DRIFT
U GYROSCOPES
U GYROSCOPIC STABILITY

GYROSCOPIC STABILITY
A comparison between theory and experiment for the yaw moment induced by a loose internal part
[AD-A187053] 09 p1131 N88-16787
An analysis of DREO's (Defence Research Establishment Ottawa) analog rebalance loops for the CSG-2 (Canadian Strapdown Gyroscope) tuned-rotor gyroscope
[AD-A188577] 12 p1629 N88-19749
What is the maximum length of a spin stabilized projectile
[PB88-130919] 13 p1728 N88-20336
Application of the Single-Axis rate Table (SAT) of the DFVLR for the evaluation of stationary and dynamic gyro properties
[DFVLR-MITT-88-09] 21 p2952 N88-27533

GYROSTABILIZERS
Gyrostabilizer system of Kvant module
08 p1006 N88-18099

GYROSTATS
U GYROSCOPES

GYROTRONS
U CYCLOTRON RESONANCE DEVICES

H

H ALPHA LINE
Contemporaneous B,V,R,I photometry and H alpha spectroscopy of YY Gem 04 p0513 N88-13155
Sensitivity of the H alpha line to expansion, geometrical extent and temperature gradient in the G and K supergiant chromospheres 04 p0514 N88-13159

H BETA LINE
The astrophysics of nebulae and active galactic nuclear emission-line regions: New methods and applications
13 p1858 N88-21111

H II REGIONS
High spatial resolution observations of dust and gas in NGC 7027 and the M8 Hourglass
06 p0801 N88-14903
Models of recombination lines in radio H2 regions
[INPE-4302-TDL/277] 12 p1710 N88-20232
Narrow-band photographic observations of the HII Region S296 in Canis Major 16 p2288 N88-23696

H LINES
NT H ALPHA LINE
NT H BETA LINE
Experimental study of the role of plasma polarization on line shape in dense laboratory plasmas
[ETN-88-92001] 13 p1844 N88-21033
Density diagnostics by hydrogen line intensity ratios: Excitation cross section between excited states
17 p2441 N88-24522

H WAVES
Input-output characterization of fiber composites by SH waves
[NASA-CR-4153] 17 p2347 N88-23986

HABITABILITY
Disturbance and recovery of Arctic Alaskan tundra terrain. A review of recent investigations
[AD-A184442] 04 p0467 N88-12887
Space station group activities habitability module study: A synopsis 12 p1651 N88-19886
Space station habitability recommendations based on a systematic comparative analysis of analogous conditions
[NASA-CR-3943] 18 p2587 N88-25372
Proceedings of the Colloquium on Space and Sea
[ESA-SP-280] 19 p2695 N88-26016
Habitability of the Space Station: From vehicle to living space 19 p2697 N88-26033
Recent research on crew wardroom habitability for the Space Station 19 p2698 N88-26039

HABITATS
Compilation of 1986 annual reports of the Navy ELF (Extremely Low Frequency) communications system ecological monitoring program, volume 2
[AD-A184562] 03 p0306 N88-11931
Compilation of 1986 annual reports of the Navy ELF (Extremely Low Frequency) communications system ecological monitoring program, volume 3
[AD-A184563] 03 p0306 N88-11932
Preliminary analysis of an integrated logistics system for OSSA payloads. Volume 4: Supportability analysis of the 1.8m centrifuge 12 p1584 N88-19481
Research on enhancing the utilization of digital multispectral data and geographic information systems in global habitability studies
[NASA-CR-182799] 17 p2368 N88-24101

HABITS
Dietary factors related to physical fitness
[AD-A190272] 15 p2103 N88-22527

HADRONS
NT BARYONS
NT KAONS
NT MESONS
NT MUONS
Parton densities from deep inelastic scattering to hadronic processes at super collider energies
[NOTA-INTERNA-885] 07 p0930 N88-15646
The high resolution spaghetti hadron calorimeter
[NIKHEF-H/87-7] 08 p0990 N88-15993
Primordial nucleosynthesis during the keV era
[DE88-002233] 08 p1104 N88-16623
Hadron-quark phase transition in dense stars
[DE88-003412] 10 p1429 N88-18532
High resolution hadron calorimetry
[NIKHEF-H/87-8] 13 p1773 N88-20605
Energy loss of particles in dense matter-calorimetry
[NIKHEF-H/87-12] 13 p1836 N88-20988
Hadronic overlap and total multiplicity distributions in high energy physics collisions
[NIKHEF-H/87-10] 13 p1838 N88-21001
Gluino branching ratio effects on the search for supersymmetry
[PREPRINT-572] 14 p1981 N88-21821
Analysis of hadron production in deep inelastic muon-proton collisions through the fire-string model
[PREPRINT-578] 14 p1981 N88-21822
Lattice QCD calculation of K yields pi nonleptonic weak transition and other hadronic weak parameters
[PREPRINT-580] 15 p2132 N88-22717
Quark core stars, quark stars and strange stars
[DE88-006991] 17 p2450 N88-24555
Experimental elementary particle physics
[DE88-007510] 18 p2572 N88-25274
Production of pi(0) mesons and charged hadrons in nu bar neon and nu neon charges current interactions
[MPI-PAE/EXP.EL.168] 22 p3150 N88-28743
Hadrons produced in atmospheric interactions
[DE88-702492] 23 p3309 N88-29712

HAFNIUM
Hafnia-rich mixed oxide ceramics of the system HfO2-ZrO2-TiO2 for heaters and heat exchangers in electrothermal thrusters: The effects of titania on selected electrical and mechanical properties of Hafnia-rich mixed oxides in the system Hafnia-Zirconia-Titania, volume 1
[NASA-CR-182800-VOL-1] 15 p2047 N88-22197

HAFNIUM COMPOUNDS
NT HAFNIUM OXIDES
Metal intercalation characteristics of n-HfS2 photoelectrodes in non-aqueous electrolytes
[AD-A184381] 03 p0383 N88-12407

HAFNIUM OXIDES
On 1064 nm and 350 nm laser damage thresholds of high index oxide films deposited from organic solutions and sols
[DE88-001636] 07 p0659 N88-15217

HAILSTORMS
The studies of physical models on hailstorms and their applications in nowcasting 02 p0207 N88-11300

HAIR
Local human skin potential: Spatial distribution, magnitude and origin
[DE87-012882] 01 p0075 N88-10480

HALF PLANES
Path integration on the upper half-plane
[DE88-751050] 12 p1682 N88-20057
Complex space monofilar approximation of diffraction currents on a conducting half plane
[NASA-CR-182883] 16 p2273 N88-23605

HALF SPACES
Electromagnetic scattering by a thick strip on a half-space
[PB87-227096] 03 p0306 N88-11928
A finite-amplitude analysis of the buoyant instability of a highly viscous film over a less viscous half-space
13 p1769 N88-20581
Exact image theory for the problem of dielectric/magnetic slab
[NASA-CR-182865] 16 p2189 N88-23055

HALIDES
NT ALUMINUM FLUORIDES
NT BORON CHLORIDES
NT BROMIDES
NT CALCIUM FLUORIDES
NT CESIUM IODIDES
NT CHLORIDES
NT CHLORINE FLUORIDES
NT COPPER CHLORIDES
NT DICHLORIDES
NT FLUORIDES
NT HYDROCHLORIC ACID
NT HYDROFLUORIC ACID
NT HYDROGEN CHLORIDES
NT LITHIUM CHLORIDES
NT LITHIUM FLUORIDES
NT MAGNESIUM CHLORIDES
NT METAL HALIDES
NT NITROGEN FLUORIDES
NT POTASSIUM BROMIDES
NT SILVER CHLORIDES
NT SILVER IODIDES
NT SODIUM CHLORIDES
NT SODIUM FLUORIDES
NT SULFUR FLUORIDES
NT URANIUM FLUORIDES
Evaluation and compilation of thermodynamic properties of high temperature chemical species
[AD-A187509] 11 p1452 N88-18654
Rare Gas Halide (RGH) kinetics
[AD-A192352] 20 p2770 N88-26425

HALL COEFFICIENT
U HALL EFFECT

HALL CURRENTS
U ELECTRIC CURRENT
U HALL EFFECT

HALL EFFECT
Complex scattering dynamics and the integer quantum Hall effect
[DE87-011790] 02 p0243 N88-11536
High pressure electronic transport in semiconductors
[AD-A187428] 11 p1555 N88-19308
Electrical characteristics of MBE (Molecular Beam Epitaxyl)-grown GaAs/sub 1-x/Sb/sub x on InP and correlation with film microstructure
[DE88-003841] 13 p1847 N88-21053
First report on InGaAs hall device
14 p1903 N88-21372
Electrical anisotropy of layered semiconductor ZrSe2
16 p2257 N88-23488
A nuclear powered space based multimegawatt MHD disc power system 17 p2432 N88-24471
Quantum transport in an electron waveguide
20 p2864 N88-27010
Thermal conductivity of isotopically pure semiconductors, superlattices, semiconductor alloys and semiconductors as a function of temperature; control of the segregation coefficient in LEC crystal growth; and photo-Hall measurements of GaAs
21 p2927 N88-27375
DARPA-URI consortium meetings on submicron heterostructures of diluted magnetic semiconductors
[AD-A193499] 23 p3206 N88-29081
Temperature dependence of conductivity and of Hall coefficients for noble metal films
[ETN-88-92981] 23 p3294 N88-29616

HALLEY'S COMET
Final phase of Project Vega 01 p0009 N88-10053
Overview of plasma observations during the Halley flybys 01 p0116 N88-10743
The status of the international Halley watch
01 p0116 N88-10744
Large-scale interaction of the solar wind with comets Halley and Giacobini-Zinner 01 p0117 N88-10745
Solar wind-cometary interaction at the ionopause and associated phenomena 01 p0117 N88-10748
Solar wind effects on the outer ion coma of Comet Halley 01 p0117 N88-10750
Plasma-tail activity and the interplanetary medium at Halley's Comet during Armada Week, 6-14 March 1986
01 p0118 N88-10752
Occultation of compact radio sources by the ion tail of Halley's Comet 01 p0118 N88-10753
Space missions to Comets Halley and Giacobini-Zinner 03 p0272 N88-11712
Comparative analysis of ultraviolet observations of Halley's comet on ASTRON astrophysical station before and after perihelion 08 p1004 N88-16086
Some ground-based optical observations of Comet Halley during its post-perihelion passage
08 p1033 N88-16259
Giotto: A mission to Halley's Comet
09 p1127 N88-16756
JPRS report: Science and technology. USSR: Space
[JPRS-USP-88-002] 13 p1724 N88-20312
Vega-1 and Vega-2 automatic stations: Functioning of landing modules in Venusian atmosphere
13 p1725 N88-20313
Vega-1 and Vega-2 automatic stations: Functioning of flyby vehicles during encounter with Halley's comet
13 p1725 N88-20314
Some periodicities in motion of Halley's Comet relative to center of mass 13 p1726 N88-20324
Results of infrared spectrometer experiment. 1: Infrared radiation of parent molecules in Halley's Comet
13 p1726 N88-20325
Results of infrared spectrometer experiment. 2: Infrared radiometry of nucleus of Halley's Comet
13 p1727 N88-20326
Analysis of hydrocarbon band 3.35 in spectrum of Halley's Comet using data from infrared spectrometer on Vega-1 spacecraft 13 p1727 N88-20327
How typical is Halley's Comet?
14 p1994 N88-21886
Solar wind observation at the time of closest encounter with Comet Halley 14 p1995 N88-21890
Variability of Comet Halley's coma: VEGA-1 and VEGA-2 magnetic field observations 14 p1995 N88-21891
Calculation of the shape of the contact surface at Comet Halley 14 p1995 N88-21892
The foreshock region upstream from the Comet Halley bow shock 14 p1995 N88-21893
Physical processes in the vicinity of the cometopause interpreted on the basis of plasma, magnetic field and plasma wave data measured on board VEGA-2 spacecraft --- Halley's comet 14 p1996 N88-21894
Some new features of plasma wave phenomena at Halley: APV-N observations --- VEGA
14 p1996 N88-21895
A comparison between wave observations performed in the environments of Comets Halley and Giacobini-Zinner 14 p1996 N88-21896
Correlation between magnetic and electric field fluctuations observed during flyby near Halley's comet
14 p1996 N88-21897
Magnetic cavity formation at Comet Halley and at the AMPTE Li release 14 p1996 N88-21898

Plasma phenomena in the vicinity of the closest approach of VEGA-1, 2 spacecraft to the Comet Halley nucleus 14 p1996 N88-21899
Energy spectra of pick-up ions recorded during the encounter of Giotto with Comet Halley 14 p1997 N88-21901
Stochastic acceleration of cometary ions: The effects of composition and source strength distributions 14 p1997 N88-21902
Observation of energetic particles (E greater than 30 keV) by the Giotto experiment EPA in the magnetic cavity of Comet Halley 14 p1997 N88-21903
Evidence for first polymer in Comet Halley: Polyoxymethylene 14 p1997 N88-21906
Photometry of P/Halley (1982i): Is what we have learned useful for other comets? 14 p1998 N88-21909
Water vapor and hydroxyl distributions in the inner coma of Comet Halley measured by the VEGA-2 three channel spectrometer TKS 14 p1998 N88-21910
CCD-observations of gas and dust jets in the coma of Comet Halley 14 p1998 N88-21912
Spatial distribution of O(supra 1D) from Comet Halley 14 p1999 N88-21913
Distribution of neutral gas molecules at large distances from Halley's comet 14 p1999 N88-21914
Halley's environments by the Japanese Suisei spacecraft 14 p1999 N88-21915
Recent observations of the OH radio lines in comets 14 p1999 N88-21917
A model of the anisotropic structure of the neutral gas coma of a comet 14 p1999 N88-21918
Profiles of the major gas emissions and distribution of dust particles in the inner coma (0 to 10,000 km) of Comet Halley 14 p1999 N88-21919
Analysis of the coma outburst of Comet Halley, March 24 to 25 (UT), 1986 14 p2000 N88-21920
Dust coma morphology of Comet Halley during the Giotto encounter 14 p2000 N88-21921
Cometary MHD and chemistry: Application to Halley 14 p2000 N88-21922
Objective-prism spectra of the Comets Honda (1968 e), Hartley-Good (1985 l) and Halley 14 p2000 N88-21924
Color fluctuations in the inner coma of Comet Halley as measured from VEGA-2 14 p2000 N88-21925
New properties of cometary dust 14 p2001 N88-21926
Comet P/Halley's near-nucleus jet activity 14 p2001 N88-21929
Dust photometry in the near nucleus region of Comet Halley from VEGA-2 observations 14 p2001 N88-21930
Dynamics of charged submicron grains in Halley's coma 14 p2001 N88-21931
Composition of cometary dust particles --- Halley 14 p2001 N88-21932
Isotopic composition of Halley dust 14 p2002 N88-21933
On the interpretation of the 3 micron emission feature in the spectrum of Comet Halley: Abundances in Comet Halley and in interstellar matter 14 p2002 N88-21935
P/Halley dust coma: Grains or rocks? 14 p2002 N88-21936
The origin of low mass particles within and beyond the dust coma envelopes of Comet Halley 14 p2002 N88-21938
Optical and hydrodynamic implications of Comet Halley dust size distribution 14 p2003 N88-21939
Cometary grains and interplanetary dust: A polarimetric sensing --- Halley 14 p2003 N88-21941
The dust around the nucleus of Comet Halley 14 p2003 N88-21942
Variation of grain properties at the dust outbursts --- Halley's comet 14 p2003 N88-21943
On orbits and association of meteor streams with Comets P/Halley and P/Encke 14 p2003 N88-21945
The evolution of the mass distribution of cometary particles 14 p2004 N88-21946
The nucleus of Comet Halley 14 p2004 N88-21947
Comparison of active regions on the nucleus of Comet Halley 14 p2004 N88-21948
Reconstruction of the orientation and shape of the nucleus of Comet Halley 14 p2004 N88-21949
Properties of the nucleus of P/Halley 14 p2004 N88-21952
Plasma tail of Comet Halley in January 1986 14 p2006 N88-21960
The evolution of CN emission in Halley's comet with heliocentric distance 14 p2006 N88-21961
Study of the ionic and neutral species in the coma of Comet Halley with an image intensifier camera 14 p2006 N88-21962
Determination of the content of CO(+) and H2O(+) ions in the tail of Comet Giacobini-Zinner and Comet Halley 14 p2006 N88-21964
Comparison of Halley's monochromatic comae with others 14 p2006 N88-21965
P/Halley activity in November 1985 14 p2006 N88-21966
Outburst of Halley's comet 14 p2007 N88-21967
Comet P/Halley: Visual magnitude estimates and gas production 14 p2007 N88-21968
Spectrophotometric observations of Comet Halley 14 p2007 N88-21972
Nature of Comet Halley's organic grains inferred from infrared spectra 14 p2007 N88-21973
The dust tail of Comet Halley 14 p2008 N88-21974
The structure of the Halley meteor stream and the orbital history of the comet 14 p2008 N88-21975
On the periodic southward jets of Comet Halley before perihelion passage 14 p2008 N88-21978
Dust tail streamers and Halley's nucleus rotation 14 p2008 N88-21979
Near-infrared imaging of Comet Halley: Discovery of a color gradient in the inner coma 14 p2009 N88-21980
Laboratory amorphous carbon: A possible analog of cometary dust 14 p2009 N88-21981
Linear and circular polarization of Comet Halley light 14 p2009 N88-21982
Image processing on VEGA pictures 14 p2009 N88-21983
The light curve of P/Halley and the rotation of its nucleus 14 p2009 N88-21984
Temperature of the nucleus of Comet Halley 14 p2009 N88-21985
Consequences of the size determination of P/Halley by space probes on the scale of sizes of cometary nuclei 14 p2009 N88-21986
The splitting of Comet Halley 1986 14 p2010 N88-21989
Three approaches to the modeling of Comet Halley's motion over long periods of time 14 p2010 N88-21992
Memoirs of the Faculty of Science, Kyoto University. Series of Physics, Astrophysics, Geophysics and Chemistry, volume 37, no. 2
[ISSN-0368-9689] 16 p2287 N88-23694
Dust and C2-contents in the coma of Halley's Comet (1986III) 16 p2288 N88-23697
The evolution of cometary activity 18 p2594 N88-25416
Processing and analysis of images transmitted by Vega space probes over Halley's comet
[ETN-88-92291] 20 p2885 N88-27131
A theoretical determination of the density at a traveling source that emitts particles
[ISAS-RN-351] 21 p3013 N88-27883

HALOCARBONS
NT CHLOROCARBONS
NT FLUOROCARBONS

HALOGEN COMPOUNDS
NT ALUMINUM FLUORIDES
NT AMMONIUM PERCHLORATES
NT BORON CHLORIDES
NT BROMIDES
NT BROMINE COMPOUNDS
NT CALCIUM FLUORIDES
NT CESIUM IODIDES
NT CHLORIDES
NT CHLORINE COMPOUNDS
NT CHLORINE FLUORIDES
NT CHLOROCARBONS
NT COPPER CHLORIDES
NT DICHLORIDES
NT DIFLUORO COMPOUNDS
NT FLUORIDES
NT FLUORINE COMPOUNDS
NT FLUORINE ORGANIC COMPOUNDS
NT FLUORO COMPOUNDS
NT FLUOROCARBONS
NT FLUOROHYDROCARBONS
NT FLUOROPOLYMERS
NT HALIDES
NT HYDROCHLORIC ACID
NT HYDROFLUORIC ACID
NT HYDROGEN CHLORIDES
NT IODIDES
NT LITHIUM CHLORIDES
NT LITHIUM FLUORIDES
NT LITHIUM IODATES
NT LITHIUM PERCHLORATES
NT MAGNESIUM CHLORIDES
NT METAL HALIDES
NT NITROGEN FLUORIDES
NT POLYTETRAFLUOROETHYLENE
NT POLYVINYL FLUORIDE
NT POTASSIUM BROMIDES
NT SILVER CHLORIDES
NT SILVER IODIDES
NT SODIUM CHLORIDES
NT SODIUM FLUORIDES
NT SULFUR FLUORIDES
NT TEFLON (TRADEMARK)
NT URANIUM FLUORIDES
Spectroscopy and energy transfer kinetics of the interhalogens
[AD-A192103] 18 p2583 N88-25344

HALOGENATION
NT BROMINATION
NT CHLORINATION
NT FLUORINATION
Measurement of vertical distributions of halogenated hydrocarbons in the stratosphere
[ETN-88-91065] 09 p1191 N88-17135

HALOGENS
NT BROMINE ISOTOPES
NT CHLORINE
NT FLUORINE
NT IODINE
NT IODINE ISOTOPES

HALOS
Experimental model of halo plasma observed in small-aspect FRC plasma
[INPE-4159-PRE/1061] 08 p1085 N88-16534
A global model for planetary nebulae, taking into account central stellar evolution and influence on halo ionization
[ETN-88-91491] 11 p1566 N88-19389

HAMILTON-JACOBI EQUATION
Fronts propagating with curvature dependent speed: Algorithms based on Hamilton-Jacobi formulations
[NASA-CR-178382] 01 p0077 N88-10495
Introduction to classical mechanics of systems with constraints, part 2
[DE88-701056] 13 p1849 N88-21072

HAMILTONIAN FUNCTIONS
A quantum theoretical study of polyimides
[NASA-CR-181495] 03 p0292 N88-11831
Equilibria, lattices and chaotic dynamics of point vortices 04 p0444 N88-12758
Recursion operator and bihamiltonian structure for integrable multi-dimensional lattices
[PREPRINT-552] 06 p0764 N88-14688
Normal form of a fully resonant Hamiltonian function
[PB88-100946] 06 p0767 N88-14711
A study to evaluate STS heads-up ascent trajectory performance employing a minimum-Hamiltonian optimization strategy
[NASA-TP-2793] 08 p0960 N88-15820
Coulomb interactions and effective strong coupling Hamiltonians in Cu-O superconductors
[DE88-002942] 08 p1090 N88-16561
The structure of the sideband spectrum in free electron lasers
[AD-A186952] 09 p1170 N88-17015
Hamiltonian approach to relativistic theory of gravity and to general relativity theory
[DE88-700404] 10 p1422 N88-18492
The Hamiltonian structure of nonlinear elasticity: The convective representation of solids, rods, and plates
[AD-A187200] 11 p1498 N88-18943
Systems near the onset and in the well-developed regimes of turbulence
[DE88-005365] 13 p1766 N88-20565
Hamiltonian description of the interaction of surface waves with mixed-layer currents 13 p1806 N88-20799
Stochasticity in nonlinear Hamiltonian systems
[DE88-005499] 13 p1826 N88-20915
Introduction to classical mechanics of systems with constraints, part 2
[DE88-701056] 13 p1849 N88-21072
The biHamiltonian formulations of integrable evolution equations in multidimensions
[PREPRINT-568] 14 p1968 N88-21745
Mixing coefficients of the lattice weak Hamiltonian with dimension five operators
[PREPRINT-576] 14 p1968 N88-21749
Periodic orbits around a satellite modelled as a triaxial ellipsoid
[AD-A190592] 15 p2022 N88-22051
Geometric methods and the gauge structure of Berry's phase
[DE88-006538] 15 p2127 N88-22682
Quantization of axial electrodynamics
[DE88-701498] 15 p2147 N88-22813
Hamiltonian formalism in the model of the relativistic string with rigidity
[DE88-701503] 15 p2147 N88-22815
Integrability of fermionic string in superfluid Hamiltonian approach
[DE88-701662] 16 p2284 N88-23678

Existence of periodic solutions in n-dimensional retarded functional differential equations
[RR-325] 17 p2392 N88-24221

Non-effective-mass matching in superlattices
20 p2872 N88-27049

Finitely many delta-interactions with supports on concentric spheres
[DE88-701834] 20 p2880 N88-27101

A minimax method for a class of Hamiltonian systems with singular potentials
[AD-A193478] 23 p3270 N88-29453

Periodic solutions of perturbed superquadratic Hamiltonian systems
[AD-A194292] 23 p3270 N88-29457

On the periodic nonlinearity and the multiplicity of solutions
[AD-A194295] 23 p3270 N88-29459

Bifurcations of periodic solutions of non-integrable Hamiltonians with two degrees of freedom: Numerical and analytical results
[DE88-702747] 23 p3272 N88-29473

HAMMERS

Size-reduction and sorting behavior in sieve hammer mills
[ETN-88-91480] 11 p1467 N88-18749

HAND (ANATOMY)

NT FINGERS

Design, development and evaluation of Stanford/Ames EVA prehensors
[NASA-CR-182688] 15 p2105 N88-22540

A standard architecture for controlling robots
[AD-A195929] 24 p3423 N88-30371

HANDBOOKS

NT USER MANUALS (COMPUTER PROGRAMS)

Middle Atmosphere Program: Handbook for MAP, volume 24
[NASA-CR-181451] 01 p0069 N88-10444

Uniform laws and regulations as adopted by the National Conference on Weights and Measures (72nd), 1987
[PB88-123724] 06 p0689 N88-14225

Development of Soviet state ergonomic standards (GOST)
[AD-A185536] 07 p0899 N88-15449

Evaluation and compilation of thermodynamic properties of high temperature chemical species
[AD-A187509] 11 p1452 N88-18654

Air traffic control
[FAA-ORDER-7110.65E] 12 p1576 N88-19426

MANPRINT handbook for RFP (Request For Proposal) development
[AD-A188321] 13 p1850 N88-21075

The official handbook of MASCOT, version 3.1, issue 1 --- software tool
[BR103975] 16 p2246 N88-23419

Soviet space program handbook
[AD-A194332] 22 p3046 N88-28077

HANDICAPS

Ergonomics of car controls for disabled people, phase 1. Part 1: Chapters 1-7. Part 2: Appendices. Part 3: References
[ISBN-0-947767-82-7] 09 p1202 N88-17204

HANDLEY PAGE AIRCRAFT

Sound transmission through the walls of light aircraft: An investigation of structure-borne noise in a Handley Page 137 Jetstream 3 aircraft
[NASA-CR-182509] 10 p1405 N88-18376

HANDLING EQUIPMENT

NT CRANES
NT GANTRY CRANES

Human factors in robotic system design discussed
02 p0158 N88-10988

Tether Elevator Crawler Systems (TECS)
07 p0927 N88-15631

HANDLING QUALITIES

U CONTROLLABILITY

HANGARS

Investigation of the nature and concentration of vapor and mist during the cleaning of aircraft
[PML-1985-29] 05 p0623 N88-13817

HANKEL FUNCTIONS

Incomplete Lipschitz-Hankel integrals of MacDonald functions
[AD-A191034] 16 p2261 N88-23515

HARDENING

The effects of thin anodic films on the cyclic microstrain/macrostrain behavior of tungsten
05 p0597 N88-13650

Study of the characteristic curve of hardening and softening during low-cycle fatigue process
06 p0719 N88-14414

Laser transformation hardening of precision V-slide way
[PB87-144028] 08 p0991 N88-15999

HARDENING (MATERIALS)

NT CARBURIZING
NT HOT ISOSTATIC PRESSING
NT HOT PRESSING
NT NITRIDING
NT PRECIPITATION HARDENING
NT PULSE HEATING
NT STRAIN HARDENING
NT WORK HARDENING

An expert system for materials design
[DE88-000191] 04 p0483 N88-12974

Master plots for predicting the case-depth in laser surface treatments
[PB87-221875] 05 p0586 N88-13574

Influence of microstructure and aging condition on the fatigue crack propagation in age hardened aluminium alloys 05 p0599 N88-13659

Analysis of stable crack growth with isotropic and kinematic hardening
[PB87-144911] 07 p0868 N88-15266

Nonlinear line-spring model for surface crack analysis with particular reference to work hardening materials
[PB87-144838] 08 p0994 N88-16016

Nondestructive magnetic testing of laser hardening parameters (hardening depth, hardness profile, retained austenite)
[ETN-88-91070] 09 p1144 N88-16857

Evolution of hardening and damage during viscoplastic deformation
[AD-A190714] 15 p2077 N88-22381

Disclination structures in carbon and graphite
[AD-A191056] 17 p2322 N88-23868

Theory of viscoplasticity based on overstress with applications 18 p2529 N88-25007

Development of fine-grained carbide-particle hardened Hadfield manganese steels
[DE88-008919] 19 p2617 N88-25523

Surface fatigue life of CBN and vitreous ground carburized and hardened AISI 9310 spur gears
[NASA-TM-100960] 19 p2677 N88-25916

HARDENING (SYSTEMS)

The electromagnetic threat to future avionic systems
17 p2305 N88-23790

Shielding effectiveness of metallic joints versus corrosion prevention 22 p3054 N88-28120

HARDNESS

NT MICROHARDNESS

Investigation of the structure of coatings of self fluxing alloys fused by laser energy
[BLL-M-37301-(5828.4)] 02 p0148 N88-10930

Ion plating: Fundamental processing studies and synthesis of high performance coatings
[AD-A184766] 03 p0303 N88-11908

Weldability of 2219-T851 and 2519-T87 aluminum armor alloys for use in Army vehicle systems
[AD-A184296] 04 p0451 N88-12792

Analysis of load-bearing capacity of nitrided layer
[PB87-144176] 08 p0968 N88-15857

Response of aluminum alloys to erosive particle impacts
[DE88-005910] 15 p2041 N88-22159

Hydrogen embrittlement susceptibility of high strength ESR 4340 steel alloys for ballistically resistant/tolerant components 17 p2319 N88-23848

Initial development of high-temperature titanium silicide alloys
[DE88-007860] 20 p2772 N88-26437

Study of the friction and wear-related properties of ceramic superconductors
[DE88-011844] 21 p3024 N88-27950

HARDNESS TESTS

Critical cooling rates on solution treatment of Cu-Cr and Cu-Be alloys
[NASA-TT-20163] 18 p2488 N88-24760

HARDWARE

Hardware fault insertion and instrumentation system: Mechanization and validation
[NASA-CR-181445] 01 p0078 N88-10497

Experimental assembly of structures in EVA: Hardware morphology and development issues
02 p0139 N88-10872

Access flight hardware design and development
02 p0139 N88-10873

The development of ODE methods: A symbiosis between hardware and numerical analysis
[DE87-014925] 03 p0370 N88-12325

Plant Growth Module (PGM) conceptual design
05 p0631 N88-13855

Benchmarking and evaluation of hardware description languages for design of VLSI systems
[PB87-134557] 06 p0758 N88-14648

Virtual image processor: A prototype implementation
[AD-A185560] 06 p0758 N88-14652

Software-implemented fault insertion: An FTMP example
[NASA-CR-178423] 06 p0761 N88-14668

Major spacecraft hardware testing in Europe
09 p1125 N88-16740

Hardware/software reliability study --- space programs
[REPT-65.5686] 09 p1218 N88-17307

An applicative programmer's approach to matrix algebra, lessons for hardware and software
10 p1382 N88-18251

A programmable global system for the manipulation of residue numbers
[ETN-88-91476] 11 p1530 N88-19139

Computer architecture for efficient algorithmic executions in real-time systems: New technology for avionics systems and advanced space vehicles
[NASA-CR-182650] 12 p1675 N88-20016

Portability of software. The use of software in the hardware mixture
[MBB/LWD-11/S/PUB/253] 16 p2246 N88-23416

An application of the Bayesian method to the estimation and forecast of system hardware components MTBF
22 p3068 N88-28211

HARMONIC ANALYSIS

NT ZONAL HARMONICS

Wave group analysis based on Kimura's method
[AD-A187610] 11 p1516 N88-19055

Comparisons of global topographic/isostatic models to the Earth's observed gravity field
[NASA-CR-182696] 13 p1798 N88-20752

HARMONIC CONTROL

Analytic investigation of helicopter rotor blade appended aeroelastic devices
[NASA-CR-166525] 03 p0266 N88-11676

Investigations on higher harmonic blade pitch control at helicopters
[DFVLR-FB-87-36] 14 p1868 N88-21165

Dual adaptive control: Design principles and applications
[NASA-CR-177485] 22 p3038 N88-28038

HARMONIC EXCITATION

A system identification technique based on the random decrement signatures. Part 1: Theory and simulation
05 p0594 N88-13625

A system identification technique based on the random decrement signatures. Part 2: Experimental results
05 p0594 N88-13626

Dynamic analysis of a structure with sliding base
08 p0998 N88-16045

Experimental and theoretical study on cavitation inception and bubbly flow dynamics. Part 1: Design, development and operation of a cavitation susceptibility meter. Part 2: Linearized dynamics of bubbly and cavitating flows with bubble dynamics effects
[AD-A187133] 09 p1160 N88-16952

Dynamic response of a geared train of rotors subjected to random support excitations 09 p1181 N88-17073

Harmonic and rectangular pulse reproduction through current transformers
[EUT-86-E-159] 14 p1907 N88-21395

HARMONIC GENERATIONS

Third-harmonic generation and multiphoton ionization spectroscopy
[DE87-013545] 03 p0281 N88-11769

Higher harmonic generation in the induced resonance electron cyclotron maser
[AD-A186236] 07 p0856 N88-15210

Enhancement of second harmonic generation on silver gratings by resonant excitation of surface plasmon
[ETN-88-92304] 17 p2439 N88-24509

HARMONIC GENERATORS

Coherent states for the damped harmonic oscillator
[AD-A186111] 07 p0922 N88-15599

Digital control of high frequency pulse-width modulated inverters
[ETN-87-90711] 09 p1157 N88-16936

Frequency doubling at 1.315 micrometers
[AD-A193902] 23 p3208 N88-29092

HARMONIC MOTION

Theory of laser cooling and spectroscopy of harmonically trapped single atoms
[AD-A189576] 13 p1775 N88-20617

HARMONIC OSCILLATION

On the pairing process in an excited, plane, turbulent mixing layer
[AD-A186[illegible]55] 07 p0850 N88-15157

A panel method based on velocity potential to compute harmonically oscillating lift surface systems
[ETN-88-91886] 15 p2061 N88-22290

Cascades with harmonically oscillating blades in supersonic flow
[NASA-TT-20323] 19 p2599 N88-25446

Off-boundary approach to the boundary element method
[AD-A192931] 20 p2815 N88-26701

HARMONIC OSCILLATORS

Visible free electron laser oscillator
[AD-A183871] 01 p0051 N88-10324

Coherent states for the damped harmonic oscillator
[AD-A186111] 07 p0922 N88-15599

Gigantic optical nonlinearity in low dimensional systems 14 p1975 N88-21786

Squeezed state in degenerate parametric amplification discussed by H. Takahasi in 1963
14 p1976 N88-21790

Thermo field dynamics and para statistical mechanics
[DE88-702057] 19 p2737 N88-26253

Research opportunities below 300 nm at the NBS Free-Electron Laser Facility
[AD-A193100] 21 p2953 N88-27538

HARMONICS

NT HARMONIC EXCITATION
NT HARMONIC GENERATIONS
NT HARMONIC OSCILLATION
NT SPHERICAL HARMONICS
NT SUPERHARMONICS
NT ZONAL HARMONICS

A deterministic approach to turbulence: Chaos in Rayleigh-Benard convection 03 p0313 N88-11975

A study of rotor broadband noise mechanisms and helicopter tail rotor noise 06 p0777 N88-14766

Characteristics of LKI-501 tunable dye laser with dyes in solid matrix 07 p0920 N88-15587

Harmonic expansion for the magnetic field of the helical solenoid
[DE88-700100] 07 p0928 N88-15638

Demonstration of efficient full aperture Type 1/Type 2 third harmonic conversion on Nova
[DE88-003834] 14 p1914 N88-21438

Subharmonic aliasing and its effects on the AFTI/F-16 digital flight control system
[AD-A190614] 15 p2020 N88-22042

Observation of synchronously transient pumped mode-locking dye laser under negative cavity detuning
16 p2187 N88-23041

Secondary instability of compressible boundary layer to subharmonic three-dimensional disturbances
[NASA-CR-4144] 16 p2200 N88-23122

Fluxons and order in long Josephson junctions
[AD-A190879] 16 p2282 N88-23665

Harmonic considerations for electrical distribution feeders
[DE88-007849] 18 p2505 N88-24860

Motor theory of auditory perception
[AD-A192095] 18 p2550 N88-25136

Analysis of the electrical harmonic characteristics of a slip recovery variable speed generating system for wind turbine applications
[DE88-001140] 19 p2687 N88-25972

Primer on coupling collective electronic oscillations to nuclei
[LA-10876] 19 p2723 N88-26170

Theoretical and experimental study of a mode-converting coupler for application to a harmonic gyrotron amplifier
[AD-A193760] 22 p3081 N88-28294

CryoSQUID: A SQUID-based magnetic field sensor
[AD-A194237] 23 p3239 N88-29275

HARNESSES

Human response to prolonged motionless suspension in four types of full body harnesses
21 p2929 N88-27387

HARRIER AIRCRAFT

Full-envelope aerodynamic modeling of the Harrier aircraft
[NASA-TM-88376] 05 p0552 N88-13363

Derivation of equipment vibration requirements for AV-8B 08 p0997 N88-16037

Manoeuvres by default, by demand and by design
12 p1580 N88-19455

HARTREE APPROXIMATION

The finite element method for electronic structure
[DE88-001708] 04 p0485 N88-12989

Theoretical studies of atomic transitions
[DE88-004719] 10 p1407 N88-18389

Numerical simulations of multiphoton processes in many electron atoms
[DE88-003293] 13 p1837 N88-20990

HARTREE-APPLETON APPROXIMATION

U HARTREE APPROXIMATION

HARTREE-FOCK APPROXIMATION

U HARTREE APPROXIMATION

HASTELLOY (TRADEMARK)

Resistance of welded joints in high temperature Hastelloy N-type nickel alloy to hot crack formation
03 p0286 N88-11798

Fatigue and uniaxial deformation behavior of Hastelloy XR at elevated temperatures
[DE88-751058] 09 p1145 N88-16862

Some implications for cyclic plastic and viscoplastic equations based on nonproportional loading experiments
14 p1931 N88-21515

Effect of strain rate on high-temperature low-cycle fatigue behavior of Hastelloy X and Hastelloy XR
[DE88-752302] 15 p2037 N88-22140

Creep behavior for Hastelloy-XR
[DE88-753428] 21 p2914 N88-27295

HATCHES

Hatch cover
[NASA-CASE-MSC-21356-1] 18 p2472 N88-24671

HAWAII

North Pacific Ocean. Tradewind region east of Hawaii, R/V Thomas G Thompson: 25 September - 1 November 1972. STD data report
[AD-A186566] 08 p1044 N88-16311

North Pacific Ocean. Subarctic front central Pacific, R/V Thomas G. Thompson: 8 September - 9 October 1975. CTD data report
[AD-A186567] 08 p1044 N88-16312

North Pacific Ocean. Central Pacific Transition Zone, R/V Thomas G. Thompson: 25 March - 3 May 1968: STD data report
[AD-A186570] 09 p1195 N88-17160

HAWKER SIDDELEY AIRCRAFT

NT HARRIER AIRCRAFT

HAZ (METALLURGY)

U HEAT AFFECTED ZONE

HAZARDOUS MATERIAL DISPOSAL (IN SPACE)

A proposed national policy concerning the reentry of space reactors 17 p2415 N88-24359

HAZARDS

NT AIRCRAFT HAZARDS
NT FLIGHT HAZARDS
NT METEOROID HAZARDS
NT RADIATION HAZARDS
NT TOXIC HAZARDS

Airborne lidar experiments at the Savannah River Plant
[NASA-TM-4007] 02 p0194 N88-11209

Human motor reactions to dangerous motions in robot operations
[PB87-222196] 03 p0361 N88-12275

Committee on Interagency Radiation Research and Policy Coordination
[DE88-003358] 09 p1188 N88-17121

Modeling of the non-auditory response to blast overpressure
[AD-A187397] 10 p1369 N88-18184

Toxic effects of man-made mineral fibers with particular reference to ceramic fibers
[AD-A187949] 11 p1519 N88-19072

Post-Challenger evaluation of space shuttle risk assessment and management
[NASA-CR-182461] 12 p1705 N88-20202

Atmospheric electrical modeling in support of the NASA F-106 storm hazards project
[NASA-CR-181639] 13 p1799 N88-20758

Bathymetric hazard survey test
[AD-A189150] 13 p1803 N88-20775

SPOT for earthquake hazard zoning in southern Italy
22 p3093 N88-28365

HAZE

Analysis of meteorological conditions and haze distribution for the Second Arctic Gas and Aerosol Sampling Program (AGASP 2), March-April 1986
[PB88-164140] 14 p1948 N88-21618

HCMM

U HEAT CAPACITY MAPPING MISSION

HCN LASERS

Electron density profile reconstruction by maximum entropy method with multichannel HCN laser interferometer system on SPAC 7
[IPPJ-858] 11 p1553 N88-19295

HEAD (ANATOMY)

NT SKULL

Analysis of head response to torso acceleration. Volume 1: Development of performance requirements
[PB88-156757] 14 p1953 N88-21640

Basic research on flame radiation
[PB88-168372] 15 p2032 N88-22105

Analysis of head response to torso acceleration. Volume 2: Description of data retrieval, analysis and display software
[PB88-156765] 15 p2104 N88-22536

HEAD DOWN TILT

Biorhythmological analysis of dynamics of pulmonary ventilation parameters during orthostatic tests
07 p0891 N88-15400

Changes in regional and central hemodynamics during seven-day water immersion 07 p0895 N88-15421

Effect of antiorthostatic position and different illumination on sensitivity of skin in upper half of the body to ultraviolet radiation 10 p1363 N88-18145

Does 7-day hindquarters unloading simulate 7 days of weightlessness exposure in rat trabecular bone?
12 p1657 N88-19928

Is ANF implied in the night attenuated renal response to central hypervolemia? 12 p1659 N88-19945

Determination of settings of a tilted head-cutter for generation of hypoid and spiral bevel gears
[NASA-CR-182138] 18 p2524 N88-24976

Human hemodynamics during water immersion as related to position during submersion
19 p2703 N88-26071

Human erykthrocyte metabolism in the presence of hyperoxygenation during antiorthostatic hypokinesia
19 p2706 N88-26092

An evaluation of flight path formats head-up and head-down
[NASA-CR-4176] 21 p2897 N88-27196

HEAD-UP DISPLAYS

The deviation of light rays passing through a curved windscreen --- aircraft
[BAE-MSC.115] 01 p0093 N88-10610

Multi-crew pictorial format display evaluation
[AD-A189349] 13 p1812 N88-20824

First flight simulator test of the head-up display for NAL QSTOL experimental aircraft (ASUKA)
[DE88-751804] 16 p2162 N88-22896

An evaluation of three linear scale radar altimeter displays
[AD-A192173] 18 p2465 N88-24636

Improvement of head-up display standards. Volume 1: Head-up display design guide, appendix
[AD-A192973] 20 p2834 N88-26809

An evaluation of flight path formats head-up and head-down
[NASA-CR-4176] 21 p2897 N88-27196

Improvement of head-up display standards. Volume 4: Head-up display dynamics flight tests
[AD-A193617] 22 p3042 N88-28060

Improvement of head-up display standards. Volume 2: Evaluation of head-up displays to enhance unusual attitude recovery
[AD-A194601] 23 p3178 N88-28921

Improvement of head-up display standards. Volume 5: Head up display ILS (Instrument Landing System) accuracy flight tests
[AD-A194602] 23 p3178 N88-28922

Vision through aircraft transparencies
23 p3242 N88-29294

Maintenance of vision-related components
23 p3242 N88-29296

Display system image quality
23 p3242 N88-29298

Improvement of head-up display standards. Volume 3: An evaluation of head-up display safety
[AD-A195787] 24 p3410 N88-30300

HEALTH

NT HEALTH PHYSICS
NT PUBLIC HEALTH

An assessment of clinical chemical sensing technology for potential use in space station health maintenance facility
[NASA-CR-172013] 04 p0475 N88-12926

Fibrous glass aerosols: A literature review
[AD-A188420] 12 p1672 N88-20008

The effects of normal and therapeutic baths on the central vascular organs of persons with healthy hearts, as measured by X-ray
[NASA-TT-20252] 13 p1811 N88-20818

The impact of hyperthermia and hypohydration on circulation, strength, endurance and health
[AD-A192657] 22 p3131 N88-28615

Physiological effects of extremely low frequency electric and magnetic fields
[DE88-752814] 22 p3132 N88-28620

Evaluation of the potential health hazards associated with the machining of carbon fiber composites
[AD-A194835] 24 p3408 N88-30286

HEALTH PHYSICS

NT PUBLIC HEALTH

Health hazards of video display terminals. A comprehensive, annotated bibliography on a critical issue of workplace health and safety with sources for obtaining items and list of terminal suppliers
[RSI-IAS-4] 03 p0355 N88-12240

Trends in research and development in the Netherlands. The influence of national science policy between 1973 and 1986
[B8701588] 08 p1094 N88-16580

HEAO

NT HEAO 2

HEAO B

U HEAO 2

HEAO 2

Soft X-ray observations of pre-main sequence stars in the chamaeleon dark cloud
[NASA-CR-181457] 02 p0250 N88-11579

Exosat results on the dMe flare Star Wolf 630AB and on VB 8 04 p0512 N88-13151

HEARING

Mechanisms mediating the perception of complex acoustic patterns
[AD-A190112] 15 p2130 N88-22705

Predicting Air Combat Maneuvering (ACM) performance: Fleet fighter ACM readiness program grades as performance criteria
[AD-A191605] 19 p2710 N88-26099

Auditory evoked magnetic fields in man
[PB88-193446] 20 p2831 N88-26796

Dissecting the visual and auditory pathways by means of the two-input technique 21 p2978 N88-27690

Neuromagnetic evidence of place mechanisms for frequency and intensity coding in the human auditory cortex 21 p2979 N88-27693

HEART

NT CARDIAC VENTRICLES
NT MYOCARDIUM

Dimensional analysis of nonlinear oscillations in brain, heart and muscle
[DE87-014749] 06 p0751 N88-14614

Ballistocardiography in weightlessness research
11 p1521 N88-19080

Response of coronary blood flow to step changes in plasma protein concentration in the isolated rat heart
12 p1651 N88-19892

The effects of normal and therapeutic baths on the central vascular organs of persons with healtny hearts, as measured by X-ray
[NASA-TT-20252] 13 p1811 N88-20818

HEART DISEASES

NT CORONARY ARTERY DISEASE
NT MYOCARDIAL INFARCTION

Relationships between coronary heart disease risk factors and serum ionized calcium in Kennedy Space Center Cohort
[NASA-TM-100979] 10 p1368 N88-18177

HEART FUNCTION

Maximal cardiorespiratory responses to one- and two-legged cycling during acute and long-term exposure to 4300m
[AD-A185730] 06 p0752 N88-14621

Cardiac contractility in weightlessness according to spatial ballistocardiography 07 p0890 N88-15393

Distinctions and mechanisms of effects of epinephrine and norepinephrine on cardiac pumping function under hypokinetic conditions 07 p0891 N88-15399

Respiratory and cardiovascular responses to cold stress following repeated cold water immersion
[AD-A186460] 08 p1050 N88-16340

Sudden in-flight incapacitation in general aviation
[AD-A187044] 09 p1115 N88-16682

Validation of a modified one-step rebreathing technique for measuring exercise cardiac output
[AD-A192600] 21 p2986 N88-27729

HEART RATE

NT ARRHYTHMIA
NT TACHYCARDIA

Assessment of physical activity intensity by heart rate during sleep limited military operations
[AD-A185913] 07 p0888 N88-15382

Distinctions and mechanisms of effects of epinephrine and norepinephrine on cardiac pumping function under hypokinetic conditions 07 p0891 N88-15399

Biorhythmic aspects of intercontinental Antarctic adaptation 08 p1046 N88-16321

The use of heart rate in the prescription and evaluation of exercise programs
[AD-A186454] 08 p1049 N88-16336

Vital signs rate meter
[AD-A187015] 09 p1198 N88-17183

Electromagnetic metrics of mental workload
[AD-A188205] 11 p1523 N88-19093

The effect of orthostatic changes in central blood volume on the heart rate response to graded Valsalva maneuvers 12 p1653 N88-19904

Desynchronization of heart rate and breathing frequency after transmeridional flight across three time zones
12 p1663 N88-19968

Interrelationship of heart rhythm indicators and resistance to hypoxia in Antarctic polar workers
12 p1664 N88-19974

Vagal tone as an index of mental state
16 p2239 N88-23373

Estimating the cost of mental loading in a bimodal divided-attention task: Combining reaction time, heart-rate variability and signal-detection theory
16 p2241 N88-23385

Cardiac rhythm of animals consuming reclaimed water differing in concentration of sodium and potassium ions
19 p2705 N88-26085

Fighter pilot performance during airborne and simulator missions: Physiological comparisons
21 p2981 N88-27704

Metabolic and cardiorespiratory parameters during three consecutive days of exhaustive running
[AD-A192598] 21 p2985 N88-27728

Validation of a modified one-step rebreathing technique for measuring exercise cardiac output
[AD-A192600] 21 p2986 N88-27729

Validation of a modified one-step rebreathing technique for non-invasive measurement of submaximal cardiac output
[AD-A192652] 21 p2987 N88-27735

Effects of psychophysical lifting training on maximal repetitive lifting capacity
[AD-A192605] 23 p3238 N88-29271

HEAT

NT DRY HEAT
NT ENTHALPY
NT GIBBS FREE ENERGY
NT HEAT OF COMBUSTION
NT HEAT OF FORMATION
NT HEAT OF FUSION
NT LATENT HEAT
NT NUCLEAR HEAT
NT SPECIFIC HEAT

Structural reliability and damage tolerance of ceramic composites for high-temperature applications
[PB87-208310] 01 p0019 N88-10119

Heat engine regenerators: Research status and needs
[DE87-013581] 01 p0054 N88-10348

Needs assessment for nondestructive testing and materials characterization for improved reliability in structural ceramics for heat engines
[DE88-000040] 02 p0153 N88-10957

Assessment of the reliability of a correction procedure for WGT (Wet Globe Thermometer) (Botsball) measurements of heat stress
[AD-A185193] 05 p0584 N88-13559

Polymer material for heat sensors
06 p0676 N88-14142

Ceramic technology for advanced heat engines program data base
[DE88-003922] 11 p1464 N88-18730

Gastric emptying during exercise: Effects of acute heat stress, acclimation and hypohydration
[AD-A188008] 11 p1519 N88-19073

HEAT ACCLIMATIZATION

Determination of the individual state of acclimatization
[IZF-1986-27] 01 p0075 N88-10478

Daily dynamics of some physiological indicators of man under desert condition 06 p0750 N88-14605

Polycythemia and hydration status: Effects on blood volume and thermoregulation during exercise-heat stress
[AD-A185946] 07 p0888 N88-15383

Gastric emptying during exercise: Effects of acute heat stress, acclimation and hypohydration
[AD-A188008] 11 p1519 N88-19073

Heat acclimatization under controlled hyperthermia
12 p1665 N88-19981

Plasma cortisol, renin and aldosterone during an intense heat acclimation program
[AD-A189387] 13 p1809 N88-20810

Physiological and hematological responses of matched older and younger men during dry-heat acclimation
[AD-A186450] 18 p2550 N88-25139

Variability in intake and dehydration in young men during a simulated desert walk
[AD-A192654] 22 p3131 N88-28613

Hormonal regulation of fluid and electrolytes: Effects of heat exposure and exercise in the heat
[AD-A192655] 22 p3131 N88-28614

HEAT AFFECTED ZONE

A physical metallurgical basis for heat-affected zone and base-plate properties of a microalloyed HSLA steel
[AD-A180200] 01 p0022 N88-10137

Effects of stress-relieving on the mechanical properties and the structure of specimens of high-temperature fine-grained structural steels heat-treated to simulate welding
[BLL-CE-TRANS-8258-(9022.09)]
04 p0417 N88-12586

Study on fracture behaviour of a joint with a crack in transverse hard layer: Effect of hard layer width on COD
[PB87-143855] 07 p0868 N88-15267

Microstructural characterization of the heat affected zone of HSLA (High Strength Low Alloy)-100 steel GMA (Gas Metal Arc)-weldment
[AD-A187825] 11 p1457 N88-18686

Transformation, metallurgical response and behavior of the weld fusion zone and heat affected zone in Cr-Mo steels for fossil energy application
[DE88-006037] 13 p1744 N88-20430

Efficiency of fusion during periodic-pulse laser-beam welding 14 p1897 N88-21324

HEAT BALANCE

Approximate solutions of heat conduction in a medium with variable properties
[AD-A186933] 10 p1326 N88-17925

The active layer of the upper Atlantic Ocean
22 p3124 N88-28566

HEAT BUDGET

NT ATMOSPHERIC HEAT BUDGET

The ocean heat budget
[AD-A186130] 07 p0881 N88-15346

Measurement from satellites of land surface parameters and fluxes in the thermal infrared bands: Problems and methods 14 p1937 N88-21557

Energy budget and ground temperatures in hot regions
[AD-A196298] 24 p3404 N88-30268

HEAT CAPACITY

U SPECIFIC HEAT

HEAT CAPACITY MAPPING MISSION

The Earthnet Heat Capacity Mapping Mission (HCMM) data-processing system at Lannion (France)
09 p1127 N88-16761

HEAT CONDUCTION

U CONDUCTIVE HEAT TRANSFER

HEAT CONTENT

U ENTHALPY

HEAT DISSIPATION

U COOLING

HEAT DISSIPATION CHILLING

U COOLING

HEAT EFFECTS

U TEMPERATURE EFFECTS

HEAT EQUATIONS

U THERMODYNAMICS

HEAT EXCHANGERS

NT TUBE HEAT EXCHANGERS

Performance of rotary regenerative heat exchanger: A numerical simulation 01 p0046 N88-10292

Comparison of different kinds of compact cross flow heat exchangers
[DFVLR-FB-86-63] 01 p0048 N88-10305

Recent progress in magma energy extraction
[DE87-013063] 01 p0066 N88-10424

Continued research on direct contact heat exchangers: Effects of crystallization
[DE87-014931] 03 p0322 N88-12035

Overview of free-piston Stirling engine technology for space power application
[NASA-TM-88886] 03 p0386 N88-12427

Two-watt, 4-Kelvin closed cycle refrigerator performance 04 p0437 N88-12709

Theory of one and two-pass cross-flow heat exchanger
[PB87-225157] 04 p0441 N88-12736

Measured performance of the heat exchanger in the NASA icing research tunnel under severe icing and dry-air conditions
[NASA-TM-100116] 04 p0451 N88-12796

Design and development of absorption heat pumps
[DE88-900082] 04 p0466 N88-12885

Advanced condensing heat exchangers
[DE88-001485] 06 p0699 N88-14288

Development of a low noise 10 K J-T refrigeration system
[AD-A186004] 07 p0838 N88-15085

Evaluation of thermal storage for solar heating systems: Executive summary
[DE88-900219] 07 p0874 N88-15304

A quasi-three-dimensional calculation procedure for the prediction of flow and heat transfer in heat exchanger passages 09 p1165 N88-16985

Microcomputer analysis of regenerative heat exchangers for oscillating flow
[DE88-001773] 10 p1329 N88-17945

A solar receiver-reactor with specularly reflecting walls for high-temperature thermoelectrochemical and thermochemical processes
[AD-A187612] 10 p1351 N88-18077

Performance evaluation of plate-fin heat exchangers
[AD-A187798] 11 p1482 N88-18845

Ultrasonic testing of heat exchanger tubes
[DE88-751172] 11 p1497 N88-18939

Growth of Cr,Nd:Gd3Sc2Al3O12 (Cr,Nd:GSAG) crystals by the Heat Exchanger Method (HEM)(trademark)
[DE88-004041] 11 p1558 N88-19326

Proceedings of the 1987 International Symposium on Condensing Heat Exchangers
[DE88-005230] 13 p1766 N88-20564

Innovative, counterflow gas/fine solids, direct contact heat exchanger
[DE88-004744] 13 p1770 N88-20585

Study on the burnout with variations of flow twisting over tube length
[DE87-703170] 14 p1909 N88-21405

Hafnia-rich mixed oxide ceramics of the system HfO2-ZrO2-TiO2 for heaters and heat exchangers in electrothermal thrusters: The effects of titania on selected electrical and mechanical properties of Hafnia-rich mixed oxides in the system Hafnia-Zirconia-Titania, volume 1
[NASA-CR-182800-VOL-1] 15 p2047 N88-22197

Basic characteristics of heat-exchanger-type steam reformer heated by high-temperature helium gas (2). Analysis by simulation model (2)
[DE87-702962] 15 p2061 N88-22291
Comparison of entropy generation and conventional design methods for heat exchangers
[AD-A190256] 15 p2064 N88-22306
A survey of oscillating flow in Stirling engine heat exchangers
[NASA-CR-182108] 15 p2067 N88-22322
An evaluation of nondestructive methods for ceramic heat exchanger applications
[DE88-006731] 15 p2068 N88-22328
Comparison of different kinds of compact crossflow heat exchangers
[ESA-TT-1076] 16 p2207 N88-23169
Computational fluid dynamics applied to the prediction of the heat-transfer, mechanical and thermal-stress behavior of heat exchangers
[CFDU/87/7] 18 p2510 N88-24893
Moving belt radiator development status
[NASA-TM-100909] 19 p2607 N88-25477
Cross flow induced vibrations in tube bundle by displaced and misaligned tube configurations
[ETN-88-92132] 20 p2801 N88-26621
The design and fabrication of a Stirling engine heat exchanger module with an integral heat pipe
[NASA-TM-101296] 20 p2820 N88-26732
Heat exchanger demonstration expert system
22 p3066 N88-28193
High effectiveness contour matching contact heat exchanger
[NASA-CASE-MSC-20840-1] 23 p3214 N88-29132
Oxidizer heat exchanger component test
[NASA-CR-182159] 24 p3339 N88-29876
Theories of comparative analysis
[AD-A196328] 24 p3427 N88-30395
Growth of GaAs crystals by the Heat Exchanger Method for microwave device applications
[AD-A196028] 24 p3433 N88-30435

HEAT FLOW
U HEAT TRANSMISSION

HEAT FLUX
Effect of NASA advanced designs on thermal behavior of Ni-H2 cells
[NASA-TM-100197] 01 p0021 N88-10132
Locating parallel numerical tasks in the solution of viscous fluid flows
[DE87-013510] 02 p0169 N88-11064
Development of heat flux sensors for turbine airfoils
02 p0184 N88-11143
Enhancement of surface-atmosphere fluxes by desert-fringe vegetation through reduction of surface albedo and of soil heat flux
[NASA-CR-181442] 02 p0197 N88-11231
Measurements of gas velocities and temperatures in a large open pool fire
[DE87-005853] 03 p0261 N88-11641
Measurements in large JP-4 pool fires
[DE87-013445] 03 p0284 N88-11783
Experimental study of thermocapillary flows in a thin liquid layer with heat fluxes imposed on the free surface
[NASA-TM-100252] 04 p0445 N88-12763
Data base on the high heat flux behaviour of metals and carbon materials for plasma facing components: Experiments at the 10 MW neutral beam injection test stand of the IPP Nagoya
[IPPJ-AM-53] 04 p0492 N88-13031
Proceedings of the Japan-US Workshop P-92 on Plasma Material Interaction/High Heat Flux Data Needs for the Next Step Ignition and Steady State Devices
[DE87-013568] 04 p0494 N88-13042
Hypersonic laminar boundary layer: Parametric study for the representation of real gas effects
05 p0532 N88-13236
Use of a local heat source for determining temperature of inlet heat section in ring channels
[DE88-700332] 07 p0854 N88-15187
The effect of asymmetric heating on flow stability and heat transfer for flow in a vertical tube
[DE88-003242] 07 p0855 N88-15193
Particle-gas temperature differentials resulting from time-dependent radiative-conductive heat flux divergences in the tenuous dust-laden atmosphere of mars
[AD-A185888] 07 p0945 N88-15747
Bidirectional electron heat flux events in space
[DE88-001791] 08 p1084 N88-16531
Heat transfer from impinging flame jets
[ETN-88-91610] 09 p1162 N88-16964
Investigation of critical heating in narrow flow channels with R12 refrigerant as model fluid
[GKSS-87/E/25] 09 p1163 N88-16972
Numerical solutions of two moving boundary problems by both finite difference and finite element methods with applications
[DE88-002867] 09 p1230 N88-17374
Approximate solutions of heat conduction in a medium with variable properties
[AD-A186933] 10 p1326 N88-17925
Experimental study of thermal loading at the wall of an industrial Diesel motor
[ISAL-IDI1-87-10] 10 p1339 N88-18000
Experimental determination of the heat flux inside a tubular projectile for the velocity range M = 3 and M = 6
[ISL-R-118/86] 11 p1443 N88-18605
Prototype thin-film thermocouple/heat-flux sensor for a ceramic-insulated diesel engine
[NASA-TM-100798] 11 p1490 N88-18892
Test methodology for infrared tubular heaters
[PB88-160916] 12 p1626 N88-19728
Current velocity and hydrographic observations in the Straits of Florida, the Caribbean Sea and offshore of the Antillean Archipelago: Subtropical Atlantic climate studies (STACS) 1984 and 1985
[PB88-149299] 12 p1649 N88-19874
Some effects of heating on the wind-driven velocity in the upper ocean 13 p1805 N88-20792
Study on the burnout with variations of flow twisting over tube length
[DE87-703170] 14 p1909 N88-21405
The turbulent heat flux in low Mach number flows with large density variations
[DE88-006445] 14 p1911 N88-21419
Mass, heat and nutrient fluxes in the Atlantic Ocean determined by inverse methods
[NASA-CR-180535] 14 p1950 N88-21626
Thermostructural analysis of simulated cowl lips
15 p2080 N88-22403
Research sensors 15 p2085 N88-22430
Magnetic fusion energy plasma interactive and high heat flux components. Volume 5: Technical assessment of critical issues in the steady state operation of fusion confinement devices
[DE88-006920] 15 p2136 N88-22744
Preliminary measurements of heat flux in a subsonic gun simulator
[AD-A191090] 16 p2208 N88-23178
REFLEX: An energy deposition code that models the effects of electron reflection during electron beam heating tests
[DE88-009789] 19 p2726 N88-26186
Vaporization studies of plasma interactive materials in simulated plasma disruption events
[DE88-010100] 19 p2731 N88-26222
Surface temperature thermal fluxmeters for shock tubes
[NASA-TT-20319] 20 p2762 N88-26381
Evaluation of surface energy and radiation balance systems for FIFE
[NASA-CR-183118] 20 p2828 N88-26778
Optical imaging diagnostics for fusion plasmas
[DE88-997572] 21 p3018 N88-27910
Development of sensors for ceramic components in advanced propulsion systems: Survey and evaluation of measurement techniques for temperature, strain and heat flux for ceramic components in advanced propulsion systems
[NASA-CR-182111] 22 p3081 N88-28299
Study on iron disilicide thermoelectric generator
[AD-A193082] 22 p3116 N88-28517
The thermal behavior of film cooled turbulent boundary layers as affected by longitudinal vortices
[AD-A195155] 24 p3374 N88-30095
Measurement of local high-level, transient surface heat flux
[NASA-TP-2840] 24 p3375 N88-30099

HEAT GAIN
U HEATING

HEAT GENERATION
Nitrogen scale-up
[AD-A185702] 06 p0709 N88-14351
Investigation of self-discharge characteristics of spacecraft nickel-cadmium cells at elevated temperatures
[AD-A186497] 08 p0979 N88-15919

HEAT MEASUREMENT
On the stressing of annealed NITINOL: The electrical resistance and calorimetric effects
[AD-A184465] 04 p0414 N88-12569
Investigation by differential scanning calorimetry of microstructure in a superplastic Al-Mg-Zr alloy
[AD-A184902] 05 p0564 N88-13439
Investigation of energy metabolism of biological systems in weightlessness 07 p0893 N88-15409
Investigation of critical heating in narrow flow channels with R12 refrigerant as model fluid
[GKSS-87/E/25] 09 p1163 N88-16972
Time-resolved heat transfer measurements and analysis in the wage region of a cylinder in crossflow
10 p1328 N88-17939
Experimental study of thermal loading at the wall of an industrial Diesel motor
[ISAL-IDI1-87-10] 10 p1339 N88-18000
Specific heat of novel thin-film material systems
10 p1415 N88-18446
Experimental determination of the heat flux inside a tubular projectile for the velocity range M = 3 and M = 6
[ISL-R-118/86] 11 p1443 N88-18605
Multilayer thermal insulation tests
[INPE-4475-PRE/1243] 12 p1626 N88-19729
A calorimetric determination of the enthalpy of formation and a description of the defect structure of the ordered beta-phase /Ni, Cu/ /1-x/ Al/x/
[NASA-TT-20157] 13 p1745 N88-20434
High resolution hadron calorimetry
[NIKHEF-H/87-8] 13 p1773 N88-20605
Anomalies in the heat-capacity signatures of submonolayer adsorbates with attractive lateral interactions
[AD-A190736] 15 p2147 N88-22817
Note on the double crystal method of measuring heat transfer coefficient
[OUEL-1710/87] 17 p2338 N88-23950
Calorimetry applied to nucleus-nucleus collisions at ultrarelativistic energies
[DE88-006173] 18 p2573 N88-25262
Surface temperature thermal fluxmeters for shock tubes
[NASA-TT-20319] 20 p2762 N88-26381
Method and device for determining heats of combustion of gaseous hydrocarbons
[NASA-CASE-LAR-13528-1] 23 p3193 N88-29002

HEAT OF COMBUSTION
Photolytic processes for measurement of combustion heats of formation and reaction rates
[DE87-014047] 02 p0144 N88-10905
Correlation between flammability and heat of combustion of polymers
[NASA-TT-20116] 08 p0973 N88-15864
Numerical simulation of turbulent flames using vortex methods
[AD-A189813] 15 p2034 N88-22116
Application of Rayleigh scattering to turbulent flow with heat transfer and combustion
[AD-A191565] 18 p2481 N88-24720
On-line measurement of heat of combustion
[NASA-CR-183076] 19 p2738 N88-26255
Method and device for determining heats of combustion of gaseous hydrocarbons
[NASA-CASE-LAR-13528-1] 23 p3193 N88-29002

HEAT OF FORMATION
A calorimetric determination of the enthalpy of formation and a description of the defect structure of the ordered beta-phase /Ni, Cu/ /1-x/ Al/x/
[NASA-TT-20157] 13 p1745 N88-20434
Evaluation of direct methane conversion to higher hydrocarbons and oxygenates
[DE88-003812] 15 p2049 N88-22204

HEAT OF FUSION
Analytical treatment of the melting and solidification of latent heat store materials in finned tube geometries
[IKE-5-223] 03 p0314 N88-11985

HEAT PIPES
Membrane heat pipe development for space radiator applications
[DE86-006015] 01 p0045 N88-10285
Transient modeling of the thermohydraulic behavior of high temperature heat pipes for space reactor applications 02 p0136 N88-10857
Applications of heat pipes to cool PWBS and hybrid microcircuits 02 p0136 N88-10858
The Proceedings of the Symposium on Mechanics for Space Flight
[ISAS-SP-5] 03 p0317 N88-12006
Heat transfer performance of axially grooved heat pipes 03 p0319 N88-12016
Heat transfer characteristics of arterial heat pipe with axial grooves 03 p0319 N88-12017
Pump assisted heat pipe 03 p0319 N88-12018
Overview of free-piston Stirling engine technology for space power application
[NASA-TM-88866] 03 p0386 N88-12427
Advanced radiator concepts utilizing honeycomb panel heat pipes
[NASA-CR-172017] 04 p0443 N88-12747
Testing of heat pipes on SPAS-01
[BMFT-FB-W-86-014] 06 p0672 N88-14119
Orbital Replaceable Unit (ORU)/cold plate thermal interface study. Volume 1: Executive Summary
[BAE-TP-8430] 07 p0855 N88-15195
Heat pipes for space use 09 p1124 N88-16736
Compressible friction coefficients in a simulated heat pipe
[AD-A188818] 12 p1627 N88-19735

Moveable thermal joints for deployable or steerable spacecraft radiator systems
[NLR-MP-87016-U] 13 p1730 N88-20347
Heat pipe transient analysis: Vapor dynamics
[DE88-005132] 13 p1767 N88-20568
Development, manufacturing and testing of a gas-loaded variable conductance methanol heat pipe
[NLR-MP-87010-U] 13 p1767 N88-20571
Design of the Sandia-Israel 20-kW reflux heat-pipe solar receiver/reactor
[DE88-001312] 13 p1794 N88-20729
Development of an integrated heat pipe-thermal storage system for a solar receiver
[NASA-TM-101099] 15 p2091 N88-22458
Solar dynamic heat rejection technology. Task 2: Heat pipe radiator development
[NASA-CR-182141] 16 p2209 N88-23182
Transient analysis of heat pipe vapor dynamics
17 p2412 N88-24341
Progress in the computer modeling of the liquid phase behavior of a liquid metal heat pipe
17 p2412 N88-24342
A compressible vapor flux model for transient heat pipe analysis 17 p2412 N88-24343
ATHENA heat pipe transient model
17 p2412 N88-24344
Detailed transient model of a liquid-metal heat pipe
17 p2412 N88-24345
Thermochemical analysis of mass transfer in a NB-1ZR-potassium heat pipe 17 p2412 N88-24346
Transient thermohydraulic heat pipe modeling
17 p2413 N88-24347
The Lewis heat pipe code with application to SP-100 GES heat pipes 17 p2421 N88-24395
HTPIPE: A steady state heat pipe analysis program
17 p2421 N88-24396
Heat pipe transient analysis: Vapor dynamics
17 p2421 N88-24397
A transient model for liquid metal heat pipes
17 p2421 N88-24398
The THROHPUT code: Thermohydraulic heat pipe modeling 17 p2421 N88-24399
MACRAD: A mass analysis code for radiators
17 p2424 N88-24418
Fabric radiators 17 p2427 N88-24435
Trade study for kWe class space reactors
17 p2430 N88-24454
Performance of vapor-fed sodium heat engine/AMTEC systems 17 p2437 N88-24502
Moving belt radiator development status
[NASA-TM-100909] 19 p2607 N88-25477
The Proceedings of the Symposium on Mechanics for Space Flight 1987
[ISAS-SP-6] 20 p2782 N88-26499
Thermostatistical estimations of vapor-state molecules affected by gravity in a heat pipe
20 p2783 N88-26505
An experimental investigation of transient characteristics in a gravity-assisted heat pipe 20 p2783 N88-26506
Heat transfer of mesh-wick heat-pipes (bottom heat mode) 20 p2783 N88-26507
A statistical treatment of accelerated life test data for copper-water heat pipes 20 p2783 N88-26509
The design and fabrication of a Stirling engine heat exchanger module with an integral heat pipe
[NASA-TM-101296] 20 p2820 N88-26732
Reflux heat-pipe solar receivers for dish-electric systems
[DE88-008671] 21 p2968 N88-27631
The heat pipe network of TDF-1/TV-SAT. Review of the development at completion
[SNIAS-881-440-103] 23 p3213 N88-29127
Development of a space deployable radiator using heat pipes
[SNIAS-881-440-104] 23 p3214 N88-29128
Polymeric heat pipe wick
[NASA-CASE-GSC-13019-1] 23 p3214 N88-29133
Unstable heat pipes
[DE88-010780] 23 p3229 N88-29217
Effect of interfacial phenomena on contact line heat Transfer-3
[AD-A194941] 24 p3343 N88-29901

HEAT PUMPS
Double-effect absorption heat pump, phase 3
[PB87-232195] 03 p0317 N88-12005
Optimized ground coupled heat pump mechanical package
[DE87-014899] 04 p0441 N88-12738
Design and development of absorption heat pumps
[DE88-900082] 04 p0466 N88-12885
Life-cycle cost analysis of residential heat pumps and alternative HVAC (Heating, Ventilating and Air-Conditioning) systems
[DE88-003701] 07 p0839 N88-15090
Feasibility of a complex compound heat pump
[PB88-113022] 07 p0853 N88-15183
Heat pump and appliance research
[PB88-102462] 07 p0853 N88-15184
Working fluids for sorption heat pumps
[DE88-900203] 07 p0874 N88-15301
Water source heat pump: How to get home heating and cooling from your own back yard
[DE88-900180] 07 p0875 N88-15306
Comparison of a thermoelectric cooling system and a groundwater heat pump
[DE88-001753] 08 p0984 N88-15950
Solar assisted absorption or motor driven heat pump with earth seasonal storage, part 1
[DE88-900191] 09 p1187 N88-17114
Free-piston Stirling engine diaphragm-coupled heat-actuated heat pump component technology program, phase 1C
[DE88-003654] 10 p1330 N88-17949
Analysis of the performance of an air-water heat pump: Regulation of intrinsic performances
[DE88-900241] 10 p1349 N88-18061
Free-piston Stirling engine diaphragm-coupled heat-actuated heat pump component technology program, phase 1B
[DE88-003653] 11 p1483 N88-18854
Open-cycle centrifugal vapor-compression heat pump
[PB88-157391] 11 p1488 N88-18885
Proceedings of the 1987 International Symposium on Condensing Heat Exchangers
[DE88-005230] 13 p1766 N88-20564
Efficiency characteristics of speed modulated drives at predicted torque conditions for air-to-air heat pumps
[DE88-005846] 13 p1770 N88-20588
Overview of 1987 moonlight project
15 p2052 N88-22231
Application and technology requirements for heat pumps at the process industries
[DE88-006740] 15 p2062 N88-22293
Advanced chemical heat pumps using liquid-vapor reactions
[DE88-006760] 16 p2205 N88-23159
Heat pump-augmented systems for spacecraft thermal management 17 p2424 N88-24419
Solar assisted absorption or motor driven heat pump with earth seasonal storage. Part 2: Tables and figures
[DE88-900226] 19 p2686 N88-25964
Heat pump augmented radiators for spacecraft thermal management
[DE88-007890] 20 p2764 N88-26392
Heat pump augmented radiator for low-temperature space applications
[DE88-008369] 20 p2765 N88-26393
Magnetic heat pump design
[DE88-007730] 20 p2798 N88-26605
The Oak Ridge Heat Pump Design Model: Mark 3 version program documentationon
[DE88-007863] 20 p2799 N88-26607
Thermodynamic analysis of chemical heat storage system for heat pump
[DE88-753121] 20 p2820 N88-26728
Magnetic heat pumps
[DE88-012058] 21 p2969 N88-27639
A comparative economic evaluation of industrial heat pumps. Part 2: Addendum
[DE88-011701] 22 p3117 N88-28519
Absorption heat pumps
[DE88-752820] 23 p3229 N88-29218

HEAT RADIATORS
NT SPACECRAFT RADIATORS
Estimating payload internal temperatures and radiator size for multimegawatt space platforms
[DE88-000244] 03 p0275 N88-11738
Adiabatic diesel engine component development: Reference engine for on-highway applications
[NASA-CR-179531] 03 p0386 N88-12428
Advanced radiator concepts utilizing honeycomb panel heat pipes
[NASA-CR-172017] 04 p0443 N88-12747
AF cryogenic and fluid management spacecraft technology program 08 p0981 N88-15925
Indirect measurement of local condensing heat-transfer coefficient around horizontal finned tubes
[AD-A186929] 09 p1160 N88-16950
Solar dynamic heat rejection technology. Task 2: Heat pipe radiator development
[NASA-CR-182141] 16 p2209 N88-23182
Thermal management for multi-modal nuclear power plants 17 p2410 N88-24331
A review of impact design criteria for space power heat rejection systems 17 p2410 N88-24333
Progress in the computer modeling of the liquid phase behavior of a liquid metal heat pipe
17 p2412 N88-24342
A generalized method for optimizing the mass of space power systems 17 p2416 N88-24369
The Curie point radiator 17 p2424 N88-24420
Development of materials for fabric radiators
17 p2429 N88-24448
High power density alkaline fuel cell technology for MMW space burst power 17 p2429 N88-24451
Trade study for kWe class space reactors
17 p2430 N88-24454

HEAT REGULATION
U TEMPERATURE CONTROL

HEAT REJECTION DEVICES
U HEAT RADIATORS

HEAT RESISTANCE
U THERMAL RESISTANCE

HEAT RESISTANT ALLOYS
NT MOLYBDENUM ALLOYS
NT NIMONIC ALLOYS
NT NIOBIUM ALLOYS
NT REFRACTORY METAL ALLOYS
NT RHENIUM ALLOYS
NT TANTALUM ALLOYS
NT TUNGSTEN ALLOYS
Investigation of rapidly-solidified dispersion strengthened titanium alloys
[AD-A183882] 01 p0022 N88-10140
The development of a high temperature static strain gage system 02 p0184 N88-11142
Constitutive modeling for single crystal superalloys
02 p0187 N88-11168
Constitutive modeling of superalloy single crystals with verification testing 02 p0188 N88-11169
Constitutive modeling for isotropic materials
02 p0188 N88-11171
Constitutive modeling for isotropic materials
02 p0188 N88-11172
Creep-fatigue behavior of NiCoCrAlY coated PWA 1480 02 p0189 N88-11176
Quantitative electron probe microanalysis investigation of the oxidation of high temperature alloys at low oxygen partial pressures
[JUEL-2120] 03 p0288 N88-11811
Investigation of the deformation behavior of ferritic two-phase Fe-Ni-Al alloys with high concentrations of the intermetallic (Fe, Ni)Al phase at high temperatures
[ETN-87-90605] 03 p0288 N88-11812
Cast iron freezing mechanisms
03 p0298 N88-11870
Influence of boron on porosity in nickel-base superalloy castings 03 p0299 N88-11877
Deformation mechanisms of thermostructural materials
[AD-A184070] 03 p0338 N88-12128
A mathematical model of high alloy nickel base high temperature alloys
[BLL-M-37381-(5828.4)] 05 p0564 N88-13436
Behavior of long and short fatigue cracks in a powder metallurgy superalloy at room and at high temperature
05 p0601 N88-13677
Fatigue strength of alloy A286 at cryogenic temperature 05 p0603 N88-13695
Low cycle fatigue behaviour of notched specimens of nickel based superalloy single crystal
05 p0605 N88-13712
An overview of fatigue 05 p0608 N88-13729
Deformation, fatigue and fracture behavior of two cast anisotropic superalloys 05 p0608 N88-13732
Characterization of the microstructures of various materials
[AD-A184961] 05 p0655 N88-14017
High temperature low cycle fatigue of oxide dispersion strengthened and single crystal nickel base superalloys
06 p0720 N88-14422
High temperature low cycle fatigue behavior and creep-fatigue interation of MA 6000 ODS alloy
06 p0720 N88-14425
The effect of temperature on fatigue crack initiation from aluminosilicate inclusions 06 p0720 N88-14427
Dependence of strainrange partitioned fatigue life at elevated temperature on monotonic stress-strain properties 06 p0721 N88-14428
An analysis of temperature effect on LCF crack growth rates in superalloy GH36 06 p0721 N88-14431
Metallurgical processes in multi-component rare earth-transition metal permanent magnet alloys
[AD-A186401] 07 p0832 N88-15045
Center for the Space Processing of Engineering Materials 07 p0838 N88-15083
Development of a new generation of high-temperature composite materials 09 p1119 N88-16702
Investigation of the deformation behavior of the intermetallic phase (Fe,Ni)Al at high temperatures
[ETN-88-91062] 09 p1143 N88-16854
Effects of ion implantation on cavitation erosion of a cobalt based metal/carbide alloy
[AD-A187239] 10 p1303 N88-17793
Hot corrosion in gas turbines: A new, unique and informative technique is EASE (Electronic Absorption Spectroscopy Experiments)
[AD-A188508] 12 p1583 N88-19470

The cyclic stress-strain behavior of a single crystal nickel-base superalloy
[NASA-TM-100269] 12 p1607 N88-19610

Development of metastable processing paths for high temperature alloys
[AD-A188682] 12 p1608 N88-19617

Gordon Conference on Intermetallic Compounds held at Tilton, New Hampshire on 20-24 July 1987
[AD-A188502] 13 p1745 N88-20435

Activities report of the Materials Department
[ETN-88-91984] 13 p1745 N88-20436

Effect of nonuniform state of thermal stress on resistance of EI826 alloy to thermal fatigue
14 p1895 N88-21313

Effect of protective coatings on high-temperature fatigue of heat-resistant alloys
14 p1895 N88-21314

Experiments on the creep behavior of semifinished X10NiCrAlTi 32 20 (Nicrofer 32 20) tubes under multiaxial loading --- nuclear reactors
[JUEL-2127] 14 p1923 N88-21464

The viscoplasticity theory based on overstress applied to the modeling of a nickel base superalloy at 815 C
14 p1928 N88-21499

Development of a unified constitutive model for an isotropic nickel base superalloy Rene 80
14 p1929 N88-21501

Modeling the viscoplastic behavior of Inconel 718 at 1200 F
14 p1929 N88-21502

A theory of viscoplasticity accounting for internal damage
14 p1930 N88-21508

A constitutive model with damage for high temperature superalloys
14 p1930 N88-21510

The effects of temperature and strain rate on the yielding behavior of the single crystal superalloy PWA 1480
14 p1931 N88-21517

Investigation and synthesis of high temperature and increased stiffness RSP aluminum alloys
[AD-A190407] 15 p2039 N88-22151

High temperature oxidation and electrochemical studies related to hot corrosion
[AD-A190699] 15 p2040 N88-22156

Characterization of HYTUF steel. Semifinished product: 160 mm dia forging block. Processor: C3f. Test Report M3-434600
[M3-434600] 15 p2041 N88-22164

Bithermal fatigue of a nickel-base superalloy single crystal
[NASA-TM-100885] 15 p2042 N88-22168

Life prediction modeling based on cyclic damage accumulation
15 p2085 N88-22426

Fatigue damage modeling for coated single crystal superalloys
15 p2085 N88-22427

Fatigue crack growth behavior of a single crystal alloy as observed through an in situ fatigue loading stage
[NASA-TM-100863] 16 p2179 N88-22986

Model study of thermal stresses in gas-turbine blades with protective coating
16 p2179 N88-22989

Effect of alloying, rapid solidification, and surface kinetics on the high temperature environmental resistance of niobium
[AD-A192093] 18 p2485 N88-24743

Isothermal and bithermal thermomechanical fatigue behavior of a NiCoCrAlY-coated single crystal superalloy
[NASA-TM-100907] 18 p2489 N88-24766

JPRS report: Science and technology. Japan
[JPRS-JST-88-005] 19 p2633 N88-25619

Research on fractography of heat-resistant alloys
19 p2634 N88-25625

New super alloys used in turbochargers
19 p2634 N88-25628

A constitutive model with damage for high-temperature superalloys
20 p2771 N88-26434

Accelerated fatigue crack growth behavior of PWA 1480 single crystal alloy and its dependence on the deformation mode
[NASA-TM-100943] 20 p2772 N88-26436

Initial development of high-temperature titanium silicide alloys
[DE88-007860] 20 p2772 N88-26437

A fundamental understanding of the interfacial compatibility in hybrid material systems
[AD-A192921] 21 p2909 N88-27264

A review of solid particle erosion of engineering materials
[DE88-010065] 22 p3054 N88-28124

Advanced processing and properties of high performance alloys
[AD-A193767] 23 p3194 N88-29010

Anisotropic constitutive modeling for nickel-base single crystal superalloys
[NASA-CR-182157] 24 p3353 N88-29961

HEAT SHIELDING

NT REENTRY SHIELDING

Raman spectra of adsorbed layers on space shuttle and AOTV thermal protection system surface
06 p0799 N88-14890

OLYMPUS shuttle specific radiator shield
14 p1879 N88-21234

New concepts for atmospheric braking deceleration in planetary atmosphere entry
[SNIAS-CAS-DECE-P003-DPAA]
16 p2168 N88-22923

Dependence of structure of stabilized ZrO2 coatings on condensation rate
16 p2180 N88-22990

Space vehicle/nuclear reactor thermal radiation integration issues
17 p2424 N88-24417

Thermal and mechanical analysis of the Faraday shield for the compact ignition tokamak
[DE88-007855] 20 p2856 N88-26962

Far infrared spectroscopy telescope (FIRST) inflatable thermal shield, phase 1
[SR/FIS/108(87)CZ] 24 p3453 N88-30552

HEAT SINKS

Low-pressure eutectic bonding of depleted uranium to copper
[DE87-014625] 02 p0181 N88-11128

The global balance of dynamic vorticity in relation to heat sources and sinks
07 p0876 N88-15316

Surface-emitting two-dimensional laser diode arrays constructed on zig-zag heat sink surface
[DE88-005215] 14 p1915 N88-21439

Assessment of energy storage concepts for use in sprint power
17 p2407 N88-24312

Transient analysis of Li and LiH thermal storage spheres
17 p2411 N88-24334

The effect of maximum allowable payload temperature on the mass of a multimegawatt space based platform
17 p2424 N88-24416

Forced-convection, liquid-cooled, microchannel heat sinks
[AD-A193337] 21 p2937 N88-27444

HEAT SOURCES

NT GEOTHERMAL RESOURCES

A 40-kW fuel cell field test summary utilities activities report
[PB88-112800] 06 p0731 N88-14496

Use of a local heat source for determining temperature of inlet heat section in ring channels
[DE88-700332] 07 p0854 N88-15187

The global balance of dynamic vorticity in relation to heat sources and sinks
07 p0876 N88-15316

Dynamics Explorer guest investigator
[NASA-CR-181494] 07 p0878 N88-15325

A case study of the development of a military specification - zirconium powder for thermal batteries
[AD-A188751] 13 p1792 N88-20717

Tropical and monsoonal studies
[AD-A188387] 14 p1947 N88-21611

Superfine grain development by laser
15 p2050 N88-22215

The Light-Weight Radioisotope Heater Unit (LWRHU): Development and application
17 p2405 N88-24299

The application of high-rate biaxial testing to the design of containment vessels for radioisotope heat sources
17 p2426 N88-24428

Milliwatt generator project
[DE88-011261] 20 p2853 N88-26939

Storage of thermal energy by means of an absorption cycle
[PB88-190614] 21 p2966 N88-27619

High temperature electric arc furnace
[NASA-CASE-MFS-28281-1] 23 p3181 N88-28938

HEAT STORAGE

DTA/DSC studies of phase equilibria in binary mixtures of barium carbonate with alkali carbonates
[DE87-001195] 02 p0194 N88-11213

Analytical treatment of the melting and solidification of latent heat store materials in finned tube geometries
[IKE-5-223] 03 p0314 N88-11985

Evaluation of thermal storage for solar heating systems: Executive summary
[DE88-900219] 07 p0874 N88-15304

Thermal energy storage by means of an absorption cycle
[ETN-88-91614] 09 p1186 N88-17106

Effect of storage thermal behavior in seasonal storage solar heating systems
[PB88-114236] 10 p1350 N88-18067

Development of encapsulated lithium hydride thermal energy storage for space power systems
[DE88-004762] 11 p1507 N88-19001

An assessment methodology for thermal energy storage evaluation
[DE88-004642] 13 p1794 N88-20732

Thermal analysis of heat storage canisters for a solar dynamic, space power system
[DE88-004199] 15 p2027 N88-22075

Structural assessment of a space station solar dynamic heat receiver thermal energy storage canister
15 p2081 N88-22406

Development of an integrated heat pipe-thermal storage system for a solar receiver
[NASA-TM-101099] 15 p2091 N88-22456

Value of energy storage in pulsed space power systems
[AD-A191311] 16 p2170 N88-22938

Material degradation in a barium hydroxide latent heat storage pilot unit
[DFVLR-FB-87-49] 16 p2175 N88-22961

Assessment of energy storage concepts for use in sprint power
17 p2407 N88-24312

Transient analysis of Li and LiH thermal storage spheres
17 p2411 N88-24334

Field experience with aquifer thermal energy storage
[DE88-007075] 18 p2538 N88-25056

Advanced heat receiver conceptual design study
[NASA-CR-180901] 19 p2688 N88-25977

Thermodynamic analysis of chemical heat storage system for heat pump
[DE88-753121] 20 p2820 N88-26726

Transient thermal analysis of three latent heat storage configurations for rapid thermal charging
[DE88-008943] 20 p2881 N88-27104

Prediction of velocity and temperature profiles in thermally driven gravity currents applied to stratified thermal storage tanks
[DE88-004452] 21 p2946 N88-27496

Transient thermal analysis of three fast-charging latent heat storage configurations for a space-based power system
[DE88-009714] 23 p3186 N88-28960

HEAT STROKE

Rapid hypothermia subsequent to oral nicotinic acid and immersion in warm (30C) water
[AD-A186458] 08 p1050 N88-16339

HEAT TESTS

U HIGH TEMPERATURE TESTS

HEAT TOLERANCE

Assessment of the reliability of a correction procedure for WGT (Wet Globe Thermometer) (Botsball) measurements of heat stress
[AD-A185193] 05 p0584 N88-13559

Effects of moderate cold and heat stress on the potential work performance of industrial workers. Part 6: The effects of increasing vapour pressure at four air temperatures on the performance and physiology of white females
[PB88-124854] 18 p2550 N88-25137

Satellite remote sensing of the wet bulb globe temperature heat stress index, phase 2
[AD-A192798] 20 p2818 N88-26717

Hyperthermia: New thoughts on an old problem
[AD-A192602] 21 p2986 N88-27731

Plasma volume expansion in rats: Effects on thermoregulation and exercise
[AD-A192656] 22 p3130 N88-28606

HEAT TRANSFER

NT AERODYNAMIC HEAT TRANSFER
NT CONDUCTIVE HEAT TRANSFER
NT CONVECTIVE HEAT TRANSFER
NT LAMINAR HEAT TRANSFER
NT RADIATIVE HEAT TRANSFER
NT TURBULENT HEAT TRANSFER

Modeling and measurement of heat transfer on turbine blade tips
01 p0006 N88-10032

Thermal Control Working Group report
01 p0016 N88-10094

Effects of forced and free convections on structural temperatures of space shuttle orbiter during reentry flight
[NASA-TM-86800] 01 p0043 N88-10275

Membrane heat pipe development for space radiator applications
[DE86-006015] 01 p0045 N88-10285

Heat engine regenerators: Research status and needs
[DE87-013581] 01 p0054 N88-10348

The reliability of numerical solutions of ordinary differential equations, obtained by implicit calculation schemes
[PTB-W-30] 01 p0085 N88-10549

Error estimates for finite element approximations of parabolic variational equations
[BONNER-MATHE-SCHR-179]
01 p0087 N88-10569

The aerothermodynamic environment for holes in hypersonic configurations
[DE87-014651] 02 p0121 N88-10767

Thermal resistance of contacting metal surfaces at helium temperatures
[BLL-RISLEY-TR-5500-(9091.9F)]
02 p0148 N88-10929

Flow and heat transfer with impinging jets and rough surfaces
[DE87-014162] 02 p0169 N88-11065

Heat transfer in a real engine environment
02 p0186 N88-11155

Film cooling heat transfer on a turbine airfoil 02 p0186 N88-11156

Coolant passage heat transfer with rotation 02 p0186 N88-11160

Prediction of turbine blade heat transfer 02 p0187 N88-11162

Flow in a model turbine stator 02 p0187 N88-11163

Component specific modeling 02 p0187 N88-11166

New directions in Vlasov plasma turbulence and anomalous transport [DE87-014425] 02 p0238 N88-11500

A heat transfer model for a heated helium airship [AD-A183786] 03 p0259 N88-11629

Heat transfer in laminar flow for mass inlet into an annular channel [DE87-702890] 03 p0314 N88-11983

A transient model for thermal detonation [IKE-2-75] 03 p0314 N88-11984

Numerical analysis of Marangoni convection in Bridgman method 03 p0319 N88-12014

Heat transfer performance of axially grooved heat pipes 03 p0319 N88-12016

Heat transfer characteristics of arterial heat pipe with axial grooves 03 p0319 N88-12017

Pump assisted heat pipe 03 p0319 N88-12018

Local heat/mass transfer and pressure drop in a two-pass rib-roughened channel for turbine airfoil cooling [NASA-CR-179635] 03 p0322 N88-12039

Heats of mixing for thermal energy storage systems. Phase 1: Selection of suitable liquid-liquid mixtures [DE87-014971] 03 p0347 N88-12196

Performance analysis of advanced spacecraft TPS [NASA-CR-181532] 04 p0399 N88-12484

Thermal analysis of electromagnetic launcher rails [DE88-000166] 04 p0405 N88-12514

Ceramic technology for advanced heat engines project [DE88-001520] 04 p0420 N88-12605

Resistor cooling in a vacuum [DE88-000696] 04 p0440 N88-12733

NACHOS 2: A finite element computer program for incompressible flow problems. Part 2: User's manual [DE88-001451] 04 p0443 N88-12750

Steady shearing in a viscoplastic solid [AD-A184341] 04 p0454 N88-12810

Theory of heat and moisture exchange between finely disperse storm-generated spray and turbulent air flow 04 p0461 N88-12851

Structure of stably stratified atmospheric surface layer in presence of heat-releasing admixture 04 p0462 N88-12856

Influence of bond dilution on the free surface and interface Potts ferromagnetism [DE87-703380] 04 p0497 N88-13061

Experimental investigations on blunt bodies and corner configurations in hypersonic flow 05 p0530 N88-13225

An evaluation of a translator for finite element data to resistor/capacitor data for the heat diffusion equation [DE87-013926] 06 p0698 N88-14285

Heat transfer investigations in a slurry bubble column [DE88-001445] 06 p0699 N88-14286

International workshop on two-phase flow fundamentals [DE88-001478] 06 p0699 N88-14287

Advanced condensing heat exchangers [DE88-001485] 06 p0699 N88-14288

Model development for induction heating [DE88-002376] 06 p0699 N88-14289

HOST turbine heat transfer program summary [NASA-TM-100280] 06 p0704 N88-14320

Role of anomalous currents in formation of ocean surface temperature field 06 p0727 N88-14474

Wall turbulence control 07 p0812 N88-14943

Numerical computations of natural convection heat transfer in irregular geometries [DE88-002358] 07 p0852 N88-15178

The effect of asymmetric heating on flow stability and heat transfer for flow in a vertical tube [DE88-003242] 07 p0855 N88-15193

A numerical study of transient heat and mass transfer in crystal growth 07 p0925 N88-15619

Particle-gas temperature differentials resulting from time-dependent radiative-conductive heat flux divergences in the tenuous dust-laden atmosphere of mars [AD-A185888] 07 p0945 N88-15747

Turbomachinery 08 p0955 N88-15792

Finite element fundamentals, part 2 08 p0985 N88-15962

Review of the equations of fluid mechanics and heat transfer 08 p0986 N88-15970

The effect of eddy distribution on momentum and heat transfer near the wall in turbulent pipe flow [NASA-TM-100257] 08 p0988 N88-15984

Comparative performance of the conjugate gradient and SOR (Successive Over Relaxation) methods for computational thermal hydraulics [DE88-002553] 08 p0988 N88-15986

Influence of skeletal muscle glycogen on passive rewarming after hypothermia [AD-A186451] 08 p1049 N88-16334

Numerical simulation of heat transfer turbulence, volume 4 [AD-A185132] 09 p1159 N88-16947

Indirect measurement of local condensing heat-transfer coefficient around horizontal finned tubes [AD-A186929] 09 p1160 N88-16950

The dynamics of heat transfer at a turbulent pipe flow [OEFZS-4400] 09 p1164 N88-16975

A quasi-three-dimensional calculation procedure for the prediction of flow and heat transfer in heat exchanger passages 09 p1165 N88-16985

Interaction of the cold conveyor belt with polar jet streaks [AD-A186774] 09 p1192 N88-17145

Investigation of thermoacoustic heat transport using a thermoacoustic couple [AD-A186889] 09 p1242 N88-17442

Two-phase reduced gravity experiments for a space reactor design [DE86-015530] 09 p1247 N88-17475

Nonequilibrium superconductivity for particle detectors [DE88-002876] 09 p1257 N88-17539

Overview of heat transfer and fluid flow problem areas encountered in Stirling engine modeling [NASA-TM-100131] 09 p1262 N88-17561

Application of Hoffman modulation contrast microscopy coupled with three-wavelength two-beam interferometry to the in situ direct observation of the growth process of a crystal in microgravity 10 p1288 N88-17704

Effect of translucence of engineering ceramics on heat transfer in diesel engines [DE88-003732] 10 p1305 N88-17804

An experiment to investigate Rankine cycle two-phase microgravity issues [DE88-004197] 10 p1308 N88-17818

Mechanistic model for void distribution in flashing flow [DE88-002948] 10 p1326 N88-17928

Time-resolved heat transfer measurements and analysis in the wage region of a cylinder in crossflow 10 p1328 N88-17939

Periodic natural convection in a rectangular enclosure of low aspect ratio 10 p1329 N88-17941

Microcomputer analysis of regenerative heat exchangers for oscillating flow [DE88-001773] 10 p1329 N88-17945

Experimental studies of heat and mass exchange in parallel-passage rotary desiccant dehumidifiers for solar cooling applications [DE88-001119] 10 p1350 N88-18069

Physiological and ecological implications of coupled heat- and water-transport mechanisms of endotherms and vegetation [DE88-004170] 10 p1352 N88-18081

Disk pumping test [AD-A187199] 11 p1440 N88-18591

Investigation of surface tension driven convection as a feasibility study for a micro-gravity experiment [NASA-CR-182504] 11 p1466 N88-18739

Laminar flow heat transfer downstream from U-bends 11 p1484 N88-18859

Two and three dimensional elliptic flows 11 p1485 N88-18866

Unsteady heat transfer in turbine blade ducts: Focus on combustor sources [NASA-TM-100815] 11 p1486 N88-18870

Thermosolutal convection in high-aspect-ratio enclosures [NASA-TM-100803] 11 p1486 N88-18871

Effect of experimental variables on flash thermal diffusivity data analysis [DE88-003631] 11 p1487 N88-18877

Effect of density change on rapid liquid-solid interface kinetics and heat flow [DE88-004286] 11 p1487 N88-18878

Ultrasonic testing of heat exchanger tubes [DE88-751172] 11 p1497 N88-18939

Effect of element size on the solution accuracies of finite-element heat transfer and thermal stress analyses of space shuttle orbiter [NASA-TM-88292] 11 p1502 N88-18971

Mechanical design and construction of a 200 mA, 100 keV, dc, negative ion accelerator [DE88-003855] 11 p1548 N88-19257

A method of calculating nonstationary heat flow in hydrogasodynamic processes in closed cryogenic systems [DE88-700884] 12 p1626 N88-19727

Vapor-mist for lightweight high voltage space insulation systems [DE87-011704] 13 p1762 N88-20538

Investigation of heat transfer to a flat plate in a shock tube [AD-A189536] 13 p1766 N88-20561

Heat pipe transient analysis. Vapor dynamics [DE88-005132] 13 p1767 N88-20568

The influence of Mach number and heat transfer on the turbulent flow wall law [NASA-TT-20230] 13 p1771 N88-20594

Estimates of ocean-atmosphere thermal interaction in Gulf Stream energy-active test range in winter of 1984 13 p1785 N88-20679

Compatibility in space reactor fuel systems [DE88-005698] 13 p1839 N88-21004

Study on the burnout with variations of flow twisting over tube length [DE87-703170] 14 p1909 N88-21405

Ocean eddies 14 p1938 N88-21566

Thermal modeling of solar central receiver cavities [DE88-004940] 14 p1943 N88-21594

Mass, heat and nutrient fluxes in the Atlantic Ocean determined by inverse methods [NASA-CR-180535] 14 p1950 N88-21626

The role of water in the thermal balance of the coma 14 p1999 N88-21916

The numerical simulation of viscous flows with change of phase and chemical reaction [DE88-003204] 15 p2062 N88-22292

Enhancement of data acquisition and numerical computation capabilities for unsteady fluid dynamics [AD-A190115] 15 p2063 N88-22302

FLOSIN: A fluid loop analyzer for SINDA 15 p2066 N88-22321

Thermal-structural analyses of Space Shuttle Main Engine (SSME) hot section components 15 p2081 N88-22404

Review and assessment of the HOST turbine heat transfer program 15 p2086 N88-22431

Performance evaluation of molten salt thermal storage systems [DE87-014645] 15 p2091 N88-22461

Peculiarities of non-stationary heat transfer to superfluid helium [DE88-701174] 16 p2200 N88-23124

Gravity currents with heat transfer effects [PB88-180047] 16 p2205 N88-23158

Preliminary measurements of heat flux in a subsonic gun simulator [AD-A191090] 16 p2208 N88-23178

Boundary layer measurements using hot-film sensors 17 p2297 N88-23743

Studies of heat and mass transfer during chemical vapor deposition 17 p2338 N88-23953

The effects of inlet turbulence and rotor/stator interactions on the aerodynamics and heat transfer of a large-scale rotating turbine model. Part 4: Aerodynamic data tabulation [NASA-CR-179469] 17 p2339 N88-23956

Heat transfer in aerospace propulsion [NASA-TM-100874] 17 p2339 N88-23957

Pumped two-phase heat transfer loop [NASA-CASE-MSC-20841-2] 17 p2339 N88-23958

Botany Facility: Test report on breadboard tests for the determination of the heat transfer at the glass disk and of the temperature distribution in the fluorescent tube [BF-TN-ER-053] 17 p2378 N88-24136

An experiment to investigate Rankine cycle two-phase microgravity issues 17 p2409 N88-24322

Transient analysis of Li and LiH thermal storage spheres 17 p2411 N88-24334

A liquid metal MHD concept for multimegawatt space power application 17 p2413 N88-24348

Development of a lightweight structure with load bearing capability and high thermal conductance 17 p2420 N88-24393

A reflux tube fabric radiator 17 p2421 N88-24394

Heat pipe transient analysis: Vapor dynamics 17 p2421 N88-24397

The Curie point radiator 17 p2424 N88-24420

The liquid droplet radiator in space: A parametric approach 17 p2427 N88-24437

Nucleate pool boiling: High gravity to reduced gravity; liquid metals to cryogens 17 p2431 N88-24464

Reduced-gravity two-phase flow experiments in the NASA KC-135 17 p2431 N88-24465

Microgravity two-phase fluid flow pattern modeling 17 p2432 N88-24467

Method and apparatus for growing crystals [NASA-CASE-MFS-28137-1] 17 p2446 N88-24544

Analytic and numerical modeling of heat and material transport in electrical hypervelocity guns [AD-A192178] 18 p2469 N88-24655

Designing to safe power limits in hybrid circuits [DE88-005533] 18 p2506 N88-24865

Heat transfer from a negatively buoyant wall jet
[PB88-181953] 18 p2507 N88-24873

Computational fluid dynamics applied to the prediction of the heat-transfer, mechanical and thermal-stress behavior of heat exchangers
[CFDU/87/7] 18 p2510 N88-24893

Similarity solutions of nonlinear partial differential equations invariant to a family of affine groups
[DE88-003404] 18 p2567 N88-25245

Modelling of thermal plasma systems
18 p2578 N88-25314

Correlations of velocity and temperature fluctuations in the stagnation-point flow of circular cylinder in turbulent flow
[NASA-TM-100930] 19 p2597 N88-25435

Liquid phase decomposition in slurry fuels
19 p2624 N88-25564

Femtosecond nonequilibrium electronic heat transport in thin gold films 19 p2659 N88-25807

Pressure drop and heat transfer in turbulent non-Newtonian pipe flow of advanced energy transmission fluids
[DE88-010021] 19 p2666 N88-25853

Design and testing of a high power spacecraft thermal management system
[NASA-TM-4051] 20 p2764 N88-26389

Heat transfer of mesh-wick heat-pipes (bottom heat mode) 20 p2783 N88-26507

Magnetic heat pump design
[DE88-007730] 20 p2798 N88-26605

Multigrid computation of practical fluid flows and heat transfer
[DE88-010064] 20 p2799 N88-26609

Boundary element method for contact heat transfer
[DE88-011013] 20 p2800 N88-26613

Overview of the TITAN-2 reversed-field pinch aqueous fusion power core design
[DE88-008170] 20 p2857 N88-26966

Development of an experimental system for studying fast transient ignition phenomena
[DE88-011917] 21 p2911 N88-27276

Ceramic technology for advanced heat engines project
[DE88-008945] 21 p2919 N88-27323

Determination of lumped-mass thermal properties associated with autoclave curing of graphite/epoxy composites 21 p2925 N88-27364

Heat and mass transfer in a transport channel
[DE88-701968] 21 p2945 N88-27493

Determination of the local heat-transfer characteristics on glaze ice accretions on a cylinder and a NACA 0012 airfoil 21 p2946 N88-27500

Heat and mass transfer in laminar wavy film absorption with the presence of non-absorbable gases
21 p2947 N88-27502

Plasma behavior in the boundary layer near a railgun surface
[DE88-008889] 21 p3017 N88-27909

On the impact of low-latitude anomalous forcing on local and remote circulation: Winters(DJF) 1978/79 to 1986/87 22 p3123 N88-28560

The effects of inlet turbulence and rotor/stator interactions on the aerodynamics and heat transfer of a large-scale rotating turbine model. Volume 3: Heat transfer data tabulation 65 percent axial spacing
[NASA-CR-179468] 23 p3180 N88-28930

Transient thermal analysis of three fast-charging latent heat storage configurations for a space-based power system
[DE88-009714] 23 p3186 N88-28960

Combustion dynamics and thermal structure of a planar spray flame 23 p3190 N88-28985

Numerical investigations in three-dimensional internal flows
[NASA-CR-183108] 23 p3210 N88-29106

Aerodynamic heating of missiles
24 p3319 N88-29764

The use of hot-film technique for boundary layer studies on a 21 percent thick airfoil
[NAE-AN-45] 24 p3321 N88-29781

The effects of inlet turbulence and rotor/stator interactions on the aerodynamics and heat transfer of a large-scale rotating turbine model. Volume 2: Heat transfer data tabulation. 15 percent axial spacing
[NASA-CR-179467] 24 p3326 N88-29804

Effect of interfacial phenomena on contact line heat Transfer-3
[AD-A194941] 24 p3343 N88-29901

Radiation from soot-containing flames
24 p3347 N88-29927

Transition at hypersonic speeds
[NASA-CR-178315] 24 p3368 N88-30058

Assessment of a 3-D boundary layer analysis to predict heat transfer and flow field in a turbine passage
[NASA-CR-174894] 24 p3370 N88-30066

The use of upwind schemes at high Reynolds number: A cautionary note
[AD-A196227] 24 p3371 N88-30074

The thermal behavior of film cooled turbulent boundary layers as affected by longitudinal vortices
[AD-A195155] 24 p3374 N88-30095

HEAT TRANSFER COEFFICIENTS

Jet impingement heat transfer: A literature study
[PNR90404] 02 p0172 N88-11083

Measurement of airfoil heat transfer coefficients on a turbine stage 02 p0186 N88-11158

Heat transfer with very high free stream turbulence
02 p0186 N88-11161

Regressed relations for forced convection heat transfer in a direct injection stratified charge rotary engine
[NASA-TM-100124] 05 p0549 N88-13345

Determination of the heat conduction coefficient of the soil from the advance of the diurnal temperature wave
08 p1015 N88-16151

Indirect measurement of local condensing heat-transfer coefficient around horizontal finned tubes
[AD-A186929] 09 p1160 N88-16950

Heat transfer modeling of jet vane Thrust Vector Control (TVC) systems
[AD-A190106] 15 p2019 N88-22034

Note on the double crystal method of measuring heat transfer coefficient
[OUEL-1710/87] 17 p2338 N88-23950

Characteristics of long size thermosyphons made of corrugated tube 20 p2784 N88-26511

Estimation of transient heat transfer coefficients in multidimensional problems by using inverse heat transfer methods 23 p3210 N88-29108

Experimental and analytical study of two-phase flow in zero gravity
[AD-A195223] 24 p3358 N88-29993

HEAT TRANSMISSION

NT AERODYNAMIC HEAT TRANSFER
NT CONDUCTIVE HEAT TRANSFER
NT CONVECTIVE HEAT TRANSFER
NT HEAT TRANSFER
NT LAMINAR HEAT TRANSFER
NT RADIATIVE HEAT TRANSFER
NT TURBULENT HEAT TRANSFER

Nitrogen scale-up
[AD-A185702] 06 p0709 N88-14351

Determining deep heat flow under complex geothermal conditions 08 p1011 N88-16130

Effect of density change on rapid liquid-solid interface kinetics and heat flow
[DE88-004286] 11 p1487 N88-18878

A method of calculating nonstationary heat flow in hydrogasodynamic processes in closed cryogenic systems
[DE88-700884] 12 p1626 N88-19727

HEAT TREATMENT

NT ANNEALING
NT LASER ANNEALING
NT NITRIDING
NT PULSE HEATING
NT TEMPERING

Outgassing data for selecting spacecraft materials
[NASA-RP-1124] 01 p0019 N88-10117

Microstructural evolution and response to double-loop reactivation testing of heat-treated pH 13-8 Mo martensitic stainless steel
[DE87-009058] 02 p0146 N88-10915

Influence of thermocyclic treatment on mobility of grain boundaries
[BLL-M-37329-(5828.4)] 02 p0149 N88-10933

High temperature superconductors
03 p0297 N88-11869

Gas tungsten arc welding of Al-10Fe-5Ce
[AD-A184202] 03 p0334 N88-12104

Effect of long-term thermal aging on coated Celion/LARC-160 composites
[NASA-TM-100495] 04 p0410 N88-12544

Effect of time and temperature on transformation toughened zirconias
[AD-A184356] 04 p0419 N88-12600

Study of the influence of mechanical - thermal treatments on the creep behavior of a niobium stainless steel
[DE87-703506] 05 p0563 N88-13431

The effect of heat treatment on fatigue crack growth in polycarbonate 05 p0606 N88-13714

Characterization of current steels. The 35 NCD 16 alloy in 30 mm diam laminated bars made by Aubert and Duval
[CEAT-41/N/76] 07 p0832 N88-15046

Rare earth elements in heat treatable steels
[PB87-144002] 08 p0968 N88-15858

Laser transformation hardening of precision V-slide way
[PB87-144028] 08 p0991 N88-15999

Modification of properties of metals by high-power ion beams 08 p1079 N88-16507

Effects of a regenerating heat treatment on the creep behavior and the lifetime during creep test loading
[ETN-88-91063] 09 p1144 N88-16855

Effect of post-cure heat-treatment on static and fatigue behaviour of XAS-914C carbon fibre composite
[AD-A186943] 10 p1294 N88-17735

Effects of thermal and thermo-mechanical treatments on the mechanical properties of centrifugally cast alloy 718
[AD-A188195] 11 p1458 N88-18690

Influence of heat treatment on the properties of boroaluminum 14 p1886 N88-21270

Increasing the rate at which ceramic castings undergo preliminary heat-treatment in an ultra-high frequency magnetic field 14 p1886 N88-21275

Cellular thermosetting fluoropolymers and process for making them
[NASA-CASE-GSC-13008-1] 17 p2326 N88-23894

A study on the precipitation and reversion behaviors of Cu-0.3 percent Cr alloy by the step annealing method
[NASA-TT-20169] 18 p2489 N88-24764

Development of protective coatings for ceramic tubular components
[PB88-197165] 20 p2776 N88-26463

Stress corrosion of C ring specimen in salt spray tests
[I-186/87] 21 p2916 N88-27307

High-speed, precision processing using an electron beam 21 p2929 N88-27391

Preparation and development of advanced battery catalysts
[AD-A193208] 21 p2937 N88-27441

HEATERS

Research and development on high strength ceramic heaters discussed 04 p0404 N88-12508

HEATING

NT AERODYNAMIC HEATING
NT ARC HEATING
NT ATMOSPHERIC HEATING
NT ELECTRON CYCLOTRON HEATING
NT GAS HEATING
NT INDUCTION HEATING
NT IONOSPHERIC HEATING
NT KINETIC HEATING
NT LASER HEATING
NT PLASMA HEATING
NT PULSE HEATING
NT RADIANT HEATING
NT RADIO FREQUENCY HEATING
NT SHOCK HEATING
NT SOLAR HEATING
NT SPACE HEATING (BUILDINGS)
NT SUPERHEATING
NT TRANSIENT HEATING
NT WATER HEATING

Millimeter wave tokamak heating and current drive with a high power free electron laser
[DE87-011324] 01 p0099 N88-10651

Thermal testing by internal IR heating of the FEP module 02 p0136 N88-10854

Overview of free-piston Stirling engine technology for space power application
[NASA-TM-88886] 03 p0386 N88-12427

A large X-ray flare on Sigma 2 coronae borealis observed with exosat 04 p0508 N88-13121

Chromospheric and coronal heating in a bias-free sample of K dwarfs 04 p0518 N88-13184

Pumping systems and flow interfaces for rapid response electronic reheat controls 10 p1282 N88-17665

The influence of the heating procedure on the oxidation behaviour of NiAl studied by XPS
[AERE-R-12498] 10 p1300 N88-17776

A study of the magnetic field annihilation process in the magnetosphere and some geotechnical applications
[DE88-004165] 10 p1355 N88-18096

Coronal heating by means of helical magnetohydrodynamic turbulence
[AD-A187064] 10 p1410 N88-18413

An application of active surface heating for augmenting lift and reducing drag of an airfoil
[NASA-TM-100563] 11 p1436 N88-18570

Removal of out-of-plane distortion in mild steel panels using flame heating, volume 1
[AD-A187802] 11 p1457 N88-18684

Removal of out-of-plane distortion in mild steel panels using flame heating, volume 2
[AD-A187803] 11 p1457 N88-18685

Some effects of heating on the wind-driven velocity in the upper ocean 13 p1805 N88-20792

Rapid e-beam heating for measuring thermodynamics of metastable materials
[DE88-003565] 13 p1849 N88-21066

Early reheating and cosmic strings
13 p1855 N88-21103

Response of aluminum alloys to erosive particle impacts
[DE88-005910] 15 p2041 N88-22159

Investigation of boundary layer disturbances caused by periodic heating of a thin ribbon
[AD-A190572] 15 p2065 N88-22314

Tactical Rubidium Frequency Standard (TRFS)
[AD-A191049] 16 p2193 N88-23078

Heating at a propagating crack tip in a viscoplastic material
[AD-A190952] 16 p2224 N88-23274

Acoustic convective system
[NASA-CASE-NPO-17278-1-CU] 18 p2498 N88-24818

Heating and evaporation of turbulent liquid films: Measurement of film thickness and the onset of nucleate boiling
[DE88-006368] 18 p2512 N88-24905

Dynamics explorer data analysis
[NASA-CR-181428] 19 p2691 N88-25996

Numerical calculations of dopent diffusion involving flashlamp heating of silicon 21 p2929 N88-27384

Thermal-sensation control: A new method of controlling cooled/heated environments 21 p2930 N88-27394

Effects of surface tension and contact angle on sensible heating and boiling incipience in dielectric falling films
[DE88-007057] 21 p2945 N88-27492

Thermocouple for heating and cooling of memory metal actuators
[NASA-CASE-NPO-17068-1-CU] 23 p3217 N88-29151

HEATING EQUIPMENT

NT BOILERS
NT EVAPORATORS
NT FURNACES
NT IMAGE FURNACES
NT SOLAR FURNACES
NT VAPORIZERS

Development of creep resistant austenitic stainless steels for advanced steam cycle superheater application
[DE87-012929] 01 p0023 N88-10147

Electrical heating method -- pipelines, metal tanks
[GB-PATENT-2-137-059-A] 01 p0043 N88-10274

Development of an innovative, low-cost solar collector
[PB87-206819] 02 p0194 N88-11210

Modified 14Cr-16Ni stainless steels with improved creep resistance at 700 C due to tailored precipitate microstructures
[DE87-014788] 03 p0290 N88-11825

SCRAM JET (Supersonic Combustion Ramjet) combustion experiments 04 p0404 N88-12512

Plant Growth Module (PGM) conceptual design 05 p0631 N88-13855

Research on fluid dynamic energy separation
[DE88-002776] 10 p1339 N88-18001

HEAVING

The impact of vertical axis characteristics on helicopter handling qualities
[AD-A188964] 12 p1583 N88-19474

HEAVY COSMIC RAY PRIMARIES

U HEAVY NUCLEI
U PRIMARY COSMIC RAYS

HEAVY ELEMENTS

Heavy element compositions and energy spectra of galactic and solar cosmic rays 03 p0272 N88-11714

New nuclear structure calculations and the astrophysical r-process
[DE88-000979] 08 p1082 N88-16518

Molecular orbital studies of the bonding in heavy element organometallics: Progress report
[DE88-007765] 19 p2723 N88-26168

HEAVY IONS

Proceedings of the Workshop on Opportunities for Atomic Physics Using Slow, Highly-Charged Ions
[DE87-013991] 02 p0231 N88-11457

Proceedings of the Workshop on Opportunities for Atomic Physics Using Slow, Highly-Charged Ions
[DE87-013991] 02 p0231 N88-11457

Relativisitic heavy ion collisions
[DE87-014292] 02 p0232 N88-11462

Irradiations. Accumulated doses. Heavy ions --- space environment 03 p0272 N88-11708

Wavelengths of the 3p-3d transitions of the Co- and Fe-like ions: The effects of electron correlation
[DE88-000219] 04 p0498 N88-13067

Heavy-ion accelerator research for inertial fusion
[DE88-000541] 05 p0653 N88-14001

Method of plasma diagnostics by a heavy ion beam for the T-15 tokamak
[DE88-700342] 07 p0935 N88-15678

Particle desorption from nonconducting surfaces by high energy heavy ions
[ETN-88-91088] 09 p1245 N88-17461

Magnetic properties of heavy fermion superconductors
[ETN-88-91078] 09 p1255 N88-17524

Cellular effects of heavy ions: Experimental results and theoretical approaches --- space radiation 12 p1658 N88-19933

Effects of heavy ions on egg-developing systems 12 p1658 N88-19935

Effects of cosmic heavy ion radiation and space microgravity on plant systems 12 p1658 N88-19936

QED description of relativistic Coulomb excitation in heavy ion collisions
[DE88-700834] 12 p1689 N88-20100

In situ TEM observations of heavy ion damage in gallium arsenide
[DE88-005984] 14 p1986 N88-21843

Stochastic acceleration of cometary ions: The effects of composition and source strength distributions 14 p1997 N88-21902

An evaluation of energy-independent heavy ion transport coefficient approximations
[NASA-TM-101158] 17 p2397 N88-24251

The precipitation of energetic heavy ions into the upper atmosphere of Jupiter
[NASA-TM-101155] 17 p2452 N88-24565

The Jovian aurora: Electron or ion precipitation
[NASA-TM-101153] 17 p2452 N88-24566

The multistring model VENUS for ultrarelativistic heavy ion collisions
[DE88-007666] 18 p2573 N88-25284

Experiments with high energy nuclear beams at Brookhaven: From AGS to RHIC (Relativistic Heavy Ion Collider)
[DE88-007042] 18 p2574 N88-25287

Heavy ion fusion system assessment: Final focus and transport model
[LBL-23040] 19 p2725 N88-26183

Heavy ion collisions with A = 10(sup 57): Aspects of nuclear stability and the nuclear equation of state in coalescing neutron-star binary systems
[DE88-008029] 19 p2741 N88-26277

Charged pion production and projectile breakup in 85A MeV(sup)12C induced heavy ion reactions
[LUIP-8802] 20 p2850 N88-26920

Fluid dynamical model of ultrarelativistic heavy ion collisions
[DE88-007905] 20 p2850 N88-26921

Studies of HZE particle interactions and transport for space radiation protection purposes
[NASA-TM-101159] 20 p2886 N88-27142

Eikonal solutions to optical model coupled-channel equations
[NASA-TP-2830] 24 p3428 N88-30402

HEAVY LIFT HELICOPTERS

General equilibrium characteristics of a dual-lift helicopter system
[NASA-TP-2615] 12 p1573 N88-19407

HEAVY LIFT LAUNCH VEHICLES

Department of Housing and Urban Development-Independent Agencies Appropriations for fiscal year 1988, Thursday, 9 April 1987: National Aeronautics and Space Administration 03 p0386 N88-12424

Department of Housing and Urban Development-Independent Agencies Appropriations for fiscal year 1988, Friday, 10 April 1987: National Aeronautics and Space Administration 03 p0386 N88-12425

Assessment of mixed fleet potential for space station launch and assembly
[NASA-TM-100550] 11 p1443 N88-18608

Space station heavy lift launch vehicle utilization
[NASA-TM-100604] 14 p1873 N88-21188

HEAVY NUCLEI

Heavy-particle collisions in the plasma edge
[DE87-012928] 02 p0237 N88-11493

Neutron capture nucleosynthesis in low mass AGB stars 04 p0517 N88-13178

Investigation of a new magnetic dipole mode in the heavy, deformed nuclei 154 Sm, 156 Gd, 158 Gd, 164 Dy, 168 Er, and 174 Yb with high resolution electron scattering
[ETN-88-91084] 09 p1245 N88-17460

Production of heavy antinuclei: Review of experimental results 16 p2269 N88-23574

Cosmions and stars
[DE88-010886] 20 p2887 N88-27145

Charge composition of primary cosmic ray nuclei with z greater than or equal to 2 in energy region greater than or equal to 2 TeV 24 p3448 N88-30519

HEIGHT

NT SCALE HEIGHT

The end height of fireball as a function of their residual kinetic energy 06 p0737 N88-14535

Some measurements of height gain at V.H.F. 12 p1617 N88-19671

WAVFLD: A program to compute ionospheric height gain functions and field strengths at VLF
[AD-A191159] 16 p2191 N88-23066

Antenna heights for the optimum utilization of the oceanic evaporation duct. Part 1: Results from the Pacific measurements. Part 2: Results from the Key West measurements, volume 1
[AD-A192358] 20 p2791 N88-26555

TE/TM (Transverse Electric/Transverse Magnetic) height profile measurements of transpolar VLF (Very Low Frequency) signals
[AD-A194503] 22 p3069 N88-28216

Determination of most probable predicted 50 kPa pattern by empirical orthogonal functions 22 p3128 N88-28593

Analysis of environmental parameters from the Panama City tower radar experiment
[AD-A194994] 24 p3404 N88-30264

HEISENBERG THEORY

A study of mechanisms of hydrogen diffusion in separation devices
[DE88-000328] 04 p0416 N88-12584

A mechanism for symmetry breaking in antiferromagnetic Heisenberg systems
[ETN-88-91320] 05 p0657 N88-14031

HELICAL ANTENNAS

Short experiment study of four-wire helical antennas (half turn half wave)
[CNES-CT/DRT/TIT/AN-249-T] 15 p2058 N88-22266

HELICAL FLOW

Computational study of three-dimensional magnetohydrodynamic equilibria in toroidal helical systems
[DE87-753007] 02 p0240 N88-11514

On helicity fluctuations and the energy cascade in turbulence
[NASA-CR-178403] 03 p0321 N88-12028

Helicity dissipation in the plasma edge
[DE87-014762] 03 p0378 N88-12376

HELICAL INDUCERS

Symmetrized magnetic field configuration of low aspect ratio helical system
[IPPJ-869] 20 p2855 N88-26956

HELICAL WINDINGS

On some asymptotics of laminar flow in a coiled pipe 10 p1328 N88-17936

HELICOPTER ATTITUDE INDICATORS

U ATTITUDE INDICATORS
U HELICOPTERS

HELICOPTER CONTROL

Engine/airframe response evaluation of the HH-60A helicopter equipped with the T700-GE-701 transient droop improvement electronic control unit
[AD-A184443] 04 p0401 N88-12492

Rotor SAR (ROSAR): A new high-resolution all-weather vision method for helicopters
[MBB-UA-1046/87] 10 p1314 N88-17855

The impact of vertical axis characteristics on helicopter handling qualities
[AD-A188964] 12 p1583 N88-19474

Automatic flight control system for modern helicopters 12 p1597 N88-19558

Servo-actuator control for sampled-data feedback disturbance rejection --- helicopters
[ESA-TT-1002] 16 p2163 N88-22903

Helicopter anti-torque system using fuselage strakes
[NASA-CASE-LAR-13630-1] 17 p2308 N88-23809

Simultaneous multiple control force exertion capabilities of males and females versus helicopter control force design limits
[AD-A191653] 18 p2553 N88-25153

Frequency domain identification of the dynamics of a scaled remotely-piloted helicopter 20 p2786 N88-26524

Minimum-complexity helicopter simulation math model
[NASA-CR-177476] 24 p3328 N88-29819

HELICOPTER DESIGN

Integration of dynamic, aerodynamic and structural optimization of helicopter rotor blades
[NASA-CR-181441] 01 p0002 N88-10012

Results of the 1986 NASA/FAA/DFVLR main rotor test entry in the German-Dutch wind tunnel (DNW)
[NASA-TM-100507] 04 p0487 N88-13003

Model helicopter rotor rig and associated strain gauge balance for performance studies
[NAL-TM-AE-8704] 05 p0552 N88-13364

Sitting posture of helicopter pilots of the Royal Netherlands Air Force; preliminary recommendations
[IZF-1986-16] 05 p0631 N88-13857

Rotorcraft transmission 08 p0956 N88-15802

Accomplishments at NASA Langley Research Center in rotorcraft aerodynamics technology 09 p1105 N88-16626

Rotorcraft aeroelastic stability 09 p1106 N88-16631

System analysis in rotorcraft design: The past decade 09 p1110 N88-16652

An integrated approach to rotorcraft human factors research 09 p1110 N88-16653

An overview of key technology thrusts at Bell Helicopter Textron 09 p1111 N88-16657

Rotorcraft technology at Boeing Vertol: Recent advances 09 p1111 N88-16658

Recent Sikorsky R and D progress 09 p1111 N88-16659

Analysis of tasks for dynamic man/machine load balancing in advanced helicopters
[DE88-003735] 09 p1117 N88-16696

Helicopter activities in Germany
[MBB-UD-487/86] 10 p1314 N88-17853

Testing of a tail rotor system in a fiber composite type of construction
[MBB-UD-472/86] 10 p1314 N88-17854

Computer program for conceptual tandem rotor helicopter design
[AD-A187832] 11 p1439 N88-18584

Verification of the momemtum theory for rotors using measurements on a model helicopter
[R-840-S] 13 p1718 N88-20275

Helicopter anti-torque system using fuselage strakes
[NASA-CASE-LAR-13630-1] 17 p2308 N88-23809

Structurally tailorable non-linear snap-through spring system
[NASA-CASE-LAR-13729-1] 18 p2523 N88-24970

Aeroelastic characteristics of the AH-64 bearingless tail rotor 21 p2891 N88-27162

Program user's manual for an unsteady helicopter rotor-fuselage aerodynamic analysis
[NASA-CR-181701] 22 p3039 N88-28047

HELICOPTER ENGINES

Efficiency testing of a helicopter transmission planetary reduction stage
[NASA-TP-2795] 07 p0861 N88-15224

Dynamic analysis of multimesh-gear helicopter transmissions
[NASA-TP-2789] 09 p1176 N88-17045

Army maintenance: Actions to reduce the likelihood of helicopter gear failures
[PB88-135256] 11 p1433 N88-18551

Artificial and natural icing tests of AH-64, phase 2
[AD-A188231] 11 p1439 N88-18585

HELICOPTER IMPULSIVE NOISE

U BLADE SLAP NOISE

HELICOPTER PERFORMANCE

An observer approach to the estimation of helicopter airspeed
[DFVLR-FB-87-13] 01 p0005 N88-10029

Engine/airframe response evaluation of the HH-60A helicopter equipped with the T700-GE-701 transient droop improvement electronic control unit
[AD-A184443] 04 p0401 N88-12492

Impact of flying qualities on mission effectiveness for helicopter air combat, volume 1
[NASA-CR-166568] 06 p0669 N88-14100

NASA/Army Rotorcraft Technology. Volume 3: Systems Integration, Research Aircraft, and Industry
[NASA-CP-2495-VOL-3] 09 p1110 N88-16650

System analysis in rotorcraft design: The past decade 09 p1110 N88-16652

Rotorcraft flight research with emphasis on rotor systems 09 p1111 N88-16656

Helicopters as test carriers for avionics systems (HETAS)
[DFVLR-IB-112-85/18] 09 p1116 N88-16692

Optimizing HF antenna systems on the Dolphin and Sea Hawk helicopters
[AD-A186552] 09 p1152 N88-16901

Rotorcraft weight trends in light of structural material characteristics
[AD-A186576] 10 p1276 N88-17642

Helicopter activities in Germany
[MBB-UD-487/86] 10 p1314 N88-17853

Robust digital model following controller for helicopters
[DFVLR-FB-88-07] 21 p2898 N88-27203

Preliminary airworthiness evaluation of the UH-60A/ESSS (External Stores Support System) with HELLFIRE launcher installed
[AD-A196187] 24 p3323 N88-29793

HELICOPTER ROTORS

U ROTARY WINGS

HELICOPTER TAIL ROTORS

A study of rotor broadband noise mechanisms and helicopter tail rotor noise 06 p0777 N88-14766

An experimental investigation of the chopping of helicopter main rotor tip vortices by the tail rotor. Part 2: High speed photographic study
[NASA-CR-177457] 09 p1114 N88-16678

Testing of a tail rotor system in a fiber composite type of construction
[MBB-UD-472/86] 10 p1314 N88-17854

HELICOPTERS

NT AH-64 HELICOPTER
NT BO-105 HELICOPTER
NT CH-46 HELICOPTER
NT COMPOUND HELICOPTERS
NT HEAVY LIFT HELICOPTERS
NT MILITARY HELICOPTERS
NT OH-58 HELICOPTER
NT RIGID ROTOR HELICOPTERS
NT TANDEM ROTOR HELICOPTERS
NT UH-1 HELICOPTER
NT UH-60A HELICOPTER

Detection of targets in the presence of clutter using target echo modulations caused by rotating structures
[REPT-12-86] 01 p0036 N88-10231

Analytical modeling of helicopter static and dynamic induced velocity in GRASP
[NASA-TM-100026] 02 p0123 N88-10777

Global positioning satellite-based automatic landing system and wind estimated feedback for the AH-64 helicopter 02 p0124 N88-10784

Improved oil-off survivability of tapered roller bearings
[NASA-CR-180804] 02 p0182 N88-11135

Helicopter main-rotor speed effects on far-field acoustic levels
[NASA-TM-100512] 02 p0230 N88-11451

Rotorcraft Design for Operations
[AGARD-CP-423] 03 p0262 N88-11649

Design requirements for future commercial operations 03 p0262 N88-11651

Mission-oriented flying qualities criteria for helicopter design via in-flight simulation 03 p0263 N88-11652

Handling qualities criterion for very low visibility rotorcraft 03 p0263 N88-11654

The flight evaluation of an advanced engine display and monitoring system 03 p0264 N88-11659

Active control of helicopter vibration using multiloop self-adaptive control 03 p0264 N88-11660

Controlling the dynamic environment during NOE flight 03 p0264 N88-11661

Minimisation of helicopter vibration through active control of structural response 03 p0264 N88-11662

New aerodynamic design of the fenestron for improved performance 03 p0264 N88-11664

System for SAR missions 03 p0265 N88-11671

The EH-101 integrated project: A naval, utility and commercial helicopter system 03 p0265 N88-11672

Analytic investigation of helicopter rotor blade appended aeroelastic devices
[NASA-CR-166525] 03 p0266 N88-11676

Integrated voice and visual systems research topics
[NASA-CR-177417] 03 p0356 N88-12246

Report of the helicopter human factors working group --- accident prevention
[CAA-PAPER-87007] 03 p0361 N88-12274

A full potential flow analysis with realistic wake influence for helicopter rotor airload prediction
[NASA-CR-4007] 04 p0393 N88-12452

A 0.15-scale study of configuration effects on the aerodynamic interaction between main rotor and fuselage
[NASA-CR-166577] 04 p0395 N88-12462

GPS vertical axis performance enhancement for helicopter precision landing approach
[NASA-CR-177443] 04 p0397 N88-12477

Hovering helicopter flight dynamics: A study of vertical motion
[AR-004-526] 04 p0399 N88-12485

Some data processing requirements for precision Nap-Of-the-Earth (NOE) guidance and control of rotorcraft
[NASA-CR-177453] 04 p0401 N88-12493

Flap-lag equations of motion of rigid, articulated rotor blades with three hinge sequences
[NASA-TM-100023] 04 p0401 N88-12495

Calculation of helicopter rotor blade/vortex interaction by Navier-Stokes procedures
[NASA-CR-177441] 05 p0540 N88-13291

Coupled elastic rotor/body vibrations with inplane degrees of freedom 05 p0596 N88-13643

Sitting posture of helicopter pilots of the Royal Netherlands Air Force; preliminary recommendations
[IZF-1986-16] 05 p0631 N88-13857

Development of an unsteady wake theory appropriate for aeroelastic analyses of rotors in hover and forward flight
[NASA-CR-182357] 06 p0664 N88-14075

Aircraft accident report: Grand Canyon Airlines, Inc., and Helitech, Inc., midair collision over Grand Canyon National Park, June 18, 1986
[PB87-910403] 06 p0666 N88-14087

Euler solution of multiblade rotor flow
[NASA-TM-100014] 06 p0704 N88-14322

Development of rotorcraft interior noise control concepts. Phase 3: Development of noise control concepts
[NASA-CR-178172] 06 p0776 N88-14702

Development of a prototype H-46 helicopter diagnostic expert system
[AD-A186077] 07 p0809 N88-14924

Lift distribution and velocity field measurements for a three-dimensional, steady blade/vortex interaction
[NASA-TM-100013] 07 p0815 N88-14962

Digital processing of flight test data without using anti-aliasing filters, using a helicopter as an example
[DFVLR-MITT-87-12] 07 p0819 N88-14981

Experimental design of a piloted helicopter off-axis-tracking simulation using a helmet mounted display
[AD-A186228] 07 p0820 N88-14982

Turbine engine supportability study for Army Aviation Systems Command (AVSCOM)
[DE88-002339] 07 p0820 N88-14984

Application of the analysis phase of the instructional system development to the MK-105 magnetic minesweeping mission of the MH-53E helicopter
[AD-A186282] 07 p0822 N88-14994

The development of laboratory vibration test schedules: Philosophies and techniques 08 p0999 N88-16049

NASA/Army Rotorcraft Technology. Volume 1: Aerodynamics, and Dynamics and Aeroelasticity
[NASA-CP-2495-VOL-1] 09 p1105 N88-16625

The development of CFD methods for rotor applications 09 p1105 N88-16627

A summary of recent NASA/Army contributions to rotorcraft vibrations and structural dynamics technology 09 p1105 N88-16628

NASA/Army Rotorcraft Technology. Volume 2: Materials and Structures, Propulsion and Drive Systems, Flight Dynamics and Control, and Acoustics
[NASA-CP-2495-VOL-2] 09 p1106 N88-16632

Review of fatigue and fracture research at NASA Langley Research Center 09 p1106 N88-16633

Helicopter crashworthiness research program 09 p1107 N88-16635

Results of NASA/Army transmission research 09 p1108 N88-16640

NASA's rotorcraft icing research program 09 p1108 N88-16641

Helicopter mathematical models and control law development for handling qualities research 09 p1108 N88-16642

Rotorcraft flight-propulsion control integration 09 p1108 N88-16643

Helicopter human factors research 09 p1109 N88-16644

Rotorcraft handling-qualities design criteria development 09 p1109 N88-16645

A decade of aeroacoustic research at NASA Ames Research Center 09 p1109 N88-16648

Aeroacoustic research programs at the Army Aviation Research and Technology Activity 09 p1109 N88-16649

Status of NASA/Army rotorcraft research and development piloted flight simulation 09 p1110 N88-16651

Helicopters as test carriers for avionics systems (HETAS)
[DFVLR-IB-112-85/18] 09 p1116 N88-16692

Optimizing HF antenna systems on the Dolphin and Sea Hawk helicopters
[AD-A186552] 09 p1152 N88-16901

Refinement of eye-point-of-regard measurement with helicopter pilots in a flight experiment
[ESA-TT-1073] 09 p1200 N88-17195

Comparison of alphanumeric data entry methods for advanced helicopter cockpits
[AD-A186934] 09 p1201 N88-17201

General Rotorcraft Aeromechanical Stability Program (GRASP) version 1.03: User's manual
[NASA-TM-100043] 09 p1219 N88-17313

Helicopter external vision requirements and visual display characteristics: A report/bibliography, revision A
[AD-A187075] 10 p1276 N88-17641

Research and development. Technical-scientific publications (1956-1987): Retrospective view and prospects. Jubilee edition on the occasion of the 75th birthday of Dipl.-Engr. Dr.-Engr. E. H. Ludwig Boelkow
[ISSN-0931-9751] 10 p1309 N88-17819

Special flight mechanical features of the bearingless helicopter rotor
[MBB-FM-315/O] 10 p1309 N88-17825

Comprehensive analysis of helicopters with bearingless rotors
[NASA-CR-182537] 10 p1390 N88-18300

The maximum entropy method for the analysis of radar echoes from hovering helicopters in clutter
[FB-2-87] 11 p1475 N88-18799

Acoustic measurements from a rotor blade-vortex interaction noise experiment in the German-Dutch Wind Tunnel (DNW)
[NASA-TM-4024] 11 p1542 N88-19218
Safety study: Commercial emergency medical service helicopter operation
[PB88-917001] 12 p1575 N88-19422
Minimum weight design of rectangular and tapered helicopter rotor blades with frequency constraints
[NASA-TM-100561] 12 p1582 N88-19465
Automatic flight control system for modern helicopters
12 p1597 N88-19558
Organization of helicopter development activities with a view toward reduction of costs and cycles
12 p1704 N88-20200
An experimental investigation of the flap-lag-torsion aeroelastic stability of a small-scale hingeless helicopter rotor in hover
[NASA-TP-2546] 13 p1715 N88-20257
Procedure for detection and identification of a helicopter
[NASA-TT-20234] 13 p1722 N88-20297
Time-domain system for identification of the natural resonant frequencies of aircraft relevant to electromagnetic compatibility testing
[PB88-164520] 13 p1759 N88-20519
Optimal placement of tuning masses for vibration reduction in helicopter rotor blades
[NASA-TM-100562] 13 p1782 N88-20665
Inflow measurement made with a laser velocimeter on a helicopter model in forward flight. Volume 2: Rectangular planform blades at an advance ratio of 0.23
[NASA-TM-100542] 14 p1864 N88-21139
Advanced transmission studies
[NASA-TM-100867] 14 p1919 N88-21454
Inflow measurement made with a laser velocimeter on a helicopter model in forward flight. Volume 3: Rectangular planform blades at an advance ratio of 0.30
[NASA-TM-100543] 15 p2015 N88-22015
The effects of torque response and time delay on rotorcraft vertical axis handling qualities
[AD-A189873] 15 p2017 N88-22023
Preliminary airworthiness evaluation of the UH-60A equipped with the XM-139 VOLCANO mine dispensing system
[AD-A190604] 15 p2018 N88-22029
Method and device for the detection and identification of a helicopter
[NASA-TT-20251] 15 p2129 N88-22698
Acoustic propagation in the low atmosphere. Experimental study and modeling by the radius method
[ISL-CO-247/86] 15 p2131 N88-22713
Inflow measurements made with a laser velocimeter on a helicopter model in forward flight. Volume 4: Tapered planform blades at an advance ratio of 0.15
[NASA-TM-100544] 16 p2156 N88-22863
Tip vortices of isolated wings and helicopter rotor blades
[AD-A191336] 16 p2158 N88-22874
Development of a flexible and, economic helicopter engine monitoring system
[PB88-165147] 16 p2160 N88-22887
Digital processing of flight data of a helicopter without using anti-aliasing filters
[ESA-TT-1094] 16 p2161 N88-22890
Minimum weight design of rotorcraft blades with multiple frequency and stress constraints
[NASA-TM-100569] 16 p2161 N88-22892
The application of linear maximum likelihood estimation of aerodynamic derivatives for the Bell-205 and Bell-206
[AD-A191279] 16 p2161 N88-22894
Airworthiness and flight characteristics test of a ski assembly for the UH-60A Black Hawk helicopter
[AD-A191414] 16 p2162 N88-22895
Experimental investigation of Hover flowfields in water at the McDonnell Douglas Research Laboratories
16 p2202 N88-23135
Acoustic characteristics of 1/20-scale model helicopter rotors
[NASA-CR-177355] 16 p2265 N88-23548
Inflow measurement made with a laser velocimeter on a helicopter model in forward flight. Volume 5: Tapered planform blades at an advance ratio of 0.23
[NASA-TM-100545] 17 p2299 N88-23755
Design and development of an avionics system adapted to helicopter missions 17 p2305 N88-23786
Competitive assessment of the U.S. civil helicopter industry
[PB88-186325] 18 p2455 N88-24574
Passive shock wave-boundary layer control for the Bell FX69-H-098 airfoil 18 p2457 N88-24588
Some rotorcraft applications of computational fluid dynamics
[NASA-TM-100066] 18 p2459 N88-24601
Inflow measurements made with a laser velocimeter on a helicopter model in forward flight. Volume 1: Rectangular planform blades at an advance ration of 0.15
[NASA-TM-100541] 18 p2460 N88-24607
Rotorcraft TCAS (traffic alert and collision avoidance system) evaluation: Group 3 results
[AD-A191719] 18 p2461 N88-24614
An enumeration of research to determine the optimal design and use of Army flight training simulators
[AD-A191242] 18 p2468 N88-24649
Design, manufacture and spin test of high contact ratio helicopter transmission utilizing Self-Aligning Bearingless Planetary (SABP)
[NASA-CR-4155] 18 p2524 N88-24975
Zero/zero rotorcraft certification issues. Volume 1: Executive summary
[NASA-CR-177483-VOL-1] 19 p2602 N88-25453
Zero/zero rotorcraft certification issues. Volume 2: Plenary session presentations
[NASA-CR-177483-VOL-2] 19 p2602 N88-25454
Zero/zero rotorcraft certification issues. Volume 3: Working group results
[NASA-CR-177483-VOL-3] 19 p2602 N88-25455
Grid generation of a helicopter rotary-wing
19 p2640 N88-25665
Aircraft accident report: Joe Foster Excavating, Inc., Bell 206B, N49606, in-flight collision with trees, Alamo, California, August 3, 1986
[PB88-910405] 20 p2755 N88-26345
Flight Mechanics Panel Symposium on Rotorcraft Design for Operations: Technical evaluation report
[AGARD-AR-243] 20 p2758 N88-26362
Computer simulation of a single pilot flying a modern high-performance helicopter
[NASA-TM-100182] 20 p2761 N88-26376
Computer simulation of multiple pilots flying a modern high performance helicopter
[NASA-TM-100183] 20 p2761 N88-26377
A high fidelity real-time simulation of a small turboshaft engine
[NASA-TM-100991] 20 p2761 N88-26378
A general-purpose approach to computer-aided dynamic analysis of a flexible helicopter
[NASA-TM-101002] 20 p2816 N88-26709
A comparison of the various helicopter mathematical models used in the methodology assessment
21 p2889 N88-27149
A comparison of theory and experiment for aeroelastic stability of a hingeless rotor model in hover
21 p2889 N88-27150
A comparison of theory and flight test of the BO 105/BMR in hover and forward flight
21 p2890 N88-27155
Comparison of experimental coupled helicopter rotor/body stability results with a simple analytical model
21 p2891 N88-27160
Transonic blade-vortex interactions
22 p3037 N88-28035
Euler equation computations for the flow over a hovering helicopter rotor
[NASA-CR-177493] 22 p3038 N88-28037
Dual adaptive control: Design principles and applications
[NASA-CR-177485] 22 p3038 N88-28038
Proceedings of the French-German Colloquium on Helicopter Detection
[ISL-R-104/87] 22 p3147 N88-28723
Acoustic helicopter positioning
22 p3148 N88-28726
Acoustic detection of helicopters: Experiments
22 p3148 N88-28727
Acoustic direction finding of flying helicopters
22 p3148 N88-28728
Detection of helicopters using ground-controlled microphones 22 p3148 N88-28730
Sensors adapted for acoustic detection
22 p3148 N88-28731
Correlation method and sensors adapted to the environment 22 p3149 N88-28732
Helicopter Warning Sensor (HWS)
22 p3149 N88-28735
Helicopter recognition using laser radars
22 p3149 N88-28736
The maximum entropy method for the analysis of short-time radar echoes from hovering helicopters
22 p3149 N88-28737
The VHF experimental radar LARA. A long-wavelength radar for helicopter detection 22 p3149 N88-28738
The radar detection of hovering helicopters
22 p3150 N88-28739
Investigation of helicopter rotor blade/wake interactive impulsive noise
[NASA-CR-177435] 23 p3171 N88-28882
JUH-1H redesigned pneumatic boot deicing system flight test evaluation
[AD-A194918] 24 p3322 N88-29785
Threat expert system technology advisor
[NASA-CR-177479] 24 p3328 N88-29816
Development and demonstration of an on-board mission planner for helicopters
[NASA-CR-177482] 24 p3328 N88-29817
A fiber optic collective flight control system for helicopters
[AD-A195406] 24 p3328 N88-29818

HELIOCENTRIC ORBITS
U SOLAR ORBITS

HELIOGRAPHS
U SPECTROHELIOGRAPHS

HELIOGRAPHY
U SPECTROHELIOGRAPHS

HELIOMAGNETISM
U SOLAR MAGNETIC FIELD

HELIOS SATELLITES
NT HELIOS 1
NT HELIOS 2
Comet West: A view from the HELIOS zodiacal light photometers 01 p0117 N88-10749

HELIOS 1
Magnetic field hourly averages from the Rome-GSFC experiment aboard Helios 1 and Helio 2
[NASA-TM-89782] 14 p2011 N88-21995

HELIOS 2
Magnetic field hourly averages from the Rome-GSFC experiment aboard Helios 1 and Helio 2
[NASA-TM-89782] 14 p2011 N88-21995

HELIOSEISMOLOGY
Perturbations of the Sun's gravitational field due to solar oscillations
[DE88-002099] 07 p0946 N88-15751
Solar oscillations, gravitational multipole field of the Sun and the solar neutrino paradox
[DE88-002100] 07 p0946 N88-15752

HELIOSPHERE
Solar modulation of the cosmic radiation in the heliosphere 01 p0112 N88-10720
Evolution of the solar wind structure in the outer heliosphere 01 p0112 N88-10721
Observations of turbulence and fluctuations in the solar wind 04 p0525 N88-13212
Observations of cosmic rays in the outer heliosphere
[NASA-CR-182942] 18 p2596 N88-25425

HELIOSTATS
Solar thermal technology
[DE87-001171] 02 p0195 N88-11218
Polymers in solar technologies
[DE88-001102] 03 p0294 N88-11849
Mean and peak wind load reduction on heliostats
[DE87-012281] 07 p0873 N88-15296
Performance evaluation of large-area glass-mirror heliostats
[DE88-011883] 21 p2969 N88-27636
Optical evaluation of prototype stretched-membrane mirror modules for solar central receivers
[DE88-011884] 21 p2969 N88-27637

HELIPORTS
Analyses of heliport system plans
[DOT/FAA/PM-87/31] 17 p2308 N88-23810
Four urban heliport case studies
[DOT/FAA/PM-87/32] 19 p2604 N88-25463

HELIUM
NT HELIUM ISOTOPES
NT LIQUID HELIUM
NT LIQUID HELIUM 2
Impact behavior of 9-Cr and 12-Cr ferritic steels after low-temperature irradiation
[DE88-000333] 03 p0291 N88-11827
Experimental study of stabilizing He-Ne laser output power with transverse magnetic field
03 p0303 N88-11906
A cold ejector for closed-cycle helium refrigerators
04 p0434 N88-12690
Design concepts for the ASTROMAG cryogenic system
[NASA-CR-181505] 04 p0497 N88-13060
A helium flare on the active G5 dwarf Kappa Ceti
04 p0519 N88-13189
An investigation into flow regimes for two-phase helium flow
[DE88-002834] 07 p0853 N88-15181
Tests of cold helium compressors at Fermilab
[DE88-002837] 07 p0862 N88-15230
A refractometer for the interferometric determination of the helium abundance in the Jupiter atmosphere
[BONN-IR-86-23] 07 p0946 N88-15749
New technique for enhancing helium production in ferritic materials
[DE88-003048] 09 p1142 N88-16847
State-to-state dynamics of molecular energy transfer
[DE88-003282] 10 p1406 N88-18382
Superfluid turbulence in He II at elevated pressures
10 p1422 N88-18493

Weldability of tritium-charged 304L stainless steel
[DP-1740] 12 p1607 N88-19611

An experimental and theoretical investigation of optogalvanic effects
[AD-A189618] 12 p1625 N88-19720

Creep behavior of consolidated rapidly solidified Type 304 stainless steel powder containing helium
[DE88-005536] 13 p1743 N88-20424

Experimental and theoretical methods for investigating helium effects in rapidly solidified metals
[DE88-005542] 13 p1743 N88-20425

Increase in influence of oxygen on the body in the presence of helium 13 p1810 N88-20816

The astrophysics of nebulae and active galactic nuclear emission-line regions: New methods and applications
13 p1858 N88-21111

Spectrographic detection of nitrogen impurity in helium
[DE88-752301] 15 p2033 N88-22111

Long-time tunneling in amorphous metals at helium temperatures
[DE88-701150] 16 p2261 N88-23654

Preliminary analysis of helium generation and its effects on the SP-100 system performance
17 p2422 N88-24406

Helium induced degradation in the weldability of an austenitic stainless steel
[DE88-009062] 20 p2773 N88-26443

HeFlow: A program for calculating pressure and temperature of helium in forced-flow superconductors. Part 1: Numerical solutions. Part 2: HeFlow user's manual
[DE88-008941] 20 p2876 N88-27071

Cosmological helium production simplified
[DE88-009578] 20 p2885 N88-27130

Improved adhesion for SiO2 particles in silica substrates using helium-ion irradiation
[DE88-008915] 21 p2920 N88-27332

Mass flow rate influence on void fraction of two-phase helium flow
[DE88-702456] 21 p2945 N88-27495

Temperature rise in superfluid helium pumps
[NASA-TM-100997] 21 p2948 N88-27507

An upper limit on the primordial He4 abundance from speckle interferometric observations of muon Cassiopeiae 23 p3298 N88-29641

Crystal structure and density of helium to 232 kbar
24 p3441 N88-30481

Evolutionary helium and CNO anomalies in the atmospheres and winds of massive hot stars
[NASA-CR-183254] 24 p3452 N88-30550

HELIUM ATOMS

Helium atom surface scattering apparatus for studies of crystalline surface dynamics
[DE88-002104] 06 p0787 N88-14826

HELIUM FILM

Dilution refrigerator with non-valve adsorption system of sup 3/He circulation
[DE88-700974] 15 p2050 N88-22209

HELIUM IONS

Experimental method for investigating helium effects in irradiated vanadium
[DE88-002891] 08 p0969 N88-15865

HELIUM ISOTOPES

Dilution refrigerator with non-valve adsorption system of sup 3/He circulation
[DE88-700974] 15 p2050 N88-22209

Basic characteristics of heat-exchanger-type steam reformer heated by high-temperature helium gas (2). Analysis by simulation model (2)
[DE87-702962] 15 p2061 N88-22291

Peculiarities of non-stationary heat transfer to superfluid helium
[DE88-701174] 16 p2200 N88-23124

Helium-3 fusion fuel resources for space power
17 p2410 N88-24330

Energy requirements for HE-3 mining operations on the Moon 17 p2420 N88-24390

HELIUM PLASMA

SOAR: Space orbiting advanced fusion power reactor
[AD-A189234] 13 p1732 N88-20356

Properties of hydrogen/helium accretion plasmas
[DE88-006831] 19 p2728 N88-26197

HELIUM STARS

U B STARS

HELIUM 2

U HELIUM ISOTOPES
U LIQUID HELIUM

HELIUM 3

U HELIUM ISOTOPES

HELIUM 4

U HELIUM ISOTOPES

HELIUM-NEON LASERS

Measuring stability of optical reference cavities by analyzing polarization spectrum
03 p0327 N88-12065

Laser system for automating topographic terrain survey 08 p1012 N88-16136

Fuels combustion research
[AD-A189114] 13 p1736 N88-20381

Failure mechanism of He-Ne lasers
14 p1902 N88-21362

Particle beam alignment system for single event upset-Van de Graaf experiments
[AD-A189695] 15 p2132 N88-22721

Fast acting optical beam detection and deflection system
[AD-A192161] 18 p2521 N88-24954

Precise beam alignment He-Ne laser tubes
[PB87-228334] 19 p2675 N88-25906

HELIUM-OXYGEN ATMOSPHERES

Structure and properties of welded joints produced between niobium parts in controllable helium atmosphere 14 p1897 N88-21326

Life in a hyperbaric environment. A new O2-H2 breathing mixture for industrial diving 19 p2695 N88-26019

HELIX TUBES

U TRAVELING WAVE TUBES

HELMET MOUNTED DISPLAYS

Experimental design of a piloted helicopter off-axis-tracking simulation using a helmet mounted display
[AD-A186228] 07 p0820 N88-14982

A piloted simulation investigating handling qualities and performance requirements of a single-pilot helicopter in air combat employing a helmet-driven turreted gun
[AD-A186878] 09 p1116 N88-16689

Refinement of eye-point-of-regard measurement with helicopter pilots in a flight experiment
[ESA-TT-1073] 09 p1200 N88-17195

Helicopter external vision requirements and visual display characteristics: A report/bibliography, revision A
[AD-A187075] 10 p1276 N88-17641

Virtual interface environment
17 p2381 N88-24153

Evaluation of the US Army fitting program for the integrated helmet unit of the integrated helmet and display sighting system
[AD-A191616] 18 p2465 N88-24635

Assessments of maneuverability with the TeleOperated Vehicle (TOV)
[AD-A191584] 21 p2993 N88-27751

Display system image quality
23 p3242 N88-29298

HELMHOLTZ EQUATIONS

On a boundary data operator and generalized exterior Robin problems for the Helmholtz equation
[AD-A185124] 05 p0640 N88-13915

HELMHOLTZ VORTICITY EQUATION

Point vortex dynamics: Recent results and open problems
[DE87-014759] 03 p0314 N88-11982

Group analysis of equations arising in ocean acoustics
04 p0472 N88-12914

Coupled FE and HIE method for exterior acoustics of axisymmetric shells --- finite element (FE) Helmholtz integral equation (HIE)
[ARE-TM(UHA)-87506] 09 p1243 N88-17448

HELOS (SATELLITE)

U EXOSAT SATELLITE

HEMATITE

Photoacoustic measurements of atmospheric aerosol absorption coefficients at ultraviolet, visible and infrared wavelengths 11 p1512 N88-19036

HEMATOLOGY

Polycythemia and hydration status: Effects on blood volume and thermoregulation during exercise-heat stress
[AD-A185946] 07 p0888 N88-15383

Changes in hemostasis system of animals under conditions of granulocytopoiesis inhibition under effect of decreased barometric pressure
12 p1651 N88-19890

Physiological and hematological responses of matched older and younger men during dry-heat acclimation
[AD-A186450] 18 p2550 N88-25139

HEMATOPOIESIS

Hypoxic hypoxia as a stimulus of erythropoiesis in vivo and in vitro 07 p0885 N88-15373

Differentiation of hemopoietic stem cells during adaptation to high altitude 07 p0893 N88-15410

HEMISPHERES

The corrosion of iron rotating hemispheres in 1 M sulfuric acid: An electrochemical impedance study
[DE87-014679] 02 p0148 N88-10925

HEMODYNAMIC RESPONSES

Effect of spaceflight factors on primate's blood circulation 10 p1359 N88-18124

Central hemodynamics in antiorthostatic hypokinesia and immersion models of weightlessness
11 p1521 N88-19081

Neuro-reflex mechanisms of circulation regulation in simulated microgravity 12 p1656 N88-19923

Physiological reactions upon controlled changes of blood distribution in humans 12 p1656 N88-19924

Is ANF implied in the night attenuated renal response to central hypervolemia? 12 p1659 N88-19945

Regulation of hemodynamics upon imitation of the transition to weightlessness (mathematical modeling)
13 p1810 N88-20817

Propranolol and the compensatory circulatory responses to orthostasis at high altitude
[AD-A192675] 22 p3131 N88-28618

Human performance and acute hypoxia, chapter 12
[AD-A192604] 23 p3238 N88-29270

HEMODYNAMICS

NT LOWER BODY NEGATIVE PRESSURE

Human metabolism and peripheral circulation during antiorthostatic hypokinesia 07 p0891 N88-15398

Acid-base equilibrium and some rat blood parameters following exposure to hyperbaric oxygenation
07 p0894 N88-15420

Changes in regional and central hemodynamics during seven-day water immersion 07 p0895 N88-15421

Comparative evaluation of orthostatic stability following immersion in horizontal and vertical positions
10 p1363 N88-18143

JPRS Report: Science and Technology. USSR: Space Biology and Aerospace Medicine, volume 21, no. 6, November - December 1987
[JPRS-USB-88-004] 10 p1364 N88-18150

Effect of exogenous cardiosynchronized counterpulsation on human regional and central hemodynamics 10 p1366 N88-18163

Hemodynamic effects of beta-adrenergic blocking with obsidan in clinostatic and orthostatic positions
10 p1367 N88-18171

Central hemodynamics in antiorthostatic hypokinesia and immersion models of weightlessness
11 p1521 N88-19081

Cardiovascular adaptation to zero-g during a long term flight (237 days) on board the Salyut 7 Soviet space station (1984) 12 p1655 N88-19920

Cardiac and peripheral circulation assessment by ultrasound on 3 astronauts during two 7-day space flights (1982 Salyut-7 - 1985 STS 51G)
12 p1656 N88-19921

Nitrogen's biological effect on oxygen transport through hematoparenchymal barrier 12 p1662 N88-19967

Effects of intense, time-constrained mental effort on hemodynamics and cardiovascular function
12 p1664 N88-19975

Human hemodynamics during water immersion as related to position during submersion
19 p2703 N88-26071

HEMOGLOBIN

Role of hemoglobin affinity for oxygen in efficiency of blood respiratory function 07 p0892 N88-15406

Air quality and human performance, chapter 16
[AD-A188335] 12 p1666 N88-19988

Effects of pulsed and CW (Continuous Wave) 2450 MHz radiation on transformation and chromosomes of human lymphocytes in vitro
[AD-A193104] 21 p2987 N88-27736

HEMORRHAGES

Hemorrhages and hemostasis in guinea pigs exposed to radiation at high altitude 19 p2705 N88-26083

HEMOSTASIS

U HEMOSTATICS

HEMOSTATICS

Role of carbon dioxide in correction of coagulation hemostasis under hypoxic conditions
10 p1365 N88-18160

Changes in hemostasis system of animals under conditions of granulocytopoiesis inhibition under effect of decreased barometric pressure
12 p1651 N88-19890

Hemostasis parameters of individuals with neurocirculatory dystonia submitted to dry immersion
19 p2703 N88-26072

Distinctive features in blood clotting and fibrinolytic properties under effect of epinephrine in presence of hypoxia and hypercapnia 19 p2705 N88-26082

Hemorrhages and hemostasis in guinea pigs exposed to radiation at high altitude 19 p2705 N88-26083

HENRY LAW

Evaluation and prediction of Henry's law constants and aqueous solubilities for solvents and hydrocarbon fuel components. Volume 1: Technical discussion
[AD-A188571] 12 p1613 N88-19643

Certain questions of thermodynamic theory of weak solutions 18 p2586 N88-25368

HERBIG-HARO OBJECTS

Finnish-Soviet Symposium on Radio Astronomy (1st) held at Otaniemi on August 26-27, 1985
[PB87-140661] 07 p0944 N88-15736

HERCULES AIRCRAFT

U C-130 AIRCRAFT

HERCULES NOVA

The 35-day cycle of Hercules X-1
[MPE-204] 11 p1571 N88-19405

HERMES MANNED SPACEPLANE
Preparation of qualification tests of a plasma generator for the feeding of a hypersonic wind tunnel
05 p0530 N88-13222
General aerodynamic-aerothermodynamic concepts for Hermes 05 p0535 N88-13251
Hermes propulsion system
[SNIAS-872-422-109] 05 p0556 N88-13363
Nonequilibrium reacting flows
08 p0965 N88-15959
The Hermes robot arm, its design and verification
12 p1588 N88-19508
The Hermes manipulation system (HERA) simulation facility development 12 p1591 N88-19524
HERMES Program: Airlock swimming pool tests
12 p1591 N88-19525
EVA, the technological challenge
12 p1592 N88-19535
Modelling and simulation of a rate controlled manipulator arm — Hermes
[NLR-TR-87010-U] 13 p1778 N88-20639
Management of large space projects. Case study: The Hermes program 22 p3162 N88-28830
Case study: The Hermes program product assurance
22 p3162 N88-28831
Ariane 5, HERMES and European vehicles for space station servicing
[SNIAS-881-422-102] 23 p3183 N88-28943
Hermes: Study of propulsion system for reusable man-rated spacecraft
[PSRM-TN-0000-00-04A] 24 p3337 N88-29866
Fuel cells for space use
[FCP-TR-DOS-SY-026] 24 p3389 N88-30183
The LTPP communication processor — Columbus and Hermes
[CL/CP/SES/FR/004] 24 p3415 N88-30328

HERMETIC SEALS
Improved glass-ceramic to metal seals in actuator and detonator applications with an aluminum-containing austenitic stainless steel
[DE88-004691] 13 p1749 N88-20458
Hermetic coating of optical fibers
[AD-A189886] 15 p2044 N88-22177
Hermetically sealable package for hybrid solid-state electronic devices and the like
[NASA-CASE-MSC-20181-1] 17 p2335 N88-23941
Sinterable ceramic powders from laser-heated gases
[AD-A194162] 23 p3197 N88-29024

HERMITIAN POLYNOMIAL
REDUCE-aided study of a problem in Hermitian matrix theory
[DE87-014331] 02 p0229 N88-11445
A taxonomy for conjugate gradient methods
[DE88-008574] 21 p3004 N88-27617

HERTZSPRUNG-RUSSELL DIAGRAM
A re-examination of the corona-wind dividing line: Diagnostics of non-coronal atmospheres
04 p0504 N88-13101

HERZBERG BANDS
Aeronomic problems of the molecular oxygen photodissociation. Part 3: Solar spectral irradiances in the region of the O2 Herzberg continuum, Schumann-Runge bands and continuum
[AERONOMICA-ACTA-A-332-1988]
24 p3343 N88-29897
Aeronomic problems of molecular oxygen photodissociation. Part 4: The various parameters for the Herzberg continuum
[AERONOMICA-ACTA-A-333-1988]
24 p3352 N88-29955

HESSIAN MATRICES
Conic algorithms for unconstrained minimization with special consideration of problems with large sparse Hessians: A summary of research performed
[DE88-002549] 13 p1616 N88-20850

HETEROCYCLIC COMPOUNDS
NT ADENOSINE TRIPHOSPHATE
NT ADENOSINES
NT ATROPINE
NT AZOLES
NT AZULENE
NT CAFFEINE
NT CARBAZOLES
NT ERGOTAMINE
NT FURANS
NT HMX
NT MORPHINE
NT NICOTINIC ACID
NT PHTHALOCYANIN
NT PYRIDINES
NT PYRROLES
NT RDX
NT THYMINE
NT URACIL
NT XANTHINES
X-ray structure analyses and molecular mechanics analyses of dense energetic materials
[AD-A185462] 06 p0779 N88-14781
Thermogravimetric analysis of polymeric materials for an intermediate temperature solid electrolyte
[DE88-004854] 10 p1306 N88-17809
Electronic and ionic transport in polymers
[AD-A187253] 11 p1452 N88-18651
Electronic and ionic transport in polymers
[AD-A190434] 15 p2045 N88-22185
High-performance polymeric materials
[AD-A190708] 15 p2046 N88-22190
High strength/sigh modulus aromatic heterocyclic ABA block copolymers
[AD-A191666] 18 p2491 N88-24774

HETERODYNING
NT OPTICAL HETERODYNING
Mid infrared LHS system packaging using flexible waveguides
[NASA-CR-181192] 01 p0093 N88-10607
Exploiting the IR: Solar and stellar spectroscopy in the IR 04 p0504 N88-13102
NO2 heterodyne frequency measurements with a tunable diode laser, a CO laser transfer oscillator and CO2 laser standards
[NASA-CR-182393] 06 p0710 N88-14353
Investigation of vibration problems with heterodyne holographic interferometer 08 p1000 N88-16058
Comparative investigation of heterodyne mixers at 1000 GHz
[FTL-068627] 09 p1156 N88-16940
Comparison of direct and heterodyne detection optical intersatellite communication links
09 p1169 N88-17013
Quantum limits of superconducting heterodyne receivers
[AD-A188014] 11 p1478 N88-18817
Diagnostics for research in atomization and turbulent two-phase flows
[AD-A187338] 11 p1482 N88-18843
Laser-heterodyne interferometry with streak camera detection
[DE88-003292] 14 p1914 N88-21437
Heterodyne spectrometer for the very high frequency range between 300 and 3000 GHz (1 mm to 0.1 mm) using a mixer in open structure
16 p2271 N88-23589
Design and calibration of a two-channel low-noise heterodyne receiver for use in a CO2 laser Thomson scattering alpha particle diagnostic
[DE88-007866] 19 p2728 N88-26201
Performance analysis of a noncoherently combined large aperture optical heterodyne receiver
22 p3065 N88-28189

HETEROGENEITY
Current experimental and theoretical understanding of detonation waves in heterogeneous solid explosives
[DE87-012177] 01 p0032 N88-10201
The calculation of thermal rate constants for gas-phase and heterogeneous reactions in combustion processes
[AD-A184435] 03 p0284 N88-11788
Heterogeneous multi-trunking queueing systems
[AD-A184255] 04 p0431 N88-12668
A date translation method for heterogeneous database systems 04 p0501 N88-13081
A raytrace method for a laterally heterogeneous environment
[AD-A186525] 08 p0978 N88-15912
Upper mantle heterogeneity and composition of primary ocean island magmas 08 p1009 N88-16120
Mechanism of and particle size effects on shock sensitivity of heterogeneous pressed explosives: Preliminary assessment of binderless RDX in fuze trains
[MRL-R-1077] 09 p1150 N88-16892
Software support for heterogeneous machines
10 p1378 N88-18224
Static dielectric breakdown strength of condensed heterogeneous high explosives
[AD-A191035] 16 p2183 N88-23014
Nanosecond laser photolysis of opaque heterogeneous photosensitizers
[AD-A191424] 16 p2213 N88-23209
Distributed mathematics in a heterogeneous environment
[DE88-009128] 19 p2716 N88-26124
Sintering of the heterogeneous MgO compacts
[DE88-010357] 20 p2767 N88-26408
Off-boundary approach to the boundary element method
[AD-A192931] 20 p2815 N88-26701
Mathematical problems of nonlinear wave propagation and of waves in heterogeneous media
[AD-A195970] 24 p3368 N88-30057

HETEROJUNCTION DEVICES
NT HIGH ELECTRON MOBILITY TRANSISTORS
NT MODFETS
Study and optimization of a technological process for the fabrication of heterojunction bipolar transistors. Applications to high speed devices
[LAAS-87-134] 02 p0246 N88-11555
Novel heterojunction devices
[DE87-013716] 05 p0656 N88-14026
AlGaAs heterojunction lasers
[NASA-CR-4119] 09 p1171 N88-17020
Positron annihilation spectroscopy of AlGaAs/GaAs interfaces in MOCVD-grown GaAs heterojunction solar cells
[DE88-003903] 11 p1508 N88-19012
Low threshold ridge waveguide single quantum well lasers 13 p1777 N88-20631
Cadmium sulfide/copper ternary heterojunction cell research
[DE88-001122] 13 p1793 N88-20727
InP/GaInAs/InP PIN photodiode with FWHM less than 18 ps 19 p2658 N88-25799
Non-stationary transport in MODFET's and heterojunction devices 19 p2659 N88-25804
Transport in GaAs heterojunction ring structures
20 p2864 N88-27011
Vertical electronic transport in novel semiconductor heterojunction structures 20 p2871 N88-27045
Theoretical investigation on heterojunction solar cell
[DE88-701837] 23 p3229 N88-29219
On 3-5 heterojunction structures and high speed devices
[AD-A195464] 24 p3433 N88-30438
Joint services electronics program
[AD-A195731] 24 p3434 N88-30439

HETEROJUNCTIONS
Metal-sensing layer-semiconductor and metal-sensing layer-metal heterostructure gas sensors
[DE87-011293] 01 p0103 N88-10674
X-ray studies of strain, interface and impurity in semiconductors
[DE87-013856] 01 p0104 N88-10678
Phase-locked semiconductor quantum well laser arrays
[AD-A185155] 05 p0588 N88-13583
Structural relaxation in strained-layer heterostructures
[DE88-002326] 07 p0868 N88-15264
Influence of arsenic superficial enrichment on the ohmicity of the n-GaAs:In/Au contact
[ECL-87-09] 08 p1089 N88-16554
Visible InGaAsP/GaAsP lasers produced by epitaxial growth from liquid phase 09 p1237 N88-17416
Solid state research
[AD-A185987] 09 p1253 N88-17508
MBE growth, characterization and electronic device processing of HgCdTe, HgZnTe related heterojunctions and HgCdTe-CdTe superlattices
[AD-A187456] 10 p1421 N88-18486
Development of a planar heterojunction bipolar transistor for very high speed logic
[AD-A188137] 11 p1476 N88-18820
MBE (Molecular Beam Epitaxial) growth characterization and electronic device processing of HgCdTe, HgZnTe related heterojunctions and HgCdTe-CdTe superlattices
[AD-A187416] 11 p1555 N88-19307
Acoustic phonons, surface plasmons and surface acoustic plasmons in a superlattice and their nonreciprocal device applications
[AD-A188918] 12 p1698 N88-20163
Silicon-germanium heterostructures
13 p1844 N88-21034
Development of Si/SiGe heterostructures
[AD-A189527] 13 p1845 N88-21044
First-principles calculations of quasiparticle energies at surfaces and interfaces: Semiconductor surface-state spectra and band offsets
[DE88-006340] 15 p2141 N88-22773
Fundamental properties and devices applications of Ge(x)Si(1-x)/Si superlattices
[AD-A190129] 15 p2143 N88-22787
MBE of HgCdTe
[AD-A191423] 16 p2283 N88-23671
Joint services electronics program research in electronics
[AD-A192206] 18 p2504 N88-24857
Optical properties of heterostructures and superlattices
[AD-A191542] 18 p2581 N88-25335
X-ray response of GaAlAs/GaAs radiation hardened double: Heterostructure photodiode compared to Si:PIN photodiodes
[DE88-007425] 19 p2733 N88-26231
Theoretical aspects of electron transport in modulated structures 20 p2865 N88-27016
Metal grid base heterojunction transistor operating at 60 and 94 GHz
[AD-A194763] 23 p3207 N88-29087

Intrinsic and extrinsic energy states of semiconductors and heterostructures using novel techniques
[DE88-008560] 23 p3289 N88-29582

Spectroscopic studies with multiple quantum well materials with applications to optical signal processing at room temperature
[AD-A194171] 24 p3429 N88-30409

HEURISTIC METHODS

Adaptive line of sight algorithms
[DE87-014275] 01 p0081 N88-10523

An expert system for aircraft conflict resolution in dense airspaces 02 p0129 N88-10810

A review of the knowledge engineering process
02 p0129 N88-10814

Autonomous Land Vehicle (ALV) planning and navigation system
[AD-A184243] 04 p0397 N88-12475

On the work needed to factor a symmetric positive definite matrix
[AD-A185781] 06 p0759 N88-14660

Heuristic control of the Utah/MIT dextrous robot hand
06 p0793 N88-14858

Heuristic search in robot configuration space using variable metric 08 p1059 N88-16389

Iterative-deepening heuristic search for optimal and semi-optimal resource allocation
08 p1062 N88-16410

Discovery and problem solving: Triangulation as a weak heuristic 08 p1062 N88-16412

Commonality analysis as a knowledge acquisition problem 08 p1062 N88-16413

Operational aspects of a spacecraft planning/scheduling expert system
08 p1062 N88-16415

Planning activities in space 08 p1063 N88-16417

Scheduling spacecraft operations
08 p1064 N88-16426

Automatic program generation from specifications using Prolog 08 p1065 N88-16437

Range and mission scheduling automation using combined AI and operations research techniques
09 p1209 N88-17249

An evaluation of project scheduling techniques in a dynamic environment
[AD-A187057] 09 p1260 N88-17554

A comparative study of heurstic algorithms for task assignment in distributed computing systems
10 p1376 N88-18211

Two new frameworks for learning
[AD-A187723] 11 p1534 N88-19162

Stochastic heuristics in network design: Parameter tuning and performance evaluation
[REPT-87-017] 11 p1541 N88-19210

Compilation of preprints
[AD-A191245] 16 p2252 N88-23460

Low altitude remote sensing data in the implementation of a mathematical model for the planning of urban equipment networks 17 p2363 N88-24074

Genetic algorithms for adaptive real-time control in space systems 17 p2388 N88-24195

Automatic program generation from specifications using PROLOG 17 p2388 N88-24196

Design of partially replicated distributed database systems: An integrated methodology
18 p2589 N88-25383

Automatic routing in symbolic IC design environment
19 p2714 N88-26112

Primer on coupling collective electronic oscillations to nuclei
[LA-10878] 19 p2723 N88-26170

Three-dimensional scene analysis using stero based imaging
[AD-A193120] 21 p2894 N88-27178

An investigation of performance improvement in knowledge-based control systems
21 p2928 N88-27382

An approach to combining heuristic and qualitative reasoning in an expert system 23 p3253 N88-29362

NOA: A Network Operator Assistant for scheduling Tracking and Data Relay Satellite System (TDRSS)
23 p3259 N88-29403

Identification and control of time-varying flexible structures: An artificial intelligence approach
23 p3265 N88-29437

HEWLETT-PACKARD COMPUTERS

A data analysis environment for HP (Hewlett-Packard) 1000 computers
[DE87-010511] 04 p0477 N88-12936

HEXAGONAL CELLS

An orthogonal oriented quadrature hexagonal image pyramid
[NASA-TM-100054] 06 p0755 N88-14630

HEXOSES

NT GLUCOSE

HF LASERS

Computer simulation of cw HF chemical laser unstable resonator performance
[AD-A185059] 05 p0587 N88-13581

An experimental study of CW HF chemical laser amplifier performance and zero power gain
[AD-A185241] 05 p0588 N88-13584

Preliminary studies of NF3+H2 production of N2(A3 sigma(+)u) in a supersonic flow
[AD-A194479] 23 p3219 N88-29162

HIBERNATION

Neurochemical changes in hibernation
08 p1046 N88-16322

HIERARCHIES

A heteroscedastic hierarchical model
[AD-A184256] 03 p0372 N88-12340

Advanced Information Processing System (AIPS) proof-of-concept system functional design I/O network system services
[NASA-CR-181488] 03 p0384 N88-12413

Source hierarchy list. Volume 1: A through D
[AD-A185900] 07 p0941 N88-15722

Source hierarchy list. Volume 2: E through O
[AD-A185901] 07 p0941 N88-15723

Cirrus: An automated protocol analysis tool
[AD-A186646] 08 p1052 N88-16348

Media independent interface. Interface control document
[NASA-CR-172032] 08 p1067 N88-16447

An approach to the hierarchical specification, design and verification of software
[RSRE-MEMO-4063] 09 p1223 N88-17332

Research and development trends for memory hierarchies --- cache memories
10 p1374 N88-18198

Hierachical object recognition using libraries of parameterized model sub-parts
[AD-A187476] 10 p1396 N88-18322

A hierarchical structure for automatic meshing and adaptive FEM analysis 11 p1527 N88-19119

The construction of a pedagogy to promote meaningful learning of strategies and tactics for solving problems of elementary combinatorics
[AD-A187928] 11 p1542 N88-19216

Update on the meso-microscale meteorological hierarchy
[DE88-009133] 21 p2975 N88-27670

An introduction to the nested sequence of tuples data model and algebra
[REPT-87-049] 22 p3145 N88-28702

Hierarchical organization for large, dynamic radio networks
[AD-A193942] 23 p3204 N88-29067

Motion planning for legged locomotion systems on uneven terrain 23 p3221 N88-29170

HIGH ALTITUDE

Maximal cardiorespiratory responses to one- and two-legged cycling during acute and long-term exposure to 4300m
[AD-A185730] 06 p0752 N88-14621

Guidance of high-altitude sounding rockets using the S19 and Spinning Rocket Altitude Control (SPINRAC) systems 08 p1034 N88-16273

Dexamethasone as prophylaxis for acute mountain sickness: Effect of dose level
[AD-A185848] 08 p1047 N88-16325

Operation Everest 2: Nutrition and body composition
[AD-A186449] 08 p1049 N88-16333

A methodology to assess the effects of high altitude electromagnetic pulse (HEMP) on electric power systems
[DE88-000338] 11 p1476 N88-18808

Results of the 1987 NASA/JPL balloon flight solar cell calibration program
[NASA-CR-182617] 12 p1574 N88-19413

High altitude chemical release systems for project BIME (Brazilian Ionospheric Modification Experiments) project IMS (Ionospheric Modification Studies) project PIIE (Polar Ionospheric Irregularities Experiment) project polar arcs
[AD-A188299] 12 p1642 N88-19833

Status of microcirculation in high-altitude blood loss
12 p1663 N88-19973

Current induced by high-altitude electromagnetic pulse (HEMP) on wire above ground
[FOA-C-30485-4.2] 22 p3072 N88-28235

Design, development, fabrication and launch support for a high altitude release of neodymium vapor
[AD-A194196] 22 p3118 N88-28527

HIGH ALTITUDE BALLOONS

NT JIMSPHERE BALLOONS

Balloon track data analysis
[AD-A184750] 03 p0350 N88-12213

Life sciences experiments on stratospheric balloons and sounding rockets 08 p1033 N88-16262

Contribution of stratospheric balloon flights in space biology 08 p1033 N88-16266

HIGH ALTITUDE BREATHING

Effects of breathing air containing contaminants such as CO2, CO and hydrocarbons at 1 and 5 atmospheres
[PB88-132915] 11 p1521 N88-19084

Acute mountain sickness at 4500 m is not altered by repeated eight-hour exposures to 3200-3550 m normobaric hypoxic equivalent
[AD-A188358] 12 p1666 N88-19990

Effect of different modes of voluntary control of breathing on human electroencephalogram with exposure to acute hypoxic hypoxia 19 p2707 N88-26093

HIGH ALTITUDE ENVIRONMENTS

Biorhythmic aspects of intercontinental Antarctic adaptation 08 p1046 N88-16321

Polar worker adaptability to Antarctic high altitudes
10 p1366 N88-18165

Medical problems related to altitude in: Human performance physiology and environmental medicine at terrestrial extremes, chapter 14
[AD-A188340] 12 p1666 N88-19989

Hemorrhages and hemostasis in guinea pigs exposed to radiation at high altitude 19 p2705 N88-26083

Alterations in upper extremity motor function in soldiers during acute high altitude exposure
[AD-A192676] 23 p3238 N88-29272

HIGH ALTITUDE FLIGHT

U HIGH ALTITUDE

HIGH ASPECT RATIO

Design verification and fabrication of active control systems for the DAST ARW-2 high aspect ratio wing, part 1
[NASA-CR-177959-PT-1] 06 p0669 N88-14101

Design verification and fabrication of active control systems for the DAST ARW-2 high aspect ratio wing Part 2: Appendices
[NASA-CR-177959-PT-2] 06 p0669 N88-14102

Testing of a schematic transport plane model in several European windtunnels
[PB87-170270] 09 p1113 N88-16671

Experimental study on the effect of fiber orientation on flutter characteristics of high-aspect-ratio transport wing
[NAL-TR-936] 09 p1120 N88-16708

Thermosolutal convection in high-aspect-ratio enclosures
[NASA-TM-100803] 11 p1486 N88-18871

A detailed description of the uncertainty analysis for high area ratio rocket nozzle tests at the NASA Lewis Research Center 19 p2626 N88-25580

HIGH ASPECT RATIO WINGS

U SLENDER WINGS

HIGH CURRENT

New concepts for high current self-sustained diffuse discharge closing switches
[DE87-011678] 01 p0040 N88-10252

High midplane accessibility stellarator windings for high current toroidal accelerators
[AD-A186235] 07 p0933 N88-15665

HIGH ECCENTRIC LUNAR OCCULTATION SATELLITE

U EXOSAT SATELLITE

HIGH ELECTRON MOBILITY TRANSISTORS

NT MODFETS

A 2.3-GHz cryogenically cooled HEMT amplifier for DSS 13 04 p0434 N88-12689

Numerical studies of the dual HEMT/algorithm development and numerical studies of Schrodinger's equation
[AD-A184471] 04 p0478 N88-12946

Microwave response of an HEMT photoconductor
[NASA-TM-100819] 11 p1480 N88-18835

Computer aided design of monolithic microwave and millimeter wave integrated circuits and subsystems
[AD-A191593] 18 p2503 N88-24852

Light-millimeter wave interactions in semiconductor devices
[AD-A195898] 24 p3432 N88-30428

HIGH ENERGY ASTRONOMY OBSERVATORY B

U HEAO 2

HIGH ENERGY ASTRONOMY OBSERVATORY 2

U HEAO 2

HIGH ENERGY ELECTRONS

NT RELATIVISTIC ELECTRON BEAMS

Simulation of tokamak runaway-electron events. Study of the response of materials by use of an electron linear accelerator
[IPPJ-841] 02 p0242 N88-11528

A generalized description of the anomalous Doppler resonance and the stabilizing role of ion dynamics
[INPE-4384-PRE/1204] 08 p1081 N88-16513

Energy distribution of Cerenkov radiation for finite frequency intervals
[AD-A186901] 09 p1244 N88-17454

Simulation and modeling of whistler mode wave growth through cyclotron resonance with energetic electrons in the magnetosphere 10 p1353 N88-18089

Investigations of stimulated Raman scattering from high density underdense plasmas irradiated by a 0.35 micron
10 p1411 N88-18421
laser

Modeling and transport in semiconductor devices
[AD-A188760] 13 p1844 N88-21037

Deep dielectric charging effects due to high energy electrons in earth's outer magnetosphere
[AD-A192154] 18 p2541 N88-25083

A study of electronic transport and breakdown in SiO2
[AD-A194258] 22 p3156 N88-28780

HIGH ENERGY INTERACTIONS

NT STRONG INTERACTIONS (FIELD THEORY)

Research program in elementary particle theory
[DE88-000159] 02 p0233 N88-11468

High energy experimental physics
[DE87-013516] 03 p0376 N88-12363

Analysis of geophysical data bases and models for spacecraft interactions
[AD-A184809] 05 p0555 N88-13375

TIBER 2 (Tokamak Ignition/Burn Experimental Reactor) parameters with neutral beams at high energies
[DE88-001891] 06 p0783 N88-14803

Scanning and measuring peculiarities with high-space resolution objects recorded at the Gabor holograms
[DE88-700373] 07 p0857 N88-15203

Energy distribution of Cerenkov radiation for finite frequency intervals
[AD-A186901] 09 p1244 N88-17454

Properties of nuclei and elementary particles at low and intermediate energies
[DE88-001913] 09 p1244 N88-17456

High Z interaction physics on Nova
[DE88-004397] 10 p1413 N88-18433

Design and fabrication of advanced hybrid circuits for high energy physics
[DE88-004392] 11 p1479 N88-18825

Pion nucleus single charge exchange reactions above the delta(1232) resonance
[LA-11004-T] 11 p1544 N88-19231

Medium high energy physics at Syracuse University
[DE88-003670] 11 p1545 N88-19235

High energy polarized electron beams
[CEBAF-R-87-002] 11 p1546 N88-19244

Induction linacs: A technology come of age for international cooperation
[DE88-003953] 11 p1548 N88-19258

Channeling and dechanneling at high energy
[DE88-003969] 11 p1548 N88-19259

Freund-Rubin type solutions for different compactifications of the eleven-dimensional space
[DE88-700869] 12 p1686 N88-20082

Energy loss of particles in dense matter-calorimetry
[NIKHEF-H/87-12] 13 p1836 N88-20988

Hadronic overlap and total multiplicity distributions in high energy physics collisions
[NIKHEF-H/87-10] 13 p1838 N88-21001

Modeling and transport in semiconductor devices
[AD-A188760] 13 p1844 N88-21037

Systematics on neutron-induced isomeric cross-section ratios at 14.5 MeV
[ECN-200] 14 p1980 N88-21815

Particle acceleration to high energies and amplification of coherent radiation by electromagnetic interactions in plasmas
[DE88-701020] 15 p2135 N88-22737

Subthreshold pion production in proton induced reactions at 180 to 201 MeV and He3 at 283 MeV
[ETN-88-92303] 17 p2397 N88-24250

Energy measurements in oxygen-induced reactions at 60 A GeV and 200 A GeV
[DE88-006420] 18 p2573 N88-25283

Products from cosmic-ray interactions in extraterrestrial matter: What they tell us about radiation backgrounds in space
[DE88-009143] 19 p2743 N88-26288

Theoretical studies in elementary particle physics
[DE88-006929] 20 p2851 N88-26926

Studying the physics and operation of multi-terminal near-micron and sub-micron length, hot electron semiconductor devices
[AD-A193380] 21 p2938 N88-27446

High energy and high intensity laser effects on aerosols: Changes in droplet morphology, surrounding temperature and vapor concentration
[AD-A193825] 23 p3220 N88-29164

Theoretical studies in high energy physics
[DE88-011606] 23 p3281 N88-29538

A coded mask telescope for observations of X and gamma ray sources in the southern sky
[INPE-4580-PRE/1314] 24 p3453 N88-30551

HIGH FREQUENCIES

High-frequency limit of the longitudinal impedance
[CEBAF-PR-87-030] 02 p0234 N88-11479

Height profile inversion of ionospheric movement from observed parameters of HF radio echoes
03 p0299 N88-11884

Target strength: An overview of some recent theoretical developments 03 p0303 N88-11910

Effect of electrostatic field on behaviour of peripheric plasma at high-frequency heating
[DE87-703328] 03 p0378 N88-12378

High frequency periodic time domain waveform measurement system
[PB87-225256] 06 p0695 N88-14264

A contribution to the realization of active filters for high frequency applications
[ETN-88-90811] 06 p0696 N88-14272

Studies on parametric instabilities in high-frequency wave heating of fusion plasmas
[PH-156] 07 p0933 N88-15667

An expert system to analyze high frequency dependent data for the space shuttle main engine turbopumps
08 p1060 N88-16399

An investigation of the equivalent circuit and carrier lifetimes of Si/SiGe heterostructure p-n diodes for frequencies between 0.5 and 18.5 MHz
[FOA-C-30469-3.2] 09 p1256 N88-17529

Wideband HF (High Frequency) modeling and simulation
[PB88-116116] 10 p1317 N88-17874

User's guide for the HF (High Frequency) broadcast antenna design and validation summary programs
[PB88-116124] 10 p1317 N88-17875

Dynamics of small and large scale irregularities at sub-auroral latitudes
[AD-A189052] 12 p1645 N88-19853

HF (High Frequency) Maximum Usable Frequency (MUF) model uncertainty assessment
[AD-A139132] 13 p1757 N88-20513

Adaptive algorithms for HF antenna arrays
[AD-A189329] 13 p1761 N88-20534

Soft decoding of recorded HF data
[FOA-C-30473-3.3] 15 p2058 N88-22269

IREPS (Integrated Refractive Effects Prediction System) 3.0, user's manual
[AD-A190398] 16 p2188 N88-23045

High frequency power distribution system
[NASA-CR-175071] 17 p2335 N88-23939

High frequency ultrasonic characterization of sintered SiC
[NASA-TM-100825] 17 p2347 N88-23985

Communications using channels formed by meteor bursts
[AD-A192058] 18 p2501 N88-24834

Radio-wave scintillations and ionospheric irregularities at high latitudes
[AD-A192140] 18 p2501 N88-24837

Improved description of base dynamics in the modeling of bipolar transistors
[PB88-181516] 19 p2732 N88-26229

Performance study of a unipole antenna with conventional and elevated radial wire ground screens
[AD-A193283] 21 p2933 N88-27413

Calculations of high-frequency parameters of disc-loaded waveguides
[DE88-702178] 21 p2933 N88-27417

Decomposition of hydrazine by high frequency glow electrical discharges
[NASA-TT-20240] 24 p3344 N88-29906

Long haul communications in the HF spectrum utilizing high speed modems
[AD-A194683] 24 p3360 N88-30003

Comparative analysis of passive communications satellites employing the SHF and HF spectrum for use in a strategic role
[AD-A194682] 24 p3362 N88-30019

Modeling and performance of HF/OTH (High-Frequency/Over-the-Horizon) radar target identification systems
[AD-A196287] 24 p3365 N88-30038

High frequency GaAlAs modulator and photodetector for phased array antenna applications
[NASA-TM-101328] 24 p3367 N88-30048

In situ fault detection by the hybrid ray mode method
[AD-A195226] 24 p3381 N88-30137

HIGH GAIN

High power phased array and tailored gain semiconductor lasers 03 p0329 N88-12078

Distributed feedback effects in lasers and high gain laser instabilities in optically pumped CH3F
03 p0329 N88-12079

Periodically pulsed excimer master oscillator-regenerative amplifier laser set
06 p0772 N88-14741

Tapered wiggler analysis of high gain free electron laser oscillators
[AD-A187997] 10 p1338 N88-17997

Research studies on extreme ultraviolet and soft X-ray lasers
[AD-A189163] 12 p1633 N88-19773

The off-axis channel macroplate
[NASA-CR-182938] 18 p2505 N88-24861

HIGH GRAVITY (ACCELERATION)

U HIGH GRAVITY ENVIRONMENTS

HIGH GRAVITY ENVIRONMENTS

The rate of adaptation to altered g in the human centrifuge: Implications for simulations of mass-discrimination in space flight
12 p1659 N88-19941

HIGH IMPULSE

Production of intensive electron beam impulsions by setup of pseudoglare discharges
[ISL-CO-210/87] 21 p3019 N88-27920

HIGH INTENSITY LASERS

U HIGH POWER LASERS

HIGH LATITUDES

U POLAR REGIONS

HIGH LEVEL LANGUAGES

NT ADA (PROGRAMMING LANGUAGE)

NT C (PROGRAMMING LANGUAGE)

Data Management Working Group report
01 p0016 N88-10097

The warp computer: Architecture, implementation, and performance
[AD-A184329] 03 p0363 N88-12286

ERIC: An object-oriented simulation language
[AD-A184757] 03 p0364 N88-12293

ADAMEASURE: An implementation of the Halstead and Henry metrics
[AD-A184005] 03 p0365 N88-12299

Comparison of pascal and the dBASE 3 PLUS language in programming an inventory management system
[AD-A184027] 03 p0365 N88-12300

A survey of object oriented languages in programming environments
[AD-A184127] 04 p0477 N88-12937

LISP: A language for stratified design
[AD-A185606] 06 p0759 N88-14654

Types and effects towards the integration of functional and imperative programming
[AD-A186930] 09 p1216 N88-17290

Occam/Ada parallel programming system
[ISAL-IDI1-87-11] 09 p1219 N88-17312

Optical symbolic processor for expert system execution
[AD-A187494] 10 p1385 N88-18268

BLITZ: Blitzen's micron-code assembly language design document, version 1.0
[TR88-14] 12 p1676 N88-20019

Design of the CONSUL programming language
[AD-A189202] 13 p1815 N88-20841

An integrated data description language for coding design knowledge
[CWI-CS-R8731] 13 p1819 N88-20871

New generation knowledge processing, volume 1
[AD-A190165] 15 p2149 N88-22826

Adapting high-level language programs for parallel processing using data flow 16 p2218 N88-23234

New generation knowledge processing, volume 2
[AD-A190166] 16 p2285 N88-23681

New generation knowledge processing, volume 3
[AD-A190167] 16 p2285 N88-23682

A software life cycle support environment
17 p2306 N88-23800

A robotic language for cooperative multi-robots
17 p2387 N88-24186

New York TRACON demonstration of program recoding requirements analysis document
[DOT/FAA/CT-87/34] 18 p2462 N88-24622

EPL (Equational Programing Language) system design: Intermediate processing steps
[AD-A191203] 18 p2556 N88-25169

Definition of an auxiliary processor dedicated to real-time operating system kernels
[NASA-CR-183070] 20 p2841 N88-26860

Subset-logic programming: Application and implementation
[AD-A193647] 22 p3138 N88-28655

Combined and-or parallel execution of logic programs
[AD-A193648] 22 p3138 N88-28656

Investigation of the use of High Order Languages (HOLs) for on-board software
[CRI/FR/HOL-C/1/87] 23 p3251 N88-29349

Archetyping: A software generation and management methodology 23 p3256 N88-29382

The FORCE
[AD-A193463] 23 p3264 N88-29429

Strategic defense initiative architecture dataflow modeling technique version 1.5
[AD-A194356] 23 p3275 N88-29494

Conversion of productions in OPS5 to their equivalent English
[ORNL/TM-10246] 24 p3411 N88-30306

HIGH MELTING COMPOUNDS

U REFRACTORY MATERIALS

HIGH PASS FILTERS

Realization of active high pass filters for group velocity correction
[MPE-IN-REPT-47] 08 p0979 N88-15918

HIGH POLYMERS

Polymer modified binders for bituminous or asphaltic paving layers
[PC-5] 02 p0153 N88-10958

JPRS report: Science and technology. Japan
[JPRS-JST-87-028] 06 p0675 N88-14130

High polymer sensor materials discussed
06 p0676 N88-14140

Synthesis of high molecular weight peptide polymers and copolymers containing L-dope residues
[AD-A186462] 08 p0973 N88-15887

Soluble polysilane derivatives: Chemistry and spectroscopy
[AD-A187889] 11 p1461 N88-18713

Photophysics and photochemistry of poly(di-n-hexylsilane) in room temperature solution
[AD-A187890] 11 p1462 N88-18714

Investigations on drag reduction in turbulent pipe flows by addition of ionic and nonionic high polymers
[ETN-88-92380] 21 p2949 N88-27515

HIGH POWER LASERS

NT NOVA LASER SYSTEM

Millimeter wave tokamak heating and current drive with a high power free electron laser
[DE87-011324] 01 p0099 N88-10651

Laser-plasma-interaction experiments using multikilojoule lasers
[DE87-013483] 01 p0100 N88-10658

Status, development of laser devices in China
03 p0303 N88-11907

High average power solid state laser power conditioning system
[DE87-013558] 03 p0328 N88-12071

Diffraction effects during materials treatment with laser beams
[ETN-87-90614] 03 p0328 N88-12075

High-power RF-pulsed modulators for the Los Alamos free-electron laser
[DE88-000514] 04 p0448 N88-12775

Phenomena at a focus in a laser system
[AD-A185442] 05 p0588 N88-13585

Lawrence Livermore National Laboratory Soft X-ray Laser Program
[DE88-001888] 07 p0659 N88-15218

Nondestructive magnetic testing of laser hardening parameters (hardening depth, hardness profile, retained austenite)
[ETN-88-91070] 09 p1144 N88-16857

Dielectric behavior of electromagnetic (EM) windows materials irradiated by a CW CO2 high-power laser --- hypersonic/reentry vehicles
[ISL-CO-239/86] 09 p1154 N88-16913

A crude scaling law for lasertrons
[DE88-003880] 09 p1173 N88-17032

Mirrors for high-power continuous-wave Ar-lasers
09 p1235 N88-17404

High-power periodic-pulse YAG:Nd3 + -laser system with telescopic unstable resonator and two-stage amplifier
09 p1237 N88-17414

Dye lasers pumped by radiation from high-power semiconductor lasers 09 p1237 N88-17417

High power, high efficiency 770 nm laser diode array
[DE88-004043] 12 p1631 N88-19762

Optical properties of compressible inhomogeneous shear layers relevant to high power lasers
[AD-A189299] 12 p1633 N88-19774

Phase preservation cleanup in a double-pass Raman amplifier SBS (Stimulated Brillouin Scattering) conjugator
[AD-A189428] 13 p1761 N88-20536

Fiber-coupled external-cavity semiconductor high power laser
[AD-A188454] 13 p1774 N88-20611

Causes of damage in multilayer dielectric coatings exposed to high average power visible laser radiation
[DE88-005363] 13 p1775 N88-20619

High power, high efficiency, 2D laser diode arrays for pumping solid state lasers
[DE88-004042] 13 p1777 N88-20632

Laser technology: CO2 lasers and laser optics
[ETN-88-91469] 14 p1915 N88-21441

JPRS report: Science and technology. China
[JPRS-CST-87-043] 15 p2053 N88-22233

Magic light high-power laser passes state certification
15 p2053 N88-22236

Coupled high power waveguide laser research
[AD-A189800] 15 p2071 N88-22345

Laser evaporation studies
[AD-A189815] 15 p2071 N88-22346

High power axial flow CO2 laser
[ETN-88-91951] 18 p2521 N88-24959

Optical coatings for high average power XeF lasers
[DE88-011356] 20 p2807 N88-26656

High energy and high intensity laser effects on aerosols: Changes in droplet morphology, surrounding temperature and vapor concentration
[AD-A193825] 23 p3220 N88-29164

Energy conversion measurements in laser-sustained argon plasmas for application to rocket propulsion
[AD-A194931] 24 p3337 N88-29861

HIGH PRESSURE

Nitrogen at high pressure
[DE87-013797] 01 p0021 N88-10130

Nitrogen at very high pressure
[DE87-013800] 01 p0021 N88-10131

Chemical equilibrium calculations for the high pressure and temperature dissociation of liquid nitrogen
[DE87-013788] 01 p0021 N88-10135

Theory of the carbon phase diagram at high pressures and temperatures
[DE87-012245] 01 p0028 N88-10180

The effect of additives on the reactivity of palladium surfaces for the chemisorption and hydrogenation of carbon monoxide: A surface science and catalytic study
[DE87-014685] 02 p0145 N88-10909

Electrical properties of high T/sub c/ superconductors under high pressures
[DE87-012818] 02 p0245 N88-11546

High pressure strand burn rate tests of polyvinylnitrate/nitramine propellants
[AD-A184178] 04 p0422 N88-12615

Studies of tunneling in metals under high pressure
06 p0775 N88-14757

Programs for calculating transient Darcian flow through non-uniform materials
[DE88-001924] 07 p0852 N88-15177

An automated flow calorimeter for heat capacity and enthalpy measurements at elevated temperatures and pressures
[DE88-002357] 07 p0857 N88-15206

Welding in high pressure CO2 atmosphere --- underwater welding
[PB87-144044] 07 p0862 N88-15232

The determination of equivalent bearing loading for the BSMT that simulate SSME high pressure oxidizer turbopump conditions using the SHABERTH/SINDA computer programs 07 p0925 N88-15623

Excess thermodynamic properties of aqueous electrolytes to high temperatures and pressures
[DE88-001768] 07 p0940 N88-15712

Superconductivity and crystal structure of high-pressure phases in V-Ru-H system 09 p1239 N88-17426

Radial compressor design using an Euler solver
10 p1283 N88-17675

Design and testing of a front stage for an advanced high pressure compressor 10 p1283 N88-17679

Gas cleaning at high temperatures and pressures for gas turbines
[DE88-751171] 11 p1440 N88-18593

Operation of electron-beam controlled CO2 laser at 6 atmospheres 11 p1468 N88-18758

High pressure electronic transport in semiconductors
[AD-A187428] 11 p1555 N88-19308

Properties of molecular solids and fluids at high pressure and temperature
[DE88-004195] 13 p1738 N88-20391

Fluids, gels and glasses under extreme conditions of pressure and temperature
[AD-A190655] 15 p2035 N88-22125

Cracking tendencies of restrained welds in high strength low alloy steels under hyperbaric conditions
[AD-A190255] 15 p2039 N88-22150

Synthesis of metastable superconductors by high dynamic pressure
[DE88-005620] 15 p2139 N88-22764

Electronic structure of matter at high compression: Isostructural transitions and approach of the Fermi-gas limit
[MPQ-124] 16 p2266 N88-23551

High pressure operation of beam diodes for generating relativistic electron beams 16 p2279 N88-23643

The high pressure sound velocity and equation of state of aqueous solutions of hydroxylammonium nitrate and triethanolammonium nitrate
[AD-A191740] 18 p2570 N88-25266

Kinetic measurements of thermal decomposition of energetic materials at high pressures
[AD-A191612] 19 p2622 N88-25552

Experimental study of protective effect of antioxidant enzymes-superoxide dismutase and catalase-when using intermittent toxic modes of hyperbaric oxygenation
19 p2707 N88-26094

Asynchronous optical sampling for laser-based combustion diagnostics in high pressure flames
[AD-A192920] 20 p2770 N88-26428

Respiration and oxygen tension in the blood of animals exposed to high pressures 20 p2830 N88-26790

Electronic structure of quantum-well states revealed under high pressures 20 p2870 N88-27038

Experimental study of planetary gases with applications to planetary interior models
[NASA-CR-183096] 20 p2886 N88-27137

Investigation of hydrogen isotope penetration through stainless steels Kh18N10T and Kh3M2BFR
[DE88-702189] 21 p2915 N88-27297

Reaction products of solid propellants after burning at pressures up to 1000 MPa: Comparison between theoretical and experimental results
[ISL-CO-227/87] 22 p3059 N88-28153

E3 10C compressor test analysis of high-speed post-stall data
[NASA-CR-179521] 23 p3179 N88-28929

Development of high temperature, high pressure rotating shaft seals
[DE88-001029] 23 p3221 N88-29172

HIGH PRESSURE OXYGEN

Effect of high pressure oxygen loading on the superconductivity of La2CuO4
[DE88-002108] 06 p0787 N88-14827

USAF hyperbaric animal transfer chamber system
[AD-A193633] 23 p3237 N88-29265

HIGH Q

U Q FACTORS •

HIGH RESOLUTION

CERGA high angular resolution optical network --- astronomical interferometry 01 p0096 N88-10633

Solar interferometry with a 4-aperture nonredundant and stabilized network 01 p0097 N88-10639

Galactic nuclei and quasars at high angular resolution
01 p0098 N88-10644

Assimilation of high resolution TOVS data into a mesoscale NWP model --- numerical weather prediction (NWP) 02 p0213 N88-11338

Present status of the high resolution spectrometers
[CEBAF-PR-87-029] 02 p0234 N88-11478

Theoretical Problems in High Resolution Solar Physics, 2
[NASA-CP-2483] 02 p0254 N88-11609

Some aspects of high resolution numerical methods for hyperbolic systems of conservation laws, with applications to gas dynamics
[DMS-86-7] 03 p0321 N88-12031

Conceptual design of a high-resolution pion (0) spectrometer
[DE87-014757] 03 p0324 N88-12047

Numerical experiments with a symmetric high-resolution shock-capturing scheme
[NASA-TM-88325] 03 p0370 N88-12332

Implementation and performance of a complex vision system on a systolic array machine
[AD-A184331] 04 p0482 N88-12971

High resolution finite volume methods on arbitrary grids via wave propagation
[NASA-CR-178397] 04 p0484 N88-12979

Exosat results on the dMe flare Star Wolf 630AB and on VB 8 04 p0512 N88-13151

New results from high angular resolution observations of alpha Ori 04 p0514 N88-13161

High resolution satellite imagery simulation --- treaty verification
[FOA-C-30462-3.3,9.3] 05 p0620 N88-13810

High resolution ultraviolet filter development
[AD-A184183] 05 p0649 N88-13979

High-spatial-resolution TOVS observations for the FIRE/SRB Wisconsin experiment region from October 14 through November 2, 1986
[NASA-TM-100522] 06 p0747 N88-14593

Use of spherical optics in high resolution soft X-ray grating monochromators
[PB87-125191] 06 p0780 N88-14788

High spatial resolution observations of dust and gas in NGC 7027 and the M8 Hourglass
06 p0801 N88-14903

High resolution simulation of turbulent flow in a channel
[AD-A186022] 07 p0848 N88-15150

Fabrication techniques used in the construction of a high resolution X-ray framing camera
[DE88-002653] 07 p0856 N88-15200

Determination of network attributes from a high resolution terrain data base
[AD-A186078] 07 p0870 N88-15279

Estimation of broadband planetary albedo from operational narrowband satellite measurements
[PB88-107644] 07 p0945 N88-15748

The high resolution spaghetti hadron calorimeter
[NIKHEF-H/87-7] 08 p0990 N88-15993

High-speed assembly language (80386/80387) programming for laser spectra scan control and data acquisition providing improved resolution water vapor spectroscopy
[NASA-CR-4117] 08 p1053 N88-16355

Application of a simple rotational spherical grating mounting to high resolution soft X-ray spectroscopy
[PB87-164836] 09 p1142 N88-16845

Investigation of a new magnetic dipole mode in the heavy, deformed nuclei 154 Sm, 156 Gd, 158 Gd, 164 Dy, 168 Er, and 174 Yb with high resolution electron scattering
[ETN-88-91084] 09 p1245 N88-17460
Rotor SAR (ROSAR): A new high-resolution all-weather vision method for helicopters
[MBB-UA-1046/87] 10 p1314 N88-17855
Experiments for the high resolution detection of moving targets using a CO2 laser radar
[MBB-UA-1044/87] 10 p1316 N88-17864
New generation imager system
[NASA-CR-180464] 10 p1408 N88-18398
High-resolution X-ray microstructural study of single crystals of YBa2Cu3O/sub 7-y/
[DE88-004856] 10 p1421 N88-18484
An evaluation of the impact of variable temporal and spatial data resolution upon IREPS (Integrated Refractive Effects Prediction System)
[AD-A187764] 11 p1470 N88-18769
General determination of Earth surface type and cloud amount using multispectral AVHRR data
[NOAA-TR-NESDIS-39] 11 p1506 N88-18997
Suggested severe local storm operational scenario for GOES I-M
[NASA-TM-100688] 11 p1515 N88-19052
High resolution hadron calorimetry
[NIKHEF-H/87-8] 13 p1773 N88-20605
Improved methods for high resolution electron microscopy
[DE88-005731] 13 p1774 N88-20609
Simulating high-resolution vertical plane array wind characteristics using lower-spatial-resolution wind measurements
[DE88-005626] 13 p1800 N88-20761
Velocity resolved far-infrared spectroscopy of galactic sources 13 p1854 N88-21099
Pre-launch calibration of channels 1 and 2 of the advanced very high resolution radiometer
[PB88-157169] 14 p1913 N88-21427
What has been done and what will be done by subnatural linewidth spectroscopy 14 p1978 N88-21807
Fluids, gels and glasses under extreme conditions of pressure and temperature
[AD-A190655] 15 p2035 N88-22125
Design, construction and performance of the ROSAT high resolution X-ray mirror assembly
[MPE-PREPRINT-101] 15 p2150 N88-22836
Navigation system from AVHRR data from NOAA series satellites 17 p2359 N88-24054
High resolution radar techniques: Five contributions to MILINF 86
[PB88-172721] 18 p2498 N88-24821
DMSP-SSM/1 NASA algorithm validation using primarily LANDSAT and secondarily DMSP and/or AVHRR visible and thermal infrared satellite imagery
[NASA-CR-182979] 18 p2532 N88-25024
New duplicating paper with high resolution for aerial photography
[PB87-228706] 19 p2685 N88-25962
Contribution of spaceborne high resolution radiometers to mapping of precoastal depths
19 p2701 N88-26063
High resolution detection of solute segregation to the cores of dislocations in grain boundaries
[DE88-009168] 20 p2877 N88-27078
Enhancement of modeling and image generation techniques for high-resolution 3-dimensional imagery
[DE88-008923] 21 p2998 N88-27782
Research for reducing the labor intensive nature of high-resolution terrain analysis feature extraction
[AD-A192661] 22 p3089 N88-28345
High resolution orthoimage quadrangle maps using SPOT satellite data 22 p3112 N88-28488
Automatic extraction of high resolution elevation data from SPOT stereo images 22 p3113 N88-28489
High definition television: Evaluation for remote task performance
[DE88-011573] 23 p3202 N88-29057
Signal processing software for ground penetrating radar, user's manual
[AD-A194286] 23 p3203 N88-29059
An analysis of results of a high-resolution world ocean circulation model
[AD-A195760] 24 p3405 N88-30272

HIGH REYNOLDS NUMBER
Wall interference tests of a CAST 10-2/DOA 2 airfoil in an adaptive-wall test section
[NASA-TM-4015] 02 p0122 N88-10772
Asymptotic form of stationary solutions of the Navier-Stokes equations for large Reynolds numbers
04 p0459 N88-12838
Practical application of two-dimensional viscous flow computation 05 p0535 N88-13257
Numerical analysis of cascade flow solving Navier-Stokes equations 05 p0536 N88-13262
The aerodynamic design of hypersonic contoured axisymmetric nozzles including real gas effects
[VKI-TM-43] 06 p0665 N88-14076
Unsteady stall penetration experiments at high Reynolds number
[AD-A186120] 07 p0814 N88-14958
Pressure distributions from high Reynolds number transonic tests of an NACA 0012 airfoil in the Langley 0.3-meter transonic cryogenic tunnel
[NASA-TM-100526] 11 p1435 N88-18565
High Reynolds number transonic tests on a NACA 0012 airfoil in the Langley 0.3-meter transonic cryogenic tunnel
[NASA-TM-100527] 11 p1436 N88-18571
High Reynolds number pump facility for cavitation research
[AD-A189310] 13 p1765 N88-20558
High Reynolds number, low Mach number, steady flow field calculations over a NACA 0012 airfoil using Navier-Stokes and interactive boundary layer theory
[AD-A189871] 15 p2013 N88-22005
Effect of freestream turbulence on a two dimensional cascade, with different surface roughness, at high Reynolds number
[AD-A190615] 15 p2065 N88-22316
High Reynolds number tests of a Douglas DLBA 032 airfoil in the Langley 0.3-meter transonic cryogenic tunnel
[NASA-TM-87663] 17 p2296 N88-23734
Velocity-pressure integrated versus penalty finite element methods for high Reynolds number flows
[NASA-CR-179357] 20 p2803 N88-26635
Analysis of experimental data for cast 10-2/DOA2 supercritical airfoil at high Reynolds numbers
[AD-A192827] 21 p2892 N88-27166
Field methods for computing high Reynolds number viscous flow
[FFA-TN-1988-01] 22 p3039 N88-28046
The use of upwind schemes at high Reynolds number: A cautionary note
[AD-A196227] 24 p3371 N88-30074

HIGH SPEED
Response of helical structures to high speed pulses or when can a helix be called an inductor
[DE87-014347] 01 p0090 N88-10587
Civil applications of high-speed rotorcraft and powered-lift aircraft configurations
[NASA-TM-100035] 03 p0261 N88-11643
Analysis of 7- X 10-foot high speed wind tunnel shaft loads in support of fan blade failure investigation
[NASA-TM-100504] 04 p0402 N88-12496
Progress in the development of niobium alloyed high speed steel
[DE87-703549] 04 p0415 N88-12576
Thermomechanical cracking in coated media due to high speed asperity excitation
[AD-A184176] 04 p0454 N88-12809
Fluctuating pressure loads under high speed boundary layers
[NASA-TM-100517] 05 p0647 N88-13962
Tribological studies on high speed steel cutting tools
[DE88-002550] 07 p0864 N88-15246
High-speed inlet research program and supporting analyses 08 p0958 N88-15811
Experimental evaluation of turning vane designs for high-speed and coupled fan-drive corners of 0.1-scale model of NASA Lewis Research Center's proposed altitude wind tunnel
[NASA-TP-2681] 10 p1285 N88-17686
Dynamics of high-speed mechanisms with elastic members 13 p1779 N88-20643
High speed, bandpass sampling of digital communications waveforms
[AD-A189842] 15 p2056 N88-22254
Application of high speed holography to aerodynamic and hydrodynamic three-dimensional velocimetry
16 p2203 N88-23144
Pressure measuring probe
[NASA-CASE-LAR-13853-1] 17 p2341 N88-23961
High-speed optical logic using GaAs
19 p2656 N88-25773
High speed opto-isolator for radar applications
19 p2658 N88-25795
Effective communication between a microVAX and a specialized high-speed subprocessor
[DE88-007967] 19 p2714 N88-26115
Development of a GaAs solid state device model for high power applications
[DE88-009048] 19 p2734 N88-26242
High speed inlet calculations with real gas effects
[NASA-CR-182167] 20 p2752 N88-26336
A high speed serial link interface for SANDAC-V
[DE88-007694] 20 p2842 N88-26861
A survey of the Ap stars for rapid variability
20 p2884 N88-27127
The MELMUX MX-7100 series high-speed digital multiplexers 21 p2930 N88-27396
E3 10C compressor test analysis of high-speed post-stall data
[NASA-CR-179521] 23 p3179 N88-28929
Proof-of-principle high speed electronic imaging system, phase 2
[AD-A193798] 23 p3181 N88-28937
Ultrafast processes and spectroscopy with free electron lasers
[AD-A195248] 24 p3379 N88-30126
On 3-5 heterojunction structures and high speed devices
[AD-A195464] 24 p3433 N88-30438

HIGH SPEED CAMERAS
NT FRAMING CAMERAS
Optically time-resolved detonation break out
[DE87-010340] 01 p0031 N88-10199
A high-speed, eight-frame image intensified electro-optic camera with 200-800mm zoom objective capability
[DE88-000229] 03 p0326 N88-12059
Simple high speed camera with CCD-sensor
[MPIS-8/1987] 18 p2518 N88-24940

HIGH SPEED FLIGHT
U HIGH SPEED

HIGH SPEED PHOTOGRAPHY
Reduction of temperature rise in high-speed photography
[NASA-TM-100222] 02 p0176 N88-11100
An ultra-high-speed cinematographic method for the study of wakes in hypersonic ballistic ranges
05 p0531 N88-13228
Analysis of photopole data reduction models
05 p0593 N88-13616
Synchronous multi-image high speed photography of welding arc by optical fibers
[PB87-143939] 07 p0857 N88-15202
Measurements of particulates in solid propellant rocket motors
[AD-A187777] 11 p1446 N88-18621
Ignition and high speed photography of energetic materials with a copper vapor laser
[DE88-004831] 12 p1631 N88-19765

HIGH SPEED TRANSPORTATION
U RAPID TRANSIT SYSTEMS

HIGH STRENGTH
Composite reliability enhancement via preloading
[AD-A185938] 07 p0826 N88-15010
Structure and surface characterizations of high strength carbon fibers
[AD-A189642] 15 p2029 N88-22087
High-strength ceramic based on tetragonal ZrO2 with Al2O3 admixture 16 p2180 N88-22996

HIGH STRENGTH ALLOYS
NT ASTROLOY (TRADEMARK)
NT HIGH STRENGTH STEELS
NT MARAGING STEELS
Investigation of rapidly-solidified dispersion strengthened titanium alloys
[AD-A183882] 01 p0022 N88-10140
The effect of temperature on the tensile properties of HSLA-100 steel
[AD-A184951] 05 p0565 N88-13441
Microstructural characterization of HSLA-100 GMA-weldments
[AD-A187782] 11 p1457 N88-18683
Microstructural characterization of the heat affected zone of HSLA (High Strength Low Alloy)-100 steel GMA (Gas Metal Arc)-weldment
[AD-A187825] 11 p1457 N88-18686
Deformation of rapidly solidified dispersion strengthened titanium alloys
[AD-A190793] 16 p2179 N88-22984
Evaluation of a diffusion/trapping model for hydrogen ingress in high-strength alloys
[AD-A194301] 23 p3194 N88-29008

HIGH STRENGTH STEELS
NT MARAGING STEELS
The fatigue properties of aerospace steels under constant amplitude and flight-by-flight simulated loading
[BAE-MSM-R-GEN-0566] 01 p0059 N88-10377
Stress corrosion cracking of high-strength steels in aqueous environments 03 p0289 N88-11818
Computational methods and results for dynamic fracture 03 p0337 N88-12123
Mechanical behavior of a controlled rolled high-strength low alloy steeel plate, microalloyed with Nb and V
[DE87-703507] 04 p0415 N88-12571
The effect of temperature on the tensile properties of HSLA-100 steel
[AD-A184951] 05 p0565 N88-13441
Fatigue characteristics of ion treated surfaces
05 p0606 N88-13713
Environmentally assisted fatigue crack growth
05 p0608 N88-13731

Numerical simulations of impact tests on a rigid wall --- armor steel
[SNIAS-872-320-102] 05 p0610 N88-13744
Effect of rare earth elements on the hydrogen-induced cracking in high strength low alloy steel
[PB87-143806] 07 p0833 N88-15052
Multipurpose corrosion inhibitors for aerospace materials in Naval environments
[AD-A186728] 09 p1143 N88-16853
Crack arrest fracture toughness of armor steels
[AD-A187711] 11 p1456 N88-18681
Microstructural characterization of HSLA-100 GMA-weldments
[AD-A187782] 11 p1457 N88-18683
The influence of strain on hydrogen entry, transport, and embrittlement of a high strength steel in aqueous sodium chloride solution
[AD-A189302] 12 p1608 N88-19619
Development of a constitutive equation for HSLA (High-Strength Low-Alloy)-100 at cryogenic temperatures
[AD-A189243] 13 p1740 N88-20408
Cracking tendencies of restrained welds in high strength low alloy steels under hyperbaric conditions
[AD-A190255] 15 p2039 N88-22150
Hydrogen embrittlement susceptibility of high strength ESR 4340 steel alloys for ballistically resistant/tolerant components 17 p2319 N88-23848
Brief evaluation of the alloy 17-4-PH (Z5 CNU 17-04). Semifinished product: 205 mm dia forged roller, test reports
[DF/NH-3616/84] 17 p2322 N88-23866
Analysis of crack arrest toughness
[AD-A193340] 21 p2913 N88-27286
Development of high strength and toughness microcomposite HSLA Fe/Cr/Mn/C steel with and without Nb
[DE88-009813] 21 p2913 N88-27290
A review of solid particle erosion of engineering materials
[DE88-010065] 22 p3054 N88-28124
Additional fracture and strength test results for A723 steel and 38644 titanium
[AD-A196329] 24 p3353 N68-29960

HIGH TEMPERATURE
Optimizing the application of high temperature corrosion resistant aluminium-silicon-base coatings
[BLL-M-37222-(5828.4)] 01 p0018 N88-10112
Oxidation of TSX graphite over the temperature range 450 to 1200°C
[DE87-012230] 01 p0020 N88-10127
Chemical equilibrium calculations for the high pressure and temperature dissociation of liquid nitrogen
[DE87-013788] 01 p0021 N88-10135
Large-strain softening of aluminum at elevated temperature
[DE87-011559] 01 p0024 N88-10153
Theory of the carbon phase diagram at high pressures and temperatures
[DE87-012245] 01 p0028 N88-10180
Effect of high-temperature annealing on the microstructure and thermoelectric properties of GaP doped SiGe
[NASA-TM-100164] 01 p0029 N88-10188
High temperature metal matrix composites for future aerospace systems
[NASA-TM-100212] 02 p0149 N88-10938
High temperature stress-strain analysis
02 p0188 N88-11170
Elevated temperature crack growth
02 p0188 N88-11174
Lewis' enhanced laboratory for research into the fatigue and constitutive behavior of high temperature materials
02 p0189 N88-11177
Organic Rankine-cycle power systems working fluids study. Topical report No. 1: Fluorinol 85
[DE87-014604] 02 p0195 N88-11217
The effect of strain rate on the yield behavior of iron-base LRO alloys at elevated temperatures
[DE87-014893] 03 p0288 N88-11806
A fundamental study of the mechanical and microstructural response of elevated temperature PM aluminum-titanium alloys 03 p0289 N88-11819
Modified 14Cr-16Ni stainless steels with improved creep resistance at 700 C due to tailored precipitate microstructures
[DE87-014788] 03 p0290 N88-11825
Impact behavior of 9-Cr and 12-Cr ferritic steels after low-temperature irradiation
[DE88-000333] 03 p0291 N88-11827
High temperature superconductors
03 p0297 N88-11869
Gas tungsten arc welding of Al-10Fe-5Ce
[AD-A184202] 03 p0334 N88-12104
Adiabatic diesel engine component development: Reference engine for on-highway applications
[NASA-CR-179531] 03 p0386 N88-12428
Research and development on high strength ceramic heaters discussed 04 p0404 N88-12508
Pipe and bend erosion by pneumatic transport of solids at high temperature
[DE88-001345] 04 p0429 N88-12658
A fundamental study of P/M processed elevated temperature aluminum alloys
[AD-A185393] 05 p0565 N88-13445
Coatings for high-temperature bearings and seals
[NASA-TM-100249] 05 p0567 N88-13453
Behavior of long and short fatigue cracks in a powder metallurgy superalloy at room and at high temperature
05 p0601 N88-13677
Thermo-mechanical behavior of high temperature fiber composites 06 p0678 N88-14149
Cyclic fatigue of ceramics at high temperatures
[PB87-127700] 06 p0685 N88-14200
Recent advances in high temperature instrumentation for hot section applications
[NASA-TM-100282] 06 p0707 N88-14339
High temperature low cycle fatigue of oxide dispersion strengthened and single crystal nickel base superalloys
06 p0720 N88-14422
Orientation effects in copper single crystals fatigued at elevated temperatures 06 p0720 N88-14423
Elevated temperature fatigue crack propagation
06 p0720 N88-14424
High temperature low cycle fatigue behavior and creep-fatigue interation of MA 6000 ODS alloy
06 p0720 N88-14425
Creep-fatigue cracking in high temperature turbine rotors 06 p0720 N88-14426
Hot piston ring tests
[NASA-TM-100256] 06 p0729 N88-14486
Precipitation in alumina-rich spinel: A transformation-toughened ceramic single crystal
[DE87-012380] 06 p0785 N88-14815
High temperature stability of superconducting YBa2Cu3O subx as characterized by X-ray diffraction
[DE88-001856] 06 p0787 N88-14824
An automated flow calorimeter for heat capacity and enthalpy measurements at elevated temperatures and pressures
[DE88-002357] 07 p0857 N88-15206
Excess thermodynamic properties of aqueous electrolytes to high temperatures and pressures
[DE88-001768] 07 p0940 N88-15712
Determination of thermodynamic function of minerals at high temperatures
[DE88-001911] 07 p0940 N88-15713
Determination of thermodynamic function of minerals at high temperatures
[DE88-002311] 07 p0940 N88-15714
High-temperature electronics
08 p0956 N88-15797
Aircraft engine hot section technology: An overview of the HOST Project 08 p0957 N88-15804
Hot piston ring/cylinder liner materials: Selection and evaluation
[NASA-TM-100276] 08 p0971 N88-15872
Sputtered silver films to improve chromium carbide based solid lubricant coatings for use to 900 C
[NASA-TM-100783] 08 p0973 N88-15885
Investigation of self-discharge characteristics of spacecraft nickel-cadmium cells at elevated temperatures
[AD-A186497] 08 p0979 N88-15919
High temperature polymer matrix composites
09 p1119 N88-16700
Development of a new generation of high-temperature composite materials 09 p1119 N88-16702
A rapid method for the computation of equilibrium chemical composition of air to 15000 K
[NASA-TP-2792] 09 p1140 N88-16830
High-temperature photoelectron spectroscopy. An increased sensitivity spectrometer for studying vapor-phase species produced at furnace temperatures greater than 2000K
[AD-A186542] 09 p1140 N88-16835
Fatigue and uniaxial deformation behavior of Hastelloy XR at elevated temperatures
[DE88-751058] 09 p1145 N88-16862
Evaluation of high temperature structural adhesives for extended service, phase 5
[NASA-CR-178176] 09 p1149 N88-16884
Molecular dynamics study of high-temperature grain-boundary stability in a (100) sigma = 29 bicrystal model
[DE88-002955] 09 p1258 N88-17546
A review of pitting corrosion in high temperature aqueous solutions
[DE88-003547] 10 p1302 N88-17787
Dynamic recrystallization during high temperature low cycle fatigue of nickel
[DE88-003224] 10 p1302 N88-17788
A solar receiver-reactor with specularly reflecting walls for high-temperature thermoelectrochemical and thermochemical processes
[AD-A187612] 10 p1351 N88-18077
High temperature processing of superconducting Y1Ba2Cu3O6.9
[DE88-003002] 10 p1416 N88-18449
Electronic structure, charge transfer excitations and high temperature superconductivity
[DE88-003096] 10 p1416 N88-18453
Innovative arrangements for industry/DOE laboratory collaboration in high temperature superconductivity
[DE88-004320] 10 p1420 N88-18482
Gas cleaning at high temperatures and pressures for gas turbines
[DE88-751171] 11 p1440 N88-18593
An electron spectroscopic investigation of high-temperature superconducting oxides
[DE88-003807] 11 p1558 N88-19325
Research briefing on high-temperature superconductivity
[PB88-133004] 11 p1561 N88-19344
To the problem of determining true volume steam content by measured values of mean density of a mixture in thermally unsteady two-phase flows
[DE88-700840] 12 p1626 N88-19726
Properties of molecular solids and fluids at high pressure and temperature
[DE88-004195] 13 p1738 N88-20391
Material parameter measurements at high temperatures
[NASA-CR-182707] 13 p1739 N88-20397
Effects of high temperature neutron irradiation on the physical, chemical and mechanical properties of fine-grained isotropic graphite 13 p1747 N88-20444
A study of the dynamics of high temperature brittle intergranular fracture by acoustic emission
[AERE-R-12479] 13 p1780 N88-20650
Power from the sun: Principles of high temperature solar thermal technology
[DE87-001104] 13 p1795 N88-20736
Discussion of radiation effects and high-temperature oxide superconductors
[DE88-001427] 13 p1846 N88-21046
Prediction of high-temperature thermodynamic properties of mixed electrolyte solutions including solubility equilibria, vapor pressure depression and boiling point elevation
[DE88-006344] 13 p1849 N88-21069
A viscoplastic constitutive theory for metal matrix composites at high temperature
14 p1929 N88-21500
Effects of state recovery on creep buckling under variable loading 14 p1933 N88-21527
On 3-D inelastic analysis methods for hot section components. Volume 1: Special finite element models
[NASA-CR-180893] 14 p1934 N88-21535
Prediction of thermodynamic properties, including solubility equilibria and vapor pressures, for mixed aqueous electrolytes to high temperatures
[DE88-006317] 14 p1990 N88-21863
Fluids, gels and glasses under extreme conditions of pressure and temperature
[AD-A190655] 15 p2035 N88-22125
Advanced B and Al combustion kinetics over wide temperature ranges
[AD-A190752] 15 p2036 N88-22128
Effect of strain rate on high-temperature low-cycle fatigue behavior of Hastelloy X and Hastelloy XR
[DE88-752302] 15 p2037 N88-22140
The thermal radiative properties of metals at high temperature
[DE88-006625] 15 p2038 N88-22141
High temperature oxidation and electrochemical studies related to hot corrosion
[AD-A190699] 15 p2040 N88-22156
Developments in ceramic superconducting materials
15 p2052 N88-22229
Fracture technology for brittle materials
15 p2083 N88-22417
Elevated temperature crack growth
15 p2084 N88-22421
Thermal stress in high temperature cylindrical fasteners
[NASA-TM-100611] 15 p2087 N88-22438
Synthesis of metastable superconductors by high dynamic pressure
[DE88-005620] 15 p2139 N88-22764
A theoretical and experimental study of the thermophysical properties of lithium hydride
[NASA-TT-20179] 16 p2175 N88-22965
The analysis of fatigue crack growth mechanism and oxidation and fatigue life at elevated temperatures
[NASA-CR-182129] 16 p2179 N88-22987

High temperature solid lubrication by catalytically generated carbon [AD-A190804] 16 p2182 N88-23004
Laser cladding of Ni, Nb and Mg alloys for improved environmental resistance at high temperature [AD-A191274] 16 p2213 N88-23208
Study of mechanisms of time-dependent crack growth at elevated temperature [DE88-006918] 16 p2223 N88-23271
Creep behavior of tungsten/niobium and tungsten/niobium-1 percent zirconium composites 17 p2425 N88-24427
Fabric radiators 17 p2427 N88-24435
The variation of torsional ductility of high-purity aluminum with temperature and strain rate [DE88-005618] 18 p2487 N88-24755
A thermally modified polymer matrix composite material with structural integrity to 371 C [NASA-TM-100922] 19 p2609 N88-25483
Extended ductility of Al and alpha-Fe alloys through dynamic recovery mechanisms [DE88-008679] 19 p2616 N88-25522
Metals and Ceramics Division [DE88-008955] 19 p2618 N88-25530
Uniaxial tensile strain measurement for ceramic testing at elevated temperature: Requirements, problems and solutions [DE88-008090] 19 p2621 N88-25550
Hot carrier effects in CMOS field effect transistors at cryogenic temperatures 19 p2662 N88-25829
Pulsatile fluidic pump performance at elevated temperatures [DE88-008046] 19 p2677 N88-25919
The adherence of nickel oxide on nickel during high temperature oxidation [DE88-011194] 20 p2774 N88-26450
Fracture resistance of a TiB2 particle/SiC matrix composite at elevated temperature [NASA-TM-100967] 20 p2779 N88-26482
Feasibility of producing jet fuel from GPGP (Great Plains Gasification Plant) by-products [DE88-010233] 20 p2781 N88-26492
Molten salt electrolytes for high-temperature lithium cells [DE88-010058] 20 p2794 N88-26581
On the chemistry of superconductivity [DE88-010714] 20 p2880 N88-27096
Creep behavior for Hastelloy-XR [DE88-753428] 21 p2914 N88-27295
Investigation of hydrogen isotope penetration through stainless steels Kh18N10T and Kh3M2BFR [DE88-702189] 21 p2915 N88-27297
Kinetic of oxidation to air of a Fe-Al-Mn alloy system at 600-800(sup 0)C temperature range [DE88-702309] 21 p2920 N88-27330
Properties of new low dimensional materials and mechanisms of high T(sub c) superconductivity [DE88-012026] 21 p3024 N88-27951
The High Temperature Materials Laboratory: A new research and user facility at the Oak Ridge National Laboratory [DE88-010792] 22 p3057 N88-28138
A new model for the simulation of interfaces at high temperature [DE88-009926] 22 p3155 N88-28772
Possible occurrence of band interplay in high Tc superconductor [PREPRINT-593] 22 p3157 N88-28789
The effects of moisture loss and elevated temperature upon the material damping of fibre reinforced polymer matrix composites [UTIAS-324] 23 p3188 N88-28970
The high temperature creep deformation of Si3N4-6Y2O3-2Al2O3 [NASA-CR-183204] 23 p3190 N88-28981
A fundamental study of P/M processed elevated temperature aluminum alloys [AD-A192958] 23 p3194 N88-29005
Development of high temperature, high pressure rotating shaft seals [DE88-001029] 23 p3221 N88-29172
Creep of carbon yarn and carbon-carbon composites at high temperatures and high stresses [AD-A195224] 24 p3340 N88-29678
A study of the critical factors controlling the synthesis of ceramic matrix composites from preceramic polymers [AD-A195405] 24 p3340 N88-29681
Electrical properties of materials for elevated temperature resistance strain gage application [NASA-CR-182214] 24 p3376 N88-30106

HIGH TEMPERATURE AIR
SCRAM JET (Supersonic Combustion Ramjet) combustion experiments 04 p0404 N88-12512

HIGH TEMPERATURE ALLOYS
U HEAT RESISTANT ALLOYS

HIGH TEMPERATURE ENVIRONMENTS
Calculation of the tribological properties of surfaces by semi-empirical methods [AD-A184283] 04 p0450 N88-12791
Daily dynamics of some physiological indicators of man under desert condition 06 p0750 N88-14605
Portable, ambient air microclimate cooling in simulated desert and tropic conditions [AD-A186457] 08 p1050 N88-16338
An integrated aero/mechanical performance approach to high technology turbine design 10 p1280 N88-17657
Johnson noise thermometer for high radiation and high temperature environments [DE88-003770] 10 p1323 N88-17911
Johnson noise thermometer for high-radiation and high-temperature environments 17 p2434 N88-24480
Effect of alloying, rapid solidification, and surface kinetics on the high temperature environmental resistance of niobium [AD-A192093] 18 p2485 N88-24743
High speed inlet calculations with real gas effects [NASA-CR-182167] 20 p2752 N88-26336
Finite-rate water condensation in combustion-heated wind tunnels [NASA-TP-2833] 22 p3046 N88-28075
Development of computer-controlled thermogravimetric instrumentation for measurement of environmental and high temperature volatilization and desorption of contaminants from polymeric materials [AD-A195934] 24 p3343 N88-29900

HIGH TEMPERATURE FLUIDS
NT HIGH TEMPERATURE AIR
NT HIGH TEMPERATURE GASES
Birch's law and the properties of high temperature fluid metals [DE87-014744] 03 p0288 N88-11807

HIGH TEMPERATURE GAS COOLED REACTORS
Effect of fuel burnup and cross sections on modular HTGR (High-Temperature Gas-cooled Reactor) reactivity coefficients [DE88-006656] 22 p3151 N88-28748

HIGH TEMPERATURE GASES
NT HIGH TEMPERATURE AIR
KR+ laser excitation of NH2 in atmospheric pressure flames [AD-A183421] 01 p0050 N88-10322
High temperature CO2 study: Anti-Stokes coherent Raman diffusion and infrared spectroscopy [ESA-TT-1048] 03 p0282 N88-11777
HOST turbine heat transfer program summary [NASA-TM-100280] 06 p0704 N88-14320
Evaluation of a temperature remote sensing technique [AD-A187885] 10 p1347 N88-18053
Evaluation and compilation of thermodynamic properties of high temperature chemical species [AD-A187509] 11 p1452 N88-18654
Basic characteristics of heat-exchanger-type steam reformer heated by high-temperature helium gas (2). Analysis by simulation model (2) [DE87-702962] 15 p2061 N88-22291
A numerical study of the hot gas environment around a STOVL aircraft in ground proximity [NASA-TM-100895] 17 p2295 N88-23729
Laser Diagnostics for combustion temperature and species measurements 17 p2330 N88-23912

HIGH TEMPERATURE LUBRICANTS
High hot-hardness gear lubricant evaluations, phase 2 [AD-A192309] 23 p3196 N88-29017

HIGH TEMPERATURE MATERIALS
U REFRACTORY MATERIALS

HIGH TEMPERATURE NUCLEAR REACTORS
NT HIGH TEMPERATURE GAS COOLED REACTORS
IAEA Specialists' Meeting on Graphite Component Structural Design [DE88-780006] 13 p1746 N88-20439

HIGH TEMPERATURE PLASMAS
Fast wave injection into high temperature tokamak plasmas in the lower-hybrid-density regime of JIPP T-IIU [ISSN-0469-4732] 01 p0099 N88-10649
Diagnostic technique for monitoring high temperature plasma dynamics [DE87-011786] 01 p0099 N88-10653
Study of ionization equilibrium of high temperature and low density plasma [DE87-703070] 02 p0238 N88-11502
Solar transition region and coronal response to heating rate perturbations 02 p0256 N88-11620
Hot plasmas in the Earth's magnetosphere 03 p0272 N88-11710
Advanced concepts theory annual report 1986 [AD-A184986] 05 p0651 N88-13991
Relativistic plasma concentration measuring by Bremsstrahlung [DE88-700560] 07 p0936 N88-15685
Simple model for hot ion plasmas [DE88-750045] 07 p0936 N88-15688
Energetics and dynamics of simple impulsive solar flares [NASA-TM-87816] 07 p0947 N88-15755
Acceleration/heating processes on auroral field lines as observed by the Viking spacecraft 08 p1096 N88-16596
X-ray lithographic research: A collection of NRL contributions [AD-A188313] 12 p1695 N88-20140
Effects of toroidal forces in current loops embedded in a background plasma [AD-A188878] 12 p1695 N88-20143
Fundamental studies and device development in beta silicon carbide [AD-A189540] 12 p1699 N88-20165
Modeling and transport in semiconductor devices [AD-A188760] 13 p1844 N88-21037
X-ray lasers: State of art and prospect [ETN-88-92003] 14 p1914 N88-21434
Ionization equilibrium and radiative energy losses in a stationary plasma [DE88-700856] 14 p1984 N88-21832
Advanced diagnostics for reacting flows [AD-A190485] 15 p2035 N88-22122
Measurement of time evolution of plasma electron component parameters on the Ogra-4 device by the Thomson scattering method [DE88-701575] 16 p2282 N88-23662
Bremsstrahlung from high Z impurities in hot plasmas [DE88-011755] 20 p2861 N88-26994
Apparatus for submillimeter laser diagnostics of high-temperature plasma [DE88-702464] 23 p3285 N88-29563

HIGH TEMPERATURE PROPELLANTS
KR+ laser excitation of NH2 in atmospheric pressure flames [AD-A183421] 01 p0050 N88-10322
Durability testing of an iridium-plated storable rocket engine injector [AD-A190707] 15 p2027 N88-22078

HIGH TEMPERATURE SUPERCONDUCTORS
Grain boundary effects in processing high T/sub c/ superconductors [DE87-009297] 01 p0103 N88-10673
Progress toward a superconducting opening switch [DE87-014170] 02 p0167 N88-11051
Electrical properties of high T/sub c/ superconductors under high pressures [DE87-012818] 02 p0245 N88-11546
High temperature superconductors 03 p0297 N88-11869
A role for national laboratories in enhancing economic competitiveness. The example of high-temperature superconductors: CNSS papers, No. 1 [DE87-013633] 03 p0379 N88-12386
Shock-induced chemical synthesis of phases similar to the high temperature superconductor oxides [DE87-013725] 03 p0380 N88-12387
Shock-induced chemical synthesis of phases similar to the high temperature superconductor oxides [DE87-013725] 03 p0380 N88-12387
Specific heat of the high T/sub c superconductors (La,M)2CuO4 and YBa2Cu3O7 in magnetic fields [DE87-014680] 03 p0380 N88-12388
The chemical bond and superconductivity [AD-A184275] 04 p0496 N88-13053
Hitachi develops ceramic superconducting device 06 p0688 N88-14214
Superconducting material development 06 p0688 N88-14217
Study of some superconducting and magnetic materials on high T sub c oxide superconductors [NASA-CR-182330] 06 p0785 N88-14813
L2,3 XANES of the high T sub c superconductor YBa2Cu3O7 with variable oxygen content [NOTA-INTERNA-888] 06 p0788 N88-14837
On the coexistence of phonon and non-phonon (plasmon) mechanisms in new high T/sub c/ superconductors [DE88-003188] 07 p0938 N88-15703
Localization of Cu 3d levels in the high Tc superconductor YBa2Cu3O approximately 7 by Cu2p X-ray photoelectron spectroscopy [NOTA-INTERNA-887] 07 p0939 N88-15710
Structural relationships in high temperature superconductors [DE88-002924] 09 p1257 N88-17534
Application of high temperature ceramic superconductors (CSC) to commercial tokamak reactors [DE88-003973] 09 p1257 N88-17538
High temperature superconductivity research at Argonne National Laboratory [DE88-003055] 09 p1258 N88-17541

The relationship of the chemical bonding topology of high critical temperature copper oxide superconductors to that of the chevrel phases and the ternary lanthanide rhodium borides
[AD-A189255] 13 p1845 N88-21042
Thermochemistry and high temperature thermodynamic properties of rare earth-alkaline earth-copper oxide superconductors
[DE88-005976] 15 p2140 N88-22770
High-T(sub c) superconducting wire fabrication and testing
[DE88-005969] 15 p2144 N88-22799
High temperature superconductors in the La(sub 1+x)Ba(sub 2-x)Cu O(sub y system
[DE88-006367] 15 p2145 N88-22802
The application of high temperature superconductors to space electrical power distribution components
[NASA-TM-100901] 16 p2171 N88-22939
High temperature superconductivity
[AD-A190259] 16 p2281 N88-23655
Materials science with muon spin rotation
[NASA-CR-182891] 17 p2396 N88-24242
Systematic variation of magnetic-field penetration depth in high-T(c) superconductors studied by muon spin relaxation 17 p2396 N88-24243
Crystalline metal-semiconductor superlattices
[DE88-007063] 18 p2581 N88-25332
Ground state properties and electronic structure of high T sub c superconductors
[DE88-007485] 18 p2585 N88-25360
Systematics of excimer laser ablation: Thin film preparation of high T(sub c) material
[DE88-010569] 19 p2675 N88-25909
Search for new high-temperature superconducting copper oxides
[DE88-009922] 19 p2735 N88-26245
Compilation of NRL publications on high temperature superconductivity
[AD-A189137] 21 p3019 N88-27921
Anharmonic model for high-Tc superconductors
[DE88-702196] 21 p3020 N88-27924
Superconducting properties of oxygen deficient YBa2Cu3O(sub 7-delta)
[DE88-009969] 22 p3155 N88-28774
La2CuO(sub 4 + delta): A superconducting superoxide
[DE88-010325] 23 p3288 N88-29578
Dependence of high critical temperature of ceramic superconductors on the nominal Cu(sup 3+)Cu(sup 2+) ratio
[DE88-702734] 23 p3293 N88-29611
Theory of superconductivity in oxides
[AD-A195647] 24 p3433 N88-30432
Theoretical model of high temperature superconductors
[DE88-702707] 24 p3434 N88-30441

HIGH TEMPERATURE TESTS
Viscosity measurements at high temperatures on a standard reference material supplied by BCR --- Bureau Communite de Reference (BCR)
[NPL-DMA(A)-146] 01 p0020 N88-10126
High temperature characterization of ceramic materials
[REPT-NT-3403] 03 p0292 N88-11837
High temperature tensile testing of ceramic composites
[NASA-CR-180888] 06 p0990 N88-15996
High temperature Young's modulus of IG-110 graphite
13 p1746 N88-20443
Development, high temperature properties, and microanalysis of nonoxide ceramics
[ETN-88-92103] 14 p1893 N88-21304
An experimental comparison of several current viscoplastic constitutive models at elevated temperature
14 p1931 N88-21516
Unified constitutive model development for metal matrix composites at high temperature
15 p2078 N88-22387
Examination of temperature effects on gate-to-drain avalanche breakdown in GaAs MESFETs (Metal-Semiconductor Field Effect Transistors) by measuring light emission under RF drive
[AD-A189634] 15 p2141 N88-22778
Strength and cracking resistance of ceramics. Report 3: SiC ceramics 16 p2180 N88-22994
Strength and failure rate of composite materials with carbon in ceramic matrix 16 p2180 N88-22995
Combustion behavior of the vitiator. Experimental results of a second test series
[VTH-LR-509] 18 p2484 N88-24734
Automated measurement of crack length and load line displacement at elevated temperature
[NLR-MP-87049-U] 20 p2816 N88-26706
Determination of multiaxial flow surfaces at elevated temperatures using the concept of dissipation potential
[ORNL/TM-10787] 24 p3383 N88-30149

HIGH THRUST
Development of circulation control technology for powered-lift STOL aircraft 10 p1272 N88-17608

HIGH VACUUM
Fatigue crack propagation of low-alloy steel in a vacuum environment
[DE87-013770] 01 p0061 N88-10393

HIGH VOLTAGES
A high-voltage multistage laser-triggered gas switch
[DE87-011725] 01 p0040 N88-10253
A tutorial on Rogowski coil theory and operation
[DE88-000006] 02 p0230 N88-11449
The LPX (Long Pulse Experiment) facility
[DE87-010493] 03 p0311 N88-11964
Measurements in an electromagnetic test laboratory
[SNIAS-872-430-102] 05 p0575 N88-13507
Low jitter laser-triggered high-voltage vacuum switch using low laser energies
[DE88-001922] 05 p0587 N88-13576
Evaluation of high-voltage, high-power, solid-state remote power controllers for amps
07 p0924 N88-15612
Vapor-mist for lightweight high voltage space insulation systems
[DE87-011704] 13 p1762 N88-20538
Partial discharges and the electrical aging of cross linked polyethene (XLPE) cable insulation
[EUT-86-E-160] 14 p1892 N88-21300
Test results of high-voltage, high-power, solid-state remote power controllers
[NASA-TM-100322] 16 p2194 N88-23085
High frequency power distribution system
[NASA-CR-175071] 17 p2335 N88-23939
Studies on the use of propylene carbonate as a high-voltage insulator
[DE88-011786] 22 p3057 N88-28141
Calibration technique and study on metrological characteristics of a high-voltage inverse square-law function generator
[DE88-702101] 22 p3072 N88-28236

HIGHLANDS
Topography of large craters on Mars: Implications for the highlands resurfacing history
23 p3306 N88-29691
Ridged and gullied terrains in the Martian uplands
23 p3307 N88-29700

HIGHLY MANEUVERABLE AIRCRAFT
HiMAT flight program: Test results and program assessment overview
[NASA-TM-86725] 01 p0005 N88-10026
Development and flight test of an experimental maneuver autopilot for a highly maneuverable aircraft
[NASA-TP-2618] 14 p1867 N88-21153

HIGHWAYS
Seasonal variation for structural strength value
[PB88-169248] 16 p2222 N88-23260

HILBERT SPACE
Stochastic integration for operator valued processes on Hilbert spaces and on nuclear spaces
[ENST-87D002] 01 p0089 N88-10580
Irreducible *-representations of the Lie superalgebra osp(1,4) with finite-degenerated vacuum
[DE87-703089] 02 p0225 N88-11420
Families of Bose rays in quantum optics
[DE87-014584] 02 p0236 N88-11489
Compactness of quasi-conforming element spaces, convergence of quasi-conforming element method
03 p0301 N88-11896
Stochastic filtering solutions for ill-posed linear problems and their extension to measurable transformations
[AD-A186016] 07 p0909 N88-15506
Strong laws of large numbers for arrays of orthogonal random variables
[AD-A186159] 07 p0910 N88-15513
Characterization of all controlled invariant sub-spaces for spectral systems
[PB88-106638] 07 p0912 N88-15532
Admissible and singular translates of stable processes
[AD-A186426] 07 p0917 N88-15571
Strong convergence and convergence rates of approximating solutions for algebraic Riccati equations in Hilbert spaces
[AD-A186190] 08 p1072 N88-16464
Computation of the zeta-function of an algebraic curve with the differentials of the first kind
[PB88-127527] 10 p1399 N88-18339
Eigenvalue problems
[AD-A188069] 10 p1401 N88-18356
The global convergence of partitioned BFGS on problems with convex decompositions and Lipschitzian gradients
[DE88-006249] 14 p1968 N88-21744
Stochastic evolution equations driven by nuclear space valued martingales
[AD-A189342] 15 p2126 N88-22677
Geometric methods and the gauge structure of Berry's phase
[DE88-006538] 15 p2127 N88-22682
Coding capacity of generalized additive channels
[AD-A190315] 15 p2127 N88-22685
On the Hilbert space of supersymmetric quantum systems
[DE88-701648] 16 p2284 N88-23677
Theory of pseudo-differential operators over C*-algebras
[DE88-701860] 20 p2845 N88-26883
Backlund transformations associated with a Riemann-Hilbert spectral problem
[PREPRINT-596] 22 p3146 N88-28712
The Hilbert space of the closed bosonic string
[USIP-88-04] 22 p3151 N88-28747
Feedback stabilization of du/dt=Au + bf in Hilbert space when the normalization function is less than or equal to r
[AD-A193510] 23 p3277 N88-29506
The Hilbert space of the open bosonic string
[USIP-88-02] 23 p3295 N88-29628

HILBERT TRANSFORMATION
Some properties of the Hilbert transform
[DE88-002465] 09 p1227 N88-17350
Approximation problems of the Hilbert transform to identify minimum phase linear systems
[FUB-42-1986] 21 p2999 N88-27790
Application of the Hilbert transform to Doppler radar signals from a hypervelocity gun
[AD-A193690] 22 p3146 N88-28716

HILLER MILITARY AIRCRAFT
U MILITARY AIRCRAFT

HIMAT
U HIGHLY MANEUVERABLE AIRCRAFT

HINDRANCE
U CONSTRAINTS

HINGE MOMENTS
U TORQUE

HINGED ROTOR BLADES
U HINGES
U ROTARY WINGS

HINGELESS ROTORS
U RIGID ROTORS

HINGES
NT FLAPPING HINGES
Locking hinge
[NASA-CASE-MSC-21056-1] 17 p2312 N88-23827
Payload deployment method and system
[NASA-CASE-MSC-21330-1] 18 p2470 N88-24660

HIP (PROCESS)
U HOT ISOSTATIC PRESSING

HIPPARCOS SATELLITE
Deep space target location with Hubble Space Telescope (HST) and Hipparcos data
[NASA-CR-182520] 10 p1427 N88-18524
Preparation of photometric measurements on a million stars in the framework of the satellite project HIPPARCOS/TYCHO
[ETN-88-91502] 13 p1853 N88-21093

HIPPOCAMPUS
Long term synaptic plasticity and learning in neuronal networks
[AD-A186834] 09 p1199 N88-17188

HISTOCHEMICAL ANALYSIS
Histomorphometric analysis of rat bones after spaceflight aboard Cosmos-1667 biosatellite
10 p1360 N88-18128
Muscle preservation in the study of bioenergetic effects of hypokinesia 10 p1362 N88-18139
Investigation of rat skeletal muscles following short-term spaceflight aboard Cosmos-1667 biosatellite
10 p1365 N88-18157

HISTOGRAMS
Necessary and sufficient conditions for the convergence of integrated and mean-integrated r-th order error of histogram density estimates
[AD-A186037] 07 p0914 N88-15550
Almost sure L(gamma)-norm convergence for data-based histogram density estimates
[AD-A189944] 17 p2393 N88-24228

HISTOLOGY
Status of microcirculation in high-altitude blood loss
12 p1663 N88-19973

HISTORIES
The history of aeroelasticity research in Germany from the beginning until 1945 --- airframes
[DFVLR-MITT-86-25] 01 p0001 N88-10003
Overview of STIP intervals 15-19
01 p0110 N88-10710
On the occasion of the 50th anniversary of the death of Professor Hugo Junkers
[MBB/LW-3016/S/PUB/201] 02 p0257 N88-11627
Hypocenters (1977-1984) around the Richton Dome and the Melvin, Alabama, 1978 earthquake
[DE87-014336] 03 p0351 N88-12214

The development of ODE methods: A symbiosis between hardware and numerical analysis
[DE87-014925] 03 p0370 N88-12325
How space, the fourth operational medium, supports operational maneuver
[AD-A184742] 03 p0373 N88-12346
Hypersonic airbreathing propulsion: Evolution and opportunities 05 p0531 N88-13231
The technical evolution of the Wilson camera: The beginnings (1895-1925)
[NOTA-INTERNA-876] 05 p0585 N88-13568
The birth of big science: Nuclear physics as advanced technology source
[NOTA-INTERNA-881] 05 p0648 N88-13967
The history and development of nonlinear stellar pulsation codes
[DE88-001828] 06 p0801 N88-14899
Measurements in centrifugal compressors
07 p0850 N88-15161
Lewis materials research and technology: An overview
09 p1119 N88-16699
A comparison of fitting techniques for the cumulative average learning curves with historical lot cost data
[AD-A187127] 09 p1227 N88-17349
The coming revolution in turbine engine technology
10 p1279 N88-17648
Airbus, the successful European cooperation
[MBB-UT-005/87] 10 p1313 N88-17847
Messerschmitt-Boelkow-Blohm: A company with a tradition 10 p1316 N88-17866
Messerschmitt-Boelkow-Blohm: Biography and history of a company 10 p1316 N88-17867
Present stage of space medicine
10 p1364 N88-18151
Antimatter: Its history and its properties
[DE88-004308] 10 p1423 N88-18498
Spacecraft fire detection and extinguishment: A bibliography
[NASA-CR-180880] 11 p1444 N88-18612
Announced United States nuclear tests: July 1945 through December 1986
[NVO-209-REV-7] 11 p1546 N88-19247
The early years of string theory: The dual resonance model
[DE88-003521] 11 p1563 N88-19359
An evaluation in a modern wind tunnel of the transonic adaptive wall adjustment strategy developed by NPL in the 1940's
[NASA-CR-181623] 12 p1575 N88-19417
Historical electromagnetic propagation condition database description
[AD-A189157] 12 p1621 N88-19695
An evaluation of historical algebras
[AD-A188350] 12 p1684 N88-20067
HISPLT: A history graphics post processor for wave propagation codes
[DE88-005507] 13 p1817 N88-20857
Electronics and communications in air traffic control: The Presidential Address
[ETN-88-92057] 14 p1865 N88-21146
Sunspot frequency and solar activity
[PUBL-17/87] 14 p2011 N88-21996
Chronology of KSC and KSC related events for 1987
[NASA-CR-182754] 14 p2012 N88-22002
Energy from the wind
[DE88-006897] 15 p2091 N88-22459
Marshall Space Flight Center 1960-1985: 25th anniversary report
[NASA-TM-100328] 15 p2153 N88-22852
Two decades of achievement in the ocean, 1968-1988
[PB88-167077] 16 p2236 N88-23356
Presentation of the METEOSAT system and the roles of EUMETSAT within the meteorological community
17 p2357 N88-24039
Sea ice kinematics: Space and time scales
[AD-A191162] 17 p2376 N88-24128
The application of hydrocarbon bioconversion technology to aerospace materials production
18 p2478 N88-24698
History of wildland fires on Vandenberg Air Force Base, California
[NASA-TM-100983] 18 p2549 N88-25134
NASA history data book. Volume 1: NASA resources 1958-1968
[NASA-SP-4012-VOL-1] 18 p2596 N88-25428
NASA historical data book. Volume 2: Programs and projects 1958-1968
[NASA-SP-4012-VOL-2] 18 p2596 N88-25429
NASA historical data book. Volume 3: Programs and projects 1969-1978
[NASA-SP-4012-VOL-3] 18 p2596 N88-25430
High-temperature superconductivity: An overview
[DE88-702051] 21 p3020 N88-27925
History of manned spaceflight
[CNES-NT-121] 21 p3032 N88-28000
Soviet space program handbook
[AD-A194332] 22 p3046 N88-28077
Review of past and current trials and uses of unmanned vehicles
[AD-A194527] 22 p3084 N88-28311
Newtonian and Einsteinian gravitation
22 p3158 N88-28791
Regional intercomparisons of General Circulation Model predictions and historical climate data: CO2
[DE88-010416] 23 p3235 N88-29248
SDI (Strategic Defense Initiative): A policy analysis
[AD-A194240] 23 p3275 N88-29493
An introduction to the historical records of China about Mars 23 p3301 N88-29664
History of aeroelasticity in Germany from the beginning to 1945
[ESA-TT-1082] 24 p3319 N88-29767
Analysis of environmental parameters from the Panama City tower radar experiment
[AD-A194994] 24 p3404 N88-30264

HLLV
U HEAVY LIFT LAUNCH VEHICLES

HMX
High pressure strand burn rate tests of polyvinylnitrate/nitramine propellants
[AD-A184178] 04 p0422 N88-12615
The correlation of HMX (cyclotetramethylenetetranitramine) particle characterization techniques to propellant burn rate
[AD-A187119] 09 p1140 N88-16833
Kinetic measurements of thermal decomposition of energetic materials at high pressures
[AD-A191612] 19 p2622 N88-25552
Temperature and species profiles in propellant ignition and combustion 19 p2633 N88-25616
Chemical kinetics modeling of HMX combustion
19 p2633 N88-25617
Descriptive characterization of propellant particles
[AD-A195176] 24 p3356 N88-29985

HOGBACKS
U RIDGES

HOHMANN TRAJECTORIES
U ELLIPTICAL ORBITS
U TRANSFER ORBITS

HOHMANN TRANSFER ORBITS
U ELLIPTICAL ORBITS
U TRANSFER ORBITS

HOLDERS
NT FLAME HOLDERS
An optically strobed sample and hold circuit
19 p2656 N88-25772
Evaluation of transfer films of Salox M on 440C for HPOTP bearing cage applications, task 119
[NASA-CR-179020] 23 p3223 N88-29184

HOLE BURNING
Applications of nonlinear hole burning spectroscopy
[AD-A184943] 05 p0587 N88-13580

HOLE DISTRIBUTION (ELECTRONICS)
Electrical and optical properties of Hg/sub 1-x/Cd/sub x/Te doped layers grown by Liquid Phase Epitaxy (LPE)
[DE88-701023] 16 p2281 N88-23653

HOLE DISTRIBUTION (MECHANICS)
Crack distribution and growth rates for critical fastener holes in Mirage wing RH79
[AD-A189080] 13 p1722 N88-20293
Stress concentration around circular hole in a composite material specimen representative of the X-29A forward-swept wing aircraft
[NASA-CR-179435] 20 p2814 N88-26694

HOLE GEOMETRY (MECHANICS)
Device for measuring hole elongation in a bolted joint
[NASA-CASE-LAR-13453-1] 06 p0712 N88-14361
Life and reliability of rotating disks
15 p2085 N88-22428
Dynamical stress concentration problems, from every side, bordered and perforated plates
[ETN-88-92128] 20 p2815 N88-26703

HOLE MOBILITY
Electrical and optical properties of Hg/sub 1-x/Cd/sub x/Te doped layers grown by Liquid Phase Epitaxy (LPE)
[DE88-701023] 16 p2281 N88-23653

HOLES
Loading rate sensitivity of open hole composites in compression
[NASA-TM-100634] 19 p2610 N88-25490
Compression creep of filamentary composites
[NASA-CR-182550] 20 p2798 N88-26601

HOLES (ELECTRON DEFICIENCIES)
Modeling and transport in semiconductor devices
[AD-A188760] 13 p1844 N88-21037
Nonlinear optical properties and subpicosecond dynamics of excitons and electron-hole plasmas in multiple quantum well structures
[AD-A191926] 19 p2727 N88-26196
Direct measurement of ultrafast electron-hole plasma expansion at high density at an asymmetric GaAs quantum well 20 p2871 N88-27044
Oxygen vacancy ordering and superconductivity in YBa2Cu3O(sub 7-x)
[DE88-010005] 20 p2877 N88-27083
Inelastic electron scattering and electron-hole excitations in iron and nickel
[DE88-011843] 21 p2915 N88-27303

HOLES (MECHANICS)
Hole diameters in plates impacted by projectiles
21 p2929 N88-27386
Two-dimensional sequential and concurrent finite element analysis of unstiffened and stiffened aluminum and composite panels with hole
[NASA-CR-183083] 22 p3086 N88-28325

HOLLAND
U NETHERLANDS

HOLLOW CATHODES
Segmented hollow cathode discharges for copper ion lasers
[ETN-87-90403] 01 p0052 N88-10333
Hollow cathode plasma coupling study, 1986
[NASA-CR-171985] 03 p0309 N88-11949
Advanced electric propulsion and space plasma contactor research
[NASA-CR-180862] 06 p0674 N88-14126
Space plasma contactor research, 1987
[NASA-CR-182148] 16 p2280 N88-23649

HOLMIUM
Magnetic phase transitions in 90-K superconductors Ho1Ba2Cu3O(7-delta) and Gd1Ba2Cu3O(7-delta) observed by ZF-muon(+)SR
[DE88-752611] 23 p3290 N88-29588

HOLOGRAPHIC INTERFEROMETRY
ISIS: Imaging Speckle Interfereometer in Space
01 p0095 N88-10625
Optical flow diagnostic measurements in turbomachinery
[PNR90396] 02 p0172 N88-11081
Development and testing of a system for the partially automated evaluation of holographic interferograms in the experimental stress analysis of reactor components
[ETN-87-90574] 02 p0175 N88-11095
The use of holographic interferometry for turbomachinery fan evaluation during rotating tests
[PNR90390] 02 p0176 N88-1109
Diffraction moire: The dynamic regime
[DE87-014883] 03 p0335 N88-12111
Determination of the origin of self-pumped phase conjugation in barium titanate
[AD-A184697] 03 p0377 N88-12372
Interferometric data for a shock-wave/boundary-layer interaction
[NASA-TM-88227] 05 p0543 N88-13306
Full field visualization of surface and bulk acoustic waves using heterodyne holographic interferometry
[AD-A185071] 05 p0646 N88-13958
Dye laser for holographic interferometry
07 p0920 N88-15588
Investigation of vibration problems with heterodyne holographic interferometer 08 p1000 N88-16058
JPRS report: Science and technology. USSR: Physics and mathematics
[JPRS-UPM-87-010] 08 p1075 N88-16485
Formation of high-coherence radiation in free-running mode ruby laser for pulse holography
08 p1077 N88-16497
Comparison of sensitivity and precision of holographic and speckle-interferometry methods with Fourier-plane recording 08 p1078 N88-16500
Holographic phase correction
[RSRE-MEMO-4036] 09 p1167 N88-17000
A review on holography, its principles and applications
[ISL-CO-242/86] 15 p2069 N88-22338
Computer tomography and hybrid optical/digital methods for aerodynamic measurements
[AD-A190909] 16 p2157 N88-22872
Dual wavelength holographic interferometry system
[NASA-CASE-MFS-28242-1] 17 p2341 N88-23960
Simultaneously time- and space-resolved spectroscopic characterization of laser-produced plasmas
[DE88-008038] 19 p2728 N88-26202
Turbulent flow field visualization with integral interferometric imaging and computed tomography
21 p2950 N88-27521
Holographic interferometry for flow visualization studies in high speed fans
[PNR90459] 22 p3045 N88-28072
Holographic flow visualization
[PNR90466] 22 p3079 N88-28283
Experimental aspects of using time-averaged holographic interferometry to detect barely visible impact damage in a graphite/epoxy composite plate
[AD-A194418] 24 p3375 N88-30097

Use of holography in vibration and flutter study of fans
[PNR90458] 24 p3375 N88-30098
HOLOGRAPHY
NT SPECKLE HOLOGRAPHY
NT WHITE LIGHT HOLOGRAPHY
Implementation of a digital optical matrix-vector multiplier using a holographic look-up table and residue arithmetic
[NASA-CR-180431] 01 p0078 N88-10496
Ultrafast holography using optical fibers
[ISL-R-101/86] 02 p0176 N88-11096
Computed neutron tomography and coded aperture holography from real time neutron images
04 p0427 N88-12645
Measurement and control of damage in composite materials: Nondestructive controls by thermography, holography, and radiography
[SNIAS-872-430-110] 05 p0559 N88-13403
The production of ultrasmall and superfine holographic diffraction gratings using synchrotron radiation and lithographic techniques
[AD-A185395] 05 p0585 N88-13562
Determination of a flow velocity field using four-exposure laser holography
[IMFL-3114-85/32] 05 p0585 N88-13565
Selection of holographic screen for projection of images reconstructed by multiaspect holograms of focused images 06 p0773 N88-14745
Online monitoring of laserpulses using the GPIB-interface of a Tektronix 2430 Digital Storage Oscilloscope
[DE88-002836] 07 p0856 N88-15201
Scanning and measuring peculiarities with high-space resolution objects recorded at the Gabor holograms
[DE88-700373] 07 p0857 N88-15203
Holography of the ionosphere at HIPAS
[AD-A186237] 07 p0877 N88-15322
Multilayer holographic functional element in analog-digital converter 07 p0921 N88-15593
Resolution of holograms produced by the fluid experiment system and the holography ground system
07 p0923 N88-15609
Cavitation inception scale effects. 1. Nuclei distributions in natural waters. 2. Cavitation inception in a turbulent shear flow
[AD-A186553] 08 p0988 N88-15987
Formation of high-coherence radiation in free-running mode ruby laser for pulse holography
08 p1077 N88-16497
A holographic investigation of particulates in metallized solid fuel ramjet combustion
[AD-A186887] 09 p1140 N88-16831
Holographic investigation of metallized solid propellant combustion in two-dimensional and three-dimensional rocket motors
[AD-A187000] 09 p1140 N88-16832
Calculation of noise in spatial speckle-field holograms under conditions of saturated photoresponse
09 p1235 N88-17403
Color shadow methods of analyzing reconstructed wave front 09 p1236 N88-17407
Kinetics and spectrum of light pulse used in picosecond holography 09 p1236 N88-17409
Measuring accuracy of 3-dimensional bodies by the GOMER-1 device
[DE87-703230] 12 p1628 N88-19744
Holographically correcting synthetic aperture aberrations
[AD-A189510] 12 p1692 N88-20123
Development of fiber optic systems for recording and transmitting holographic information
[AD-A189406] 13 p1773 N88-20603
ONR Far East Scientific Bulletin, volume 12, number 3, July-September 1987
[AD-A188554] 13 p1851 N88-21081
Holographic disk for data storage
14 p1972 N88-21771
MIG-1 on-line measuring holographic microscope
[DE88-701103] 15 p2068 N88-22332
Focused image holography abberations
[DE88-701105] 15 p2068 N88-22333
A review on holography, its principles and applications
[ISL-CO-242/86] 15 p2069 N88-22338
Space-variant optical systems
[AD-A189967] 15 p2133 N88-22724
The use of a water towing tank for aerodynamic testing and methods for quantitative evaluation of photographs
16 p2202 N88-23140
Flow measurements in a water tunnel using a holocinematographic velocimeter
16 p2203 N88-23141
Application of high speed holography to aerodynamic and hydrodynamic three-dimensional velocimetry
16 p2203 N88-23144
Study of flow tracer behavior models and experimental validation with multiple exposure holographic velocimetry
[IMFL-87/30] 20 p2801 N88-26622
Interferometric recording of holographic optical elements using partially coherent light
20 p2805 N88-26636
Active phase compensation system for fiber optic holography
[NASA-TM-101295] 20 p2805 N88-26641
Optical data processing
[AD-A193024] 20 p2839 N88-26841
Precise rotational alignment of X-ray transmission diffraction gratings
[DE88-010599] 21 p2911 N88-27273
Holographic determination of droplet size distributions
[DFVLR-MITT-88-05] 22 p3074 N88-28250
Noise generation and boundary layer effects in vortex-airfoil interaction and methods of digital hologram analysis for these flow fields
[AD-A194191] 23 p3171 N88-28883
Hologram representation of design data in an expert system knowledge base 23 p3251 N88-29354
Automatic data retrieval from rocket motor holograms
[AD-A195586] 24 p3337 N88-29864
Evaluation of multi-focus holographic lenses
[AD-A196167] 24 p3377 N88-30110
High-resolution (30 m) lunar radar images
24 p3442 N88-30486
HOLOMORPHISM
U ANALYTIC FUNCTIONS
HOMEOSTASIS
Physicochemical correlates of human adaptation to extreme environments 06 p0750 N88-14607
Mother-fetus system as object for investigation of mechanisms of physiological effect of weightlessness
07 p0891 N88-15402
Spleen lymphocyte nucleic acids in pregnant rats flown in space and their offspring 07 p0892 N88-15403
Role of testing total gas (O2 and CO2) tension of blood plasma in the study of human gas homeostasis
07 p0894 N88-15419
JPRS Report: Science and Technology. USSR: Space Biology and Aerospace Medicine, volume 21, no. 5, September - October 1987
[JPRS-USB-88-003] 10 p1359 N88-18122
Effect of spaceflight factors on primate hydration homeostasis 10 p1360 N88-18126
Discrete adaptation to sensory conflict
10 p1363 N88-18146
The influence of space flight on water-salt homeostasis in man and animals 12 p1659 N88-19943
Human adaptation to various hypercapnic conditions in relation to salivary electrolyte dynamics and renal function 12 p1664 N88-19977
HOMING
Optimal guidance of homing missiles
06 p0671 N88-14111
Effects of closing speed uncertainty on optimal guidance 12 p1597 N88-19556
HOMING DEVICES
The impact of environmental factors on the performance of millimeter wave seekers in smart munitions
[DE87-014277] 03 p0270 N88-11697
Optimal guidance of homing missiles
06 p0671 N88-14111
Advanced guidance algorithms for homing missiles with bearings-only measurements
[AD-A190435] 15 p2017 N88-22026
HOMODYNE RECEPTION
Coherent infrared detection, volume B --- CO2 laser intersatellite data link
[ESA-CR(P)-2392-VOL-1] 01 p0034 N88-10218
Coherent infrared detection, volume D --- CO2 laser intersatellite data link
[ESA-CR(P)-2392-VOL-2] 01 p0034 N88-10219
HOMOGENEITY
The dishomogeneity of the degree of sensitization in large recirculation pipes in Boiling Water Reactor (BWR) power plants
[CISE-3955] 09 p1247 N88-17473
The h-p version of the finite element method for problems with nonhomogeneous essential boundary condition
[AD-A187356] 10 p1400 N88-18348
Inversion of parabolic and paraboloidal projections
[AD-A187538] 10 p1405 N88-18380
Notes on a class of homogeneous space-times
[DE88-700138] 11 p1562 N88-19353
Decomposition of hypochlorite in the presence of copper in a homogeneous medium
[NASA-TT-20199] 13 p1740 N88-20403
Local structure of intercomponent energy transfer in homogeneous turbulent shear flow
16 p2197 N88-23103
Kinetics of homogeneous nucleation in superheated F-11 and F-21 liquid freons
[NASA-TT-20286] 19 p2613 N88-25503
Off-boundary approach to the boundary element method
[AD-A192931] 20 p2815 N88-26701
Homogeneity of glasses: Experiment WL-IHF-05 in D1 mission --- Spacelab
[ETN-88-92339] 21 p2924 N88-27353
HOMOGENEOUS TURBULENCE
Center for Turbulence Research 1987 activities
[NASA-CR-182693] 13 p1769 N88-20583
Dense-spray structure and phenomena. Part 1. Turbulence/dispersed-phase interactions
[AD-A190606] 15 p2065 N88-22315
Reynolds stress models of homogeneous turbulence
16 p2197 N88-23106
Evaluation of a theory for pressure-strain rate
16 p2198 N88-23108
Relations between two-point correlations and pressure strain terms 16 p2198 N88-23109
Coherent structures: Comments on mechanisms
16 p2199 N88-23118
On the prediction of equilibrium states in homogeneous turbulence
[NASA-CR-181659] 16 p2207 N88-23174
Numerical simulation of compressible homogeneous turbulence: Effects of fluid compressibility
[PB88-127154] 19 p2597 N88-25433
Development of a more general Reynolds stress closure for swirling flow
[AD-A195121] 24 p3374 N88-30092
HOMOGENIZATION
U HOMOGENIZING
HOMOGENIZING
Homogenization study of matrix behavior in a composite material
[ONERA-RT-1/7256-RY-060-R]
16 p2172 N88-22943
Functional and mechanical analysis of continuous media-application to the study of elastic composites with periodic structure: Homogenization
[NASA-TT-20188] 18 p2480 N88-24710
HOMOMORPHISMS
NT AUTOMORPHISMS
HOMOTOPY THEORY
A polynomial approach to the H sub infinity control design method
[MEMO-662] 14 p1962 N88-21701
Edge-disjoint homotopic paths in straight-line planar graphs
[CWI-OS-R8718] 16 p2264 N88-23537
Decomposition of graphs on surfaces and a homotopic circulation theorem
[CWI-OS-R8719] 16 p2264 N88-23538
HONEYCOMB CORES
Core material --- honeycombs
[EP-PATENT-0-196-926-A2] 05 p0558 N88-13393
HONEYCOMB STRUCTURES
NT HONEYCOMB CORES
Solar converging method 04 p0403 N88-12504
Advanced radiator concepts utilizing honeycomb panel heat pipes
[NASA-CR-172017] 04 p0443 N88-12747
Influence of bonding shop moisture on metal-honeycomb junctions bonded with ultra-thin adhesive films
[SNIAS-872-422-112] 05 p0558 N88-13399
A comparison of experimental and theoretical results for labyrinth gas seals with honeycomb stators
[NASA-CR-182441] 08 p0993 N88-16006
Experimental rotordynamic coefficient results for honeycomb seals
[NASA-CR-182440] 08 p0993 N88-16007
HOOKES LAW
Kinematics of Hooke universal joint robot wrists
[NASA-TM-100567] 20 p2843 N88-26870
HOOP COLUMN ANTENNAS
Studies of the structural dynamic behavior of satellite antenna system
[AD-A185526] 06 p0673 N88-14121
The 15-meter diameter hoop/column antenna surface control actuator system 14 p1924 N88-21469
HOPPERS
Energy efficient continuous flow ash lockhopper
[NASA-CASE-NPO-16985-1-CU]
18 p2497 N88-24814
HORIZON
Satellite autonomous navigation with SHAD (Stellar Horizon Atmospheric Dispersion)
[AD-A184988] 05 p0544 N88-13313
HORIZON SCANNERS
High lifetime mechanisms implemented in infrared horizon scanning sensors --- SPOT
14 p1877 N88-21214
HORIZON SENSING
U HORIZON SCANNERS

HORIZONTAL FLIGHT
Flap-lag-torsion aeroelastic stability of a circulation control rotor in forward flight 10 p1271 N88-17600
HORIZONTAL ORIENTATION
Large-scale horizontal flows from SOUP observations of solar granulation 02 p0256 N88-11621
Effects of combining vertical and horizontal information into a primary flight display [NASA-TP-2783] 04 p0399 N88-12487
Aircraft engine exhaust plume dynamics [AD-A184238] 04 p0400 N88-12488
Study on a rotor speed control system for a horizontal axis windmill [NAL-TR-931] 10 p1349 N88-18062
State-of-the-art for assessing earthquake hazards in the US. Parameters for specifying intensity-related earthquake ground motions [AD-A188230] 11 p1512 N88-19032
A polarization diversity meteorological radar system [AD-A189291] 13 p1758 N88-20515
Fatigue load measurements and evaluation of the 25m Horizontal Axis Wind Turbine (HAWT) at Petten, The Netherlands [NLR-MP-86054-U] 13 p1782 N88-20660
HORIZONTAL STABILIZERS
U STABILIZERS (FLUID DYNAMICS)
HORMONE METABOLISMS
Is ANF implied in the night attenuated renal response to central hypervolemia? 12 p1659 N88-19945
Renal effects of anti-gravity suit inflation in man in relation to cardiovascular and hormonal changes 12 p1661 N88-19959
HORMONES
NT ALDOSTERONE
NT CORTICOSTEROIDS
NT PITUITARY HORMONES
Cosmonauts' hormonal responses after brief spaceflights 07 p0890 N88-15394
Effect of steroid hormones on biogenic amine levels in lungs during development of pulmonary hypertension in rats submitted to chronic hypobaric hypoxia 07 p0896 N88-15430
Certain aspects of human metabolism during spaceflights of varying duration [NASA-TT-20215] 10 p1369 N88-18181
Endocrine responses to resistance exercise [AD-A188681] 12 p1667 N88-19993
Hormonal regulation of fluid and electrolytes: Effects of heat exposure and exercise in the heat [AD-A192655] 22 p3131 N88-28614
HORNS
Horn design equations for the NBS (National Bureau of Standards) horn-type noise standards [PB88-110226] 07 p0844 N88-15122
HOSES
Variable collision frequency effects on hose and sausage instabilities in relativistic electron beams [AD-A184206] 04 p0490 N88-13021
HOT AIR
U HIGH TEMPERATURE AIR
HOT CORROSION
Optimizing the application of high temperature corrosion resistant aluminium-silicon-base coatings [BLL-M-37222-(5828.4)] 01 p0018 N88-10112
Turbine airfoil deposition models and their hot corrosion implications 02 p0189 N88-11178
Experimental verification of vapor deposition rate theory in high velocity burner rigs 02 p0189 N88-11179
Effects of surface chemistry on hot corrosion life 02 p0189 N88-11180
Reaction mechanism of sulfur dioxide with single crystal cobalt and chromium and CoCrAlY coatings [AD-A185989] 09 p1253 N88-17509
High temperature oxidation and electrochemical studies related to hot corrosion [AD-A190699] 15 p2040 N88-22156
Corrosion Research Center, University of Minnesota [DE88-006681] 15 p2041 N88-22160
High temperature corrosion of ceramics [DE88-006567] 15 p2046 N88-22193
Vanadic hot corrosion of gas turbine blade coating materials 17 p2321 N88-23864
Molten salt corrosion of SiC and Si3N4 17 p2325 N88-23885
Guide to the control of high temperature corrosion and protection of gas turbine materials [PB88-107412] 20 p2760 N88-26370
HOT ELECTRONS
Long wavelength vortices of low frequency interchange modes [IPPJ-844] 02 p0241 N88-11525
A ray-tracing study of electron cyclotron resonance heating in tokamak plasmas with a superthermal electron tail [INPE-4381-PRE/1201] 08 p1085 N88-16536
Absorption of electron cyclotron radiation in tokamak plasmas with a superthermal tail in the electron velocity distribution [INPE-4391-PRE/1211] 08 p1086 N88-16541
Investigations of stimulated Raman scattering from high density underdense plasmas irradiated by a 0.35 micron laser 10 p1411 N88-18421
Hot electron diagnostics using X-ray imaging on GAMMA10 17 p2443 N88-24530
Resonant tunneling electron spectroscopy 19 p2660 N88-25811
Third International Conference on Superlattices, Microstructures and Microdevices [AD-A191416] 20 p2861 N88-26995
Hot electron transistors grown by MOCVD 20 p2861 N88-26996
Hot electrons in silicon dioxide: Ballistic to steady-state transport 20 p2871 N88-27042
Recent applications of Monte Carlo methods for semiconductor microdevice simulation 20 p2871 N88-27046
Studying the physics and operation of multi-terminal near-micron and sub-micron length, hot electron semiconductor devices [AD-A193380] 21 p2938 N88-27446
Hot electron emission in semiconductors [AD-A194101] 23 p3292 N88-29601
HOT EXTRUDING
U EXTRUDING
HOT FORMING
U HOT WORKING
HOT GAS SYSTEMS
U HIGH TEMPERATURE GASES
HOT GASES
U HIGH TEMPERATURE GASES
HOT ISOSTATIC PRESSING
Hot isostatic pressing of nickel aluminide powders [DE88-009677] 19 p2617 N88-25525
HOT JET EXHAUST
U HIGH TEMPERATURE GASES
U JET EXHAUST
HOT JETS
U JET FLOW
HOT PLASMAS
U HIGH TEMPERATURE PLASMAS
HOT PRESSING
NT HOT ISOSTATIC PRESSING
Isothermal forging and its effect on the microstructure of powder route nickel alloy AP1 [RAE-TM-P-1094] 01 p0022 N88-10138
Characterization and thermal conductivity of hot-pressed silicon carbide [DKG-25] 03 p0292 N88-11834
Deformation mechanisms of thermostructural materials [AD-A184070] 03 p0338 N88-12128
Fabrication and materials evaluation of high performance aligned ceramic fibre reinforced glass matrix composite [AERE-R-12517] 10 p1294 N88-17736
Molybdenum-base cermet fuel development [DE88-005529] 13 p1839 N88-21003
Processing, physical metallurgy and creep of NiAl + Ta and NiAl + Nb alloys [NASA-CR-182113] 14 p1890 N88-21295
Processing, microstructure, and mechanical properties of silicon carbide particulate reinforced aluminum alloys [AD-A188981] 15 p2037 N88-22136
Strength optimization of alpha-SiC by improved processing 17 p2324 N88-23880
Improved silicon nitride for advanced heat engines 17 p2324 N88-23881
Molybdenum-base cermet fuel development 17 p2434 N88-24481
Martensitic transformation and microstructures in sintered NiAl alloys [NASA-TT-20178] 18 p2488 N88-24761
Martensitic transformation and microstructures in sintered NiAl alloys [NASA-TT-20192] 19 p2616 N88-25519
Hot isostatic pressing of tungsten-nickel-iron composites [FOA-C-20698-2.1] 22 p3056 N88-28135
HOT STARS
NT A STARS
NT B STARS
NT O STARS
NT WHITE DWARF STARS
NT WOLF-RAYET STARS
Literature survey relating to the absorption properties of ozone in the near ultraviolet [ESRO-SM-81] 09 p1190 N88-17129
Time-dependent mass loss from hot stars with and without radiative driving [DE88-008899] 20 p2884 N88-27128
Evolutionary helium and CNO anomalies in the atmospheres and winds of massive hot stars [NASA-CR-183254] 24 p3452 N88-30550
HOT SURFACES
Recent advances in high temperature instrumentation for hot section applications [NASA-TM-100282] 06 p0707 N88-14339
Structural analysis methods development for turbine hot section components [NASA-TM-100298] 11 p1501 N88-18967
On 3-D inelastic analysis methods for hot section components. Volume 1: Special finite element models [NASA-CR-180893] 14 p1934 N88-21535
Diamond film by hot filament CVD method [NASA-TT-20335] 23 p3294 N88-29618
Constitutive modeling for isotropic materials [NASA-CR-182132] 24 p3327 N88-29811
HOT WORKING
Advances in processing techniques for nickel aluminides [DE87-014571] 05 p0566 N88-13449
Method of obtaining of fire resistant polyacrylonitrile fiber or cloth from it [AD-A185941] 07 p0836 N88-15071
Statistical analysis of feasibility of non-destructive inspection of mechanical properties of hot worked pipes of alloy steels [BLL-M-37598-(5828.4)] 14 p1922 N88-21455
HOT-FILM ANEMOMETERS
The design and use of a temperature-compensated hot-film anemometer system for boundary-layer flow transition detection on supersonic aircraft [NASA-TM-100421] 13 p1723 N88-20304
Crossflow vorticity sensor [NASA-CASE-LAR-13436-1-CU] 17 p2300 N88-23759
Method of forming a multiple layer dielectric and a hot film sensor therewith [NASA-CASE-LAR-13678-1] 18 p2584 N88-25355
The use of hot-film technique for boundary layer studies on a 21 percent thick airfoil [NAE-AN-45] 24 p3321 N88-29781
HOT-WIRE ANEMOMETERS
Turbulence measurement in hypersonic flow 05 p0530 N88-13224
Hot wire and laser velocimeter studies of turbulent flow at supersonic velocities [ETN-88-91172] 05 p0585 N88-13566
Studies of supersonic turbulence and hot-wire response using Laser-Induced Fluorescence (LIF) 06 p0664 N88-14072
Flow field measurements using hotwire anemometry [AD-A187029] 09 p1160 N88-16951
Calibration of a hot-wire/hot-film anemometer over a range of temperatures, velocities and pressures [AD-A189717] 14 p1913 N88-21430
Development of a hot-wire measurement technique for moderate intensity three-dimensional flows 22 p3080 N88-28289
Calibration of a triple wire probe for turbulence measurements [AD-A193956] 22 p3081 N88-28296
HOT-WIRE FLOWMETERS
Development of subminiature multi-sensor hot-wire probes [NASA-TM-100052] 15 p2069 N88-22336
On experiences with two hot-wire instruments for measuring the liquid water content in clouds [ESA-TT-1085] 23 p3236 N88-29255
HOT-WIRE TURBULENCE METERS
U HOT-WIRE FLOWMETERS
U TURBULENCE METERS
HOTOL LAUNCH VEHICLE
Hypersonic aerodynamics: Applications for HOTOL 05 p0535 N88-13252
HOTSHOT WIND TUNNELS
The aerodynamic design of hypersonic contoured axisymmetric nozzles including real gas effects [VKI-TM-43] 06 p0665 N88-14076
HOUSEKEEPING (SPACECRAFT)
Contamination control of the space shuttle Orbiter crew compartment 02 p0133 N88-10834
Development of response models for the Earth Radiation Budget Experiment (ERBE) sensors. Part 3: ERBE scanner measurement accuracy analysis due to reduced housekeeping data [NASA-CR-178294] 05 p0583 N88-13553
HOUSINGS
NT COWLINGS
Gas erosion of impeller housing in the operation of a high-temperature, high-pressure helium circulator [DE88-002607] 09 p1175 N88-17041
Cast iron-base alloy for cylinder/regenerator housing [NASA-CR-182116] 12 p1608 N88-19613

A review of gear housing dynamics and acoustics literature
[NASA-CR-183110] 20 p2811 N88-26675

HOVERCRAFT
U GROUND EFFECT MACHINES

HOVERING

Detection of targets in the presence of clutter using target echo modulations caused by rotating structures
[REPT-12-86] 01 p0036 N88-10231

Investigation of vertical axis handling qualities for helicopter hover and NOE flight
03 p0263 N88-11653

Handling qualities criterion for very low visibility rotorcraft 03 p0263 N88-11654

Modeling XV-15 tilt-rotor aircraft dynamics by frequency and time-domain identification techniques
03 p0263 N88-11657

Hovering helicopter flight dynamics: A study of vertical motion
[AR-004-526] 04 p0399 N88-12485

Solution procedure for the Navier-Stokes equations applied to rotors 05 p0579 N88-13533

Development of an unsteady wake theory appropriate for aeroelastic analyses of rotors in hover and forward flight
[NASA-CR-182357] 06 p0664 N88-14075

Preliminary airworthiness evaluation of a UH-1 equipped with a terrain mapping receiver antenna
[AD-A186274] 07 p0819 N88-14980

A dynamic simulation and feedback control scheme for the U.S. Marine Corps' Airborne Remotely Operated Device (AROD)
[AD-A186597] 08 p0953 N88-15784

The maximum entropy method for the analysis of radar echoes from hovering helicopters in clutter
[FB-2-87] 11 p1475 N88-18799

An experimental investigation of the flap-lag-torsion aeroelastic stability of a small-scale hingeless helicopter rotor in hover
[NASA-TP-2546] 13 p1715 N88-20257

Experimental investigation of Hover flowfields in water at the McDonnell Douglas Research Laboratories
16 p2202 N88-23135

Method for prediction and determination of takeoff performance for vectored thrust vehicles
[AD-A191809] 18 p2463 N88-24626

Operational noise data for CH-47D and AH-64 army helicopters
[AD-A191059] 18 p2570 N88-25263

Hover performance tests of baseline metal and Advanced Technology Blade (ATB) rotor systems for the XV-15 tilt rotor aircraft
[NASA-CR-177436] 20 p2759 N88-26367

A comparison of theory and experiment for coupled rotor-body stability of a hingeless rotor model in hover
21 p2889 N88-27152

A comparison of theory and experiment for coupled rotor body stability of a bearingless rotor model in hover and forward flight 21 p2890 N88-27154

Effects of static equilibrium and higher-order nonlinearities on rotor blade stability in hover
21 p2890 N88-27157

A conceptual design study of a hovering system controller for an autonomous underwater vehicle
[AD-A193423] 21 p2930 N88-27399

Euler equation computations for the flow over a hovering helicopter rotor
[NASA-CR-177493] 22 p3038 N88-28037

The maximum entropy method for the analysis of short-time radar echoes from hovering helicopters
22 p3149 N88-28737

The radar detection of hovering helicopters
22 p3150 N88-28739

HR DIAGRAM
U HERTZSPRUNG-RUSSELL DIAGRAM

HRB-1 HELICOPTER
U CH-46 HELICOPTER

HTGR
U HIGH TEMPERATURE GAS COOLED REACTORS

HTPB PROPELLANTS

Review of research concerning Solid Fuel Ramjet (SOFRAM) at the Research Institute of National Defence (FOA) 2
[FOA-C-20714-2.1] 24 p3327 N88-29813

Thermomechanical computations for GAP, a high energy binder for composite propellants
[FOA-C-20718-2.1] 24 p3357 N88-29988

HU-1 HELICOPTER
U UH-1 HELICOPTER

HUBBLE CONSTANT

Crucial cosmological observations
[DE87-703081] 02 p0251 N88-11587

String driven inflation
[DE88-006994] 15 p2151 N88-22841

HUBBLE SPACE TELESCOPE

Department of Housing and Urban Development-Independent Agencies Appropriations for fiscal year 1988, Friday, 10 April 1987: National Aeronautics and Space Administration
03 p0386 N88-12425

HSTDEK: Developing a methodology for construction of large-scale, multi-use knowledge bases
08 p1057 N88-16377

Knowledge-based monitoring of the pointing control system on the Hubble space telescope
08 p1057 N88-16378

A distributed architecture for intelligent monitoring and anomaly diagnosis of the Hubble Space Telescope
08 p1057 N88-16379

A knowledge-based system for monitoring the electrical power system of the Hubble Space Telescope
08 p1058 N88-16380

Artificial intelligence and space power systems automation 08 p1058 N88-16381

A multiprocessing architecture for real-time monitoring
08 p1059 N88-16390

ESA Bulletin No. 8
[ETN-87-90513] 09 p1122 N88-16718

The 2.4 m Space Telescope and ESA participation in the program 09 p1123 N88-16721

Deep space target location with Hubble Space Telescope (HST) and Hipparcos data
[NASA-CR-182520] 10 p1427 N88-18524

TALOS: A distributed architecture for intelligent monitoring and anomaly diagnosis of the Hubble Space Telescope 17 p2388 N88-24193

Automated generation of spacecraft activity plans
23 p3258 N88-29396

Knowledge based tools for Hubble Space Telescope planning and scheduling: Constraints and strategies
24 p3417 N88-30338

The proposal entry processor: Telescience applications for Hubble Space Telescope science operations
24 p3417 N88-30339

Lisp Object State Saver (LOSS): A facility used to save partial schedules of the Hubble Space Telescope
24 p3421 N88-30360

HUBS

Impacts of rotor hub design criteria on the operational capabilities of rotorcraft systems
03 p0264 N88-11663

A129 advanced solutions for meeting today's combat helicopter requirement 03 p0265 N88-11669

A comparison of theory and flight test of the BO 105/BMR in hover and forward flight
21 p2890 N88-27155

HUGHES AIRCRAFT
NT AH-64 HELICOPTER

HUGHES MILITARY AIRCRAFT
U MILITARY AIRCRAFT

HULLS (STRUCTURES)
NT SHIP HULLS

Response of SMA (Shielded Metal Arc) and narrow gap HY80 weldments to explosive shock loading
[AD-A195994] 24 p3385 N88-30162

HUMAN BEHAVIOR

Studies of the processing of single words using positron tomographic measures of cerebral blood flow change
[AD-A184058] 03 p0356 N88-12244

Human adaptation to isolated and confined environments
[NASA-CR-181502] 03 p0357 N88-12248

A simulation study of a speed control system for autonomous on-road operation of automotive vehicles
[AD-A184030] 03 p0362 N88-12279

Complex sound processing: An interdisciplinary approach
[AD-A189782] 15 p2102 N88-22523

The representational code of the internal model of dynamic systems: An individual differences and dual task approach
[AD-A190876] 16 p2244 N88-23403

Performance effectiveness and the work/rest cycle
[AD-A191448] 18 p2551 N88-25145

Attitudes towards the cold: Effects on psychological mood and subjective reports of illness during cold weather training
[AD-A194777] 23 p3239 N88-29274

Contributions to engineering models of human-computer interaction, volume 1
[AD-A195590] 24 p3409 N88-30295

HUMAN BEINGS

Cirrus: An automated protocol analysis tool
[AD-A186646] 08 p1052 N88-16348

Experimental measurements of the uptake of ozone in rats and human subjects
[PB88-125422] 10 p1364 N88-18149

Certain aspects of human metabolism during spaceflights of varying duration
[NASA-TT-20215] 10 p1369 N88-18181

Modeling of the non-auditory response to blast overpressure
[AD-A187397] 10 p1369 N88-18184

Methods of eliciting information from experts
[AD-A187468] 10 p1372 N88-18189

Critical phenomena and electromagnetic effects in biological membranes
[AD-A188156] 11 p1518 N88-19064

Motor control in man and monkey
11 p1518 N88-19065

Motion sickness: A study of its effects on human physiology
[AD-A188821] 12 p1667 N88-19995

Pursuit tracking performance decrements associated with decreasing ambient illumination
[AD-A189336] 13 p1809 N88-20809

Evaluation of existing total human exposure models
[PB88-146840] 15 p2101 N88-22517

Auditory pattern memory: Mechanisms of tonal sequence discrimination by human observers
[AD-A190337] 15 p2104 N88-22534

Extension of computer based algorithms by operator analysts
[NASA-CR-182798] 15 p2111 N88-22575

The event-related brain potential as an index of information processing and cognitive activity: A program of basic research
[AD-A191244] 16 p2243 N88-23400

Activation, strength and endurance of human respiratory and limb muscles 17 p2361 N88-24158

Effects of pulsed and CW (Continuous Wave) 2450 MHz radiation on transformation and chromosomes of human lymphocytes in vitro
[AD-A193104] 21 p2987 N88-27736

Demodulation processes in auditory perception
[AD-A193421] 21 p2988 N88-27740

SQUID (superconducting quantum interference device) arrays for simultaneous magnetic measurements: Calibration and source localization performance
[AD-A193815] 23 p3216 N88-29143

Currents induced in a human being for electromagnetic fields to 10 kHz-50 MHz
[AD-A191977] 23 p3238 N88-29268

Human auditory and visual continuous evoked potentials 23 p3238 N88-29269

Limits of pattern discrimination in human vision
[AD-A193449] 23 p3239 N88-29273

Methods and instrumentation for biomagnetism
[AD-A193811] 23 p3239 N88-29278

Visual motion perception and visual attentive processes
[AD-A193640] 23 p3241 N88-29288

Multilevel computational theory of stereoscopic visual image processing
[AD-A195331] 24 p3408 N88-30288

Eye movements and spatial pattern vision
[AD-A195496] 24 p3408 N88-30290

Haptic exploration in humans and machines: Attribute integration and machine recognition/implementation
[AD-A193692] 24 p3410 N88-30299

HUMAN BODY

Human physical fields 06 p0750 N88-14609

Proceedings and program draft in Gravitational Biology in the Federal Republic of Germany --- Effects of Weightlessness on the Human Organism
[ESA-TT-988] 07 p0884 N88-15363

Operation Everest 2: Nutrition and body composition
[AD-A186449] 08 p1049 N88-16333

Lifting and carrying capacities relative to physical fitness measures
[AD-A189305] 13 p1809 N88-20808

Anthropomorphic phantom radiation dosimetry at the NATO standard reference point at Aberdeen Proving Ground
[AD-A190508] 15 p2103 N88-22528

Experimental research on skin reflection, transmission, absorption of light rays 16 p2187 N88-23039

Physiological effects on man of long duration confinement in a carbon dioxide enriched environment
19 p2695 N88-26017

Behavioral, psychological and demographic predictors of physical fitness
[AD-A192697] 21 p2986 N88-27733

HUMAN CENTRIFUGES

The rate of adaptation to altered g in the human centrifuge: Implications for simulations of mass-discrimination in space flight
12 p1659 N88-19941

Physiological monitoring methodology in the USAFSAM centrifuge 21 p2924 N88-27356

HUMAN ENGINEERING
U HUMAN FACTORS ENGINEERING

HUMAN FACTORS ENGINEERING
NT MOTION SIMULATION

Human factors in robotic system design discussed
02 p0158 N88-10988

A research on pilot performance in a flight incident situation
[ETN-87-90653] 02 p0217 N88-11370

Computer-controlled testing of visual-spatial ability
[AD-A183971] 03 p0357 N88-12249

Report of the helicopter human factors working group --- accident prevention
[CAA-PAPER-87007] 03 p0361 N88-12274

A scientific workstation operator-interface for accelerator control
[DE87-014689] 03 p0362 N88-12278

Research papers and publications (1981-1987): Workload research program
[NASA-TM-100016] 04 p0474 N88-12924

Human engineering laboratory grounding analysis (HELGA)-2
[AD-A185367] 05 p0578 N88-13524

Sitting posture of helicopter pilots of the Royal Netherlands Air Force; preliminary recommendations
[IZF-1986-16] 05 p0631 N88-13857

Research and development of anti-G life support systems. Part 1: Development and evaluation of uniform-pressure anti-G suits
[AD-A185658] 06 p0754 N88-14628

Tools and technologies for expert systems: A human factors perspective 06 p0797 N88-14882

New US book on aviation psychology reviewed
07 p0896 N88-15433

Human performance data needed for training device design decisions
[AD-A185988] 07 p0898 N88-15441

Using multiple dialog modes in a user-system interface to accomodate different levels of user experience: An experimental study
[AD-A186115] 07 p0899 N88-15444

Development of Soviet state ergonomic standards (GOST)
[AD-A185536] 07 p0899 N88-15449

Soviet state ergonomic standards (GOST)
[AD-A185537] 07 p0900 N88-15450

Proceedings of the DOD Workload Assessment Workshop on Workload Assessment Techniques and Tools held in Dayton, Ohio on 27-28 September 1986
[AD-A185650] 08 p1052 N88-16352

Development of a menu of performance tests self-administered on a portable microcomputer
[NASA-CR-172040] 08 p1067 N88-16452

Helicopter human factors research
09 p1109 N88-16644

An integrated approach to rotorcraft human factors research 09 p1110 N88-16653

Dynamic function allocation in fighter cockpits
[AD-A185397] 09 p1201 N88-17199

Air Force Human Resources Laboratory technical reports and technical papers
[AD-A186830] 09 p1201 N88-17200

Comparison of alphanumeric data entry methods for advanced helicopter cockpits
[AD-A186934] 09 p1201 N88-17201

Ergonomics of car controls for disabled people, phase 1. Part 1: Chapters 1-7. Part 2: Appendices. Part 3: References
[ISBN-0-947767-82-7] 09 p1202 N88-17204

Systems integrated human engineering on the Navy's rapid acquisition of manufactured parts/test and integration facility 09 p1206 N88-17226

User engineering: A new look at system engineering
09 p1206 N88-17231

Surrogate measures: A proposed alternative in human factors assessment of operational measures of performance 09 p1215 N88-17281

Information transfer in the National Airspace System
10 p1275 N88-17634

Cockpit data management
[NASA-CR-178407] 11 p1438 N88-18579

Spacecraft fire detection and extinguishment: A bibliography
[NASA-CR-180880] 11 p1444 N88-18612

A worked example of an application of the SAINT simulation program
[AD-A188198] 11 p1524 N88-19097

Night Vision: Current Research and Future Directions, symposium proceedings
[PB88-132006] 11 p1550 N88-19274

Characteristics of the thermal environment
[AD-A186359] 12 p1641 N88-19827

Space Station Human Factors Research Review. Volume 3: Space Station Habitability and Function: Architectural Research
[NASA-CP-2426-VOL-3] 12 p1650 N88-19883

Space station architectural elements model study. Space station human factors research review
12 p1650 N88-19884

Space station group activities habitability module study: A synopsis 12 p1651 N88-19886

Full scale architectural simulation techniques for space stations 12 p1651 N88-19887

Social factors in space station interiors
12 p1651 N88-19888

Human factor in engineering work
12 p1663 N88-19970

JPRS report: Science and technology. USSR: Life sciences
[JPRS-ULS-88-002] 12 p1665 N88-19982

User perceptions of side-arm flight control in rotary-wing aircraft
[AD-A188519] 12 p1672 N88-20009

Multi-crew pictorial format display evaluation
[AD-A189349] 13 p1812 N88-20824

Advanced human factors engineering tool technologies
[AD-A189390] 13 p1812 N88-20825

Incorporation of privacy elements in space station design
[NASA-CR-182748] 14 p1881 N88-21242

Human interfaces in remote driving
[DE88-006843] 14 p1953 N88-21643

Napping and human functioning during prolonged work
[AD-A190228] 15 p2102 N88-22525

Psychosensory cockpit ergonomics, advantages of intelligent information systems 17 p2304 N88-23784

Designing for design effectiveness of complex avionics systems 17 p2305 N88-23788

Experience in the integration of human engineering effort with avionics systems development
17 p2305 N88-23793

A look toward the future of complex avionics systems development using the USAF Test Pilot School's avionics systems test training aircraft 17 p2306 N88-23797

Space Station Human Factors Research Review. Volume 1: EVA Research and Development
[NASA-CP-2426-VOL-1] 17 p2379 N88-24145

Space Station Human Factors Research Review. Volume 4: Inhouse Advanced Development and Research
[NASA-CP-2426-VOL-4] 17 p2380 N88-24148

Teleoperator human factors study
[NASA-CR-178930] 17 p2382 N88-24162

SP-100 ground engineering systems test facility control systems 17 p2436 N88-24496

Space station architectural elements model study
[NASA-CR-4027] 18 p2464 N88-24632

Evaluation of the US Army fitting program for the integrated helmet unit of the integrated helmet and display sighting system
[AD-A191616] 18 p2465 N88-24635

Human problem solving in complex dynamic environments
[AD-A190788] 18 p2551 N88-25142

An advanced prototyping tool for human factors design
[AD-A187290] 18 p2552 N88-25149

Human performance issues arising from manned space station missions
[NASA-CR-3942] 18 p2553 N88-25156

Space station habitability recommendations based on a systematic comparative analysis of analogous conditions
[NASA-CR-3943] 18 p2587 N88-25372

Similarities between diving operations and space missions 19 p2697 N88-26027

Ergonomy and interior furnishing of the cabins of deep diving manned submarines: The Nautile example --- couch 19 p2697 N88-26032

Habitability of the Space Station: From vehicle to living space 19 p2697 N88-26033

Recent research on crew wardroom habitability for the Space Station 19 p2698 N88-26039

Introduction to human factors
[DE88-009021] 19 p2711 N88-26103

Computer simulation of multiple pilots flying a modern high performance helicopter
[NASA-TM-100183] 20 p2761 N88-26377

A human factors evaluation of the Advanced Visual Technology System (AVTS) eye tracking oculometer
21 p2925 N88-27361

The human element in space: Lessons from Antarctica
[AD-A193440] 21 p2988 N88-27741

The assessment of human/computer performance using human productivity measures: MIPS and BIPS are MEGAFLOPS
[DE87-013491] 21 p2993 N88-27750

Issues in computer-assisted interpretation of graphs and quantitative information
[PB88-116280] 21 p2998 N88-27783

NASA information sciences and human factors program
[NASA-TM-4064] 22 p3166 N88-28856

Visual Effects in the High Performance Aircraft Cockpit
[AGARD-LS-156] 23 p3241 N88-29291

Advances in Flying Qualities
[AGARD-LS-157] 24 p3314 N88-29735

Pilot modeling 24 p3314 N88-29736

Human factors report on information management requirements for next-generation manned bombers
[AD-A195870] 24 p3409 N88-30296

Study of human factors engineering criteria for extravehicular activity (EVA) systems, volume 1
[STF23-F87025-VOL-1] 24 p3410 N88-30298

Haptic exploration in humans and machines: Attribute integration and machine recognition/implementation
[AD-A193692] 24 p3410 N88-30299

Space station proximity operations windows: Human factors design guidelines
[NASA-TM-88233] 24 p3410 N88-30301

HUMAN PATHOLOGY

Further investigation of tests for susceptibility to noise-induced hearing loss
[ISVR-TR-149] 14 p1952 N88-21633

HUMAN PERFORMANCE

NT ASTRONAUT PERFORMANCE
NT OPERATOR PERFORMANCE
NT PILOT PERFORMANCE

Modeling of human judgement in multicriteria analysis using pairwise comparison
[REPT-87-01] 01 p0076 N88-10484

Masking effects of fine and coarse grain pictorial noise
[IZF-1985-21] 01 p0076 N88-10485

Loss of performance due to military clothing and equipment
[IZF-1986-13] 01 p0077 N88-10490

Integrated voice and visual systems research topics
[NASA-CR-177417] 03 p0356 N88-12246

Research papers and publications (1981-1987): Workload research program
[NASA-TM-100016] 04 p0474 N88-12924

Examining the relative efficiency of Part- versus whole-task practice for multiple-task situations
[AD-A185056] 05 p0631 N88-13856

Vision of details in space and time
[B8711402] 06 p0753 N88-14624

Stress effects and the optimum format of a scrolling seven-line VDT text window
[AD-A185559] 06 p0758 N88-14651

Regulation of energy metabolism during parachute jumps 07 p0896 N88-15428

Evoked brain activity and personnel performance
[AD-A185922] 07 p0897 N88-15436

Human performance data needed for training device design decisions
[AD-A185988] 07 p0898 N88-15441

Antarctica as a model for the human exploration of Mars
[AD-A185835] 08 p1051 N88-16342

Overlearning and positive thinking alleviate negative effects of stress on performance
[FOA-C-50051-5.3] 08 p1051 N88-16344

Stability, reliability and cross-mode correlations of tests in a recommended 8-minute performance assessment battery
[NASA-CR-172039] 08 p1052 N88-16351

Team problem solving: Effects of communication and function overlap
[AD-A187010] 09 p1152 N88-16898

Air Force Human Resources Laboratory technical reports and technical papers
[AD-A186830] 09 p1201 N88-17200

Tutoring electronic troubleshooting in a simulated maintenance work environment
09 p1204 N88-17215

A human performance modelling approach to intelligent decision support systems 09 p1208 N88-17242

Surrogate measures: A proposed alternative in human factors assessment of operational measures of performance 09 p1215 N88-17281

Second All-Union Conference on Physiology of Extreme States and Individual Protection of Man
10 p1363 N88-18147

Development of a coping strategies questionnaire to assess endurance performance
[AD-A188010] 11 p1520 N88-19074

Influence of a 6 hr head-out water immersion on different tests of endurance performance capacity
12 p1653 N88-19903

JPRS report: Science and technology. USSR: Life sciences
[JPRS-ULS-88-002] 12 p1665 N88-19982

Measuring functional feasibility of human visual system 12 p1665 N88-19983

Training in time interval discrimination using verbal feedback 12 p1665 N88-19985

Efficiency of human workers and means to increase it
12 p1666 N88-19986

Air quality and human performance, chapter 16
[AD-A188335] 12 p1666 N88-19988

Medical problems related to altitude in: Human performance physiology and environmental medicine at terrestrial extremes, chapter 14
[AD-A188340] 12 p1666 N88-19989

Human efficiency for visual detection of targets on CRT displays using a two-level multiple channel time history format
[AD-A188419] 12 p1670 N88-20001

Task allocation for efficient performance of a decentralized organization
[AD-A188699] 12 p1705 N88-20204

Management information systems design implications: The effect of cognitive style and information presentation on problem solving
[AD-A188850] 12 p1705 N88-20205

Lifting and carrying capacities relative to physical fitness measures
[AD-A189305] 13 p1809 N88-20808

Proceedings of the Workshop on the Assessment of Crew Workload Measurements Methods, Techniques and Procedures. Volume 1: Preliminary Selection of Measures
[AD-A189004] 13 p1812 N88-20827

A comparison of two chord keyboard coding systems for alphanumeric data entry
[AD-A189230] 13 p1813 N88-20834

Construction of a multidimensional questionnaire to determine interindividual differences in controlling attention
[DFVLR-FB-87-45] 14 p1952 N88-21637

Masking of motion cues by random motion: Comparison of human performance with a signal detection model
[UTIAS-313] 14 p1953 N88-21639

Age, alcohol, and simulated altitude: Effects on performance and breathalyzer scores
[AD-A190642] 15 p2103 N88-22531

An evaluation of the effects of high visual taskload on the separate behaviors involved in complex monitoring performance
[AD-A190641] 15 p2105 N88-22536

Dynamic properties of human brightness perception
[ETN-88-92243] 16 p2238 N88-23366

Mental-State Estimation, 1987
[NASA-CP-2504] 16 p2239 N88-23370

Challenges of physiological monitoring in a Navy operational setting 16 p2239 N88-23374

The N2-P3 complex of the evoked potential and human performance 16 p2241 N88-23388

The relationship between group process and performance 17 p2448 N88-24549

Effects of moderate cold and heat stress on the potential work performance of industrial workers. Part 6: The effects of increasing vapour pressure at four air temperatures on the performance and physiology of white females
[PB88-124854] 18 p2550 N88-25137

Eye and head response to an attention cue in a dual task paradigm
[AD-A191052] 18 p2551 N88-25143

Optimizing feedback utilization in motor skill training
[AD-A191559] 18 p2552 N88-25146

Performance estimates for operations conducted while wearing individual protective equipment: User manual
[AD-A191871] 18 p2553 N88-25154

Modeling and evaluation of variable structure organizations
[AD-A191947] 18 p2586 N88-25381

Monitoring of divers/astronauts during missions
19 p2698 N88-26036

Contra- and ipsilateral auditory stimuli produce different activation patterns at the human auditory cortex: A neuromagnetic study
[PB88-181490] 19 p2708 N88-26098

Proceedings of the Workshop on the Assessment of Crew Workload Measurement Methods, Techniques and Procedures. Volume 2: Library references
[AD-A191209] 19 p2710 N88-26101

Electric and Magnetic Activity of the Central Nervous System: Research and Clinical Applications in Aerospace Medicine
[AGARD-CP-432] 21 p2977 N88-27683

Studies of the intact human brain: Implications for performance 21 p2977 N88-27684

The effects of hypoxia on P300 and reaction time
[DCIEM-87-RR-12] 21 p2979 N88-27697

Can CNV amplitude predict ability to accomplish a demanding task? 21 p2980 N88-27700

Physiological responses to acute exercise-heat stress
[AD-A192606] 21 p2986 N88-27732

Determinants of dual-task interference and resource theories in cognitive psychology
[DFVLR-FB-88-14] 21 p2992 N88-27748

The effects of acute cold exposure on exercise performance
[AD-A192650] 22 p3130 N88-28610

Human acclimatization and physical performance at high altitude
[AD-A192651] 22 p3130 N88-28611

The impact of hyperthermia and hypohydration on circulation, strength, endurance and health
[AD-A192657] 22 p3131 N88-28615

Effects of air polution on human exercise performance
[AD-A192660] 22 p3131 N88-28617

Engineering data compendium. Human perception and performance, volume 2
[LC-87-19560] 22 p3134 N88-28631

Engineering data compendium. Human perception and performance, volume 3
[LC-87-19560] 22 p3134 N88-28632

Human performance and acute hypoxia, chapter 12
[AD-A192604] 23 p3238 N88-29270

Literature review: Validity and potential usefulness of psychomotor ability tests for personnel selection and classification
[AD-A193558] 23 p3241 N88-29287

HUMAN REACTIONS

Human motor reactions to dangerous motions in robot operations
[PB87-222196] 03 p0361 N88-12275

Life sciences experiments on stratospheric balloons and sounding rockets 06 p1033 N88-16262

The ESA Anthrorack project: Integrated research in human physiology 06 p1033 N88-16265

Evidence for human adaptive response to dehydration: Increase of circulating protein mass
[AD-A186225] 08 p1048 N88-16328

White blood cells in space: An experiment for the first Spacelab mission 09 p1127 N88-16757

Cardiovascular adaptation to zero-g during a long term flight (237 days) on board the Salyut 7 Soviet space station (1984) 12 p1655 N88-19920

Load and control of the cardiocirculatory system in weightlessness 12 p1656 N88-19922

Computer simulation of a single pilot flying a modern high-performance helicopter
[NASA-TM-100182] 20 p2761 N88-26376

Effect of microgravity on lymphocyte activation --- Spacelab D1 mission 22 p3061 N88-28163

HUMAN RELATIONS

A comparison of the effects of group dynamics on individuals assigned to integral and non-integral aircrews
[AD-A186467] 08 p1051 N88-16345

HUMAN RESOURCES

A software planning and development methodology with resource allocation capability
[AD-A186088] 07 p0902 N88-15462

HUMAN TOLERANCES

Determination of the individual state of acclimatization
[IZF-1986-27] 01 p0075 N88-10478

Measurement of suspension and ride characteristics of the M1 main battle tank 05 p0596 N88-13637

Investigation of the exposure to harmful compounds in the workshop of nondestructive materials testing at Gilze-Rijen (Netherlands)
[PML-1985-42] 05 p0623 N88-13816

Improvement of human tolerance to head-pelvis (+Gz) accelerations by increasing hydration
10 p1364 N88-18153

Influence of a 6 hr head-out water immersion on different tests of endurance performance capacity
12 p1653 N88-19903

Advanced turboprop aircraft flyover noise: Annoyance to counter-rotating-propeller configurations with an equal number of blades on each rotor, preliminary results
[NASA-TM-100612] 16 p2265 N88-23547

Human response to prolonged motionless suspension in four types of full body harnesses
21 p2929 N88-27387

HUMAN WASTES

NT URINE

Specific organic compounds in excreta
07 p0895 N88-15422

HUMAN-COMPUTER INTERFACE

U MAN-COMPUTER INTERFACE

HUMIDITY

The effect of organic inhibitors on the atmospheric corrosion and solderability of copper
[DE88-000261] 04 p0414 N88-12565

Estimation of marine boundary layer depth and relative humidity with multispectral satellite measurements
[AD-A184881] 05 p0620 N88-13804

Controlled ecological life support systems: Development of a plant growth module 05 p0630 N88-13854

Corrosion and deterioration testing in humid tropic environments
[AD-A186917] 10 p1302 N88-17783

Determination of atmospheric moisture structure from high resolution MAMS radiance data
11 p1515 N88-19049

Review of recent developments in evaporation ducting assessment 12 p1616 N88-19684

Remote sensing of meteorological parameters with the aid of a clear-air Doppler radar
[PB88-142518] 12 p1647 N88-19864

Perspectives in microclimate cooling involving protective clothing in hot environments
[AD-A188370] 12 p1671 N88-20007

The effects of humidity on the profile of photographic plates
[NPL-DMOM-88] 14 p1913 N88-21429

Aerodynamic aspects of the Amazon Forest
[INPE-4445-TDL/313] 15 p2098 N88-22501

Intercomparison of NMC (National Meteorological Center) and ECMWF (European Centre for Medium Range Weather Forecasts) global analyses: 1980-1986
[PB88-196548] 21 p2974 N88-27669

Corrosion problems associated with computer disk packs 22 p3054 N88-28121

Advancements in oxygen generation and humidity control by water vapor electrolysis
[NASA-CR-172073] 22 p3134 N88-28633

Real-time measurements of the size fractionation of ambient black carbon aerosols at elevated humidities
[DE88-010870] 23 p3215 N88-29138

Fatigue crack growth characteristics of ARALL (trademark)-1
[AD-A196185] 24 p3341 N88-29869

HUMIDITY MEASUREMENT

Lidar-radiometric method for determining liquid-water content of cirrus clouds 04 p0461 N88-12854

Estimation of marine boundary layer depth and relative humidity with multispectral satellite measurements
[AD-A184881] 05 p0620 N88-13804

Method of determining atmospheric moisture content by measurement of upward radiation intensity in near IR
08 p1007 N88-16106

Ion content and infrared absorption of moist atmospheric air
[AD-A188839] 12 p1643 N88-19838

Thermodynamic study of hygroscopic polymers using surface acoustic waves 19 p2672 N88-25882

HUNGARY

Proceedings of the 17th International Conference on Phenomena in Ionized Gases held in Budapest, Hungary, July 8-12, 1985: Invited papers
[DE87-703562] 05 p0651 N88-13987

HURRICANES

Hurricane Elena storm surge data
[AD-A184573] 03 p0353 N88-12228

Hurricane Danny storm surge data, report 4
[AD-A186373] 07 p0879 N88-15334

Hurricane Kate storm surge data, report 5
[AD-A186374] 07 p0880 N88-15335

Hurricane climatology for the Atlantic and Gulf coasts of the United States
[PB88-114857] 08 p1039 N88-16288

Annual data summary and climatological evaluation CERC (Coastal Engineering Research Center) field research facility, 1985. Volume 1. Main text and appendixes A and B
[AD-A186442] 08 p1039 N88-16289

Forecast of Atlantic seasonal hurricane activity for 1988 15 p2098 N88-22500

Suggested hurricane operational scenario for GOES I-M
[NASA-TM-89729] 19 p2692 N88-26002

Observational/numerical study of the upper ocean response to hurricanes
[AD-A193592] 22 p3126 N88-28598

HYBRID CIRCUITS

Wire interconnection reliability and moisture levels in hybrid microcircuits with epoxy-attached components
[DE87-012987] 01 p0039 N88-10247

Applications of heat pipes to cool PWBS and hybrid microcircuits 02 p0136 N88-10858

Generic specifications for hybrid microcircuits
[ESA-PSS-01-608-ISSUE-2] 06 p0696 N88-14273

Evaluation of solder flux solvents in a vapor-degreasing application for hybrid microcircuits
[BDX-613-3638] 11 p1468 N88-18752

Design and fabrication of advanced hybrid circuits for high energy physics
[DE88-004392] 11 p1479 N88-18825

Hermetically sealable package for hybrid solid-state electronic devices and the like
[NASA-CASE-MSC-20181-1] 17 p2335 N88-23941

Designing to safe power limits in hybrid circuits
[DE88-005533] 18 p2506 N88-24865

HYBRID COMPUTERS

Simulation of real time problem solving
[AD-A193436] 21 p2907 N88-27778

HYBRID PROPULSION
The convertible engine: A dual-mode propulsion system 09 p1108 N88-16639
HYBRID STRUCTURES
Design description report for a photovoltaic power system for a remote satellite earth terminal
[NASA-CR-179586] 04 p0465 N88-12875
Fatigue behaviour of hybrid composites
[BR102236] 09 p1136 N88-16819
The strength of hybrid composites
[BR101991] 09 p1138 N88-16821
Outlook for the fusion hybrid and tritium-breeding fusion reactors
[PB88-149261] 13 p1843 N88-21029
HYBRIDS (BIOLOGY)
U GENETIC ENGINEERING
HYDRATES
Development of highly porous calcium silicate hydrate materials with extremely low thermal conductivity
[BMFT-FB-T-86-164] 02 p0150 N88-10941
Gas hydrate model development and validation
[DE88-001004] 10 p1298 N88-17762
Geological evolution and analysis of confirmed or suspected gas hydrate localities. Volume 9: Formation and stability of gas hydrates of the Middle America Trench
[DE88-001007] 10 p1347 N88-18050
Geological evolution and analysis of confirmed or suspected gas hydrate localities. Volume 2: Basin analysis, formation and stability of gas hydrates in the Black Sea
[DE88-001052] 18 p2532 N88-25023
HYDRATION
Effect of spaceflight factors on primate hydration homeostasis 10 p1360 N88-18126
Improvement of human tolerance to head-pelvis (+Gz) accelerations by increasing hydration
10 p1364 N88-18153
Morphological and functional state of the hypothalamo-hypophyseal neurosecretory system of rats flown aboard Cosmos-1667 10 p1365 N88-18156
Gastric emptying during exercise: Effects of acute heat stress, acclimation and hypohydration
[AD-A188008] 11 p1519 N88-19073
The impact of hyperthermia and hypohydration on circulation, strength, endurance and health
[AD-A192657] 22 p3131 N88-28615
HYDRAULIC ACTUATORS
U ACTUATORS
U HYDRAULIC EQUIPMENT
HYDRAULIC CONTROL
Adaptive control of hydraulic devices
[FB-1/85] 01 p0084 N88-10543
Control system simulation for a single-link flexible arm
[AD-A187037] 09 p1174 N88-17035
HYDRAULIC EQUIPMENT
Adaptive control of hydraulic devices
[FB-1/85] 01 p0084 N88-10543
RE-1000 free-piston Stirling engine hydraulic output system description
[NASA-TM-100185] 01 p0108 N88-10700
Human factors in robotic system design discussed
02 p0158 N88-10988
The axisymmetric sealing gap with variable viscosity. A variable hydraulic resistance
[ETN-87-90604] 03 p0314 N88-11987
Calculation of the three dimensional flow in the impeller of hydraulic turbomachines using a finite element method
[ETN-87-90612] 03 p0315 N88-11988
A cost and benefit analysis of hydraulic fluid systems for the next generation of tactical aircraft
[AD-A186911] 09 p1116 N88-16690
Control system simulation for a single-link flexible arm
[AD-A187037] 09 p1174 N88-17035
Reduction of residual stresses and distortion in girth welded pipes
[AD-A187728] 11 p1494 N88-18920
Electrical/pneudraulic design considerations
[AD-A188097] 12 p1581 N88-19462
High Reynolds number pump facility for cavitation research
[AD-A189310] 13 p1765 N88-20558
Modelling of a hydraulic motor and servo-valve to produce a desired system response using analogue and digital compensation techniques
[ETN-88-92079] 14 p1899 N88-21337
A 150,000 pounds per square inch dynamic pressure calibrator
[AD-A190659] 15 p2069 N88-22335
Hydraulic pumps and hydraulic equipment at low temperatures
[DE88-752871] 21 p2958 N88-27570
HYDRAULIC FLUIDS
A cost and benefit analysis of hydraulic fluid systems for the next generation of tactical aircraft
[AD-A186911] 09 p1116 N88-16690
Evaluation of the acute toxicity of a synthetic polyalphaolefin-based hydraulic fluid
[AD-A190412] 15 p2045 N88-22184
Experimental determination of the coefficients of the hydraulic resistance of apertures in the rotary disks
[AD-A190627] 15 p2066 N88-22317
Hydraulic pumps and hydraulic equipment at low temperatures
[DE88-752871] 21 p2958 N88-27570
HYDRAULIC HEATING SOURCES
U HEAT SOURCES
U HYDRAULIC EQUIPMENT
HYDRAULIC JETS
Pressure distributions and losses in a waterjet propulsion system
[AD-A188423] 12 p1633 N88-19777
Dense-spray structure and phenomena. Part 2: Pressure-atomized sprays
[AD-A190312] 15 p2064 N88-22307
Deflection of a circular liquid jet on a flat plate perpendicular to the flow direction
[NASA-TT-20279] 16 p2207 N88-23173
Hydroacoustic pulsating jet generator
[MPIS-7/1987] 18 p2510 N88-24891
HYDRAULIC PUMPS
U HYDRAULIC EQUIPMENT
U PUMPS
HYDRAULIC SYSTEMS
U HYDRAULIC EQUIPMENT
HYDRAULIC TEST TUNNELS
Main features of the 0.43m x 0.43m wind tunnel
[AXM-132] 14 p1870 N88-21175
Aerodynamic and Related Hydrodynamic Studies Using Water Facilities
[AGARD-CP-413] 16 p2200 N88-23125
Vortex breakdown and control experiments in the Ames-Dryden water tunnel 16 p2200 N88-23127
The use of the NRC/NAE water facilities in Canadian aeronautical research and development
16 p2201 N88-23132
Description of a water tank facility: Study of a missile at high incidence 16 p2201 N88-23133
The ONERA water tunnels test possibilities for flow visualization in aeronautical and Naval domains
16 p2202 N88-23139
A new laminar water tunnel to study the transition process in a blasius layer and in a separation bubble and a new tool for industrial aerodynamics and hydrodynamic research 16 p2204 N88-23150
A comparative study of vortex flows in wind and water tunnels 16 p2204 N88-23151
HYDRAULIC VALVES
U HYDRAULIC EQUIPMENT
U VALVES
HYDRAZINE ENGINES
Development and qualification of an Augmented Electro-Thermal Hydrazine-Thruster (AEHT) with 0.1 to 0.2 N vacuum thrust
[BMFT-FB-W-86-012] 16 p2169 N88-22931
HYDRAZINE NITRATE
Detonation velocity of the hydrazinum nitrate-hydrazine water system
[NASA-TT-20213] 13 p1770 N88-20590
HYDRAZINES
Products of the neutralization of hydrazine fuels with hypochlorite, 2
[DE87-011454] 01 p0030 N88-10193
A life test of a 22-Newton (5-lbf) hydrazine rocket
[NASA-TM-100232] 03 p0278 N88-11750
Low-g propellant gaging 08 p0982 N88-15937
The chemistry of the hypochlorite neutralization of hydrazine fuels
[DE88-002971] 10 p1307 N88-17812
Decomposition of hydrazine by high frequency glow electrical discharges
[NASA-TT-20240] 24 p3344 N88-29906
HYDRAZINIUM COMPOUNDS
Detonation velocity of the hydrazinum nitrate-hydrazine water system
[NASA-TT-20213] 13 p1770 N88-20590
HYDRIDES
NT BORANES
NT BORON HYDRIDES
NT LITHIUM HYDRIDES
NT METAL HYDRIDES
NT NITROGEN HYDRIDES
NT SILANES
NT SODIUM HYDRIDES
Hydride generation from the Exide load-leveling cells
[DE87-011361] 01 p0041 N88-10259
Metal hydrides
[DE88-005083] 10 p1299 N88-17766
Quantitative determination of a hydrogen impurity in a sodium coolant by hydride thermal dissociation
[NASA-TT-20239] 13 p1740 N88-20402
HYDROACOUSTICS
U UNDERWATER ACOUSTICS
HYDROAEROMECHANICS
U AERODYNAMICS
HYDROBALLISTICS
Investigation and implementation of an algorithm for computing optimal search paths
[AD-A185927] 07 p0902 N88-15461
HYDROBAROPHONES
U HYDROPHONES
HYDROCARBON COMBUSTION
Detailed kinetic modeling of autoignition chemistry
[DE87-013226] 03 p0283 N88-11782
Laser probes of propellant combustion chemistry
[AD-A184854] 05 p0561 N88-13415
Investigation of fuel additive effects on sooting flames
[AD-A186403] 07 p0829 N88-15026
Combustion of hydrogen and hydrocarbons in fluorine
[AD-A188018] 11 p1453 N88-18662
Chemical kinetics of nitramine propellant combustion
[AD-A191556] 18 p2495 N88-24802
Laser probes of natural gas ignition chemistry
[PB88-212568] 21 p2910 N88-27271
HYDROCARBON FUEL PRODUCTION
Research on hydrotreating catalysts to hydrodeoxygenate biocrude oils
18 p2536 N88-25046
HYDROCARBON FUELS
NT CRUDE OIL
NT DIESEL FUELS
NT FOSSIL FUELS
NT GASOLINE
NT JET ENGINE FUELS
NT JP-4 JET FUEL
NT JP-5 JET FUEL
NT JP-8 JET FUEL
NT LIQUEFIED NATURAL GAS
NT NATURAL GAS
Detection of vapors of flammable liquids in air by atmospheric sampling mass spectrometry/mass spectrometry
[DE88-000030] 02 p0196 N88-11227
An experimental investigation of the ignition and flammability limits of various hydrocarbon fuels in a two-dimensional solid fuel ramjet
[AD-A184968] 05 p0549 N88-13342
Evaluation and prediction of Henry's law constants and aqueous solubilities for solvents and hydrocarbon fuel components. Volume 1: Technical discussion
[AD-A188571] 12 p1613 N88-19643
Dual-fuel, dual-mode rocket engine
[NASA-CASE-LAR-13773-1] 18 p2475 N88-24685
Production costs of hydrocarbon fuels from biomass
[DE88-006667] 18 p2495 N88-24804
Motor vehicles as sources of compounds important to tropospheric and stratospheric ozone
[PB88-195219] 18 p2540 N88-25076
Combustion rate limits of hydrogen plus hydrocarbon fuel: Air diffusion flames from an opposed jet burner technique 19 p2624 N88-25567
Mach 2 combustion characteristics of hydrogen/hydrocarbon fuel mixtures
19 p2625 N88-25568
Pollutant formation in heterogeneous mixtures of fuel drops and air
[DOE/CE-50052/H1] 19 p2689 N88-25986
Carbon deposition model for oxygen-hydrocarbon combustion, volume 1
[NASA-CR-179375] 21 p2908 N88-27254
Carbon deposition model for oxygen-hydrocarbon combustion, volume 2
[NASA-CR-179376] 21 p2908 N88-27255
Hydrocarbon fuel spill dispersion on water: Literature review
[AD-A192486] 21 p2922 N88-27346
Experiments and modeling of multi-component fuel behavior in combustion
[AD-A195011] 24 p3343 N88-29896
HYDROCARBONS
NT ACETYLENE
NT ALKANES
NT ALKENES
NT ANTHRACENE
NT BENZENE
NT BUTADIENE
NT BUTANES
NT BUTENES
NT CAROTENE
NT CETANE
NT CUBANE
NT CYCLIC HYDROCARBONS
NT CYCLOBUTANE
NT CYCLOHEXANE
NT ETHANE
NT ETHYLENE
NT LIQUEFIED NATURAL GAS

best copy available

NT METHANE
NT METHYLENE
NT NAPHTHALENE
NT NAPHTHENES
NT NATURAL GAS
NT OXYACETYLENE
NT PARAFFINS
NT POLYBUTADIENE
NT PROPANE
NT PROPYLENE
NT PYRENES
NT TOLUENE
NT VINYLIDENE
The photophysics and chemistry of PAH (Polycyclic Aromatic Hydrocarbons) compounds
[DE87-014455] 02 p0153 N88-10954
The structure of adsorbed sulfur and carbon on molybdenum and rhenium single crystal surfaces, and their influence on carbon monoxide and hydrocarbon chemisorption
[DE88-001393] 04 p0499 N88-13073
Development of a low noise 10 K J-T refrigeration system
[AD-A185258] 05 p0571 N88-13484
Molecular dynamics studies of aromatic hydrocarbon liquids
[DE88-001473] 05 p0648 N88-13973
Summary and analysis of comments on the recommended practice for the measurement of refueling emissions
[PB88-101530] 07 p0876 N88-15313
Van der Waals clusters of aromatic molecules studied using supersonic molecular jet spectroscopy
[AD-A186087] 07 p0929 N88-15644
A review of methanol vehicles and air quality impacts
[DE88-002646] 08 p1023 N88-16194
Measurement of vertical distributions of halogenated hydrocarbons in the stratosphere
[ETN-88-91065] 09 p1191 N88-17135
Degradation of jet and missile fuels by aquatic microbial communities
[AD-A188065] 11 p1465 N88-18737
Effects of breathing air containing contaminants such as CO2, CO and hydrocarbons at 1 and 5 atmospheres
[PB88-132915] 11 p1521 N88-19084
Analysis of hydrocarbon band 3.35 in spectrum of Halley's Comet using data from infrared spectrometer on Vega-1 spacecraft 13 p1727 N88-20327
On the interpretation of the CH cometary spectrum
14 p2007 N88-21969
The application of hydrocarbon bioconversion technology to aerospace materials production
18 p2478 N88-24698
Diamond like carbon coatings: Categorization by atomic number density
[NASA-CR-174895] 22 p3059 N88-28151
Method and device for determining heats of combustion of gaseous hydrocarbons
[NASA-CASE-LAR-13528-1] 23 p3193 N88-29002
Nonseismic, surface geophysical and geochemical prospecting technology
[PB88-196613] 23 p3227 N88-29207
Determination of relative flammability of materials by pyrolysis and gas-chromatographic light hydrocarbon analysis
[DE88-012449] 24 p3343 N88-29896
Rates of formation of soot from hydrocarbon flames and its destruction 24 p3349 N88-29933

HYDROCHLORIC ACID
Monitoring biological impacts of space shuttle launches from Vandenberg Air Force Base: Establishment of baseline conditions
[NASA-TM-100982] 18 p2549 N88-25133

HYDROCRACKING
High-density jet fuels from coal syncrudes, appendix 4
[DE88-003132] 10 p1307 N88-17813
Research on hydrotreating catalysts to hydrodeoxygenate biocrude oils
18 p2536 N88-25046

HYDRODYNAMIC COEFFICIENTS
Free Lagrange reconnection algorithms for hydrocodes using a quadrilateral mesh
[DE88-001580] 05 p0611 N88-13752

HYDRODYNAMIC EQUATIONS
NT HELMHOLTZ VORTICITY EQUATION
Lattice gas hydrodynamics 03 p0313 N88-11978
Induced turbulence in aerosol-loaded atmospheres, Jun. 1987
[DE87-014724] 09 p1192 N88-17141
Hydrodynamical regimes in molten metals under a horizontal temperature gradient
14 p1988 N88-21859

HYDRODYNAMIC STABILITY
U FLOW STABILITY

HYDRODYNAMICS
NT ELASTOHYDRODYNAMICS
NT ELECTROHYDRODYNAMICS
NT MAGNETOHYDRODYNAMICS
NASA-VOF3D: A three-dimensional computer program for incompressible flows with free surfaces
[DE87-011849] 01 p0045 N88-10288
Research on one-dimensional two-phase flow. Theory on hydrodynamic balance in two fluid model and its application
[DE87-702615] 01 p0045 N88-10290
Two-phase non-Newtonian hydrodynamic modeling of slurries
[DE87-011519] 01 p0047 N88-10298
Phase dynamics: A review and a perspective
[DE87-013173] 01 p0048 N88-10306
Technical evaluation report on the Fluid Dynamics Panel Symposium on aerodynamic and related hydrodynamic studies using water facilities
[AGARD-AR-225] 03 p0312 N88-11968
Lattice gas hydrodynamics 03 p0313 N88-11978
The evolution of HOBO
[DE87-014742] 03 p0313 N88-11980
Nonequilibrium fluctuations and transport in sheared fluids 03 p0316 N88-11999
Breaking wave forces on vertical cylinders
[RR-CE71] 03 p0338 N88-12126
Coastal dynamics of the mouth of the Saloum (Senegal) --- SPOT imagery 03 p0345 N88-12177
Kinematics and dynamics of barred spiral galaxies
03 p0388 N88-12440
Three-dimensional, free-Lagrange hydrodynamics
[DE88-000494] 04 p0443 N88-12749
Observations on the hydrodynamic flow visualization at ONERA
[PD-FM-8718] 04 p0444 N88-12753
Dynamics of isolated intrathermocline eddy
04 p0460 N88-12845
Variations of the vertical and horizontal velocities of the small-scale structures and the physical problems related to overshoot layers 04 p0507 N88-13115
A complete linearized theory for the analysis and design of two-dimensional hydrofoils near a free surface
[UTIAS-TN-264] 05 p0579 N88-13531
Advanced concepts theory annual report 1986
[AD-A184986] 05 p0651 N88-13991
Hydroburst test of a carbon-carbon involute exit cone
[NASA-TP-2556] 06 p0671 N88-14112
Methods for reducing computational costs of typical finite element unsteady hydrodynamic models
[AD-A185499] 06 p0702 N88-14312
Method of two-time Green functions in molecular hydrodynamics of superfluid liquid
06 p0771 N88-14735
Fundamental studies of surfaces processes and trace analysis using solid electrodes
[AD-A186156] 07 p0826 N88-15024
A variational formulation of a hydrodynamic lubrication problem
[MEMO-642] 08 p0987 N88-15979
The use of optical fibers for shock pressure and timing measurements at high pressures
[DE88-004012] 10 p1334 N88-17971
Energy transfers for multilayer hydrodynamic ocean models: General formulation and specific examples
[AD-A187604] 10 p1358 N88-18116
A method of calculating nonstationary heat flow in hydrogasodynamic processes in closed cryogenic systems
[DE88-700884] 12 p1626 N88-19727
Dynamic modelling of flexible rotor shafts mounted on hydrodynamic bearings 13 p1779 N88-20641
Model of hydrodynamic adjustment of temperature, salinity and current fields 13 p1789 N88-20700
Proceedings of the Seminar on Hydrodynamics and Crystal Growth
[ETN-88-92025] 14 p1987 N88-21853
Optical and hydrodynamic implications of Comet Halley dust size distribution 14 p2003 N88-21939
PLASMOR: A laser-plasma simulation code, part 2
[DE88-701289] 15 p2135 N88-22736
Hydrodynamical equations for spherical gravitational collapse in terms of a generalized theory of gravitation with higher derivatives
[DE87-703027] 15 p2151 N88-22838
Aerodynamic and Related Hydrodynamic Studies Using Water Facilities
[AGARD-CP-413] 16 p2200 N88-23125
Water facilities in retrospect and prospect: An illuminating tool for vehicle design
16 p2200 N88-23126
Application of high speed holography to aerodynamic and hydrodynamic three-dimensional velocimetry
16 p2203 N88-23144
Use of water towing tanks for aerodynamics and hydrodynamics 16 p2204 N88-23149
A new laminar water tunnel to study the transition process in a blasius layer and in a separation bubble and a new tool for industrial aerodynamics and hydrodynamic research 16 p2204 N88-23150
Initial condition effect on pressure waves in an axisymmetric jet
[NASA-TM-100915] 16 p2209 N88-23184
Pump rod forces due to hydrodynamic effects in piston pumps
[PB88-164850] 16 p2214 N88-23212
Periodic response of nonlinear systems
16 p2217 N88-23226
Self-similar expansions in ion beam fusion
16 p2276 N88-23605
The structure and stability of spherically expanding flames 17 p2318 N88-23842
Specific features of emanation, temperature and hydrodynamic fields in the epicentral zone of tectonic earthquake
[DE88-701140] 17 p2373 N88-24114
The influence of cathodic protection on erosion-corrosion of metals and model alloys
[AD-A191613] 18 p2485 N88-24742
Dynamics and control of turbulent shear flows
[AD-A191527] 18 p2506 N88-24879
Heating and evaporation of turbulent liquid films: Measurement of film thickness and the onset of nucleate boiling
[DE88-006388] 18 p2512 N88-24905
LLNL granular solids flow project
[DE88-007492] 18 p2513 N88-24906
Droplet formation for liquid monopropellant jets
19 p2623 N88-25557
Dissipative relativistic radiation hydrodynamics
[DE88-702092] 19 p2686 N88-25846
Electron-acoustic waves in a beam-plasma system
[DE88-702053] 19 p2729 N88-26207
Ludwig Prandtl collected treatises on applied mechanics, hydro- and aerodynamics, part 2, IV interfaces and resistance
[NASA-TT-20315] 20 p2752 N88-26338
Modelling of premixed combustion using a thin flame sheet and the effect of the hydrodynamic instability
[DE88-009467] 20 p2770 N88-26423
Numerical modeling of the effect of particle size of explosives on shock initiation properties
[DE88-010479] 20 p2780 N88-26461
Vertical ship motions and sea loads considering nonlinear effects
[TAE-592] 20 p2784 N88-26515
Freely expanding detonation products: Scaling of rate processes
[DE88-007627] 20 p2790 N88-26606
A study of fluid-structure problems
21 p2941 N88-27468
Numerical simulation of fuel droplet interactions and breakup
[AD-A192431] 21 p2941 N88-27470
Research on ocean forecasting and nonlinear wave propagation and numerical hydrodynamics in the ocean
[AD-A193363] 21 p2976 N88-27680
Surface tension and viscosity with Lagrangian hydrodynamics on a triangular mesh
[AD-A194120] 22 p3075 N88-28258
Nonseismic, surface geophysical and geochemical prospecting technology
[PB88-196613] 23 p3227 N88-29207
Piecewise-parabolic methods for systems of hyperbolic conservation laws in multiprocessing environments
[DE88-010202] 23 p3248 N88-29329
Gaseous premixed flames in non-uniform flows
24 p3351 N88-29945

HYDROELASTICITY
Traction model development
[AD-A188450] 15 p2073 N88-22359
Nonlinear hydroelastic vibrations in rectangular containers
[LRT-WE-9-FB-7(1987)] 22 p3088 N88-28340

HYDROELECTRIC POWER STATIONS
Utilization of LANDSAT-TM imagery in the hydroenergetic inventory of the Paraibe de Sul River Basin 17 p2364 N88-24077

HYDROFLUORIC ACID
Evaluation of the sensidyne toxic gas sensor for HF (Hydrogen Fluoride) vapor
[DE88-000647] 04 p0446 N88-12767

HYDROFOILS
NT KEELS
A complete linearized theory for the analysis and design of two-dimensional hydrofoils near a free surface
[UTIAS-TN-264] 05 p0579 N88-13531

HYDROFORMING
A finite element analysis for the hydroforming of aluminum
[DE88-008050] 20 p2784 N88-26516

HYDROGEN
NT DEUTERIUM
NT HYDROGEN ISOTOPES
NT LIQUID HYDROGEN
NT TRITIUM
Hydrogen annealing of P(sub) b and E prime defect centers in oxidized silicon wafers
[DE87-014293] 02 p0152 N88-10951
Flame acceleration and transition to detonation in channels
[DE87-014193] 03 p0284 N88-11786
Characterization of catalysts with metal-support effects and of the species adsorbed on their surfaces
[DE87-014636] 04 p0414 N88-12564
A hydrogen/nickel oxide battery for remote applications
[DE87-009048] 04 p0484 N88-12872
Excess emission in the wings of the Hydrogen Balmer lines during a flare on the late-type dMe star YZ CMi
04 p0511 N88-13146
Hydrogen and deuterium in the local interstellar medium 04 p0521 N88-13204
Fatigue crack growth behavior in hydrogen gas environment 06 p0716 N88-14391
Threshold behaviour of semi-elliptic hydrogen-induced and fatigue-induced cracks 06 p0717 N88-14397
Experimental observation of photoresonance of electrons localized above surface of solid hydrogen
06 p0774 N88-14756
Hydrogen retention and release from uranium dioxide
[DE88-002042] 07 p0829 N88-15030
The carbon dioxide chaperon efficiency for the reaction H + O2 + M yields HO2 + M from ignition delay times behind reflected shock waves
[NASA-TM-100125] 07 p0830 N88-15036
Helium-ion-induced release of hydrogen from graphite
[DE88-002599] 09 p1142 N88-16846
Hydrogen in niobium-tantalum superlattices
09 p1146 N88-16867
Blast waves generated by planar detonations
[DE88-002219] 09 p1164 N88-16979
Feasibility of chemical lasers based on chain reaction involving hydrogen fluorination with thermal branching mechanism 09 p1238 N88-17420
Oscillations of solar models with internal element diffusion
[DE88-003156] 09 p1264 N88-17573
Hydrogen Energy Coordinating Committee: Summary of DOE hydrogen programs for FY 1987
[DE88-003960] 10 p1306 N88-17811
Two-photon (VUV and visible) resonant ionization spectroscopy of atoms and molecules
[DE88-004332] 10 p1407 N88-18386
Combustion of hydrogen and hydrocarbons in fluorine
[AD-A188018] 11 p1453 N88-18662
Calculations of rate constants for the three-body recombination of H2 in the presence of H2
[NASA-CR-182548] 11 p1454 N88-18664
Spatial and temporal monitoring of the Jovian atmosphere 12 p1711 N88-20240
Uncertainties in hydrogen combustion
[DE88-005354] 13 p1739 N88-20395
Quantitative determination of a hydrogen impurity in a sodium coolant uy hydride thermal dissociation
[NASA-TT-20239] 13 p1740 N88-20402
Hydrogen induced cracks in armor steel weldments fabricated with austenitic filler alloys
[AD-A188733] 13 p1740 N88-20406
Influence of hydrogen on crack formation tendency in heat-affected zone with stress concentrator
14 p1887 N88-21276
Use of nonporous metals membranes for the separation of hydrogen from gas mixtures
[BMFT-FB-T-86-206] 14 p1888 N88-21280
The effect of H2S concentration and pH on hydrogen permeation in AISI 410 stainless steel in 5 percent NaCl
[NPL-DMA(A)-148] 14 p1890 N88-21293
Theory of Muon method for study of solid and liquid hydrogen 14 p1972 N88-21770
The role of hydrogen thermalization in shaping the Lyman-alpha coma -- comets 14 p2007 N88-21971
The structure of the boron-hydrogen complex in silicon
[DE88-005433] 15 p2144 N88-22795
Some visualization studies on turbulent boundary levers using multiwire hydrogen bubble generation
16 p2204 N88-23153
Hydrogen turbines for space power systems: A simplified axial flow gas turbine model 17 p2419 N88-24385
Effect of hydrogen, deuterium and oxygen on the anelastic properties of refractory alloys
[DE88-007349] 18 p2484 N88-24736
The response of ultrathin palladium gate sensors to hydrogen and carbon monoxide
19 p2672 N88-25885
Life in a hyperbaric environment. A new O2-H2 breathing mixture for industrial diving 19 p2695 N88-26019
Ultraviolet imaging of hydrogen flames
[DE88-009152] 20 p2769 N88-26422
Production of powdered sodium hydride with large specific surface by the catalyzed reaction of molten sodium with hydrogen-1
[NASA-TT-20185] 20 p2776 N88-26462
Shock wave compression and metallization of simple molecules
[DE88-008031] 20 p2851 N88-26925
Enhancement of volume H(-) production by vibrationally pre-exciting the hydrogen molecules
[DE88-010783] 20 p2853 N88-26937
A method for determining the solubility of hydrogen in molten aluminum-lithium alloys
[DE88-009807] 21 p2910 N88-27270
Theory of the dissociation dynamics of small molecules on metal surfaces: Finite temperature studies
[DE88-007763] 21 p3013 N88-27882
Hydrogen storage by molecular polyhydrides
[AD-A194207] 23 p3191 N88-28989
Measure of hydrogen concentration profile in materials by resonant nuclear reactions
[DE86-702599] 23 p3193 N88-28999
Hydrogen permeation through metallic foils
[DE88-702600] 23 p3193 N88-29000
Kinetic of martensitic transformations induced by hydrogen in the austenite
[DE88-701623] 23 p3194 N88-29007
N2(A3epsilon u+) by reaction of N2F4+H2 in a supersonic flow
[AD-A194493] 23 p3219 N88-29163
Chemical kinetics of hydrogen and P(sub b) centers
[DE88-010528] 23 p3291 N88-29594
Theoretical investigation of image states of the hydrogen covered Cu (100)
[DE88-702662] 23 p3292 N88-29604
Extended atmospheres of outer planet satellites and comets
[NASA-CR-183157] 24 p3457 N88-30572

HYDROGEN AIR FUEL CELLS
U HYDROGEN OXYGEN FUEL CELLS

HYDROGEN ATOMS
Design study for measurement of neutral hydrogen atom density by laser induced fluorescence method
[DE87-752964] 02 p0179 N88-11114
A study of mechanisms of hydrogen diffusion in separation devices
[DE88-000326] 04 p0416 N88-12564
Atomic data for hydrogens in collisions with electrons: Addenda
[IPPJ-AM-55-ADD] 09 p1252 N88-17502
On the dynamical supersymmetry of atomic hydrogen
[DE88-700713] 10 p1422 N88-18495
The astrophysics of nebulae and active galactic nuclear emission-line regions: New methods and applications
13 p1858 N88-21111
Determination of beam orientation of optical diagnostics of excited 200-MeV hydrogen atoms resulting from photodetachment of H(-)ions
[AD-A189976] 14 p1981 N88-21823
Analysis of reversible and irreversible hydrogen trapping in metals
[NPL-DMA(A)-154] 16 p2177 N88-22977
Stark effect in intense field. Perturbation theory and 1/n-expansion
[DE87-702947] 16 p2266 N88-23550
Associative two-body condensation in laser-cooled sodium and hydrogen 16 p2267 N88-23559
Electromagnetic manipulation of atomic hydrogen
16 p2268 N88-23568
Magnetic traps for an anti-hydrogen gas
16 p2268 N88-23572
Key problems and hydrogen atom formation
16 p2268 N88-23573
Small molecule and small cluster ion formation in a low-density containerless mixture of electrons, protons and hydrogen atoms 16 p2269 N88-23577
Nascent vibrational/rotational distribution produced by hydrogen atom recombination
[AD-A193005] 20 p2852 N88-26933
Electronic states of the Xe(sub n)HCl systems in gas and condensed phases
[AD-A193881] 23 p3192 N88-28997
Computed potential energy surfaces for chemical reactions
[NASA-CR-183168] 24 p3342 N88-29893

HYDROGEN BONDS
High pressure strand burn rate tests of polyvinylnitrate/nitramine propellants
[AD-A184178] 04 p0422 N88-12615
Observing effect of laser radiation of low-frequency Raman scattering of light 06 p0772 N88-14742
Van der Waals clusters of aromatic molecules studied using supersonic molecular jet spectroscopy
[AD-A186087] 07 p0929 N88-15644

HYDROGEN CHLORIDES
NT HYDROCHLORIC ACID
Hydrogen chloride measurements in launch-vehicle exhaust clouds
[DE87-011552] 08 p0964 N88-15837

HYDROGEN CLOUDS
NT H II REGIONS
NT ORION NEBULA
Detection of abundant molecular gas in the UV-excess quasar Mrk 1014 22 p3164 N88-28842

HYDROGEN COMPOUNDS
NT BORANES
NT BORON HYDRIDES
NT DEUTERIUM COMPOUNDS
NT HYDRIDES
NT HYDROGEN PEROXIDE
NT HYDROGEN SULFIDE
NT LITHIUM HYDRIDES
NT METAL HYDRIDES
NT NITROGEN HYDRIDES
NT SILANES
NT SODIUM HYDRIDES

HYDROGEN CYANIDE LASERS
U HCN LASERS

HYDROGEN EMBRITTLEMENT
Environmentally assisted cracking: Overview of evidence for an adsorption-induced localised-slip process
[AD-A185175] 05 p0565 N88-13443
The influence of crack conditions on hydrogen uptake by steels 05 p0604 N88-13702
the influence of temper embrittlement on fatigue crack growth in hydrogen 05 p0605 N88-13709
Crack initiation studies in hydrogen embrittled spring steel strip 05 p0605 N88-13710
Embrittling effect of the plastic zone
05 p0607 N88-13721
The factors which govern the acceleration of corrosion fatigue crack growth rate of a ferritic stainless steel
06 p0717 N88-14402
Effect of rare earth elements on the hydrogen-induced cracking in high strength low alloy steel
[PB87-143806] 07 p0833 N88-15052
Multipurpose corrosion inhibitors for aerospace materials in Naval environments
[AD-A186728] 09 p1143 N88-16853
Detection of hydrogen-assisted-cracking in U-0.8Ti alloy weldments by acoustic emission monitoring
[DE88-003221] 09 p1184 N88-17093
Influence of grain boundary phosphorus segregation on hydrogen embrittlement in steel
[DE88-700176] 11 p1459 N88-18696
The influence of strain on hydrogen entry, transport, and embrittlement of a high strength steel in aqueous sodium chloride solution
[AD-A189302] 12 p1608 N88-19619
Hydrogen embrittlement of gun steel
[AD-A188972] 13 p1740 N88-20407
Dependence of hydrogen embrittlement of austenitic stainless steels on structural state of grain boundaries
14 p1896 N88-21316
Hydrogen embrittlement susceptibility of high strength ESR 4340 steel alloys for ballistically resistant/tolerant components 17 p2319 N88-23848
Investigation of structure and surface state effect on hydrogen embrittlement of steels, under consideration of acoustic emission analysis
[ETN-88-92350] 20 p2775 N88-26457
Research on the kinetics of phase changes in solids
[AD-A192222] 20 p2814 N88-26696
Evaluation of a diffusion/trapping model for hydrogen ingress in high-strength alloys
[AD-A194301] 23 p3194 N88-29008
Hydrogen embrittlement of iron-nickel alloys
[AD-A195909] 24 p3353 N88-29956

HYDROGEN ENGINES
Advanced fabrication techniques for hydrogen-cooled engine structures
[NASA-CR-3949] 06 p0723 N88-14447

HYDROGEN FLUORIDES
U HYDROFLUORIC ACID

HYDROGEN FUELS
Hydrogen Energy Coordinating Committee: Summary of DOE hydrogen programs for FY 1987
[DE88-003960] 10 p1306 N88-17811
Fusion, and advanced fuel, reaction bibliography: Particle reactions from H1 to B11
[AD-A187420] 11 p1552 N88-19286
Electrochemical hydrogen concentrator for phosphoric acid fuel cells
[AD-A191355] 16 p2229 N88-23317
Ultra high temperature direct propulsion
17 p2401 N88-24275

Performance of a hydrogen pulsed electrothermal thruster. Strategic defense initiative organization innovative science and technology. SBIR, phase 1
[AD-A191999] 18 p2475 N88-24679

Dual-fuel, dual-mode rocket engine
[NASA-CASE-LAR-13773-1] 18 p2475 N88-24685

Catalytic ignition of hydrogen and oxygen propellants
[NASA-TM-100957] 18 p2476 N88-24689

Mach 2 combustion characteristics of hydrogen/hydrocarbon fuel mixtures
19 p2625 N88-25568

Numerical simulation of ignition of hydrogen jet in hot air 19 p2637 N88-25647

Chemical/hydrogen energy systems
[DE88-007013] 19 p2687 N88-25969

HYDROGEN IONS

Dynamic effects of stellar winds and associated HII regions on the interstellar medium
[ETN-87-90421] 01 p0109 N88-10706

Studies on surface chemical states of some metals and ceramics bombarded with energetic light-ions
[DE87-752975] 02 p0145 N88-10910

The dc conductivity studies of an hydroxide ion conductor at intermediate temperatures
[AD-A186044] 07 p0847 N88-15142

Atomic data for hydrogens in collisions with electrons: Addenda
[IPPJ-AM-55-ADD] 09 p1252 N88-17502

Optimization of volume produced H(-) ions in a low-pressure hydrogen plasma
[IPPJ-853] 09 p1252 N88-17505

An infra-red investigation of HAN (Hydroxylammonium Nitrate)-based liquid propellants
[AD-A187226] 10 p1307 N88-17815

The magnitude of secondary electron contributions in photon stimulated desorption
[AD-A189094] 13 p1835 N88-20980

Determination of beam orientation of optical diagnostics of excited 200-MeV hydrogen atoms resulting from photodetachment of H(-)ions
[AD-A189976] 14 p1981 N88-21823

Proceedings of the Cooling, Condensation, and Storage of Hydrogen Cluster Ions Workshop
[AD-A189857] 16 p2266 N88-23555

Overview of hydrogen clusters
16 p2267 N88-23557

Large hydrogen cluster ions 16 p2267 [illegible]23558

Formation and reactivity of small hydrog[illegible] ions 16 p2267 N88-2[illegible]

Electronic structure and stability of small cation and anion hydrogen clusters 16 p2267 N88-23562

Photon-assisted formation and cooling of molecular hydrogen
[MP-87-102] 16 p2267 N88-23563

Vibrational spectroscopy of the hydrogen and hydrated hydronium cluster ions 16 p2268 N88-23566

First capture of antiprotons in an ion trap and the possibility of antihydrogen 16 p2268 N88-23569

Analysis of containerless condensation of polyatomic hydrogen ions, with emphasis on H3(+,-) association channels and a future workshop to study related topics
16 p2269 N88-23576

An optical technique for measuring divergence, beam profile, and aiming direction, of relativistic negative hydrogen ions
[DE88-007049] 18 p2572 N88-25278

Development of high current and high brightness negative hydrogen ion sources
[DE88-010682] 20 p2852 N88-26934

HYDROGEN ISOTOPES
NT DEUTERIUM
NT TRITIUM

Impact-induced devolatilization and hydrogen isotopic fractionation of serpentine: Implications for planetary accretion
[NASA-CR-182877] 16 p2175 N88-22966

Investigation of hydrogen isotope penetration through stainless steels Kh18N10T and Kh3M2BFR
[DE88-702189] 21 p2915 N88-27297

HYDROGEN MASERS

Fast autotuning of a hydrogen maser by cavity Q modulation 04 p0436 N88-12707

Study and construction of a compact hydrogen maser with a high-degree of frequency stability
[PB87-151122] 07 p0859 N88-15216

Atomic clocks research: An overview
[AD-A185567] 07 p0930 N88-15648

Hydrogen maser
[PB87-171617] 09 p1172 N88-17025

HYDROGEN OXYGEN ENGINES

Space station propulsion
[NASA-TM-100216] 03 p0277 N88-11746

Auxiliary propulsion technology for advanced Earth-to-orbit vehicles
[NASA-TM-100237] 06 p0674 N88-14127

Equilibrium retention in the nozzle of oxygen hydrogen propulsion systems 07 p0924 N88-15616

Space station propulsion technology
[NASA-CR-179260] 08 p0964 N88-15835

An analytical study of the hydrogen-air reaction mechanism with application to scramjet combustion
[NASA-TP-2791] 08 p0966 N88-15846

Recent advances in low-thrust propulsion technology
[NASA-TM-100959] 18 p2569 N88-25260

HYDROGEN OXYGEN FUEL CELLS

Electrochemical characteristics of acid electrolytes for fuel cells
[PB88-104641] 06 p0731 N88-14497

Regenerative fuel cell energy storage system for a low earth orbit space station
[NASA-CR-174802] 24 p3389 N88-30184

HYDROGEN PEROXIDE

The redox chemistry of some peroxo and superoxo metal ion complexes
[AD-A189159] 12 p1606 N88-19606

Sulfur dioxide-hydrogen peroxide relationships in clean air, clouds, and precipitation
[DE88-006352] 19 p2690 N88-25990

Liquid-phase oxidation of acetone with hydrogen peroxide on oxide catalysts 19 p2706 N88-26091

HYDROGEN PLASMA
NT DEUTERIUM PLASMA

Theoretical studies of kinetic mechanisms of negative ion formation in plasmas
[AD-A185735] 06 p0784 N88-14812

Hydrogen pumping and release by graphite under high flux plasma bombardment
[DE88-005880] 13 p1842 N88-21021

Properties of hydrogen/helium accretion plasmas
[DE88-006831] 19 p2728 N88-26197

Plasma armature formation in high-pressure, high-velocity hydrogen
[DE88-008347] 20 p2857 N88-26967

HYDROGEN PRODUCTION

The developmental status of solar thermochemical hydrogen production
[DE88-001778] 04 p0466 N88-12884

Intramolecular energy transfer reactions as a method for metal complex assisted production of hydrogen
[DE88-001621] 05 p0562 N88-13425

Nitrogen scale-up
[AD-A185702] 06 p0709 N88-14351

Study of the vapor-liquid equilibria used in the fabrication process of hydrogen by thermochemistry
[DE88-900239] 07 p0830 N88-15035

Organic coatings to improve the storageability and safety of pyrotechnic compositions
[AD-A187158] 09 p1150 N88-16889

Optimization of volume produced H(-) ions in a low-pressure hydrogen plasma
[IPPJ-853] 09 p1252 N88-17505

Solar-assisted hydrogen generation by photoelectrocatalysis
[PB88-160932] 12 p1605 N88-19597

Basic characteristics of heat-exchanger-type steam reformer heated by high-temperature helium gas (2). Analysis by simulation model (2)
[DE87-702962] 15 p2061 N88-22291

Chemical/hydrogen energy systems
[DE88-007013] 19 p2687 N88-25969

Photosynthetic water splitting
[DE88-007809] 20 p2830 N88-26791

HYDROGEN RECOMBINATIONS

Test summary for advanced H2 cycle NI-CD cell
02 p0165 N88-11040

Nascent vibrational/rotational distribution produced by hydrogen atom recombination
[AD-A193005] 20 p2852 N88-26933

HYDROGEN SULFIDE

The effect of H2S concentration and pH on hydrogen permeation in AISI 410 stainless steel in 5 percent NaCl
[NPL-DMA(A)-148] 14 p1890 N88-21293

The effect of H2S concentration and pH on the cracking resistance of AISI 410 stainless steel in 5 percent brine
[NPL-DMA(A)-149] 14 p1890 N88-21294

HYDROGEN 2
U DEUTERIUM

HYDROGEN 3
U TRITIUM

HYDROGENATION

The effect of additives on the reactivity of palladium surfaces for the chemisorption and hydrogenation of carbon monoxide: A surface science and catalytic study
[DE87-014685] 02 p0145 N88-10909

Characterization of catalysts with metal-support effects and of the species adsorbed on their surfaces
[DE87-014636] 04 p0414 N88-12564

Detection of minimum-ionizing particles in hydrogenated amorphous silicon
[DE88-002769] 07 p0837 N88-15081

Surface composition-reactivity relationships in heterogeneous catalysis
[DE87-003450] 09 p1140 N88-16804

Superconductivity and crystal structure of high-pressure phases in V-Ru-H system 09 p1239 N88-17426

High-density jet fuels from coal syncrudes, appendix 4
[DE88-003132] 10 p1307 N88-17813

A new polymer-based hydrogen getter
[DE88-004538] 13 p1751 N88-20467

Investigations of the origins of metastable, light-induced changes in hydrogenated amorphous silicon
[DE88-001117] 13 p1846 N88-21051

Improvements to Raney copper zinc methanol synthesis catalysts 17 p2318 N88-23844

Surface composition-reactivity relationships in heterogeneous catalysis
[DE88-006679] 18 p2480 N88-24714

Research on hydrotreating catalysts to hydrodeoxygenate biocrude oils
18 p2536 N88-25046

Hydrogenated amorphous silicon-germanium alloys
[DE88-001147] 19 p2620 N88-25546

HYDROGENOLYSIS
NT HYDROCRACKING

HYDROGEOLOGY

Study of Earth from space and strengthening of economy 01 p0010 N88-10055

The contribution of remote sensing to hydrology and hydrogeology 22 p3090 N88-28347

The use of SPOT images for water resources surveys in the Kasserine Basin (Tunisia)
22 p3090 N88-28348

HYDROGRAPHY

Varifront 3 expedition data report (USNS DE STEIGUER CRUISE 1202-82). Bioluminescence, hydrographic, nutrient, and satellite data from the Gulf of California (November-December 1981)
[AD-A185011] 05 p0620 N88-13805

Hurricane Danny storm surge data, report 4
[AD-A186373] 07 p0879 N88-15334

Hurricane Kate storm surge data, report 5
[AD-A186374] 07 p0880 N88-15335

North Pacific Ocean. Subtropical front north of Hawaii, R/V Thomas G. Thompson: 7 January - 10 February 1974. CTD data report
[AD-A186565] 08 p1044 N88-16310

North Pacific Ocean. Tradewind region east of Hawaii, R/V Thomas G Thompson: 25 September - 1 November 1972. STD data report
[AD-A186566] 08 p1044 N88-16311

North Pacific Ocean. Subarctic front central Pacific, R/V Thomas G. Thompson: 8 September - 9 October 1975. CTD data report
[AD-A186567] 08 p1044 N88-16312

North Pacific Ocean. Central Pacific Transition Zone, R/V Thomas G. Thompson: 25 March - 3 May 1968. STD data report
[AD-A186570] 09 p1195 N88-17160

North Pacific Ocean. Northeast Pacific Transition Zone, R/V Thomas G. Thompson: 1 November - 6 December 1969. STD data report
[AD-A186574] 09 p1195 N88-17161

Hydrographic and current measurements in the North-East Atlantic Ocean. Data report on F.S. Meteor cruises 69/5 and 69/6, October to November 1984
[REPT-166] 09 p1196 N88-17164

Current velocity and hydrographic observations in the Straits of Florida, the Caribbean Sea and offshore of the Antillean Archipelago: Subtropical Atlantic climate studies (STACS) 1984 and 1985
[PB88-149299] 12 p1649 N88-19874

Mass, heat and nutrient fluxes in the Atlantic Ocean determined by inverse methods
[NASA-CR-180535] 14 p1950 N88-21626

Hydrographic data from the OPTOMA (Ocean Prediction Through Observation, Modeling and Analysis) program: OPTOMA 23, 9-19 November 1986
[AD-A189868] 15 p2099 N88-22506

Physical, chemical and CTD (Conductivity/Temperature/Depth) data from the Marathon 2 expedition
[AD-A189930] 15 p2099 N88-22507

Hydrographic observations in the northwestern Weddell Sea Marginal Ice Zone during March 1986
[PB88-173240] 16 p2237 N88-23359

The impact of hemp production on the development of the municipalities of Araras, Leme, Santa Cruz da Conceicao and Pirassununga 19 p2683 N88-25948

Aerial photography as an instrument of atmospheric analysis: Maps of the middle atmosphere and its dynamics, Baixada Santista (SP) 19 p2684 N88-25955

Beaufort sea mesoscale circulation study: Hydrography helicopter operations, April 1987
[PB88-203658] 21 p2976 N88-27681

Utilization of SPOT in hydrography
22 p3108 N88-28438

A method for determining absolute velocities from hydrographic data: The numerical code
[AD-A193997] 22 p3129 N88-28603
An analysis of results of a high-resolution world ocean circulation model
[AD-A195760] 24 p3405 N88-30272

HYDROKINETICS
U HYDROMECHANICS

HYDROLOGICAL CYCLE
Report of the Workshop on Space Systems Possibilities for a Global Energy and Water Cycle Experiment
[WCP-137] 09 p1193 N88-17147

HYDROLOGY
NT HYDROGEOLOGY
Remote Sensing-Arid Lands Workshop, Page, Arizona, June 10-12, 1986
[DE87-012368] 01 p0064 N88-10412
Description of NCAR (National Center for Atmospheric Research) Community Climate Model (CCM1)
[PB87-203782] 01 p0072 N88-10462
Study of evolution of Gulf Stream cyclinic eddy
06 p0727 N88-14473
Errors in retrieving hydrological fields and fields of their differential characteristics by method of approximation by orthogonal functions 06 p0727 N88-14475
Hydrochemical structure of Gulf Stream frontal zone waters 06 p0727 N88-14476
Modern concept concerning transport of bottom sediments in abyssal regions of world ocean
06 p0728 N88-14478
Tropical hydrology
[WMO-655] 06 p0745 N88-14584
Evaluation of the flooding areas of the Sao Goncalo Canal through LANDSAT 5 thematic mapper images
[INPE-4118-PRE/1039] 08 p1020 N88-16185
Hydrological models 14 p1937 N88-21559
The Hapex-Mobilhy program 14 p1938 N88-21560
Project CODEAMA/FUNCATE (test-area of Barreirinha-AM): Field report
[INPE-4500-RPE/563] 15 p2090 N88-22455
A core hole into the hydrothermal system of the Long Valley caldera
[DE88-006335] 16 p2231 N88-23325
Evaluation of the floodable area of the canal of Sao Goncalo through TM-LANDSAT 5 imagery
17 p2364 N88-24078
Evaluation of a flood period (June, 1984) in the southern region of Laguna dos Patos, through remote sensing data, meteorological and oceanographic
17 p2365 N88-24083
Aerial photography as an instrument of atmospheric analysis: Maps of the middle atmosphere and its dynamics, Baixada Santista (SP) 19 p2684 N88-25955
Surface hydrology, sediment transport dynamics and remote sensing of disturbed watersheds in a humid temperate region
[DE88-008719] 20 p2817 N88-26715
Vegetation studies on Vandenberg Air Force Base, California
[NASA-TM-100985] 20 p2831 N88-26795
Use of SPOT satellite in agrohydrology: Detection of spring water excess in a grassland region
22 p3091 N88-28357
The world's water resources: A major neglect. A study in remote sensing in hydrology and water management
[ESA-BR-40] 22 p3116 N88-28511
Use of LANDSAT images of vegetation cover to estimate effective hydraulic properties of soils
[NASA-CR-183185] 22 p3116 N88-28514

HYDROLOGY MODELS
Regularity properties of a doubly degenerate equation in hydrology
[REPT-87-07] 01 p0064 N88-10409
Use of the thermodynamic evaporation formula of Hoffmann in energy balance models for flowing water
08 p1013 N88-16143
Hydrologic models for land-atmosphere retrospective studies of the use of LANDSAT and AVHRR data
[NASA-CR-182861] 20 p2817 N88-26712
Hydrologic models for land-atmosphere retrospective studies of the use of LANDSAT and AVHRR data
[NASA-CR-182862] 20 p2818 N88-26716

HYDROLYSIS
Preparation of oxide glasses from metal alkoxides by sol-gel method
[NASA-TT-20124] 02 p0154 N88-10965
Effects of hydrolysis on metallo-organic solution deposition of PZT films
[ATR-86(8443)-1] 06 p0679 N88-14160
On copper peroxide
[NASA-TT-20263] 15 p2037 N88-22135
Identification of hydroxypropyl starch hydrolysate components 17 p2315 N88-23832
Saccharification of cellulose by combined fungal and bacterial preparations 17 p2316 N88-23833
Complexation and hydrolysis reactions of iron(III)
17 p2322 N88-23867
A study of solvent effects on the synthesis of pure component and composite ceramic powders by metal alkoxide hydrolysis
[DE88-008381] 20 p2777 N88-26470

HYDROMAGNETIC FLOW
U MAGNETOHYDRODYNAMIC FLOW

HYDROMAGNETIC STABILITY
U MAGNETOHYDRODYNAMIC STABILITY

HYDROMAGNETIC WAVES
U MAGNETOHYDRODYNAMIC WAVES

HYDROMAGNETICS
U MAGNETOHYDRODYNAMICS

HYDROMAGNETISM
U MAGNETOHYDRODYNAMICS

HYDROMECHANICS
NT ELASTOHYDRODYNAMICS
NT ELECTROHYDRODYNAMICS
NT HYDRODYNAMICS
NT HYDROSTATICS
NT MAGNETOHYDRODYNAMICS
A review of the NATO special group of experts on Naval hydromechanics and related problems
16 p2205 N88-23157

HYDROMETEOROLOGY
NT MARINE METEOROLOGY
The application of doubly-truncated hydrometeor distributions to numerical cloud models
[AD-A185273] 05 p0627 N88-13636
Influence of hydrometeorological factors on visibility of objects detected by radar 13 p1790 N88-20707

HYDRONIUM IONS
Vibrational spectroscopy of the hydrogen and hydrated hydronium cluster ions 16 p2268 N88-23566

HYDROPHONES
Bodies in unsteady flow
[AD-A190416] 15 p2064 N88-22308
Remote sensing of acoustic properties of shallow water sediments: A review
[AD-A192107] 18 p2570 N88-25267

HYDROPOWER STATIONS
U HYDROELECTRIC POWER STATIONS

HYDROSTATIC PRESSURE
Experimental studies on the tripping behavior of narrow T-stiffened flat plates subjected to hydrostatic pressure and underwater shock 05 p0592 N88-13613
Quantum wells and bulk AlGaAs under hydrostatic pressure 20 p2862 N88-27000
Pressure-dependent measurement on n+GaAs (Si, Sn): The effect of deep donor (DX) states on the electrical properties and presistent photoconductivity effects
20 p2866 N88-27020

HYDROSTATICS
Composites strengthening
[AD-A189258] 13 p1734 N88-20364
Active control and system identification of rotordynamic structure 16 p2218 N88-23230

HYDROTHERMAL STRESS ANALYSIS
STAEBL/general composites with hygrothermal effects (STAEBL/GENCOM)
[NASA-TM-100266] 05 p0611 N88-13754

HYDROTHERMAL SYSTEMS
Tapping the earth's geothermal resources: Hydrothermal today, magma tomorrow
[DE87-014716] 02 p0196 N88-11223
Effective use of principal component analysis with high resolution remote sensing data to delineate hydrothermal alteration and carbonate rocks 05 p0612 N88-13758
Evaluation of AIS-2 (1986) data over hydrothermally altered granitoid rocks of the Singatse Range (Yerington) Nevada and comparison with 1985 AIS-1 data
05 p0613 N88-13767
Mapping hydrothermally altered rocks in the Northern Grapevine Mountains, Nevada and California with the airborne imaging spectrometer 05 p0614 N88-13772
Experimental and theoretical constraints on the origin of mid-ocean ridge geothermal fluids
13 p1804 N88-20784
A core hole into the hydrothermal system of the Long Valley caldera
[DE88-006335] 16 p2231 N88-23325
Geothermal energy technology: Issues, R and D (Research and Development) and cooperative arrangements
[PB88-193107] 21 p2967 N88-27626

HYDROX ENGINES
U HYDROGEN OXYGEN ENGINES

HYDROXIDES
NT LITHIUM HYDROXIDES
NT SODIUM HYDROXIDES
Toughening of alpha-alumina: Preliminary results
[DE87-702776] 01 p0028 N88-10178
Hydroxide ion conductors as possible electrolytes in intermediate temperature fuel cells
[AD-A185508] 06 p0731 N88-14495
Investigation of OH reaction products. Excimer laser photolysis/slab laser fluorescence under tropospheric conditions
[REPT-8] 09 p1191 N88-17137
Electron transfer to iron(3) oxide colloids
[DE88-002685] 10 p1416 N88-18448
Dynamics of production and oxidation of boranes
[AD-A188968] 12 p1606 N88-19605
Characterization of redox states of nickel hydroxide film electrodes by in-situ Raman spectroscopy
[AD-A189268] 13 p1741 N88-20411
Material degradation in a barium hydroxide latent heat storage pilot unit
[DFVLR-FB-87-49] 16 p2175 N88-22961
Transition probabilities in OH A 2 sigma + - X 2 pi i: Bands with v prime = 0 and 1, v double prime = 0 to 4
[NASA-CR-182946] 18 p2584 N88-25353
Crystallization of aluminum hydroxide in the aluminum-air battery: Literature review, crystallizer design and results of integrated system tests
[DE88-010510] 20 p2797 N88-26594

HYDROXYL COMPOUNDS
NT ALCOHOLS
NT ETHYL ALCOHOL
NT GLYCOLS
NT ISOPROPYL ALCOHOL
NT METHYL ALCOHOL
NT PHENOLS
NT POLYVINYL ALCOHOL
High pressure strand burn rate tests of polyvinylnitrate/nitramine propellants
[AD-A184178] 04 p0422 N88-12615
An infra-red investigation of HAN (Hydroxylammonium Nitrate)-based liquid propellants
[AD-A187226] 10 p1307 N88-17815
Identification of hydroxypropyl starch hydrolysate components 17 p2315 N88-23832
The burning of HAN-based (hydroxylammonium nitrate) liquid propellants
[DE88-006863] 18 p2494 N88-24600

HYDROXYL EMISSION
Lyman-alfa/OH-resonance-absorbtion measurements and simulation calculations for the investigation of the induction behavior of methane/ethane/oxygen mixtures in reflected shock waves
[ETN-88-90606] 07 p0831 N88-15042
VLBI research on OH-maser IN W33
08 p1001 N88-16064

HYDROXYL RADICALS
Preparation of polymer polyols
[EP-PATENT-0-162-589-A1] 01 p0102 N88-10665
Investigations of extragalactic hydroxyl
03 p0389 N88-12441
Photon stimulated desorption from oxidized Al(110)
[DE88-002209] 06 p0787 N88-14828
Measurement of rate constants of elementary gas reactions of importance to upper atmosphere and combustion systems
[AD-A189432] 13 p1737 N88-20386
Ground-based column abundance measurements of atmospheric hydroxyl
[NASA-CR-182676] 14 p1944 N88-21599
Water vapor and hydroxyl distributions in the inner coma of Comet Halley measured by the VEGA-2 three channel spectrometer TKS 14 p1998 N88-21910
Ultraviolet measurements: Measurements of photolysis rates 18 p2539 N88-25065
Laboratory experiments on atmospheric OH reactions
18 p2539 N88-25066
Effect of carbohydrate oxidation on the tropospheric HOx-system 18 p2539 N88-25067
Measurement of atmospheric OH with laser differential optical absorption spectroscopy (LDOAS)
18 p2539 N88-25068
Tropospheric OH measurements by long path absorption with rapid spectral concordance
18 p2539 N88-25069
Determination of tropospheric H concentrations by a double-pulsed UV laser method
18 p2539 N88-25070
Tropospheric OH measurement by Laser Induced Fluorescence (LIF) 18 p2540 N88-25071
Development of continuous wave laser frequency modulation of OH in tropospheric concentrations range
18 p2540 N88-25073
The evolution of cometary activity
18 p2594 N88-25416
Ground level hydroxyl (OH) concentration measurements by long path differential optical laser absorption
[ETN-88-92124] 20 p2855 N88-26952
Distribution of hydroxyl clouds in the galaxy
[DE88-702415] 22 p3164 N88-28844

HYGRAL PROPERTIES
STAEBL/general composites with hygrothermal effects (STAEBL/GENCOM)
[NASA-TM-100266] 05 p0611 N88-13754
HYGROSCOPICITY
Thermodynamic study of hygroscopic polymers using surface acoustic waves 19 p2672 N88-25882
HYPERBARIC CHAMBERS
Space station internal environmental and safety concerns 04 p0407 N88-12527
USAF hyperbaric animal transfer chamber system
[AD-A193633] 23 p3237 N88-29265
HYPERBOLIC COORDINATES
Two dimensional hyperbolic grid generation
[VKI-TN-162] 18 p2511 N88-24897
HYPERBOLIC DIFFERENTIAL EQUATIONS
A study of numerical methods for hyperbolic conservation laws with stiff source terms
[NASA-TM-100075] 10 p1399 N88-18343
Accurate boundary conditions for exterior problems in gas dynamics
[NASA-TM-100807] 11 p1537 N88-19182
Conservative finite volume solutions of a linear hyperbolic transport equation in two and three dimensions using multiple grids
[NASA-CR-182715] 13 p1828 N88-20934
Feedback control of a hyperbolic partial-differential equation with viscoelastic damping
[AD-A192806] 21 p3003 N88-27810
HYPERBOLIC FUNCTIONS
Inhomogeneous conditions at open boundaries for wave propagation problems
[AD-A183847] 01 p0033 N88-10214
Smooth dynamics on the interval (with an emphasis on unimodal maps)
[REPT-87-09] 01 p0086 N88-10555
Stability of semidiscrete approximations for hyperbolic initial-boundary-value problems: An eigenvalue analysis
[NASA-TM-88328] 02 p0227 N88-11434
Some aspects of high resolution numerical methods for hyperbolic systems of conservation laws, with applications to gas dynamics
[DMS-86-7] 03 p0321 N88-12031
Nonlinear hyperbolic conservation laws
[AD-A184963] 05 p0580 N88-13538
Stability analysis of finite difference schemes for hyperbolic systems, and problems in applied and computational linear algebra
[AD-A185624] 07 p0908 N88-15499
Hyperbolicity and invariant measures for general C sq interval maps satisfying the Misiurewicz condition
[REPT-87-46] 14 p1966 N88-21733
La Recherche Aerospatiale, bimonthly bulletin, no. 1986-5, 234/September-October
[ESA-TT-1032] 19 p2641 N88-25671
Stability of semidiscrete approximations for hyperbolic initial-boundary-value problems: Stationary modes
[NASA-TM-100994] 23 p3270 N88-29455
HYPERBOLIC NAVIGATION
NT LORAN C
HYPERBOLIC SPACE
U HYPERBOLIC COORDINATES
HYPERBOLIC TRAJECTORIES
Solution of the hyperbolic Kepler's equation
[RAE-TR-87042] 09 p1229 N88-17368
HYPERCAPNIA
Effect of intermittent hypercapnia on visual analyzer function 07 p0896 N88-15431
Effect of hypercapnic-hypoxic test on cardiorespiratory parameters of individuals with neurocirculatory dystonia
10 p1367 N88-18169
Human adaptation to various hypercapnic conditions in relation to salivary electrolyte dynamics and renal function 12 p1664 N88-19977
Physiological effects on man of long duration confinement in a carbon dioxide enriched environment
19 p2695 N88-26017
Distinctive features in blood clotting and fibrinolytic properties under effect of epinephrine in presence of hypoxia and hypercapnia 19 p2705 N88-26082
HYPERCUBE MULTIPROCESSORS
A portable hypercube simulator
[DE87-013369] 04 p0478 N88-12947
Implementation of a 3-D nonlinear MHD calculation on the Intel hypercube
[DE87-014837] 04 p0479 N88-12949
Parallelization of hydrocodes on the Intel Hypercube, part 2
[DE88-001591] 04 p0480 N88-12957
Performance analysis of parallel branch and bound search with the hypercube architecture
09 p1206 N88-17229
The next generation of hypercube computers
10 p1376 N88-18226
Investigations on the usefulness of the Massively Parallel Processor for study of electronic properties of atomic and condensed matter systems
[NASA-CR-182514] 10 p1383 N88-18259
Experiences with serial and parallel algorithms for channel routing using simulated annealing
[NASA-CR-182530] 10 p1388 N88-18289
Implementation of a 3-D nonlinear MHD (magnetohydrodynamics) calculation on the Intel hypercube
[DE88-000625] 13 p1816 N88-20848
Cholesky downdating on a hypercube
[DE88-006780] 15 p2113 N88-22586
Simulation of fault tolerance in a hypercube arrangement of discrete processors
[AD-A189682] 15 p2114 N88-22594
Implementation and performance analysis of parallel assignment algorithms on a hypercube computer
[AD-A190678] 15 p2115 N88-22600
Multi-sensor integration on the NCUBE hypercube computer
[DE88-007472] 18 p2554 N88-25162
QR factorization of a dense matrix on a hypercube multiprocessor
[DE88-009187] 19 p2716 N88-26129
Relay approach message routing in hypercube multiprocessors
[DE88-009973] 20 p2835 N88-26814
Distributed fault tolerant embeddings of binary trees in hypercubes
[AD-A192929] 20 p2839 N88-26840
Motor-response learning at a process control panel by an autonomous robot
[DE88-005055] 21 p2955 N88-27554
Parallel implementation of the boundary element method
[DE88-011846] 21 p3007 N88-27839
Solving the symmetric tridiagonal eigenvalue problem on the hypercube
[AD-A193905] 23 p3250 N88-29344
A performance study of the hypercube architecture
[AD-A194361] 23 p3264 N88-29433
HYPERFINE STRUCTURE
Fundamental properties of spin-polarized quantum systems
[DE88-004425] 10 p1423 N88-18499
Sources of polarized ions and atoms
[DE88-010910] 20 p2852 N88-26931
Experimental and theoretical investigations of isotope shift and hyperfine structure on 5d elements (especially platinum, iridium and rhenium)
[ETN-88-93121] 24 p3353 N88-29957
HYPERGEOMETRIC FUNCTIONS
Peetre's Theorem and generalized functions
[MEMO-661] 14 p1967 N88-21742
Jacobi polynomials as generalized Faber polynomials
[CWI-PM-R8706] 16 p2258 N88-23496
Incomplete Lipschitz-Hankel integrals of MacDonald functions
[AD-A191034] 16 p2261 N88-23515
HYPERGEOMETRY
U HYPERSPACES
HYPERNUCLEI
Physics of few-body lambda hypernuclei
[DE87-014746] 03 p0375 N88-12357
Few body hypernuclear systems: Weak decays
[DE87-014920] 04 p0486 N88-13010
Experimental aspects of hypernuclear physics at CEBAF
[CEBAF-R-86-013] 11 p1546 N88-19245
HYPEROXIA
Human metabolism and peripheral circulation during antiorthostatic hypokinesia 07 p0891 N88-15396
Effect of oxygen inhalation on respiratory function during exercise and exposure to added resistance to respiration
10 p1366 N88-18164
Increase in influence of oxygen on the body in the presence of helium 13 p1810 N88-20816
The evolution of glutathione metabolism in phototrophic microorganisms
[NASA-CR-182902] 19 p2695 N88-26015
Human erykthrocyte metabolism in the presence of hyperoxygenation during antiorthostatic hypokinesia
19 p2706 N88-26092
HYPERPLANES
On the volume of a n-dimensional simplex
[REPT-87-16] 01 p0086 N88-10557
HYPERSONIC AIRCRAFT
Experimental aerothermodynamic research of hypersonic aircraft
[NASA-CR-181533] 04 p0399 N88-12483
The off-design performance of hypersonic waveriders
05 p0533 N88-13244
Numerical optimization of conical flow waveriders including detailed viscous effects
05 p0533 N88-13245
Dynamic stability of hypersonic conical lifting vehicles according to Newton-Busemann theory
05 p0534 N88-13247
Lifting bodies: An attractive aerodynamic configuration choice for hypervelocity vehicles
05 p0534 N88-13248
Aeropropulsion '87. Session 6: High-Speed Propulsion Technology
[NASA-CP-10003-SESS-6] 08 p0957 N88-15807
Hypersonic propulsion research
08 p0958 N88-15812
Accuracies of southwell and force/stiffness methods in the prediction of buckling strength of hypersonic aircraft wing tubular panels
[NASA-TM-88295] 09 p1183 N88-17090
Aerothermal tests of quilted dome models on a flat plate at a Mach number of 6.5
[NASA-TP-2804] 15 p2067 N88-22325
National aero-space plane: A technology development and demonstration program to build the X-30
[GAO/NSIAD-88-122] 17 p2301 N88-23764
Application of integrated fluid-thermal-structural analysis methods
[NASA-TM-100625] 17 p2350 N88-24001
Supersonic transport/hypersonic transport (SST/HST) development
[REPT-881-111-101] 21 p2896 N88-27192
HYPERSONIC BOUNDARY LAYER
Turbulence in hypersonic flow
[AD-A185624] 07 p0815 N88-14961
Shock wave/turbulent boundary layer interaction in high-Reynolds-number hypersonic flows
[AD-A186029] 11 p1434 N88-18555
Hypersonic turbulent wall boundary layer computations
[NASA-CR-182147] 18 p2514 N88-24917
Low density real gas flows about hypersonic vehicles
[AD-A194251] 22 p3075 N88-28253
The effects of incoming boundary layer thickness on unsteady shock-induced turbulent separations induced by cylinders
[AD-A196190] 24 p3368 N88-30060
HYPERSONIC FLIGHT
Shock tunnels for real gas hypersonics
05 p0530 N88-13223
Driving mechanism of unsteady separation shock motion in hypersonic interactive flow 05 p0530 N88-13226
Upgrading of NASA-Ames high-energy hypersonic facilities: A Study
[NASA-CR-182475] 09 p1122 N88-16717
Review of convectively cooled structures for hypersonic flight
[NASA-TM-87740] 17 p2310 N88-23817
Compressible boundary layers — atmospheric reentry
[CERT-OA-13/5005-AYD] 20 p2801 N88-26623
Hypersonic flight testing
[DE88-001655] 21 p3015 N88-27894
HYPERSONIC FLOW
Fast shock tube assemblies
[DE87-011732] 01 p0008 N88-10042
The aerothermodynamic environment for holes in hypersonic configurations
[DE87-014651] 02 p0121 N88-10767
Similar solutions for viscous hypersonic flow over a slender three-fourths-power body of revolution
[NASA-TM-100205] 04 p0443 N88-12752
Experimental investigations on blunt bodies and corner configurations in hypersonic flow
05 p0530 N88-13225
An ultra-high-speed cinematographic method for the study of wakes in hypersonic ballistic ranges
05 p0531 N88-13228
Numerical simulation of the hypersonic flow around lifting vehicles 05 p0532 N88-13234
Hypersonic laminar boundary layer: Parametric study for the representation of real gas effects
05 p0532 N88-13236
On the numerical simulation of three-dimensional hypersonic flow 05 p0532 N88-13237
Numerical experiments with hypersonic flows beneath a cone-delta-wing combination 05 p0532 N88-13238
A spatial marching technique for the inviscid blunt body problem 05 p0533 N88-13239
A 3-D Euler solution for hypersonic Mach numbers
05 p0533 N88-13240
Computation of flow past conical hypersonic wings using a second order Godunov method
05 p0533 N88-13241
Time-dependent hypersonic viscous interactions
[AD-A185764] 06 p0665 N88-14082
Turbulence in hypersonic flow
[AD-A185624] 07 p0815 N88-14961
Three-dimensional Euler solutions for hypersonic Mach numbers
[MBB-UR-944/87] 10 p1315 N88-17859

A study of numerical methods for hyperbolic conservation laws with stiff source terms
[NASA-TM-100075] 10 p1399 N88-18343
Hypersonic blunt body computations including real gas effects
[NASA-TM-100074] 10 p1400 N88-18344
Analysis of shear-layer probe data for holes in hypersonic configurations
[DE88-003992] 11 p1435 N88-18564
Topology and grid adaption for high-speed flow computations
[NASA-CR-182586] 11 p1487 N88-18875
A new parabolized Navier-Stokes code for chemically reacting flow fields 12 p1625 N88-19721
Documentation and installation of the hypersonic arbitrary-body computer program (Mark 3 version) of A.E. Gentry on the IBM computer system
[MBB/LKE-127/S/PUB/256] 13 p1719 N88-20276
High-resolution shock-capturing schemes for inviscid and viscous hypersonic flows
[NASA-TM-100097] 15 p2122 N88-22651
Experimental investigation of the hypersonic flow over a six finned configuration
[AD-A190670] 16 p2157 N88-22871
Application of integrated fluid-thermal-structural analysis methods
[NASA-TM-100625] 17 p2350 N88-24001
Boundary layer transition
[CERT-OA-37/5018-AYD] 18 p2458 N88-24595
Hypersonic turbulent wall boundary layer computations
[NASA-CR-182147] 18 p2514 N88-24917
Aerodynamics of lifting bodies with combined transverse and longitudinal curvature 19 p2598 N88-25436
Two-dimensional viscous flow computations of hypersonic scramjet nozzle flowfields at design and off-design conditions
[NASA-CR-182150] 19 p2603 N88-25459
The Proceedings of the Symposium on Mechanics for Space Flight 1987
[ISAS-SP-6] 20 p2782 N88-26499
Numerical computation of space shuttle orbiter flow field
[NASA-CR-183193] 22 p3040 N88-28046
Fellowships in hypersonic aerodynamics
[AD-A194265] 23 p3172 N88-28885
A numerical study of the test time in a hypersonic shock tunnel
[AD-A194057] 23 p3172 N88-28888

HYPERSONIC REENTRY
The aerodynamic design of hypersonic contoured axisymmetric nozzles including real gas effects
[VKI-TM-43] 06 p0665 N88-14076
Three-dimensional Euler solutions for hypersonic Mach numbers
[MBB-UR-944/87] 10 p1315 N88-17859
Study of hypersonic boundary layers
[CERT-RSF-OA-17/5005-AYD]
23 p3213 N88-29121

HYPERSONIC SHOCK
A numerical study of the test time in a hypersonic shock tunnel
[AD-A194057] 23 p3172 N88-28888

HYPERSONIC SPEED
SCRAM JET (Supersonic Combustion Ramjet) combustion experiments 04 p0404 N88-12512
Aerodynamic characteristics of wings designed with a combined-theory method to cruise at a Mach number of 4.5
[NASA-TP-2799] 12 p1575 N88-19420
Numerical study of unsteady viscous hypersonic blunt body flows with an impinging shock
[NASA-TM-100096] 15 p2122 N88-22650
A computational analysis of under-expanded jets in the hypersonic regime
[NASA-TM-101319] 21 p2893 N88-27174
Fellowships in hypersonic aerodynamics
[AD-A194265] 23 p3172 N88-28885
Transition at hypersonic speeds
[NASA-CR-178315] 24 p3368 N88-30058

HYPERSONIC VEHICLES
NT HYPERSONIC AIRCRAFT
NT X-30 VEHICLE
The aerothermodynamic environment for holes in hypersonic configurations
[DE87-014651] 02 p0121 N88-10767
The effects of sweep and bluntness on a glancing shock wave turbulent boundary layer interaction
05 p0531 N88-13227
Hypersonic static and dynamic stability of axisymmetric shapes: A comparison of prediction methods and experiment 05 p0534 N88-13246
Hypervelocity Technology (HVT) crew escape
09 p1214 N88-17280
Thermal stress in high temperature cylindrical fasteners
[NASA-TM-100611] 15 p2087 N88-22438
Aerodynamics of Hypersonic Lifting Vehicles: Fluid Dynamics Panel AGARD Symposium
[AGARD-AR-246] 21 p2943 N88-27480
Low density real gas flows about hypersonic vehicles
[AD-A194251] 22 p3075 N88-28253
Fellowships in hypersonic aerodynamics
[AD-A194265] 23 p3172 N88-28885

HYPERSONIC WIND TUNNELS
NT CASCADE WIND TUNNELS
NT HOTSHOT WIND TUNNELS
NT SHOCK TUNNELS
The 0.6m x 0.6m trisonic test section (TMK) of DFVLR in Cologne-Porz, Federal Republic of Germany (status 1986)
[ESA-TT-1052] 03 p0267 N88-11681
A survey of existing hypersonic ground test facilities: North America 05 p0529 N88-13220
European hypersonic wind tunnels
05 p0530 N88-13221
Preparation of qualification tests of a plasma generator for the feeding of a hypersonic wind tunnel
05 p0530 N88-13222
Turbulence measurement in hypersonic flow
05 p0530 N88-13224
The drag of slender axisymmetric cones in rarefied hypersonic flow 05 p0531 N88-13229
Low Reynolds number influence on aerodynamic performance of hypersonic lifting vehicles
05 p0531 N88-13230
Aerothermodynamics research at NASA Ames
05 p0533 N88-13242
The performance of the VKI longshot hypersonic wind tunnel
[VKI-TN-161] 18 p2466 N88-24650
A numerical study of the test time in a hypersonic shock tunnel
[AD-A194057] 23 p3172 N88-28888
Quantitative surface temperature measurement using two-color thermographic phosphors and video equipment
[NASA-CASE-LAR-13740-1] 24 p3376 N88-30105

HYPERSPACES
Group theoretic interpretations of Askey's scheme of hypergeometric orthogonal polynomials
[CWI-PM-R8703] 13 p1831 N88-20954
Hyperelliptic statsums in superstring theory
[DE83-701646] 16 p2284 N88-23676

HYPERTENSION
Effect of steroid hormones on biogenic amine levels in lungs during development of pulmonary hypertension in rats submitted to chronic hypobaric hypoxia
07 p0896 N88-15430
Hemodynamic effects of beta-adrenergic blocking with obsidan in clinostatic and orthostatic positions
10 p1367 N88-18171
Risk of hypertension and functional cerebral laterality in oil expedition works in far north
12 p1665 N88-19980

HYPERTHERMIA
Heat acclimatization under controlled hyperthermia
12 p1665 N88-19981
Analysis of annular microstrip antennas for hyperthermic applicators
[PB88-181508] 19 p2643 N88-25679
Hyperthermia: New thoughts on an old problem
[AD-A192602] 21 p2986 N88-27731
The impact of hyperthermia and hypohydration on circulation, strength, endurance and health
[AD-A192657] 22 p3131 N88-28615
Improvements in techniques of microwave thermography
[AD-A193620] 23 p3239 N88-29276

HYPERTONIA
U OSMOSIS

HYPERTROPHY
U GROWTH

HYPERVELOCITY ACCELERATORS
U HYPERVELOCITY GUNS

HYPERVELOCITY CRATERING
U HYPERVELOCITY PROJECTILES
U PROJECTILE CRATERING

HYPERVELOCITY FLOW
Acceleration to hypervelocities using minimum energy concepts
[DE87-011796] 01 p0089 N88-10583

HYPERVELOCITY GUNS
Effects of barrel joints on hypervelocity projectiles
[DE87-013447] 02 p0157 N88-10983
Current-filamentation instability in railgun arcs
[AD-A184616] 03 p0269 N88-11693
Experimental investigation of a three-stage railgun incorporating puff-switching
[MRL-R-1056] 09 p1130 N88-16785
Pulsed current transformer for low inductive loads
[AD-A187224] 10 p1324 N88-17913
A laboratory railgun for terminal ballistics and arc armature research studies
[AD-A187225] 11 p1442 N88-18603
Structural integrity of metallic armature rail guns
[AD-A188735] 13 p1726 N88-20333
Launchability of base-driven electromagnetic projectiles
[AD-A189635] 15 p2023 N88-22055
Ultrasonic Time-Of-Flight Diffraction (TOFD) measurements of crack depths in an acceleration reservoir of a high velocity research gun
[DE88-006644] 16 p2164 N88-22907
Experimental investigation of a three-stage railgun incorporating puff-switching
[AD-A191044] 16 p2166 N88-22918
Analytic and numerical modeling of heat and material transport in electrical hypervelocity guns
[AD-A192178] 18 p2469 N88-24655
STARFIRE: Hypervelocity railgun development for high-pressure research
[DE88-008348] 19 p2605 N88-25469
Application of the Hilbert transform to Doppler radar signals from a hypervelocity gun
[AD-A193690] 22 p3146 N88-28716

HYPERVELOCITY IMPACT
Shock-wave studies using plastic flyers driven by an electric gun for hypervelocity impact on selected materials
[DE87-012631] 01 p0008 N88-10046
Computations of hypervelocity impact using the CTH shock wave physics code
[DE87-013067] 02 p0169 N88-11062
Measurements of iridium and the meteoric impact hypothesis at cretaceous end
[DE87-703765] 04 p0521 N88-13200
Conditions for geomagnetically trapping sub-micron lunar ejecta between L = 1.2 and L = 3.1
04 p0521 N88-13203
An investigation of oblique hypervelocity impact
07 p0927 N88-15629
An analysis of penetration and ricochet phenomena in oblique hypervelocity impact
[NASA-TM-100319] 10 p1339 N88-18004
Sub-scaling of projectile/target system damaged by hypervelocity
[AD-A188683] 12 p1634 N88-19779
Effects of meteoroids and space debris on the particulate environment for space station 18 p2591 N88-25399
Hypervelocity impact analysis with supercomputers
[DE88-008907] 21 p3001 N88-2779[illegible]
The effect of the near earth micrometeoroid environment on a highly reflective mirror surface
[NASA-TM-101307] 24 p3332 N88-29833

HYPERVELOCITY LAUNCHERS
A feasibility study of a hypersonic real-gas facility
[NASA-CR-180423] 01 p0008 N88-10043
Ultimate velocities for induction launchers
[DE87-012360] 04 p0404 N88-12513
Analysis of a series of electromagnetic launcher firings
[AR-005-131] 04 p0405 N88-12516
The railgun and its power source
[MRL-R-1058] 09 p1130 N88-16786
Continuous measurements of in-bore projectile velocity
[DE88-006841] 15 p2023 N88-22056
A chemical method for achieving acceleration of macroparticles to ultrahigh velocities
[DE88-006377] 15 p2128 N88-22695
Power and energy requirements for electromagnetic launchers 17 p2420 N88-24391
Fabrication issues and technology development for HELEOS (Hypervelocity Electromagnetic Launcher for Equation Of State)
[DE88-007419] 18 p2470 N88-24658
Application of superconducting technology to earth-to-orbit electromagnetic launch systems
[NASA-TM-101134] 20 p2763 N88-26385
Application of superconducting technology to earth-to-orbit electromagnetic launch systems
[DE88-010022] 20 p2763 N88-26386

HYPERVELOCITY PROJECTILES
Effects of barrel joints on hypervelocity projectiles
[DE87-013447] 02 p0157 N88-10983
Efficiency aspects of short, low velocity railguns
[AR-004-847] 04 p0405 N88-12517
A laboratory railgun for terminal ballistics and arc armature research studies
[AD-A187225] 11 p1442 N88-18603
Experimental determination of the heat flux inside a tubular projectile for the velocity range M = 3 and M = 6
[ISL-R-118/86] 11 p1443 N88-18605
Numerical simulation of the perforation of thin plates
[ISL-R-122/86] 11 p1495 N88-18926

Trajectory characteristics and heating of hypervelocity projectiles having large ballistic coefficients
[NASA-TP-2614] 12 p1574 N88-19412
Aerodynamic possibilities for the realization of trajectory corrections
[ISL-CO-251/86] 14 p1862 N88-21120
Variable Mach number wall jets for control/propulsion on hypervelocity projectiles/interceptors: Tests with an existing model
[AD-A192645] 21 p2892 N88-27167

HYPERVELOCITY WIND TUNNELS
NT CASCADE WIND TUNNELS
NT HOTSHOT WIND TUNNELS
NT SHOCK TUNNELS
Experience about the application and valuation of roughness strips for boundary layer transition control in wind tunnel tests in the high-speed range
[ESA-TT-1029] 01 p0044 N88-10278

HYPERVENTILATION
Detection of hyperventilation of parachutists
[DFVLR-FB-87-11] 01 p0075 N88-10482

HYPNOSIS
Hypnosis: Possible applications for cosmonauts
12 p1665 N88-19984

HYPOBARIC ATMOSPHERES
Cooling electronic equipment at simulated high altitude in hypobaric chambers
[AD-A185196] 05 p0584 N88-13560
Dexamethasone as prophylaxis for acute mountain sickness: Effect of dose level
[AD-A185848] 08 p1047 N88-16325
Operation Everest 2: Alterations in the immune system at high altitude
[AD-A188011] 11 p1520 N88-19075
Changes in hemostasis system of animals under conditions of granulocytopoiesis inhibition under effect of decreased barometric pressure
12 p1651 N88-19890
Acute mountain sickness at 4500 m is not altered by repeated eight-hour exposures to 3200-3550 m normobaric hypoxic equivalent
[AD-A188358] 12 p1666 N88-19990
Visual sensitivities under reduced oxygen
[AD-A195628] 24 p3406 N88-30279

HYPOCAPNIA
Biofeedback control of alveolar carbon dioxide tension to eliminate hypocapnia in man in the presence of hypoxia 07 p0892 N88-15405

HYPOGLYCEMIA
Spontaneous cerebral electrical activity during prolonged hypoglycemia: A quantitative study in humans
21 p2983 N88-27717

HYPOKINESIA
Human metabolism and peripheral circulation during antiorthostatic hypokinesia 07 p0891 N88-15398
Distinctions and mechanisms of effects of epinephrine and norepinephrine on cardiac pumping function under hypokinetic conditions 07 p0891 N88-15399
Circulatory response of males 45-52 years of age to antiorthostatic hypokinesia 07 p0894 N88-15416
Morphometric analysis of rat aorta endothelium during long-term hypokinesia 07 p0894 N88-15417
Nucleic acid content of skeletal muscles during hypokinesia and in the recovery period
07 p0894 N88-15418
JPRS Report: Science and Technology. USSR: Space Biology and Aerospace Medicine, volume 21, no. 5, September - October 1987
[JPRS-USB-88-003] 10 p1359 N88-18122
Isotope methods of determining distribution and movement of blood in the body
10 p1362 N88-18138
JPRS Report: Science and Technology. USSR: Space Biology and Aerospace Medicine, volume 21, no. 6, November - December 1987
[JPRS-USB-88-004] 10 p1364 N88-18150
Morphological study of early changes in rat bones in simulated weightlessness 10 p1365 N88-18158
Lipid peroxidation in rat tissues with exposure to antiorthostatic hypokinesia, exercise and immobilization stress 10 p1365 N88-18159
New book on metabolic aspects of spaceflight stress
10 p1367 N88-18172
Central hemodynamics in antiorthostatic hypokinesia and immersion models of weightlessness
11 p1521 N88-19081
Regulation of calcium metabolism during prolonged antiorthostatic hypokinesia
[NASA-TT-20219] 11 p1521 N88-19085
Use of diphosphonates to correct disorders in calcium metabolism and mineral composition of bone tissue with 60-day hypokinesia in rats
[NASA-TT-20220] 13 p1809 N88-20807
Changes in the status of the human tibia during antiorthostatic hypokinesia
[NASA-TT-20221] 13 p1810 N88-20813
JPRS report: Science and technology. USSR: Space Biology and Aerospace Medicine, volume 22, no. 1, January - February 1988
[JPRS-USB-88-005] 19 p2702 N88-26069
Noninvasive examination of bones during long-term hypokinesia 19 p2704 N88-26077
Human erykthrocyte metabolism in the presence of hyperoxygenation during antiorthostatic hypokinesia
19 p2706 N88-26092

HYPOPHYSIS
U PITUITARY GLAND

HYPOTHALAMUS
Neurophysiological analysis of hypothalamic regulation mechanisms of primary sleep and hypobiosis
06 p0751 N88-14611
Morphological and functional state of the hypothalamo-hypophyseal neurosecretory system of rats flown aboard Cosmos-1667 10 p1365 N88-18156
Hypothalamic-pituitary-adrenal responses to short duration high intensity cycle exercise
[AD-A192597] 21 p2985 N88-27727

HYPOTHERMIA
Influence of skeletal muscle glycogen on passive rewarming after hypothermia
[AD-A186451] 08 p1049 N88-16334
Rapid hypothermia subsequent to oral nicotinic acid and immersion in warm (30C) water
[AD-A186458] 08 p1050 N88-16339
Respiratory and cardiovascular responses to cold stress following repeated cold water immersion
[AD-A186460] 08 p1050 N88-16340
The role of hydration on peripheral response to cold
[AD-A186448] 09 p1199 N88-17186
Accidental hypothermia
[AD-A194967] 24 p3406 N88-30278

HYPOTHESES
NT EXPECTANCY HYPOTHESIS
NT LAGRANGE SIMILARITY HYPOTHESIS
Lower bounds on bearing accuracy for closely spaced sources
[AD-A184258] 04 p0486 N88-12997
Measurements of iridium and the meteoric impact hypothesis at cretaceous end
[DE87-703765] 04 p0521 N88-13200
Testing and interval estimation in a change-point model allowing at most one change
[AD-A185525] 06 p0767 N88-14716
Changing the layers of mind
[AD-A186648] 08 p1052 N88-16350
Exploring hypotheses in attitude control fault diagnosis
08 p1058 N88-16384
Discovery and problem solving: Triangulation as a weak heuristic 08 p1062 N88-16412
Practical applicability of exact and approximate forms of the randomization test for two independent samples
[AD-A186815] 09 p1231 N88-17381
An application of fuzzy set theory to statistical hypothesis testing
[AD-A186705] 09 p1232 N88-17386
Natural object categorization
[AD-A194103] 22 p3139 N88-28662

HYPOVOLEMIA
Human and animal hypovolemic reactions to increasing +Gz accelerations 07 p0890 N88-15395

HYPOXIA
Superoxide dismutase assays
[AD-A183972] 03 p0356 N88-12242
Scotopic sensitivity with 10 percent oxygen
[AD-A183973] 03 p0356 N88-12243
Hypoxic hypoxia as a stimulus of erythropoiesis in vivo and in vitro 07 p0885 N88-15373
Trace-element metabolism in man and animals in the presence of hypoxic states of diverse etiology
07 p0889 N88-15390
Biofeedback control of alveolar carbon dioxide tension to eliminate hypocapnia in man in the presence of hypoxia 07 p0892 N88-15405
Differentiation of hemopoietic stem cells during adaptation to high altitude 07 p0893 N88-15410
Effect of pyrocetam on mouse resistance to hypoxic hypoxia 2-3 months after exposure to X-radiation
07 p0895 N88-15425
Effect of steroid hormones on biogenic amine levels in lungs during development of pulmonary hypertension in rats submitted to chronic hypobaric hypoxia
07 p0896 N88-15430
Mononuclear phagocytes during adaptation of essentially healthy people to high altitudes
07 p0896 N88-15432
Effects of extreme hypoxia on phospholipid metabolism in subcellular structures of rat brain
08 p1046 N88-16323
Operation Everest 2: Nutrition and body composition
[AD-A186449] 08 p1049 N88-16333
Role of carbon dioxide in correction of coagulation hemostasis under hypoxic conditions
10 p1365 N88-18180
Polar worker adaptability to Antarctic high altitudes
10 p1366 N88-18185
Combined effect of ionizing radiation and altered gas atmosphere on central nervous system
10 p1367 N88-18188
Effect of hypercapnic-hypoxic test on cardiorespiratory parameters of individuals with neurocirculatory dystonia
10 p1367 N88-18189
Operation Everest 2: Alterations in the immune system at high altitude
[AD-A188011] 11 p1520 N88-19075
Interrelationship of heart rhythm indicators and resistance to hypoxia in Antarctic polar workers
12 p1664 N88-19974
Human adaptation to various hypercapnic conditions in relation to salivary electrolyte dynamics and renal function 12 p1664 N88-19977
Medical problems related to altitude in: Human performance physiology and environmental medicine at terrestrial extremes, chapter 14
[AD-A188340] 12 p1666 N88-19989
Acute mountain sickness at 4500 m is not altered by repeated eight-hour exposures to 3200-3550 m normobaric hypoxic equivalent
[AD-A188358] 12 p1666 N88-19990
Distinctive features in blood clotting and fibrinolytic properties under effect of epinephrine in presence of hypoxia and hypercapnia 19 p2705 N88-26082
Effect of different modes of voluntary control of breathing on human electroencephalogram with exposure to acute hypoxic hypoxia 19 p2707 N88-26093
Experimental study of protective effect of antioxidant enzymes-superoxide dismutase and catalase-when using intermittent toxic modes of hyperbaric oxygenation
19 p2707 N88-26094
The effects of hypoxia on P300 and reaction time
[DCIEM-87-RR-12] 21 p2979 N88-27097
The effect of mild hypoxia on the vestibular evoked response 21 p2982 N88-27713
Alterations in cutaneous vasomotor regulation during acute and chronic hypoxia
[AD-A192653] 22 p3131 N88-28612
Biomedical aspects of military operations at high altitude
[AD-A192677] 22 p3132 N88-28619
Human performance and acute hypoxia, chapter 12
[AD-A192604] 23 p3238 N88-29270
Visual sensitivities under reduced oxygen
[AD-A195628] 24 p3406 N88-30279

HYPSOGRAPHY
Vectorization of raster algorithms for elevation data processing 18 p2534 N88-25036

HYSTERESIS
Temperature hysteresis and magnetic transitions in amorphous Fe-Ni-Zr alloys
[DE88-000228] 03 p0294 N88-11848
Applications of a theory of ferromagnetic hysteresis
[DE87-014725] 03 p0373 N88-12348
The consequences of intergrain Josephson coupling in ceramic high-temperature superconductors
[DE87-013713] 06 p0785 N88-14816
RCL model for the development of hysteresis in superconductors
[DE88-702061] 19 p2733 N88-26234
Experimental and theoretical study of the dynamic operational behavior of a three stage radial compressor
[ETN-88-92129] 20 p2811 N88-26876
Mathematical theory and calculations of magnetic hysteresis curves
[DE88-011055] 23 p3277 N88-29510
The aspect ratio dependence of the attractor dimension in Taylor-Couette flow
[AD-A196297] 24 p3369 N88-30065
Nonlinear stress-strain and inelastic rebound with exponential stiffness
[AD-A195667] 24 p3384 N88-30159
Behaviour and hysteresis losses of irreversible type-2 superconducting cylindrical shell
[DE88-702708] 24 p3433 N88-304

I

I BEAMS
Partially braced inelastic beam buckling experiments
[PB87-133831] 06 p0723 N88-14444

IBM COMPUTERS
A CAMAC system controlled by an IBM AT computer for time-resolved spectroscopy
[DE87-010111] 01 p0060 N88-10514
FORTRAN compiler performance benchmarks for the IBM personal computer
[LA-10663-MS] 03 p0363 N88-12284

An IBM PC version of ASENT
[DE88-004244] 11 p1532 N88-19150
Documentation and installation of the hypersonic arbitrary-body computer program (Mark 3 version) of A.E. Gentry on the IBM computer system
[MBB/UKE-127/S/PUB/256] 13 p1719 N88-20276
The PC/AT compatible computer as a mission control center display processor at Ames-Dryden Flight Research Facility
[NASA-TM-100428] 14 p1955 N88-21654
Specification for IBM/IBM compatible 3480 tape cartridge
[NASA-TM-100702] 17 p2364 N88-24168
Aircraft noise prediction program propeller analysis system IBM-PC version user's manual version 2.0
[NASA-CR-181689] 24 p3428 N88-30399
ICE
NT GLACIERS
NT ICE FLOES
NT ICEBERGS
NT LAND ICE
NT PRESSURE ICE
NT SEA ICE
On the surging potential of polar ice streams. Antarctic surges: A clear and present danger
[DE87-013980] 02 p0216 N88-11363
Altered and enhanced iodargyrite with bismuth triiodide for use in precipitation enhancement operations
[AD-A185229] 05 p0561 N88-13419
Automated satellite cloud analysis: A multispectral approach to the problem of snow/cloud discrimination
[AD-A185672] 06 p0746 N88-14591
Planetary science 07 p0883 N88-15356
Atmospheric science 07 p0883 N88-15357
Recommendations for a US ice coring program
[PB88-115043] 09 p1185 N88-17102
Radar reflectivity and attenuation of radio waves in the melting layer of precipitation
[PB88-121553] 10 p1318 N88-17882
Aircraft and ground vehicle friction correlation test results obtained under winter runway conditions during joint FAA/NASA Runway Friction Program
[NASA-TM-100506] 11 p1438 N88-18582
Multiple scattering of polarized light in cirrus clouds
13 p1801 N88-20768
Predictions and studies with a one-dimensional ice/ocean model
[AD-A189158] 13 p1803 N88-20776
Diversity of comets, synergic temperature effects and the stability of organic compounds in icy nuclei
14 p2005 N88-21955
Different trapping mechanisms of gases by water ice and their relevance for comet nuclei
14 p2007 N88-21970
Sublimation characteristics of H2O comet nucleus with CO2 impurities 14 p2010 N88-21988
Thermal instability and heat transfer characteristics in water/ice systems
[AD-A189827] 15 p2062 N88-22297
Microgravity thaw experiment (MITEX)
17 p2427 N88-24439
Analysis of dust grain properties in two star forming regions through comparison of theoretical models to observations 17 p2451 N88-24559
MIZPAC (marginal ice zone Pacific) 84-86 CTD (Conductivity, Temperature, Depth) data report
[AD-A192476] 21 p2976 N88-27679
Reduce uncertainty in projection of future sea-level changes due to ice wastage
[DE88-009683] 22 p3129 N88-28601
Ice detector
[NASA-CASE-LAR-13776-1] 23 p3217 N88-29149
General equations for the motions of ice crystals and water drops in gravitational and electric fields
[NASA-CR 183229] 24 p3370 N88-30070
ICE ENVIRONMENTS
Blade excitation criteria developed for aero derived engines in Arctic Alaska
[PNR90368] 02 p0182 N88-11131
JPRS report: Science and technology. USSR: Earth sciences
[JPRS-UES-88-001] 13 p1784 N88-20674
Real-time environmental Arctic monitoring (R-TEAM)
[AD-A189948] 15 p2099 N88-22508
ICE FLOES
Underwater acoustic backscatter from a model of arctic ice open leads and pressure ridges
[AD-A184693] 03 p0354 N88-12234
Navarin Basin Ice Drift Program
[PB88-104021] 06 p0748 N88-14599
ICE FORMATION
NT CLOUD GLACIATION
Conception and discussion of a model describing ice formation on various obstacles
[ONERA-NT-1986-6] 01 p0072 N88-10460
The dependence of the normalized ice accretion thickness on cloud-physical parameters
[DFVLR-FB-87-08] 01 p0072 N88-10464
Stability relationship for water droplet crystallization with the NASA Lewis icing spray
[NASA-TM-100220] 02 p0125 N88-10790
On the role of convective motion during dendrite growth: Experiments under variable gravity, revised
[NASA-CR-179213] 02 p0156 N88-10979
Analysis of counting errors in the phase/Doppler particle analyzer
[NASA-TM-100231] 03 p0323 N88-12043
Icing detector with early warning capability
[AOA-4.1.0055] 03 p0325 N88-12050
Experimental evidence for modifying the current physical model for ice accretion on aircraft surfaces
[NASA-TM-87184] 04 p0397 N88-12473
Measured performance of the heat exchanger in the NASA icing research tunnel under severe icing and dry-air conditions
[NASA-TM-100116] 04 p0451 N88-12796
Computation of rime ice accretion on airfoils
[FFA-TN-1987-08] 05 p0542 N88-13301
Measurement of local convective heat transfer coefficients from a smooth and roughened NACA-0012 airfoil: Flight test data
[NASA-TM-100284] 05 p0582 N88-13552
Operating envelopes of particle sizing instrumentation used for icing research
[NASA-CR-180870] 05 p0586 N88-13573
The ice conditions in the Greenland waters, 1981
[ISBN-87-7478-276-2] 05 p0629 N88-13844
A flow visualization study of the leading edge separation bubble on a NACA 0012 airfoil with simulated glaze ice
[NASA-CR-180846] 07 p0816 N88-14966
An experimental mapping of the flow field behind a glaze ice shape on a NACA 0012 airfoil
[NASA-CR-180847] 08 p0950 N88-15766
The NASA aircraft icing research program
08 p0957 N88-15803
NASA's rotorcraft icing research program
09 p1108 N88-16641
Calibration of the ARL (Aeronautical Research Laboratories) rain and icing facility
[AD-A186776] 09 p1121 N88-16710
Evaluation of the magnetic induction conductivity method for detecting frazil ice deposits
[AD-A186940] 09 p1194 N88-17157
Physical and structural characteristics of Weddell Sea pack ice
[AD-A186189] 10 p1358 N88-18119
Three-dimensional trajectory analyses of two drop sizing instruments: PMS OAP and PMS FSSP
[NASA-CR-4113] 11 p1437 N88-18574
Artificial and natural icing tests of AH-64, phase 2
[AD-A188231] 11 p1439 N88-18585
Layered-capacitor method for dielectric bridge measurements. Algorithms for inversion and parameter fitting: Documentation, verification, data analysis
[PB88-131479] 11 p1505 N88-18989
An experimental and theoretical study of the ice accretion process during artificial and natural icing conditions
[NASA-CR-182119] 14 p1865 N88-21143
Bibliography of icing on aircraft (status 1987)
[DFVLR-MITT-87-18] 16 p2158 N88-22876
Reclamation of water contaminated with fuel system icing inhibitor. Phase 1: Literature review and information compilation
[DE88-006575] 16 p2183 N88-23013
Investigation of air transportation technology at Massachusetts Institute of Technology, 1986
17 p2293 N88-23716
In-flight measurement of ice growth on an airfoil using an array of ultrasonic transducers
[AIAA-PAPER-87-0178] 17 p2293 N88-23717
Experimental measurements of heat transfer from an iced surface during artificial and natural cloud icing conditions
[AIAA-PAPER-86-1352] 17 p2293 N88-23718
Ice formation on aircraft
[ETN-88-92154] 18 p2545 N88-25104
National plans for aircraft icing and improved aircraft icing forecasts and associated warning services
18 p2546 N88-25113
Determination of the local heat-transfer characteristics on glaze ice accretions on a cylinder and a NACA 0012 airfoil 21 p2946 N88-27500
New ice detection system 22 p3037 N88-28030
JUH-1H redesigned pneumatic boot deicing system flight test evaluation
[AD-A194918] 24 p3322 N88-29785
Cloud/mesoscale model development and application studies
[AFGL-TR-87-0219] 24 p3404 N88-30269
ICE MAPPING
Navarin Basin Ice Drift Program
[PB88-104021] 06 p0748 N88-14599
Marginal Ice Zone Experiment (MIZEX) 1984 VARAN-S data set
[ETN-88-92032] 14 p1950 N88-21625
ICE OBSERVATION
U ICE REPORTING
ICE PACKS
U SEA ICE
ICE PREVENTION
Boundary layer profile investigations downstream of an aero-engine intake anti-icing air exhaust slot
[PNR90378] 02 p0171 N88-11080
Theoretical analysis of the electrical aspects of the basic electro-impulse problem in aircraft de-icing applications
[NASA-CR-180845] 05 p0543 N88-13310
Laminar flow control leading edge glove flight test article development
[NASA-CR-172137] 07 p0815 N88-14960
Effects of aircraft deicing/anticing fluids on airfoil characteristics 08 p0952 N88-15776
NASA's rotorcraft icing research program
09 p1108 N88-16641
Artificial and natural icing tests of AH-64, phase 2
[AD-A188231] 11 p1439 N88-18585
ICE REPORTING
Eastern - western Arctic Sea ice analysis 1986
[AD-A184016] 03 p0355 N88-12235
The ice conditions in the Greenland waters, 1981
[ISBN-87-7478-276-2] 05 p0629 N88-13844
The Greenland Sea Project: The Arctemiz project
14 p1939 N88-21573
ERS-1 data products and services and their value for tropical countries 17 p2357 N88-24040
Ice conditions along the Ohio River as observed on LANDSAT images, 1972-1985
[AD-A191172] 18 p2531 N88-25018
An experimental study of the coherent under-ice reflectivity of sound in the Greenland Sea Marginal Ice Zone 18 p2548 N88-25125
ICE SHELVES
U LAND ICE
ICEBERGS
Arctic ice island and sea ice movements and mechanical properties
[DE88-004267] 20 p2829 N88-26782
ICELAND
SeaSoar profiles in the Iceland-Scotland area, May 1987
[IOS-253] 18 p2548 N88-25124
Meteorological features during the marginal ice zone experiment from 20 March to 10 April 1987
[AD-A193960] 23 p3235 N88-29251
ICING
U ICE FORMATION
ICOSAHEDRONS
Structural relationship between icosahedral and Frank-Kasper phases of Al-Li-Cu
[AD-A193768] 23 p3195 N88-29011
ICY SATELLITES
NT TITANIA
IDEAL FLUIDS
Instability of steady flow with constant vorticity in vessels with elliptical cross-section 02 p0159 N88-10997
Torsion as a source of expansion in a Bianchi type I universe in the self-consistent Einstein-Cartan theory of a perfect fluid with spin density
[AD-A184200] 03 p0322 N88-12037
Mass transport in annular spherical system
[LRT-WE-9-FB-11(1987)] 22 p3077 N88-28271
IDEAL GAS
Method of calculations for flow of ideal gas through plane and axisymmetric nozzles with broken-line contour
06 p0771 N88-14737
Some performance comparisons for a fluid dynamics code
[PB88-113709] 07 p0852 N88-15175
A new parabolized Navier-Stokes code for chemically reacting flow fields 12 p1625 N88-19721
IDENTIFYING
NT CROP IDENTIFICATION
NT PARAMETER IDENTIFICATION
NT SYSTEM IDENTIFICATION
Foreign language identification: First step in the translation process
[DE87-011065] 02 p0248 N88-11565
Recognition of isolated non-speech sounds
[AD-A184600] 03 p0306 N88-11933
A search for X-ray luminous late type stars in NIPSS data 04 p0511 N88-13143
Bar code document accountability system performance update
[DE88-002256] 06 p0791 N88-14849

Application of knowledge based systems to the maintenance of inertial system electronics
12 p1578 N88-19441
A texture analysis approach to computer vision for identification of roads in aerial photographs
[AD-A189340] 12 p1639 N88-19815
Estimation-correlation, modeling, and identification in adaptive array processors
[AD-A189130] 13 p1757 N88-20512
A comparison of terrain association and resection as methods of position location
[AD-A189480] 13 p1790 N88-20710
Passive DF: A tutorial, part 1
[NASA-CR-182669] 13 p1815 N88-20846
On categorizing sounds
[AD-A189784] 15 p2129 N88-22700
K-pulse estimation from incomplete multiple-frequency scattering data and target identification
[AD-A190827] 16 p2190 N88-23061
An approximation theory for the identification of nonlinear distributed parameter systems
[NASA-CR-181658] 16 p2260 N88-23510
Modeling and performance of HF/OTH (High-Frequency/Over-the-Horizon) radar target identification systems
[AD-A196287] 24 p3365 N88-30038

IDENTITIES
Effects of divided attention on identity and semantic priming
[AD-A184289] 03 p0357 N88-12250
Decoupling identities and predictable transformations in exchangeability
[AD-A186013] 07 p0913 N88-15540

IFR (RULES)
U INSTRUMENT FLIGHT RULES

IGFET
U FIELD EFFECT TRANSISTORS

IGNEOUS ROCKS
NT ANORTHOSITE
NT BASALT
NT ECLOGITE
NT GRANITE
NT PERIDOTITE
Abundance and distribution of ultramafic microbreccia in Moses Rock Dike: Quantitative application of AIS data
05 p0613 N88-13766
Weathering of sulfides on Mars
23 p3301 N88-29662
Volcano evolution on Mars 23 p3305 N88-29686
Pluton emplacement and magmatic arc construction: A model from the Patagonian batholith
24 p3393 N88-30206

IGNIMBRITE
U IGNEOUS ROCKS

IGNITERS
NT BOOSTERS (EXPLOSIVES)
NT DETONATORS
NT INITIATORS (EXPLOSIVES)
NT PRIMERS (EXPLOSIVES)
Pulsed plasma jet igniters: Species measurements in methane combustion
[DE88-001389] 05 p0562 N88-13422
Ignition studies in a two-stage closed vessel using various igniter materials
[ISL-CO-231/86] 09 p1142 N88-16843
An electro-optic explosive igniter
[DE88-004728] 11 p1466 N88-18738
Catalytic ignition of hydrogen and oxygen propellants
[NASA-TM-100957] 18 p2476 N88-24689
Some properties of ignition gases. Review of measuring results in the years 1981-1986)
[PB88-106968] 21 p2908 N88-27259

IGNITION
NT ELECTRIC IGNITION
NT SOLID PROPELLANT IGNITION
NT SPARK IGNITION
Laser probes of natural gas ignition chemistry
[PB87-208699] 01 p0021 N88-10129
Pyrotechnic component development at Sandia National Laboratory
[DE87-006899] 02 p0154 N88-10967
System studies of compact ignition tokamaks
[DE87-014976] 02 p0239 N88-11508
Planning for US ion cyclotron heating research relevant to the compact ignition tokamak and Alcator C-Mod
[DE88-000022] 02 p0241 N88-11520
Relative merits of size, field, and current on ignited Tokamak performance: A comparison of CITs and Super-JETs
[DE88-000038] 02 p0241 N88-11521
Detailed mechanism of benzene oxidation
[NASA-TM-100202] 03 p0282 N88-11775
Photochemical ignition studies. 3: Ignition by efficient and resonant multiphoton photochemical formation of microplasmas
[AD-A184844] 03 p0283 N88-11780
Detailed kinetic modeling of autoignition chemistry
[DE87-013226] 03 p0283 N88-11782
High pressure autoignition of natural gas/air mixtures and the problem of engine knock
[DE87-013799] 03 p0284 N88-11784
Ignition and combustion of metals in oxygen
04 p0407 N88-12530
Proceedings of the Japan-US Workshop P-92 on Plasma Material Interaction/High Heat Flux Data Needs for the Next Step Ignition and Steady State Devices
[DE87-013568] 04 p0494 N88-13042
An experimental investigation of the ignition and flammability limits of various hydrocarbon fuels in a two-dimensional solid fuel ramjet
[AD-A184968] 05 p0549 N88-13342
Ignition and flameholding in supersonic flow by injection of dissociated hydrogen 05 p0560 N88-13410
Pulsed plasma jet igniters: Species measurements in methane combustion
[DE88-001389] 05 p0562 N88-13422
Detailed mechanism of toluene oxidation and comparison with benzene
[NASA-TM-100261] 05 p0563 N88-13428
Jet initiation of PBX 9502
[DE88-000493] 05 p0571 N88-13481
A study of the interaction of laser light with liquid propellant drops
[AD-A185117] 05 p0587 N88-13582
Edge plasmas and plasma/wall interactions in an ignition-class reversed field pinch
[DE88-001825] 06 p0782 N88-14799
TIBER 2 (Tokamak Ignition/Burn Experimental Reactor) parameters with neutral beams at high energies
[DE88-001891] 06 p0783 N88-14803
Overview of the TIBER 2 (Thermal Ignition/Burn Experimental Reactor) design
[DE88-001892] 06 p0783 N88-14804
The carbon dioxide chaperon efficiency for the reaction H + O2 + M yields HO2 + M from ignition delay times behind reflected shock waves
[NASA-TM-100125] 07 p0830 N88-15036
Dimensions of ignition zones in blow-outs of combustible gases from rectangular and circular ports
07 p0918 N88-15577
Poloidal magnetics of compact ignition tokamaks
[DE88-001774] 07 p0934 N88-15672
Calculation evaluation of the boundary conditions of autoinflammation of propulsive charges
[PB87-139044] 08 p0974 N88-15890
DSC (Differential Scanning Calorimeter) stability test for liquid propellants: A preliminary report
[AD-A187115] 09 p1150 N88-16888
EXPLO: Explosives thermal analysis computer code
[DE88-001938] 10 p1307 N88-17814
Flash threshold of shocked aluminum silicofluoride
[DE88-003978] 10 p1339 N88-18005
D-3He fuels in a field-reversed configuration
[IPPJ-855] 10 p1411 N88-18419
On the possibility of high velocity deflagration front propagation by radiative energy transfer
[AD-A189022] 12 p1613 N88-19645
J85-21 fuel nozzle atomization tests
[AD-A189394] 12 p1613 N88-19647
CIT (Compact Ignition Tokamak) fueling
[DE88-002709] 12 p1692 N88-20125
A pyrotechnic delay ignition system for a submarine launched marine signal
[MRL-R-1079] 13 p1754 N88-20487
Numerical modeling of divergent detonation wave
14 p1903 N88-21373
Environmental assessment for the compact ignition Tokamak
[DE88-005633] 15 p2135 N88-22740
Transport simulations of ohmic ignition experiment: IGNITEX
[DE88-006055] 15 p2138 N88-22757
Laser induced ignition of propellants
[AD-A191100] 16 p2168 N88-22927
Laser induced ignition of propellants
[AD-A191099] 16 p2213 N88-23206
Numerical analysis for effects of irradiation nonuniformities on target implosion
16 p2276 N88-23621
Pusherless implosion, pulse tailoring and ignition scaling law for laser fusion 16 p2277 N88-23629
Stability requirement FOT ignition and high gain implosion = 2-D simulation for high neutron yield experiment = 16 p2278 N88-23633
On selfsimilar thermonuclear ignition of a plasma in necks of zeta devices
[DE88-701640] 16 p2280 N88-23647
Catalytic ignition of hydrogen and oxygen propellants
[NASA-TM-100957] 18 p2476 N88-24689
The burning of HAN-based (hydroxylammonium nitrate) liquid propellants
[DE88-006863] 18 p2494 N88-24800
On the use of thermal degradation data to predict cable ignition performance
[DE88-002276] 19 p2621 N88-25549
The 24th JANNAF Combustion Meeting, volume 2
[AD-A190164] 19 p2622 N88-25554
The combustion of hydroxylammonium nitrate based liquid propellants 19 p2622 N88-25555
Comparison of calculated and measured ignition times for boron agglomerates 19 p2624 N88-25563
Recent advances in photochemical techniques for ignition and combustion enhancement
19 p2625 N88-25570
Ignition and flammability characteristics of solid fuel ramjets 19 p2626 N88-25575
The 24th JANNAF Combustion Meeting, volume 1
[AD-A190163] 19 p2627 N88-25585
Dynamics of propellant ignition
19 p2628 N88-25590
How much do edges affect the ignition of a homogeneous reactive solid: Summary to date
19 p2631 N88-25606
Theoretical studies of the chemical reactions involved in the ignition of nitramines 19 p2632 N88-25615
Temperature and species profiles in propellant ignition and combustion 19 p2633 N88-25616
Ignition and flame spread of PMMA
[NASA-TT-20290]. 20 p2771 N88-26431
Thermal and mechanical analysis of the Faraday shield for the compact ignition tokamak
[DE88-007855] 20 p2856 N88-26962
Effects of ceramic surfaces on autoignition in a constant volume combustion apparatus
[AD-A193055] 21 p2909 N88-27266
Laser probes of natural gas ignition chemistry
[PB88-212566] 21 p2910 N88-27271
Development of an experimental system for studying fast transient ignition phenomena
[DE88-011917] 21 p2911 N88-27276
Shock initiation studies on heterogeneous explosives
[DE88-008581] 21 p2923 N88-27351
Diode laser ignition of high explosives and pyrotechnics
[DE88-008771] 21 p2923 N88-27352
Combustion dynamics and thermal structure of a planar spray flame 23 p3190 N88-28985
Semiconductor bridge (SCB) igniter studies. 1: Comparison of SCB and hot-wire pyrotechnic actuators
[DE88-008802] 23 p3200 N88-29046
Ignition and extinguishing of a Solid Fuel Ramjet (SOFRAM)
[FOA-C-20713-2.1] 24 p3337 N88-29865
Gas phase combustion chemistry of nitramine propellants
[AD-A195082] 24 p3344 N88-29902
Flamespreading processes in obliquely loaded stick propellant beds
[AD-A195081] 24 p3352 N88-29956

IGNITION LIMITS
An experimental investigation of the ignition and flammability limits of various hydrocarbon fuels in a two-dimensional solid fuel ramjet
[AD-A184968] 05 p0549 N88-13342
Numerical simulation of ignition of hydrogen jet in hot air 19 p2637 N88-25647

IGNITION SYSTEMS
High pressure autoignition of natural gas/air mixtures and the problem of engine knock
[DE87-013799] 03 p0284 N88-11784
An electro-optic explosive igniter
[DE88-004728] 11 p1466 N88-18738
Flamespreading processes in obliquely loaded stick propellant beds
[AD-A195081] 24 p3352 N88-29956

IGNITION TEMPERATURE
NT FLASH POINT
Ignition and flame propagation in sprays
[AD-A184679] 03 p0283 N88-11781
A neutral-beam diagnostic for fast confined alpha particles in a burning plasma: Applicatoin on CIT (Compact Ignition Tokamak)
[DE88-004890] 11 p1554 N88-19301

ILLINOIS
TABLET: The personal computer of the year 2000
[NASA-CR-182528] 10 p1384 N88-18267

ILLUMINANCE
Monte Carlo method calculation of spectral brightness coefficient of vegetation cover as function of illumination conditions 08 p1006 N88-16113
Influence of solar illumination conditions on TM/Landsat data
[INPE-4463-TDL/320] 12 p1638 N88-19806
Analysis of the parameters responsible for the variations of the illumination conditions in the LANSAT data
17 p2362 N88-24070

ILLUMINATING

The optimum illumination conditions for EXELFS studies in a CTEM [USIP-87-08] 01 p0092 N88-10600

Photoinduced low-temperature changes in optical losses in fiber optics based on chalcogenide glasses 06 p0770 N88-14731

Fish as a tool for testing fitness in space 12 p1662 N88-19963

Botany Facility: Breadboarding results of the illumination system [SIRA-A/7373/WP110/MAC003] 17 p2378 N88-24137

Optical system of laser illuminated streamer chamber [DE88-702127] 18 p2577 N88-25306

Maintenance of vision-related components 23 p3242 N88-29296

Night lighting and night vision goggle compatibility 23 p3242 N88-29297

ILLUMINATION

Plant Growth Module (PGM) conceptual design 05 p0631 N88-13855

ILLUSIONS

Eye movements and spatial pattern vision [AD-A195496] 24 p3408 N88-30290

ILS (LANDING SYSTEMS)

U INSTRUMENT LANDING SYSTEMS

IMAGE ANALYSIS

Masking effects of fine and coarse grain pictorial noise [IZF-1985-21] 01 p0076 N88-10485

Input/output technologies: An overview of image scanning, storage, and display [DE87-014837] 04 p0476 N88-12833

On the recognition of curved objects [AD-A184441] 04 p0478 N88-12845

Determination of the fiber ratio in carbon fiber/resin composites by means of image analysis [SNIAS-872-422-101] 05 p0558 N88-13398

Land cover/use classification of Cairns, Queensland, Australia: A remote sensing study involving the conjunctive use of the airborne imaging spectrometer, the large format camera and the thematic mapper simulator 05 p0612 N88-13759

A unified mathematical approach to image analysis [AD-A185719] 06 p0765 N88-14703

Some vision algorithms 06 p0795 N88-14871

An investigation of offshore circulation using satellite data and feature tracking techniques [AD-A186271] 07 p0861 N88-15347

A knowledge-based object recognition system for applications in the space station [NASA-CR-182411] 08 p0989 N88-15991

Space photographs of the Onega-Ladoga isthmus and prediction of useful minerals 08 p1006 N88-16106

Study of relief of ore regions using space images (on the example of Eastern Yakutia) 08 p1008 N88-16111

Processing of radar images of Venus on the Magiscan-2 analyzer 08 p1009 N88-16117

Thematic mapper research in the earth sciences: Small scale patches of suspended matter and phytoplankton in the Elbe River Estuary, German Bight and Tidal Flats [NASA-CR-182378] 08 p1019 N88-16180

Textural features for image classification in remote sensing [INPE-4169-PRE/1066] 08 p1020 N88-16181

Digital image processing [INPE-4131-TDL/264] 08 p1083 N88-16527

Nature and origin of mineral coatings on volcanic rocks of the Black Mountain, Stonewall Mountain, and Kane Springs Wash volcanic centers, Southern Nevada [NASA-CR-181437] 09 p1191 N88-17140

A procedure for automatic classification of crop areas [INPE-4467-PRE/1240] 13 p1790 N88-20706

Exact image method for Gaussian beam problems involving a planar interface [NASA-CR-182702] 14 p1905 N88-21380

Classification of small image areas by digital correlation for the connection of different images in photogrammetry and long-range reconnaissance [ETN-88-91506] 14 p1940 N88-21578

On the geometric interpretation of image contours [RR-647-I-IMAG-57-LIFIA] 15 p2109 N88-22563

Conversational Analysis of Color Images (CAICOU): An interactive development system for the analysis of color images [RR-641-I-IMAG-39-LIFIA] 17 p2342 N88-23964

Textural features for image classification in remote sensing 17 p2354 N88-24027

Practical image analysis using personal computers: The Canadian experience 17 p2356 N88-24037

A proposal of adaptation of a knowledge-based scene analysis model to some remote sensing problems 17 p2362 N88-24068

Interpretation of MSS/LANDSAT data for evaluation of physical distribution of mangroves in Cananeia-Iguape (SP) 17 p2363 N88-24072

An update on remote measurement of soil moisture over vegetation using infrared temperature measurements: A FIFE perspective [NASA-CR-182926] 17 p2370 N88-24109

Generic cueing in image understanding [RSRE-MEMO-4109] 17 p2386 N88-24181

Linguistic definition of generic models in computer vision [RSRE-MEMO-4110] 17 p2386 N88-24182

Mathematical morphology for structures without translation symmetry [CWI-AM-R8803] 18 p2566 N88-25241

Real-time image difference detection using a polarization rotation spacial light modulator [NASA-CASE-NPO-17144-1-CU] 18 p2576 N88-25305

Separability of cultivation through digital analysis of SPOT and TM data [INPE-4541-PRE/1287] 19 p2685 N88-25963

Bathymetry estimation by analyzing swell on SPOT images 19 p2701 N88-26062

Image pyramid motion detection applied to sea ice 20 p2817 N88-26713

Processing and analysis of images transmitted by Vega space probes over Halley's comet [ETN-88-92291] 20 p2885 N88-27131

Automatic line network extraction from aerial imagery of urban areas through knowledge based image analysis [AD-A193067] 21 p2965 N88-27615

Remote sensing of wetlands: Applications overview [DE88-010895] 21 p2966 N88-27618

Mapping of streamflow and soil infiltration of a Sahelian catchment area by SPOT image interpretation: The Oursi pond catchment area in Burkino Faso 22 p3090 N88-28348

Evaluation of automatic texture analysis for increased crop identification accuracy with SPOT data 22 p3094 N88-28373

Digital and visual analysis of SPOT and TM data for crop discrimination in southern Brazil 22 p3096 N88-28385

Discrimination methods of traditional fields in a humid tropical region (Shaba, Zaire) using digital classification on SPOT data 22 p3096 N88-28387

Identification of farming systems in the cotton area of West Burkina Faso from SPOT-1 data 22 p3097 N88-28389

Monitoring urban land cover changes at the urban fringe from SPOT HRV imagery in south-east England 22 p3099 N88-28406

Analysis of SPOT multispectral data concerning a border zone between two geographical regions in southern Belgium 22 p3100 N88-28411

Applications of SPOT data for urban real estate investment information systems 22 p3101 N88-28414

Mapping and urban multi-experimental assessment of SPOT: Urban results 22 p3101 N88-28415

SPOT-1 over New Zealand: Analysis of SPOT imagery for land use investigations 22 p3101 N88-28416

Comparison of SPOT, LANDSAT TM and combined data for urban studies 22 p3101 N88-28417

Utilization of SPOT multispectral data for urban planning 22 p3101 N88-28418

First results of international investigations of the applications of SPOT-1 data to geologic problems, mineral and energy exploration 22 p3101 N88-28419

Rate of slip on the Altin Dagh Fault (North Tibet, China) 22 p3102 N88-28420

Karst and submarine fresh water discharge in the Antalya area, southern Turkey 22 p3102 N88-28421

Results of the Geosat program to evaluate SPOT data for petroleum and mineral exploration 22 p3102 N88-28422

The application of SPOT data to the structural geology of western Nevada 22 p3102 N88-28423

Application SPOT-1 data to mining activity: Example of the Imiter Silver Mine, Morocco 22 p3102 N88-28424

Evaluation of SPOT imagery contribution to petroleum exploration: The Suez Rift (Egypt) 22 p3102 N88-28425

Evaluation of SPOT imagery for discriminating vegetation communities associated with surficial and bedbrock geology and identifying anomalous and stressed vegetation associated with mineralization 22 p3103 N88-28426

SPOT imagery as an aid to understanding volcanism and tectonics: Examples from the Chilean Andes and the Tibetan Plateau 22 p3103 N88-28427

Role of SPOT in geological application of remote sensing 22 p3103 N88-28428

SPOT imagery preliminary contribution to cartography and geodynamics in the Benue trough (Nigeria) 22 p3103 N88-28429

An evaluation of SPOT imagery for Earth science studies in the Antarctic. Preliminary Evaluation Program (PEPS) 289 for SPOT 22 p3103 N88-28430

Structural analysis of the Jura mountains-Rhine Graben intersection (Switzerland) for petroleum exploration using SPOT stereoscopic data 22 p3103 N88-28431

Methodology for the use of SPOT imagery in petroleum exploration. Example of the Bas-Languedoc area (France) 22 p3104 N88-28432

Analyzing the stratigraphy, tectonism, and mineralization at the Spanish side of the pyrite belt, Huelva province, Spain, using SPOT imagery 22 p3104 N88-28433

Geologic applications of SPOT-1, TM, and NOAA-7 data: Finding and defining unmapped structural features 22 p3104 N88-28434

Spectral and spatial attribute evaluation of SPOT data in geological mapping of precambrian terrains in semiarid environment of Brazil 22 p3104 N88-28436

Geologic results obtained from the use of SPOT imagery along plate boundaries: Examples in the East African rift and of the northern-Caribbean collision 22 p3105 N88-28437

SPOT images and geochemical mapping of lateritic covers in southern Mali 22 p3105 N88-28438

Analysis of the multispectral content and of SPOT subscenes in two regions of Burundi. Lithologic and tectonic interpretations 22 p3105 N88-28439

SPOT imagery for landslide cartography in mountainous areas. Example of the French Maritime Alps 22 p3105 N88-28440

SPOT for slope instability survey in Nepal 22 p3105 N88-28441

Detailed geological mapping of the massif of Sainte Victoire (Provence, France) using SPOT imagery. Comparison with other multisource data. New tectonic interpretation of this region 22 p3105 N88-28442

An evaluation of the utility of SPOT and Thematic Mapper data for providing forest inventory information 22 p3106 N88-28444

SPOT-1 satellite imagery for forest inventory in Sweden 22 p3106 N88-28445

Forest mapping by visual interpretation of SPOT images 22 p3106 N88-28446

SPOT multispectral data and maritime pine stands in southwest of France 22 p3106 N88-28448

Stand-based forestry inventory from SPOT image 22 p3106 N88-28449

Potential of SPOT imagery as a tool for forest mapping in Quebec 22 p3107 N88-28450

Assessment of large area forest disturbances caused by biotic and abiotic factors on the basis of SPOT images 22 p3107 N88-28451

Study of deforestation in the Vosges (France) by remote sensing 22 p3107 N88-28452

Contribution to the mapping of forests in an intensively divided area, with the help of SPOT image data 22 p3107 N88-28453

SPOT 1: Image utilization, assessment, results. A study of the Elburgon Forest area (Kenya) showing the spectral responses of different forest tree species 22 p3107 N88-28454

SPOT investigations of estuaries and coastal zones. An overview 22 p3107 N88-28455

SPOT: A tool to aid preselection of sites favorable for aquiculture. Evaluation and perspectives of the Preliminary Evaluation Program for SPOT (PEPS) ALIAS Caledonie 22 p3108 N88-28456

The monitoring of sediment transport, water circulation and mixing in estuaries and coastal waters 22 p3108 N88-28457

Evaluation of SPOT data for remote sensing of physical and biological properties of estuaries and coastal zones 22 p3108 N88-28458

Physiography and kinematics of the western coast of the province of Huelva (Andaloucia, Spain) 22 p3109 N88-28465

The use of SPOT imagery on analytical photogrammetric instruments 22 p3110 N88-28471

SPOT images features extraction 22 p3114 N88-28496

SEP/VIPS 32 geographic information system. Processing and thematic analysis of images, maps, and associated data 22 p3114 N88-28499

Summary of analysis and processing techniques used on SPOT imagery 22 p3115 N88-28503

Automatic line network extraction from aerial imagery of urban areas through knowledge-based image analysis [AD-A192399] 23 p3227 N88-29208

Evaluation of LANDSAT-TM data for geomorphological mapping [INPE-4593-PRE/1324] 24 p3386 N88-30168

Autonomous image data reduction by analysis and interpretation 24 p3418 N88-30347

IMAGE CONTRAST

Performances of an Actively Stabilized Stellar Interferometer (ASSI): Faint magnitudes, low fringe contrast measurements and operationality
01 p0097 N88-10641

Development and validation of transmission measurements techniques of image contrast, utilizing existing IR imagers
[AD-A191471] 18 p2541 N88-25079

The FEL CCD-camera: Experimental system for camera and image processing research
[FEL-1987-34] 21 p2952 N88-27532

IMAGE CONVERTERS

NT IMAGE TUBES

Multilayered foils as radiation entrance windows and spectral filters for image converters in the ultrasoft X-ray wavelength region
[MPE-PREPRINT-90] 02 p0176 N88-11099

Dynamics Explorer guest investigator
[NASA-CR-181494] 07 p0878 N88-15325

Suspension of small metallic plates: A versatile sensor
[PB88-130901] 11 p1487 N88-18874

IMAGE CORRELATORS

Statistical investigations of the behavior of a product correlator and an edge detector in critical situations
[MBB-UA-1034/87] 06 p0781 N88-14793

Image correlation on an IBM-PC for characterization of advanced ceramics
[DE88-002629] 09 p1149 N88-16865

Classification of small image areas by digital correlation for the connection of different images in photogrammetry and long-range reconnaissance
[ETN-88-91506] 14 p1940 N88-21578

A high dynamic range acousto-optic image correlator for real-time pattern recognition
[DE88-007933] 19 p2726 N88-26191

IMAGE DISSECTOR TUBES

Visual display representation of multidimensional systems: The effect of information correlation and display integrality
[AD-A188655] 12 p1672 N88-20010

IMAGE ENHANCEMENT

A general solution to the silhouette problem
[NASA-TP-2695] 06 p0755 N88-14629

Digital enhancement of flow field images
[NASA-TP-2770] 13 p1813 N88-20833

Weighted averaging method for image smoothing reported 14 p1901 N88-21352

Utilization of space color transformation, linear contrast and filtration for enhancement of colored digital images
[INPE-4310-PRE/1176] 14 p1983 N88-21831

Dynamic range compression/expansion of light beams by photorefractive crystals
[NASA-CASE-NPO-17140-1-CU]
17 p2438 N88-24508

Enhancement of modeling and image generation techniques for high-resolution 3-dimensional imagery
[DE88-008923] 21 p2998 N88-27782

IMAGE FILTERS

Multilayered foils as radiation entrance windows and spectral filters for image converters in the ultrasoft X-ray wavelength region
[MPE-PREPRINT-90] 02 p0176 N88-11099

Parallel algorithms for computer vision on the connection machine
[AD-A185842] 07 p0901 N88-15456

Optimization of imaging energy filters for analytical electron microscopy
[ETN-88-91079] 09 p1248 N88-17483

Photographic filters
[INPE-4446-RPE/558] 12 p1692 N88-20124

IMAGE FURNACES

Zone crystallization experiments in mirror heating facilities
[BMFT-FB-W-86-023] 16 p2184 N88-23016

IMAGE INTENSIFIERS

Development, testing and evaluation of a night vision goggle compatible BO-105 for night low level operation
03 p0265 N88-11668

A high-speed, eight-frame image intensified electro-optic camera with 200-800mm zoom objective capability
[DE88-000229] 03 p0326 N88-12059

Determination of the origin of self-pumped phase conjugation in barium titanate
[AD-A184697] 03 p0377 N88-12372

Increased gain of channel intensifier tubes by pulsed biasing
[DE88-000512] 04 p0490 N88-13019

A focussed MCP (microchannel plate) image intensifier type for high speed gating
[DE88-000480] 05 p0583 N88-13555

Streak camera dynamic range optimization
[DE88-001632] 05 p0586 N88-13571

High-resolution Real-Time Radiography (RTR) system design
[AD-A187107] 09 p1186 N88-16992

Signal processing studies program optical signal amplification, volume 1
[AD-A188055] 10 p1321 N88-17897

Performance of a photon counting microchannel plate intensifier with wedge and strip image readout
[DE88-003831] 10 p1334 N88-17970

Study of the ionic and neutral species in the coma of Comet Halley with an image intensifier camera
14 p2006 N88-21962

Four-frame gated optical imager with 120-ps resolution
[DE88-011735] 22 p3080 N88-28288

The application of an image intensifier to atmospheric Cerenkov gamma ray astronomy
[MPE-PREPRINT-115] 22 p3163 N88-28839

IMAGE MOTION COMPENSATION

Self calibration of motion and stereo vision for mobile robot navigation
[AD-A185602] 06 p0781 N88-14794

A directed method for locating the focus of expansion
[AD-A185840] 07 p0906 N88-15491

Relaxing the brightness constancy assumption in computing optical flow
[AD-A187437] 10 p1410 N88-18410

IMAGE PROCESSING

NT GEOMETRIC RECTIFICATION (IMAGERY)

Study, design, and evaluation of data reduction by encoding or information extraction. Part 1: Data generation analysis — multispectral satellite imagery
[NLR-TR-85094-L-PT-1] 01 p0078 N88-10501

Study, design and evaluation of data reduction by encoding or information extraction. Part 2: Operational considerations — multispectral satellite imagery
[NLR-TR-85094-L-PT-2] 01 p0079 N88-10502

Study, design and evaluation of data reduction by encoding or information extraction. Part 4: Performance demonstration — multispectral satellite imagery
[NLR-TR-85094-L-PT-4] 01 p0079 N88-10504

Estimation of the position and orientation of objects using associative memories
[ESA-TT-1034] 01 p0079 N88-10507

Report outline of a programming variable and application through example
[INPE-4211-PRE/1092] 01 p0081 N88-10521

Unified Sun and sky illumination for shadows under trees
[DE87-014232] 01 p0083 N88-10535

Imaging at radio wavelengths
01 p0094 N88-10616

Diagnostic technique for monitoring high temperature plasma dynamics
[DE87-011786] 01 p0099 N88-10653

Personal Computer (PC) based image processing applied to fluid mechanics
[NASA-TM-100024] 02 p0172 N88-11087

How we get pictures from space, revised edition
[NF-151/7-87-REV] 02 p0193 N88-11203

Operational cloud-clearing techniques of VAS radiance data — Visible and Infrared Spin Scan Radiometer Atmospheric Sounder (VAS) 02 p0201 N88-11256

Automated detection of severe thunderstorms using geosynchronous infrared data 02 p0201 N88-11257

The use of McIDAS as a Mesoscale forecasting tool during the Canadian Atlantic storms programs — Man-computer Interactive Data Access System (McIDAS) 02 p0205 N88-11264

A preliminary taxonomy of visible surface algorithms
[DE87-013559] 02 p0220 N88-11386

Projection-space iterative interpolation for limited-angle tomography in parallel- and fan-beam geometry, part 1
[DE87-013965] 02 p0221 N88-11391

Pyroelectric line scanner for remote IR imaging of vehicles
[DE87-012127] 02 p0235 N88-11484

Description of a multiframe optical probing system
[DE87-014255] 02 p0236 N88-11487

Fundamentals and techniques of nonimaging optics research
[DE87-014544] 02 p0236 N88-11488

Preliminary estimation of color inhomogeneities on the surface of Venus according to the television images obtained by the VENERA-13 and VENERA-14 automated space probes
[NASA-TT-20114] 02 p0254 N88-11606

Dynamic image interpretation for autonomous vehicle navigation
[AD-A184043] 03 p0262 N88-11647

Helicopter fire control: Advantages of an automatic target tracker 03 p0264 N88-11667

Delay-Doppler radar imaging
[AD-A184165] 03 p0306 N88-11943

SPOT 1: First In-Flight Results — conferences
[ISBN-2-85428-177-2] 03 p0340 N88-12143

Results of the satellite and the Toulouse (France) receiving station operator — SPOT
03 p0341 N88-12149

Detector normalization — SPOT remote sensors
03 p0341 N88-12151

Registration of SPOT images
03 p0341 N88-12155

Adaptation of numerical SPOT data to an urban environment 03 p0342 N88-12158

Geological interpretation of a SPOT image over Kenya: The Gregory rift network of faults
03 p0343 N88-12164

SPOT data for crop discrimination in southern Brazil
03 p0343 N88-12169

A review of computer-assisted photo interpretation research at USAETL (US Army Engineer Topographic Laboratories)
[AD-A184034] 03 p0346 N88-12186

Algorithms and hardware for efficient image smoothing
[TR-149] 03 p0365 N88-12296

Issues in image processing software development for a multi-user, multi-programming environment
[DE88-000358] 03 p0365 N88-12298

End of year report for parallel vision algorithm design and implementation
[AD-A184327] 03 p0366 N88-12301

Recognizing rigid objects by aligning them with an image
[AD-A184253] 03 p0368 N88-12318

Low-level vision on warp and the apply programming model
[AD-A184330] 03 p0369 N88-12320

Image processing for optical engineering applications
[PB87-210035] 03 p0376 N88-12364

An application of a gradient relaxation method to noisy infrared images
[AD-A184666] 03 p0377 N88-12371

Programmable real-time digital video image processing
[PB87-104162] 04 p0430 N88-12661

Design of source coders and joint source/channel coders for noisy channels
[NASA-CR-181547] 04 p0432 N88-12678

Tracking through turbulence at the Tonopah Test Range
[DE88-001448] 04 p0446 N88-12766

Cloud cover determination in polar regions from satellite imagery
[NASA-CR-181544] 04 p0471 N88-12906

Input/output technologies: An overview of image scanning, storage, and display
[DE87-014837] 04 p0476 N88-12933

Computer-aided X-ray image system design and evaluation
[DE88-000997] 04 p0481 N88-12965

Correction of inertial navigation system drift errors for an autonomous land vehicle using optical radar terrain data
[AD-A184973] 05 p0544 N88-13311

Television motion measurement for DATV and other applications
[BBC-RD-1987/11] 05 p0573 N88-13496

Italy's Institute of Research on Electromagnetic Waves--the Istituto di Ricerca sulle Onde Elettromagnetiche
[AD-A185020] 05 p0574 N88-13501

Study on data compression systems for operational remote sensing — meteosat imagery
[NLR-TR-86029-L] 05 p0620 N88-13808

Matching segments from a map and an aerial image using relaxation techniques
[SNIAS-872-422-103] 05 p0620 N88-13809

Learning a color algorithm from examples
[AD-A184385] 05 p0632 N88-13852

A prototype ray tracer
[AD-A184863] 05 p0634 N88-13874

The use of color in electronic maps. Part 1: Generation and analysis of color on the Gould/DeAnza image processing system
[IZF-1986-32] 05 p0635 N88-13882

The maximum likelihood estimator method of image reconstruction: Its fundamental characteristics and their origin
[DE88-000462] 05 p0636 N88-13892

Full field visualization of surface and bulk acoustic waves using heterodyne holographic interferometry
[AD-A185071] 05 p0648 N88-13958

X-ray imaging: Status and trends
[DE88-000758] 05 p0649 N88-13960

Two digital X-ray imaging systems for applications in X-ray diffraction
[PB87-123683] 06 p0669 N88-14103

Optical seam tracking in robotic arc welding
[VTT-RR-463] 06 p0713 N88-14378

A general solution to the silhouette problem
[NASA-TP-2695] 06 p0755 N88-14629

An orthogonal oriented quadrature hexagonal image pyramid
[NASA-TM-100054] 06 p0755 N88-14630

Algorithms and programming tools for image processing on the MPP-3
[NASA-CR-182349] 06 p0757 N88-14841
Virtual image processor: A prototype implementation
[AD-A185580] 06 p0758 N88-14852
A unified mathematical approach to image analysis
[AD-A185719] 06 p0765 N88-14703
New description of Lau effect based on theory of raster image forming process 06 p0772 N88-14744
Selection of holographic screen for projection of images reconstructed by multiaspect holograms of focused images 06 p0773 N88-14745
Self calibration of motion and stereo vision for mobile robot navigation
[AD-A185602] 06 p0781 N88-14794
Characterization of microstructure in metallic and composite materials
[AD-A186193] 07 p0826 N88-15012
Texture study of Synthetic Aperture Radar (SAR) images of ocean surfaces
[AD-A186021] 07 p0841 N88-15101
Electronic imaging technique for welding and other high-luminosity processes
[DE88-002199] 07 p0862 N88-15227
Model-based building verification in aerial photographs
[AD-A186010] 07 p0870 N88-15278
Optimization of photogrammetric image adjustment
[SER-C-323] 07 p0872 N88-15288
Theory and research on the disjunction of cross passage errors and systematic image errors in photogrammetric point determination
[SER-C-324] 07 p0872 N88-15290
Parallel algorithms for computer vision on the connection machine
[AD-A185842] 07 p0901 N88-15456
Proceedings of Image Understanding Workshop, volume 1
[AD-A186103] 07 p0902 N88-15463
Proceedings of Image Understanding Workshop, volume 2
[AD-A186104] 07 p0902 N88-15464
Image processing language development
[AD-A186251] 07 p0903 N88-15467
Sound pressure distribution in front of a serrated boundary: Standing wave suppression and diffusion
07 p0928 N88-15639
Feasibility studies of optical processing of image bandwidth compression schemes
[AD-A186073] 07 p0932 N88-15660
Active control of jet flowfields
[AD-A186736] 08 p0989 N88-15969
A knowledge-based object recognition system for applications in the space station
[NASA-CR-182411] 08 p0989 N88-15991
Modeling of architecture of a problem-oriented on-board processor 08 p1006 N88-16114
Textural features for image classification in remote sensing
[INPE-4169-PRE/1066] 08 p1020 N88-16181
Evaluation of the flooding areas of the Sao Goncalo Canal through LANDSAT 5 thematic mapper images
[INPE-4118-PRE/1039] 08 p1020 N88-16185
The power of neural nets 08 p1064 N88-16430
Digital image processing: A summary of main techniques
[INPE-4404-PRE/1220] 08 p1068 N88-16454
Digital image processing
[INPE-4131-TDL/264] 08 p1083 N88-16527
Earthnet's experience with Seasat SAR image processing 09 p1127 N88-16760
The Earthnet Heat Capacity Mapping Mission (HCMM) data-processing system at Lannion (France)
09 p1127 N88-16761
Parallel-processing computer systems and their possible applications in the agency 09 p1128 N88-16774
Technical assessment of the joint CSIRO/Bureau of Meteorology proposal for a geostationary imager/sounder over the Australian region
[RTP-15] 09 p1135 N88-16811
Image correlation on an IBM-PC for characterization of advanced ceramics
[DE88-002629] 09 p1149 N88-16885
Backscattering signal analysis concerning a three-dimensional object configuration on the basis of object motion
[ESA-TT-1044] 09 p1154 N88-16915
Unsteady behavior of three-dimensional vortices relevant to turbulent boundary layers
[AD-A186767] 09 p1161 N88-16958
Techniques of flow visualization
[AGARD-AG-302] 09 p1164 N88-16977
Flat-field responses and geometric distortion measurements of optical streak cameras
[DE88-002394] 09 p1168 N88-17005
Performance of a digital real time radiographic imaging system
[MRL-R-1068] 09 p1169 N88-17011
Nature and origin of mineral coatings on volcanic rocks of the Black Mountain, Stonewall Mountain, and Kane Springs Wash volcanic centers, Southern Nevada
[NASA-CR-181437] 09 p1191 N88-17140
Meteorological Information Extraction Center (MIEC) processing — Meteosat imagery
[ESA-STR-224] 09 p1192 N88-17143
Sea surface current estimates off central California as derived from enhanced AVHRR (Advanced Very High Resolution Radiometer) infrared images
[AD-A186867] 09 p1194 N88-17155
Image chunking: Defining spatial building blocks for scene analysis
[AD-A187072] 09 p1200 N88-17191
Vision algorithms and psychophysics
[AD-A186773] 09 p1200 N88-17193
Handbook of the GEMS image processing system
[RAE-TR-86062] 09 p1219 N88-17310
A comparison of algorithms for the analysis of images generated by two-dimensional electrophoresis
[DE88-003730] 09 p1220 N88-17319
Comparison of a few methods of restoring images distorted by atmospheric turbulence
[ESA-TT-1065] 09 p1248 N88-17481
Transport delay compensation for computer-generated imagery systems
[NASA-TM-100084] 10 p1277 N88-17645
Instrumentation and quantitative methods of evaluation
[DE87-013639] 10 p1342 N88-18017
A smart, mapping, charting and geodesy control generator, phase 1
[AD-A188184] 10 p1347 N88-18055
Autocorrelation of control points on 11-band multispectral imagery
[AD-A188185] 10 p1348 N88-18056
Image texture classification with an optical crossbar interconnected processor 10 p1375 N88-18202
New generation imager system
[NASA-CR-180464] 10 p1408 N88-18398
Multidimensional system analysis of electro-optic sensors with sampled deterministic output
[AD-A187083] 10 p1408 N88-18399
Simulation and processing of high resolution images of defects and interfaces in superconducting YBa2Cu3O7
[DE88-003856] 10 p1420 N88-18480
Air Force geographic information and analysis system
[DE88-001420] 10 p1424 N88-18505
Fixed and adaptive interframe image prediction for remote piloting application
[AD-A187987] 11 p1471 N88-18771
Imaging methods for nondestructive materials testing
[ETN-88-91477] 11 p1497 N88-18940
Three-dimensional image generation from an aerial photograph
[AD-A188039] 11 p1503 N88-18979
The Quick Response Multicolor Printer (QRMP) system
[AD-A188140] 11 p1504 N88-18982
Geophysical diffraction tomography for imaging isolated subsurface inclusions
[DE88-003918] 11 p1505 N88-18990
Ideal shrinking and expansion of discrete sequences
[NASA-TM-88202] 11 p1524 N88-19100
A unified approach for digital image processing problems: Mathematical morphology
[INPE-4311-TDL/278] 11 p1537 N88-19183
Solar radiomage restoration
[INPE-4312-TDL/279] 11 p1571 N88-19402
Three-dimensional information from stereovision process 12 p1593 N88-19540
Measuring accuracy of 3-dimensional bodies by the GOMER-1 device
[DE87-703230] 12 p1626 N88-19744
Automated stereophotogrammetry
[AD-A188617] 12 p1630 N88-19757
Report on phase 1 of the project estimate development of a model for yield estimation of sugar cane based on LANDSAT and agromet data
[INPE-4466-RPE/560] 12 p1636 N88-19807
Automatic knowledge acquisition for aerial image interpretation
[AD-A188616] 12 p1638 N88-19810
Visual display representation of multidimensional systems: The effect of information correlation and display integrality
[AD-A188855] 12 p1672 N88-20010
Procedure for initial data input and checkup in the system for film data mathematical processing
[DE88-700826] 12 p1676 N88-20022
Image segmentation via fractal dimension
[AD-A188625] 12 p1678 N88-20033
Applications of mathematical morphology to range imagery
[AD-A189316] 12 p1684 N88-20072
Three-dimensional image reconstruction in object space
[DE88-900279] 12 p1712 N88-20248
Recent developments in nondestructive evaluation for structural ceramics
[DE88-005889] 13 p1751 N88-20473
A hybrid transform/DPCM encoder for data compression
[DE87-014852] 13 p1758 N88-20518
Dynamics of high-speed mechanisms with elastic members 13 p1779 N88-20643
Analysis for architecture for image processing
[INPE-4294-PRE/1165] 13 p1791 N88-20715
Bathymetric hazard survey test
[AD-A189150] 13 p1803 N88-20775
Retinotopic mapping of the human visual system with magnetoencephalography
[AD-A189557] 13 p1810 N88-20811
Digital enhancement of flow field images
[NASA-TP-2770] 13 p1813 N88-20833
On relaxation algorithms based on Markov random fields
[AD-A189043] 13 p1814 N88-20840
Method to evaluate image-recovery algorithms based on task performance
[DE88-005382] 13 p1816 N88-20853
Parallel graphical output from dialogue cells
[CWI-CS-R8719] 13 p1818 N88-20867
On effectively labeling planar projections of polyhedra
[CWI-CS-R8715] 13 p1826 N88-20917
Passive autonomous infrared sensor technology
[AD-A188698] 13 p1839 N88-21005
Weighted averaging method for image smoothing reported 14 p1901 N88-21352
Classification of small image areas by digital correlation for the connection of different images in photogrammetry and long-range reconnaissance
[ETN-88-91506] 14 p1940 N88-21578
Generalised threshold selection for edge detection
[RAE-TR-87035] 14 p1941 N88-21581
Oceanographic export system development, year 1
[AD-A189134] 14 p1950 N88-21623
Definition and display of profiled sweep-objects — computer graphics
[REPT-87-45] 14 p1957 N88-21665
Proposal for a parallel system with image processing applications
[INPE-4293-PRE/1164] 14 p1961 N88-21696
The application of thermal imaging sensors and image processing techniques to a short range surface-to-air missile system
[ETN-88-92080] 14 p1982 N88-21829
Utilization of space color transformation, linear contrast and filtration for enhancement of colored digital images
[INPE-4310-PRE/1176] 14 p1983 N88-21831
Image processing on VEGA pictures
14 p2009 N88-21983
Focused image holography abberations
[DE88-701105] 15 p2066 N88-22333
Systems for ultrasonic scanning, analysis and imagery
15 p2082 N88-22414
Satellite UV image processing
[AD-A190466] 15 p2089 N88-22451
Method for restoration and resampling of TM sensor imagery
[INPE-4491-PRE/1255] 15 p2090 N88-22454
A hardware/software system for implementing geophysical diffraction tomography
[DE88-006411] 15 p2094 N88-22480
Calibration and processing of AVHRR data for temperature estimation
[INPE-4493-PRE/1257] 15 p2095 N88-22486
Multiple-transform pipelines for image coding
[REPT-87-038] 15 p2108 N88-22561
On the geometric interpretation of image contours
[RR-647-I-IMAG-57-LIFIA] 15 p2109 N88-22563
Rapid feature extraction via the radon transform
[AD-A190032] 15 p2110 N88-22573
Design and implementation of VLSI prime factor algorithm processor
[AD-A190483] 15 p2112 N88-22580
Contour interactive extraction using image numerical treatment
[ISL-R-114/86] 15 p2113 N88-22587
Modeling a parallel architecture for image processing
[RR-648-I] 15 p2114 N88-22593
Finding texture boundaries in images
[AD-A190554] 15 p2117 N88-22609
Multi-disciplinary techniques for understanding time-varying space-based imagery
[AD-A190711] 15 p2117 N88-22610

Concurrent algorithms for a mobile robot vision system
[DE88-005850] 15 p2117 N88-22614

Rigidity and smoothness of motion
[AD-A190555] 15 p2128 N88-22694

ROVER: A prototype active vision system
[AD-A189246] 15 p2133 N88-22722

Flow velocity measurements by image processing of optically modulated traces 16 p2203 N88-23147

The radiometric processing of SLAR measuring values using the PARES program
[BCRS-86-04] 16 p2227 N88-23301

Results of the testing of the segmentation program on RESEDA
[BCRS-87-01] 16 p2228 N88-23304

Stochastic approach of image segmentation: A model of cooperation between region primitives and boundaries
[ETN-88-92192] 16 p2262 N88-23523

Activities report of the imagery Department
[ENST-87D008] 16 p2273 N88-23604

Visual enhancement of digital color imagery utilizing transformation in color coordinates (IHS transformation)
[INPE-4482-PRE/1248] 16 p2273 N88-23606

Adaptive segmentation evaluation
[AD-A190965] 16 p2274 N88-23609

Sensitivity of F-106B leading-edge-vortex images to flight and vapor-screen parameters
[NASA-TP-2818] 17 p2300 N88-23760

Nondestructive Evaluation (NDE) of structural ceramics by photoacoustic microscopy 17 p2325 N88-23884

Conversational Analysis of Color Images (CAICOU): An interactive development system for the analysis of color images
[RR-641-I-IMAG-39-LIFIA] 17 p2342 N88-23964

Some problems with regard to the TOVS processing detected by using NOAA-HRPT data check program
17 p2351 N88-24009

Enhanced infra-red picture of LR-FAX for spring and autumn seasons 17 p2351 N88-24011

Latin American Symposium on Remote Sensing. 4th Brazilian Remote Sensing Symposium and 6th SELPER Plenary Meeting, volume 1 17 p2352 N88-24013

Textural features for image classification in remote sensing 17 p2354 N88-24027

The USSR space systems for remote sensing of earth resources and the environment (sensor systems, processing techniques, applications)
17 p2356 N88-24035

Evolution of a family of image processing systems at INPE 17 p2361 N88-24065

Study of methods of post-processing applied to a problem of standard classification
17 p2362 N88-24067

Interpretation of MSS/LANDSAT data for evaluation of physical distribution of mangroves in Cananeia-Iguape (SP) 17 p2363 N88-24072

COMTAL vision one/20 programming processor system from the VAX 11/780 17 p2364 N88-24079

Automatic registration of satellite imagery
17 p2364 N88-24080

Application of its transformation in color enhancement of LANDSAT imagery 17 p2365 N88-24082

Restrictions in activity monitoring through remote sensing 17 p2365 N88-24084

Preliminary study on the application of digital processing of TM-LANDSAT data in the mapping of apple orchards in Fraiburgo (SC) 17 p2367 N88-24093

Evaluation of TM false color composites for crop discrimination 17 p2367 N88-24096

Terrain classification using SPOT images and the computer system GOP-300
[FOA-C-20677-2.7] 17 p2368 N88-24102

Adjustment in photogrammetry: Methods, programs and applications
[B8735130] 17 p2369 N88-24105

Image management research
17 p2380 N88-24150

Generic cueing in image understanding
[RSRE-MEMO-4109] 17 p2386 N88-24181

Orbital navigation, docking and obstacle avoidance as a form of three dimensional model-based image understanding 17 p2388 N88-24194

Application of spline functions to digital image processing
[ETN-88-92194] 17 p2392 N88-24218

Analysis of binarized Hartley phase-only filter performance with respect to stochastic noise
[DE88-007604] 18 p2519 N88-24945

High-energy laser-assisted imaging through vaporizing aerosols
[DE88-007911] 18 p2521 N88-24957

Visual information processing in the perception of features and objects
[AD-A192026] 18 p2552 N88-25148

CIMAG2: The computer program to generate color images
[AD-A191847] 18 p2557 N88-25175

System overview: Teragon 4000, an image processing equipment at FOA 3
[FOA-C-30465-3.3] 18 p2557 N88-25179

Shape from shading, occlusion and texture
[AD-A184840] 18 p2571 N88-25269

Optical system of laser illuminated streamer chamber
[DE88-702127] 18 p2577 N88-25306

An image processing system for research in solar physics
[AD-A191673] 18 p2595 N88-25421

Analysis and modeling of complex non-stationary flows
[PB88-127188] 19 p2664 N88-25842

A concurrent on-board vision system for a mobile robot
[DE88-007475] 19 p2676 N88-25914

Model-based computed tomography for nondestructive evaluation: An overview and proposal
[DE88-010600] 19 p2679 N88-25926

Model-based computed tomography for nondestructive evaluation: An overview and proposal
[DE88-010600] 19 p2679 N88-25926

Separability of cultivation through digital analysis of SPOT and TM data
[INPE-4541-PRE/1287] 19 p2685 N88-25963

Underwater optical trajectography and video image mosaics 19 p2700 N88-26051

Image processing applied to quantitative numerical cartography of ocean circulation
19 p2702 N88-26065

Methods for processing satellite images and their application to underwater operations
19 p2702 N88-26066

Intermediate level computer vision processing algorithm development for the content addressable array parallel processor
[AD-A192086] 19 p2714 N88-26111

PHOTODIGITIZE: A software/hardware system
[DE88-009575] 19 p2716 N88-26125

An instrument control and data analysis program for NMR imaging and spectroscopy
[DE88-007377] 19 p2717 N88-26132

SLAPP: A special multiprocessor array for signal processing and linear algebra
[AD-A191587] 19 p2719 N88-26146

Data volume reduction for imaging radar polarimetry
[NASA-CASE-NPO-17184-1-CU]
20 p2788 N88-26541

Microwave image understanding and its application to radar cross section management
20 p2788 N88-26542

Microfocus X-ray techniques for flaw location
[DE88-008636] 20 p2812 N88-26680

The interaction of sensory and perceptual variables: Spatial, temporal and orientation response to figure and ground
[AD-A192897] 20 p2832 N88-26798

Research in computer science 1985/6
[PB88-113840] 20 p2835 N88-26815

Automated system for mathematical processing of the data from a hybrid spectrometer
[DE87-702995] 20 p2836 N88-26820

Common Data Format (CDF) to store images
[NASA-CR-179366] 20 p2836 N88-26825

SEGMERGE: A scanline visible surface algorithm with adaptive span selection and inexpensive antialiasing
[DE88-009186] 20 p2836 N88-26826

A new approach to machine-based perception of monocular images
[DE88-002418] 20 p2853 N88-26942

Digital image processing from speckle interferograms by correlation methods: Application in atmospheric optics, astronomy, and biology
[ETN-88-92125] 20 p2855 N88-26953

Direct imaging of the columnar structure of GaAs quantum wells 20 p2868 N88-27030

Methods for indirect imaging through the atmosphere
[ONERA-NT-1987-4] 20 p2884 N88-27124

The application of imaging to the atmospheric Cerenkov technique: Observations of the Crab nebula
20 p2884 N88-27126

Processing and analysis of images transmitted by Vega space probes over Halley's comet
[ETN-88-92291] 20 p2885 N88-27131

Three-dimensional scene analysis using stero based imaging
[AD-A193120] 21 p2894 N88-27178

Applications of differential geometry to the shape analysis of gray-value images 21 p2924 N88-27358

Optical interconnections for digital image coding
21 p2928 N88-27381

Linear feature extraction from radar imagery. Phase 2: Base contract report
[AD-A192828] 21 p2931 N88-27404

The design of a digital Eprom oscillator for electrical impedance tomography
[DE88-012243] 21 p2940 N88-27462

The FEL CCD-camera: Experimental system for camera and image processing research
[FEL-1987-34] 21 p2952 N88-27532

Phase comparator for range imaging laser radar
[DE88-008109] 21 p2954 N88-27545

Interface control using low frequency (3 to 20 MHz) acoustic microscopy
[REPT-48-411/F] 21 p2959 N88-27577

Automatic line network extraction from aerial imagery of urban areas through knowledge based image analysis
[AD-A193067] 21 p2965 N88-27615

Review of geographic processing techniques applicable to regional analysis
[DE88-010759] 21 p2970 N88-27643

Photon limited image processing in the space-time domain
[AD-A193142] 21 p2972 N88-27655

Effects of pulsed and CW (Continuous Wave) 2450 MHz radiation on transformation and chromosomes of human lymphocytes in vitro
[AD-A193104] 21 p2987 N88-27736

Texture perception and shape from texture
[AD-A192923] 21 p2996 N88-27771

Research into the architecture of CAD based robot vision systems
[AD-A193330] 21 p2997 N88-27776

Enhancement of modeling and image generation techniques for high-resolution 3-dimensional imagery
[DE88-008923] 21 p2998 N88-27782

Maximum entropy signal restoration with linear programming
[DE88-011740] 21 p2999 N88-27787

Contribution to almost realistic picture processing by a computer graphics procedure
[ETN-88-92372] 21 p2999 N88-27789

Image processing using a parallel architecture
[AD-A192833] 21 p3002 N88-27803

Optical method to measure the deformations of structures loaded by hydraulic pressure
[SNIAS-881-430-111] 22 p3088 N88-28338

Methodological developments on crop inventories using SPOT and ground surveys 22 p3094 N88-28371

An evaluation of multidate SPOT data for agriculture and land use mapping in the United Kingdom
22 p3094 N88-28375

Topographic suppression and advances in classification for land cover mapping using SPOT-1 HRV imagery
22 p3099 N88-28404

Assessment of SPOT satellite based system in humid tropical vegetation identification, classification and monitoring 22 p3100 N88-28408

SPOT-1 satellite imagery for forest inventory in Sweden 22 p3106 N88-28445

Rigorous stereophotogrammetric treatment of SPOT images 22 p3111 N88-28482

Automatic extraction of high resolution elevation data from SPOT stereo images 22 p3113 N88-28489

Digital SPOT stereoplotting: An original approach to the formation of epipolar images and matching
22 p3113 N88-28493

Summary of analysis and processing techniques used on SPOT imagery 22 p3115 N88-28503

Research on wide area workstations
[AD-A192529] 22 p3136 N88-28643

Natural object categorization
[AD-A194103] 22 p3139 N88-28662

Implementation of nonsquare tilings on an image processing system
[FOA-C-30487-3.3] 22 p3140 N88-28669

Survey of neural net paradigms for specification of discrete networks
[AD-A192682] 22 p3141 N88-28674

Rendering of surfaces from volume data
[AD-A193649] 22 p3143 N88-28689

Direct visualization of surfaces from computed tomography data
[AD-A193646] 22 p3153 N88-28758

Noise generation and boundary layer effects in vortex-airfoil interaction and methods of digital hologram analysis for these flow fields
[AD-A194191] 23 p3171 N88-28883

Three-dimensional vortex interactions
[AD-A194066] 23 p3172 N88-28889

Analysis of edge detection techniques for radiographic image measurement
[AD-A193650] 23 p3186 N88-28961

Comparison of 2-D Fourier and spatial techniques for removing noise in real-time X-ray radiography
[AD-A193700] 23 p3187 N88-28962

Visual motion perception and visual attentive processes
[AD-A193640] 23 p3241 N88-29268
Automatic object recognition
23 p3254 N88-29368
Two dimensional convolute integers for machine vision and image recognition 23 p3254 N88-29369
Object discrimination via bulk temperature/velocity filtering, phase 1
[AD-A194533] 23 p3274 N88-29487
Accuracy of satellite data navigation
[AD-A195877] 24 p3322 N88-29787
Automatic data retrieval from rocket motor holograms
[AD-A195586] 24 p3337 N88-29864
Degradation of protective coatings on steel in corrosive environments 24 p3354 N88-29969
Integrating multispectral imagery and ground level hyperspectral signature data
[AD-A195976] 24 p3386 N88-30166
LANDSAT-TM data to map flooded areas
[INPE-4594-PRE/1324] 24 p3387 N88-30177
Multilevel computational theory of stereoscopic visual image processing
[AD-A195331] 24 p3408 N88-30268
Using primal sketch primitives as the basis for the Hough transform
[INPE-4564-PRE/1305] 24 p3412 N88-30310
A digital terrain model system for a microcomputer
[INPE-4610-PRE/1333] 24 p3413 N88-30316
Compression and decompression of imaging sensor signals (CADISS): A multiprocessor system for image compression/decompression on board scientific satellites
[NLR-TR-87076-L] 24 p3414 N88-30323
The 1988 Goddard Conference on Space Applications of Artificial Intelligence
[NASA-CP-3009] 24 p3415 N88-30330
Low level image processing techniques using the pipeline image processing engine in the flight telerobotic servicer 24 p3418 N88-30346
An interactive testbed for development of expert tools for pattern recognition 24 p3419 N88-30349
The combinatorics of object recognition in cluttered environments using constrained search
[AD-A196224] 24 p3422 N88-30364
Symbolic construction of a 2D scale-space image
[AD-A195926] 24 p3423 N88-30374
Image focusing in space and time
[AD-A195839] 24 p3429 N88-30410
Activities in astrophysics
[INPE-4582-PRE/1316] 24 p3456 N88-30570

IMAGE RECONSTRUCTION
Imaging strategies for a spaceborne interferometer
01 p0094 N88-10617
ISIS: Image reconstruction methods and signal-to-noise ratio investigations --- spaceborne interferometry
01 p0094 N88-10619
ISIS: Image reconstruction experiments and comparison of various array configurations --- spaceborne interferometry 01 p0095 N88-10620
Milliarcsecond ground-based imaging with single telescopes 01 p0097 N88-10637
Three dimensional reconstruction of optical microscope pictures using the three dimensional microscopic inverse point spread function
[ETN-87-90420] 01 p0098 N88-10646
Study of the distribution of a multi-electrode circular system sensitivity for the reconstruction of bioelectrical impedance images
[ISAL-IDI1-87-01] 02 p0217 N88-11368
The maximum likelihood estimator method of image reconstruction: Its fundamental characteristics and their origin
[DE88-000462] 05 p0636 N88-13892
Computing 3-D structure of rigid objects using stereo and motion 08 p1061 N88-16407
Comparison of a few methods of restoring images distorted by atmospheric turbulence
[ESA-TT-1065] 09 p1248 N88-17481
Ideal shrinking and expansion of discrete sequences
[NASA-TM-88202] 11 p1524 N88-19100
Solar radioimage restoration
[INPE-4312-TDL/279] 11 p1571 N88-19402
Three-dimensional image reconstruction in object space
[DE88-900279] 12 p1712 N88-20246
Restoration techniques for redisplay of LANDSAT-5 satellite imagery
[INPE-4189-PRE/1076] 13 p1791 N88-20712
Method to evaluate image-recovery algorithms based on task performance
[DE88-005382] 13 p1816 N88-20853
Rainbow holographic image reconstructed by spatially extended white light source 15 p2055 N88-22249
Focused image holography abberations
[DE88-701105] 15 p2066 N88-22333
Geometric restoration of satellite image data
[AD-A190462] 15 p2089 N88-22450
Stochastic approach of image segmentation. A model of cooperation between region primitives and boundaries
[ETN-88-92192] 16 p2262 N88-23523
Activities report of the Imagery Department
[ENST-87D008] 16 p2273 N88-23604
Application of dynamic programming to image registration
[ENST-87E022] 18 p2557 N88-25180
A fast and efficient procedure for generalized cross-validation with large data sets. Application to image reconstruction
[RR-669-M] 18 p2563 N88-25220
Display and processing of multidimensional signals with the aid of fractal image sequences
[ETN-88-92131] 20 p2806 N88-26642
A new approach to machine-based perception of monocular images
[DE88-002418] 20 p2853 N88-26942
Reconstruction of multidimensional signals from multiple level threshold crossings
[AD-A195561] 24 p3425 N88-30383

IMAGE RESOLUTION
On the concept of resolution ellipse in aperture synthesis matched deconvolution with error analysis --- astronomical interferometry 01 p0095 N88-10621
Galactic nuclei and quasars at high angular resolution
01 p0098 N88-10644
Intrinsic and extrinsic geometric quality --- SPOT images 03 p0341 N88-12154
Registration of SPOT images
03 p0341 N88-12155
Input/output technologies: An overview of image scanning, storage, and display
[DE87-014837] 04 p0476 N88-12933
High resolution ultraviolet filter development
[AD-A184133] 05 p0649 N88-13979
Study of synthetic aperture radar data compression and encoding. Part 1: SAR image data analysis
[NLR-TR-85085-L-PT-1] 07 p0843 N88-15115
Multiple-object motion estimation by maximal matching of 3-D point and line features 09 p1220 N88-17322
Investigations of high resolution imaging through the Earth's atmosphere using speckle interferometry
[AD-A189295] 12 p1692 N88-20121
Generalised threshold selection for edge detection
[RAE-TR-87035] 14 p1941 N88-21581
Rainbow holographic image reconstructed by spatially extended white light source 15 p2055 N88-22249
An investigation into the precision of a digital camera
[B8735054] 16 p2210 N88-23193
Instrumentation for turbulent reacting flows
[AD-A191671] 18 p2515 N88-24923
Ultraviolet imaging of hydrogen flames
[DE88-009152] 20 p2769 N88-26422
Interpreting forest biome productivity and cover utilizing nested scales of image resolution and biogeographical analysis
[NASA-CR-183036] 20 p2817 N88-26711
Comparison of 2-D Fourier and spatial techniques for removing noise in real-time X-ray radiography
[AD-A193700] 23 p3187 N88-28962
High definition television: Evaluation for remote task performance
[DE88-011573] 23 p3202 N88-29057

IMAGE ROTATION
Position, scale, and rotation invariant target recognition using range imagery
[AD-A188828] 12 p1633 N88-19772

IMAGE TRANSDUCERS
Cryogenic acoustic microscopy
[AD-A187274] 10 p1299 N88-17767

IMAGE TUBES
Resolution limitations and optimization of the LLNL streak camera focus
[DE88-001633] 05 p0586 N88-13572
Resolution limitations and optimization of the ITT F4157 streak tube focus for fast (10 ps) operation
[DE88-003727] 09 p1169 N88-17007
The 5-GHz operation of the ITT and RCA streak tubes with a 7.5-ns time window
[DE88-003342] 09 p1169 N88-17008

IMAGERY
NT AERIAL PHOTOGRAPHY
NT ASTRONOMICAL PHOTOGRAPHY
NT AUTORADIOGRAPHY
NT BLACK AND WHITE PHOTOGRAPHY
NT CINEMATOGRAPHY
NT CLOUD PHOTOGRAPHY
NT COLOR PHOTOGRAPHY
NT COMPUTER AIDED TOMOGRAPHY
NT ELECTRO-OPTICAL PHOTOGRAPHY
NT HOLOGRAPHY
NT INFRARED IMAGERY
NT INFRARED PHOTOGRAPHY
NT MICROWAVE IMAGERY
NT NEUTRON RADIOGRAPHY
NT PHOTOMICROGRAPHY
NT PHOTORECONNAISSANCE
NT PIXELS
NT RADAR IMAGERY
NT RADAR PHOTOGRAPHY
NT RADIOGRAPHY
NT REPRODUCTION (COPYING)
NT SATELLITE IMAGERY
NT SATELLITE-BORNE PHOTOGRAPHY
NT SCHLIEREN PHOTOGRAPHY
NT SHADOWGRAPH PHOTOGRAPHY
NT SPACEBORNE PHOTOGRAPHY
NT SPECKLE HOLOGRAPHY
NT SPECTROHELIOGRAPHS
NT SPECTROPHOTOGRAPHY
NT STEREOPHOTOGRAPHY
NT STEREOSCOPY
NT TOMOGRAPHY
NT ULTRAVIOLET PHOTOMETRY
NT WHITE LIGHT HOLOGRAPHY
NT X RAY IMAGERY
NT XEROGRAPHY
Two dimensional imaging observations of meter-decameter bursts associated with the February 1986 flare activity 01 p0113 N88-10723
Modeling cloudy and clear interval length probabilities using space shuttle imagery
[AD-A185290] 05 p0627 N88-13837
Range imagery algorithms for the detection of obstacles by autonomous vehicles
[AD-A185421] 05 p0659 N88-14045
Imaging subtle microstructural variations in ceramics with precision ultrasonic velocity and attenuation measurements
[NASA-TM-100129] 07 p0867 N88-15257
Theory and research on the disjunction of cross passage errors and systematic image errors in photogrammetric point determination
[SER-C-324] 07 p0872 N88-15290
Proceedings of Image Understanding Workshop, volume 2
[AD-A186104] 07 p0902 N88-15464
Orbital navigation, docking and obstacle avoidance as a form of three dimensional model-based image understanding 08 p1061 N88-16406
Computing 3-D structure of rigid objects using stereo and motion 08 p1061 N88-16407
Comparison of UNL laser imaging and sizing system and a phase/Doppler system for analyzing sprays from a NASA nozzle
[NASA-CR-182437] 09 p1161 N88-16956
Performance of a photon counting microchannel plate intensifier with wedge and strip image readout
[DE88-003831] 10 p1334 N88-17970
Autocorrelation of control points on 11-band multispectral imagery
[AD-A188185] 10 p1348 N88-18056
Three-dimensional image generation from an aerial photograph
[AD-A188039] 11 p1503 N88-18979
Applications of mathematical morphology to range imagery
[AD-A189316] 12 p1684 N88-20072
Multi-disciplinary techniques for understanding time-varying space-based imagery
[AD-A190711] 15 p2117 N88-22610
Television monitor field shifter and an opto-electronic method for obtaining a stereo image of optimal depth resolution and reduced depth distrotion on a single screen
[NASA-CASE-NPO-17249-1-CU]
17 p2332 N88-23924
Atmospheric autorotating imaging device
[NASA-CASE-NPO-17390-1-CU]
18 p2519 N88-24944
Investigation of the diffuse ultraviolet background with DE data
[NASA-CR-182863] 19 p2741 N88-26271
Description of a tool for the simulation of imagery systems 22 p3147 N88-28724
Determining vehicle motion from stereo image sequences
[AD-A194371] 23 p3216 N88-29140
Microcircuit trace cutting with focused ion beams
[AD-A196030] 24 p3367 N88-30050
Integrating multispectral imagery and ground level hyperspectral signature data
[AD-A195976] 24 p3386 N88-30166
Symbolic construction of a 2D scale-space image
[AD-A195926] 24 p3423 N88-30374
Kalman filter-based algorithms for estimating depth from image sequences
[AD-A195816] 24 p3424 N88-30380

Diffraction imaging (topography) with monochromatic synchrotron radiation
[NASA-CR-183264] 24 p3433 N88-30431
Applications of synchrotron radiation to materials science: Diffraction imaging (topography) and microradiography
[NASA-CR-183265] 24 p3434 N88-30440
IMAGES
Design of source coders and joint source/channel coders for noisy channels
[NASA-CR-181547] 04 p0432 N88-12678
Interaction of different modules in depth perception: Stereo and shading
[AD-A185607] 06 p0759 N88-14655
Three dimensional display of meteorological scientific data
[DE88-000776] 07 p0880 N88-15339
Research on visual information processing with special reference to oculomotor behavior in the areas of exploration, recognition and search
[AD-A186598] 08 p1051 N88-16346
Image correlation on an IBM-PC for characterization of advanced ceramics
[DE88-002829] 09 p1149 N88-16885
Fractal images: Procedure and theory
[AD-A187014] 09 p1217 N88-17293
The role of photodetectors in optical signal processing
[AD-A186804] 09 p1247 N88-17476
Management Information and Downloader Interface System (MIDIS)
[AD-A186976] 09 p1261 N88-17557
Visual integration and detection of discontinuities: The key role of intensity edges
[AD-A188012] 11 p1520 N88-19076
Soft maps for US Army electronic map background applications
[AD-A188427] 12 p1638 N88-19809
Reduced tolerance imaging 2, volume 2
[AD-A189604] 13 p1829 N88-20939
Aberrations: Their effect on off-axis beam steering
[AD-A189601] 13 p1840 N88-21008
Finding texture boundaries in images
[AD-A190554] 15 p2117 N88-22609
Finding wheels of vehicles in stereo images
[AD-A194372] 22 p3080 N88-28292
Transformations of short-term visual memory
[AD-A193873] 23 p3241 N88-29290
Particle sizing in combustion systems, using scattered laser light
[AD-A196231] 24 p3352 N88-29953
Comparative aspects of multiple processes of attention
[AD-A195805] 24 p3408 N88-30291
Dynamical systems and motion vision
[AD-A195932] 24 p3422 N88-30366
Symbolic construction of a 2D scale-space image
[AD-A195926] 24 p3423 N88-30374
Kalman filter-based algorithms for estimating depth from image sequences
[AD-A195818] 24 p3424 N88-30380
Streaking images that appear only in the plane of diffraction in undoped GaAs single crystals: Diffraction imaging (topography) by monochromatic synchrotron radiation
[NASA-CR-183267] 24 p3433 N88-30437
IMAGING RADAR
Principal space programs in the area of microwaves
[INPE-4164-PRE/1064] 12 p1618 N88-19677
The superconducting phase shifter in the development of a terahertz imaging radar system
[AD-A190666] 16 p2188 N88-23046
Investigation of the usefulness of speckle analysis in imaging radar systems
[BCRS-86-05] 16 p2227 N88-23302
The role of space borne imaging radars in environmental monitoring: Some shuttle imaging radar results in Asia
[NASA-TM-101178] 18 p2502 N88-24844
Data volume reduction for imaging radar polarimetry
[NASA-CASE-NPO-17184-1-CU]
20 p2788 N88-26541
Phase comparator for range imaging laser radar
[DE88-006109] 21 p2954 N88-27545
A submillimeter wavelength space-based imaging radar
[AD-A195846] 24 p3364 N88-30033
IMAGING SPECTROMETERS
Radiometric calibration of the Earth observing system's imaging sensors
[NASA-CR-181542] 04 p0463 N88-12665
Proceedings of the Third Airborne Imaging Spectrometer Data Analysis Workshop
[NASA-CR-181552] 05 p0611 N88-13755
The Portable Instant Display and Analysis Spectrometer (PIDAS) 05 p0611 N88-13756
AIS-2 radiometry and a comparison of methods for the recovery of ground reflectance
05 p0611 N88-13757
Effective use of principal component analysis with high resolution remote sensing data to delineate hydrothermal alteration and carbonate rocks 05 p0612 N88-13758
Land cover/use classification of Cairns, Queensland, Australia: A remote sensing study involving the conjunctive use of the airborne imaging spectrometer, the large format camera and the thematic mapper simulator
05 p0612 N88-13759
Calibrating AIS images using the surface as a reference 05 p0612 N88-13760
The use of airborne imaging spectrometer data to determine experimentally induced variation in coniferous canopy chemistry 05 p0612 N88-13761
Overview of Austrian Airborne Imaging Spectrometer (AIS) programme and first results
05 p0612 N88-13762
AIS-2 spectra of California wetland vegetation
05 p0613 N88-13763
Toward detecting California shrubland canopy chemistry with AIS data 05 p0613 N88-13764
Measuring near infrared spectral reflectance changes from water stressed conifer stands with AIS-2
05 p0613 N88-13765
Abundance and distribution of ultramafic microbreccia in Moses Rock Dike: Quantitative application of AIS data
05 p0613 N88-13766
Evaluation of AIS-2 (1986) data over hydrothermally altered granitoid rocks of the Singatse Range (Yerington) Nevada and comparison with 1985 AIS-1 data
05 p0613 N88-13767
Preliminary results from an investigation of AIS-1 data over an area of epithermal alteration: Plateau, Northern Queensland, Australia 05 p0613 N88-13768
Causes of spurious features in spectral reflectance data 05 p0614 N88-13769
Automatic continuum analysis of reflectance spectra
05 p0614 N88-13770
Analysis of airborne imaging spectrometer data for the Ruby Mountains, Montana, by use of absorption-band-depth images 05 p0614 N88-13771
Mapping hydrothermally altered rocks in the Northern Grapevine Mountains, Nevada and California with the airborne imaging spectrometer 05 p0614 N88-13772
A geostationary imaging spectrometer TOMS instrument 05 p0619 N88-13802
HIRIS (High-Resolution Imaging Spectrometer: Science opportunities for the 1990s. Earth observing system. Volume 2C: Instrument panel report
[NASA-TM-89703] 07 p0871 N88-15282
Technical assessment of the joint CSIRO/Bureau of Meteorology proposal for a geostationary imager/sounder over the Australian region
[RTP-15] 09 p1135 N88-16811
IMAGING TECHNIQUES
NT RASTER SCANNING
NT SPECKLE HOLOGRAPHY
Laser probes of natural gas ignition chemistry
[PB87-209599] 01 p0021 N88-10129
Imaging of planar defects with synthetic aperture focusing technique (LSAFT) --- ultrasonic inspection
[VTT-468] 01 p0058 N88-10370
Image sharpening observations of active galactic nuclei 01 p0098 N88-10643
How we get pictures from space, revised edition
[NF-151/7-87-REV] 02 p0193 N88-11203
Study of the distribution of a multi-electrode circular system sensitivity for the reconstruction of bioelectrical impedance images
[ISAL-IDI1-87-01] 02 p0217 N88-11368
A preliminary taxonomy of visible surface algorithms
[DE87-013559] 02 p0220 N88-11386
Fundamentals and techniques of nonimaging optics research
[DE87-014544] 02 p0236 N88-11488
Delay-Doppler radar imaging
[AD-A184165] 03 p0308 N88-11943
Planning for future operational sensors and other priorities
[PB87-220802] 03 p0325 N88-12056
Some new ideas in liquid detectors
[DE88-000732] 04 p0446 N88-12768
Simultaneous, cospatial imaging of the Sun in cyanogen and singly-ionized calcium 04 p0507 N88-13114
Doppler snapshots 04 p0508 N88-13125
Photon counting image sensor development for astronomical applications
[NASA-CR-181507] 05 p0660 N88-14049
Statistical investigations of the behavior of a product correlator and an edge detector in critical situations
[MBB-UA-1034/87] 06 p0781 N88-14793
Time-domain robotic vision application
06 p0798 N88-14886
Scanning and measuring peculiarities with high-space resolution objects recorded at the Gabor holograms
[DE88-700373] 07 p0857 N88-15203
Electronic imaging technique for welding and other high-luminosity processes
[DE88-002199] 07 p0862 N88-15227
Recognition of polyhedral objects under structured illumination
[PB88-106703] 07 p0932 N88-15861
The use of NMR imaging to measure porosity and binder distributions in green-state and partially sintered ceramics
[DE88-003099] 08 p0972 N88-15881
Textural features for image classification in remote sensing
[INPE-4169-PRE/1066] 08 p1020 N88-16181
Developments in instrumental techniques for observations of magnetospheric and ionospheric shaped charge releases 08 p1031 N88-16248
Computing 3-D structure of rigid objects using stereo and motion 08 p1061 N88-16407
Crystal diffraction lenses for imaging gamma-ray telescope
[DE88-003064] 08 p1083 N88-16529
Future television systems: Comparison of sequential and interlaced scanning
[BBC-RD-1987/18] 09 p1155 N88-16923
Thermal wave imaging
[AD-A186810] 09 p1177 N88-17046
Comparison of a few methods of restoring images distorted by atmospheric turbulence
[ESA-TT-1065] 09 p1248 N88-17481
Some present limitations on the lattice imaging of grain boundaries
[DE87-014665] 09 p1256 N88-17530
NMR (Nuclear Magnetic Resonance) imaging for detecting binder/plasticizers in green-state structural ceramics
[DE88-003111] 10 p1304 N88-17800
Digital imaging techniques for single- and multi-phase reacting flowfields 10 p1327 N88-17933
Instrumentation and quantitative methods of evaluation
[DE87-013639] 10 p1342 N88-18017
Investigation of a ray-mode representation of the Green's function in a rectangular cavity
[PB88-131677] 11 p1469 N88-18783
Multisource context classification methods in remote sensing 11 p1504 N88-18985
Geophysical diffraction tomography for imaging isolated subsurface inclusions
[DE88-003918] 11 p1505 N88-18990
Scanning tunneling microscopy of silver, gold, and aluminium monomers and small clusters on graphite
[DE88-003871] 11 p1562 N88-19349
Spectral images and multi-component models of the chromospheres of AR Lacertae
11 p1568 N88-19384
A method to detect and digitize small plant movements 12 p1654 N88-19912
Image segmentation via fractal dimension
[AD-A188825] 12 p1678 N88-20033
Investigations of high resolution imaging through the Earth's atmosphere using speckle interferometry
[AD-A189295] 12 p1692 N88-20121
Photographic filters
[INPE-4448-RPE/558] 12 p1692 N88-20124
The imaging of extra-galactic low-energy gamma-ray sources prospects, techniques, and instrumentation
[NASA-CR-182536] 12 p1713 N88-20251
Bathymetric hazard survey test
[AD-A189150] 13 p1803 N88-20775
Parallel image compression
[NASA-CR-180758] 13 p1814 N88-20837
Reduced tolerance imaging 2, volume 2
[AD-A189604] 13 p1829 N88-20939
Effects of update and refresh rates on flight simulation visual displays
[NASA-TM-100415] 15 p2018 N88-22033
Polarimetric ISAR imaging using either measured or calculated transient signatures
[AD-A190077] 15 p2056 N88-22259
Range image segmentation and surface parameter extraction for a mobile robot
[DE87-013877] 15 p2073 N88-22360
Systems for ultrasonic scanning, analysis and imagery
15 p2082 N88-22414
Method for restoration and resampling of TM sensor imagery
[INPE-4491-PRE/1255] 15 p2090 N88-22454
Comparative utilization of analog and digital processes in the treatment of MSS-LANDSAT data for studying the national parks of Brazil
[INPE-4011-TDL/240] 15 p2090 N88-22456

Stochastic approach of image segmentation. A model of cooperation between region primitives and boundaries
[ETN-88-92192] 16 p2262 N88-23523

Activities report of the Imagery Department
[ENST-87D008] 16 p2273 N88-23604

Latin American Symposium on Remote Sensing. 4th Brazilian Remote Sensing Symposium and 6th SELPER Plenary Meeting, volume 1 17 p2352 N88-24013

The geometric workstation, a new approach for geometric corrections of remotely sensed data
17 p2352 N88-24017

Subsurface morphology and geoarchaeology revealed by spaceborne and airborne radar
17 p2353 N88-24022

Mapping soil and rock variation from satellite images in the Sahel 17 p2354 N88-24023

Textural features for image classification in remote sensing 17 p2354 N88-24027

Shape detection in remote sensing through graph isomorphism 17 p2354 N88-24028

The modeling of error budget analysis and tolerance specifications for BRESEX multiband linear array CCD camera 17 p2355 N88-24029

Practical image analysis using personal computers: The Canadian experience 17 p2356 N88-24037

Comparison of the solar radiation estimation method by satellites 17 p2360 N88-24055

Study of methods of post-processing applied to a problem of standard classification
17 p2362 N88-24067

Analysis of the parameters responsible for the variations of the illumination conditions in the LANSAT data
17 p2362 N88-24070

COMTAL vision one/20 programming processor system from the VAX 11/780 17 p2364 N88-24079

Automatic registration of satellite imagery
17 p2364 N88-24080

Application of its transformation in color enhancement of LANDSAT imagery 17 p2365 N88-24082

Evaluation of TM false color composites for crop discrimination 17 p2367 N88-24096

Novel silicon Schottky barrier infrared imaging arrays
17 p2439 N88-24510

Delay-doppler radar imaging
[AD-A191509] 18 p2499 N88-24826

High-energy laser-assisted imaging through vaporizing aerosols
[DE88-007911] 18 p2521 N88-24957

Utilization of the IR telescope gimbaling system as a stabilized pointing platform for balloon payloads. Volume 1: Technical results
[NASA-CR-179339] 18 p2522 N88-24962

Instantaneous two-dimensional multiple particle sizing diagnostic 19 p2630 N88-25600

Design and preliminary evaluation of an underwater laser-based imaging system
[DE88-010560] 19 p2675 N88-25908

The use of satellite imagery for municipal conditions in rural recording in Pereira Barreto (SP)
19 p2682 N88-25944

The impact of disorganized occupation of urban sub-basins: Sub-basin of the Cabucu River, metropolitan area of Sao Paulo (SP) 19 p2682 N88-25945

Application of 35mm EM aerial reconnaissance photographic format of the municipality of Ubatuba (SP)
19 p2684 N88-25953

An instrument control and data analysis program for NMR imaging and spectroscopy
[DE88-007377] 19 p2717 N88-26132

Ultraviolet imaging of hydrogen flames
[DE88-009152] 20 p2769 N88-26422

Methods for indirect imaging through the atmosphere
[ONERA-NT-1987-4] 20 p2884 N88-27124

Optical diagnostics for metallurgical processes
[DE88-009255] 21 p2913 N88-27289

Ellipsometric imaging of drying sol-gel films
[DE88-011785] 21 p2921 N88-27335

Turbulent flow field visualization with integral interferometric imaging and computed tomography
21 p2950 N88-27521

Optical imaging diagnostics for fusion plasmas
[DE88-997572] 21 p3018 N88-27910

Application of two-dimensional imaging to very high energy gamma ray astronomy
[DE88-010120] 21 p3030 N88-27983

Characterization of new FPS (Focus Projection and Scale) vidicons for scientific imaging applications
[DE88-011213] 22 p3080 N88-28290

Proof-of-principle high speed electronic imaging system, phase 2
[AD-A193798] 23 p3181 N88-28937

Visual Effects in the High Performance Aircraft Cockpit
[AGARD-LS-156] 23 p3241 N88-29291

Display system image quality
23 p3242 N88-29298

Optimization-driven machine-oriented motion measurement 23 p3245 N88-29312

ZT imaging system for layered thin wall structures
[AD-A195466] 24 p3352 N88-29954

Quantitative surface temperature measurement using two-color thermographic phosphors and video equipment
[NASA-CASE-LAR-13740-1] 24 p3376 N88-30105

Method for combined image interpolation-restoration through a fir filter design technique
[INPE-4561-PRE/1302] 24 p3413 N88-30315

A coded mask telescope for observations of X and gamma ray sources in the southern sky
[INPE-4580-PRE/1314] 24 p3453 N88-30551

IMBEDDINGS (MATHEMATICS)
NT INVARIANT IMBEDDINGS

IMCC (CONTROL CENTER)
U INTEGRATED MISSION CONTROL CENTER

IMIDES
Aromatic cyclotriphosphazenes
[NASA-CASE-ARC-11428-3] 18 p2477 N88-24692

IMINES
Polymerization of azaethylenes (imines) and aza-1,3-dienes: Potential reactive monomers
[AD-A194717] 23 p3197 N88-29028

IMMERSION
U SUBMERGING

IMMISCIBILITY
U SOLUBILITY

IMMITTANCE
U ELECTRICAL IMPEDANCE

IMMOBILIZATION
Lipid peroxidation in rat tissues with exposure to antiorthostatic hypokinesia, exercise and immobilization stress 10 p1365 N88-18159

New book on metabolic aspects of spaceflight stress
10 p1367 N88-18172

Human response to prolonged motionless suspension in four types of full body harnesses
21 p2929 N88-27387

IMMUNE SYSTEMS
Mononuclear phagocytes during adaptation of essentially healthy people to high altitudes
07 p0896 N88-15432

White blood cells in space: An experiment for the first Spacelab mission 09 p1127 N88-16757

Operation Everest 2: Alterations in the immune system at high altitude
[AD-A188011] 11 p1520 N88-19075

Direct interaction between autonomic nerves and the immune system
[AD-A188576] 12 p1667 N88-19991

Immunofluorescence localization of dissociation supernatant and extracellular matrix components in Lytechinus pictus sectioned embryos
[NASA-CR-183137] 24 p3406 N88-30276

IMMUNITY
Mononuclear phagocytes during adaptation of essentially healthy people to high altitudes
07 p0896 N88-15432

Operation Everest 2: Alterations in the immune system at high altitude
[AD-A188011] 11 p1520 N88-19075

IMMUNOASSAY
A solid phase enzyme-linked immunosorbent assay for the antigenic detection of Legionella pneumophila (serogroup 1): A compliment for the space station diagnostic capability 06 p0795 N88-14868

Effects of anti-g suit inflation on renin and aldosterone response physical exercise 12 p1659 N88-19944

Is ANF implied in the night attenuated renal response to central hypervolemia? 12 p1659 N88-19945

Photochrome from green plants: Assay, purification and characterization
[DE88-007511] 19 p2702 N88-26067

IMMUNOLOGY
JPRS report: Science and technology. USSR: Life sciences
[JPRS-ULS-87-009] 04 p0473 N88-12915

TOMS as a monitor of the ultraviolet radiation environment: Applications to photobiology
05 p0617 N88-13785

Physiological and immunological aspects of human adaptation to temperature elevation in a closed environment 07 p0895 N88-15424

Supersonic and subsonic aircraft noise effects on animals: A literature survey
[AD-A186922] 10 p1404 N88-18373

Neurohumoral aspects of sleep
[AD-A188653] 12 p1667 N88-19992

JPRS report: Science and technology. USSR: Life sciences
[JPRS-ULS-88-004] 13 p1810 N88-20815

Bioeffects of electromagnetic waves
24 p3364 N88-30032

IMP-H
U EXPLORER 47 SATELLITE

IMP-7
U EXPLORER 47 SATELLITE

IMPACT
NT ECONOMIC IMPACT
NT ELECTRON IMPACT
NT HYPERVELOCITY IMPACT
NT POINT IMPACT

Assessment of the impacts of transferring certain nuclear reactor technologies to the Soviet Union and Eastern Europe
[DE87-014388] 02 p0249 N88-11576

The impact of environmental factors on the performance of millimeter wave seekers in smart munitions
[DE87-014277] 03 p0270 N88-11697

Simulation of effect on biological systems of impact wave from heavy charged particle track
07 p0896 N88-15429

A review of methanol vehicles and air quality impacts
[DE88-002846] 08 p1023 N88-16194

Factors affecting the sticking of insects on modified aircraft wings
[NASA-CR-182451] 09 p1148 N88-16878

A substructure method for dynamic simulation of flexible mechanical systems with geometric nonlinearities
09 p1176 N88-17044

Quantitative and qualitative assessments of the impact of linguistic theory on information science
10 p1424 N88-18507

The concept of an impact resonance diagram for characterizing the nonlinear response of impact vibration
[DE88-005475] 15 p2086 N88-22432

Revised Impact Dynamic Design-Analysis Method (RIDDAM)
[AD-A190479] 16 p2217 N88-23225

Survey of impact damper performance
16 p2217 N88-23227

Nineteenth Lunar and Planetary Science Conference. Press abstracts
[NASA-CR-183037] 24 p3440 N88-30473

Exotic minerals in 3,500 million year old rocks: Evidence for large meteorite impacts 24 p3440 N88-30475

LSU scientists discover evidence of large meteorite impacts on the early earth 24 p3441 N88-30480

IMPACT ACCELERATION
Peak Acceleration Device (PAD)
[AD-A191639] 18 p2461 N88-24611

IMPACT DAMAGE
NT METEORITIC DAMAGE
NT RAIN IMPACT DAMAGE

Effect of adhesive layers on impact damage and dynamic response in composite laminates
02 p0141 N88-10887

Simulation of tokamak runaway-electron events. Study of the response of materials by use of an electron linear accelerator
[IPPJ-841] 02 p0242 N88-11528

Impact of solids on composite materials
[NASA-CR-182395] 07 p0827 N88-15015

Behavior of a steel cylinder under the influence of a local load in the elastic and elasto-plastic area
[PB87-154787] 07 p0869 N88-15272

Investigation of low velocity impact damage on filamentary composite materials
07 p0923 N88-15607

Through-transmission/pulse-echo ultrasonic equipment evaluation
[AD-A186340] 07 p0929 N88-15641

Space station integrated wall damage and penetration damage control. Task 5: Space debris measurement, mapping and characterization system
[NASA-CR-179281] 10 p1285 N88-17688

An analysis of penetration and ricochet phenomena in oblique hypervelocity impact
[NASA-TM-100319] 10 p1339 N88-18004

Analysis of impact crater arrangement on the Venutian surface (from photographic materials of the Venera-15 and -16 spacecraft)
[NASA-TT-20211] 11 p1571 N88-19401

Simulated impact damage in a thick graphite/epoxy laminate using spherical indenters
[NASA-TM-100539] 13 p1733 N88-20363

Studies of traverse impact damage in composite materials using a Hopkinson pressure-bar technique
[OUEL-1706/87] 14 p1883 N88-21255

Analysis of head response to torso acceleration. Volume 1: Development of performance requirements
[PB88-156757] 14 p1953 N88-21640

Impact damage in composite laminates
15 p2080 N88-22402

Bilateral symmetry elements of the Zhamanshin impact crater
[NASA-TT-20288] 15 p2096 N88-22490

Surface crack analysis applied to impact damage in a thick graphite-epoxy composite
[NASA-TM-100600] 16 p2173 N88-22950
GARTEUR TP-037: Impact damage tolerance of carbon fiber and hybrid laminates
[RAE-TR-87057] 17 p2316 N88-23837
The application of high-rate biaxial testing to the design of containment vessels for radioisotope heat sources
17 p2426 N88-24428
Design manual for impact damage tolerant aircraft structure, addendum
[AGARD-AG-238-ADD] 21 p2895 N88-27185
Hole diameters in plates impacted by projectiles
21 p2929 N88-27386
Assessment of the effects of space debris and meteoroids environment on the space station solar array assembly
[NASA-TM-101315] 23 p3185 N88-28959
Wave and fracture phenomena in impacted ceramics
[AD-A192946] 23 p3196 N88-29020
Experimental aspects of using time-averaged holographic interferometry to detect barely visible impact damage in a graphite/epoxy composite plate
[AD-A194418] 24 p3375 N88-30097
A compilation of information and data on the Manson impact structure
[NASA-CR-183169] 24 p3401 N88-30258

IMPACT DECELERATION
U DECELERATION
U IMPACT ACCELERATION

IMPACT LOADS
Time-resolved measurements of shock-induced vapor-pressure profiles
[DE87-012972] 01 p0045 N88-10289
Fabrication of standardized piezoelectric polymer shock gauges by the Bauer method
[DE87-012738] 01 p0049 N88-10315
Experimental measurements and numerical simulations of metal spallation by detonating solid explosives
[DE87-013227] 01 p0054 N88-10347
Experimental molecular spectroscopy in shock-compressed materials
[DE87-013139] 02 p0144 N88-10903
Rarefaction velocities in shocked lead
[DE87-013141] 02 p0146 N88-10917
Computations of hypervelocity impact using the CTH shock wave physics code
[DE87-013067] 02 p0169 N88-11062
Shock-chemistry in natural materials and evolution of planetary surfaces
[DE87-012737] 02 p0254 N88-11604
Conservatism implications of shock test tailoring for multiple design environments
[DE87-013927] 03 p0338 N88-12127
The nonlinear dynamic response of an elastic-plastic thin plate under impulse loading
[AD-A182147] 08 p0994 N88-16013
Dynamic finite element with diagonalized consistent mass matrix and elastic-plastic impact calculation
[PB87-143376] 08 p0995 N88-16020
Mechanical impact: Theoretical simulation and correlation 09 p1179 N88-17060
Spatial pressure variations and three-dimensional effects on liquid sloshing loads
[PB88-120134] 10 p1326 N88-17926
Use of the LLNL 40 kV electric gun to study the shock response of 21-6-9 stainless steel
[DE87-014550] 13 p1742 N88-20418
An investigation of the spray produced by a yawed wheel, including measurement of impact forces --- aircraft wheels
[BU-363] 14 p1866 N88-21150
Inertia welding with variable magnitude of impact load
14 p1897 N88-21328
Response of aluminum alloys to erosive particle impacts
[DE88-005910] 15 p2041 N88-22159
Impact damage in composite laminates
15 p2080 N88-22402
Behavior of a two-layered beam under impact loading
[OUEL-1716/87] 17 p2349 N88-23993
Interfacial shear phenomena in graphite epoxy composites under impact loading using dynamic moire interferometry
[DE88-006773] 18 p2479 N88-24709
Contact force history and dynamic response due to the impact of a soft projectile
[NASA-TM-100961] 20 p2811 N88-26679
Control systems for platform landings cushioned by air bags
[AD-A196154] 24 p3358 N88-29996
Impact force as a part of the total breaking wave force on a vertical cylinder
[RR-CE78] 24 p3384 N88-30154

IMPACT MELTS
Spray deposition: A fundamental study of droplet impingement, spreading and consolidation
[AD-A186627] 08 p0970 N88-15869

IMPACT PREDICTION
Utilization of dynamic characteristics of materials to optimize military explosive charges. Application to antiship devices
[SNIAS-872-320-101] 05 p0610 N88-13743
Survey of impact damper performance
16 p2217 N88-23227

IMPACT PRESSURES
U IMPACT LOADS

IMPACT RESISTANCE
Impact behavior of 9-Cr and 12-Cr ferritic steels after low-temperature irradiation
[DE88-000333] 03 p0291 N88-11827
Development of an impact- and solvent-resistant thermoplastic composite matrix, phase 4
[NASA-CR-178413] 06 p0677 N88-14145
Behavior of a steel cylinder under the influence of a local load in the elastic and elasto-plastic area
[PB87-154787] 07 p0869 N88-15272
Abrasion and impact resistant coatings
[DE88-003562] 13 p1750 N88-20464
KRASH parametric sensitivity study: Transport category airplanes
[AD-A189962] 15 p2017 N88-22024
Evaluation of the US Army fitting program for the integrated helmet unit of the integrated helmet and display sighting system
[AD-A191616] 18 p2465 N88-24635
Improved procedure for impact probability computation of aircraft crash based on Balfanz model
[JUEL-SPEZ-425] 21 p2894 N88-27176
Deformation, fracture and explosive properties of reactive materials
[AD-A193060] 21 p2923 N88-27348

IMPACT SENSITIVITY
U IMPACT RESISTANCE

IMPACT STRENGTH
Laminated ferrous composites based on ultrahigh carbon (UHC) steels
[AD-A184617] 03 p0280 N88-11764
Impact behavior of 9-Cr and 12-Cr ferritic steels after low-temperature irradiation
[DE88-000333] 03 p0291 N88-11827
Models for penetration of thin plates
[DE87-013727] 03 p0332 N88-12090
Computer simulations of ballistic experiments
[DE87-005835] 07 p0862 N88-15226
Effect of low velocity impact on compression strength of a quasi-isotropic laminate
[FFA-TN-1987-38] 09 p1138 N88-16822
Effect of low-temperature aging on the mechanical properties of cast stainless steels
[DE88-002872] 10 p1300 N88-17774
A direct correlation of strength with impact velocity
[AD-A189251] 13 p1741 N88-20409
Structure and properties of welded joints produced between niobium parts in controllable helium atmosphere 14 p1897 N88-21326
A study of damage tolerance in curved composite panels
[AD-A190617] 15 p2029 N88-22092
Relation between the mechanical characteristics of carbon-resin composites and their impact strength
[REPT-48-284/F] 21 p2907 N88-27249

IMPACT TESTS
NT CHARPY IMPACT TEST
Full-scale transport controlled impact demonstration program
[NASA-TM-89642] 01 p0004 N88-10021
Shock-wave studies using plastic flyers driven by an electric gun for hypervelocity impact on selected materials
[DE87-012631] 01 p0008 N88-10046
High velocity erosion of metal interfaces
[DE87-013937] 01 p0025 N88-10155
Computations of hypervelocity impact using the CTH shock wave physics code
[DE87-013067] 02 p0169 N88-11062
A direct method to obtain constitutive model constants from cylinder impact test results
04 p0427 N88-12647
High explosive moulding powders from RDX and aqueous polyurethane dispersions
[AD-A185C26] 05 p0568 N88-13458
Numerical simulations of impact tests on a rigid wall --- armor steel
[SNIAS-872-320-102] 05 p0610 N88-13744
New mechanism of the high temperature (reversible) temper brittleness of alloy steels
[PB87-143954] 07 p0833 N88-15056
Study on the cryogenic toughness of stainless steel weld metals
[PB87-143830] 07 p0834 N88-15067
Residual stiffness and strength of Kevlar/epoxy laminated impulsively loaded to 7.9 ktaps
[DE88-003724] 09 p1149 N88-16886
High-velocity reverse ballistic rocket sled testing at Sandia National Laboratories 09 p1179 N88-17059
A direct correlation of strength with impact velocity
[AD-A189251] 13 p1741 N88-20409
Mechanical design of a ultrahigh gravity UHV facility to launch and recover a low-speed projectile tested on board KC 135 14 p1877 N88-21216
Studies of traverse impact damage in composite materials using a Hopkinson pressure-bar technique
[OUEL-1706/87] 14 p1883 N88-21255
Environmental effects on the post-impact compressive strength of CFC
[RAE-TM-MAT-STR-1086] 14 p1884 N88-21258
An investigation of the mechanical properties of improved carbon fibre composite materials
[RAE-TR-86021] 14 p1884 N88-21259
Phenomenological piercing characteristics of composite materials 14 p1895 N88-21315
Impact shock generator from explosively driven plates
[DE88-003596] 14 p1918 N88-21452
KRASH parametric sensitivity study: Transport category airplanes
[AD-A189962] 15 p2017 N88-22024
Response of aluminum alloys to erosive particle impacts
[DE88-005910] 15 p2041 N88-22159
Finite element simulation of perforation of aluminum plates
[DE88-002092] 15 p2073 N88-22362
Behaviour of fibre-reinforced composites under dynamic loading
[AD-A191310] 16 p2174 N88-22955
Peak Acceleration Device (PAD)
[AD-A191639] 18 p2461 N88-24611
Fuel containment and damage tolerance in large composite primary aircraft structures. Phase 2: Testing
[NASA-CR-172519] 19 p2601 N88-25452
Contact force history and dynamic response due to the impact of a soft projectile
[NASA-TM-100961] 20 p2811 N88-26679
Analysis of the perforation of monolithic and simple laminate aluminium targets as a test of analytical deformation models
[MRL-R-1111] 20 p2813 N88-26686
Milliwatt generator project
[DE88-011261] 20 p2853 N88-26939
Hypervelocity impact analysis with supercomputers
[DE88-006907] 21 p3001 N88-27797
Decomposition of energetic materials on the drop-weight impact machine
[DE88-009154] 22 p3059 N88-28152
Calibration of quartz load cells: An in-situ procedure for instrumented falling weight impact machines
[NPL-DMA(A)-155] 22 p3081 N88-28297
Experimental aspects of using time-averaged holographic interferometry to detect barely visible impact damage in a graphite/epoxy composite plate
[AD-A194418] 24 p3375 N88-30097

IMPACT TOLERANCES
Fuel containment, lightning protection and damage tolerance in large composite primary aircraft structures
[NASA-CR-3875] 17 p2317 N88-23839
Design manual for impact damage tolerant aircraft structure, addendum
[AGARD-AG-238-ADD] 21 p2895 N88-27185

IMPACTORS
Measurement of combustion aerosol size distributions with multistage inertial impactors
[DE88-751101] 11 p1454 N88-18669

IMPATT DIODES
U AVALANCHE DIODES

IMPEDANCE
NT ACOUSTIC IMPEDANCE
NT CONTACT RESISTANCE
NT ELECTRICAL IMPEDANCE
NT ELECTRICAL RESISTANCE
NT MECHANICAL IMPEDANCE
NT SKIN RESISTANCE
NT TRANSCONDUCTANCE
Impedance of passive lithium anodes in SOCl2 solutions under low-field polarization
[DE88-000922] 04 p0439 N88-12728
Interior impedance wedge diffraction with surface waves
[NASA-CR-182405] 07 p0854 N88-15186
Minimum necessary intensity of source of preionization for stabilization of a self-sustaining laser discharge with mean power raised by electron beam or X-rays
[PB87-178158] 09 p1171 N88-17024

Model-scale sound propagation experiment
[NASA-TM-100602] 15 p2130 N88-22709
Study on the flashover ion diode with cryogenic anode
16 p2279 N88-23642
AC impedance analysis of corrosion fatigue in naval aircraft alloys
[AD-A190822] 17 p2322 N88-23885
Scattering patterns of dihedral corner reflectors with impedance surface impedances
[NASA-CR-183078] 20 p2789 N88-26545
Some equivalent circuit models for AC impedance analysis of pyrite/solution interface
[DE88-010574] 21 p2939 N88-27452
Power supply conditioning circuit
[NASA-CASE-NPO-17233-1-CU]
23 p3208 N88-29095

IMPEDANCE MATCHING
Electromagnetic tests
[SNIAS-672-430-103] 05 p0575 N88-13506
The design of Impedance- matching networks for broadband antennas
[AD-A187600] 10 p1320 N88-17895
Vortices in long Josephson junctions
[AD-A190338] 15 p2059 N88-22279

IMPEDANCE MEASUREMENT
High-frequency limit of the longitudinal impedance
[CEBAF-PR-87-030] 02 p0234 N88-11479
Operators manual for a computer controlled impedance measurement system
[AD-A187513] 10 p1324 N88-17917
Estimation of body fluid shift by electrical impedance in various postures 12 p1661 N88-19956
A simulation analysis of errors in the measurement of standard electrochemical rate constants from phase-selective impedance data
[AD-A192739] 20 p2770 N88-26426
Ultrasonic detection of diffusion and adhesion loss
24 p3354 N88-29967

IMPEDANCE PROBES
Evaluation of a multi-point method for determining acoustic impedance
[NASA-TM-100637] 20 p2849 N88-26913

IMPELLER BLADES
U ROTOR BLADES (TURBOMACHINERY)

IMPELLERS
NT PUMP IMPELLERS
Calculation of the three dimensional flow in the impeller of hydraulic turbomachines using a finite element method
[ETN-87-90612] 03 p0315 N88-11988
Centrifugal compressors 07 p0850 N88-15162
Gas erosion of impeller housing in the operation of a high-temperature, high-pressure helium circulator
[DE88-002607] 09 p1175 N88-17041
Secondary flow measurements with L2F-technique in centrifugal compressors 10 p1283 N88-17676
A study of fluid-structure problems
21 p2941 N88-27468
JTDE 1 XTE34 materials research and development report
[AD-A194268] 22 p3044 N88-28063

IMPERFECTIONS
U DEFECTS

IMPINGEMENT
NT JET IMPINGEMENT
Performance of supersonic impingement radial turbines 06 p0712 N88-14367
Spray deposition: A fundamental study of droplet impingement, spreading and consolidation
[AD-A186627] 08 p0970 N88-15869
Studies on rocket exhaust plumes and impingement effects related to the Columbus Space Station program: Executive summary
[DFVLR-IB-222-88-A-12] 24 p3337 N88-29862

IMPLANTATION
NT ION IMPLANTATION
Design considerations for the development of an implantable sensor for the continuous measurement of glucose in the diabetic patient 17 p2382 N88-24159
Investigation of photoconductive picosecond microstripline switches on self-implanted Silicon On Sapphire (SOS) 19 p2657 N88-25789
Transport study on Si/Si(1-x)Ge(x) superlattices selectively doped by secondary implantation of Sb
20 p2867 N88-27027
NDP (Neutron Depth Profiling) evaluations of boron-implanted compound semiconductors
[AD-A192306] 21 p2934 N88-27425

IMPLICATION
Conservatism implications of shock test tailoring for multiple design environments
[DE87-013927] 03 p0336 N88-12127
Phenomenological implications of the blown-up orbifolds
[DE87-014608] 03 p0373 N88-12347
Implications of the trapping-desorption and direct inelastic scattering channels on Dicke-narrowed lineshapes
[AD-A191410] 16 p2270 N88-23581
The cost and performance implications of reliability improvements in the F-16A/B
[AD-A195096] 24 p3324 N88-29796

IMPLOSIONS
Time-resolved ablation measurements of imploding targets
[DE87-014464] 02 p0178 N88-11111
Time-resolved absorption measurements on OMEGA
[DE87-014465] 02 p0179 N88-11112
Analytic model of an imploding Z-pinch plasma colliding inelastically with a thin-shelled cylindrical target
[DE88-000051] 03 p0378 N88-12379
Advanced concepts theory annual report 1986
[AD-A184986] 05 p0651 N88-13991
Analysis for high compressible supersonic flow in converging nozzle
[IPPJ-860] 16 p2157 N88-22869
Proceedings of Symposium on Physics of Target Implosion and Pulsed Power Techniques
[IPPJ-859] 16 p2276 N88-23619
Analysis for fuel implosion in ICF target and pellet gain 16 p2276 N88-23620
Numerical analysis for effects of irradiation nonuniformities on target implosion
16 p2276 N88-23621
Numerical analysis of target implosion in LIB ICF
16 p2277 N88-23628
Pusherless implosion, pulse tailoring and ignition scaling law for laser fusion 16 p2277 N88-23629
Efficient shell implosion and target design
16 p2277 N88-23630
Stability requirement FOT ignition and high gain implosion = 2-D simulation for high neutron yield experiment = 16 p2278 N88-23633
Finite ion-relaxation and nonequilibrium radiation effects on laser-driven implosions 16 p2278 N88-23636
The application of Rutherford backscattering for analyzing multilayered structure change induced by pulsed ion beam bombardment 16 p2278 N88-23638

IMPROVEMENT
Performance improvements of an F-15 airplane with an integrated engine-flight control system
[NASA-TM-100431] 14 p1867 N88-21159
Parameter identification methods for improving structural dynamic models
[NASA-TM-100812] 17 p2349 N88-23994

IMPULSE GENERATORS
Development of a repetitive 1-MV, 22-kJ Marx generator
[DE87-011286] 01 p0038 N88-10242
The light pulse generator 869 for high speed investigations
[MPIS-9/1987] 11 p1491 N88-18898

IMPULSES
Structural frequency functions for an impulsive, distributed forcing function
[DE87-013811] 03 p0333 N88-12101
Analysis of photopole data reduction models
05 p0593 N88-13616
Dynamic evolution of the source volumes of gradual and impulsive solar flare emissions
[NASA-TM-87815] 08 p1102 N88-16621
Fiber-optics used to record high-speed photographs inside a pressurized tank during lethality testing
[DE88-011283] 21 p2951 N88-27529

IMPURITIES
X-ray studies of strain, interface and impurity in semiconductors
[DE87-013856] 01 p0104 N88-10678
Interaction between defects and the formation of dissipative structures in irradiated impure crystals
[DE87-703125] 02 p0246 N88-11552
Far infrared Fourier transform spectroscopy of semiconductors
[DE88-000188] 04 p0499 N88-13072
Chemical analysis for excimer laser systems
[DE88-001941] 05 p0589 N88-13591
Vibrational properties of disordered solids. Far infrared studies: Performance report
[DE88-001474] 06 p0786 N88-14821
Computer simulation of impurities and interfaces in body centered cubic metals
[PB88-108162] 07 p0832 N88-15047
Investigation of impurity defects in alpha-iron by molecular dynamics method
[DE88-700355] 07 p0834 N88-15058
Interface characteristics and the mechanical properties of metal matrix composites
[AD-A186441] 08 p0966 N88-15845
Effect of extraneous factors on optical one-phonon transitions in impurity centers with cubic symmetry
08 p1077 N88-16496
Impurity bands in quantum wells
[INPE-4250-PRE/1123] 08 p1089 N88-16552
Diagonal and off-diagonal disorder in doped quantum wells
[INPE-4255-PRE/1128] 08 p1089 N88-16556
Density of states of electrons bound to impurities in quantum wells of GaAlAs/GaAs
[INPE-4257-PRE/1130] 08 p1089 N88-16557
Modeling considerations for selected rf-plasma edge effects
[DE88-003285] 09 p1252 N88-17500
Superconductivity in La/sub 1.85-x/Nd/sub x/Sr/sub .15/CuO
[DE88-003014] 09 p1258 N88-17540
Mechanisms of intergranular attack and stress corrosion cracking of alloy 600 by high-temperature caustic solutions containing impurities
[DE87-012820] 10 p1300 N88-17773
Influence of non-metallic elements in the mechanical properties of 20 Mn Mo Ni 55 steel
[DE88-700412] 10 p1300 N88-17775
The effect of magnetic impurities and barriers on the magnetization and critical current of fine filament NbTi composites
[DE88-004443] 10 p1419 N88-18472
Deactivation of alumina based catalysts
11 p1455 N88-18673
Study of adherent oxide scales
[AD-A187366] 11 p1456 N88-18680
Influence of grain boundary phosphorus segregation on hydrogen embrittlement in steel
[DE88-700176] 11 p1459 N88-18696
Atomistic studies of the structure and properties of grain boundaries with substitutional impurities
[DE88-004161] 11 p1545 N88-19237
Spatial distribution of carbon and native defects in large-diameter bulk grown GaAs
[DE88-003870] 11 p1562 N88-19348
Laser raman studies related to liquid propellants: Structural characteristics inferred from the nitrate anion spectra
[AD-A188462] 12 p1612 N88-19641
Thermal oxide growth on silicon: Intrinsic stress and silicon cleaning effects
[AD-A188790] 13 p1736 N88-20377
Quantitative determination of a hydrogen impurity in a sodium coolant by hydride thermal dissociation
[NASA-TT-20239] 13 p1740 N88-20402
Study of activationless reactions of point defects with impurities and impurity-defect complexes in alpha-iron
[DE88-701028] 13 p1745 N88-20433
Research on multibandgap solar cells
[DE87-012261] 13 p1792 N88-20721
Evolution of poloidal variation of impurity density and ambipolar potential in rotating tokamak plasma, part 1
[DE88-006263] 13 p1842 N88-21022
Effect of Mg impurity on local vibrations of U-centers in LiF lattice 14 p1969 N88-21753
Magnetic impurities in superconductors
[DE88-006917] 14 p1986 N88-21846
Sublimation characteristics of H2O comet nucleus with CO2 impurities 14 p2010 N88-21988
Spectrographic detection of nitrogen impurity in helium
[DE88-752301] 15 p2033 N88-22111
Activities of As, Sb, Bi and Pb in copper mattes and their effects on impurity elimination
[TKK-V-A10(1988)] 15 p2041 N88-22165
High temparature corrosion of ceramics
[DE88-006567] 15 p2046 N88-22193
Long-time impurity confinement as a precursor to disruptions in ohmically heated tokamaks
[DE88-006183] 15 p2136 N88-22742
Observation of injected silicon in heliotron E
17 p2441 N88-24524
Flux density measurements of neutral iron in TEXTOR with laser induced fluorescence
17 p2442 N88-24528
Recent data on Si:As impurity band conduction multiplexed arrays
[AD-A191752] 18 p2582 N88-25340
Advanced development of double-injection, deep-impurity semiconductor switches
[NASA-CR-182118] 18 p2583 N88-25346
A general qualitative study of point and extended defects and their interactions in non-metallic systems
[AD-A191687] 19 p2618 N88-25532
Zero-dimensional calculation for ZT-H
[DE88-009175] 19 p2731 N88-26217
Evolution of poloidal variation of impurity density and ambipolar potential in rotating tokamak plasma, part 2
[DE88-009882] 19 p2731 N88-26218
Structural and magnetic properties of Fe impurities in YBa2Cu3O(sub 7-delta)
[DE88-009961] 19 p2735 N88-26247

Impurity transport calculations for a drift-dependent tokamak scrape-off plasma
[DE88-010053] 20 p2859 N88-26984
Bremsstrahlung from high Z impurities in hot plasmas
[DE88-011755] 20 p2881 N88-26994
Diffusion and solubility of some interstitial impurities in deformed metals
[DE88-701859] 21 p2914 N88-27296
Application of Auger electron spectroscopy to the study of trace element effects on weldability
[DE88-010457] 21 p2915 N88-27301
Prediction of deep levels and equilibrium concentrations of defects in semiconductors 21 p3023 N88-27945
X-ray studies of strain, interface and impurities in semiconductors
[DE88-012460] 21 p3025 N88-27954
Determination of impurities in silicon carbide by ICP AES (inductively coupled plasma atomic emission spectrometry) after coprecipitation with lanthanum hydroxide
[NASA-TT-20332] 23 p3193 N88-29003
Vibration spectra induced by impurities in 3-5-compounds semiconductors
[DE88-702730] 23 p3293 N88-29610
Impurity analysis in SIMOX samples by high-efficiency resonance ionization time-of-flight mass spectrometry
[DE88-012061] 24 p3367 N88-30051

IN-FLIGHT MONITORING
Acquisition of gust statistics from Aircraft Integrated Data Systems (AIDS) recorded data
[NLR-MP-86046-U-ISS-2] 06 p0745 N88-14586
Measurement and modification of sensorimotor system function during visual-motor performance
[AD-A186351] 07 p0869 N88-15387
Refinement of eye-point-of-regard measurement with helicopter pilots in a flight experiment
[ESA-TT-1073] 09 p1200 N88-17195
Flight testing of fighter aircraft
[MBB/LKE-62/S/PUB/292] 10 p1312 N88-17844
A system status monitor for the National Aerospace Plane
[AD-A190681] 18 p2463 N88-24624
In-flight load measurements of the Robot-X canards
[AD-A193428] 21 p2695 N88-27187
Robust digital model following controller for helicopters
[DFVLR-FB-88-07] 21 p2696 N88-27203
Proceedings of the 14th Symposium on Aircraft Integrated Monitoring Systems
[DFVLR-MITT-88-04] 22 p3033 N88-28001
From turboprop aircraft to multi-engined jet aircraft Aircraft Integrated Monitoring Systems (AIMS)
22 p3033 N88-28003
Aircraft component health monitoring: An effective approach 22 p3033 N88-28006
German Air Force requirements for the on-board life monitoring system (OLMOS) on Tornado
22 p3033 N88-28007
Onboard Life Monitoring System (OLMOS), hardware equipment onboard and on ground
22 p3034 N88-28009
A solution to improve a military aircraft's Onboard-Checkout-And-Monitoring-System (OCAMS)
22 p3034 N88-28013
Proposal for the on-board part of a future aircraft integrated monitoring system 22 p3035 N88-28016
V2500 Condition Monitoring and Performance Analysis Software System (COMPASS): Overview of system --- aircraft engine
[PNR90418] 22 p3139 N88-28666
Acquisition of gust statistics from AIDS-recorded data
24 p3313 N88-29733
The development of acoustic emission for structural integrity monitoring of aircraft
[AD-A196264] 24 p3427 N88-30398

INACTIVATION
U DEACTIVATION

INCENDIARY AMMUNITION
Granulation of pyrotechnic tracer composition R284T
[MRL-TN-528] 20 p2780 N88-26490

INCENTIVE TECHNIQUES
Anatomy of an organizational change effort at the Lewis Research Center
[NASA-CR-4146] 19 p2739 N88-26264

INCIDENCE
NT GRAZING INCIDENCE
Effects of free stream turbulence, Reynolds number and incidence angle on axial turbine cascade performance
05 p0548 N88-13339
An investigation of oblique hypervelocity impact
07 p0927 N88-15629
Influence of solar illumination conditions on TM/Landsat data
[INPE-4463-TDL/320] 12 p1638 N88-19806
Experimental investigation of the transonic flow at the leeward side of a delta wing at high incidence
[LR-518] 16 p2156 N88-22861
Description of a water tank facility: Study of a missile at high incidence 16 p2201 N88-23133
Curvature of blended rolled edge reflectors at the shadow boundary contour
[NASA-CR-182974] 18 p2576 N88-25300
On the global radiation incident variously orientated surfaces on the South Coast of Finland
[FMI-5] 20 p2823 N88-26748
A calculation of the turbulent boundary layer on a slender ellipsoid at low incidence
[FFA-TN-1988-02] 23 p3213 N88-29126

INCIDENT RADIATION
A method of long-term radar shower data analysis
06 p0738 N88-14541
Incident meteoroid flux density
06 p0739 N88-14542
On meteor stream spatial structure theory
06 p0739 N88-14544
Scattering of longitudinal wave normally incident on discal cavity in elastic body 08 p1077 N88-16492
Radiation balance components above the tropical evergreen Amazon forests (3rd campaign of data collection)
[INPE-4195-PRE/1079] 11 p1513 N88-19039

INCINERATION
U INCINERATORS

INCINERATORS
Government research on ceramics coating technology
16 p2184 N88-23019

INCLUSIONS
The effect of temperature on fatigue crack initiation from aluminosilicate inclusions
[PNR90377] 02 p0154 N88-10962
The effect of non-metallic inclusions on fatigue and fatigue thresholds of 25Mn-5Cr-1Ni steel
06 p0718 N88-14410
A comparison of film-based tomography and computed tomography for advanced ceramic materials
[DE88-003114] 07 p0837 N88-15079
Acoustic emission-microstructural relations in ferritic steels. Part 3: The effect of inclusion content
[AERE-R-12041] 10 p1341 N88-18015
Geophysical diffraction tomography for imaging isolated subsurface inclusions
[DE88-003918] 11 p1505 N88-18990
Resolution of the magnetotelluric method for determining local inhomogeneities in the sedimentary cover 13 p1789 N88-20701
An evaluation of nondestructive methods for ceramic heat exchanger applications
[DE88-006731] 15 p2068 N88-22328

INCOHERENCE
Theory of induced spatial incoherence
[AD-A185005] 05 p0651 N88-13992

INCOHERENT SCATTER RADAR
NT EISCAT RADAR SYSTEM (EUROPE)
High latitude problems to be studied by incoherent scatter radars
[DMI-GEOPHYS-PAPERS-R-77]
03 p0350 N88-12211
Radar observations of high-latitude lower-thermospheric and upper-mesospheric winds and their response to geomagnetic activity 06 p0742 N88-14563
EISCAT (European incoherent scatter radar) electron density studies
[AD-A185998] 07 p0841 N88-15099
Investigation of the Sun-aligned F-region walls and related phenomena in the auroral latitude range
[AFGL-TR-87-0248] 19 p2692 N88-26000

INCOHERENT SCATTERING
Lower bounds on bearing accuracy for closely spaced sources
[AD-A184258] 04 p0486 N88-12997
The solution of large linear inverse problems
06 p0691 N88-14238
Incoherent radar spectra 06 p0691 N88-14239
Characteristics of coherent and incoherent waves in snow at microwave and millimeter wave frequencies
[AD-A188990] 12 p1620 N88-19692
Spectrophotometric remote sensing of the diffuse aurora
[AD-A188599] 12 p1643 N88-19837
Dynamics of small and large scale irregularities at sub-auroral latitudes
[AD-A189052] 12 p1645 N88-19853
The effects of optical smoothing techniques on filamentation in laser plasmas
[AD-A188719] 16 p2275 N88-23614
Multiple scattering of waves in discrete random media
[AD-A191068] 18 p2499 N88-24823
Ionospheric radio and propagation: Waves in plasmas
24 p3364 N88-30030

INCOMPRESSIBILITY
A critical review of the development of several viscoplastic constitutive theories
[AD-A185652] 07 p0867 N88-15262
Generalized displacement method in the finite element analysis of incompressible material
[PB87-143434] 08 p0995 N88-16018
Vibrations of shells containing fluid
12 p1635 N88-19787
Equilibrium shocks in plane deformations of incompressible elastic materials
[AD-A188696] 12 p1636 N88-19796

INCOMPRESSIBLE BOUNDARY LAYER
Breakdown of steady and unsteady interacting boundary layers
[NLR-MP-86047-U] 01 p0045 N88-10284
A method for the approximate calculation of the skin friction coefficient of horizontal wavy plates
[VKI-TN-160] 07 p0851 N88-15172
Boundary layer calculation using digital computers
[REPT-MM-4] 10 p1309 N88-17821
Study of the boundary layer of a flow pulsed by acoustic waves
[ETN-88-91998] 16 p2206 N88-23163
Nonlinear Tollmien-Schlichting/vortex interaction in boundary layers
[NASA-CR-181698] 24 p3311 N88-29715

INCOMPRESSIBLE FLOW
NT STOKES FLOW
An inviscid model of planar, separated flows of finite extent
[RAE-TR-86070] 01 p0044 N88-10279
ARSPNS: A method to calculate steady and unsteady potential flow about fixed and rotational lifting and nonlifting bodies
[NLR-TR-85114-U] 01 p0044 N88-10282
NASA-VOF3D: A three-dimensional computer program for incompressible flows with free surfaces
[DE87-011849] 01 p0045 N88-10288
Instability of steady flow with constant vorticity in vessels with elliptical cross-section 02 p0159 N88-10997
Point vortex dynamics: Recent results and open problems
[DE87-014759] 03 p0314 N88-11982
The diffusion-convection vortex method for solving two-dimensional incompressible Navier-Stokes equation
03 p0317 N88-12001
The dynamics of bubble growth for Rayleigh-Taylor unstable interfaces
[AD-A184752] 03 p0321 N88-12027
On the instability of thin circular shear layers
04 p0395 N88-12467
Calculation of aerodynamic characteristics of three-dimensional finite span wings in potential incompressible flow 04 p0425 N88-12631
Studies of pressure-velocity coupling schemes for analysis of incompressible and compressible flows
[NASA-CR-181526] 04 p0443 N88-12748
NACHOS 2: A finite element computer program for incompressible flow problems. Part 2: User's manual
[DE88-001451] 04 p0443 N88-12750
Analytical studies of axially symmetric motion of an incompressible viscous fluid between two concentric rotating spheres 04 p0444 N88-12757
INS3D: An incompressible Navier-Stokes code in generalized three-dimensional coordinates
[NASA-TM-100012] 04 p0485 N88-12991
Numerical prediction of turbulent flows in dump diffusers 05 p0537 N88-13265
Computation of flow around 2-D circular cylinder
05 p0539 N88-13284
The development of a computer code (U2DIIF) for the numerical solution of unsteady, inviscid and incompressible flow over an airfoil
[AD-A185033] 05 p0541 N88-13293
Delta wing in incompressible flow. Experimental study in F2
[ONERA-RT-36/1147-AN-249-G]
05 p0541 N88-13298
Statistical theory of turbulent incompressible multimaterial flow
[DE88-000435] 05 p0579 N88-13535
Incompressible viscous flow simulations of the NFAC wind tunnel
[NASA-CR-177431] 07 p0816 N88-14969
Analysis of three-dimensional viscous internal flows
[AD-A186254] 07 p0849 N88-15155
Spectral methods: Analysis and applications to flow problems
[AD-A186265] 07 p0850 N88-15156
Nonlinear and nonparallel stability problems
[AD-A186406] 07 p0850 N88-15159
Mean velocities and Reynolds stresses in the juncture flow and in the shear layer downstream of an appendage
[AD-A185619] 08 p0960 N88-15923
Navier-Stokes solutions for laminar incompressible flow over a NACA 0012 airfoil and a backward facing step
[FFA-TN-1987-50] 09 p1162 N88-16966

A project to experimentally and theoretically examine fluid interfacial wave phenomena in a rotating cylindrical geometry: Current results and future plans
[DE88-003738] 09 p1165 N88-16984

Implicit solution of the incompressible Navier-Stokes equations in primitive variables on non-staggered grids
10 p1326 N88-17930

On the smallest scale for the incompressible Navier-Stokes equations
[NASA-CR-181626] 11 p1434 N88-18558

A hydrodynamic analysis of fluid flow between meshing spur gear teeth
[AD-A187671] 11 p1482 N88-18844

A new computational technique for generating algorithms, with application to the solution of the time-dependent incompressible Navier-Stokes equations
11 p1485 N88-18864

Transient radiative energy transfer in incompressible laminar flows
[NASA-CR-182605] 11 p1488 N88-18883

Three-dimensional incompressible Navier-Stokes computations of internal flows
[NASA-TM-100076] 12 p1576 N88-19425

High Reynolds number pump facility for cavitation research
[AD-A189310] 13 p1765 N88-20558

Potential applications of computational fluid dynamics to biofluid analysis
[NASA-TM-100069] 14 p1911 N88-21422

On the use of nonstaggered pressure-velocity arrangement for the numerical solution of incompressible flows
[KU-SFB-210/T/35] 16 p2206 N88-23165

Investigation of subgrid models in homogeneous incompressible turbulence
[ONERA-RSF-13/3419-AY-106-A]
16 p2209 N88-23183

The exact calculation of quadrupole sources for some incompressible flows
[NASA-TM-100623] 17 p2395 N88-24240

Incompressible Euler solution on a multiblock grid around a car configuration
[FFA-TN-1987-65] 18 p2457 N88-24586

Prediction of laminar and turbulent flows past single and twin airfoils 18 p2457 N88-24589

Continuum theories for fluid-particle flows: Some aspects of lift forces and turbulence
[DE88-007038] 18 p2511 N88-24898

Theoretical analysis of laminar incompressible flow in slender channels
[VTH-LR-517] 18 p2513 N88-24909

Finite element analysis of incompressible viscous flow around multi-element aerofoils 19 p2635 N88-25634

Computational boundary conditions for the incompressible Navier-Stokes equations in channels and pipes
[AD-A193356] 21 p2944 N88-27487

Numerical treatment of the pressure singularity at a re-entrant corner
[AD-A193357] 21 p2944 N88-27488

A fast vortex code for computing 2-D flow in a box
[DE88-011732] 21 p2946 N88-27498

Numerical methods for incompressible viscous flows with engineering applications
[NASA-CR-183143] 21 p2948 N88-27506

Surface tension and viscosity with Lagrangian hydrodynamics on a triangular mesh
[AD-A194120] 22 p3075 N88-28258

Steady and unsteady internal flow computations via the solution of the compressible Navier Stokes equations for low Mach numbers 23 p3209 N88-29100

Computation of the eigenvalues for perturbations of Poiseuille flow using a two-point boundary value method
[AD-A193479] 23 p3210 N88-29104

An exponential decay estimate for the stationary perturbation of Poiseuille flow
[AD-A193480] 23 p3210 N88-29105

Computational fluid dynamics methods for low Reynolds number precessing/spinning incompressible flows
[AD-A193891] 23 p3212 N88-29119

Numerical simulation of unsteady incompressible flow in a partially-filled rotating cylinder
[AD-A196001] 24 p3371 N88-30073

Numerical simulation of unsteady incompressible viscous flows in generalized coordinate systems
[NASA-TM-101016] 24 p3373 N88-30085

INCOMPRESSIBLE FLUIDS
NT MICROPOLAR FLUIDS

Determination of the dynamic parameters of annular clearances with turbulent flow and incompressible media
[ETN-87-90434] 01 p0047 N88-10303

Viscous damped space structure for reduced jitter
05 p0594 N88-13623

Well-posedness and spectral estimation for infinite dimensional systems
[AD-A187621] 10 p1401 N88-18354

Vibrations of shells containing fluid
12 p1635 N88-19767

Incompressible theory of interaction between moving bodies and vorticity field: Force on moving bodies by vorticity field 14 p1863 N88-21132

Theoretical studies of solar lasers and converters
[NASA-CR-182927] 17 p2344 N88-23972

Higher order vortex methods with rezoning
[DE88-010777] 21 p2947 N88-27505

Distributive iteration for indefinite systems as smoothing method in multigrid process on example of Stokes and Navier-Stokes equations with emphasis on incomplete decompositions
[ETN-88-92127] 21 p2948 N88-27509

Nonlinear oscillations of a nonviscous cylindrical liquid system in weightlessness condition
[LRT-WE-9-FB-14(1987)] 22 p3063 N88-28175

Nonlinear liquid motion in conical containers
[LRT-WE-9-FB-10(1987)] 22 p3077 N88-28270

Nonlinear oscillations in paraboloidal containers
[LRT-WE-9-FB-3(1988)] 22 p3078 N88-28275

INCONEL (TRADEMARK)

Near-threshold fatigue crack growth behavior at cryogenic temperature 06 p0718 N88-14409

Grain refinement during primary breakdown of alloy 718
[DE88-005193] 13 p1743 N88-20423

Modeling the viscoplastic behavior of Inconel 718 at 1200 F 14 p1929 N88-21502

An experimental comparison of several current viscoplastic constitutive models at elevated temperature
14 p1931 N88-21516

Milliwatt generator project
[DE88-011261] 20 p2853 N88-26939

INDEPENDENT VARIABLES
NT LATTICE PARAMETERS

Group analysis of equations arising in ocean acoustics
04 p0472 N88-12914

Investigation, development and application of optimal output feedback theory. Vol. 4: Measures of eigenvalue/eigenvector sensitivity to system parameters and unmodeled dynamics
[NASA-CR-4108] 04 p0482 N88-12969

The bimodality of large scale averaged flow parameters --- statistical weather forecasting
08 p1016 N88-16159

On error equations for determining Earth rotation parameters with VLBI network 13 p1756 N88-20500

Comperative analysis
[AD-A190556] 15 p2065 N88-22313

Effects of randomness of parameters on mean wave propagation in a viscoelastic medium
[REPT-87-60] 16 p2206 N88-23166

Improved estimators in simultaneous estimation of scale parameters
[AD-A191108] 17 p2392 N88-24216

Studies of HZE particle interactions and transport for space radiation protection purposes
[NASA-TM-101159] 20 p2886 N88-27142

Superconducting thin films, composites and junctions
[AD-A193123] 21 p2937 N88-27440

A minitab macro for the Kaplan-Meier product limit estimator and the Tarone-Ware class of tests
[AD-A194298] 23 p3248 N88-29331

A nonparametric multidimensional IRT approach with applications to ability estimation and test bias
[AD-A194212] 23 p3273 N88-29483

High power storage system based on thin film solid ionics
[AD-A193623] 23 p3291 N88-29598

Canonical variables and canonical integrals for motion in near-circular orbits 24 p3446 N88-30512

INDEXES (DOCUMENTATION)

Master index for the carbon dioxide research state-of-the-art report series
[DE87-012757] 01 p0072 N88-10459

Source header list. Volume 1: A through K
[AD-A184000] 04 p0501 N88-13086

USSR Space Life Sciences Digest index to issues 10-14
[NASA-CR-3922(17)] 07 p0883 N88-15361

TeXting the FORMULARY: A collection of examples of the use of TeX to produce ruled tables and displayed equations
[AD-A185920] 07 p0921 N88-15598

Source hierarchy list. Volume 1: A through D
[AD-A185900] 07 p0941 N88-15722

Source hierarchy list. Volume 2: E through O
[AD-A185901] 07 p0941 N88-15723

Source hierarchy list. Volume 3: P through Z
[AD-A185902] 07 p0942 N88-15724

A performance index approach to aerodynamic design with the use of analysis codes only
[NASA-TP-2805] 11 p1433 N88-18552

NASA scientific and technical publications: A catalog of Special Publications, Reference Publications, Conference Publications, and Technical Papers, 1987
[NASA-SP-7063(02)] 15 p2149 N88-22830

Engine structures: A bibliography of Lewis Research Center's research for 1980-1987
[NASA-TM-100842] 17 p2350 N88-24002

NASA combined file postings statistics based on NASA thesaurus, Jan. 1968 - July 1988
[NASA-CR-182965] 18 p2569 N88-25384

An assessment of index term ranking
21 p3028 N88-27974

A design for a ground-based data management system 24 p3420 N88-30355

INDEXES (RATIOS)
NT LEAF AREA INDEX

Vagal tone as an index of mental state
16 p2239 N88-23373

INDIA

Director of R and D institutions (Government of India)
[PB88-127162] 10 p1285 N88-17685

Science and technology in India
[PB88-134747] 11 p1564 N88-19362

District information system of National Information Centre
[PB88-134739] 11 p1565 N88-19373

National Informatics Centre: Profile of services
[PB88-134135] 12 p1706 N88-20211

Indian monsoon rainfall, 1986-1987
22 p3120 N88-28536

Differences in radiation budget parameters over Asia in relation to contrasting Indian monsoons
22 p3125 N88-28574

On climate prediction for India
22 p3127 N88-28590

INDIAN OCEAN

Interactions between the Asian monsoons, the tropical Pacific and the southern hemisphere extratropics
04 p0470 N88-12907

Modes of surface circulation and climate over the tropical Atlantic, Eastern Pacific, and Indian Oceans
06 p0742 N88-14564

New data on structure of earth's crust and seismicity of basins in Atlantic and Indian Oceans
08 p1010 N88-16123

Oceanographic features of the east and southeast Indian Ocean for June 1983
[AD-A186948] 09 p1195 N88-17158

Interannual variability in the Atlantic and Indian Oceans and its relationship to the southern oscillation
22 p3121 N88-28548

Indian Ocean validation
[AD-A194458] 23 p3175 N88-28902

INDIAN SPACECRAFT

Radio frequency compatibility between IRS and SPOT 3: Preliminary study
[CNES-86/CT/DRT/TIT/TR/011]
14 p1905 N88-21383

INDICATING INSTRUMENTS
NT ATTITUDE INDICATORS
NT CLOUD HEIGHT INDICATORS
NT POSITION INDICATORS
NT TACHOMETERS
NT WEIGHT INDICATORS

The P delta V fundamental gas leak calibration system qualification report
[DE88-008964] 21 p2951 N88-27526

INDIUM

Visible InGaAsP/GaAsP lasers produced by epitaxial growth from liquid phase 09 p1237 N88-17416

Strength and structure of Ga sub 1-xin sub xAs alloys
[AD-A188092] 10 p1303 N88-17795

Silicon and indium doping of GaAs: Measurements of the effect of duping on mechanical behavior and relation with dislocation formation
[DE88-003862] 11 p1554 N88-19303

New method of examining micrononhomogeneity of local centers in high-resistivity semiconductor materials under scanning electron microscope 14 p1969 N88-21754

Giant Josephson signal in wide superconducting films
14 p1973 N88-21777

Device physics related to the granular nature of CuInSe2 solar cells
[DE88-001159] 21 p2967 N88-27622

Studies on strained (In,Ga)As/GaAs semiconductors and optical devices 23 p3287 N88-29575

Muon-spin rotation experiment (micro + SR) on aluminum and indium after low temperature electron irradiation
[ETN-88-92985] 23 p3294 N88-29617

INDIUM ALLOYS

Nonlinear absorption of CO2 laser radiation in p-type InSb
[DE88-004055] 11 p1492 N88-18906

Studies of transverse phonon modes in premartensitic indium-thallium alloys
[DE88-003481] 13 p1744 N88-20428
Aluminum alloy
[NASA-CASE-LAR-13924-1-CU]
18 p2487 N88-24753

INDIUM ANTIMONIDES
MBE of HgCdTe
[AD-A191423] 16 p2283 N88-23671
Spectroscopy of one-dimensional subbands on InSb
20 p2864 N88-27007

INDIUM ARSENIDES
MBE growth of InAsSb strained-layer superlattices
[DE88-000365] 05 p0654 N88-14011
Development of a high speed InGaAs/InP Schottky barrier photodetector for millimeter-wave fiber optical links
[AD-A188594] 12 p1629 N88-19750
First report on InGaAs hall device
14 p1903 N88-21372
Photoluminescence studies of InGaAlAs quaternary alloys
[DE88-007197] 20 p2874 N88-27062
Photodiodes for optical communication in the near infrared
[ETN-88-92379] 21 p3016 N88-27900

INDIUM COMPOUNDS
NT INDIUM ANTIMONIDES
NT INDIUM ARSENIDES
NT INDIUM PHOSPHATES
NT INDIUM PHOSPHIDES
Deposition of device quality epitaxial layers of gallium nitride and indium nitride for electronic applications
[AD-A188001] 11 p1453 N88-18661
The synthesis, characterization and structural studies of In(C5H4Me) by X-ray diffraction and electron diffraction techniques and a reinvestigation of the crystaline state of In(C5H5) by X-ray diffraction studies
[AD-A189110] 13 p1844 N88-21038

INDIUM PHOSPHATES
Design and evaluation of single-lobed far-field pattern laser arrays: AlGaAs/GaAs and InGaAsP/InP systems --- optical communication
[LAAS-88-023] 16 p2214 N88-23211
Power MISFETs on OnP
[AD-A195242] 24 p3433 N88-30436

INDIUM PHOSPHIDES
Photoluminescence study of InP surfaces and InP-insulator interfaces
[ECL-87-13] 08 p1089 N88-16555
Progress in InP solar cell research
[NASA-TM-100914] 18 p2507 N88-24870
Planar fully ion-implanted high power InP MISFETs
[AD-A191589] 18 p2582 N88-25338
InP/GaInAs/InP PIN photodiode with FWHM less than 18 ps 19 p2658 N88-25799
Quantum-confined stark effect in InGaAs/InP quantum wells grown by metal-organic chemical vapor deposition
19 p2660 N88-25814
Investigations on the MBE (Molecular Beam Epitaxy) growth and properties of Al(sub y)Ga(sub y)In(sub 1-x-y)AsInP and InGaAs-InAlAs superlattices
[DE88-009105] 21 p3022 N88-27941

INDONESIA
Spatial and spectral registration of Javanese landscape units with SPOT 22 p3092 N88-28362
Thematic mapping of central Java (Indonesia)
22 p3100 N88-28412

INDOOR AIR POLLUTION
Committee on Interagency Radiation Research and Policy Coordination
[DE88-003358] 09 p1188 N88-17121

INDUCED FLUID FLOW
U FLUID FLOW

INDUCTANCE
NT PROXIMITY EFFECT (ELECTRICITY)
Inductance effects in the high-power transmitter crowbar system 04 p0433 N88-12687
Pulsed current transformer for low inductive loads
[AD-A187224] 10 p1324 N88-17913
Comparative evaluation of resistive and inductive techniques for measuring temperature of superconducting transition
[DE88-700603] 10 p1417 N88-18457
Inductive spurious coupling of a dc-SQUID to resonant input circuit
[NOTA-INTERNA-894] 14 p1908 N88-21401
Linear thyratron
[AD-A194111] 23 p3208 N88-29094

INDUCTION (MATHEMATICS)
Constructive version of the approximation induction principle
[PB88-165477] 15 p2122 N88-22647
The use of rule induction to assist in the diagnosis of avionic circuit board defects
[ETN-88-92077] 16 p2162 N88-22899
Induction of models under uncertainty
[NASA-TM-101173] 17 p2394 N88-24230
Induction instrument for logic conclusion
[LRT-WE-9-FB-5(1987)] 22 p3144 N88-28697

INDUCTION HEATING
A finite element model for induction heating of a metal crucible
[DE87-014246] 02 p0246 N88-11551
Model development for induction heating
[DE88-002376] 06 p0699 N88-14289

INDUCTION MOTORS
Process support compressor motor electromagnetic design summary
[DE87-014359] 02 p0167 N88-11048
The theory and implementation of a high quality pulse width modulated waveform synthesiser applicable to voltage FED inverters
[ETN-87-90712] 09 p1157 N88-16937
Industrial electric motors and controllers
[PB88-139589] 14 p1907 N88-21394
Analysis of induction motors based on the numerical solution of the magnetic field and circuit equations
[EL-59] 14 p1907 N88-21398

INDUCTION SYSTEMS
U INTAKE SYSTEMS

INDUCTORS
Response of helical structures to high speed pulses or when can a helix be called an inductor
[DE87-014347] 01 p0090 N88-10587
Advanced thermionic converter technology for inductive output coupling 17 p2407 N88-24311

INDUSTRIAL MANAGEMENT
NT ENGINEERING MANAGEMENT
NT INVENTORY CONTROLS
NT INVENTORY MANAGEMENT
NT PERSONNEL MANAGEMENT
The ESA centralized management system for satellite electronic test and checkout instrumentation
09 p1124 N88-16731
Research, development, and growth strategy
10 p1309 N88-17820
Operations research in management?
[MBB-Z-136/87] 10 p1311 N88-17835
Messerschmitt-Boelkow-Blohm, the company today. Data, numbers and facts 10 p1316 N88-17868
Soviet high-technology restructuring drive: the MNTK network
[AD-A168138] 11 p1565 N88-19370
Managing and controlling change
[PNR90419] 22 p3159 N88-28801
Human organization --- space projects
22 p3160 N88-28808

INDUSTRIAL PLANTS
Contribution to the design of flexible manufacturing systems: Modeling, simulation, and evaluation of parameters
[ISAL-IDI1-87-04] 09 p1151 N88-16894
Stable discrete-time adaptive control
19 p2719 N88-26142

INDUSTRIAL SAFETY
Safety guidelines and procedures for bioscience-based industry and other applied microbiology
[PB87-140521] 08 p1045 N88-16316
Toxic effects of man-made mineral fibers with particular reference to ceramic fibers
[AD-A187949] 11 p1519 N88-19072
Spectroradiometry in industrial safety
16 p2272 N88-23600
Evaluation of the potential health hazards associated with the machining of carbon fiber composites
[AD-A194835] 24 p3408 N88-30286

INDUSTRIAL WASTES
Global mixed-layer natural and anthropogenic fluxes
13 p1807 N88-20803
Waste destruction by plasma
[SNIAS-881-430-113] 21 p2971 N88-27651

INDUSTRIES
NT AEROSPACE INDUSTRY
NT AIRCRAFT INDUSTRY
NT DEFENSE INDUSTRY
Japanese industrial research on lean combustion: A case study: International Research Monitoring Program
[DE87-013839] 02 p0144 N88-10904
Spinoff, 1987
[NASA-TM-89652] 02 p0250 N88-11577
Composite materials in western Europe
[PB87-102943] 03 p0279 N88-11759
A national model at Howard University demonstrating private sector interrelationships that facilitate research in predominantly Black colleges and universities
[DE88-000160] 04 p0502 N88-13089
Impacts of world development on selected characteristics of the atmosphere: An integrative approach. Volume 1: Main report
[DE88-001495] 07 p0875 N88-15309
Impacts of world development on selected characteristics of the atmosphere: An integrative approach. Volume 2: Appendices
[DE88-001496] 07 p0875 N88-15310
An extended Cobb-Douglas form for use in production economics
[AD-A186372] 07 p0943 N88-15733
The development of emission tomography for the nuclear industry
[AERE-R-12319] 10 p1341 N88-18014
International Conference on Industrial and Applied Mathematics
[AD-A188251] 11 p1483 N88-18851
Status of emerging technologies: An economic/technological assessment to the year 2000
[PB88-155775] 11 p1567 N88-19381
Safety study: Commercial emergency medical service helicopter operation
[PB88-917001] 12 p1575 N88-19422
Basic research in ceramic and semiconductor science at selected Japanese laboratories, based on a September 1986 visit: Highlights, summary and overview and detailed notes from selected Japanese laboratories
[DOE/ER-0314] 12 p1696 N88-20150
A project to transfer technology from NASA centers in support of industrial innovation in the midwest
[NASA-CR-180360] 12 p1708 N88-20224
Development of a nationwide network for technology transfer
[NASA-CR-181058] 12 p1709 N88-20225
Technology transfer from US Federal laboratories: Report of a roundtable
[PB88-144803] 12 p1709 N88-20228
Some properties of Australian produced explosive composition H-6
[MRL-TN-525] 13 p1754 N88-20490
Industrial electric motors and controllers
[PB88-139589] 14 p1907 N88-21394
Lasers: Invention to application
[PB88-161583] 14 p1914 N88-21436
Preliminary market analysis for large zeolite crystals
[NASA-CR-182882] 15 p2049 N88-22207
The necessity of automation in Brazil
[INPE-4346-PRE/1183] 15 p2150 N88-22832
Status of CAD/CAM in medium-sized industries described 16 p2184 N88-23022
DOE (Department of Energy) national laboratories and the semiconductor industry: Continuing the joint planning
[PB88-170295] 16 p2281 N88-23657
Data management strategies in the industrial environment
[NLR-MP-87002-U] 16 p2286 N88-23684
Defense Small Business Innovation Research Program (SBIR). Volume 3: Air Force abstracts of phase 1 awards, 1987 17 p2448 N88-24548
Competitive assessment of the U.S. civil helicopter industry
[PB88-186325] 18 p2455 N88-24574
The application of hydrocarbon bioconversion technology to aerospace materials production
18 p2478 N88-24698
Determining system maintainability as a probability
[DE88-007722] 19 p2679 N88-25927
Photointerpretation with instrumentation for evaluation of environmental impact: Mata Atlantica in Cubatao
19 p2683 N88-25946
Study of evolution of vegetal cover and slide scars in the Cubatao municipality-Sao Paulo
19 p2683 N88-25947
Workshop report and presentations from the Semiconductor Research Corporation-DOE Semiconductor Task Force Workshop
[DE88-007690] 19 p2733 N88-26232
Resources: NASA for entrepreneurs
[NASA-CR-182152] 20 p2883 N88-27119
Federal Council on Science, Engineering and Technology: Committee on Computer Research and Applications, Subcommittee on Science and Engineering Computing: The US Supercomputer Industry
[DE88-011262] 21 p2994 N88-27756
Absorption heat pumps
[DE88-752820] 23 p3229 N88-29218

INELASTIC BODIES
U RIGID STRUCTURES

INELASTIC COLLISIONS
An interactive computer program for materials analysis by means of ion scattering
[MRL-R-1040] 01 p0091 N88-10596
Physics and chemistry 07 p0883 N88-15359
Particle-dynamics calculations of gravity flow of inelastic, frictional spheres
[DE88-005224] 13 p1770 N88-20586
Survey of impact damper performance
16 p2217 N88-23227
Forbidden transitions as ion-temperature sensitive lines 17 p2441 N88-24520

INELASTIC SCATTERING
Experimental studies of electromagnetic properties of few body systems
[DE87-014810] 02 p0161 N88-11008
Electron interactions with nuclei
[DE87-014587] 02 p0232 N88-11460
Consistency question in the renormalization group analysis of deep inelastic scattering
[DE87-703372] 04 p0487 N88-12999
Parton densities from deep inelastic scattering to hadronic processes at super collider energies
[NOTA-INTERNA-885] 07 p0930 N88-15646
Pion elastic and inelastic scattering near N=28
[LA-10968-T] 11 p1544 N88-19232
Advanced electron optics for vibrational spectroscopy
[AD-A188469] 12 p1629 N88-19747
On (p,n) systematics and the cosmological connection
[DE88-005031] 12 p1712 N88-20245
Analysis of hadron production in deep inelastic muon-proton collisions through the fire-string model
[PREPRINT-578] 14 p1981 N88-21822
Implications of the trapping-desorption and direct inelastic scattering channels on Dicke-narrowed lineshapes
[AD-A191410] 16 p2270 N88-23581
Memoirs of the Faculty of Science, Kyoto University. Series of Physics, Astrophysics, Geophysics and Chemistry, volume 37, no. 2
[ISSN-0368-9689] 16 p2287 N88-23694
Nuclear structure studies at intermediate energies
[DE88-006683] 18 p2571 N88-25271
Influence of scattering on seismic waves: Physical mechanisms contributing to attenuation in the crust
[AD-A191699] 19 p2690 N88-25992
Inelastic ion-surface collisions
[AFGL-TR-87-0206] 19 p2724 N88-26174
Half collision studies of inelastic energy transfer processes
[DE88-008096] 19 p2724 N88-26178
Inelastic two composite particle systems scattering at high energy
[DE88-701841] 20 p2851 N88-26928
Inelastic electron scattering and electron-hole excitations in iron and nickel
[DE88-011843] 21 p2915 N88-27303
Tagging of gamma yields qq bar events and direct measurement of the gluon structure function at HERA
[NOTA-INTERNA-910] 22 p3151 N88-28745
Effect of a laser field in the electron inelastic scattering into plasma fields
[DE88-702295] 23 p3218 N88-29157
On selection rules and inelastic electron scattering at intermediate energies
[DE88-701833] 23 p3280 N88-29526
Eikonal solutions to optical model coupled-channel equations
[NASA-TP-2830] 24 p3428 N88-30402
INELASTIC STRESS
Experimental determination of flow potential surfaces supporting a multiaxial formulation of viscoplasticity
02 p0187 N88-11167
Constitutive modeling of superalloy single crystals with verification testing 02 p0188 N88-11169
Unified constitutive models for high-temperature structural applications 14 p1932 N88-21523
A constitutive model for an overlay coating
14 p1933 N88-21525
On 3-D inelastic analysis methods for hot section components. Volume 1: Special finite element models
[NASA-CR-180893] 14 p1934 N88-21535
Experiments investigating advanced materials under thermomechanical loading 15 p2077 N88-22385
Three-dimensional inelastic approximate analysis code (MOMM) 15 p2079 N88-22392
Specialty three-dimensional finite element analysis codes 15 p2079 N88-22393
MHOST: An efficient finite element program for inelastic analysis of solids and structures
15 p2079 N88-22394
An experimental study of biaxial yield in modified 9Cr-1Mo steel at room temperature
[NASA-CR-175012] 24 p3385 N88-30164
INEQUALITIES
NT SCHWARTZ INEQUALITY
Feedback in LQCP (Linear Quadratic Control Problem) with a terminal inequality constraint
[PB87-220034] 06 p0762 N88-14676
On hypercontractivity of alpha-stable random variables, 0 less than alpha less than 2
[AD-A186425] 07 p0915 N88-15559
Norm inequalities for derivatives and differences
[DE88-002920] 09 p1230 N88-17371
Some majorization inequalities for functions of exchangeable random variables
[AD-A188207] 11 p1536 N88-19178
Additive prophet inequalities for transforms of uniformly bounded pairwise independent random variables
[PB88-173513] 18 p2568 N88-25250
Conditions for finite convergence of algorithms for nonlinear programs and variational inequalities
[AD-A192355] 20 p2838 N88-26834
INERT ATMOSPHERE
Spacecraft Fire Safety
[NASA-CP-2476] 04 p0406 N88-12520
Fire extinguishment and inhibition in spacecraft environments 04 p0406 N88-12523
Inerting and atmospheres 04 p0406 N88-12524
INERT GASES
U RARE GASES
INERTIA
WKBJ method and strained coordinates for high frequency inertial wave filtering
[INPE-4214-PRE/1095] 11 p1537 N88-19186
Horizontal scales of wind forced inertial motions
13 p1806 N88-20795
The buckling and vibration of composite plates using the Levy method considering shear deformation and rotary inertia
[AD-A189743] 15 p2076 N88-22374
Napping and human functioning during prolonged work
[AD-A190228] 15 p2102 N88-22525
A new method for the estimation of aircraft inertia characteristics 20 p2787 N88-26530
INERTIA BONDING
Inertia welding with variable magnitude of impact load
14 p1897 N88-21328
INERTIA MOMENTS
U MOMENTS OF INERTIA
INERTIA WHEELS
U REACTION WHEELS
INERTIAL CONFINEMENT FUSION
Status of inertial fusion
[DE87-010988] 01 p0099 N88-10654
Laser-plasma-interaction experiments using multikilojoule lasers
[DE87-013483] 01 p0100 N88-10658
Compact torus studies
[DE87-014254] 02 p0237 N88-11496
Filamentation instability of rotating light ion beams in fusion target chambers
[IPPJ-839] 02 p0242 N88-11530
Analysis of an induction linac driver system for inertial fusion
[DE88-000681] 03 p0379 N88-12384
Interplanetary propulsion using inertial fusion
[NASA-TM-89661] 04 p0409 N88-12540
The VISTA spacecraft: Advantages of ICF (Inertial Confinement Fusion) for interplanetary fusions propulsion applications
[NASA-CR-181549] 04 p0491 N88-13024
Inertial confinement fusion reactor cavity analysis
[DE88-000788] 04 p0492 N88-13028
ICRF launcher studies
[DE88-001710] 04 p0495 N88-13046
The Rayleigh-Taylor instability in ablatively accelerated targets with 1, 1/2 and 1/4 micrometers laser light
[AD-A185945] 07 p0858 N88-15208
Laser Program
[DE87-011009] 07 p0858 N88-15212
High Z interaction physics on Nova
[DE88-004397] 10 p1413 N88-18433
The stability of free-electron lasers against filamentation
[DE88-004712] 10 p1414 N88-18435
Diagnostics for ATF
[DE88-004175] 10 p1414 N88-18438
ATF experimental plans
[DE88-004177] 10 p1414 N88-18439
ICF research at Los Alamos
[DE88-005394] 11 p1493 N88-18916
ICF special studies
[DE88-004057] 11 p1551 N88-19281
Magnetic and inertial fusion status and development plans
[DE88-004405] 11 p1552 N88-19288
Potential benefits of a broad magnetic fusion R and D program
[DE88-003288] 11 p1553 N88-19297
The Magnetically Insulated Inertial Confinement Fusion (MICF): A novel approach
[DE88-005460] 13 p1842 N88-21026
Activities report in laser-matter interaction
[ETN-88-92007] 15 p2129 N88-22696
Environmental assessment for the compact ignition Tokamak
[DE88-005633] 15 p2135 N88-22740
Magnetic fusion energy plasma interactive and high heat flux components. Volume 5: Technical assessment of critical issues in the steady state operation of fusion confinement devices
[DE88-006920] 15 p2136 N88-22744
Rayleigh-Taylor instability in inertial confinement fusion
[DE88-701411] 15 p2137 N88-22750
Development of Electromagnetic PIC code for LIB diode 16 p2276 N88-23622
Kinetic theoretical analysis for propagation of rotating ion beam in ICF 16 p2276 N88-23623
Hybrid particle simulation for focusing of rotating and propagating LIB 16 p2276 N88-23624
Simulation code for ICF including radiative energy transfer 16 p2277 N88-23627
Efficient shell implosion and target design
16 p2277 N88-23630
Microinstabilities in ion beam propagation
16 p2277 N88-23631
Self-similar expansions in ion beam fusion
16 p2278 N88-23635
Two-dimensional focusing of self-magnetically insulated plasma focus diode 16 p2278 N88-23639
Research on anode plasma behavior of flashover pulsed ion sources 16 p2279 N88-23640
Study on the flashover ion diode with cryogenic anode
16 p2279 N88-23642
Interplanetary propulsion using inertial fusion
17 p2401 N88-24273
Inertial fusion in the nineties
[DE88-007913] 19 p2730 N88-26214
Pulsed power driver technologies for inertial confinement fusion power reactors
[DE88-009260] 19 p2731 N88-26221
The effect of ICRF on the Alcator C Scrape-Off Layer plasma
[DE88-009821] 20 p2858 N88-26972
INERTIAL FORCES
U INERTIA
INERTIAL FUSION (REACTOR)
Status of inertial fusion
[DE87-010988] 01 p0099 N88-10654
LLE Review, volume 30
[DE87-014469] 02 p0178 N88-11109
Analysis of an induction linac driver system for inertial fusion
[DE88-000681] 03 p0379 N88-12384
Interplanetary propulsion using inertial fusion
[NASA-TM-89661] 04 p0409 N88-12540
Heavy-ion accelerator research for inertial fusion
[DE88-000541] 05 p0653 N88-14001
Particle transport in microdetonations — inertial confinement fusion pellets
[OEFZS-4402] 09 p1164 N88-16976
Magneto-Inertia Confinement Approach (MICA) to fusion in dynamic Z-pinch formed from a frozen deuterium-tritium tube
[IPPJ-856] 09 p1252 N88-17504
Design issues for a laboratory high gain fusion facility
[DE88-004406] 10 p1413 N88-18434
Interplanetary propulsion using inertial fusion
17 p2401 N88-24273
INERTIAL GUIDANCE
NT STRAPDOWN INERTIAL GUIDANCE
Optical alignment of Centaur's inertial guidance system
[NASA-TM-88844] 04 p0405 N88-12515
Gyrostabilizer system of Kvant module
08 p1006 N88-16099
Development of a facility using robotics for testing automation of inertial instruments
09 p1213 N88-17271
Reference position vector 12 p1577 N88-19432
Rate and dynamic tests on the Canadian Strapdown Gyroscope (CSG-2) 12 p1578 N88-19439
Convective heat transfer and its effect on inertial measurement units 12 p1578 N88-19442
Features of Soyuz TM spacecraft
13 p1727 N88-20329
Inertial reference system with Global Positioning System (GPS) support 18 p2518 N88-24936
INERTIAL MEASURING UNITS
U INERTIAL PLATFORMS
INERTIAL NAVIGATION
Test equipment with fiber optic data bus and laser gyro strapdown system LTN-90 for the helicopter BO-105
[ESA-TT-1038] 01 p0005 N88-10025
NAVSIM 2: A computer program for simulating aided-inertial navigation for aircraft
[NASA-CR-177438] 04 p0398 N88-12478
Correction of inertial navigation system drift errors for an autonomous land vehicle using optical radar terrain data
[AD-A184973] 05 p0544 N88-13311

A conceptual design of an inertial navigation system for an autonomous submersible testbed vehicle
[AD-A188038] 11 p1438 N88-18578
Thirteenth Biennial Guidance Test Symposium, volume 1
[AD-A185782] 12 p1576 N88-19427
Calibration of a ring laser gyro inertial navigation system 12 p1576 N88-19428
Simultaneous estimation and detection of bias shifts for inertial navigation systems 12 p1576 N88-19429
Covariance analysis and post-processing of gravity compensation effects for aided multi-state navigation systems
[PAPER-87-13] 12 p1577 N88-19430
Commonality in the design and production of the H-423 (F3) and H-770 (F-15) RLG inertial navigation systems
12 p1577 N88-19431
The global positioning system as an aid to the testing of inertial navigation units (volume 1, addendum 1)
[AD-A185783] 12 p1578 N88-19443
An evaluation of perceptions of form, fit, function (F3) standardization on the Standard Inertial Navigation Unit (STD INU) program
[AD-A188955] 12 p1579 N88-19446
Optics: Perspectives for Measurement Techniques and Signal Processing for Flight Guidance — conference
[DFVLR-MITT-87-21] 18 p2516 N88-24928
Laboratory tests of laser gyroscopes for future utilization in multifunction systems for precision navigation and flight guidance 18 p2517 N88-24932
The optical accelerometer: A novel sensor for vertical flight guidance 18 p2518 N88-24935
On-board data processing of navigation data at high latitudes in Antarctica 22 p3036 N88-28027
Performance of GPS-aided INS during high-dynamic maneuvers
[AD-A194624] 23 p3175 N88-28903
Angle of attack and sideslip estimation using an inertial reference platform
[AD-A194876] 24 p3319 N88-29769
Observed track-keeping performance of DC10 aircraft equipped with the Collins AINS-70 area navigation system: Karlsruhe and Masstricht UACs (Upper Area Control centres)
[EEC-202] 24 p3323 N88-29786
Estimation of short-wavelength gravity on a dense grid using digital terrain elevation data
[AD-A196325] 24 p3391 N88-30196

INERTIAL PLATFORMS
Application of the Single-Axis rate Table (SAT) of the DFVLR for the evaluation of stationary and dynamic gyro properties
[DFVLR-MITT-88-09] 21 p2952 N88-27533
Angle of attack and sideslip estimation using an inertial reference platform
[AD-A194876] 24 p3319 N88-29769

INERTIAL REFERENCE SYSTEMS
The global positioning system as an aid to the testing of inertial navigation units (volume 1, addendum 1)
[AD-A185783] 12 p1578 N88-19443
A study on local level inertial surveying systems. Error model for the stationary system
[B8736714] 16 p2229 N88-23312
Laboratory tests of laser gyroscopes for future utilization in multifunction systems for precision navigation and flight guidance 18 p2517 N88-24932
Inertial reference system with Global Positioning System (GPS) support 18 p2518 N88-24936

INERTIAL UPPER STAGE
Qualification by analysis of IUS plume deflectors
09 p1179 N88-17063

INFARCTION
NT MYOCARDIAL INFARCTION

INFECTIONS
U INFECTIOUS DISEASES

INFECTIOUS DISEASES
NT BACTERIAL DISEASES
NT FUNGAL DISEASES
NT PARASITIC DISEASES
Illustrations of a density-equalizing map projection technique
[DE87-013992] 03 p0339 N88-12130

INFERENCE
Analogical inference and analogical access
[AD-A184345] 03 p0369 N88-12321
Statistical inference: Computer oriented algorithmic approach
[DE87-013874] 04 p0478 N88-12948
An APL workspace for conducting nonparametric statistical inference
[AD-A184971] 05 p0634 N88-13877
Genie inference engine rule writer's guide
[AD-A185709] 06 p0762 N88-14675
An inference engine for embedded diagnostic systems
08 p1056 N88-16367
The empirical accuracy of uncertain inference models
09 p1208 N88-17243
TYPICAL: A knowledge representation system for automated discovery and inference
[AD-A187483] 11 p1533 N88-19160
Expert systems: Their impact on performance and cognitive strategies in diagnostic inference
[AD-A188518] 12 p1677 N88-20027
Knowledge retrieval as specialized inference
[AD-A189042] 13 p1823 N88-20899
Inference engine for expert systems
[INPE-4465-TDL/321] 15 p2113 N88-22590
Statistical inference for stochastic processes
[AD-A190491] 15 p2126 N88-22673
Studies in reliability and inference
[AD-A191389] 16 p2217 N88-23223
Capitalizing on failure through case-based inference
[AD-A190927] 16 p2255 N88-23480
Inference for a nonlinear semimartingale regression model
[AD-A190857] 16 p2262 N88-23527
Induction of models under uncertainty
[NASA-TM-101173] 17 p2394 N88-24230
User's guide to the Fault Inferring Nonlinear Detection System (FINDS) computer program
[NASA-CR-178410] 18 p2462 N88-24619
Adaptive time series analysis using predictive inference and entropy
[AD-A191858] 18 p2560 N88-25199
A network approach to the certainty factor model — expert systems
[CWI-CS-R8757] 20 p2840 N88-26852
Topics in adaptive control and inference
[AD-A194718] 23 p3266 N88-29443
Theories of comparative analysis
[AD-A196328] 24 p3427 N88-30395

INFILTRATION
Ceramic composites by chemical vapor infiltration
[DE87-009128] 01 p0029 N88-10185
Cast iron freezing mechanisms
03 p0298 N88-11870

INFINITY
Equivalence of input-output stability and exponential stability for infinite dimensional systems
[TW-276] 05 p0638 N88-13903
Conditions at infinity for theories of oscillating wings and propellers in subsonic flow
[NAL-TR-937] 11 p1434 N88-18556
Algorithm for accounting the conditions in infinity for two-dimensional magnetostatics problems
[DE88-701673] 16 p2264 N88-23541

INFLATABLE DEVICES
U INFLATABLE STRUCTURES

INFLATABLE STRUCTURES
NT BALLOONS
NT GAS BAGS
NT HIGH ALTITUDE BALLOONS
NT JIMSPHERE BALLOONS
Far infrared spectroscopy telescope (FIRST) inflatable thermal shield, phase 1
[SR/FIS/108(87)CZ] 24 p3453 N88-30552

INFLATING
Rheological behaviors of an elastomeric membrane
[DE87-013105] 01 p0061 N88-10392
Renal effects of anti-gravity suit inflation in man in relation to cardiovascular and hormonal changes
12 p1661 N88-19959

INFLECTION POINTS
Boundary value problems for ordinary differential equations with multiple turning points
[CWI-AM-R8701] 09 p1228 N88-17354

INFLUENCE COEFFICIENT
NT STRUCTURAL INFLUENCE COEFFICIENTS
An initial investigation into methods of computing transonic aerodynamics sensitivity coefficients
[NASA-CR-182444] 09 p1112 N88-16663
The experimental verification of wall movement influence coefficients for an adaptive walled test section
[NASA-CR-181681] 19 p2596 N88-25439
Investigation of oscillating cascade aerodynamics by an experimental influence coefficient technique
[NASA-TM-101313] 22 p3039 N88-28041
Comparison of the influence of different gust models on structural design 24 p3312 N88-29722
An experimental study of an adaptive-wall wind tunnel
[NASA-CR-183152] 24 p3329 N88-29821

INFORMATION
Summaries of the FY 1987 applied mathematical sciences research program
[DE87-014447] 02 p0225 N88-11416
Wave and wind data sources, environmental conditions committee report, International Ship and Offshore Structures Congress
[PB87-234902] 06 p0746 N88-14588
Conceptual information processing: A robust approach to KBS-DBMS integration 08 p1063 N88-16422
Resonance, information, and the primacy of process: Ancient light on modern information and communication theory and technology 10 p1424 N88-18506
The optimum solution to instrument quantization effects 12 p1577 N88-19434
Interfacing and integrating hardware and software design systems 17 p2306 N88-23796

INFORMATION ADAPTIVE SYSTEM
An interactive computer graphics network monitor for a tactical communications network
[AD-A184131] 04 p0477 N88-12938

INFORMATION DISSEMINATION
NT MESSAGES
Spacecraft 2000 program overview
01 p0015 N88-10085
NASA's new technology reporting system: A review and future prospects
[NASA-CR-180954] 01 p0105 N88-10686
Freedom of Information Act: Fee waiver practices at the FBI (Federal Bureau of Investigation)
[PB87-216727] 02 p0249 N88-11573
Automatic photometric monitoring of cool stars
04 p0504 N88-13103
Role of technical information in innovation
[PB87-235388] 05 p0656 N88-14039
Role of the technical report in technological innovation
[PB87-232500] 05 p0658 N88-14040
Inexpensive solution for the mass distribution of satellite images
[PB88-114038] 10 p1317 N88-17873
NASA/UK TAP
[NASA-CR-180350] 12 p1706 N88-20223
Applicability of aerospace thermal insulation technologies to the civilian sector
[DE88-003717] 13 p1852 N88-21086
Sigma system: Overview, prospects
15 p2052 N88-22230
Presentation of the METEOSAT system and the roles of EUMETSAT within the meteorological community
17 p2357 N88-24039
Computer resource management technology program (PE 64740F). Task no. 9: Advanced user authentication
[PB88-183066] 18 p2555 N88-25163
Technology transfer, Sandia National Laboratories
[DE88-009790] 19 p2740 N88-26268
Context of national information systems in developing countries: India and China in a comparative perspective
[PB88-109954] 20 p2882 N88-27111
Flight information publication (FLIP) feedback
[AD-A194462] 23 p3174 N88-28897
Barriers to Information Transfer and Approaches Toward Their Reduction
[AGARD-CP-430] 24 p3437 N88-30458
Linguistic and cultural barriers to the transfer of information 24 p3437 N88-30459

INFORMATION FLOW
Application of artificial intelligence to impulsive orbital transfers 08 p1066 N88-16439
Data flow graph optimization in IF1
[DE88-004396] 11 p1532 N88-19151
Rapid prototyping of complex avionic system architectures 17 p2302 N88-23771
A multiprocessor data flow accelerator module
[DE88-007587] 18 p2554 N88-25161
Technology transfer, Sandia National Laboratories
[DE88-009790] 19 p2740 N88-26268
Context of national information systems in developing countries: India and China in a comparative perspective
[PB88-109954] 20 p2882 N88-27111
Hiding in stream semantics of uniform concurrency
[PB88-121579] 20 p2882 N88-27114
Large-grain pipelining on distributed-memory multiprocessors
[DE88-009974] 23 p3264 N88-29432

INFORMATION MANAGEMENT
Implementing and managing change: A guide for assessing information technology
[DE88-000035] 02 p0249 N88-11571
Advanced Information Processing System (AIPS) proof-of-concept system functional design I/O network system services
[NASA-CR-181486] 03 p0384 N88-12413
Electronic Records Administration at the Savannah River Plant
[DE87-014842] 03 p0384 N88-12415
Information analysis centers in the department of defense, revision
[AD-A184002] 03 p0385 N88-12420
Foundation: Transforming data bases into knowledge bases 08 p1063 N88-16423
The intelligent user interface for NASA's advanced information management systems
08 p1063 N88-16424
Media independent interface. Interface control document
[NASA-CR-172032] 08 p1067 N88-16447

Information handling architecture and software for CIM (Computer Integrated Manufacturing)
[PB88-105820] 08 p1067 N88-16453
Distributed transaction processing and the Camelot system
[AD-A188614] 13 p1821 N88-20885
Laboratory Information Management System (LIMS): A case study
[NASA-TM-100835] 14 p1961 N88-21697
Information systems for quality. Experience at the Nerviano Aeritalia plant. Avionic systems and equipment group
[ETN-88-92274] 15 p2148 N88-22821
Crewstation Information and Development System (CIDS) 17 p2304 N88-23781
Designing for design effectiveness of complex avionics systems 17 p2305 N88-23788
Space Power Reference Source (SPRS): A user's guide to SDI Space Power Technology Programs
17 p2427 N88-24440
Developing a connector selection DBMS (database management system) using NIAM (Nijssen's Information Analysis Methodology)
[DE88-008110] 21 p3028 N88-27972
Pattern information processing and multimedia database system: Current research on multimedia information system
[PB88-131917] 21 p3028 N88-27973
Information retrieval systems evolve-advances for easier and more successful use 24 p3438 N88-30462

INFORMATION PROCESSING (BIOLOGY)
A survey of artificial neural systems
[AD-A184759] 03 p0368 N88-12312
Taskomat, a task battery for information processing
[IZF-1987-2] 05 p0630 N88-13851
Genie inference engine rule writer's guide
[AD-A185709] 06 p0762 N88-14675
Probabilistic neural networks: In or out of equilibrium
[DE88-002907] 09 p1201 N88-17198
A situation-response model for intelligent pilot aiding
09 p1208 N88-17241
A conceptual framework for intelligent real-time information processing 09 p1211 N88-17257
Two attentional models of classical conditioning: Variations in CS effectiveness revisited
[AD-A187697] 11 p1522 N88-19088
Electromagnetic metrics of mental workload
[AD-A188205] 11 p1523 N88-19093
When decision aids fail
[AD-A187531] 11 p1523 N88-19095
A personalized and prescriptive decision aid for choice from a database of options
[AD-A188726] 13 p1811 N88-20820
Synapses that compute motion
[AD-A190389] 15 p2116 N88-22607
Processing deficits in monitoring analog and digital displays: Implications for attentional theory and mental-state estimation research
16 p2241 N88-23389
Information processing deficits in psychiatric populations: Implications for normal workload assessment 16 p2241 N88-23390
Novel nonlinear signal processing principles
[AD-A191644] 19 p2707 N88-26097
Contra- and ipsilateral auditory stimuli produce different activation patterns at the human auditory cortex: A neuromagnetic study
[PB88-181490] 19 p2708 N88-26098
Working memory capacity: An individual differences approach
[AD-A192359] 20 p2833 N88-26803
A review of workload measurement in relation to verbal comprehension 21 p2925 N88-27360
The effects of increased cognitive demands on autonomic self-regulation: An indicator of parallel processing in the brain 21 p2925 N88-27362
Mitsubishi Electric Advance (R and D Edition), Volume 41
[PB88-194162] 21 p2929 N88-27386
Basic research on optical neural computers
21 p2929 N88-27389
Electric and Magnetic Activity of the Central Nervous System: Research and Clinical Applications in Aerospace Medicine
[AGARD-CP-432] 21 p2977 N88-27683
Dissecting the visual and auditory pathways by means of the two-input technique 21 p2978 N88-27690
Electric and magnetic brain activity related to cognitive performance 21 p2979 N88-27692
Neuromagnetic evidence of place mechanisms for frequency and intensity coding in the human auditory cortex 21 p2979 N88-27693
A study of sources in the human brain associated with stereopsis 21 p2979 N88-27695
The effects of hypoxia on P300 and reaction time
[DCIEM-87-RR-12] 21 p2979 N88-27697
Using ERPS to study human information processing
21 p2980 N88-27698
The effect of mild hypoxia on the vestibular evoked response 21 p2982 N88-27713
Transformations of short-term visual memory
[AD-A193873] 23 p3241 N88-29290
Nested neural networks
[NASA-TM-101032] 24 p3423 N88-30373

INFORMATION RETRIEVAL
A parallel model of the kinetic depth effect using local computations
[AD-A181945] 01 p0083 N88-10536
On perfect hash functions
[ENST-88D008] 01 p0087 N88-10565
High performance clause indexing
[DE87-011309] 01 p0106 N88-10688
Optical laser technology, specifically CD-ROM (Compact Disc - Read Only Memory) and its application to the storage and retrieval of information
[AD-A184111] 03 p0330 N88-12086
Electronic Records Administration at the Savannah River Plant
[DE87-014842] 03 p0384 N88-12415
Source header list. Volume 2: L through Z
[AD-A184001] 03 p0385 N88-12419
Towards automated consulting: Design feedback from the performance of online documentation
[DE87-012243] 04 p0501 N88-13082
Subjective probability, combination of expert opinion and probabilistic approaches to information retrieval
04 p0501 N88-13085
Storing and retrieving data in a parallel distributed memory system
[AD-A185177] 05 p0637 N88-13897
Status, outlook of optical technology in information equipment field 06 p0689 N88-14222
Using user models and automatic expertise acquisition in data base interactions
[PB87-234357] 06 p0791 N88-14848
A review of hypertext in a NASA project management context 06 p0793 N88-14859
Source hierarchy list. Volume 1: A through D
[AD-A185900] 07 p0941 N88-15722
Source hierarchy list. Volume 2: E through O
[AD-A185901] 07 p0941 N88-15723
Source hierarchy list. Volume 3: P through Z
[AD-A185902] 07 p0942 N88-15724
Problem solving as intelligent retrieval from distributed knowledge sources 08 p1059 N88-16392
User's guide to a data base of current environmental monitoring projects in the US-Canadian transboundary region
[DE88-002476] 09 p1188 N88-17119
Recovery using virtual memory
[AD-A187098] 09 p1217 N88-17296
Inexpensive solution for the mass distribution of satellite images
[PB88-114036] 10 p1317 N88-17873
A hypertext writing environment and its cognitive basis
[AD-A188179] 10 p1389 N88-18298
Using SIR (Scientific Information Retrival) system for data management during a field program
[DE88-001555] 10 p1424 N88-18506
The acoustic-modeling problem in automatic speech recognition
[AD-A188529] 13 p1757 N88-20510
Knowledge retrieval as specialized inference
[AD-A189042] 13 p1823 N88-20899
A menu-driven knowledge retrieval system accessing ASCII data
[DE88-001742] 13 p1851 N88-21079
Baseline observing system experiments using the AFGL global data assimilation system
[AD-A188861] 15 p2024 N88-22062
Relationship of encoding speed and memory tests to flight training performance
[AD-A190670] 15 p2105 N88-22539
The Scientific and Technical Information Network (STINET). Foundation for evolution
[AD-A189750] 15 p2148 N88-22822
The Engineer Studies Center guide to research and data collection
[AD-A189971] 16 p2285 N88-23680
Translations of scientific and technical literature: A guide to their location 16 p2286 N88-23686
Extracting information from problem solving experience
[AD-A191331] 16 p2286 N88-23688
Defense Technical Information Center cataloging guidelines
[AD-A192200] 18 p2589 N88-25382
Engineering drawings and changes: Storing and controlling by the tens of terrabytes
[DE88-007605] 18 p2589 N88-25387
Computer-aided research
[DE88-007771] 19 p2714 N88-26114
MVS (Multiple Virtual Storage) batch computing and data management at ANL
[DE88-007342] 19 p2718 N88-26137
A cockpit natural language study - selected transcripts
[AD-A192972] 20 p2834 N88-26808
Use of optical disk technology at the Air Command and Staff College
[AD-A192424] 21 p3027 N88-27969
Capitalizing on experience with intelligence gateway software
[AD-A193362] 21 p3028 N88-27971
An assessment of index term ranking
21 p3028 N88-27974
Walter user's manual (Version 1.0)
[AD-A192542] 22 p3136 N88-28644
Optimization techniques for relational database systems 22 p3137 N88-28650
Distributed knowledge base systems for diagnosis and information retrieval
[AD-A193107] 23 p3296 N88-29633
Experiments in automatic phrase indexing for document retrieval: A comparison of syntactic and non-syntactic methods 23 p3296 N88-29634
Information retrieval systems evolve-advances for easier and more successful use 24 p3438 N88-30462

INFORMATION SYSTEMS
NT GEOGRAPHIC INFORMATION SYSTEMS
NT INFORMATION ADAPTIVE SYSTEM
NT MANAGEMENT INFORMATION SYSTEMS
NT NUMERICAL DATA BASES
Compilation and analysis of air quality data in support of acid deposition research
[DE87-014428] 02 p0196 N88-11226
The microcomputer as an engineering management tool
[DE87-014882] 02 p0219 N88-11378
Design and development of a database for spectral data and analysis results
[DE87-011323] 02 p0247 N88-11564
Implementing and managing change: A guide for assessing information technology
[DE88-000035] 02 p0249 N88-11571
Lewis Information Network (LINK): Background and overview
[NASA-TM-100162] 03 p0305 N88-11925
Advanced Information Processing System (AIPS) proof-of-concept system functional requirements I/O network system services
[NASA-CR-181481] 03 p0384 N88-12412
Advanced Information Processing System (AIPS) proof-of-concept system functional design I/O network system services
[NASA-CR-181488] 03 p0384 N88-12413
The impact of information technology on research in science and engineering
[DE88-000342] 03 p0385 N88-12417
Information analysis centers in the department of defense, revision
[AD-A184002] 03 p0385 N88-12420
Advanced techniques for the storage and use of very large, heterogeneous spatial databases. The representation of geographic knowledge: Toward a universal framework — relations (mathematics)
[NASA-CR-181517] 03 p0385 N88-12421
Materials sciences programs: Fiscal Year 1987
[DE88-000672] 04 p0429 N88-12659
Space station software reliability analysis based on failures observed during testing at the multisystem integration facility 06 p0798 N88-14884
Facility design validation of the information systems laboratory
[AD-A186309] 07 p0906 N88-15488
Compilation and development of K-6 aerospace materials for implementation in NASA spacelink electronic information system 07 p0922 N88-15605
DoD Gateway Information System (DGIS) common command language: The first prototyping and the decision for artificial intelligence
[AD-A185950] 07 p0942 N88-15725
DoD Gateway Information System (DGIS): Common command language mapping
[AD-A185951] 07 p0942 N88-15726
Problem solving as intelligent retrieval from distributed knowledge sources 08 p1059 N88-16392
Conceptual information processing: A robust approach to KBS-DBMS integration 08 p1063 N88-16422
The intelligent user interface for NASA's advanced information management systems
08 p1063 N88-16424
DOD Gateway Information System (DGIS) common command language: Prolog knowledge base profile. Common command language report no. 3
[AD-A188150] 08 p1092 N88-16574
Critical issues in NASA information systems
[NASA-CR-182380] 08 p1093 N88-16577

IMIS: Integrated Maintenance Information System. A maintenance information delivery concept
09 p1203 N88-17207
Interchange of electronic design through VHDL and EIS 09 p1205 N88-17222
Management of complex information in support of evolving autonomous expert systems
[AD-A186680] 09 p1224 N88-17337
Wind turbine acoustics research bibliography with selected annotation
[NASA-TM-100528] 09 p1243 N88-17450
Code division multiple access applied to fiber optic data transmission
[AD-A186873] 09 p1247 N88-17477
Information needs analysis for the Aeronautical Systems Division Executive Information System
[AD-A186912] 09 p1261 N88-17556
Wide band data transmission system using optical fibers
[DE88-004555] 10 p1319 N88-17889
Methods of eliciting information from experts
[AD-A187468] 10 p1372 N88-18189
Automated data flow diagram verification
10 p1382 N88-18255
Air Force geographic information and analysis system
[DE88-001420] 10 p1424 N88-18505
Computer-Aided Design Information System (CADIS): User's manual
[DE88-004365] 10 p1424 N88-18509
Guidelines for exchanging computerized information
[DE88-004736] 10 p1425 N88-18510
International geosphere-biosphere program: A study of global change
[PB88-142393] 11 p1510 N88-19021
AITI Test Report 87-002: Pratt and Whitney technical order transfer tests
[DE88-004045] 11 p1564 N88-19363
AITI Report 87-003: Honeywell technical order transfer tests
[DE88-004046] 11 p1564 N88-19364
District information system of National Information Centre
[PB88-134739] 11 p1565 N88-19373
Application of ARIADNE: A data bank-based information system for human physiology research --- Spacelab Anthrorack 12 p1662 N88-19962
KREME (Knowledge Representation, Editing and Modeling Environment): A user's introduction, phase 1
[AD-A188908] 12 p1681 N88-20052
Defending secrets, sharing data: New locks and keys for electronic information
[PB88-143185] 12 p1706 N88-20210
National Informatics Centre: Profile of services
[PB88-134135] 12 p1706 N88-20211
Design methodology for allocating data in a distributed database
[AD-A188826] 12 p1706 N88-20215
Implementing information systems/office automation in an Air Force environment
[AD-A188956] 12 p1707 N88-20218
A comparison of information system development methodologies
[AD-A188957] 12 p1707 N88-20219
Towards a tribology information system: The results of a Planning Workshop held at the National Bureau of Standards, July-August 1985
[PB88-168604] 14 p1918 N88-21448
Geometric modeling of flight information for graphical cockpit display
[AD-A190484] 15 p2021 N88-22043
Information systems for quality. Experience at the Nerviano Aeritalia plant. Avionic systems and equipment group
[ETN-88-92274] 15 p2148 N88-22821
The Scientific and Technical Information Network (STINET). Foundation for evolution
[AD-A189750] 15 p2148 N88-22822
Sources of digital spatial data for geographic information systems
[AD-A189788] 15 p2148 N88-22824
Data base design and implementation
[AD-A190414] 15 p2149 N88-22827
PPDS compas-primer
[DE88-701589] 16 p2266 N88-23554
Information and stochastic systems
[AD-A192167] 18 p2501 N88-24838
The human genome: Computational challenges
[DE88-006465] 18 p2549 N88-25131
Application of interactive graphic system (CAD/CAM) in the determination of process evolution in land use in the Ribeirao Preto municipality 19 p2684 N88-25956
The role of working memory in language comprehension
[AD-A192721] 20 p2833 N88-26805
SIMS: Single Interface to Multiple Systems
[AD-A192264] 20 p2837 N88-26832
Computer-aided writing
[AD-A192516] 20 p2838 N88-26837
Context of national information systems in developing countries: India and China in a comparative perspective
[PB88-109954] 20 p2882 N88-27111
Capitalizing on experience with intelligence gateway software
[AD-A193362] 21 p3028 N88-27971
Walter user's manual (Version 1.0)
[AD-A192542] 22 p3136 N88-28644
NASA information sciences and human factors program
[NASA-TM-4064] 22 p3166 N88-28856
A comparison of typical meteorological year solar radiation information with the SOLMET data base
[DE88-009242] 23 p3234 N88-29247
Advanced information processing system: Input/output network management software
[NASA-CR-181678] 23 p3264 N88-29431
Experiments in automatic phrase indexing for document retrieval: A comparison of syntactic and non-syntactic methods 23 p3296 N88-29634
EMPTAC (Electromagnetic Pulse Test Aircraft) user's guide
[AD-A195072] 24 p3360 N88-30006
Human factors report on information management requirements for next-generation manned bombers
[AD-A195870] 24 p3409 N88-30296
Telescience testbed pilot program
[NASA-CR-183207] 24 p3412 N88-30309
A shared-world conceptual model for integrating space station life sciences telescience operations
24 p3416 N88-30333
The second generation intelligent user interface for the crustal dynamics data information system
24 p3419 N88-30352
Knowledge-based integrated information systems engineering: Highlights and bibliography. Knowledge-Based Integrated Information Systems Engineering (KBIISE) Project, volume 1
[AD-A195850] 24 p3435 N88-30449
Technical opinions regarding knowledge-based integrated information systems engineering, volume 8
[AD-A195857] 24 p3436 N88-30454
Knowledge-Based Integrated Information Systems Development Methodologies Plan. Knowledge-Based Integrated Information Systems Engineering (KBIISE) report, volume 2
[AD-A195851] 24 p3436 N88-30455
Strategic, organizational and standardization aspects of integrated information systems, volume 6
[AD-A195855] 24 p3437 N88-30457
Integrating information systems in a major decentralized international organization, volume 7
[AD-A195856] 24 p3439 N88-30468

INFORMATION THEORY
Study, design, and evaluation of data reduction by encoding or information extraction. Part 1: Data generation analysis --- multispectral satellite imagery
[NLR-TR-85094-L-PT-1] 01 p0078 N88-10501
Study, design and evaluation of data reduction by encoding or information extraction. Part 2: Operational considerations --- multispectral satellite imagery
[NLR-TR-85094-L-PT-2] 01 p0079 N88-10502
Study, design and evaluation of data reduction by encoding or information extraction. Part 3: Algorithm design --- multispectral satellite imagery
[NLR-TR-85094-L-PT-3] 01 p0079 N88-10503
Study, design and evaluation of data reduction by encoding or information extraction. Part 4: Performance demonstration --- multispectral satellite imagery
[NLR-TR-85094-L-PT-4] 01 p0079 N88-10504
Study, design and evaluation of data reduction by encoding or information extraction. Part 5: Algorithm implementation aspects --- multispectral satellite imagery
[NLR-TR-85094-L-PT-5] 01 p0079 N88-10505
General potential surfaces and neural networks
[AD-A184484] 03 p0367 N88-12311
Bandwidth efficient block codes for M-ary PSK modulation
[NASA-CR-181543] 04 p0437 N88-12712
On detection of change points using mean vectors
[AD-A185581] 06 p0767 N88-14717
Local likelihood method in the problems related to change points
[AD-A185604] 06 p0768 N88-14718
Variable selection in logistic regression
[AD-A186032] 07 p0914 N88-15547
Discovery and problem solving: Triangulation as a weak heuristic 08 p1062 N88-16412
Conceptual information processing: A robust approach to KBS-DBMS integration 08 p1063 N88-16422
The linear dependency structure of covariance nonstationary time series
[AD-A186548] 09 p1232 N88-17383
Strong consistency of certain information theoretic criteria for model selection in calibration, discriminant analysis and canonical correlation analysis
[AD-A186584] 09 p1232 N88-17385
Resonance, information, and the primacy of process: Ancient light on modern information and communication theory and technology 10 p1424 N88-18506
Quantitative and qualitative assessments of the impact of linguistic theory on information science
10 p1424 N88-18507
Two new frameworks for learning
[AD-A187723] 11 p1534 N88-19182
A comparison of information system development methodologies
[AD-A188957] 12 p1707 N88-20219
Research in applied mathematics ralated to identification of noisy systems
[AD-A189355] 13 p1825 N88-20908
Instrumentation for scientific computing in neural networks, information science, artificial intelligence and applied mathematics
[AD-A189981] 15 p2106 N88-22549
Information and coding capacities of mismatched Gaussian channels
[AD-A190321] 15 p2124 N88-22665
Information capacity of Gaussian channels
[AD-A190316] 15 p2127 N88-22686
Coding capacity of discrete-time Gaussian and nonGaussian channels
[AD-A190318] 15 p2127 N88-22688
Error control techniques for satellite and space communications
[NASA-CR-182886] 17 p2332 N88-23922
Analysis and synthesis of decision-making organizations
[AD-A191948] 19 p2738 N88-26258
Modeling and evaluation of expert systems in decisionmaking organizations
[AD-A191951] 19 p2739 N88-26260
Survey of neural net paradigms for specification of discrete networks
[AD-A192682] 22 p3141 N88-28674
NASA information sciences and human factors program
[NASA-TM-4064] 22 p3166 N88-28856
On the design and optimization of distributed signal detection and parameter estimation systems
[AD-A193934] 23 p3266 N88-29448
Signals and systems 24 p3363 N88-30026
The bounded rationality constraint: Experimental and analytical results
[AD-A195897] 24 p3413 N88-30318

INFORMATION TRANSFER
Impressions, observations and comments on science and technology in Japan
[PB87-235743] 06 p0799 N88-14893
Computer aided design for Petri Nets
[AD-A186109] 07 p0902 N88-15465
DOE data exchange format specification, mechanical products/drafting: Version 1.2.2: CADCAM-045
[DE88-001923] 07 p0904 N88-15477
Information needs analysis for the Aeronautical Systems Division Executive Information System
[AD-A186912] 09 p1261 N88-17556
Airborne Wind Shear Detection and Warning Systems: First Combined Manufacturers' and Technologists' Conference
[NASA-CP-10006] 10 p1273 N88-17616
Information transfer in the National Airspace System
10 p1275 N88-17634
Minutes of the meeting of the Indo-US Subcommission on Science and Technology (8th) held at Washington, D.C. on September 22-24, 1986
[PB88-130158] 10 p1423 N88-18503
District information system of National Information Centre
[PB88-134739] 11 p1565 N88-19373
Design and implementation of VLSI prime factor algorithm processor
[AD-A190483] 15 p2112 N88-22580
Sky radiance distributions for thermal imaging backgrounds
[AD-A191135] 17 p2373 N88-24115
A cockpit natural language study - selected transcripts
[AD-A192972] 20 p2834 N88-26808
Barriers to Information Transfer and Approaches Toward Their Reduction
[AGARD-CP-430] 24 p3437 N88-30458
Linguistic and cultural barriers to the transfer of information 24 p3437 N88-30459
Political and economic barriers to information transfer
24 p3437 N88-30460
Information retrieval systems evolve-advances for easier and more successful use 24 p3438 N88-30462
Words: Keys or barriers to information transfer
24 p3438 N88-30464

Technical change needs organizational change
24 p3438 N88-30486

Using standards to break down information transfer barriers
24 p3439 N88-30487

INFORMATION TRANSMISSION
U DATA TRANSMISSION

INFRARED ABSORPTION

Reduction of temperature rise in high-speed photography
[NASA-TM-100222] 02 p0176 N88-11100

Direct infrared absorption of clusters in pulsed molecular beams
[DE87-014802] 02 p0236 N88-11490

Absorption of far IR-radiation by H2O-N2 complexes under atmospheric conditions 04 p0462 N88-12855

Radiation absorption in the infrared spectral range: A comparison between laboratory measurements and theoretical calculation illustrated by a H2O 2.7 micrometer 08 p1018 N88-16170

Ion content and infrared absorption of moist atmospheric air
[AD-A188639] 12 p1643 N88-19838

Infrared absorption spectroscopy and chemical kinetics of free radicals
[DE88-008536] 15 p2033 N88-22112

Infrared differential absorption lidar for vapor detection
[AD-A190600] 15 p2098 N88-22497

Calculation of far infrared absorption in B poly(dA).poly(dT)
[AD-A193128] 21 p2918 N88-27318

Survey of material for an infrared-opaque coating
[NASA-TM-88204] 22 p3153 N88-28757

INFRARED ASTRONOMY

Circumstellar radio molecular lines
02 p0252 N88-11595

Study of solid state photomultiplier
[NASA-CR-177465] 05 p0583 N88-13556

Activities report in interplanetary space physics
[IFSI-86-5] 05 p0659 N88-14047

A new liquid helium-cooled Fabry-Perot spectrometer used in a far infrared astronomical balloon experiment
08 p1028 N88-16224

Justification and prospects of observations of interstellar, far-infrared emission lines, using a small-sized balloon-borne telescope 08 p1032 N88-16254

PRONAOS: A submillimeter facility --- astronomical balloon 08 p1032 N88-16255

ESA Bulletin No. 8
[ETN-87-90513] 09 p1122 N88-16718

Infrared astronomy: Why and how?
09 p1123 N88-16722

Experiment control and data system for an infrared detector array with maximum sensitivity
[ETN-88-91497] 09 p1136 N88-16813

Integrated focal plane star sensor
[OG-RT/86-0156] 09 p1262 N88-17562

Workshop on Technology Development Issues for the Large Deployable Reflector (LDR)
[NASA-CP-2407] 12 p1710 N88-20235

Advanced components for spaceborne infrared astronomy
[NASA-CR-177470] 13 p1772 N88-20601

Analysis of deep sky sources found by the infrared astronomy satellite
[AD-A189605] 13 p1853 N88-21089

Far-infrared (120-300 micron) observations of the Carina Nebula 14 p1993 N88-21876

The galactic nucleus at mm-, sub-mm and far-infrared wavelengths
[MPE-PREPRINT-102] 16 p2288 N88-23700

Submillimeter and far infrared line observations of M17 SW: A clumpy molecular cloud penetrated by UV radiation
[NASA-CR-182866] 16 p2288 N88-23701

Balloon-borne three-meter telescope for far-infrared and submillimeter astronomy
[NASA-CR-182924] 17 p2449 N88-24550

Infrared astronomy at extremely faint light levels in support of the LAIRTS program
[AD-A191497] 18 p2592 N88-25404

Study of a safe attitude for the Infrared Space Observatory (ISO) during perigee pass
[SNIAS-881-440-113] 23 p3185 N88-28954

Far infrared supplement: Catalog of infrared observations, second edition
[NASA-RP-1205] 24 p3452 N88-30545

INFRARED ASTRONOMY SATELLITE

Optical spectroscopy of IRAS sources with infrared emission bands. 1: IRAS 21282+5050 and the diffuse interstellar bands
[NASA-CR-181387] 01 p0094 N88-10611

Emission features in IRAS LRS spectra of MS, S and CS stars 04 p0514 N88-13163

IRAS and cool stellar mass loss
04 p0515 N88-13166

Study of interactional effects in the chemisorbed layer by Infrared Reflection Absorption Spectroscopy (IRAS)
[DE88-001808] 06 p0680 N88-14164

Analysis of deep sky sources found by the infrared astronomy satellite
[AD-A189605] 13 p1853 N88-21089

INFRARED DETECTORS
NT FLIR DETECTORS

Coherent infrared detection, volume B --- CO2 laser intersatellite data link
[ESA-CR(P)-2392-VOL-1] 01 p0034 N88-10218

Coherent infrared detection, volume D --- CO2 laser intersatellite data link
[ESA-CR(P)-2392-VOL-2] 01 p0034 N88-10219

Automatic seam welding with infrared sensor feedback
[DE87-013556] 01 p0055 N88-10332

A study of infrared missile seekers and the countermeasure techniques employed to defeat them
[ETN-87-90927] 02 p0131 N88-10822

Monitored background radiometer
02 p0133 N88-10831

Exosat results on the dMe flare Star Wolf 630AB and on VB 8 04 p0512 N88-13151

Evaluation of a cryogenic refrigerator for cooling focal plane instrumentation --- satellite instruments
[BAE-TP-8095-VOL-1] 05 p0572 N88-13485

Evaluation of a cryogenic refrigerator for cooling focal plane instrumentation. Appendix B: Accommodation study --- satellite instruments
[BAE-TP-8095-VOL-2] 05 p0572 N88-13486

Integrated photo-responsive metal oxide semiconductor circuit
[NASA-CASE-GSC-12782-1] 06 p0696 N88-14271

Visible and infrared linear detector arrays for the Airborne Visible/Infrared imaging Spectrometer (AVIRIS)
06 p0706 N88-14329

AVHRR/HIRS (Advanced Very High Resolution Radiometer/High Resolution Infra-Red Sounder) operational method for satellite based sea surface temperature determination
[PB88-107594] 06 p0708 N88-14340

Description of data on the Nimbus 7 LIMS map archive tape: Water vapor and nitrogen dioxide
[NASA-TP-2761] 06 p0744 N88-14572

Experiment control and data system for an infrared detector array with maximum sensitivity
[ETN-88-91497] 09 p1136 N88-16813

Fabrication and packaging of discontinuous MIM (Metal-Insulator-Metal) film arrays for efficient MM wave and IR detection and mixing
[AD-A186809] 09 p1146 N88-16869

IRAC test report. Gallium doped silicon band 2: Read noise and dark current
[NASA-TM-87813] 09 p1159 N88-16945

Integrated focal plane star sensor
[OG-RT/86-0156] 09 p1262 N88-17562

Depolarized infrared reflectance from dry and wetted surfaces
[AD-A188213] 11 p1492 N88-18903

Project SKYLITE: A design exploration
[AD-A187906] 11 p1511 N88-19030

HP-41CX programs for HgCdTe detectors and IR systems
[AD-A188935] 12 p1692 N88-20120

Procedure for detection and identification of a helicopter
[NASA-TT-20234] 13 p1722 N88-20297

Advanced components for spaceborne infrared astronomy
[NASA-CR-177470] 13 p1772 N88-20601

Passive autonomous infrared sensor technology
[AD-A188698] 13 p1839 N88-21005

Analysis of deep sky sources found by the infrared astronomy satellite
[AD-A189605] 13 p1853 N88-21089

Laser pulse detection with infrared range semiconductor detectors
[DE88-700857] 14 p1914 N88-21432

Mid infrared multichannel focal plane breadboard --- pushbroom sensors
[RT-87/014] 14 p1982 N88-21827

Hybrid PV HgCdTe IR detectors technology reliability and failure program: Environmental stress testing plan
[AD-A191165] 16 p2211 N88-23195

Novel silicon Schottky barrier infrared imaging arrays
17 p2439 N88-24510

Infrared detectors based on the photon drag effect and intersubband absorption by a two-dimensional electron gas 20 p2867 N88-27024

Photodiodes for optical communication in the near infrared
[ETN-88-92379] 21 p3016 N88-27900

Development of 30 micrometers extrinsic silicon multiplexed infrared detector array
[NASA-CR-177446] 22 p3082 N88-28301

Infrared detection using Rydberg atoms
[AD-A194308] 23 p3191 N88-28990

Evaluation of atmospheric effects for operational tactical decision aid
[AD-A194205] 23 p3232 N88-29236

Multi-sensory tracking mount control
[AD-A194675] 23 p3246 N88-29339

Integration of LANTIRN (Low Altitude Navigation and Targeting Infrared for Night) into operational fighter training
[AD-A194906] 24 p3325 N88-29799

Development of a unit cell for a Ge:Ga detector array
[NASA-CR-177445] 24 p3375 N88-30100

A system study with an infrared sensitive microelectronic image sensor
[FOA-C-30481-3.1] 24 p3429 N88-30407

Principles of the optical differential thermal analysis
[AD-A195951] 24 p3429 N88-30408

Estimation of soil temperature profile from remote microwave and IR measurements
24 p3450 N88-30532

INFRARED HORIZON SCANNERS
U HORIZON SCANNERS
U INFRARED SCANNERS

INFRARED IMAGERY

Tropical cyclone center locations from enhanced infrared satellite imagery
[PB87-213450] 01 p0071 N88-10455

Psychophysical considerations in measuring MRTD with staring arrays --- minimum resolvable temperature difference (MRTD)
[RSRE-MEMO-4031] 01 p0076 N88-10487

The use of satellite IR data in the enhancement of surface thermal fields 02 p0202 N88-11260

Pyroelectric line scanner for remote IR imaging of vehicles
[DE87-012127] 02 p0235 N88-11484

An application of a gradient relaxation method to noisy infrared images
[AD-A184666] 03 p0377 N88-12371

Aircraft engine exhaust plume dynamics
[AD-A184238] 04 p0400 N88-12488

Airborne Visible/Infrared Imaging Spectrometer (AVIRIS). A description of the sensor, ground data processing facility, laboratory calibration, and first results
[NASA-CR-182365] 06 p0705 N88-14325

A system overview of the Airborne Visible/Infrared Imaging Spectrometer (AVIRIS)
06 p0705 N88-14326

AVIRIS ground data-processing system
06 p0707 N88-14333

Spectral and radiometric calibration of the Airborne Visible/Infrared Imaging Spectrometer
06 p0707 N88-14334

First results from the Airborne Visible/Infrared Imaging Spectrometer (AVIRIS) 06 p0707 N88-14335

Experimental design of a piloted helicopter off-axis-tracking simulation using a helmet mounted display
[AD-A186228] 07 p0820 N88-14982

Commercial applications and scientific research requirements for thermal-infrared observations of terrestrial surfaces
[NASA-TM-89704] 08 p1019 N88-16179

Technical assessment of the joint CSIRO/Bureau of Meteorology proposal for a geostationary imager/sounder over the Australian region
[RTP-15] 09 p1135 N88-16811

Thermal wave imaging
[AD-A186810] 09 p1177 N88-17046

Sea surface current estimates off central California as derived from enhanced AVHRR (Advanced Very High Resolution Radiometer) infrared images
[AD-A186867] 09 p1194 N88-17155

Passive autonomous infrared sensor technology
[AD-A188698] 13 p1839 N88-21005

The application of thermal imaging sensors and image processing techniques to a short range surface-to-air missile system
[ETN-88-92080] 14 p1982 N88-21829

Infrared-sensitive spatial light modulator
[AD-A190391] 15 p2134 N88-22729

Validate algorithms for the determination of rainfall rates from SSM/I microwave satellite imagery
[AD-A188769] 16 p2233 N88-23317

Infrared radiometric technique in temperature measurement 17 p2330 N88-23913

Real time thermal imaging of high temperature semiconductor melts 17 p2330 N88-23914

Enhanced infra-red picture of LR-FAX for spring and autumn seasons 17 p2351 N88-24011

An update on remote measurement of soil moisture over vegetation using infrared temperature measurements: A FIFE perspective
[NASA-CR-182926] 17 p2370 N88-24109

Sky radiance distributions for thermal imaging backgrounds
[AD-A191135] 17 p2373 N88-24115
Thermographic detection of buried debonds
[AD-A192115] 18 p2475 N88-24680
Stress analysis using infrared thermography
[ETN-88-92169] 20 p2816 N88-26705
Cyrogenic test facilities for an optical cryomechanism qualification
[REPT-831-440-116] 21 p2901 N88-27219
IR (infrared) sky radiance distributions in the marine boundary layer
[AD-A193683] 22 p3119 N88-28531
A probabilistic model of the apparent radiance of a rough sea
[AD-A193867] 22 p3129 N88-28602
An objective technique for Arctic cloud analysis using multispectral AVHRR (Advanced Very High Resolution Radiometer) satellite imagery
[AD-A194732] 23 p3235 N88-29250
A system study with an infrared sensitive microelectronic image sensor
[FOA-C-30481-3.1] 24 p3429 N88-30407
Common modules: A success story
[AD-A195937] 24 p3430 N88-30415

INFRARED INSTRUMENTS
NT FLIR DETECTORS
NT INFRARED DETECTORS
NT INFRARED INTERFEROMETERS
NT INFRARED SCANNERS
NT INFRARED SPECTROMETERS
NT INFRARED SPECTROPHOTOMETERS
Scene simulation for passive IR systems
02 p0137 N88-10861
Infrared low-level wind shear work
10 p1275 N88-17628
Specification for an infrared satellite surveillance system for the detection of aircraft
[AD-A189592] 13 p1797 N88-20746
Infrared simulation model Sensor Atmosphere Target (SENSAT)-2A
[DFVLR-FB-88-01] 16 p2165 N88-22910
A disposable liquid microcell for near-infrared reflectance analysis
[AD-A192190] 18 p2575 N88-25298
Infrared devices using semiconductor quantum wells
[RSRE-MEMO-4018] 22 p3157 N88-28788
Common modules: A success story
[AD-A195937] 24 p3430 N88-30415

INFRARED INTERFEROMETERS
A two-wavelength infrared interferometer/polarimeter system for CIT (Compact Ignition Tokamak)
[DE88-007681] 18 p2579 N88-25321

INFRARED LASERS
IR laser excitation in molecules: Chaos and diffusive energy growth
[DE87-013147] 02 p0178 N88-11105
Distributed feedback effects in lasers and high gain laser instabilities in optically pumped CH3F
03 p0329 N88-12079
Dynamic restructuring of pulsed CO2 laser frequency and multiple-peak generation in a cell with IR-absorbing gas in the resonator 07 p0919 N88-15580
Dielectric behavior of electromagnetic (EM) windows materials irradiated by a CW CO2 high-power laser --- hypersonic/reentry vehicles
[ISL-CO-239/86] 09 p1154 N88-16913
Continuously frequency-tunable high-pressure CO2-laser with plasmatic cathode
09 p1236 N88-17418
Energy transfer studies with lasers
[DE88-004864] 10 p1337 N88-17991
Influence of nonlinear spectroscopic effects on atmospheric propagation of intense laser radiation at 10.6 microns wavelength 13 p1780 N88-20705
Effect of atmospheric turbulence on the bit error probability of a space to ground near infrared laser communications link using binary pulse position modulation and an avalanche photodiode detector
[NASA-TM-100699] 14 p1873 N88-21189
Laser technology: CO2 lasers and laser optics
[ETN-88-91469] 14 p1915 N88-21441
Nonlinearly tunable wideband emission of infrared radiation by Al2O3:Ti laser 14 p1970 N88-21758
Diode laser spectroscopy of chemical moieties at surfaces
[AD-A190710] 15 p2036 N88-22127
Generation of tunable coherent radiation in 3 micrometers-5 micrometers region using semiconductor lasers in external cavities
[AD-A190860] 16 p2212 N88-23202
The new UCSB (University of California, Santa Barbara) compact far-infrared FEL
[AD-A190864] 16 p2212 N88-23203
Infrared and far-infrared laser development for plasma diagnostics at Oak Ridge National Laboratory
[DE88-007262] 19 p2674 N88-25904
Predicting the durability of adhesives and coatings by remote detection of hidden defects and coating-thickness irregularities: A theoretical and numerical study
24 p3355 N88-29972

INFRARED MASERS
U INFRARED LASERS

INFRARED PHOTOGRAPHY
IRAC test report. Gallium doped silicon band 2: Read noise and dark current
[NASA-TM-87813] 09 p1159 N88-16945

INFRARED PHOTOMETRY
A search for very low mass (brown dwarf) stars as wide binaries using a seven element infrared camera-photometer 04 p0512 N88-13150
IRAS and near IR observations of active binaries
04 p0518 N88-13186
Tailorable infrared sensing device with strain layer superlattice structure
[NASA-CASE-NPO-16807-1-CU]
06 p0788 N88-14836
Infrared constraints on the nature of dark matter
13 p1855 N88-21102
Near-infrared observations of cepheids: The distance to M33 15 p2152 N88-22846

INFRARED RADAR
A very wide frequency band pulsed/IF radar system
[NASA-CR-182889] 16 p2190 N88-23059

INFRARED RADIATION
NT FAR INFRARED RADIATION
NT NEAR INFRARED RADIATION
Status of the solar and infrared radiation submodels in the LLNL 1-D and 2-D chemical-transport models
[DE87-014320] 01 p0069 N88-10441
GOES observations for the FIRE/SRB Wisconsin experiment region from October 11 through November 2, 1986
[NASA-TM-100485] 01 p0071 N88-10453
Mid infrared LHS system packaging using flexible waveguides
[NASA-CR-181192] 01 p0093 N88-10607
Infra-red lamp panel study and assessment application to thermal vacuum testing of sigma telescope
02 p0132 N88-10830
Thermal testing by internal IR heating of the FEP module 02 p0136 N88-10854
A new type of lamp and reflector for I.R. simulation
02 p0136 N88-10855
Evaluation of the infrared test method for the olympus thermal balance tests 02 p0136 N88-10856
IR laser excitation in molecules: Chaos and diffusive energy growth
[DE87-013147] 02 p0178 N88-11105
The effects of minor trace gases on the transfer of thermal infrared radiation through the Earth's atmosphere 04 p0468 N88-12893
The giant spot on II Peg in 1986
04 p0506 N88-13120
Macroscopic distribution of fiber finish
[DCQ/L-48-283/F] 07 p0827 N88-15013
Satellite techniques of solar resource assessment for focusing and non-focusing solar collector systems
[DE88-001657] 07 p0874 N88-15298
Intracavity spectrum analyzer with NaF:F2(+):F3(-) crystal laser for long-wave IR wave band
07 p0919 N88-15584
Infrared emission and tidal interactions of spiral galaxies 07 p0923 N88-15611
Catalog of infrared observations. Part 2: Appendixes
[NASA-RP-1196-PT-2-ED-2] 08 p1099 N88-16615
Development of infrared techniques for testing spacecraft 09 p1128 N88-16772
Radiant power degradation of silicon-doped gallium arsenide and gallium aluminum arsenide infrared light-emitting diodes
[AD-A186726] 09 p1157 N88-16935
Variable band gap materials for thermophotovoltaic generators
[AD-A186858] 09 p1186 N88-17104
PbSnTe photovoltaic detectors for operation in the 2-14 micron band
[INPE-4252-PRE/1125] 11 p1508 N88-19008
Some applications of surface Raman and infrared spectroscopies to mechanistic electrochemistry involved adsorbed species
[AD-A188777] 12 p1606 N88-19602
Test methodology for infrared tubular heaters
[PB88-160916] 12 p1626 N88-19728
DIRBE External Calibrator (DEC)
[NASA-CR-180761] 12 p1631 N88-19760
Results of infrared spectrometer experiment. 1: Infrared radiation of parent molecules in Halley's Comet
13 p1726 N88-20325
Analysis of hydrocarbon band 3.35 in spectrum of Halley's Comet using data from infrared spectrometer on Vega-1 spacecraft 13 p1727 N88-20327
Dynamical modeling of marine boundary layer convection 13 p1797 N88-20750
Analysis of deep sky sources found by the infrared astronomy satellite
[AD-A189605] 13 p1853 N88-21089
Infrared differential absorption lidar for vapor detection
[AD-A190600] 15 p2098 N88-22497
Studies of surfaces using optical sum-frequency generation
[DE88-006334] 15 p2131 N88-22715
Dispersion measurements of microcrystals in the near ultraviolet and infrared
[DE88-006234] 15 p2145 N88-22800
Tunable optical sources/growth and characterization of nonlinear optical materials
[AD-A190674] 16 p2274 N88-23608
Estimation of total Outgoing Longwave Radiation (OLR) flux from geostationary meteorological satellite infrared window radiance 17 p2351 N88-24006
Bimolecular reactions and energy-transfer processes of highly vibrationally excited molecules related to energetic materials
[AD-A189013] 18 p2571 N88-25270
Calculation of space station infrared irradiance from atmosphere-induced emissions
18 p2591 N88-25396
Regulatory biochemical and metabolic responses in photoreceptors
[AD-A192898] 20 p2831 N88-26794
Far- and mid-infrared properties of metal-insulator composite materials
[AD-A193227] 21 p2905 N88-27236
Development of radiation and cloud parameterization programs for AFGL (Air Force Geophysics Laboratory) global models
[AD-A193369] 21 p2973 N88-27658
A probabilistic model of the apparent radiance of a rough sea
[AD-A193867] 22 p3129 N88-28602
MIDIR (Mid-Infrared) laser, phase 1
[AD-A193935] 23 p3220 N88-29166
Miniature respiratory sensor
[AD-A193430] 23 p3243 N88-29300
Principles of the optical differential thermal analysis
[AD-A195951] 24 p3429 N88-30406
Radio and infrared properties of young stars
[NASA-CR-183252] 24 p3459 N88-30579

INFRARED RADIOMETERS
NT ADVANCED VERY HIGH RESOLUTION RADIOMETER
Forward looking wind shear detection
10 p1275 N88-17629
Noncontact Temperature Measurement
[NASA-CP-2503] 17 p2327 N88-23895
Radiation thermometry: The measurement problem
17 p2328 N88-23896
The role of fiberoptics in remote temperature measurement 17 p2329 N88-23909
Infrared radiometric technique in temperature measurement 17 p2330 N88-23913

INFRARED REFLECTION
Reduction of temperature rise in high-speed photography
[NASA-TM-100222] 02 p0176 N88-11100
Study of interactional effects in the chemisorbed layer by Infrared Reflection Absorption Spectroscopy (IRAS)
[DE88-001808] 06 p0680 N88-14164
Some applications of surface Raman and infrared spectroscopies to mechanistic electrochemistry involved adsorbed species
[AD-A188777] 12 p1606 N88-19602

INFRARED SCANNERS
Improved geostationary satellite soundings for the mesoscale weather analysis/forecast operation
02 p0200 N88-11252
VAS products as indices of thunderstorms and severe local storm potential --- Visible and Infrared Spin Scan Radiometer Atmospheric Sounder (VAS)
02 p0201 N88-11253
Operational cloud-clearing techniques of VAS radiance data --- Visible and Infrared Spin Scan Radiometer Atmospheric Sounder (VAS) 02 p0201 N88-11256
Measurement from satellites of land surface parameters and fluxes in the thermal infrared bands: Problems and methods 14 p1937 N88-21557

INFRARED SIGNATURES
A probabilistic model of the apparent radiance of a rough sea
[AD-A193867] 22 p3129 N88-28602

INFRARED SOURCES (ASTRONOMY)
NT INFRARED STARS

Optical spectroscopy of IRAS sources with infrared emission bands. 1: IRAS 21282+5050 and the diffuse interstellar bands
[NASA-CR-181387] 01 p0094 N88-10611
Catalog of infrared observations. Part 1: Data
[NASA-RP-1196-PT-1-ED-2] 07 p0944 N88-15738
Catalog of infrared observations. Part 2: Appendixes
[NASA-RP-1196-PT-2-ED-2] 08 p1099 N88-16615
Far infrared supplement: Catalog of infrared observations, second edition
[NASA-RP-1205] 24 p3452 N88-30545

INFRARED SPACE OBSERVATORY (ISO)
Development of a cryogenic stepping drive for ISO/LWS 14 p1878 N88-21220
Cryogenic mechanism for ISO camera
14 p1878 N88-21221

INFRARED SPECTRA
Picosecond CO2 laser interactions with polyatomic molecules
[DE87-012072] 01 p0051 N88-10327
Development of many-body methods for flame chemistry and large molecule applications
[AD-A184451] 03 p0284 N88-11789
Spectroscopic and retrieval studies in support of SCRIBE (Stratospheric Cryogenic Interferometer Balloon Experiment)
[AD-A184037] 03 p0351 N88-12216
Far-infrared spectra of lithium deposited on a gold electrode: Interpretation using a cluster model
[AD-A184231] 04 p0495 N88-13050
Infrared excesses of barium stars
04 p0516 N88-13174
The contribution of accretion luminosity to the infrared spectra of T Tauri stars: A possible test
04 p0518 N88-13183
IRAS and near IR observations of active binaries
04 p0518 N88-13186
Measuring near infrared spectral reflectance changes from water stressed conifer stands with AIS-2
05 p0613 N88-13765
High energy molecules of high symmetry
[AD-A185385] 05 p0647 N88-13965
Extinction by dielectric particles at optical and infrared wavelength
[AD-A184818] 05 p0650 N88-13981
Study of interactional effects in the chemisorbed layer by Infrared Reflection Absorption Spectroscopy (IRAS)
[DE88-001808] 06 p0680 N88-14164
Lightning spectra in the near infrared
[DE88-002218] 07 p0880 N88-15341
Christiansen effect in infrared spectra of soil-derived atmospheric dusts
[AD-A187071] 09 p1248 N88-17479
Memory effects on infrared adsorbate spectra
[AD-A186976] 09 p1253 N88-17512
Crystalline sulfur dioxide: Crystal field splittings, absolute band intensities and complex refractive indices derived from infrared spectra
[NASA-CR-182502] 09 p1258 N88-17547
Simulation of infrared spectra
[AD-A187881] 11 p1453 N88-18658
Growth and characteristics of materials for tunable lasers in the near infrared spectral region
[NASA-CR-182501] 11 p1491 N88-18901
In-situ vibrational spectroscopy of specifically adsorbed azide on silver electrodes
[AD-A188511] 12 p1605 N88-19600
FTIR (Fourier Transform Infrared) and FTNMR (Fourier Transform Nuclear Magnetic Resonance) study of organophosphorus surface reactions
[AD-A188337] 12 p1609 N88-19625
Synchronous measurements of effective photon path length in visible and near-IR spectral regions in real cloud systems 13 p1790 N88-20706
Stratospheric trace gas distributions from fair infrared thermal emission spectroscopy
13 p1797 N88-20749
An investigation of the infrared emission spectra of carbon condensates 14 p1886 N88-21272
Measurement of the water content of soil from space and application to the regional water balance
14 p1938 N88-21561
Effect of Mg impurity on local vibrations of U-centers in LiF lattice 14 p1969 N88-21753
Optical and hydrodynamic implications of Comet Halley dust size distribution 14 p2003 N88-21939
Nature of Comet Halley's organic grains inferred from infrared spectra 14 p2007 N88-21973
Extension of the vegetation mission to thermal infrared spectral bands
[CNES-T-86/224-CT/DRT/TIT/IO]
16 p2227 N88-23299
Time-resolved studies of free radicals and laser-initiated chain reactions
[DE88-006569] 16 p2266 N88-23553
Optical constants of minerals and other materials from the millimeter to the ultraviolet
[AD-A192210] 18 p2482 N88-24724
Development of an experimental system for studying fast transient ignition phenomena
[DE88-011917] 21 p2911 N88-27276

INFRARED SPECTROMETERS
Balloon-based infrared solar occultation measurements of stratospheric O3, H2O, HNO3 and CFC-12
[NOAA-TR-NESDIS-34] 01 p0068 N88-10438
Direct infrared absorption of clusters in pulsed molecular beams
[DE87-014802] 02 p0236 N88-11490
Complementary information between UV and IR for remote sensing of total ozone 05 p0619 N88-13800
Airborne Visible/Infrared Imaging Spectrometer (AVIRIS) spectrometer design and performance
06 p0706 N88-14327
AVIRIS foreoptics, fiber optics and on-board calibrator
06 p0706 N88-14328
Visible and infrared linear detector arrays for the Airborne Visible/Infrared Imaging Spectrometer (AVIRIS)
06 p0706 N88-14329
AVIRIS scan drive design and performance
06 p0706 N88-14330
Signal chain for the Airborne Visible/Infrared Imaging Spectrometer (AVIRIS) 06 p0706 N88-14331
AVIRIS onboard data handling and control
06 p0706 N88-14332
AVIRIS ground data-processing system
06 p0707 N88-14333
Spectral and radiometric calibration of the Airborne Visible/Infrared Imaging Spectrometer
06 p0707 N88-14334
First results from the Airborne Visible/Infrared Imaging Spectrometer (AVIRIS) 06 p0707 N88-14335
A new liquid helium-cooled Fabry-Perot spectrometer used in a far infrared astronomical balloon experiment
08 p1026 N88-16224
The Cryogenic Infrared Spectrometer and Telescope for the Atmosphere (CRISTA) experiment on Astro-SPAS
08 p1034 N88-16270
Characteristics of an Ebert monochromator for an infrared spectrometer in the wavelength range 1 micrometer to 15 micrometers
[AD-A186945] 09 p1166 N88-16991
Results of infrared spectrometer experiment. 1: Infrared radiation of parent molecules in Halley's Comet
13 p1726 N88-20325
Velocity resolved far-infrared spectroscopy of galactic sources 13 p1854 N88-21099
Calibration and data reduction techniques for the AFGL infrared array spectrometer 21 p2927 N88-27374

INFRARED SPECTROPHOTOMETERS
NBS (National Bureau of Standards) measurement services: Spectral reflectance
[PB88-109905] 06 p0779 N88-14785
Extension of the vegetation mission to thermal infrared spectral bands
[CNES-T-86/224-CT/DRT/TIT/IO]
16 p2227 N88-23299

INFRARED SPECTROSCOPY
Far infrared Fourier transform spectroscopy of semiconductors
[DE88-000188] 04 p0499 N88-13072
Time series infrared spectroscopy of long period variables 04 p0516 N88-13172
Use of lasers with F sub A(II)-color center KCl:Li crystals in the intraresonator laser spectroscopy method
06 p0769 N88-14729
Photoacoustic infrared laser spectroscopy for analyzing gaseous contaminants
[ETN-88-90805] 07 p0831 N88-15041
Long range reconnaissance of trace gases: A special aspect of emission spectroscopy
08 p1018 N88-16172
Monolayer films prepared by the spontaneous self-assembly of symmetrical and unsymmetrical dialkyl sulfides from solution onto gold substrates: Structure, properties, and reactivity of constituent functional groups
[AD-A186717] 09 p1137 N88-16814
An infra-red investigation of HAN (Hydroxylammonium Nitrate)-based liquid propellants
[AD-A187226] 10 p1307 N88-17815
Study of the vibrational modes of subsurface oxygen on Al (111) using diode laser infrared reflection-absorption spectroscopy
[AD-A188322] 12 p1632 N88-19769
Results of infrared spectrometer experiment. 2: Infrared radiometry of nucleus of Halley's Comet
13 p1727 N88-20326
Analysis of hydrocarbon band 3.35 in spectrum of Halley's Comet using data from infrared spectrometer on Vega-1 spacecraft 13 p1727 N88-20327
Molecular collision processes in gases and at surfaces
[AD-A189518] 13 p1836 N88-20982
Infrared reflection-absorption spectroscopy of hyperfine layers on surfaces of semiconductors and dielectrics
14 p1969 N88-21755
The spectroscopy and reaction kinetics of coordinatively unsaturated metal carbonyls
[AD-A190533] 15 p2035 N88-22124
Diode laser spectroscopy of chemical moieties at surfaces
[AD-A190710] 15 p2036 N88-22127
Excitations in magnetic low-dimensional systems: A spectroscopic study
[ETN-88-92230] 15 p2129 N88-22697
Infrared spectroscopy of H3(+)
16 p2268 N88-23565
Spectral radiometry: Methods, measuring techniques, and applications --- conference
[PTB-OPT-24] 16 p2271 N88-23585
Multiplex methods in infrared spectrometry
16 p2271 N88-23588
Spectroscopy of one-dimensional subbands on InSb
20 p2864 N88-27007
Attenuated total reflectance FT-IR spectroscopy to measure interfacial reaction kinetics at silica surfaces
[AD-A196330] 24 p3344 N88-29908
Photoacoustic Fourier transform infrared spectroscopy. An early detection technique for coatings degradation
24 p3354 N88-29968

INFRARED STARS
A search for very low mass (brown dwarf) stars as wide binaries using a seven element infrared camera-photometer 04 p0512 N88-13150
Analysis of deep sky sources found by the infrared astronomy satellite
[AD-A189605] 13 p1853 N88-21089

INFRARED SUPPRESSION
A technique for wing suppressed IR sampling
19 p2658 N88-25794

INFRARED TELESCOPES
NT SPACE INFRARED TELESCOPE FACILITY
PRONAOS: A submillimeter facility --- astronomical balloon 08 p1032 N88-16255
The Cryogenic Infrared Spectrometer and Telescope for the Atmosphere (CRISTA) experiment on Astro-SPAS
08 p1034 N88-16270
Multisurface control mechanism for a deployable antenna: Far Infrared and Submillimeter Space Telescope (FIRST) technology study
[RP-FA-D003] 09 p1135 N88-16807
Workshop on Technology Development Issues for the Large Deployable Reflector (LDR)
[NASA-CP-2407] 12 p1710 N88-20235
Design of a linear actuator and breadboard test result --- far IR telescope 14 p1877 N88-21217
Photoelastic model tests of the Dornier linear actuator --- far IR telescope 14 p1877 N88-21218
Fine adjustment mechanism for FIRST
14 p1878 N88-21219
Far-infrared (120-300 micron) observations of the Carina Nebula 14 p1993 N88-21876
Telescope illumination and beam measurements for submillimeter astronomy
[MPE-PREPRINT-88] 16 p2288 N88-23699
Balloon-borne three-meter telescope for far-infrared and submillimeter astronomy
[NASA-CR-182924] 17 p2449 N88-24550
Utilization of the IR telescope gimbaling system as a stabilized pointing platform for balloon payloads. Volume 1: Technical results
[NASA-CR-179339] 18 p2522 N88-24962
Far infrared spectroscopy telescope (FIRST) inflatable thermal shield, phase 1
[SR/FIS/108(87)CZ] 24 p3453 N88-30552

INFRARED TRACKING
Passive autonomous infrared sensor technology
[AD-A188698] 13 p1839 N88-21005

INFRARED WINDOWS
A rapid polishing method for KBr and NaCl infrared windows
[DE88-002480] 07 p0862 N88-15229
Estimation of total Outgoing Longwave Radiation (OLR) flux from geostationary meteorological satellite infrared window radiance 17 p2351 N88-24006
Growth and characterization of CuGaS2, CuAlS2 and CuGa0.9Al0.1S2 single crystals
[AD-A192963] 21 p3021 N88-27930
An organometallic route to micron-sized whiskers of zinc sulfide
[AD-A195889] 24 p3430 N88-30414

INFRASONIC FREQUENCIES
Mechanisms mediating the perception of complex acoustic patterns
[AD-A190112] 15 p2130 N88-22705
Surface disturbances produced by low-level, subsonic B-1 aircraft
[AD-A192257] 20 p2824 N88-26752

INGESTION (BIOLOGY)
NT DRINKING
NT GRAZING
INGESTION (ENGINES)
A numerical study of the hot gas environment around a STOVL aircraft in ground proximity
[NASA-TM-100895] 17 p2295 N88-23729
INGOTS
Compositional redistribution during casting of Hg sub 0.8 Cd sub 0.2 Te alloys
[NASA-TM-101151] 17 p2326 N88-23893
INHALATION
U RESPIRATION
INHIBITION (PSYCHOLOGY)
Distraction and inhibition in continuous CRT performance: A replication and some new findings
[PB88-150941] 13 p1811 N88-20821
INHIBITORS
NT WEAR INHIBITORS
Proceedings of the 1987 Tri-Service Conference on Corrosion, Volume 2
[AD-A189660] 17 p2319 N88-23847
Development of microencapsulated DNBM quaternary ammonium inhibitors for paints
17 p2319 N88-23851
Low doses of atropine sulfate impair retention of a well-learned spatial task
[AD-A194065] 23 p3237 N88-29266
INHOMOGENEITY
Eddy current density in wedge-shaped conducting cylinders with inhomogeneous conductivity
[ETN-87-90404] 01 p0042 N88-10268
Effect of optical inhomogeneities on space coherence of radiation emitted by laser with unstable resonator
06 p0771 N88-14738
Evolution of spectral densities in weakly inhomogeneous plasmas
[PB87-137402] 06 p0784 N88-14811
Analysis of electromagnetic wave propagation in slightly inhomogeneous hollow waveguides
[DFVLR-FB-87-23] 09 p1152 N88-16904
New method of examining micrononhomogeneity of local centers in high-resistivity semiconductor materials under scanning electron microscope 14 p1969 N88-21754
Wave energy flow conservation for propagation in inhomogeneous Vlasov-Maxwell equilibria
[DE88-006705] 15 p2055 N88-22251
Parametric instabilities of inhomogeneous plasma near the lower-hybrid resonance
[DE88-701201] 15 p2137 N88-22748
Statistical fine structure in the inhomogeneously broadened electronic origin of pentacene in p-terphenyl
[AD-A191211] 16 p2176 N88-22968
Experimental investigation of simplest inhomogeneities in cylindrical slit line
[DE88-702388] 21 p2933 N88-27418
INITIAL VALUE PROBLEMS
U BOUNDARY VALUE PROBLEMS
INITIATION
A nondissipative Pyrotechnic Arming and Firing Unit (PAFU)
[CRA/REPO/8019] 02 p0155 N88-10974
Shock initiation studies on heterogeneous explosives
[DE88-008681] 21 p2923 N88-27351
INITIATORS (EXPLOSIVES)
NT BOOSTERS (EXPLOSIVES)
NT DETONATORS
NT PRIMERS (EXPLOSIVES)
Development and verification of NASA Standard Initiator-2 (NSI-2)
[NASA-CR-172069] 23 p3200 N88-29044
Development and verification of NASA Standard Initiator-2 (NSI-2): Appendix
[NASA-CR-172070] 23 p3200 N88-29045
INJECTION
NT CARRIER INJECTION
NT FLUID INJECTION
NT FUEL INJECTION
NT GAS INJECTION
NT ION INJECTION
NT WATER INJECTION
The injector for the CEBAF CW superconducting linac
[CEBAF-PR-87-011] 11 p1546 N88-19241
Application of railgun principle to high-velocity hydrogen pellet injection for magnetic fusion reactor refueling
[DE88-005830] 13 p1728 N88-20334
Design of divertor plate and measurements of double-null open divertor plasma in the JFT-2M tokamak
[DE88-753130] 21 p3018 N88-27914
Influence of plasma parameters on VLF radiation in near-rocket region 24 p3448 N88-30518
INJECTION CARBURETORS
U CARBURETORS
U FUEL INJECTION
INJECTION LOCKING
An analytical and experimental study of injection-locked two-port oscillators
[NASA-TM-100119] 04 p0439 N88-12727
INJECTION MOLDING
Fabrication of microstructures with extreme structural heights by vacuum reaction injection molding and electroforming
[KFK-4267] 01 p0033 N88-10210
Development of a statistically proven injection molding method for reaction bonded silicon nitride, sintering reaction bonded silicon nitride, and sintered silicon nitride
[ETN-87-90575] 02 p0160 N88-11002
Improved silicon nitride for advanced heat engines
[NASA-CR-175006] 08 p0973 N88-15886
Processing of glass to aluminum (low melting metals) seals via an injection molding technique
[DE88-004689] 13 p1751 N88-20468
Improved silicon carbide for advanced heat engines
17 p2324 N88-23879
Improved silicon nitride for advanced heat engines
17 p2324 N88-23881
High temperature resins for injection. High temperature pre-impregnated
[RC-648676] 20 p2780 N88-26486
INJECTORS
Aerothermal modeling program, phase 2
02 p0185 N88-11149
Fuel-injector/air-swirl characterization
02 p0185 N88-11150
A three-barrel repeating pneumatic pellet injector for plasma fueling of the Joint European Torus
[DE88-000330] 04 p0491 N88-13026
RIIM two-pulse injector experiments
[DE88-000926] 05 p0653 N88-14005
Preliminary injector, accelerator, and beamline design for rf-linac-driven XUV free-electron lasers
[DE88-003185] 10 p1336 N88-17983
Proposal for construction of an Energetic Particle Injector (EPI)
[INPE-4242-RPE/546] 12 p1690 N88-20112
Durability testing of an indium-plated storable rocket engine injector
[AD-A190707] 15 p2027 N88-22078
Development of a laboratory test for multiport injector deposits: Approaches 1 and 2
[AD-A190697] 15 p2048 N88-22203
Dense-spray structure and phenomena. Part 2: Pressure-atomized sprays
[AD-A190312] 15 p2064 N88-22307
Program to research laser-driven thermionic electron sources for free electron lasers
[AD-A190473] 15 p2072 N88-22353
Film cooling effectiveness on a flat plate in high free-stream turbulence using a single row of 30 deg slant-hole injectors
[AD-A190500] 15 p2147 N88-22816
Application of pulse compression and shaping to the FEL photoelectric injector
[DE88-007906] 19 p2675 N88-25910
Initial electron distributions for free-electron lasers generated by injector and accelerator simulations
[DE88-007022] 21 p2953 N88-27540
INJURIES
NT BACK INJURIES
NT BRAIN DAMAGE
NT LESIONS
NT NOISE INJURIES
NT RADIATION INJURIES
Modeling of the non-auditory response to blast overpressure
[AD-A187397] 10 p1369 N88-18184
Causes and prevention of occupational Repetition Strain Injuries (RSI) 11 p1521 N88-19083
Analysis of head response to torso acceleration. Volume 1: Development of performance requirements
[PB88-156757] 14 p1953 N88-21640
INLAND WATERS
NT GROUND WATER
An exploratory study of inland water and land altimetry using Seasat data
[ESA-CR(P)-2433] 02 p0193 N88-11208
Research in Switzerland on ocean and inland-water colour monitoring 08 p1043 N88-16301
INLET FLOW
Numerical computation of transonic potential flow about 3-dimensional inlets
[NAL-TR-924] 02 p0122 N88-10770
Combustor-diffuser interaction program
02 p0185 N88-11152
Measurement of airfoil heat transfer coefficients on a turbine stage 02 p0186 N88-11158
Heat transfer in laminar flow for mass inlet into an annular channel
[DE87-702890] 03 p0314 N88-11983
Analysis and performance prediction of scramjet inlets utilizing a three-dimensional Navier-Stokes code
07 p0811 N88-14936
Aeropropulsion '87. Session 3: Internal Fluid Mechanics Research
[NASA-CP-10003-SESS-3] 08 p0954 N88-15790
Propulsion challenges and opportunities for high-speed transport aircraft 08 p0958 N88-15809
Supersonic throughflow fans for high-speed aircraft
08 p0958 N88-15810
High-speed inlet research program and supporting analyses 08 p0958 N88-15811
Parametric study of choke flutter with a linear theory
10 p1283 N88-17673
Experimental investigation of a supercritical compressor rotor blade section 10 p1284 N88-17680
Numerical simulation of scramjet inlet flow fields
[NASA-TP-2517] 17 p2296 N88-23735
Low frequency pressure oscillations in a model ramjet combustor 19 p2625 N88-25571
Effects of Mach number on acoustic-vortex interactions in a ramjet 19 p2625 N88-25573
High speed inlet calculations with real gas effects
[NASA-CR-182167] 20 p2752 N88-26336
The calculation of the flow through a two-dimensional faired diffuser
[PNR90433] 22 p3076 N88-28259
Prediction of the pressure distribution for radial inflow between co-rotating discs
[PNR90464] 22 p3076 N88-28261
The use of fins to reduce the pressure drop in a rotating cavity with a radial flow
[PNR90465] 22 p3079 N88-28282
The effects of inlet turbulence and rotor/stator interactions on the aerodynamics and heat transfer of a large-scale rotating turbine model. Volume 3: Heat transfer data tabulation 65 percent axial spacing
[NASA-CR-179468] 23 p3180 N88-28930
The effects of inlet turbulence and rotor/stator interactions on the aerodynamics and heat transfer of a large-scale rotating turbine model. Volume 2: Heat transfer data tabulation. 15 percent axial spacing
[NASA-CR-179467] 24 p3326 N88-29804
INLET NOZZLES
Test stand performance of a convertible engine for advanced V/STOL and rotorcraft propulsion
[NASA-TM-100211] 03 p0266 N88-11679
Theoretical and experimental study of flow-control devices for inlets of indraft wind tunnels
03 p0268 N88-11684
Electromagnetic fields backscattered from an s-shaped inlet cavity with an absorber coating on its inner walls
[NASA-CR-182401] 07 p0845 N88-15130
Low pressure gas flow analysis through an effusive inlet using mass spectrometry
[NASA-CR-182712] 14 p1910 N88-21413
The effects of inlet turbulence and rotor/stator interactions on the aerodynamics and heat transfer of a large-scale rotating turbine model. Part 4: Aerodynamic data tabulation
[NASA-CR-179469] 17 p2339 N88-23956
Rotation symmetric inside flow with diametric expansion resolution
[ILR-MITT-193] 23 p3213 N88-29123
INLET PRESSURE
Soot and radiation in a gas turbine combustor
[AD-A191991] 23 p3179 N88-28924
Simulation of Vulcain engine operation at low inlet pressure
[ETN-88-93083] 24 p3339 N88-29875
INLET TEMPERATURE
Use of a local heat source for determining temperature of inlet heat section in ring channels
[DE88-700332] 07 p0854 N88-15187
Effect of spatial inlet temperature and pressure distortion on turbofan engine stability
[NASA-TM-100850] 14 p1868 N88-21162
INLETS (DEVICES)
U INTAKE SYSTEMS
INNER RADIATION BELT
Approximate analytical formulae for electron density and collision frequency in the natural and nuclear-disturbed ionosphere and inner magnetosphere
[AD-A193129] 21 p2972 N88-27654
INORGANIC COATINGS
NT ANODIC COATINGS
NT CERAMIC COATINGS
INORGANIC COMPOUNDS
NT AMMONIA
NT LIQUID AMMONIA
INORGANIC MATERIALS
Highly Non-Linear Optical (NLO) organic crystals and films. Electrooptical organic materials
03 p0297 N88-11886

INORGANIC NITRATES
NT AMMONIUM NITRATES
NT HYDRAZINE NITRATE
NT SODIUM NITRATES
INORGANIC PEROXIDES
NT HYDROGEN PEROXIDE
INORGANIC SULFIDES
NT BISMUTH SULFIDES
NT CADMIUM SULFIDES
NT COPPER SULFIDES
NT HYDROGEN SULFIDE
NT LEAD SULFIDES
NT MOLYBDENUM DISULFIDES
NT MOLYBDENUM SULFIDES
NT POLYSULFIDES
NT ZINC SULFIDES
INPUT
Equivalence of input-output stability and exponential stability for infinite dimensional systems
[TW-276] 05 p0638 N88-13903
Modeling and generating input processes
[DE87-013162] 05 p0645 N88-13948
A queueing system with independent Markov input streams
[AD-A187601] 10 p1402 N88-18363
High bit rate serial input mutipliers
[REPT-87-012] 11 p1530 N88-19140
A serial input pipelined multiplier
[REPT-87-030] 11 p1530 N88-19141
On serial-input multipliers for two-complement numbers
[REPT-86-035] 11 p1536 N88-19181
Logical input devices and interaction --- computer graphics
[CWI-CS-R8738] 13 p1814 N88-20836
Why is it difficult to program in von Neumann languages
[AD-A192830] 20 p2838 N88-26839
A study of the effect of random input motion on low Reynolds number flows
[AD-A195559] 24 p3316 N88-29747
INPUT/OUTPUT ROUTINES
Integrated voice and visual systems research topics
[NASA-CR-177417] 03 p0356 N88-12246
Advanced Information Processing System (AIPS) proof-of-concept system functional requirements I/O network system services
[NASA-CR-181481] 03 p0384 N88-12412
Advanced Information Processing System (AIPS) proof-of-concept system functional design I/O network system services
[NASA-CR-181488] 03 p0384 N88-12413
Rationale for the design of the Ada (tradename) programming language
[AD-A187106] 09 p1217 N88-17297
Data acquisition and processing for surface plate calibration
[AD-A187264] 11 p1564 N88-19366
The TempIS Project: Performance analysis of temporal queries
[AD-A188354] 12 p1706 N88-20213
A comparison of two chord keyboard coding systems for alphanumeric data entry
[AD-A189230] 13 p1813 N88-20834
A proof of the Kahn principle for input/output automata
[AD-A194454] 23 p3248 N88-29333
INSAT SATELLITES
U INDIAN SPACECRAFT
INSECTICIDES
NT CARBAMATES (TRADENAME)
NT URETHANES
INSECTS
NT DROSOPHILA
Insect contamination protection for laminar flow surfaces 07 p0814 N88-14954
Factors affecting the sticking of insects on modified aircraft wings
[NASA-CR-182451] 09 p1148 N88-16878
Factors affecting the sticking of insects on modified aircraft wings
[NASA-CR-182615] 12 p1575 N88-19421
INSENSITIVITY
U SENSITIVITY
INSERTION
Hardware fault insertion and instrumentation system: Mechanization and validation
[NASA-CR-181445] 01 p0078 N88-10497
Software-implemented fault insertion: An FTMP example
[NASA-CR-178423] 06 p0761 N88-14668
Insertions using geometric analysis and hybrid force-position control: Method and analysis
[DE87-013652] 15 p2117 N88-22611
INSERTS
A low volume insert for solid state magic angle spinning NMR of small samples
[AD-A184359] 04 p0419 N88-12601
Increasing strength of graphite/epoxy bolted joints by introducing an adhesively bonded metallic insert
[FFA-TN-1987-45] 15 p2088 N88-22442
Insert design handbook
[ESA-PSS-03-1202-ISSUE-1] 17 p2311 N88-23822
INSOLATION
A quasi-physical model for converting hourly global horizontal to direct normal insolation
[DE87-012273] 03 p0349 N88-12204
Calendar year 1985 solar and weather data for Austin, Texas
[PB87-220174] 03 p0352 N88-12219
Satellite techniques of solar resource assessment for focusing and non-focusing solar collector systems
[DE88-001657] 07 p0874 N88-15298
Short Reference Years: Short weather data sets for faster simulations of solar energy systems and energy consumption in buildings
[DE88-900198] 07 p0881 N88-15343
The use of the direct measurement of solar radiation for the determination of Pasquill Stability Parameter
[AD-A186084] 07 p0946 N88-15750
Calibration of the solar radiation estimation method by satellites
[INPE-4349-PRE/1185] 12 p1646 N88-19861
Global solar radiation in Sierra Leone (West Africa)
[DE88-702725] 23 p3235 N88-29252
INSPECTION
NT X RAY INSPECTION
Technology survey for a robot which will investigate the condition of underground pipe
[PB87-209979] 01 p0055 N88-10351
Nondestructive inspection of the pressure vessel in Stuttgart. ALOK part. Phase 1: ALOK combined with conventional probes
[REPT-860113-TW] 01 p0057 N88-10367
Needs assessment for NDT and characterization of ceramics: Assessment of inspection technology for green state and sintered ceramics
[DE87-013550] 02 p0151 N88-10947
Ultrasonic method of inspecting austenitic weld joints in nuclear power station equipment
[BLL-CE-TRANS-8281-(9022.09)] 04 p0453 N88-12806
Pulsed eddy-current inspection of thin-walled stainless steel tubing
[DE88-001492] 04 p0457 N88-12830
Computerized certification of digital ultrasonic instrumentation
[DE88-000820] 04 p0488 N88-13008
A pulsed eddy current method for examining thin-walled stainless steel tubing
[DE88-002294] 07 p0866 N88-15255
Through-transmission/pulse-echo ultrasonic equipment evaluation
[AD-A186340] 07 p0929 N88-15641
Analysis of the reliability of Royal Australian Air force non-destructive inspection
[AD-A186979] 09 p1177 N88-17049
Micro PAVER concept and development airport pavement management system
[AD-A187360] 11 p1441 N88-18598
Ultrasonic inspection of irregular surfaces
[AERE-R-12465] 13 p1780 N88-20648
Quick actuating closure and handling system
14 p1925 N88-21476
Eddy current nondestructive inspection of graphite epoxy using ferrite cup core probes
[AD-A189823] 15 p2074 N88-22365
Nondestructive evaluation of large scale composite components
[AD-A190998] 16 p2173 N88-22954
Method of radiographic inspection of wooden members
[NASA-CASE-LAR-13724-1] 17 p2346 N88-23983
Knowledge based systems in nondestructive evaluation
[DE88-006653] 18 p2525 N88-24981
The inspection of metallurgical bounds in electronic systems
[AD-A192064] 18 p2582 N88-25343
Inspection methods in programming: Cliches and plans
[AD-A192782] 21 p2996 N88-27767
Use of Moessbauer spectroscopy to study implanted surfaces
[DE88-010452] 21 p3023 N88-27942
Evaluation of bond testing equipment for inspection of Army advanced composite airframe structures
[AD-A195795] 24 p3341 N88-29885
INSPIRATION
Discovery and problem solving: Triangulation as a weak heuristic 08 p1062 N88-16412
INSTABILITY
U STABILITY
INSTALLATION
U INSTALLING
INSTALLING
Advanced turboprop wing installation effects measured by unsteady blade pressure and noise
[NASA-TM-100200] 01 p0002 N88-10008
Airframe/store compatibility 05 p0545 N88-13323
Human engineering laboratory grounding analysis (HELGA)-2
[AD-A185367] 05 p0578 N88-13524
Facility design validation of the information systems laboratory
[AD-A186309] 07 p0906 N88-15488
The design and implementation of the Technical Facilities Controller (TFC) for the Goldstone deep space communications complex 11 p1474 N88-18794
Airworthiness and flight characteristics test of a ski assembly for the UH-60A Black Hawk helicopter
[AD-A191414] 16 p2162 N88-22895
The Environment for Application Software Integration and Execution (EASIE) version 1.0. Volume 4: System installation and maintenance guide
[NASA-TM-100576] 17 p2386 N88-24185
Aircraft avionics and missile system installation cost study. Volume 2: Appendices F and G
[AD-A195372] 24 p3325 N88-29801
Electronic materials and devices prepared by molecular beam epitaxy
[AD-A195694] 24 p3433 N88-30433
INSTANTONS
Instanton in supersymmetric theory with static disorder
[DE88-700357] 07 p0940 N88-15716
Recent developments in the path integral approach to anomalies
[DE87-703032] 15 p2118 N88-22616
INSTRUCTIONS
U EDUCATION
INSTRUCTORS
Elementary and middle school science improvement project
[NASA-CR-179328] 16 p2285 N88-23679
US civil airmen statistics, 1987
[AD-A191714] 18 p2455 N88-24577
INSTRUMENT APPROACH
Boeing 727 MLS (Microwave Landing System) terminal instrument procedures (TERPS) approach data collection and processing, data report
[AD-A185523] 06 p0667 N88-14090
Investigation of air transportation technology at Massachusetts Institute of Technology, 1986
17 p2293 N88-23716
Loran-C monitor correlation over a 92-mile baseline in Ohio 17 p2293 N88-23720
Cessna 172 MLS (Microwave Landing System) terminal instrument procedures (TERPS) approach data collection and processing data report
[AD-A191241] 18 p2461 N88-24613
INSTRUMENT COMPENSATION
NT TEMPERATURE COMPENSATION
CGI delay compensation
[NASA-TM-86703] 04 p0476 N88-12932
Corner compensation structures for (110) oriented silicon
[DE88-003300] 10 p1417 N88-18455
INSTRUMENT DRIFT
U DRIFT (INSTRUMENTATION)
INSTRUMENT ERRORS
Effect of installation and calibration errors of sensors on system identification results of an aircraft
[ESA-TT-1059] 03 p0266 N88-11678
Flightpath reconstruction and systematic radar error estimation from multiradar range-azimuth measurements
[NLR-MP-85064-U] 06 p0693 N88-14251
Determination of cloud base height and emissivity from downwelling angular radiances
[AD-A185985] 07 p0879 N88-15331
Zeroshift of piezoelectric accelerometers in pyroshock measurements 08 p0997 N88-16039
Common but unappreciated sources of error in one, two, and multiple-color pyrometry 17 p2329 N88-23907
INSTRUMENT FLIGHT RULES
Estimates of potential increases in airport capacity through ATC (Air Traffic Control) system improvements in the airport and terminal areas
[AD-A188533] 12 p1578 N88-19444
Rule-based fault-tolerant flight control
17 p2294 N88-23725
Aircraft accident/incident, Copperhill, Tennessee, February 22, 1986
[PB88-910407] 18 p2461 N88-24612

Improvement of head-up display standards. Volume 3: An evaluation of head-up display safety
[AD-A195787] 24 p3410 N88-30300

INSTRUMENT LANDING SYSTEMS
NT AUTOMATIC LANDING CONTROL

Improvement of head-up display standards. Volume 5: Head up display ILS (Instrument Landing System) accuracy flight tests
[AD-A194602] 23 p3178 N88-28922

INSTRUMENT PACKAGES
NT EREP

Instrumentation package for a shrouded SWERVE/EPW rocket sled test
[DE87-014267] 01 p0006 N88-10045

INSTRUMENT TRANSFORMERS

Low frequency IF transformer designs having variable coupling
[RAE-TM-RAD-NAV-291] 01 p0043 N88-10272

INSTRUMENTAL ANALYSIS
U AUTOMATION

INSULATING MATERIALS
U INSULATION

INSULATION
NT ELECTRICAL INSULATION
NT MULTILAYER INSULATION
NT THERMAL INSULATION

Elimination of subboundaries in 0.5-micron-thick Si-on-insulation films produced by ZMR
[AD-A184590] 03 p0381 N88-12396

The assessment of the sound insulation requirements for a large broadcasting studio, using a scale model: Theoretical considerations
[BBC-RD-1987/20] 09 p1155 N88-16921

Some investigations of electrical discharges at the surfaces of solid cathodes immersed in aqueous electrolyte solutions
[PB87-166209] 09 p1159 N88-16946

Indirect measurement of local condensing heat-transfer coefficient around horizontal finned tubes
[AD-A186929] 09 p1160 N88-16950

The assessment of the sound insulation requirements for a large broadcasting studio, using a scale model: Practical details
[BBC-RD-1987/21] 10 p1318 N88-17878

Prototype thin-film thermocouple/heat-flux sensor for a ceramic-insulated diesel engine
[NASA-TM-100798] 11 p1490 N88-18892

Review of the state of the art and projected technology of low heat rejection engines
[PB88-131255] 11 p1496 N88-18934

Safety research of insulating materials of cable for nuclear power generating station
[NASA-TT-20202] 13 p1752 N88-20477

Aging properties of cable polmers (2)
[NASA-TT-20228] 13 p1752 N88-20479

The Magnetically Insulated Inertial Confinement Fusion (MICF): A novel approach
[DE88-005460] 13 p1842 N88-21026

Experiments on insulation of relativistic electron flows in oblique and tapered magnetic fields
[DE88-007199] 19 p2724 N88-26176

SIS (Superconductor-Insulator-Superconductor) mixer research
[AD-A192908] 20 p2879 N88-27092

Far- and mid-infrared properties of metal-insulator composite materials
[AD-A193227] 21 p2905 N88-27236

INSULATORS

Gases released by surface flashover of insulators
[DE87-013651] 01 p0039 N88-10249

Thermionic Technology Program. A: Insulator test and evaluation
[DE88-004707] 13 p1795 N88-20735

Generation of high brightness ion beam from insuleted anode PED 16 p2276 N88-23637

Development of the field-induced electron injection and impact ionization (F4I) technique for radiation hardness testing of MOS (Metal-Oxide-Semiconductor) gate insulators
[AD-A192114] 18 p2583 N88-25345

Data compilation for radiation damage on ceramic insulators. Revised with updated data and reviews
[DE88-753426] 21 p2920 N88-27329

Studies on the use of propylene carbonate as a high-voltage insulator
[DE88-011766] 22 p3057 N88-28141

INSURANCE (CONTRACTS)

Review of commercial spacecraft: Recovery and repair experiences. Implications for future spacecraft designs and operations 12 p1591 N88-19528

The role and the place of insurance of large space projects 22 p3161 N88-28826

INTAKE SYSTEMS
NT AIR INTAKES
NT ENGINE INLETS
NT HELICAL INDUCERS
NT SIDE INLETS
NT SUPERSONIC INLETS

Theoretical and experimental study of flow-control devices for inlets of indraft wind tunnels
03 p0268 N88-11684

Dynamics of reverse flows at pump inlet
04 p0425 N88-12636

Fundamentals of fighter aircraft design: Engine intake and afterbody 05 p0545 N88-13322

Fluid mass and thermal loading effects on the modal characteristics of space shuttle main engine liquid oxygen inlet splitter vanes 05 p0594 N88-13628

Inlets, ducts and nozzles 08 p0955 N88-15791

The advantage of variable geometry for turbine engines at low power 10 p1280 N88-17653

Investigation of dihedral effects in compressor cascades 10 p1282 N88-17672

Wake interaction effects on the transition process on turbine blades
[AD-A188020] 10 p1332 N88-17962

Measurement and analysis of the noise radiated by low Mach numbers centrifugal blowers
[AD-A189226] 13 p1833 N88-20966

Flow/acoustic interaction in duct inflow
[AD-A189264] 13 p1833 N88-20967

Inflow measurement made with a laser velocimeter on a helicopter model in forward flight. Volume 2: Rectangular planform blades at an advance ratio of 0.23
[NASA-TM-100542] 14 p1864 N88-21139

Inflow measurements made with a laser velocimeter on a helicopter model in forward flight. Volume 4: Tapered planform blades at an advance ratio of 0.15
[NASA-TM-100544] 16 p2156 N88-22863

A numerical study of the hot gas environment around a STOVL aircraft in ground proximity
[NASA-TM-100895] 17 p2295 N88-23729

Inflow measurement made with a laser velocimeter on a helicopter model in forward flight. Volume 5: Tapered planform blades at an advance ratio of 0.23
[NASA-TM-100545] 17 p2299 N88-23755

Inflow measurements made with a laser velocimeter on a helicopter model in forward flight. Volume 1: Rectangular planform blades at an advance ration of 0.15
[NASA-TM-100541] 18 p2460 N88-24607

The effects of different combinations of inlet air conditions used for cooling as measured on a heated manikin
[AD-A191116] 18 p2552 N88-25151

Air intake aerodynamics 24 p3318 N88-29762

INTEGERS

Discrete generalized networks: Application to integer constrained flow problems
[AD-A190823] 16 p2190 N88-23060

A mixed-integer linear programming problem which is efficiently solvable
[AD-A191028] 18 p2556 N88-25168

Factorization of large integers on a massively parallel computer
[DE88-011625] 21 p2999 N88-27786

Multicriteria integer programming for problems involving linear and nonlinear utility functions
[AD-A194530] 23 p3249 N88-29336

Two dimensional convolute integers for machine vision and image recognition 23 p3254 N88-29369

Bifurcations of periodic solutions of non-integrable Hamiltonians with two degrees of freedom: Numerical and analytical results
[DE88-702747] 23 p3272 N88-29473

INTEGRAL CALCULUS

An algebraic approach to a calculus of functional differences: Fixed differences and integrals
[AD-A187079] 09 p1227 N88-17346

Martingale representation and the Malliavin calculus
[AD-A189721] 15 p2119 N88-22626

INTEGRAL EQUATIONS
NT FREDHOLM EQUATIONS
NT J INTEGRAL
NT SINGULAR INTEGRAL EQUATIONS
NT VOLTERRA EQUATIONS

On oscillation of a kind of integro-differential equation with delay
[DE87-703059] 02 p0225 N88-11417

Parallel methods for ordinary differential equations
[DE87-014667] 02 p0226 N88-11425

Numerical modeling: Integral equation method
03 p0304 N88-11919

An integral equation analysis of inelastic shells
03 p0336 N88-12118

Mutual admittance between slots in cylinders of arbitrary shape
[AD-A184254] 04 p0439 N88-12723

Steady waves in a nonlinear theory of viscoelasticity
[AD-A185548] 06 p0723 N88-14448

On the convergence of the p-version of the boundary element Galerkin method
[AD-A186198] 07 p0910 N88-15514

Computational analysis of propagation properties of integrated-optical waveguides using a domain integral equation
[PB87-163358] 09 p1154 N88-16917

Retarded potential technique applied for shock wave loading of doubly symmetric submerged structures
09 p1179 N88-17058

Theory of the generalized Abel integral equations
[ETN-88-91066] 09 p1229 N88-17382

Conjugate gradient spectral iterative technique
[PB88-126917] 10 p1398 N88-18337

Small degree solutions for the polynomial Bezout equation
[AD-A187630] 10 p1401 N88-18355

Integral equations with modified fundamental solutions for exterior boundary value problems from electromagnetic wave theory
[ETN-88-91483] 11 p1475 N88-18600

A discretization of the integral equation for the time dependent linearized subsonic potential flow over a wing
[AD-A188534] 12 p1574 N88-19411

Study of inhomogeneously filled cylindrical resonant cavities by the finite integration technique
[PB88-133707] 12 p1697 N88-20156

Computational technique for compressible vortex flows using the integral equation solution
[NASA-CR-182695] 13 p1716 N88-20271

Integral equation theory of homopolymer melts
[DE88-005304] 13 p1751 N88-20470

Integral equation theory of polymer blends
[DE88-005305] 13 p1751 N88-20471

Inversion algorithms for geophysical problems
[AD-A189252] 13 p1815 N88-20645

WKB theory of wave tunneling for Hermitian vector systems of integral equations
[DE88-005332] 13 p1831 N88-20951

Global spatial periodic solutions to the Ginzburg-Landau equations
[DE88-006424] 15 p2119 N88-22623

An integral equation for the linearized supersonic flow over a wing
[AD-A191408] 16 p2158 N88-22675

Determination of characteristic radiation properties of a torus antenna: Integral equation method
[DFVLR-FB-87-46] 16 p2188 N88-23049

Parameter estimation for boundary value problems by integral equations of the second kind
[NASA-CR-181660] 17 p2332 N88-23918

A new collocation-type method for the numerical solution of Hammerstein equations 17 p2393 N88-24226

Joint services electronics program
[AD-A191749] 18 p2504 N88-24853

Cross stream differencing for integral boundary layer equations
[AD-A191744] 18 p2509 N88-24866

Integral equation for the laser field: Multimode description of a free-electron laser oscillator
[DE88-007050] 18 p2521 N88-24956

Fracture mechanics analysis for short cracks
[AD-A192002] 18 p2527 N88-24992

Information analysis of integral equations in remote sensing of atmospheric aerosols
18 p2532 N88-25022

A mixed min-max control problem governed by integral equations 18 p2564 N88-25228

Optimal processes governed by integral equations with unilateral constraint 18 p2565 N88-25231

Numerical solution of random Love's integral equation
18 p2565 N88-25235

New hybrid method for solving time-domain integral equations (one-dimensional scattering problems)
[PB88-186192] 20 p2789 N88-26547

Time-domain boundary element analysis of dynamic near-tip fields for impact-loaded collinear cracks
[AD-A192930] 20 p2815 N88-26700

A new boundary integral equation formulation for elastodynamic and elastostatic crack analysis
[AD-A192967] 20 p2815 N88-26702

Ill-posed problems and integral equations
[AD-A193709] 22 p3143 N88-28691

An integral equation for the linearized unsteady supersonic flow over a wing
[AD-A193773] 23 p3172 N88-28867

Resonance excitation of linear and non-linear spiral density waves in a gaseous disk
23 p3299 N88-29643

Initial value problems in viscoelasticity
[AD-A196052] 24 p3382 N88-30145

INTEGRAL FUNCTIONS
U ENTIRE FUNCTIONS

INTEGRAL TRANSFORMATIONS
NT FAST FOURIER TRANSFORMATIONS
NT FOURIER TRANSFORMATION
NT FOURIER-BESSEL TRANSFORMATIONS
NT HILBERT TRANSFORMATION
NT LAPLACE TRANSFORMATION

Thermomechanical cracking in coated media due to high speed asperity excitation
[AD-A184176] 04 p0454 N88-12809

Theory of the generalized Abel integral equations
[ETN-88-91086] 09 p1229 N88-17362

INTEGRALS
NT CONVOLUTION INTEGRALS

Elevated temperature crack growth
02 p0188 N88-11174

Method estimating integral mean value of enhancement factor and path latitude for whistlers below magnetic latitude 10 deg 03 p0300 N88-11885

Operator foundation of functional integral in non-Abelian gauge theory
[DE88-700508] 07 p0941 N88-15719

Theory of the generalized Abel integral equations
[ETN-88-91086] 09 p1229 N88-17362

Path integration on the upper half-plane
[DE88-751050] 12 p1682 N88-20057

Product-integrals and counting processes
[CWI-MS-R8707] 14 p1965 N88-21727

Recent developments in the path integral approach to anomalies
[DE87-703032] 15 p2118 N88-22616

Remarks on the time transformation of path-integral measures
[DE87-703040] 15 p2118 N88-22617

Path integral, BRS symmetry, and string and membrane theories
[DE88-752300] 15 p2146 N88-22810

Computation of a complete elliptic integral of the first kind using q-expansion 16 p2257 N88-23490

Incomplete Lipschitz-Hankel integrals of MacDonald functions
[AD-A191034] 16 p2261 N88-23515

Evaluation of quantum mechanics path integrals by the approximations exact on a class of polynomial functionals
[DE88-702434] 21 p3011 N88-27865

An asymptotic evaluation of the tail of a multiple symmetric alpha-stable integral
[AD-A194570] 23 p3270 N88-29460

Numerical calculations of the response of a spinning spheroidal payload to coning motion
[AD-A195890] 24 p3368 N88-30059

On the Nash point equilibria in the calculus of variations
[AD-A194959] 24 p3424 N88-30381

Canonical variables and canonical integrals for motion in near-circular orbits 24 p3446 N88-30512

INTEGRATED CIRCUITS
NT ENCAPSULATED MICROCIRCUITS
NT LARGE SCALE INTEGRATION
NT LINEAR INTEGRATED CIRCUITS
NT VERY LARGE SCALE INTEGRATION
NT VHSIC (CIRCUITS)

Physics and device design of vacuum integrated circuits 01 p0039 N88-10251

An interactive optimization procedure for the computer aided dimensioning of integrated circuits
[ETN-87-90414] 01 p0082 N88-10531

Understanding the transport properties of silicon grain boundaries and how they relate to I.C. applications of polysilicon
[DE87-013809] 01 p0104 N88-10677

Voltammetric investigation of porous silicon for integrated circuit applications
[DE87-009287] 02 p0166 N88-11042

Low noise-low power monolithic multiplexing readout electronics for silicon strip detectors
[MPI-PAE/EXP.EL.178] 02 p0168 N88-11057

Some 2-D WSI array architectures --- wafer scale integration (WSI)
[OUEL-1672/87] 02 p0219 N88-11381

Development of standard cells in NMOS technology for the design of digital integrated circuits
[FI-62-TB-6] 03 p0310 N88-11953

Integrated circuit design
[AD-A184486] 03 p0311 N88-11960

Research in monolithic signal-processing circuits
[AD-A184680] 03 p0311 N88-11962

Dramatically improved radiation hardness for CMOS silicon gate integrated circuits even down to cryogenic temperatures
[AD-A184672] 03 p0381 N88-12398

A procedural method for the efficient implementation of full-custom VLSI designs 04 p0436 N88-12701

Programmable Logic Arrays (PLA's) design for testability
[PB87-102935] 04 p0438 N88-12718

Electromagnetics and electrothermal approach to evaluate failures in microelectronic devices caused by electrostatic discharges: Stochastical aspects of the device reliability
[AD-A184906] 05 p0577 N88-13522

An extension to the multilevel logic simulator for microcomputers
[AD-A185032] 05 p0634 N88-13879

Computer modeling of complete IC fabrication process
[AD-A184807] 05 p0654 N88-14012

Technology upgrade of a silicon compiler
[AD-A184873] 05 p0655 N88-14016

Integrated photo-responsive metal oxide semiconductor circuit
[NASA-CASE-GSC-12782-1] 06 p0696 N88-14271

An analysis of simplified feed architectures for MMIC (Monolithic Microwave Integrated Circuit) T/R (Transmit/Receive) module arrays
[AD-A185474] 06 p0697 N88-14275

Investigations on an RF plasma related to plasma etching
[ETN-88-91366] 06 p0784 N88-14809

Correctness proofs for systolic algorithms: Palindromes and sorting
[PB88-106075] 07 p0912 N88-15534

GaAs MMIC yield evaluation --- monolithic microwave integrated circuits (MMIC)
[ESA-CR(P)-2470] 08 p0979 N88-15916

Single-layer wire routing
[AD-A186990] 09 p1157 N88-16932

Plasma and ion etching for failure analysis. Part 2. The etching of plastic encapsulant and other semiconductor device materials, using the Technics Giga Etch 100-E plasma etch system
[AERE-R-12212] 09 p1177 N88-17050

Interchange of electronic design through VHDL and EIS 09 p1205 N88-17222

Effect of the gate oxide thickness on the speed of MOS integrated circuits
[PB88-155783] 10 p1323 N88-17910

Time domain wave propagation in multilayered integrated circuits
[AD-A187462] 10 p1324 N88-17916

Formal multilevel hierarchical verification of synchronous MOS VLSI circuits
[AD-A187532] 10 p1324 N88-17918

The soft/hard wet anodization of aluminum oxide and its use in a thin film multilayered capacitor
[AD-A187575] 10 p1325 N88-17919

Signal processing studies program VLSI designs for unary functions
[AD-A188053] 10 p1325 N88-17922

The arithmetic cube and its associated algorithms
10 p1374 N88-18195

Voltammetric investigation of porous silicon for integrated circuit applications
[DE88-004024] 11 p1456 N88-18677

RELIC: A reliability simulator for integrated circuits
[AD-A187493] 11 p1477 N88-18811

Modules of nanosecond logic electronics system with computer control
[DE88-700190] 11 p1479 N88-18828

Polymeric materials for electro-optic testing
[AD-A188382] 12 p1610 N88-19627

Intergrated circuit design, phase 2
[AD-A189060] 13 p1760 N88-20530

Laser programming integrated circuits
[AD-A189590] 13 p1762 N88-20537

Optical RF distribution links for MMIC phased array antennas
[NASA-TM-100841] 13 p1764 N88-20555

Monolithic microwave integrated circuit technology for advanced space communication
[NASA-TM-100829] 14 p1906 N88-21389

Monolithic phase shifter study
[AD-A190213] 15 p2059 N88-22278

Fabrication and electrical characterization of multilevel aluminum interconnects used to achieve silicon-hybrid wafer-scale integration
[AD-A190519] 15 p2060 N88-22282

Fast analog-to-digital converter
[DE88-701488] 15 p2106 N88-22543

Beam assisted fabrication of 3-5/Si monolithic devices
[AD-A189979] 15 p2142 N88-22785

Present, future of automotive hybrid IC applications discussed 16 p2185 N88-23024

Algorithms and architectures for acoustic phonetical detection of continuous speech
[ENST-87E016] 16 p2189 N88-23054

Instrumentation for ultrafast electronics
[AD-A191379] 16 p2193 N88-23060

A 30 GHz monolithic receive module technology assessment
[NASA-CR-180825] 16 p2194 N88-23064

Computer aided design tools for integrated silicon system structures
[ETN-88-92186] 16 p2247 N88-23424

Contribution to the automatic generation of floor plan placing --- integrated circuit design
[ETN-88-92193] 16 p2247 N88-23426

Millimeter and submillimeter waves and frequency selective surfaces
[AD-A191511] 18 p2500 N88-24827

Joint services electronics program
[AD-A190239] 18 p2503 N88-24848

Computer aided design of monolithic microwave and millimeter wave integrated circuits and subsystems
[AD-A191593] 18 p2503 N88-24852

The inspection of metallurgical bounds in electronic systems
[AD-A192064] 18 p2582 N88-25343

A non-contact picosecond prober for integrated circuit testing 19 p2655 N88-25766

Picosecond sampling of integrated circuits
19 p2655 N88-25767

Electro-optic sampling of high-speed, InP-based integrated circuits 19 p2655 N88-25769

Millimeter-wave integrated circuits
19 p2656 N88-25774

Enhanced performance ultrabroadband distributed amplifiers 19 p2656 N88-25775

Thermionic integrated circuit program
[DE88-010119] 19 p2662 N88-25833

The 1986 IEEE Solid-State Sensor Workshop
[AD-A190922] 19 p2668 N88-25860

An integrated on-chip pressure sensor for accurate control applications 19 p2671 N88-25880

Resonant structures for integrated sensors
19 p2673 N88-25893

Zinc-oxide thin films for integrated-sensor applications
19 p2673 N88-25896

Effects of cosmic rays on single event upsets
[NASA-CR-183053] 20 p2793 N88-26569

Analysis of networks with parameters S: Generalization of junction matrix
[INPE-4535-PRE/1282] 20 p2793 N88-26570

Integrated optoelectronic circuits utilizing InGaAsP grown by molecular beam epitaxy (erbium doping of MBE GaAs)
[AD-A192269] 20 p2795 N88-26584

An integrated circuit for error protection in modern data communication systems conforming to Eurocom specifications
[FEL-1987-48] 20 p2796 N88-26593

Research in VLSI computer systems
[AD-A192[illegible]15] 20 p2835 N88-26816

Defects in high-mobility semiconductor systems
[AD-A192298] 20 p2879 N88-27090

Picosecond optoelectronic sampling of electrical waveforms produced by an optically excited field effect transistor
[AD-A192384] 21 p2935 N88-27428

A planar IC-compatible transferred electron device for millimeter-wave operation
[AD-A192692] 21 p2936 N88-27433

Guided wave interactions in millimeter-wave integrated circuits
[AD-A193017] 21 p2936 N88-27437

Very High Speed Integrated Circuits (VHSIC)
[AD-A193225] 21 p2937 N88-27442

Silicon-on-insulator pin diodes
[AD-A193359] 21 p2937 N88-27445

STAR: Sandia Timing Analyzer Routine
[DE88-012412] 21 p2940 N88-27463

Molecular beam epitaxy of GaP films on Si substrates
[PB88-131974] 21 p3020 N88-27923

Dose-enhancement effects in TaSi/Al- and Al-gate MOS devices
[DE88-005483] 21 p3020 N88-27926

Array trade-off study using multilayer parasitic subarrays
[NASA-TM-101321] 22 p3070 N88-28222

Time domain wave propagation in multilayered integrated circuits
[AD-A193821] 22 p3073 N88-28241

Signals and systems 24 p3363 N88-30026

Electronic and optical devices and applications
24 p3363 N88-30027

Circuit design criteria for stable lateral inhibition neural networks
[AD-A195066] 24 p3366 N88-30046

Impurity analysis in SIMOX samples by high-efficiency resonance ionization time-of-flight mass spectrometry
[DE88-012061] 24 p3367 N88-30051

Stress related failures causing open metallization
[AD-A195061] 24 p3383 N88-30150

INTEGRATED ENERGY SYSTEMS

Integrated analysis and applications
08 p0954 N88-15789

Assessment of VAS-derived products created by a simultaneous algorithm on a convectively active day
[AD-A186158] 08 p1054 N88-16359

INTEGRATED MISSION CONTROL CENTER
Optimization of the dilation characteristic on the control jurisdiction of an area control facility
[AD-A191720] 18 p2461 N88-24615

INTEGRATED OPTICS
Computational analysis of propagation properties of integrated-optical waveguides using a domain integral equation
[PB87-163358] 09 p1154 N88-16917
Monolithic integration on a GaAs substrate of a quarter ring laser and an optical guide coupled by an evanescent wave
[ETN-88-92308] 17 p2344 N88-23969
Nonlinear surface polaritons
[AD-A191046] 18 p2499 N88-24822
Research in the optical sciences
[AD-A192175] 18 p2575 N88-25297
Investigations on periodically perturbed optical waveguides
[B8712725] 23 p3283 N88-29548
Ion exchange processes for fabrication of integrated optical waveguide structures into glass substrates
[VTT-46] 24 p3429 N88-30405

INTEGRATION (REAL VARIABLES)
U MEASURE AND INTEGRATION

INTEGRATORS
Rotorcraft flight-propulsion control integration: An eclectic design concept
[NASA-TP-2815] 12 p1584 N88-19475

INTEGRITY
NT COMPUTER PROGRAM INTEGRITY

INTEGRODIFFERENTIAL EQUATIONS
U DIFFERENTIAL EQUATIONS
U INTEGRAL EQUATIONS

INTELLIGENCE
NT ARTIFICIAL INTELLIGENCE
NT EXPERT SYSTEMS
NT EXTRATERRESTRIAL INTELLIGENCE
Intelligent tutoring systems as tools for investigating individual differences in learning
09 p1204 N88-17216
An intelligent processing environment for real-time simulation
[NASA-CR-183056] 19 p2715 N88-26119
Reliability and construct validity of reaction time, inspection time and machine-paced tests of cognitive speed
[AD-A193779] 23 p3241 N88-29289

INTELLIGIBILITY
NT SPEECH RECOGNITION

INTENSIFICATION
U AMPLIFICATION

INTENSIFIER TUBES
U IMAGE INTENSIFIERS

INTENSIFIERS
NT IMAGE INTENSIFIERS

INTERACTIONAL AERODYNAMICS
Breakdown of steady and unsteady interacting boundary layers
[NLR-MP-86047-U] 01 p0045 N88-10294
An experimental investigation of the chopping of helicopter main rotor tip vortices by the tail rotor. Part 2: High speed photographic study
[NASA-CR-177457] 09 p1114 N88-16678
Propulsion and airframe aerodynamic interactions of supersonic V/STOL configurations. Volume 1: Wind tunnel test pressure data report
[NASA-CR-177343-VOL-1] 16 p2157 N88-22866
Propulsion and airframe aerodynamic interactions of supersonic V/STOL configurations. Volume 2: Wind tunnel test force and moment data report
[NASA-CR-177343-VOL-2] 16 p2157 N88-22867
Propulsion and airframe aerodynamic interactions of supersonic V/STOL configurations. Volume 4: Summary
[NASA-CR-177343-VOL-4] 16 p2157 N88-22868
Forced response unsteady aerodynamics in a multistage compressor 18 p2512 N88-24903
Research investigation of helicopter main rotor/tail rotor interaction noise
[NASA-CR-4143] 19 p2722 N88-26165
Theory of sound production by vortex-airfoil interaction
[AD-A193386] 21 p3012 N88-27875
An unsteady helicopter rotor: Fuselage interaction analysis
[NASA-CR-4178] 23 p3171 N88-28880
Experience with three dimensional composite grids
23 p3247 N88-29324
Three-dimensional Navier-Stokes simulations of turbine rotor-stator interaction
[NASA-TM-100081] 24 p3316 N88-29750
Experimental and numerical investigation of the effect of distributed suction on oblique shock wave/turbulent boundary layer interaction
[NASA-TM-101334] 24 p3372 N88-30084

INTERACTIONS
Interaction between a module cluster and a plasma in a magnetic field
[PB87-148276] 07 p0934 N88-15675
Process migration in UNIX environments
[NASA-CR-182951] 23 p3245 N88-29311

INTERACTIVE CONTROL
An interactive optimization procedure for the computer aided dimensioning of integrated circuits
[ETN-87-90414] 01 p0082 N88-10531
Interactive Design of Accelerators (IDA)
[DE87-013296] 02 p0234 N88-11476
Microcomputer control of spectroscopic instruments
[ATR-86(8431)-4] 03 p0326 N88-12058
A computer code to process and plot laser altimetry data interactively on a microcomputer
[NASA-TM-100687] 05 p0554 N88-13371
GENLPLOT: An interactive program for display and analysis of data, user's manual
[DE88-002292] 07 p0905 N88-15485
Development and testing of an interactive procedure for the improvement of objective analyses
[AD-A186595] 08 p1040 N88-16290
An interactive user-friendly approach to surface-fitting three-dimensional geometries
[NASA-CR-4126] 12 p1682 N88-20058
A description of an automated database comparison program
[NASA-TM-100609] 16 p2253 N88-23463
EnviroNET: An interactive space-environment information resource
[NASA-TM-101137] 17 p2309 N88-23812
A computer-aided approach to nonlinear control systhesis
[NASA-CR-179391] 22 p3140 N88-28673
Mesh generation for industrial application of Euler and Navier Stokes solvers 23 p3247 N88-29323
Numerical simulation of nozzle flows
[AD-A195144] 24 p3369 N88-30064

INTERACTIVE GRAPHICS
U COMPUTER GRAPHICS

INTERATOMIC FORCES
Investigation of impurity defects in alpha-iron by molecular dynamics method
[DE88-700355] 07 p0834 N88-15058

INTERCALATION
Metal intercalation characteristics of n-HfS2 photoelectrodes in non-aqueous electrolytes
[AD-A184381] 03 p0383 N88-12407
Neutron and X-ray scattering studies of layered solids
09 p1246 N88-17469

INTERCEPTION
Optimal thrust vector control of coplanar orbital evasive maneuvers
[AD-A189544] 13 p1730 N88-20346
Passive DF: A tutorial, part 1
[NASA-CR-182669] 13 p1815 N88-20846

INTERCEPTOR AIRCRAFT
U FIGHTER AIRCRAFT

INTERCONNECTION
U JOINING

INTERCONTINENTAL BALLISTIC MISSILES
NT MX MISSILE

INTERCOSMOS SATELLITES
Intershock observations during STIP intervals 17 and 18 01 p0119 N88-10759

INTERDIGITAL TRANSDUCERS
MESFET compatible IMSM detectors
19 p2659 N88-25801

INTERFACE STABILITY
Lithium/polymer electrolyte interfacial instability
[AD-A187164] 09 p1147 N88-16874
Microscopic control of metallization stability
[AD-A187553] 10 p1421 N88-18487
CdTe(110)-Mn interface reaction and the formation of non-equilibrium ternary semimagnetic semiconductor alloys
[AD-A187593] 10 p1422 N88-18491
The influence of current stressing on the structure of Ag contacts to GaAs
[DE88-005968] 15 p2140 N88-22771
Agenda for advancing electrochemical science and technology 17 p2321 N88-23861
The morphological stability of continuous intergranular phases: Thermodynamic considerations
[DE88-006328] 18 p2584 N88-25350
Stability of a coastal upwelling front over topography
[AD-A192354] 20 p2829 N88-26784
Natural frequencies and stability of immiscible spherical liquid systems
[LRT-WE-9-FB-2(1987)] 22 p3053 N88-28113
Natural frequencies and stability of circular cylindrical immiscible liquid systems
[LRT-WE-9-FB-3(1987)] 22 p3062 N88-28172

INTERFACES
NT FLUID BOUNDARIES
NT LIQUID-LIQUID INTERFACES
NT LIQUID-SOLID INTERFACES
NT LIQUID-VAPOR INTERFACES
NT SOLID-SOLID INTERFACES
Polyitaconic acid macromolecule primer for adhesive bonding and corrosion control of aluminum
[DE87-013306] 01 p0027 N88-10173
Si - SiO2 interfaces: A High Resolution Transmission Electron Microscopy (HRTEM) study
[DE87-012255] 01 p0028 N88-10181
A simulation study of interfaces in Ni, Al and Ni3Al with and without boron
[DE87-013156] 01 p0102 N88-10667
X-ray studies of strain, interface and impurity in semiconductors
[DE87-013856] 01 p0104 N88-10676
Photocatalytic electrochemistry at a biological-membrane metal-colloid interface
[DE87-009122] 02 p0166 N88-11041
Surface topography and electrical response of metal-electrolyte interface
[DE87-013553] 02 p0166 N88-11046
Tutorial and hands-on demonstration of a fluent interpreter for CARE 3
[NASA-TM-4011] 02 p0220 N88-11383
Taper sectioning to magnify the interface thickness of a dissimilar metal joint
[RFP-3890-REV] 03 p0333 N88-12099
Gas tungsten arc welding of Al-10Fe-5Ce
[AD-A184202] 03 p0334 N88-12104
Durability (lifetime) predictions adhesively bonded structures
[AD-A184069] 03 p0335 N88-12110
A scientific workstation operator-interface for accelerator control
[DE87-014689] 03 p0362 N88-12278
Materials sciences programs: Fiscal Year 1987
[DE88-000672] 04 p0429 N88-12659
On computing environments in data analysis
[DE88-000078] 04 p0480 N88-12961
Influence of bond dilution on the free surface and interface Potts ferromagnetism
[DE87-703360] 04 p0497 N88-13061
Non-lattice matched metallic superlattices
[DE87-011512] 04 p0497 N88-13062
Development of an interface for an ultrareliable fault-tolerant control system and an electronic servo-control unit
[NASA-TM-88236] 05 p0553 N88-13367
Reactions of porphyrins in surfactant assemblies, microemulsions and in solutions
[AD-A184797] 05 p0560 N88-13412
Water disbondment characterization of organic Coating/metal substrate systems
[AD-A184847] 05 p0567 N88-13454
Molecular-level synthesis and characterization of metal-polymer interfaces
[AD-A184956] 05 p0567 N88-13455
Bending of a bonded beam as a test method for adhesive properties
[AD-A184813] 05 p0609 N88-13736
Molecular beam epitaxial growth and characterization of 3-5 compound semiconductor single and multiple interface structures
[AD-A185400] 05 p0656 N88-14021
Reactions and bonding between glasses and titanium
[DE88-000603] 06 p0685 N88-14195
Some investigations of molecular beam epitaxial growth of 3-5 semiconductor films via Monte-Carlo computer simulations, carrier tunnelling and spectroscopic ellipsometry
[AD-A185520] 06 p0789 N88-14839
Scientific data manipulation in a relational database system
[PB87-124400] 06 p0791 N88-14850
Interface effects on the mechanical properties of ceramic composites
[AD-A185899] 07 p0826 N88-15009
Orbital Replaceable Unit (ORU)/cold plate thermal interface study. Volume 1. Executive Summary
[BAE-TP-8430] 07 p0855 N88-15195
Online monitoring of laserpulses using the GPIB-interface of a Tektronix 2430 Digital Storage Oscilloscope
[DE88-002636] 07 p0856 N88-15201
An interactive visual interface for Fastbus diagnostics
[DE88-002569] 07 p0900 N88-15453
The feasibility of using TAE as the UIL for the space station and for other internal NASA tasks and projects
07 p0925 N88-15618

Interface between astrophysical datasets and distributed database management systems (DAVID)
[NASA-CR-182394] 07 p0942 N88-15731

Interfacing the expert: Characteristics and requirements for the user interface in expert systems
08 p1063 N88-16419

Media independent interface
[NASA-CR-172033] 08 p1066 N88-16446

Media independent interface. Interface control document
[NASA-CR-172032] 08 p1067 N88-16447

Moving Target Indicator (MTI) interface for simple radar
[FOA-C-30463-3.2] 09 p1154 N88-16914

Study of pattern formation at liquid interfaces
[DE88-001399] 09 p1160 N88-16954

User interface devices for mission control
09 p1205 N88-17224

The desktop interface in intelligent tutoring systems
09 p1205 N88-17225

Interfacing slave designs to Fastbus: Practical experience
[DE88-002807] 09 p1215 N88-17286

A proposal for a feasibility study on the design of software interfaces in large systems
[NPL-DITC-89/87] 09 p1222 N88-17330

Electronic and chemical structure of 3-5/metal and Si/metal interfaces
[AD-A186579] 09 p1254 N88-17518

Surface and interface electronic structure
[DE88-003363] 09 p1258 N88-17545

Molecular dynamics study of high-temperature grain-boundary stability in a (100) sigma = 29 bicrystal model
[DE88-002955] 09 p1258 N88-17546

POCC capabilities document. Payload support capabilities description: MCC, JSC POCC, remote POCC interface
[NASA-TM-89708] 09 p1260 N88-17555

Crew interface with windshear systems
10 p1275 N88-17631

Short fiber reinforced thermoplastic composites for armor applications: Interfacial bonding
[DE88-004007] 10 p1295 N88-17742

Ytterbium monolayer diffusion barriers at Hg(1-x)Cd(x)Te/Al junctions
[AD-A188013] 10 p1299 N88-17768

A detailed microstructural examination of the cause of HAZ cracking in type 316 steel
[AERE-R-12428] 10 p1301 N88-17777

Monitoring interfacial dynamics by pulsed laser techniques
[DE88-003362] 10 p1335 N88-17976

Energy transfers for multilayer hydrodynamic ocean models: General formulation and specific examples
[AD-A187604] 10 p1358 N88-18116

Chips: A tool for developing software interfaces interactively
[AD-A187499] 10 p1389 N88-18295

Application of Onsager's reciprocity relations to interface motion
[DE88-003286] 10 p1397 N88-18327

Local stoichiometry and atomic interdiffusion during reactive metal/mercury-cadmium-telluride junction formation
[AD-A187554] 10 p1421 N88-18488

Nonmonotonic evolution and thermodynamic trends at metal/(Hg,Cd)Te interfaces: Yb/Hg0.78Cd0.22Te
[AD-A187591] 10 p1422 N88-18490

CdTe(110)-Mn interface reaction and the formation of non-equilibrium ternary semimagnetic semiconductor alloys
[AD-A187593] 10 p1422 N88-18491

Void formation in solidification
[DE88-003895] 11 p1452 N88-18650

Parallel pseudospectral domain decomposition techniques
[NASA-CR-181629] 11 p1524 N88-19101

Theoretical studies of the interface electronic properties of tetrahedrally coordinated semiconductors
[AD-A187216] 11 p1555 N88-19306

Formation of buried nitride layers in (110) silicon
[DE88-003255] 11 p1557 N88-19323

Interfacial adhesion: Theory and experiment
[NASA-TM-100830] 13 p1742 N88-20417

Interfacial chemistry-structure and fracture of ceramic composites
[DE88-005516] 13 p1750 N88-20461

Component mode synthesis using experimental modes enhanced by mass loading
[DE88-006097] 13 p1781 N88-20657

An interface between object-oriented systems
[AD-A189245] 13 p1815 N88-20844

Exploring the relation between interface structure and mechanical properties in multilayer structures
[DE88-005428] 13 p1848 N88-21060

Human interfaces in remote driving
[DE88-006843] 14 p1953 N88-21643

Proceedings of the Seminar on Hydrodynamics and Crystal Growth
[ETN-88-92025] 14 p1987 N88-21853

Problems appearing at interface balances --- flames
14 p1987 N88-21855

Common database interface for heterogeneous software engineering tools
[AD-A189628] 14 p1991 N88-21870

Vapor phase deposition and growth of polyimide films on copper
[AD-A189969] 15 p2044 N88-22178

Thermal instability and heat transfer characteristics in water/ice systems
[AD-A189627] 15 p2062 N88-22297

CK-LOG system conversion (user's manual and user interface)
[AD-A190273] 15 p2111 N88-22577

Studies of surfaces using optical sum-frequency generation
[DE88-006334] 15 p2131 N88-22715

Interface formation and precursory dynamics
[AD-A190741] 15 p2144 N88-22794

Surface and interfacial properties of carbon fibers
[NASA-CR-182690] 16 p2173 N88-22951

High temperature solid lubrication by catalytically generated carbon
[AD-A190604] 16 p2182 N88-23004

Laser cladding of Ni, Nb and Mg alloys for improved environmental resistance at high temperature
[AD-A191274] 16 p2213 N88-23208

Microscopic control of semiconductor interface reactivity
[AD-A191193] 16 p2283 N88-23668

Test philosophy of the EH101 integrated avionic
17 p2303 N88-23775

Interfacing and integrating hardware and software design systems 17 p2306 N88-23796

Polyitaconic acid macromolecule primer for adhesive bonding and corrosion control of aluminum
17 p2319 N88-23849

Service offerings and interfaces for the ACTS network of Earth stations
[NASA-TM-100609] 18 p2471 N88-24663

Interfacial shear phenomena in graphite epoxy composites under impact loading using dynamic moire interferometry
[DE88-006773] 18 p2479 N88-24709

Auger analysis of a fiber/matrix interface in a ceramic matrix composite
[NASA-TM-100892] 19 p2610 N88-25487

The development of an intelligent interface to a computational fluid dynamics flow-solver code
[NASA-TM-100908] 19 p2716 N88-26127

Report on the Second Catalog Interoperability Workshop
[NASA-TM-100701] 19 p2718 N88-26135

Ludwig Prandtl collected treatises on applied mechanics, hydro- and aerodynamics, part 2, IV interfaces and resistance
[NASA-TT-20315] 20 p2752 N88-26338

Interface modification in Nicalon (trademark)/SiC composites
[DE88-009708] 20 p2767 N88-26409

Surface phases and their influence on metal-oxide interfaces
[DE88-007936] 20 p2769 N88-26420

Direct manipulation and the design of user interfaces
[PB88-126354] 20 p2834 N88-26810

Common Data Format (CDF) to store images
[NASA-CR-179366] 20 p2836 N88-26825

A high speed serial link interface for SANDAC-V
[DE88-007694] 20 p2842 N88-26861

Superlattice doping interfaces
20 p2866 N88-27019

Fermi level dependent native defect formation: Consequences for metal-semiconductor and semiconductor-semiconductor interfaces
[DE88-008247] 20 p2875 N88-27066

Fundamental optical studies of competitive adsorption and thin film phenomena
[DE88-008780] 20 p2875 N88-27068

Twin boundaries and heterophase interfaces in ferroelastic martensites
[DE88-011894] 21 p2916 N88-27304

Effects of near interfacial microstructure on toughness and subcritical crack growth in ceramic/metal systems
[DE88-009842] 21 p2919 N88-27325

Application of controlled interfacial pore structures to kinetic studies in alumina
[DE88-010884] 21 p2919 N88-27326

Some equivalent circuit models for AC impedance analysis of pyrite/solution interface
[DE88-010574] 21 p2939 N88-27452

Synopsis of a computer program designed to interface a personal computer with the fast data acquisition system of a time-of-flight mass spectrometer
[NASA-CR-177474] 21 p3001 N88-27798

X-ray studies of strain, interface and impurities in semiconductors
[DE88-012460] 21 p3025 N88-27954

Capitalizing on experience with intelligence gateway software
[AD-A193362] 21 p3028 N88-27971

Interface techniques and systems for standard aircraft data buses 22 p3036 N88-28028

Corrosion control through a better understanding of the metallic substrate/organic coating/interface
[AD-A193981] 22 p3056 N88-28132

Chemistry of adhesion at the polyimide-metal interface
[AD-A194647] 22 p3058 N88-28143

An interface for the connection of the SCP2160A pulse analyser to a Hewlett-Packard desk-top computer
[RSRE-MEMO-4030] 22 p3073 N88-28245

Review of past and current trials and uses of unmanned vehicles
[AD-A194527] 22 p3084 N88-28311

A new model for the simulation of interfaces at high temperature
[DE88-009926] 22 p3155 N88-28772

Influence of the interface on the crystallization of amorphous Ge in Pb/Ge multilayers
[DE88-010072] 22 p3156 N88-28776

Model for bimetallic interfaces, part 2
[DE88-702672] 22 p3157 N88-28787

Expandable pallet for space station interface attachments
[NASA-CASE-MSC-21117-1] 23 p3185 N88-28958

Elastic behavior of a rubber layer bonded between two rigid spheres
[AD-A193698] 23 p3198 N88-29030

Experimental investigation of the effects of underwater exposure on the damping characteristics of bolted structural connections for plates and shells
[AD-A194486] 23 p3226 N88-29200

The gradient method for interface tracking
[AD-A194477] 23 p3248 N88-29334

Definition of common support equipment and space station interface requirements for IOC model technology experiments
[NASA-TM-100656] 24 p3336 N88-29856

INTERFACIAL ENERGY

On rotating sphere-on-a-plate experiments and the questions of whether high angle grain boundaries melt below bulk melting temperatures
[DE88-006627] 15 p2038 N88-22142

First-principles calculations of quasiparticle energies at surfaces and interfaces: Semiconductor surface-state spectra and band offsets
[DE88-006340] 15 p2141 N88-22773

Adhesion of hydrated silicate films
[DE88-011250] 21 p2920 N88-27333

INTERFACIAL STRAIN

U INTERFACIAL TENSION

INTERFACIAL TENSION

Calculation of the eigenvibrations of axisymmetric fluid configurations with a singularity method, taking into account surface tension effects under reduced gravity
[ETN-87-90438] 01 p0048 N88-10304

The infiltration kinetics of aluminum in silicon carbide compacts
[AD-A184682] 03 p0290 N88-11823

Double-effect absorption heat pump, phase 3
[PB87-232195] 03 p0317 N88-12005

Numerical analysis of Marangoni convection in Bridgman method 03 p0319 N88-12014

Interfacial strength development in thermoplastic resins and fiber-reinforced thermoplastic composites
[NASA-CR-181525] 04 p0411 N88-12549

Effect of interface on mechanical properties of graphite/201 aluminum composites
05 p0606 N88-13717

Crack opening displacement test in tension
[PB87-143848] 08 p0996 N88-16026

Investigation of surface tension driven convection as a feasibility study for a micro-gravity experiment
[NASA-CR-182504] 11 p1466 N88-18739

The effect of surface tension in the weld pool on seam formation when welding thin sheet with light rays
14 p1898 N88-21334

Electrohydrodynamic migration of charged droplets in an insulating fluid
[NASA-TM-100849] 14 p1912 N88-21424

Selective growth velocity in needle crystals
14 p1968 N88-21858

Methods of measurement for the evaluation of monolayer properties. Development and applications --- lung surfactants
[ETN-88-92229] 15 p2104 N88-22532

A study of surface tension driven segregation in monotectic alloy systems
[NASA-CR-182894] 16 p2178 N88-22983
Dendritic growth in the presence of convection
18 p2580 N88-25328
Interfacial tension of immiscible polymer blends: Temperature and molecular weight dependence
[AD-A192463] 21 p2917 N88-27312
Rubber-modified epoxies: Interfacial tension and morphology
[AD-A192464] 21 p2917 N88-27313
Plasma treatment of polymers for improved adhesion
[DE88-011623] 21 p2921 N88-27334
Effects of surface tension and contact angle on sensible heating and boiling incipience in dielectric falling films
[DE88-007057] 21 p2945 N88-27492
Surface tension and viscosity with Lagrangian hydrodynamics on a triangular mesh
[AD-A194120] 22 p3075 N88-28258
Orbital Propulsion Module (OPM). Study on coni-spherical surface tension tanks (COSTA)
[MBB-URV-170/87] 23 p3187 N88-28963
Surface Tension Confined Liquid Cryogen Cooler (STCLCC)
[NASA-CASE-GSC-13112-1] 23 p3201 N88-29050
Shear stress at a film-substrate interface due to mismatch strain
[AD-A193461] 23 p3288 N88-29577
A test for interfacial effects and stress transfer in ceramic matrix composites
[NASA-CR-182873] 24 p3340 N88-29880
Some theoretical considerations of the surface tension of liquid metals for metal matrix composites
[AD-A195999] 24 p3340 N88-29882
Effect of interfacial phenomena on contact line heat Transfer-3
[AD-A194941] 24 p3343 N88-29901

INTERFERENCE
Wind tunnel wall interference
07 p0811 N88-14938
Status of magnetic suspension technology
07 p0811 N88-14939
Effect of a model support strut on measurement of aerodynamic longitudinal and lateral coefficients
[PB87-170288] 09 p1113 N88-16670
Wideband HF (High Frequency) modeling and simulation
[PB88-116116] 10 p1317 N88-17874
Simulated performance of an order statistic threshold strategy for detection of narrowband signals
11 p1474 N88-18796
Wind tunnel wall interference (January 1980 - May 1988): A selected, annotated bibliography
[NASA-TM-4061] 19 p2604 N88-25466

INTERFERENCE DRAG
Laser velocimeter measurements in a wing-fuselage type juncture
[NASA-TM-100588] 15 p2014 N88-22012

INTERFERENCE FIT
A finite element procedure for interference-fit and cold-working problems with limited yielding
[AR-004-517] 04 p0485 N88-12992
Computed stress and strain distributions under interference fit and after coldworking
[AD-A186950] 10 p1342 N88-18024

INTERFERENCE GRATING
An infrared grating spectrometer for GIRL
[ETN-88-91071] 09 p1167 N88-16997

INTERFERENCE IMMUNITY
Electromagnetic compatibility. View of the near future
[SNIAS-881-422-104] 22 p3071 N88-28229

INTERFERENCE LIFT
An engineering study of hybrid adaptation of wind tunnel walls for three-dimensional testing
[NASA-CR-178374] 07 p0814 N88-14957

INTERFERENCE MONOCHROMATIZATION
U DIFFRACTION

INTERFEROGRAMS
U INTERFEROMETRY

INTERFEROMETERS
NT ETALONS
NT FABRY-PEROT INTERFEROMETERS
NT INFRARED INTERFEROMETERS
NT MACH-ZEHNDER INTERFEROMETERS
NT MICHELSON INTERFEROMETERS
NT MICROWAVE INTERFEROMETERS
NT PHASE SWITCHING INTERFEROMETERS
NT RADIO INTERFEROMETERS
Description of a multiframe optical probing system
[DE87-014255] 02 p0236 N88-11487
Vibrational properties of disordered solids. Far infrared studies: Performance report
[DE88-001474] 06 p0786 N88-14821
Middle atmospheric wind measurements using a medium frequency radar
[AD-A185931] 07 p0879 N88-15330
Optical Fourier transformation by lensless method with perforated mask and with modified Talbot interferometer for analysis of interferograms 09 p1236 N88-17408
Electron density profile reconstruction by maximum entropy method with multichannel HCN laser interferometer system on SPAC 7
[IPPJ-858] 11 p1553 N88-19295
Applications of the lateral shearing interferometer in measurement of synchrotron radiation optical elements
[DE88-005184] 13 p1840 N88-21011
Development of an optical diagnostic instrument. Part 2: Instrument development --- space laboratories
[NLR-TR-87079-L-PT-2] 13 p1841 N88-21016
Synthetic-aperture radars viewed as interferometers with matched filter processing of the collected data
[AD-A190608] 15 p2057 N88-22262
Equipment for an advanced electron beam lithography system
[AD-A192956] 21 p2936 N88-27435
Optical bistable behavior of a planar quasi-waveguide interferometer made with a conjugated organic polymer film
[AD-A194349] 22 p3152 N88-28756

INTERFEROMETRY
NT DIFFERENTIAL INTERFEROMETRY
NT HOLOGRAPHIC INTERFEROMETRY
NT LASER INTERFEROMETRY
NT MOIRE INTERFEROMETRY
NT SPECKLE INTERFEROMETRY
NT VERY LONG BASE INTERFEROMETRY
Time-resolved measurements of shock-induced vapor-pressure profiles
[DE87-012972] 01 p0045 N88-10289
ESA Workshop on Optical Interferometry in Space
[ESA-SP-273] 01 p0094 N88-10613
A comparison of interferometry from space and ground 01 p0094 N88-10614
About the interest of solar interferometric observations
01 p0094 N88-10615
Imaging strategies for a spaceborne interferometer
01 p0094 N88-10617
Imaging at radio wavelengths
01 p0094 N88-10618
ISIS: Image reconstruction methods and signal-to-noise ratio investigations --- spaceborne interferometry
01 p0094 N88-10619
ISIS: Image reconstruction experiments and comparison of various array configurations --- spaceborne interferometry 01 p0095 N88-10620
On the concept of resolution ellipse in aperture synthesis matched deconvolution with error analysis --- astronomical interferometry 01 p0095 N88-10621
OASIS: A mission concept --- Optical Aperture Synthesis Space Interferometry (OASIS) 01 p0095 N88-10622
COSMIC --- Coherent Optical System of Modular Image Collectors (COSMIC); spaceborne telescope
01 p0095 N88-10623
Binary Star Explorer 01 p0095 N88-10624
Fiber-linked telescope arrays on the ground and in space 01 p0095 N88-10626
Space station based interferometry
01 p0096 N88-10628
ESA technological research activities on lightweight mirrors --- spaceborne interferometry
01 p0096 N88-10629
NASA/JPL study on optical imaging interferometry in space 01 p0096 N88-10630
Ground-based optical interferometry
01 p0096 N88-10631
Ground-based interferometry with the European Very Large Telescope (VLT) 01 p0096 N88-10632
CERGA high angular resolution optical network --- astronomical interferometry 01 p0096 N88-10633
Practical limits to ground based interferometry and its impact on space interferometry
01 p0096 N88-10634
Solar interferometry with a 4-aperture nonredundant and stabilized network 01 p0097 N88-10639
Diagnostics of solar coronal loops at interferometric angular resolution 01 p0098 N88-10642
Short baseline phase delay interferometry
04 p0433 N88-12683
Interferometry theory for the block 2 processor
[NASA-CR-181551] 04 p0440 N88-12730
An optical interferometry technique to evaluate closure along a crack front 05 p0607 N88-13726
Realization of an instrument to measure temperature and concentration gradients in fluids --- microgravity
[CISE-3128] 09 p1168 N88-17003
Application of Hoffman modulation contrast microscopy coupled with three-wavelength two-beam interferometry to the in situ direct observation of the growth process of a crystal in microgravity 10 p1288 N88-17704
Interferometric study of natural convection heat transfer from a vertical flat plate with transverse roughness elements 10 p1327 N88-17935
Diagnostics for research in atomization and turbulent two-phase flows
[AD-A187338] 11 p1482 N88-19843
An interferometric investigation of the diffraction of planar shock waves over a half-diamond cylinder in air
[UTIAS-322] 13 p1768 N88-20575
Passive DF: A tutorial, part 1
[NASA-CR-182669] 13 p1815 N88-20846
Optics for large telescope 13 p1840 N88-21014
Continuous measurements of in-bore projectile velocity
[DE88-006841] 15 p2023 N88-22056
Development and applications of optical interferometric micrometrology in the angstrom and subangstrom range
[NASA-TM-100299] 16 p2211 N88-23196
Geodesy by radio interferometry: Optimization of wet path delay algorithms using microwave radiometer data
[PB88-167739] 18 p2498 N88-24820
Interferometric recording of holographic optical elements using partially coherent light
20 p2805 N88-26636
Digital image processing from speckle interferograms by correlation methods: Application in atmospheric optics, astronomy, and biology
[ETN-88-92125] 20 p2855 N88-26953
Is the 3C273 quasar Mach nearer
[DE88-702235] 21 p3030 N88-27988
Interferometric tomography of continuous fields with incomplete projections
[NASA-CR-183181] 22 p306 N88-28295

INTERGALACTIC MEDIA
Royal Observatory, Edinburgh: Research and Facilities
[ISSN-0267-6281] 14 p1993 N88-21881

INTERGRANULAR CORROSION
Microstructural evolution and response to double-loop reactivation testing of heat-treated pH 13-8 Mo martensitic stainless steel
[DE87-009058] 02 p0146 N88-10915
Study of stainless steel time-temperature sensitization diagrams, part 1
[ETN-87-90762] 03 p0289 N88-11815
The influence of grain boundary chemistry and structure on the intergranular attack and intergranular stress corrosion cracking of austenitic alloys
[DE88-002436] 07 p0835 N88-15063
Mechanisms of intergranular attack and stress corrosion cracking of alloy 600 by high-temperature caustic solutions containing impurities
[DE87-012820] 10 p1300 N88-17773
Stress corrosion cracking properties of Al-Li alloys
17 p2320 N88-23853
The effect of titanium reinforcement on the life of positive grids in lead-acid batteries 17 p2320 N88-23857
Hydrogen embrittlement of iron-nickel alloys
[AD-A195909] 24 p3353 N88-29958

INTERIM STAGES (SPACECRAFT)
NT INERTIAL UPPER STAGE

INTERIM UPPER STAGE (STS)
U INERTIAL UPPER STAGE

INTERIOR BALLISTICS
A study of the interaction of laser light with liquid propellant drops
[AD-A185117] 05 p0587 N88-13582
Experimental determination of the heat flux inside a tubular projectile for the velocity range M = 3 and M = 6
[ISL-R-118/86] 11 p1443 N88-18805
Continued studies of programmed-splitting stick propellant
[AD-A188987] 12 p1613 N88-19844
A study of combustion and flow behaviour in solid-propellant rocket motors
[UTIAS-280] 13 p1732 N88-20357
Two-phase flows in the wake of in-cylinder projectiles
[AD-A189422] 13 p1765 N88-20559
Flamespreading processes in obliquely loaded stick propellant beds
[AD-A195081] 24 p3352 N88-29956

INTERLACING DRAINAGE
U DRAINAGE PATTERNS

INTERLAYERS
NT MULTILAYER INSULATION
Effect of adhesive layers on impact damage and dynamic response in composite laminates
02 p0141 N88-10887
Improving the interlaminar shear strength of carbon fiber-epoxy composites through carbon fiber bromination
[NASA-TM-100248] 07 p0827 N88-15018
Interlaminar fracture toughness of thermoplastic composites
[NASA-TM-100532] 15 p2030 N88-22097
Dimensional crossover in layered superconductors
19 p2734 N88-26237

INTERLOCKING
U LOCKING

INTERMEDIATE FREQUENCIES
Low frequency IF transformer designs having variable coupling
[RAE-TM-RAD-NAV-291] 01 p0043 N88-10272
Performance study of a unipole antenna with conventional and elevated radial wire ground screens
[AD-A193283] 21 p2933 N88-27413

INTERMETALLICS
High temperature metal matrix composites for future aerospace systems
[NASA-TM-100212] 02 p0149 N88-10938
Modelling and theories of alloy phase behavior
[DE87-014399] 03 p0287 N88-11804
Investigation of the deformation behavior of ferritic two-phase Fe-Ni-Al alloys with high concentrations of the intermetallic (Fe, Ni)Al phase at high temperatures
[ETN-87-90605] 03 p0298 N88-11812
Welding and weldability of ductile intermetallic alloys
[DE87-014061] 04 p0416 N88-12582
Experimental perspectives on heavy electron metals
[DE87-014766] 04 p0416 N88-12583
Investigation of the deformation behavior of the intermetallic phase (Fe,Ni)Al at high temperatures
[ETN-88-91062] 09 p1143 N88-16854
Superconductivity of thin film intermetallic compounds
[AD-A187563] 10 p1421 N88-18489
The intergranular segregation of boron in substoichiometric Ni3Al
[DE88-004783] 11 p1462 N88-18720
Thermodynamics of wetting by liquid metals
[DE88-003634] 11 p1563 N88-19360
Development of metastable processing paths for high temperature alloys
[AD-A188682] 12 p1608 N88-19617
Elevated temperature crack growth studies of advanced titanium aluminides
[AD-A189025] 12 p1608 N88-19618
Gordon Conference on Intermetallic Compounds held at Tilton, New Hampshire on 20-24 July 1987
[AD-A188502] 13 p1745 N88-20435
Processing, physical metallurgy and creep of NiAl + Ta and NiAl + Nb alloys
[NASA-CR-182113] 14 p1890 N88-21295
Brillouin scattering and transmission electron microscopy studies of radiation-induced elastic softening, disordering and amorphization of intermetallic compounds
[DE88-005927] 14 p1987 N88-21850
Coexisting static magnetic ordering and superconductivity in CeCu2.1Si2 found by muon spin relaxation 17 p2396 N88-24245
Static magnetic ordering of CeCu2.1Si2 found by muon spin relaxation 17 p2396 N88-24246
Chemical compatibility between silicon carbide and a nickel aluminide
[DE88-006188] 18 p2479 N88-24706
Martensitic transformation and microstructures in sintered NiAl alloys
[NASA-TT-20178] 18 p2488 N88-24761
Martensitic transformation and microstructures in sintered NiAl alloys
[NASA-TT-20192] 19 p2616 N88-25519
Extended ductility of Al and alpha-Fe alloys through dynamic recovery mechanisms
[DE88-008679] 19 p2616 N88-25522
Exploratory development in the system Al-Sc-X
[DE88-008242] 19 p2618 N88-25529
Phase stability and alloy design of ordered intermetallics
[DE88-007479] 20 p2772 N88-26435
Nickel aluminides: A new family of nickel + aluminum alloys featuring simple composition, low density, excellent oxidation resistance and high yield strength that increases with temperature
[DE88-010692] 20 p2776 N88-26461
Superconductivity of heavy-electron uranium compounds
[DE88-007901] 20 p2875 N88-27065
A fundamental understanding of the interfacial compatibility in hybrid material systems
[AD-A192921] 21 p2909 N88-27264
Microchemical analysis of polycrystalline Ni3Al and other ordered alloys using the field-ion microscope atom probe
[DE88-011519] 21 p2914 N88-27294

INTERMITTENCY
Anomalous scaling laws in multifractal objects
[NOTA-INTERNA-883] 07 p0916 N88-15565
Intermittency of atmospheric turbulence--applicatin of Lyapunov exponents and fractional dimension
14 p1900 N88-21348

INTERMODULATION
A GaAs MESFET balanced mixer with very low intermodulation
[AD-A184848] 05 p0655 N88-14015

INTERMONTANE FLOORS
U VALLEYS

INTERNAL COMBUSTION ENGINES
NT CONVERTIBLE FAN-SHAFT ENGINES
NT DIESEL ENGINES
NT GAS TURBINE ENGINES
NT HELICOPTER ENGINES
NT HYDROGEN ENGINES
NT J-57 ENGINE
NT JET ENGINES
NT RAMJET ENGINES
NT ROTARY ENGINES
NT SUPERSONIC COMJUSTION RAMJET ENGINES
NT TF-30 ENGINE
NT TURBOFAN ENGINES
NT TURBOJET ENGINES
NT TURBOPROP ENGINES
NT WANKEL ENGINES
Multidimensional modeling of convective heat transfer with application to IC engines
[DE87-011048] 01 p0055 N88-10353
Japanese industrial research on lean combustion: A case study: International Research Monitoring Program
[DE87-013839] 02 p0144 N88-10904
Needs assessment for nondestructive testing and materials characterization for improved reliability in structural ceramics for heat engines
[DE88-000040] 02 p0153 N88-10957
Development of a light duty gas engine for cogeneration service
[PB87-221297] 02 p0180 N88-11119
Coatings for Advanced Heat Engines Workshop: Book of abstracts
[DE87-012623] 02 p0180 N88-11121
High pressure autoignition of natural gas/air mixtures and the problem of engine knock
[DE87-013799] 03 p0284 N88-11784
Multidimensional modeling of convective heat transfer with application to I.C. engines
[DE87-014983] 03 p0322 N88-12036
Numerical simulation of internal combustion engine flows: Development and users guide for MAGIC radial-azmuthal version
[DE87-014453] 03 p0332 N88-12091
Development, construction and testing of a novel internal combustion engine with conical rotating slide valve
[DE88-900071] 05 p0589 N88-13593
The development and evaluation of three-dimensional models of cold flow in internal combustion engines
[DE88-900077] 05 p0589 N88-13594
The role of low temperature chemistry in the autoignition of n-butane
[DE88-002385] 07 p0829 N88-15031
Multidimensional modeling of convective heat transfer with application to IC engines
[DE88-003398] 10 p1330 N88-17948
An evaluation of effectiveness of PTFE (polytetrafluoroethylene) type friction reducers on reducing friction and wear
[AD-A187440] 10 p1340 N88-18010
Fuel cell/battery hybrid vehicle assessment
[DE88-005087] 10 p1427 N88-18520
Review of the state of the art and projected technology of low heat rejection engines
[PB88-131255] 11 p1496 N88-18934
Status of alcohol fuels utilization technology for highway transportation: A 1986 perspective. Volume 2: Compression ignition engines
[DE88-006059] 13 p1753 N88-20485
Combustion and performance characteristics of methanol plus higher alcohols in a spark ignition engine
[PB88-147962] 14 p1918 N88-21451
JPRS report: Science and technology. Japan
[JPRS-JST-87-030] 16 p2185 N88-23026
Status, trends in research on internal combustion engines 16 p2185 N88-23027
Composite piston
[NASA-CASE-LAR-13435-1] 17 p2346 N88-23981
Multidimensional modeling of convective heat transfer with application to I.C. engines
[DE88-007446] 19 p2738 N88-26257
The outlook for ceramics in heat engines, 1990-2010: Results of a worldwide Delphi survey
[DE88-010075] 20 p2778 N88-26475
Ceramic Technology for Advanced Heat Engines Program data base
[DE88-008954] 20 p2780 N88-26489
Analytical and experimental investigation of ringless piston concept
[AD-A193213] 21 p2956 N88-27559

INTERNAL CONVERSION
The effect of internal relaxation on optoacoustic conversion in liquids
[AD-A191307] 16 p2176 N88-22970

INTERNAL ENERGY
Product kinetic and internal energy distributions via velocity-aligned Doppler spectroscopy
[DE88-003510] 10 p1298 N88-17764

INTERNAL PRESSURE
Durability of compound cylinder under static internal-pressure repeat load of long duration
16 p2180 N88-22991

INTERNAL STRESS
U RESIDUAL STRESS

INTERNAL WAVES
NT PLANETARY WAVES
The effect of ocean fluctuations on sound transmission in the ocean
[AD-A184362] 03 p0355 N88-12236
AFAR (Azores Fixed Acoustic Range) measurements of intensity and intensity moments
[AD-A184431] 03 p0355 N88-12237
A study of the mechanism of internal gravity wave generation by quasigeostrophic meteorological motions
06 p0735 N88-14520
Study of internal gravity waves in the meteor zone
06 p0735 N88-14521
Numerical modeling of troposphere-induced gravity wave propagation 06 p0735 N88-14522
A statistical study of variations of internal gravity wave energy characteristics in meteor zone
06 p0735 N88-14523
Internal gravity waves in the meteor zone in the Tbilisi Region 06 p0736 N88-14528
An analysis of apparent-motion vectors in, and the structure of, A mid-latitude sporadic E layer using a 2.66 MHz radar
[AD-A186126] 07 p0877 N88-15321
Interpretation of equatorial current meter data as internal waves
[PB88-108113] 08 p1044 N88-16309
Wind forcing and observed oceanic wavenumber spectra 13 p1806 N88-20797
Nonlinear surface and internal waves on shear flow
[PREPRINT-584] 22 p3129 N88-28604

INTERNATIONAL COMETARY EXPLORER
U INTERNATIONAL SUN EARTH EXPLORER 3

INTERNATIONAL COOPERATION
Space station: Leadership for the future
[NASA-PAM-509/8-87] 01 p0013 N88-10072
The criterion of equal integrated quality: An improved method of planning DBS systems
[BBC-RD-1987/10] 02 p0161 N88-11012
Materials studies for magnetic fusion energy applications at low temperatures-X
[PB87-232575] 03 p0381 N88-12395
Solar energy: European research and development
[PB87-107645] 04 p0463 N88-12866
Technology transfer to China
[PB87-223418] 04 p0502 N88-13087
The A320 Airbus program
[SNIAS-872-111-105] 05 p0529 N88-13215
Dutch-German wind tunnel's tenth anniversary
[ETN-88-91350] 06 p0670 N88-14105
EISCAT research in Finland in 1986
06 p0691 N88-14234
Current status of world weather service
06 p0725 N88-14459
Integrated Global Background Monitoring Network
[DE88-001503] 06 p0731 N88-14499
Interim review of the possibilities and opportunities for the ONR tropical cyclone motion research initiative
[AD-A185679] 06 p0746 N88-14592
The results of the 1984/1985 Round-Robin Calibration of Reference Solar Cells for the Summit Working Group on Technology, Growth and Employment
[DE88-900215] 07 p0874 N88-15303
International role of US geoscience
[NASA-CR-182407] 08 p1035 N88-16261
The European space physics analysis network
08 p1099 N88-16613
The 2.4 m Space Telescope and ESA participation in the program 09 p1123 N88-16721
A policy for international relations
09 p1123 N88-16724
Unispace 82 09 p1128 N88-16766
Entry into force of the ESA convention
09 p1128 N88-16768
Satellite power systems under consideration by the United Nations 09 p1128 N88-16773
The NORSTAR Program: Space shuttle to space station 10 p1289 N88-17710
Cooperation know-how in high-tech products
[MBB-Z-101/86] 10 p1311 N88-17833
Airbus, the successful European cooperation
[MBB-UT-005/87] 10 p1313 N88-17847
Messerschmitt-Boelkow-Blohm, the company today. Data, numbers and facts 10 p1316 N88-17868
Minutes of the meeting of the Indo-US Subcommission on Science and Technology (8th) held at Washington, D.C. on September 22-24, 1986
[PB88-130158] 10 p1423 N88-18503

Journal of Research of the National Bureau of Standards, volume 92, number 5, September-October 1987
[PB88-124409] 10 p1426 N88-18518
Journal of Research of the National Bureau of Standards, volume 92, number 6, November-December 1987
[PB88-138516] 10 p1426 N88-18519
International geosphere-biosphere program: A study of global change
[PB88-142393] 11 p1510 N88-19021
Proceedings of the First International Symposium on Physical and Technical Problems of Superconductivity Application in Power Generation
[DE88-700818] 11 p1559 N88-19332
Science and technology in India
[PB88-134747] 11 p1564 N88-19362
System-wide medium-term environment programme for the period 1990-1995: Strategies of the United Nations system for the environment
[UNEP/GCSS.I/2] 12 p1641 N88-19826
The influence of infrastructure on the costs and timescales of collaborative programmes
12 p1704 N88-20201
Space projects for the 90's relevant to climatology
14 p1935 N88-21539
The International Satellite Land-Surface Climatology Project (ISLSCP) 14 p1937 N88-21558
Japanese space station module
15 p2052 N88-22224
Overview of 1987 moonlight project
15 p2052 N88-22231
A review of the NATO special group of experts on Naval hydromechanics and related problems
16 p2205 N88-23157
International cooperation in remote sensing: The ESA experience 17 p2356 N88-24038
Discussions and agreements in the United Nations on important issues associated with nuclear power in space
17 p2423 N88-24411
CFD benefits, goals, stepping-stones and techniques. Proposals for the scientific programme of the European Research Centre on flow, turbulence and combustion --- computational fluid dynamics
[CFDU/88/1] 18 p2510 N88-24894
Centre for International Co-Operation and Approriate Technology (CICAT)
[PB88-165501] 18 p2590 N88-25389
Mobile satellite services: International co-ordination, co-operation and competition 19 p2644 N88-25691
International and domestic regulator issues facing the Canadian MSAT system 19 p2644 N88-25692
Satellites at sea --- INMARSAT
19 p2700 N88-26054
Realistic planning scenarios
[AD-A191640] 19 p2740 N88-26267
An agenda for the strategic defense initiative
[RAND-P-7404] 20 p2847 N88-26896
Simulation of the neutronic characteristics of large fast neutron reactors
[ETN-88-92305] 20 p2853 N88-26940
European transonic wind tunnel project: Assistance to the design group
[ONERA-RSF-11/0694-GY-010-G]
21 p2900 N88-27208
Studies concerning the European transonic wind tunnel
[ONERA-RSF-10/0694-GY-010-G]
21 p2900 N88-27209
Metrology in France: Industrial aspects and its status in the world
[SNIAS-881-430-109] 22 p3146 N88-28713
Using standards to break down information transfer barriers 24 p3439 N88-30467

INTERNATIONAL GEOSPHERE-BIOSPHERE PROGRAM
International geosphere-biosphere program: A study of global change
[PB88-142393] 11 p1510 N88-19021

INTERNATIONAL LAW
NT SPACE LAW

INTERNATIONAL PRACTICAL TEMPERATURE
U TEMPERATURE SCALES

INTERNATIONAL RELATIONS
NT INTERNATIONAL COOPERATION
SDI (Strategic Defense Initiative). Where do we go from here
[AD-A194544] 23 p3275 N88-29497

INTERNATIONAL SATS FOR IONOSPHERIC STUDY
U ISIS SATELLITES

INTERNATIONAL SOLAR POLAR MISSION
U ULYSSES MISSION

INTERNATIONAL SUN EARTH EXPLORER 3
Space missions to Comets Halley and Giacobini-Zinner 03 p0272 N88-11712
A comparison between wave observations performed in the environments of Comets Halley and Giacobini-Zinner 14 p1996 N88-21896

INTERNATIONAL SUN EARTH EXPLORERS
NT INTERNATIONAL SUN EARTH EXPLORER 3
Nuclear and ionic charge distribution experiment on ISEE-1 and ISEE-3
[NASA-CR-180776] 23 p3183 N88-28947

INTERNATIONAL SYSTEM OF UNITS
Metrology in France: Industrial aspects and its status in the world
[SNIAS-881-430-109] 22 p3146 N88-28713

INTERNATIONAL TRADE
Aircraft accident reports: Brief format, US Civil and Foreign Aviation, Issue Number 5 of 1986 accidents
[PB87-916907] 06 p0952 N88-15780
Aircraft accident reports: Brief format, US Civil and Foreign Aviation, Issue Number 8 of 1986 accidents
[PB87-916910] 06 p0953 N88-15782
Cooperation know-how in high-tech products
[MBB-Z-101/86] 10 p1311 N88-17833
Status of emerging technologies: An economic/technological assessment to the year 2000
[PB88-155775] 11 p1567 N88-19381
Oceanographic export system development, year 1
[AD-A189134] 14 p1950 N88-21623
Competitive assessment of the U.S. civil helicopter industry
[PB88-186325] 18 p2455 N88-24574
A basis of settlement: Economic foundations of permanent pioneer communities
[DE88-010907] 20 p2762 N88-26382
Commercialization and export --- aerospace industry
22 p3161 N88-28824

INTERNATIONAL ULTRAVIOLET EXPLORER
U IUE

INTERPERSONAL RELATIONS
U HUMAN RELATIONS

INTERPLANETARY DUST
NT ZODIACAL DUST
Analysis of laser extracted volatiles in carbonaceous chondrites 06 p0793 N88-14861
Planetary science 07 p0883 N88-15356
Mass loss from evolved stars
11 p1569 N88-19394
Cometary evolution: Clues from chondritic interplanetary dust particles 14 p2002 N88-21934
Cometary grains and interplanetary dust: A polarimetric sensing --- Halley 14 p2003 N89-21941
Particles injected by comets 14 p2003 N88-21944
Doppler distortion of solar Fraunhofer lines in zodiacal light by reflection from interplanetary dust
19 p2740 N88-26270

INTERPLANETARY FLIGHT
Preliminary estimates of galactic cosmic ray exposures for manned interplanetary missions
[NASA-TM-100519] 05 p0661 N88-14058
Trade study for kWe class space reactors
17 p2430 N88-24454
Preliminary estimates of radiation exposures for manned interplanetary missions from anomalously large solar flare events
[NASA-TM-100620] 18 p2596 N88-25427
Interplanetary travel: Is gravity needed to close the loop
[NASA-TM-101013] 22 p3132 N88-28622
JPRS report: Science and technology. USSR: Space
[JPRS-USP-88-001] 24 p3444 N88-30498

INTERPLANETARY GAS
Mass loss from evolved stars
11 p1569 N88-19394
Extended atmospheres of outer planet satellites and comets
[NASA-CR-183157] 24 p3457 N88-30572

INTERPLANETARY MAGNETIC FIELDS
Dynamics of magnetic clouds in interplanetary space
01 p0115 N88-10736
Model of solar-wind magnetosphere coupling
04 p0525 N88-13211
Observations of turbulence and fluctuations in the solar wind 04 p0525 N88-13212
The polar ionosphere and interplanetary field
[AD-A185386] 05 p0624 N88-13622
Magnetic field draping about coronal mass ejecta
[DE88-001805] 05 p0661 N88-14057
Interplanetary magnetic field effects on the interaction of the solar wind with Venus 06 p0805 N88-14910
A compilation of Sudden Storm Commencements (SSCs), associated interplanetary disturbances, and cosmic ray variations
[IFSI-86-11] 06 p0807 N88-14923
Monitoring of Pc3 pulsations in solar wind and at Earth by interplanetary magnetic field
08 p1002 N88-16069
Criteria of interplanetary parameters causing intense magnetic storms (Dst less than -100nT)
[NASA-CR-182423] 08 p1024 N88-16200
Polar cusp electrodynamics 08 p1030 N88-16242
Interplanetary Magnetic Field (IMF) influence on the magnetic configuration and particle fluxes at geostationary orbit and on the substorm onset
08 p1031 N88-16247
Bidirectional electron heat flux events in space
[DE88-001791] 08 p1064 N88-16531
Proceedings of the 21st ESLAB Symposium on Small Scale Processes in the Chromosphere/Corona, Interplanetary Medium and Planetary Magnetospheres
[ESA-SP-275] 08 p1094 N88-16582
Interplanetary and geophysical effects of a coronal transient 08 p1095 N88-16587
Transverse flow deflections associated with fast coronal mass ejecta in interplanetary space
[DE88-003180] 09 p1263 N88-17566
Electric fields in Earth orbital space. Magnetospheric structural dynamic response to external variables
[AD-A188592] 12 p1643 N88-19836
Variability of Comet Halley's coma: VEGA-1 and VEGA-2 magnetic field observations 14 p1995 N88-21891
Correlation between magnetic and electric field fluctuations observed during flyby near Halley's comet
14 p1996 N88-21897
Magnetic cavity formation at Comet Halley and at the AMPTE Li release 14 p1996 N88-21898
Time dependent MHD models for the cometary magnetosphere 14 p1997 N88-21900
Observation of energetic particles (E greater than 30 keV) by the Giotto experiment EPA in the magnetic cavity of Comet Halley 14 p1997 N88-21903
Dynamics Explorer-2 measurements during an isolated auroral substorm
[AD-A191202] 18 p2543 N88-25091
On the conjugacy of the aurora: High and low latitudes
[AD-A193008] 20 p2824 N88-26755

INTERPLANETARY MEDIUM
NT INTERPLANETARY DUST
NT INTERPLANETARY GAS
NT ZODIACAL DUST
STIP Symposium on Physical Interpretation of Solar/Interplanetary and Cometary Intervals
[NASA-CR-181201] 01 p0110 N88-10709
Solar-terrestrial observations during STIP interval 15 (12-21 February 1984) 01 p0111 N88-10711
Overview of the MONSEE UAG report on STIP intervals No. 15 and 16: The 24-25 April 1984 Forbush decrease period 01 p0111 N88-10712
The largest white light flare ever observed: 25 April 1984, 0001 UT 01 p0111 N88-10714
Probable detection of solar neutrons by ground-level neutron monitors during STIP interval 16
01 p0111 N88-10715
Solar energetic particles events observed by Prognoz-10 Intercosmos (May-October 1985)
01 p0111 N88-10716
The large Type 4 radio burst event of 24 April 1985 interpreted by dynamic spectral recordings and associated recordings 01 p0112 N88-10717
Propagating shocks in the corona
01 p0112 N88-10718
Change in interplanetary shock acceleration preceding STIP interval 17 01 p0112 N88-10719
Solar modulation of the cosmic radiation in the heliosphere 01 p0112 N88-10720
Comparison of MHD simulation for the February 1986 events with interplanetary observations by the spacecraft Sakigake 01 p0113 N88-10722
Two dimensional imaging observations of meter-decameter bursts associated with the February 1986 flare activity 01 p0113 N88-10723
Solar origins of coronal mass ejections
01 p0113 N88-10726
Radio studies of large scale structures of the Sun's corona and transient activity 01 p0114 N88-10728
Observations of the brightness temperature distribution of the quiet solar corona at decametric wavelengths
01 p0114 N88-10729
Meter-wave observations of a coronal hole
01 p0114 N88-10730
Coronal and interplanetary Type 2 radio emission
01 p0114 N88-10731
Coronal mass ejections: The long-term variation of their occurrence rate and the solar wind mass flux
01 p0114 N88-10732
Was the eclipse comet of 1893 a disconnected coronal transient? 01 p0115 N88-10733
Solar events and their influence on the interplanetary medium 01 p0115 N88-10734
Solar activity, magnetic clouds, and geomagnetic storms 01 p0115 N88-10735
Dynamics of magnetic clouds in interplanetary space
01 p0115 N88-10736
The expansion of magnetic clouds
01 p0115 N88-10737
A numerical study of transient, thermally-conductive solar wind 01 p0115 N88-10738

A two-fluid model for solar wind fluid with higher order moments 01 p0116 N88-10739
Interaction of interplanetary shocks with nonuniform ambient solar wind 01 p0116 N88-10740
An overview of STIP interval 18: September 1985, the G-Z encounter 01 p0116 N88-10741
Comparative plasma tails of Venus and comets 01 p0116 N88-10742
Overview of plasma observations during the Halley flybys 01 p0116 N88-10743
The status of the international Halley watch 01 p0116 N88-10744
Large-scale interaction of the solar wind with comets Halley and Giacobini-Zinner 01 p0117 N88-10745
The global interaction of comets with the solar wind 01 p0117 N88-10746
Solar-terrestrial research in the space station era 01 p0117 N88-10747
Solar wind-cometary interaction at the ionopause and associated phenomena 01 p0117 N88-10748
Comet West: A view from the HELIOS zodiacal light photometers 01 p0117 N88-10749
Solar wind effects on the outer ion coma of Comet Halley 01 p0117 N88-10750
The solar wind interaction with comets: A post encounter view 01 p0118 N88-10751
Plasma-tail activity and the interplanetary medium at Halley's Comet during Armada's Week: 6-14 March 1986 01 p0118 N88-10752
Occultation of compact radio sources by the ion tail of Halley's Comet 01 p0118 N88-10753
Equilibrium and tearing stability of thin current layers in magnetic arcades 01 p0118 N88-10754
A simulation of the IPS variations from a magnetohydrodynamical simulation 01 p0118 N88-10755
Study of the mechanism for solar wind formation 01 p0118 N88-10756
An account of a flare related shock event recorded by the energetic particle detector EPONA of the Giotto spacecraft during September 1985 (STIP interval 18) 01 p0118 N88-10757
Interactions of oblique interplanetary discontinuities and their manifestations during STIP intervals 15-19 01 p0119 N88-10758
Intershock observations during STIP intervals 17 and 18 01 p0119 N88-10759
Research in particles and fields [NASA-CR-180412] 01 p0119 N88-10763
Media calibrations of the Doppler signal for a gravitational wave experiment --- interplanetary medium [IFSI-86-13] 05 p0625 N88-13825
JPRS report: Science and technology. USSR: Space [JPRS-USP-87-006] 08 p1001 N88-16063
Flare doublet: Interplanetary and geomagnetic effects 08 p1001 N88-16066
Unusually strong density decrease in near-Earth interplanetary plasma and magnetically quiet day as effects of isolated solar flare 08 p1002 N88-16072
Extended atmospheres of outer planet satellites and comets [NASA-CR-181449] 10 p1430 N88-18540
Physical processes in the vicinity of the cometopause interpreted on the basis of plasma, magnetic field and plasma wave data measured on board VEGA-2 spacecraft --- Halley's comet 14 p1996 N88-21894

INTERPLANETARY PROPULSION
U INTERPLANETARY SPACECRAFT
U ROCKET ENGINES

INTERPLANETARY SPACE
Overview of STIP intervals 15-19 01 p0110 N88-10710
Satellite environment: Polar orbits 03 p0272 N88-11713
Environmental interactions of solar generators in space 03 p0274 N88-11730
Activities report in interplanetary space physics [IFSI-86-5] 05 p0659 N88-14047
Low-frequency VLBI in space and interstellar refraction [PB87-127643] 06 p0696 N88-14267
Personal overview of solar wind 6 [DE88-003147] 10 p1430 N88-18543
Activities report of the Institute for Extraterrestrial Physics [MPE-206] 21 p3029 N88-27961
Solar flares and magnetospheric particles: Investigations based upon the ONR-602 and ONR-604 experiments [AD-A193396] 21 p3031 N88-27994

INTERPLANETARY SPACECRAFT
NT GALILEO PROBE
NT GALILEO SPACECRAFT
NT MARS OBSERVER
NT MARS PROBES
NT PIONEER VENUS SPACECRAFT
The VISTA spacecraft: Advantages of ICF (Inertial Confinement Fusion) for interplanetary fusions propulsion applications [NASA-CR-181549] 04 p0491 N88-13024
A technique for capture analysis of low thrust missions in a planetary system [AD-A188934] 12 p1594 N88-19544

INTERPLANETARY TRAJECTORIES
Design study for asteroidal exploitation 03 p0369 N88-12445

INTERPOLATION
BIMOND3: Monotone piecewise bicubic Hermite interpolation code [DE87-014612] 02 p0229 N88-11442
A shape preserving interpolant which has tension controls [DE87-014615] 02 p0229 N88-11443
Robust prediction and interpolation for vector stationary processes, 2d enriched version [AD-A185875] 07 p0865 N88-15247
Fast and practical parallel polynomial interpolation [DE88-003530] 10 p1397 N88-18328
Contour-to-grid interpolation with nonlinear finite elements: A feasibility study [AD-A188108] 11 p1503 N88-18980
Interpolation algorithms for digital terrain models [INPE-4373-PRE/1196] 13 p1820 N88-20877
Synthetic-aperture radars viewed as interferometers with matched filter processing of the collected data [AD-A190608] 15 p2057 N88-22262
Derivation of consistent surface fixed fields for use in a global NWP model [AD-A190131] 15 p2093 N88-22475
Multigrid for structures analysis 16 p2218 N88-23232
High degree interpolation polynomial in Newton form [NASA-CR-181677] 18 p2567 N88-25249
A practical shifted Adams algorithm [DE88-008573] 20 p2837 N88-26830
Prolongation, restriction and coarse grid approximation in a three-dimensional cell-centered multigrid method [REPT-88-02] 20 p2846 N88-26889
Two families of graphs satisfying the cycle basis interpolation property [PB88-127808] 20 p2846 N88-26890
Analytical surfaces and grids 23 p3247 N88-29322
Radial basis functions, multi-variable functional interpolation and adaptive networks [RSRE-MEMO-4148] 23 p3265 N88-29436
Method for combined image interpolation-restoration through a fir filter design technique [INPE-4561-PRE/1302] 24 p3413 N88-30315
Reconstruction of multidimensional signals from multiple level threshold crossings [AD-A195561] 24 p3425 N88-30383

INTERPOLATORS
U REPEATERS

INTERPROCESSOR COMMUNICATION
Data Management Working Group report 01 p0016 N88-10097
Study and design of a communication processor unit [RIDU/TREP/1002/SAAB] 01 p0083 N88-10538
Communications for the DTroll distributed database system [AD-A185579] 06 p0791 N88-14853
Study of communication options in a distributed data handling system and survey of advanced man machine communications schemes. Work package 1: Interprocess communication [ESA-CR(P)-2447] 07 p0843 N88-15114
DoD Gateway Information System (DGIS) common command language: The first prototyping and the decision for artificial intelligence [AD-A185950] 07 p0942 N88-15725
DoD Gateway Information System (DGIS): Common command language mapping [AD-A185951] 07 p0942 N88-15726
SAHAYOG: A testbed for load sharing under failure [AD-A186615] 08 p1069 N88-16460
Interdisciplinary research in applied mathematics [AD-A186793] 09 p1226 N88-17344
Multi-processor reduction machines 10 p1382 N88-18253
Air Force Institute of Technology (AFIT) Local Area Network (LAN) performance evaluation model: An analytic model for assessing the impact of changing LAN hardware and software configurations [AD-A187191] 11 p1469 N88-18764
Experience with Berkeley UNIX interprocess communications [AD-A188353] 12 p1680 N88-20041
MultiRPC: A parallel remote procedure call mechanism [AD-A188613] 12 p1680 N88-20046
Locality, communication and interconnect length in multicomputers [CWI-CS-R8708] 13 p1822 N88-20890
Atomic multireader register --- computer storage [CWI-CS-R8722] 14 p1954 N88-21648
Enhancement of data acquisition and numerical computation capabilities for unsteady fluid dynamics [AD-A190115] 15 p2063 N88-22302
Alpha structure based B-HIVE multicomputer [AD-A188708] 16 p2244 N88-23405
Reasoning about networks with many identical finite-state processes [AD-A188743] 16 p2245 N88-23413
IPC for modular software requires a third party connect [AD-A189199] 16 p2246 N88-23414
Intelligent systems interconnection: What should come after open systems interconnection? [CWI-CS-R8742] 16 p2253 N88-23465
Locality, communication and interconnect length in multicomputers [CWI-CS-R8743] 16 p2254 N88-23466
A five-layer Open Systems Interconnection (OSI) implementation 17 p2390 N88-24204
Interconnection of high-speed local area networks 17 p2390 N88-24205
Cellular Array Processor (CAP) and its application to computer graphics 19 p2641 N88-25667
Effective communication between a microVAX and a specialized high-speed subprocessor [DE88-007967] 19 p2714 N88-26115
Real time data base management [AD-A191758] 19 p2739 N88-26265
Relay approach message routing in hypercube multiprocessors [DE88-009973] 20 p2835 N88-26814
Correctness criteria for process migration [NASA-CR-182939] 20 p2836 N88-26823
Constructing a highly-available location service for a distributed environment [AD-A192723] 21 p3001 N88-27801
A modular proof of correctness for a network synchronizer [AD-A192726] 21 p3002 N88-27802
LO-CO-GRAF (low cost graphics): Generating maps to support command and control/crisis management using small computers [AD-A193964] 22 p3139 N88-28661
Random-access algorithms for environments with capture [AD-A194303] 23 p3203 N88-29060
Process migration in UNIX environments [NASA-CR-182951] 23 p3245 N88-29311
Design of a self-timed VLSI multicomputer communication controller [AD-A194567] 24 p3361 N88-30014

INTERSTELLAR CHEMISTRY
Circumstellar chemistry 02 p0253 N88-11598
On the interpretation of the 3 micron emission feature in the spectrum of Comet Halley: Abundances in Comet Halley and in interstellar matter 14 p2002 N88-21935
A spectroscopic study of absorption and emission features of interstellar dust components [B8681462] 16 p2289 N88-23706
Observations of star formation 24 p3451 N88-30538

INTERSTELLAR EXTINCTION
A spectroscopic study of absorption and emission features of interstellar dust components [B8681462] 16 p2289 N88-23706

INTERSTELLAR GAS
NT NEUTRAL GASES
Dynamic effects of stellar winds and associated HII regions on the interstellar medium [ETN-87-90421] 01 p0109 N88-10706

INTERSTELLAR MASERS
The distance to the center of the galaxy: H2O maser proper motions in Sgr B2(N) [MPE-PREPRINT-104] 16 p2286 N88-23702

INTERSTELLAR MATTER
NT DARK MATTER
NT INTERSTELLAR GAS
NT NEUTRAL GASES
Composition, structure and chemistry of interstellar dust [NASA-TM-88350] 02 p0253 N88-11603
Adiabatic supernova expansion into the circumstellar medium [DE87-014241] 03 p0387 N88-12433
Hydrogen and deuterium in the local interstellar medium 04 p0521 N88-13204
Galactic interstellar abundance surveys with IUE and IRAS 04 p0522 N88-13206
Exobiology and life science 07 p0883 N88-15358

Molecular clouds at high galactic latitudes
11 p1569 N88-19392
HNC: A detector to study ultraheavy cosmic rays
12 p1713 N88-20252
On the interpretation of the 3 micron emission feature in the spectrum of Comet Halley: Abundances in Comet Halley and in interstellar matter
14 p2002 N88-21935
A spectroscopic study of absorption and emission features of interstellar dust components
[B8681462] 16 p2289 N88-23706
Optical and infrared observations of high latitude dust clouds --- interstellar matter
[B8621135] 16 p2289 N88-23709
Probing the possibility of a (12)C/(13)C abundance gradient from observations of interstellar CH+
[DE88-008908] 20 p2684 N88-27125
Catalog of open clusters and associated interstellar matter
[NASA-RP-1202] 23 p3300 N88-29652

INTERSTELLAR MICROWAVE SPECTRA
U INTERSTELLAR RADIATION
U MICROWAVE SPECTRA

INTERSTELLAR RADIATION
Optical spectroscopy of IRAS sources with infrared emission bands. 1: IRAS 21282+5050 and the diffuse interstellar bands
[NASA-CR-181387] 01 p0094 N88-10611
Photoabsorption and photodissociation of molecules important in the interstellar medium
[NASA-CR-182435] 08 p1100 N88-16617
Observations of the large scale anisotropy in the cosmic background radiation at 3 mm
[INPE-4425-PRE/1229] 12 p1712 N88-20249

INTERSTELLAR REDDENING
U INTERSTELLAR EXTINCTION

INTERSTELLAR SPACE
Justification and prospects of observations of interstellar, far-infrared emission lines, using a small-sized balloon-borne telescope 08 p1032 N88-16254

INTERSTELLAR SPACECRAFT
Advanced space propulsion study - antiproton and beamed power propulsion
[AD-A189218] 13 p1732 N88-20355

INTERSTELLAR TRAVEL
Engineering planetary lasers for interstellar communication
[NASA-CR-180780] 17 p2311 N88-23825

INTERSTITIALS
Theory of interstitial solutions
[BLL-M-37314-(5828.4)] 02 p0233 N88-11469
Diffusion studies in amorphous NiZr alloys
[DE88-003009] 10 p1301 N88-17781
The intergranular segregation of boron in substoichiometric Ni3Al
[DE88-004783] 11 p1462 N88-18720
Does the pipe diffusion of self-interstitials in crystals under stresses exist
[DE88-701027] 15 p2139 N88-22762
Migration and stability of HgCdTe lattice defects
[AD-A193293] 21 p3021 N88-27935

INTERVALS
STIP Symposium on Physical Interpretation of Solar/Interplanetary and Cometary Intervals
[NASA-CR-181201] 01 p0110 N88-10709
Solar energetic particles events observed by Prognoz-10 Intercosmos (May-October 1985)
01 p0111 N88-10716
The large Type 4 radio burst event of 24 April 1985 interpreted by dynamic spectral recordings and associated recordings 01 p0112 N88-10717
Propagating shocks in the corona
01 p0112 N88-10718
Change in interplanetary shock acceleration preceding STIP Interval 17 01 p0112 N88-10719
Solar modulation of the cosmic radiation in the heliosphere 01 p0112 N88-10720
Comparison of MHD simulation for the February 1986 events with interplanetary observations by the spacecraft Sakigake 01 p0113 N88-10722
Solar origins of coronal mass ejections
01 p0113 N88-10726
Radio studies of large scale structures of the Sun's corona and transient activity 01 p0114 N88-10728
Observations of the brightness temperature distribution of the quiet solar corona at decametric wavelengths
01 p0114 N88-10729
Meterwave observations of a coronal hole
01 p0114 N88-10730
Coronal and interplanetary Type 2 radio emission
01 p0114 N88-10731
Coronal mass ejections: The long-term variation of their occurrence rate and the solar wind mass flux
01 p0114 N88-10732
Was the eclipse comet of 1893 a disconnected coronal transient? 01 p0115 N88-10733
Solar events and their influence on the interplanetary medium 01 p0115 N88-10734
Solar activity, magnetic clouds, and geomagnetic storms 01 p0115 N88-10735
Dynamics of magnetic clouds in interplanetary space
01 p0115 N88-10736
The expansion of magnetic clouds
01 p0115 N88-10737
A numerical study of transient, thermally-conductive solar wind 01 p0115 N88-10738
A two-fluid model for solar wind fluid with higher order moments 01 p0116 N88-10739
Interaction of interplanetary shocks with nonuniform ambient solar wind 01 p0116 N88-10740
An overview of STIP interval 18: September 1985, the G-Z encounter 01 p0116 N88-10741
Comparative plasma tails of Venus and comets
01 p0116 N88-10742
Overview of plasma observations during the Halley flybys 01 p0116 N88-10743
The status of the international Halley watch
01 p0116 N88-10744
Large-scale interaction of the solar wind with comets Halley and Giacobini-Zinner 01 p0117 N88-10745
The global interaction of comets with the solar wind
01 p0117 N88-10746
Solar-terrestrial research in the space station era
01 p0117 N88-10747
Solar wind-cometary interaction at the ionopause and associated phenomena 01 p0117 N88-10748
Comet West: A view from the HELIOS zodiacal light photometers 01 p0117 N88-10749
Solar wind effects on the outer ion coma of Comet Halley 01 p0117 N88-10750
The solar wind interaction with comets: A post encounter view 01 p0118 N88-10751
Occultation of compact radio sources by the ion tail of Halley's Comet 01 p0118 N88-10753
Equilibrium and tearing stability of thin current layers in magnetic arcades 01 p0118 N88-10754
A simulation of the IPS variations from a magnetohydrodynamical simulation
01 p0118 N88-10755
Study of the mechanism for solar wind formation
01 p0118 N88-10756
An account of a flare related shock event recorded by the energetic particle detector EPONA of the Giotto spacecraft during September 1985 (STIP interval 18)
01 p0118 N88-10757
Interactions of oblique interplanetary discontinuities and their manifestations during STIP intervals 15-19
01 p0119 N88-10758
Intershock observations during STIP intervals 17 and 18 01 p0119 N88-10759
Testing and interval estimation in a change-point model allowing at most one change
[AD-A185525] 06 p0767 N88-14716
Detecting and interval estimation about a slope change point
[AD-A186030] 07 p0909 N88-15509
Training in time interval discrimination using verbal feedback 12 p1665 N88-19965
The total interval of a graph
[AD-A189648] 15 p2119 N88-22625

INTERVERTEBRAL DISKS
Hierarchical structure in polymeric solids and its influence on properties
[AD-A194720] 23 p3197 N88-29029

INTESTINES
Use of bifidumbacterin for correction of intestinal dysbacteriosis 07 p0895 N88-15427

INTOXICATION
Age, alcohol, and simulated altitude: Effects on performance and breathalyzer scores
[AD-A190642] 15 p2103 N88-22531

INTRACRANIAL PRESSURE
Neuropeptides in experimental head injury
[AD-A188067] 11 p1520 N88-19077

INTRAMOLECULAR STRUCTURES
Intramolecular dynamics: A study of molecules at high levels of vibrational excitation
[AD-A195285] 24 p3428 N88-30400

INTRUSION
Volcanic contribution to crustal growth in the Central Andes: A new estimate and a discussion of uncertainties
24 p3401 N88-30255

INVALIDITY
U ERRORS

INVARIANCE
NT GAUGE INVARIANCE
Superconformal invariance and superstring in background fields
[DE87-703097] 02 p0247 N88-11561
Carbon-fiber reinforced plastics
04 p0403 N88-12506
Global bifurcation of periodic solutions with symmetry
[AD-A185881] 07 p0908 N88-15501
Relativistic Calogero-Moser systems and solutions
[CWI-PM-R8702] 08 p1092 N88-16570
Status of the electroweak theory
[DE88-002342] 10 p1422 N88-18494
Topics in string theory: Task D
[DE88-004532] 12 p1699 N88-20167
Invariant characteristics of acoustic field in stratified ocean 13 p1788 N88-20698
Chronometrically invariant formulation of electrodynamics equation
[DE88-701030] 13 p1849 N88-21071
Efficient monotone sequential design
[CWI-MS-R8705] 14 p1962 N88-21707
Hyperbolicity and invariant measures for general C sq interval maps satisfying the Misiurewicz condition
[REPT-87-46] 14 p1966 N88-21730
Absolutely continuous invariant measures for C sq unimodal maps satisfying the Collet-Eckmann conditions
[REPT-87-55] 14 p1966 N88-21735
Similarity solutions of nonlinear partial differential equations invariant to a family of affine groups
[DE88-003404] 18 p2567 N88-25245
Rigid symmetries and BRST-invariance in gauge theories
[PB88-180948] 18 p2572 N88-25280
Gravitation and polarization properties of electromagnetic field
[DE88-702166] 19 p2654 N88-25761
Generalized Jordan chains and two bifurcation theorems of Krasnoselski
[AD-A192353] 21 p3008 N88-27845
On the estimation of a variance ratio
[AD-A193190] 21 p3009 N88-27854
On the computation of finite invariant sets of mappings
[AD-A193670] 22 p3143 N88-28690
Theory of quark mixing matrix and invariant functions of mass matrices
[USIP-87-14] 22 p3159 N88-28800
A nonparametric multidimensional IRT approach with applications to ability estimation and test bias
[AD-A194212] 23 p3273 N88-29480
Invariant ideals of multiplicity free algebraic group actions
[B8803517] 23 p3277 N88-29509
Non-linear scale invariance in a cold-dark-matter universe
[DE88-011725] 23 p3299 N88-29644

INVARIANT IMBEDDINGS
Vortices on the world sheet and string's critical dynamics
[DE88-702116] 21 p3026 N88-27961

INVENTIONS
Identifying areas of leading edge Japanese science and technology: Activity analysis using SIC (Standard Industrial Classes) categories and scientific subfields
[PB87-204087] 02 p0249 N88-11574
Identifying areas of leading edge Japanese science and technology: Patent activity and citation analysis using US POC (Patent Office Classification) classification
[PB87-204095] 02 p0249 N88-11575
Metals. Preliminary study for an Innovation-Oriented research Program (IOP)
[ETN-88-91317] 14 p1889 N88-21290
Innovation-Oriented research Program (IOP) metals. Annexes
[ETN-88-91318] 14 p1889 N88-21291

INVENTORIES
NT CROP INVENTORIES
NT TIMBER INVENTORY
The Aquarack as a potential instrument for basic research work in space biology: Inventory and scientific dispositions 01 p0073 N88-10470
A general approach to error propagation
[DE87-014287] 02 p0224 N88-11412
Inventory of weather stations. Climatological data from Dutch stations, no. 26
[KNMI-150-26] 05 p0628 N88-13841
Investigations on the application of space photographs (Spacelab metric camera) for routine inventories of extensively managed forest areas
[DFVLR-FB-87-22] 09 p1185 N88-17098
Inventory of topographic mapping and standardization of geographic names as the basis of a Geographic Information System (GIS) 16 p2225 N88-23281
Utilization of LANDSAT-TM imagery in the hydroenergetic inventory of the Paraiba de Sul River Basin 17 p2364 N88-24077
Application of SPOT multidate data to wheat yield estimation in Beauce (France) 22 p3094 N88-28374
An evaluation of the utility of SPOT and Thematic Mapper data for providing forest inventory information
22 p3106 N88-28444

Stand-based forestry inventory from SPOT image
22 p3106 N88-28449
The dynamics of transuranics and other radionuclides in natural environments, December 1985
[DE87-014456] 24 p3390 N88-30189

INVENTORY CONTROLS
Comparison of pascal and the dBASE 3 PLUS language in programming an inventory management system
[AD-A184027] 03 p0365 N88-12300
Application of a database system for inventory management of classified material
[AD-A186986] 09 p1261 N88-17558

INVENTORY MANAGEMENT
NT INVENTORY CONTROLS
Comparison of pascal and the dBASE 3 PLUS language in programming an inventory management system
[AD-A184027] 03 p0365 N88-12300
Inventory behavior at remote sites
06 p0796 N88-14873
Application of a database system for inventory management of classified material
[AD-A186986] 09 p1261 N88-17558
A robotic system for automation of logistics functions on the Space Station 23 p3260 N88-29407

INVERSE SCATTERING
Theoretical aspects of target classification: Physical optics and radon transform methods
03 p0304 N88-11915
Elastodynamic ray theory and asymptotic methods for direct and inverse scattering problems
03 p0335 N88-12108
Inverse scattering analysis of diffraction limited SAR
[FOA-C-30459-3.2] 05 p0576 N88-13512
Solitons in stimulated Raman scattering: Generation and control of ultrashort optical pulses
[AD-A185141] 05 p0650 N88-13983
The inverse back scattering problem for the Schroedinger equation in two space dimensions
[AD-A185603] 06 p0765 N88-14701
Direct scattering of electromagnetic waves by one- and two-dimensional objects and its use for inverse profiling
[PB88-126909] 10 p1319 N88-17887
An efficient numerical algorithm for solving scattering and inverse scattering problems of electromagnetic waves
[AD-A188479] 12 p1619 N88-19684
Born-type reconstruction of material parameters of an inhomogeneous, lossy dielectric slab from reflected-field data
[PB88-188356] 18 p2569 N88-25261
Fields and waves 24 p3363 N88-30025

INVERSIONS
NT POPULATION INVERSION
NT TEMPERATURE INVERSIONS
Review of inversion techniques for spaceborne lidar systems
[AD-A184164] 04 p0447 N88-12772
Lower bounds on bearing accuracy for closely spaced sources
[AD-A184258] 04 p0486 N88-12997
Comparing hard and soft prior bounds in geophysical inverse problems
[NASA-CR-181557] 05 p0624 N88-13820
The solution of large linear inverse problems
06 p0691 N88-14238
Development of direct-inverse 3-D methods for applied aerodynamic design and analysis
[NASA-CR-182436] 08 p0950 N88-15767
Inversion of simulated satellite signals
08 p1017 N88-16168
Aerosol size distribution from measurements of the radiance in the solar aureole 08 p1019 N88-16176
Improved canopy reflectance modeling and scene inference through improved understanding of scene pattern
[NASA-CR-182488] 10 p1347 N88-18049
Inversion of parabolic and paraboloidal projections
[AD-A187538] 10 p1405 N88-18380
Regional wave attenuation and seismic moment from the inversion of NORESS spectra
[AD-A187399] 11 p1510 N88-19023
Recursive inversion of externally defined linear systems
[NASA-TM-100070] 11 p1541 N88-19215
The inverse problem and the pseudo-empirical orthogonal function method of solution. Part 1: Theory; Part 2: Application
[AD-A188894] 12 p1684 N88-20069
Electronic properties of semiconductor inversion layers in sub-micron structures
[AD-A188635] 12 p1698 N88-20161
Tectonics and three-dimensional structure of spreading centers: Microearthquake studies and tomographic inversions
[PB88-163290] 14 p1945 N88-21602
Mass, heat and nutrient fluxes in the Atlantic Ocean determined by inverse methods
[NASA-CR-180535] 14 p1950 N88-21626
Seismic inversion by a RMS (Root-Mean-Square) Born approximation in the space-time domain
[PB88-165402] 15 p2131 N88-22711
A diagonally inverted LU implicit multigrid scheme
[NASA-TM-100911] 20 p2753 N88-26340
Sidelobe level of an adaptive array using the SMI (Sampled Matrix Inversion) algorithm
[AD-A193131] 21 p2932 N88-27409
A method for determining absolute velocities from hydrographic data: The numerical code
[AD-A193997] 22 p3129 N88-28633

INVERTEBRATES
NT ARTEMIA
NT DROSOPHILA
NT INSECTS
NT MOLLUSKS
NT SEA URCHINS
NT SNAILS
Five New South Wales barrier lagoons: Their macrobenthic fauna and seagrass communities
11 p1517 N88-19059

INVERTED CONVERTERS (DC TO AC)
Digital control of a direct current converter for a hybrid vehicle
[LAAS-87-266] 05 p0578 N88-13527
Mathematical model for the dc-ac inverter for the Space Shuttle 06 p0793 N88-14860
Costs and benefits of AC propulsion
[PB88-173380] 16 p2287 N88-23691

INVERTERS
Evaluation of stand-alone inverters for remote applications
[DE87-010957] 01 p0040 N88-10257
Digital control of high frequency pulse-width modulated inverters
[ETN-87-90711] 09 p1157 N88-16936
The operational behavior of microprocessor-controlled and pulsed inverter-fed synchronous machines with permanent magnet excitation
[ETN-88-91479] 11 p1480 N88-18833
A high performance inverter-fed drive system of an interior permanent magnet synchronous machine
[DE88-006753] 15 p2061 N88-22288
A microcomputer-based control and simulation of an advanced IPM (interior Permanent Magnet) synchronous machine drive system for electric vehicle propulsion
[DE88-006735] 18 p2505 N88-24859
Reduced order modeling of grid-connected photovoltaic inverter systems
[DE88-010603] 21 p2969 N88-27635

INVESTIGATION
NT ACCIDENT INVESTIGATION
NT AIRCRAFT ACCIDENT INVESTIGATION
Analysis of 7- X 10-foot high speed wind tunnel shaft loads in support of fan blade failure investigation
[NASA-TM-100504] 04 p0402 N88-12496
The effect of mass, wind angle and erection technique on the aeroelastic behaviour of a cable-stayed bridge model
[NAE-AN-46] 04 p0455 N88-12819
Method for investigating the formation of crystals in a transparent material
[NASA-CASE-MFS-26008-1-CU]
06 p0798 N88-14835
CTD observations in the coastal transition zone off northern California, 16-25 February 1987
[AD-A187283] 10 p1357 N88-18111
Experimental and theoretical methods for investigating helium effects in rapidly solidified metals
[DE88-005542] 13 p1743 N88-20425
A defect investigation of Thunderflash MK N5 (Navy)
[MRL-TN-522] 13 p1754 N88-20488

INVESTMENT CASTING
Investment foundry melting stock. Rolls Royce requirements and demands in terms of quality and the relationship to end product performance
[PNR90397] 02 p0160 N88-11003

INVESTMENTS
The judgement and evaluation of long-term investments demonstrated by means of a civil aircraft program
12 p1701 N88-20180

INVISCID FLOW
NT STAGNATION FLOW
An inviscid model of planar, separated flows of finite extent
[RAE-TR-86070] 01 p0044 N88-10279
Mechanical and flow excited vibrations of elastic plates and cylindrical shells in dense fluids
03 p0316 N88-11996
Some experiences with the viscous-inviscid interaction approach
[NASA-TM-100015] 04 p0395 N88-12466
Solution of the two-dimensional Euler equations on unstructured triangular meshes
04 p0396 N88-12469
Optimization of explicit time-stepping algorithms and Stream-Function-Coordinate (SFC) concept for fluid dynamics problems 04 p0445 N88-12762
Mesoscale eddy dynamics by the method of point vortices 04 p0463 N88-12863
A spatial marching technique for the inviscid blunt body problem 05 p0533 N88-13239
Numerical optimization of conical flow waveriders including detailed viscous effects
05 p0533 N88-13245
The role of computation fluid dynamics in aeronautical engineering (4). The development and applications of implicit TVD finite volume code
05 p0536 N88-13259
The development of a computer code (U2DIIF) for the numerical solution of unsteady, inviscid and incompressible flow over an airfoil
[AD-A185033] 05 p0541 N88-13293
A Cartesian finite-volume method for the Euler equations 05 p0579 N88-13532
A note on the use of symmetric line Gauss-Seidel for the steady upwind differenced Euler equations
[AD-A185223] 05 p0580 N88-13540
Investigation of viscous/inviscid interaction in transonic flow over airfoils with suction 06 p0664 N88-14074
Numerical simulation of flows in axial and radial turbomachines using Euler solvers
06 p0713 N88-14372
Turbulence in hypersonic flow
[AD-A185624] 07 p0815 N88-14961
Inviscid flows, part 1: Formulation of inviscid rotational flow problems by velocity potential and stream function methods. Applications to turbomachines
08 p0985 N88-15964
Viscous flows, part 1 08 p0986 N88-15967
Supersonic aerodynamics of delta wings
[NASA-TP-2771] 10 p1273 N88-17615
The unsteady gas flow through stator and rotor of a turbomachine 10 p1281 N88-17660
Well-posedness and spectral estimation for infinite dimensional systems
[AD-A187621] 10 p1401 N88-18354
Vibrations of shells containing fluid
12 p1635 N88-19757
Application of a flux vector splitting methodology towards the solution of unsteady transonic flows, with future emphasis on the blade flutter problem
[AD-A189500] 13 p1716 N88-20260
Multigrid solution of the Euler equations
13 p1789 N88-20582
Utilization of parallel processing in solving the inviscid form of the average-passage equation system for multistage turbomachinery
[NASA-TM-89845] 14 p1868 N88-21160
Splitting of inviscid fluxes for real gases
[NASA-TM-100956] 14 p1964 N88-21717
Enhanced viscous flow drag reduction using acoustic excitation
[NASA-CR-182734] 15 p2062 N88-22295
High-resolution shock-capturing schemes for inviscid and viscous hypersonic flows
[NASA-TM-100097] 15 p2122 N88-22651
User's manual for EULER3DS
[AD-A191048] 16 p2208 N88-23177
Numerical method for unsteady viscous-inviscid interaction to calculate buffeting
[ONERA-RSF-02/3617-AY-008-A]
17 p2338 N88-23949
Accurate multigrid solution of the Euler equations on unstructured and adaptive meshes
[NASA-CR-181679] 18 p2490 N88-24808
Composite reduced Navier-Stokes procedures for flow problems with strong pressure interactions
[AD-A191127] 18 p2508 N88-24875
Theoretical investigation of 3-D shock wave-turbulent boundary layer interactions, part 6
[AD-A191546] 18 p2509 N88-24882
Axisymmetric viscid-inviscid interaction by a frozen vorticity approximation
[AD-A191743] 18 p2509 N88-24885
Open channel flow near the resonance speed
18 p2514 N88-24918
A study of flow separation in transonic flow using inviscid and viscous computational fluid dynamics (CFD) schemes
[NASA-CR-183119] 20 p2801 N88-26618
Higher order vortex methods with rezoning
[DE88-010777] 21 p2947 N88-27505
Nonlinear oscillations of an inviscid liquid column under zero-gravity
[LRT-WE-9-FB-8(1987)] 22 p3063 N88-28173

Stability of parallel inviscid shear flow with mean spanwise variation
[FFA-TN-1987-57] 22 p3079 N88-28285
Numerical solutions of unsteady inviscid transonic turbine cascade flows
[AD-A196111] 24 p3316 N88-29748

INVISIBILITY
U VISIBILITY

IO
A modeling analysis program for the JPL table mountain Io sodium cloud data
[NASA-CR-182555] 11 p1570 N88-19400
The Io sulfur torus in 1981
[NASA-TM-101139] 18 p2595 N88-25419
The interaction of Io with the plasma torus
23 p3308 N88-29704

IODATES
NT LITHIUM IODATES

IODIDES
NT CESIUM IODIDES
NT SILVER IODIDES
Altered and enhanced iodargyrite with bismuth triiodide for use in precipitation enhancement operations
[AD-A185229] 05 p0561 N88-13419
The kinetics and dynamics of iodine monofluoride formation in gas-phase collisions
[AD-A185715] 06 p0709 N88-14352

IODINE
NT IODINE ISOTOPES
State-to-state dynamics of molecular energy transfer
[DE88-003282] 10 p1406 N88-18382
Preparation and characterization of Cu2Zn1-xMnxGeS4
[AD-A188113] 11 p1556 N88-19315
Measurement of pressure fluctuations in a resonant chamber with laser-induced iodine fluorescence
[DFVLR-FB-87-53] 21 p2955 N88-27551
Growth and characterization of CuGaS2, CuAlS2 and CuGa0.9Al0.1S2 single crystals
[AD-A192963] 21 p3021 N88-27930

IODINE COMPOUNDS
NT CESIUM IODIDES
NT IODIDES
NT LITHIUM IODATES
NT SILVER IODIDES

IODINE ISOTOPES
The Moessbauer effect of SnI4 at high pressure
[DE87-014771] 04 p0495 N88-13048

IODINE LASERS
Theoretical studies of solar lasers and converters
[NASA-CR-181569] 05 p0587 N88-13577
O2-I laser (Oxygen-iodine) mixing studies using LIF (Laser Induced Fluorescence)
[AD-A186667] 09 p1171 N88-17018
Theoretical studies of solar lasers and converters
[NASA-CR-182927] 17 p2344 N88-23972
Frequency doubling at 1.315 micrometers
[AD-A193902] 23 p3208 N88-29092

ION ACCELERATORS
Mechanical design and construction of a 200 mA, 100 keV, dc, negative ion accelerator
[DE88-003855] 11 p1548 N88-19257
Bevalac external beamline optics
[LBL-23240] 19 p2727 N88-26194
Plasma theory and simulation
[AD-A194674] 23 p3286 N88-29565

ION ACOUSTIC WAVES
Observations of an ion acoustic oscillation near a pulsed sheath
[INPE-4386-PRE/1206] 08 p0979 N88-15915
Experiments on ion-acoustic rarefactive solitons in a multi-component plasma with negative ions
[INPE-4393-PRE/1213] 08 p1086 N88-16542
Double layer formed by beam driven ion-acoustic turbulence
[INPE-4292-PRE/1163] 08 p1086 N88-16543
Experimental investigation of double layers formed by ion-acoustic turbulence
[INPE-4296-PRE/1167] 08 p1086 N88-16544
Basic physics of laser-plasma interactions
[ETN-88-92055] 14 p1984 N88-21838

ION BEAMS
Direct formation of thin films and epitaxial overlayers at low temperatures using a low-energy (10-500 eV) ion beam deposition system
[DE87-012291] 01 p0103 N88-10675
Degradation mechanisms of materials for large space systems in low Earth orbit
[NASA-CR-181472] 02 p0143 N88-10896
Multidimensional elemental analysis with the Sandia nuclear microprobe
[DE87-014158] 02 p0183 N88-11136
Fusion reactivity enhancement due to ion tail formation by beam and ion cyclotron heating
[DE87-753018] 02 p0240 N88-11518
Filamentation instability of rotating light ion beams in fusion target chambers
[IPPJ-839] 02 p0242 N88-11530
Analysis of an induction linac driver system for inertial fusion
[DE88-000681] 03 p0379 N88-12384
Negative ion beams for heating and current-drive in NET
[AD-A184390] 04 p0489 N88-13012
PISCES: Plasma-surface interactions and materials research
[DE88-001323] 04 p0494 N88-13044
ICRF launcher studies
[DE88-001710] 04 p0495 N88-13046
Extreme ultraviolet beam-foil spectroscopy of highly ionized neon and argon
[AD-A185197] 05 p0561 N88-13418
The effect of ion beam mixed Ni-Al surface layers on PSB extrusion morphology in fatigued nickel
05 p0598 N88-13652
Ion-beam nitriding of steels
[NASA-CASE-LEW-14104-2] 06 p0682 N88-14179
Surface modification using ion beams: Recent developments at ORNL
[DE88-000951] 06 p0786 N88-14819
Extending the range of Low Energy Electron Diffraction (LEED) surface structure determination: Co-adsorbed molecules, incommensurate overlayers and alloy surface order studied by new video and electron counting LEED techniques
[DE88-001401] 06 p0786 N88-14820
Structure of layered crystals studied by high energy ion beams
[DE88-001675] 06 p0786 N88-14822
Ion mixing and surface modification in metal-semiconductor systems
[DE88-001702] 06 p0786 N88-14823
On a possibility of ion acceleration up to high energies in a high-current electron beam
[DE88-700532] 07 p0931 N88-15657
Method of plasma diagnostics by a heavy ion beam for the T-15 tokamak
[DE88-700342] 07 p0935 N88-15678
Evolution of radiation-induced voids and dislocations at low temperature
[DE88-700350] 07 p0939 N88-15704
Modification of properties of metals by high-power ion beams 08 p1079 N88-16507
Design considerations for a negative ion source for DC operation of high-power, multi-megaelectron-volt neutral beams
[DE88-002692] 08 p1083 N88-16525
Conceptual design of a radio-frequency driven compact tokamak
[INPE-4364-PRE/1190] 08 p1085 N88-16535
Magnetically insulated ion diode with a gas-breakdown plasma anode
[INPE-4382-PRE/1202] 08 p1085 N88-16537
Double layer formed by beam driven ion-acoustic turbulence
[INPE-4292-PRE/1163] 08 p1086 N88-16543
Experimental investigation of double layers formed by ion-acoustic turbulence
[INPE-4296-PRE/1167] 08 p1086 N88-16544
Energy disposal in ion-molecule reactions
[AD-A186772] 09 p1171 N88-17019
Determination of molecular-ion structures through the use of accelerated beams
[DE88-002960] 09 p1246 N88-17467
Application of ECR ion source beams in atomic physics
[DE88-003767] 10 p1406 N88-18384
Optimization of outlet channel of plasma ion source
[DE88-700471] 10 p1410 N88-18415
Composition and thickness of multilayer foils using MeV ion-beam techniques
[DE88-004360] 11 p1448 N88-18629
Ion energy diagnostics for voltage determinations in plasma-erosion-opening-switch experiments
[DE88-004822] 11 p1479 N88-18827
Charge exchange in low energy (keV) and hyperthermal energy (10-100 eV) ion scattering
[AD-A187643] 11 p1543 N88-19222
Ion beam modification of film stress and the effectiveness of thin film encapsulants on GaAs
[DE88-004458] 11 p1558 N88-19328
Silicon containing photoresists
[AD-A188666] 12 p1605 N88-19601
Focused ion beam fabrication of graded channel FET's in GaAs and Si
[AD-A189166] 13 p1845 N88-21040
A novel method for sputter-deposition of high T(sub c) superconductor films via a computer-controlled mass analyzed ion beam
[DE88-006001] 13 p1848 N88-21064
Improvements in end point detection — semiconductor fabrication
[RSRE-MEMO-4035/A] 14 p1899 N88-21336
In situ TEM observations of heavy ion damage in gallium arsenide
[DE88-005984] 14 p1986 N88-21843
Ion-beam mixing and amorphization in Au/Zr bilayers
[DE88-005999] 15 p2140 N88-22767
Question on the measurement of the metal work function in an electron spectrometer by the secondary-electron emission threshold method
[NASA-TT-20190] 16 p2178 N88-22979
Proceedings of Symposium on Physics of Target Implosion and Pulsed Power Techniques
[IPPJ-850] 16 p2276 N88-23619
Numerical analysis for effects of irradiation nonuniformities on target implosion
16 p2276 N88-23621
Kinetic theoretical analysis for propagation of rotating ion beam in ICF 16 p2276 N88-23623
Hybrid particle simulation for focusing of rotating and propagating LIB 16 p2276 N88-23624
Electron current effect on stability of plasma channel
16 p2276 N88-23625
Numerical analysis of target implosion in LIB ICF
16 p2277 N88-23628
Microinstabilities in ion beam propagation
16 p2277 N88-23631
Self-similar expansions in ion beam fusion
16 p2278 N88-23635
Generation of high brightness ion beam from insulated anode PED 16 p2278 N88-23637
The application of Rutherford backscattering for analyzing multilayered structure change induced by pulsed ion beam bombardment 16 p2278 N88-23638
Two-dimensional focusing of self-magnetically insulated plasma focus diode 16 p2278 N88-23639
Time-resolved spectroscopic measurement of anode plasma in magnetically-insulated diode
16 p2279 N88-23641
Study on the flashover ion diode with cryogenic anode
16 p2279 N88-23642
Ion beam alloying of aluminum for corrosion resistance 17 p2321 N88-23860
A multi-frame ion pinhole camera for intense ion beam transport and focusing experiments
[DE88-007283] 18 p2516 N88-24926
A new approach to generating negative ion beams
[AD-A191119] 18 p2572 N88-25276
An optical technique for measuring divergence, beam profile, and aiming direction, of relativistic negative hydrogen ions
[DE88-007049] 18 p2572 N88-25278
Trochoidal analysis of scattered electrons in a merged electron-ion beam
[NASA-CASE-NPO-16789-1-CU]
18 p2573 N88-25281
Experiments with high energy nuclear beams at Brookhaven: From AGS to RHIC (Relativistic Heavy Ion Collider)
[DE88-007042] 18 p2574 N88-25287
Propagation of neutralized ion beams
[AD-A191599] 18 p2574 N88-25289
Intense ion beam diagnostics for particle beam fusion experiments on PBFA 2
[DE88-007279] 18 p2577 N88-25308
Rutherford magnetic spectrograph for intense ion beam measurements on PBFA 2
[DE88-007281] 19 p2725 N88-26181
Pulsed power driver technologies for inertial confinement fusion power reactors
[DE88-009260] 19 p2731 N88-26221
Equipment for building and testing superconductive flux flow electronic devices
[AD-A192959] 21 p2936 N88-27436
Propagation of charged particle beams in the atmosphere
[AD-A193185] 21 p3014 N88-27887
Plasmoid propagation
[AD-A192376] 23 p3284 N88-29555
Nonlinear analysis of non-neutral plasmas
[AD-A192506] 23 p3284 N88-29556
An HVEM study of displacement cascade damage in Nb3Sn at 13 K
[DE88-009997] 23 p3289 N88-29584
Ion gun generated electromagnetic interference on the SCATHA satellite
[AD-A195179] 24 p3335 N88-29853
Microcircuit trace cutting with focused ion beams
[AD-A196030] 24 p3367 N88-30050
The Single Event Upset (SEU) test facility on the Harwell tandem generator for cosmic ray simulation
[AERE-R-12896] 24 p3459 N88-30580

ION CHAMBERS
U IONIZATION CHAMBERS

ION CHARGE
Measurements of vacuum arc ion charge state distributions
[DE88-006249] 23 p3284 N88-29558

ION CONCENTRATION
Ion composition measurements in the upper stratosphere --- parachute-borne mass spectrometer
[ETN-87-90423] 01 p0069 N88-10442
The formation and thermochemical properties of multiligand complexes
[AD-A184935] 05 p0561 N88-13416
Activated metal oxide surfaces as highly basic and reducing environments
[AD-A184958] 05 p0561 N88-13417

ION CURRENTS
NT ION BEAMS
High ionic conductivity in PEO.PPG block polymer and salt solutions
[AD-A183502] 01 p0026 N88-10168
New materials for electrochemical cells
[AD-A183659] 01 p0037 N88-10238
Ionically conductive polymers: Application to solid state batteries
[AD-A183733] 01 p0037 N88-10239
Dielectric response of ionic conductors
[DE87-013552] 02 p0166 N88-11045
Applications of multivalent ionic conductors to polymeric electrolyte batteries
[AD-A184252] 04 p0439 N88-12722
Effect of sidechain length and crosslinking on ionic conductivity in polyphosphazene solid electrolytes
[AD-A184419] 04 p0497 N88-13058
Ionically conducting polymers: Principles and properties of solid electrolytes
[DE88-001552] 06 p0684 N88-14190
Conductivity studies on hydroxide ion conductors in the Li-Al-O-H system at intermediate temperatures
[AD-A185714] 06 p0697 N88-14279
Phase behavior in the Li-Al-O-H system at intermediate temperatures
[AD-A185732] 06 p0697 N88-14280
The dc conductivity studies of an hydroxide ion conductor at intermediate temperatures
[AD-A186044] 07 p0847 N88-15142
Studies of model ion channels in defect-free multibilayers of phospholipids
[AD-A188740] 16 p2238 N88-23365
Internal erosion rates of a 10-kW xenon ion thruster
[NASA-TM-100954] 18 p2476 N88-24688
Electrical and chemical sensors for biological cell research 19 p2669 N88-25866
Ion thermal conductivity and ion distribution function in the banana regime
[IPPJ-865] 19 p2729 N88-26208
Polymeric electrolytes
[AD-A193766] 23 p3198 N88-29031

ION CYCLOTRON RADIATION
Fusion reactivity enhancement due to ion tail formation by beam and ion cyclotron heating
[DE87-753018] 02 p0240 N88-11518
Planning for US ion cyclotron heating research relevant to the compact ignition tokamak and Alcator C-Mod
[DE88-000022] 02 p0241 N88-11520
Applications of neutral beam and rf technologies
[DE87-014936] 03 p0379 N88-12382
Theoretical atomic and molecular physics
[DE88-001625] 05 p0649 N88-13974
Parallel gradient effects on ICRH (Ion Cyclotron Resonance Heating) in tokamaks
[DE88-009038] 19 p2730 N88-26216

ION DENSITY (CONCENTRATION)
NT IONOSPHERIC ION DENSITY
NT MAGNETOSPHERIC ION DENSITY
NT PROTON DENSITY (CONCENTRATION)
Self-consistent modification of a fast tail distribution by resonant fields in nonuniform plasmas
[AD-A183790] 01 p0099 N88-10650
The effect of object potentials on the wake of a flowing plasma
[AD-A184038] 03 p0379 N88-12385
Data processing of the JPA instrument. Part 1: Data management
[IFSI-86-15-PT-1] 06 p0757 N88-14645
Ionic mechanisms of soot formation in flames
[AD-A186195] 08 p0966 N88-15848
Anthropogenic effects on the droplet formation process, and ion concentrations in droplets --- clouds
08 p1018 N88-16175
Characteristics of laser-plasma X-radiation source (review) 09 p1239 N88-17428
Electrosorptive detection based on double-layer capacitance for selective anion monitoring in ion chromatography. Part 1: Mercury electrodes
[AD-A188780] 12 p1606 N88-19603
Nonlinear resonance of two-dimensional ion layers
[AD-A188890] 12 p1695 N88-20145
Spectral diagnostics for temperature and density measurements on ATF 17 p2442 N88-24525

ION DISTRIBUTION
Measurement of parallel ion energy distribution function in PISCES plasma
[DE88-000108] 03 p0378 N88-12380
Ion thermal conductivity and ion distribution function in the banana regime
[IPPJ-865] 19 p2729 N88-26208
Moment approach to neoclassical flows, currents and transport in auxiliary heated tokamaks
[DE88-008024] 21 p3016 N88-27901
Nuclear and ionic charge distribution experiment on ISEE-1 and ISEE-3
[NASA-CR-180776] 23 p3183 N88-28947

ION EMISSION
Characterization of Er,Cr:YSGG
[AD-A185885] 07 p0932 N88-15650
Observation of nonlinear wave decay processes in the solar wind by the AMPTE IRM plasma wave experiment
[AD-A191409] 16 p2290 N88-23713
Ion gun generated electromagnetic interference on the SCATHA satellite
[AD-A195179] 24 p3335 N88-29853

ION ENGINES
NT MERCURY ION ENGINES
An 8-cm ion thruster characterization
[NASA-CR-180819] 01 p0017 N88-10106
Megawatt level electric propulsion perspectives
17 p2404 N88-24294
Electric propulsion options for the SP-100 reference mission 17 p2404 N88-24296
TR CE design, evaluation and feasibility tests
17 p2437 N88-24498
Internal erosion rates of a 10-kW xenon ion thruster
[NASA-TM-100954] 18 p2476 N88-24688
Performance of 10-kW class xenon ion thrusters
[NASA-TM-101292] 22 p3049 N88-28088
The NASA Electric Propulsion Program
[NASA-TM-101324] 24 p3336 N88-29859

ION EXCHANGE MEMBRANE ELECTROLYTES
Studies of transport processes in porous and ion exchange membranes
[ISBN-951-99847-0-4] 01 p0021 N88-10133

ION EXCHANGING
Heterogeneous isotope exchange between solid cesium iodide and gaseous methyl iodide
[ETN-88-91085] 09 p1141 N88-16840
Molecular and electronic mechanism in the control of Na+ and K+ permeability of excitable cell membrane by ligand binding on receptor sites
[AD-A188725] 13 p1808 N88-20805
Solid-state electrochemical processes in dye films
[AD-A188756] 13 p1844 N88-21036
Electronic and ionic transport in polymers
[AD-A190434] 15 p2045 N88-22185
Computer simulation of uphill diffusion in ternary ionic system
[NASA-TT-20194] 18 p2573 N88-25285
Dual mechanism bifunctional polymers: Design, synthesis and application of a new category of metal ion complexing agents
[DE88-008233] 20 p2777 N88-26468
Ion exchange processes for fabrication of integrated optical waveguide structures into glass substrates
[VTT-46] 24 p3429 N88-30405

ION EXTRACTION
Application of magnetic barrier for increasing the efficiency of laser ion source
[DE88-701669] 16 p2212 N88-23200
Ion generator and ion application system
[NASA-CASE-MFS-28122-1] 17 p2397 N88-24253

ION GAGES
U IONIZATION GAGES

ION IMPLANTATION
Ion-implantation-induced stress in glasses: Variation of damage mode efficiency with changes in glass structure
[DE87-013523] 01 p0028 N88-10175
Electrical behavior of layers implanted with low energy pions in Si
[INPE-4199-PRE/1051] 01 p0102 N88-10670
Studies on surface chemical states of some metals and ceramics bombarded with energetic light-ions
[DE87-752975] 02 p0145 N88-10910
DSA RuO2/TiO2 electrode modeled by ion implantation: An in situ characterization by photoacoustic and photocurrent spectroscopy
[DE87-009129] 02 p0245 N88-11545
Modeling of irradiation-induced amorphization in a titanate ceramic
[DE87-014751] 03 p0292 N88-11833
Microstructural change of Al on H implantation
[IPPJ-847] 04 p0493 N88-13036
Fatigue characteristics of ion treated surfaces
05 p0606 N88-13713
Develop techniques for ion implantation of (lead-lanthanum-zirconate-titanate) for adaptive optics
[DE88-000642] 05 p0650 N88-13986
Structural characterization of ion implanted beta-SiC thin films
[DE87-014567] 05 p0656 N88-14027
Basic energy sciences research in the Metals and Ceramics Division of Oak Ridge National Laboratory
[DE87-013538] 06 p0681 N88-14171
The effect of ion implantation on the corrosion behavior of a high-density sintered tungsten alloy
[AD-A185713] 06 p0683 N88-14185
Theoretical aspects of channeling, damage, and range distributions for low (keV) and high (MeV) energy implantation
[DE88-000949] 06 p0786 N88-14818
Surface modification using ion beams: Recent developments at ORNL
[DE88-000951] 06 p0786 N88-14819
Ion mixing and surface modification in metal-semiconductor systems
[DE88-001702] 06 p0786 N88-14823
X-ray measurements of phason distortion in ion-implanted Al-Mn
[DE87-014566] 07 p0937 N88-15694
Analysis of load-bearing capacity of nitrided layer
[PB87-144176] 08 p0966 N88-15857
Control of solid-excitation-based photochemical dry etching of semiconductors by ion-bombardment-induced damage
[DE88-003214] 09 p1257 N88-17537
Effects of ion implantation on cavitation erosion of a cobalt based metal/carbide alloy
[AD-A187239] 10 p1303 N88-17793
Metal modification for improved glass-ceramic to metal seals: 1. Auger results on ion implantation and vapor deposition films
[DE88-005244] 10 p1339 N88-18006
Formation of optical waveguides by ion implantation
[DE88-003894] 10 p1409 N88-18407
Electrochemical and optical investigations on ion-implanted TiO2 samples
[ETN-88-91485] 11 p1455 N88-18670
In situ ultrahigh vacuum friction measurement and wear track analysis of ion implanted 304 stainless steel
[DE88-004537] 11 p1494 N88-18922
Optical waveguide formation by ion implantation of Ti or Ag
[DE88-004595] 11 p1551 N88-19278
Formation of buried nitride layers in (110) silicon
[DE88-003255] 11 p1557 N88-19323
Ion beam modification of film stress and the effectiveness of thin film encapsulants on GaAs
[DE88-004458] 11 p1558 N88-19328
An in situ annealing study of lead implanted single crystal calcium titanate
[DE88-005435] 11 p1562 N88-19351
Fundamental studies and device development in beta silicon carbide
[AD-A189540] 12 p1699 N88-20165
Temperature dependence of Kr precipitation in Ni
[DE88-005953] 13 p1744 N88-20429
Focused ion beam fabrication of graded channel FET's in GaAs and Si
[AD-A189166] 13 p1845 N88-21040
Optical study of germanium, germanium plus arsenic, and germanium plus gallium implants in gallium arsenide
[AD-A189600] 13 p1845 N88-21045
Secondary electron emission characteristics improved by ion implantation 14 p1903 N88-21370
Effect of P implantation on the corrosion behavior of Fe-Cr alloys
[DE88-005732] 15 p2040 N88-22158
Ion-beam mixing and amorphization in Au/Zr bilayers
[DE88-005999] 15 p2140 N88-22767
High density ion implanted contiguous disk bubble technology
[AD-A190169] 15 p2143 N88-22789
Microelectronics the next fifteen years
17 p2305 N88-23792
Ion beam alloying of aluminum for corrosion resistance 17 p2321 N88-23860
Planar fully ion-implanted high power InP MISFETs
[AD-A191589] 18 p2582 N88-25338
Studies of boron implantation through photochemically deposited SiO2 films on Hg(sub 1-x)Cd(sub x)Te
[SD-TR-87-26] 19 p2621 N88-25548
Carrier lifetime versus ion-implantation dose in Silicon On Sapphire 19 p2658 N88-25791
High dose uranium ion implantation into silicon
[LBL-23509] 19 p2725 N88-26182
Ion implantation processing of 3-5 strained-layer semiconductors
[DE88-005270] 19 p2734 N88-26240

Development of high current and high brightness negative hydrogen ion sources
[DE88-010882] 20 p2852 N88-26934
A fundamental understanding of the interfacial compatibility in hybrid material systems
[AD-A192921] 21 p2909 N88-27264
Thin film and near-surface characterization using a mechanical properties microprobe
[DE88-011399] 21 p2915 N88-27302
Focused ion beam fabrication of graded channel FETs in GaAs and Si
[AD-A193096] 21 p2936 N88-27439
Friction, wear and electrical contact resistance of precious metal alloys
[DE88-011244] 21 p2938 N88-27450
Use of Moessbauer spectroscopy to study implanted surfaces
[DE88-010452] 21 p3023 N88-27942
Rivista Tecnica Selenia, volume 10, no. 3, 1987
[ETN-88-92717] 22 p3068 N88-28210
A 400 kV ion implanter: Operating principles and applications 22 p3069 N88-28213
Rapid thermal annealing of silicon layers amorphized by ion implantation
[DE88-702307] 23 p3290 N88-29591
Electrical conductivity of GaAs layers implanted on semi-insulator nondoped substrates
[CERT-422000/RF] 23 p3294 N88-29614

ION INJECTION
Particle injection and cosmic ray acceleration at collisionless parallel shocks
[DE88-000507] 04 p0430 N88-12665
Status of RF superconductivity at Argonne National Laboratory
[DE88-005913] 15 p2144 N88-22796
Dynamics explorer data analysis
[NASA-CR-181428] 19 p2691 N88-25996

ION IRRADIATION
NT DEUTERON IRRADIATION
NT PROTON IRRADIATION
Monte Carlo calculations for the simulation of channeling experiments on irradiated aluminum alloys. Calculation of angle-dependent efficiency curves
[HMI-B-433] 01 p0092 N88-10597
Ion-beam nitriding of steels
[NASA-CASE-LEW-14104-2] 06 p0682 N88-14179
Theoretical aspects of channeling, damage, and range distributions for low (keV) and high (MeV) energy implantation
[DE88-000949] 06 p0786 N88-14818
Laser fluorescence spectroscopy of zinc neutrals originating from laser-irradiated and ion-bombarded zinc sulfide and zinc surfaces
[DE88-006033] 13 p1776 N88-20620

ION MICROSCOPES
Field ion microscope studies of surface reconstructions
[DE87-014644] 02 p0147 N88-10924
Atomic-level studies of superconducting YBa2Cu3O sub 7-x
[DE88-002522] 06 p0788 N88-14831
Characterization of duplex stainless steel by TEM (Transmission Electron Microscopy), SANS (Small-Angle Neutron Scattering) and APFIM (Atom-Probe Field Ion Microscopy) techniques
[DE88-002916] 09 p1145 N88-16865
SHaRE: Collaborative materials science research
[DE88-007175] 18 p2467 N88-24646

ION MOTION
Nuclear magnetic resonance studies of ion motion in solid electrolytes
[DE87-014547] 02 p0232 N88-11464
A generalized description of the anomalous Doppler resonance and the stabilizing role of ion dynamics
[INPE-4384-PRE/1204] 08 p1081 N88-16513
Advanced studies of integrable systems
[AD-A186792] 09 p1151 N88-16895
Theory of laser cooling and spectroscopy of harmonically trapped single atoms
[AD-A189576] 13 p1775 N88-20617

ION OSCILLATION
U PLASMA OSCILLATIONS

ION PLATING
Ion plating: Fundamental processing studies and synthesis of high performance coatings
[AD-A184766] 03 p0303 N88-11908
Ion plating for corrosion control
[AD-A185061] 05 p0565 N88-13442
Tin activated reactive ion plating and its application
[PB87-144036] 08 p0970 N88-15871
Structure and properties of titanium nitride and zirconium nitride thin films prepared by reactive ion plating --- cutting tools
[ETN-88-92218] 15 p2042 N88-22167
Status and directions of modified tribological surfaces by ion processes
[NASA-TM-101304] 22 p3063 N88-28176

ION PROBES
Studies of fluorine combustion
[AD-A187646] 11 p1452 N88-18656
Electronic and ionic transport in polymers
[AD-A190434] 15 p2045 N88-22185
Laser spectoscopy of plasmas
[AD-A193009] 20 p2861 N88-26991
Role of zircon in tracing crustal growth and recycling
24 p3394 N88-30211

ION PRODUCTION RATES
On formulating a simple D-region model
[AD-A195841] 24 p3392 N88-30197

ION PROPULSION
An 8-cm ion thruster characterization
[NASA-CR-180819] 01 p0017 N88-10106
Auxiliary propulsion system flight package
[NASA-CR-180828] 02 p0141 N88-10886
Design study for asteroidal exploitation
03 p0389 N88-12445
High power ion thruster performance
[NASA-TM-100127] 04 p0409 N88-12542
Intelligent on board control for field emission electric propulsion system 12 p1589 N88-19513
Plasma-gas interaction studies in a hybrid plume plasma rocket
[AD-A190310] 15 p2138 N88-22755
Advanced electric propulsion research
[NASA-CR-182130] 16 p2170 N88-22937
A cyclic ground test of an ion auxiliary propulsion system: Description and operational considerations
[NASA-TM-100870] 17 p2313 N88-23829
High power ion thruster performance
17 p2404 N88-24295

ION RECOMBINATION
Wavelength scaling of lithium-like recombination scheme for X-UV gain production --- X-ray lasers
[ETN-88-92002] 13 p1778 N88-20634

ION SCATTERING
An interactive computer program for materials analysis by means of ion scattering
[MRL-R-1040] 01 p0091 N88-10596
Atomic physics with highly charged ions
[DE88-000894] 05 p0648 N88-13972
Charge exchange in low energy (keV) and hyperthermal energy (10-100 eV) ion scattering
[AD-A187643] 11 p1543 N88-19222
Studies of model ion channels in defect-free multibilayers of phospholipids
[AD-A188740] 16 p2238 N88-23365
Inelastic ion-surface collisions
[AFGL-TR-87-0206] 19 p2724 N88-26174

ION SELECTIVE ELECTRODES
Thin films for geothermal sensing
[DE88-000154] 03 p0326 N88-12061
High polymer sensor materials discussed
06 p0676 N88-14140
Chemical multisensors with selective encapsulation of ion-selective membranes 19 p2670 N88-25869
Silver multi-layers for planar Ag/AgCl reference electrodes 19 p2672 N88-25883
Functional study of the Si/SiO2 structures. Application to the implementation of an integrated ion sensor
[ECL-87-16] 22 p3073 N88-28246

ION SHEATHS
Irradiation test results on thermionic fuel element sheath insulators 17 p2402 N88-24280

ION SOURCES
Theoretical atomic and molecular physics
[DE88-001625] 05 p0649 N88-13974
Design considerations for a negative ion source for DC operation of high-power, multi-megaelectron-volt neutral beams
[DE88-002692] 08 p1083 N88-16525
A fiber-optic link for pressure control of ion sources
[DE88-001782] 09 p1248 N88-17484
Application of ECR ion source beams in atomic physics
[DE88-003767] 10 p1406 N88-18384
Optimization of outlet channel of plasma ion source
[DE88-700471] 10 p1410 N88-18415
Magnetic and inertial fusion status and development plans
[DE88-004405] 11 p1552 N88-19288
A moment approach to modeling negative ion sources
[AD-A188858] 12 p1691 N88-20114
Application of magnetic barrier for increasing the efficiency of laser ion source
[DE88-701669] 16 p2212 N88-23200
Multiply stripped ion generation in the metal vapor vacuum arc
[DE88-008416] 19 p2725 N88-26179
A low divergence, high brightness lithium ion source for plasma diagnostics
[DE88-008063] 19 p2729 N88-26203
Sources of polarized ions and atoms
[DE88-010910] 20 p2852 N88-26931
Development of high current and high brightness negative hydrogen ion sources
[DE88-010882] 20 p2852 N88-26934
Enhancement of volume H(-) production by vibrationally pre-exciting the hydrogen molecules
[DE88-010783] 20 p2853 N88-26937
Field-enhanced lithium ion sources for PBFA 2
[DE88-007195] 20 p2856 N88-26960

ION SPECTROMETERS
U MASS SPECTROMETERS

ION STORAGE
Ion traps for large storage capacity
16 p2268 N88-23570

ION STRIPPING
Neutral beam propagation through the atmosphere
[AD-A188984] 12 p1691 N88-20115

ION TEMPERATURE
High ionic conductivity in PEO/PPG block polymer and salt solutions
[AD-A183502] 01 p0026 N88-10168
Hydroxide ion conductors as possible electrolytes in intermediate temperature fuel cells
[AD-A185508] 06 p0731 N88-14495
Magnetic and inertial fusion status and development plans
[DE88-004405] 11 p1552 N88-19288
Alfven waves in plasma with finite ion temperatures
14 p1972 N88-21769
Ion temperature measurement with spectroscopy in JT-60 17 p2439 N88-24513
Ion temperature profile measurement using charge exchange recombination spectroscopy on JIPP T-IIU
17 p2440 N88-24518
Spectroscopic measurements of ion temperature, rotation speed and beam deposition profile on DIII-D
17 p2440 N88-24519
Forbidden transitions as ion-temperature sensitive lines 17 p2441 N88-24520
Spectroscopic study of heliotron E plasmas: Stark profile, CXR, poloidal rotation and carbon coating
17 p2441 N88-24523
Spectral diagnostics for temperature and density measurements on ATF 17 p2442 N88-24525
Properties of hydrogen/helium accretion plasmas
[DE88-006831] 19 p2728 N88-26197
Effects of secondary electron emission on the collector and source sheaths of a finite ion temperature plasma
[DE88-008930] 20 p2858 N88-26971
Effects of low reflection on the collector and source sheaths of a finite ion temperature plasma
[DE88-008929] 21 p3017 N88-27908
Collector and source sheaths of a finite ion temperature plasma
[DE88-008934] 23 p3286 N88-29564

ION TRAPS (INSTRUMENTATION)
Large hydrogen cluster ions 16 p2267 N88-23558
First capture of antiprotons in an ion trap and the possibility of antihydrogen 16 p2268 N88-23569
Ion traps for large storage capacity
16 p2268 N88-23570
Long duration coherent Lyman-alpha sources
16 p2268 N88-23571
Magnetic traps for an anti-hydrogen gas
16 p2269 N88-23572
Examination of the termalization of confined ions
[PB87-227815] 19 p2723 N88-26171

IONIC COLLISIONS
Radiation induced collapse of the crystalline structure
[DE87-014407] 04 p0498 N88-13064
Atomic physics with highly charged ions
[DE88-000894] 05 p0648 N88-13972
The approach to equilibrium in a quark-gluon plasma
[DE88-002117] 09 p1251 N88-17499
Control of solid-excitation-based photochemical dry etching of semiconductors by ion-bombardment-induced damage
[DE88-003214] 09 p1257 N88-17537
Large hydrogen cluster ions 16 p2267 N88-23558
Associative two-body condensation in laser-cooled sodium and hydrogen 16 p2267 N88-23559
Distorted-wave-method calculation of electron-impact excitation of atomic ions 17 p2443 N88-24532
Plasma neutralizer work at BNL (Brookhaven National Laboratory)
[DE88-007046] 18 p2579 N88-25317
Inelastic ion-surface collisions
[AFGL-TR-87-0206] 19 p2724 N88-26174
Theoretical atomic and molecular physics
[DE88-007122] 19 p2724 N88-26175
Atomic physics of strongly correlated systems
[DE88-007789] 19 p2724 N88-26177

Fluid dynamical model of ultrarelativistic heavy ion collisions
[DE88-007905] 20 p2850 N88-26921

Eikonal solutions to optical model coupled-channel equations
[NASA-TP-2830] 24 p3428 N88-30402

IONIC CONDUCTIVITY
U ION CURRENTS

IONIC DIFFUSION

GAS 450: A space payload for the People Central Coast Student Experimenters 10 p1289 N88-17709

Anisotropy of light absorption by color centers in waveguides produced on photochromic glasses by diffusion 14 p1896 N88-21320

Computer simulation of uphill diffusion in ternary ionic system
[NASA-TT-20194] 18 p2573 N88-25285

Inner-shell X-ray line spectra of highly ionized titanium, chromium, iron and nickel and their appliation to laboratory plasmas
[PB87-225181] 19 p2730 N88-26212

IONIC MOBILITY

Ionic transport and electrical relaxation in glass
[DE88-000867] 05 p0657 N88-14028

Ionically conducting polymers: Principles and properties of solid electrolytes
[DE88-001552] 06 p0684 N88-14190

Some aspects of metallic ion chemistry and dynamics in the mesosphere and thermosphere
06 p0737 N88-14534

High power storage system based on thin film solid ionics
[AD-A193623] 23 p3291 N88-29598

IONIC PROPELLANTS
U ION ENGINES

IONIC REACTIONS

Relativisitic heavy ion collisions
[DE87-014292] 02 p0232 N88-11462

Atomic physics with highly charged ions
[DE88-000894] 05 p0648 N88-13972

Studies in solid state ionics
[DE88-700830] 11 p1559 N88-19333

IONIC WAVES

A possible role for ionospheric ions in triggering a geomagnetic substorm onset 08 p1096 N88-16594

Low frequency waves and small scale solitary structures observed by Viking --- Swedish satellite; auroras
08 p1099 N88-16611

IONIZATION
NT ATMOSPHERIC IONIZATION
NT AURORAL IONIZATION
NT AUTOIONIZATION
NT FLAME IONIZATION
NT GAS IONIZATION
NT ION PRODUCTION RATES
NT NONEQUILIBRIUM IONIZATION
NT PHOTOIONIZATION
NT SURFACE IONIZATION

Study of ionization equilibrium of high temperature and low density plasma
[DE87-703070] 02 p0238 N88-11502

JPRS report: Science and technology. China
[JPRS-CST-87-031] 03 p0299 N88-11880

XeCl excimer laser induced multiphoton ionization of ammonia molecule 03 p0299 N88-11883

Equilibrium calculations of ionization in tracer flames
[PB87-104154] 04 p0412 N88-12555

High efficiency generation of 130-nm radiation from sum-frequency mixing in Hg
[DE87-013714] 04 p0431 N88-12674

Radio continuum emission from the ionized stellar winds of the cool supergiants in zeta Aurigae-like systems
04 p0514 N88-13160

Anti-Stokes generation of 226 nm light
[DE88-001612] 05 p0589 N88-13590

Ionization losses in BGO
[NOTA-INTERNA-889] 07 p0856 N88-15198

Method of plasma diagnostics by a heavy ion beam for the T-15 tokamak
[DE88-700342] 07 p0935 N88-15678

Minimum necessary intensity of source of preionization for stabilization of a self-sustaining laser discharge with mean power raised by electron beam or X-rays
[PB87-178156] 09 p1171 N88-17024

An analytic model for ionization distributions produced in nanometer sites by protons
[DE88-003943] 10 p1406 N88-18385

Chemical activation of molecules by metals: Experimental studies of electron distributions and bonding
[DE88-004465] 10 p1407 N88-18393

Synthesis and characterization of thin films
[AD-A187335] 10 p1421 N88-18485

Numerical simulation of the propagation and absorption due to air breakdown of long microwave pulses
[DE88-005227] 11 p1475 N88-18798

Resonantly-enhanced, four-photon ionization of krypton at laser intensities exceeding 10(12) W/sq cm
[DE88-005038] 11 p1544 N88-19229

Spectroscopic determinations of surface gravities of giant stars, and ultraviolet observations of RR Lyrae and X Arietis 11 p1569 N88-19391

Discharge excitation of dye vapors
[AD-A188428] 12 p1632 N88-19770

Kinetic mechanisms for ionization and afterburning suppression
[AD-A189219] 13 p1737 N88-20383

Studies of compound states of negative ions using laser beams
[DE88-004708] 13 p1777 N88-20627

Ionization equilibrium and radiative energy losses in a stationary plasma
[DE88-700856] 14 p1984 N88-21832

Narrow-band photographic observations of the HII Region S296 in Canis Major 16 p2288 N88-23696

Ion generator and ion application system
[NASA-CASE-MFS-28122-1] 17 p2397 N88-24253

Contributions of autoionizing resonances to the electron collisional excitation rates for Be-like ions
[AD-A190924] 18 p2572 N88-25275

High-fidelity in isotope ratio measurements for resonance ionization mass spectrometry
[DE88-009129] 19 p2613 N88-25506

A mass spectrometer for the analysis of thermally labile compounds 19 p2668 N88-25859

Space and sea: Is there a place for ionization?
19 p2699 N88-26043

Interactions of molecules with surfaces
[DE88-007950] 19 p2723 N88-26169

Theoretical atomic and molecular physics
[DE88-007122] 19 p2724 N88-26175

Rare Gas Halide (RGH) kinetics
[AD-A192352] 20 p2770 N88-26425

Laser desorption/ablation studies by resonance ionization mass spectrometry
[DE88-009124] 20 p2807 N88-26650

A 10 microns photoexcited avalanche gain due to electron impact ionization from GaAs quantum well superlattices 20 p2867 N88-27026

Multiphoton ionization of alkaline earth atoms in an intense laser field
[DE88-008078] 21 p3014 N88-27884

The influence of ionization within a plasma opening switch
[AD-A193147] 21 p3017 N88-27906

The 2D Rydberg series in Al I
[NASA-TM-101189] 22 p3150 N88-28740

Breakdown of molecular oxygen by brief pulses of laser radiation
[DE88-702687] 23 p3220 N88-29168

Electron impact ionization cross-section of some organic compounds
[DE88-702044] 23 p3280 N88-29525

The kinematics of Milky Way halo gas
23 p3299 N88-29648

Impurity analysis in SIMOX samples by high-efficiency resonance ionization time-of-flight mass spectrometry
[DE88-012061] 24 p3367 N88-30051

Cluster beam studies
[AD-A195182] 24 p3434 N88-30443

IONIZATION CHAMBERS
NT BUBBLE CHAMBERS
NT CLOUD CHAMBERS
NT PROPORTIONAL COUNTERS
NT SPARK CHAMBERS

Development and evaluation of a Monte Carlo code system for analysis of ionization chamber responses
[AD-A183970] 03 p0375 N88-12359

High efficiency generation of 130-nm radiation from sum-frequency mixing in Hg
[DE87-013714] 04 p0431 N88-12674

Single wire drift chamber design
[DE87-011002] 07 p0857 N88-15205

IONIZATION COEFFICIENTS

Detection of minimum-ionizing particles in hydrogenated amorphous silicon
[DE88-002769] 07 p0837 N88-15081

On formulating a simple D-region model
[AD-A195841] 24 p3392 N88-30197

IONIZATION COUNTERS
U IONIZATION CHAMBERS
U RADIATION COUNTERS

IONIZATION CROSS SECTIONS

Photoionization of atoms and ions: Application of time-dependent response method within the density functional theory
[AD-A185686] 07 p0930 N88-15649

Neutral beam propagation through the atmosphere
[AD-A188984] 12 p1691 N88-20115

Photoionization dynamics and abundance patterns in laser vaporized tin and lead clusters
[AD-A191604] 18 p2482 N88-24722

Molecular sources of ionospheric holes
[AD-A191857] 18 p2541 N88-25082

High-order multiphoton ionization of the noble gases
[DE88-007489] 18 p2571 N88-25273

A new approach to generating negative ion beams
[AD-A191119] 18 p2572 N88-25276

Trochoidal analysis of scattered electrons in a merged electron-ion beam
[NASA-CASE-NPO-16789-1-CU]
18 p2573 N88-25281

Electron impact ionization cross-section of some organic compounds
[DE88-702044] 23 p3280 N88-29525

IONIZATION FREQUENCIES

On the role of the ionization frequency to gyrofrequency ratio in the critical ionization velocity interaction
[TRITA-EPP-86-10] 10 p1410 N88-18414

Photoionization dynamics and abundance patterns in laser vaporized tin and lead clusters
[AD-A191604] 18 p2482 N88-24722

IONIZATION GAGES

TOTAL: A new instrument to study turbulent parameters in the mesosphere and lower thermosphere
08 p1029 N88-16234

IONIZATION POTENTIALS

Critical Ionization Velocity (CIV) interaction: Some unsolved questions
[TRITA-EPP-87-12] 09 p1250 N88-17491

IONIZED GASES

Proceedings of the 17th International Conference on Phenomena in Ionized Gases held in Budapest, Hungary, July 8-12, 1985: Invited papers
[DE87-703562] 05 p0651 N88-13987

A plasma wave instrument on the AMPTE/IRM (Active Magnetospheric Particle Tracing Explorers/Ion Release Module) spacecraft
[AD-A191216] 16 p2233 N88-23336

IONIZED PLASMAS
U PLASMAS (PHYSICS)

IONIZING RADIATION
NT ALPHA PARTICLES
NT BETA PARTICLES
NT COSMIC RAY SHOWERS
NT COSMIC RAYS
NT COSMIC X RAYS
NT EXTREME ULTRAVIOLET RADIATION
NT FAR ULTRAVIOLET RADIATION
NT GALACTIC COSMIC RAYS
NT GAMMA RAY BURSTS
NT GAMMA RAYS
NT LYMAN ALPHA RADIATION
NT NEAR ULTRAVIOLET RADIATION
NT PRIMARY COSMIC RAYS
NT SOLAR COSMIC RAYS
NT SOLAR X-RAYS
NT ULTRAVIOLET RADIATION
NT X RAYS

Ion-implantation-induced stress in glasses: Variation of damage mode efficiency with changes in glass structure
[DE87-013523] 01 p0028 N88-10175

Instrument for radiation testing/screening electronic devices over an extended temperature range
[AD-A184245] 03 p0326 N88-12060

Reevaluating the worst-case radiation response of MOS transistors
[DE87-014157] 04 p0497 N88-13059

Karyometric evaluation of neuronal reactions of rat cerebral cortex to the combined effect of ionizing radiation, longitudinal accelerations and vibration
07 p0890 N88-15396

Combined effect of microwaves and ionizing radiation
07 p0893 N88-15413

Simulation of effect on biological systems of impact wave from heavy charged particle track
07 p0896 N88-15429

Combined effect of ionizing radiation and altered gas atmosphere on central nervous system
10 p1367 N88-18168

Characterization of space radiation environment in terms of the energy deposition in functionally important volumes
[DE88-005627] 15 p2100 N88-22513

Point defects in irradiated silicates
17 p2408 N88-24319

Modeling of radiation dose dependence of MOSFETs
17 p2416 N88-24370

Extremely Low Frequency (ELF) communications program: Non-ionizing electromagnetic radiation literature evaluation and assessment, 1986-1987 literature review
[AD-A192024] 19 p2642 N88-25677

Stress corrosion of ceramic materials
[AD-A191979] 23 p3195 N88-29016

Emetic mechanism in acute radiation sickness
[AD-A194102] 23 p3238 N88-29267

IONOGRAMS
Trajectory synthesis of ionograms in presence of artificial ionospheric inhomogeneities 08 p1002 N88-16067
Trajectory synthesis of ionograms in presence of artificial ionospheric inhomogeneities 13 p1789 N88-20703
IONOSONDES
Height profile inversion of ionospheric movement from observed parameters of HF radio echoes 03 p0299 N88-11884
Ionospheric convection and structure using ground-based digital ionosondes [AD-A194246] 23 p3233 N88-29237
Ionosonde studies of field-aligned irregularities during high-power HF heating at Arecibo [AD-A195848] 24 p3401 N88-30256
IONOSPHERE-MAGNETOSPHERE COUPLING
U MAGNETOSPHERE-IONOSPHERE COUPLING
IONOSPHERES
Solar wind effects on the outer ion coma of Comet Halley 01 p0117 N88-10750
Processes in the quiet and disturbed equatorial-low latitude ionosphere: Sundial campaign, 1984 [INPE-4152-PRE/1057] 08 p1036 N88-16282
A proposal for the establishment of a center of excellence in theoretical geoplasma research [AD-A189742] 16 p2231 N88-23327
The effects of solar cycle and latitude dependence on the formation of ionospheric C layer [INPE-4342-TDL/293] 16 p2232 N88-23332
IONOSPHERIC ABSORPTION
U ELECTROMAGNETIC ABSORPTION
U IONOSPHERIC PROPAGATION
IONOSPHERIC COMPOSITION
The new CP3 06 p0691 N88-14237
Investigations into the properties, conditions and effects of the ionosphere [AD-A194245] 22 p3118 N88-28528
Photochemistry of ionospheric D-region with injection of nitrogen oxides 24 p3444 N88-30499
IONOSPHERIC CURRENTS
NT AURORAL ELECTROJETS
NT EQUATORIAL ELECTROJET
Area of reduced electron concentration in terrestrial plasmasphere 08 p1003 N88-16078
IONOSPHERIC DISTURBANCES
NT SUDDEN IONOSPHERIC DISTURBANCES
NT TRAVELING IONOSPHERIC DISTURBANCES
Height profile inversion of ionospheric movement from observed parameters of HF radio echoes 03 p0299 N88-11884
High latitude F-region drift studies [AD-A184466] 04 p0467 N88-12889
Internal gravity waves in the meteor zone in the Tbilisi Region 06 p0736 N88-14528
Electron acceleration by wave processes in the earth's ionosphere [AD-A186110] 07 p0877 N88-15320
Trajectory synthesis of ionograms in presence of artificial ionospheric inhomogeneities 08 p1002 N88-16067
High altitude chemical release systems for project BIME (Brazilian Ionospheric Modification Experiments) project IMS (Ionospheric Modification Studies) project PIIE (Polar Ionospheric Irregularities Experiment) project polar arcs [AD-A186299] 12 p1642 N88-19833
Trajectory synthesis of ionograms in presence of artificial ionospheric inhomogeneities 13 p1789 N88-20703
Support for FY87 midlatitude electron-density calibration campaign [AD-A190174] 15 p2094 N88-22476
Radio-wave scintillations and ionospheric irregularities at high latitudes [AD-A192140] 18 p2501 N88-24837
The Effect of the Ionosphere on Communication, Navigation and Surveillance Systems Based on Ionospheric Effects Symposium held on 5-7 May 1987 in Springfield, Virginia [AD-A191855] 18 p2541 N88-25081
Approximate analytical formulae for electron density and collision frequency in the natural and nuclear-disturbed ionosphere and inner magnetosphere [AD-A193129] 21 p2972 N88-27654
The effect of equatorial ionospheric irregularities on the performance of a south-looking OTH-B (Over-The-Horizon-Backscatter) radar [AD-A195090] 24 p3362 N88-30018
IONOSPHERIC DRIFT
High latitude F-region drift studies [AD-A184466] 04 p0467 N88-12889
On connection between evolution of troposphere fronts and changes of circulation regime in meteor zone 06 p0735 N88-14519
Atmosphere dynamic processes structure at 80-105 km altitude 06 p0736 N88-14527
Studies of ionosphere/magnetosphere dynamics using SABRE and HILAT [AD-A190947] 16 p2232 N88-23333
High latitude ionospheric radio studies [AD-A192270] 20 p2824 N88-26753
Ionospheric convection and structure using ground-based digital ionosondes [AD-A194246] 23 p3233 N88-29237
IONOSPHERIC ELECTRON DENSITY
Trajectory synthesis of ionograms in presence of artificial ionospheric inhomogeneities 08 p1002 N88-16067
Electrostatic VLF emission determined from rocket and satellite experiments 08 p1002 N88-16068
Longitudinal variations of equatorial ionosphere determined from Intercosmos-19 artificial Earth satellite data 08 p1003 N88-16074
Area of reduced electron concentration in terrestrial plasmasphere 08 p1003 N88-16078
Application of correlation method of reception of direct and reflected cosmic radiation to study of plasmaspheres of planet and distribution of radiation brightness 08 p1004 N88-1[illegible]085
Distribution of electron concentration in nightime atmosphere of Venus based on radio transmission data 08 p1005 N88-16092
Multispectral optical observations of ionospheric F-region storm effects at low latitude [INPE-4231-PRE/1105] 08 p1024 N88-16198
Trajectory synthesis of ionograms in presence of artificial ionospheric inhomogeneities 13 p1789 N88-20703
Effect of nitrogen dioxide release on thermosphere 13 p1789 N88-20704
A model of the ionosphere in the altitude interval 50 to 4000 km. Part 2: Molecular ions (N2(+), NO(+), O2(+)) and electron density [DFVLR-FB-88-12-PT-2] 23 p3234 N88-29242
One equatorial anomaly in nighttime ionospheric F region 24 p3447 N88-30517
IONOSPHERIC HEATING
The effects of a geomagnetic storm on thermospheric circulation [AD-A186638] 09 p1190 N88-17128
Role of ordinary to extraordinary mode wave coupling in ionospheric heating experiments [AD-A195335] 24 p3362 N88-30017
IONOSPHERIC ION DENSITY
A possible role for ionospheric ions in triggering a geomagnetic substorm onset 08 p1096 N88-16594
Rocket-borne low energy ion measurements in space 18 p2593 N88-25412
A model of the ionosphere in the altitude interval 50 to 4000 km. Part 1: Atomic ions (H(+), He(+), N(+), O(+)) [DFVLR-FB-88-11-PT-1] 23 p3233 N88-29241
A model of the ionosphere in the altitude interval 50 to 4000 km. Part 2: Molecular ions (N2(+), NO(+), O2(+)) and electron density [DFVLR-FB-88-12-PT-2] 23 p3234 N88-29242
IONOSPHERIC NOISE
NT WHISTLERS
Ionospheric research in Antarctica [INPE-4521-PRE/1273] 16 p2232 N88-23331
IONOSPHERIC PROPAGATION
Report of the 3rd Finnish EISCAT Workshop --- European Incoherent Scatter Radar (EISCAT) [REPT-111] 06 p0691 N88-14233
Finnish contributions to EISCAT science in 1986 06 p0691 N88-14235
CP-1-H analysis tests 06 p0691 N88-14236
EISCAT research programs for 1987 06 p0692 N88-14244
Polar Geophysical Institute's studies of magnetosphere, ionosphere 06 p0728 N88-14480
Wideband HF (High Frequency) modeling and simulation [PB88-116116] 10 p1317 N88-17874
User's guide for the HF (High Frequency) broadcast antenna design and validation summary programs [PB88-116124] 10 p1317 N88-17875
Correcting ray field failures caused by focusing in an inhomogeneous duct: A critical look at the Gaussian beam method 12 p1616 N88-19663
An assessment of the application of in situ ion-density data from DMSP to modeling of transionospheric scintillation [AD-A188919] 12 p1643 N88-19840
Upward propagating electric fields from thunderstorms and VLF transmitters 13 p1801 N88-20767
Radial track of moving objects determined by HF backscatter technique 14 p1901 N88-21354
WAVFLD: A program to compute ionospheric height gain functions and field strengths at VLF [AD-A191159] 16 p2191 N88-23066
The Effect of the Ionosphere on Communication, Navigation and Surveillance Systems Based on Ionospheric Effects Symposium held on 5-7 May 1987 in Springfield, Virginia [AD-A191855] 18 p2541 N88-25081
Role of ordinary to extraordinary mode wave coupling in ionospheric heating experiments [AD-A195335] 24 p3362 N88-30017
Review of Radio Science, 1984-1986 24 p3363 N88-30023
Ionospheric radio and propagation: Waves in plasmas 24 p3364 N88-30030
IONOSPHERIC REFLECTION
U IONOSPHERIC PROPAGATION
IONOSPHERIC SOUNDING
First results from the Viking associated Aureld-VIP rocket and EISCAT campaign --- auroras; Swedish satellite 08 p1026 N88-16211
A model of the ionosphere in the altitude interval 50 to 4000 km. Part 1: Atomic ions (H(+), He(+), N(+), O(+)) [DFVLR-FB-88-11-PT-1] 23 p3233 N88-29241
Ionospheric radio and propagation: Waves in plasmas 24 p3364 N88-30030
IONOSPHERIC STORMS
NT SUDDEN IONOSPHERIC DISTURBANCES
IONOSPHERIC TEMPERATURE
Support for FY87 midlatitude electron-density calibration campaign [AD-A190174] 15 p2094 N88-22476
IONS
NT ANIONS
NT CATIONS
NT CESIUM IONS
NT DEUTERONS
NT FERRIC IONS
NT HEAVY IONS
NT HELIUM IONS
NT HYDROGEN IONS
NT HYDRONIUM IONS
NT LIGHT IONS
NT METAL IONS
NT MOLECULAR IONS
NT NEGATIVE IONS
NT NITROGEN IONS
NT OXYGEN IONS
NT POSITIVE IONS
NT RECOIL IONS
NT TRITONS
Study of pickup of cometary ions in turbulent solar winds 01 p0113 N88-10725
The analysis of metal finishing solutions by ion chromatography [AD-A184812] 05 p0561 N88-13414
Survey state of the art: Electrical load management techniques and equipment [AD-A184083] 05 p0577 N88-13517
Atomic physics with highly charged ions [DE88-000894] 05 p0648 N88-13972
Ionic transport and electrical relaxation in glass [DE88-000887] 05 p0657 N88-14028
Self-alignment of ions drifting in plasma 06 p0774 N88-14752
Ion mixing and surface modification in metal-semiconductor systems [DE88-001702] 06 p0786 N88-14823
Correlation effects on double electron capture in highly-charged, low-energy ion-atom collisions [DE87-013179] 07 p0930 N88-15651
EISCAT measurements of ion velocities during Coordinated Auroral Experiment using Scatter And Rockets (CAESAR) campaign 08 p1031 N88-16251
Ion flows in magnetospheric flux transfer events 08 p1098 N88-16607
Models for ionic transport in glass [DE88-002860] 10 p1304 N88-17799
Ion chromatography in the manufacture of multilayer circuit boards [DE88-002428] 10 p1322 N88-17902
A study of the magnetic field annihilation process in the magnetosphere and some geotechnical applications [DE88-004165] 10 p1355 N88-18096
Lithium fast-ion conductors: Polymer based materials [AD-A187879] 11 p1461 N88-18712
The JPL trapped mercury ion frequency standard 11 p1471 N88-18776
Ion energy diagnostics for voltage determinations in plasma-erosion-opening-switch experiments [DE88-004822] 11 p1479 N88-18827
Spectral line-broadening codes for hydrogen-, helium- and lithium-like ions in plasmas [DE88-005238] 11 p1552 N88-19289
The redox chemistry of some peroxo and superoxo metal ion complexes [AD-A189159] 12 p1606 N88-19606
Ion content and infrared absorption of moist atmospheric air [AD-A188839] 12 p1643 N88-19838
Laser photoelectron spectroscopy of ions [DE88-006860] 15 p2033 N88-22113

Angular resolved energy analysis of (69)Ga + ions from a gallium liquid metal ion source
[AERE-R-12649] 15 p2139 N88-22760
Universal detection of ions by replacement-ion chromatography employing an anion-replacement method and an ultraviolet-visible spectrophotometric detector
[AD-A191326] 16 p2176 N88-22971
Studies of model ion channels in defect-free multibilayers of phospholipids
[AD-A188740] 16 p2238 N88-23365
A new fiber-optic-based ion sensor
[AD-A191322] 16 p2274 N88-23612
Centrifugal acceleration of ions in the polar magnetosphere
[NASA-TM-101148] 17 p2374 N88-24120
Contributions of autoionizing resonances to the electron collisional excitation rates for Be-like ions
[AD-A190924] 18 p2572 N88-25275
Contaminant ions and waves in the space station environment 18 p2590 N88-25393
Rocket-borne low energy ion measurements in space
18 p2593 N88-25412
A mass spectrometer for the analysis of thermally labile compounds 19 p2668 N88-25859
Dynamics explorer data analysis
[NASA-CR-181428] 19 p2691 N88-25996
Sources of polarized ions and atoms
[DE88-010910] 20 p2852 N88-26931
Recent advances in atom-probe field ion microscopy
[DE88-008799] 20 p2876 N88-27070
Ion Bernstein modes in current-carrying plasmas
21 p3017 N88-27903
Theory and simulation of relaxed plasmoids
[AD-A192884] 21 p3032 N88-27997
Hydrogen concentration cells as converters of heat into electricity
[DE88-009662] 23 p3229 N88-29216
Large ionic species in sooting acetylene and benzene flames 24 p3348 N88-29932
Particle trajectories and potentials in a plane sheath moving in a magnetoplasma
[AD-A196226] 24 p3390 N88-30190
Ion kinetics in silane plasmas
[AD-A196202] 24 p3431 N88-30423
Ring current role in dynamics of fluctuating electron and ion fluxes in low-latitude magnetosphere
24 p3447 N88-30514

IP (IMPACT PREDICTION)
U COMPUTERIZED SIMULATION

IRAS
U INFRARED ASTRONOMY SATELLITE

IRASERS
U INFRARED LASERS

IRIDIUM
NT IRIDIUM ISOTOPES
Measurements of iridium and the meteoric impact hypothesis at cretaceous end
[DE87-703765] 04 p0521 N88-13200
Oxide-bound transition metal complexes for methane activation
[PB88-169719] 14 p1887 N88-21277
Weldability of general purpose heat source iridium capsules 17 p2426 N88-24429
The structure and properties of RF reactive sputtered IrO2 films 19 p2672 N88-25884
Catalytic activation of carbon dioxide by metal complexes
[AD-A192310] 21 p2909 N88-27262
Iridium-coated rhenium thrusters by CVD
[NASA-TM-101309] 24 p3339 N88-29874

IRIDIUM ISOTOPES
Experimental and theoretical investigations of isotope shift and hyperfine structure on 5d elements (especially platinum, iridium and rhenium)
[ETN-88-93121] 24 p3353 N88-29957

IRON
NT IRON ISOTOPES
NT IRON 57
Lithium/iron sulfide batteries: Development and demonstration
[DE87-014222] 01 p0042 N88-10265
The corrosion of iron rotating hemispheres in 1 M sulfuric acid: An electrochemical impedance study
[DE87-014679] 02 p0148 N88-10925
Wear of iron and nickel in corrosive liquid environments
[NASA-TM-100246] 03 p0289 N88-11817
Post-test analyses of aqueous batteries developed for electric propulsion
[DE88-000655] 03 p0311 N88-11965
Plasticity of aluminum and iron at high shear strain rate and high pressure 05 p0563 N88-13430
The mechanism by which sigma-phase forms in Fe-Cr-Ni system alloys
[BLL-M-37380-(5828.4)] 05 p0564 N88-13437
Effect of grain orientation on the origination and the initial growth of fatigue cracks in pure iron
05 p0597 N88-13647
Surface deformation and fatigue crack initiation of alpha-iron 05 p0598 N88-13651
Determination, by X-ray fluorescence, of platinum, palladium, ruthenium, iron and chromium in special steels
[PB87-132114] 06 p0683 N88-14183
Cyclic deformation behaviour of cast irons with various graphite shapes in the temperature range 20 C less than or = T less than or = 500 C 06 p0715 N88-14384
The relationship between microstructural size and fatigue threshold in iron and steel
06 p0716 N88-14396
Threshold and crack-growth tests on pre-cracked specimens produced in cyclic compression
06 p0718 N88-14412
Investigation of impurity defects in alpha-iron by molecular dynamics method
[DE88-700355] 07 p0834 N88-15058
Seasonal cycling of sulfur and iron in porewaters of a Delaware salt marsh
[NASA-CR-182385] 07 p0876 N88-15311
Studies of the electron spectrum with reference to the clean surfaces of iron, cobalt and nickel and their subsequent exposure to oxygen
11 p1459 N88-18700
Study of activationless reactions of point defects with impurities and impurity-defect complexes in alpha-iron
[DE88-701028] 13 p1745 N88-20433
Use of long-distance pair potentials in calculations of defect characteristics in metals
[DE88-701039] 15 p2037 N88-22138
Effect of P implantation on the corrosion behavior of Fe-Cr alloys
[DE88-005732] 15 p2040 N88-22158
Complexation and hydrolysis reactions of iron(III)
17 p2322 N88-23867
Flux density measurements of neutral iron in TEXTOR with laser induced fluorescence
17 p2442 N88-24528
Calculation of oxidation rates for iron in CO-CO2
[DE88-007313] 18 p2487 N88-24757
Epitaxial iron films
[AD-A191815] 19 p2732 N88-26225
Inelastic electron scattering and electron-hole excitations in iron and nickel
[DE88-011843] 21 p2915 N88-27303
Kinetic of oxidation to air of a Fe-Al-Mn alloy system at 600-800(sup 0)C temperature range
[DE88-702309] 21 p2920 N88-27330
Perfluoropolyalkylether lubricants under boundary conditions: Iron catalysis of lubricant degradation
[AD-A193241] 21 p2956 N88-27560
Study on iron disilicide thermoelectric generator
[AD-A193082] 22 p3116 N88-28517
Radial velocity measurements of a sample of northern metal-deficient stars
[SER-C-PREPUBL-FASC-25] 24 p3455 N88-30564

IRON ALLOYS
NT AUSTENITIC STAINLESS STEELS
NT BAINITIC STEEL
NT CARBON STEELS
NT CHROMIUM STEELS
NT FERRITIC STAINLESS STEELS
NT HIGH STRENGTH STEELS
NT LOW CARBON STEELS
NT MARAGING STEELS
NT MARTENSITIC STAINLESS STEELS
NT NICKEL STEELS
NT STAINLESS STEELS
NT STEELS
Relationships governing change in density in liquid ferrous alloys
[BLL-M-37305-(5828.4)] 02 p0149 N88-10935
The effect of strain rate on the yield behavior of iron-base LRO alloys at elevated temperatures
[DE87-014893] 03 p0288 N88-11808
Microstructural effects on the fatigue behavior of Fe-C-X alloys
[DE88-000155] 03 p0288 N88-11809
Investigations of crystallization velocity and boron diffusion in glassy iron-boron alloys and of activity coefficients of boron in crystalline iron-boron alloys
[ETN-87-90613] 03 p0381 N88-12393
A comparison of high damping shape memory alloys with Cu-Mn-based and Fe-Cr-based alloys
[AD-A184110] 04 p0414 N88-12566
Fatigue strength of alloy A286 at cryogenic temperature 05 p0603 N88-13695
Undercooling and nucleation in iron nickel alloys
[AD-A185500] 06 p0683 N88-14184
Structural relaxation and mechanical properties of amorphous Fe-Zr alloys 07 p0840 N88-15094
Response of Fe-Cr-Mn austenitic alloys to thermal aging neutron irradiation
[DE88-003415] 10 p1302 N88-17785
Cast iron-base alloy for cylinder/regenerator housing
[NASA-CR-182116] 12 p1608 N88-19613
Magnetic studies of iron-rare-earth-metalloid alloys
[DE88-006801] 16 p2282 N88-23660
On the abnormal phenomena observed in the electrical resistivity measurement during the decomposition process of saturated Cu-Fe alloys
[NASA-TT-20183] 18 p2507 N88-24869
Reduced-activation austenitic stainless steels: The Fe-Cr-C system
[DE88-008091] 20 p2773 N88-26442
Hot isostatic pressing of tungsten-nickel-iron composites
[FOA-C-20698-2.1] 22 p3056 N88-28135
The influence of solute segregation on the dislocation structure of small and large angle (001) twist boundaries in Fe-Sb alloys
[DE88-009166] 22 p3155 N88-28770
Hydrogen embrittlement of iron-nickel alloys
[AD-A195909] 24 p3353 N88-29958

IRON COMPOUNDS
NT FERRITES
NT FERROCENES
NT HEMATITE
NT IRON OXIDES
NT PYRITES
Development of iron aluminides
[AD-A185190] 05 p0568 N88-13461
Electron microscopy study of morphology and composition of a ferrisilicate catalyst
[DE88-005754] 11 p1562 N88-19352

IRON ISOTOPES
NT IRON 57
New technique for enhancing helium production in ferritic materials
[DE88-003048] 09 p1142 N88-16847

IRON METEORITES
Moessbauer study of shock induced effects in the Fe-Ni 50/50 ordered alloy in meteorites
[DE87-703364] 04 p0521 N88-13199

IRON ORES
NT HEMATITE

IRON OXIDES
NT HEMATITE
Grain boundary and surface diffusion in oxides
[DE88-002348] 07 p0938 N88-15697
Electron transfer to iron(3) oxide colloids
[DE88-002885] 10 p1416 N88-18448
High Tc superconducting HoBa2Cu(sub 1-x)Fe(sub x)3O(sub 7-y)
[DE88-008909] 22 p3155 N88-28768
Reflectance pattern and the physical and chemical characteristics of three Brazilian Oxisols
[INPE-4590-PRE/1320] 24 p3387 N88-30172

IRON 57
A sup 57 Fe Mossbauer study of the superconductor YBa sub 2 (Fe sub x Cu sub 1-x) sub 3 O sub y
[DE88-701543] 16 p2282 N88-23661

IROQUOIS HELICOPTER
U UH-1 HELICOPTER

IRRADIANCE
NT ILLUMINANCE
NT SOLAR CONSTANT
Radiometric calibration of the Earth observing system's imaging sensors
[NASA-CR-181542] 04 p0463 N88-12865
Statistical distribution of solar radiation (hourly sums): Cumulative frequency curves preparation of a European data set and direction for use
[PB87-107454] 04 p0467 N88-12886
Short-term temporal variations of Nimbus-7 measurements of the solar UV spectral irradiance
[PB88-102132] 07 p0946 N88-15753
Bright source lasers and experiments at very high irradiance
[DE88-004317] 10 p1337 N88-17988
Calculation of space station infrared irradiance from atmosphere-induced emissions
18 p2591 N88-25396
The propagation of irradiance moments of an aberrated, apodized FEL beam
[DE88-008972] 20 p2806 N88-26648
Short term variability between 120 and 300 mm from Solar Mesosphere Explorer (SME) observations
[AERONOMICA-ACTA-A-328-1988]
23 p3308 N88-29709
Aeronomic problems of the molecular oxygen photodissociation. Part 3: Solar spectral irradiances in the region of the O2 Herzberg continuum, Schumann-Runge bands and continuum
[AERONOMICA-ACTA-A-332-1988]
24 p3343 N88-29897

IRRADIATION
NT DEUTERON IRRADIATION
NT ELECTRON IRRADIATION
NT ION IRRADIATION
NT NEUTRON IRRADIATION
NT PROTON IRRADIATION
NT X RAY IRRADIATION
Surface modification by metal deposition and laser irradiation 01 p0023 N88-10148
Effects of electron and proton irradiations on n/p and p/n GaAs cells grown by MOCVD
[NASA-TM-100199] 01 p0042 N88-10266
Electron beam irradiation effects on carbon fiber reinforced PEEK composite
[DE87-753001] 02 p0142 N88-10690
Degradation mechanisms of materials for large space systems in low Earth orbit
[NASA-CR-181472] 02 p0143 N88-10696
Time-resolved absorption measurements on OMEGA
[DE87-014465] 02 p0179 N88-11112
Effects of radiation damage in optical fibers: A tutorial
[PB87-210308] 02 p0235 N88-11482
Time-resolved temperature and density measurements in ionizing, uniformly irradiated UV-laser-produced plasmas
[DE87-014649] 02 p0238 N88-11504
Irradiations. Accumulated doses. Heavy ions — space environment 03 p0272 N88-11708
Effect of irradiation on the tensile properties of niobium-base alloys
[DE87-002409] 03 p0285 N88-11790
Superconductivity of pseudobinary compounds Al5 (V-Cr)3Si, (V-MO)3Si, Mo3(Si-Re), bombarded with fast neutrons 03 p0285 N88-11792
Effect of helium on irradiation creep in an austenitic stainless steel
[DE87-013754] 03 p0290 N88-11824
Impact behavior of 9-Cr and 12-Cr ferritic steels after low-temperature irradiation
[DE88-000333] 03 p0291 N88-11827
Impact behavior of 9-Cr and 12-Cr ferritic steels after low-temperature irradiation
[DE88-000333] 03 p0291 N88-11827
Microstructural characterization of irradiated PWR steels using the atom probe field-ion microscope
[DE88-000341] 03 p0291 N88-11828
Temperature hysteresis and magnetic transitions in amorphous Fe-Ni-Zr alloys
[DE88-000228] 03 p0294 N88-11848
Computerized system for studies on creep of irradiated materials in the BR-10 reactor. Control system for electric motor
[DE87-702888] 03 p0310 N88-11952
Utilization of potatoes in bioregenerative life support systems 03 p0360 N88-12269
Performance of GaAs and silicon concentrator cells under 37 MeV proton irradiation
[NASA-TM-100144] 04 p0465 N88-12877
PISCES: Plasma-surface interactions and materials research
[DE88-001323] 04 p0494 N88-13044
Reevaluating the worst-case radiation response of MOS transistors
[DE87-014157] 04 p0497 N88-13059
An investigation of unipolar arcing at atmospheric pressure in aluminum 2024 and aluminum coated glass slides
[AD-A184903] 05 p0577 N88-13521
Raman microprobe characterization of dielectric films following high-energy pulsed laser irradiation
[DE88-000559] 05 p0588 N88-13587
Pure dephasing of a vibrational adbond
[AD-A185222] 05 p0609 N88-13740
Controlled ecological life support systems: Development of a plant growth module 05 p0630 N88-13854
Irradiation preservation of seafood: Literature review
[DE88-001691] 05 p0631 N88-13858
Fractographic and microstructural aspects of fracture toughness testing in irradiated 304 stainless steel
[DE88-000795] 06 p0681 N88-14172
Combined effect of microwaves and ionizing radiation 07 p0893 N88-15413
Effect of irradiation on the diffusion evolution of void ensemble in crystals
[DE88-700558] 07 p0939 N88-15706
Space environmental effects on polymeric materials
[NASA-CR-182454] 09 p1148 N88-16879
Food irradiation seminar: Asia and the Pacific
[DE88-700432] 09 p1202 N88-17203
Irradiation effects in metals
[DE88-004272] 10 p1303 N88-17789
International cooperative effort to establish ASTM (American Society for Testing and Materials) standards for the measurement of radiation dose for food processing
[DE88-002702] 10 p1372 N88-18190
NBS (National Bureau of Standards) measurement services: Spectral irradiance calibrations
[PB88-123781] 10 p1408 N88-18401
Investigations of stimulated Raman scattering from high density underdense plasmas irradiated by a 0.35 micron laser 10 p1411 N88-18421
Effects of X irradiation and high field electron injection on the electrical properties of rapid thermal oxides
[DE88-002642] 10 p1417 N88-18461
The effects of low doses of 14 MeV neutrons on the tensile properties of three binary copper alloys
[DE88-003400] 11 p1458 N88-18691
Crystallization and glass formation in electron and laser beam irradiated Cu-Zr alloys
[DE88-003390] 11 p1464 N88-18729
Ceramic decomposition under irradiation
[DE88-004327] 11 p1464 N88-18732
Metastable materials by laser irradiation
[PB88-130364] 11 p1493 N88-18912
An economic analysis of a multi-commodity fruit and vegetable irradiator
[DE88-003425] 11 p1524 N88-19098
Studies in solid state ionics
[DE88-700830] 11 p1559 N88-19333
Radiation response of thin oxides grown by rapid thermal oxidation and rapid thermal annealing techniques
[DE88-003632] 11 p1561 N88-19347
Food Irradiation Newsletter, Vol. 11, No. 1
[DE88-700808] 12 p1671 N88-20004
Hydrogen pumping and release by graphite under high flux plasma bombardment
[DE88-005880] 13 p1842 N88-21021
Coronal fluid-dynamics in laser fusion 16 p2278 N88-23634
The application of Rutherford backscattering for analyzing multilayered structure change induced by pulsed ion beam bombardment 16 p2278 N88-23638
Effects of irradiation on thermal coalescence of pores in real crystals
[DE88-701683] 16 p2282 N88-23663
Irradiation test results on thermionic fuel element sheath insulators 17 p2402 N88-24280
The effect of elevated temperature on irradiated MOS devices 17 p2406 N88-24308
An irradiation performance data base for nitride fuels 17 p2427 N88-24438
Material property and irradiation performance correlations for nitride fuels 17 p2434 N88-24483
Arcing and rf signal generation during target irradiation by a high-energy, pulsed neutral particle beam
[DE88-007169] 18 p2471 N88-24664
Behavioral response of rats exposed to high-power microwave radiation
[AD-A192199] 18 p2548 N88-25128
Self shielding of surfaces irradiated by intense energy fluxes
[DE88-007094] 18 p2579 N88-25318
Molecular characterization of structure and bonding in thin film materials
[DE88-006811] 18 p2584 N88-25351
High-speed phenomena in GaAs multiple-quantum-wells 19 p2660 N88-25812
Laser fluorescence spectroscopy of zinc neutrals originating from laser-irradiated and ion-bombarded zinc sulfide and zinc surfaces
[DE88-008037] 20 p2769 N88-26418
Fast atom bombardment study on interaction of anticodonic nucleotides and their cognate amino acid
[ISAS-RN-355] 20 p2850 N88-26918
Effects of electron beam irradiation on mechanical properties at low and high temperature of fiber reinforced composites using PEEK as matrix material
[DE88-753134] 21 p2905 N88-27239
Improved adhesion for SiO2 particles in silica substrates using helium-ion irradiation
[DE88-008915] 21 p2920 N88-27332
Assessment of cochlear damage after microwave irradiation
[AD-A193237] 21 p2987 N88-27737
Short pulse X-ray diffraction studies of shocked and annealed crystals using the JANUS research laser
[DE88-011329] 23 p3288 N88-29579
Functional assessment of laser irradiation
[AD-A195735] 24 p3408 N88-30287
IRREGULAR GALAXIES
Asymptotic giant branch populations in composite stellar systems 13 p1854 N88-21098
Infrared astronomy at extremely faint light levels in support of the LAIRTS program
[AD-A191497] 18 p2592 N88-25404
IRREGULARITIES
Numerical solution of partial differential equations on irregular grids
[DE87-014760] 03 p0369 N88-12324
Dynamics of small and large scale irregularities at sub-auroral latitudes
[AD-A189052] 12 p1645 N88-19853
Ultrasonic inspection of irregular surfaces
[AERE-R-12465] 13 p1780 N88-20848
IRREVERSIBLE PROCESSES
Two studies of nonlinear processes in irreversible thermodynamics
[DE88-005794] 13 p1849 N88-21067
Applications of some new ideas on irreversible processes to particular fluids
[AD-A191610] 19 p2683 N88-25836
Behaviour and hysteresis losses of irreversible type-2 superconducting cylindrical shell
[DE88-702708] 24 p3433 N88-30434
IRRIGATION
Stirling engines and irrigation pumping
[DE88-000020] 02 p0181 N88-11125
Use of energy emission for detecting the necessity of irrigation in wheat in field conditions
[INPE-4461-TDL/318] 16 p2229 N88-23315
Evaluation of an estimation system for an irrigated area in a tropical region through TM-LANDSAT imagery 17 p2363 N88-24075
Evaluation of SPOT imagery for monitoring irrigated lands 22 p3090 N88-28352
IRRITATION
NT TOXICITY AND SAFETY HAZARD
IRROTATIONAL FLOW
U POTENTIAL FLOW
IRS (INDIAN SPACECRAFT)
U INDIAN SPACECRAFT
ISCHEMIA
Diagnostic value of some load tests in evaluation of nonspecific electrocardiographic changes 07 p0895 N88-15426
ISEE
U INTERNATIONAL SUN EARTH EXPLORERS
ISENTROPE
Isentropic analysis and interpretation: Operational applications to synoptic and mesoscale forecast problems
[AD-A184814] 05 p0626 N88-13830
ISENTROPIC PROCESSES
An isentropic mesoscale analysis system 02 p0212 N88-11332
An isentropic coordinate model used in a mesoscale data assimilation system 02 p0212 N88-11333
A semigroup for Lagrangian 1D isentropic flow
[DE88-006464] 18 p2513 N88-24912
ISIS SATELLITES
Alouette-ISIS program summary
[NASA-CR-180747] 08 p1023 N88-16195
ISLAND ARCS
Pluton emplacement and magmatic arc construction: A model from the Patagonian batholith 24 p3393 N88-30206
An illustration of the complexity of continent formation 24 p3393 N88-30207
ISLANDS
NT ALEUTIAN ISLANDS (US)
NT GREENLAND
NT HAWAII
NT ICELAND
NT INDONESIA
NT JAPAN
NT MALDIVE ISLANDS
NT NEW ZEALAND
Coastal winds of the southeast Alaska Peninsula
[PB87-206173] 02 p0215 N88-11354
Upper mantle heterogeneity and composition of primary ocean island magmas 08 p1009 N88-16120
Zonal wind observations at Christmas Island (2 deg N, 157 deg W) during the 1986-1987 El-Nino 22 p3120 N88-28539
ISOBUTANE
U BUTANES
ISOBUTYLENE
U BUTENES
ISOCYANATES
Research in energetic compounds
[AD-A192953] 20 p2781 N88-26494
ISOLATION
NT SOCIAL ISOLATION
Human adaptation to isolated and confined environments
[NASA-CR-181502] 03 p0357 N88-12248
Analytical study of the effect of early warning on optimal shock isolation 08 p0998 N88-16047
Antarctica as a model for the human exploration of Mars
[AD-A185835] 08 p1051 N88-16342
Expanded envelope concepts for aircraft control-element failure detection and identification
[NASA-CR-181664] 16 p2160 N88-22886

Biological rhythms, sleep, and wakefulness in prolonged confinement 19 p2696 N88-26022
Selection and training of subjects to live and work in hostile and unusual environments
19 p2696 N88-26026
Selection of isolated space crews
19 p2697 N88-26028
The human element in space: Lessons from Antarctica
[AD-A193440] 21 p2988 N88-27741

ISOLATORS
NT VIBRATION ISOLATORS
Development of isostatic mounts and associated guidelines --- spacecraft payloads
[CASA-IM-WP-301] 13 p1731 N88-20354
Low-loss, high-isolation, fiber-optic isolator
[NASA-CASE-NPO-17207-1-CU]
18 p2576 N88-25304
High speed opto-isolator for radar applications
19 p2658 N88-25795

ISOMERIZATION
New polyisoimides: An approach to in situ rigid-rod polyimide formation
[AD-A191665] 18 p2490 N88-24773
Active sites and roles of solid acid base catalysts
[NASA-TT-20333] 24 p3345 N88-29909

ISOMERS
NT ISOPROPYL ALCOHOL
Development of FTMS methods for the detection of trace chemical species and development of FTMS methods for the analysis of various chemical species
[AD-A185857] 07 p0828 N88-15023
Shape isomers as candidates for the gamma ray laser storage state
[DE88-005228] 11 p1492 N88-18909
Systematics on neutron-induced isomeric cross-section ratios at 14.5 MeV
[ECN-200] 14 p1980 N88-21815
Fundamental studies of separation processes
[DE88-007487] 19 p2611 N88-25494

ISOMORPHISM
Complexity of some problems in module algebra
[PB88-165386] 15 p2122 N88-22648

ISOPARAMETRIC FINITE ELEMENTS
Finite element mesh generation and isoparametric elements
[NPL-DITC-97/87] 09 p1229 N88-17365
Mathematical stress analysis of composite materials
14 p1900 N88-21349
Distortion effects in isoparametric elements, an analytic approach
[PNR90454] 22 p3145 N88-28703
Investigation of the higher-order elements in the SAMSON2 code
[AD-A193638] 23 p3271 N88-29465

ISOPROPYL ALCOHOL
Characterization of catalysts with metal-support effects and of the species adsorbed on their surfaces
[DE87-014636] 04 p0414 N88-12564

ISOPROPYL COMPOUNDS
NT ISOPROPYL ALCOHOL

ISOPYCNIC PROCESSES
Contribution to theory of quasigeostrophic motions of finite amplitude in viscous stratified ocean
13 p1788 N88-20695

ISOSTASY
Comparisons of global topographic/isostatic models to the Earth's observed gravity field
[NASA-CR-182696] 13 p1798 N88-20752

ISOSTATIC PRESSURE
Deformation mechanisms of thermostructural materials
[AD-A184070] 03 p0338 N88-12128
Strength optimization of alpha-SiC by improved processing 17 p2324 N88-23880
Improved silicon nitride for advanced heat engines
17 p2324 N88-23881
Fabrication of reactor shields at the Y-12 plant
17 p2402 N88-24283

ISOSTERIC PROCESSES
U ISOPYCNIC PROCESSES

ISOTHERMAL FLOW
Determining Langmuir circulation parameters on basis of similarity theory 13 p1785 N88-20680
Heat transfer from a negatively buoyant wall jet
[PB88-181953] 18 p2507 N88-24873
Liquid crystals for unsteady surface shear stress visualization
[DE88-010570] 21 p2951 N88-27527

ISOTHERMAL PROCESSES
Equation of state of condensed materials physical principles and applications
[NASA-TT-20007] 08 p0968 N88-15855
Isothermal and bithermal thermomechanical fatigue behavior of a NiCoCrAlY-coated single crystal superalloy
[NASA-TM-100907] 18 p2489 N88-24766
Isothermal measurement and thermal desorption using SAW devices 19 p2671 N88-25881
The crystallization of tough thermoplastic resins in the presence of carbon fibers
[NASA-CR-182984] 20 p2776 N88-26464

ISOTOPE EFFECT
Fusion, and advanced fuel, reaction bibliography: Particle reactions from H1 to B11
[AD-A187420] 11 p1552 N88-19286
XUV source for ultra-high resolution photoionization spectroscopy
[DE88-007531] 19 p2614 N88-25510
Thermal conductivity of isotopically pure semiconductors, superlattices, semiconductor alloys and semiconductors as a function of temperature; control of the segregation coefficient in LEC crystal growth; and photo-Hall measurements of GaAs
21 p2927 N88-27375
Experimental and theoretical investigations of isotope shift and hyperfine structure on 5d elements (especially platinum, iridium and rhenium)
[ETN-88-93121] 24 p3353 N88-29957

ISOTOPE SEPARATION
A study of mechanisms of hydrogen diffusion in separation devices
[DE88-000328] 04 p0416 N88-12584
Plasma centrifuge development at INPE
[INPE-4243-PRE/1117] 08 p1087 N88-16546
Isotope separation using tuned laser and electron beam
[NASA-CASE-NPO-16907-1-CU]
18 p2483 N88-24732

ISOTOPE SHIFT
U ISOTOPE EFFECT

ISOTOPES
NT ARGON ISOTOPES
NT BORON ISOTOPES
NT BROMINE ISOTOPES
NT CALCIUM ISOTOPES
NT CARBON 12
NT CARBON 13
NT COBALT 60
NT DEUTERIUM
NT HELIUM ISOTOPES
NT HYDROGEN ISOTOPES
NT IODINE ISOTOPES
NT IRIDIUM ISOTOPES
NT IRON ISOTOPES
NT IRON 57
NT KRYPTON ISOTOPES
NT LAWRENCIUM
NT LEAD ISOTOPES
NT LITHIUM ISOTOPES
NT MAGNESIUM ISOTOPES
NT MERCURY ISOTOPES
NT NEODYMIUM ISOTOPES
NT NEPTUNIUM
NT NIOBIUM ISOTOPES
NT NITROGEN ISOTOPES
NT OXYGEN ISOTOPES
NT PLATINUM ISOTOPES
NT PLUTONIUM ISOTOPES
NT PLUTONIUM 238
NT RADIOACTIVE ISOTOPES
NT RADON ISOTOPES
NT RUBIDIUM ISOTOPES
NT SAMARIUM ISOTOPES
NT TELLURIUM
NT TRITIUM
NT URANIUM ISOTOPES
NT URANIUM 238
Electron scattering off palladium isotopes. An investigation of the equivalence of the anharmonic vibrator model and the interacting boson model
[B8671274] 07 p0931 N88-15654
Heterogeneous isotope exchange between solid cesium iodide and gaseous methyl iodide
[ETN-88-91085] 09 p1141 N88-16840
Analysis of gases in the earth's crust
[PB88-141619] 10 p1354 N88-18093
Isotopic and chemical studies of early crustal metasedimentary rocks
[NASA-CR-182711] 14 p1944 N88-21601
The dynamic isotope power system: Technology status and demonstration program 17 p2422 N88-24400
Characteristics of the closed Brayton cycle for dynamic isotope power systems 17 p2422 N88-24401
Dynamic isotope power system critical component verification 17 p2425 N88-24421
SNAP-DYN: Proven technology for wear-term, higher power in space 17 p2425 N88-24422
The application of high-rate biaxial testing to the design of containment vessels for radioisotope heat sources
17 p2426 N88-24428
High-fidelity in isotope ratio measurements for resonance ionization mass spectrometry
[DE88-009129] 19 p2613 N88-25506
Lithospheric evolution of the Northern Arabian Shield: Chemical and isotopic evidence from basalts, xenoliths and granites 24 p3399 N88-30242
The growth of the continental crust: Constraints from radiogenic isotope geochemistry
24 p3399 N88-30245
Noble gases, C,N, and Si isotopes in interstellar SiC form the Murchison carbonaceous chondrite
24 p3442 N88-30483

ISOTOPIC ENRICHMENT
New nuclear structure calculations and the astrophysical r-process
[DE88-000979] 08 p1082 N88-16518
Vacuum-arc plasma centrifuge experiment
[INPE-4509-PRE/1263] 15 p2138 N88-22758

ISOTOPIC LABELING
The effect of wind and currents on gas exchange in an estuarine system
[NASA-CR-181424] 01 p0073 N88-10468
Applications and limitations of deuterium labeling methods to neutron scattering studies of polymers
[DE87-012936] 02 p0151 N88-10945
Isotope methods of determining distribution and movement of blood in the body
10 p1362 N88-18138
Method for the isotopically selective detection of inert gases
[DE88-008370] 20 p2769 N88-26421
The timing and mechanism of depletion in Lewisian granulites 24 p3394 N88-30209
Genesis of archean granitoids in the Pilbara block and implications for crustal growth 24 p3394 N88-30210
Decoupled Rb-Sr and Sm-Nd isotopic evolution of the continental crust 24 p3395 N88-30216
The early archaean crustal history of West Greenland as recorded by detrital zircons 24 p3395 N88-30221

ISOTOPIC SPIN
Few body hypernuclear systems: Weak decays
[DE87-014920] 04 p0488 N88-13010
Double beta decay and nuclear structure
[DE88-001966] 07 p0931 N88-15652

ISOTROPIC MEDIA
Existence of absolutely closed universe
08 p1080 N88-16503
Ultrasonic beam distortion in transversely isotropic media
[DE88-005937] 15 p2129 N88-22699
Acousto-ultrasonic input-output characterization of unidirectional fiber composite plate by SV waves
[NASA-CR-4152] 16 p2217 N88-23224
Wave propagation in locally isotropic turbulent medium with smoothly changing characteristics
[NASA-TT-20312] 20 p2800 N88-26617
A transversely isotropic thermoelastic theory
[NASA-TM-101302] 22 p3087 N88-28332
Constitutive modeling for isotropic materials
[NASA-CR-182132] 24 p3327 N88-29811

ISOTROPIC TURBULENCE
The generation of nearly isotropic turbulence by means of grids
[PNR90411] 02 p0172 N88-11084
Center for Turbulence Research 1987 activities
[NASA-CR-182693] 13 p1769 N88-20583
EDQNM closure: A homogeneous simulation to support it. A quasi-homogeneous simulation to disprove it
16 p2195 N88-23091
Angular distribution of turbulence in wave space
16 p2195 N88-23093
Big whorls carry little whorls 16 p2195 N88-23094
Analysis of non-premixed turbulent reacting flows
16 p2196 N88-23100
The decay of isotropic turbulence in a rapidly rotating frame 16 p2197 N88-23107
Wave propagation in locally isotropic turbulent medium with smoothly changing characteristics
[NASA-TT-20312] 20 p2800 N88-26617

ISOTROPISM
Equilibrium shocks in plane deformations of incompressible elastic materials
[AD-A188696] 12 p1636 N88-19796
Wave curves for simple isotropic elastic solids
[AD-A188865] 12 p1636 N88-19798
The two isotropic asymptotes of fiber composites
[AD-A192305] 21 p2904 N88-27231

ISOTROPY
NT ISOTROPIC MEDIA
Low cycle fatigue on isotropic fine-grained graphite
[DE87-702627] 01 p0028 N88-10177
Effect of low velocity impact on compression strength of a quasi-isotropic laminate
[FFA-TN-1987-38] 09 p1138 N88-16822
Wave curves for simple isotropic elastic solids
[AD-A188865] 12 p1636 N88-19798

Changes in seismic velocity and apparent attenuation due to isotropic and anisotropic scattering: Results from physical modeling 19 p2691 N88-25997

Failure analysis of quasi-isotropic composite laminates with free edges under off-axis loading
22 p3049 N88-28092

ISRAEL

Design of the Sandia-Israel 20-kW reflux heat-pipe solar receiver/reactor
[DE88-001312] 13 p1794 N88-20729

ITALY

Italian activities in ocean colour remote sensing
08 p1043 N88-16304

The 1985 Meteorological Yearbook of Ispra (27th)
[PB88-125729] 20 p2828 N88-26777

Utilization of a satellite communication system to protect the national communication network
[FUB-33-1986] 21 p2934 N88-27423

SPOT for earthquake hazard zoning in southern Italy
22 p3093 N88-28365

ITERATION

NT CONJUGATE GRADIENT METHOD
NT ITERATIVE SOLUTION
NT NEWTON METHODS

An exponential example for Terlaky's pivoting rule for the criss-cross simplex method
[REPT-87-18] 01 p0080 N88-10512

Nonlinear parametric least-squares adjustment
[AD-A184039] 03 p0371 N88-12336

A new method to real-normalize measured complex modes 05 p0593 N88-13618

Near-horn prolog
[AD-A185172] 05 p0634 N88-13880

Research and development of finite elements and iterative algorithms for elliptic partial differential equations
[DE88-001381] 05 p0643 N88-13934

Freidlin-Wentzell type estimates and the law of the iterated logarithm for a class of stochastic processes related to symmetric statistics
[AD-A185366] 05 p0644 N88-13944

Spectral- and spatial-domain filtering and sampling approach to the numerical solution of electromagnetic scattering problems
[PB88-106711] 06 p0694 N88-14261

Study of extended least-square iterative techniques in electromagnetic scattering by penetrable objects
[PB88-105879] 06 p0694 N88-14262

Computing block-angular Karmarker projections with applications to stochastic programming, revision
[AD-A185647] 06 p0759 N88-14656

A multicut algorithm for two-stage stochastic linear programs
[AD-A186148] 07 p0903 N88-15466

A Schur-complement method for sparse quadratic programming
[DE88-002520] 07 p0904 N88-15479

An O(n3L) interior point algorithm for convex quadratic programming
[AD-A186001] 07 p0909 N88-15504

Remark on the multiple Wiener integral
[AD-A186015] 07 p0913 N88-15541

The iterative radiance model of the Meteorological Institute of the University of Munich (West Germany)
08 p1019 N88-16178

Iterative-deepening heuristic search for optimal and semi-optimal resource allocation
08 p1062 N88-16410

Method of iterative coupling between periodic aerodynamic and dynamic fields
[PB87-169934] 09 p1113 N88-16669

Theory of elementary particle studies in weak iteration and grand unification and studies in accelerator design
[DE88-004261] 11 p1545 N88-19238

An improved data reduction procedure for accelerometer centrifuge data 12 p1577 N88-19436

Statistical signal processing using a class of iterative estimation algorithms
[AD-A189050] 13 p1757 N88-20511

Nonlinear differential equations
[DE88-006047] 13 p1828 N88-20933

Iteration of transformation passes over attributed program trees --- compilers
[INF-87-28] 14 p1956 N88-21661

Application of Moment Iteration Method (MIM) to electromagnetic field computation
[PB88-194139] 20 p2789 N88-26546

SARLAC: A relativistic electron beam code
[AD-A193134] 21 p2932 N88-27411

KRYSI, an ODE solver combining a semi-implicit Runge-Kutta method and a preconditioned Krylov method
[DE88-012245] 21 p3008 N88-27841

ITERATIVE NETWORKS

Contribution to optimal flow in networks. A experimental multiprocessor for asynchronous iteration implementation
[LAAS-87-269] 05 p0576 N88-13510

Investigation and implementation of an algorithm for computing optimal search paths
[AD-A185927] 07 p0902 N88-15461

ITERATIVE SOLUTION

Exact solution of the inverse problem for a six-link manipulator with a mechanical offset
[DE87-702646] 01 p0054 N88-10349

S-step iterative methods for symmetric linear systems
[DE87-010819] 01 p0086 N88-10559

Preconditioned iterative methods applied to singularly perturbed elliptic boundary value problems: Volume 2
[DE87-014337] 02 p0225 N88-11415

Parallel methods for ordinary differential equations
[DE87-014667] 02 p0226 N88-11425

Iterative solution of a nonlinear system arising in phase change problems
[DE87-014672] 02 p0226 N88-11426

Efficient numerical approaches for predicting supersonic flows with viscous/inviscid interaction
03 p0260 N88-11637

Three-dimensional finite element based, interative approach for analysis of laminated composites
03 p0280 N88-11763

Steady waves in a nonlinear theory of viscoelasticity
[AD-A185548] 06 p0723 N88-14448

Solution of non-symmetric linear systems by biconjugate gradients or conjugate gradients squared
[PB87-226387] 06 p0763 N88-14679

On the parabolized Navier-Stokes equations without sublayer assumptions
[AD-A186127] 07 p0849 N88-15152

The k-grid Fourier analysis of multigrid-type iterative methods
[AD-A186315] 07 p0910 N88-15520

Investigation of iterative and spectral Galerkin techniques for solving electromagnetic boundary value problems 09 p1155 N88-16925

Improving the stability of predictor-corrector methods by residue smoothing
[CWI-NM-R8707] 09 p1228 N88-17359

Solution of the hyperbolic Kepler's equation
[RAE-TR-87042] 09 p1229 N88-17368

Preconditioned iterative methods for partial differential equations
[DE88-003071] 09 p1230 N88-17372

Optimal application of Morrison's iterative noise removal for deconvolution. Appendices
[NASA-CR-182477] 09 p1231 N88-17376

Centerplane source distribution for slender bodies
10 p1328 N88-17940

Quasigroup approach to solution of linear algebraic equation systems
[DE88-700595] 10 p1398 N88-18330

Leapfrog variants of iterative methods for linear algebra equations
[NASA-CR-181616] 10 p1398 N88-18332

Conjugate gradient spectral iterative technique
[PB88-126917] 10 p1398 N88-18337

Spectral iterative technique with Gram-Schmidt orthoganalization
[PB88-127451] 10 p1399 N88-18338

The application of the hybrid iterative method to scattering by perfectly conducting bodies of revolution
11 p1475 N88-18802

Further refinement and applications of the mixed computational algorithm for plane elastic contact problems
[AD-A188308] 12 p1663 N88-20065

Data traffic reduction schemes for sparse Cholesky factorizations
[NASA-CR-181626] 13 p1813 N88-20831

Inversion algorithms for geophysical problems
[AD-A189252] 13 p1815 N88-20845

A constitutive material model for nonlinear finite element structural analysis using an iterative matrix approach
14 p1932 N88-21521

Assimilation of meteorological observations
14 p1936 N88-21544

Contraction design for small low-speed wind tunnels
[NASA-CR-182747] 15 p2021 N88-22045

Smoothing technique to resolve X-ray spectra in laser nuclear fusion 15 p2053 N88-22235

Relative orientation
[AD-A190385] 15 p2089 N88-22449

Trust regions and projected gradients
[DE88-005829] 15 p2122 N88-22646

Efficiency of some computational techniques for electromagnetic scattering problems
[PB88-148895] 16 p2187 N88-23043

Iterative finite element solver on transputer networks
16 p2218 N88-23235

Vectorization of the odd-even hopscotch scheme and the alternating direction implicit scheme for the two-dimensional Burgers' equations
[CWI-NM-R8720] 16 p2249 N88-23440

Parallelization of Gauss-Seidel algorithms as an example of parallel iterative equation solving
[REPT-87-76] 16 p2254 N88-23471

Residual smoothing for accelerating the Alternating Direction Implicit (ADI) iteration method for elliptic difference equations
[CWI-NM-R8721] 16 p2259 N88-23500

A practical termination criterion for the conjugate gradient method
[REPT-87-62] 16 p2259 N88-23506

Algorithm for accounting the conditions in infinity for two-dimensional magnetostatics problems
[DE88-701673] 16 p2264 N88-23541

Electromagnetic scattering from nonlinear anisotropic cylinders 17 p2333 N88-23930

Fitting a circle to radially suppressed data
[NPL-DITC-103/87] 17 p2392 N88-24223

Adaptive local grid refinement in computational fluid mechanics
[AD-A192215] 18 p2510 N88-24890

Two domain decomposition techniques for Stokes problems
[DE88-008724] 19 p2720 N88-26149

Distributive iteration for indefinite systems as smoothing method in multigrid process on example of Stokes and Navier-Stokes equations with emphasis on incomplete decompositions
[ETN-88-92127] 21 p2948 N88-27509

Grid generation around transport aircraft configurations using a multi-block structured computational domain
23 p3247 N88-29325

Convergence acceleration for vector sequences and applications to computational fluid dynamics
[NASA-TM-101327] 24 p3424 N88-30377

IUE

Active phases on II Peg 04 p0507 N88-13119

The onset of chromospheric activity among the A- and F- type stars 04 p0511 N88-13144

IUE/Optical/VLA flares on AD Leo
04 p0512 N88-13152

A flash spectrum of Cl I, C I, N I, and Ni II absorption in 31 Cygni: A direct observation of the reversing layer
04 p0513 N88-13158

Hydrogen and deuterium in the local interstellar medium 04 p0521 N88-13204

IUE evidence on the nature of the innermost broad-line region in Seyfert 1 galaxies 17 p2450 N88-24552

International ultraviolet explorer observatory operations
[NASA-CR-180775] 22 p3145 N88-28708

International ultraviolet explorer spectral atlas of planetary nebulae, central stars, and related objects
[NASA-RP-1203] 22 p3164 N88-28843

Beyond the visible: A decade of observations with the International Ultraviolet Explorer (IUE)
[ESA-F09] 24 p3331 N88-29828

IUS

U INERTIAL UPPER STAGE

IZSAK ELLIPSOID

U ELLIPSOIDS
U GEODESY

J

J INTEGRAL

Determination of the critical crack length a (sub IC) in turbine discs
[PB87-144812] 07 p0820 N88-14986

J-estimation procedure based on moire interferometry data
[AD-A185965] 07 p0867 N88-15258

The J-integral concept for elastic-plastic material behavior
[W-5/87] 08 p1000 N88-16059

Fracture mechanics and creep crack growth of 1 percent Cr 1/2 percent Mo steel with and without prior exposure to creep conditions
[NLR-TR-86051-U] 13 p1743 N88-20426

The Nordic J-R curve round robin test program --- reactor steel
[VTT-RR-510] 14 p1923 N88-21459

A simplified key-curve approach for J-R-curve testing of CT specimens
[VTT-RR-503] 15 p2088 N88-22444

Method and models for R-curve instability calculations
[NASA-TM-100935] 16 p2224 N88-23278

Analysis and developments of failure concepts in fracture mechanics based on research results in the field of component safety topics: J-integral concept; crack resistance curves; dynamic criterion
[V-19/86] 18 p2530 N88-25009

Experimental investigation of ductile fracture by white light moire interferometry 22 p3087 N88-28329
J-integral measurement using moire interferometry
[AD-A193751] 23 p3226 N88-29202

J-57 ENGINE
Operation of gas turbine engines in dust-laden environments 10 p1280 N88-17654

JACKS (ELECTRICAL)
U ELECTRIC CONNECTORS

JACOBI MATRIX METHOD
Analysis of smoothing matrices for the preconditioning of elliptic difference equations
[CWI-NM-R8705] 09 p1228 N88-17357
Problems in fluid dynamics
[NASA-CR-182678] 14 p1909 N88-21410

JACOBI POLYNOMIALS
U HYPERGEOMETRIC FUNCTIONS

JAMMING
Monitoring of harmful interference to the HF (High Frequency) broadcasting service. 3: Results of the June 1986 coordinated monitoring period
[PB87-210274] 01 p0036 N88-10229
Radar ECCM's new area: Anti-STEALTH and anti-ARM 03 p0299 N88-11881
Performance analysis of coded frequency-hopped spread-spectrum systems with unknown interference
[AD-A186069] 07 p0841 N88-15103
Adaptive spread spectrum networks
[AD-A187154] 09 p1152 N88-16900
Static and dynamic jamming of networks
[AD-A188921] 12 p1620 N88-19690
Visual recognition training: Effectiveness of computer graphics
[AD-A188302] 12 p1669 N88-19997
Distortions in processed signals and their application in electronic design. Part 3: An automated generator of communication jamming signals
[DE88-702733] 23 p3205 N88-29072
MIDIR (Mid-Infrared) laser, phase 1
[AD-A193935] 23 p3220 N88-29166

JAPAN
Japanese industrial research on lean combustion: A case study: International Research Monitoring Program
[DE87-013839] 02 p0144 N88-10904
JPRS report: Science and technology. Japan
[JPRS-JST-87-025] 04 p0403 N88-12502
Impressions, observations and comments on science and technology in Japan
[PB87-235743] 06 p0799 N88-14893
North Pacific Ocean. Northwest Pacific Transition Zone, R/V Thomas G. Thompson: 19 March - 1 May 1971. STD data report
[AD-A186568] 08 p1044 N88-16313
NASDA's new test facilities for satellites and rockets
11 p1499 N88-18951
Proceedings of US-Japan Heliotron-Stellarator Workshop, volume 3
[DE88-004788] 11 p1554 N88-19299
Proceedings of US-Japan Heliotron-Stellarator Workshop, volume 2
[DE88-004789] 11 p1554 N88-19300
Directory of Japanese technical resources, 1987
[PB87-205258] 12 p1706 N88-20212
Sunshine project for FY 1987 outlined
16 p2184 N88-23021
Survey on utility technology of a tidal and ocean current energy
[DE88-770148] 20 p2819 N88-26722

JAPANESE SPACE PROGRAM
Space missions to Comets Halley and Giacobini-Zinner 03 p0272 N88-11712
An overview of the current Earth observation programs (Europe, USA, and Japan) 09 p1129 N88-16778
Space utilization plans 15 p2051 N88-22219
Space experiment plan FMPT
15 p2051 N88-22220
Japanese space station module
15 p2052 N88-22224
High speed and high angle of attack wind tunnel test results of the winged space vehicle C-2
[ISAS-RN-623] 20 p2751 N88-26329

JAPANESE SPACECRAFT
Comparison of MHD simulation for the February 1986 events with interplanetary observations by the spacecraft Sakigake 01 p0113 N88-10722
Investigation of European remote sensing user needs in accessing MOS-1 payload
[ESA-CR(P)-2535] 14 p1940 N88-21580
Halley's environments by the Japanese Suisei spacecraft 14 p1999 N88-21915

JARRING
U MECHANICAL SHOCK

JC-130 AIRCRAFT
U C-130 AIRCRAFT

JEEPS
U AUTOMOBILES

JET AIRCRAFT
NT A-300 AIRCRAFT
NT A-320 AIRCRAFT
NT B-57 AIRCRAFT
NT B-70 AIRCRAFT
NT BOEING 737 AIRCRAFT
NT BOEING 747 AIRCRAFT
NT C-130 AIRCRAFT
NT C-135 AIRCRAFT
NT CONCORDE AIRCRAFT
NT DC 9 AIRCRAFT
NT EUROPEAN AIRBUS
NT F-4 AIRCRAFT
NT F-14 AIRCRAFT
NT F-15 AIRCRAFT
NT F-16 AIRCRAFT
NT F-18 AIRCRAFT
NT F-27 AIRCRAFT
NT F-106 AIRCRAFT
NT F-111 AIRCRAFT
NT MIRAGE AIRCRAFT
NT OV-1 AIRCRAFT
NT P-3 AIRCRAFT
NT T-33 AIRCRAFT
NT TURBOFAN AIRCRAFT
NT TURBOPROP AIRCRAFT
NT U-2 AIRCRAFT
NT VC-10 AIRCRAFT
Effect of empennage arrangement on single-engine nozzle/afterbody static pressures at transonic speeds
[NASA-TP-2753] 02 p0122 N88-10771
Soviet aviation technology's state of the art SU-27 fighter
[AD-A184121] 03 p0259 N88-11628
Improvements to the adaptive maneuvering logic program
[NASA-CR-3985] 03 p0262 N88-11648
Aircraft engine exhaust plume dynamics
[AD-A184238] 04 p0400 N88-12488
Computation of nacelle interference using boundary element method 05 p0537 N88-13267
AFRAPT (Air Force Research in Aero Propulsion Technology) trainee program
[AD-A190525] 15 p2035 N88-22123
Pilot report: AFTI (Advanced Fighter Technology Integration) F-111
[AD-A192937] 21 p2895 N88-27184
Integration of LANTIRN (Low Altitude Navigation and Targeting Infrared for Night) into operational fighter training
[AD-A194906] 24 p3325 N88-29799

JET AIRCRAFT NOISE
Shock structure and noise of supersonic jets in simulated flight to Mach 0.4
[NASA-TP-2785] 08 p1080 N88-16510
Annoyance caused by advanced turboprop aircraft flyover noise: Single-rotating propeller configuration
[NASA-TP-2782] 09 p1242 N88-17441
Noise levels from a jet-engined aircraft measured at ground level and at 1.2 m above the ground
[NPL-AC-114] 23 p3279 N88-29524

JET AIRSTREAMS
U JET STREAMS (METEOROLOGY)

JET AUGMENTED WING FLAPS
U JET FLAPS
U WING FLAPS

JET CONTROL
Active control of jet flowfields
[AD-A186736] 08 p0989 N88-15989
Research on flow control
[AD-A189014] 12 p1627 N88-19736
Aerodynamic possibilities for the realization of trajectory corrections
[ISL-CO-251/86] 14 p1862 N88-21120
Experimental investigation of two-dimensional confined jet thrust vector control
[AD-A189845] 15 p2027 N88-22077
Variable Mach number wall jets for control/propulsion on hypervelocity projectiles/interceptors: Tests with an existing model
[AD-A192845] 21 p2892 N88-27167

JET DAMPING
U DAMPING
U SPIN REDUCTION

JET DRIVE
U JET PROPULSION

JET ENGINE FUELS
NT JP-4 JET FUEL
NT JP-5 JET FUEL
NT JP-8 JET FUEL
Study of electrostatic modulation of fuel sprays to enhance combustion performance in an aviation gas turbine
[AD-A184967] 05 p0548 N88-13341
An experimental investigation of the ignition and flammability limits of various hydrocarbon fuels in a two-dimensional solid fuel ramjet
[AD-A184968] 05 p0549 N88-13342
Production of jet fuels from coal derived liquids. Volume 1: Market assessment for liquid by-products from the Great Plains gasification plant
[AD-A184846] 05 p0570 N88-13475
Aviation turbine fuels from tar sands bitumen and heavy oils. Part 2: Laboratory sample production
[AD-A185744] 06 p0687 N88-14211
Military jet fuels, 1944-1987
[AD-A186752] 09 p1150 N88-16890
High-density jet fuels from coal syncrudes, appendix 4
[DE88-003132] 10 p1307 N88-17813
Degradation of jet and missile fuels by aquatic microbial communities
[AD-A188065] 11 p1485 N88-18737
Flammability characteristics of distillate fuels
[AD-A188497] 12 p1612 N88-19642
Availability and cost estimate of a high naphthene, modified aviation turbine fuel
[NASA-TM-100823] 13 p1749 N88-20455
Aviation turbine fuels from tar sands bitumen and heavy oils. Part 3: Laboratory sample production
[AD-A189278] 13 p1753 N88-20484
Turbine fuels from tar sands bitumen and heavy oil. Volume 2, phase 3: Process design specifications for a turbine fuel refinery charging San Ardo heavy crude oil
[AD-A190120] 16 p2183 N88-23011
Development of a laboratory test for multiport fuel injector deposits - evaluation of the Jet Fuel Thermal Oxidation Test apparatus (JFTOT)
[AD-A191313] 16 p2183 N88-23015
Selective detection in gas chromatography
[AD-A191499] 18 p2481 N88-24718
Reference filters for electrostatic charging tendency measurements of fuels
[AD-A191717] 18 p2495 N88-24803
Feasibility of producing jet fuel from GPGP (Great Plains Gasification Plant) by-products
[DE88-010233] 20 p2781 N88-26492
Biodegradation of JP-5 aviation fuel by subsurface microbial communities
[AD-A192743] 20 p2781 N88-26493
A study relating to the fog oil replacement program
[AD-A192536] 21 p2923 N88-27347
Development of a test method to determine potential peroxide content in turbine fuels. Part 2
[AD-A192244] 23 p3199 N88-29042
Fuel property effects on the US Navy's TF30 engine
24 p3345 N88-29911
Determination of the hydroperoxide potential of jet fuels
[AD-A195975] 24 p3357 N88-29991

JET ENGINES
NT CONVERTIBLE FAN-SHAFT ENGINES
NT J-57 ENGINE
NT RAMJET ENGINES
NT SUPERSONIC COMBUSTION RAMJET ENGINES
NT TF-30 ENGINE
NT TURBOFAN ENGINES
NT TURBOJET ENGINES
NT TURBOPROP ENGINES
First article test noise survey of the A/F32T-9 large turbo fan engine enclosed noise suppressor system, Sky Harbor IAP (International Airport), Phoenix, Arizona
[AD-A183799] 01 p0090 N88-10588
Effect of empennage arrangement on single-engine nozzle/afterbody static pressures at transonic speeds
[NASA-TP-2753] 02 p0122 N88-10771
The use of Kevlar on aero-engine fan containment casings
[PNR90410] 02 p0182 N88-11134
Qualitative and temporal reasoning in engine behavior analysis 08 p1058 N88-16383
Optimisation of military compressors for weight and volume 10 p1279 N88-17649
An examination of the impact of potential advances in component technology for future military engines
10 p1279 N88-17650
Specification of an engine and its components starting from a consideration of aircraft missions
10 p1279 N88-17651
Application of highly loaded single-stage mixed-flow compressors in small jet-engines
10 p1280 N88-17652
Aerodynamic performance of a scale-model, counter-rotating unducted fan 10 p1282 N88-17666
Design and development of an advanced F100 compressor 10 p1283 N88-17678
Noise assessment of unsuppressed TF-34-GE-100A engine at Warfield ANG, Baltimore, Maryland
[AD-A189966] 15 p2129 N88-22702

Engine component retirement for cause. Volume 1: Executive summary
[AD-A192730] 20 p2760 N88-26371
A fundamental understanding of the interfacial compatibility in hybrid material systems
[AD-A192921] 21 p2909 N88-27264
An investigation of constitutive models for predicting viscoplastic response during cyclic loading
[AD-A194875] 24 p3385 N88-30163

JET EXHAUST
Optical sizing of soot in gas turbine combustors and exhaust augmentor tubes
[AD-A183785] 01 p0006 N88-10034
Aircraft engine exhaust plume dynamics
[AD-A184238] 04 p0400 N88-12488
Influence of base modifications on in-flight base drag in the presence of jet exhaust for Mach numbers from 0.7 to 1.5
[NASA-TP-2802] 11 p1488 N88-18881
Fully-coupled analysis of jet mixing problems. Three-dimensional PNS model, SCIP3D
[NASA-CR-4139] 13 p1715 N88-20256
Techniques utilized in the simulated altitude testing of a 2D-CD vectoring and reversing nozzle
[NASA-TM-100872] 19 p2604 N88-25464

JET FLAMES
U FLAMES
U JET FLOW

JET FLAPS
Investigations of aircraft control with jet spoilers
[ISL-R-112/87] 21 p2898 N88-27202

JET FLIGHT
U JET AIRCRAFT

JET FLOW
NT AIR JETS
NT SUPERSONIC JET FLOW
Experimental and theoretical studies of vertical annular liquid jets
[DE87-013907] 01 p0047 N88-10299
Flow and heat transfer with impinging jets and rough surfaces
[DE87-014162] 02 p0169 N88-11065
A calculation method for the propulsive jet and its aerodynamic interaction with an afterbody
[ESA-TT-1039] 03 p0259 N88-11632
On the instability of thin circular shear layers
04 p0395 N88-12467
Comparative studies in the near-field of turbulent transports of heated and unheated jets normal to a cross stream 04 p0444 N88-12756
Mesoscale eddy dynamics by the method of point vortices 04 p0463 N88-12863
Combustion related shear-flow dynamics in elliptic supersonic jets 05 p0531 N88-13232
Jet initiation of PBX 9502
[DE88-000493] 05 p0571 N88-13481
Trajectory control using laterally ejected jets. Literature review
[ISL-R-117/85] 05 p0581 N88-13544
Raman spectra of adsorbed layers on space shuttle and AOTV thermal protection system surface
06 p0799 N88-14890
Experimental study of secondary flow in the presence of two jet arrays on the wall of a turbine blade
[ECL-87-11] 08 p0987 N88-15981
On the correlation of plume centerline velocity decay of turbulent acoustically excited jets
[NASA-TM-100193] 09 p1114 N88-16681
Wind tunnel studies of circulation control elliptical airfoils 10 p1270 N88-17598
Investigation of non-symmetric jets in cross flow
10 p1327 N88-17932
Droplet formation for liquid monopropellant jets
[AD-A187172] 10 p1331 N88-17956
Numerical simulations of the California current: Filament formation as related to baroclinic instability
[AD-A187573] 10 p1358 N88-18115
A hydrodynamic analysis of fluid flow between meshing spur gear teeth
[AD-A187671] 11 p1482 N88-18844
Studies on homogeneous and heterogeneous reactive flows 11 p1484 N88-18861
Reynold stress closure in jet flows using wave models
[NASA-CR-182662] 12 p1628 N88-19741
Mushroom-shaped currents (eddy dipoles) under rotation and stratification conditions
13 p1784 N88-20678
Interaction of a two-dimensional bluff body and incompressible jet and annulus flows
[AD-A190503] 15 p2064 N88-22310
The structure of sonic underexpanded turbulent air jets in still air
[AD-A190856] 16 p2157 N88-22870
Numerical analysis of critical penetration velocity for jet perpendicular penetration 16 p2186 N88-23037
Initial condition effect on pressure waves in an axisymmetric jet
[NASA-TM-100915] 16 p2209 N88-23184
Acoustically excited heated jets. 1: Internal excitation
[NASA-CR-4129-PT-1] 17 p2298 N88-23751
Acoustically excited heated jets. 2: In search of a better understanding
[NASA-CR-4129-PT-2] 17 p2299 N88-23752
Heat transfer from a negatively buoyant wall jet
[PB88-181953] 18 p2507 N88-24873
Hydroacoustic pulsating jet generator
[MPIS-7/1987] 18 p2510 N88-24891
Numerical solutions of the complete Navier-Stokes equations
[NASA-CR-183023] 18 p2514 N88-24914
Aerodynamic focusing of particles and heavy molecules
[DE88-007145] 19 p2598 N88-25440
Numerical simulations of astrophysical jets
19 p2636 N88-25635
Three-dimensional viscous flow computations of a circular jet in subsonic and supersonic cross flow
[NASA-CR-182153] 20 p2800 N88-26616
A computational analysis of under-expanded jets in the hypersonic regime
[NASA-TM-101319] 21 p2893 N88-27174
Coupled experimental and theoretical investigations of instability, chaos and turbulence in an axisymmetric jet flow
[AD-A192943] 21 p2942 N88-27476
Turbulence structure of mixing swirling flows
[AD-A193063] 21 p2943 N88-27478
A numerical study of turbulent plane jets in still and flowing environments employing two-equation k-epsilon model 23 p3211 N88-29109
The influence of delay effects on the decay of liquid jets
[MPIS-14/1987] 23 p3214 N88-29130
Modelling of CO oxidation in dilution jet flows
24 p3351 N88-29947

JET FUELS
U JET ENGINE FUELS

JET IMPINGEMENT
Flow and heat transfer with impinging jets and rough surfaces
[DE87-014162] 02 p0169 N88-11065
Jet impingement heat transfer: A literature study
[PNR90404] 02 p0172 N88-11083
Heat transfer from impinging flame jets
[ETN-88-91610] 09 p1162 N88-16964

JET LAG
Pharmacological resetting of the Circadian sleep-wake cycle
[AD-A186194] 07 p0889 N88-15385
Desynchronization of heart rate and breathing frequency after transmeridional flight across three time zones
12 p1663 N88-19968

JET LIFT
A jet in a crossflow
[NASA-CR-182469] 09 p1113 N88-16674
Numerical study of delta wing leading edge blowing
[NASA-CR-183101] 20 p2752 N88-26335

JET MIXING FLOW
Dilution jet mixing program, phase 3
02 p0185 N88-11153
On the mixing of a row of jets with a confined crossflow 02 p0185 N88-11154
A numerical study of the effects of curvature and convergence on dilution jet mixing
[NASA-TM-89878] 05 p0549 N88-13347
Chemical reactions in turbulent mixing flows
[AD-A186141] 07 p0849 N88-15153
Fully-coupled analysis of jet mixing problems. Three-dimensional PNS model, SCIP3D
[NASA-CR-4139] 13 p1715 N88-20256
Control of structure in turbulent flows: Bifurcating and blooming jets
[AD-A189607] 13 p1766 N88-20562
Chemically reacting turbulent flow
[AD-A190522] 15 p2065 N88-22311
Saturation and the limit of jet mixing enhancement by single frequency plane wave excitation: Experiment and theory
[NASA-TM-100882] 17 p2295 N88-23732
Acoustically excited heated jets. 1: Internal excitation
[NASA-CR-4129-PT-1] 17 p2298 N88-23751
Acoustically excited heated jets. 2: In search of a better understanding
[NASA-CR-4129-PT-2] 17 p2299 N88-23752
Acoustically excited heated jets. 3: Mean flow data
[NASA-CR-4129-PT-3] 17 p2299 N88-23753
Effect of initial tangential velocity distribution on the mean evolution of a swirling turbulent free jet
[NASA-TM-100934] 18 p2458 N88-24592
An empirical model of the effects of curvature and convergence on dilution jet mixing
[NASA-TM-100896] 18 p2466 N88-24840
Numerical simulation of ignition of hydrogen jet in hot air 19 p2637 N88-25647
Three-dimensional vortex interactions
[AD-A194066] 23 p3172 N88-28889
Small scale mixing in the initial region of a jet
[AD-A193500] 23 p3192 N88-28994

JET NOISE
U JET AIRCRAFT NOISE

JET NOZZLES
Design of supersonic Coanda jet nozzles
10 p1270 N88-17590

JET PILOTS
U AIRCRAFT PILOTS

JET PROPULSION
A calculation method for the propulsive jet and its aerodynamic interaction with an afterbody
[ESA-TT-1039] 03 p0259 N88-11632
Rocket and airjet propulsion for ballistic and aerodynamic space probes
[REPT-TR-527] 10 p1310 N88-17826
Pressure distributions and losses in a waterjet propulsion system
[AD-A188423] 12 p1633 N88-19777
Variable Mach number wall jets for control/propulsion on hypervelocity projectiles/interceptors: Tests with an existing model
[AD-A192845] 21 p2892 N88-27167

JET STREAMS (METEOROLOGY)
Ozone, jet streaks and severe weather
05 p0616 N88-13781
Northern winter circulations for the period 1974-1983
[AD-A187779] 11 p1511 N88-19028

JET THRUST
Aircraft engine exhaust plume dynamics
[AD-A184238] 04 p0400 N88-12488
Pressure measurements of impinging jet with asymmetric nozzle
[NASA-CR-182759] 15 p2014 N88-22011
Experimental investigation of two-dimensional confined jet thrust vector control
[AD-A189845] 15 p2027 N88-22077

JET VANES
Effects of the installation and operation of jet-exhaust yaw vanes on the longitudinal and lateral-directional characteristics of the F-14 airplane
[NASA-TP-2769] 04 p0393 N88-12455
Heat transfer modeling of jet vane Thrust Vector Control (TVC) systems
[AD-A190106] 15 p2019 N88-22034
TVC (Thrust Vector Control) jet vane thermal modeling using parametric system identification
[AD-A191518] 18 p2474 N88-24678

JETAVATORS
U GUIDE VANES

JETS
Jet formation and characterization of a conical shaped charge
[DE87-012102] 02 p0155 N88-10969

JETTIES
U BREAKWATERS

JFET
Advanced components for spaceborne infrared astronomy
[NASA-CR-177470] 13 p1772 N88-20601
JFET/SOS (Junction Field-Effect Transistor/Silicon-on-Sapphire) devices: Gamma-radiation-induced effects
[AD-A193001] 20 p2795 N88-26586

JIMSPHERE BALLOONS
Analysis of the bivariate parameter wind differences between Jimsphere and Windsonde
[NASA-TM-4014] 01 p0072 N88-10461

JITTER
U VIBRATION

JOBS
U TASKS

JOINING
Optically interconnected phased arrays
[NASA-TM-100855] 14 p1908 N88-21400

JOINT EUROPEAN TORUS
Comparison of high purity fine grain graphites from different suppliers with regard to physical, mechanical, and thermal properties --- Joint European Torus wall protection
[JUEL-SPEZ-401] 02 p0154 N88-10963
A three-barrel repeating pneumatic pellet injector for plasma fueling of the Joint European Torus
[DE88-000330] 04 p0491 N88-13026
The JET (Joint European Torus) multipellet launcher and fueling of JET plasmas by multipellet injection
[DE88-008367] 19 p2729 N88-26206

JOINTS (ANATOMY)
NT WRIST

Joint angle sensors for closed-loop control
19 p2673 N88-25891

JOINTS (JUNCTIONS)
NT BOLTED JOINTS
NT BUTT JOINTS
NT INTERFERENCE FIT
NT LAP JOINTS
NT METAL JOINTS
NT RIVETED JOINTS
NT SEAMS (JOINTS)
NT SOLDERED JOINTS
NT SPOT WELDS
NT WELDED JOINTS
Joints in carbon fibre reinforced composites
[BR99969] 01 p0019 N88-10114
Metallic superlattices with monolayer modulation
[DE87-012724] 01 p0023 N88-10145
Superconducting properties of metallic superlattices
[DE87-012725] 01 p0023 N88-10146
Exact solution of the inverse problem for a six-link manipulator with a mechanical offset
[DE87-702646] 01 p0054 N88-10349
Effects of barrel joints on hypervelocity projectiles
[DE87-013447] 02 p0157 N88-10983
Process and equipment capabilities materials joining laboratory, 1987
[DE87-014534] 02 p0180 N88-11122
Low-pressure eutectic bonding of depleted uranium to copper
[DE87-014625] 02 p0181 N88-11128
Assessment of structural integrity from forced vibration testing
[DE87-014642] 02 p0191 N88-11195
Direction dependent connections of complex manifolds and their submanifolds
[DE87-703073] 02 p0225 N88-11419
Stability of mechanical joints in launching vehicles: Local and global stationary values of energy density
03 p0270 N88-11696
Considerations concerning a thermal joint for a deployable or steerable battery radiator for the Columbus Polar Platform
[NLR-TR-86055-U] 03 p0276 N88-11739
Joining of silicon carbide reinforced ceramics
[DE87-014881] 03 p0294 N88-11847
Durability (lifetime) predictions adhesively bonded structures
[AD-A184069] 03 p0335 N88-12110
Overview of free-piston Stirling engine technology for space power application
[NASA-TM-88886] 03 p0386 N88-12427
Reduced complexity structural modeling for automated airframe synthesis
[NASA-CR-177440] 04 p0393 N88-12453
Influence of bond dilution on the free surface and interface Potts ferromagnetism
[DE87-703360] 04 p0497 N88-13061
Advanced joining concepts for passive vibration control 05 p0596 N88-13638
Behavior of bolted joints in composite laminates
06 p0677 N88-14148
Pin joints, gears, springs, cranks and other novel micromechanical structures
[DE88-002504] 07 p0864 N88-15245
Through-transmission/pulse-echo ultrasonic equipment evaluation
[AD-A186340] 07 p0929 N88-15641
Effect of peel angle on peel force
[AD-A186117] 08 p0972 N88-15878
Two-phase flow forms and pressure drop in horizontal T tube joints with vertical branch
[GKSS-87/E/12] 09 p1163 N88-16969
Development of methods for low temperature diffusion bonding
[AD-A186875] 09 p1174 N88-17033
A finite element analysis of adhesively bonded composite joints including geometric nonlinearity, nonlinear viscoelasticity moisture diffusion and delayed failure
[AD-A187455] 10 p1296 N88-17747
Design conditions and workspace for the generally-proportioned 3-hinge spherical wrist for robots
10 p1339 N88-18003
Computed stress and strain distributions under interference fit and after coldworking
[AD-A186950] 10 p1342 N88-18024
Finite element analysis of adhesively bonded composite joints including geometric nonlinearity, nonlinear viscoelasticity, moisture diffusion and delayed failure
[PB88-147822] 11 p1451 N88-18648
Characterization of damped structural connections for multi-component systems
[NASA-TM-100801] 11 p1502 N88-18974
The Shock and Vibration Digest, volume 20, no. 3
12 p1635 N88-19786
Further refinement and applications of the mixed computational algorithm for plane elastic contact problems
[AD-A188308] 12 p1683 N88-20065
Reduction of erosion in elbows due to flow modifications, phase 1
[DE88-001028] 13 p1769 N88-20584
Structural clearances and internal friction: Simulation by Eigen distortions
[ISSN-0208-5658] 13 p1779 N88-20640
Robotic joint prototype for space applications
14 p1878 N88-21222
An efficient gradient projection optimization scheme for a seven-degree-of-freedom redundant robot with spherical wrist
[DE88-005440] 14 p1919 N88-21453
Robotic joint experiments under ultravacuum
14 p1927 N88-21490
Ammonia transfer across rotating joints in space
14 p1927 N88-21492
Space shuttle solid rocket motor Profile Measuring Device (PMD) 14 p1928 N88-21495
Fracture toughness of silicon nitride-silicon nitride joints bonded with oxynitride glass
[DE88-005548] 15 p2043 N88-22172
Ultrasonic characterization of ceramic joints
[DE88-005844] 15 p2043 N88-22173
Stabilization and control problems in structural dynamics
[AD-A190197] 15 p2073 N88-22361
Increasing strength of graphite/epoxy bolted joints by introducing an adhesively bonded metallic insert
[FFA-TN-1987-45] 15 p2088 N88-22442
A three dimensional non-singular modelling of rigid manipulators
[AD-A189707] 15 p2116 N88-22604
Design and test of a new coaxial air joints
[DE88-751808] 16 p2164 N88-22908
Characterization of structural connections for multicomponent systems 16 p2220 N88-23251
On the calculation of stresses in pin-loaded anisotropic plates
[LR-529] 16 p2223 N88-23268
Manufacturing requirements 17 p2297 N88-23745
Bearing-bypass material system test
[NASA-CASE-LAR-13458-1] 17 p2342 N88-23967
The inspection of metallurgical bounds in electronic systems
[AD-A192064] 18 p2582 N88-25343
Optimization of performance criteria with bounded joint velocities for robots with one degree of redundancy
[DE88-003915] 20 p2810 N88-26670
FEB structural analysis, revision H
[AD-A192302] 20 p2814 N88-26698
Kinematics of Hooke universal joint robot wrists
[NASA-TM-100567] 20 p2843 N88-26870
General expression of manipulator kinematics
[DE88-753430] 21 p2957 N88-27567
Chemistry of adhesion at the polyimide-metal interface
[AD-A194647] 22 p3058 N88-28143
Critical joints in large composite primary aircraft structures. Volume 2: Technology demonstration test report
[NASA-CR-172587] 23 p3177 N88-28915
Critical joints in large composite primary aircraft structures. Volume 3: Ancillary test results
[NASA-CR-172588] 23 p3177 N88-28916
Soot and radiation in a gas turbine combustor
[AD-A191991] 23 p3179 N88-28924
Critical joints in large composite primary aircraft structures. Volume 1: Technical summary
[NASA-CR-3914] 23 p3190 N88-28983
Elastic behavior of a rubber layer bonded between two rigid spheres
[AD-A193698] 23 p3198 N88-29030
Stability control of leakage flow channels
[DE88-009995] 23 p3210 N88-29107
Recursive mass matrix factorization and inversion: An operator approach to open- and closed-chain multibody dynamics
[NASA-CR-182516] 23 p3247 N88-29328
Criteria for matrix dominated failure
[AD-A196263] 24 p3341 N88-29887

JOSEPHSON JUNCTIONS
Abrikosov vortex motion and elementary pinning force in a SNS Josephson junction
[DE87-013607] 01 p0105 N88-10683
Hitachi develops ceramic superconducting device
06 p0688 N88-14214
The consequences of intergrain Josephson coupling in ceramic high-temperature superconductors
[DE87-013713] 06 p0785 N88-14816
Macroscopic quantum effects in a Josephson tunnel junction
[DE88-002239] 06 p0787 N88-14830
Comparative investigation of heterodyne mixers at 1000 GHz
[FTL-068627] 09 p1158 N88-16940
Studies of nonlinear and chaotic phenomena in solid state systems
[DE88-002330] 09 p1254 N88-17515
Effect of the subgap conductance on the metastable states in a Josephson tunnel junction
[DE88-003102] 09 p1258 N88-17543
Bloch oscillations in small Josephson junctions: Their manifestation in switching effects
14 p1969 N88-21756
Vortices in long Josephson junctions
[AD-A190338] 15 p2059 N88-22279
Preparation of large area NbN/AlN/NbN Josephson junctions
[DE88-006074] 15 p2145 N88-22799
Fluxons and order in long Josephson junctions
[AD-A190879] 16 p2282 N88-23665
Picosecond switching in Josephson tunnel junctions
19 p2657 N88-25780
Noise and chaos in driven Josephson junctions
19 p2734 N88-26238
Phase sensitive amplification with SIS (Superconductor-Insulator-Superconductor) quasiparticle mixers
[AD-A194594] 23 p3291 N88-29596
Planar thin film SQUID with integral flux concentrator
[NASA-CASE-MFS-28282-1] 23 p3292 N88-29602

JOUKOWSKI TRANSFORMATION
An efficient patched grid Navier-Stokes solution for multiple bodies, phase 1
[AD-A194166] 23 p3211 N88-29110

JOULE HEATING
U OHMIC DISSIPATION

JOULE-THOMSON EFFECT
Development of a low noise 10 K J-T refrigeration system
[AD-A185258] 05 p0571 N88-13484
Cryocooler systems demonstration
[AD-A188025] 11 p1467 N88-18745

JOURNAL BEARINGS
Determination of the fatigue strength of mechanically, thermally and corrosively loaded multilayer materials
[ETN-87-90375] 01 p0058 N88-10372
On the performance of finite journal bearings lubricated with micropolar fluids
[NASA-TM-100293] 08 p0988 N88-15983
The use of multigrid techniques in the solution of the Elrod algorithm for a dynamically loaded journal bearing
[NASA-CR-180873] 10 p1331 N88-17954
Table with aerostatic bearings for simulation in one degree of freedom attitude control systems of artificial satellites
[INPE-4272-PRE/1144] 12 p1595 N88-19552
Dynamic modelling of flexible rotor shafts mounted on hydrodynamic bearings 13 p1779 N88-20641
The solution of the Elrod algorithm for a dynamically loaded journal bearing using multigrid techniques
[NASA-TM-100941] 19 p2666 N88-25854
A lubrication study of engine bearings
21 p2958 N88-27574

JOURNALS (DOCUMENTS)
U PERIODICALS

JOURNALS (SHAFTS)
U SHAFTS (MACHINE ELEMENTS)

JP-4 JET FUEL
Measurements in large JP-4 pool fires
[DE87-013445] 03 p0284 N88-11783
The performance of a surrogate blend in simulating JP-4 in a spray-fueled combustor 24 p3347 N88-29926

JP-5 JET FUEL
Biodegradation of JP-5 aviation fuel by subsurface microbial communities
[AD-A192743] 20 p2781 N88-26493

JP-8 JET FUEL
Cost savings possible with Air Force conversion to JP-8 as its primary fuel
[AD-A183784] 01 p0030 N88-10192

JUDGMENTS
Effects of stress on judgement and decision making in dynamic tasks
[AD-A188203] 11 p1523 N88-19092
Space vehicle approach velocity judgments under simulated visual space conditions
[NASA-TM-89437] 11 p1523 N88-19094
Training in time interval discrimination using verbal feedback 12 p1665 N88-19985
Science, technology and the Constitution: Background paper
[PB88-142534] 12 p1708 N88-20222
On categorizing sounds
[AD-A189784] 15 p2129 N88-22700
A framework for a theory of mapping
[AD-A191071] 18 p2551 N88-25144

Rules, schema and decision making
[AD-A193389] 21 p3027 N88-27967
JUNCTION DIODES
NT MIM DIODES
Metal-sensing layer-semiconductor and metal-sensing layer-metal heterostructure gas sensors
[DE87-011293] 01 p0103 N88-10674
JUNCTION FIELD EFFECT TRANSISTORS
U JFET
JUNCTION TRANSISTORS
NT JFET
Mechanically stacked multijunction solar cells: An update on Sandia programs
[DE87-014641] 03 p0347 N88-12190
JUNGLES
U TROPICAL REGIONS
JUPITER (PLANET)
A Jupiter Data Analysis Program (JDAP) research grant on wave accessibility and attributes
[NASA-CR-182348] 06 p0804 N88-14908
Ray tracing of Jovian low frequency radiation
[NASA-CR-179262] 08 p1101 N88-16620
The precipitation of energetic heavy ions into the upper atmosphere of Jupiter
[NASA-TM-101155] 17 p2452 N88-24565
The Jovian aurora: Electron or ion precipitation
[NASA-TM-101153] 17 p2452 N88-24566
Interpretation of the polarimetric observations of Jupiter
[DE88-702414] 21 p3031 N88-27991
JUPITER ATMOSPHERE
A refractometer for the interferometric determination of the helium abundance in the Jupiter atmosphere
[BONN-IR-86-23] 07 p0946 N88-15749
Study of descent of probes with high lift-drag ratio into the atmosphere of Jupiter 08 p1006 N88-16101
Spatial and temporal monitoring of the Jovian atmosphere 12 p1711 N88-20240
Model of Jovian F region ionosphere
[NASA-CR-182587] 13 p1855 N88-21105
The precipitation of energetic heavy ions into the upper atmosphere of Jupiter
[NASA-TM-101155] 17 p2452 N88-24565
JUPITER PROBES
NT GALILEO PROBE
NT GALILEO SPACECRAFT
JUPITER SATELLITES
NT IO
A modeling analysis program for the JPL table mountain Io sodium cloud data
[NASA-CR-182555] 11 p1570 N88-19400
The 1985 mutual phenomena of Jupiter's satellites observed in Brazil
[INPE-4526-PRE/1276] 15 p2152 N88-22848

K

K BAND
U EXTREMELY HIGH FREQUENCIES
K LINES
Simultaneous, cospatial imaging of the Sun in cyanogen and singly-ionized calcium 04 p0507 N88-13114
K STARS
Magnetic fields on K and M stars
04 p0510 N88-13137
An analysis of the photospheric line profiles in F, G, and K supergiants 04 p0513 N88-13157
Sensitivity of the H alpha line to expansion, geometrical extent and temperature gradient in the G and K supergiant chromospheres 04 p0514 N88-13159
Chromospheric and coronal heating in a bias-free sample of K dwarfs 04 p0518 N88-13184
Observations and analysis of the photospheric magnetic fields on dwarf G, K and M stars
04 p0520 N88-13196
Spectral images and multi-component models of the chromospheres of AR Lacertae
11 p1568 N88-19384
Spectroscopic determinations of surface gravities of giant stars, and ultraviolet observations of RR Lyrae and X Arietis 11 p1569 N88-19391
K-EPSILON TURBULENCE MODEL
A numerical study of turbulent plane jets in still and flowing environments employing two-equation k-epsilon model 23 p3211 N88-29109
Three-dimensional gas turbine combustor modelling
24 p3349 N88-29937
Numerical modeling of combustion processes in gas turbines 24 p3350 N88-29939
Three-dimensional combustor predictors: A comparison of equilibrium and laminar flamelet chemistry models
24 p3350 N88-29940
Analysis of the flow through double swirl airblast atomizers 24 p3351 N88-29949
K-MESONS
U KAONS
KA BAND
U EXTREMELY HIGH FREQUENCIES
KALMAN FILTERS
Estimation filters with adaptive scanning time for flying target tracking
[ETN-87-90401] 01 p0036 N88-10232
Development of response models for the Earth Radiation Budget Experiment (ERBE) sensors. Part 4: Preliminary nonscanner models and count conversion algorithms
[NASA-CR-178295] 01 p0050 N88-10317
GPS vertical axis performance enhancement for helicopter precision landing approach
[NASA-CR-177443] 04 p0397 N88-12477
Investigation, development, and application of optimal output feedback theory. Volume 3: The relationship between dynamic compensators and observers and Kalman filters
[NASA-CR-4107] 05 p0638 N88-13900
Optimal guidance of homing missiles
06 p0671 N88-14111
Improved understanding of the loss-of-symmetry phenomenon in the conventional Kalman filter
[NASA-TM-100041] 06 p0766 N88-14709
Tracking procedure for non-normally distributed measurement errors
[AD-A186287] 07 p0903 N88-15468
Simultaneous estimation and detection of bias shifts for inertial navigation systems 12 p1576 N88-19429
Covariance analysis and post-processing of gravity compensation effects for aided multi-state navigation systems
[PAPER-87-13] 12 p1577 N88-19430
A cause of divergence in the Kalman gain equation
12 p1578 N88-19438
Utilization of strapdown inertial and non-inertial sensors in determination of satellite attitude by Kalman filters
[INPE-4313-TDL/280] 13 p1731 N88-20349
Robustifying the Kalman filter
[AD-A189240] 13 p1825 N88-20907
Kalman filter residual expert system
[AD-A190520] 15 p2020 N88-22041
Moving-bank multiple model adaptive estimation applied to flexible spacestructure control
[AD-A190761] 15 p2026 N88-22071
New stable, vectorisable Kalman filter algorithms based on orthogonal transformations
[DFVLR-FB-87-52] 16 p2258 N88-23494
A positioning system based on NAVSAT
[NLR-MP-87018-U] 20 p2757 N88-26358
Control, stability and filter for a discrete linear stochastic system with correlated noise
[PB88-109525] 21 p3004 N88-27816
Estimation forces acting on an underwater vehicle with G.P.S. (Global Positioning System) and Kalman filtering
[AD-A194339] 23 p3175 N88-28901
Estimation of aircraft parameters using filter error methods and extended Kalman filter
[DFVLR-FB-88-15] 23 p3176 N88-28911
Multi-sensory tracking mount control
[AD-A194675] 23 p3249 N88-29339
Dynamical systems and motion vision
[AD-A195932] 24 p3422 N88-30366
Kalman filter-based algorithms for estimating depth from image sequences
[AD-A195818] 24 p3424 N88-30380
KANSAS
Evaluation of surface energy and radiation balance systems on the Konza Prairie
[NASA-CR-182534] 10 p1355 N88-18097
KAONS
Study of the production of Ko mesons in proton antiproton interactions at 630 GeV
[NOTA-INTERNA-908] 21 p3015 N88-27892
KAPPA-EPSILON TURBULENCE MODEL
U K-EPSILON TURBULENCE MODEL
KARMAN VORTEX STREET
The phenomenology of Karman vortex streets via sound in oscillatory flow
[MPIS-MITT-84-1987] 02 p0122 N88-10775
Dynamics of the von Karman vortex street
03 p0316 N88-11998
ESA Bulletin No. 25
[ISSN-0376-4265] 09 p1128 N88-16767
Meteosat tracks Karman vortex streets in the atmosphere 09 p1128 N88-16770
KC-130 AIRCRAFT
U C-130 AIRCRAFT
KC-135 AIRCRAFT
U C-135 AIRCRAFT
KEELS
Ray scattering from a collection of ice keels
[AD-A191757] 19 p2722 N88-26163
Reflection and scattering of acoustic rays computed for parabolic ice keel models
[AD-A193898] 23 p3278 N88-29517
KELP
U SEAWEEDS
KELVIN-HELMHOLTZ INSTABILITY
Numerical simulation of solar wind and magnetospheric phenomena 08 p1097 N88-16600
The Kelvin-Helmholtz instability in a stratified shear flow
[CFD/88/2] 22 p3076 N88-28265
Vortex formation and particle transport in a cross-field plasma sheath
[AD-A194838] 24 p3432 N88-30425
KENTUCKY
NASA/UK TAP
[NASA-CR-180350] 12 p1708 N88-20223
KENYA
Use of SPOT imagery for vegetation/biomass mapping, geotechnical mapping, catchment area determination, and settlement location in the Turkana district, northern Kenya 22 p3096 N88-28384
KEPLER LAWS
Solution of the hyperbolic Kepler's equation
[RAE-TR-87042] 09 p1229 N88-17368
KERNEL FUNCTIONS
Steady waves in a nonlinear theory of viscoelasticity
[AD-A185548] 06 p0723 N88-14448
Pseudodifferential operators on the circle and finite differences
[PB87-222352] 06 p0763 N88-14681
A modified kernel quantile estimator under censoring
[AD-A186364] 07 p0911 N88-15525
A smooth nonparametric quantile estimator from right-censored data
[AD-A186180] 07 p0915 N88-15552
Admissible and singular translates of stable processes
[AD-A186426] 07 p0917 N88-15571
A note on the analyticity of the Neumann Kernel and an associated quadrature problem in two-dimensional boundary element methods
[ETN-88-92054] 14 p1964 N88-21719
Inference for a nonlinear semimartingale regression model
[AD-A190857] 16 p2262 N88-23527
Symmetrized nearest neighbor regression estimates
[AD-A191998] 18 p2568 N88-25254
Definition of an auxiliary processor dedicated to real-time operating system kernels
[NASA-CR-183070] 20 p2841 N88-26860
KEROSENE
High-density jet fuels from coal syncrudes, appendix 4
[DE88-003132] 10 p1307 N88-17813
Availability and cost estimate of a high naphthene, modified aviation turbine fuel
[NASA-TM-100823] 13 p1749 N88-20455
Antimisting kerosene: Low temperature degradation and blending
[NASA-CR-182725] 20 p2781 N88-26495
KERR ELECTROOPTICAL EFFECT
Double layer polarization of nonconducting spheroidal particles and its application to Kerr effect
[ISSN-0208-5658] 13 p1832 N88-20960
KERR MAGNETOOPTICAL EFFECT
Studies of coherent beam processing concepts, phase 1
[AD-A194749] 22 p3083 N88-28306
KETONES
NT ACETONE
KEVLAR (TRADEMARK)
An experimental and theoretical study of the bending behavior of Kevlar 49/epoxy beams and rings
[DE87-010430] 01 p0061 N88-10394
The use of Kevlar on aero-engine fan containment casings
[PNR90410] 02 p0182 N88-11134
Flammability test on aircraft seats equipped with fire barrier fabrics for the Porcher company
[CEAT-M5-525200] 06 p0666 N88-14084
Flammability, smoke and toxicity test on fire barrier fabric from the Porcher company --- Airbus aircraft
[ETN-88-91168] 06 p0666 N88-14085
Comparison of ultrasonic flaw detection analysis for spherical composite test specimens using two data acquisition techniques
[DE88-005002] 12 p1634 N88-19782
Fracture characteristics of carbon and aramid unidirectional composites in interlaminar shear and open hole tensile tests
[NLR-TR-86083-U] 13 p1735 N88-20371
Thermoviscoelastic characterization and predictions of Kevlar/epoxy composite laminates
[NASA-CR-182878] 16 p2172 N88-22946
On the bending response of Kevlar 49/epoxy beams and rings
[DE88-006824] 18 p2530 N88-25012

NDE performance in predicting failure strength of spherical composite specimens with implanted flaws
[DE88-008223] 21 p2959 N88-27575
Use of microwave measuring systems for the nondestructive control of resins and composites
[REPT-881-430-123] 21 p2959 N88-27576
Nondestructive tests and high performance composite structures
[SNIAS-881-430-119] 23 p3188 N88-28969
KEYING
NT FREQUENCY SHIFT KEYING
NT PHASE SHIFT KEYING
Reconfigurable work station for a video display unit and keyboard
[NASA-CASE-MFS-26009-1-SB]
17 p2382 N88-24163
WIPP (Wave Induced Particle Precipitation) experiment logistic support
[AD-A191184] 18 p2499 N88-24824
KIDNEYS
Nutrient requirements and other factors involved in the culture of human kidney cells on microcarrier beads
09 p1197 N88-17176
KILOMETRIC WAVES
A Jupiter Data Analysis Program (JDAP) research grant on wave accessibility and attributes
[NASA-CR-182348] 06 p0804 N88-14908
KIMBERLITE
U BIOTITE
U PERIDOTITE
KINEMATIC EQUATIONS
Structure-dependent matrix representation of manipulator kinematics and its inverse solution
[DE87-752966] 02 p0229 N88-11447
KINEMATICS
NT BODY KINEMATICS
Use of simulated satellite radiances from a mesoscale numerical model to understand kinematic and dynamic processes 02 p0202 N88-11261
Spectroscopy and nonthermal processes
02 p0252 N88-11594
Kinematics and dynamics of barred spiral galaxies
03 p0388 N88-12440
Kinematics and galactic structure
[PREPRINT-18] 03 p0389 N88-12442
Static standing and dynamic walking of a practical biped robot
[DE88-001367] 04 p0451 N88-12795
Kinematic formulation of finite elements for plate bending 04 p0455 N88-12821
Extremum methods of structural analysis for system reliability assessment 04 p0456 N88-12824
Non-linear maximum likelihood estimation of stability derivatives from range data
[NAL-TM-SE-8608] 05 p0552 N88-13365
SHARP simulation of discontinuities in highly convective steady flow
[NASA-TM-100240] 05 p0642 N88-13931
Robot accuracy improvement through kinematic parameter identification 06 p0712 N88-14363
Dynamics, control and sensor issues pertinent to robotic hands for the EVA retriever system
06 p0796 N88-14876
Analysis of stable crack growth with isotropic and kinematic hardening
[PB87-144911] 07 p0868 N88-15266
Theory of deformation. Part 1: Kinematics
[DE88-003007] 08 p1001 N88-16062
Goal driven kinematic simulation of flexible arm robot for space station missions 08 p1059 N88-16388
Kinematic optimization of mechanisms, a finite element approach
[ISBN-90-370-0012-6] 09 p1175 N88-17039
A substructure method for dynamic simulation of flexible mechanical systems with geometric nonlinearities
09 p1176 N88-17044
An optimal resolved rate law for kinematically redundant manipulators 09 p1212 N88-17268
Considerations of acceleration effects in relativistic kinematics 09 p1260 N88-17553
Kinematic and dynamic analyses of the Stanford/JPL robot hand
[DE88-004637] 11 p1495 N88-18923
Real-time kinematic and dynamic analysis and adaptive model-following control of manipulator arms
11 p1495 N88-18927
Improvement in robot positioning accuracy by a kinematic identification model 11 p1496 N88-18931
Electro-mechanical vibratory system
11 p1500 N88-18958
Mass loss from evolved stars
11 p1569 N88-19394
Synthesis of finite displacements and displacements in continental margins
[NASA-CR-182616] 12 p1642 N88-19832
Force distribution and trajectory control for closed kinematic chains with applications to walking machines
13 p1779 N88-20642
Subduction 13 p1806 N88-20796
New representation for kinematics of manipulator
[DE88-751446] 14 p1917 N88-21445
Kinematic support using elastic elements
14 p1926 N88-21481
Analysis of head response to torso acceleration. Volume 1: Development of performance requirements
[PB88-156757] 14 p1953 N88-21640
The striae in the dust tails of great comets: A formal comparison of the goodness of fit by various theories, and a new proposal 14 p2002 N88-21937
A three dimensional non-singular modelling of rigid manipulators
[AD-A189707] 15 p2116 N88-22604
Wave-growth associated with turbulent spot in plane Poiseuille flow 16 p2199 N88-23116
Base reaction optimization of manipulators with redundant kinematics 16 p2219 N88-23238
Sea ice kinematics: Space and time scales
[AD-A191162] 17 p2376 N88-24128
Kinematics, dynamics and control of a closed chain mechanism manipulator 18 p2523 N88-24967
Real-time implementation of a kinematic optimization scheme for seven-degree-of-freedom redundant robots with spherical wrists
[DE88-006785] 18 p2524 N88-24974
Determination of settings of a tilted head-cutter for generation of hypoid and spiral bevel gears
[NASA-CR-182138] 18 p2524 N88-24976
MHD bending waves in a current sheet
[NASA-TM-101149] 18 p2579 N88-25323
Automatic calibration of space based manipulators and mechanisms
[NASA-CP-182804] 19 p2676 N88-25912
Spatial dynamics of deformable multibody systems with variable kinematic structure 20 p2813 N88-26687
Kinematics of Hooke universal joint robot wrists
[NASA-TM-100567] 20 p2843 N88-26870
Theory of relativity and super-light-speeds-I: Kinematical part
[DE88-701832] 20 p2880 N88-27100
Aeroelastic modeling of rotor blades with spanwise variable elastic axis offset: Classic issues revisited and new formulations 21 p2890 N88-27158
Control and use of unsteady flows: Insect use of various wing kinematics and related pressure measurements using a pitching airfoil 21 p2926 N88-27366
Control of free-flying space robot manipulator systems
[NASA-CR-183017] 21 p2956 N88-27562
General expression of manipulator kinematics
[DE88-753430] 21 p2957 N88-27567
Dexterous hands: Optimizing grasp by design and planning 21 p2958 N88-27572
Flow dynamics stimulated by hairpin-like vortices in initially laminar boundary layers
[AD-A194253] 22 p3075 N88-28254
The analysis and control of robotic manipulators operating at or near kinematically singular configurations
22 p3084 N88-28315
A comparison: Static and future kinematic GPS (Global Positioning System) surveys
[AD-A194666] 23 p3175 N88-28904
Shock waves in unsteady flows
[NASA-TT-20329] 23 p3214 N88-29134
Sea ice processes
[AD-A193980] 23 p3237 N88-29262
The kinematics of Milky Way halo gas
23 p3299 N88-29648
A review: Quantitative models for lava flows on Mars
23 p3301 N88-29656
Approximation of viscoelastic stresses from Newtonian turbulent kinematics
[AD-A194317] 24 p3371 N88-30077
The kinematics of late-type supergiants
[SER-C-PREPUBL-FASC-28] 24 p3454 N88-30560
KINESTHESIS
U PROPRIOCEPTION
KINETIC ENERGY
Apparatus for storing kinetic energy
[EP-PATENT-0-181-736-A1] 01 p0066 N88-10422
Navier-Stokes cascade analysis with a stiff Kappa-Epsilon turbulence solver
[NASA-TM-100218] 02 p0123 N88-10778
A multiple-time-scale turbulence model based on variable partitioning of turbulent kinetic energy spectrum
[NASA-CR-179222] 04 p0444 N88-12754
Mechanical property evaluation of a series of commercial tungsten alloys
[AD-A185440] 05 p0565 N88-13446
The end height of fireball as a function of their residual kinetic energy 06 p0737 N88-14535
Theoretical aspects of channeling, damage, and range distributions for low (keV) and high (MeV) energy implantation
[DE88-000949] 06 p0786 N88-14818
New model to estimate the perforation power of kinetic energy projectiles
[PB87-166757] 09 p1175 N88-17040
Product kinetic and internal energy distributions via velocity-aligned Doppler spectroscopy
[DE88-003510] 10 p1298 N88-17764
Energy transfers for multilayer hydrodynamic ocean models: General formulation and specific examples
[AD-A187604] 10 p1358 N88-18116
Unsteady shallowing mixed layer
13 p1805 N88-20791
Launchability of base-driven electromagnetic projectiles
[AD-A189635] 15 p2023 N88-22055
Rocket measurements of ionospheric electron temperature over Natal
[INPE-4485-PRE/1250] 15 p2096 N88-22489
Experimental investigation of a three-stage railgun incorporating puff-switching
[AD-A191044] 16 p2166 N88-22918
Coherent structures and modeling: Some background comments 16 p2199 N88-23120
Inevitable inflation in Einstein-Cartan theory with improved energy-momentum tensor with spin
[NASA-TM-101146] 18 p2586 N88-25365
KINETIC EQUATIONS
NT HELMHOLTZ VORTICITY EQUATION
NT HYDRODYNAMIC EQUATIONS
NT KINEMATIC EQUATIONS
Equations for determining CVD tungsten-rhenium alloy composition and plating rate
[DE87-008831] 01 p0024 N88-10152
Computer models for kinetic equations of magnetically confined plasmas
[DE87-011571] 02 p0236 N88-11492
Current generation and induced conductivity of a plasma under common action of constant electric field and lower-hybrid or ECR waves
[DE88-700345] 07 p0935 N88-15680
Application of Onsager's reciprocity relations to interface motion
[DE88-003286] 10 p1397 N88-18327
Applied mathematics of transport theory
[DE88-004098] 10 p1404 N88-18369
Kinetic and turbulence models for granular and two-phase flows 11 p1484 N88-18862
Plasma rotation in a tokamak
[DE88-700855] 12 p1693 N88-20128
Consistent transport coefficients in astrophysics
[NASA-TM-101154] 17 p2451 N88-24560
KINETIC FRICTION
NT SLIDING FRICTION
KINETIC HEATING
NT AERODYNAMIC HEATING
NT SHOCK HEATING
Sinterable ceramic powders from laser-heated gases
[AD-A194162] 23 p3197 N88-29024
KINETIC THEORY
NT MIXING LENGTH FLOW THEORY
NT TRANSPORT THEORY
Physics and chemistry 07 p0883 N88-15359
Resonance cones in nonthermal plasmas: Laboratory experiments 08 p1027 N88-16223
Kinetic theory for plane flows of rough, inelastic, circular disks 21 p2946 N88-27499
Kinetic theory for electrostatic waves due to transverse velocity shears
[AD-A193404] 23 p3284 N88-29557
KINETICS
NT ELECTROKINETICS
NT KINETIC ENERGY
NT NEWTON SECOND LAW
NT NEWTON THEORY
NT REACTION KINETICS
Exact solution of the inverse problem for a six-link manipulator with a mechanical offset
[DE87-702646] 01 p0054 N88-10349
A parallel model of the kinetic depth effect using local computations
[AD-A181945] 01 p0083 N88-10536
The infiltration kinetics of aluminum in silicon carbide compacts
[AD-A184682] 03 p0290 N88-11823
Molecular engineering of ceramics
[DE88-000174] 04 p0420 N88-12603
An analysis of the effect of system variables on the quality of thin films and powders produced by laser-breakdown chemical vapor deposition
[DE88-001793] 06 p0708 N88-14342
Fundamental studies of surfaces processes and trace analysis using solid electrodes
[AD-A186156] 07 p0828 N88-15024

TEA-TE: Powerful nitrogen-based laser system
07 p0919 N88-15583
Study of kinetics of intracavity absorption in pulsed dye lasers 07 p0919 N88-15585
Investigations in field of surface forces in metallurgy
[BLL-M-47406-(5828.4)] 08 p0969 N88-15860
Kinetics and mechanism of thermal aging embrittlement of duplex stainless steels
[DE88-002987] 08 p0969 N88-15866
Influence of skeletal muscle glycogen on passive rewarming after hypothermia
[AD-A186451] 08 p1049 N88-16334
Kinetics and spectrum of light pulse used in picosecond holography 09 p1236 N88-17409
Deactivation of alumina based catalysts
11 p1455 N88-18673
Effect of density change on rapid liquid-solid interface kinetics and heat flow
[DE88-004286] 11 p1467 N88-18873
Thermodynamic theory of fluctuations and Rayleigh light scattering in solutions 13 p1785 N88-20681
Kinetics of combustion of finely divided solid fuel in granules
[BLL-M-37626-(5828.4)] 14 p1888 N88-21283
Kinetics of slow electrons in excimer laser with electron-beam pumping 14 p1970 N88-21760
Free carrier nonlinear optics 14 p1977 N88-21796
Reactions of N2(A sup 3 sigma sup + sub u) candidates for short wavelength lasers
[DE88-007018] 15 p2070 N88-22342
The kinetics of contact noise in NaBeta alumina
[AD-A190651] 15 p2130 N88-22707
Theoretical calculations of XeF ground state kinetics
[AD-A191398] 16 p2270 N88-23580
Kinetic theoretical analysis for propagation of rotating ion beam in ICF 16 p2276 N88-23623
Thomson scattering for determining electron concentrations and temperatures in an inductively coupled plasma. 2: Description and evaluation of a multichannel instrument
[AD-A191324] 16 p2280 N88-23652
Effect of alloying, rapid solidification, and surface kinetics on the high temperature environmental resistance of niobium
[AD-A192093] 18 p2485 N88-24743
Kinetics of homogeneous nucleation in superheated F-11 and F-21 liquid freons
[NASA-TT-20286] 19 p2613 N88-25503
Kinetics of CO oxidation over a deactivated Rh(111) single crystal catalyst
[DE88-003000] 19 p2613 N88-25504
Irreversible dissolution of solid solutions: A kinetic and stoichiometric model
[DE88-009194] 19 p2614 N88-25513
The crystallization of tough thermoplastic resins in the presence of carbon fibers
[NASA-CR-182984] 20 p2776 N88-26464
Research on the kinetics of phase changes in solids
[AD-A192222] 20 p2814 N88-26696
Proceedings of the 2nd US-Japan Workshop on Advanced Plasma Modeling, volume 3
[IPPJ-867] 20 p2855 N88-26957
Modeling of subtle kinetic processes in plasma simulation 20 p2856 N88-26959
Kinetic of oxidation to air of a Fe-Al-Mn alloy system at 600-800(sup 0)C temperature range
[DE88-702309] 21 p2920 N88-27330
Sol-gel kinetics: Si(sup)29 NMR and a statistical reaction model
[DE88-011545] 23 p3191 N88-28988
Kinetic of martensitic transformations induced by hydrogen in the austenite
[DE88-701623] 23 p3194 N88-29007
Reaction-theoretical aspects of the thermal behavior of lubricating oils and working fluids
[NASA-TT-20304] 23 p3199 N88-29041
Chemical kinetics of hydrogen and P(sub b) centers
[DE88-010528] 23 p3291 N88-29594
Ion kinetics in silane plasmas
[AD-A196202] 24 p3431 N88-30423

KIRCHHOFF LAW OF RADIATION
Beam quality of stable and unstable resonators: A theoretical approach
[DFVLR-FB-87-35] 14 p1962 N88-21826

KIRCHHOFF-HELMHOLTZ FLOW
U PIPE FLOW

KIRCHHOFF-HUYGENS PRINCIPLE
U DIFFRACTION
U WAVE PROPAGATION

KLYSTRONS
Performance of high power S-band klystrons focused with permanent magnet
[DE87-753024] 02 p0167 N88-11053
Development of a high-energy crowbar for the Los Alamos free-electron laser
[DE87-014748] 02 p0179 N88-11113
Inductance effects in the high-power transmitter crowbar system 04 p0433 N88-12687
Microwave system for the microwave Tokamak experiment (MTX)
[DE88-002391] 09 p1250 N88-17487
The numerical simulation of accelerator components
[DE87-011597] 10 p1412 N88-18423
RF pulse compression development
[DE88-004818] 11 p1479 N88-18826
Accelerator research studies
[DE88-008236] 19 p2726 N88-26187

KNIGHT SHIFT
U NUCLEAR MAGNETIC RESONANCE

KNOWLEDGE
NT PARADOXES
NT PHILOSOPHY
Data Model of Objects and Relations (DAMOR): A data model for knowledge representation
[REPT-87-05] 01 p0085 N88-10553
Towards the unmanned cockpit
02 p0129 N88-10812
Generating diagnostic knowledge from a structural and functional description 02 p0129 N88-10813
A review of the knowledge engineering process
02 p0129 N88-10814
Third Conference on Artificial Intelligence for Space Applications, part 1
[NASA-CP-2492-Pt-1] 08 p1055 N88-16360
Methodology for testing and validating knowledge bases 08 p1055 N88-16364
HSTDEK: Developing a methodology for construction of large-scale, multi-use knowledge bases
08 p1057 N88-16377
Interactive knowledge acquisition tools
08 p1060 N88-16401
Knowledge-based simulation
08 p1061 N88-16404
Similarity networks as a knowledge representation for space applications 08 p1062 N88-16411
Commonality analysis as a knowledge acquisition problem 08 p1062 N88-16413
Qualitative models for planning: A gentle introduction
08 p1062 N88-16414
Interfacing the expert: Characteristics and requirements for the user interface in expert systems
08 p1063 N88-16419
Foundation: Transforming data bases into knowledge bases 08 p1063 N88-16423
Case-based reasoning for space applications: Utilization of prior experience in knowledge-based systems
08 p1065 N88-16433
Substructure discovery in executed action sequences
[AD-A186446] 08 p1069 N88-16462
Simplifying the construction of domain-specific automatic programming systems: The NASA automated software development workstation project
09 p1204 N88-17212
Tutoring electronic troubleshooting in a simulated maintenance work environment
09 p1204 N88-17215
The representation of knowledge within model-based control systems
[DE88-004863] 10 p1396 N88-18319
Automatic knowledge acquisition for aerial image interpretation
[AD-A188616] 12 p1638 N88-19810
Rapid prototyping of simulations in artificial intelligence environments
[DE88-004295] 15 p2117 N88-22612
Minimum disclosure proofs of knowledge
[CWI-PM-R8710] 20 p2840 N88-26854
Knowledge representation in geographic information systems
[ETN-88-92470] 20 p2882 N88-27112
A model of information growth
23 p3265 N88-29440

KNOWLEDGE ENGINEERING
U EXPERT SYSTEMS

KNOWLEDGE REPRESENTATION
A survey of artificial neural systems
[AD-A184759] 03 p0368 N88-12312
Advanced techniques for the storage and use of very large, heterogeneous spatial databases. The representation of geographic knowledge: Toward a universal framework --- relations (mathematics)
[NASA-CR-181517] 03 p0385 N88-12421
The characterization of diagnostic tasks for engineering systems
[DE88-000093] 04 p0483 N88-12973
Investigation of candidate data structures and search algorithms to support a knowledge based fault diagnosis system 07 p0923 N88-15606
Expert system technology 07 p0926 N88-15628
A formal approach to validation and verification for knowledge-based control systems
09 p1207 N88-17233
Building validation tools for knowledge-based systems
09 p1207 N88-17235
Diagnoses: Reasoning from first principles and experiential knowledge 09 p1207 N88-17236
Beyond rules: The next generation of expert systems
09 p1210 N88-17256
An efficient representation of spatial information for expert reasoning in robotic vehicles
09 p1214 N88-17278
KBGIS-II: A knowledge-based geographic information system
[NASA-CR-182492] 09 p1261 N88-17559
Knowledge base refinement by monitoring abstract control knowledge, revision 1
[AD-A187502] 10 p1397 N88-18323
Research in knowledge representation for natural language communication and planning assistance
[AD-A187355] 11 p1522 N88-19087
KR: An efficient knowledge representation system
[AD-A187705] 11 p1529 N88-19129
KREME (Knowledge Representation, Editing and Modeling Environment): A user's introduction, phase 1
[AD-A188906] 12 p1681 N88-20052
A knowledge system for automatic finite element mesh generation: AMEKS
[DE87-014894] 13 p1826 N88-20914
Conception of a knowledge-based system for designing distributed systems
[DFVLR-MITT-87-16] 14 p1961 N88-21694
Representing knowledge in two distinct descriptions: Extensional vs. intensional
[CWI-CS-R8728] 14 p1961 N88-21699
Memory-based expert systems
[AD-A190203] 15 p2116 N88-22606
Knowledge engineering in design
[CWI-CS-R8745] 16 p2248 N88-23432
Representation and decision mechanisms in artificial intelligence
[AD-A191083] 18 p2560 N88-25197
Application of flight systems methodologies to the validation of knowledge-based systems
[NASA-TM-100442] 18 p2561 N88-25207
An expert system model using predicate transition nets
[AD-A191953] 19 p2718 N88-26141
The knowledge based automatic extraction of the machinable surfaces for automatic CAD-CAM system
[INPE-4542-PRE/1288] 20 p2836 N88-26824
Delfi-3 as a development environment for expert systems
[REPT-8767] 20 p2839 N88-26845
Computer science and technology: Knowledge-based system for physical database design
[PB88-193289] 20 p2882 N88-27109
Knowledge-based cost estimating vs traditional software cost models
[DE88-009707] 20 p2883 N88-27116
Cooperating knowledge-based systems
[NASA-CR-183109] 23 p3247 N88-29327
Hologram representation of design data in an expert system knowledge base 23 p3251 N88-29354
Knowledge-based fault diagnosis on future space vehicles 23 p3254 N88-29374
AI and simulation: What can they learn from each other 23 p3257 N88-29391
Knowledge acquisition and rapid protyping of an expert system: Dealing with real world problems
23 p3258 N88-29394
Requirements for a tool to aid in the development of expert systems for space station applications
23 p3258 N88-29398
A methodology for multiple rule system integration and resolution within a singular knowledge base
23 p3261 N88-29413
Semantic based man-machine interface for real-time communication 23 p3262 N88-29421
Distributed knowledge base systems for diagnosis and information retrieval
[AD-A193107] 23 p3296 N88-29633
Knowledge-based flow field zoning
[NASA-TM-101023] 24 p3412 N88-30314
Knowledge based simulation: An artificial intelligence approach to system modeling and automating the simulation life cycle
[AD-A195838] 24 p3423 N88-30372

KOLMOGOROFF THEORY
The velocity structure and turbulence at the center of the Orion Nebula 04 p0521 N88-13201
An elementary approach to the Daniell-Kolmogorov theorem and some related results
[AD-A186011] 07 p0909 N88-15505

KONDO EFFECT
Heavy Fermions and coherence in Kondo lattices: Specific heat of low energy excitation in Ce: systems
[ETN-88-91080] 09 p1255 N88-17525

Interactions between superconductivity and Kondo-grid properties in CeCu2Si2. Measurement results of specific heat under high pressure
[ETN-88-92377] 21 p3025 N88-27958
Possible occurrence of band interplay in high Tc superconductor
[PREPRINT-593] 22 p3157 N88-28789

KORTEWEG-DEVRIES EQUATION
Variation of wave action. Modulations of the phase shift for strongly nonlinear dispersive waves with weak dissipation. A new adiabatic invariant involving the modulated phase shift for strongly nonlinear, slowly varying, and weakly damped oscillators. The modulated phase shift for weakly dissipated nonlinear oscillatory waves of the Korteweg-de vries type
[AD-A185630] 06 p0765 N88-14702
Baecklund transformation and the Schwarzian derivative
[AD-A190277] 15 p2127 N88-22684
Nonlinear surface and internal waves on shear flow
[PREPRINT-584] 22 p3129 N88-28604

KRAMERS-KRONIG FORMULA
Optical constants of minerals and other materials from the millimeter to the ultraviolet
[AD-A192210] 18 p2482 N88-24724

KRONECKER PRODUCT
U ORTHOGONALITY

KRYPTON
NT KRYPTON ISOTOPES
KR + laser excitation of NH2 in atmospheric pressure flames
[AD-A183421] 01 p0050 N88-10322
Two-photon (VUV and visible) resonant ionization spectroscopy of atoms and molecules
[DE88-004332] 10 p1407 N88-18388
Resonantly enhanced, four-photon ionization of krypton at laser intensities exceeding 10(12) W/sq cm
[DE88-005038] 11 p1544 N88-19229
Temperature dependence of Kr precipitation in Ni
[DE88-005953] 13 p1744 N88-20429
Electron stimulated desorption and coherent electron scattering
[AD-A189091] 13 p1835 N88-20978
Numerical modelling specific energy charcteristics of excimer KrF lasers with electron beam excitation
[DE88-701525] 15 p2070 N88-22344
Krypton based adsorption type cryogenic refrigerator
[NASA-CASE-NPO-17334-1-CU]
17 p2331 N88-23917

KRYPTON FLUORIDE LASERS
Operational performance of repetitive KrF, XeCl excimer lasers 03 p0327 N88-12068
Narrow linewidth gain measurements in a KrF excimer amplifier pumped longitudinally by a high-power electron beam
[DE88-001365] 05 p0586 N88-13575
ICF research at Los Alamos
[DE88-005394] 11 p1493 N88-18916
Pulse-train amplification of subnanosecond near-transform-limited KrF laser pulses
[DE88-004460] 12 p1631 N88-19764
The development of high power KrF laser systems for plasma research by the application of stimulated Raman scattering
[ETN-88-92220] 15 p2073 N88-22358
Aurora status and plans
[DE88-006476] 18 p2521 N88-24955

KRYPTON ISOTOPES
Prospects for large dynamic range isotope analysis using photon burst mass spectrometry
[DE88-009110] 19 p2613 N88-25505

KU BAND
U SUPERHIGH FREQUENCIES

KUTTA-JOUKOWSKI CONDITION
On the Kutta condition for flows around lifting airfoils and wings
[DFVLR-FB-87-40] 13 p1717 N88-20268

L

L BAND
U ULTRAHIGH FREQUENCIES

L-SAT
The role of the L-Sat program in the evolution of European communications satellites
09 p1127 N88-16758
Qualification of the OLYMPUS reaction wheel
14 p1878 N88-21226
Development and qualification of the OLYMPUS antenna pointing mechanism 14 p1879 N88-21227
OLYMPUS shuttle specific radiator shield
14 p1879 N88-21234
A 30/20 GHz multibeam array antenna suitable for future high rate TDMA European satellite networks
[ETN-88-93079] 24 p3365 N88-30037

LABELING (MARKING)
U MARKING

LABOR
An extended Cobb-Douglas form for use in production economics
[AD-A186372] 07 p0943 N88-15733

LABORATORIES
NT ENVIRONMENTAL LABORATORIES
NT MANNED ORBITAL LABORATORIES
NT SPACE LABORATORIES
NT SPACELAB
Dynamics of spacecraft control laboratory experiment (SCOLE) slew maneuvers
[NASA-CR-4098] 01 p0014 N88-10082
Transactions of the 4th Army Conference on Applied Mathematics and Computing
[AD-A183544] 01 p0085 N88-10547
Stirling engine research at national and university laboratories in Japan
[DE87-014622] 02 p0180 N88-11123
The Lewis Strain Gauge Laboratory: Status and plans
02 p0184 N88-11146
Lewis' enhanced laboratory for research into the fatigue and constitutive behavior of high temperature materials
02 p0189 N88-11177
Control design challenges of large space systems and spacecraft control laboratory experiment (SCOLE)
[NASA-CR-178392] 03 p0275 N88-11735
Electronics engineering thrust area report, FY86
[DE87-014616] 03 p0309 N88-11950
LLE (Laboratory for Laser Energetics) review, volume 31
[DE87-013732] 03 p0328 N88-12072
Materials sciences programs: Fiscal Year 1987
[DE88-000672] 04 p0429 N88-12659
Realization of the immediate objectives of the Aero-Gas Dynamics and Vibration Laboratory (LAGG) at the National Center for Research, Science and Technology (PUSPIPTEK) at Serpong, Java (indonesia). Project TTA-79
[GG/QPR-10] 08 p1092 N88-16572
Experience of developing an integrated nondestructive assay system
[DE88-003149] 09 p1184 N88-17092
A study of federal technology transfer to the commercial sector
[AD-A187017] 09 p1262 N88-17560
Helsinki University of Technology Communications Laboratory
[PB88-112974] 10 p1318 N88-17881
Laboratory evaluation and analysis of advanced lead-acid load-leveling batteries
[DE88-002851] 10 p1349 N88-18064
Engineering thrust areas, 1988
[DE88-005103] 11 p1468 N88-18753
Aviation turbine fuels from tar sands bitumen and heavy oils. Part 3: Laboratory sample production
[AD-A189278] 13 p1753 N88-20484
Laboratory Information Management System (LIMS): A case study
[NASA-TM-100835] 14 p1961 N88-21697
Study of lightning and lightning protection (selected pages)
[AD-A190623] 15 p2098 N88-22498
DOE (Department of Energy) national laboratories and the semiconductor industry: Continuing the joint planning
[PB88-170295] 16 p2281 N88-23657
An overview of advanced battery development at Sandia National Laboratories
[DE88-006823] 18 p2506 N88-24867
Inference and discovery in an exploratory laboratory
[AD-A192231] 20 p2832 N88-26801
Experimental study of planetary gases with applications to planetary interior models
[NASA-CR-183098] 20 p2886 N88-27137
Development of radiation and cloud parameterization programs for AFGL (Air Force Geophysics Laboratory) global models
[AD-A193[illegible]9] 21 p2973 N88-27658
Activities report of the Werner-Heisenberg Institute of Physics
[ETN-88-92946] 21 p3015 N88-27893
An evaluation of Interactive Laboratory System software, ILS-PC/DOS: A digital signal processing software package
[AD-A193838] 22 p3138 N88-28657
Laboratory feasibility study of a composite embedded fiber optic sensor for measurement of structural vibrations
[AD-A194270] 22 p3152 N88-28754
Center for opto-electronic systems research
[AD-A195159] 24 p3429 N88-30411
Electronic materials and devices prepared by molecular beam epitaxy
[AD-A195694] 24 p3433 N88-30433

LABORATORY EQUIPMENT
NT IMAGE FURNACES
A preliminary study of a fluid science laboratory for space station (Columbus). Part 4: Executive summary
[NLR-TR-87023-L-PT-4] 02 p0170 N88-11072
A low volume insert for solid state magic angle spinning NMR of small samples
[AD-A184359] 04 p0419 N88-12601
Measurements in an electromagnetic test laboratory
[SNIAS-872-430-102] 05 p0575 N88-13507
Electromagnetic tests
[SNIAS-872-430-103] 05 p0575 N88-13508
Controlled Ecological Life Support System: Design, Development, and Use of a Ground-Based Plant Growth Module
[NASA-CP-2479] 05 p0630 N88-13852
CELSS Program Meeting 05 p0630 N88-13853
Metrology and calibrating laboratories
[ETN-88-90761] 06 p0670 N88-14104
Data analysis at the Oulu (Finland) EISCAT laboratory
06 p0691 N88-14241
Practical photochemistry: General considerations
[PB87-123386] 06 p0730 N88-14491
Design of a velocity and position control laboratory servo system
[AD-A186596] 08 p0990 N88-15997
The ESA Anthrorack project: integrated research in human physiology 08 p1033 N88-16265
A laboratory railgun for terminal ballistics and arc armature research studies
[AD-A187225] 11 p1442 N88-18603
ESA's facility for research in human physiology in space: Anthrorack 12 p1652 N88-19896
The ESA facility Biorack 12 p1652 N88-19897
Exobiology and botany facilities for EURECA
12 p1652 N88-19898
BIOTEX, a project for biotechnological basic experiments under microgravity --- Spacelab
12 p1652 N88-19899
Life science techonology --- space applications
12 p1653 N88-19900
Second-generation respiratory monitoring system for microgravity studies in man 12 p1653 N88-19906
Development of an optical diagnostic instrument. Part 2: Instrument development --- space laboratories
[NLR-TR-87079-L-PT-2] 13 p1841 N88-21016
Environment test laboratory
[ETN-88-91885] 14 p1869 N88-21166
Interfacial structure-property relationships at the fiber-matrix interphase in advanced composites
[AD-A190649] 15 p2030 N88-22093
The CRREL (Cold Regions Research and Engineering Laboratory) Hopkinson bar apparatus
[AD-A190599] 15 p2077 N88-22380
Mechanisms mediating perception of complex acoustic patterns
[AD-A189765] 15 p2102 N88-22520
Laboratory equipment update
[AD-A189781] 15 p2102 N88-22522
Microgravity mechanisms and robotics program
16 p2219 N88-23237
Spectroradiometry in the industrial test laboratory
16 p2272 N88-23598
Impact of control errors on the volume/weight demand of the Ventilation and Dryer (VAD) concept --- EURECA Botany Facility
[TN-RB524-006/87] 17 p2377 N88-24132
Botany Facility pre-phase C/D: Core payload for EURECA, volume 1
[BF-RP-ER-015-VOL-1] 17 p2379 N88-24144
SHaRE: Collaborative materials science research
[DE88-007175] 18 p2467 N88-24646
Laboratory experiments on atmospheric OH reactions
18 p2539 N88-25066
Hanging drop crystal growth apparatus and method
[NASA-CASE-MFS-28206-1-SB]
18 p2585 N88-25356
Biorack on Spacelab D1: An overview of the first flight of Biorack, an ESA facility for life sciences research in microgravity
[ESA-SP-1091] 22 p3059 N88-28154
A brief overview of the results of the experiments using the ESA Biorack Facility on the German Spacelab D1 mission 22 p3060 N88-28155
The Biorack facility and its performance during the D1 Spacelab mission 22 p3060 N88-28156
Dosimetric mapping inside Biorack --- Spacelab D1 mission 22 p3062 N88-28169
Biorack thermal performance during the D1 mission --- Spacelab 22 p3062 N88-28170
A 400 kV ion implanter: Operating principles and applications 22 p3069 N88-28213
An evaluation of Interactive Laboratory System software, ILS-PC/DOS: A digital signal processing software package
[AD-A193838] 22 p3138 N88-28657

Research and development objectives: Installation, startup, and test operation of a remote and program controlled measuring table for the calibration of EGRET experiment
[ETN-88-92105] 22 p3152 N88-28752
Biosample: Preservation, handling and observation system synthesis and breadboarding --- Spacelab
[ESA-CR(P)-2609] 24 p3336 N88-29857
Crystal structures of ordered carbon metal alloys
[AD-A195597] 24 p3353 N88-29959
Accommodation concept for fluid physics facilities, volume 2 --- Spacelab
[SG-TN-AI-027-VOL-2] 24 p3358 N88-29994

LABYRINTH
NT COCHLEA
NT OTOLITH ORGANS
NT SEMICIRCULAR CANALS
NT VESTIBULES

LABYRINTH SEALS
Three-dimensional dynamic labyrinth seal analysis
[AD-A185353] 05 p0590 N88-13599
Flow in labyrinth seals and its influence on rotor stability of turbocompressors 07 p0851 N88-15168
A comparison of experimental and theoretical results for labyrinth gas seals with honeycomb stators
[NASA-CR-182441] 08 p0993 N88-16006
Experimental rotordynamic coefficient results for honeycomb seals
[NASA-CR-182440] 08 p0993 N88-16007

LACE (ENGINE)
U LIQUID AIR CYCLE ENGINES

LACTATES
Oxygen transport during exercise at extreme simulated altitude: Operation Everest 2
[AD-A185720] 06 p0752 N88-14620

LAG (DELAY)
U TIME LAG

LAGEOS (SATELLITE)
The Monte Generoso-Zimmerwald (Switzerland) baseline from satellite laser ranging data using various analysis techniques
[LR-533] 14 p1940 N88-21576
Determining earth's rotation from laser observations of Lageos artificial earth satellite (during period of main merit campaign) 24 p3449 N88-30528

LAGOONS
Five New South Wales barrier lagoons: Their macrobenthic fauna and seagrass communities
11 p1517 N88-19059

LAGRANGE COORDINATES
The evolution of HOBO
[DE87-014742] 03 p0313 N88-11980
A Lagrangian moving grid scheme for one-dimensional evolutionary partial differential equations
[CWI-NM-R8713] 13 p1827 N88-20922
Singular Lagrangians. Classical dynamics and quantization. Lectures for young scientists
[DE88-701158] 15 p2146 N88-22806
A nonlinear computation for composite structures
[ONERA-RT-15/3542-RY-062-R]
16 p2222 N88-23265
Classical non-Abelian solutions for nonstandard Lagrangians
[DE88-701305] 16 p2263 N88-23532

LAGRANGE EQUATIONS OF MOTION
U EULER-LAGRANGE EQUATION

LAGRANGE MULTIPLIERS
Generalized hybrid variational principle, corresponding finite element model 03 p0301 N88-11895
Lagrangian procedures for higher order field equations
[DE87-703365] 05 p0640 N88-13911
A substructure method for dynamic simulation of flexible mechanical systems with geometric nonlinearities
09 p1176 N88-17044
A concurrent neural network algorithm for the traveling salesman problem
[DE88-006981] 18 p2562 N88-25208
The use of Lagrange multipliers and Kuhn-Tucker's theory in optimization problems
18 p2565 N88-25236
Surface tension and viscosity with Lagrangian hydrodynamics on a triangular mesh
[AD-A194120] 22 p3075 N88-28258
Lagrangian of the self-duality equation and d = 10, N = 2b supergravity
[DE88-701554] 24 p3455 N88-30563

LAGRANGE SIMILARITY HYPOTHESIS
Fully Lagrangian Renormalized Approximation theory of fluid turbulence
[DE88-004960] 10 p1330 N88-17952
Center for Turbulence Research 1987 activities
[NASA-CR-182693] 13 p1769 N88-20583

LAGRANGIAN EQUILIBRIUM POINTS
Single-burn transfer to nominally periodic orbit in the vicinity of point L2 of Earth-Sun system and related problems 08 p1006 N88-16100

LAGUERRE FUNCTIONS
Generalizations of Laguerre (type) polynomials
[REPT-87-58] 14 p1963 N88-21714

LAKE ICE
NT ICE FLOES

LAKES
Using space photography of the Earth in the classroom: Drought in Africa
[NASA-CR-182948] 19 p2685 N88-25960
Eigenmatrix representations of radiance distributions in layered natural waters with wind-roughened surfaces
[PB88-188701] 20 p2828 N88-26780
SPOT on land and lakes in the Hubei Province (China)
22 p3090 N88-28351

LAMB WAVES
Different ways of looking at the electromagnetic vacuum
[DE87-013150] 01 p0089 N88-10584
Thin-membrane Lamb-mode acoustic oscillators for chemical detection 19 p2673 N88-25895
Relativistic theory of the Lamb shift based on self energy
[DE88-702658] 23 p3295 N88-29626

LAMINA
U LAYERS

LAMINAR BOUNDARY LAYER
Excitation of natural oscillations of a boundary layer by an external acoustic field 04 p0425 N88-12634
Hypersonic laminar boundary layer: Parametric study for the representation of real gas effects
05 p0532 N88-13236
Navier-Stokes analysis of laminar flow control of a two-dimensional airfoil 05 p0540 N88-13286
Structural tests and development of a laminar flow control wing surface composite chordwise joint
[NASA-CR-172462] 06 p0663 N88-14066
Investigation of viscous/inviscid interaction in transonic flow over airfoils with suction 06 p0664 N88-14074
Upwind relaxation algorithms for Euler/Navier-Stokes equations 07 p0810 N88-14931
Numerical simulation of a controlled boundary layer
07 p0810 N88-14933
Computational design of natural laminar flow wings for transonic transport application 07 p0813 N88-14948
Flight research on natural laminar flow
07 p0813 N88-14950
Design and experimental evaluation of a swept supercritical Laminar Flow Control (LFC) airfoil
07 p0813 N88-14951
Laminar flow integration: Flight tests status and plans
07 p0813 N88-14952
Roughness and waviness requirements for laminar flow surfaces 07 p0813 N88-14953
Nonlinear and nonparallel stability problems
[AD-A186406] 07 p0850 N88-15159
A computationally efficient modelling of laminar separation bubbles
[NASA-CR-182417] 08 p0984 N88-15949
Numerical simulation of the interaction of pressure waves with laminar and turbulent boundary layers
[DFVLR-FB-87-18] 09 p1161 N88-16960
Boundary layer calculation using digital computers
[REPT-MM-4] 10 p1309 N88-17821
Velocity measurements in a 3D (three dimensional) shock wave laminar boundary layer interaction
[AD-A187334] 10 p1332 N88-17959
A simplified streamline swallowing procedure for the windward meridian of axisymmetric blunt bodies
[AD-A188413] 12 p1626 N88-19732
Development of disturbances in swept wing flows
[NASA-CR-182675] 13 p1768 N88-20574
The NASA Langley Laminar-Flow-Control (LFC) experiment on a swept, supercritical airfoil: Design overview
[NASA-TP-2809] 14 p1861 N88-21117
Application of hybrid laminar flow control to global range military transport aircraft
[NASA-CR-181638] 14 p1862 N88-21124
Modifications to the Langley 8-foot transonic pressure tunnel for the laminar flow control experiment
[NASA-TM-4032] 15 p2021 N88-22047
Investigation of boundary layer disturbances caused by periodic heating of a thin ribbon
[AD-A190572] 15 p2065 N88-22314
Aerothermal tests of quilted dome models on a flat plate at a Mach number of 6.5
[NASA-TP-2804] 15 p2067 N88-22325
Design method for laminar flow control of two-dimensional airfoils in incompressible flow. Numerical study of LFC design concepts
[DE88-751809] 16 p2155 N88-22859
The simulation of coherent structures in a laminar boundary layer 16 p2198 N88-23111
A new laminar water tunnel to study the transition process in a blasius layer and in a separation bubble and a new tool for industrial aerodynamics and hydrodynamic research 16 p2204 N88-23150
Solution of the compressible Navier-Stokes equations of motion by Chebyshev polynomials for laminar shock-boundary layer flow
[AD-A191033] 16 p2208 N88-23176
Boundary-layer stability and airfoil design
17 p2296 N88-23738
Numerical simulations of the flat-plate laminar boundary layer in subsonic and supersonic flow
[PDR/CFDU/IC/36] 18 p2511 N88-24895
Aerodynamic analysis of natural laminar flow airfoil
19 p2634 N88-25624
Active control of 2-D instability waves on an axisymmetric body
[AD-A191578] 19 p2663 N88-25835
Comparison of the wall pressure fluctuations in artificially generated turbulent spots, natural transition and turbulent boundary layers
[AD-A191777] 19 p2663 N88-25838
Boundary layer development as a function of chamber pressure in the NASA Lewis 1030:1 area ratio rocket nozzle
[NASA-TM-100917] 19 p2664 N88-25841
Analysis of experimental data for cast 10-2/DOA2 supercritical airfoil at high Reynolds numbers
[AD-A192827] 21 p2892 N88-27186
Flow dynamics stimulated by hairpin-like vortices in initially laminar boundary layers
[AD-A194253] 22 p3075 N88-28254
Solution to the compressible Navier-Stokes equations of motion by Chebyshev polynomials with implicit time stepping
[AD-A194119] 22 p3075 N88-28257
Coupled inviscid - boundary layer methods for turbomachinery blading design
[PNR90437] 22 p3076 N88-28260
Techniques for boundary layer tripping and control
23 p3168 N88-28863
Numerical simulation of the interaction of pressure waves with laminar and turbulent boundary layers
[ESA-TT-1089] 24 p3371 N88-30075

LAMINAR BOUNDARY LAYER SEPARATION
U BOUNDARY LAYER SEPARATION
U LAMINAR BOUNDARY LAYER

LAMINAR FLAMES
U FLAMES
U LAMINAR FLOW

LAMINAR FLOW
NT BLASIUS FLOW
NT STRATIFIED FLOW
Laminar flow over a spinning projectile at an angle of attack 02 p0121 N88-10766
Radiative and free-convective heat transfer from a finite horizontal plate inside an enclosure
02 p0133 N88-10833
Transition to turbulence via spatio-temporal intermittency 03 p0313 N88-11976
Heat transfer in laminar flow for mass inlet into an annular channel
[DE87-702890] 03 p0314 N88-11983
Numerical study of the entrance flow and its transition in a circular pipe (2) 03 p0318 N88-12011
Experiments on densely loaded non-Newtonian slurries in laminar and turbulent pipe flows
[DE88-000719] 04 p0442 N88-12746
Studies of pressure-velocity coupling schemes for analysis of incompressible and compressible flows
[NASA-CR-181526] 04 p0443 N88-12748
On the numerical simulation of three-dimensional hypersonic flow 05 p0532 N88-13237
Structural tests and development of a laminar flow control wing surface composite chordwise joint
[NASA-CR-172462] 06 p0663 N88-14066
Visible boundary layer transition points through flight tests 06 p0675 N88-14136
Numerical simulation of boundary layers. Part 3: Turbulence and relaminarization in sink flows
[NASA-TM-88220] 06 p0698 N88-14283
Experimental investigation of heterogeneous compressible shear layers 06 p0700 N88-14294
Three-dimensional structure of boundary layers in transition to turbulence
[AD-A185466] 06 p0702 N88-14311
A multistage time-stepping scheme for the thin-layer Navier-Stokes equations 07 p0810 N88-14932
Flow diagnostics and visualization in wind tunnels and flight 07 p0811 N88-14940
Overview of the Langley viscous drag reduction program 07 p0812 N88-14946
Advanced natural laminar flow airfoil with high lift to drag ratio 07 p0812 N88-14947
Natural laminar flow nacelle for transport aircraft
07 p0813 N88-14949

Flight research on natural laminar flow
07 p0813 N88-14950
Laminar flow integration: Flight tests status and plans
07 p0813 N88-14952
Insect contamination protection for laminar flow surfaces 07 p0814 N88-14954
Laminar flow control leading edge glove flight test article development
[NASA-CR-172137] 07 p0815 N88-14960
Viscous drag reduction of horizontal plates
[VKI-TN-159] 07 p0851 N88-15171
Experimental and theoretical study on cavitation inception and bubbly flow dynamics. Part 1: Design, development and operation of a cavitation susceptibility meter. Part 2: Linearized dynamics of bubbly and cavitating flows with bubble dynamics effects
[AD-A187133] 09 p1160 N88-16952
Navier-Stokes solutions for laminar incompressible flow over a NACA 0012 airfoil and a backward facing step
[FFA-TN-1987-50] 09 p1162 N88-16966
Solution of the three-dimensional Navier-Stokes equations for transonic flow using a multigrid method
10 p1267 N88-17579
On some asymptotics of laminar flow in a coiled pipe
10 p1328 N88-17936
An experimental investigation of the hydrodynamic and heat-transfer behavior of aqueous foam in laminar tube flow
[DE88-004954] 11 p1483 N88-18855
Laminar flow heat transfer downstream from U-bends
11 p1484 N88-18859
A velocity-pressure integrated, mixed interpolation, Galerkin finite element method for high Reynolds number laminar flows
[NASA-CR-179264] 11 p1486 N88-18868
Transient radiative energy transfer in incompressible laminar flows
[NASA-CR-182605] 11 p1488 N88-18883
Solution of a rotating Navier-Stokes problem by a nonlinear multigrid algorithm 11 p1536 N88-19194
The NASA Langley Laminar-Flow-Control (LFC) experiment on a swept, supercritical airfoil: Design overview
[NASA-TP-2809] 14 p1861 N88-21117
Application of hybrid laminar flow control to global range military transport aircraft
[NASA-CR-181638] 14 p1862 N88-21124
Constructing Gloved wings for aerodynamic studies
[NASA-TM-100440] 14 p1863 N88-21128
Duct flow nonuniformities: Effect of struts in SSME HGM II(+)
[NASA-CR-179285] 15 p2062 N88-22296
Experiments on densely-loaded non-Newtonian slurries in laminar and turbulent pipe flows
[DE88-006209] 15 p2067 N88-22323
Wave-growth associated with turbulent spot in plane Poiseuille flow 16 p2199 N88-23116
Experimental study of vortex sheets in plane flow
16 p2203 N88-23142
Simulation of laminar-turbulent transition in the vicinity of a wall
[AD-A191380] 16 p2208 N88-23160
Laminar Flow Aircraft Certification
[NASA-CP-2413] 17 p2296 N88-23737
Boundary-layer stability and airfoil design
17 p2296 N88-23738
High-flaps for natural laminar flow airfoils
17 p2296 N88-23739
Computational wing design studies relating to natural laminar flow 17 p2297 N88-23740
Wind tunnel testing of low-drag airfoils
17 p2297 N88-23741
Flight experiences with laminar flow
17 p2297 N88-23744
Manufacturing requirements 17 p2297 N88-23745
Preliminary aerodynamic design considerations for advanced laminar flow aircraft configurations
17 p2297 N88-23746
Natural laminar flow and airplane stability and control
17 p2298 N88-23747
Operational considerations for laminar flow aircraft
17 p2298 N88-23748
Certification aspects of airplanes which may operate with significant natural laminar flow 17 p2298 N88-23749
Wave growth associated with turbulent spots in plane Poiseuille flow
[FFA-TN-1988-08] 18 p2457 N88-24587
Prediction of laminar and turbulent flows past single and twin airfoils 18 p2457 N88-24589
Theoretical analysis of laminar incompressible flow in slender channels
[VTH-LR-517] 18 p2513 N88-24909
Method and apparatus for detecting laminar flow separation and reattachment
[NASA-CASE-LAR-13952-1-SB]
18 p2513 N88-24910
Method of forming a multiple layer dielectric and a hot film sensor therewith
[NASA-CASE-LAR-13678-1] 18 p2584 N88-25355
Drag measurements on a laminar flow body of revolution in Langley's 13 inch magnetic suspension and balance system
[NASA-CR-182909] 19 p2597 N88-25432
Structure of laminar, premixed flames of CH2O/NO2/O2 mixtures 19 p2632 N88-25613
Finite element analysis of incompressible viscous flow around multi-element aerofoils 19 p2635 N88-25634
Numerical simulation of transition to turbulence in plane Poiseuille flow by a spectral method
19 p2640 N88-25661
Boundary layer development as a function of chamber pressure in the NASA Lewis 1030:1 area ratio rocket nozzle
[NASA-TM-100917] 19 p2664 N88-25841
Numerical simulation studies of laminar-turbulent transition in the plan channel 19 p2665 N88-25850
Navier-Stokes code NS3D for blunt bodies. Part 1: Analysis, results and verification
[DE88-010105] 19 p2666 N88-25855
Experiments on densely-loaded non-Newtonian slurries in laminar and turbulent pipe flows
[DE88-010579] 20 p2800 N88-26612
Velocity-pressure integrated versus penalty finite element methods for high Reynolds number flows
[NASA-CR-179357] 20 p2803 N88-26635
The structure and stability of nonpremixed gas jet flames 21 p2908 N88-27257
Turbulent flow field visualization with integral interferometric imaging and computed tomography
21 p2950 N88-27521
Runge-Kutta finite-volume simulation of laminar transonic flow over the ONERA M6 wing using the Navier-Stokes equations
[FFA-TN-1987-06] 22 p3039 N88-28045
Theoretical study and numerical simulation of flame fronts
[PB88-122932] 22 p3051 N88-28104
Application of rectangular co-ordinates to the problem of laminar combined convection in a straight horizontal tube whose circumference is heated nonuniformly
[PDR/CFDU/IC/33] 22 p3076 N88-28263
The Kelvin-Helmholtz instability in a stratified shear flow
[CFD/88/2] 22 p3076 N88-28265
Mass transport in annular spherical system
[LRT-WE-9-FB-11(1987)] 22 p3077 N88-28271
Variable Sweep Transition Flight Experiment (VSTFE)-parametric pressure distribution boundary layer stability study and wing glove design task
[NASA-CR-3992] 23 p3173 N88-28894
Pressure distributions from subsonic tests of an advanced laminar-flow-control wing with leading- and trailing-edge flaps
[NASA-TM-4040-PT-2] 24 p3321 N88-29776
Radiation from soot-containing flames
24 p3347 N88-29927
Techniques used in the F-14 variable-sweep transition flight experiment
[NASA-TM-100444] 24 p3374 N88-30093
LAMINAR FLOW AIRFOILS
Wind-tunnel investigation of a full-scale general aviation airplane equipped with an advanced natural laminar flow wing
[NASA-TP-2772] 01 p0002 N88-10009
Wind tunnel results for a high-speed, natural laminar-flow airfoil designed for general aviation aircraft
[NASA-TM-87602] 06 p0665 N88-14078
Oscillating airfoils: Achievements and conjectures
[AD-A190490] 15 p2014 N88-22008
Design method for laminar flow control of two-dimensional airfoils in incompressible flow. Numerical study of LFC design concepts
[DE88-751809] 16 p2155 N88-22859
Laminar Flow Aircraft Certification
[NASA-CP-2413] 17 p2296 N88-23737
Pressure distributions from subsonic tests of an advanced laminar-flow-control wing with leading- and trailing-edge flaps
[NASA-TM-4040-PT-1] 17 p2300 N88-23758
Instability of laminar separation bubbles: Causes and effects
[AD-A191168] 18 p2508 N88-24876
Calibration of averaging total pressure flight wake rake and natural-laminar-flow airfoil drag certification
[NASA-CR-181630] 19 p2599 N88-25443
JPRS report: Science and technology. Japan
[JPRS-JST-88-005] 19 p2633 N88-25619
Aerodynamic analysis of natural laminar flow airfoil
19 p2634 N88-25624
Solution to the compressible Navier-Stokes equations of motion by Chebyshev polynomials with implicit time stepping
[AD-A194119] 22 p3075 N88-28257
LAMINAR FLOW CONTROL
U BOUNDARY LAYER CONTROL
U LAMINAR BOUNDARY LAYER
LAMINAR HEAT TRANSFER
Heat transfer in laminar flow for mass inlet into an annular channel
[DE87-702890] 03 p0314 N88-11983
An experimental investigation of the hydrodynamic and heat-transfer behavior of aqueous foam in laminar tube flow
[DE88-004954] 11 p1483 N88-18855
Heat transfer modeling of jet vane Thrust Vector Control (TVC) systems
[AD-A190106] 15 p2019 N88-22034
Forced-convection, liquid-cooled, microchannel heat sinks
[AD-A193337] 21 p2937 N88-27444
LAMINAR JETS
U JET FLOW
U LAMINAR FLOW
LAMINAR WAKES
A mapping of the viscous flow behavior in a controlled diffusion compressor cascade using laser Doppler velocimetry and preliminary evaluation of codes for the prediction of stall
[AD-A194490] 23 p3211 N88-29112
LAMINATED MATERIALS
U LAMINATES
LAMINATES
Joints in carbon fibre reinforced composites
[BR99969] 01 p0019 N88-10114
Effect of adhesive layers on impact damage and dynamic response in composite laminates
02 p0141 N88-10887
A stochastic delamination growth model for fatigue loaded laminated composite materials
02 p0141 N88-10888
Cumulative fatigue and life prediction of fibre composites. Part 1: Literature reviews
[BR101013] 02 p0142 N88-10893
Cumulative fatigue and life prediction of fibre composites. Part 2: Experimental techniques and results
[BR101014] 02 p0142 N88-10894
Contribution to the study of composite materials and their damage
[NASA-TT-20107] 02 p0143 N88-10897
Theoretical investigation of stress concentrations in damaged carbon fibre reinforced plastic plate structures. Volume 1: Main text
[BR99872-VOL-1] 03 p0280 N88-11761
Theoretical investigation of stress concentrations in damaged carbon fibre reinforced plastic plate structures. Volume 2: Tables, figures and plates
[BR99873-VOL-2] 03 p0280 N88-11762
Carbon-fiber reinforced plastics
04 p0403 N88-12506
Thixotropic surface composition for phenolaldehyde resin laminates
[GB-PATENT-2-180-251-A] 04 p0410 N88-12545
Study of zero CTE (Coefficients of Thermal Expansion) of graphite/epoxy composites
[DE87-013557] 04 p0412 N88-12554
Spatial strength variation and statistical size effect of laminated orthotropic composite materials
04 p0427 N88-12646
A refined nonlinear analysis of laminated composite plates and shells
[AD-A184436] 04 p0454 N88-12811
Vibration and buckling of geometrically imperfect laminated cylindrical shells 04 p0456 N88-12822
Dynamic response of laminated composite plates using a three-dimensional hybrid-stress finite-element formulation 05 p0596 N88-13639
Fatigue mechanisms in ARALL, a fatigue resistant hybrid aluminum aramid composite material
05 p0605 N88-13711
Behavior of bolted joints in composite laminates
06 p0677 N88-14148
Evaluation of closed cubic failure criterion for graphite/epoxy laminates
[NASA-CR-182375] 06 p0679 N88-14158
Stresses and displacements in two, three and four layered structures submitted to flexible or rigid loads
[AD-A185707] 06 p0723 N88-14450
Experimental and theoretical investigation of mechanically fastened composites
[AD-A185896] 07 p0826 N88-15008
Investigation of low velocity impact damage on filamentary composite materials
07 p0923 N88-15607
Postbuckling of laminated anisotropic panels
[NASA-TM-100509] 08 p0994 N88-16011

Failure modes of laminate structures
[DE88-002579] 08 p0996 N88-16033
Sublaminate damage mechanisms in composite structures
[AD-A186807] 09 p1137 N88-16815
Fatigue and damage tolerance design data for carbon fibre composites
[BAE-MSM-R-GEN-0454] 09 p1138 N88-16818
Fatigue behaviour of hybrid composites
[BR102236] 09 p1138 N88-16819
Effects of processing variables on the behavior of E-glass/913 and XAS carbon fibre/913 laminates subjected to hot/wet environmental conditions
[BR101940] 09 p1138 N88-16820
Effect of low velocity impact on compression strength of a quasi-isotropic laminate
[FFA-TN-1987-38] 09 p1138 N88-16822
Finite element analysis of damaged cross-ply composite laminates
[CCMS-87-10] 09 p1139 N88-16829
An analytical study of the effects of transverse shear deformation and anisotropy on natural vibration frequencies of laminated cylinders
[NASA-TM-100554] 10 p1295 N88-17739
Analytical and experimental characterization of damage processes in composite laminates
[AD-A187221] 10 p1296 N88-17746
Piezoelectric laminates for torsional and bending model control: Theory and experiment
10 p1343 N88-18029
Ultrasonic characterization of layered composite systems 10 p1404 N88-18374
On delamination of (+ or - theta sub m/90 sub n/2) sub s laminates subject to tensile loading
[AD-A188095] 11 p1447 N88-18626
Colloquium on damage mechanics of graphite/expoxy laminates during fatigue
[DFVLR-MITT-87-08] 11 p1448 N88-18630
Influence of different parameters on damage development --- carbon fiber reinforced plastics
11 p1448 N88-18632
Initiation and propagation of damage in notched unidirectional and multidirectional CFRE resin laminates
11 p1449 N88-18633
Damage initiation and growth in sateen laminates under static and cyclic loading 11 p1449 N88-18634
Damage mechanisms of CFRP riveted joints
11 p1449 N88-18636
Damage mechanisms and fatigue life prediction of graphite/epoxy laminates 11 p1449 N88-18637
Innovative design of composite structures: Further studies in the use of a curvilinear fiber format to improve structural efficiency
[NASA-CR-182576] 11 p1450 N88-18641
An experimental and numerical study of notch sensitivity of ARALL laminates
[CCMS-88-04] 11 p1450 N88-18644
Analysis of composite laminates with matrix cracks
[CCMS-88-03] 11 p1451 N88-18645
A nonlinear computational model for the strength and failure of composite plates and shells
11 p1501 N88-18964
An experimental measurement of metal multilayer X-ray reflectivity degradation due to intense X-ray flux
[LA-10989-T] 11 p1547 N88-19255
Wave propagation in laminated composite plates
[AD-A188999] 12 p1604 N88-19594
Ultrasonic-velocity studies of composite and heterogeneous materials
[AD-A189000] 12 p1604 N88-19595
Multilayer thermal insulation tests
[INPE-4475-PRE/1243] 12 p1626 N88-19729
Simulated impact damage in a thick graphite/epoxy laminate using spherical indenters
[NASA-TM-100539] 13 p1733 N88-20363
Transient dynamics of fibre reinforced composite plates
[IIT-B/CE/RR/87-1] 13 p1734 N88-20370
Delamination stresses in semicircular laminated composite bars
[NASA-TM-4026] 13 p1735 N88-20375
Nondestructive evaluation of carbon-carbon coatings
[AD-A189524] 13 p1748 N88-20453
Exploring the relation between interface structure and mechanical properties in multilayer structures
[DE88-005428] 13 p1848 N88-21060
Studies of traverse impact damage in composite materials using a Hopkinson pressure-bar technique
[OUEL-1706/87] 14 p1883 N88-21255
Environmental effects on the post-impact compressive strength of CFC
[RAE-TM-MAT-STR-1088] 14 p1884 N88-21258
Strength and failure analysis of composite laminate containing a circular hole with reinforcement
[AD-A189629] 14 p1884 N88-21260
Crack resistance of multilayer ceramic-based composite material 14 p1885 N88-21265
Influence of heat treatment on the properties of boroaluminum 14 p1886 N88-21270
Stress-strain behaviour of a bolt hole in carbon fibre composite plates
[BU-354] 14 p1923 N88-21460
An investigation of the failure response of laminates under biaxial stress
[AD-A190039] 15 p2029 N88-22090
Interlaminar fracture toughness of thermoplastic composites
[NASA-TM-100532] 15 p2030 N88-22097
A system to measure damage in composite materials by the ultrasonic method
[ONERA-RT-2/7256-RY-061-R]
15 p2031 N88-22103
Donor acceptor polymerization chemistry as a vehicle to low energy cure matrix resins
[AD-A190119] 15 p2044 N88-22179
The buckling and vibration of composite plates using the Levy method considering shear deformation and rotary inertia
[AD-A189743] 15 p2076 N88-22374
Impact damage in composite laminates
15 p2080 N88-22402
Design studies of primary aircraft structures in ARALL laminates
[LR-520] 16 p2160 N88-22888
A study of failure characteristics in thermoplastic composite material
[AD-A190613] 16 p2171 N88-22940
Fatigue damage development of various CFRP-laminates
[NASA-TT-20247] 16 p2172 N88-22945
Behaviour of fibre-reinforced composites under dynamic loading
[AD-A191310] 16 p2174 N88-22955
On the calculation of stresses in pin-loaded anisotropic plates
[LR-529] 16 p2223 N88-23268
GARTEUR TP-037: Impact damage tolerance of carbon fiber and hybrid laminates
[RAE-TR-87057] 17 p2316 N88-23837
Local delamination buckling in layered structures
18 p2480 N88-24711
Damage by creep fatigue: Influence of the visco-elasticity of the matrix
[PB88-124706] 18 p2528 N88-24998
On the bending response of Kevlar 49/epoxy beams and rings
[DE88-006824] 18 p2530 N88-25012
Method of forming a multiple layer dielectric and a hot film sensor therewith
[NASA-CASE-LAR-13678-1] 18 p2584 N88-25355
Metastability in SiGe/Si strained-layer structures
[DE88-007603] 18 p2585 N88-25361
Fuel containment and damage tolerance in large composite primary aircraft structures. Phase 2: Testing
[NASA-CR-172519] 19 p2601 N88-25452
Fracture physics of delamination of composite materials
[AD-A192021] 19 p2609 N88-25482
Loading rate sensitivity of open hole composites in compression
[NASA-TM-100634] 19 p2610 N88-25490
Silver multi-layers for planar Ag/AgCl reference electrodes 19 p2672 N88-25883
Stiffness degradation of composite laminates
20 p2767 N88-26405
Instability-related delamination growth of embedded and edge delaminations 20 p2767 N88-26406
Computation equipment for damage simulation in laminated composites
[AD-A193013] 20 p2768 N88-26412
A micromechanics model of the stiffness and strength of laminates with fiber waviness
[NASA-CR-181670] 20 p2768 N88-26413
Compression creep of filamentary composites
[NASA-CR-182550] 20 p2798 N88-26601
Three-dimensional analysis of a postbuckled embedded delamination
[NASA-TP-2823] 20 p2812 N88-26684
Analysis of the perforation of monolithic and simple laminate aluminium targets as a test of analytical deformation models
[MRL-R-1111] 20 p2813 N88-26686
Properties of multilayers for soft X-ray optics
20 p2867 N88-27025
The two isotropic asymptotes of fiber composites
[AD-A192305] 21 p2904 N88-27231
An experimental and analytical evaluation of a biaxial test for determining shear properties of composite materials
[NASA-CR-182928] 21 p2962 N88-27593
Failure analysis of quasi-isotropic composite laminates with free edges under off-axis loading
22 p3049 N88-28092
Analysis of stiffness reduction, failure and stress concentration in fiber composite laminates
[AD-A193519] 22 p3050 N88-28096
Micromechanics of composite laminate compression failures
[NASA-CR-183179] 22 p3050 N88-28098
Wave propagation and vibration of fibre reinforced laminates
[AD-A194144] 22 p3051 N88-28101
Array trade-off study using multilayer parasitic subarrays
[NASA-TM-101321] 22 p3070 N88-28222
Elastic wave dispersion in laminated composite plate
[AD-A192269] 23 p3188 N88-28967
A comprehensive study on damage tolerance properties of notched composite laminates
[AD-A192952] 23 p3188 N88-28968
Thermal stress analysis in PMR-15 carbon fibre laminates
[ETN-88-93123] 24 p3341 N88-29886
ZT imaging system for layered thin wall structures
[AD-A195466] 24 p3352 N88-29954
Modeling of micromechanisms of fatigue and fracture in hybrid materials
[AD-A195604] 24 p3382 N88-30142
Large displacement and rotational formulation for laminated cylindrical shells including parabolic transverse shear
[AD-A194871] 24 p3384 N88-30158

LAMINATIONS
U LAMINATES

LAMPS
U LUMINAIRES

LAN (COMPUTER NETWORKS)
U LOCAL AREA NETWORKS

LAND
NT ARID LANDS
NT COASTAL PLAINS
NT DESERTS
NT FARMLANDS
NT FLOOD PLAINS
NT GRASSLANDS
NT MARSHLANDS
NT PARKS
NT PLAINS
NT PLAYAS
NT SAHARA DESERT (AFRICA)
NT TUNDRA
NT WETLANDS
An exploratory study of inland water and land altimetry using Seasat data
[ESA-CR(P)-2433] 02 p0193 N88-11208
Automated satellite cloud analysis: A multispectral approach to the problem of snow/cloud discrimination
[AD-A185672] 06 p0746 N88-14591
The role of anisotropy in the long range reconnaissance of the albedo of land surfaces 08 p1017 N88-16169
The anisotropy of reflected solar radiation over several types of land surface 08 p1018 N88-16171
Assessment of the differential technique for land navigation within 1000 km of Omega Australia
[AD-A191036] 16 p2160 N88-22885
Non-Gaussian models for surface clutter
22 p3068 N88-28212
Global-scale temperature changes to August 1987 and a comparison of satellite and conventional data
22 p3125 N88-28572

LAND ICE
Large ice masses: Characteristics, behaviour and relation to climate 14 p1939 N88-21569
The role of remote sensing in the study of polar ice sheets 14 p1939 N88-21570

LAND MANAGEMENT
Characterization, topology, and cartography of grasslands for the development of fodder resources (Preliminary Evaluation Program for SPOT number 26)
22 p3095 N88-28377

LAND MOBILE SATELLITE SERVICE
Communication satellite technology trends
01 p0015 N88-10088
Study of mobile communications payload for Columbus Polar Platforms
[ITS-TR-056A/86] 01 p0034 N88-10220
Study of the feasiblity of a satellite communication system for road transportation home office to vehicle communication. Volume 1: Conceptual analysis
[SC/87-E/6-VOL-1] 05 p0575 N88-13505
Study of the feasibility of a satellite communication system for road transportation home office to vehicle communication. Volume 2: Market study
[SC/87-E/6-VOL-2] 05 p0575 N88-13506

Receiver susceptibility measurements relating to interference between UHF (Ultra High Frequency) television and land mobile radio services
[PB87-228029] 06 p0690 N88-14228
Land mobile satellite transmission measurements at 869 MHz. A comparison of error probabilities for various message block durations and fade margins as a function of vegetation shadowing
[NASA-CR-179929] 06 p0693 N88-14255
Multicarrier demodulator design, volume 1 --- communication satellites
[ESA-CR(P)-2468-VOL-1] 09 p1158 N88-16941
Multicarrier demodulator design. Volume 2: Executive summary --- communication satellites
[ESA-CR(P)-2468-VOL-2] 09 p1158 N88-16942
A microstrip array feed for MSAT spacecraft reflector antenna 19 p2652 N88-25747

LAND USE
NT RURAL LAND USE
Vegetation classification, land systems and mapping using SPOT multispectral data: Preliminary results
03 p0342 N88-12160
Land cover/use classification of Cairns, Queensland, Australia: A remote sensing study involving the conjunctive use of the airborne imaging spectrometer, the large format camera and the thematic mapper simulator
05 p0612 N88-13759
Overview of Austrian Airborne Imaging Spectrometer (AIS) programme and first results
05 p0612 N88-13762
Design and implementation of a data base system for Digital Land Mass System (DLMS) data
[FEL-IR-1987-19] 09 p1185 N88-17101
Air Force geographic information and analysis system
[DE88-001420] 10 p1424 N88-18505
Land-use classification in a region north-west of Wuerzburg (Federal Republic of Germany) using digital, multispectral LANDSAT 5 Thematic Mapper data
[DFVLR-FB-87-37] 14 p1940 N88-21579
Updating of the municipal official register of real estate through a geographical information system
[INPE-4459-PRE/1238] 15 p2090 N88-22453
Comparative utilization of analog and digital processes in the treatment of MSS-LANDSAT data for studying the national parks of Brazil
[INPE-4011-TDL/240] 15 p2090 N88-22456
Orbital remote sensing: An instrument for monitoring urban growth
[INPE-4456-PRE/1287] 15 p2150 N88-22833
Applications of multitemporal compositions obtained from LANDSAT data in the study of urban growth
[INPE-4480-PRE/1246] 16 p2287 N88-23692
Updating land-use of the Sao Jose dos Campos municipality through remote sensing data
[INPE-4479-RPE/562] 16 p2287 N88-23693
Landuse and landform studies of the Mahanadi River Delta with the help of satellite MSS band
17 p2355 N88-24033
Remote sensing techniques in the estimation of the area cultivated with beans, corn, and castor beans in the Irece County (Bahia State) 17 p2358 N88-24045
CANASATE: Sugar cane mapping by satellite
17 p2358 N88-24046
Utilization of LANDSAT-TM imagery in the hydroenergetic inventory of the Paraiba de Sul River Basin 17 p2364 N88-24077
Preliminary study on the application of digital processing of TM-LANDSAT data in the mapping of apple orchards in Fraiburgo (SC) 17 p2367 N88-24093
Research on enhancing the utilization of digital multispectral data and geographic information systems in global habitability studies
[NASA-CR-182799] 17 p2368 N88-24101
Coupling of satellite remote sensing to digitized topographic map to detect changes in land use
[B8735129] 17 p2369 N88-24104
National Meeting on Remote Sensing Applied to Municipal Planning 19 p2681 N88-25939
Mapping of land use in Sao Jose dos Campos municipality by remote sensing, an aid for the elaboration of its PDDI 19 p2681 N88-25940
Remote sensing techniques applied to the study of metropolitan regions: The west sector of the Sao Paulo metropolitan area 19 p2681 N88-25941
The use of satellite imagery for municipal conditions in rural recording in Pereira Barreto (SP)
19 p2682 N88-25944
The impact of disorganized occupation of urban sub-basins: Sub-basin of the Cabucu River, metropolitan area of Sao Paulo (SP) 19 p2682 N88-25945
The impact of hemp production on the development of the municipalities of Araras, Leme, Santa Cruz da Conceicao and Pirassununga 19 p2683 N88-25948
Application of interactive graphic system (CAD/CAM) in the determination of process evolution in land use in the Ribeirao Preto municipality 19 p2684 N88-25956
Hydrologic models for land-atmosphere retrospective studies of the use of LANDSAT and AVHRR data
[NASA-CR-182861] 20 p2817 N88-26712
SPOT on land and lakes in the Hubei Province (China)
22 p3090 N88-28351
Review of the studies of geography and environment and studies on spectral characteristics of SPOT HRV data 22 p3091 N88-28358
Comparison between the respective contributions of the TM LANDSAT-4 and HRV SPOT-1 data to the land use mapping of Mediterranean coastal zone
22 p3092 N88-28363
Evaluation of annual crop surfaces and territorial inventory in the Paris basin by combining classic statistical inquiries and SPOT data (Preliminary Evaluation Program for SPOT 127) 22 p3094 N88-28372
SPOT-1 HRV data and vegetation amount
22 p3095 N88-28379
Use of SPOT imagery for vegetation/biomass mapping, geotechnical mapping, catchment area determination, and settlement location in the Turkana district, northern Kenya 22 p3096 N88-28384
An evaluation of the applicability of SPOT stereoscopic imagery to the Canada Land Use Monitoring Program (CLUMP) 22 p3099 N88-28403
Topographic suppression and advances in classification for land cover mapping using SPOT-1 HRV imagery
22 p3099 N88-28404
Accuracy of land use classification for SPOT image data 22 p3100 N88-28410
Utilization of SPOT-1 multispectral data for mapping land cover and phytohygiene monitoring in the central zone of the Mercantour National Park (France)
22 p3100 N88-28413
Applications of SPOT data for urban real estate investment information systems
22 p3101 N88-28414
Mapping and urban multi-experimental assessment of SPOT: Urban results 22 p3101 N88-28415
Utilization of SPOT multispectral data for urban planning 22 p3101 N88-28418
An analysis of time and space requirements for aircraft turnrounds
[TT-8705] 24 p3322 N88-29783

LANDAU DAMPING
Fast wave injection into high temperature tokamak plasmas in the lower-hybrid-density regime of JIPP T-IIU
[ISSN-0469-4732] 01 p0099 N88-10649
Plasma wave radiative damping of a new type in a relativistic one-dimensional plasma
[DE88-701191] 15 p2135 N88-22739
Improvement of plasma confinement due to electron Landau damping in tokamaks
[DE88-752339] 15 p2136 N88-22747

LANDAU-GINZBURG EQUATIONS
Global spatial periodic solutions to the Ginzburg-Landau equations
[DE88-006424] 15 p2119 N88-22623

LANDFORMS
NT ALEUTIAN ISLANDS (US)
NT ALPS MOUNTAINS (EUROPE)
NT ANDES MOUNTAINS (SOUTH AMERICA)
NT CALDERAS
NT CAPE HATTERAS (NC)
NT CARPATHIAN MOUNTAINS (EUROPE)
NT DELAWARE RIVER BASIN (US)
NT DELTAS
NT DUNES
NT GREAT BASIN (US)
NT GREENLAND
NT HAWAII
NT ICELAND
NT INDONESIA
NT ISLAND ARCS
NT ISLANDS
NT JAPAN
NT LAGOONS
NT MALDIVE ISLANDS
NT MARS VOLCANOES
NT MOUNTAINS
NT NEW ZEALAND
NT PIEDMONTS
NT PLATEAUS
NT PLAYAS
NT RIVER BASINS
NT SIERRA NEVADA MOUNTAINS (CA)
NT STEPPES
NT STRUCTURAL BASINS
NT TUNDRA
NT VOLCANOES
NT WATERSHEDS
Tectonics and magmatism of Walvis Ridge and Discovery Rise (Atlantic Ocean)
06 p0726 N88-14463
The digital landmass simulation production overview
[AD-A187978] 11 p1503 N88-18978

LANDING
NT AIRCRAFT LANDING
NT CRASH LANDING
NT DITCHING (LANDING)
NT GLIDE LANDINGS
NT MARS LANDING
NT PLANETARY LANDING
NT SPACECRAFT LANDING
NT VERTICAL LANDING
Effect of motion cues during complex curved approach and landing tasks: A piloted simulation study
[NASA-TP-2773] 04 p0398 N88-12480
High speed propeller performance and noise predictions at takeoff/landing conditions
[NASA-TM-100267] 05 p0646 N88-13960
Aerodynamic and acoustic characteristics of an advanced propeller under take-off and landing conditions
[NAL-TR-935] 09 p1243 N88-17453
Radar returns from ground clutter in vicinity of airports
10 p1274 N88-17624

LANDING AIDS
NT ARRESTING GEAR
NT AUTOMATIC LANDING CONTROL
NT INSTRUMENT LANDING SYSTEMS
NT MICROWAVE LANDING SYSTEMS
Boeing 727 MLS (Microwave Landing System) terminal instrument procedures (TERPS) approach data collection and processing, data report
[AD-A185523] 06 p0667 N88-14090
First flight simulator test of the head-up display for NAL QSTOL experimental aircraft (ASUKA)
[DE88-751804] 16 p2162 N88-22896
Cessna 172 MLS (Microwave Landing System) terminal instrument procedures (TERPS) approach data collection and processing data report
[AD-A191241] 18 p2461 N88-24613
Microwave landing system mathematical modeling study for Midway Airport Runway 22L, Chicago, Illinois
[AD-A191721] 18 p2462 N88-24616
Simulator evaluation of lineup visual landing aids for night carrier landing
[AD-A191212] 18 p2468 N88-24648
Control systems for platform landings cushioned by air bags
[AD-A196154] 24 p3358 N88-29996

LANDING GEAR
Cornering characteristics of the main-gear tire of the space shuttle orbiter
[NASA-TP-2790] 11 p1438 N88-18583
Metallurgical analysis of fractured F-27 aircraft landing gear
[DE88-005885] 11 p1460 N88-18705
An investigation of classical dynamic scaling techniques applied to an oleo-pneumatic landing gear strut
[AD-A187664] 13 p1721 N88-20292
Aircraft corrosion problems and research in the Netherlands
[NLR-MP-86066-U] 13 p1744 N88-20427
In-service measurements of SAAB SF-340 landing gear loads
[FFA-TN-1987-48] 15 p2018 N88-22032
Soft-ground aircraft arresting systems
[AD-A190838] 16 p2165 N88-22912

LANDING LOADS
In-service measurements of SAAB SF-340 landing gear loads
[FFA-TN-1987-48] 15 p2018 N88-22032
Control systems for platform landings cushioned by air bags
[AD-A196154] 24 p3358 N88-29996

LANDING MODULES
NT LUNAR LANDING MODULES
Mars Lander/Rover vehicle development: An advanced space design project for USRA and NASA/OAST
[NASA-CR-182570] 11 p1567 N88-19380
Mars Lander/Rover vehicle development: An advanced space design project for USRA and NASA/OAST
[NASA-CR-182562] 12 p1709 N88-20226

LANDING SIMULATION
Additional investigations in landing process of aircraft: Test distributions
[DFVLR-MITT-87-13] 09 p1115 N88-16686
First flight simulator test of the head-up display for NAL QSTOL experimental aircraft (ASUKA)
[DE88-751804] 16 p2162 N88-22896
Automatic landing by computer vision
[ETN-88-92991] 23 p3175 N88-28905
Additional investigations into the aircraft landing process: Test distributions
[ESA-TT-1099] 23 p3177 N88-28913

LANDING SITES
A Workshop on Desert Processes, September 24-28, 1984: Report on the conference
[AD-A184599] 03 p0345 N88-12184

The Viking landing sites: A cartographic perspective
[NASA-CR-177486] 19 p2742 N88-26282

LANDING SYSTEMS
U LANDING AIDS

LANDSAT SATELLITES
NT LANDSAT 5
Object-dependent atmospheric influence on LANDSAT recordings 01 p0065 N88-10420
Remote sensing in mineral exploration
[PB87-138558] 06 p0729 N88-14484
LANDSAT thematic mapper radiometric calibration study
[NASA-CR-182410] 07 p0872 N88-15287
Space-based remote sensing of the Earth: A report to the Congress
[NASA-TM-89709] 10 p1346 N88-18046
Thematic mapper study of Alaskan ophiolites
[NASA-CR-182554] 11 p1504 N88-18984
An application of digital cartography updating middle and small scale thematic maps using orbital data
[INPE-4460-TDL/317] 12 p1637 N88-19805
The use of LANDSAT-TM pictures for the detection of space-limiting elements for the benefit of landscape photomapping
[BCRS-87-02] 16 p2228 N88-23305
Applications of multitemporal compositions obtained from LANDSAT data in the study of urban growth
[INPE-4480-PRE/1246] 16 p2287 N88-23692
Mapping soil and rock variation from satellite images in the Sahel 17 p2354 N88-24023
DMSP-SSM/1 NASA algorithm validation using primarily LANDSAT and secondarily DMSP and/or AVHRR visible and thermal infrared satellite imagery
[NASA-CR-182979] 18 p2532 N88-25024
Comparative study of crop and soil mapping using multitemporal and multispectral SPOT and LANDSAT data 22 p3091 N88-28354
Monitoring of agricultural production in West Africa. The need to integrate different satellite platforms
22 p3096 N88-28383
Use of SPOT imagery for vegetation/biomass mapping, geotechnical mapping, catchment area determination, and settlement location in the Turkana district, northern Kenya 22 p3096 N88-28384
Accuracy of land use classification for SPOT image data 22 p3100 N88-28410
Utilization of SPOT-1 multispectral data for mapping land cover and phytohygiene monitoring in the central zone of the Mercantour National Park (France)
22 p3100 N88-28413
Use of LANDSAT images of vegetation cover to estimate effective hydraulic properties of soils
[NASA-CR-183185] 22 p3116 N88-28514

LANDSAT 5
Remote sensing with LANDSAT 5 Thematic Mapper (TM) and its application to various planning levels: A case study from the Wuerzburg area, West Germany
[DFVLR-FB-86-62] 01 p0065 N88-10421
Evaluation of digital, multitemporal LANDSAT 5 thematic mapper data for the determination of the aerial snowcover extent and spectral separation of various surface types in the inner Oetztal (West Germany) with special regard to the significance of aerial snowcover information for water resources management
[DFVLR-FB-86-46] 03 p0345 N88-12180
Land-use classification in a region north-west of Wuerzburg (Federal Republic of Germany) using digital, multispectral LANDSAT 5 Thematic Mapper data
[DFVLR-FB-87-37] 14 p1940 N88-21579
Comparison between the respective contributions of the TM LANDSAT-4 and HRV SPOT-1 data to the land use mapping of Mediterranean coastal zone
22 p3092 N88-28363

LANDSCAPE
U TERRAIN
U TOPOGRAPHY

LANDSLIDES
Photointerpretation with instrumentation for evaluation of environmental impact: Mata Atlantica in Cubatao
19 p2683 N88-25946
Study of evolution of vegetal cover and slide scars in the Cubatao municipality Sao Paulo
19 p2683 N88-25947
SPOT imagery for landslide cartography in mountainous areas. Example of the French Maritime Alps
22 p3105 N88-28440
SPOT for slope instability survey in Nepal
22 p3105 N88-28441

LANES
U PATHS

LANGEVIN FORMULA
Weak solution of the Langevin equation on a generalized functional space
[AD-A194290] 23 p3270 N88-29456

LANGMUIR PROBES
U ELECTROSTATIC PROBES

LANGUAGE PROGRAMMING
Applicative parallelism: Potential and challenge
[DE87-011885] 08 p1068 N88-16459
Design for a TPL compiler system: A system for retargeting high level language programs
10 p1381 N88-18248

LANGUAGES
NT ADA (PROGRAMMING LANGUAGE)
NT APL (PROGRAMMING LANGUAGE)
NT ASSEMBLY LANGUAGE
NT BASIC (PROGRAMMING LANGUAGE)
NT C (PROGRAMMING LANGUAGE)
NT COBOL
NT COMMAND LANGUAGES
NT CONTEXT FREE LANGUAGES
NT ENGLISH LANGUAGE
NT FORTRAN
NT HIGH LEVEL LANGUAGES
NT LISP (PROGRAMMING LANGUAGE)
NT NATURAL LANGUAGE (COMPUTERS)
NT PASCAL (PROGRAMMING LANGUAGE)
NT PROGRAMMING LANGUAGES
NT PROLOG (PROGRAMMING LANGUAGE)
NT QUERY LANGUAGES
NT SYLLABLES
NT WORDS (LANGUAGE)
Foreign language identification: First step in the translation process
[DE87-011065] 02 p0248 N88-11565
Errors associated with Russian name transliteration
[DE87-011717] 02 p0248 N88-11566
LISP as a rapid prototyping environment: The chinese tutor
[AD-A184328] 03 p0369 N88-12319
Space languages 08 p1063 N88-16420
Linguistic-technical aspects of machine translation
24 p3438 N88-30461
Linguistic barriers: Translation problems
24 p3438 N88-30465

LANTHANIDE SERIES METALS
U RARE EARTH ELEMENTS

LANTHANUM
Develop techniques for ion implantation of (lead-lanthanum-zirconate-titanate) for adaptive optics
[DE88-000642] 05 p0650 N88-13986
Theory of the tetragonal-to-orthorhombic structural phase transition in La2CuO4
[AD-A187141] 09 p1254 N88-17514
Paramagnetic spins in oxygen-loaded ceramic La2CuO4/sub 4 + delta/
[DE88-007114] 19 p2619 N88-25539
PLZT (Lead-Lathanium-Zirconium-Titanium) electro-optic photographic system
[AD-A193473] 23 p3215 N88-29137

LANTHANUM COMPOUNDS
NT LANTHANUM OXIDES
NT LANTHANUM TELLURIDES
A synthetic plasma source
[TRITA-EPP-86-15] 05 p0652 N88-13995
Properties of lanthanide oxides as supports for transition metal catalysts
[DE88-004520] 11 p1456 N88-18678
High-current density, high-brightness electron beams from large-area lanthanum hexaboride cathodes
[AD-A187700] 11 p1477 N88-18813
Compilation of NRL publications on high temperature superconductivity
[AD-A189137] 21 p3019 N88-27921
Anharmonic model for high-Tc superconductors
[DE88-702196] 21 p3020 N88-27924

LANTHANUM OXIDES
Superconductivity in La/sub 1.85-x/Nd/sub x/Sr/sub .15/CuO
[DE88-003014] 09 p1258 N88-17540
Single-crystal structural study of La2Cu/sub 0.95/Li/sub 0.05/O4
[DE88-003482] 11 p1554 N88-19302
High temperature superconductors in the La(sub 1 + x)Ba(sub 2-x)Cu O(sub y system
[DE88-006367] 15 p2145 N88-22802
Comparison between muon spin rotation and neutron scattering studies on the 3-dimensional magnetic ordering of La2CuO(4-y) 17 p2396 N88-24244
Superconducting properties of LaBa2Cu3O(sub x) and YBa2Cu3O(sub y)
[DE88-012038] 21 p3024 N88-27952
Possible mechanism for high-temperature superconductivity in the BaSr-La(Y)-CuO systems
[DE88-702060] 23 p3288 N88-29576
La2CuO(sub 4 + delta): A superconducting superoxide
[DE88-010325] 23 p3288 N88-29578
Theory of superconductivity in oxides
[AD-A195647] 24 p3433 N88-30432

LANTHANUM TELLURIDES
Crystalline metal-semiconductor superlattices
[DE88-007063] 18 p2581 N88-25332

LAOS
A comparative thematic mapping analysis of SPOT data: The Vientiane Plain (Lao PDR)
22 p3096 N88-28386

LAP JOINTS
Device for measuring hole elongation in a bolted joint
[NASA-CASE-LAR-13453-1] 06 p0712 N88-14361

LAPLACE EQUATION
Contributions to a numerical library in Ada
[NPL-DITC-98/87] 09 p1219 N88-17309
Finite element mesh generation and isoparametric elements
[NPL-DITC-97/87] 09 p1229 N88-17365
Performance of a multigrid method on parallel architecture 11 p1539 N88-19200
Double layer polarization of nonconducting spheroidal particles and its application to Kerr effect
[ISSN-0208-5658] 13 p1832 N88-20960
The calculation of transonic flow over the shuttle orbiter using slender body theory 18 p2460 N88-24606
Theory of Laplacian fractals: Diffusion limited aggregation and dielectric breakdown model
[PREPRINT-590] 22 p3144 N88-28701

LAPLACE OPERATORS
U LAPLACE TRANSFORMATION

LAPLACE TRANSFORMATION
Frozen-field, rigid-beam, uniform-conductivity-channel tracking force calculation
[DE87-012510] 02 p0190 N88-11190
Numerica calculation in the Laplace domain for subsonic unsteady aerodynamic forces acting on a finite wing
05 p0535 N88-13256
Symbolic, algebraic, and numeric solutions to heat conduction problems using Green's functions
09 p1165 N88-16987
Free Laplacian with attractive boundary conditions
[DE87-702971] 16 p2256 N88-23482

LARGE SCALE INTEGRATION
Introducing new technology into onboard handling systems 09 p1124 N88-16733
Characteristics of LSI-wiring expert system discussed
15 p2052 N88-22226
Progress and challenges in HEMT LSI technology
19 p2656 N88-25779
Diffraction by a simple deep phase object — integrated circuit measurement
[RSRE-MEMO-4039] 22 p3070 N88-28224

LARGE SPACE STRUCTURES
Assessment of the COFSI/MAST I project
[NASA-CR-181366] 01 p0053 N88-10340
A DMAP for updating dynamic mathematical models with measured data
[NLR-MP-86027-U] 01 p0060 N88-10387
Recent advances in structural dynamics of large space structures
[NASA-TM-100513] 02 p0138 N88-10867
Structural Assembly Demonstration Experiment (SADE)
[NASA-CR-179205] 02 p0138 N88-10868
Experimental assembly of structures in EVA: Hardware morphology and development issues
02 p0139 N88-10872
Marshall Space Flight Center's role in EASE/ACCESS mission management 02 p0139 N88-10875
A monograph of the National Space Transportation System Office (NSTSO) integration activities conducted at the NASA Lyndon B. Johnson Space Center for the EASE/ACCESS payload flown on STS 61-B
02 p0139 N88-10876
Research and development at the Marshall Space Flight Center Neutral Buoyancy Simulator
02 p0139 N88-10878
A synopsis of the EVA training conducted on EASE/ACCESS for STS-61-B 02 p0140 N88-10879
Results of the ACCESS experiment
02 p0140 N88-10880
EASE (Experimental Assembly of Structures in EVA) overview of selected results 02 p0140 N88-10881
Overview of crew member energy expenditure during Shuttle Flight 61-B EASE/ACCESS task performance
02 p0140 N88-10882
Pinhole occulter experiment
[NASA-CR-179206] 02 p0235 N88-11481
Control design challenges of large space systems and spacecraft control laboratory experiment (SCOLE)
[NASA-CR-178392] 03 p0275 N88-11735
Adaptive control of Large Space Structure (LSS)
[ISAS-R-621] 03 p0276 N88-11740
Wavefront error sensing
[NASA-CR-181504] 03 p0321 N88-12030

Stochastic model of the NASA/MSFC ground facility for large space structures with uncertain parameters: The maximum entropy approach
[NASA-CR-181489] 03 p0372 N88-12343
New feedback design methodologies for large space structures: A multi-criterion optimization approach
04 p0408 N88-12535
Computational methods for problems in aerodynamics and large space structure using parallel and vector architectures
[AD-A185401] 05 p0541 N88-13294
Survey on large scale system control methods
[NASA-CR-181556] 05 p0554 N88-13374
Design of low order controllers for robust disturbance rejection in large space structures
[AD-A185202] 05 p0555 N88-13376
Modeling and control of large flexible vehicles in the atmosphere and space
[AD-A185368] 05 p0555 N88-13377
Potential for on-orbit manufacture of large space structures using the pultrusion process
[NASA-TM-4016] 05 p0557 N88-13388
Optimal control of large space structures via generalized inverse matrix
[NASA-CR-182336] 05 p0639 N88-13907
Approaches and possible improvements in the area of multibody dynamics modeling
[NASA-CR-179227] 06 p0663 N88-14067
Investigation of design concepts for large space structures to support military applications
[AD-A186098] 07 p0824 N88-15000
Natural frequencies and structural integrity assessment of large space structures
[AD-A186139] 07 p0824 N88-15001
Wave propagation experiments on 22-bay lattice
[AD-A186140] 07 p0824 N88-15002
Maximum entropy/optimal projection design synthesis for decentralized control of large space structures
[AD-A186359] 07 p0824 N88-15003
Large-angle slewing maneuvers for flexible spacecraft
[NASA-CR-4123] 08 p1000 N88-16060
Emulating a flexible space structure: Modeling
[NASA-TM-100320] 09 p1135 N88-16812
Optimized structure design using reanalysis techniques 09 p1180 N88-17067
Sensitivity of active vibration control to structural changes and model reduction 10 p1284 N88-17683
Formulation methods of rigid multibody systems for large space structures and some results of computer simulation
[NAL-TR-942] 10 p1293 N88-17730
Preliminary investigation of stability of a fin-stiffened slender strut
[NASA-TM-4034] 12 p1599 N88-19568
Cost effective development of a national test bed
[NASA-TM-100321] 12 p1601 N88-19585
Workshop on Technology Development Issues for the Large Deployable Reflector (LDR)
[NASA-CP-2407] 12 p1710 N88-20235
Robust decentralized control of large flexible structures
[DE88-005416] 13 p1824 N88-20902
A sequentially deployable structure for space applications 14 p1875 N88-21202
Optimal control and identification of space structures
[AD-A190033] 15 p2025 N88-22065
Wave propagation and dynamics of lattice structures
[AD-A190037] 15 p2025 N88-22066
Feedback control of distributed parameter systems with applications to large space structures
[AD-A190536] 15 p2025 N88-22068
Wave propagation and dynamics of lattice structures
[AD-A190611] 15 p2025 N88-22069
Vibrations of structures with parametric uncertainties
[AD-A190400] 15 p2076 N88-22378
Travelling wave concepts for the modeling and control of space structures
[AD-A191235] 17 p2310 N88-23819
Soviet spacecraft engineering research
[FASAC-TAR-3090] 17 p2311 N88-23823
LDR structural experiment definition
[NASA-TM-100618] 17 p2312 N88-23826
Space spider crane
[NASA-CASE-LAR-13411-1-SB]
17 p2312 N88-23828
Continuum modeling and dynamic analysis of large truss structures 17 p2349 N88-23995
Electromagnetic damping and vibration isolation of space structures
[AD-A191492] 18 p2471 N88-24665
Estimation and control of distributed models for certain elastic systems arising in large space structures
[AD-A192120] 18 p2472 N88-24666
Low authority control of large space structures using a constrained threshold control formulation
18 p2472 N88-24667
Experimental study of active vibration control
[AD-A191454] 18 p2526 N88-24989
Large antenna experiments aboard the space shuttle: Application of nonuniform sampling techniques
19 p2652 N88-25745
The 15-meter antenna performance optimization using an interdisciplinary approach 19 p2652 N88-25746
Adaptive residual mode filter control of distributed parameter systems for large space structure applications
19 p2719 N88-26143
L(sub infinity symbol)-approximations of complex functions and robust controllers for large flexible space structures
[PB88-186226] 20 p2764 N88-26390
Mobile remote manipulator system for a tetrahedral truss
[NASA-CASE-MSC-20985-1] 20 p2765 N88-26398
Experimental and theoretical investigation of passive damping concepts for member forced and free vibration
[NASA-CR-183082] 20 p2814 N88-26693
Spacecraft applications of advanced global positioning system technology
[NASA-CR-172055] 21 p2894 N88-27180
Technology for large space systems: A bibliography with indexes (supplement 18)
[NASA-SP-7046(18)] 21 p2901 N88-27214
Vibration control of large structures
[AD-A193317] 21 p2961 N88-27587
Sensor and actuator selection for large space structure control
[AD-A194912] 24 p3333 N88-29842
Space structure (dynamics and control) theme development
[NASA-TM-100597] 24 p3335 N88-29850
Theory of filtering and control with application to control of large space structures
[AD-A195500] 24 p3335 N88-29851
Clevis joint for deployable space structures
[NASA-CASE-LAR-13898-1] 24 p3380 N88-30130
Robust design of distributed controllers for large flexible space structures
[NASA-CR-183202] 24 p3380 N88-30134

LARGE SPACE TELESCOPE
U HUBBLE SPACE TELESCOPE

LARVAE
Embryogenesis and organogenesis of Carausius morosus under spaceflight conditions
22 p3061 N88-28167

LARYNX
NT GLOTTIS
Visualization of the air flowing through a dynamic model of the vocal folds
[ISVR-TR-154] 14 p1952 N88-21634

LASER ALTIMETERS
Considering refraction in leveling with laser plane
04 p0462 N88-12857
A computer code to process and plot laser altimetry data interactively on a microcomputer
[NASA-TM-100687] 05 p0554 N88-13371

LASER ANEMOMETERS
Optical flow diagnostic measurements in turbomachinery
[PNR90396] 02 p0172 N88-11081
The four spot time-of-flight laser anemometer
02 p0184 N88-11145
Three-dimensional calculation in high subsonic axial compressor rotor and its comparison with L2F velocity measurement 03 p0300 N88-11886
A FORTRAN code for the calculation of probe volume geometry changes in a laser anemometry system caused by window refraction
[NASA-TM-100210] 03 p0364 N88-12288
Turbulence measurement in hypersonic flow
05 p0530 N88-13224
Optical measurement systems
08 p0955 N88-15796
Correlation and spectral density measurements by LDA --- flow measurement
[ISL-CO-244/86] 14 p1910 N88-21412
Matched index laser anemometry systems for flow studies in complex geometries 16 p2203 N88-23145
Laser Doppler anemometry
[NASA-TM-100072] 16 p2210 N88-23187
Study of the local behavior of a flame
[ETN-88-92300] 20 p2771 N88-26433

LASER ANNEALING
Nondestructive magnetic testing of laser hardening parameters (hardening depth, hardness profile, retained austenite)
[ETN-88-91070] 09 p1144 N88-16857
Laser spectroscopy investigations of materials for solid state laser systems
[AD-A192514] 21 p2952 N88-27535

LASER APPLICATIONS
NT LASER CUTTING
NT LASER FUSION
Experimental investigation in a wind tunnel of the stability and vorticity of the vortex breakdown phenomenon above delta wings, using the ultrasonic laser method
[DFVLR-FB-87-06] 01 p0003 N88-10017
Low temperature deposition by laser induced breakdown in the vapor phase
[DE87-007509] 01 p0024 N88-10151
Laser chemically vapor deposited silicon-carbide: Growth features, topography, microstructure, and composition
[DE87-013767] 01 p0029 N88-10184
A high-voltage multistage laser-triggered gas switch
[DE87-011725] 01 p0040 N88-10253
Monocrystalline silicon gradiometer for gravity experiments in space
[NASA-CR-181452] 01 p0050 N88-10321
KR + laser excitation of NH2 in atmospheric pressure flames
[AD-A183421] 01 p0050 N88-10322
Diode pumped solid-state laser oscillators for spectroscopic applications
[NASA-CR-180576] 01 p0052 N88-10331
Mid infrared LHS system packaging using flexible waveguides
[NASA-CR-181192] 01 p0093 N88-10607
Improving coherent visualization by means of film optical filtering --- projectile visualization
[ISL-R-116/86] 02 p0176 N88-11097
Method for single-shot measurement of picosecond laser pulse-lengths without electronic time dispersion
[DE87-013171] 02 p0178 N88-11107
A study of the performance of airborne laser radar systems and techniques
[ETN-87-90928] 02 p0179 N88-11117
Description of a multiframe optical probing system
[DE87-014255] 02 p0236 N88-11487
JPRS report: Science and technology. China
[JPRS-CST-87-026] 03 p0269 N88-11688
China report: Science and technology
[JPRS-CST-87-015] 03 p0298 N88-11873
JPRS report: Science and technology. China
[JPRS-CST-87-025] 03 p0300 N88-11888
Study of IR laser photoacoustic spectra of organic molecules adsorbed on metal surface
03 p0301 N88-11891
Ultra-short pulse laser system used for lageos range finding 03 p0301 N88-11893
Performance and operating envelope of imaging and scattering particle sizing instruments
[NASA-CR-180859] 03 p0323 N88-12042
JPRS Report: Science and Technology. China
[JPRS-CST-87-033] 03 p0326 N88-12062
Single-periodic multilayer grating laser Doppler vibrometer 03 p0327 N88-12066
Laser sources today and tomorrow
[DE87-014247] 03 p0330 N88-12083
Optical laser technology, specifically CD-ROM (Compact Disc - Read Only Memory) and its application to the storage and retrieval of information
[AD-A184111] 03 p0330 N88-12086
A simplified CARS measurement system for rapid determination of temperature and oxygen concentration
[NASA-TM-100498] 03 p0374 N88-12353
High efficiency generation of 130-nm radiation from sum-frequency mixing in Hg
[DE87-013714] 04 p0431 N88-12674
Lasers measure atmosphere
04 p0461 N88-12849
Multiwave laser soundings of atmospheric aerosol: Experimental research (review)
04 p0461 N88-12852
JPRS report: Science and technology. USSR: Life sciences
[JPRS-ULS-87-009] 04 p0473 N88-12915
Theoretical plasma physics
[DE88-001475] 04 p0492 N88-13029
An ultra-high-speed cinematographic method for the study of wakes in hypersonic ballistic ranges
05 p0531 N88-13228
Master plots for predicting the case-depth in laser surface treatments
[PB87-221875] 05 p0586 N88-13574
Measurement of particle size distribution in a solid propellant rocket motor using light scattering
[AD-A184875] 06 p0673 N88-14124
Recording materials for optical disk memory discussed
06 p0684 N88-14193
JPRS report: Science and technology. Japan
[JPRS-JST-87-027] 06 p0688 N88-14213
Developments in optical sensor technologies described 06 p0689 N88-14220
Laser development, evolution of applied technologies described 06 p0689 N88-14221
Status, outlook of optical technology in information equipment field 06 p0689 N88-14222

USSR report: Physics and mathematics
[JPRS-UPM-87-006] 06 p0708 N88-14344
Uses of airborne laser Chayka-1 for probing water, land surfaces 06 p0725 N88-14461
Super-short yttrium aluminate pulse generator with controlled resonator Q-factor 06 p0772 N88-14740
Nonuniformity of electromagnetic field at Lambda = 10.6 micron wavelength inside atmospheric aerosol particles
06 p0772 N88-14743
Development of crack under periodically pulsed laser radiation 06 p0774 N88-14754
Analysis of laser extracted volatiles in carbonaceous chondrites 06 p0793 N88-14861
Lawrence Livermore National Laboratory Soft X-ray Laser Program
[DE88-001886] 07 p0859 N88-15218
Intracavity spectrum analyzer with NaF:F2(+):F3(-) crystal laser for long-wave IR wave band
07 p0919 N88-15584
Laser thermal propulsion
[AD-A186407] 07 p0933 N88-15666
The application of photoconductive detectors to the measurement of X-ray production in laser produced plasmas
[DE88-001630] 07 p0934 N86 15671
Laser transformation hardening of precision V-slide way
[PB87-144028] 08 p0991 N88-15999
Laser system for automating topographic terrain survey 08 p1012 N88-16136
High-speed assembly language (80386/80387) programming for laser spectra scan control and data acquisition providing improved resolution water vapor spectroscopy
[NASA-CR-4117] 08 p1053 N88-16355
Pulsed laser stereophotography of plasmas and dynamically moving surfaces
[DE88-003170] 09 p1173 N88-17031
Laser simulation of light and plasma action on comets and planets 09 p1237 N88-17413
Energy transmission using coherent, quasimonochromatic light beams
09 p1241 N88-17436
Solid antimatter
[PB87-166146] 09 p1259 N88-17549
Laser investigations for payload G-652 prior to filing pre-flight accommodation requirements
10 p1286 N88-17694
High resolution electron and ion microscopy
[AERE-R-12502] 10 p1297 N88-17754
A ring model of the lasertron
[DE88-004656] 10 p1323 N88-17908
Digital imaging techniques for single- and multi-phase reacting flowfields 10 p1327 N88-17933
Monitoring interfacial dynamics by pulsed laser techniques
[DE88-003362] 10 p1335 N88-17976
Overview of applications of Laser-Induced Breakdown Spectroscopy (LIBS)
[DE88-004314] 10 p1336 N88-17987
Optically controlled devices and ultrafast laser sources for signal processing
[AD-A187417] 10 p1338 N88-17995
Evaluation of a temperature remote sensing technique
[AD-A187885] 10 p1347 N88-18053
A laser communication experiment utilizing the ACT satellite and an airborne laser transceiver
[NASA-TM-100792] 11 p1492 N88-18910
The Quick Response Multicolor Printer (QRMP) system
[AD-A188140] 11 p1504 N88-18982
JPRS report. Science and technology: Europe and Latin America
[JPRS-ELS-87-054] 12 p1573 N88-19406
JPRS report. Science and technology: Europe and Latin America
[JPRS-ELS-87-055] 12 p1686 N88-20086
Optically stimulated sound from gas bubbles in water
12 p1686 N88-20087
Molecular dynamics of laser ablation of a polymer coating
[DE88-004337] 13 p1750 N88-20466
Studies of compound states of negative ions using laser beams
[DE88-004708] 13 p1777 N88-20627
Noncontact thermometry via laser pumped, thermographic phosphors: Characterization of systematic errors and industrial applications
[DE88-005599] 13 p1777 N88-20628
Low threshold ridge waveguide single quantum well lasers 13 p1777 N88-20631
Study of photochromic materials for use in optical signal processing
[AD-A189066] 13 p1839 N88-21006
Vortex flow over a delta wing with apex flaps using laser flow visualisation
[BU-356] 14 p1862 N88-21121
Influence of hydrogen on crack formation tendency in heat-affected zone with stress concentrator
14 p1887 N88-21276
Measurement of species concentrations in flames by laser-induced fluorescence
[DE88-007096] 14 p1889 N88-21286
JPRS report: Science and technology. China
[JPRS-CST-87-038] 14 p1901 N88-21350
Applications of lasers to semiconductor studies
14 p1901 N88-21356
JPRS report: Science and technology. China
[JPRS-CST-87-041] 14 p1902 N88-21365
Laser surface melting
[BMFT-FB-T-86-072] 14 p1914 N88-21435
Lasers: Invention to application
[PB88-161583] 14 p1914 N88-21436
Lidar active remote sensing. Applications to the atmosphere 14 p1936 N88-21547
Optical cooling and trapping 14 p1974 N88-21782
Optical trapping of neutral atoms and dielectric particles by radiation pressure 14 p1974 N88-21783
Laser cooling of neon metastable states
14 p1975 N88-21785
Femtosecond studies in hot carrier relaxation in GaAs and AlGaAs 14 p1977 N88-21801
Diode laser spectroscopy of chemical moieties at surfaces
[AD-A190710] 15 p2036 N88-22127
Laser enhanced adhesion of copper films to sapphire substrates
[DE88-006802] 15 p2038 N88-22144
Laser photodeposition and etching study
[AD-A190535] 15 p2040 N88-22153
Oxide optical coatings prepared by metal-organic vapor deposition
[DE88-006809] 15 p2043 N88-22175
JPRS report: Science and technology. Japan
[JPRS-JST-88-002] 15 p2050 N88-22210
Laser processing-status, perspectives
15 p2050 N88-22211
Compound ceramic processing
15 p2050 N88-22212
Fine grain development by laser CVD
15 p2050 N88-22214
Material surface improvement by laser
15 p2051 N88-22217
Laser evaporation studies
[AD-A189815] 15 p2071 N88-22346
Research on certain aspects of laser diffraction particle sizing relevant to autonomous self-diagnosing instrumentation
[AD-A190220] 15 p2071 N88-22348
A laser-based photoacoustic spectrometer for direct breath C-13O2/C-12O2 measurement
[DE88-004915] 15 p2101 N88-22516
Activities report in laser-matter interaction
[ETN-88-92007] 15 p2129 N88-22696
Characteristics of distributed feedback lasers discussed 16 p2185 N88-23028
Three-dimensional flow visualization using laser-sheet scanning 16 p2203 N88-23143
Comparison of electrically driven lasers for space power transmission
[NASA-TM-4045] 16 p2212 N88-23197
Laser induced ignition of propellants
[AD-A191099] 16 p2213 N88-23206
Laser cladding of Ni, Nb and Mg alloys for improved environmental resistance at high temperature
[AD-A191274] 16 p2213 N88-23208
Proceedings of the Cooling, Condensation, and Storage of Hydrogen Cluster Ions Workshop
[AD-A189857] 16 p2266 N88-23555
Pusherless implosion, pulse tailoring and ignition scaling law for laser fusion 16 p2277 N88-23629
Efficient shell implosion and target design
16 p2277 N88-23630
Research on anode plasma behavior of flashover pulsed ion sources 16 p2279 N88-23640
Laser pyrometry 17 p2330 N88-23910
Noncontact true temperature measurement, 2
17 p2330 N88-23911
Laser Diagnostics for combustion temperature and species measurements 17 p2330 N88-23912
Research investigation directed toward extending the useful range of the electromagnetic spectrum
[AD-A190198] 17 p2332 N88-23920
Research investigation directed toward extending the useful range of the electromagnetic spectrum, appendix
[AD-A190199] 17 p2332 N88-23921
Cascade fluorescences from laser-excited lithium atom for plasma diagnostics 17 p2442 N88-24526
Flux density measurements of neutral iron in TEXTOR with laser induced fluorescence
17 p2442 N88-24528
Isotope separation using tuned laser and electron beam
[NASA-CASE-NPO-16907-1-CU]
18 p2483 N88-24732
Bibliography of Soviet laser developments, number 83, May - June 1986
[AD-A190969] 18 p2520 N88-24950
Optical diagnostics for a high power, rf-inductively coupled plasma
[DE88-007822] 18 p2579 N88-25322
Propellant combustion response to oscillatory radiant heat flux 19 p2628 N88-25589
Minimum ignition energy measurements using laser induced spark initiation 19 p2632 N88-25610
Laser-RDX aerosol pyrolysis with matrix isolation of unstable intermediates 19 p2632 N88-25614
Organization of a Topical Meeting on Picosecond Electronics and Optoelectronics
[AD-A187136] 19 p2655 N88-25765
Picosecond electrical pulses for VLSI electronics characterization 19 p2655 N88-25768
A mass spectrometer for the analysis of thermally labile compounds 19 p2668 N88-25859
Asynchronous optical sampling for laser-based combustion diagnostics in high pressure flames
[AD-A192920] 20 p2770 N88-26428
Interferometric recording of holographic optical elements using partially coherent light
20 p2805 N88-26636
Study of feasibility and optimization conditions of laser treatments: Application of the local recrystallization of aluminum
[ISAL-87-0048] 21 p2916 N88-27309
Attachable interferometric strain gages
[AD-A192390] 21 p2950 N88-27522
Measurement of pressure fluctuations in a resonant chamber with laser-induced iodine fluorescence
[DFVLR-FB-87-53] 21 p2955 N88-27551
Laser and electrochemical studies of metallizations in electronic devices
[AD-A193786] 23 p3208 N88-29090
Flow visualization by laser sheet
[AD-A194481] 23 p3211 N88-29111
N2(A3epsilon u+) by reaction of N2F4+H2 in a supersonic flow
[AD-A194493] 23 p3219 N88-29163
Optical measurements of soot and temperature profiles in premixed propane-oxygen flames
[NASA-TM-101343] 24 p3358 N88-29997
Optical measurements of soot in premixed flames
[NASA-TM-101305] 24 p3373 N88-30090
Spontaneous force optical traps
[AD-A196103] 24 p3377 N88-30114
Bibliography of Soviet laser developments, number 88, March - April 1987
[AD-A195978] 24 p3378 N88-30116
Laser sensing for identification and control of distributed parameter systems
[AD-A195886] 24 p3379 N88-30124

LASER BEAM DEFOCUSING
U THERMAL BLOOMING

LASER BEAMS
Laser CO2/TEA frequency-stabilized by phase conjugation 22 p3082 N88-28303
Application of optical correlation techniques to particle imaging velocimetry
[NASA-TM-101306] 23 p3218 N88-29152

LASER CAVITIES
JPRS report: Science and technology. China
[JPRS-CST-87-034] 03 p0301 N88-11897
Measuring stability of optical reference cavities by analyzing polarization spectrum
03 p0327 N88-12065
Nonconventional optical techniques for optical wavefront processing
[AD-A185099] 05 p0650 N88 13982
Active medium formation in lasers using mixtures of inert gases and optical breakdown pumping
06 p0709 N88-14347
Dynamic restructuring of pulsed CO2 laser frequency and multiple-peak generation in a cell with IR-absorbing gas in the resonator 07 p0919 N88-15580
Study of kinetics of intracavity absorption in pulsed dye lasers 07 p0919 N88-15585
Characteristics of LKI-501 tunable dye laser with dyes in solid matrix 07 p0920 N88-15587
High peak power Ka-band gyrotron oscillator experiments with slotted and unslotted cavities
[AD-A188109] 11 p1476 N88-18819
Soft X-ray beamsplitters and highly dispersive multilayer mirrors for use as soft X-ray laser cavity components
[DE88-004003] 11 p1549 N88-19270

Fiber-coupled external-cavity semiconductor high power laser
[AD-A188454] 13 p1774 N88-20611
Resonator coupling of two ring cavity, argon-ion lasers
[AD-A189558] 13 p1775 N88-20616
JPRS report: Science and technology. China
[JPRS-CST-87-038] 14 p1901 N88-21350
A picosecond tunable ultrashort cavity dye laser
14 p1902 N88-21361
Generation of tunable coherent radiation in 3 micrometers-5 micrometers region using semiconductor lasers in external cavities
[AD-A190860] 16 p2212 N88-23202
Mode locking of semiconductor laser with external cavity
[AD-A196018] 24 p3378 N88-30117

LASER COMMUNICATION
U OPTICAL COMMUNICATION

LASER CUTTING
Geometry and reproducibility of a plasma-supported removal of material by laser radiation
[ETN-87-90436] 01 p0052 N88-10335
Diffraction effects during materials treatment with laser beams
[ETN-87-90614] 03 p0328 N88-12075
Laser programming integrated circuits
[AD-A189590] 13 p1762 N88-20537

LASER DAMAGE
Optical damage in polymers by millisecond light pulses
[DE87-013106] 02 p0151 N88-10943
Long-range pulselength scaling of 351nm laser damage thresholds
[DE87-014754] 04 p0448 N88-12777
Dependence of acoustical characteristics of laser-induced breakdown in dielectric materials on shape of inelastic region 06 p0774 N88-14753
On 1064 nm and 350 nm laser damage thresholds of high index oxide films deposited from organic solutions and sols
[DE88-001636] 07 p0859 N88-15217
Dielectric behavior of electromagnetic (EM) windows materials irradiated by a CW CO2 high-power laser --- hypersonic/reentry vehicles
[ISL-CO-239/86] 09 p1154 N88-16913
Psychophysical, biochemical and histological studies of spectrally selective photic damage to primate retina
[AD-A188115] 11 p1517 N88-19063
Causes of damage in multilayer dielectric coatings exposed to high average power visible laser radiation
[DE88-005363] 13 p1775 N88-20619
Database of average-power damage thresholds at 1064 nm
[DE88-004352] 13 p1776 N88-20626
Protection against laser damage to human body reviewed 15 p2053 N88-22237
A preliminary comparison of the transient effects of single versus multiple q-switched doubled-neodymium laser pulses
[AD-A189855] 15 p2071 N88-22347
Advanced programming and control techniques for complex mechanical systems
[AD-A190238] 15 p2071 N88-22349
A comparison of visual evoked potential and behavioral measures of flashblindness in humans
[AD-A189757] 15 p2101 N88-22519
New acousto-ultrasonic techniques applied to aerospace materials
[NASA-TM-101299] 22 p3086 N88-28323
Spallation and dynamic fracture as an effect of laser induced shock-waves
[AD-A193513] 23 p3188 N88-28971
Functional assessment of laser irradiation
[AD-A195735] 24 p3408 N88-30287

LASER DOPPLER VELOCIMETERS
Laser Doppler measurements in a turbulent free jet
[ESA-TT-1067] 03 p0315 N88-11994
Methods for a coherent CO2 laser heterodyne radar system
[ESA-TT-1035] 03 p0328 N88-12076
A FORTRAN code for the calculation of probe volume geometry changes in a laser anemometry system caused by window refraction
[NASA-TM-100210] 03 p0364 N88-12288
Determination of a flow velocity field using four-exposure laser holography
[IMFL-3114-85/32] 05 p0585 N88-13565
Hot wire and laser velocimeter studies of turbulent flow at supersonic velocities
[ETN-88-91172] 05 p0585 N88-13566
Dual cylindrical wave Laser-Doppler method for measurement of skin friction in fluid flow
06 p0700 N88-14297
Dual mode laser velocimeter
[NASA-CASE-ARC-11634-1] 06 p0709 N88-14350
Velocity interferometry in shock tubes and shock tunnels
[ISL-CO-203/87] 09 p1122 N88-16713
Investigation of dynamic stall using LDV (Laser Doppler Velocimetry): Mean flow studies
[AD-A187629] 10 p1272 N88-17611
Laser velocimeter measurements of solids in multiphase flow
[DE88-000196] 11 p1487 N88-18876
New monostatic balanced Doppler velocimeter using a polarization preserving fiber
[PB88-130869] 11 p1490 N88-18895
Laser fluorescence velocimeter
[AD-A189010] 12 p1630 N88-19753
Laser Doppler velocimetry primer
[NASA-CR-177386] 12 p1631 N88-19761
Inflow measurement made with a laser velocimeter on a helicopter model in forward flight. Volume 2: Rectangular planform blades at an advance ratio of 0.23
[NASA-TM-100542] 14 p1864 N88-21139
Correlation and spectral density measurements by LDA --- flow measurement
[ISL-CO-244/86] 14 p1910 N88-21412
Laser velocimeter measurements in a wing-fuselage type juncture
[NASA-TM-100588] 15 p2014 N88-22012
Inflow measurement made with a laser velocimeter on a helicopter model in forward flight. Volume 3: Rectangular planform blades at an advance ratio of 0.30
[NASA-TM-100543] 15 p2015 N88-22015
Unsteady flow field measurements using LDV (Laser Doppler Velocimetry)
[AD-A189907] 15 p2063 N88-22298
Instruments for use in experimental studies of complex turbulent shear flow: Three component LDVs
[AD-A190526] 15 p2065 N88-22312
Inflow measurements made with a laser velocimeter on a helicopter model in forward flight. Volume 4: Tapered planform blades at an advance ratio of 0.15
[NASA-TM-100544] 16 p2156 N88-22863
Flow measurements in a water tunnel using a holocinematographic velocimeter
16 p2203 N88-23141
Experimental studies of vortex flows
[NASA-CR-182874] 16 p2207 N88-23171
Inflow measurement made with a laser velocimeter on a helicopter model in forward flight. Volume 5: Tapered planform blades at an advance ratio of 0.23
[NASA-TM-100545] 17 p2299 N88-23755
Inflow measurements made with a laser velocimeter on a helicopter model in forward flight. Volume 1: Rectangular planform blades at an advance ratio of 0.15
[NASA-TM-100541] 18 p2460 N88-24607
Propellant combustion response to oscillatory radiant heat flux 19 p2628 N88-25589
Influence of rear body geometry on the velocity characteristics of the near wake
[ISL-R-113/87] 20 p2753 N88-26339
Experiments on densely-loaded non-Newtonian slurries in laminar and turbulent pipe flows
[DE88-010579] 20 p2800 N88-26612
Study of flow tracer behavior models and experimental validation with multiple exposure holographic velocimetry
[IMFL-87/30] 20 p2801 N88-26622
A microcomputer based frequency-domain processor for laser Doppler anemometry
[NASA-TM-100998] 20 p2803 N88-26634
Laser-Doppler measurements of turbulence structures in free streams behind flat and rotation symmetrical profiles
[ETN-88-92336] 21 p2948 N88-27510
Velocity measurements downstream of a sudden expansion using the Laser Doppler Velocimeters (LDV) technique. Part 1: Method of measurement and experimental facility
[FOA-C-20700-2.1-PT-1] 22 p3076 N88-28262
Hot-wire measurements of compressor blade wakes in a cascade wind tunnel
[AD-A194737] 23 p3181 N88-28936
Three-dimensional laser Doppler velocimeter studies of flow in a 90 deg curved duct having a square cross-section 23 p3209 N88-29101
Construction of a laser Doppler anemometer and its use for the testing of a novel probe for the measurement of the variations of the lateral component of the vortex vector
[MPIS-13/1987] 23 p3217 N88-29147
Laser Doppler Velocimeter (LDV) and pressure measurements of gas particle flows in bends
[VKI-TN-163] 24 p3372 N88-30083

LASER FUSION
Laser-plasma-interaction experiments using multikilojoule lasers
[DE87-013483] 01 p0100 N88-10658
Investigation of the structure of coatings of self fluxing alloys fused by laser energy
[BLL-M-37301-(5828.4)] 02 p0148 N88-10930
LLE Review, volume 30
[DE87-014469] 02 p0178 N88-11109
X-ray emission from high-Z spherical laser plasmas: Implications for plasma dynamics
[DE87-014722] 02 p0239 N88-11506
Interplanetary propulsion using inertial fusion
[NASA-TM-89661] 04 p0409 N88-12540
Thermal stress in the edge cladding of Nova glass laser disks
[DE88-000425] 04 p0448 N88-12780
Inertial confinement fusion reactor cavity analysis
[DE88-000788] 04 p0492 N88-13028
Theory of induced spatial incoherence
[AD-A185005] 05 p0651 N88-13992
The Rayleigh-Taylor instability in ablatively accelerated targets with 1, 1/2 and 1/4 micrometers laser light
[AD-A185945] 07 p0858 N88-15208
High Z interaction physics on Nova
[DE88-004397] 10 p1413 N88-18433
Smoothing technique to resolve X-ray spectra in laser nuclear fusion 15 p2053 N88-22235
Magic light high-power laser passes state certification
15 p2053 N88-22236
Coronal fluid-dynamics in laser fusion
16 p2278 N88-23634
Finite ion-relaxation and nonequilibrium radiation effects on laser-driven implosions 16 p2278 N88-23636
Interplanetary propulsion using inertial fusion
17 p2401 N88-24273

LASER GEODYNAMIC SATELLITE
U LAGEOS (SATELLITE)

LASER GUIDANCE
Range imagery algorithms for the detection of obstacles by autonomous vehicles
[AD-A185421] 05 p0659 N88-14045
Optics: Perspectives for Measurement Techniques and Signal Processing for Flight Guidance --- conference
[DFVLR-MITT-87-21] 18 p2516 N88-24928
Tracking a monochromatic light source
[DE88-011260] 20 p2807 N88-26653

LASER GYROSCOPES
Test equipment with fiber optic data bus and laser gyro strapdown system LTN-90 for the helicopter BO-105
[ESA-TT-1038] 01 p0005 N88-10025
Investigation of the fabrication parameters of laser mirrors with hard oxide interference coatings
[ESA-TT-1064] 03 p0329 N88-12077
Study on a unidirectional ring laser gyro. Part 1: Proposition of the principle and studies on the components
[NAL-TR-933] 09 p1169 N88-17010
Laser gyro attitude control system feasibility
[AD-A189368] 13 p1720 N88-20285
Principles of a low-cost laser gyro for rotating vehicles and platforms
[DFVLR-MITT-87-15] 14 p1912 N88-21425
Optimization of metal-dielectric laser mirrors of TiO2/SiO2 and silver
[ESA-TT-1068] 16 p2212 N88-23199
Concepts for a laser gyroscope of the highest precision 18 p2517 N88-24929
Laser gyroscopes using the rate-bias technique
18 p2517 N88-24930
Development of mirrors for high-precision laser gyroscopes 18 p2517 N88-24931
Laboratory tests of laser gyroscopes for future utilization in multifunction systems for precision navigation and flight guidance 18 p2517 N88-24932
Precision measurement of the Fresnel drag coefficient using a ring laser
[AD-A196025] 24 p3366 N88-30043

LASER HEATING
Mechanisms in thermal mechanical forming of plates
[AD-A187797] 11 p1466 N88-18744
Effect of experimental variables on flash thermal diffusivity data analysis
[DE88-003631] 11 p1487 N88-18877
Particle simulation research by plasma parametric heating caused by strong laser
14 p1903 N88-21368
Laser surface melting
[BMFT-FB-T-86-072] 14 p1914 N88-21435
Superfine grain development by laser
15 p2050 N88-22215
Material surface improvement by laser
15 p2051 N88-22217
Laser-RDX aerosol pyrolysis with matrix isolation of unstable intermediates 19 p2632 N88-25614
Laser-heated CVD process for depositing thin films for low-cost solar-cell applications
[DE88-001162] 21 p2967 N88-27623

LASER INDUCED FLUORESCENCE

Design study for measurement of neutral hydrogen atom density by laser induced fluorescence method
[DE87-752964] 02 p0179 N88-11114

Laser induced fluorescent study of relativistic electron beams
[AD-A184456] 04 p0447 N88-12774

Calibration of a laser-pumped, thermographic phosphor remote thermometry system
[DE88-000452] 04 p0449 N88-12781

Nitrogen energy transfer study
[AD-A184457] 04 p0464 N88-12869

Laser probes of propellant combustion chemistry
[AD-A184854] 05 p0561 N88-13415

Studies of supersonic turbulence and hot-wire response using Laser-Induced Fluorescence (LIF)
06 p0664 N88-14072

The kinetics and dynamics of iodine monofluoride formation in gas-phase collisions
[AD-A185715] 06 p0709 N88-14352

The use of chlorophyll fluorescence measurements from space for separating constituents of sea water. Volume 1: Summary
[ESA-CR(P)-2444-VOL-1] 07 p0873 N88-15294

The use of chlorophyll fluorescence measurements from space for separating constituents of sea water. Volume 2: Appendices
[ESA-CR(P)-2444-VOL-2] 07 p0873 N88-15295

O2-I laser (Oxygen-iodine) mixing studies using LIF (Laser Induced Fluorescence)
[AD-A186667] 09 p1171 N88-17018

The YAlO(sub 3):Er laser
[PB88-130877] 11 p1493 N88-18911

Dynamics of production and oxidation of boranes
[AD-A188988] 12 p1606 N88-19605

Laser fluorescence velocimeter
[AD-A189010] 12 p1630 N88-19753

An experimental method for species concentration measurements in a welding arc using laser-induced fluorescence
[DE88-005638] 13 p1778 N88-20636

Measurement of species concentrations in flames by laser-induced fluorescence
[DE88-007096] 14 p1889 N88-21286

Application of laser-induced fluorescence in an atmospheric-pressure boron-seeded flame
[AD-A189631] 14 p1889 N88-21287

Turbulent reacting flows and supersonic combustion
[AD-A189690] 15 p2034 N88-22115

Advanced diagnostics for reacting flows
[AD-A190485] 15 p2035 N88-22122

Visualization of flows in turbomachinery
[AD-A189927] 15 p2063 N88-22299

Instrumentation for turbulent reacting flows
[AD-A191671] 18 p2515 N88-24923

Tropospheric OH measurement by Laser Induced Fluorescence (LIF) 18 p2540 N88-25071

Quantitative use of exciplex-based vapor/liquid visualization systems, users' manual
[AD-A191649] 19 p2610 N88-25491

Developing diagnostic methods for plasma-particle interaction
[DE88-007726] 20 p2858 N88-26973

Velocity measurements and flow visualization in turbulent three-dimensional supersonic flows using oxygen flow tagging
[AD-A192551] 21 p2892 N88-27165

Laser probes of natural gas ignition chemistry
[PB88-212568] 21 p2910 N88-27271

Measurement of pressure fluctuations in a resonant chamber with laser-induced iodine fluorescence
[DFVLR-FB-87-53] 21 p2955 N88-27551

LASER INTERFEROMETRY

Microstructural effects in shock initiation of granular explosives
[DE87-011282] 01 p0031 N88-10200

Proposed studies of a 30 meter imaging interferometer concept -- spaceborne astronomy
01 p0096 N88-10627

Optical flow diagnostic measurements in turbomachinery
[PNR90396] 02 p0172 N88-11081

LLE (Laboratory for Laser Energetics) review, volume 31
[DE87-013732] 03 p0328 N88-12072

Phase-coherent astrometric interferometry
[AD-A184428] 04 p0439 N88-12725

Velocity interferometry in shock tubes and shock tunnels
[ISL-CO-203/87] 09 p1122 N88-16713

Determination of the equilibrium concentration of characteristic defects by the measurement of thermal expansion using neutron scattering and laser interferometry
[ETN-88-91400] 11 p1490 N88-18890

A rubidium-stabilised laser diode for interferometry
[NPL-MOM-85] 14 p1914 N88-21433

Laser-heterodyne interferometry with streak camera detection
[DE88-003292] 14 p1914 N88-21437

Attachable interferometric strain gages
[AD-A192390] 21 p2950 N88-27522

LASER MATERIALS

Laser sources today and tomorrow
[DE87-014247] 03 p0330 N88-12083

JPRS report: Science and technology. USSR: Life sciences
[JPRS-ULS-87-012] 03 p0355 N88-12238

400-nm photoluminescence of a color center in undoped YAG grown under reducing atmosphere
[DE88-001760] 07 p0858 N88-15213

Development of composite polymer-glass edge claddings for Nova laser disks
[DE88-002389] 07 p0860 N88-15220

Photodetachment neutralizer development: Laser window design study. Volume 2: Window design details
[DE88-000783] 09 p1170 N88-17014

JPRS report: Science and technology. USSR: Physics and mathematics
[JPRS-UPM-87-009] 09 p1233 N88-17395

Efficiency of ionic noble gas and alkali metal molecules as ultraviolet and far-ultraviolet lasers
09 p1238 N88-17419

A nuclear structure study of the proposed gamma-ray laser candidate nucleus Re-186
[DE88-004299] 10 p1336 N88-17986

Growth and characteristics of materials for tunable lasers in the near infrared spectral region
[NASA-CR-182501] 11 p1491 N88-18901

Fracture mechanisms and strengthening of slab lasers
[DE88-004002] 11 p1493 N88-18914

High power, high efficiency 770 nm laser diode array
[DE88-004043] 12 p1631 N88-19762

Reactions of N2(A(3)(SIGMA)/sub u/(+)) and candidates for short wavelength lasers
[DE88-005366] 12 p1632 N88-19767

Phosphorus oxynitride glass for laser applications
[DE88-005413] 12 p1632 N88-19768

Database of average-power damage thresholds at 1064 nm
[DE88-004352] 13 p1776 N88-20626

Design studies for a solar pumped laser device
[DFVLR-FB-87-39] 13 p1777 N88-20629

Guidelines for estimation and characterization of the thermo-mechanical properties of new optical materials
[DE88-004359] 13 p1840 N88-21010

Reactions of N2(A sup 3 sigma sup + sub u) candidates for short wavelength lasers
[DE88-007018] 15 p2070 N88-22342

Solid hosts for dye laser rods. Part 1: Criteria for choosing a host material
[DE88-006478] 15 p2072 N88-22355

Development program for 1.93-micron lasers
[NASA-CR-4148] 16 p2212 N88-23198

Laser comparison study of Nd:BEL and Nd:YAG
[AD-A191084] 16 p2213 N88-23205

Fracture of solid state lasers
[DE88-007023] 18 p2522 N88-24961

Liquid crystal optics for laser systems
[DE88-008475] 20 p2854 N88-26948

Nonlinear materials for frequency conversion
[DE88-008343] 20 p2875 N88-27067

Growth and characterization of materials for tunable lasers in the near infrared spectral region
[NASA-CR-183132] 24 p3377 N88-30113

Bibliography of Soviet laser developments, number 88, March - April 1987
[AD-A195978] 24 p3378 N88-30116

LASER MICROSCOPY

Flaw characterization in structural ceramics using scanning laser acoustic microscopy
15 p2082 N88-22415

Nondestructive evaluation of sintered ceramics
15 p2083 N88-22416

LASER MODE LOCKING

A mode-locked ruby laser with chlorophyll d as saturable absorber 03 p0327 N88-12064

Mode locking in Nd-laser by means of Gd-Sc-Ga-garnet shutter 09 p1237 N88-17412

Theoretical study of colliding pulse mode-locking in dye lasers 14 p1903 N88-21366

Laser gyroscopes using the rate-bias technique
18 p2517 N88-24930

LASER MODES

Distributed feedback effects in lasers and high gain laser instabilities in optically pumped CH3F
03 p0329 N88-12079

Lasers with wavefront-reversing mirrors (review article)
06 p0709 N88-14349

Burst mode Nd:YLF laser oscillator
[DE88-004040] 11 p1492 N88-18905

Beam quality of stable and unstable resonators: A theoretical approach
[DFVLR-FB-87-35] 14 p1982 N88-21826

Discussion of two-mode two-photon CW laser oscillation 16 p2187 N88-23042

Distributed feedback lasers
[NASA-CR-4154] 18 p2520 N88-24948

Spectral properties of semiconductor lasers with external resonators
[ETN-88-93119] 24 p3379 N88-30125

LASER OUTPUTS

Thermo-optical modeling of flashlamp-pumped zig-zag slabs
[DE87-011878] 01 p0051 N88-10326

Models of high spatial frequency thermal blooming instabilities
[DE87-014280] 01 p0052 N88-10330

High energy efficient solid state laser sources
[NASA-CR-181362] 01 p0052 N88-10332

Optical damage in polymers by millisecond light pulses
[DE87-013106] 02 p0151 N88-10943

Quantum-mechanical aspects of classically chaotic driven systems
[DE87-013152] 02 p0178 N88-11106

An acoustic emission digital data acquisition workstation
[DE87-012425] 02 p0191 N88-11191

Feasibility of alpha particle measurement in a magnetically confined plasma by CO2 laser Thomson scattering
[DE88-000039] 02 p0241 N88-11522

Ultra-short pulse laser system used for lageos range finding 03 p0301 N88-11893

Large-aperture high-efficiency frequency doubling using tandem KDP crystals 03 p0301 N88-11894

A 10 W transverse flow excimer laser
03 p0302 N88-11901

Excimer laser cell with longitudinal electron-beam excitation 03 p0302 N88-11903

Experimental study of stabilizing He-Ne laser output power with transverse magnetic field
03 p0303 N88-11906

Thrust and specific impulse of repetitively-pulsed-laser propulsion rocket 03 p0318 N88-12012

Instrument for radiation testing/screening electronic devices over an extended temperature range
[AD-A184245] 03 p0326 N88-12060

Powerful picosecond ultraviolet laser output at 354.7 nanometers 03 p0327 N88-12063

Gas dynamic characteristics in past axial flow CO2 laser 03 p0327 N88-12067

Investigation of two laser beam coupling and amplification in Ce-doped SBN single crystals
03 p0327 N88-12069

Production of atom flows at materials evaporation by laser radiation
[DE87-703327] 03 p0328 N88-12074

Distributed feedback effects in lasers and high gain laser instabilities in optically pumped CH3F
03 p0329 N88-12079

Plume mechanics and aerosol growth processes
[AD-A184467] 04 p0442 N88-12742

The lasertron RF generator for FEL (Free-Electron Laser) applications
[DE88-000515] 04 p0448 N88-12776

Low jitter laser-triggered high-voltage vacuum switch using low laser energies
[DE88-001922] 05 p0587 N88-13576

Theoretical studies of solar lasers and converters
[NASA-CR-181569] 05 p0587 N88-13577

A study of the interaction of laser light with liquid propellant drops
[AD-A185117] 05 p0587 N88-13582

An experimental study of CW HF chemical laser amplifier performance and zero power gain
[AD-A185241] 05 p0588 N88-13584

Raman microprobe characterization of dielectric films following high-energy pulsed laser irradiation
[DE88-000559] 05 p0588 N88-13587

Development of a data analysis system for the detection of lower level atmospheric turbulence with an acoustic sounder
[AD-A184972] 05 p0624 N88-13821

Repetitively pulsed and continuous wave CO2 lasers pumped by a pulsed self-sustained discharge for thermal processing 06 p0709 N88-14346

Observation of instabilities in time during dynamic self-diffraction of light in anisotropic nonhomogeneous medium 06 p0769 N88-14730

Effect of optical inhomogeneities on space coherence of radiation emitted by laser with unstable resonator
06 p0771 N88-14738

Super-short yttrium aluminate pulse generator with controlled resonator Q-factor 06 p0772 N88-14740

Periodically pulsed excimer master oscillator-regenerative amplifier laser set
06 p0772 N88-14741

Observing effect of laser radiation of low-frequency Raman scattering of light 06 p0772 N88-14742

The Rayleigh-Taylor instability in ablatively accelerated targets with 1, 1/2 and 1/4 micrometers laser light
[AD-A185945] 07 p0856 N88-15208

Laser action from syn-(methyl,methyl) bimane
[AD-A186314] 07 p0858 N88-15211

Chapter 2: Threshold for Raman conversion of FEL laser pulses in the atmosphere
[DE88-002470] 07 p0859 N88-15215

Lawrence Livermore National Laboratory Soft X-ray Laser Program
[DE88-001888] 07 p0859 N88-15218

Phase phenomena in parametric generators and amplifiers of ultrashort light pulses
07 p0918 N88-15576

Effect of multiplication of spectral components of multi-frequency lasing of pulsed tunable laser
07 p0920 N88-15586

Characteristics of LKI-501 tunable dye laser with dyes in solid matrix 07 p0920 N88-15587

Explosive absorption of laser beam of finite diameter
07 p0921 N88-15597

Characterization of Er,Cr:YSGG
[AD-A185885] 07 p0932 N88-15659

Laser thermal propulsion
[AD-A186407] 07 p0933 N88-15666

Effect of the band-gap characteristics on laser-induced dry etching of semiconductors
[DE88-001853] 07 p0937 N88-15695

Characteristics of thermooptical sound excitation in metals 08 p1076 N88-16486

Instability of strong-absorption domain in semiconductor 08 p1077 N88-16495

Stimulated Raman scattering of picosecond light pulses in long dispersive medium 08 p1078 N88-16498

Electron acceleration by laser fields in a gas
[DE88-003337] 08 p1082 N88-16523

Analysis of the decomposition of transparent polymer materials (blocks) under the action of laser beams in free generation mode
[AD-A187090] 09 p1147 N88-16873

Studies on nonlinear mechanisms of excimer laser propagation in fused silica fibers
[AD-A186822] 09 p1156 N88-16929

Comparison of UNL laser imaging and sizing system and a phase/Doppler system for analyzing sprays from a NASA nozzle
[NASA-CR-182437] 09 p1161 N88-16956

Solar pumped, alkali vapor laser
[AD-A187156] 09 p1170 N88-17016

Nuclear excitation via the motion of electrons in a strong laser field
[AD-A187166] 09 p1171 N88-17017

Investigations of solid state slab lasers
[ETN-88-91055] 09 p1171 N88-17022

Minimum necessary intensity of source of preionization for stabilization of a self-sustaining laser discharge with mean power raised by electron beam or X-rays
[PB87-178158] 09 p1171 N88-17024

Semiconductor laser with electron-beam pumping and fiber-optic output waveguide 09 p1235 N88-17405

Parametric interaction of optical modes in fiber-optic light guide 09 p1235 N88-17406

Statistics of breakdown centers appearing during propagation of laser radiation through turbulent atmosphere 09 p1236 N88-17411

High-power periodic-pulse YAG:Nd3 + -laser system with telescopic unstable resonator and two-stage amplifier
09 p1237 N88-17414

Spatially resolved X-ray laser spectra and demonstration of gain in nickel-like systems
[DE88-003957] 10 p1335 N88-17979

Dynamics of coupled electron-nucleon motion in a laser field
[DE88-005063] 10 p1337 N88-17994

Evaluation of a temperature remote sensing technique
[AD-A187885] 10 p1347 N88-18053

Laser-induced desorption determinations of surface diffusion on Rh(111)
[DE88-005159] 11 p1454 N88-18667

Operation of electron-beam controlled CO2 laser at 6 atmospheres 11 p1468 N88-18758

Burst mode Nd:YLF laser oscillator
[DE88-004040] 11 p1492 N88-18905

Metastable materials by laser irradiation
[PB88-130364] 11 p1493 N88-18912

Surface free energy of laser-produced bond percolators
[PB88-130885] 11 p1493 N88-18913

Quenched-laser operation of a Littman dye oscillator
[DE88-004020] 11 p1493 N88-18915

Project SKYLITE: A design exploration
[AD-A187906] 11 p1511 N88-19030

Laser flash effects on chromatic discrimination in monkeys
[AD-A187703] 11 p1517 N88-19061

An experimental and theoretical investigation of optogalvanic effects
[AD-A189618] 12 p1625 N88-19720

Non-linear materials (TAS)
[AD-A189197] 12 p1633 N88-19775

Magnetic trapping of neutral atoms
[AD-A188473] 12 p1689 N88-20103

Advanced space propulsion study - antiproton and beamed power propulsion
[AD-A189218] 13 p1732 N88-20355

Laser ignition of nitramine composite propellants and crack propagation and branching in burning solid propellants
[AD-A189260] 13 p1753 N88-20483

Laser fluorescence spectroscopy of zinc neutrals originating from laser-irradiated and ion-bombarded zinc sulfide and zinc surfaces
[DE88-006033] 13 p1776 N88-20620

Refractive index gradients in nuclear-reactor-pumped lasers: Gasdynamic effects
[DE88-006099] 13 p1776 N88-20621

Multimode-waveguide laser beam deflector
[DE88-006222] 13 p1776 N88-20622

Database of average-power damage thresholds at 1064 nm
[DE88-004352] 13 p1776 N88-20626

Studies of compound states of negative ions using laser beams
[DE88-004708] 13 p1777 N88-20627

Direct solar-pumped iodine laser amplifier
[NASA-CR-182674] 13 p1777 N88-20630

Low threshold ridge waveguide single quantum well lasers 13 p1777 N88-20631

Doubly periodic output from a dye laser pumped by a free-running argon laser
[DE88-005027] 13 p1778 N88-20633

Initial stages of silicon growth on the (100) surface of silicon by localized laser CVD
[DE88-005420] 13 p1848 N88-21059

Folded long-pulse XeCl excimer laser described
14 p1901 N88-21357

Theoretical study of colliding pulse mode-locking in dye lasers 14 p1903 N88-21366

Exact image method for Gaussian beam problems involving a planar interface
[NASA-CR-182702] 14 p1905 N88-21380

Nonlinearly tunable wideband emission of infrared radiation by Al2O3:Ti laser 14 p1970 N88-21758

Time characteristics of ultrashort light pulses from dye lasers with distributed feedback
14 p1970 N88-21759

Emission characteristics of XeCl-laser excited by electron beam of microsecond duration
14 p1970 N88-21762

Effects of emission energy transient in periodic-pulse XeCl excimer laser of approximately 400 W average power 14 p1971 N88-21763

Nonlinear stage of ultrashort-pulse formation in solid-state laser 14 p1971 N88-21765

High-efficiency Y-Sc-Ga:Cr (sup)3 + ,Tu (sup)3 + ,Ho (sup)3 + garnet laser (gl = 2.088 gmm at room temperature 14 p1971 N88-21766

Space-time structure of ultrashort light pulses formed during stimulated backscattering of laser beam
14 p1972 N88-21767

Free carrier nonlinear optics 14 p1977 N88-21796

Beam quality of stable and unstable resonators: A theoretical approach
[DFVLR-FB-87-35] 14 p1982 N88-21826

Laser processing-status, perspectives
15 p2050 N88-22211

Magic light high-power laser passes state certification
15 p2053 N88-22236

A preliminary comparison of the transient effects of single versus multiple q-switched doubled-neodymium laser pulses
[AD-A189855] 15 p2071 N88-22347

Research on certain aspects of laser diffraction particle sizing relevant to autonomous self-diagnosing instrumentation
[AD-A190220] 15 p2071 N88-22348

Characterization of space radiation environment in terms of the energy deposition in functionally important volumes
[DE88-005627] 15 p2100 N88-22513

Collective rotation of molecules driven by the angular momentum of light in a nematic film
[FUB-6-1986] 15 p2131 N88-22714

Particle beam alignment system for single event upset-Van de Graaf experiments
[AD-A189695] 15 p2132 N88-22721

Optical switching and control techniques using nonlinear optical wave mixing
[AD-A190467] 15 p2134 N88-22730

Characteristics of distributed feedback lasers discussed 16 p2185 N88-23028

Experimental investigation on stimulated Raman scattering in high-pressure hydrogen by ruby laser
16 p2186 N88-23034

Efficient narrow linewidth waveguide dye laser pumped by CuCl laser 16 p2187 N88-23038

Investigation of ultrashort traveling-wave amplified spontaneous emission 16 p2187 N88-23040

Observation of synchronously transient pumped mode-locking dye laser under negative cavity detuning
16 p2187 N88-23041

Discussion of two-mode two-photon CW laser oscillation 16 p2187 N88-23042

Development program for 1.93-micron lasers
[NASA-CR-4148] 16 p2212 N88-23198

Application of magnetic barrier for increasing the efficiency of laser ion source
[DE88-701669] 16 p2212 N88-23200

Realization of an XeCl laser producing 100W on average
[ETN-88-92541] 17 p2344 N88-23970

Magnetically switched power supply system for lasers
[NASA-CASE-NPO-16402-2] 18 p2505 N88-24862

Distributed feedback lasers
[NASA-CR-4154] 18 p2520 N88-24948

An optical preamplifier for detection of CO2 laser radiation
[AD-A190790] 18 p2520 N88-24949

Atmospheric propagation of laser beams
[AD-A191447] 18 p2520 N88-24952

Fast acting optical beam detection and deflection system
[AD-A192161] 18 p2521 N88-24954

Integral equation for the laser field: Multimode description of a free-electron laser oscillator
[DE88-007050] 18 p2521 N88-24956

An optical technique for measuring divergence, beam profile, and aiming direction, of relativistic negative hydrogen ions
[DE88-007049] 18 p2572 N88-25278

Optical system of laser illuminated streamer chamber
[DE88-702127] 18 p2577 N88-25306

Characteristics, packaging and physics of ultra high speed diode lasers and detectors
19 p2658 N88-25797

A new optoelectronic CW microwave source
19 p2660 N88-25818

A twin-mirrored galvanometer laser light sheet generator
[NASA-TM-100587] 19 p2674 N88-25901

Precise beam alignment He-Ne laser tubes
[PB87-228334] 19 p2675 N88-25906

Laser induced surface emission of neutral species and its relationship to optical surface damage processes
[DE88-008035] 19 p2726 N88-26192

The use of liquid films for spacecraft survivability to laser radiation
[AD-A192954] 20 p2765 N88-26395

Laser fluorescence spectroscopy of zinc neutrals originating from laser-irradiated and ion-bombarded zinc sulfide and zinc surfaces
[DE88-008037] 20 p2769 N88-26418

Electron-impact-ionization and electron-attachment cross sections of radicals important in transient gaseous discharges
[AD-A192248] 20 p2770 N88-26424

Results from the SLAC lasertron
[DE88-007816] 20 p2806 N88-26647

The propagation of irradiance moments of an aberrated, apodized FEL beam
[DE88-008972] 20 p2806 N88-26648

Laser desorption/ablation studies by resonance ionization mass spectrometry
[DE88-009124] 20 p2807 N88-26650

Poloidal field measurements using laser enhanced attenuation of an energetic lithium beam
[DE88-008360] 20 p2856 N88-26963

Predicting optical degradation of a laser beam through a turbulent shear layer 21 p2927 N88-27376

Wave equations for pulse propagation
[DE88-011760] 21 p2954 N88-27548

Multiphoton ionization of alkaline earth atoms in an intense laser field
[DE88-008078] 21 p3014 N88-27884

Theory and simulation of relaxed plasmoids
[AD-A192884] 21 p3032 N88-27997

Frequency doubling at 1.315 micrometers
[AD-A193902] 23 p3208 N88-29092

Flow visualization by laser sheet
[AD-A194481] 23 p3211 N88-29111

Coupling between radiation and gas dynamics
[AD-A194593] 23 p3211 N88-29113

Effect of a laser field in the electron inelastic scattering into plasma fields
[DE88-702295] 23 p3218 N88-29157

Analysis of free electron laser performance utilizing the National Bureau of Standards CW microtron
[AD-A194217] 23 p3219 N88-29160

High energy and high intensity laser effects on aerosols: Changes in droplet morphology, surrounding temperature and vapor concentration
[AD-A193825] 23 p3220 N88-29164

Evidence for laser emission from the TICT exciplex of coumarin dyes
[DE88-702544] 23 p3220 N88-29167

Theory of filtering and control with application to control of large space structures
[AD-A195500] 24 p3335 N88-29851

Bibliography of Soviet laser developments, number 88, March - April 1987
[AD-A195978] 24 p3378 N88-30116

Transverse CO2 laser two-dimensional gain distributions
[AD-A196240] 24 p3378 N88-30119

Nonlinear optical phase conjugation techniques to reduce the physical size of lasers
[AD-A196170] 24 p3379 N88-30122

Functional assessment of laser irradiation
[AD-A195735] 24 p3408 N88-30287

Spectroscopic studies with multiple quantum well materials with applications to optical signal processing at room temperature
[AD-A194171] 24 p3429 N88-30409

LASER PLASMA INTERACTIONS

Transient absorption behavior of metals at the onset of the laser welding process
[DFVLR-FB-87-12] 01 p0025 N88-10160

Laser-plasma-interaction experiments using multikilojoule lasers
[DE87-013483] 01 p0100 N88-10658

Laser blow-off experiments on ASDEX --- tokamak
[IPP-III/119] 02 p0243 N88-11535

Relativistic electromagnetic waves in an electron-ion plasma
[NASA-CR-182421] 08 p1085 N88-16532

Activities report in quantum optics
[ISSN-0177-0101] 09 p1248 N88-17482

Basic physics of laser-plasma interactions
[ETN-88-92055] 14 p1984 N88-21838

The development of high power KrF laser systems for plasma research by the application of stimulated Raman scattering
[ETN-88-92220] 15 p2073 N88-22358

Activities report in laser-matter interaction
[ETN-88-92007] 15 p2129 N88-22696

Unified study of plasma/surface interactions for space power and propulsion
[AD-A195971] 24 p3338 N88-29870

LASER PLASMAS

Geometry and reproducibility of a plasma-supported removal of material by laser radiation
[ETN-87-90436] 01 p0052 N88-10335

Enhanced noise and Raman scattering in plasma
[DE87-014466] 02 p0238 N88-11501

Enhanced Thomson scattering from laser plasmas
[DE87-014463] 02 p0238 N88-11503

X-ray emission from high-Z spherical laser plasmas: Implications for plasma dynamics
[DE87-014722] 02 p0239 N88-11506

Review of X-ray spectroscopy from laser-produced plasmas
[DE88-000755] 04 p0494 N88-13043

An investigation of unipolar arcing at atmospheric pressure in aluminum 2024 and aluminum coated glass slides
[AD-A184903] 05 p0577 N88-13521

Active medium formation in lasers using mixtures of inert gases and optical breakdown pumping
06 p0709 N88-14347

The application of photoconductive detectors to the measurement of X-ray production in laser produced plasmas
[DE88-001630] 07 p0934 N88-15671

Pulsed laser stereophotography of plasmas and dynamically moving surfaces
[DE88-003170] 09 p1173 N88-17031

Characteristics of laser-plasma X radiation source (review) 09 p1239 N88-17428

Activities report in quantum optics
[ISSN-0177-0101] 09 p1248 N88-17482

Spatially resolved X-ray laser spectra and demonstration of gain in nickel-like systems
[DE88-003957] 10 p1335 N88-17979

Overview of applications of Laser-Induced Breakdown Spectroscopy (LIBS)
[DE88-004314] 10 p1336 N88-17987

Spectroscopic studies of a laser-produced carbon plasma in the near and extreme ultraviolet
11 p1553 N88-19292

Photoenhanced attachment for optical control of diffuse discharges
[AD-A188980] 12 p1696 N88-20147

Wavelength scaling of lithium-like recombination scheme for X-UV gain production --- X-ray lasers
[ETN-88-92002] 13 p1778 N88-20634

Experimental study of the role of plasma polarization on line shape in dense laboratory plasmas
[ETN-88-92001] 13 p1844 N88-21033

Progress in X-ray laser experiments
[ETN-88-92004] 14 p1915 N88-21442

Review of X-ray laser studies at the GRECO: Laser-matter interaction
[ETN-88-92005] 14 p1915 N88-21443

Kinetics of slow electrons in excimer laser with electron-beam pumping 14 p1970 N88-21760

One dimensional calculation model for laser produced plasmas expanding in vacuum
[ISL-R-126/86] 14 p1984 N88-21836

PLASMOR: A laser-plasma simulation code, part 2
[DE88-701269] 15 p2135 N88-22736

Particle acceleration to high energies and amplification of coherent radiation by electromagnetic interactions in plasmas
[DE88-701020] 15 p2135 N88-22737

Application of magnetic barrier for increasing the efficiency of laser ion source
[DE88-701669] 16 p2212 N88-23200

The effects of optical smoothing techniques on filamentation in laser plasmas
[AD-A188719] 16 p2275 N88-23614

Thomson scattering for determining electron concentrations and temperatures in an inductively coupled plasma. 2: Description and evaluation of a multichannel instrument
[AD-A191324] 16 p2280 N88-23652

Laser measurement of particle velocities in vacuum plasma spray deposition
[DE88-007111] 19 p2726 N88-26198

On the self-focusing of electric helicons
[DE88-701870] 20 p2848 N88-26905

Thermal inhibition by megagauss field due to variation of electron temperature in laser plasma
[DE88-701887] 20 p2859 N88-26977

Megagauss field variation along axis of wire target in laser produced plasma
[DE88-701895] 20 p2859 N88-26979

Ultraviolet-visible spectroscopy of laser-produced aluminum plasmas
[AD-A193004] 20 p2860 N88-26990

Laser spectoscopy of plasmas
[AD-A193009] 20 p2861 N88-26991

Target designs for plasma-implosion-driven, photoionization-pumped soft X-ray lasers
[DE88-011278] 21 p2954 N88-27547

Introduction to laser plasma diagnostics
[DE88-011056] 23 p3285 N88-29560

Apparatus for submillimeter laser diagnostics of high-temperature plasma
[DE88-702464] 23 p3285 N88-29563

Modeling of atomic processes in X-ray laser plasmas
[AD-A194118] 23 p3286 N88-29567

Energy conversion measurements in laser-sustained argon plasmas for application to rocket propulsion
[AD-A194931] 24 p3337 N88-29861

Bibliography of Soviet laser developments, number 88, March - April 1987
[AD-A195978] 24 p3378 N88-30116

Structuring processes in expanding laser-produced plasmas
[AD-A195249] 24 p3431 N88-30424

LASER PROPULSION

Thrust and specific impulse of repetitively-pulsed-laser propulsion rocket 03 p0318 N88-12012

Proceedings: SDIO/DARPA Workshop on Laser Propulsion. Volume 3: Viewgraphs
[DE88-000964] 04 p0450 N88-12790

Strategic Defense Initiative Organization/DARPA (Defense Advanced Research Projects Agency) workshop on laser propulsion. Volume 1: Executive summary
[DE87-003254] 06 p0768 N88-14722

Laser thermal propulsion
[AD-A186407] 07 p0933 N88-15666

Solar pumped, alkali vapor laser
[AD-A187156] 09 p1170 N88-17016

Advanced energy conversion concept for beamed-energy propulsion
[AD-A187336] 10 p1324 N88-17914

Advanced space propulsion study - antiproton and beamed power propulsion
[AD-A189218] 13 p1732 N88-20355

Possibilities and limits for use of laser propulsion systems in interorbital space flight
[ILR-MITT-185] 18 p2475 N88-24683

A numerical analysis of flow characteristics in laser propulsion system 19 p2637 N88-25645

LASER PUMPING

Diode pumped solid-state laser oscillators for spectroscopic applications
[NASA-CR-180576] 01 p0052 N88-10331

High energy efficient solid state laser sources
[NASA-CR-181362] 01 p0052 N88-10332

Generation of IR stimulated radiation, UV visible violet coherent radiation by two-photon resonance pumping in K vapor 03 p0301 N88-11892

Operational performance of repetitive KrF, XeCl excimer lasers 03 p0327 N88-12068

Distributed feedback effects in lasers and high gain laser instabilities in optically pumped CH3F
03 p0329 N88-12079

Nonconventional optical techniques for optical wavefront processing
[AD-A185099] 05 p0650 N88-13982

Theory of induced spatial incoherence
[AD-A185005] •05 p0651 N88-13992

Compensation of small-scale phase distortions by means of a Fourier phase corrector
06 p0706 N88-14345

Active medium formation in lasers using mixtures of inert gases and optical breakdown pumping
06 p0709 N88-14347

Periodically pulsed excimer master oscillator-regenerative amplifier laser set
06 p0772 N88-14741

Time characteristics of travelling wave lasing with two-photon picosecond optical pumping
07 p0918 N88-15578

Study of kinetics of intracavity absorption in pulsed dye lasers 07 p0919 N88-15585

High-sensitivity recording of weak reflected or scattered radiation by method of coherent intracavity reception with YAG:Nd(3+) laser 08 p1078 N88-16502

Energy disposal in ion-molecule reactions
[AD-A186772] 09 p1171 N88-17019

Investigations of solid state slab lasers
[ETN-88-91055] 09 p1171 N88-17022

The suppression of stimulated hyper-Raman emission in Na due to parametric four-wave mixing
[DE88-003290] 09 p1172 N88-17030

Dye lasers pumped by radiation from high-power semiconductor lasers 09 p1237 N88-17417

Diode pumped fiber laser
[AD-A187694] 11 p1491 N88-18902

Reactions of N2(A(3)(SIGMA)/sub u/(+)) and candidates for short wavelength lasers
[DE88-005366] 12 p1632 N88-19767

Instrumentation for collisional energy transfer studies
[AD-A188495] 12 p1689 N88-20105

Proof of the feasibility of coherent and incoherent schemes for pumping a gamma-ray laser
[AD-A189236] 13 p1774 N88-20613

Design studies for a solar pumped laser device
[DFVLR-FB-87-39] 13 p1777 N88-20629

XeF excimer laser pumped by high-intensity relativistic electron beam 14 p1901 N88-21355

Folded long-pulse XeCl excimer laser described
14 p1901 N88-21357

XeCl laser-pumped nanosecond dye lasers
14 p1902 N88-21359

A picosecond tunable ultrashort cavity dye laser
14 p1902 N88-21361

X-ray lasers: State of art and prospect
[ETN-88-92003] 14 p1914 N88-21434

Review of X-ray laser studies at the GRECO: Laser-matter interaction
[ETN-88-92005] 14 p1915 N88-21443

Nonlinearly tunable wideband emission of infrared radiation by Al2O3:Ti laser 14 p1970 N88-21758

Kinetics of slow electrons in excimer laser with electron-beam pumping 14 p1970 N88-21760

High-efficiency Y-Sc-Ga:Cr (sup)3+,Tu (sup)3+,Ho (sup)3+ garnet laser (gl= 2.088 gmm at room temperature 14 p1971 N88-21766

Pulsed squeezed light 14 p1976 N88-21792

Fundamental noise processes in a laser excited optical filter
[DE88-006460] 15 p2070 N88-22340

Investigation of ultrashort traveling-wave amplified spontaneous emission 16 p2187 N88-23040

Comparison of electrically driven lasers for space power transmission
[NASA-TM-4045] 16 p2212 N88-23197

Effects of translational and rotational nonequilibrium on CW (Continuous Wave) chemical laser performance
[AD-A191425] 16 p2214 N88-23210

The effects of optical smoothing techniques on filamentation in laser plasmas
[AD-A188719] 16 p2275 N88-23614

Space based nuclear-pumped laser/reactor concepts
17 p2403 N88-24289

Application of particle simulations to the NRL laser experiment
[AD-A191641] 18 p2520 N88-24953

A plasma ultraviolet source for short wavelength lasers
[AD-A192844] 21 p2952 N88-27537

Overview and future direction for blackbody solar-pumped lasers
[NASA-TM-100621] 21 p2955 N88-27553

Spectroscopic studies with multiple quantum well materials with applications to optical signal processing at room temperature
[AD-A194171] 24 p3429 N88-30409

LASER RADAR

U OPTICAL RADAR

LASER RADIATION

U LASER BEAMS

LASER RANGE FINDERS

Ultra-short pulse laser system used for lageos range finding 03 p0301 N88-11893

Evaluation of a satellite laser ranging technique using pseudonoise code modulated laser diodes
[NASA-CR-182347] 06 p0706 N88-14343

The Monte Generoso-Zimmerwald (Switzerland) baseline from satellite laser ranging data using various analysis techniques
[LR-533] 14 p1940 N88-21576

Limits of accuracy and range of laser radars
18 p2517 N88-24934

Range and range rate system
[NASA-CASE-MSC-20867-1] 18 p2521 N88-24958

Laser ranging data analysis
[NASA-CR-183115] 20 p2792 N88-26567

Phase comparator for range imaging laser radar
[DE88-008109] 21 p2954 N88-27545

IEMIS (Integrated Emergency Management Information System) floodplain mapping based on a LIDAR derived data set
[AD-A193071] 21 p2966 N88-27616

Determining earth's rotation from laser observations of Lageos artificial earth satellite (during period of main merit campaign) 24 p3449 N88-30528

LASER RANGER/TRACKER

Orbital navigation, docking and obstacle avoidance as a form of three dimensional model-based image understanding 08 p1061 N88-16406

Baseline estimation from simultaneous satellite laser tracking
[NASA-CR-182750] 15 p2022 N88-22052

Solid Earth mission end-to-end data system study
[C04825.08/FR] 17 p2309 N88-23811

LASER SPECTROMETERS

On the multiple grating spectrometer resolving power
[PREPRINT-585] 22 p3153 N88-28761

The 1985-86 measurements with the tunable diode laser absorption spectrometer
[PB88-214002] 23 p3231 N88-29226

LASER SPECTROSCOPY

Laser spectroscopy and gas-phase chemistry in CVD
[DE87-013715] 03 p0281 N88-11770

Energy transformation in molecular electronic systems
[DE87-013916] 03 p0282 N88-11771

Ro-vibrational laser spectroscopy of ESD neutrals from chemisorbed species
[DE87-013011] 04 p0447 N88-12770

Use of lasers with F sub A(II)-color center KCl:Li crystals in the intraresonator laser spectroscopy method
06 p0769 N88-14729

TEA-TE: Powerful nitrogen-based laser system
07 p0919 N88-15583

Laser post-ionization secondary neutral mass spectroscopy
[DE88-002979] 09 p1172 N88-17027

Picosecond laser spectroscopy of charge-separation in photosynthetic model systems
[DE88-003122] 09 p1172 N88-17028

Energy transfer studies with lasers
[DE88-004864] 10 p1337 N88-17991

Two-photon (VUV and visible) resonant ionization spectroscopy of atoms and molecules
[DE88-004332] 10 p1407 N88-18388

Pulsed laser photothermal spectroscopy of liquids and solids
[DE88-003839] 11 p1455 N88-18675

Study of the vibrational modes of subsurface oxygen on Al (111) using diode laser infrared reflection-absorption spectroscopy
[AD-A188322] 12 p1632 N88-19769

Research studies on extreme ultraviolet and soft X-ray lasers
[AD-A189163] 12 p1633 N88-19773

Resonance energy transfer between carbon monoxide and oxygen molecules using dye laser intracavity absorption spectroscopy
[AD-A188488] 12 p1589 N88-20104

Theory of laser cooling and spectroscopy of harmonically trapped single atoms
[AD-A189576] 13 p1775 N88-20617

Laser fluorescence spectroscopy of zinc neutrals originating from laser-irradiated and ion-bombarded zinc sulfide and zinc surfaces
[DE88-006033] 13 p1776 N88-20620

What has been done and what will be done by subnatural linewidth spectroscopy 14 p1978 N88-21807

Laser spectroscopy and dynamics of combustion intermediates
[DE88-006541] 15 p2033 N88-22110

Infrared absorption spectroscopy and chemical kinetics of free radicals
[DE88-006536] 15 p2033 N88-22112

Laser photoelectron spectroscopy of ions
[DE88-006860] 15 p2033 N88-22113

The spectroscopy and reaction kinetics of coordinatively unsaturated metal carbonyls
[AD-A190533] 15 p2035 N88-22124

Diode laser spectroscopy of chemical moieties at surfaces
[AD-A190710] 15 p2036 N88-22127

Statistical line structure in the inhomogeneously broadened electronic origin of pentacene in p-terphenyl
[AD-A191211] 16 p2176 N88-22968

Laser Diagnostics for combustion temperature and species measurements 17 p2330 N88-23912

Time resolved spectroscopy facility for the study of nonlinear optical properties of semiconducting polymers
[AD-A191221] 18 p2490 N88-24768

Stress measurements in graphite fibers by laser raman spectroscopy
[AD-A191710] 18 p2491 N88-24779

Workshop on Atmospheric OH
[BPT-7/87] 18 p2538 N88-25063

Determination of tropospheric H concentrations by a double-pulsed UV laser method
18 p2539 N88-25070

Tropospheric OH measurement by Laser Induced Fluorescence (LIF) 18 p2540 N88-25071

Trace gas measurements in the troposphere using tunable diode lasers 18 p2540 N88-25072

Development of continuous wave laser frequency modulation of OH in tropospheric concentrations range
18 p2540 N88-25073

Laser fluorescence spectroscopy of zinc neutrals originating from laser-irradiated and ion-bombarded zinc sulfide and zinc surfaces
[DE88-008037] 20 p2769 N88-26418

Laser diagnostics applied to advanced combustion systems
[DE88-753119] 20 p2806 N88-26649

Ground level hydroxyl (OH) concentration measurements by long path differential optical laser absorption
[ETN-88-92124] 20 p2855 N88-26952

An elliptical spectrograph/gated microchannel plate detector for time-resolved spectral measurements in the X-ray region
[DE88-007590] 20 p2856 N88-26961

Laser spectroscopy investigations of materials for solid state laser systems
[AD-A192514] 21 p2952 N88-27535

Laser spectroscopy of quantum well and superlattice structures
[AD-A193336] 21 p3022 N88-27937

Particle sizing in combustion systems, using scattered laser light
[AD-A196231] 24 p3352 N88-29953

LASER STABILITY

Experimental study of stabilizing He-Ne laser output power with transverse magnetic field
03 p0303 N88-11906

Measuring stability of optical reference cavities by analyzing polarization spectrum
03 p0327 N88-12065

Distributed feedback effects in lasers and high gain laser instabilities in optically pumped CH3F
03 p0329 N88-12079

High-power periodic-pulse YAG:Nd3+-laser system with telescopic unstable resonator and two-stage amplifier
09 p1237 N88-17414

Semiclassical theory of injected lasers with arbitrary stable and unstable resonators
[AD-A189514] 13 p1775 N88-20615

A rubidium-stabilised laser diode for interferometry
[NPL-MOM-85] 14 p1914 N88-21433

Analysis of free electron laser performance utilizing the National Bureau of Standards CW microtron
[AD-A194217] 23 p3219 N88-29160

LASER TARGET INTERACTIONS

Geometry and reproducibility of a plasma-supported removal of material by laser radiation
[ETN-87-90436] 01 p0052 N88-10335

Time-resolved ablation measurements of imploding targets
[DE87-014464] 02 p0178 N88-11111

Time-resolved absorption measurements on OMEGA
[DE87-014465] 02 p0179 N88-11112

Numerical simulation of laser filamentation experiments
[ETN-87-90959] 02 p0179 N88-11118

Transient processes in the interaction between pulsed laser radiation and matter
[ISL-R-115/86] 05 p0588 N88-13586

Review of X-ray laser studies at the GRECO Laser-matter interaction
[ETN-88-92005] 14 p1915 N88-21443

Activities report in laser-matter interaction
[ETN-88-92007] 15 p2129 N88-22696

Spallation and dynamic fracture as an effect of laser induced shock-waves
[AD-A193513] 23 p3188 N88-28971

Interaction of high power laser radiation with metals in laser welding
[ISL-PU-304/87] 24 p3381 N88-30135

LASER TARGETS

LLE Review, volume 30
[DE87-014469] 02 p0178 N88-11109

Low jitter laser-triggered high-voltage vacuum switch using low laser energies
[DE88-001922] 05 p0587 N88-13576

Proceedings of Symposium on Physics of Target Implosion and Pulsed Power Techniques
[IPPJ-859] 16 p2276 N88-23619

Efficient shell implosion and target design
16 p2277 N88-23630

Coronal fluid-dynamics in laser fusion
16 p2278 N88-23634

Finite ion-relaxation and nonequilibrium radiation effects on laser-driven implosions 16 p2278 N88-23636

Aurora status and plans
[DE88-006476] 18 p2521 N88-24955

Target designs for plasma-implosion-driven, photoionization-pumped soft X-ray lasers
[DE88-011278] 21 p2954 N88-27547

LLE (Laboratory for Laser Energetics) review
[DE88-008065] 23 p3219 N88-29158

LASER WEAPONS

Large-scale stimulated rotational Raman scattering experiments using the LLNL Nova laser
[DE87-012661] 01 p0051 N88-10328

Relating service doctrine to space system requirements
[AD-A186620] 08 p1074 N88-16483

Where directed energy stands in strategic defense
[DE88-005092] 10 p1403 N88-18365

Constellation sizing for modest directed energy platforms
[DE88-007033] 15 p2070 N88-22343

Power source selection for neutral particle beam systems 17 p2407 N88-24314

Nuclear reactor magnetohydrodynamic power generator for directed energy weapons 17 p2411 N88-24336

Fundamental analysis of space nuclear-MHD generator for gigawatt-level power 17 p2411 N88-24337

Rotating-hoop, pulsed-energy converter
17 p2426 N88-24433

Space Power Reference Source (SPRS): A user's guide to SDI Space Power Technology Programs
17 p2427 N88-24440

Monolithic fuel cell based power source for burst power generation 17 p2429 N88-24450

Laser countermeasure impacts and penalties
[DE88-006871] 18 p2520 N88-24947

High spatial frequency thermal blooming instability: A linear stability analysis
[DE88-010711] 20 p2807 N88-26655

SDI (Strategic Defense Initiative) battle management/C3 (Command, Control and Communications) algorithms technology program plan
[AD-A194357] 23 p3275 N88-29495

Looking beyond the strategic defense initiative
[AD-A195079] 24 p3427 N88-30394

LASER WELDING

NT BRAZING

NT FUSION WELDING

NT GAS WELDING

Transient absorption behavior of metals at the onset of the laser welding process
[DFVLR-FB-87-12] 01 p0025 N88-10160

Effect of rapid solidification on stainless steel weld metal microstructures and its implications on the Schaeffler diagram
[DE88-001489] 05 p0566 N88-13451

Production-process CO2 laser with amplified pulse-repetition operation 06 p0771 N88-14739
Study of combination type CO2 laser welding system
[PB87-143764] 08 p0992 N88-16002
Microstructural modification during laser welding
[DE88-002344] 09 p1144 N88-16860
Joining of dissimilar materials with the pulsed Nd-YAG laser
[DE88-003757] 11 p1458 N88-18693
Calibration of beam power monitors for laser welding
[DE88-004687] 11 p1492 N88-18908
Modeling of laser ultrasound generation in a weld pool
[DE88-005546] 13 p1834 N88-20971
The technical feasibility of using spiked-radiation lasers to cut out and weld metals 14 p1898 N88-21332
Reduced thermal input by proper selection of YAG laser welding parameters
[DE88-000730] 15 p2072 N88-22356
Process control improvements in pulsed Nd:YAG laser closure welding of electromechanical relays
[DE88-006275] 21 p2957 N88-27564
Interaction of high power laser radiation with metals in laser welding
[ISL-PU-304/87] 24 p3381 N88-30135

LASER WINDOWS
Photodetachment neutralizer development: Laser window design study. Volume 2: Window design details
[DE88-000783] 09 p1170 N88-17014

LASERS
NT AIRBORNE LASERS
NT ARGON LASERS
NT ATMOSPHERIC LASERS
NT CARBON DIOXIDE LASERS
NT CARBON MONOXIDE LASERS
NT CHEMICAL LASERS
NT CONTINUOUS WAVE LASERS
NT DISTRIBUTED FEEDBACK LASERS
NT DYE LASERS
NT EXCIMER LASERS
NT FREE ELECTRON LASERS
NT GALLIUM ARSENIDE LASERS
NT GAMMA RAY LASERS
NT GAS LASERS
NT GASDYNAMIC LASERS
NT GLASS LASERS
NT HCN LASERS
NT HELIUM-NEON LASERS
NT HF LASERS
NT HIGH POWER LASERS
NT INFRARED LASERS
NT IODINE LASERS
NT KRYPTON FLUORIDE LASERS
NT LIQUID LASERS
NT METAL VAPOR LASERS
NT NEODYMIUM LASERS
NT NITROGEN LASERS
NT NOVA LASER SYSTEM
NT NUCLEAR PUMPED LASERS
NT PULSED LASERS
NT Q SWITCHED LASERS
NT RAMAN LASERS
NT RARE GAS-HALIDE LASERS
NT RING LASERS
NT RUBY LASERS
NT SEMICONDUCTOR LASERS
NT SOLAR-PUMPED LASERS
NT SOLID STATE LASERS
NT SPACEBORNE LASERS
NT TEA LASERS
NT TUNABLE LASERS
NT TWO-WAVELENGTH LASERS
NT ULTRASHORT PULSED LASERS
NT ULTRAVIOLET LASERS
NT WAVEGUIDE LASERS
NT X RAY LASERS
NT XENON CHLORIDE LASERS
NT XENON FLUORIDE LASERS
NT YAG LASERS
LLE Review, volume 30
[DE87-014469] 02 p0178 N88-11109
LLE review
[DE87-014468] 02 p0178 N88-11110
Quantum well laser diodes: Modeling and realization of GaAs/GaAlAs
[LAAS-87-165] 02 p0179 N88-11116
JPRS report: Science and technology. China
[JPRS-CST-87-025] 03 p0300 N88-11888
Experimental study of stabilizing He-Ne laser output power with transverse magnetic field
03 p0303 N88-11906
LLE (Laboratory for Laser Energetics) review, volume 31
[DE87-013732] 03 p0328 N88-12072
Storing photomicrographs on optical laser disks
[DE87-013747] 04 p0449 N88-12785
Lasers measure atmosphere
04 p0461 N88-12849
An analysis of the effect of system variables on the quality of thin films and powders produced by laser-breakdown chemical vapor deposition
[DE88-001793] 06 p0708 N88-14342
JPRS report: Science and technology. USSR: Physics and mathematics
[JPRS-UPM-87-006] 06 p0769 N88-14727
USSR report: Physics and mathematics
[JPRS-UPM-87-002] 07 p0918 N88-15575
Bright source lasers and experiments at very high irradiance
[DE88-004317] 10 p1337 N88-17988
Laser studies of the dynamics of free radical reactions
[DE88-004431] 10 p1337 N88-17989
Absolute rate measurements of two-photon process of gases, liquids, and solids
[DE88-003800] 10 p1407 N88-18391
Investigations of stimulated Raman scattering from high density underdense plasmas irradiated by a 0.35 micron laser 10 p1411 N88-18421
Atomic and molecular gas phase spectrometry
[AD-A187562] 11 p1452 N88-18655
Laser velocimeter measurements of solids in multiphase flow
[DE88-000196] 11 p1487 N88-18876
Calibration of beam power monitors for laser welding
[DE88-004687] 11 p1492 N88-18908
Reactions of N2(A(3)(SIGMA)/sub u/(+)) and candidates for short wavelength lasers
[DE88-005366] 12 p1632 N88-19767
JPRS report: Science and technology. USSR: Life sciences
[JPRS-ULS-88-002] 12 p1665 N88-19982
Superconductors with structured surfaces: Fields and currents
[AD-A189353] 12 p1699 N88-20164
Solid state research
[AD-A188388] 12 p1699 N88-20166
Laser programming integrated circuits
[AD-A189590] 13 p1762 N88-20537
Proof of the feasibility of coherent and incoherent schemes for pumping a gamma-ray laser
[AD-A189238] 13 p1774 N88-20613
Semiclassical theory of injected lasers with arbitrary stable and unstable resonators
[AD-A189514] 13 p1775 N88-20615
Lasers: Invention to application
[PB88-161583] 14 p1914 N88-21436
Demonstration of efficient full aperture Type 1/Type 2 third harmonic conversion on Nova
[DE88-003834] 14 p1914 N88-21438
Surface-emitting two-dimensional laser diode arrays constructed on zig-zag heat sink surface
[DE88-005215] 14 p1915 N88-21439
Nonlinearly tunable wideband emission of infrared radiation by Al2O3:Ti laser 14 p1970 N88-21758
High-efficiency Y-Sc-Ga:Cr (sup)3+,Tu (sup)3+,Ho (sup)3+ garnet laser (gl= 2.088 gmm at room temperature 14 p1971 N88-21766
United States - Japan Seminar on Quantum Mechanical Aspects of Quantum Electronics
[AD-A186938] 14 p1974 N88-21781
Pulsed squeezed light 14 p1976 N88-21792
Quantum nondemolition detection and squeezing in optical fibers 14 p1976 N88-21793
Recent progress in optical bistability and tristability
14 p1979 N88-21809
Investigation of laser diagnostics of PACVD processes for depositing hard face coatings
[DE88-007083] 15 p2043 N88-22176
JPRS report: Science and technology. Japan
[JPRS-JST-87-030] 16 p2185 N88-23026
Noncondensing round turbulent gas jets in liquids
[AD-A191191] 16 p2208 N88-23179
Theoretical studies of Resonance Enhanced Stimulated Raman Scattering (RESRS) of frequency doubled Alexandrite laser wavelength in cesium vapor
[NASA-CR-182871] 17 p2317 N88-23841
Magnetically switched power supply system for lasers
[NASA-CASE-NPO-16402-2] 18 p2505 N88-24862
Bibliography of Soviet laser developments, number 83, May - June 1986
[AD-A190969] 18 p2520 N88-24950
Laser desorption/ablation studies by resonance ionization mass spectrometry
[DE88-009124] 20 p2807 N88-26650
Liquid crystal optics for laser systems
[DE88-008475] 20 p2854 N88-26948
Direct measurement of solids: High temperature sensing. Experimental development and testing of high temperature pulsed EMATs
[DE88-009859] 21 p2954 N88-27546
Finite element methodology for integrated flow-thermal-structural analysis
[NASA-CR-183144] 21 p2964 N88-27606
Future SDI (Strategic Defense Initiative) decision making
[AD-A192794] 21 p3010 N88-27880
Application of laser diffraction techniques to particle sizing in solid propellant rocket motors
[AD-A193841] 22 p3049 N88-28089
Apparent brightness of stars and lasers
22 p3065 N88-28188
Effect of fiber diameter on the reliability of composites - automated laser diffraction implementation
[AD-A193524] 23 p3188 N88-28972
Tolerances for phase locking of semiconductor laser arrays
[AD-A195974] 24 p3378 N88-30120
Nonlinear optical phase conjugation techniques to reduce the physical size of lasers
[AD-A196170] 24 p3379 N88-30122
The study of hydromagnetic waves and RF heating using the TORTUS tokamak, the development of diagnostic techniques based on submillimeter lasers and the gyrotron, and gas discharge 24 p3431 N88-30419

LASING
XeCl excimer laser with magnetic compressor
03 p0299 N88-11879
Intracavity absorption spectroscopy with ring traveling-wave dye laser 03 p0300 N88-11890
Distributed feedback effects in lasers and high gain laser instabilities in optically pumped CH3F
03 p0329 N88-12079
Repetitively pulsed and continuous wave CO2 lasers pumped by a pulsed self-sustained discharge for thermal processing 06 p0709 N88-14346
The suppression of stimulated hyper-Raman emission in Na due to parametric four-wave mixing
[DE88-003290] 09 p1172 N88-17030
Progress in X-ray laser experiments
[ETN-88-92004] 14 p1915 N88-21442
Recent progress in optical bistability and tristability
14 p1979 N88-21809
Characteristics of distributed feedback lasers discussed 16 p2185 N88-23028
Isotope separation using tuned laser and electron beam
[NASA-CASE-NPO-16907-1-CU]
18 p2483 N88-24732
Characteristics, packaging and physics of ultra high speed diode lasers and detectors
19 p2658 N88-25797

LASV
U F-111 AIRCRAFT

LATCH-UP
Electric design rules related to latch-up and radiation --- simulation
[FOA-E-30006-3.1] 08 p0979 N88-15917
High density CMOS technology
11 p1561 N88-19342

LATCHES
Docking/Berthing Subsystem (DBS). Development part 1: Latching analysis --- Columbus
[ESA-CR(P)-2479] 08 p0962 N88-15825
Centaur G Prime modal test 09 p1181 N88-17075
System and concept design of the SSRMS latching end effector --- Space Station 14 p1875 N88-21204
Latching mechanisms for IOC --- EURECA
14 p1875 N88-21205
Structural latches for modular assembly of spacecraft and space mechanisms 14 p1925 N88-21471
Toggle release
[NASA-CASE-MSC-21354-1] 18 p2523 N88-24969

LATE STARS
NT CARBON STARS
NT COOL STARS
NT FLARE STARS
NT K STARS
NT M STARS
NT MIRA VARIABLES
NT S STARS
Circumstellar radio molecular lines
02 p0252 N88-11595
Measurements of stellar magnetic fields
04 p0503 N88-13093
Magnetic fields on K and M stars
04 p0510 N88-13137
Broadband linear polarization and chromospheric Call H and K line emission in late-type main sequence stars
04 p0511 N88-13140
A search for X-ray luminous late type stars in NIPSS data 04 p0511 N88-13143
Excess emission in the wings of the Hydrogen Balmer lines during a flare on the late-type dMe star YZ CMi
04 p0511 N88-13146
MHD energy fluxes for late type dwarfs
04 p0512 N88-13148

Sensitivity of the H alpha line to expansion, geometrical extent and temperature gradient in the G and K supergiant chromospheres 04 p0514 N88-13159

The delta upsilon = 1 fundamental bands of carbon monoxide in late-type stars 04 p0517 N88-13177

A comprehensive exploration of late-type stars in the far-ultraviolet 04 p0520 N88-13194

Hydrogen and deuterium in the local interstellar medium 04 p0521 N88-13204

Duplicity in the solar neighborhood. Part 3: New spectroscopic elements fo: nine solar-type binary stars [SER-C-PREPUBL-FASC-18-PT-3] 18 p2592 N88-25405

Asymptotic giant branch stars in the Infrared Astronomical Satellite (IRAS) catalogs: Selection and analysis of the population characteristics [MPE-PREPRINT-116] 22 p3163 N88-28840

The kinematics of late-type supergiants [SER-C-PREPUBL-FASC-28] 24 p3454 N88-30560

LATENT HEAT

NT HEAT OF FUSION

Transient thermal analysis of three latent heat storage configurations for rapid thermal charging [DE88-008943] 20 p2681 N88-27104

LATENT HEAT OF FUSION

U HEAT OF FUSION

LATERAL CONTROL

Investigation of interactions between limb-manipulator dynamics and effective vehicle roll control characteristics [NASA-CR-3983] 01 p0007 N88-10039

A preliminary investigation into the feasibility of implementing a direct sideforce control system on the Astra Hawk by means of an active control surface --- aircraft control [ETN-87-90924] 02 p0126 N88-10795

A study into the effects and viability of applying lateral force control to an air to ground rocket [ETN-87-90925] 02 p0131 N88-10821

Determination of the drag of missiles with variable lateral accleration possibility [REPT-FM15] 10 p1310 N88-17831

Lateral and longitudinal stability and control parameters for the space shuttle discovery as determined from flight test data [NASA-TM-100555] 13 p1724 N88-20309

Control law parameterization for an aeroelastic wind-tunnel model equipped with an active roll control system and comparison with experiment [NASA-TM-100593] 17 p2308 N88-23807

LATERAL STABILITY

Effects of the installation and operation of jet-exhaust yaw vanes on the longitudinal and lateral-directional characteristics of the F-14 airplane [NASA-TP-2769] 04 p0393 N88-12455

Effect of a model support strut on measurement of aerodynamic longitudinal and lateral coefficients [PB87-170288] 09 p1113 N88-16670

Lateral stability and control derivatives extracted from space shuttle Challenger flight data [NASA-TM-100520] 09 p1132 N88-16788

Investigation of dihedral effects in compressor cascades 10 p1282 N88-17672

Natural laminar flow and airplane stability and control 17 p2298 N88-23747

LATERALITY

U LATERAL STABILITY

LATERALIZATION

U LATERAL CONTROL

LATERITES

SPOT images and geochemical mapping of lateritic covers in southern Mali 22 p3105 N88-28438

LATEX

The morphology of emulsion polymerized latex particles [DE88-002672] 08 p0972 N88-15879

LATHES

Universal precision sine bar attachment [NASA-CASE-MFS-28253-1] 18 p2523 N88-24971

LATITUDE

Method estimating integral mean value of enhancement factor and path latitude for whistlers below magnetic latitude 10 deg 03 p0300 N88-11885

Radar observations of high-latitude lower-thermospheric and upper-mesospheric winds and their response to geomagnetic activity 06 p0742 N88-14563

The effect of latitude on the development of tropical cyclones [AD-A185670] 06 p0746 N88-14590

The solar radiation incident at the top of the atmosphere of Uranus and Neptune [AERONOMICA-ACTA-A-317-1987] 07 p0878 N88-15323

Effect of neutral wind on the latitudinal variation of nighttime F-layer vertical movements 08 p1030 N88-16244

Latitudinal and seasonal variation of the cloud characteristic parameters and their effects on the cloud classification 17 p2351 N88-24005

Navigation system from AVHRR data from NOAA series satellites 17 p2359 N88-24054

LATTICE IMPERFECTIONS

U CRYSTAL DEFECTS

LATTICE PARAMETERS

Interaction between defects and the formation of dissipative structures in irradiated impure crystals [DE87-703125] 02 p0246 N88-11552

Effect of point defects on graphite lattice parameters [DE88-700340] 07 p0827 N88-15019

Change of europium crystallographic symmetry at helicoidal magnetic ordering [DE88-700559] 07 p0939 N88-15707

Bulk superconductivity in La2CuO4 [DE88-002509] 09 p1254 N88-17516

Structural studies on La/sub 2/CuO/sub 4+delta/ [DE88-006828] 18 p2581 N88-25330

LATTICE VIBRATIONS

Improper ferroelectricity: A theoretical and experimental study [AD-A184614] 03 p0381 N88-12397

Pure dephasing of a vibrational adbond [AD-A185222] 05 p0609 N88-13740

Computation of natural frequencies of planar lattice structure [AD-A185387] 05 p0641 N88-13920

Study of boundary structures [AD-A184808] 05 p0655 N88-14013

Geometric structure, pseudoband gaps, and surface vibrational resonances on metal surfaces [AD-A187001] 09 p114[illegible] [illegible]8-16851

The convergence rate for the strong law of large numbers: General lattice distributions [AD-A187560] 10 p1402 N88-18362

Order-disorder transition of Au and Pt (110) surfaces: The significance of relaxations and vibrations [DE88-004651] 10 p1419 N88-18473

Vibration spectra of oxygen and vanadium atoms in vanadium-oxygen disordered interstitial alloys [DE87-703166] 13 p1740 N88-20404

Effect of Mg impurity on local vibrations of U-centers in LiF lattice 14 p1969 N88-21753

Defects and disorder in amorphous and damaged silicon [AD-A19227[illegible]] 20 p2879 N88-27089

Coupled even-parity superconducting states: Square lattice [AD-A193432] 21 p3022 N88-27938

LATTICES

Continuum modeling of large lattice structures: Status and projections [NASA-TP-2767] 06 p0672 N88-14115

An orthogonal oriented quadrature hexagonal image pyramid [NASA-TM-100054] 06 p0755 N88-14630

LATTICES (MATHEMATICS)

NT BOOLEAN ALGEBRA

NT BOOLEAN FUNCTIONS

A microstructural lattice model for strain oriented problems: A combined Monte Carlo finite element technique [NASA-TM-100215] 02 p0150 N88-10939

Finite size scaling and lattice gauge theory [DE87-014139] 02 p0245 N88-11549

Transition to turbulence via spatio-temporal intermittency 03 p0313 N88-11976

Lattice gas hydrodynamics 03 p0313 N88-11978

Application of lattice filtering techniques to CW measured time domain data [AD-A184351] 04 p0431 N88-12671

Recursion operator and bihamiltonian structure for integrable multi-dimensional lattices [PREPRINT-552] 06 p0764 N88-14688

Darboux transformation and special solutions for the two-dimensional Toda-lattice [PREPRINT-562] 06 p0764 N88-14692

Integrable quantum systems and classical Lie algebras [DE88-700872] 12 p1683 N88-20063

Mixing properties for random walk in random scenery [REPT-87-48] 14 p1966 N88-21734

The two-dimensional Toda-lattice and its recursion operators [PREPRINT-571] 14 p1968 N88-21746

Mixing coefficients of the lattice weak Hamiltonian with dimension five operators [PREPRINT-576] 14 p1968 N88-21749

Recursion operator and Backlund Transformation for the Ruijsenaars-Toda lattice [PREPRINT-577] 14 p1968 N88-21750

Lattice QCD calculation of K yields pi nonleptonic weak transition and other hadronic weak parameters [PREPRINT-580] 15 p2132 N88-22717

A numerical model of unsteady, subsonic aeroelastic behavior [NASA-TM-101126] 16 p2156 N88-22862

Fixpoint representations of characteristic sets of linear-time temporal formulas [CWI-CS-R8754] 20 p2840 N88-26849

Eigenmodes of a random walk on a 2-D lattice torus with one trap [DE88-007830] 20 p2844 N88-26874

Challenge equality problems in lattice theory [DE88-010094] 20 p2876 N88-27072

An overview of lattice QCD [DE88-010867] 21 p3026 N88-27963

Lax representation and complete integrability for the periodic relativistic Toda lattice [PREPRINT-594] 22 p3146 N88-28711

LAUNCH COMPLEXES

U LAUNCHING BASES

LAUNCH VEHICLE CONFIGURATIONS

ESA Bulletin No. 15: Ariane, the European launcher for the 1980's [ESA-BULLETIN-NO-15] 09 p1125 N88-16741

The Ariane launcher and its progress 09 p1125 N88-16742

Increased performance for Ariane 09 p1125 N88-16744

The Ariane-3 program 09 p1128 N88-16771

LAUNCH VEHICLES

NT ARIANE LAUNCH VEHICLE

NT CENTAUR LAUNCH VEHICLE

NT HEAVY LIFT LAUNCH VEHICLES

NT HOTOL LAUNCH VEHICLE

NT RECOVERABLE LAUNCH VEHICLES

NT REUSABLE LAUNCH VEHICLES

NT TITAN LAUNCH VEHICLES

Configuration evaluation and criteria plan. Volume 2: Evaluation criteria plan (update). Space Transportation Main Engine (STME) configuration study [NASA-CR-181429] 03 p0270 N88-11699

Control of an unstable launcher in atmospheric flight using minimax optimal control laws [SNIAS-872-422-107] 05 p0638 N88-13901

The ILV: A new commercial expendable launch vehicle --- Industrial Launch Vehicle (ILV) 08 p1035 N88-16275

Soviet space transport systems 13 p1727 N88-20328

Expected value analysis for an unmanned expendable launch vehicle payload escape system [AD-A189494] 13 p1728 N88-20337

Satellite acquisition: Global positioning system acquisition changes after Challenger's accident [PB88-155536] 14 p1880 N88-21236

Application of superconducting technology to earth-to-orbit electromagnetic launch systems [DE88-010022] 20 p2763 N88-26386

In-flight motor torque estimates for the second-stage Strypi 9 launch vehicle [DE88-010833] 21 p2902 N88-27222

LRS-2: A specialized knowledge system for launch resource scheduling [AD-A194625] 23 p3182 N88-28941

Wind measurements by electromagnetic probes [NASA-TM-4066] 23 p3236 N88-29256

Reduced flexibility in processing Titan 4 space launch vehicles at Cape Canaveral Air Force Station [AD-A194908] 24 p3332 N88-29834

LAUNCHERS

NT GUN LAUNCHERS

NT HYPERVELOCITY LAUNCHERS

NT MISSILE LAUNCHERS

Thermal analysis of electromagnetic launcher rails [DE88-000166] 04 p0405 N88-12514

ICRF launcher studies [DE88-001710] 04 p0495 N88-13046

Experimental investigation of a three-stage railgun incorporating puff-switching [AD-A191044] 16 p2166 N88-22918

The JET (Joint European Torus) multipellet launcher and fueling of JET plasmas by multipellet injection [DE88-008367] 19 p2729 N88-26206

LAUNCHING

NT AIR LAUNCHING

NT ORBITAL LAUNCHING

NT ROCKET LAUNCHING

NT SEA LAUNCHING

NT SPACECRAFT LAUNCHING

Non-linear shipboard shock analysis of the Tomahawk missile shock isolation system 05 p0592 N88-13614

Operational activity and improvements in the services and facilities of the balloon launch centers in France 08 p1030 N88-16238

A pyrotechnic delay ignition system for a submarine launched marine signal [MRL-R-1079] 13 p1754 N88-20487

Simulations of a missile with liquid payload under launch conditions
[AD-A191479] 18 p2463 N88-24625
Design, development, fabrication and launch support for a high altitude release of neodymium vapor
[AD-A194196] 22 p3118 N88-28527
LAUNCHING BASES
NT CAPE KENNEDY LAUNCH COMPLEX
Esrange (Sweden): New installations, future plans and investments --- rocket range 08 p1029 N88-16235
Facilities and plans for improvements at Andoya (Norway) rocket range 08 p1029 N88-16236
The DFVLR-German Space Operations Center (GSOC) mobile rocket base 08 p1029 N88-16237
The Ariane launch base 09 p1126 N88-16746
Description of MSFC engineering photographic analysis
[NASA-TM-4035] 11 p1491 N88-18900
Chronology of KSC and KSC related events for 1987
[NASA-CR-182754] 14 p2012 N88-22002
Lunar base launch and landing facility conceptual design, 2nd edition
[NASA-CR-172049] 20 p2885 N88-27135
Space shuttle natural environment analysis
[NASA-CR-179337] 21 p2976 N88-27676
LAUNCHING DEVICES
U LAUNCHERS
LAUNCHING PADS
Orbiter processing facility service platform failure and redesign 14 p1928 N88-21494
LAUNCHING SITES
NT LAUNCHING PADS
The Ariane launch base 09 p1126 N88-16746
Description of MSFC engineering photographic analysis
[NASA-TM-4035] 11 p1491 N88-18900
High altitude chemical release systems for project BIME (Brazilian Ionospheric Modification Experiments) project IMS (Ionospheric Modification Studies) project PIIE (Polar Ionospheric Irregularities Experiment) project polar arcs
[AD-A188299] 12 p1642 N88-19833
Soil erosion and causative factors at Vandenberg Air Force Base, California
[NASA-TM-100981] 17 p2381 N88-24156
LAVA
A review: Quantitative models for lava flows on Mars
23 p3301 N88-29656
Mapping of volcanic units at Alba Patera, Mars
23 p3301 N88-29663
Lava flow-field morphology: A case study from Mount Etna, Sicily 23 p3303 N88-29676
Lava thicknesses: Implications for rheological and crustal development 24 p3443 N88-30490
Simulations of lava flows on Mars
24 p3443 N88-30495
Small-scale volcanic landforms indicative of distributary tube systems 24 p3444 N88-30496
Volcanic styles at Alba Patera, Mars: Implications of lava flow morphology to the volcanic history
24 p3444 N88-30497
LAW (JURISPRUDENCE)
NT LEGAL LIABILITY
NT SPACE LAW
Science, technology and the Constitution: Background paper
[PB88-142534] 12 p1708 N88-20222
LAWRENCIUM
Bulk superconductivity in La2CuO4
[DE88-002509] 09 p1254 N88-17516
LAWS
NT CLOSURE LAW
NT CONSERVATION LAWS
NT HOOKES LAW
NT KEPLER LAWS
NT KIRCHHOFF LAW OF RADIATION
NT NEWTON SECOND LAW
NT OHMS LAW
NT SCALING LAWS
NT SIMILITUDE LAW
Three-halves law in sunspot cycle shape
[NASA-CR-181520] 04 p0525 N88-13210
LAY-UP
Factors affecting strength in composite materials used for aircraft
[DT-212/87] 21 p2907 N88-27248
LAYERS
Formation of buried nitride layers in (110) silicon
[DE88-003255] 11 p1557 N88-19323
Equilibrium stability of strained epitaxial layers on a rigid substrate
[INPE-4254-PRE/1127] 15 p2145 N88-22804
Ion implantation processing of 3-5 strained-layer semiconductors
[DE88-005270] 19 p2734 N88-26240
Eigenmatrix representations of radiance distributions in layered natural waters with wind-roughened surfaces
[PB88-188701] 20 p2828 N88-26780
LAYOUTS
A procedural method for the efficient implementation of full-custom VLSI designs 04 p0436 N88-12701
Very thin VLSI-layouts (Very Large Scale Integration-Layouts) of complete binary trees
[PB88-100847] 06 p0789 N88-14841
A quantitative method for evaluating sensor layouts
09 p1178 N88-17056
Aerodynamic aspects of the configurational systems layout of a dispenser
[MBB-UA-1047/87] 10 p1315 N88-17863
Gridless routing for generalized cell assemblies: Report and user manual
[EUT-87-E-180] 13 p1764 N88-20549
GM: A gate matrix layout generator
[EUT-87-E-179] 13 p1820 N88-20875
Generating layouts for random logic: Cell generation schemes
[EUT-86-E-164] 14 p1956 N88-21658
Computer aided design tools for integrated silicon system structures
[ETN-88-92186] 16 p2247 N88-23424
LEACHING
Improvements to Raney copper zinc methanol synthesis catalysts 17 p2318 N88-23844
LEAD (METAL)
NT LEAD ISOTOPES
Rarefaction velocities in shocked lead
[DE87-013141] 02 p0146 N88-10917
Analysis of free cutting brass by A.C. polarography
[PD-MT-8726] 04 p0417 N88-12587
Develop techniques for ion implantation of (lead-lanthanum-zirconate-titanate) for adaptive optics
[DE88-000642] 05 p0650 N88-13986
Effect of hold time on fatigue of lead rich PbSn solder
06 p0715 N88-14387
Weldability of a leaded carbon steel
[PB88-110341] 07 p0861 N88-15225
Photoionization dynamics and abundance patterns in laser vaporized tin and lead clusters
[AD-A191604] 18 p2482 N88-24722
Influence of the interface on the crystallization of amorphous Ge in Pb/Ge multilayers
[DE88-010072] 22 p3156 N88-28776
PLZT (Lead-Lathanium-Zirconium-Titanium) electro-optic photographic system
[AD-A193473] 23 p3215 N88-29137
LEAD ACID BATTERIES
Hydride generation from the Exide load-leveling cells
[DE87-011361] 01 p0041 N88-10259
DOT fuel-cell-powered bus feasibility study
[DE87-012705] 01 p0107 N88-10699
Results of a wind turbine/sealed lead-acid battery experiment
[DE87-012720] 02 p0166 N88-11044
Post-test analyses of aqueous batteries developed for electric propulsion
[DE88-000655] 03 p0311 N88-11965
Research and development of advanced lead-acid batteries for electric vehicle propulsion
[DE87-014661] 07 p0873 N88-15297
Laboratory evaluation and analysis of advanced lead-acid load-leveling batteries
[DE88-002851] 10 p1349 N88-18064
Lead-acid load-leveling battery testing at Argonne National Laboratory
[DE88-002853] 11 p1480 N88-18837
Evaluation of advanced lead-acid batteries developed for load-leveling applications
[DE88-002871] 11 p1481 N88-18838
The effect of titanium reinforcement on the life of positive grids in lead-acid batteries 17 p2320 N88-23857
LEAD ALLOYS
Thermomechanical fatigue of lead-base low tin solder
06 p0721 N88-14432
PbSnTe photovoltaic detectors for operation in the 2-14 micron band
[INPE-4252-PRE/1125] 11 p1508 N88-19008
Fraction eutectic measurements in slowly cooled Pb - 15 wt percent Sn alloys
[NASA-CR-180830] 19 p2618 N88-25531
LEAD COMPOUNDS
NT LEAD OXIDES
NT LEAD SULFIDES
NT LEAD TELLURIDES
NT LEAD TITANATES
LEAD ISOTOPES
The elastic scattering of intermediate energy protons from (40)Ca and (208)Pb 01 p0092 N88-10599
Pb isotope constaints on the extent of crustal recycling into a steady state mantle 24 p3394 N88-30215
Geochronological and lead-isotope evidences for rapid crust formation in middle-proterozoic time: The Labrador example 24 p3398 N88-30239
LEAD OXIDES
Properties of superconductors with strong electron-phonon interaction 14 p1974 N88-21779
LEAD SULFIDES
Integrated photo-responsive metal oxide semiconductor circuit
[NASA-CASE-GSC-12782-1] 06 p0696 N88-14271
Activities of As, Sb, Bi and Pb in copper mattes and their effects on impurity elimination
[TKK-V-A10(1988)] 15 p2041 N88-22165
LEAD TELLURIDES
Fabrication and characterization of semiconductor lasers of Pb(1-x)Sn(x)Te
[INPE-4253-PRE/1126] 15 p2072 N88-22357
Growth of Pb/sub 1-x/Eu/sub x/Te epitaxial layers by the liquid phase epitaxy technique
[DE88-701022] 15 p2139 N88-22763
Preparation of improved PbSnTe thermoelectric alloys and evaluation of their figure of merit
[AD-A191346] • 17 p2445 N88-24538
Crystalline metal-semiconductor superlattices
[DE88-007063] 18 p2561 N88-25332
LEAD TITANATES
An in situ annealing study of lead implanted single crystal calcium titanate
[DE88-005435] 11 p1562 N88-19351
LEAD ZIRCONATE TITANATES
Effects of hydrolysis on metallo-organic solution deposition of PZT films
[ATR-86(8443)-1] 06 p0679 N88-14160
LEADERSHIP
Space station: Leadership for the future
[NASA-PAM-509/8-87] 01 p0013 N88-10072
Networking requirements and future alternatives
[NASA-TM-89711] 10 p1426 N88-18517
First encounters of the close kind: The formation process of airline flight crews
[AD-A187977] 11 p1523 N88-19091
Meta-analysis of leadership differences between males and females and the effect on performance
[AD-A187769] 11 p1564 N88-19361
Report of the Defense Science Board Summer Study on Technology Base Management
[AD-A188560] 13 p1851 N88-21078
Management and the executive
[AD-A190778] 18 p2587 N88-25374
Stress/fatigue and the ARNG (Army National Guard) aviator
[AD-A194184] 22 p3132 N88-28621
The time of leaders 22 p3160 N88-28809
LEADING EDGE FLAPS
High-flaps for natural laminar flow airfoils
17 p2296 N88-23739
Pressure distributions from subsonic tests of an advanced laminar-flow-control wing with leading- and trailing-edge flaps
[NASA-TM-4040-PT-1] 17 p2300 N88-23758
A low speed wind tunnel investigation of Reynolds number effects on a 60-deg swept wing configuration with leading and trailing edge flaps
[NASA-CR-181684] 19 p2598 N88-25441
Pressure distributions from subsonic tests of an advanced laminar-flow-control wing with leading- and trailing-edge flaps
[NASA-TM-4040-PT-2] 24 p3321 N88-29776
LEADING EDGE SWEEP
Large-Scale Advanced Prop-Fan (LAP)
[NASA-CR-182112] 13 p1723 N88-20306
LEADING EDGES
NT SHARP LEADING EDGES
The structure of separated flow regions occurring near the leading edge of airfoils including transition
[NASA-CR-181434] 01 p0002 N88-10011
Vortex interaction with a leading-edge of finite thickness
[NASA-CR-182341] 05 p0543 N88-13307
A theory for the core flow of leading-edge vortices
07 p0810 N88-14935
Insect contamination protection for laminar flow surfaces 07 p0814 N88-14954
Laminar flow control leading edge glove flight test article development
[NASA-CR-172137] 07 p0815 N88-14960
A flow visualization study of the leading edge separation bubble on a NACA 0012 airfoil with simulated glaze ice
[NASA-CR-180846] 07 p0816 N88-14966
Three-dimensional unsteady flow elicited by finite wings and complex configurations
[AD-A186464] 08 p0951 N88-15770
Mean velocities and Reynolds stresses in the juncture flow and in the shear layer downstream of an appendage
[AD-A185819] 08 p0960 N88-15923

On the effect of leading edge blowing on circulation control airfoil aerodynamics 10 p1270 N88-17595
The international vortex flow experiment: A test case for compressible Euler codes
[NLR-MP-86076-U] 13 p1717 N88-20267
Fluid-thermal-structural study of aerodynamically heated leading edges
[NASA-TM-100579] 13 p1783 N88-20666
Wave interactions in a three-dimensional attachment line boundary layer
[NASA-CR-181653] 14 p1910 N88-21414
Thermostructural analysis of simulated cowl lips
15 p2080 N88-22403
Structure of unsteady flows at leading- and trailing-edges: Flow visualization and its interpretation
16 p2205 N88-23154
Operational considerations for laminar flow aircraft
17 p2298 N88-23748
Sensitivity of F-106B leading-edge-vortex images to flight and vapor-screen parameters
[NASA-TP-2818] 17 p2300 N88-23760
A comparison of experimental and calculated thin-shell leading-edge buckling due to thermal stresses
[NASA-TM-100416] 17 p2349 N88-23999
Numerical study of delta wing leading edge blowing
[NASA-CR-183101] 20 p2752 N88-26335

LEAF AREA INDEX
Estimating scattered and absorbed radiation in plant canopies by remote sensing
[NASA-CR-181390] 02 p0193 N88-11205

LEAKAGE
Experimental rotordynamic coefficient results for honeycomb seals
[NASA-CR-182440] 08 p0993 N88-16007
One-dimensional leakage-flow vibration instabilities
[DE88-002875] 10 p1330 N88-17947
The use of least squares in undetermined problems
[DE88-004473] 12 p1682 N88-20059
Ammonia transfer across rotating joints in space
14 p1927 N88-21492
Development of a rotary fluid transfer coupling and support mechanism for space station
14 p1928 N88-21493
Visualization of flows in turbomachinery
[AD-A189927] 15 p2063 N88-22299
Reduced thermal input by proper selection of YAG laser welding parameters
[DE88-000730] 15 p2072 N88-22356
Study on shaft seals for potassium turbine
[EL-891] 15 p2074 N88-22364
Monte Carlo analysis of lateral collection diode arrays
[RSRE-MEMO-4080] 17 p2335 N88-23938
Fuel containment and damage tolerance in large composite primary aircraft structures. Phase 2: Testing
[NASA-CR-172519] 19 p2601 N88-25452
Investigation of leaks in fiberglass-reinforced pressure vessels by direct observation of hollow fibers in glass cloth
[DE88-006936] 19 p2609 N88-25485
Evaluation of engineering leak before break assessment methods by piping tests
[PB88-126982] 20 p2788 N88-26538
Remote sensing and satellite applications to the needs of the gas and pipeline industry
[PB88-202668] 20 p2817 N88-26714
The P delta V fundamental gas leak calibration system qualification report
[DE88-008964] 21 p2951 N88-27526
Stability control of leakage flow channels
[DE88-009995] 23 p3210 N88-29107

LEARNING
NT ASTRONAUT TRAINING
NT CONDITIONING (LEARNING)
NT MAZE LEARNING
NT TRANSFER OF TRAINING
Analogical inference and analogical access
[AD-A184345] 03 p0369 N88-12321
Learning a color algorithm from examples
[AD-A184385] 05 p0632 N88-13862
A learning model as a basis for investigations of the effects of gravity on the learning processes and memory formulation 07 p0886 N88-15374
Computing support for basic research in perception and cognition
[AD-A186192] 07 p0897 N88-15437
Roles of knowledge in motor learning
[AD-A186420] 07 p0897 N88-15438
Substructure discovery in executed action sequences
[AD-A186446] 08 p1069 N88-16462
Long term synaptic plasticity and learning in neuronal networks
[AD-A186834] 09 p1199 N88-17188
Intelligent tutoring systems as tools for investigating individual differences in learning
09 p1204 N88-17216
Computer assisted instruction: Two decades in perspective
[AD-A186813] 09 p1216 N88-17289
Experiments with the back propagation algorithm: A systematic look at a small problem
[RSRE-MEMO-4049] 09 p1224 N88-17340
Analysis and synthesis of adaptive neural elements
[AD-A187047] 10 p1395 N88-18316
The choice of learning strategy in an autonomous system
[AD-A187707] 11 p1534 N88-19161
Two new frameworks for learning
[AD-A187723] 11 p1534 N88-19162
Learning functions from examples
[AD-A187725] 11 p1534 N88-19163
Soar: An architecture for general intelligence
[AD-A188742] 13 p1823 N88-20898
Optimizing feedback utilization in motor skill training
[AD-A191559] 18 p2552 N88-25146
Models of incremental concept formation
[AD-A191597] 18 p2552 N88-25147
Visual information processing in the perception of features and objects
[AD-A192026] 18 p2552 N88-25148
Representation and decision mechanisms in artificial intelligence
[AD-A191083] 18 p2560 N88-25197
Generalization and the backward propagation neural network
[AD-A191634] 19 p2710 N88-26100
Inference and discovery in an exploratory laboratory
[AD-A192231] 20 p2832 N88-26801
Script editor: An editor for the specification phase in the development of computer based learning
[REPT-87-68] 20 p2839 N88-26846
The sine and cosine function for class 4-VWO. Exploration of possible bottlenecks
[REPT-87-72] 20 p2881 N88-27105
Motor-response learning at a process control panel by an autonomous robot
[DE88-005055] 21 p2955 N88-27554
What's on the menu? Friendlier computers
[AD-A194393] 22 p3135 N88-28637
Effect of hypoxia on speech recognition in noise
[AD-A193943] 23 p3240 N88-29280
Some learnability results for analogical generation
[AD-A193669] 23 p3250 N88-29342
Design of a feeling-thinking machine
[AD-A194107] 23 p3267 N88-29448

LEARNING CURVES
A comparison of fitting techniques for the cumulative average learning curves with historical lot cost data
[AD-A187127] 09 p1227 N88-17349
Analysis of learning curve fitting techniques
[AD-A187680] 11 p1535 N88-19173

LEARNING MACHINES
Analysis and synthesis of abstract data types through generalization from examples
[NASA-CR-178369] 01 p0081 N88-10519
The structure-mapping engine: Algorithm and examples
[AD-A184042] 03 p0368 N88-12315
Deriving descriptions of the mind
[AD-A186647] 08 p1052 N88-16349
Neural network based speech synthesizer: A preliminary report 08 p1064 N88-16429
The power of neural nets 08 p1064 N88-16430
The choice of learning strategy in an autonomous system
[AD-A187707] 11 p1534 N88-19161
Learning by experimentation
[AD-A188912] 12 p1681 N88-20053
Generalizing the structure of explanations in explanation-based learning
[AD-A191327] 16 p2256 N88-23481
Radial basis functions, multi-variable functional interpolation and adaptive networks
[RSRE-MEMO-4148] 23 p3265 N88-29436
Active explanation reduction: An approach to the multiple explanations problem
[AD-A194127] 23 p3276 N88-29501

LEARNING THEORY
Knowledge base refinement by monitoring abstract control knowledge, revision 1
[AD-A187502] 10 p1397 N88-18323
The construction of a pedagogy to promote meaningful learning of strategies and tactics for solving problems of elementary combinatorics
[AD-A187928] 11 p1542 N88-19216
Text organization and comprehensibility in technical writing
[AD-A188913] 12 p1707 N88-20217
Topics in adaptive control and inference
[AD-A194718] 23 p3266 N88-29443

LEAST SQUARES METHOD
A generalized least-squares determination of triaxial stress states by X-ray diffraction and the associated errors
[AD-A183851] 01 p0058 N88-10371
The use of splines in the modelling of a photodiode response
[NPL-DITC-88/87] 01 p0085 N88-10550
Computational behavior of Gauss-Newton methods
[DE87-014486] 02 p0224 N88-11413
Solution of nonlinear least-squares problems
[AD-A184010] 03 p0371 N88-12335
Nonlinear parametric least-squares adjustment
[AD-A184039] 03 p0371 N88-12336
A computational examination of orthogonal distance regression
[AD-A184374] 03 p0371 N88-12337
Least squares linear lags and limited memory filters
[NASA-CR-178381] 03 p0372 N88-12339
Model-based motion estimation and its application to restoration and interpolation of motion pictures
[AD-A185054] 05 p0584 N88-13558
A system identification technique based on the random decrement signatures. Part 1: Theory and simulation
05 p0594 N88-13625
A system identification technique based on the random decrement signatures. Part 2: Experimental results
05 p0594 N88-13626
Multidimensional least squares fitting of fuzzy models
[AD-A185148] 05 p0640 N88-13916
Least squares for fuzzy vector data regression
[AD-A185156] 05 p0640 N88-13917
Study of extended least-square iterative techniques in electromagnetic scattering by penetrable objects
[PB88-105879] 06 p0694 N88-14262
Knot selection for least squares thin plate splines
[AD-A185681] 06 p0759 N88-14657
Interactive nonlinear least squares program
[PB88-109855] 06 p0760 N88-14661
Stabilized Galerkin method for convection-diffusion problems
[PB87-234985] 06 p0764 N88-14694
Round-off error propagation in four generally applicable, recursive, least-squares-estimation schemes
[NASA-TM-100055] 06 p0766 N88-14708
A survey study of energy distribution in component stars of Algol-type binary systems 06 p0801 N88-14901
On the least squares estimator in moving average models of order one
[AD-A186028] 07 p0909 N88-15508
A simultaneous M-ary channel hypothesis test with least-mean-square signal amplitude estimation
[AD-A186526] 08 p0978 N88-15913
Estimation and comparison of changes in the presence of information right censoring by modeling the censoring process
[AD-A186320] 08 p1074 N88-16478
A note on computing robust regression estimates via iteratively reweighted least squares
[AD-A186709] 09 p1227 N88-17352
Fitting a generalized parabola to data
[NPL-DITC-96/87] 09 p1229 N88-17364
Strategies for knot placement in least squares data fitting by splines
[NPL-DITC-101/87] 09 p1229 N88-17366
Analysis of learning curve fitting techniques
[AD-A187680] 11 p1535 N88-19173
Position finding and tolerances
[AD-A187685] 11 p1540 N88-19205
Realtime pilot model parameter identification
[AD-A188873] 12 p1584 N88-19476
The use of least squares in undetermined problems
[DE88-004473] 12 p1682 N88-20059
Computation of LMS (Least-Mean-Square) and matched digital filters for optical clutter suppression
[AD-A188885] 12 p1687 N88-20093
Analysis of pre-flight modulator voltage calibration data for the Voyager plasma science experiment
[NASA-CR-182577] 12 p1710 N88-20236
Two dimensional uncorrelated bias in fix algorithms
[NASA-CR-182683] 13 p1815 N88-20847
Survival analysis using additive risk models
[AD-A189053] 13 p1825 N88-20906
Identification of nonlinear output-affine systems using an orthogonal least squares algorithm
[RR-313] 14 p1958 N88-21678
Motion sickness: Quantitative, algorithmic malaise indication in real time
[AD-A189674] 15 p2101 N88-22518
Cholesky downdating on a hypercube
[DE88-006780] 15 p2113 N88-22586
The 1 and 2D symmetric Helmert transformation: An exact nonlinear least squares solution
[REPT-87-1] 16 p2259 N88-23503
Calculation of root-mean-square loads
[BLL-M-37776-(5828.4)] 18 p2531 N88-25015

Asymptotic theory for weighted least squares estimators in Aalen's additive risk model
[AD-A191085] 18 p2562 N88-25210
New mixed finite element methods
18 p2567 N88-25248
Signal processing computational needs
[AD-A191756] 19 p2642 N88-25674
Parameter estimation of dynamical systems
20 p2785 N88-26519
A deconvolution technique using least-squares model-fitting and its application to optical pulse measurement
[NPL-DES-87] 22 p3144 N88-28694
Automatic classification of digitally modulated signals
[AD-A194623] 23 p3203 N88-29064
Obtaining stress intensity factors on cracks, by means of fitting techniques on numerical results calculated with the finite element method 24 p3384 N88-30153
Algorithms for nonlinear least-squares problems
[AD-A196071] 24 p3411 N88-30305
New methods for nonlinear optimization
[AD-A195982] 24 p3412 N88-30313

LEAVES
Estimation of aerial deposition and foliar uptake of xenobiotics: Assessment of current models
[DE88-000993] 09 p1188 N88-17117
Sources of scattering in vegetarian and other surfaces and objects
[NASA-CR-182975] 20 p2816 N88-26710

LEBESGUE THEOREM
A study on Lebesgue decomposition of measures induced by stable processes
[AD-A192893] 21 p3009 N88-27850

LECTURES
A lecture on detonation-shock dynamics
[DE88-004313] 11 p1487 N88-18879
A practical guide to modern high energy particle accelerators
[DE88-004035] 11 p1548 N88-19260

LED (DIODES)
U LIGHT EMITTING DIODES

LEE WAVES
Simulation of a lee cyclogenesis using a numerical model 08 p1016 N88-16162

LEG (ANATOMY)
Determination of the effect of walking on the forced convective heat transfer coefficient using an articulated mannikin
[AD-A186452] 08 p1049 N88-16335
Morphological manifestations of primate adaptation to orthograde statics and walking erect
10 p1366 N88-18162
Currents induced in a human being for electromagnetic fields to 10 kHz-50 MHz
[AD-A191977] 23 p3238 N88-29268

LEGAL LIABILITY
New technologies and intellectual property: An economic analysis
[N-2601-NSF] 01 p0107 N88-10695

LEGENDRE CODE
U COMPUTER PROGRAMMING
U NEUTRON SCATTERING

LEGUMINOUS PLANTS
NT SOYBEANS
Remote sensing techniques in the estimation of the area cultivated with beans, corn, and castor beans in the Irece County (Bahia State) 17 p2358 N88-24045
TM/LANDSAT-5 data to evaluate wheat and bean percent soil cover and leaf area index
[INPE-4609-PRE/1332] 24 p3385 N88-30165

LEMMAS
U THEOREMS

LENGTH
NT DIFFUSION LENGTH
The effect of microstructure on the surface crack length: Crack depth relationship for short cracks
05 p0600 N88-13670
Mixing and combustion of pulsed gas jets
[PB88-108014] 06 p0680 N88-14170
Development and calibration of Direct Current Potential Difference (DCPD) crack length measurement equipment
[VTT-RR-480] 09 p1182 N88-17083
Locality, communication and interconnect length in multicomputers
[CWI-CS-R8708] 13 p1822 N88-20890
Automated measurement of crack length and load line displacement at elevated temperature
[AGARD-R-751] 20 p2814 N88-26695

LENNARD-JONES POTENTIAL
Free energy calculation via MD (molecular dynamics): Methodology and application to bicrystals
[DE88-002902] 09 p1256 N88-17532

LENSES
NT CONTACT LENSES
NT FRESNEL LENSES
NT GRAVITATIONAL LENSES
NT MAGNETIC LENSES
NT WIDE ANGLE LENSES
NT ZOOM LENSES
Design concepts to improve high performance solar simulator 02 p0136 N88-10852
Dual mode laser velocimeter
[NASA-CASE-ARC-11634-1] 06 p0709 N88-14350
Selection of polymer materials for manufacturing optical parts
[AD-A185898] 07 p0836 N88-15069
Optical Fourier transformation by lensless method with perforated mask and with modified Talbot interferometer for analysis of interferograms 09 p1236 N88-17408
Aberrations: Their effect on off-axis beam steering
[AD-A189601] 13 p1840 N88-21008
Nonlinear wave and diffusion equations
[AD-A191421] 16 p2265 N88-23544
Evaluation of multi-focus holographic lenses
[AD-A196167] 24 p3377 N88-30110

LEO ENVIRONMENTS
U EARTH ORBITAL ENVIRONMENTS

LEPTONS
NT ANTINEUTRINOS
NT CONDUCTION ELECTRONS
NT ELECTRONS
NT MUONS
NT NEUTRINOS
NT POSITRONS
NT SOLAR NEUTRINOS
Study of tau pairs and search for new particles
[B8680488] 07 p0931 N88-15655
Semileptonic weak interactions in nuclei: A relativistic analysis
[CEBAF-PR-87-024] 11 p1547 N88-19249

LESIONS
Relation between VEP and visual function in lesions of the optic nerve and visual pathway
21 p2983 N88-27718

LETHALITY
Switching devices used in the Lethality Test System
[DE87-011734] 01 p0011 N88-10062
Reaming experiments for the lethality test system
[DE88-007902] 20 p2763 N88-26383
Fiber-optics used to record high-speed photographs inside a pressurized tank during lethality testing
[DE88-011283] 21 p2951 N88-27529

LETTERS (SYMBOLS)
U SYMBOLS

LEUKOCYTES
NT LYMPHOCYTES
Mononuclear phagocytes during adaptation of essentially healthy people to high altitudes
07 p0896 N88-15432
White blood cells in space: An experiment for the first Spacelab mission 09 p1127 N88-16757
Effects of whole-body irradiation with low-intensity microwaves on morphological, functional and cytochemical characteristics of leukocytes 12 p1663 N88-19971

LEVEL (QUANTITY)
NT ATOMIC ENERGY LEVELS
NT ELECTRON STATES
NT ENERGY LEVELS
NT GROUND STATE
NT MOLECULAR ENERGY LEVELS
Rain attenuation at 35 GHz over an 18 km path
[AD-A194504] 22 p3069 N88-28217
Exact lower confidence limits for the reliability of k of n systems for zero failures and nonconservativeness of the maximus method
[AD-A194299] 23 p3274 N88-29485
Validate algorithms for the determination of rainfall rates from SSM/I microwave satellite imagery
[AD-A195428] 24 p3404 N88-30270

LEVITATION
NT ACOUSTIC LEVITATION
The interaction of small particles with laser beams
[AD-A190716] 15 p2072 N88-22354

LIABILITIES
NT LEGAL LIABILITY

LIAPUNOV FUNCTIONS
The periodic Lyapunov equations
[REPT-86-007] 01 p0087 N88-10567
Closed-loop system analysis using Lyapunov stability theory 04 p0483 N88-12978
Investigation of the spin stability of the NPS (Naval Postgraduate School) mini-satellite (Orion)
[AD-A187781] 11 p1445 N88-18613
Intermittency of atmospheric turbulence--applicatin of Lyapunov exponents and fractional dimension
14 p1900 N88-21348
Markov processes applied to control, replacement and signal analysis
[AD-A190563] 15 p2126 N88-22674
Finite dimensionality in the complex Ginzburg-Landau equation
[DE88-006480] 16 p2263 N88-23534
Dynamic stability of elastic rotor-bearing systems via Liapunov's direct method 21 p2958 N88-27571
Generalized Jordan chains and two bifurcation theorems of Krasnoselskii
[AD-A192353] 21 p3008 N88-27845
Stability, stochastic stationarity and generalized Lyapunov equations for two-point boundary-value descriptor systems
[AD-A195645] 24 p3425 N88-30385

LIBRARIES
Information analysis centers in the department of defense, revision
[AD-A184002] 03 p0385 N88-12420
The SUPRENUM communications subroutine library for grid-oriented problems
[DE88-000137] 04 p0479 N88-12950
LISP: A language for stratified design
[AD-A185606] 06 p0759 N88-14654
Bibliographic relationships: Toward a conceptual structure of bibliographic information used in cataloging
06 p0791 N88-14852
Treatment of small wire loops in the method of moments code NEC (Numerical Electromagnetics Code)
[DE88-002995] 07 p0846 N88-15136
Prospectus for the development of a linear algebra library for high-performance computers
[DE88-003715] 08 p1068 N88-16457
Hierachical object recognition using libraries of parameterized model sub-parts
[AD-A187476] 10 p1396 N88-18322
DataViews: A personalizable, interactive, data display system for the decisionmaker
[AD-A188509] 14 p1991 N88-21868
Data base design and implementation
[AD-A190414] 15 p2149 N88-22827
A standard library for modeling satellite orbits on a microcomputer
[AD-A195759] 24 p3331 N88-29830

LIBRATION
Relative motion near the triangular libration points in the Earth-Moon system 01 p0097 N88-10636
Study on orbits near the triangular libration points in the perturbed restricted three body problem
[ESA-CR(P)-2440] 07 p0944 N88-15741
Limitation of spacecraft orbit near colinear libration center of limited elliptical three body problem
08 p1003 N88-16075
The dust ring of the Earth
[RAE-TRANS-2163] 22 p3119 N88-28530
Plane periodic satellite motions relative to center of mass in neighborhood of collinear libration point
24 p3445 N88-30507

LIBRATIONAL MOTION
Study on orbits near the triangular libration points in the perturbed restricted three body problem
[ESA-CR(P)-2440] 07 p0944 N88-15741
Periodic orbits of limited elliptical three body problem
08 p1004 N88-16081
Families of periodic solutions in problem of solid body rotation at triangular libration point in restricted three-body problem 24 p3446 N88-30508

LIDAR
U OPTICAL RADAR

LIE GROUPS
Irreducible *-representations of the Lie superalgebra osp(1,4) with finite-degenerated vacuum
[DE87-703089] 02 p0225 N88-11420
Class of N-associative rings
[PB87-230421] 06 p0769 N88-14724
Lie algebraic method in filtering and identification
[CWI-PM-R8606] 08 p1072 N88-16467
The r-rank of the groups of exceptional Lie type
[CWI-PM-R8607] 08 p1072 N88-16468
Applications of Lie group methods to the equations of magnetohydrodynamics 10 p1411 N88-18422
Integrable quantum systems and classical Lie algebras
[DE88-700872] 12 p1683 N88-20063
Freund-Rubin type solutions for different compactifications of the eleven-dimensional space
[DE88-700869] 12 p1686 N88-20082
On the equivalence of four-dimensional self-duality equations to continual analog of the main chiral field problem
[DE88-700871] 12 p1686 N88-20083
Nonlinear differential equations
[DE88-006047] 13 p1828 N88-20933
Galilei relativity principle in classical electrodynamics
[DE87-703203] 14 p1904 N88-21376
Lie groups in prolongation theory
[B8721781] 14 p1967 N88-21743
Algebraic structure of linear and nonlinear models of open quantum systems
[PREPRINT-573] 14 p1968 N88-21747
On generalized lie-like algebras
[PREPRINT-574] 14 p1968 N88-21748

Markov processes applied to control, replacement and signal analysis
[AD-A190563] 15 p2126 N88-22674

Lumped model generation and evaluation: Sensitivity and Lie algebraic techniques with applications to combustion
[AD-A190402] 15 p2127 N88-22689

Introduction to nilpotent approximation filtering
[CWI-PM-R8709] 16 p2262 N88-23524

Canonical construction of differential operators intertwining representations of real semisimple Lie groups
[DE88-701852] 20 p2845 N88-26882

Superalgebras with Grassmann algebra-valued structure constants from superfields
[DE88-702239] 21 p3011 N88-27862

LIF (FLUORESCENCE)
U LASER INDUCED FLUORESCENCE

LIFE (BIOLOGY)
U LIFE SCIENCES

LIFE (DURABILITY)
NT CARRIER LIFETIME
NT FATIGUE LIFE
NT SATELLITE LIFETIME
NT SERVICE LIFE
NT STORAGE STABILITY

High intensity 5 eV O-atom exposure facility for material degradation studies 02 p0135 N88-10847

Advances in nickel hydrogen technology at Yardney Battery Division 02 p0164 N88-11029

International Ultraviolet Explorer (IUE) spacecraft battery performance update 02 p0164 N88-11033

Life prediction and constitutive models for engine hot section anisotropic materials program
02 p0188 N88-11175

Lewis' enhanced laboratory for research into the fatigue and constitutive behavior of high temperature materials
02 p0189 N88-11177

Turbine airfoil deposition models and their hot corrosion implications 02 p0189 N88-11178

Effects of surface chemistry on hot corrosion life
02 p0189 N88-11180

Coating life prediction 02 p0189 N88-11181

Thermal barrier coating life prediction model development 02 p0190 N88-11183

Thermal barrier coating life prediction model development 02 p0190 N88-11184

Thermal barrier coating life prediction model development 02 p0190 N88-11185

Airworthiness of long-life jet transport structures
03 p0265 N88-11674

A low-power arcjet cyclic lifetest
[NASA-TM-100233] 03 p0278 N88-11748

A life test of a 22-Newton (5-lbf) hydrazine rocket
[NASA-TM-100232] 03 p0278 N88-11750

Materials preparation and longevity in hyperthermal atomic oxygen 03 p0297 N88-11862

Advanced natural gas fueled engine development. Part 2: Materials investigation
[PB87-223160] 03 p0331 N88-12088

Durability (lifetime) predictions adhesively bonded structures
[AD-A184069] 03 p0335 N88-12110

Reliability of Li/SO2 cells for long-life applications
[DE88-001360] 04 p0440 N88-12735

Fiber composite structural durability and damage tolerance: Simplified predictive methods
[NASA-TM-100179] 05 p0560 N88-13409

Significance of fatigue crack closure under spectrum loading 05 p0599 N88-13662

Further studies in estimation of life distribution characteristics from censored data
[AD-A184862] 05 p0643 N88-13937

Life prediction of steel cords
06 p0715 N88-14386

Life modeling of thermal barrier coatings for aircraft gas turbine engines
[NASA-TM-100283] 07 p0834 N88-15060

Life prediction of thermomechanical fatigue using total strain version of strainrange partitioning (SRP): A proposal
[NASA-TP-2779] 07 p0867 N88-15263

Documentation in a software maintenance environment
[AD-A185892] 07 p0901 N88-15459

Life prediction technologies for aeronautical propulsion systems 08 p0954 N88-15788

Rotorcraft transmission 08 p0956 N88-15802

Aircraft engine hot section technology: An overview of the HOST Project 08 p0957 N88-15804

Space Infrared Telescope Facility (SIRTF) design and thermal analysis 08 p0982 N88-15934

KBS V and V as related to automation of space station subsystems: Rationale for a KBS lifecycle
08 p1057 N88-16375

Delamination durability of composite materials for rotorcraft 09 p1107 N88-16634

Creep and fatigue research efforts on advanced materials 09 p1119 N88-16701

Ceramics for engines 09 p1119 N88-16704

Mechanics of composite materials: Past, present and future
[NASA-TM-100793] 10 p1295 N88-17744

Lead-acid load-leveling battery testing at Argonne National Laboratory
[DE88-002853] 11 p1480 N88-18837

Review of the state of the art and projected technology of low heat rejection engines
[PB88-131255] 11 p1496 N88-18934

Improve the lifetime of the hollow fiber sodium sulfur cell
[DE88-004881] 13 p1751 N88-20469

In situ fatigue loading stage inside scanning electron microscope 15 p2083 N88-22419

Cumulative fatigue damage models
15 p2084 N88-22422

Life prediction modeling based on strainrange partitioning 15 p2084 N88-22425

Life prediction modeling based on cyclic damage accumulation 15 p2085 N88-22426

Fatigue damage modeling for coated single crystal superalloys 15 p2085 N88-22427

Life and reliability of rotating disks
15 p2085 N88-22428

Status, trends in research on internal combustion engines 16 p2185 N88-23027

Seasonal variation for structural strength value
[PB88-169248] 16 p2222 N88-23260

Rainfall rates and drop-size distributions for environmental testing
[AD-A191342] 16 p2236 N88-23354

Lifetime of pristine optical fibers
[ETN-88-92246] 16 p2273 N88-23602

Ceramics for turbine engines
17 p2323 N88-23873

Thermal cyclic durability testing of ceramic materials for turbine engines 17 p2325 N88-23886

Fractographic and microstructural evaluation of 3500-hour durability specimens
17 p2325 N88-23887

Space reactor end of life issues
17 p2424 N88-24413

Internal erosion rates of a 10-kW xenon ion thruster
[NASA-TM-100954] 18 p2476 N88-24688

Environment assisted degradation mechanisms in advanced light metals
[NASA-CR-182907] 18 p2486 N88-24746

The relationship between observed fatigue damage and life estimation models
[NASA-CR-182191] 21 p2965 N88-27611

Thermal barrier coating life-prediction model development
[NASA-CR-179507] 22 p3058 N88-28142

Vapor Compression Distillation Subsystem (VCDS) component enhancement, testing and expert fault diagnostics development, volume 1
[NASA-CR-172072] 22 p3134 N88-28634

Influence of the temperature-dependence of recombination life-time of free carriers in amorphous semiconductors on thermostimulated photocurrent spectra
[DE88-702728] 23 p3293 N88-29609

Performance and lifetime assessment of MPD arc thruster technology
[NASA-TM-101293] 24 p3336 N88-29860

Successful completion of a cyclic ground test of a mercury ion auxiliary propulsion system
[NASA-TM-101351] 24 p3339 N88-29873

Morphological changes in polymer electrolyte cells
[AD-A195821] 24 p3368 N88-30054

A static scheduler for the computer aided prototyping system: An implementation guide
[AD-A194340] 24 p3414 N88-30322

Knowledge based simulation. An artificial intelligence approach to system modeling and automating the simulation life cycle
[AD-A195838] 24 p3423 N88-30372

Space systems cost study
[AD-A196024] 24 p3439 N88-30469

LIFE CYCLE COSTS

DOT fuel-cell-powered bus feasibility study
[DE87-012705] 01 p0107 N88-10699

A design methodology for the utilization of metrics within various phases of software lifecycle models
[DE87-010519] 02 p0220 N88-11385

Determination of life cycle costs in astronautics
[MBB-UR-E-910/86-PUB] 02 p0249 N88-11572

Optimized ground coupled heat pump mechanical package
[DE87-014899] 04 p0441 N88-12738

Technology Base Research Project for electrochemical energy storage
[DE88-000649] 04 p0464 N88-12868

Simulated service test behavior of various internal and external coatings applied on CF6-50 first stage turbine blades
[NLR-MP-86018-U] 05 p0549 N88-13343

Life-cycle cost analysis of residential heat pumps and alternative HVAC (Heating, Ventilating and Air-Conditioning) systems
[DE88-003701] 07 p0839 N88-15090

Documentation in a software maintenance environment
[AD-A185892] 07 p0901 N88-15459

Supportability in aircraft systems through technology and acquisition strategy applications
[AD-A186465] 08 p0949 N88-15759

Proposal of a methodology for the conceptual design of the Distributed Data Base
[INPE-4315-TDL/282] 08 p1093 N88-16576

A cost and benefit analysis of hydraulic fluid systems for the next generation of tactical aircraft
[AD-A186911] 09 p1116 N88-16690

STS propellant scavenging systems study. Part 2, volume 2: Cost and WBS/dictionary
[NASA-CR-179276] 10 p1290 N88-17717

Future directions in computer architecture
10 p1383 N88-18257

The space station assembly phase: Flight telerobotic servicer feasibility. Volume 2: Methodology and case study
[NASA-CR-182690] 13 p1731 N88-20352

Costs and benefits of AC propulsion
[PB88-173380] 16 p2287 N88-23691

The multi-disciplinary design study: A life cycle cost algorithm
[NASA-CR-4156] 17 p2385 N88-24172

Engine component retirement for cause. Volume 1: Executive summary
[AD-A192730] 20 p2760 N88-26371

PAX ECONOPACK economic analysis package users manual
[AD-A192949] 20 p2883 N88-27117

LIFE SCIENCES
NT EXTRATERRESTRIAL LIFE
NT MOLECULAR BIOLOGY

JPRS report: Science and technology. USSR: Life sciences
[JPRS-ULS-87-009] 04 p0473 N88-12915

JPRS report: Science and technology. USSR: Life sciences
[JPRS-ULS-87-011] 06 p0749 N88-14601

Life sciences flight experiments microcomputer
06 p0792 N88-14857

USSR Space Life Sciences Digest index to issues 10-14
[NASA-CR-3922(17)] 07 p0883 N88-15361

USSR Space Life Sciences Digest, issue 14
[NASA-CR-3922(16)] 08 p1045 N88-16317

USSR report: Life sciences. Biomedical and behavioral sciences
[JPRS-UBB-86-022] 08 p1046 N88-16318

Trends in research and development in the Netherlands. The influence of national science policy between 1973 and 1986
[B8701588] 08 p1094 N88-16580

System analysis study of space platform and station accommodations for life sciences research facilities. Volume 1: Executive summary. Phase A: Conceptual design and programmatics
[NASA-CR-179268] 10 p1291 N88-17721

System analysis study of space platform and station accommodations for life sciences research facilities. Volume 2: Study results, attachment 2. Phase A: Conceptual design and programmatics
[NASA-CR-179272] 10 p1291 N88-17722

System analysis study of space platform and station accommodations for life sciences research facilities. Volume 2: Study results. Appendix E: Work breakdown structure and dictionary
[NASA-CR-179274] 10 p1292 N88-17723

System analysis study of space platform and station accommodations for life sciences research facilities. Volume 2: Study results. Appendix D: Life sciences research facility requirements
[NASA-CR-179273] 10 p1292 N88-17724

USSR Space Life Sciences Digest, issue 15
[NASA-CR-3922(18)] 10 p1368 N88-18175

Minutes of the meeting of the Indo-US Subcommission on Science and Technology (8th) held at Washington, D.C. on September 22-24 1986
[PB88-130158] 10 p1423 N88-18503

JPRS report: Science and technology. USSR: Life sciences
[JPRS-ULS-88-001] 11 p1520 N88-19079

Conceptual design and programmatics studies of space station accommodations for Life Sciences Research Facilities (LSRF)
[NASA-CR-179270] 12 p1598 N88-19567
Space station accommodations for life sciences research facilities: Phase A conceptual design and programmatics studies for Missions SAAX0307, SAAX0302 and the transition from SAAX0307 to SAAX0302. Volume 1: Executive summary
[NASA-CR-179267] 12 p1599 N88-19571
Proceedings of the 3rd European Symposium on Life Sciences Research in Space
[ESA-SP-271] 12 p1652 N88-19893
The European Space Agency's role in life sciences and research in space 12 p1652 N88-19894
Life sciences in the framework of the ESA microgravity program and future flight opportunities
12 p1652 N88-19895
Life science techonology --- space applications
12 p1653 N88-19900
Why life science in space? The next step to go beyond 12 p1661 N88-19954
Application of ARIADNE: A data bank-based information system for human physiology research --- Spacelab Anthrorack 12 p1662 N88-19962
JPRS report: Science and technology. USSR: Life sciences
[JPRS-ULS-88-004] 13 p1810 N88-20815
JPRS report: Science and technology. China
[JPRS-CST-87-041] 14 p1902 N88-21365
USSR Space Life Sciences Digest, issue 16
[NASA-CR-3922(19)] 15 p2101 N88-22515
JPRS report: Science and technology. China
[JPRS-CST-88-001] 16 p2186 N88-23036
USSR Space Life Sciences Digest, Issue 17
[NASA-CR-3922(20)] 17 p2381 N88-24155
USSR space life sciences digest, issue 18
[NASA-CR-3922(21)] 19 p2707 N88-26096
A shared-world conceptual model for integrating space station life sciences telescience operations
24 p3416 N88-30333

LIFE SPAN
Drosophila geotaxis as a tool for the study of aging
10 p1288 N88-17706

LIFE SUPPORT SYSTEMS
NT CLOSED ECOLOGICAL SYSTEMS
The usefulness of microalgal structures as an element of closed ecological systems like Aquarack and CELSS --- Controlled Ecological Life Support System (CELSS)
01 p0074 N88-10476
Life support systems for biological experiments under weightlessness in the German and European space programs 01 p0074 N88-10477
Controlled Ecological Life Support Systems (CELSS) conceptual design option study
[NASA-CR-177421] 06 p0754 N88-14625
Research and development of anti-G life support systems. Part 1: Development and evaluation of uniform-pressure anti-G suits
[AD-A185658] 06 p0754 N88-14628
Development of a graphical display on the DMS test bed 06 p0794 N88-14864
Monitoring of space station life support systems with miniature mass spectrometry and artificial intelligence
08 p1057 N88-16376
Prototype space station automation system delivered and demonstrated at NASA 08 p1066 N88-16442
Aspects of bioregenerative life support systems
12 p1655 N88-19917
Regenerative life support system research
[NASA-CR-182606] 12 p1671 N88-20006
Life Support Subsystem (LSS). Concept for the Botany Facility --- EURECA
[TN-RB524-107/86] 17 p2377 N88-24131
Summary of the activities performed during the Botany Facility (BF) predevelopment phase for the Life Support S/S (LSS)
[TB-RB524-002/87] 17 p2378 N88-24133
Subsea approach to work systems development
17 p2379 N88-24146
Advanced life support control/monitor instrumentation concepts for flight application
[NASA-CR-177378] 20 p2833 N88-26807
Advanced EMU electrochemically regenerable CO2 and moisture absorber module breadboard
[NASA-CR-172054] 21 p2993 N88-27754
ARGES: An expert system for fault diagnosis within space-based ECLS systems 23 p3255 N88-29380
Maintenance and supply options
[NASA-CR-172062] 24 p3332 N88-29637

LIFETIME (DURABILITY)
U LIFE (DURABILITY)

LIFT
NT INTERFERENCE LIFT
NT JET LIFT
NT ZERO LIFT
On the prospects for increasing dynamic lift
[RAE-TM-AERO-2068] 01 p0003 N88-10018
A heat transfer model for a heated helium airship
[AD-A183786] 03 p0259 N88-11629
An experimental evaluation of advanced rotorcraft airfoils in the NASA Ames eleven-foot transonic wind tunnel
[NASA-CR-166587] 03 p0261 N88-11640
Aerodynamic sensitivities from subsonic, sonic and supersonic unsteady, nonplanar lifting-surface theory
[NASA-TM-100502] 04 p0394 N88-12459
Nonlinear lift control at high speed and high angle of attack using vortex flow technology
05 p0545 N88-13319
Prediction of wing aeroelastic effects on aircraft life and pitching moment characteristics
05 p0551 N88-13356
Wind tunnel results for a high-speed, natural laminar-flow airfoil designed for general aviation aircraft
[NASA-TM-87602] 06 p0665 N88-14078
Lift distribution and velocity field measurements for a three-dimensional, steady blade/vortex interaction
[NASA-TM-100013] 07 p0815 N88-14962
Wind tunnel studies of circulation control elliptical airfoils 10 p1270 N88-17598
Lifting-surface theory of oscillating propellers in compressible flow
[NAL-TR-943] 10 p1273 N88-17613
Calculation of the distributed loads on the blades of individual multiblade propellers in axial flow using linear and nonlinear lifting surface theories
[NASA-TT-20173] 13 p1719 N88-20278
Zero-lift drag predictions in supersonic flow for complex configurations 15 p2054 N88-22246
Stall flutter analysis of propfans
16 p2221 N88-23256
Propulsive performance of a lifting flapping wing
17 p2295 N88-23733
Continuum theories for fluid-particle flows: Some aspects of lift forces and turbulence
[DE88-007038] 18 p2511 N88-24898
FEB (Multifilter Electronics Box) lifting device analysis, revision A
[AD-A192313] 21 p2935 N88-27427
Effects of psychophysical lifting training on maximal repetitive lifting capacity
[AD-A192605] 23 p3238 N88-29271

LIFT AUGMENTATION
On the prospects for increasing dynamic lift
[RAE-TM-AERO-2068] 01 p0003 N88-10018
Validation elements of the computation methods and measurement techniques for high lift aerodynamic systems
[SNIAS-872-111-101] 05 p0541 N88-13299
Propulsion-induced effects caused by out-of-ground effects
[NASA-TM-100032] 06 p0666 N88-14088
Evaluation of a research circulation control airfoil using Navier-Stokes methods 10 p1269 N88-17591
On the effect of leading edge blowing on circulation control airfoil aerodynamics 10 p1270 N88-17595
The impact of circulation control on rotary aircraft controls systems 10 p1271 N88-17601
Analysis of a fixed-pitch X-wing rotor employing lower surface blowing 10 p1271 N88-17602
An aerodynamic comparison of blown and mechanical high lift airfoils 10 p1272 N88-17606
Fixed wing CCW aerodynamics with and without supplementary thrust deflection
10 p1272 N88-17607
Circulation control STOL aircraft design aspects
10 p1272 N88-17610
An application of active surface heating for augmenting lift and reducing drag of an airfoil
[NASA-TM-100563] 11 p1436 N88-18570
Performance optimization of a cruise missile using dynamic-stall induced lift augmentation
[AD-A190497] 15 p2017 N88-22027
Analysis of a fixed-pitch X-wing rotor employing lower surface blowing
[AD-A187379] 24 p3321 N88-29779

LIFT COEFFICIENTS
U AERODYNAMIC COEFFICIENTS
U LIFT

LIFT DEVICES
Aircraft dynamic response calculation based on discrete-continual model 04 p0424 N88-12624
Studies of unsteadiness in boundary layers
[AD-A185662] 06 p0703 N88-14315
On the Kutta condition for flows around lifting airfoils and wings
[DFVLR-FB-87-40] 13 p1717 N88-20268
A panel method based on velocity potential to compute harmonically oscillating lift surface systems
[ETN-88-91886] 15 p2061 N88-22290
High-flaps for natural laminar flow airfoils
17 p2296 N88-23739
The identification of the direct lift control flap system of the research aircraft ATTAS
20 p2786 N88-26527

LIFT DISTRIBUTION
U FORCE DISTRIBUTION
U LIFT

LIFT DRAG RATIO
Conical wing with maximum lift-to-drag ratio in supersonic gas flow 04 p0425 N88-12633
Airframe/store compatibility 05 p0545 N88-13323
Study of descent of probes with high lift-drag ratio into the atmosphere of Jupiter 08 p1006 N88-16101
Investigation into the effects of flap end modifications on the performance of a wing with a single slotted flap
[BU-357] 14 p1866 N88-21148

LIFT FANS
Airborne remote operated device
[DE88-010324] 21 p2895 N88-27188

LIFT FORCES
U LIFT

LIFTING BODIES
NT LIFTING REENTRY VEHICLES
Aerodynamics of Hypersonic Lifting Vehicles
[AGARD-CP-428] 05 p0529 N88-13219
Numerical experiments with hypersonic flows beneath a cone-delta-wing combination 05 p0532 N88-13238
Numerical optimization of conical flow waveriders including detailed viscous effects
05 p0533 N88-13245
Dynamic stability of hypersonic conical lifting vehicles according to Newton-Busemann theory
05 p0534 N88-13247
Lifting bodies: An attractive aerodynamic configuration choice for hypervelocity vehicles
05 p0534 N88-13248
Aerodynamics of lifting bodies with combined transverse and longitudinal curvature 19 p2598 N88-25436
Aerodynamics of Hypersonic Lifting Vehicles: Fluid Dynamics Panel AGARD Symposium
[AGARD-AR-246] 21 p2943 N88-27480
VSAERO analysis of tip planforms for the free-tip rotor
[NASA-CR-177487] 22 p3038 N88-28036
Fellowships in hypersonic aerodynamics
[AD-A194265] 23 p3172 N88-28685

LIFTING REENTRY VEHICLES
European hypersonic wind tunnels
05 p0530 N88-13221
Shock tunnels for real gas hypersonics
05 p0530 N88-13223
Low Reynolds number influence on aerodynamic performance of hypersonic lifting vehicles
05 p0531 N88-13230

LIFTING ROTORS
NT BEARINGLESS ROTORS

LIFTING SURFACES
U LIFT DEVICES
U LIFTING BODIES
U SURFACES

LIGANDS
The formation and thermochemical properties of multiligand complexes
[AD-A184935] 05 p0561 N88-13416
Intramolecular energy transfer reactions as a method for metal complex assisted production of hydrogen
[DE88-001621] 05 p0562 N88-13425
Soluble metal chelate polymers of coordination numbers six, seven and eight
[AD-A185094] 05 p0568 N88-13459
The role of electronic structure calculation in mechanistic analysis of electron transfer reactions in the liquid phase
[DE87-014395] 05 p0647 N88-13963
Feasibility of a complex compound heat pump
[PB88-113022] 07 p0853 N88-15183
Coupling of vibrational modes of adsorbates: Application to field induced shifts for CO and CN on Cu(100)
[AD-A187891] 11 p1453 N88-18659
An investigation of metal complexes of some 2-substituted and 2,6-disubstituted pyridine N-oxides
11 p1460 N88-18701
Molecular and electronic mechanism in the control of Na+ and K+ permeability of excitable cell membrane by ligand binding on receptor sites
[AD-A188725] 13 p1808 N88-20805

LIGHT (VISIBLE RADIATION)
NT AIRGLOW
NT COHERENT LIGHT
NT DAYGLOW
NT GEOCORONAL EMISSIONS
NT NIGHTGLOW
NT POLARIZED LIGHT
NT SKY RADIATION
NT SUNLIGHT
NT ZODIACAL LIGHT

The largest white light flare ever observed: 25 April 1984, 0001 UT 01 p0111 N88-10714
New physical explanation of phase-conjugate waves produced in backward stimulated scattering 03 p0302 N88-11900
Solitons in stimulated Raman scattering: Generation and control of ultrashort optical pulses
[AD-A185141] 05 p0650 N88-13983
Airborne Visible/Infrared Imaging Spectrometer (AVIRIS). A description of the sensor, ground data processing facility, laboratory calibration, and first results
[NASA-CR-182365] 06 p0705 N88-14325
A system overview of the Airborne Visible/Infrared Imaging Spectrometer (AVIRIS) 06 p0705 N88-14326
Airborne Visible/Infrared Imaging Spectrometer (AVIRIS) spectrometer design and performance 06 p0706 N88-14327
AVIRIS foreoptics, fiber optics and on-board calibrator 06 p0706 N88-14328
Visible and infrared linear detector arrays for the Airborne Visible/Infrared Imaging Spectrometer (AVIRIS) 06 p0706 N88-14329
AVIRIS scan drive design and performance 06 p0706 N88-14330
Signal chain for the Airborne Visible/Infrared Imaging Spectrometer (AVIRIS) 06 p0706 N88-14331
AVIRIS onboard data handling and control 06 p0706 N88-14332
AVIRIS ground data-processing system 06 p0707 N88-14333
Spectral and radiometric calibration of the Airborne Visible/Infrared Imaging Spectrometer 06 p0707 N88-14334
First results from the Airborne Visible/Infrared Imaging Spectrometer (AVIRIS) 06 p0707 N88-14335
New description of Lau effect based on theory of raster image forming process 06 p0772 N88-14744
Parametric and resonance interaction of ultrashort light pulses in nonlinear multilevel medium 06 p0773 N88-14746
Total light flux and colour of solar corona
[PB87-143335] 07 p0946 N88-15754
Joint services electronics program
[AD-A188173] 11 p1478 N88-18822
Solid-state ring laser with acoustooptical phase nonreciprocity of opposing waves 14 p1970 N88-21761
Squeezed states of light 14 p1976 N88-21791
Pulsed squeezed light 14 p1976 N88-21792
Nonclassical lights 14 p1979 N88-21810
Open questions in closed-loop photodetection 14 p1979 N88-21812
Relationship between optical transfer function and natural light field in sea or atmosphere 15 p2054 N88-22247
Infrared-sensitive spatial light modulator
[AD-A190391] 15 p2134 N88-22729
Experimental research on skin reflection, transmission, absorption of light rays 16 p2187 N88-23039
Nonlinear wave and diffusion equations
[AD-A191421] 16 p2265 N88-23544
Research investigation directed toward extending the useful range of the electromagnetic spectrum
[AD-A190198] 17 p2332 N88-23920
Light propagation through gravitationally perturbed Friedmann universes 18 p2577 N88-25307
A twin-mirrored galvanometer laser light sheet generator
[NASA-TM-100587] 19 p2674 N88-25901
Precision measurement of the Fresnel drag coefficient using a ring laser
[AD-A196025] 24 p3366 N88-30043

LIGHT ABSORPTION
U ELECTROMAGNETIC ABSORPTION

LIGHT ADAPTATION
Electroencephalographic changes during equilibrium test in the presence of rhythmic photic interference 19 p2703 N88-26075

LIGHT AIRCRAFT
NT DO-28 AIRCRAFT
NT OH-58 HELICOPTER
Modern materials for light constructions --- aircraft
[MBB-Z-136/86] 10 p1312 N88-17839
Determination of canopy loads for a light aircraft by wind tunnel testing and computer modelling
[BU-353] 14 p1869 N88-21167
It's time to reinvent the general aviation airplane 17 p2294 N88-23726
An interim comparison of operational CG records in turbulence on small and large civil aircraft 24 p3313 N88-29729

LIGHT ALLOYS
NT ALUMINUM ALLOYS
NT BERYLLIUM ALLOYS
NT MAGNESIUM ALLOYS
Materials for fighter aircraft 05 p0546 N88-13325
Application of the ONERA model to the life estimation under fatigue cracking of a Al-Li alloy. Parameter identification and test-experiment comparison under FALSTAFF loading
[ONERA-RT-32/7169-RY-063-R] 16 p2222 N88-23264
Crack retardation under load spectra. Experimental study and numerical simulation using the simplified K constant model --- light alloys, aircraft construction materials
[ONERA-RT-30/7169-RY-054-R] 16 p2222 N88-23266

LIGHT AMPLIFIERS
An experimental study of CW HF chemical laser amplifier performance and zero power gain
[AD-A185241] 05 p0588 N88-13584
Periodically pulsed excimer master oscillator-regenerative amplifier laser set 06 p0772 N88-14741
Phase phenomena in parametric generators and amplifiers of ultrashort light pulses 07 p0918 N88-15576
TEA-TE: Powerful nitrogen-based laser system 07 p0919 N88-15583
Generation of coherent soft X-rays using a single-pass free-electron laser amplifier
[DE88-009137] 19 p2675 N88-25907
Optical guiding in the separable beam limit
[AD-A192452] 21 p2952 N88-27534
Nonlinear optical phase conjugation techniques to reduce the physical size of lasers
[AD-A196170] 24 p3379 N88-30122

LIGHT BEAMS
NT LASER BEAMS
The deviation of light rays passing through a curved windscreen --- aircraft
[BAE-MSC.115] 01 p0093 N88-10610
Optoelectronic measurement methods for ballistic experiments
[PB87-110706] 05 p0583 N88-13554
Periodically pulsed excimer master oscillator-regenerative amplifier laser set 06 p0772 N88-14741
Energy transmission using coherent, quasimonochromatic light beams 09 p1241 N88-17436
Continuous collective molecule rotation of a nematic liquid crystal induced from light angular momentum
[FUB-17-1986] 14 p1986 N88-21845
An optical technique for measuring divergence, beam profile, and aiming direction, of relativistic negative hydrogen ions
[DE88-007049] 18 p2572 N88-25278

LIGHT BULBS
U LUMINAIRES

LIGHT COMMUNICATION
U OPTICAL COMMUNICATION

LIGHT CURVE
Basic properties and variability 02 p0252 N88-11593
The giant spot on II Peg in 1986 04 p0508 N88-13120
The short-period RS CVn stars: Starspots and fundamental properties 04 p0508 N88-13124
The X-ray orbital lightcurves of AR Lac and TY Pyx 04 p0509 N88-13129
Differential B and V light curves of the bright BY Draconis star HD80715 04 p0509 N88-13130
Light curve behaviour in the near IR of the CG Cyg system 04 p0513 N88-13156
Pre-main sequence activity: How far is magnetism involved 04 p0517 N88-13179
Stromgren photometry of RSCVn and HD108102 04 p0519 N88-13187
The type Ia supernova 1986G in NGC5128: Optical photometry and spectra
[INPE-4426-PRE/1230] 12 p1710 N88-20231
The light curve of P/Halley and the rotation of its nucleus 14 p2009 N88-21984
To the opportunities of cluster analysis of light curves of supernovae
[DE88-701642] 21 p3030 N88-27982
The ultrashort period dwarf nova SW Ursae Majoris 24 p3453 N88-30553

LIGHT DURATION
U PULSE DURATION

LIGHT EMISSION
NT BIOLUMINESCENCE
NT CHEMILUMINESCENCE
NT ELECTROLUMINESCENCE
NT FLUORESCENCE
NT LASER INDUCED FLUORESCENCE
NT LUMINESCENCE
NT OPTICAL RESONANCE
NT PHOSPHORESCENCE
NT PHOTOLUMINESCENCE
NT RESONANCE FLUORESCENCE
NT SPACECRAFT GLOW
NT X RAY FLUORESCENCE
The largest white light flare ever observed: 25 April 1984, 0001 UT 01 p0111 N88-10714
IUE/Optical/VLA flares on AD Leo 04 p0512 N88-13152
Laser thermal propulsion
[AD-A186407] 07 p0933 N88-15666
Linear theory of generation of longitudinal sound waves in semiconductors upon interband absorption of optical radiation 09 p1234 N88-17397
Scattering of optical radiation by bursting water particles in fog 09 p1236 N88-17410
The analytical exponential decay coefficient of the submarine light field
[AD-A187215] 11 p1548 N88-19261
Merit of Hadamard transform active absorption spectrometer described 15 p2053 N88-22232
Development of liquid metal field-emission sources for use in fast repetitive opening switches
[AD-A192230] 20 p2795 N88-26583
Optical emission behavior and radiation resistance of epoxy resins
[DE88-752629] 23 p3196 N88-29023
Optical emission from surface waves supported in thin metal films 23 p3282 N88-29540

LIGHT EMITTING DIODES
Development of an optical feedback based high accuracy beam transmissometer
[AD-A189396] 12 p1692 N88-20122
Atmospheric attenuation of near infrared radiation propagating through fog 14 p1899 N88-21342
Excitation of single-mode glass fiber by partially coherent sources
[ETN-88-92121] 20 p2854 N88-26951

LIGHT GAS GUNS
Ideal-viscoplastic extrusion model with application to deforming pistons in light-gas guns
[UTIAS-TN-266] 04 p0429 N88-12657
An investigation of soft launch and instability breakup with a two-stage light gas gun
[DE88-010371] 21 p2901 N88-27218

LIGHT INTENSITY
U LUMINOUS INTENSITY

LIGHT IONS
Studies on surface chemical states of some metals and ceramics bombarded with energetic light-ions
[DE87-752975] 02 p0145 N88-10910
Energy dependence of ion-induced sputtering yields of monatomic solids in the low energy region
[IPPJ-AM-52] 05 p0651 N88-13988
Two-dimensional focusing of self-magnetically insulated plasma focus diode 16 p2278 N88-23639
Time-resolved spectroscopic measurement of anode plasma in magnetically-insulated diode 16 p2279 N88-23641
Pulsed power driver technologies for inertial confinement fusion power reactors
[DE88-009260] 19 p2731 N88-26221

LIGHT MODULATION
Development of optical modulators for measurements of solar magnetic fields
[NASA-TM-100315] 04 p0490 N88-13016
Phase phenomena in parametric generators and amplifiers of ultrashort light pulses 07 p0918 N88-15576
Joint services electronics program
[AD-A188173] 11 p1478 N88-18822
A numerical analysis of the dynamics of PRIZ operation
[AD-A188853] 12 p1678 N88-20035
Study of photochromic materials for use in optical signal processing
[AD-A189068] 13 p1839 N88-21006
Infrared-sensitive spatial light modulator
[AD-A190391] 15 p2134 N88-22729
Research on materials and components for opto-electronic signal processing and computing
[AD-A190130] 15 p2143 N88-22788
Research investigation directed toward extending the useful range of the electromagnetic spectrum, appendix
[AD-A190199] 17 p2332 N88-23921
Optical modulation above 20 GHz using a waveguide electrooptic switch 19 p2660 N88-25819
Use of depletion edge translation for high-speed modulation and switching of lightwaves
[AD-A195611] 24 p3430 N88-30417

LIGHT PRESSURE
U ILLUMINANCE

LIGHT PROBES
U LIGHT BEAMS

LIGHT SCATTERING
NT HALOS

Light scattering by oriented and randomly dispersed chiral particles
[DE87-014758] 03 p0376 N88-12368
All-optical beam control by forced Rayleigh scattering
[AD-A184315] 04 p0490 N88-13018
Extinction by dielectric particles at optical and infrared wavelength
[AD-A184818] 05 p0650 N88-13981
Measurement of particle size distribution in a solid propellant rocket motor using light scattering
[AD-A184875] 06 p0673 N88-14124
Observing effect of laser radiation of low-frequency Raman scattering of light 06 p0772 N88-14742
Research on acoustical scattering, diffraction catastrophes, optics of bubbles, photoacoustics, and acoustical phase conjugation
[AD-A185785] 06 p0776 N88-14761
Chemical reactions in turbulent mixing flows
[AD-A186141] 07 p0849 N88-15153
Monte Carlo method calculation of spectral brightness coefficient of vegetation cover as function of illumination conditions 08 p1008 N88-16113
Stimulated Mandelstam-Brillouin scattering during forward scattering of light 08 p1078 N88-16499
A review of some flow visualization experiments carried out at the Institut Franco-Allemand de Recherches (ISL) shock tubes
[ISL-CO-243/86] 09 p1163 N88-16974
Digital imaging techniques for single- and multi-phase reacting flowfields 10 p1327 N88-17933
Advances in calculating macroionic solution structure
[DE88-003799] 10 p1409 N88-18406
Diagnostics for research in atomization and turbulent two-phase flows
[AD-A187338] 11 p1482 N88-18843
Depolarized infrared reflectance from dry and wetted surfaces
[AD-A188213] 11 p1492 N88-18903
Optical characterization of tropospheric aerosols
[AD-A187839] 11 p1511 N88-19029
Vibrational, mechanical and thermal properties of 3-5 semiconductors
[AD-A187569] 11 p1556 N88-19316
Thermodynamic theory of fluctuations and Rayleigh light scattering in solutions 13 p1785 N88-20681
Multiple scattering of polarized light in cirrus clouds
13 p1801 N88-20768
Additional peak of light scattering by sound under conditions of acoustic instability
14 p1968 N88-21752
A new class of multiple dispersion grating spectrometers
[PREPRINT-569] 14 p1983 N88-21830
Linear and circular polarization of Comet Halley light
14 p2009 N88-21982
Research on certain aspects of laser diffraction particle sizing relevant to autonomous self-diagnosing instrumentation
[AD-A190220] 15 p2071 N88-22348
The interaction of small particles with laser beams
[AD-A190716] 15 p2072 N88-22354
Multiple scattering from nonspherical targets
[AD-A189939] 15 p2133 N88-22723
Light scattering of intracellular gas vacuoles: Anomalous behavior of forward and perpendicular light scattering of a cyanobacterium due to intracellular gas vacuoles
[BCRS-87-08] 16 p2228 N88-23308
Enhanced backscattering from rough surfaces
[AD-A191089] 16 p2274 N88-23610
Analysis of dust grain properties in two star forming regions through comparison of theoretical models to observations 17 p2451 N88-24559
Molecular characterization of structure and bonding in thin film materials
[DE88-006811] 18 p2584 N88-25351
Effects of atmospheric model layering on LOWTRAN 6 calculations of 8-12 micrometers near-horizon sky radiances
[AD-A192969] 20 p2791 N88-26559
Light scattering by charged spheres
[AD-A193753] 22 p3153 N88-28759
Beam combining by phase transition nonlinear media
[AD-A194116] 23 p3283 N88-29547
Particle sizing in combustion systems, using scattered laser light
[AD-A196231] 24 p3352 N88-29953

LIGHT SCATTERING METERS
Study of the properties of a new detector class for liquid chromatography
[DE88-001666] 05 p0563 N88-13426

LIGHT SOURCES
National Synchrotron Light Source users manual: Guide to the VUV and X-ray beam lines
[DE88-001464] 04 p0490 N88-13020
Anti-Stokes generation of 226 nm light
[DE88-001612] 05 p0589 N88-13590
Soliton mode of propagation of light pulses through single-mode optical fibers and problems of its experimental realization 07 p0920 N88-15592
Pulsed laser stereophotography of plasmas and dynamically moving surfaces
[DE88-003170] 09 p1173 N88-17031
Signal processing studies program optical signal amplification, volume 2
[AD-A188054] 10 p1320 N88-17896
The light pulse generator 869 for high speed investigations
[MPIS-9/1987] 11 p1491 N88-18898
Coherent VUV source at 130 nm: Theory and modeling
[DE88-003874] 11 p1549 N88-19269
Rainbow holographic image reconstructed by spatially extended white light source 15 p2055 N88-22249
Tracking a monochromatic light source
[DE88-011260] 20 p2807 N88-26653
Fiber optic sensing systems using high frequency resonant sensing heads with intensity sensors
[NASA-TM-101318] 22 p3080 N88-28293
Eye movements and spatial pattern vision
[AD-A195496] 24 p3408 N88-30290

LIGHT SPEED
Superluminal velocities within relativity theory
[ETN-87-90958] 02 p0247 N88-11563
Theory of relativity and super-light-speeds-I: Kinematical part
[DE88-701832] 20 p2880 N88-27100

LIGHT TRANSMISSION
NT HALOS
NT LIGHT SCATTERING
Radiation-induced transient attenuation of optical fibers at 800 and 1300 nm
[DE87-013165] 02 p0235 N88-11485
Optical probe
[EP-PATENT-0-210-869-A1] 05 p0650 N88-13984
Effect of clarifying the atmosphere in relation to quasi-monochromatic CO2 laser radiation
06 p0709 N88-14348
Photoinduced low-temperature changes in optical losses in fiber optics based on chalcogenide glasses
06 p0770 N88-14731
Determination of cloud base height and emissivity from downwelling angular radiances
[AD-A185985] 07 p0879 N88-15331
Soliton mode of propagation of light pulses through single-mode optical fibers and problems of its experimental realization 07 p0920 N88-15592
Characterization of transparent insulation materials --- solar energy absorbers
[ETN-88-91052] 09 p1163 N88-16970
Signal processing for an optical wide band data transmission system
[DE88-003854] 10 p1319 N88-17888
The analytical exponential decay coefficient of the submarine light field
[AD-A187215] 11 p1548 N88-19261
Remote sensing of atmospheric optical thickness and sea-water attenuation when submerged: Wavelength selection and anticipated errors
[AD-A187609] 11 p1548 N88-19262
Analysis of the inter-layer independence of stellar scintillometer profiles of Cn2
[AD-A189372] 12 p1645 N88-19854
Development of an optical feedback based high accuracy beam transmissometer
[AD-A189396] 12 p1692 N88-20122
Influence of nonlinear spectroscopic effects on atmospheric propagation of intense laser radiation at 10.6 microns wavelength 13 p1789 N88-20705
Coherence effects in optical physics with special reference to spectroscopy
[AD-A189520] 13 p1840 N88-21007
Atmospheric attenuation of near infrared radiation propagating through fog 14 p1899 N88-21342
Advanced programming and control techniques for complex mechanical systems
[AD-A190238] 15 p2071 N88-22349
Atmospheric propagation of laser beams
[AD-A191447] 18 p2520 N88-24952
Study of light transmission methods from scintillators to optical fiber with wave length shifter
[DE88-701587] 18 p2574 N88-25292
Low-loss, high-isolation, fiber-optic isolator
[NASA-CASE-NPO-17207-1-CU]
18 p2576 N88-25304
Stress-related phenomena in transient radiation-induced absorption in optical fibers
[DE88-010956] 20 p2854 N88-26949
Multichannel data transmission through a fiber optic cable
[AD-A193842] 22 p3070 N88-28221
Metal halide optical glasses
[AD-A193794] 23 p3198 N88-29032

LIGHT WATER REACTORS
A model for stationary and dynamic impression of undercooled boiling in coupled thermohydraulic and neutron physics calculations of nuclear reactors
[IKE-6-171] 09 p1247 N88-17472
Development of fast breeder reactors in China
16 p2186 N88-23032
Statistical evaluation of light water reactor piping damping data for use in PRA (Probabilistic Risk Assessment) analyses
[DE88-007708] 19 p2661 N88-25828

LIGHTING
U ILLUMINATING

LIGHTING EQUIPMENT
NT ARC LAMPS
NT FLASH LAMPS
NT LUMINAIRES
NT QUARTZ LAMPS
Failure of filament lamps subjected to vibration with special reference to the 26 volt 5 Watt tank lamp
[EL-135] 09 p1158 N88-16938

LIGHTNING
The physics of charge separation preceding lightning strokes in thunderclouds
[NASA-CR-178371] 01 p0071 N88-10452
Production of NO by galactic cosmic rays and lightning
[DE87-014613] 02 p0197 N88-11230
Short-term forecasting of lightning based on the surface wind field at Kennedy Space Center
02 p0208 N88-11306
Experimental and analytic studies of the triggered lightning environment of the F106B
[NASA-CR-4104] 04 p0469 N88-12897
Lightning discharge protection rod
[NASA-CASE-LAR-13470-1] 06 p0666 N88-14083
Atmospheric electricity
[NASA-CR-179239] 06 p0744 N88-14575
Radar observations of changes in precipitation size spectra associated with lightning
06 p0744 N88-14576
Lightning spectra in the near infrared
[DE88-002218] 07 p0880 N88-15341
Astrophysics and the solar nebula
07 p0883 N88-15355
Applicability of extremely low frequency global resonances for study of Venusian storm activity
08 p1005 N88-16093
Return stroke velocities and currents using a solid state silicon detector system 11 p1515 N88-19050
Validation of GEMACS (General Electromagnetic Model for the Analysis of Complex Systems) for modeling lightning-induced electromagnetic fields
[AD-A188822] 12 p1620 N88-19687
Atmospheric electrical modeling in support of the NASA F-106 storm hazards project
[NASA-CR-181639] 13 p1799 N88-20758
Characteristics of the positive lighting flash
[DE88-005854] 13 p1800 N88-20760
Upward propagating electric fields from thunderstorms and VLF transmitters 13 p1801 N88-20767
Activities report of the Physics Department
[ETN-88-91985] 13 p1833 N88-20964
Equipment test methods for externally produced electromagnetic transients
[RAE-TM-FS(F)-457] 14 p1865 N88-21140
Distribution of summertime lightning as a function of low-level wind flow in central Florida
[PB88-160759] 14 p1948 N88-21619
Experimental comparison of lightning simulation techniques to CV-580 airborne lightning strike measurements
[AD-A190576] 15 p2098 N88-22496
Study of lightning and lightning protection (selected pages)
[AD-A190623] 15 p2098 N88-22498
Proceedings of the Lightning Threat Warning Workshop
[DE88-006607] 15 p2098 N88-22499
Atmospheric Science and Remote Sensing Laboratory
[NASA-CR-179290] 16 p2236 N88-23355
Finite element simulation of the atmosphere's electromagnetic response to charge perturbations associated with lightning 17 p2375 N88-24124
Theoretical basis for an experimental test with regard to the origin of VHF (Very High Frequency) radiation from natural lightning
[DE88-007535] 18 p2544 N88-25102
Analysis of lightning field changes during active thunderstorms in Florida 18 p2545 N88-25103
Lightning detection and locating systems
18 p2546 N88-25112
Voltages induced by lightning on electric power distribution lines: Field data and analysis results for the period July 1984-1986
[DE88-007841] 19 p2693 N88-26006

Computer controlled data acquisition system for the NASA 1986 Rocket Triggered Lightning Program
[DE88-008335] 20 p2826 N88-26766
A radar study of the interaction between lightning and precipitation
[DE88-009120] 20 p2827 N88-26770
Investigations into the triggered lightning response of the F106B thunderstorm research aircraft
[NASA-CR-3902] 23 p3236 N88-29258
The 1983 direct strike lightning data, part 1
[NASA-TM-86426-PT-1] 23 p3237 N88-29259
The 1983 direct strike lightning data, part 2
[NASA-TM-86426-PT-2] 23 p3237 N88-29260
The 1983 direct strike lightning data, part 3
[NASA-TM-86426-PT-3] 23 p3237 N88-29261

LIGHTNING SUPPRESSION
Fuel containment, lightning protection and damage tolerance in large composite primary aircraft structures
[NASA-CR-3875] 17 p2317 N88-23839
An interagency working group on lightning threat warning
[DE88-009828] 20 p2826 N88-26767
The first synthesis of chem-prep varistor LAC (Lightning Arrestor Connector) granules
[DE88-008005] 21 p2936 N88-27438

LIGHTS
U LUMINAIRES

LIKELIHOOD RATIO
A note on extended quasi-likelihood
[AD-A186318] 07 p0915 N88-15555
A likelihood based grouping method for multidimensional observations. An interactive method used on large transportation data bases
[REPT-87-74] 16 p2286 N88-23685

LIMB DARKENING
Asymmetry and variations of solar limb darkening along the diameter defined by diurnal motion in April 1981
04 p0506 N88-13111
Calibration of the Ca II K line-core density and the magnetic flux density in stars using solar data
04 p0507 N88-13116

LIMBS (ANATOMY)
NT ARM (ANATOMY)
NT FINGERS
NT HAND (ANATOMY)
NT LEG (ANATOMY)
Dynamics and stability of bipedal locomotion robots
03 p0333 N88-12096
Limb regeneration in amphibians, a suitable model for investigations of the effects of weightlessness as regards evolution and modifications 07 p0885 N88-15369

LIME
U CALCIUM OXIDES

LIMITATIONS
U CONSTRAINTS

LIMITERS (FUSION REACTORS)
Technical evaluation of major candidate blanket systems for fusion power reactor
[DE87-752989] 02 p0239 N88-11512
Modular pump limiter systems for large tokamaks
[DE88-001487] 04 p0494 N88-13045
ALT-1 pump limiter experiments
[DE88-000822] 05 p0651 N88-13989
Pump limiter experiments and analysis in the TEXTOR tokamak 09 p1252 N88-17506
Stability of an RFP (Reversed-Field Pinch) with resistive and distant boundaries
[DE88-004155] 10 p1413 N88-18431
Analyses and experiments on the integrity and lifetime predictions of plasma-facing components in fusion reactors
[DE87-702957] 15 p2135 N88-22735
Erosion/redeposition modeling and calculations for carbon
[DE88-010382] 22 p3057 N88-28139
Tokamak plasma interaction with limiters
[UTIAS-325] 23 p3286 N88-29566

LIMITS (MATHEMATICS)
Stochastic filtering solutions for ill-posed linear problems and their extension to measurable transformations
[AD-A186016] 07 p0909 N88-15506
Mathematical foundations of signal processing. 2: The role of group theory
[AD-A188482] 12 p1620 N88-19685
The partially observed stochastic minimum principle
[AD-A189787] 15 p2124 N88-22658
A central limit theorem for M-estimators by the von Mises method
[CWI-MS-R8713] 16 p2262 N88-23525
Computation of filters by sampling and quantization
[AD-A192839] 21 p3005 N88-27826
Approximations and implementations of nonlinear filtering schemes
[AD-A194685] 23 p3271 N88-29462

LIMNOLOGY
The effect of wind and currents on gas exchange in an estuarine system
[NASA-CR-181424] 01 p0073 N88-10468

LINE CURRENT
Optical power line voltage and current measurement systems. Volume 1: Limits to the precision of electro-optic and magneto-optic sensors
[DE87-014558] 02 p0175 N88-11092
On the potential role of concentrated field-aligned currents in solar physics 08 p1099 N88-16614
Complex space monofilar approximation of diffraction currents on a conducting half plane
[NASA-CR-182883] 16 p2273 N88-23605

LINE OF SIGHT
Adaptive line of sight algorithms
[DE87-014275] 01 p0081 N88-10523

LINE OF SIGHT COMMUNICATION
Identification of microwave line-of-sight multipath components 12 p1616 N88-19665
Refractive index, meteorology and fading in line-of-sight transmission paths 12 p1616 N88-19666
Radio and radar holes and multipath zones: The global and local influences on atmospheric refractive structure and resulting adverse radio and radar performance
12 p1617 N88-19667
Space-diversity effects on line-of-sight propagation paths 12 p1617 N88-19670
An EHF telecommunication system engineering model
12 p1618 N88-19674

LINE SHAPE
Calculation of the line shapes of radiators immersed in plasma 19 p2729 N88-26210
Molecular line shape effects on atmospheric window absorption
[AD-A196316] 24 p3342 N88-29894

LINE SPECTRA
NT BALMER SERIES
NT ELECTRONIC SPECTRA
NT FRAUNHOFER LINES
NT H ALPHA LINE
NT H BETA LINE
NT H LINES
NT K LINES
NT LYMAN SPECTRA
NT RYDBERG SERIES
Evidence of a new spectral line intensity formula for optical emission
[KGI-PREPRINT-098] 01 p0090 N88-10585
Spectrograms of the visible region in the JT-60 tokamak (wavelength range from 2210 A to 5250 A)
[DE87-753002] 02 p0240 N88-11513
Relaxation effect of stark split levels for two-level system interacting with symmetrical strong resonant bichromatic field 03 p0299 N88-11882
Comparison of global and nuclear properties of starburst and Seyfert 1 galaxies 03 p0388 N88-12438
Investigations of extragalactic hydroxyl
03 p0389 N88-12441
Active phases on II Peg 04 p0507 N88-13119
H alpha and Ca II emission line variability of FK comae 04 p0509 N88-13128
Magnetic fields on K and M stars
04 p0510 N88-13137
Broadband linear polarization and chromospheric CaII H and K line emission in late-type main sequence stars
04 p0511 N88-13140
An analysis of the photospheric line profiles in F, G, and K supergiants 04 p0513 N88-13157
The Wilson-Bappu relationship: A barometric effect
04 p0516 N88-13170
Synthetic spectra for the N-type carbon star TX Psc
04 p0516 N88-13173
Infrared excesses of barium stars
04 p0516 N88-13174
The delta upsilon = 1 fundamental bands of carbon monoxide in late-type stars 04 p0517 N88-13177
A helium flare on the active G5 dwarf Kappa Ceti
04 p0519 N88-13189
A computer code to calculate line by line atmospheric transmission spectra on a microcomputer
[NASA-TM-100686] 05 p0554 N88-13372
Narrow linewidth gain measurements in a KrF excimer amplifier pumped longitudinally by a high-power electron beam
[DE88-001365] 05 p0586 N88-13575
An adaptive lattice algorithm for spectral line estimation
[AD-A184970] 05 p0634 N88-13876
Main results of atmospheric fine structure parameter observation in the lower thermosphere
06 p0735 N88-14518
Optical electronics for meteor observations
06 p0741 N88-14559
Justification and prospects of observations of interstellar, far-infrared emission lines, using a small-sized balloon-borne telescope 08 p1032 N88-16254
Gamma-ray imaging observations of the Crab and Cygnus regions 10 p1427 N88-18522
An analysis of longitude variations in the equatorial spectrum of Saturn 10 p1430 N88-18539
Spectral line-broadening codes for hydrogen-, helium- and lithium-like ions in plasmas
[DE88-005238] 11 p1552 N88-19289
An interpretation of the ethylenic, carbidic, and graphite auger lineshapes of chemisorbed carbon species
[AD-A189092] 13 p1736 N88-20379
The astrophysics of nebulae and active galactic nuclear emission-line regions: New methods and applications
13 p1858 N88-21111
Effect of Mg impurity on local vibrations of U-centers in LiF lattice 14 p1969 N88-21753
The observability of carbon monoxide in planetary nebulae
[ETN-88-91498] 14 p2011 N88-21994
Statistical fine structure in inhomogeneously broadened absorption lines in solids
[AD-A190341] 16 p2174 N88-22957
Implications of the trapping-desorption and direct inelastic scattering channels on Dicke-narrowed lineshapes
[AD-A191410] 16 p2270 N88-23581
Total photoionization cross sections of atomic oxygen from threshold to 44.3A
[NASA-CR-182992] 17 p2397 N88-24252
Helium-like titanium spectra from tokamak plasmas
17 p2440 N88-24516
Forbidden transitions as ion-temperature sensitive lines 17 p2441 N88-24520
Tokamak studies of density sensitive line ratios
17 p2441 N88-24521
Intensity calibration of a VUV system by branching line pairs 17 p2443 N88-24533
The gamma 1 and gamma 3 bands of (16)O3: Line positions and intensities
[NASA-TM-101162] 17 p2445 N88-24541
Line positions and intensities for the gamma 1 + gamma 2 and gamma 2 + gamma 3 bands of (16)O3
[NASA-TM-101161] 17 p2446 N88-24542
An optical preamplifier for detection of CO2 laser radiation
[AD-A190790] 18 p2520 N88-24949
Observations of wave number dependent spectral line ratio fluctuations in the atmospheric emissions
[IRF-PREPRINT-101] 18 p2542 N88-25085
Studies of spectral line ratio fluctuations using Inductively Coupled Plasma (ICP) light
[IRF-PREPRINT-100] 18 p2578 N88-25311
Recent data on Si:As impurity band conduction multiplexed arrays
[AD-A191752] 18 p2582 N88-25340
Inner-shell X-ray line spectra of highly ionized titanium, chromium, iron and nickel and their appliation to laboratory plasmas
[PB87-225181] 19 p2730 N88-26212
Detection of absorption lines in the spectra of X-ray bursts from X1608-52
[ISAS-RN-360] 20 p2887 N88-27143
Spectral line shapes from highly ionized sodium plasmas
[AD-A193401] 21 p3017 N88-27907
Paramagnetic point defects in boron-implanted HgO.7CdO.3Te
[AD-A193276] 21 p3021 N88-27934
The electromagnetic spectrum: The information mine
[AD-A194316] 22 p3069 N88-28215
First detection of HCN J=9 to 8 (797 GHz) line emission: Very high densities in the Orion core
[MPE-PREPRINT-110] 22 p3165 N88-28847
On selection rules and inelastic electron scattering at intermediate energies
[DE88-701833] 23 p3280 N88-29526
The optical spectroscopy of copper-blue luminescence in zinc sulfide crystals. Zero-phonon line spectra under the influence of magnetic field, temperature and excitation intensity
[ETN-88-93122] 24 p3344 N88-29903

LINEAMENT
U STRUCTURAL PROPERTIES (GEOLOGY)

LINEAR ACCELERATORS
Visible free electron laser oscillator
[AD-A183871] 01 p0051 N88-10324
Induction linac-driven free-electron lasers: Status and future prospects
[DE87-012914] 01 p0051 N88-10329
Open accelerating structures
[DE87-010540] 01 p0092 N88-10603
Transverse focussing using plasma wake fields
[DE87-011503] 01 p0099 N88-10652

Status of inertial fusion
[DE87-010988] 01 p0099 N88-10654
A simple self-breaking 2 MV gas switch
[DE87-014346] 02 p0166 N88-11047
A high-power RF linear accelerator for FELs (Free-Electron Lasers)
[DE87-011795] 02 p0177 N88-11104
The nature of beamstrahlung
[DE87-012837] 02 p0234 N88-11474
A conceptual design of Final Focus Systems for linear colliders
[DE87-012840] 02 p0234 N88-11475
Interactive Design of Accelerators (IDA)
[DE87-013298] 02 p0234 N88-11476
Simulation of tokamak runaway-electron events. Study of the response of materials by use of an electron linear accelerator
[IPPJ-841] 02 p0242 N88-11528
Proceedings: SDIO/DARPA Workshop on Laser Propulsion. Volume 3: Viewgraphs
[DE88-000964] 04 p0450 N88-12790
Development of a laced electromagnetic wiggler
[DE88-000972] 05 p0646 N88-13953
Heavy-ion accelerator research for inertial fusion
[DE88-000541] 05 p0653 N88-14001
A qualitative study of wake fields for very short bunches
[DE88-002565] 09 p1164 N88-16980
CEBAF design overview and project status
[CEBAF-PR-88-001] 09 p1246 N88-17470
Preliminary injector, accelerator, and beamline design for rf-linac-driven XUV free-electron lasers
[DE88-003185] 10 p1336 N88-17983
Medium high energy physics at Syracuse University
[DE88-003670] 11 p1545 N88-19235
The injector for the CEBAF CW superconducting linac
[CEBAF-PR-87-011] 11 p1546 N88-19241
Perturbation effects in the CEBAF beam transport system
[CEBAF-PR-87-010] 11 p1546 N88-19242
Investigation of multiple particle final states at CEBAF (Continuous Electron Beam Accelerator Facility)
[CEBAF-PR-87-026] 11 p1547 N88-19250
RF steering in the CEBAF CW superconducting linac
[CEBAF-PR-87-013] 11 p1547 N88-19251
The CEBAF project and its few-body research program
[CEBAF-PR-87-014] 11 p1547 N88-19253
Two dimensional simulations of multipass beam breakup
[CEBAF-PR-87-008] 11 p1547 N88-19254
Induction linacs: A technology come of age for international cooperation
[DE88-003953] 11 p1548 N88-19258
Big Bang Nucleosynthesis: Accelerator tests and can (UC OMEGA)(sub B) really be large
[DE88-003405] 11 p1570 N88-19396
Application of radio frequency superconductivity to recirculating linacs
[CEBAF-PR-88-002] 12 p1690 N88-20107
On (e,e'N) reactions
[CEBAF-PR-87-028] 12 p1690 N88-20109
Optics of the CEBAF CW superconducting accelerator
[CEBAF-PR-87-012] 12 p1690 N88-20110
Multipass beam breakup in recirculating linacs
[CEBAF-PR-87-007] 12 p1690 N88-20111
Projected performance of RF-linac-driven free-electron lasers in the VUV and soft X-ray regions
[DE88-004294] 13 p1776 N88-20625
The continuous electron beam accelerator facility
[CEBAF-PR-87-017] 13 p1838 N88-20996
Status of RF superconductivity at Argonne National Laboratory
[DE88-005913] 15 p2144 N88-22796
Heavy ion fusion system assessment: Final focus and transport model
[LBL-23040] 19 p2725 N88-26183
Accelerator research studies
[DE88-006236] 19 p2726 N88-26187
Results from the SLAC lasertron
[DE88-007816] 20 p2806 N88-26647
Research opportunities below 300 nm at the NBS Free-Electron Laser Facility
[AD-A193100] 21 p2953 N88-27538

LINEAR ARRAYS
Spectrometric test of a linear array sensor
[NASA-TM-100676] 01 p0064 N88-10414
Ground-based interferometry with the European Very Large Telescope (VLT) 01 p0096 N88-10632
Visible and infrared linear detector arrays for the Airborne Visible/Infrared Imaging Spectrometer (AVIRIS)
06 p0706 N88-14329
High bit rate serial input mutipliers
[REPT-87-012] 11 p1530 N88-19140
On serial-input multipliers for two-complement numbers
[REPT-86-035] 11 p1536 N88-19181
Optimal and conventional space-time processing in flow noise
[AD-A189104] 13 p1833 N88-20965
Mid infrared multichannel focal plane breadboard --- pushbroom sensors
[RT-87/014] 14 p1982 N88-21827
Space time processing, environmental-acoustic effects
[AD-A190764] 15 p2130 N88-22708
Software development for the reconstruction of source parameters using research and development arrays
[REPT-840445-TW] 16 p2246 N88-23417
Flexible tactile sensing arrays for robotics: Architectural robustness and yield considerations
19 p2671 N88-25878

LINEAR CIRCUITS
Piecewise linear approach for timing simulation of VLSI (Very-Large-Scale-Integrated) circuits on serial and parallel computers
[AD-A191328] 16 p2252 N88-23462

LINEAR EQUATIONS
NT RICCATI EQUATION
Solution methods for bidiagonal and tridiagonal linear systems for parallel and vector computers
[REPT-87-04] 01 p0085 N88-10552
Nonequilibrium fluctuations and transport in sheared fluids 03 p0316 N88-11999
Polynomial compensation, inversion, and approximation of discrete time linear systems
[NASA-TM-100027] 03 p0372 N88-12344
Eigenvalue projection theory for linear operator equations of electromagnetics
[AD-A185434] 05 p0575 N88-13504
Stability analysis of finite difference schemes for hyperbolic systems, and problems in applied and computational linear algebra
[AD-A185824] 07 p0908 N88-15499
Techniques in linear and nonlinear partial differential equations
[AD-A187109] 09 p1227 N88-17347
Advances in reliable numerical computation: A summary --- conference
[NPL-DITC-102/87] 09 p1229 N88-17367
PSolve: A concurrent algorithm for solving sparse systems of linear equations
[DE88-003584] 10 p1386 N88-18275
Quasigroup approach to solution of linear algebraic equation systems
[DE88-700595] 10 p1398 N88-18330
Leapfrog variants of iterative methods for linear algebra equations
[NASA-CR-181616] 10 p1398 N88-18332
Schwarz splitting and template operators
[AD-A187956] 10 p1404 N88-18370
Method of reduction of polynomially nonlinear equations to linear equations
[DE88-700922] 12 p1683 N88-20064
Conservative finite volume solutions of a linear hyperbolic transport equation in two and three dimensions using multiple grids
[NASA-CR-182715] 13 p1828 N88-20934
Pointwise stabilization for coupled quasilinear and linear wave equations
[AD-A190031] 15 p2120 N88-22632
Iterative finite element solver on transputer networks
16 p2218 N88-23235
A new block solver for large, full, unsymmetric, complex systems of linear algebraic equations
[AD-A190590] 16 p2256 N88-23483
Solving bidiagonal systems of linear equations on the CDC CYBER 205
[CWI-NM-R8725] 18 p2558 N88-25187
Model reduction methods for control design
[NASA-CR-179434] 19 p2719 N88-26144
Parallel quasi-Newton methods for unconstrained optimization
[AD-A193250] 21 p3003 N88-27812
A review of parallel methods for solving sets of linear equations and their application within optimisation algorithms
[AD-A193137] 21 p3006 N88-27830
The computation of stationary distributions on Markov chains through perturbations
[AD-A193191] 21 p3009 N88-27855
Rational Newton algorithms to compute formal solutions of linear differential equations in an irregular singular point
[RR-704-M] 22 p3140 N88-28670
Second order differential equations in the complex domain
[RR-674-M] 22 p3144 N88-28695

LINEAR FILTERS
NT KALMAN FILTERS
Passage from two-parameters to infinite dimension
[ENST-87C002] 01 p0086 N88-10577
A generalization of order statistic filters: The alpha-trimmed linear filter
[AD-A188125] 07 p0842 N88-15107
Optical correlation using the magneto-optic device
[AD-A192342] 20 p2854 N88-26950
Analytical methods in stochastic control and nonlinear filtering
[AD-A194272] 24 p3426 N88-30388

LINEAR INTEGRATED CIRCUITS
Description, analysis and simulation of a new realization of digital filters
[AD-A187763] 11 p1477 N88-18814

LINEAR OPERATORS
Coordinate-momentum probability operator for point particles in a stationary electromagnetic field
[DE88-701165] 16 p2188 N88-23044
Multicontinuations method and strong regular perturbations of linear operators
[DE88-701375] 16 p2263 N88-23533
Recursive mass matrix factorization and inversion: An operator approach to open- and closed-chain multibody dynamics
[NASA-CR-182516] 23 p3247 N88-29328

LINEAR POLARIZATION
Spectroscopy and nonthermal processes
02 p0252 N88-11594
Observation of instabilities in time during dynamic self-diffraction of light in anisotropic nonhomogeneous medium 06 p0769 N88-14730
Polarization properties of SiO masers
13 p1858 N88-21113
Polarization of molecular fluorescence bands in comets: Recent observations and interpretation
14 p1996 N88-21907
Linear and circular polarization of Comet Halley light
14 p2009 N88-21982

LINEAR PREDICTION
On rate of convergence of equivariation linear prediction estimates of the number of signals and frequencies of multiple sinusoids
[AD-A186034] 07 p0914 N88-15549
Large-aperture sparse array antenna systems of moderate bandwidth for multiple emitter location
[AD-A188409] 12 p1619 N88-19683
Evaluating the performance of the LPC (Linear Predictive Coding) 2.4 kbps (kilobits per second) processor with bit errors using a sentence verification task
[AD-A188573] 12 p1620 N88-19686
Spire based speaker-independent continuous speech recognition using mixed feature sets
[AD-A188834] 12 p1620 N88-19688
Multichannel 2-D power spectral estimation and applications
[AD-A191273] 16 p2191 N88-23068
Analysis and improvement of the vector quantization in SELP (Stochastically Excited Linear Prediction)
19 p2653 N88-25756
An analysis of the efficiency and directivity of the sound generated by a moving laser source
[AD-A192220] 20 p2849 N88-26914
Two biased estimation techniques in linear regression: Application to aircraft
[NASA-TM-100649] 23 p3274 N88-29489

LINEAR PROGRAMMING
A new pivoting rule for the dual network simplex method
[REPT-87-17] 01 p0080 N88-10511
The box method for linear programming. Part 1: Basic theory
[DE87-011029] 01 p0080 N88-10515
A look at the evolution of mathematical software for dense matrix problems over the past fifteen years
[DE87-011485] 01 p0081 N88-10517
Report outline of a programming variable and application through example
[INPE-4211-PRE/1092] 01 p0081 N88-10521
S-step iterative methods for symmetric linear systems
[DE87-010619] 01 p0086 N88-10559
Parallel computation of a domain decomposition method
[DE87-011444] 01 p0086 N88-10560
An analysis of an available set of linear programming test problems
[DE87-014578] 02 p0221 N88-11392
Methods for design and evaluation of integrated hardware/software systems for concurrent computation
[NASA-CR-181522] 04 p0479 N88-12953
Parallel superconvergent multigrid
[DE87-013153] 04 p0480 N88-12960
Computing block-angular Karmarker projections with applications to stochastic programming, revision
[AD-A185647] 06 p0759 N88-14656
Progress in mathematical programming
[AD-A185729] 06 p0759 N88-14658

A multicut algorithm for two-stage stochastic linear programs
[AD-A186148] 07 p0903 N88-15466

Parallel LU-factorization algorithms for dense matrices
[DE88-002179] 07 p0904 N88-15478

Explicit construction and analysis of some efficient empirical production functions in data envelopment analysis
[AD-A185907] 07 p0908 N88-15502

A modal control based limiting performance formulation for shock excited systems 08 p0998 N88-16046

Analytical study of the effect of early warning on optimal shock isolation 08 p0998 N88-16047

Task allocation in a distributed computing system
09 p1206 N88-17230

The impact of hierarchical memory systems on linear algebra algorithm design
[DE88-003574] 10 p1385 N88-18274

Eliminating columns in the simplex method for linear programming
[DE88-004191] 10 p1386 N88-18277

Performance studies of a parallel processor for large linear programming problems
[PB88-121611] 10 p1393 N88-18310

Primal-dual parallel solution of very large sparse linear programs
[AD-A188500] 12 p1680 N88-20045

Linear programming along the trajectory of the problem
[REPT-87-41] 14 p1956 N88-21662

On the trajectory of a linear programming problem
[REPT-87-53] 16 p2250 N88-23442

A mixed-integer linear programming problem which is efficiently solvable
[AD-A191026] 18 p2556 N88-25168

Decomposition of linear programs using parallel computation
[AD-A191716] 18 p2556 N88-25173

A centered projective algorithm for linear programming
[AD-A192100] 18 p2557 N88-25178

A new trajectory following polynomial-time algorithm for the linear programming problem
[REPT-87-87] 20 p2840 N88-26848

A linear-programming method inspired by the neural networks framework
[DE88-008688] 20 p2842 N88-26862

Linear programming in R sup 3 and the skeleton and largest incircle of a convex polygon
[PB88-124664] 20 p2846 N88-26892

Linear programming for Air Force decision aiding
21 p2928 N88-27378

Maximum entropy signal restoration with linear programming
[DE88-011740] 21 p2999 N88-27787

Linear goal programming as a military decision aid
[AD-A194276] 22 p3137 N88-28652

LINEAR QUADRATIC GAUSSIAN CONTROL

A linear quadratic Gaussian with loop transfer recovery proximity operations autopilot for spacecraft
[NASA-CR-172026] 02 p0227 N88-11433

New feedback design methodologies for large space structures: A multi-criterion optimization approach
04 p0408 N88-12535

Closed-loop system analysis using Lyapunov stability theory 04 p0483 N88-12978

Design of low order controllers for robust disturbance rejection in large space structures
[AD-A185202] 05 p0555 N88-13376

Feedback in LQCP (Linear Quadratic Control Problem) with a terminal inequality constraint
[PB87-220034] 06 p0762 N88-14676

Large-angle slewing maneuvers for flexible spacecraft
[NASA-CR-4123] 08 p1000 N88-16060

Attitude control of an artificial satellite through the extension of the linear quadratic regulator theory
[INPE-4407-TDL/304] 12 p1600 N88-19577

Analysis and design of gain scheduled control systems
[NASA-CR-182867] 16 p2163 N88-22904

State covariance assignment of discrete systems: Development and applications 17 p2393 N88-24225

Experiments in adaptive control of a very flexible one link manipulator 20 p2842 N88-26865

Robust finite-dimensional LQG (Linear Quadric Gaussian)-based controllers for a class of distributed parameter systems
[AD-A194872] 24 p3425 N88-30382

LINEAR QUADRATIC REGULATOR

NT LINEAR QUADRATIC GAUSSIAN CONTROL

The design of a turboshaft speed governor using modern control techniques
[NASA-CR-175046] 01 p0053 N88-10339

A LQG regulator for the angular motion of the rotor at a tuned gyroscope
[INPE-4280-PRE/1152] 12 p1631 N88-19759

Optimal discrete-time LQR problems for parabolic systems with unbounded input: Approximation and convergence
[NASA-CR-181673] 18 p2567 N88-25247

LINEAR REGULATOR

U LINEAR QUADRATIC REGULATOR

LINEAR SYSTEMS

Maximum likelihood estimates of parameters in linear systems with process and measurement noise
[DFVLR-FB-87-20] 01 p0083 N88-10532

Extraction and evaluation of Boolean relations for the solution of linear programs in 0-1 variables, volume 1
[ENST-86E023-VOL-1] 02 p0227 N88-11430

Polynomial compensation, inversion, and approximation of discrete time linear systems
[NASA-TM-100027] 03 p0372 N88-12344

A new state space model for the NASA/JPL 70-meter antenna servo controls 04 p0436 N88-12702

Parallel superconvergent multigrid
[DE87-013153] 04 p0480 N88-12960

Closed-loop system analysis using Lyapunov stability theory 04 p0483 N88-12978

Oscillation theory for linear second-order differential systems
[DE87-011393] 04 p0484 N88-12983

The linear characteristic method in XYZ geometry
[DE87-011668] 04 p0484 N88-12984

Tridiagonal approximate factorization method: A preconditioning technique for solving nonsymmetric linear systems suitable to supercomputers
05 p0537 N88-13271

Equivalence of input-output stability and exponential stability for infinite dimensional systems
[TW-276] 05 p0638 N88-13903

Robustness of linear systems
[PB87-220042] 05 p0639 N88-13909

Development of a technique for estimating noise covariances using multiple observers
[NASA-TM-4020] 06 p0669 N88-14098

The solution of large linear inverse problems
06 p0691 N88-14238

Strong consistency of M-estimates for the linear model
[AD-A185487] 06 p0764 N88-14696

Asymptotic normality of poly-t densities with Bayesian applications
[AD-A185718] 06 p0768 N88-14719

The design and implementation of surface acoustic wave devices for linear FM and a new non-linear FM pulse compression technique for radar applications
[AD-A186741] 08 p0980 N88-15922

A direct approach to almost disturbance and almost input-output decoupling
[MEMO-641] 08 p1072 N88-16471

Tensorial calibration. Part 1: First order tensorial calibration
[AD-A186708] 09 p1167 N88-16995

System characterization in nonlinear random vibration
09 p1180 N88-17071

Multicolor numbering of irregular triangular meshes
[AD-A186559] 09 p1217 N88-17298

A method for designing robust multivariable feedback systems
[NASA-CR-182459] 09 p1225 N88-17341

Applications of nonlinear systems theory to control design
[NASA-CR-182485] 09 p1231 N88-17377

Linear theory of generation of longitudinal sound waves in semiconductors upon interband absorption of optical radiation 09 p1234 N88-17397

Dynamic observers as asymptotic limits of recursive filters: Special cases
[AD-A187578] 10 p1397 N88-18324

Linear prediction of stationary vector sequences
[NASA-TM-100069] 10 p1403 N88-18366

Innovative design of composite structures: Further studies in the use of a curvilinear fiber format to improve structural efficiency
[NASA-CR-182576] 11 p1450 N88-18641

A semianalytical technique for sensitivity analysis of unsteady aerodynamic computations
[NASA-TM-100810] 11 p1503 N88-18976

Deterministic equivalent for a continuous linear-convex stochastic control problem
[AD-A187818] 11 p1540 N88-19206

Recursive inversion of externally defined linear systems
[NASA-TM-100070] 11 p1541 N88-19215

A hybrid-stress finite element approach for stress and vibration analysis in linear anisotropic elasticity
[NASA-CR-179311] 12 p1634 N88-19784

Efficient parallel architecture for highly coupled real-time linear system applications
[NASA-CR-182649] 12 p1675 N88-20015

Analysis, estimation, and control for perturbed and singular systems and for systems subject to discrete events
[AD-A188496] 12 p1677 N88-20026

Preconditioned conjugate gradient algorithms and software for solving large sparse linear systems
[DE88-002180] 13 p1816 N88-20849

Further results on the McMillan degree and the Kronecker indices of ARMA models --- input-output relations of linear systems
[EUT-87-E-175] 13 p1827 N88-20925

Regional Conference on the Analysis of the Unbalanced Mixed Model
[AD-A188747] 13 p1830 N88-20943

A new approach to almost decoupling problems for linear and nonlinear systems
[MEMO-660] 14 p1962 N88-21700

Bilinear systems in the frequency domain and an application to optimal control
[RR-320] 14 p1962 N88-21704

Boundary stabilization of the reaction-diffusion equation with unilateral conditions
[RR-315] 14 p1964 N88-21720

Parametric methods of analysing linear and nonlinear systems
[RR-318] 14 p1967 N88-21741

The theory of flotation
[NASA-TT-20278] 16 p2207 N88-23172

Feedback decoupling and stabilization for linear systems with multiple exogenous variables
[ETN-88-92245] 16 p2255 N88-23474

Optimal control, estimation compensation of linear discrete-time systems with stochastic parameters
[REPT-87-56] 16 p2255 N88-23478

Formal solution of differential linear systems in the proximity of a singularity
[ETN-88-92190] 16 p2258 N88-23495

Derivative arrays, geometric control theory and realizations of linear descriptor systems
[AD-A190882] 16 p2260 N88-23513

The LDCM actuator for vibration suppression
[NASA-CR-182898] 17 p2335 N88-23940

State covariance assignment of discrete systems: Development and applications 17 p2393 N88-24225

Robust adaptive regulation without persistent excitation
[NASA-TM-100571] 18 p2561 N88-25204

Linear and nonlinear acoustic wave propagation in the atmosphere
[NASA-CR-4157] 18 p2571 N88-25268

Structural properties of multivariable linear systems
[PB88-181375] 19 p2717 N88-26134

Characterization of accelerating pipe flow
[AD-A193065] 21 p2943 N88-27481

Approximation problems of the Hilbert transform to identify minimum phase linear systems
[FUB-42-1986] 21 p2999 N88-27790

Asymptotic orders of reachability in perturbed linear systems
[AD-A192718] 22 p3143 N88-28688

Linear thyratron
[AD-A194111] 23 p3208 N88-29094

Improved finite strip Mindlin plate bending element using assumed shear strain distributions
[NASA-TM-100928] 23 p3225 N88-29195

Robust control of multivariable and large scale systems
[AD-A194250] 23 p3266 N88-29441

Topics in adaptive control and inference
[AD-A194718] 23 p3266 N88-29443

Linearized model matching for single-imput nonlinear systems
[AD-A193642] 23 p3266 N88-29445

Feedback stabilization of du/dt=Au + bf in Hilbert space when the normalization function is less than or equal to r
[AD-A193510] 23 p3277 N88-29506

Performance of DS/SSMA communications in impulsive channels. Part 1: Correlation receivers
[AD-A195712] 24 p3362 N88-30021

Increasing accuracy in evaluating vector of state under conditions of incomplete observability of expanded system 24 p3446 N88-30511

LINEAR TRANSFORMATIONS

Stochastic filtering solutions for ill-posed linear problems and their extension to measurable transformations
[AD-A186016] 07 p0909 N88-15506

Study of microcomputer-based real-time programmable optical signal processor and application
[AD-A190076] 15 p2133 N88-22726

LINEAR VIBRATION

Vibration and buckling of geometrically imperfect laminated cylindrical shells 04 p0456 N88-12822

Theoretical investigations of chaotic dynamics
[AD-A186404] 07 p0867 N88-15261

Parametric and experimental analysis using a power flow approach
[NASA-CR-182460] 09 p1116 N88-16693
Method for finding principal modes of nonlinear vibration systems and their stabilities 14 p1899 N88-21340

LINEARITY
NT COLLINEARITY
Linear emittance damper with megagauss fields
[DE87-013562] 01 p0093 N88-10606
Total linearisation method for solving viscous free boundary flow problems by the finite element method
[PB87-222337] 04 p0441 N88-12737
Numerical methods for reaction-diffusion problems with non-differentiable kinetics
[AD-A185405] 05 p0641 N88-13923
Comments on the theory of absolute and convective instabilities
[PB87-124624] 06 p0783 N88-14808
Estimation and testing in truncated and nontruncated linear median-regression models
[AD-A186317] 07 p0911 N88-15522
Conditionally unbiased bounded influence robust regression with applications to generalized linear models
[AD-A186319] 07 p0915 N88-15556
Test of linearity in general regression models
[AD-A186036] 08 p1073 N88-16477
Consistent linearization of the element-independent corotational formulation for the structural analysis of general shells
[NASA-CR-178418] 09 p1181 N88-17078
Application of empirical and linear methods to VSTOL powered-lift aerodynamics
[NASA-TM-100048] 10 p1267 N88-17581
Parametric study of choke flutter with a linear theory
10 p1283 N88-17673
On the stability of the supersonic boundary layer
11 p1435 N88-18561
Estimation in linear models with censored data
[AD-A187209] 11 p1540 N88-19203
Linear state space modeling of a turbofan engine
[AD-A190110] 15 p2019 N88-22035
An integral equation for the linearized supersonic flow over a wing
[AD-A191408] 16 p2158 N88-22875
The application of linear maximum likelihood estimation of aerodynamic derivatives for the Bell-205 and Bell-206
[AD-A191279] 16 p2161 N88-22894
Automated cartographic generalization for linear map features 18 p2532 N88-25021
Linear spaces, absolute retracts and the compact extension property
[PB88-181110] 18 p2564 N88-25225
A full but elementary treatment of systems of homogeneous ordinary linear differential equations with constant coefficients
[REPT-87-82] 20 p2845 N88-26887
On linear relationship between shock velocity and particle velocity
[DE88-701827] 20 p2880 N88-27099
On solvability of an equation arising in the theory of M-estimates
[AD-A193059] 21 p3006 N88-27828
An integral equation for the linearized unsteady supersonic flow over a wing
[AD-A193773] 23 p3172 N88-28887
Automatic classification of digitally modulated signals
[AD-A194623] 23 p3203 N88-29064
A linear-time algorithm for finding a minimum spanning pseudoforest
[AD-A194029] 23 p3250 N88-29346
Wigner distribution function: Relation to short-term spectral estimation, smoothing and performance in noise
[AD-A193865] 23 p3275 N88-29492
Formulation and solution of economic equilibrium problems
[AD-A196034] 24 p3439 N88-30470

LINEARIZATION
Linearized aeroelastic analysis of a wind turbine with a two-bladed rotor
[ETN-87-90600] 03 p0347 N88-12192
Numerical analysis of supersonic flows using panel method 05 p0537 N88-13266
Prediction of the response and optimal control of stochastic parametrically and externally excited nonlinear systems 11 p1496 N88-18930
Nonlinear input-output systems
[NASA-CR-182484] 11 p1535 N88-19171
Method of reduction of polynomially nonlinear equations to linear equations
[DE88-700922] 12 p1683 N88-20064
Transport and stability properties of free shear flows
13 p1768 N88-20577
User's manual for LINEAR, a FORTRAN program to derive linear aircraft models
[NASA-TP-2768] 14 p1967 N88-21740
Some numerical methods for the computation of capillary free boundaries governed by the Navier-Stokes equations
[REPT-87-69] 16 p2206 N88-23167
Linearization along invariant manifolds and a generalization of the Hartman-Grobman theorems for degenerate singularities of vector fields in R cubed
[REPT-87-80] 20 p2845 N88-26886
On the pseudo-linearization problem for nonlinear systems
[AD-A194021] 22 p3142 N88-28683
An approach to CMG steering using feedback linearization
[NASA-CR-183172] 24 p3422 N88-30369

LINERS
U LININGS

LINES (GEOMETRY)
NT GEODESIC LINES
Development of a line-drawing algorithm
[CS-8701] 01 p0082 N88-10530
Computing the bounded region determined by finitely many lines in the plane
[CS-8703] 01 p0086 N88-10558

LINES OF FORCE
Acceleration of auroral particles by magnetic field-aligned electric fields 08 p1031 N88-16246
Acceleration/heating processes on auroral field lines as observed by the Viking spacecraft
08 p1096 N88-16596
Simultaneous observation of upward moving field aligned energetic electrons and ions on auroral zone field lines
[IRF-PREPRINT-102] 16 p2231 N88-23326

LINGUISTICS
NT MACHINE TRANSLATION
NT SEMANTICS
NT SYLLABLES
NT SYNTAX
NT WORDS (LANGUAGE)
Antithesis: A study in clause combining and discourse structure
[AD-A184789] 03 p0368 N88-12313
Space languages 08 p1063 N88-16420
Quantitative and qualitative assessments of the impact of linguistic theory on information science
10 p1424 N88-18507
Linguistic and cultural barriers to the transfer of information 24 p3437 N88-30459
Linguistic-technical aspects of machine translation
24 p3438 N88-30461
Linguistic barriers: Translation problems
24 p3438 N88-30465

LININGS
Turbine Engine Hot Section Technology, 1985
[NASA-CP-2405] 02 p0184 N88-11140
An analysis of sound absorbing linings for the interior of the NASA Ames 80 x 120-foot wind tunnel
[NASA-CR-177396] 04 p0488 N88-13006
Fabric space radiators
[DE88-005569] 14 p1880 N88-21237
High-temperature combustor liner tests in structural component response test facility
15 p2077 N88-22383
Life assessment of combustor liner using unified constitutive models 15 p2077 N88-22384
Compositional redistribution during casting of Hg sub 0.8 Cd sub 0.2 Te alloys
[NASA-TM-101151] 17 p2326 N88-23893
Basic mechanisms of diesel lubrication correlation of bench and engine tests
[AD-A193360] 21 p2956 N88-27561

LINKAGES
Assessment of the COFSI/MAST I project
[NASA-CR-181366] 01 p0053 N88-10340
Kinematic optimization of mechanisms, a finite element approach
[ISBN-90-370-0012-6] 09 p1175 N88-17039
Dynamic response of a geared train of rotors subjected to random support excitations 09 p1181 N88-17073
The dynamics of an oscillating four-bar linkage
09 p1181 N88-17074
Adaptive control of a manipulator with a flexible link
[NASA-CR-181637] 11 p1476 N88-18807
Improvement in robot positioning accuracy by a kinematic identification model 11 p1496 N88-18931
Dynamics of high-speed mechanisms with elastic members 13 p1779 N88-20643
A three dimensional non-singular modelling of rigid manipulators
[AD-A189707] 15 p2116 N88-22604
Payload deployment method and system
[NASA-CASE-MSC-21330-1] 18 p2470 N88-24660
Skin friction balance
[NASA-CASE-LAR-13710-1] 23 p3216 N88-29145

LINKING
U JOINING

LIOUVILLE THEOREM
Systems near the onset and in the well-developed regimes of turbulence
[DE88-005365] 13 p1766 N88-20565

LIPIDS
NT ALDOSTERONE
NT CORTICOSTEROIDS
Development of microencapsulation techniques
[AD-A185019] 05 p0567 N88-13457
Effects of extreme hypoxia on phospholipid metabolism in subcellular structures of rat brain
08 p1046 N88-16323
Factors governing light driven electron and proton translocation in proteins across membranes
[DE88-002716] 08 p1082 N88-16519
Lipid peroxidation in rat tissues with exposure to antiorthostatic hypokinesia, exercise and immobilization stress 10 p1365 N88-18159
Studies of model ion channels in defect-free multibilayers of phospholipids
[AD-A188740] 16 p2238 N88-23365
Significance of nutrition to change in human carbohydrate and lipid metabolism under emotional stress 19 p2703 N88-26073

LIPSCHITZ CONDITION
Convergence of Runge-Kutta methods on classes of stiff initial value problems
[CWI-NM-R8717] 13 p1827 N88-20924
The global convergence of partitioned BFGS on problems with convex decompositions and Lipschitzian gradients
[DE88-006249] 14 p1968 N88-21744
Detection of the number, locations and magnitudes of jumps
[AD-A190328] 15 p2125 N88-22671
Incomplete Lipschitz-Hankel integrals of MacDonald functions
[AD-A191034] 16 p2261 N88-23515
Perturbation theory for dual semigroups. Part 3: Nonlinear Lipschitz continuous perturbations in the Sun-reflexive case
[CWI-AM-R8706-PT-3] 16 p2263 N88-23535

LIQUEFACTION
NT COAL LIQUEFACTION
Proceedings of the 1987 Biomass Thermochemical Conversion Contractors' Review Meeting
[DE88-006730] 18 p2535 N88-25041
An advanced extruder-feeder biomass liquefaction reactor system 18 p2535 N88-25042

LIQUEFIED GASES
NT LIQUEFIED NATURAL GAS
NT LIQUID AMMONIA
NT LIQUID HELIUM
NT LIQUID HELIUM 2
NT LIQUID HYDROGEN
NT LIQUID NITROGEN
NT LIQUID OXYGEN

LIQUEFIED NATURAL GAS
An investigation of high pressure/late cycle injection of CNG (Compressed Natural Gas) as a fuel for rail applications
[DE88-009000] 19 p2677 N88-25917

LIQUID AIR CYCLE ENGINES
Auxiliary propulsion technology for advanced Earth-to-orbit vehicles
[NASA-TM-100237] 06 p0674 N88-14127

LIQUID ALLOYS
Liquid alloys: New perspectives and challenges
[DE88-005935] 13 p1750 N88-20463
Fluid flow modeling in casting processes and its implications
[DE88-010009] 20 p2810 N88-26671

LIQUID AMMONIA
Ammonia transfer across rotating joints in space
14 p1927 N88-21492
Ammonia cleanup of lithium containing components
17 p2403 N88-24287
Ammonia boiling in long tubes. Heat transfer and charge loss in vertical and horizontal tubes
[NASA-TT-20313] 19 p2667 N88-25858

LIQUID ATOMIZATION
Stability relationship for water droplet crystallization with the NASA Lewis icing spray
[NASA-TM-100220] 02 p0125 N88-10790
Droplet formation for liquid monopropellant jets
[AD-A187172] 10 p1331 N88-17956
Dense-spray structure and phenomena. Part 2: Pressure-atomized sprays
[AD-A190312] 15 p2064 N88-22307
Effect of mass-velocity on liquid jet atomization in Mach 1 gasflow
[NASA-TM-100813] 16 p2211 N88-23194
Atomization of alternative fuels
24 p3345 N88-29913
Turbulence effects on the droplet distribution behind airblast atomizers 24 p3346 N88-29915

Influence of operating conditions on the atomization and distribution of fuel by air blast atomizers
24 p3346 N88-29918
Spray performance of a vaporizing fuel injector
24 p3346 N88-29919
The characterizatin of combustion by fuel composition: Measurements in a small conventional combustor
24 p3346 N88-29920
The performance of a surrogate blend in simulating JP-4 in a spray-fueled combustor 24 p3347 N88-29926

LIQUID CHROMATOGRAPHY
Application of high performance liquid chromatography to the fast determination of bitumen generic composition
[PC-2] 02 p0145 N88-10911
Study of the properties of a new detector class for liquid chromatography
[DE88-001666] 05 p0563 N88-13426
Chromatographic and related reactors
[AD-A188452] 12 p1605 N88-19599
Electrosorptive detection of simple organic compounds in liquid chromatography
[AD-A188757] 13 p1736 N88-20376
Fuels combustion research
[AD-A189114] 13 p1736 N88-20381
Determination of the partition coefficients of organophosphorus compounds using high-performance liquid chromatography
[AD-A189276] 13 p1737 N88-20385
Development and evaluation of supercritical fluid chromatography-mass spectrometry
[DE88-005122] 13 p1738 N88-20394
Instrumental aspects of capillary supercritical fluid chromatography
[ETN-88-92242] 16 p2174 N88-22960
Determination of low molecular weight thiols using monobromobimane fluorescent labeling and high-performance liquid chromatography
[NASA-CR-182932] 19 p2608 N88-25478

LIQUID COOLED REACTORS
NT BOILING WATER REACTORS
NT EXPERIMENTAL BREEDER REACTOR 2
NT LIGHT WATER REACTORS
NT LIQUID METAL COOLED REACTORS
NT PRESSURIZED WATER REACTORS
NT ZERO POWER REACTORS
Gas-cooled reactor power systems for space
17 p2413 N88-24350

LIQUID COOLING
NT FILM COOLING
Water source heat pump: How to get home heating and cooling from your own back yard
[DE88-900180] 07 p0875 N88-15306
Single phase liquid immersion cooling of discrete heat sources in a vertical channel
[AD-A191224] 17 p2337 N88-23944
The liquid droplet radiator in space: A parametric approach 17 p2427 N88-24437
Forced-convection, liquid-cooled, microchannel heat sinks
[AD-A193337] 21 p2937 N88-27444

LIQUID CRYSTALS
The development of a new and novel Hadamard transform infrared spectrometer for analytical chemistry
[DE87-014804] 02 p0175 N88-11094
Near-infrared dichroism of a mesogenic transition metal complex and its solubility in nematic hosts
[DE87-014471] 03 p0287 N88-11805
New theory for competing interactions and microstructures in partially-ordered (liquid-crystalline) phases
[DE87-014739] 03 p0380 N88-12389
Boundary effects on the drag of an oscillating sphere: Applications to the magnetic sphere rheometer. Attenuation and dispersion of acoustic waves in nematic liquid crystals 04 p0488 N88-13007
Guest-host interactions in thermotropic and lyotropic liquid crystals
[AD-A184402] 04 p0496 N88-13057
Observation of instabilities in time during dynamic self-diffraction of light in anisotropic nonhomogeneous medium 06 p0769 N88-14730
Thermoplastic elastomers as LOVA binders
[AD-A185865] 07 p0835 N88-15068
X-ray diffraction study of thermotropic liquid crystalline polyesters and diester model compounds
[AD-A186788] 09 p1255 N88-17521
Brightness contrast and character height of five flat panel computer displays
[AD-A187743] 11 p1524 N88-19096
Continuous collective molecule rotation of a nematic liquid crystal induced from light angular momentum
[FUB-17-1986] 14 p1986 N88-21845
Electronic and ionic transport in polymers
[AD-A190434] 15 p2045 N88-22185
Collective rotation of molecules driven by the angular momentum of light in a nematic film
[FUB-6-1986] 15 p2131 N88-22714
Basic design studies for the realization of liquid crystal display systems in aircraft
[VA-87-001] 16 p2163 N88-22900
Electrochemistry in liquid crystals
[AD-A191554] 18 p2481 N88-24719
Liquid crystal optics for laser systems
[DE88-008475] 20 p2854 N88-26948
Liquid crystals for unsteady surface shear stress visualization
[DE88-010570] 21 p2951 N88-27527
Interactions in miscible polymer blends
[AD-A193824] 22 p3058 N88-28144
Quasi-liquid crystalline materials with special electro-optic properties
[AD-A194579] 23 p3282 N88-29544
Thermodynamical, optical and X-rays studies of some thermotropic liquid crystals
[DE88-702301] 23 p3290 N88-29590

LIQUID DROPS
U DROPS (LIQUIDS)

LIQUID FILLED SHELLS
Internal fluid dynamics within a nonspinning partially liquid-filled shell due to burster rupture
[AD-A191055] 18 p2507 N88-24874
Theoretical investigation of the development of the normal fluid and superfluid velocity distributions during spin-up for a He2-filled cylinder
[MPIS-6/1987] 18 p2510 N88-24892
Liquid motions in partially filled containers: Preliminary results of the D-1 mission --- Spacelab
[NLR-MP-86042-U] 20 p2802 N88-26629
Nonlinear oscillations of a nonviscous cylindrical liquid system in weightlessness condition
[LRT-WE-9-FB-14(1987)] 22 p3063 N88-28175
Nonlinear liquid motion in conical containers
[LRT-WE-9-FB-10(1987)] 22 p3077 N88-28270
Nonlinear hydroelastic vibrations in rectangular containers
[LRT-WE-9-FB-7(1987)] 22 p3088 N88-28340
Computational fluid dynamics methods for low Reynolds number precessing/spinning incompressible flows
[AD-A193891] 23 p3212 N88-29119
Numerical calculations of the response of a spinning spheroidal payload to coning motion
[AD-A195890] 24 p3368 N88-30059

LIQUID FLOW
NT OPEN CHANNEL FLOW
NT WATER FLOW
Gas diffusion studies in steady and nonsteady cavities
[AD-A185795] 06 p0704 N88-14318
An investigation into flow regimes for two-phase helium flow
[DE88-002834] 07 p0853 N88-15181
Experimental and numerical study of liquid distribution in dispersive-annular flow
[DE88-700844] 14 p1909 N88-21406
Dense-spray structure and phenomena. Part 1: Turbulence/dispersed-phase interactions
[AD-A190606] 15 p2065 N88-22315
Fluid motion in a spinning, coning cylinder via spatial eigenfunction expansion
[AD-A190758] 15 p2066 N88-22319
Development of a liquid-fed water resistojet
[NASA-TM-100927] 18 p2523 N88-24968

LIQUID FUELS
NT AIRCRAFT FUELS
NT ANTIMISTING FUELS
NT AUTOMOBILE FUELS
NT DIESEL FUELS
NT GASOLINE
NT HYDROGEN FUELS
NT JET ENGINE FUELS
NT JP-4 JET FUEL
NT JP-5 JET FUEL
NT JP-8 JET FUEL
NT KEROSENE
Droplet formation for liquid monopropellant jets
[AD-A187172] 10 p1331 N88-17956
Dense-spray structure and phenomena. Part 2: Pressure-atomized sprays
[AD-A190312] 15 p2064 N88-22307
The burning of HAN-based (hydroxylammonium nitrate) liquid propellants
[DE88-006863] 18 p2494 N88-24800
Electrical ignition of HAN-based liquid propellants
[AD-A191349] 18 p2495 N88-24801
Low pressure entrained flow pyrolysis of biomass to produce liquid fuels 18 p2535 N88-25043
Low-temperature thermochemical conversion of high moisture biomass feedstocks 18 p2536 N88-25047
Chemical/hydrogen energy systems
[DE88-007013] 19 p2687 N88-25969
An outdoor test facility for the large-scale production of microalgae
[DE88-001146] 21 p2984 N88-27723
Combustion studies of acoustically suspended liquid droplets
[AD-A193892] 23 p3192 N88-28998

LIQUID HELIUM
NT LIQUID HELIUM 2
Components for cryostat --- spaceborne
[MBB/ISO-TN-CD00.003-REV-A]
01 p0032 N88-10207
Study of helium transfer technology for STICCR: Fluid management
[NASA-CR-177463] 10 p1291 N88-17720
Development of a motorized cryovalve for the control of superfluid liquid helium 14 p1925 N88-21477
Calorimetric technique for measuring liquid helium flow rate
[DE88-701308] 16 p2200 N88-23123
Peculiarities of non-stationary heat transfer to superfluid helium
[DE88-701174] 16 p2200 N88-23124
Preliminary study of niobium alloy contamination by transport through helium 17 p2402 N88-24279
Superfluid turbulence in counterflowing helium II
19 p2665 N88-25849
Superfluid Helium On-Orbit Transfer (SHOOT) operatons
[NASA-TM-101009] 22 p3048 N88-28084
An experimental setup for the study of polarized He3 and dilute He3-He4 mixtures
[B8705589] 23 p3193 N88-29001

LIQUID HELIUM 2
Theoretical investigation of the development of the normal fluid and superfluid velocity distributions during spin-up for a He2-filled cylinder
[MPIS-6/1987] 18 p2510 N88-24892

LIQUID HYDROGEN
Advanced fabrication techniques for hydrogen-cooled engine structures
[NASA-CR-3949] 06 p0723 N88-14447
Development of on-orbit fluid gaging techniques
08 p0982 N88-15936
Some problems of the theory of bubble growth and condensation in bubble chambers
[NASA-TT-20232] 13 p1771 N88-20593
Theory of Muon method for study of solid and liquid hydrogen 14 p1972 N88-21770
Rotor self-lubricating axial stop
[NASA-CASE-MFS-28273-1] 17 p2344 N88-23974

LIQUID INJECTION
NT WATER INJECTION

LIQUID LASERS
Bibliography of Soviet laser developments, number 88, March - April 1987
[AD-A195978] 24 p3378 N88-30116

LIQUID LITHIUM
Corrosion of ferritic steels by molten lithium: Influence of competing thermal gradient mass transfer and surface product reactions
[DE88-000334] 04 p0417 N88-12585
Ammonia cleanup of lithium containing components
17 p2403 N88-24287
Transient analysis of Li and LiH thermal storage spheres 17 p2411 N88-24334
Fabrication of a niobium 1 percent zirconium containment for SP-100 primary lithium system materials mass transfer studies 17 p2417 N88-24373
Liquid metal testing at ETEC for the SP-100 program
17 p2428 N88-24446
An evaluation of some thermodynamic and transport properties of solid and liquid lithium over the temperature range 200 to 1700 K
[DE88-008947] 19 p2614 N88-25512

LIQUID MERCURY
U MERCURY (METAL)

LIQUID METAL COOLED REACTORS
NT EXPERIMENTAL BREEDER REACTOR 2
Fast critical experiment data for space reactors
[DE87-007005] 01 p0093 N88-10605
Detecting the gas bubbles in a liquid metal coolant by means of magnetic flowmeters
[DE88-701427] 15 p2062 N88-22294
Status of CEA design and simulation studies of a 200 KWe turboelectric space power system
17 p2400 N88-24268
Conceptual design of the SP-100 GES test site
17 p2402 N88-24284
Selection of a handling and maintenance option for the SP-100 ground engineering system test
17 p2402 N88-24285
Fast critical experiment data for space reactors
17 p2403 N88-24286
A review of diffusion barrier technology for application in SP-100 fuel pins 17 p2410 N88-24328

Liquid-metal MHD power conversion for space electric systems 17 p2411 N88-24338
Studies for the definition of a Faraday converter for space nuclear systems 17 p2411 N88-24339
A liquid metal MHD concept for multimegawatt space power application 17 p2413 N88-24348
Nuclear Rankine/flywheel MMW space power concept
17 p2413 N88-24349
A dynamic model for the aft accumulator in the TE SP-100 system 17 p2414 N88-24354
Parametric analyses of the TE SP-100 system performance 17 p2415 N88-24358
Advanced LMMHD space power generation concept
17 p2415 N88-24364
Transient analyses of multimegawatt space reactors
17 p2430 N88-24456

LIQUID METAL FAST BREEDER REACTORS
Computation of failure probability of fatigue loaded cracked structures
[ETN-88-92360] 21 p2964 N88-27607

LIQUID METALS
NT LIQUID LITHIUM
NT LIQUID POTASSIUM
NT LIQUID SODIUM
NT MERCURY (METAL)
NT MERCURY VAPOR
Formation of amorphous alloys by solid state reactions
[DE87-013175] 02 p0146 N88-10918
Thermodynamics of interaction between nitrogen and molten nickel alloys
[BLL-M-37309-(5828.4)] 02 p0149 N88-10934
Relationships governing change in density in liquid ferrous alloys
[BLL-M-37305-(5828.4)] 02 p0149 N88-10935
Birch's law and the properties of high temperature fluid metals
[DE87-014744] 03 p0288 N88-11807
Cast iron freezing mechanisms
03 p0298 N88-11870
Corrosion strength of niobium and its alloys
[DE87-703693] 04 p0416 N88-12578
Inertial confinement fusion reactor cavity analysis
[DE88-000788] 04 p0492 N88-13028
The use of alloy 117 as a liquid metal current collector
[AD-A185740] 06 p0698 N88-14281
Spray deposition: A fundamental study of droplet impingement, spreading and consolidation
[AD-A186627] 08 p0970 N88-15869
The application of liquid-metal MHD (magnetohydrodynamics) to renewable energy sources
[DE88-003083] 09 p1251 N88-17495
Thermodynamics of wetting by liquid metals
[DE88-003634] 11 p1563 N88-19360
Liquid alloys: New perspectives and challenges
[DE88-005935] 13 p1750 N88-20463
Hydrodynamical regimes in molten metals under a horizontal temperature gradient
14 p1988 N88-21859
Electrical resistivities of some compound forming liquid metal alloys
[PB88-145172] 15 p2037 N88-22137
Angular resolved energy analysis of (69)Ga+ ions from a gallium liquid metal ion source
[AERE-R-12649] 15 p2139 N88-22760
A theoretical and experimental study of the thermophysical properties of lithium hydride
[NASA-TT-20179] 16 p2175 N88-22965
Detailed transient model of a liquid-metal heat pipe
17 p2412 N88-24345
A transient model for liquid metal heat pipes
17 p2421 N88-24398
The THROHPUT code: Thermohydraulic heat pipe modeling 17 p2421 N88-24399
Possible creep studies of lithium with a compact device 17 p2422 N88-24404
Review of alkali metal and refractory alloy compatibility for Rankine cycle applications 17 p2428 N88-24447
Nucleate pool boiling: High gravity to reduced gravity; liquid metals to cryogens 17 p2431 N88-24464
Liquid metal thermal electric converter theoretical and experimental studies
[DE88-008806] 19 p2688 N88-25974
MHD (magnetohydrodynamic) thermal hydraulic analysis of three-dimensional liquid metal flows in fusion blanket ducts
[DE88-009929] 19 p2731 N88-26219
Blanket technology experiments at Argonne National Laboratory
[DE88-010006] 19 p2731 N88-26220
Development of liquid metal field-emission sources for use in fast repetitive opening switches
[AD-A192230] 20 p2795 N88-26583
A method for determining the solubility of hydrogen in molten aluminum-lithium alloys
[DE88-009807] 21 p2910 N88-27270
Liquid metal thermal-electric converter electrode development
[DE88-009252] 23 p3230 N88-29221
Some theoretical considerations of the surface tension of liquid metals for metal matrix composites
[AD-A195999] 24 p3340 N88-29882

LIQUID NITROGEN
Chemical equilibrium calculations for the high pressure and temperature dissociation of liquid nitrogen
[DE87-013786] 01 p0021 N88-10135
The dissociation of dense liquid nitrogen and shock cooling
[DE87-013490] 01 p0022 N88-10136
Vibrational spectroscopy of shock-compressed fluid N2 and O2
[DE87-013138] 03 p0313 N88-11979
Hot carrier effects in CMOS field effect transistors at cryogenic temperatures 19 p2662 N88-25829

LIQUID OXIDIZERS
Bipropellant combustion in a liquid rocket combustion chamber 13 p1733 N88-20359

LIQUID OXYGEN
Vibrational spectroscopy of shock-compressed fluid N2 and O2
[DE87-013138] 03 p0313 N88-11979
Seal technology for liquid oxygen (LOX) turbopumps
[NASA-CR-174866] 05 p0591 N88-13603
Fluid mass and thermal loading effects on the modal characteristics of space shuttle main engine liquid oxygen inlet splitter vanes 05 p0594 N88-13628
Oxygen chemisorption cryogenic refrigerator
[NASA-CASE-NPO-16734-1-CU]
06 p0689 N88-14223
The determination of equivalent bearing loading for the BSMT that simulate SSME high pressure oxidizer turbopump conditions using the SHABERTH/SINDA computer programs 07 p0925 N88-15623
Development of on-orbit fluid gaging techniques
08 p0982 N88-15936
A lunar transportation system
[NASA-CR-182561] 11 p1567 N88-19379
Rotor self-lubricating axial stop
[NASA-CASE-MFS-28273-1] 17 p2344 N88-23974
Carbon deposition model for oxygen-hydrocarbon combustion, volume 2
[NASA-CR-179376] 21 p2908 N88-27255

LIQUID PHASE EPITAXY
Growth of HgZnTe layers by LPE technique
[AD-A186723] 09 p1255 N88-17520
Investigation of defect and electronic interactions associated with GaAs device processing
[AD-A188021] 11 p1556 N88-19313
Growth of Pb/sub 1-x/Eu/sub x/Te epitaxial layers by the liquid phase epitaxy technique
[DE88-701022] 15 p2139 N88-22763
Electrical and optical properties of Hg/sub 1-x/Cd/sub x/Te doped layers grown by Liquid Phase Epitaxy (LPE)
[DE88-701023] 16 p2281 N88-23653
Lattice-matched HgZnTe epitaxy development
[AD-A193677] 23 p3292 N88-29600

LIQUID PHASES
Physical properties of immiscible polymers
03 p0297 N88-11868
The role of electronic structure calculation in mechanistic analysis of electron transfer reactions in the liquid phase
[DE87-014395] 05 p0647 N88-13963
Visible InGaAsP/GaAsP lasers produced by epitaxial growth from liquid phase 09 p1237 N88-17416
Progress in the computer modeling of the liquid phase behavior of a liquid metal heat pipe
17 p2412 N88-24342
Microgravity thaw experiment (MITEX)
17 p2427 N88-24439
Liquid-phase oxidation of acetone with hydrogen peroxide on oxide catalysts 19 p2706 N88-26091
Electronic states of the Xe(sub n)HCl systems in gas and condensed phases
[AD-A193881] 23 p3192 N88-28997

LIQUID POTASSIUM
Design of a high-power-density Ljungstroem turbine using potassium as a working fluid
17 p2409 N88-24323
Nuclear Rankine/flywheel MMW space power concept
17 p2413 N88-24349

LIQUID PROPELLANT ROCKET ENGINES
NT HYDRAZINE ENGINES
NT HYDROGEN OXYGEN ENGINES
NT LIQUID AIR CYCLE ENGINES
NT SPACE SHUTTLE MAIN ENGINE
Space station resistojet system requirements and interface definition study
[NASA-CR-180832] 04 p0409 N88-12541
Zero-G thermodynamic vent system for shuttle/Centaur 08 p0983 N88-15943
Durability testing of an iridium-plated storable rocket engine injector
[AD-A190707] 15 p2027 N88-22078
The 24th JANNAF Combustion Meeting, volume 2
[AD-A190164] 19 p2622 N88-25554
Development of a generic combustion stability code for liquid propellant rocket engines
19 p2626 N88-25576
Breadboard RL10-2B low-thrust operating mode (second iteration) test report
[NASA-CR-182160] 24 p3338 N88-29867
Oxidizer heat exchanger component test
[NASA-CR-182159] 24 p3339 N88-29876

LIQUID ROCKET PROPELLANTS
NT CRYOGENIC ROCKET PROPELLANTS
NT GELLED ROCKET PROPELLANTS
NT MONOPROPELLANTS
NT RP-1 ROCKET PROPELLANTS
NT SLURRY PROPELLANTS
Performance analysis of advanced spacecraft TPS
[NASA-CR-181532] 04 p0399 N88-12484
Space station resistojet system requirements and interface definition study
[NASA-CR-180832] 04 p0409 N88-12541
Dynamics of propellant feedline systems
[AD-A184865] 05 p0580 N88-13537
Computational prediction of propellant reorientation
08 p0982 N88-15940
Low gravity liquid motions in spacecraft
08 p0982 N88-15941
Peacekeeper tank slosh model
08 p0983 N88-15942
An infra-red investigation of HAN (Hydroxylammonium Nitrate)-based liquid propellants
[AD-A187226] 10 p1307 N88-17815
Bipropellant combustion in a liquid rocket combustion chamber 13 p1733 N88-20359
Performance of a hydrogen pulsed electrothermal thruster. Strategic defense initiative organization innovative science and technology. SBIR, phase 1
[AD-A191999] 18 p2475 N88-24679
A dynamic model of liquid propellant combustion
19 p2622 N88-25556
Dynamical properties of a collapsing spherical cavity
19 p2623 N88-25562
Pressure/temperature sensitive inorganic phosphors
19 p2627 N88-25583
Liquid Engine Jet Atomization Workshop report
19 p2627 N88-25584

LIQUID ROTATION
U ROTATING LIQUIDS

LIQUID SLOSHING
Calculation of the eigenvibrations of axisymmetric fluid configurations with a singularity method, taking into account surface tension effects under reduced gravity
[ETN-87-90438] 01 p0048 N88-10304
Computational prediction of propellant reorientation
08 p0982 N88-15940
Low gravity liquid motions in spacecraft
08 p0982 N88-15941
Peacekeeper tank slosh model
08 p0983 N88-15942
Spatial pressure variations and three-dimensional effects on liquid sloshing loads
[PB88-120134] 10 p1326 N88-17926
The nonlinear dynamics of a spacecraft coupled to the vibration of a contained fluid
[DE88-007035] 16 p2168 N88-22925
Axisymmetric liquid sloshing under low-g conditions: Numerical simulation method (reference manual)
[NLR-TR-86057-U] 20 p2802 N88-26627
Liquid oscillations in a prolate spheroidal container
[LRT-WE-9-FB-4(1988)] 22 p3078 N88-28276

LIQUID SODIUM
Sodium heat engine/AMTEC system experiments
17 p2409 N88-24325

LIQUID SURFACES
New equilibrium forms of free surface of confined magnetic fluid 06 p0770 N88-14734
Liquid motions in partially filled containers: Preliminary results of the D-1 mission --- Spacelab
[NLR-MP-86042-U] 20 p2802 N88-26629
Development of computer-controlled thermogravimetric instrumentation for measurement of environmental and high temperature volatilization and desorption of contaminants from polymeric materials
[AD-A195934] 24 p3343 N88-29900
Effect of interfacial phenomena on contact line heat Transfer-3
[AD-A194941] 24 p3343 N88-29901

LIQUID WASTES
NT URINE
NT WASTE WATER
Space station resistojet system requirements and interface definition study
[NASA-CR-180832] 04 p0409 N88-12541

LIQUID-GAS MIXTURES
NT AEROSOLS
NT FOG

Thermodynamic properties for natural gas binaries
[PB87-226833] 04 p0500 N88-13074

Theoretical and experimental investigation of swirl flow phase separators for microgravity applications
17 p2411 N88-24335

Experimental investigation of a microgravity separator for two phase mixtures containing small volumes of gas/vapor 17 p2432 N88-24468

LIQUID-LIQUID INTERFACES

Natural frequencies and stability of immiscible spherical liquid systems
[LRT-WE-9-FB-2(1987)] 22 p3053 N88-28113

Natural frequencies and stability of circular cylindrical immiscible liquid systems
[LRT-WE-9-FB-3(1987)] 22 p3062 N88-28172

Nonlinear oscillations of axially independent liquid column under zero-gravity environment
[LRT-WE-9-FB-12(1987)] 22 p3063 N88-28174

LIQUID-SOLID INTERFACES

An advanced microcomputer design for processing of semiconductor materials 10 p1288 N85-17703

Effect of density change on rapid liquid-solid interface kinetics and heat flow
[DE88-004286] 11 p1487 N88-18878

Variable-energy positron studies on liquids and liquid-solid interfaces
[DE88-006356] 15 p2033 N88-22109

Arctic ice attenuation model study
[AD-A193382] 22 p3146 N88-28715

Attenuated total reflectance FT-IR spectroscopy to measure interfacial reaction kinetics at silica surfaces
[AD-A196330] 24 p3344 N88-29908

LIQUID-VAPOR EQUILIBRIUM

Study of the vapor-liquid equilibria used in the fabrication process of hydrogen by thermochemistry
[DE88-900239] 07 p0830 N88-15035

Feasibility of a complex compound heat pump
[PB88-113022] 07 p0853 N88-15183

Phase equilibria and density calculations in the critical region: A phenomenological correction for a classical equation of state
[PB88-185335] 19 p2723 N88-26167

LIQUID-VAPOR INTERFACES

Review of nucleation and incipient boiling under pool and forced convection conditions
08 p0982 N88-15938

Vapor condensation on a turbulent liquid interface
08 p0982 N88-15939

Investigation of real-time two-dimensional visualization of fuel spray liquid/vapor distribution via exciplex fluorescence
[AD-A188268] 10 p1307 N88-17816

An experiment to investigate Rankine cycle two-phase microgravity issues 17 p2409 N88-24322

The combustion of hydroxylammonium nitrate based liquid propellants 19 p2622 N88-25555

LIQUIDS
NT CRYOGENIC FLUIDS
NT FERMI LIQUIDS
NT HYDRAULIC FLUIDS
NT LIQUEFIED NATURAL GAS
NT LIQUID AMMONIA
NT LIQUID HELIUM
NT LIQUID HELIUM 2
NT LIQUID HYDROGEN
NT LIQUID LITHIUM
NT LIQUID METALS
NT LIQUID NITROGEN
NT LIQUID OXIDIZERS
NT LIQUID OXYGEN
NT LIQUID POTASSIUM
NT LIQUID SODIUM
NT MERCURY (METAL)
NT MERCURY ISOTOPES
NT MERCURY VAPOR
NT ORGANIC LIQUIDS
NT POTABLE WATER
NT ROTATING LIQUIDS

Theoretical approaches to chemical dynamics in highly compressed fluids
[DE87-012242] 01 p0046 N88-10296

Application of new conformal solution of theories
[PB87-214557] 01 p0105 N88-10684

Electrical conductivity and equation of state measurements on planetary fluids at high pressures and temperatures
[DE87-013787] 01 p0110 N88-10708

Application of new conformal solution theories
[PB87-211934] 02 p0247 N88-11558

Vacuum ultraviolet electronic properties of liquids
[DE88-000165] 03 p0282 N88-11772

Wear of iron and nickel in corrosive liquid environments
[NASA-TM-100246] 03 p0289 N88-11817

Novel macrocyclic carriers for proton-coupled liquid membrane transport
[DE88-000636] 04 p0413 N88-12560

Experimental study of thermocapillary flows in a thin liquid layer with heat fluxes imposed on the free surface
[NASA-TM-100252] 04 p0445 N88-12763

Some new ideas in liquid detectors
[DE88-000732] 04 p0446 N88-12768

Statistical process control applied to the liquid-fed ceramic melter process
[DE88-000271] 05 p0569 N88-13471

Molecular dynamics studies of aromatic hydrocarbon liquids
[DE88-001473] 05 p0648 N88-13973

Experimental and theoretical studies of dense fluid mixtures
[DE88-002710] 07 p0831 N88-15039

The generalized van der Waals theory of pure fluids and mixtures
[DE88-002380] 07 p0855 N88-15192

The properties of sound propagation in liquid constrained viscoelastic and polymeric structures
[AD-A185944] 07 p0929 N88-15640

Equation of state of condensed materials physical principles and applications
[NASA-TT-20007] 08 p0968 N88-15855

Liquid spring design methodology for shock isolation system applications 08 p0998 N88-16043

DSC (Differential Scanning Calorimeter) stability test for liquid propellants: A preliminary report
[AD-A187115] 09 p1150 N88-16888

Study of pattern formation at liquid interfaces
[DE88-001399] 09 p1160 N88-16954

Design and characteristics of a liquid aerosol generator
[AD-A186942] 09 p1174 N88-17034

Attenuation of ultrasonic waves in nonmagnetized magnetic fluids 09 p1234 N88-17398

Pulsed laser photothermal spectroscopy of liquids and solids
[DE88-003839] 11 p1455 N88-18675

Liquid ventilation: New data and possible use in space medicine 12 p1654 N88-19908

Contrasting conductance/viscosity relations in liquid states of vitreous and polymer solid electrolytes
[AD-A189378] 13 p1748 N88-20452

Mathematical models of sound waves in fluids
[AD-A189270] 13 p1834 N88-20968

Techniques for studying fast reactions in liquids
[DE88-005917] 14 p1888 N88-21285

Variable-energy positron studies on liquids and liquid-solid interfaces
[DE88-006356] 15 p2033 N88-22109

Density measurements on solids and liquids
[PB88-164934] 15 p2036 N88-22129

Nucleation in super-saturated products
[NASA-TT-20275] 15 p2037 N88-22134

The effect of internal relaxation on optoacoustic conversion in liquids
[AD-A191307] 16 p2176 N88-22970

Noncondensing round turbulent gas jets in liquids
[AD-A191191] 16 p2208 N88-23179

Direct emissivity measurements on liquids and corrections to multi-color pyrometers
17 p2329 N88-23906

Liquid carbon
[AD-A191707] 18 p2491 N88-24776

Kinetics of homogeneous nucleation in superheated F-11 and F-21 liquid freons
[NASA-TT-20286] 19 p2613 N88-25503

Observation of metallic conductivity in liquid carbon
[AD-A191723] 19 p2618 N88-25533

The use of liquid films for spacecraft survivability to laser radiation
[AD-A192954] 20 p2765 N88-26395

Extension of Boltzmann's theory to a liquid
[DE88-009153] 20 p2880 N88-27097

Natural frequencies and stability of immiscible cylindrical z-independent liquid systems
[LRT-WE-9-FB-1(1987)] 22 p3053 N88-28112

Natural convection immersion cooling of an array of simulated chips in an enclosure filled with dielectric liquid
[AD-A193594] 23 p3207 N88-29088

Liquid thickness gauge
[NASA-CASE-LAR-13826-1] 23 p3217 N88-29150

The dc power control for a liquid-fed resistojet
[NASA-TM-101326] 24 p3338 N88-29869

Design criteria for extraction with chemical reaction and liquid membrane permeation
[NASA-TT-20352] 24 p3343 N88-29899

Titrimetric analysis of HAN-based liquid propellants
[AD-A196225] 24 p3357 N88-29990

LISP (PROGRAMMING LANGUAGE)

LISP as a rapid prototyping environment: The chinese tutor
[AD-A184328] 03 p0369 N88-12319

The desktop interface in intelligent tutoring systems
09 p1205 N88-17225

A rule-based Lisp dialect translator using paramodulation 10 p1380 N88-18238

SimPL: A simulator for parallel LISP
[AD-A189831] 15 p2109 N88-22566

CK-LOG system conversion (user's manual and user interface)
[AD-A190273] 15 p2111 N88-22577

Simulating futures in extended common LISP
[NASA-TM-101000] 18 p2559 N88-25192

The concurrent common Lisp development environment 23 p3263 N88-29422

Scheme86: A system for interpreting SCHEME
[AD-A195931] 24 p3413 N88-30319

Lisp Object State Saver (LOSS): A facility used to save partial schedules of the Hubble Space Telescope
24 p3421 N88-30360

LISTS

Source header list. Volume 2: L through Z
[AD-A184001] 03 p0385 N88-12419

Source hierarchy list. Volume 1: A through D
[AD-A185900] 07 p0941 N88-15722

Source hierarchy list. Volume 2: E through O
[AD-A185901] 07 p0941 N88-15723

Source hierarchy list. Volume 3: P through Z
[AD-A185902] 07 p0942 N88-15724

On the productivity of recursive list definitions
[CS-8707] 14 p1960 N88-21692

LITERATURE
NT BIOGRAPHY
NT DOCUMENTATION

Translations of scientific and technical literature: A guide to their location 16 p2286 N88-23686

Publications of the Jet Propulsion Laboratory 1987
[NASA-CR-181198] 24 p3436 N88-30453

LITHIUM
NT LIQUID LITHIUM
NT LITHIUM ISOTOPES

Corrosion susceptibility study of candidate pin materials for ALTC (Active Lithium/Thionyl Chloride) batteries
[DE88-001449] 04 p0440 N88-12734

Technical evaluation of a solar-powered absorption cooling system (LiBr-H2O)
[PB87-108254] 04 p0463 N88-12867

Far-infrared spectra of lithium deposited on a gold electrode: Interpretation using a cluster model
[AD-A184231] 04 p0495 N88-13050

Survey state of the art: Electrical load management techniques and equipment
[AD-A184083] 05 p0577 N88-13517

A fluid simulation of the AMPTE lithium gas releases in the solar wind
[TRITA-EPP-87-06] 05 p0661 N88-14056

Interfacial effects in thin Li/PEO cells at room temperature
[AD-A186974] 09 p1157 N88-16931

Environment assisted degradation mechanisms in aluminum-lithium alloys
[NASA-CR-182482] 10 p1301 N88-17782

Polymeric electrolytes for ambient temperature lithium batteries
[DE88-004896] 13 p1763 N88-20547

Wavelength scaling of lithium-like recombination scheme for X-UV gain production --- X-ray lasers
[ETN-88-92002] 13 p1778 N88-20634

Magnetic cavity formation at Comet Halley and at the AMPTE Li release 14 p1996 N88-21898

A transient model for liquid metal heat pipes
17 p2421 N88-24398

The THROHPUT code: Thermohydraulic heat pipe modeling 17 p2421 N88-24399

Possible creep studies of lithium with a compact device 17 p2422 N88-24404

A low divergence, high brightness lithium ion source for plasma diagnostics
[DE88-008063] 19 p2729 N88-26203

Optimizing superplastic response in lithium containing aluminum-magnesium alloys
[AD-A192217] 20 p2774 N88-26451

Ambient temperature secondary lithium batteries using LiAl lithium insertion anodes
[DE88-008394] 20 p2793 N88-26574

Molten salt electrolytes for high-temperature lithium cells
[DE88-010058] 20 p2794 N88-26581

Field-enhanced lithium ion sources for PBFA 2
[DE88-007195] 20 p2856 N88-26960

Poloidal field measurements using laser enhanced attenuation of an energetic lithium beam
[DE88-008360] 20 p2856 N88-26963

Generation of Adlam-Allen waves by plasma release experiments in the solar wind
[PB88-106000] 20 p2886 N88-27140
Morphological changes in polymer electrolyte cells
[AD-A195821] 24 p3368 N88-30054

LITHIUM ALLOYS
On the role of crack tip shielding in influencing the behavior of long and small fatigue cracks in aluminum-lithium alloy 2090 05 p0600 N88-13671
Variable amplitude fatigue crack growth in aluminum alloys 2090-T8E41 and 7075-T651
05 p0602 N88-13687
The age hardening response of thermomechanically processed Al-Mg-Li alloys
[AD-A189870] 15 p2039 N88-22147
Stress corrosion cracking properties of Al-Li alloys
17 p2320 N88-23853
Aluminum alloy
[NASA-CASE-LAR-13924-1-CU]
18 p2487 N88-24753
Nondestructive evaluation methods for determination of thermal history and mechanical properties of aluminum-lithium alloys
[DE88-007352] 19 p2615 N88-25516
Inelastic ion-surface collisions
[AFGL-TR-87-0206] 19 p2724 N88-26174
Fatigue of lithium-aluminum alloys: An example of localization of the plastic deformation
[ETN-88-92309] 20 p2775 N88-26456
A method for determining the solubility of hydrogen in molten aluminum-lithium alloys
[DE88-009807] 21 p2910 N88-27270
Structural relationship between icosahedral and Frank-Kasper phases of Al-Li-Cu
[AD-A193768] 23 p3195 N88-29011

LITHIUM CHLORIDES
Optimization of reserve lithium thionyl chloride battery electrochemical design parameters
[DE88-007109] 18 p2506 N88-24868

LITHIUM COMPOUNDS
NT LITHIUM CHLORIDES
NT LITHIUM FLUORIDES
NT LITHIUM HYDRIDES
NT LITHIUM HYDROXIDES
NT LITHIUM IODATES
NT LITHIUM NIOBATES
NT LITHIUM OXIDES
NT LITHIUM PERCHLORATES
NT ORGANIC LITHIUM COMPOUNDS
Study of the micromechanical behavior of a SiO2-Al2O3-Li2O glass ceramic and its relation to the microstructure
[ISAL-ITC1-87-01] 02 p0153 N88-10960
Steady-state deformation of some lithium ceramics
[DE88-003116] 08 p0972 N88-15882
Lithium fast-ion conductors: Polymer based materials
[AD-A187879] 11 p1461 N88-18712
The synthesis, characterization and structural studies of In(C5H4Me) by X-ray diffraction and electron diffraction techniques and a reinvestigation of the crystalline state of In(C5H5) by X-ray diffraction studies
[AD-A189110] 13 p1844 N88-21038
Structure and dynamics of solutions of lithium salts relevant to battery construction
[AD-A195399] 24 p3366 N88-30044

LITHIUM FLUORIDES
Growth and characteristics of materials for tunable lasers in the near infrared spectral region
[NASA-CR-182501] 11 p1491 N88-18901
Effect of Mg impurity on local vibrations of U-centers in LiF lattice 14 p1969 N88-21753

LITHIUM HYDRIDES
Development of encapsulated lithium hydride thermal energy storage for space power systems
[DE88-004762] 11 p1507 N88-19001
A theoretical and experimental study of the thermophysical properties of lithium hydride
[NASA-TT-20179] 16 p2175 N88-22965
Fabrication of lithium hydride shields for space nuclear power systems 17 p2402 N88-24282
Fabrication of reactor shields at the Y-12 plant
17 p2402 N88-24283
Transient analysis of Li and LiH thermal storage spheres 17 p2411 N88-24334
Energy storage for nuclear burst power systems
17 p2426 N88-24431

LITHIUM HYDROXIDES
DC conductivity studies in Li5AlO4 at intermediate temperatures and its possible application for the electrolysis of water
[AD-A185489] 06 p0697 N88-14276
Phase behavior in the Li-Al-O-H system at intermediate temperatures
[AD-A185732] 06 p0697 N88-14280
Hydroxide ion conductors as possible electrolytes in intermediate temperature fuel cells
[AD-A185508] 06 p0731 N88-14495

LITHIUM IODATES
High ionic conductivity in PEO.PPG block polymer and salt solutions
[AD-A183502] 01 p0026 N88-10168

LITHIUM ISOTOPES
Development and applications of new technical advances to problems of fluid/electrolyte/mineral imbalance in military personnel
[AD-A186437] 07 p0889 N88-15388

LITHIUM NIOBATES
Optical frequency doubling in Ti:LiMbO3 waveguide resonators
[ETN-88-91486] 11 p1550 N88-19271

LITHIUM OXIDES
Growth and characteristics of materials for tunable lasers in the near infrared spectral region
[NASA-CR-182501] 11 p1491 N88-18901
Single-crystal structural study of La2Cu/sub 0.95/Li/sub 0.05/O4
[DE88-003482] 11 p1554 N88-19302

LITHIUM PERCHLORATES
Lithium/polymer electrolyte interfacial instability
[AD-A187164] 09 p1147 N88-16874

LITHIUM SULFUR BATTERIES
Lithium/iron sulfide batteries: Development and demonstration
[DE87-014222] 01 p0042 N88-10265
The 1986 Goddard Space Flight Center Battery Workshop
[NASA-CP-2486] 02 p0163 N88-11021
Computer simulation of thermal modeling of primary lithium cells 02 p0163 N88-11022
The 250AH/90A active lithium-thionyl chloride cell for Centaur-G application 02 p0163 N88-11023
The MOLICEL(R) rechargeable lithium system: Multicell battery aspects 02 p0163 N88-11024
Fault tree safety analysis of a large Li/SOCl(sub)2 spacecraft battery 02 p0163 N88-11025
Chemical analysis of charged Li/SO(sub)2 cells
02 p0163 N88-11026
Impedance of passive lithium anodes in SOCl2 solutions under low-field polarization
[DE88-000922] 04 p0439 N88-12728
Reliability of Li/SO2 cells for long-life applications
[DE88-001360] 04 p0440 N88-12735
Ionically conducting polymers: Principles and properties of solid electrolytes
[DE88-001552] 06 p0684 N88-14190
Lithium/disulfide battery R and D
[DE88-003032] 11 p1481 N88-18839
All inorganic ambient temperature rechargeable lithium battery
[DE88-008425] 19 p2662 N88-25834
The kinetics of charge-transfer reactions on passive lithium electrodes
[DE88-009256] 21 p2939 N88-27454

LITHIUM 4
U LITHIUM ISOTOPES

LITHIUM 6
U LITHIUM ISOTOPES

LITHOGRAPHY
NT PHOTOLITHOGRAPHY
Basic research in ceramic and semiconductor science at selected Japanese laboratories, based on a September 1986 visit: Highlights, summary and overview and detailed notes from selected Japanese laboratories
[DOE/ER-0314] 12 p1696 N88-20150
Electronic properties of semiconductor inversion layers in sub-micron structures
[AD-A188635] 12 p1698 N88-20161
Content of natural radioactive elements in Venusian rocks determined using data from Vega-1 and Vega-2 stations 13 p1726 N88-20323
Practical constraints on sources for pulsed beam lithographies
[DE88-006594] 13 p1776 N88-20623
High-speed electron beam lithography devices discussed 16 p2185 N88-23023
Microelectronics the next fifteen years
17 p2305 N88-23792
Department of Defense statement on the X-ray Lithography Program to the Research and Development Subcommittee of the House Armed Services Committee of 100th Congress, second session
[AD-A191854] 18 p2582 N88-25341
Excitonic properties of GaAs-AlGaAs nanostructures
20 p2867 N88-27023
Precise rotational alignment of X-ray transmission diffraction gratings
[DE88-010599] 21 p2911 N88-27273
High-speed, precision processing using an electron beam 21 p2929 N88-27391
Equipment for an advanced electron beam lithography system
[AD-A192956] 21 p2936 N88-27435
The Kerala Khondalite Belt (KKB) of Southern India: An ensialic mobile belt 24 p3393 N88-30208
The timing and mechanism of depletion in Lewisian granulites 24 p3394 N88-30209

LITHOLOGY
Nature and origin of mineral coatings on volcanic rocks of the Black Mountain, Stonewall Mountain, and Kane Springs Wash volcanic centers, Southern Nevada
[NASA-CR-181437] 09 p1191 N88-17140
Geological evolution and analysis of confirmed or suspected gas hydrate localities. Volume 10: Basin analysis, formation and stability of gas hydrates of the Aleutian Trench and the Bering Sea
[DE88-001008] 10 p1346 N88-18048
Geological evolution and analysis of confirmed or suspected gas hydrate localities. Volume 9: Formation and stability of gas hydrates of the Middle America Trench
[DE88-001007] 10 p1347 N88-18050
Data-base of Antarctic pre-Pleistocene sediment cores
[PB88-124151] 10 p1354 N88-18094
Martian geomorphology and its relation to subsurface volatiles
[NASA-CR-182428] 12 p1711 N88-20237
Analysis and interpretation of image lithostructure: An application of the multiconcept in the metamorphic belt of Sul de Santana da Boa Vista (RS)
17 p2359 N88-24051
Some geological aspects of the Pirapemas Lineament Belt 17 p2368 N88-24099
Lithostructural interpretation of Chapda do Cachimbo (Pa-Am-Mt), based on radar and LANDSAT imagery
17 p2368 N88-24100
A sedimentological and mineralogical study of the Koogah Formation, New South Wales
18 p2542 N88-25087
Analysis of the multispectral content and of SPOT subscenes in two regions of Burundi. Lithologic and tectonic interpretations 22 p3105 N88-28439

LITHOSPHERE
NT EARTH CORE
NT EARTH CRUST
NT EARTH MANTLE
NT EARTH SURFACE
Ocean floor magmatism and problems of lithosphere formation 08 p1009 N88-16121
Thematic mapper study of Alaskan ophiolites
[NASA-CR-182554] 11 p1504 N88-18984
Synthesis of finite displacements and displacements in continental margins
[NASA-CR-182616] 12 p1642 N88-19832
Effects of a temperature-dependent rheology on large scale continental extension
[NASA-CR-183117] 20 p2825 N88-26759
Intraplate deformation, stress in the lithosphere and the driving mechanism for plate motions
[NASA-CR-183121] 23 p3231 N88-29231
Lithospheric evolution of the Northern Arabian Shield: Chemical and isotopic evidence from basalts, xenoliths and granites 24 p3399 N88-30242

LITTORAL CURRENTS
U COASTAL CURRENTS

LITTORAL TRANSPORT
Nearshore wave transformation study of sites near Port Canaveral Inlet, Florida
[AD-A186965] 09 p1195 N88-17159

LIVER
Effect of weightlessness on replicative function of rat hepatocyte DNA 10 p1360 N88-18129
RNA-synthesizing activity in rat liver following flight aboard Cosmos-1667 10 p1360 N88-18130

LIVERWORTS
U BRYOPHYTES

LMCR (REACTORS)
U LIQUID METAL COOLED REACTORS

LMFBR
U LIQUID METAL FAST BREEDER REACTORS

LNG
U LIQUEFIED NATURAL GAS

LOAD DISTRIBUTION (FORCES)
Physiological determinants of load bearing capacity
[AD-A184977] 05 p0629 N88-13848
Behavior of a steel cylinder under the influence of a local load in the elastic and elasto-plastic area
[PB87-154787] 07 p0869 N88-15272
Cubic spline solution of symmetric buckling problems of clamped shallow spherical shells
15 p2053 N88-22239
Development of a lightweight structure with load bearing capability and high thermal conductance
17 p2420 N88-24393

Wind tunnel investigation of wing and control panel loads at transonic and supersonic speeds on some schematic cruciform missile configurations
[FFA-TN-1986-43-SUPPL-1] 22 p3039 N88-28044
Tripping of stiffened plates using a refined beam theory
[AD-A193989] 22 p3087 N88-28333

LOAD FACTORS
U LOADS (FORCES)

LOAD TESTING MACHINES
Device for measuring hole elongation in a bolted joint
[NASA-CASE-LAR-13453-1] 06 p0712 N88-14361
User's guide: Lower neck transducer for the Hybrid 3 dummy
[PB88-133319] 12 p1628 N88-19743
Evaluation tests of lower neck transducer for the Hybrid 3 Dummy
[PB88-133327] 12 p1628 N88-19745
Bearing-bypass material system test
[NASA-CASE-LAR-13458-1] 17 p2342 N88-23967
Automated measurement of crack length and load line displacement at elevated temperature
[NLR-MP-87049-U] 20 p2816 N88-26706

LOAD TESTS
Requirements for a test stand for plastic rollers for the verification of nonequilibrium force laws
[ILR-MITT-176] 01 p0008 N88-10040
Cumulative fatigue and life prediction of fibre composites. Part 2: Experimental techniques and results
[BR101014] 02 p0142 N88-10894
A study of the crack tip parameters that govern environmentally assisted cracking by use of the rising displacement test 04 p0427 N88-12649
Durability of powdered aluminum structures
04 p0429 N88-12655
Control of a flexible one-link manipulator
[AD-A185035] 05 p0590 N88-13598
An optical interferometry technique to evaluate closure along a crack front 05 p0607 N88-13726
Deformation, fatigue and fracture behavior of two cast anisotropic superalloys 05 p0608 N88-13732
A summary of experimental results on square plates and stiffened panels subjected to air-blast loading
09 p1178 N88-17057
To determine the stress distribution in the vicinity of GRP end pads where the specimen is held and loaded (CFC coupon specimens) --- glass reinforced plastic (GRP) carbon fiber composite (CFC)
[BAE-WST-R-RES-CFC-12023]
09 p1182 N88-17080
Further tests to determine the stress distribution in the vicinity of GRP end pads where the specimen is held and loaded (CFC coupon specimens) --- glass reinforced plastic (GRP) carbon fiber composite (CFC)
[BAE-WST-R-RES-CFC-12023-ADD-1]
09 p1182 N88-17081
Application of ISRM testing methods to fracture toughness testing of graphite 13 p1747 N88-20446
European approaches in standard spectrum development --- aircraft load spectra
[NLR-MP-87007-U] 13 p1782 N88-20661
Determination of canopy loads for a light aircraft by wind tunnel testing and computer modelling
[BU-353] 14 p1869 N88-21167
Some structural aspects of crack propagation in heat-resistant steels under cyclic thermal and mechanical load 14 p1896 N88-21317
Controlled-strain rate tests at very low strain rates of 2618 aluminum at 200 C 14 p1931 N88-21513
Some implications for cyclic plastic and viscoplastic equations based on nonproportional loading experiments
14 p1931 N88-21515
A unified creep-plasticity model suitable for thermo-mechanical loading 14 p1932 N88-21518
Constitutive response of Rene 80 under thermal mechanical loads 14 p1932 N88-21524
Experiments investigating advanced materials under thermomechanical loading 15 p2077 N88-22385
MHOST: An efficient finite element program for inelastic analysis of solids and structures
15 p2079 N88-22394
Characterization of Mode 1 and Mode 2 delamination growth and thresholds in graphite/peek composites
[NASA-TM-100577] 16 p2172 N88-22947
Development of a biaxial test system for thin-walled metal tubes using tensile-compressive axial load and internal-external pressure
[DE88-011279] 21 p2962 N88-27592
Modal testing in the design evaluation of wind turbines
[DE88-010374] 21 p2968 N88-27632
Wind tunnel investigation of wing and control panel loads at transonic and supersonic speeds on some schematic cruciform missile configurations
[FFA-TN-1986-43-SUPPL-1] 22 p3039 N88-28044
Stress corrosion evaluation of powder metallurgy aluminum alloy 7091 with the breaking load test method
22 p3053 N88-28115
Calibration of quartz load cells: An in-situ procedure for instrumented falling weight impact machines
[NPL-DMA(A)-155] 22 p3081 N88-28297

LOADING FORCES
U LOADS (FORCES)

LOADING MOMENTS
Kinematic support using elastic elements
14 p1926 N88-21481

LOADING OPERATIONS
The composition of the gas in the loading inlet of the Space Shuttle Orbiter
[ETN-87-90430] 01 p0012 N88-10069
Modification of integrated partial payload lifting assembly
[NASA-CR-182573] 11 p1443 N88-18607

LOADING RATE
Composite materials applications program at the US Army Ballistic Research Laboratory: Work in progress
04 p0428 N88-12651
Loading rate sensitivity of open hole composites in compression
[NASA-TM-100634] 19 p2610 N88-25490
Cold worked reinforcing bars in tensile test under high loading rate and low temperatures
[DE88-752993] 21 p2964 N88-27610
An investigation of constitutive models for predicting viscoplastic response during cyclic loading
[AD-A194875] 24 p3385 N88-30163

LOADING WAVES
U ELASTIC WAVES
U LOADS (FORCES)

LOADS (FORCES)
NT AERODYNAMIC LOADS
NT AXIAL COMPRESSION LOADS
NT AXIAL LOADS
NT BLAST LOADS
NT COMPRESSION LOADS
NT CONTACT LOADS
NT CRITICAL LOADING
NT CYCLIC LOADS
NT DYNAMIC LOADS
NT EDGE LOADING
NT GUST LOADS
NT IMPACT LOADS
NT LANDING LOADS
NT RANDOM LOADS
NT ROLLING CONTACT LOADS
NT SHOCK LOADS
NT STATIC LOADS
NT TRANSIENT LOADS
NT VIBRATORY LOADS
NT WING LOADING
Calculation of the damage of highly loaded gas turbine disks under real flight conditions
[ETN-87-90416] 01 p0007 N88-10036
Assessment of the COFSI/MAST I project
[NASA-CR-181366] 01 p0053 N88-10340
Analysis of shell-type structures subjected to time-dependent mechanical and thermal loading
[NASA-CR-181409] 01 p0060 N88-10388
Nonsteady-state vibrations in acoustic medium of elastic elliptical shell subjected to instantaneously applied uniform pressure 02 p0160 N88-11000
Frozen-field, rigid-beam, uniform-conductivity-channel tracking force calculation
[DE87-012510] 02 p0190 N88-11190
Operational load measurements on service helicopters
03 p0263 N88-11658
Pump assisted heat pipe 03 p0319 N88-12018
Bearing loads in slider crank mechanisms
[PB87-216495] 03 p0332 N88-12089
Computational methods and results for dynamic fracture 03 p0337 N88-12123
Kinetics of crack growth: Thermal/mechanical interaction 03 p0337 N88-12124
Ideal-viscoplastic extrusion model with application to deforming pistons in light-gas guns
[UTIAS-TN-266] 04 p0429 N88-12657
The effect of mass, wind angle and erection technique on the aeroelastic behaviour of a cable-stayed bridge model
[NAE-AN-46] 04 p0455 N88-12819
A comparison of structural frequency response functions measured with forces from 500 to 250,000 lb
[DE88-000668] 04 p0457 N88-12829
Static aeroelastic considerations in the definition of design loads for fighter airplanes
05 p0550 N88-13351
An analytical study of the effects of transverse shear deformation and anisotropy on buckling loads of laminated cylinders
[NASA-TM-100508] 05 p0557 N88-13387
The simulation of the viscous flow around a cylinder by the random vortex method 05 p0579 N88-13534
A dislocation model for fatigue crack propagation under variable amplitude loading 05 p0602 N88-13683
Observations on the effect of overloads on fatigue crack growth 05 p0602 N88-13684
Variable amplitude fatigue crack growth in aluminum alloys 2090-T8E41 and 7075-T651
05 p0602 N88-13687
Fatigue of 30CrMnSiNi2A notched specimens under spectrum loading 05 p0602 N88-13689
Damping analysis of flexural waves in fluid-loaded single and constrained plates
[AD-A185116] 05 p0609 N88-13739
Fluctuating pressure loads under high speed boundary layers
[NASA-TM-100517] 05 p0647 N88-13962
Behavior of bolted joints in composite laminates
06 p0677 N88-14148
The effects of loading history on fatigue crack growth threshold 06 p0718 N88-14406
Beam and column buckling under directed loading
[PB87-124004] 06 p0722 N88-14436
A loading system for creep testing under constant compressive stress
[NASA-TT-20119] 06 p0722 N88-14441
Wave propagation experiments on 22-bay lattice
[AD-A186140] 07 p0824 N88-15002
Load carriage induced alterations of pulmonary function
[AD-A186227] 07 p0889 N88-15386
Integral equation method for the analysis of plates and shells
[PB87-144788] 08 p0996 N88-16030
TECOM's research efforts in the dynamic environments 08 p0999 N88-16048
Evaluation of vibration specifications for acoustic environments 08 p0999 N88-16053
Design procedures for fiber composite box beams
[NASA-TM-100296] 09 p1139 N88-16828
A research program on the aerodynamics of a highly loaded turbine stage 10 p1280 N88-17655
Tactile sensing and inverse problems
[AD-A187464] 10 p1340 N88-18011
Study of the mechanical behavior of a 2-D carbon-carbon composite
[NASA-CR-182594] 11 p1451 N88-18649
Fracture characteristics of a viscoelastic polymer under constant load: Experiments and analysis
11 p1501 N88-18963
Dynamic analysis of plane frames by microcomputer
11 p1531 N88-19143
Determination of design loads for modern combat aircraft 12 p1580 N88-19457
Mechanical response of unidirectional boron/aluminum under combined loading
[NASA-CR-182595] 12 p1604 N88-19591
Ply-level failure analysis of a graphite/epoxy laminate under bearing-bypass loading
[NASA-TM-100578] 13 p1735 N88-20372
Dynamic modelling of flexible rotor shafts mounted on hydrodynamic bearings 13 p1779 N88-20641
Component mode synthesis using experimental modes enhanced by mass loading
[DE88-006097] 13 p1781 N88-20657
Analysis of shell-type structures subjected to time-dependent mechanical and thermal loading
[NASA-CR-182705] 13 p1783 N88-20668
Quick actuating closure and handling system
14 p1925 N88-21476
Effects of state recovery on creep buckling under variable loading 14 p1933 N88-21527
Practical considerations for structural control: System uncertainty, system time delay and truncation of small control forces
[PB88-163738] 14 p1933 N88-21528
Determination of the commutation and angle and load response for a continuous-current, single phase controlled rectifier
[AD-A190602] 15 p2060 N88-22285
Fatique crack growth behavior of a single crystal alloy as observed through an in situ fatigue loading stage
[NASA-TM-100863] 16 p2179 N88-22986
Crack retardation under load spectra. Experimental study and numerical simulation using the simplified K constant model --- light alloys, aircraft construction materials
[ONERA-RT-30/7169-RY-054-R]
16 p2222 N88-23266
Calculation of root-mean-square loads
[BLL-M-37776-(5828.4)] 18 p2531 N88-25015
Vertical ship motions and sea loads considering nonlinear effects
[TAE-592] 20 p2784 N88-26515

Instrumentation for the measurement of penetrator dynamic response to permit force estimation
[DE88-010608] 20 p2809 N88-26666
A comparison of the various helicopter mathematical models used in the methodology assessment
21 p2889 N88-27149
Wind tunnel tests of the influence of airfoil-thickness on normal force and pitching moment of two slender wings at transonic and supersonic Mach numbers
[DFVLR-FB-88-17] 21 p2893 N88-27171
Thermo-viscoelastic analysis of composite materials, volume 1
[NASA-CR-183048-VOL-1] 21 p2904 N88-27230
Analysis of crack arrest toughness
[AD-A193340] 21 p2913 N88-27286
A study of fluid-structure problems
21 p2941 N88-27468
The influence of weld metal properties, weld geometry and applied load on weld system performance
[AD-A193403] 21 p2961 N88-27588
Method to predict external store carriage characteristics at transonic speeds
[NASA-CR-4170] 22 p3037 N88-28034
Wave propagation and vibration of fibre reinforced laminates
[AD-A194144] 22 p3051 N88-28101
Estimation forces acting on an underwater vehicle with G.P.S. (Global Positioning System) and Kalman filtering
[AD-A194339] 23 p3175 N88-28901
Plastic flow and failure modeling under high strain rate loading
[AD-A194223] 23 p3226 N88-29199

LOCAL AREA NETWORKS
Space lab system analysis
[NASA-CR-179207] 02 p0138 N88-10869
Lewis Information Network (LINK): Background and overview
[NASA-TM-100162] 03 p0305 N88-11925
Applications of the hybrid automated reliability predictor
[NASA-TP-2760] 04 p0475 N88-12928
Introduction to local area network design on Ariane 5 and future launchers
[SNIAS-872-422-102] 05 p0635 N88-13886
On real-time systems using local area networks
[AD-A185475] 06 p0694 N88-14256
A new library of CAMAC routines for the control of the system CRATE by a microVAX in the VAXELN environment
[NOTA-INTERNA-893] 06 p0761 N88-14667
Facility design validation of the information systems laboratory
[AD-A186309] 07 p0906 N88-15488
Media independent interface
[NASA-CR-172033] 08 p1066 N88-16446
Media independent interface. Interface control document
[NASA-CR-172032] 08 p1067 N88-16447
MPAD MCC workstation system: ADDAM and EEVE
09 p1203 N88-17209
A classified bibliography on publications relevant to data security in LANs --- local area networks (LANS)
[NPL-DITC-99/87] 09 p1223 N88-17331
The design of load balancing strategies for distributed systems 10 p1376 N88-18216
Experiments with parallel program execution on a network of workstations 10 p1377 N88-18217
An Ethernet local area network controller with supporting operating system software
[DE88-003534] 10 p1392 N88-18304
Air Force Institute of Technology (AFIT) Local Area Network (LAN) performance evaluation model: An analytic model for assessing the impact of changing LAN hardware and software configurations
[AD-A187191] 11 p1469 N88-18764
Performance analysis of slotted ring protocols in High Speed Local Area Networks (HSLANS)
[INF-87-31] 14 p1955 N88-21652
Passive coupler, network adapter, and network acquisition procedure for optical local networks
[ETN-88-92130] 14 p1961 N88-21695
Exact analyses of slotted ring protocols for local area networks with one transmitting station
[MEMO-650] 14 p1967 N88-21737
DATAC bus monitor 17 p2294 N88-23721
Development of a generic architecture
17 p2303 N88-23774
Interconnection of high-speed local area networks
17 p2390 N88-24205
An investigation of a distributed clock for local area networks with ring topology 18 p2516 N88-24924
The high speed local area network
19 p2717 N88-26133
A state-of-the-art survey of low-cost security in local area networks
[NPL-DITC-113/88] 22 p3141 N88-28678
Intelligent resource management for local area networks: Approach and evolution
23 p3256 N88-29385

LOCAL GROUP (ASTRONOMY)
NT MILKY WAY GALAXY
Duplicity in the solar neighborhood. Part 3: New spectroscopic elements for nine solar-type binary stars
[SER-C-PREPUBL-FASC-18-PT-3]
18 p2592 N88-25405
Duplicity in the solar neighborhood: Part 4: Spectroscopic orbits for four dwarf M stars
[SER-C-PREPUBL-FASC-21] 24 p3454 N88-30561
Duplicity in the solar neighborhood: Part 5: Spectroscopic orbit for the nearby double-lined solar-type star HR 8581
[SER-C-PREPUBL-FASC-23] 24 p3455 N88-30562

LOCALIZATION
U POSITION (LOCATION)

LOCATION
U POSITION (LOCATION)

LOCKHEED AIRCRAFT
NT C-130 AIRCRAFT
NT P-3 AIRCRAFT
NT T-33 AIRCRAFT
NT U-2 AIRCRAFT

LOCKHEED U-2 AIRCRAFT
U U-2 AIRCRAFT

LOCKING
NT LASER MODE LOCKING
Frequency locking of two lasers
[FOA-C-30456-3.1] 08 p0992 N88-16000
Locking hinge
[NASA-CASE-MSC-21056-1] 17 p2312 N88-23827
Mode locking of semiconductor laser with external cavity
[AD-A196018] 24 p3378 N88-30117

LOCKS (FASTENERS)
Modification and development of the external tank hydrogen vent umbilical system for the space shuttle vehicle 14 p1928 N88-21496
Collet lock joint for space station truss
[NASA-CASE-MSC-21207-1] 23 p3222 N88-29180

LOCOMOTION
NT ASTRONAUT LOCOMOTION
NT WALKING
Dynamics and stability of bipedal locomotion robots
03 p0333 N88-12096
Some remarks on gravitational biology
07 p0884 N88-15366
Investigations of Paramecium cells analyzed under microgravity conditions 07 p0884 N88-15367
Questions on the evolution of the development program of the vertebrate inner ear under long term zero-g conditions 07 p0886 N88-15379

LOCOMOTIVES
Application of Kalker's rolling contact theory to the simulation of rail vehicles
[DFVLR-FB-87-07] 01 p0057 N88-10363

LOG PERIODIC ANTENNAS
The use of coaxial transmission line elements in log-periodic dipole arrays
[AD-A184864] 05 p0574 N88-13499
A computer model investigation of a half square log-periodic array
[AD-A190955] 16 p2190 N88-23062

LOGARITHMS
Freidlin-Wentzell type estimates and the law of the iterated logarithm for a class of stochastic processes related to symmetric statistics
[AD-A185366] 05 p0644 N88-13944
On selecting the best of k lognormal distributions
[AD-A185628] 07 p0916 N88-15567
High speed transcendental elementary function architecture in support of the Vector Wave Equation (VWE)
[AD-A189746] 15 p2119 N88-22627
Research on algebraic manipulation
[AD-A190149] 15 p2120 N88-22634

LOGGING (INDUSTRY)
Applicability of SPOT for forest inventory, mapping and change monitoring 03 p0344 N88-12174

LOGIC
Induction instrument for logic conclusion
[LRT-WE-9-FB-5(1987)] 22 p3144 N88-28697

LOGIC CIRCUITS
Programmable Logic Arrays (PLA's) design for testability
[PB87-102935] 04 p0438 N88-12718
Mental models in expert physics reasoning
[AD-A184106] 04 p0500 N88-13075
An exact analysis and performance of framed ALOHA with capture
[AD-A185006] 05 p0574 N88-13500
New breakthrough in Chinese integrated circuits: Successful development of high-speed CMOS circuits
[AD-A185381] 05 p0578 N88-13525
Implementation of an FIR band pass filter using a bit-slice processor
[AD-A184895] 05 p0634 N88-13875
Interfacing slave designs to Fastbus: Practical experience
[DE88-002807] 09 p1215 N88-17286
Vertical charge transport in junction charge-coupled devices
[ETN-88-91613] 09 p1255 N88-17523
Signal processing studies program VLSI designs for unary functions
[AD-A188053] 10 p1325 N88-17922
New mode switching algorithm for the JPL 70-meter antenna servo controller 11 p1474 N88-18791
Modules of nanosecond logic electronics system with computer control
[DE88-700190] 11 p1479 N88-18828
Fast serial input-serial output pipelined inner product units
[REPT-87-031] 11 p1530 N88-19142
A methodology for hardware verification based on logic simulation
[AD-A188553] 12 p1622 N88-19704
A digital circuit design environment
[AD-A188831] 12 p1623 N88-19709
MOBICALC: An integrated and interactive system for development of administrative models
[INPE-4335-TDL/291] 12 p1679 N88-20038
Ultra-high speed integrated optical waveguide devices for optical computing
[AD-A188470] 12 p1691 N88-20118
Describing constraints on a digital circuit's behavior
[AD-A189200] 13 p1761 N88-20531
A fault injection experiment using the AIRLAB Diagnostic Emulation Facility
[NASA-CR-178390] 13 p1823 N88-20895
An expert system for discrete component digital circuit design
[AD-A189680] 15 p2059 N88-22274
Applications of optical computing to problems with symbolic computations
[AD-A189772] 15 p2106 N88-22548
Joint services electronics program research in electronics
[AD-A192206] 18 p2504 N88-24857
SYMBL: A new Boolean compiler
18 p2554 N88-25160
High-speed optical logic using GaAs
19 p2656 N88-25773
The design of a digital Eprom oscillator for electrical impedance tomography
[DE88-012243] 21 p2940 N88-27462
STAR: Sandia Timing Analyzer Routine
[DE88-012412] 21 p2940 N88-27463
Nanosequencer digital logic controller
[NASA-CASE-NPO-16116-2] 23 p3245 N88-29310
Use of depletion edge translation for high-speed modulation and switching of lightwaves
[AD-A195611] 24 p3430 N88-30417

LOGIC DESIGN
Mental models in expert physics reasoning
[AD-A184106] 04 p0500 N88-13075
Software program validity: A survey
[PB87-170593] 09 p1219 N88-17315
A framework for evaluating computer architectures to support systems with security requirements, with applications
[AD-A187082] 10 p1392 N88-18303
Fast serial input-serial output pipelined inner product units
[REPT-87-031] 11 p1530 N88-19142
A logical structuration for an administration of space projects
[INPE-4435-TDL/310] 12 p1585 N88-19482
A new approach on test generation for array structures using the behavior of the system --- VLSI chips
[INF-87-27] 14 p1907 N88-21397
An optimal CMOS structure for the design of a cell library
[EUT-87-E-166] 14 p1985 N88-21841
HIFI: A design method for implementing signal processing algorithms on VLSI processor arrays
[ETN-88-92238] 16 p2247 N88-23421
Identification of control structures --- expert systems
[REPT-87-66] 16 p2255 N88-23479
SYMBL: A new Boolean compiler
18 p2554 N88-25160
Knowledge elicitation for an operator assistant system in process control tasks 23 p3253 N88-29366

LOGIC NETWORKS
U LOGIC CIRCUITS

LOGIC PROGRAMMING
Improvements to the adaptive maneuvering logic program
[NASA-CR-3985] 03 p0262 N88-11648

Programmable Logic Arrays (PLA's) design for testability
[PB87-102935] 04 p0438 N88-12718
PROVER: A first-order logic system in Ada
[DE88-000220] 04 p0479 N88-12951
Near-horn prolog
[AD-A185172] 05 p0634 N88-13880
Parallel logic programming and ZMOB and parallel systems software and hardware
[AD-A186300] 07 p0903 N88-15470
Methodology for testing and validating knowledge bases 08 p1055 N88-16364
DOD Gateway Information System (DGIS) common command language: Prolog knowledge base profile. Common command language report no. 3
[AD-A186150] 08 p1092 N88-16574
An investigation of parallelism in rule based systems
10 p1377 N88-18223
Experimenting with parallel programing in logic
10 p1380 N88-18240
Parallel architectures for logic programming
10 p1380 N88-18241
Implementing logical variables on a graph reduction architecture 10 p1382 N88-18252
Deriving abstractions from a software object network
[AD-A187472] 10 p1389 N88-18294
A digital logic simulator with concurrent programming considerations
[AD-A188823] 12 p1678 N88-20032
MOBICALC: An integrated and interactive system for development of administrative models
[INPE-4335-TDL/291] 12 p1679 N88-20038
Northeast Artificial Intelligence Consortium (NAIC) administrative matters and ancillary functions, volume 1
[AD-A189466] 12 p1682 N88-20055
Towards a solution to the proper integration of a logic programming system and a large knowledge based management system
[AD-A188949] 12 p1705 N88-20207
Semantics for Prolog via term rewrite systems
[CWI-CS-R8739] 16 p2247 N88-23428
Semantics for logic programs without occur check
[CWI-CS-R8740] 16 p2248 N88-23429
Introduction to logic programming
[CWI-CS-R8741] 16 p2248 N88-23430
Towards fully abstract semantics for local variables: Preliminary report
[AD-A191065] 16 p2251 N88-23456
Subset-logic programming: Application and implementation
[AD-A193647] 22 p3138 N88-28655
Combined and-or parallel execution of logic programs
[AD-A193648] 22 p3138 N88-28656
Unification and set-valued functions for functional and logic programming
[AD-A193643] 23 p3250 N88-29341
Practical higher-order functional and logic programming based on lambda-calculus and set-abstraction
[AD-A193645] 23 p3271 N88-29466

LOGICAL ELEMENTS
Logical input devices and interaction --- computer graphics
[CWI-CS-R8738] 13 p1814 N88-20836

LOGISTICS
NT LUNAR LOGISTICS
NT SPACE LOGISTICS
Naval Aviation Integrated Logistics: Technical users guide version 1.0
[DE87-013368] 01 p0001 N88-10001
A functional interpretation of the logistic equation
[REPT-87-037] 05 p0645 N88-13946
A space transportation system operations model
[NASA-TM-100481] 07 p0823 N88-14999
Variable selection in logistic regression
[AD-A186032] 07 p0914 N88-15547
An elimination type two-stage procedure for selecting the population with the largest mean from k logistic populations
[AD-A185614] 07 p0916 N88-15566
Prototype resupply scheduler
08 p1064 N88-16428
Replication and reconfiguration in a distributed mail repository
[AD-A186967] 09 p1151 N88-16897
First Annual Workshop on Space Operations Automation and Robotics (SOAR 87)
[NASA-CP-2491] 09 p1203 N88-17206
Preliminary analysis of an integrated logistics system for OSSA payloads
[NASA-CR-4114] 12 p1584 N88-19477
Preliminary analysis of an integrated logistics system for OSSA payloads. Volume 1: Executive summary
12 p1584 N88-19478
Preliminary analysis of an integrated logistics system for OSSA payloads. Volume 2: OSSA integrated logistics support strategy 12 p1584 N88-19479
Preliminary analysis of an integrated logistics system for OSSA payloads. Volume 3: OSSA integrated logistics support planning document 12 p1584 N88-19480
Preliminary analysis of an integrated logistics system for OSSA payloads. Volume 4: Supportability analysis of the 1.8m centrifuge 12 p1584 N88-19481
Space station heavy lift launch vehicle utilization
[NASA-TM-100604] 14 p1873 N88-21188
A model of intrazonal trip distribution considering centrality index 16 p2257 N88-23486
Lunar base surface mission operations. Lunar Base Systems Study (LBSS) task 4.1
[NASA-CR-172050] 18 p2594 N88-25415
The assessment of human/computer performance using human productivity measures: MIPS and BIPS are MEGAFLOPS
[DE87-013491] 21 p2993 N88-27750
Introduction to artificial intelligence and expert systems
[SNIAS-881-320-101] 21 p3004 N88-27814
Expert system contribution to logistics improvement
[SNIAS-881-320-102] 21 p3004 N88-27815
An evaluation of SPOT imagery for Earth science studies in the Antarctic. Preliminary Evaluation Program (PEPS) 289 for SPOT 22 p3103 N88-28430
Inflight rearming
[AD-A193564] 23 p3176 N88-28909
Dirichlet prior in Bayesian estimation of item response curves
[AD-A195311] 24 p3426 N88-30392

LOGISTICS MANAGEMENT
NT INVENTORY CONTROLS
NT INVENTORY MANAGEMENT
Optimum dimensioning of field service centers: Analysis of the problem and solutions thereof
01 p0012 N88-10066
Introduction to artificial intelligence and expert systems
[SNIAS-881-320-101] 21 p3004 N88-27814
Expert system contribution to logistics improvement
[SNIAS-881-320-102] 21 p3004 N88-27815
Reliability and Maintainability (R and M)
[AD-A193857] 23 p3224 N88-29187

LOMONOSOV CURRENT
Propagation of subsurface salinity maximum in tropical Atlantic 13 p1786 N88-20686

LONG DURATION SPACE FLIGHT
Use of bifidumbacterin for correction of intestinal dysbacteriosis 07 p0895 N88-15427
Air Force cryocooler development for spacecraft
08 p0983 N88-15945
Zero gravity and living organism
08 p1046 N88-16320
Analysis of water recovered after being used for washing by men and women 10 p1361 N88-18135
Present stage of space medicine
10 p1364 N88-18151
Effect of spaceflight factors on biological material flown aboard Cosmos-1514 biosatellite
10 p1364 N88-18154
Basic results of medical studies during prolonged manned flights on-board the Salyut-7/Soyuz-T orbital complex
[NASA-TT-20217] 10 p1369 N88-18182
Hemolysis in runners as evidenced by low serum haptoglobin: Implications for preflight monitoring of astronauts
[NASA-TM-100304] 11 p1518 N88-19067
Results of medical research conducted in 1985 during long-term spaceflights 19 p2702 N88-26070
Studies of HZE particle interactions and transport for space radiation protection purposes
[NASA-TM-101159] 20 p2886 N88-27142

LONG PERIOD VARIABLES
U MIRA VARIABLES

LONG RANGE WEATHER FORECASTING
Sea ice observations and models
14 p1939 N88-21572

LONG TERM EFFECTS
Space technology to meet future needs
[NASA-CR-181473] 02 p0130 N88-10819
Effects of long term storage on aerospace nickel cadmium cell performance 02 p0165 N88-11035
Effect of long-term thermal aging on coated Celion/LARC-160 composites
[NASA-TM-100495] 04 p0410 N88-12544
Influence of creep on the precipitate structure under conditions of long-term creep. 4: Experiments on 10 CrMo 9 10 steel
[BLL-CE-TRANS-8256-(9022.09)]
04 p0417 N88-12589
Lifting bodies: An attractive aerodynamic configuration choice for hypervelocity vehicles
05 p0534 N88-13248
A study of charged particles/radiation damage to VLSI device materials
[NASA-CR-172036] 05 p0577 N88-13518
Contributions of lidar measurements to the study of long term variations of the middle atmosphere
[ETN-88-91237] 05 p0625 N88-13824
Carbon Dioxide observational platform system (CO-OPS) Feasibility Study
[NASA-CR-179225] 06 p0671 N88-14113
Morphometric analysis of rat aorta endothelium during long-term hypokinesia 07 p0894 N88-15417
Changes in functional parameters of animals during long-term inhalation of acetic acid
07 p0895 N88-15423
Long-term variation of total ozone
[INPE-4307-PRE/1173] 08 p1023 N88-16192
Long-term aging of cast stainless steels: Mechanisms and resulting properties
[DE88-002888] 09 p1145 N88-16864
Short- and long-term effects of nonlethal levels of fast high-energy helium ions on retention of developed and formation of new behavioral patterns in rats
10 p1362 N88-18140
Results of long-term electrocardiographic monitoring of cosmonauts 10 p1364 N88-18152
Research briefing on high-temperature superconductivity
[PB88-133004] 11 p1561 N88-19344
Conceptualization and design of a variable-gravity research facility
[NASA-CR-182574] 12 p1595 N88-19550
Sea ice observations and models
14 p1939 N88-21572
Fractographic and microstructural evaluation of 3500-hour durability specimens
17 p2325 N88-23887
Environment assisted degradation mechanisms in advanced light metals
[NASA-CR-182907] 18 p2486 N88-24746
Effect of long-term inhalation of acetic acid vapor on some functional parameters of man
19 p2705 N88-26084
Aging of CFRP due to longterm storage in heated air
[DFVLR-FB-88-05] 21 p2922 N88-27345
Physiology of prolonged bed rest
[NASA-TM-101010] 22 p3130 N88-28607
Long-term behavior of energy production systems with the example of HELIOS and SYMPHONIE
[ETN-88-92988] 23 p3230 N88-29223

LONG WAVE RADIATION
Numerical modeling of radiation fog
08 p1017 N88-16166
Application of satellite data in observational and theoretical studies of the evolving structure of baroclinic waves
[NASA-CR-179277] 10 p1354 N88-18091
Radiation balance components above the tropical evergreen Amazon forests (3rd campaign of data collection)
[INPE-4195-PRE/1079] 11 p1513 N88-19039
Tropical circulations and the associated rainfall anomalies during two contrasting years
[INPE-4506-PRE/1261-REV] 15 p2098 N88-22502
Estimation of total Outgoing Longwave Radiation (OLR) flux from geostationary meteorological satellite infrared window radiance 17 p2351 N88-24006
Nonlinear waves
[AD-A192148] 18 p2510 N88-24889
On the impact of low-latitude anomalous forcing on local and remote circulation: Winters(DJF) 1978/79 to 1986/87 22 p3123 N88-28560
An observational study of interaction between large scale tropical cumulus convection and the equatorial circulation anomalies 22 p3124 N88-28564
Proof of the feasibility of coherent and incoherent schemes for pumping a gamma-ray laser
[AD-A193856] 23 p3220 N88-29165

LONG WAVES (METEOROLOGY)
U PLANETARY WAVES

LONGERONS
The X-beam as a deployable boom for the space station 14 p1925 N88-21473

LONGITUDE
Navigation system from AVHRR data from NOAA series satellites 17 p2359 N88-24054
Vertical directionality of ambient noise at 32 deg N as a function of longitude: Tape number 86180
[AD-A193228] 21 p3012 N88-27872

LONGITUDINAL CONTROL
Lateral and longitudinal stability and control parameters for the space shuttle discovery as determined from flight test data
[NASA-TM-100555] 13 p1724 N88-20309
Investigations on higher harmonic blade pitch control at helicopters
[DFVLR-FB-87-36] 14 p1868 N88-21165

Steady and unsteady transonic pressure measurements on a clipped delta wing for pitching and control-surface oscillations
[NASA-TP-2594] 23 p3173 N88-28895
Low-speed longitudinal flying qualities of modern transport aircraft 24 p3314 N88-29738

LONGITUDINAL STABILITY
Effects of the installation and operation of jet-exhaust yaw vanes on the longitudinal and lateral-directional characteristics of the F-14 airplane
[NASA-TP-2769] 04 p0393 N88-12455
Natural laminar flow and airplane stability and control
17 p2296 N88-23747
Experiment investigation on longitudinal characteristics of the forward swept wing
[AD-A191553] 18 p2456 N88-24582
Calculation of aerodynamic characteristics of airplane configurations at high angles of attack
[NASA-CR-4182] 23 p3172 N88-28891

LONGITUDINAL WAVES
NT PLANE WAVES
High-frequency limit of the longitudinal impedance
[CEBAF-PR-87-030] 02 p0234 N88-11479
Plane longitudinal waves in solutions of Maxwell equations
[DE88-700347] 07 p0846 N88-15135
An analysis of longitude variations in the equatorial spectrum of Saturn 10 p1430 N88-18539
Generation of flux tube waves in stellar convection zones. 1: Longitudinal tube waves
[NASA-TM-101152] 17 p2451 N88-24561
Experimental proof of quasilongitudinal propagation of low-frequency waves in middle latitudes in upper ionosphere 24 p3447 N88-30516

LONGSHORE CURRENTS
U COASTAL CURRENTS

LOOP ANTENNAS
A MININEC model of the miniloop antenna
[AD-A191759] 18 p2500 N88-24830
MSAT-X phased array antenna adaptions to airborne applications 19 p2647 N88-25713
Research in electromagnetic shielding theory. Part 2: EMP (electromagnetic pulse) simulation using small loops
[AD-A192882] 20 p2791 N88-26558

LOOPS
Timing variation in dual loop benchmarks
[AD-A185697] 06 p0707 N88-14338
Performance evaluation of a loop interconnection structure 10 p1378 N88-18229
Loop coalescing: A compiler transformation for parallel machines
[DE88-003571] 10 p1392 N88-18307
Deadlock prevention in processor self-scheduling for parallel nested loops
[DE88-003573] 10 p1393 N88-18313
Effects of toroidal forces in current loops embedded in a background plasma
[AD-A188878] 12 p1695 N88-20143
Tactical Rubidium Frequency Standard (TRFS)
[AD-A191049] 16 p2193 N88-23078
Phase length optical phase-locked-loop sensor
[NASA-CASE-LAR-13387-1] 18 p2576 N88-25302
Polymeric heat pipe wick
[NASA-CASE-GSC-13019-1] 23 p3214 N88-29133

LORAN
NT LORAN C

LORAN C
Alaska Loran C probe test results
[AD-A189131] 13 p1720 N88-20284
Investigation of air transportation technology at Massachusetts Institute of Technology, 1986
17 p2293 N88-23716
Investigation of air transportation technology at Ohio University, 1986 17 p2293 N88-23719
Loran-C monitor correlation over a 92-mile baseline in Ohio 17 p2293 N88-23720
Integrated multisensor navigation systems
17 p2294 N88-23722
Descriptions of HF and VHF Loran-C buoys and evaluations as potential datum marker buoys
[AD-A192069] 18 p2462 N88-24618
Research project Loran-C of the Geometric Service of the Ministry of Public Works
[B8735055] 20 p2757 N88-26356

LORENTZ CONTRACTION
Analysis of absolute space-time Lorentz theories
[DE87-703371] 04 p0500 N88-13076

LORENTZ FORCE
Covariant Lorentz anomalies in higher dimensional space
[DE87-753021] 02 p0230 N88-11448
Difficulties with interpretation of underground muons from Cygnus X-3
[DE88-701645] 23 p3309 N88-29710

LORENTZ TRANSFORMATIONS
The entropy of the Lorentz model
08 p1015 N88-16153
Spin precession in stationary gravitational fields
[DE88-701107] 15 p2093 N88-22470
Recent developments in the path integral approach to anomalies
[DE87-703032] 15 p2118 N88-22616
Local time displacement as a symmetry of nature in flat space-time
[NASA-TM-100610] 16 p2264 N88-23542

LOS ALAMOS TURRET REACTOR
U HIGH TEMPERATURE NUCLEAR REACTORS

LOSS OF COOLANT
Development of a rotary fluid transfer coupling and support mechanism for space station
14 p1928 N88-21493
Inherently safe space reactors
17 p2415 N88-24363

LOSSES
Blade loss transient dynamics analysis, volume 1. Task 2: TETRA 2 theoretical development
[NASA-CR-179632] 02 p0125 N88-10791
Blade loss transient dynamics analysis, volume 2. Task 2: TETRA 2 user's manual
[NASA-CR-179633] 02 p0126 N88-10792
Static magnetization and microwave loss in shock-modified ferrites
[DE87-012362] 02 p0146 N88-10916
Mass loss 02 p0253 N88-11597
Circumstellar chemistry 02 p0253 N88-11598
A new method for measuring waveguide propagation losses
[DE87-011305] 03 p0307 N88-11938
Empirical relations between photospheric magnetic fields and atmospheric radiative losses for cool dwarf stars 04 p0511 N88-13145
IRAS and cool stellar mass loss
04 p0515 N88-13166
Improved understanding of the loss-of-symmetry phenomenon in the conventional Kalman filter
[NASA-TM-100041] 06 p0766 N88-14709
Status of microcirculation in high-altitude blood loss
12 p1663 N88-19973
Eddy current losses induced by rotation of magnetisation
[BLL-M-37634-(5828.4)] 14 p1890 N88-21298
The loss parameters for very short bunches
[CEBAF-PR-88-005] 18 p2574 N88-25291
Characteristics of shielded microstrip lines on GaAs-Si at millimeter-wave frequencies 19 p2657 N88-25787
Loss evaluation of self-commutated power conditioner for battery energy storage system
[DE88-752075] 20 p2794 N88-26575
The effects of moisture loss and elevated temperature upon the material damping of fibre reinforced polymer matrix composites
[UTIAS-324] 23 p3188 N88-28970
Conductor loss in superconducting power transmission cables
[DE88-011414] 23 p3290 N88-29586
Behaviour and hysteresis losses of irreversible type-2 superconducting cylindrical shell
[DE88-702708] 24 p3433 N88-30434

LOSSY MEDIA
Measurement of the properties of lossy materials inside a finite conducting cylinder
[NASA-CR-182664] 13 p1832 N88-20962
Born-type reconstruction of material parameters of an inhomogeneous, lossy dielectric slab from reflected-field data
[PB88-188958] 18 p2569 N88-25261

LOST WAX PROCESS
U INVESTMENT CASTING

LOUVERS
The acoustic source created by turbulent flow over orifices and louvers
[REPT-97674] 06 p0776 N88-14764
Describing the source created by turbulent flow over orifices and louvers
[AD-A190254] 15 p2130 N88-22706

LOW ALLOY STEELS
U HIGH STRENGTH STEELS

LOW ALTITUDE
Dispersion in the wake of aircraft: An investigation of the effects of a ground plane on trailing vortices. Literature survey
[IC-AERO-REP-86-04] 01 p0003 N88-10014
Evaluation of a mesoscale prediction system with surface weather observations and comparison with a large-scale prediction system 02 p0210 N88-11319
Development, testing and evaluation of a night vision goggle compatible BO-105 for night low level operation
03 p0265 N88-11668
Development of an acoustic echosounder for detection of lower level atmospheric turbulence
[AD-A184877] 05 p0626 N88-13831
State-of-the-art technologies for construction in space: A review
[AD-A188412] 12 p1585 N88-19483
The low-latitude auroral boundary: Steady-state and time-dependent representations
[AD-A193200] 21 p2972 N88-27656
Low altitude: A new dimension in air refueling
[AD-A193819] 23 p3176 N88-28910
Integration of LANTIRN (Low Altitude Navigation and Targeting Infrared for Night) into operational fighter training
[AD-A194906] 24 p3325 N88-29799

LOW ASPECT RATIO
Periodic natural convection in a rectangular enclosure of low aspect ratio 10 p1329 N88-17941
Computational design of low aspect ratio wing-winglet configurations for transonic wind-tunnel tests
[NASA-CR-183021] 18 p2464 N88-24630
Design studies of low aspect-ratio torsatrons
[DE88-007562] 18 p2579 N88-25320
Symmetrized magnetic field configuration of low aspect ratio helical system
[IPPJ-869] 20 p2855 N88-26956

LOW ASPECT RATIO WINGS
NT DELTA WINGS
Theoretical-numerical study of feasibility of use of winglets on low aspect ration wings at subsonic and transonic Mach numbers at reduce drag
[NASA-CR-4174] 21 p2892 N88-27168

LOW CARBON STEELS
Wear of hard steel in rolling lubricated contact
[RP-699] 03 p0332 N88-12094
The growth behavior of small fatigue cracks; the effect of microstructure and crack closure
05 p0600 N88-13673
A study of fatigue crack growth life under random stresses 05 p0602 N88-13685
Influence of cleavage on fatigue propagation rates in a low carbon steel 06 p0716 N88-14389
Notch-geometry effect on propagation threshold of short fatigue cracks in notched components
06 p0716 N88-14393
Sulfur-induced ductility-dip cracking in weld metal of low-carbon steel
[PB87-143814] 07 p0833 N88-15051
Investigation of the auto-tempering of low-carbon martensite
[PB87-143970] 07 p0833 N88-15053
New mechanism of the high temperature (reversible) temper brittleness of alloy steels
[PB87-143954] 07 p0833 N88-15056
An investigation of the influence of dislocation substructures on the deformation behavior of AK, DQ steel sheets
[DE88-006337] 14 p1889 N88-21289
Studies on hot-dip zinc-aluminum coated sheet steels
[ETN-88-92217] 15 p2042 N88-22166

LOW COST
Development of an innovative, low-cost solar collector
[PB87-206819] 02 p0194 N88-11210
Configuration evaluation and criteria plan. Volume 2: Evaluation criteria plan (update). Space Transportation Main Engine (STME) configuration study
[NASA-CR-181429] 03 p0270 N88-11699
Lightsats and their attraction to budget oriented Federal agencies 10 p1289 N88-17711
Low cost telemetry and telecommand system for remote measurement of magnitude character
[INPE-4273-PRE/1145] 12 p1598 N88-19564
Alternative program approaches for the advanced satellite technology program
[AD-A188917] 12 p1600 N88-19576
Low cost mobile robot
[AD-A188507] 12 p1633 N88-19778
Principles of a low-cost laser gyro for rotating vehicles and platforms
[DFVLR-MITT-87-15] 14 p1912 N88-21425
Laser-heated CVD process for depositing thin films for low-cost solar-cell applications
[DE88-001162] 21 p2967 N88-27623
Finding minimum-cost circulations by successive approximation
[AD-A192724] 21 p3005 N88-27824
Finding minimum-cost circulations by canceling negative cycles
[AD-A192727] 21 p3005 N88-27825
LO-CO-GRAF (low cost graphics): Generating maps to support command and control/crisis management using small computers
[AD-A193964] 22 p3139 N88-28661
Finding minimum-cost circulations by canceling negative cycles
[AD-A194027] 23 p3271 N88-29468

Finding minimum-cost circulations by successive approximation
[AD-A194028] 23 p3272 N88-29469
A multiprocessor avionics system for an unmanned research vehicle
[AD-A194806] 24 p3325 N88-29800
Low cost satellite
[ESA-CR(P)-2560] 24 p3334 N88-29844
Interim Flight Opportunity (IFO). Volume 1: Executive summary --- space platform
[SE/LS/AP-36-818/CN-VOL-1]
24 p3334 N88-29849
Space systems cost study
[AD-A196024] 24 p3439 N88-30469

LOW CURRENTS
Low-current behavior and current chopping of vacuum arcs
[ISBN-90-9001649-X] 05 p0578 N88-13529

LOW DENSITY GASES
U RAREFIED GASES

LOW EARTH ORBITAL ENVIRONMENTS
U EARTH ORBITAL ENVIRONMENTS

LOW FREQUENCIES
NT VERY LOW FREQUENCIES
ELF/VLF/LF propagation and system design
[AD-A183261] 01 p0033 N88-10212
Compilation of 1986 annual reports of the Navy ELF (Extremely Low Frequency) communications system ecological monitoring program, volume 1
[AD-A184561] 03 p0306 N88-11930
Application of ray theory to propagation of low frequency noise from wind turbines
[NASA-CR-178367] 03 p0373 N88-12349
Low-frequency VLBI in space and interstellar refraction
[PB87-127643] 06 p0696 N88-14267
Observing effect of laser radiation of low-frequency Raman scattering of light 06 p0772 N88-14742
Low-frequency oscillations in nonideal plasma
06 p0774 N88-14751
Low frequency VLBI in space using GAS-Can satellites: Report on the May 1987 JPL Workshop
[NASA-CR-182362] 06 p0801 N88-14904
Acoustic scattering from composite wind-wave surfaces 3: Forward scatter intensities and spatial coherence at low and high frequencies and small grazing angles for Bubble-free regimes
[AD-A185908] 07 p0881 N88-15345
A proposed metric for assessing the potential of community annoyance from wind turbine low-frequency noise emissions
[DE88-001113] 08 p1022 N88-16187
Low frequency electrostatic waves observed on board the Coordinated Auroral Experiment using Scatter And Rockets (CAESAR) 2 payload 08 p1032 N88-16253
Low frequency waves and small scale solitary structures observed by Viking --- Swedish satellite; auroras
08 p1099 N88-16611
Ray tracing of Jovian low frequency radiation
[NASA-CR-179262] 08 p1101 N88-16620
Subharmonic aliasing and its effects on the AFTI/F-16 digital flight control system
[AD-A190614] 15 p2020 N88-22042
Low frequency ocean ambient noise: Measurements and theory
[AD-A191188] 16 p2237 N88-23362
Practical VLF/LF radio test system
[AD-A191768] 18 p2500 N88-24831
Aircraft interior noise reduction by alternate resonance tuning
[NASA-CR-182540] 20 p2849 N88-26909
The polarization of radio galaxies: Its structure at low frequencies
[B8681611] 20 p2884 N88-27123
Airborne measurement of low frequency atmospheric noise ALFAN 1
[AD-A193056] 21 p2931 N88-27405
The observed dynamical structure of low frequency variabilities 22 p3120 N88-28541
Physiological effects of extremely low frequency electric and magnetic fields
[DE88-752814] 22 p3132 N88-28620

LOW FREQUENCY BANDS
NT VERY LOW FREQUENCIES

LOW GRAVITY
U REDUCED GRAVITY

LOW GRAVITY MANUFACTURING
Center for the Space Processing of Engineering Materials 07 p0838 N88-15083
Analysis of low gravity tolerance of model experiments for space station: Preliminary results for directional solidification
[NASA-CR-182657] 12 p1614 N88-19648
Preparation for microgravity: The role of the microgravity materials science laboratory
[NASA-TM-100906] 18 p2497 N88-24811
Optimization of low gravity materials processing experiments using expert systems
23 p3252 N88-29361

LOW LATITUDES
U TROPICAL REGIONS

LOW LEVEL TURBULENCE
Numerical calculation of appendage, flat plate junction flow
[AD-A186371] 07 p0850 N88-15158
Turbulence structure during high wind
08 p1014 N88-16149
Utilization of dense packed planar acoustic echosounders to identify turbulence structure in the lowest levels of the atmosphere
[AD-A191006] 16 p2233 N88-23335
Measurement and analysis of low altitude atmospheric turbulence obtained using a specially instrumented Gnat aircraft 24 p3313 N88-29728

LOW MASS
U MASS

LOW NOISE
Low noise-low power monolithic multiplexing readout electronics for silicon strip detectors
[MPI-PAE/EXP.EL.178] 02 p0168 N88-11057
Research in monolithic signal-processing circuits
[AD-A184680] 03 p0311 N88-11962
Low-noise cryogenic transmission line
04 p0434 N88-12688
The 8.4-GHz low-noise maser pump source assembly
04 p0436 N88-12705
Development of a low noise 10 K J-T refrigeration system
[AD-A186004] 07 p0838 N88-15085
Low noise cryogenic dielectric resonator oscillator
[NASA-CASE-NPO-17157-1-CU]
20 p2797 N88-26596

LOW PASS FILTERS
A digital low pass filter for the reduction of large quantities of data
[ESA-TT-1058] 03 p0363 N88-12281
On a circular correlation technique for filtering randomly noisy data
[AD-A184317] 04 p0431 N88-12669
Error reduction in two-dimensional pulse-area modulation, with application to computer-generated transparencies --- optical field synthesis
[EUT-87-E-172] 14 p1982 N88-21825
High speed, bandpass sampling of digital communications waveforms
[AD-A189842] 15 p2056 N88-22254
A notch filter instrument for measuring ELF (Extremely Low Frequency) MSK (Minimum Shift Keying) signals
[AD-A193324] 21 p2933 N88-27414
Anti-aliasing filters for dynamics and control experiments
[AD-A193758] 23 p3226 N88-29203

LOW PRESSURE
An illustrative example of the nowcasting challenge
02 p0199 N88-11243
Forecasting polar lows using a numerical mesoscale model 02 p0210 N88-11321
Typhoon structural evolution
[AD-A186090] 07 p0879 N88-15333
Low pressure gas flow analysis through an effusive inlet using mass spectrometry
[NASA-CR-182712] 14 p1910 N88-21413
Study of surface discharges
[ONERA-12/7236-PY] 15 p2026 N88-22073
Low pressure entrained flow pyrolysis of biomass to produce liquid fuels 18 p2535 N88-25043
Microlaminate composite structures by low pressure plasma spray deposition
[DE88-006453] 19 p2610 N88-25488
Genesis of Atlantic lows experiment NASA electra boundary layer flights data report
[NASA-TM-100703] 22 p3126 N88-28597
Simulation of Vulcain engine operation at low inlet pressure
[ETN-88-93083] 24 p3339 N88-29875

LOW PRESSURE CHAMBERS
U VACUUM CHAMBERS

LOW REYNOLDS NUMBER
International Conference on the Aerodynamics at Low Reynolds Numbers between 10(4) and 10(6)
[ONRL-7-023-C] 01 p0002 N88-10010
Low Reynolds number influence on aerodynamic performance of hypersonic lifting vehicles
05 p0531 N88-13230
Two-equation low-Reynolds-number turbulence modeling of transitional boundary layer flows characteristic of gas turbine blades
[NASA-CR-4145] 16 p2209 N88-23185
Computational fluid dynamics methods for low Reynolds number precessing/spinning incompressible flows
[AD-A193891] 23 p3212 N88-29119
A study of the effect of random input motion on low Reynolds number flows
[AD-A195559] 24 p3316 N88-29747

LOW SPEED
On the prospects for increasing dynamic lift
[RAE-TM-AERO-2068] 01 p0003 N88-10018
Investigation of low-speed turbulent separated flow around airfoils
[NASA-CR-177450] 04 p0396 N88-12471
A swept wing panel in a low speed flexible walled test section
[NASA-CR-4106] 05 p0540 N88-13292
Advanced natural laminar flow airfoil with high lift to drag ratio 07 p0812 N88-14947
Preliminary airworthiness evaluation of a UH-1 equipped with a terrain mapping receiver antenna
[AD-A186274] 07 p0819 N88-14980
Planetary science 07 p0883 N88-15356
Investigation of low velocity impact damage on filamentary composite materials
07 p0923 N88-15607
Effect of low velocity impact on compression strength of a quasi-isotropic laminate
[FFA-TN-1987-38] 09 p1138 N88-16822
A review of technologies applicable to low-speed flight of high-performance aircraft investigated in the Langley 14- x 22-foot subsonic tunnel
[NASA-TP-2796] 13 p1717 N88-20264
The effect of sting interference at low speeds on the drag coefficient of an ellipsoidal body using a magnetic suspension and balance system
[NASA-CR-181611] 13 p1718 N88-20274

LOW SPEED STABILITY
Low-speed longitudinal flying qualities of modern transport aircraft 24 p3314 N88-29738

LOW SPEED WIND TUNNELS
NT SUBSONIC WIND TUNNELS
The 5.5 m low speed wind tunnel. Introduction to the facilities
[ARG-205] 14 p1870 N88-21172
Main features of Warton (United Kingdom) 2.7 x 2.1 m low speed wind tunnel
[AXM-124] 14 p1870 N88-21173
Details of low speed intake test facility at the Warton (United Kingdom) 2.7m x 2.1m wind tunnel
[AXM-127] 14 p1870 N88-21174
Contraction design for small low-speed wind tunnels
[NASA-CR-182747] 15 p2021 N88-22045
Summary of low-speed wind tunnel results of several high-speed counterrotation propeller configurations
[NASA-TM-100945] 18 p2458 N88-24597
A low speed wind tunnel investigation of Reynolds number effects on a 60-deg swept wing configuration with leading and trailing edge flaps
[NASA-CR-181684] 19 p2598 N88-25441
Effects of independent variation of Mach and Reynolds numbers on the low-speed aerodynamic characteristics of the NACA 0012 airfoil section
[NASA-TM-4074] 23 p3170 N88-28879

LOW TEMPERATURE
NT CRYOGENIC TEMPERATURE
Low temperature deposition by laser induced breakdown in the vapor phase
[DE87-007509] 01 p0024 N88-10151
The development of a friction model predicting the sliding behavior of materials pairs, especially at low temperatures: Progress report and renewal proposal
[DE87-013941] 01 p0055 N88-10354
Direct formation of thin films and epitaxial overlayers at low temperatures using a low-energy (10-500 eV) ion beam deposition system
[DE87-012291] 01 p0103 N88-10675
Near-threshold fatigue crack growth behavior at cryogenic temperature 06 p0718 N88-14409
The effect of non-metallic inclusions on fatigue and fatigue thresholds of 25Mn-5Cr-1Ni steel
06 p0718 N88-14410
Photoinduced low-temperature changes in optical losses in fiber optics based on chalcogenide glasses
06 p0770 N88-14731
The role of low temperature chemistry in the autoignition of n-butane
[DE88-002385] 07 p0829 N88-15031
Prediction of human thermoregulatory responses and endurance time in water at 20 and 24C
[AD-A186223] 08 p1048 N88-16326
Effect of low-temperature aging on the mechanical properties of cast stainless steels
[DE88-002872] 10 p1300 N88-17774
The Shubnikov de Haas effect in narrow-gap semimagnetic semiconductors
[ETN-88-92249] 14 p1988 N88-21861
Cellular thermosetting fluoropolymers and process for making them
[NASA-CASE-GSC-13008-1] 17 p2326 N88-23894

Update of low temperature catalyst development
[DE88-007032] 18 p2480 N88-24715
Antimisting kerosene: Low temperature degradation and blending
[NASA-CR-182725] 20 p2781 N88-26495
Superconducting electronic film structures
[AD-A192907] 20 p2879 N88-27091
Preparation and development of advanced battery catalysts
[AD-A193208] 21 p2937 N88-27441
Cold worked reinforcing bars in tensile test under high loading rate and low temperatures
[DE89-752993] 21 p2964 N88-27610
Low temperature film growth of the oxides of zinc, aluminum and vanadium (and related systems, oxides of gold and germanium, nitrides of aluminum and tungsten) by reactive sputter deposition
[AD-A193497] 23 p3191 N88-28986
Muon-spin rotation experiment (micro + SR) on aluminum and indium after low temperature electron irradiation
[ETN-88-92985] 23 p3294 N88-29617
Discovery of a low temperature form of TAGN (Triaminoguanidinium Nitrate)
[AD-A196059] 24 p3357 N88-29989

LOW TEMPERATURE ENVIRONMENTS
The initiation and growth of small fatigue cracks in copper at room and cryogenic temperatures
05 p0600 N88-13668
Polar worker adaptability to Antarctic high altitudes
10 p1366 N88-18165
The CRREL (Cold Regions Research and Engineering Laboratory) Hopkinson bar apparatus
[AD-A190599] 15 p2077 N88-22380
Hydraulic pumps and hydraulic equipment at low temperatures
[DE88-752871] 21 p2958 N88-27570
Accidental hypothermia
[AD-A194967] 24 p3406 N88-30278

LOW TEMPERATURE PHYSICS
Interactions between superconductivity and Kondo-grid properties in CeCu2Si2. Measurement results of specific heat under high pressure
[ETN-88-92377] 21 p3025 N88-27958

LOW TEMPERATURE PLASMAS
U COLD PLASMAS

LOW TEMPERATURE TESTS
Instrument for radiation testing/screening electronic devices over an extended temperature range
[AD-A184245] 03 p0326 N88-12060
A test facility for the in-vacuo assessment of dry lubricants and small mechanisms at cryogenic temperatures 14 p1878 N88-21224
Cryogenic test facilities for an optical cryomechanism qualification 14 p1879 N88-21228
Materials testing at cryogenic temperatures
[BU-359] 14 p1923 N88-21462
The CRREL (Cold Regions Research and Engineering Laboratory) Hopkinson bar apparatus
[AD-A190599] 15 p2077 N88-22380

LOW THRUST
Breadboard RL10-2B low-thrust operating mode (second iteration) test report
[NASA-CR-182160] 24 p3338 N88-29867

LOW THRUST PROPULSION
NT ELECTROMAGNETIC PROPULSION
NT ELECTROSTATIC PROPULSION
NT ION PROPULSION
NT PLASMA PROPULSION
NT SOLAR THERMAL PROPULSION
A technique for capture analysis of low thrust missions in a planetary system
[AD-A188934] 12 p1594 N88-19544
Recent advances in low-thrust propulsion technology
[NASA-TM-100959] 18 p2569 N88-25260

LOW VACUUM
Low jitter laser-triggered high-voltage vacuum switch using low laser energies
[DE88-001922] 05 p0587 N88-13576

LOW VELOCITY
U LOW SPEED

LOW VISIBILITY
Flight simulator experiments concerning take-off visibility minima
[NLR-TR-86050-U] 13 p1719 N88-20281

LOW VOLTAGE
High density CMOS technology
11 p1561 N88-19342
Extinction behavior of low voltage switching arc under consideration of cathodic coatings and dynamic arc column
[ETN-88-92384] 20 p2796 N88-26591

LOWER ATMOSPHERE
NT TROPOPAUSE
NT TROPOSPHERE
Experimental study of the propagation of an acoustic wave in the low atmosphere
[ISL-R-111/86] 02 p0231 N88-11454
Geochemistry of the middle and lower atmosphere: Environmental impact through the deterioration of the ozone layer
[INPE-4477-PRE/1241] 16 p2230 N88-23321

LOWER BODY NEGATIVE PRESSURE
Blood redistribution in man with lower body negative pressure 07 p0891 N88-15397
Leg volume change under Lower Body Negative Pressure (LBNP) in dependence on stratification
[DFVLR-FB-87-47] 16 p2238 N88-23367

LOWER IONOSPHERE
NT D REGION
Ionospheric research in Antarctica
[INPE-4521-PRE/1273] 16 p2232 N88-23331

LOX (OXYGEN)
U LIQUID OXYGEN

LOX-HYDROGEN ENGINES
U HYDROGEN OXYGEN ENGINES

LQG CONTROL
U LINEAR QUADRATIC GAUSSIAN CONTROL

LQR
U LINEAR QUADRATIC REGULATOR

LSI
U LARGE SCALE INTEGRATION

LST
U HUBBLE SPACE TELESCOPE

LUBRICANT TESTS
Activities report in tribology
[ESA-ESTL-79] 09 p1174 N68-17037
Standardization of lubricity test
[AD-A187776] 11 p1465 N88-18736
The SPOT solar array. Box opening mechanisms physical vapor deposition (PVD)-MoS2: Lubricated slides. Functional evaluation 14 p1876 N88-21211
A test facility for the in-vacuo assessment of dry lubricants and small mechanisms at cryogenic temperatures 14 p1878 N88-21224
Characterization of lubricants in terms of transition diagram data
[AD-A191264] 23 p3197 N88-29025
The lubricating properties of magnetron sputtered MoS2
[ESA-ESTL-76] 24 p3381 N88-30136

LUBRICANTS
NT GAS LUBRICANTS
NT HIGH TEMPERATURE LUBRICANTS
NT LUBRICATING OILS
NT SOLID LUBRICANTS
Boundary lubrication. Experiments with boundary lubrication and plain bearings at +60...-60 deg C temperatures
[DE87-752869] 02 p0180 N88-11124
Analysis of wear metals in engine oils using the atomic absorption spectrophotometric method
[NAL-TM-MT-8704] 05 p0564 N88-13435
Film thicknesses in circular elastohydrodynamic contacts
[PB87-123725] 06 p0710 N88-14354
Research study for materials/properties test results database
[NASA-CR-178923] 07 p0861 N88-15222
Evaluation of load tracks and wear of two sets of bearings from space shuttle main engine high pressure oxygen turbopumps
[NASA-CR-178969] 07 p0861 N88-15223
Improved perfluoroalkylether fluid development
[NASA-CR-180872] 08 p0967 N88-15851
On the performance of finite journal bearings lubricated with micropolar fluids
[NASA-TM-100293] 08 p0988 N88-15983
Technology developments for a compound cycle engine 09 p1107 N88-16637
Activities report in tribology
[ESA-ESTL-79] 09 p1174 N88-17037
An evaluation of effectiveness of PTFE (polytetrafluoroethylene) type friction reducers on reducing friction and wear
[AD-A187440] 10 p1340 N88-18010
Tribological properties of alumina-boria-silicate fabric from 25 to 850 C
[NASA-TM-100806] 11 p1464 N88-18726
Evaluation of centrifugal barrel tumbling process for impregnation of molybdenum disulfide powder lubricant
[BDX-613-3696] 11 p1464 N88-18727
Carbon residue studies of polyphenyl ethers and ester-based lubricants using a microcarbon residue tester
[AD-A188585] 12 p1611 N88-19632
Lubricating properties of molybdenum disulfide. Part 3: Performance of molybdenum disulfide-containing oils in fluid lubrication
[NASA-TT-20156] 13 p1752 N88-20480
A new approach to highly fluorinated lubricants
[AD-A190523] 15 p2045 N88-22188
Studies of dynamic contact of ceramics and alloys for advanced heat engines
[DE88-008996] 21 p2919 N88-27324
Perfluoropolyalkylether lubricants under boundary conditions: Iron catalysis of lubricant degradation
[AD-A193241] 21 p2956 N88-27560
The 000 stage equipment bearing performance with a lower viscosity lubricant
[DE88-011827] 21 p2957 N88-27566
Development of high temperature, high pressure rotating shaft seals
[DE88-001029] 23 p3221 N88-29172

LUBRICATING OILS
Piston ring friction and vehicle fuel economy
[DE87-014536] 02 p0181 N88-11127
High shear rate rheometry of low-viscosity liquids
[AD-A188447] 12 p1627 N88-19733
Corrosion-wear process under rolling-sliding motion
[AD-A189603] 13 p1778 N88-20635
A new method of measuring multigrade oil shear elasticity and viscosity at high shear rates
[AD-A190145] 15 p2064 N88-22304
Calibration of the portable wear metal analyzer
[AD-A192971] 21 p2950 N88-27524
Reaction-theoretical aspects of the thermal behavior of lubricating oils and working fluids
[NASA-TT-20304] 23 p3199 N88-29041

LUBRICATION
NT BOUNDARY LUBRICATION
NT SELF LUBRICATION
NT SPACECRAFT LUBRICATION
Boundary lubrication. Experiments with boundary lubrication and plain bearings at +60...-60 deg C temperatures
[DE87-752869] 02 p0180 N88-11124
Piston ring friction and vehicle fuel economy
[DE87-014536] 02 p0181 N88-11127
Improved oil-off survivability of tapered roller bearings
[NASA-CR-180804] 02 p0182 N88-11135
Film thicknesses in circular elastohydrodynamic contacts
[PB87-123725] 06 p0710 N88-14354
The numerical solution of the elastohydrodynamically lubricated line and point contact problem, using multigrid techniques
[ISBN-90-9001583-3] 06 p0714 N88-14377
Investigation of instability, dynamic forces, and effect of dynamic loading on strength of cages for the bearings in the high pressure oxygen turbopumps for the space shuttle main engine
[NASA-CR-178970] 06 p0714 N88-14378
A variational formulation of a hydrodynamic lubrication problem
[MEMO-642] 08 p0987 N88-15979
Activities report in tribology
[ESA-ESTL-79] 09 p1174 N88-17037
A comparison of measurements from the A/E35U-3 and PWMA (Portable Wear Metal Analyzer) spectrometers
[AD-A186855] 09 p1177 N88-17047
Characteristics and use of lubricating greases
[DE88-751103] 11 p1463 N88-18723
Standardization of lubricity test
[AD-A187776] 11 p1465 N88-18736
A hydrodynamic analysis of fluid flow between meshing spur gear teeth
[AD-A187671] 11 p1482 N88-18844
Overview of the DOE-ECUT Tribology Program
[DE88-002878] 13 p1778 N88-20637
Experience with duplex bearings in narrow angle oscillating applications 14 p1926 N88-21484
A new method of measuring multigrade oil shear elasticity and viscosity at high shear rates
[AD-A190145] 15 p2064 N88-22304
Traction model development
[AD-A188450] 15 p2073 N88-22359
High temperature solid lubrication by catalytically generated carbon
[AD-A190804] 16 p2182 N88-23004
Basic mechanisms of diesel lubrication correlation of bench and engine tests
[AD-A193360] 21 p2956 N88-27561
The 000 stage equipment bearing performance with a lower viscosity lubricant
[DE88-011827] 21 p2957 N88-27566
A lubrication study of engine bearings
21 p2958 N88-27574
Status and directions of modified tribological surfaces by ion processes
[NASA-TM-101304] 22 p3063 N88-28176

LUBRICATION SYSTEMS
Literature review of solid lubrication mechanisms
[AD-A185010] 05 p0567 N88-13456
Traction model development
[AD-A188450] 15 p2073 N88-22359

LUCITE (TRADEMARK)
U POLYMETHYL METHACRYLATE
LUDER BANDS
U PLASTIC DEFORMATION
U YIELD POINT
LUMBERING AREAS
U FORESTS
LUMINAIRES
NT ARC LAMPS
NT FLASH LAMPS
NT QUARTZ LAMPS
Evidence of a new spectral line intensity formula for optical emission
[KGI-PREPRINT-098] 01 p0090 N88-10585
Design concepts to improve high performance solar simulator 02 p0136 N88-10852
A defect investigation of Thunderflash MK N5 (Navy)
[MRL-TN-522] 13 p1754 N88-20488
Laser induced ignition of propellants
[AD-A191099] 16 p2213 N88-23206
Spectroradiometry in the industrial test laboratory
16 p2272 N88-23598
LUMINANCE
Target size and luminance effects on accommodation and vergence
[AD-A185861] 08 p1051 N88-16343
Pursuit tracking performance decrements associated with decreasing ambient illumination
[AD-A189336] 13 p1809 N88-20809
Design and testing of a luminance and chrominance stabilization system for a computer-controlled color display
[AD-A191922] 18 p2554 N88-25159
LUMINESCENCE
NT BIOLUMINESCENCE
NT CHEMILUMINESCENCE
NT ELECTROLUMINESCENCE
NT FLUORESCENCE
NT LASER INDUCED FLUORESCENCE
NT OPTICAL RESONANCE
NT PHOSPHORESCENCE
NT PHOTOLUMINESCENCE
NT RESONANCE FLUORESCENCE
NT SPACECRAFT GLOW
NT X RAY FLUORESCENCE
The influence of polymer structure on triplet luminescence
[DE87-014431] 02 p0152 N88-10952
A physico-chemical study of some areas of fundamental significance to biophysics
[DE87-013457] 02 p0217 N88-11365
Performance characteristics of magnesium-sodium nitrate flares in oxygen-nitrogen atmospheres
[AD-A185274] 05 p0570 N88-13476
Multicomponent analysis using synchronous-excitation phase-resolved fluorescence spectroscopy
[AD-A188883] 12 p1606 N88-19604
Electronic and ionic transport in polymers
[AD-A190434] 15 p2045 N88-22185
Superthermal electron processes in the upper atmosphere of Uranus. Aurora and electroglow
[NASA-TM-101150] 18 p2594 N88-25417
Laser spectroscopy of quantum well and superlattice structures
[AD-A193336] 21 p3022 N88-27937
The optical spectroscopy of copper-blue luminescence in zinc sulfide crystals. Zero-phonon line spectra under the influence of magnetic field, temperature and excitation intensity
[ETN-88-93122] 24 p3344 N88-29903
LUMINESCENT INTENSITY
U LUMINOUS INTENSITY
LUMINOSITY
NT STELLAR LUMINOSITY
Modes, masses, metallicities, and magnitudes of RR Lyrae variables
[DE87-013149] 01 p0109 N88-10703
Neutrinos in supernovae
[DE87-014295] 03 p0387 N88-12434
Comparison of global and nuclear properties of starburst and Seyfert 1 galaxies 03 p0388 N88-12438
Stellar cycle variability of solar-like stars: A sneak preview 04 p0510 N88-13136
A search for X-ray luminous late type stars in NIPSS data 04 p0511 N88-13143
Solar Dynamics and G-modes
[NASA-CR-180737] 06 p0605 N88-14911
Global properties of star formation in spiral galaxies
14 p1994 N88-21883
Hydrodynamical models of supernova SN 1987 A in the LMC
[DE88-701123] 15 p2151 N88-22837
Cosmological parameters and evolution of the galaxy luminosity function
[NASA-CR-183081] 21 p3030 N88-27986
The stability of disk galaxies and constraints on their mass-luminosity ratio
[SER-C-PREPUBL-FASC-27] 24 p3455 N88-30565
LUMINOUS FLUX DENSITY
U LUMINOUS INTENSITY
LUMINOUS INTENSITY
NT ILLUMINANCE
NT LUMINANCE
Trickle water and feeding system in plant culture and light-dark cycle effects on plant growth
03 p0361 N88-12273
Analysis of dust grain properties in two star forming regions through comparison of theoretical models to observations 17 p2451 N88-24559
Fiber optic sensors 19 p2670 N88-25870
Fiber optic sensing systems using high frequency resonant sensing heads with intensity sensors
[NASA-TM-101318] 22 p3080 N88-28293
LUMPING
Determination of lumped-mass thermal properties associated with autoclave curing of graphite/epoxy composites 21 p2925 N88-27364
LUNAR BASES
Space station accommodations for lunar base elements: A study
[NASA-TM-100501] 06 p0804 N88-14907
Advantages of manned lunar base
08 p1009 N88-16118
Critical issues for establishment of a permanently-occupied lunar base
[AD-A187128] 09 p1263 N88-17567
Lunar fiberglass: Properties and process design
[NASA-CR-182580] 11 p1466 N88-18740
Multimegawatt nuclear power system for lunar base applications 17 p2416 N88-24367
Applications of nuclear power to lunar and Mars missions 17 p2417 N88-24377
Electromagnetic powered vehicles (EMPV) for Mars exploration 17 p2419 N88-24388
Lunar base surface mission operations. Lunar Base Systems Study (LBSS) task 4.1
[NASA-CR-172050] 18 p2594 N88-25415
Advanced photovoltaic power system technology for lunar base applications
[NASA-TM-100965] 20 p2766 N88-26402
Lunar base launch and landing facility conceptual design, 2nd edition
[NASA-CR-172049] 20 p2885 N88-27135
Steps toward lunar settlement
[DE88-009141] 21 p2900 N88-27213
Space transportation nodes assumptions and requirements: Lunar base systems study task 2.1
[NASA-CR-172052] 23 p3183 N88-28944
Maintenance and supply options
[NASA-CR-172062] 24 p3332 N88-29837
LUNAR CRATERS
Conditions for geomagnetically trapping sub-micron lunar ejecta between L = 1.2 and L = 3.1
04 p0521 N88-13203
LUNAR CRUST
Chronology of early lunar crust
24 p3394 N88-30212
The complexity, depth, and rapidity of processes that formed the lunar crust 24 p3398 N88-30237
LUNAR EFFECTS
Orbital evolution of distant artificial earth satellites
24 p3445 N88-30506
LUNAR EVOLUTION
Chronology of early lunar crust
24 p3394 N88-30212
Nineteenth Lunar and Planetary Science Conference. Press abstracts
[NASA-CR-183037] 24 p3440 N88-30473
The origin of the moon: Further studies of the giant impact 24 p3440 N88-30474
LUNAR GRAVITATION
Resonance effects accompanying motion with low thrust in earth-moon system 24 p3446 N88-30510
LUNAR LANDING MODULES
A lunar transportation system
[NASA-CR-182561] 11 p1567 N88-19379
Lunar lander conceptual design: Lunar base systems study task 2.2
[NASA-CR-172051] 24 p3335 N88-29854
LUNAR LOGISTICS
Maintenance and supply options
[NASA-CR-172062] 24 p3332 N88-29837
LUNAR OCCULTATION
NT SOLAR ECLIPSES
LUNAR PERTURBATION
U LUNAR EFFECTS
LUNAR ROCKS
Chronology of early lunar crust
24 p3394 N88-30212
LUNAR SCATTERING
U DIFFUSE RADIATION
LUNAR SOIL
Photochemical conversion of nucleic acid components catalyzed by lunar soil 06 p0750 N88-14604
Uses of lunar sulfur
[DE88-009119] 21 p3031 N88-27990
LUNAR SPACECRAFT
NT LUNAR LANDING MODULES
Possibilities of economical improvements for Moon based rocket propulsion using lunar propellants
[ILR-MITT-196] 24 p3338 N88-29871
LUNAR SURFACE
Space station accommodations for lunar base elements: A study
[NASA-TM-100501] 06 p0804 N88-14907
Lunar fiberglass: Properties and process design
[NASA-CR-182580] 11 p1466 N88-18740
Energy requirements for HE-3 mining operations on the Moon 17 p2420 N88-24390
Lunar base launch and landing facility conceptual design, 2nd edition
[NASA-CR-172049] 20 p2885 N88-27135
Growth of planetary crusts 24 p3400 N88-30247
High-resolution (30 m) lunar radar images
24 p3442 N88-30486
LUNEBERG LENSES
U RADAR CORNER REFLECTORS
LUNG MORPHOLOGY
Lung function in simulated microgravity
12 p1654 N88-19907
LUNGS
NT ALVEOLI
Effect of exogenous cardiosynchronized counterpulsation on human regional and central hemodynamics 10 p1366 N88-18163
Liquid ventilation: New data and possible use in space medicine 12 p1654 N88-19908
Methods of measurement for the evaluation of monolayer properties. Development and applications --- lung surfactants
[ETN-88-92229] 15 p2104 N88-22532
LUTETIUM COMPOUNDS
Electrochromic cells with lutetium diphthalocyanine and semisolid polymer electrolytes
[AD-A188031] 10 p1352 N88-18078
LYAPUNOV FUNCTIONS
U LIAPUNOV FUNCTIONS
LYMAN ALPHA RADIATION
Lyman alpha SMM/UVSP absolute calibration and geocoronal correction
[NASA-TM-100314] 03 p0389 N88-12446
Hydrogen and deuterium in the local interstellar medium 04 p0521 N88-13204
Lyman-alfa/OH-resonance-absorbtion measurements and simulation calculations for the investigation of the induction behavior of methane/ethane/oxygen mixtures in reflected shock waves
[ETN-88-90806] 07 p0831 N88-15042
IUE program SUGSD: Varability time scale of H Ly-alpha from Uranus
[NASA-CR-182706] 13 p1856 N88-21107
The role of hydrogen thermalization in shaping the Lyman-alpha coma --- comets 14 p2007 N88-21971
Long duration coherent Lyman-alpha sources
16 p2268 N88-23571
A theoretical determination of the density at a traveling source that emitts particles
[ISAS-RN-351] 21 p3013 N88-27883
LYMAN SPECTRA
Experimental study of the role of plasma polarization on line shape in dense laboratory plasmas
[ETN-88-92001] 13 p1844 N88-21033
LYMPHOCYTES
Spleen lymphocyte nucleic acids in pregnant rats flown in space and their offspring 07 p0892 N88-15403
White blood cells in space: An experiment for the first Spacelab mission 09 p1127 N88-16757
Effects of pulsed and CW (Continuous Wave) 2450 MHz radiation on transformation and chromosomes of human lymphocytes in vitro
[AD-A193104] 21 p2987 N88-27736
Effect of microgravity on lymphocyte activation --- Spacelab D1 mission 22 p3061 N88-28163
LYOPHILIZATION
U COLLOIDING
LYOPHILS
U COLLOIDS
LYRA CONSTELLATION
Modes, masses, metallicities, and magnitudes of RR Lyrae variables
[DE87-013149] 01 p0109 N88-10703
The distances and absolute magnitudes of RR Lyrae variable stars 11 p1568 N88-19386

M

M STARS
The M-type stars
[NASA-SP-492] 02 p0252 N88-11592
Basic properties and variability
02 p0252 N88-11593
Spectroscopy and nonthermal processes
02 p0252 N88-11594
Mass loss 02 p0253 N88-11597
Circumstellar chemistry 02 p0253 N88-11598
Thermal atmospheric models
02 p0253 N88-11599
Quasi-thermal models 02 p0253 N88-11600
The atmospheres of M dwarfs: Observations
02 p0253 N88-11601
M dwarfs: Theoretical work 02 p0253 N88-11602
Evidence for an additional source of opacity during the impulsive phase of stellar flares
04 p0510 N88-13133
Magnetic fields on K and M stars
04 p0510 N88-13137
Carbon abundances and C12/C13 ratios in M giants
04 p0515 N88-13167
M dwarfs from the Einstein medium sensitivity survey
04 p0519 N88-13188
Asymptotic giant branch populations in composite stellar systems 13 p1854 N88-21098
Analysis of emission features in IRAS LRS spectra
21 p2928 N88-27380
Duplicity in the solar neighborhood: Part 4: Spectroscopic orbits for four dwarf M stars
[SER-C-PREPUBL-FASC-21] 24 p3454 N88-30561

M WINGS
U VARIABLE SWEEP WINGS

MAARS
U CRATERS

MACH NUMBER
Fundamentals of fighter aircraft design: Engine intake and afterbody 05 p0545 N88-13322
Static force and moment test of the Holloman narrow-gage rocket sled at Mach numbers from 3.5 to 5.5
[AD-A186291] 07 p0822 N88-14995
Shock structure and noise of supersonic jets in simulated flight to Mach 0.4
[NASA-TP-2785] 08 p1080 N88-16510
Mach number effects on transonic aeroelastic forces and flutter characteristics
[NASA-TM-100547] 09 p1113 N88-16675
Influence of base modifications on in-flight base drag in the presence of jet exhaust for Mach numbers from 0.7 to 1.5
[NASA-TP-2802] 11 p1488 N88-18881
Galileo probe parachute test program: Wake properties of the Galileo probe at Mach numbers from 0.25 to 0.95
[NASA-RP-1130] 11 p1488 N88-18884
Nonaxisymmetric body supersonic, aerodynamic prediction
[AD-A189338] 13 p1716 N88-20259
The influence of Mach number and heat transfer on the turbulent flow wall law
[NASA-TT-20230] 13 p1771 N88-20594
Preliminary in-flight boundary layer transition measurements on a 45 deg swept wing at Mach Numbers between 0.9 and 1.8
[NASA-TM-100412] 13 p1772 N88-20598
Measurement and analysis of the noise radiated by low Mach numbers centrifugal blowers
[AD-A189226] 13 p1833 N88-20966
The turbulent heat flux in low Mach number flows with large density variations
[DE88-006445] 14 p1911 N88-21419
High Reynolds number, low Mach number, steady flow field calculations over a NACA 0012 airfoil using Navier-Stokes and interactive boundary layer theory
[AD-A189871] 15 p2013 N88-22005
Flow quality of NAL two-dimensional transonic wind tunnel. Part 1: Mach number distributions, flow angularities and preliminary study of side wall boundary layer suction
[NASA-TT-20209] 16 p2165 N88-22911
Aeropropulsive characteristics of isolated combined turbojet/ramjet nozzles at Mach numbers from 0 to 1.20
[NASA-TP-2814] 17 p2299 N88-23757
Spatial stability of a compressible mixing layer
[NASA-CR-181671] 18 p2514 N88-24916
Effects of Mach number on acoustic-vortex interactions in a ramjet 19 p2625 N88-25573
The effects of RCS jet firing on the isolated Orbiter and mated coast phases of the glide return to launch site maneuver at Mach number 6 (IA302B)
[NASA-CR-180223] 20 p2766 N88-26403
Analysis of experimental data for cast 10-2/DOA2 supercritical airfoil at high Reynolds numbers
[AD-A192827] 21 p2892 N88-27166
Theoretical-numerical study of feasibility of use of winglets on low aspect ration wings at subsonic and transonic Mach numbers at reduce drag
[NASA-CR-4174] 21 p2892 N88-27168
Wind tunnel tests of elliptical missile body configurations at Mach numbers 0.4 to 5.0
[AD-A193525] 22 p3038 N88-28040

MACH REFLECTION
Analytical investigation of reflection of a regular or mach reflection over a secondary wedge
[AD-A185690] 06 p0703 N88-14316
The effect of collision angle on mach reflection
[AD-A185798] 06 p0704 N88-14319

MACH-ZEHNDER INTERFEROMETERS
Fiber optic single mode sensors
[FOA-C-30453-3.1] 06 p0780 N88-14790

MACHINE LEARNING
U LEARNING MACHINES

MACHINE LIFE
U SERVICE LIFE

MACHINE RECOGNITION
U ARTIFICIAL INTELLIGENCE

MACHINE STORAGE
U COMPUTER STORAGE DEVICES

MACHINE TOOLS
NT GRINDING MACHINES
NT LATHES
NT MILLING MACHINES
A passive vibration-cancelling isolation mount
05 p0595 N88-13636
Selected aspects of microelectronics technology and applications: Numerically controlled machine tools. Technology trends series no. 2
[PB87-132973] 06 p0696 N88-14268
Alignment and assembly tool for very large diameter cylinders
[NASA-CASE-MFS-28001-2] 06 p0711 N88-14360
Identification and feedback control of machine tool vibrations
[PB88-109715] 08 p0976 N88-15902
A problem of machine repair with a variable number of heterogeneous servers
[INPE-4245-PRE/1118] 08 p1074 N88-16482
Fiber-reinforced plastic composites. Possibilities and limitations of applications as machine-construction materials
[NASA-TT-20159] 15 p2031 N88-22102
Contribution to the study of modern materials for cutting tools
[ISAL-IDI1-87-17] 16 p2185 N88-23029
Determination of settings of a tilted head-cutter for generation of hypoid and spiral bevel gears
[NASA-CR-182138] 18 p2524 N88-24976

MACHINE TRANSLATION
Program translation via abstraction and reimplementation
[AD-A185845] 07 p0901 N88-15458
The Ada compiler: On the design and implementation of an Ada compiler
[ETN-88-91594] 09 p1215 N88-17284
Linguistic-technical aspects of machine translation
24 p3438 N88-30461
Linguistic barriers: Translation problems
24 p3438 N88-30465

MACHINERY
Optimization of a controlled two-server maintenance system
[INPE-4202-PRE/1083] 01 p0107 N88-10694

MACHINING
NT MILLING (MACHINING)
NT SPARK MACHINING
Components for measuring robots
[KFK-PFT-126] 03 p0332 N88-12092
Interactions between science and precision engineering
[DE87-010873] 04 p0426 N88-12643
Diamond turning of silicon for optics applications
[DE88-002501] 07 p0840 N88-15095
The mechanism of anisotropic silicon etching and its relevance for micromachinings
[MBB-UA-1013/86] 10 p1311 N88-17838
Government research on ceramics coating technology
16 p2184 N88-23019
Spur gears: Optimal geometry, methods for generation and Tooth Contact Analysis (TCA) program
[NASA-CR-4135] 16 p2215 N88-23216
Frequency Analysis of Acoustic Emission - Application to machining and welding
[DE88-701478] 18 p2570 N88-25262
The use of micromachined structures for the management of mechanical properties and adhesion of thin films 19 p2674 N88-25899
Ductile-brittle transition of cutting behavior in diamond turning of single crystal Si
[DE88-008890] 20 p2809 N88-26664
The knowledge based automatic extraction of the machinable surfaces for automatic CAD-CAM system
[INPE-4542-PRE/1288] 20 p2836 N88-26824
Surface properties in electric discharge machining
[NASA-TT-20243] 23 p3223 N88-29182
Evaluation of the potential health hazards associated with the machining of carbon fiber composites
[AD-A194835] 24 p3408 N88-30286

MACROCLIMATE
U CLIMATE

MACROMOLECULES
U MOLECULES

MACULAR VISION
U VISION

MAGAZINES (SUPPLY CHAMBERS)
Organic coatings to improve the storageability and safety of pyrotechnic compositions
[AD-A187158] 09 p1150 N88-16889

MAGELLANIC CLOUDS
Data recorded by the Rome room temperature gravitational wave antenna, during the supernova SN 1987 A in the Large Magellanic Cloud
[NOTA-INTERNA-879] 06 p0806 N88-14922
Color-magnitude diagrams of star clusters in the Magellanic clouds from wide-field electronography. Part 3: NGC 1841
[PUBL-SER-C-FASC-14] 07 p0944 N88-15740
Investigation of nuclei of active galaxies as well as sources in the Large Magellanic Cloud using the X-ray astronomy satellite EXOSAT
[ETN-88-91494] 11 p1570 N88-19399
Astron observations of supernova 1987A in large magellanic cloud 24 p3445 N88-30504
Gamma radiation expected from supernova 1987A in large magellanic cloud 24 p3445 N88-30505

MAGMA
Recent progress in magma energy extraction
[DE87-013083] 01 p0066 N88-10424
Petrogenesis of basalts from the Archean Matachewan Dike Swarm Superior Province of Canada
06 p0796 N88-14878
Upper mantle heterogeneity and composition of primary ocean island magmas 08 p1009 N88-16120
Ocean floor magmatism and problems of lithosphere formation 08 p1009 N88-16121
Status of the Magma Energy Project
[DE88-002413] 13 p1792 N88-20719
Advanced geothermal technologies
[DE88-004307] 15 p2091 N88-22463
Carbon analysis in natural olivine crystals of deep origin
[NASA-TT-20311] 19 p2734 N88-26239
Fine-scale traverses in cumulate rocks, Stillwater Complex: A lunar analogue study
[NASA-CR-183066] 20 p2823 N88-26747
Geothermal energy technology: Issues, R and D (Research and Development) and cooperative arrangements
[PB88-193107] 21 p2967 N88-27626
Time-dependent thermal convection of Earth mantle and double diffusive convection in magma chambers
[MITT-52] 21 p2974 N88-27663
What SNC meteorites tell us about Martian magmatism 23 p3303 N88-29679
Growth of continental crust: Clues from Nd isotopes and Nb-Th relationships in mantle-derived magmas
24 p3393 N88-30205
Pluton emplacement and magmatic arc construction: A model from the Patagonian batholith
24 p3393 N88-30206
Does subduction zone magmatism produce average continental crust 24 p3394 N88-30214
Evidence for crustal recycling during the Archean: The parental magmas of the stillwater complex
24 p3396 N88-30226
Mid to late proterozoic magmatism within Northeastern North America and its iplications for the growth of the continental crust 24 p3397 N88-30229
Late-Archaean crustal growth in the Lewisian Complex of Northwest Scotland: Diachroneity in magmatic accretion and implications for models of crustal growth
24 p3401 N88-30253
Volcanic contribution to crustal growth in the Central Andes: A new estimate and a discussion of uncertainties
24 p3401 N88-30255

MAGNESIUM
NT MAGNESIUM ISOTOPES
Investigation by differential scanning calorimetry of microstructure in a superplastic Al-Mg-Zr alloy
[AD-A184902] 05 p0564 N88-13439
The influence of slip mechanism on fatigue of Mg and Mg-2.3Li 05 p0600 N88-13672
Effect of Mg impurity on local vibrations of U-centers in LiF lattice 14 p1969 N88-21753

Microplasticity phenomena in graphite/magnesium metal matrix composites
[DE88-006772] 15 p2029 N88-22086
AGNESIUM ALLOYS
Cyclic deformation of an extruded AlMgSi alloy
05 p0598 N88-13654
The influence of microstructure and residual stresses on the initiation and propagation of short surface cracks on AlMgSi1 05 p0601 N88-13674
Characterization of the microstructures of various materials
[AD-A184961] 05 p0655 N88-14017
A fundamental understanding of the effect of alloying elements on the corrosion resistance of rapidly solidified Mg alloys
[AD-A189385] 13 p1741 N88-20413
Diffusion welding of aluminomagnesium alloys to ceramics 14 p1898 N88-21333
The age hardening response of thermomechanically processed Al-Mg-Li alloys
[AD-A189870] 15 p2039 N88-22147
Corrosion and electrochemical behavior of binary magnesium alloys
[AD-A190624] 15 p2040 N88-22154
Laser cladding of Ni, Nb and Mg alloys for improved environmental resistance at high temperature
[AD-A191274] 16 p2213 N88-23208
Strain hardening at large strains in aluminum alloys
[DE88-007415] 18 p2484 N88-24737
Effect of Zr or Cr content on the fracture toughness of the high purity Al-Zn-Mg alloys
[NASA-TT-20294] 19 p2616 N88-25518
Optimizing superplastic response in lithium containing aluminum-magnesium alloys
[AD-A192217] 20 p2774 N88-26451
Analysis of grain refinement and superplasticity in aluminum-magnesium alloys
[AD-A193029] 21 p2912 N88-27283
MAGNESIUM CHLORIDES
Influence of some parameters on the stress corrosion of a ABNT 304 stainless steel in MgCl/sub 2/
[DE87-703707] 04 p0416 N88-12580
MAGNESIUM COMPOUNDS
NT CHLOROPHYLLS
NT MAGNESIUM CHLORIDES
NT MAGNESIUM OXIDES
Performance characteristics of magnesium-sodium nitrate flares in oxygen-nitrogen atmospheres
[AD-A185274] 05 p0570 N88-13476
MAGNESIUM ISOTOPES
Prospects for large dynamic range isotope analysis using photon burst mass spectrometry
[DE88-009110] 19 p2613 N88-25505
MAGNESIUM OXIDES
Brittle to ductile transition to cleavage fracture
[DE88-004074] 10 p1420 N88-18481
Sintering of the heterogeneous MgO compacts
[DE88-010357] 20 p2767 N88-26408
MAGNESYN (TRADEMARK)
U SERVOMOTORS
MAGNET COILS
Development of a strong electromagnet wiggler
[DE88-000971] 05 p0645 N88-13952
The TITAN magnet configuration
[DE88-001826] 06 p0782 N88-14800
Proceedings of the International Workshop on Engineering Design of Next Step Reversed Field Pinch Devices
[DE88-001915] 09 p1251 N88-17494
Plasma physics design and major specifications of candidate reactors for FER design studies. Conceptual design study of FY86 FER
[DE88-751066] 10 p1411 N88-18416
Electromechanical timing measurement technique
[DE88-005098] 11 p1489 N88-18889
Development activities for a 21-T superconducting magnet and cryostat
[DE88-004370] 11 p1558 N88-19327
Quench detection by fluid dynamic means in cable-in-conduit superconductors
[DE88-007269] 18 p2585 N88-25359
MAGNETIC ABSORPTION
U ELECTROMAGNETIC ABSORPTION
MAGNETIC ANOMALIES
Area of reduced electron concentration in terrestrial plasmasphere 08 p1003 N88-16078
MAGNETIC BEARINGS
Model adaptation and imbalance compensation in rotors with active magnetic bearings
[ETN-87-90440] 01 p0056 N88-10361
Design feasibility report on investigation of magnetic bearings for the ocean colour monitor radiometer scanner
[BAE-TP-7849] 09 p1174 N88-17036
Modelling and control of an annular momentum control device
[NASA-CR-4138] 13 p1754 N88-20491
An advanced low-cost 2-axis active magnetic bearing flywheel --- satellite attitude control
14 p1877 N88-21213
Vibration and control of flexible rotor supported by magnetic bearings
[NASA-TM-100888] 17 p2345 N88-23977
MAGNETIC CIRCUITS
Test results on dual resonant power supply with flat top and flat bottom current
[DE87-007506] 09 p1157 N88-16933
Electromechanical timing measurement technique
[DE88-005098] 11 p1489 N88-18889
Influence of magnetic material on the transient of a controle electrovalve
[INPE-4418-PRE/1223] 12 p1624 N88-19713
MAGNETIC CLOUDS
Solar activity, magnetic clouds, and geomagnetic storms 01 p0115 N88-10735
Dynamics of magnetic clouds in interplanetary space
01 p0115 N88-10736
The expansion of magnetic clouds
01 p0115 N88-10737
MAGNETIC COILS
NT MAGNET COILS
Design and testing of electrical insulation for superconducting coils
[DE87-012256] 01 p0039 N88-10246
XeCl excimer laser with magnetic compressor
03 p0299 N88-11879
Scaling the electromagnetically driven explosive shock simulator 05 p0592 N88-13612
MAGNETIC COMPRESSION
Proceedings of the Energy Independence Conference: Fusion Energy and Plasma Physics
[DE88-700657] 09 p1253 N88-17507
MAGNETIC CONTROL
Magnetic control of low pressure discharges
[AD-A186794] 10 p1322 N88-17900
MAGNETIC COOLING
Magnetic anomalies in the rare earth oxide superconductors GdBa2Cu3O(7-x) and YbBa2Cu3O(7-x)
[AD-A190713] 15 p2144 N88-22793
Study of a magnetic refrigerator for space applications for temperatures under 20 K
[NASA-TT-20283] 19 p2641 N88-25668
MAGNETIC DIFFUSION
Influence of a magnetic field on the diffusion of small particles in a turbulent flow
[DE87-702877] 01 p0046 N88-10291
Vortex dynamics and transport to the wall in a crossed-field plasma sheath
[DE87-013286] 01 p0100 N88-10657
MAGNETIC DIPOLES
Modeling of proximity coupling between superconducting filaments in superconducting dipole magnets
[DE87-014684] 03 p0382 N88-12403
Rotation of magnetized particle in electrically conducting viscous medium 06 p0770 N88-14733
Properties of a magnetic dipole
[AD-A186128] 07 p0922 N88-15600
Magnetic field of planet Uranus: Predictions, measurements, interpretations 08 p1005 N88-16094
investigation of a new magnetic dipole mode in the heavy, deformed nuclei 154 Sm, 156 Gd, 158 Gd, 164 Dy, 168 Er, and 174 Yb with high resolution electron scattering
[ETN-88-91084] 09 p1245 N88-17460
Modeling the behavior of oriented permanent magnet material using current double theory
[DE88-004446] 13 p1833 N88-20963
SSC (Superconducting Super Collider) magnet technology
[DE88-007386] 19 p2733 N88-26230
Far- and mid-infrared properties of metal-insulator composite materials
[AD-A193227] 21 p2905 N88-27236
Passage of relativistic magnetic dipole moments through magnetic fields
[DE88-702640] 23 p3295 N88-29624
MAGNETIC DISKS
High density ion implanted contiguous disk bubble technology
[AD-A190169] 15 p2143 N88-22789
Corrosion problems associated with computer disk packs 22 p3054 N88-28121
MAGNETIC DISPERSION
Time-domain reciprocity theorems for electromagnetic fields in dispersive media
[PB88-126925] 10 p1319 N88-17886
MAGNETIC DISTURBANCES
NT MAGNETIC STORMS
The large Type 4 radio burst event of 24 April 1985 interpreted by dynamic spectral recordings and associated recordings 01 p0112 N88-10717
New results from high angular resolution observations of alpha Ori 04 p0514 N88-13161
Characteristics of atmospheric disturbances with a quasi-two day period 06 p0734 N88-14515
A compilation of Sudden Storm Commencements (SSCs), associated interplanetary disturbances, and cosmic ray variations
[IFSI-86-11] 06 p0807 N88-14923
Flare doublet: Interplanetary and geomagnetic effects
08 p1001 N88-16066
Unusually strong density decrease in near-Earth interplanetary plasma and magnetically quiet day as effects of isolated solar flare 08 p1002 N88-16072
Relationship between characteristics of low-energy electrons and geomagnetic disturbance in geostationary orbit 24 p3444 N88-30501
MAGNETIC EFFECTS
Electrodynamic tether system study
[NASA-CR-172024] 03 p0275 N88-11737
Magnetic field dependence of the specific heat of some high-T/sub c/ superconductors
[DE87-014078] 04 p0497 N88-13063
Study of some superconducting and magnetic materials on high T sub c oxide superconductors
[NASA-CR-182330] 06 p0785 N88-14813
Criteria of interplanetary parameters causing intense magnetic storms (Dst less than -100nT)
[NASA-CR-182423] 08 p1024 N88-16200
The Shubnikov de Haas effect in narrow-gap semimagnetic semiconductors
[ETN-88-92249] 14 p1988 N88-21861
Embryonic development of the newt Cynops pyrrhogaster in very weak magnetic fields
[ISAS-RN-357] 19 p2702 N88-26068
Effect of a weak magnetic field on high temperature superconductivity in Y-Ba-Cu-O ceramics
[DE88-702192] 19 p2733 N88-26235
Energy levels and magneto-electric effects in some quasi uni-dimensional semiconductor heterostructures
20 p2864 N88-27009
MAGNETIC FIELD CONFIGURATIONS
On tokamak equilibrium
[DE87-014811] 02 p0239 N88-11507
Magnetic field morphology in the upper layers
02 p0255 N88-11610
Laser induced fluorescent study of relativistic electron beams
[AD-A184456] 04 p0447 N88-12774
Large scale solar and stellar magnetic fields
04 p0507 N88-13117
Model of solar-wind magnetosphere coupling
04 p0525 N88-13211
Reversed field pinch plasmas with various boundary conditions
[DE88-000832] 05 p0653 N88-14004
A fluid simulation of the AMPTE lithium gas releases in the solar wind
[TRITA-EPP-87-06] 05 p0661 N88-14056
Magnetic field draping about coronal mass ejecta
[DE88-001805] 05 p0661 N88-14057
Observations of field-aligned current structures during the Coordinated Auroral Experiment using Scatter And Radar (CAESAR) flight 2 08 p1031 N88-16250
Experimental model of halo plasma observed in small-aspect FRC plasma
[INPE-4159-PRE/1061] 08 p1085 N88-16534
Design, construction and operation of a small RFP for turbulent plasma studies
[INPE-4241-PRE/1116] 08 p1087 N88-16545
Magnetic reconnection and solar flare loops
08 p1094 N88-16583
The effects of viscosity on resistive ballooning modes in line-tied coronal magnetic fields
08 p1097 N88-16599
Influence of viscosity on the structure of a magnetic neutral layer 08 p1098 N88-16605
D-3He fuels in a field-reversed configuration
[IPPJ-855] 10 p1411 N88-18419
Applications of Lie group methods to the equations of magnetohydrodynamics 10 p1411 N88-18422
Evaluation of magnetic coordinates in finite-beta asymmetric plasmas
[DE88-003665] 10 p1412 N88-18424
Magnetic and inertial fusion status and development plans
[DE88-004405] 11 p1552 N88-19288
Fully implicit three-dimensional MHD (magnetohydrodynamics) stability and evolution in toroidal geometry
[DE88-000624] 13 p1842 N88-21023
Magnetic cavity formation at Comet Halley and at the AMPTE Li release 14 p1996 N88-21898

Plasmapause formation
[AERONOMICA-ACTA-A-319-1987]
15 p2138 N88-22759
A mode-transforming polarization-rotatable launcher for the ATF (Advanced Toroidal Facility) fusion experiment
[DE88-005070] 19 p2730 N88-26213
Parallel gradient effects on ICRH (Ion Cyclotron Resonance Heating) in tokamaks
[DE88-009038] 19 p2730 N88-26216
MACH2: A two-dimensional magnetohydrodynamic simulation code for complex experimental configurations
[AD-A192285] 20 p2860 N88-26988
Global and local magnetohydrodynamic relaxations
[DE88-752602] 21 p3018 N88-27913
Millimeter wave generation by relativistic electron beams
[AD-A195683] 24 p3362 N88-30016

MAGNETIC FIELD INTENSITY
U MAGNETIC FLUX

MAGNETIC FIELD RECONNECTION
Numerical modeling of slow shocks
[DE87-014768] 04 p0454 N88-12808
Model of solar-wind magnetosphere coupling
04 p0525 N88-13211
Magnetic reconnection and solar flare loops
08 p1094 N88-16583
Coupling of microscopic and macroscopic processes in the Earth's magnetotail 08 p1095 N88-16588
Emerging flux, magnetic reconnection, plasma turbulence and waves in the transition zone of the solar atmosphere 08 p1096 N88-16597
Evidence of small-scale reconnection in the magnetosphere 08 p1097 N88-16601
An unusual magnetopause encounter by AMPTE-UKS
08 p1097 N88-16602

MAGNETIC FIELDS
NT BIOMAGNETISM
NT FORCE-FREE MAGNETIC FIELDS
NT GEOMAGNETISM
NT INTERPLANETARY MAGNETIC FIELDS
NT MAGNETIC CLOUDS
NT MAGNETOSTATIC FIELDS
NT PALEOMAGNETISM
NT PLANETARY MAGNETIC FIELDS
NT SOLAR MAGNETIC FIELD
NT STELLAR MAGNETIC FIELDS
NT TRAPPED MAGNETIC FIELDS
Recovery of vacuum gaps after arcing
[DE87-013852] 01 p0039 N88-10250
Influence of a magnetic field on the diffusion of small particles in a turbulent flow
[DE87-702877] 01 p0046 N88-10291
Visible free electron laser oscillator
[AD-A183871] 01 p0051 N88-10324
Plasma properties
[DE87-013662] 01 p0101 N88-10663
Electrical conductivity and equation of state measurements on planetary fluids at high pressures and temperatures
[DE87-013787] 01 p0110 N88-10708
Magnetic field twist driven by remote convective motions: Characteristics and twist rates 01 p0113 N88-10724
Study of pickup of cometary ions in turbulent solar winds 01 p0113 N88-10725
Dynamics of magnetic clouds in interplanetary space
01 p0115 N88-10736
The expansion of magnetic clouds
01 p0115 N88-10737
Equilibrium and tearing stability of thin current layers in magnetic arcades 01 p0118 N88-10754
Solar-geophysical data number 513, May 1987. Part 1: (Prompt reports). Data for April, March 1987 and late data
[PB87-204939] 01 p0119 N88-10760
Complex scattering dynamics and the integer quantum Hall effect
[DE87-011790] 02 p0243 N88-11536
Method estimating integral mean value of enhancement factor and path latitude for whistlers below magnetic latitude 10 deg 03 p0300 N88-11885
Excimer laser cell with longitudinal electron-beam excitation 03 p0302 N88-11903
Experimental study of stabilizing He-Ne laser output power with transverse magnetic field
03 p0303 N88-11906
Analysis of undulator field errors for XUV FELs (Extreme Ultraviolet Free Electron Laser)
[DE87-014734] 03 p0326 N88-12073
A tapered poloidal gap for the reduction of field errors
[DE87-014750] 03 p0377 N88-12375
Specific heat of the high T/sub c superconductors (La,M)2CuO4 and YBa2Cu3O7 in magnetic fields
[DE87-014660] 03 p0380 N88-12388
The impact of varves on solar physics
[NASA-CR-181519] 03 p0390 N88-12448
Relativistic electron precipitations in a pulsating aurora
04 p0468 N88-12894
Magnetic field dependence of the specific heat of some high-T/sub c/ superconductors
[DE87-014078] 04 p0497 N88-13063
Resistivity of EuBa2(Cu/sub 1-y/Zn/sub y/)3O/sub x/ as a ffunction of temperature, magnetic field, pressure and Zn concentration
[DE87-014740] 04 p0499 N88-13069
The dynamics of solar magnetic flux tubes subjected to resonant foot point shaking 04 p0507 N88-13118
Completely magnetically contained electrothermal thrusters
[AD-A185674] 06 p0674 N88-14129
Ferromagnetic mitigation of electromagnetic pulse effects
[AD-A185685] 06 p0694 N88-14258
The TITAN oscillating-field current-drive system
[DE88-001823] 06 p0782 N88-14798
Nature and the nonlinear evolution of electrostatic waves associated with the AMPTE (Active Magnetosphere Particle Tracer Explorers) solar wind releases
[AD-A185471] 06 p0806 N88-14920
Metallurgical processes in multi-component rare earth-transition metal permanent magnet alloys
[AD-A186401] 07 p0832 N88-15045
Harmonic expansion for the magnetic field of the helical solenoid
[DE88-700100] 07 p0928 N88-15636
Poloidal magnetics of compact ignition tokamaks
[DE88-001774] 07 p0934 N88-15672
Study on the model of a toroidal magnet for a tokamak with a strong field
[DE88-700346] 07 p0935 N88-15681
Simulation an experiment on plasma instability investigation in a tokamak with a divertor
[DE88-700352] 07 p0935 N88-15683
Possibility of calculation of magnetic surface function gradient and related quantities
[DE88-700561] 07 p0936 N88-15686
FTE like variations in the geomagnetic field at ground based conjugate stations in the cusp regions
[INPE-4345-PRE/1182] 08 p1024 N88-16199
Magnetic investigations of superconductive, polycrystalline (RE)1Ba2Cu3O(7-x) compounds (RE = Y, Gd, Ho, Dy)
[DE88-002537] 08 p1090 N88-16558
Acceleration of auroral particles by magnetic field-aligned electric fields
[TRITA-EPP-87-08] 09 p1190 N88-17131
Mechanism of change of vortex structure orientation in type-2 superconductors 09 p1239 N88-17425
Suppression of the mass enhancement in CeB6 in high magnetic fields
[DE88-002946] 09 p1241 N88-17439
Magneto-Inertia Confinement Approach (MICA) to fusion in dynamic Z-pinch formed from a frozen deuterium-tritium tube
[IPPJ-856] 09 p1252 N88-17504
X-ray diffraction study of thermotropic liquid crystalline polyesters and diester model compounds
[AD-A186788] 09 p1255 N88-17521
Realistic conductivity geometry model of the human head for interpretation of neuromagnetic data
[PB88-112230] 10 p1369 N88-18179
Evaluation of magnetic coordinates in finite-beta, asymmetric plasmas
[DE88-003665] 10 p1412 N88-18424
The relation of solar wind structure to hydromagnetic discontinuities
[DE88-004304] 10 p1431 N88-18546
Computer-aided modeling and prediction of performance of the modified Lundell class of alternators in space station solar dynamic power systems
[NASA-CR-182538] 11 p1507 N88-19000
Potential benefits of a broad magnetic fusion R and D program
[DE88-003288] 11 p1553 N88-19297
Toward a comprehensive theory for the sweeping of trapped radiation by inert orbiting matter
[NASA-CR-182584] 11 p1569 N88-19395
The effects of a dc electric field on the current driven ion cyclotron instability
[AD-A188877] 12 p1695 N88-20142
Effects of toroidal forces in current loops embedded in a background plasma
[AD-A188878] 12 p1695 N88-20143
Solar flares and magnetic topology
[AD-A188692] 12 p1712 N88-20244
Wiggler taper optimization for free-electron-laser amplifiers with moderate space-charge effects
[DE88-003758] 13 p1775 N88-20618
Experience with and ways to upgrade accuracy of hydromagnetic surveys in ocean
13 p1787 N88-20692
The Magnetically Insulated Inertial Confinement Fusion (MICF): A novel approach
[DE88-005460] 13 p1842 N88-21028
Helical ripple transport in stellarators at low collision frequency
[DE88-006431] 13 p1843 N88-21031
Increasing the rate at which ceramic castings undergo preliminary heat-treatment in an ultra-high frequency magnetic field 14 p1886 N88-21275
Eddy current losses induced by rotation of magnetisation
[BLL-M-37634-(5828.4)] 14 p1890 N88-21298
Research on variable-period wiggler type free electr lasers 14 p1902 N88-21360
Pulsed magnet fields for free-electron lasers
14 p1903 N88-21367
Analysis of induction motors based on the numerical solution of the magnetic field and circuit equations
[EL-59] 14 p1907 N88-21398
Statistical analysis of feasibility of non-destructive inspection of mechanical properties of hot worked pipes of alloy steels
[BLL-M-37598-(5828.4)] 14 p1922 N88-21455
Chaotic diffusion across magnetic field in a model of electrostatic turbulent plasma
[PREPRINT-566] 14 p1985 N88-21839
Analysis of anomalous resistivity during the conduction phase of the plasma erosion opening switch
[DE88-006382] 15 p2061 N88-22286
On the acceleration of electrons and positive ions in the same direction along magnetic field lines by parallel electric fields
[IRF-PREPRINT-103] 15 p2096 N88-22488
Electrical circuit modeling of reversed field pinches
[DE88-006942] 15 p2136 N88-22745
Parametric instabilities of inhomogeneous plasma near the lower-hybrid resonance
[DE88-701201] 15 p2137 N88-22748
Quantization of axial electrodynamics
[DE88-701498] 15 p2147 N88-22813
Application of magnetic barrier for increasing the efficiency of laser ion source
[DE88-701669] 16 p2212 N88-23200
Magnetic traps for an anti-hydrogen gas
16 p2269 N88-23572
Numerical research of dispersion properties of plasma cylindrical waveguides located in magnetic field
[DE87-703009] 16 p2275 N88-23615
Corpuscular plasma diagnostics complex on a tokamak with a strong field
[DE88-701576] 16 p2279 N88-23646
Solar-geophysical data number 520, December 1987. Part 1: (Prompt reports). Data for November 1987, October 1987 and late data
[PB88-164199] 16 p2290 N88-23712
Magnetic drive coupling
[NASA-CASE-MSC-21171-1] 17 p2344 N88-23973
Systematic variation of magnetic-field penetration depth in high-T(c) superconductors studied by muon spin relaxation 17 p2396 N88-24243
Electromagnetic penetration into a conducting circular cylinder through a narrow slot, TE case
[AD-A191602] 18 p2500 N88-24828
Application of particle simulations to the NRL laser experiment
[AD-A191641] 18 p2520 N88-24953
Solving time-dependent two-dimensional eddy current problems
[NASA-TM-100875] 18 p2566 N88-25239
Propagation of neutralized ion beams
[AD-A191599] 18 p2574 N88-25289
Basic processes of plasma propulsion
[AD-A192117] 18 p2577 N88-25310
Design studies of low aspect-ratio torsatrons
[DE88-007562] 18 p2579 N88-25320
Influence of alternating magnetic fields on Zn-67 Moessbauer resonance in ZnO
[PB88-186432] 18 p2584 N88-25352
Space station induced electromagnetic effects
18 p2591 N88-25394
Anomalous temperature-dependent negative magnetoresistance in pregraphitic carbons
[AD-A191725] 19 p2619 N88-25535
Theoretical study of the folded waveguide
[DE88-007877] 19 p2654 N88-25759
Optical sensing of magnetic fields
19 p2670 N88-25871
Experiments on insulation of relativistic electron flows in oblique and tapered magnetic fields
[DE88-007199] 19 p2724 N88-26176
Rutherford magnetic spectrograph for intense ion beam measurements on PBFA 2
[DE88-007281] 19 p2725 N88-26181
ECRH current drive in tokamak plasmas
[IPPJ-864] 19 p2729 N88-26209

The effects of magnetic nozzle configurations on plasma thrusters
[NASA-CR-183096] 19 p2732 N88-26223
Superconductive analogue of spin glasses
[DE88-702059] 19 p2733 N88-26233
Effect of a weak magnetic field on high temperature superconductivity in Y-Ba-Cu-O ceramics
[DE88-702192] 19 p2733 N88-26235
Application of superconducting technology to earth-to-orbit electromagnetic launch systems
[NASA-TM-101134] 20 p2763 N88-26385
Magnetic heat pump design
[DE88-007730] 20 p2798 N88-26605
Magnetohydrodynamic squeeze film
[DE88-701876] 20 p2810 N88-26669
Interaction of biological systems with static and ELF electric and magnetic fields
[DE88-007951] 20 p2831 N88-26792
Sources of polarized ions and atoms
[DE88-010910] 20 p2852 N88-26931
Symmetrized magnetic field configuration of low aspect ratio helical system
[IPPJ-869] 20 p2855 N88-26956
Thermal inhibition by megagauss field due to variation of electron temperature in laser plasma
[DE88-701887] 20 p2859 N88-26977
Megagauss field variation along axis of wire target in laser produced plasma
[DE88-701895] 20 p2859 N88-26979
An interferometric measurement technique for railgun structures
[AD-A192851] 21 p2901 N88-27217
Magnetic excitations in transition metal systems
[DE88-011022] 21 p2912 N88-27279
Electric and Magnetic Activity of the Central Nervous System: Research and Clinical Applications in Aerospace Medicine
[AGARD-CP-432] 21 p2977 N88-27683
Studies of the intact human brain: Implications for performance 21 p2977 N88-27684
Squid instrumentation for neuromagnetic study of complex brain activity 21 p2978 N88-27691
Electric and magnetic brain activity related to cognitive performance 21 p2979 N88-27692
Neuromagnetic evidence of place mechanisms for frequency and intensity coding in the human auditory cortex 21 p2979 N88-27693
Staggered-grid finite element solution technique for the Maxwell's equations in the time domain
[DE88-011731] 21 p3007 N88-27838
Tokamak magnetic turbulence over the safety factor range 0.6 less than q less than 3
[DE88-008421] 21 p3017 N88-27904
TE/TM (Transverse Electric/Transverse Magnetic) height profile measurements of transpolar VLF (Very Low Frequency) signals
[AD-A194503] 22 p3069 N88-28216
The far field from a hybrid electromagnetic pulse (HPD) simulator
[FOA-C-30480-4.2] 22 p3071 N88-28231
Physiological effects of extremely low frequency electric and magnetic fields
[DE88-752814] 22 p3132 N88-28620
CryoSQUID: A SQUID-based magnetic field sensor
[AD-A194237] 23 p3239 N88-29275
Waves and instabilities in an electron-positron plasma in an ultra-strong magnetic field
23 p3283 N88-29551
High-T(sub c) superconductor and its use in superconducting magnets
[DE88-008403] 23 p3289 N88-29581
Activity-rotation relations for lower main sequence stars 23 p3298 N88-29640
Resonant spin-flavor procession of solar and supernova neutrinos
[DE88-752604] 23 p3308 N88-29707
More than a solar cycle of synoptic solar and coronal data: A video presentation
[NASA-CR-181459] 23 p3308 N88-29708
NASA Marshall Space Flight Center solar observatory
[NASA-TM-100339] 24 p3332 N88-29832
Relationships among earth's gravity field, magnetic field, crustal structure and the magnetic character of crustal rocks
[AD-A195539] 24 p3392 N88-30198
Structuring processes in expanding laser-produced plasmas
[AD-A195249] 24 p3431 N88-30424
Stability of Venusian ionopause
24 p3448 N88-30523

MAGNETIC FLUX
The method of rigid armature flux orientation for the field-oriented control of highly dynamic drives with synchronous machines
[ETN-87-90405] 01 p0042 N88-10269
Theoretical Problems in High Resolution Solar Physics, 2
[NASA-CP-2483] 02 p0254 N88-11609
Magnetic field morphology in the upper layers
02 p0255 N88-11610
Magnetic fields in the overshoot zone: The great escape 02 p0256 N88-11616
Theoretical modelling of the fine structures in sunspots 02 p0256 N88-11617
Observational constraints and evidence for saturation
04 p0503 N88-13097
Magnetic flux tubes as sources of wave generation
04 p0505 N88-13108
Calibration of the Ca II K line-core density and the magnetic flux density in stars using solar data
04 p0507 N88-13116
The dynamics of solar magnetic flux tubes subjected to resonant foot point shaking 04 p0507 N88-13118
Reversed field pinch plasmas with various boundary conditions
[DE88-000832] 05 p0653 N88-14004
The appearance and disappearance of magnetic flux on the quiet sun
[AD-A185432] 05 p0661 N88-14055
Electrodynamics of midnight sector of auroral oval in period of slight disturbance 08 p1003 N88-16077
Flux tubes and loops in the solar chromosphere and corona 08 p1095 N88-16591
Emerging flux, magnetic reconnection, plasma turbulence and waves in the transition zone of the solar atmosphere 08 p1096 N88-16597
Evidence of small-scale reconnection in the magnetosphere 08 p1097 N88-16601
Ion flows in magnetospheric flux transfer events
08 p1098 N88-16607
Observations of small scale structures using data from the wave experiment on the AMPTE-UKS spacecraft
08 p1099 N88-16612
Magnetic emissions testing of the space station engineering model resistojet
[NASA-TM-100788] 10 p1292 N88-17728
Magnetic control of low pressure discharges
[AD-A186794] 10 p1322 N88-17900
Research on variable-period wiggler type free electron lasers 14 p1902 N88-21360
Properties of superconductors with strong electron-phonon interaction 14 p1974 N88-21779
Generation of flux tube waves in stellar convection zones. 1: Longitudinal tube waves
[NASA-TM-101152] 17 p2451 N88-24561
Permanent magnet excitation of axial flow synchronous machines with high rotation moment
[ETN-88-92385] 20 p2796 N88-26592

MAGNETIC INDUCTION
Electromagnetic induction in spherical earth containing oceans and continents in electrical contact with underlying section: Theory, method, example
08 p1011 N88-16127
Theoretical and experimental investigations on a linear, permanently excited stepping motor
[ETN-88-91061] 09 p1158 N88-16939
Evaluation of the magnetic induction conductivity method for detecting frazil ice deposits
[AD-A186940] 09 p1194 N88-17157
Magnetic drive coupling
[NASA-CASE-MSC-21171-1] 17 p2344 N88-23973
Integrated magnetic field sensor using high magnetotransistors
[ETN-88-92356] 21 p2941 N88-27465

MAGNETIC INDUCTION PROBES
U MAGNETIC PROBES

MAGNETIC LENSES
Bevalac external beamline optics
[LBL-23240] 19 p2727 N88-26194

MAGNETIC LEVITATION VEHICLES
Repulsive force support system feasibility study
[NASA-CR-178400] 04 p0402 N88-12497
The MBB propulsion concepts for magnetic suspension railways: Retrospective view and prospects
[MBB-Z-141/87] 10 p1316 N88-17865

MAGNETIC MATERIALS
NT FERROMAGNETIC MATERIALS
Magnetic diffuse scattering
[DE87-013539] 04 p0489 N88-13014
Rotation of magnetized particle in electrically conducting viscous medium 06 p0770 N88-14733
New equilibrium forms of free surface of confined magnetic fluid 06 p0770 N88-14734
Application of high temperature ceramic superconductors (CSC) to commercial tokamak reactors
[DE88-003973] 09 p1257 N88-17538
CdTe(110)-Mn interface reaction and the formation of non-equilibrium ternary semimagnetic semiconductor alloys
[AD-A187593] 10 p1422 N88-18491
Study of the production of some superconducting and magnetic materials by solidification in the drop tube and drop tower
[NASA-CR-182494] 11 p1461 N88-18708
Influence of magnetic material on the transient of a controle electrovalve
[INPE-4418-PRE/1223] 12 p1624 N88-19713
Exact image theory for the problem of dielectric/magnetic slab
[NASA-CR-182865] 16 p2189 N88-23055
Magnetic superlattices
[AD-A191450] 18 p2581 N88-25334
Use of magnetic materials in excimer laser circuits
[DE88-006449] 19 p2674 N88-25903
Novel magnetic materials research using free electron lasers
[DE88-009989] 20 p2807 N88-26652
An undulator radiation source for spin-polarized photoemission studies of novel magnetic materials
[AD-A193756] 22 p3083 N88-28307
Investigation of magnetic anisotropy and spin wave modes in transition metal multilayers
[DE88-009007] 22 p3154 N88-28765
DARPA-URI consortium meetings on submicron heterostructures of diluted magnetic semiconductors
[AD-A193499] 23 p3206 N88-29081
Mathematical theory and calculations of magnetic hysteresis curves
[DE88-011055] 23 p3277 N88-29510

MAGNETIC MEASUREMENT
Narsarsuaq (Greenland) Geophysical Observatory. Magnetic results, 1984
[ISBN-87-7478-281-9] 02 p0198 N88-11235
Measurements of stellar magnetic fields
04 p0503 N88-13093
The photospheric magnetic fields of cool stars: Recent results of survey and time-variability programs
04 p0503 N88-13094
Hitachi develops ceramic superconducting device
06 p0588 N88-14214
Viking quick look plots: A short description --- Swedish satellite 06 p0692 N88-14243
Effective methods of gravimetric and magnetometric data processing 06 p0728 N88-14479
Study of the technique of stress determination by measuring magnetism
[PB87-143905] 08 p0996 N88-16028
Magnetic field of planet Uranus: Predictions, measurements, interpretations 08 p1005 N88-16094
Report on ground-based activity at Andoya (Norway) in relation to the Aureld-VIP high rocket and to the Viking satellite --- Swedish satellite 08 p1026 N88-16212
Observations of field-aligned current structures during the Coordinated Auroral Experiment using Scatter And Radar (CAESAR) flight 2 08 p1031 N88-16250
Spaceborne magnetometry 12 p1644 N88-19846
Magnetic results, 1985
[ISBN-8-77-478282-7] 14 p1944 N88-21600
Excitations in magnetic low-dimensional systems: A spectroscopic study
[ETN-88-92230] 15 p2129 N88-22697
The SAMEX vector magnetograph: A design study for a space-based solar vector magnetograph
[NASA-TM-4048] 18 p2596 N88-25424
Rutherford magnetic spectrograph for intense ion beam measurements on PBFA 2
[DE88-007281] 19 p2725 N88-26181
Tokamak magnetic turbulence over the safety factor range 0.6 less than q less than 3
[DE88-008421] 21 p3017 N88-27904

MAGNETIC METALS
U MAGNETIC MATERIALS
U METALS

MAGNETIC MIRRORS
NT TANDEM MIRRORS
Fusion reactor physics and technology studies
[DE87-013691] 01 p0101 N88-10664
MHD stability and control for mirror machines
04 p0493 N88-13038
Curvature driven drift mirror instability in the magnetosphere
[IFSI-86-14] 06 p0742 N88-14568
Mirror theory applied to toroidal systems
[DE88-003832] 07 p0933 N88-15669
New methods of confinement and heating of plasma in magnetic fields
[DE88-701021] 15 p2135 N88-22738

MAGNETIC MOMENTS
Rotation of magnetized particle in electrically conducting viscous medium 06 p0770 N88-14733
TRISTAN research on neutron rich nuclei: Magnetic moments and nuclear structure
[DE88-002122] 06 p0783 N88-14807
Superconductivity in La/sub 1.85-x/Nd/sub x/Sr/sub .15/CuO
[DE88-003014] 09 p1258 N88-17540

best copy available

High temperature processing of superconducting Y1Ba2Cu3O6.9
[DE88-003002] 10 p1416 N88-18449
Neutrino magnetic moment and time variation of solar neutrino flux
[DE88-700687] 10 p1430 N88-18542
Passage of relativistic magnetic dipole moments through magnetic fields
[DE88-702640] 23 p3295 N88-29624

MAGNETIC PERMEABILITY
The effect of magnetic impurities and barriers on the magnetization and critical current of fine filament NbTi composites
[DE88-004443] 10 p1419 N88-18472

MAGNETIC POLES
Theoretical investigations of drift waves in a magnetic quadrupole 18 p2578 N88-25312

MAGNETIC PROBES
Thin superconducting film characterization by surface acoustic waves
[AD-A190417] 15 p2143 N88-22791

MAGNETIC PROPERTIES
NT ANTIFERROMAGNETISM
NT BIOMAGNETISM
NT CURIE TEMPERATURE
NT DIAMAGNETISM
NT FERROMAGNETISM
NT GEOMAGNETISM
NT GYROFREQUENCY
NT MAGNETIC EFFECTS
NT MAGNETIC FIELD RECONNECTION
NT MAGNETIC INDUCTION
NT MAGNETIC MOMENTS
NT MAGNETIC PERMEABILITY
NT MAGNETIC SUSPENSION
NT MAGNETOACOUSTICS
NT MAGNETORESISTIVITY
NT MAGNETOSTRICTION
NT PALEOMAGNETISM
NT PARAMAGNETISM
NT POLARIZATION CHARACTERISTICS
NT SPIN-LATTICE RELAXATION
Application of spin-sensitive electron spectroscopies to investigations of electronic and magnetic properties of solid surfaces and epitaxial systems
[DE87-014235] 02 p0245 N88-11550
Temperature hysteresis and magnetic transitions in amorphous Fe-Ni-Zr alloys
[DE88-000226] 03 p0294 N88-11848
Effect of rapid solidification on short-range order: A magnetic study
[AD-A185216] 05 p0565 N88-13444
Integrated systems with applications to the multi-phases of the ephemerides, physics and methematics of the upper atmosphere
[AD-A185748] 06 p0743 N88-14570
Study of some superconducting and magnetic materials on high T sub c oxide superconductors
[NASA-CR-182330] 06 p0785 N88-14813
The consequences of intergrain Josephson coupling in ceramic high-temperature superconductors
[DE87-013713] 06 p0785 N88-14816
Microstructure and magnetic properties of cobalt-chromium alloys
[DE88-002762] 07 p0835 N88-15064
Properties of a magnetic dipole
[AD-A186128] 07 p0922 N88-15600
Low field characterization of YBa2Cu3O sub 7-delta single crystals
[DE88-002695] 07 p0938 N88-15700
Magnetic investigations of superconductive, polycrystalline (RE)1Ba2Cu3O(7-x) compounds (RE = Y, Gd, Ho, Dy)
[DE88-002537] 08 p1090 N88-16558
Attenuation of ultrasonic waves in nonmagnetized magnetic fluids 09 p1234 N88-17398
Magnetic investigations of the one-dimensional Heisenberg magnet Gd2Cl3
[ETN-88-91063] 09 p1241 N88-17438
Magnetic properties of heavy fermion superconductors
[ETN-88-91076] 09 p1255 N88-17524
Superconducting and magnetic properties of Fe-doped oxide superconductors
[DE88-003024] 10 p1416 N88-18451
The physics of metallic superlattices: An experimental point of view
[DE88-003080] 10 p1416 N88-18452
Magnetic rare earth superlattices
[DE88-003483] 10 p1418 N88-18465
Brillouin scattering from collective spin waves in magnetic superlattices
[DE88-005347] 12 p1697 N88-20154
Theoretical studies on the electronic structure and properties of complex ceramic crystals and glasses
[DE88-005837] 13 p1846 N88-21049
A qualitative approach to electricity
[AD-A189854] 15 p2128 N88-22693
Magnetic anomalies in the rare earth oxide superconductors GdBa2Cu3O(7-x) and YbBa2Cu3O(7-x)
[AD-A190713] 15 p2144 N88-22793
Magnetic studies of iron-rare-earth-metalloid alloys
[DE88-006801] 16 p2282 N88-23660
Coexisting static magnetic ordering and superconductivity in CeCu2.1Si2 found by muon spin relaxation 17 p2396 N88-24245
Static magnetic ordering of CeCu2.1Si2 found by muon spin relaxation 17 p2396 N88-24246
Electromagnetic damping and vibration isolation of space structures
[AD-A191492] 18 p2471 N88-24665
The theory of random alloys
[DE88-006406] 18 p2487 N88-24756
Physical properties of f electron systems
[DE88-006886] 18 p2581 N88-25331
Magnetic superlattices
[AD-A191450] 18 p2581 N88-25334
Epitaxial iron films
[AD-A191815] 19 p2732 N88-26225
Structural and magnetic properties of Fe impurities in YBa2Cu3O(sub 7-delta)
[DE88-009961] 19 p2735 N88-26247
Magneto-optical studies of GaInAs-InP quantum wells
20 p2870 N88-27039
Influence of interfaces on electronic and magnetic properties of MnSe/ZnSe superlattices near monolayer limit 20 p2872 N88-27050
Characterization of structural and magnetic order of Er/Y superlattices 20 p2873 N88-27056
Investigation of magnetic anisotropy and spin wave modes in transition metal multilayers
[DE88-009007] 22 p3154 N88-28765
CryoSQUID: A SQUID-based magnetic field sensor
[AD-A194237] 23 p3239 N88-29275
Particle trajectories and potentials in a plane sheath moving in a magnetoplasma
[AD-A196228] 24 p3390 N88-30190

MAGNETIC RECORDING
Simulation of the perpendicular magnetic recording process
[B8713537] 05 p0586 N88-13570

MAGNETIC RELAXATION
NT SPIN-LATTICE RELAXATION

MAGNETIC RESONANCE
NT ELECTRON PARAMAGNETIC RESONANCE
NT NUCLEAR MAGNETIC RESONANCE
NT PARAMAGNETIC RESONANCE
Nuclear magnetic resonance studies of ion motion in solid electrolytes
[DE87-014547] 02 p0232 N88-11464

MAGNETIC SHIELDING
Magnet shielding analysis for SOAR: A space fusion reactor 17 p2400 N88-24269

MAGNETIC SIGNALS
SQUID (superconducting quantum interference device) arrays for simultaneous magnetic measurements: Calibration and source localization performance
[AD-A193615] 23 p3216 N88-29143

MAGNETIC SIGNATURES
Narssarssuaq Geophysical Observatory: Magnetic results, 1980-83. Instrumentation and formulas
[ISBN-87-7478-280-0] 03 p0350 N88-12209

MAGNETIC SPECTROSCOPY
Excitations in magnetic low-dimensional systems: A spectroscopic study
[ETN-88-92230] 15 p2129 N88-22697

MAGNETIC STARS
Ultraviolet spectra of two magnetic white dwarfs and ultraviolet spectra of subluminous objects found in the Kiso Schmidt survey
[NASA-CR-183051] 18 p2593 N88-25406

MAGNETIC STORAGE
NT BUBBLE MEMORY DEVICES
NT MAGNETIC DISKS

MAGNETIC STORMS
Solar activity, magnetic clouds, and geomagnetic storms 01 p0115 N88-10735
Magnetospheric storms 03 p0272 N88-11711
Modeling of environmentally-induced effects within satellites. Part 1: NASCAP modeling of satellites
03 p0273 N88-11721
Configurations of the quiet polar cap and its response to a sudden increase of the energy input rate epsilon
[DMI-GEOPHYS-PAPERS-R-74]
03 p0350 N88-12210
A compilation of Sudden Storm Commencements (SSCs), associated interplanetary disturbances, and cosmic ray variations
[IFSI-86-11] 06 p0807 N88-14923
Multispectral optical observations of ionospheric F-region storm effects at low latitude
[INPE-4231-PRE/1105] 08 p1024 N88-16198
Criteria of interplanetary parameters causing intense magnetic storms (Dst less than -100nT)
[NASA-CR-182423] 08 p1024 N88-16200
Balloon measurement of magnetic field during substorms in auroral zone 08 p1026 N88-16213
Interplanetary Magnetic Field (IMF) influence on the magnetic configuration and particle fluxes at geostationary orbit and on the substorm onset
08 p1031 N88-16247
A possible role for ionospheric ions in triggering a geomagnetic substorm onset 08 p1096 N88-16594
Field-aligned fluxes of energetic electrons related to the onset of magnetospheric substorms
08 p1096 N88-16595
The effects of a geomagnetic storm on thermospheric circulation
[AD-A186638] 09 p1190 N88-17128
Dynamics of small and large scale irregularities at sub-auroral latitudes
[AD-A189052] 12 p1645 N88-19863
Dynamics Explorer-2 measurements during an isolated auroral substorm
[AD-A191202] 18 p2543 N88-25081
Field-aligned structure of the storm time Pc 5 wave of November 14-15, 1979
[AD-A193022] 21 p2972 N88-27653
On the dynamics of the auroral ionosphere during the breakup of a substorm
[AD-A193368] 21 p2972 N88-27657
Corona-solar wind coupling review
[AFGL-TR-87-0203] 24 p3458 N88-30575

MAGNETIC SUBSTORMS
U MAGNETIC STORMS

MAGNETIC SURVEYS
Experience with and ways to upgrade accuracy of hydromagnetic surveys in ocean
13 p1787 N88-20682
Resolution of the magnetotelluric method for determining local inhomogeneities in the sedimentary cover 13 p1789 N88-20701

MAGNETIC SUSCEPTIBILITY
U MAGNETIC PERMEABILITY

MAGNETIC SUSPENSION
Repulsive force support system feasibility study
[NASA-CR-176400] 04 p0402 N88-12497
Status of magnetic suspension technology
07 p0811 N88-14809
The effect of sting interference at low speeds on the drag coefficient of an ellipsoidal body using a magnetic suspension and balance system
[NASA-CR-181611] 13 p1718 N88-20274
The 22nd Aerospace Mechanisms Symposium
[NASA-CP-2506] 14 p1924 N88-21468
Development of a magnetically suspended, tetrahedron-shaped antenna pointing system
14 p1926 N88-21470
Drag measurements on a laminar flow body of revolution in Langley's 13 inch magnetic suspension and balance system
[NASA-CR-182909] 19 p2597 N88-25432
Nutational stability of a satellite equipped with an active magnetic momentum wheel 20 p2784 N88-26513

MAGNETIC SWITCHING
Investigations into the design of multi-terawatt magnetic switches
[DE87-012014] 01 p0040 N88-10254
Magnetically switched power supply system for lasers
[NASA-CASE-NPO-16402-2] 18 p2505 N88-24862

MAGNETIC TAPE RECORDERS
U MAGNETIC RECORDING
U TAPE RECORDERS

MAGNETIC TAPES
Specification for IBM/IBM compatible 3480 tape cartridge
[NASA-TM-100702] 17 p2384 N88-24169
A guide to good magnetic tape management practice for MODAS users --- modular airborne data acquisition system (MODAS)
[RAE-TM-IT-212] 22 p3162 N88-28834

MAGNETIC TRANSDUCERS
Comparison of five readout techniques for an integrated magnetometer 19 p2671 N88-25976

MAGNETIC VARIATIONS
NT GEOMAGNETIC MICROPULSATIONS
NT GEOMAGNETIC PULSATIONS
NT NOCTURNAL VARIATIONS
Narssarssuaq Geophysical Observatory: Magnetic results, 1980-83. Instrumentation and formulas
[ISBN-87-7478-280-0] 03 p0350 N88-12209
Development of high stability fiber optic spectrophotometric systems for study of solar/stellar magnetic activity
[AD-A188327] 13 p1852 N88-21089
Magnetic field hourly averages from the Rome-GSFC experiment aboard Helios 1 and Helio 2
[NASA-TM-89782] 14 p2011 N88-21895

DOD 1985 world magnetic model: Charts and grid values
[AD-A191484] 18 p2541 N88-25080
MAGNETICALLY TRAPPED PARTICLES
NT INNER RADIATION BELT
NT RADIATION BELTS
Conditions for geomagnetically trapping sub-micron lunar ejecta between L = 1.2 and L = 3.1
04 p0521 N88-13203
Magnetic trapping of neutral atoms
[AD-A188473] 12 p1689 N88-20103
Helical ripple transport in stellarators at low collision frequency
[DE88-006431] 13 p1843 N88-21031
Magnetic traps for an anti-hydrogen gas
16 p2269 N88-23572
On the self-trapping of an electromagnetic wave in magnetized plasma
[DE88-701872] 20 p2858 N88-26974
MAGNETIZATION
Static magnetization and microwave loss in shock-modified ferrites
[DE87-012362] 02 p0146 N88-10916
Bulk superconductivity in La2CuO4
[DE88-002509] 09 p1254 N88-17516
Improved magnetization for YBa2Cu3O/sub 7-delta annealed in oxygen above 1000 C
[DE88-003934] 10 p1418 N88-18469
The effect of magnetic impurities and barriers on the magnetization and critical current of fine filament NbTi composites
[DE88-004443] 10 p1419 N88-18472
Magnetization studies of multifilamentary Nb3Sn wires
[DE88-009103] 19 p2735 N88-26243
Superconducting properties of oxygen deficient YBa2Cu3O(sub 7-delta)
[DE88-009969] 22 p3155 N88-28774
Effect of neutron irradiation on critical magnetization current in single crystal YBa2Cu3O(sub 7-delta)
[DE88-009970] 22 p3156 N88-28775
MAGNETO-OPTICS
Limits to the precision of electro-optic and magneto-optic sensors
[PB87-212536] 03 p0323 N88-12040
Optical correlation using the magneto-optic device
[AD-A192342] 20 p2854 N88-26950
MAGNETOACOUSTIC WAVES
Method and apparatus for non-destructive testing of temper embrittlement in steels
[NASA-CASE-LAR-13817-1] 23 p3195 N88-29012
MAGNETOACOUSTICS
The measurement of stress in steels of varying microstructure by Barkhausen and magneto-acoustic emission
[AERE-R-12387] 10 p1343 N88-18027
MAGNETOACTIVITY
NT MAGNETIC FIELD RECONNECTION
NT MAGNETORESISTIVITY
MAGNETOCARDIOGRAPHY
Methods and instrumentation for biomagnetism
[AD-A193811] 23 p3239 N88-29278
MAGNETOELASTIC WAVES
NT MAGNETOACOUSTIC WAVES
MAGNETOELASTICITY
U MAGNETOSTRICTION
MAGNETOGASDYNAMICS
U MAGNETOHYDRODYNAMICS
MAGNETOGRAMS
U MAGNETIC SIGNATURES
MAGNETOHYDRODYNAMIC ACCELERATION
U PLASMA ACCELERATION
MAGNETOHYDRODYNAMIC FLOW
Evolution of the solar wind structure in the outer heliosphere 01 p0112 N88-10721
Comparative plasma tails of Venus and comets
01 p0116 N88-10742
Solar transition region and coronal response to heating rate perturbations 02 p0256 N88-11620
Large-scale horizontal flows from SOUP observations of solar granulation 02 p0256 N88-11621
Sunspot observations from the SOUP instrument on Spacelab 2 02 p0257 N88-11623
The effect of object potentials on the wake of a flowing plasma
[AD-A184038] 03 p0379 N88-12385
Flux tube dynamics and solar/stellar redshift measurements 04 p0503 N88-13095
Subcommittee for MHD theory
[DE88-000596] 05 p0653 N88-14003
Numerical models for high beta magnetohydrodynamic flow
[DE88-001650] 05 p0654 N88-14006
Ultraviolet rocket-spectra of a sunspot
08 p1032 N88-16257
Experimental model of halo plasma observed in small-aspect FRC plasma
[INPE-4159-PRE/1061] 08 p1065 N88-16534
The formation of boundary layers by the entry of low-energy electrons and energetic ions into the Earth's magnetosphere 08 p1095 N88-16590
Evidence of small-scale reconnection in the magnetosphere 08 p1097 N88-16601
Influence of viscosity on the structure of a magnetic neutral layer 08 p1098 N88-16605
A study of single and binary ion plasma expansion into laboratory-generated plasma wakes
[NASA-CR-4125] 10 p1412 N88-18427
An adaptive grid finite difference method for time-dependent Magnetohydrodynamic (MHD) flows and its astrogeophysical applications
11 p1553 N88-19294
Investigation of low energy space plasma
[NASA-CR-182611] 12 p1694 N88-20138
Calculation of the shape of the contact surface at Comet Halley 14 p1985 N88-21892
Advanced diagnostics for reacting flows
[AD-A190485] 15 p2035 N88-22122
MPD (magnetoplasmadynamic) thrust chamber flow dynamics
[AD-A189940] 15 p2137 N88-22751
Basic processes of plasma propulsion
[AD-A192117] 18 p2577 N88-25310
Full-wave calculations in flux coordinates for toroidal geometry
[DE88-010131] 20 p2860 N88-26985
MAGNETOHYDRODYNAMIC GENERATORS
MHD (magnetohydrodynamics) channel development
[DE87-014126] 02 p0237 N88-11498
Gasdynamic effects in linear MHD generators
[ETN-88-91372] 06 p0784 N88-14810
Pulsed power sources based on MHD generators (a state-of-art review)
[DE88-700298] 07 p0935 N88-15677
Laser production and heating of plasma for MHD application
[NASA-TP-2798] 10 p1415 N88-18443
Arcs in cesium seeded noble gases resulting from a magnetically induced electric field
[EUT-87-E-177] 13 p1843 N88-21028
A general 2D electrical model for diagonally connected MHD generators
[DE88-004283] 14 p1984 N88-21835
Acoustical gas core reactor with MHD power generation for burst power in a bimodal system
17 p2403 N88-24290
Fluid dynamics of spherical cavity reactors
17 p2403 N88-24291
Nuclear reactor magnetohydrodynamic power generator for directed energy weapons 17 p2411 N88-24336
Fundamental analysis of space nuclear-MHD generator for gigawatt-level power 17 p2411 N88-24337
Liquid-metal MHD power conversion for space electric systems 17 p2411 N88-24338
Studies for the definition of a Faraday converter for space nuclear systems 17 p2411 N88-24339
A liquid metal MHD concept for multimegawatt space power application 17 p2413 N88-24348
Advanced LMMHD space power generation concept
17 p2415 N88-24364
A multimegawatt space power source radiator design
17 p2427 N88-24436
A nuclear powered space based multimegawatt MHD disc power system 17 p2432 N88-24471
Burst power gas core reactor with MHD power generation 17 p2433 N88-24472
Unified study of plasma/surface interactions for space power and propulsion
[AD-A195971] 24 p3338 N88-29870
MAGNETOHYDRODYNAMIC STABILITY
Equilibrium and tearing stability of thin current layers in magnetic arcades 01 p0118 N88-10754
Numerical simulation of Tokamaks: Ideal MHD equilibrium and stability
[DE87-013452] 02 p0218 N88-11373
Compact torus studies
[DE87-014254] 02 p0237 N88-11496
New directions in Vlasov plasma turbulence and anomalous transport
[DE87-014425] 02 p0238 N88-11500
Field-reversing electron and ion rings for the confinement and heating of plasmas
[DE87-014869] 02 p0238 N88-11505
Vectorization of MHD equilibrium and stability codes
[DE87-753013] 02 p0240 N88-11516
Stability of spheroidal spheromak plasma by use of force-free approximation
[IPPJ-846] 02 p0241 N88-11523
Magnetohydrodynamic stability of spheromak plasma in toroidal flux conserver with rectangular cross section 3. Stability for symmetric modes
[IPPJ-845] 02 p0241 N88-11524
Long wavelength vortices of low frequency interchange modes
[IPPJ-844] 02 p0241 N88-11525
Wavepacket propagation and current startup near the lower hybrid frequency in the torus
[IPPJ-840] 02 p0242 N88-11529
Limit of possible operation of crescent and bean shaped Tokamaks
[IPPJ-837] 02 p0242 N88-11532
Current-filamentation instability in railgun arcs
[AD-A184618] 03 p0269 N88-11693
Stability of low-shear Tokamaks
[DE88-000305] 03 p0379 N88-12383
The role of stellarators in the advanced toroidal program
[DE87-014815] 04 p0491 N88-13025
Transport simulations of the oscillating field current drive experiment in the ZT-40M reversed field pinch
[DE88-000538] 04 p0491 N88-13027
Magnetic fluctuation behaviour of current termination in reversed field pinch
[IPPJ-849] 04 p0492 N88-13034
MHD stability and control for mirror machines
04 p0493 N88-13038
A review of the experimental and theoretical status of the reversed-field pinch
[DE88-000529] 05 p0652 N88-14000
Reversed field pinch plasmas with various boundary conditions
[DE88-000832] 05 p0653 N88-14004
Curvature driven drift mirror instability in the magnetosphere
[IFSI-86-14] 06 p0742 N88-14568
Comments on the theory of absolute and convective instabilities
[PB87-124624] 06 p0783 N88-14808
Experimental research of electron beam instability on the Doppler anomalous effect
[DE88-700565] 07 p0932 N88-15658
Studies on parametric instabilities in high-frequency wave heating of fusion plasmas
[PH-156] 07 p0933 N88-15667
Free-boundary equilibrium problem for helically symmetric plasmas
[DE88-700101] 07 p0934 N88-15674
Simulation an experiment on plasma instability investigation in a tokamak with a divertor
[DE88-700352] 07 p0935 N88-1[illegible]3
Experimental evaluation for efficiency of excitation s[illegible] plasma and cyclotron waves in collective accelerators
[DE88-700566] 07 p0936 N88-15687
The rocket and scatter experiment ROSE: Presentation of the scientific payload 08 p1034 N88-16269
A generalized description of the anomalous Doppler resonance and the stabilizing role of ion dynamics
[INPE-4384-PRE/1204] 08 p1081 N88-16513
Experimental model of halo plasma observed in small-aspect FRC plasma
[INPE-4159-PRE/1061] 08 p1065 N88-16534
Design, construction and operation of a small RFP for turbulent plasma studies
[INPE-4241-PRE/1116] 08 p1087 N88-16545
The effects of viscosity on resistive ballooning modes in line-tied coronal magnetic fields
08 p1097 N88-16599
Conditional sampling in plasma turbulence
08 p1097 N88-16603
Data reduction and analysis of HELIOS plasma wave data
[NASA-CR-182466] 09 p1264 N88-17572
Tokamak with highly elongated cross-section of a plasma
[DE88-700356] 10 p1410 N88-18412
Plasma confinement calculations for TIBER-2
[DE88-004044] 10 p1412 N88-18425
Stability of an RFP (Reversed-Field Pinch) with resistive and distant boundaries
[DE88-004155] 10 p1413 N88-18431
The stability of free-electron lasers against filamentation
[DE88-004712] 10 p1414 N88-18435
Formation of high-Beta plasmas in various modes of operation in TPE-2 12 p1693 N88-20132
The stability of a screw-pinch plasma to global MHD modes 12 p1694 N88-20133
Improved confinement of screw pinch plasmas in SPICA 2 12 p1694 N88-20137
Large scale plasma irregularities observed in the nighttime ionosphere over Natal using a rocket-borne Langmuir probe
[INPE-4422-PRE/1226] 12 p1694 N88-20139

The effects of a dc electric field on the current driven ion cyclotron instability
[AD-A188877] 12 p1695 N88-20142
Effects of toroidal forces in current loops embedded in a background plasma
[AD-A188878] 12 p1695 N88-20143
Fully implicit three-dimensional MHD (magnetohydrodynamics) stability and evolution in toroidal geometry
[DE88-000624] 13 p1842 N88-21023
Magnetohydrodynamic (MHD) simulation of solar prominence formation 13 p1858 N88-21109
Particle simulation research by plasma parametric heating caused by strong laser
14 p1903 N88-21368
Ionization equilibrium and radiative energy losses in a stationary plasma
[DE88-700856] 14 p1984 N88-21832
Preliminary analysis on plasma equilibrium control. Conceptual design study of FY86 FER
[DE88-751441] 14 p1984 N88-21834
Analyses and experiments on the integrity and lifetime predictions of plasma-facing components in fusion reactors
[DE87-702957] 15 p2135 N88-22735
A proposal for the establishment of a center of excellence in theoretical geoplasma research
[AD-A189742] 16 p2231 N88-23327
Proceedings of Symposium on Physics of Target Implosion and Pulsed Power Techniques
[IPPJ-859] 16 p2276 N88-23619
The 2-D magnetohydrostatic configurations leading to flares or quiescent filament eruptions
[NASA-TM-101147] 18 p2595 N88-25423
Electron-acoustic waves in a beam-plasma system
[DE88-702053] 19 p2729 N88-26207
Stability of spheromak against current driven modes: Effects of flux hole on stability
[IPPJ-868] 19 p2730 N88-26211
Modulational instability of electric helicons in a magnetized collisional plasma
[DE88-701885] 20 p2858 N88-26976
Kinetic modulational instability of electron cyclotron waves in plasmas
[DE88-701893] 20 p2859 N88-26978
Reminimization of energy integral and stability limit for non-ideal MHD (magnetohydrodynamic) plasma
[DE88-008422] 21 p3018 N8[illegible]11
On plasma stability under anisotropic random [illegible] field influence
[DE88-702422] 21 p3019 N88-27918
Density fluctuations in currentless high beta plasmas in Heliotron E
[DE88-752310] 23 p3283 N88-29550
A survey of the current experimental database for lower hybrid current-drive and heating
[DE88-009830] 23 p3283 N88-29552
Numerical simulations of resistive magnetohydrodynamic instabilities in a poloidal divertor tokamak
[DE88-010768] 23 p3285 N88-29559

MAGNETOHYDRODYNAMIC TURBULENCE
NT PLASMA TURBULENCE
Evolution of mean square magnetic vector potential in compressible, two-dimensional, magnetofluid turbulence
[AD-A184985] 05 p0651 N88-13990
Coronal heating by means of helical magnetohydrodynamic turbulence
[AD-A187084] 10 p1410 N88-18413
Study of resistive pressure-gradient-driven turbulence
[DE88-005062] 10 p1414 N88-18441

MAGNETOHYDRODYNAMIC WAVES
NT ELECTROSTATIC WAVES
NT PLASMA WAVES
Interactions of oblique interplanetary discontinuities and their manifestations during STIP intervals 15-19
01 p0119 N88-10758
The acceleration of winds by MHD waves in open magnetic structures 04 p0506 N88-13109
MHD energy fluxes for late type dwarfs
04 p0512 N88-13148
Solar corona and solar wind 08 p1094 N88-16584
Small scale MHD wave processes in the solar atmosphere and solar wind 08 p1098 N88-16608
MHD waves in the solar atmosphere
08 p1098 N88-16609
Hydromagnetic cavity eigenmodes in a non-uniform plasma 08 p1098 N88-16610
Observation of a hydromagnetic wave in the earth's magnetosphere
[AD-A188942] 12 p1644 N88-19841
Shear Alfven spectrum of analytic high-Beta equilibria
12 p1694 N88-20136
Resonant Alfven wave instabilities driven by streaming fast particles 13 p1855 N88-21104
Alfven waves in plasma with finite ion temperatures
14 p1972 N88-21769
MHD bending waves in a current sheet
[NASA-TM-101149] 18 p2579 N88-25323
Magnetohydrodynamic wave propagation in the solar wind
[DE88-702411] 21 p3032 N88-27995
The study of hydromagnetic waves and RF heating using the TORTUS tokamak, the development of diagnostic techniques based on submillimeter lasers and the gyrotron, and gas discharge 24 p3431 N88-30419

MAGNETOHYDRODYNAMICS
Fundamentals of numerical magnetohydrodynamics
[DE87-011769] 01 p0100 N88-10656
Plasma properties
[DE87-013662] 01 p0101 N88-10663
Comparison of MHD simulation for the February 1986 events with interplanetary observations by the spacecraft Sakigake 01 p0113 N88-10722
A simulation of the IPS variations from a magnetohydrodynamical simulation
01 p0118 N88-10755
Compact torus studies
[DE87-014254] 02 p0237 N88-11496
Computational study of three-dimensional magnetohydrodynamic equilibria in toroidal helical systems
[DE87-753007] 02 p0240 N88-11514
Numerical modeling of slow shocks
[DE87-014768] 04 p0454 N88-12808
Implementation of a 3-D nonlinear MHD calculation on the intel hypercube
[DE87-014637] 04 p0479 N88-12949
Numerical simulation of the Reversed Field Pinch
[AD-A184353] 04 p0491 N88-13023
Rotation of magnetized particle in electrically conducting viscous medium 06 p0770 N88-14733
Coupling of microscopic and macroscopic processes in the Earth's magnetotail 08 p1095 N88-16588
The application of liquid-metal MHD (magnetohydrodynamics) to renewable energy sources
[DE88-003083] 09 p1251 N88-17495
Two-dimensional analysis for a scrapeoff and divertor regions with an MHD model. Conceptual design study of FY86 FER
[DE88-751069] 09 p1251 N88-17497
Applications of Lie group methods to the equations of magnetohydrodynamics 10 p1411 N88-18422
Self-similar solutions of MHD equations of plasma filament in the case of complete degenerated ultrarelativistic electron gas
[DE88-700684] 10 p1412 N88-18426
The relation of solar wind structure to hydromagnetic discontinuities
[DE88-004304] 10 p1431 N88-18546
Plasma rotation in a tokamak
[DE88-700855] 12 p1693 N88-20128
Experience with and ways to upgrade accuracy of hydromagnetic surveys in ocean
13 p1787 N88-20692
Implementation of a 3-D nonlinear MHD (magnetohydrodynamics) calculation on the Intel hypercube
[DE88-000625] 13 p1816 N88-20848
Time dependent MHD models for the cometary magnetosphere 14 p1997 N88-21900
Cometary MHD and chemistry: Application to Halley
14 p2000 N88-21922
ALEX results: A comparison of measurements from a round and a rectangular duct with 3-D code predictions
[DE88-005947] 15 p2135 N88-22741
Gigawatt, closed cycle, vapor core-MHD space power system conceptual design study
17 p2433 N88-24473
Generation of flux tube waves in stellar convection zones. 1: Longitudinal tube waves
[NASA-TM-101152] 17 p2451 N88-24561
MHD (magnetohydrodynamic) thermal hydraulic analysis of three-dimensional liquid metal flows in fusion blanket ducts
[DE88-009929] 19 p2731 N88-26219
Blanket technology experiments at Argonne National Laboratory
[DE88-010006] 19 p2731 N88-26220
Magnetohydrodynamic squeeze film
[DE88-701876] 20 p2810 N88-26669
Proceedings of the 2nd US-Japan Workshop on Advanced Plasma Modeling, volume 3
[IPPJ-867] 20 p2855 N88-26957
MACH2: A two-dimensional magnetohydrodynamic simulation code for complex experimental configurations
[AD-A192285] 20 p2860 N88-26988
Global and local magnetohydrodynamic relaxations
[DE88-752602] 21 p3018 N88-27913
Piecewise-parabolic methods for systems of hyperbolic conservation laws in multiprocessing environments
[DE88-010202] 23 p3248 N88-29029
The interaction of Io with the plasma torus
23 p3308 N88-29704
Theoretical modeling of accelerating arc plasmas
[AD-A195606] 24 p3432 N88-30426

MAGNETOIONIC PLASMA
U PLASMAS (PHYSICS)

MAGNETOMETERS
NT VARIOMETERS
Interplanetary magnetic field effects on the interaction of the solar wind with Venus 06 p0805 N88-14910
Comparison of five readout techniques for an integrated magnetometer 19 p2671 N88-25676
Carrier transport in semiconductor magnetic sensors under nonuniform fields 19 p2672 N88-25686
Studies of the intact human brain: Implications for performance 21 p2977 N88-27684

MAGNETOMETRY
U MAGNETIC MEASUREMENT

MAGNETOPAUSE
The formation of boundary layers by the entry of low-energy electrons and energetic ions into the Earth's magnetosphere 08 p1095 N88-16590
Evidence of small-scale reconnection in the magnetosphere 08 p1097 N88-16601
An unusual magnetopause encounter by AMPTE-UKS
08 p1097 N88-16602
Experimental evidence of micro-nonequilibrium on the magnetopause and further predictions
08 p1098 N88-16606
A study of the magnetic field annihilation process in the magnetosphere and some geotechnical applications
[DE88-004165] 10 p1355 N88-18096

MAGNETOPLASMADYNAMICS
Plasma thruster development
[AD-A184173] 04 p0408 N88-12536
MPD (magnetoplasmadynamic) thrust chamber flow dynamics
[AD-A189940] 15 p2137 N88-22751
Fundamental studies on MPD thrusters
[AD-A190307] 15 p2137 N88-22753
Physical fluid mechanics in MPD thrusters
[AD-A190309] 15 p2138 N88-22754
MPD (magnetoplasmadynamic) thruster advanced pumping system concepts
[AD-A190513] 15 p2138 N88-22756
Basic processes of plasma propulsion
[AD-A192117] 18 p2577 N88-25310
The effects of magnetic nozzle configurations on plasma thrusters
[NASA-CR-183096] 19 p2732 N88-26223
Performance and lifetime assessment of MPD arc thruster technology
[NASA-TM-101293] 24 p3336 N88-29880

MAGNETOPLASMAS
U PLASMAS (PHYSICS)

MAGNETORESISTIVITY
Nature of gigantic resistance fluctuations in metal-oxide-semiconductor wires
[DE88-002905] 09 p1256 N88-17530
Spin disorder resistivity and bare Curie temperature in the ferromagnetic superconductor ErRh4B4
[DE88-003016] 10 p1415 N88-18445
Normal and superconducting state properties of La2-xSr/sub x/CuO4
[DE88-003013] 10 p1416 N88-18450
Magnetic impurities in superconductors
[DE88-006917] 14 p1986 N88-21846
The Shubnikov de Haas effect in narrow-gap semimagnetic semiconductors
[ETN-88-92249] 14 p1988 N88-21861
Electrical conduction in thin film carbons
[AD-A191726] 18 p2491 N88-24780
Electron-Rayleigh wave interaction in thin film carbons
[AD-A191727] 18 p2492 N88-24781
Anomalous temperature-dependent negative magnetoresistance in pregraphitic carbons
[AD-A191725] 19 p2619 N88-25535
Anomalous RF magnetoresistance in copper at 4 K
[DE88-010232] 19 p2722 N88-26162

MAGNETOSPHERE-IONOSPHERE COUPLING
Model of solar-wind magnetosphere coupling
04 p0525 N88-13211
Studies of ionosphere/magnetosphere dynamics using SABRE and HILAT
[AD-A190947] 16 p2232 N88-23333
Investigations of magnetosphere-ionosphere coupling relevant to operational systems
[AD-A195972] 24 p3391 N88-30195
Corona-solar wind coupling review
[AFGL-TR-87-0203] 24 p3458 N88-30575

MAGNETOSPHERES
MAXIE 1
[AD-A189688] 14 p1882 N88-21247

Characteristics of solitary waves and weak double layers in the magnetospheric plasma
[IRF-PREPRINT-105] 24 p3431 N88-30418

MAGNETOSPHERIC ELECTRON DENSITY
Electrostatic VLF emission determined from rocket and satellite experiments 08 p1002 N88-16068
Field-aligned fluxes of energetic electrons related to the onset of magnetospheric substorms
08 p1096 N88-16595
Approximate analytical formulae for electron density and collision frequency in the natural and nuclear-disturbed ionosphere and inner magnetosphere
[AD-A193129] 21 p2972 N88-27654

MAGNETOSPHERIC ION DENSITY
The polar ionosphere and interplanetary field
[AD-A185386] 05 p0624 N88-13822

MAGNETOSTATIC FIELDS
Boundary element method for three-dimensional magnetostatic fields in terms of vector variables
[EL-61] 15 p2122 N88-22649

MAGNETOSTATICS
Boundary element method for three-dimensional magnetostatic fields in terms of vector variables
[EL-61] 15 p2122 N88-22649
Algorithm for accounting the conditions in infinity for two-dimensional magnetostatics problems
[DE88-701673] 16 p2264 N88-23541

MAGNETOSTRICTION
Static magnetization and microwave loss in shock-modified ferrites
[DE87-012362] 02 p0146 N88-10916
Ferromagnetic mitigation of electromagnetic pulse effects
[AD-A185685] 06 p0694 N88-14258
High density ion implanted contiguous disk bubble technology
[AD-A190169] 15 p2143 N88-22789
Research work completed at the Naval Surface Warfare Center Solid State Group of the Radiation Division
[AD-A191627] 18 p2582 N88-25339

MAGNETOTELLURIC PROFILING
U MAGNETIC SURVEYS

MAGNETOVARIOGRAPHS
U VARIOMETERS

MAGNETRON SPUTTERING
Method of producing high T(subc) superconducting NBN films
[NASA-CASE-NPO-16881-1-CU]
17 p2446 N88-24543
Equipment for building and testing superconductive flux flow electronic devices
[AD-A192959] 21 p2936 N88-27436
Preparation of superconducting YBa2Cu3O(sub 7-x) films by magnetron sputtering
[DE88-009977] 23 p3289 N88-29583
The lubricating properties of magnetron sputtered MoS2
[ESA-ESTL-76] 24 p3381 N88-30136

MAGNETRONS
Initial operation of a high-power whispering-gallery-mode gyrotron
[DE88-002500] 07 p0857 N88-15207

MAGNETS
NT ELECTROMAGNETS
NT FERRIMAGNETS
NT PERMANENT MAGNETS
NT SUPERCONDUCTING MAGNETS
NT WIGGLER MAGNETS
Present status of the high resolution spectrometers
[CEBAF-PR-87-029] 02 p0234 N88-11478

MAGNIFICATION
Taper sectioning to magnify the interface thickness of a dissimilar metal joint
[RFP-3890-REV] 03 p0333 N88-12099
Application of magnification xeroradiography to advanced ceramics
[DE88-009965] 20 p2778 N88-26473

MAGNIFIERS
U MAGNIFICATION

MAGNITUDE
NT STELLAR MAGNITUDE
The absolute total magnitudes of periodic comets and their variations 14 p1994 N88-21887
Cometary magnitude distribution: The tabulated data
14 p1995 N88-21888
Comet P/Halley: Visual magnitude estimates and gas production 14 p2007 N88-21968

MAGNONS
Non-lattice matched metallic superlattices
[DE87-011512] 04 p0497 N88-13062
Brillouin scattering from collective spin waves in magnetic superlattices
[DE88-005347] 12 p1697 N88-20154

MAGSAT SATELLITES
Spaceborne magnetometry 12 p1644 N88-19846

MAIN SEQUENCE STARS
NT DWARF NOVAE
NT DWARF STARS
NT FLARE STARS
NT RED DWARF STARS
NT SUN
PG 0308 + 096: A short-period white dwarf + dM binary with strongly modulated H-alpha emission
04 p0509 N88-13132
Stellar cycle variability of solar-like stars: A sneak preview 04 p0510 N88-13136
Relations between chromospheric and coronal structure, flux-flux correlations and convective zone properties
04 p0510 N88-13138
Broadband linear polarization and chromospheric CaII H and K line emission in late-type main sequence stars
04 p0511 N88-13140
Activity in warm stars 04 p0511 N88-13142
Emission features in IRAS LRS spectra of MS, S and CS stars 04 p0514 N88-13163
Spin-up and spin-down on the way to the main sequence 04 p0518 N88-13181
Mass loss from evolved stars
11 p1569 N88-19394
Activity-rotation relations for lower main sequence stars 23 p3298 N88-29640

MAINE
Revised Uniform Summary of Surface Weather Observations, Loring AFB, Maine, Parts A - F
[AD-A188201] 14 p1947 N88-21610

MAINTAINABILITY
Improving repairability of gears
02 p0158 N88-10989
An independent evaluation of the CH-46 Safety Reliability and Maintainability Program (SR and M)
[AD-A186310] 07 p0817 N88-14971
Supportability in aircraft systems through technology and acquisition strategy applications
[AD-A186465] 08 p0949 N88-15759
Preliminary analysis of an integrated logistics system for OSSA payloads. Volume 4: Supportability analysis of the 1.8m centrifuge 12 p1584 N88-19481
Statistical aspects of reliability, maintainability and availability
[AD-A188491] 12 p1634 N88-19783
Determining system maintainability as a probability
[DE88-007722] 19 p2679 N88-25927
Behavioral, psychological and demographic predictors of physical fitness
[AD-A192697] 21 p2986 N88-27733
Reliability and Maintainability (R and M)
[AD-A193857] 23 p3224 N88-29187

MAINTENANCE
NT AIRCRAFT MAINTENANCE
NT FILE MAINTENANCE (COMPUTERS)
NT SPACE MAINTENANCE
NT SPACECRAFT MAINTENANCE
Naval Aviation Integrated Logistics: Technical users guide version 1.0
[DE87-013368] 01 p0001 N88-10001
Rivista Tecnica Selenia, volume 10, number 2
[ETN-87-90763] 01 p0011 N88-10064
Optimum dimensioning of field service centers: Analysis of the problem and solutions thereof
01 p0012 N88-10066
Space Assembly, Maintenance, and Servicing Study (SAMSS) 01 p0015 N88-10089
Spacecraft Systems Working Group report
01 p0015 N88-10091
Space station assembly/servicing capabilities
01 p0016 N88-10100
Wet deposition and snowpack monitoring operations and quality assurance manual
[PB87-212817] 01 p0064 N88-10413
Optimization of a controlled two-server maintenance system
[INPE-4202-PRE/1083] 01 p0107 N88-10694
DEDALE: An expert system for analog circuit maintenance 02 p0128 N88-10809
Airworthiness of long-life jet transport structures
03 p0265 N88-11674
Diagnostics aid for mass spectrometer trouble-shooting
[DE88-000350] 03 p0324 N88-12049
Software maintenance in scientific and engineering environments: An introduction and guide
[NASA-CR-177409] 04 p0479 N88-12954
Avionic corrosion 05 p0547 N88-13332
US Naval Air Force avionic and electrical system corrosion prevention and control maintenance
05 p0547 N88-13334
Turbine engine supportability study for Army Aviation Systems Command (AVSCOM)
[DE88-002339] 07 p0820 N88-14984
Documentation in a software maintenance environment
[AD-A185892] 07 p0901 N88-15459
Rotorcraft transmission 08 p0956 N88-15802
Embedded expert system for space shuttle main engine maintenance 08 p1058 N88-16382
Expert systems relations in space applications
08 p1059 N88-16391
Verification of a micro-thrusting model to maintain satellites in low orbit
[AD-A186874] 09 p1133 N88-16793
The knowledge-based software assistant
09 p1204 N88-17213
Concept of a programmable maintenance processor applicable to multiprocessing systems
[NASA-TM-100406] 09 p1223 N88-17333
Micro PAVER concept and development airport pavement management system
[AD-A187360] 11 p1441 N88-18598
Profilometer for bomb-damage-repaired airfield pavements and measurement of pavement upheaval. Report 1: Technology evaluation
[AD-A187985] 11 p1442 N88-18601
Long term measurement network for FIFE
[NASA-CR-182491] 12 p1546 N88-19857
Turnaround operations analysis for OTV. Volume 1: Executive summary
[NASA-CR-179316] 13 p1729 N88-20340
Turnaround operations analysis for OTV. Volume 3: Technology development plan
[NASA-CR-179318] 13 p1729 N88-20342
Remote maintenance design activities and research and development accomplishments for the compact ignition tokamak
[DE88-006980] 16 p2279 N88-23645
Costs and benefits of AC propulsion
[PB88-173380] 16 p2287 N88-23691
The Environment for Application Software Integration and Execution (EASIE) version 1.0. Volume 4: System installation and maintenance guide
[NASA-TM-100576] 17 p2386 N88-24165
Aerospace energy systems laboratory: Requirements and design approach
[NASA-TM-100423] 17 p2390 N88-24206
Selection of a handling and maintenance option for the SP-100 ground engineering system test
17 p2402 N88-24285
Predictive corrosion modeling, volume 1
[AD-A191229] 18 p2485 N88-24739
A perspective of PC-based probabilistic risk assessment
[DE88-006715] 18 p2568 N88-25251
Mutually exclusive alternatives by clustering
[DE88-007707] 20 p2882 N88-27115
Evaluation of explosive bonding for patching aluminum with aluminum
[AD-A193303] 21 p2913 N88-27285
Avionic and electrical system corrosion prevention and control maintenance 22 p3054 N88-28119
Maintenance of vision-related components
23 p3242 N88-29296
Maintenance and supply options
[NASA-CR-172062] 24 p3332 N88-29837
Fuel effects on flame radiation and hot-section durability 24 p3347 N88-29925

MAINTENANCE TRAINING
Field evaluation of interactive simulation for maintenance training: SH-3 helicopter electro-mechanical bladefold system
[AD-A185923] 07 p0821 N88-14991
Air Force Human Resources Laboratory technical reports and technical papers
[AD-A186830] 09 p1201 N88-17200

MALDIVE ISLANDS
Application of SPOT data to renewable resources in the Maldives 22 p3109 N88-28469

MALES
Meta-analysis of leadership differences between males and females and the effect on performance
[AD-A187769] 11 p1564 N88-19361
Human factor in engineering work
12 p1663 N88-19970
Individual functional typology of sympathoadrenal system as indicator of physiological status in adverse environments 12 p1665 N88-19979

MALFUNCTIONS
A research on pilot performance in the case of aircraft malfunction
[ETN-87-90652] 02 p0217 N88-11369
A framework for real-time distributed expert systems: On-orbit spacecraft fault diagnosis, monitoring and control 08 p1066 N88-16440
TES: A modular systems approach to expert system development for real time space applications
08 p1066 N88-16441

Long term measurement network for FIFE
[NASA-CR-182491] 12 p1646 N88-19857

TALOS: A distributed architecture for intelligent monitoring and anomaly diagnosis of the Hubble Space Telescope 17 p2388 N88-24193

MALI

SPOT images and geochemical mapping of lateritic covers in southern Mali 22 p3105 N88-28438

MAMMALS

NT CATS
NT DOGS
NT HUMAN BEINGS
NT MICE
NT MONKEYS
NT PRIMATES
NT RATS

General biological character of adaptive capacity of mammalian metabolism in response to diverse and extreme environmental factors 08 p1047 N88-16324

Some process control/design considerations in the development of a microgravity mammalian cell bioreactor 09 p1197 N88-17174

Physiological and ecological implications of coupled heat- and water-transport mechanisms of endotherms and vegetation
[DE88-004170] 10 p1352 N88-18081

MAN

U HUMAN BEINGS

MAN ENVIRONMENT INTERACTIONS

Desertification in the Sahelian and Sudanian Zones of West Africa
[PB87-217063] 03 p0345 N88-12183

Disturbance and recovery of Arctic Alaskan tundra terrain. A review of recent investigations
[AD-A184442] 04 p0467 N88-12887

International geosphere-biosphere program: A study of global change
[PB86-142393] 11 p1510 N88-19021

System-wide medium-term environment programme for the period 1990-1995: Strategies of the United Nations system for the environment
[UNEP/GCSS.I/2] 12 p1641 N88-19826

An efficient model for changes of global climate and composition of the atmosphere due to human activities
[ETN-88-92359] 20 p2827 N88-26775

MAN MACHINE SYSTEMS

NT MAN-COMPUTER INTERFACE

A methodology for dynamic task allocation in a man-machine system
[DE87-007373] 01 p0077 N88-10492

System adaptivity and the modelling of stereotypes --- human-computer interaction
[NPL-DITC-91/87] 01 p0077 N88-10494

Input devices for tasks using interactive video
[NPL-DITC-87/87] 01 p0080 N88-10510

A rule-based system for arrival sequencing and scheduling in air traffic control 02 p0129 N88-10815

Nowcasting microbursts using Doppler radar in a forecaster-computer environment
02 p0200 N88-11246

A research on pilot performance in the case of aircraft malfunction
[ETN-87-90852] 02 p0217 N88-11369

A review of computer-assisted photo interpretation research at USAETL (US Army Engineer Topographic Laboratories)
[AD-A184034] 03 p0346 N88-12186

Architecture for dynamic task allocation in a man-robot symbiotic system
[DE87-013872] 03 p0362 N88-12277

A scientific workstation operator-interface for accelerator control
[DE87-014689] 03 p0362 N88-12278

Ground vehicle convoying
[DE88-000360] 04 p0502 N88-13088

A general architecture for intelligent training systems
06 p0796 N88-14875

Tools and technologies for expert systems: A human factors perspective 06 p0797 N88-14882

FAA air traffic control operations concepts. Volume 1: ATC background and analysis methodology
[AD-A185979] 07 p0818 N88-14973

Measurement and modification of sensorimotor system function during visual-motor performance
[AD-A186351] 07 p0889 N88-15387

Development and testing of an interactive procedure for the improvement of objective analyses
[AD-A186595] 08 p1040 N88-16290

Third Conference on Artificial Intelligence for Space Applications, part 1
[NASA-CP-2492-Pt-1] 08 p1055 N88-16360

Intelligent man/machine interfaces on the space station 08 p1063 N88-16418

Interfacing the expert: Characteristics and requirements for the user interface in expert systems
08 p1063 N88-16419

Space languages 08 p1063 N88-16420

Case-based reasoning for space applications: Utilization of prior experience in knowledge-based systems
08 p1065 N88-16433

A framework for real-time distributed expert systems: On-orbit spacecraft fault diagnosis, monitoring and control 08 p1066 N88-16440

Helicopter human factors research
09 p1109 N88-16644

Rotorcraft handling-qualities design criteria development 09 p1109 N88-16645

A piloted simulation investigating handling qualities and performance requirements of a single-pilot helicopter in air combat employing a helmet-driven turreted gun
[AD-A186878] 09 p1116 N88-16689

Analysis of tasks for dynamic man/machine load balancing in advanced helicopters
[DE88-003735] 09 p1117 N88-16696

Dynamic function allocation in fighter cockpits
[AD-A185397] 09 p1201 N88-17199

Comparison of alphanumeric data entry methods for advanced helicopter cockpits
[AD-A186934] 09 p1201 N88-17201

First Annual Workshop on Space Operations Automation and Robotics (SOAR 87)
[NASA-CP-2491] 09 p1203 N88-17206

Development of a comprehensive software engineering environment 09 p1203 N88-17211

An intelligent training system for payload-assist module deploys 09 p1204 N88-17214

Development and experimentation of an eye/brain/task testbed 09 p1205 N88-17219

Crew interface with a telerobotic control station
09 p1213 N88-17273

Crew interface with windshear systems
10 p1275 N88-17631

Medical and psychological problems of assuring flight safety under present conditions
10 p1359 N88-18123

Motion planning and control of robot manipulators via application of a computer graphics animated display
11 p1496 N88-18932

A worked example of an application of the SAINT simulation program
[AD-A188196] 11 p1524 N88-19097

Realtime pilot model parameter identification
[AD-A188873] 12 p1584 N88-19476

The ESA/Fokker service end-effector subsystem. A robotic/man-compatible servicing approach
12 p1587 N88-19502

Ground based supervisory and programming system for automatic experiment execution in orbit
12 p1590 N88-19519

Man-tended options for European space robotics
12 p1593 N88-19538

OMV man/system simulation integration: A preliminary analysis and recommendation
[NASA-CR-182602] 12 p1671 N88-20005

NAVLAB: An autonomous navigation testbed
[AD-A189049] 13 p1720 N88-20283

A personalized and prescriptive decision aid for choice from a database of options
[AD-A188726] 13 p1811 N88-20820

Mental models of mechanical systems: Individual differences in qualitative and quantitative reasoning
[AD-A189035] 13 p1812 N88-20823

Human problem solving in dynamic environments. Understanding and supporting operators in large-scale, complex systems
[AD-A189539] 13 p1812 N88-20826

F-16 simulator for man-in-the-loop testing of aircraft control systems (SIMTACS)
[AD-A189675] 14 p1870 N88-21178

Construction of a multidimensional questionnaire to determine interindividual differences in controlling attention
[DFVLR-FB-87-45] 14 p1952 N88-21637

Improving the man-machine interface to robotic systems
[NPL-DITC-100/87] 14 p1953 N88-21641

Human interfaces in remote driving
[DE88-006843] 14 p1953 N88-21643

Conflict resolution in cooperative systems
[AD-A190351] 15 p2104 N88-22535

Toward a mathematical formalism of performance, task difficulty, and activation 16 p2239 N88-23372

Capitalizing on failure through case-based inference
[AD-A190927] 16 p2255 N88-23480

Development and testing of a predictive methodology for optimization of man-machine interface in future avionics systems 17 p2304 N88-23780

Crewstation Information and Development System (CIDS) 17 p2304 N88-23781

A change in system design emphasis: From machine to man 17 p2304 N88-23782

Psychosensory cockpit ergonomics, advantages of intelligent information systems 17 p2304 N88-23784

Experience in the integration of human engineering effort with avionics systems development
17 p2305 N88-23793

A look toward the future of complex avionics systems development using the USAF Test Pilot School's avionics systems test training aircraft 17 p2306 N88-23797

Teleoperator human factors study
[NASA-CR-178930] 17 p2382 N88-24162

Dialog design: General requirements and analysis of an Ada system --- user interface design
[FOA-C-20691-2.7] 17 p2385 N88-24177

Human problem solving in complex dynamic environments
[AD-A190788] 18 p2551 N88-25142

Eye and head response to an attention cue in a dual task paradigm
[AD-A191052] 18 p2551 N88-25143

An advanced prototyping tool for human factors design
[AD-A187290] 18 p2552 N88-25149

A graphical, intelligent interface for discrete-event simulations
[DE88-000522] 18 p2557 N88-25181

Man versus machine: The role of astronauts in extravehicular activity 19 p2699 N88-26045

Introduction to human factors
[DE88-009021] 19 p2711 N88-26103

Preliminary study within a project for the development of intelligent assistance to piloting: Formal description of combat pilot expertise and implementation of an interactive system to represent operations
[CERMA-87-31] 20 p2833 N88-26806

Interaction management in CAD systems with a history mechanism
[CWI-CS-R8756] 20 p2840 N88-26851

Review of past and current trials and uses of unmanned vehicles
[AD-A194527] 22 p3084 N88-28311

General operational and training visual concerns
23 p3242 N88-29295

Artificial intelligence applied to process signal analysis
23 p3252 N88-29359

Prediction and measurement of human pilot dynamic characteristics in a manned rotorcraft simulation
[NASA-CR-183246] 24 p3410 N88-30297

Haptic exploration in humans and machines: Attribute integration and machine recognition/implementation
[AD-A193682] 24 p3410 N88-30299

Artificial intelligence in a mission operations and satellite test environment 24 p3416 N88-30334

Integrated resource scheduling in a distributed scheduling environment 24 p3417 N88-30342

Barriers to Information Transfer and Approaches Toward Their Reduction
[AGARD-CP-430] 24 p3437 N88-30458

MAN-COMPUTER INTERFACE

Gender and cognitive style differences at the human-computer interface
[NPL-DITC-90/87] 01 p0077 N88-10493

System adaptivity and the modelling of stereotypes --- human-computer interaction
[NPL-DITC-91/87] 01 p0077 N88-10494

Concepts and techniques for support of real time distributed operating systems
[AD-A184491] 03 p0367 N88-12307

Advanced Information Processing System (AIPS) proof-of-concept system functional requirements I/O network system services
[NASA-CR-181481] 03 p0384 N88-12412

SDVS (State Delta Verification System) 5 users' manual
[AD-A184339] 04 p0478 N88-12943

The ISI (Information Sciences Institute) grapher: A portable tool for displaying graphs pictorially
[AD-A184354] 04 p0478 N88-12944

User interface for a partially incompatible system software environment with non-ADP users
[DE88-001518] 04 p0482 N88-12988

Window system: A toolbox for interactive computer graphics
[PB87-234282] 06 p0756 N88-14637

Communications for the DTroll distributed database system
[AD-A185579] 06 p0791 N88-14853

A review of hypertext in a NASA project management context 06 p0793 N88-14859

A general architecture for intelligent training systems
06 p0796 N88-14875

Using multiple dialog modes in a user-system interface to accomodate different levels of user experience: An experimental study
[AD-A186115] 07 p0889 N88-15444

The crustal dynamics intelligent user interface anthology
[NASA-TM-100693] 08 p1067 N88-16448
User engineering: A new look at system engineering
09 p1206 N88-17231
Crew interface with a telerobotic control station
09 p1213 N88-17273
Methods of eliciting information from experts
[AD-A187468] 10 p1372 N88-18169
A digital circuit design environment
[AD-A188831] 12 p1623 N88-19709
Online aiding for human-computer interfaces
[AD-A189239] 13 p1815 N88-20842
A model for graphical interaction --- computer graphics
[CWI-CS-R8718] 13 p1818 N88-20866
Parallel graphical output from dialogue cells
[CWI-CS-R8719] 13 p1818 N88-20867
Application of expert systems in project management decision aiding
[NASA-CR-180762] 13 p1850 N88-21074
Applicability of nonlinear programming in decision support systems: Realization of user-friendly software
[REPT-87-42] 14 p1957 N88-21663
DataViews: A personalizable, interactive, data display system for the decisionmaker
[AD-A188509] 14 p1991 N88-21868
Investigation into the development of computer aided design software for space based sensors
[NASA-CR-180772] 15 p2107 N88-22552
Extension of computer based algorithms by operator analysts
[NASA-CR-182798] 15 p2111 N88-22575
The Scientific and Technical Information Network (STINET). Foundation for evolution
[AD-A189750] 15 p2148 N88-22822
Toward a mathematical formalism of performance, task difficulty, and activation 16 p2239 N88-23372
Resource management in dialog cell specification (DICE) method
[CWI-CS-R8746] 16 p2248 N88-23433
Virtual interface environment
17 p2381 N88-24153
An advanced prototyping tool for human factors design
[AD-A187290] 18 p2552 N88-25149
Knowledge acquisition tool implementation
[AD-A190415] 18 p2555 N88-25164
Development of training implying man-machine interface: From the aircraft to the spacecraft
19 p2700 N88-26052
Introduction to human factors
[DE88-009021] 19 p2711 N88-26103
The relationship between system response time, working memory, and task complexity: An empirical investigation
[DE88-000976] 19 p2711 N88-26105
SIMS: Single Interface to Multiple Systems
[AD-A192264] 20 p2837 N88-26832
The assessment of human/computer performance using human productivity measures: MIPS and BIPS are MEGAFLOPS
[DE87-013491] 21 p2993 N88-27750
The effect of input device on user performance with a menu-based natural language interface
[AD-A193095] 21 p2996 N88-27772
Image processing using a parallel architecture
[AD-A192833] 21 p3002 N88-27803
What's on the menu? Friendlier computers
[AD-A194393] 22 p3135 N88-28637
Knowledge elicitation for an operator assistant system in process control tasks 23 p3253 N88-29366
Intelligent interfaces for expert systems
23 p3258 N88-29397
A space station onboard scheduling assistant
23 p3259 N88-29402
Intelligent interface design and evaluation
23 p3260 N88-29405
MANIP --- spacecraft modeling program
[MANIP-217A] 24 p3335 N88-29855
Contributions to engineering models of human-computer interaction, volume 1
[AD-A195590] 24 p3409 N88-30295

MANAGEMENT
NT CONFIGURATION MANAGEMENT
NT CONTRACT MANAGEMENT
NT DATA MANAGEMENT
NT ENGINEERING MANAGEMENT
NT ENVIRONMENT MANAGEMENT
NT FINANCIAL MANAGEMENT
NT FOREST MANAGEMENT
NT INDUSTRIAL MANAGEMENT
NT INFORMATION MANAGEMENT
NT INVENTORY CONTROLS
NT INVENTORY MANAGEMENT
NT LAND MANAGEMENT
NT LOGISTICS MANAGEMENT
NT PERSONNEL MANAGEMENT
NT PROJECT MANAGEMENT
NT RESEARCH MANAGEMENT
NT RESOURCES MANAGEMENT
NT SAFETY MANAGEMENT
NT SYSTEMS MANAGEMENT
NT WATER MANAGEMENT
NT WEAPON SYSTEM MANAGEMENT
Issues in air transport and airport management
[PB87-204509] 02 p0124 N88-10782
Evaluating software testing methods to reduce testing duplication in US Army communications equipment acquisition
[AD-A186961] 09 p1216 N88-17292
Report of the Defense Science Board Summer Study on Technology Base Management
[AD-A188560] 13 p1851 N88-21078
Management: A bibliography for NASA managers
[NASA-SP-7500(22)] 14 p1991 N88-21867
Napping and human functioning during prolonged work
[AD-A190228] 15 p2102 N88-22525
Models and metrics for software management and engineering
[NASA-CR-182953] 17 p2389 N88-24200
Management and the executive
[AD-A190778] 18 p2587 N88-25374
Department of Defense Statement on the Balanced Technology Initiative to the Committee on Armed Services, United States Senate, 100th Congress, second session
[AD-A191841] 18 p2588 N88-25378
Idea processing for creativity and management
[DE88-006110] 19 p2714 N88-26113
Anatomy of an organizational change effort at the Lewis Research Center
[NASA-CR-4146] 19 p2739 N88-26264

MANAGEMENT ANALYSIS
FAA air traffic control operations concepts. Volume 1: ATC background and analysis methodology
[AD-A185979] 07 p0818 N88-14973
Field dependence-independence and its relationship to flight training performance
[AD-A188888] 12 p1670 N88-20003

MANAGEMENT INFORMATION SYSTEMS
CNET (Chief of Naval Education and Training) Program Automated Tracking System (CPATS): A comprehensive study
[AD-A184694] 03 p0385 N88-12418
University research initiative research program summaries
[AD-A184876] 05 p0658 N88-14035
Information needs analysis for the Aeronautical Systems Division Executive Information System
[AD-A186912] 09 p1261 N88-17556
Management Information and Downloader Interface System (MIDIS)
[AD-A186978] 09 p1261 N88-17557
Management information systems design implications: The effect of cognitive style and information presentation on problem solving
[AD-A188850] 12 p1705 N88-20205
Report of the Defense Science Board Summer Study on Technology Base Management
[AD-A188560] 13 p1851 N88-21078
Management and the executive
[AD-A190778] 18 p2587 N88-25374
IEMIS (Integrated Emergency Management Information System) floodplain mapping based on a LIDAR derived data set
[AD-A193071] 21 p2966 N88-27616
Database design and management in engineering optimization
[AD-A193325] 21 p3003 N88-27813
Developing a connector selection DBMS (database management system) using NIAM (Nijssen's Information Analysis Methodology)
[DE88-008110] 21 p3028 N88-27972
Reliability and Maintainability (R and M)
[AD-A193857] 23 p3224 N88-29187
The P-3 Scheduling Support System (P-3 S3)
[AD-A194824] 24 p3436 N88-30450

MANAGEMENT METHODS
NT DELPHI METHOD (FORECASTING)
Cost savings possible with Air Force conversion to JP-8 as its primary fuel
[AD-A183784] 01 p0030 N88-10192
A study of the Department of Defense configuration management policies and procedures as applied to the FA-18 Strike/Fighter program
[AD-A184872] 05 p0657 N88-14034
Design and management of research projects
[PB88-106380] 07 p0941 N88-15721
Operations research in management?
[MBB-Z-138/87] 10 p1311 N88-17835
Using SIR (Scientific Information Retrival) system for data management during a field program
[DE88-001555] 10 p1424 N88-18508
Distributed transaction processing and the Camelot system
[AD-A188614] 13 p1821 N88-20885
Application of expert systems in project management decision aiding
[NASA-CR-180762] 13 p1850 N88-21074
Management: A bibliography for NASA managers
[NASA-SP-7500(22)] 14 p1991 N88-21867
Propagation management for no-acknowledge HF communications links 18 p2502 N88-24843
Management and the executive
[AD-A190778] 18 p2587 N88-25374
Weight savings in aerospace vehicles through propellant scavenging
[NASA-TM-100900] 19 p2605 N88-25470
Engineering research centers and their evaluation
[PB88-180054] 19 p2739 N88-26262
Overview of the TITAN-2 reversed-field pinch aqueous fusion power core design
[DE88-008170] 20 p2857 N88-26966
Integration of SPOT data into a geocoded information system 22 p3098 N88-28400
Carrying out space projects 22 p3160 N88-28811
The Ariane line 22 p3161 N88-28828
Advanced information processing system: Input/output network management software
[NASA-CR-181678] 23 p3264 N88-29431
SDI (Strategic Defense Initiative) battle management/C3 (Command, Control and Communications) algorithms technology program plan
[AD-A194357] 23 p3275 N88-29495
Technical change needs organizational change
24 p3438 N88-30466

MANAGEMENT PLANNING
NT PRODUCTION PLANNING
NT PROJECT PLANNING
Documentation as a management strategy for reaching goals in high-risk research-oriented projects
[DE87-012394] 01 p0105 N88-10685
Space Construction
[NASA-CP-2490] 02 p0138 N88-10870
Marshall Space Flight Center's role in EASE/ACCESS mission management 02 p0139 N88-10875
An allotment planning concept and related computer software for planning the fixed satellite service at the 1988 space WARC
[NASA-TM-100244] 03 p0308 N88-11944
Comparison of pascal and the dBASE 3 PLUS language in programming an inventory management system
[AD-A184027] 03 p0365 N88-12300
Experimental use of artificial intelligence for (future) ATC systems
[PB87-108449] 04 p0482 N88-12970
Strategic management of research and development: A literature search
[NASA-CR-182337] 06 p0790 N88-14847
An evaluation of project scheduling techniques in a dynamic environment
[AD-A187057] 09 p1260 N88-17554
Information needs analysis for the Aeronautical Systems Division Executive Information System
[AD-A186912] 09 p1261 N88-17556
State of the art of natural language processing
[AD-A188112] 11 p1530 N88-19136
Science and technology in India
[PB88-134747] 11 p1564 N88-19362
District information system of National Information Centre
[PB88-134739] 11 p1565 N88-19373
A logical structuration for an administration of space projects
[INPE-4435-TDL/310] 12 p1585 N88-19482
Prototype manufacturing techniques for reducing cost, schedule, and technical risk 12 p1702 N88-20189
Minimizing development flight test time and cost in the US Air Force 12 p1703 N88-20192
Implementing information systems/office automation in an Air Force environment
[AD-A186956] 12 p1707 N88-20216
Management: A bibliography for NASA managers
[NASA-SP-7500(22)] 14 p1991 N88-21867
The challenges and opportunities of supersonic transport propulsion technology
[NASA-TM-100921] 17 p2307 N88-23806
Anatomy of an organizational change effort at the Lewis Research Center
[NASA-CR-4146] 19 p2739 N88-26264
Engine component retirement for cause. Volume 1: Executive summary
[AD-A192730] 20 p2760 N88-26371
Managing microcomputer applications: A primer and guide to good practice
[AD-A192992] 20 p2835 N88-26817
Large space projects --- management
22 p3159 N88-28805

Development and demonstration of an on-board mission planner for helicopters
[NASA-CR-177482] 24 p3328 N88-29817
Reduced flexibility in processing Titan 4 space launch vehicles at Cape Canaveral Air Force Station
[AD-A194908] 24 p3332 N88-29834

MANAGEMENT SYSTEMS
NT FLIGHT MANAGEMENT SYSTEMS
NT MANAGEMENT INFORMATION SYSTEMS
Comparison of pascal and the dBASE 3 PLUS language in programming an inventory management system
[AD-A184027] 03 p0365 N88-12300
Chicago's O'Hare Runway Configuration Management System (RCMS). Volume 1: Description of the operational software
[AD-A185886] 07 p0821 N88-14990
Chicago's O'Hare Runway Configuration Management System (RCMS). Volume 2: Users guide
[AD-A186222] 08 p0953 N88-15783
Using SIR (Scientific Information Retrival) system for data management during a field program
[DE88-001555] 10 p1424 N88-18508
Micro PAVER concept and development airport pavement management system
[AD-A187360] 11 p1441 N88-18598
RIAR automated research and management systems
[DE88-700934] 12 p1706 N88-20209
GTE battery management system: State of charge indicator evaluation
[DE88-006800] 15 p2058 N88-22272
A timestamp ordering mechanism with dynamic selection of rollback objects 16 p2257 N88-23489
Background to the UK military requirements for engine usage, condition and maintenance management systems
22 p3033 N88-28004

MANDELSTAM REPRESENTATION
Stimulated Mandelstam-Brillouin scattering during forward scattering of light 08 p1078 N88-16499
Secondary gauge conditions in field theory
[DE88-701499] 15 p2147 N88-22814

MANEUVERABILITY
Airframe/store compatibility 05 p0545 N88-13323
Future fighter maneuverability for air combat
[MBB/LKE-1/S/PUB/120] 10 p1312 N88-17843
On the maneuvering of vehicles
[AD-A187632] 10 p1427 N88-18521
Assessments of maneuverability with the TeleOperated Vehicle (TOV)
[AD-A191584] 21 p2993 N88-27751
Passive multipath target tracking in an inhomogeneous acoustic medium
[AD-A193284] 21 p3012 N88-27873
A second look at MIL prime flying qualities requirements 24 p3314 N88-29740

MANEUVERABLE REENTRY BODIES
NT LIFTING REENTRY VEHICLES
Maneuverable reentry vehicle trajectory footprints: Calculation and properties
[DE88-004726] 10 p1292 N88-17726

MANEUVERABLE SPACECRAFT
NT AEROSPACE PLANES
NT HOTOL LAUNCH VEHICLE
NT X-30 VEHICLE
National aero-space plane: A technology development and demonstration program to build the X-30
[GAO/NSIAD-88-122] 17 p2301 N88-23764

MANEUVERS
NT AIRCRAFT MANEUVERS
NT EVASIVE ACTIONS
NT HOVERING
NT ORBITAL MANEUVERS
NT ORBITAL RENDEZVOUS
NT SIDESLIP
NT SPACECRAFT DOCKING
NT SPACECRAFT MANEUVERS
Dynamics of spacecraft control laboratory experiment (SCOLE) slew maneuvers
[NASA-CR-4098] 01 p0014 N88-10082
Approach trajectory planning system for maximum concealment
[NASA-TM-88258] 02 p0227 N88-11435
How space, the fourth operational medium, supports operational maneuver
[AD-A184742] 03 p0373 N88-12346
Analytical investigation of the dynamics of tethered constellations in Earth orbit (phase 2)
[NASA-CR-179218] 04 p0408 N88-12533
Combined problem of slew maneuver control and vibration suppression
[NASA-CR-181537] 04 p0455 N88-12817
Aircraft flight test trajectory control
[NASA-CR-179428] 09 p1120 N88-16707
ADAM (Acquisition Deployment and Maneuvering): The space game
[AD-A189512] 12 p1685 N88-20078
Nonlinear flying quality parameters based on dynamic inversion
[AD-A192146] 18 p2464 N88-24627
Large planar maneuvers for articulated flexible manipulators
[NASA-CR-183079] 19 p2711 N88-26104
The effects of RCS jet firing on the isolated Orbiter and mated coast phases of the glide return to launch site maneuver at Mach number 6 (IA302B)
[NASA-CR-180223] 20 p2766 N88-26403
Performance of GPS-aided INS during high-dynamic maneuvers
[AD-A194624] 23 p3175 N88-28903
The principles of mass and maneuver applied to space operations
[AD-A194037] 23 p3276 N88-29500

MANGANESE
Sintered steels of high resistance alloyed to Nb, Mo, Mn and Si
[DE87-703546] 04 p0415 N88-12573
Effects of MN dispersoids on near threshold fatigue crack growth in 2134 type alloys
05 p0603 N88-13692
Concentration coefficients of elements in ferromanganese nodules relative to ocean sediments
06 p0726 N88-14464
Remote acoustic sounding of ferromanganese nodules
06 p0727 N88-14471
Ferromanganese nodules of Antarctic sector in Pacific Ocean 06 p0727 N88-14472
CdTe(110)-Mn interface reaction and the formation of non-equilibrium ternary semimagnetic semiconductor alloys
[AD-A187593] 10 p1422 N88-18491
Preparation and characterization of Cu2Zn1-xMnxGeS4
[AD-A188113] 11 p1556 N88-19315
Electron paramagnetic resonance studies of Mn(2+) in 2-6 semiconductor alloys 11 p1560 N88-19340
An experimental method for species concentration measurements in a welding arc using laser-induced fluorescence
[DE88-005638] 13 p1778 N88-20636
Kinetic of oxidation to air of a Fe-Al-Mn alloy system at 600-800(sup 0)C temperature range
[DE88-702309] 21 p2920 N88-27330

MANGANESE ALLOYS
Development of ultrafine grains and related properties in Hadfield manganese steels
[DE87-011884] 01 p0024 N88-10154
A comparison of high damping shape memory alloys with Cu-Mn-based and Fe-Cr-based alloys
[AD-A184110] 04 p0414 N88-12566
X-ray measurements of phason distortion in ion-implanted Al-Mn
[DE87-014566] 07 p0937 N88-15694
Influence of non-metallic elements in the mechanical properties of 20 Mn Mo Ni 55 steel
[DE88-700412] 10 p1300 N88-17775
Response of Fe-Cr-Mn austenitic alloys to thermal aging neutron irradiation
[DE88-003415] 10 p1302 N88-17785
The role of composition and microstructure gradients on weld metal properties and behavior
[DE88-004956] 10 p1303 N88-17791
Evaporation characteristics of elements during vacuum arc remelting of alloy A-286 15 p2055 N88-22248
Strain hardening at large strains in aluminum alloys
[DE88-007415] 18 p2484 N88-24737
Development of fine-grained carbide-particle hardened Hadfield manganese steels
[DE88-008919] 19 p2617 N88-25523
Reduced-activation austenitic stainless steels: The Fe-Cr-C system
[DE88-008091] 20 p2773 N88-26442

MANGANESE COMPOUNDS
NT MANGANESE OXIDES
Structure and function of the manganese complex involved in photosynthetic oxygen evolution determined by X-ray adsorption spectroscopy and electron paramagnetic resonance spectroscopy
[DE88-010360] 21 p2985 N88-27725

MANGANESE OXIDES
An investigation of the rechargability of certain modified forms of MnO2
[AD-A185919] 07 p0847 N88-15140

MANIFOLDS (MATHEMATICS)
NT RIEMANN MANIFOLD
Direction dependent connections of complex manifolds and their submanifolds
[DE87-703073] 02 p0225 N88-11419
A theory for the articulation of robot manipulators
03 p0333 N88-12097
Phenomenological implications of the blown-up orbifolds
[DE87-014606] 03 p0373 N88-12347
Transient periodic behavior related to a saddle-node bifurcation
[ETN-88-91321] 05 p0642 N88-13
There exists a C sup infinity symbol Kupka-Smale diffeomorphism of S sup 2 with neither sinks nor sources
[PB87-225967] 06 p0769 N88-14725
Error questions in the computation of solution manifolds of parametrized equations
[AD-A188648] 12 p1684 N88-200
Multicontinuations method and strong regular perturbations of linear operators
[DE88-701375] 16 p2263 N88-2353
Linearization along invariant manifolds and a generalization of the Hartman-Grobman theorems for degenerate singularities of vector fields in R cubed
[REPT-87-80] 20 p2845 N88-2
Geometry of superconformal manifolds, part 1
[DE88-702405] 21 p3011 N88-278
Geometry of superconformal manifolds, part 2
[DE88-702406] 21 p3011 N88-27864

MANIPULATION
U MANIPULATORS

MANIPULATORS
NT REMOTE MANIPULATOR SYSTEM
Telepresence work station system definition study, part 2
[NASA-CR-172006] 01 p0013 N88-10071
Telerobotics 01 p0015 N88-100
Traction-drive seven degrees-of-freedom telerobot arm: A concept for manipulation in space
[DE87-010895] 01 p0054 N88-10348
Exact solution of the inverse problem for a six-link manipulator with a mechanical offset
[DE87-702646] 01 p0054 N88-10349
Augmenting the control of a flexible manipulator with passive mechanical damping 01 p0055 N88-10350
A methodology for dynamic task allocation in a man-machine system
[DE87-007373] 01 p0077 N88-10492
Human factors in robotic system design discussed
02 p0158 N88-10
Robotics and Intelligent Systems Program
[DE87-014561] 02 p0223 N88-1140
Structure-dependent matrix representation of manipulator kinematics and its inverse solution
[DE87-752966] 02 p0229 N88-11447
A theory for the articulation of robot manipulators
03 p0333 N88-12097
Architecture for dynamic task allocation in a man-robot symbiotic system
[DE87-013872] 03 p0362 N88-12277
Modeling and control of large flexible vehicles in the atmosphere and space
[AD-A185368] 05 p0556 N88-13377
Control of a flexible one-link manipulator
[AD-A185035] 05 p0590 N88-135
Trajectory control of robot manipulators with closed-kinematic chain mechanism
[NASA-TM-89305] 05 p0591 N88-13
Cartesian path control of a two-degree-of-freedom robot manipulator
[NASA-CR-182331] 05 p0639 N88-139
Heuristic control of the Utah/MIT dextrous robot hand
06 p0793 N88-14
Dynamics, control and sensor issues pertinent to robotic hands for the EVA retriever system
06 p0796 N88-148
Goal driven kinematic simulation of flexible arm robot for space station missions 08 p1059 N88-16
Solid modelling for the manipulative robot arm (power) and adaptive vision control for space station missions
08 p1061 N88-164
Control system simulation for a single-link flexible arm
[AD-A187037] 09 p1174 N88-170
Robotic planner expert system (RPLANES)
09 p1209 N88-172
An optimal resolved rate law for kinematically redundant manipulators 09 p1212 N88-172
Telerobotic research at NASA Langley Research Center 09 p1213 N88-172
Manipulator arm design for the Extravehicular Teleoperator Assist Robot (ETAR): Applications on the space station 09 p1213 N88-1727
Telerobotic truss assembly 09 p1213 N88-1727
Design conditions and workspace for the generally-proportioned 3-hinge spherical wrist for robots
10 p1339 N88-18
Recursive forward dynamics for multiple robot arms moving a common task object
[NASA-CR-182526] 10 p1340 N88-18
Tactile sensing and inverse problems
[AD-A187464] 10 p1340 N88-18011
Parameter identification and sensitivity analysis for a robotic manipulator arm
[NASA-CR-181608] 10 p1385 N88-182

Adaptive control of a manipulator with a flexible link
[NASA-CR-181637] 11 p1476 N88-18807
Changes in the turbulent boundary layer structure associated with net drag reduction by outer layer manipulators
[NASA-CR-178152] 11 p1483 N88-18853
Time varying controller design for robot manipulator control
[AD-A188094] 11 p1494 N88-18919
Kinematic and dynamic analyses of the Stanford/JPL robot hand
[DE88-004637] 11 p1495 N88-18923
Real-time kinematic and dynamic analysis and adaptive model following control of manipulator arms
11 p1495 N88-18927
Motion planning and control of robot manipulators via application of a computer graphics animated display
11 p1496 N88-18932
Free boundary problems arising in the control of a flexible robot arm
[AD-A189124] 12 p1634 N88-19781
Intelligent control of robot manipulators in hazardous environments
[DE88-003305] 13 p1778 N88-20638
Modelling and simulation of a rate controlled manipulator arm --- Hermes
[NLR-TR-87010-U] 13 p1778 N88-20639
Force distribution and trajectory control for closed kinematic chains with applications to walking machines
13 p1779 N88-20642
Dynamics of high-speed mechanisms with elastic members 13 p1779 N88-20643
The dynamic control of robotic manipulators in space
[NASA-CR-182710] 13 p1779 N88-20646
New representation for kinematics of manipulator
[DE88-751446] 14 p1917 N88-21445
An efficient gradient projection optimization scheme for a seven-degree-of-freedom redundant robot with spherical wrist
[DE88-005440] 14 p1919 N88-21453
Telerobotic operation of conventional robot manipulators
[DE88-005718] 15 p2073 N88-22363
Design, development and evaluation of Stanford/Ames EVA prehensors
[NASA-CR-182688] 15 p2105 N88-22540
A three dimensional non-singular modelling of rigid manipulators
[AD-A189707] 15 p2116 N88-22604
Path following robot
[AD-A190960] 16 p2215 N88-23217
Microgravity mechanisms and robotics program
16 p2219 N88-23237
Base reaction optimization of manipulators with redundant kinematics 16 p2219 N88-23238
Microgravity manipulator demonstration
16 p2219 N88-23242
Accurate positioning of long, flexible ARM's (Articulated Robotic Manipulator) 16 p2219 N88-23243
Contribution to the adaptive dynamic control of a robot manipulator
[LAAS-87-350] 16 p2255 N88-23475
Remote maintenance design activities and research and development accomplishments for the compact ignition tokamak
[DE88-006980] 16 p2270 N88-23645
Space sprier crane
[NASA-CASE-LAR-13411-1-SB]
17 p2312 N88-23828
A design analysis for an automated robotic workpiece manipulator 17 p2344 N88-23975
Point accessibility and primary workspace of simple six-link robots 17 p2345 N88-23976
Precise computer controlled positioning of robot end effectors using force sensors
[NASA-CR-182887] 17 p2391 N88-24213
Energy optimal trajectory planning for robot manipulators and autonomous vehicles 17 p2437 N88-24497
The coordination of multiple robotic manipulators
[AD-A190869] 18 p2522 N88-24963
Kinematics, dynamics and control of a closed chain mechanism manipulator 18 p2523 N88-24967
Real-time implementation of a kinematic optimization scheme for seven-degree-of-freedom redundant robots with spherical wrists
[DE88-006785] 18 p2524 N88-24974
A computational model of motor behavior
[AD-A191179] 18 p2553 N88-25152
The efficacy of using human myoelectric signals to control the limbs of robots in space
[NASA-CR-182901] 18 p2553 N88-25155
Introduction to compliance in programming of robots
[ETN-88-92189] 18 p2561 N88-25201
Analysis of a closed-kinematic chain robot manipulator
[NASA-CR-183034] 18 p2561 N88-25206
Flexible tactile sensing arrays for robotics: Architectural robustness and yield considerations
19 p2671 N88-25878
Automatic calibration of space based manipulators and mechanisms
[NASA-CR-182804] 19 p2676 N88-25912
Underwater simulation for space teleoperation
19 p2698 N88-26040
Man versus machine: The role of astronauts in extravehicular activity 19 p2699 N88-26045
Underwater robotics in the service of oil field exploitation: The Running and Interconnecting Tool (RIT) in the East Frigg field (North Sea) 19 p2699 N88-26049
Large planar maneuvers for articulated flexible manipulators
[NASA-CR-183079] 19 p2711 N88-26104
Mobile remote manipulator system for a tetrahedral truss
[NASA-CASE-MSC-20985-1] 20 p2765 N88-26398
Design of a controller to reduce residual vibration in the positioning control of flexible robotic manipulators
20 p2806 N88-26658
Optimization of performance criteria with bounded joint velocities for robots with one degree of redundancy
[DE88-003915] 20 p2810 N88-26670
An introduction to robot joint control methods
[NLR-TR-86060-U] 20 p2811 N88-26677
Simulation of space manipulator operations (EUROSIM)
[NLR-MP-87017-U] 20 p2811 N88-26678
Experiments in adaptive control of a very flexible one link manipulator 20 p2842 N88-26865
Development of a hybrid simulator for robotic manipulators
[AD-A193119] 21 p2956 N88-27557
Control of free-flying space robot manipulator systems
[NASA-CR-183017] 21 p2956 N88-27562
Control of free-flying space robot manipulator systems
[NASA-CR-183104] 21 p2957 N88-27563
General expression of manipulator kinematics
[DE88-753430] 21 p2957 N88-27567
Dexterous hands: Optimizing grasp by design and planning 21 p2958 N88-27572
The VITE model: A neutral command circuit for a generating arm and articulator trajectories
[AD-A192715] 21 p2987 N88-27734
The analysis and control of robotic manipulators operating at or near kinematically singular configurations
22 p3084 N88-28315
Motion planning with obstacles and dynamic constraints 23 p3222 N88-29175
Study on design and control of torque-controlled manipulators
[NASA-TT-20197] 23 p3223 N88-29183
Implementation of a flexible link model in a designed robot system, using the finite element method
[ETN-88-92902] 23 p3243 N88-29303
A robotic system for automation of logistics functions on the Space Station 23 p3260 N88-29407
Next-generation space manipulator
23 p3263 N88-29428
Low-speed longitudinal flying qualities of modern transport aircraft 24 p3314 N88-29738
Modeling robot flexibility for endpoint force control
[AD-A195923] 24 p3380 N88-30132
Adaptive control in positioning a rigid-flexible robot arm
[AD-A195194] 24 p3422 N88-30367
Simulation of a two link robot manipulator with elastic members
[AD-A196014] 24 p3422 N88-30368
A standard architecture for controlling robots
[AD-A195929] 24 p3423 N88-30371

MANNED MANEUVERING UNITS
Personnel occupied woven envelope robot power
[NASA-CR-182367] 07 p0856 N88-15196
Personnel occupied woven envelope robot
23 p3260 N88-29406

MANNED MARS MISSIONS
Aeroassisted-vehicle design studies for a manned Mars mission
[NASA-TM-100031] 03 p0271 N88-11700
Aeroassisted manned transfer vehicle (TAXI) for advanced Mars Transportation: NASA/USRA 1987 Senior Design Project
[NASA-CR-181478] 03 p0275 N88-11736
Manned Mars mission accommodation: Sprint mission
[NASA-TM-100588] 16 p2290 N88-23711
Applications of nuclear power to lunar and Mars missions 17 p2417 N88-24377

MANNED ORBITAL LABORATORIES
NT SPACELAB
Metallurgy laboratory for Columbus, executive summary
[SNIAS-813-CA/TS] 02 p0157 N88-10980
Thermophysical Properties Measurement Facility (TPMF) --- Columbus space station
[ESA-CR(P)-2417] 02 p0157 N88-10981
A preliminary study of a fluid science laboratory for space station (Columbus). Part 4: Executive summary
[NLR-TR-87023-L-PT-4] 02 p0170 N88-11072
Man-Tended Free Flyer operational design features
12 p1585 N88-19485
Mission profiles of the MTFF co-orbiting with the US Space Station 12 p1585 N88-19487
Analysis of RVD operations in manned space missions
12 p1586 N88-19494
On a knowledge based assisted system for highly autonomous control of experiment-manipulators in the Man-Tended Free Flyer 12 p1588 N88-19505
Microgravity User Support Center (MUSC) for EURECA, Spacelab and Columbus missions
12 p1660 N88-19947
Arguments for manned or unmanned spacecraft activities
[REPT-46/87] 17 p2309 N88-23813

MANNED ORBITAL SPACE STATIONS
U SPACE STATIONS

MANNED SPACE FLIGHT
NT SPACE SHUTTLE MISSION 31-A
NT SPACE SHUTTLE MISSION 31-B
NT SPACE SHUTTLE MISSION 41-C
NT SPACE SHUTTLE MISSION 51-L
NT SPACE SHUTTLE MISSION 61-B
NT SPACE SHUTTLE MISSIONS
USSR report: Space
[JPRS-USP-87-003] 01 p0009 N88-10050
A matter-antimatter propulsion system for manned interstellar flight
[DE87-013311] 02 p0141 N88-10885
Progress in European CELSS activities
03 p0358 N88-12252
National Aeronautics and Space Administration space station proposal, fiscal year 1988
[S-HRG-100-328] 05 p0659 N88-14043
Preliminary estimates of galactic cosmic ray exposures for manned interplanetary missions
[NASA-TM-100519] 05 p0661 N88-14058
JPRS report: Science and technology. USSR: Space Biology and Aerospace Medicine, volume 21, no. 4, July - August 1987
[JPRS-USB-88-002] 07 p0893 N88-15412
Bibliography of space biology and medicine
07 p0897 N88-1543
Safety philosophy, policy, and requirements for manned spaceflight. Volume 1: Executive summary
[HEG-0886/1036-VOL-1] 08 p0982 N88-15826
Electrochemical processing of solid waste
[NASA-CR-182413] 08 p0987 N88-15852
JPRS report: Science and technology. USSR: Space
[JPRS-USP-87-006] 08 p1001 N88-16063
Integrity control of carbon fiber reinforced plastics (CFRP) structural elements. Conclusion with respect to the control methodology of CFRP primary structures in manned space flight and the implications to the design, analysis and testing of CFRP structural elements, executive summary
[MBB-TR-RB517-014/85] 09 p1139 N88-16824
Study on long term evolution towards European manned space flight. Volume 1: Executive summary
[MBB-RA3-004/87-VOL-1] 10 p1296 N88-17689
Present stage of space medicine
10 p1364 N88-18151
Certain aspects of human metabolism during spaceflights of varying duration
[NASA-TT-20215] 10 p1369 N88-18181
Basic results of medical studies during prolonged manned flights on-board the Salyut-7/Soyuz-T orbital complex
[NASA-TT-20217] 10 p1369 N88-18182
Liquid ventilation: New data and possible use in space medicine 12 p1654 N88-19908
Fluid volume changes in astronauts: How they fit our understanding of physiology 12 p1655 N88-19919
Radiation problems in manned space flight with a view to the Space Station 12 p1658 N88-19934
The influence of space flight on water-salt homeostasis in man and animals 12 p1659 N88-19943
JPRS report: Science and technology. USSR: Space
[JPRS-USP-88-002] 13 p1724 N88-20312
Study on long term evolution Towards European Autonomous Manned Spaceflight (STEAMS)
[SNIAS-SE/LS/AP-35-073] 13 p1727 N88-20330
Aeronautics and space report of the President: 1986 activities 13 p1852 N88-21087
International manned flight, USSR-SAR
[NASA-TT-20260] 16 p2166 N88-22914
Human performance issues arising from manned space station missions
[NASA-CR-3942] 18 p2553 N88-25156

Preliminary estimates of radiation exposures for manned interplanetary missions from anomalously large solar flare events
[NASA-TM-100620] 18 p2596 N88-25427
Proceedings of the Colloquium on Space and Sea
[ESA-SP-280] 19 p2685 N88-26016
Similarities between diving operations and space missions 19 p2687 N88-26027
Contribution of ultrasonic Doppler detection of circulating bubbles to human interventions under the sea and in space 19 p2687 N88-26029
History of manned spaceflight
[CNES-NT-121] 21 p3032 N88-28000
Study of biological effects and radiation protection to future European manned space flights
[DGT-33061] 23 p3281 N88-29535
Study on long-term evolution towards European manned spaceflight. Volume 1: Executive summary
[ERNO-OX1-002/88-VOL-1] 24 p3330 N88-29827
JPRS report: Science and technology. USSR: Space
[JPRS-USP-88-001] 24 p3444 N88-30498

MANNED SPACECRAFT
NT AEROSPACE PLANES
NT CHALLENGER (ORBITER)
NT COLUMBUS SPACE STATION
NT DISCOVERY (ORBITER)
NT HERMES MANNED SPACEPLANE
NT HOTOL LAUNCH VEHICLE
NT MANNED ORBITAL LABORATORIES
NT MIR SPACE STATION
NT SALYUT SPACE STATION
NT SOYUZ SPACECRAFT
NT SPACE SHUTTLE ORBITERS
NT SPACE SHUTTLES
NT SPACELAB
NT X-30 VEHICLE
Design study for asteroidal exploitation
03 p0389 N88-12445
Techniques for fire detection
04 p0406 N88-12521
Space station accommodations for lunar base elements: A study
[NASA-TM-100501] 06 p0804 N88-14907
A systems analysis of fire suppression alternatives for the US space station
[AD-A189847] 15 p2025 N88-22064
Arguments for manned or unmanned spacecraft activities
[REPT-46/87] 17 p2300 N88-23813
Hatch cover
[NASA-CASE-MSC-21356-1] 18 p2472 N88-24671
The human element in space: Lessons from Antarctica
[AD-A193440] 21 p2988 N88-27741

MANPOWER
NT SCIENTISTS
MANPRINT handbook for RFP (Request For Proposal) development
[AD-A188321] 13 p1850 N88-21075

MANTLE (EARTH STRUCTURE)
U EARTH MANTLE

MANUAL CONTROL
The optimal control pilot model and applications
24 p3315 N88-29741

MANUALS
NT USER MANUALS (COMPUTER PROGRAMS)
Naval Aviation Integrated Logistics: Technical users guide version 1.0
[DE87-013368] 01 p0001 N88-10001
Wet deposition and snowpack monitoring operations and quality assurance manual
[PB87-212817] 01 p0064 N88-10413
DOE explosives safety manual
[DE88-000831] 04 p0422 N88-12616
A portable hypercube simulator
[DE87-013369] 04 p0476 N88-12947
National Synchrotron Light Source users manual: Guide to the VUV and X-ray beam lines
[DE88-001464] 04 p0490 N88-13020
US Naval Air Force avionic and electrical system corrosion prevention and control maintenance
05 p0547 N88-13334
Development of a prototype H-46 helicopter diagnostic expert system
[AD-A186077] 07 p0809 N88-14924
Standardization of software development
[INPE-4330-NTE/272] 08 p1088 N88-16455
Temperament Structure Scales (TSS). Test manual
[ESA-TT-1069] 09 p1201 N88-17197
ZAP user's manual
[LBL-21270] 11 p1546 N88-19248
User's manual for EULER3DS
[AD-A191048] 16 p2208 N88-23177
Users guide to CAESAR
[BCRS-87-04] 16 p2229 N88-23306
Concurrency efficiency user's manual
[AD-A190884] 16 p2251 N88-23450
Advisory circular: Noise certification handbook
[FAA-AC-36-4B] 17 p2394 N88-24234
Defense Technical Information Center cataloging guidelines
[AD-A192200] 18 p2589 N88-25382
MVS (Multiple Virtual Storage) batch computing and data management at ANL
[DE88-007342] 19 p2718 N88-26137
Technical instructions for a control operating system of the gas flow installation for the solid fuel combustion chamber
[LR-507] 20 p2788 N88-26537
Engineering data compendium. Human perception and performance. User's guide
[LC-87-19560] 21 p2993 N88-27749
SERI standard broadband format: A solar and meteorological data archival format
[DE88-001145] 21 p3028 N88-27975
Avionic and electrical system corrosion prevention and control maintenance 22 p3054 N88-28119
Engineering data compendium. Human perception and performance, volume 1
[LC-87-19560] 22 p3134 N88-28630
Engineering data compendium. Human perception and performance, volume 2
[LC-87-19560] 22 p3134 N88-28631
Engineering data compendium. Human perception and performance, volume 3
[LC-87-19560] 22 p3134 N88-28632

MANUFACTURING
NT COMPUTER AIDED MANUFACTURING
NT LOW GRAVITY MANUFACTURING
NT SPACE MANUFACTURING
Spacecraft Systems Working Group report
01 p0015 N88-10091
NBS (National Bureau of Standards) research reports (April 1987)
[PB87-210258] 01 p0018 N88-10111
Statistically determined nickel cadmium performance relationships 02 p0165 N88-11039
Improved cathode life testing
[REPT-3189-T] 02 p0168 N88-11056
A 1987 progress report of manufacturing techniques for Gravity Probe B gyroscope rotors
[NASA-TM-100312] 02 p0176 N88-11101
Silicon oxidation photoassisted with a continuous wave CO2 laser beam and contribution to the study of silica layers obtained
[LAAS-87-158] 02 p0179 N88-11115
Elevated temperature strain gages
02 p0184 N88-11144
Precision metrology comparing ultrasonic and other techniques for the determination of steel thickness
[DE87-011051] 02 p0230 N88-11452
Study and optimization of a technological process for the fabrication of heterojunction bipolar transistors. Applications to high speed devices
[LAAS-87-134] 02 p0246 N88-11555
Spinoff, 1987
[NASA-TM-89652] 02 p0250 N88-11577
Airworthiness of long-life jet transport structures
03 p0265 N88-11674
Status of titanium alloys R and D described
03 p0298 N88-11876
Requirements for the calibration of mechanical shock transducers
[PB87-227591] 03 p0325 N88-12054
Activities at government research laboratories reported 04 p0403 N88-12503
Research and development on high strength ceramic heaters discussed 04 p0404 N88-12508
Thixotropic surface composition for phenolaldehyde resin laminates
[GB-PATENT-2-180-251-A] 04 p0410 N88-12545
Avionics and corrosion 05 p0547 N88-13336
Development of strength in cements
[PB87-232971] 06 p0684 N88-14189
Design, fabrication and delivery of a miniature Cassegrainian concentrator solar array system
[NASA-CR-179237] 06 p0730 N88-14493
Selection of polymer materials for manufacturing optical parts
[AD-A185898] 07 p0836 N88-15069
Activities report in metal manufacturing
[ISSN-0524-7705] 07 p0839 N88-15086
Powder metallurgical preparation of A15 superconductors
[ETN-88-91072] 09 p1144 N88-16858
Contribution to the design of flexible manufacturing systems: Modeling, simulation, and evaluation of parameters
[ISAL-IDI1-87-04] 09 p1151 N88-16894
Systems integrated human engineering on the Navy's rapid acquisition of manufactured parts/test and integration facility 09 p1206 N88-17228
Software for integrated manufacturing systems, part 1
09 p1211 N88-17261
Software for integrated manufacturing systems, part 2
09 p1211 N88-17262
Communication and control in an integrated manufacturing system 09 p1212 N88-17263
Development of Moire machine vision
09 p1212 N88-17264
Automated Composites, First International Conference, September 10-12, 1986, University of Nottingham, England
[PB87-126199] 10 p1294 N88-17734
Ion chromatography in the manufacture of multilayer circuit boards
[DE88-002428] 10 p1322 N88-17802
Measurements as a process
[DE88-005275] 11 p1497 N88-18808
JPRS report. Science and technology: Europe and Latin America
[JPRS-ELS-87-054] 12 p1573 N88-19406
Presentation of structural component designs for the family of commuter airplanes
[NASA-CR-182568] 12 p1581 N88-19483
JPRS report. Science and technology: Europe and Latin America
[JPRS-ELS-87-055] 12 p1686 N88-20088
Basic research in ceramic and semiconductor science at selected Japanese laboratories, based on a September 1986 visit: Highlights, summary and overview and detailed notes from selected Japanese laboratories
[DOE/ER-0314] 12 p1696 N88-20150
Reducing rotary wing aircraft development time/cost through the use of simulation 12 p1702 N88-20186
The design of aircraft using the decision support problem technique
[NASA-CR-4134] 13 p1721 N88-20291
Development of a manufacturing unit for selective coating of solar absorbers made out of aluminum
[BMFT-FB-T-86-204] 14 p1942 N88-21590
Manufacturing of ultrasonic focused probes
[VTT-RR-487] 15 p2074 N88-22368
Insertions using geometric analysis and hybrid force-position control: Method and analysis
[DE87-013652] 15 p2117 N88-22611
Multivariate analysis and its application
[AD-A189983] 15 p2124 N88-22661
Computer aided design tools for integrated silicon system structures
[ETN-88-92186] 16 p2247 N88-23424
Manufacturing requirements 17 p2297 N88-23745
Preliminary aerodynamic design considerations for advanced laminar flow aircraft configurations
17 p2297 N88-23746
Manufacturing of a ceramic-ceramic composite matrix using the sol-gel procedure
[ETN-88-92157] 20 p2768 N88-26414
Preparation technology for thin film solid electrolyte fuel cells
[PB88-131925] 20 p2821 N88-26735
Application of sol-gel procedures to ceramic composites
[ETN-88-92741] 21 p2921 N88-27308
A small annular combustor of high power density, wide operating range and low manufacturing cost
24 p3351 N88-29951
Advanced planar array development for space station
[NASA-CR-179373] 24 p3389 N88-30181

MANURES
Evaluation of manure as a feedstock for gas turbines
18 p2536 N88-25050

MANY BODY PROBLEM
FDM-FEM zonal method for viscous flow computations over multiple-bodies
[NAL-TR-925T] 02 p0170 N88-11088
Development of many-body methods for flame chemistry and large molecule applications
[AD-A184451] 03 p0284 N88-11789
A periodic small-cluster approach to many-body problems
[DE88-002235] 06 p0763 N88-14683
Whither many-body theory. A summary of the Oslo Conference
[DE88-003095] 11 p1583 N88-19358
Very large vortex calculations in two dimensions
[DE88-005748] 13 p1770 N88-20587
Numerical solution of multibody systems in space applications 14 p1875 N88-21200
Monte Carlo modified method for Green function. Algorithm and computer code for calculations in equal mass many-body system
[DE88-701114] 14 p1957 N88-21687
Corrosion Research Center, University of Minnesota
[DE88-006681] 15 p2041 N88-22160

On new solvable many-body dynamical systems with velocity dependent forces
[PREPRINT-581] 15 p2127 N88-22683

An electron-scattering study of N-15
[ETN-88-92479] 16 p2266 N88-23552

Spatial dynamics of deformable multibody systems with variable kinematic structure 20 p2813 N88-26687

Atomistic simulation of stability, metastability and growth of strained layer structures 20 p2873 N88-27053

Dynamics of interacting galaxies
23 p3299 N88-29647

MANY PARTICLE THEORY
U MANY BODY PROBLEM

MAP MATCHING GUIDANCE

The integration of digital maps in vehicle navigation systems 16 p2225 N88-23286

MAPPING
NT CADASTRAL MAPPING
NT COMPUTER AIDED MAPPING
NT ICE MAPPING
NT PHOTOMAPPING
NT PLANETARY MAPPING
NT SOIL MAPPING
NT THEMATIC MAPPING
NT THERMAL MAPPING

Study of Earth from space and strengthening of economy 01 p0010 N88-10055

NBS (National Bureau of Standards) research reports (April 1987)
[PB87-210258] 01 p0018 N88-10111

Smooth dynamics on the interval (with an emphasis on unimodal maps)
[REPT-87-09] 01 p0086 N88-10555

Correlation between aircraft MSS and LIDAR remotely sensed data on a forested wetland in South Carolina
[NASA-TM-89843] 02 p0193 N88-11204

Components and cycles of a random function
[DE87-014155] 02 p0228 N88-11437

Illustrations of a density-equalizing map projection technique
[DE87-013992] 03 p0339 N88-12130

SPOT 1: First In-Flight Results --- conferences
[ISBN-2-85428-177-2] 03 p0340 N88-12143

A review of computer-assisted photo interpretation research at USAETL (US Army Engineer Topographic Laboratories)
[AD-A184034] 03 p0346 N88-12186

East coast gravity validation study
[AD-A184292] 03 p0351 N88-12217

Mapping a battlefield simulation onto message-passing parallel architectures
[NASA-CR-178396] 03 p0363 N88-12287

Phase transition of multifractals
[DE87-014344] 03 p0383 N88-12409

Principles for problem aggregation and assignment in medium scale multiprocessors
[NASA-CR-178379] 04 p0476 N88-12935

Foundations of O-theory 2: Measurements and relation to fuzzy set theory
[DE88-000013] 04 p0485 N88-12986

Scientific and Operational Requirements for TOMS Data
[NASA-CP-2497] 05 p0615 N88-13774

Observation guidelines for a Total Ozone Mapping Spectrometer (TOMS) in geosynchronous orbit
05 p0619 N88-13801

Research needs for hydrocarbon fuels
[DE87-014555] 06 p0667 N88-14209

Mathematical-cartographic modeling of economic utilization of Atlantic Ocean 06 p0726 N88-14469

Fast, colour displays of digital terrain elevation data
[AD-A185596] 06 p0729 N88-14485

Description of data on the Nimbus 7 LIMS map archive tape: Water vapor and nitrogen dioxide
[NASA-TP-2761] 06 p0744 N88-14572

Optimal pre-scheduling of problem remappings
[NASA-CR-178378] 06 p0756 N88-14633

There exists a C sup infinity symbol Kupka-Smale diffeomorphism of S sup 2 with neither sinks nor sources
[PB87-225967] 06 p0769 N88-14725

Preliminary airworthiness evaluation of a UH-1 equipped with a terrain mapping receiver antenna
[AD-A186274] 07 p0819 N88-14980

Determination of network attributes from a high resolution terrain data base
[AD-A186078] 07 p0870 N88-15279

An experimental mapping of the flow field behind a glaze ice shape on a NACA 0012 airfoil
[NASA-CR-180847] 08 p0950 N88-15786

Photogrammetric principles for combining remote sounding and three-dimensional mapping
08 p1012 N88-16135

Laser system for automating topographic terrain survey 08 p1012 N88-16136

Construction of airborne radars for remote sensing
[PB88-113063] 09 p1154 N88-16916

An automatic finite element mesh generator
[AD-A186939] 09 p1216 N88-17291

Navigation planning using quadtrees
[DE88-003706] 09 p1225 N88-17343

A smart, mapping, charting and geodesy control generator, phase 1
[AD-A188184] 10 p1347 N88-18055

An overview of the transactional interpretation of quantum mechanics
[DE88-004236] 10 p1423 N88-18497

Chaos, mappings and spatial complexity in fluids
11 p1484 N88-18860

Contour-to-grid interpolation with nonlinear finite elements: A feasibility study
[AD-A188108] 11 p1503 N88-18980

A digital terrain system for microcomputers
[INPE-4170-PRE/1067] 11 p1505 N88-18987

Reports on cartography and geodesy. Series 1, report 96
[ISSN-0469-4236] 11 p1506 N88-18993

A sky temperature survey at 19.2 GHz using a balloon borne Dicke radiometer for anisotropy tests of the cosmic microwave background 11 p1571 N88-19403

Department of Defense World Geodetic System 1984: Its definition and relationships with local geodetic systems
[AD-A188815] 12 p1639 N88-19811

Comparison of simulation modeling and satellite techniques for monitoring ecological processes
[NASA-CR-182592] 12 p1641 N88-19825

Proceedings of US-Japan Heliotron-Stellarator Workshop, volume 4
[DE88-004787] 12 p1693 N88-20126

Development of an interactive real-time graphics system for the display of vehicle space positioning
[NASA-TM-100429] 13 p1730 N88-20344

The 1987 Airborne Antarctic Ozone Experiment: The Nimbus-7 TOMS data atlas
[NASA-RP-1201] 13 p1791 N88-20714

Bathymetric hazard survey test
[AD-A189150] 13 p1803 N88-20775

Retinotopic mapping of the human visual system with magnetoencephalography
[AD-A189557] 13 p1810 N88-20811

Vegetation mapping using high resolution MSS (multispectral scanner) data: Canopy reflectance and shadow problems encountered and possible solutions
[DE88-004273] 14 p1939 N88-21574

Parallel algorithms for mapping pipelined and parallel computations
[NASA-CR-181655] 14 p1960 N88-21687

Enhanced viscous flow drag reduction using acoustic excitation
[NASA-CR-182734] 15 p2062 N88-22295

Fatigue damage mapping 15 p2084 N88-22423

Geometric restoration of satellite image data
[AD-A190462] 15 p2089 N88-22450

Matched index laser anemometry systems for flow studies in complex geometries 16 p2203 N88-23145

Contributions to geodesy, photogrammetry and cartography. Series 1, number 46 --- conference
[ISSN-0469-4244] 16 p2225 N88-23279

Report on the cartographic activities of the Federal Republic of Germany in the period 1984 - 1987
16 p2225 N88-23280

Do we need a new cartography?
16 p2225 N88-23283

Down-to-Earth approach for final projects in Karlsruhe (Federal Republic of Germany)
16 p2226 N88-23292

Urban cartography: A book review
16 p2227 N88-23297

Near-real-time TOMS, telecommunications and meteorological support for the 1987 Airborne Antarctic Ozone Experiment
NASA-CR-4133] 16 p2233 N88-23338

Updating land-use of the Sao Jose dos Campos municipality through remote sensing data
[INPE-4479-RPE/562] 16 p2287 N88-23693

A proposal for a project entitled assessment of forest resources in Uruguay submitted to the United Nations Industrial Development Organization (UNIDO)
17 p2352 N88-24016

The geometric workstation, a new approach for geometric corrections of remotely sensed data
17 p2352 N88-24017

Mapping from LANDSAT and SPOT satellite imagery
17 p2352 N88-24018

Airborne and spaceborne radar images for geologic and environmental mapping in the Amazon rain forest, Brazil
17 p2353 N88-24021

Mapping soil and rock variation from satellite images in the Sahel 17 p2354 N88-24023

Remote sensing and data integration: Practical solutions for resource managers 17 p2356 N88-24034

Utilization of TM/LANDSAT images in the implanted forests mapping in the Mogi-Guacu Region (SP-Brazil)
17 p2357 N88-24042

CANASATE: Sugar cane mapping by satellite
17 p2358 N88-24046

Structure and dynamics of vegetation in the middle semi-and tropics. Quixaba's Caatinga (PE): Terrain analysis of MSS/LANDSAT data 17 p2358 N88-24049

Study of fracturing for groundwater research in the Sergipe state with remote sensing products
17 p2359 N88-24052

Implantation of a geo-cartographical information system through microcomputers 17 p2361 N88-24064

Detection of biomass burning and smoke plumes in the Amazon region through NOAA satellite imagery
17 p2365 N88-24085

The 35 mm vertical aerial photographs for mapping stands of bracatinga in different age classes
17 p2366 N88-24087

The breaked anticlines, cuesta and crest homoclines, ortoclinal valleys, and other forms of relief outcrops delineated with the help of remote sensing imagery
17 p2366 N88-24089

Current stage of remote sensing system for cartographic application 17 p2366 N88-24090

Mapping of plant associations and the variation of surface water in the Pantanal Mato-Grossense National Park, through remote sensing techniques
17 p2366 N88-24092

Characteristics of drainage determinations in aerial photographs and relief determination on different scales planialtimetric charts for three soils in the state of Sao Paulo 17 p2367 N88-24095

Criteria for planimetric and altimetric correction of maps restituted from aerial photographs in 1:100,000 scale
17 p2367 N88-24097

Geomorphologic sector maps of Niquizanga-Mayares, province of San Juan, Argentina
17 p2368 N88-24098

Research on enhancing the utilization of digital multispectral data and geographic information systems in global habitability studies
[NASA-CR-182799] 17 p2368 N88-24101

Automated cartographic generalization for linear map features 18 p2532 N88-25021

Drilling investigation of a young magmatic intrusion beneath the Inyo Domes, Long Valley, California: Structural and textural studies
[DE88-006613] 18 p2541 N88-25078

A framework for a theory of mapping
[AD-A191071] 18 p2551 N88-25144

Territorial management program
19 p2682 N88-25942

The impact of hemp production on the development of the municipalities of Araras, Leme, Santa Cruz da Conceicao and Pirassununga 19 p2683 N88-25948

Remote sensing technique applied to vegetation as an aid to municipal planning 19 p2683 N88-25951

Application of 35mm EM aerial reconnaissance photographic format of the municipality of Ubatuba (SP)
19 p2684 N88-25953

Aerial photography as an instrument of atmospheric analysis: Maps of the middle atmosphere and its dynamics, Baixada Santista (SP) 19 p2684 N88-25955

Remote sensing applied to integrated regional development programs 19 p2685 N88-25958

Generalization and the backward propagation neural network
[AD-A191634] 19 p2710 N88-26100

Solar microwave radiation maps measured at Metsaehovi Radio Research Station in 1980-1981
[PB88-193453] 19 p2741 N88-26276

The Viking landing sites: A cartographic perspective
[NASA-CR-177486] 19 p2742 N88-26282

Efficient bit-level, word-level and block-level systolic arrays for matrix-matrix multiplication
[DE88-011331] 20 p2841 N88-26856

IEMIS (Integrated Emergency Management Information System) floodplain mapping based on a LIDAR derived data set
[AD-A193071] 21 p2966 N88-27616

Review of geographic processing techniques applicable to regional analysis
[DE88-010759] 21 p2970 N88-27643

CEEG dynamic brain mapping: A new method to evaluate brain function in different psychological and drug conditions 21 p2977 N88-27685

Geologic applications of SPOT-1, TM, and NOAA-7 data: Finding and defining unmapped structural features
22 p3104 N88-28434

The use of SPOT imagery for topographic mapping
22 p3110 N88-28473

Topographic mapping with SPOT 1 data. A practical approach by the Ordnance Survey
22 p3111 N88-28479

Mapping and urban multi-experimental assessment of SPOT: Mapping results 22 p3112 N88-28483

Production of satellite image maps based on SPOT data 22 p3113 N88-28491

SPOT: A data capture and data updating tool for the French National Geographic Institute's (IGN's) cartographic data base 22 p3114 N88-28497

Some remarks on geodesics in gauge groups and harmonic maps
[DE88-702665] 22 p3115 N88-28510

On the computation of finite invariant sets of mappings
[AD-A193670] 22 p3143 N88-28690

Monotone recurrence relations, their Birkhoff orbits and topological entropy
[AD-A193461] 23 p3276 N88-29504

Mapping of volcanic units at Alba Patera, Mars
23 p3301 N88-29663

Sub-kilometer rampart craters in the equatorial region of Mars: Possible implications for the state and distribution of regolith H2O 23 p3302 N88-29666

Chemical and spectroscopic characterization of a suite of Mars soil analogs 23 p3302 N88-29667

The Martian sedimentary record
23 p3302 N88-29669

Progress in determining the thickness and distribution of volcanic materials on Mars 23 p3302 N88-29670

Geology of six possible Martian landing sites
23 p3304 N88-29682

Spectral reflectance of SNC meteorites: Relationships to Martian surface composition
23 p3304 N88-29683

Evaluation of LANDSAT-TM data for geomorphological mapping
[INPE-4593-PRE/1324] 24 p3386 N88-30168

The use of orbital remote sensing data for low cost ground-water survey
[INPE-4587-PRE/1318] 24 p3386 N88-30170

Use of digital images as a mineral prospecting tool in the tin province of Goias, Brazil
[INPE-4537-PRE/1284] 24 p3387 N88-30173

Implementation of the NCAR (National Centre for Atmospheric Research) graphics package at ARL (Aeronautical Research Laboratory)
[AD-A195163] 24 p3391 N88-30193

Structure of Southwestern Michipicoten Greenstone Belt, Ontario: Evidence for Archean accretion
24 p3397 N88-30226

Supermap for Cray FORTRAN: A user's guide
[NASA-CR-177410] 24 p3412 N88-30308

A digital terrain model system for a microcomputer
[INPE-4610-PRE/1333] 24 p3413 N88-30316

Faulting and its relation to volcanism: Mars western equatorial region 24 p3443 N88-30489

MAPS
NT ASTRONOMICAL MAPS
NT METEOROLOGICAL CHARTS
NT RADAR CLUTTER MAPS
NT RADAR MAPS
NT RELIEF MAPS

X-rays, color, and the Vaughan-Preston gap
04 p0510 N88-13135

Fatigue damage maps 06 p0715 N88-14382

Mathematical-cartographic modeling of economic utilization of Atlantic Ocean 06 p0726 N88-14469

Fast, colour displays of digital terrain elevation data
[AD-A185598] 06 p0729 N88-14485

Protected areas with enhanced bird-aircraft collision risk in the Federal Republic of Germany
[GEOPHYSBDBW-FM-209] 11 p1437 N88-18576

Terrain Analyst Work Station (TAWS) demonstrations
[AD-A188139] 11 p1504 N88-18981

A digital terrain system for microcomputers
[INPE-4170-PRE/1067] 11 p1505 N88-18987

The US Army Electronic Map Data (EMD) initiative
[AD-A188209] 11 p1565 N88-19372

Development of a ground-conductivity map for the area of the Federal Republic of Germany from measured field-strength contours 12 p1615 N88-19656

Mono- and bistatic radar coverage diagrams including diffractive wave propagation 12 p1616 N88-19660

An application of digital cartography updating middle and small scale thematic maps using orbital data
[INPE-4460-TDL/317] 12 p1637 N88-19805

Digital Topographic Support System (DTSS)
[AD-A188304] 12 p1638 N88-19808

Soft maps for US Army electronic map background applications
[AD-A188427] 12 p1638 N88-19809

Relative orientation
[AD-A190385] 15 p2089 N88-22449

PLOT3D (version-5): A computer code for drawing three dimensional graphs, maps and histograms, in single or multiple colours, for mono or stereoscopic viewing
[DE88-701410] 15 p2108 N88-22558

Regularity of the Albanese map for nonoriented surfaces
[DE88-006428] 15 p2126 N88-22679

Contributions to geodesy, photogrammetry and cartography. Series 1, number 46 --- conference
[ISSN-0469-4244] 16 p2225 N88-23279

Report on the cartographic activities of the Federal Republic of Germany in the period 1984 - 1987
16 p2225 N88-23280

Developments in the design of topographic maps in the Federal Republic of Germany: Activities and suggestions
16 p2226 N88-23290

The atlas of regional development
16 p2226 N88-23291

Thailand in maps. Application of the mapping system THEMAK2 for specific purpose atlas preparation
16 p2226 N88-23295

Maps for tourists. A systematic approach to tourist cartography 16 p2227 N88-23296

Urban cartography: A book review
16 p2227 N88-23297

Maps for the blind and methods of their production
16 p2227 N88-23298

Research in enumeration and graph theory with applications to computer science
[AD-A191567] 18 p2556 N88-25171

LO-CO-GRAF (low cost graphics): Generating maps to support command and control/crisis management using small computers
[AD-A193964] 22 p3139 N88-28661

Distortion estimates for negative Schwarzian maps
[AD-A193172] 23 p3228 N88-29200

Polynomial definition of discrete field points of map of diffusion equation, part 1
[AD-A193697] 23 p3271 N88-29467

MARAGING STEELS

Metallography of maraging 350 steel
[DE87-013746] 04 p0416 N88-12581

MARANGONI CONVECTION

Numerical analysis of Marangoni convection in Bridgman method 03 p0319 N88-12014

Flight results of the ESA experiment modules in Materials Science Experiment Rocket (MASER) 1
08 p1033 N88-16261

Marangoni convection in finite cylindrical liquid bridges
[LRT-WE-9-FB-5(1988)] 22 p3078 N88-28277

MARECS MARITIME SATELLITES

A conformal aircraft phased array antenna for airplane-satellite communication in the L band
[ESA-TT-1057] 03 p0305 N88-11926

MARINE BIOLOGY

Compilation of 1986 annual reports of the Navy ELF (Extremely Low Frequency) communications system ecological monitoring program, volume 3
[AD-A184563] 03 p0306 N88-11932

Vanfront 3 expedition data report (USNS DE STEIGUER CRUISE 1202-82). Bioluminescence, hydrographic, nutrient, and satellite data from the Gulf of California (November-December 1981)
[AD-A185011] 05 p0620 N88-13805

Remote sensing of ocean colour for studies of biological productivity and biochemical cycles
08 p1042 N88-16296

Relationships between remotely-sensed surface properties and subsurface structure in the ocean
[AD-A189317] 12 p1650 N88-19881

Remote determination of chlorophyll concentration in the ocean using an optical pulse radar
[NASA-TT-20301] 19 p2694 N88-26014

MARINE CHEMISTRY

Satellite and synoptic studies of chemical fronts in the California current and coastal upwelling zone
[AD-A183909] 01 p0073 N88-10466

Remote sensing of ocean colour for studies of biological productivity and biochemical cycles
08 p1042 N88-16296

The use of chlorophyll fluorescence measurements from space for separating constituents of sea water
08 p1043 N88-16307

Physical oceanography and tracer chemistry of the southern ocean
[DE88-006852] 20 p2828 N88-26779

MARINE ENVIRONMENTS

Modelling of crack-tip deformation and transient electrochemical processes in relation to corrosion fatigue of steels cathodically protected in marine environments
[NPL-DMA(A)-145] 01 p0059 N88-10379

NOAA's (National Oceanic and Atmospheric Administration's) Northeast Monitoring Program (NEMP). A report on progress of the first five years (1979-84) and a plan for the future
[PB87-210100] 02 p0196 N88-11225

Properties of the atmospheric boundary layer above a subtropical oceanic front
[AD-A184006] 03 p0351 N88-12215

Estimation of marine boundary layer depth and relative humidity with multispectral satellite measurements
[AD-A184881] 05 p0620 N88-13804

The ocean heat budget
[AD-A186130] 07 p0881 N88-15340

Formation of sediments in fuels containing added sulphonic acids --- marine diesel fuels
[RAE-TM-NAV-ENG-1163] 09 p1150 N88-16891

Corrosion performance of high damping alloys in 3.5 percent sodium chloride environment
[AD-A188048] 11 p1457 N88-18687

A propagation campaign in a marine environment utilizing a digital system at 36 GHz 12 p1618 N88-19675

The effects of atmospheric and thermohaline variability on the validation of the GEOSAT altimeter oceanographic signal between Scotland and Iceland
[AD-A189324] 12 p1650 N88-19882

Cavitation inception
[AD-A189220] 13 p1765 N88-20557

The corrosion resistance of an aluminum alloy coated with polysilazane derived ceramics
[AD-A190703] 15 p2046 N88-22189

Derivation of consistent surface fixed fields for use in a global NWP model
[AD-A190131] 15 [illegible] N88-22475

Real-time environmental Arctic [illegible] (R-TEAM)
[AD-A189848] 15 [illegible] N88-22509

Corrosion of tungsten alloys in marine environments
17 p2320 N88-23854

The effects of better environmental inputs in estimating sea clutter
[AD-A192058] 19 p2643 N88-25678

Doppler radar analysis of coastal marine atmospheric boundary layer structure during a cold air outbreak
[AD-A196023] 24 p3403 N88-30261

MARINE METEOROLOGY

A proposal of the nowcasting system for sea fog
02 p0202 N88-11264

A one-dimensional model of thermally-driven coastal front evolution 02 p0204 N88-11274

Australian East Coast cyclones 3: Case study of the storm of August 1986 02 p0204 N88-11276

A short-range forecasting experiment conducted during the Canadian Atlantic storms program
02 p0205 N88-11285

An hourly analysis, updating and short-range forecasting system --- numerical weather forecasting
02 p0206 N88-11288

Statistical relationships between the mesoscale organization of convection and the large-scale wind profiles during GATE --- GARP Atlantic Tropical Experiment (GATE) 02 p0208 N88-11302

Mesoscale analysis and forecasting for the 1987 America's Cup, Fremantle, Western Australia
02 p0214 N88-11350

Properties of the atmospheric boundary layer above a subtropical oceanic front
[AD-A184006] 03 p0351 N88-12215

New precipitation map of world ocean
04 p0458 N88-12804

Review of the potential of satellite remote sensing for marine flood protection
[IOS-237] 07 p0870 N88-15280

Annual data summary and climatological evaluation, CERC (Coastal Engineering Research Center) field research facility, 1985, volume 2, appendix C
[AD-A185894] 07 p0881 N88-15344

Mariners Weather Log, Volume 31, Number 3, Summer 1987
[PB87-234894] 08 p1039 N88-16284

North Pacific Ocean. Tradewind region east of Hawaii. R/V Thomas G Thompson: 25 September - 1 November 1972. STD data report
[AD-A186586] 08 p1044 N88-16311

US Navy climatic study of the Mediterranean Sea
[AD-A188264] 10 p1356 N88-18107

Study of cations in the precipitation of Estacao Antartica Comandante Ferraz
[INPE-4377-PRE/1187] 12 p1644 N88-19843

Worldwide distributions of shipboard surface meteorological observations for EM propagation analysis
[AD-A188771] 12 p1648 N88-19871

Dynamical modeling of marine boundary layer convection 13 p1797 N88-20750

Predictions and studies with a one-dimensional ice/ocean model
[AD-A189158] 13 p1803 N88-20778

Mariners weather log, volume 32, number 1, Winter 1988
[PB88-173869] 18 p2544 N88-25087

Mariners weather log, volume 31, number 4, Fall 1987
[PB88-173851] 20 p2825 N88-26761

Stability of a coastal upwelling front over topography
[AD-A192354] 20 p2829 N88-26784
Genesis of Atlantic lows experiment NASA electra boundary layer flights data report
[NASA-TM-100703] 22 p3126 N88-28597
Meteorological features during the marginal ice zone experiment from 20 March to 10 April 1987
[AD-A193960] 23 p3235 N88-29251
MARINE NAVIGATION
U SURFACE NAVIGATION
MARINE PROPULSION
Calculations of the turbulent wake behind a slender self-propelled double-body and comparisons with experiment
[AD-A185661] 06 p0703 N88-14314
Formation of sediments in fuels containing added sulphonic acids — marine diesel fuels
[RAE-TM-NAV-ENG-1163] 09 p1150 N88-16891
A comparative study of various electric propulsion systems and their impact on a nominal ship design
[AD-A187600] 11 p1477 N88-18616
Design features of small Brayton cycles for autonomous underwater vehicles
[AD-A187799] 11 p1506 N88-18999
Cavitation inception
[AD-A189220] 13 p1765 N88-20557
MARINE RESOURCES
Remote sensing of ocean colour for studies of biological productivity and biochemical cycles
08 p1042 N88-16296
MARINE TECHNOLOGY
Marine gas turbines - engine health monitoring, new approaches
[PNR90369] 02 p0182 N88-11132
Integrating syntax, semantics, and discourse DARPA (Defense Advanced Research Projects Agency) Natural Language Understanding Program
[AD-A184505] 03 p0364 N88-12269
JPRS report: Science and technology. Japan
[JPRS-JST-87-023] 06 p0684 N88-14191
Trends in research and development in the Netherlands. The influence of national science policy between 1973 and 1986
[B8701588] 08 p1094 N88-16580
Analysis of wind turbines on offshore support structures excited by random wind and random waves
[DE88-004772] 10 p1351 N88-18074
Digital correlator for the portable channel prober measurement instrument
[AD-A189065] 14 p1904 N88-21377
Naval research reviews, volume 39, number 3
[AD-A191392] 16 p2264 N88-23543
Marine techniques: R and D axes, identification of areas of common interest with space techniques
19 p2699 N88-26047
Materials qualification in oceanology and the offshore industry 19 p2700 N88-26050
MARISAT SATELLITES
The JPL mechanically steered antenna
19 p2647 N88-25715
MARITIME SATELLITES
NT ERS-1 (ESA SATELLITE)
NT MARECS MARITIME SATELLITES
NROSS (Navy Remote Ocean Sensing System): A force multiplier
[AD-A188853] 10 p1346 N88-18045
Proceedings of the Colloquium on Space and Sea
[ESA-SP-280] 19 p2695 N88-26016
Satellites at sea — INMARSAT
19 p2700 N88-26054
The contribution of space to maritime activities
19 p2700 N88-26055
MARKERS
Descriptions of HF and VHF Loran-C buoys and evaluations as potential datum marker buoys
[AD-A192060] 18 p2462 N88-24618
MARKET RESEARCH
Study of the feasibility of a satellite communication system for road transportation home office to vehicle communication. Volume 2: Market study
[SC/87-E/6-VOL-2] 05 p0575 N88-13506
National Point Of Contact (NPOC)-SPOT inquiry 1986
[NLR-MP-86055-U] 05 p0620 N88-13807
Data base management in CAD/CAM systems: Requirements for CAD/CAM data bases, actual market offer, advice for an efficient data base management, development tendencies
[MBB/LWD-11/S/PUB/254] 16 p2285 N88-23683
MARKETING
JPRS report: Science and technology. China
[JPRS-CST-87-026] 03 p0269 N88-11666
Production of jet fuels from coal derived liquids. Volume 1: Market assessment for liquid by-products from the Great Plains gasification plant
[AD-A184846] 05 p0570 N88-13475
Research briefing on high-temperature superconductivity
[PB88-133004] 11 p1561 N88-19344
Selling to NASA
[NASA-TM-89724] 12 p1705 N88-20208
High temperature materials: What's available
[AERE-R-12632] 15 p2028 N88-22081
Preliminary market analysis for large zeolite crystals
[NASA-CR-182882] 15 p2049 N88-22207
Function of Japan Fine Ceramics Center described
15 p2052 N88-22227
Commercialization and export — aerospace industry
22 p3161 N88-28824
MARKING
NT ISOTOPIC LABELING
A labeling procedure for linear finite-state codes
11 p1472 N88-18781
Study of flow tracer behavior models and experimental validation with multiple exposure holographic velocimetry
[IMFL-87/30] 20 p2811 N88-26622
Velocity measurements and flow visualization in turbulent three-dimensional supersonic flows using oxygen flow tagging
[AD-A192551] 21 p2992 N88-27165
Development of automatic names placement software
[AD-A192786] 21 p2996 N88-27770
MARKOV CHAINS
Contribution to the study of circuit switched networks. Modeling and numerical solutions
[LAAS-87-174] 02 p0162 N88-11017
On the approximation of the output process of multi-user random access communication networks
[AD-A186197] 07 p0842 N88-15108
Power series for stationary distributions of coupled processor models
[REPT-87-70] 16 p2254 N88-23470
Colored stochastic Petri nets. Application to real time distributed systems
[ENST-87E017] 20 p2839 N88-26843
Asymptotically efficient adaptive allocation schemes for controlled Markov chains: Finite parameter space
[AD-A192228] 20 p2846 N88-26893
Markov chain computations to a solution of the mutual-exclusion problem in concurrency
[REPT-87-89] 20 p2847 N88-26896
MARKOV PROCESSES
NT MARKOV CHAINS
Passage from two-parameters to infinite dimension
[ENST-87C002] 01 p0088 N88-10577
White noise calculus for two-parameter filtering
[ENST-87C003] 01 p0088 N88-10578
Optimization of a controlled two-server maintenance system
[INPE-4202-PRE/1083] 01 p0107 N88-10694
Real-time expert systems: A status report
02 p0129 N88-10817
Electronic system reliability and effectiveness
[AD-A184522] 03 p0311 N88-11961
Overlooked potential of systems with Markovian coefficients
[NLR-MP-86049-U] 05 p0552 N88-13366
Stationary regenerative sets and subordinators
[AD-A186298] 07 p0918 N88-15573
Formal grammars and Markov models
[RSRE-MEMO-4051] 09 p1219 N88-17311
Experiments with the back propagation algorithm: A systematic look at a small problem
[RSRE-MEMO-4049] 09 p1224 N88-17340
SURE reliability analysis: Program and mathematics
[NASA-TP-2764] 09 p1231 N88-17380
Random truncation models and Markov processes
[CWI-MS-R8702] 09 p1232 N88-17389
A queueing system with independent Markov input streams
[AD-A187601] 10 p1402 N88-18363
Estimation of the probability of a long time to the first entrance to a state in a semi-Markov model
[AD-A188960] 12 p1685 N88-20074
An optimal branch-and-bound procedure for the constrained path, moving target search problem
[AD-A188962] 12 p1685 N88-20075
The acoustic-modeling problem in automatic speech recognition
[AD-A188529] 13 p1757 N88-20510
On relaxation algorithms based on Markov random fields
[AD-A189043] 13 p1814 N88-20840
Nonstationary solution in random vibration theory
[PB88-163746] 14 p1933 N88-21529
Analysis and testing of the SURE program
[NASA-TP-2817] 15 p2123 N88-22653
Filtering of jump processes
[AD-A189701] 15 p2123 N88-22656
Structural decomposition of multiple time scale Markov processes
[AD-A189739] 15 p2123 N88-22657
The partially observed stochastic minimum principle
[AD-A189787] 15 p2124 N88-22658
Markov processes applied to control, replacement and signal analysis
[AD-A190563] 15 p2126 N88-22674
EDQNM closure: A homogeneous simulation to support it. A quasi-homogeneous simulation to disprove it
16 p2195 N88-23091
Validation of EDQNM for subgrid and supergrid models 16 p2195 N88-23092
Angular distribution of turbulence in wave space
16 p2195 N88-23093
Experimental evaluation of algorithms for connected speech recognition using hidden Markov models
[RSRE-MEMO-4099] 17 p2333 N88-23928
Poisson functionals of Markov processes and queueing networks
[AD-A191217] 18 p2568 N88-25252
Semi-Markov adjunction to the Computer-Aided Markov Evaluator (CAME)
[NASA-CR-181645] 19 p2678 N88-25924
Distributed algorithms for probabilistic solution of computational vision problems
[AD-A193150] 21 p2997 N88-27773
Performability analysis: Measures, an algorithm and a case study
[AD-A192477] 21 p3001 N88-27800
Free boundary control of the Markov process
[AD-A192401] 21 p3008 N88-27846
The computation of stationary distributions on Markov chains through perturbations
[AD-A193191] 21 p3009 N88-27855
Importance sampling for stochastic simulations
[AD-A193585] 22 p3138 N88-28654
Poisson functionals of Markov processes and queueing networks
[AD-A194289] 22 p3145 N88-28705
Use of Markov probability and reliability model generation methods in the analysis of reliability of a fault tolerant hardware and software based system with flexible repair policies
[PNR90467] 22 p3145 N88-28706
Approximate evaluation of semi-Markov chain reliability models
[AD-A194669] 23 p3223 N88-29185
Dynamic analysis of computer and communications sytems: Semi-Markov approach
23 p3244 N88-29305
Hidden Markov models for automatic speech recognition: Theory and application
[RSRE-MEMO-4135] 23 p3251 N88-29350
Approximations and implementations of nonlinear filtering schemes
[AD-A194685] 23 p3271 N88-29462
On stable Markov processes
[AD-A192892] 23 p3273 N88-29482
Range data description based on multiple characteristics 24 p3419 N88-30351
MARS
Interplanetary mission design handbook. Volume 1, Part 5: Mars-to-Earth ballistic mission opportunities, 1992-2007
[NASA-CR-182525] 10 p1430 N88-18538
MARS (PLANET)
Possible dynamical mechanisms for the Martian polar warming phenomenon
[NASA-CR-181454] 02 p0254 N88-11605
A near-earth optical communications terminal with a corevolving planetary sun shield
04 p0434 N88-12693
An evolutionary communications scenario for Mars exploration
[NASA-TM-100263] 05 p0576 N88-13515
Mars: High resolution VLA observations at wavelengths of 2 and 6 cm and derived properties
06 p0804 N88-14909
Frozen orbit analysis in the Martian system
[AD-A189574] 13 p1856 N88-21106
Periodic orbits around a satellite modelled as a triaxial ellipsoid
[AD-A190592] 15 p2022 N88-22051
Engineering planetary lasers for interstellar communication
[NASA-CR-180780] 17 p2311 N88-23825
Electromagnetic powered vehicles (EMPV) for Mars exploration 17 p2419 N88-24388
Power requirements for mining and microwave processing of extraterrestrial resources
17 p2420 N88-24389
A design study of onboard navigation and guidance during aerocapture at Mars
[NASA-CR-172053] 18 p2469 N88-24654
The Viking landing sites: A cartographic perspective
[NASA-CR-177486] 19 p2742 N88-26292
A bibliography of dunes: Earth, Mars, and Venus
[NASA-CR-4149] 20 p2685 N88-27134

Mars: Near-infrared comparative spectroscopy during the 1986 opposition 23 p3301 N88-29658
An introduction to the historical records of China about Mars 23 p3301 N88-29664
How dirty is Mars' North Polar cap, and why isn't it black 23 p3303 N88-29677
Preliminary analysis of recent 2.2-4.2 micrometers telescopic observations of Elysium, Mars: Implications for crystallinity and hydration state of surface materials
23 p3306 N88-29692
Mars earth-based radar: 1986 results and 1988-1990 opportunities 23 p3306 N88-29697
Nineteenth Lunar and Planetary Science Conference. Press abstracts
[NASA-CR-183037] 24 p3440 N88-30473

MARS ATMOSPHERE
Possible dynamical mechanisms for the Martian polar warming phenomenon
[NASA-CR-181454] 02 p0254 N88-11605
The atmosphere of Mars and optical communications
04 p0434 N88-12692
Particle-gas temperature differentials resulting from time-dependent radiative-conductive heat flux divergences in the tenuous dust-laden atmosphere of mars
[AD-A185888] 07 p0945 N88-15747
Aerosols in Martian Atmosphere and Natural Dust Observation (AMANDO). Proposal for the Mars orbiter balloon and rover to study the Martian atmosphere, its thermal content, and its interaction with the soil
[IFSI-87-9] 08 p1100 N88-16619
Development of an engineering model atmosphere for Mars
[NASA-CR-182462] 09 p1263 N88-17568
Mars Lander/Rover vehicle development: An advanced space design project for USRA and NASA/OAST
[NASA-CR-182571] 12 p1709 N88-20227
Martian Clouds Data Workshop
[NASA-CR-182431] 12 p1711 N88-20238
Diurnal variations in optical depth at Mars: Observations and interpretations
[NASA-TM-100057] 18 p2595 N88-25420
Chemical interactions between the present-day Martian atmosphere and surface minerals
23 p3305 N88-29689
Volatiles on Mars
[NASA-CR-183113] 24 p3456 N88-30571

MARS ENVIRONMENT
NT MARS ATMOSPHERE
Mars Lander/Rover vehicle development: An advanced space design project for USRA and NASA/OAST
[NASA-CR-182562] 12 p1709 N88-20226

MARS GEOSCIENCE CLIMATOLOGY ORBITER
U MARS OBSERVER

MARS LANDING
Mars Lander/Rover vehicle development: An advanced space design project for USRA and NASA/OAST
[NASA-CR-182562] 12 p1709 N88-20226
Energy storage considerations for a robotic Mars surface sampler
[NASA-TM-100969] 22 p3166 N88-28853

MARS OBSERVER
Mars Lander/Rover vehicle development: An advanced space design project for USRA and NASA/OAST
[NASA-CR-182562] 12 p1709 N88-20226

MARS PROBES
NT MARS OBSERVER
Mars Lander/Rover vehicle development: An advanced space design project for USRA and NASA/OAST
[NASA-CR-182570] 11 p1567 N88-19380
Mars rover/sample return mission requirements affecting space station
[NASA-CR-172048] 18 p2594 N88-25414

MARS SATELLITES
NT DEIMOS
NT PHOBOS

MARS SURFACE
An evolutionary communications scenario for Mars exploration
[NASA-TM-100263] 05 p0576 N88-13515
Gamma-ray and neutron spectroscopy of planetary surfaces and atmospheres
[DE88-004287] 10 p1430 N88-18541
Martian geomorphology and its relation to subsurface volatiles
[NASA-CR-182428] 12 p1711 N88-20237
Groundwater sapping valleys: Experimental studies, geological controls and implications to the interpretation of valley networks on Mars
[NASA-CR-182718] 15 p2152 N88-22847
The Viking landing sites: A cartographic perspective
[NASA-CR-177486] 19 p2742 N88-26282
MEVTV Workshop on Nature and Composition of Surface Units on Mars
[NASA-CR-183075] 23 p3300 N88-29654
Surface composition of Mars: A Viking multispectral view 23 p3300 N88-29655
A review: Quantitative models for lava flows on Mars
23 p3301 N88-29656
Mars: Spectral signatures seen and unseen
23 p3301 N88-29659
Selective weathering of shocked minerals and chondritic enrichment of the Martian fines
23 p3301 N88-29660
Intercrater plains deposits and the origin of Martian valleys 23 p3301 N88-29661
Weathering of sulfides on Mars
23 p3301 N88-29662
Elemental composition of the Martian surface
23 p3302 N88-29665
Sub-kilometer rampart craters in the equatorial region of Mars: Possible implications for the state and distribution of regolith H2O 23 p3302 N88-29666
Chemical and spectroscopic characterization of a suite of Mars soil analogs 23 p3302 N88-29667
The Martian sedimentary record
23 p3302 N88-29669
Gamma-ray/neutron spectroscopy from the Mars observer 23 p3302 N88-29671
Aqueous alteration in S-N-C meteorites and implications for weathering products on Mars
23 p3303 N88-29673
Distribution and timing of thick transient air-fall deposits in Electris: Implications for the nature of the upland plains 23 p3303 N88-29674
Photogeological inferences of Martian surface composition 23 p3303 N88-29675
Some probable characteristics of the Martian regolith
23 p3303 N88-29678
Surface units on Mars: The assemblage in the Valles Marineris 23 p3304 N88-29680
Morphologic contrasts between Nirgal and Auqakuh Valles, Mars: Evidence of different crustal properties
23 p3304 N88-29681
Geology of six possible Martian landing sites
23 p3304 N88-29682
Spectral reflectance of SNC meteorites: Relationships to Martian surface composition
23 p3304 N88-29683
Constraints on the origin of fractured terrane, Northern Martian plains 23 p3304 N88-29684
Viking Landers and remote sensing
23 p3304 N88-29685
Origin of northern lowland plains: Constraints from boundary morphology 23 p3305 N88-29687
Episodic vs. epochal release of SO2 on Mars
23 p3305 N88-29688
Chemical interactions between the present-day Martian atmosphere and surface minerals
23 p3305 N88-29689
Stratigraphy of the Kasei Valles region, Mars
23 p3305 N88-29690
Topography of large craters on Mars: Implications for the highlands resurfacing history
23 p3306 N88-29691
Early cratering rates and the nature of the Martian cratered uplands 23 p3306 N88-29694
Documenting volcano-tectonic episodes in Mars' stratigraphic record 23 p3306 N88-29695
The surface composition of Mars from earthbased observations 23 p3306 N88-29696
Crystal fractionation in the SNC meteorites: Implications for surface units on Mars 23 p3307 N88-29698
Martian surface analogs: Laboratory spectral studies in the mid infrared 23 p3307 N88-29699
Ridged and gullied terrains in the Martian uplands
23 p3307 N88-29700
Variation in the thickness of ejecta cover on Mars with increasing crater density 23 p3307 N88-29701
Coadsorption of H2O and CO2 on the Martian surface
23 p3307 N88-29702
High resolution Viking Orbiter images: A useful data source for testing the viability of geomorphic processes attributed to Martian landforms
23 p3307 N88-29703
Debris flows of the Simud-Tiu outflow system of Mars
24 p3442 N88-30485
Faulting and its relation to volcanism: Mars western equatorial region 24 p3443 N88-30489
Physical properties of surface materials on Martian volcanoes: Dust-covered lava and ash
24 p3443 N88-30493
Simulations of lava flows on Mars
24 p3443 N88-30495
Volatiles on Mars
[NASA-CR-183113] 24 p3456 N88-30571

MARS VOLCANOES
MEVTV Workshop on Nature and Composition of Surface Units on Mars
[NASA-CR-183075] 23 p3300 N88-29654
The history of Martian volcanism determined from a revised relative chronology 23 p3301 N88-29657
Weathering of sulfides on Mars
23 p3301 N88-29662
Mapping of volcanic units at Alba Patera, Mars
23 p3301 N88-29663
Small Martian valcanoes 23 p3302 N88-29668
The Martian sedimentary record
23 p3302 N88-29669
Progress in determining the thickness and distribution of volcanic materials on Mars 23 p3302 N88-29670
Variability in spectral signatures of terrestrial volcanic rocks and implications for volcanology on Mars
23 p3303 N88-29672
What SNC meteorites tell us about Martian magmatism 23 p3303 N88-29679
Volcano evolution on Mars 23 p3305 N88-29686
Episodic vs. epochal release of SO2 on Mars
23 p3305 N88-29688
Documenting volcano-tectonic episodes in Mars' stratigraphic record 23 p3306 N88-29695
NASA MEVTV Program Working Group Meeting Volcanism on Mars
[NASA-CR-183074] 24 p3442 N88-30487
Mars: Volcanism in the Valles Marineris overlooked
24 p3443 N88-30491
The Martian highland paterae: Evidence for explosive volcanism on Mars 24 p3443 N88-30492
Physical properties of surface materials on Martian volcanoes: Dust-covered lava and ash
24 p3443 N88-30493
Rifts of deeply eroded Hawaiian basaltic shields: A structural analog for large Martian volcanoes
24 p3443 N88-30494
Simulations of lava flows on Mars
24 p3443 N88-30495
Small-scale volcanic landforms indicative of distributary tube systems 24 p3444 N88-30496
Volcanic styles at Alba Patera, Mars: Implications of lava flow morphology to the volcanic history
24 p3444 N88-30497

MARSHES
U MARSHLANDS

MARSHLANDS
Seasonal cycling of sulfur and iron in porewaters of a Delaware salt marsh
[NASA-CR-182385] 07 p0876 N88-15311
Relevance of a thematic map (SPOT data) with regards to the real flora and structure of the vegetation covering of salt marshes (Mont Saint Michel Bay, France)
22 p3109 N88-28488

MARTENSITE
Low activation ferritic alloys for nuclear fusion reactors
[DE87-010711] 03 p0286 N88-11801
A comparison of high damping shape memory alloys with Cu-Mn-based and Fe-Cr-based alloys
[AD-A184110] 04 p0414 N88-12586
Fracture analysis of drawn composite dual-phase steel wire
[DE88-001396] 06 p0681 N88-14173
Fatigue, fracture and strain hardening of high carbon hardened alloy steel
[AD-A186101] 07 p0831 N88-15043
Investigation of the auto-tempering of low-carbon martensite
[PB87-143970] 07 p0833 N88-15053
Propagation of fatigue crack in the medium-carbon steel containg both martensite and ferrite
[PB87-143962] 07 p0869 N88-15273
Studies of transverse phonon modes in premartensitic indium-thallium alloys
[DE88-003481] 13 p1744 N88-20428
Irradiation effects on tungsten stabilized martensitic steels
[DE88-007074] 18 p2486 N88-24748
Twin boundaries and heterophase interfaces in ferroelastic martensites
[DE88-011694] 21 p2916 N88-27304

MARTENSITIC STAINLESS STEELS
Microstructural evolution and response to double-loop reactivation testing of heat-treated pH 13-8 Mo martensitic stainless steel
[DE87-009058] 02 p0146 N88-10915
Swelling behavior of ferritic/martensitic steels
[DE88-001757] 06 p0682 N88-14177
Data requirements to model creep in 9Cr-1Mo-V steel
14 p1931 N88-21512

MARTENSITIC TRANSFORMATION
Soliton twin boundaries of the cubic-tetragonal martensitic transformations in ferroelastic materials
[DE87-014741] 04 p0495 N88-13047
Martensitic transformation and microstructures in sintered NiAl alloys
[NASA-TT-20178] 18 p2488 N88-24761
Martensitic transformation and microstructures in sintered NiAl alloys
[NASA-TT-20192] 19 p2616 N88-25519

Kinetic of martensitic transformations induced by hydrogen in the austenite
[DE88-701623] 23 p3194 N88-29007
MARTIN AIRCRAFT
NT B-57 AIRCRAFT
MARTINGALES
Stochastic integration for operator valued processes on Hilbert spaces and on nuclear spaces
[ENST-87D002] 01 p0089 N88-10580
On the relations between increasing functions associated with two-parameter continuous martingales
[AD-A185572] 06 p0765 N88-14699
Point processes in the plane
[AD-A186017] 07 p0913 N88-15542
Martingale representation and the Malliavin calculus
[AD-A189721] 15 p2119 N88-22626
Stochastic evolution equations driven by nuclear space valued martingales
[AD-A189342] 15 p2126 N88-22677
A Wong-Zakai type theorem for certain discontinuous semimartingales
[AD-A192713] 21 p3005 N88-27822
MASER RESONATORS
U MASERS
MASERS
NT HYDROGEN MASERS
NT INTERSTELLAR MASERS
NT TRAVELING WAVE MASERS
NT WATER MASERS
The 8.4-GHz low-noise maser pump source assembly
04 p0436 N88-12705
Traveling-wave maser closed-cycle refrigerator data acquisition and display system 04 p0437 N88-12708
Two-watt, 4-Kelvin closed cycle refrigerator performance 04 p0437 N88-12709
Nonthermal phenomena in stellar coronae: Evidence from radio observations 04 p0503 N88-13096
Higher harmonic generation in the induced resonance electron cyclotron maser
[AD-A186236] 07 p0858 N88-15210
VLBI research on OH-maser IN W33
08 p1001 N88-16064
Physics modeling support contract
[DE88-004039] 10 p1335 N88-17980
Polarization properties of SiO masers
13 p1858 N88-21113
MASKS
NT OXYGEN MASKS
Optical Fourier transformation by lensless method with perforated mask and with modified Talbot interferometer for analysis of interferograms 09 p1236 N88-17408
Smoke hoods: Net safety benefit analysis --- aircraft accidents
[CAA-PAPER-87017] 23 p3174 N88-28898
MASS
NT CENTER OF MASS
NT CRITICAL MASS
NT GALACTIC MASS
NT MISSING MASS (ASTROPHYSICS)
NT PARTICLE MASS
NT PLANETARY MASS
NT STELLAR MASS
Aqueous-phase reactions in clouds
[DE88-005249] 01 p0069 N88-10445
Modes, masses, metallicities, and magnitudes of RR Lyrae variables
[DE87-013149] 01 p0109 N88-10703
Phase 3 study of selected tether applications in space. Volume 2: Study results
[NASA-CR-179186] 02 p0132 N88-10828
Physics of few-body lambda hypernuclei
[DE87-014746] 03 p0375 N88-12357
Gravitational accretion of hot dark matter
03 p0388 N88-12439
Effect of permissible variations of center-of-gravity locations of cargo airplane on its mass
04 p0424 N88-12625
A search for very low mass (brown dwarf) stars as wide binaries using a seven element infrared camera-photometer 04 p0512 N88-13150
The effect of maximum-allowable payload temperature on the mass of a multimegawatt space-based platform
[DE88-001921] 05 p0555 N88-13381
Fluid mass and thermal loading effects on the modal characteristics of space shuttle main engine liquid oxygen inlet splitter vanes 05 p0594 N88-13628
Pressure and mass velocity measurements in solids subjected to dynamic loadings 07 p0921 N88-15595
Finite element method with continuous mass elements
[PB87-143384] 08 p0995 N88-16019
Dynamic finite element with diagonalized consistent mass matrix and elastic-plastic impact calculation
[PB87-143376] 08 p0995 N88-16020
Suppression of the mass enhancement in CeB6 in high magnetic fields
[DE88-002946] 09 p1241 N88-17439
Renormalization group analysis of the temperature dependent coupling constant in massless theory
[DE88-751059] 09 p1259 N88-17552
Spacecraft telecommunications system mass estimates 11 p1473 N88-18784
The rate of adaptation to altered g in the human centrifuge: Implications for simulations of mass-discrimination in space flight
12 p1659 N88-19941
Optimal placement of tuning masses for vibration reduction in helicopter rotor blades
[NASA-TM-100562] 13 p1782 N88-20665
To the field theory with a fundamental mass
[DE88-701159] 15 p2146 N88-22807
Effect of mass-velocity on liquid jet atomization in Mach 1 gasflow
[NASA-TM-100813] 16 p2211 N88-23194
The effect of maximum allowable payload temperature on the mass of a multimegawatt space based platform
17 p2424 N88-24416
MACRAD: A mass analysis code for radiators
17 p2424 N88-24418
Energy storage for nuclear burst power systems
17 p2426 N88-24431
Hydrogen turbines for space power systems: A simplified axial flow gas turbine model
[DE88-009585] 19 p2677 N88-25920
A Vlasov ion zero mass electron model for plasma simulations 20 p2855 N88-26958
Electromagnetic theory of the gravitation
22 p3158 N88-28793
The principles of mass and maneuver applied to space operations
[AD-A194037] 23 p3276 N88-29500
Spacecraft mass estimation, relationships and engine data: Task 1.1 of the lunar base systems study
[NASA-CR-172061] 24 p3332 N88-29836
The stability of disk galaxies and constraints on their mass-luminosity ratio
[SER-C-PREPUBL-FASC-27] 24 p3455 N88-30565
MASS DISTRIBUTION
Aerosol sensor: Real time determination of aerosol mass size distributors using filtering quartz oscillators
[ETN-87-90397] 01 p0049 N88-10311
Identification of linear structural models
03 p0337 N88-12121
The role of fragmentation in interaction of meteoroids with the Earth's atmosphere 06 p0737 N88-14532
A method of long-term radar shower data analysis
06 p0738 N88-14541
Incident meteoroid flux density
06 p0739 N88-14542
Analysis of the mass formula dependence of spallation product distribution
[DE88-750297] 07 p0864 N88-15243
Evidence for human adaptive response to dehydration: Increase of circulating protein mass
[AD-A186225] 08 p1048 N88-16328
On the time delay of the ultrahigh-energy radiation signal from the source Cygnus X-3
[DE88-700649] 10 p1431 N88-18547
The evolution of the mass distribution of cometary particles 14 p2004 N88-21946
Estimates of masses, volumes and densities of short-period comet nuclei 14 p2004 N88-21950
Angular resolved energy analysis of (69)Ga + ions from a gallium liquid metal ion source
[AERE-R-12649] 15 p2139 N88-22760
A review of the Initial Mass Function (IMF) --- stellar mass
[MPE-PREPRINT-112] 22 p3165 N88-28848
Laser sensing for identification and control of distributed parameter systems
[AD-A195886] 24 p3379 N88-30124
MASS DRIVERS (PAYLOAD DELIVERY)
Design study for asteroidal exploitation
03 p0389 N88-12445
MASS FILTERS
U FLUID FILTERS
MASS FLOW
Studies of transport processes in porous and ion exchange membranes
[ISBN-951-99847-0-4] 01 p0021 N88-10133
IRAS and cool stellar mass loss
04 p0515 N88-13166
Combustion characteristics of gas turbine alternative fuels
[NASA-TM-100247] 05 p0548 N88-13338
Speed control of a missile with throttleable ducted rocket propulsion 12 p1597 N88-19561
Mass transport in flow of sources
[LRT-WE-9-FB-4(1987)] 22 p3077 N88-28268
Mass transfer instabilities due to angular momentum flows in close binaries --- stars
[MPE-PREPRINT-113] 22 p3165 N88-28849
MASS FLOW FACTORS
Mass transport in flow of sources
[LRT-WE-9-FB-4(1987)] 22 p3077 N88-28268
Mass transport in annular spherical system
[LRT-WE-9-FB-11(1987)] 22 p3077 N88-28271
Analysis of a feed device for the pneumatic transport of noncohesive particles
[VKI-TM-44] 24 p3369 N88-30062
MASS FLOW RATE
Equipment for mass flow measurements in the low-speed wind tunnel at DFVLR in Brunswick, West Germany
[DFVLR-MITT-88-02] 21 p2900 N88-27212
Turbulence structure of mixing swirling flows
[AD-A193063] 21 p2943 N88-27478
Mass flow rate influence on void fraction of two-phase helium flow
[DE88-702456] 21 p2945 N88-27495
Mass transport in flow of sources
[LRT-WE-9-FB-4(1987)] 22 p3077 N88-28268
MASS RATIOS
NT PAYLOAD MASS RATIO
NT PROPELLANT MASS RATIO
A review of the Initial Mass Function (IMF) --- stellar mass
[MPE-PREPRINT-112] 22 p3165 N88-28848
MASS SPECTRA
Real time analysis of detonation products
[DE87-007453] 01 p0031 N88-10195
Trace analysis by MS/MS on a double focussing mass spectrometer
[AD-A187954] 10 p1334 N88-17973
Accuracy of analytic energy level formulas applied to hadronic spectroscopy of heavy mesons
[NASA-TM-4042] 19 p2725 N88-26185
MASS SPECTROMETERS
Ion composition measurements in the upper stratosphere --- parachute-borne mass spectrometer
[ETN-87-90423] 01 p0069 N88-10442
Research relative to an advanced rod control system for quadrupole mass spectrometry applications
[NASA-CR-181458] 02 p0167 N88-11050
Mass spectroscopic facility 03 p0296 N88-11861
Diagnostics aid for mass spectrometer trouble-shooting
[DE88-000350] 03 p0324 N88-12049
The tail lobe ion spectrometer: Theory and observations
[IFSI-86-12] 05 p0585 N88-13569
Trace analysis by MS/MS on a double focussing mass spectrometer
[AD-A187954] 10 p1334 N88-17973
Energy spectra of pick-up ions recorded during the encounter of Giotto with Comet Halley
14 p1997 N88-21901
Evidence for first polymer in Comet Halley: Polyoxymethylene 14 p1997 N88-21906
High-voltage inverse-square function generator
[DE88-701109] 15 p2058 N88-22270
Stratospheric positive ion composition measurements and acetonitrile detection: A consistent picture
[AERONOMICA-ACTA-A-326-1987]
18 p2542 N88-25084
A mass spectrometer for the analysis of thermally labile compounds 19 p2668 N88-25859
Evaluation of the ion trap mass spectrometer for potential application in the space station
[DE88-008940] 19 p2674 N88-25902
Synopsis of a computer program designed to interface a personal computer with the fast data acquisition system of a time-of-flight mass spectrometer
[NASA-CR-177474] 21 p3001 N88-27798
MASS SPECTROMETRY
U MASS SPECTROSCOPY
MASS SPECTROSCOPY
Simultaneous TG/DSC (thermogravimetry/Differential Scanning Calorimetry) and TG/MS (thermogravimetry/Mass Spectrometry) analyses of polymeric and energetic materials
[DE88-000727] 04 p0413 N88-12561
Supersonic beam observations of semiconductor clusters
[AD-A184991] 05 p0655 N88-14018
Atomic-level studies of superconducting YBa2Cu3O sub 7-x
[DE88-002522] 06 p0788 N88-14831
Development of FTMS methods for the detection of trace chemical species and development of FTMS methods for the analysis of various chemical species
[AD-A185857] 07 p0828 N88-15023
Monitoring of space station life support systems with miniature mass spectrometry and artificial intelligence
08 p1057 N88-16376
Laser post-ionization secondary neutral mass spectroscopy
[DE88-002979] 09 p1172 N88-17027

A chemical precursor to optical damage. Studies by laser ionization mass spectrometry
[DE88-004321] 10 p1409 N88-18408

Determining chemical composition of aerosol in Venusian cloud layer on Vega-1 automatic interplanetary station using Malakhit mass spectrum analyzer
13 p1726 N88-20321

Development and evaluation of supercritical fluid chromatography-mass spectrometry
[DE88-005122] 13 p1738 N88-20394

A mass spectrometer evolved gas analysis experiment for in-situ analysis of cometary dust volatiles
13 p1854 N88-21097

Low pressure gas flow analysis through an effusive inlet using mass spectrometry
[NASA-CR-182712] 14 p1910 N88-21413

Chromatographic and mass spectrometric separation and analysis
[AD-A190113] 16 p2174 N88-22958

Molecular-beam, mass-spectrometric studies of wood vapor and model compounds over HZSM-5 catalyst
18 p2535 N88-25044

Mass spectrometric high temperature measurements of the barium oxide-zirconium dioxide system and the determination of thermodynamic data for barium zirconate. Clarification of the counter-stopping capacity of coated particles for solid fission products by zirconium dioxide addition
[NASA-TT-20187] 19 p2611 N88-25496

Prospects for large dynamic range isotope analysis using photon burst mass spectrometry
[DE88-009110] 19 p2613 N88-25505

High-fidelity in isotope ratio measurements for resonance ionization mass spectrometry
[DE88-009129] 19 p2613 N88-25506

Simultaneous thermogravimetric modulated beam mass spectrometry and time-of-flight velocity spectra measurements: Thermal decomposition mechanisms of RDX and HMX 19 p2632 N88-25612

Laser desorption/ablation studies by resonance ionization mass spectrometry
[DE88-009124] 20 p2807 N88-26650

Recent advances in atom-probe field ion microscopy
[DE88-006799] 20 p2876 N88-27070

Measurement of Beta-decay energies of short-lived neutron-rich nuclei in the vicinity of mass number between 101 and 106, and A = 109
[ETN-88-92376] 21 p3014 N88-27890

Impurity analysis in SIMOX samples by high-efficiency resonance ionization time-of-flight mass spectrometry
[DE88-012061] 24 p3367 N88-30051

Ion kinetics in silane plasmas
[AD-A196202] 24 p3431 N88-30423

MASS TRANSFER

Flow and heat transfer with impinging jets and rough surfaces
[DE87-014162] 02 p0169 N88-11065

On the surging potential of polar ice streams. Antarctic surges: A clear and present danger
[DE87-013980] 02 p0216 N88-11363

Mass transport by diffusion 03 p0297 N88-11864

Heat transfer in laminar flow for mass inlet into an annular channel
[DE87-702890] 03 p0314 N88-11983

Local heat/mass transfer and pressure drop in a two-pass rib-roughened channel for turbine airfoil cooling
[NASA-CR-179635] 03 p0322 N88-12039

Novel macrocyclic carriers for proton-coupled liquid membrane transport
[DE88-000636] 04 p0413 N88-12560

Corrosion of ferritic steels by molten lithium: Influence of competing thermal gradient mass transfer and surface product reactions
[DE88-000334] 04 p0417 N88-12565

Heat and moisture transport in the atmospheric boundary layer
[AD-A184222] 04 p0470 N88-12904

Study of the effect of mass transfer on a transonic boundary layer. Application to flow relaminarization
[ETN-88-91169] 05 p0541 N88-13296

Systematic stratospheric-tropospheric exchange viewed from isentropic coordinates 05 p0615 N88-13777

Modern concept concerning transport of bottom sediments in abyssal regions of world ocean
06 p0726 N88-14476

The adaption and use of research codes for performance assessment
[DE88-000552] 06 p0756 N88-14639

EXOSAT guest observer program. Binary parameters of the X-ray Pulsar 4U1626-67
[NASA-CR-182374] 06 p0802 N88-14905

Examination of the development of a compressible turbulent boundary layer on a rough and porous wall
[PB87-148266] 07 p0815 N88-14964

A numerical study of transient heat and mass transfer in crystal growth 07 p0925 N88-15619

The paradoxical asymptotic status of massless springs
[AD-A185625] 07 p0928 N88-15637

Investigations in field of surface forces in metallurgy
[BLL-M-47406-(5828.4)] 08 p0969 N88-15860

Determination of the effect of walking on the forced convective heat transfer coefficient using an articulated mannikin
[AD-A186452] 08 p1049 N88-16335

Application of Hoffman modulation contrast microscopy coupled with three-wavelength two-beam interferometry to the in situ direct observation of the growth process of a crystal in microgravity 10 p1268 N88-17704

Experimental studies of heat and mass exchange in parallel-passage rotary desiccant dehumidifiers for solar cooling applications
[DE88-001119] 10 p1350 N88-18069

Physiological and ecological implications of coupled heat- and water-transport mechanisms of endotherms and vegetation
[DE88-004170] 10 p1352 N88-18081

Mass transport phenomena between bubbles and dissolved gases in liquids under reduced gravity conditions
[NASA-TM-100273] 11 p1455 N88-18672

Effect of density change on rapid liquid-solid interface kinetics and heat flow
[DE88-004286] 11 p1487 N88-18878

Mass transport and chemical demixing of Y-Ba-Cu-O compounds during sintering in temperature gradients
[DE88-004887] 12 p1696 N88-20151

Mass, heat and nutrient fluxes in the Atlantic Ocean determined by inverse methods
[NASA-CR-180535] 14 p1950 N88-21626

The mass loss rates of periodic comets
14 p2010 N88-21991

Mass transfer mechanisms for water adsorbed on silica gel
[DE88-005993] 15 p2032 N88-22107

The numerical simulation of viscous flows with change of phase and chemical reaction
[DE88-003204] 15 p2062 N88-22292

Studies of heat and mass transfer during chemical vapor deposition 17 p2338 N88-23953

Thermochemical analysis of mass transfer in a NB-1ZR-potassium heat pipe 17 p2412 N88-24346

Fabrication of a niobium 1 percent zirconium containment for SP-100 primary lithium system materials mass transfer studies 17 p2417 N88-24373

Irreversible dissolution of solid solutions: A kinetic and stoichiometric model
[DE88-009194] 19 p2614 N88-25513

Parametric methodologies of cloud vertical transport for acid deposition models
[PB88-191374] 20 p2825 N88-26762

Development of an experimental system for studying fast transient ignition phenomena
[DE88-011917] 21 p2911 N88-27276

Heat and mass transfer in a transport channel
[DE88-701968] 21 p2945 N88-27493

Heat and mass transfer in laminar wavy film absorption with the presence of non-absorbable gases
21 p2947 N88-27502

Mass transport in flow of sources
[LRT-WE-9-FB-4(1987)] 22 p3077 N88-28268

Mass transport in sector and annular sector tubes
[LRT-WE-9-FB-9(1987)] 22 p3077 N88-28269

Mass transport in annular spherical system
[LRT-WE-9-FB-11(1987)] 22 p3077 N88-28271

Mass transport in a parabolic conduit
[LRT-WE-9-FB-1(1988)] 22 p3077 N88-28273

Mass transfer instabilities due to angular momentum flows in close binaries --- stars
[MPE-PREPRINT-113] 22 p3165 N88-28849

The evolution of low-mass X-ray binaries
[MPE-PREPRINT-118] 22 p3165 N88-28851

Global vertical mass transport by clouds: A two-dimensional model study
[CM-74] 24 p3391 N88-30192

MASSACHUSETTS

Tide- and wind-forced currents in Buzzards Bay, Massachusetts
[PB88-110580] 07 p0682 N88-15350

MATCHED FILTERS

Detection of signals by the digital integrate-and-dump filter with offset sampling 04 p0435 N88-12695

Detection of signals by weighted integrate-and-dump filter 04 p0435 N88-12696

On the design of suboptimal matched filters for three-dimensional moving target detection
[AD-A186364] 12 p1619 N88-19682

Computation of LMS (Least-Mean-Square) and matched digital filters for optical clutter suppression
[AD-A188885] 12 p1687 N88-20093

Synthetic-aperture radars viewed as interferometers with matched filter processing of the collected data
[AD-A190606] 15 p2057 N88-22262

Spatial matched processing for multipath propagation
[AD-A189790] 15 p2129 N88-22701

A numerically efficient digital matched filter for periodic and windowed periodic radar waveforms
[AD-A193132] 21 p2932 N88-27410

Maximum dynamic responses using matched filter theory and random process theory
[NASA-TM-100653] 22 p3042 N88-28059

MATCHING

Multiple-object motion estimation by maximal matching of 3-D point and line features 09 p1220 N88-17322

Digital SPOT stereoplotting: An original approach to the formation of epipolar images and matching
22 p3113 N88-28483

Cleanability of aircraft polyurethane topcoats
[AD-A193456] 23 p3170 N88-28878

On broadband matching of multiport electrical networks with applications
[AD-A194224] 23 p3207 N88-29086

Linearized model matching for single-imput nonlinear systems
[AD-A193642] 23 p3266 N88-29445

MATERIAL ABSORPTION

Microwave dispersion and absorption in tissues: Molecular mechanisms
[AD-A190118] 15 p2100 N88-22512

Bimolecular reactions and energy-transfer processes of highly vibrationally excited molecules related to energetic materials
[AD-A189013] 18 p2571 N88-25270

MATERIAL BALANCE
NT WATER BALANCE

Design of an elemental analysis system for CELSS research 03 p0360 N88-12266

Mass balances for a biological life support system simulation model 03 p0361 N88-12272

Problems appearing at interface balances --- flames
14 p1987 N88-21955

MATERIAL REMOVAL (MACHINING)
U MACHINING

MATERIAL STRENGTH
U MECHANICAL PROPERTIES

MATERIALS HANDLING
NT GROUND HANDLING
NT PROPELLANT TRANSFER
NT REMOTE HANDLING

The development of a friction model predicting the sliding behavior of materials pairs, especially at low temperatures: Progress report and renewal proposal
[DE87-013941] 01 p0055 N88-10354

Experimental molecular spectroscopy in shock-compressed materials
[DE87-013139] 02 p0144 N88-10900

DOE explosives safety manual
[DE88-000831] 04 p0422 N88-12616

Nuclear techniques in studies of condensed matter
[NASA-RP-1195] 04 p0489 N88-13015

To determine the stress distribution in the vicinity of GRP end pads where the specimen is held and loaded (CFC coupon specimens) --- glass reinforced plastic (GRP) carbon fiber composite (CFC)
[BAE-WST-R-RES-CFC-12023]
09 p1182 N88-17090

Non-proprietary research projects of the Center for the Space Processing of Engineering Materials
[AR-2] 10 p1426 N88-18516

Selection of a handling and maintenance option for the SP-100 ground engineering system test
17 p2402 N88-24285

Proposed quality assurance/quality control plan
[AD-A191490] 18 p2525 N88-24978

RRSAS (Robotic Radiation Survey and Analysis System) Project: A real time sensor driven robotic system
[DE88-006825] 20 p2808 N88-26661

Expert system application education project
[NASA-CR-183069] 20 p2843 N88-26867

Aircraft refueling demonstrator using a microbot alpha 2 robot 21 p2926 N88-27367

Mobile robotics R and D at the Savannah River Laboratory
[DE88-011665] 22 p3083 N88-28310

A guide to good magnetic tape management practice for MODAS users --- moduler airborne data acquisition system (MODAS)
[RAE-TM-IT-212] 22 p3162 N88-28834

A robotic system for automation of logistics functions on the Space Station 23 p3260 N88-29407

Vanderbilt free electron laser project in biomedical and materials research
[AD-A195961] 24 p3378 N88-30121

Applications of synchrotron radiation to materials science: Diffraction imaging (topography) and microradiography
[NASA-CR-183265] 24 p3434 N88-30440

MATERIALS RECOVERY
NT SOLVOLYSIS
NT WATER RECLAMATION
Separation of anionic from nonionic alkoxy compounds using silica gel
[GB-PATENT-2-140-415-A] 01 p0020 N88-10122
A large-scale perspective on ecosystems
03 p0360 N88-12265
An overview of Japanese CELSS research activities
03 p0360 N88-12267
Design study for asteroidal exploitation
03 p0389 N88-12445
STS propellant scavenging systems study. Part 2, volume 1: Executive summary and study results
[NASA-CR-179275] 10 p1290 N88-17716
Evaluation of bituminous materials used in pavement recycling projects at Tyndall, MacDill, and Hurlburt Air Force Bases
[AD-A188068] 10 p1317 N88-17871
MATERIALS SCIENCE
JPRS report: Science and technology. USSR: Materials science
[JPRS-UMS-87-006] 03 p0285 N88-11791
The contribution of electron microscopy of materials science to society
[DE88-006341] 15 p2028 N88-22082
MATERIALS TESTING REACTORS
U NUCLEAR RESEARCH AND TEST REACTORS
MATERIALS TESTS
Spectroradiometry in materials testing
16 p2273 N88-23601
MATHEMATICAL ANALYSIS
U APPLICATIONS OF MATHEMATICS
MATHEMATICAL LOGIC
NT ALGORITHMS
NT AXIOMS
NT BOOLEAN ALGEBRA
NT BOOLEAN FUNCTIONS
NT BOREL SETS
NT EQUIVALENCE
NT FORMULAS (MATHEMATICS)
NT LATTICES (MATHEMATICS)
NT PARSING ALGORITHMS
NT SET THEORY
NT SIMPLEX METHOD
Extraction and evaluation of Boolean relations for the solution of linear programs in 0-1 variables, volume 1
[ENST-86E023-VOL-1] 02 p0227 N88-11430
Extraction and evaluation of Boolean relations for the solution of linear programs in 0-1 variables, volume 2
[ENST-86E023-VOL-2] 02 p0227 N88-11431
Maintaining state constraints in relational databases: A proof theoretic basis
[DE87-014329] 02 p0248 N88-11569
An exact penalization viewpoint of constrained optimization
[DE88-001477] 04 p0486 N88-12995
The implementation of artificial intelligence in control systems
[DE88-003497] 10 p1396 N88-18318
The representation of knowledge within model-based control systems
[DE88-004863] 10 p1396 N88-18319
Measures of similarity between fuzzy concepts: A comparative analysis
[AD-A189430] 13 p1825 N88-20910
Abstraction and empty process in process algebra
[CWI-CS-R8721] 13 p1826 N88-20919
ONTIC: A knowledge representation system for mathematics
[AD-A190553] 15 p2121 N88-22643
Improving the performance of AI algorithms
[AD-A192848] 21 p3003 N88-27809
MATHEMATICAL MODELS
NT ANALOG SIMULATION
NT BIOLOGICAL MODELS (MATHEMATICS)
NT DIGITAL SIMULATION
NT K-EPSILON TURBULENCE MODEL
NT MANDELSTAM REPRESENTATION
NT PETRI NETS
NT THOMAS-FERMI MODEL
NT TURBULENCE MODELS
The numerical simulation of an idealised one-dimensional, steady monopropellant rocket
[PDR/CFDU/IC/31] 01 p0018 N88-10107
The dissociation of dense liquid nitrogen and shock cooling
[DE87-013490] 01 p0022 N88-10136
A quantitative statistical model for cleavage fracture initiation in carbide strengthened steels
[ETN-87-90735] 01 p0025 N88-10157
Current experimental and theoretical understanding of detonation waves in heterogeneous solid explosives
[DE87-012177] 01 p0032 N88-10201
Performance of rotary regenerative heat exchanger: A numerical simulation 01 p0046 N88-10292
Cooling effect of a single evaporating droplet on a hot semi-infinite metal body
[PB87-201802] 01 p0046 N88-10294
Experimental and theoretical studies of vertical annular liquid jets
[DE87-013907] 01 p0047 N88-10299
Problem specifications and collated solutions of the two-phase numerical-benchmark exercise 1986-7 --- two phase flow
[CFDU/87/1] 01 p0047 N88-10300
Phase dynamics: A review and a perspective
[DE87-013173] 01 p0048 N88-10306
Development of response models for the Earth Radiation Budget Experiment (ERBE) sensors. Part 4: Preliminary nonscanner models and count conversion algorithms
[NASA-CR-178295] 01 p0050 N88-10317
The development of a friction model predicting the sliding behavior of materials pairs, especially at low temperatures: Progress report and renewal proposal
[DE87-013941] 01 p0055 N88-10354
Analysis of shell-type structures subjected to time-dependent mechanical and thermal loading
[NASA-CR-181409] 01 p0060 N88-10388
High-efficiency silicon solar cells: Numerical modeling, transient measurements, efficiency goals, and v-shaped grooves
[DE87-012842] 01 p0066 N88-10423
Status of the solar and infrared radiation submodels in the LLNL 1-D and 2-D chemical-transport models
[DE87-014320] 01 p0069 N88-10441
Experimental study and modeling of the physical mechanisms of the gliding spark
[ESA-TT-1029] 01 p0070 N88-10447
Conception and discussion of a model describing ice formation on various obstacles
[ONERA-NT-1986-6] 01 p0072 N88-10460
Contributions to the modeling of wind shear for danger studies
[ETN-87-90442] 01 p0072 N88-10463
The box method for linear programming. Part 1: Basic theory
[DE87-011029] 01 p0080 N88-10515
Language modelling for automatic speech recognition: A review
[RSRE-MEMO-4038] 01 p0084 N88-10544
The use of splines in the modelling of a photodiode response
[NPL-DITC-88/87] 01 p0085 N88-10550
Data Model of Objects and Relations (DAMOR): A data model for knowledge representation
[REPT-87-05] 01 p0085 N88-10553
Steady state theta pinch concept for slow formation of FRC
[ISSN-0469-4732] 01 p0098 N88-10648
Optimization of SIS mixer elements
[NASA-CR-180710] 01 p0104 N88-10680
Spontaneous symmetry breaking in N=2 supergravity
[DE87-702749] 01 p0109 N88-10704
Spontaneous symmetry breaking in N=3 supergravity
[DE87-702753] 01 p0109 N88-10705
Real-time expert systems: A status report
02 p0129 N88-10817
Mathematical modelling of solar ultraviolet radiation induced optical degradation in anodized aluminum
02 p0135 N88-10846
Structural Assembly Demonstration Experiment (SADE)
[NASA-CR-179205] 02 p0138 N88-10868
Numerical simulation of a supersonic chemically reacting mixing layer 02 p0143 N88-10900
Computer modeling of metal forming
[DE87-013804] 02 p0157 N88-10984
Modeling and performance evaluation of the DPS25 packet switching multiprocessor system --- communication networks
[ENST-87E009] 02 p0162 N88-11016
Contribution to the study of circuit switched networks: Modeling and numerical solutions
[LAAS-87-174] 02 p0162 N88-11017
On the modelling of non-reactive and reactive turbulent combustor flows 02 p0169 N88-11061
An approximate solution to the problem of heating massive bodies by both radiation and convection
[BLL-M-37315-(5828.4)] 02 p0170 N88-11068
Impact of turbulence modeling on numerical accuracy and efficiency of compressible flow simulations
[NASA-TM-88333] 02 p0173 N88-11088
Turbine Engine Hot Section Technology, 1985
[NASA-CP-2405] 02 p0184 N88-11140
Aerothermal modeling program, phase 2
02 p0185 N88-11149
Constitutive modeling for single crystal superalloys
02 p0187 N88-11168
Life prediction and constitutive models for engine hot section anisotropic materials program
02 p0188 N88-11175
Coating life prediction 02 p0189 N88-11181
Thermal barrier coating life prediction model development 02 p0190 N88-11184
Thermal barrier coating life prediction model development 02 p0190 N88-11185
Estimating scattered and absorbed radiation in plant canopies by remote sensing
[NASA-CR-181390] 02 p0193 N88-11205
A real-data numerical study and four-dimensional data assimilation application for mesobeta-scale flow in complex terrain 02 p0212 N88-11329
On the surging potential of polar ice streams. Antarctic surges: A clear and present danger
[DE87-013980] 02 p0216 N88-11363
Numerical simulation of Tokamaks: Ideal MHD equilibrium and stability
[DE87-013452] 02 p0218 N88-11373
Software reliability models for fault-tolerant avionics computers and related topics
[NASA-CR-181440] 02 p0220 N88-11382
Projection-space iterative interpolation for limited-angle tomography in parallel- and fan-beam geometry, part 1
[DE87-013965] 02 p0221 N88-11391
A treatment of jw-axis model-matching transformation zeros in the optimal H squared and H infinity control designs
[OUEL-1673/87] 02 p0223 N88-11407
On the relational modeling of discrete PDE problems
[DE87-013336] 02 p0224 N88-11409
An adaptive pseudo-spectral method for reaction diffusion problems
[NASA-CR-178394] 02 p0224 N88-11414
Parallel methods for ordinary differential equations
[DE87-014667] 02 p0226 N88-11425
An empirical investigation of the use of ranks in pips sampling
[DE87-010609] 02 p0228 N88-11438
Measures of diversity based on fuzzy multinomial distributions
[DE87-010617] 02 p0228 N88-11439
Evaluation of a scale-model experiment to investigate long-range acoustic propagation
[NASA-TP-2748] 02 p0230 N88-11450
Pinhole occulter experiment
[NASA-CR-179206] 02 p0235 N88-11481
Computer models for kinetic equations of magnetically confined plasmas
[DE87-011571] 02 p0236 N88-11492
Thin film microstructures: Simulation and theory
[DE87-014732] 02 p0246 N88-11553
The Shock and Vibration Digest, Volume 19, No. 11
03 p0265 N88-11673
Analytical average model of studies on orbital resonance 03 p0269 N88-11689
Stability of mechanical joints in launching vehicles: Local and global stationary values of energy density
03 p0270 N88-11696
Three-dimensional finite element based, interative approach for analysis of laminated composites
03 p0280 N88-11763
Combustion in turbulent jets and buoyant flames
[PB87-232674] 03 p0283 N88-11779
Ignition and flame propagation in sprays
[AD-A184679] 03 p0283 N88-11781
Numerical simulation of turbulent premixed combustion and decay of turbulent swirling flow
[DE87-014253] 03 p0284 N88-11787
Crevice corrosion of stainless steels and related alloys. Part 2: Summary of experimental test data for input to mathematical model
[BR99871-PT-2] 03 p0289 N88-11816
Generalized coupled-mode equations, applications to fiber couplers 03 p0298 N88-11875
Generalized hybrid variational principle, corresponding finite element model 03 p0301 N88-11895
Compactness of quasi-conforming element spaces, convergence of quasi-conforming element method
03 p0301 N88-11896
Numerical modeling: Integral equation method
03 p0304 N88-11919
Hollow cathode plasma coupling study, 1986
[NASA-CR-171985] 03 p0309 N88-11949
Computation of turbulent flows using an extended k-epsilon turbulence closure model
[NASA-CR-179204] 03 p0312 N88-11969
Special Course on Modern Theoretical and Experimental Approaches to Turbulent Flow Structure and its Modelling
[AGARD-R-755] 03 p0312 N88-11970
Turbulence modelling through one point closures-applications-enlightening by large eddy simulation 03 p0312 N88-11972
Transition to turbulence via spatio-temporal intermittency 03 p0313 N88-11976
Lattice gas hydrodynamics 03 p0313 N88-11978

A transient model for thermal detonation
[IKE-2-75] 03 p0314 N88-11984

Stochastic model of the motion of suspended particles in turbulent flow
[HSBW-MITT-21/1987] 03 p0315 N88-11990

Conjugated heat transfer from a radiating fluid in a rectangular channel 03 p0317 N88-12003

Thrust and specific impulse of repetitively-pulsed-laser propulsion rocket 03 p0318 N88-12012

Heat transfer performance of axially grooved heat pipes 03 p0319 N88-12016

Heat transfer characteristics of arterial heat pipe with axial grooves 03 p0319 N88-12017

On the root locus method applied to flexural vibration control systems 03 p0320 N88-12022

Unsteady flow about cambered plates
[AD-A184725] 03 p0320 N88-12025

A study of chaos and mixing in Rayleigh-Taylor and Richtmyer-Meshkov unstable interfaces
[AD-A184751] 03 p0320 N88-12026

The dynamics of bubble growth for Rayleigh-Taylor unstable interfaces
[AD-A184752] 03 p0321 N88-12027

Continued research on direct contact heat exchangers: Effects of crystallization
[DE87-014931] 03 p0322 N88-12035

Multidimensional modeling of convective heat transfer with application to I.C. engines
[DE87-014983] 03 p0322 N88-12036

Bearing loads in slider crank mechanisms
[PB87-216495] 03 p0332 N88-12089

Models for conducting economic analysis of alternative fuel vehicles
[AD-A184028] 03 p0334 N88-12103

Teleoperator and robotics system analysis
[NASA-CR-179220] 03 p0334 N88-12105

Effects of state recovery on creep buckling induced by thermomechanical loading 03 p0336 N88-12116

Dynamic response of a 330 KW horizontal axis wind turbine generator
[DE87-014867] 03 p0347 N88-12195

Heats of mixing for thermal energy storage systems. Phase 1: Selection of suitable liquid-liquid mixtures
[DE87-014971] 03 p0347 N88-12196

An algorithmic approach to crustal deformation analysis
[NASA-CR-181497] 03 p0349 N88-12203

Earthquake source mechanisms and transform fault tectonics in the Gulf of California
03 p0349 N88-12206

Kinds of bootstraps and kinds of jackknives, discussed in terms of a year of weather-related data
[AD-A184495] 03 p0353 N88-12227

A simulation study of a speed control system for autonomous on-road operation of automotive vehicles
[AD-A184030] 03 p0362 N88-12279

Nonlinear parametric least-squares adjustment
[AD-A184039] 03 p0371 N88-12336

Stochastic model of the NASA/MSFC ground facility for large space structures with uncertain parameters: The maximum entropy approach
[NASA-CR-181489] 03 p0372 N88-12343

Mathematical models for the S.D.I.
[AD-A184667] 03 p0373 N88-12345

Applications of a theory of ferromagnetic hysteresis
[DE87-014725] 03 p0373 N88-12348

A hybrid numerical technique for predicting the aerodynamic and acoustic fields of advanced turboprops
[NASA-CR-174926] 03 p0374 N88-12352

Monte Carlo simulation of primitive atom-transfer reactions in solution
[AD-A183977] 03 p0375 N88-12360

Mathematical models of plasma discharge control in a tokamak
[DE87-702891] 03 p0378 N88-12377

Stability of low-shear Tokamaks
[DE88-000305] 03 p0379 N88-12383

The itinerant resonating-valence-bond model for superconductivity
[DE87-014794] 03 p0380 N88-12391

Modeling of proximity coupling between superconducting filaments in superconducting dipole magnets
[DE87-014684] 03 p0382 N88-12403

Hovering helicopter flight dynamics: A study of vertical motion
[AR-004-526] 04 p0399 N88-12485

An integrated study of structures, aerodynamics and controls on the forward swept wing X-29A and the oblique wing research aircraft
[NASA-CR-181548] 04 p0399 N88-12486

Aircraft engine exhaust plume dynamics
[AD-A184238] 04 p0400 N88-12488

Efficiency aspects of short, low velocity railguns
[AR-004-647] 04 p0405 N88-12517

Analytical investigation of the dynamics of tethered constellations in Earth orbit (phase 2)
[NASA-CR-179218] 04 p0408 N88-12533

A study of mechanisms of hydrogen diffusion in separation devices
[DE88-000328] 04 p0416 N88-12584

Microgravity nucleation and particle coagulation experiments support
[NASA-CR-181540] 04 p0423 N88-12618

Microgravity nucleation and particle coagulation experiments support
[NASA-CR-181541] 04 p0423 N88-12619

Aircraft dynamic response calculation based on discrete-continual model 04 p0424 N88-12624

A direct method to obtain constitutive model constants from cylinder impact test results
04 p0427 N88-12647

Ideal-viscoplastic extrusion model with application to deforming pistons in light-gas guns
[UTIAS-TN-266] 04 p0429 N88-12657

Heterogeneous multi-trunking queueing systems
[AD-A184255] 04 p0431 N88-12668

Programmable Logic Arrays (PLA's) design for testability
[PB87-102935] 04 p0438 N88-12718

An analytical and experimental study of injection-locked two-port oscillators
[NASA-TM-100119] 04 p0439 N88-12727

The Pierce diode with an external circuit. Part 1: Simulations in the linear regime
[DE88-000413] 04 p0440 N88-12731

Fully developed turbulence via Feigenbaum's period-doubling bifurcations
[DE88-000242] 04 p0441 N88-12739

Numerical simulation of unsteady separated flows
[AD-A184132] 04 p0442 N88-12741

Tracking through turbulence at the Tonopah Test Range
[DE88-001448] 04 p0446 N88-12766

Analysis of sideband spectra from untapered undulator using analytical technique
[DE87-014763] 04 p0448 N88-12778

The modelling of orientation in planar polymer welding flows
[AD-A184404] 04 p0451 N88-12793

Nonlinear axial stiffness characteristics of axisymmetric bolted joints 04 p0452 N88-12799

Creep life prediction based on stochastic model of microstructurally short crack growth
[NASA-TM-100245] 04 p0456 N88-12825

Two-layer stratified flow analysis of gravity currents and turbidity currents in lakes, reservoirs and the ocean
04 p0463 N88-12864

Statistics of the geomagnetic secular variation for the past 5Ma
[NASA-CR-181556] 04 p0467 N88-12890

An algorithmic approach to crustal deformation analysis 04 p0468 N88-12891

The effects of minor trace gases on the transfer of thermal infrared radiation through the Earth's atmosphere 04 p0468 N88-12893

Experimental and analytic studies of the triggered lightning environment of the F106B
[NASA-CR-4104] 04 p0469 N88-12897

Estimation of a multivariate continuous variable panel model
[AD-A184472] 04 p0484 N88-12982

The shifted Adams method for ordinary differential equations
[DE88-000810] 04 p0486 N88-12994

Radiation induced collapse of the crystalline structure
[DE87-014407] 04 p0498 N88-13064

Subjective probability, combination of expert opinion and probabilistic approaches to information retrieval
04 p0501 N88-13085

The acceleration of winds by MHD waves in open magnetic structures 04 p0506 N88-13109

Cosmological applications of singular hypersurfaces in general relativity 04 p0521 N88-13202

Gamma ray lines from novae
04 p0526 N88-13214

Computation of rime ice accretion on airfoils
[FFA-TN-1987-08] 05 p0542 N88-13301

Non-linear maximum likelihood estimation of stability derivatives from range data
[NAL-TM-SE-8608] 05 p0552 N88-13365

Development of an integrated BEM approach for hot fluid structure interaction
[NASA-CR-181577] 05 p0556 N88-13384

OH(A-X) fluorescence from photodissociative excitation of HO2 at 157.5 nm
[NASA-CR-181580] 05 p0563 N88-13429

A mathematical model of high alloy nickel base high temperature alloys
[BLL-M-37381-(5828.4)] 05 p0564 N88-13436

Noise modelling in the time domain with the aid of Spice
[PB87-221941] 05 p0573 N88-13492

Large bandwidth ground scattering model --- radar scattering
[FOA-C-30458-3.2] 05 p0576 N88-13511

Conditional second order closure for turbulent shear flows
[AD-A185369] 05 p0581 N88-13542

Active and passive plume distribution models in the convective boundary layer using a large eddy simulation model
[KNMI-TR-90] 05 p0581 N88-13546

Model-based motion estimation and its application to restoration and interpolation of motion pictures
[AD-A185054] 05 p0584 N88-13558

Simulation of the perpendicular magnetic recording process
[B8713537] 05 p0586 N88-13570

Theoretical studies of solar lasers and converters
[NASA-CR-181569] 05 p0587 N88-13577

Control of a flexible one-link manipulator
[AD-A185035] 05 p0590 N88-13598

Non-linear shipboard shock analysis of the Tomahawk missile shock isolation system 05 p0592 N88-13614

Analysis of photopole data reduction models
05 p0593 N88-13616

Initial dynamic load estimates during configuration design 05 p0593 N88-13621

Significance of fatigue crack closure under spectrum loading 05 p0599 N88-13662

Low cycle fatigue life predictions of a 1CrMoV steel in terms of a J-controlled short crack growth model
05 p0599 N88-13665

A unified model for fatigue crack initiation, short crack growth, long crack propagation, and closure effects
05 p0601 N88-13680

A dislocation model for fatigue crack propagation under variable amplitude loading 05 p0602 N88-13683

Observations on the effect of overloads on fatigue crack growth 05 p0602 N88-13684

Computer aided modeling and fatigue failure forecast under stochastic loading 05 p0607 N88-13720

Fatigue under nonnormal random stresses using Monte Carlo method 05 p0607 N88-13723

Applications of fatigue analyses: Transportation
05 p0608 N88-13733

The application of doubly-truncated hydrometeor distributions to numerical cloud models
[AD-A185273] 05 p0627 N88-13836

Modeling cloudy and clear interval length probabilities using space shuttle imagery
[AD-A185290] 05 p0627 N88-13837

Human thermoregulatory model for whole body immersion in water at 20 and 28 C
[AD-A185052] 05 p0629 N88-13849

Optimal control of large space structures via generalized inverse matrix
[NASA-CR-182336] 05 p0639 N88-13907

Multidimensional least squares fitting of fuzzy models
[AD-A185148] 05 p0640 N88-13916

The estimation of basic matrices using travel intensity theorems
[REPT-87-13] 05 p0642 N88-13926

SHARP simulation of discontinuities in highly convective steady flow
[NASA-TM-100240] 05 p0642 N88-13931

Sample reuse in statistical remodeling
[AD-A184916] 05 p0643 N88-13938

Presentation of a computer program permitting the exploitation of tests designed to determine the sensitivity of one shot devices to a parameter. Application to a degenerate one shot sequence
[SNIAS-872-430-117] 05 p0644 N88-13945

The interaction of DC plasma jet with a melting metal: Experimental measurements and mathematical description
[AD-A185173] 05 p0651 N88-13993

Numerical models for high beta magnetohydrodynamic flow
[DE88-001850] 05 p0654 N88-14008

A numerical model of unsteady, subsonic aeroelastic behavior
[NASA-TM-100487] 06 p0663 N88-14064

Integration of a supersonic unsteady aerodynamic code into the NASA FASTEX system
[NASA-CR-182329] 06 p0663 N88-14068

Post stall behavior in axial-flow compressors
[AD-A185712] 06 p0665 N88-14081

Performance-limiting factors in MPD thrusters
[AD-A185605] 06 p0674 N88-14128

An overview of metal plasticity
[DE88-001658] 06 p0681 N88-14175

The effective elastic properties of low-density foams
[DE87-014629] 06 p0684 N88-14194

Theory of displaced phase center antenna for space based radar applications
[PB87-229837] 06 p0690 N88-14227

Advanced numerical modeling of microwave penetration and coupling for complex structures
[DE88-001873] 06 p0690 N88-14231

A model for ultra-low fatigue crack growth
06 p0717 N88-14404

Crack closure phenomena in modes 1 and 2 interactions 06 p0719 N88-14417

Fatigue life prediction modeling for turbine hot section materials
[NASA-TM-100291] 06 p0724 N88-14453

Mathematical-cartographic modeling of economic utilization of Atlantic Ocean 06 p0726 N88-14469

Numerical modeling of troposphere-induced gravity wave propagation 06 p0735 N88-14522

Meteor velocity distribution and an optimum monitoring mathematical model 06 p0739 N88-14546

Monte Carlo modeling and meteor showers
06 p0740 N88-14549

Some models of the Geminids meteor stream formation 06 p0740 N88-14551

Estimation of rainfall rates in tropical cyclones by passive microwave radiometry 06 p0744 N88-14577

Interim review of the possibilities and opportunities for the ONR tropical cyclone motion research initiative
[AD-A185679] 06 p0746 N88-14592

Forecast of current patterns for an eddy tracking experiment in the Norwegian coastal current
[PB87-224853] 06 p0747 N88-14595

Dimensional analysis of nonlinear oscillations in brain, heart and muscle
[DE87-014749] 06 p0751 N88-14614

Model based monitoring of human sleep stages
[ISBN-90-9001448-9] 06 p0752 N88-14618

A taxonomy of analytical computer performance models for computer design
[AD-A185561] 06 p0755 N88-14632

The adaption and use of research codes for performance assessment
[DE88-000552] 06 p0756 N88-14639

Diffusion first passage times: Approximations and related differential equations
[AD-A185592] 06 p0765 N88-14700

A unified mathematical approach to image analysis
[AD-A185719] 06 p0765 N88-14703

Characteristic trajectories of generalized Lanchester equations
[AD-A185762] 06 p0766 N88-14705

Asymptotic normality of poly-t densities with Bayesian applications
[AD-A185718] 06 p0768 N88-14719

Sound propagation over uneven ground and irregular topography
[NASA-CR-182352] 06 p0776 N88-14763

A long term radiological risk model for plutonium-fueled and fission reactor space nuclear system
[DE87-010466] 06 p0779 N88-14782

Mathematical model for the dc-ac inverter for the Space Shuttle 06 p0793 N88-14860

Prediction of physical workload in reduced gravity environments 06 p0794 N88-14867

Inventory behavior at remote sites
06 p0796 N88-14873

Modeling the growth dynamics of four candidate crops for Controlled Ecological Life Support Systems (CELSS)
06 p0799 N88-14889

Consistent spherical Nonlocal Thermal Equilibrium (NLTE) models for objects with B-star-like luminosities
[ETN-88-90601] 06 p0800 N88-14897

Observation and interpretation of solar S-component radiation at millimetre waves
[PB87-225207] 06 p0805 N88-14916

A theory for the core flow of leading-edge vortices
07 p0810 N88-14935

Microwave Landing System (MLS) mathematical model installation manual
[AD-A185612] 07 p0819 N88-14978

Mathematical models of continuous flow electrophoresis: Electrophoresis technology
[NASA-CR-179241] 07 p0828 N88-15021

SRB combustion dynamics analysis computer program (CDA-1)
[NASA-CR-182404] 07 p0830 N88-15032

Catalog of compartment fire model algorithms and associated computer subroutines
[PB88-110861] 07 p0839 N88-15087

Channel access protocols for multihop packet radio networks
[AD-A186074] 07 p0842 N88-15105

Chemical reactions in turbulent mixing flows
[AD-A186141] 07 p0849 N88-15153

Microcomputer controlled arc welding power source: Its steady state and transient performance
[PB87-143921] 07 p0863 N88-15233

Behavior of a steel cylinder under the influence of a local load in the elastic and elasto-plastic area
[PB87-154787] 07 p0869 N88-15272

Hurricane Danny storm surge data, report 4
[AD-A186373] 07 p0879 N88-15334

Hurricane Kate storm surge data, report 5
[AD-A186374] 07 p0880 N88-15335

The ocean heat budget
[AD-A186130] 07 p0881 N88-15346

New methods for numerical solution of one class of strongly nonlinear partial differential equations with applications
[AD-A186166] 07 p0899 N88-15445

Modelling of clustering effects in point processes: An application to failures in SPC-systems (stored program control-systems)
[PB87-149241] 07 p0904 N88-15480

On two methods of identifying influential sets of observations
[AD-A186270] 07 p0910 N88-15518

The information metric for univariate linear elliptic models
[AD-A186385] 07 p0911 N88-15527

Maximum likelihood principle and model selection when the true model is unspecified
[AD-A186027] 07 p0914 N88-15544

A simplified model of elementary particles
[NOTA-INTERNA-890] 07 p0930 N88-15647

Model for plasma equilibrium configuration evolution in a tokamak with adiabatic compression
[DE88-700354] 07 p0936 N88-15684

Simple model for hot ion plasmas
[DE88-750045] 07 p0936 N88-15688

Numerical modelling of the classical nova outburst
[NASA-TM-89707] 07 p0945 N88-15746

Energetics and dynamics of simple impulsive solar flares
[NASA-TM-87816] 07 p0947 N88-15755

Rotorcraft transmission 08 p0956 N88-15802

The dynamics and control of large-flexible space structures, part 10
[NASA-CR-182426] 08 p0963 N88-15830

Contribution to modeling flexion fatigue damage in unidirectional composite materials
[ECL-87-12] 08 p0965 N88-15843

Velocity and density measurements in a turbulent nonpremixed flame with comparison to numerical model predictions
[DE87-014695] 08 p0967 N88-15854

A continuous oxidizer regression model for the combustion of composite solid propellants
[AD-A186742] 08 p0974 N88-15894

Peacekeeper tank slosh model
08 p0983 N88-15942

A computationally efficient modelling of laminar separation bubbles
[NASA-CR-182417] 08 p0984 N88-15949

Time accurate techniques using characteristic flux averaging with application to unsteady aerodynamics
08 p0985 N88-15957

Nonequilibrium reacting flows
08 p0985 N88-15959

Introduction to the Modeling of Turbulence
[VKI-LS-81-06] 08 p0986 N88-15972

Examples of turbulence-model applications
08 p0987 N88-15975

Turbulence modeling for compressible flows
08 p0987 N88-15978

Modeling the unsteady flow found in axial turbomachinery
[ECL-87-07] 08 p0987 N88-15980

Dynamic analysis of a structure with sliding base
08 p0998 N88-16045

Summary of HSST wide-plate crack-arrest tests and analyses
[DE88-002601] 08 p1000 N88-16061

Theory of deformation. Part 1: Kinematics
[DE88-003007] 08 p1001 N88-16062

Gyrostabilizer system of Kvant module
08 p1006 N88-16099

Selection of efficient correcting motor for an artificial Earth satellite 08 p1007 N88-16102

Statistical model of interaction of electromagnetic waves with natural objects being sensed
08 p1008 N88-16112

Modeling of architecture of a problem-oriented on-board processor 08 p1008 N88-16114

Geomechanical model of seismofocal zone of active continental margin 08 p1011 N88-16128

The entropy of the Lorentz model
08 p1015 N88-16153

Model calculations of the behavior of orographically influenced cold fronts 08 p1015 N88-16155

The iterative radiance model of the Meteorological Institute of the University of Munich (West Germany)
08 p1019 N88-16178

Nonlinear, relativistic Langmuir waves in astrophysical magnetospheres
[NASA-CR-182422] 08 p1024 N88-16197

Wave acceleration of auroral electrons
08 p1031 N88-16245

Prediction of human thermoregulatory responses and endurance time in water at 20 and 24C
[AD-A186223] 08 p1048 N88-16326

Short pseudorandom test sequences
[AD-A185863] 08 p1054 N88-16357

Automatic mathematical modeling for space application 08 p1060 N88-16402

LISP based simulation generators for modeling complex space processes 08 p1061 N88-16403

Rapid prototyping and AI programming environments applied to payload modeling 08 p1061 N88-16405

Qualitative models for planning: A gentle introduction
08 p1062 N88-16414

Development of a computer model for missile simulation, or simulation of a kinetic coverage area for a target detection missile
[FOA-C-20666-2.5] 08 p1067 N88-16449

Development of a computer model for missile simulation, or simulation of a kinetic coverage area for a collimation guided missile
[FOA-C-20667-2.5] 08 p1067 N88-16450

Effects of uniform target density on random search
[AD-A186468] 08 p1073 N88-16473

Test of linearity in general regression models
[AD-A186036] 08 p1073 N88-16477

Estimation and comparison of changes in the presence of information right censoring by modeling the censoring process
[AD-A186320] 08 p1074 N88-16478

Numerical analysis of motion of solid bodies in atmosphere 08 p1079 N88-16505

Digital image processing
[INPE-4131-TDL/264] 08 p1083 N88-16527

Interpretation of the temperature dependence of conductivity in superconducting oxides
[DE88-003028] 08 p1091 N88-16565

Comprehensive rotorcraft analysis methods
09 p1106 N88-16630

Rotorcraft aeroelastic stability
09 p1106 N88-16631

Helicopter mathematical models and control law development for handling qualities research
09 p1108 N88-16642

An initial investigation into methods of computing transonic aerodynamics sensitivity coefficients
[NASA-CR-182444] 09 p1112 N88-16663

Verification of obstacle accountability areas using a simple mathematical model. Part 1: Description of general model and application for a specific case --- engine failure at takeoff
[NLR-TR-85069-U] 09 p1115 N88-16683

Communications satellite systems operations with the space station. Volume 3: Supplementary technical report
[NASA-CR-180875] 09 p1133 N88-16794

Kinetic isolation tether experiment
[NASA-CR-182458] 09 p1135 N88-16810

Helium-ion-induced release of hydrogen from graphite
[DE88-002599] 09 p1142 N88-16846

The effects of fuel composition on ignition delay in homogeneous charge and direct injection compression ignition engines
[DE88-003691] 09 p1143 N88-16849

Dynamical characteristics of weak turbulence
[AD-A186724] 09 p1161 N88-16957

Numerical modeling of multidimensional flow in seals and bearings used in rotating machinery
[NASA-TM-100779] 09 p1165 N88-16988

Modeling of pulsed gas flow lasers
[DFVLR-FB-87-19] 09 p1171 N88-17021

New model to estimate the perforation power of kinetic energy projectiles
[PB87-166757] 09 p1175 N88-17040

Maximum likelihood estimates for the discrete application of the AMSAA growth model
[AD-A186921] 09 p1177 N88-17048

Mechanical impact: Theoretical simulation and correlation 09 p1179 N88-17060

Dynamic stress at critical locations of a structure as a criterion for mathematical model modification
09 p1180 N88-17066

Statistics of two-dimensional structure elements of mountainous ranges (mosaic model) for calculating three-dimensional reflection functions
[DFVLR-FB-87-33] 09 p1185 N88-17099

VAWT (Vertical-Axis Wind Turbine) stochastic loads produced by atmospheric turbulence
[DE88-001355] 09 p1187 N88-17110

A comparison of different module configurations for multibandgap solar cells
[DE88-002718] 09 p1187 N88-17113

Simulation of global wet and dry deposition of nitric acid in a three-dimensional chemistry-transport model
[DE87-009647] 09 p1188 N88-17116

Numerical investigation of orographically enhanced instability
[AD-A186841] 09 p1189 N88-17125

Induced turbulence in aerosol-loaded atmospheres, Jun. 1987
[DE87-014724] 09 p1192 N88-17141

Application of satellite data in variational analysis for global cyclonic systems
[NASA-CR-182468] 09 p1193 N88-17152

Development of a physically-based general circulation model parameterization of clouds and their radiative interactions
[DE88-004060] 09 p1194 N88-17154

GAVID and ACQUIR, two Operations-Research (OR) models for visual detection
[FEL-1985-72] 09 p1200 N88-17194

A situation-response model for intelligent pilot aiding
09 p1208 N88-17241

A human performance modeling approach to intelligent decision support systems 09 p1208 N88-17242

Autonomous control procedures for shuttle rendezvous proximity operations 09 p1208 N88-17244

Artificial Intelligence (AI), Operations Research (OR), and Decision Support Systems (DSS): A conceptual framework 09 p1209 N88-17245

Methodological and structural principles for flexible geometric modeling in computer aided design
[MA-48] 09 p1218 N88-17306

Modification of a successive corrections objective analysis for improved higher order calculations
[NASA-CR-182467] 09 p1230 N88-17370

SURE reliability analysis: Program and mathematics
[NASA-TP-2764] 09 p1231 N88-17380

Prediction of polytomous events: Model description, algorithm development and methodological aspects, with an application
[AD-A186549] 09 p1232 N88-17384

Numerical fluid mechanics 09 p1240 N88-17434

A model for stationary and dynamic impression of undercooled boiling in coupled thermohydraulic and neutron physics calculations of nuclear reactors
[IKE-6-171] 09 p1247 N88-17472

Modeling considerations for selected rf-plasma edge effects
[DE88-003285] 09 p1252 N88-17500

Optimization of volume produced H(-) ions in a low-pressure hydrogen plasma
[IPPJ-853] 09 p1252 N88-17505

Effect of the subgap conductance on the metastable states in a Josephson tunnel junction
[DE88-003102] 09 p1258 N88-17543

Oscillations of solar models with internal element diffusion
[DE88-003156] 09 p1264 N88-17573

Navier-Stokes calculations and turbulence modeling in the trailing edge region of a circulation control airfoil
10 p1268 N88-17587

Wall jet analysis for circulation control aerodynamics. Part 1: Fundamental CFD and turbulence modeling concepts 10 p1269 N88-17588

A theory for turbulent curved wall jets
10 p1269 N88-17590

Wall jet analysis for circulation control aerodynamics. Part 2: Zonal modeling concepts for wall jet/potential flow coupling 10 p1269 N88-17593

Frequency-response identification of XV-15 tilt-rotor aircraft dynamics 10 p1277 N88-17643

Maneuverable reentry vehicle trajectory footprints: Calculation and properties
[DE88-004726] 10 p1292 N88-17726

Insights into the mechanisms of chemical reactions: Reaction paths for chemical reactions
[DE88-003041] 10 p1297 N88-17755

Gas hydrate model development and validation
[DE88-001004] 10 p1298 N88-17762

A large strain thermomechanical forming model for elastic-viscoplastic behavior in metals
10 p1301 N88-17780

The mathematization of the military sciences
[MBB-Z-139/87] 10 p1311 N88-17834

Radar reflectivity and attenuation of radio waves in the melting layer of precipitation
[PB88-121553] 10 p1318 N88-17882

Pulsed current transformer for low inductive loads
[AD-A187224] 10 p1324 N88-17913

Leeside crossflow modeling in Euler space-marching computations
[NASA-TM-89710] 10 p1325 N88-17924

Centerplane source distribution for slender bodies
10 p1328 N88-17940

Periodic natural convection in a rectangular enclosure of low aspect ratio 10 p1329 N88-17941

Three-dimensional incompressible flowfield analysis for establishing rotor designs which optimize power extraction 10 p1329 N88-17943

A review of flow-induced vibration in two-phase flow
[DE88-002873] 10 p1329 N88-17946

Capacitive charge division in centroid finding cathode readouts in MWPCs
[DE88-003545] 10 p1333 N88-17969

Physics modeling support contract
[DE88-004039] 10 p1335 N88-17980

Analysis and application of the constant tensile load test for polyethylene gas pipe materials
[DE88-002868] 10 p1345 N88-18037

Turbulence loads on the Howden 26-m-diameter wind turbine
[DE88-001118] 10 p1351 N88-18075

Evaluation of regional-scale air quality models: Chairmen reports from four workshops
[DE88-001397] 10 p1352 N88-18080

Simulation and modeling of whistler mode wave growth through cyclotron resonance with energetic electrons in the magnetosphere 10 p1353 N88-18089

Analysis of gases in the earth's crust
[PB88-141619] 10 p1354 N88-18093

Systematic errors of the FSU global spectral model
10 p1356 N88-18103

Membrane model of cupula or vestibular semicircular canals 10 p1361 N88-18132

Two-dimensional static otolith model
10 p1367 N88-18167

Scaling physiological pharmacokinetic models by physiological time
[DE88-000335] 10 p1368 N88-18173

Modeling of the non-auditory response to blast overpressure
[AD-A187397] 10 p1369 N88-18184

Parameter identification and sensitivity analysis for a robotic manipulator arm
[NASA-CR-181608] 10 p1385 N88-18272

Identifiability of multivariate ARMA models
[AD-A187394] 10 p1400 N88-18350

Well-posedness and spectral estimation for infinite dimensional systems
[AD-A187621] 10 p1401 N88-18354

A component synthesis method using Lanczos vectors
[DE88-002263] 10 p1403 N88-18366

Applied mathematics of transport theory
[DE88-004098] 10 p1404 N88-18369

Semiempirical studies of atomic structure
[DE88-004096] 10 p1407 N88-18392

Advances in calculating macroionic solution structure
[DE88-003799] 10 p1409 N88-18406

Coronal heating by means of helical magnetohydrodynamic turbulence
[AD-A187064] 10 p1410 N88-18413

Positron-annihilation 2D-ACAR studies of disordered and defected alloys
[DE88-003118] 10 p1416 N88-18454

An experimental investigation of straight and curved annular wall jets
[NASA-CR-182546] 11 p1434 N88-18557

Matrix-fiber stress transfer in composite materials: Elasto-plastic model with an interphase layer
[PB88-136635] 11 p1450 N88-18643

Finite element analysis of adhesively bonded composite joints including geometric nonlinearity, nonlinear viscoelasticity, moisture diffusion and delayed failure
[PB88-147822] 11 p1451 N88-18648

Reactions of some thiol collectors at noble-metal and pyrite electrodes
[PB88-138318] 11 p1455 N88-18674

Experimental set-up and mathematical modeling of H-shaped beam type structure
[AD-A187196] 11 p1466 N88-18743

Investigation of a ray-mode representation of the Green's function in a rectangular cavity
[PB88-131677] 11 p1469 N88-18763

Air Force Institute of Technology (AFIT) Local Area Network (LAN) performance evaluation model: An analytic model for assessing the impact of changing LAN hardware and software configurations
[AD-A187191] 11 p1469 N88-18764

The coaxial colinear antenna: Theoretical and experimental models 11 p1475 N88-18803

Numerical and analytical study of fluid dynamic forces in seals and bearings
[NASA-TM-100268] 11 p1485 N88-18867

Further development of a finite element model of orthogonal metal cutting
[DE88-004048] 11 p1494 N88-18921

Improvement in robot positioning accuracy by a kinematic identification model 11 p1496 N88-18931

Mathematical modeling of the postbuckling behavior of structural elements 11 p1500 N88-18960

A nonlinear computational model for the strength and failure of composite plates and shells
11 p1501 N88-18964

Numerical fracture mechanics using finite element method 11 p1501 N88-18966

Multisource context classification methods in remote sensing 11 p1504 N88-18985

Status of the special-purpose airfoil families
[DE88-001124] 11 p1506 N88-18988

Computer-aided modeling and prediction of performance of the modified Lundell class of alternators in space station solar dynamic power systems
[NASA-CR-182538] 11 p1507 N88-19000

Energetic particle drift motions in the outer dayside magnetosphere
[DE88-005007] 11 p1512 N88-19034

Five New South Wales barrier lagoons: Their macrobenthic fauna and seagrass communities
11 p1517 N88-19059

Center for nonlinear dynamics of the brain
[AD-A187245] 11 p1518 N88-19066

Center for the study of rhythmic processes
[AD-A188204] 11 p1520 N88-19078

Two attentional models of classical conditioning: Variations in CS effectiveness revisited
[AD-A187697] 11 p1522 N88-19086

Integration of finite element modeling with solid modeling through a dynamic interface 11 p1526 N88-19112

Integration of geometric modeling and advanced finite element preprocessing 11 p1526 N88-19114

Finite element meshing of ANSYS (trademark) solid models 11 p1526 N88-19115

Solid/FEM integration at SNLA
[SAND-87-0682A] 11 p1526 N88-19116

Geometrical and topological issues in octree based automatic meshing 11 p1527 N88-19118

Finite octree meshing through topologically driven geometric operators 11 p1527 N88-19121

Design modeling for shape optimization
11 p1527 N88-19122

Postprocessing techniques for 3D non-linear structures 11 p1528 N88-19124

Geometric versus finite element modeling current and future trends at Northrop 11 p1528 N88-19125

Estimation in linear models with censored data
[AD-A187209] 11 p1540 N88-19203

Irreducible tensor operators and multiple-quantum NMR 11 p1542 N88-19217

Theory of two-photon emission from atomic inner shells
[AD-A187742] 11 p1543 N88-19223

Problems in modeling TF ripple loss of fast alphas from a tokamak reactor
[DE88-000612] 11 p1553 N88-19296

Thermodynamics of wetting by liquid metals
[DE88-003634] 11 p1563 N88-19380

A comparative survey of mathematical models for dynamic simulation of in-orbit manipulation operations
12 p1592 N88-19533

Dynamics modeling, simulation, and control of a spacecraft/manipulator system
12 p1592 N88-19534

Modeling of a nutation damper for satellite stabilization through rotation
[INPE-4275-PRE/1147] 12 p1601 N88-19584

Linear and nonlinear acoustics with nonuniform entropy in combustion chambers 12 p1607 N88-19609

Analysis of low gravity tolerance of model experiments for space station: Preliminary results for directional solidification
[NASA-CR-182657] 12 p1614 N88-19648

Reliability analyses of a surface mounted package using finite element simulation
[AD-A189488] 12 p1624 N88-19717

Accelerating the computation of steady state solutions for non-equilibrium, chemically reacting flow fields
12 p1625 N88-19724

Compressible friction coefficients in a simulated heat pipe
[AD-A188818] 12 p1627 N88-19735

A simulation of void lining during ductile fracture
[AD-A188404] 12 p1635 N88-19792

Report on phase 1 of the project estimate development of a model for yield estimation of sugar cane based on LANDSAT and agromet data
[INPE-4466-RPE/560] 12 p1638 N88-19807

Department of Defense World Geodetic System 1984: Its definition and relationships with local geodetic systems
[AD-A188815] 12 p1639 N88-19811

Measuring and modeling near surface reflected and emitted radiation fluxes at the FIFE site
[NASA-CR-182660] 12 p1640 N88-19818

Systems approach to energy quality and efficiency
[PB88-139506] 12 p1640 N88-19823

Numerical simulation of near-surface environments and particulate clouds generated by large-area fires
[AD-A188375] 12 p1641 N88-19828

Estimating the solar irradiance of an intermountain region using GOES (Geostationary Operational Environmental Satellite) satellite data. A test of two statistical models
[AD-A188414] 12 p1642 N88-19834

Mesoscale monitoring of the soil freeze/thaw boundary from orbital microwave radiometry
[NASA-CR-182659] 12 p1645 N88-19855

Human factor in engineering work
12 p1663 N88-19970

A neuronal model of classical conditioning
[AD-A188378] 12 p1670 N88-19999

Regenerative life support system research
[NASA-CR-182606] 12 p1671 N88-20006

An experiment in software reliability: Additional analyses using data from automated replications
[NASA-CR-178395] 12 p1676 N88-20017

Procedure for initial data input and checkup in the system for film data mathematical processing
[DE88-700926] 12 p1676 N88-20022

Image segmentation via fractal dimension
[AD-A188825] 12 p1678 N88-20033

A numerical analysis of the dynamics of PRIZ operation
[AD-A188853] 12 p1678 N88-20035

Further refinement and applications of the mixed computational algorithm for plane elastic contact problems
[AD-A188308] 12 p1683 N88-20065

Structural-acoustic interior noise modeling and analysis from experimental data
[PB88-141775] 12 p1687 N88-20088

A study of methods to predict and measure the transmission of sound through the walls of light aircraft
[NASA-CR-182656] 12 p1687 N88-20090

Pion absorption in nuclei: The pion(+ or -).proton reactions
[LA-10997-T] 12 p1688 N88-20098

Multipass beam breakup in recirculating linacs
[CEBAF-PR-87-007] 12 p1690 N88-20111

Improved zero dimensional model of a reversed field pinch fusion device
[DE88-005212] 12 p1693 N88-20127

Phase transitions in two-dimensional superconducting arrays in a transverse magnetic field
[INPE-4457-RPE/559] 12 p1697 N88-20157

Task allocation for efficient performance of a decentralized organization
[AD-A188699] 12 p1705 N88-20204

The TempIS Project: Performance analysis of temporal queries
[AD-A188354] 12 p1706 N88-20213

HNC: A detector to study ultraheavy cosmic rays
12 p1713 N88-20252

Fully-coupled analysis of jet mixing problems. Three-dimensional PNS model, SCIP3D
[NASA-CR-4139] 13 p1715 N88-20256

A study of combustion and flow behaviour in solid-propellant rocket motors
[UTIAS-280] 13 p1732 N88-20357

Bipropellant combustion in a liquid rocket combustion chamber 13 p1733 N88-20359

Numerical model of the time independent mean flow in a rotating rocket motor 13 p1733 N88-20360

Erosion in dual-phase microstructures
[DE88-004507] 13 p1743 N88-20421

PNL-1 improved ceramic composites through controlled fiber matrix interaction
[DE88-005680] 13 p1750 N88-20462

Molecular dynamics of laser ablation of a polymer coating
[DE88-004337] 13 p1750 N88-20466

Computer-aided transformation of descriptive mode of mathematical models of a control system
13 p1756 N88-20503

Theoretical investigation of EM wave generation and radiation in the ULF, ELF and VLF bands by the electrodynamic orbiting tether
[NASA-CR-182720] 13 p1760 N88-20529

Aluminum-air battery development
[DE88-006617] 13 p1762 N88-20542

Development, manufacturing and testing of a gas-loaded variable conductance methanol heat pipe
[NLR-MP-87010-U] 13 p1767 N88-20571

Transport and stability properties of free shear flows
13 p1768 N88-20577

Calculations of viscous flows with a multigrid method
13 p1769 N88-20580

Direct solar-pumped iodine laser amplifier
[NASA-CR-182674] 13 p1777 N88-20630

Modelling and simulation of a rate controlled manipulator arm --- Hermes
[NLR-TR-87010-U] 13 p1778 N88-20639

Dynamic modelling of flexible rotor shafts mounted on hydrodynamic bearings 13 p1779 N88-20641

Finite element methods for quasi-prismatic bodies with application to gears 13 p1779 N88-20644

Numerical modeling of wave migration of seismic data
13 p1786 N88-20684

Numerical model of Rayleigh instability and spin-off eddies on fronts 13 p1788 N88-20696

Model of hydrodynamic adjustment of temperature, salinity and current fields 13 p1789 N88-20700

Performance and cost benefits associated with nonimaging secondary concentrators used in point-focus dish solar thermal applications
[DE88-001104] 13 p1792 N88-20718

Correlation of data on strain accumulation adjacent to the San Andreas Fault with available models
[NASA-CR-180757] 13 p1796 N88-20742

Ultrasonic physical modeling of seismic wave propagation from graben-like structures
[AD-A189066] 13 p1796 N88-20744

The pressure drag and momentum flux during a cold frontal passage over the Alps 13 p1800 N88-20763

Planetary scale barotropic spectral model
13 p1801 N88-20766

The use of a barotropic finite element model for the study of circulation on the continental shelf of the southeast coast of Brazil
[INPE-4401-PRE/1218] 13 p1802 N88-20774

Studies toward observing and modelling large energetic ocean regions
[AD-A189267] 13 p1803 N88-20778

Evaluation of wave calculations using GONO in the period October 1985 - April 1986
[KNMI-TR-96] 13 p1807 N88-20804

A model for graphical interaction --- computer graphics
[CWI-CS-R8718] 13 p1818 N88-20866

Interpolation algorithms for digital terrain models
[INPE-4373-PRE/1196] 13 p1820 N88-20877

Mathematic modeling of visual perception problems
[INPE-4355-PRE/1186] 13 p1823 N88-20897

A Darwinian approach to artificial neural systems
[DE87-013184] 13 p1824 N88-20900

Further results on the McMillan degree and the Kronecker indices of ARMA models --- input-output relations of linear systems
[EUT-87-E-175] 13 p1827 N88-20925

Model structure selection for multivariable systems by cross-validation methods
[EUT-87-E-176] 13 p1827 N88-20926

Regional Conference on the Analysis of the Unbalanced Mixed Model
[AD-A188747] 13 p1830 N88-20943

The automated symbolic derivation of state equations for dynamic systems
[DE88-000968] 13 p1830 N88-20945

Double layer polarization of nonconducting spheroidal particles and its application to Kerr effect
[ISSN-0208-5658] 13 p1832 N88-20960

Modeling the behavior of oriented permanent magnet material using current double theory
[DE88-004446] 13 p1833 N88-20963

Mathematical models of sound waves in fluids
[AD-A189270] 13 p1834 N88-20968

Modeling of laser ultrasound generation in a weld pool
[DE88-005546] 13 p1834 N88-20971

Optics for large telescope 13 p1840 N88-21014

Electrical characteristics of MBE (Molecular Beam Epitaxyl)-grown GaAs/sub 1-x/Sb/sub x on InP and correlation with film microstructure
[DE88-003841] 13 p1847 N88-21053

The thermodynamic properties of organic oxygen compounds
[DE88-001208] 13 p1849 N88-21065

Review of selenium thermodynamic data
[DE88-006194] 13 p1849 N88-21068

On the role of complete reducibility in general competitive equilibrium models
[DE88-005693] 13 p1851 N88-21083

Magnetohydrodynamic (MHD) simulation of solar prominence formation 13 p1858 N88-21109

Comparison of methods for the calculation of thermal contact resistance of the first Brazilian satellite
[NASA-TT-20180] 14 p1880 N88-21239

Spacecraft dielectric surface charging property determination
[NASA-CR-180879] 14 p1881 N88-21243

Finite area combustor theoretical rocket performance
[NASA-TM-100785] 14 p1883 N88-21252

Numerical modeling of divergent detonation wave
14 p1903 N88-21373

Potential applications of computational fluid dynamics to biofluid analysis
[NASA-TM-100089] 14 p1911 N88-21422

Accuracy requirements and benchmark experiments for CFD validation
[NASA-TM-100087] 14 p1911 N88-21423

Nonlinear Constitutive Relations for High Temperature Applications, 1986
[NASA-CP-10010] 14 p1928 N88-21498

Development of a unified constitutive model for an isotropic nickel base superalloy Rene 80
14 p1929 N88-21501

Modeling the viscoplastic behavior of Inconel 718 at 1200 F 14 p1929 N88-21502

An internal variable constitutive model for the large deformation of metals at high temperatures
14 p1929 N88-21503

Constitutive modeling and thermoviscoplasticity
14 p1930 N88-21506

A theory of viscoplasticity accounting for internal damage 14 p1930 N88-21508

A constitutive model with damage for high temperature superalloys 14 p1930 N88-21510

An automated procedure for material parameter evaluation for viscoplastic constitutive models
14 p1932 N88-21520

A constitutive material model for nonlinear finite element structural analysis using an iterative matrix approach
14 p1932 N88-21521

Nonlinear structural analysis of a turbine airfoil using the Walker viscoplastic material model for B1900 + Hf
14 p1932 N88-21522

Unified constitutive models for high-temperature structural applications 14 p1932 N88-21523

A constitutive model for an overlay coating
14 p1933 N88-21525

Non-isothermal elastoviscoplastic analysis of planar curved beams 14 p1933 N88-21526

Simulation of thermo-mechanical forming processes: A mixed Eulerian-Langrangian finite element method
[PB88-155247] 14 p1933 N88-21530

Large-scale ocean dynamics
14 p1938 N88-21562

The 25 m horizontal-axis turbine as a test case for standard Dutch aerodynamic calculation methods for high-speed rotors
[R-762-D] 14 p1942 N88-21589

Thermal modeling of solar central receiver cavities
[DE88-004940] 14 p1943 N88-21594

Report of Atmospheric-Canopy Exchange Panel
[DE88-004478] 14 p1944 N88-21597

Masking of motion cues by random motion: Comparison of human performance with a signal detection model
[UTIAS-313] 14 p1953 N88-21639

On a bound of the modeling errors of black-box transfer function estimates
[EUT-87-E-173] 14 p1963 N88-21708

Procedures for updating dynamic mathematical models
[EMSB-23/86] 14 p1964 N88-21716

Application of the NARMAX method to nonlinear frequency response estimation
[RR-319] 14 p1964 N86-21721

Additional peak of light scattering by sound under conditions of acoustic instability
14 p1968 N88-21752

Thermal model describing development of normal region in superconductor film carrying electric current
14 p1973 N88-21776

Comprehensive model for laser instability in a CO2 laser with gaseous saturable absorber
14 p1979 N88-21808

Analysis of hadron production in deep inelastic muon-proton collisions through the fire-string model
[PREPRINT-578] 14 p1981 N88-21822

A general 2D electrical model for diagonally connected MHD generators
[DE88-004283] 14 p1984 N88-21835

Linear state space modeling of a turbofan engine
[AD-A190110] 15 p2019 N88-22035

Baseline estimation from simultaneous satellite laser tracking
[NASA-CR-182750] 15 p2022 N88-22052

Moving-bank multiple model adaptive estimation applied to flexible spacestructure control
[AD-A190761] 15 p2026 N88-22071

Numerical simulation of turbulent flames using vortex methods
[AD-A189813] 15 p2034 N88-22116

Duct flow nonuniformities: Effect of struts in SSME HGM II(+)
[NASA-CR-179285] 15 p2062 N88-22296

On the prediction of highly vortical flows using an Euler equation model, part 2
[AD-A190245] 15 p2064 N88-22305

Numerical modelling specific energy charcteristics of excimer KrF lasers with electron beam excitation
[DE88-701525] 15 p2070 N88-22344

Life assessment of combustor liner using unified constitutive models 15 p2077 N88-22384

Biaxial experiments supporting the development of constitutive theories for advanced high-temperature materials 15 p2078 N88-22386

Unified constitutive model development for metal matrix composites at high temperature 15 p2078 N88-22387

Unified constitutive model for single crystal deformation behavior with applications 15 p2078 N88-22388

Finite element (MARC) solution technologies for viscoplastic analyses 15 p2078 N88-22389

Continuous fiber ceramic matrix composites for heat engine components 15 p2082 N88-22411

Cumulative fatigue damage models 15 p2084 N88-22422

Life prediction modeling based on strainrange partitioning 15 p2084 N88-22425

Fatigue damage modeling for coated single crystal superalloys 15 p2085 N88-22427

Review and assessment of the HOST turbine heat transfer program 15 p2086 N88-22431

Atmospheric carbon dioxide and the global carbon cycle: The key uncertainties
[DE88-005059] 15 p2092 N88-22465

A survey of denser-than-air atmospheric dispersion models
[DE88-006626] 15 p2092 N88-22467

Description of ground motion data processing codes, volume 2
[DE88-007137] 15 p2095 N88-22481

Proceedings of the Lightning Threat Warning Workshop
[DE88-006607] 15 p2098 N88-22499

SEARCH: An interactive computer program for optimizing two-variable, unconstrained experiments or simulation
[AD-A190593] 15 p2112 N88-22583

Artificial neural networks: An introduction with an annotated bibliography
[DE88-007003] 15 p2116 N88-22603

Higher order crossings
[AD-A190489] 15 p2121 N88-22641

Analysis and testing of the SURE program
[NASA-TP-2817] 15 p2123 N88-22653

Statistical inference for stochastic processes
[AD-A190491] 15 p2126 N88-22673

Lumped model generation and evaluation: Sensitivity and Lie algebraic techniques with applications to combustion
[AD-A190402] 15 p2127 N88-22689

Model-scale sound propagation experiment
[NASA-TM-100602] 15 p2130 N88-22709

Electrical circuit modeling of reversed field pinches
[DE88-006942] 15 p2136 N88-22745

Plasma-gas interaction studies in a hybrid plume plasma rocket
[AD-A190310] 15 p2138 N88-22755

A method for estimating and controlling the cost of extending technology
[AD-A190717] 15 p2150 N88-22831

Design method for laminar flow control of two-dimensional airfoils in incompressible flow. Numerical study of LFC design concepts
[DE88-751809] 16 p2155 N88-22859

A numerical model of unsteady, subsonic aeroelastic behavior
[NASA-TM-101126] 16 p2156 N88-22862

Development of a digital sun sensor for a spin-stabilized satellite
[INPE-4508-TDL/327] 16 p2169 N88-22929

Dynamic fracture toughness evaluation by measurement of CTOD
[WNS/ASD-88-02] 16 p2178 N88-22962

Finite elements for the computation of three-dimensional electromagnetic fields in inhomogeneous media (revised)
[PB88-173471] 16 p2190 N88-23057

Studying Turbulence Using Numerical Simulation Databases. Proceedings of the 1987 Summer Program
[NASA-CR-182692] 16 p2194 N88-23086

A low dimensional dynamical system for the wall layer 16 p2194 N88-23088

Self similarity of two point correlations in wall bounded turbulent flows 16 p2195 N88-23089

EDQNM closure: A homogeneous simulation to support it. A quasi-homogeneous simulation to disprove it 16 p2195 N88-23091

Validation of EDQNM for subgrid and supergrid models 16 p2195 N88-23092

Angular distribution of turbulence in wave space 16 p2195 N88-23093

Modeling scalar flux and the energy and dissipation equations 16 p2196 N88-23096

Premixed turbulent flame calculation 16 p2196 N88-23098

Modeling of turbulent transport as a volume process 16 p2196 N88-23099

Analysis of non-premixed turbulent reacting flows 16 p2196 N88-23100

A statistical investigation of the single-point pdf of velocity and vorticity based on direct numerical simulations 16 p2196 N88-23101

On local approximations of the pressure-strain term in turbulence models 16 p2197 N88-23102

Local structure of intercomponent energy transfer in homogeneous turbulent shear flow 16 p2197 N88-23103

Test code for the assessment and improvement of Reynolds stress models 16 p2197 N88-23105

Reynolds stress models of homogeneous turbulence 16 p2197 N88-23106

The decay of isotropic turbulence in a rapidly rotating frame 16 p2197 N88-23107

Evaluation of a theory for pressure-strain rate 16 p2198 N88-23108

Relations between two-point correlations and pressure strain terms 16 p2198 N88-23109

Shear-layer structures in near-wall turbulence 16 p2198 N88-23110

Inflectional instabilities in the wall region of bounded turbulent shear flows 16 p2199 N88-23114

Active layer model for wall-bounded turbulence 16 p2199 N88-23115

Wave-growth associated with turbulent spot in plane Poiseuille flow 16 p2199 N88-23116

Coherent structures and modeling: Some background comments 16 p2199 N88-23120

Fast algorithms for Euler and Navier-Stokes simulations
[AD-A190897] 16 p2208 N88-23175

Investigation of subgrid models in homogeneous incompressible turbulence
[ONERA-RSF-13/3419-AY-106-A] 16 p2209 N88-23183

Two-equation low-Reynolds-number turbulence modeling of transitional boundary layer flows characteristic of gas turbine blades
[NASA-CR-4145] 16 p2209 N88-23185

Pump rod forces due to hydrodynamic effects in piston pumps
[PB88-164850] 16 p2214 N88-23212

Automatic control of robot motion
[AD-A191012] 16 p2215 N88-23218

Periodic response of nonlinear systems 16 p2217 N88-23228

Multigrid for structures analysis 16 p2218 N88-23232

Aeroelastic forced response analysis of turbomachinery 16 p2220 N88-23247

Stall flutter analysis of propfans 16 p2221 N88-23256

Models in nonlinear thermomechanics. Finite element models and constitutive models for large deformation elastoplasticity
[ETN-88-92240] 16 p2222 N88-23262

Application of the ONERA model to the life estimation under fatigue cracking of a Al-Li alloy. Parameter identification and test-experiment comparison under FALSTAFF loading
[ONERA-RT-32/7169-RY-063-R] 16 p2222 N88-23264

Effects of axial load on elastomeric isolation bearings
[PB88-179015] 16 p2223 N88-23269

Method and models for R-curve instability calculations
[NASA-TM-100935] 16 p2224 N88-23278

Computer assisted generalization of buildings for digital landscape models by classification methods 16 p2226 N88-23294

The spreading and mixing of dense gas clouds in still air
[KNMI-WR-87-12] 16 p2230 N88-23320

A three-dimensional gravity model of the geologic structure of Long Valley caldera
[DE88-006331] 16 p2231 N88-23324

A proposal for the establishment of a center of excellence in theoretical geoplasma research
[AD-A189742] 16 p2231 N88-23327

Modeling and estimation of a low degree geopotential model from terrestrial gravity data
[NASA-CR-182808] 16 p2232 N88-23330

Towards fully abstract semantics for local variables: Preliminary report
[AD-A191065] 16 p2251 N88-23456

Algorithms and intuition
[NASA-CR-182900] 16 p2252 N88-23459

A model of intrazonal trip distribution considering centrality index 16 p2257 N88-23486

Inference for a nonlinear semimartingale regression model
[AD-A190857] 16 p2262 N88-23527

Proceedings of Symposium on Physics of Target Implosion and Pulsed Power Techniques
[IPPJ-859] 16 p2276 N88-23619

Development of Electromagnetic PIC code for LIB diode 16 p2276 N88-23622

Simulation code for ICF including radiative energy transfer 16 p2277 N88-23627

Efficient shell implosion and target design 16 p2277 N88-23630

Some aspects of the unified model of non-ideal high-parameter plasmas: Electron EOS and conduction coefficients 16 p2277 N88-23632

Coronal fluid-dynamics in laser fusion 16 p2278 N88-23634

Finite ion-relaxation and nonequilibrium radiation effects on laser-driven implosions 16 p2278 N88-23636

High pressure operation of beam diodes for generating relativistic electron beams 16 p2279 N88-23643

Propulsive performance of a lifting flapping wing 17 p2295 N88-23733

Travelling wave concepts for the modeling and control of space structures
[AD-A191235] 17 p2310 N88-23819

Preventing aircraft corrosion by predictive corrosion modeling 17 p2321 N88-23863

Modeling, filtering and control of stochastic processes --- communication networks
[ENST-87E021] 17 p2333 N88-23925

Numerical modelling of flows using phoenics 17 p2339 N88-23955

Theory of neutron moisture probes and interpretation of measurements in complex soil and water systems 17 p2342 N88-23965

Theoretical studies of solar-pumped lasers
[NASA-CR-182929] 17 p2344 N88-23971

Parameter identification methods for improving structural dynamic models
[NASA-TM-100812] 17 p2349 N88-23994

Three-dimensional curved shell and solid-shell transition finite elements with temperature and temperature gradients as primary variables for steady state heat conduction 17 p2349 N88-23997

Navigation system from AVHRR data from NOAA series satellites 17 p2359 N88-24054

Low altitude remote sensing data in the implementation of a mathematical model for the planning of urban equipment networks 17 p2363 N88-24074

Visualization of digital terrain models 17 p2364 N88-24081

Digital monoplotting, part 1
[B8735122-PT-1] 17 p2369 N88-24106

Digital monoplotting, part 2
[B8735122-PT-2] 17 p2369 N88-24107

An update on remote measurement of soil moisture over vegetation using infrared temperature measurements: A FIFE perspective
[NASA-CR-182926] 17 p2370 N88-24109

Evaluation of a model of the Earth's gravity field
[EPSHOM-003/87] 17 p2373 N88-24116

A theoretical model of the washout of trace gases by raindrops in the atmosphere 17 p2375 N88-24125

Mathematical modelling of the heat and water vapour transport in the human respiratory tract 17 p2382 N88-24160

Separability and security models --- software
[RSRE-87020] 17 p2386 N88-24180

Adjusting a finite element model using vibration type experimental data. Concept and error detection
[ONERA-RT-7/3313-RY-060-R] 17 p2392 N88-24220

A recursive prediction error parameter estimator for nonlinear models
[RR-326] 17 p2392 N88-24222

On Hotelling's approach to testing for a nonlinear parameter in regression
[AD-A191189] 17 p2393 N88-24229

A thermal equilibrium model for multi-megawatt space platforms 17 p2410 N88-24332

Progress in the computer modeling of the liquid phase behavior of a liquid metal heat pipe 17 p2412 N88-24342

A compressible vapor flux model for transient heat pipe analysis 17 p2412 N88-24343

ATHENA heat pipe transient model 17 p2412 N88-24344

Detailed transient model of a liquid-metal heat pipe 17 p2412 N88-24345

Transient thermohydraulic heat pipe modeling 17 p2413 N88-24347

RSMASS: A simple model for estimating reactor/shield masses 17 p2414 N88-24355

SP-100 control system modeling 17 p2414 N88-24356

Expert systems approach to modeling systems with the ATHENA thermal-hydraulics code 17 p2416 N88-24365

A generalized method for optimizing the mass of space power systems 17 p2416 N88-24369

Modeling of radiation dose dependence of MOSFETs 17 p2416 N88-24370

SP-100 system modeling: SNPSAM update 17 p2417 N88-24372

Microgravity two-phase fluid flow pattern modeling 17 p2432 N88-24467

Experimental evaluation of the MIT-SNL period-generated minimum time control laws for the rapid adjustment of reactor power 17 p2436 N88-24494

Consistent transport coefficients in astrophysics [NASA-TM-101154] 17 p2451 N88-24560

A model for the X-ray binery 4U1820-30 [NASA-TM-101143] 17 p2451 N88-24562

The Jovian aurora: Electron or ion precipitation [NASA-TM-101153] 17 p2452 N88-24566

A benchmark for galactic cosmic ray transport codes [NASA-TM-101157] 17 p2453 N88-24571

An analytic model for aerodynamic shapes [AD-A191573] 18 p2456 N88-24583

Compressible flow in a pie-shaped cylinder rotating about the vertex 18 p2460 N88-24604

Microwave landing system mathematical modeling study for Midway Airport Runway 22L, Chicago, Illinois [AD-A191721] 18 p2462 N88-24616

Nonlinear flying quality parameters based on dynamic inversion [AD-A192146] 18 p2464 N88-24627

Particle-laden weakly swirling free jets: Measurements and predictions [NASA-TM-100920] 18 p2466 N88-24639

An enumeration of research to determine the optimal design and use of Army flight training simulators [AD-A191242] 18 p2468 N88-24649

Analytic and numerical modeling of heat and material transport in electrical hypervelocity guns [AD-A192178] 18 p2469 N88-24655

Fundamental limits to the velocity of solid armatures in railguns 18 p2469 N88-24656

Thermodynamic modeling of the no-vent fill methodology for transferring cryogens in low gravity [NASA-TM-100932] 18 p2476 N88-24686

Interaction of ultrasonic waves with composite plates [AD-A191879] 18 p2478 N88-24702

Shape stability in composites 18 p2479 N88-24706

The influence of cathodic protection on erosion-corrosion of metals and model alloys [AD-A191613] 18 p2485 N88-24742

Delay-doppler radar imaging [AD-A191509] 18 p2499 N88-24826

Internal fluid dynamics within a nonspinning partially liquid-filled shell due to burster rupture [AD-A191055] 18 p2507 N88-24874

Transient particle deposition in a boundary layer of impulsive flow over a flat plate [AD-A191537] 18 p2508 N88-24880

Research in nonlinear wave motion [AD-A191686] 18 p2509 N88-24884

Gas diffusion studies in steady and nonsteady cavities 18 p2512 N88-24902

Numerical solutions of the complete Navier-Stokes equations [NASA-CR-183023] 18 p2514 N88-24914

Experimental study of active vibration control [AD-A191454] 18 p2526 N88-24989

Self-consistent model for the brittle response of solids 18 p2528 N88-24999

Reduced order modelling and analytical model modification for structural dynamics and control 18 p2529 N88-25006

Theory of viscoplasticity based on overstress with applications 18 p2529 N88-25007

Multishaker modal testing [NASA-CR-179355] 18 p2530 N88-25010

Fatigue crack growth due to random loading 18 p2531 N88-25017

Yaw dynamics of horizontal axis wind turbines [DE88-001137] 18 p2537 N88-25055

Photovoltaic Advanced Research and Development Project, solar radiation research [DE88-001143] 18 p2537 N88-25056

Drilling investigation of a young magmatic intrusion beneath the Inyo Domes, Long Valley, California: Structural and textural studies [DE88-006613] 18 p2541 N88-25078

DOD 1985 world magnetic model: Charts and grid values [AD-A191484] 18 p2541 N88-25080

Report on project WIND: Preliminary experiments with the UK Meteorological Office mesoscale model, September 1987 [AD-A191621] 18 p2544 N88-25099

Analysis of lightning field changes during active thunderstorms in Florida 18 p2545 N88-25103

A computational model of motor behavior [AD-A191179] 18 p2553 N88-25152

A concurrent neural network algorithm for the traveling salesman problem [DE88-006981] 18 p2562 N88-25208

Mathematical models for VLSI device simulation [AD-A191125] 18 p2562 N88-25212

Theoretical investigation of optical computing based on neural network models [AD-A191668] 18 p2563 N88-25214

Direct numerical simulations of the PDF's (Probability Density Functions) of a passive scalar in a forced mixing layer [AD-A192134] 18 p2568 N88-25256

Transmitting boundary for finite-difference calculations with finite modeling of an infinite medium [AD-A191441] 18 p2570 N88-25264

Computer simulation of uphill diffusion in ternary ionic system [NASA-TT-20194] 18 p2573 N88-25285

Para-ortho abundance ratio of molecular hydrogen in NGC2023 [ISAS-RN-352] 18 p2573 N88-25286

Modelling of thermal plasma systems 18 p2578 N88-25314

Study of data distributions and functions for the development of thermodynamic equations of state [PB88-196365] 18 p2587 N88-25370

Superthermal electron processes in the upper atmosphere of Uranus: Aurora and electroglow [NASA-TM-101150] 18 p2594 N88-25417

Cluster analysis of multiple planetary flow regimes [NASA-CR-182931] 18 p2594 N88-25418

Diurnal variations in optical depth at Mars: Observations and interpretations [NASA-TM-100057] 18 p2595 N88-25420

Development of a computerized analysis for solid propellant combustion instability with turbulence [NASA-CR-182351] 19 p2611 N88-25497

Coal particle behaviour in a counter-current combustor [TAE-606] 19 p2612 N88-25498

An assessment of the state of the art in predicting the failure of ceramics [DE88-008998] 19 p2621 N88-25551

Droplet formation for liquid monopropellant jets 19 p2623 N88-25557

Comparison of calculated and measured ignition times for boron agglomerates 19 p2624 N88-25563

Liquid phase decomposition in slurry fuels 19 p2624 N88-25564

Effects of Mach number on acoustic-vortex interactions in a ramjet 19 p2625 N88-25573

Development of a generic combustion stability code for liquid propellant rocket engines 19 p2626 N88-25576

Numerical grid generation and flow simulation in SSME thrust chamber 19 p2626 N88-25577

Fuel droplet vaporization and temperature distributions of axisymmetric unsteady sprays 19 p2626 N88-25579

Boundary layer simulator (BLIMPJ) improvement 19 p2627 N88-25582

Liquid Engine Jet Atomization Workshop report 19 p2627 N88-25584

One person's view of velocity-coupled instability 19 p2629 N88-25595

The scaling of the threshold conditions for solid propellant erosive burning 19 p2630 N88-25601

Effect of burn-path tortuosity on the burn rate of composite propellants 19 p2630 N88-25602

Solid rocket motor performance: A workshop report 19 p2631 N88-25607

How much do edges affect the ignition of a homogeneous reactive solid: Summary to date 19 p2631 N88-25608

Minimum ignition energy measurements using laser induced spark initiation 19 p2632 N88-25610

Chemical kinetics modeling of HMX combustion 19 p2633 N88-25617

A multiple chamber volume-filling model for prediction of transient solid rocket motor ballistic performance 19 p2633 N88-25618

Numerical simulation of turbulent flow using the exponential expression of k-Epsilon equation 19 p2640 N88-25662

Color charge motion in non-Abelian fields [DE88-701306] 19 p2642 N88-25672

System capacity and economic modeling computer tool for satellite mobile communications systems 19 p2644 N88-25686

Mobile satellite propagation measurements and modeling: A review of results for systems engineers 19 p2645 N88-25696

Quantum transport calculation of resonant-tunneling response time 19 p2659 N88-25810

Photocurrent modeling of modern microcircuit PN junctions [DE88-007037] 19 p2662 N88-25832

The propagation of pressure perturbations in bubbly air/water flows 19 p2664 N88-25843

Thermal management of integrated microsensors 19 p2670 N88-25875

Automatic calibration of space based manipulators and mechanisms [NASA-CR-182804] 19 p2676 N88-25912

Energy dissipation in a rolling aircraft tire [NASA-CR-182978] 19 p2676 N88-25913

Semi-Markov adjunction to the Computer-Aided Markov Evaluator (CAME) [NASA-CR-181645] 19 p2678 N88-25924

Determining system maintainability as a probability [DE88-007722] 19 p2679 N88-25927

Study of probabilistic fatigue crack growth and associated scatter under constant-and-variable amplitude loading spectrum [AD-A192027] 19 p2679 N88-25929

Timing regulations to prevent stratospheric-ozone depletion [R-3495-JMO/RC] 19 p2690 N88-25987

Sulfur dioxide-hydrogen peroxide relationships in clean air, clouds, and precipitation [DE88-006352] 19 p2690 N88-25990

Theory on conductivity measurement technique for Langmuir probes in the stratosphere [INPE-4514-PRE/1268] 19 p2692 N88-25999

Voltages induced by lightning on electric power distribution lines: Field data and analysis results for the period July 1984-1986 [DE88-007841] 19 p2693 N88-26006

Bathymetry estimation by analyzing swell on SPOT images 19 p2701 N88-26062

Method of assessing changes in biorhythmological structure of human physiological functions 19 p2706 N88-26088

Adaptive residual mode filter control of distributed parameter systems for large space structure applications 19 p2719 N88-26143

Model reduction methods for control design [NASA-CR-179434] 19 p2719 N88-26144

The Potts model in a random field 19 p2721 N88-26159

Acoustic wave dispersion in a viscous, compressible, liquid-filled cylindrical elastic tube 19 p2722 N88-26164

Phase equilibria and density calculations in the critical region: A phenomenological correction for a classical equation of state [PB88-185335] 19 p2723 N88-26167

Primer on coupling collective electronic oscillations to nuclei [LA-10878] 19 p2723 N88-26170

Heavy ion fusion system assessment: Final focus and transport model [LBL-23040] 19 p2725 N88-26183

REFLEX: An energy deposition code that models the effects of electron reflection during electron beam heating tests [DE88-009789] 19 p2726 N88-26186

Superstrings [DE87-702982] 19 p2737 N88-26249

Quantum gravity and new forces [DE88-007829] 19 p2737 N88-26250

Multidimensional modeling of convective heat transfer with application to I.C. engines [DE88-007446] 19 p2738 N88-26257

The solar flare of 18 August 1979: Incoherent scatter radar data and photochemical model comparisons [DE88-007616] 19 p2743 N88-26286

Finite element approximation to a model problem of transonic flow [DE88-701835] 20 p2752 N88-26333

Stiffness degradation of composite laminates 20 p2767 N88-26405

Experimental and theoretical analysis of the radiative transfer within a sooty pool fire [DE88-007099] 20 p2769 N88-26419

A constitutive model with damage for high-temperature superalloys 20 p2771 N88-26434

A numerical study of Rayleigh-Taylor instability in aluminum and steel plates [DE88-010475] 20 p2774 N88-26449

Numerical modeling of the effect of particle size of explosives on shock initiation properties [DE88-010479] 20 p2780 N88-26491

Dynamics of satellites with radial wire antennas 20 p2784 N88-26514

Vertical ship motions and sea loads considering nonlinear effects [TAE-592] 20 p2784 N88-26515

Modeling and parameter identification of motor vehicles 20 p2785 N88-26521

A two-point aerodynamic model for identification 20 p2786 N88-26526

Utilization of identification methods in the time and frequency domain for the determination of the XV-15 (tilt-rotor) dynamics for lateral motion in hover flight
20 p2787 N88-26532

A random access algorithm for environments with capture and limited feedback capabilities
[AD-A192233] 20 p2790 N88-26552

Modeling and thermal management of advanced batteries
[DE88-010023] 20 p2794 N88-26580

Microwave amplifiers
[AD-A192974] 20 p2795 N88-26585

The Oak Ridge Heat Pump Design Model: Mark 3 version program documentationon
[DE88-007863] 20 p2799 N88-26607

Nonlinear equation of state effects and the momentum-dilution trade-off in a turbulent buoyant jet
[DE88-701839] 20 p2799 N88-26610

Axisymmetric liquid sloshing under low-g conditions: Numerical simulation method (reference manual)
[NLR-TR-86057-U] 20 p2802 N88-26627

Vibration frequencies of tapered bars with nonclassical boundary conditions
[NASA-CR-183059] 20 p2813 N88-26688

Microstructural effects in static and dynamic numerical experiments
[DE88-004289] 20 p2813 N88-26690

Random vibration analysis of rattling structures
[DE88-007196] 20 p2813 N88-26691

An assessment of modelling techniques for the finite element analysis of reinforced concrete plate and shell structures
[AD-A192263] 20 p2814 N88-26697

Interpreting forest biome productivity and cover utilizing nested scales of image resolution and biogeographical analysis
[NASA-CR-183036] 20 p2817 N88-26711

Surface hydrology, sediment transport dynamics and remote sensing of disturbed watersheds in a humid temperate region
[DE88-008719] 20 p2817 N88-26715

Development of a model procedure for the determination of volume diffusion lengths by transient measurements on monocrystal silicon solar cells
[ETN-88-92119] 20 p2821 N88-26733

Development of an atmospheric diffusion evaluation method incorporating topographical effects. Part 1: Literature review of atmospheric diffusion models incorporating terrain effects
[DE88-753104] 20 p2822 N88-26742

Effects of a temperature-dependent rheology on large scale continental extension
[NASA-CR-183117] 20 p2825 N88-26759

Parametric methodologies of cloud vertical transport for acid deposition models
[PB88-191374] 20 p2825 N88-26762

Synoptic patterns related to tropical cyclone recurvature
[AD-A192338] 20 p2827 N88-26771

Evaluation of surface energy and radiation balance systems for FIFE
[NASA-CR-183118] 20 p2828 N88-26778

Prediction of continental shelf sediment transport using a theoretical model of the wave-current boundary layer
[AD-A192272] 20 p2829 N88-26783

Stability of a coastal upwelling front over topography
[AD-A192354] 20 p2829 N88-26784

Aircraft interior noise reduction by alternate resonance tuning
[NASA-CR-182540] 20 p2849 N88-26909

A modal approach to Arctic noise modelling with implied vertical coherence
[AD-A192966] 20 p2850 N88-26916

Proceedings of the 2nd US-Japan Workshop on Advanced Plasma Modeling, volume 3
[IPPJ-867] 20 p2855 N88-26957

A Vlasov ion zero mass electron model for plasma simulations 20 p2855 N88-26958

Modeling of subtle kinetic processes in plasma simulation 20 p2856 N88-26959

Atomistic simulation of stability, metastability and growth of strained layer structures 20 p2873 N88-27053

Superconductivity of Cr/V superlattices
20 p2874 N88-27057

Integrated Technology Rotor Methodology Assessment Workshop
[NASA-CP-10007] 21 p2889 N88-27148

A comparison of the various helicopter mathematical models used in the methodology assessment
21 p2889 N88-27149

A comparison of theory and experiment for coupled rotor-body stability of a hingeless rotor model in hover under simulated vacuum conditions
21 p2889 N88-27151

A comparison of theory and experiment for coupled rotor-body stability of a hingeless rotor model in hover
21 p2889 N88-27152

A comparison of theory and experiment for the aeroelastic stability of a bearingless model rotor in hover
21 p2890 N88-27153

The importance of steady and dynamic inflow on the stability of rotor-body systems 21 p2890 N88-27156

Effects of static equilibrium and higher-order nonlinearities on rotor blade stability in hover
21 p2890 N88-27157

Aeroelastic modeling of rotor blades with spanwise variable elastic axis offset: Classic issues revisited and new formulations 21 p2890 N88-27158

Comparison of experimental coupled helicopter rotor/body stability results with a simple analytical model
21 p2891 N88-27160

Aeromechanical stability analysis of COPTER
21 p2891 N88-27161

Improved procedure for impact probability computation of aircraft crash based on Balfanz model
[JUEL-SPEZ-425] 21 p2894 N88-27176

Contribution to the numerical solution of airplane spin motion
[ETN-88-92368] 21 p2896 N88-27190

In-flight motor torque estimates for the second-stage Strypi 9 launch vehicle
[DE88-010833] 21 p2902 N88-27222

Evaluation and improvement of liquid propellant rocket chugging analysis techniques. Part 2: A study of low frequency combustion instability in rocket engine preburners using a heterogeneous stirred tank reactor model
[NASA-CR-182724] 21 p2903 N88-27225

Probabilistic anisotropic failure criteria for composite materials
[AD-A193046] 21 p2904 N88-27232

Analysis of transverse strength of composites using percolation theory
[AD-A193204] 21 p2904 N88-27234

The structure and stability of nonpremixed gas jet flames 21 p2908 N88-27257

Laser probes and numerical modeling as process diagnostics in chemical vapor deposition
[DE88-011622] 21 p2911 N88-27275

Computer modeling for surface properties of carbon fibers 21 p2928 N88-27383

Basic research on optical neural computers
21 p2929 N88-27389

Model for dynamically structured communicating systems
[PB88-105283] 21 p2931 N88-27402

Dependence effects in unique signal transmission
[DE88-010331] 21 p2933 N88-27419

Numerical experiments on turbulent mixing
[AD-A192572] 21 p2942 N88-27473

User's manual for C-HEMP: A two-dimensional wave propagation code. Volume 1: Description and derivations of the code
[AD-A193197] 21 p2944 N88-27486

A comparison of analytical techniques for modeling the Rayleigh-Taylor response of elastic-plastic solids
[DE88-010372] 21 p2962 N88-27596

Reduced order modeling of grid-connected photovoltaic inverter systems
[DE88-010603] 21 p2969 N88-27635

Prediction of regional pollutant dispersion using a nested-grid, three-dimensional numerical model
21 p2971 N88-27649

An empirical surface temperature model
[AD-A192737] 21 p2974 N88-27665

Angular radiation models for Earth-atmosphere system. Volume 1: Shortwave radiation
[NASA-RP-1184] 21 p2976 N88-27677

Dissecting the visual and auditory pathways by means of the two-input technique 21 p2978 N88-27690

Contribution to almost realistic picture processing by a computer graphics procedure
[ETN-88-92372] 21 p2999 N88-27789

Benefits of an object approach in a computer aided design environment
[SNIAS-881-440-102] 21 p3000 N88-27791

Modeling and approximate performance analysis of multiuser computer systems
[ETN-88-92137] 21 p3002 N88-27806

Feedback control of a hyperbolic partial-differential equation with viscoelastic damping
[AD-A192896] 21 p3003 N88-27810

A zoomable and adaptable hidden fine-mesh approach to solving advection-dispersion equations
[DE88-006174] 21 p3004 N88-27816

Parallel solutions to geometric problems on the scan model of computation
[AD-A192321] 21 p3004 N88-27819

Measuring dispersion effects of factors in factorial experiments
[AD-A193216] 21 p3006 N88-27831

Asymptotic normality of minimum L1-norm estimates in linear models
[AD-A193399] 21 p3006 N88-27835

Matrix substructuring, domain decomposition and particle methods: Current trends for solving PDEs in parallel
[DE88-009826] 21 p3007 N88-27836

Reminimization of energy integral and stability limit for non-ideal MHD (magnetohydrodynamic) plasma
[DE88-008422] 21 p3018 N88-27911

Cascade model of gamma-ray bursts: Power-law and annihilation-line components
[NASA-TM-101176] 21 p3032 N88-27998

Literal dynamic modeling
[REPT-881-440-114] 22 p3048 N88-28083

Interactions between coherent structures and premixed flame fronts
[ETN-88-92885] 22 p3053 N88-28111

A review of solid particle erosion of engineering materials
[DE88-010065] 22 p3054 N88-28124

Thermal barrier coating life-prediction model development
[NASA-CR-179507] 22 p3058 N88-28142

Non-Gaussian models for surface clutter
22 p3068 N88-28212

Large-signal modeling of gallium arsenide field-effect transistors 22 p3073 N88-28242

The calculation of the flow through a two-dimensional faired diffuser
[PNR90433] 22 p3076 N88-28259

Modeling of spray combustion in direct injection diesel engine
[AD-A193787] 22 p3084 N88-28314

Modeling discrete bathtub and upside down bathtub mean residual life functions
[AD-A192000] 22 p3085 N88-28320

Determination of the residual stresses in welded structures using the elastoplastodynamic method
[ETN-88-92745] 22 p3087 N88-28330

Parametric identification of mechanical structures
[ETN-88-92881] 22 p3088 N88-28339

Aspects of the 30-60 day oscillation in a GCM simulation 22 p3121 N88-28545

Systematic behavior of NMC medium range forecasts and the effect of model changes 1985-87
22 p3125 N88-28575

The impact of the El Nino event on the ECMWF model performance 22 p3125 N88-28576

Application of Dynamic Extended Range Forecasting (DERF) to the monthly forecast problem
22 p3125 N88-28578

Analysis of the dynamic extended range forecast experiment 22 p3126 N88-28581

Experimental 30-day forecasts from several spectral general circulation models 22 p3126 N88-28582

Correction of systematic errors in NMC medium range forecasts 22 p3126 N88-28584

Theoretical and practical limits of predictability of the NMC medium-range model 22 p3127 N88-28586

The predictability of low frequency patterns in the NMC MRF 22 p3127 N88-28587

Reduce uncertainty in projection of future sea-level changes due to ice wastage
[DE88-009883] 22 p3129 N88-28601

A probabilistic model of the apparent radiance of a rough sea
[AD-A193867] 22 p3129 N88-28602

Models for motion perception
22 p3133 N88-28629

VAXGAP: A code for the routine analysis of gamma-ray pulse-height spectra on a VAX computer
[DE88-011702] 22 p3137 N88-28648

Connectionist models and artificial intelligence
[RR-684-I-IMAG-66-LIFIA] 22 p3142 N88-28684

Refining finite element models. Numerical application to a lattice structure. Study of a macroelement of Timoshenko beam type
[ONERA-RT-8/3313-RY-070-R]
22 p3144 N88-28686

An introduction to the nested sequence of tuples data model and algebra
[REPT-87-049] 22 p3145 N88-28702

Numerical modeling results for mode propagation in a wedge
[AD-A193998] 22 p3147 N88-28718

Sound propagation at low altitude
22 p3148 N88-28725

Customizing Space Nuclear Power System Analysis Model (SNPSAM): Introducing a secondary coolant loop
[AD-A194620] 22 p3151 N88-28750

Development and analysis of turbulent non-equilibrium boundary layers 23 p3169 N88-28872

Vortex flows 23 p3170 N88-28875

Environmental effects on transition and boundary layer characteristics 23 p3170 N88-28876

Contributions to the modeling of wind shear for danger studies
[NASA-TT-20293] 23 p3174 N88-28900

Structural dynamics of maneuvering aircraft
[AD-A192376] 23 p3176 N88-28906

Progress on a Monte Carlo shuttle contamination model
[AD-A193694] 23 p3183 N88-28945

SRB/SLEEC (Solid Rocket Booster/Shingle Lap Extendible Exit Cone) feasibility study, volume 2. Appendix A: Design study for a SLEEC actuation system
[NASA-CR-178974] 23 p3187 N88-28965

Phenomena of the ionic transport in the stress corrosion of metals
[DE88-702502] 23 p3195 N88-29013

Thin film-residual stress assessment
[AD-A193205] 23 p3196 N88-29018

Development of creep fracture modelling in ceramics
[PB88-202825] 23 p3196 N88-29021

Open bosonic string in background electromagnetic field
[DE88-702140] 23 p3201 N88-29053

Development and experimental verification of a two-dimensional numerical model of piezoelectrically induced threshold voltage shifts in GaAs MESFETs
[AD-A193462] 23 p3206 N88-29080

Numerical investigations in three-dimensional internal flows
[NASA-CR-183108] 23 p3210 N88-29106

Stability control of leakage flow channels
[DE88-009995] 23 p3210 N88-29107

Modeling of large stall in axial compressors
[VKI-TN-164] 23 p3213 N88-29124

Modeling of momentum transport of axially parallel turbulent flows in rod cascades
[ETN-88-92978] 23 p3214 N88-29131

Solid-state laser research report: Energy transfer in non-uniform codoped crystals
[AD-A194358] 23 p3219 N88-29161

Modeling of pulsed gas flow lasers
[ESA-TT-1090] 23 p3220 N88-29169

Development of the Simplified Compressor Model (SCM) for performance analysis of gaseous diffusion compressors
[DE88-009066] 23 p3221 N88-29173

Approximate evaluation of semi-Markov chain reliability models
[AD-A194669] 23 p3223 N88-29185

Nonlinear dynamic analysis and optimal control of shallow shells 23 p3224 N88-29191

Mechanics of thrust fault formation
23 p3231 N88-29229

Intraplate deformation, stress in the lithosphere and the driving mechanism for plate motions
[NASA-CR-183121] 23 p3231 N88-29231

Analysis of the hopfield neural networks and their application to pattern recognition
[AD-A193827] 23 p3239 N88-29279

Optimization-driven machine-oriented motion measurement 23 p3245 N88-29312

Piecewise-parabolic methods for systems of hyperbolic conservation laws in multiprocessing environments
[DE88-010202] 23 p3248 N88-29329

Hidden Markov models for automatic speech recognition: Theory and application
[RSRE-MEMO-4135] 23 p3251 N88-29350

AI and simulation: What can they learn from each other 23 p3257 N88-29391

Large-grain pipelining on distributed-memory multiprocessors
[DE88-009974] 23 p3264 N88-29432

Computer-Aided-Control Engineering (CACE) primitives for robust and adaptive control systems, phase 1
[AD-A192446] 23 p3265 N88-29439

Easy Bayes estimation for Rasch-type models
[AD-A193628] 23 p3274 N88-29491

Mathematical theory and calculations of magnetic hysteresis curves
[DE88-011055] 23 p3277 N88-29510

Fusion product spectra
[DE88-010912] 23 p3284 N88-29554

Electrical conductivity of GaAs layers implanted on semi-insulator nondoped substrates
[CERT-422000/RF] 23 p3294 N88-29614

A review: Quantitative models for lava flows on Mars
23 p3301 N88-29656

Origin of northern lowland plains: Constraints from boundary morphology 23 p3305 N88-29687

Coadsorption of H2O and CO2 on the Martian surface
23 p3307 N88-29702

Status review of atmosphere turbulence and aircraft response
24 p3312 N88-29726

Extreme gusts distribution 24 p3314 N88-29734

Advances in Flying Qualities
[AGARD-LS-157] 24 p3314 N88-29735

Pilot modeling 24 p3314 N88-29736

Pilot modeling applications 24 p3314 N88-29737

Advances in flying qualities: Concepts and criteria for a mission oriented flying qualities specification
24 p3314 N88-29739

The optimal control pilot model and applications
24 p3315 N88-29741

Prediction of dynamic derivatives
24 p3318 N88-29761

Prediction of base-flows 24 p3319 N88-29765

Computational methods for the problems of the tip vortex
[NASA-CR-181438] 24 p3320 N88-29775

Minimum-complexity helicopter simulation math model
[NASA-CR-177476] 24 p3328 N88-29819

Procedures for updating dynamic mathematical models, test phase --- spacecraft hardware
[MEBS-38/87] 24 p3335 N88-29852

Some theoretical considerations of the surface tension of liquid metals for metal matrix composites
[AD-A195999] 24 p3340 N88-29882

Combustion and fuels in gas turbine engines
[AGARD-CP-422] 24 p3345 N88-29910

Flamelet chemistry modelling of soot formation for radiation 24 p3348 N88-29928

Numerical models for analytical predictions of combustor aerothermal performance characteristics
24 p3349 N88-29935

Gas turbine combustion modeling
24 p3349 N88-29936

Three-dimensional gas turbine combustor modelling
24 p3349 N88-29937

Flamelet modeling of turbulent premixed flames
24 p3350 N88-29942

Numerical modelling of premixed flames in gaseous media 24 p3350 N88-29944

Modelling of CO oxidation in dilution jet flows
24 p3351 N88-29947

Influence of the convection on evaporation and combustion of a fuel droplet 24 p3351 N88-29948

Numerical field model simulation of full scale fire tests in a closed spherical/cylindrical vessel
[AD-A195067] 24 p3359 N88-29998

The use of upwind schemes at high Reynolds number: A cautionary note
[AD-A196227] 24 p3371 N88-30074

Transition mixing study empirical model report
[NASA-CR-182139] 24 p3371 N88-30076

Numerical simulation of the function of scientific instrumentation for measuring the speed of electron devices
[AD-A194969] 24 p3376 N88-30103

Fatigue crack propagation: Probabilistic modeling and statistical analysis
[AD-A195885] 24 p3384 N88-30155

Relief effect correction on LANDSAT imagery for forest applications using digital terrain models
[INPE-4611-PRE/1334] 24 p3388 N88-30179

LANDSAT TM and agrometeorological data for wheat yield estimation at the farm level
[INPE-4591-PRE/1321] 24 p3388 N88-30180

Nd isotopes and crustal growth rate
24 p3392 N88-30203

Construction of mass-age curves for the continental crust: An empirical model and an example from the western US 24 p3394 N88-30213

Temperature profile construction methods: An evaluation
[AD-A195919] 24 p3403 N88-30262

Some results from the Amazon Forest micrometeorological experiment
[INPE-4631-PRE/1346] 24 p3403 N88-30263

Cloud/mesoscale model development and application studies
[AFGL-TR-87-0219] 24 p3404 N88-30269

A digital terrain model system for a microcomputer
[INPE-4610-PRE/1333] 24 p3413 N88-30316

Range data description based on multiple characteristics 24 p3419 N88-30351

Automatic mathematical modeling for real time simulation system 24 p3420 N88-30356

Adaptive control in positioning a rigid-flexible robot arm
[AD-A195194] 24 p3422 N88-30367

Nested neural networks
[NASA-TM-101032] 24 p3423 N88-30373

Generation of surface grids through elliptic partial differential equations for aircraft and missile configurations
[AD-A195639] 24 p3424 N88-30378

Dirichlet prior in Bayesian estimation of item response curves
[AD-A195311] 24 p3426 N88-30392

Theoretical modeling of accelerating arc plasmas
[AD-A195606] 24 p3432 N88-30426

The origin of the moon: Further studies of the giant impact 24 p3440 N88-30474

Volatiles on Mars
[NASA-CR-183113] 24 p3456 N88-30571

MATHEMATICAL PROGRAMMING
NT DYNAMIC PROGRAMMING
NT LINEAR PROGRAMMING
NT NONLINEAR PROGRAMMING
NT QUADRATIC PROGRAMMING

On the exact solution of large-scale simple plant location problems
[FI-032-TB-22E] 02 p0229 N88-11441

Computing block-angular Karmarker projections with applications to stochastic programming, revision
[AD-A185647] 06 p0759 N88-14656

Progress in mathematical programming
[AD-A185729] 06 p0759 N88-14658

Local and global techniques for the tracking of periodic solutions of parameter-dependent functional differential equations
[AD-A185756] 06 p0766 N88-14704

Bounding the expectation of convex functions with limited distribution information
[AD-A186147] 07 p0910 N88-15512

Sublinear upper bounds for stochastic programs with recourse, revision
[AD-A186436] 07 p0916 N88-15564

Tutorial on GAMS (Generalized Algebraic Modeling System): A modeling language for optimization
[AD-A189867] 15 p2109 N88-22568

Discrete generalized networks: Application to integer constrained flow problems
[AD-A190823] 16 p2190 N88-23060

Towards fully abstract semantics for local variables: Preliminary report
[AD-A191065] 16 p2251 N88-23456

Experimental design and structural optimization
[ETN-88-92232] 16 p2257 N88-23492

Optimal design of viscoelastic structures
21 p2959 N88-27579

Motion planning with obstacles and dynamic constraints 23 p3222 N88-29175

Multicriteria integer programming for problems involving linear and nonlinear utility functions
[AD-A194530] 23 p3249 N88-29336

Computer systems for the representation and manipulation of mathematical knowledge
[AD-A193547] 23 p3249 N88-29340

MATHEMATICS

Interdisciplinary research in mathematics, science and technology education
[PB88-131446] 10 p1388 N88-18333

JPRS report: Science and technology. USSR: Physics and mathematics
[JPRS-UPM-88-001] 14 p1968 N88-21751

MATRICES (CIRCUITS)

Photodiode matrix for the analysis of two-beam interferences
[PTB-OPT-23] 01 p0048 N88-10310

Reducing the parallel solution time of sparse circuit matrices using reordered Gaussian elimination and relaxation
[AD-A195152] 24 p3366 N88-30045

MATRICES (MATHEMATICS)
NT ADJOINTS
NT CANONICAL FORMS
NT EIGENVALUES
NT EIGENVECTORS
NT HESSIAN MATRICES
NT STIFFNESS MATRIX

Implementation of a digital optical matrix-vector multiplier using a holographic look-up table and residue arithmetic
[NASA-CR-180431] 01 p0078 N88-10496

The box method for linear programming. Part 1: Basic theory
[DE87-011029] 01 p0080 N88-10515

Finite-dimensional matrix representation of the differential operator, determinental form and zeros of special functions
[DE87-703091] 02 p0225 N88-11421

Structure-dependent matrix representation of manipulator kinematics and its inverse solution
[DE87-752966] 02 p0229 N88-11447

QR factorization of a dense matrix on a shared-memory multiprocessor
[DE88-001506] 04 p0480 N88-12956

Two classes of preconditioners computed using block matrix factorization techniques
[DE88-001313] 04 p0485 N88-12988

Reduced order optimal command applied to longitudinal automatic pilots
[SNIAS-872-111-114] 05 p0552 N88-13362

Mechanics of anisotropic media. Study of the boundary conditions --- stratified composites
[SNIAS-872-430-112] 05 p0559 N88-13404

The matrix exponential in transient structural analysis
05 p0593 N88-13619

Simultaneous structural and control optimization via linear quadratic regulator eigenstructure assignment
05 p0594 N88-13622

Illustrative examples of principal component analysis using BMDP/4M
[AD-A185179] 05 p0635 N88-13881

Structuring data for concurrent vectorized processing in a transient dynamics finite element program
[DE87-013082] 05 p0636 N88-13890

Optimal control of large space structures via generalized inverse matrix
[NASA-CR-182336] 05 p0639 N88-13907

Eigenvectors of distance-regular graphs
[AD-A185375] 05 p0641 N88-13919

Computation of natural frequencies of planar lattice structure
[AD-A185387] 05 p0641 N88-13920

The estimation of basic matrices using travel intensity theorems
[REPT-87-13] 05 p0642 N88-13926

Illustrative examples of principal component analysis using SYSTAT/FACTOR
[AD-A184920] 05 p0644 N88-13939

On the work needed to factor a symmetric positive definite matrix
[AD-A185781] 06 p0759 N88-14660

Parallel pivoting combined with parallel reduction
[NASA-CR-178422] 06 p0760 N88-14662

Analysis of a parallel solution method for tridiagonal systems
[PB87-230538] 06 p0762 N88-14678

Parallel LU-factorization algorithms for dense matrices
[DE88-002179] 07 p0904 N88-15478

Parallel LU-factorization algorithms for dense matrices
[DE88-002179] 07 p0904 N88-15478

A Schur-complement method for sparse quadratic programming
[DE88-002520] 07 p0904 N88-15479

The effect of response scaling on the detection of singularities in multiresponse estimation
[AD-A185964] 07 p0908 N88-15503

Strong laws of large numbers for arrays of orthogonal random variables
[AD-A186159] 07 p0910 N88-15513

On the asymptotic joint distributions of the eigenvalues of random matrices which arise under components of covariance model
[AD-A186387] 07 p0915 N88-15558

Method for joint adjustment of satellite and surface geodetic networks 08 p1007 N88-16105

A parallel algorithm for the general LU-factorization
[DE88-002177] 08 p1066 N88-16444

Matrix functions in the stability of higher-order numerical schemes
[INPE-4246-PRE/1119] 08 p1073 N88-16472

An efficient method for computing leading Eigenvalues and Eigenvectors of large asymmetric matrices
09 p1159 N88-16949

Mesospheric dynamics and chemistry from SME data
[NASA-CR-182465] 09 p1191 N88-17139

Multicolor numbering of irregular triangular meshes
[AD-A186559] 09 p1217 N88-17298

An applicative programmer's approach to matrix algebra, lessons for hardware and software
10 p1382 N88-18251

A multigrid preconditioner applied to a two-dimensional convection-diffusion problem
[DE88-004765] 10 p1397 N88-18329

Identifiability of multivariate ARMA models
[AD-A187394] 10 p1400 N88-18350

Status of the electroweak theory
[DE88-002342] 10 p1422 N88-18494

Multipass beam breakup in recirculating linacs
[CEBAF-PR 87-007] 12 p1690 N88-20111

Further results on the McMillan degree and the Kronecker indices of ARMA models --- input-output relations of linear systems
[EUT-87-E-175] 13 p1827 N88-20925

The parameterization of orthogonal matrices: A review mainly for statisticians
[AD-A189144] 13 p1829 N88-20936

Optimization of the real level 2 BLAS on the Cyber 205
[CWI-NM-R8715] 14 p1956 N88-21657

A parallel algorithm for computing the singular value decomposition of a matrix
[DE88-007059] 14 p1958 N88-21673

Split-coefficient matrix solution and experimental study of axisymmetric underexpanded exhaust plumes
15 p2054 N88-22242

Sufficient matrices and the linear complementarity problem
[AD-A190429] 15 p2128 N88-22690

Homogenization study of matrix behavior in a composite material
[ONERA-RT-1/7256-RY-060-R]
16 p2172 N88-22943

Systolic algorithm for matrix-vector multiplication
[PB88-165394] 16 p2256 N88-23484

Minimal parameter solution of the orthogonal matrix differential equation
[NASA-TM-4043] 17 p2383 N88-24165

Nonequilibrium phonons and disorder in Al sub x Ga sub 1-x As 19 p2657 N88-25788

QR factorization of a dense matrix on a hypercube multiprocessor
[DE88-009187] 19 p2716 N88-26129

A diagonally inverted LU implicit multigrid scheme
[NASA-TM-100911] 20 p2753 N88-26340

Eigenmatrix representations of radiance distributions in layered natural waters with wind-roughened surfaces
[PB88-188701] 20 p2828 N88-26780

Computing small singular values of bidiagonal matrices with guaranteed high relative accuracy: LAPACK working note number 3
[DE88-008465] 20 p2837 N88-26829

A matroid algorithm and its application to the efficient solution of two optimization problems on graphs, revision
[AD-A192709] 20 p2838 N88-26838

Derivation of space groups in mm2, 222 and mmm crystal classes
[DE88-701881] 20 p2876 N88-27076

Sidelobe level of an adaptive array using the SMI (Sampled Matrix Inversion) algorithm
[AD-A193131] 21 p2932 N88-27409

A programmable systolic array for factorial analysis. Part 2: The symmetric eigenvalue problem
[AD-A192396] 21 p2995 N88-27762

A unified approach to estimation in linear models with fixed and mixed effects
[AD-A193060] 21 p3006 N88-27829

On matrix pencil equivalents of a general polynomial matrix
[MATH-REPT-207] 23 p3273 N88-29479

On Wiener-Masani's algorithm for finding the generating function of multivariate stochastic processes
[NASA-CR-182905] 23 p3273 N88-29481

Invariant ideals of multiplicity free algebraic group actions
[B8803517] 23 p3277 N88-29509

MATRIX ANALYSIS
U MATRICES (MATHEMATICS)

MATRIX MATERIALS

Calculation methods of atomic number density for various nuclear materials
[DE87-753006] 02 p0233 N88-11467

Ion-matrix coupling in polymer electrolytes from relaxation time studies
[AD-A184632] 03 p0293 N88-11841

Carbon fiber reinforced glass matrix composites for space based applications
[AD-A184355] 04 p0410 N88-12546

Composite materials with glass matrix
[SGR/PR-4305/86-SV/JC] 05 p0558 N88-13394

Fabrication of composites by chemical vapor deposition
[DE87-014565] 05 p0559 N88-13408

Development of an impact- and solvent-resistant thermoplastic composite matrix, phase 4
[NASA-CR-178413] 06 p0677 N88-14145

Sintering and densification of particulate composites: Inclusion size and clustering
[DE88-002230] 06 p0685 N88-14199

Characterization of mechanical damage mechanisms in ceramic composite materials
[AD-A185549] 06 p0686 N88-14205

Dynamic finite element with diagonalized consistent mass matrix and elastic-plastic impact calculation
[PB87-143376] 08 p0995 N88-16020

Analysis of composite laminates with matrix cracks
[CCMS-88-03] 11 p1451 N88-18645

Effect of rigid inclusions on sintering
[DE88-005745] 12 p1609 N88-19623

Interface structure and properties of alumina/glass ceramic composites
[DE88-006219] 14 p1892 N88-21302

Physical-mechanical properties of matrices on the comet nuclei surface models 14 p2010 N88-21987

Cement paste matrix composite materials center
[AD-A188657] 15 p2028 N88-22083

Microplasticity phenomena in graphite/magnesium metal matrix composites
[DE88-006772] 15 p2029 N88-22086

Singlet oxygen behavior in solid polymer matrices
[DE88-005171] 15 p2043 N88-22171

Donor acceptor polymerization chemistry as a vehicle to low energy cure matrix resins
[AD-A190119] 15 p2044 N88-22179

A test for interfacial effects and stress transfer in ceramic matrix composites
[NASA-CR-182758] 15 p2046 N88-22194

Investigation of non-linear optical behavior of semiconductors for optical switching, volume 1
[AD-A191297] 16 p2274 N88-23811

Carbon matrix composites prospective roles for biotechnology 18 p2477 N88-24694

Sol/gel processing techniques for glass matrix composites
[AD-A191748] 18 p2478 N88-24701

Effects of electron beam irradiation on mechanical properties at low and high temperature of fiber reinforced composites using PEEK as matrix material
[DE88-753134] 21 p2905 N88-27239

Fabrication of SiC fiber reinforced glass matrix by extrusion process and investigation of its mechanical properties
[ETN-88-92367] 21 p2906 N88-27244

Programs for preliminary design of composite materials which were developed by the design group of Aerospatiale Aquitaine
[REPT-881-430-112] 21 p2907 N88-27251

Determination of impurities in silicon carbide by ICP AES (inductively coupled plasma atomic emission spectrometry) after coprecipitation with lanthanum hydroxide
[NASA-TT-20332] 23 p3193 N88-28603

Creep of carbon yarn and carbon-carbon composites at high temperatures and high stresses
[AD-A195224] 24 p3340 N88-29878

Criteria for matrix dominated failure
[AD-A196263] 24 p3341 N88-29887

MATRIX METHODS

A DMAP for updating dynamic mathematical models with measured data
[NLR-MP-86027-U] 01 p0060 N88-10387

Relaxation effect of stark split levels for two-level system interacting with symmetrical strong resonant bichromatic field 03 p0299 N88-11882

Structural optimization in the design process -- aircraft
[SNIAS-872-111-115] 05 p0635 N88-13865

An efficient sparse matrix multiplication scheme for the CYBER 205 computer
[NASA-TM-4029] 10 p1390 N88-18302

A constitutive material model for nonlinear finite element structural analysis using an iterative matrix approach
14 p1932 N88-21521

Coupled bending-torsion steady-state response of pretwisted, nonuniform rotating beams using a transfer-matrix method
[NASA-TM-100596] 15 p2086 N88-22435

Efficient bit-level, word-level and block-level systolic arrays for matrix-matrix multiplication
[DE88-011331] 20 p2841 N88-26856

Effective buffering schemes for performing matrix operations for numerical databases
21 p3027 N88-27968

MATRIX STRESS CALCULATION
U MATRIX METHODS

MATRIX THEORY

REDUCE-aided study of a problem in Hermitian matrix theory
[DE87-014331] 02 p0229 N88-11445

Graph partitioning by eigenvectors
[AD-A184430] 03 p0372 N88-12338

The matrix exponential in transient structural analysis
05 p0593 N88-13619

Strong representation of weak convergence
[AD-A186433] 07 p0916 N88-15583

Relativistic corrections for one- and two-photon matrix elements of weakly-bound systems
[NOTA-INTERNA-884] 07 p0929 N88-15845

Predicting oscillatory finite difference solutions to the heat equation: A comparative study of the coefficient and matrix methods
[AD-A189591] 13 p1825 N88-20811

Sufficient matrices and the linear complementarity problem
[AD-A190429] 15 p2128 N88-22690

Computing partial correlations from the data matrix
[AD-A193904] 22 p3138 N88-28659

MATTER (PHYSICS)
NT DARK MATTER

Gravitational accretion of hot dark matter
03 p0388 N88-12439

Beta limitation of matter-antimatter boundary layers
[TRITA-EPP-87-11] 09 p1250 N88-17489

The origin of the diffuse X-ray background and the formation of galaxies and voids
10 p1428 N88-18527

Quark matter in astrophysics and cosmology
[DE88-003406] 10 p1429 N88-18534

Atomic processes in matter-antimatter interactions
[DE88-008911] 19 p2723 N88-26172
N=2 supergravity in superspace: different versions and matter couplings
[DE88-702137] 19 p2741 N88-26274
Inelastic mean free paths of electrons and positrons in matter
[DE88-008086] 20 p2851 N88-26929

MATURING
U GROWTH

MAXIMA
Additional peak of light scattering by sound under conditions of acoustic instability
14 p1968 N88-21752
Structural dynamics of high-latitude magnetosphere determined from solar electron data
24 p3444 N88-30500

MAXIMUM ENTROPY METHOD
Stochastic model of the NASA/MSFC ground facility for large space structures with uncertain parameters: The maximum entropy approach
[NASA-CR-181489] 03 p0372 N88-12343
Restoration of particle pitch angle distribution functions by a maximum entropy algorithm
[ATR-86(7098)-3] 05 p0648 N88-13969
The maximum entropy method for the analysis of radar echoes from hovering helicopters in clutter
[FB-2-87] 11 p1475 N88-18799
Electron density profile reconstruction by maximum entropy method with multichannel HCN laser interferometer system on SPAC 7
[IPPJ-858] 11 p1553 N88-19295
A maximum entropy solution for the underdetermined electromagnetic field within a volume
[DE88-007020] 20 p2790 N88-26550
Maximum entropy signal restoration with linear programming
[DE88-011740] 21 p2999 N88-27787
The maximum entropy method for the analysis of short-time radar echoes from hovering helicopters
22 p3149 N88-28737

MAXIMUM LIKELIHOOD ESTIMATES
Maximum likelihood estimates of parameters in linear systems with process and measurement noise
[DFVLR-FB-87-20] 01 p0083 N88-10532
Exploiting auxiliary information about items in the estimation of Rasch item difficulty parameters
[AD-A184383] 03 p0372 N88-12341
Tau ranging revisited 04 p0437 N88-12710
Estimation of a multivariate continuous variable panel model
[AD-A184472] 04 p0484 N88-12982
An urn model for the multi-sample capture/recapture sequential tagging process
[AD-A184470] 04 p0486 N88-12998
Non-linear maximum likelihood estimation of stability derivatives from range data
[NAL-TM-SE-8608] 05 p0552 N88-13365
Approximating multivariate normal orthant probabilities using the Clark algorithm
[AD-A184855] 05 p0634 N88-13873
The maximum likelihood estimator method of image reconstruction: Its fundamental characteristics and their origin
[DE88-000462] 05 p0638 N88-13892
Presentation of a computer program permitting the exploitation of tests designed to determine the sensitivity of one shot devices to a parameter. Application to a degenerate one shot sequence
[SNIAS-872-430-117] 05 p0644 N88-13945
A three-parameter generalisation of the beta-binomial distribution with applications
[AD-A185733] 06 p0768 N88-14720
Discrete reliability growth models using failure discounting
[AD-A186380] 07 p0866 N88-15252
Strong consistency of maximum likelihood parameter estimation of superimposed exponential signals in noise
[AD-A186384] 07 p0911 N88-15526
Maximum likelihood principle and model selection when the true model is unspecified
[AD-A186027] 07 p0914 N88-15544
A simultaneous M-ary channel hypothesis test with least-mean-square signal amplitude estimation
[AD-A186526] 08 p0978 N88-15913
Short data length effects in an asymptotically efficient ARMA (AutoRegressive Moving Average) spectral estimator
[AD-A186561] 08 p1068 N88-16458
Estimation and comparison of changes in the presence of information right censoring by modeling the censoring process
[AD-A186320] 08 p1074 N88-16478
Lateral stability and control derivatives extracted from space shuttle Challenger flight data
[NASA-TM-100520] 09 p1132 N88-16788
Maximum likelihood estimates for the discrete application of the AMSAA growth model
[AD-A186921] 09 p1177 N88-17048
Random truncation models and Markov processes
[CWI-MS-R8702] 09 p1232 N88-17389
A maximum likelihood parameter estimation program for general non-linear systems
[ARL-AERO-TM-392] 11 p1532 N88-19154
Optimal recursive maximum likelihood estimation
[AD-A187980] 11 p1536 N88-19176
Statistical signal processing using a class of iterative estimation algorithms
[AD-A189050] 13 p1757 N88-20511
Estimating system and component reliabilities under partial information on cause of failure
[AD-A189107] 13 p1780 N88-20653
Non- and semi-parametric maximum likelihood estimators and the von Misis Method, part 1
[CWI-MS-R8709] 13 p1829 N88-20941
The application of linear maximum likelihood estimation of aerodynamic derivatives for the Bell-205 and Bell-206
[AD-A191279] 16 p2161 N88-22894
Maximum likelihood parameter identification of flexible spacecraft
[LR-508] 16 p2168 N88-22924
Multichannel 2-D power spectral estimation and applications
[AD-A191273] 16 p2191 N88-23068
Partial likelihood analysis of time series models with application to rainfall-runoff data
[AD-A191157] 16 p2261 N88-23516
Leave-K-Out diagnostics for time series
[AD-A191343] 16 p2261 N88-23518
A central limit theorem for M-estimators by the von Mises method
[CWI-MS-R8713] 16 p2262 N88-23525
A comparison of supervised maximum likelihood and decision tree classification for crop cover estimation from multitemporal LANDSAT MSS data
17 p2352 N88-24014
Generation of thematic maps for updating aeronautical pilot charts utilizing LANDSAT-TM images
17 p2361 N88-24062
Adaptive time series analysis using predictive inference and entropy
[AD-A191858] 18 p2560 N88-25199
Recursive maximum likelihood identification of a nonlinear output-affine model
[RR-322] 18 p2569 N88-25257
System identification in vehicle dynamics
[DFVLR-MITT-87-22] 20 p2785 N88-26518
Parameter estimation of dynamical systems
20 p2785 N88-26519
Parametric estimation of aerodynamic nonlinearities in rolling moment due to sideslip using maximum likelihood method 20 p2786 N88-26528
Tuning a major part of a clustering algorithm
[AD-A191446] 20 p2836 N88-26821
Spectral estimation of received phase in the presence of amplitude scintillation 22 p3064 N88-28180
Easy Bayes estimation for Rasch-type models
[AD-A193628] 23 p3274 N88-29491
Maximum-likelihood multichannel deconvolution of P waves at seismic arrays
[AD-A194990] 24 p3391 N88-30191
Advancement of latent trait theory
[AD-A194302] 24 p3408 N88-30289

MAXIMUM PRINCIPLE
Conference on Maximum Principles and Eigenvalue Problems in Partial Differential Equations
[AD-A187870] 11 p1536 N88-19175

MAXIMUM USABLE FREQUENCY
HF (High Frequency) Maximum Usable Frequency (MUF) model uncertainty assessment
[AD-A189132] 13 p1757 N88-20513
The MUF (Maximum Usable Frequency) (3000) as an indicator for F-region variations
[AD-A191655] 19 p2690 N88-25991

MAXWELL EQUATION
Trajectory versus PIC methods in diode design
[DE87-012135] 02 p0166 N88-11043
On the collective variables description of a high gain free electron laser
[DE87-013315] 02 p0178 N88-11108
Spectral evolution equation for the sideband instability in a free-electron laser oscillator
[DE88-000510] 04 p0447 N88-12771
Plane longitudinal waves in solutions of Maxwell equations
[DE88-700347] 07 p0846 N88-15135
A moment approach to modeling negative ion sources
[AD-A188858] 12 p1691 N88-20114
Study of inhomogeneously filled cylindrical resonant cavities by the finite integration technique
[PB88-133707] 12 p1697 N88-20156
Chronometrically invariant formulation of electrodynamics equation
[DE88-701030] 13 p1849 N88-21071
Topics in curved and flat space electromagnetism
13 p1854 N88-21100
Galilei relativity principle in classical electrodynamics
[DE87-703203] 14 p1904 N88-21376
A general 2D electrical model for diagonally connected MHD generators
[DE88-004283] 14 p1984 N88-21835
Wave energy flow conservation for propagation in inhomogeneous Vlasov-Maxwell equilibria
[DE88-006705] 15 p2055 N88-22251
High speed transcendental elementary function architecture in support of the Vector Wave Equation (VWE)
[AD-A189746] 15 p2119 N88-22627
Microinstabilities in ion beam propagation
16 p2277 N88-23631
Coronal fluid-dynamics in laser fusion
16 p2278 N88-23634
The MAFIA approach to solving Maxwell's equations in three dimensions
[DE88-007826] 19 p2720 N88-26155
Stochastic modeling of EM scattering from foliage
[AD-A192258] 20 p2790 N88-26553
SARLAC: A relativistic electron beam code
[AD-A193134] 21 p2932 N88-27411
Kinetic theory for plane flows of rough, inelastic, circular disks 21 p2946 N88-27499
Wave equations for pulse propagation
[DE88-011760] 21 p2954 N88-27548
Staggered-grid finite element solution technique for the Maxwell's equations in the time domain
[DE88-011731] 21 p3007 N88-27836
On the self-consistent equation for the microscopic local electric field in dielectric systems
[PREPRINT-589] 22 p3074 N88-28247
Research on a two-stage free electron laser oscillator
[AD-A195991] 24 p3377 N88-30115

MAXWELL-BOLTZMANN DENSITY FUNCTION
Effects of low reflection on the collector and source sheaths of a finite ion temperature plasma
[DE88-008929] 21 p3017 N88-27906

MAXWELLIAN DISTRIBUTION (DENSITY)
U MAXWELL-BOLTZMANN DENSITY FUNCTION

MAZE LEARNING
Path planning and path following for the Amsterdam autonomous cart
[FVI-86-22] 24 p3380 N88-30133

MCDONNELL AIRCRAFT
NT F-4 AIRCRAFT
NT RF-4 AIRCRAFT

MCDONNELL DOUGLAS AIRCRAFT
NT DC 9 AIRCRAFT
NT F-4 AIRCRAFT
NT F-18 AIRCRAFT
NT RF-4 AIRCRAFT
McDonnell Douglas Helicopter Company independent research and development: Preparing for the future
09 p1111 N88-16660

MEADOWLANDS
U GRASSLANDS

MEAN
Testing and interval estimation in a change-point model allowing at most one change
[AD-A185525] 06 p0767 N88-14716
On detection of change points using mean vectors
[AD-A185581] 06 p0767 N88-14717
An elimination type two-stage procedure for selecting the population with the largest mean from k logistic populations
[AD-A185614] 07 p0916 N88-15566
Modeling discrete bathtub and upside down bathtub mean residual life functions
[AD-A192000] 22 p3085 N88-28320

MEAN FREE PATH
Study of mean free path effects on growth of ultrafine metallic aerosols
[AD-A190206] 15 p2039 N88-22149
Inelastic mean free paths of electrons and positrons in matter
[DE88-008086] 20 p2851 N88-26929

MEAN SQUARE VALUES
Evolution of mean square magnetic vector potential in compressible, two-dimensional, magnetofluid turbulence
[AD-A184985] 05 p0651 N88-13990
A simultaneous M-ary channel hypothesis test with least-mean-square signal amplitude estimation
[AD-A186526] 08 p0978 N88-15913

MEAN TIME BETWEEN FAILURES
U MTBF

MEASURE AND INTEGRATION
NT BINARY INTEGRATION
NT BOREL SETS
NT INTEGRAL CALCULUS

NT J INTEGRAL
NT LEBESGUE THEOREM
NT NUMERICAL INTEGRATION
NT RUNGE-KUTTA METHOD
NT WEIGHTING FUNCTIONS
The precision of limits on bodily fluids when using beta-expectation inner tolerance limits
[AD-A187966] 10 p1369 N88-18185
Path integration on the upper half-plane
[DE88-751050] 12 p1682 N88-20057
Remarks on the time transformation of path-integral measures
[DE87-703040] 15 p2118 N88-22617
Why are certain nonlinear Partial Differential Equations (PDE) both widely applicable and integrable
[PREPRINT-582] 22 p3144 N88-28698
MEASURE THEORY
U MEASURE AND INTEGRATION
MEASUREMENT
Group quantization of constrained systems
[PREPRINT-564] 06 p0790 N88-14844
MEASURING
U MEASUREMENT
MEASURING INSTRUMENTS
NT ACCELEROMETERS
NT ADVANCED VERY HIGH RESOLUTION RADIOMETER
NT ALTIMETERS
NT ANALYZERS
NT ANEMOMETERS
NT ATOMIC CLOCKS
NT ATTITUDE INDICATORS
NT BALLOON-BORNE INSTRUMENTS
NT BAROMETERS
NT BATHYMETERS
NT BATHYTHERMOGRAPHS
NT BOLOMETERS
NT BOMB CALORIMETERS
NT CALORIMETERS
NT CERENKOV COUNTERS
NT CLOCKS
NT CLOUD HEIGHT INDICATORS
NT COMPARATORS
NT COUNTERS
NT DENSIMETERS
NT DENSITOMETERS
NT DICKE RADIOMETERS
NT DIFFRACTOMETERS
NT DISTANCE MEASURING EQUIPMENT
NT DOSIMETERS
NT DYNAMOMETERS
NT EBERT SPECTROMETERS
NT ELECTRICAL CONDUCTIVITY METERS
NT ELECTRON COUNTERS
NT ELECTRON PROBES
NT ELECTROPHOTOMETERS
NT ELECTROSTATIC PROBES
NT ELLIPSOMETERS
NT ENGINE ANALYZERS
NT ENGINE MONITORING INSTRUMENTS
NT ERGOMETERS
NT ETALONS
NT EXTENSOMETERS
NT FABRY-PEROT INTERFEROMETERS
NT FABRY-PEROT SPECTROMETERS
NT FLAME PROBES
NT FLIGHT RECORDERS
NT FLIR DETECTORS
NT FLOWMETERS
NT GALVANOMETERS
NT GAMMA RAY SPECTROMETERS
NT GONIOMETERS
NT GRAVIMETERS
NT GRAVITY GRADIOMETERS
NT HOT-FILM ANEMOMETERS
NT HOT-WIRE ANEMOMETERS
NT HOT-WIRE FLOWMETERS
NT IMAGING SPECTROMETERS
NT IMPEDANCE PROBES
NT INDICATING INSTRUMENTS
NT INFRARED DETECTORS
NT INFRARED INSTRUMENTS
NT INFRARED INTERFEROMETERS
NT INFRARED RADIOMETERS
NT INFRARED SCANNERS
NT INFRARED SPECTROMETERS
NT INFRARED SPECTROPHOTOMETERS
NT INTERFEROMETERS
NT ION PROBES
NT ION TRAPS (INSTRUMENTATION)
NT IONIZATION GAGES
NT IONOSONDES
NT LASER ALTIMETERS
NT LASER ANEMOMETERS
NT LASER DOPPLER VELOCIMETERS
NT LASER RANGE FINDERS
NT LASER SPECTROMETERS
NT LIGHT SCATTERING METERS
NT MACH-ZEHNDER INTERFEROMETERS
NT MAGNETIC PROBES
NT MAGNETOMETERS
NT MASS SPECTROMETERS
NT METEOROLOGICAL INSTRUMENTS
NT MICHELSON INTERFEROMETERS
NT MICRODENSITOMETERS
NT MICROMETERS
NT MICROWAVE INTERFEROMETERS
NT MICROWAVE RADIOMETERS
NT MICROWAVE SENSORS
NT MICROWAVE SPECTROMETERS
NT MOISTURE METERS
NT MONOCHROMATORS
NT NEUTRON COUNTERS
NT NEUTRON SPECTROMETERS
NT OCULOMETERS
NT OMEGA NAVIGATION SYSTEM
NT OPTICAL MEASURING INSTRUMENTS
NT OPTICAL PYROMETERS
NT OXYGEN ANALYZERS
NT PARTICLE TELESCOPES
NT PHASE SWITCHING INTERFEROMETERS
NT PHOTOMETERS
NT PIEZOELECTRIC GAGES
NT PLASMA PROBES
NT PNEUMATIC PROBES
NT POLARIMETERS
NT POSITION INDICATORS
NT PRESSURE GAGES
NT PROFILOMETERS
NT PROPORTIONAL COUNTERS
NT PYROMETERS
NT RADIATION COUNTERS
NT RADIATION DETECTORS
NT RADIATION MEASURING INSTRUMENTS
NT RADIATION PYROMETERS
NT RADIO ALTIMETERS
NT RADIO INTERFEROMETERS
NT RADIOMETERS
NT RADIOSONDES
NT RAIN GAGES
NT RANGE FINDERS
NT RAWINSONDES
NT REFRACTOMETERS
NT RESISTANCE THERMOMETERS
NT SATELLITE-BORNE INSTRUMENTS
NT SCATTEROMETERS
NT SCINTILLATION COUNTERS
NT SEISMOGRAPHS
NT SIGNAL ANALYZERS
NT SILICON RADIATION DETECTORS
NT SOLAR BACKSCATTER UV SPECTROMETER
NT SOLAR SPECTROMETERS
NT SONDES
NT SPARK CHAMBERS
NT SPECTROHELIOGRAPHS
NT SPECTROMETERS
NT SPECTROPHOTOMETERS
NT SPECTRORADIOMETERS
NT STRAIN GAGE ACCELEROMETERS
NT STRAIN GAGES
NT TACHOMETERS
NT TEMPERATURE MEASURING INSTRUMENTS
NT THEODOLITES
NT THERMOMETERS
NT THRESHOLD DETECTORS (DOSIMETERS)
NT TILTMETERS
NT TIME OF FLIGHT SPECTROMETERS
NT TIMING DEVICES
NT TORQUEMETERS
NT TOTAL OZONE MAPPING SPECTROMETER
NT TRANSMISSOMETERS
NT TURBULENCE METERS
NT ULTRAVIOLET SPECTROMETERS
NT ULTRAVIOLET SPECTROPHOTOMETERS
NT VACUUM GAGES
NT VARIOMETERS
NT VIBRATION METERS
NT VISCOMETERS
NT VOLTMETERS
NT WATTMETERS
NT WEIGHT INDICATORS
Nonintrusive ultrasonic flow measurement techniques and their applications to BTU metering
[DE87-011390] 01 p0045 N88-10286
NBS (National Bureau of Standards) calibration services users guide: Fee schedule
[PB87-210654] 01 p0090 N88-10586
The use of fiber optics in the determination of temperature and extent of reaction in detonating explosives
[DE87-012632] 01 p0094 N88-10612
Simple instrumentation for testing of ceramic superconductors
[DE87-013849] 01 p0103 N88-10672
Further development of the dynamic gas temperature measurement system 02 p0184 N88-11141
Description of a multiframe optical probing system
[DE87-014255] 02 p0236 N88-11487
Combustion control with smart sensors
[DE87-013688] 03 p0281 N88-11768
Particle velocity and stress gage measurements in spherical diverging flow
[DE87-007333] 03 p0321 N88-12033
Components for measuring robots
[KFK-PFT-126] 03 p0332 N88-12092
Proceedings of the Fifth Symposium on Energy Engineering Sciences: Instrumentation, Diagnostics, and Material Behavior
[DE88-001479] 04 p0429 N88-12680
Non-linearity in measurement systems: Evaluation method and application to microwave radiometers
04 p0433 N88-12684
Evaluation of the sensidyne toxic gas sensor for HF (Hydrogen Fluoride) vapor
[DE88-000647] 04 p0446 N88-12767
Optimization of dilatometer test procedures
[DE87-014998] 04 p0447 N88-12769
Use of electron beam instruments to determine fluctuations in vertical refraction partial angle
04 p0461 N88-12853
Computerized certification of digital ultrasonic instrumentation
[DE88-000820] 04 p0488 N88-13008
New approach to telemetry development will significantly increase productivity of Joint Test Assembly (JTA) teams
[DE88-001676] 05 p0554 N88-13373
Research for electric energy systems
[DE88-001733] 06 p0695 N88-14265
Recent advances in high temperature instrumentation for hot section applications
[NASA-TM-100282] 06 p0707 N88-14339
Quick measurement of individual stress reaction level: Development of the Emotional Stress Reaction Questionnaire (ESRQ)
[FOA-C-50050-5.3] 06 p0752 N88-14617
Investigation of the performance of a novel double crystal X-ray monochromator measurements
[PB87-125167] 06 p0788 N88-14834
Survey of electronic measurement needs below 10 MHz
[PB88-110366] 07 p0844 N88-15121
Scientific research in the field of measurement and control technology
[SMBT-322] 07 p0907 N88-15493
Fiber optics refractometer for absorption machines
[DE88-002296] 07 p0932 N88-15662
Aeropropulsion '87. Session 4: Instrumentation and Controls Research
[NASA-CP-10003-SESS-4] 08 p0955 N88-15794
Research sensors 08 p0955 N88-15795
Development of on-orbit fluid gaging techniques
08 p0982 N88-15936
Effectiveness of oceanographic method in earthquake prediction 08 p1010 N88-16124
Surface acoustic wave deposition sensor
[DE87-006527] 09 p1243 N88-17452
A technique for low level, wide range CW microwave power meter calibrations
[DE88-004147] 10 p1333 N88-17966
Into the thermosphere: The atmosphere explorers
[NASA-SP-490] 10 p1353 N88-18084
Developments in National Weather Service meteorological data collection programs as related to EPA (Environmetal Protection Agency) air pollution models
[PB88-130240] 10 p1356 N88-18104
Cleanliness tests with the Omega Meter: A comparative study for solder flux removal
[DE88-004634] 11 p1460 N88-187
LiNbO3:Ti directional-coupler modulators for high-bandwidth, single-shot instrumentation systems operating at 800 nm
[DE88-003830] 11 p1479 N88-18823
Measurement of velocity and temperature profiles in low-speed, turbulent non-isothermal flows
[PB88-155833] 11 p1486 N88-18872
Measurements as a process
[DE88-005275] 11 p1497 N88-18938
Ultrasonic testing of heat exchanger tubes
[DE88-751172] 11 p1497 N88-18939
Applications of lower cost computers to dimensional gaging
[BDX-613-3606] 11 p1525 N88-19106
Long term measurement network for FIFE
[NASA-CR-182491] 12 p1646 N88-19857

The Joint NASA/Goddard-University of Maryland Research Program in Charged Particle and High Energy Photon Detector Technology
[NASA-CR-182612] 12 p1712 N88-20247

Development of a torsion balance for adhesion measurements
[NASA-TM-100799] 13 p1748 N88-20454

Digital correlator for the portable channel prober measurement instrument
[AD-A189065] 14 p1904 N88-21377

Density measurements on solids and liquids
[PB88-164934] 15 p2036 N88-22129

A 150,000 pounds per square inch dynamic pressure calibrator
[AD-A190659] 15 p2069 N88-22335

Research sensors 15 p2085 N88-22430

Proceedings of the Lightning Threat Warning Workshop
[DE88-006607] 15 p2098 N88-22499

Development of a digital sun sensor for a spin-stabilized satellite
[INPE-4508-TDL/327] 16 p2169 N88-22929

French evaluation of Japanese biosensors
16 p2184 N88-23020

A compact high resolution piezoresistive digital tactile sensor
[DE88-000430] 16 p2210 N88-23188

Cylindrical surface profile and diameter measuring tool and method
[NASA-CASE-MFS-28287-1] 17 p2341 N88-23959

Apparatus for the measurement of resistivity of glasses and ceramics 17 p2431 N88-24460

Electrostatic discharge test apparatus
[NASA-CASE-MSC-21094-1] 18 p2518 N88-24941

Universal precision sine bar attachment
[NASA-CASE-MFS-28253-1] 18 p2523 N88-24971

A non-contact picosecond prober for integrated circuit testing 19 p2655 N88-25766

Fast GaAs photoconductive detectors with high sensitivity integrated in coplanar systems onto GaAs substrates 19 p2658 N88-25790

A technique for wing suppressed IR sampling
19 p2658 N88-25794

MESFET compatible IMSM detectors
19 p2659 N88-25801

Surface temperature thermal fluxmeters for shock tubes
[NASA-TT-20319] 20 p2762 N88-26381

Instrumentation for the measurement of penetrator dynamic response to permit force estimation
[DE88-010608] 20 p2809 N88-26666

Acoustic emission calibration instrumentation
[DE88-010817] 21 p2951 N88-27528

Components of an atmospheric lidar system
[AD-A193366] 21 p2953 N88-27539

Direct measurement of solids: High temperature sensing. Experimental development and testing of high temperature pulsed EMATs
[DE88-009659] 21 p2954 N88-27546

Atmospheric nitrogen oxides: Their detection and chemistry
[PB88-193057] 21 p2970 N88-27642

Apparent brightness of stars and lasers
22 p3065 N88-28188

A wideband, high-resolution spectrum analyzer
22 p3066 N88-28194

Langley Research Center Metrology Program status for fiscal year 1987
[NASA-TM-100651] 22 p3086 N88-28324

Aerodynamics of seeing on large transport aircraft
[NASA-CR-183122] 23 p3174 N88-28896

Skin friction balance
[NASA-CASE-LAR-13710-1] 23 p3216 N88-29145

Ice detector
[NASA-CASE-LAR-13776-1] 23 p3217 N88-29149

Liquid thickness gauge
[NASA-CASE-LAR-13826-1] 23 p3217 N88-29150

MECHANICAL DEVICES

Tape wrapping apparatus and method
[EP-PATENT-0-181-747-A2] 01 p0053 N88-10336

Mechanical design of the ac bracket package for the RETE experiment
[IFSI-87-4] 05 p0555 N88-13379

Utilization of FEP energetics
[NASA-CR-182373] 06 p0714 N88-14379

ESA Bulletin No. 10
[ETN-87-90514] 09 p1123 N88-16728

Why mechanisms are critical to spacecraft performance 09 p1125 N88-16737

Seven year thermal vacuum real life test of a medium speed (despin) mechanism manufactured by Dornier System
[ESA-ESTL-64] 09 p1175 N88-17036

A substructure method for dynamic simulation of flexible mechanical systems with geometric nonlinearities
09 p1176 N88-17044

Tactile sensing and inverse problems
[AD-A187464] 10 p1340 N88-18011

Understanding machines from text and diagrams
[AD-A189034] 13 p1755 N88-20493

Mental models of mechanical systems: Individual differences in qualitative and quantitative reasoning
[AD-A189035] 13 p1812 N88-20823

The SPOT solar array. Box opening mechanisms physical vapor deposition (PVD)-MoS2: Lubricated slides. Functional evaluation 14 p1876 N88-21211

Nonlinear analysis and optimal design of dynamic mechanical systems for spacecraft application
[AD-A190644] 15 p2026 N88-22070

A technique for measuring area under a curve
[AD-A193559] 23 p3271 N88-29463

MECHANICAL DRAWINGS
U ENGINEERING DRAWINGS

MECHANICAL DRIVES
NT PROPELLER DRIVE
NT TRANSMISSIONS (MACHINE ELEMENTS)

Improvements to the precision pan and tilt head
[RSRE-MEMO-3996] 01 p0057 N88-10365

Adaptive control of hydraulic devices
[FB-1/85] 01 p0084 N88-10543

Pulse width modulator controller design for a brushless DC motor position servo
[AD-A186618] 08 p0980 N88-15921

Why mechanisms are critical to spacecraft performance 09 p1125 N88-16737

Theoretical and experimental investigations on a linear, permanently excited stepping motor
[ETN-88-91061] 09 p1158 N88-16939

Analysis of possible transmission arrangements applicable for driving single or twin counterrotating fans on propfan engines 10 p1282 N88-17670

Hemispherical pointing mechanism drive unit --- satellite payloads antennas 14 p1874 N88-21193

Development of a cryogenic stepping drive for ISO/LWS 14 p1878 N88-21220

Qualification testing of the EUROSTAR Solar Array Drive Mechanism (SADM) 14 p1879 N88-21229

Advanced transmission studies
[NASA-TM-100867] 14 p1919 N88-21454

The 22nd Aerospace Mechanisms Symposium
[NASA-CP-2506] 14 p1924 N88-21468

Development of drive mechanism for an oscillating airfoil 14 p1926 N88-21482

A high performance inverter-fed drive system of an interior permanent magnet synchronous machine
[DE88-006753] 15 p2061 N88-22288

Evaluation of a high-torque backlash-free roller actuator 16 p2219 N88-23239

Roller drive materials performance
16 p2219 N88-23241

A microcomputer-based control and simulation of an advanced IPM (Interior Permanent Magnet) synchronous machine drive system for electric vehicle propulsion
[DE88-006735] 18 p2505 N88-24859

Optimization of planetary gears
[ETN-88-92375] 21 p2958 N88-27573

MECHANICAL ENGINEERING

National Science Foundation
[PB87-228375] 03 p0384 N88-12410

Interactions between science and precision engineering
[DE87-010873] 04 p0426 N88-12643

COLA2: A computer program for the structural synthesis of two components using general modal coordinates
[DE88-001457] 04 p0481 N88-12963

Bulletin of the Yamagata University (Engineering), Volume 20, No. 1, January 1988
[ISSN-0085-834X] 07 p0839 N88-15091

Why mechanisms are critical to spacecraft performance 09 p1125 N88-16737

Kinematic optimization of mechanisms, a finite element approach
[ISBN-90-370-0012-6] 09 p1175 N88-17039

Mechanical design and construction of a 200 mA, 100 keV, dc, negative ion accelerator
[DE88-003855] 11 p1548 N88-19257

DARM: A new deployment and retraction mechanism which does not need electric power
14 p1876 N88-21206

MECHANICAL FINGERS
U END EFFECTORS

MECHANICAL HANDS
U END EFFECTORS

MECHANICAL IMPEDANCE

Analyses by equivalent mechanical circuits of bending vibration bars with load-impedance at one end
07 p0840 N88-15093

Dynamic response of plates to moving loads: Structural impedance and finite element methods
18 p2528 N88-25000

MECHANICAL MEASUREMENT
NT DISPLACEMENT MEASUREMENT
NT DRAG MEASUREMENT
NT FLOW MEASUREMENT
NT FRICTION MEASUREMENT
NT PRESSURE MEASUREMENT
NT STRESS MEASUREMENT
NT THRUST MEASUREMENT
NT VELOCITY MEASUREMENT
NT VIBRATION MEASUREMENT
NT WIND MEASUREMENT
NT WIND VELOCITY MEASUREMENT

In-service measurements of SAAB SF-340 landing gear loads
[FFA-TN-1987-48] 15 p2018 N88-22032

MECHANICAL OSCILLATORS
NT PENDULUMS

Equivalent circuit consideration on the rotation of resonant modes of double resonant vibrators
07 p0839 N88-15092

Analyses by equivalent mechanical circuits of bending vibration bars with load-impedance at one end
07 p0840 N88-15093

MECHANICAL PROPERTIES
NT ABRASION RESISTANCE
NT AEROELASTICITY
NT ANELASTICITY
NT BRITTLENESS
NT BULK MODULUS
NT COMPRESSIBILITY
NT COMPRESSIVE STRENGTH
NT CREEP PROPERTIES
NT CREEP RUPTURE STRENGTH
NT CREEP STRENGTH
NT DIMENSIONAL STABILITY
NT DUCTILITY
NT ELASTIC PROPERTIES
NT ELASTOPLASTICITY
NT ELECTROSTRICTION
NT FATIGUE LIFE
NT FIBER STRENGTH
NT FLEXIBILITY
NT FRACTURE STRENGTH
NT HARDNESS
NT HIGH STRENGTH
NT HYDROELASTICITY
NT IMPACT STRENGTH
NT MAGNETOSTRICTION
NT MICROHARDNESS
NT MODULUS OF ELASTICITY
NT NOTCH SENSITIVITY
NT NOTCH STRENGTH
NT PHOTOELASTICITY
NT PIEZOELECTRICITY
NT PLASTIC PROPERTIES
NT POISSON RATIO
NT PROPORTIONAL LIMIT
NT SHEAR CREEP
NT SHEAR PROPERTIES
NT SHEAR STRENGTH
NT SHELL STABILITY
NT STIFFNESS
NT STRESS CYCLES
NT STRESS RELAXATION
NT STRUCTURAL STABILITY
NT SUPERPLASTICITY
NT TENSILE PROPERTIES
NT TENSILE STRENGTH
NT THERMAL RESISTANCE
NT THERMOELASTICITY
NT THERMOPLASTICITY
NT THERMOVISCOELASTICITY
NT TOUGHNESS
NT VISCOELASTICITY
NT VISCOPLASTICITY
NT WEAR RESISTANCE
NT WELD STRENGTH
NT YIELD POINT
NT YIELD STRENGTH

Structural reliability and damage tolerance of ceramic composites for high-temperature applications
[PB87-208310] 01 p0019 N88-10119

Mechanical properties characterization of composite sandwich materials intended for space antenna applications
[NASA-TM-88893] 01 p0020 N88-10121

Development of ultrafine grains and related properties in Hadfield manganese steels
[DE87-011884] 01 p0024 N88-10154

Evaluation of mechanical and technological parameters of different steel states by nondestructive micro- and macromagnetic measuring quantities as well as ultrasonic techniques
[MPA-810-079] 01 p0057 N88-10366

An experimental and theoretical study of the bending behavior of Kevlar 49/epoxy beams and rings
[DE87-010430] 01 p0061 N88-10394

Measurement of agglomerate strength distributions in agglomerated powders
[DE87-013605] 01 p0090 N88-10591

Colloidal structure of bitumens. Relationship between composition-structure behavior
[PC-4] 02 p0146 N88-10912

Needs assessment for nondestructive testing and materials characterization for improved reliability in structural ceramics for heat engines
[DE88-000040] 02 p0153 N88-10957

Study of the micromechanical behavior of a SiO2-Al2O3-Li2O glass ceramic and its relation to the microstructure
[ISAL-ITC1-87-01] 02 p0153 N88-10960

Elevated temperature strain gages
02 p0184 N88-11144

Effect of irradiation on the tensile properties of niobium-base alloys
[DE87-002409] 03 p0285 N88-11790

Development and application of composites
03 p0286 N88-11795

Low activation ferritic alloys for nuclear fusion reactors
[DE87-010711] 03 p0286 N88-11801

Birch's law and the properties of high temperature fluid metals
[DE87-014744] 03 p0288 N88-11807

Modified 14Cr-16Ni stainless steels with improved creep resistance at 700 C due to tailored precipitate microstructures
[DE87-014788] 03 p0290 N88-11825

Microstructural characterization of irradiated PWR steels using the atom probe field-ion microscope
[DE88-000341] 03 p0291 N88-11828

High temperature characterization of ceramic materials
[REPT-NT-3403] 03 p0292 N88-11837

Indentation damage in ceramics
[AD-A184686] 03 p0294 N88-11844

Joining of silicon carbide reinforced ceramics
[DE87-014861] 03 p0294 N88-11847

Wittig synthesis of conductive segmented block polymer compositions
[AD-A184018] 03 p0295 N88-11850

Effects of cure pressure on resin flow, voids, and mechanical properties
[AD-A184267] 03 p0295 N88-11853

Status of titanium alloys R and D described
03 p0298 N88-11876

Gas tungsten arc welding of Al-10Fe-5Ce
[AD-A184202] 03 p0334 N88-12104

Investigation of reliability of strength values measured on CFRP test bars by statistical methods. Part 1: Probability distributions for strength analysis
[ESA-TT-1036] 03 p0336 N88-12115

Scaling of size/time/temperature associated with dilatation and distortion in uniaxial specimens
03 p0336 N88-12117

Materials studies for magnetic fusion energy applications at low temperatures-X
[PB87-232575] 03 p0381 N88-12395

Research and development on high strength ceramic heaters discussed 04 p0404 N88-12508

Parachute materials
[DE87-014845] 04 p0411 N88-12550

Mechanical properties of a microalloyed steel with high niobium content
[DE87-703545] 04 p0415 N88-12572

Mechanical properties of an acicular ferrite steel microalloyed to niobium and vanadium
[DE87-703547] 04 p0415 N88-12574

Mechanical strength and niobium and niobium-base alloys substructures
[DE87-703692] 04 p0415 N88-12577

Effects of stress-relieving on the mechanical properties and the structure of specimens of high-temperature fine-grained structural steels heat-treated to simulate welding
[BLL-CE-TRANS-8258-(9022.09)]
04 p0417 N88-12586

The aging behavior of types 308 and 308CRE stainless steels and its effect on mechanical properties
[DE87-012541] 04 p0417 N88-12590

Development of advanced fiber reinforced ceramics
[DE88-000779] 04 p0420 N88-12604

Thermomechanical cracking in coated media due to high speed asperity excitation
[AD-A184176] 04 p0454 N88-12809

Micromechanics of the degradation of composite materials
[SNIAS-872-430-113] 05 p0559 N88-13405

Mechanical property evaluation of a series of commercial tungsten alloys
[AD-A185440] 05 p0565 N88-13446

The evolution of local mechanical properties of Al 2219-T851 during fatigue 05 p0598 N88-13653

An investigation of physical properties of thermoplastic polyimides
[NASA-TM-100530] 06 p0678 N88-14151

Study of surface treatment before bonding of light alloys
[DCQ/L-48-287/F] 06 p0682 N88-14181

Development of strength in cements
[PB87-232971] 06 p0684 N88-14189

The effective elastic properties of low-density foams
[DE87-014629] 06 p0684 N88-14194

Characterization of mechanical damage mechanisms in ceramic composite materials
[AD-A185549] 06 p0686 N88-14205

Waves and vibrations in elastic superlattice composites 06 p0776 N88-14765

Precipitation in alumina-rich spinel: A transformation-toughened ceramic single crystal
[DE87-012380] 06 p0785 N88-14815

Natural frequencies and structural integrity assessment of large space structures
[AD-A186139] 07 p0824 N88-15001

Interface effects on the mechanical properties of ceramic composites
[AD-A185899] 07 p0826 N88-15009

Composite reliability enhancement via preloading
[AD-A185938] 07 p0826 N88-15010

Characterization of current steels. The 35 NCD 16 alloy in 30 mm diam laminated bars made by Aubert and Duval
[CEAT-41/N/76] 07 p0832 N88-15046

Microstructural observations of the Sn-Pb solder/Cu system and thermal fatigue of the solder joint
[DE88-001392] 07 p0832 N88-15048

Study on substructures of martensite in steels containing rare earth metals
[PB87-143996] 07 p0833 N88-15050

Method of obtaining of fire resistant polyacrylonitrile fiber or cloth from it
[AD-A185941] 07 p0836 N88-15071

Center for the Space Processing of Engineering Materials 07 p0838 N88-15083

Weldability of a leaded carbon steel
[PB88-110341] 07 p0861 N88-15225

Computer-aided analysis for the Mechanics of Granular Materials (MGM) experiment, part 2
07 p0925 N88-15626

Effects of aviation fluids on fiber composite material
[FOA-C-20674-2.6] 08 p0965 N88-15840

Interface characteristics and the mechanical properties of metal matrix composites
[AD-A186441] 08 p0966 N88-15845

Methods of improving compacting quality of intricately shaped powder components
[BLL-M-37412-(5828.4)] 08 p0968 N88-15859

Kinetics and mechanism of thermal aging embrittlement of duplex stainless steels
[DE88-002987] 08 p0969 N88-15866

Mechanical properties of steel-to-steel adhesive bonds
[PB88-111299] 08 p0971 N88-15877

Laser transformation hardening of precision V-slide way
[PB87-144028] 08 p0991 N88-15999

Solid mechanics research for quantitative non-destructive evaluation
[AD-A186599] 08 p0993 N88-16010

Group 2A metastable collision complexes: Spectroscopy and behavior in intense radiation fields
[AD-A186737] 08 p1082 N88-16524

High temperature polymer matrix composites
09 p1119 N88-16700

Sublaminate damage mechanisms in composite structures
[AD-A186807] 09 p1137 N88-16815

Study of the temperature dependence of the mechanical characteristics of the steels GX 5 CrNi 13 4 and GGG 40 in tensile and bending tests
[DE88-001469] 09 p1143 N88-16850

Correlations of norbornenyl crosslinked polyimide resin structures with resin thermo-oxidative stability, resin glass transition temperature and composite initial mechanical properties
[NASA-TM-100791] 09 p1147 N88-16877

Residual stiffness and strength of Kevlar/epoxy laminated impulsively loaded to 7.9 ktaps
[DE88-003724] 09 p1149 N88-16886

Detection of hydrogen-assisted-cracking in U-0.8Ti alloy weldments by acoustic emission monitoring
[DE88-003221] 09 p1184 N88-17093

Effect of post-cure heat-treatment on static and fatigue behaviour of XAS-914C carbon fibre composite
[AD-A186943] 10 p1294 N88-17735

Mechanics of composite materials: Past, present and future
[NASA-TM-100793] 10 p1295 N88-17744

Influence of non-metallic elements in the mechanical properties of 20 Mn Mo Ni 55 steel
[DE88-700412] 10 p1300 N88-17775

Effects of the neutron spectrum on mechanical property changes in low dose irradiations
[DE88-003429] 10 p1302 N88-17786

The role of composition and microstructure gradients on weld metal properties and behavior
[DE88-004956] 10 p1303 N88-17791

Bias, internal stress and substrate effects on the microstructure and properties of PVD-wear resistant coatings
[AERE-R-12360] 10 p1304 N88-17796

Adhesion, friction and micromechanical properties of ceramics
[NASA-TM-100782] 10 p1305 N88-17801

Mechanisms of wear in single- and two-phase materials
[DE88-003846] 10 p1306 N88-17806

Physical and structural characteristics of Weddell Sea pack ice
[AD-A188189] 10 p1358 N88-18119

Study of the mechanical behavior of a 2-D carbon-carbon composite
[NASA-CR-182594] 11 p1451 N88-18649

Fracture mechanisms and strengthening of slab lasers
[DE88-004002] 11 p1493 N88-18914

The place for thermoplastic composites in structural components
[AD-A189149] 12 p1604 N88-19586

An interdisciplinary approach to predictive modeling of structural adhesive bonding: Factors affecting the durability of titanium/epoxy bonds
[AD-A189503] 12 p1611 N88-19636

Advanced durability analysis. Volume 1: Analytical methods
[AD-A188341] 12 p1635 N88-19789

Nonaxisymmetric body supersonic, aerodynamic prediction
[AD-A189338] 13 p1716 N88-20259

Viscoelastic behavior of a polyetheretherketone (PEEK) composite
[AD-A189545] 13 p1734 N88-20368

The influence of the fiber-matrix bond on the mechanical behavior of NICALON/SiC composites
[DE88-006155] 13 p1734 N88-20369

A fundamental understanding of the effect of alloying elements on the corrosion resistance of rapidly solidified Mg alloys
[AD-A189385] 13 p1741 N88-20413

Gordon Conference on Intermetallic Compounds held at Tilton, New Hampshire on 20-24 July 1987
[AD-A188502] 13 p1745 N88-20435

PNL-1 improved ceramic composites through controlled fiber matrix interaction
[DE88-005680] 13 p1750 N88-20462

Analysis of shell-type structures subjected to time-dependent mechanical and thermal loading
[NASA-CR-182705] 13 p1783 N88-20688

Mechanical properties of sea ice and sea ice deformation in the near-shore zone
[PB88-147889] 13 p1804 N88-20782

On the structure of pulsed plasma jets
13 p1843 N88-21030

Exploring the relation between interface structure and mechanical properties in multilayer structures
[DE88-005428] 13 p1848 N88-21060

Static mechanical properties of 30 x 11.5 - 14.5, type 8 aircraft tires of bias-ply and radial-belted design
[NASA-TP-2810] 14 p1867 N88-21157

Influence of heat treatment on the properties of boroaluminum 14 p1886 N88-21270

Processing, texture and mechanical properties of sintered silicon carbide
[NASA-TT-20253] 14 p1893 N88-21305

Effect of oxidation on strength and thermal stability of material based on Si3N4 14 p1896 N88-21319

Statistical analysis of feasibility of non-destructive inspection of mechanical properties of hot worked pipes of alloy steels
[BLL-M-37598-(5828.4)] 14 p1922 N88-21455

Applications of elastic-viscoplastic constitutive models in dynamic analyses of crack run-arrest events
14 p1930 N88-21507

High temperature materials: What's available
[AERE-R-12632] 15 p2028 N88-22081

Galvanic corrosion initiatives
[AD-A190658] 15 p2040 N88-22155

Transformation toughening of ceramics
[AD-A190399] 15 p2045 N88-22183

Mechanical behaviour of particle filled thermoplastics
[PB88-169297] 15 p2047 N88-22196

Hafnia-rich mixed oxide ceramics of the system HfO2-ZrO2-TiO2 for heaters and heat exchangers in electrothermal thrusters. The effects of titania on selected electrical and mechanical properties of Hafnia-rich mixed oxides in the system Hafnia-Zirconia-Titania, volume 1
[NASA-CR-182800-VOL-1] 15 p2047 N88-22197

Developments in ceramic superconducting materials
15 p2052 N88-22229

Features and applications of the integrated composites analyzer (ICAN) code 15 p2078 N88-22391

Structural decomposition of multiple time scale Markov processes
[AD-A189739] 15 p2123 N88-22657

Experimental studies on electronic properties of HgTe/CdTe and Hg sub 1-x Cd sub x Te/CdTe heterostructures and superlattices
[AD-A189826] 15 p2142 N88-22783

Fundamental studies of the mechanical behavior of microelectronic thin film materials
[AD-A190038] 15 p2143 N88-22786

Delamination analysis in crossed layer composites
[REPT-48-447/F] 16 p2171 N88-22942

Test procedures and standards for mechanical property measurements on metal matrix composites
[NPL-DMA(A)-153] 16 p2172 N88-22944

Thermoviscoelastic characterization and predictions of Kevlar/epoxy composite laminates
[NASA-CR-182878] 16 p2172 N88-22946

Strength and failure rate of composite materials with carbon in ceramic matrix 16 p2180 N88-22995

Small-scale cleavage test of polymer products
[PB88-165360] 16 p2181 N88-23001

Seasonal variation for structural strength value
[PB88-169248] 16 p2222 N88-23260

Technology Reports of Kyushu University, volume 61, no. 2
[ISSN-0023-2718] 16 p2256 N88-23485

Travelling wave concepts for the modeling and control of space structures
[AD-A191235] 17 p2310 N88-23819

Structural ceramics research
17 p2324 N88-23878

Improved silicon carbide for advanced heat engines
17 p2324 N88-23879

Improved silicon nitride for advanced heat engines
17 p2324 N88-23881

Improved processing of Si3N4
17 p2325 N88-23882

Colloidal characterization of silicon nitride and silicon carbide 17 p2325 N88-23883

SiC fiber analysis 17 p2326 N88-23891

Improved GaP doped SiGe thermoelectric material
17 p2437 N88-24503

Carbon matrix composites prospective roles for biotechnology 18 p2477 N88-24694

Interaction of ultrasonic waves with composite plates
[AD-A191879] 18 p2478 N88-24702

Fundamental studies of beta phase decomposition modes in titanium alloys
[AD-A191495] 18 p2485 N88-24740

Environment assisted degradation mechanisms in advanced light metals
[NASA-CR-182907] 18 p2486 N88-24746

Characterization of 7090 and 7091 profiles made with Cegedur powder --- powder metallurgy, aircraft construction materials
[REPT-48-441/F] 18 p2487 N88-24752

Effect of size of precipitates on recrystallization temperatures in Cu-Cr, Cu-Zr, and Cu-Zr-Cr alloys
[NASA-TT-20166] 18 p2489 N88-24763

Stress measurements in graphite fibers by laser raman spectroscopy
[AD-A191710] 18 p2491 N88-24779

The influence of the chemical nature of resins on their reticulation kinetics and the consequences for their nonelastic mechanical properties
[ETN-88-92539] 18 p2493 N88-24788

Characterization of aluminum/RP-1 gel propellant properties
[NASA-TM-100951] 18 p2496 N88-24808

Microlaminate composite structures by low pressure plasma spray deposition
[DE88-006453] 19 p2610 N88-25488

Nondestructive evaluation methods for determination of thermal history and mechanical properties of aluminum-lithium alloys
[DE88-007352] 19 p2615 N88-25516

Optimization of mechanical/corrosion properties of TI-CODE 12 plate and sheet. Part 2: Thermomechanical processing effects
[DE88-007493] 19 p2616 N88-25517

Extended ductility of Al and alpha-Fe alloys through dynamic recovery mechanisms
[DE88-008679] 19 p2616 N88-25522

Development of fine-grained carbide-particle hardened Hadfield manganese steels
[DE88-008919] 19 p2617 N88-25523

Dimensional analysis and experimental observation of the coupling phenomena between cnmbustion and fracture of damaged propellant samples
19 p2630 N88-25603

Interface modification in Nicalon (trademark)/SiC composites
[DE88-009708] 20 p2767 N88-26409

A constitutive model with damage for high-temperature superalloys 20 p2771 N88-26434

Phase stability and alloy design of ordered intermetallics
[DE88-007479] 20 p2772 N88-26435

Investigation of structure and surface state effect on hydrogen embrittlement of steels, under consideration of acoustic emission analysis
[ETN-88-92350] 20 p2775 N88-26457

Application of electron microscopy for the analysis of the mechanical behavior of advanced ceramics
[DE88-005049] 20 p2777 N88-26469

Resistance of polyamide-6 against long time effects of various media at various temperatures
[NASA-TT-20297] 20 p2779 N88-26484

Polymerization of epoxy matrix composites using pulsed microwaves
[CERT-3/1324-MO] 20 p2780 N88-26487

A finite element analysis for the hydroforming of aluminum
[DE88-008050] 20 p2784 N88-26516

Electrodynamic driver for the space thermoacoustic refrigerator (STAR)
[AD-A192337] 20 p2785 N88-26517

Research on the kinetics of phase changes in solids
[AD-A192222] 20 p2814 N88-26696

Analysis of transverse strength of composites using percolation theory
[AD-A193204] 21 p2904 N88-27234

Fabrication of SiC fiber reinforced glass matrix by extrusion process and investigation of its mechanical properties
[ETN-88-92367] 21 p2906 N88-27244

Rocket motor case materials. An evaluation of new fibers for composites
[FOA-C-20696-2.1] 21 p2906 N88-27245

Factors affecting strength in composite materials used for aircraft
[DT-212/87] 21 p2907 N88-27248

Development of high strength and toughness microcomposite HSLA Fe/Cr/Mn/C steel with and without Nb
[DE88-009813] 21 p2913 N88-27290

Thin film and near-surface characterization using a mechanical properties microprobe
[DE88-011399] 21 p2915 N88-27302

Superconducting oxides with high critical temperatures
21 p2930 N88-27392

FEB (Multifilter Electronics Box) lifting device analysis, revision A
[AD-A192313] 21 p2935 N88-27427

The influence of weld metal properties, weld geometry and applied load on weld system performance
[AD-A193403] 21 p2961 N88-27588

Corrosion fatigue of small cracks: Mechanics and chemistry
[DE88-012121] 21 p2964 N88-27605

Durability of continuous fiber reinforced metal matrix composites
[AD-A193868] 22 p3050 N88-28097

An endochronic rate-sensitive constitutive equation for metals, application to generalized creep and large deformations
[AD-A194167] 22 p3055 N88-28125

An investigation into the metallurgical aspects of joining rapidly-solidified aluminum alloys
[AD-A194677] 23 p3194 N88-29009

Relation between strength, creep and relaxation behavior in Cu and Al at room temperature
[ETN-88-92982] 23 p3195 N88-29015

Thin film-residual stress assessment
[AD-A193205] 23 p3196 N88-29018

The mechanical behavior of surface modified ceramics
[DE88-010564] 23 p3196 N88-29022

Experimental investigation of the effects of underwater exposure on the damping characteristics of bolted structural connections for plates and shells
[AD-A194486] 23 p3226 N88-29200

Fatigue crack growth characteristics of ARALL (trademark)-1
[AD-A196185] 24 p3341 N88-29889

Attenuated total reflectance FT-IR spectroscopy to measure interfacial reaction kinetics at silica surfaces
[AD-A196330] 24 p3344 N88-29908

Additional fracture and strength test results for A723 steel and 38644 titanium
[AD-A196329] 24 p3353 N88-29960

Initial value problems in viscoelasticity
[AD-A196052] 24 p3382 N88-30145

MECHANICAL RESONANCE
U RESONANT VIBRATION

MECHANICAL SHOCK

Requirements for the calibration of mechanical shock transducers
[PB87-227591] 03 p0325 N88-12054

Mechanical shock test specification using nonstationary random excitation models
[DE87-013650] 04 p0454 N88-12812

The 58th Shock and Vibration Symposium, volume 1
[NASA-CP-2488-VOL-1] 05 p0592 N88-13609

Conservatism implications of shock test tailoring for multiple design environments 05 p0592 N88-13611

Scaling the electromagnetically driven explosive shock simulator 05 p0592 N88-13612

Initial dynamic load estimates during configuration design 05 p0593 N88-13621

Optimal shock isolation with minimum settling time
05 p0595 N88-13633

The Shock and Vibration Digest, Volume 20, No. 1
08 p0975 N88-15897

The Shock and Vibration Bulletin. Part 4: Structural Dynamics and Modal Test and Analysis
[AD-A186751] 09 p1179 N88-17062

The Shock and Vibration Digest, volume 20, no. 2
10 p1417 N88-18459

Design and dynamic testing of an instrumented spacecraft component 11 p1499 N88-18952

The Shock and Vibration Digest, volume 20, no. 4
17 p2391 N88-24214

Peak Acceleration Device (PAD)
[AD-A191639] 18 p2461 N88-24611

Selective weathering of shocked minerals and chondritic enrichment of the Martian fines
23 p3301 N88-29660

MECHANIZATION

Ultrasonic mechanized checking of weld joints of nuclear power plant equipment 02 p0158 N88-10987

MEDIA
NT ANISOTROPIC FLUIDS
NT ANISOTROPIC MEDIA
NT ELASTIC MEDIA
NT INTERGALACTIC MEDIA
NT INTERPLANETARY DUST
NT INTERPLANETARY GAS
NT INTERPLANETARY MEDIUM
NT ZODIACAL DUST

Mathematical problems of nonlinear wave propagation and of waves in heterogeneous media
[AD-A195970] 24 p3368 N88-30057

MEDIAN (STATISTICS)

PROGRESS: A program for robust regression analysis on the IBM PC
[REPT-85-14] 01 p0088 N88-10576

Embedding topological median algebras in products of dendrons
[PB88-100888] 06 p0767 N88-14713

Contour interactive extraction using image numerical treatment
[ISL-R-114/86] 15 p2113 N88-22587

MEDICAL EQUIPMENT
NT ENDOSCOPES
NT PROSTHETIC DEVICES
NT X RAY APPARATUS
NT X RAY TUBES

Spinoff, 1987
[NASA-TM-89652] 02 p0250 N88-11577

Photonic temperature and pressure sensors for biosystems/pulsed microwave. Part 1: Interaction studies
[AD-A188887] 12 p1629 N88-19751

Low altitude remote sensing data in the implementation of a mathematical model for the planning of urban equipment networks 17 p2363 N88-24074

Analysis of annular microstrip antennas for hyperthermic applicators
[PB88-181508] 19 p2643 N88-25679

Miniature radiation dosimeter for in vivo radiation measurements 19 p2672 N88-25889

MEDICAL PERSONNEL

Satellite communications experiment for the Ontario air ambulance service 19 p2646 N88-25705

Central serous chorioretinopathy in USAF aviators: A review
[AD-A195697] 24 p3407 N88-30280

MEDICAL PHENOMENA

Experience in occupational medicine, derived from 16 operational deep saturation trimix 5 dives in GUSI from 150 to 600 m 19 p2695 N88-26018

MEDICAL SCIENCE
NT CARDIOLOGY
NT CLINICAL MEDICINE
NT ENDOCRINOLOGY
NT EPIDEMIOLOGY
NT HISTOLOGY
NT HUMAN PATHOLOGY
NT IMMUNOLOGY
NT NEUROLOGY
NT NEUROPSYCHIATRY
NT NUCLEAR MEDICINE
NT OPHTHALMOLOGY
NT PATHOLOGY
NT PSYCHIATRY
NT RADIOBIOLOGY
USSR report: Life sciences. Biomedical and behavioral sciences
[JPRS-UBB-86-022] 08 p1046 N88-16318
Using IMSL mathematical and statistical computer subroutines in physiological and biomechanical research
[AD-A192594] 21 p2995 N88-27765
The NBS/NRL (National Bureau of Standards/Naval Research Laboratory) free electron laser facility
[AD-A194214] 23 p3219 N88-29159
Vanderbilt free electron laser project in biomedical and materials research
[AD-A195961] 24 p3378 N88-30121
MEDICAL SERVICES
Safety study: Commercial emergency medical service helicopter operation
[PB88-917001] 12 p1575 N88-19422
Satellite communications experiment for the Ontario air ambulance service 19 p2646 N88-25705
Activities report in aerospace medicine
[ETN-88-92906] 23 p3240 N88-29283
MEDITERRANEAN SEA
NT ADRIATIC SEA
Accuracy of GPS surveying technique and its possible application to the Wegener project --- Mediterranean tectonics
[REPT-85.3] 01 p0063 N88-10407
Large balloon development and trans-Mediterranean flights 08 p1030 N88-16239
Italian activities in ocean colour remote sensing
08 p1043 N88-16304
US Navy climatic study of the Mediterranean Sea
[AD-A188264] 10 p1356 N88-18107
The physical oceanography of the Alboran Sea
[AD-A189027] 12 p1650 N88-19880
Deep water mass circulation in the Alboran Basin. Measurements - January to April 1982: ALBORAN 2
[AD-A189205] 13 p1803 N88-20777
The interpretation of crustal dynamics data in terms of plate interactions and active tectonics of the Anatolian Plate and surrounding regions in the Middle East
[NASA-CR-183024] 18 p2543 N88-25092
MEETINGS
U CONFERENCES
MEGALOPOLISES
Spread of large tropical conurbations
22 p3098 N88-28398
MEISSNER EFFECT
U DIAMAGNETISM
U SUPERCONDUCTIVITY
MELLIN TRANSFORMS
Theory of the generalized Abel integral equations
[ETN-88-91086] 09 p1229 N88-17362
MELT SPINNING
Development of metastable processing paths for high temperature alloys
[AD-A188682] 12 p1608 N88-19617
Hydrodynamic simulation of forced convection in the Czochralski process
[INPE-4471-TDL/323] 12 p1697 N88-20158
MELTING
NT ARC MELTING
NT FUSION (MELTING)
NT VACUUM MELTING
Formation of amorphous alloys by solid state reactions
[DE87-013175] 02 p0146 N88-10918
Thermodynamics of interaction between nitrogen and molten nickel alloys
[BLL-M-37309-(5828.4)] 02 p0149 N88-10934
Shock-induced melting and rapid solidification
[DE88-000226] 03 p0288 N88-11810
Data base on the high heat flux behaviour of metals and carbon materials for plasma facing components: Experiments at the 10 MW neutral beam injection test stand of the IPP Nagoya
[IPPJ-AM-53] 04 p0492 N88-13031
Advances in processing techniques for nickel aluminides
[DE87-014571] 05 p0566 N88-13449
Statistical process control applied to the liquid-fed ceramic melter process
[DE88-000271] 05 p0569 N88-13471
Results from the melting of tungsten composites under microgravity (TEXUS 10 flight)
[FOA-C-20676-2.1] 05 p0571 N88-13482
Exploitation of the sol-gel route in processing of ceramics and composites
[AD-A185482] 06 p0686 N88-14204
Radar reflectivity and attenuation of radio waves in the melting layer of precipitation
[PB88-121553] 10 p1318 N88-17882
Mesoscale monitoring of the soil freeze/thaw boundary from orbital microwave radiometry
[NASA-CR-182659] 12 p1645 N88-19855
Integral equation theory of homopolymer melts
[DE88-005304] 13 p1751 N88-20470
Rapid e-beam heating for measuring thermodynamics of metastable materials
[DE88-003565] 13 p1849 N88-21066
Laser surface melting
[BMFT-FB-T-86-072] 14 p1914 N88-21435
Brillouin scattering and transmission electron microscopy studies of radiation-induced elastic softening, disordering and amorphization of intermetallic compounds
[DE88-005927] 14 p1987 N88-21850
On rotating sphere-on-a-plate experiments and the questions of whether high angle grain boundaries melt below bulk melting temperatures
[DE88-006627] 15 p2038 N88-22142
Directed-energy electron-beam processing of a hypoeutectic Cr90Ta10 alloy
[DE88-005621] 15 p2040 N88-22157
Melt processing ceramic YBa2Cu3O(sub 6.9)
[DE88-007039] 15 p2047 N88-22198
Microgravity thaw experiment (MITEX)
17 p2427 N88-24439
The viscosity of molten TNT
[MRL-R-1100] 19 p2622 N88-25553
Component stress during freeze/thaw cycling
[DE88-011204] 21 p2938 N88-27449
Effect of thermal cycling on CSPL (Chloride Silent Power Ltd.) sodium/sulfur cells
[DE88-011205] 21 p2939 N88-27455
Theory of surface melting and non-melting
[DE88-702652] 22 p3157 N88-28785
Initiation of explosive molten aluminum-water interactions at wet or underwater surfaces
[DE88-004686] 23 p3194 N88-29006
Evidence of the in situ decay of Al-26 in a Semarkona chondrule 24 p3441 N88-30479
MELTING POINTS
The use of alloy 117 as a liquid metal current collector
[AD-A185740] 06 p0698 N88-14281
Determination of the melting and decomposition points of different materials in an oxygen stream
[INFORME-I-158/86] 09 p1142 N88-16844
Research and development to acquire and reduce melting layer cloud physics and evaluate a prototype M-meter
[AD-A188390] 12 p1648 N88-19873
Processing of glass to aluminum (low melting metals) seals via an injection molding technique
[DE88-004689] 13 p1751 N88-20468
The crystallization of tough thermoplastic resins in the presence of carbon fibers
[NASA-CR-182984] 20 p2776 N88-26464
MELTS (CRYSTAL GROWTH)
NT CONTAINERLESS MELTS
NT IMPACT MELTS
NT MELT SPINNING
Raman spectroscopic investigations of Hg-Cd-Te melts 07 p0926 N88-15625
Investigation of defect and electronic interactions associated with GaAs device processing
[AD-A188021] 11 p1556 N88-19313
Real time thermal imaging of high temperature semiconductor melts 17 p2330 N88-23914
A review of melt and vapor growth techniques for polydiacetylene thin films for nonlinear optical applications
[NASA-TM-100340] 24 p3430 N88-30412
MEMBRANE ANALOGY
U MEMBRANE STRUCTURES
U STRUCTURAL ANALYSIS
MEMBRANE STRUCTURES
NT SKIN (STRUCTURAL MEMBER)
Large change-of-curvature effects in quadratic finite elements for CAD of membrane structures
04 p0480 N88-12958
Optimization of the southern electrophoretic transfer method
[DE88-004527] 10 p1299 N88-17765
Use of nonporous metals membranes for the separation of hydrogen from gas mixtures
[BMFT-FB-T-86-206] 14 p1888 N88-21280
MEMBRANE THEORY
U STRUCTURAL ANALYSIS
MEMBRANES
NT ION EXCHANGE MEMBRANE ELECTROLYTES
NT MEMBRANE STRUCTURES
NT SKIN (STRUCTURAL MEMBER)
Membrane heat pipe development for space radiator applications
[DE86-006015] 01 p0045 N88-10285
Rheological behaviors of an elastomeric membrane
[DE87-013105] 01 p0061 N88-10392
Photocatalytic electrochemistry at a biological-membrane metal-colloid interface
[DE87-009122] 02 p0166 N88-11041
Investigation of structure-permeability relationships of silicone polymer membranes
[PB87-230181] 03 p0293 N88-11839
Vapor compression distiller and membrane technology for water revitalization 03 p0359 N88-12262
The formation of optical membrane reflector surfaces using uniform pressure loading
[DE87-012275] 03 p0376 N88-12367
Novel macrocyclic carriers for proton-coupled liquid membrane transport
[DE88-000636] 04 p0413 N88-12560
Photochemical solar energy conversion utilizing semiconductors localized in membrane mimetic systems
[DE88-002887] 10 p1349 N88-18065
Critical phenomena and electromagnetic effects in biological membranes
[AD-A188156] 11 p1518 N88-19064
Molecular and electronic mechanism in the control of Na+ and K+ permeability of excitable cell membrane by ligand binding on receptor sites
[AD-A188725] 13 p1808 N88-20805
Enzyme-based fiber optic sensors
[DE88-005674] 13 p1840 N88-21013
Synthesis and analysis of novel polymers with potential for providing both high permselectivity and permeability in gas separation applications
[DE88-006533] 15 p2043 N88-22174
Mechanisms of gas permeation through polymer membranes: Renewal proposal for period December 1, 1986 - November 30, 1989
[DE88-007436] 18 p2494 N88-24796
The flying characteristics of the membrane slider bearing 18 p2522 N88-24965
Employment of porous polytetrafluoroethylene Membrane with a hydrophilic and hydrophobic strata structure for construction of an enzyme electrode
[NASA-TT-20296] 19 p2620 N88-25543
Chemical multisensors with selective encapsulation of ion-selective membranes 19 p2670 N88-25869
Air loading effects on a capacitively sensed membrane supported silicon accelerometer
19 p2672 N88-25886
Optical evaluation of prototype stretched-membrane mirror modules for solar central receivers
[DE88-011884] 21 p2969 N88-27637
Factors governing light driven electron and proton translocation in proteins across membranes
[DE88-011120] 21 p2984 N88-27724
Hyperthermia: New thoughts on an old problem
[AD-A192602] 21 p2986 N88-27731
Method of forming dynamic membrane on stainless steel support
[NASA-CASE-MSC-18172-3] 23 p3201 N88-29052
Hydrogen concentration cells as converters of heat into electricity
[DE88-009662] 23 p3229 N88-29216
Design criteria for extraction with chemical reaction and liquid membrane permeation
[NASA-TT-20352] 24 p3343 N88-29890
MEMORY
A learning model as a basis for investigations of the effects of gravity on the learning processes and memory formulation 07 p0886 N88-15374
Stability, reliability and cross-mode correlations of tests in a recommended 8-minute performance assessment battery
[NASA-CR-172039] 08 p1052 N88-16351
Relationship of encoding speed and memory tests to flight training performance
[AD-A190670] 15 p2105 N88-22539
On categorizing sounds
[AD-A189784] 15 p2129 N88-22700
Short-term memory load and pronunciation rate
16 p2241 N88-23386
Processing deficits in monitoring analog and digital displays: Implications for attentional theory and mental-state estimation research
16 p2241 N88-23390

Information processing deficits in psychiatric populations: Implications for normal workload assessment 16 p2241 N88-23390
Working memory capacity: An individual differences approach [AD-A192359] 20 p2833 N88-26803
Cognitive and neural bases of skilled performance [AD-A193392] 21 p2992 N88-27747
Skilled memory and expertise: Mechanisms of exceptional performance [AD-A193829] 22 p3133 N88-28628
Thermocouple for heating and cooling of memory metal actuators [NASA-CASE-NPO-17068-1-CU] 23 p3217 N88-29151
Analysis of the hopfield neural networks and their application to pattern recognition [AD-A193827] 23 p3239 N88-29279
Transformations of short-term visual memory [AD-A193873] 23 p3241 N88-29290
Nested neural networks [NASA-TM-101032] 24 p3423 N88-30373

MEMORY (COMPUTERS)
Memory systems for single bus multiprocessor architecture. Application to the SCQM system [ENST-86E022] 02 p0219 N88-11379
Hardware-assisted multiprocessor performance measurements [PB87-226908] 03 p0363 N88-12262
General potential surfaces and neural networks [AD-A184484] 03 p0367 N88-12311
Least squares linear lags and limited memory filters [NASA-CR-178381] 03 p0372 N88-12339
An approach to implementing state space searches on heterogeneous systems of multiprocessors [DE88-001321] 04 p0482 N88-12967
A rudimentary database for three-dimensional objects using structural representation [CSE-87-00004] 05 p0590 N88-13597
Storing and retrieving data in a parallel distributed memory system [AD-A185177] 05 p0637 N88-13897
Recording materials for optical disk memory discussed 06 p0684 N88-14193
A comparison of the Cray-2 performance before and after the installation of memory pseudo-banking [NASA-CR-177462] 09 p1215 N88-17287
The effectiveness of caches and data prefetch buffers in large-scale shared memory multiprocessors [DE88-003594] 09 p1223 N88-17334
Research and development trends for memory hierarchies --- cache memories 10 p1374 N88-18198
Vector performance of register-to-register vector computers [DE88-004013] 10 p1384 N88-18265
The impact of hierarchical memory systems on linear algebra algorithm design [DE88-003574] 10 p1385 N88-18274
Debugging FORTRAN on a shared memory machine [DE88-003589] 10 p1386 N88-18276
Using program structure to achieve prefetching for cache memories [DE88-003599] 10 p1387 N88-18282
The performance of software-managed multiprocessor caches on parallel numerical programs [DE88-003590] 10 p1393 N88-18308
Data prefetching in shared memory multiprocessors [DE88-003576] 10 p1394 N88-18314
Measurement and analysis of memory conflicts on vector multiprocessors [AD-A188206] 11 p1525 N88-19104
A shared memory algorithm and proof for the alternative construct in CSP (Communicating Sequential Processes) [AD-A187820] 11 p1533 N88-19156
Gaussian techniques on shared memory multiprocessor computers [DE88-005426] 13 p1817 N88-20855
Implementation and evaluation of a combined test-error correction procedure for memories with defects [EUT-87-E-169] 14 p1955 N88-21651
Characteristics of LSI-wiring expert system discussed 15 p2052 N88-22226
Application of static memory for data acquisition and transmission into a computer [DE88-701491] 15 p2106 N88-22544
Coding for write-unidirectional memories and conflict resolution [ENST-87C005] 16 p2245 N88-23408
Effective use of shared memory multiprocessors [DE88-007019] 18 p2560 N88-25195
On the implementation of applicative on shared-memory, MIMD multiprocessors [DE88-005367] 19 p2718 N88-26136
Content-addressable memory storage by neural networks: A general model and global Liapunov method [AD-A192716] 21 p3002 N88-27807
Large-grain pipelining on distributed-memory multiprocessors [DE88-009974] 23 p3264 N88-29432

MENSTRUATION
Temperature regulation at rest and exercise during the human menstrual cycle [AD-A186461] 08 p1050 N88-16341

MENTAL PERFORMANCE
Computer-controlled testing of visual-spatial ability [AD-A183971] 03 p0357 N88-12249
Analogical inference and analogical access [AD-A184345] 03 p0369 N88-12321
Mental models in expert physics reasoning [AD-A184106] 04 p0500 N88-13075
Taskomat, a task battery for information processing [IZF-1987-2] 05 p0630 N88-13851
Cirrus: An automated protocol analysis tool [AD-A186646] 08 p1052 N88-16348
Measuring mental workload: A performance battery [AD-A187116] 09 p1200 N88-17192
Intelligent tutoring systems as tools for investigating individual differences in learning 09 p1204 N88-17216
Cardiovascular and subjective measures of task demand in a low workload monitoring task [REPT-8804] 10 p1366 N88-18176
Center for nonlinear dynamics of the brain [AD-A187245] 11 p1518 N88-19068
Electromagnetic metrics of mental workload [AD-A188205] 11 p1523 N88-19093
When decision aids fail [AD-A187531] 11 p1523 N88-19095
Effects of intense, time-constrained mental effort on hemodynamics and cardiovascular function 12 p1664 N88-19975
Neurocognitive predictions of performance [AD-A188323] 12 p1669 N88-19998
A comparison of the Army's Project A: Cognitive and psychomotor tests to analogous Air Force and Navy tests [AD-A188636] 12 p1670 N88-20002
Understanding machines from text and diagrams [AD-A189034] 13 p1755 N88-20493
A comparison of terrain association and resection as methods of position location [AD-A189480] 13 p1790 N88-20710
Distraction and inhibition in continuous CRT performance: A replication and some new findings [PB88-150941] 13 p1811 N88-20821
Identification of visual evoked response parameters sensitive to pilot mental state [NASA-CR-4140] 13 p1811 N88-20822
Mental models of mechanical systems: Individual differences in qualitative and quantitative reasoning [AD-A189035] 13 p1812 N88-20823
Knowledge retrieval as specialized inference [AD-A189042] 13 p1823 N88-20899
Relationship of encoding speed and memory tests to flight training performance [AD-A190670] 15 p2105 N88-22539
Mental-State Estimation, 1987 [NASA-CP-2504] 16 p2239 N88-23370
Vagal tone as an index of mental state 16 p2239 N88-23373
Primary task event-related potentials related to different aspects of information processing 16 p2240 N88-23382
Defining and measuring pilot mental workload 16 p2240 N88-23383
Estimating the cost of mental loading in a bimodal divided-attention task: Combining reaction time, heart-rate variability and signal-detection theory 16 p2241 N88-23385
Short-term memory load and pronunciation rate 16 p2241 N88-23386
Processing deficits in monitoring analog and digital displays: Implications for attentional theory and mental-state estimation research 16 p2241 N88-23389
Information processing deficits in psychiatric populations: Implications for normal workload assessment 16 p2241 N88-23390
Neurophysiological predictors of quality of performance 16 p2242 N88-23391
Brainstem response and state-trait variables 16 p2242 N88-23394
The event-related brain potential as an index of information processing and cognitive activity: A program of basic research [AD-A191244] 16 p2243 N88-23400
The representational code of the internal model of dynamic systems: An individual differences and dual task approach [AD-A190876] 16 p2244 N88-23403
A framework for a theory of mapping [AD-A191071] 18 p2551 N88-25144
Proceedings of the Workshop on the Assessment of Crew Workload Measurement Methods, Techniques and Procedures. Volume 2: Library references [AD-A191209] 19 p2710 N88-26101
Method for observing changes in functional state of human operator 20 p2830 N88-26789
The effects of increased cognitive demands on autonomic self-regulation: An indicator of parallel processing in the brain 21 p2925 N88-27362
Thermal stress and its effects on fine motor skill and decoding tasks 21 p2926 N88-27369
Event-related brain potentials as indices of mental workload and attentional allocation 21 p2979 N88-27696
Cognitive and neural bases of skilled performance [AD-A193392] 21 p2992 N88-27747
WORDNET: An electronic lexical reference system based on theories of lexical memory [AD-A193086] 21 p3027 N88-27970
Human performance and acute hypoxia, chapter 12 [AD-A192604] 23 p3238 N88-29270
Visual motion perception and visual attentive processes [AD-A193640] 23 p3241 N88-29286
Pilot modeling applications 24 p3314 N88-29737
Central adrenergic receptors as mediators of central response to stress: Study with Positron Emission Tomography (PET) [AD-A194947] 24 p3407 N88-30284
Venture theory: A model of decision weights [AD-A194809] 24 p3426 N88-30391

MENTAL STRESS
U STRESS (PSYCHOLOGY)

MERCAPTAN
U THIOLS

MERCAPTO COMPOUNDS
U THIOLS

MERCURY (METAL)
NT MERCURY ISOTOPES
NT MERCURY VAPOR
The JPL trapped mercury ion frequency standard 11 p1471 N88-18776
Lattice-matched HgZnTe epitaxy development [AD-A193677] 23 p3292 N88-29600

MERCURY CADMIUM TELLURIDES
Growth of solid solution single crystals [NASA-TP-2787] 06 p0688 N88-14212
Raman spectroscopic investigations of Hg-Cd-Te melts 07 p0926 N88-15625
Growth of HgZnTe layers by LPE technique [AD-A186723] 09 p1255 N88-17520
Ytterbium monolayer diffusion barriers at Hg(1-x)Cd(x)Te/Al junctions [AD-A188013] 10 p1299 N88-17768
MBE growth, characterization and electronic device processing of HgCdTe, HgZnTe related heterojunctions and HgCdTe-CdTe superlattices [AD-A187456] 10 p1421 N88-18486
Local stoichiometry and atomic interdiffusion during reactive metal/mercury-cadmium-telluride junction formation [AD-A187554] 10 p1421 N88-18488
Nonmonotonic evolution and thermodynamic trends at metal/(Hg,Cd)Te interfaces: Yb/Hg0.78Cd0.22Te [AD-A187591] 10 p1422 N88-18490
MBE (Molecular Beam Epitaxial) growth characterization and electronic device processing of HgCdTe, HgZnTe related heterojunctions and HgCdTe-CdTe superlattices [AD-A187416] 11 p1555 N88-19307
Optical absorption in doped CdxHg1-xTe [AD-A187434] 11 p1560 N88-19338
HP-41CX programs for HgCdTe detectors and IR systems [AD-A188935] 12 p1692 N88-20120
Research on mercury cadmium telluride [AD-A189155] 13 p1845 N88-21039
Study for the determination of general and specific properties of wide energy-band gap HgHdTe in the 1-2 micrometer wavelength range [AD-A189177] 13 p1845 N88-21041
Experimental studies on electronic properties of HgTe/CdTe and Hg sub 1-z Cd sub x Te/CdTe heterostructures and superlattices [AD-A189826] 15 p2142 N88-22783
Hybrid PV HgCdTe IR detectors technology reliability and failure program. Environmental stress testing plan [AD-A191165] 16 p2211 N88-23195
MBE of HgCdTe [AD-A191423] 16 p2283 N88-23671

Compositional redistribution during casting of Hg sub 0.8 Cd sub 0.2 Te alloys
[NASA-TM-101151] 17 p2326 N88-23893
Study for the determination of general and specific properties of wide energy-band gap HgCdTe in the 1 to 2 micrometer wavelength range
[AD-A191091] 17 p2334 N88-23934
Studies of boron implantation through photochemically deposited SiO2 films on Hg(sub 1-x)Cd(sub x)Te
[SD-TR-87-26] 19 p2621 N88-25548
Paramagnetic point defects in boron-implanted HgO.7CdO.3Te
[AD-A193276] 21 p3021 N88-27934
Migration and stability of HgCdTe lattice defects
[AD-A193293] 21 p3021 N88-27935
New method for preparation of (Cd, Hg)Te thin films
[DE88-702727] 23 p3293 N88-29608

MERCURY COMPOUNDS
NT MERCURY TELLURIDES
Grace DAKASEP alkaline battery separator
02 p0164 N88-11031
Organic metal (ET)4Hg3Br8A quasi-two-dimensional superconductor 14 p1974 N88-21778

MERCURY ION ENGINES
The design and development of mercury vaporisers for use with electron-bombardment ion engines
[RAE-TR-70042] 01 p0018 N88-10108
An experimental comparison of two designs of mercury propellant tank for use with an electric propulsion engine
[RAE-TR-75109] 01 p0018 N88-10109
Auxiliary propulsion system flight package
[NASA-CR-180828] 02 p0141 N88-10886
Successful completion of a cyclic ground test of a mercury ion auxiliary propulsion system
[NASA-TM-101351] 24 p3339 N88-29873

MERCURY ISOTOPES
Shape isomers as candidates for the gamma ray laser storage state
[DE88-005226] 11 p1492 N88-18909

MERCURY TELLURIDES
Electrical and optical properties of Hg/sub 1-x/Cd/sub x/Te doped layers grown by Liquid Phase Epitaxy (LPE)
[DE88-701023] 16 p2281 N88-23653
MBE growth of HgTe/CdTe superlattices on Si(100) substrates 20 p2869 N88-27033
Type 3 - type 1 transition and strain effect in Hg(1-x)Cd(x)Te-CdTe and Hg(1-x)Zn(x)Te-CdTe superlattices 20 p2872 N88-27052
Tunnelling currents in reverse biased CMT photodiodes
[RSRE-MEMO-4137] 23 p3209 N88-29097

MERCURY VAPOR
High efficiency generation of 130-nm radiation from sum-frequency mixing in Hg
[DE87-013714] 04 p0431 N88-12674
Coherent VUV source at 130 nm: Theory and modeling
[DE88-003874] 11 p1549 N88-19269

MERGING ROUTINES
Merge and termination in process algebra
[CWI-CS-R8716] 13 p1826 N88-20918

MERIDIONAL FLOW
Systematic stratospheric-tropospheric exchange viewed from isentropic coordinates 05 p0615 N88-13777
The lower thermosphere wind regime from simultaneous observations over Euroasia (Collm, Dushanbe, Frunze)
06 p0733 N88-14510
Wind regime peculiarities in the lower thermosphere in the winter of 1983/84 06 p0733 N88-14511
Longitudinal peculiarities of meridional circulation in lower thermosphere and mesosphere
06 p0736 N88-14525
Lower thermosphere wind regime according to radiometeor measurements in Kazan
06 p0736 N88-14526
Atmosphere dynamic processes structure at 80-105 km altitude 06 p0736 N88-14527
Large-scale dynamics of the mean flow breakdown in the stratosphere and mesosphere during the winter 1983/84 08 p1028 N88-16228
Numerical simulation of the ocean front response to the mesoscale atmospheric forcing
[INPE-4473-TDL/324] 12 p1648 N88-19868
Seasonal variations and excitation mechanisms of the equatorially trapped waves 13 p1798 N88-20751
JPRS report: Science and technology. China
[JPRS-CST-87-042] 14 p1899 N88-21338
Physical processes for maintaining mean meridional and zonal circulation of atmosphere in middle latitudes, volume 1 14 p1900 N88-21343
Numerical simulation of generation of mesoscale convective systems in large-scale environment
14 p1900 N88-21344
Physical process for maintenance of mean meridional and zonal circulation of atmosphere in middle latitudes, volume 2 14 p1900 N88-21345

MEROMORPHIC FUNCTIONS
NT ELLIPTIC FUNCTIONS
Systems near the onset and in the well-developed regimes of turbulence
[DE88-005365] 13 p1766 N88-20565

MESFETS
U FIELD EFFECT TRANSISTORS

MESH
The generation of nearly isotropic turbulence by means of grids
[PNR90411] 02 p0172 N88-11084
The integration of a mesh reflector to a 15-foot box truss structure. Task 3: Box truss analysis and technology development
[NASA-CR-178229] 11 p1497 N88-18941
Fatigue failure of regenerator screens in a high frequency Stirling engine 17 p2436 N88-24491
Accurate, productive aerodynamic simulation on patched mesh systems
[AD-A192040] 19 p2714 N88-26110

MESH (MATHEMATICS)
U COMPUTATIONAL GRIDS

MESH GENERATION (MATHEMATICS)
U GRID GENERATION (MATHEMATICS)

MESOMETEOROLOGY
Research work at the Meteorological Institute of the University of Munich (Federal Republic of Germany)
[MITT-56] 08 p1013 N88-16141
Results of the experiment MERKUR: Structural change of a weak cold front in the sphere of influence of the Alps — mesoscale experiment 08 p1014 N88-16146
Numerical simulation of thermally generated mountain-foreland circulation
[DFVLR-FB-87-30] 09 p1190 N88-17132
The accuracy of the radiation parameterization in mesoscale models
[DFVLR-IB-553-85/11] 09 p1190 N88-17133

MESON RESONANCE
Search for bound states of the eta-meson in light nuclei 17 p2397 N88-24248

MESONS
NT KAONS
NT MESON RESONANCE
NT MUONS
NT PIONS
Two-photon exclusive meson production at large angles
[NIKHEF-H/87-4] 08 p1081 N88-16515
Basic physics program for a low energy antiproton source in North America
[DE88-003148] 08 p1082 N88-16522
Search for bound states of the eta-meson in light nuclei 17 p2397 N88-24248
Accuracy of analytic energy level formulas applied to hadronic spectroscopy of heavy mesons
[NASA-TM-4042] 19 p2725 N88-26185

MESOPAUSE
Long-period variations of wind parameters in the mesopause region and the solar cycle dependence
06 p0733 N88-14509
Rocket experiments and payloads for Super CAMP — Cold Arctic Mesopause Project (CAMP)
08 p1034 N88-16271

MESOSCALE PHENOMENA
NT JET STREAMS (METEOROLOGY)
Mesoscale Analysis and Forecasting: Incorporating Nowcasting
[ESA-SP-282] 02 p0199 N88-11239
Applications and benefits of short period weather forecasts 02 p0199 N88-11240
Mesoscale forecasting today and tomorrow: Problems and opportunities. A position paper
02 p0199 N88-11244
The use of advanced data sets in the short-range forecasting of the development of a tornadic thunderstorm along a mesoscale convergence zone
02 p0200 N88-11250
Improved geostationary satellite soundings for the mesoscale weather analysis/forecast operation
02 p0200 N88-11252
The combined use of diagnosed mesoscale frontogenesis and satellite imagery in forecasting squall line formation 02 p0201 N88-11258
Observation of the development of mesoscale systems by operational meteorological satellites
02 p0201 N88-11259
Use of simulated satellite radiances from a mesoscale numerical model to understand kinematic and dynamic processes 02 p0202 N88-11261
The numerical simulation of the mesoscale characteristics associated with Baiu front. Part 1: Structure, low-level jet and radiation characteristics
02 p0203 N88-11272
The importance of mesoscale waves in the upper troposphere for formation of cloud and precipitation areas 02 p0203 N88-11273
On the interaction between radar and satellite image nowcasting systems and mesoscale numerical models
02 p0204 N88-11277
Satellite imagery and conceptual models in mesoscale forecasting 02 p0205 N88-11282
The use of McIDAS as a Mesoscale forecasting tool during the Canadian Atlantic storms programs — Man-computer Interactive Data Access System (McIDAS) 02 p0205 N88-11284
A short-range forecasting experiment conducted during the Canadian Atlantic storms program
02 p0205 N88-11285
Simplified models for use in an operational short range forecasting system 02 p0206 N88-11289
Statistical remote sensing algorithm development: A complementary process to mesoscale numerical models
02 p0206 N88-11292
Mesoscale thunderstorm forecasting using RAOB data, surface mesonet observations, and an expert system
02 p0206 N88-11293
Analysis of squall line based on conventional data
02 p0207 N88-11295
Detailed analysis of a mesoscale convective complex situation in the Carpathian Basin (Europe)
02 p0207 N88-11296
Effects of the large scale motion and horizontal inhomogeneity of the moist static instability on development of the mesoscale convective systems in the midlatitudes 02 p0207 N88-11297
Statistical relationships between the mesoscale organization of convection and the large-scale wind profiles during GATE — GARP Atlantic Tropical Experiment (GATE) 02 p0208 N88-11302
Toward operational forecasting and detection of weather-producing gravity waves
02 p0208 N88-11303
Two-dimensional numerical modeling of the life cycle of fog 02 p0209 N88-11311
Mesoscale MOS forecast support for 1988 winter Olympics ski events — model output statistics (MOS)
02 p0209 N88-11312
Mesoscale surface field analysis from routine observations — pressure, wind fields
02 p0209 N88-11315
Evaluation of a mesoscale prediction system with surface weather observations and comparison with a large-scale prediction system 02 p0210 N88-11319
The Norwegian mesoscale Numerical Weather Prediction (NWP) system 02 p0210 N88-11320
Forecasting polar lows using a numerical mesoscale model 02 p0210 N88-11321
Preliminary results from real data experiments with the NRL mesoscale numerical model
02 p0211 N88-11323
Short range forecasting of sea breeze generated thunderstorms at the Kennedy Space Center: A real-time experiment using a primitive equation mesoscale numerical model 02 p0211 N88-11324
Validation of a three dimensional numerical model of the sea breeze in complex terrain
02 p0211 N88-11325
The mesoscale numerical model for heavy rainfall forecasting in Yangtze River Valley, China
02 p0211 N88-11326
The impact on short-term precipitation forecast skill of time-dependent lateral and lower boundary conditions within a meso-beta numerical cloud prediction model
02 p0211 N88-11327
Mesoscale analysis and nowcasting via a numerical model coupled with satellite sounder data
02 p0211 N88-11328
A real-data numerical study and four-dimensional data assimilation application for mesobeta-scale flow in complex terrain 02 p0212 N88-11329
Opportunities and problems in mesoscale objective analysis 02 p0212 N88-11331
An isentropic mesoscale analysis system
02 p0212 N88-11332
An isentropic coordinate model used in a mesoscale data assimilation system 02 p0212 N88-11333
Strategies for using mesoscale data in an operational mesoscale model 02 p0212 N88-11335
Methods of incorporating satellite data into mesoscale numerical forecast models 02 p0212 N88-11336
Toward optimizing the use of data for operational mesoscale forecasting at the National Meteorological Center 02 p0213 N88-11337
Assimilation of high resolution TOVS data into a mesoscale NWP model — numerical weather prediction (NWP) 02 p0213 N88-11338
Use of four-dimensional data assimilation to improve a mesoscale-model precipitation forecast: A case study
02 p0213 N88-11340
Mesoscale very short-range numerical prediction with dynamical initialization including condensation heating
02 p0213 N88-11341

The future of data in mesoscale numerical models 02 p0214 N88-11344

Simulation of mesoscale satellite sounder data from a mesoscale numerical model 02 p0214 N88-11345

The challenge of using mesoscale data in mesoscale numerical models 02 p0214 N88-11346

The challenge of using mesoscale data in mesoscale numerical models: A position paper 02 p0214 N88-11347

Comments on the challenge of using mesoscale data in mesoscale numerical models 02 p0214 N88-11348

Four-dimensional initialization of mesoscale models 02 p0214 N88-11349

Mesoscale analysis and forecasting for the 1987 America's Cup, Fremantle, Western Australia 02 p0214 N88-11350

Windfield simulations from a hierarchy of nested meso- and micrometeorological models 02 p0215 N88-11351

Mesoscale forecasting with satellite data: Challanges and opportunities for today and tomorrow 02 p0215 N88-11353

Documentation of the regional climate model based on FITNAH [DFVLR-MITT-87-07] 02 p0216 N88-11358

Mesoscale eddy dynamics by the method of point vortices 04 p0463 N88-12863

Mesoscale applications of high resolution imagery [AD-A185039] 05 p0627 N88-13833

Mesoscale aerosol clouds 08 p1013 N88-16140

Spectral analysis of an orographically structured area in the forefield of mesoscale flow simulations 08 p1016 N88-16160

Numerical simulation of thermally generated mountain-foreland circulation [DFVLR-FB-87-30] 09 p1190 N88-17132

Simulations of thermally induced winds and cross flow situations [MITT-57] 09 p1193 N88-17148

The retardation of cold fronts at high mesoscale mountains 09 p1241 N88-17437

Analysis of quasi-geostrophic forcing during the AIMCS (Airborne Investigations of Mesoscale Convective Systems) Project. Volume 2: Results for June 14 through July 16, 1984 [PB88-123807] 10 p1354 N88-18092

Mesoscale coastal ocean dynamics 11 p1517 N88-19060

Analysis of quasi-geostrophic forcing during the AIMCS (Airborne Investigations of Mesoscale Convective System) Project. Volume 1: Discussion [PB88-133095] 12 p1646 N88-19860

National Severe Storms Laboratory, fiscal year 1987 [PB88-140108] 12 p1647 N88-19863

Numerical simulation of the ocean front response to the mesoscale atmospheric forcing [INPE-4473-TDL/324] 12 p1648 N88-19868

Phenomenological description of eddy registered in Gulf Stream 13 p1787 N88-20694

JPRS report: Science and technology. China [JPRS-CST-87-042] 14 p1899 N88-21338

Numerical simulation of generation of mesoscale convective systems in large-scale environment 14 p1900 N88-21344

Numerical simulation of medium scale disturbance on meiyu front 14 p1900 N88-21346

Ocean eddies 14 p1938 N88-21566

Taiwan area mesoscale experiment: Daily operations summary [PB88-169081] 16 p2235 N88-23348

Taiwan area mesoscale experiment: P-3 aircraft operations summary [PB88-169073] 18 p2544 N88-25098

Report on project WIND: Preliminary experiments with the UK Meteorological Office mesoscale model, September 1987 [AD-A191621] 18 p2544 N88-25099

Determination of mesoscale variability of sea surface temperature and attenuation in the North Atlantic from satellite measurement [REPT-162] 18 p2548 N88-25127

MM4 (Penn State/NCAR (National Center for Atmospheric Research)) mesoscale model version 4 documentation [PB88-173232] 19 p2688 N88-25979

Composite, meso-gamma scale diagnostic modeling [DE88-006189] 19 p2689 N88-25983

Satellite observed Mesoscale Convective System (MCS) propagation characteristics and a 3-12 hour heavy precipitation forecast index [PB88-180161] 19 p2692 N88-26004

Modelling and forecasting deep ocean and near surface mesoscale eddies: Hindcasting and forecasting with, and coupling a surface boundary layer model to, the Harvard quasigeostrophic model 19 p2694 N88-26013

Beaufort sea mesoscale circulation study: Hydrography helicopter operations, April 1987 [PB88-203658] 21 p2976 N88-27661

MESOSPHERE

NT MESOPAUSE

Theoretical and lidar studies of the seasonal and nocturnal variations of the mesospheric sodium layer at Urbana, Illinois 01 p0068 N88-10435

Circulation in the mesosphere and lower thermosphere during the MAP (Middle Atmosphere Program)/WINE (Winter in the Northern Europe) period 06 p0734 N88-14514

Longitudinal peculiarities of meridional circulation in lower thermosphere and mesosphere 06 p0736 N88-14525

Mesoscale density variability in the mesosphere and thermosphere: Effects of vertical flow accelerations 06 p0736 N88-14529

Some aspects of metallic ion chemistry and dynamics in the mesosphere and thermosphere 06 p0737 N88-14534

Lidar investigations of M-zone 06 p0741 N88-14558

Observations of inertial period waves and vertical velocities in the tropical middle atmosphere using the MST radar technique 06 p0742 N88-14562

Radar observations of high-latitude lower-thermospheric and upper-mesospheric winds and their response to geomagnetic activity 06 p0742 N88-14563

Middle atmospheric wind measurements using a medium frequency radar [AD-A185931] 07 p0879 N88-15330

Comparison of simultaneous MST radar and electron density probe measurements in the polar mesosphere --- Mesospheric, Stratospheric, Tropospheric (MST) 08 p1028 N88-16226

Large-scale dynamics of the mean flow breakdown in the stratosphere and mesosphere during the winter 1983/84 08 p1028 N88-16228

Observational evidence for saturation of gravity waves and the production of turbulence in the mesosphere 08 p1028 N88-16229

TOTAL: A new instrument to study turbulent parameters in the mesosphere and lower thermosphere 08 p1029 N88-16234

Rayleigh lidar observations of gravity wave activity in the stratosphere and lower mesosphere [NASA-CR-182384] 09 p1189 N88-17123

Mesospheric dynamics and chemistry from SME data [NASA-CR-182465] 09 p1191 N88-17139

Polar mesospheric cloud experiment [AD-A188936] 12 p1648 N88-19872

MESSAGE PROCESSING

Token execution strategies for distributed algorithms: Simulation studies [AD-A184792] 03 p0365 N88-12294

An interactive computer graphics network monitor for a tactical communications network [AD-A184131] 04 p0477 N88-12938

On real-time systems using local area networks [AD-A185475] 06 p0694 N88-14256

Voice technology using personal computers [AD-A186743] 09 p1218 N88-17300

Optical symbolic processor for expert system execution [AD-A187494] 10 p1385 N88-18268

Theory and practice of fault tolerance in distributed systems [AD-A187559] 11 p1540 N88-19204

Experience with Berkeley UNIX interprocess communications [AD-A188353] 12 p1680 N88-20041

A simulation study of a parallel processor with unbalanced loads [AD-A189573] 13 p1822 N88-20887

Deadlock-free message routing in processor networks [CS-8706] 14 p1960 N88-21691

Performance of data compression codes in channels with errors [AD-A189667] 15 p2055 N88-22253

Implementation of a distributed adaptive routing algorithm on the Intel iPSC (Intel Personal Super-Computer) [AD-A189849] 15 p2109 N88-22567

Alpha structure based B-HIVE multicomputer [AD-A188708] 16 p2244 N88-23405

Motor theory of auditory perception [AD-A192095] 18 p2550 N88-25136

Automatic discovery of optimal classes [NASA-TM-101174] 18 p2566 N88-25238

Narrative compression coding for a channel with errors [AD-A191577] 19 p2642 N88-25673

A cockpit natural language study - selected transcripts [AD-A192972] 20 p2834 N88-26808

Relay approach message routing in hypercube multiprocessors [DE88-009973] 20 p2835 N88-26814

Method for Veterbi decoding of large constraint length convolutional codes [NASA-CASE-NPO-17310-1-CU] 23 p3183 N88-28946

Coding for meteor-burst communications channel and side information for channels with block-interference 23 p3202 N88-29054

An overview of technology for spoken interaction with machines [AD-A194153] 23 p3202 N88-29058

A performance study of the hypercube architecture [AD-A194361] 23 p3264 N88-29433

Performance analysis of k-ary n-cube interconnection networks [AD-A195542] 24 p3361 N88-30010

Integrated resource scheduling in a distributed scheduling environment 24 p3417 N88-30342

Integrating information systems in a major decentralized international organization, volume 7 [AD-A195856] 24 p3439 N88-30466

MESSAGES

Technical characteristics of the OmniTRACS: The first operation mobile Ku-band satellite communications system 19 p2647 N88-25709

METABOLIC WASTES

NT HUMAN WASTES

NT URINE

METABOLISM

NT CALCIUM METABOLISM

NT CARBOHYDRATE METABOLISM

NT CATABOLISM

NT ELECTROLYTE METABOLISM

NT ENZYME ACTIVITY

NT FERMENTATION

NT HORMONE METABOLISMS

NT HYPOGLYCEMIA

NT NITROGEN METABOLISM

NT OXYGEN METABOLISM

NT PHOSPHORUS METABOLISM

Long term investigations of the growth, metabolism, and reproduction of fish under conditions close to weightlessness 01 p0074 N88-10473

The influence of weightlessness on the metabolism of the Biomphalaria glabrata 01 p0074 N88-10475

Fundamental study on gas monitoring in CELSS 03 p0359 N88-12263

The toxicology and metabolism of nickel compounds [DE87-014801] 04 p0474 N88-12921

Human thermoregulatory model for whole body immersion in water at 20 and 28 C [AD-A185052] 05 p0629 N88-13849

Trace-element metabolism in man and animals in the presence of hypoxic states of diverse etiology 07 p0889 N88-15390

Human metabolism and peripheral circulation during antiorthostatic hypokinesia 07 p0891 N88-15398

Investigation of energy metabolism of biological systems in weightlessness 07 p0893 N88-15409

Third Soviet-French Symposium on Space Cytology 07 p0893 N88-15411

Experiments with rats flown aboard Cosmos-1667 biosatellite (main objectives, conditions and results) 07 p0893 N88-15414

Regulation of energy metabolism during parachute jumps 07 p0896 N88-15428

Rational considerations for modelling human thermoregulation during cold water immersion [AD-A186226] 08 p1048 N88-16329

Temperature regulation at rest and exercise during the human menstrual cycle [AD-A186461] 08 p1050 N88-16341

Some process control/design considerations in the development of a microgravity mammalian cell bioreactor 09 p1197 N88-17174

Role of body fat in the prediction of the metabolic response for immersion in cold water [AD-A186914] 09 p1198 N88-17182

Human blood glutamic acid level with exposure to high ambient concentrations of ammonia 10 p1361 N88-18134

New book on metabolic aspects of spaceflight stress 10 p1367 N88-18172

Certain aspects of human metabolism during spaceflights of varying duration [NASA-TT-20215] 10 p1369 N88-18181

The evolution of glutathione metabolism in phototrophic microorganisms [NASA-CR-182902] 19 p2695 N88-26015

The US space programme spacewalk/extravehicular activity experience: Past, present and future 19 p2697 N88-26031

Human erykthrocyte metabolism in the presence of hyperoxygenation during antiorthostatic hypokinesia
19 p2706 N88-26092
Regulatory biochemical and metabolic responses in photoreceptors
[AD-A192898] 20 p2831 N88-26794
Metabolic and cardiorespiratory parameters during three consecutive days of exhaustive running
[AD-A192598] 21 p2985 N88-27728
Software modifications to total data reporting accessory for metabolic measurement cart
[AD-A193641] 22 p3132 N88-28623

METABOLITES
Specific organic compounds in excreta
07 p0895 N88-15422
Effect of low-frequency whole-body vertical vibration on the serotoninergic system of the brain and spinal cord
19 p2704 N88-26081

METAGALAXY
U UNIVERSE

METAL AIR BATTERIES
NT ZINC-OXYGEN BATTERIES
Extended abstracts: Eighth Battery and Electrochemical Contractors' Conference
[DE88-000960] 06 p0730 N88-14489
Aluminum-air battery development
[DE88-006617] 13 p1762 N88-20542
Aluminum-air battery development
[DE88-006618] 13 p1762 N88-20543
Technology base research on zinc/air battery systems
[DE88-004893] 13 p1763 N88-20546
Aluminum-air battery development
[DE88-006620] 15 p2061 N88-22287
Crystallization of aluminum hydroxide in the aluminum-air battery: Literature review, crystallizer design and results of integrated system tests
[DE88-010510] 20 p2797 N88-26594
Metal-air battery assessment
[DE88-011361] 21 p2940 N88-27459

METAL BONDING
NT METAL-METAL BONDING
Bonding and coupling of C sub 1 fragments on metal surfaces
[AD-A184186] 03 p0295 N88-11852
Valence bond cluster studies of alkali metal/semiconductor bonding
[AD-A184276] 04 p0496 N88-13054
Analysis of end stresses in glass-metal bimaterial strips
[DE87-007848] 05 p0610 N88-13750
Behavior of metal ceramic interfaces
[PB87-147500] 07 p0837 N88-15076
Improved glass-ceramic to metal seals in actuator and detonator applications with an aluminum-containing austenitic stainless steel
[DE88-004691] 13 p1749 N88-20458
The relationship of the chemical bonding topology of high critical temperature copper oxide superconductors to that of the chevrel phases and the ternary lanthanide rhodium borides
[AD-A189255] 13 p1845 N88-21042
Composite piston
[NASA-CASE-LAR-13435-1] 17 p2346 N88-23981
Composite repair of cracked aluminum alloy aircraft structure
[AD-A190514] 18 p2455 N88-24573
A scientific basis for an alternate cathode architecture
[AD-A191498] 18 p2481 N88-24717
Environmental integrity of coating/metal interface
[AD-A192184] 18 p2492 N88-24786

METAL COATINGS
NT ALUMINUM COATINGS
NT NICKEL COATINGS
NT ZINC COATINGS
Corrosion-resistant amorphous metallic coatings: Engineering development
[NASA-CR-181487] 03 p0287 N88-11802
Bond character at a silicon/copper surface
[AD-A184167] 03 p0295 N88-11851
Investigation of the fabrication parameters of laser mirrors with hard oxide interference coatings
[ESA-TT-1064] 03 p0329 N88-12077
Deformation mechanisms of thermostructural materials
[AD-A184070] 03 p0338 N88-12128
The analysis of metal finishing solutions by ion chromatography
[AD-A184812] 05 p0561 N88-13414
Ion plating for corrosion control
[AD-A185061] 05 p0565 N88-13442
Development of methods for low temperature diffusion bonding
[AD-A186875] 09 p1174 N88-17033
Reaction mechanism of sulfur dioxide with single crystal cobalt and chromium and CoCrAlY coatings
[AD-A185969] 09 p1253 N88-17500
Study of adherent oxide scales
[AD-A187368] 11 p1456 N88-18680
Adhesion of PVD titanium coatings to beryllium substrates
[DE88-005147] 11 p1463 N88-18721
Technical applications of solar energy. Project: Selective coatings
[BMFT-FB-T-86-213] 14 p1943 N88-21591
Corrosion of electroless nickel-coated steel
[AD-A191045] 16 p2179 N88-22985
Dependence of structure of stabilized ZrO2 coatings on condensation rate 16 p2180 N88-22990
Recent advances in metallic/ceramic coatings for corrosion control in military applications
17 p2320 N88-23858
Vanadic hot corrosion of gas turbine blade coating materials 17 p2321 N88-23864
Development of reliable fuel pins for space reactor applications 17 p2409 N88-24326
Corrosion control through a better understanding of the metallic substrate/organic coating/interface
[AD-A193981] 22 p3056 N88-28132
Zinc filled coatings 24 p3355 N88-29978

METAL COMBUSTION
Measurement of combustion aerosol size distributions with multistage inertial impactors
[DE88-751101] 11 p1454 N88-18669

METAL CORROSION
U CORROSION

METAL CRYSTALS
Computer simulations of knock-on processes in bcc Ta crystal
[DE87-752980] 02 p0246 N88-11554
Production of metallic monocrystals described
03 p0286 N88-11796
Progress toward a crystal streak camera using tungsten bronze crystals for the electrooptic material
[DE87-013110] 03 p0323 N88-12044
Measurements of the scintillation time constants of inorganic crystals for the development of a triple-Phoswich detector for high-energy X-ray quanta
[ETN-88-91501] 14 p1993 N88-21875

METAL CUTTING
Analysis of free cutting brass by A.C. polarography
[PD-MT-8728] 04 p0417 N88-12587
Identification and feedback control of machine tool vibrations
[PB88-109715] 06 p0976 N88-15902
Further development of a finite element model of orthogonal metal cutting
[DE88-004048] 11 p1494 N88-18921
Optimization of oxygen cutting process for titanium alloys 14 p1897 N88-21323
Friction welding: Advanced method of producing end cutting tool 14 p1897 N88-21327
The technical feasibility of using spiked-radiation lasers to cut out and weld metals 14 p1898 N88-21332

METAL FATIGUE
The effect of fretting corrosion on the fatigue strength of steel and cast iron under sinusoidal and random loading
[LBF-FB-177] 01 p0023 N88-10142
Modelling of crack-tip deformation and transient electrochemical processes in relation to corrosion fatigue of steels cathodically protected in marine environments
[NPL-DMA(A)-145] 01 p0059 N88-10379
Fatigue crack propagation of low-alloy steel in a vacuum environment
[DE87-013770] 01 p0061 N88-10393
Turbine Engine Hot Section Technology, 1985
[NASA-CP-2405] 02 p0184 N88-11140
Constitutive modeling for single crystal superalloys
02 p0187 N88-11168
Microstructural effects on the fatigue behavior of Fe-C-X alloys
[DE88-000155] 03 p0288 N88-11809
Fatigue failure of thin porous strips
04 p0426 N88-12640
Welded joint fatigue of a AISI 304 L type stainless steel
[DE87-703530] 05 p0592 N88-13607
Fatigue 87, volume 1
[AD-A184045] 05 p0597 N88-13645
Cyclic deformation and crack initiation
05 p0597 N88-13646
Effect of grain orientation on the origination and the initial growth of fatigue cracks in pure iron
05 p0597 N88-13647
The growth of persistent slip bands
05 p0597 N88-13648
The mechanics of fatigue-crack nucleation in a low-alloy steel under fretting conditions 05 p0597 N88-13649
Surface deformation and fatigue crack initiation of alpha-iron 05 p0598 N88-13651
The effect of ion beam mixed Ni-Al surface layers on PSB extrusion morphology in fatigued nickel
05 p0598 N88-13652
The evolution of local mechanical properties of Al 2219-T851 during fatigue 05 p0598 N88-13653
Cyclic deformation of an extruded AlMgSi alloy
05 p0598 N88-13654
Closure behavior under constant effective stress intensity loading conditions 05 p0598 N88-13656
Growth of short fatigue cracks in a squeeze formed aluminum alloy 05 p0598 N88-13658
Influence of microstructure and aging condition on the fatigue crack propagation in age hardened aluminium alloys 05 p0599 N88-13659
Fatigue crack growth behavior of A356-T6 cast aluminum alloy 05 p0599 N88-13660
Striations and the fatigue growth mechanism in a micro-alloyed steel 05 p0599 N88-13661
Significance of fatigue crack closure under spectrum loading 05 p0599 N88-13662
Near-threshold short crack growth behavior in Nimonic 105 05 p0599 N88-13663
Fatigue crack propagation of short and long cracks: Phys. basis, prediction methods and engineering significance 05 p0599 N88-13664
Low cycle fatigue life predictions of a 1CrMoV steel in terms of a J-controlled short crack growth model
05 p0599 N88-13665
The statistics of the shape of small fatigue cracks
05 p0599 N88-13666
The effect of alpha platelet morphology and beta-grain size on the initiation and growth of short fatigue cracks in Ti65S 05 p0600 N88-13667
The initiation and growth of small fatigue cracks in copper at room and cryogenic temperatures
05 p0600 N88-13668
On the role of crack tip shielding in influencing the behavior of long and small fatigue cracks in aluminum-lithium alloy 2090 05 p0600 N88-13671
The influence of slip mechanism on fatigue of Mg and Mg-2.3Li 05 p0600 N88-13672
The growth behavior of small fatigue cracks: the effect of microstructure and crack closure
05 p0600 N88-13673
The influence of microstructure and residual stresses on the initiation and propagation of short surface cracks on AlMgSi1 05 p0601 N88-13674
Threshold stress for fatigue crack initiation from a small crack 05 p0601 N88-13675
An experimental study of closure behavior of naturally initiated small cracks 05 p0601 N88-13676
Behavior of long and short fatigue cracks in a powder metallurgy superalloy at room and at high temperature
05 p0601 N88-13677
Propagation of small fatigue cracks in 2024-T3 aluminum alloy 05 p0601 N88-13678
Closure and propagation behavior of short fatigue cracks at different R-ratios 05 p0601 N88-13679
A unified model for fatigue crack initiation, short crack growth, long crack propagation, and closure effects
05 p0601 N88-13680
Fatigue crack retardation in aluminium alloys
05 p0602 N88-13681
Fatigue crack growth under random overloads
05 p0602 N88-13682
A dislocation model for fatigue crack propagation under variable amplitude loading 05 p0602 N88-13683
Observations on the effect of overloads on fatigue crack growth 05 p0602 N88-13684
A study of fatigue crack growth life under random stresses 05 p0602 N88-13685
Crack growth in contrasting titanium alloys under the conjoint action of high and low cycle fatigue
05 p0602 N88-13686
Variable amplitude fatigue crack growth in aluminum alloys 2090-T8E41 and 7075-T651
05 p0602 N88-13687
Fatigue of 30CrMnSiNi2A notched specimens under spectrum loading 05 p0602 N88-13689
The how and why of variable amplitude testing
05 p0603 N88-13690
Near-threshold growth of defects in engineering materials 05 p0603 N88-13691
Interaction of microstructure and fatigue in tool steels
05 p0603 N88-13693
Tensile mean stress effects on uniaxial fatigue behavior of 1045 HR steel 05 p0603 N88-13694
Fatigue strength of alloy A286 at cryogenic temperature 05 p0603 N88-13695
The initiation and growth of fatigue cracks in carburised 9Cr1Mo steel 05 p0603 N88-13696
Fretting wear and fretting fatigue damage
05 p0603 N88-13697
The role of inclusions in corrosion fatigue crack initiation in Q1N 05 p0604 N88-13699

A study of corrosion fatigue crack initiation, growth and the threshold condition under variable amplitude loading 05 p0604 N88-13701

The influence of crack conditions on hydrogen uptake by steels 05 p0604 N88-13702

Occurance and growth of fatigue cracks in corrosion environment 05 p0604 N88-13704

The effect of environment on low cycle fatigue properties in HSLA steel 05 p0605 N88-13705

Coupling effects between the ferrite and austenite phases during corrosion fatigue of a ferrite/austenite duplex stainless steel 05 p0605 N88-13706

Development of research on fatigue of spot-weld in automobile structures in Japan 05 p0608 N88-13728

Environmentally assisted fatigue crack growth 05 p0608 N88-13731

Deformation, fatigue and fracture behavior of two cast anisotropic superalloys 05 p0608 N88-13732

Fatigue crack growth 05 p0608 N88-13734

Temperature dependent mechanical properties of an alumina fiber reinforced aluminum composite 06 p0677 N88-14147

Fatigue damage maps 06 p0715 N88-14382

An investigation of fatigue crack growth in a ductile material at high growth rates 06 p0715 N88-14383

Cyclic deformation behaviour of cast irons with various graphite shapes in the temperature range 20 C less than or = T less than or = 500 C 06 p0715 N88-14384

Life prediction of steel cords 06 p0715 N88-14386

Effect of hold time on fatigue of lead rich PbSn solder 06 p0715 N88-14387

On cleavage in fatigue for rail steels 06 p0716 N88-14388

Influence of cleavage on fatigue propagation rates in a low carbon steel 06 p0716 N88-14389

Effect of metal surface properties on the fatigue crack growth behavior 06 p0716 N88-14390

Fatigue crack growth behavior in hydrogen gas environment 06 p0716 N88-14391

Near-threshold fatigue 06 p0716 N88-14392

Notch-geometry effect on propagation threshold of short fatigue cracks in notched components 06 p0716 N88-14393

Influence of crack closure on fatigue crack propagation and threshold 06 p0716 N88-14394

An explanation of the fractography of near-threshold fatigue in FCC metals 06 p0716 N88-14395

The relationship between microstructural size and fatigue threshold in iron and steel 06 p0716 N88-14396

Threshold behaviour of semi-elliptic hydrogen-induced and fatigue-induced cracks 06 p0717 N88-14397

Effect of compressive portion of loading cycles on the near threshold fatigue closure behavior 06 p0717 N88-14398

Absolute fatigue thresholds in metallic materials 06 p0717 N88-14399

Thermometrical investigations on the near threshold fatigue crack propagation behavior 06 p0717 N88-14400

A re-evaluation of fatigue threshold test methods 06 p0717 N88-14401

The factors which govern the acceleration of corrosion fatigue crack growth rate of a ferritic stainless steel 06 p0717 N88-14402

Fatigue thresholds of C.Mn steels in saline environments 06 p0717 N88-14403

Influence of stress ratio R on fatigue threshold delta K(th) for 40Cr steel 06 p0718 N88-14405

The effects of loading history on fatigue crack growth threshold 06 p0718 N88-14406

Threshold stress intensity for stable crack growth in high strength steel at ambient temperature and below 06 p0718 N88-14407

The effect of shear lips on fatigue crack growth in Al-2024 sheet material 06 p0718 N88-14408

Near-threshold fatigue crack growth behavior at cryogenic temperature 06 p0718 N88-14409

The effect of non-metallic inclusions on fatigue and fatigue thresholds of 25Mn-5Cr-1Ni steel 06 p0718 N88-14410

Role of interstitials and precipitates in initiation and propagation of L.C.F. cracks in austenitic stainless steels 06 p0718 N88-14411

Threshold and crack-growth tests on pre-cracked specimens produced in cyclic compression 06 p0718 N88-14412

Micromechanics of fatigue crack initiation under axial and torsional loadings 06 p0719 N88-14413

Study of the characteristic curve of hardening and softening during low-cycle fatigue process 06 p0719 N88-14414

The effect of prestraining on fatigue crack growth in nickel-base alloys 06 p0719 N88-14415

Mixed mode fatigue crack growth using the Brasilian disc 06 p0719 N88-14416

Crack closure phenomena in modes 1 and 2 interactions 06 p0719 N88-14417

Multiaxial fatigue failure criterion: A new approach 06 p0719 N88-14418

Profiles of self stress and of load stress at notches 06 p0719 N88-14419

Fatigue oxidation interaction in low cycle fatigue 06 p0719 N88-14420

Effect of temperature exposure on fatigue crack propagation 06 p0720 N88-14421

High temperature low cycle fatigue of oxide dispersion strengthened and single crystal nickel base superalloys 06 p0720 N88-14422

Orientation effects in copper single crystals fatigued at elevated temperatures 06 p0720 N88-14423

Elevated temperature fatigue crack propagation 06 p0720 N88-14424

High temperature low cycle fatigue behavior and creep-fatigue interation of MA 6000 ODS alloy 06 p0720 N88-14425

Creep-fatigue cracking in high temperature turbine rotors 06 p0720 N88-14426

The effect of temperature on fatigue crack initiation from aluminosilicate inclusions 06 p0720 N88-14427

Dependence of strainrange partitioned fatigue life at elevated temperature on monotonic stress-strain properties 06 p0721 N88-14428

Thermal mechanical low cycle fatigue of 25CDV4-10 steel 06 p0721 N88-14429

Axial creep-fatigue damage assessment in type 316 SS material 06 p0721 N88-14430

An analysis of temperature effect on LCF crack growth rates in superalloy GH36 06 p0721 N88-14431

Thermomechanical fatigue of lead-base low tin solder 06 p0721 N88-14432

Fatigue life prediction modeling for turbine hot section materials [NASA-TM-100291] 06 p0724 N88-14453

Transients in elevated temperature crack growth [DE87-013189] 06 p0724 N88-14454

Fatigue, fracture and strain hardening of high carbon hardened alloy steel [AD-A186101] 07 p0831 N88-15043

Effect of overload ratios on fatigue crack growth behavior in Ti-6Al-4V alloy [PB87-147062] 07 p0833 N88-15055

Propagation of fatigue crack in the medium-carbon steel containg both martensite and ferrite [PB87-143962] 07 p0869 N88-15273

Review of fatigue and fracture research at NASA Langley Research Center 09 p1106 N88-16633

Fatigue crack growth due to random loading [DE88-004641] 10 p1345 N88-18038

Thermal fatigue of stainless steel [DE88-004146] 11 p1458 N88-18694

Thermal-mechanical fatigue testing of a titanium-aluminide alloy [AD-A189555] 12 p1609 N88-19620

Advanced durability analysis. Volume 1: Analytical methods [AD-A188341] 12 p1635 N88-19789

A simulation of void lining during ductile fracture [AD-A188404] 12 p1635 N88-19792

Non-destructive evaluation techniques applied to the study of fatigue microcrack growth in steel alloys [DE88-004090] 13 p1742 N88-20420

The fatigue behavior of ferritic and austenitic steels at elevated temperatures [DE88-006304] 13 p1744 N88-20431

Investigation of the use of horizontally polarised shear waves for TOFD studies on austenitic steel [AERE-R-12145] 13 p1780 N88-20649

JPRS report: Science and technology. USSR: Materials science [JPRS-UMS-87-007] 14 p1895 N88-21312

Some structural aspects of crack propagation in heat-resistant steels under cyclic thermal and mechanical load 14 p1896 N88-21317

The growth of corner cracks under the conjoint action of high and low cycle fatigue [AD-A190510] 15 p2076 N88-22379

Lewis Structures Technology, 1988. Volume 3: Structural Integrity Fatigue and Fracture Wind Turbines HOST [NASA-CP-3003-VOL-3] 15 p2081 N88-22408

Life prediction modeling based on cyclic damage accumulation 15 p2085 N88-22426

Fatigue damage modeling for coated single crystal superalloys 15 p2085 N88-22427

Development of a flexible and economic helicopter engine monitoring system [PB88-165147] 16 p2160 N88-22887

Fatigue crack growth under full-scale cyclic plasticity [DFVLR-FB-87-48] 16 p2222 N88-23263

Study of mechanisms of time-dependent crack growth at elevated temperature [DE88-006918] 16 p2223 N88-23271

AC impedance analysis of corrosion fatigue in naval aircraft alloys [AD-A190822] 17 p2322 N88-23865

The application of high-rate biaxial testing to the design of containment vessels for radioisotope heat sources 17 p2426 N88-24428

Environment assisted degradation mechanisms in advanced light metals [NASA-CR-182907] 18 p2486 N88-24746

Isothermal and bithermal thermomechanical fatigue behavior of a NiCoCrAlY-coated single crystal superalloy [NASA-TM-100907] 18 p2489 N88-24766

Cyclic fatigue damage characteristics observed for simple loadings extended to multiaxial life prediction [NASA-CR-182126] 18 p2531 N88-25016

Characterization of fatigue crack initiation and propagation in Ti-6Al-4V with electrical potential drop technique [NASA-TM-100877] 19 p2661 N88-25937

Analyses and correlations of environment assisted fatigue crack propagation for attachment lugs 22 p3053 N88-28116

Load interaction effects on compression fatigue crack growth in ductile solids [FFA-TN-1986-12] 22 p3089 N88-28342

AGARD engine disc cooperative test programme [AGARD-R-766] 23 p3179 N88-28926

METAL FIBERS

Magnetization studies of multifilamentary Nb3Sn wires [DE88-009103] 19 p2735 N88-26243

METAL FILMS

Simulation of the layer-growth dynamics in silver films: Dynamics of adatom clusters and vacancy clusters on Ag(100) [DE87-014764] 03 p0380 N88-12390

Superconducting switch program [AD-A185682] 07 p0848 N88-15144

Optical measurements of surface oxide layer formation on metal films [DE88-003163] 10 p1409 N88-18405

Characterization of redox states of nickel hydroxide film electrodes by in-situ Raman spectroscopy [AD-A189288] 13 p1741 N88-20411

Properties of reactively sputtered WNx films Zhao, X. -A. [AD-A188711] 13 p1835 N88-20976

Laser enhanced adhesion of copper films to sapphire substrates [DE88-006802] 15 p2038 N88-22144

Vapor phase deposition and growth of polyimide films on copper [AD-A189969] 15 p2044 N88-22178

Ion-beam mixing and amorphization in Au/Zr bilayers [DE88-005999] 15 p2140 N88-22767

Femtosecond nonequilibrium electronic heat transport in thin gold films 19 p2659 N88-25807

Epitaxial iron films [AD-A191815] 19 p2732 N88-26225

Aharonov-Bohm effects in disordered metals 20 p2864 N88-27008

PECVD of amorphous nickel--phosphorus films [DE88-011088] 21 p2915 N88-27299

Status and directions of modified tribological surfaces by ion processes [NASA-TM-101304] 22 p3063 N88-28176

Optical emission from surface waves supported in thin metal films 23 p3282 N88-29540

Temperature dependence of conductivity and of Hall coefficients for noble metal films [ETN-88-92981] 23 p3294 N88-29616

The lubricating properties of magnetron sputtered MoS2 [ESA-ESTL-76] 24 p3381 N88-30136

METAL FINISHING

The analysis of metal finishing solutions by ion chromatography [AD-A184812] 05 p0561 N88-13414

METAL FLUORIDES

NT ALUMINUM FLUORIDES
NT CALCIUM FLUORIDES
NT LITHIUM FLUORIDES
NT SODIUM FLUORIDES
NT URANIUM FLUORIDES

METAL FOILS

High-temperature properties of ceramic fibers and insulations for thermal protection of atmospheric entry and hypersonic cruise vehicles [NASA-TM-100059] 10 p1295 N88-17743

Composition and thickness of multilayer foils using MeV ion-beam techniques [DE88-004360] 11 p1448 N88-18629

Erosion of metals exposed to hot, dense gases [AD-A193708] 22 p3056 N88-28131

Hydrogen permeation through metallic foils
[DE88-702600] 23 p3193 N88-29000

METAL FORGING
U FORGING

METAL FORMING
U FORMING TECHNIQUES
U METAL WORKING

METAL HALIDES
NT ALUMINUM FLUORIDES
NT CALCIUM FLUORIDES
NT CESIUM IODIDES
NT COPPER CHLORIDES
NT LITHIUM CHLORIDES
NT LITHIUM FLUORIDES
NT POTASSIUM BROMIDES
NT SILVER CHLORIDES
NT SILVER IODIDES
NT SODIUM CHLORIDES
NT SODIUM FLUORIDES
NT URANIUM FLUORIDES
An investigation of metal complexes of some 2-substituted and 2,6-disubstituted pyridine N-oxides
11 p1460 N88-18701
Metal halide optical glasses
[AD-A193794] 23 p3198 N88-29032

METAL HARDENING
U HARDENING (MATERIALS)

METAL HYDRIDES
NT LITHIUM HYDRIDES
NT SODIUM HYDRIDES
Performance analysis of advanced spacecraft TPS
[NASA-CR-181532] 04 p0399 N88-12484
Method for preparing hydride configurations and reactive metal surfaces
[DE88-000845] 06 p0679 N88-14161
Electronic structure calculations and binding analyses for selected binary and ternary metal hydrides
[ETN-88-91087] 09 p1256 N88-17527
Metal hydrides
[DE88-005083] 10 p1299 N88-17766
Chemical activation of molecules by metals: Experimental studies of electron distributions and bonding
[DE88-004465] 10 p1407 N88-18393
Materials science with muon spin rotation
[NASA-CR-182891] 17 p2396 N88-24242
Muon motion in titanium hydride
17 p2396 N88-24247
Super hydrides
[AD-A193710] 23 p3192 N88-28995

METAL INSULATOR SEMICONDUCTORS
U MIS (SEMICONDUCTORS)

METAL IONS
NT FERRIC IONS
Segmented hollow cathode discharges for copper ion lasers
[ETN-87-90403] 01 p0052 N88-10333
Some aspects of metallic ion chemistry and dynamics in the mesosphere and thermosphere
06 p0737 N88-14534
Meteor matter interaction with the Earth's atmosphere and the ionospheric E-region structure
06 p0738 N88-14537
Development of FTMS methods for the detection of trace chemical species and development of FTMS methods for the analysis of various chemical species
[AD-A185857] 07 p0828 N88-15023
Electrosorptive detection based on double-layer capacitance for selective anion monitoring in ion chromatography. Part 1: Mercury electrodes
[AD-A188780] 12 p1606 N88-19603
Transition metal cluster chemistry
[AD-A188731] 13 p1740 N88-20405
Wavelength scaling of lithium-like recombination scheme for X-UV gain production --- X-ray lasers
[ETN-88-92002] 13 p1778 N88-20634
Determination of aquo-complexes of chromium and iron in chromium plating and polishing solutions by ion chromatography
[AD-A190168] 15 p2039 N88-22148
Ion beam alloying of aluminum for corrosion resistance 17 p2321 N88-23860
Complexation and hydrolysis reactions of iron(III)
17 p2322 N88-23867
Self shielding of surfaces irradiated by intense energy fluxes
[DE88-007094] 18 p2579 N88-25318
Field-enhanced lithium ion sources for PBFA 2
[DE88-007195] 20 p2856 N88-26960
Storing bits on a DNA polymer chain
[AD-A195701] 24 p3356 N88-29981

METAL JOINTS
NT SOLDERED JOINTS
NT SPOT WELDS
NT WELDED JOINTS
Taper sectioning to magnify the interface thickness of a dissimilar metal joint
[RFP-3890-REV] 03 p0333 N88-12099
Investigation of Super*Zip separation joint
[NASA-TM-4031] 15 p2026 N88-22072
Stress relaxation of a titanium (Ti-6Al-4V) threaded joint
[DE88-010102] 21 p2961 N88-27590
Shielding effectiveness of metallic joints versus corrosion prevention 22 p3054 N88-28120

METAL MATRIX COMPOSITES
NT ALUMINUM BORON COMPOSITES
NT ALUMINUM GRAPHITE COMPOSITES
NT EUTECTIC COMPOSITES
An investigation of the high strain rate deformation of SiCw/2124 Al composite
[OUEL-1675/87] 02 p0142 N88-10895
High temperature metal matrix composites for future aerospace systems
[NASA-TM-100212] 02 p0149 N88-10938
Composite structural materials
[NASA-CR-181416] 02 p0190 N88-11186
Plasticity of fibrous composites
[AD-A184637] 03 p0280 N88-11765
Corrosion resistance of silver-plated carbon-aluminum composite 03 p0285 N88-11793
Corrosion-electrochemical and mechanical properties of composite graphite-carbide metal materials based on titanium and its alloys 03 p0285 N88-11794
The infiltration kinetics of aluminum in silicon carbide compacts
[AD-A184682] 03 p0290 N88-11823
Damping characteristics of a composite-reinforced stainless-steel plate
[DE88-000303] 04 p0457 N88-12826
Plasma joining of metal matrix composites
[AD-A184828] 05 p0557 N88-13390
Micromechanisms of fatigue crack growth and fracture toughness in metal matrix composites
[AD-A185200] 05 p0558 N88-13392
Time-temperature-stress capabilities of composite materials for advanced supersonic technology application
[NASA-CR-178272] 06 p0677 N88-14144
Thermo-mechanical behavior of high temperature fiber composites 06 p0678 N88-14149
Bending properties of aluminum base composite with CVD-fiber
[PB87-130878] 06 p0678 N88-14156
Interface characteristics and the mechanical properties of metal matrix composites
[AD-A186441] 08 p0966 N88-15845
Aeropropulsion '87. Session 1: Aeropropulsion Materials Research
[NASA-CP-10003-SESS-1] 09 p1118 N88-16697
Development of a new generation of high-temperature composite materials 09 p1119 N88-16702
Micromechanisms of fatigue crack growth and fracture toughness in metal matrix composites
[AD-A186941] 09 p1137 N88-16816
Micro-mechanisms of deformation in SiC/Al composites
[AD-A188282] 10 p1296 N88-17749
Creep behavior of tungsten/niobium and tungsten/niobium-1 percent zirconium composites
[NASA-TM-100804] 11 p1460 N88-18707
Mechanical response of unidirectional boron/aluminum under combined loading
[NASA-CR-182595] 12 p1604 N88-19591
Plasma joining of metal matrix composites
[AD-A188559] 12 p1604 N88-19593
Composites strengthening
[AD-A189258] 13 p1734 N88-20364
High-temperature metal matrix composites
[AD-A189516] 13 p1734 N88-20367
Processing, structure and properties of heavily deformed in situ composites
[AD-A189611] 13 p1742 N88-20416
Fracture criteria for discontinuously reinforced metal matrix composites
[NASA-CR-182665] 13 p1782 N88-20662
Structure and strength of boron-aluminum composites
14 p1885 N88-21264
A viscoplastic constitutive theory for metal matrix composites at high temperature
14 p1929 N88-21500
Microplasticity phenomena in graphite/magnesium metal matrix composites
[DE88-006772] 15 p2029 N88-22086
Drilling metal matrix composites
[AD-A190480] 15 p2029 N88-22091
Interfacial structure-property relationships at the fiber-matrix interphase in advanced composites
[AD-A190649] 15 p2030 N88-22093
Specimen preparation techniques for the examination of ceramic and metal-matrix composites
[DE88-005157] 15 p2030 N88-22094
Thermal expansion behavior of randomly oriented short carbon fiber reinforced copper composites
[NASA-TT-20175] 15 p2031 N88-22099
Reciprocating sliding wear characteristics of copper-carbon fiber composites
[NASA-TT-20176] 15 p2031 N88-22100
Application of copper-carbon fiber composites to power semiconductor devices
[NASA-TT-20171] 15 p2031 N88-22101
Joints in fiber-reinforced aluminum alloys
[NASA-TT-20160] 15 p2031 N88-22104
Processing, microstructure, and mechanical properties of silicon carbide particulate reinforced aluminum alloys
[AD-A188981] 15 p2037 N88-22136
Investigation and synthesis of high temperature and increased stiffness RSP aluminum alloys
[AD-A190407] 15 p2039 N88-22151
Growth and deformation mechanisms of refractory alloy hybrid materials
[AD-A190492] 15 p2039 N88-22152
Unified constitutive model development for metal matrix composites at high temperature
15 p2078 N88-22387
METCAN: The metal matrix composite analyzer
15 p2079 N88-22395
Test procedures and standards for mechanical property measurements on metal matrix composites
[NPL-DMA(A)-153] 16 p2172 N88-22944
Thermal conductivity, electrical conductivity and specific heat of copper-carbon fiber composite
[NASA-TT-20172] 16 p2172 N88-22948
Structure and mechanical properties of metal matrix composites made using semi-solid processes: The case of the system Al-Si/SiC
[ETN-88-92299] 17 p2316 N88-23836
Strain intensity factor approach for predicting the strength of continuously reinforced metal matrix composites
[NASA-TM-100617] 17 p2317 N88-23838
Analysis of notched metal matrix composites under tension loading
[NASA-TM-100629] 18 p2480 N88-24713
Research work completed at the Naval Surface Warfare Center Solid State Group of the Radiation Division
[AD-A191627] 18 p2582 N88-25339
Fatigue testing and damage development in continuous fiber reinforced metal matrix composites
[NASA-TM-100628] 19 p2610 N88-25489
Fracture resistance of a TiB2 particle/SiC matrix composite at elevated temperature
[NASA-TM-100967] 20 p2779 N88-26482
Damping characteristics of metal matrix composites
[AD-A193144] 21 p2904 N88-27233
Analysis of transverse strength of composites using percolation theory
[AD-A193204] 21 p2904 N88-27234
Refractory metal alloys and composites for space power systems
[NASA-TM-100946] 21 p2916 N88-27310
The composite aeroengine
[PNR90451] 22 p3045 N88-28070
Durability of continuous fiber reinforced metal matrix composites
[AD-A193668] 22 p3050 N88-28097
Plasma joining of metal matrix composites
[AD-A193939] 22 p3051 N88-28100
Investigation of a SiC/Ti-24Al-11Nb composite
[NASA-TM-100956] 23 p3190 N88-28980
A fundamental study of P/M processed elevated temperature aluminum alloys
[AD-A192958] 23 p3194 N88-29005
Some theoretical considerations of the surface tension of liquid metals for metal matrix composites
[AD-A195999] 24 p3340 N88-29682

METAL NITRIDES
NT ALUMINUM NITRIDES
NT GALLIUM NITRIDES
NT TITANIUM NITRIDES
NT ZIRCONIUM NITRIDES
Process for preparing transition metal nitrides and transition metal carbonitrides and their reaction intermediates
[DE88-000849] 06 p0679 N88-14162

METAL OXIDE SEMICONDUCTORS
NT CMOS
NT SOS (SEMICONDUCTORS)
Hydrogen annealing of P(sub) b and E prime defect centers in oxidized silicon wafers
[DE87-014293] 02 p0152 N88-10951
A review of the semiconductor storage of television signals. Part 2: Applications 1975-1986
[BBC-RD-1987/6] 02 p0161 N88-11009

Development of standard cells in NMOS technology for the design of digital integrated circuits
[FI-62-TB-6] 03 p0310 N88-11953
Research in monolithic signal-processing circuits
[AD-A184680] 03 p0311 N88-11962
Reevaluating the worst-case radiation response of MOS transistors
[DE87-014157] 04 p0497 N88-13059
A study of charged particles/radiation damage to VLSI device materials
[NASA-CR-172036] 05 p0577 N88-13518
Integrated photo-responsive metal oxide semiconductor circuit
[NASA-CASE-GSC-12782-1] 06 p0696 N88-14271
The role of hydrogen in radiation-induced defect formation in polysilicon gate MOS devices
[DE87-012374] 06 p0785 N88-14814
Further study of inversion layer MOS solar cells
07 p0925 N88-15621
Extraction of MOS VLSI (Very-Large-Scale-Integrated) circuit models including critical interconnect parasitics
[AD-A185847] 08 p0979 N88-15914
Impurity bands in quantum wells
[INPE-4250-PRE/1123] 08 p1089 N88-16552
Dispersive hole transport in SiO2
[AD-A187077] 09 p1254 N88-17513
Nature of gigantic resistance fluctuations in metal-oxide-semiconductor wires
[DE88-002905] 09 p1256 N88-17533
Formal multilevel hierarchical verification of synchronous MOS VLSI circuits
[AD-A187532] 10 p1324 N88-17918
RELIC: A reliability simulator for integrated circuits
[AD-A187493] 11 p1477 N88-18811
Radiation response of thin oxides grown by rapid thermal oxidation and rapid thermal annealing techniques
[DE88-003632] 11 p1561 N88-19347
Metal oxide varistor polarization from an initial transient
[AD-A189012] 12 p1623 N88-19711
Response characteristics of dual MOSFET gamma-ray sensors produced by Mitel Corporation
[AD-A189026] 12 p1630 N88-19755
Fundamental studies and device development in beta silicon carbide
[AD-A189540] 12 p1699 N88-20165
GM: A gate matrix layout generator
[EUT-87-E-179] 13 p1820 N88-20875
Two papers on a symbolic analyzer for MOS (Metal-Oxide Semiconductors) circuits
[AD-A188617] 15 p2139 N88-22761
Modeling the effects of heavy charged particles on MOSFETs (Metal-Oxide-Semiconductor Field Effect Transistors)
[AD-A190575] 15 p2143 N88-22792
The effect of elevated temperature on irradiated MOS devices 17 p2406 N88-24308
Development of the field-induced electron injection and impact ionization (F4I) technique for radiation hardness testing of MOS (Metal-Oxide-Semiconductor) gate insulators
[AD-A192114] 18 p2583 N88-25345
The response of ultrathin palladium gate sensors to hydrogen and carbon monoxide
19 p2672 N88-25885
Zinc-oxide thin films for integrated-sensor applications
19 p2673 N88-25896
Extended and local plasmons in a lateral superlattice
20 p2870 N88-27041
Dose-enhancement effects in TaSi/Al- and Al-gate MOS devices
[DE88-005483] 21 p3020 N88-27926
Sol-gel processing of metal-oxide-semiconductor structures
[DE88-009853] 22 p3156 N88-28778
Electrical properties of metal-oxide-silicon structures with sol-gel oxides
[DE88-011791] 22 p3156 N88-28779
Evaluation of silicon-on-insulator MOS (Metal-Oxide-Semiconductor) transistor response to 10-keV X-ray and cobalt-60 irradiation
[DE88-006102] 23 p3206 N88-29082
Waveform relaxation applied to transient device simulation
[AD-A194992] 24 p3432 N88-30429
Joint services electronics program
[AD-A195731] 24 p3434 N88-30439

METAL OXIDES
NT ALKALINE EARTH OXIDES
NT ALUMINUM OXIDES
NT BARIUM OXIDES
NT BERYLLIUM OXIDES
NT BISMUTH OXIDES
NT CALCIUM OXIDES
NT CERIUM OXIDES
NT CHROMIUM OXIDES
NT COBALT OXIDES
NT COPPER OXIDES
NT HAFNIUM OXIDES
NT HEMATITE
NT IRON OXIDES
NT LANTHANUM OXIDES
NT LEAD OXIDES
NT LITHIUM OXIDES
NT MAGNESIUM OXIDES
NT MANGANESE OXIDES
NT MOLYBDENUM OXIDES
NT NICKEL OXIDES
NT NIOBIUM OXIDES
NT RUTILE
NT SAPPHIRE
NT TANTALUM OXIDES
NT TIN OXIDES
NT TITANIUM OXIDES
NT VANADIUM OXIDES
NT YTTRIUM OXIDES
NT ZINC OXIDES
NT ZIRCONIUM OXIDES
Slip casting and extruding shapes of rhenium with metal oxide additives. Part 2: Development of grain stabilized rhenium parts for resistojets
[NASA-CR-180851] 03 p0278 N88-11749
Shock-induced chemical synthesis of phases similar to the high temperature superconductor oxides
[DE87-013725] 03 p0380 N88-12387
Activated metal oxide surfaces as highly basic and reducing environments
[AD-A184958] 05 p0561 N88-13417
Effect of the gate oxide thickness on the speed of MOS integrated circuits
[PB88-155783] 10 p1323 N88-17910
Gas-phase photoelectron spectroscopy of metals and metal oxides of importance in the upper atmosphere
[AD-A187771] 11 p1511 N88-19027
Composite ceramic superconducting filaments for superconducting cable
[AD-A187833] 11 p1556 N88-19312
Metal oxide varistor polarization from an initial transient
[AD-A189012] 12 p1623 N88-19711
Compound ceramic processing
15 p2050 N88-22212
The structure and properties of RF reactive sputtered IrO2 films 19 p2672 N88-25884
Surface phases and their influence on metal-oxide interfaces
[DE88-007938] 20 p2769 N88-26420
Defect characterization of the redox behavior and stability of conducting oxides
[DE88-010799] 20 p2876 N88-27088

METAL PARTICLES
NT METAL POWDER
NT POWDERED ALUMINUM
NT SINTERED ALUMINUM POWDER
Rotation of magnetized particle in electrically conducting viscous medium 06 p0770 N88-14733
Characterization of the arc/spark excitation sources used in the spectrometric oil analysis program
[AD-A187131] 10 p1297 N88-17758
Suspension of small metallic plates: A versatile sensor
[PB88-130901] 11 p1487 N88-18874
The percolation approach as a basis for experimental research on the mechanical properties of composite materials 14 p1886 N88-21271
Study of mean free path effects on growth of ultrafine metallic aerosols
[AD-A190206] 15 p2039 N88-22149
Far- and mid-infrared properties of metal-insulator composite materials
[AD-A193227] 21 p2905 N88-27236
Calibration of the portable wear metal analyzer
[AD-A192971] 21 p2950 N88-27524

METAL PLATES
Evaluation of mechanical and technological parameters of different steel states by nondestructive micro- and macromagnetic measuring quantities as well as ultrasonic techniques
[MPA-810-079] 01 p0057 N88-10366
Experiments: Test range facilities, part 2
03 p0305 N88-11921
Fatigue failure of thin porous strips
04 p0426 N88-12640
Water disbondment characterization of organic Coating/metal substrate systems
[AD-A184847] 05 p0567 N88-13454
Numerical simulations of impact tests on a rigid wall --- armor steel
[SNIAS-872-320-102] 05 p0610 N88-13744
A summary of experimental results on square plates and stiffened panels subjected to air-blast loading
09 p1178 N88-17057
A detailed microstructural examination of the cause of HAZ cracking in type 316 steel
[AERE-R-12428] 10 p1301 N88-17777
Effects of commercial cladding on the fracture behavior of pressure vessel steel plates
[DE88-004333] 10 p1303 N88-17790
Removal of out-of-plane distortion in mild steel panels using flame heating, volume 1
[AD-A187802] 11 p1457 N88-18684
Removal of out-of-plane distortion in mild steel panels using flame heating, volume 2
[AD-A187803] 11 p1457 N88-18685
Mechanisms in thermal mechanical forming of plates
[AD-A187797] 11 p1466 N88-18744
Performance evaluation of plate-fin heat exchangers
[AD-A187798] 11 p1482 N88-18845
Investigation of constrained-layer technique using exact elasticity theory
[AD-A188664] 12 p1636 N88-19795
Mechanical design of a ultrahigh gravity UHV facility to launch and recover a low-speed projectile tested on board KC 135 14 p1877 N88-21216
Impact shock generator from explosively driven plates
[DE88-003596] 14 p1918 N88-21452
The effective fracture toughness of aluminum at rapid heating rates
[AD-A189745] 15 p2036 N88-22146
Finite element simulation of perforation of aluminum plates
[DE88-002092] 15 p2073 N88-22362
Processing defects and strength of alumina substrates
[W-10/87] 15 p2087 N88-22441
Plate response analysis using shock tube
[AD-A190828] 18 p2526 N88-24987
Optimization of mechanical/corrosion properties of TI-CODE 12 plate and sheet. Part 2: Thermomechanical processing effects
[DE88-007493] 19 p2616 N88-25517
A numerical study of Rayleigh-Taylor instability in aluminum and steel plates
[DE88-010475] 20 p2774 N88-26449
Analysis of the perforation of monolithic and simple laminate aluminium targets as a test of analytical deformation models
[MRL-R-1111] 20 p2813 N88-26686
Vibration response of constrained viscoelastically damped plates: Analyses and experiments
[AD-A192329] 20 p2815 N88-26659
Finite element method for plate structures with inclined angles
[ILR-MITT-182] 21 p3008 N88-27842
High effectiveness contour matching contact heat exchanger
[NASA-CASE-MSC-20840-1] 23 p3214 N88-29132

METAL POWDER
NT POWDERED ALUMINUM
NT SINTERED ALUMINUM POWDER
Development and production of new and modified powders for sprayed coatings and components for saving important raw materials
[BMFT-FB-T-86-129] 01 p0025 N88-10159
GSSR powder metallurgy research, production expanding 03 p0286 N88-11797
Cast iron freezing mechanisms
03 p0298 N88-11870
Fatigue failure of thin porous strips
04 p0426 N88-12640
Improved silicon nitride for advanced heat engines
[NASA-CR-175006] 08 p0973 N88-15886
A case study of the development of a military specification - zirconium powder for thermal batteries
[AD-A188751] 13 p1792 N88-20717
Microprobe examination of composite materials produced by burning of Ti, Cr, C powders with powder of any one Fe-group metal 14 p1886 N88-21269
Grain growth behavior of extrusion consolidated centrifugally atomized Type 304 stainless steel powder
[DE88-006788] 15 p2038 N88-22143
Laboratory scale inert gas atomizer for producing rapidly solidified powders
[DE88-006734] 18 p2497 N88-24812
Hot isostatic pressing of nickel aluminide powders
[DE88-009677] 19 p2617 N88-25525
Assessment of opportunities for gas-fired sintering in the advanced ceramics and powdered metals industries
[PB88-197157] 19 p2620 N88-25545
Plasma joining of metal matrix composites
[AD-A193939] 22 p3051 N88-28100

METAL PROPELLANTS
Metal containing polymers as fuel cell catalysts
[AD-A184605] 03 p0347 N88-12194
A holographic investigation of particulates in metallized solid fuel ramjet combustion
[AD-A186887] 09 p1140 N88-16831

Holographic investigation of metalized solid propellant combustion in two-dimensional and three-dimensional rocket motors
[AD-A187000] 09 p1140 N88-16832

Characterization of aluminum/RP-1 gel propellant properties
[NASA-TM-100951] 18 p2496 N88-24808

Possibilities of economical improvements for Moon based rocket propulsion using lunar propellants
[ILR-MITT-196] 24 p3338 N88-29871

METAL SHEETS

Superplastic deformation and post forming tensile properties of Ti-6Al-4V sheet
[RAE-TR-86015] 01 p0023 N88-10144

Fatigue failure of thin porous strips
04 p0426 N88-12640

Behavior of short cracks in a 2024 aluminum alloy sheet tested at several stress ratios 05 p0600 N88-13669

The effect of shear lips on fatigue crack growth in Al-2024 sheet material 06 p0718 N88-14408

An investigation of the influence of dislocation substructures on the deformation behavior of AK, DC steel sheets
[DE88-006337] 14 p1889 N88-21289

Studies on hot-dip zinc-aluminum coated sheet steels
[ETN-88-92217] 15 p2042 N88-22166

Weldability of general purpose heat source iridium capsules 17 p2426 N88-24429

Optimization of mechanical/corrosion properties of TI-CODE 12 plate and sheet. Part 2: Thermomechanical processing effects
[DE88-007493] 19 p2616 N88-25517

Constant amplitude fatigue life data for notched and unnotched annealed Ti-6Al-4V sheet
[AD-A193420] 21 p2913 N88-27287

Ultrasonic detection of diffusion and adhesion loss
24 p3354 N88-29967

METAL SHELLS

Vibration-absorbing characteristics of metal-polymer shells 02 p0158 N88-10991

METAL STRIPS

Method for maintaining precise suction strip porosities
[NASA-CASE-LAR-13638-1] 23 p3201 N88-29051

METAL SURFACES

A surface science investigation of potential intermediates, catalysts, and promoters in the synthesis of higher alcohols by metals
[DE87-014188] 02 p0144 N88-10906

Studies on surface chemical states of some metals and ceramics bombarded with energetic light-ions
[DE87-752975] 02 p0145 N88-10910

Studies on temporal field emission from stainless steel surfaces
[DE87-014237] 02 p0147 N88-10919

On the interaction of a planar metal surface with a charge and with a molecule
[DE87-703083] 02 p0147 N88-10920

Thermal resistance of contacting metal surfaces at helium temperatures
[BLL-RISLEY-TR-5500-(9091.9F)]
02 p0148 N88-10929

Experimental determination of flow potential surfaces supporting a multiaxial formulation of viscoplasticity
02 p0187 N88-11167

A theoretical analysis of the deactivation of metal surfaces upon carburization
[AD-A184556] 03 p0290 N88-11821

Bonding and coupling of C sub 1 fragments on metal surfaces
[AD-A184186] 03 p0295 N88-11852

Study of field adsorption using pulsed-laser field ion microscopy
[DE88-000310] 03 p0330 N88-12085

The structure of adsorbed sulfur and carbon on molybdenum and rhenium single crystal surfaces, and their influence on carbon monoxide and hydrocarbon chemisorption
[DE88-001393] 04 p0499 N88-13073

Master plots for predicting the case-depth in laser surface treatments
[PB87-221875] 05 p0586 N88-13574

The effect of ion beam mixed Ni-Al surface layers on PSB extrusion morphology in fatigued nickel
05 p0598 N88-13652

The influence of the topography of fracture surfaces on crack closure 05 p0598 N88-13657

Atomic beam studies of the interaction of hydrogen with transition metal surfaces
[DE88-000208] 05 p0648 N88-13970

Method for preparing hydride configurations and reactive metal surfaces
[DE88-000845] 06 p0679 N88-14161

Surface gouging by hypervelocity sliding contact between metallic materials
[DE88-001937] 06 p0682 N88-14178

Ion-beam nitriding of steels
[NASA-CASE-LEW-14104-2] 06 p0682 N88-14179

Profiles of self stress and of load stress at notches
06 p0719 N88-14419

Partial analysis of experiment LDEF A-0114
[NASA-CR-179236] 06 p0780 N88-14787

Ion mixing and surface modification in metal-semiconductor systems
[DE88-001702] 06 p0786 N88-14823

Wind tunnel model surface gauge for measuring roughness
[NASA-CR-182392] 07 p0822 N88-14996

Processing and interfacial analysis of glass-ceramic to metal seals
[DE88-002999] 08 p0971 N88-15873

Review of nucleation and incipient boiling under pool and forced convection conditions
08 p0982 N88-15938

Geometric structure, pseudoband gaps, and surface vibrational resonances on metal surfaces
[AD-A187001] 09 p1143 N88-16851

Local stoichiometry and atomic interdiffusion during reactive metal/mercury-cadmium-telluride junction formation
[AD-A187554] 10 p1421 N88-18488

Laser measurements of state-resolved Ga and in atom sticking and desorption on metal and semiconductor surfaces
[AD-A187644] 11 p1555 N88-19310

Thermodynamics of wetting by liquid metals
[DE88-003634] 11 p1563 N88-19360

Chemical cleaning of metal surfaces in vacuum systems by exposure to reactive gases
[AD-A188588] 12 p1608 N88-19616

Correlations between photons in resonance fluorescence emitted by an atom near a metal surface
[AD-A188365] 12 p1689 N88-20102

A study of the interaction of light with sub-micron metallic surfaces
[DE88-003138] 12 p1776 N88-20624

Spontaneous decay and atomic fluorescence near a metal surface of an absorbing dielectric
[AD-A187508] 13 p1835 N88-20975

Recent progress in structure determination by LEED (Low-Energy Electron Diffraction) measure the properties of the deep donors (DX-cent)
[DE88-003851] 13 p1846 N88-21048

Development of a laboratory test for multiport injector deposits: Approaches 1 and 2
[AD-A190697] 15 p2048 N88-22203

Theory of the dissociation dynamics of small molecules on metal surfaces: Finite temperature studies
[DE88-006495] 15 p2132 N88-22716

Auger electron spectroscopy of contrast-forming layers on metals
[NASA-TT-20182] 16 p2178 N88-22960

Enhanced emittance of oxidized 304 stainless steel
17 p2423 N88-24408

Specular steel surfaces for solar mirror substrates
[DE88-001153] 21 p2968 N88-27630

Theory of the dissociation dynamics of small molecules on metal surfaces: Finite temperature studies
[DE88-007763] 21 p3013 N88-27882

Dynamics of a plasma produced under effect of the XeCl-laser radiation on metallic surface
[DE88-701983] 21 p3017 N88-27902

Reaction dynamics on semiconductor surfaces
[AD-A194305] 22 p3156 N88-28781

Influence of local volume forces on surface relaxation of pure metals and alloys: Applications to Ni, Al, Ni3Al
[DE88-702718] 23 p3195 N88-29014

Storing bits on a DNA polymer chain
[AD-A195701] 24 p3356 N88-29981

METAL VAPOR LASERS

Ignition and high speed photography of energetic materials with a copper vapor laser
[DE88-004831] 12 p1631 N88-19765

Electronic energy transfer processes in the alkali/alkaline earth metal vapors
[AD-A190035] 15 p2034 N88-22119

Alkali metal diffuse band lasers
[AD-A190244] 15 p2071 N88-22350

METAL VAPORS
NT MERCURY VAPOR
NT SODIUM VAPOR

Generation of IR stimulated radiation, UV visible violet coherent radiation by two-photon resonance pumping in K vapor 03 p0301 N88-11892

Microgravity nucleation and particle coagulation experiments support
[NASA-CR-181541] 04 p0423 N88-12619

Behavior and structure of metal vapor arc plasma between molten electrodes
[DE88-001854] 06 p0782 N88-14801

TiN coatings on M2 steel produced by plasma assisted chemical vapor deposition
[DE88-003189] 08 p0970 N88-15867

The band systems of alkali vapors
[NASA-TT-20206] 10 p1417 N88-18462

Multiply stripped ion generation in the metal vapor vacuum arc
[DE88-008418] 19 p2725 N88-26179

METAL WHISKER REINFORCEMENT
U WHISKER COMPOSITES

METAL WORKING
NT CLADDING
NT EXPLOSIVE FORMING
NT FORGING
NT HYDROFORMING
NT SIZING (SHAPING)

Superplastic deformation and post forming tensile properties of Ti-6Al-4V sheet
[RAE-TR-86015] 01 p0023 N88-10144

Hardening of metal during production of bent shapes
[BLL-M-37250-(5828.4)] 02 p0149 N88-10928

Activities report in metal manufacturing
[ISSN-0524-7705] 07 p0839 N88-15086

Contribution to the study of wrinkling in metal stamping
[ISAL-IDI1-87-08] 08 p0976 N88-15900

Modification of properties of metals by high-power ion beams 08 p1079 N88-16507

Metals. Preliminary study for an Innovation-Oriented research Program (IOP)
[ETN-88-91317] 14 p1889 N88-21290

Innovation-Oriented research Program (IOP) metals. Annexes
[ETN-88-91318] 14 p1889 N88-21291

Simulation of thermo-mechanical forming processes: A mixed Eulerian-Langrangian finite element method
[PB88-155247] 14 p1933 N88-21530

METAL-GAS SYSTEMS

Studies for the definition of a Faraday converter for space nuclear systems 17 p2411 N88-24339

Evaluation of a diffusion/trapping model for hydrogen ingress in high-strength alloys
[AD-A194301] 23 p3194 N88-29008

METAL-INSULATOR-METAL DIODES
U MIM DIODES

METAL-INSULATOR-METAL SEMICONDUCTORS
U MIM (SEMICONDUCTORS)

METAL-METAL BONDING

Investigation on diffusion reaction brazing of aluminum
[PB87-143368] 08 p0992 N88-16001

Composite/metal jointing technology for vehicle weight reduction
[DE88-900228] 08 p0992 N88-16005

Evaluation of high temperature structural adhesives for extended service, phase 5
[NASA-CR-178176] 09 p1149 N88-16884

New scientific findings on the morphology of aluminum oxide layers, serving as an adhesive basis
[MBB-Z-137/86] 10 p1312 N88-17840

Surface free energy of laser-produced bond percolators
[PB88-130885] 11 p1493 N88-18913

The relationship of the chemical bonding topology of high critical temperature copper oxide superconductors to that of the chevrel phases and the ternary lanthanide rhodium borides
[AD-A189255] 13 p1845 N88-21042

Optimum duration of steady-state stage in friction welding of metals without artificial braking
14 p1898 N88-21330

Interface characterization of Cu-Cu and Cu-Ag-Cu low temperature solid state bonds
[AD-A191015] 16 p2283 N88-23667

Evaluation of explosive bonding for patching aluminum with aluminum
[AD-A193303] 21 p2913 N88-27295

Shielding effectiveness of metallic joints versus corrosion prevention 22 p3054 N88-28120

Static and dynamic metal-metal friction at plastic stress levels
[DE88-011281] 23 p3222 N88-29176

METAL-SEMICONDUCTOR-METAL SEMICONDUCTORS
U MSM (SEMICONDUCTORS)

METAL-WATER REACTIONS

Corrosion problems associated with computer disk packs 22 p3054 N88-28121

METALLIC GLASSES

Studies on some Ge-Se-Te glasses
[PD-MT-8721] 04 p0420 N88-12607

Structural investigations of some metallic glasses
[ECN-198] 06 p0686 N88-14203

Neutron- and X-ray-small angle scattering with Fe-base metallic glasses
[DE88-002538] 09 p1147 N88-16876

Anodic behavior of Ni-P and Ni-Cr-P metallic glasses
[DE88-005334] 11 p1463 N88-18722
Metastable materials by laser irradiation
[PB88-130364] 11 p1493 N88-18912
Corrosion and fatigue properties of FeCrB/Si metallic glass wires in aqueous environments
17 p2320 N88-23855
Oxidation behavior and microstructural studies of melt-spun glassy Fe-Al-Zr metal
[DE88-009964] 19 p2617 N88-25526

METALLIC PLASMAS
NT CESIUM PLASMA
Behavior and structure of metal vapor arc plasma between molten electrodes
[DE88-001654] 06 p0782 N88-14801
X-ray source model for Z-pinch aluminum plasmas
[AD-A189509] 12 p1696 N88-20148
Ultraviolet-visible spectroscopy of laser-produced aluminum plasmas
[AD-A193004] 20 p2860 N88-26990
Spectral line shapes from highly ionized sodium plasmas
[AD-A193401] 21 p3017 N88-27907

METALLICITY
Modes, masses, metallicities, and magnitudes of RR Lyrae variables
[DE87-013149] 01 p0109 N88-10703
A geometrical model for determining the physicochemical properties of ternary metallic systems
[BLL-M-37303-(5828.4)] 02 p0149 N88-10931
Molecular hydrogen in galaxies
23 p3299 N88-29645

METALLIZING
Microscopic control of metalization stability
[AD-A187553] 10 p1421 N88-18487
UV-Laser reactions of molecular adsorbates
[AD-A190796] 16 p2212 N88-23201
Microscopic control of semiconductor interface reactivity
[AD-A191193] 16 p2283 N88-23668
Shock wave compression and metallization of simple molecules
[DE88-008031] 20 p2851 N88-26925
Laser and electrochemical studies of metallizations in electronic devices
[AD-A193786] 23 p3208 N88-29090
Stress related failures causing open metallization
[AD-A195061] 24 p3383 N88-30150

METALLOGRAPHY
Evaluation of cracking in aluminum cylinders
[PB87-201398] 01 p0024 N88-10149
Precision metrology comparing ultrasonic and other techniques for the determination of steel thickness
[DE87-011051] 02 p0230 N88-11452
Study of stainless steel time-temperature sensitization diagrams, part 1
[ETN-87-90762] 03 p0289 N88-11815
International Conference on Microstructology held in Gainesville, Florida on 7-9 May 1986
[AD-A184604] 03 p0290 N88-11822
Calibration standard for metallographic microscopes
[RFP-3956-REV] 03 p0326 N88-12057
Metallography of maraging 350 steel
[DE87-013748] 04 p0418 N88-12591
A detailed microstructural examination of the cause of HAZ cracking in type 316 steel
[AERE-R-12428] 10 p1301 N88-17777
Metallurgical analysis of fractured F-27 aircraft landing gear
[DE88-005885] 11 p1460 N88-18705
Processing, structure and properties of heavily deformed in situ composites
[AD-A189611] 13 p1742 N88-20416
Auger electron spectroscopy of contrast-forming layers on metals
[NASA-TT-20182] 16 p2178 N88-22980
The adherence of nickel oxide on nickel during high temperature oxidation
[DE88-011194] 20 p2774 N88-26450
As-received microstructure of a SiC/Ti-15-3 composite
[NASA-TM-100938] 22 p3050 N88-28095

METALLOIDS
NT AMORPHOUS SILICON
NT ARSENIC
NT BORON
NT BORON ISOTOPES
NT GERMANIUM
NT SILICON
NT TELLURIUM

METALLORGANIC COMPOUNDS
U ORGANOMETALLIC COMPOUNDS

METALLURGY
Metallurgy laboratory for Columbus, executive summary
[SNIAS-813-CA/TS] 02 p0157 N88-10980
Investigations in field of surface forces in metallurgy
[BLL-M-47406-(5828.4)] 08 p0969 N88-15860

METALS
NT ALKALI METALS
NT ALKALINE EARTH METALS
NT ALUMINUM
NT BARIUM
NT BERYLLIUM
NT BISMUTH
NT CADMIUM
NT CALCIUM
NT CALCIUM ISOTOPES
NT CERIUM
NT CESIUM
NT CHROMIUM
NT COBALT
NT COBALT 60
NT DYSPROSIUM
NT ERBIUM
NT EUROPIUM
NT FERROUS METALS
NT GADOLINIUM
NT GALLIUM
NT GOLD
NT HAFNIUM
NT HOLMIUM
NT INDIUM
NT IRIDIUM
NT IRIDIUM ISOTOPES
NT IRON
NT IRON ISOTOPES
NT IRON 57
NT LANTHANUM
NT LAWRENCIUM
NT LEAD (METAL)
NT LEAD ISOTOPES
NT LIQUID LITHIUM
NT LIQUID METALS
NT LIQUID POTASSIUM
NT LIQUID SODIUM
NT LITHIUM
NT LITHIUM ISOTOPES
NT MAGNESIUM
NT MAGNESIUM ISOTOPES
NT MANGANESE
NT MERCURY (METAL)
NT MERCURY ISOTOPES
NT MERCURY VAPOR
NT METAL VAPORS
NT MOLYBDENUM
NT NEODYMIUM
NT NEODYMIUM ISOTOPES
NT NEPTUNIUM
NT NICKEL
NT NIOBIUM
NT NIOBIUM ISOTOPES
NT NOBLE METALS
NT OSMIUM
NT PALLADIUM
NT PLATINUM
NT PLATINUM ISOTOPES
NT PLUTONIUM ISOTOPES
NT PLUTONIUM 238
NT POTASSIUM
NT RARE EARTH ELEMENTS
NT REFRACTORY METALS
NT RHENIUM
NT RHENIUM ISOTOPES
NT RHODIUM
NT RUBIDIUM
NT RUBIDIUM ISOTOPES
NT RUTHENIUM
NT SAMARIUM ISOTOPES
NT SILVER
NT SODIUM
NT SODIUM VAPOR
NT STRONTIUM
NT TANTALUM
NT THORIUM
NT TIN
NT TITANIUM
NT TRANSITION METALS
NT TUNGSTEN
NT ULTRAPURE METALS
NT URANIUM
NT URANIUM ISOTOPES
NT URANIUM 238
NT VANADIUM
NT YTTERBIUM
NT YTTRIUM
NT ZINC
NT ZIRCONIUM
Transient absorption behavior of metals at the onset of the laser welding process
[DFVLR-FB-87-12] 01 p0025 N88-10160
Electrical heating method — pipelines, metal tanks
[GB-PATENT-2-137-059-A] 01 p0043 N88-10274
Analysis of shell-type structures subjected to time-dependent mechanical and thermal loading
[NASA-CR-181409] 01 p0060 N88-10388
Channeled particle acceleration by plasma waves in metals
[DE87-010541] 01 p0093 N88-10604
Metal-sensing layer-semiconductor and metal-sensing layer-metal heterostructure gas sensors
[DE87-011280] 01 p0103 N88-10674
Grain boundary phase equilibria in metallic systems
[DE87-014123] 01 p0104 N88-10679
Reduction of CO2 to methanol and methane by photo and dark reactions on semiconductor and metal electrodes
[PB87-226825] 02 p0156 N88-10975
Computer modeling of metal forming
[DE87-013804] 02 p0157 N88-10984
Photocatalytic electrochemistry at a biological-membrane metal-colloid interface
[DE87-009122] 02 p0166 N88-11041
Electron capture from solids by positrons
[DE87-014355] 02 p0232 N88-11463
Birch's law and the properties of high temperature fluid metals
[DE87-014744] 03 p0288 N88-11807
Shock-induced melting and rapid solidification
[DE88-000226] 03 p0288 N88-11810
Surface coatings and catalyst production by electrodeposition 03 p0297 N88-11863
Gas tungsten arc welding of Al-10Fe-5Ce
[AD-A184202] 03 p0334 N88-12104
Activities at government research laboratories reported 04 p0403 N88-12503
Ignition and combustion of metals in oxygen
04 p0407 N88-12530
Topological aspects of infinite metal clusters and superconductors
[AD-A184104] 04 p0495 N88-13049
Analysis of wear metals in engine oils using the atomic absorption spectrophotometric method
[NAL-TM-MT-8704] 05 p0564 N88-13435
Molecular-level synthesis and characterization of metal-polymer interfaces
[AD-A184956] 05 p0567 N88-13455
Photocurrent generation from basic metals, utilizing a short pulsed ArF excimer laser
[AD-A184928] 05 p0587 N88-13579
The orientations of dipolar walls produced by cyclic deformation 05 p0598 N88-13655
The interaction of DC plasma jet with a melting metal: Experimental measurements and mathematical description
[AD-A185173] 05 p0651 N88-13993
Singularities in X-ray spectra of metals
[DE88-001440] 06 p0681 N88-14174
An overview of metal plasticity
[DE88-001658] 06 p0681 N88-14175
Characterization of microstructure in metallic and composite materials
[AD-A186193] 07 p0826 N88-15012
Studies of metal/carbon surface chemistry
[DE87-009545] 07 p0829 N88-15029
Studies of supported metal catalysts
[DE88-002546] 07 p0831 N88-15038
Computer simulation of impurities and interfaces in body centered cubic metals
[PB88-108162] 07 p0832 N88-15047
Computer simulation of pencil glide in B.C.C. metals
[DE88-001802] 07 p0834 N88-15062
Study of the embedded atom method of atomistic calculations for metals and alloys
[DE88-002798] 07 p0835 N88-15065
Life prediction of thermomechanical fatigue using total strain version of strainrange partitioning (SRP): A proposal
[NASA-TP-2779] 07 p0867 N88-15263
Phonon dispersion for several surfaces with ordered overlayers: A lattice dynamical study
07 p0876 N88-15315
Atomic oxygen effects on metals
07 p0924 N88-15617
Interrelation and measurement of formability, strengthening, and thermomechanical processing under metalworking conditions
[DE88-002485] 08 p0967 N88-15850
Critical analysis of the dynamic behavior laws for metallic materials — ballistics
[ISL-NB-401/86] 08 p0969 N88-15862
Submerged arc flux welding with CaF2-CaO-SiO2 fluxes: Possible electrochemical effects on weld metal
[DE88-003107] 08 p0992 N88-16004
Characteristics of thermooptical sound excitation in metals 08 p1076 N88-16486

A comparison of measurements from the A/E35U-3 and PWMA (Portable Wear Metal Analyzer) spectrometers
[AD-A186855] 09 p1177 N88-17047
Electronic and chemical structure of 3-5/metal and Si/metal interfaces
[AD-A186579] 09 p1254 N88-17518
A large strain thermomechanical forming model for elastic-viscoplastic behavior in metals
10 p1301 N88-17780
Irradiation effects in metals
[DE88-004272] 10 p1303 N88-17789
Metal modification for improved glass-ceramic to metal seals: 1. Auger results on ion implantation and vapor deposition films
[DE88-005244] 10 p1339 N88-18006
Chemical activation of molecules by metals: Experimental studies of electron distributions and bonding
[DE88-004465] 10 p1407 N88-18393
Non-proprietary research projects of the Center for the Space Processing of Engineering Materials
[AR-2] 10 p1426 N88-18516
Deactivation of alumina based catalysts
11 p1455 N88-18673
Reference standards for nondestructive tests
[AD-A187766] 11 p1497 N88-18936
Gas-phase photoelectron spectroscopy of metals and metal oxides of importance in the upper atmosphere
[AD-A187771] 11 p1511 N88-19027
Atomistic studies of the structure and properties of grain boundaries with substitutional impurities
[DE88-004161] 11 p1545 N88-19237
An experimental measurement of metal multilayer X-ray reflectivity degradation due to intense X-ray flux
[LA-10989-T] 11 p1547 N88-19255
Microstructure characterization with a pulsed laser ultrasonic source
[DE88-005207] 12 p1632 N88-19766
Photochemistry at structured surfaces: A classical electromagnetic approach
[AD-A189519] 13 p1737 N88-20387
Material instabilities in solids
[AD-A189525] 13 p1738 N88-20388
The coordination cluster theory for metallic solutions
[DE88-005934] 13 p1738 N88-20389
Formation of nuclei during precipitation in metallic mixed crystals
[NASA-TT-20248] 13 p1745 N88-20437
Spontaneous decay and atomic fluorescence near a metal surface of an absorbing dielectric
[AD-A187508] 13 p1835 N88-20975
Image charge, coherent scattering, and symmetry effects in electron stimulated desorption: O(-) from O sub 2 condensed on metals
[AD-A189093] 13 p1835 N88-20979
Annihilation momentum density of positrons trapped at vacancy-type defects in metals and alloys
[DE88-005936] 15 p2144 N88-22797
Surface enhanced Raman scattering applied to surface chemical kinetics
[AD-A191275] 16 p2176 N88-22969
Question on the measurement of the metal work function in an electron spectrometer by the secondary-electron emission threshold method
[NASA-TT-20190] 16 p2178 N88-22979
Friction and wear of ceramics
17 p2323 N88-23874
Noncontact temperature measurement: Requirements and applications for metals and alloys research
17 p2328 N88-23899
The influence of cathodic protection on erosion-corrosion of metals and model alloys
[AD-A191613] 18 p2485 N88-24742
Arc-textured metal surfaces for high thermal emittance space radiators
[NASA-TM-100894] 18 p2487 N88-24754
The stress analysis of ceramic, polymeric, and metallic composite systems by the finite element method
18 p2529 N88-25004
Metals and Ceramics Division
[DE88-008955] 19 p2618 N88-25530
Observation of metallic conductivity in liquid carbon
[AD-A191723] 19 p2618 N88-25533
Plastic deformation and roughness of free metal surfaces
[PB88-196621] 20 p2772 N88-26439
Abnormal diffusion of vacancies in metals
[DE88-701880] 20 p2773 N88-26441
Shock wave compression and metallization of simple molecules
[DE88-006031] 20 p2851 N88-26925
Metallic superlattices 20 p2864 N88-27012
Pure metallic bridge and point-contact tunneling into single- and polycrystal YBa2Cu3O(sub 7-y)
[DE88-010030] 20 p2878 N88-27084
On the systematics of phase transformation in metallic alloys
[DE88-008041] 21 p2913 N88-27288
Oxidation-erosion of metals and alloys: Models, verification, and prediction
[DE88-010016] 21 p2915 N88-27300
Soluble metal chelate polymers of coordination numbers six, seven and eight
[AD-A192485] 21 p2917 N88-27314
Effects of near interfacial microstructure on toughness and subcritical crack growth in ceramic/metal systems
[DE88-009842] 21 p2919 N88-27325
The influence of weld metal properties, weld geometry and applied load on weld system performance
[AD-A193403] 21 p2961 N88-27588
Amorphous silicon solar cells using a metal substrate
[PB88-131941] 21 p2968 N88-27628
An endochronic rate-sensitive constitutive equation for metals, application to generalized creep and large deformations
[AD-A194167] 22 p3055 N88-28125
Equipment for the pressure welding of metals and alloys utilising the effects of superplasticity
[RAE-TRANS-2162] 22 p3055 N88-28129
Chemistry of adhesion at the polyimide-metal interface
[AD-A194647] 22 p3058 N88-28143
Stress intensity factors for cracked metallic structures under rapid thermal loading
[AD-A191219] 23 p3193 N88-29004
Phenomena of the ionic transport in the stress corrosion of metals
[DE88-702502] 23 p3195 N88-29013
Thermocouple for heating and cooling of memory metal actuators
[NASA-CASE-NPO-17068-1-CU]
23 p3217 N88-29151
System suitable for observing surface plasmon in a semi-infinite semiconductor superlattice
[DE88-702686] 23 p3293 N88-29606

METAMORPHISM (GEOLOGY)
Isotopic and chemical studies of early crustal metasedimentary rocks
[NASA-CR-182711] 14 p1944 N88-21601
The timing and mechanism of depletion in Lewisian granulites 24 p3394 N88-30209
Decoupled Rb-Sr and Sm-Nd isotopic evolution of the continental crust 24 p3395 N88-30216
Metamorphic P-T paths and Precambrian crustal growth in East Antarctica 24 p3395 N88-30218
The early archaean crustal history of West Greenland as recorded by detrital zircons 24 p3395 N88-30221
Reappraisal of the geology of Kangimut Sammisoq, Ameralik Fjord, Southern West Greenland: Crustal structure and interpretation of isotopic data
24 p3398 N88-30234
Growth of the lower continental crust
24 p3398 N88-30236
Late-Archaean crustal growth in the Lewisian Complex of Northwest Scotland: Diachroneity in magmatic accretion and implications for models of crustal growth
24 p3401 N88-30253

METASTABILITY
U METASTABLE STATE

METASTABLE ATOMS
Group 2A metastable collision complexes: Spectroscopy and behavior in intense radiation fields
[AD-A186737] 08 p1082 N88-16524

METASTABLE STATE
Application of spin-sensitive electron spectroscopies to investigations of electronic and magnetic properties of solid surfaces and epitaxial systems
[DE87-014235] 02 p0245 N88-11550
The gamma-ray laser project
[AD-A184824] 05 p0587 N88-13578
Structural relaxation in strained-layer heterostructures
[DE88-002326] 07 p0868 N88-15264
Group 2A metastable collision complexes: Spectroscopy and behavior in intense radiation fields
[AD-A186737] 08 p1082 N88-16524
Relaxation of metastable semiconductor strained-layer structures by plastic flow
[DE88-002729] 08 p1090 N88-16560
Effect of the subgap conductance on the metastable states in a Josephson tunnel junction
[DE88-003102] 09 p1258 N88-17543
Stability and metastability in semiconductor strained-layer structures
[DE88-003306] 09 p1258 N88-17544
Metastable materials by laser irradiation
[PB88-130364] 11 p1493 N88-18912
Development of metastable processing paths for high temperature alloys
[AD-A188682] 12 p1608 N88-19617
Quantum Monte Carlo study of the MIES associated with H2 (X 1 sigma sub g (+)) and H2 (B 1 sigma sub u (+))
[AD-A189063] 13 p1835 N88-20977
Investigations of the origins of metastable, light-induced changes in hydrogenated amorphous silicon
[DE88-001117] 13 p1846 N88-21051
Laser cooling of neon metastable states
14 p1975 N88-21785
Stability limits in the monoclinic-tetragonal transformations of zirconia
[DE88-005924] 14 p1986 N88-21849
Effect of vibrational excitation on rate parameters of atmospheric reactions
[AD-A190464] 15 p2094 N88-22477
Synthesis of metastable superconductors by high dynamic pressure
[DE88-005620] 15 p2139 N88-22764
Magnetic anomalies in the rare earth oxide superconductors GdBa2Cu3O(7-x) and YbBa2Cu3O(7-x)
[AD-A190713] 15 p2144 N88-22793
Metastability in SiGe/Si strained-layer structures
[DE88-007603] 18 p2585 N88-25361
Formation of metastable structures and amorphous phases in Cu-W alloys using the triod sputtering technique
[DE88-009051] 21 p2915 N88-27298
Proof of the feasibility of coherent and incoherent schemes for pumping a gamma-ray laser
[AD-A193856] 23 p3220 N88-29165

METAZOA
U ANIMALS

METEOR BURSTS
U METEOROID SHOWERS

METEOR CRATERS
U CRATERS

METEOR HAZARDS
U METEOROID HAZARDS

METEOR TRAILS
Meteor-burst communications: Is this what the Navy needs?
[AD-A184433] 04 p0431 N88-12672
Middle Atmosphere Program. Handbook for MAP, volume 25
[NASA-CR-181571] 06 p0732 N88-14502
Elementary process and meteor train spectra
06 p0732 N88-14504
Atmosphere dynamic processes structure at 80-105 km altitude 06 p0736 N88-14527
Internal gravity waves in the meteor zone in the Tbilisi Region 06 p0736 N88-14528
On the wave excitation in the turbulent meteor trace
06 p0737 N88-14530
Methods and first results of plasma non-isothermal parameters measurements in meteor trails
06 p0737 N88-14531
On the meteor trail spectra 06 p0737 N88-14533
Ozone formation due to interaction of meteoroids with Earth's atmosphere 06 p0738 N88-14536
Meteor matter interaction with the Earth's atmosphere and the ionospheric E-region structure
06 p0738 N88-14537
Incident meteoroid flux density
06 p0739 N88-14542
On meteor stream spatial structure theory
06 p0739 N88-14544
Meteor velocity distribution and an optimum monitoring mathematical model 06 p0739 N88-14546
Optical electronics for meteor observations
06 p0741 N88-14559

METEORITE COLLISIONS
Measurements of iridium and the meteoric impact hypothesis at cretaceous end
[DE87-703765] 04 p0521 N88-13200
Conditions for geomagnetically trapping sub-micron lunar ejecta between L = 1.2 and L = 3.1
04 p0521 N88-13203

METEORITE COMPRESSION TESTS
U COMPRESSION TESTS
U MECHANICAL PROPERTIES
U METEORITES

METEORITE CRATERS
Early intense cratering: Effects on growth of earth's crust 24 p3395 N88-30219
A compilation of information and data on the Manson impact structure
[NASA-CR-183169] 24 p3401 N88-30258

METEORITES
NT ACHONDRITES
NT CARBONACEOUS CHONDRITES
NT CARBONACEOUS METEORITES
NT CHONDRITES
NT IRON METEORITES
Moessbauer study of shock induced effects in the Fe-Ni 50/50 ordered alloy in meteorites
[DE87-703364] 04 p0521 N88-13199

The archiving of meteor research information 06 p0732 N88-14505

The nonlinear thermodynamics of meteors, noctilucent clouds, enhanced airglow and global atmospheric circulation 06 p0738 N88-14538

The distribution of evaporitic weathering products on Antarctic meteorites 06 p0798 N88-14888

Products from cosmic-ray interactions in extraterrestrial matter: What they tell us about radiation backgrounds in space
[DE88-009143] 19 p2743 N88-26288

MEVTV Workshop on Nature and Composition of Surface Units on Mars
[NASA-CR-183075] 23 p3300 N88-29654

Selective weathering of shocked minerals and chondritic enrichment of the Martian fines 23 p3301 N88-29660

Aqueous alteration in S-N-C meteorites and implications for weathering products on Mars 23 p3303 N88-29673

What SNC meteorites tell us about Martian magmatism 23 p3303 N88-29679

Spectral reflectance of SNC meteorites: Relationships to Martian surface composition 23 p3304 N88-29683

Origin of SNC kaersutitic amphibole: Experimental data 23 p3306 N88-29693

Crystal fractionation in the SNC meteorites: Implications for surface units on Mars 23 p3307 N88-29698

Nineteenth Lunar and Planetary Science Conference. Press abstracts
[NASA-CR-183037] 24 p3440 N88-30473

Exotic minerals in 3,500 million year old rocks: Evidence for large meteorite impacts 24 p3440 N88-30475

Evidence of the in situ decay of Al-26 in a Semarkona chondrule 24 p3441 N88-30479

LSU scientists discover evidence of large meteorite impacts on the early earth 24 p3441 N88-30480

Lewis Cliff 86010, a unique Antarctic meteorite: Possible new clues to the early history of the solar system 24 p3442 N88-30482

Did the greenhouse effect kill the dinosaurs 24 p3442 N88-30484

Antarctic Meteorite Newsletter, Volume 11, Number 2, August 1988
[NASA-TM-89801] 24 p3457 N88-30573

METEORITIC COMPOSITION

The end height of fireball as a function of their residual kinetic energy 06 p0737 N88-14535

Meteor matter interaction with the Earth's atmosphere and the ionospheric E-region structure 06 p0738 N88-14537

A processing method and results of meteor shower radar observations 06 p0738 N88-14539

Optical electronics for meteor observations 06 p0741 N88-14559

Nineteenth Lunar and Planetary Science Conference. Press abstracts
[NASA-CR-183037] 24 p3440 N88-30473

Ureilites are not igneous differentiates 24 p3441 N88-30477

New type of primitive meteorite found in Antarcitca 24 p3441 N88-30478

Physical processes and timescales in planet and small-body accretion 24 p3451 N88-30540

Nebular processes recorded in chondritic meteorites 24 p3451 N88-30541

METEORITIC DAMAGE

Space environmental considerations for a long-term cryogenic storage vessel 08 p0981 N88-15933

A review of impact design criteria for space power heat rejection systems 17 p2410 N88-24333

The effect of the near earth micrometeoroid environment on a highly reflective mirror surface
[NASA-TM-101307] 24 p3332 N88-29833

METEORITIC DUST

U MICROMETEOROIDS

METEORITIC IONIZATION

U ATMOSPHERIC IONIZATION

U METEOR TRAILS

METEOROID CONCENTRATION

A method of long-term radar shower data analysis 06 p0738 N88-14541

Models of sporadic meteor body distributions 06 p0739 N88-14543

Density variations of meteor flux along the Earth's orbit 06 p0739 N88-14545

METEOROID CRATERS

U METEORITE CRATERS

METEOROID DUST CLOUDS

NT ZODIACAL DUST

METEOROID HAZARDS

Space environmental considerations for a long-term cryogenic storage vessel 08 p0981 N88-15933

Assessment of the effects of space debris and meteoroids environment on the space station solar array assembly
[NASA-TM-101315] 23 p3185 N88-28959

METEOROID PROTECTION

Optimization techniques applied to passive measures for in-orbit spacecraft survivability
[NASA-CR-179216] 04 p0408 N88-12532

Space suit extravehicular hazards protection development
[NASA-TM-100458] 04 p0475 N88-12927

Space environmental considerations for a long-term cryogenic storage vessel 08 p0981 N88-15933

Space station integrated wall damage and penetration damage control. Task 5: Space debris measurement, mapping and characterization system
[NASA-CR-179281] 10 p1285 N88-17688

An analysis of penetration and ricochet phenomena in oblique hypervelocity impact
[NASA-TM-100319] 10 p1339 N88-18004

A review of impact design criteria for space power heat rejection systems 17 p2410 N88-24333

METEOROID SHOWERS

NT AQUARID METEOROIDS

NT GEMINID METEOROIDS

NT ORIONID METEOROIDS

NT PERSEID METEOROIDS

NT QUADRANTID METEOROIDS

NT TAURID METEOROIDS

Meteor-burst communications: Is this what the Navy needs?
[AD-A184433] 04 p0431 N88-12672

Middle Atmosphere Program. Handbook for MAP, volume 25
[NASA-CR-181571] 06 p0732 N88-14502

Dynamics of meteor streams 06 p0732 N88-14503

Elementary process and meteor train spectra 06 p0732 N88-14504

Main results of atmospheric fine structure parameter observation in the lower thermosphere 06 p0735 N88-14518

On connection between evolution of troposphere fronts and changes of circulation regime in meteor zone 06 p0735 N88-14519

Study of internal gravity waves in the meteor zone 06 p0735 N88-14521

The role of fragmentation in interaction of meteoroids with the Earth's atmosphere 06 p0737 N88-14532

On the meteor trail spectra 06 p0737 N88-14533

A processing method and results of meteor shower radar observations 06 p0738 N88-14539

Photographic fireball networks 06 p0738 N88-14540

On meteor stream spatial structure theory 06 p0739 N88-14544

The Valec fireball and predicted meteorite fall 06 p0739 N88-14547

Results of observations of the Eta Aquarid and Orionid meteor showers in 1980-1984 06 p0740 N88-14548

Monte Carlo modeling and meteor showers 06 p0740 N88-14549

On the spatial structure of the Perseids meteor stream 06 p0740 N88-14550

Some models of the Geminids meteor stream formation 06 p0740 N88-14551

Structural peculiarities of the Quadrantid meteor shower 06 p0740 N88-14552

On the possible origin of meteoroid generating asteroid orbits 06 p0740 N88-14553

New approaches to some methodological problems of meteor science 06 p0741 N88-14557

Hard- and software problems of spaced meteor observations by optical electronics 06 p0741 N88-14560

The evolution of the mass distribution of cometary particles 14 p2004 N88-21946

Communications using channels formed by meteor bursts
[AD-A192088] 18 p2501 N88-24834

A study of a meteor burst communication system 21 p2934 N88-27421

METEOROIDS

NT AQUARID METEOROIDS

NT BOLIDES

NT GEMINID METEOROIDS

NT MICROMETEOROIDS

NT ORIONID METEOROIDS

NT PERSEID METEOROIDS

NT QUADRANTID METEOROIDS

NT SPORADIC METEOROIDS

NT TAURID METEOROIDS

NT ZODIACAL DUST

Ozone formation due to interaction of meteoroids with Earth's atmosphere 06 p0738 N88-14536

Meteor detection on ST (MST) radars 06 p0740 N88-14554

The Cyclone meteor radar system for routine wind measurements in the lower thermosphere 06 p0741 N88-14555

Optical electronics for meteor observations 06 p0741 N88-14559

Effects of meteoroids and space debris on the particulate environment for space station 18 p2591 N88-25399

METEOROLOGICAL BALLOONS

NT JIMSPHERE BALLOONS

METEOROLOGICAL CHARTS

New precipitation map of world ocean 04 p0458 N88-12834

Mariners weather log, volume 31, number 4, Fall 1987
[PB88-173851] 20 p2825 N88-26761

Meteorological atlas of the Southern Hemisphere lower stratosphere for August and September 1987
[NASA-TM-4049] 20 p2825 N88-26763

The 1985 Meteorological Yearbook of Ispra (27th)
[PB88-125729] 20 p2828 N88-26777

Intercomparison of NMC (National Meteorological Center) and ECMWF (European Centre for Medium Range Weather Forecasts) global analyses: 1980-1986
[PB88-196548] 21 p2974 N88-27668

METEOROLOGICAL FLIGHT

Definition and use of sensors for measuring electrical conductivity in thunderclouds
[ESA-TT-1047] 03 p0352 N88-12222

METEOROLOGICAL INSTRUMENTS

NT BAROMETERS

NT CLOUD HEIGHT INDICATORS

NT IONOSONDES

NT RADIOSONDES

NT RAIN GAGES

NT RAWINSONDES

BARS-1M meteorological complex carried on IL-18 airplane 06 p0725 N88-14458

On-site meteorological program guidance for regulatory modeling applications
[PB87-227542] 06 p0731 N88-14498

Air temperature shield tests
[AD-A187459] 11 p1514 N88-19043

MRS-3000 meteorological rocket probe for the MMR-06 dart integrated meteorological rocket system
[NASA-TT-20303] 19 p2693 N88-26010

The pneumatic wind shear sensor: A tool for meteorological investigations and flight management 22 p3036 N88-28024

METEOROLOGICAL PARAMETERS

Effects on electromagnetic wave propagation at frequencies over 10 GHz due to inhomogeneities of the complex refraction index
[REPT-86-025] 01 p0036 N88-10228

Conception and discussion of a model describing ice formation on various obstacles
[ONERA-NT-1986-6] 01 p0072 N88-10460

A mini system for nowcasting 02 p0204 N88-11278

Use of time changes of surface data parameters in short range forecasting 02 p0206 N88-11291

An isentropic mesoscale analysis system 02 p0212 N88-11332

Experimental study of the propagation of an acoustic wave in the low atmosphere
[ISL-R-111/86] 02 p0231 N88-11454

The CNR/PSN Advanced Microwave Imaging Radiometer (AMIR) -- satellite-borne 03 p0340 N88-12141

Application of multitemporal SPOT data for crop monitoring: Effects of frost and drought 03 p0344 N88-12171

Documentation of NCAR (National Center for Atmospheric Research) CCM1 program modules
[PB87-213567] 03 p0352 N88-12220

Global atmospheric circulation statistics: Four year averages
[NASA-TM-100690] 05 p0628 N88-13842

Results on the low elevation angle propagation experiment, part 1
[TUD-R-328] 06 p0693 N88-14250

Middle Atmosphere Program. Handbook for MAP, volume 25
[NASA-CR-181571] 06 p0732 N88-14502

The climatic wind regime in the lower thermosphere from meteor radar observations 06 p0733 N88-14506

Report of the second session of the CAS/JSC working group on numerical experimentation --- weather forecasting
[WMO/TD-168] 06 p0745 N88-14579

Eighth Session of the Commission for Aeronautical Meteorology (abridged)
[WMO-673] 06 p0745 N88-14585

Facilities for research and weather observations on the 213 m tower at Cabauw (Netherlands) and at remote locations
[KNMI-WR-87-5] 06 p0746 N88-14587

Three dimensional display of meteorological scientific data
[DE88-000776] 07 p0880 N88-15339

Influence of Environmental Factors on Aircraft Wing Performance
[VKI-LS-1987-03] 08 p0951 N88-15771

Characterization of meteorological phenomena influencing aircraft operations 08 p0951 N88-15772

The influence of wind shear, downdraft, and turbulence in aircraft performance 08 p0952 N88-15773

The potential influence of rain on airfoil performance
08 p0952 N88-15774

Revised uniform summary of surface weather observations. Parts A-F: Carswell AFB, Texas
[AD-A186820] 09 p1192 N88-17144

Modification of a successive corrections objective analysis for improved higher order calculations
[NASA-CR-182467] 09 p1230 N88-17370

Development of an engineering model atmosphere for Mars
[NASA-CR-182462] 09 p1263 N88-17568

NASA Oceanic Processes Program
[NASA-TM-4025] 10 p1357 N88-18109

Long term measurement network for FIFE
[NASA-CR-182491] 12 p1646 N88-19857

Calibration of the solar radiation estimation method by satellites
[INPE-4349-PRE/1185] 12 p1646 N88-19861

Quality control of upper air conventional data (TEMP and PILOT)
[INPE-4223-RPE/546] 12 p1647 N88-19862

Remote sensing of meteorological parameters with the aid of a clear-air Doppler radar
[PB88-142518] 12 p1647 N88-19864

Worldwide distributions of shipboard surface meteorological observations for EM propagation analysis
[AD-A188771] 12 p1648 N88-19871

Climatology and space observations
[ISBN-2-85-428179-9] 14 p1935 N88-21536

Global meteorological data facility for real-time field experiments support and guidance
[NASA-TM-4023] 14 p1947 N88-21608

Local meteorological processes and air mass origin during a cloud chemical field experiment on Areskutan, Sweden, in summer 1986
[AP-28] 14 p1948 N88-21615

Analysis of meteorological conditions and haze distribution for the Second Arctic Gas and Aerosol Sampling Program (AGASP 2), March-April 1986
[PB88-164140] 14 p1948 N88-21618

Tropic heat MR (Meteorological Recorder) meteorological data (April 1984 - June 1985)
[PB88-161286] 14 p1948 N88-21620

A study on electric fields and conductivity associated with electrified clouds in the region of South America
[INPE-4487-TDL/325] 15 p2096 N88-22486

A multivariate variational objective analysis-assimilation method. Part 1: Development of the basic model
[NASA-CR-182651] 15 p2097 N88-22491

Acoustic propagation in the low atmosphere. Experimental study and modeling by the radius method
[ISL-CO-247/86] 15 p2131 N88-22713

Use of energy emission for detecting the necessity of irrigation in wheat in field conditions
[INPE-4461-TDL/318] 16 p2229 N88-23315

Spectroradiometry in meteorology
16 p2272 N88-23599

Ice formation on aircraft
[ETN-88-92154] 18 p2545 N88-25104

Effects of atmospheric model layering on LOWTRAN 6 calculations of 8-12 micrometers near-horizon sky radiances
[AD-A192969] 20 p2791 N88-26559

The 1985 Meteorological Yearbook of Ispra (27th)
[PB88-125729] 20 p2828 N88-26777

Intercomparison of NMC (National Meteorological Center) and ECMWF (European Centre for Medium Range Weather Forecasts) global analyses: 1980-1986
[PB88-196548] 21 p2974 N88-27668

The Hanford meteorological data collection system and data base
[DE88-008632] 21 p2975 N88-27672

Space shuttle natural environment analysis
[NASA-CR-179337] 21 p2976 N88-27676

SERI standard broadband format: A solar and meteorological data archival format
[DE88-001145] 21 p3028 N88-27975

The effects of changes in observation and data assimilation systems on CAC climate data sets
22 p3124 N88-28568

Evaluation of global data sets for climate studies
22 p3124 N88-28569

A method to adjust climatological time series for discontinuous inhomogeneities
22 p3124 N88-28570

A comparison of typical meteorological year solar radiation information with the SOLMET data base
[DE88-009242] 23 p3234 N88-29247

Microwave remote sensing at INPE (Institute for Space Research) Brazil: Concepts and future prospects of soil moisture studies
[INPE-4569-PRE/1310] 24 p3388 N88-30178

METEOROLOGICAL PROBES
U SONDES

METEOROLOGICAL RADAR

COST-73 and its application in very short range forecasting 02 p0199 N88-11242

New nowcasting opportunities using modern meteorological radar 02 p0199 N88-11245

Nowcasting microbursts using Doppler radar in a forecaster-computer environment
02 p0200 N88-11246

Use of a 5 cm Doppler radar to detect and forecast severe thunderstorms in a real time forecast operation
02 p0200 N88-11247

Thunderstorm nowcasting using Doppler radar and soundings 02 p0200 N88-11248

A real-time system for automatic single-Doppler wind field analysis 02 p0200 N88-11249

Diagnosing short term changes in temperature and moisture profiles from single Doppler radar
02 p0200 N88-11251

On the interaction between radar and satellite image nowcasting systems and mesoscale numerical models
02 p0204 N88-11277

Evaluation of the Rainsat precipitation analysis system in real-time use 02 p0205 N88-11283

The Pacific Weather Center Satellite Facility: An overview 02 p0205 N88-11286

Specification of predictors necessary for the determination of over or underestimation of radar derived total rainfall
[AD-A185363] 05 p0628 N88-13838

Waveform for short-dwell-time meteorological Doppler radars
[PB88-102199] 07 p0845 N88-15126

Development of a Doppler wind lidar system for atmospheric wind measurements
08 p1027 N88-16217

Improved resolution atmospheric density measurements based on simulations 08 p1027 N88-16221

Meteorological radar and its usage in the Navy
[AD-A186650] 09 p1152 N88-16902

Airborne Doppler radar technology for wind shear detection 10 p1274 N88-17622

Status of FAA terminal Doppler weather radar programs 10 p1275 N88-17632

Information transfer in the National Airspace System
10 p1275 N88-17634

Research and development to acquire and reduce melting layer cloud physics and evaluate a prototype M-meter
[AD-A188390] 12 p1648 N88-19873

A polarization diversity meteorological radar system
[AD-A189291] 13 p1758 N88-20515

TDWR (Terminal Doppler Weather Radar) clutter residue map generation and usage
[AD A191148] 16 p2235 N88-23352

Observation of stratiform rain with 94 GHz and s-b and Doppler radar
[AD-A192013] 18 p2544 N88-25100

Remote sensing of temperature profiles. Performance test of PASS
[DE88-753108] 20 p2826 N88-26768

A radar study of the interaction between lightning and precipitation
[DE88-009120] 20 p2827 N88-26770

TDWR (Terminal Doppler Weather Radar) PRF (Pulse Repetition Frequency) selection criteria
[AD-A193089] 21 p2932 N88-27407

Utilization of a single clear-air Doppler radar beam to measure vertical divergence
[AD-A195543] 24 p3405 N88-30271

METEOROLOGICAL ROCKETS
U SOUNDING ROCKETS

METEOROLOGICAL SATELLITES
NT DMSP SATELLITES
NT METEOSAT SATELLITE
NT NIMBUS 7 SATELLITE
NT NOAA SATELLITES
NT NOAA 7 SATELLITE
NT TIROS N SERIES SATELLITES
NT TIROS SATELLITES

Improved geostationary satellite soundings for the mesoscale weather analysis/forecast operation
02 p0200 N88-11252

Impact of a direct assimilation of satellite-inferred precipitation rates into a regional meteorological model
02 p0213 N88-11342

Fabricate, calibrate and test a dosimeter for integration into the CRRES (Combined Release and Radiation Effects Satellite) satellite
[AD-A185439] 05 p0585 N88-13564

Estimation of marine boundary layer depth and relative humidity with multispectral satellite measurements
[AD-A184881] 05 p0620 N88-13804

Country plans three-axis weather satellite
06 p0688 N88-14218

Regional weather satellite data processing center opens in Tashkent 06 p0725 N88-14457

Suggested severe local storm operational scenario for GOES I-M
[NASA-TM-100688] 11 p1515 N88-19052

Space projects for the 90's relevant to climatology
14 p1935 N88-21539

Satellite rainfall retrieval by logistic regression
[NASA-CR-180485] 14 p1946 N88-21607

Global meteorological data facility for real-time field experiments support and guidance
[NASA-TM-4023] 14 p1947 N88-21608

Baseline observing system experiments using the AFGL global data assimilation system
[AD-A188861] 15 p2024 N88-22062

A multivariate variational objective analysis-assimilation method. Part 2: Case study results with and without satellite data
[NASA-CR-182653] 15 p2097 N88-22492

Meteorological Satellite Center Technical Note No 16
[ISSN-0388-9653] 17 p2350 N88-24003

Prospects of satellite wind sensing systems in the years 1995-2000 17 p2350 N88-24004

Outline of the GPCP strategy
17 p2351 N88-24007

VISSR line number monitoring system
17 p2351 N88-24008

Contribution of space to marine activities
19 p2700 N88-26057

Meteorological satellite product support and research for project GALE
[NASA-CR-180989] 19 p2727 N88-26193

Satellite remote sensing of the wet bulb globe temperature heat stress index, phase 2
[AD-A192798] 20 p2818 N88-26717

The effects of changes in observation and data assimilation systems on CAC climate data sets
22 p3124 N88-28568

Global-scale temperature changes to August 1987 and a comparison of satellite and conventional data
22 p3125 N88-28572

Investigations of magnetosphere-ionosphere coupling relevant to operational systems
[AD-A195972] 24 p3391 N88-30195

Passive microwave measurements of water vapor fields and rain for locating fronts in cyclonic storms
[AD-A195632] 24 p3404 N88-30267

Analytical method for approximate geodetic referencing of scanner images of meteorological artificial earth satellites using control points 24 p3449 N88-30527

METEOROLOGICAL SERVICES

Applications and benefits of short period weather forecasts 02 p0199 N88-11240

Mesoscale forecasting today and tomorrow: Problems and opportunities. A position paper
02 p0199 N88-11244

Meteorological systems support to critical shuttle requirements on the Eastern Test Range --- STS
02 p0205 N88-11281

The Pacific Weather Center Satellite Facility: An overview 02 p0205 N88-11286

Mesoscale analysis and forecasting for the 1987 America's Cup, Fremantle, Western Australia
02 p0214 N88-11350

Regional weather satellite data processing center opens in Tashkent 06 p0725 N88-14457

Current status of world weather service
06 p0725 N88-14459

Wave and wind data sources, environmental conditions committee report, International Ship and Offshore Structures Congress
[PB87-234902] 06 p0746 N88-14586

Federal plan for meteorological services and supporting research, fiscal year 1988
[PB88-118716] 07 p0880 N88-15336

WMO Region 2/Region 5 Training Seminar on Climate Data Management and User Services
[WCP-133] 16 p2234 N88-23344

A drought watch system
[WCP-134] 16 p2234 N88-23345

METEOROLOGICAL STATIONS
U WEATHER STATIONS

METEOROLOGY
NT AEROLOGY
NT AGROMETEOROLOGY
NT ALPINE METEOROLOGY
NT AVIATION METEOROLOGY
NT HYDROMETEOROLOGY
NT LONG RANGE WEATHER FORECASTING
NT MARINE METEOROLOGY
NT MESOMETEOROLOGY
NT MICROBURSTS (METEOROLOGY)
NT MICROMETEOROLOGY
NT NOWCASTING
NT NUCLEAR METEOROLOGY
NT NUMERICAL WEATHER FORECASTING
NT POLAR METEOROLOGY
NT RADIO METEOROLOGY
NT STATISTICAL WEATHER FORECASTING
NT SYNOPTIC METEOROLOGY
NT TROPICAL METEOROLOGY
NT WEATHER FORECASTING
Diagnostics of atmospheric chemistry through ozone measurement
[INPE-4230-PRE/1105] 01 p0068 N88-10437
Solar Energy Meteorological Research and Training Site, Alaska
[DE87-013706] 01 p0069 N88-10440
Hanford Meteorological Station computer codes. Volume 1: The GEN computer code
[DE87-012816] 01 p0071 N88-10456
Hanford Meteorological Station computer codes. Volume 2: The PROD computer code
[DE87-014807] 02 p0215 N88-11355
Convective cross section analysis
[PB87-204566] 02 p0216 N88-11361
Publications and final reports on contracts and grants, 1986 (National Environmental Satellite, Data and Information Service)
[PB87-220810] 03 p0352 N88-12218
Short reference year
[PB87-107470] 03 p0352 N88-12221
Study of an airborne Doppler radar: Project Astenx
[BLL-MO-TRANS-1667-(9022.552)]
04 p0432 N88-12675
USSR report: Earth sciences
[JPRS-UES-86-006] 04 p0458 N88-12831
Application of TOMS data to weather analysis models
05 p0617 N88-13787
USSR report: Earth sciences
[JPRS-UES-87-004] 06 p0725 N88-14455
AN-30M cloud-seeding airplane in international exhibition 06 p0725 N88-14456
Current status of world weather service
06 p0725 N88-14459
CTD/02 measurements during 1984 and 1985 as part of the Equatorial Pacific Ocean Climate Studies (EPOCS)
[PB88-102082] 06 p0748 N88-14600
USSR report: Earth sciences
[JPRS-UES-87-003] 08 p1009 N88-16119
Application of satellite data in variational analysis for global cyclonic systems
[NASA-CR-182468] 09 p1193 N88-17152
NASA wind shear model: Summary of model analyses
10 p1273 N88-17617
Cape Blanco wind farm feasibility study
[DE88-003748] 10 p1348 N88-18059
Wake effects in a Fayette 95-IIS wind turbine array
[DE88-001103] 10 p1349 N88-18063
The structure and dynamics of monsoon depressions
10 p1355 N88-18102
Developments in National Weather Service meteorological data collection programs as related to EPA (Environmetal Protection Agency) air pollution models
[PB88-130240] 10 p1356 N88-18104
Refractive index, meteorology and fading in line-of-sight transmission paths 12 p1616 N88-19666
The correlation between methodological and low-level angle-of-arrival measurements 12 p1617 N88-19668
Historical electromagnetic propagation condition database description
[AD-A189157] 12 p1621 N88-19695
A study of satellite emission computed tomography
[AD-A189567] 13 p1797 N88-20745
A multivariate variational objective analysis-assimilation method. Part 2: Case study results with and without satellite data
[NASA-CR-182653] 15 p2097 N88-22492
The collection of statistics on the frequency of cloud cover over North America
[AD-A190456] 15 p2097 N88-22495
Evaluation of NMC (National Meteorological Center) global analyses: 1979-1987
[PB88-178157] 18 p2544 N88-25096
Taiwan area mesoscale experiment: P-3 aircraft operations summary
[PB88-169073] 18 p2544 N88-25098
NOAA (National Oceanic and Atmospheric Administration) Meteorology Division support to the Environmental Protection Agency
[PB88-179866] 19 p2689 N88-25980
Meteorological satellite product support and research for project GALE
[NASA-CR-180989] 19 p2727 N88-26193
Our climate in danger
[DE88-701824] 20 p2822 N88-26743
An evaluation of two millimeter wave propagation models for horizontal atmospheric attenuation at 70-115 GHZ
[AD-A192699] 21 p2931 N88-27403
Update on the meso-microscale meteorological hierarchy
[DE88-009133] 21 p2975 N88-27670
A comparison of typical meteorological year solar radiation information with the SOLMET data base
[DE88-009242] 23 p3234 N88-29247
Activities report of the World Meteorological Organization
[WMO-689] 24 p3404 N88-30265

METEORS
U METEOROIDS

METEOSAT SATELLITE
Study on data compression systems for operational remote sensing --- meteosat imagery
[NLR-TR-86029-L] 05 p0620 N88-13808
The Meteosat operational program
09 p1127 N88-16759
Meteorological Information Extraction Center (MIEC) processing --- Meteosat imagery
[ESA-STR-224] 09 p1192 N88-17143
Introduction to the Meteosat system
[ESA-SP-1041] 09 p1193 N88-17146
La Recherche Aerospatiale, bimonthly bulletin, number 1987-2, 237/March-April
[ESA-TT-1074] 11 p1433 N88-18550
Presentation of the METEOSAT system and the roles of EUMETSAT within the meteorological community
17 p2357 N88-24039

METERS
U MEASURING INSTRUMENTS

METHACRYLATE RESINS
U ACRYLIC RESINS

METHANE
Reduction of CO2 to methanol and methane by photo and dark reactions on semiconductor and metal electrodes
[PB87-226825] 02 p0156 N88-10975
Pulsed plasma jet igniters: Species measurements in methane combustion
[DE88-001389] 05 p0562 N88-13422
A process study of the biothermal conversion of water hyacinths to methane
[DE88-000554] 06 p0730 N88-14488
Catalytic combustion of methane
[PB88-123112] 07 p0829 N88-15028
Gas hydrate model development and validation
[DE88-001004] 10 p1298 N88-17762
Geological evolution and analysis of confirmed or suspected gas hydrate localities. Volume 9: Formation and stability of gas hydrates of the Middle America Trench
[DE88-001007] 10 p1347 N88-18050
Novel catalysts for methane activation
[DE88-003637] 13 p1738 N88-20390
Oxide-bound transition metal complexes for methane activation
[PB88-169719] 14 p1887 N88-21277
Basic research on natural gas combustion phenomena
[PB88-168380] 14 p1887 N88-21278
Evaluation of direct methane conversion to higher hydrocarbons and oxygenates
[DE88-003812] 15 p2049 N88-22204
A theoretical model of the washout of trace gases by raindrops in the atmosphere 17 p2375 N88-24125
Probing the possibility of a (12)C/(13)C abundance gradient from observations of interstellar CH^+
[DE88-008908] 20 p2884 N88-27125
On the bond distance in methane
[NASA-CR-181436] 22 p3150 N88-28741
Molecular composites processing and properties, 1
[AD-A194113] 23 p3189 N88-28974
The design of methane activation catalysts
[DE88-002265] 23 p3199 N88-29043
Ultraviolet absorption cross sections of chloro- and chlorofluoromethanes at stratospheric temperatures
[AERONOMICA-ACTA-A-324-1988]
23 p3231 N88-29228

METHANOL
U METHYL ALCOHOL

METHOD OF CHARACTERISTICS
The linear characteristic method in XYZ geometry
[DE87-011668] 04 p0484 N88-12984
Analysis and optimization of truncated scarf nozzles subject to external flow conditions
[NASA-TM-100955] 24 p3316 N88-29746

METHOD OF MOMENTS
Treatment of small wire loops in the method of moments code NEC (Numerical Electromagnetics Code)
[DE88-002995] 07 p0846 N88-15136
Electromagnetic scattering from and natural resonances of the circular strip 13 p1759 N88-20523
The new MININEC (version 3): A mini-numerical electromagnetic code
[AD-A191778] 19 p2642 N88-25675

METHODOLOGY
A design methodology for the utilization of metrics within various phases of software lifecycle models
[DE87-010519] 02 p0220 N88-11385
A flight-test methodology for identification of an aerodynamic model for a V/STOL aircraft
[NASA-TM-100067] 09 p1117 N88-16694
Approaches to the verification of rule-based expert systems 09 p1206 N88-17232
A methodology for the synthesis of robust feedback systems
[NASA-CR-182455] 09 p1225 N88-17342
Space station operating system study
[NASA-CR-179308] 11 p1446 N88-18619
Structural analysis methods development for turbine hot section components
[NASA-TM-100298] 11 p1501 N88-18967
The formal specification of computer systems
[AD-A188947] 12 p1675 N88-20013
Design of feedback control systems for stable plants with saturating actuators
[NASA-CR-182613] 12 p1681 N88-20050
Avionics acquisition, trends and future approaches
12 p1702 N88-20184
A comparison of information system development methodologies
[AD-A188957] 12 p1707 N88-20219
Active cooling design for scramjet engines using optimization methods
[NASA-TM-100581] 13 p1783 N88-20669

METHODS
U METHODOLOGY
U PROCEDURES

METHYL ALCOHOL
Reduction of CO2 to methanol and methane by photo and dark reactions on semiconductor and metal electrodes
[PB87-226825] 02 p0156 N88-10975
Alternative fuels: Information on DOD's (Department of Defense's) methanol vehicle program
[PB87-213328] 02 p0156 N88-10976
Application of electronic fuel injection to the optimum engine for methanol utilization
[PB87-201950] 02 p0180 N88-11120
Model Cu/ZnO catalysts for methanol synthesis: The role of surface structure
[DE88-002354] 07 p0830 N88-15037
Fuel cell/battery hybrid vehicle assessment
[DE88-005087] 10 p1427 N88-18520
Practical system for the use of alcohol in diesel engines
[PB88-147863] 12 p1612 N88-19638
Alternative fuels: Information on DOE's (Department of Energy's) methanol vehicle demonstration program
[PB88-118203] 13 p1753 N88-20481
Combustion and performance characteristics of methanol plus higher alcohols in a spark ignition engine
[PB88-147962] 14 p1918 N88-21451
Technical highlights of the Alternative Fuels Utilization Program
[DE88-005064] 15 p2049 N88-22205
Improvements to Raney copper zinc methanol synthesis catalysts 17 p2318 N88-23844
Update of low temperature catalyst development
[DE88-007032] 18 p2480 N88-24715

METHYL COMPOUNDS
NT ACETONITRILE
Thermally stable aromatic structures from acyclic precursors. 1: Para polyphenylene model compounds from 3-Dimethyl amino hex-5-EN-1-YNES
[AD-A185300] 05 p0568 N88-13462
Heterogeneous isotope exchange between solid cesium iodide and gaseous methyl iodide
[ETN-88-91085] 09 p1141 N88-16840
Ultraviolet absorption cross sections of methylbromide at stratospheric temperatures
[AERONOMICA-ACTA-A-320-1987]
15 p2036 N88-22132
Corrosion and corrosion inhibition of metals/alloys in methyphosphonic difluoride 17 p2319 N88-23850
Modification of polymers by photografting processes
17 p2323 N88-23871
Preferential surface adsorption in miscible blends of polystyrene and poly(vinyl methyl ether)
[AD-A191451] 18 p2490 N88-24769

Stratospheric positive ion composition measurements and acetonitrile detection: A consistent picture
[AERONOMICA-ACTA-A-326-1987] 18 p2542 N88-25084

Dissolution rates of polymers and copolymers based on methyl, ethyl and butyl methacrylate
[AD-A194713] 23 p3197 N88-29027

METHYL CYANIDE
U ACETONITRILE

METHYLENE
Evidence for first polymer in Comet Halley: Polyoxymethylene 14 p1997 N88-21906

METRIC CONVERSION
U METRICATION

METRIC PHOTOGRAPHY
Accuracy potential of non-metric cameras in close-range photogrammetry 04 p0463 N88-12862

Investigations on the application of space photographs (Spacelab metric camera) for routine inventories of extensively managed forest areas
[DFVLR-FB-87-22] 09 p1185 N88-17098

METRIC SPACE
NT HILBERT SPACE

Nonsymmetric metrics in nonlinear field theory
[DE88-700509] 07 p0913 N88-15537

Heuristic search in robot configuration space using variable metric 08 p1059 N88-16389

Solving reflexive domain equations in a category of complete metric spaces
[CWI-CS-R8709] 13 p1832 N88-20956

On the Fefferman class of metrics associated with a 3-dimensional Cauchy-Riemann (CR)-space
[PREPRINT-579] 14 p1991 N88-21865

Einstein metrics and Brans-Dicke superfields
[DE88-006992] 15 p2146 N88-22809

Pairwise complete regularity as a separation axiom
[REPT-87-57] 16 p2264 N88-23539

METRIC SYSTEM
U INTERNATIONAL SYSTEM OF UNITS

METRICATION
ADAMEASURE: An implementation of the Halstead and Henry metrics
[AD-A184005] 03 p0365 N88-12299

METROLOGY
Precision metrology comparing ultrasonic and other techniques for the determination of steel thickness
[DE87-011051] 02 p0230 N88-11452

Metrology and calibrating laboratories
[ETN-88-90761] 06 p0670 N88-14104

Temperature Metrology '86
[DE88-700236] 08 p0989 N88-15990

Results from a questionnaire on particulate metrology in the UK
[NPL-MOM-81] 09 p1141 N88-16841

Evaluation of a miniature horizontal pendulum tilt transducer 12 p1577 N88-19435

The effects of humidity on the profile of photographic plates
[NPL-DMOM-88] 14 p1913 N88-21429

Development and applications of optical interferometric micrometrology in the angstrom and subangstrom range
[NASA-TM-100299] 16 p2211 N88-23196

Calibration technique and study on metrological characteristics of a high-voltage inverse square-law function generator
[DE88-702101] 22 p3072 N88-28236

Langley Research Center Metrology Program status for fiscal year 1987
[NASA-TM-100651] 22 p3086 N88-28324

Metrology in France: Industrial aspects and its status in the world
[SNIAS-881-430-109] 22 p3146 N88-28713

Electromagnetic metrology 24 p3363 N88-30024

METROPOLITAN AREAS
U CITIES

MEXICO
Vanfront 3 expedition data report (USNS DE STEIGUER CRUISE 1202-82). Bioluminescence, hydrographic, nutrient, and satellite data from the Gulf of California (November-December 1981)
[AD-A185011] 05 p0620 N88-13805

Land use systems and rural landscapes in the center of Veracruz State (Mexico): First results
22 p3092 N88-28364

MGCO
U MARS OBSERVER

MICA
NT BIOTITE

MICE
A learning model as a basis for investigations of the effects of gravity on the learning processes and memory formulation 07 p0886 N88-15374

Changes in functional parameters of animals during long-term inhalation of acetic acid
07 p0895 N88-15423

Effect of pyrocetam on mouse resistance to hypoxic hypoxia 2-3 months after exposure to X-radiation
07 p0895 N88-15425

Scaling physiological pharmacokinetic models by physiological time
[DE88-000335] 10 p1368 N88-18173

Life sciences research in space: The requirement for animal models 12 p1654 N88-19909

The effect of microgravity on mammalian cell polarization at the ultrastructural level --- Spacelab D1 mission
22 p3061 N88-28164

MICHELSON INTERFEROMETERS
Photodiode matrix for the analysis of two-beam interferences
[PTB-OPT-23] 01 p0048 N88-10310

Milliarcsecond ground-based imaging with single telescopes 01 p0097 N88-10637

A test-bed for space interferometry: Space Platform Interferometer (SPI) 01 p0097 N88-10640

Performances of an Actively Stabilized Stellar Interferometer (ASSI): Faint magnitudes, low fringe contrast measurements and operationality
01 p0097 N88-10641

Optical fiber interferometric sensor to measure temperature in gas flow
[ENST-87E006] 02 p0170 N88-11071

On the theory of the Michelson-Morley experiment in the Earth's gravitational field
[DE87-703077] 02 p0198 N88-11233

Optical determination of the virial coefficients of the gases C2H4, C2H6 and SF6
[ETN-87-90610] 03 p0282 N88-11776

Phase-coherent astrometric interferometry
[AD-A184428] 04 p0439 N88-12725

Fiber optic single mode sensors
[FOA-C-30453-3.1] 06 p0780 N88-14790

Telescope design for Michelson Interferometer for Passive Atmospheric Sounding (MIPAS) B
08 p1017 N88-16167

Computerized evaluation of interferograms of the Michelson Interferometer for Passive Atmospheric Sounding (MIPAS) Laboratory Model (LM)
08 p1019 N88-16177

Modern pulsed wavemeters
[DE88-003875] 10 p1335 N88-17978

Investigations in electro-optical multistability for signal processing 18 p2518 N88-24938

An interferometric measurement technique for railgun structures
[AD-A192851] 21 p2901 N88-27217

Investigations on Mie and Rayleigh scattering as basis for the development of Rayleigh temperature lidars with aid of Michelson interferometry
[GKSS-87/E/62] 21 p2976 N88-27675

Piezoelectric and electrostrictive materials for transducer applications, volume 2
[AD-A194956] 24 p3376 N88-30104

MICHIGAN
Aircraft accident report: Northwest Airlines, Inc., McDonnell Douglas DC-9-82, N312RC, Detroit Metropolitan Wayne County Airport, Romulus, Michigan, August 16, 1987
[PB88-910406] 19 p2601 N88-25449

MICROANALYSIS
Electron sputtering in the analytical electron microscope: Calculations and experimental data
[DE87-011457] 01 p0049 N88-10312

Multidimensional elemental analysis with the Sandia nuclear microprobe
[DE87-014158] 02 p0183 N88-11136

Development of an X-ray fluorescence microprobe at the National Synchrotron Light Source, Brookhaven National Laboratory: Early results: Comparison with data from other techniques
[NASA-CR-181468] 02 p0236 N88-11486

Quantitative electron probe microanalysis investigation of the oxidation of high temperature alloys at low oxygen partial pressures
[JUEL-2120] 03 p0288 N88-11811

X-ray microfluorescence analysis of thin- and thick-sectioned geologic materials
[DE87-009803] 09 p1189 N88-17126

Atom probe microanalysis of superconducting YBa2Cu3O(sub 7-x)
[DE88-003203] 11 p1557 N88-19322

Development, high temperature properties, and microanalysis of nonoxide ceramics
[ETN-88-92103] 14 p1893 N88-21304

Advances in geochemistry and cosmochemistry: Trace element microdistributions with the synchrotron X-ray fluorescence microprobe
[DE88-006355] 15 p2032 N88-22108

Microchemical analysis of polycrystalline Ni3Al and other ordered alloys using the field-ion microscope atom probe
[DE88-011519] 21 p2914 N88-27294

Thin film and near-surface characterization using a mechanical properties microprobe
[DE88-011399] 21 p2915 N88-27302

Superconducting oxides with high critical temperatures
21 p2930 N88-27392

MICROBE
U MICROORGANISMS

MICROBIOLOGY
NT BACTERIOLOGY

JPRS report: Science and technology. USSR: Life sciences
[JPRS-ULS-87-009] 04 p0473 N88-12915

Review of cytoskeleton research in cell differentiation and development
[AD-A185832] 07 p0882 N88-15353

Safety guidelines and procedures for bioscience-based industry and other applied microbiology
[PB87-140521] 08 p1045 N88-16316

USSR report: Life sciences. Biomedical and behavioral sciences
[JPRS-UBB-87-010] 12 p1651 N88-19889

JPRS report: Science and technology. USSR: Life sciences
[JPRS-ULS-88-002] 12 p1665 N88-19982

Digital image processing from speckle interferograms by correlation methods: Application in atmospheric optics, astronomy, and biology
[ETN-88-92125] 20 p2855 N88-26953

Quality control in microbiology: CDC lab manual
[PB88-179890] 23 p3237 N88-29263

MICROBURSTS (METEOROLOGY)
Study of microburst detection performance during 1985 in Memphis, Tennessee
[AD-A184013] 03 p0354 N88-12231

Power spectral density analysis of wind-shear turbulence for related flight simulations
[NASA-CR-182721] 13 p1802 N88-20773

Flight penetration of wind shear: Control strategies
17 p2294 N88-23727

The Federal Aviation Administration/Massachusetts Institute of Technology (FAA/MIT) Lincoln Laboratory Doppler weather radar program
18 p2547 N88-25118

Flight-management strategies for escape from microburst encounters
[NASA-TM-4057] 19 p2603 N88-25461

Influence of wind shear on the aerodynamic characteristics of airplanes
[NASA-TP-2827] 20 p2755 N88-26344

Control of flight through microburst wind shear using deterministic trajectory optimization
20 p2761 N88-26375

MICROCALORIMETERS
U CALORIMETERS

MICROCHANNEL PLATES
A neutron detector based on microchannel plates
[DE87-014703] 02 p0232 N88-11466

A high-speed, eight-frame image intensified electro-optic camera with 200-800mm zoom objective capability
[DE88-000229] 03 p0326 N88-12059

Performance of a photon counting microchannel plate intensifier with wedge and strip image readout
[DE88-003831] 10 p1334 N88-17970

Conception and realization of components for a microchannel-plate detector, and testing of the detector system in the laboratory and in astronomical use
[ETN-88-91495] 11 p1491 N88-18899

The off-axis channel macroplate
[NASA-CR-182938] 18 p2505 N88-24861

An elliptical spectrograph/gated microchannel plate detector for time-resolved spectral measurements in the X-ray region
[DE88-007590] 20 p2856 N88-26961

MICROCHANNELS
A focussed MCP (microchannel plate) image intensifier type for high speed gating
[DE88-000480] 05 p0583 N88-13555

Forced-convection, liquid-cooled, microchannel heat sinks
[AD-A193337] 21 p2937 N88-27444

MICROCIRCUITS
U MICROELECTRONICS

MICROCLIMATOLOGY
Portable, ambient air microclimate cooling in simulated desert and tropic conditions
[AD-A186457] 08 p1050 N88-16338

Perspectives in microclimate cooling involving protective clothing in hot environments
[AD-A188370] 12 p1671 N88-20007

The effects of different combinations of inlet air conditions used for cooling as measured on a heated manikin
[AD-A191116] 18 p2552 N88-25151

MICROCOMPUTERS
NT PERSONAL COMPUTERS

The microcomputer as an engineering management tool
[DE87-014882] 02 p0219 N88-11378

Microcomputer control of spectroscopic instruments
[ATR-86(8431)-4] 03 p0326 N88-12058

The MicroVAX-based data acquisition system for D0
[DE87-014475] 03 p0366 N88-12303

A computer code to calculate line by line atmospheric transmission spectra on a microcomputer
[NASA-TM-100686] 05 p0554 N88-13372

An extension to the multilevel logic simulator for microcomputers
[AD-A185032] 05 p0634 N88-13879

Data analysis at the Oulu (Finland) EISCAT laboratory
06 p0691 N88-14241

MINIX: A UNIX clone with source code
[PB88-100862] 06 p0760 N88-14664

Life sciences flight experiments microcomputer
06 p0792 N88-14857

Microcomputer controlled arc welding power source: Its steady state and transient performance
[PB87-143921] 07 p0863 N88-15233

Study on automatic detection and identification of defects in weld by microcomputer
[PB87-143897] 07 p0863 N88-15237

Data acquisition, reduction and analysis of shock and vibration testing using a super microcomputer
[AD-A186123] 07 p0867 N88-15260

Version description document for the Ada compiler validation capability (version 1.9) (for microcomputer)
[AD-A186390] 07 p0903 N88-15471

Preliminary evaluation of a micro-based repeated measures testing system
[NASA-CR-172038] 08 p1048 N88-16331

Stability, reliability and cross-mode correlations of tests in a recommended 8-minute performance assessment battery
[NASA-CR-172039] 08 p1052 N88-16351

Development of a menu of performance tests self-administered on a portable microcomputer
[NASA-CR-172040] 08 p1067 N88-16452

Measuring mental workload: A performance battery
[AD-A187118] 09 p1200 N88-17192

Design of a neural network simulator on a transputer array 09 p1205 N88-17221

The desktop interface in intelligent tutoring systems
09 p1205 N88-17225

An advanced microcomputer design for processing of semiconductor materials 10 p1288 N88-17703

Microcomputer analysis of regenerative heat exchangers for oscillating flow
[DE88-001773] 10 p1329 N88-17945

Parallelism at the microlevel: Cooperative microcontrollers with real time considerations
10 p1381 N88-18246

Applications of lower cost computers to dimensional gaging
[BDX-613-3606] 11 p1525 N88-19108

Interfacing of a microcomputer with a simultaneous atomic-emission spectrometer
[PB88-139571] 11 p1526 N88-19109

Report on desktop publishing
[AD-A187698] 11 p1528 N88-19128

Computer aided tactics for air combat
12 p1597 N88-19559

Development of a digital terrain modeling system for microcomputers
[INPE-4406-TDL/303] 12 p1639 N88-19816

Automatic data acquisition system utilizing microcomputers: Automatic Meteorological Stations (AMS)
[INPE-4215-PRE/1096] 12 p1646 N88-19859

A simplified computer code for reduction to burning rates of closed bomb pressure-time data (MINICB)
[AD-A189112] 13 p1736 N88-20380

Interactive automated system for testing analog units of digital seismic stations 13 p1789 N88-20702

Study of microcomputer-based real-time programmable optical signal processor and application
[AD-A190076] 15 p2133 N88-22726

Fundamentals of microprocessor-based design: A tutorial, second edition
[DE88-006761] 16 p2244 N88-23406

DATAC bus monitor 17 p2294 N88-23721

Implantation of a geo-cartographical information system through microcomputers 17 p2361 N88-24064

Effective communication between a microVAX and a specialized high-speed subprocessor
[DE88-007967] 19 p2714 N88-26115

On-line measurement of heat of combustion
[NASA-CR-183076] 19 p2738 N88-26255

A microcomputer based frequency-domain processor for laser Doppler anemometry
[NASA-TM-100998] 20 p2803 N88-26634

Managing microcomputer applications: A primer and guide to good practice
[AD-A192992] 20 p2835 N88-26817

Design of high performance microcomputers for numerical data processing
[ETN-88-92371] 20 p2835 N88-26818

A multiprocess operating system for 16 bit microcomputers or porting Unix (trademark) to a NS32016 with enhancements 20 p2836 N88-26822

What's on the menu? Friendlier computers
[AD-A194393] 22 p3135 N88-28637

Microsupercomputers: Design and implementation
[AD-A194712] 22 p3135 N88-28638

LO-CO-GRAF (low cost graphics): Generating maps to support command and control/crisis management using small computers
[AD-A193964] 22 p3139 N88-28661

Finite Element Composite Analysis Program (FECAP) for a microcomputer
[NASA-TM-100670] 23 p3190 N88-28982

A computer program package for introductory one-dimensional digital signal processing applications
[AD-A194656] 23 p3249 N88-29338

A standard library for modeling satellite orbits on a microcomputer
[AD-A195759] 24 p3331 N88-29830

MICROCRACKS

Transply crack density detection by acousto-ultrasonics
[NASA-TM-100224] 03 p0279 N88-11758

Environmentally assisted cracking: Overview of evidence for an adsorption-induced localised-slip process
[AD-A185175] 05 p0565 N88-13443

The orientations of dipolar walls produced by cyclic deformation 05 p0598 N88-13655

Crack propagation properties of sintered steel
05 p0604 N88-13698

The effect of environment on low cycle fatigue properties in HSLA steel 05 p0605 N88-13705

X-ray fatigue failure prediction based on plasticity response to microcracks 05 p0607 N88-13725

Development of crack under periodically pulsed laser radiation 06 p0774 N88-14754

Deformation induced cracking in steel girder bridges and retrofit guidelines
[PB88-102710] 07 p0868 N88-15265

Study on the correlation of polystyrene (PS) film craze to its fracture behaviour by TEM (Transmission Electron Microscopy)
[PB87-143343] 08 p0970 N88-15870

La Recherche Aerospatiale, bimonthly bulletin, number 1987-2, 237/March-April
[ESA-TT-1074] 11 p1433 N88-18550

Study of the effects of metallurgical factors on the growth of fatigue microcracks
[AD-A188475] 12 p1608 N88-19615

Stress analysis in elastic solids with many cracks
[AD-A189015] 12 p1636 N88-19799

Non-destructive evaluation techniques applied to the study of fatigue microcrack growth in steel alloys
[DE88-004090] 13 p1742 N88-20420

Bimodular behavior and crack closure in compression in a brittle material
[AD-A191267] 16 p2224 N88-23275

Time-domain boundary element analysis of dynamic near-tip fields for impact-loaded collinear cracks
[AD-A192930] 20 p2815 N88-26700

Kinetic of martensitic transformations induced by hydrogen in the austenite
[DE88-701623] 23 p3194 N88-29007

The use of a surface acoustic wave technique to study the growth behavior of small cracks in a high strength steel alloy 23 p3225 N88-29193

MICROCRYSTALS

Amorphous or microcrystalline semiconductor memory device
[EP-PATENT-0-162-529-A1] 01 p0026 N88-10167

Gigantic optical nonlinearity in low dimensional systems 14 p1975 N88-21786

Enhanced excitonic optical nonlinearity and exciton dynamics in semiconductor microstructures
14 p1977 N88-21795

Optical characterization of microcrystals
[DE88-006622] 15 p2141 N88-22775

Dispersion measurements of microcrystals in the near ultraviolet and infrared
[DE88-006234] 15 p2145 N88-22800

Semiconductor microcrystallites in porous glass and their applications in optics 20 p2863 N88-27005

MICROCYSTIS

Light scattering of intracellular gas vacuoles: Anomalous behavior of forward and perpendicular light scattering of a cyanobacterium due to intracellular gas vacuoles
[BCPS-87-08] 16 p2228 N88-23308

MICRODENSITOMETERS

Method of digital surface photometry of galaxies and its application to the edge-on galaxy NGC 5907
16 p2287 N88-23695

MICROELECTRONICS

NT LARGE SCALE INTEGRATION
NT VERY LARGE SCALE INTEGRATION

Use of sol-gels in the application of ceramic oxide thin films
[DE87-013610] 01 p0028 N88-10176

Wire interconnection reliability and moisture levels in hybrid microcircuits with epoxy-attached components
[DE87-012987] 01 p0039 N88-10247

Physics and device design of vacuum integrated circuits 01 p0039 N88-10251

Applications of heat pipes to cool PWBS and hybrid microcircuits 02 p0136 N88-10858

Study and realization of Schottky diodes for forthcoming integrated hyperfrequency devices
[LAAS-87-062] 02 p0167 N88-11054

Silicon oxidation photoassisted with a continuous wave CO2 laser beam and contribution to the study of silica layers obtained
[LAAS-87-158] 02 p0179 N88-11115

Study and optimization of a technological process for the fabrication of heterojunction bipolar transistors. Applications to high speed devices
[LAAS-87-134] 02 p0246 N88-11555

Molecular beam heteroepitaxy: (Ca,Sr)F2-GaAs system
[LAAS-87-168] 02 p0246 N88-11556

RADC/NBS (Rome Air Development Center/National Bureau of Standards) Workshop: Moisture Measurement and Control for Microelectronics (4)
[PB87-224614] 03 p0309 N88-11947

Research in monolithic signal-processing circuits
[AD-A184680] 03 p0311 N88-11962

Chemically modified microelectrode arrays: New kinds of electronic devices
[AD-A184389] 04 p0439 N88-12724

Electromagnetics and electrothermal approach to evaluate failures in microelectronic devices caused by electrostatic discharges: Stochastical aspects of the device reliability
[AD-A184906] 05 p0577 N88-13522

Developments in electronics ceramics reported
06 p0684 N88-14192

Selected aspects of microelectronics technology and applications: Numerically controlled machine tools. Technology trends series no. 2
[PB87-132973] 06 p0696 N88-14268

Generic specifications for hybrid microcircuits
[ESA-PSS-01-608-ISSUE-2] 06 p0696 N88-14273

An analysis of simplified feed architectures for MMIC (Monolithic Microwave Integrated Circuit) T/R (Transmit/Receive) module arrays
[AD-A185474] 06 p0697 N88-14275

Assessment of electroceramics research in Europe and the Middle East
[AD-A186377] 07 p0836 N88-15074

Properties of superconducting tunnel structures in microwave radiation field 09 p1239 N88-17424

Solid state research
[AD-A185987] 09 p1253 N88-17508

Superlattice photodetectors
[AD-A186956] 09 p1253 N88-17511

Random vibration (stress screening) of printed wiring assemblies 11 p1499 N88-18953

Microelectronic applications of the conductor-thin insulator-semiconductor (CIS) structure
11 p1560 N88-19341

JPRS report: Science and technology: Europe and Latin America
[JPRS-ELS-87-054] 12 p1573 N88-19406

JPRS report: Science and technology: Europe and Latin America
[JPRS-ELS-88-001] 12 p1614 N88-19649

Emerging technologies program 3-5: Microelectronics Panel report
[AD-A189463] 12 p1624 N88-19716

JPRS report: Science and technology: Europe and Latin America
[JPRS-ELS-87-055] 12 p1686 N88-20086

Solid state research
[AD-A188388] 12 p1699 N88-20166

Advanced packaging for VLSI/VHSIC (Very Large Scale Integrated Circuits/Very High Speed Integrated Circuits) applications: Electrical, thermal and mechanical considerations, an IR and D report
[AD-A189666] 14 p1965 N88-21724

JPRS report: Science and technology. Japan
[JPRS-JST-88-001] 15 p2051 N88-22218

Nondestructive moisture measurement in microelectronics
[AD-A190515] 15 p2060 N88-22281

The Department of Defense Superconductivity Research and Development (DSRD) options. A study of possible directions for exploitation of superconductivity in military applications
[AD-A189747] 15 p2142 N88-22780
Fundamental studies of the mechanical behavior of microelectronic thin film materials
[AD-A190038] 15 p2143 N88-22786
JPRS report: Science and technology. Japan
[JPRS-JST-87-026] 16 p2184 N88-23018
Local density of states in double-barrier resonant tunneling structures
[AD-A190673] 16 p2281 N88-23656
Microelectronics the next fifteen years
17 p2305 N88-23792
Photocurrent modeling of modern microcircuit PN junctions
[DE88-007037] 19 p2662 N88-25832
Anomalous emissivity from periodic micro-machined silicon surfaces 19 p2670 N88-25872
Thermal management of integrated microsensors
19 p2670 N88-25875
Application-specific packaging for custom micromechanical structures 19 p2671 N88-25879
An integrated on-chip pressure sensor for accurate control applications 19 p2671 N88-25880
Silver multi-layers for planar Ag/AgCl reference electrodes 19 p2672 N88-25883
Solid state research
[AD-A192837] 21 p3020 N88-27929
Electronic and optical devices and applications
24 p3363 N88-30027
Microcircuit trace cutting with focused ion beams
[AD-A196030] 24 p3367 N88-30050
A system study with an infrared sensitive microelectronic image sensor
[FOA-C-30481-3.1] 24 p3429 N88-30407

MICROGRAPHY
U PHOTOMICROGRAPHY

MICROGRAVITY
U REDUCED GRAVITY

MICROHARDNESS
Welding and weldability of ductile intermetallic alloys
[DE87-014061] 04 p0416 N88-12582
Tribological studies on high speed steel cutting tools
[DE88-002550] 07 p0864 N88-15246
Effects of cold working on precipitation in age hardenable alloys: On the copper alloys
[NASA-TT-20164] 16 p2177 N88-22973
Microstructural characterization and properties of 3Cr-1.5Mo-O.1V thick section electron beam welds
[DE88-004330] 18 p2486 N88-24747
Characterization of coating wear phenomena in nitride and carbide coated tool inserts
[DE88-011196] 20 p2779 N88-26478

MICROINDENTATION
U MICROHARDNESS

MICROINSTRUMENTATION
A monolithic gas flow sensor with polyimide as thermal insulator 19 p2669 N88-25864

MICROMECHANICS
A quantitative statistical model for cleavage fracture initiation in carbide strengthened steels
[ETN-87-90735] 01 p0025 N88-10157
Pin joints, gears, springs, cranks and other novel micromechanical structures
[DE88-002504] 07 p0864 N88-15245
Micromechanisms of fatigue crack growth and fracture toughness in metal matrix composites
[AD-A186941] 09 p1137 N88-16816
A fiber-resin micromechanics analysis of the delamination front in a DCB specimen
[NASA-TM-100540] 10 p1294 N88-17737
Mechanics of composite materials: Past, present and future
[NASA-TM-100793] 10 p1295 N88-17744
Adhesion, friction and micromechanical properties of ceramics
[NASA-TM-100782] 10 p1305 N88-17801
The mechanism of anisotropic silicon etching and its relevance for micromachinings
[MBB-UA-1013/86] 10 p1311 N88-17838
Mechanical response of unidirectional boron/aluminum under combined loading
[NASA-CR-182595] 12 p1604 N88-19591
Micromechanical and microstructural studies of ceramic superplasticity
[DE86-005793] 13 p1751 N88-20472
Microplasticity phenomena in graphite/magnesium metal matrix composites
[DE88-006772] 15 p2029 N88-22086
Whisker-reinforced ceramic composites for heat engine components 15 p2082 N88-22410
A micromechanics model of the stiffness and strength of laminates with fiber waviness
[NASA-CR-181670] 20 p2768 N88-26413
Micromechanics of composite laminate compression failures
[NASA-CR-183179] 22 p3050 N88-28098
Modeling of micromechanisms of fatigue and fracture in hybrid materials
[AD-A195604] 24 p3382 N88-30142

MICROMETEOROIDS
NT ZODIACAL DUST
Atmospheric entry heating of cosmic dust
06 p0794 N88-14865
Assessment of the effects of space debris and meteoroids environment on the space station solar array assembly
[NASA-TM-101315] 23 p3185 N88-28959
The effect of the near earth micrometeoroid environment on a highly reflective mirror surface
[NASA-TM-101307] 24 p3332 N88-29833

MICROMETEOROLOGY
NT MICROBURSTS (METEOROLOGY)
An update on remote measurement of soil moisture over vegetation using infrared temperature measurements: A FIFE perspective
[NASA-CR-182926] 17 p2370 N88-24109
Some results from the Amazon Forest micrometeorological experiment
[INPE-4631-PRE/1346] 24 p3403 N88-30263
Microphysical processes in cloud layers of Venus
24 p3448 N88-30522

MICROMETEORS
U MICROMETEOROIDS

MICROMETERS
Study for the determination of general and specific properties of wide energy-band gap HgHdTe in the 1-2 micrometer wavelength range
[AD-A189177] 13 p1845 N88-21041

MICROMINIATURIZATION
Development of a low noise 10 K J-T refrigeration system
[AD-A186004] 07 p0838 N88-15085
The 1986 IEEE Solid-State Sensor Workshop
[AD-A190922] 19 p2668 N88-25860
Microminiature fluidic amplifier
19 p2669 N88-25865
Electrical and chemical sensors for biological cell research 19 p2669 N88-25866
Resonant structures for integrated sensors
19 p2673 N88-25893
Tin oxide microsensors on thin silicon membranes
19 p2673 N88-25897

MICROMINIATURIZED ELECTRONIC DEVICES
Study and realization of Schottky diodes for forthcoming integrated hyperfrequency devices
[LAAS-87-062] 02 p0167 N88-11054

MICROORGANISMS
NT AMOEBA
NT BACILLUS
NT BACTERIA
NT ESCHERICHIA
NT PARAMECIA
NT PSEUDOMONAS
NT STAPHYLOCOCCUS
Exobiology and life science 07 p0883 N88-15358
Physiological and immunological aspects of human adaptation to temperature elevation in a closed environment 07 p0895 N88-15424
Design concepts for bioreactors in space
09 p1198 N88-17179
Degradation of jet and missile fuels by aquatic microbial communities
[AD-A188065] 11 p1465 N88-18737
Ecological risk factors related to environmental uses of genetically engineered organisms
[DE88-006674] 18 p2549 N88-25132
Biodegradation of JP-5 aviation fuel by subsurface microbial communities
[AD-A192743] 20 p2781 N88-26493
An outdoor test facility for the large-scale production of microalgae
[DE88-001146] 21 p2964 N88-27723

MICROPARTICLES
The effect of Ca(OH)2-treated ceramic microspheres on the mechanical properties of high-temperature lightweight cement composites
[DE88-004590] 13 p1749 N88-20457
A chemical method for achieving acceleration of macroparticles to ultrahigh velocities
[DE88-006377] 15 p2128 N88-22695
Distribution of chain ends inside the polybutadiene microspheres of SB diblock copolymers
[AD-A191257] 16 p2162 N88-23007

MICROPHONES
Vital signs rate meter
[AD-A187015] 09 p1198 N88-17183
Experimental study on the influence of wind on acoustic pressure sensors
[ISL-R-121/86] 15 p2131 N88-22712
Outdoor sound propagation, its implications for unattended ground sensors
[FEL-1986-64] 20 p2850 N88-26917
Detection of helicopters using ground-controlled microphones 22 p3148 N88-28730
Noise levels from a jet-engined aircraft measured at ground level and at 1.2 m above the ground
[NPL-AC-114] 23 p3279 N88-29524

MICROPHOTOGRAPHS
Method for measuring absolute linear parameters of chromosomes 19 p2707 N88-26095

MICROPHOTOMETERS
U PHOTOMETERS

MICROPOLAR FLUIDS
On the performance of finite journal bearings lubricated with micropolar fluids
[NASA-TM-100293] 08 p0988 N88-15983

MICROPOROSITY
Ultrasonic characterization of non-uniform porosity distributions in SiC ceramic
[DE88-004814] 13 p1749 N88-20459

MICROPROCESSORS
The impact of new computer technology on accelerator control
[DE87-014021] 02 p0219 N88-11376
The pros and cons of using a CAI package on a central computer as opposed to a microprocessor: What's your CAI MO, mainframe or micro
[DE87-011123] 04 p0475 N88-12929
Test and evaluation of the transputer in a multi-transputer system
[AD-A184969] 05 p0631 N88-13859
Reserach on microprocessor controller for spot welding
[PB87-143913] 07 p0863 N88-15240
Microprocessor emulating the intermediate code for FORTRAN compiler
[DE88-700540] 07 p0900 N88-15452
High performance data buses: Progress and evolution
[DE88-002570] 09 p1215 N88-17285
Multitasking and microtasking experience on the NAS Cray-2 and ACF Cray X-MP
[NASA-CR-177464] 09 p1221 N88-17325
Microcomputer analysis of regenerative heat exchangers for oscillating flow
[DE88-001773] 10 p1329 N88-17945
High-performance CPU implementation of the nebula instruction set architecture 10 p1373 N88-18194
The design of ultra high-speed numeric intensive systems (having fault tolerant and load balancing capabilities) 10 p1374 N88-18196
Hardware implementation for special functions. An application for combat simulation
10 p1374 N88-18197
MICRO system for control, acquisition and processing of experimental data
[DE88-700724] 10 p1386 N88-18278
Implementation of encoders and decoders for Reed-Solomon codes
[PB88-126628] 10 p1387 N88-18286
Modular CAMAC system, 2
[DE88-700237] 11 p1525 N88-19106
Efficient instruction level simulation of computers
[AD-A187821] 11 p1529 N88-19130
A microprocessor-based real-time simulator of a turbofan engine
[NASA-TM-100889] 14 p1868 N88-21163
Microprocessors in space instrumentation
[RR-321] 14 p1955 N88-21655
MIG-1 on-line measuring holographic microscope
[DE88-701103] 15 p2068 N88-22332
Fundamentals of microprocessor-based design: A tutorial, second edition
[DE88-006761] 16 p2244 N88-23406
Design of high yield microprocessors
[ETN-88-92184] 16 p2245 N88-23410
Automatic layout generation of data processing sections of VLSI microprocessor-like circuits
[ETN-88-92185] 16 p2245 N88-23411
SP-100 ground engineering systems test facility control systems 17 p2436 N88-24496
Sensors for process control requirements for design and test 19 p2671 N88-25877
The relationship between system response time, working memory, and task complexity: An empirical investigation
[DE88-000976] 19 p2711 N88-26105
Idea processing for creativity and management
[DE88-006110] 19 p2714 N88-26113
FASTRUN phase sequencer descriptor language (PDL)
[DE88-007966] 20 p2837 N88-26828
Mutually exclusive alternatives by clustering
[DE88-007707] 20 p2882 N88-27115
SP-100 Ground Engineering Systems: Test facility control systems
[DE88-009195] 21 p3015 N88-27695

DSS 13 microprocessor antenna controller
22 p3066 N88-28192

Multichannel data transmission through a fiber optic cable
[AD-A193842] 22 p3070 N88-28221

The VIPER microprocessor
[RSRE-87014] 22 p3135 N88-28640

Feasibility study of a microprocessor controlled actuator test mechanism
[AD-A194654] 23 p3249 N88-29337

Heavy ion and proton tests for subsystem upset
[AD-A195267] 24 p3434 N88-30442

MICROPROGRAMMING

The UMAC simulator 20 p2834 N88-26811

MICROPULSATIONS

NT GEOMAGNETIC MICROPULSATIONS

MICROSCOPES

NT ACOUSTIC MICROSCOPES
NT ELECTRON MICROSCOPES
NT ION MICROSCOPES
NT OPTICAL MICROSCOPES

Calibration standard for metallographic microscopes
[RFP-3956-REV] 03 p0326 N88-12057

MICROSCOPY

NT ELECTRON MICROSCOPY
NT LASER MICROSCOPY
NT PHOTOACOUSTIC MICROSCOPY

Structural characterization of undoped and doped GaAs: A comparative study of four techniques
[DE88-004552] 11 p1555 N88-19304

Scanning tunneling microscopy of silver, gold, and aluminium monomers and small clusters on graphite
[DE88-003871] 11 p1562 N88-19349

Computer software for the computation of the scattered field and the optical microscope image of line objects patterned in thick layers
[PB88-153705] 13 p1814 N88-20838

Microprobe examination of composite materials produced by burning of Ti, Cr, C powders with powder of any one Fe-group metal 14 p1886 N88-21269

Recent advances in atom-probe field ion microscopy
[DE88-008799] 20 p2876 N88-27070

Progress in diagnostic techniques for SC (superconducting) cavities
[DE88-008600] 20 p2876 N88-27077

Scanning tunneling microscopy as a surface chemical probe
[AD-A192710] 21 p2909 N88-27263

MICROSPORES

Ultraviolet (180 to 300 nm) action spectra for inactivation and DNA photoproduct formation of Bacillus subtilis spores under ultrahigh vacuum 12 p1657 N88-19931

MICROSTRIP ANTENNAS

Investigation of surface wave blindness in microstrip phased array antennas
[AD-A189326] 12 p1621 N88-19696

Conformal microstrip slot antenna and antenna array
[AD-A189623] 15 p2055 N88-22252

Investigation of radiating and guiding structures in microstrip patch antennas
[AD-A191445] 16 p2193 N88-23082

Analysis of annular microstrip antennas for hyperthermic applicators
[PB88-181508] 19 p2643 N88-25679

A microstrip array feed for MSAT spacecraft reflector antenna 19 p2652 N88-25747

Array trade-off study using multilayer parasitic subarrays
[NASA-TM-101321] 22 p3070 N88-28222

MICROSTRIP DEVICES

NT MICROSTRIP ANTENNAS
NT MICROSTRIP TRANSMISSION LINES

The silicon microstrip detector --- particle position measurement
[ETN-88-92235] 16 p2210 N88-23189

Investigation of photoconductive picosecond microstripline switches on self-implanted Silicon On Sapphire (SOS) 19 p2657 N88-25789

MICROSTRIP TRANSMISSION LINES

Simple, low-profile, circularly polarized arrays
19 p2647 N88-25716

An optically strobed sample and hold circuit
19 p2656 N88-25772

Characteristics of shielded microstrip lines on GaAs-Si at millimeter-wave frequencies 19 p2657 N88-25787

Picosecond optoelectronic study of a thin film transmission line structure 19 p2661 N88-25823

MICROSTRUCTURE

NBS (National Bureau of Standards) research reports (April 1987)
[PB87-210258] 01 p0018 N88-10111

Isothermal forging and its effect on the microstructure of powder route nickel alloy AP1
[RAE-TM-P-1094] 01 p0022 N88-10138

Development of creep resistant austenitic stainless steels for advanced steam cycle superheater application
[DE87-012929] 01 p0023 N88-10147

Fatigue and thermal fatigue of Pb-Sn solder joints
[DE87-012881] 01 p0024 N88-10150

Laser chemically vapor deposited silicon-carbide: Growth features, topography, microstructure, and composition
[DE87-013767] 01 p0029 N88-10184

Effect of high-temperature annealing on the microstructure and thermoelectric properties of GaP doped SiGe
[NASA-TM-100164] 01 p0029 N88-10188

Microstructural effects in shock initiation of granular explosives
[DE87-011282] 01 p0031 N88-10200

Fabrication of microstructures with extreme structural heights by vacuum reaction injection molding and electroforming
[KFK-4267] 01 p0033 N88-10210

Analytical electron microscopy characterization of boron in sintered alpha-SiC
[DE87-012532] 02 p0142 N88-10889

Microstructural evolution and response to double-loop reactivation testing of heat-treated pH 13-8 Mo martensitic stainless steel
[DE87-009058] 02 p0146 N88-10915

Investigation of the structure of coatings of self fluxing alloys fused by laser energy
[BLL-M-37301-(5828.4)] 02 p0148 N88-10930

Analysis of phase equilibria in NiTi-C system in high nickel regions
[BLL-M-37304-(5828.4)] 02 p0149 N88-10932

Study of the microscopic mechanisms of cyclic deformation. Development of a new approach: The case of aluminum
[ISAL-87-0003] 02 p0149 N88-10936

A microstructural lattice model for strain oriented problems: A combined Monte Carlo finite element technique
[NASA-TM-100215] 02 p0150 N88-10939

Study of the micromechanical behavior of a SiO2-Al2O3-Li2O glass ceramic and its relation to the microstructure
[ISAL-ITC1-87-01] 02 p0153 N88-10960

Need for composites, new materials discussed
02 p0160 N88-11001

Thin film microstructures: Simulation and theory
[DE87-014732] 02 p0246 N88-11553

Resistance of welded joints in high temperature Hastelloy N-type nickel alloy to hot crack formation
03 p0286 N88-11798

Microstructural effects on the fatigue behavior of Fe-C-X alloys
[DE88-000155] 03 p0288 N88-11809

Stress corrosion cracking of high-strength steels in aqueous environments 03 p0289 N88-11818

A fundamental study of the mechanical and microstructural response of elevated temperature PM aluminum-titanium alloys 03 p0289 N88-11819

Ultra-fine grained alloy material
[AD-A184500] 03 p0290 N88-11820

International Conference on Microstructology held in Gainesville, Florida on 7-9 May 1986
[AD-A184604] 03 p0290 N88-11822

Modified 14Cr-16Ni stainless steels with improved creep resistance at 700 C due to tailored precipitate microstructures
[DE87-014788] 03 p0290 N88-11825

Reduced-activation ferritic steels: A comparison with Cr-Mo steels
[DE88-000332] 03 p0290 N88-11826

Microstructural characterization of irradiated PWR steels using the atom probe field-ion microscope
[DE88-000341] 03 p0291 N88-11828

The correlation between microstructure and thermomechanical properties of two-phase materials and porous sintered materials
[KFK-4205] 03 p0292 N88-11835

Indentation damage in ceramics
[AD-A184686] 03 p0294 N88-11844

Flaw imaging and ultrasonic techniques for characterizing sintered silicon carbide
[NASA-TM-100177] 03 p0334 N88-12106

Monte Carlo simulation of modulated phases
[NASA-TM-89654] 03 p0369 N88-12323

New theory for competing interactions and microstructures in partially-ordered (liquid-crystalline) phases
[DE87-014739] 03 p0380 N88-12389

Corrosion behavior of P/M mechanically alloyed IN-9052.1: An electro-chemical investigation
[AD-A184191] 04 p0414 N88-12567

The nature of metallurgical reactions in underwater welding
[AD-A184464] 04 p0414 N88-12568

Mechanical properties of a microalloyed steel with high niobium content
[DE87-703545] 04 p0415 N88-12572

Mechanical strength and niobium and niobium-base alloys substructures
[DE87-703692] 04 p0415 N88-12577

Welding and weldability of ductile intermetallic alloys
[DE87-014061] 04 p0416 N88-12582

The accommodation of precipitate plates modelled as a tensile test
[DE88-000207] 04 p0454 N88-12814

Characterization of thin layers for optics
[PB87-217949] 04 p0490 N88-13017

Microstructural change of Al on H implantation
[IPPJ-847] 04 p0493 N88-13036

Theory and simulations of Zone 2 microstructures in thin films
[DE87-014752] 04 p0499 N88-13071

Study of the influence of mechanical - thermal treatments on the creep behavior of a niobium stainless steel
[DE87-703506] 05 p0563 N88-13431

Investigation by differential scanning calorimetry of microstructure in a superplastic Al-Mg-Zr alloy
[AD-A184902] 05 p0564 N88-13439

Ion plating for corrosion control
[AD-A185061] 05 p0565 N88-13442

Effect of rapid solidification on short-range order: A magnetic study
[AD-A185216] 05 p0565 N88-13444

Effect of rapid solidification on stainless steel weld metal microstructures and its implications on the Schaeffler diagram
[DE88-001489] 05 p0566 N88-13451

United States - Japan Workshop on Dielectric and Piezoelectric Ceramics (3rd) held in Toyama, Japan on November 9-12, 1986
[AD-A185113] 05 p0568 N88-13460

Fatigue 87, volume 1
[AD-A184045] 05 p0597 N88-13645

The influence of the topography of fracture surfaces on crack closure 05 p0598 N88-13657

Influence of microstructure and aging condition on the fatigue crack propagation in age hardened aluminium alloys 05 p0599 N88-13659

The effect of microstructure on the surface crack length: Crack depth relationship for short cracks
05 p0600 N88-13670

The growth behavior of small fatigue cracks; the effect of microstructure and crack closure
05 p0600 N88-13673

The influence of microstructure and residual stresses on the initiation and propagation of short surface cracks on AlMgSi1 05 p0601 N88-13674

Propagation of small fatigue cracks in 2024-T3 aluminum alloy 05 p0601 N88-13678

Interaction of microstructure and fatigue in tool steels
05 p0603 N88-13693

Deformation mechanisms and crack initiation in fatigue 05 p0608 N88-13730

Environmentally assisted fatigue crack growth
05 p0608 N88-13731

Fatigue crack growth 05 p0608 N88-13734

Characterization of the microstructures of various materials
[AD-A184961] 05 p0655 N88-14017

Basic energy sciences research in the Metals and Ceramics Division of Oak Ridge National Laboratory
[DE87-013538] 06 p0681 N88-14171

Fractographic and microstructural aspects of fracture toughness testing in irradiated 304 stainless steel
[DE88-000795] 06 p0681 N88-14172

Fracture analysis of drawn composite dual-phase steel wire
[DE88-001396] 06 p0681 N88-14173

The effect of neutron irradiation on the tensile properties and microstructure of several vanadium alloys
[DE88-001755] 06 p0682 N88-14176

Electron microscopy studies of tensile cyclic fatigue-tested silicon nitride ceramics
[DE88-001438] 06 p0685 N88-14196

Characterization of mechanical damage mechanisms in ceramic composite materials
[AD-A185549] 06 p0686 N88-14205

The relationship between microstructural size and fatigue threshold in iron and steel
06 p0716 N88-14396

Crack closure phenomena in modes 1 and 2 interactions 06 p0719 N88-14417

The microstructure and texture of torsion-reverse torsion experiments
[DE88-001801] 06 p0721 N88-14434

Dynamic high pressure process for fabricating superconducting and permanent magnetic materials
[DE88-000848] 06 p0785 N88-14817

Interface effects on the mechanical properties of ceramic composites
[AD-A185899] 07 p0826 N88-15009

Characterization of microstructure in metallic and composite materials
[AD-A186193] 07 p0826 N88-15012

Fatigue, fracture and strain hardening of high carbon hardened alloy steel
[AD-A186101] 07 p0831 N88-15043

Metallurgical processes in multi-component rare earth-transition metal permanent magnet alloys
[AD-A186401] 07 p0832 N88-15045

Characterization of current steels. The 35 NCD 16 alloy in 30 mm diam laminated bars made by Aubert and Duval
[CEAT-41/N/76] 07 p0832 N88-15046

Microstructural observations of the Sn-Pb solder/Cu system and thermal fatigue of the solder joint
[DE88-001392] 07 p0832 N88-15048

The influence of grain boundary chemistry and structure on the intergranular attack and intergranular stress corrosion cracking of austenitic alloys
[DE88-002436] 07 p0835 N88-15063

Microstructure and magnetic properties of cobalt-chromium alloys
[DE88-002762] 07 p0835 N88-15064

Imaging subtle microstructural variations in ceramics with precision ultrasonic velocity and attenuation measurements
[NASA-TM-100129] 07 p0867 N88-15257

Processing and interfacial analysis of glass-ceramic to metal seals
[DE88-002999] 08 p0971 N88-15873

The mechanism of stereo regulation during anionic polymerization of polar monomers
[AD-A186530] 08 p0973 N88-15888

Experimental aspects of high-T/sub c/ superconductors
[DE88-003019] 08 p1090 N88-16564

Microstructure modifications of micron thick NbN films to improve J/sub c/ and H/sub c2/
[DE88-003078] 08 p1091 N88-16567

Monolayer films prepared by the spontaneous self-assembly of symmetrical and unsymmetrical dialkyl sulfides from solution onto gold substrates: Structure, properties, and reactivity of constituent functional groups
[AD-A186717] 09 p1137 N88-16814

Investigation of microstructural factors that cause low fracture toughness in silicon carbide whisker/Al alloy composites
[AD-A186443] 09 p1137 N88-16817

Microstructures and properties of SiC whisker-reinforced mullite composites
[DE88-002611] 09 p1139 N88-16826

Microstructural modification during laser welding
[DE88-002344] 09 p1144 N88-16860

Long-term-aging embrittlement of cast duplex stainless steels: Mechanism and kinetics
[DE88-002929] 09 p1145 N88-16861

Study of molecular mobility of noncrystaline polymer alloys of different compatibility using mechanical spectrometry
[ISAL-87-0032] 09 p1149 N88-16883

The effect of varying sputtering parameters on the microstructure and mechanical properties of 10 percent Ni + TiB2 thin films
[DE88-002600] 09 p1254 N88-17517

Micro-mechanisms of deformation in SiC/Al composites
[AD-A188282] 10 p1296 N88-17749

A detailed microstructural examination of the cause of HAZ cracking in type 316 steel
[AERE-R-12428] 10 p1301 N88-17777

Influence of convection on microstructure
[NASA-CR-182489] 10 p1302 N88-17784

Response of Fe-Cr-Mn austenitic alloys to thermal aging neutron irradiation
[DE88-003415] 10 p1302 N88-17785

Irradiation effects in metals
[DE88-004272] 10 p1303 N88-17789

The role of composition and microstructure gradients on weld metal properties and behavior
[DE88-004956] 10 p1303 N88-17791

Bias, internal stress and substrate effects on the microstructure and properties of PVD-wear resistant coatings
[AERE-R-12360] 10 p1304 N88-17798

Mechanisms of wear in single- and two-phase materials
[DE88-003846] 10 p1305 N88-17806

Durability and damage tolerance of aluminum castings
[AD-A186444] 10 p1341 N88-18013

Acoustic emission-microstructural relations in ferritic steels. Part 3: The effect of inclusion content
[AERE-R-12041] 10 p1341 N88-18015

The measurement of stress in steels of varying microstructure by Barkhausen and magneto-acoustic emission
[AERE-R-12387] 10 p1343 N88-18027

Relationship between fatigue life in the creep-fatigue region and stress-strain response
[NASA-TM-100796] 10 p1345 N88-18040

Optical characterization of GaAs/sub 1-x/Sb/sub x/ and GaAs/sub 1-x/Sb/sub x/GaAs strained layer superlattices
[DE88-003393] 10 p1418 N88-18464

The structure and properties of twin boundaries in superconducting YBa2Cu3O7
[DE88-003864] 10 p1418 N88-18468

Freestanding films of YBa2Cu3O/sub 6.9/
[DE88-003995] 10 p1419 N88-18471

Simulation and processing of high resolution images of defects and interfaces in superconducting YBa2Cu3O7
[DE88-003856] 10 p1420 N88-18480

High-resolution X-ray microstructural study of single crystals of YBa2Cu3O/sub 7-y/
[DE88-004856] 10 p1421 N88-18484

The metallurgical database of Aladin: An alloy de sign system
[AD-A187724] 11 p1457 N88-18682

Microstructural characterization of HSLA-100 GMA-weldments
[AD-A187782] 11 p1457 N88-18683

Microstructural characterization of the heat affected zone of HSLA (High Strength Low Alloy)-100 steel GMA (Gas Metal Arc)-weldment
[AD-A187825] 11 p1457 N88-18686

Thermal fatigue of stainless steel
[DE88-004146] 11 p1458 N88-18694

Institute for Materials Science and Engineering, Metallurgy: Technical activities 1987
[PB88-157722] 11 p1460 N88-18702

Photoacoustic studies of surface plasmons in metallic microstructures
[DE88-004423] 11 p1460 N88-18703

Crystallization and glass formation in electron and laser beam irradiated Cu-Zr alloys
[DE88-003390] 11 p1464 N88-18729

In situ ultrahigh vacuum friction measurement and wear track analysis of ion implanted 304 stainless steel
[DE88-004537] 11 p1494 N88-18922

Novel analytical X-ray Non-Destructive Evaluation (NDE) tool for quality control of energetic materials
[AD-A187737] 11 p1497 N88-18935

Plasma joining of metal matrix composites
[AD-A188559] 12 p1604 N88-19593

Ultrasonic-velocity studies of composite and heterogeneous materials
[AD-A189000] 12 p1604 N88-19595

Study of the effects of metallurgical factors on the growth of fatigue microcracks
[AD-A188475] 12 p1608 N88-19615

Microdesigning of lightweight/high strength ceramic materials
[AD-A188526] 12 p1610 N88-19631

Microstructure characterization with a pulsed laser ultrasonic source
[DE88-005207] 12 p1632 N88-19766

The effect of microstructure on the fatigue crack growth resistance of nickel base superalloys
[AD-A189526] 13 p1741 N88-20414

Processing, structure and properties of heavily deformed in situ composites
[AD-A189611] 13 p1742 N88-20416

Use of the LLNL 40 kV electric gun to study the shock response of 21-6-9 stainless steel
[DE87-014550] 13 p1742 N88-20418

Non-destructive evaluation techniques applied to the study of fatigue microcrack growth in steel alloys
[DE88-004090] 13 p1742 N88-20420

Erosion in dual-phase microstructures
[DE88-004507] 13 p1743 N88-20421

Grain refinement during primary breakdown of alloy 718
[DE88-005193] 13 p1743 N88-20423

Advances in X-ray line profile analysis to determine microstructure information about ceramics
[DE88-003938] 13 p1750 N88-20465

Micromechanical and microstructural studies of ceramic superplasticity
[DE88-005793] 13 p1751 N88-20472

Mixing of viscous fluids: Behavior of microstructures and chaos
[DE88-006287] 13 p1766 N88-20566

Ductile failure
[AD-A189429] 13 p1781 N88-20654

Anisotropy of microstructural eddy motion in surface layer during calm 13 p1784 N88-20677

Electrical characteristics of MBE (Molecular Beam Epitaxyl)-grown GaAs/sub 1-x/Sb/sub x on InP and correlation with film microstructure
[DE88-003841] 13 p1847 N88-21053

Microprobe examination of composite materials produced by burning of Ti, Cr, C powders with powder of any one Fe-group metal 14 p1886 N88-21269

The unique characteristics of the structure of composite materials made on a base of sphalerite-analogous boron nitride 14 p1886 N88-21273

Development, high temperature properties, and microanalysis of nonoxide ceramics
[ETN-88-92103] 14 p1893 N88-21304

Processing, texture and mechanical properties of sintered silicon carbide
[NASA-TT-20253] 14 p1893 N88-21305

New method of examining micrononhomogeneity of local centers in high-resistivity semiconductor materials under scanning electron microscope 14 p1969 N88-21754

Dynamic and spectral properties of semiconductor lasers with quantum well, quantum wire, and quantum box structures 14 p1975 N88-21788

Enhanced excitonic optical nonlinearity and exciton dynamics in semiconductor microstructures
14 p1977 N88-21795

The contribution of electron microscopy of materials science to society
[DE88-006341] 15 p2028 N88-22082

Processing, microstructure, and mechanical properties of silicon carbide particulate reinforced aluminum alloys
[AD-A188981] 15 p2037 N88-22136

Segregation effects in welded stainless steels
[DE88-701224] 15 p2037 N88-22139

The age hardening response of thermomechanically processed Al-Mg-Li alloys
[AD-A189870] 15 p2039 N88-22147

Directed-energy electron-beam processing of a hypoeutectic Cr90Ta10 alloy
[DE88-005621] 15 p2040 N88-22157

Transformation toughening of ceramics
[AD-A190399] 15 p2045 N88-22183

Strength and microstructure of ceramics
[AD-A190712] 15 p2046 N88-22191

A three-dimensional model for the elastic properties of a foam
[DE88-006197] 15 p2046 N88-22192

High temperature corrosion of ceramics
[DE88-006567] 15 p2046 N88-22193

The growth of corner cracks under the conjoint action of high and low cycle fatigue
[AD-A190510] 15 p2076 N88-22379

Evolution of hardening and damage during viscoplastic deformation
[AD-A190714] 15 p2077 N88-22381

Characterization of sintered SiC by using NDE
15 p2082 N88-22413

The weldability of consolidated rapidly solidified Type 304 SS powders
[DE88-006738] 16 p2178 N88-22978

Deformation of rapidly solidified dispersion strengthened titanium alloys
[AD-A190793] 16 p2179 N88-22984

Dependence of structure of stabilized ZrO2 coatings on condensation rate 16 p2180 N88-22990

Applications research studies of microtubules
[AD-A190855] 16 p2182 N88-23005

Laser cladding of Ni, Nb and Mg alloys for improved environmental resistance at high temperature
[AD-A191274] 16 p2213 N88-23208

Investigation of non-linear optical behavior of semiconductors for optical switching, volume 1
[AD-A191297] 16 p2274 N88-23611

Radiation effects in silicon
[DE88-006642] 16 p2282 N88-23659

Magnetic studies of iron-rare-earth-metalloid alloys
[DE88-006801] 16 p2282 N88-23660

Structure and mechanical properties of metal matrix composites made using semi-solid processes. The case of the system Al-Si/SiC
[ETN-88-92299] 17 p2316 N88-23835

Improved processing of Si3N4
17 p2325 N88-23882

Fractographic and microstructural evaluation of 3500-hour durability specimens
17 p2325 N88-23887

The role of oxygen on the mechanical behavior of molybdenum alloys 17 p2401 N88-24278

Chemical compatibility between silicon carbide and a nickel aluminide
[DE88-006188] 18 p2479 N88-24708

Superplasticity: A fundamental investigation on deformation mechanism and cavitation phenomena
[AD-A191548] 18 p2485 N88-24741

Dynamic consolidation of metal powders
[AD-A192126] 18 p2485 N88-24744

Microstructural characterization and properties of 3Cr-1.5Mo-O.1V thick section electron beam welds
[DE88-004330] 18 p2486 N88-24747
High temperature embrittleness of Cu-Cr alloy
[NASA-TT-20184] 18 p2488 N88-24759
An investigation of 2-6 superlattice deposition by laser photochemical techniques
[AD-A191547] 18 p2581 N88-25336
Electronic and structural studies of carbon/carbon composites
[AD-A191729] 19 p2609 N88-25481
Microlaminate composite structures by low pressure plasma spray deposition
[DE88-006453] 19 p2610 N88-25488
The postirradiation tensile properties and microstructure of several vanadium alloys
[DE88-007140] 19 p2615 N88-25515
Influence of strain rate on the substructure evolution and yield behavior of Ti-6Al-4V
[DE88-006457] 19 p2616 N88-25520
Development of fine-grained carbide-particle hardened Hadfield manganese steels
[DE88-008919] 19 p2617 N88-25523
Low-chromium reduced-activation ferritic steels
[DE88-009060] 19 p2617 N88-25524
Hot isostatic pressing of nickel aluminide powders
[DE88-009677] 19 p2617 N88-25525
Oxidation behavior and microstructural studies of melt-spun glassy Fe-Al-Zr metal
[DE88-009964] 19 p2617 N88-25526
Mechanical testing and microscopic analysis of structure of extruded powder aluminum
[DE88-007193] 19 p2617 N88-25528
Microstructure of thin intercalated benezene derived graphite fibers
[AD-A191724] 19 p2618 N88-25534
The structure and properties of RF reactive sputtered IrO2 films 19 p2672 N88-25884
Initial development of high-temperature titanium silicide alloys
[DE88-007860] 20 p2772 N88-26437
Helium induced degradation in the weldability of an austenitic stainless steel
[DE88-009062] 20 p2773 N88-26443
The structure and properties of grain boundaries in B2 ordered alloys
[DE88-009890] 20 p2773 N88-26447
Application of electron microscopy for the analysis of the mechanical behavior of advanced ceramics
[DE88-005049] 20 p2777 N88-26469
Microstructural effects in static and dynamic numerical experiments
[DE88-004289] 20 p2813 N88-26690
Third International Conference on Superlattices, Microstructures and Microdevices
[AD-A191416] 20 p2861 N88-26995
Hot electron transistors grown by MOCVD
20 p2861 N88-26996
Spectroscopy of one-dimensional subbands on InSb
20 p2864 N88-27007
Metallic superlattices 20 p2864 N88-27012
Quantum interference and transport in microstructures
20 p2866 N88-27022
EXAFS studies of the microstructure of semiconductor alloys, defects and semiconductor-metal interfaces
20 p2868 N88-27031
The theory of electron-polar phonon scattering rates in semiconductor micro-structures
20 p2871 N88-27043
Influence of interfaces on electronic and magnetic properties of MnSe/ZnSe superlattices near monolayer limit 20 p2872 N88-27050
Type 3 - type 1 transition and strain effect in Hg(1-x)Cd(x)Te-CdTe and Hg(1-x)Zn(x)Te-CdTe superlattices 20 p2872 N88-27052
Damping characteristics of metal matrix composites
[AD-A193144] 21 p2904 N88-27233
Gaseous tracer techniques for pore structure characterization of granular materials
[DE88-011542] 21 p2911 N88-27274
Thermomechanical processing of Al alloy 2090 for grain refinement and superplasticity
[AD-A192333] 21 p2912 N88-27281
Processing and properties of advanced aluminum alloys
[AD-A193224] 21 p2912 N88-27284
On the systematics of phase transformation in metallic alloys
[DE88-008041] 21 p2913 N88-27288
Development of high strength and toughness microcomposite HSLA Fe/Cr/Mn/C steel with and without Nb
[DE88-009813] 21 p2913 N88-27290
Controlling phase formation and stability to improve the high temperature creep resistance of austenitic stainless steels
[DE88-011401] 21 p2914 N88-27293
Processing and additive effects of ZrO2 on microstructure and dielectric porperties of BaTiO3 ceramics
[AD-A193126] 21 p2917 N88-27316
Preparation and properties of high Q microwave dielectrics in the (CA, SR, BA) zirconate system
[AD-A193127] 21 p2918 N88-27317
Effects of near interfacial microstructure on toughness and subcritical crack growth in ceramic/metal systems
[DE88-009842] 21 p2919 N88-27325
Influence of microstructure and microdamage processes on fracture at high loading rates
[AD-A192957] 21 p2960 N88-27583
Ultrafast physics in semiconductor microstructures
[AD-A193300] 21 p3022 N88-27936
X-ray studies of strain, interface and impurities in semiconductors
[DE88-012460] 21 p3025 N88-27954
As-received microstructure of a SiC/Ti-15-3 composite
[NASA-TM-100938] 22 p3050 N88-28095
Study of fatigue cracks in aluminum alloys. Influence of microstructure
[REPT-48-553] 22 p3056 N88-28134
High temperature electric arc furnace
[NASA-CASE-MFS-28281-1] 23 p3181 N88-28938
Ultrafine microstructure composites prepared by chemical vapor deposition
[AD-A193849] 23 p3189 N88-28973
Low temperature film growth of the oxides of zinc, aluminum and vanadium (and related systems, oxides of gold and germanium, nitrides of aluminum and tungsten) by reactive sputter deposition
[AD-A193497] 23 p3191 N88-28986
An investigation into the metallurgical aspects of joining rapidly-solidified aluminum alloys
[AD-A194677] 23 p3194 N88-29009
Effects of metal substitutions (Fe and Ga) in YBa2Cu3O7 on its superconducting properties and microstructures
[DE88-007393] 23 p3287 N88-29572
An HVEM study of displacement cascade damage in Nb3Sn at 13 K
[DE88-009997] 23 p3289 N88-29584
Creep of carbon yarn and carbon-carbon composites at high temperatures and high stresses
[AD-A195224] 24 p3340 N88-29878
Modeling of micromechanisms of fatigue and fracture in hybrid materials
[AD-A195604] 24 p3382 N88-30142

MICROTRONS
Analysis of free electron laser performance utilizing the National Bureau of Standards CW microtron
[AD-A194217] 23 p3219 N88-29160

MICROWAVE AMPLIFIERS
NT CYCLOTRON RESONANCE DEVICES
Initial operation of a high-power whispering-gallery-mode gyrotron
[DE88-002500] 07 p0857 N88-15207
GaAs MMIC yield evaluation --- monolithic microwave integrated circuits (MMIC)
[ESA-CR(P)-2470] 08 p0979 N88-15916
Low-noise cryogenically cooled broad-band microwave preamplifiers
[DE88-004561] 10 p1324 N88-17912
Wiggler taper optimization for free-electron-laser amplifiers with moderate space-charge effects
[DE88-003758] 13 p1775 N88-20618
Construction of a 60 GHz Traveling Wave Tube (TWT) for intersatellite link on geostationary orbit (ISL/TWT)
[BMFT-FB-W-86-015] 16 p2192 N88-23076
Monolithic GaAs Ku-band one watt constant phase variable power amplifier
[DE88-006272] 18 p2506 N88-24866
Microwave amplifiers
[AD-A192974] 20 p2795 N88-26585
Recent advances in high-power microwave amplifiers
[DE88-007820] 23 p3206 N88-29083
Space-charge-wave solid state microwave amplifier
[AD-A193792] 23 p3208 N88-29091

MICROWAVE ANTENNAS
The 8.4-GHz low-noise maser pump source assembly
04 p0436 N88-12705
An evaluation of equivalent models for design of rectangular microstrip antennas
[FOA-C-30451-3.2] 08 p0977 N88-15905

MICROWAVE ATTENUATION
Numerical simulation of the propagation and absorption due to air breakdown of long microwave pulses
[DE88-005227] 11 p1475 N88-18798
Research and development to acquire and reduce melting layer cloud physics and evaluate a prototype M-meter
[AD-A188390] 12 p1648 N88-19873
Microwave dispersion and absorption in tissues: Molecular mechanisms
[AD-A190118] 15 p2100 N88-22512
An evaluation of two millimeter wave propagation models for horizontal atmospheric attenuation at 70-115 GHZ
[AD-A192699] 21 p2931 N88-27403
Rain attenuation at 35 GHz over an 18 km path
[AD-A194504] 22 p3069 N88-28217

MICROWAVE CIRCUITS
An analysis of simplified feed architectures for MMIC (Monolithic Microwave Integrated Circuit) T/R (Transmit/Receive) module arrays
[AD-A185474] 06 p0697 N88-14275
GaAs varactor diode MMIC fabrication technology --- monolithic microwave integrated circuit (MMIC)
[RSRE-MEMO-4022] 09 p1158 N88-16943
Optical RF distribution links for MMIC phased array antennas
[NASA-TM-100841] 13 p1764 N88-20555
Monolithic microwave integrated circuit technology for advanced space communication
[NASA-TM-100829] 14 p1906 N88-21389
Instrumentation for ultrafast electronics
[AD-A191379] 16 p2193 N88-23080
A 30 GHz monolithic receive module technology assessment
[NASA-CR-180825] 16 p2194 N88-23084
Identification of cascaded microwave circuits with moderate reflections using reflections and transmission measurements
[PB88-171921] 18 p2503 N88-24849
Computer aided design of monolithic microwave and millimeter wave integrated circuits and subsystems
[AD-A191593] 18 p2503 N88-24852
Active feed array compensation for reflector antenna surface distortions
[NASA-TM-100826] 19 p2654 N88-25762
Analysis of networks with parameters S: Generalization of junction matrix
[INPE-4535-PRE/1282] 20 p2793 N88-26570
Guided wave interactions in millimeter-wave integrated circuits
[AD-A193017] 21 p2936 N88-27437
Array trade-off study using multilayer parasitic subarrays
[NASA-TM-101321] 22 p3070 N88-28222
Electronic and optical devices and applications
24 p3363 N88-30027

MICROWAVE COUPLING
Advanced numerical modeling of microwave penetration and coupling for complex structures
[DE88-001873] 06 p0690 N88-14231
Microwave polymerization of composite structures
[REPT-881-430-116] 21 p2922 N88-27343
Nonlinear dynamics of coupled oscillator arrays
[AD-A194888] 24 p3367 N88-30053

MICROWAVE EMISSION
Meterwave observations of a coronal hole
01 p0114 N88-10730
VLA observations of the X-ray bright Hyades M-dwarfs
04 p0512 N88-13147
Microwave observations of red dwarf flare stars
04 p0513 N88-13153
Current status of high power microwave effects and simulation
[DE87-004112] 06 p0751 N88-14615
Techniques for ceramic sintering using microwave energy
[DE88-001416] 07 p0837 N88-15080
Phase control of the microwave radiation in free electron laser two-beam accelerator
[DE88-001460] 07 p0859 N88-15219
Dynamic evolution of the source volumes of gradual and impulsive solar flare emissions
[NASA-TM-87815] 08 p1102 N88-16621
Research relative to angular distribution of snow reflectance/snow cover characterization and microwave emission
[NASA-CR-182733] 14 p1941 N88-21582
High power, high frequency radiation from beam-plasma interactions
[AD-A190207] 15 p2137 N88-22752

MICROWAVE EQUIPMENT
NT CYCLOTRON RESONANCE DEVICES
NT KLYSTRONS
NT MAGNETRONS
NT MICROWAVE AMPLIFIERS
NT MICROWAVE ANTENNAS
NT MICROWAVE FILTERS
NT MICROWAVE INTERFEROMETERS
NT MICROWAVE OSCILLATORS
NT MICROWAVE RADIOMETERS
NT MICROWAVE TUBES
NT THYRATRONS
NT TRAVELING WAVE TUBES

Anechoic Chamber test of the Electromagnetic Measurement System ground test unit
[DE87-012998] 01 p0035 N88-10226

Microwave refractive index structure function profiles (Cn2) measured from a small aircraft
[AD-A184343] 04 p0431 N88-12670

The lasertron RF generator for FEL (Free-Electron Laser) applications
[DE88-000515] 04 p0448 N88-12776

Evaluation of device figure of merit in microwave switching circuit design
[AD-A184896] 05 p0577 N88-13520

Observation guidelines for a Total Ozone Mapping Spectrometer (TOMS) in geosynchronous orbit
05 p0619 N88-13801

An analysis of simplified feed architectures for MMIC (Monolithic Microwave Integrated Circuit) T/R (Transmit/Receive) module arrays
[AD-A185474] 06 p0697 N88-14275

Microwave system for the microwave Tokamak experiment (MTX)
[DE88-002391] 09 p1250 N88-17487

Thermal analysis of transistor packages, part 2
[DE88-005091] 10 p1323 N88-17909

The bit-error rate performance of a satellite microwave matrix switch
[NASA-TM-100285] 16 p2167 N88-22920

The off-axis channel macroplate
[NASA-CR-182938] 18 p2505 N88-24861

The effects of better environmental inputs in estimating sea clutter
[AD-A192058] 19 p2643 N88-25678

Study and implementation of ultrahigh frequency coupling devices using the fin line technology --- millimeter waves
[ETN-88-92307] 20 p2796 N88-26588

Microwave polymerization of composite structures
[REPT-881-430-116] 21 p2922 N88-27343

Use of microwave measuring systems for the nondestructive control of resins and composites
[REPT-881-430-123] 21 p2959 N88-27576

Solid state research
[AD-A192837] 21 p3020 N88-27929

SSVCO feed characteristics
[DE88-011322] 22 p3068 N88-28208

HPM (High Power Microwave) simulation fidelity studies
[DE88-012229] 22 p3068 N88-28209

HPM (High-Power Microwave) coupling into realistic targets
[DE88-011788] 23 p3207 N88-29084

Millimeter wave generation by relativistic electron beams
[AD-A195683] 24 p3362 N88-30016

Growth of GaAs crystals by the Heat Exchanger Method for microwave device applications
[AD-A196028] 24 p3433 N88-30435

Estimation of soil temperature profile from remote microwave and IR measurements
24 p3450 N88-30532

The Deep Space Network: An instrument for radio astronomy research
[NASA-CR-183219] 24 p3453 N88-30554

MICROWAVE FILTERS

Band pass with cavity resonators by use of three oscillation types
[ETN-88-92984] 23 p3209 N88-29096

MICROWAVE FREQUENCIES

NT EXTREMELY HIGH FREQUENCIES
NT SUPERHIGH FREQUENCIES

Study and realization of Schottky diodes for forthcoming integrated hyperfrequency devices
[LAAS-87-062] 02 p0167 N88-11054

Deformation effects on microwave reflectivity
[AD-A185684] 07 p0844 N88-15120

Microwave response of an HEMT photoconductor
[NASA-TM-100819] 11 p1480 N88-18835

Polymerization of epoxy matrix composites using pulsed microwaves
[CERT-3/1324-MO] 20 p2780 N88-26487

Microwave frequency nondestructive control
[CERT-2/1355-MO] 23 p3189 N88-28976

Coupling between radiation and gas dynamics
[AD-A194593] 23 p3211 N88-29113

Microwave remote sensing in the French industries
[ETN-88-93081] 24 p3387 N88-30171

MICROWAVE IMAGERY

Validate algorithms for the determination of rainfall rates from SSM/I microwave satellite imagery
[AD-A188769] 16 p2233 N88-23337

Validate algorithms for the determination of rainfall rates from SSM/I microwave satellite imagery
[AD-A191337] 16 p2236 N88-23353

Microwave image understanding and its application to radar cross section management
20 p2788 N88-26542

Validate algorithms for the determination of rainfall rates from SSM/I microwave satellite imagery
[AD-A192299] 21 p2974 N88-27664

Validate algorithms for the determination of rainfall rates from SSM/I microwave satellite imagery
[AD-A195428] 24 p3404 N88-30270

MICROWAVE INTERFEROMETERS

Testing a very good microwave interferometer
[TRITA-EPP-86-09] 09 p1167 N88-16996

Geodesy by radio interferometry: Optimization of wet path delay algorithms using microwave radiometer data
[PB88-167739] 18 p2498 N88-24820

MICROWAVE LANDING SYSTEMS

Effect of motion cues during complex curved approach and landing tasks: A piloted simulation study
[NASA-TP-2773] 04 p0398 N88-12480

Boeing 727 MLS (Microwave Landing System) terminal instrument procedures (TERPS) approach data collection and processing, data report
[AD-A185523] 06 p0667 N88-14090

Microwave Landing System (MLS) mathematical model installation manual
[AD-A185612] 07 p0819 N88-14978

Crew procedures for microwave landing system operations
[NASA-CR-178359] 09 p1116 N88-16688

Flight simulations of MLS interception procedures applicable to laterally segmented approach paths
[NLR-MP-86037-U] 13 p1721 N88-20288

Analysis of a range estimator which uses MLS angle measurements
[NASA-CR-182896] 16 p2160 N88-22884

Development of an airborne facility for advanced avionics research 17 p2307 N88-23801

Cessna 172 MLS (Microwave Landing System) terminal instrument procedures (TERPS) approach data collection and processing data report
[AD-A191241] 18 p2461 N88-24613

Microwave landing system mathematical modeling study for Midway Airport Runway 22L, Chicago, Illinois
[AD-A191721] 18 p2462 N88-24616

Development of an airborne facility for advanced avionics research
[NLR-MP-87012-U] 20 p2760 N88-26368

MICROWAVE OSCILLATORS

NT MAGNETRONS

Optically tuned MM-wave IMPATT source
[AD-A185250] 05 p0577 N88-13523

High peak power ka-band gyrotron oscillator experiment
[AD-A185424] 05 p0585 N88-13563

High peak power Ka-band gyrotron oscillator experiments with slotted and unslotted cavities
[AD-A188109] 11 p1478 N88-18819

Low noise cryogenic dielectric resonator oscillator
[NASA-CASE-NPO-17157-1-CU]
20 p2797 N88-26596

MICROWAVE RADIATION

U MICROWAVES

MICROWAVE RADIOMETERS

Study of a payload for Columbus Polar Platform Earth observation demonstration mission, executive summary
[ESA-CR(P)-2412] 01 p0014 N88-10079

The CNR/PSN Advanced Microwave Imaging Radiometer (AMIR) --- satellite-borne
03 p0340 N88-12141

Non-linearity in measurement systems: Evaluation method and application to microwave radiometers
04 p0433 N88-12684

A multibody dynamic analysis of the N-ROSS (Navy Remote Ocean Sensing System) satellite rotating flexible reflector using Kane's method
[AD-A184452] 04 p0462 N88-12860

Cloud cover determination in polar regions from satellite imagery
[NASA-CR-181544] 04 p0471 N88-12908

In-orbit calibration adjustment of the Nimbus-7 SMMR
[NASA-TM-100678] 05 p0614 N88-13773

Estimation of rainfall rates in tropical cyclones by passive microwave radiometry 06 p0744 N88-14577

Characterization of 6 soils in the X-band, through measurements of complex permittivity
[INPE-4376-TDL/302] 12 p1639 N88-19814

Contribution of spaceborne high resolution radiometers to mapping of precoastal depths
19 p2701 N88-26063

Passive microwave measurements of water vapor fields and rain for locating fronts in cyclonic storms
[AD-A195632] 24 p3404 N88-30267

MICROWAVE SCATTERING

Active and passive remote sensing of ice
[AD-A1866[illegible]] 09 p1195 N88-17162

Characteristics of coherent and incoherent waves in snow at microwave and millimeter wave frequencies
[AD-A188990] 12 p1620 N88-19692

Almond test body --- for microwave anechoic chambers
[NASA-CASE-LAR-13747-1] 18 p2502 N88-24845

Microwave amplifiers
[AD-A192974] 20 p2795 N88-26585

Transient interaction of electromagnetic pulses in dielectrics and microwave biophysics
[AD-A195687] 24 p3360 N88-30008

MICROWAVE SENSORS

Fundamental aspects of the physics of remote sensing
[ESA-TT-1045] 09 p1185 N88-17100

Principal space programs in the area of microwaves
[INPE-4164-PRE/1064] 12 p1618 N88-19677

Microwave calibration system 2
[AD-A192976] 20 p2805 N88-26639

Active and passive remote sensing of ice
[AD-A193307] 21 p2966 N88-27617

Microwave instrument for planetary mission (Titan/CASSINI mission orbiter spacecraft)
[BAE-CS/TP-8359] 24 p3375 N88-30102

MICROWAVE SOUNDING ●

Determination of total ozone from HIRS2/MSU sounding data 05 p0619 N88-13799

Multifilter spectrometer (FEB) for microwave atmospheric sounder
[AD-A192312] 21 p2935 N88-27426

MICROWAVE SPECTRA

Microwave observations of nonthermal phenomena in pre-main sequence stars 04 p0505 N88-13107

Microwave dielectric spectrum of rocks
[NASA-TM-89719] 12 p1642 N88-19831

Microwave spectroscopy and gravitational collapse
18 p2594 N88-25413

Mode locking of semiconductor laser with external cavity
[AD-A196018] 24 p3378 N88-30117

MICROWAVE SPECTROMETERS

Precise measurement of refractive index and absorption coefficient of near millimeter wave and far infrared materials
[AD-A184538] 03 p0293 N88-11840

MICROWAVE SWITCHING

Loss measurement of 3-port ferrite switches in the 90 GHz range
[ESA-TT-1054] 03 p0310 N88-11958

Evaluation of device figure of merit in microwave switching circuit design
[AD-A184896] 05 p0577 N88-13520

RF-switches: Application and design --- satellite communication 14 p1877 N88-21215

MICROWAVE TRANSMISSION

Operation of the TEMPO machine
[DE87-011285] 01 p0038 N88-10241

An evaluation of equivalent models for design of rectangular microstrip antennas
[FOA-C-30451-3.2] 08 p0977 N88-15905

A review of the role of surface reflection in multipath propagation over terrestrial microwave links
12 p1615 N88-19655

Identification of cascaded microwave circuits with moderate reflections using reflections and transmission measurements
[PB88-171921] 18 p2503 N88-24849

MICROWAVE TUBES

NT CYCLOTRON RESONANCE DEVICES
NT KLYSTRONS
NT MAGNETRONS
NT TRAVELING WAVE TUBES

Microwave tubes: Literature study no. 8 comprising the year 1986
[FOA-C-30467-3] 09 p1159 N88-16944

A crude scaling law for lasertrons
[DE88-003880] 09 p1173 N88-17032

MICROWAVES

NT CENTIMETER WAVES
NT DECIMETER WAVES
NT MICROWAVE EMISSION
NT MILLIMETER WAVES

Static magnetization and microwave loss in shock-modified ferrites
[DE87-012362] 02 p0146 N88-10916

Laboratory evaluation and application of microwave absorption properties under simulated conditions for planetary atmospheres
[NASA-CR-181466] 02 p0254 N88-11606

Measurement of solid propellant combustion velocity by means of microwaves
[CERT-1/1316-MO] 03 p0283 N88-11778

Automated microwave dielectric constant measurement
[AD-A184182] 04 p0431 N88-12667

United States - Japan Workshop on Dielectric and Piezoelectric Ceramics (3rd) held in Toyama, Japan on November 9-12, 1986
[AD-A185113] 05 p0568 N88-13460

Microwave challenges to the thermoregulatory system
[AD-A185391] 05 p0629 N88-13847
Microwave superheaters for fusion
[DE88-001656] 05 p0653 N88-14007
Propagation effects on satellite systems at frequencies below 10 GHz: A handbook for satellite systems design
[NASA-RP-1108/2] 06 p0690 N88-14226
Time-domain robotic vision application
06 p0798 N88-14886
Modulation of an intense beam by an external microwave source: Theory and simulation
[AD-A185683] 07 p0848 N88-15145
Combined effect of microwaves and ionizing radiation
07 p0893 N88-15413
Construction of airborne radars for remote sensing
[PB88-113063] 09 p1154 N88-16916
Properties of superconducting tunnel structures in microwave radiation field 09 p1239 N88-17424
Fundamental cyclotron frequency generation from a cusptron oscillator
[AD-A188187] 10 p1321 N88-17898
A technique for low level, wide range CW microwave power meter calibrations
[DE88-004147] 10 p1333 N88-17966
Numerical simulation of the propagation and absorption due to air breakdown of long microwave pulses
[DE88-005227] 11 p1475 N88-18798
Microwave radiation from rotating, annular electron beams 11 p1475 N88-18801
Experimental results of a high-gain microwave FEL operating at 140 GHz
[DE88-004358] 11 p1492 N88-18907
A sky temperature survey at 19.2 GHz using a balloon borne Dicke radiometer for anisotropy tests of the cosmic microwave background 11 p1571 N88-19403
Two-dimensional electron fluid computer calculations of nanosecond pulse, low pressure microwave air breakdown in a rectangular waveguide and their verification by experimental measurement
[DE88-004407] 12 p1618 N88-19678
Microwave generation from a cusptron oscillator with a six-vane circuit
[AD-A188377] 12 p1619 N88-19680
Solid-state travelling wave amplifiers based on multi-stream instability
[AD-A189566] 12 p1624 N88-19718
Photonic temperature and pressure sensors for biosystems/pulsed microwave. Part 1: Interaction studies
[AD-A188887] 12 p1629 N88-19751
Effects of whole-body irradiation with low-intensity microwaves on morphological, functional and cytochemical characteristics of leukocytes 12 p1663 N88-19971
Microwave and structural properties of saline ice
[AD-A189307] 13 p1803 N88-20779
Design of electron beam accelerator for microwave application
[DE88-005252] 13 p1838 N88-20999
Solar microwave radiation maps measured at Metsaehovi Radio Research Station in 1978-1979
[PB88-127543] 13 p1857 N88-21108
Tabulation of Mie scattering calculation results for microwave radiative transfer modeling
[NASA-CR-4130] 14 p1947 N88-21612
Generating squeezed microwave radiation with a Josephson parametric amplifier
14 p1978 N88-21805
Microwave sintering of alumina-SiC composites at 2.45 and 60 GHz
[DE88-006455] 15 p2030 N88-22095
Preparing the Alcator C bolometer system for use on MTX (Microwave Tokamak Experiment)
[DE88-006724] 15 p2134 N88-22733
Validate algorithms for the determination of rainfall rates from SSM/I microwave satellite imagery
[AD-A188769] 16 p2233 N88-23337
Power requirements for mining and microwave processing of extraterrestrial resources
17 p2420 N88-24389
The radar cross section of some simple reflectors at short wavelengths
[FOA-C-30472-3.3] 18 p2501 N88-24839
Behavioral response of rats exposed to high-power microwave radiation
[AD-A192199] 18 p2548 N88-25128
Analysis of microwave burner measurement system using a microwave network analysis computer program
19 p2631 N88-25604
A simple technique to generate or gate microwave pulses with picosecond speeds 19 p2657 N88-25784
Radar and EW applications of multi-gigahertz optical components and systems 19 p2660 N88-25816
The ratio of microwaves to X-rays in solar flares: The case for the thick target model
[NASA-CR-183102] 19 p2743 N88-26287
Antenna heights for the optimum utilization of the oceanic evaporation duct. Part 3: Results from the Mediterranean measurements, volume 2
[AD-A192311] 20 p2791 N88-26554
MTX (Microwave Tokamak Experiment) plasma diagnostic system
[DE88-011326] 20 p2861 N88-26993
Preparation and properties of high Q microwave dielectrics in the (CA, SR, BA) zirconate system
[AD-A193127] 21 p2918 N88-27317
A method for estimating the susceptibility of electronic systems to HPM (High Power Microwave)
[DE88-012246] 21 p2934 N88-27422
Genetic effects of low level microwave radiation
[AD-A192687] 21 p2984 N88-27722
Effects of pulsed and CW (Continuous Wave) 2450 MHz radiation on transformation and chromosomes of human lymphocytes in vitro
[AD-A193104] 21 p2987 N88-27736
Assessment of cochlear damage after microwave irradiation
[AD-A193237] 21 p2987 N88-27737
Behavioral effects of exposure to the tempo high-power microwave system
[AD-A193305] 21 p2987 N88-27738
Experiments applications guide: Advanced Communications Technology Satellite (ACTS)
[NASA-TM-100265] 22 p3048 N88-28082
Improvements in techniques of microwave thermography
[AD-A194613] 23 p3203 N88-29062
Improvements in techniques of microwave thermography
[AD-A193620] 23 p3239 N88-29276
The surface evaporative duct height product: An evaluation
[AD-A195918] 24 p3392 N88-30199

MICROWEIGHING
U WEIGHT MEASUREMENT

MIDAIR COLLISIONS
NT BIRD-AIRCRAFT COLLISIONS
UK airmiss statistics
[CAP-530] 03 p0261 N88-11642
Aircraft accident report: Midair collision of Cessna-340A, N8716K, and North American SNJ-4N, N711SQ, Orlando, Florida, May 1, 1987
[PB88-910402] 13 p1720 N88-20282
UK airmiss statistics
[REPT-3/87] 14 p1865 N88-21141
Aircraft accident report: Midair collision of US Army U-21A, Army 18061 and Sachs Electric Company Piper PA-31-350, N60SE, Independence, Missouri, January 20, 1987
[PB88-910401] 16 p2159 N88-22877
UK airmiss statistics
[CAA-1/87] 17 p2300 N88-23761
Aircraft accident report: Midair collision of SkyWest Airlines Swearingen METRO 2, N163SW, and Mooney M20, N6485U, Kearns, Utah, January 15, 1987
[PB88-910404] 20 p2755 N88-26346
UK airmisses involving commercial air transport
[CAA-1/88] 23 p3176 N88-28907

MIDCOURSE GUIDANCE
Report to congress on the strategic defense system architecture
[AD-A195476] 24 p3426 N88-30393

MIDDLE ATMOSPHERE
NT MESOPAUSE
NT MESOSPHERE
NT OZONOSPHERE
NT STRATOPAUSE
NT STRATOSPHERE
Contributions of lidar measurements to the study of long term variations of the middle atmosphere
[ETN-88-91237] 05 p0625 N88-13824
Latitude coverage of observations of the middle atmosphere by solar absorption spectrometry from a heliosynchronous orbit
[AERONOMICA-ACTA-A-316-1987]
06 p0742 N88-14566
New techniques for rocket and balloon-borne instrumentation for investigations of the structure, dynamics and electrodynamics of the middle atmosphere 08 p1027 N88-16220
Electrodynamics of the high latitude middle atmosphere 08 p1028 N88-16225
Dynamic modeling of the middle atmosphere
08 p1028 N88-16227
Project CONDOR: Middle atmosphere wind structure obtained with lightweight inflatable spheres near the equatorial electrojet 08 p1028 N88-16230
ROCOZ-A (improved rocket launched ozone sensor) for middle atmosphere ozone measurements
08 p1029 N88-16233
The Cryogenic Infrared Spectrometer and Telescope for the Atmosphere (CRISTA) experiment on Astro-SPAS
08 p1034 N88-16270
Geochemistry of the middle and lower atmosphere: Environmental impact through the deterioration of the ozone layer
[INPE-4477-PRE/1241] 16 p2230 N88-23321
Finite element simulation of the atmosphere's electromagnetic response to charge perturbations associated with lightning 17 p2375 N88-24124
Aerial photography as an instrument of atmospheric analysis: Maps of the middle atmosphere and its dynamics, Baixada Santista (SP) 19 p2684 N88-25955
Diffusion of slight solar induced disturbances in the middle atmosphere
[MITT-53] 20 p2825 N88-26758

MIDDLE EAR
Novel nonlinear signal processing principles
[AD-A191644] 19 p2707 N88-26097

MIDLATITUDE ATMOSPHERE
Physical processes for maintaining mean meridional and zonal circulation of atmosphere in middle latitudes, volume 1 14 p1900 N88-21343
Physical process for maintenance of mean meridional and zonal circulation of atmosphere in middle latitudes, volume 2 14 p1900 N88-21345
Experimental proof of quasilongitudinal propagation of low-frequency waves in middle latitudes in upper ionosphere 24 p3447 N88-30516

MIDLATITUDES
U TEMPERATE REGIONS

MIE SCATTERING
NT RAYLEIGH SCATTERING
Extinction by dielectric particles at optical and infrared wavelength
[AD-A184818] 05 p0650 N88-13981
Tabulation of Mie scattering calculation results for microwave radiative transfer modeling
[NASA-CR-4130] 14 p1947 N88-21612
Advanced diagnostics for reacting flows
[AD-A190485] 15 p2035 N88-22122
Investigations on Mie and Rayleigh scattering as basis for the development of Rayleigh temperature lidars with aid of Michelson interferometry
[GKSS-87/E/62] 21 p2976 N88-27675

MIE THEORY
U MIE SCATTERING

MIG AIRCRAFT
Proposal for a new aggressor aircraft
[AD-A194311] 22 p3041 N88-28056

MIGRATION
Migration and transfer of triplet energy in selected polymer systems
[DE87-014432] 02 p0152 N88-10953
The migration of grain boundaries in ceramic materials with particular reference to the sintering process
[DE88-004085] 10 p1306 N88-17808
Electrohydrodynamic migration of charged droplets in an insulating fluid
[NASA-TM-100849] 14 p1912 N88-21424
Energy migration, motion and order in synthetic polymers
[AD-A193334] 21 p2918 N88-27320
Migration and stability of HgCdTe lattice defects
[AD-A193293] 21 p3021 N88-27935

MILANKOVITCH THEORY
U CLIMATOLOGY

MILITARY AIR FACILITIES
ZEUS: A knowledge-based expert system that assists in predicting visibility at airbases
[AD-A184197] 05 p0626 N88-13829
Evaluation of bituminous materials used in pavement recycling projects at Tyndall, MacDill, and Hurlburt Air Force Bases
[AD-A188068] 10 p1317 N88-17871
Revised Uniform Summary of Surface Weather Observations, Loring AFB, Maine, Parts A - F
[AD-A188201] 14 p1947 N88-21610
Vegetation studies on Vandenberg Air Force Base, California
[NASA-TM-100985] 20 p2831 N88-26795
Reduced flexibility in processing Titan 4 space launch vehicles at Cape Canaveral Air Force Station
[AD-A194908] 24 p3332 N88-29834
EMPTAC (Electromagnetic Pulse Test Aircraft) user's guide
[AD-A195072] 24 p3360 N88-30006

MILITARY AIRCRAFT
The EH-101 integrated project: A naval, utility and commercial helicopter system 03 p0265 N88-11672
Aircraft field degradation and electromagnetic compatibility
[PB88-183975] 19 p2602 N88-25456
Background to the UK military requirements for engine usage, condition and maintenance management systems
22 p3033 N88-28004

MILITARY HELICOPTERS
NT AH-64 HELICOPTER
NT CH-46 HELICOPTER
NT HEAVY LIFT HELICOPTERS
NT OH-58 HELICOPTER
NT UH-1 HELICOPTER
NT UH-60A HELICOPTER
The influence of operational requirements on LHX concept formulation 03 p0262 N88-11650
Investigation of vertical axis handling qualities for helicopter hover and NOE flight 03 p0263 N88-11653
MBB simulation facilities applied for rotorcraft research 03 p0263 N88-11655
Impacts of rotor hub design criteria on the operational capabilities of rotorcraft systems 03 p0264 N88-11663
Helicopter (performance) management 03 p0264 N88-11666
Helicopter fire control: Advantages of an automatic target tracker 03 p0264 N88-11667
Development, testing and evaluation of a night vision goggle compatible BO-105 for night low level operation 03 p0265 N88-11668
A129 advanced solutions for meeting today's combat helicopter requirement 03 p0265 N88-11669
Advanced helicopter cockpit and control configurations for helicopter combat missions
[NASA-TM-100017] 07 p0821 N88-14988
A piloted simulation investigating handling qualities and performance requirements of a single-pilot helicopter in air combat employing a helmet-driven turreted gun
[AD-A186878] 09 p1116 N88-16689
Helicopter activities in Germany
[MBB-UD-487/86] 10 p1314 N88-17853
Artificial and natural icing tests of AH-64, phase 2
[AD-A188231] 11 p1439 N88-18585
User perceptions of side-arm flight control in rotary-wing aircraft
[AD-A188519] 12 p1672 N88-20009
AVSCOM'S modifications to Teledyne Systems Company's air-to-air fire control system simulation model
[AD-A189136] 13 p1722 N88-20294
An investigation of the ability to recover from transients following failures for single-pilot rotorcraft
[NASA-TM-100078] 16 p2164 N88-22905
Test philosophy of the EH101 integrated avionic 17 p2303 N88-23775
Operation and performance of an integrated helicopter communication system 17 p2305 N88-23787
Operational noise data for CH-47D and AH-64 army helicopters
[AD-A191059] 18 p2570 N88-25263
Helicopter transmission research at NASA Lewis Research Center
[NASA-TM-100962] 24 p3379 N88-30128
MILITARY OPERATIONS
NT COMBAT
NT ELECTRONIC WARFARE
Automation strategy and results for an airbase command and control information system
[NLR-MP-86031-U] 01 p0035 N88-10223
How space, the fourth operational medium, supports operational maneuver
[AD-A184742] 03 p0373 N88-12346
High resolution satellite imagery simulation --- treaty verification
[FOA-C-30462-3.3,9.3] 05 p0620 N88-13810
Assessment of physical activity intensity by heart rate during sleep limited military operations
[AD-A185913] 07 p0888 N88-15382
Analysis of the reliability of Royal Australian Air force non-destructive inspection
[AD-A186979] 09 p1177 N88-17049
Computer assisted instruction: Two decades in perspective
[AD-A186813] 09 p1216 N88-17289
The evolution of naval warfare technology and the impact of space systems
[AD-A186900] 09 p1233 N88-17392
The mathematization of the military sciences
[MBB-Z-139/87] 10 p1311 N88-17834
Development of a graphics based two-attribute utility assessment program with application to mission planning
[AD-A187276] 10 p1388 N88-18292
State-of-the-art technologies for construction in space: A review
[AD-A188412] 12 p1585 N88-19483
Alternative program approaches for the advanced satellite technology program
[AD-A188917] 12 p1600 N88-19576
Emerging technologies program 3-5: Microelectronics Panel report
[AD-A189463] 12 p1624 N88-19716
Selected aspects of triazolam in relation to aviator performance in naval flight operations
[AD-A189322] 12 p1667 N88-19996
Knowledge-based system analysis and control
[AD-A188163] 12 p1681 N88-20049
Expert systems for decision support in military aircraft mission preparation
[NLR-MP-87013-U] 13 p1830 N88-20946
MANPRINT handbook for RFP (Request For Proposal) development
[AD-A188321] 13 p1850 N88-21075
Soviet military power, 1987 13 p1858 N88-21114
Application of hybrid laminar flow control to global range military transport aircraft
[NASA-CR-181638] 14 p1862 N88-21124
An overview of the army GIS (Geographic Information Systems) Research Program
[AD-A189711] 14 p1992 N88-21871
Department of Defense statement on the X-ray Lithography Program to the Research and Development Subcommittee of the House Armed Services Committee of 100th Congress, second session
[AD-A191854] 18 p2582 N88-25341
Real time data base management
[AD-A191758] 19 p2739 N88-26265
NAVSTAR global positioning system
[AD-A192609] 20 p2757 N88-26354
The strategic defense initiative: Strategic implications
[AD-A192341] 20 p2847 N88-26902
Launch operations to support future space forces
[AD-A192679] 20 p2881 N88-27107
Aerospace applications studies, 1971-1987
[AGARD-R-759] 21 p2889 N88-27147
Army space systems for terrestrial applications
[AD-A192735] 21 p2965 N88-27613
Analysis of ATCRBS (Air Traffic Control Radar Beacon System), mode select (Mode S) in combat operations
[AD-A193140] 22 p3040 N88-28050
Biomedical aspects of military operations at high altitude
[AD-A192677] 22 p3132 N88-28619
Tactical air force night/adverse weather training
[AD-A194243] 22 p3133 N88-28625
Linear goal programming as a military decision aid
[AD-A194276] 22 p3137 N88-28652
Inflight rearming
[AD-A193564] 23 p3176 N88-28909
Low altitude: A new dimension in air refueling
[AD-A193819] 23 p3176 N88-28910
Defensive platform size and survivability
[DE88-011634] 23 p3184 N88-28948
Remotely Operated Vehicle (ROV) reliability study, phase 1
[AD-A194367] 23 p3222 N88-29177
SDI (Strategic Defense Initiative): A policy analysis
[AD-A194240] 23 p3275 N88-29493
The problem of space in Soviet operational art
[AD-A194150] 23 p3276 N88-29502
Centralized class A flight mishap investigation
[AD-A194397] 24 p3322 N88-29786
Integration of LANTIRN (Low Altitude Navigation and Targeting Infrared for Night) into operational fighter training
[AD-A194906] 24 p3325 N88-29799
Long haul communications in the HF spectrum utilizing high speed modems
[AD-A194683] 24 p3360 N88-30003
Looking beyond the strategic defense initiative
[AD-A195079] 24 p3427 N88-30394
Antisatellite weapons and satellite deployment strategies
[AD-A195014] 24 p3427 N88-30396
MILITARY PSYCHIATRY
U MILITARY PSYCHOLOGY
MILITARY PSYCHOLOGY
New US book on aviation psychology reviewed 07 p0896 N88-15433
MILITARY SPACECRAFT
NT DMSP SATELLITES
NT RECONNAISSANCE SPACECRAFT
An introduction to military satellite communications
[RSRE-MEMO-3976] 09 p1153 N88-16911
NROSS (Navy Remote Ocean Sensing System): A force multiplier
[AD-A186853] 10 p1346 N88-18045
Alternative program approaches for the advanced satellite technology program
[AD-A188917] 12 p1600 N88-19576
Alternative force structuring strategies for military satellite communication systems
[AD-A189492] 13 p1758 N88-20516
Air Force space power requirements and nuclear power assessment methodology 17 p2418 N88-24378
Comparison of a direct thrust nuclear engine, nuclear electric engine and a chemical engine for future space missions 17 p2418 N88-24379
The Army's role in space: Support for the battlefield commander
[RAND-P-7396] 19 p2721 N88-26159
Launch operations to support future space forces
[AD-A192679] 20 p2881 N88-27107
The principles of mass and maneuver applied to space operations
[AD-A194037] 23 p3276 N88-29500
The problem of space in Soviet operational art
[AD-A194150] 23 p3276 N88-29502
Antisatellite weapons and satellite deployment strategies
[AD-A195014] 24 p3427 N88-30396
MILITARY TECHNOLOGY
Soviet aviation technology's state of the art SU-27 fighter
[AD-A184121] 03 p0259 N88-11628
Fuel cells --- military applications
[PML-1986-43] 05 p0622 N88-13813
University research initiative research program summaries
[AD-A184876] 05 p0658 N88-14035
Investigation of design concepts for large space structures to support military applications
[AD-A186098] 07 p0824 N88-15000
A summary of the Naval Postgraduate School research program
[AD-A186362] 07 p0942 N88-15727
AGARD reports: A quarterly listing, 1 July through September 30, 1987
[AD-A186572] 08 p1093 N88-16579
Advanced composite airframe program: Today's technology 09 p1107 N88-16636
Cooperative analysis expert situation assessment research 09 p1206 N88-17228
The evolution of naval warfare technology and the impact of space systems
[AD-A186900] 09 p1233 N88-17392
The military techniques of tomorrow: A contribution to active peace assurance
[MBB-UA-1049/87] 10 p1315 N88-17860
Optical memory cards: A comparison with other current technologies and potential military applications
[AD-A187287] 10 p1425 N88-18512
Soviet high-technology restructuring drive: the MNTK network
[AD-A188138] 11 p1565 N88-19370
Soviet military power, 1987 13 p1858 N88-21114
JPRS report: Science and technology. Japan
[JPRS-JST-87-029] 15 p2052 N88-22228
Laser comparison study of Nd:BEL and Nd:YAG
[AD-A191084] 16 p2213 N88-23205
Development of a C3 generic workstation: System overview 16 p2242 N88-23396
C3 generic workstation: Performance metrics and applications 16 p2242 N88-23397
Department of Defense statement on defense agency research and development to the Subcommittee on Defense of the Committee on Appropriations, United States House of Representatives, 100th Congress, second session
[AD-A191840] 18 p2588 N88-25377
The FY 1989 Department of Defense statement on the Science and Technology Program to 100th Congress, second session
[AD-A191843] 18 p2588 N88-25380
Radar and EW applications of multi-gigahertz optical components and systems 19 p2660 N88-25816
On 3-5 transistors for MM-wave applications
[AD-A191580] 19 p2661 N88-25825
The Army's role in space: Support for the battlefield commander
[RAND-P-7396] 19 p2721 N88-26159
Air Force technical objective document, FY89
[AD-A193110] 21 p2896 N88-27194
Intelligent Mobile Autonomous System (IMAS)
[AD-A193181] 21 p3003 N88-27811
Dynamically reconfigurable distributed database systems
[AD-A194716] 23 p3297 N88-29636
MILKY WAY GALAXY
The astrophysics of nebulae and active galactic nuclear emission-line regions: New methods and applications 13 p1858 N88-21111
Royal Observatory, Edinburgh: Research and Facilities
[ISSN-0267-6281] 14 p1993 N88-21881
The galactic nucleus at mm-, sub-mm and far-infrared wavelengths
[MPE-PREPRINT-102] 16 p2288 N88-23700
The distance to the center of the galaxy: H2O maser proper motions in Sgr B2(N)
[MPE-PREPRINT-104] 16 p2288 N88-23702
The velocity field of the outer galaxy
[B8681472] 20 p2885 N88-27132

Gamma radiation from center of the galaxy of the order of MeV values
[MPE-207] 21 p3032 N88-27999
Distribution of hydroxyl clouds in the galaxy
[DE88-702415] 22 p3164 N88-28844
The kinematics of Milky Way halo gas
23 p3299 N88-29648

MILLIMETER WAVES
Millimeter wave tokamak heating and current drive with a high power free electron laser
[DE87-011324] 01 p0099 N88-10651
The impact of environmental factors on the performance of millimeter wave seekers in smart munitions
[DE87-014277] 03 p0270 N88-11697
Precise measurement of refractive index and absorption coefficient of near millimeter wave and far infrared materials
[AD-A184538] 03 p0293 N88-11840
Millimeter-wave studies of moist air
[AD-A184681] 03 p0306 N88-11935
Investigation of hexagonal ferrite film growth techniques for millimeter-wave systems applications
[AD-A184335] 03 p0383 N88-12406
An investigation of millimeter wave propagation in the atmosphere: Measurement program
[AD-A184837] 05 p0574 N88-13498
Optically tuned MM-wave IMPATT source
[AD-A185250] 05 p0577 N88-13523
Observation and interpretation of solar S-component radiation at millimetre waves
[PB87-225207] 06 p0805 N88-14916
Horn design equations for the NBS (National Bureau of Standards) horn-type noise standards
[PB88-110226] 07 p0844 N88-15122
An adiabatic demagnetization cooled bolometer system for millimeter continuum astronomy
07 p0943 N88-15735
Finnish-Soviet Symposium on Radio Astronomy (1st) held at Otaniemi on August 26-27, 1985
[PB87-140661] 07 p0944 N88-15736
ESA Bulletin No. 10
[ETN-87-90514] 09 p1123 N88-16728
Technology developments to meet tomorrow's need for higher satellite frequencies 09 p1124 N88-16732
Fabrication and packaging of discontinuous MIM (Metal-Insulator-Metal) film arrays for efficient MM wave and IR detection and mixing
[AD-A186809] 09 p1146 N88-16869
MM-wave propagation and application in military communication systems 12 p1617 N88-19669
Millimeter and submillimeter wave research: Spectroscopy, energy transfer, and techniques
[AD-A188952] 12 p1620 N88-19691
Characteristics of coherent and incoherent waves in snow at microwave and millimeter wave frequencies
[AD-A188990] 12 p1620 N88-19692
Development of a high speed InGaAs/InP Schottky barrier photodetector for millimeter-wave fiber optical links
[AD-A188594] 12 p1629 N88-19750
Observations of the large scale anisotropy in the cosmic background radiation at 3 mm
[INPE-4425-PRE/1229] 12 p1712 N88-20249
Millimeter-wave properties of the atmosphere: Laboratory studies and propagation modeling
[PB88-164215] 14 p1905 N88-21387
Millimeter-wave pulse distortion by a single adsorption line simulating the terrestrial atmosphere
[PB88-161237] 14 p1906 N88-21388
Calculation of the efficiency of a resonant cyclotronic electron maser (gyrotrons)
[INPE-4387-PRE/1207] 14 p1915 N88-21444
Some models for rain and cloud attenuation of millimeter waves
[PB88-160809] 14 p1948 N88-21616
Instrumentation for the characterization and development of millimeter wave components compatible with monolithic integration
[AD-A189724] 15 p2059 N88-22275
The superconducting phase shifter in the development of a terahertz imaging radar system
[AD-A190666] 16 p2188 N88-23046
UV-Laser reactions of molecular adsorbates
[AD-A190796] 16 p2212 N88-23201
The galactic nucleus at mm-, sub-mm and far-infrared wavelengths
[MPE-PREPRINT-102] 16 p2288 N88-23700
Submillimeter and far infrared line observations of M17 SW: A clumpy molecular cloud penetrated by UV radiation
[NASA-CR-182866] 16 p2288 N88-23701
Operation and performance of an integrated helicopter communication system 17 p2305 N88-23787
Optical constants of minerals and other materials from the millimeter to the ultraviolet
[AD-A192210] 18 p2482 N88-24724
Millimeter and submillimeter waves and frequency selective surfaces
[AD-A191511] 18 p2500 N88-24827
Computer aided design of monolithic microwave and millimeter wave integrated circuits and subsystems
[AD-A191593] 18 p2503 N88-24852
Millimeter-wave integrated circuits
19 p2656 N88-25774
Characteristics of shielded microstrip lines on GaAs-Si at millimeter-wave frequencies 19 p2657 N88-25787
Picosecond response of an optically controlled millimeter wave phase shifter 19 p2660 N88-25820
On 3-5 transistors for MM-wave applications
[AD-A191580] 19 p2661 N88-25825
Study and implementation of ultrahigh frequency coupling devices using the fin line technology --- millimeter waves
[ETN-88-92307] 20 p2796 N88-26588
An evaluation of two millimeter wave propagation models for horizontal atmospheric attenuation at 70-115 GHZ
[AD-A192699] 21 p2931 N88-27403
Multifilter spectrometer (FEB) for microwave atmospheric sounder
[AD-A192312] 21 p2935 N88-27426
A planar IC-compatible transferred electron device for millimeter-wave operation
[AD-A192692] 21 p2936 N88-27433
Guided wave interactions in millimeter-wave integrated circuits
[AD-A 93017] 21 p2936 N88-27437
Rapid-scanning Fourier transform spectrometer for studies of propagation of near-millimeter-wave radiation through clear air and fog
[AD-A193752] 22 p3070 N88-28219
A millimeter-wave tunneLadder TWT
[NASA-CR-182184] 22 p3072 N88-28239
Multi-sensory tracking mount control
[AD-A194675] 23 p3249 N88-29339
Laboratory evaluation and application of microwave absorption properties under simulated conditions for planetary atmospheres
[NASA-CR-182443] 23 p3300 N88-29653
Millimeter wave generation by relativistic electron beams
[AD-A195683] 24 p3362 N88-30016
Dielectric millimeter waveguides: A feasibility study for a novel dielectric millimeter waveguide
[AD-A195104] 24 p3366 N88-30042
Light-millimeter wave interactions in semiconductor devices
[AD-A195898] 24 p3432 N88-30428

MILLING (MACHINING)
Size-reduction and sorting behavior in sieve hammer mills
[ETN-88-91480] 11 p1467 N88-18749
An automatic system for extraction of information from a Computer Aided Design (CAD), selection, sequencing, and execution of turning processes
[INPE-4350-TDL/294] 12 p1676 N88-20020
Improvements in end point detection --- semiconductor fabrication
[RSRE-MEMO-4035/A] 14 p1899 N88-21336

MILLING MACHINES
Structure and properties of titanium nitride and zirconium nitride thin films prepared by reactive ion plating --- cutting tools
[ETN-88-92218] 15 p2042 N88-22167

MIM (SEMICONDUCTORS)
Fabrication and packaging of discontinuous MIM (Metal-Insulator-Metal) film arrays for efficient MM wave and IR detection and mixing
[AD-A186809] 09 p1146 N88-16869

MIM DIODES
Studies of tunneling in metals under high pressure
06 p0775 N88-14757

MIMD (COMPUTERS)
Performance of a multigrid method on parallel architecture 11 p1539 N88-19200
An analysis of multiple grain CHiP architectures
[AD-A189942] 15 p2110 N88-22570
Transformations of concurrent algorithms for highly parallel systems: A one year project summary report
[AD-A190236] 15 p2111 N88-22576
Multidimensional nodal transport methods for multiple-instruction multiple-data distributed memory machines
[DE88-004732] 19 p2713 N88-26108
Basic database operations on the butterfly parallel processor: Experiment results
[AD-A193199] 21 p3002 N88-27804
What have we learnt from using real parallel machines to solve real problems
[DE88-011227] 22 p3135 N88-28636

MINERAL DEPOSITS
A mineral reconnaissance sampling manual for Costa Rica: Central American energy and resource project
[DE87-014997] 04 p0462 N88-12859
Proceedings of the Third Airborne Imaging Spectrometer Data Analysis Workshop
[NASA-CR-181552] 05 p0611 N88-13755
Preliminary results from an investigation of AIS-1 data over an area of epithermal alteration: Plateau, Northern Queensland, Australia 05 p0613 N88-13768
Space photographs of the Onega-Ladoga isthmus and prediction of useful minerals 08 p1008 N88-16108
Study of relief of ore regions using space images (on the example of Eastern Yakutia)
08 p1008 N88-16111
Character of five selected LANDSAT lineaments in southwestern Pennsylvania: Report of investigations, 1987
[PB88-133517] 11 p1505 N88-18988

MINERAL EXPLORATION
Study of Earth from space and strengthening of economy 01 p0010 N88-10055
Marine minerals: Exploring our new ocean frontier
[PB87-217725] 02 p0216 N88-11364
Application of SPOT-1 data to mineral exploration in Nevada 03 p0343 N88-12163
Evolution of remote sensing utilization in geological mapping and ore exploration: Example in Zimbabwe
03 p0343 N88-12165
A mineral reconnaissance sampling manual for Costa Rica: Central American energy and resource project
[DE87-014997] 04 p0462 N88-12859
Remote sensing in mineral exploration
[PB87-138558] 06 p0729 N88-14484
Study of relief of ore regions using space images (on the example of Eastern Yakutia)
08 p1008 N88-16111
International role of US geoscience
[NASA-CR-182407] 08 p1035 N88-16281
Three-dimensional transient electromagnetic modeling for exploration geophysics 10 p1346 N88-18047
An integrated study of the Alto Paranaiba Kimberlite Province, Minas Gerais, Brazil: A possible tool for diamond exploration 17 p2355 N88-24031
Lithostructural interpretation of Chapda do Cachimbo (Pa-Am-Mt), based on radar and LANDSAT imagery
17 p2368 N88-24100
Remote sensing applied to the monitoring of mineral extraction in the proximity of urban areas: Pros and cons
19 p2684 N88-25954
First results of international investigations of the applications of SPOT-1 data to geologic problems, mineral and energy exploration 22 p3101 N88-28419
Results of the Geosat program to evaluate SPOT data for petroleum and mineral exploration
22 p3102 N88-28422
Evaluation of SPOT imagery for discriminating vegetation communities associated with surficial and bedbrock geology and identifying anomalous and stressed vegetation associated with mineralization
22 p3103 N88-28426
Use of digital images as a mineral prospecting tool in the tin province of Goias, Brazil
[INPE-4537-PRE/1284] 24 p3387 N88-30173
Oblique metallogenic zones recognized by interpreting space photographs of southern Tien Shan
24 p3450 N88-30529

MINERAL OILS
The wear process during the RUNNING-IN of steel in lubricated sliding
[NAL-TR-922T] 02 p0181 N88-11130
Lubricating properties of molybdenum disulfide. Part 3: Performance of molybdenum disulfide-containing oils in fluid lubrication
[NASA-TT-20156] 13 p1752 N88-20480
A study relating to the fog oil replacement program
[AD-A192536] 21 p2923 N88-27347

MINERALOGY
The distribution of evaporitic weathering products on Antarctic meteorites 06 p0798 N88-14888
A sedimentological and mineralogical study of the Koogah Formation, New South Wales
18 p2542 N88-25087
Analyzing the stratigraphy, tectonism, and mineralization at the Spanish side of the pyrite belt, Huelva province, Spain, using SPOT imagery 22 p3104 N88-28433
Volcano evolution on Mars 23 p3305 N88-29686
Nineteenth Lunar and Planetary Science Conference. Press abstracts
[NASA-CR-183037] 24 p3440 N88-30473
Exotic minerals in 3,500 million year old rocks: Evidence for large meteorite impacts 24 p3440 N88-30475

MINERALS
NT AMPHIBOLES
NT ASBESTOS
NT BIOTITE

NT CALCITE
NT GARNETS
NT GRAPHITE
NT HEMATITE
NT OLIVINE
NT PEROVSKITES
NT PYRITES
NT PYROLYTIC GRAPHITE
NT QUARTZ
NT SERPENTINE
NT SPINEL
NT VERMICULITE
NT YTTRIUM-ALUMINUM GARNET

Determination of thermodynamic function of minerals at high temperatures
[DE88-001911] 07 p0940 N88-15713

Determination of thermodynamic function of minerals at high temperatures
[DE88-002311] 07 p0940 N88-15714

Characteristics and climatic relevance of the atmospheric aerosol components
08 p1017 N88-16164

X-ray microfluorescence analysis of thin- and thick-sectioned geologic materials
[DE87-009803] 09 p1189 N88-17126

Experimental and theoretical constraints on the origin of mid-ocean ridge geothermal fluids
13 p1804 N88-20784

An investigation of the crystalchemistry and thermochemistry of selected mineral systems
[AD-A189758] 15 p2142 N88-22781

Optical constants of minerals and other materials from the millimeter to the ultraviolet
[AD-A192210] 18 p2482 N88-24724

Selective weathering of shocked minerals and chondritic enrichment of the Martian fines
23 p3301 N88-29660

Mineralization through geologic time Evolution of continental crust 24 p3400 N88-30250

MINES

Criteria for planimetric and altimetric correction of maps restituted from aerial photographs in 1:100,000 scale
17 p2367 N88-24097

MINES (EXCAVATIONS)

Mining volume measurement system
[NASA-CASE-LAR-13519-1] 17 p2342 N88-23963

Remote sensing applied to the monitoring of mineral extraction in the proximity of urban areas: Pros and cons
19 p2684 N88-25954

MINES (ORDNANCE)

Application of the analysis phase of the instructional system development to the MK-105 magnetic minesweeping mission of the MH-53E helicopter
[AD-A186282] 07 p0822 N88-14994

Preliminary airworthiness evaluation of the UH-60A equipped with the XM-139 VOLCANO mine dispensing system
[AD-A190604] 15 p2018 N88-22029

MINIATURE ELECTRONIC EQUIPMENT

Development of the field-induced electron injection and impact ionization (F4I) technique for radiation hardness testing of MOS (Metal-Oxide-Semiconductor) gate insulators
[AD-A192114] 18 p2583 N88-25345

Miniature radiation dosimeter for in vivo radiation measurements 19 p2672 N88-25889

The effects of incoming boundary layer thickness on unsteady shock-induced turbulent separations induced by cylinders
[AD-A196190] 24 p3368 N88-30060

MINIATURIZATION

NT MICROMINIATURIZATION
NT SUBMINIATURIZATION

TABLET: The personal computer of the year 2000
[NASA-CR-182528] 10 p1384 N88-18267

Concentrating photovoltaic collectors: Fabrication design
[PB88-148051] 12 p1640 N88-19821

French evaluation of Japanese biosensors
16 p2184 N88-23020

Miniature traveling wave tube and method of making
[NASA-CASE-LEW-14520-1] 17 p2335 N88-23936

Tactical Rubidium Frequency Standard (TRFS), volume 2
[AD-A191190] 18 p2503 N88-24850

Tactical Rubidium Frequency Standard (TRFS), volume 1
[AD-A192981] 20 p2805 N88-26640

MINICOMPUTERS

A data analysis environment for HP (Hewlett-Packard) 1000 computers
[DE87-010511] 04 p0477 N88-12936

Error propagation in a digital avionic mini processor
[NASA-CR-181565] 05 p0633 N88-13872

SAHAYOG: A testbed for load sharing under failure
[AD-A186615] 08 p1069 N88-16460

Rocketdyne automated dynamics data analysis and management system 11 p1499 N88-18954

The PC/AT compatible computer as a mission control center display processor at Ames-Dryden Flight Research Facility
[NASA-TM-100426] 14 p1955 N88-21654

Introduction to the VMS (DEC) operating system
[ENST-87D006] 16 p2245 N88-23409

MINIMA

The partially observed stochastic minimum principle
[AD-A189787] 15 p2124 N88-22658

A linear-time algorithm for finding a minimum spanning pseudoforest
[AD-A194029] 23 p3250 N88-29346

Faster algorithms for the shortest path problem
[AD-A194031] 23 p3250 N88-29347

MINIMAL SURFACES

Computer graphics tools for the study of minimal surfaces
[DE88-006421] 15 p2108 N88-22557

Complete minimal surfaces in R^3 of low total curvature
[DE88-006425] 15 p2118 N88-22619

Embedded minimal sufaces with an infinite number of ends
[DE88-006429] 15 p2126 N88-22680

MINIMAX TECHNIQUE

Control of an unstable launcher in atmospheric flight using minimax optimal control laws
[SNIAS-872-422-107] 05 p0638 N88-13901

Min-max bias robust regression
[AD-A191345] 16 p2263 N88-23529

A mixed min-max control problem governed by integral equations 18 p2564 N88-25228

Mixed min-max optimization problem with restrictions
18 p2565 N88-25232

A minimax method for a class of Hamiltonian systems with singular potentials
[AD-A193478] 23 p3270 N88-29453

MINIMIZATION

U OPTIMIZATION

MINING

Marine minerals: Exploring our new ocean frontier
[PB87-217725] 02 p0216 N88-11364

Character of five selected LANDSAT lineaments in southwestern Pennsylvania: Report of investigations, 1987
[PB88-133517] 11 p1505 N88-18986

Power requirements for mining and microwave processing of extraterrestrial resources
17 p2420 N88-24399

Energy requirements for HE-3 mining operations on the Moon 17 p2420 N88-24330

Lunar base surface mission operations. Lunar Base Systems Study (LBSS) task 4.1
[NASA-CR-172050] 18 p2594 N88-25415

Application SPOT-1 data to mining activity: Example of the Imiter Silver Mine, Morocco
22 p3102 N88-28424

MINKOWSKI SPACE

To the field theory with a fundamental mass
[DE88-701159] 15 p2146 N88-22807

Finite width corrections to the Nambu action for the Nielsen-Olesen string
[DE88-006996] 15 p2147 N88-22812

Using Clifford algebras for the geometry of a tube domain (and its corresponding bounded domain) in the complexified Minkowski space of arbitrary dimension
[REPT-87-64] 16 p2264 N88-23540

On the GKP and BS constructions of C-boundary
[DE88-702643] 22 p3159 N88-28799

MINORITIES

A national model at Howard University demonstrating private sector interrelationships that facilitate research in predominantly Black colleges and universities
[DE88-000160] 04 p0502 N88-13089

A study of the minority college programs at the NASA Johnson Space Center 06 p0798 N88-14887

MINORITY CARRIERS

Picosecond carrier transport in GaAs quantum wells
19 p2660 N88-25813

MIR SPACE STATION

USSR report: Space
[JPRS-USP-87-003] 01 p0009 N88-10050

Blagov commentary on Mir station, first manning
01 p0009 N88-10051

X-ray astronomy instruments to operate on Mir station
01 p0009 N88-10052

Gyrostabilizer system of Kvant module
08 p1006 N88-16099

Medilab: A project of a medical laboratory in space
12 p1660 N88-19946

The Soviet MIR space station
[AD-A194040] 23 p3184 N88-28951

MIRA VARIABLES

Basic properties and variability
02 p0252 N88-11593

Spectroscopy and nonthermal processes
02 p0252 N88-11594

Mass loss 02 p0253 N88-11597

Quasi-thermal models 02 p0253 N88-11600

Application of dynamic atmosphere models to the analysis of angular diameter observations of Mira variables 04 p0515 N88-13168

MIRAGE AIRCRAFT

Airplane load drop and missile firing: Experimental methods for predicting trajectories
[PB87-170494] 09 p1117 N88-16695

Testing complex avionics software: A practical experience 17 p2306 N88-23794

Development of complex avionics systems: Experience from French military programs 17 p2307 N88-23804

Supplements to the study of the wake of a Mirage G8 model at F2 --- wind tunnel
[CERT-RT-OA-20/5025-AYD] 18 p2458 N88-24596

MIRROR FUSION

Mirror theory applied to toroidal systems
[DE88-003832] 07 p0933 N88-15669

SOAR: Space orbiting advanced fusion power reactor
17 p2416 N88-24366

MIRRORS

NT ETALONS
NT MAGNETIC MIRRORS
NT TANDEM MIRRORS

ESA technological research activities on lightweight mirrors --- spaceborne interferometry
01 p0096 N88-10629

Multilayer monochromators for neutron spectrometers
[DE87-014291] 02 p0175 N88-11080

Investigation of the fabrication parameters of laser mirrors with hard oxide interference coatings
[ESA-TT-1064] 03 p0329 N88-12077

Solar converging method 04 p0403 N88-12504

Long-range pulselength scaling of 351nm laser damage thresholds
[DE87-014754] 04 p0448 N88-12777

USSR report: Physics and mathematics
[JPRS-UPM-87-006] 06 p0708 N88-14344

Lasers with wavefront-reversing mirrors (review article)
06 p0709 N88-14349

Performance of highly concentrating mirror collectors and collector systems
[DFVLR-FB-87-29] 09 p1186 N88-17107

Mirrors for high-power continuous-wave Ar-lasers
09 p1235 N88-17404

Polymer reflectors research during FY86
[DE88-001101] 11 p1508 N88-19005

Soft X-ray beamsplitters and highly dispersive multilayer mirrors for use as soft X-ray laser cavity components
[DE88-004003] 11 p1549 N88-19270

Multilayer-coated mirrors as power filters in synchrotron radiation beamlines
[DE88-003872] 11 p1550 N88-19276

Optics for large telescope 13 p1840 N88-21014

Chemical vapor deposited silica coatings for solar mirror protection
[NASA-TM-100834] 14 p1893 N88-21306

Constellation sizing for modest directed energy platforms
[DE88-007033] 15 p2070 N88-22343

Optimization of metal-dielectric laser mirrors of TiO2/SiO2 and silver
[ESA-TT-1068] 16 p2212 N88-23199

Development of mirrors for high-precision laser gyroscopes 18 p2517 N88-24931

A twin-mirrored galvanometer laser light sheet generator
[NASA-TM-100587] 19 p2674 N88-25901

X-ray and optical analysis of surface properties of metal optics
[DE88-004033] 19 p2727 N88-26195

Specular steel surfaces for solar mirror substrates
[DE88-001153] 21 p2968 N88-27630

Performance evaluation of large-area glass-mirror heliostats
[DE88-011883] 21 p2969 N88-27636

Planarization of metal substrates for solar mirrors
[DE88-011492] 23 p3229 N88-29214

The effect of the near earth micrometeoroid environment on a highly reflective mirror surface
[NASA-TM-101307] 24 p3332 N88-29833

MIS (SEMICONDUCTORS)

Analysis of the voltage-current characteristics of metal-isolator-tin-telluride sandwich structures
[ETN-88-91089] 09 p1256 N88-17528

Steady state and transient behavior of the Pd-SnO(sub x) MIS oxygen sensors 19 p2672 N88-25890

MISCIBILITY

U SOLUBILITY

MISFETS

U FIELD EFFECT TRANSISTORS

MISMATCH (ELECTRICAL)
Information and coding capacities of mismatched Gaussian channels
[AD-A190321] 15 p2124 N88-22665
Coding capacity of generalized additive channels
[AD-A190315] 15 p2127 N88-22685
Atomistic simulation of stability, metastability and growth of strained layer structures 20 p2873 N88-27053
MISSILE BODIES
Empirical formulas for the base pressure of missile bodies with a central propulsive jet
[ESA-TT-1046] 03 p0270 N88-11694
Base pressure measurements on a missile body with cruciform tail
[ESA-TT-1062] 03 p0270 N88-11695
Flow visualization on an ogive-nosed circular cylinder body at high incidence using the laser light sheet method
[ESA-TT-1066] 03 p0315 N88-11993
Wind tunnel tests of elliptical missile body configurations at Mach numbers 0.4 to 5.0
[AD-A193525] 22 p3038 N88-28040
MISSILE CASES
U MISSILE BODIES
MISSILE COMPONENTS
NT MISSILE BODIES
Nonaxisymmetric body supersonic aerodynamic prediction
[AD-A189338] 13 p1716 N88-20259
MISSILE CONFIGURATIONS
Utilization of dynamic characteristics of materials to optimize military explosive charges. Application to antiship devices
[SNIAS-872-320-101] 05 p0610 N88-13743
Generation of surface grids through elliptic partial differential equations for aircraft and missile configurations
[AD-A186631] 11 p1535 N88-19169
Zero-lift drag predictions in supersonic flow for complex configurations 15 p2054 N88-22246
Submunitions simulations, volume 2
[TR-CR-RD-SS-87-7-VOL-2] 19 p2641 N88-25669
Wind tunnel investigation of wing and control panel loads at transonic and supersonic speeds on some schematic cruciform missile configurations
[FFA-TN-1986-43-SUPPL-1] 22 p3039 N88-28044
Prediction of dynamic derivatives
24 p3318 N88-29761
Semiempirical methods for airbreathing missiles
24 p3318 N88-29763
Aerodynamic heating of missiles
24 p3319 N88-29764
Next generation missile design
24 p3319 N88-29766
Generation of surface grids through elliptic partial differential equations for aircraft and missile configurations
[AD-A195639] 24 p3424 N88-30378
MISSILE CONTROL
A study into the effects and viability of applying lateral force control to an air to ground rocket
[ETN-87-90925] 02 p0131 N88-10821
Empirical formulas for the base pressure of missile bodies with a central propulsive jet
[ESA-TT-1046] 03 p0270 N88-11694
Optimal guidance of homing missiles
06 p0671 N88-14111
An inexpensive real-time interactive three dimensional flight simulation system
[AD-A184868] 07 p0821 N88-14989
POLYPHEM, a universal defensive missile with optical waveguides guidance
[MBB-UA-1045/87] 10 p1315 N88-17862
Covariance analysis and post-processing of gravity compensation effects for aided multi-state navigation systems
[PAPER-87-13] 12 p1577 N88-19430
Advances in Air-Launched Weapon Guidance and Control
[AGARD-CP-431] 12 p1596 N88-19553
A prototype fibre optic gyroscope for missile guidance applications 12 p1596 N88-19554
Effects of closing speed uncertainty on optimal guidance 12 p1597 N88-19556
Guidance and control of air-launched armaments: An aeroengineer's perspective 12 p1597 N88-19557
A fiber optic gyro strapdown reference system for guided weapons 12 p1597 N88-19560
The use of hardware-in-the-loop-techniques in the development of a modern air-to-surface missile system
12 p1597 N88-19562
Advanced guidance algorithms for homing missiles with bearings-only measurements
[AD-A190435] 15 p2017 N88-22026
Memory efficient evaluations of nonlinear stochastic equations and C3 applications
[AD-A189872] 15 p2110 N88-22569
IREPS (Integrated Refractive Effects Prediction System) 3.0, user's manual
[AD-A190398] 16 p2188 N88-23045
Optical data processing
[AD-A193024] 20 p2839 N88-26841
Feasibility study of a microprocessor controlled actuator test mechanism
[AD-A194654] 23 p3249 N88-29337
Special Course on Missile Aerodynamics
[AGARD-R-754] 24 p3317 N88-29755
The present status and the future of missile aerodynamics
[NASA-TM-100063] 24 p3320 N88-29773
MISSILE DEFENSE
Where directed energy stands in strategic defense
[DE88-005092] 10 p1403 N88-18365
SEAT: A strategic engagement analysis tool
[DE88-000498] 13 p1830 N88-20944
Free electron lasers in strategic defense
[DE88-007024] 17 p2394 N88-24231
A simulation of post boost vehicle deployment of multiple reentry vehicles
[DE88-009537] 20 p2764 N88-26391
SDI: Myth or reality
[DE88-009121] 20 p2847 N88-26901
An overview of the development of a linear broadband analog fiber optic link
[DE88-008668] 20 p2854 N88-26945
MISSILE DESIGN
Determination of the drag of missiles with variable lateral acceleration possibility
[REPT-FM15] 10 p1310 N88-17831
Calculation and design of a ramjet missile
[REPT-TR-500] 10 p1311 N88-17832
Guidance and control of air-launched armaments: An aeroengineer's perspective 12 p1597 N88-19557
Special Course on Missile Aerodynamics
[AGARD-R-754] 24 p3317 N88-29755
Accuracy criteria for evaluating supersonic aerodynamic coefficient predictions 24 p3317 N88-29756
Survey on nonlinear effects 24 p3317 N88-29757
Semi-empirical methods for conventional and unconventional missiles 24 p3318 N88-29758
Space marching Euler solvers
24 p3318 N88-29759
Numerical methods: Euler time dependent solver
24 p3318 N88-29760
Semiempirical methods for airbreathing missiles
24 p3318 N88-29763
Aerodynamic heating of missiles
24 p3319 N88-29764
Next generation missile design
24 p3319 N88-29766
MISSILE DETECTION
NT RADAR DETECTION
A cockpit natural language study - selected transcripts
[AD-A192972] 20 p2834 N88-26808
MISSILE ENGINE CASES
U ROCKET ENGINE CASES
MISSILE GUIDANCE
U MISSILE CONTROL
MISSILE LAUNCHERS
Store separation and missile firing from aircraft: Experimental methods for trajectory projection
[NASA-TT-20214] 11 p1439 N88-18589
Expert system contribution to logistics improvement
[SNIAS-881-320-102] 21 p3004 N88-27815
Preliminary airworthiness evaluation of the UH-60A/ESSS (External Stores Support System) with HELLFIRE launcher installed
[AD-A196187] 24 p3323 N88-29793
MISSILE STABILIZATION
U MISSILE CONTROL
U STABILIZATION
MISSILE SYSTEMS
Aircraft avionics and missile system installation cost study. Volume 1: Technical report and appendices A through E
[AD-A194605] 23 p3178 N88-28923
Aircraft avionics and missile system installation cost study. Volume 2: Appendices F and G
[AD-A195372] 24 p3325 N88-29801
MISSILE TRACKING
Use of the global positioning system for trajectory determination of SRAM 2 missiles at the Eastern Test Range
[AD-A185266] 05 p0544 N88-13314
Strategic Defense Initiative Program: Status of space surveillance and tracking system
[PB88-150438] 14 p1967 N88-21739
MISSILE TRAJECTORIES
Use of the global positioning system for trajectory determination of SRAM 2 missiles at the Eastern Test Range
[AD-A185266] 05 p0544 N88-13314
Airplane load drop and missile firing: Experimental methods for predicting trajectories
[PB87-170494] 09 p1117 N88-16695
Store separation and missile firing from aircraft: Experimental methods for trajectory projection
[NASA-TT-20214] 11 p1439 N88-18589
Effect of rotation on the lateral stability of a free-flying column subjected to an axial thrust with directional control
[AD-A188690] 13 p1728 N88-20338
Advanced guidance algorithms for homing missiles with bearings-only measurements
[AD-A190435] 15 p2017 N88-22026
MISSILES
NT AIR TO AIR MISSILES
NT AIR TO SURFACE MISSILES
NT ANTIAIRCRAFT MISSILES
NT ANTIMISSILE MISSILES
NT ANTISHIP MISSILES
NT ANTITANK MISSILES
NT BALLISTIC MISSILES
NT CRUISE MISSILES
NT MX MISSILE
NT RAMJET MISSILES
NT SURFACE TO AIR MISSILES
NT SURFACE TO SURFACE MISSILES
NT TOMAHAWK MISSILES
High resolution ultraviolet filter development
[AD-A184183] 05 p0649 N88-13979
Peacekeeper tank slosh model
08 p0983 N88-15942
Leeside crossflow modeling in Euler space-marching computations
[NASA-TM-89710] 10 p1325 N88-17924
A prototype fibre optic gyroscope for missile guidance applications 12 p1596 N88-19554
A fiber optic gyro strapdown reference system for guided weapons 12 p1597 N88-19560
Speed control of a missile with throttleable ducted rocket propulsion 12 p1597 N88-19561
Advanced guidance algorithms for homing missiles with bearings-only measurements
[AD-A190435] 15 p2017 N88-22026
Efficient, high resolution computations of projectile and missile flow fields
[AD-A191086] 16 p2158 N88-22873
Description of a water tank facility: Study of a missile at high incidence 16 p2201 N88-23133
Wind tunnel investigation of wing and control panel loads at transonic and supersonic speeds on some schematic cruciform missile configurations
[FFA-TN-1986-43] 18 p2457 N88-24585
Launch operations to support future space forces
[AD-A192679] 20 p2881 N88-27107
Missiles, fuselage and similar bodies
23 p3167 N88-28858
Missiles, fuselages and similar bodies
23 p3169 N88-28869
Air intake aerodynamics 24 p3318 N88-29762
Prediction of base-flows 24 p3319 N88-29765
MISSING MASS (ASTROPHYSICS)
Comments on H. Arp: The persistent problem of spiral galaxies
[TRITA-EPP-87-05] 05 p0660 N88-14052
Finnish-Soviet Symposium on Radio Astronomy (1st) held at Otaniemi on August 26-27, 1985
[PB87-140661] 07 p0944 N88-15736
MISSION PLANNING
Space Station Mission Planning System (MPS) development study. Volume 2
[NASA-CR-179200] 01 p0009 N88-10048
Space Station Mission Planning Study (MPS) development study. Volume 3: Software development plan
[NASA-CR-179203] 01 p0009 N88-10049
Planning and execution of the NAVEX experiment in the Spacelab Mission D1
[DFVLR-FB-87-03] 01 p0010 N88-10056
Columbus preparatory program. Payload element study on a technology demonstration mission, executive summary
[CS-RP-AI-016] 01 p0014 N88-10080
Military needs and forecast, 2
01 p0015 N88-10087
Automation strategy and results for an airbase command and control information system
[NLR-MP-86031-U] 01 p0035 N88-10223
Space technology to meet future needs
[NASA-CR-181473] 02 p0130 N88-10819
Space Construction
[NASA-CP-2490] 02 p0138 N88-10870

The flight demonstration program and selection process 02 p0138 N88-10871
Mission Peculiar Equipment Support Structure: A platform for space construction
02 p0139 N88-10874
Marshall Space Flight Center's role in EASE/ACCESS mission management 02 p0139 N88-10875
Helicopter (performance) management
03 p0264 N88-11666
High power ion thruster performance
[NASA-TM-100127] 04 p0409 N88-12542
Mission requirements and aircraft sizing
05 p0545 N88-13317
Space station systems: A bibliography with indexes
[NASA-SP-7056(05)] 05 p0556 N88-13382
Impact of flying qualities on mission effectiveness for helicopter air combat, volume 1
[NASA-CR-166566] 06 p0669 N88-14100
Simulation and analysis of a geopotential research mission
[NASA-CR-182354] 06 p0670 N88-14109
Rendezvous and Docking Verification (RVDV) and in-orbit demonstration, executive summary
[RVD-RVDV-FR-AS-01] 06 p0673 N88-14120
Tethers in space handbook
[NASA-CR-181371] 06 p0673 N88-14123
Controlled Ecological Life Support Systems (CELSS) conceptual design option study
[NASA-CR-177421] 06 p0754 N88-14625
Max '91: Flare research at the next solar maximum
[NASA-TM-89700] 06 p0806 N88-14919
A space transportation system operations model
[NASA-TM-100481] 07 p0823 N88-14999
Advancing automation and robotics technology for the space station and for the US economy: Submitted to the United States Congress May 15, 1987
[NASA-TM-89811] 08 p0959 N88-15817
Studies for future scientific projects
09 p1123 N88-16720
Numerical arc segmentation algorithm for a radio conference-NASARC, version 2.0: User's manual
[NASA-TM-100161] 09 p1156 N88-16928
Expert system verification concerns in an operations environment 09 p1207 N88-17234
Expert mission planning and replanning scheduling system for NASA KSC payload operations
09 p1209 N88-17247
Management of complex information in support of evolving autonomous expert systems
[AD-A186680] 09 p1224 N88-17337
POCC capabilities document. Payload support capabilities description: MCC, JSC POCC, remote POCC interface
[NASA-TM-89708] 09 p1260 N88-17555
The 1987 Get Away Special Experimenter's Symposium
[NASA-CP-2500] 10 p1286 N88-17691
Planet X probe: A fresh new look at an old familiar place 10 p1287 N88-17699
America plans for space
[AD-A187465] 10 p1289 N88-17713
Rendezvous and docking verification and demonstration in orbit, executive summary
[MBB-303-16/86] 10 p1291 N88-17719
Development of a graphics based two-attribute utility assessment program with application to mission planning
[AD-A187276] 10 p1388 N88-18292
Interplanetary mission design handbook. Volume 1, Part 5: Mars-to-Earth ballistic mission opportunities, 1992-2007
[NASA-CR-182525] 10 p1430 N88-18538
A two stage launch vehicle for use as an advanced space transportation system for logistics support of the space station
[NASA-CR-182572] 11 p1443 N88-18606
Search problems in mission planning and navigation of autonomous aircraft
[NASA-CR-182666] 12 p1579 N88-19448
Rendezvous and docking (RVD) verification and demonstration in-orbit 12 p1592 N88-19531
Conceptual design and programmatics studies of space station accommodations for Life Sciences Research Facilities (LSRF)
[NASA-CR-179270] 12 p1598 N88-19567
The integration of artificial intelligence techniques to improve the effectiveness of electronic countermeasure strategies in a tactical environment
[AD-A189483] 12 p1682 N88-20056
Mars Lander/Rover vehicle development: An advanced space design project for USRA and NASA/OAST
[NASA-CR-182562] 12 p1709 N88-20226
Mars Lander/Rover vehicle development: An advanced space design project for USRA and NASA/OAST
[NASA-CR-182571] 12 p1709 N88-20227
Orbital transfer vehicle concept definition and system analysis study. Volume 2: OTV concept definition and evaluation. Book 1: Mission and system requirements
[NASA-CR-179321] 13 p1729 N88-20339
Turnaround operations analysis for OTV. Volume 1: Executive summary
[NASA-CR-179316] 13 p1729 N88-20340
Turnaround operations analysis for OTV. Volume 2: Detailed technical report
[NASA-CR-179317] 13 p1729 N88-20341
Turnaround operations analysis for OTV. Volume 3: Technology development plan
[NASA-CR-179318] 13 p1729 N88-20342
Development of an interactive real-time graphics system for the display of vehicle space positioning
[NASA-TM-100429] 13 p1730 N88-20344
Expert systems for decision support in military aircraft mission preparation
[NLR-MP-87013-U] 13 p1830 N88-20946
Johnson Space Center's strategic game plan: Charting a course to the year 2000 and beyond
[NASA-TM-89733] 13 p1850 N88-21076
The German Spacelab mission D1: Payload integration
[ETN-88-91507] 14 p1871 N88-21179
Satellite acquisition: Global positioning system acquisition changes after Challenger's accident
[PB88-155536] 14 p1880 N88-21236
The PC/AT compatible computer as a mission control center display processor at Ames-Dryden Flight Research Facility
[NASA-TM-100426] 14 p1955 N88-21654
The comet rendezvous asteroid flyby mission
14 p2005 N88-21956
The Giotto extended mission
14 p2005 N88-21957
Rosetta: A mission to sample the nucleus of a comet
14 p2005 N88-21958
Retrieving samples from comet nuclei
14 p2006 N88-21959
Alternative cometary targets for the Giotto extended mission 14 p2010 N88-21990
Orbital transfer vehicle: Concept definition and system analysis study
[NASA-CR-179315] 15 p2024 N88-22060
Space utilization plans 15 p2051 N88-22219
External tank gamma ray imaging telescope study. Final review, phase 2
[NASA-CR-179320] 15 p2150 N88-22834
The NAVEX experiment in the Spacelab D1 mission: Planning and execution
[ESA-TT-1078] 16 p2166 N88-22913
Manned Mars mission accommodation: Sprint mission
[NASA-TM-100598] 16 p2290 N88-23711
Civil missions applications study
17 p2417 N88-24376
Human performance issues arising from manned space station missions
[NASA-CR-3942] 18 p2553 N88-25156
Modeling and evaluation of variable structure organizations
[AD-A191947] 18 p2588 N88-25381
Mars rover/sample return mission requirements affecting space station
[NASA-CR-172048] 18 p2594 N88-25414
Lunar base surface mission operations. Lunar Base Systems Study (LBSS) task 4.1
[NASA-CR-172050] 18 p2594 N88-25415
Flight Mechanics Panel Symposium on Rotorcraft Design for Operations: Technical evaluation report
[AGARD-AR-243] 20 p2758 N88-26362
The Telecommunications and Data Acquisition Report
[NASA-CR-183131] 22 p3063 N88-28178
Mark IV-85 mission support planning and future mission set 22 p3067 N88-28202
Inflight rearming
[AD-A193564] 23 p3176 N88-28909
Analyst-centered models for systems design, analysis, and development 23 p3253 N88-29364
A plan for time-phased incorporation of automation and robotics on the US space station
23 p3255 N88-29377
A scheduling and resource management system for space applications 23 p3256 N88-29383
Two implementations of the Expert System for the Flight Analysis System (ESFAS) project
23 p3259 N88-29400
Experiment scheduling for Spacelab missions
23 p3259 N88-29404
Blackboard architectures and their relationship to autonomous space systems 23 p3261 N88-29414
Development and demonstration of an on-board mission planner for helicopters
[NASA-CR-177482] 24 p3328 N88-29817
Definition of common support equipment and space station interface requirements for IOC model technology experiments
[NASA-TM-100656] 24 p3336 N88-29856
The 1988 Goddard Conference on Space Applications of Artificial Intelligence
[NASA-CP-3009] 24 p3415 N88-30330
Contingency rescheduling of spacecraft operations
24 p3416 N88-30337
Knowledge based tools for Hubble Space Telescope planning and scheduling: Constraints and strategies
24 p3417 N88-30338
Candidate functions for advanced technology implementation in the Columbus mission planning environment 24 p3417 N88-30340
A rule-based systems approach to spacecraft communications configuration optimization
24 p3417 N88-30341
Integrated resource scheduling in a distributed scheduling environment 24 p3417 N88-30342

MISSISSIPPI
Hypocenters (1977-1984) around the Richton Dome and the Melvin, Alabama, 1978 earthquake
[DE87-014336] 03 p0351 N88-12214

MIST
Investigation of the nature and concentration of vapor and mist during the cleaning of aircraft
[PML-1985-29] 05 p0623 N88-13817

MITOSIS
Zero gravity and living organism
08 p1046 N88-16320

MIXED CRYSTALS
Calibration constants for the 1986 BGO crystals matrix
[NOTA-INTERNA-886] 07 p0856 N88-15197
Formation of nuclei during precipitation in metallic mixed crystals
[NASA-TT-20248] 13 p1745 N88-20437
Statistical fine structure in the inhomogeneously broadened electronic origin of pentacene in p-terphenyl
[AD-A191211] 16 p2176 N88-22968

MIXED FLOW
U MULTIPHASE FLOW

MIXERS
A GaAs MESFET balanced mixer with very low intermodulation
[AD-A184848] 05 p0655 N88-14015
Dual-fuel, dual-mode rocket engine
[NASA-CASE-LAR-13773-1] 18 p2475 N88-24685
SIS (Superconductor-Insulator-Superconductor) mixer research
[AD-A192908] 20 p2879 N88-27092

MIXING
NT COLLOIDING
NT DISSOLVING
NT HOMOGENIZING
NT PREMIXING
NT SIGNAL MIXING
NT SUSPENDING (MIXING)
NT TURBULENT MIXING
Numerical simulation of a supersonic chemically reacting mixing layer 02 p0143 N88-10900
Combustion in turbulent jets and buoyant flames
[PB87-232674] 03 p0283 N88-11779
Generation of IR stimulated radiation, UV visible violet coherent radiation by two-photon resonance pumping in K vapor 03 p0301 N88-11692
A study of chaos and mixing in Rayleigh-Taylor and Richtmyer-Meshkov unstable interfaces
[AD-A184751] 03 p0320 N88-12026
Heats of mixing for thermal energy storage systems. Phase 1: Selection of suitable liquid-liquid mixtures
[DE87-014971] 03 p0347 N88-12196
Activities at government research laboratories reported 04 p0403 N88-12503
Atomic and electronic structure of surfaces and chemisorbed layers
[DE87-014987] 04 p0498 N88-13085
The effect of ion beam mixed Ni-Al surface layers on PSB extrusion morphology in fatigued nickel
05 p0596 N88-13652
Mixing and combustion of pulsed gas jets
[PB88-112834] 06 p0680 N88-14169
Mixing and combustion of pulsed gas jets
[PB88-108014] 06 p0680 N88-14170
Ion mixing and surface modification in metal-semiconductor systems
[DE88-001702] 06 p0786 N88-14823
Structural study of the impregnating resins of the type TGMDA/DDS --- expoxy resins
[ETN-88-91616] 08 p0965 N88-15842
O2-I laser (Oxygen-iodine) mixing studies using LIF (Laser Induced Fluorescence)
[AD-A186667] 09 p1171 N88-17018
A computational study of thrust augmenting ejectors based on a viscous-inviscid approach
10 p1326 N88-17929

Radial mixing in turbomachines
[AD-A188028] 11 p1482 N88-18847

Investigations into shock-induced enhancement of mixing and combustion in supersonic burners
[AD-A189609] 12 p1607 N88-19608

Mass transport and chemical demixing of Y-Ba-Cu-O compounds during sintering in temperature gradients
[DE88-004887] 12 p1696 N88-20151

Mixing of viscous fluids: Behavior of microstructures and chaos
[DE88-006287] 13 p1766 N88-20566

Structures and fluxes in a deep convecting mixed layer 13 p1804 N88-20786

Equatorial turbulence: Mixed layer and thermocline
13 p1804 N88-20787

The mixed layer of the western equatorial Pacific Ocean
[HIG-1861] 13 p1805 N88-20789

Squeezing via travelling-wave forward four-wave mixing in atomic vapors: Comparison with nondegenerate theory 14 p1978 N88-21804

Experimental investigation of a spanwise forced mixing layer
[AD-A190136] 15 p2013 N88-22007

Effect of moisture level in PBXW-109(E) (plastic-bonded explosive) mixes on the aging of the cured explosive
[AD-A190200] 15 p2048 N88-22202

Mixing: Stretching, breakup and chaos
[DE88-006699] 15 p2067 N88-22327

Optical switching and control techniques using nonlinear optical wave mixing
[AD-A190467] 15 p2134 N88-22730

Ion-beam mixing and amorphization in Au/Zr bilayers
[DE88-005909] 15 p2140 N88-22767

Analysis of molecular mixing and chemical reaction in mixing layer
[AD-A191600] 18 p2482 N88-24721

Signal processing with degenerate four-wave mixing
[AD-A191496] 18 p2499 N88-24825

Spatial stability of a compressible mixing layer
[NASA-CR-181671] 18 p2514 N88-24916

Direct numerical simulations of the PDF's (Probability Density Functions) of a passive scalar in a forced mixing layer
[AD-A192134] 18 p2568 N88-25256

Turbulence structure of mixing swirling flows
[AD-A193063] 21 p2943 N88-27478

Burn-in with mixed populations
[AD-A194651] 22 p3085 N88-28321

Soot and radiation in a gas turbine combustor
[AD-A191991] 23 p3179 N88-28924

Strong law for mixing sequence
[AD-A193615] 23 p3274 N88-29490

MIXING CIRCUITS

Comparative investigation of heterodyne mixers at 1000 GHz
[FTL-068627] 09 p1158 N88-16940

Supercomputer-aided generalized mixer analysis and optimization
[FUB-15-1986] 14 p1957 N88-21668

Heterodyne spectrometer for the very high frequency range between 300 and 3000 GHz (1 mm to 0.1 mm) using a mixer in open structure
16 p2271 N88-23589

MIXING LENGTH FLOW THEORY

Velocity and density measurements in a turbulent nonpremixed flame with comparison to numerical model predictions
[DE87-014695] 08 p0967 N88-15654

Turbulent reacting flows and supersonic combustion
[AD-A189690] 15 p2034 N88-22115

An investigation of flow structure, mixing and chemical reaction in combusting turbulent flows
[AD-A189980] 15 p2034 N88-22117

Numerical predictions for the flow induced by an enclosed rotating disc
[PNR90463] 22 p3078 N88-28281

MIXTURES
NT ADMIXTURES
NT AEROSOLS
NT AIR
NT ALVEOLAR AIR
NT AQUEOUS SOLUTIONS
NT BINARY MIXTURES
NT COLLOIDS
NT DETONABLE GAS MIXTURES
NT DISPERSIONS
NT EMULSIONS
NT EUTECTIC ALLOYS
NT EUTECTICS
NT FOG
NT GAS MIXTURES
NT HIGH TEMPERATURE AIR
NT LIQUID-GAS MIXTURES
NT SIALON
NT SLURRIES
NT SMOKE
NT SOLID SOLUTIONS
NT SOLID SUSPENSIONS
NT SOLUTIONS

Application of new conformal solution theories
[PB87-211934] 02 p0247 N88-11558

Annotated computer output for illustrative examples of clustering using the mixture method and two comparable methods from SAS
[AD-A184687] 03 p0364 N88-12292

Thermodynamic properties of supercritical mixtures
[DE88-000809] 04 p0413 N88-12562

A laboratory study of asphalt concrete mix designs for high-contact pressure aircraft traffic
[AD-A185753] 06 p0670 N88-14106

Experimental and theoretical study of condensation in multicomponent mixtures
[DE88-002715] 07 p0830 N88-15033

Experimental and theoretical studies of dense fluid mixtures
[DE88-002710] 07 p0831 N88-15039

Theoretical studies of multicomponent mixtures: Phase equilibrium and transport
[DE88-002717] 07 p0831 N88-15040

The generalized van der Waals theory of pure fluids and mixtures
[DE88-002380] 07 p0855 N88-15192

Realization of an instrument to measure temperature and concentration gradients in fluids --- microgravity
[CISE-3128] 09 p1168 N88-17003

Predicting transforms of stable noise and other Gaussian mixtures
[AD-A189260] 12 p1684 N88-20071

Prediction of high-temperature thermodynamic properties of mixed electrolyte solutions including solubility equilibria, vapor pressure depression and boiling point elevation
[DE88-006344] 13 p1849 N88-21069

Noise generation by air bubbles in water: An experimental study of creation and splitting
[AD-A192063] 19 p2664 N88-25839

Interactions in miscible polymer blends
[AD-A193824] 22 p3058 N88-28144

Blends of crystallizable polybutadienes
[AD-A194536] 23 p3197 N88-29026

MNEMONICS

Long term synaptic plasticity and learning in neuronal networks
[AD-A186834] 09 p1199 N88-17188

MOBILE COMMUNICATION SYSTEMS
NT LAND MOBILE SATELLITE SERVICE

Measured characteristics of 800/900 MHz mobile radio channels with high-angle propagation through moderately dense foliage
[CRC-1398] 05 p0573 N88-13493

Two-signal cross modulation effects, half-IF effects and interference criteria in land mobile sharing with UHF (Ultra High Frequency) television
[PB87-228037] 05 p0576 N88-13514

A multi user random access communication system for users with different priorities
[AD-A186041] 07 p0841 N88-15102

Spread spectrum mobile radio communications
[AD-A187487] 11 p1470 N88-18765

Spatial distribution of traffic in a cellular mobile data network
[EUT-87-E-168] 14 p1904 N88-21378

Development of a mobile research flight test support capability
[NASA-TM-100428] 16 p2159 N88-22883

MSAT-X: A technical introduction and status report
[NASA-CR-182921] 17 p2334 N88-23933

Proceedings of the Mobile Satellite Conference
[NASA-CR-182964] 19 p2643 N88-25680

The AMSC mobile satellite system
19 p2643 N88-25681

NASA's mobile satellite development program
19 p2643 N88-25682

Mobile satellite service for Canada
19 p2643 N88-25683

AUSSAT mobile satellite services
19 p2643 N88-25684

A satellite system for land-mobile communications in Europe 19 p2643 N88-25685

System capacity and economic modeling computer tool for satellite mobile communications systems
19 p2644 N88-25686

World-wide aeronautical satellite communications
19 p2644 N88-25688

An overview of the OmniTRACS: The first operational mobile Ku-band satellite communications
19 p2644 N88-25689

International and domestic mobile satellite regulatory proceedings: A comparison of outcomes and discussion of implications 19 p2644 N88-25690

Mobile satellite services: International co-ordination, co-operation and competition 19 p2644 N88-25691

International and domestic regulator issues facing the Canadian MSAT system 19 p2644 N88-25692

Propagation effects by roadside trees measured at UHF and L-band for mobile satellite systems
19 p2644 N88-25693

Propagation modeling for land mobile satellite systems
19 p2645 N88-25694

Attenuated direct and scattered wave propagation on simulated land mobile satellite service paths in the presence of trees 19 p2645 N88-25695

Mobile satellite propagation measurements and modeling: A review of results for systems engineers
19 p2645 N88-25696

Propagation measurements for an Australian land mobile satellite system 19 p2645 N88-25697

Land mobile satellite propagation results
19 p2645 N88-25698

Propagation effects on spread-spectrum mobile satellite systems 19 p2645 N88-25699

Multipath measurements for land mobile satellite service using global positioning system signals
19 p2645 N88-25700

Development of a mobile satellite communication unit
19 p2646 N88-25701

Development of the network architecture of the Canadian MSAT system 19 p2646 N88-25702

System architecture for the Canadian interim mobile satellite system 19 p2646 N88-25703

Satellite communications experiment for the Ontario air ambulance service 19 p2646 N88-25705

Land mobile satellite demonstration system
19 p2646 N88-25706

Mobilestar field test program
19 p2646 N88-25707

The JPL MSAT mobile laboratory and the pilot field experiments 19 p2646 N88-25708

Technical characteristics of the OmniTRACS: The first operation mobile Ku-band satellite communications system 19 p2647 N88-25709

An adaptive array antenna for mobile satellite communications 19 p2647 N88-25710

MSAT mobile electronically steered phased array antenna development 19 p2647 N88-25711

MSAT-X electronically steered phased array antenna system 19 p2647 N88-25712

MSAT-X phased array antenna adaptions to airborne applications 19 p2647 N88-25713

Adaptive interference techniques for mobile antennas
19 p2647 N88-25714

The JPL mechanically steered antenna
19 p2647 N88-25715

Simple, low-profile, circularly polarized arrays
19 p2647 N88-25716

Omni-directional L-band antenna for mobile communications 19 p2648 N88-25717

Trellis-coded CPM for satellite-based mobile communications 19 p2648 N88-25718

Interleaver design for trellis-coded differential 8-PSK modulation with non-coherent detection
19 p2648 N88-25719

Codes for QPSK modulation with invariance under 90 degrees rotation 19 p2648 N88-25720

Trellis-coded MPSK modulation techniques for MSAT-X(sup)1 19 p2648 N88-25721

Modulation and coding for fast fading mobile satellite communication channels 19 p2648 N88-25722

Comparison of CDMA and FDMA for the MobileStar(sm) system 19 p2649 N88-25724

An 8-DPSK TCM modem for MSAT-X
19 p2649 N88-25725

Modem for the land mobile satellite channel
19 p2649 N88-25727

Pilot-aided modulation for narrow-band satellite communications 19 p2649 N88-25728

A study on the co- and adjacent channel protection requirements for mobile satellite ACSSB modulation
19 p2650 N88-25732

A framework for implementing data services in multi-service mobile satellite systems
19 p2650 N88-25733

L-band and SHF multiple access schemes for the MSAT system 19 p2650 N88-25734

Rearrangement procedures in regenerative multibeammobile communications satellites with frequency reuse 19 p2650 N88-25735

Design mobile satellite system architecture as an integral part of the cellular access digital network
19 p2650 N88-25736

An access alternative for mobile satellite networks
19 p2651 N88-25737

An operational open-end file transfer protocol for mobile satellite communications 19 p2651 N88-25738

Integrated voice/data protocols for satellite channels
19 p2651 N88-25739

Evaluation of CDMA system capacity for mobile satellite system applications 19 p2651 N88-25740
Considerations for spacecraft design for MSAT 19 p2651 N88-25741
Antenna system for MSAT mission 19 p2651 N88-25742
Antenna technology for advanced mobile communication systems 19 p2651 N88-25743
Frequency addressable beams for land mobile communications 19 p2652 N88-25744
Speech coding at 4800 bps for mobile satellite communications 19 p2652 N88-25749
Real-time speech encoding based on Code-Excited Linear Prediction (CELP) 19 p2653 N88-25751
Development of an 8000 bps voice codec for AvSat 19 p2653 N88-25755
Mobile satellite communications in the Forest Service 19 p2654 N88-25757
Mobile satellite service in the United States 19 p2654 N88-25758
Random-access algorithms for environments with capture [AD-A194303] 23 p3203 N88-29060

MOBILITY
NT CARRIER MOBILITY
NT ELECTRON MOBILITY
NT HOLE MOBILITY
NT IONIC MOBILITY
Influence of thermocyclic treatment on mobility of grain boundaries [BLL-M-37329-(5828.4)] 02 p0149 N88-10933
Dealing with unanticipated events in autonomous navigation [DE88-000590] 05 p0590 N88-13602
An investigation of classical dynamic scaling techniques applied to an oleo-pneumatic landing gear strut [AD-A187664] 13 p1721 N88-20292
Examples of ice pack rigidity and mobility characteristics determined from ice motion [AD-A191163] 17 p2377 N88-24129

MODAL RESPONSE
Mode purity measurements on gyrotrons for plasma heating at the stellarator W 7-AS [IPF-87-3] 01 p0101 N88-10660
Modal survey of the space shuttle solid rocket motor using multiple input methods 05 p0593 N88-13617
A new method to real-normalize measured complex modes 05 p0593 N88-13618
Improvement of modal scaling factors using mass additive technique 05 p0593 N88-13620
Viscous damped space structure for reduced jitter 05 p0594 N88-13623
On the glitches in the force transmitted by an electrodynamic exciter to a structure 05 p0594 N88-13624
Modal analyses of the Kernville diagnostic canister [DE88-003268] 07 p0870 N88-15277
Modal analysis using frequency response measurement data 08 p0976 N88-15899
Finite element method with continuous mass elements [PB87-143384] 08 p0995 N88-16019
Centaur G Prime modal test 09 p1181 N88-17075
An adaptive filtering technique for removing periodic noise from modal response data [DE88-002347] 10 p1322 N88-17903
A component synthesis method using Lanczos vectors [DE88-002263] 10 p1403 N88-18368
Overview of multi-input frequency domain modal testing methods with an emphasis on sine testing 11 p1499 N88-18949
Modal forced response of propfans in yawed flow 16 p2221 N88-23253
Dynamic characteristics of a vibrating beam with periodic variation in bending stiffness [NASA-TP-2697] 17 p2348 N88-23988
Reduced order modelling and analytical model modification for structural dynamics and control 18 p2529 N88-25006
Multishaker modal testing [NASA-CR-179355] 18 p2530 N88-25010
Modal synthesis by use of substructures with fixed or free coupling points [ILR-MITT-191] 22 p3089 N88-28341
Asymptotic modal analysis and statistical energy analysis [NASA-CR-183077] 23 p3278 N88-29514

MODE (STATISTICS)
The bimodality of large scale averaged flow parameters --- statistical weather forecasting 08 p1016 N88-16159

MODE COUPLING
U COUPLED MODES

MODE OF VIBRATION
U VIBRATION MODE

MODE SHAPES
U MODAL RESPONSE

MODE TRANSFORMERS
Optimization of mode converters for generating the fundamental TE(06) gyrotron output at 140 GHz [IPF-87-1] 01 p0043 N88-10273
Harmonic and rectangular pulse reproduction through current transformers [EUT-86-E-159] 14 p1907 N88-21395

MODEL REFERENCE ADAPTIVE CONTROL
Adaptive control of scientific balloon-borne gondola attitude 13 p1755 N88-20497

MODELS
NT AIRCRAFT MODELS
NT ANALOG SIMULATION
NT ASTRONOMICAL MODELS
NT ATMOSPHERIC MODELS
NT BIOLOGICAL MODELS (MATHEMATICS)
NT BREADBOARD MODELS
NT DENSITY WAVE MODEL
NT DIGITAL SIMULATION
NT DYNAMIC MODELS
NT ENVIRONMENT MODELS
NT HYDROLOGY MODELS
NT K-EPSILON TURBULENCE MODEL
NT MANDELSTAM REPRESENTATION
NT MATHEMATICAL MODELS
NT NUCLEAR MODELS
NT OCEAN MODELS
NT PETRI NETS
NT QUARK MODELS
NT REFERENCE ATMOSPHERES
NT SCALE MODELS
NT SEMISPAN MODELS
NT SPACECRAFT MODELS
NT STATIC MODELS
NT STELLAR MODELS
NT THOMAS-FERMI MODEL
NT THREE DIMENSIONAL MODELS
NT TURBULENCE MODELS
NT TWO DIMENSIONAL MODELS
NT WIND TUNNEL MODELS
Modeling and measurement of heat transfer on turbine blade tips 01 p0006 N88-10032
HF (High Frequency) broadcasting planning model: A comparison of two versions [PB87-210282] 01 p0036 N88-10230
Two-phase non-Newtonian hydrodynamic modeling of slurries [DE87-011519] 01 p0047 N88-10298
Multidimensional modeling of convective heat transfer with application to IC engines [DE87-011046] 01 p0055 N88-10353
Thermal stress analysis of space shuttle orbiter subjected to reentry aerodynamic heating [NASA-TM-88286] 01 p0061 N88-10389
Self-consistent modification of a fast tail distribution by resonant fields in nonuniform plasmas [AD-A183790] 01 p0099 N88-10650
A simulation of the IPS variations from a magnetohydrodynamical simulation 01 p0118 N88-10755
Reliability modeling of fault-tolerant computer based systems 02 p0127 N88-10801
A stochastic delamination growth model for fatigue loaded laminated composite materials 02 p0141 N88-10888
Models of degradation of stratified composite structures [ONERA-RT-13/3542-RY-061-R] 02 p0142 N88-10892
A numerical method for the treatment of kinked cracks in finite bodies 02 p0190 N88-11189
A design methodology for the utilization of metrics within various phases of software lifecycle models [DE87-010519] 02 p0220 N88-11385
Application of new conformal solution theories [PB87-211934] 02 p0247 N88-11558
A heat transfer model for a heated helium airship [AD-A183786] 03 p0259 N88-11629
The effects of corona on current surges induced on conducting lines by EMP: A comparison of experiment data with results of analytic corona models [DE87-014970] 03 p0305 N88-11924
Visualization of the flow field around a generic destroyer model in a simulated turbulent atmospheric boundary layer [AD-A184658] 03 p0320 N88-12023
Conservation and transport properties of turbulence with large density variations [LA-10911-MS] 03 p0321 N88-12032
Interseismic deformation for normal fault earthquakes 03 p0349 N88-12207
Transform fault earthquakes in the North Atlantic: Source mechanisms and depth of faulting 03 p0350 N88-12208
Microcomputer control of a hydraulically actuated piston [AD-A184130] 03 p0366 N88-12317
Number count-redshift relation in universe models with nonzero cosmological constant [DE87-703043] 03 p0388 N88-12435
Reduced complexity structural modeling for automated airframe synthesis [NASA-CR-177440] 04 p0393 N88-12453
Experimental evidence for modifying the current physical model for ice accretion on aircraft surfaces [NASA-TM-87184] 04 p0397 N88-12473
A multiple-time-scale turbulence model based on variable partitioning of turbulent kinetic energy spectrum [NASA-CR-179222] 04 p0444 N88-12754
On dynamic loads in parallel shaft transmissions. 1: Modelling and analysis [NASA-TM-100180] 04 p0451 N88-12797
On dynamic loads in parallel shaft transmissions. 2: Parameter study [NASA-TM-100181] 04 p0452 N88-12798
User's guide to NCAR (National Center for Atmospheric Research) CCM1 [PB87-224366] 04 p0469 N88-12[illegible]
A tight upper bound for the speed-up of parallel best-first branch-and-bound algorithms [AD-A184246] 04 p0477 N88-12939
Mental models in expert physics reasoning [AD-A184106] 04 p0500 N88-13075
Full-envelope aerodynamic modeling of the Harrier aircraft [NASA-TM-88376] 05 p0552 N88-13363
Model helicopter rotor rig and associated strain gauge balance for performance studies [NAL-TM-AE-8704] 05 p0552 N88-13364
Damping analysis of flexural waves in fluid-loaded single and constrained plates [AD-A185116] 05 p0609 N88-13739
Performability modeling based on real data: A casestudy [NASA-CR-181563] 05 p0633 N88-13870
Example of correlation between space and spin coordinates [DE87-703366] 05 p0657 N88-14030
Approaches and possible improvements in the area of multibody dynamics modeling [NASA-CR-179227] 06 p0663 N88-14067
Balanced realizations: Canonical form, parametrization, model reduction [PB87-123360] 06 p0757 N88-14642
Model of earlier stage of universe's evolution 06 p0775 N88-14756
Unsteady stall penetration experiments at high Reynolds number [AD-A186120] 07 p0814 N88-14958
A space transportation system operations model [NASA-TM-100481] 07 p0823 N88-14999
Treatment of small wire loops in the method of moments code NEC (Numerical Electromagnetics Code) [DE88-002995] 07 p0846 N88-15136
User manual for ATILA, a finite-element code for modeling piezoelectric transducers [AD-A185948] 07 p0847 N88-15141
Reynolds-stress and dissipation rate budgets in a turbulent channel flow [NASA-TM-89451] 07 p0852 N88-15174
Numerical solution of turbulent flow past a backward facing step using a nonlinear K-epsilon model [NASA-CR-178421] 07 p0854 N88-15189
A software planning and development methodology with resource allocation capability [AD-A186088] 07 p0902 N88-15462
Estimation and testing in truncated and nontruncated linear median-regression models [AD-A186317] 07 p0911 N88-15522
Development of an emulation-simulation thermal control model for space station application [NASA-CR-182409] 08 p0962 N88-15823
Nonlinear line-spring model for surface crack analyses with particular reference to work hardening materials [PB87-144838] 08 p0994 N88-16016
Expert systems relations in space applications 08 p1059 N88-16391
Emulating a flexible space structure: Modeling [NASA-TM-100320] 09 p1135 N88-16812
Experimental identification of nonlinear structural models [DE88-001795] 09 p1184 N88-17094
Solid modelling with faceted primitives [ETN-88-91593] 09 p1218 N88-17305
Phenomenological model of superconductivity of heavy fermions in U(sub 1-x)ThsubxBesub13 09 p1238 N88-17423
Theory of the tetragonal-to-orthorhombic structural phase transition in La2CuO4 [AD-A187141] 09 p1254 N88-17514

Research in theoretical physics [DE88-003201] 09 p1259 N88-17548

Overview of heat transfer and fluid flow problem areas encountered in Stirling engine modeling [NASA-TM-100131] 09 p1262 N88-17561

Modeling of some coplanar waveguide discontinuities [NASA-TM-100808] 10 p1318 N88-17880

Improved canopy reflectance modeling and scene inference through improved understanding of scene pattern [NASA-CR-182488] 10 p1347 N88-18049

A paradigm for concurrency control performance evaluation 10 p1377 N88-18220

Machine models and simulations [PB88-118690] 10 p1386 N88-18280

Analysis and synthesis of adaptive neural elements [AD-A187047] 10 p1395 N88-18316

Hierachical object recognition using libraries of parameterized model sub-parts [AD-A187476] 10 p1396 N88-18322

Zero-dimensional model of a reversed field pinch fusion reactor [DE88-005213] 10 p1414 N88-18442

Procedures for quantitative sensitivity and performance validation studies of a deterministic fire safety model [NBS/GCR-88/544] 11 p1469 N88-18762

Turbulence modeling in non-inertial frames of reference [NASA-CR-181646] 11 p1488 N88-18880

Characterization of damped structural connections for multi-component systems [NASA-TM-100801] 11 p1502 N88-18974

A digital terrain system for microcomputers [INPE-4170-PRE/1067] 11 p1505 N88-18987

Target-reflectivity models for various terrain types [DE88-005510] 11 p1505 N88-18992

Concepts and nomenclature in the world modeling system (a lesson in applied metaphysics) [AD-A188246] 11 p1534 N88-19166

MCT crystal growth [NASA-CR-179297] 11 p1557 N88-19318

Notes on a class of homogeneous space-times [DE88-700138] 11 p1562 N88-19353

The early years of string theory: The dual resonance model [DE88-003521] 11 p1563 N88-19359

A modeling analysis program for the JPL table mountain lo sodium cloud data [NASA-CR-182555] 11 p1570 N88-19400

Modeling of limit cycle stall flutter oscillations 12 p1583 N88-19472

Mathematical foundations of signal processing. 2: The role of group theory [AD-A188482] 12 p1620 N88-19685

Validation of GEMACS (General Electromagnetic Model for the Analysis of Complex Systems) for modeling lightning-induced electromagnetic fields [AD-A188822] 12 p1620 N88-19687

Electromagnetic modeling of a control valve [INPE-4140-PRE/1048] 12 p1622 N88-19700

KREME (Knowledge Representation, Editing and Modeling Environment): A user's introduction, phase 1 [AD-A188906] 12 p1681 N88-20052

Motion in a random gyrotropic environment in D dimensions [PB87-170650] 12 p1685 N88-20079

A moment approach to modeling negative ion sources [AD-A188858] 12 p1691 N88-20114

Development savings through parametric modeling of program costs 12 p1700 N88-20175

Nonaxisymmetric body supersonic, aerodynamic prediction [AD-A189338] 13 p1716 N88-20259

Understanding machines from text and diagrams [AD-A189034] 13 p1755 N88-20493

Estimation-correlation, modeling, and identification in adaptive array processors [AD-A189130] 13 p1757 N88-20512

Numerical methods in the resolution of control electrovalve model [INPE-4154-RPE/540] 13 p1764 N88-20554

Improvement of the Reynolds-stress model by a new pressure-strain correlation [NASA-CR-182699] 13 p1783 N88-20667

Atmospheric electrical modeling in support of the NASA F-106 storm hazards project [NASA-CR-181639] 13 p1799 N88-20758

Broadband correlation analysis [AD-A188732] 13 p1814 N88-20839

Relativistic jet models for the BL Lacertae object Mrk 421 during three epochs of observation [NASA-TM-89727] 13 p1853 N88-21090

Modeling surface exchanges: The soil-vegetation-atmosphere continuum 14 p1937 N88-21553

Hydrological models 14 p1937 N88-21559

Tabulation of Mie scattering calculation results for microwave radiative transfer modeling [NASA-CR-4130] 14 p1947 N88-21612

Some models for rain and cloud attenuation of millimeter waves [PB88-160809] 14 p1948 N88-21616

Aero/structural tailoring of engine blades (AERO/STAEBL) [NASA-CR-180805] 14 p1959 N88-21682

Strings in four dimensions [DE88-006435] 14 p1990 N88-21864

Geometric modeling of flight information for graphical cockpit display [AD-A190484] 15 p2021 N88-22043

A model for nitrogen atom recombination on a silicon dioxide surface [AD-A189843] 15 p2142 N88-22784

Georelational data model [INPE-4490-PRE/1254] 15 p2149 N88-22829

Inflow measurements made with a laser velocimeter on a helicopter model in forward flight. Volume 4: Tapered planform blades at an advance ratio of 0.15 [NASA-TM-100544] 16 p2156 N88-22863

On the validation of a code and a turbulence model appropriate to circulation control airfoils [NASA-TM-100090] 16 p2156 N88-22864

Measurements of the time dependent velocity field surrounding a model propeller in uniform water flow 16 p2205 N88-23155

On the prediction of equilibrium states in homogeneous turbulence [NASA-CR-181659] 16 p2207 N88-23174

User's manual for EULER3DS [AD-A191048] 16 p2208 N88-23177

Computerized life and reliability modelling for turboprop transmissions [NASA-TM-100918] 16 p2215 N88-23220

Characterization of structural connections for multicomponent systems 16 p2220 N88-23251

Computer based modeling of thematic mapping 16 p2225 N88-23285

The event-related brain potential as an index of information processing and cognitive activity: A program of basic research [AD-A191244] 16 p2243 N88-23400

On 2-D versus 3-D: Sine of squared angular error and weighted perpendicular fixing [NASA-CR-182899] 16 p2252 N88-23458

Flight testing a V/STOL aircraft to identify a full-envelope aerodynamic model [NASA-TM-100996] 17 p2301 N88-23762

The Systeme d'Analyse Geographique (SAGE) geographic analysis system 17 p2353 N88-24019

A proposal of adaptation of a knowledge-based scene analysis model to some remote sensing problems 17 p2354 N88-24026

Three-dimensional models of conventional and vertical junction laser-photovoltaic energy converters [NASA-TM-4039] 17 p2370 N88-24111

Models and metrics for software management and engineering [NASA-CR-182953] 17 p2389 N88-24200

Induction of models under uncertainty [NASA-TM-101173] 17 p2394 N88-24230

Analytical modeling of the structureborne noise path on a small twin-engine aircraft [NASA-CR-4136] 17 p2394 N88-24233

Hydrogen turbines for space power systems: A simplified axial flow gas turbine model 17 p2419 N88-24385

A transient model for liquid metal heat pipes 17 p2421 N88-24398

Analysis of dust grain properties in two star forming regions through comparison of theoretical models to observations 17 p2451 N88-24559

Dynamic consolidation of metal powders [AD-A192126] 18 p2485 N88-24744

Computational Fluid Mechanics [NASA-CR-183022] 18 p2514 N88-24915

An investigation of a distributed clock for local area networks with ring topology 18 p2516 N88-24924

The Effect of the Ionosphere on Communication, Navigation and Surveillance Systems Based on Ionospheric Effects Symposium held on 5-7 May 1987 in Springfield, Virginia [AD-A191855] 18 p2541 N88-25081

Energy measurements in oxygen-induced reactions at 60 A GeV and 200 A GeV [DE88-006420] 18 p2573 N88-25283

Modeling and evaluation of variable structure organizations [AD-A191947] 18 p2588 N88-25381

F-14 modeling study [NASA-CR-4164] 19 p2603 N88-25462

Next-generation fire extinguishing agent. Phase 1: Suppression concepts [AD-A192279] 19 p2614 N88-25514

Structure and refinement of ordered aromatic heterocyclic polymers by diffraction methods: Application of results to electro-optic phenomena [AD-A191859] 19 p2619 N88-25537

Entrance and exit region friction factor models for annular seal analysis [NASA-CR-183084] 19 p2678 N88-25921

Improved description of base dynamics in the modeling of bipolar transistors [PB88-181516] 19 p2732 N88-26229

Development of a GaAs solid state device model for high power applications [DE88-009048] 19 p2734 N88-26242

Analysis and synthesis of decision-making organizations [AD-A191948] 19 p2738 N88-26258

Voyager imaging photometry and radiative transfer modeling of the spoke-like features in Saturn's outer B-ring 19 p2742 N88-26278

Stochastic modeling of EM scattering from foliage [AD-A192258] 20 p2790 N88-26553

Modeling and optimum time performance for concurrent processing [NASA-CR-4167] 20 p2797 N88-26595

Numerical model for the computation of radiance distributions in natural waters with wind-roughened surfaces [PB88-192703] 20 p2826 N88-26765

Prediction of continental shelf sediment transport using a theoretical model of the wave-current boundary layer [AD-A192272] 20 p2829 N88-26783

Experimental study of planetary gases with applications to planetary interior models [NASA-CR-183098] 20 p2886 N88-27137

Carbon deposition model for oxygen-hydrocarbon combustion, volume 1 [NASA-CR-179375] 21 p2908 N88-27254

Carbon deposition model for oxygen-hydrocarbon combustion, volume 2 [NASA-CR-179376] 21 p2908 N88-27255

Surface-wave model uncertainty assessment [AD-A193094] 21 p2932 N88-27408

Evaluation of fracture models through pressurized-thermal-shock testing [DE88-011834] 21 p2963 N88-27603

The relationship between observed fatigue damage and life estimation models [NASA-CR-182191] 21 p2965 N88-27611

Solar cell modeling and simulation [AD-A193249] 21 p2966 N88-27620

Enhancement of modeling and image generation techniques for high-resolution 3-dimensional imagery [DE88-008923] 21 p2998 N88-27782

Some stability criteria in fluid and solid mechanics 21 p3027 N88-27966

Modeling, designing and simulating a pointing control system for balloon-borne solar experiments [NASA-TM-100337] 22 p3082 N88-28300

An overview of technology for spoken interaction with machines [AD-A194153] 23 p3202 N88-29058

A statistical rain attenuation prediction model with application to the advanced communication technology satellite project. 1: Theoretical development and application to yearly predictions for selected cities in the United States [NASA-CR-179498] 23 p3205 N88-29077

Regional intercomparisons of General Circulation Model predictions and historical climate data. CO2 [DE88-010416] 23 p3235 N88-29248

Conjunctive measurement theory: Cognitive research prospects [AD-A193627] 23 p3239 N88-29277

A model of information growth 23 p3265 N88-29440

Linearized model matching for single-imput nonlinear systems [AD-A193642] 23 p3266 N88-29445

An analysis of heat transfer after loss of primary coolant in the SP-100 reactor system [AD-A194619] 23 p3281 N88-29539

Can we calculate the fundamental dimensionless constants of physics [DE88-702641] 23 p3295 N88-29625

Constitutive modeling for isotropic materials [NASA-CR-182132] 24 p3327 N88-29811

Gas phase combustion chemistry of nitramine propellants [AD-A195082] 24 p3344 N88-29902

Attenuated total reflectance FT-IR spectroscopy to measure interfacial reaction kinetics at silica surfaces [AD-A196330] 24 p3344 N88-29908

Synchronous response modelling and control of an annular momentum control device [NASA-CR-4166] 24 p3358 N88-29995

Track performance considerations for monopulse radars
[AD-A196232] 24 p3360 N88-30007
Measurement and interpretation of North Atlantic Ocean marine radar sea scatter
[AD-A196239] 24 p3364 N88-30036
An improvement in the numerical integration procedure used in the NASA Marshall engineering thermosphere model
[NASA-CR-179389] 24 p3392 N88-30200
Thermal models pertaining to continental growth
24 p3397 N88-30230
Continental crustal formation and recycling: Evidence from oceanic basalts 24 p3398 N88-30238
Physical processes in the growth of the continental crust 24 p3398 N88-30240
Trace element differences between Archean, Proterozoic and Phanerozoic crustal components: Implications for crustal growth processes
24 p3399 N88-30243
The growth of the continental crust: Constraints from radiogenic isotope geochemistry
24 p3399 N88-30245
Crustal growth in the Archean: The geochemical evidence 24 p3400 N88-30246
Growth of the continental crust: A planetary-mantle perspective 24 p3400 N88-30251
Late-Archaean crustal growth in the Lewisian Complex of Northwest Scotland: Diachroneity in magmatic accretion and implications for models of crustal growth
24 p3401 N88-30253
The effect of thicker oceanic crust in the Archaean on the growth of continental crust through time
24 p3401 N88-30254
An analysis of results of a high-resolution world ocean circulation model
[AD-A195760] 24 p3405 N88-30272
Contributions to engineering models of human-computer interaction, volume 1
[AD-A195590] 24 p3409 N88-30295
A model for architectural comparison
[AD-A195993] 24 p3411 N88-30302
A shared-world conceptual model for integrating space station life sciences telescience operations
24 p3416 N88-30333
Automatic qualitative analysis of ordinary differential equations using piecewise linear approximations
[AD-A196310] 24 p3424 N88-30379
Orbital evolution of distant artificial earth satellites
24 p3445 N88-30506

MODEMS
Digital receiver structures and methods for the determination of the scanning frequency in modems for fast data transmission via telephone channels
[ETN-87-90429] 01 p0037 N88-10235
High data rate modem simulation for the space station multiple-access communications system
06 p0795 N88-14870
Modem for digital phase modulation: Results and summary
[PB87-149233] 07 p0845 N88-15129
Compilation and development of K-6 aerospace materials for implementation in NASA spacelink electronic information system 07 p0922 N88-15605
An 8-DPSK TCM modem for MSAT-X
19 p2649 N88-25725
Development of a coded 16-ary CPFSK coherent demodulator 19 p2649 N88-25726
Modem for the land mobile satellite channel
19 p2649 N88-25727
A mixed-modem solution for sensitive data segregation on a broadband network
[DE88-001765] 19 p2718 N88-26139
Performance of a rapid carrier acquisition circuit for satellite ground terminal modems
[RSRE-TEST-REPORT-87/CC3/2]
22 p3071 N88-28227
An OKQPSK modem incorporating numerically controlled carrier synthesis
[DE88-009536] 23 p3244 N88-29304

MODERATION (ENERGY ABSORPTION)
NT THERMALIZATION (ENERGY ABSORPTION)
Particle bed reactor scaling relationships
17 p2400 N88-24267

MODES
NT AXIAL MODES
NT BALLOONING MODES
NT COUPLED MODES
NT FAILURE MODES
NT LASER MODES
NT PROPAGATION MODES
NT PUSHBROOM SENSOR MODES
NT VIBRATION MODE
Fully plastic analysis of mixed mode plane-strain crack problems
[PB87-144929] 08 p0994 N88-16015
New mode conversion process and overdense plasma heating in the electron cyclotron range of frequencies
[IPPJ-854] 10 p1411 N88-18420

MODFETS
Enhanced performance ultrabroadband distributed amplifiers 19 p2656 N88-25775
High performance quarter-micron-gate MODFETs
19 p2656 N88-25776
Progress and challenges in HEMT LSI technology
19 p2656 N88-25779
Modulation efficiency limited high frequency performance of the MODFET 19 p2657 N88-25786
Non-stationary transport in MODFET's and heterojunction devices 19 p2659 N88-25804

MODIFICATION
U REVISIONS

MODULARITY
Modular CAMAC system, 2
[DE88-700237] 11 p1525 N88-19106
Multimission Modular Spacecraft (MMS). A serviceable design spacecraft 12 p1587 N88-19501
Status of modular RTG technology
17 p2422 N88-24403
Loading and linking in a modular language, an exercise in verification by unification
[INF-87-30] 22 p3136 N88-28642
Modularity in the PASCAL model compiler
[NPL-DITC-111/88] 22 p3139 N88-28664
The SMITE modular compilation system
[RSRE-MEMO-4145] 23 p3244 N88-29307

MODULATED CONTINUOUS RADIATION
Discussion on the modelling and processing of signals from an acousto-optic spectrum analyzer
[AD-A185639] 06 p0694 N88-14257

MODULATION
NT AMPLITUDE MODULATION
NT DELTA MODULATION
NT DIFFERENTIAL PULSE CODE MODULATION
NT FREQUENCY MODULATION
NT FREQUENCY SHIFT KEYING
NT INTERMODULATION
NT LIGHT MODULATION
NT PHASE MODULATION
NT PHASE SHIFT KEYING
NT PULSE AMPLITUDE MODULATION
NT PULSE CODE MODULATION
NT PULSE DURATION MODULATION
NT PULSE MODULATION
NT PULSE POSITION MODULATION
NT TRAVELING WAVE MODULATION
Metallic superlattices with monolayer modulation
[DE87-012724] 01 p0023 N88-10145
Reception of pseudo noise-modulated signals using digital correlators for satellite navigation tasks
[ETN-87-90426] 01 p0037 N88-10234
Phase dynamics: A review and a perspective
[DE87-013173] 01 p0048 N88-10306
Solar modulation of the cosmic radiation in the heliosphere 01 p0112 N88-10720
A digital audio link to the Channel Islands in the UHF television band: Protection of television signals from digitally modulated interference
[BBC-RD-1987/7] 02 p0161 N88-11010
Study of a coding and modulation system for the V32 call of the CCITT
[ENST-87E007] 02 p0162 N88-11015
High-power RF-pulsed modulators for the Los Alamos free-electron laser
[DE88-000514] 04 p0448 N88-12775
Study of electrostatic modulation of fuel sprays to enhance combustion performance in an aviation gas turbine
[AD-A184967] 05 p0548 N88-13341
Two-signal cross modulation effects, half-IF effects and interference criteria in land mobile sharing with UHF (Ultra High Frequency) television
[PB87-228037] 05 p0576 N88-13514
Evaluation of a satellite laser ranging technique using pseudonoise code modulated laser diodes
[NASA-CR-182347] 06 p0708 N88-14343
Response of a sequential damper to shock inputs
08 p0998 N88-16042
LiNbO3:Ti directional-coupler modulators for high-bandwidth, single-shot instrumentation systems operating at 800 nm
[DE88-003830] 11 p1479 N88-18823
Atomic monolayer metallic superlattices
[DE88-005348] 12 p1607 N88-19612
A concatenated coded modulation scheme for error control
[NASA-CR-182639] 12 p1621 N88-19697
Signal-filter design and system performance for polarimetric radar
[AD-A189257] 13 p1758 N88-20514
Efficiency characteristics of speed modulated drives at predicted torque conditions for air-to-air heat pumps
[DE88-005848] 13 p1770 N88-20588
Nonlinear dynamics of interaction between charged particles modulated beam and bounded plasma regular oscillations
[DE88-701681] 16 p2280 N88-23648
Doppler radar with multiphase modulation of transmitted and reflected signal
[NASA-CASE-MSC-18808-1] 17 p2332 N88-23923
Dynamic characteristics of a vibrating beam with periodic variation in bending stiffness
[NASA-TP-2697] 17 p2348 N88-23988
Interleaver design for trellis-coded differential 8 PSK modulation with non-coherent detection
19 p2648 N88-25719
Pilot-aided modulation for narrow-band satellite communications 19 p2649 N88-25728
ACSB: A minimum performance assessment
19 p2649 N88-25731
Kinetic modulational instability of electron cyclotron waves in plasmas
[DE88-701893] 20 p2859 N88-26976
Modulated-splitting-ratio fiber-optic temperature sensor
[NASA-TM-101332] 22 p3042 N88-28062
Direct bit detection receiver performance analyses for 8-DPSK (Differential Phase Shift Keyed) modulated signals operating with improper carrier phase synchronization
[AD-A193839] 22 p3070 N88-28220
Automatic classification of digitally modulated signals
[AD-A194623] 23 p3203 N88-29064
Long haul communications in the HF spectrum utilizing high speed modems
[AD-A194683] 24 p3360 N88-30003

MODULATION DOPED FETS
U MODFETS

MODULATION TRANSFER FUNCTION
Modulation transfer function — SPOT
03 p0341 N88-12153
High-energy laser-assisted imaging through vaporizing aerosols
[DE88-007911] 18 p2521 N88-24957

MODULATORS
NT MODEMS
The 8.4-GHz low-noise maser pump source assembly
04 p0436 N88-12705
Pulse width modulator controller design for a brushless DC motor position servo
[AD-A186618] 08 p0980 N88-15921
LiNbO3:Ti directional-coupler modulators for high-bandwidth, single-shot instrumentation systems operating at 800 nm
[DE88-003830] 11 p1479 N88-18823
Analysis of pre-flight modulator voltage calibration data for the Voyager plasma science experiment
[NASA-CR-182577] 12 p1710 N88-20236
Characteristics and application of wideband guided-wave devices 19 p2660 N88-25817
Error performance of voice band data signals with an overloaded delta modulator
[FEL-1987-05] 20 p2792 N88-26562
A high frequency GaAlAs traveling wave electro-optic modulator at 0.82 micrometers
[NASA-TM-100970] 22 p3073 N88-28240
High frequency GaAlAs modulator and photodetector for phased array antenna applications
[NASA-TM-101328] 24 p3367 N88-30048

MODULATORS-DEMODULATORS
U MODEMS

MODULES
NT CHEMICAL RELEASE MODULES
NT COMMAND MODULES
NT ELECTRONIC MODULES
NT LANDING MODULES
NT LUNAR LANDING MODULES
NT PAYLOAD ASSIST MODULE
NT POWER MODULES (STS)
NT SPACECRAFT MODULES
Columbus pressurized module verification
02 p0134 N88-10842
Documentation of NCAR (National Center for Atmospheric Research) CCM1 program modules
[PB87-213567] 03 p0352 N88-12220
A modular BLSS simulation model
03 p0359 N88-12260
Modular pump limiter systems for large tokamaks
[DE88-001487] 04 p0494 N88-13045
An analysis of simplified feed architectures for MMIC (Monolithic Microwave Integrated Circuit) T/R (Transmit/Receive) module arrays
[AD-A185474] 06 p0697 N88-14275
Interaction of different modules in depth perception: Stereo and shading
[AD-A185607] 06 p0759 N88-14655

Evaluate the application of modal test and analysis processes to structural fault detection in MSFC - STS project elements 07 p0927 N88-15630
The German Honeywell ring laser gyro: Development and test results 12 p1578 N88-19440
Parts-R-Us
[AD-A188621] 12 p1622 N88-19705
Optics of the CEBAF CW superconducting accelerator
[CEBAF-PR-87-012] 12 p1690 N88-20110
Component mode synthesis using experimental modes enhanced by mass loading
[DE88-006097] 13 p1781 N88-20657
Advanced avionics system analysis. Modular avionics cost benefit study formulation
[AD-A189019] 14 p1867 N88-21158
Thermophotovoltaic space power system, phase 3
[NASA-CR-179327] 14 p1942 N88-21585
Japanese space station module
15 p2052 N88-22224
Solar cell cover glasses for satellites
15 p2052 N88-22225
Investigation into the development of computer aided design software for space based sensors
[NASA-CR-180772] 15 p2107 N88-22552
Complexity of some problems in module algebra
[PB88-165386] 15 p2122 N88-22648
A 30 GHz monolithic receive module technology assessment
[NASA-CR-180825] 16 p2194 N88-23084
IPC for modular software requires a third party connect
[AD-A189199] 16 p2246 N88-23414
Systems for the 21st century
17 p2302 N88-23769
Design for interoperability (interchangeability)
17 p2305 N88-23789
EMPTAC (Electromagnetic Pulse Test Aircraft) user's guide
[AD-A195072] 24 p3360 N88-30006
Advanced planar array development for space station
[NASA-CR-179373] 24 p3389 N88-30181
The design of an intelligent multidisk control module for VME bus based systems
[AD-A195587] 24 p3411 N88-30303

MODULUS OF ELASTICITY
Elastic moduli of copper under compression
[DE87-013137] 02 p0147 N88-10922
Anelastic behaviour of materials under multiaxial strains. Part 3: Order-disorder transition. Shoek effect and Poisson's ratio in AISI-1080 steel
[DE87-703087] 02 p0191 N88-11193
Ion-matrix coupling in polymer electrolytes from relaxation time studies
[AD-A184632] 03 p0293 N88-11841
Effects of cure pressure on resin flow, voids, and mechanical properties
[AD-A184267] 03 p0295 N88-11853
Carbon fiber reinforced glass matrix composites for space based applications
[AD-A184255] 04 p0410 N88-12546
Determination of through-plane shear moduli for glass-reinforced plastics
[PB87-106274] 04 p0418 N88-12592
High temperature low cycle fatigue of oxide dispersion strengthened and single crystal nickel base superalloys
06 p0720 N88-14422
Structural relaxation and mechanical properties of amorphous Fe-Zr alloys 07 p0840 N88-15094
Investigation of low velocity impact damage on filamentary composite materials
07 p0923 N88-15607
Applications and limitations of the spectral-analysis-of-surface-waves method
[PB88-136619] 11 p1513 N88-19038
A continuum damage model for viscoelastic materials
[AD-A189426] 12 p1637 N88-19800
High temperature Young's modulus of IG-110 graphite
13 p1746 N88-20443
Effects of high temperature neutron irradiation on the physical, chemical and mechanical properties of fine-grained isotropic graphite 13 p1747 N88-20444
Determination of the modulus of elasticity of structural silicone sealants
[PB88-157458] 14 p1893 N88-21307
The age hardening response of thermomechanically processed Al-Mg-Li alloys
[AD-A189870] 15 p2039 N88-22147
The sensitivity of boundary layer instability growth rates to compliant wall properties
[AD-A190433] 15 p2064 N88-22309
The mechanical behavior of particle filled thermoplastics
[ETN-88-92234] 16 p2181 N88-22999
The use of micromachined structures for the management of mechanical properties and adhesion of thin films 19 p2674 N88-25899

MOHAWK AIRCRAFT
U OV-1 AIRCRAFT

MOHR CIRCLES
U FRACTURE MECHANICS

MOIRE EFFECTS
The mechanical properties of card measured by photographic Moire
[NPL-DMOM-87] 14 p1923 N88-21463

MOIRE FRINGES
Optical deformation measurement on shells following the raster principle
[ETN-88-90608] 05 p0609 N88-13741
Transient welding strain measurement by Moire technique: A comparison between experimental measurement and numerical analysis for strain-stress cycles during GTA spot-welding
[PB87-143871] 07 p0868 N88-15269

MOIRE INTERFEROMETRY
Diffraction moire: The dynamic regime
[DE87-014883] 03 p0335 N88-12111
A composite grating for moire interferometry
[AD-A186330] 07 p0832 N88-15044
J-estimation procedure based on moire interferometry data
[AD-A185965] 07 p0867 N88-15258
Development of Moire machine vision
09 p1212 N88-17264
The magic of carrier patterns in moire interferometry
[AD-A187582] 10 p1296 N88-17748
The analysis of deformations and strains in composites by moire interferometry
[AD-A187482] 10 p1345 N88-18043
Interfacial shear phenomena in graphite epoxy composites under impact loading using dynamic moire interferometry
[DE88-006773] 18 p2479 N88-24709
Experimental investigation of ductile fracture by white light moire interferometry 22 p3087 N88-28329
J-integral measurement using moire interferometry
[AD-A193751] 23 p3226 N88-29202

MOISTURE
NT ATMOSPHERIC MOISTURE
NT SOIL MOISTURE
RADC/NBS (Rome Air Development Center/National Bureau of Standards) Workshop. Moisture Measurement and Control for Microelectronics (4)
[PB87-224614] 03 p0309 N88-11947
Theory of heat and moisture exchange between finely disperse storm-generated spray and turbulent air flow
04 p0461 N88-12851
A finite element analysis of adhesively bonded composite joints including geometric nonlinearity, nonlinear viscoelasticity moisture diffusion and delayed failure
[AD-A187455] 10 p1296 N88-17747
Suggested severe local storm operational scenario for GOES I-M
[NASA-TM-100688] 11 p1515 N88-19052
Effects of moisture, elevated temperature, and fatigue loading on the behavior of graphite/epoxy buffer strip panels with center cracks
[NASA-TM-100558] 12 p1603 N88-19590
Temperature, moisture and strain rate effects on the compressive mechanical behavior of Nylon 6/6
[DE88-010734] 21 p2961 N88-27591
The effects of moisture loss and elevated temperature upon the material damping of fibre reinforced polymer matrix composites
[UTIAS-324] 23 p3188 N88-28970

MOISTURE CONTENT
NT ATMOSPHERIC MOISTURE
Moisture determinations in and under vegetation canopies. Part 2: Results after parameterization of the CLOUD model
[FEL-1986-63] 01 p0064 N88-10410
A method for remote sensing of precipitable water vapor and liquid in the atmosphere using a 22-ghz radiometer
[AD-A184204] 03 p0354 N88-12232
Lidar-radiometric method for determining liquid-water content of cirrus clouds 04 p0461 N88-12854
Variations of tropical circulation and associated rainfall anomalies, during 2 years of contrast
[INPE-4359-TDL/300] 08 p1039 N88-16286
Moisture plotting of carbon fiber composite in flight operations
[MBB-UT-119/87] 09 p1138 N88-16823
Detection of soil erosion with Thematic Mapper (TM) satellite data within Pinyon-Juniper woodlands
[NASA-CR-182476] 09 p1185 N88-17103
Measuring and modeling near surface reflected and emitted radiation fluxes at the FIFE site
[NASA-CR-182660] 12 p1640 N88-19818
Ion content and infrared absorption of moist atmospheric air
[AD-A188839] 12 p1643 N88-19838
Environmental effects on the post-impact compressive strength of CFC
[RAE-TM-MAT-STR-1088] 14 p1884 N88-21258
Effect of moisture level in PBXW-109(E) (plastic-bonded explosive) mixes on the aging of the cured explosive
[AD-A190200] 15 p2048 N88-22202
Use of energy emission for detecting the necessity of irrigation in wheat in field conditions
[INPE-4461-TDL/318] 16 p2229 N88-23315
Low-temperature thermochemical conversion of high moisture biomass feedstocks 18 p2536 N88-25047
Studies of the mechanisms and rates with which nitrogen species are incorporated into cloud water and precipitation
[PB88-193065] 20 p2826 N88-26764
Simulation of moisture diffusion of fiber reinforced components of aircraft for general air transportation
[IFL-IB-87-05] 21 p2907 N88-27253
On experiences with two hot-wire instruments for measuring the liquid water content in clouds
[ESA-TT-1085] 23 p3236 N88-29255

MOISTURE DETECTORS
U MOISTURE METERS

MOISTURE METERS
High polymer sensor materials discussed
06 p0676 N88-14140
Nondestructive moisture measurement in microelectronics
[AD-A190515] 15 p2060 N88-22281

MOISTURE RESISTANCE
The analysis of moisture absorption in multi-layered media
[NPL-DMA(A)-147] 01 p0019 N88-10115
The water absorption of model epoxy resin networks cured with aromatic diamines
[BR100722] 01 p0027 N88-10169
Stability of uncapsulated weight cells with thin film elongation measurement bands under influence of humidity, temperature and operation voltage
[ETN-88-92383] 21 p2951 N88-27531

MOL (ORBITAL LABORATORIES)
U MANNED ORBITAL LABORATORIES

MOLDING MATERIALS
High explosive moulding powders from RDX and aqueous polyurethane dispersions
[AD-A185026] 05 p0568 N88-13458
Intelligent process development of foam molding for the Thermal Protection System (TPS) of the space shuttle external tank 08 p1060 N88-16397
Development of a shell system for DS moulds at RR precision casting facility --- directional solidification (DS)
[PNR90400] 09 p1151 N88-16893

MOLDS
Process for producing sandwich mouldings
[EP-PATENT-0-191-623-A2] 04 p0426 N88-12642
Intelligent process development of foam molding for the Thermal Protection System (TPS) of the space shuttle external tank 08 p1060 N88-16397
Development of a shell system for DS moulds at RR precision casting facility --- directional solidification (DS)
[PNR90400] 09 p1151 N88-16893
Injection compression for short fiber reinforced plastics
[SNIAS-881-430-118] 21 p2922 N88-27344

MOLECULAR ABSORPTION
MODTRAN: A moderate resolution model for LOWTRAN
[AD-A185384] 05 p0574 N88-13503
Statistical fine structure in inhomogeneously broadened absorption lines in solids
[AD-A190341] 16 p2174 N88-22957
Molecular line shape effects on atmospheric window absorption
[AD-A196316] 24 p3342 N88-29894

MOLECULAR BEAM EPITAXY
Quantum well laser diodes: Modeling and realization of GaAs/GaAlAs
[LAAS-87-165] 02 p0179 N88-11116
Molecular beam heteroepitaxy: (Ca,Sr)F2-GaAs system
[LAAS-87-168] 02 p0246 N88-11556
JPRS report: Science and technology. China
[JPRS-CST-87-026] 03 p0269 N88-11688
Raman scattering spectrum along a bevel etched GaAs on Si, TEM (Transmission Electron Microscope) study and GaAs P-I-N photodetector on Si
[DE88-000210] 04 p0498 N88-13066
MBE growth of InAsSb strained-layer superlattices
[DE88-000365] 05 p0654 N88-14011
Molecular beam epitaxial growth and characterization of 3-5 compound semiconductor single and multiple interface structures
[AD-A185400] 05 p0656 N88-14021

Some investigations of molecular beam epitaxial growth of 3-5 semiconductor films via Monte-Carlo computer simulations, carrier tunneling and spectroscopic ellipsometry
[AD-A185520] 06 p0789 N88-14839

Molecular beam epitaxy for research on quantum well structures
[AD-A186791] 09 p1255 N88-17522

Epitaxial growth and new phase of single crystal Dy by molecular beam epitaxy
[DE88-002850] 09 p1256 N88-17531

Microwave semiconductor research-materials, devices and circuits
[AD-A187121] 10 p1415 N88-18444

Grazing incidence X-ray scattering study of defect structures in MBE GaAs/Si using synchrotron radiation
[DE88-004556] 10 p1420 N88-18483

MBE growth, characterization and electronic device processing of HgCdTe, HgZnTe related heterojunctions and HgCdTe-CdTe superlattices
[AD-A187456] 10 p1421 N88-18486

Theoretical studies of the interface electronic properties of tetrahedrally coordinated semiconductors
[AD-A187216] 11 p1555 N88-19306

MBE (Molecular Beam Epitaxial) growth characterization and electronic device processing of HgCdTe, HgZnTe related heterojunctions and HgCdTe-CdTe superlattices
[AD-A187416] 11 p1555 N88-19307

Comparison of low temperature photoluminescence of bulk MBE (Molecular Beam Epitaxy) grown AlGaAs and GaAs using a graphite generated dimer versus a standard tetramer arsenic group-V source
[DE88-004939] 11 p1558 N88-19320

Characterization of enhanced Schottky-barrier InGaAs/Al(1-x)As strained channel modulation-doped field-effect transistors
[AD-A188820] 12 p1698 N88-20162

Research on multibandgap solar cells
[DE87-012261] 13 p1792 N88-20721

Development of Si/SiGe heterostructures
[AD-A189527] 13 p1845 N88-21044

Electrical characteristics of MBE (Molecular Beam Epitaxyl)-grown GaAs/sub 1-x/Sb/sub x on InP and correlation with film microstructure
[DE88-003841] 13 p1847 N88-21053

Gas source MBE (Molecular Beam Epitaxy)
[AD-A189763] 15 p2142 N88-22782

Beam assisted fabrication of 3-5/Si monolithic devices
[AD-A189979] 15 p2142 N88-22785

Microelectronics the next fifteen years
17 p2305 N88-23792

Molecular Beam Epitaxy (MBE) for high speed devices
19 p2656 N88-25770

Epitaxial iron films
[AD-A191815] 19 p2732 N88-26225

Center for thin film studies
[AD-A191996] 19 p2732 N88-26226

Analysis of the performance of the space ultravacuum research facility in attached and free-flyer mode
[NASA-TM-100325] 20 p2763 N88-26387

Integrated optoelectronic circuits utilizing InGaAsP grown by molecular beam epitaxy (erbium doping of MBE GaAs)
[AD-A192269] 20 p2795 N88-26584

MBE growth of HgTe/CdTe superlattices on Si(100) substrates 20 p2869 N88-27033

Preparation of high-T(sub)c Y1Ba2Cu3O(sub 7-Delta) superconducting thin films by MBE (Molecular-Beam-Epitaxy) techniques
[DE88-009999] 20 p2877 N88-27082

Molecular beam epitaxy of GaP films on Si substrates
[PB88-131974] 21 p3020 N88-27923

Investigations on the MBE (Molecular Beam Epitaxy) growth and properties of Al(sub y)Ga(sub y)In(sub 1-x-y)AsInP and InGaAs-InAlAs superlattices
[DE88-009105] 21 p3022 N88-27941

Spectroscopic studies with multiple quantum well materials with applications to optical signal processing at room temperature
[AD-A194171] 24 p3429 N88-30409

Electronic materials and devices prepared by molecular beam epitaxy
[AD-A195694] 24 p3433 N88-30433

MOLECULAR BEAMS

Direct infrared absorption of clusters in pulsed molecular beams
[DE87-014802] 02 p0236 N88-11490

Materials preparation and longevity in hyperthermal atomic oxygen 03 p0297 N88-11862

Ceramics thin film 04 p0403 N88-12505

Reactive sticking coefficients of silane on silicon
[DE88-000601] 05 p0570 N88-13473

Supersonic beam observations of semiconductor clusters
[AD-A184991] 05 p0655 N88-14018

Determination of molecular-ion structures through the use of accelerated beams
[DE88-002960] 09 p1246 N88-17467

Apparatus for the study of silicon film deposition and silicon etching
[AD-A187616] 10 p1334 N88-17972

Self-pumped phase conjugation in a supersonically flowing medium
[AD-A188281] 10 p1338 N88-17998

Development of a planar heterojunction bipolar transistor for very high speed logic
[AD-A188137] 11 p1478 N88-18820

A study of the interaction of light with sub-micron metallic surfaces
[DE88-003136] 13 p1776 N88-20624

Crossed molecular beam studies of substitution and exchange reactions
[DE88-006322] 14 p1980 N88-21814

Molecular-beam, mass-spectrometric studies of wood vapor and model compounds over HZSM-5 catalyst
18 p2535 N88-25044

Interactions of molecules with surfaces
[DE88-007950] 19 p2723 N88-26169

Electron-impact-ionization and electron-attachment cross sections of radicals important in transient gaseous discharges
[AD-A192248] 20 p2770 N88-26424

Reaction dynamics on semiconductor surfaces
[AD-A194305] 22 p3156 N88-28781

MOLECULAR BIOLOGY

Molecular mechanisms of neuronal responsivity
[AD-A187061] 09 p1199 N88-17185

Biology and Medicine Division
[DE87-009280] 14 p1952 N88-21632

Studies of molecular biology
[DE88-005906] 15 p2101 N88-22514

ECUT (Energy Conversion and Utilization Technologies) program: Biocatalysis Project
[NASA-CR-182917] 17 p2370 N88-24110

MOLECULAR BONDS

U CHEMICAL BONDS

MOLECULAR CHAINS

Applications and limitations of deuterium labeling methods to neutron scattering studies of polymers
[DE87-012936] 02 p0151 N88-10945

Estimations of gravitational effects on thermal denaturation process in a biopolymer
03 p0318 N88-12013

Feasibility of chemical lasers based on chain reaction involving hydrogen fluorination with thermal branching mechanism 09 p1238 N88-17420

Basic research on macromolecular dynamics
[PB88-141643] 10 p1305 N88-17805

Storing bits on a DNA polymer chain
[AD-A195701] 24 p3356 N88-29981

Novel ladder polymers for use as high temperature stable resins or coatings
[NASA-CASE-LEW-14203-1] 24 p3356 N88-29984

MOLECULAR CLOUDS

Soft X-ray observations of pre-main sequence stars in the chamaeleon dark cloud
[NASA-CR-181457] 02 p0250 N88-11579

Composition, structure and chemistry of interstellar dust
[NASA-TM-88350] 02 p0253 N88-11603

Molecular clouds at high galactic latitudes
11 p1569 N88-19392

Submillimeter and far infrared line observations of M17 SW: A clumpy molecular cloud penetrated by UV radiation
[NASA-CR-182866] 16 p2288 N88-23701

Optical and infrared observations of high latitude dust clouds --- interstellar matter
[B8621135] 16 p2289 N88-23709

Analysis of dust grain properties in two star forming regions through comparison of theoretical models to observations 17 p2451 N88-24559

Microwave spectroscopy and gravitational collapse
18 p2594 N88-25413

High spatial resolution observations of neutral atomic carbon in the molecular clouds M17 and W51
[MPE-PREPRINT-109] 22 p3164 N88-28846

First detection of HCN J = 9 to 8 (797 GHz) line emission: Very high densities in the Orion core
[MPE-PREPRINT-110] 22 p3165 N88-28847

Star formation and molecular clouds
24 p3451 N88-30537

Observations of star formation
24 p3451 N88-30538

Comparisons of solar nebula models
24 p3451 N88-30539

MOLECULAR COLLISIONS

Ab initio methods for electron-molecule collisions
[DE87-011728] 01 p0092 N88-10598

The Conference on the Dynamics of Molecular Collisions held in Oglebay Park, Wheeling, West Virginia on 12-17 July 1987
[AD-A184690] 03 p0374 N88-12354

Theoretical atomic and molecular physics
[DE88-001625] 05 p0649 N88-13974

Molecular collision processes in gases and at surfaces
[AD-A189518] 13 p1836 N88-20982

Excimer laser photolysis studies of T-V (Translation-to-Vibration) energy transfer
[AD-A189613] 13 p1837 N88-20989

Molecular reaction and energy transfer rate estimation for chemical-laser analysis
[AD-A190664] 15 p2035 N88-22126

Energy transfer processes in free radicals: A collaborative experimental and theoretical investigation
[AD-A191264] 16 p2269 N88-23578

Theoretical calculations of XeF ground state kinetics
[AD-A191398] 16 p2270 N88-23580

Bimolecular reactions and energy-transfer processes of highly vibrationally excited molecules related to energetic materials
[AD-A189013] 18 p2571 N88-25270

Energy-transfer properties and mechanisms
[DE88-007107] 18 p2571 N88-25272

Theoretical studies of dynamics combustion
[DE88-007565] 19 p2611 N88-25495

Interactions of molecules with surfaces
[DE88-007950] 19 p2723 N88-26169

Low energy molecular collisions
[ISAS-RN-366] 20 p2850 N88-26919

MOLECULAR DIFFUSION

The modelling of orientation in planar polymer welding flows
[AD-A184404] 04 p0451 N88-12793

Does the pipe diffusion of self-interstitials in crystals under stresses exist
[DE88-701027] 15 p2139 N88-22762

Mechanisms of gas permeation through polymer membranes: Renewal proposal for period December 1, 1986 - November 30, 1989
[DE88-007436] 18 p2494 N88-24796

Study of mixing and reaction in the field of a vortex
[AD-A191489] 18 p2508 N88-24876

Molecular composites processing and properties, 1
[AD-A194113] 23 p3189 N88-28974

MOLECULAR DISSOCIATION

U DISSOCIATION

MOLECULAR ELECTRONICS

A strategy to determine the transition state of an electron transfer reaction
[AD-A183976] 03 p0382 N88-12404

MOLECULAR ENERGY LEVELS

Intramolecular energy transfer reactions as a method for metal complex assisted production of hydrogen
[DE88-001621] 05 p0562 N88-13425

Molecular-level synthesis and characterization of metal-polymer interfaces
[AD-A184956] 05 p0567 N88-13455

Sequential excitation preparation of molecular energy levels with special structural and chemical properties
[AD-A190041] 15 p2132 N88-22718

Energy-transfer properties and mechanisms
[DE88-007107] 18 p2571 N88-25272

Study of energy levels and decay mechanisms for singlet Rydberg states of molecular nitrogen
[AD-A192505] 21 p3014 N88-27886

MOLECULAR EXCITATION

Picosecond CO2 laser interactions with polyatomic molecules
[DE87-012072] 01 p0051 N88-10327

Ro-vibrational laser spectroscopy of ESD neutrals from chemisorbed species
[DE87-013011] 04 p0447 N88-12770

Intramolecular energy transfer reactions as a method for metal complex assisted production of hydrogen
[DE88-001621] 05 p0562 N88-13425

Pure dephasing of a vibrational adbond
[AD-A185222] 05 p0609 N88-13740

Explosive absorption of laser beam of finite diameter
07 p0921 N88-15597

Molecular and electronic mechanism in the control of Na+ and K+ permeability of excitable cell membrane by ligand binding on receptor sites
[AD-A188725] 13 p1808 N88-20805

Quantum Monte Carlo study of the MIES associated with H2 (X 1 sigma sub g (+)) and H2 (B 1 sigma sub u (+))
[AD-A189063] 13 p1835 N88-20977

Excimer laser photolysis studies of T-V (Translation-to-Vibration) energy transfer
[AD-A189613] 13 p1837 N88-20989

Molecular reaction and energy transfer rate estimation for chemical-laser analysis
[AD-A190664] 15 p2035 N88-22126

Reactions of N2(A sup 3 sigma sup + sub u) candidates for short wavelength lasers
[DE88-007018] 15 p2070 N88-22342
Experiments on reactions of the electronically excited molecule nitron NH (a sup 1 delta) and carbon CH2 (a bar sup 1 A(1)) in gas phase
[MPIS-3/1987] 17 p2397 N88-24249
Steady-state approximations in Raman excitation equations
[DE88-011759] 21 p3014 N88-27889
Molecular fluorescence measurements with a charge-coupled device detector
[AD-A194221] 22 p3080 N88-28291
Charge storage and switching phenomena in metal complexes
[AD-A193778] 23 p3192 N88-28996
Molecular fluorescence measurements with a charge-coupled device detector
[AD-A194437] 23 p3216 N88-29141
Intramolecular dynamics: A study of molecules at high levels of vibrational excitation
[AD-A195285] 24 p3428 N88-30400

MOLECULAR FLOW
NT SLIP FLOW
NT TRANSITION FLOW
Three dimensional Monte Carlo simulation of molecular movement and heat radiation in vacuum devices: Computer code MOVAK3D --- fusion reactors
[KFK-4292] 09 p1246 N88-17471
Analysis of molecular mixing and chemical reaction in mixing layer
[AD-A191600] 18 p2482 N88-24721

MOLECULAR GASES
NT DIATOMIC GASES
Atomic and molecular gas phase spectrometry
[AD-A187562] 11 p1452 N88-18655
Molecular collision processes in gases and at surfaces
[AD-A189518] 13 p1836 N88-20982
Solar generation and storage of O2 (a 1 delta g)
[NASA-CR-4127] 14 p1913 N88-21431
Kinetics of electrons and molecules at plasma-beam discharge in molecular gases
[DE88-701196] 16 p2275 N88-23616
Molecular gas in Virgo cluster spiral galaxies
17 p2450 N88-24557
Thermostatistical estimations of vapor-state molecules affected by gravity in a heat pipe
20 p2783 N88-26505
Molecular hydrogen in galaxies
23 p3299 N88-29645

MOLECULAR INTERACTIONS
NT MOLECULAR COLLISIONS
On the interaction of a planar metal surface with a charge and with a molecule
[DE87-703083] 02 p0147 N88-10920
Modeling shockwave deformation via molecular dynamics
[DE87-013157] 02 p0169 N88-11063
Systematic studies of molecular vibrational anharmonicity and vibration-rotation interaction by self-consistent-field higher derivative methods: Applications to asymmetric and symmetric top and linear polyatomic molecules
[DE87-014691] 02 p0232 N88-11465
New theory for competing interactions and microstructures in partially-ordered (liquid-crystalline) phases
[DE87-014739] 03 p0380 N88-12389
Soluble metal chelate polymers of coordination numbers six, seven and eight
[AD-A185094] 05 p0568 N88-13459
Investigation of impurity defects in alpha-iron by molecular dynamics method
[DE88-700355] 07 p0834 N88-15058
Van der Waals clusters of aromatic molecules studied using supersonic molecular jet spectroscopy
[AD-A186087] 07 p0929 N88-15644
Energy disposal in ion-molecule reactions
[AD-A188772] 09 p1171 N88-17019
Free energy calculation via MD (molecular dynamics): Methodology and application to bicrystals
[DE88-002902] 09 p1256 N88-17532
Rovibrational spectroscopy of ArCO van der Waals complex
[DE88-004291] 10 p1406 N88-18387
Soluble polysilane derivatives: Chemistry and spectroscopy
[AD-A187889] 11 p1461 N88-18713
Photochemistry at structured surfaces: A classical electromagnetic approach
[AD-A189519] 13 p1737 N88-20387
Molecular reaction and energy transfer rate estimation for chemical-laser analysis
[AD-A190664] 15 p2035 N88-22126
Fast atom bombardment study on interaction of anticodonic nucleotides and their cognate amino acid
[ISAS-RN-355] 20 p2850 N88-26918
Low energy molecular collisions
[ISAS-RN-366] 20 p2850 N88-26919
Precise ultraviolet absorbance study of the interaction of amino acids and mononucleosides in aqueous solution
[ISAS-RN-356] 21 p2908 N88-27256
Corrosion control through a better understanding of the metallic substrate/organic coating/interface
[AD-A193981] 22 p3056 N88-28132
Interactions in miscible polymer blends
[AD-A193824] 22 p3058 N88-28144
Cytochrome electron transfer and biomolecular electronics
[AD-A195482] 24 p3406 N88-30277

MOLECULAR IONS
NT HYDRONIUM IONS
Ionic mechanisms of soot formation in flames
[AD-A186195] 08 p0966 N88-15848
Efficiency of ionic noble gas and alkali metal molecules as ultraviolet and far-ultraviolet lasers
09 p1238 N88-17419
Determination of molecular-ion structures through the use of accelerated beams
[DE88-002960] 09 p1246 N88-17467
The role of electron-ion recombination in bulk antimatter production 16 p2268 N88-23567

MOLECULAR ORBITALS
Accurate ab initio calculations which demonstrate a 3 Pi u ground state for Al2
[NASA-TM-89302] 01 p0102 N88-10666
Clusters: Link between molecules and solids
[AD-A188170] 11 p1543 N88-19224
Molecular orbital studies of the bonding in heavy element organometallics: Progress report
[DE88-007765] 19 p2723 N88-26168

MOLECULAR OSCILLATIONS
Pure dephasing of a vibrational adbond
[AD-A185222] 05 p0609 N88-13740
The 1,2,3-triaminoguanidinium nitrate: An alternate explanation of the nitrate anion disorder
[AD-A188386] 12 p1612 N88-19640
Instrumentation for collisional energy transfer studies
[AD-A188495] 12 p1689 N88-20105

MOLECULAR RELAXATION
Relaxation effect of stark split levels for two-level system interacting with symmetrical strong resonant bichromatic field 03 p0299 N88-11882
Study of vibration relaxation in active medium of CO2-laser using phase-absorption method
07 p0919 N88-15582
Exciton relaxation phenomena in a disordered system
14 p1978 N88-21802
Reactions of N2(A sup 3 sigma sup + sub u) candidates for short wavelength lasers
[DE88-007018] 15 p2070 N88-22342
Monte Carlo investigation of hot photoexcited electron relaxation in GaAs 19 p2659 N88-25805
Monte Carlo simulations of femtosecond relaxation of photoexcited electrons in AlGaAs/GaAs quantum wells
20 p2869 N88-27036
Reaction dynamics on semiconductor surfaces
[AD-A194305] 22 p3156 N88-28781

MOLECULAR ROTATION
Ro-vibrational laser spectroscopy of ESD neutrals from chemisorbed species
[DE87-013011] 04 p0447 N88-12770
Dynamical analysis of molecular decay at spherical surfaces
[AD-A184908] 05 p0647 N88-13964
Rovibrational spectroscopy of ArCO van der Waals complex
[DE88-004291] 10 p1406 N88-18387
The 1,2,3-triaminoguanidinium nitrate: An alternate explanation of the nitrate anion disorder
[AD-A188386] 12 p1612 N88-19640
Continuous collective molecule rotation of a nematic liquid crystal induced from light angular momentum
[FUB-17-1986] 14 p1986 N88-21845
Rotational structure and absorption cross sections from 300 to 190 K of the Schumann-Runge bands
[AERONOMICA-ACTA-A-318-1987]
15 p2036 N88-22131
Collective rotation of molecules driven by the angular momentum of light in a nematic film
[FUB-6-1986] 15 p2131 N88-22714
Sequential excitation preparation of molecular energy levels with special structural and chemical properties
[AD-A190041] 15 p2132 N88-22718
Time-resolved studies of free radicals and laser-initiated chain reactions
[DE88-006569] 16 p2266 N88-23553
Low energy molecular collisions
[ISAS-RN-366] 20 p2850 N88-26919

MOLECULAR SPECTRA
NT ELECTRONIC SPECTRA
NT RAMAN SPECTRA
NT VIBRATIONAL SPECTRA
CARS measurements of combustion. 2: Gas species concentration measurements
[NAL-TR-940] 11 p1453 N88-18663

MOLECULAR SPECTROSCOPY
NT RAMAN SPECTROSCOPY
Experimental molecular spectroscopy in shock-compressed materials
[DE87-013139] 02 p0144 N88-10903
Supersonic beam observations of semiconductor clusters
[AD-A184991] 05 p0655 N88-14018
On the signal strength dependency on pressure in laser sub-Doppler saturation spectroscopy with special attention to gaseous diatomic molecules
[USIP-87-13] 09 p1171 N88-17023
Polarization of molecular fluorescence bands in comets: Recent observations and interpretation
14 p1998 N88-21907
Reaction dynamics on semiconductor surfaces
[AD-A194305] 22 p3156 N88-28781
Molecular fluorescence measurements with a charge-coupled device detector
[AD-A194437] 23 p3216 N88-29141

MOLECULAR STRUCTURE
The influence of polymer structure on triplet luminescence
[DE87-014431] 02 p0152 N88-10952
The Conference on the Dynamics of Molecular Collisions held in Oglebay Park, Wheeling, West Virginia on 12-17 July 1987
[AD-A184690] 03 p0374 N88-12354
Improper ferroelectricity: A theoretical and experimental study
[AD-A184614] 03 p0381 N88-12397
Molecular engineering of ceramics
[DE88-000174] 04 p0420 N88-12603
Advances in inherently conducting polymers
[DE88-000501] 04 p0421 N88-12610
The Moessbauer effect of SnI4 at high pressure
[DE87-014771] 04 p0495 N88-13048
Molecular and supramolecular orientation in conducting polymers
[DE88-000533] 05 p0569 N88-13472
Pressure induced phase transitions, superconductivity of phosphorus described 06 p0675 N88-14134
Observing effect of laser radiation of low-frequency Raman scattering of light 06 p0772 N88-14742
X-ray structure analyses and molecular mechanics analyses of dense energetic materials
[AD-A185462] 06 p0779 N88-14781
Structure-property relationships in thermoplastic elastomers. 4: Dynamic mechanical relaxations in poly(dioxolane), poly(butyltrioxocane) and poly(propylene oxide) polyurethanes
[AD-A186278] 07 p0836 N88-15073
The Coupled Cluster Single and Double excitation (CCSD) method in quantum chemistry: An efficient formulation of the theory and application to closed shell molecular systems
[DE88-000475] 07 p0930 N88-15650
Determination of molecular-ion structures through the use of accelerated beams
[DE88-002960] 09 p1246 N88-17467
Electronic and chemical structure of 3-5/metal and Si/metal interfaces
[AD-A186579] 09 p1254 N88-17518
Copper oxidation states, vacancy ordering and their effect on high temperature superconductivity
[DE88-003079] 09 p1258 N88-17542
Application of inverse gas chromatography to fluidity studies
[DE88-002896] 10 p1296 N88-17750
Investigations on the usefulness of the Massively Parallel Processor for study of electronic properties of atomic and condensed matter systems
[NASA-CR-182514] 10 p1383 N88-18259
Energy-related atomic and molecular structure and scattering studies
[DE88-004246] 10 p1406 N88-18386
Absolute rate measurements of two-photon process of gases, liquids, and solids
[DE88-003800] 10 p1407 N88-18391
Effect of density change on rapid liquid-solid interface kinetics and heat flow
[DE88-004286] 11 p1487 N88-18878
Clusters: Link between molecules and solids
[AD-A188170] 11 p1543 N88-19224
Raman enhancement methods for molecular structure characterization of optical thin films
[DE88-003421] 11 p1558 N88-19324

The 1,2,3-triaminoguanidinium nitrate: An alternate explanation of the nitrate anion disorder
[AD-A188386] 12 p1612 N88-19640
A procedure for estimating the crystal densities of organic explosives
[AD-A189023] 12 p1613 N88-19646
Novel catalysts for methane activation
[DE88-003637] 13 p1738 N88-20390
Properties of molecular solids and fluids at high pressure and temperature
[DE88-004195] 13 p1738 N88-20391
Gordon Conference on Intermetallic Compounds held at Tilton, New Hampshire on 20-24 July 1987
[AD-A188502] 13 p1745 N88-20435
Thermodynamic theory of fluctuations and Rayleigh light scattering in solutions 13 p1785 N88-20681
Sequential excitation preparation of molecular energy levels with special structural and chemical properties
[AD-A190041] 15 p2132 N88-22718
Chromatographic and mass spectrometric separation and analysis
[AD-A190113] 16 p2174 N88-22958
Synthesis and properties of novel cluster phases
[DE88-006816] 16 p2175 N88-22964
Correlation between dielectric and structural properties during epoxy cure
[AD-A190696] 16 p2181 N88-22997
Distribution of chain ends inside the polybutadiene microspheres of SB diblock copolymers
[AD-A191257] 16 p2182 N88-23007
Studies of model ion channels in defect-free multibilayers of phospholipids
[AD-A188740] 16 p2238 N88-23365
Disclination structures in carbon and graphite
[AD-A191056] 17 p2322 N88-23868
Topological stereochemistry
[AD-A191867] 18 p2477 N88-24691
Structural study of the TGMDA-DDS system — epoxy system
[ONERA-RT-4/3346-M] 18 p2493 N88-24792
A compatible encapsulant for explosives
[DE88-007212] 18 p2495 N88-24806
A constraint algorithm for maintaining rigid bonds in molecular dynamics simulations of large molecules
[AD-A191663] 18 p2572 N88-25277
Neutron diffraction refinement of CsHSO4 superionic phase structure
[DE88-701496] 18 p2580 N88-25326
Molecular characterization of structure and bonding in thin film materials
[DE88-006811] 18 p2584 N88-25351
Structure and refinement of ordered aromatic heterocyclic polymers by diffraction methods: Application of results to electro-optic phenomena
[AD-A191859] 19 p2619 N88-25537
High resolution spectroscopy of dissociating molecules
[DE88-007959] 20 p2851 N88-26924
Spatial organization of homopolymer chains inside spherical polybutadiene domains of SB diblock copolymers
[AD-A193390] 21 p2918 N88-27321
Experiments in microgravity environment: Protein crystallization
[REPT-881-430-101] 21 p2924 N88-27354
Chemistry of adhesion at the polyimide-metal interface
[AD-A194647] 22 p3058 N88-28143
Raman spectroscopy on simple molecular systems at very high density
[DE88-010947] 23 p3191 N88-28987
Hydrogen storage by molecular polyhydrides
[AD-A194207] 23 p3191 N88-28989
Blends of crystallizable polybutadienes
[AD-A194536] 23 p3197 N88-29026
Nonlinear optical processes in molecular systems
[AD-A193871] 23 p3282 N88-29546
Localized excitations in one-dimensional molecular crystal with structural defect
[DE88-702691] 23 p3293 N88-29607
Discovery of a low temperature form of TAGN (Triaminoguanidinium Nitrate)
[AD-A196056] 24 p3357 N88-29989

MOLECULAR TRAJECTORIES
Theoretical calculations of XeF ground state kinetics
[AD-A191398] 16 p2270 N88-23580

MOLECULAR WEIGHT
Synthesis of high molecular weight peptide polymers and copolymers containing L-dope residues
[AD-A186462] 08 p0973 N88-15887
Ordered polymers for space applications
[AD-A188480] 12 p1610 N88-19630
North Carolina Biomolecular Engineering and Materials Applications Center (NC-BEMAC)
[AD-A190923] 16 p2237 N88-23364
Interfacial tension of immiscible polymer blends: Temperature and molecular weight dependence
[AD-A192463] 21 p2917 N88-27312

MOLECULES
NT DIATOMIC MOLECULES
NT MONATOMIC MOLECULES
NT POLYATOMIC MOLECULES
Polyitaconic acid macromolecule primer for adhesive bonding and corrosion control of aluminum
[DE87-013306] 01 p0027 N88-10173
An investigation of the behavior of outgassed molecules in thermal vacuums 02 p0133 N88-10836
IR laser excitation in molecules: Chaos and diffusive energy growth
[DE87-013147] 02 p0178 N88-11105
Quantum-mechanical aspects of classically chaotic driven systems
[DE87-013152] 02 p0178 N88-11106
Development of many-body methods for flame chemistry and large molecule applications
[AD-A184451] 03 p0284 N88-11789
Theory of atomic additivity in molecular hyperpolizabilities 03 p0297 N88-11867
Wake shield 03 p0298 N88-11871
JPRS report: Science and technology. China
[JPRS-CST-87-031] 03 p0299 N88-11880
XeCl excimer laser induced multiphoton ionization of ammonia molecule 03 p0299 N88-11883
Study of IR laser photoacoustic spectra of organic molecules adsorbed on metal surface
03 p0301 N88-11891
Tetrahedral carbon and interstitial electrons in Li cluster: CLi4 and (LiCH3)4
[AD-A184277] 04 p0496 N88-13055
The formation and thermochemical properties of multiligand complexes
[AD-A184935] 05 p0561 N88-13416
High energy molecules of high symmetry
[AD-A185385] 05 p0647 N88-13965
First flight of the ATMOS instrument during the Spacelab 3 Mission, April 29 through May 6, 1985
[NASA-CR-182360] 06 p0728 N88-14482
Photoabsorption and photodissociation of molecules important in the interstellar medium
[NASA-CR-182435] 08 p1100 N88-16617
Photoionization dynamics of excited molecular states
[DE88-002982] 09 p1246 N88-17468
Molecular dynamics study of high-temperature grain-boundary stability in a (100) sigma = 29 bicrystal model
[DE88-002955] 09 p1258 N88-17546
Clusters: Link between molecules and solids
[AD-A188170] 11 p1543 N88-19224
Mass loss from evolved stars
11 p1569 N88-19394
Resonance energy transfer between carbon monoxide and oxygen molecules using dye laser intracavity absorption spectroscopy
[AD-A188488] 12 p1689 N88-20104
Results of infrared spectrometer experiment. 1: Infrared radiation of parent molecules in Halley's Comet
13 p1726 N88-20325
MOPAC manual: A general molecular orbital package, fourth edition
[AD-A188623] 13 p1733 N88-20362
New polyisoimides: An approach to in situ rigid-rod polyimide formation
[AD-A191665] 18 p2490 N88-24773
Bimolecular reactions and energy-transfer processes of highly vibrationally excited molecules related to energetic materials
[AD-A189013] 18 p2571 N88-25270
Modeling the primary events of photosynthesis using chlorophyll containing fixed distance donor-acceptor molecules
[DE88-010033] 20 p2831 N88-26793
Shock wave compression and metallization of simple molecules
[DE88-008031] 20 p2851 N88-26925
Equilibrium distribution functions for limited plasma-molecular systems
[DE88-702412] 21 p3018 N88-27916
Semi-microdroplet assay for cell adhesion molecules
[NASA-CR-183139] 24 p3406 N88-30274

MOLIERE FORMULA
U COSMIC RAY SHOWERS
U SPATIAL DISTRIBUTION

MOLLUSKS
NT SNAILS
Synthesis of high molecular weight peptide polymers and copolymers containing L-dope residues
[AD-A186462] 08 p0973 N88-15887

MOLTEN SALT ELECTROLYTES
Determination of optimum electrolyte composition for molten carbonate fuel cells literature review
[DE88-001015] 10 p1348 N88-18058
Molten salt electrolytes for high-temperature lithium cells
[DE88-010058] 20 p2794 N88-26581

MOLTEN SALTS
Electronic conduction in molten sodium chloride
[DE87-010063] 02 p0144 N88-10901
Direct Absorption Receiver (DAR) systems assessment
[DE87-012277] 02 p0196 N88-11222
Quantitative determination of a hydrogen impurity in a sodium coolant by hydride thermal dissociation
[NASA-TT-20239] 13 p1740 N88-20402
Thermal modeling of solar central receiver cavities
[DE88-004940] 14 p1943 N88-21594
Fast ion conducting glasses
[AD-A191412] 16 p2183 N88-23010
Production of powdered sodium hydride with large specific surface by the catalyzed reaction of molten sodium with hydrogen-1
[NASA-TT-20185] 20 p2776 N88-26402
Nuclear magnetic resonance spectrometer
[AD-A192928] 21 p2950 N88-27523

MOLYBDENUM
Metallic superlattices with monolayer modulation
[DE87-012724] 01 p0023 N88-10145
Superconducting properties of metallic superlattices
[DE87-012725] 01 p0023 N88-10146
Sintered steels of high resistance alloyed to Nb, Mo, Mn and Si
[DE87-703546] 04 p0415 N88-12573
Data base on the high heat flux behaviour of metals and carbon materials for plasma facing components. Experiments at the 10 MW neutral beam injection test stand of the IPP Nagoya
[IPPJ-AM-53] 04 p0492 N88-13031
Development of encapsulated lithium hydride thermal energy storage for space power systems
[DE88-004762] 11 p1507 N88-19001
The effect of microstructure on the fatigue crack growth resistance of nickel base superalloys
[AD-A189526] 13 p1741 N88-20414
The relationship of the chemical bonding topology of high critical temperature copper oxide superconductors to that of the chevrel phases and the ternary lanthanide rhodium borides
[AD-A189255] 13 p1845 N88-21042
AMTEC electrode development
17 p2409 N88-24324
An experimental study of biaxial yield in modified 9Cr-1Mo steel at room temperature
[NASA-CR-175012] 24 p3385 N88-30164

MOLYBDENUM ALLOYS
Investigation of creep crack growth in heat resistant tube steels
[ETN-87-90606] 03 p0288 N88-11813
Effect of low-temperature aging on the mechanical properties of cast stainless steels
[DE88-002872] 10 p1300 N88-17774
The role of oxygen on the mechanical behavior of molybdenum alloys 17 p2401 N88-24278

MOLYBDENUM COMPOUNDS
NT MOLYBDENUM DISULFIDES
NT MOLYBDENUM OXIDES
Surface modification by metal deposition and laser irradiation 01 p0023 N88-10148

MOLYBDENUM DISULFIDES
Evaluation of centrifugal barrel tumbling process for impregnation of molybdenum disulfide powder lubricant
[BDX-613-3698] 11 p1464 N88-18727
Lubricating properties of molybdenum disulfide. Part 3: Performance of molybdenum disulfide-containing oils in fluid lubrication
[NASA-TT-20150] 13 p1752 N88-20480
The SPOT solar array. Box opening mechanisms physical vapor deposition (PVD)-MoS2: Lubricated slides. Functional evaluation 14 p1876 N88-21211
The effects of Hertzian stress and test ambient on the friction coefficient of MsS2 coatings
[DE88-008118] 20 p2777 N88-26467
The lubricating properties of magnetron sputtered MoS2
[ESA-ESTL-76] 24 p3381 N88-30136

MOLYBDENUM OXIDES
The tribological properties of MoS2 coatings in vacuum, low relative humidity and high relative humidity environments
[DE88-001611] 06 p0711 N88-14356

MOLYBDENUM SULFIDES
NT MOLYBDENUM DISULFIDES
The tribological properties of MoS2 coatings in vacuum, low relative humidity and high relative humidity environments
[DE88-001611] 06 p0711 N88-14356
Electron tunneling microscopy
[AD-A187426] 11 p1452 N88-18852

Schottky-barrier formation on a covalent semiconductor without Fermi-level pinning: The Metal-MoS2(0001) interface
[AD-A193044] 21 p3021 N88-27931

MOMENT DISTRIBUTION

An introduction to single point closure methodology
08 p0986 N88-15973

MOMENTS

NT BENDING MOMENTS
NT DIPOLE MOMENTS
NT DISTRIBUTION MOMENTS
NT ELECTRIC MOMENTS
NT LOADING MOMENTS
NT MAGNETIC MOMENTS
NT MEAN
NT MOMENTS OF INERTIA
NT ORTHOGONALITY
NT PITCHING MOMENTS
NT ROLLING MOMENTS
NT STABILITY DERIVATIVES
NT STANDARD DEVIATION
NT TORQUE
NT YAWING MOMENTS

Semiempirical method for prediction of aerodynamic forces and moments on a steadily spinning light airplane
[NASA-TM-4009] 04 p0393 N88-12456

Measurement of forces and moments on, and velocity about a body of revolution with an attached fin at angles of attack
[AD-A187796] 11 p1433 N88-18554

Regional wave attenuation and seismic moment from the inversion of NORESS spectra
[AD-A187399] 11 p1510 N88-19023

Joint moments of the maximum in a critical branching process
[AD-A188157] 11 p1541 N88-19209

A moment approach to modeling negative ion sources
[AD-A188858] 12 p1691 N88-20114

Application of Moment Iteration Method (MIM) to electromagnetic field computation
[PB88-194139] 20 p2789 N88-26546

Moment invariants for particle beams
[DE88-011052] 23 p3281 N88-29537

MOMENTS OF INERTIA

What is the maximum length of a spin stabilized projectile
[PB88-130919] 13 p1728 N88-20336

A new method for the estimation of aircraft inertia characteristics 20 p2787 N88-26530

MOMENTUM

NT ANGULAR MOMENTUM

Predictive momentum management for a space station measurement and computation requirements
[NASA-CR-172026] 02 p0138 N88-10866

Efficient numerical techniques for complex fluid flows
02 p0185 N88-11151

Momentum transport and particle dynamics in turbulent shear flows 03 p0317 N88-12002

Lagrangian procedures for higher order field equations
[DE87-703365] 05 p0640 N88-13911

Theory of neutron scattering experiments on momentum distributions in quantum fluids
[DE87-01369] 05 p0648 N88-13968

The pressure drag and momentum flux during a cold frontal passage over the Alps 13 p1800 N88-20763

Energy and momentum fluxes through the sea surface
13 p1806 N88-20798

Large momentum pairing in one-dimensional systems
[AD-A189228] 13 p1835 N88-20981

Inflation in Einstein-Cartan theory with energy-momentum tensor with spin
[NASA-TM-101164] 17 p2447 N88-24547

Symmetry problem of energy-momentum tensor and the creation of gravitational field
[DE88-702442] 21 p3026 N88-27964

MOMENTUM ENERGY

U KINETIC ENERGY

MOMENTUM THEORY

Parametric dependence in the equilibrium dynamics of rotating structures
[AD-A187817] 11 p1498 N88-18945

MOMENTUM TRANSFER

Variable collision frequency effects on hose and sausage instabilities in relativistic electron beams
[AD-A184206] 04 p0490 N88-13021

Spin-up and spin-down on the way to the main sequence 04 p0518 N88-13181

Statistical theory of turbulent incompressible multimaterial flow
[DE88-000435] 05 p0579 N88-13535

Approximate solutions for the momentum transport in turbulent flows in narrow rod array bundles using the finite element method
[ETN-88-90810] 06 p0701 N88-14306

The effect of eddy distribution on momentum and heat transfer near the wall in turbulent pipe flow
[NASA-TM-100257] 08 p0988 N88-15984

Design issues for a laboratory high gain fusion facility
[DE88-004406] 10 p1413 N88-18434

Studies in finite time thermodynamics
[DE88-004531] 10 p1423 N88-18500

On (p,n) systematics and the cosmological connection
[DE88-005031] 12 p1712 N88-20245

Turbulent transfer of momentum and heat in boundary layer of fluid beyond an obstacle. 1: Hydrodynamic characteristics 13 p1787 N88-20690

On the zonal momentum balance at the equator
13 p1805 N88-20788

Energy and momentum fluxes through the sea surface
13 p1806 N88-20798

Fragmentation and flow in central collisions
[DE88-005386] 13 p1837 N88-20991

Continuum theories for fluid-particle flows: Some aspects of lift forces and turbulence
[DE88-007038] 18 p2511 N88-24898

Comparison of exclusive reactions at large momentum transfer
[DE88-007544] 20 p2851 N88-26922

Modeling of momentum transport of axially parallel turbulent flows in rod cascades
[ETN-88-92978] 23 p3214 N88-29131

Development of a more general Reynolds stress closure for swirling flow
[AD-A195121] 24 p3374 N88-30092

MONATOMIC GASES

Mechanisms of polymer degradation using an oxygen plasma generator
[NASA-TM-100681] 01 p0018 N88-10110

Atomic oxygen effects on metals
07 p0924 N88-15617

Atomic and molecular gas phase spectrometry
[AD-A187562] 11 p1452 N88-18655

Solar generation and storage of O2 (a 1 delta g)
[NASA-CR-4127] 14 p1913 N88-21431

Total photoionization cross sections of atomic oxygen from threshold to 44.3A
[NASA-CR-182992] 17 p2397 N88-24252

Design and demonstration of a system for the deposition of atomic-oxygen durable coatings for reflective solar dynamic power system concentrators
[NASA-CR-4158] 19 p2606 N88-25474

Breakdown of molecular oxygen by brief pulses of laser radiation
[DE88-702687] 23 p3220 N88-29168

Theoretical investigation of image states of the hydrogen covered Cu (100)
[DE88-702662] 23 p3292 N88-29604

MONATOMIC MOLECULES

Breakdown of molecular oxygen by brief pulses of laser radiation
[DE88-702687] 23 p3220 N88-29168

MONITORS

Rapid toxicity detection in water quality control utilizing automated multispecies biomonitoring for permanent space stations 02 p0135 N88-10848

Development of an acoustic emission monitor and monitoring techniques for long-term monitoring of U-0.8Ti electron-beam weldments for postweld cracking
[DE88-000819] 04 p0453 N88-12804

An interactive computer graphics network monitor for a tactical communications network
[AD-A184131] 04 p0477 N88-12938

Plant Growth Module (PGM) conceptual design
05 p0631 N88-13855

Monitoring corrosion and process physical-chemical parameters in electric power plants
[CISE-3708] 06 p0682 N88-14182

Welding monitoring system
[NASA-CASE-MFS-29177-1] 06 p0712 N88-14362

Online monitoring of laserpulses using the GPIB-interface of a Tektronix 2430 Digital Storage Oscilloscope
[DE88-002836] 07 p0856 N88-15201

On line instrument systems for monitoring steam turbogenerators
[CISE-3860] 08 p0990 N88-15995

Monitoring of space station life support systems with miniature mass spectrometry and artificial intelligence
08 p1057 N88-16376

Knowledge-based monitoring of the pointing control system on the Hubble space telescope
08 p1057 N88-16378

A distributed architecture for intelligent monitoring and anomaly diagnosis of the Hubble Space Telescope
08 p1057 N88-16379

A knowledge-based system for monitoring the electrical power system of the Hubble Space Telescope
08 p1058 N88-16380

Qualitative and temporal reasoning in engine behavior analysis 08 p1058 N88-16383

A multiprocessing architecture for real-time monitoring
08 p1059 N88-16390

Space shuttle main engine anomaly data and inductive knowledge based systems: Automated corporate expertise 08 p1060 N88-16398

Space shuttle onboard navigation console expert/trainer system 09 p1203 N88-17208

Knowledge based jet engine diagnostics
09 p1203 N88-17210

Pattern-recognition software detecting the onset of failures in complex systems
[DE88-002861] 09 p1220 N88-17318

Results of long-term electrocardiographic monitoring of cosmonauts 10 p1364 N88-18152

Acoustic wave electroless deposition monitor
[DE88-004023] 11 p1489 N88-18887

Calibration of beam power monitors for laser welding
[DE88-004687] 11 p1492 N88-18906

Real-time environmental Arctic monitoring (R-TEAM)
[AD-A189948] 15 p2099 N88-22508

DATAC bus monitor 17 p2294 N88-23721

Television monitor field shifter and an opto-electronic method for obtaining a stereo image of optimal depth resolution and reduced depth distrotion on a single screen
[NASA-CASE-NPO-17249-1-CU]
17 p2332 N88-23924

TES: A modular systems approach to expert system development for real-time space applications
17 p2388 N88-24197

Airplane runway performance monitoring system
[NASA-CASE-LAR-13854-1-CU]
18 p2462 N88-24621

Aircraft emissions characterization: TF41-A2, TF30-P103 and TF30-P109 engines
[AD-A192053] 18 p2466 N88-24638

Automated test device for FASR (Fixed Array Surveillance Radar) beam steering componentry
[AD-A191650] 18 p2500 N88-24829

Radio Frequency (RF) strain monitor
[NASA-CASE-LAR-13705-1] 18 p2530 N88-25011

Monitoring of divers/astronauts during missions
19 p2698 N88-26036

Performance evaluation for multiprocessors programmed using monitors
[DE88-010056] 19 p2718 N88-26138

Low cost corrosion sensors 22 p3054 N88-28123

MONKEYS

Microwave challenges to the thermoregulatory system
[AD-A185391] 05 p0629 N88-13847

Effect of spaceflight factors on primate's blood circulation 10 p1359 N88-18124

Inflight simian circadian rhythms and temperature homeostasis aboard Cosmos-1514 biosatellite
10 p1359 N88-18125

Effect of spaceflight factors on primate hydration homeostasis 10 p1360 N88-18126

Motor control in man and monkey
11 p1518 N88-19065

Life sciences research in space: The requirement for animal models 12 p1654 N88-19909

Biological patterns of growth in postnatal ontogenesis of lower primates 19 p2705 N88-26087

Evoked potential analysis of impact acceleration experiments 21 p2981 N88-27708

MONOCHROMATIC RADIATION

Effect of clarifying the atmosphere in relation to quasi-monochromatic CO2 laser radiation
06 p0709 N88-14348

Energy transmission using coherent, quasimonochromatic light beams
09 p1241 N88-17436

Comparison of Halley's monochromatic comae with others 14 p2006 N88-21965

Diffraction imaging (topography) with monochromatic synchrotron radiation
[NASA-CR-183264] 24 p3433 N88-30431

Streaking images that appear only in the plane of diffraction in undoped GaAs single crystals: Diffraction imaging (topography) by monochromatic synchrotron radiation
[NASA-CR-183267] 24 p3433 N88-30437

MONOCHROMATORS

Multilayer monochromators for neutron spectrometers
[DE87-014291] 02 p0175 N88-11093

Use of spherical optics in high resolution soft X-ray grating monochromators
[PB87-125191] 06 p0780 N88-14788

Investigation of the performance of a novel double crystal X-ray monochromator measurements
[PB87-125167] 06 p0788 N88-14834

Thermal stress analysis of a cooled monochromator crystal
[DE88-002116] 07 p0937 N88-15696

Application of a simple rotational spherical grating mounting to high resolution soft X-ray spectroscopy
[PB87-164836] 09 p1142 N88-16845
Characteristics of an Ebert monochromator for an infrared spectrometer in the wavelength range 1 micrometer to 15 micrometers
[AD-A186945] 09 p1166 N88-16991
UHV (Ultra-High Vacuum) double crystal monochromator design
[DE88-003904] 11 p1456 N88-18676
Multilayer-coated mirrors as power filters in synchrotron radiation beamlines
[DE88-003872] 11 p1550 N88-19276
A new class of multiple dispersion grating spectrometers
[PREPRINT-569] 14 p1983 N88-21630
Intensity calibration of a VUV system by branching line pairs 17 p2443 N88-24533
Instrumentation for turbulent reacting flows
[AD-A191671] 18 p2515 N88-24923
The detection and interpretation of long-term changes in ozone from space
[NASA-TM-101135] 21 p2971 N88-27650

MONOCRYSTALS
U SINGLE CRYSTALS

MONOCULAR VISION
Biorhythms of binocular vision
20 p2830 N88-26788
A new approach to machine-based perception of monocular images
[DE88-002418] 20 p2853 N88-26942

MONOLITHIC CIRCUITS
U INTEGRATED CIRCUITS

MONOMERS
Ion-matrix coupling in polymer electrolytes from relaxation time studies
[AD-A184632] 03 p0293 N88-11841
The mechanism of stereo regulation during anionic polymerization of polar monomers
[AD-A186530] 08 p0973 N88-15888
Pressure induced ageing of polymers
14 p1929 N88-21504
Synthesis and characterization of new phosphazene polymers
[AD-A191508] 18 p2490 N88-24771
Substituted 1,1,1-Triaryl-2,2,2-Trifluoroethanes and processes for their synthesis
[NASA-CASE-LEW-14345-1] 20 p2767 N88-26404
Synthesis of model polymers and related structures in support of vinyl monomer grafting studies
[DE88-010245] 20 p2778 N88-26476
Charge storage and switching phenomena in metal complexes
[AD-A193778] 23 p3192 N88-28996
Polymerization of azaethylenes (imines) and aza-1,3-dienes: Potential reactive monomers
[AD-A194717] 23 p3197 N88-29028

MONOMOLECULAR FILMS
Ceramics thin film 04 p0403 N88-12505
Methods of measurement for the evaluation of monolayer properties. Development and applications --- lung surfactants
[ETN-88-92229] 15 p2104 N88-22532

MONOPLANES
NT B-57 AIRCRAFT
NT B-70 AIRCRAFT
NT BOEING 737 AIRCRAFT
NT C-130 AIRCRAFT
NT C-135 AIRCRAFT
NT DO-28 AIRCRAFT
NT F-4 AIRCRAFT
NT F-27 AIRCRAFT
NT F-106 AIRCRAFT
NT MIRAGE AIRCRAFT
NT OV-1 AIRCRAFT
NT P-3 AIRCRAFT
NT RF-4 AIRCRAFT
NT T-33 AIRCRAFT
NT U-2 AIRCRAFT
NT VC-10 AIRCRAFT

MONOPOLE ANTENNAS
Land mobile satellite propagation results
19 p2645 N88-25698
An adaptive array antenna for mobile satellite communications 19 p2647 N88-25710
Evaluation of vertical monopole antennas with elevated radials
[DE88-008339] 19 p2654 N88-25760
Performance study of a unipole antenna with conventional and elevated radial wire ground screens
[AD-A193283] 21 p2933 N88-27413

MONOPOLES
Electronics for the External Muon Detector (EMD) of ICARUS
[NOTA-INTERNA-880] 07 p0847 N88-15143

MONOPROPELLANTS
The numerical simulation of an idealised one-dimensional, steady monopropellant rocket
[PDR/CFDU/IC/31] 01 p0018 N88-10107
Orbital Spacecraft Consumables Resupply System (OSCRS): Monopropellant application to space station and OMV automatic refueling impacts of an ELV launch, volume 4
[NASA-CR-172029] 03 p0276 N88-11741
Droplet formation for liquid monopropellant jets
[AD-A187172] 10 p1331 N88-17956
Electrical ignition of HAN-based liquid propellants
[AD-A191349] 18 p2495 N88-24801
The combustion of hydroxylammonium nitrate based liquid propellants 19 p2622 N88-25555
Droplet formation for liquid monopropellant jets
19 p2623 N88-25557
Mixing and thermodynamic critical phenomena of combusting monopropellant sprays
19 p2623 N88-25558

MONOPULSE RADAR
Track performance considerations for monopulse radars
[AD-A196232] 24 p3360 N88-30007

MONOSACCHARIDES
NT GLUCOSE

MONOTECTIC ALLOYS
Cellular solidification in a monotectic system
[NASA-TM-100317] 07 p0829 N88-15027
Transparent metal model study of the use of a cellular growth front to form aligned monotectic composite materials
[NASA-CR-182414] 08 p0969 N88-15861
A study of surface tension driven segregation in monotectic alloy systems
[NASA-CR-182894] 16 p2178 N88-22983

MONOTONE FUNCTIONS
Software reliability models for fault-tolerant avionics computers and related topics
[NASA-CR-181440] 02 p0220 N88-11382
Efficient monotone sequential design
[CWI-MS-R8705] 14 p1962 N88-21707
Periodic solutions of perturbed superquadratic Hamiltonian systems
[AD-A194292] 23 p3270 N88-29457
Monotone recurrence relations, their Birkhoff orbits and topological entropy
[AD-A193481] 23 p3276 N88-29504

MONSOONS
Observational analysis of the interaction between fronts and the orography in Taiwan during the late winter monsoon season 02 p0203 N88-11270
The mesoscale numerical model for heavy rainfall forecasting in Yangtze River Valley, China
02 p0211 N88-11326
Interactions between the Asian monsoons, the tropical Pacific and the southern hemisphere extratropics
04 p0470 N88-12907
The structure and dynamics of monsoon depressions
10 p1355 N88-18102
Study of passages of cross-equatorial current during southern monsoon 14 p1900 N88-21347
Tropical and monsoonal studies
[AD-A188387] 14 p1947 N88-21611
Indian monsoon rainfall, 1986-1987
22 p3120 N88-28536
Differences in radiation budget parameters over Asia in relation to contrasting Indian monsoons
22 p3125 N88-28574
On climate prediction for India
22 p3127 N88-28590

MONTE CARLO METHOD
The importance sampling and its application to radar simulation 01 p0012 N88-10065
Feature selection applied to radar target identification
[AD-A183880] 01 p0034 N88-10215
Monte Carlo calculations for the simulation of channeling experiments on irradiated aluminum alloys. Calculation of angle-dependent efficiency curves
[HMI-B-433] 01 p0092 N88-10597
A microstructural lattice model for strain oriented problems: A combined Monte Carlo finite element technique
[NASA-TM-100215] 02 p0150 N88-10939
A relativistic Monte Carlo binary collision model for use in plasma particle simulation codes
[DE87-013287] 02 p0237 N88-11494
Two dimensional neutral transport analysis in tokamak plasma
[DE87-752984] 02 p0239 N88-11510
Solute segregation to phase interfaces and grain boundaries: Studies by analytical electron microscopy and profile deconvolution
[DE87-012129] 02 p0243 N88-11537
Wake shield 03 p0298 N88-11871
Monte Carlo simulation of modulated phases
[NASA-TM-89654] 03 p0369 N88-12323
A computational examination of orthogonal distance regression
[AD-A184374] 03 p0371 N88-12337
Development and evaluation of a Monte Carlo code system for analysis of ionization chamber responses
[AD-A183970] 03 p0375 N88-12359
Monte Carlo simulation of primitive atom-transfer reactions in solution
[AD-A183977] 03 p0375 N88-12360
Gravitational accretion of hot dark matter
03 p0388 N88-12439
Creep life prediction based on stochastic model of microstructurally short crack growth
[NASA-TM-100245] 04 p0456 N88-12825
Final (n,l) state-resolved electron capture by multiply charged ions from neutral atoms
[IPPJ-AM-54] 04 p0492 N88-13030
Monte Carlo analysis of neoclassical transport for a compact helical system
[IPPJ-850] 04 p0492 N88-13033
The statistics of the shape of small fatigue cracks
05 p0599 N88-13666
Fatigue under nonnormal random stresses using Monte Carlo method 05 p0607 N88-13723
Approximating multivariate normal orthant probabilities using the Clark algorithm
[AD-A184855] 05 p0634 N88-13873
Monte Carlo modeling and meteor showers
06 p0740 N88-14549
The adaption and use of research codes for performance assessment
[DE88-000552] 06 p0756 N88-14639
Some investigations of molecular beam epitaxial growth of 3-5 semiconductor films via Monte-Carlo computer simulations, carrier tunnelling and spectroscopic ellipsometry
[AD-A185520] 06 p0789 N88-14839
Estimating system reliability: Monte Carlo methods, sensitivity and errors in input parameters
[AD-A186182] 07 p0865 N88-15248
Discrete reliability growth models using failure discounting
[AD-A186380] 07 p0866 N88-15252
Monte Carlo photon transport on vector and parallel supercomputers
[DE88-002503] 07 p0905 N88-15486
Monte Carlo simulation of triangulated random surfaces grand canonical ensemble
[DE88-700378] 07 p0941 N88-15718
Frequency response functions of a nonlinear system
09 p1180 N88-17070
Three dimensional Monte Carlo simulation of molecular movement and heat radiation in vacuum devices: Computer code MOVAK3D --- fusion reactors
[KFK-4292] 09 p1246 N88-17471
Plasma theory and simulation
[AD-A187100] 09 p1249 N88-17486
Two-dimensional analysis for a scrapeoff and divertor regions with an MHD model. Conceptual design study of FY86 FER
[DE88-751069] 09 p1251 N88-17497
Unidimensional Rasch model and multidimensional data: An analytic approach
[PB88-105861] 10 p1372 N88-18187
The hybrid Monte Carlo Algorithm and the chiral transition
[DE88-004305] 10 p1399 N88-18341
An analytic model for ionization distributions produced in nanometer sites by protons
[DE88-003943] 10 p1406 N88-18385
Algorithmic alternatives
[DE88-003905] 11 p1531 N88-19149
Robustness in cost performance models
[AD-A187183] 11 p1566 N88-19374
Analysis of simulated annealing type algorithms
[AD-A189382] 12 p1679 N88-20037
Estimating system and component reliabilities under partial information on cause of failure
[AD-A189107] 13 p1780 N88-20653
Performance and cost benefits associated with nonimaging secondary concentrators used in point-focus dish solar thermal applications
[DE88-001104] 13 p1792 N88-20718
Biophysical applications of solid state and tritium NMR
[DE88-005328] 13 p1808 N88-20806
The physical structure of concurrent problems and concurrent computers
[DE88-005812] 13 p1814 N88-20835
A simulation study of a parallel processor with unbalanced loads
[AD-A189573] 13 p1822 N88-20887

Quantum Monte Carlo study of the MIES associated with H2 (X 1 sigma sub g (+)) and H2 (B 1 sigma sub u (+))
[AD-A189063] 13 p1835 N88-20977
Modeling and transport in semiconductor devices
[AD-A188760] 13 p1844 N88-21037
Monte Carlo modified method for Green function. Algorithm and computer code for calculations in equal mass many-body system
[DE88-701114] 14 p1957 N88-21667
Monte Carlo reliability analysis
[AD-A189972] 15 p2074 N88-22366
Quantum Monte Carlo study of the MIES associated with H2(X 1 sigma g +) and H2(B 1 sigma u +)
16 p2268 N88-23564
Computational quantum field theory
[DE88-700918] 16 p2284 N88-23672
Monte Carlo analysis of lateral collection diode arrays
[RSRE-MEMO-4080] 17 p2335 N88-23938
Multiple scattering of waves in discrete random media
[AD-A191068] 18 p2499 N88-24823
Sensitivity analysis for the system reliability function
[AD-A191648] 18 p2525 N88-24979
The development of KENO and the calculation of differential parameters with KENO
[DE88-006176] 18 p2555 N88-25166
A fast and efficient procedure for generalized cross-validation with large data sets. Application to image reconstruction
[RR-669-M] 18 p2563 N88-25220
Introduction to lattice gauge theory
[DE88-006073] 18 p2584 N88-25349
Non-stationary transport in MODFET's and heterojunction devices 19 p2659 N88-25804
Monte Carlo investigation of hot photoexcited electron relaxation in GaAs 19 p2659 N88-25805
Statistical mechanics of polymer systems
[DE88-011172] 20 p2778 N88-26477
Theoretical studies in elementary particle physics
[DE88-006929] 20 p2851 N88-26926
Monte Carlo simulations of femtosecond relaxation of photoexcited electrons in AlGaAs/GaAs quantum wells
20 p2869 N88-27036
Hot electrons in silicon dioxide: Ballistic to steady-state transport 20 p2871 N88-27042
Recent applications of Monte Carlo methods for semiconductor microdevice simulation
20 p2871 N88-27046
Atomistic simulation of stability, metastability and growth of strained layer structures 20 p2873 N88-27053
Sampling strategies for Monte-Carlo forecasting methods 22 p3126 N88-28583
Importance sampling for stochastic simulations
[AD-A193585] 22 p3138 N88-28654
Progress on a Monte Carlo shuttle contamination model
[AD-A193694] 23 p3183 N88-28945
Variation in the thickness of ejecta cover on Mars with increasing crater density 23 p3307 N88-29701
Monte-Carlo estimation of the influence of plant architecture parameters on spectral brightness
24 p3450 N88-30533

MOODS

Computer response time measurements of mood, fatigue and symptom scale items: Implications for scale response time uses
[AD-A186093] 07 p0888 N88-15384

MOON

Computing basic solar and lunar data from the Air Almanac
[AD-A190777] 16 p2290 N88-23710
A basis of settlement: Economic foundations of permanent pioneer communities
[DE88-010907] 20 p2762 N88-26382
Steps toward lunar settlement
[DE88-009141] 21 p2900 N88-27213

MOORING

SEQUAL (seasonal Equatorial Atlantic) meteorological data from Moorings S2, S5 and S6 (March 1983 - March 1985)
[PB88-108048] 07 p0880 N88-15337
Moored current meter data from the Canary Basin near 32 deg N, 24 W (84-1986), volume 40
[PB88-108105] 07 p0882 N88-15351
Real-time environmental Arctic monitoring (R-TEAM)
[AD-A189948] 15 p2099 N88-22508
An FSK (Frequency Shift Keying) telemetry module for vector measuring current meters
[AD-A192142] 18 p2470 N88-24661

MOORINGS

U MOORING

MORAINES

U GLACIAL DRIFT

MORALE

A comparison of the effects of group dynamics on individuals assigned to integral and non-integral aircrews
[AD-A186467] 08 p1051 N88-16345

MORL

U MANNED ORBITAL LABORATORIES

MORPHINE

Protection from stress 12 p1664 N88-19978

MORPHOLOGY

NT GEOMORPHOLOGY
NT ISOMORPHISM
NT LUNG MORPHOLOGY
Experimental assembly of structures in EVA: Hardware morphology and development issues
02 p0139 N88-10872
Magnetic field morphology in the upper layers
02 p0255 N88-11610
Morphology of the Earth's environment
03 p0272 N88-11706
Factors determining the morphology of precipitation in aluminum-germanium and aluminum-silicon alloys
[DE87-014682] 03 p0287 N88-11806
Cure and properties of thermosetting polymers
[AD-A184669] 03 p0293 N88-11843
Wittig synthesis of conductive segmented block polymer compositions
[AD-A184018] 03 p0295 N88-11850
Corrosion behavior of P/M mechanically alloyed IN-9052.1: An electro-chemical investigation
[AD-A184191] 04 p0414 N88-12567
Steady shearing in a viscoplastic solid
[AD-A184341] 04 p0454 N88-12810
Banded ion morphology 04 p0468 N88-12892
Study of certain biological characteristics of bacteria during the French-Soviet CYTOS-2 space experiment
04 p0473 N88-12917
Molecular and supramolecular orientation in conducting polymers
[DE88-000533] 05 p0569 N88-13472
The effect of alpha platelet morphology and beta-grain size on the initiation and growth of short fatigue cracks in Ti6SS 05 p0600 N88-13667
Characterization of the microstructures of various materials
[AD-A184961] 05 p0655 N88-14017
Comparative anatomic analysis of seedling organs of pisum sativum (fabaceae) cultivated under space flight conditions 06 p0749 N88-14603
High spatial resolution observations of dust and gas in NGC 7027 and the M8 Hourglass
06 p0801 N88-14903
Study on substructures of martensite in steels containing rare earth metals
[PB87-143996] 07 p0833 N88-15050
Experiments with rats flown aboard Cosmbs-1667 biosatellite (main objectives, conditions and results)
07 p0893 N88-15414
Brain morphogenesis in rats developing in weightlessness 07 p0894 N88-15415
Morphometric analysis of rat aorta endothelium during long-term hypokinesia 07 p0894 N88-15417
Examination of the physical processes associated with the keyhole region of variable polarity plasma arc welds in aluminum alloy 2219 07 p0927 N88-15634
The morphology of emulsion polymerized latex particles
[DE88-002672] 08 p0972 N88-15879
A new technique for rocket and space-borne investigations of time-dependant auroral morphology
08 p1030 N88-16241
Morphology control and reinforcing mechanisms using an elastomer in an epoxy network based on diamine menthane
[ISAL-IDI1-87-09] 09 p1148 N88-16881
Bias, internal stress and substrate effects on the microstructure and properties of PVD-wear resistant coatings
[AERE-R-12360] 10 p1304 N88-17798
New scientific findings on the morphology of aluminum oxide layers, serving as an adhesive basis
[MBB-Z-137/86] 10 p1312 N88-17840
Collaborative studies of polar cap ionospheric dynamics
[AD-A187888] 10 p1355 N88-18098
Histomorphometric analysis of rat bones after spaceflight aboard Cosmos-1667 biosatellite
10 p1360 N88-18128
JPRS Report: Science and Technology. USSR: Space Biology and Aerospace Medicine, volume 21, no. 6, November - December 1987
[JPRS-USB-88-004] 10 p1364 N88-18150
Morphological and functional state of the hypothalamo-hypophyseal neurosecretory system of rats flown aboard Cosmos-1667 10 p1365 N88-18156
Investigation of rat skeletal muscles following short-term spaceflight aboard Cosmos-1667 biosatellite
10 p1365 N88-18157
Morphological study of early changes in rat bones in simulated weightlessness 10 p1365 N88-18158
Morphological manifestations of primate adaptation to orthograde statics and walking erect
10 p1366 N88-18162
Local stoichiometry and atomic interdiffusion during reactive metal/mercury-cadmium-telluride junction formation
[AD-A187554] 10 p1421 N88-18488
Synthesis and structure property studies of toughened epoxy resins via functionalized polysiloxanes
[AD-A187984] 11 p1462 N88-18715
A unified approach for digital image processing problems: Mathematical morphology
[INPE-4311-TDL/278] 11 p1537 N88-19183
Electron microscopy study of morphology and composition of a ferrisilicate catalyst
[DE88-005754] 11 p1562 N88-19352
Elevated temperature crack growth studies of advanced titanium aluminides
[AD-A189025] 12 p1608 N88-19618
Morphological studies of conductive polymers
[AD-A188456] 12 p1610 N88-19629
Applications of mathematical morphology to range imagery
[AD-A189316] 12 p1684 N88-20072
Dependence of hydrogen embrittlement of austenitic stainless steels on structural state of grain boundaries
14 p1896 N88-21316
Dust coma morphology of Comet Halley during the Giotto encounter 14 p2000 N88-21921
Reconstruction of the orientation and shape of the nucleus of Comet Halley 14 p2004 N88-21949
Laser enhanced adhesion of copper films to sapphire substrates
[DE88-006802] 15 p2038 N88-22144
Fracture morphologies of carbon-black-loaded SBR (Styrene-Butadiene Rubber) subjected to low-cycle, high-stress fatigue
[DE88-006808] 16 p2181 N88-23002
Mathematical morphology: An algebraic approach
[CWI-AM-R8707] 16 p2258 N88-23497
Study of fracturing for groundwater research in the Sergipe state with remote sensing products
17 p2359 N88-24052
Dune fields in central Western Argentina
17 p2366 N88-24058
Molecular gas in Virgo cluster spiral galaxies
17 p2450 N88-24557
Dynamic consolidation of metal powders
[AD-A192126] 18 p2485 N88-24744
Mathematical morphology for structures without translation symmetry
[CWI-AM-R8803] 18 p2566 N88-25241
NASA research Program: The roles of fluid motion and other transport phenomena in the morphology of materials
[NASA-CR-182801] 18 p2580 N88-25327
The morphological stability of continuous intergranular phases: Thermodynamic considerations
[DE88-006328] 18 p2584 N88-25350
The Io sulfur torus in 1981
[NASA-TM-101139] 18 p2595 N88-25419
Method for measuring absolute linear parameters of chromosomes 19 p2707 N88-26095
Damping characteristics of metal matrix composites
[AD-A193144] 21 p2904 N88-27233
Rubber-modified epoxies: Interfacial tension and morphology
[AD-A192464] 21 p2917 N88-27313
Plasma treatment of polymers for improved adhesion
[DE88-011623] 21 p2921 N88-27334
Analysis of remotely sensed imagery using digital morphology
[AD-A192738] 21 p2965 N88-27614
Mechanics of thrust fault formation
23 p3231 N88-29229
Mars: Near-infrared comparative spectroscopy during the 1986 opposition 23 p3301 N88-29658
Sub-kilometer rampart craters in the equatorial region of Mars: Possible implications for the state and distribution of regolith H2O 23 p3302 N88-29666
Small Martian volcanoes 23 p3302 N88-29668
Distribution and timing of thick transient air-fall deposits in Electris: Implications for the nature of the upland plains 23 p3303 N88-29674
Lava flow-field morphology: A case study from Mount Etna, Sicily 23 p3303 N88-29676
Constraints on the origin of fractured terrane, Northern Martian plains 23 p3304 N88-29684
Volcano evolution on Mars 23 p3305 N88-29686
Origin of northern lowland plains: Constraints from boundary morphology 23 p3305 N88-29687

Ridged and gullied terrains in the Martian uplands
23 p3307 N88-29700
Morphological changes in polymer electrolyte cells
[AD-A195821] 24 p3368 N88-30054
Volcanic styles at Alba Patera, Mars: Implications of lava flow morphology to the volcanic history
24 p3444 N88-30497
MORPHOTROPISM
U ISOMORPHISM
MOS (JAPANESE SPACECRAFT)
U JAPANESE SPACECRAFT
MOS (SEMICONDUCTORS)
U METAL OXIDE SEMICONDUCTORS
MOSAICS
Implementation of nonsquare tilings on an image processing system
[FOA-C-30487-3.3] 22 p3140 N88-28669
MOSFET
U FIELD EFFECT TRANSISTORS
MOSS (SPACE STATIONS)
U SPACE STATIONS
MOSSBAUER EFFECT
Temperature hysteresis and magnetic transitions in amorphous Fe-Ni-Zr alloys
[DE88-000228] 03 p0294 N88-11848
The Moessbauer effect of SnI4 at high pressure
[DE87-014771] 04 p0495 N88-13048
Moessbauer study of shock induced effects in the Fe-Ni 50/50 ordered alloy in meteorites
[DE87-703364] 04 p0521 N88-13199
SDIO/IST ultrashort wavelength laser: Novel experimental schemes for observing the Mossbauer effect in long-lived nuclear levels
[AD-A190275] 15 p2072 N88-22351
SDIO/IST ultrashort wavelength laser. Mossbauer effect in gamma-ray lasers
[AD-A190306] 15 p2072 N88-22352
A sup 57 Fe Mossbauer study of the superconductor YBa sub 2 (Fe sub x Cu sub 1-x) sub 3 O sub y
[DE88-701543] 16 p2282 N88-23661
A scientific basis for an alternate cathode architecture
[AD-A191498] 18 p2481 N88-24717
Influence of alternating magnetic fields on Zn-67 Moessbauer resonance in ZnO
[PB88-186432] 18 p2584 N88-25352
Structural and magnetic properties of Fe impurities in YBa2Cu3O(sub 7-delta)
[DE88-009961] 19 p2735 N88-26247
Phase modulation of recoilless gamma radiation in Mossbauer spectroscopy
[ETN-88-92648] 24 p3428 N88-30403
MOSSES
U BRYOPHYTES
MOTILITY
U LOCOMOTION
MOTION
Effect of motion cues during complex curved approach and landing tasks: A piloted simulation study
[NASA-TP-2773] 04 p0398 N88-12480
Computing 3-D structure of rigid objects using stereo and motion 08 p1061 N88-16407
Motion planning for legged locomotion systems on uneven terrain 23 p3221 N88-29170
Motion planning with obstacles and dynamic constraints 23 p3222 N88-29175
Passive damping concepts for free and forced member and grillage vibration
[NASA-CR-183114] 23 p3225 N88-29196
Optimization-driven machine-oriented motion measurement 23 p3245 N88-29312
MOTION EQUATIONS
U EQUATIONS OF MOTION
MOTION PERCEPTION
Television motion measurement for DATV and other applications
[BBC-RD-1987/11] 05 p0573 N88-13496
Massively parallel implementations of theories for apparent motion
[AD-A185841] 07 p0901 N88-15455
Perception and control of simulated self motion
[AD-A187444] 10 p1372 N88-18188
A method to detect and digitize small plant movements 12 p1654 N88-19912
Computerised measurement of human horizontal smooth pursuit eye movements
13 p1811 N88-20819
Masking of motion cues by random motion: Comparison of human performance with a signal detection model
[UTIAS-313] 14 p1953 N88-21639
Designing for design effectiveness of complex avionics systems 17 p2305 N88-23788
Visual information processing in the perception of features and objects
[AD-A192026] 18 p2552 N88-25148
Image pyramid motion detection applied to sea ice
20 p2817 N88-26713
Influence of moving visual environment on saccadic eye movements and fixation 21 p2926 N88-27368
Perception of motion in statistically-defined displays
[AD-A193076] 21 p2991 N88-27745
Models for motion perception
22 p3133 N88-28629
Determining vehicle motion from stereo image sequences
[AD-A194371] 23 p3216 N88-29140
Visual motion perception and visual attentive processes
[AD-A193640] 23 p3241 N88-29288
Dynamical systems and motion vision
[AD-A195932] 24 p3422 N88-30366
MOTION PICTURES
Cineradiography
[DE87-013158] 03 p0324 N88-12045
Model-based motion estimation and its application to restoration and interpolation of motion pictures
[AD-A185054] 05 p0584 N88-13558
MOTION SICKNESS
Motion and space sickness 04 p0404 N88-12510
Change in functional activity of cortical brain structures and their blood supply in alert rabbits in response to rocking 04 p0473 N88-12916
Long-term adaptation of the otolith organs
07 p0886 N88-15375
Development of methods for the study of space motion sickness 07 p0892 N88-15408
Discrete adaptation to sensory conflict
10 p1363 N88-18146
Summary of Payload Integration Plan (PIP) for Starlab-1 flight experiment, enclosure 3
[NASA-TM-89713] 11 p1522 N88-19086
Gastric emptying assessment by echography after a stress (rotating chair) 12 p1661 N88-19955
Studies of the vestibulo-ocular reflex on STS 4, 5 and 6
[NASA-TM-100461] 12 p1666 N88-19987
Motion sickness: A study of its effects on human physiology
[AD-A188821] 12 p1667 N88-19995
An analysis of physiological data related to motion sickness for use in a real-time motion sickness indicator
[AD-A189589] 13 p1810 N88-20812
Motion sickness: Quantitative, algorithmic malaise indication in real time
[AD-A189674] 15 p2101 N88-22518
The relationship between preflight underwater training and space motion sickness 19 p2695 N88-26025
Significance of sensory signal phase mismatch in mechanisms of motion sickness development
20 p2830 N88-26787
Simulator sickness in the AH-64 Apache combat mission simulator
[AD-A193419] 21 p2988 N88-27739
MOTION SIMULATION
Application of Kalker's rolling contact theory to the simulation of rail vehicles
[DFVLR-FB-87-07] 01 p0057 N88-10363
Determination of the effect of walking on the forced convective heat transfer coefficient using an articulated mannikin
[AD-A186452] 08 p1049 N88-16335
Motion simulation for in-orbit operations
12 p1589 N88-19514
Dynamics of high-speed mechanisms with elastic members 13 p1779 N88-20643
Effects of update and refresh rates on flight simulation visual displays
[NASA-TM-100415] 15 p2018 N88-22033
Fast algorithm development for large-eddy simulation of circular-jet turbulence
[AD-A192044] 18 p2509 N88-24887
Parameter identification of the passenger simulation model MADYMO: Methods and experience
20 p2788 N88-26536
Motion evoked vestibular potentials
21 p2982 N88-27712
Interactive, networked moving platform simulators
[AD-A192374] 23 p3182 N88-28940
MOTION SIMULATORS
Measurement and effects of transport delays in a state-of-the-art F-16C flight simulator
[AD-A187367] 11 p1441 N88-18599
EPOS: European Proximity Operations Simulation
12 p1589 N88-19515
Dynamic testing of a docking system --- ground-based simulator 12 p1589 N88-19516
MOTION STABILITY
NT AERODYNAMIC STABILITY
NT AIRCRAFT STABILITY
NT BOUNDARY LAYER STABILITY
NT DIRECTIONAL STABILITY
NT FLAME STABILITY
NT FLOW STABILITY
NT GYROSCOPIC STABILITY
NT LATERAL STABILITY
NT LONGITUDINAL STABILITY
NT LOW SPEED STABILITY
NT MAGNETOHYDRODYNAMIC STABILITY
NT ROTARY STABILITY
NT SPACECRAFT STABILITY
Stability of a coastal upwelling front over topography
[AD-A192354] 20 p2829 N88-26784
An efficient patched grid Navier-Stokes solution for multiple bodies, phase 1
[AD-A194166] 23 p3211 N88-29110
Utilizing dynamic stability of orient parts
[AD-A195730] 24 p3427 N88-30397
Orbital stability in rotating triaxial stellar systems
[SEP C-PREPUBL-FASC-24] 24 p3455 N88-30560
MOTIVATION
A comparison of the effects of group dynamics on individuals assigned to integral and non-integral aircrews
[AD-A186467] 08 p1051 N88-16345
MOTOR SYSTEMS (BIOLOGY)
U EFFERENT NERVOUS SYSTEMS
MOTOR VEHICLES
NT AUTOMOBILES
NT ELECTRIC AUTOMOBILES
NT ELECTRIC MOTOR VEHICLES
NT TRACKED VEHICLES
NT TRUCKS
Evaluation of vision systems for teleoperated land vehicles
[DE87-013066] 03 p0333 N88-12100
Ground vehicle convoying
[DE88-000360] 04 p0502 N88-13088
Experiences in teleoperation of land vehicles
[DE88-000429] 06 p0711 N88-14355
Pollution from motor vehicles and aircraft at Stapleton International Airport (abbreviated report), revision 2
[AD-A185916] 07 p0875 N88-15307
Creating title blocks for vehicle animations
[AD-A185620] 07 p0904 N88-15473
TECOM's research efforts in the dynamic environments 08 p0999 N88-16048
The development of laboratory vibration test schedules: Philosophies and techniques 08 p0999 N88-16049
Laboratory vibration test schedules development beyond MIL-STD-810D 08 p0999 N88-16050
Aircraft and ground vehicle friction correlation test results obtained under winter runway conditions during joint FAA/NASA Runway Friction Program
[NASA-TM-100506] 11 p1438 N88-18582
Alternative fuels: Information on DOE's (Department of Energy's) methanol vehicle demonstration program
[PB88-118203] 13 p1753 N88-20481
Human interfaces in remote driving
[DE88-006843] 14 p1953 N88-21643
Propagation effects by roadside trees measured at UHF and L-band for mobile satellite systems
19 p2644 N88-25693
Propagation modeling for land mobile satellite systems
19 p2645 N88-25694
Propagation measurements for an Australian land mobile satellite system 19 p2645 N88-25697
The JPL MSAT mobile laboratory and the pilot field experiments 19 p2646 N88-25708
System identification in vehicle dynamics
[DFVLR-MITT-87-22] 20 p2785 N88-26518
Modeling and parameter identification of motor vehicles 20 p2785 N88-26521
Identification methods for transport dynamical investigations 20 p2787 N88-26531
Parameter identification of the passenger simulation model MADYMO: Methods and experience
20 p2788 N88-26536
MOTORS
NT ASYNCHRONOUS MOTORS
NT ELECTRIC MOTORS
NT INDUCTION MOTORS
NT SERVOMOTORS
NT STEPPING MOTORS
NT SYNCHRONOUS MOTORS
NT TORQUE MOTORS
Design verification tests for an axial gap permanent magnet compressor motor
[DE87-014360] 02 p0167 N88-11049
Dynamics of high-speed mechanisms with elastic members 13 p1779 N88-20643
Performance test results: AXIAL-GAP, permanent magnet compressor motor
[DE88-006857] 15 p2061 N88-22289
A universal computer control system for motors
[NASA-CASE-NPO-17134-1-CU]
18 p2506 N88-24864

MOUNTAINS
NT ALPS MOUNTAINS (EUROPE)
NT ANDES MOUNTAINS (SOUTH AMERICA)
NT CARPATHIAN MOUNTAINS (EUROPE)
NT SIERRA NEVADA MOUNTAINS (CA)
Description of the Mountain Cloud Chemistry Program version of the PLUVIUS MOD 5.0 reactive storm simulation model
[DE87-012846] 01 p0070 N88-10450
Mesoscale MOS forecast support for 1988 winter Olympics ski events --- model output statistics (MOS)
02 p0209 N88-11312
Measurements of vapor flux, liquid water contents, precipitation rates and riming in a Utah mountain cloud system
[PB87-224945] 04 p0469 N88-12900
Wind and temperature structure on the slopes of a mountain valley
[DE88-000080] 07 p0860 N88-15338
Density flows at the mountain edge
08 p1016 N88-16156
Operation Everest 2: Nutrition and body composition
[AD-A186449] 08 p1049 N88-16333
Numerical investigation of orographically enhanced instability
[AD-A186841] 09 p1189 N88-17125
Numerical simulation of thermally generated mountain-foreland circulation
[DFVLR-FB-87-30] 09 p1190 N88-17132
Surface ozone measurements at a Swedish mountain site
[CM-72] 09 p1191 N88-17138
The retardation of cold fronts at high mesoscale mountains 09 p1241 N88-17437
Thematic mapper study of Alaskan ophiolites
[NASA-CR-182554] 11 p1504 N88-18984
Local meteorological processes and air mass origin during a cloud chemical field experiment on Areskutan, Sweden, in summer 1986
[AP-28] 14 p1948 N88-21615
Geometric modeling of flight information for graphical cockpit display
[AD-A190484] 15 p2021 N88-22043
Photointerpretation with instrumentation for evaluation of environmental impact: Mata Atlantica in Cubatao
19 p2683 N88-25946
Study of evolution of vegetal cover and slide scars in the Cubatao municipality-Sao Paulo
19 p2683 N88-25947
Structure of eastern Turkestan Ridge based on space photographs 24 p3450 N88-30530

MOUNTING
Dynamic analysis of a structure with sliding base
08 p0998 N88-16045
A study of the TCAS 2 collision avoidance system mounted on a Boeing 737 aircraft
[NASA-CR-182457] 09 p1116 N88-16687
Application of a simple rotational spherical grating mounting to high resolution soft X-ray spectroscopy
[PB87-164836] 09 p1142 N88-16845
To determine the stress distribution in the vicinity of GRP end pads where the specimen is held and loaded (CFC coupon specimens) --- glass reinforced plastic (GRP) carbon fiber composite (CFC)
[BAE-WST-R-RES-CFC-12023]
09 p1182 N88-17080
Further tests to determine the stress distribution in the vicinity of GRP end pads where the specimen is held and loaded (CFC coupon specimens) --- glass reinforced plastic (GRP) carbon fiber composite (CFC)
[BAE-WST-R-RES-CFC-12023-ADD-1]
09 p1182 N88-17081
Microgravity isolation mount
[ESA-CR(P)-2480] 11 p1443 N88-18604
Structural analysis of the space shuttle solid rocket booster/external tank attach ring
[NASA-TM-100510] 11 p1446 N88-18618
Almond test body --- for microwave anechoic chambers
[NASA-CASE-LAR-13747-1] 18 p2502 N88-24845
Thermal compensating mount
[NASA-CASE-LAR-13794-1] 18 p2519 N88-24942

MOUNTS
U SUPPORTS

MOVEMENT
U MOTION

MOVING TARGET INDICATORS
Investigation and implementation of an algorithm for computing optimal search paths
[AD-A185927] 07 p0902 N88-15461
Moving Target Indicator (MTI) interface for simple radar
[FOA-C-30463-3.2] 09 p1154 N88-16914
Experiments for the high resolution detection of moving targets using a CO2 laser radar
[MBB-UA-1044/87] 10 p1316 N88-17864
An optimal branch-and-bound procedure for the constrained path, moving target search problem
[AD-A188962] 12 p1685 N88-20075
Passive multipath target tracking in an inhomogeneous acoustic medium
[AD-A193284] 21 p3012 N88-27873
Autoregressive moving average modeling of radar target signatures
[AD-A194612] 22 p3069 N88-28218

MRAC (SYSTEMS)
U MODEL REFERENCE ADAPTIVE CONTROL

MRCA AIRCRAFT
German Air Force requirements for the on-board life monitoring system (OLMOS) on Tornado
22 p3033 N88-28007
Event monitoring functions introduced by the Onboard Life Monitoring System (OLMOS) into a German aircraft
22 p3034 N88-28008
Onboard Life Monitoring System (OLMOS), hardware equipment onboard and on ground
22 p3034 N88-28009
Onboard Life Monitoring System (OLMOS): Engine life cycle calculation and trending 22 p3034 N88-28010
Tornado: Airframe fatigue life monitoring
22 p3034 N88-28011

MSM (SEMICONDUCTORS)
MESFET compatible IMSM detectors
19 p2659 N88-25801

MTBF
Explicit formulate for the distributions of stopping variables under Wald's truncated SPRT (Sequential Probability Radio Tests) for a poisson process
[AD-A185053] 05 p0640 N88-13914
Rivista Tecnica Selenia, volume 10, n[illegible] 1987
[ETN-88-92717] 22 p30[illegible] [illegible]8-28210
An application of the Bayesian method to the estimation and forecast of system hardware components MTBF
22 p3068 N88-28211

MTF
U MODULATION TRANSFER FUNCTION

MTI RADAR
U MOVING TARGET INDICATORS

MULLITES
Microstructures and properties of SiC whisker-reinforced mullite composites
[DE88-002611] 09 p1139 N88-16826
Superplastic flow of mullite-zirconia composites
[DE88-005905] 15 p2028 N88-22085

MULTI-ROLE COMBAT AIRCRAFT
U MRCA AIRCRAFT

MULTIBEAM ANTENNAS
Multiple-beam ground station reflector antenna system: A preliminary study
[EUT-87-E-171] 14 p1904 N88-21379
Rearrangement procedures in regenerative multibeammobile communications satellites with frequency reuse 19 p2650 N88-25735
Antenna system for MSAT mission
19 p2651 N88-25742
Antenna technology for advanced mobile communication systems 19 p2651 N88-25743
Frequency addressable beams for land mobile communications 19 p2652 N88-25744

MULTICHANNEL COMMUNICATION
Multi-channel communications system analyzer
[AD-A184756] 03 p0307 N88-11937
In-orbit calibration adjustment of the Nimbus-7 SMMR
[NASA-TM-100678] 05 p0614 N88-13773
Multicarrier demodulator design, volume 1 --- communication satellites
[ESA-CR(P)-2468-VOL-1] 09 p1158 N88-16941
Multicarrier demodulator design. Volume 2: Executive summary --- communication satellites
[ESA-CR(P)-2468-VOL-2] 09 p1158 N88-16942
Code division multiple access applied to fiber optic data transmission
[AD-A186873] 09 p1247 N88-17477
Multichannel data transmission through a fiber optic cable
[AD-A193842] 22 p3070 N88-28221

MULTICHANNEL PLATES
U MICROCHANNEL PLATES

MULTILAYER INSULATION
Radiative heat transfer solutions in plane-parallel participating media: Application to multilayer insulations for space vehicles
[INPE-4221-PRE/1101] 08 p0962 N88-15824
High-temperature properties of ceramic fibers and insulations for thermal protection of atmospheric entry and hypersonic cruise vehicles
[NASA-TM-100059] 10 p1295 N88-17743

MULTILAYER STRUCTURES
U LAMINATES

MULTILOOP SYSTEMS
U CASCADE CONTROL

MULTIPATH TRANSMISSION
Multipath time-delay estimation via the EM algorithm
[PB88-106851] 07 p0845 N88-15124
Wideband HF (High Frequency) modeling and simulation
[PB88-116116] 10 p1317 N88-17874
Terrestrial Propagation Characteristics in Modern Systems of Communications, Surveillance, Guidance and Control
[AGARD-CP-407] 12 p1614 N88-19653
An investigation of terrain related variables for predicting the multipath fade depth distribution on terrestrial microwave lines 12 p1615 N88-19654
A review of the role of surface reflection in multipath propagation over terrestrial microwave links
12 p1615 N88-19655
Identification of microwave line-of-sight multipath components 12 p1616 N88-19665
Radio and radar holes and multipath zones: The global and local influences on atmospheric refractive structure and resulting adverse radio and radar performance
12 p1617 N88-19667
The 6 GHz propagation measurements over a 51 km path in the UK 12 p1617 N88-19673
Spatial matched processing for multipath propagation
[AD-A189790] 15 p2129 N88-22701
Miltipath measurements for land mobile satellite service using global positioning system signals
19 p2645 N88-25700
A random access algorithm for environments with capture and limited feedback capabilities
[AD-A192233] 20 p2790 N88-26552
Description of the MPTR system: Multi Path Transmissometer Radiometer
[FEL-1987-14] 20 p2855 N88-26954
Passive multipath target tracking in an inhomogeneous acoustic medium
[AD-A193284] 21 p3012 N88-27873
Random-access algorithms for environments with capture
[AD-A194303] 23 p3203 N88-29060

MULTIPHASE FLOW
NT TWO PHASE FLOW
A guide to the transient three phase porous flow model implemented in the two-dimensional CRAY-TENSOR code: Physics, numerics, and code description
[DE88-003709] 09 p1165 N88-16983
Turbulence interactions in single- and multi-phase turbulent mixing and combustion processes
[AD-A187505] 10 p1332 N88-17960
Laser velocimeter measurements of solids in multiphase flow
[DE88-000196] 11 p1487 N88-18876
Noncondensing round turbulent gas jets in liquids
[AD-A191191] 16 p2208 N88-23179
Study of a water-steam two phase flow in a T-branch
[ETN-88-92306] 20 p2801 N88-26624

MULTIPHOTON ABSORPTION
Third-harmonic generation and multiphoton ionization spectroscopy
[DE87-013545] 03 p0281 N88-11769
Interaction of intense electromagnetic fields with SF/sub 6/ molecules and clusters in supersonic expansion
[DE88-700310] 07 p0846 N88-15132
Photoionization dynamics of excited molecular states
[DE88-002982] 09 p1246 N88-17468
Memory effects on infrared adsorbate spectra
[AD-A186976] 09 p1253 N88-17512
High-order multiphoton ionization of the noble gases
[DE88-007489] 18 p2571 N88-25273
Multiphoton transitions in semiconductors in the non-perturbative approach
[DE88-702664] 22 p3157 N88-28786

MULTIPLE ACCESS
NT ALOHA SYSTEM
NT CODE DIVISION MULTIPLE ACCESS
NT DEMAND ASSIGNMENT MULTIPLE ACCESS
NT FREQUENCY DIVISION MULTIPLE ACCESS
NT TIME DIVISION MULTIPLE ACCESS
High data rate modem simulation for the space station multiple-access communications system
06 p0795 N88-14870
Channel access protocols for multihop packet radio networks
[AD-A186074] 07 p0842 N88-15105
On the approximation of the output process of multi-user random access communication networks
[AD-A186197] 07 p0842 N88-15108
Measured noise performance of a direct-sequence spread-spectrum system and a comparison of single vice dual-channel delay-lock loops
[AD-A186288] 07 p0843 N88-15110
Coding for spread-spectrum communications networks
[AD-A185667] 07 p0844 N88-15119

Accessing hierarchical databases via SQL transactions in a multi-model database system
[AD-A187878] 11 p1565 N88-19369
An access alternative for mobile satellite networks
19 p2651 N88-25737
Integrated voice/data protocols for satellite channels
19 p2651 N88-25739
The emergence of multi-user expert systems
23 p3260 N88-29406
Optical multiple access intersatellite links
[BAE-TP-8502] 24 p3361 N88-30013
Performance of DS/SSMA communications in impulsive channels. Part 1: Correlation receivers
[AD-A195712] 24 p3362 N88-30021

MULTIPLE INSTRUCTION MULTIPLE DATA STREAM
U MIMD (COMPUTERS)

MULTIPLETS
U FINE STRUCTURE

MULTIPLEX TRANSMISSION
U MULTIPLEXING

MULTIPLEXERS
U MULTIPLEXING

MULTIPLEXING
NT FREQUENCY DIVISION MULTIPLEXING
NT TIME DIVISION MULTIPLEXING
NT WAVELENGTH DIVISION MULTIPLEXING
Low noise-low power monolithic multiplexing readout electronics for silicon strip detectors
[MPI-PAE/EXP.EL.178] 02 p0168 N88-11057
A129 advanced solutions for meeting today's combat helicopter requirement 03 p0265 N88-11669
Development of a multiplexer module for use in a spaceborne cryogenic environment based on GaAs MESFET technology
[RPT/CRY/62463/BOP] 11 p1559 N88-19335
Applications of optical computing to problems with symbolic computations
[AD-A189772] 15 p2106 N88-22548
Multiplex methods in infrared spectrometry
16 p2271 N88-23588
Adaptive data acquisition multiplexing system and method
[NASA-CASE-MSC-21170-1] 18 p2471 N88-24662
The MELMUX MX-7100 series high-speed digital multiplexers 21 p2930 N88-27396
Multichannel data transmission through a fiber optic cable
[AD-A193842] 22 p3070 N88-28221
Development of 30 micrometers extrinsic silicon multiplexed infrared deterctor array
[NASA-CR-177446] 22 p3082 N88-28301
On broadband matching of multiport electrical networks with applications
[AD-A194224] 23 p3207 N88-29086

MULTIPLICATION
Efficient multiplication algorithms over the finite fields GF(q sup m), where q equals 3,5
22 p3066 N88-28191
Sequential approach to Colombeau's theory of generalized functions
[DE88-701869] 23 p3276 N88-29503

MULTIPLIER PHOTOTUBES
U PHOTOMULTIPLIER TUBES

MULTIPLIERS
Implementation of a digital optical matrix-vector multiplier using a holographic look-up table and residue arithmetic
[NASA-CR-180431] 01 p0078 N88-10496
High bit rate serial input mutipliers
[REPT-87-012] 11 p1530 N88-19140
A serial input pipelined multiplier
[REPT-87-030] 11 p1530 N88-19141
On serial-input multipliers for two-complement numbers
[REPT-86-035] 11 p1536 N88-19181

MULTIPOLES
Solar oscillations, gravitational multipole field of the Sun and the solar neutrino paradox
[DE88-002100] 07 p0946 N88-15752
Application of state-multipole Heisenberg equations to Raman excitation dynamics
[DE88-003828] 10 p1335 N88-17977
On the efficient implementation of the fast multipole algorithm
[AD-A191167] 17 p2385 N88-24173

MULTIPROCESSING (COMPUTERS)
Memory systems for single bus multiprocessor architecture. Application to the SCOM system
[ENST-86E022] 02 p0219 N88-11379
Multi-processor architectures for artificial intelligence processing
[OUEL-1671/87] 02 p0219 N88-11380
Concurrent algorithms for transient nonlinear FE analysis
[NASA-CR-181455] 02 p0221 N88-11389
Semantic network processing systems --- artificial intelligence
[OUEL-1677/87] 02 p0223 N88-11401
QUICKSILVER: A 3D, electromagnetic, PIC code
[DE87-013013] 02 p0245 N88-11547
On the control of a compliant robot arm
03 p0332 N88-12095
Hardware-assisted multiprocessor performance measurements
[PB87-226908] 03 p0363 N88-12282
Delft parallel processor 84/16
[PB87-226254] 03 p0366 N88-12305
Comparing barrier algorithms
[NASA-CR-178377] 04 p0476 N88-12934
Principles for problem aggregation and assignment in medium scale multiprocessors
[NASA-CR-178379] 04 p0476 N88-12935
An approach to implementing state space searches on heterogeneous systems of multiprocessors
[DE88-001321] 04 p0482 N88-12967
Contribution to optimal flow in networks. A experimental multiprocessor for asynchronous iteration implementation
[LAAS-87-269] 05 p0576 N88-13510
Set of multi-process primitives for stack based machines
[PB87-234381] 06 p0756 N88-14636
Life sciences flight experiments microcomputer
06 p0792 N88-14857
A multiprocessing architecture for real-time monitoring
08 p1059 N88-16390
Numerical experiments with a parallel conjugate gradient method
[DE88-002178] 08 p1066 N88-16445
Communications patterns in a symbolic multiprocessor
[AD-A186896] 09 p1215 N88-17282
Types and effects towards the integration of functional and imperative programming
[AD-A186930] 09 p1216 N88-17290
Algorithm design for scientific computation for highly parallel multiprocessor systems
[AD-A186713] 09 p1217 N88-17299
Twisted cube
[PB87-162814] 09 p1220 N88-17316
Multitasking and microtasking experience on the NA S Cray-2 and ACF Cray X-MP
[NASA-CR-177464] 09 p1221 N88-17325
Concept of a programmable maintenance processor applicable to multiprocessing systems
[NASA-TM-100406] 09 p1223 N88-17333
Role of broadcasting in multiprocessor systems
10 p1374 N88-18201
Multiple-bus interconnection for future multiprocessor systems 10 p1375 N88-18203
Implementation of a buddy failure recovery concept in the NOVAC system 10 p1375 N88-18205
The case for a shared address space
10 p1378 N88-18225
Performance evaluation of a loop interconnection structure 10 p1378 N88-18229
Aspects of a multiprocessor architecture
10 p1379 N88-18232
Parallelism at the microlevel: Cooperative microcontrollers with real time considerations
10 p1381 N88-18246
A VLSI implementable block oriented data driven multiprocessor 10 p1381 N88-18249
Multi-processor reduction machines
10 p1382 N88-18253
A measurement-based study of concurrency in a multiprocessor
[DE88-003536] 10 p1383 N88-18260
A performance analysis of architectural scalability
[DE88-003537] 10 p1383 N88-18261
A multiprocessor scheme for the singular value decomposition
[DE88-003591] 10 p1388 N88-18288
Data prefetching in shared memory multiprocessors
[DE88-003576] 10 p1394 N88-18314
Measurement and analysis of memory conflicts on vector multiprocessors
[AD-A188206] 11 p1525 N88-19104
Implementing dynamic arrays: A challenge for high-performance machines
[AD-A188142] 11 p1533 N88-19157
Accessing hierarchical databases via SQL transactions in a multi-model database system
[AD-A187878] 11 p1565 N88-19369
Evaluation of network communication multiprocessor fault tolerance
[INPE-4305-PRE/1171] 12 p1674 N88-20011
Architecture with parallel processing for incremental computation
[INPE-4326-PRE/1178] 12 p1675 N88-20012
An emulation tool for simulating matrix operations on an SIMD (Single Instruction Multiple Data stream) multiprocessor
[AD-A188654] 12 p1678 N88-20030
A laboratory facility for research in parallel computation
[AD-A188499] 12 p1680 N88-20044
Primal-dual parallel solution of very large sparse linear programs
[AD-A188500] 12 p1680 N88-20045
NAVLAB: An autonomous navigation testbed
[AD-A189049] 13 p1720 N88-20283
Very large vortex calculations in two dimensions
[DE88-005748] 13 p1770 N88-20587
Data traffic reduction schemes for sparse Cholesky factorizations
[NASA-CR-181626] 13 p1813 N88-20831
Gaussian techniques on shared memory multiprocessor computers
[DE88-005426] 13 p1817 N88-20855
Locality, communication and interconnect length in multicomputers
[CWI-CS-R8708] 13 p1822 N88-20890
Evaluation of a parallel chart parser
[AD-A189172] 14 p1959 N88-21685
Distributed operating systems: An overview
[INF-87-29] 14 p1960 N88-21688
Parallel memory addressing using coincident optical pulses
[AD-A189767] 15 p2106 N88-22547
An analysis of multiple grain CHiP architectures
[AD-A189942] 15 p2110 N88-22570
Comparative analysis of multistage interconnection networks
[AD-A190436] 15 p2115 N88-22596
A methodolgy, based on analytical modeling, for the design of parallel and distributed architectures for relational database query processors
[AD-A189844] 15 p2149 N88-22825
New generation knowledge processing, volume 1
[AD-A190165] 15 p2149 N88-22826
Fast algorithms for Euler and Navier-Stokes simulations
[AD-A190897] 16 p2208 N88-23175
Multiprocessor graphics computation and display using transputers 16 p2218 N88-23236
Program profiling in Cedar
[AD-A190883] 16 p2250 N88-23449
VPC: A proposal for a vector parallel C programming language
[AD-A190885] 16 p2251 N88-23451
Supercomputer programming environments
[AD-A190887] 16 p2251 N88-23452
Locality, communication and interconnect length in multicomputers
[CWI-CS-R8743] 16 p2254 N88-23466
New generation knowledge processing, volume 2
[AD-A190166] 16 p2285 N88-23681
New generation knowledge processing, volume 3
[AD-A190167] 16 p2285 N88-23682
A multiprocessor data flow accelerator module
[DE88-007587] 18 p2554 N88-25161
Decomposition of linear programs using parallel computation
[AD-A191718] 18 p2556 N88-25173
Effective use of shared memory multiprocessors
[DE88-007019] 18 p2560 N88-25195
Gaussian techniques on shared-memory multiprocessors
[DE88-010594] 19 p2716 N88-26126
On the implementation of applicative on shared-memory, MIMD multiprocessors
[DE88-005367] 19 p2718 N88-26136
Performance evaluation for multiprocessors programmed using monitors
[DE88-010056] 19 p2718 N88-26138
SLAPP: A special multiprocessor array for signal processing and linear algebra
[AD-A191587] 19 p2719 N88-26146
A multiprocess operating system for 16 bit microcomputers or porting Unix (trademark) to a NS32016 with enhancements 20 p2836 N88-26822
Definition of an auxiliary processor dedicated to real-time operating system kernels
[NASA-CR-183070] 20 p2841 N88-26860
An evaluation methodology for dependable multiprocessors
[AD-A192799] 20 p2842 N88-26863
Dynamic modelling and estimation of the error due to asynchronism in a redundant asynchronous multiprocessor system
[NASA-CR-177427] 21 p2898 N88-27205
FTMP data acquisition environment
[NASA-TM-100636] 21 p2938 N88-27447
MINIAC: A small embedded computer
[DE88-008142] 21 p2994 N88-27757

The sub-implicit method: New multiprocessor algorithms for old implicit codes
[DE88-011345] 21 p2999 N88-27785

Performability analysis: Measures, an algorithm and a case study
[AD-A192477] 21 p3001 N88-27800

Constructing a highly-available location service for a distributed environment
[AD-A192723] 21 p3001 N88-27801

Modeling and approximate performance analysis of multiuser computer systems
[ETN-88-92137] 21 p3002 N88-27806

Dynamic resource allocation in a hierarchical multiprocessor system: A preliminary study
[NASA-CR-183177] 22 p3141 N88-28675

Partitioning of regular computation on multiprocessor systems
[NASA-CR-183176] 22 p3141 N88-28676

Piecewise-parabolic methods for systems of hyperbolic conservation laws in multiprocessing environments
[DE88-010202] 23 p3248 N88-29329

The FORCE
[AD-A193463] 23 p3264 N88-29429

Programming language concepts for multiprocessors
[AD-A193465] 23 p3264 N88-29430

Large-grain pipelining on distributed-memory multiprocessors
[DE88-009974] 23 p3264 N88-29432

Parallel real-time expert systems
[AD-A193673] 23 p3264 N88-29434

Compression and decompression of imaging sensor signals (CADISS): A multiprocessor system for image compression/decompression on board scientific satellites
[NLR-TR-87076-L] 24 p3414 N88-30323

The triangle: A multiprocessor architecture for fast curve and surface generation
[AD-A195882] 24 p3414 N88-30324

Reification without evaluation
[AD-A195928] 24 p3414 N88-30326

MULTIPROPELLANTS
U ROCKET PROPELLANTS

MULTIRADAR TRACKING
U RADAR NETWORKS

MULTISENSOR APPLICATIONS

From pattern to process: The strategy of the Earth Observing System. Volume 2: EOS Science Steering Committee report
[NASA-TM-89702] 07 p0871 N88-15283

Development of subminiature multi-sensor hot-wire probes
[NASA-TM-100052] 15 p2069 N88-22336

Multi-sensor integration on the NCUBE hypercube computer
[DE88-007472] 18 p2554 N88-25162

Path planning and path following for the Amsterdam autonomous cart
[FVI-86-22] 24 p3380 N88-30133

MULTISPECTRAL BAND CAMERAS

Land cover/use classification of Cairns, Queensland, Australia: A remote sensing study involving the conjunctive use of the airborne imaging spectrometer, the large format camera and the thematic mapper simulator
05 p0612 N88-13759

Development of a CCD characterization system
[INPE-4361-TDL/301] 12 p1623 N88-19712

MULTISPECTRAL BAND SCANNERS
NT THEMATIC MAPPERS (LANDSAT)

Study, design, and evaluation of data reduction by encoding or information extraction. Part 1: Data generation analysis --- multispectral satellite imagery
[NLR-TR-85094-L-PT-1] 01 p0078 N88-10501

Study, design and evaluation of data reduction by encoding or information extraction. Part 2: Operational considerations --- multispectral satellite imagery
[NLR-TR-85094-L-PT-2] 01 p0079 N88-10502

Study, design and evaluation of data reduction by encoding or information extraction. Part 3: Algorithm design --- multispectral satellite imagery
[NLR-TR-85094-L-PT-3] 01 p0079 N88-10503

Study, design and evaluation of data reduction by encoding or information extraction. Part 4: Performance demonstration --- multispectral satellite imagery
[NLR-TR-85094-L-PT-4] 01 p0079 N88-10504

Study, design and evaluation of data reduction by encoding or information extraction. Part 5: Algorithm implementation aspects --- multispectral satellite imagery
[NLR-TR-85094-L-PT-5] 01 p0079 N88-10505

MBB-ERNO view of remote sensing commercialization
03 p0340 N88-12140

Development of a method for forest damage inventory using multispectral scanner data
[KFK-PEF-25] 03 p0345 N88-12182

Cloud cover determination in polar regions from satellite imagery
[NASA-CR-181544] 04 p0471 N88-12908

Commercial applications and scientific research requirements for thermal-infrared observations of terrestrial surfaces
[NASA-TM-89704] 08 p1019 N88-16179

Autocorrelation of control points on 11-band multispectral imagery
[AD-A188185] 10 p1348 N88-18056

NIMBUS-7 CZCS. Coastal Zone Color Scanner imagery for selected coastal regions. North America - Europe. South America - Africa - Antarctica. Level 2 photographic product
[NASA-CR-180755] 15 p2089 N88-22447

Turbidity patterns in the delta waters of southwest Netherlands on Thematic Mapper (TM) and multispectral scanner (MSS) satellite images
[BCRS-86-06] 16 p2227 N88-23303

Applications of multitemporal compositions obtained from LANDSAT data in the study of urban growth
[INPE-4480-PRE/1246] 16 p2287 N88-23692

MULTISPECTRAL PHOTOGRAPHY
NT INFRARED PHOTOGRAPHY
NT RADAR PHOTOGRAPHY

Vegetation classification, land systems and mapping using SPOT multispectral data: Preliminary results
03 p0342 N88-12160

Coastal dynamics of the mouth of the Saloum (Senegal) --- SPOT imagery 03 p0345 N88-12177

Development of a method for forest damage inventory using multispectral scanner data
[KFK-PEF-25] 03 p0345 N88-12182

Multistep component analysis of correlations
08 p1009 N88-16115

Commercial applications and scientific research requirements for thermal-infrared observations of terrestrial surfaces
[NASA-TM-89704] 08 p1019 N88-16179

A variant of the ISODATA algorithm for application to agricultural targets
[INPE-4436-PRE/1235] 12 p1676 N88-20023

Study of methods of post-processing applied to a problem of standard classification
17 p2362 N88-24067

Remote sensing of wetlands: Applications overview
[DE88-010895] 21 p2966 N88-27618

Comparative study of crop and soil mapping using multitemporal and multispectral SPOT and LANDSAT data 22 p3091 N88-28354

Pilot study of rice culture in sub-tropical high population density region (Madagascar) with SPOT 1 multispectral data 22 p3097 N88-28392

Utilization of SPOT-1 multispectral data for mapping land cover and phytohygiene monitoring in the central zone of the Mercantour National Park (France)
22 p3100 N88-28413

MULTISTAGE COMPRESSORS
U TURBOCOMPRESSORS

MULTISTAGE ROCKET VEHICLES
NT ARIANE LAUNCH VEHICLE
NT SKYLARK ROCKET VEHICLE
NT TITAN LAUNCH VEHICLES

Multi-stage plasma thruster
[AD-A183635] 01 p0017 N88-10105

MULTISTATIC RADAR

Airborne bistatic radar applications
[ETN-87-90930] 02 p0163 N88-11020

Mono- and bistatic radar coverage diagrams including diffractive wave propagation 12 p1616 N88-19660

DSS 14 antenna calibrations for GSSR/VLA Saturn radar experiments 22 p3068 N88-28207

MULTITEMPORAL ANALYSIS
U TEMPORAL RESOLUTION

MULTIVARIATE STATISTICAL ANALYSIS
NT BIVARIATE ANALYSIS
NT COVARIANCE
NT ORTHOGONALITY
NT REGRESSION ANALYSIS

Breakdown points of affine equivariant estimators of multivariate location and covariance matrices
[REPT-87-14] 01 p0088 N88-10574

Horizontal shape matching applied to VAS data --- Visible and Infrared Spin Scan Radiometer Atmospheric Sounder (VAS) 02 p0201 N88-11254

Estimation of a multivariate continuous variable panel model
[AD-A184472] 04 p0484 N88-12982

Approximating multivariate normal orthant probabilities using the Clark algorithm
[AD-A184855] 05 p0634 N88-13873

Illustrative examples of principal component analysis using BMDP/4M
[AD-A185179] 05 p0635 N88-13881

Illustrative examples of principal component analysis using SYSTAT/FACTOR
[AD-A184920] 05 p0644 N88-13939

Illustrative examples of principal component analysis using GENSTAT/PCP
[AD-A185085] 05 p0644 N88-13941

Modeling and generating input processes
[DE87-013162] 05 p0645 N88-13948

Asymptotic normality of poly-t densities with Bayesian applications
[AD-A185718] 06 p0768 N88-14719

Control charts when the observations are correlated
[AD-A186388] 07 p0866 N88-15253

On the least squares estimator in moving average models of order one
[AD-A186028] 07 p0909 N88-15508

A new method of estimation in a moving average model of order one
[AD-A186039] 07 p0909 N88-15510

On the extreme points of the set of all 2xn bivariate positive quadrant dependent distributions with fixed marginals and some applications
[AD-A186316] 07 p0911 N88-15521

The information metric for univariate linear elliptic models
[AD-A186385] 07 p0911 N88-15527

Estimation of multivariate binary density using orthonormal functions
[AD-A186386] 07 p0912 N88-15528

Strategies of data analysis
[AD-A186033] 07 p0914 N88-15548

Some new approaches to multivariate probability distributions
[AD-A186038] 07 p0914 N88-15551

A weighting sequence approach to the analysis and design of multivariable control systems
[AD-A186086] 07 p0917 N88-15570

Test of linearity in general regression models
[AD-A186036] 08 p1073 N88-16477

New directions for multivariate statistical computation and data analysis
[AD-A186523] 08 p1074 N88-16480

Tensorial calibration. 2. Second order tensorial calibration
[AD-A186614] 09 p1167 N88-16994

Tensorial calibration. Part 1: First order tensorial calibration
[AD-A186708] 09 p1167 N88-16995

Modification of a successive corrections objective analysis for improved higher order calculations
[NASA-CR-182467] 09 p1230 N88-17370

The linear dependency structure of covariance nonstationary time series
[AD-A186548] 09 p1232 N88-17383

Strong consistency of certain information theoretic criteria for model selection in calibration, discriminant analysis and canonical correlation analysis
[AD-A186584] 09 p1232 N88-17385

Identifiability of multivariate ARMA models
[AD-A187394] 10 p1400 N88-18350

Statistical aspects of reliability, maintainability and availability
[AD-A188491] 12 p1634 N88-19783

Visual display representation of multidimensional systems: The effect of information correlation and display integrality
[AD-A188655] 12 p1672 N88-20010

A variant of the ISODATA algorithm for application to agricultural targets
[INPE-4436-PRE/1235] 12 p1676 N88-20023

Force distribution and trajectory control for closed kinematic chains with applications to walking machines
13 p1779 N88-20642

A multivariate variational objective analysis-assimilation method. Part 1: Development of the basic model
[NASA-CR-182651] 15 p2097 N88-22491

A multivariate variational objective analysis-assimilation method. Part 2: Case study results with and without satellite data
[NASA-CR-182653] 15 p2097 N88-22492

Some comments on quadrant dependence in higher dimensions
[AD-A190329] 15 p2121 N88-22639

Multivariate analysis and its application
[AD-A189983] 15 p2124 N88-22661

Detection of the number, locations and magnitudes of jumps
[AD-A190328] 15 p2125 N88-22671

Very short range statistical forecasting of automated weather observations
[AD-A190803] 16 p2235 N88-23349

The display of multivariate information: The effects of auto- and cross-correlation, reliability and heterogeneity
[AD-A191070] 16 p2243 N88-23398

An innovation approach to goodness of fit tests in R sup m
[CWI-MS-R8712] 16 p2259 N88-23501

Improved estimators in simultaneous estimation of scale parameters
[AD-A191108] 17 p2392 N88-24216
Almost sure L(gamma)-norm convergence for data-based histogram density estimates
[AD-A189944] 17 p2393 N88-24228
Parameter-adaptive model-following for in-flight simulation
[AD-A190567] 18 p2467 N88-24645
Poisson functionals of Markov processes and queueing networks
[AD-A191217] 18 p2568 N88-25252
Structural properties of multivariable linear systems
[PB88-181375] 19 p2717 N88-26134
On solvability of an equation arising in the theory of M-estimates
[AD-A1930[illegible]9] 21 p3006 N88-27828
Further extensions of the choquet-deny and deny theorems with applications in characterization theory
[AD-A193358] 21 p3006 N88-27834
Asymptotic normality of minimum L1-norm estimates in linear models
[AD-A193399] 21 p3008 N88-27835
Joint asymptotic distribution of marginal quantiles and quantile functions in samples from a multivariate population
[AD-A193385] 21 p3010 N88-27856
Poisson functionals of Markov processes and queueing networks
[AD-A194289] 22 p3145 N88-28705
An expert system for reliability modeling
23 p3252 N88-29355
Robust control of multivariable and large scale systems
[AD-A194250] 23 p3266 N88-29441
Reconstruction of multidimensional signals from multiple level threshold crossings
[AD-A195561] 24 p3425 N88-30383

MUON SPIN ROTATION
Wrong helicity events induced by the CERN-SPS wide band muonic (anti)neutrino beam
[NIKHEF-H/87-2] 06 p0779 N88-14779
Materials science with muon spin rotation
[NASA-CR-182891] 17 p2396 N88-24242
Systematic variation of magnetic-field penetration depth in high-T(c) superconductors studied by muon spin relaxation 17 p2396 N88-24243
Comparison between muon spin rotation and neutron scattering studies on the 3-dimensional magnetic ordering of La2CuO(4-y) 17 p2396 N88-24244
Coexisting static magnetic ordering and superconductivity in CeCu2.1Si2 found by muon spin relaxation 17 p2396 N88-24245
Static magnetic ordering of CeCu2.1Si2 found by muon spin relaxation 17 p2396 N88-24246
Muon motion in titanium hydride
17 p2396 N88-24247
Muon-spin rotation experiment (micro + SR) on aluminum and indium after low temperature electron irradiation
[ETN-88-92985] 23 p3294 N88-29617

MUONS
Electronics for the External Muon Detector (EMD) of ICARUS
[NOTA-INTERNA-880] 07 p0847 N88-15143
Characteristics of multimuon events from fourth generation quarks at the SSC (Superconducting Super Collider)
[DE88-002954] 09 p1257 N88-17535
A combined cosmic ray muon spectrometer and high energy air shower array
[DE88-003057] 09 p1264 N88-17574
Theory of Muon method for study of solid and liquid hydrogen 14 p1972 N88-21770
Analysis of hadron production in deep inelastic muon-proton collisions through the fire-string model
[PREPRINT-578] 14 p1981 N88-21822
High energy cosmic muons and the calibration of the L3 electromagnetic calorimeter
[NOTA-INTERNA-895] 14 p2011 N88-21999
Muon motion in titanium hydride
17 p2396 N88-24247
Difficulties with interpretation of underground muons from Cygnus X-3
[DE88-701645] 23 p3309 N88-29710

MUSCLES
NT MYOCARDIUM
Motion and space sickness 04 p0404 N88-12510
Dimensional analysis of nonlinear oscillations in brain, heart and muscle
[DE87-014749] 06 p0751 N88-14614
Model based monitoring of human sleep stages
[ISBN-90-9001448-9] 06 p0752 N88-14618
Nucleic acid content of skeletal muscles during hypokinesia and in the recovery period
07 p0894 N88-15418
Muscle preservation in the study of bioenergetic affects of hypokinesia 10 p1362 N88-18139
Investigation of rat skeletal muscles following short-term spaceflight aboard Cosmos-1667 biosatellite
10 p1365 N88-18157
Morphological manifestations of primate adaptation to orthograde statics and walking erect
10 p1366 N88-18162
P-31 Magnetic Resonance Spectroscopy (MRS) of limb muscles during bedrest with exercise countermeasures
12 p1656 N88-19925
Endocrine responses to resistance exercise
[AD-A188681] 12 p1667 N88-19993
A program for the study of skeletal muscle catabolism following physical trauma
[AD-A189771] 15 p2102 N88-22521
Activation, strength and endurance of human respiratory and limb muscles 17 p2381 N88-24158
Dexamethasone regulates glutamine synthetase expression in rat skeletal muscles
[NASA-CR-182935] 18 p2549 N88-25129

MUSCULAR FATIGUE
Activation, strength and endurance of human respiratory and limb muscles 17 p2381 N88-24158

MUSCULAR FUNCTION
Investigation of interactions between limb-manipulator dynamics and effective vehicle roll control characteristics
[NASA-CR-3983] 01 p0007 N88-10039
Results of research with biological satellites
08 p1006 N88-16097
Models describing muscle behavior and control
[LR-522] 16 p2238 N88-23368
Activation, strength and endurance of human respiratory and limb muscles 17 p2381 N88-24158
Motor theory of auditory perception
[AD-A192095] 18 p2550 N88-25136

MUSCULAR STRENGTH
Ergonomics of car controls for disabled people, phase 1. Part 1: Chapters 1-7. Part 2: Appendices. Part 3: References
[ISBN-0-947767-82-7] 09 p1202 N88-17204
Activation, strength and endurance of human respiratory and limb muscles 17 p2381 N88-24158
The effects of acute cold exposure on exercise performance
[AD-A192650] 22 p3130 N88-28610

MUSCULAR TONUS
Oxidative enzyme activity in healthy subjects and individuals with neurocirculatory dystonia during graded exercise 10 p1367 N88-18170
Hemostasis parameters of individuals with neurocirculatory dystonia submitted to dry immersion
19 p2703 N88-26072

MUSCULOSKELETAL SYSTEM
NT BONE MARROW
NT BONES
NT COLLAGENS
NT JOINTS (ANATOMY)
NT MUSCLES
NT SKULL
NT TIBIA
NT WRIST
Physiological determinants of load bearing capacity
[AD-A184977] 05 p0629 N88-13848
The origin of the spicule skeleton of fresh water sponges (Spongillides) 07 p0885 N88-15368
Xiphophorus: A system to recognize radiation-induced mutations and to study the effects of zero-gravity environment on embryo development
07 p0885 N88-15372
Functional development of gravity receptors in insects and amphibians 07 p0886 N88-15376
Influence of skeletal muscle glycogen on passive rewarming after hypothermia
[AD-A186451] 08 p1049 N88-16334
A program for the study of skeletal muscle catabolism following physical trauma
[AD-A189771] 15 p2102 N88-22521

MUTAGENS
Genetic effects of low level microwave radiation
[AD-A192687] 21 p2984 N88-27722

MUTATIONS
Xiphophorus as an experimental system for genetic and biological development studies under microgravity conditions 01 p0074 N88-10472
Xiphophorus: A system to recognize radiation-induced mutations and to study the effects of zero-gravity environment on embryo development
07 p0885 N88-15372
Investigation of genetic structures of rat germ cells following flight aboard Cosmos-1514 biosatellite during their prenatal development 10 p1364 N88-18155

MX MISSILE
Convective heat transfer and its effect on inertial measurement units 12 p1578 N88-19442

MYOCARDIAL INFARCTION
Aircraft accident report: Joe Foster Excavating, Inc., Bell 206B, N49606, in-flight collision with trees, Alamo, California, August 3, 1986
[PB88-910405] 20 p2755 N88-26345

MYOCARDIUM
Myosin Ca sup (2+), Mg sup (2+)-adenosine triphosphatase activity in ray myocardium following 30-day expose to 1.1 and 2.0 G 10 p1362 N88-18141
Effect of cardioactive compounds on rat myocardium actomyosin following exposure to accelerations
10 p1365 N88-18161

MYOELECTRICITY
The efficacy of using human myoelectric signals to control the limbs of robots in space
[NASA-CR-182901] 18 p2553 N88-25155

MYOPIA
Does the knife open perspectives for the myopic pilot?
[ETN-87-90166] 09 p1199 N88-17187

N

N-BODY PROBLEM
U MANY BODY PROBLEM

N-P JUNCTIONS
U P-N JUNCTIONS

N-P-N JUNCTIONS
Vertical charge transport in junction charge-coupled devices
[ETN-88-91613] 09 p1255 N88-17523
Neutron effects on the electrical and switching characteristics of NPN bipolar power transistors
17 p2431 N88-24463

N-TYPE SEMICONDUCTORS
Integrated fiber-optic coupler
[AD-A184494] 03 p0377 N88-12369
Point defect structure of Cr2O3
[AD-A187620] 11 p1556 N88-19317
Fundamental studies and device development in beta silicon carbide
[AD-A189540] 12 p1699 N88-20165
Calculating depletion region carrier concentrations with capacitance-voltage measurements and etching
[AD-A189630] 15 p2141 N88-22777
Electrical anisotropy of layered semiconductor ZrSe2
16 p2257 N88-23488
Photovoltaic cells with n-silicon and conductive polymers
[ETN-88-92133] 20 p2821 N88-26734
Electrical properties of p-type and n-type ZnSe-ZnTe strained-layer superlattices 20 p2868 N88-27029
Growth and characterization of CuGaS2, CuAlS2 and CuGa0.9Al0.1S2 single crystals
[AD-A192963] 21 p3021 N88-27930

NACELLES
Numerical computation of transonic potential flow about 3-dimensional inlets
[NAL-TR-924] 02 p0122 N88-10770
Computation of transonic flows with nacelle simulation
[SNIAS-872-111-117] 05 p0542 N88-13300
Low speed wind tunnel investigation of propeller slipstream aerodynamic effects on different nacelle/wing combinations. Part 1: Total forces and moments and pressure distributions on nacelle/wing at different angles of attack and yaw and at different thrust coefficients
[FFA-TN-1987-22] 05 p0542 N88-13302
Aerodynamic and propeller performance characteristics of a propfan-powered, semispan model
[NASA-TM-86705] 06 p0667 N88-14002
Natural laminar flow nacelle for transport aircraft
07 p0813 N88-14949
Flight research on natural laminar flow
07 p0813 N88-14950
Roughness and waviness requirements for laminar flow surfaces 07 p0813 N88-14953
Testing of the engine compartment fire extinguishing system in the F/EF-111 aircraft
[AD-A188801] 12 p1576 N88-19423

NAMIBIA
Evolution of thermal structure of Benguela upswelling system according to satellite and shipboard data
24 p3449 N88-30525

NAMING
NT NORMS
Contributions to geodesy, photogrammetry, and cartography. Series 2, number 45
[ISSN-0469-4244] 01 p0065 N88-10416
Digital Name Data Base Antarctic as a component of a landscape data base of the Antarctic
01 p0065 N88-10419
Inventory of topographic mapping and standardization of geographic names as the basis of a Geographic Information System (GIS) 16 p2225 N88-23281

NAP-OF-THE-EARTH NAVIGATION
Investigation of vertical axis handling qualities for helicopter hover and NOE flight
03 p0263 N88-11653
Handling qualities criterion for very low visibility rotorcraft 03 p0263 N88-11654
Some data processing requirements for precision Nap-Of-the-Earth (NOE) guidance and control of rotorcraft
[NASA-CR-177453] 04 p0401 N88-12493
Low altitude: A new dimension in air refueling
[AD-A193819] 23 p3176 N88-28910
LANTIRN simulator training in the F-16C
[AD-A195201] 24 p3330 N88-29826

NAPHTHALENE
Transport and relaxation processes in supercritical fluids
[DE88-004804] 10 p1419 N88-18474

NAPHTHENES
Availability and cost estimate of a high naphthene, modified aviation turbine fuel
[NASA-TM-100823] 13 p1749 N88-20455

NARCOTICS
NT MORPHINE

NARROWBAND
Improving the method of calculating electronic properties of narrow bandgap semiconductors
07 p0926 N88-15627
Estimation of broadband planetary albedo from operational narrowband satellite measurements
[PB88-107644] 07 p0945 N88-15748
Simulated performance of an order statistic threshold strategy for detection of narrowband signals
11 p1474 N88-18796
Optimal and conventional space-time processing in flow noise
[AD-A189104] 13 p1833 N88-20965
A study on the co- and adjacent channel protection requirements for mobile satellite ACSSB modulation
19 p2650 N88-25732

NASA PROGRAMS
NT ACEE PROGRAM
NT EARTH RESOURCES PROGRAM
NT GALILEO PROJECT
NT NASA SPACE PROGRAMS
NT NATIONAL AEROSPACE PLANE PROGRAM
NT PROJECT SETI
NT QUIET ENGINE PROGRAM
NT ROVER PROJECT
NT SKYLAB PROGRAM
NT SUPERSONIC CRUISE AIRCRAFT RESEARCH
NT TILT ROTOR RESEARCH AIRCRAFT PROGRAM
Middle Atmosphere Program: Handbook for MAP, volume 24
[NASA-CR-181451] 01 p0069 N88-10444
Budget reimbursements: The National Aeronautics and Space Administration's reimbursable work
[PB87-207296] 01 p0107 N88-10696
Space technology to meet future needs
[NASA-CR-181473] 02 p0130 N88-10819
Report from the MPP Working Group to the NASA Associate Administrator for Space Science and Applications
[NASA-TM-87819] 02 p0223 N88-11402
Spinoff, 1987
[NASA-TM-89552] 02 p0250 N88-11577
Materials processing in space program support
[NASA-CR-179217] 03 p0298 N88-11872
Natinnal Aeronautics and Space Administration Authorization Act, 1988
[PUB-LAW-100-147] 03 p0385 N88-12422
Department of Housing and Urban Development, and Certain Independent Agencies Appropriations, 1988, Part 2
[S-HRG-100-106-PT-2] 03 p0385 N88-12423
Department of Housing and Urban Development-Independent Agencies Appropriations for fiscal year 1988, Thursday, 9 April 1987: National Aeronautics and Space Administration
03 p0386 N88-12424
Department of Housing and Urban Development-Independent Agencies Appropriations for fiscal year 1988, Friday, 10 April 1987: National Aeronautics and Space Administration
03 p0386 N88-12425
Spinoff
[NASA-TM-89651] 03 p0386 N88-12426
FY 1985 scientific and technical reports, articles, papers and presentations
[NASA-TM-86521] 04 p0501 N88-13083
National Aeronautics and Space Administration space station proposal, fiscal year 1988
[S-HRG-100-328] 05 p0659 N88-14043
The 1988 NASA (National Aeronautics and Space Administration) authcrization
[GPO-80-245] 05 p0659 N88-14044
University program management information system, fiscal year 1985
[NASA-TM-88381] 06 p0790 N88-14846
The 1988 National Aeronautics and Space Administration (NASA) authorization
[GFO-76-600] 06 p0792 N88-14854
National Aeronautics and Space Administration (NASA)/American Society for Engineering Education (ASEE) Summer Faculty Fellowship Program, 1987. Volume 1
[NASA-CR-172009-VOL-1] 06 p0792 N88-14855
A study of the minority college programs at the NASA Johnson Space Center 06 p0798 N88-14887
Research reports: 1987 NASA/ASEE Summer Faculty Fellowship Program
[NASA-CR-179219] 07 p0922 N88-15601
Risk analysis methodology survey
07 p0922 N88-15604
Compilation and development of K-6 aerospace materials for implementation in NASA spacelink electronic information system 07 p0922 N88-15605
NASA patent abstracts bibliography: A continuing bibliography. Section 1: Abstracts (supplement 32)
[NASA-SP-7039(32)-SECT-1-ABST]
07 p0943 N88-15732
Future plans for the NASA suborbital program
08 p1034 N88-16267
NASA thesaurus supplement: A four part cumulative supplement to the 1985 edition of the NASA Thesaurus
[NASA-SP-7053(SUPP-4)] 08 p1093 N88-16575
Research and technology 1987
[NASA-TM-4021] 09 p1265 N88-17577
Report of the Committee on the Space Station of the National Research Council
[NASA-CR-181602] 10 p1292 N88-17727
Into the thermosphere: The atmosphere explorers
[NASA-SP-490] 10 p1353 N88-18084
NASA patent abstracts bibliography: A continuing bibliography. Section 2: Indexes (supplement 32)
[NASA-SP-7039(32)-SECT-2] 10 p1425 N88-18511
Preliminary analysis of an integrated logistics system for OSSA payloads. Volume 1: Executive summary
12 p1584 N88-19478
Preliminary analysis of an integrated logistics system for OSSA payloads. Volume 2: OSSA integrated logistics support strategy 12 p1584 N88-19479
Communication satellites: Guidelines for a strategic plan
[NASA-TM-89306] 12 p1599 N88-19569
Selling to NASA
[NASA-TM-89724] 12 p1705 N88-20208
NASA/UK TAP
[NASA-CR-180350] 12 p1708 N88-20223
A project to transfer technology from NASA centers in support of industrial innovation in the midwest
[NASA-CR-180360] 12 p1708 N88-20224
Development of a nationwide network for technology transfer
[NASA-CR-181058] 12 p1709 N88-20225
The Joint NASA/Goddard-University of Maryland Research Program in Charged Particle and High Energy Photon Detector Technology
[NASA-CR-182612] 12 p1712 N88-20247
Research and technology, 1987
[NASA-TM-100323] 12 p1713 N88-20253
The Deep Space Network
[NASA-CR-182700] 13 p1759 N88-20524
Application of expert systems in project management decision aiding
[NASA-CR-180762] 13 p1850 N88-21074
Johnson Space Center's strategic game plan: Charting a course to the year 2000 and beyond
[NASA-TM-89733] 13 p1850 N88-21076
NASA advanced turboprop research and concept validation program
[NASA-TM-100891] 16 p2163 N88-22902
Department of Housing and Urban Development independent agencies appropriations for 1989. Part 7. National Aeronautics and Space Administration
[GPO-85-166] 16 p2286 N88-23689
PAN AIR analysis of the NASA/MCAIR 279-3: An advanced supersonic V/STOL fighter/attack aircraft
[NASA-TM-86838] 17 p2298 N88-23750
Structural ceramics research
17 p2324 N88-23878
Structures and Dynamics Division research and technology plans for FY 1988 and accomplishments for FY 1987
[NASA-TM-100585] 17 p2350 N88-24000
NAS: The first year
[NASA-TM-101006] 18 p2560 N88-25196
Financial reporting: NASA (National Aeronautics and Space Administration) can improve compliance with GAO (General Accounting Office) standards and treasury requirements
[PB88-172523] 18 p2587 N88-25373
NASA combined file postings statistics based on NASA thesaurus, Jan. 1968 - July 1988
[NASA-CR-182985] 18 p2589 N88-25384
NASA patent abstracts bibliography: A continuing bibliography. Section 1: Abstracts
[NASA-SP-7039(33)] 18 p2590 N88-25388
NASA history data book. Volume 1: NASA resources 1958-1968
[NASA-SP-4012-VOL-1] 18 p2596 N88-25428
NASA historical data book. Volume 2: Programs and projects 1958-1968
[NASA-SP-4012-VOL-2] 18 p2596 N88-25429
NASA historical data book. Volume 3: Programs and projects 1969-1978
[NASA-SP-4012-VOL-3] 18 p2596 N88-25430
Overview of NASA research in fiber optics for aircraft controls
[NASA-TM-100919] 19 p2603 N88-25458
Resources: NASA for entrepreneurs
[NASA-CR-182152] 20 p2883 N88-27119
Bibliography of Lewis Research Center technical publications announced in 1987
[NASA-TM-100910] 22 p3162 N88-28832
SR-7A aeroelastic model design report
[NASA-CR-174791] 23 p3179 N88-28928
Development and verification of NASA Standard Initiator-2 (NSI-2)
[NASA-CR-172069] 23 p3200 N88-29044
Development and verification of NASA Standard Initiator-2 (NSI-2): Appendix
[NASA-CR-172070] 23 p3200 N88-29045

NASA SPACE PROGRAMS
NT EARTH RESOURCES PROGRAM
NT GALILEO PROJECT
NT PROJECT SETI
NT ROVER PROJECT
NT SKYLAB PROGRAM
Columbus preparatory program. Payload element study on a technology demonstration mission, executive summary
[CS-RP-AI-016] 01 p0014 N88-10080
NASA/JPL study on optical imaging interferometry in space 01 p0096 N88-10630
Space station. National Aeronautics and Space Administration's 1987 cost estimate
[PB87-220760] 02 p0140 N88-10883
The Telecommunications and Data Acquisition Report
[NASA-CR-181546] 04 p0432 N88-12679
Expert system development for commonality analysis in space programs 07 p0928 N88-15635
NASA (National Aeronautics and Space Administration) ADP (Automated Data Processing) system: Information on the automated mission and the payload tracking system
[PB88-104989] 07 p0942 N88-15730
Update of NASA's ocean colour activities
08 p1042 N88-16295
The European space physics analysis network
08 p1099 N88-16613
An overview of the current Earth observation programs (Europe, USA, and Japan) 09 p1129 N88-16778
America plans for space
[AD-A187465] 10 p1289 N88-17713
Relationships between coronary heart disease risk factors and serum ionized calcium in Kennedy Space Center Cohort
[NASA-TM-100979] 10 p1368 N88-18177
Research and technology 1987 annual report of the Kennedy Space Center
[NASA-TM-100303] 10 p1431 N88-18548
Columbus feasibility studies. Volume 4: Integration, test, and operations
[ETN-88-90576] 11 p1445 N88-18614
NASA (National Aeronautics and Space Administration) procurement: The 1973 space shuttle solid rocket motor contractor selection
[PB88-135264] 11 p1447 N88-18623
NASA Office of Space Flight (OSF) in-orbit servicing program 12 p1587 N88-19498
NASA's geodynamics program
12 p1644 N88-19845
Aeronautics and space report of the President: 1986 activities 13 p1852 N88-21087
Chronology of KSC and KSC related events for 1987
[NASA-CR-182754] 14 p2012 N88-22002
Science at NASA field centers: Findings and recommendations on the scope, strength and interactions of science and science-related technology programs
[NASA-TM-101188] 24 p3459 N88-30581
Research and technology of the Lyndon B. Johnson Space Center
[NASA-TM-100463] 24 p3460 N88-30583

NASA STRUCTURAL ANALYSIS PROGRAM
U NASTRAN

NASTRAN
Qualification by analysis of IUS plume deflectors
09 p1179 N88-17063

Optimized structure design using reanalysis techniques 09 p1180 N88-17067

Dynamic substructuring for shock spectrum analysis using component mode synthesis
11 p1499 N88-18950

Sixteenth NASTRAN (trademark) Users' Colloquium
[NASA-CP-2505] 13 p1780 N88-20652

A preliminary investigation of finite-element modeling for composite rotor blades
[NASA-TM-100559] 13 p1781 N88-20656

Thermostructural analysis of simulated cowl lips
15 p2080 N88-22403

Lewis Structures Technology, 1988. Volume 1: Structural Dynamics
[NASA-CP-3003-VOL-1] 16 p2217 N88-23226

Analysis of rotating flexible blades using MSC/NASTRAN 16 p2222 N88-23259

Interactive plotting of NASTRAN aerodynamic models using NPLOT and DISSPLA
[AD-A194115] 23 p3226 N88-29204

Computer programs for generation of NASTRAN and VIBRA-6 aircraft models
[AD-A195467] 24 p3323 N88-29792

NATIONAL AEROSPACE PLANE PROGRAM

Hypersonic propulsion research
08 p0958 N88-15812

Numerical investigations in three-dimensional internal flows
[NASA-CR-183108] 23 p3210 N88-29106

NATIONAL AIRSPACE SYSTEM

FAA (Federal Aviation Administration) technical center: Mission and role in natinal airspace system plan implementation
[PB88-169818] 18 p2460 N88-24609

NATIONAL SEVERE STORMS PROJECT

Verification of severe local storm forecasts issued by the National Severe Storms Forecast Center, 1986
[PB88-101407] 06 p0747 N88-14594

NATIONS
NT ALABAMA
NT ALASKA
NT ARIZONA
NT AUSTRALIA
NT BELGIUM
NT BRAZIL
NT BRITISH COLUMBIA
NT BURKINA
NT BURUNDI
NT CALIFORNIA
NT CANADA
NT CHAD
NT CHINA
NT COLOMBIA
NT CONNECTICUT
NT CZECHOSLOVAKIA
NT DELAWARE
NT EGYPT
NT ENGLAND
NT FINLAND
NT FLORIDA
NT FRANCE
NT HAWAII
NT HUNGARY
NT ICELAND
NT ILLINOIS
NT INDIA
NT INDONESIA
NT ISRAEL
NT ITALY
NT JAPAN
NT KANSAS
NT KENTUCKY
NT KENYA
NT LAOS
NT MAINE
NT MALDIVE ISLANDS
NT MALI
NT MASSACHUSETTS
NT MEXICO
NT MICHIGAN
NT MISSISSIPPI
NT NEPAL
NT NETHERLANDS
NT NEVADA
NT NEW MEXICO
NT NEW YORK
NT NEW ZEALAND
NT NORTH CAROLINA
NT NORTH DAKOTA
NT NORWAY
NT SCOTLAND
NT SIERRA LEONE
NT SPAIN
NT SRI LANKA
NT SWEDEN
NT SWITZERLAND
NT SYRIA
NT TAIWAN
NT TEXAS
NT THAILAND
NT TIBET
NT TUNISIA
NT TURKEY
NT U.S.S.R.
NT UNITED KINGDOM
NT UNITED STATES
NT WEST GERMANY
NT WISCONSIN
NT WYOMING
NT YEMEN
NT ZIMBABWE

NATURAL FREQUENCIES
U RESONANT FREQUENCIES

NATURAL GAS

Laser probes of natural gas ignition chemistry
[PB87-209599] 01 p0021 N88-10129

Endurance testing of a natural gas-fueled rotary engine
[PB87-215703] 01 p0055 N88-10356

Development of a light duty gas engine for cogeneration service
[PB87-221297] 02 p0180 N88-11119

Use of natural gas diesel engines in mechanical pulp production: A preliminary study
[DE87-753065] 02 p0181 N88-11129

High pressure autoignition of natural gas/air mixtures and the problem of engine knock
[DE87-013799] 03 p0284 N88-11784

Advanced natural gas fueled engine development. Part 1: Design and analyses
[PB87-224804] 03 p0331 N88-12087

Advanced natural gas fueled engine development. Part 2: Materials investigation
[PB87-223160] 03 p0331 N88-12088

Thermodynamic properties for natural gas binaries
[PB87-226833] 04 p0500 N88-13074

Projects within the Center for Advanced Materials
[PB88-123054] 06 p0677 N88-14143

Advanced communication systems: A report on fiber optic technology and its possible applications in the gas industry
[PB88-112792] 07 p0845 N88-15125

Geological evolution and analysis of confirmed or suspected gas hydrate localities. Volume 9: Formation and stability of gas hydrates of the Middle America Trench
[DE88-001007] 10 p1347 N88-18050

Basic research on natural gas combustion phenomena
[PB88-168380] 14 p1887 N88-21278

Assessment of opportunities for gas-fired sintering in the advanced ceramics and powdered metals industries
[PB88-197157] 19 p2620 N88-25545

Direct gas injection with glow plug ignition
[PB88-187323] 19 p2676 N88-25911

Advanced energy system program
[PB88-183025] 19 p2686 N88-25965

Development of an equation of state for computation of supercompressibility factors, critical flow factors and other properties for wet, sour natural gases, synthetic gases and admixtures
[PB88-202676] 20 p2798 N88-26602

Laser probes of natural gas ignition chemistry
[PB88-212568] 21 p2910 N88-27271

Absorption heat pumps
[DE88-752820] 23 p3229 N88-29218

NATURAL LANGUAGE (COMPUTERS)

Intelligent man/machine interfaces on the space station 08 p1063 N88-16418

SWAN: An expert system with natural language interface for tactical air capability assessment
09 p1210 N88-17253

Voice/natural language interfacing for robotic control
[AD-A187765] 11 p1494 N88-18917

Research in knowledge representation for natural language communication and planning assistance
[AD-A187355] 11 p1522 N88-19087

State of the art of natural language processing
[AD-A188112] 11 p1530 N88-19136

Realization of natural language style robot task instruction by using the object oriented concept
16 p2257 N88-23487

A cockpit natural language study - selected transcripts
[AD-A192972] 20 p2834 N88-26808

The effect of input device on user performance with a menu-based natural language interface
[AD-A193095] 21 p2996 N88-27772

An expert system for natural language processing
23 p3263 N88-29426

Exploiting lexical regularities in designing natural language systems
[AD-A195922] 24 p3423 N88-30375

NATURAL LASERS
U LASERS

NATURAL SATELLITES
NT DEIMOS
NT IO
NT JUPITER SATELLITES
NT MOON
NT PHOBOS
NT SATURN SATELLITES
NT TITAN
NT TITANIA
NT URANUS SATELLITES

A technique for capture analysis of low thrust missions in a planetary system
[AD-A188934] 12 p1594 N88-19544

Extended atmospheres of outer planet satellites and comets
[NASA-CR-183157] 24 p3457 N88-30572

NAUTICAL CHARTS

Generation of thematic maps for updating aeronautical pilot charts utilizing LANDSAT-TM images
17 p2361 N88-24062

Contribution of spaceborne high resolution radiometers to mapping of precoastal depths
19 p2701 N88-26063

NAVIER-STOKES EQUATION

Accurate, stable, explicit solution of the parabolized Navier-Stokes equations 01 p0043 N88-10276

Laminar flow over a spinning projectile at an angle of attack 02 p0121 N88-10766

Navier-Stokes cascade analysis with a stiff Kappa-Epsilon turbulence solver
[NASA-TM-100218] 02 p0123 N88-10778

Characteristics and boundary elements for three dimensional nonstationary Navier Stokes flows
[PREPRINT-1051] 02 p0172 N88-11086

Personal Computer (PC) based image processing applied to fluid mechanics
[NASA-TM-100024] 02 p0172 N88-11087

Computation of transonic separated wing flows using an Euler/Navier-Stokes zonal approach
[NASA-TM-88311] 02 p0173 N88-11089

Flow in a model turbine stator
02 p0187 N88-11163

Efficient numerical approaches for predicting supersonic flows with viscous/inviscid interaction
03 p0260 N88-11637

Application of an upwind algorithm to the parabolized Navier-Stokes equations 03 p0316 N88-12000

The diffusion-convection vortex method for solving two-dimensional incompressible Navier-Stokes equation
03 p0317 N88-12001

Development and application of computational aerothermodynamics flowfield computer codes
[NASA-CR-181534] 04 p0395 N88-12465

Blowup for a nonlinear evolution equation and self-reproducing strained shear layers
04 p0444 N88-12755

Cauchy problem for linearized system of Navier-Stokes equations considering compressibility
04 p0459 N88-12837

Asymptotic form of stationary solutions of the Navier-Stokes equations for large Reynolds numbers
04 p0459 N88-12838

On operator splitting for unsteady boundary value problems
[AD-A184281] 04 p0484 N88-12981

INS3D: An incompressible Navier-Stokes code in generalized three-dimensional coordinates
[NASA-TM-100012] 04 p0483 N88-12991

Numerical analysis of flow through scramjet engine inlets 05 p0532 N88-13233

Numerical simulation of the hypersonic flow around lifting vehicles 05 p0532 N88-13234

Solution of some 3-D viscous and inviscid supersonic flow problems by finite-volume space-marching schemes
05 p0532 N88-13235

Numerical experiments with hypersonic flows beneath a cone-delta-wing combination 05 p0532 N88-13236

Numerical analysis of cascade flow solving Navier-Stokes equations 05 p0536 N88-13262

Relaxation method for the compressible Navier-Stokes equations using upwind schemes
05 p0539 N88-13263

Navier-Stokes analysis of laminar flow control of a two-dimensional airfoil 05 p0540 N88-13286

Navier-Stokes simulation of transonic transportation aircraft configurations. 1: Flow-field simulation over wing-fuselage combinations 05 p0540 N88-13288

Numerical simulation of transonic aircraft in comparison to wind tunnel test 05 p0540 N88-13289

Calculation of helicopter rotor blade/vortex interaction by Navier-Stokes procedures
[NASA-CR-177441] 05 p0540 N88-13291

Solution procedure for the Navier-Stokes equations applied to rotors 05 p0579 N88-13533

Physical analysis and numerical simulation of coherent turbulent structures in mixed layers, jets, and wakes [ETN-88-91183] 05 p0581 N88-13548

Low thrust viscous nozzle flow fields prediction [NASA-CR-182334] 05 p0582 N88-13551

The interaction of DC plasma jet with a melting metal: Experimental measurements and mathematical description [AD-A185173] 05 p0651 N88-13993

Transonic Navier-Stokes computations of strake-generated vortex interactions for a fighter-like configuration 06 p0664 N88-14073

Post stall behavior in axial-flow compressors [AD-A185712] 06 p0665 N88-14081

Vectorization of a multigrid method for the compressible Navier-Stokes equations [PB87-230496] 06 p0698 N88-14284

Computational fluid dynamics overview 07 p0809 N88-14927

Upwind relaxation algorithms for Euler/Navier-Stokes equations 07 p0810 N88-14931

A multistage time-stepping scheme for the thin-layer Navier-Stokes equations 07 p0810 N88-14932

Numerical simulation of a controlled boundary layer 07 p0810 N88-14933

Viscous vortex flows 07 p0810 N88-14934

Analysis and performance prediction of scramjet inlets utilizing a three-dimensional Navier-Stokes code 07 p0811 N88-14936

Boundary layer transition 07 p0811 N88-14942

The numerical and analytical study of bifurcation and multicellular flow instability due to natural convection between narrow horizontal isothermal cylindrical annuli at high Rayleigh numbers [AD-A186113] 07 p0849 N88-15151

On the parabolized Navier-Stokes equations without sublayer assumptions [AD-A186127] 07 p0849 N88-15152

Analysis of three-dimensional viscous internal flows [AD-A186254] 07 p0849 N88-15155

Multitasked embedded multigrid for three-dimensional flow simulation [NASA-CR-182398] 07 p0852 N88-15173

Consistent boundary conditions for Reduced Navier-Stokes (RNS) scheme applied to 3-dimensional internal viscous flows [NASA-CR-180874] 08 p0950 N88-15762

The simulation of three-dimensional viscous supersonic flow past blunt bodies with a hybrid implicit/explicit finite difference method [DFVLR-FB-87-32] 08 p0950 N88-15765

Inlets, ducts and nozzles 08 p0955 N88-15791

Turbomachinery 08 p0955 N88-15792

Integration of Navier-Stokes equations in finite volume formulation 08 p0984 N88-15954

Viscous flows. Part 3: Formulation of the Navier-Stokes equations by stream function vorticity methods 08 p0986 N88-15969

Navier-Stokes solutions for laminar incompressible flow over a NACA 0012 airfoil and a backward facing step [FFA-TN-1987-50] 09 p1162 N88-16966

A project to experimentally and theoretically examine fluid interfacial wave phenomena in a rotating cylindrical geometry: Current results and future plans [DE88-003738] 09 p1165 N88-16984

Numerical modeling of multidimensional flow in seals and bearings used in rotating machinery [NASA-TM-100779] 09 p1165 N88-16988

Numerical solutions of three-dimensional Navier-Stokes equations for closed-bluff bodies [NASA-CR-182359] 09 p1166 N88-16990

Solution of the three-dimensional Navier-Stokes equations for transonic flow using a multigrid method 10 p1267 N88-17579

Navier-Stokes simulation of wind-tunnel flow using LU-ADI factorization algorithm [NASA-TM-100042] 10 p1268 N88-17584

Navier-Stokes calculations and turbulence modeling in the trailing edge region of a circulation control airfoil 10 p1268 N88-17587

Evaluation of a research circulation control airfoil using Navier-Stokes methods 10 p1269 N88-17591

Navier-Stokes computations for circulation control airfoils 10 p1269 N88-17592

Implicit solution of the incompressible Navier-Stokes equations in primitive variables on non-staggered grids 10 p1326 N88-17930

A numerical study of unsteady two-dimensional subsonic compressible base flow 10 p1327 N88-17931

The numerical and analytical study of bifurcation and multicellular flow instability due to natural convection between narrow horizontal isothermal cylindrical annuli at high Rayleigh numbers 10 p1328 N88-17937

Instability and transition in curved channel flow 10 p1328 N88-17938

Three-dimensional incompressible flowfield analysis for establishing rotor designs which optimize power extraction 10 p1329 N88-17943

Free-surface flow phenomena ahead of a two-dimensional body in a viscous fluid 10 p1329 N88-17944

A visual programming environment for the Navier-Stokes computer [NASA-CR-181615] 10 p1390 N88-18299

Implementation and analysis of a Navier-Stokes algorithm on parallel computers [NASA-CR-181614] 10 p1390 N88-18301

On the smallest scale for the incompressible Navier-Stokes equations [NASA-CR-181628] 11 p1434 N88-19558

Fluctuations and massive separation in three-dimensional shock-wave/boundary-layer interactions [NASA-TM-89224] 11 p1434 N88-18559

Comparisons of Monte-Carlo and PNS (Parabolized Navier-Stokes) calculations for rarefied flow over reentry vehicle configurations [DE88-004937] 11 p1435 N88-18560

High performance Solid Rocket Motor (SRM) submerged nozzle/combustion cavity flowfield assessment [NASA-CR-179307] 11 p1446 N88-18622

A code development system for computational fluid dynamics [AD-A188050] 11 p1482 N88-18848

A new computational technique for generating algorithms, with application to the solution of the time-dependent incompressible Navier-Stokes equations 11 p1485 N88-18864

Numerical and analytical study of fluid dynamic forces in seals and bearings [NASA-TM-100268] 11 p1485 N88-18867

A velocity-pressure integrated, mixed interpolation, Galerkin finite element method for high Reynolds number laminar flows [NASA-CR-179264] 11 p1486 N88-18868

Estimates of green tensors for certain boundary value problems [NASA-TT-20203] 11 p1535 N88-19172

Solution of a rotating Navier-Stokes problem by a nonlinear multigrid algorithm 11 p1538 N88-19194

Applications of a multigrid finite volume method with Runge-Kutta time integrations for solving the Euler and Navier-Stokes equations 11 p1539 N88-19201

Three-dimensional incompressible Navier-Stokes computations of internal flows [NASA-TM-100076] 12 p1576 N88-19425

A new parabolized Navier-Stokes code for chemically reacting flow fields 12 p1625 N88-19721

Time-accurate simulations of a shear layer forced at a single frequency [NASA-TM-100836] 12 p1628 N88-19740

Fully-coupled analysis of jet mixing problems. Three-dimensional PNS model, SCIP3D [NASA-CR-4139] 13 p1715 N88-20256

The construction of a three-dimensional finite volume grid generator for a wing in a wind tunnel with application to Navier-Stokes flow solvers [FFA-TN-1987-58] 13 p1719 N88-20277

Numerical model of the time independent mean flow in a rotating rocket motor 13 p1733 N88-20360

Calculations of viscous flows with a multigrid method 13 p1769 N88-20580

Numerical experiments on the stability of controlled boundary layers [NASA-CR-181649] 13 p1771 N88-20591

Numerical analysis of three-dimensional viscous internal flows [NASA-TM-100878] 14 p1861 N88-21116

High-speed flow calculations past 3-D configurations based on the Reynolds averaged Navier-Stokes equations [NASA-TM-100082] 14 p1911 N88-21421

Choice of implicit and explicit operators for the upwind differencing method [NASA-TM-100857] 14 p1964 N88-21718

High Reynolds number, low Mach number, steady flow field calculations over a NACA 0012 airfoil using Navier-Stokes and interactive boundary layer theory [AD-A189871] 15 p2013 N88-22005

Transonic Navier-Stokes computations of strake-generated vortex interactions for a fighter-like configuration [NASA-TM-100009] 15 p2014 N88-22010

Random processes, turbulence and disordering fields [AD-A190123] 15 p2063 N88-22303

Review and assessment of the HOST turbine heat transfer program 15 p2086 N88-22431

Numerical study of unsteady viscous hypersonic blunt body flows with an impinging shock [NASA-TM-100096] 15 p2122 N88-22650

High-resolution shock-capturing schemes for inviscid and viscous hypersonic flows [NASA-TM-100097] 15 p2122 N88-22651

A low dimensional dynamical system for the wall layer 16 p2194 N88-23088

Test code for the assessment and improvement of Reynolds stress models 16 p2197 N88-23105

Numerical treatment of Navier-Stokes equations [REPT-87-22] 16 p2206 N88-23162

Application of a multigrid method for solving the Navier-Stokes equation in two-dimensional flow problems [KU-SFB-210/T/32] 16 p2206 N88-23164

Some numerical methods for the computation of capillary free boundaries governed by the Navier-Stokes equations [REPT-87-69] 16 p2206 N88-23167

Fast algorithms for Euler and Navier-Stokes simulations [AD-A190897] 16 p2208 N88-23175

Solution of the compressible Navier-Stokes equations of motion by Chebyshev polynomials for laminar shock-boundary layer flow [AD-A191033] 16 p2208 N88-23176

Reduced order models for nonlinear aerodynamics 16 p2220 N88-23248

Application of Navier-Stokes analysis to stall flutter 16 p2220 N88-23249

Research in nonlinear partial differential equations and bifurcation theory [AD-A190986] 16 p2260 N88-23514

Numerical simulation of scramjet inlet flow fields [NASA-TP-2517] 17 p2296 N88-23735

An efficient parallel algorithm for the simulation of three-dimensional compressible transition on a 20 processor Flex/32 multicomputer [NASA-CR-178340] 17 p2337 N88-23943

Prediction of laminar and turbulent flows past single and twin airfoils 18 p2457 N88-24589

Some rotorcraft applications of computational fluid dynamics [NASA-TM-100066] 18 p2459 N88-24601

Applications of the Navier-Stokes equations to wings and complex configurations using a zonal approach [NASA-TM-100080] 18 p2459 N88-24602

Computation and characteristics of pulsatile multi-bifurcation flow 18 p2483 N88-24729

Composite reduced Navier-Stokes procedures for flow problems with strong pressure interactions [AD-A191127] 18 p2508 N88-24875

Two dimensional hyperbolic grid generation [VKI-TN-162] 18 p2511 N88-24897

Finite element solution of 3-D turbulent Navier-Stokes equations for propeller-driven slender bodies 18 p2515 N88-24919

Characteristic time correlations to liquid fuel ramjet combustion efficiency 19 p2624 N88-25566

Numerical investigation of acoustic energy exchange through flow turning 19 p2629 N88-25593

Aerodynamic analysis of natural laminar flow airfoil 19 p2634 N88-25624

Numerical calculation of supersonic flow by the PNS equations 19 p2636 N88-25636

Navier-Stokes analysis of transonic transport aircraft empennage 19 p2636 N88-25637

Numerical simulation of the shock tube flows by TVD scheme 19 p2638 N88-25648

Numerical calculation of three dimensional flow by TVD scheme 19 p2638 N88-25649

Numerical analysis of three dimensional cascade flow by solving Navier-Stokes equations 19 p2638 N88-25650

Numerical analysis of duct flow using three-dimensional parabolized Navier-Stokes equation 19 p2638 N88-25652

The role of computational fluid dynamics in aeronautical engineering (5). Improvements and applications of implicit TVD finite volume code 19 p2638 N88-25653

Scaling laws for homogeneous turbulent shear flows in a rotating frame [NASA-CR-181672] 19 p2665 N88-25847

Numerical simulation studies of laminar-turbulent transition in the plan channel 19 p2665 N88-25850

Navier-Stokes code NS3D for blunt bodies. Part 1: Analysis, results and verification [DE88-010105] 19 p2666 N88-25855

A Navier-Stokes solver for cascade flows [NASA-CR-181682] 19 p2666 N88-25856

Vortex methods for separated flows [NASA-TM-100068] 20 p2753 N88-26342

Numerical analysis of reconnection of vortex rings 20 p2782 N88-26500

Navier-Stokes simulation of shock tube flows over a wedge-type step by finite volume method [ISAS-RN-628] 20 p2797 N88-26599

Spectra' resolution of the Navier-Stokes equations in multi-domain curved complex geometries
[ONERA-NT-1987-2] 20 p2802 N88-26631

An h-p adaptive finite element method for steady compressible flow 21 p2941 N88-27467

A Navier-Stokes study of cascade flow fields including inlet distortion and rotating stall
[AD-A193109] 21 p2943 N88-27483

Computational boundary conditions for the incompressible Navier-Stokes equations in channels and pipes
[AD-A193356] 21 p2944 N88-27487

Numerical treatment of the pressure singularity at a re-entrant corner
[AD-A193357] 21 p2944 N88-27488

Stream function-vorticity finite elements and the resolution of the Navier-Stokes equations
[DE88-702318] 21 p2945 N88-27494

Determination of the local heat-transfer characteristics on glaze ice accretions on a cylinder and a NACA 0012 airfoil 21 p2946 N88-27500

Distributive iteration for indefinite systems as smoothing method in multigrid process on example of Stokes and Navier-Stokes equations with emphasis on incomplete decompositions
[ETN-88-92127] 21 p2948 N88-27509

Numerical integration of Navier-Stokes equations by application of multigrid concept
[ETN-88-92365] 21 p2949 N88-27513

The three-dimensional stress field around a cylindrical inclusion in a plate of arbitrary thickness
21 p2963 N88-27602

Runge-Kutta finite-volume simulation of laminar transonic flow over the ONERA M6 wing using the Navier-Stokes equations
[FFA-TN-1987-06] 22 p3039 N88-28045

Numerical computation of space shuttle orbiter flow field
[NASA-CR-183193] 22 p3040 N88-28048

A study of the vortex sheet method for solving the Prandtl boundary layer equations
[DE88-011346] 22 p3074 N88-28249

Solution to the compressible Navier-Stokes equations of motion by Chebyshev polynomials with implicit time stepping
[AD-A194119] 22 p3075 N88-28257

Steady and unsteady internal flow computations via the solution of the compressible Navier Stokes equations for low Mach numbers 23 p3209 N88-29100

Three-dimensional laser Doppler velocimeter studies of flow in a 90 deg curved duct having a square cross-section 23 p3209 N88-29101

Computation of the eigenvalues for perturbations of Poiseuille flow using a two-point boundary value method
[AD-A193479] 23 p3210 N88-29104

An exponential decay estimate for the stationary perturbation of Poiseuille flow
[AD-A193480] 23 p3210 N88-29105

An efficient patched grid Navier-Stokes solution for multiple bodies, phase 1
[AD-A194166] 23 p3211 N88-29110

Navier-Stokes calculations of transonic flows past cavities
[NASA-CR-180484] 23 p3212 N88-29116

Computational fluid dynamics methods for low Reynolds number processing/spinning incompressible flows
[AD-A193891] 23 p3212 N88-29119

Lessons learned in the mesh generation for PN/S calculations 23 p3245 N88-29314

Mesh generation for industrial application of Euler and Navier Stokes solvers 23 p3247 N88-29323

Experience with three dimensional composite grids
23 p3247 N88-29324

Three-dimensional Navier-Stokes simulations of turbine rotor-stator interaction
[NASA-TM-100081] 24 p3316 N88-29750

A streamwise upwind algorithm for the Euler and Navier-Stokes equations applied to transonic flows
[NASA-TM-101019] 24 p3316 N88-29751

Application of unsteady aerodynamic methods for transonic aeroelastic analysis
[NASA-TM-100665] 24 p3317 N88-29754

Aerodynamic heating of missiles
24 p3319 N88-29764

Computational aerodynamic analysis for a range-limited 25mm training round
[AD-A185270] 24 p3320 N88-29772

The computation of flow past an oblique wing using the thin-layer Navier-Stokes equations
[NASA-TM-88317] 24 p3320 N88-29774

On the application of finite-difference techniques for the computation of the flow field in gas turbine combustors with complex geometries 24 p3349 N88-29938

Modeling the stability of a turbulent premixed flame, downstream from a step by a Lagrangian method
24 p3350 N88-29943

Numerical simulation of unsteady incompressible viscous flows in generalized coordinate systems
[NASA-TM-101016] 24 p3373 N88-30085

NAVIGATION

NT AIR NAVIGATION
NT ALL-WEATHER AIR NAVIGATION
NT AREA NAVIGATION
NT DEAD RECKONING
NT DIGITAL NAVIGATION
NT INERTIAL NAVIGATION
NT LORAN C
NT NAP-OF-THE-EARTH NAVIGATION
NT OMEGA NAVIGATION SYSTEM
NT RADIO NAVIGATION
NT SPACE NAVIGATION
NT SURFACE NAVIGATION

Calendar of selected aeronautical and space meetings
[AGARD-CAL-87/1] 05 p0657 N88-14033

The power of neural nets 08 p1064 N88-16430

Navigation planning using quadtrees
[DE88-003706] 09 p1225 N88-17343

An overview of vision-based navigation for autonomous land vehicles 1986
[AD-A188186] 10 p1276 N88-17640

Search problems in mission planning and navigation of autonomous aircraft
[NASA-CR-182666] 12 p1579 N88-19448

Alaska Loran C probe test results
[AD-A189131] 13 p1720 N88-20284

The visit problem: Visibility graph-based solution
[DE88-000343] 15 p2108 N88-22556

A design study of onboard navigation and guidance during aerocapture at Mars
[NASA-CR-172053] 18 p2469 N88-24654

Ice conditions along the Ohio River as observed on LANDSAT images, 1972-1985
[AD-A191172] 18 p2531 N88-25018

Robot navigation using simple sensor fusion
[DE88-006184] 18 p2561 N88-25203

Aircraft accident report: Midair collision of SkyWest Airlines Swearingen METRO 2, N163SW, and Mooney M20, N6485U, Kearns, Utah, January 15, 1987
[PB88-910404] 20 p2755 N88-26346

Treatment of systematic errors in the processing of wide angle sonar sensor data for robotic navigation
[DE88-008961] 20 p2756 N88-26352

Spacecraft applications of advanced global positioning system technology
[NASA-CR-172063] 20 p2757 N88-26359

Sensor fusion for robot navigation
[DE88-008383] 20 p2809 N88-26663

Kalman filter-based algorithms for estimating depth from image sequences
[AD-A195818] 24 p3424 N88-30380

NAVIGATION AIDS

NT ATTITUDE INDICATORS
NT BEACONS
NT NAVIGATION INSTRUMENTS
NT RADAR BEACONS
NT RADIO BEACONS

Advanced dead reckoning navigation for mobile robots
03 p0262 N88-11646

Comparison of alphanumeric data entry methods for advanced helicopter cockpits
[AD-A186934] 09 p1201 N88-17201

Navigation recovery block design description
[NASA-CR-182473] 10 p1342 N88-18022

Optimal selection of global positioning system set to minimize emitter location errors
[AD-A189559] 12 p1579 N88-19447

Assessment of the differential technique for land navigation within 1000 km of Omega Australia
[AD-A191036] 16 p2160 N88-22885

The integration of digital maps in vehicle navigation systems 16 p2225 N88-23286

Refraction in underwater acoustics --- navigation systems
[B8735053] 17 p2395 N88-24236

Search and rescue satellite system (SERES), phase AD
[ETN-88-92335] 18 p2472 N88-24669

Digital maps for an electronic traffic guide
18 p2534 N88-25033

Geographical information for design purposes
[NLR-MP-87014-U] 20 p2818 N88-26719

Accuracy of satellite data navigation
[AD-A195877] 24 p3322 N88-29787

The guide star catalog
[NASA-CR-183253] 24 p3452 N88-30547

NAVIGATION INSTRUMENTS

NT ATTITUDE INDICATORS

Simple 2-D navigation for wheeled vehicles
[DE88-007115] 20 p2756 N88-26351

Observed track-keeping performance of DC10 aircraft equipped with the Collins AINS-70 area navigation system: Karlsruhe and Masstricht UACs (Upper Area Control centres)
[EEC-202] 24 p3323 N88-29788

NAVIGATION SATELLITES

NT NAVSTAR SATELLITES

Accurate position measuring spacecraft package
[ESA-CR(P)-2398-VOL-1] 01 p0004 N88-10022

Accurate position measuring spacecraft package, executive summary
[ESA-CR(P)-2398-VOL-2] 01 p0004 N88-10023

Implications of a simplified signal structure for Navsat
[REPT-63/1439] 01 p0005 N88-10024

Planning and execution of the NAVEX experiment in the Spacelab Mission D1
[DFVLR-FB-87-03] 01 p0010 N88-10056

Dynamic positioning at sea using the global positioning system
[AD-A184453] 04 p0397 N88-12476

Use of the global positioning system for trajectory determination of SRAM 2 missiles at the Eastern Test Range
[AD-A185266] 05 p0544 N88-13314

Determination of TRANET (tracking station coordinates for tracking network) and SMTP (Special Mission Tracking Program) tracking station coordinates for use in the WGS (World Geodetic System) 84
[AD-A185863] 07 p0817 N88-14972

NAVARES: A prototype expert system for NAVSTAR anomaly resolution
[AD-A189491] 12 p1600 N88-19579

The NAVEX experiment in the Spacelab D1 mission: Planning and execution
[ESA-TT-1078] 16 p2166 N88-22913

NAVIGATORS

US civil airmen statistics, 1987
[AD-A191714] 18 p2455 N88-24577

NAVSTAR SATELLITES

Mobile test fixture system for use in a thermal vacuum facility 02 p0134 N88-10843

On-orbit frequency stability analysis of the GPS NAVSTAR 8 rubidium clock and NAVSTARs 9 and 10 cesium clocks
[AD-A184984] 05 p0544 N88-13312

NAVARES: A prototype expert system for NAVSTAR anomaly resolution
[AD-A189491] 12 p1600 N88-19579

Satellite acquisition: Global positioning system acquisition changes after Challenger's accident
[PB88-155536] 14 p1880 N88-21236

Global Positioning System (GPS) exploitation by ODOT (Ohio Department of Transportation)
[PB88-172796] 16 p2159 N88-22882

NAVSTAR global positioning system
[AD-A192609] 20 p2757 N88-26354

NAVY

Naval Aviation Integrated Logistics: Technical users guide version 1.0
[DE87-013368] 01 p0001 N88-10001

CNET (Chief of Naval Education and Training) Program Automated Tracking System (CPATS): A comprehensive study
[AD-A184694] 03 p0385 N88-12418

Avionic corrosion 05 p0547 N88-13332

A summary of the Naval Postgraduate School research program
[AD-A186362] 07 p0942 N88-15727

Meteorological radar and its usage in the Navy
[AD-A186650] 09 p1152 N88-16902

The evolution of naval warfare technology and the impact of space systems
[AD-A186900] 09 p1233 N88-17392

NROSS (Navy Remote Ocean Sensing System): A force multiplier
[AD-A186853] 10 p1346 N88-18045

US Navy climatic study of the Mediterranean Sea
[AD-A188264] 10 p1356 N88-18107

The accommodative status in the dark of US Navy fighter pilots
[AD-A188188] 10 p1370 N88-18186

Worldwide distributions of shipboard surface meteorological observations for EM propagation analysis
[AD-A188771] 12 p1648 N88-19871

A review of the NATO special group of experts on Naval hydromechanics and related problems
16 p2205 N88-23157

Challenges of physiological monitoring in a Navy operational setting 16 p2239 N88-23374

Naval research reviews, volume 39, number 3
[AD-A191392] 16 p2264 N88-23543

Analysis of gas turbine test cell number 1, Lemoore Naval Air Station, California
[AD-A192870] 20 p2762 N88-26380

Multiple-Purpose Subsonic Naval Aircraft (MPSNA): Multiple Application Propfan Study (MAPS)
[NASA-CR-175104] 23 p3177 N88-28917

The spatial and temporal variability of the arctic atmospheric boundary layer and its effect on electromagnetic (EM) propagation
[AD-A193958] 23 p3204 N88-29068

NC-130 AIRCRAFT
U C-130 AIRCRAFT

NEAR FIELDS

The effect of object potentials on the wake of a flowing plasma
[AD-A184038] 03 p0379 N88-12385

Power density measurements in the near field of the DSS 13 26-meter antenna 04 p0437 N88-12711

Regional wave attenuation and seismic moment from the inversion of NORESS spectra
[AD-A187399] 11 p1510 N88-19023

State-of-the-art for assessing earthquake hazards in the US. Parameters for specifying intensity-related earthquake ground motions
[AD-A188230] 11 p1512 N88-19032

Fast algorithm development for large-eddy simulation of circular-jet turbulence
[AD-A192044] 18 p2509 N88-24887

Effects of tectonic release on broadband regional distance bodywaves
[AD-A194247] 22 p3119 N88-28529

Application of sampling techniques to near-field far-field transformation
[ESA-CR(P)-2546] 24 p3359 N88-30002

NEAR INFRARED RADIATION

Near-infrared dichroism of a mesogenic transition metal complex and its solubility in nematic hosts
[DE87-014471] 03 p0287 N88-11805

Precise measurement of refractive index and absorption coefficient of near millimeter wave and far infrared materials
[AD-A184538] 03 p0293 N88-11840

A search for X-ray luminous late type stars in NIPSS data 04 p0511 N88-13143

Light curve behaviour in the near IR of the CG Cyg system 04 p0513 N88-13156

The angular diameter of alpha Scorpii in the near-infrared Ca II triplet 04 p0514 N88-13162

Measuring near infrared spectral reflectance changes from water stressed conifer stands with AIS-2
05 p0613 N88-13765

Lightning spectra in the near infrared
[DE88-002218] 07 p0880 N88-15341

Method of determining atmospheric moisture content by measurement of upward radiation intensity in near IR
08 p1007 N88-16106

Signal and data processing for IR sensors
10 p1374 N88-18199

Growth and characteristics of materials for tunable lasers in the near infrared spectral region
[NASA-CR-182501] 11 p1491 N88-18901

Global solar oscillations observed in the visible to near infrared continuum 13 p1858 N88-21110

Effect of atmospheric turbulence on the bit error probability of a space to ground near infrared laser communications link using binary pulse position modulation and an avalanche photodiode detector
[NASA-TM-100699] 14 p1873 N88-21189

Atmospheric attenuation of near infrared radiation propagating through fog 14 p1899 N88-21342

Near-infrared imaging of Comet Halley: Discovery of a color gradient in the inner coma
14 p2009 N88-21980

Near-infrared observations of cepheids: The distance to M33 15 p2152 N88-22846

A disposable liquid microcell for near-infrared reflectance analysis
[AD-A192190] 18 p2575 N88-25298

Infrared astronomy at extremely faint light levels in support of the LAIRTS program
[AD-A191497] 18 p2592 N88-25404

A new near-infrared tunable-room temperature solid state laser La3Ga5SiO14:Cr(3+)
[DE88-011341] 21 p2953 N88-27543

Growth and characterization of materials for tunable lasers in the near infrared spectral region
[NASA-CR-183132] 24 p3377 N88-30113

NEAR ULTRAVIOLET RADIATION

Literature survey relating to the absorption properties of ozone in the near ultraviolet
[ESRO-SM-81] 09 p1190 N88-17129

Spectroscopic studies of a laser-produced carbon plasma in the near and extreme ultraviolet
11 p1553 N88-19292

Dispersion measurements of microcrystals in the near ultraviolet and infrared
[DE88-006234] 15 p2145 N88-22800

NEAR WAKES

Investigation of large-scale structures in the near wake of a parallel flat plate
[DFVLR-FB-87-31] 09 p1162 N88-16967

Mean flow structure in the near wake of a turbulent junction vortex
[PB88-150115] 14 p1910 N88-21416

Influence of rear body geometry on the velocity characteristics of the near wake
[ISL-R-113/87] 20 p2753 N88-26339

Investigation of large-scale structures in the near wake of a parallel flat plate
[ESA-TT-1100] 24 p3372 N88-30080

NEARSHORE WATER
NT COASTAL WATER

NEBULAE
NT CRAB NEBULA
NT H II REGIONS
NT HERBIG-HARO OBJECTS
NT ORION NEBULA
NT PLANETARY NEBULAE

The astrophysics of nebulae and active galactic nuclear emission-line regions: New methods and applications
13 p1858 N88-21111

Far-infrared (120-300 micron) observations of the Carina Nebula 14 p1993 N88-21876

Para-ortho abundance ratio of molecular hydrogen in NGC2023
[ISAS-RN-352] 18 p2573 N88-25286

Cometary nucleus as aggregate of planetesimals
[ISAS-RN-364] 19 p2741 N88-26275

Comparisons of solar nebula models
24 p3451 N88-30539

Physical processes and timescales in planet and small-body accretion 24 p3451 N88-30540

Nebular processes recorded in chondritic meteorites
24 p3451 N88-30541

Cosmochemical trends of volatile elements in the solar system 24 p3451 N88-30542

Terrestrial versus giant planet formation
24 p3451 N88-30543

NECK (ANATOMY)

Motion and space sickness 04 p0404 N88-12510

Neck receptor stimulation in 0 and 1 g
12 p1658 N88-19938

Basic research on flame radiation
[PB88-168372] 15 p2032 N88-22105

Analysis of head response to torso acceleration. Volume 2: Description of data retrieval, analysis and display software
[PB88-156765] 15 p2104 N88-22536

NEEDLES

Selective growth velocity in needle crystals
14 p1988 N88-21858

NEGATIVE IONS
NT ANIONS

Negative ion beams for heating and current-drive in NET
[AD-A184390] 04 p0489 N88-13012

Theoretical studies of kinetic mechanisms of negative ion formation in plasmas
[AD-A185735] 06 p0784 N88-14812

Experiments on ion-acoustic rarefactive solitons in a multi-component plasma with negative ions
[INPE-4393-PRE/1213] 08 p1086 N88-16542

Gas phase reactions of electrons, negative ions and free-radicals with transition metal complexes
11 p1560 N88-19339

A moment approach to modeling negative ion sources
[AD-A188858] 12 p1691 N88-20114

Photoenhanced attachment for optical control of diffuse discharges
[AD-A188989] 12 p1696 N88-20147

Studies of compound states of negative ions using laser beams
[DE88-004708] 13 p1777 N88-20627

A new approach to generating negative ion beams
[AD-A191119] 18 p2572 N88-25276

An optical technique for measuring divergence, beam profile, and aiming direction, of relativistic negative hydrogen ions
[DE88-007049] 18 p2572 N88-25278

Plasma neutralizer work at BNL (Brookhaven National Laboratory)
[DE88-007046] 18 p2579 N88-25317

Development of high current and high brightness negative hydrogen ion sources
[DE88-010882] 20 p2852 N88-26934

NEGATIVE RESISTANCE DEVICES

Quantum transport theory of resonant-tunneling heterostructure devices 20 p2865 N88-27017

Resonant tunneling transistors and resonant tunneling hot electron spectroscopy 20 p2866 N88-27018

Excellent negative differential resistance of InGaAs/InAlAs resonant tunneling barrier structures and applications to a new functional device, RHET
20 p2872 N88-27048

NEMESIS (STAR)

An astrometric search for a stellar companion to the sun 04 p0520 N88-13195

NEODYMIUM

Effects of galactic chemical evolution on thorium/neodymium cosmochronology
[DE88-003829] 11 p1570 N88-19397

Design, development, fabrication and launch support for a high altitude release of neodymium vapor
[AD-A194196] 22 p3118 N88-28527

Absorption spectra and energy levels of Gd(3+), Nd(3+) and Cr(3+) in the garnet Gd3Sc2Ga3O12
[AD-A193634] 23 p3292 N88-29599

NEODYMIUM COMPOUNDS

Superconductivity in La/sub 1.85-x/Nd/sub x/Sr/sub .15/CuO
[DE88-003014] 09 p1258 N88-17540

NEODYMIUM ISOTOPES

Nd isotopes and crustal growth rate
24 p3392 N88-30203

Growth of continental crust: Clues from Nd isotopes and Nb-Th relationships in mantle-derived magmas
24 p3393 N88-30205

Changing styles of crustal growth in Southern Africa: Constraints from geochemical and Sr-Nd isotope studies in Archaean to Pan African terrains
24 p3396 N88-30227

NEODYMIUM LASERS

Large-scale stimulated rotational Raman scattering experiments using the LLNL Nova laser
[DE87-012661] 01 p0051 N88-10328

Saturable absorbers for colliding pulse-locked Nd:YAG lasers 03 p0302 N88-11902

Physical design of parameters of Nd:YAG disk laser
03 p0302 N88-11904

Status, development of laser devices in China
03 p0303 N88-11907

An investigation of unipolar arcing at atmospheric pressure in aluminum 2024 and aluminum coated glass slides
[AD-A184903] 05 p0577 N88-13521

Super-short yttrium aluminate pulse generator with controlled resonator Q-factor 06 p0772 N88-14740

Investigations of solid state slab lasers
[ETN-88-91055] 09 p1171 N88-17022

Mode locking in Nd-laser by means of Gd-Sc-Ga-garnet shutter 09 p1237 N88-17412

Polarization effects in laser-pumped Nd:YAG lasers
[DE88-004019] 11 p1492 N88-18904

Burst mode Nd:YLF laser oscillator
[DE88-004040] 11 p1492 N88-18905

Magnetic and inertial fusion status and development plans
[DE88-004405] 11 p1552 N88-19288

Phosphorus oxynitride glass for laser applications
[DE88-005413] 12 p1632 N88-19768

Radiation absorption in neodymium glasses during passage of strong laser pulse 14 p1969 N88-21757

Solid-state ring laser with acoustooptical phase nonreciprocity of opposing waves
14 p1970 N88-21761

Nonlinear stage of ultrashort-pulse formation in solid-state laser 14 p1971 N88-21765

A preliminary comparison of the transient effects of single versus multiple q-switched doubled-neodymium laser pulses
[AD-A189855] 15 p2071 N88-22347

Observation of synchronously transient pumped mode-locking dye laser under negative cavity detuning
16 p2187 N88-23041

Graphite as a picosecond laser activated opening switch 19 p2657 N88-25783

Coupling of a spark source mass spectrograph and a ND-YAG laser
[DE88-012116] 21 p2951 N88-27530

Radial compression of picosecond electrical pulses
[DE88-008440] 21 p2953 N88-27544

Process control improvements in pulsed Nd:YAG laser closure welding of electromechanical relays
[DE88-006275] 21 p2957 N88-27564

Short pulse X-ray diffraction studies of shocked and annealed crystals using the JANUS research laser
[DE88-011329] 23 p3288 N88-29579

NEON

Experimental study of stabilizing He-Ne laser output power with transverse magnetic field
03 p0303 N88-11906

Extreme ultraviolet beam-foil spectroscopy of highly ionized neon and argon
[AD-A185197] 05 p0561 N88-13418

Equation of state of solid neon from X-ray diffraction measurements to 110 GPa
[DE88-006723] 19 p2734 N88-26241

NEOPLASMS
NT CANCER
Radon Research Program, FY-1987
[DE88-002633] 09 p1188 N88-17120

NEPAL
SPOT for slope instability survey in Nepal
22 p3105 N88-28441

NEPHANALYSIS
Cloud climatology derived from the AFGWC (Air Force Global Weather Central) 3D-nephanalysis for January and July 1979
[AD-A183686] 01 p0070 N88-10446

NEPTUNE (PLANET)
Electrical conductivity and equation of state measurements on planetary fluids at high pressures and temperatures
[DE87-013787] 01 p0110 N88-10708
A noise-adding radiometer for the Parkes antenna
11 p1473 N88-18788

NEPTUNE ATMOSPHERE
The solar radiation incident at the top of the atmosphere of Uranus and Neptune
[AERONOMICA-ACTA-A-317-1987]
07 p0878 N88-15323

NEPTUNIUM
Atlas of atomic spectral lines of neptunium emitted by an inductively coupled plasma
[DE88-000640] 06 p0782 N88-14796

NERVA (ENGINE)
U NUCLEAR ENGINE FOR ROCKET VEHICLES

NERVES
NT OCULOMOTOR NERVES
Motion and space sickness 04 p0404 N88-12510
Relation between VEP and visual function in lesions of the optic nerve and visual pathway
21 p2983 N88-27718

NERVOUS SYSTEM
NT AUTONOMIC NERVOUS SYSTEM
NT BRAIN
NT CENTRAL NERVOUS SYSTEM
NT CEREBELLUM
NT CEREBRAL CORTEX
NT CEREBRUM
NT EFFERENT NERVOUS SYSTEMS
NT HIPPOCAMPUS
NT HYPOTHALAMUS
NT NERVES
NT OCULOMOTOR NERVES
NT SPINAL CORD
NT SYMPATHETIC NERVOUS SYSTEM
NT THALAMUS
Function-dependent plasticity in the nervous system
07 p0886 N88-15377
Analysis and synthesis of adaptive neural elements
[AD-A187047] 10 p1395 N88-18316
A neuronal model of classical conditioning
[AD-A188378] 12 p1670 N88-19999
A program for the study of skeletal muscle catabolism following physical trauma
[AD-A189771] 15 p2102 N88-22521
Hemostasis parameters of individuals with neurocirculatory dystonia submitted to dry immersion
19 p2703 N88-26072
Interplanetary travel: Is gravity needed to close the loop
[NASA-TM-101013] 22 p3132 N88-28622
New method for the study of spontaneous brain activity
[AD-A193813] 22 p3132 N88-28624

NETHERLANDS
Civil aeronautics
[ETN-88-90616] 05 p0543 N88-13309
Inventory of weather stations. Climatological data from Dutch stations, no. 26
[KNMI-150-26] 05 p0628 N88-13841
National Remote Sensing Program (NRSP) of the Netherlands 08 p1043 N88-16305
Trends in research and development in the Netherlands. The influence of national science policy between 1973 and 1986
[B8701568] 08 p1094 N88-16580
Activities report in civil aeronautics
[ETN-88-91344] 13 p1715 N88-20255
Study of the plan for a national data center for the European Remote Sensing Satellite ERS-1
[BCRS-87-11] 16 p2228 N88-23309
Advice for astronomical research
[ISBN-9-03-460977-4] 16 p2289 N88-23703

NETS
NT NEURAL NETS
NT PETRI NETS
The significance of orientation unknowns in station and net adjustments 11 p1506 N88-18994

NETWORK ANALYSIS
Development of methods for the analysis of the frequency and voltage statics of electricity users and electrical networks
[ETN-87-90412] 01 p0043 N88-10271
Study into a data relay satellite mission analysis tool
[ESA-CR(P)-2422] 02 p0220 N88-11384
Network reconstitution protocol
[AD-A184755] 03 p0367 N88-12309
On real-time systems using local area networks
[AD-A185475] 06 p0694 N88-14256
A note on the partitioning shortest path algorithm
[CWI-OS-R8703] 08 p1067 N88-16451
Approximating the size of a dynamically growing asynchronous distributed network
[AD-A187011] 09 p1152 N88-16899
Calibration of neural networks using genetic algorithms, with application to optimal path planning
09 p1214 N88-17277
Experiments with the back propagation algorithm: A systematic look at a small problem
[RSRE-MEMO-4049] 09 p1224 N88-17340
Air Force Institute of Technology (AFIT) Local Area Network (LAN) performance evaluation model: An analytic model for assessing the impact of changing LAN hardware and software configurations
[AD-A187191] 11 p1469 N88-18764
Photoconductor switch and circuit analysis
[AD-A188168] 11 p1478 N88-18821
Stochastic heuristics in network design: Parameter tuning and performance evaluation
[REPT-87-017] 11 p1541 N88-19210
A computer code for the solution of large scale network reliability analysis problems
[AD-A188455] 12 p1680 N88-20042
An extension of the MS pivoting rule to capacitated network flow problems
[REPT-87-33] 14 p1963 N88-21711
Exact analyses of slotted ring protocols for local area networks with one transmitting station
[MEMO-650] 14 p1967 N88-21737
Instrumentation for the characterization and development of millimeter wave components compatible with monolithic integration
[AD-A189724] 15 p2059 N88-22275
ECP (Electrical Circuitry Program): A proposed program for electrical circuitry analysis
[AD-A190494] 15 p2060 N88-22280
Analysis of microwave burner measurement system using a microwave network analysis computer program
19 p2631 N88-25604
Fault diagnosis in distributed computer networks
[AD-A192406] 19 p2718 N88-26140
Analysis of networks with parameters S: Generalization of junction matrix
[INPE-4535-PRE/1282] 20 p2793 N88-26570
A network approach to the certainty factor model --- expert systems
[CWI-CS-R8757] 20 p2840 N88-26852
Some equivalent circuit models for AC impedance analysis of pyrite/solution interface
[DE88-010574] 21 p2939 N88-27452
Automatic line network extraction from aerial imagery of urban areas through knowledge based image analysis
[AD-A193067] 21 p2965 N88-27615
Automatic line network extraction from aerial imagery of urban areas through knowledge-based image analysis
[AD-A192399] 23 p3227 N88-29208
An analysis of heat transfer after loss of primary coolant in the SP-100 reactor system
[AD-A194619] 23 p3281 N88-29539
Performance analysis of k-ary n-cube interconnection networks
[AD-A195542] 24 p3361 N88-30010

NETWORK CONTROL
Design, manufacture and testing of an elegant breadboard model communications processor
[D/2244] 01 p0034 N88-10217
Advanced Information Processing System (AIPS) proof-of-concept system functional requirements I/O network system services
[NASA-CR-181481] 03 p0384 N88-12412
Advanced Information Processing System (AIPS) proof-of-concept system functional design I/O network system services
[NASA-CR-181486] 03 p0384 N88-12413
Multicast gateway design considerations
[PB87-219960] 04 p0430 N88-12663
Survey on large scale system control methods
[NASA-CR-181556] 05 p0554 N88-13374
An analysis of simplified feed architectures for MMIC (Monolithic Microwave Integrated Circuit) T/R (Transmit/Receive) module arrays
[AD-A185474] 06 p0697 N88-14275
A new library of CAMAC routines for the control of the system CRATE by a microVAX in the VAXELN environment
[NOTA-INTERNA-893] 06 p0761 N88-14667
Channel access protocols for multihop packet radio networks
[AD-A186074] 07 p0842 N88-15105
Throughput analysis of a flow-contoured communication network with buffer space limitations
[CWI-OS-R8702] 08 p0977 N88-15908
Waiting times in discrete-time cyclic-service systems --- communication networks
[CWI-OS-R8707] 08 p0977 N88-15909
Knowledge-based system analysis and control
[AD-A188163] 12 p1681 N88-20049
Sojourn times in feedback queues
[CWI-OS-R8710] 13 p1830 N88-20947
Two queues with alternating service and switching times
[CWI-OS-R8712] 13 p1831 N88-20949
Deadlock-free message routing in processor networks
[CS-8706] 14 p1960 N88-21691
Impact of blocking policies in closed, exponential and symmetrical ring networks
[FUB-8-1986] 14 p1960 N88-21693
Passive coupler, network adapter, and network acquisition procedure for optical local networks
[ETN-88-92130] 14 p1961 N88-21695
Exact analyses of slotted ring protocols for local area networks with one transmitting station
[MEMO-650] 14 p1967 N88-21737
Implementation of a distributed adaptive routing algorithm on the Intel iPSC (Intel Personal Super-Computer)
[AD-A189849] 15 p2109 N88-22567
Software structuring principles for VLSI CAD
[AD-A190386] 15 p2112 N88-22579
Problems in integrated networks
[AD-A191391] 16 p2191 N88-23069
Reasoning about networks with many identical finite-state processes
[AD-A188743] 16 p2245 N88-23413
Distributed matchmaking
[CWI-CS-R8750] 16 p2254 N88-23467
Modeling, filtering and control of stochastic processes --- communication networks
[ENST-87E021] 17 p2333 N88-23925
The MELMUX MX-7100 series high-speed digital multiplexers 21 p2930 N88-27396
Optimum-Path-to-Go guidance of command adjusted trajectory projectiles
[AD-A193377] 22 p3040 N88-28051
Experiments applications guide: Advanced Communications Technology Satellite (ACTS)
[NASA-TM-100265] 22 p3048 N88-28082
Design of a self-timed VLSI multicomputer communication controller
[AD-A194567] 24 p3361 N88-30014

NETWORK SYNTHESIS
Synthesizing controllers for uncertain systems by a quantitative pole-placement
[PB87-195590] 02 p0223 N88-11403

NEUMANN PROBLEM
IMPSOR: A fully vectorized FORTRAN code for three dimensional moving boundary problems with Dirichlet or Neumann boundary conditions
[DE87-014964] 02 p0226 N88-11427
Diffraction of sound at junction of two waveguides
08 p1076 N88-16491
On an overdetermined Neumann problem
[AD-A187451] 10 p1401 N88-18352
A note on the analyticity of the Neumann Kernel and an associated quadrature problem in two-dimensional boundary element methods
[ETN-88-92054] 14 p1964 N88-21719
On a class of functionals invariant under a Z(sup n) action
[AD-A193474] 23 p3269 N88-29451

NEURAL NETS
General potential surfaces and neural networks
[AD-A184484] 03 p0367 N88-12311
A survey of artificial neural systems
[AD-A184759] 03 p0368 N88-12312
Large-scale neuronal circuits for selective storage and recognition of complex stimuli, a pilot study
[AD-A184134] 04 p0474 N88-12920
Dynamics, control and sensor issues pertinent to robotic hands for the EVA retriever system
06 p0796 N88-14876
Improved input representation for enhancement of neural network performance
[DE88-001830] 07 p0907 N88-15496
Neural network based speech synthesizer: A preliminary report 08 p1064 N88-16429
The power of neural nets 08 p1064 N88-16430

Neural networks as a possible architecture for the distributed control of space systems
08 p1064 N88-16431
Long term synaptic plasticity and learning in neuronal networks
[AD-A186834] 09 p1199 N88-17188
Probabilistic neural networks: In or out of equilibrium
[DE88-002907] 09 p1201 N88-17198
First Annual Workshop on Space Operations Automation and Robotics (SOAR 87)
[NASA-CP-2491] 09 p1203 N88-17206
Neural network based architectures for aerospace applications 09 p1204 N88-17218
NASA JSC neural network survey results
09 p1205 N88-17220
Design of a neural network simulator on a transputer array 09 p1205 N88-17221
Teaching artificial neural systems to drive: Manual training techniques for autonomous systems
09 p1207 N88-17238
Calibration of neural networks using genetic algorithms, with application to optimal path planning
09 p1214 N88-17277
Experiments with the back propagation algorithm: A systematic look at a small problem
[RSRE-MEMO-4049] 09 p1224 N88-17340
Introduction to a system for implementing neural net connections on SIMD architectures
[NASA-CR-181612] 10 p1386 N88-18279
Orthogonal patterns in binary neural networks
[NASA-TM-100060] 10 p1396 N88-18320
Automated radar target recognition based on models of neural nets 11 p1476 N88-18804
Center for the study of rhythmic processes
[AD-A188204] 11 p1520 N88-19078
Optical computing research
[AD-A187862] 11 p1549 N88-19264
Neurocognitive predictions of performance
[AD-A188323] 12 p1669 N88-19998
A neuronal model of classical conditioning
[AD-A188378] 12 p1670 N88-19999
A Darwinian approach to artificial neural systems
[DE87-013184] 13 p1824 N88-20900
Adaptive neural network architecture
[AD-A190114] 15 p2104 N88-22533
Instrumentation for scientific computing in neural networks, information science, artificial intelligence and applied mathematics
[AD-A189981] 15 p2106 N88-22549
Optical Conceptual Computing and Associative Memory (OCCAM)
[AD-A190030] 15 p2107 N88-22550
Rapid feature extraction via the radon transform
[AD-A190032] 15 p2110 N88-22573
Artificial neural networks: An introduction with an annotated bibliography
[DE88-007003] 15 p2116 N88-22603
Nonlinear signal processing using neural networks: Prediction and system modelling
[DE88-006479] 15 p2118 N88-22621
Genetic algorithms for adaptive real-time control in space systems 17 p2388 N88-24195
The efficacy of using human myoelectric signals to control the limbs of robots in space
[NASA-CR-182901] 18 p2553 N88-25155
A concurrent neural network algorithm for the traveling salesman problem
[DE88-006981] 18 p2562 N88-25208
Theoretical investigation of optical computing based on neural network models
[AD-A191668] 18 p2563 N88-25214
Optical computing based on neuronal models
[AD-A191481] 18 p2575 N88-25293
Generalization and the backward propagation neural network
[AD-A191634] 19 p2710 N88-26100
An extension of the Hopfield-Tank model for solution of the multiple traveling salesmen problem
[DE88-008377] 19 p2715 N88-26122
A linear-programming method inspired by the neural networks framework
[DE88-006688] 20 p2842 N88-26862
Basic research on optical neural computers
21 p2929 N88-27389
Content-addressable memory storage by neural networks: A general model and global Liapunov method
[AD-A192716] 21 p3002 N88-27807
Neural network research: A personal perspective
[AD-A192717] 21 p3003 N88-27808
A virtual statistical mechanical neural computer
[AD-A193962] 22 p3139 N88-28660
Survey of neural net paradigms for specification of discrete networks
[AD-A192682] 22 p3141 N88-28674
Analysis of the hopfield neural networks and their application to pattern recognition
[AD-A193827] 23 p3239 N88-29279
Design of a feeling-thinking machine
[AD-A194107] 23 p3267 N88-29448
Circuit design criteria for stable lateral inhibition neural networks
[AD-A195066] 24 p3366 N88-30046
Autonomous image data reduction by analysis and interpretation 24 p3418 N88-30347
Parallel and distributed computation for fault-tolerant object recognition 24 p3419 N88-30350
Nested neural networks
[NASA-TM-101032] 24 p3423 N88-30373

NEUROLOGY
Neurochemical changes in hibernation
08 p1046 N88-16322
Molecular mechanisms of neuronal responsivity
[AD-A187061] 09 p1199 N88-17185
Three-dimensional computer graphics brain-mapping project
[AD-A187202] 11 p1528 N88-19126
Direct interaction between autonomic nerves and the immune system
[AD-A188576] 12 p1667 N88-19991
Neurocognitive predictions of performance
[AD-A188323] 12 p1669 N88-19998
Computing with structured connections networks
[AD-A189244] 13 p1821 N88-20886
Normative developmental equations for the EEG and their sensitivity to neurological and psychiatric disorders
21 p2977 N88-27687
Models of cerebral-body perfusion and cerebral chemical transport
[AD-A194945] 24 p3407 N88-30283
Central adrenergic receptors as mediators of central response to stress: Study with Positron Emission Tomography (PET)
[AD-A194947] 24 p3407 N88-30284

NEUROMUSCULAR TRANSMISSION
Biophysical and biochemical mechanisms in synaptic transmitter release
[AD-A187059] 09 p1199 N88-17184
Long term synaptic plasticity and learning in neuronal networks
[AD-A186834] 09 p1199 N88-17188
Facilitory effects of voluntary movements on vestibulomotor reaction 12 p1664 N88-19976
Evaluation of the endogenous glucocorticoid hypothesis of denervation atrophy
[NASA-CR-182848] 17 p2381 N88-24157
A systems engineering based methodology for analyzing human electrocortical responses
[AD-A190809] 18 p2550 N88-25135
The VITE model: A neutral command circuit for a generating arm and articulator trajectories
[AD-A192715] 21 p2987 N88-27734

NEURON TRANSMISSION
U BIOELECTRICITY

NEURONS
Function-dependent plasticity in the nervous system
07 p0886 N88-15377
Karyometric evaluation of neuronal reactions of rat cerebral cortex to the combined effect of ionizing radiation, longitudinal accelerations and vibration
07 p0890 N88-15396
Molecular mechanisms of neuronal responsivity
[AD-A187061] 09 p1199 N88-17185
Analysis and synthesis of adaptive neural elements
[AD-A187047] 10 p1395 N88-18316
Center for nonlinear dynamics of the brain
[AD-A187245] 11 p1518 N88-19068
Synapses that compute motion
[AD-A190389] 15 p2116 N88-22607

NEUROPHYSIOLOGY
Functional plasticity of the nervous system of vertebrates 01 p0074 N88-10474
Visual evoked responses to sinusoidal gratings presented in central and right visual fields: 1
[DE87-014731] 04 p0473 N88-12919
Large-scale neuronal circuits for selective storage and recognition of complex stimuli, a pilot study
[AD-A184134] 04 p0474 N88-12920
Neurophysiological analysis of hypothalamic regulation mechanisms of primary sleep and hypobiosis
06 p0751 N88-14611
Functional development of gravity receptors in insects and amphibians 07 p0886 N88-15376
The filtering problem for infinite dimensional stochastic processes
[AD-A186431] 07 p0916 N88-15562
Molecular mechanisms of neuronal responsivity
[AD-A187061] 09 p1199 N88-17185
Long term synaptic plasticity and learning in neuronal networks
[AD-A186834] 09 p1199 N88-17188
Neuro-reflex mechanisms of circulation regulation in simulated microgravity 12 p1656 N88-19923
Vestibular integrated function and microgravity
12 p1658 N88-19937
Synopsis of the Spacelab D-1 frog statolith experiment STATEX 12 p1659 N88-19940
A neuronal model of classical conditioning
[AD-A188378] 12 p1670 N88-19999
Complex sound processing: An interdisciplinary approach
[AD-A189782] 15 p2102 N88-22523
Neurophysiological predictors of quality of performance 16 p2242 N88-23391
Electric and Magnetic Activity of the Central Nervous System: Research and Clinical Applications in Aerospace Medicine
[AGARD-CP-432] 21 p2977 N88-27683
Fourth generation neurocognitive pattern analysis system 21 p2977 N88-27686
Neurophysiological patterns of operational fatigue: Preliminary results 21 p2981 N88-27703
Neurophysiological precursors of accurate visuomotor performance 21 p2981 N88-27706
The neuroelectric selection of Naval aviation personnel: An evaluation 21 p2981 N88-27707
Electroencephalographic correlates of pilot performance: Simulation and in-flight studies
21 p2982 N88-27711
Spontaneous cerebral electrical activity during prolonged hypoglycemia: A quantitative study in humans
21 p2983 N88-27717
Relation between VEP and visual function in lesions of the optic nerve and visual pathway
21 p2983 N88-27718
Models for motion perception
22 p3133 N88-28629
Comparative aspects of multiple processes of attention
[AD-A195805] 24 p3408 N88-30291

NEUROPSYCHIATRY
Attention, effort, and fatigue: Neuropsychological perspectives 16 p2241 N88-23387

NEUROSCIENCE
U NEUROLOGY

NEUROTRANSMITTERS
Large-scale neuronal circuits for selective storage and recognition of complex stimuli, a pilot study
[AD-A184134] 04 p0474 N88-12920
Neurohumoral aspects of sleep
[AD-A188653] 12 p1667 N88-19992

NEUTRAL ATOMS
Improvement of energy confinement of neutral beam heated plasma by lower hybrid current drive in JT-60
[DE87-752983] 02 p0239 N88-11509
Ro-vibrational laser spectroscopy of ESD neutrals from chemisorbed species
[DE87-013011] 04 p0447 N88-12770
Forces on neutral atoms due to electromagnetic fields
[AD-A187461] 10 p1408 N88-18396
Magnetic trapping of neutral atoms
[AD-A188473] 12 p1689 N88-20103
Optical trapping of neutral atoms and dielectric particles by radiation pressure 14 p1974 N88-21783
Electromagnetic manipulation of atomic hydrogen
16 p2268 N88-23568
Corpuscular plasma diagnostics complex on a tokamak with a strong field
[DE88-701576] 16 p2279 N88-23646
Flux density measurements of neutral iron in TEXTOR with laser induced fluorescence
17 p2442 N88-24528

NEUTRAL BEAMS
NT MOLECULAR BEAMS
NT NEUTRON BEAMS
Improvement of energy confinement of neutral beam heated plasma by lower hybrid current drive in JT-60
[DE87-752983] 02 p0239 N88-11509
Applications of neutral beam and rf technologies
[DE87-014936] 03 p0379 N88-12382
TIBER 2 (Tokamak Ignition/Burn Experimental Reactor) parameters with neutral beams at high energies
[DE88-001891] 06 p0783 N88-14803
A calorimeter for measuring the neutral beam power reaching the plasma
[DE88-001412] 07 p0937 N88-15691
Design considerations for a negative ion source for DC operation of high-power, multi-megaelectron-volt neutral beams
[DE88-002692] 08 p1083 N88-16525
Benchmarks of neutral beam injection codes for stellarators
[DE88-003786] 10 p1412 N88-18428
Neutral beam propagation through the atmosphere
[AD-A188984] 12 p1691 N88-20115

A segmented calorimeter for low-energy particle beams in space
[DE88-001806] 13 p1838 N88-20997
Power source selection for neutral particle beam systems 17 p2407 N88-24314
Ion temperature profile measurement using charge exchange recombination spectroscopy on JIPP T-IIU
17 p2440 N88-24518
Spectroscopic measurements of ion temperature, rotation speed and beam deposition profile on DIII-D
17 p2440 N88-24519
Arcing and rf signal generation during target irradiation by a high-energy, pulsed neutral particle beam
[DE88-007169] 18 p2471 N88-24664
Propagation of neutralized ion beams
[AD-A191599] 18 p2574 N88-25289
Requirements for neutral beam current drive in tokamaks
[DE88-006180] 20 p2859 N88-26980

NEUTRAL BUOYANCY SIMULATION
Structural Assembly Demonstration Experiment (SADE)
[NASA-CR-179205] 02 p0138 N88-10868
Research and development at the Marshall Space Flight Center Neutral Buoyancy Simulator
02 p0139 N88-10878
EASE (Experimental Assembly of Structures in EVA) overview of selected results 02 p0140 N88-10881

NEUTRAL CURRENTS
Determination of the neutral current chiral coupling constants u sublsq, u subrsq, d sublsq and d subrsq from an (anti)neutrino-deuterium experiment
[B8715857] 06 p0779 N88-14780

NEUTRAL GASES
Design study for measurement of neutral hydrogen atom density by laser induced fluorescence method
[DE87-752964] 02 p0179 N88-11114
Kinematics and dynamics of barred spiral galaxies
03 p0388 N88-12440
Upper-thermospheric observations and neutral-gas dynamics at high latitudes during solar maximum
[AD-A188058] 11 p1512 N88-19031
Distribution of neutral gas molecules at large distances from Halley's comet 14 p1999 N88-21914
A model of the anisotropic structure of the neutral gas coma of a comet 14 p1999 N88-21918

NEUTRAL PARTICLES
NT FAST NEUTRONS
NT NEUTRONS
NT SOLAR NEUTRONS
NT THERMAL NEUTRONS
Neutral environment for space station
18 p2590 N88-25391
Space station neutral external environment
18 p2590 N88-25392

NEUTRAL SHEETS
The solar wind 03 p0271 N88-11705
Hot plasmas in the Earth's magnetosphere
03 p0272 N88-11710
Influence of viscosity on the structure of a magnetic neutral layer 08 p1098 N88-16605
A quadratic-form analysis of the collisionless tearing mode
[AD-A188886] 12 p1695 N88-20144

NEUTRALIZERS
Products of the neutralization of hydrazine fuels with hypochlorite, 2
[DE87-011454] 01 p0030 N88-10193
Photodetachment neutralizer development: Laser window design study. Volume 2: Window design details
[DE88-000783] 09 p1170 N88-17014
Plasma neutralizer work at BNL (Brookhaven National Laboratory)
[DE88-007046] 18 p2579 N88-25317

NEUTRINO BEAMS
Wrong helicity events induced by the CERN-SPS wide band muonic (anti)neutrino beam
[NIKHEF-H/87-2] 06 p0779 N88-14779
Determination of the neutral current chiral coupling constants u sublsq, u subrsq, d sublsq and d subrsq from an (anti)neutrino-deuterium experiment
[B8715857] 06 p0779 N88-14780

NEUTRINOS
NT SOLAR NEUTRINOS
Summary and conclusions of the 6th Moriond workshop --- standard electroweak model
[USIP-87-11] 01 p0092 N88-10602
Quantification of the background signal to solar neutrino detection from cosmogenic activation of the atmosphere
[DE87-013830] 01 p0119 N88-10762
Neutrinos in supernovae
[DE87-014295] 03 p0387 N88-12434
A theoretical model for neutrino masses and mixing
[PREPRINT-553] 06 p0778 N88-14777
Event classification in (anti)neutrino experiments using an Internal Picket Fence-External Muon Identifier (IPF-EMI) detector system
[NIKHEF-H/87-6] 09 p1245 N88-17457
Oscillations of solar models with internal element diffusion
[DE88-003156] 09 p1264 N88-17573
A research program in neutrino physics, cosmic rays and elementary particles
[DE88-003507] 09 p1264 N88-17575
A look at Supernova 1987A
[DE88-003411] 10 p1429 N88-18531
Neutrino magnetic moment and time variation of solar neutrino flux
[DE88-700687] 10 p1430 N88-18542
Intermediate energy neutrino physics
[DE88-005378] 13 p1836 N88-20984
Strange, quark and metastable neutron stars
[DE88-702404] 21 p3030 N88-27984
Neutrino detection primer
[AD-A193805] 23 p3280 N88-29529
On neutrino fields in Einstein-Cartan theory
[MATH-REPT-208] 23 p3295 N88-29629

NEUTRON ABSORBERS
Fabrication of lithium hydride shields for space nuclear power systems 17 p2402 N88-24282

NEUTRON ACTIVATION ANALYSIS
Cryogenic cell --- neutron borehole logging
[GB-PATENT-2-139-745-A] 01 p0048 N88-10308
Characterization of yttrium aluminum garnet/YAG/using 14 MeV neutron activation
[AD-A191925] 18 p2582 N88-25342

NEUTRON BEAMS
A layered scintillation detector for solar neutron observations
[DE87-011354] 01 p0049 N88-10314
Multilayer monochromators for neutron spectrometers
[DE87-014291] 02 p0175 N88-11093
Interaction of slow neutrons with Ge74 single crystals
[DE87-703010] 17 p2445 N88-24536
Tracking a monochromatic light source
[DE88-011260] 20 p2807 N88-26653

NEUTRON COUNTERS
NT NEUTRON SPECTROMETERS
A layered scintillation detector for solar neutron observations
[DE87-011354] 01 p0043 N88-10314
Probable detection of solar neutrons by ground-level neutron monitors during STIP interval 16
01 p0111 N88-10715
A neutron detector based on microchannel plates
[DE87-014703] 02 p0232 N88-11466
Cosmic ray NM-64 neutron monitor data 14, Rome, Italy, January - December 1985
[IFSI-87-8] 05 p0661 N88-14060
Rome Neutron Monitor (NM) - 64 data for 5 solar particle ground-level events
[IFSI-86-7] 06 p0806 N88-14918
Properties of nuclei and elementary particles at low and intermediate energies
[DE88-001913] 09 p1244 N88-17456
A combined cosmic ray muon spectrometer and high energy air shower array
[DE88-003057] 09 p1264 N88-17574

NEUTRON CROSS SECTIONS
Computer programs for calculating group cross-section covariances from uncertainty parameters in the ENDF/B-V format. UNC 32/33 --- neutron physics
[ECN-202] 13 p1837 N88-20995
Systematics on neutron-induced isomeric cross-section ratios at 14.5 MeV
[ECN-200] 14 p1980 N88-21815
Effects of space-dependent cross sections on core physics parameters for compact fast spectrum space power reactors 17 p2399 N88-24263
Nucleon-nucleus interaction data base: Total nuclear and absorption cross sections
[NASA-TM-4053] 20 p2852 N88-26935

NEUTRON DECAY
Measurement of Beta-decay energies of short-lived neutron-rich nuclei in the vicinity of mass number between 101 and 106, and A = 109
[ETN-88-92376] 21 p3014 N88-27890

NEUTRON DETECTORS
U NEUTRON COUNTERS

NEUTRON DIFFRACTION
Characterization of the dimensions of colloidal calcium carbonate dispersions in toluene with neutron small-angle scattering
[ECN-197] 06 p0680 N88-14167
Nondestructive characterization of ceramic composite whiskers with neutron diffraction and ultrasonic techniques
[DE88-003075] 08 p0965 N88-15844
High-temperature charge-density studies of CeO/sub 2-x/ using X-ray and neutron diffraction techniques
[DE88-002988] 09 p1257 N88-17536
Magnetic rare earth superlattices
[DE88-003483] 10 p1418 N88-18465
Single-crystal structural study of La2Cu/sub 0.95/Li/sub 0.05/O4
[DE88-003482] 11 p1554 N88-19302
The structural analysis of some crystalline and semi-crystalline substances using X-ray and neutron diffraction 17 p2445 N88-24540
Neutron diffraction refinement of CsHSO4 superionic phase structure
[DE88-701496] 18 p2580 N88-25326
Structural studies on La/sub 2/CuO/sub 4+delta/
[DE88-006828] 18 p2581 N88-25330
Structural and magnetic properties of Fe impurities in YBa2Cu3O(sub 7-delta)
[DE88-009961] 19 p2735 N88-26247
Observations on residual stresses in ceramic composites by neutron diffraction techniques
[DE88-009937] 20 p2778 N88-26472

NEUTRON EMISSION
Probable detection of solar neutrons by ground-level neutron monitors during STIP interval 16
01 p0111 N88-10715
Solar-geophysical data number 514, June 1987. Part 1: (Prompt reports). Data for May 1987, April 1987 and late data
[PB87-217261] 02 p0257 N88-11626
Properties of hydrogen/helium accretion plasmas
[DE88-006831] 19 p2728 N88-26197

NEUTRON FLUX
U FLUX (RATE)

NEUTRON FLUX DENSITY
Application of the reactivity constraint approach to the transient control of spacecraft reactors
17 p2406 N88-24305

NEUTRON IRRADIATION
Computed neutron tomography and coded aperture holography from real time neutron images
04 p0427 N88-12645
The effect of neutron irradiation on the tensile properties and microstructure of several vanadium alloys
[DE88-001755] 06 p0682 N88-14176
Experimental method for investigating helium effects in irradiated vanadium
[DE88-002891] 08 p0969 N88-15865
A report on the effects of neutron irradiation of GaAs semiconductors
[AD-A186816] 09 p1253 N88-17510
Response of Fe-Cr-Mn austenitic alloys to thermal aging neutron irradiation
[DE88-003415] 10 p1302 N88-17785
Influence of neutron irradiation on the Charpy impact properties of V-15Cr-5Ti
[DE88-003430] 11 p1458 N88-18692
Effects of high temperature neutron irradiation on the physical, chemical and mechanical properties of fine-grained isotropic graphite 13 p1747 N88-20444
Degradations of thermal shock resistance and the fracture toughness of reactor graphite subjected to neutron irradiation 13 p1747 N88-20445
Anthropomorphic phantom radiation dosimetry at the NATO standard reference point at Aberdeen Proving Ground
[AD-A190508] 15 p2103 N88-22528
Material tradeoffs to minimize flooding reactivity
17 p2399 N88-24265
Neutron radiation tolerance of Au-activated silicon
17 p2408 N88-24316
Defects in cubic silicon carbide on silicon
17 p2408 N88-24317
Point defects in irradiated silicates
17 p2408 N88-24319
MMW shielding design and analysis
17 p2430 N88-24457
Neutron effects on the electrical and switching characteristics of NPN bipolar power transistors
17 p2431 N88-24463
Development of refractory thermocouples for space nuclear power tests 17 p2434 N88-24478
Effect of neutron irradiation on critical magnetization current in single crystal YBa2Cu3O(sub 7-delta)
[DE88-009970] 22 p3156 N88-28775

NEUTRON PHYSICS
A model for stationary and dynamic impression of undercooled boiling in coupled thermohydraulic and neutron physics calculations of nuclear reactors
[IKE-6-171] 09 p1247 N88-17472
Systematics on neutron-induced isomeric cross-section ratios at 14.5 MeV
[ECN-200] 14 p1980 N88-21815

NEUTRON RADIOGRAPHY

Computed neutron tomography and coded aperture holography from real time neutron images 04 p0427 N88-12645

NEUTRON SCATTERING

Applications and limitations of deuterium labeling methods to neutron scattering studies of polymers [DE87-012936] 02 p0151 N88-10945

Small-Angle Neutron Scattering (SANS) from polymers and colloids [DE87-013548] 02 p0151 N88-10946

Applied nuclear science research and development [LA-10915-PR] 03 p0374 N88-12355

Theory of neutron scattering experiments on momentum distributions in quantum fluids [DE87-01369] 05 p0648 N88-13968

Characterization of the dimensions of colloidal calcium carbonate dispersions in toluene with neutron small-angle scattering [ECN-197] 06 p0680 N88-14167

Characterization of duplex stainless steel by TEM (Transmission Electron Microscopy), SANS (Small-Angle Neutron Scattering) and APFIM (Atom-Probe Field Ion Microscopy) techniques [DE88-002916] 09 p1145 N88-16865

Neutron- and X-ray-small angle scattering with Fe-base metallic glasses [DE88-002538] 09 p1147 N88-16876

Neutron and X-ray scattering studies of layered solids 09 p1246 N88-17469

Structural analysis using X-ray scattering and neutron scattering on binary amorphous (Co,Cu)Ti alloys [ETN-88-91487] 11 p1459 N88-18699

Determination of the equilibrium concentration of characteristic defects by the measurement of thermal expansion using neutron scattering and laser interferometry [ETN-88-91489] 11 p1490 N88-18890

Theory of neutron moisture probes and interpretation of measurements in complex soil and water systems 17 p2342 N88-23965

Comparison between muon spin rotation and neutron scattering studies on the 3-dimensional magnetic ordering of La2CuO(4-y) 17 p2396 N88-24244

Calculation of far infrared absorption in B poly(dA).poly(dT) [AD-A193128] 21 p2918 N88-27318

NEUTRON SPECTRA

Effects of the neutron spectrum on mechanical property changes in low dose irradiations [DE88-003429] 10 p1302 N88-17786

Computer programs for calculating group cross-section covariances from uncertainty parameters in the ENDF/B-V format. UNC 32/33 --- neutron physics [ECN-202] 13 p1837 N88-20995

Systematics on neutron-induced isomeric cross-section ratios at 14.5 MeV [ECN-200] 14 p1980 N88-21815

The development of KENO and the calculation of differential parameters with KENO [DE88-006176] 18 p2555 N88-25166

NEUTRON SPECTROMETERS

Multilayer monochromators for neutron spectrometers [DE87-014291] 02 p0175 N88-11093

Investigation of the evolution of the fusion processes in the plasma focus using time-resolved neutron spectroscopy [IPF-87-4] 09 p1251 N88-17493

Gamma-ray/neutron spectroscopy from the Mars observer 23 p3302 N88-29671

NEUTRON STARS

NT PULSARS

Neutrinos in supernovae [DE87-014295] 03 p0387 N88-12434

Core bounce supernovae [DE87-014910] 04 p0520 N88-13137

Neutron stars observations as astrophysical probes 06 p0800 N88-14896

EXOSAT guest observer program. Binary parameters of the X-ray Pulsar 4U1626-67 [NASA-CR-182374] 06 p0802 N88-14905

HEAO-1 observations of gamma-ray bursts 07 p0947 N88-15756

Stellar energy loss and anomalous contributions to the (photon photon) (neutrino antineutrino) interaction [DE88-700618] 10 p1428 N88-18529

Hadron-quark phase transition in dense stars [DE88-003412] 10 p1429 N88-18532

Photohydrodynamical processes near compact objects 11 p1569 N88-19390

Thermal radiation from neutron stars [MPE-203] 11 p1571 N88-19404

Generation and propagation of sound waves in a collapsing or anti-collapsing star with uniform density [DE87-703034] 15 p2151 N88-22839

Quark core stars, quark stars and strange stars [DE88-006991] 17 p2450 N88-24555

A model for the X-ray binary 4U1820-30 [NASA-TM-101143] 17 p2451 N88-24562

Spectral modelling of the soft gamma ray repeater [DE88-007027] 17 p2453 N88-24570

Nuclear and astrophysical evidence on the equation of state [DE88-007397] 18 p2572 N88-25279

Heavy ion collisions with A = 10(sup 57): Aspects of nuclear stability and the nuclear equation of state in coalescing neutron-star binary systems [DE88-008029] 19 p2741 N88-26277

Detection of absorption lines in the spectra of X-ray bursts from X1608-52 [ISAS-RN-360] 20 p2887 N88-27143

Strange, quark and metastable neutron stars [DE88-702404] 21 p3030 N88-27984

EXOSAT observations of Hercules X-1 [MPE-PREPRINT-119] 22 p3164 N88-28841

On the origin of gamma ray bursts [MPE-PREPRINT-120] 22 p3166 N88-28855

NEUTRON TRANSMUTATION

U NUCLEAR REACTIONS

NEUTRONS

NT FAST NEUTRONS

NT SOLAR NEUTRONS

NT THERMAL NEUTRONS

TRISTAN research on neutron rich nuclei: Magnetic moments and nuclear structure [DE88-002122] 06 p0783 N88-14807

New nuclear structure calculations and the astrophysical r-process [DE88-000979] 08 p1082 N88-16518

Two-dimensional analysis for a scrapeoff and divertor regions with an MHD model. Conceptual design study of FY86 FER [DE88-751069] 09 p1251 N88-17497

The effects of low doses of 14 MeV neutrons on the tensile properties of three binary copper alloys [DE88-003400] 11 p1458 N88-18691

Emission of gamma rays from various materials pulsed with 14-MeV neutrons [DE88-003837] 11 p1544 N88-19227

Symmetry problems in particle physics [DE88-004927] 12 p1688 N88-20099

Reference nuclear data for space applications [DE88-007041] 16 p2270 N88-23583

Stability requirement FOT ignition and high gain implosion = 2-D simulation for high neutron yield experiment = 16 p2278 N88-23633

Observation of ferromagnetism in ultrathin f.c.c. films by spin polarised neutron reflection 20 p2865 N88-27015

NEVADA

Delineation of ephemeral fluvial networks on low-relief Piedmont surfaces, Plutonium Valley, Nevada, USA 22 p3093 N88-28367

The application of SPOT data to the structural geology of western Nevada 22 p3102 N88-28423

The dynamics of transuranics and other radionuclides in natural environments, December 1985 [DE87-014456] 24 p3390 N88-30189

NEW ENGLAND (US)

NOAA's (National Oceanic and Atmospheric Administration's) Northeast Monitoring Program (NEMP): A report on progress of the first five years (1979-84) and a plan for the future [PB87-210100] 02 p0196 N88-11225

NEW MEXICO

Transactions of the Fifth Symposium on Space Nuclear Power Systems [DE88-006165] 17 p2417 N88-24374

NEW YORK

New York TRACON demonstration of program recoding requirements analysis document [DOT/FAA/CT-87/34] 18 p2462 N88-24622

NEW ZEALAND

Numerical simulation of the flow about New Zealand 08 p1017 N88-16163

Wind energy resource survey of New Zealand: National resource assessment [PB88-139365] 12 p1640 N88-19822

Systems approach to energy quality and efficiency [PB88-139506] 12 p1640 N88-19823

Ozonesonde observations at Lauder, New Zealand during the Spring and early Summer of 1986 [PB88-173273] 16 p2232 N88-23328

NEWTON METHODS

NT NEWTON-RAPHSON METHOD

Computational behavior of Gauss-Newton methods [DE87-014486] 02 p0224 N88-11413

A tool for the analysis of quasi-Newton methods with application to unconstrained minimization [DE88-005783] 11 p1532 N88-19153

Some numerical methods for the computation of capillary free boundaries governed by the Navier-Stokes equations [REPT-87-69] 16 p2206 N88-23167

High degree interpolation polynomial in Newton form [NASA-CR-181677] 13 p2567 N88-25249

Parallel quasi-Newton methods for unconstrained optimization [AD-A193250] 21 p3003 N88-27812

Optimisation algorithms for highly parallel computer architectures. The performance of the truncated Newton, conjugate gradient algorithm in FORTRAN and Ada [AD-A193940] 23 p3265 N88-29435

Generating semi-Gaussian two dimensional quadrature rules [REPT-205] 23 p3272 N88-29476

NEWTON SECOND LAW

A comparative survey of mathematical models for dynamic simulation of in-orbit manipulation operations 12 p1592 N88-19533

NEWTON THEORY

Some considerations on measuring the Newtonian gravitational constant G in an orbiting laboratory 07 p0922 N88-15603

Post-Newtonian equations of motion in an expanding universe [DE88-750303] 07 p0945 N88-15744

Non-Newtonian gravity or gravity anomalies? [NASA-TM-4030] 17 p2374 N88-24118

Transcending Newton's legacy [DE88-010784] 19 p2738 N88-26254

NEWTON-RAPHSON METHOD

Efficient numerical techniques for complex fluid flows 02 p0185 N88-11151

Computational behavior of Gauss-Newton methods [DE87-014486] 02 p0224 N88-11413

Numerical methods in the resolution of control electrovalve model [INPE-4154-RPE/540] 13 p1764 N88-20554

An analytical investigation of geared system dynamics containing spur and helical gears 22 p3085 N88-28317

Rational Newton algorithms to compute formal solutions of linear differential equations in an irregular singular point [RR-704-M] 22 p3140 N88-28670

NEWTONIAN FLUIDS

Review of the equations of fluid mechanics and heat transfer 08 p0986 N88-15970

Boundary effects on the drag of a cylinder in axial motion at low Reynolds number 13 p1768 N88-20578

Extrema principles of entrophy production and energy dissipation in fluid mechanics [NASA-TM-100992] 18 p2519 N88-24946

A computer model for the flow of a molten polymer in a narrow cavity [NPL-DMA(A)-157] 22 p3058 N88-28146

NICKEL

A simulation study of interfaces in Ni, Al and Ni3Al with and without boron [DE87-013156] 01 p0102 N88-10667

The water permeability of multi-layer coatings [BLL-M-37252-(5828.4)] 02 p0148 N88-10927

Low-pressure eutectic bonding of depleted uranium to copper [DE87-014625] 02 p0181 N88-11128

Constitutive modeling for isotropic materials 02 p0185 N88-11171

Kinetics of CO adsorption on nickel using time resolved vibration spectroscopy [ETN-87-90615] 03 p0289 N88-11814

Wear of iron and nickel in corrosive liquid environments [NASA-TM-100246] 03 p0289 N88-11817

Studies on estimation of nickel in zinc base die casting by D.C. polarography [PD-MT-8729] 04 p0417 N88-12588

Moessbauer study of shock induced effects in the Fe-Ni 50/50 ordered alloy in meteorites [DE87-703364] 04 p0521 N88-13199

The mechanism by which sigma-phase forms in Fe-Cr-Ni system alloys [BLL-M-37380-(5828.4)] 05 p0564 N88-13437

Advances in processing techniques for nickel aluminides [DE87-014571] 05 p0566 N88-13449

Contrast between the chemical, structural and electronic properties of thin films of Cu and Ni on the Ru(0001) surface [DE88-002360] 07 p0938 N88-15698

TiN coatings on M2 steel produced by plasma assisted chemical vapor deposition [DE88-003189] 08 p0970 N88-15867

Study on the fracture behavior of 9 percent Ni steel welded joint [PB87-143863] 08 p0995 N88-16023

Dynamic recrystallization during high temperature low cycle fatigue of nickel
[DE88-003224] 10 p1302 N88-17788

Effects of ion implantation on cavitation erosion of a cobalt based metal/carbide alloy
[AD-A187239] 10 p1303 N88-17793

Growth and electronic properties of strained metal overlayers
[DE87-010956] 10 p1417 N88-18463

Studies of the electron spectrum with reference to the clean surfaces of iron, cobalt and nickel and their subsequent exposure to oxygen
11 p1459 N88-18700

The effect of microstructure on the fatigue crack growth resistance of nickel base superalloys
[AD-A189526] 13 p1741 N88-20414

Temperature dependence of Kr precipitation in Ni
[DE88-005953] 13 p1744 N88-20429

The unique characteristics of the structure of composite materials made on a base of sphalerite-analogous boron nitride 14 p1886 N88-21273

Bithermal fatigue of a nickel-base superalloy single crystal
[NASA-TM-100885] 15 p2042 N88-22168

Performance of lightweight nickel electrodes
[NASA-TM-100958] 20 p2771 N88-26430

Grain boundary structure in Ni3Al
[DE88-009164] 20 p2773 N88-26444

The adherence of nickel oxide on nickel during high temperature oxidation
[DE88-011194] 20 p2774 N88-26450

A fundamental understanding of the interfacial compatibility in hybrid material systems
[AD-A192921] 21 p2909 N88-27264

Inelastic electron scattering and electron-hole excitations in iron and nickel
[DE88-011843] 21 p2915 N88-27303

NICKEL ALLOYS
NT ASTROLOY (TRADEMARK)
NT HASTELLOY (TRADEMARK)
NT INCONEL (TRADEMARK)
NT NITINOL ALLOYS

Isothermal forging and its effect on the microstructure of powder route nickel alloy AP1
[RAE-TM-P-1094] 01 p0022 N88-10138

Structure of rapidly solidified Ni-Ti
[DE87-012252] 02 p0147 N88-10921

Thermodynamics of interaction between nitrogen and molten nickel alloys
[BLL-M-37309-(5828.4)] 02 p0149 N88-10934

The effect of sulfur and zirconium Co-doping on the oxidation of NiCrAl
[NASA-TM-100209] 02 p0150 N88-10940

Influence of boron on porosity in nickel-base superalloy castings 03 p0299 N88-11877

A mathematical model of high alloy nickel base high temperature alloys
[BLL-M-37381-(5828.4)] 05 p0564 N88-13436

The effect of ion beam mixed Ni-Al surface layers on PSB extrusion morphology in fatigued nickel
05 p0598 N88-13652

Low cycle fatigue behaviour of notched specimens of nickel based superalloy single crystal
05 p0605 N88-13712

An overview of fatigue 05 p0608 N88-13729

Basic energy sciences research in the Metals and Ceramics Division of Oak Ridge National Laboratory
[DE87-013538] 06 p0681 N88-14171

Undercooling and nucleation in iron nickel alloys
[AD-A185500] 06 p0683 N88-14184

The effect of prestraining on fatigue crack growth in nickel-base alloys 06 p0719 N88-14415

High temperature low cycle fatigue of oxide dispersion strengthened and single crystal nickel base superalloys
06 p0720 N88-14422

High temperature low cycle fatigue behavior and creep-fatigue interation of MA 6000 ODS alloy
06 p0720 N88-14425

The effect of temperature on fatigue crack initiation from aluminosilicate inclusions 06 p0720 N88-14427

Dependence of strainrange partitioned fatigue life at elevated temperature on monotonic stress-strain properties 06 p0721 N88-14428

The effect of varying sputtering parameters on the microstructure and mechanical properties of 10 percent Ni + TiB2 thin films
[DE88-002600] 09 p1254 N88-17517

Diffusion studies in amorphous NiZr alloys
[DE88-003009] 10 p1301 N88-17781

The role of composition and microstructure gradients on weld metal properties and behavior
[DE88-004956] 10 p1303 N88-17791

Friction and wear of monolithic and fiber reinforced silicon-ceramics sliding against IN-718 alloy at 25 to 800 C in atmospheric air at ambient pressure
[NASA-TM-100294] 10 p1304 N88-17796

Study of adherent oxide scales
[AD-A187368] 11 p1456 N88-18680

High temperature oxidation studies on alloys containing dispersed phase particles and clarification of the mechanism of growth of SiO2
[AD-A188158] 11 p1457 N88-18688

Effects of thermal and thermo-mechanical treatments on the mechanical properties of centrifugally cast alloy 718
[AD-A188195] 11 p1458 N88-18690

Corrosion resistance of electrodeposited amorphous Ni-Cr-P alloys
[DE88-005116] 11 p1459 N88-18695

Anodic behavior of Ni-P and Ni-Cr-P metallic glasses
[DE88-005334] 11 p1463 N88-18722

The cyclic stress-strain behavior of a single crystal nickel-base superalloy
[NASA-TM-100269] 12 p1607 N88-19610

The effect of microstructure on the fatigue crack growth resistance of nickel base superalloys
[AD-A189526] 13 p1741 N88-20414

Processing, physical metallurgy and creep of NiAl + Ta and NiAl + Nb alloys
[NASA-CR-182113] 14 p1890 N88-21295

Electron diffraction evidence for the ordering of excess nickel atoms by relation to stoichiometry in nickel-rich beta'-NiAl formation of a nickel-aluminum (Ni2Al) superlattices
[NASA-TT-20177] 14 p1890 N88-21297

Effect of nonuniform state of thermal stress on resistance of EI826 alloy to thermal fatigue
14 p1895 N88-21313

Growth of fatigue cracks in nickel alloys at high temperatures 14 p1896 N88-21318

The viscoplasticity theory based on overstress applied to the modeling of a nickel base superalloy at 815 C
14 p1928 N88-21499

Development of a unified constitutive model for an isotropic nickel base superalloy Rene 80
14 p1929 N88-21501

Constitutive response of Rene 80 under thermal mechanical loads 14 p1932 N88-21524

Characterization of an explosively consolidated rapidly solidified Fe-16Ni-9Cr-5Mo-2Cu alloy powder
[DE88-006733] 15 p2041 N88-22162

Atomic beam study of crystalline order and precipitation in nickel based alloys
[ETN-88-91994] 16 p2177 N88-22975

Laser cladding of Ni, Nb and Mg alloys for improved environmental resistance at high temperature
[AD-A191274] 16 p2213 N88-23208

Martensitic transformation and microstructures in sintered NiAl alloys
[NASA-TT-20178] 18 p2488 N88-24761

Rapidly solidified lightweight durable disk material
[AD-A191697] 18 p2491 N88-24775

Martensitic transformation and microstructures in sintered NiAl alloys
[NASA-TT-20192] 19 p2616 N88-25519

Electrodeposition of amorphous Ni-Cr-P alloys
[DE88-006868] 19 p2616 N88-25521

Hot isostatic pressing of nickel aluminide powders
[DE88-009677] 19 p2617 N88-25525

New super alloys used in turbochargers
19 p2634 N88-25628

Glass forming ranges of amorphous alloys
[DE88-007897] 20 p2772 N88-26438

Precipitation study by electrical resistivity measurement in Ni-Al alloys
[DE88-701877] 20 p2773 N88-26440

Shape memory alloys: New materials for future engineering
[NASA-TT-20193] 20 p2775 N88-26455

The preparation of mechanically alloyed powders for TEM (Transmission Electron Microscopy) examination
[DE88-008043] 20 p2775 N88-26460

Nickel aluminides: A new family of nickel + aluminum alloys featuring simple composition, low density, excellent oxidation resistance and high yield strength that increases with temperature
[DE88-010692] 20 p2776 N88-26461

PECVD of amorphous nickel--phosphorus films
[DE88-011088] 21 p2915 N88-27299

Hot isostatic pressing of tungsten-nickel-iron composites
[FOA-C-20698-2.1] 22 p3056 N88-28135

Development of Nb-Ti multifilamentar superconducting wires
[DE88-702324] 23 p3290 N88-29592

Hydrogen embrittlement of iron-nickel alloys
[AD-A195909] 24 p3353 N88-29958

Anisotropic constitutive modeling for nickel-base single crystal superalloys
[NASA-CR-182157] 24 p3353 N88-29961

NICKEL CADMIUM BATTERIES

The 1986 Goddard Space Flight Center Battery Workshop
[NASA-CP-2486] 02 p0163 N88-11021

Battery development and testing at ESA
02 p0164 N88-11027

BRASILSAT A2: Ground and in-orbit anomalies
02 p0164 N88-11032

International Ultraviolet Explorer (IUE) spacecraft battery performance update 02 p0164 N88-11033

Effects of long term storage on aerospace nickel cadmium cell performance 02 p0165 N88-11035

Qualification testing of General Electric 50 Ah nickel-cadmium cells with Pellon 2536 separator and passivated positive plates 02 p0165 N88-11036

Flight experience of solar mesosphere explorer's power system over high temperatures ranges
02 p0165 N88-11037

Real time charge efficiency monitoring for nickel electrodes in NICD and NIH2 cells
02 p0165 N88-11038

Statistically determined nickel cadmium performance relationships 02 p0165 N88-11039

Test summary for advanced H2 cycle NI-CD cell
02 p0165 N88-11040

High energy density rechargeable batteries for aerospace power requirements
[AD-A184883] 05 p0577 N88-13519

Investigation of self-discharge characteristics of spacecraft nickel-cadmium cells at elevated temperatures
[AD-A186497] 08 p0979 N88-15919

ESL batteries and multi-segment applications --- ESA Simulation Language (ESL)
[CS-1029/00-QFIN4] 10 p1322 N88-17901

Effects of cadmium electrode properties on nickel-cadmium cell performance
[AD-A191394] 16 p2193 N88-23081

Aerospace energy systems laboratory: Requirements and design approach
[NASA-TM-100423] 17 p2390 N88-24206

Results from life test in progress on eagle-picher nickel cadmium cells
[AD-A192816] 21 p2936 N88-27434

Aircraft battery state of charge and charge control system
[AD-A194979] 24 p3367 N88-30052

NICKEL COATINGS

Corrosion of electroless nickel-coated steel
[AD-A191045] 16 p2179 N88-22985

NICKEL COMPOUNDS
NT NICKEL OXIDES

Analysis of phase equilibria in NiTi-C system in high nickel regions
[BLL-M-37304-(5828.4)] 02 p0149 N88-10932

The toxicology and metabolism of nickel compounds
[DE87-014801] 04 p0474 N88-12921

Phase purity of NiCo2O4, a catalyst candidate for electrolysis of water
[NASA-TM-100239] 05 p0556 N88-13385

An investigation of metal complexes of some 2-substituted and 2,6-disubstituted pyridine N-oxides
11 p1460 N88-18701

Characterization of redox states of nickel hydroxide film electrodes by in-situ Raman spectroscopy
[AD-A189288] 13 p1741 N88-20411

NICKEL HYDROGEN BATTERIES

Effect of NASA advanced designs on thermal behavior of Ni-H2 cells
[NASA-TM-100197] 01 p0021 N88-10132

The 1986 Goddard Space Flight Center Battery Workshop
[NASA-CP-2486] 02 p0163 N88-11021

Battery development and testing at ESA
02 p0164 N88-11027

Nickel hydrogen low Earth orbit test program update and status 02 p0164 N88-11028

Advances in nickel hydrogen technology at Yardney Battery Division 02 p0164 N88-11029

Failure analysis of a 3.5 inch, 50 ampere-hour nickel-hydrogen cell 02 p0164 N88-11030

Real time charge efficiency monitoring for nickel electrodes in NICD and NIH2 cells
02 p0165 N88-11038

Effects of pressure fluctuations on nickel electrodes
[AD-A184293] 03 p0311 N88-11967

Making space nickel/hydrogen batteries lighter and less expensive
[DE88-000168] 05 p0578 N88-13530

Nickel hydrogen low earth orbit life testing
[AD-A191946] 18 p2504 N88-24855

Small scale bipolar nickel-hydrogen testing
[NASA-TM-100936] 18 p2538 N88-25059

Effect of LEO cycling at shallow depths of discharge on MANTECH IPV nickel-hydrogen cells
[NASA-TM-101300] 19 p2688 N88-25978

Performance of lightweight nickel electrodes
[NASA-TM-100958] 20 p2771 N88-26430
Nickel hydrogen cell positive-electrode studies: Cobalt segregation in reducing environments
[AD-A193025] 20 p2796 N88-26587
Recent developments in nickel hydrogen technology
[DE88-011248] 21 p2939 N88-27456
The effect of compression on individual pressure vessel nickel/hydrogen components
[NASA-TM-101312] 22 p3052 N88-28109

NICKEL IRON BATTERIES
Post-test analyses of aqueous batteries developed for electric propulsion
[DE88-000655] 03 p0311 N88-11965

NICKEL OXIDES
A hydrogen/nickel oxide battery for remote applications
[DE87-009048] 04 p0464 N88-12872
The migration of grain boundaries in ceramic materials with particular reference to the sintering process
[DE88-004085] 10 p1306 N88-17808
The adherence of nickel oxide on nickel during high temperature oxidation
[DE88-011194] 20 p2774 N88-26450

NICKEL PLATE
Analysis of nickel sulphamate bath using charging current compensated D.C. polarography
[NAL-TM-MT-8705] 05 p0564 N88-13433

NICKEL STEELS
Modified 14Cr-16Ni stainless steels with improved creep resistance at 700 C due to tailored precipitate microstructures
[DE87-014788] 03 p0290 N88-11825
Impact behavior of 9-Cr and 12-Cr ferritic steels after low-temperature irradiation
[DE88-000333] 03 p0291 N88-11827
Texture profile in thermomechanically processed 2-inch-thick 5 Ni-steel armor plate
[AD-A189275] 13 p1741 N88-20410

NICKEL ZINC BATTERIES
Grace DAKASEP alkaline battery separator
02 p0164 N88-11031

NICOTINIC ACID
Rapid hypothermia subsequent to oral nicotinic acid and immersion in warm (30C) water
[AD-A186458] 08 p1050 N88-16339

NIGHT
Pyroelectric line scanner for remote IR imaging of vehicles
[DE87-012127] 02 p0235 N88-11484
Distribution of electron concentration in nighttime atmosphere of Venus based on radio transmission data
08 p1005 N88-16092
Biorhythmic aspects of intercontinental Antarctic adaptation 08 p1046 N88-16321
Tactical air force night/adverse weather training
[AD-A194243] 22 p3133 N88-28625

NIGHT AIRGLOW
U NIGHTGLOW

NIGHT E LAYER
U E REGION
U NIGHT SKY

NIGHT F LAYER
U F REGION
U NIGHT SKY

NIGHT FLIGHTS (AIRCRAFT)
The accommodative status in the dark of US Navy fighter pilots
[AD-A188188] 10 p1370 N88-18186
Simulator evaluation of lineup visual landing aids for night carrier landing
[AD-A191212] 18 p2468 N88-24648
Integration of LANTIRN (Low Altitude Navigation and Targeting Infrared for Night) into operational fighter training
[AD-A194906] 24 p3325 N88-29799
LANTIRN simulator training in the F-16C
[AD-A195201] 24 p3330 N88-29826

NIGHT SKY
Ionospheric convection and structure using ground-based digital ionosondes
[AD-A194246] 23 p3233 N88-29237
One equatorial anomaly in nighttime ionospheric F region 24 p3447 N88-30517

NIGHT VISION
Development, testing and evaluation of a night vision goggle compatible BO-105 for night low level operation
03 p0265 N88-11668
Scotopic sensitivity with 10 percent oxygen
[AD-A183973] 03 p0356 N88-12243
Management Information and Downloader Interface System (MIDIS)
[AD-A186978] 09 p1261 N88-17557
The accommodative status in the dark of US Navy fighter pilots
[AD-A188188] 10 p1370 N88-18186
Night Vision: Current Research and Future Directions, symposium proceedings
[PB88-132006] 11 p1550 N88-19274
Mechanisms of early light and dark adaptations
12 p1663 N88-19972
Fast Algorithm Simulation and Test (FAST) facility
[AD-A191183] 16 p2252 N88-23457
Night lighting and night vision goggle compatibility
23 p3242 N88-29297
Visual sensitivities under reduced oxygen
[AD-A195628] 24 p3406 N88-30279
Common modules: A success story
[AD-A195937] 24 p3430 N88-30415

NIGHTGLOW
Electrodynamics of midnight sector of auroral oval in period of slight disturbance 08 p1003 N88-16077
Multispectral optical observations of ionospheric F-region storm effects at low latitude
[INPE-4231-PRE/1105] 08 p1024 N88-16198
The photons payload, G-494: A learning experience
10 p1288 N88-17701

NIMBUS SATELLITES
NT NIMBUS 7 SATELLITE

NIMBUS 7 SATELLITE
In-orbit calibration adjustment of the Nimbus-7 SMMR
[NASA-TM-100678] 05 p0614 N88-13773
Volcanic eruption detection with TOMS
05 p0618 N88-13793
Selection of optimum wavelengths for ozone mapping from satellites 05 p0619 N88-13798
Determination of total ozone from HIRS2/MSU sounding data 05 p0619 N88-13799
Description of data on the Nimbus 7 LIMS map archive tape: Water vapor and nitrogen dioxide
[NASA-TP-2761] 06 p0744 N88-14572
Nimbus 7 Solar Backscatter Ultraviolet (SBUV) spectral scan solar irradiance and Earth radiance product user's guide
[NASA-RP-1199] 09 p1184 N88-17096
The 1987 Airborne Antarctic Ozone Experiment: The Nimbus-7 TOMS data atlas
[NASA-RP-1201] 13 p1791 N88-20714
NIMBUS-7 CZCS. Coastal Zone Color Scanner imagery for selected coastal regions. North America - Europe. South America - Africa - Antarctica. Level 2 photographic product
[NASA-CR-180755] 15 p2089 N88-22447

NIMONIC ALLOYS
Near-threshold short crack growth behavior in Nimonic 105 05 p0599 N88-13663

NIMPHE (ENGINE)
U HYDRAZINE ENGINES

NIOBATES
NT LITHIUM NIOBATES
The role of point defects on structural phase transitions
[DE88-005209] 12 p1696 N88-20152

NIOBIUM
NT NIOBIUM ISOTOPES
Mechanical properties of a microalloyed steel with high niobium content
[DE87-703545] 04 p0415 N88-12572
Sintered steels of high resistance alloyed to Nb, Mo, Mn and Si
[DE87-703546] 04 p0415 N88-12573
Mechanical properties of an acicular ferrite steel microalloyed to niobium and vanadium
[DE87-703547] 04 p0415 N88-12574
Partial substitution of vanadium by niobium in AISI H13 steel
[DE87-703548] 04 p0415 N88-12575
Progress in the development of niobium alloyed high speed steel
[DE87-703549] 04 p0415 N88-12576
Hadfield steels with Nb and Ti carbides
[DE87-703706] 04 p0416 N88-12579
Study of the influence of mechanical - thermal treatments on the creep behavior of a niobium stainless steel
[DE87-703506] 05 p0563 N88-13431
Nb3Al formation in sputter-deposited Nb/Al mutli-layer samples
[DE88-003192] 08 p0970 N88-15868
Creep behavior of tungsten/niobium and tungsten/niobium-1 percent zirconium composites
[NASA-TM-100804] 11 p1460 N88-18707
The effects of various conductor components on Nb3Sn filament prestrain in cable-in-conduit conductors
[DE88-003956] 11 p1479 N88-18824
Use of nonporous metals membranes for the separation of hydrogen from gas mixtures
[BMFT-FB-T-86-206] 14 p1888 N88-21280
Structure and properties of welded joints produced between niobium parts in controllable helium atmosphere 14 p1897 N88-21326
Superconducting transition temperature of Cu-Nb microcomposites 14 p1973 N88-21775
Thermal model describing development of normal region in superconductor film carrying electric current
14 p1973 N88-21776
Creep behavior of tungsten/niobium and tungsten/niobium-1 percent zirconium composites
17 p2425 N88-24427
Effect of alloying, rapid solidification, and surface kinetics on the high temperature environmental resistance of niobium
[AD-A192093] 18 p2485 N88-24743
Magnetization studies of multifilamentary Nb3Sn wires
[DE88-009103] 19 p2735 N88-26243
Rocket-propellant burn tests of silicide-coated niobium and tantalum
[DE88-010729] 20 p2781 N88-26496
Investigation of a SiC/Ti-24Al-11Nb composite
[NASA-TM-100956] 23 p3190 N88-28980

NIOBIUM ALLOYS
Strain rate effects in fast-gas-cooled uranium-titanium and uranium-niobium alloys
[OUEL-1683/87] 02 p0149 N88-10937
Effect of irradiation on the tensile properties of niobium-base alloys
[DE87-002409] 03 p0285 N88-11790
Mechanical strength and niobium and niobium-base alloys substructures
[DE87-703692] 04 p0415 N88-12577
Corrosion strength of niobium and its alloys
[DE87-703693] 04 p0416 N88-12578
Characteristics of joint formation during friction welding of Ti alloys to Nb alloys 14 p1898 N88-21329
Superconducting transition temperature of Cu-Nb microcomposites 14 p1973 N88-21775
Growth and deformation mechanisms of refractory alloy hybrid materials
[AD-A190492] 15 p2039 N88-22152
Characterization of precipitates in a niobium-zirconium-carbon alloy
[NASA-TM-100848] 16 p2178 N88-22981
Laser cladding of Ni, Nb and Mg alloys for improved environmental resistance at high temperature
[AD-A191274] 16 p2213 N88-23208
Preliminary study of niobium alloy contamination by transport through helium 17 p2402 N88-24279
Fabrication of a niobium 1 percent zirconium containment for SP-100 primary lithium system materials mass transfer studies 17 p2417 N88-24373
The preparation of mechanically alloyed powders for TEM (Transmission Electron Microscopy) examination
[DE88-008043] 20 p2775 N88-26460
An HVEM study of displacement cascade damage in Nb3Sn at 13 K
[DE88-009997] 23 p3289 N88-29584

NIOBIUM CARBIDES
Contributions to the investigation of mechanical behavior of gamma/gamma NbC Cotac composites at medium and at high temperature
[ESA-TT-1031] 03 p0280 N88-11760

NIOBIUM COMPOUNDS
NT LITHIUM NIOBATES
NT NIOBATES
NT NIOBIUM CARBIDES
NT NIOBIUM OXIDES
NT NIOBIUM STANNIDES
Microstructure modifications of micron thick NbN films to improve J/sub c/ and H/sub c2/
[DE88-003078] 08 p1091 N88-16567
Hydrogen in niobium-tantalum superlattices
09 p1146 N88-16867
Method of producing high T(subc) superconducting NBN films
[NASA-CASE-NPO-16681-1-CU]
17 p2446 N88-24543

NIOBIUM ISOTOPES
Bulk plasmon enhanced photoemission from Nb(100) surface resonances
[AD-A192711] 22 p3154 N88-28767

NIOBIUM OXIDES
Growth and characteristics of materials for tunable lasers in the near infrared spectral region
[NASA-CR-182501] 11 p1491 N88-18901

NIOBIUM STANNIDES
Properties of Nb3Sn superconductor wires with composite cores
[KFK-4263] 02 p0246 N88-11557
Powder-metallurgical preparation of A15 superconductors
[ETN-87-90584] 03 p0380 N88-12392
Powder metallurgical preparation of A15 superconductors
[ETN-88-91072] 09 p1144 N88-16858

NITINOL ALLOYS
On the stressing of annealed NITINOL: The electrical resistance and calorimetric effects
[AD-A184465] 04 p0414 N88-12569

NITRAMINE PROPELLANTS
High pressure strand burn rate tests of polyvinylnitrate/nitramine propellants
[AD-A184178] 04 p0422 N88-12615
Laser ignition of nitramine composite propellants and crack propagation and branching in burning solid propellants
[AD-A189260] 13 p1753 N88-20483
Structure/property/reactivity relations among nitramine and other energetic materials
[AD-A190878] 18 p2481 N88-24716
Chemical kinetics of nitramine propellant combustion
[AD-A191556] 18 p2495 N88-24802
The 24th JANNAF Combustion Meeting, volume 1
[AD-A190163] 19 p2627 N88-25585
Deuterium isotope effects in the combustion of formulated nitramine propellants
19 p2632 N88-25611
Discovery of a low temperature form of TAGN (Triaminoguanidinium Nitrate)
[AD-A196059] 24 p3357 N88-29989

NITRATES
NT AMMONIUM NITRATES
NT HYDRAZINE NITRATE
NT PETN
NT SODIUM NITRATES
Comparison of three aerosol sampling techniques and the differences in the nitrate determined by each
[DE87-0'1456] 03 p0348 N88-12200
High pressure strand burn rate tests of polyvinylnitrate/nitramine propellants
[AD-A184178] 04 p0422 N88-12615
The 1,2,3-triaminoguanidinium nitrate: An alternate explanation of the nitrate anion disorder
[AD-A186386] 12 p1612 N88-19640
The unique characteristics of the structure of composite materials made on a base of sphalerite-analogous boron nitride 14 p1886 N88-21273
Meteorological aspects of wet deposition in Southern Finland
[FMI-3] 19 p2693 N88-26007
Studies of the mechanisms and rates with which nitrogen species are incorporated into cloud water and precipitation
[PB88-193065] 20 p2826 N88-26764
Foliar nitrate reductase: A marker for assimilation of atmospheric nitrogen oxides
[DE88-010453] 21 p2971 N88-27648
Atmospheric deposition of nitrate to the ocean surface
23 p3231 N88-29227
Some effects of nitrates on the tensile properties of Al 7075-T7351
[AD-A195118] 24 p3354 N88-29965
Discovery of a low temperature form of TAGN (Triaminoguanidinium Nitrate)
[AD-A196059] 24 p3357 N88-29989

NITRATION
Research in energetic compounds
[AD-A192953] 20 p2781 N88-26494

NITRIC ACID
Simulation of global wet and dry deposition of nitric acid in a three-dimensional chemistry-transport model
[DE87-009847] 09 p1188 N88-17116
Mechanism of the nitric oxide-carbon monoxide-oxygen reaction over a single crystal rhodium catalyst
[DE88-006274] 21 p2910 N88-27268

NITRIDES
NT ALUMINUM NITRIDES
NT BORON NITRIDES
NT GALLIUM NITRIDES
NT METAL NITRIDES
NT OXYNITRIDES
NT SILICON NITRIDES
NT TITANIUM NITRIDES
NT ZIRCONIUM NITRIDES
High temperature oxidation studies on alloys containing dispersed phase particles and clarification of the mechanism of growth of SiO2
[AD-A188158] 11 p1457 N88-18688
Formation of buried nitride layers in (110) silicon
[DE88-003255] 11 p1557 N88-19323
Properties of reactively sputtered WNx films Zhao, X. -A.
[AD-A188711] 13 p1835 N88-20976
Uranium nitride fuel swelling and thermal conductivity correlations 17 p2409 N88-24327
An irradiation performance data base for nitride fuels
17 p2427 N88-24438
Material property and irradiation performance correlations for nitride fuels 17 p2434 N88-24483
A comparison of uranium nitride and mixed carbide fuels swelling 17 p2435 N88-24485
Method of producing high T(subc) superconducting NBN films
[NASA-CASE-NPO-16681-1-CU]
17 p2446 N88-24543

NITRIDING
Fatigue characteristics of ion treated surfaces
05 p0606 N88-13713
Ion-beam nitriding of steels
[NASA-CASE-LEW-14104-2] 06 p0682 N88-14179
Analysis of load-bearing capacity of nitrided layer
[PB87-144176] 08 p0968 N88-15857
Antistokes coherent Raman diffusion of a nitriding plasma
[ONERA-RF-6/3644-PY] 16 p2175 N88-22962
SiC fiber reinforced reaction-bonded Si3N4 composites 17 p2326 N88-23892

NITRILES
NT ACETONITRILE
NT ACRYLONITRILES
Transparent metal model study of the use of a cellular growth front to form aligned monotectic composite materials
[NASA-CR-182414] 08 p0969 N88-15861
Development of a nitrile rubber for dynamic damping
[AD-A194060] 22 p3058 N88-28145

NITRO COMPOUNDS
NT NITROMETHANE
NT TETRYL
NT TRINITROTOLUENE
Theoretical investigations of nitrocubane decomposition
[AD-A194556] 23 p3200 N88-29047

NITROBENZENES
NT TRINITROTOLUENE

NITROGEN
NT LIQUID NITROGEN
NT NITROGEN ISOTOPES
Nitrogen at high pressure
[DE87-013797] 01 p0021 N88-10130
Nitrogen at very high pressure
[DE87-013800] 01 p0021 N88-10131
Rocket nozzle thermal shock tests in an arc heater facility 02 p0133 N88-10832
Thermodynamics of interaction between nitrogen and molten nickel alloys
[BLL-M-37309-(5828.4)] 02 p0149 N88-10934
Shock-induced cooling in dense fluids
[DE87-014343] 02 p0170 N88-11067
Absorption of far IR-radiation by H2O-N2 complexes under atmospheric conditions 04 p0462 N88-12855
Nitrogen energy transfer study
[AD-A184457] 04 p0464 N88-12869
Development of a low noise 10 K J-T refrigeration system
[AD-A185258] 05 p0571 N88-13484
Fuel nitrogen conversion in a supercharged spark ignition engine
[DE88-003739] 08 p0974 N88-15893
CARS measurements of combustion. 1: Precision of thermometry
[NAL-TR-939] 10 p1299 N88-17769
Effects of ion implantation on cavitation erosion of a cobalt based metal/carbide alloy
[AD-A187239] 10 p1303 N88-17793
Investigations of surface coatings based on silicon and nitrogen: From amorphous Si to silicon nitride
[DE88-004995] 12 p1609 N88-19622
Nitrogen's biological effect on oxygen transport through hematoparenchymal barrier 12 p1662 N88-19967
Spectrographic detection of nitrogen impurity in helium
[DE88-752301] 15 p2033 N88-22111
Reactions of N2(A sup 3 sigma sup + sub u) candidates for short wavelength lasers
[DE88-007018] 15 p2070 N88-22342
Thermal conductivity of selected foams and systems from 100 to 300 K
[PB88-201553] 20 p2777 N88-26466
A shock-tube experiment on gases mixing processes associated with CO2/N2 mixing gasdynamic laser
[ISAS-RN-350] 20 p2797 N88-26598
Study of energy levels and decay mechanisms for singlet Rydberg states of molecular nitrogen
[AD-A192505] 21 p3014 N88-27886
Chemically-produced N2(A) to NO(X) energy transfer in a supersonic flow
[AD-A192501] 22 p3082 N88-28302
NF (a 1 delta) production in a supersonic flow using N2F4 + H2 in a BCL-16 nozzle
[AD-A194478] 22 p3082 N88-28304
Computed potential energy surfaces for chemical reactions
[NASA-CR-183168] 24 p3342 N88-29893

NITROGEN ATOMS
A model for nitrogen atom recombination on a silicon dioxide surface
[AD-A189843] 15 p2142 N88-22784

NITROGEN COMPOUNDS
NT ALUMINUM NITRIDES
NT AMIDES
NT AMMONIA
NT AMMONIUM NITRATES
NT ATROPINE
NT AZIDES (INORGANIC)
NT AZIDES (ORGANIC)
NT BORON NITRIDES
NT CAFFEINE
NT CYANO COMPOUNDS
NT ERGOTAMINE
NT GALLIUM NITRIDES
NT HMX
NT HYDRAZINE NITRATE
NT HYDRAZINIUM COMPOUNDS
NT IMIDES
NT IMINES
NT ISOCYANATES
NT LIQUID AMMONIA
NT METAL NITRIDES
NT MORPHINE
NT NITRATES
NT NITRIC ACID
NT NITRIDES
NT NITRO COMPOUNDS
NT NITROGEN DIOXIDE
NT NITROGEN FLUORIDES
NT NITROGEN HYDRIDES
NT NITROGEN OXIDES
NT NITROGEN POLYMERS
NT NITROMETHANE
NT NITROUS OXIDES
NT OXYNITRIDES
NT PETN
NT POLYIMIDES
NT QUINOLINE
NT RDX
NT SILICON NITRIDES
NT SODIUM NITRATES
NT TETRYL
NT THYMINE
NT TITANIUM NITRIDES
NT TRINITROTOLUENE
NT URACIL
NT UREAS
NT XANTHINES
NT ZIRCONIUM NITRIDES
Investigations of the influence of chemical reactions of the vertical flow of gaseous and particulate compounds
08 p1017 N88-16165

NITROGEN DIOXIDE
NO2 heterodyne frequency measurements with a tunable diode laser, a CO laser transfer oscillator and CO2 laser standards
[NASA-CR-182393] 06 p0710 N88-14353
Effect of nitrogen dioxide release on thermosphere
13 p1789 N88-20704
Pyrolyzed organic polymer nitrogen dioxide sensor
19 p2669 N88-25868

NITROGEN FIXATION
U NITROGENATION

NITROGEN FLUORIDES
N2(A3epsilon u +) by reaction of N2F4 + H2 in a supersonic flow
[AD-A194493] 23 p3219 N88-29163

NITROGEN HYDRIDES
Experiments on reactions of the electronically excited molecule nitron NH (a sup 1 delta) and carbon CH2 (a bar sup 1 A(1)) in gas phase
[MPIS-3/1987] 17 p2397 N88-24249

NITROGEN IONS
The effect of object potentials on the wake of a flowing plasma
[AD-A184038] 03 p0379 N88-12385
The magnitude of secondary electron contributions in photon stimulated desorption
[AD-A189094] 13 p1835 N88-20980

NITROGEN ISOTOPES
The atomic weight and isotopic composition of nitrogen and their variation in nature
[DE87-012867] 02 p0144 N88-10902

NITROGEN LASERS
TEA-TE: Powerful nitrogen-based laser system
07 p0919 N88-15583

NITROGEN METABOLISM
Comparison of morning with afternoon nitrogen elimination in resting subjects breathing 100 percent oxygen
[AD-A196191] 24 p3407 N88-30282

NITROGEN OXIDES
NT NITROGEN DIOXIDE
NT NITROUS OXIDES
Production of NO by galactic cosmic rays and lightning
[DE87-014613] 02 p0197 N88-11230
Study of polyatomic dynamics in the atmosphere
[AD-A190964] 16 p2233 N88-23334

Atmospheric nitrogen oxides: Their detection and chemistry
[PB88-193057] 21 p2970 N88-27642
Chemically-produced N2(A) to NO(X) energy transfer in a supersonic flow
[AD-A192501] 22 p3082 N88-28302
A study of the interaction of NO2 with carbon particles
[DE88-010778] 22 p3118 N88-28524
Photochemistry of ionospheric D-region with injection of nitrogen oxides 24 p3444 N88-30499

NITROGEN PLASMA
Nonequilibrium characteristics of nitrogen plasmas appropriate to an AOTV flight 03 p0319 N88-12019
The effect of object potentials on the wake of a flowing plasma
[AD-A184038] 03 p0379 N88-12385

NITROGEN POLYMERS
Interfacial shear strength of pitch and high strain pan fibers in an epoxy matrix
[AD-A185966] 07 p0826 N88-15011
Electronic and ionic transport in polymers
[AD-A187253] 11 p1452 N88-18651
MOPAC manual: A general molecular orbital package, fourth edition
[AD-A188623] 13 p1733 N88-20362

NITROGENATION
Application of photosynthetic N(2)-fixing cyanobacteria to the CELSS program 03 p0358 N88-12257

NITROMETHANE
Kinetic measurements of thermal decomposition of energetic materials at high pressures
[AD-A191612] 19 p2622 N88-25552

NITROUS OXIDES
Formation and destruction of nitrous oxide in lean, premixed combustion
[DE88-001390] 05 p0562 N88-13423

NMR
U NUCLEAR MAGNETIC RESONANCE

NOAA SATELLITES
NT NOAA 7 SATELLITE
Observation of the development of mesoscale systems by operational meteorological satellites
02 p0201 N88-11259
TOMS and the NOAA/FAA volcano support plan
05 p0618 N88-13796
An overview of the current Earth observation programs (Europe, USA, and Japan) 09 p1129 N88-16778
Processing of HRPT data from the NOAA series satellites 17 p2359 N88-24053

NOAA 7 SATELLITE
Analysis of thickness fields retrieved from NOAA-7 observations through the 3I (Improved Initialization Inversion) method. Interest for weather forecasting
02 p0201 N88-11255

NOBLE GASES
U RARE GASES

NOBLE METALS
NT GOLD
NT RUTHENIUM
NT SILVER
Reactions of some thiol collectors at noble-metal and pyrite electrodes
[PB88-138318] 11 p1455 N88-18674
Temperature dependence of conductivity and of Hall coefficients for noble metal films
[ETN-88-92981] 23 p3294 N88-29616

NOCTILUCENCE
U LUMINESCENCE

NOCTILUCENT CLOUDS
The nonlinear thermodynamics of meteors, noctilucent clouds, enhanced airglow and global atmospheric circulation 06 p0738 N88-14538

NOCTURNAL VARIATIONS
Theoretical and lidar studies of the seasonal and nocturnal variations of the mesospheric sodium layer at Urbana, Illinois 01 p0068 N88-10435
Effect of neutral wind on the latitudinal variation of nighttime F-layer vertical movements
08 p1030 N88-16244
Is ANF implied in the night attenuated renal response to central hypervolemia? 12 p1659 N88-19945
Computer simulation of tropospheric chemistry
[JUEL-2144] 13 p1798 N88-20756

NODES (STANDING WAVES)
Five-point form of the nodal diffusion method and comparison with finite-difference
[DE88-004141] 19 p2720 N88-26154
A nodal method for time-dependent transport equation
[DE88-004285] 20 p2844 N88-26876

NODULES
Concentration coefficients of elements in ferromanganese nodules relative to ocean sediments
06 p0726 N88-14464
Remote acoustic sounding of ferromanganese nodules
06 p0727 N88-14471
Ferromanganese nodules of Antarctic sector in Pacific Ocean 06 p0727 N88-14472

NOE NAVIGATION
U NAP-OF-THE-EARTH NAVIGATION

NOISE
Application of ray theory to propagation of low frequency noise from wind turbines
[NASA-CR-178367] 03 p0373 N88-12349
Development of a technique for estimating noise covariances using multiple observers
[NASA-TM-4020] 06 p0669 N88-14098
A new method of boundary parameter estimation for a two-dimensional diffusion system under noisy observations
[NASA-CR-178405] 06 p0767 N88-14714
IRAC test report. Gallium doped silicon band 2: Read noise and dark current
[NASA-TM-87813] 09 p1159 N88-16945
Research in applied mathematics ralated to identification of noisy systems
[AD-A189355] 13 p1825 N88-20908
Fundamental noise processes in a laser excited optical filter
[DE88-006460] 15 p2070 N88-22340

NOISE (SOUND)
NT AERODYNAMIC NOISE
NT AIRCRAFT NOISE
NT BLADE SLAP NOISE
NT ENGINE NOISE
NT JET AIRCRAFT NOISE
NT SONIC BOOMS
NT THERMAL NOISE
Activities report of the Institute of Sound and Vibration Research
[ETN-87-90685] 01 p0090 N88-10589
Noise modelling in the time domain with the aid of Spice
[PB87-221941] 05 p0573 N88-13492
A study of rotor broadband noise mechanisms and helicopter tail rotor noise 06 p0777 N88-14766
Brain potentials and personality: A new look at stress susceptibility
[AD-A186931] 09 p1199 N88-17189
Structural-acoustic interior noise modeling and analysis from experimental data
[PB88-141775] 12 p1687 N88-20088
Auditory perception of complex sounds
[AD-A190528] 15 p2103 N88-22529
Low frequency ocean ambient noise: Measurements and theory
[AD-A191188] 16 p2237 N88-23362
Overground Excess Sound Attenuation (ESA). Volume 1: Experimental study for flat grassy terrains
[AD-A191289] 16 p2265 N88-23549
Higher frequency ambient noise in the arctic ocean
[AD-A192203] 18 p2547 N88-25122
Noise and chaos in driven Josephson junctions
19 p2734 N88-26238
A modal approach to Arctic noise modelling with implied vertical coherence
[AD-A192966] 20 p2850 N88-26916
Vertical directionality of ambient noise at 32 deg N as a function of longitude: Tape number 86180
[AD-A193228] 21 p3012 N88-27872
Signal, noise, and reverberation in bistatic sonar systems
[FOA-C-20703-2.7] 22 p3147 N88-28721
CryoSQUID: A SQUID-based magnetic field sensor
[AD-A194237] 23 p3239 N88-29275
An investigation of acoustic cavitation produced by pulsed ultrasound
[AD-A193523] 23 p3278 N88-29516

NOISE ATTENUATION
U NOISE REDUCTION

NOISE ELIMINATION
U NOISE REDUCTION

NOISE GENERATORS
Noise emission of civil and military aero-engines. Sources of generation and measures for attenuation
[ETN-87-91021] 01 p0091 N88-10595
A digital control system for high level acoustic noise generation 02 p0138 N88-10865
An experimental investigation of noise generation and noise reduction in a pipe flow downstream of a discontinuous area enlargement
[ESA-TT-1027] 03 p0374 N88-12351
Higher frequency ambient noise in the arctic ocean
[AD-A192203] 18 p2547 N88-25122
Noise generation by air bubbles in water: An experimental study of creation and splitting
[AD-A192063] 19 p2664 N88-25839
Noise generation and boundary layer effects in vortex-airfoil interaction and methods of digital hologram analysis for these flow fields
[AD-A194191] 23 p3171 N88-28883

NOISE HAZARDS
U HAZARDS
U NOISE (SOUND)

NOISE INJURIES
Further investigation of tests for susceptibility to noise-induced hearing loss
[ISVR-TR-149] 14 p1952 N88-21633

NOISE INTENSITY
First article test noise survey of the A/F32T-9 large turbo fan engine enclosed noise suppressor system, Sky Harbor IAP (International Airport), Phoenix, Arizona
[AD-A183799] 01 p0090 N88-10588
Helicopter main-rotor speed effects on far-field acoustic levels
[NASA-TM-100512] 02 p0230 N88-11451
AFAR (Azores Fixed Acoustic Range) measurements of intensity and intensity moments
[AD-A184431] 03 p0355 N88-12237
Development of rotorcraft interior noise control concepts. Phase 2: Full scale testing, revision 1
[NASA-CR-172594-REV-1] 06 p0777 N88-14769
Measuring the annoyance of aircraft noise
[AD-A185494] 06 p0777 N88-14770
Annoyance caused by advanced turboprop aircraft flyover noise: Single-rotating propeller configuration
[NASA-TP-2782] 09 p1242 N88-17441
Wideband HF (High Frequency) modeling and simulation
[PB88-116116] 10 p1317 N88-17874
Operational noise data for CH-47D and AH-64 army helicopters
[AD-A191059] 18 p2570 N88-25263
Sound power measurements in situ using a reference sound source
[PB88-182571] 20 p2849 N88-26910
Discrimination studies using short-period P waves at upper mantle distances
[AD-A195468] 24 p3401 N88-30257

NOISE MEASUREMENT
Noise levels from propeller-driven aircraft measured at ground level and at 1.2 m above the ground
[NPL-AC-110] 01 p0091 N88-10594
An experimental investigation of noise generation and noise reduction in a pipe flow downstream of a discontinuous area enlargement
[ESA-TT-1027] 03 p0374 N88-12351
Overview of NASA PTA propfan flight test program
08 p0957 N88-15805
Advanced propeller research
08 p0957 N88-15806
Identification and proposed control of helicopter transmission noise at the source
09 p1109 N88-16647
Wind turbine acoustics research bibliography with selected annotation
[NASA-TM-100528] 09 p1243 N88-17450
Analysis of in-flight acoustic data for a twin-engined turboprop airplane
[NASA-CR-178389] 11 p1543 N88-19220
Experimental study on the influence of wind on acoustic pressure sensors
[ISL-R-121/86] 15 p2131 N88-22712
Advisory circular: Noise certification handbook
[FAA-AC-36-4B] 17 p2394 N88-24234
Sound power measurements in situ using a reference sound source
[PB88-182571] 20 p2849 N88-26910
Aeroacoustic investigation on the noise from ultralight aircraft
[DFVLR-FB-88-03] 21 p3013 N88-27879
Minimizing escape probabilities: A large deviations approach
[AD-A194534] 23 p3275 N88-29496
Noise levels from a jet-engined aircraft measured at ground level and at 1.2 m above the ground
[NPL-AC-114] 23 p3279 N88-29524

NOISE POLLUTION
A proposed metric for assessing the potential of community annoyance from wind turbine low-frequency noise emissions
[DE88-001113] 08 p1022 N88-16187
Cape Blanco wind farm feasibility study
[DE88-003749] 10 p1349 N88-18060
Supersonic and subsonic aircraft noise effects on animals: A literature survey
[AD-A186922] 10 p1404 N88-18373
Noise assessment of unsuppressed TF-34-GE-100A engine at Warfield ANG, Baltimore, Maryland
[AD-A189966] 15 p2129 N88-22702
The MOD-2 wind turbine: Aeroacoustical noise sources, emissions, and potential impact
[DE88-001132] 19 p2687 N88-25971
Aircraft noise: A review
[PNR90450] 22 p3147 N88-28719

NOISE PREDICTION
Surface effects and low frequency noises in GaAs field effect transistors
[LAAS-87-179] 02 p0168 N88-11055
High speed propeller performance and noise predictions at takeoff/landing conditions
[NASA-TM-100267] 05 p0646 N88-13960
Comparison of two transonic noise prediction formulations using the aircraft noise prediction program
[NASA-CR-181609] 12 p1688 N88-20095
Aircraft noise prediction program propeller analysis system IBM-PC version user's manual version 2.0
[NASA-CR-181689] 24 p3428 N88-30399
NOISE PREDICTION (AIRCRAFT)
Compressor large bandwidth noise emission mechanisms
[ETN-88-91177] 05 p0646 N88-13959
Development of rotorcraft interior noise control concepts. Phase 3: Development of noise control concepts
[NASA-CR-178172] 06 p0776 N88-14762
A comparison of simple analytical models for representing propeller aircraft structural and acoustic responses
[ISVR-TR-153] 23 p3279 N88-29523
NOISE PROPAGATION
A new method for determining acoustic properties of the seabed from the ambient noise field in the ocean
[RAE-TR-86035] 01 p0090 N88-10590
Noise emission of civil and military aero-engines. Sources of generation and measures for attenuation
[ETN-87-91021] 01 p0091 N88-10595
Sound propagation over uneven ground and irregular topography
[NASA-CR-182956] 20 p2849 N88-26911
Investigation of helicopter rotor blade/wake interactive impulsive noise
[NASA-CR-177435] 23 p3171 N88-28882
NOISE REDUCTION
Masking effects of fine and coarse grain pictorial noise
[IZF-1985-21] 01 p0076 N88-10485
First article test noise survey of the A/F32T-9 large turbo fan engine enclosed noise suppressor system, Sky Harbor IAP (International Airport), Phoenix, Arizona
[AD-A183799] 01 p0090 N88-10588
Active minimisation of acoustic fields. A review of research into the active control of sound undertaken at ISVR from 1983 to 1986
[ISVR-TR-146] 01 p0091 N88-10593
Noise emission of civil and military aero-engines. Sources of generation and measures for attenuation
[ETN-87-91021] 01 p0091 N88-10595
An experimental investigation of noise generation and noise reduction in a pipe flow downstream of a discontinuous area enlargement
[ESA-TT-1027] 03 p0374 N88-12351
On a circular correlation technique for filtering randomly noisy data
[AD-A184317] 04 p0431 N88-12669
Design of source coders and joint source/channel coders for noisy channels
[NASA-CR-181547] 04 p0432 N88-12678
Aircraft interior noise reduction by alternate resonance tuning
[NASA-CR-181530] 04 p0488 N88-13005
Noise of a model counterrotation propeller with reduced aft rotor diameter at simulated takeoff/approach conditions (F7/A3)
[NASA-TM-100254] 05 p0647 N88-13961
A computer decision-making process for the elimination of noise from data
[AD-A185746] 06 p0759 N88-14659
Development of rotorcraft interior noise control concepts. Phase 3: Development of noise control concepts
[NASA-CR-178172] 06 p0776 N88-14762
Propulsion challenges and opportunities for high-speed transport aircraft 08 p0958 N88-15809
Recent Langley helicopter acoustics contributions
09 p1109 N88-16646
Identification and proposed control of helicopter transmission noise at the source
09 p1109 N88-16647
A decade of aeroacoustic research at NASA Ames Research Center 09 p1109 N88-16648
Rotorcraft technology at Boeing Vertol: Recent advances 09 p1111 N88-16658
Optimal application of Morrison's iterative noise removal for deconvolution. Appendices
[NASA-CR-182477] 09 p1231 N88-17376
Measured and calculated acoustic attenuation rates of tuned resonator arrays for two surface impedance distribution models with flow
[NASA-TP-2766] 09 p1241 N88-17440
Silencium resonators (Silators) for the attenuation and elimination of sound
[MBB-Z-546/83] 10 p1312 N88-17841
The assessment of the sound insulation requirements for a large broadcasting studio, using a scale model: Practical details
[BBC-RD-1987/21] 10 p1318 N88-17878
An adaptive filtering technique for removing periodic noise from modal response data
[DE88-002347] 10 p1322 N88-17903
Advanced propfan analysis for the family of commuter airplanes
[NASA-CR-182566] 12 p1582 N88-19468
A study of methods to predict and measure the transmission of sound through the walls of light aircraft
[NASA-CR-182656] 12 p1687 N88-20090
Evaluation of chemical and atmospheric sciences research
[AD-A188468] 12 p1687 N88-20091
Design, optimization and construction of a dc-SQUID with complete flux transformer circuits
[PB88-160742] 14 p1907 N88-21399
Ultrahigh coherent semiconductor lasers and their applications to Rb atomic clock
14 p1976 N88-21789
Generation of number-phase minimum uncertainty states 14 p1978 N88-21803
Investigation of aeroacoustic mechanisms by remote thermal imaging
[DE88-002612] 15 p2021 N88-22046
Noise assessment of unsuppressed TF-34-GE-100A engine at Warfield ANG, Baltimore, Maryland
[AD-A189966] 15 p2129 N88-22702
Experimental study on the influence of wind on acoustic pressure sensors
[ISL-R-121/86] 15 p2131 N88-22712
The calculation of casually constrained optima in the active control of sound
[ISVR-TR-147] 17 p2395 N88-24237
Evaluation of the US Army fitting program for the integrated helmet unit of the integrated helmet and display sighting system
[AD-A191616] 18 p2465 N88-24635
First article noise survey of the A/F32T-9 large turbo fan engine enclosed noise suppressor system, far-field noise, Ellsworth AFB, South Dakota
[AD-A191938] 19 p2602 N88-25457
Signal processing in digital speech transmission systems
[ETN-88-92122] 20 p2792 N88-26561
A review of gear housing dynamics and acoustics literature
[NASA-CR-183110] 20 p2811 N88-26675
Aircraft interior noise reduction by alternate resonance tuning
[NASA-CR-182540] 20 p2849 N88-26909
Electromagnetic compatibility. View of the near future
[SNIAS-881-422-104] 22 p3071 N88-28229
Aircraft noise: A review
[PNR90450] 22 p3147 N88-28719
A comparison of simple analytical models for representing propeller aircraft structural and acoustic responses
[ISVR-TR-153] 23 p3279 N88-29523
NOISE SPECTRA
Compressor large bandwidth noise emission mechanisms
[ETN-88-91177] 05 p0646 N88-13959
HOC spectral analysis of an almost periodic random sequence in noise
[AD-A185528] 06 p0765 N88-14697
The acoustic source created by turbulent flow over orifices and louvers
[REPT-97674] 06 p0776 N88-14764
Universal power spectra for wave turbulence: Applications to wind waves, flicker noise, solar wind spectrum and classical second sound
10 p1318 N88-17879
Determination of distributed resistance of base of bipolar transistors measuring noise spectral densities
[DE88-700197] 11 p1479 N88-18829
Regional wave attenuation and seismic moment from the inversion of NORESS spectra
[AD-A187399] 11 p1510 N88-19023
Optimal and conventional space-time processing in flow noise
[AD-A189104] 13 p1833 N88-20965
Describing the source created by turbulent flow over orifices and louvers
[AD-A190254] 15 p2130 N88-22706
Sound power measurements in situ using a reference sound source
[PB88-182571] 20 p2849 N88-26910
Application of pattern recognition techniques to the identification of aerospace acoustic sources
[NASA-CR-183116] 21 p3013 N88-27877
Aeroacoustic investigation on the noise from ultralight aircraft
[DFVLR-FB-88-03] 21 p3013 N88-27879
High performance charge transfer device detectors
[AD-A194409] 23 p3192 N88-28993
NOISE SUPPRESSORS
U NOISE REDUCTION
NOISE TEMPERATURE
Capacitive resonant transducer for the Frascati gravitational antenna
[IFSI-86-9] 05 p0578 N88-13528
DSS 14 64-meter antenna S- and X-band efficiency and system noise temperature calibrations, September 1987
11 p1473 N88-18790
A study of satellite emission computed tomography
[AD-A189567] 13 p1797 N88-20745
Generating squeezed microwave radiation with a Josephson parametric amplifier
14 p1978 N88-21805
The kinetics of contact noise in NaBeta alumina
[AD-A190651] 15 p2130 N88-22707
Fluxons and order in long Josephson junctions
[AD-A190879] 16 p2282 N88-23665
X-band noise temperature near the Sun at a 34-meter high efficiency antenna 22 p3067 N88-28200
NOISE TOLERANCE
Annoyance caused by advanced turboprop aircraft flyover noise: Single-rotating propeller configuration
[NASA-TP-2782] 09 p1242 N88-17441
Electroencephalographic changes during equilibrium test in the presence of rhythmic photic interference
19 p2703 N88-26075
NOMENCLATURES
Abregrams or deleweds: A forty-year view of acronyms
[DE87-010808] 01 p0106 N88-10690
NOMINAL VALUES
U APPROXIMATION
NONADIABATIC PROCESSES
U HEAT TRANSFER
NONAQUEOUS ELECTROLYTES
Metal intercalation characteristics of n-HfS2 photoelectrodes in non-aqueous electrolytes
[AD-A184381] 03 p0383 N88-12407
Re-usable thin-layer spectroelectrochemical cell for non-aqueous solvent systems
[AD-A186951] 09 p1248 N88-17478
NONCONDUCTORS
U ELECTRICAL INSULATION
NONCONSERVATIVE FORCES
Contribution to the dynamical analysis of rheolinear nonconservative, gyroscopic systems using finite element methods
[ETN-87-90410] 01 p0050 N88-10320
Examples of nonconservatism in the CARE 3 program
[NASA-TM-100524] 09 p1233 N88-17390
NONDESTRUCTIVE TESTS
NT NEUTRON RADIOGRAPHY
Compendium of post-failure analysis techniques for composite materials
[AD-A183783] 01 p0018 N88-10113
X-ray tomography and nuclear magnetic resonance imaging applications for advanced ceramic materials
[DE87-011534] 01 p0027 N88-10171
Evaluation of mechanical and technological parameters of different steel states by nondestructive micro- and macromagnetic measuring quantities as well as ultrasonic techniques
[MPA-810-079] 01 p0057 N88-10366
Nondestructive inspection of the pressure vessel in Stuttgart. ALOK part. Phase 1: ALOK combined with conventional probes
[REPT-860113-TW] 01 p0057 N88-10367
Model-based ultrasonic tomography
[DE87-013786] 01 p0058 N88-10369
Needs assessment for NDT and characterization of ceramics: Assessment of inspection technology for green state and sintered ceramics
[DE87-013550] 02 p0151 N88-10947
Needs assessment for nondestructive testing and materials characterization for improved reliability in structural ceramics for heat engines
[DE88-000040] 02 p0153 N88-10957
Ultrafast holography using optical fibers
[ISL-R-101/86] 02 p0176 N88-11096
Development of an X-ray fluorescence microprobe at the National Synchrotron Light Source, Brookhaven National Laboratory: Early results: Comparison with data from other techniques
[NASA-CR-181468] 02 p0236 N88-11486
Transply crack density detection by acousto-ultrasonics
[NASA-TM-100224] 03 p0279 N88-11758
Ultrasonic characterization of the nonlinear elastic properties of unidirectional graphite/epoxy composites
[NASA-CR-4100] 03 p0281 N88-11767

NDE (Nondestructive Evaluation) of advanced structural ceramics
[DE87-014417] 03 p0292 N88-11832

Flaw imaging and ultrasonic techniques for characterizing sintered silicon carbide
[NASA-TM-100177] 03 p0334 N88-12106

Real time analysis of the results from mechanized ultrasonic testing
[DE87-752511] 03 p0334 N88-12107

Elastodynamic ray theory and asymptotic methods for direct and inverse scattering problems
03 p0335 N88-12108

Failure analysis of composite structure materials
[AD-A184468] 04 p0410 N88-12548

Detection of defects on structures
[EP-PATENT-0-210-794-A2] 04 p0453 N88-12807

Philosophy and practice of nondestructive tests of composite material structures at Aerospatiale Aquitaine
[SNIAS-872-430-105] 05 p0559 N88-13400

Utilization of microwave measuring systems for nondestructive control of composite materials
[SNIAS-872-430-109] 05 p0559 N88-13402

Measurement and control of damage in composite materials: Nondestructive controls by thermography, holography, and radiography
[SNIAS-872-430-110] 05 p0559 N88-13403

Contribution of acoustic analysis to assess damage in fluid storage tanks under high pressure --- composite materials, filament winding
[SNIAS-872-430-119] 05 p0559 N88-13407

Water disbondment characterization of organic Coating/metal substrate systems
[AD-A184847] 05 p0567 N88-13454

First International Week of Adhesive Bonding and Assembling
[SNIAS-872-430-106] 05 p0569 N88-13468

Investigation of the exposure to harmful compounds in the workshop of nondestructive materials testing at Gilze-Rijen (Netherlands)
[PML-1985-42] 05 p0623 N88-13816

Comparative study of nondestructive pavement testing, MacDill Air Force Base, Florida
[AD-A186082] 07 p0822 N88-14993

Natural frequencies and structural integrity assessment of large space structures
[AD-A186139] 07 p0824 N88-15001

Macroscopic distribution of fiber finish
[DCQ/L-48-283/F] 07 p0827 N88-15013

Improvement of deep resolution in ultrasonic echographic nondestructive evaluation using signal processing methods
[PB87-147658] 07 p0866 N88-15256

Through-transmission/pulse-echo ultrasonic equipment evaluation
[AD-A186340] 07 p0929 N88-15641

Determining structural performance
08 p0954 N88-15787

Nondestructive characterization of ceramic composite whiskers with neutron diffraction and ultrasonic techniques
[DE88-003075] 08 p0965 N88-15844

Nondestructive control: Modeling of electromagnetic phenomena, defect characterization, and sensor optimization
[ECL-86-14] 08 p0993 N88-16008

Solid mechanics research for quantitative non-destructive evaluation
[AD-A186599] 08 p0993 N88-16010

Study of the technique of stress determination by measuring magnetism
[PB87-143905] 08 p0996 N88-16028

Nondestructive magnetic testing of laser hardening parameters (hardening depth, hardness profile, retained austenite)
[ETN-88-91070] 09 p1144 N88-16857

Nondestructive evaluation of structural ceramics by photoacoustic microscopy
[NASA-CR-180858] 09 p1146 N88-16868

Image correlation on an IBM-PC for characterization of advanced ceramics
[DE88-002829] 09 p1149 N88-16885

Thermal wave imaging
[AD-A186810] 09 p1177 N88-17046

Analysis of the reliability of Royal Australian Air force non-destructive inspection
[AD-A186979] 09 p1177 N88-17049

Experience of developing an integrated nondestructive assay system
[DE88-003149] 09 p1184 N88-17092

Durability and damage tolerance of aluminum castings
[AD-A186444] 10 p1341 N88-18013

The development of emission tomography for the nuclear industry
[AERE-R-12319] 10 p1341 N88-18014

Training guidelines in non-destructive testing techniques
[DE88-700613] 10 p1342 N88-18019

Institute for Materials Science and Engineering, nondestructive evaluation: Technical activities 1987
[PB88-153655] 10 p1342 N88-18020

Application of nondestructive testing techniques to materials testing
[AD-A187645] 10 p1342 N88-18021

Institute for Materials Science and Engineering, Fracture and Deformation Division: Technical activities, 1987
[PB88-153622] 10 p1345 N88-18039

Ultrasonic characterization of layered composite systems 10 p1404 N88-18374

Scattering of impulsive acoustic waves by a semi-infinite crack in the plane interface of a half-space and a layer
[PB88-126396] 10 p1405 N88-18377

Quantitative non-destructive evaluation of porous composite materials based on ultrasonic wave propagation
[NASA-CR-182544] 11 p1447 N88-18627

Quality assurance of ceramic materials and gas turbine components
[IZFP-850303-TW] 11 p1465 N88-18735

Novel analytical X-ray Non-Destructive Evaluation (NDE) tool for quality control of energetic materials
[AD-A187737] 11 p1497 N88-18935

Reference standards for nondestructive tests
[AD-A187766] 11 p1497 N88-18936

STA-2A NDT testing
[NASA-CR-179301] 11 p1497 N88-18937

Imaging methods for nondestructive materials testing
[ETN-88-91477] 11 p1497 N88-18940

Non-destructive evaluation techniques applied to the study of fatigue microcrack growth in steel alloys
[DE88-004090] 13 p1742 N88-20420

High temperature Young's modulus of IG-110 graphite
13 p1746 N88-20443

Nondestructive testings of HTGR graphites
13 p1747 N88-20448

Nondestructive evaluation of carbon-carbon coatings
[AD-A189524] 13 p1748 N88-20453

Recent developments in nondestructive evaluation for structural ceramics
[DE88-005889] 13 p1751 N88-20473

X-ray computed tomography for structural ceramic applications: Beam hardening corrections
[DE88-005891] 13 p1752 N88-20474

Noncontact thermometry via laser pumped, thermographic phosphors: Characterization of systematic errors and industrial applications
[DE88-005599] 13 p1777 N88-20628

Thermionic Technology Program. A: Insulator test and evaluation
[DE88-004707] 13 p1795 N88-20735

Statistical analysis of feasibility of non-destructive inspection of mechanical properties of hot worked pipes of alloy steels
[BLL-M-37598-(5828.4)] 14 p1922 N88-21455

A system to measure damage in composite materials by the ultrasonic method
[ONERA-RT-2/7256-RY-061-R]
15 p2031 N88-22103

Electromagnetic sensor arrays for nondestructive evaluation and robot control
[AD-A190210] 15 p2056 N88-22260

Nondestructive moisture measurement in microelectronics
[AD-A190515] 15 p2060 N88-22281

An evaluation of nondestructive methods for ceramic heat exchanger applications
[DE88-006731] 15 p2068 N88-22328

Eddy current nondestructive inspection of graphite epoxy using ferrite cup core probes
[AD-A189823] 15 p2074 N88-22365

Manufacturing of ultrasonic focused probes
[VTT-RR-487] 15 p2074 N88-22368

A 3-D solid rendering of NDT data
[DE88-006199] 15 p2076 N88-22373

Impact damage in composite laminates
15 p2080 N88-22402

Lewis Structures Technology, 1988. Volume 3: Structural Integrity Fatigue and Fracture Wind Turbines HOST
[NASA-CP-3003-VOL-3] 15 p2081 N88-22408

Nondestructive evaluation by acousto-ultrasonics
15 p2082 N88-22412

Characterization of sintered SiC by using NDE
15 p2082 N88-22413

Nondestructive evaluation of sintered ceramics
15 p2083 N88-22416

Nondestructive evaluation of large scale composite components
[AD-A190998] 16 p2173 N88-22954

Detection sensitivity in thick assemblies --- eddy currents, light alloys, aircraft construction materials
[REPT-48-912/F] 16 p2216 N88-23221

Utility NDE personnel qualification/certification: Enhanced personnel qualification requirements for ASME (American Society for Mechanical Engineers) Code Section 11 examinations
[DE88-006748] 16 p2216 N88-23222

Acousto-ultrasonic input-output characterization of unidirectional fiber composite plate by SV waves
[NASA-CR-4152] 16 p2217 N88-23224

Structural Ceramics
[NASA-CP-2427] 17 p2323 N88-23872

Nondestructive evaluation of structural ceramics
17 p2324 N88-23876

Nondestructive Evaluation (NDE) of structural ceramics by photoacoustic microscopy 17 p2325 N88-23884

Acoustic emission frequency discrimination
[NASA-CASE-MSC-20467-1] 17 p2342 N88-23966

Method of radiographic inspection of wooden members
[NASA-CASE-LAR-13724-1] 17 p2346 N88-23983

Input-output characterization of fiber composites by SH waves
[NASA-CR-4153] 17 p2347 N88-23986

Characterization of noncontact piezoelectric transducer with conically shaped piezoelement
[NASA-CR-4151] 17 p2347 N88-23987

Stress measurements in graphite fibers by laser raman spectroscopy
[AD-A191710] 18 p2491 N88-24779

Defect detection and classification in VLSI pattern inspection 18 p2507 N88-24871

Knowledge based systems in nondestructive evaluation
[DE88-006653] 18 p2525 N88-24981

Nondestructive testing using ultrahigh frequencies
[CERT-5/1333-MO] 18 p2526 N88-24984

Nondestructive evaluation methods for determination of thermal history and mechanical properties of aluminum-lithium alloys
[DE88-007352] 19 p2615 N88-25516

Model-based computed tomography for nondestructive evaluation: An overview and proposal
[DE88-010600] 19 p2679 N88-25926

Sensitivity to crack initiation in thick assemblies. Test report 48-444
[REPT-48-444] 20 p2758 N88-26365

Microfocus X-ray techniques for flaw location
[DE88-008636] 20 p2812 N88-26680

Development of an automated X-ray gauge for nondestructive quantitative analysis
[DE88-008633] 20 p2812 N88-26681

Methods and techniques of NDA (nondestructive assay)
[DE88-009145] 20 p2812 N88-26682

Principles of a nondestructive evaluation process for damage location, damage profile, and damage extension in welded joints by radiometric measurements
[MPA-86-02] 20 p2812 N88-26683

Stress analysis using infrared thermography
[ETN-88-92169] 20 p2816 N88-26705

Assembly Test Article (ATA)
[NASA-CR-179361] 21 p2903 N88-27226

Design and implementation of contact ultrasonic sensors to assess internal damage
[I-177/87] 21 p2906 N88-27247

Balance of X-ray radioscopy application to nondestructive tests of composite materials
[SNIAS-881-430-110] 21 p2907 N88-27250

NDE performance in predicting failure strength of spherical composite specimens with implanted flaws
[DE88-008223] 21 p2959 N88-27575

Interface control using low frequency (3 to 20 MHz) acoustic microscopy
[REPT-48-411/F] 21 p2959 N88-27577

Genetic effects of low level microwave radiation
[AD-A192687] 21 p2984 N88-27722

Use of penetrating radiations for the dynamic examination of aero gas turbines
[PNR90470] 22 p3045 N88-28073

Optimization of nondestructive control of ceramic pieces for aeronautical turbines
[ETN-88-92884] 22 p3059 N88-28149

Direct and inverse diffraction problems for QNDE (Quantitative Non-Destructive Evaluation) applications
[AD-A194721] 22 p3085 N88-28322

New acousto-ultrasonic techniques applied to aerospace materials
[NASA-TM-101299] 22 p3086 N88-28323

Comparison of 2-D Fourier and spatial techniques for removing noise in real-time X-ray radiography
[AD-A193700] 23 p3187 N88-28962

Nondestructive tests and high performance composite structures
[SNIAS-881-430-119] 23 p3188 N88-28969

Microwave frequency nondestructive control
[CERT-2/1355-MO] 23 p3189 N88-28976

Contribution to the study of materials behavior in space environment
[SNIAS-881-430-104] 23 p3169 N88-28977
Method and apparatus for non-destructive testing of temper embrittlement in steels
[NASA-CASE-LAR-13817-1] 23 p3195 N88-29012
Radioactivity as a means of nondestructive testing
[DE88-702778] 23 p3224 N88-29188
Nondestructive investigations for space use
[SNIAS-881-430-105] 23 p3224 N88-29189
A generic expert system for materials processing in space 23 p3255 N88-29376
Evaluation of bond testing equipment for inspection of Army advanced composite airframe structures
[AD-A195795] 24 p3341 N88-29885
In situ fault detection by the hybrid ray mode method
[AD-A195226] 24 p3381 N88-30137
Application of nondestructive testing techniques to materials testing
[AD-A195716] 24 p3381 N88-30138
Automated early fatigue damage sensing system
[AD-A195717] 24 p3382 N88-30143
Report on an overseas visit to USA relating to the thermoelastic measurement of stresses, 16-21 August 1987
[AD-A195313] 24 p3385 N88-30161

NONEQUILIBRIUM CONDITIONS
Requirements for a test stand for plastic rollers for the verification of nonequilibrium force laws
[ILR-MITT-176] 01 p0008 N88-10040
Development of the non-equilibrium reactive chemical transport code CHMTRNS
[DE88-000682] 04 p0481 N88-12964
Studies in finite time thermodynamics
[DE88-004531] 10 p1423 N88-18500
Nonequilibrium phonons and disorder in Al sub x Ga sub 1-x As 19 p2657 N88-25788
Femtosecond nonequilibrium electronic heat transport in thin gold films 19 p2659 N88-25807
Non-equilibrium phases and phase diagrams
[DE88-008896] 20 p2860 N88-27098

NONEQUILIBRIUM DRAG
U FRICTION DRAG

NONEQUILIBRIUM FLOW
Interface characteristics and the mechanical properties of metal matrix composites
[AD-A186441] 08 p0966 N88-15845
Nonequilibrium reacting flows
08 p0985 N88-15959
Experimental evidence of micro-nonequilibrium on the magnetopause and further predictions
08 p1098 N88-16606
A study of numerical methods for hyperbolic conservation laws with stiff source terms
[NASA-TM-100075] 10 p1399 N88-18343
Accelerating the computation of steady state solutions for non-equilibrium, chemically reacting flow fields
12 p1625 N88-19724
Low density real gas flows about hypersonic vehicles
[AD-A194251] 22 p3075 N88-28253
Development and analysis of turbulent non-equilibrium boundary layers 23 p3169 N88-28872
Nonequilibrium flow of a radiating gas in a vertical channel with axial temperature variation
[DE88-702535] 23 p3212 N88-29120
Beam combining by phase transition nonlinear media
[AD-A194116] 23 p3283 N88-29547
Nonequilibrium flow of a dissociating gas in a horizontal channel with axial temperature variation
[DE88-702536] 24 p3373 N88-30089
Nonequilibrium flow computations. 1: An analysis of numerical formulations of conservation laws
[NASA-CR-177489] 24 p3425 N88-30384

NONEQUILIBRIUM IONIZATION
Nonequilibrium ionization of pregalactic plasma and lessening of relic radiation anisotropy
08 p1002 N88-16071
Nonequilibrium superconductivity for particle detectors
[DE88-002676] 09 p1257 N88-17539

NONEQUILIBRIUM PLASMAS
Nonequilibrium ionization of pregalactic plasma and lessening of relic radiation anisotropy
08 p1002 N88-16071
Experimental evidence of micro-nonequilibrium on the magnetopause and further predictions
08 p1098 N88-16606
Ionization equilibrium and radiative energy losses in a stationary plasma
[DE88-700856] 14 p1984 N88-21832

NONEQUILIBRIUM RADIATION
Consistent spherical Nonlocal Thermal Equilibrium (NLTE) models for objects with B-star-like luminosities
[ETN-88-90601] 06 p0800 N88-14897

NONEQUILIBRIUM THERMODYNAMICS
Nonequilibrium characteristics of nitrogen plasmas appropriate to an AOTV flight 03 p0319 N88-12019

NONEUCLIDIAN GEOMETRY
U DIFFERENTIAL GEOMETRY

NONHOMOGENEITY
U INHOMOGENEITY

NONISOTHERMAL PROCESSES
Methods and first results of plasma non-isothermal parameters measurements in meteor trails
06 p0737 N88-14531
Bithermal fatigue: A simplified alternative to thermomechanical fatigue 15 p2084 N88-22424

NONISOTROPIC PLATES
U ANISOTROPIC PLATES

NONISOTROPY
U ANISOTROPY

NONLINEAR EQUATIONS
NT CUBIC EQUATIONS
NT NONLINEAR EVOLUTION EQUATIONS
NT QUADRATIC EQUATIONS
An asymptotic theory for a class of initial-boundary value problems for weakly nonlinear wave equations with an application to a model of the galloping oscillations of overhead transmission lines
[REPT-87-12] 01 p0086 N88-10556
Nonlinear fluid equations for a low collisionality toroidal plasma
[DE87-013006] 01 p0100 N88-10655
Extending Green's function formalism to general nonlinear equations
[DE87-013541] 02 p0224 N88-11411
Long wavelength vortices of low frequency interchange modes
[IPPJ-844] 02 p0241 N88-11525
New physical explanation of phase-conjugate waves produced in backward stimulated scattering
03 p0302 N88-11900
Blowup for a nonlinear evolution equation and self-reproducing strained shear layers
04 p0444 N88-12755
Solution of three-dimensional inverse problem of gravimetry in contact surfaces class by local corrections method 04 p0460 N88-12848
Steady waves in a nonlinear theory of viscoelasticity
[AD-A185548] 06 p0723 N88-14448
Development of symbolic computation methods for nonlinear dynamics
[AD-A185562] 06 p0758 N88-14653
Characteristic trajectories of generalized Lanchester equations
[AD-A185762] 06 p0766 N88-14705
Nonlinear reflection of sound wave in gas mixture
06 p0769 N88-14728
New methods for numerical solution of one class of strongly nonlinear partial differential equations with applications
[AD-A186166] 07 p0899 N88-15445
Nonlinear diffusion in the presence of a time-dependent external electric field
[INPE-4378-PRE/1198] 08 p1085 N88-16533
Techniques in linear and nonlinear partial differential equations
[AD-A187109] 09 p1227 N88-17347
Straightening and the Stanley decomposition for the (2;n)-nilpotent vectorfield
[PB88-126685] 10 p1398 N88-18336
Method of reduction of polynomially nonlinear equations to linear equations
[DE88-700922] 12 p1683 N88-20064
Nonlinear differential equations
[DE88-006047] 13 p1828 N88-20933
The biHamiltonian formulations of integrable evolution equations in multidimensions
[PREPRINT-568] 14 p1968 N88-21745
Memory efficient evaluations of nonlinear stochastic equations and C3 applications
[AD-A189872] 15 p2110 N88-22569
Almost-periodic solutions of nonlinear parabolic equations
[DE88-006423] 15 p2118 N88-22618
Numerical solution of nonlinear algebraic equations in stiff ODE solving
[DE88-006634] 15 p2118 N88-22622
New methods for numerical solution of one class of strongly nonlinear partial differential equations with applications
[AD-A189945] 15 p2119 N88-22630
Research in nonlinear partial differential equations and bifurcation theory
[AD-A190986] 16 p2260 N88-23514
On a generalization of renormalization group equations to quantum field theories of an arbitrary type
[DE88-701143] 16 p2263 N88-23531
Similarity solutions of nonlinear partial differential equations invariant to a family of affine groups
[DE88-003404] 18 p2567 N88-25245
Semi-discrete approximations to nonlinear systems of conservation laws; consistency and L(infinity)-stability imply convergence
[NASA-CR-181683] 19 p2721 N89-26157
Initial value problems for nonlinear heat equations
[DE88-702021] 19 p2737 N88-26251
Nonlinear equation of state effects and the momentum-dilution trade-off in a turbulent buoyant jet
[DE88-701839] 20 p2799 N88-26610
Numerical optimization
[AD-A193032] 21 p3005 N88-27827
Cauchy problem for the nonlinear Schroedinger equation
[DE88-702454] 21 p3011 N88-27867
Initial boundary value problems of nonlinear wave equations in an exterior domain
[DE88-701883] 21 p3026 N88-27962
The construction of implicit and explicit solitary wave solutions of nonlinear partial differential equations
[AD-A193475] 23 p3269 N88-29452
MACSYMA program for the painleve test of nonlinear ordinary and partial differential equations
[AD-A194293] 23 p3270 N88-29458
On nonlinear equations admitting soliton solutions with a deBroglie phase
[DE88-702694] 23 p3277 N88-29508
New methods for nonlinear optimization
[AD-A195982] 24 p3412 N88-30313
Convergence acceleration for vector sequences and applications to computational fluid dynamics
[NASA-TM-101327] 24 p3424 N88-30377
Convergence of Galerkin approximations for operator Riccati equations: A nonlinear evolution equation approach
[NASA-CR-181706] 24 p3425 N88 30386

NONLINEAR EVOLUTION EQUATIONS
The Eckhaus Partial Differential Equation (PDE) I psi t + psi xx + 2(psi/sq)x psi + 2(/psi/) to the 4th power psi = 0
[PREPRINT-546] 06 p0763 N88-14686
Equations of nonlinear Schroedinger type in 1 + 1 and 2 + 1 dimensions, obtained from integrable Partial Differential Equations (PDEs)
[PREPRINT-548] 06 p0764 N88-14687
Recursion operator and bihamiltonian structure for integrable multi-dimensional lattices
[PREPRINT-552] 06 p0764 N88-14688
Nonlinear evolution equatons, rescalings, model partial differential equations (PDES) and their integrability, 2
[PREPRINT-560] 06 p0764 N88-14691
Algebraic structure of linear and nonlinear models of open quantum systems
[PREPRINT-573] 14 p1968 N88-21747
Perturbation theory for dual semigroups. Part 3: Nonlinear Lipschitz continuous perturbations in the Sun-reflexive case
[CWI-AM-R8706-PT-3] 16 p2263 N88-23535
Nonlinear wave propagaton
[AD-A192104] 18 p2501 N88-24835
Nonlinear waves
[AD-A192148] 18 p2510 N88-24889
Why are certain nonlinear Partial Differential Equations (PDE) both widely applicabe and integrable
[PREPRINT-582] 22 p3144 N88-28698

NONLINEAR FEEDBACK
Approximation methods for the identification and control of distributed parameter systems
[AD-A190201] 15 p2124 N88-22662
Problems in nonlinear continuum dynamics
[AD-A190538] 15 p2128 N88-22691
A feedback linearization approach to spacecraft control using momentum exchange devices
[NASA-CR-172057] 18 p2472 N88-24666
Robust control of multivariable and large scale systems
[AD-A194250] 23 p3266 N88-29441
Feedback stabilization of du/dt = Au + bf in Hilbert space when the normalizaton function is less than or equal to r
[AD-A193510] 23 p3277 N88-29506

NONLINEAR FILTERS
White noise calculus for two-parameter filtering
[ENST-87C003] 01 p0088 N88-10578
Nonlinear techniques for detection and filtering of discrete-time signals 02 p0160 N88-11004
Statistical techniques for signal processing
[AD-A185774] 06 p0694 N88-14259
The filtering problem for infinite dimensional stochastic processes
[AD-A186431] 07 p0916 N88-15562
Lie algebraic method in filtering and identification
[CWI-PM-R8606] 08 p1072 N88-16467
Nonlinear filtering and large deviations: A PDE-Control theoretic approach
[AD-A187436] 10 p1396 N88-18321

Dynamic observers as asymptotic limits of recursive filters: Special cases
[AD-A187578] 10 p1397 N88-18324

Advanced guidance algorithms for homing missiles with bearings-only measurements
[AD-A190435] 15 p2017 N88-22026

Introduction to nilpotent approximation filtering
[CWI-PM-R8709] 16 p2262 N88-23524

Investigation of non-linear optical behavior of semiconductors for optical switching, volume 1
[AD-A191297] 16 p2274 N88-23611

A nonlinear filtering process diagnostic system for the Space Station 23 p3262 N88-29417

Approximations and implementations of nonlinear filtering schemes
[AD-A194685] 23 p3271 N88-29462

Analytical methods in stochastic control and nonlinear filtering
[AD-A194272] 24 p3426 N88-30388

NONLINEAR OPTICS

Phase equilibrium and crystal growth studies on AgGaSe2 and related nonlinear optical materials
[AD-A184768] 03 p0382 N88-12400

Anti-Stokes generation of 226 nm light
[DE88-001612] 05 p0589 N88-13590

Parametric and resonance interaction of ultrashort light pulses in nonlinear multilevel medium
06 p0773 N88-14746

Nonlinear optics with broad-band lasers
[DE88-005026] 10 p1337 N88-17992

Subpicosecond optical digital computation using phase conjugate parametric generators
[AD-A188279] 10 p1410 N88-18411

Optical signal processing using nonlinear optics
[AD-A188461] 12 p1691 N88-20117

Solid state research
[AD-A188388] 12 p1699 N88-20166

Influence of nonlinear spectroscopic effects on atmospheric propagation of intense laser radiation at 10.6 microns wavelength 13 p1789 N88-20705

United States - Japan Seminar on Quantum Mechanical Aspects of Quantum Electronics
[AD-A186938] 14 p1974 N88-21781

Gigantic optical nonlinearity in low dimensional systems 14 p1975 N88-21786

Quantum nondemolition detection and squeezing in optical fibers 14 p1976 N88-21793

Optical properties of quantum well structures with electric field. Life time free switching of luminescence intensity and virtual charge-induced ultrafast optical nonlinearity 14 p1976 N88-21794

Enhanced excitonic optical nonlinearity and exciton dynamics in semiconductor microstructures
14 p1977 N88-21795

Free carrier nonlinear optics 14 p1977 N88-21796

Collective rotation of molecules driven by the angular momentum of light in a nematic film
[FUB-6-1986] 15 p2131 N88-22714

Studies of surfaces using optical sum-frequency generation
[DE88-006334] 15 p2131 N88-22715

Theory of interactions of intense light with nonlinear, inhomogeneous and periodic structures and its applications to optical bistability, optic gyroscopes, nonlinear spectroscopy, radiation protection, X-ray emission and related fields
[AD-A190040] 15 p2133 N88-22725

Optical switching and control techniques using nonlinear optical wave mixing
[AD-A190467] 15 p2134 N88-22730

Unstable behavior of lasers and other optical systems
[AD-A190875] 16 p2213 N88-23204

Enhancement of second harmonic generation on silver gratings by resonant excitation of surface plasmon
[ETN-88-92304] 17 p2439 N88-24509

Nonlinear surface polaritons
[AD-A191046] 18 p2499 N88-24822

Nonlinear waves
[AD-A192148] 18 p2510 N88-24889

Research in the optical sciences
[AD-A192175] 18 p2575 N88-25297

Liquid crystal optics for laser systems
[DE88-008475] 20 p2854 N88-26948

Solid state research
[AD-A192837] 21 p3020 N88-27929

High energy and high intensity laser effects on aerosols: Changes in droplet morphology, surrounding temperature and vapor concentration
[AD-A193825] 23 p3220 N88-29164

Nonlinear optical processes in molecular systems
[AD-A193871] 23 p3282 N88-29546

Nonlinear optical phase conjugation techniques to reduce the physical size of lasers
[AD-A196170] 24 p3379 N88-30122

A review of melt and vapor growth techniques for polydiacetylene thin films for nonlinear optical applications
[NASA-TM-100340] 24 p3430 N88-30412

NONLINEAR PROGRAMMING

Using MINOS (Modular In-core Nonlinear Optimization System) as a subroutine for decomposition
[DE87-013086] 02 p0221 N88-11390

Performance analysis of coded frequency-hopped spread-spectrum systems with unknown interference
[AD-A186069] 07 p0841 N88-15103

A Schur-complement method for sparse quadratic programming
[DE88-002520] 07 p0904 N88-15479

Search rearrangement backtracking often requires exponential time to verify unsatisfiability
[AD-A186121] 07 p0909 N88-15511

Research on algorithms for nonlinear programming
[AD-A188326] 12 p1677 N88-20024

Constrained nonlinear programming
[DE88-005695] 13 p1817 N88-20860

Applicability of nonlinear programming in decision support systems: Realization of user-friendly software
[REPT-87-42] 14 p1957 N88-21663

Efficient method for structural optimization
15 p2054 N88-22240

On the capacity of channels with unknown interference
[AD-A191160] 16 p2191 N88-23067

Nonlinear programming extensions to rational function approximation methods for unsteady aerodynamic forces
[NASA-TP-2776] 18 p2463 N88-24623

The Sizing and Optimization Language, (SOL): Computer language for design problems
[NASA-TM-100565] 18 p2559 N88-25190

Conditions for finite convergence of algorithms for nonlinear programs and variational inequalities
[AD-A192355] 20 p2838 N88-26834

NONLINEAR SYSTEMS

Geometrically nonlinear rod mechanism analogy of axisymmetrically loaded spherical shells based on a comprehensive approach to the stability of circular arches
[ETN-87-90419] 01 p0062 N88-10398

Dimension densities for turbulent systems with spatially decaying correlation functions
[DE87-010119] 02 p0169 N88-11066

Iterative solution of a nonlinear system arising in phase change problems
[DE87-014672] 02 p0226 N88-11426

Solution of nonlinear least-squares problems
[AD-A184010] 03 p0371 N88-12335

A refined nonlinear analysis of laminated composite plates and shells
[AD-A184436] 04 p0454 N88-12811

Nonlinear acoustics
[AD-A184271] 04 p0488 N88-13004

Supertracks: The building blocks of chaos
[DE88-001513] 04 p0522 N88-13207

On the correlation free forms for nonlinear stochastic systems
[DE87-011169] 05 p0645 N88-13947

Nonlinear aerodynamic wing design
[NASA-CR-3950] 06 p0665 N88-14079

Steady waves in a nonlinear theory of viscoelasticity
[AD-A185548] 06 p0723 N88-14448

Nature and the nonlinear evolution of electrostatic waves associated with the AMPTE (Active Magnetosphere Particle Tracer Explorers) solar wind releases
[AD-A185471] 06 p0806 N88-14920

Numerical solution of turbulent flow past a backward facing step using a nonlinear K-epsilon model
[NASA-CR-178421] 07 p0854 N88-15189

Theoretical investigations of chaotic dynamics
[AD-A186404] 07 p0867 N88-15261

The design and implementation of surface acoustic wave devices for linear FM and a new non-linear FM pulse compression technique for radar applications
[AD-A186741] 08 p0980 N88-15922

Some aspects of control for semilinear distributed parameter systems
[INPE-4147-PRE/1054] 08 p1075 N88-16484

Studies on nonlinear mechanisms of excimer laser propagation in fused silica fibers
[AD-A186822] 09 p1156 N88-16929

Reliability of structures with stiffness and strength degradation 09 p1180 N88-17068

Frequency response functions of a nonlinear system
09 p1180 N88-17070

Regulation of nonlinear and generalized linear systems
[AD-A186706] 09 p1224 N88-17338

Applications of nonlinear systems theory to control design
[NASA-CR-182485] 09 p1231 N88-17377

Numerical fluid mechanics 09 p1240 N88-17434

The role of photodetectors in optical signal processing
[AD-A186804] 09 p1247 N88-17476

A finite element analysis of adhesively bonded composite joints including geometric nonlinearity, nonlinear viscoelasticity moisture diffusion and delayed failure
[AD-A187455] 10 p1296 N88-17747

Design sensitivity analysis of nonlinear structural systems and numerical implementation with established finite element codes 10 p1344 N88-18032

Nonlinear dynamic maximum power theorem
[AD-A187491] 11 p1477 N88-18810

Symmetries in nonlinear control systems and their applications 11 p1496 N88-18929

Prediction of the response and optimal control of stochastic parametrically and externally excited nonlinear systems 11 p1496 N88-18930

Optimal control theory of load-following and parameter-tracking of nonlinear systems: An application of Pontryagin Maximum Principle to reactor dynamics
[DE88-004770] 11 p1532 N88-19152

A maximum likelihood parameter estimation program for general non-linear systems
[ARL-AERO-TM-392] 11 p1532 N88-19154

Nonlinear input-output systems
[NASA-CR-182484] 11 p1535 N88-19171

Optimal recursive maximum likelihood estimation
[AD-A187980] 11 p1536 N88-19176

Advanced nonlinear theory: Long-term stability at the SSC
[CEBAF-PR-87-027] 11 p1546 N88-19246

Non-linear materials (TAS)
[AD-A189197] 12 p1633 N88-19775

A numerical study of automated dynamic relaxation for nonlinear static tensioned structures
[AD-A188372] 12 p1635 N88-19790

On analysis of viscoelastic structures
[AD-A188445] 12 p1636 N88-19793

NFEARS (Nonlinear Finite Element Adaptive Research Solver): A nonlinear adaptive finite element solver. Part 2: User's manual
[AD-A189009] 12 p1684 N88-20070

Nonlinear optical principles and the photorefractive effect applied to optical phase conjugation
[AD-A188856] 12 p1691 N88-20119

Nonlinear resonance of two-dimensional ion layers
[AD-A188890] 12 p1695 N88-20145

Stability and uniqueness in nonlinear continuum mechanics
[AD-A189616] 12 p1699 N88-20172

Robustifying the Kalman filter
[AD-A189240] 13 p1825 N88-20907

Stochasticity in nonlinear Hamiltonian systems
[DE88-005499] 13 p1826 N88-20915

Period-doubling universality in multidimensional dissipative and conservative systems
[PB88-148812] 13 p1832 N88-20961

Method for finding principal modes of nonlinear vibration systems and their stabilities 14 p1899 N88-21340

Identification of nonlinear output-affine systems using an orthogonal least squares algorithm
[RR-313] 14 p1958 N88-21678

A prediction-error estimation algorithm for nonlinear output-affine systems
[RR-314] 14 p1959 N88-21679

Identification of nonlinear rational systems using a prediction-error estimation algorithm
[RR-317] 14 p1959 N88-21680

A new approach to almost decoupling problems for linear and nonlinear systems
[MEMO-660] 14 p1962 N88-21700

Some maximum norm estimates for the finite element method applied to nonlinear two dimensional boundary value problems
[ETN-88-91505] 14 p1964 N88-21715

An orthogonal parameter estimation algorithm for nonlinear stochastic systems
[RR-307] 14 p1966 N88-21736

Parametric methods of analysing linear and nonlinear systems
[RR-318] 14 p1967 N88-21741

Three-wave parametric resonance in plasma of relativistic electron flux 14 p1972 N88-21772

Nonlinear analysis and optimal design of dynamic mechanical systems for spacecraft application
[AD-A190644] 15 p2026 N88-22070

Random processes, turbulence and disordering fields
[AD-A190123] 15 p2063 N88-22303

Buckling of blast loaded cylinder
[AD-A190124] 15 p2076 N88-22376

The analysis of non-linear dynamic behavior (including snap-through) of postbuckled plates by simple analytical solution
[NASA-TM-89165] 15 p2087 N88-22439

Memory efficient evaluations of nonlinear stochastic equations and C3 applications
[AD-A189872] 15 p2110 N88-22569

Nonlinear signal processing using neural networks: Prediction and system modelling
[DE88-006479] 15 p2118 N88-22621

Numerical methods for linear and nonlinear optimization
[AD-A190029] 15 p2120 N88-22631

Symmetry and global bifurcation in nonlinear solid mechanics
[AD-A190521] 15 p2121 N88-22642

Applications research studies of microtubules
[AD-A190855] 16 p2182 N88-23005

On the computation of stationary deterministic behavior of nonlinear dynamic systems with applications to rotor-bearing structures
[ETN-88-92241] 16 p2214 N88-23213

Periodic response of nonlinear systems
16 p2217 N88-23228

A multigrid approach for the solution of a nonlinear diffusion equation in a time-dependent area using Cartesian coordinates
[GMD-STUDIEN-122] 16 p2257 N88-23491

An approximation theory for the identification of nonlinear distributed parameter systems
[NASA-CR-181658] 16 p2260 N88-23510

Inference for a nonlinear semimartingale regression model
[AD-A190857] 16 p2262 N88-23527

Nonlinear wave and diffusion equations
[AD-A191421] 16 p2265 N88-23544

Time-domain frequency-selective optical memories: A study of the basic mechanisms and potential systems
[AD-A190854] 16 p2274 N88-23607

Observation of nonlinear wave decay processes in the solar wind by the AMPTE IRM plasma wave experiment
[AD-A191409] 16 p2290 N88-23713

Parallel processors and nonlinear structural dynamics algorithms and software
[NASA-CR-182925] 17 p2387 N88-24187

A recursive prediction error parameter estimator for nonlinear models
[RR-326] 17 p2392 N88-24222

User's guide to the Fault Inferring Nonlinear Detection System (FINDS) computer program
[NASA-CR-178410] 18 p2462 N88-24619

Signal processing with degenerate four-wave mixing
[AD-A191496] 18 p2499 N88-24825

Research in nonlinear wave motion
[AD-A191686] 18 p2509 N88-24884

Calculation of root-mean-square loads
[BLL-M-37776-(5828.4)] 18 p2531 N88-25015

On frequency response for nonlinear systems
[RR-323] 18 p2563 N88-25221

Galerkin approximation for inverse problems for nonautonomous nonlinear distributed systems
[NASA-CR-181676] 18 p2567 N88-25246

Linear and nonlinear acoustic wave propagation in the atmosphere
[NASA-CR-4157] 18 p2571 N88-25268

Parametric estimation of aerodynamic nonlinearities in rolling moment due to sideslip using maximum likelihood method 20 p2786 N88-26528

Identification of lateral operation dynamics of rail vehicles using roll test stand tests
20 p2787 N88-26534

Nonlinear identification of an aircraft for the direct calculation of an anticipatory control
20 p2787 N88-26535

Studying materials using acoustic waves
[AD-A192234] 20 p2850 N88-26915

Determination of Tafel constants in nonlinear polarization curves
[AD-A192335] 21 p2912 N88-27282

Nonlinear vibrations of periodically stiffened plates
21 p2963 N88-27598

Periodic oscillations in nonlinear mechanical systems
21 p2963 N88-27599

The robust tracking control of nonlinear systems with uncertain dynamics 21 p2999 N88-27788

Effects of applied stress and temperature on the nonlinear elastic properties of graphite fibers
[AD-A194469] 22 p3050 N88-28093

Studies of coherent beam processing concepts, phase 1
[AD-A194749] 22 p3083 N88-28306

A computer-aided approach to nonlinear control systhesis
[NASA-CR-179391] 22 p3140 N88-28673

Nonlinear dynamic analysis and optimal control of shallow shells 23 p3224 N88-29191

Linearized model matching for single-imput nonlinear systems
[AD-A193642] 23 p3266 N88-29445

Approximations and implementations of nonlinear filtering schemes
[AD-A194685] 23 p3271 N88-29462

Finite element analysis of steady and transiently moving/rolling nonlinear viscoelastic structure. Part 1: Theory
[NASA-CR-179886] 23 p3273 N88-29480

Limiting distributions of non-linear vector functions of stationary Gaussian processes
[AD-A194569] 23 p3274 N88-29488

Beam combining by phase transition nonlinear media
[AD-A194116] 23 p3283 N88-29547

Nonlinear analysis of non-neutral plasmas
[AD-A192506] 23 p3284 N88-29556

The construction of the thermoelasticity equations on the basis of contemporary notions of nonlinear continua mechanics
[NASA-TT-20307] 23 p3296 N88-29631

Resonance excitation of linear and non-linear spiral density waves in a gaseous disk
23 p3299 N88-29643

Nonlinear Tollmien-Schlichting/vortex interaction in boundary layers
[NASA-CR-181698] 24 p3311 N88-29715

The strong nonlinear interaction of Tollmien-Schlichting waves and Taylor-Goertler vortices in curved channel flow
[NASA-CR-181697] 24 p3311 N88-29716

Nonlinear dynamics of coupled oscillator arrays
[AD-A194888] 24 p3367 N88-30053

Mathematical problems of nonlinear wave propagation and of waves in heterogeneous media
[AD-A195970] 24 p3368 N88-30057

Initial value problems in viscoelasticity
[AD-A196052] 24 p3382 N88-30145

Algorithms for nonlinear least-squares problems
[AD-A196071] 24 p3411 N88-30305

K(sup th)-order extended linearization
[AD-A194786] 24 p3421 N88-30363

Automatic qualitative analysis of ordinary differential equations using piecewise linear approximations
[AD-A196310] 24 p3424 N88-30379

Multiple solutions and bifurcation for a class of nonlinear Sturm-Liouville eigenvalue problems on an unbounded domain
[AD-A195954] 24 p3426 N88-30389

NONLINEARITY

Concurrent algorithms for transient nonlinear FE analysis
[NASA-CR-181455] 02 p0221 N88-11389

Using MINOS (Modular In-core Nonlinear Optimization System) as a subroutine for decomposition
[DE87-013086] 02 p0221 N88-11390

Ultrasonic characterization of the nonlinear elastic properties of unidirectional graphite/epoxy composites
[NASA-CR-4100] 03 p0281 N88-11767

Highly Non-Linear Optical (NLO) organic crystals
03 p0297 N88-11865

Highlv Non-Linear Optical (NLO) organic crystals and films. Electrooptical organic materials
03 p0297 N88-11866

Perturbation and characterization of nonlinear processes
[DE87-014580] 03 p0369 N88-12322

Nonlinear parametric least-squares adjustment
[AD-A184039] 03 p0371 N88-12336

Non-linearity in measurement systems: Evaluation method and application to microwave radiometers
04 p0433 N88-12684

Implementation of a 3-D nonlinear MHD calculation on the Intel hypercube
[DE87-014637] 04 p0479 N88-12949

Non-linear maximum likelihood estimation of stability derivatives from range data
[NAL-TM-SE-8608] 05 p0552 N88-13365

HF sidebands in the ionosphere
05 p0574 N88-13497

Nonlinear hyperbolic conservation laws
[AD-A184963] 05 p0580 N88-13538

Applications of nonlinear hole burning spectroscopy
[AD-A184943] 05 p0587 N88-13580

Dynamics of cables and chains
05 p0610 N88-13747

Geometrically nonlinear analysis of stiffened panels
06 p0722 N88-14440

Development of symbolic computation methods for nonlinear dynamics
[AD-A185562] 06 p0758 N88-14653

The history and development of nonlinear stellar pulsation codes
[DE88-001828] 06 p0801 N88-14899

Nonsymmetric metrics in nonlinear field theory
[DE88-700509] 07 p0913 N88-15537

The design and implementation of surface acoustic wave devices for linear FM and a new non-linear FM pulse compression technique for radar applications
[AD-A186741] 08 p0980 N88-15922

Nonlinear line-spring model for surface crack analysis with particular reference to work hardening materials
[PB87-144838] 08 p0994 N88-16016

Steady ship waves at low Froude numbers, part 2
[AD-A176805] 09 p1160 N88-16953

A substructure method for dynamic simulation of flexible mechanical systems with geometric nonlinearities
09 p1176 N88-17044

Experimental identification of nonlinear structural models
[DE88-001795] 09 p1184 N88-17094

Nonlinear and diffraction effects in sound beams with random transverse structure 09 p1235 N88-17402

Explicit approximations for strictly nonlinear oscillators with slowly varying parameters with applications to free electron lasers
[DE88-004116] 10 p1336 N88-17984

Nonlinear dynamic maximum power theorem
[AD-A187491] 11 p1477 N88-18810

Nonlinear absorption of CO2 laser radiation in p-type InSb
[DE88-004055] 11 p1492 N88-18906

Numerical-experimental investigation of singularity at a crack in nonlinear rubber elasticity
11 p1500 N88-18961

Contour-to-grid interpolation with nonlinear finite elements: A feasibility study
[AD-A188108] 11 p1503 N88-18980

Postprocessing techniques for 3D non-linear structures 11 p1528 N88-19124

Design for performance enhancement in feedback control systems with multiple saturating nonlinearities
[NASA-CR-182614] 11 p1535 N88-19168

An improved data reduction procedure for accelerometer centrifuge data 12 p1577 N88-19436

The lattice nonlinearities and the long term stability of the SSC
[CEBAF-PR-87-009] 12 p1690 N88-20108

Finite element methodology for nonlinear free and harmonic forced vibrations of beam and plate structures
13 p1782 N88-20663

Algorithms with conic termination for nonlinear optimization
[DE88-005893] 13 p1816 N88-20851

Nonlinear refractive index measurements of glasses and crystals
[DE88-005673] 13 p1840 N88-21009

Energy transfer and non-linear optical properties at near ultraviolet wavelengths: Rare earth 4f yields 5d transitions in crystals and glasses
[DE88-005403] 13 p1840 N88-21012

Two studies of nonlinear processes in irreversible thermodynamics
[DE88-005794] 13 p1849 N88-21067

Nonlinear acoustic parameter and its application in ultrasonic imaging 14 p1902 N88-21364

Nonlinear stage of ultrashort-pulse formation in solid-state laser 14 p1971 N88-21765

Numerical methods for linear and nonlinear optimization
[AD-A190029] 15 p2120 N88-22631

Symmetry and global bifurcation in nonlinear solid mechanics
[AD-A190521] 15 p2121 N88-22642

Nonlinear effects in plasma wake field acceleration
[DE88-700972] 15 p2134 N88-22734

Nonlinear wave interactions in swept wing flows
[NASA-CR-4142] 16 p2206 N88-23160

Multigrid for structures analysis
16 p2218 N88-23232

Reduced order models for nonlinear aerodynamics
16 p2220 N88-23248

The 1 and 2D symmetric Helmert transformation: An exact nonlinear least squares solution
[REPT-87-1] 16 p2259 N88-23503

Investigation of non-linear optical behavior of semiconductors for optical switching, volume 1
[AD-A191297] 16 p2274 N88-23611

Nonlinear dynamics of interaction between charged particles modulated beam and bounded plasma regular oscillations
[DE88-701681] 16 p2280 N88-23648

Electromagnetic scattering from nonlinear anisotropic cylinders 17 p2333 N88-23930

On Hotelling's approach to testing for a nonlinear parameter in regression
[AD-A191189] 17 p2393 N88-24229

Electronic structure of Zintl phase compounds by nonlinear optimization
[DE88-009998] 19 p2613 N88-25508

Nonlinear mechanisms of solid propellant combustion instability 19 p2628 N88-25588

Electron tunneling in junctions doped with semiconductors and metals 19 p2734 N88-26236

Finite element welding computations using general purpose nonlinear analysis codes [DE88-005398] 20 p2808 N88-26659

Comparison theorems and their use in the analysis of some nonlinear diffusion problems [DE88-010032] 20 p2845 N88-26884

Ultrafast optical nonlinearity in quantum well structures with electric field 20 p2863 N88-27003

Nonlinear materials for frequency conversion [DE88-008343] 20 p2875 N88-27067

Effects of static equilibrium and higher-order nonlinearities on rotor blade stability in hover 21 p2890 N88-27157

Nonlinear dynamics of the electron self-field interaction [DE88-010597] 21 p2934 N88-27420

Nonlinear interaction between overall and local buckling of stiffened panels with symmetric cross-sections [PB88-104054] 21 p2960 N88-27580

Nonlinear liquid motion in conical containers [LRT-WE-9-FB-10(1987)] 22 p3077 N88-28270

Regularity of solutions for nonlinear degenerate elliptic boundary value problems [DE88-702646] 22 p3146 N88-28710

A singular perturbation analysis of the weakly nonlinear evolution of long and short water waves and waves in boundary layers 23 p3209 N88-29102

Nonlinear vibrations of imperfect thin walled cylindrical shells [ETN-88-92904] 23 p3227 N88-29205

On the periodic nonlinearity and the multiplicity of solutions [AD-A194295] 23 p3270 N88-29459

Investigation of non-classical effects in two-photon interference processes 23 p3282 N88-29541

Non-linear scale invariance in a cold-dark-matter universe [DE88-011725] 23 p3299 N88-29644

Survey on nonlinear effects 24 p3317 N88-29757

Nonlinear optical phase conjugation techniques to reduce the physical size of lasers [AD-A196170] 24 p3379 N88-30122

Geometric and material nonlinear analysis of structures comprising rectangular hollow sections [CE-79] 24 p3382 N88-30141

NONNEWTONIAN FLOW

Theoretical and experimental analysis of pressure pulse transmission in non-Newtonian pipe flow 11 p1485 N88-18863

NONNEWTONIAN FLUIDS

Two-phase non-Newtonian hydrodynamic modeling of slurries [DE87-011519] 01 p0047 N88-10298

A review of approaches to the study of turbulence modification by means of non-Newtonian additives [AD-A188799] 12 p1627 N88-19734

Approximation of viscoelastic stresses from Newtonian turbulent kinematics [AD-A194317] 24 p3371 N88-30077

NONOSCILLATORY ACTION

Non-oscillatory spectral Fourier methods for shock wave calculations [NASA-CR-181675] 19 p2720 N88-26148

NONPARAMETRIC STATISTICS

Feature selection applied to radar target identification [AD-A183880] 01 p0034 N88-10215

An APL workspace for conducting nonparametric statistical inference [AD-A184971] 05 p0634 N88-13877

Further studies in estimation of life distribution characteristics from censored data [AD-A184862] 05 p0643 N88-13937

Sample reuse in statistical remodeling [AD-A184916] 05 p0643 N88-13938

Quantile statistical data analysis [AD-A185181] 05 p0644 N88-13943

A unified mathematical approach to image analysis [AD-A185719] 06 p0765 N88-14703

Robust prediction and interpolation for vector stationary processes, 2d enriched version [AD-A185875] 07 p0865 N88-15247

Nonparametric estimation of the generalized variance [AD-A186029] 07 p0914 N88-15545

A smooth nonparametric quantile estimator from right-censored data [AD-A186180] 07 p0915 N88-15552

On determining the weight for obtaining a large number of items [AD-A186181] 07 p0915 N88-15553

Practical applicability of exact and approximate forms of the randomization test for two independent samples [AD-A186815] 09 p1231 N88-17381

A generalized quantile estimator under censoring [AD-A188280] 10 p1402 N88-18364

Analysis of learning curve fitting techniques [AD-A187680] 11 p1535 N88-19173

Nonparametric discriminant analysis applied to the extraction and selection of radar target signature features [AD-A191849] 18 p2501 N88-24833

Symmetrized nearest neighbor regression estimates [AD-A191998] 18 p2568 N88-25254

Joint asymptotic distribution of marginal quantiles and quantile functions in samples from a multivariate population [AD-A193385] 21 p3010 N88-27856

A nonparametric multidimensional IRT approach with applications to ability estimation and test bias [AD-A194212] 23 p3273 N88-29483

NONREFLECTION
U ENERGY ABSORPTION

NONRELATIVISTIC ELECTRONS
U ELECTRONS

NONRIGIDITY
U FLEXIBILITY

NONTHERMAL EMISSION
U NONTHERMAL RADIATION

NONTHERMAL RADIATION
NT CYCLOTRON RADIATION
NT ION CYCLOTRON RADIATION
NT SYNCHROTRON RADIATION

Microwave observations of nonthermal phenomena in pre-main sequence stars 04 p0505 N88-13107

Spherical models of QSO/AGN emission line clouds 06 p0806 N88-14921

High density femtosecond excitation of nonthermal carrier distributions in intrinsic and modulation doped GaAs quantum wells 14 p1977 N88-21798

Experimental and theoretical studies of coherent and nonthermal processes in semiconductors probed by femtosecond laser techniques 14 p1977 N88-21800

NONUNIFORM FLOW

The spatially nonuniform convergence of the numerical solution of flows [NASA-TM-100037] 02 p0226 N88-11429

Turbulence modelling of flows with non-uniform density 22 p3075 N88-28256

Gaseous premixed flames in non-uniform flows 24 p3351 N88-29945

NONUNIFORM PLASMAS

Self-consistent modification of a fast tail distribution by resonant fields in nonuniform plasmas [AD-A183790] 01 p0099 N88-10650

Electron acceleration by wave processes in the earth's ionosphere [AD-A186110] 07 p0877 N88-15320

NONUNIFORMITY

Interaction of interplanetary shocks with nonuniform ambient solar wind 01 p0116 N88-10740

Programs for calculating transient Darcian flow through non-uniform materials [DE88-001924] 07 p0852 N88-15177

NONVISCOUS FLOW
U INVISCID FLOW

NOREPINEPHRINE

Distinctions and mechanisms of effects of epinephrine and norepinephrine on cardiac pumping function under hypokinetic conditions 07 p0891 N88-15399

Individual functional typology of sympathoadrenal system as indicator of physiological status in adverse environments 12 p1665 N88-19979

Direct interaction between autonomic nerves and the immune system [AD-A188576] 12 p1667 N88-19991

NORMAL DENSITY FUNCTIONS

Statistics of the geomagnetic secular variation for the past 5Ma [NASA-CR-181558] 04 p0467 N88-12890

Local likelihood method in the problems related to change points [AD-A185604] 06 p0768 N88-14718

Asymptotic normality of poly-t densities with Bayesian applications [AD-A185718] 06 p0768 N88-14719

The information metric for univariate linear elliptic models [AD-A186385] 07 p0911 N88-15527

On selecting the best of k lognormal distributions [AD-A185628] 07 p0916 N88-15567

An APL function for bivariate normal probabilities [AD-A186535] 09 p1232 N88-17382

On two-stage allocation procedures for selection problems [AD-A190766] 15 p2126 N88-22675

Analysis of means in some nonstandard situations [ETN-88-92247] 16 p2262 N88-23522

Weak solution of the Langevin equation on a generalized functional space [AD-A194290] 23 p3270 N88-29456

NORMAL DISTRIBUTIONS
U NORMAL DENSITY FUNCTIONS

NORMAL FORCE DISTRIBUTION
U FORCE DISTRIBUTION

NORMALITY

Asymptotic normality of minimum L1-norm estimates in linear models [AD-A193399] 21 p3006 N88-27835

NORMALIZING (STATISTICS)

Detector normalization --- SPOT remote sensors 03 p0341 N88-12151

Consistency question in the renormalization group analysis of deep inelastic scattering [DE87-703372] 04 p0487 N88-12999

On the extreme order statistics for a stationary sequence [AD-A186426] 07 p0916 N88-15561

A small concentration expansion for the effective heat conductivity of a random disperse two-component material, an assessment of Batchelor's renormalization method [REPT-87-71] 16 p2207 N88-23168

Feedback stabilization of $du/dt = Au + bf$ in Hilbert space when the normalization function is less than or equal to r [AD-A193510] 23 p3277 N88-29506

NORMS

Norm inequalities for derivatives and differences [DE88-002920] 09 p1230 N88-17371

On the norm equivalence of singularly perturbed elliptic difference operators [DE88-006353] 13 p1826 N88-20913

Contribution to the study of modern materials for cutting tools [ISAL-IDI1-87-17] 16 p2185 N88-23029

Asymptotic of Peanokerns of finite fixed order [ETN-88-92381] 21 p3008 N88-27843

NORTH AMERICA

Theory and methods for design of pulse shapes for broadcast teletext [CRC-1405] 02 p0162 N88-11013

A survey of existing hypersonic ground test facilities: North America 05 p0529 N88-13220

Mid-tertiary volcano-tectonic development of the Southwestern Cordillera of North America 06 p0797 N88-14879

Biogeochemical cycling in the ocean. Part 1: Introduction to the effects of upwelling along the west coast of North America [NASA-TM-88230] 07 p0882 N88-15349

Meteorological and aerosol measurements from the NOAA WP-3D aircraft during WATOX-86, January 4-9, 1986 [PB88-120860] 10 p1352 N88-18079

Synthesis of finite displacements and displacements in continental margins [NASA-CR-182616] 12 p1642 N88-19832

Northern Hemisphere circulation and the principal components of subsequent summer patterns in North America and West Africa 13 p1801 N88-20765

The collection of statistics on the frequency of cloud cover over North America [AD-A190456] 15 p2097 N88-22495

DATATRAN: Datum transformation software [AD-A195723] 24 p3387 N88-30175

Gravity anomalies, plate tectonics and the lateral growth of Precambrian North America 24 p3400 N88-30248

NORTH AMERICAN AIRCRAFT
NT B-1 AIRCRAFT
NT B-70 AIRCRAFT

NORTH ATLANTIC TREATY ORGANIZATION (NATO)

Special Course on Fundamentals of Fighter Aircraft Design [AGARD-R-740] 05 p0544 N88-13315

Calendar of selected aeronautical and space meetings [AGARD-CAL-88/1] 05 p0658 N88-14037

AGARD reports: A quarterly listing, 1 July through September 30, 1987 [AD-A186572] 08 p1093 N88-16579

Anthropomorphic phantom radiation dosimetry at the NATO standard reference point at Aberdeen Proving Ground [AD-A190508] 15 p2103 N88-22528

A review of the NATO special group of experts on Naval hydromechanics and related problems 16 p2205 N88-23157

NORTH CAROLINA

Annual data summary and climatological evaluation CERC (Coastal Engineering Research Center) field research facility, 1985. Volume 1. Main text and appendixes A and B [AD-A186442] 08 p1039 N88-16289

NORTH DAKOTA

Feasibility of producing jet fuel from GPGP (Great Plains Gasification Plant) by-products [DE88-010233] 20 p2781 N88-26492

NORTH SEA
An hourly analysis, updating and short-range forecasting system --- numerical weather forecasting
02 p0206 N88-11288
Forecast of current patterns for an eddy tracking experiment in the Norwegian coastal current
[PB87-224853] 06 p0747 N88-14595
Climatological data of the Netherlands lightvessels over the period 1949-1980 --- North Sea
[KNMI-WR-87-9] 14 p1947 N88-21613
NORTHERN HEMISPHERE
NT ARCTIC REGIONS
Mean pressure distribution and geostrophic circulation in the meteor zone 06 p0734 N88-14513
Objective prediction of monthly mean surface temperature and climatological relationships to mid-tropospheric heights
[DE88-000908] 07 p0880 N88-15340
Upper-thermospheric observations and neutral-gas dynamics at high latitudes during solar maximum
[AD-A188058] 11 p1512 N88-19031
Northern Hemisphere circulation and the principal components of subsequent summer patterns in North America and West Africa 13 p1801 N88-20765
Health and environmental consequences of the Chernobyl nuclear power plant accident
[DOE/ER-0332] 19 p2689 N88-25985
Some evidence for a Northern Hemispheric extratropic trigger mechanism of ENSO events
22 p3123 N88-28558
Persistence of North Pacific Sea surface temperature and atmospheric flow patterns 22 p3123 N88-28559
Northern Hemisphere 700 mb teleconnections based on half-monthly mean anomaly data stratified by season and by sign 22 p3123 N88-28561
Interannual variability of 850 mb temperatures during the Northern Hemisphere winter
22 p3123 N88-28562
Dependence of medium range forecast errors upon the large-scale initial state 22 p3126 N88-28585
NORTHROP AIRCRAFT
NT F-18 AIRCRAFT
NORWAY
The Norwegian scientific balloon and sounding rocket program 1987-1990 08 p1025 N88-16204
Facilities and plans for improvements at Andoya (Norway) rocket range 08 p1029 N88-16236
NOSE CAPS
U NOSE CONES
NOSE CONES
NT ABLATIVE NOSE CONES
NT ROCKET NOSE CONES
Numerical study of supersonic flow around blunt bodies with extended needle nose 04 p0425 N88-12635
A spatial marching technique for the inviscid blunt body problem 05 p0533 N88-13239
A simplified streamline swallowing procedure for the windward meridian of axisymmetric blunt bodies
[AD-A188413] 12 p1626 N88-19732
NOSES (FOREBODIES)
NT ABLATIVE NOSE CONES
NT NOSE CONES
NT ROCKET NOSE CONES
An experimental investigation of appendage-flat plate junction flow. Volume 2. Elliptical nose appendage data base
[AD-A184974] 05 p0580 N88-13539
NOTATION
U CODING
NOTCH SENSITIVITY
Fatigue strength of alloy A286 at cryogenic temperature 05 p0603 N88-13695
An experimental and numerical study of notch sensitivity of ARALL laminates
[CCMS-88-04] 11 p1450 N88-18644
Notch sensitivity of graphite materials for VHTR
13 p1747 N88-20447
Cyclic crack growth emanating at a round notch considering viscoplasticity
[AD-A189577] 13 p1781 N88-20655
NOTCH STRENGTH
Estimation multiaxial elastic-plastic notch stresses and strains in combined loading
[FB-2/1986] 01 p0060 N88-10382
The use of Hencky's equations for the estimation of multiaxial elastic-plastic notch stresses and strains
[FB-3/1986] 01 p0060 N88-10383
Crack initiation life estimations for notched specimens with residual stresses based on local strains
[FF-17/1986] 01 p0060 N88-10385
Laminated ferrous composites based on ultrahigh carbon (UHC) steels
[AD-A184617] 03 p0280 N88-11764
Influence of strain rate and notch depth on tensile properties of HITCO 6250
[DE88-001324] 04 p0455 N88-12816
Low cycle fatigue behaviour of notched specimens of nickel based superalloy single crystal
05 p0605 N88-13712
Profiles of self stress and of load stress at notches
06 p0719 N88-14419
Hybrid FEM (Finite Element Method) approach to stress distribution in the vicinity of a notch in non-homogeneous materials
[PB87-143392] 07 p0868 N88-15268
A comprehensive study on damage tolerance properties of notched composite laminates
[AD-A192952] 23 p3188 N88-28968
The effect of notch root radius on the determination of toughness in ultrahigh strength steel friction welds
[AD-A195952] 24 p3384 N88-30156
NOTCH TESTS
NT CHARPY IMPACT TEST
The effect of size and surface on the lifetime prediction of StE 460 notched bars
[FD-6/1986] 01 p0058 N88-10374
Closure and propagation behavior of short fatigue cracks at different R-ratios 05 p0601 N88-13679
Crack growth in contrasting titanium alloys under the conjoint action of high and low cycle fatigue
05 p0602 N88-13686
Fatigue of 30CrMnSiNi2A notched specimens under spectrum loading 05 p0602 N88-13689
Initiation and propagation of damage in notched unidirectional and multidirectional CFRE resin laminates
11 p1449 N88-18633
Application of ISRM testing methods to fracture toughness testing of graphite 13 p1747 N88-20446
Notch sensitivity of graphite materials for VHTR
13 p1747 N88-20447
An investigation of the mechanical properties of improved carbon fibre composite materials
[RAE-TR-86021] 14 p1884 N88-21259
Analysis of notched metal matrix composites under tension loading
[NASA-TM-100629] 18 p2480 N88-24713
NOTCHED METALS
U NOTCH TESTS
NOTCHES
Spread of plastic deformation in notched and cracked plates 03 p0337 N88-12122
Influence of strain rate and notch depth on tensile properties of HITCO 6250
[DE88-001324] 04 p0455 N88-12816
Notch-geometry effect on propagation threshold of short fatigue cracks in notched components
06 p0716 N88-14393
Profiles of self stress and of load stress at notches
06 p0719 N88-14419
Cyclic crack growth emanating at a round notch considering viscoplasticity
[AD-A189577] 13 p1781 N88-20655
NOVA LASER SYSTEM
Large-scale stimulated rotational Raman scattering experiments using the LLNL Nova laser
[DE87-012661] 01 p0051 N88-10328
Thermal stress in the edge cladding of Nova glass laser disks
[DE88-000425] 04 p0448 N88-12780
Design of the Backscatter Spectroscopy System for the Nova Laser Facility
[DE88-001880] 07 p0859 N88-15214
High Z interaction physics on Nova
[DE88-004397] 10 p1413 N88-18433
NOVAE
NT DWARF NOVAE
NT HERCULES NOVA
Gamma ray lines from novae
04 p0526 N88-13214
The classical nova outburst
[DE88-009138] 21 p3030 N88-27987
NOWCASTING
Mesoscale Analysis and Forecasting: Incorporating Nowcasting
[ESA-SP-282] 02 p0199 N88-11239
Nowcasting for the national economy needs
02 p0199 N88-11241
An illustrative example of the nowcasting challenge
02 p0199 N88-11243
New nowcasting opportunities using modern meteorological radar 02 p0199 N88-11245
Nowcasting microbursts using Doppler radar in a forecaster-computer environment
02 p0200 N88-11246
Thunderstorm nowcasting using Doppler radar and soundings 02 p0200 N88-11248
The use of advanced data sets in the short-range forecasting of the development of a tornadic thunderstorm along a mesoscale convergence zone
02 p0200 N88-11250
The use of satellite IR data in the enhancement of surface thermal fields 02 p0202 N88-11260
Forecasting and nowcasting cumulus convection with soundings released from a storm-intercept vehicle
02 p0202 N88-11262
Structure and modification of winter mountain clouds in the Sierra Nevada: Nowcasting/forecasting the onset of supercooled liquid water 02 p0202 N88-11263
A proposal of the nowcasting system for sea fog
02 p0202 N88-11264
Nowcasting rain/snow transitions and freezing rain
02 p0202 N88-11265
On the interaction between radar and satellite image nowcasting systems and mesoscale numerical models
02 p0204 N88-11277
A mini system for nowcasting
02 p0204 N88-11278
FRONTIERS: An operational system for nowcasting precipitation 02 p0204 N88-11279
Operational experiment in very short range forecast of precipitation 02 p0204 N88-11280
Satellite imagery and conceptual models in mesoscale forecasting 02 p0205 N88-11282
The studies of physical models on hailstorms and their applications in nowcasting 02 p0207 N88-11300
Toward operational forecasting and detection of weather-producing gravity waves
02 p0208 N88-11303
Opportunities for nowcasting air pollution episodes and accidental toxic and radioactive releases
02 p0210 N88-11317
Mesoscale analysis and nowcasting via a numerical model coupled with satellite sounder data
02 p0211 N88-11328
Opportunities and problems in mesoscale objective analysis 02 p0212 N88-11331
Mesoscale forecasting with satellite data: Challanges and opportunities for today and tomorrow
02 p0215 N88-11353
NOXIOUS MATERIALS
U CONTAMINANTS
NOZZLE COEFFICIENT
U NOZZLE FLOW
NOZZLE DESIGN
The aerodynamic design of hypersonic contoured axisymmetric nozzles including real gas effects
[VKI-TM-43] 06 p0665 N88-14076
Investigation of the need for in-use dispensing rate limits and fuel nozzle geometry standardization
[PB88-102611] 07 p0839 N88-15089
Design of supersonic Coanda jet nozzles
10 p1270 N88-17599
Analysis for high compressible supersonic flow in converging nozzle
[IPPJ-860] 16 p2157 N88-22869
The effects of magnetic nozzle configurations on plasma thrusters
[NASA-CR-183096] 19 p2732 N88-26223
Variable Mach number wall jets for control/propulsion on hypervelocity projectiles/interceptors. Tests with an existing model
[AD-A192845] 21 p2892 N88-27167
Numerical investigations in three-dimensional internal flows
[NASA-CR-183108] 23 p3210 N88-29106
Analysis and optimization of truncated scarf nozzles subject to external flow conditions
[NASA-TM-100955] 24 p3316 N88-29746
Stresses in cylindrical shells with tangential nozzles submitted to external loads and internal pressure
[CRIF-MT-172] 24 p3382 N88-30146
NOZZLE EFFICIENCY
Aeropropulsive characteristics of isolated combined turbojet/ramjet nozzles at Mach numbers from 0 to 1.20
[NASA-TP-2814] 17 p2299 N88-23757
Analysis and optimization of truncated scarf nozzles subject to external flow conditions
[NASA-TM-100955] 24 p3316 N88-29746
NOZZLE FLOW
Rayleigh scattering measurements of a freejet with homogeneous condensation 03 p0319 N88-12020
Numerical simulation and visualization of a flowfield by interaction of two parallel two-dimensional freejets
03 p0320 N88-12021
Method of calculations for flow of ideal gas through plane and axisymmetric nozzles with broken-line contour
06 p0771 N88-14737
Experimental evaluation of a translating nozzle sidewall radial turbine 10 p1280 N88-17656
Laval nozzle flow of a binary, retrograde mixture
[MPIS-1/1987] 11 p1488 N88-18882
J85-21 fuel nozzle atomization tests
[AD-A189394] 12 p1613 N88-19647
Application of a flux vector splitting methodology towards the solution of unsteady transonic flows, with future emphasis on the blade flutter problem
[AD-A189500] 13 p1716 N88-20280

An adaptive grid technique for solution of the Euler equations 13 p1768 N88-20579

Effect of flow convergence on turbulence level in stream 14 p1973 N88-21773

Tests on oscillating flows in a pipe nozzle with an abrupt diameter variation [MPIS-2/1987] 17 p2337 N88-23947

Fast algorithm development for large-eddy simulation of circular-jet turbulence [AD-A192044] 18 p2509 N88-24887

Nozzle lip effects on gas expansion into the plume backflow region [AD-A192806] 21 p2942 N88-27475

Aerodynamics in ground effect and predicted landing ground roll of a fighter configuration with a secondary-nozzle thrust reverser [NASA-TP-2834] 24 p3317 N88-29752

Nozzle airflow influences on fuel patternation 24 p3346 N88-29916

Numerical simulation of nozzle flows [AD-A195144] 24 p3369 N88-30064

NOZZLE GEOMETRY

Development and application of computational aerothermodynamics flowfield computer codes [NASA-CR-181534] 04 p0395 N88-12465

Combustion related shear-flow dynamics in elliptic supersonic jets 05 p0531 N88-13232

An experimental and numerical investigation of swirling flows in a rectangular nozzle 06 p0700 N88-14295

Investigation of the need for in-use dispensing rate limits and fuel nozzle geometry standardization [PB88-102611] 07 p0839 N88-15089

Experimental evaluation of a translating nozzle sidewall radial turbine 10 p1280 N88-17656

High performance Solid Rocket Motor (SRM) submerged nozzle/combustion cavity flowfield assessment [NASA-CR-179307] 11 p1446 N88-18622

Aeropropulsive characteristics of isolated combined turbojet/ramjet nozzles at Mach numbers from 0 to 1.20 [NASA-TP-2814] 17 p2299 N88-23757

Nozzle fabrication technique [NASA-CASE-MSC-21299-1] 18 p2475 N88-24684

A detailed description of the uncertainty analysis for high area ratio rocket nozzle tests at the NASA Lewis Research Center 19 p2626 N88-25580

Extensive verification of blade-to-blade flow code based on Denton scheme 19 p2638 N88-25654

NOZZLE THRUST COEFFICIENTS

Comparison of wind tunnel and flight test afterbody and nozzle pressures for a twin-jet fighter aircraft at transonic speeds [NASA-TP-2588] 02 p0121 N88-10765

NOZZLE WALLS

Experimental evaluation of a translating nozzle sidewall radial turbine 10 p1280 N88-17656

NOZZLELESS ROCKET ENGINES

Evaluation of techniques for direct measurement of burning rates in nozzleless motors 19 p2631 N88-25609

NOZZLES

Effect of empennage arrangement on single-engine nozzle/afterbody static pressures at transonic speeds [NASA-TP-2753] 02 p0122 N88-10771

Verification of FANTASTIC integrated code 07 p0924 N88-15613

Equilibrium retention in the nozzle of oxygen hydrogen propulsion systems 07 p0924 N88-15616

Aeropropulsion '87. Session 3: Internal Fluid Mechanics Research [NASA-CP-10003-SESS-3] 08 p0954 N88-15790

Inlets, ducts and nozzles 08 p0955 N88-15791

Comparison of UNL laser imaging and sizing system and a phase/Doppler system for analyzing sprays from a NASA nozzle [NASA-CR-182437] 09 p1161 N88-16956

SRB/SLEEC (Solid Rocket Booster/Shingle Lap Extendible Exit Cone) feasibility study, volume 1 [NASA-CR-178973] 23 p3187 N88-28964

NUCLEAR ASTROPHYSICS

Influences of the astrophysical environment on nuclear decay rates [DE88-001461] 04 p0522 N88-13208

New nuclear structure calculations and the astrophysical r-process [DE88-000979] 08 p1082 N88-16518

An introduction to nuclear astrophysics [DE88-002761] 08 p1100 N88-16618

NUCLEAR AUXILIARY POWER UNITS

NT FISSION ELECTRIC CELLS
NT SNAP
NT SNAP 19
NT SPACE POWER REACTORS

Creep behavior of tungsten/niobium and tungsten/niobium-1 percent zirconium composites [NASA-TM-100804] 11 p1460 N88-18707

NUCLEAR BINDING ENERGY

Schottky-barrier formation on a covalent semiconductor without Fermi-level pinning: The Metal-MoS2(0001) interface [AD-A193044] 21 p3021 N88-27931

NUCLEAR CAPTURE

NT ELECTRON CAPTURE

Neutron capture nucleosynthesis in low mass AGB stars 04 p0517 N88-13178

First capture of antiprotons in an ion trap and the possibility of antihydrogen 16 p2268 N88-23569

NUCLEAR ELECTRIC POWER GENERATION

NT FISSION ELECTRIC CELLS
NT NUCLEAR AUXILIARY POWER UNITS
NT NUCLEAR POWER PLANTS
NT NUCLEAR POWER REACTORS
NT SNAP
NT SNAP 19
NT SPACE POWER REACTORS
NT THERMONUCLEAR POWER GENERATION

Procedure and program used for data processing in a poll on nuclear energy utilization [IFSI-87-3] 05 p0649 N88-13977

Starpower: The US and the international quest for fusion energy [PB88-128731] 11 p1551 N88-19283

Benefits of 20 kHz PMAD in a nuclear space station 17 p2398 N88-24256

Nuclear electric power for multimegawatt orbit transfer vehicles 17 p2399 N88-24261

NUCLEAR ELECTRIC PROPULSION

Nuclear electric propulsion system: Nuclear plant and thermomechanical conversion system 17 p2405 N88-24298

Comparison of a direct thrust nuclear engine, nuclear electric engine and a chemical engine for future space missions 17 p2418 N88-24379

NUCLEAR ENERGY

USSR report: Engineering and equipment [JPRS-UEQ-87-008] 04 p0423 N88-12621

Power systems for production, construction, life support and operations in space [NASA-TM-100838] 14 p1883 N88-21254

Analytical Chemistry Division [DE88-701236] 16 p2174 N88-22956

NUCLEAR ENGINE FOR ROCKET VEHICLES

History of some direct nuclear propulsion developments since 1946 17 p2400 N88-24270

A critique of NERVA based nuclear reactor design and performance for MMW space propulsion applications 17 p2404 N88-24297

Nuclear propulsion: Past, present and future 17 p2427 N88-24441

The NERVA derivative reactor and a systematic approach to multiple space power requirements 17 p2430 N88-24458

NUCLEAR EXPLOSION EFFECT

Buckling of blast loaded cylinder [AD-A190124] 15 p2076 N88-22376

Effects of tectonic release on broadband regional distance bodywaves [AD-A194247] 22 p3119 N88-28529

NUCLEAR EXPLOSIONS

Historical catalog of Southern Great Basin earthquakes, 1868-1978 [DE87-014340] 02 p0198 N88-11232

The development of low level coastal flow fields when solar radiation is blocked by smoke [DE87-014348] 03 p0354 N88-12230

NORSAR detection processing system [AD-A185968] 07 p0877 N88-15318

A methodology to assess the effects of high altitude electromagnetic pulse (HEMP) on electric power systems [DE88-000338] 11 p1476 N88-18808

Announced United States nuclear tests: July 1945 through December 1986 [NVO-209-REV-7] 11 p1546 N88-19247

Characteristics of seismic sources of some Asian earthquakes and Soviet underground explosions from Gauribidanur array records [DE88-701233] 15 p2093 N88-22472

An approximation technique for solving a system of Fredholm integral equations for asymmetric detector response functions [AD-A190577] 15 p2121 N88-22645

Research and development activities of the Seismology Section [DE88-701235] 16 p2231 N88-23323

Acute radiation syndrones and their management [DE88-009839] 20 p2831 N88-26797

Approximate analytical formulae for electron density and collision frequency in the natural and nuclear-disturbed ionosphere and inner magnetosphere [AD-A193129] 21 p2972 N88-27654

Effects of tectonic release on broadband regional distance bodywaves [AD-A194247] 22 p3119 N88-28529

Maximum-likelihood multichannel deconvolution of P waves at seismic arrays [AD-A194990] 24 p3391 N88-30191

NUCLEAR FISSION

Space based nuclear-pumped laser/reactor concepts 17 p2403 N88-24289

Influence of pairing correlations on the probability and dynamics of tunneling through the barrier in fission and fusion of complex nuclei [DE88-701500] 23 p3286 N88-29570

NUCLEAR FUEL BURNUP

Effect of fuel burnup and cross sections on modular HTGR (High-Temperature Gas-cooled Reactor) reactivity coefficients [DE88-006656] 22 p3151 N88-28748

NUCLEAR FUEL ELEMENTS

Review of diffusion barrier technology for application in SP-100 fuel pins [DE88-000021] 02 p0234 N88-11480

Material tradeoffs to minimize flooding reactivity 17 p2399 N88-24265

Particle bed reactor scaling relationships 17 p2400 N88-24267

Irradiation test results on thermionic fuel element sheath insulators 17 p2402 N88-24280

Development of reliable fuel pins for space reactor applications 17 p2409 N88-24326

A review of diffusion barrier technology for application in SP-100 fuel pins 17 p2410 N88-24328

Evaluation of UN fuel pin failure modes and motion of fuel during severe accidents for reactors in space 17 p2425 N88-24424

Research and development of electrical insulators for thermionic applications 17 p2429 N88-24449

SNAP fuel performance 17 p2435 N88-24484

Methods and techniques of NDA (nondestructive assay) [DE88-009145] 20 p2812 N88-26682

Effect of fuel burnup and cross sections on modular HTGR (High-Temperature Gas-cooled Reactor) reactivity coefficients [DE88-006656] 22 p3151 N88-28748

NUCLEAR FUELS

NT CERAMIC NUCLEAR FUELS
NT SPENT FUELS

Experience of developing an integrated nondestructive assay system [DE88-003149] 09 p1184 N88-17092

Fusion, and advanced fuel, reaction bibliography: Particle reactions from H1 to B11 [AD-A187420] 11 p1552 N88-19286

Studies in solid state ionics [DE88-700830] 11 p1559 N88-19333

CIT (Compact Ignition Tokamak) fueling [DE88-002709] 12 p1692 N88-20125

Compatibility in space reactor fuel systems [DE88-005698] 13 p1839 N88-21004

Analysis for high compressible supersonic flow in converging nozzle [IPPJ-860] 16 p2157 N88-22869

Analysis for fuel implosion in ICF target and pellet gain 16 p2276 N88-23620

Pusherless implosion, pulse tailoring and ignition scaling law for laser fusion 16 p2277 N88-23629

Fully passive space reactor conceptual design 17 p2403 N88-24288

Uranium nitride fuel swelling and thermal conductivity correlations 17 p2409 N88-24327

Helium-3 fusion fuel resources for space power 17 p2410 N88-24330

Fabrication of SP-100 fuel barrier structures by chemical vapor deposition 17 p2416 N88-24371

Critical nuclear launch issues: A perspective from the State of Florida 17 p2423 N88-24412

A novel plant protection strategy for transient reactors 17 p2425 N88-24423

Evaluation of UN fuel pin failure modes and motion of fuel during severe accidents for reactors in space 17 p2425 N88-24424

Weldability of general purpose heat source iridium capsules 17 p2426 N88-24429

An irradiation performance data base for nitride fuels 17 p2427 N88-24438

A high power density radial-in-flow reactor split core design for space power systems 17 p2430 N88-24455

Molybdenum-base cermet fuel development 17 p2434 N88-24481

Test plan and facilities for qualifying nuclear rocket fuel elements 17 p2434 N88-24482

Material property and irradiation performance correlations for nitride fuels 17 p2434 N88-24483

SNAP fuel performance 17 p2435 N88-24484

A comparison of uranium nitride and mixed carbide fuels swelling 17 p2435 N88-24485

The JET (Joint European Torus) multipellet launcher and fueling of JET plasmas by multipellet injection

[DE88-008367] 19 p2729 N88-26206

The hole of a blanket tritium system on the fusion fuel cycle

[DE88-010007] 20 p2859 N88-26983

NUCLEAR FUSION

NT CONTROLLED FUSION

System studies of compact ignition tokamaks

[DE87-014976] 02 p0239 N88-11508

Feasibility of alpha particle measurement in a magnetically confined plasma by CO2 laser Thomson scattering

[DE88-000039] 02 p0241 N88-11522

Volume produced H(-),D(-) ion source for proton accelerator and thermo-nuclear fusion research by sheet plasma (III)

[IPPJ-838] 02 p0242 N88-11531

Measurement of parallel ion energy distribution function in PISCES plasma

[DE88-000108] 03 p0378 N88-12380

Interchange stability of noncircular reversed field pinches

[DE88-000177] 03 p0378 N88-12381

The attitudes of science policy, environmental, and utility leaders on US energy issues and fusion

[DE88-000784] 04 p0494 N88-13041

Neutron capture nucleosynthesis in low mass AGB stars 04 p0517 N88-13178

A review of the experimental and theoretical status of the reversed-field pinch

[DE88-000529] 05 p0652 N88-14000

Mirror theory applied to toroidal systems

[DE88-003832] 07 p0933 N88-15669

Summary of the report of the Senior Committee on Environmental, Safety and Economic Aspects of Magnetic Fusion Energy

[DE88-003270] 07 p0937 N88-15692

Primordial nucleosynthesis during the keV era

[DE88-002233] 08 p1104 N88-16623

Investigation of the evolution of the fusion processes in the plasma focus using time-resolved neutron spectroscopy

[IPF-87-4] 09 p1251 N88-17493

Understanding and accepting fusion as an alternative energy source

[DE88-004356] 10 p1413 N88-18432

Starpower: The US and the international quest for fusion energy

[PB88-128731] 11 p1551 N88-19283

Low aspect ratio torsatrons

[DE88-004173] 11 p1552 N88-19284

Fusion, and advanced fuel, reaction bibliography: Particle reactions from H1 to B11

[AD-A187420] 11 p1552 N88-19286

Intermixing processes in massive stars and their influence on stellar evolution and nucleosynthesis

[ETN-88-91484] 11 p1568 N88-19388

Big Bang Nucleosynthesis: Accelerator tests and can (UC OMEGA)(sub B) really be large

[DE88-003405] 11 p1570 N88-19396

Application of railgun principle to high-velocity hydrogen pellet injection for magnetic fusion reactor refueling

[DE88-005830] 13 p1728 N88-20334

SOAR: Space orbiting advanced fusion power reactor

[AD-A189234] 13 p1732 N88-20356

JPRS report: Science and technology. China

[JPRS-CST-87-043] 15 p2053 N88-22233

Smoothing technique to resolve X-ray spectra in laser nuclear fusion 15 p2053 N88-22235

Magnetic fusion energy plasma interactive and high heat flux components. Volume 5: Technical assessment of critical issues in the steady state operation of fusion confinement devices

[DE88-006920] 15 p2136 N88-22744

Soviet magnetic confinement fusion research

[PB88-182316] 16 p2279 N88-23644

Helium-3 fusion fuel resources for space power

17 p2410 N88-24330

Intense ion beam diagnostics for particle beam fusion experiments on PBFA 2

[DE88-007279] 18 p2577 N88-25306

A mode-transforming polarization-rotatable launcher for the ATF (Advanced Toroidal Facility) fusion experiment

[DE88-005070] 19 p2730 N88-26213

Heavy ion collisions with A = 10(sup 57): Aspects of nuclear stability and the nuclear equation of state in coalescing neutron-star binary systems

[DE88-008029] 19 p2741 N88-26277

Fusion programs in applied plasma physics and development and technology at GA Technologies, Inc.

[DE88-008406] 20 p2856 N88-26964

Overview of the TITAN-2 reversed-field pinch aqueous fusion power core design

[DE88-008170] 20 p2857 N88-26966

Influence of pairing correlations on the probability and dynamics of tunneling through the barrier in fission and fusion of complex nuclei

[DE88-701500] 23 p3286 N88-29570

NUCLEAR HEAT

Basic characteristics of heat-exchanger-type steam reformer heated by high-temperature helium gas (2). Analysis by simulation model (2)

[DE87-702962] 15 p2061 N88-22291

NUCLEAR INTERACTIONS

NT ELECTRON CAPTURE

NT NUCLEAR CAPTURE

NT WEAK INTERACTIONS (FIELD THEORY)

Cosmic-ray nuclear event with an anomalously strong concentration of energy and particles in the central region

[DE87-703376] 04 p0526 N88-13213

Nucleon-nucleus interaction data base: Total nuclear and absorption cross sections

[NASA-TM-4053] 20 p2852 N88-26935

NUCLEAR MAGNETIC RESONANCE

X-ray tomography and nuclear magnetic resonance imaging applications for advanced ceramic materials

[DE87-011534] 01 p0027 N88-10171

Nuclear magnetic resonance studies of ion motion in solid electrolytes

[DE87-014547] 02 p0232 N88-11464

Evaluation of one-sided nuclear magnetic resonance for remote detection of explosives

[AD-A184490] 03 p0296 N88-11857

Synthesis, NMR characterization and electrical properties of siloxane-based polymer electrolytes

[AD-A184184] 04 p0418 N88-12596

Solid state C-13 NMR characterization of textiles: Qualitative and quantitative analysis

[AD-A184349] 04 p0419 N88-12598

A low volume insert for solid state magic angle spinning NMR of small samples

[AD-A184359] 04 p0419 N88-12601

Alternating current circuit theory and pulsed NMR (Nuclear Magnetic Resonance)

[DE88-000641] 04 p0440 N88-12732

The use of NMR imaging to measure porosity and binder distributions in green-state and partially sintered ceramics

[DE88-003099] 06 p0972 N88-15881

A 13C and 15N solid state NMR characterization of aramid-containing nylon-6 polymers synthesized by in situ polymerization of caprolactam with benzoyl caprolactam derivatives

[AD-A187067] 09 p1147 N88-16872

NMR (Nuclear Magnetic Resonance) imaging for detecting binder/plasticizers in green-state structural ceramics

[DE88-003111] 10 p1304 N88-17800

Instrumentation and quantitative methods of evaluation

[DE87-013639] 10 p1342 N88-18017

Irreducible tensor operators and multiple-quantum NMR 11 p1542 N88-19217

FTIR (Fourier Transform Infrared) and FTNMR (Fourier Transform Nuclear Magnetic Resonance) study of organophosphorus surface reactions

[AD-A188337] 12 p1609 N88-19625

Recent developments in nondestructive evaluation for structural ceramics

[DE88-005889] 13 p1751 N88-20473

Velocity and concentration measurements in flowing suspensions by nuclear magnetic resonance

[DE88-006225] 13 p1770 N88-20589

Biophysical applications of solid state and tritium NMR

[DE88-005328] 13 p1808 N88-20806

Biology and Medicine Division

[DE87-009280] 14 p1952 N88-21632

Structure of sol-gel silica

[DE88-006870] 15 p2033 N88-22114

Fluids, gels and glasses under extreme conditions of pressure and temperature

[AD-A190655] 15 p2035 N88-22125

NMR analysis of a fluorocarbon copolymer

[DE88-002364] 15 p2043 N88-22170

Chromatographic and mass spectrometric separation and analysis

[AD-A190113] 16 p2174 N88-22958

Structural study of the TGMDA-DDS system — epoxy system

[ONERA-RT-4/3346-M] 18 p2493 N88-24792

An instrument control and data analysis program for NMR imaging and spectroscopy

[DE88-007377] 19 p2717 N88-26132

Determination of binder distributions in green-state ceramics by NMR imaging

[DE88-009990] 20 p2778 N88-26474

Nuclear magnetic resonance spectrometer

[AD-A192928] 21 p2950 N88-27523

Sol-gel kinetics: Si(sup)29 NMR and a statistical reaction model

[DE88-011545] 23 p3191 N88-28988

Static and dynamic behavior of a quasi one-dimensional Heisenberg antiferromagnet in the long-range ordered state. A nuclear magnetic resonance study performed with a He3-He4 dilution refrigerator

[B8705564] 23 p3281 N88-29533

NUCLEAR MEDICINE

NT RADIOBIOLOGY

South African Association of Physicists in Medicine and Biology: 26th Annual Congress

[DE88-700824] 11 p1521 N88-19082

Nuclear health and safety: Radiation exposures for some cloud-sampling personnel need to be reexamined

[PB88-130497] 12 p1662 N88-19965

JPRS report: Science and technology. USSR: Life sciences

[JPRS-ULS-88-002] 12 p1665 N88-19982

Technology '87: Research and Development Laboratory Technology Transfer Program

[DE88-003142] 13 p1852 N88-21084

Biology and Medicine Division

[DE87-009280] 14 p1952 N88-21632

NUCLEAR METEOROLOGY

Opportunities for nowcasting air pollution episodes and accidental toxic and radioactive releases

02 p0210 N88-11317

Nuclear health and safety: Radiation exposures for some cloud-sampling personnel need to be reexamined

[PB88-130497] 12 p1662 N88-19965

Health and environmental consequences of the Chernobyl nuclear power plant accident

[DOE/ER-0332] 19 p2689 N88-25885

NUCLEAR MODELS

Development and evaluation of a Monte Carlo code system for analysis of ionization chamber responses

[AD-A183970] 03 p0375 N88-12359

New nuclear structure calculations and the astrophysical r-process

[DE88-000979] 08 p1082 N88-16518

Simulation of nuclear collisions at high energies in the frames of quark-gluon string model

[DE88-700914] 12 p1690 N88-20113

Development of nuclear models for higher energy calculations

[DE88-010919] 20 p2852 N88-26932

NUCLEAR PARTICLES

NT ALPHA PARTICLES

NT ANTINEUTRINOS

NT ANTINUCLEONS

NT ANTIPARTICLES

NT ANTIPROTONS

NT BETA PARTICLES

NT BOSONS

NT KAONS

NT MESON RESONANCE

NT MESONS

NT MUONS

NT NUCLEONS

NT PHOTOELECTRONS

NT PHOTONS

NT PIONS

NT POSITRONS

Theory of double beta decay

[DE88-002285] 07 p0931 N88-15653

Large area nuclear particle detectors using ET materials

[NASA-CR-180777] 23 p3215 N88-29136

NUCLEAR PHYSICS

NT NUCLEAR ASTROPHYSICS

NT REACTOR PHYSICS

Mathematics applied to nuclear geophysics

[INPE-4234-PRE/1109] 01 p0066 N88-10561

Experimental nuclear physics

[DE87-014586] 02 p0231 N88-11459

Electron interactions with nuclei

[DE87-014587] 02 p0232 N88-11460

Future directions in interplays between particle and nuclear physics: Summary session

[DE87-011791] 04 p0489 N88-13013

Nuclear techniques in studies of condensed matter

[NASA-RP-1195] 04 p0489 N88-13015

Research in elementary particle physics

[DE88-002130] 06 p0777 N88-14771

USSR report: Physics and mathematics

[JPRS-UPM-87-002] 07 p0918 N88-15575

Theoretical nuclear physics

[DE87-004504] 09 p1244 N88-17455

Activities report in nuclear physics

[ETN-88-91609] 09 p1245 N88-17458

Semiclassical theory of the nuclear response function. Quasielastic electron scattering

[ETN-88-91082] 09 p1245 N88-17459

Technical activities 1987, Center for Radiation Research
[PB88-129325] 09 p1245 N88-17464
The development of emission tomography for the nuclear industry
[AERE-R-12319] 10 p1341 N88-18014
Research in experimental nuclear physics
[DE88-004100] 10 p1408 N88-18397
Experimental elementary particle physics at the University of Pittsburgh
[DE88-003542] 11 p1545 N88-19234
Experimental aspects of hypernuclear physics at CEBAF
[CEBAF-R-86-013] 11 p1546 N88-19245
Channeling and dechanneling at high energy
[DE88-003989] 11 p1548 N88-19259
Reports and contributions of the Max-Planck Institute of Chemistry (Otto Hahn Institute)
[REPT-1/87] 11 p1570 N88-19398
Intermediate energy neutrino physics
[DE88-005378] 13 p1836 N88-20984
Research in high energy elementary particle physics
[DE88-006065] 13 p1837 N88-20994
Particle physics and cosmology
[DE88-004944] 13 p1854 N88-21096
Experimental elementary particle physics
[DE88-007510] 18 p2572 N88-25274

NUCLEAR POWER GENERATION
U NUCLEAR ELECTRIC POWER GENERATION

NUCLEAR POWER PLANTS
Reinforced flexural elements for TEMP-STRESS Program
[DE87-012961] 01 p0061 N88-10391
USSR Report: Engineering and Equipment
[JPRS-UEQ-87-007] 02 p0157 N88-10985
Ultrasonic mechanized checking of weld joints of nuclear power plant equipment 02 p0158 N88-10987
Real-time evaluation and prediction of coastal dispersion near the SW tip of Africa --- effluents
02 p0210 N88-11318
Expert robots in nuclear plants
[DE87-014839] 04 p0452 N88-12800
Ultrasonic method of inspecting austenitic weld joints in nuclear power station equipment
[BLL-CE-TRANS-8281-(9022.09)]
04 p0453 N88-12806
Computer code simulations of explosions in flow networks and comparison with experiments
[DE88-001946] 05 p0573 N88-13401
Effects of commercial cladding on the fracture behavior of pressure vessel steel plates
[DE88-004333] 10 p1303 N88-17790
Understanding and accepting fusion as an alternative energy source
[DE88-004356] 10 p1413 N88-18432
Proceedings of the 19th DOE/NRC Airborne Waste Management and Air Cleaning Conference
[NUREG/CP-0086-VOL-1] 11 p1509 N88-19018
Proceedings of the 19th DOE/NRC Airborne Waste Management and Air Cleaning Conference
[NUREG/CP-0086-VOL-2] 11 p1509 N88-19019
Uncertainties in hydrogen combustion
[DE88-005354] 13 p1739 N88-20395
Small and medium power reactors 1987
[DE88-701435] 15 p2132 N88-22720
JPRS report: Science and technology. Japan
[JPRS-JST-87-030] 16 p2185 N88-23026
Design of nuclear heat, power co-generation plant detailed 16 p2186 N88-23033
Nuclear electric propulsion system: Nuclear plant and thermomechanical conversion system
17 p2405 N88-24298
Thermal management for multi-modal nuclear power plants 17 p2410 N88-24331
Knowledge based systems in nondestructive evaluation
[DE88-006653] 18 p2525 N88-24981
Health and environmental consequences of the Chernobyl nuclear power plant accident
[DOE/ER-0332] 19 p2689 N88-25985
Qualification of expansion and welding procedures of tube-to-tubesheet joints for heat exchangers in nuclear power plants
[DE88-701621] 23 p3221 N88-29174

NUCLEAR POWER REACTORS
NT FISSION ELECTRIC CELLS
NT SPACE POWER REACTORS
Small reactor power systems for manned planetary surface bases
[NASA-TM-100223] 04 p0524 N88-13209
Small and medium power reactors 1987
[DE88-701435] 15 p2132 N88-22720
Development of fast breeder reactors in China
16 p2186 N88-23032
Operational concerns involving a shadow-shielded nuclear reactor for space station applications
17 p2398 N88-24257
Nuclear electric power for multimegawatt orbit transfer vehicles 17 p2399 N88-24261
Gigawatt, closed cycle, vapor core-MHD space power system conceptual design study
17 p2433 N88-24473
Critical issues for SOAR: The space orbiting advanced fusion power reactor 17 p2433 N88-24474
Comparison of 20-kWe space nuclear power systems: Impact of reactor temperature and technology upon system design and performances 17 p2433 N88-24475
Potassium Rankine power system for space power
17 p2433 N88-24476
Low cross-section Mo-Nb thermocouples for nuclear application: The state-of-the-art
17 p2433 N88-24477
Material property and irradiation performance correlations for nitride fuels 17 p2434 N88-24483
Health and environmental consequences of the Chernobyl nuclear power plant accident
[DOE/ER-0332] 19 p2689 N88-25985
Pulsed power driver technologies for inertial confinement fusion power reactors
[DE88-009260] 19 p2731 N88-26221

NUCLEAR PROPULSION
NT NUCLEAR ELECTRIC PROPULSION
Fusion, and advanced fuel, reaction bibliography: Particle reactions from H1 to B11
[AD-A187420] 11 p1552 N88-19286
Nuclear electric power for multimegawatt orbit transfer vehicles 17 p2399 N88-24261
History of some direct nuclear propulsion developments since 1946 17 p2400 N88-24270
Direct nuclear propulsion for Earth-to-orbit vehicles
17 p2400 N88-24271
Nuclear propulsion systems for orbit transfer based on the particle bed reactor 17 p2401 N88-24272
Ultra high temperature direct propulsion
17 p2401 N88-24275
Safety constraints and considerations in the development of nuclear powered propulsion
17 p2401 N88-24276
Comparison of a direct thrust nuclear engine, nuclear electric engine and a chemical engine for future space missions 17 p2418 N88-24379
Nuclear propulsion: Past, present and future
17 p2427 N88-24441
Gas core reactors for direct nuclear propulsion
17 p2428 N88-24442
Noncryogenic propellants for a nuclear orbit transfer vehicle 17 p2428 N88-24444

NUCLEAR PUMPED LASERS
Refractive index gradients in nuclear-reactor-pumped lasers: Gasdynamic effects
[DE88-006099] 13 p1776 N88-20621

NUCLEAR RADIATION
NT BETA PARTICLES
NT FAST NEUTRONS
NT GAMMA RAY BURSTS
NT GAMMA RAYS
NT NEUTRON BEAMS
NT SPALLATION
NT THERMAL NEUTRONS

NUCLEAR RADIATION SPECTROSCOPY
Phase modulation of recoilless gamma radiation in Mossbauer spectroscopy
[ETN-88-92648] 24 p3428 N88-30403

NUCLEAR REACTIONS
NT ALPHA DECAY
NT CONTROLLED FUSION
NT ELECTRON CAPTURE
NT NEUTRON EMISSION
NT NEUTRON SCATTERING
NT NUCLEAR CAPTURE
NT NUCLEAR FISSION
NT NUCLEAR FUSION
NT NUCLEAR INTERACTIONS
NT NUCLEAR SCATTERING
NT NUCLEAR TRANSFORMATIONS
NT PHOTONUCLEAR REACTIONS
NT PROTON SCATTERING
NT PROTON-PROTON REACTIONS
NT RADIOACTIVE DECAY
NT RESONANCE SCATTERING
NT SPALLATION
NT THERMONUCLEAR REACTIONS
NT TRANSMUTATION
NT WEAK INTERACTIONS (FIELD THEORY)
Experimental nuclear physics
[DE87-014586] 02 p0231 N88-11459
The development of diagnostic fuses
[SAND-86-0395] 03 p0311 N88-11963
Applied nuclear science research and development
[LA-10915-PR] 03 p0374 N88-12355
Computer simulations of fragmentation
[DE87-900985] 03 p0375 N88-12358
Anomalous phonon behavior of superconductor Y-Ba-Cu-O
[DE87-703401] 05 p0654 N88-14010
Analysis of the mass formula dependence of spallation product distribution
[DE88-750297] 07 p0864 N88-15243
An introduction to nuclear astrophysics
[DE88-002761] 08 p1100 N88-16618
Theoretical nuclear physics
[DE87-004504] 09 p1244 N88-17455
Measurements of astrophysical reaction rates for radioactive samples
[DE88-004309] 10 p1429 N88-18537
Gamma-ray and neutron spectroscopy of planetary surfaces and atmospheres
[DE88-004287] 10 p1430 N88-18541
Ion energy diagnostics for voltage determinations in plasma-erosion-opening-switch experiments
[DE88-004822] 11 p1479 N88-18827
Emission of gamma rays from various materials pulsed with 14-MeV neutrons
[DE88-003837] 11 p1544 N88-19227
Fusion, and advanced fuel, reaction bibliography: Particle reactions from H1 to B11
[AD-A187420] 11 p1552 N88-19286
On (p,n) systematics and the cosmological connection
[DE88-005031] 12 p1712 N88-20245
Theory of Muon method for study of solid and liquid hydrogen 14 p1972 N88-21770
Reference nuclear data for space applications
[DE88-007041] 16 p2270 N88-23583
Search for bound states of the eta-meson in light nuclei 17 p2397 N88-24248
Nuclear and astrophysical evidence on the equation of state
[DE88-007397] 18 p2572 N88-25279
Automated system for mathematical processing of the data from a hybrid spectrometer
[DE87-702995] 20 p2836 N88-26820
Development of nuclear models for higher energy calculations
[DE88-010919] 20 p2852 N88-26932
Measure of hydrogen concentration profile in materials by resonant nuclear reactions
[DE88-702599] 23 p3193 N88-28999
Hadrons produced in atmospheric interactions
[DE88-702492] 23 p3300 N88-29712

NUCLEAR REACTOR CONTROL
Application of the reactivity constraint approach to the transient control of spacecraft reactors
17 p2406 N88-24305
Reactor instrumentation and control design and performance simulation for SP-100
17 p2406 N88-24306
An adaptive load-following control system for a space nuclear power system 17 p2406 N88-24307
Benchmark physics experiments for SP-100
17 p2429 N88-24453
A high power density radial-in-flow reactor split core design for space power systems
17 p2430 N88-24455
Transient analyses of multimegawatt space reactors
17 p2430 N88-24456
Silicon-on-insulator electronics for a space nuclear power system 17 p2431 N88-24461

NUCLEAR REACTORS
NT BOILING WATER REACTORS
NT BREEDER REACTORS
NT EXPERIMENTAL BREEDER REACTOR 2
NT FAST NUCLEAR REACTORS
NT FISSION ELECTRIC CELLS
NT FUSION REACTORS
NT FUSION-FISSION HYBRID REACTORS
NT GAS COOLED REACTORS
NT GASEOUS FISSION REACTORS
NT HIGH TEMPERATURE GAS COOLED REACTORS
NT HIGH TEMPERATURE NUCLEAR REACTORS
NT JOINT EUROPEAN TORUS
NT LIGHT WATER REACTORS
NT LIQUID COOLED REACTORS
NT LIQUID METAL COOLED REACTORS
NT LIQUID METAL FAST BREEDER REACTORS
NT NUCLEAR POWER REACTORS
NT NUCLEAR RESEARCH AND TEST REACTORS
NT PEBBLE BED REACTORS
NT PLASMA CORE REACTORS
NT PRESSURIZED WATER REACTORS
NT SPACE POWER REACTORS
NT SPHEROMAKS
NT STELLARATORS
NT THERMAL REACTORS
NT TOKAMAK DEVICES
NT ZERO POWER REACTORS

best copy available

Oxidation of TSX graphite over the temperature range 450 to 1200°C
[DE87-012230] 01 p0020 N88-10127

Transient modeling of the thermohydraulic behavior of high temperature heat pipes for space reactor applications 02 p0136 N88-10857

Assessment of the impacts of transferring certain nuclear reactor technologies to the Soviet Union and Eastern Europe
[DE87-014368] 02 p0249 N88-11576

Computerized system for studies on creep of irradiated materials in the BR-10 reactor. Control system for electric motor
[DE87-702888] 03 p0310 N88-11952

Shielding analysis of a small compact space nuclear reactor
[AD-A185566] 06 p0779 N88-14784

Effects of the neutron spectrum on mechanical property changes in low dose irradiations
[DE88-003429] 10 p1302 N88-17786

Ballistic deficits in pulse shaping amplifiers
[DE88-003908] 11 p1481 N88-18840

Optimal control theory of load-following and parameter-tracking of nonlinear systems: An application of Pontryagin Maximum Principle to reactor dynamics
[DE88-004770] 11 p1532 N88-19152

The use of least squares in undetermined problems
[DE88-004473] 12 p1662 N88-20059

Requirements and cost considerations for a combined space nuclear reactor test facility
17 p2401 N88-24277

The role of integral experiments and nuclear cross section evaluations in space nuclear reactor design
17 p2404 N88-24293

Nuclear reactor magnetohydrodynamic power generator for directed energy weapons 17 p2411 N88-24336

EETAP (End-to-End Transient Analysis Program) for space nuclear power system simulation
17 p2418 N88-24381

Relating design and environmental variables to reliability 17 p2418 N88-24383

Theoretical prediction of single phase turbulent flow distribution in particulate bed reactors
17 p2419 N88-24386

Monolithic fuel cell based power source for burst power generation 17 p2429 N88-24450

High power density alkaline fuel cell technology for MMW space burst power 17 p2429 N88-24451

Computer aided remote control: A general concept for intervention in the nuclear, underwater, and space domains 19 p2699 N88-26046

The safety designs for the TITAN reversed-field pinch reactor study
[DE88-008169] 19 p2729 N88-26205

Principles of a nondestructive evaluation process for damage location, damage profile, and damage extension in welded joints by radiometric measurements
[MPA-86-02] 20 p2812 N88-26683

Fusion programs in applied plasma physics and development and technology at GA Technologies, Inc.
[DE88-006406] 20 p2856 N88-26964

TIBER (Tokamak Ignition/Burn Experimental Reactor) 2 as a precursor to an international thermonuclear experimental reactor
[DE88-008806] 20 p2858 N88-26970

NUCLEAR RELAXATION

A review of the experimental and theoretical status of the reversed-field pinch
[DE88-000529] 05 p0652 N88-14000

NUCLEAR RESEARCH

Applied nuclear science research and development
[LA-10915-PR] 03 p0374 N88-12355

The birth of big science: Nuclear physics as advanced technology source
[NOTA-INTERNA-861] 05 p0648 N88-13967

Technology security, volume 1
[DE88-008612] 21 p3029 N88-27976

NUCLEAR RESEARCH AND TEST REACTORS

NT EXPERIMENTAL BREEDER REACTOR 2

NT HIGH TEMPERATURE NUCLEAR REACTORS

Radiation effects testing capabilities of the Texas A and M Nuclear Science Center 17 p2416 N88-24368

NUCLEAR ROCKET ENGINES

TRICE design, evaluation and feasibility tests
17 p2437 N88-24496

Advanced nuclear rocket engine mission analysis
[DE88-006797] 18 p2475 N88-24681

NUCLEAR SCATTERING

NT NEUTRON SCATTERING

NT RESONANCE SCATTERING

Status of cross section data for photon scattering by atoms
[DE87-011291] 08 p1081 N88-16517

Pion elastic and inelastic scattering near N=28
[LA-10966-T] 11 p1544 N88-19232

Eikonal solutions to optical model coupled-channel equations
[NASA-TP-2830] 24 p3428 N88-30402

NUCLEAR SHIELDING

U RADIATION SHIELDING

NUCLEAR SPIN

Theory of Muon method for study of solid and liquid hydrogen 14 p1972 N88-21770

NUCLEAR STRUCTURE

Electron interactions with nuclei
[DE87-014587] 02 p0232 N88-11460

TRISTAN research on neutron rich nuclei: Magnetic moments and nuclear structure
[DE88-002122] 06 p0783 N88-14807

Double beta decay and nuclear structure
[DE88-001966] 07 p0931 N88-15652

New nuclear structure calculations and the astrophysical r-process
[DE88-000979] 08 p1082 N88-16518

Theoretical nuclear physics
[DE87-004504] 09 p1244 N88-17455

Extension of nuclear structure data base searches for gamma-ray laser candidates
[DE88-004288] 10 p1336 N88-17985

A nuclear structure study of the proposed gamma-ray laser candidate nucleus Re-186
[DE88-004299] 10 p1336 N88-17986

Nuclear structure at intermediate energies
[DE88-002796] 10 p1407 N88-18390

Nuclear structure studies by the scattering of medium-energy electrons
[DE88-003603] 11 p1545 N88-19236

Presentations to the SuperHILAC Program Advisory Committee
[DE88-003653] 11 p1547 N88-19256

Ground-state correlations in C12 and the mechanism of the (e,e'p) reaction
[B8729349] 14 p1980 N88-21816

Nuclear structure studies at intermediate energies
[DE88-006683] 18 p2571 N88-25271

Tagging of gamma yields qq bar events and direct measurement of the gluon structure function at HERA
[NOTA-INTERNA-910] 22 p3151 N88-28745

Nuclear magnetic ordering and paramagnetic relaxation of diatomic molecules in Ca (OH)2
[B8681469] 23 p3281 N88-29532

Fluctuation and relaxation phenomena studied by means of nuclear orientation
[B8679671] 23 p3281 N88-29534

NUCLEAR TEST REACTORS

U NUCLEAR RESEARCH AND TEST REACTORS

NUCLEAR TRANSFORMATIONS

NT TRANSMUTATION

Nuclear transitions induced by atomic excitations
[DE88-004311] 11 p1545 N88-19239

NUCLEAR VULNERABILITY

The strategic defense initiative: Strategic implications
[AD-A192341] 20 p2847 N88-26902

NUCLEAR WARFARE

SDI (Strategic Defense Initiative). Where do we go from here
[AD-A194544] 23 p3275 N88-29497

NUCLEAR WASTES

U RADIOACTIVE WASTES

NUCLEAR WEAPONS

Anechoic Chamber test of the Electromagnetic Measurement System ground test unit
[DE87-012986] 01 p0035 N88-10226

Store separation of nuclear weapons
[DE87-010778] 02 p0124 N88-10785

The effects of corona on current surges induced on conducting lines by EMP: A comparison of experiment data with results of analytic corona models
[DE87-014970] 03 p0305 N88-11924

An excitation-term modification for a certain class of electromagnetic aperture-coupling problems
[DE88-000260] 04 p0437 N88-12713

New approach to telemetry development will significantly increase productivity of Joint Test Assembly (JTA) teams
[DE88-001676] 05 p0554 N88-13373

Announced United States nuclear tests: July 1945 through December 1986
[NVO-209-REV-7] 11 p1546 N88-19247

Characteristics of the positive lighting flash
[DE88-005854] 13 p1800 N88-20760

An agenda for the strategic defense initiative
[RAND-P-7404] 20 p2847 N88-26898

Monitoring space weaponry: Detection and verification issues
[DE88-008726] 20 p2847 N88-26900

SDI and/or arms control
[RAND-P-7357] 20 p2848 N88-26903

Technology security, volume 1
[DE88-008612] 21 p3029 N88-27976

Looking beyond the strategic defense initiative
[AD-A195079] 24 p3427 N88-30394

NUCLEATE BOILING

An experiment to investigate Rankine cycle two-phase microgravity issues
[DE88-004197] 10 p1308 N88-17816

Nucleate pool boiling: High gravity to reduced gravity; liquid metals to cryogens 17 p2431 N88-24484

Heating and evaporation of turbulent liquid films: Measurement of film thickness and the onset of nucleate boiling
[DE88-006388] 18 p2512 N88-24905

Forced-convective boiling in small diameter tube
20 p2783 N88-26510

NUCLEATION

NT CLOUD SEEDING

Abrikosov vortex motion and elementary pinning force in a SNS Josephson junction
[DE87-013607] 01 p0105 N88-10683

Experimental and theoretical study of condensation in multicomponent vapors
[DE87-013663] 02 p0145 N88-10807

Continued research on direct contact heat exchangers: Effects of crystallization
[DE87-014931] 03 p0322 N88-12035

Experimental and theoretical study of condensation in multicomponent mixtures
[DE88-000897] 04 p0413 N88-12907

Microgravity nucleation and particle coagulation experiments support
[NASA-CR-181540] 04 p0423 N88-12818

Microgravity nucleation and particle coagulation experiments support
[NASA-CR-181541] 04 p0423 N88-12819

Plume mechanics and aerosol growth processes
[AD-A184467] 04 p0442 N88-12742

The mechanics of fatigue-crack nucleation in a low-alloy steel under fretting conditions 05 p0587 N88-13849

Undercooling and nucleation in iron nickel alloys
[AD-A185500] 06 p0663 N88-14184

Astrophysics and the solar nebula
07 p0883 N88-15335

Atmospheric science 07 p0883 N88-15357

Ionic mechanisms of soot formation in flames
[AD-A186195] 08 p0966 N88-15948

Kinetics and mechanism of thermal aging embrittlement of duplex stainless steels
[DE88-002987] 08 p0969 N88-15866

TiN coatings on M2 steel produced by plasma assisted chemical vapor deposition
[DE88-003189] 08 p0970 N88-1586

Review of nucleation and incipient boiling under pool and forced convection conditions
08 p0982 N88-15939

Mechanistic model for void distribution in flashing flow
[DE88-002948] 10 p1326 N88-17928

Deactivation of alumina based catalysts
11 p1455 N88-18673

Crystallization and glass formation in electron and laser beam irradiated Cu-Zr alloys
[DE88-003390] 11 p1464 N88-18729

Nucleation and growth of calcium carbonate crystals on surface-modified polyethylene and polystyrene
[DE88-005126] 11 p1465 N88-18733

Cavitation inception
[AD-A189220] 13 p1765 N88-20557

Ductile failure
[AD-A189429] 13 p1781 N88-20654

Stability limits in the monoclinic-tetragonal transformations of zirconia
[DE88-005924] 14 p1986 N88-21849

Nucleation in super-saturated products
[NASA-TT-20275] 15 p2037 N88-22134

Optical monitoring of protein crystal growth
[NASA-CR-182969] 18 p2484 N88-24738

Kinetics of homogeneous nucleation in superheated F-11 and F-21 liquid freons
[NASA-TT-20266] 19 p2613 N88-25580

Studies of metal-silicon, silicon-metal and silicide based interfaces: Synchrotron radiation photo emission and inverse photoemission investigations of interface formation and compound nucleation
[AD-A191808] 19 p2619 N88-25536

Center for thin film studies
[AD-A191996] 19 p2732 N88-25228

Cloud simulation warm cloud experiments: Droplet growth and aerosol scavenging
[AD-A192944] 21 p2974 N88-27980

Atomic layer epitaxy of ZnS and ZnSe
[AD-A192307] 21 p3020 N88-27628

Finite-rate water condensation in combustion-heated wind tunnels
[NASA-TP-2833] 22 p3046 N88-28075

NUCLEI (NUCLEAR PHYSICS)
NT ALPHA PARTICLES
NT DEUTERONS
NT EVEN-EVEN NUCLEI
NT HEAVY NUCLEI
NT HYPERNUCLEI
NT ODD-ODD NUCLEI
NT TRITONS
Experimental nuclear physics
[DE87-014586] 02 p0231 N88-11459
TRISTAN research on neutron rich nuclei: Magnetic moments and nuclear structure
[DE88-002122] 06 p0783 N88-14807
Pion nucleus single charge exchange reactions above the delta(1232) resonance
[LA-11004-T] 11 p1544 N88-19231
Nucleon resonances and nuclei: Experimental aspects
[CEBAF-PR-87-025] 11 p1545 N88-19233
Nucleation in super-saturated products
[NASA-TT-20275] 15 p2037 N88-22134
Search for bound states of the eta-meson in light nuclei 17 p2397 N88-24248
NUCLEIC ACID DENATURATION
U BIOPOLYMER DENATURATION
NUCLEIC ACIDS
NT DEOXYRIBONUCLEIC ACID
NT RIBONUCLEIC ACIDS
Photochemical conversion of nucleic acid components catalyzed by lunar soil 06 p0750 N88-14604
Biopolymers: Protein and nucleic acids
[AD-A185837] 07 p0835 N88-15066
Nucleic acid content of skeletal muscles during hypokinesia and in the recovery period
07 p0894 N88-15418
NUCLEON-NUCLEON INTERACTIONS
An electron-scattering study of N-15
[ETN-88-92479] 16 p2266 N88-23552
Computer program for parameterization of nucleus-nucleus electromagnetic dissociation cross sections
[NASA-TM-4038] 16 p2270 N88-23584
Nuclear structure studies at intermediate energies
[DE88-006683] 18 p2571 N88-25271
Energy measurements in oxygen-induced reactions at 60 A GeV and 200 A GeV
[DE88-006420] 18 p2573 N88-25283
NUCLEONS
Dynamics of coupled electron-nucleon motion in a laser field
[DE88-005063] 10 p1337 N88-17994
Nucleon resonances and nuclei: Experimental aspects
[CEBAF-PR-87-025] 11 p1545 N88-19233
Single nucleon coincidence cross sections in a relativistic mean field theory
[CEBAF-PR-87-016] 11 p1546 N88-19243
Theoretical studies in few-body intermediate energy physics
[DE88-004101] 12 p1689 N88-20106
On (e,e'N) reactions
[CEBAF-PR-87-028] 12 p1690 N88-20109
Production of pi(0) mesons and charged hadrons in nu bar neon and nu neon charges current interactions
[MPI-PAE/EXP EL 188] 22 p3150 N88-28743
NUCLEOSIDES
Precise ultraviolet absorbance study of the interaction of amino acids and mononucleosides in aqueous solution
[ISAS-RN-356] 21 p2908 N88-27256
NUCLEOSYNTHESIS
U NUCLEAR FUSION
NUCLEOTIDES
NT ADENOSINE TRIPHOSPHATE
NT ADENOSINES
Fed-batch control based upon the measurement of intracellular NADH 09 p1197 N88-17175
Fast atom bombardment study on interaction of anticodonic nucleotides and their cognate amino acid
[ISAS-RN-355] 20 p2850 N88-26918
NUCLIDES
NT ARGON ISOTOPES
NT BORON ISOTOPES
NT BROMINE ISOTOPES
NT CALCIUM ISOTOPES
NT CARBON 12
NT CARBON 13
NT COBALT 60
NT DEUTERIUM
NT HELIUM ISOTOPES
NT HYDROGEN ISOTOPES
NT IODINE ISOTOPES
NT IRIDIUM ISOTOPES
NT IRON ISOTOPES
NT IRON 57
NT ISOTOPES
NT KRYPTON ISOTOPES
NT LAWRENCIUM
NT LEAD ISOTOPES
NT LITHIUM ISOTOPES
NT MERCURY ISOTOPES
NT NEODYMIUM ISOTOPES
NT NEPTUNIUM
NT NIOBIUM ISOTOPES
NT NITROGEN ISOTOPES
NT OXYGEN ISOTOPES
NT PLATINUM ISOTOPES
NT PLUTONIUM ISOTOPES
NT PLUTONIUM 238
NT RADIOACTIVE ISOTOPES
NT RADON ISOTOPES
NT RUBIDIUM ISOTOPES
NT TELLURIUM
NT TRITIUM
NT URANIUM ISOTOPES
NT URANIUM 238
Calculation methods of atomic number density for various nuclear materials
[DE87-753006] 02 p0233 N88-11467
NULL ZONES
Null steering applications of polynomials with unimodular coefficients
[AD-A191087] 18 p2562 N88-25211
Polynomials with restricted coefficients and their applications
[AD-A192589] 23 p3202 N88-29055
NUMBER THEORY
NT ARITHMETIC
NT DIVIDING (MATHEMATICS)
NT EXPONENTS
NT FLOATING POINT ARITHMETIC
NT INDUCTION (MATHEMATICS)
NT INTEGERS
NT MULTIPLICATION
The design of ultra high-speed numeric intensive systems (having fault tolerant and load balancing capabilities) 10 p1374 N88-18196
On a classification of problems on sets of bilinear forms by formal polynomials
[RR-642-I-IMAG-53-LIFIA] 17 p2392 N88-24219
Some properties of modular equations and the partition function 18 p2564 N88-25224
NUMERICAL ANALYSIS
NT APPROXIMATION
NT BORN APPROXIMATION
NT BORN-OPPENHEIMER APPROXIMATION
NT BOUNDARY INTEGRAL METHOD
NT CHEBYSHEV APPROXIMATION
NT COMPUTATIONAL CHEMISTRY
NT COMPUTATIONAL FLUID DYNAMICS
NT CONJUGATE GRADIENT METHOD
NT DIFFERENCE EQUATIONS
NT ERROR ANALYSIS
NT FINITE DIFFERENCE THEORY
NT FINITE ELEMENT METHOD
NT FINITE VOLUME METHOD
NT FLUX VECTOR SPLITTING
NT HARTREE APPROXIMATION
NT INTERPOLATION
NT ITERATION
NT ITERATIVE SOLUTION
NT LEAST SQUARES METHOD
NT MEAN SQUARE VALUES
NT MONTE CARLO METHOD
NT NEWTON METHODS
NT NEWTON-RAPHSON METHOD
NT NUMERICAL INTEGRATION
NT PADE APPROXIMATION
NT PARTICLE IN CELL TECHNIQUE
NT RAYLEIGH-RITZ METHOD
NT RELAXATION METHOD (MATHEMATICS)
NT RITZ AVERAGING METHOD
NT RUNGE-KUTTA METHOD
NT TRUNCATION ERRORS
Laser probes of natural gas ignition chemistry
[PB87-209599] 01 p0021 N88-10129
Transactions of the 4th Army Conference on Applied Mathematics and Computing
[AD-A183544] 01 p0085 N88-10547
Finite difference solution of a generic differential equation
[PB87-205878] 01 p0087 N88-10568
Fundamentals of numerical magnetohydrodynamics
[DE87-011789] 01 p0100 N88-10656
A numerical study of transient, thermally-conductive solar wind 01 p0115 N88-10738
Numerical simulation of a supersonic chemically reacting mixing layer 02 p0143 N88-10900
Impact of turbulence modeling on numerical accuracy and efficiency of compressible flow simulations
[NASA-TM-88333] 02 p0173 N88-11068
A numerical method for the treatment of kinked cracks in finite bodies 02 p0190 N88-11189
Numerical simulation of Tokamaks: Ideal MHD equilibrium and stability
[DE87-013452] 02 p0218 N88-11373
The spatially nonuniform convergence of the numerical solution of flows
[NASA-TM-100037] 02 p0226 N88-11429
Analytic investigation of helicopter rotor blade appended aeroelastic devices
[NASA-CR-166525] 03 p0266 N88-11676
Electromagnetic scattering by a thick strip on a half-space
[PB87-227096] 03 p0306 N88-11928
Performance evaluation of a half-wave resonant slot antenna over perfect ground using NEC (Numerical Electromagnetic Code)
[AD-A184004] 03 p0308 N88-11942
Computation of turbulent flows using an extended k-epsilon turbulence closure model
[NASA-CR-179204] 03 p0312 N88-11969
Momentum transport and particle dynamics in turbulent shear flows 03 p0317 N88-12002
Numerical study of the entrance flow and its transition in a circular pipe (2) 03 p0318 N88-12011
Numerical analysis of Marangoni convection in Bridgman method 03 p0319 N88-12014
Numerical simulation and visualization of a flowfield by interaction of two parallel two-dimensional freejets
03 p0320 N88-12021
On the root locus method applied to flexural vibration control systems 03 p0320 N88-12022
The dynamics of bubble growth for Rayleigh-Taylor unstable interfaces
[AD-A184752] 03 p0321 N88-12027
Some aspects of high resolution numerical methods for hyperbolic systems of conservation laws, with applications to gas dynamics
[DMS-86-7] 03 p0321 N88-12031
Adaptation of numerical SPOT data to an urban environment 03 p0342 N88-12158
Numerical solution of partial differential equations on irregular grids
[DE87-014760] 03 p0369 N88-12324
The development of ODE methods: A symbiosis between hardware and numerical analysis
[DE87-014925] 03 p0370 N88-12325
Institute for Computational Mechanics in Propulsion (ICOMP) first year summary
[NASA-TM-100225] 03 p0370 N88-12330
Numerical experiments with a symmetric high-resolution shock-capturing scheme
[NASA-TM-88325] 03 p0370 N88-12332
Numerical solution of bound constrained problems
[DE88-000653] 03 p0371 N88-12334
Concepts for radically increasing the numerical convergence rate of the Euler equations
[NASA-CR-177456] 04 p0395 N88-12463
Natural control of flexible space structures
04 p0408 N88-12534
An analytical and experimental study of injection-locked two-port oscillators
[NASA-TM-100119] 04 p0439 N88-12727
Numerical simulation of unsteady separated flows
[AD-A184132] 04 p0442 N88-12741
Methods for design and evaluation of integrated hardware/software systems for concurrent computation
[NASA-CR-181522] 04 p0479 N88-12953
Flux tube dynamics and solar/stellar redshift measurements 04 p0503 N88-13095
Numerical analysis of flow through scramjet engine inlets 05 p0532 N88-13233
Eigenvalue projection theory for linear operator equations of electromagnetics
[AD-A185434] 05 p0575 N88-13504
Numerical analysis, computing and fundamental studies in fluid mechanics
[DE88-001912] 05 p0582 N88-13550
The numerical and analytic of implicit differential equations and their application to control and circuit problems
[AD-A185404] 05 p0641 N88-13922
Numerical methods for reaction-diffusion problems with non-differentiable kinetics
[AD-A185405] 05 p0641 N88-13923
Numerical simulation of boundary layers. Part 3: Turbulence and relaminarization in sink flows
[NASA-TM-88220] 06 p0698 N88-14283
Theoretical and numerical analysis of shock wave propagation through different dusty-gas mixture layers
06 p0699 N88-14292
Development of symbolic computation methods for nonlinear dynamics
[AD-A185562] 06 p0758 N88-14653
Local and global techniques for the tracking of periodic solutions of parameter-dependent functional differential equations
[AD-A185756] 06 p0766 N88-14704

Characteristic trajectories of generalized Lanchester equations
[AD-A185762] 06 p0766 N88-14705

Analytical investigations of bulk wave resonators in the piezoelectric thin film on gallium-arsenide configuration
[AD-A185716] 06 p0789 N88-14840

Numerical simulation of a controlled boundary layer
07 p0810 N88-14933

Boundary layer transition 07 p0811 N88-14942

Packet error probabilities in frequency-hopped spread spectrum packet radio networks. Markov frequency hopping patterns considered
[AD-A186071] 07 p0841 N88-15104

User manual for ATILA, a finite-element code for modeling piezoelectric transducers
[AD-A185948] 07 p0847 N88-15141

On the parabolized Navier-Stokes equations without sublayer assumptions
[AD-A186127] 07 p0849 N88-15152

Numerical calculation of appendage, flat plate junction flow
[AD-A186371] 07 p0850 N88-15158

Numerical solution of turbulent flow past a backward facing step using a nonlinear K-epsilon model
[NASA-CR-178421] 07 p0854 N88-15189

Numerical methods for fluid flow problems
[DE88-000156] 07 p0854 N88-15190

Transient welding strain measurement by Moire technique: A comparison between experimental measurement and numerical analysis for strain-stress cycles during GTA spot-welding
[PB87-143871] 07 p0866 N88-15269

Bending analysis of thin plates with openings
[PB87-143400] 07 p0869 N88-15274

Recent developments in the numerical solution of differential/algebraic systems
[DE88-001885] 07 p0912 N88-15535

A numerical study of transient heat and mass transfer in crystal growth 07 p0925 N88-15619

Simple model for hot ion plasmas
[DE88-750045] 07 p0936 N88-15686

Acta Aerodynamica Sinica (selected articles)
[AD-A185723] 08 p0949 N88-15757

A multistage mesh generator for solving the average-passage equation system
[NASA-CR-179539] 08 p0951 N88-15769

Numerical solution methods for viscoelastic orthotropic materials
[NASA-CR-182381] 08 p0971 N88-1

The single particle and collective descriptions of [illegible] anomalous Doppler resonance and the role of ion dynamics
[INPE-4390-PRE/1210] 08 p0976 N88-15904

Scanning finite element calculation method
[PB87-143442] 08 p0995 N88-16017

Mixed method of finite strip and finite element
[PB87-143467] 08 p0996 N88-16027

Integral equation method for the analysis of plates and shells
[PB87-144788] 08 p0996 N88-16030

A study of finite difference and finite element vertical discretization schemes for baroclinic prediction equations
[AD-A186617] 08 p1040 N88-16291

Research in progress at the Institute for Computer Applications in Science and Engineering
[NASA-CR-181607] 08 p1053 N88-16354

Matrix functions in the stability of higher-order numerical schemes
[INPE-4246-PRE/1119] 08 p1073 N88-16472

FOR3D: A computer model for solving the LSS (Lee-Saad-Schultz) three-dimensional, wide angle wave equation
[AD-A186649] 08 p1080 N88-16511

Comprehensive rotorcraft analysis methods
09 p1106 N88-16630

Computational analysis of propagation properties of integrated-optical waveguides using a domain integral equation
[PB87-163358] 09 p1154 N88-16917

Numerical simulation of heat transfer turbulence, volume 4
[AD-A185132] 09 p1159 N88-16947

Steady ship waves at low Froude numbers, part 2
[AD-A176805] 09 p1160 N88-16953

A guide to the transient three phase porous flow model implemented in the two-dimensional CRAY-TENSOR code: Physics, numerics, and code description
[DE88-003709] 09 p1165 N88-16983

Numerical solutions of three-dimensional Navier-Stokes equations for closed-bluff bodies
[NASA-CR-182359] 09 p1166 N88-16990

Numerical investigation of orographically enhanced instability
[AD-A186841] 09 p1189 N88-17125

Numerical simulation of axisymmetric turbulent flow in combustors and diffusors
[NASA-CR-4115] 10 p1268 N88-17582

A finite element analysis of adhesively bonded composite joints including geometric nonlinearity, nonlinear viscoelasticity moisture diffusion and delayed failure
[AD-A187455] 10 p1296 N88-17747

Flame propagation in the approximation of straight-line trajectories of burning products
[DE88-700675] 10 p1297 N88-17756

A numerical study of unsteady two-dimensional subsonic compressible base flow 10 p1327 N88-17931

The numerical and analytical study of bifurcation and multicellular flow instability due to natural convection between narrow horizontal isothermal cylindrical annuli at high Rayleigh numbers 10 p1328 N88-17937

Instability and transition in curved channel flow
10 p1328 N88-17938

Periodic natural convection in a rectangular enclosure of low aspect ratio 10 p1329 N88-17941

Recent progress in the p and h-p version on the finite element method
[AD-A187254] 10 p1400 N88-18347

Eigenvalue problems
[AD-A188069] 10 p1401 N88-18356

Coronal - heating by means of helical magnetohydrodynamic turbulence
[AD-A187084] 10 p1410 N88-18413

An experimental investigation of straight and curved annular wall jets
[NASA-CR-182546] 11 p1434 N88-18557

Analysis of shear-layer probe data for holes in hypersonic configurations
[DE88-003992] 11 p1435 N88-18564

Backscattering from three dimensional conducting bodies
[AD-A187570] 11 p1470 N88-18768

Analytical and numerical analysis of finite amplitude Rayleigh-Taylor instability
[DE88-004056] 11 p1474 N88-18797

Two and three dimensional elliptic flows
11 p1485 N88-18866

A posteriori error estimates in computational fluid mechanics 11 p1486 N88-18869

Transient radiative energy transfer in incompressible laminar flows
[NASA-CR-182605] 11 p1488 N88-18883

Multisource context classification methods in remote sensing 11 p1504 N88-18985

Cumulative reports and publications through December 31, 1987
[NASA-CR-181624] 11 p1524 N88-19099

Compact high order schemes for the Euler equations
[NASA-CR-181625] 11 p1530 N88-19138

Generation of surface grids through elliptic partial differential equations for aircraft and missile configurations
[AD-A186631] 11 p1535 N88-19169

Simulation of the plasma interaction with thin dust clouds 11 p1552 N88-19291

Numerical analysis, computing and fundamental studies in fluid mechanics
[DE88-005343] 12 p1625 N88-19725

Compressible friction coefficients in a simulated heat pipe
[AD-A188618] 12 p1627 N88-19735

Reynold stress closure in jet flows using wave models
[NASA-CR-182662] 12 p1628 N88-19741

Sub-scaling of projectile/target system damaged by hypervelocity
[AD-A188683] 12 p1634 N88-19779

A numerical study of automated dynamic relaxation for nonlinear static tensioned structures
[AD-A188372] 12 p1635 N88-19790

Numerical simulation of near-surface environments and particulate clouds generated by large-area fires
[AD-A188375] 12 p1641 N88-19828

Geophysical study of the structure and processes of the continental convergence zones: Alpine-Himalayan Belt
[NASA-CR-182647] 12 p1644 N88-19842

Gradiometer mission spectral analysis and simulation studies: Past and future 12 p1645 N88-19851

A numerical analysis of the dynamics of PRIZ operation
[AD-A188853] 12 p1678 N88-20035

Object-oriented design in numerical linear algebra
[AD-A189427] 12 p1685 N88-20073

Three-dimensional scattering of impulsive acoustic waves by a semi-infinite crack in the plane interface of a half space and a layer
[PB88-146996] 12 p1687 N88-20089

Numerical simulation of subsonic and transonic propeller flow
[NASA-TM-100163] 13 p1716 N88-20262

Detection and angle estimation of coherent plane waves 13 p1759 N88-20522

Numerical methods in the resolution of control electrovalve model
[INPE-4154-RPE/540] 13 p1764 N88-20554

Control of structure in turbulent flows: Bifurcating and blooming jets
[AD-A189607] 13 p1766 N88-20562

Center for Turbulence Research 1987 activities
[NASA-CR-182693] 13 p1769 N88-20563

Numerical experiments on the stability of controlled boundary layers
[NASA-CR-181649] 13 p1771 N88-20591

Structural clearances and internal friction: Simulation by Eigen distortions
[ISSN-0208-5658] 13 p1779 N88-20640

Dynamical modeling of marine boundary layer convection 13 p1797 N88-20750

Multiple scattering of polarized light in cirrus clouds
13 p1801 N88-20768

Computer aided surface representation
[DE88-005408] 13 p1817 N88-20854

Numerical solution of ill posed problems in partial differential equations
[AD-A189383] 13 p1825 N88-20909

Elimination of quantifiers of linear variables and corresponding transfer principles
[DE88-005692] 13 p1826 N88-20912

Numerical simulations of multiphoton processes in many electron atoms
[DE88-003293] 13 p1837 N88-20990

Silicon-germanium heterostructures
13 p1844 N88-21034

Numerical analysis of three-dimensional viscous internal flows
[NASA-TM-100878] 14 p1861 N88-21116

Numerical solution of multibody systems in space applications 14 p1875 N88-21200

Practical considerations for structural control: System uncertainty, system time delay and truncation of small control forces
[PB88-163738] 14 p1933 N88-21528

Estimation of geopotential from satellite-to-satellite range rate data: Numerical results
[NASA-CR-180771] 14 p1941 N88-21583

Numerical orbit propagation methods for earth artifical satellites
[INPE-4405-RPE/556] 15 p2023 N88-22053

Nonlinear analysis and optimal design of dynamic mechanical systems for spacecraft application
[AD-A190644] 15 p2026 N88-22070

Numerical simulation of turbulent flames using vortex methods
[AD-A189813] 15 p2034 N88-22116

Mode 2 fracture mechanics 15 p2083 N88-22418

Numerical solution of nonlinear algebraic equations in stiff ODE solving
[DE88-006634] 15 p2118 N88-22622

Numerical methods for singularly perturbed differential equations with applications
[AD-A189786] 15 p2119 N88-22628

New methods for numerical solution of one class of strongly nonlinear partial differential equations with applications
[AD-A189945] 15 p2119 N88-22630

Numerical methods for linear and nonlinear optimization
[AD-A190029] 15 p2120 N88-22631

Expressing mathematical subroutines constructively
[AD-A190559] 15 p2121 N88-22644

Numerical study of unsteady viscous hypersonic blunt body flows with an impinging shock
[NASA-TM-100096] 15 p2122 N88-22650

Approximation methods for the identification and control of distributed parameter systems
[AD-A190201] 15 p2124 N88-22662

Design method for laminar flow control of two-dimensional airfoils in incompressible flow. Numerical study of LFC design concepts
[DE88-751609] 16 p2155 N88-22859

Thermoviscoelastic characterization and predictions of Kevlar/epoxy composite laminates
[NASA-CR-182678] 16 p2172 N88-22946

Theoretical and numerical solution of the forward-scattering problem in a circularly cylindrical configuration
[PB88-173489] 16 p2189 N88-23056

A computer model investigation of a half square log-periodic array
[AD-A190955] 16 p2190 N88-23062

Calculation of displacement, constraints and eigenmodes of rotating blades
[ETN-88-92296] 16 p2224 N88-23277

Numerical simulation of coastal upwelling phenomena in Cabo Frio (RJ) through a two layer finite element model
[INPE-4502-RPE/561] 16 p2237 N88-23361
Supercomputer programming environments
[AD-A190887] 16 p2251 N88-23452
Research in nonlinear partial differential equations and bifurcation theory
[AD-A190986] 16 p2260 N88-23514
Analysis for fuel implosion in ICF target and pellet gain 16 p2276 N88-23620
Numerical analysis for effects of irradiation nonuniformities on target implosion
16 p2276 N88-23621
Numerical analysis of target implosion in LIB ICF
16 p2277 N88-23628
Unsteady flow about cambered plates
[AD-A191226] 17 p2337 N88-23945
Activities of the Institute for Computer Applications in Science and Engineering (ICASE)
[NASA-CR-181666] 17 p2384 N88-24166
Scientific computing environments
[AD-A191239] 17 p2385 N88-24175
Consistent transport coefficients in astrophysics
[NASA-TM-101154] 17 p2451 N88-24560
Dynamics of a flexible orbiting platform with MRMS
[ISSN-0285-6808] 18 p2473 N88-24673
Internal fluid dynamics within a nonspinning partially liquid-filled shell due to burster rupture
[AD-A191055] 18 p2507 N88-24874
SOLA-DM: A numerical solution algorithm for transient three-dimensional flows
[DE88-007159] 18 p2514 N88-24913
NAS: The first year
[NASA-TM-101006] 18 p2560 N88-25196
Mathematical models for VLSI device simulation
[AD-A191125] 18 p2562 N88-25212
Computational sciences
[AD-A190826] 18 p2564 N88-25226
Numerical solution of a system of random Volterra integral equations. 1: Successive approximation method
18 p2564 N88-25227
Numerical solutions to stochastic difference equations
18 p2564 N88-25229
Numerical solution to a system of random Volterra integral equations 18 p2565 N88-25230
A method for the numerical solution of random Cauchy singular integral equation 18 p2565 N88-25234
Numerical solution of random Love's integral equation
18 p2565 N88-25235
High degree interpolation polynomial in Newton form
[NASA-CR-181677] 18 p2567 N88-25249
The 2-D magnetohydrostatic configurations leading to flares or quiescent filament eruptions
[NASA-TM-101147] 18 p2595 N88-25423
Improved numerical methods for turbulent viscous recirculating flows
[NASA-CR-180852] 19 p2599 N88-25445
Comparison of calculated and measured ignition times for boron agglomerates 19 p2624 N88-25563
Proceedings of the 5th NAL Symposium on Aircraft Computational Aerodynamics
[NAL-SP-8] 19 p2635 N88-25630
Numerical simulations of aerodynamic contribution of flows about a space-plane-type configuration
19 p2635 N88-25632
Numerical simulations of astrophysical jets
19 p2636 N88-25635
A numerical analysis of flow characteristics in laser propulsion system 19 p2637 N88-25645
Numerical calculation of three dimensional flow by TVD scheme 19 p2638 N88-25649
Numerical analysis of three dimensional cascade flow by solving Navier-Stokes equations
19 p2638 N88-25650
Numerical analysis of duct flow using three-dimensional parabolized Navier-Stokes equation
19 p2638 N88-25652
Picosecond response of an optically controlled millimeter wave phase shifter 19 p2660 N88-25820
Study of the structure of turbulence in accelerating transitional boundary layers
[AD-A191686] 19 p2663 N88-25837
A Navier-Stokes solver for cascade flows
[NASA-CR-181682] 19 p2666 N88-25856
Static analysis of thin plates using the finite strip-element method 19 p2679 N88-25931
Changes in seismic velocity and apparent attenuation due to isotropic and anisotropic scattering: Results from physical modeling 19 p2691 N88-25997
Scaling laws for geomagnetic tail current sheet acceleration
[AD-A193379] 19 p2691 N88-25998
Solution of Faddeev-Yakubovsky differential equations by the finite-dimensional approximation method for four spinless particles in the 1+3 scattering problem
[DE87-702983] 19 p2719 N88-26145
Analysis of gas turbine test cell number 1, Lemoore Naval Air Station, California
[AD-A192870] 20 p2762 N88-26380
Numerical analysis of reconnection of vortex rings
20 p2782 N88-26500
Numerical solution of weak forms of conservation laws on optimal unstructured triangular grids
20 p2797 N88-26597
Navier-Stokes simulation of shock-tube flows over a wedge-type step by finite volume method
[ISAS-RN-628] 20 p2797 N88-26599
A numerical simulation of two-dimensional transient shear flow
[ISAS-RN-627] 20 p2797 N88-26600
Off-boundary approach to the boundary element method
[AD-A192931] 20 p2815 N88-26701
Numerical model for the computation of radiance distributions in natural waters with wind-roughened surfaces
[PB88-192703] 20 p2826 N88-26765
Prediction of continental shelf sediment transport using a theoretical model of the wave-current boundary layer
[AD-A192272] 20 p2829 N88-26783
Superconductivity of Cr/V superlattices
20 p2874 N88-27057
A computational analysis of under-expanded jets in the hypersonic regime
[NASA-TM-101319] 21 p2893 N88-27174
Evaluation and improvement of liquid propellant rocket chugging analysis techniques. Part 1: A one-dimensional analysis of low frequency combustion instability in the fuel preburner of the space shuttle main engine
[NASA-CR-183106] 21 p2903 N88-27224
The structure and stability of nonpremixed gas jet flames 21 p2908 N88-27257
Analytical approximation of a distorted reflector surface defined by a discrete set of points
[NASA-TM-101323] 21 p2934 N88-27424
Numerical simulation of fuel droplet interactions and breakup
[AD-A192431] 21 p2941 N88-27470
Numerical experiments on turbulent mixing
[AD-A192572] 21 p2942 N88-27473
Effects of numerical dissipation on finite-volume solutions of compressible flow problems
[AD-A193173] 21 p2944 N88-27485
Numerical treatment of the pressure singularity at a re-entrant corner
[AD-A193357] 21 p2944 N88-27486
Numerical methods for incompressible viscous flows with engineering applications
[NASA-CR-183143] 21 p2948 N88-27506
Three-dimensional aspects of fatigue crack closure
[AD-A192296] 21 p2960 N88-27581
A zoomable and adaptable hidden fine-mesh approach to solving advection-dispersion equations
[DE88-006174] 21 p3004 N88-27816
Research in applied mathematics
[AD-A192385] 21 p3004 N88-27820
A numerical treatment of the fluid/elastic interface under range-dependent environments
[AD-A192478] 21 p3005 N88-27821
Numerical optimization
[AD-A193032] 21 p3005 N88-27827
On the estimation of a variance ratio
[AD-A193190] 21 p3009 N88-27854
VSAERO analysis of tip planforms for the free-tip rotor
[NASA-CR-177487] 22 p3038 N88-28036
Theoretical study and numerical simulation of flame fronts
[PB88-122932] 22 p3051 N88-28104
Time domain wave propagation in multilayered integrated circuits
[AD-A193821] 22 p3073 N88-28241
Observational/numerical study of the upper ocean response to hurricanes
[AD-A193592] 22 p3128 N88-28598
A method for determining absolute velocities from hydrographic data: The numerical code
[AD-A193997] 22 p3129 N88-28603
A fast algorithm for the numerical evaluation of conformal mappings
[AD-A193903] 22 p3138 N88-28658
Ill-posed problems and integral equations
[AD-A193709] 22 p3143 N88-28691
A numerical study of the test time in a hypersonic shock tunnel
[AD-A194057] 23 p3172 N88-28868
Random-access algorithms for environments with capture
[AD-A194303] 23 p3203 N88-29060
Stability and drag reduction in a boundary layer with microbubbles
[AD-A191975] 23 p3209 N88-29099
Steady and unsteady internal flow computations via the solution of the compressible Navier Stokes equations for low Mach numbers 23 p3209 N88-29100
Computational fluid dynamics methods for low Reynolds number precessing/spinning incompressible flows
[AD-A193891] 23 p3212 N88-29119
Thickness effects on the stability of shell like structures 23 p3224 N88-29192
Wigner distribution function: Relation to short-term spectral estimation, smoothing and performance in noise
[AD-A193865] 23 p3275 N88-29492
Numerical simulations of resistive magnetohydrodynamic instabilities in a poloidal divertor tokamak
[DE88-010766] 23 p3285 N88-29559
Numerical solutions of unsteady inviscid transonic turbine cascade flows
[AD-A196111] 24 p3316 N88-29748
Space marching Euler solvers
24 p3318 N88-29759
Simulation of Vulcain engine operation at low inlet pressure
[ETN-88-93083] 24 p3339 N88-29875
Analysis of the flow through double swirl airblast atomizers 24 p3351 N88-29949
Numerical field model simulation of full scale fire tests in a closed spherical/cylindrical vessel
[AD-A195067] 24 p3359 N88-29998
Transition at hypersonic speeds
[NASA-CR-178315] 24 p3368 N88-30058
Transition mixing study empirical model report
[NASA-CR-182139] 24 p3371 N88-30076
Numerical simulation of the function of scientific instrumentation for measuring the speed of electron devices
[AD-A194969] 24 p3376 N88-30103
A detection theory analysis of visual display performance
[AD-A196291] 24 p3409 N88-30292
Nonequilibrium flow computations. 1: An analysis of numerical formulations of conservation laws
[NASA-CR-177489] 24 p3425 N88-30384
Regularity and numerical solution of eigenvalue problems with piecewise analytic data
[AD-A194993] 24 p3425 N88-30387
Orbital evolution of distant artificial earth satellites
24 p3445 N88-30506
The atmospheres of the earth and the other planets: Origin, evolution and composition
24 p3452 N88-30544
Study of modern instrumentation and methods for astronomic positioning in the field
[AD-A196173] 24 p3452 N88-30548
Numerical evidence that the motion of Pluto is chaotic
[AD-A195920] 24 p3455 N88-30568

NUMERICAL CONTROL
Telerobotics 01 p0015 N88-10090
Microcomputer control of a hydraulically actuated piston
[AD-A184130] 03 p0368 N88-12317
Digital control of a direct current converter for a hybrid vehicle
[LAAS-87-266] 05 p0578 N88-13527
The numerical and analytic of implicit differential equations and their application to control and circuit problems
[AD-A185404] 05 p0641 N88-13922
Selected aspects of microelectronics technology and applications: Numerically controlled machine tools. Technology trends series no. 2
[PB87-132973] 06 p0696 N88-14268
Microcomputer controlled arc welding power source: Its steady state and transient performance
[PB87-143921] 07 p0863 N88-15233
Reserach on microprocessor controller for spot welding
[PB87-143913] 07 p0863 N88-15240
Intelligent controllers
[DE88-001862] 07 p0904 N88-15475
Regulation of nonlinear and generalized linear systems
[AD-A186706] 09 p1224 N88-17336
Instrumentation and quantitative methods of evaluation
[DE87-013639] 10 p1342 N88-18017
Automatic riveting machine for spherically-formed airframe structures
[ETN-88-91024] 11 p1495 N88-18924
Control test and validation for a large diameter high stability centrifuge 12 p1577 N88-19437
Intelligent control of robot manipulators in hazardous environments
[DE88-003305] 13 p1778 N88-20638

A novel method for sputter-deposition of high T(sub c) superconductor films via a computer-controlled mass analyzed ion beam
[DE88-006001] 13 p1848 N88-21064
On the use of nonstaggered pressure-velocity arrangement for the numerical solution of incompressible flows
[KU-SFB-210/T/35] 16 p2206 N88-23165
A timing evaluator for C programs generated by the model system
[AD-A191204] 17 p2385 N88-24174
A universal computer control system for motors
[NASA-CASE-NPO-17134-1-CU]
18 p2506 N88-24864
Design and testing of a luminance and chrominance stabilization system for a computer-controlled color display
[AD-A191922] 18 p2554 N88-25159
Ultrasonic and video computerized data acquisition for automated welding
[DE88-006741] 19 p2677 N88-25918
Compliant robotic structures, part 3
[AD-A192426] 21 p2955 N88-27556
IEMIS (Integrated Emergency Management Information System) floodplain mapping based on a LIDAR derived data set
[AD-A193071] 21 p2966 N88-27616

NUMERICAL DATA BASES
Stochastic estimation of conditional eddies in turbulent channel flow 16 p2194 N88-23087
Theory of numerical information environment and its applications 19 p2640 N88-25686
Effective buffering schemes for performing matrix operations for numerical databases
21 p3027 N88-27968

NUMERICAL FLOW VISUALIZATION
Efficient implementation of essentially non-oscillatory shock capturing schemes, 2
[NASA-CR-181656] 17 p2392 N88-24217

NUMERICAL INTEGRATION
NT RUNGE-KUTTA METHOD
Stochastic integration for operator valued processes on Hilbert spaces and on nuclear spaces
[ENST-87D002] 01 p0089 N88-10580
Preliminary results from real data experiments with the NRL mesoscale numerical model
02 p0211 N88-11323
Propagation of random initial conditions in time
04 p0486 N88-12993
VHF/UHF propagation by diffraction: Calculation by numerical integration 12 p1615 N88-19659
Vibration protection of inelastic structures by means of active and passive control 18 p2528 N88-25001
Analysis of gas turbine test cell number 1, Lemoore Naval Air Station, California
[AD-A192870] 20 p2762 N88-26380
Numerical integration of Navier-Stokes equations by application of multigrid concept
[ETN-88-92365] 21 p2940 N88-27513
Multiple integration with respect to Poisson and Levy processes
[AD-A192895] 21 p3009 N88-27851
Approximate and numerical methods in acousto-optics. Part 1: Normal incidence of the light
[AD-A194294] 22 p3152 N88-28755
An improvement in the numerical integration procedure used in the NASA Marshall engineering thermosphere model
[NASA-CR-179389] 24 p3392 N88-30200

NUMERICAL STABILITY
Numerical and analytical methods in nonlinear partial differential equations
[AD-A185210] 05 p0641 N88-13918
The numerical and analytical study of bifurcation and multicellular flow instability due to natural convection between narrow horizontal isothermal cylindrical annuli at high Rayleigh numbers
[AD-A186113] 07 p0849 N88-15151
Some stability results for the hopscotch difference method when applied to convection-diffusion equations
[CWI-NM-R8711] 08 p1072 N88-16465
Improving the stability of predictor-corrector methods by residue smoothing
[CWI-NM-R8707] 09 p1226 N88-17359
Stability results for theta methods applied to a class of stiff differential-algebraic equations
[CWI-NM-R8708] 09 p1226 N88-17360
Boundary layer calculation using digital computers
[REPT-MM-4] 10 p1309 N88-17821
Transport and stability properties of free shear flows
13 p1768 N88-20577
Stabilization of explicit difference schemes by smoothing techniques
[CWI-NM-R8714] 13 p1827 N88-20923
Nonlinear differential equations
[DE88-006047] 13 p1828 N88-20933
Boundary stabilization of the reaction-diffusion equation with unilateral conditions
[RR-315] 14 p1964 N88-21720
Global spatial periodic solutions to the Ginzburg-Landau equations
[DE88-006424] 15 p2119 N88-22623
Continuity of symmetric stable processes
[AD-A190324] 15 p2125 N88-22667
Stability and convergence of the Peaceman-Rachford ADI method for initial-boundary value problems
[CWI-NM-R8724] 18 p2566 N88-25243
New mixed finite element methods
18 p2567 N88-25248
QN3D: A 3-dimensional quasi-neutral hybrid particle-in-cell code with applications to the tilt mode instability in field reversed configurations
18 p2580 N88-25325
Semi-discrete approximations to nonlinear systems of conservation laws; consistency and L(infinity)-stability imply convergence
[NASA-CR-181683] 19 p2721 N88-26157
Semilinear elliptic problems on domains with corners
[REPT-87-83] 20 p2846 N88-26888
Two classes of self-similar stable processes with stationary increments
[AD-A192842] 20 p2846 N88-26894
A study on Lebesgue decomposition of measures induced by stable processes
[AD-A192693] 21 p3009 N88-27850
Method to predict external store carriage characteristics at transonic speeds
[NASA-CR-4170] 22 p3037 N88-28034
Stability and convergence in the numerical solution of stiff initial value problems
[B8861460] 23 p3272 N88-29474
On stable Markov processes
[AD-A192892] 23 p3273 N88-29482
Stability, stochastic stationarity and generalized Lyapunov equations for two-point boundary-value descriptor systems
[AD-A195645] 24 p3425 N88-30385

NUMERICAL WEATHER FORECASTING
Mesoscale Analysis and Forecasting: Incorporating Nowcasting
[ESA-SP-282] 02 p0199 N88-11239
Use of simulated satellite radiances from a mesoscale numerical model to understand kinematic and dynamic processes 02 p0202 N88-11261
An hourly analysis, updating and short-range forecasting system --- numerical weather forecasting
02 p0206 N88-11286
Statistical remote sensing algorithm development: A complementary process to mesoscale numerical models
02 p0206 N88-11292
The application of divergence equation in the analysis of heavy rainfall 02 p0207 N88-11299
Forecasting boundary layer clouds and fog: A review of operational numerical models
02 p0208 N88-11307
Operational practice of an air mass transformation model 02 p0208 N88-11308
Two-dimensional numerical modeling of the life cycle of fog 02 p0209 N88-11311
Evaluation of a mesoscale prediction system with surface weather observations and comparison with a large-scale prediction system 02 p0210 N88-11319
The Norwegian mesoscale Numerical Weather Prediction (NWP) system 02 p0210 N88-11320
Forecasting polar lows using a numerical mesoscale model 02 p0210 N88-11321
Development and testing of a vertically-nested regional prediction system --- weather forecasting
02 p0210 N88-11322
Preliminary results from real data experiments with the NRL mesoscale numerical model
02 p0211 N88-11323
Short range forecasting of sea breeze generated thunderstorms at the Kennedy Space Center: A real-time experiment using a primitive equation mesoscale numerical model 02 p0211 N88-11324
Validation of a three dimensional numerical model of the sea breeze in complex terrain
02 p0211 N88-11325
The mesoscale numerical model for heavy rainfall forecasting in Yangtze River Valley, China
02 p0211 N88-11326
The impact on short-term precipitation forecast skill of time-dependent lateral and lower boundary conditions within a meso-beta numerical cloud prediction model
02 p0211 N88-11327
Mesoscale analysis and nowcasting via a numerical model coupled with satellite sounder data
02 p0211 N88-11328
A preliminary demonstration of the use of boundary-layer models of flow in complex terrain for high resolution surface wind forecasting 02 p0212 N88-11330
Opportunities and problems in mesoscale objective analysis 02 p0212 N88-11331
An isentropic coordinate model used in a mesoscale data assimilation system 02 p0212 N88-11333
Strategies for using mesoscale data in an operational mesoscale model 02 p0212 N88-11335
Methods of incorporating satellite data into mesoscale numerical forecast models 02 p0212 N88-11336
Toward optimizing the use of data for operational mesoscale forecasting at the National Meteorological Center 02 p0213 N88-11337
Assimilation of high resolution TOVS data into a mesoscale NWP model --- numerical weather prediction (NWP) 02 p0213 N88-11338
A VAS-numerical model impact study using the Gal-Chen variational approach --- Visible Infrared Spin-Scan Radiometer Atmospheric Sounder (VAS)
02 p0213 N88-11339
Use of four-dimensional data assimilation to improve a mesoscale-model precipitation forecast: A case study
02 p0213 N88-11340
Mesoscale very short-range numerical prediction with dynamical initialization including condensation heating
02 p0213 N88-11341
Impact of a direct assimilation of satellite-inferred precipitation rates into a regional meteorological model
02 p0213 N88-11342
Initialization experiments with the NMC nested grid model --- National Meteorological Center (NMC)
02 p0213 N88-11343
The future of data in mesoscale numerical models
02 p0214 N88-11344
Simulation of mesoscale satellite sounder data from a mesoscale numerical model 02 p0214 N88-11345
The challenge of using mesoscale data in mesoscale numerical models 02 p0214 N88-11346
The challenge of using mesoscale data in mesoscale numerical models: A position paper
02 p0214 N88-11347
Comments on the challenge of using mesoscale data in mesoscale numerical models
02 p0214 N88-11348
Four-dimensional initialization of mesoscale models
02 p0214 N88-11349
Study of isolated convective clouds in the lower Alps in summer 1984, using radar and a simple Weinstein numerical model
[ESA-TT-1061] 03 p0353 N88-12224
Report of the second session of the CAS/JSC working group on numerical experimentation --- weather forecasting
[WMO/TD-168] 06 p0745 N88-14579
Prognosis using spectral embedding --- weather forecasting 08 p1016 N88-16157
On the dynamic estimation of relative weights for observation and forecast in numerical weather prediction
[NASA-CR-182531] 10 p1356 N88-18106
Quality control of upper air conventional data (TEMP and PILOT)
[INPE-4223-RPE/546] 12 p1647 N88-19862
Assimilation of meteorological observations
14 p1936 N88-21544
Nonlinear normal mode initialization of a limited area model using nonstationary Rossby modes --- numerical weather forecasting
[KNMI-WR-87-10] 14 p1947 N88-21614
Analysis of a six-component barotropic spectral model: Chaotic motion, predictability and vacillation --- atmospheric circulation
[CWI-AM-R8710] 18 p2542 N88-25090
Adaptive grid refinement for numerical weather prediction
[AD-A192172] 18 p2544 N88-25101
Bracknell Meteorological Office
18 p2545 N88-25107
Applications products of aviation forecast models
18 p2546 N88-25109
Computer and model changes at National Meteorological Center (NWC) 18 p2547 N88-25116
The Federal Aviation Administration/Massachusetts Institute of Technology (FAA/MIT) Lincoln Laboratory Doppler weather radar program
18 p2547 N88-25118
Proceedings of the Twelfth Annual Climate Diagnostics Workshop
[PB88-191747] 22 p3119 N88-28534
Extratropical response to tropical heating as a function of period of model integrations
22 p3125 N88-28577
Application of Dynamic Extended Range Forecasting (DERF) to the monthly forecast problem
22 p3125 N88-28578
Another approach for forecasting forecast skill
22 p3126 N88-28580
Experimental 30-day forecasts from several spectral general circulation models 22 p3126 N88-28582

Sampling strategies for Monte-Carlo forecasting methods 22 p3126 N88-28583
Correction of systematic errors in NMC medium range forecasts 22 p3126 N88-28584
Dependence of medium range forecast errors upon the large-scale initial state 22 p3126 N88-28585
Theoretical and practical limits of predictability of the NMC medium-range model 22 p3127 N88-28586
The predictability of low frequency patterns in the NMC MRF 22 p3127 N88-28587
The relative utility of persistence and medium-range dynamical forecasts of monthly mean 700 mb heights 22 p3127 N88-28588
Some screening experiments in objective prediction of monthly mean temperature over the United States during the winter season 22 p3127 N88-28589
On climate prediction for India 22 p3127 N88-28590
Characteristics of regression equations for specifying monthly precipitation amounts over the United States from the field of concurrent mean 700 mb heights 22 p3127 N88-28591
Operational multifield analog forecasting of US seasonal temperatures for non-winter seasons 22 p3127 N88-28592
Determination of most probable predicted 50 kPa pattern by empirical orthogonal functions 22 p3128 N88-28593

NUSSELT NUMBER
Experimental study of local natural convection heat transfer in inclined and rotating enclosures 09 p1165 N88-16986

NUTATION
Preliminary design of the ORION attitude control system [AD-A187179] 10 p1292 N88-17729
Observation model and parameter partials for the JPL VLBI parameter estimation software MASTERFIT-1987 [NASA-CR-182524] 10 p1427 N88-18523
Separation dynamics for the last stage of a launch vehicle and satellite [INPE-4281-PRE/1153] 12 p1601 N88-19582
Rotational evolution of dynamically symmetric gyrostat with internal friction 24 p3446 N88-30509

NUTATION DAMPERS
Effect of void gas lying between fluid slugs in nutation dampers 03 p0319 N88-12015
Modeling of a nutation damper for satellite stabilization through rotation [INPE-4275-PRE/1147] 12 p1601 N88-19584
Nutational stability of a satellite equipped with an active magnetic momentum wheel 20 p2784 N88-26513

NUTATIONAL OSCILLATION
U NUTATION

NUTRITION
Study of the relationship between photosynthesis, respiration, transpiration, and mineral nutrition in wheat 03 p0360 N88-12268
Controlled ecological life support systems: Development of a plant growth module 05 p0630 N88-13854
Plant Growth Module (PGM) conceptual design 05 p0631 N88-13855
Trace-element metabolism in man and animals in the presence of hypoxic states of diverse etiology 07 p0889 N88-15390
Operation Everest 2: Nutrition and body composition [AD-A186449] 08 p1049 N88-16333
Dietary factors related to physical fitness [AD-A190272] 15 p2103 N88-22527
Significance of nutrition to change in human carbohydrate and lipid metabolism under emotional stress 19 p2703 N88-26073

NUTRITIONAL REQUIREMENTS
NT CALORIC REQUIREMENTS
Design of an elemental analysis system for CELSS research 03 p0360 N88-12266
The determination of nutritional requirements for Safe Haven Food Supply System (emergency/survival foods) 06 p0792 N88-14856
Fed-batch control based upon the measurement of intracellular NADH 09 p1197 N88-17175
Nutrient requirements and other factors involved in the culture of human kidney cells on microcarrier beads 09 p1197 N88-17176
Botany Facility: Problems of water supply, plant nutrients and soil in the Botany Facility [SIRA-A/7373/WP220/RJS/003] 17 p2379 N88-24141
Supply and distribution of plant nutrients in the Botany Facility [SIRA-A/7373/WP220/RJS/004] 17 p2379 N88-24142
Nutrient requirements for high stress environments [AD-A194595] 23 p3243 N88-29301

NYLON (TRADEMARK)
Optimization of the southern electrophoretic transfer method [DE88-004527] 10 p1299 N88-17765
Temperature, moisture and strain rate effects on the compressive mechanical behavior of Nylon 6/6 [DE88-010734] 21 p2961 N88-27591

NYLON RESINS
U POLYAMIDE RESINS

NYSTAGMUS
NT VESTIBULAR NYSTAGMUS
Nystagmometric distinctions of individuals regularly exposed to vibration 07 p0891 N88-15401

O

O RING SEALS
Results of the development motor 8 test firing [GPO-78-692] 03 p0278 N88-11751
Design and test of a spacecraft instrument shock isolator 08 p0998 N88-16044

O STARS
The effects of rotation on the winds from hot stars 11 p1569 N88-19393

OBESITY
Prediction of physical fitness: Estimated percent body fat using body circumferences versus weight-height measures [AD-A190233] 15 p2103 N88-22526

OBJECT PROGRAMS
ERIC: An object-oriented simulation language [AD-A184757] 03 p0364 N88-12293
Realization of natural language style robot task instruction by using the object oriented concept 16 p2257 N88-23487
Mentat: An object-oriented macro data flow system [NASA-TM-101165] 17 p2388 N88-24199
Towards knowledge bases: semantics, rules and object-oriented programming [PB88-106154] 20 [illegible] N88-27110

OBLATE SPHEROIDS
Investigation of the feasibility of an analytical method of accounting for the effects of atmospheric drag on satellite motion 07 p0923 N88-15608

OBLIQUE SHOCK WAVES
Experimental and numerical investigation of the effect of distributed suction on oblique shock wave/turbulent boundary layer interaction [NASA-TM-101334] 24 p3372 N88-30084

OBLIQUE WINGS
An integrated study of structures, aerodynamics and controls on the forward swept wing X-29A and the oblique wing research aircraft [NASA-CR-181548] 04 p0399 N88-12486
Conceptual final paper on the preliminary design of an oblique flying wing SST [NASA-CR-182879] 16 p2161 N88-22891
The computation of flow past an oblique wing using the thin-layer Navier-Stokes equations [NASA-TM-88317] 24 p3320 N88-29774

OBLIQUENESS
An investigation of oblique hypervelocity impact 07 p0927 N88-15629
An analysis of penetration and ricochet phenomena in oblique hypervelocity impact [NASA-TM-100319] 10 p1339 N88-18004

OBSCURATION
U OCCULTATION

OBSERVABILITY (SYSTEMS)
Optimal detection of sensor failures in flight control systems using deterministic observers 02 p0128 N88-10803
Closed-loop system analysis using Lyapunov stability theory 04 p0483 N88-12978
Development of a technique for estimating noise covariances using multiple observers [NASA-TM-4020] 06 p0669 N88-14098
Optimal observers for ARMA models [OUEL-1659/86] 07 p0907 N88-15495
Increasing accuracy in evaluating vector of state under conditions of incomplete observability of expanded system 24 p3446 N88-30511

OBSERVATION
NT EARTH OBSERVATIONS (FROM SPACE)
NT SATELLITE OBSERVATION
NT SKY SURVEYS (ASTRONOMY)
NT SPACE OBSERVATIONS (FROM EARTH)
NT SPOT (FRENCH SATELLITE)
NT VISUAL OBSERVATION
Method for investigating the formation of crystals in a transparent material [NASA-CASE-MFS-26008-1-CU] 06 p0788 N88-14835
On observer problems for systems governed by partial differential equations [AD-A187430] 10 p1400 N88-18351
A two-stage isolated-word recognition system using discriminant analysis [AD-A187425] 10 p1402 N88-18360
Editing master oceanographic observation data set 4 [AD-A188405] 12 p1649 N88-19876
Revised Uniform Summary of Surface Weather Observations, Loring AFB, Maine, Parts A - F [AD-A188201] 14 p1947 N88-21610
Observation of nonlinear wave decay processes in the solar wind by the AMPTE IRM plasma wave experiment [AD-A191409] 16 p2290 N88-23713

OBSERVATION AIRCRAFT
NT MIRAGE AIRCRAFT
NT OV-1 AIRCRAFT
NT RF-4 AIRCRAFT
NT U-2 AIRCRAFT

OBSERVATORIES
NT ASTRONOMICAL OBSERVATORIES
NT ASTRONOMICAL SATELLITES
NT GAMMA RAY OBSERVATORY
NT GEOPHYSICAL OBSERVATORIES
NT HEAO 2
NT HUBBLE SPACE TELESCOPE
NT INFRARED ASTRONOMY SATELLITE
NT INFRARED SPACE OBSERVATORY (ISO)
NT IUE
NT PINHOLE OCCULTER FACILITY
NT ROSAT MISSION
NT SAS
NT SOLAR OBSERVATORIES
NT SPACE INFRARED TELESCOPE FACILITY
NT X RAY ASTROPHYSICS FACILITY
Astrophysics observatory in Byurakan [AD-A185144] 05 p0660 N88-14050

OBSTACLES
U BARRIERS

OBSTRUCTING
U BLOCKING

OCCLUSION
Local versus global minima in visual pattern completion [PB87-234803] 07 p0897 N88-15439
Shape from shading, occlusion and texture [AD-A184840] 18 p2571 N88-25269

OCCULTATION
NT RADIO OCCULTATION
NT SOLAR ECLIPSES
Balloon-based infrared solar occultation measurements of stratospheric O3, H2O, HNO3 and CFC-12 [NOAA-TR-NESDIS-34] 01 p0068 N88-10438
Occultation of compact radio sources by the ion tail of Halley's Comet 01 p0118 N88-10753
Manual for obscuration code with space station applications [NASA-CR-178099] 17 p2334 N88-23931
A study relating to the fog oil replacement program [AD-A192536] 21 p2923 N88-27347

OCCUPATIONAL DISEASES
Radon Research Program, FY-1987 [DE88-002633] 09 p1188 N88-17120

OCEAN BOTTOM
Geoacoustic models of the Hudson Canyon area [AD-A183535] 01 p0073 N88-10465
A new method for determining acoustic properties of the seabed from the ambient noise field in the ocean [RAE-TR-86035] 01 p0090 N88-10590
Marine minerals: Exploring our new ocean frontier [PB87-217725] 02 p0216 N88-11364
RRS DISCOVERY cruise 160, 30 June-25 July, 1986. Geochemical sampling over the Madeira and Porcupine Abyssal Plains [PB87-222030] 04 p0471 N88-12910
USSR report: Earth sciences [JPRS-UES-87-004] 06 p0725 N88-14455
Tectonics of the Caroline Oceanic Step (southwestern Pacific Ocean) 06 p0725 N88-14462
Tectonics and magmatism of Walvis Ridge and Discovery Rise (Atlantic Ocean) 06 p0726 N88-14463
Tectonics of sedimentary cover and basement of Labrador Sea 06 p0726 N88-14468
Remote acoustic sounding of ferromanganese nodules 06 p0727 N88-14471
Modern concept concerning transport of bottom sediments in abyssal regions of world ocean 06 p0728 N88-14478
RRS DISCOVERY Cruise 161, 15 August (227)-19 September (262) 1986. Portuguese Ocean-continent boundary, plate boundaries west of Iberia and seismic structure of sediments off Madeira [PB87-222006] 06 p0747 N88-14596
Ocean floor magmatism and problems of lithosphere formation 08 p1009 N88-16121

Acoustic backscattering from bottom sediment at normal incidence in the laboratory
[AD-A186905] 09 p1242 N88-17443

A deep-water OBS (Ocean Bottom Seismometer) array with real-time telemetry
[AD-A187404] 10 p1357 N88-18112

Rapid underway sediment classification by electrical methods
[AD-A187477] 10 p1357 N88-18114

On the barotropic model of the ocean circulation
[AD-A188148] 10 p1358 N88-18118

Thematic mapper study of Alaskan ophiolites
[NASA-CR-182554] 11 p1504 N88-18984

Sea duct: A deep-sea computer-controlled recirculating flume for the study of sea floor stability
[AD-A187734] 11 p1516 N88-19056

Relationship between oceanic geological formations and tectonic structures 13 p1785 N88-20683

Experience with and ways to upgrade accuracy of hydromagnetic surveys in ocean
13 p1787 N88-20692

Research on turbulence in bottom boundary layer in ocean 13 p1788 N88-20697

Bathymetric hazard survey test
[AD-A189150] 13 p1803 N88-20775

Experimental and theoretical constraints on the origin of mid-ocean ridge geothermal fluids
13 p1804 N88-20784

A computerized investigation using the method of images to predict the sound field in a fluid wedge overlying a slow fluid half-space
[AD-A190013] 15 p2130 N88-22704

The representation of the sea-bottom in deep sea areas by the Digital Terrain Model (DTM) program TASH
16 p2226 N88-23293

To relate measurements of gravity and geoid anomalies over the oceans to near surface density distributions
[AD-A192168] 18 p2547 N88-25120

Evaluation of the biot coefficients
[AD-A191643] 18 p2570 N88-25265

Remote sensing of acoustic properties of shallow water sediments: A review
[AD-A192107] 18 p2570 N88-25267

Evaluation of the contribution of SPOT in the framework of the mineral exploration program of the Aitutaki Atoll (Cook Islands). Preliminary study of the impact of the passage of Hurricane Sally 22 p3109 N88-28463

Acoustic pressure distribution on the bottom of a wedge-shaped ocean
[AD-A193961] 23 p3278 N88-29518

The growth of continents and some consequences since 1.5 Ga 24 p3395 N88-30220

The tectonic setting of the Seychelles, Mascarene and Amirante Plateaus in the Western Equatorial Indian Ocean 24 p3396 N88-30225

The petrogenesis of oceanic kimberlites and included mantle megacrysts: The Malaitan alnoite
24 p3397 N88-30232

Continental crustal formation and recycling: Evidence from oceanic basalts 24 p3398 N88-30238

Solid earth as a recycling systems and the lateral growth of Precambrian North America 24 p3400 N88-30249

The effect of thicker oceanic crust in the Archaean on the growth of continental crust through time
24 p3401 N88-30254

OCEAN COLOR SCANNER

The distinction between different water masses using optical remote sensing applied to data from the Alboran Sea Experiment 1982
[DFVLR-FB-86-48] 03 p0345 N88-12181

Design feasibility report on investigation of magnetic bearings for the ocean colour monitor radiometer scanner
[BAE-TP-7849] 09 p1174 N88-17036

OCEAN CURRENTS

NT COASTAL CURRENTS
NT EL NINO
NT GULF STREAM
NT LOMONOSOV CURRENT

Satellite and synoptic studies of chemical fronts in the California current and coastal upwelling zone
[AD-A183909] 01 p0073 N88-10466

Vertical profiles of wind-induced current --- North Sea
[IOS-238] 02 p0193 N88-11207

Experimental study of turbulent diffusion parameters in ocean 04 p0459 N88-12840

Intensive synoptic eddies and quasigeostrophic approximation 04 p0460 N88-12844

Dynamics of isolated intrathermocline eddy
04 p0460 N88-12845

Influence of secondary eddy currents on scattering of admixture in zonal flow 04 p0460 N88-12846

Two-layer model of circulation in world ocean with detailed description of seasonal evolution of upper quasihomogeneous layer 06 p0727 N88-14470

Role of anomalous currents in formation of ocean surface temperature field 06 p0727 N88-14474

Modern concept concerning transport of bottom sediments in abyssal regions of world ocean
06 p0728 N88-14478

Forecast of current patterns for an eddy tracking experiment in the Norwegian coastal current
[PB87-224853] 06 p0747 N88-14595

Preliminary report of hydrological measurements carried out in the southern Adriatic Sea: Palma 86 campaign
[PREPRINT-555] 06 p0748 N88-14597

Statistical analyses of measured directional wave and current data
[PB87-144523] 07 p0853 N88-15185

An investigation of offshore circulation using satellite data and feature tracking techniques
[AD-A186271] 07 p0881 N88-15347

Moored current meter data from the Canary Basin near 32 deg N, 24 W (84-1986), volume 40
[PB88-108105] 07 p0882 N88-15351

On estimating the basin-scale ocean circulation from satellite altimetry. Part 1: Straightforward spherical harmonic expansion
[NASA-CR-182387] 07 p0882 N88-15352

North Pacific Ocean. Tradewind region east of Hawaii, R/V Thomas G Thompson: 25 September - 1 November 1972. STD data report
[AD-A186566] 08 p1044 N88-16311

North Pacific Ocean. Gulf of Alaska, R/V Thomas G. Thompson: 1 February - 8 March 1967. STD data report
[AD-A186569] 08 p1045 N88-16314

Sea surface current estimates off central California as derived from enhanced AVHRR (Advanced Very High Resolution Radiometer) infrared images
[AD-A186867] 09 p1194 N88-17155

Oceanographic features of the east and southeast Indian Ocean for June 1983
[AD-A186948] 09 p1195 N88-17158

North Pacific Ocean. Northeast Pacific Transition Zone, R/V Thomas G. Thompson: 1 November - 6 December 1969. STD data report
[AD-A186574] 09 p1195 N88-17161

Hydrographic and current measurements in the North-East Atlantic Ocean. Data report on F.S. Meteor cruises 69/5 and 69/6, October to November 1984
[REPT-166] 09 p1196 N88-17164

Analysis of low frequency current fluctuations in the North-East Atlantic Ocean
[REPT-170] 09 p1196 N88-17165

Numerical simulations of the California current: Filament formation as related to baroclinic instability
[AD-A187573] 10 p1358 N88-18115

Energy transfers for multilayer hydrodynamic ocean models: General formulation and specific examples
[AD-A187604] 10 p1358 N88-18116

On the barotropic model of the ocean circulation
[AD-A188148] 10 p1358 N88-18118

Sea duct: A deep-sea computer-controlled recirculating flume for the study of sea floor stability
[AD-A187734] 11 p1516 N88-19056

Mesoscale coastal ocean dynamics
11 p1517 N88-19060

Current velocity and hydrographic observations in the Straits of Florida, the Caribbean Sea and offshore of the Antillean Archipelago: Subtropical Atlantic climate studies (STACS) 1984 and 1985
[PB88-149299] 12 p1649 N88-19874

Research on the physical oceanography of the Gulf Stream
[AD-A188512] 12 p1649 N88-19877

The physical oceanography of the Alboran Sea
[AD-A189027] 12 p1650 N88-19880

Relationships between remotely-sensed surface properties and subsurface structure in the ocean
[AD-A189317] 12 p1650 N88-19881

Anisotropy of microstructural eddy motion in surface layer during calm 13 p1784 N88-20677

Mushroom-shaped currents (eddy dipoles) under rotation and stratification conditions
13 p1784 N88-20678

Determining Langmuir circulation parameters on basis of similarity theory 13 p1785 N88-20680

Space-time analysis of oceanographic fields by modified empirical orthogonal functions method
13 p1786 N88-20687

Intrathermocline lens of Mediterranean water in tropical North Atlantic 13 p1786 N88-20688

Dynamics of synoptic ocean eddies
13 p1786 N88-20689

Contribution to theory of quasigeostrophic motions of finite amplitude in viscous stratified ocean
13 p1788 N88-20695

Research on turbulence in bottom boundary layer in ocean 13 p1788 N88-20697

Study of spectra of sea waves on horizontally nonuniform current in rip zone 13 p1788 N88-20699

Model validation research: Comparison of simulated and observed climate patterns for the past 18,000 years
[DE88-004945] 13 p1800 N88-20759

Deep water mass circulation in the Alboran Basin. Measurements - January to April 1982: ALBORAN 2
[AD-A189205] 13 p1803 N88-20777

Survey of acoustic techniques for monitoring El Nino
[PB88-157615] 13 p1804 N88-20783

Dynamics of the Oceanic Surface Mixed Layer
[AD-A188348] 13 p1804 N88-20785

Equatorial turbulence: Mixed layer and thermocline
13 p1804 N88-20787

On the zonal momentum balance at the equator
13 p1805 N88-20788

The mixed layer of the western equatorial Pacific Ocean
[HIG-1861] 13 p1805 N88-20789

Observations of waves and Langmuir circulation with Doppler sonars 13 p1805 N88-20790

Some effects of heating on the wind-driven velocity in the upper ocean 13 p1805 N88-20792

Mixed-layer shear related to wind stress in the central equatorial Pacific 13 p1805 N88-20793

Mixed-layer fronts in the California current
13 p1805 N88-20794

Horizontal scales of wind forced inertial motions
13 p1806 N88-20795

Subduction 13 p1806 N88-20796

Wind forcing and observed oceanic wavenumber spectra 13 p1806 N88-20797

Hamiltonian description of the interaction of surface waves with mixed-layer currents
13 p1806 N88-20799

Large-scale ocean dynamics
14 p1938 N88-21562

Wind and buoyancy driven ocean circulation
14 p1938 N88-21564

Climatological data of the Netherlands lightvessels over the period 1949-1980 --- North Sea
[KNMI-WR-87-9] 14 p1947 N88-21613

Current velocity and hydrographic observations in the Straits of Florida, the Caribbean Sea and offshore of the Antillean Archipelago: Subtropical Atlantic Climate Studies (STACS) 1986
[PB88-160767] 14 p1951 N88-21628

Ocean general circulation models: Report on proceedings of a meeting of ocean and climate modelers
[DE88-005530] 15 p2099 N88-22504

Hydrographic data from the OPTOMA (Ocean Prediction Through Observation, Modeling and Analysis) program: OPTOMA 23, 9-19 November 1986
[AD-A189868] 15 p2099 N88-22506

The physical oceanography of the northern Baffin Bay-Nares Strait region
[AD-A190015] 15 p2100 N88-22509

Changes in the California current system observed off northern California during July-August 1986
[AD-A190027] 15 p2100 N88-22510

The effects of time-dependent winds and ocean eddies on ice motion in a marginal ice zone
[AD-A190105] 15 p2100 N88-22511

The WOCE Core Project Planning Meeting on the Gyre Dynamics Experiment --- ocean dynamics
[WCP-139] 16 p2236 N88-23358

Near surface current determined from INPE's satellite-tracked buoy, during 6-26 November, 1985
17 p2360 N88-24058

Determination of the ocean circulation by spaceborne radar altimeter 19 p2701 N88-26080

Image processing applied to quantitative numerical cartography of ocean circulation
19 p2702 N88-26085

Survey on utility technology of a tidal and ocean current energy
[DE88-770148] 20 p2819 N88-26722

The 1986-87 Pacific warm episode: Oceanic and Atmospheric features 22 p3120 N88-28535

Interannual variability in the Atlantic and Indian Oceans and its relationship to the southern oscillation
22 p3121 N88-28548

Atlantic SST variability and high latitude climate fluctuations 22 p3122 N88-28551

Low frequency variability of SST and its relationship to atmospheric forcing 22 p3122 N88-28554

Observational/numerical study of the upper ocean response to hurricanes
[AD-A193582] 22 p3128 N88-28588

Application of acoustic-Doppler current profiler and expendable bathythermograph measurements to the study of the velocity structure and transport of the Gulf Stream
[NASA-CR-183188] 22 p3129 N88-28605

An analysis of results of a high-resolution world ocean circulation model
[AD-A195780] 24 p3405 N88-30272

KOSPAS-SARSAT satellites used for ocean current study 24 p3450 N88-30534

OCEAN DATA ACQUISITIONS SYSTEMS

Complex for ocean study from space and hydroacoustic stations 04 p0458 N88-12836

A multibody dynamic analysis of the N-ROSS (Navy Remote Ocean Sensing System) satellite rotating flexible reflector using Kane's method [AD-A184452] 04 p0462 N88-12860

Status and prospects of the Joint Research Commitee (JRC) work on the application of ocean colour monitoring from space 08 p1043 N88-16299

NROSS (Navy Remote Ocean Sensing System): A force multiplier [AD-A188853] 10 p1346 N88-18045

Basic networks of TOGA: Determination of thermal profiles by XBT and of sea level by tide gage 14 p1939 N88-21568

From satellite altimetry to ocean topography, a survey of data processing techniques [ETN-88-91841] 14 p1939 N88-21575

Hydrographic data from the OPTOMA (Ocean Prediction Through Observation, Modeling and Analysis) program: OPTOMA 23, 9-19 November 1986 [AD-A189868] 15 p2099 N88-22506

Overview of space missions and techniques for ocean monitoring 19 p2700 N88-26053

Sensors in spaceborne oceanography 19 p2700 N88-26056

The French spaceborne oceanography program 19 p2701 N88-26058

SPOT: A satellite for oceanography 22 p3108 N88-28462

OCEAN DATA PLATFORMS

U OCEAN DATA ACQUISITIONS SYSTEMS

OCEAN DATA STATIONS

U OCEAN DATA ACQUISITIONS SYSTEMS

OCEAN DYNAMICS

The distinction between different water masses using optical remote sensing applied to data from the Alboran Sea Experiment 1982 [DFVLR-FB-86-48] 03 p0345 N88-12181

Dynamics of isolated intrathermocline eddy 04 p0460 N88-12845

Influence of secondary eddy currents on scattering of admixture in zonal flow 04 p0460 N88-12846

Studies of thin surface films aim at seeing deep ocean processes 04 p0460 N88-12847

Ocean colour applications in ocean dynamics and coastal processes 08 p1042 N88-16297

Interpretation of equatorial current meter data as internal waves [PB88-108113] 08 p1044 N88-16309

The physical oceanography of the Alboran Sea [AD-A189027] 12 p1650 N88-19880

Negative viscosity in global circulations 13 p1786 N88-20685

Propagation of subsurface salinity maximum in tropical Atlantic 13 p1786 N88-20686

Intrathermocline lens of Mediterranean water in tropical North Atlantic 13 p1786 N88-20688

Dynamics of synoptic ocean eddies 13 p1786 N88-20689

Structures and fluxes in a deep convecting mixed layer 13 p1804 N88-20786

Equatorial turbulence: Mixed layer and thermocline 13 p1804 N88-20787

On the zonal momentum balance at the equator 13 p1805 N88-20788

The mixed layer of the western equatorial Pacific Ocean [HIG-1861] 13 p1805 N88-20789

Some effects of heating on the wind-driven velocity in the upper ocean 13 p1805 N88-20792

Subduction 13 p1806 N88-20796

Introduction to the dynamics of the ocean and the atmosphere 14 p1935 N88-21537

Ocean eddies 14 p1938 N88-21566

Study of the dynamic topography of oceans by means of satellite altimetry 14 p1938 N88-21567

Hydrographic data from the OPTOMA (Ocean Prediction Through Observation, Modeling and Analysis) program: OPTOMA 23, 9-19 November 1986 [AD-A189868] 15 p2099 N88-22506

The physical oceanography of the northern Baffin Bay-Nares Strait region [AD-A190015] 15 p2100 N88-22509

The WOCE Core Project Planning Meeting on the Gyre Dynamics Experiment — ocean dynamics [WCP-139] 16 p2236 N88-23358

Physical oceanography and tracer chemistry of the southern ocean [DE88-006852] 20 p2828 N88-26779

OCEAN MODELS

Ocean model processor for climate studies [PB87-224713] 03 p0353 N88-12226

Intensive synoptic eddies and quasigeostrophic approximation 04 p0460 N88-12844

Coupled acoustic and ocean thermodynamic model [AD-A184357] 04 p0472 N88-12911

Influence of gas exchange between ocean and atmosphere on formation of atmospheric pressure field 06 p0726 N88-14467

Two-layer model of circulation in world ocean with detailed description of seasonal evolution of upper quasihomogeneous layer 06 p0727 N88-14470

NASA Oceanic Processes Program [NASA-TM-4025] 10 p1357 N88-18109

Numerical simulations of the California current: Filament formation as related to baroclinic instability [AD-A187573] 10 p1358 N88-18115

Energy transfers for multilayer hydrodynamic ocean models: General formulation and specific examples [AD-A187604] 10 p1358 N88-18116

On the barotropic model of the ocean circulation [AD-A188148] 10 p1358 N88-18118

Spatial-temporal variability of North Pacific sea surface temperature anomaly patterns 11 p1516 N88-19058

Model validation research: Comparison of simulated and observed climate patterns for the past 18,000 years [DE88-004945] 13 p1800 N88-20759

Predictions and studies with a one-dimensional ice/ocean model [AD-A189158] 13 p1803 N88-20776

Wind forcing and observed oceanic wavenumber spectra 13 p1806 N88-20797

Evaluation of wave calculations using GONO in the period October 1985 - April 1986 [KNMI-TR-96] 13 p1807 N88-20804

The main ocean thermocline 14 p1938 N88-21563

Wind and buoyancy driven ocean circulation 14 p1938 N88-21564

Sea ice observations and models 14 p1939 N88-21572

An improved wind input source term for third generation ocean wave modeling [KNMI-WR-87-8] 14 p1950 N88-21624

Ocean general circulation models: Report on proceedings of a meeting of ocean and climate modelers [DE88-005530] 15 p2099 N88-22504

A study of the dynamics of the Intertropical Convergence Zone (ITCZ) in a symmetric atmosphere-ocean model [NASA-TM-86220] 19 p2693 N88-26005

Modelling and forecasting deep ocean and near surface mesoscale eddies: Hindcasting and forecasting with, and coupling a surface boundary layer model to, the Harvard quasigeostrophic model 19 p2694 N88-26013

Air-sea interaction in the vicinity of a land-sea boundary in the presence of upwelling 21 p2973 N88-27661

Research on ocean forecasting and nonlinear wave propagation and numerical hydrodynamics in the ocean [AD-A193363] 21 p2976 N88-27680

On the energy source of 1982-83 ENSO episode simulated by the NCAR community climate model 22 p3122 N88-28556

The active layer of the upper Atlantic Ocean 22 p3124 N88-28566

Observational/numerical study of the upper ocean response to hurricanes [AD-A193592] 22 p3128 N88-28598

A method for determining absolute velocities from hydrographic data: The numerical code [AD-A193997] 22 p3129 N88-28603

An analysis of results of a high-resolution world ocean circulation model [AD-A195760] 24 p3405 N88-30272

OCEAN SURFACE

Study on propagation and inverse scattering --- sea studies [ESA-CR(P)-2394] 01 p0063 N88-10405

Precise orbit computation, gravity model adjustment and altimeter data processing for the ERS-1 altimetry mission [ESA-CR(P)-2436] 02 p0130 N88-10820

High resolution determination of true surface winds at sea from wind and pressure data 02 p0210 N88-11316

Spherical harmonic expansion of the Levitus Sea surface topography [NASA-CR-181448] 02 p0216 N88-11362

GEOSAT altimeter geophysical data record user handbook [PB87-213336] 03 p0276 N88-11743

Studies of thin surface films aim at seeing deep ocean processes 04 p0460 N88-12847

Theory of heat and moisture exchange between finely disperse storm-generated spray and turbulent air flow 04 p0461 N88-12851

Radial orbit error reduction and sea surface topography determination using satellite altimetry 04 p0462 N88-12861

Sea level changes [DE87-014357] 04 p0472 N88-12913

Varifront 3 expedition data report (USNS DE STEIGUER CRUISE 1202-82). Bioluminescence, hydrographic, nutrient, and satellite data from the Gulf of California (November-December 1981) [AD-A185011] 05 p0620 N88-13805

Correlation between refraction over sea and nature of radar reflections from sea surface 06 p0728 N88-14477

Texture study of Synthetic Aperture Radar (SAR) images of ocean surfaces [AD-A186021] 07 p0841 N88-15101

Foam generation and air entrainment near a free surface [AD-A185986] 07 p0848 N88-15149

Acoustic scattering from composite wind-wave surfaces 3: Forward scatter intensities and spatial coherence at low and high frequencies and small grazing angles for Bubble-free regimes [AD-A185908] 07 p0881 N88-15345

The ocean heat budget [AD-A186130] 07 p0881 N88-15346

Interaction of a vortex pair with a free surface [AD-A186619] 08 p0988 N88-15988

Limiting accuracy of scatterometer determination of wind speed over ocean from satellite 08 p1007 N88-16107

Sea surface current estimates off central California as derived from enhanced AVHRR (Advanced Very High Resolution Radiometer) infrared images [AD-A186867] 09 p1194 N88-17155

Investigation of the quantitative determination of two dimensional sea surface wave spectra from shipborne radar measurements [GKSS-87/E/10] 09 p1195 N88-17163

Radar returns from ground clutter in vicinity of airports 10 p1274 N88-17624

Numerical simulations of the California current: Filament formation as related to baroclinic instability [AD-A187573] 10 p1358 N88-18115

Estimation of sea surface wave spectra using acoustic tomography [AD-A187837] 11 p1516 N88-19057

Observations of the upper ocean using a multi-beam Doppler sonar [AD-A188896] 12 p1649 N88-19878

Relationships between remotely-sensed surface properties and subsurface structure in the ocean [AD-A189317] 12 p1650 N88-19881

The effects of atmospheric and thermohaline variability on the validation of the GEOSAT altimeter oceanographic signal between Scotland and Iceland [AD-A189324] 12 p1650 N88-19882

Spectral reflective characteristics of sea surface 13 p1784 N88-20676

Anisotropy of microstructural eddy motion in surface layer during calm 13 p1784 N88-20677

Vertical turbulent transfer of matter in thin ocean surface layer during daytime heating 13 p1787 N88-20693

Dynamics of the Oceanic Surface Mixed Layer [AD-A188348] 13 p1804 N88-20785

Structures and fluxes in a deep convecting mixed layer 13 p1804 N88-20786

Equatorial turbulence: Mixed layer and thermocline 13 p1804 N88-20787

Observations of waves and Langmuir circulation with Doppler sonars 13 p1805 N88-20790

Unsteady shallowing mixed layer 13 p1805 N88-20791

Some effects of heating on the wind-driven velocity in the upper ocean 13 p1805 N88-20792

Mixed-layer shear related to wind stress in the central equatorial Pacific 13 p1805 N88-20793

Mixed-layer fronts in the California current 13 p1805 N88-20794

Horizontal scales of wind forced inertial motions 13 p1806 N88-20795

Energy and momentum fluxes through the sea surface 13 p1806 N88-20796

Monitoring ocean surface layer processes 13 p1806 N88-20801

Global mixed-layer natural and anthropogenic fluxes 13 p1807 N88-20803

From satellite altimetry to ocean topography, a survey of data processing techniques [ETN-88-91841] 14 p1939 N88-21575

Climatic summaries of ocean weather stations [PB88-162820] 14 p1948 N88-21617

Relationship between optical transfer function and natural light field in sea or atmosphere 15 p2054 N88-22247

Models for electromagnetic scattering from the sea at extremely low grazing angles
[AD-A190472] 15 p2057 N88-22261
NIMBUS-7 CZCS. Coastal Zone Color Scanner imagery for selected coastal regions. North America - Europe. South America - Africa - Antarctica. Level 2 photographic product
[NASA-CR-180755] 15 p2089 N88-22447
Derivation of consistent surface fixed fields for use in a global NWP model
[AD-A190131] 15 p2093 N88-22475
The effects of better environmental inputs in estimating sea clutter
[AD-A192058] 19 p2643 N88-25678
Bathymetry estimation by analyzing swell on SPOT images 19 p2701 N88-26062
Image processing applied to quantitative numerical cartography of ocean circulation
19 p2702 N88-26065
Definition of long ocean wave slope for radar applications
[AD-A193198] 21 p2933 N88-27412
Research on ocean forecasting and nonlinear wave propagation and numerical hydrodynamics in the ocean
[AD-A193363] 21 p2976 N88-27680
Non-Gaussian models for surface clutter
22 p3068 N88-28212
IR (infrared) sky radiance distributions in the marine boundary layer
[AD-A193683] 22 p3119 N88-28531
Interannual variability in the Atlantic and Indian Oceans and its relationship to the southern oscillation
22 p3121 N88-28548
ENSO, sea-surface temperatures and African rainfall
22 p3122 N88-28550
Atlantic SST variability and high latitude climate fluctuations 22 p3122 N88-28551
Sub-Saharan rainfall anomalies and global sea-surface temperature relationships for the recent fifteen year (1970-1984) period 22 p3122 N88-28552
Simulation studies of the influence of sea-surface temperature anomalies on the Sahelian circulation and rainfall 22 p3122 N88-28553
Low frequency variability of SST and its relationship to atmospheric forcing 22 p3122 N88-28554
On the energy source of 1982-83 ENSO episode simulated by the NCAR community climate model
22 p3122 N88-28556
Persistence of North Pacific Sea surface temperature and atmospheric flow patterns 22 p3123 N88-28559
The active layer of the upper Atlantic Ocean
22 p3124 N88-28566
A probabilistic model of the apparent radiance of a rough sea
[AD-A193867] 22 p3129 N88-28602
Atmospheric deposition of nitrate to the ocean surface
23 p3231 N88-29227
Measurement and interpretation of North Atlantic Ocean marine radar sea scatter
[AD-A196239] 24 p3384 N88-30036
Analysis of environmental parameters from the Panama City tower radar experiment
[AD A194994] 24 p3404 N88-30264
Determining near-water wind speed using radar data from Cosmos-1500 artificial earth satellite
24 p3449 N88-30524

OCEAN TEMPERATURE
NT SEA SURFACE TEMPERATURE
Detection of CO2-induced climate change
[DE87-013127] 01 p0071 N88-10457
Role of anomalous currents in formation of ocean surface temperature field 06 p0727 N88-14474
Moored current meter data from the Canary Basin near 32 deg N, 24 W (84-1986), volume 40
[PB88-108105] 07 p0882 N88-15351
Editing master oceanographic observation data set 4
[AD-A188405] 12 p1649 N88-19876
Determination of mean thermohaline characteristics of the ocean 13 p1784 N88-20675
Estimates of ocean-atmosphere thermal interaction in Gulf Stream energy-active test range in winter of 1984
13 p1785 N88-20679
Propagation of subsurface salinity maximum in tropical Atlantic 13 p1786 N88-20686
Space-time analysis of oceanographic fields by modified empirical orthogonal functions method
13 p1786 N88-20687
Intrathermocline lens of Mediterranean water in tropical North Atlantic 13 p1786 N88-20688
Model of hydrodynamic adjustment of temperature, salinity and current fields 13 p1789 N88-20700
Dynamics of the Oceanic Surface Mixed Layer
[AD-A188348] 13 p1804 N88-20785
Structures and fluxes in a deep convecting mixed layer 13 p1804 N88-20786
Equatorial turbulence: Mixed layer and thermocline
13 p1804 N88-20787
The mixed layer of the western equatorial Pacific Ocean
[HIG-1861] 13 p1805 N88-20789
Mixed-layer fronts in the California current
13 p1805 N88-20794
Wind forcing and observed oceanic wavenumber spectra 13 p1806 N88-20797
Radiative processes affecting ocean mixed-layer heat content and their monitoring from satellite
13 p1806 N88-20800
Monitoring ocean surface layer processes
13 p1806 N88-20801
Sea surface temperatures of winter 1982-83 and their effect on atmospheric circulation
14 p1936 N88-21546
Climatological data of the Netherlands lightvessels over the period 1949-1980 — North Sea
[KNMI-WR-87-9] 14 p1947 N88-21613
The physical oceanography of the northern Baffin Bay-Nares Strait region
[AD-A190015] 15 p2100 N88-22509
Evaluating evaporation with satellite thermal data
[AD-A192042] 18 p2531 N88-25019
The 1986-87 Pacific warm episode: Oceanic and Atmospheric features 22 p3120 N88-28535
Interannual variability in the Atlantic and Indian Oceans and its relationship to the southern oscillation
22 p3121 N88-28548
ENSO, sea-surface temperatures and African rainfall
22 p3122 N88-28550
Atlantic SST variability and high latitude climate fluctuations 22 p3122 N88-28551
Sub-Saharan rainfall anomalies and global sea-surface temperature relationships for the recent fifteen year (1970-1984) period 22 p3122 N88-28552
Simulation studies of the influence of sea-surface temperature anomalies on the Sahelian circulation and rainfall 22 p3122 N88-28553
Low frequency variability of SST and its relationship to atmospheric forcing 22 p3122 N88-28554
On the energy source of 1982-83 ENSO episode simulated by the NCAR community climate model
22 p3122 N88-28556
Persistence of North Pacific Sea surface temperature and atmospheric flow patterns 22 p3123 N88-28559

OCEAN THERMAL ENERGY CONVERSION
Federal Ocean Energy Technology
[DE87-012279] 13 p1792 N88-20722
Ocean, Wave, and Tidal Energy Systems: Current abstracts
[DE88-006299] 19 p2687 N88-25973

OCEANOGRAPHIC PARAMETERS
NT OCEAN TEMPERATURE
NT SEA SURFACE TEMPERATURE
Regime dependent analysis experiments — sea level pressure field 02 p0209 N88-11314
The CNR/PSN Advanced Microwave Imaging Radiometer (AMIR) — satellite-borne
03 p0340 N88-12141
Eastern - western Arctic Sea ice analysis 1986
[AD-A184016] 03 p0355 N88-12235
The influence of yellow substances on remote sensing of sea water constituents from space. Volume 1: Summary
[ESA-CR(P)-2443-VOL-1] 07 p0872 N88-15292
The influence of yellow substances on remote sensing of sea water constituents from space. Volume 2: Appendices
[ESA-CR(P)-2443-VOL-2] 07 p0873 N88-15293
SEQUAL (seasonal Equatorial Atlantic) meteorological data from Moorings S2, S5 and S6 (March 1983 - March 1985)
[PB88-108048] 07 p0880 N88-15337
Annual data summary and climatological evaluation, CERC (Coastal Engineering Research Center) field research facility, 1985, volume 2, appendix C
[AD-A185894] 07 p0881 N88-15344
An investigation of offshore circulation using satellite data and feature tracking techniques
[AD-A186271] 07 p0881 N88-15347
Mariners Weather Log, Volume 31, Number 3, Summer 1987
[PB87-234894] 08 p1039 N88-16284
Annual data summary and climatological evaluation CERC (Coastal Engineering Research Center) field research facility, 1985. Volume 1. Main text and appendixes A and B
[AD-A186442] 08 p1039 N88-16289
Ocean Colour Workshop — conference
[ESA-SP-1083] 08 p1042 N88-16292
Europe's position concerning ocean colour activities
08 p1042 N88-16293
Overview of ESA's activities in ocean colour remote sensing 08 p1042 N88-16294
Update of NASA's ocean colour activities
08 p1042 N88-16295
Remote sensing of ocean colour for studies of biological productivity and biochemical cycles
08 p1042 N88-16296
Ocean colour applications in ocean dynamics and coastal processes 08 p1042 N88-16297
Technical aspects of future ocean colour remote sensing 08 p1042 N88-16298
Status and prospects of the Joint Research Committee (JRC) work on the application of ocean colour monitoring from space 08 p1043 N88-16299
Canadian activities and goals in remote sensing of ocean colour and fluorescence from space
08 p1043 N88-16300
Federal Republic of Germany's interests, activities and goals in remote sensing of ocean colour/fluorescence from space 08 p1043 N88-16302
French activities in ocean colour observations
08 p1043 N88-16303
Developments in ocean colour research in the United Kingdom 08 p1043 N88-16306
North Pacific Ocean. Subtropical front north of Hawaii, R/V Thomas G. Thompson: 7 January - 10 February 1974. CTD data report
[AD-A186565] 08 p1044 N88-16310
North Pacific Ocean. Tradewind region east of Hawaii, R/V Thomas G Thompson: 25 September - 1 November 1972. STD data report
[AD-A186566] 08 p1044 N88-16311
North Pacific Ocean. Subarctic front central Pacific, R/V Thomas G. Thompson: 8 September - 9 October 1975. CTD data report
[AD-A186567] 08 p1044 N88-16312
North Pacific Ocean. Northwest Pacific Transition Zone, R/V Thomas G. Thompson: 19 March - 1 May 1971. STD data report
[AD-A186568] 08 p1044 N88-16313
Oceanographic features of the east and southeast Indian Ocean for June 1983
[AD-A186948] 09 p1195 N88-17158
North Pacific Ocean. Central Pacific Transition Zone, R/V Thomas G. Thompson: 25 March - 3 May 1968. STD data report
[AD-A186570] 09 p1195 N88-17160
North Pacific Ocean. Northeast Pacific Transition Zone, R/V Thomas G. Thompson: 1 November - 6 December 1969. STD data report
[AD-A186574] 09 p1195 N88-17161
NROSS (Navy Remote Ocean Sensing System): A force multiplier
[AD-A186853] 10 p1346 N88-18045
CTD observations in the coastal transition zone off northern California, 16-25 February 1987
[AD-A187283] 10 p1357 N88-18111
Editing master oceanographic observation data set 4
[AD-A188405] 12 p1649 N88-19876
The effects of atmospheric and thermohaline variability on the validation of the GEOSAT altimeter oceanographic signal between Scotland and Iceland
[AD-A189324] 12 p1650 N88-19882
Predictions and studies with a one-dimensional ice/ocean model
[AD-A189158] 13 p1803 N88-20776
Oceanographic export system development, year 1
[AD-A189134] 14 p1950 N88-21623
Hydrographic data from the OPTOMA (Ocean Prediction Through Observation, Modeling and Analysis) program: OPTOMA 23, 9-19 November 1986
[AD-A188868] 15 p2099 N88-22506
The physical oceanography of the northern Baffin Bay-Nares Strait region
[AD-A190015] 15 p2100 N88-22509
ERS-1 data products and services and their value for tropical countries 17 p2357 N88-24040
SeaSoar profiles in the Iceland-Scotland area, May 1987
[IOS-253] 18 p2548 N88-25124
Overview of space missions and techniques for ocean monitoring 19 p2700 N88-26053
MIZPAC (marginal ice zone Pacific) 84-86 CTD (Conductivity, Temperature, Depth) data report
[AD-A192478] 21 p2976 N88-27679
A method for determining absolute velocities from hydrographic data: The numerical code
[AD-A193997] 22 p3129 N88-28600
A study of the feasibility of using sea and wind information from the ERS-1 satellite. Part 1: Wind scatterometer data
[NASA-CR-182833] 24 p3386 N88-30167
A study of the feasibility of using sea and wind information from the ERS-1 satellite. Part 2: Use of scatterometer and altimeter data in wave modeling and assimilation
[ESA-CR(P)-2604-PT-2] 24 p3387 N88-30176

OCEANOGRAPHY

The effect of wind and currents on gas exchange in an estuarine system
[NASA-CR-181424] 01 p0073 N88-10468

Publications and final reports on contracts and grants, 1986 (National Environmental Satellite, Data and Information Service)
[PB87-220810] 03 p0352 N88-12218

USSR report: Earth sciences
[JPRS-UES-86-006] 04 p0458 N88-12831

Experimental study of turbulent diffusion parameters in ocean 04 p0459 N88-12840

Effects of rainfall on the seasonal thermocline
[AD-A184432] 04 p0472 N88-12912

USSR report: Earth sciences
[JPRS-UES-87-004] 06 p0725 N88-14455

Tectonics of the Caroline Oceanic Step (southwestern Pacific Ocean) 06 p0725 N88-14462

Tectonics and magmatism of Walvis Ridge and Discovery Rise (Atlantic Ocean)
06 p0726 N88-14463

Study of evolution of Gulf Stream cyclinic eddy
06 p0727 N88-14473

Wave and wind data sources, environmental conditions committee report, International Ship and Offshore Structures Congress
[PB87-234902] 06 p0746 N88-14588

Preliminary report of hydrological measurements carried out in the southern Adriatic Sea: Palma 86 campaign
[PREPRINT-555] 06 p0748 N88-14597

WOCE Core Project 2 Planning Meeting: The Southern Ocean
[WCP-138] 07 p0882 N88-15348

USSR report: Earth sciences
[JPRS-UES-87-003] 08 p1009 N88-16119

Sea surface current estimates off central California as derived from enhanced AVHRR (Advanced Very High Resolution Radiometer) infrared images
[AD-A185867] 09 p1194 N88-17155

Oceanographic features of the east and southeast Indian Ocean for June 1983
[AD-A186948] 09 p1195 N88-17158

Continental shelf processes affecting the oceanography of the South Atlantic Bight
[DE88-004102] 09 p1196 N88-17166

NASA Oceanic Processes Program
[NASA-TM-4025] 10 p1357 N88-18109

Coordination: Southeast continental shelf studies
[DE88-003680] 10 p1357 N88-18110

Mesoscale coastal ocean dynamics
11 p1517 N88-19060

Current velocity and hydrographic observations in the Straits of Florida, the Caribbean Sea and offshore of the Antillean Archipelago: Subtropical Atlantic climate studies (STACS) 1984 and 1985
[PB88-149299] 12 p1649 N88-19874

JEDA (Joint Environmental Data Analysis) Center report on tropical Pacific subsurface thermal data management, 1986
[PB88-140090] 12 p1649 N88-19875

Editing master oceanographic observation data set 4
[AD-A188405] 12 p1649 N88-19876

Research on the physical oceanography of the Gulf Stream
[AD-A188512] 12 p1649 N88-19877

The physical oceanography of the Alboran Sea
[AD-A189027] 12 p1650 N88-19880

The effects of atmospheric and thermohaline variability on the validation of the GEOSAT altimeter oceanographic signal between Scotland and Iceland
[AD-A189324] 12 p1650 N88-19882

JPRS report: Science and technology. USSR: Earth sciences
[JPRS-UES-88-001] 13 p1784 N88-20674

Studies toward observing and modelling large energetic ocean regions
[AD-A189267] 13 p1803 N88-20778

Dynamics of the Oceanic Surface Mixed Layer
[AD-A188348] 13 p1804 N88-20785

Inversion algorithms for geophysical problems
[AD-A188252] 13 p1815 N88-20845

ONR Far East Scientific Bulletin, volume 12, number 3, July-September 1987
[AD-A188554] 13 p1851 N88-21081

Introduction to the dynamics of the ocean and the atmosphere 14 p1935 N88-21537

Large-scale ocean dynamics
14 p1938 N88-21562

The main ocean thermocline
14 p1938 N88-21563

Basic networks of TOGA: Determination of thermal profiles by XBT and of sea level by tide gage
14 p1939 N88-21568

Oceanographic export system development, year 1
[AD-A189134] 14 p1950 N88-21623

Biological processes in the water column of the South Atlantic bight: Zooplankton responses
[DE88-004811] 14 p1951 N88-21630

Definition and implementation study for the Varan-S radar
[CNES-CT/DRT/TIT/RL-143-T]
15 p2056 N88-22267

Instruments for use in experimental studies of complex turbulent shear flow: Three component LDVs
[AD-A190526] 15 p2065 N88-22312

Ocean general circulation models: Report on proceedings of a meeting of ocean and climate modelers
[DE88-005530] 15 p2099 N88-22504

Hydrographic data from the OPTOMA (Ocean Prediction Through Observation, Modeling and Analysis) program: OPTOMA 23, 9-19 November 1986
[AD-A189868] 15 p2099 N88-22506

Two decades of achievement in the ocean, 1968-1988
[PB88-167077] 16 p2236 N88-23356

Investigation of the imaging of ocean surface waves using a synthetic aperture radar
[SER-A-WISS-ABHANDL-84] 16 p2236 N88-23357

The WOCE Core Project Planning Meeting on the Gyre Dynamics Experiment --- ocean dynamics
[WCP-139] 16 p2236 N88-23358

Research and Technology, 1987, Goddard Space Flight Center
[NAS 1.15:101097] 17 p2453 N88-24572

Mariners weather log, volume 32, number 1, Winter 1988
[PB88-173869] 18 p2544 N88-25097

Sensors in spaceborne oceanography
19 p2700 N88-26056

The French spaceborne oceanography program
19 p2701 N88-26058

Mariners weather log, volume 31, number 4, Fall 1987
[PB88-173851] 20 p2825 N88-26761

Physical oceanography and tracer chemistry of the southern ocean
[DE88-006852] 20 p2828 N88-26779

An analysis of horizontal temperature gradients and heat content in the mixed layer and the surface forcing during PATCHEX
[AD-A192330] 21 p2976 N88-27678

Beaufort sea mesoscale circulation study: Hydrography helicopter operations, April 1987
[PB88-203658] 21 p2976 N88-27681

ERS-1: A satellite with an oceanographic mission
[NLR-MP-86072-U] 24 p3333 N88-29838

OCEANS

NT ANTARCTIC OCEAN
NT ARCTIC OCEAN
NT ATLANTIC OCEAN
NT INDIAN OCEAN
NT PACIFIC OCEAN

The effect of ocean fluctuations on sound transmission in the ocean
[AD-A184382] 03 p0355 N88-12236

New method of estimating continentality of climate on global scale 06 p0725 N88-14460

Uses of airborne laser Chayka-1 for probing water, land surfaces 06 p0725 N88-14461

Concentration coefficients of elements in ferromanganese nodules relative to ocean sediments
06 p0726 N88-14464

Two-layer model of circulation in world ocean with detailed description of seasonal evolution of upper quasihomogeneous layer 06 p0727 N88-14470

Modern concept concerning transport of bottom sediments in abyssal regions of world ocean
06 p0729 N88-14478

Wave and wind data sources, environmental conditions committee report, International Ship and Offshore Structures Congress
[PB87-234902] 06 p0746 N88-14588

Cavitation inception scale effects. 1. Nuclei distributions in natural waters. 2. Cavitation inception in a turbulent shear flow
[AD-A185553] 08 p0988 N88-15967

Sea resonance vibrational source of seismic waves
08 p1010 N88-16126

Numerical studies of propagation of Lg waves across ocean continent boundaries using the Representation Theorem (RT) 10 p1353 N88-18085

Review of recent developments in evaporation ducting assessment 12 p1616 N88-19664

Determination of mean thermohaline characteristics of the ocean 13 p1784 N88-20675

Structures and fluxes in a deep convecting mixed layer 13 p1804 N88-20786

On the zonal momentum balance at the equator
13 p1805 N88-20788

Subduction 13 p1806 N88-20796

Wind forcing and observed oceanic wavenumber spectra 13 p1806 N88-20797

Energy and momentum fluxes through the sea surface
13 p1806 N88-20798

Global mixed-layer natural and anthropogenic fluxes
13 p1807 N88-20803

Low frequency ocean ambient noise: Measurements and theory
[AD-A191188] 16 p2237 N88-23362

Identification and acoustic characterization of seamounts
[AD-A192204] 18 p2548 N88-25123

Construction of approximations to acoustic Green's functions for nonhomogeneous oceans using transmutation
[PB88-185384] 18 p2548 N88-25126

The distribution of some chemical elements between dissolved and particulate phases in the ocean
[DE88-010181] 21 p2977 N88-27682

Simulation studies of the influence of sea-surface temperature anomalies on the Sahelian circulation and rainfall 22 p3122 N88-28553

MIZEX (marginal ice zone experiment) 1987 SAR (Synthetic Aperture Radar) data summary
[AD-A195560] 24 p3364 N88-30035

Rossby waves in mid-latitude oceans
24 p3405 N88-30273

OCTANE NUMBER

The effect of weathering on octane quality for winter-grade and summer-grade gasolines
[AD-A190640] 16 p2183 N88-23012

OCULOMETERS

A human factors evaluation of the Advanced Visual Technology System (AVTS) eye tracking oculometer
21 p2925 N88-27361

OCULOMOTOR NERVES

Research on visual information processing with special reference to oculomotor behavior in the areas of exploration, recognition and search
[AD-A186598] 08 p1051 N88-16346

ODAS

U OCEAN DATA ACQUISITIONS SYSTEMS

ODD-ODD NUCLEI

Influence of pairing correlations on the probability and dynamics of tunneling through the barrier in fission and fusion of complex nuclei
[DE88-701500] 23 p3286 N88-29570

OFF-ON CONTROL

Control design challenges of large space systems and spacecraft control laboratory experiment (SCOLE)
[NASA-CR-178392] 03 p0275 N88-11735

OFFSHORE PLATFORMS

High performance composite tubes for offshore applications
[SNIAS-872-430-116] 05 p0572 N88-13488

A system identification technique based on the random decrement signatures. Part 2: Experimental results
05 p0584 N88-13626

Experimental studies on acoustic emission monitoring of crack propagation in offshore structures: A literature survey 05 p0610 N88-13748

Hurricane Danny storm surge data, report 4
[AD-A186373] 07 p0879 N88-15334

Geological evolution and analysis of confirmed or suspected gas hydrate localities. Volume 9: Formation and stability of gas hydrates of the Middle America Trench
[DE88-001007] 10 p1347 N88-18050

Analysis of wind turbines on offshore support structures excited by random wind and random waves
[DE88-004772] 10 p1351 N88-18074

The effect of H2S concentration and pH on hydrogen permeation in AISI 410 stainless steel in 5 percent NaCl
[NPL-DMA(A)-148] 14 p1890 N88-21293

The effect of H2S concentration and pH on the cracking resistance of AISI 410 stainless steel in 5 percent brine
[NPL-DMA(A)-149] 14 p1890 N88-21294

Underwater robotics in the service of oil field exploitation: The Running and Interconnecting Tool (RIT) in the East Frigg field (North Sea) 19 p2699 N88-26049

OFT 4

U SPACE TRANSPORTATION SYSTEM 4 FLIGHT

OGEE WINGS

U VARIABLE SWEEP WINGS

OGIVES

Flow visualization on an ogive-nosed circular cylinder body at high incidence using the laser light sheet method
[ESA-TT-1066] 03 p0315 N88-11993

Calculation of symmetric and asymmetric vortex seperation on cones and tangent ogives based on discrete vortex models
[NASA-CR-4122] 08 p0950 N88-15768

OH-58 HELICOPTER

Identification and proposed control of helicopter transmission noise at the source
09 p1109 N88-16647

OHIO RIVER (US)
Ice conditions along the Ohio River as observed on LANDSAT images, 1972-1985
[AD-A191172] 18 p2531 N88-25018
OHMIC DISSIPATION
Use of polarimetry to measure the current profile in MTX
[DE87-013835] 02 p0237 N88-11495
Helicity dissipation in the plasma edge
[DE87-014762] 03 p0378 N88-12376
On the potential role of concentrated field-aligned currents in solar physics 08 p1099 N88-16614
Transport simulations of ohmic ignition experiment: IGNITEX
[DE88-006055] 15 p2138 N88-22757
Dissipative relativistic radiation hydrodynamics
[DE88-702092] 19 p2685 N88-25846
OHMS LAW
Aging behavior of Au-based ohmic contacts to GaAs
[NASA-CR-182146] 19 p2662 N88-25831
OIL ADDITIVES
The performance of perfluoropolyalkylether oils under boundary lubrication conditions
[AD-A191057] 17 p2323 N88-23869
OIL EXPLORATION
Research needs for hydrocarbon fuels
[DE87-014555] 06 p0687 N88-14209
Three-dimensional transient electromagnetic modeling for exploration geophysics 10 p1346 N88-18047
Utilizing SPOT data for seismic shot-line mapping and environmental monitoring in oil and gas exploration
22 p3098 N88-28401
First results of international investigations of the applications of SPOT-1 data to geologic problems, mineral and energy exploration 22 p3101 N88-28419
Results of the Geosat program to evaluate SPOT data for petroleum and mineral exploration
22 p3102 N88-28422
Evaluation of SPOT imagery contribution to petroleum exploration: The Suez Rift (Egypt)
22 p3102 N88-28425
Structural analysis of the Jura mountains-Rhine Graben intersection (Switzerland) for petroleum exploration using SPOT stereoscopic data 22 p3103 N88-28431
Methodology for the use of SPOT imagery in petroleum exploration. Example of the Bas-Languedoc area (France) 22 p3104 N88-28432
OIL FIELDS
Underwater robotics in the service of oil field exploitation: The Running and Interconnecting Tool (RIT) in the East Frigg field (North Sea) 19 p2699 N88-26049
OIL POLLUTION
Application of SPOT imagery for oil spill contingency planning 22 p3108 N88-28460
OILS
NT CRUDE OIL
NT LUBRICATING OILS
NT MINERAL OILS
Low extractable wipers for cleaning space flight hardware 02 p0137 N88-10863
Boundary lubrication. Experiments with boundary lubrication and plain bearings at +60...-60 deg C temperatures
[DE87-752869] 02 p0180 N88-11124
Analysis of wear metals in engine oils using the atomic absorption spectrophotometric method
[NAL-TM-MT-8704] 05 p0564 N88-13435
A comparison of measurements from the A/E35U-3 and PWMA (Portable Wear Metal Analyzer) spectrometers
[AD-A186855] 09 p1177 N88-17047
Characterization of the arc/spark excitation sources used in the spectrometric oil analysis program
[AD-A187131] 10 p1297 N88-17758
Oil flow patterns on a series of capsule-type re-entry vehicles at hypersonic speeds
[DE88-751805] 16 p2155 N88-22858
Boundary layer flow visualization for flight testing
17 p2297 N88-23742
Low pressure entrained flow pyrolysis of biomass to produce liquid fuels 18 p2535 N88-25043
Research on hydrotreating catalysts to hydrodeoxygenate biocrude oils
18 p2536 N88-25046
Measurement of the radiative properties of gas and oil flames
[NASA-TT-20299] 19 p2612 N88-25502
Study of experimental technique of oil flow with emphasis on quantitative determination of the flow position parameters on the surface
[NASA-TT-20341] 23 p3215 N88-29135
OLEFINS
U ALKENES
OLIVINE
Carbon analysis in natural olivine crystals of deep origin
[NASA-TT-20311] 19 p2734 N88-26239
OMEGA NAVIGATION SYSTEM
Assessment of the differential technique for land navigation within 1000 km of Omega Australia
[AD-A191036] 16 p2160 N88-22885
Western Pacific Omega validation: Project description
[AD-A191753] 18 p2462 N88-24617
Automatic omega station and LOP (Line Of Position) selection
[AD-A193302] 21 p2894 N88-27179
Indian Ocean validation
[AD-A194458] 23 p3175 N88-28902
OMNIDIRECTIONAL ANTENNAS
NT MONOPOLE ANTENNAS
The AMSC mobile satellite system
19 p2643 N88-25681
Omni-directional L-band antenna for mobile communications 19 p2648 N88-25717
ON-LINE SYSTEMS
The VAXONLINE software system at Fermilab
[DE87-013565] 02 p0220 N88-11387
Towards automated consulting: Design feedback from the performance of online documentation
[DE87-012243] 04 p0501 N88-13082
Online monitoring of laserpulses using the GPIB-interface of a Tektronix 2430 Digital Storage Oscilloscope
[DE88-002836] 07 p0856 N88-15201
DoD Gateway Information System (DGIS): Common command language mapping
[AD-A185951] 07 p0942 N88-15726
MICRO system for control, acquisition and processing of experimental data
[DE88-700724] 10 p1386 N88-18278
Modules of nanosecond logic electronics system with computer control
[DE88-700190] 11 p1479 N88-18828
Neurocognitive predictions of performance
[AD-A188323] 12 p1669 N88-19998
Improved flight test productivity using advanced on line data systems 12 p1703 N88-20193
Parallel image compression
[NASA-CR-180758] 13 p1814 N88-20837
Online aiding for human-computer interfaces
[AD-A189239] 13 p1815 N88-20842
MIG-1 on-line measuring holographic microscope
[DE88-701103] 15 p2068 N88-22332
Argus reference manual
[AD-A190382] 15 p2111 N88-22578
IPC for modular software requires a third party connect
[AD-A189199] 16 p2246 N88-23414
On-line measurement of heat of combustion
[NASA-CR-183076] 19 p2738 N88-26255
WORDNET: An electronic lexical reference system based on theories of lexical memory
[AD-A193086] 21 p3027 N88-27970
Geometric modeling for computer aided design
[NASA-CR-183161] 24 p3413 N88-30320
ONBOARD COMPUTERS
U AIRBORNE/SPACEBORNE COMPUTERS
ONBOARD DATA PROCESSING
Design, manufacture and testing of an elegant breadboard model communications processor
[D/2244] 01 p0034 N88-10217
Study, design and evaluation of data reduction by encoding or information extraction. Part 2: Operational considerations — multispectral satellite imagery
[NLR-TR-85094-L-PT-2] 01 p0079 N88-10502
Digital bus unit engineering model: Design, manufacture and test
[MRM/TREP/1003/SAAB] 01 p0083 N88-10537
Study and design of a communication processor unit
[RIDU/TREP/1002/SAAB] 01 p0083 N88-10538
Calibration of attitude control sensors
02 p0159 N88-10995
Prototype Rendezvous Onboard Software (PROBS)
[MATRA-EPT-DT-PRB-2A-00068]
02 p0222 N88-11396
Study of fault tolerant techniques for satellite data handling
[FTT/REP/0001/SAAB] 05 p0632 N88-13860
Data processing of the JPA instrument. Part 1: Data management
[IFSI-86-15-PT-1] 06 p0757 N88-14645
Expert system study for spacecraft management
[TL-2699-ISS-1] 07 p0824 N88-15004
Packet telecommand: System performance assessment study — onboard data handling
[PTC/TNOT/0015/SAAB] 07 p0843 N88-15113
Study of communication options in a distributed data handling system and survey of advanced man machine communications schemes. Work package 1: Interprocess communication
[ESA-CR(P)-2447] 07 p0843 N88-15114
ESA Bulletin No. 10
[ETN-87-90514] 09 p1123 N88-16726
Introducing new technology into onboard handling systems 09 p1124 N88-16730
An expert system to support the verification/validation of flight-critical software
[MBB-UT-102/87] 10 p1314 N88-17852
The RVD mission: The on-board data processing requirements 12 p1585 N88-19495
Prototype on-board software for rendezvous and docking 12 p1586 N88-19496
On-board processing for mobile satellite communications
[ESA-CR(P)-2519] 14 p1905 N88-21382
Development of a flexible and economic helicopter engine monitoring system
[PB88-165147] 16 p2160 N88-22887
On-board data processing of navigation data at high latitudes in Antarctica 22 p3036 N88-28027
Study of standard generic approach for spacecraft (S/C) autonomy and automation (phase 3). Book A: Autonomy concept description
[ESA-CR(P)-2555-VOL-1] 23 p3185 N88-28955
Study of standard generic approach for spacecraft (S/C) autonomy and automation (phase 3). Book B: Autonomy concept application example
[ESA-CR(P)-2555-VOL-2] 23 p3185 N88-28956
Study of standard generic approach for spacecraft (S/C) autonomy and automation (phase 3). Book C: Autonomy concept summary
[ESA-CR(P)-2555-VOL-3] 23 p3185 N88-28957
Investigation of the use of High Order Languages (HOLs) for on-board software
[CRI/FR/HOL-C/1/87] 23 p3251 N88-29349
An expert systems application to space base data processing 23 p3256 N88-29384
Compression and decompression of imaging sensor signals (CADISS): A multiprocessor system for image compression/decompression on board scientific satellites
[NLR-TR-87076-L] 24 p3414 N88-30323
ONBOARD EQUIPMENT
NT AIRBORNE EQUIPMENT
NT AIRBORNE LASERS
NT AIRBORNE/SPACEBORNE COMPUTERS
NT AIRCRAFT EQUIPMENT
NT SPACECRAFT ELECTRONIC EQUIPMENT
NT SPACECRAFT EQUIPMENT
An assessment of clinical chemical sensing technology for potential use in space station health maintenance facility
[NASA-CR-172013] 04 p0475 N88-12626
A project of an intelligent system to help on-line trouble shooting — aircraft maintenance
[SNIAS-872-111-106] 05 p0529 N88-13216
Definition and implementation study for the Varan-S radar
[CNES-CT/DRT/TIT/RL-143-T]
15 p2058 N88-22287
Systems for the 21st century
17 p2302 N88-23769
On-orbit technology experiment facility definition
[NASA-TM-100614] 17 p2311 N88-23824
Digital maps for an electronic traffic guide
18 p2534 N88-25033
Generic supervisor: A knowledge-based tool for control of space station on-board systems
23 p3257 N88-29389
A space station onboard scheduling assistant
23 p3259 N88-29402
Flight test equipment for the on-board measurement of wind turbulence 24 p3311 N88-29719
ONE DIMENSIONAL FLOW
Relaxation method for the compressible Navier-Stokes equations using upwind schemes
05 p0539 N88-13280
TOPP: A post-processor for TOPAZ, the one dimensional pipe flow analysis code
[DE88-003711] 09 p1164 N88-16981
One dimensional calculation model for laser [illegible] plasmas expanding in vacuum
[ISL-R-128/86] 14 p1904 8-21838
ONE-PHASE FLOW
U SINGLE-PHASE FLOW
ONISOTROPY
U ANISOTROPY
ONSAGER RELATIONSHIP
Application of Onsager's reciprocity relations to interface motion
[DE88-003286] 10 p1397 N88-18327
ONTOGENESIS
U ONTOGENY
ONTOGENY
Some remarks on gravitational biology
07 p0864 N88-15366
Biological patterns of growth in postnatal ontogenesis of lower primates 19 p2705 N88-26087

OPACITY

Evidence for an additional source of opacity during the impulsive phase of stellar flares
04 p0510 N88-13133

Computer program in BASIC language for computation of spectrochemical analytical data
[DE88-701229] 15 p2032 N88-22106

Survey of material for an infrared-opaque coating
[NASA-TM-88204] 22 p3153 N88-28757

OPEN CHANNEL FLOW

Open channel flow near the resonance speed
18 p2514 N88-24918

Recent insights into instability and transition to turbulence in open-flow systems
[NASA-CR-181693] 24 p3372 N88-30079

OPENINGS

NT APERTURES
NT PORTS (OPENINGS)
NT SLITS
NT SYNTHETIC APERTURES

Superconducting switch program
[AD-A185682] 07 p0848 N88-15144

Theoretical and observational problems with Holes in the far UV dayglow
[AD-A188190] 10 p1355 N88-18100

Strength and failure analysis of composite laminate containing a circular hole with reinforcement
[AD-A189629] 14 p1884 N88-21260

OPERATING COSTS

Requirements and cost considerations for a Combined Space Nuclear Reactor Test Facility
[DE88-006763] 15 p2132 N88-22719

Costs and benefits of AC propulsion
[PB88-173380] 16 p2287 N88-23891

A contribution to the quantitative analysis of the influence of design parameters on the optimal design of passenger aircraft
[ETN-88-92979] 23 p3176 N88-28912

OPERATING SYSTEMS (COMPUTERS)

UNIX benchmark system
[AD-A184492] 03 p0367 N88-12306

Connecting RPC (Remote Procedure Call)-based distributed systems using wide-area networks
[PB87-234423] 05 p0658 N88-14041

MINIX: A UNIX clone with source code
[PB88-100862] 06 p0760 N88-14864

Clouds: A support architecture for fault tolerant, distributed systems 10 p1375 N88-18206

The mapping of parallel algorithms to reconfigurable parallel architectures 10 p1376 N88-18209

Performance and evaluation at the Center for Supercomputing Research and Development
[DE88-003563] 10 p1417 N88-18456

Space station operating system study
[NASA-CR-179309] 11 p1446 N88-18619

Applicability of Ada (trademark) tasking for avionics executives
[AD-A188827] 12 p1578 N88-19445

A production-quality UNIX Very High Speed Integrated Circuit (VHSIC) Hardware Description Language (VHDL) subset analyzer
[AD-A188832] 12 p1623 N88-19710

Experience with Berkeley UNIX interprocess communications
[AD-A188353] 12 p1680 N88-20041

MultiRPC: A parallel remote procedure call mechanism
[AD-A188613] 12 p1680 N88-20046

An interface between object-oriented systems
[AD-A189245] 13 p1815 N88-20844

An amoeba replicated service organisation -- Amoeba operating system
[CWI-CS-R8723] 13 p1822 N88-20892

Distributed operating systems: An overview
[INF-87-29] 14 p1960 N88-21686

Sigma system: Overview, prospects
15 p2052 N88-22230

Introduction to the VMS (DEC) operating system
[ENST-87D006] 16 p2245 N88-23409

Concurrency efficiency user's manual
[AD-A190884] 16 p2251 N88-23450

Design, implementation and evaluation of an operating system for a network of transputers
[AD-A186593] 18 p2558 N88-25193

The MELCOM PSI 2 AI workstation
21 p2930 N88-27395

Process migration in UNIX environments
[NASA-CR-182951] 23 p3245 N88-29311

A rule-based systems approach to spacecraft communications configuration optimization
24 p3417 N88-30341

OPERATING TEMPERATURE

Evaluating and testing thermographic phosphors for turbine-engine temperature measurements
[DE87-011772] 02 p0174 N88-11090

Blade excitation criteria developed for aero derived engines in Arctic Alaska
[PNR90368] 02 p0182 N88-11131

The effect of operating temperature on open, multimegawatt space power systems
17 p2414 N88-24352

The effect of operating temperature and turbine blade cooling on Brayton cycle space power systems
17 p2435 N88-24489

OPERATIONS RESEARCH

Workshop on AI (Artificial Intelligence) and Simulation (2nd) held in Seattle, Washington on 14 July 1987
[AD-A183736] 01 p0084 N88-10542

Extraction and evaluation of Boolean relations for the solution of linear programs in 0-1 variables, volume 1
[ENST-86E023-VOL-1] 02 p0227 N88-11430

Extraction and evaluation of Boolean relations for the solution of linear programs in 0-1 variables, volume 2
[ENST-86E023-VOL-2] 02 p0227 N88-11431

Potential applications of expert systems and operations research to space station logistics functions
[NASA-CR-180473] 03 p0372 N88-12342

Inventory behavior at remote sites
06 p0796 N88-14873

Estimating system reliability: Monte Carlo methods, sensitivity and errors in input parameters
[AD-A186182] 07 p0885 N88-15248

A multicut algorithm for two-stage stochastic linear programs
[AD-A186148] 07 p0903 N88-15486

Explicit construction and analysis of some efficient empirical production functions in data envelopment analysis
[AD-A185907] 07 p0906 N88-15502

GAVID and ACQUIR, two Operations-Research (OR) models for visual detection
[FEL-1985-72] 09 p1200 N88-17194

Artificial intelligence (AI), Operations Research (OR), and Decision Support Systems (DSS): A conceptual framework 09 p1209 N88-17245

Range and mission scheduling automation using combined AI and operations research techniques
09 p1209 N88-17249

Operations research in management?
[MBB-Z-138/87] 10 p1311 N88-17835

Perspectives on parallel computing
[CWI-OS-R8709] 13 p1822 N88-20889

SEARCH: An interactive computer program for optimizing two-variable, unconstrained experiments or simulation
[AD-A190580] 15 p2112 N88-22583

Optical symbolic processor for expert system execution
[AD-A192005] 18 p2575 N88-25296

Realistic planning scenarios
[AD-A191640] 19 p2740 N88-26267

A fast parametric maximum flow algorithm, revision
[AD-A194026] 23 p3250 N88-29345

Faster scaling algorithms for network problems
[AD-A194032] 23 p3251 N88-29348

Finding minimum-cost circulations by canceling negative cycles
[AD-A194027] 23 p3271 N88-29468

Finding minimum-cost circulations by successive approximation
[AD-A194028] 23 p3272 N88-29469

Improved time bounds for the maximum flow problem
[AD-A194034] 23 p3272 N88-29471

OPERATOR PERFORMANCE

Report of safety survey: Human integration of approach charts
[DOT/FAA/PM-87/15] 01 p0076 N88-10498

Gender and cognitive style differences at the human-computer interface
[NPL-DITC-90/87] 01 p0077 N88-10483

Input devices for tasks using interactive video
[NPL-DITC-87/87] 01 p0080 N88-10510

Assessment of fatigue in aviation crews
[AD-A184129] 03 p0356 N88-12245

Proceedings of the DOD Workload Assessment Workshop on Workload Assessment Techniques and Tools held in Dayton, Ohio on 27-28 September 1986
[AD-A185650] 08 p1052 N88-16352

Crew procedures for microwave landing system operations
[NASA-CR-178359] 09 p1116 N88-16686

A human performance modelling approach to intelligent decision support systems 09 p1208 N88-17242

Investigation of effects of short-term exposure to high concentrations of carbon monoxide on operator's psychophysiological functions 10 p1361 N88-18133

Risk of hypertension and functional cerebral laterality in oil expedition works in far north
12 p1665 N88-19880

OMV man/system simulation integration: A preliminary analysis and recommendation
[NASA-CR-182602] 12 p1671 N88-20005

Human problem solving in dynamic environments. Understanding and supporting operators in large-scale, complex systems
[AD-A189539] 13 p1812 N88-20826

Mental-State Estimation, 1987
[NASA-CP-2504] 16 p2239 N88-23370

An overview of current approaches and future challenges in physiological monitoring
16 p2239 N88-23371

Toward a mathematical formalism of performance, task difficulty, and activation 16 p2239 N88-23372

Challenges of physiological monitoring in a Navy operational setting 16 p2239 N88-23374

Predicting operator workload during system design
16 p2239 N88-23375

POPEYE: A production rule-based model of multitask supervisory control (POPCORN)
16 p2240 N88-23384

A correlational approach to predicting operator status
16 p2242 N88-23393

Development of a C3 generic workstation: System overview 16 p2242 N88-23396

C3 generic workstation: Performance metrics and applications 16 p2242 N88-23397

The biomorphic model of the human operator controlling a single or a double integrator
[LR-505] 16 p2243 N88-23402

The representational code of the internal model of dynamic systems: An individual differences and dual task approach
[AD-A190676] 16 p2244 N88-23403

Spatial cognition 17 p2380 N88-24152

Teleoperator human factors study
[NASA-CR-178930] 17 p2382 N88-24162

An advanced prototyping tool for human factors design
[AD-A187290] 18 p2552 N88-25149

Method for observing changes in functional state of human operator 20 p2830 N88-26789

Neurophysiological patterns of operational fatigue: Preliminary results 21 p2981 N88-27703

Display system image quality
23 p3242 N88-29296

OPERATORS (MATHEMATICS)

NT LINEAR OPERATORS

Semidiscrete Galerkin method for semilinear evolution equations with a differential operator of third order
[BONNER-MATHE-SCHR-181]
01 p0087 N88-10570

Processing of fractal functions by linear and nonlinear operators
[RAE-TR-85079] 01 p0088 N88-10571

Spectral and structural properties of nonnegative reducible operators in Banach relations
[ETN-87-90402] 01 p0089 N88-10581

Finite-dimensional matrix representation of the differential operator, determinantal form and zeros of special functions
[DE87-703091] 02 p0225 N88-11421

On operator splitting for unsteady boundary value problems
[AD-A184291] 04 p0484 N88-12981

Eigenvalue projection theory for linear operator equations of electromagnetics
[AD-A185434] 05 p0575 N88-13504

On a boundary data operator and generalized exterior Robin problems for the Helmholtz equation
[AD-A185124] 05 p0640 N88-13915

Introduction to string field theory
[DE87-014583] 05 p0657 N88-14032

Pseudodifferential operators on the circle and finite differences
[PB87-222352] 06 p0783 N88-14681

Recursion operator and bihamiltonian structure for integrable multi-dimensional lattices
[PREPRINT-552] 06 p0784 N88-14686

Nonisospectral deformations and Darboux transformations for the 3rd order spectral problem
[PREPRINT-558] 06 p0784 N88-14690

Embedding topological median algebras in products of dendrons
[PB88-100888] 06 p0787 N88-14713

Operator foundation of functional integral in non-Abelian gauge theory
[DE88-700508] 07 p0941 N88-15710

A learning apprentice for software parts composition
08 p1065 N88-16436

Developments related to scattering eigen elements in Schroedinger operators for particles with spin
[ETN-88-91077] 09 p1229 N88-17361

Application of state-multipole Heisenberg equations to Raman excitation dynamics
[DE88-003826] 10 p1335 N88-17977

Schwarz splitting and template operators
[AD-A187956] 10 p1404 N88-18370
Canonical coordinates for partial differential equations
[NASA-CR-182486] 11 p1535 N88-19170
Irreducible tensor operators and multiple-quantum NMR 11 p1542 N88-19217
On the norm equivalence of singularly perturbed elliptic difference operators
[DE88-006353] 13 p1826 N88-20913
Choice of implicit and explicit operators for the upwind differencing method
[NASA-TM-100857] 14 p1964 N88-21718
Peetre's Theorem and generalized functions
[MEMO-881] 14 p1967 N88-21742
The two-dimensional Toda-lattice and its recursion operators
[PREPRINT-571] 14 p1968 N88-21746
Algebraic structure of linear and nonlinear models of open quantum systems
[PREPRINT-573] 14 p1968 N88-21747
Mixing coefficients of the lattice weak Hamiltonian with dimension five operators
[PREPRINT-576] 14 p1968 N88-21749
Recursion operator and Backlund Transformation for the Ruijsenaars-Toda lattice
[PREPRINT-577] 14 p1968 N88-21750
Coding capacity of generalized additive channels
[AD-A190315] 15 p2127 N88-22685
Systolic algorithm for matrix-vector multiplication
[PB88-165394] 16 p2256 N88-23484
On the efficient implementation of the fast multipole algorithm
[AD-A191167] 17 p2365 N88-24173
Canonical construction of differential operators intertwining representations of real semisimple Lie groups
[DE88-701852] 20 p2845 N88-26882
Theory of pseudo-differential operators over C*-algebras
[DE88-701860] 20 p2845 N88-26883

OPERATORS (PERSONNEL)
NT AIRCRAFT PILOTS
NT PILOTS (PERSONNEL)
Measurement of suspension and ride characteristics of the M1 main battle tank 05 p0596 N88-13637
Using multiple dialog modes in a user-system interface to accomodate different levels of user experience: An experimental study
[AD-A186115] 07 p0899 N88-15444
Interfacing the expert: Characteristics and requirements for the user interface in expert systems
08 p1063 N88-16419
Space languages 08 p1063 N88-16420
Human problem solving in dynamic environments. Understanding and supporting operators in large-scale, complex systems
[AD-A189539] 13 p1812 N88-20826
Extension of computer based algorithms by operator analysts
[NASA-CR-182798] 15 p2111 N88-22575

OPHTHALMOLOGY
Does the knife open perspectives for the myopic pilot?
[ETN-87-90166] 09 p1199 N88-17167
Microesotropia patients performa well as military jet pilots 21 p2925 N88-27363

OPTICAL ABSORPTION
U ELECTROMAGNETIC ABSORPTION
U LIGHT TRANSMISSION

OPTICAL ACTIVITY
Image processing for optical engineering applications
[PB87-210035] 03 p0376 N88-12364

OPTICAL AMPLIFIERS
U LIGHT AMPLIFIERS

OPTICAL BISTABILITY
Ultrafast intrinsic bistable devices
[PB87-109310] 05 p0649 N88-13978
Dependence of formation of radiative color centers in optical glass fibers on technological factors
14 p1896 N88-21321
Theory of interactions of intense light with nonlinear, inhomogeneous and periodic structures and its applications to optical bistability, optic gyroscopes, nonlinear spectroscopy, radiation protection, X-ray emission and related fields
[AD-A190040] 15 p2133 N88-22725
Cooperative effects and intrinsic optical bistability in collections of atoms
[AD-A193993] 23 p3280 N88-29530

OPTICAL COMMUNICATION
Coherent infrared detection, volume B --- CO2 laser intersatellite data link
[ESA-CR(P)-2392-VOL-1] 01 p0034 N88-10218
Coherent infrared detection, volume D --- CO2 laser intersatellite data link
[ESA-CR(P)-2392-VOL-2] 01 p0034 N88-10219
The design and testing of an analog optical communication link capable of the simultaneous transmission of four frequency division multiplexed audio signals
[AD-A184695] 03 p0307 N88-11936
Frequency doubling conversion efficiencies for deep space optical communications 04 p0434 N88-12691
The atmosphere of Mars and optical communications
04 p0434 N88-12692
A near-earth optical communications terminal with a corevolving planetary sun shield
04 p0434 N88-12693
Electro-optical studies of semiconductor compounds for electroluminescent and laser devices
[PH-155] 07 p0937 N88-15693
Optical communication with semiconductor laser diodes
[NASA-CR-182464] 09 p1154 N88-16918
Signal processing studies program optical signal amplification, volume 1
[AD-A188055] 10 p1321 N88-17897
Design and implementation of a fiber optic RS232 link
[AD-A187319] 10 p1409 N88-18409
Microwave semiconductor research-materials, devices and circuits
[AD-A187121] 10 p1415 N88-18444
A laser communication experiment utilizing the ACT satellite and an airborne laser transceiver
[NASA-TM-100792] 11 p1492 N88-18910
Computation of LMS (Least-Mean-Square) and matched digital filters for optical clutter suppression
[AD-A188685] 12 p1687 N88-20093
Effect of atmospheric turbulence on the bit error probability of a space to ground near infrared laser communications link using binary pulse position modulation and an avalanche photodiode detector
[NASA-TM-100699] 14 p1873 N88-21169
Continued design of a Pointing, Acquisition, and Tracking (PAT) subsystem for InterSatellite Laser links (ISL2)
[TELDIX-15-093-178] 14 p1905 N88-21364
Characteristics of distributed feedback lasers discussed 16 p2185 N88-23028
Design and evaluation of single-lobed far-field pattern laser arrays: AlGaAs/GaAs and InGaAsP/InP systems --- optical communication
[LAAS-88-023] 16 p2214 N88-23211
Engineering planetary lasers for interstellar communication
[NASA-CR-180780] 17 p2311 N88-23825
Interaction of solitons in single model optical fibres
17 p2439 N88-24511
Assessment of optical communications systems for Data Relay Satellite. Volume 1: Executive summary
[ESA-CR(P)-2488-VOL-1] 18 p2502 N88-24641
Assessment of optical communications systems for the Data Relay Satellite
[ESA-CR(P)-2488-VOL-2] 18 p2502 N88-24642
Activities report of the Division of Optical Technology
[FOA-C-30477-3] 18 p2576 N88-25299
New semiconductor laser structure for an optical communication system
[ETN-88-92353] 20 p2807 N88-26654
Use of fiber optic equipment for security
[DE88-007898] 20 p2853 N88-26943
Strawman Optical Reception Development Antenna (SORDA) 22 p3065 N88-28187
Effect of detector dead time on the performance of optical direct-detection communication links
22 p3065 N88-28190
Multichannel data transmission through a fiber optic cable
[AD-A193842] 22 p3070 N88-28221
Optical multiple access intersatellite links
[BAE-TP-8502] 24 p3361 N88-30013

OPTICAL COMPUTERS
Optical symbolic processor for expert system execution
[AD-A187494] 10 p1385 N88-18266
Integrated optical synthetic aperture radar processor
[AD-A188019] 11 p1471 N88-18772
Optical symbolic processor for expert system execution
[AD-A187882] 11 p1525 N88-19103
Optical computing research
[AD-A187862] 11 p1549 N88-19264
Ultra-high speed integrated optical waveguide devices for optical computing
[AD-A188470] 12 p1691 N88-20118
Applications of optical computing to problems with symbolic computations
[AD-A189772] 15 p2106 N88-22548
Optical Conceptual Computing and Associative Memory (OCCAM)
[AD-A190030] 15 p2107 N88-22550
Optical computer and optical methods for data processing 18 p2518 N88-24939
Theoretical investigation of optical computing based on neural network models
[AD-A191668] 18 p2563 N88-25214
Optical computing based on neuronal models
[AD-A191481] 18 p2575 N88-25293
Optical symbolic processor for expert system execution
[AD-A192005] 18 p2575 N88-25296
Mitsubishi Electric Advance (R and D Edition), Volume 41
[PB88-194162] 21 p2929 N88-27388
Basic research on optical neural computers
21 p2929 N88-27389
Architecture for optical digital computers
[AD-A195477] 24 p3430 N88-30416

OPTICAL CORRECTION PROCEDURE
Corrections for differential scattering by aerosols in the measurement of ozone by DIAL --- differential absorption lidar (DIAL)
[NPL-QU-78] 14 p1945 N88-21603

OPTICAL COUNTERMEASURES
MIDIR (Mid-Infrared) laser, phase 1
[AD-A193935] 23 p3220 N88-29166

OPTICAL COUPLING
Research on acoustical scattering, diffraction catastrophes, optics of bubbles, photoacoustics, and acoustical phase conjugation
[AD-A185785] 06 p0776 N88-14761
Passive coupler, network adapter, and network acquisition procedure for optical local networks
[ETN-88-92130] 14 p1961 N88-21695
Discussion of two-mode two-photon CW laser oscillation 16 p2187 N88-23042

OPTICAL DATA PROCESSING
NT SCENE ANALYSIS
Implementation of a digital optical matrix-vector multiplier using a holographic look-up table and residue arithmetic
[NASA-CR-180431] 01 p0078 N88-10486
Nonconventional optical techniques for optical wavefront processing
[AD-A185099] 05 p0650 N88-13982
The role of photodetectors in optical signal processing
[AD-A186804] 09 p1247 N88-17476
Image texture classification with an optical crossbar interconnected processor 10 p1375 N88-18202
Integrated optical synthetic aperture radar processor
[AD-A188019] 11 p1471 N88-18772
Optical symbolic processor for expert system execution
[AD-A187882] 11 p1525 N88-19103
Optical computing research
[AD-A187862] 11 p1549 N88-19264
Optical signal processing using nonlinear optics
[AD-A188461] 12 p1691 N88-20117
Ultra-high speed integrated optical waveguide devices for optical computing
[AD-A188470] 12 p1691 N88-20118
Study of photochromic materials for use in optical signal processing
[AD-A189068] 13 p1839 N88-21006
Gigantic optical nonlinearity in low dimensional systems 14 p1975 N88-21786
Error reduction in two-dimensional pulse-area modulation, with application to computer-generated transparencies --- optical field synthesis
[EUT-87-E-172] 14 p1982 N88-21825
Applications of optical computing to problems with symbolic computations
[AD-A189772] 15 p2106 N88-22548
Optical Conceptual Computing and Associative Memory (OCCAM)
[AD-A190030] 15 p2107 N88-22550
Space-variant optical systems
[AD-A189967] 15 p2133 N88-22724
Sky radiance distributions for thermal imaging backgrounds
[AD-A191135] 17 p2373 N88-24115
Nonlinear surface polaritons
[AD-A191046] 18 p2499 N88-24822
Theoretical investigation of optical computing based on neural network models
[AD-A191668] 18 p2563 N88-25214
Optical computing based on neuronal models
[AD-A191481] 18 p2575 N88-25293
Activities report of the Division of Optical Technology
[FOA-C-30477-3] 18 p2576 N88-25299
Optical nonlinearities in GaAs/GaAlAs multiple quantum wells fabricated by metalorganic chemical vapor deposition for use in optical signal processing
[AD-A191558] 18 p2582 N88-25337
Optical data processing
[AD-A193024] 20 p2839 N88-26841
Investigation of the potential impact of new photonic materials on optical processing systems
21 p2924 N88-27359

Optical interconnections for digital image coding
21 p2928 N88-27381
An optical 2-dimensional correlator for pattern recognition in embedded computing
[DE88-007198] 21 p2998 N88-27780
Optical symbolic computing
[AD-A195680] 24 p3429 N88-30406
Spectroscopic studies with multiple quantum well materials with applications to optical signal processing at room temperature
[AD-A194171] 24 p3429 N88-30409
Use of depletion edge translation for high-speed modulation and switching of lightwaves
[AD-A195611] 24 p3430 N88-30417

OPTICAL DATA STORAGE MATERIALS
Holographic disk for data storage
14 p1972 N88-21771
Evaluation of multi-focus holographic lenses
[AD-A196167] 24 p3377 N88-30110

OPTICAL DENSITY
Study of kinetics of intracavity absorption in pulsed dye lasers 07 p0919 N88-15585
Perception and control of simulated self motion
[AD-A187444] 10 p1372 N88-18188
Characteristics of coherent and incoherent waves in snow at microwave and millimeter wave frequencies
[AD-A188990] 12 p1620 N88-19692
The visiocellometer and its tactical applications
[AD-A188216] 12 p1647 N88-19866

OPTICAL DEPTH
U OPTICAL THICKNESS

OPTICAL DISKS
Storing photomicrographs on optical laser disks
[DE87-013747] 04 p0449 N88-12785
Recording materials for optical disk memory discussed
06 p0684 N88-14193
Holographic disk for data storage
14 p1972 N88-21771
Use of optical disk technology at the Air Command and Staff College
[AD-A192424] 21 p3027 N88-27969

OPTICAL EMISSION
U LIGHT EMISSION

OPTICAL EMISSION SPECTROSCOPY
NT LASER SPECTROSCOPY
Evidence of a new spectral line intensity formula for optical emission
[KGI-PREPRINT-098] 01 p0090 N88-10585
Optical spectroscopy of IRAS sources with infrared emission bands. 1: IRAS 21282 + 5050 and the diffuse interstellar bands
[NASA-CR-181387] 01 p0094 N88-10611
On the signal strength dependency on pressure in laser sub-Doppler saturation spectroscopy with special attention to gaseous diatonic molecules
[USIP-87-13] 09 p1171 N88-17023
The relationship between low activity comets and more active comets 14 p1997 N88-21904
The optical spectroscopy of copper-blue luminescence in zinc sulfide crystals. Zero-phonon line spectra under the influence of magnetic field, temperature and excitation intensity
[ETN-88-93122] 24 p3344 N88-29903

OPTICAL EQUIPMENT
NT CAMERAS
NT COLLIMATORS
NT DIFFRACTION LIMITED CAMERAS
NT DIFFRACTOMETERS
NT EBERT SPECTROMETERS
NT ELECTROPHOTOMETERS
NT ELLIPSOMETERS
NT ENDOSCOPES
NT ETALONS
NT FAINT OBJECT CAMERA
NT FRAMING CAMERAS
NT HIGH SPEED CAMERAS
NT IMAGE CONVERTERS
NT IMAGE TUBES
NT INFRARED SPECTROMETERS
NT INFRARED SPECTROPHOTOMETERS
NT LASER DOPPLER VELOCIMETERS
NT LASER RANGE FINDERS
NT LIGHT SCATTERING METERS
NT MICRODENSITOMETERS
NT MULTISPECTRAL BAND CAMERAS
NT MULTISPECTRAL BAND SCANNERS
NT OCULOMETERS
NT OPTICAL GYROSCOPES
NT OPTICAL MEASURING INSTRUMENTS
NT OPTICAL MICROSCOPES
NT OPTICAL PYROMETERS
NT OPTICAL RADAR
NT OPTICAL SCANNERS
NT PERISCOPES
NT PHOTOMETERS
NT PINHOLE CAMERAS
NT POLARIMETERS
NT PRISMS
NT REFRACTOMETERS
NT SPECTROHELIOGRAPHS
NT SPECTROPHOTOMETERS
NT STREAK CAMERAS
NT TELEVISION CAMERAS
NT THEMATIC MAPPERS (LANDSAT)
NT THEODOLITES
NT TOTAL OZONE MAPPING SPECTROMETER
NT TRANSMISSOMETERS
NT ULTRAVIOLET SPECTROMETERS
NT ULTRAVIOLET SPECTROPHOTOMETERS
NT WIDE ANGLE LENSES
Optically time-resolved detonation break out
[DE87-010340] 01 p0031 N88-10199
Test of the Hipparcos payload in the Liege vacuum facility focal 02 p0135 N88-10850
Fundamentals and techniques of nonimaging optics research
[DE87-014544] 02 p0236 N88-11488
Storing photomicrographs on optical laser disks
[DE87-013747] 04 p0449 N88-12785
Development of optical modulators for measurements of solar magnetic fields
[NASA-TM-100315] 04 p0490 N88-13016
Airborne Visible/Infrared Imaging Spectrometer (AVIRIS) spectrometer design and performance
06 p0706 N88-14327
Optical electronics for meteor observations
06 p0741 N88-14559
Hard- and software problems of spaced meteor observations by optical electronics
06 p0741 N88-14560
Use of spherical optics in high resolution soft X-ray grating monochromators
[PB87-125191] 06 p0780 N88-14788
Investigation of the performance of a novel double crystal X-ray monochromator measurements
[PB87-125167] 06 p0788 N88-14834
Laser Program
[DE87-011009] 07 p0856 N88-15212
Design of the Backscatter Spectroscopy System for the Nova Laser Facility
[DE88-001880] 07 p0859 N88-15214
The magic of carrier patterns in moire interferometry
[AD-A187582] 10 p1296 N88-17748
Remote sensing of atmospheric crosswinds by utilizing speckle-turbulence interaction and optical heterodyne detection
[AD-A187580] 10 p1347 N88-18052
Fabrication and evaluation of transmissive multilayer optics for 8 keV X-rays
[DE88-003999] 10 p1409 N88-18402
A chemical precursor to optical damage. Studies by laser ionization mass spectrometry
[DE88-004321] 10 p1409 N88-18408
Subpicosecond optical digital computation using phase conjugate parametric generators
[AD-A188279] 10 p1410 N88-18411
Microwave semiconductor research-materials, devices and circuits
[AD-A187121] 10 p1415 N88-18444
Optical memory cards: A comparison with other current technologies and potential military applications
[AD-A187287] 10 p1425 N88-18512
Multiaperture optical system research
[AD-A188211] 11 p1549 N88-19267
Radiation effects on gallium arsenide integrated optical devices
[DE88-004107] 11 p1551 N88-19277
Optical waveguide formation by ion implantation of Ti or Ag
[DE88-004595] 11 p1551 N88-19278
Holographically correcting synthetic aperture aberrations
[AD-A189510] 12 p1692 N88-20123
Laser gyro attitude control system feasibility
[AD-A189368] 13 p1720 N88-20285
Aberrations: Their effect on off-axis beam steering
[AD-A189601] 13 p1840 N88-21006
Applications of the lateral shearing interferometer in measurement of synchrotron radiation optical elements
[DE88-005184] 13 p1840 N88-21011
Cryogenic test facilities for an optical cryomechanism qualification 14 p1879 N88-21228
Laser technology: CO2 lasers and laser optics
[ETN-88-91469] 14 p1915 N88-21441
Preliminary airworthiness evaluation of the UH-60A with Advanced Digital Optical Control System (ADOCS)
[AD-A190674] 15 p2018 N88-22030
Applications of optical computing to problems with symbolic computations
[AD-A189772] 15 p2106 N88-22548
Computer tomography and hybrid optical/digital methods for aerodynamic measurements
[AD-A190909] 16 p2157 N88-22872
Applications research studies of microtubules
[AD-A190855] 16 p2182 N88-23005
Tunable optical sources/growth and characterization of nonlinear optical materials
[AD-A190874] 16 p2274 N88-23608
Joint services electronics program
[AD-A192076] 18 p2504 N88-24856
Optical symbolic processor for expert system execution
[AD-A192005] 18 p2575 N88-25296
Research in the optical sciences
[AD-A192175] 18 p2575 N88-25297
Investigation of the Sun-aligned F-region walls and related phenomena in the auroral latitude range
[AFGL-TR-87-0248] 19 p2692 N88-26000
Use of fiber optic equipment for security
[DE88-007898] 20 p2853 N88-26943
In-situ reactive of X-ray optics by glow discharge
[DE88-009840] 20 p2854 N88-26947
Fabrication technology
[DE88-010598] 20 p2855 N88-26955
Novel quantum well optical devices
20 p2868 N88-27028
An optical 2-dimensional correlator for pattern recognition in embedded computing
[DE88-007198] 21 p2998 N88-27780
Four-frame gated optical imager with 120-ps resolution
[DE88-011735] 22 p3080 N88-28288
Beam optics test stand
[AD-A193901] 23 p3216 N88-29144
Center for opto-electronic systems research instrumentation grant
[AD-A193711] 23 p3282 N88-29545
A fiber optic collective flight control system for helicopters
[AD-A195406] 24 p3328 N88-29818
Optoelectronic gain control of a microwave single stage GaAs MESFET amplifier
[NASA-CR-182201] 24 p3368 N88-30055
Application of nondestructive testing techniques to materials testing
[AD-A195716] 24 p3381 N88-30138

OPTICAL FIBERS
Ultrafast holography using optical fibers
[ISL-R-101/86] 02 p0176 N88-11096
Effects of radiation damage in optical fibers: A tutorial
[PB87-210308] 02 p0235 N88-11482
Radiation-induced transient attenuation of optical fibers at 800 and 1300 nm
[DE87-013165] 02 p0235 N88-11485
Photoinduced low-temperature changes in optical losses in fiber optics based on chalcogenide glasses
06 p0770 N88-14731
Synchronous multi-image high speed photography of welding arc by optical fibers
[PB87-143939] 07 p0857 N88-15202
Transversely anisotropic curved optical fibres: Variational analysis of a nonstandard Eigenproblem
[PB88-112966] 08 p1083 N88-16528
Studies on nonlinear mechanisms of excimer laser propagation in fused silica fibers
[AD-A186822] 09 p1156 N88-16929
Turbine flow meter with optical fiber pick-up
[NAL-TR-923] 09 p1169 N88-17009
Wide band data transmission system using optical fibers
[DE88-004555] 10 p1319 N88-17889
The use of optical fibers for shock pressure and timing measurements at high pressures
[DE88-004012] 10 p1334 N88-17971
Optically controlled phased-array antenna technology for space communication systems
[NASA-TM-100852] 11 p1476 N88-18809
New monostatic balanced Doppler velocimeter using a polarization preserving fiber
[PB88-130869] 11 p1490 N88-18895
Diode pumped fiber laser
[AD-A187694] 11 p1491 N88-18902
Quantum nondemolition detection and squeezing in optical fibers 14 p1976 N88-21793
Berry's phase in fiber optics 14 p1977 N88-21797
Hermetic coating of optical fibers
[AD-A189886] 15 p2044 N88-22177
Clinical measurements using fiber optic sensors
[DE88-005624] 15 p2134 N88-22731
Lifetime of pristine optical fibers
[ETN-88-92246] 16 p2273 N88-23602
Interaction of solitons in single model optical fibres
17 p2439 N88-24511
Study of light transmission methods from scintillators to optical fiber with wave length shifter
[DE88-701587] 18 p2574 N88-25292

Novel fiber preforms: Rare earth doping
[AD-A191549] 18 p2575 N88-25294

Optical sensing of magnetic fields
19 p2670 N88-25871

Peturbational analysis of the curved anisotropic optical fiber for the birefringence due to the geometry
[PB88-171848] 19 p2726 N88-26189

Stress-related phenomena in transient radiation-induced absorption in optical fibers
[DE88-010956] 20 p2854 N88-26949

Multi-mode optical fibers for simultaneous 13-position measurements Thomson scattering apperatus in the JFT-2M tokamak
[DE88-753133] 21 p3015 N88-27897

Fiber optic sensing systems using high frequency resonant sensing heads with intensity sensors
[NASA-TM-101318] 22 p3080 N88-28293

OPTICAL FILTERS

Improving coherent visualization by means of film optical filtering --- projectile visualization
[ISL-R-116/86] 02 p0176 N88-11097

Reduction of temperature rise in high-speed photography
[NASA-TM-100222] 02 p0176 N88-11100

Sideband suppression by an intracavity optical filter in the Los Alamos free-electron laser oscillator
[DE87-011740] 02 p0177 N88-11103

Multilayer-coated mirrors as power filters in synchrotron radiation beamlines
[DE88-003872] 11 p1550 N88-19276

Raman enhancement methods for molecular structure characterization of optical thin films
[DE88-003421] 11 p1556 N88-19324

Photographic filters
[INPE-4448-RPE/558] 12 p1692 N88-20124

Study of photochromic materials for use in optical signal processing
[AD-A189068] 13 p1839 N88-21006

Fundamental noise processes in a laser excited optical filter
[DE88-006460] 15 p2070 N88-22340

Advanced programming and control techniques for complex mechanical systems
[AD-A190238] 15 p2071 N88-22349

Fabry-Perot etalons as prefilters for astronomical far infrared Fourier transform spectroscopy
[MPE-205] 16 p2273 N88-23603

Analysis of binarized Hartley phase-only filter performance with respect to stochastic noise
[DE88-007604] 18 p2519 N88-24945

Optical correlation using the magneto-optic device
[AD-A192342] 20 p2654 N88-26950

OPTICAL GENERATORS
U LASER CAVITIES

OPTICAL GYROSCOPES

Navigation using the Teldix fiber-optic gyroscope
18 p2517 N88-24933

OPTICAL HETERODYNING

Methods for a coherent CO2 laser heterodyne radar system
[ESA-TT-1035] 03 p0328 N88-12076

Remote sensing of atmospheric crosswinds by utilizing speckle-turbulence interaction and optical heterodyne detection
[AD-A187580] 10 p1347 N88-18052

OPTICAL IMAGES
U IMAGES

OPTICAL MASER MODULATION
U LIGHT MODULATION

OPTICAL MASERS
U LASERS

OPTICAL MATERIALS

Phase equilibrium and crystal growth studies on AgGaSe2 and related nonlinear optical materials
[AD-A193763] 22 p3157 N88-28783

OPTICAL MEASUREMENT
NT ASTRONOMICAL PHOTOMETRY
NT COLORIMETRY
NT ELECTROPHOTOMETRY
NT INFRARED PHOTOMETRY
NT PHOTOMETRY
NT POLARIMETRY
NT SPECTROPHOTOMETRY
NT STELLAR SPECTROPHOTOMETRY
NT ULTRAVIOLET PHOTOMETRY
NT VISUAL PHOTOMETRY

An instrument for the quasi-continuous determination of atmospheric soot content
[DFVLR-FB-87-04] 01 p0068 N88-10433

Optical power line voltage and current measurement systems. Volume 1: Limits to the precision of electro-optic and magneto-optic sensors
[DE87-014558] 02 p0175 N88-11092

Description of a multiframe optical probing system
[DE87-014255] 02 p0236 N88-11487

Microcomputer control of spectroscopic instruments
[ATR-86(8431)-4] 03 p0326 N88-12058

Lidar-radiometric method for determining liquid-water content of cirrus clouds 04 p0461 N88-12854

Optical deformation measurement on shells following the raster principle
[ETN-88-90608] 05 p0609 N88-13741

Optical measurement systems
08 p0955 N88-15796

Evaluation of a temperature remote sensing technique
[AD-A187885] 10 p1347 N88-18053

Diagnostics for research in atomization and turbulent two-phase flows
[AD-A187338] 11 p1482 N88-18843

Ion content and infrared absorption of moist atmospheric air
[AD-A188839] 12 p1643 N88-19838

Computer software for the computation of the scattered field and the optical microscope image of line objects patterned in thick layers
[PB88-153705] 13 p1814 N88-20838

Technical applications of solar energy. Project: Selective coatings
[BMFT-FB-T-86-213] 14 p1943 N88-21591

Ray tracing optical analysis of offset solar collector for space station solar dynamic system
[NASA-TM-100853] 15 p2027 N88-22080

Development and applications of optical interferometric micrometrology in the angstrom and subangstrom range
[NASA-TM-100299] 16 p2211 N88-23196

Air Force ultrafast optical electronics center
[AD-A191491] 17 p2438 N88-24507

Measurements of Z(sub eff) profile with a visible bremsstrahlung continuum detector array
17 p2443 N88-24529

Optical monitoring of protein crystal growth
[NASA-CR-182869] 18 p2484 N88-24738

Instrumentation for turbulent reacting flows
[AD-A191671] 18 p2515 N88-24923

An optical preamplifier for detection of CO2 laser radiation
[AD-A190790] 18 p2520 N88-24949

An optical technique for measuring divergence, beam profile, and aiming direction, of relativistic negative hydrogen ions
[DE88-007049] 18 p2572 N88-25278

Fiber optic sensors 19 p2670 N88-25870

Optical sensing of magnetic fields
19 p2670 N88-25871

Optical measurement of propeller blade deflections
[NASA-TP-2841] 22 p3079 N88-28286

Metal halide optical glasses
[AD-A193794] 23 p3198 N88-29032

Optical measurement of unducted fan blade deflections
[NASA-TM-100966] 23 p3216 N88-29142

Volumetric measurement of vorticity vectors by optical probe
[AD-A195997] 24 p3369 N88-30061

Optical measurements of soot in premixed flames
[NASA-TM-101305] 24 p3373 N88-30090

OPTICAL MEASURING INSTRUMENTS
NT DIFFRACTOMETERS
NT EBERT SPECTROMETERS
NT ELECTROPHOTOMETERS
NT ELLIPSOMETERS
NT ETALONS
NT INFRARED SPECTROMETERS
NT INFRARED SPECTROPHOTOMETERS
NT LASER RANGE FINDERS
NT LIGHT SCATTERING METERS
NT MICRODENSITOMETERS
NT OCULOMETERS
NT OPTICAL PYROMETERS
NT PHOTOMETERS
NT POLARIMETERS
NT REFRACTOMETERS
NT SPECTROPHOTOMETERS
NT THEODOLITES
NT TOTAL OZONE MAPPING SPECTROMETER
NT TRANSMISSOMETERS
NT ULTRAVIOLET SPECTROMETERS
NT ULTRAVIOLET SPECTROPHOTOMETERS

Surface scattering characteristics and the measurement of particulate contamination 02 p0137 N88-10862

Optical instrumentation and study of gas-solid suspension flows
[DE88-000147] 04 p0442 N88-12744

Determination of the fiber ratio in carbon fiber/resin composites by means of image analysis
[SNIAS-872-422-101] 05 p0558 N88-13398

Developments in optical sensor technologies described 06 p0689 N88-14220

Optical seam tracking in robotic arc welding
[VTT-RR-463] 06 p0713 N88-14376

Integrated systems with applications to the multi-phases of the ephemerides, physics and mathematics of the upper atmosphere
[AD-A185748] 06 p0743 N88-14570

Wind tunnel model surface gauge for measuring roughness
[NASA-CR-182392] 07 p0822 N88-14996

Fundamental aspects of the physics of remote sensing
[ESA-TT-1045] 09 p1185 N88-17100

Multichannel anisotropic single-mode fiber optics for transducers 09 p1240 N88-17429

Computer modeling for optical waveguide sensors
[AD-A187702] 11 p1549 N88-19263

Cramer-Rao bounds on the accuracy of location and velocity estimations using CCD optical sensors
[AD-A188481] 12 p1629 N88-19748

Activities report of the Physics Department
[ETN-88-91985] 13 p1833 N88-20964

Research on certain aspects of laser diffraction particle sizing relevant to autonomous self-diagnosing instrumentation
[AD-A190220] 15 p2071 N88-22346

Optical sensors for the measurement of electric current and voltage
[PB88-172945] 16 p2193 N88-23077

Low-cost optical data acquisition system for blade vibration measurement 16 p2219 N88-23240

Phase length optical phase-locked-loop sensor
[NASA-CASE-LAR-13387-1] 18 p2576 N88-25302

IPS guidestar selection for stellar mode (ASTRO)
[NASA-TM-100336] 21 p2894 N88-27181

Diffraction by a simple deep phase object --- integrated circuit measurement
[RSRE-MEMO-4039] 22 p3070 N88-28224

Optical method to measure the deformations of structures loaded by hydraulic pressure
[SNIAS-881-430-111] 22 p3088 N88-28339

Research and development objectives: Installation, startup, and test operation of a remote and program controlled measuring table for the calibration of EGRET experiment
[ETN-88-92105] 22 p3152 N88-28752

Investigations on periodically perturbed optical waveguides
[B8712725] 23 p3283 N88-29549

OPTICAL MEMORY (DATA STORAGE)

Optical laser technology, specifically CD-ROM (Compact Disc - Read Only Memory) and its application to the storage and retrieval of information
[AD-A184111] 03 p0330 N88-12086

Optical memory cards. A comparison with other current technologies and potential military applications
[AD-A187287] 10 p1425 N88-18512

Rapid feature extraction via the radon transform
[AD-A190032] 15 p2110 N88-22573

Time-domain frequency-selective optical memories: A study of the basic mechanisms and potential systems
[AD-A190854] 16 p2274 N88-23607

Optical computing based on neuronal models
[AD-A191481] 18 p2575 N88-25293

Evaluation of multi-focus holographic lenses
[AD-A196167] 24 p3377 N88-30110

OPTICAL METHODS
U OPTICS

OPTICAL MICROSCOPES

Three dimensional reconstruction of optical microscope pictures using the three dimensional microscopic inverse point spread function
[ETN-87-90420] 01 p0098 N88-10646

Computer software for the computation of the scattered field and the optical microscope image of line objects patterned in thick layers
[PB88-153705] 13 p1814 N88-20838

MIG-1 on-line measuring holographic microscope
[DE88-701103] 15 p2068 N88-22332

OPTICAL MODULATION
U LIGHT MODULATION

OPTICAL PATHS

Uniform geometrical theory of diffraction
03 p0303 N88-11911

All-optical beam control by forced Rayleigh scattering
[AD-A184315] 04 p0490 N88-13018

Program to development an optical transistor and switch
[AD-A185666] 06 p0697 N88-14278

Navigation planning using quadtrees
[DE88-003706] 09 p1225 N88-17343

Applications of optical computing to problems with symbolic computations
[AD-A189772] 15 p2106 N88-22548

Phase length optical phase-locked-loop sensor
[NASA-CASE-LAR-13387-1] 18 p2576 N88-25302

OPTICAL POLARIZATION

Determination of the origin of self-pumped phase conjugation in barium titanate
[AD-A184697] 03 p0377 N88-12372

Research on acoustical scattering, diffraction catastrophes, optics of bubbles, photoacoustics, and acoustical phase conjugation
[AD-A185785] 06 p0776 N88-14761

New monostatic balanced Doppler velocimeter using a polarization preserving fiber
[PB88-130869] 11 p1490 N88-18895

Optical characterization of tropospheric aerosols
[AD-A187839] 11 p1511 N88-19029

Nonlinear optical principles and the photorefractive effect applied to optical phase conjugation
[AD-A188856] 12 p1691 N88-20119

Spontaneous decay and atomic fluorescence near a metal surface of an absorbing dielectric
[AD-A187508] 13 p1835 N88-20975

Real-time image difference detection using a polarization rotation spacial light modulator
[NASA-CASE-NPO-17144-1-CU] 18 p2576 N88-25305

OPTICAL PROPERTIES

NT ABSORPTIVITY
NT BIDIRECTIONAL REFLECTANCE
NT BIREFRINGENCE
NT BRIGHTNESS
NT BRIGHTNESS DISTRIBUTION
NT COLOR
NT DICHROISM
NT KERR ELECTROOPTICAL EFFECT
NT LUMINOSITY
NT OPACITY
NT OPTICAL BISTABILITY
NT OPTICAL REFLECTION
NT PHOSPHORESCENCE
NT PHOTOCONDUCTIVITY
NT RADIANCE
NT REFLECTANCE
NT REFRACTIVITY
NT SKY BRIGHTNESS
NT SPECTRAL REFLECTANCE
NT STELLAR LUMINOSITY
NT STIGMATISM
NT TRANSLUCENCE
NT TRANSMISSIVITY
NT TRANSMITTANCE
NT TRANSPARENCE
NT TURBIDITY
NT WATER COLOR

Optical sizing of soot in gas turbine combustors and exhaust augmentor tubes
[AD-A183785] 01 p0006 N88-10034

Calorimetric Absorption Spectroscopy (CAS): A new method for the characterization of the optical properties of semiconductor systems
[ETN-87-90407] 01 p0098 N88-10645

Direct detection of optical radiation through a sampling orifice for inductively coupled plasma atomic emission spectroscopy
[DE87-013609] 01 p0101 N88-10662

An evaluation of the LEC-460 solar collector
[DE88-000052] 02 p0196 N88-11224

Composition, structure and chemistry of interstellar dust
[NASA-TM-88350] 02 p0253 N88-11603

Near-infrared dichroism of a mesogenic transition metal complex and its solubility in nematic hosts
[DE87-014471] 03 p0287 N88-11805

Highly Non-Linear Optical (NLO) organic crystals
03 p0297 N88-11865

Theory of atomic additivity in molecular hyperpolizabilities 03 p0297 N88-11867

Advances in inherently conducting polymers
[DE88-000501] 04 p0421 N88-12610

Conducting hybrid polymeric systems
[DE88-000527] 04 p0421 N88-12611

Measurement of cirrus cloud optical properties by high spectral resolution lidar 04 p0470 N88-12906

Characterization of thin layers for optics
[PB87-217949] 04 p0490 N88-13017

Fundamental studies in the OM-CVD growth of Ga-In-As-Sb
[AD-A184822] 05 p0655 N88-14014

Material design of high performance glasses discussed 06 p0688 N88-14216

Coherence, propagation and fluctuations of light: A generalized ray approach
[DE88-001669] 06 p0780 N88-14786

Selection of polymer materials for manufacturing optical parts
[AD-A185898] 07 p0836 N88-15069

Astrophysics and the solar nebula
07 p0883 N88-15355

Development of a physically-based general circulation model parameterization of clouds and their radiative interactions
[DE88-004080] 09 p1194 N88-17154

Optical Fourier transformation by lensless method with perforated mask and with modified Talbot interferometer for analysis of interferograms 09 p1236 N88-17408

Molecular beam epitaxy for research on quantum well structures
[AD-A186791] 09 p1255 N88-17522

Relaxing the brightness constancy assumption in computing optical flow
[AD-A187437] 10 p1410 N88-18410

Optical characterization of GaAs/sub 1-x/Sb/sub x/ and GaAs/sub 1-x/Sb/sub x/GaAs strained layer superlattices
[DE88-003393] 10 p1418 N88-18464

Photoconductor switch and circuit analysis
[AD-A188166] 11 p1478 N88-18821

Nonlinear optical waveguides containing a transition metal-based dye molecule
[DE88-003257] 11 p1550 N88-19275

Raman enhancement methods for molecular structure characterization of optical thin films
[DE88-003421] 11 p1558 N88-19324

Spatial distribution of carbon and native defects in large-diameter bulk grown GaAs
[DE88-003870] 11 p1562 N88-19348

Investigations of surface coatings based on silicon and nitrogen: From amorphous Si to silicon nitride
[DE88-004995] 12 p1609 N88-19622

Experimental and analytical investigation on a proposed embedded fiber optic displacement sensor
[AD-A189030] 12 p1630 N88-19756

Optical properties of compressible inhomogeneous shear layers relevant to high power lasers
[AD-A189299] 12 p1633 N88-19774

A continued study of optical sound generation and amplification
[AD-A188362] 12 p1691 N88-20116

Development of an optical feedback based high accuracy beam transmissometer
[AD-A189396] 12 p1692 N88-20122

Tungsten-carbon multilayer system studied with X-ray scattering
[DE88-005749] 13 p1735 N88-20373

Materials Research Laboratory at Brown University
[AD-A188006] 13 p1739 N88-20396

Optical studies of dynamical processes in disordered system
[DE88-005965] 13 p1837 N88-20993

Energy transfer and non-linear optical properties at near ultraviolet wavelengths: Rare earth 4f yields 5d transitions in crystals and glasses
[DE88-005403] 13 p1840 N88-21012

Optical properties of quantum well structures with electric field: Life time free switching of luminescence intensity and virtual charge-induced ultrafast optical nonlinearity 14 p1976 N88-21794

High density femtosecond excitation of nonthermal carrier distributions in intrinsic and modulation doped GaAs quantum wells 14 p1977 N88-21798

Recent progress in optical bistability and tristability
14 p1979 N88-21809

Oxide optical coatings prepared by metal-organic vapor deposition
[DE88-006809] 15 p2043 N88-22175

Research on stable processible conducting polymers for electronic applications
[AD-A190246] 15 p2044 N88-22180

A 104-km unrepeatered bidirectional fiber optic demonstration link
[AD-A190282] 15 p2134 N88-22728

Optical characterization of microcrystals
[DE88-006622] 15 p2141 N88-22775

The effect of internal relaxation on optoacoustic conversion in liquids
[AD-A191307] 16 p2176 N88-22970

The optical properties of aerosols
[AD-A191420] 16 p2176 N88-22972

Nonlinear wave and diffusion equations
[AD-A191421] 16 p2265 N88-23544

Tunable optical sources/growth and characterization of nonlinear optical materials
[AD-A190874] 16 p2274 N88-23608

Investigation of non-linear optical behavior of semiconductors for optical switching, volume 1
[AD-A191297] 16 p2274 N88-23611

Air Force ultrafast optical electronics center
[AD-A191491] 17 p2438 N88-24507

Time resolved spectroscopy facility for the study of nonlinear optical properties of semiconducting polymers
[AD-A191221] 18 p2490 N88-24768

Stress measurements in graphite fibers by laser raman spectroscopy
[AD-A191710] 18 p2491 N88-24779

Studies of optical matrix multiplication and reconfigurable optical interconnect concepts
[AD-A191635] 18 p2575 N88-25295

Research in the optical sciences
[AD-A192175] 18 p2575 N88-25297

Electronic structure, elementary excitations, optical and transport properties of semiconductor superlattices
[AD-A190795] 18 p2581 N88-25333

Optical properties of heterostructures and superlattices
[AD-A191542] 18 p2581 N88-25335

Dual Stokes cars measurements in supersonic combusting flow 19 p2625 N88-25569

Selective radiation absorption in aluminized composite propellant combustion 19 p2630 N88-25598

X-ray and optical analysis of surface properties of metal optics
[DE88-004033] 19 p2727 N88-26195

Nonlinear optical properties and subpicosecond dynamics of excitons and electron-hole plasmas in multiple quantum well structures
[AD-A191926] 19 p2727 N88-26196

Development of liquid metal field-emission sources for use in fast repetitive opening switches
[AD-A192230] 20 p2795 N88-26583

Interferometric recording of holographic optical elements using partially coherent light
20 p2805 N88-26636

Optical coatings for high average power XeF lasers
[DE88-011356] 20 p2807 N88-26656

Determination and application of bidirectional solar-optical properties of fenestration systems
[DE88-010364] 20 p2820 N88-26727

Stress-related phenomena in transient radiation-induced absorption in optical fibers
[DE88-010956] 20 p2854 N88-26949

Ultrafast optical nonlinearity in quantum well structures with electric field 20 p2863 N88-27003

Semiconductor microcrystallites in porous glass and their applications in optics 20 p2863 N88-27005

Properties of multilayers for soft X-ray optics
20 p2867 N88-27025

Magneto-optical studies of GaInAs-InP quantum wells
20 p2870 N88-27039

On a-Si:H/a-SiN(x):H superlattices: Confinement or contamination 20 p2870 N88-27040

Performance evaluation of large-area glass-mirror heliostats
[DE88-011863] 21 p2969 N88-27636

The collection of statistics on the frequency of cloud cover over North America
[AD-A193093] 21 p2974 N88-27667

Atomic layer epitaxy of ZnS and ZnSe
[AD-A192307] 21 p3020 N88-27928

Studies of coherent beam processing concepts, phase 1
[AD-A194749] 22 p3083 N88-28306

Recent advances in optical spectroscopy using high performance array detectors
[AD-A194219] 22 p3152 N88-28753

Optical bistable behavior of a planar quasi-waveguide interferometer made with a conjugated organic polymer film
[AD-A194349] 22 p3152 N88-28756

Phase equilibrium and crystal growth studies on AgGaSe2 and related nonlinear optical materials
[AD-A193763] 22 p3157 N88-28783

Aerodynamics of seeing on large transport aircraft
[NASA-CR-183122] 23 p3174 N88-28896

Optical emission behavior and radiation resistance of epoxy resins
[DE88-752629] 23 p3196 N88-29023

Metal halide optical glasses
[AD-A193794] 23 p3198 N88-29032

LLE (Laboratory for Laser Energetics) review
[DE88-008065] 23 p3219 N88-29158

Proof of the feasibility of coherent and incoherent schemes for pumping a gamma-ray laser
[AD-A193856] 23 p3220 N88-29165

Planarization of metal substrates for solar mirrors
[DE88-011492] 23 p3229 N88-29214

Vision through aircraft transparencies
23 p3242 N88-29294

Quasi-liquid crystalline materials with special electro-optic properties
[AD-A194579] 23 p3282 N88-29544

Nonlinear optical processes in molecular systems
[AD-A193871] 23 p3282 N88-29546

Growth and characterization of materials for tunable lasers in the near infrared spectral region
[NASA-CR-183132] 24 p3377 N88-30113

Spontaneous force optical traps
[AD-A196103] 24 p3377 N88-30114

Bibliography of Soviet laser developments, number 88, March - April 1987
[AD-A195978] 24 p3378 N88-30116

Atmospheric corrections for in-flight satellite radiometric calibration
[AD-A196124] 24 p3391 N88-30194

An organometallic route to micron-sized whiskers of zinc sulfide
[AD-A195889] 24 p3430 N88-30414

On 3-5 heterojunction structures and high speed devices
[AD-A195464] 24 p3433 N88-30438

OPTICAL PUMPING

NT LASER PUMPING

Thermo-optical modeling of flashlamp-pumped zig-zag slabs
[DE87-011878] 01 p0051 N88-10326

Nonconventional optical techniques for optical wavefront processing
[AD-A185099] 05 p0650 N88-13982

Solitons in stimulated Raman scattering: Generation and control of ultrashort optical pulses
[AD-A185141] 05 p0650 N88-13983

Lasers with wavefront-reversing mirrors (review article)
06 p0709 N88-14349

Population inversion in gapless semiconductors as result of interband pumping 06 p0770 N88-14732

Time characteristics of travelling wave lasing with two-photon picosecond optical pumping
07 p0918 N88-15578

Atomic clocks research: An overview
[AD-A185567] 07 p0930 N88-15648

Tunable Al2O3:Ti3 + -laser with optical pumping
09 p1237 N88-17415

High power, high efficiency, 2D laser diode arrays for pumping solid state lasers
[DE88-004042] 13 p1777 N88-20632

Squeezing via travelling-wave forward four-wave mixing in atomic vapors: Comparison with nondegenerate theory 14 p1978 N88-21804

Generation of tunable coherent radiation in 3 micrometers-5 micrometers region using semiconductor lasers in external cavities
[AD-A190860] 16 p2212 N88-23202

High-speed phenomena in GaAs multiple-quantum-wells 19 p2660 N88-25812

Sources of polarized ions and atoms
[DE88-010910] 20 p2852 N88-26931

Far-infrared studies of doped AlGaAs/GaAs multiple-quantum-well structures
20 p2862 N88-26998

OPTICAL PYROMETERS

Noncontact Temperature Measurement
[NASA-CP-2503] 17 p2327 N88-23895

Direct emissivity measurements on liquids and corrections to multi-color pyrometers
17 p2329 N88-23906

Common but unappreciated sources of error in one, two, and multiple-color pyrometry 17 p2329 N88-23907

Fast optical pyrometry 17 p2329 N88-23908

OPTICAL RADAR

Investigation of lidar backscatter including depolarization and higher scattering orders
[ETN-87-90431] 01 p0052 N88-10334

Theoretical and lidar studies of the seasonal and nocturnal variations of the mesospheric sodium layer at Urbana, Illinois 01 p0068 N88-10435

Airborne lidar studies of Arctic polar stratospheric clouds 01 p0069 N88-10443

A study of the performance of airborne laser radar systems and techniques
[ETN-87-90928] 02 p0179 N88-11117

Correlation between aircraft MSS and LIDAR remotely sensed data on a forested wetland in South Carolina
[NASA-TM-89643] 02 p0193 N88-11204

Airborne lidar experiments at the Savannah River Plant
[NASA-TM-4007] 02 p0194 N88-11209

The Avionics Flight Evaluation System (AFES) of the DFVLR
[ESA-TT-1037] 03 p0266 N88-11677

Methods for a coherent CO2 laser heterodyne radar system
[ESA-TT-1035] 03 p0328 N88-12076

Review of inversion techniques for spaceborne lidar systems
[AD-A184164] 04 p0447 N88-12772

Multiwave laser soundings of atmospheric aerosol: Experimental research (review)
04 p0461 N88-12852

Lidar-radiometric method for determining liquid-water content of cirrus clouds 04 p0461 N88-12854

Measurement of cirrus cloud optical properties by high spectral resolution lidar 04 p0470 N88-12906

Italy's Institute of Research on Electromagnetic Waves--the Istituto di Ricerca sulle Onde Elettromagnetiche
[AD-A185020] 05 p0574 N88-13501

Contributions of lidar measurements to the study of long term variations of the middle atmosphere
[ETN-88-91237] 05 p0625 N88-13824

Lidar investigations of M-zone
06 p0741 N88-14558

Problems and possible solutions involved in hard target calibration of coherent Doppler lidar
07 p0922 N88-15602

Inversion of simulated satellite signals
08 p1017 N88-16168

A backscatter lidar proposed for the second German Spacelab mission 08 p1018 N88-16173

Development of a Doppler wind lidar system for atmospheric wind measurements
08 p1027 N88-16217

The sodium layer at 69 N latitude in wintertime
08 p1027 N88-16218

Lidar metal density measurements in the upper atmosphere 08 p1027 N88-16219

Rayleigh lidar observations of gravity wave activity in the stratosphere and lower mesosphere
[NASA-CR-182384] 09 p1189 N88-17123

Concept, construction, and experimental testing of a polychromator for a Raman lidar for the simultaneous telemetering of carbon dioxide and water vapor, relative to oxygen
[GKSS-87/E/20] 09 p1191 N88-17134

Airborne Wind Shear Detection and Warning Systems: First Combined Manufacturers' and Technologists' Conference
[NASA-CP-10006] 10 p1273 N88-17616

Lidar windshear detection and avoidance: Performance and technical assessment 10 p1274 N88-17626

Airborne Doppler lidar detection of wind shear. Results of performance analysis 10 p1275 N88-17627

Experiments for the high resolution detection of moving targets using a CO2 laser radar
[MBB-UA-1044/87] 10 p1316 N88-17864

Integrated optical synthetic aperture radar processor
[AD-A188019] 11 p1471 N88-18772

Atmospheric backscatter at 10.6 microns; a compendium of measurements made outside the United Kingdom by the airborne LATAS coherent laser radar velocimeter
[RSRE-87002] 12 p1631 N88-19763

Distortion of wideband carbon dioxide laser radar waveforms due to atmospheric dispersion and absorption
[AD-A188687] 12 p1632 N88-19771

Position, scale, and rotation invariant target recognition using range imagery
[AD-A188828] 12 p1633 N88-19772

Coherent laser radar system theory
[AD-A188759] 13 p1774 N88-20612

Lidar active remote sensing. Applications to the atmosphere 14 p1936 N88-21547

Corrections for differential scattering by aerosols in the measurement of ozone by DIAL --- differential absorption lidar (DIAL)
[NPL-QU-78] 14 p1945 N88-21603

Optical properties of Southern Hemisphere aerosols: Report of the joint CSIRO/NASA study
[NASA-CR-179287] 14 p1945 N88-21605

Aerosol lidar for environment protection and meteorology
[DFVLR-FB-87-43] 14 p1982 N88-21828

Infrared differential absorption lidar for vapor detection
[AD-A190600] 15 p2098 N88-22497

Optics: Perspectives for Measurement Techniques and Signal Processing for Flight Guidance --- conference
[DFVLR-MITT-87-21] 18 p2516 N88-24928

Limits of accuracy and range of laser radars
18 p2517 N88-24934

Aircraft/lidar turbulence comparison
18 p2546 N88-25111

High speed opto-isolator for radar applications
19 p2658 N88-25795

Remote determination of chlorophyll concentration in the ocean using an optical pulse radar
[NASA-TT-20301] 19 p2694 N88-26014

Components of an atmospheric lidar system
[AD-A193366] 21 p2953 N88-27539

IEMIS (Integrated Emergency Management Information System) floodplain mapping based on a LIDAR derived data set
[AD-A193071] 21 p2966 N88-27616

Investigations on Mie and Rayleigh scattering as basis for the development of Rayleigh temperature lidars with aid of Michelson interferometry
[GKSS-87/E/62] 21 p2976 N88-27675

South Pole lidar: Brief description of the instrument
[NOTA-INTERNA-907] 22 p3083 N88-28308

Atmospheric Lidar Experiment In Space (ALEXIS)
[DFVLR-MITT-88-10] 22 p3118 N88-28526

Genesis of Atlantic lows experiment NASA electra boundary layer flights data report
[NASA-TM-100703] 22 p3128 N88-28597

Helicopter recognition using laser radars
22 p3149 N88-28736

Program to increase the measurement capabilities of the AFGL (Air Force Geophysics Laboratory) fixed and mobile high altitude lidar systems
[AD-A194614] 23 p3203 N88-29063

Large aperture multi-dimensional laser radar testbed
[AD-A193447] 23 p3218 N88-29155

Forty-eight-inch lidar aerosol measurements taken at the Langley Research Center, May 1974 to December 1987
[NASA-RP-1209] 23 p3232 N88-29234

Spaceborne lidar: Development of a laboratory test system
[BF-R-66.090-1] 24 p3378 N88-30118

OPTICAL RANGE FINDERS

NT LASER RANGE FINDERS

OPTICAL REFLECTION

Space-time structure of ultrashort light pulses formed during stimulated backscattering of laser beam
14 p1972 N88-21767

Phase length optical phase-locked-loop sensor
[NASA-CASE-LAR-13387-1] 18 p2576 N88-25302

OPTICAL RELAY SYSTEMS

Coherent infrared detection, volume B --- CO2 laser intersatellite data link
[ESA-CR(P)-2392-VOL-1] 01 p0034 N88-10218

Coherent infrared detection, volume D --- CO2 laser intersatellite data link
[ESA-CR(P)-2392-VOL-2] 01 p0034 N88-10219

OPTICAL RESONANCE

Ultrafast intrinsic bistable devices
[PB87-109310] 05 p0649 N88-13978

Experimental observation of photoresonance of electrons localized above surface of solid hydrogen
06 p0774 N88-14756

Enhancement of second harmonic generation on silver gratings by resonant excitation of surface plasmon
[ETN-88-92304] 17 p2439 N88-24509

Laser desorption/ablation studies by resonance ionization mass spectrometry
[DE88-009124] 20 p2807 N88-26650

OPTICAL RESONATORS

Computer simulation of cw HF chemical laser unstable resonator performance
[AD-A185059] 05 p0587 N88-13561

Effect of optical inhomogeneities on space coherence of radiation emitted by laser with unstable resonator
06 p0771 N88-14738

Super-short yttrium aluminate pulse generator with controlled resonator Q-factor 06 p0772 N88-14740

High-power periodic-pulse YAG:Nd3 + -laser system with telescopic unstable resonator and two-stage amplifier
09 p1237 N88-17414

The 80 fsec soliton-like pulses from an optical-nonlinear fiber resonator
[PB88-127303] 10 p1409 N88-18403

Optical frequency doubling in Ti:LiNbO3 waveguide resonators
[ETN-88-91486] 11 p1550 N88-19271

Squeezed states of light 14 p1976 N88-21791

Beam quality of stable and unstable resonators: A theoretical approach
[DFVLR-FB-87-35] 14 p1982 N88-21826

High power axial flow CO2 laser
[ETN-88-91951] 18 p2521 N88-24959

Analytical description of noise in phase-conjugate resonators
[PB88-171947] 19 p2726 N88-26186

Spectral properties of semiconductor lasers with external resonators
[ETN-88-93119] 24 p3379 N88-30125

OPTICAL SCANNERS

NT MULTISPECTRAL BAND SCANNERS

NT THEMATIC MAPPERS (LANDSAT)

Applications of nonlinear hole burning spectroscopy
[AD-A184943] 05 p0587 N88-13580

Range imagery algorithms for the detection of obstacles by autonomous vehicles
[AD-A185421] 05 p0659 N88-14045

Joint services electronics program
[AD-A186173] 11 p1478 N88-18822

Application of new technologies to DTIC document processing
[AD-A189778] 15 p2148 N88-22823

Users guide to CAESAR
[BCRS-87-04] 16 p2228 N88-23306

Development of an automated X-ray gauge for nondestructive quantitative analysis
[DE88-008633] 20 p2812 N88-26681

Five channel auroral photometer
[REPT-112] 24 p3375 N88-30101

Application of nondestructive testing techniques to materials testing
[AD-A195716] 24 p3381 N88-30138

OPTICAL SENSORS
U OPTICAL MEASURING INSTRUMENTS

OPTICAL SIGNALS
U OPTICAL COMMUNICATION

OPTICAL SPECTRUM
U LIGHT (VISIBLE RADIATION)
U SPECTRA

OPTICAL SWITCHING
The design and construction of a thermally controlled single mode fiber switch
[ETN-87-90929] 02 p0236 N88-11491
Theory of interactions of intense light with nonlinear, inhomogeneous and periodic structures and its applications to optical bistability, optic gyroscopes, nonlinear spectroscopy, radiation protection, X-ray emission and related fields
[AD-A190040] 15 p2133 N88-22725
Optical switching and control techniques using nonlinear optical wave mixing
[AD-A190467] 15 p2134 N88-22730
Investigation of non-linear optical behavior of semiconductors for optical switching, volume 1
[AD-A191297] 16 p2274 N88-23611

OPTICAL THICKNESS
Aerosol optical depth and ratios of diffuse-sky to total solar irradiance measured from aircraft following the eruption of El Chichon
[PB88-100789] 07 p0878 N88-15326
Remote sensing of atmospheric optical thickness and sea-water attenuation when submerged: Wavelength selection and anticipated errors
[AD-A187609] 11 p1548 N88-19262
Diurnal variations in optical depth at Mars: Observations and interpretations
[NASA-TM-100057] 18 p2595 N88-25420

OPTICAL TRACKING
Resources, confusions and compatibility in dual axis tracking: Displays, controls and dynamics
[AD-A185871] 07 p0898 N88-15440
Intelligent robotic tracker 09 p1214 N88-17276
Multiaperture optical system research
[AD-A188211] 11 p1549 N88-19267
Pursuit tracking performance decrements associated with decreasing ambient illumination
[AD-A189336] 13 p1809 N88-20809
Real-time optical multiple object recognition and tracking system and method
[NASA-CASE-NPO-17139-1-CU]
16 p2576 N88-25301
Tracking a monochromatic light source
[DE88-011260] 20 p2807 N88-26653

OPTICAL TRANSFER FUNCTION
Imaging interferometry with non-redundant arrays
02 p0257 N88-11624
Relationship between optical transfer function and natural light field in sea or atmosphere
15 p2054 N88-22247

OPTICAL TRANSITION
Program to development an optical transistor and switch
[AD-A185666] 06 p0697 N88-14278
Effect of extraneous factors on optical one-phonon transitions in impurity centers with cubic symmetry
08 p1077 N88-16496
Infrared devices using semiconductor quantum wells
[RSRE-MEMO-4018] 22 p3157 N88-28788

OPTICAL WAVEGUIDES
NT OPTICAL FIBERS
Coupling and absorption phenomena in semiconductor-clad dielectric optical waveguides
[DE87-013446] 03 p0307 N88-11939
Ultrafast intrinsic bistable devices
[PB87-109310] 05 p0649 N88-13978
Design, production, and characterization of broadband optical waveguides
[DFVLR-FB-85-52] 06 p0780 N88-14791
A surface plasmon waveguide sensor: A new type of chemical transducer based on optical phenomena
[ETN-88-91322] 06 p0780 N88-14792
Surface modification using ion beams: Recent developments at ORNL
[DE88-000951] 06 p0786 N88-14819
Pressure and tension dependence of phase shift of polarization modes in birefringent single-mode fiber-optic waveguide 08 p1078 N88-16501
Computational analysis of propagation properties of integrated-optical waveguides using a domain integral equation
[PB87-163358] 09 p1154 N88-16917
Semiconductor laser with electron-beam pumping and fiber-optic output waveguide 09 p1235 N88-17405
Multichannel anisotropic single-mode fiber optics for transducers 09 p1240 N88-17429
Light Electronic Control System (LECOS): A proposal for a interconnected error-tolerant, optoelectronic control system
[MBB-UT-004/87] 10 p1311 N88-17836
POLYPHEM, a universal defensive missile with optical waveguides guidance
[MBB-UA-1045/87] 10 p1315 N88-17862
Formation of optical waveguides by ion implantation
[DE88-003894] 10 p1409 N88-18407
Computer modeling for optical waveguide sensors
[AD-A187702] 11 p1549 N88-19263
Optical frequency doubling in Ti:LiMbO3 waveguide resonators
[ETN-88-91486] 11 p1550 N88-19271
Nonlinear optical waveguides containing a transition metal-based dye molecule
[DE88-003257] 11 p1550 N88-19275
Optical waveguide formation by ion implantation of Ti or Ag
[DE88-004595] 11 p1551 N88-19278
Ultra-high speed integrated optical waveguide devices for optical computing
[AD-A188470] 12 p1691 N88-20118
Coupled high power waveguide laser research
[AD-A189800] 15 p2071 N88-22345
Monolithic integration on a GaAs substrate of a quarter ring laser and an optical guide coupled by an evanescent wave
[ETN-88-92308] 17 p2344 N88-23969
Silicon-sapphire waveguides
[AD-A191754] 18 p2504 N88-24854
A high frequency GaAlAs travelling wave electro-optic modulator at 0.82 micrometers
[NASA-TM-100970] 22 p3073 N88-28240
Investigations on periodically perturbed optical waveguides
[B8712725] 23 p3283 N88-29548
Ion exchange processes for fabrication of integrated optical waveguide structures into glass substrates
[VTT-46] 24 p3429 N88-30405
Use of depletion edge translation for high-speed modulation and switching of lightwaves
[AD-A195611] 24 p3430 N88-30417

OPTICS
JPRS report: Science and technology. USSR: Physics and mathematics
[JPRS-UPM-87-008] 06 p0769 N88-14727
JPRS report: Science and technology. USSR: Physics and mathematics
[JPRS-UPM-87-009] 09 p1233 N88-17395
Optically interconnected phased arrays
[NASA-TM-100855] 14 p1908 N88-21400
Computing X-ray effects in optics
[DE88-006722] 15 p2134 N88-22732
Flow velocity measurements by image processing of optically modulated traces 16 p2203 N88-23147
Optics and symbolic computing
[AD-A195119] 24 p3360 N88-30004

OPTIMAL CONTROL
NT LINEAR QUADRATIC GAUSSIAN CONTROL
NT LINEAR QUADRATIC REGULATOR
NT TIME OPTIMAL CONTROL
A treatment of jw-axis model-matching transformation zeros in the optimal H squared and H infinity control designs
[OUEL-1673/87] 02 p0223 N88-11407
Stochastic model of the NASA/MSFC ground facility for large space structures with uncertain parameters: The maximum entropy approach
[NASA-CR-181489] 03 p0372 N88-12343
Local-optimal control in systems with delay
04 p0421 N88-12627
Investigation, development and application of optimal output feedback theory. Volume 3: The relationship between dynamic compensators and observers and Kalman filters
[NASA-CR-4107] 05 p0638 N88-13900
Control of an unstable launcher in atmospheric flight using minimax optimal control laws
[SNIAS-872-422-107] 05 p0638 N88-13901
Guidance and control strategies for aerospace vehicles
[NASA-CR-181579] 05 p0643 N88-13935
Optimal guidance of homing missiles
06 p0671 N88-14111
Feedback in LQCP (Linear Quadratic Control Problem) with a terminal inequality constraint
[PB87-220034] 06 p0762 N88-14676
Optimal repeated measurements designs for comparing test treatments with a control
[AD-A185999] 07 p0917 N88-15569
Analytical study of the effect of early warning on optimal shock isolation 08 p0998 N88-16047
Optimal control of windpowered plants
[FOA-C-20610-2.7] 08 p1022 N88-16188
Control variate selection for multiresponse simulation
[AD-A186637] 08 p1069 N88-16463
Nonlinear filtering and large deviations: A PDE-Control theoretic approach
[AD-A187436] 10 p1396 N88-18321
Viscosity methods in optimal control of distributed systems
[AD-A188086] 10 p1401 N88-18357
Symmetries in nonlinear control systems and their applications 11 p1496 N88-18929
Prediction of the response and optimal control of stochastic parametrically and externally excited nonlinear systems 11 p1496 N88-18930
Optimal control theory of load-following and parameter-tracking of nonlinear systems: An application of Pontryagin Maximum Principle to reactor dynamics
[DE88-004770] 11 p1532 N88-19152
Deterministic equivalent for a continuous linear-convex stochastic control problem
[AD-A187818] 11 p1540 N88-19206
Effects of closing speed uncertainty on optimal guidance 12 p1597 N88-19556
Bilinear systems in the frequency domain and an application to optimal control
[RR-320] 14 p1962 N88-21704
Advanced guidance algorithms for homing missiles with bearings-only measurements
[AD-A190435] 15 p2017 N88-22026
Optimal control and identification of space structures
[AD-A190033] 15 p2025 N88-22065
The adjoint process in stochastic optimal control
[AD-A189720] 15 p2116 N88-22605
An algorithm for super-optimal H sup inf design: The 2-block case
[OUEL-1711/87] 17 p2391 N88-24210
A state-space approach to discrete-time super-optimal H sup inf control problems
[OUEL-1712/87] 17 p2391 N88-24211
Energy optimal trajectory planning for robot manipulators and autonomous vehicles 17 p2437 N88-24497
Estimation and control of distributed models for certain elastic systems arising in large space structures
[AD-A192120] 18 p2472 N88-24666
Low authority control of large space structures using a constrained threshold control formulation
18 p2472 N88-24667
Optimal processes governed by integral equations with unilateral constraint 18 p2565 N88-25231
Optimal control of the wing rock phenomenon
21 p2927 N88-27373
Computer aided design for linear control State Variable System (SVS)
[AD-A193282] 21 p2997 N88-27775
Free boundary control of the Markov process
[AD-A192401] 21 p3008 N88-27846
Approximations and optimal control for the pathwise average cost per unit time and discounted problems for wideband noise driven systems
[AD-A192712] 21 p3008 N88-27847
Motion planning with obstacles and dynamic constraints 23 p3222 N88-29175
Nonlinear dynamic analysis and optimal control of shallow shells 23 p3224 N88-29191
Convex duality approach to the optimal control of diffusions
[AD-A194535] 23 p3266 N88-29442
The optimal control pilot model and applications
24 p3315 N88-29741
Sensor and actuator selection for large space structure control
[AD-A194912] 24 p3333 N88-29842
Theory of filtering and control with application to control of large space structures
[AD-A195500] 24 p3335 N88-29851
Analytical methods in stochastic control and nonlinear filtering
[AD-A194272] 24 p3426 N88-30388
Increasing accuracy in evaluating vector of state under conditions of incomplete observability of expanded system 24 p3446 N88-30511

OPTIMIZATION
NT DYNAMIC PROGRAMMING
NT FLIGHT OPTIMIZATION
NT LINEAR PROGRAMMING
NT LINEAR QUADRATIC GAUSSIAN CONTROL
NT LINEAR QUADRATIC REGULATOR
NT MATHEMATICAL PROGRAMMING
NT NONLINEAR PROGRAMMING
NT OPERATIONS RESEARCH
NT OPTIMAL CONTROL
NT QUADRATIC PROGRAMMING
NT SIMPLEX METHOD
NT TIME OPTIMAL CONTROL
NT TRAJECTORY OPTIMIZATION
Shape optimization of linear antennas
[ETN-87-90413] 01 p0036 N88-10233

Optimum size of staged flux compression generators
[DE87-011741] 01 p0038 N88-10244

An interactive optimization procedure for the computer aided dimensioning of integrated circuits
[ETN-87-90414] 01 p0082 N88-10531

Spectral and structural properties of nonnegative reducible operators in Banach relations
[ETN-87-90402] 01 p0089 N88-10581

Optimization of a controlled two-server maintenance system
[INPE-4202-PRE/1083] 01 p0107 N88-10694

Using MINOS (Modular In-core Nonlinear Optimization System) as a subroutine for decomposition
[DE87-013086] 02 p0221 N88-11390

A treatment of jw-axis model-matching transformation zeros in the optimal H squared and H infinity control designs
[OUEL-1673/87] 02 p0223 N88-11407

Irreducible *-representations of the Lie superalgebra osp(1,4) with finite-degenerated vacuum
[DE87-703089] 02 p0225 N88-11420

Numerical solution of bound constrained problems
[DE88-000653] 03 p0371 N88-12334

Mathematical models of plasma discharge control in a tokamak
[DE87-702891] 03 p0378 N88-12377

Reduced complexity structural modeling for automated airframe synthesis
[NASA-CR-177440] 04 p0393 N88-12453

New feedback design methodologies for large space structures: A multi-criterion optimization approach
04 p0408 N88-12535

Performance optimization of electronic networks in the frequency domain
[PB87-123873] 04 p0438 N88-12720

Optimization of explicit time-stepping algorithms and Stream-Function-Coordinate (SFC) concept for fluid dynamics problems 04 p0445 N88-12762

Optimization of dilatometer test procedures
[DE87-014998] 04 p0447 N88-12769

Parallel superconvergent multigrid
[DE87-013153] 04 p0480 N88-12960

Investigation, development and application of optimal output feedback theory. Vol. 4: Measures of eigenvalue/eigenvector sensitivity to system parameters and unmodeled dynamics
[NASA-CR-4108] 04 p0482 N88-12969

An exact penalization viewpoint of constrained optimization
[DE88-001477] 04 p0486 N88-12995

Techniques for performance optimisation in cruise and manoeuverability 05 p0545 N88-13321

Aeroelasticity and optimization in fighter aircraft design
05 p0546 N88-13324

Reduced order optimal command applied to longitudinal automatic pilots
[SNIAS-872-111-114] 05 p0552 N88-13362

Design of low order controllers for robust disturbance rejection in large space structures
[AD-A185202] 05 p0555 N88-13376

Digital video bit-rate reduction: DPCM for sub-Nyquist PAL
[BBC-RD-1987/16] 05 p0573 N88-13494

Contribution to optimal flow in networks. A experimental multiprocessor for asynchronous iteration implementation
[LAAS-87-269] 05 p0576 N88-13510

Establishment of complete minimum test sets for digital circuits with safety engineering significance
[ETN-88-90599] 05 p0578 N88-13526

Finite-element grid improvement by minimization of stiffness matrix trace
[NASA-TM-100255] 05 p0591 N88-13604

Simultaneous structural and control optimization via linear quadratic regulator eigenstructure assignment
05 p0594 N88-13622

Shape optimization of damping layers
05 p0595 N88-13635

STAEBL/general composites with hygrothermal effects (STAEBL/GENCOM)
[NASA-TM-100266] 05 p0611 N88-13754

Structural optimization in the design process --- aircraft
[SNIAS-872-111-115] 05 p0635 N88-13885

Aerodynamic design and test performance of supersonic turbines for the Vulcain rocket engine
06 p0713 N88-14373

Fast algorithms for structural optimization and least squares
[AD-A185766] 06 p0724 N88-14452

Meteor velocity distribution and an optimum monitoring mathematical model 06 p0739 N88-14546

Parallel algorithms for unconstrained and constrained nonlinear optimization
[PB87-230454] 06 p0756 N88-14634

Stress effects and the optimum format of a scrolling seven-line VDT text window
[AD-A185559] 06 p0758 N88-14651

Composite reliability enhancement via preloading
[AD-A185938] 07 p0826 N88-15010

Investigation of fuel additive effects on sooting flames
[AD-A186403] 07 p0829 N88-15026

Optimization of charged particle acceleration rate over wave parameters in the scheme with acceleration by surface electromagnetic waves
[DE88-700320] 07 p0846 N88-15134

Optimization of photogrammetric image adjustment
[SER-C-323] 07 p0872 N88-15289

Image processing language development
[AD-A186251] 07 p0903 N88-15467

On stochastic optimality of policies in first passage problems
[AD-A186293] 07 p0915 N88-15554

Integrated analysis and applications
08 p0954 N88-15789

A study to evaluate STS heads-up ascent trajectory performance employing a minimum-Hamiltonian optimization strategy
[NASA-TP-2793] 08 p0960 N88-15820

A modal control based limiting performance formulation for shock excited systems 08 p0996 N88-16046

Method of iterative coupling between periodic aerodynamic and dynamic fields
[PB87-169934] 09 p1113 N88-16669

Effect of an optimized fiber orientation on transonic flutter characteristics of a high-aspect-ratio composite wing
[NAL-TR-930] 09 p1120 N88-16709

Contribution to the design of flexible manufacturing systems: Modeling, simulation, and evaluation of parameters
[ISAL-IDI1-87-04] 09 p1151 N88-16894

A project to experimentally and theoretically examine fluid interfacial wave phenomena in a rotating cylindrical geometry: Current results and future plans
[DE88-003738] 09 p1165 N88-16984

High-resolution Real-Time Radiography (RTR) system design
[AD-A187107] 09 p1166 N88-16992

Resolution limitations and optimization of the ITT F4157 streak tube focus for fast (10 ps) operation
[DE88-003727] 09 p1169 N88-17007

Kinematic optimization of mechanisms, a finite element approach
[ISBN-90-370-0012-6] 09 p1175 N88-17039

The Shock and Vibration Bulletin. Part 4: Structural Dynamics and Modal Test and Analysis
[AD-A186751] 09 p1179 N88-17062

Optimized structure design using reanalysis techniques 09 p1180 N88-17067

Algorithms for transitive reduction of an acyclic graph
[PB87-162822] 09 p1220 N88-17317

On line search termination criteria for and convergence of conic algorithms for minimization
[DE88-002844] 09 p1227 N88-17351

Optimal application of Morrison's iterative noise removal for deconvolution. Appendices
[NASA-CR-182477] 09 p1231 N88-17376

Optimization of imaging energy filters for analytical electron microscopy
[ETN-88-91079] 09 p1248 N88-17483

Optimisation of military compressors for weight and volume 10 p1279 N88-17649

Specification of an engine and its components starting from a consideration of aircraft missions
10 p1279 N88-17651

The design of Impedance- matching networks for broadband antennas
[AD-A187600] 10 p1320 N88-17895

Optimal design and parameter identification of flexible rotor-bearing systems 10 p1339 N88-18002

Applications of energy density theory in cyclic plasticity
[AD-A186947] 10 p1342 N88-18023

Continuous deformation algorithm on the product space of unit simplices, revised version
[PB88-114210] 10 p1387 N88-18281

Graph transformation algorithms for array memory optimization in applicative languages
[DE88-004727] 10 p1387 N88-18283

Experiences with serial and parallel algorithms for channel routing using simulated annealing
[NASA-CR-182530] 10 p1388 N88-18289

A parallel quasi-Newton method for partially separable large scale minimization
[DE88-003592] 10 p1393 N88-18309

Strongly sequential term rewriting systems
[PB88-126[illegible]3] 10 p1398 N88-18334

Viscosity methods in optimal control of distributed systems
[AD-A188086] 10 p1401 N88-18357

Optimization of outlet channel of plasma ion source
[DE88-700471] 10 p1410 N88-18415

On the maneuvering of vehicles
[AD-A187632] 10 p1427 N88-18521

The aerodynamic design optimisation of a forward swept wing fighter aircraft
[CAR-87-18] 11 p1433 N88-18553

Improving battery reliability by using regression trees
[DE88-004539] 11 p1481 N88-18841

Design modeling for shape optimization
11 p1527 N88-19122

Shape optimization of three-dimensional stamped and solid automotive components
[GMR-5168] 11 p1528 N88-19123

EqL: The language and its implementation
[AD-A188161] 11 p1530 N88-19137

Data flow graph optimization in IF1
[DE88-004396] 11 p1532 N88-19151

A tool for the analysis of quasi-Newton methods with application to unconstrained minimization
[DE88-005783] 11 p1532 N88-19153

Parallel processing in nonlinear programming
[INPE-4298-PRE/1169] 11 p1533 N88-19158

Research on output feedback control
[NASA-CR-182543] 11 p1534 N88-19167

Optimal recursive maximum likelihood estimation
[AD-A187980] 11 p1536 N88-19176

Multigrid methods in convex optimization
11 p1538 N88-19190

Deterministic equivalent for a continuous linear-convex stochastic control problem
[AD-A187818] 11 p1540 N88-19206

Solution of the Lloyd-Max quantizer parameters by the method of successive substitution
[AD-A187829] 11 p1540 N88-19207

Optimal arrangement of components via pairwise rearrangements
[AD-A187633] 11 p1541 N88-19213

Structural shape optimization in multidisciplinary system synthesis
[NASA-TM-100538] 12 p1614 N88-19650

Optimum filters and smoothers design for carrier phase and frequency tracking
[NASA-CR-182654] 12 p1618 N88-19679

On the design of suboptimal matched filters for three-dimensional moving target detection
[AD-A188384] 12 p1619 N88-19682

A technique for local refinement of the stress field by finite element method
[INPE-4219-PRE/1099] 12 p1683 N88-20061

Method of reduction of polynomially nonlinear equations to linear equations
[DE88-700922] 12 p1683 N88-20064

A view of unconstrained optimization
[AD-A188327] 12 p1684 N88-20066

Optimizing powerplant design and development cycles
12 p1701 N88-20183

Control augmented structural synthesis
[NASA-CR-4132] 13 p1721 N88-20290

The design of aircraft using the decision support problem technique
[NASA-CR-4134] 13 p1721 N88-20291

Optimization of binary pigment coatings
[AD-A189103] 13 p1748 N88-20450

Optimal placement of tuning masses for vibration reduction in helicopter rotor blades
[NASA-TM-100562] 13 p1782 N88-20665

Active cooling design for scramjet engines using optimization methods
[NASA-TM-100581] 13 p1783 N88-20669

On the sensitivity of complex, internally coupled systems
[NASA-TM-100537] 13 p1813 N88-20829

A new algorithm for general multiobjective optimization
[NASA-TM-100536] 13 p1813 N88-20830

Conic algorithms for unconstrained minimization with special consideration of problems with large sparse Hessians: A summary of research performed
[DE88-002549] 13 p1816 N88-20850

Algorithms with conic termination for nonlinear optimization
[DE88-005693] 13 p1816 N88-20851

Constrained nonlinear programming
[DE88-005695] 13 p1817 N88-20860

Deterministic uncertainty analysis
[DE88-006139] 13 p1829 N88-20942

Optimal and conventional space-time processing in flow noise
[AD-A189104] 13 p1833 N88-20965

Design, optimization and construction of a dc-SQUID with complete flux transformer circuits
[PB88-160742] 14 p1907 N88-21339

An efficient gradient projection optimization scheme for a seven-degree-of-freedom redundant robot with spherical wrist
[DE88-005440] 14 p1919 N88-21453

Sensitivity of control-augmented structure obtained by a system decomposition method
[NASA-TM-100535] 14 p1954 N88-21647

Optimization of the real level 2 BLAS on the Cyber 205
[CWI-NM-R8715] 14 p1956 N88-21657

Multiextremal optimization via adaptive partition algorithms
[REPT-87-44] 14 p1957 N88-21664

Aero/structural tailoring of engine blades (AERO/STAEBL)
[NASA-CR-180805] 14 p1959 N88-21682

Unsteady aerodynamics of a Wortmann FX-63-137 wing in a fluctuating wind field
[AD-A190128] 15 p2013 N88-22006

Nonlinear analysis and optimal design of dynamic mechanical systems for spacecraft application
[AD-A190644] 15 p2026 N88-22070

Efficient method for structural optimization
15 p2054 N88-22240

Optimum signal processing in distributed sensor systems
[AD-A189443] 15 p2055 N88-22250

Structural tailoring of high-speed turbine blades (SSME/STAEBL) 15 p2080 N88-22398

Structural tailoring of advanced turboprops
15 p2080 N88-22400

Experimental design and structural optimization
[PB88-168255] 15 p2087 N88-22436

SEARCH: An interactive computer program for optimizing two-variable, unconstrained experiments or simulation
[AD-A190593] 15 p2112 N88-22583

Numerical methods for linear and nonlinear optimization
[AD-A190029] 15 p2120 N88-22631

Lumped model generation and evaluation: Sensitivity and Lie algebraic techniques with applications to combustion
[AD-A190402] 15 p2127 N88-22689

Dynamical optimization techniques for the calculation of electronic structure in solids
[DE88-006010] 15 p2140 N88-22768

Minimum weight design of rotorcraft blades with multiple frequency and stress constraints
[NASA-TM-100569] 16 p2161 N88-22892

Vibration control of large structures
[AD-A191358] 16 p2168 N88-22928

On the capacity of channels with unknown interference
[AD-A191160] 16 p2191 N88-23067

Problems in integrated networks
[AD-A191391] 16 p2191 N88-23069

Spur gears: Optimal geometry, methods for generation and Tooth Contact Analysis (TCA) program
[NASA-CR-4135] 16 p2215 N88-23216

Mixed finite element formulation applied to shape optimization 16 p2221 N88-23252

Variable speed optimal control of a wind turbine generator
[LAAS-87-358] 16 p2229 N88-23316

STRUTEX: A prototype knowledge-based system for initially configuring a structure to support point loads in two dimensions
[NASA-TM-100613] 16 p2250 N88-23448

Parallel computing in combinatorial optimization
[CWI-OS-R8720] 16 p2254 N88-23468

Convergence qualification of partition algorithms in global optimization
[REPT-87-61] 16 p2259 N88-23505

Sensitivity analysis and multidisciplinary optimization for aircraft design: Recent advances and results
[NASA-TM-100630] 17 p2302 N88-23766

A generalized method for optimizing the mass of space power systems 17 p2416 N88-24369

Optimization of SP-100 thermoelectric electromagnetic pump 17 p2418 N88-24382

Optimization of organic Rankine cycles for space station applications 17 p2423 N88-24407

Small particle bed reactors: Sensitivity to Brayton cycle parameters 17 p2435 N88-24487

Energy conversion system optimization study for multimegawatt space nuclear power application
17 p2436 N88-24492

Superconducting thin film vertex detector for SSC (Superconducting Super Collider) applications
[DE88-005951] 17 p2445 N88-24535

Nonlinear programming extensions to rational function approximation methods for unsteady aerodynamic forces
[NASA-TP-2776] 18 p2463 N88-24623

Guidance and control strategies for aerospace vehicles
[NASA-CR-183032] 18 p2467 N88-24644

A feedback linearization approach to spacecraft control using momentum exchange devices
[NASA-CR-172057] 18 p2472 N88-24668

Optimization of reserve lithium thionyl chloride battery electrochemical design parameters
[DE88-007109] 18 p2506 N88-24868

Applications of fault tree analysis to the design process
[DE88-007048] 18 p2525 N88-24982

A mixed-integer linear programming problem which is efficiently solvable
[AD-A191028] 18 p2556 N88-25168

Solving bidiagonal systems of linear equations on the CDC CYBER 205
[CWI-NM-R8725] 18 p2558 N88-25187

The Sizing and Optimization Language, (SOL): Computer language for design problems
[NASA-TM-100565] 18 p2559 N88-25190

Gram-Schmidt implementation of a linearly constrained adaptive array
[AD-A191651] 18 p2560 N88-25198

Mixed min-max optimization problem with restrictions
18 p2565 N88-25232

The use of Lagrange multipliers and Kuhn-Tucker's theory in optimization problems
18 p2565 N88-25236

Optimal discrete-time LQR problems for parabolic systems with unbounded input: Approximation and convergence
[NASA-CR-181673] 18 p2567 N88-25247

Electronic structure of Zintl phase compounds by nonlinear optimization
[DE88-009998] 19 p2613 N88-25508

Fluid dynamics of high performance turbomachines
[AD-A192073] 19 p2664 N88-25840

An extension of the Hopfield-Tank model for solution of the multiple traveling salesmen problem
[DE88-008377] 19 p2715 N88-26122

Model reduction methods for control design
[NASA-CR-179434] 19 p2719 N88-26144

The Oak Ridge National Laboratory strategic defense initiative shield optimization program
[DE88-008946] 19 p2721 N88-26160

Structural optimization of fiber composite turbomachine blades
[ETN-88-92351] 20 p2760 N88-26372

Modeling and optimum time performance for concurrent processing
[NASA-CR-4167] 20 p2797 N88-26595

Optimization of performance criteria with bounded joint velocities for robots with one degree of redundancy
[DE88-003915] 20 p2810 N88-26670

A matroid algorithm and its application to the efficient solution of two optimization problems on graphs, revision
[AD-A192709] 20 p2838 N88-26838

Using common subexpressions to optimize multiple queries
[DE88-008210] 20 p2844 N88-26877

Combining expert opinions: An optimization framework
[REPT-87-84] 20 p2846 N88-26895

Visible tunable source
[DE88-006442] 20 p2854 N88-26944

A feasibility study in path planning using optimization techniques
[AD-A193030] 21 p2894 N88-27177

Numerical optimization, system theoretic and software tools for the integrated design of flexible structures and their control systems
[AD-A192927] 21 p2895 N88-27183

Optimal rheological characteristics in dynamic stability of polymer flow through porous media
[DE88-001225] 21 p2918 N88-27322

An aspect graph-based control strategy for 3-D object recognition 21 p2927 N88-27377

Efficiency optimization for FEL oscillators
[AD-A192541] 21 p2952 N88-27536

Dexterous hands: Optimizing grasp by design and planning 21 p2958 N88-27572

An investigation of techniques for determination of optimum/self-optimizing systems
21 p2963 N88-27600

Parallel quasi-Newton methods for unconstrained optimization
[AD-A193250] 21 p3003 N88-27812

Database design and management in engineering optimization
[AD-A193325] 21 p3003 N88-27813

Finding minimum-cost circulations by successive approximation
[AD-A192724] 21 p3005 N88-27824

Finding minimum-cost circulations by canceling negative cycles
[AD-A192727] 21 p3005 N88-27825

Numerical optimization
[AD-A193032] 21 p3005 N88-27827

Optimization of fatigue and friction properties of titanium by means of surface treatments
[ECL-87-22] 22 p3056 N88-28133

Optimization and scale-up performance of polymer electrolyte batteries
[AD-A193987] 22 p3073 N88-28243

Optimization techniques for relational database systems 22 p3137 N88-28650

Design of multirate control systems via parameter optimization
[REPT-87-013] 22 p3142 N88-28666

Refining finite element models. Numerical application to a lattice structure. Study of a macroelement of Timoshenko beam type
[ONERA-RT-8/3313-RY-070-R]
22 p3144 N88-28696

A contribution to the quantitative analysis of the influence of design parameters on the optimal design of passenger aircraft
[ETN-88-92979] 23 p3176 N88-28912

Small scale mixing in the initial region of a jet
[AD-A193500] 23 p3192 N88-28994

Free electron lasers with small period wigglers
[DE88-011627] 23 p3218 N88-29156

Optimization-driven machine-oriented motion measurement 23 p3245 N88-29312

Faster scaling algorithms for network problems
[AD-A194032] 23 p3251 N88-29348

Optimization of low gravity materials processing experiments using expert systems
23 p3252 N88-29361

Design consideration in constructing high performance embedded Knowledge-Based Systems (KBS)
23 p3261 N88-29415

Optimisation algorithms for highly parallel computer architectures. The performance of the truncated Newton, conjugate gradient algorithm in FORTRAN and Ada
[AD-A193940] 23 p3265 N88-29435

Analysis and optimization of truncated scarf nozzles subject to external flow conditions
[NASA-TM-100955] 24 p3316 N88-29746

New methods for nonlinear optimization
[AD-A195982] 24 p3412 N88-30313

A rule-based systems approach to spacecraft communications configuration optimization
24 p3417 N88-30341

Formulation and solution of economic equilibrium problems
[AD-A196034] 24 p3439 N88-30470

OPTIMUM CONTROL
U OPTIMAL CONTROL

OPTIMUM THRUST PROGRAMMING
U THRUST PROGRAMMING

OPTOELECTRONIC DEVICES
NT PHOTODIODES

Optoelectronic measurement methods for ballistic experiments
[PB87-110706] 05 p0583 N88-13554

Light Electronic Control System (LECOS): A proposal for a interconnected error-tolerant, optoelectronic control system
[MBB-UT-004/87] 10 p1311 N88-17836

A laser communication experiment utilizing the ACT satellite and an airborne laser transceiver
[NASA-TM-100792] 11 p1492 N88-18910

Concept of an Opto-electronic Accelerometer System (OAS) 12 p1645 N88-19852

Mid infrared multichannel focal plane breadboard --- pushbroom sensors
[RT-87/014] 14 p1982 N88-21827

Television monitor field shifter and an opto-electronic method for obtaining a stereo image of optimal depth resolution and reduced depth distrotion on a single screen
[NASA-CASE-NPO-17249-1-CU]
17 p2332 N88-23924

Electronic and optical devices and applications
24 p3363 N88-30027

Optoelectronic gain control of a microwave single stage GaAs MESFET amplifier
[NASA-CR-182201] 24 p3368 N88-30055

OPTOELECTRONIC SWITCHING
U OPTICAL SWITCHING

OR-GATES
U GATES (CIRCUITS)

ORBIT CALCULATION

Satellite orbits: Plot routines
[UIO-SR-87-02] 01 p0011 N88-10060

Precise orbit computation, gravity model adjustment and altimeter data processing for the ERS-1 altimetry mission
[ESA-CR(P)-2436] 02 p0130 N88-10820

A demonstration of high precision GPS orbit determination for geodetic applications
04 p0432 N88-12680

Determination of TRANET (tracking station coordinates for tracking network) and SMTP (Special Mission Tracking Program) tracking station coordinates for use in the WGS (World Geodetic System) 84
[AD-A185863] 07 p0817 N88-14972

An orbit simulation study of a geopotential research mission including satellite-to-satellite tracking and disturbance compensation systems
[NASA-CR-182353] 07 p0823 N88-14997

Error assessments of widely-used orbit error approximations in satellite altimetry
[NASA-CR-182390] 07 p0823 N88-14998

Limitation of spacecraft orbit near colinear libration center of limited elliptical three body problem
08 p1003 N88-16075

Selection of efficient correcting motor for an artificial Earth satellite 08 p1007 N88-16102

Mission profiles of the MTFF co-orbiting with the US Space Station 12 p1585 N88-19487

Preliminary orbit determination algorithms: Application to the Brazilian satellite
[INPE-4411-NTE/276] 12 p1594 N88-19546

Orbit correction requirements for a natural resources satellite
[INPE-4286-PRE/1158] 12 p1594 N88-19548

Analysis of orbital geometry and orbit maintenance of an Earth observation satellite
[INPE-4276-PRE/1148] 12 p1594 N88-19549

Orbit correction strategy for an Earth observation satellite
[INPE-4287-PRE/1159] 13 p1727 N88-20331

Orbit accuracy requirement of GPS for precise positioning and orbit determination within local area
13 p1756 N88-20499

Seasat orbit determination experiments in preparation for the ERS-1 altimetry mission
[ETN-88-91842] 14 p1871 N88-21182

Analysis of the orbit of Cosmos 1335 (1982-07A) at 3:12 resonance
[RAE-TR-87041] 14 p1872 N88-21185

Numerical orbit propagation methods for earth artificial satellites
[INPE-4405-RPE/556] 15 p2023 N88-22053

Analytical orbit propagation of artificial satellites
[INPE-4454-TDL/315] 16 p2166 N88-22915

Orbit determination of 1965-09A for analysis of the eccentricity at 15th-order resonance
[RAE-TR-87059] 22 p3047 N88-28081

ORBIT DECAY

The contraction of satellite orbits under the influence of air drag. Part 8: Orbital lifetime in an oblate atmosphere, when perigee distance is perturbed by odd zonal harmonics in the geopotential
[RAE-TR-86069-PT-8] 01 p0010 N88-10058

Verification of a micro-thrusting model to maintain satellites in low orbit
[AD-A186874] 09 p1133 N88-16793

Mission profiles of the MTFF co-orbiting with the US Space Station 12 p1585 N88-19487

Orbit correction requirements for a natural resources satellite
[INPE-4286-PRE/1158] 12 p1594 N88-19548

Analysis of the orbit of Cosmos 1335 (1982-07A) at 3:12 resonance
[RAE-TR-87041] 14 p1872 N88-21185

The prediction of satellite lifetimes
[RAE-TR-87030] 17 p2310 N88-23818

ORBIT EQUATIONS

U ORBITAL MECHANICS

ORBIT PERTURBATION

NT SATELLITE PERTURBATION

Electrodynamic tether system study
[NASA-CR-172024] 03 p0275 N88-11737

Orbit correction strategy for an Earth observation satellite
[INPE-4287-PRE/1159] 13 p1727 N88-20331

How typical is Halley's Comet?
14 p1994 N88-21886

ORBIT TRANSFER VEHICLES

Aeroassisted-vehicle design studies for a manned Mars mission
[NASA-TM-100031] 03 p0271 N88-11700

Aeroassisted manned transfer vehicle (TAXI) for advanced Mars Transportation: NASA/USRA 1987 Senior Design Project
[NASA-CR-181478] 03 p0275 N88-11736

Nonequilibrium characteristics of nitrogen plasmas appropriate to an AOTV flight 03 p0319 N88-12019

Study of fault tolerant techniques for satellite data handling
[FTT/REP/0001/SAAB] 05 p0632 N88-13860

An analysis of the effect of aeroassist maneuvers on orbital transfer vehicle performance
[NASA-TM-89117] 06 p0672 N88-14116

AF cryogenic and fluid management spacecraft technology program 08 p0981 N88-15925

SAMSS: An in-progress review of the Spacecraft Assembly, Maintenance, and Servicing Study
08 p0981 N88-15930

Orbital transfer vehicle studies overview
08 p0981 N88-15931

Large capacity cryopropellant orbital storage facility
08 p0981 N88-15932

Orbiter transfer vehicle concept definition and system analysis study. Volume 4: Space station accommodations. Revision 1
[NASA-CR-179293] 11 p1444 N88-18609

Orbital transfer vehicle concept definition and system analysis study. Volume 4, Appendix A: Space station accommodations. Revision 1
[NASA-CR-179294] 11 p1444 N88-18610

A lunar transportation system
[NASA-CR-182561] 11 p1567 N88-19379

Automatic in-orbit payload deployment mechanisms, logistic operations and transport vehicle design compatibilities 12 p1586 N88-19493

Aeroassisted orbit transfer vehicle trajectory analysis
[NASA-TM-89138] 12 p1599 N88-19575

Orbital transfer vehicle concept definition and system analysis study. Volume 2: OTV concept definition and evaluation. Book 1: Mission and system requirements
[NASA-CR-179321] 13 p1729 N88-20339

Turnaround operations analysis for OTV. Volume 1: Executive summary
[NASA-CR-179316] 13 p1729 N88-20340

Turnaround operations analysis for OTV. Volume 2: Detailed technical report
[NASA-CR-179317] 13 p1729 N88-20341

Turnaround operations analysis for OTV. Volume 3: Technology development plan
[NASA-CR-179318] 13 p1729 N88-20342

Turnaround operations analysis for OTV. Volume 4: WBS and dictionary and cost methodology
[NASA-CR-179319] 13 p1729 N88-20343

Space station mobile transporter
14 p1927 N88-21488

Space station full-scale docking/berthing mechanisms development 14 p1927 N88-21491

Orbital transfer vehicle: Concept definition and system analysis study
[NASA-CR-179315] 15 p2024 N88-22060

Nuclear electric power for multimegawatt orbit transfer vehicles 17 p2399 N88-24261

Analysis of a nuclear orbital transfer vehicle reentry accident 17 p2425 N88-24426

Noncryogenic propellants for a nuclear orbit transfer vehicle 17 p2428 N88-24444

Solar thermal propulsion for orbit transfer vehicles
17 p2428 N88-24445

Advanced nuclear rocket engine mission analysis
[DE88-006797] 18 p2475 N88-24681

Centaur operations at the space station
[NASA-CR-179593] 19 p2606 N88-25473

Centaur operations at the space station: Cost and transportation analysis
[NASA-CR-182128] 24 p3332 N88-29835

Orbital transfer vehicle 3000 LBF thrust chamber assembly hot fire test program
[NASA-CR-182145] 24 p3336 N88-29858

ORBITAL ASSEMBLY

Potential for on-orbit manufacture of large space structures using the pultrusion process
[NASA-TM-4016] 05 p0557 N88-13388

Definition and economic evaluation of Space Solar Power Systems (SSPS), part 2
[ILR-MITT-184-2(1987)] 08 p1022 N88-16190

Planning and scheduling for robotic assembly
08 p1062 N88-16416

ESA Bulletin No. 25
[ISSN-0376-4265] 09 p1128 N88-16767

Satellite assembly in geostationary orbit: A plug-and-socket concept 09 p1128 N88-16769

Space station structures development
[NASA-CR-179261] 09 p1133 N88-16792

Telerobotic truss assembly 09 p1213 N88-17272

Assessment of mixed fleet potential for space station launch and assembly
[NASA-TM-100550] 11 p1443 N88-18608

Orbital transfer vehicle concept definition and system analysis study. Volume 4, Appendix A: Space station accommodations. Revision 1
[NASA-CR-179294] 11 p1444 N88-18610

State-of-the-art technologies for construction in space: A review
[AD-A188412] 12 p1585 N88-19483

Proceedings of the 1st European In-Orbit Operations Technology Symposium
[ESA-SP-272] 12 p1585 N88-19484

Assembly of user systems at Space Station
12 p1586 N88-19490

In-orbit automatic assembly of reticular structures
12 p1586 N88-19491

Assembly and servicing of a European Space Station
12 p1586 N88-19492

A knowledge-based approach for sensory-controlled assembly operations 12 p1588 N88-19506

Remote manipulation in orbital construction, servicing and repair missions: Is one arm enough? A comparative evaluation of the performance features of robots with one or more arms 12 p1588 N88-19509

Utilization of robotics and teleoperation for future in-orbit operations 12 p1591 N88-19527

External payload servicing: Operational requirements and technology 12 p1593 N88-19541

Space station heavy lift launch vehicle utilization
[NASA-TM-100604] 14 p1873 N88-21188

A 60-meter erectable assembly concept for a control of flexible structures flight experiment
[NASA-TM-100497] 14 p1873 N88-21190

Structural latches for modular assembly of spacecraft and space mechanisms 14 p1925 N88-21471

Space spider crane
[NASA-CASE-LAR-13411-1-SB]
* 17 p2312 N88-23828

Bi-stem gripping apparatus
[NASA-CASE-MFS-28185-1] 17 p2345 N88-23979

Design guidelines for robotically serviceable hardware
[NASA-TM-100700] 19 p2606 N88-25472

Mobile remote manipulator system for a tetrahedral truss
[NASA-CASE-MSC-20985-1] 20 p2765 N88-26398

Centaur operations at the space station: Cost and transportation analysis
[NASA-CR-182128] 24 p3332 N88-29835

Study of robotics spacecraft servicing and assembly in space. Volume 1: Executive summary
[ESA-CR(P)-2612-VOL-1] 24 p3333 N88-29839

ORBITAL ELEMENTS

Numerical arc segmentation algorithm for a radio conference-NASARC (version 2.0) technical manual
[NASA-TM-100160] 08 p0977 N88-15910

Numerical arc segmentation algorithm for a radio conference-NASARC, version 2.0: User's manual
[NASA-TM-100161] 09 p1156 N88-16928

Universal procedures for conversion of orbital elements to and from position and velocity (unperturbed orbits)
[RAE-TR-87043] 14 p1872 N88-21184

On orbits and association of meteor streams with Comets P/Halley and P/Encke
14 p2003 N88-21945

Duplicity in the solar neighborhood: Part 4: Spectroscopic orbits for four dwarf M stars
[SER-C-PREPUBL-FASC-21] 24 p3454 N88-30561

ORBITAL FLIGHT TEST 4 (SHUTTLE)

U SPACE TRANSPORTATION SYSTEM 4 FLIGHT

ORBITAL LAUNCHING

Department of Housing and Urban Development-Independent Agencies Appropriations for fiscal year 1988, Thursday, 9 April 1987: National Aeronautics and Space Administration
03 p0386 N88-12424

The determination of exhaust cloud dimensions from films of space shuttle launches
[NASA-CR-4103] 06 p0732 N88-14500

Alternative program approaches for the advanced satellite technology program
[AD-A188917] 12 p1600 N88-19576

Interplanetary propulsion using inertial fusion
17 p2401 N88-24273

Centaur operations at the space station
[NASA-CR-179593] 19 p2606 N88-25473

LRS-2: A specialized knowledge system for launch resource scheduling
[AD-A194625] 23 p3182 N88-28941

ORBITAL LIFETIME

The contraction of satellite orbits under the influence of air drag. Part 8: Orbital lifetime in an oblate atmosphere, when perigee distance is perturbed by odd zonal harmonics in the geopotential
[RAE-TR-86069-PT-8] 01 p0010 N88-10058

Electric propulsion: A controversial must for long-lived applications satellites 09 p1124 N88-16735

The prediction of satellite lifetimes
[RAE-TR-87030] 17 p2310 N88-23818

An extended life and performance test of a low-power arcjet
[NASA-TM-100942] 18 p2476 N88-24687

Attitude and orbit control for the AMPTE-UKS (Active Magnetospheric Particle Tracer Explores-UK Subsatellite): Evaluation of the in-flight performance
[PB87-225199] 19 p2604 N88-25467

ORBITAL MANEUVERING VEHICLES

Telepresence work station system definition study, part 2
[NASA-CR-172006] 01 p0013 N88-10071

Orbital Spacecraft Consumables Resupply System (OSCRS). Volume 4: Extended study results Part 1: Executive Summary
[NASA-CR-172012] 03 p0268 N88-11686
Orbital Spacecraft Consumables Resupply System (OSCRS): Monopropellant application to space station and OMV automatic refueling impacts of an ELV launch, volume 4
[NASA-CR-172029] 03 p0276 N88-11741
Teleoperator and robotics system analysis
[NASA-CR-179220] 03 p0334 N88-12105
Orbital Spacecraft Consumables Resupply System (OSCRS). Volume 1: Executive summary
[NASA-CR-172010] 05 p0553 N88-13368
Servicer system demonstration plan and capability development
[NASA-CR-179246] 08 p0975 N88-15895
OMV man/system simulation integration: A preliminary analysis and recommendation
[NASA-CR-182602] 12 p1671 N88-20005
Space station mobile transporter
14 p1927 N88-21488
OMV docking simulator 23 p3255 N88-29379

ORBITAL MANEUVERS
Study of Plasma Motor Generator (PMG) tether system for orbit reboost
[NASA-CR-172016] 04 p0403 N88-12501
Orbit correction strategy for an Earth observation satellite
[INPE-4287-PRE/1159] 13 p1727 N88-20331
Optimal thrust vector control of coplanar orbital evasive maneuvers
[AD-A189544] 13 p1730 N88-20346
Docking/berthing subsystem: Design and breadboard test 14 p1879 N88-21233
Study of Plasma Motor Generator (PMG) tether system for orbit reboost
[NASA-CR-172074] 23 p3184 N88-28949
Machine vision for real time orbital operations
23 p3253 N88-29367
Automated generation of spacecraft activity plans
23 p3258 N88-29396
The eivaN: A forward-looking interactive orbital trajectory plotting tool for use with proximity operations (PROX OPS) and other maneuvers: Description and user's manual
[NASA-CR-177490] 24 p3414 N88-30327

ORBITAL MECHANICS
NT KEPLER LAWS
A study of a satellite-to-satellite tracking configuration by application of linear perturbation theory
[REPT-86.3] 01 p0011 N88-10059
Estimability of potential coefficients from orbit perturbations --- satellite geodesy
[REPT-86.1] 01 p0064 N88-10408
Analytical average model of studies on orbital resonance 03 p0269 N88-11689
Computational method for orbit improvement for short arc observations of artificial satellites
03 p0269 N88-11690
On air-drag perturbation of transit satellite and selection of parameters in orbit improvement
03 p0269 N88-11691
Adaptive control of Large Space Structure (LSS)
[ISAS-R-621] 03 p0276 N88-11740
Phenomenological implications of the blown-up orbifolds
[DE87-014608] 03 p0373 N88-12347
Radial orbit error reduction and sea surface topography determination using satellite altimetry
04 p0462 N88-12861
Engineering calculations for the Delta S method of solving the orbital allotment problem
[NASA-CR-182372] 06 p0671 N88-14110
An analysis of the effect of aeroassist maneuvers on orbital transfer vehicle performance
[NASA-TM-89117] 06 p0672 N88-14116
Geosat crossover analysis in the tropical Pacific. Part 1: Constrained sinusoidal crossover adjustment
[NASA-CR-182391] 07 p0871 N88-15285
Study on orbits near the triangular libration points in the perturbed restricted three body problem
[ESA-CR(P)-2440] 07 p0944 N88-15741
Selection of efficient correcting motor for an artificial Earth satellite 08 p1007 N88-16102
Application of artificial intelligence to impulsive orbital transfers 08 p1066 N88-16439
Verification of a micro-thrusting model to maintain satellites in low orbit
[AD-A186874] 09 p1133 N88-16793
Numerical arc segmentation algorithm for a radio conference-NASARC, version 2.0: User's manual
[NASA-TM-100161] 09 p1156 N88-16928
An intelligent tutor for the space domain
09 p1204 N88-17217
Orbit correction requirements for a natural resources satellite
[INPE-4286-PRE/1158] 12 p1594 N88-19548
Analysis of orbital geometry and orbit maintenance of an Earth observation satellite
[INPE-4276-PRE/1148] 12 p1594 N88-19549
Simulation and tests of a satellite attitude and orbit control system. General considerations concerning an example case (INPE) and design of a servo rate table
[INPE-4282-PRE/1154] 12 p1599 N88-19572
Orbit correction strategy for an Earth observation satellite
[INPE-4287-PRE/1159] 13 p1727 N88-20331
Study of the optimization of satellite system design for transfer orbit
[MBB-URV-135] 13 p1727 N88-20332
Frozen orbit analysis in the Martian system
[AD-A189574] 13 p1856 N88-21106
Universal procedures for conversion of orbital elements to and from position and velocity (unperturbed orbits)
[RAE-TR-87043] 14 p1872 N88-21184
Estimation of geopotential from satellite-to-satellite range rate data: Numerical results
[NASA-CR-180771] 14 p1941 N88-21583
How typical is Halley's Comet?
14 p1994 N88-21886
The structure of the Halley meteor stream and the orbital history of the comet 14 p2008 N88-21975
Three approaches to the modeling of Comet Halley's motion over long periods of time
14 p2010 N88-21992
A model of the nongravitational motion of Comet P/Encke 14 p2010 N88-21993
Numerical orbit propagation methods for earth artificial satellites
[INPE-4405-RPE/556] 15 p2023 N88-22053
Spacecraft trajectories
[ISBN-2-85-428166-7] 15 p2023 N88-22054
A generic multibody simulation
[NASA-CR-182949] 17 p2368 N88-24198
Stochasticity in elliptical galaxies
[SER-C-PREPUBL-FASC-20] 17 p2450 N88-24556
The limits of direct satellite tracking with the Global Positioning System (GPS) 22 p3064 N88-28179
Study of Plasma Motor Generator (PMG) tether system for orbit reboost
[NASA-CR-172074] 23 p3184 N88-28949
Investigation of the validity of the non-rotating planet assumption for three-dimensional earth atmospheric entry
[AD-A194877] 24 p3331 N88-29829
Orbital evolution of distant artificial earth satellites
24 p3445 N88-30506
Plane periodic satellite motions relative to center of mass in neighborhood of collinear libration point
24 p3445 N88-30507
Orbital stability in rotating triaxial stellar systems
[SER-C-PREPUBL-FASC-24] 24 p3455 N88-30569

ORBITAL MOTION
U ORBITS

ORBITAL POSITION ESTIMATION
Precise near-earth navigation with GPS: A survey of techniques 04 p0433 N88-12682
Short baseline phase delay interferometry
04 p0433 N88-12683
Long range sensor for rendezvous and docking missions 12 p1587 N88-19497
Geodetic positioning by employment of the GPS-NAVSTAR satellites applying the techniques of VLBI and sequential recursive optimal estimation
[INPE-4438-TDL/311] 12 p1594 N88-19547
Seasat orbit determination experiments in preparation for the ERS-1 altimetry mission
[ETN-88-91842] 14 p1871 N88-21182
Universal procedures for conversion of orbital elements to and from position and velocity (unperturbed orbits)
[RAE-TR-87043] 14 p1872 N88-21184
Baseline estimation from simultaneous satellite laser tracking
[NASA-CR-182750] 15 p2022 N88-22052
Approximation of atmospheric density by Chebyshev polynomials in predicting motion of low artificial earth satellites 24 p3445 N88-30503

ORBITAL RENDEZVOUS
Proceedings of the 1st European In-Orbit Operations Technology Symposium
[ESA-SP-272] 12 p1585 N88-19484
Safe rendezvous approach to a space station by impulsive transfers and continuous thrust arcs
12 p1585 N88-19486
Safe and fuel minimum reference trajectories for closed loop controlled approaches --- space stations
12 p1585 N88-19488
Analysis of RVD operations in manned space missions
12 p1586 N88-19494
Rendezvous and docking (RVD) verification and demonstration in-orbit 12 p1592 N88-19531
Space transportation nodes assumptions and requirements: Lunar base systems study task 2.1
[NASA-CR-172052] 23 p3183 N88-28944

ORBITAL RESONANCES (CELESTIAL MECHANICS)
Analytical average model of studies on orbital resonance 03 p0269 N88-11689

ORBITAL SERVICING
Telepresence work station system definition study, part 2
[NASA-CR-172006] 01 p0013 N88-10071
Robotic sensors and actuators for a service manipulator system. Volume 1: Executive summary
[MATRA-EPT/DT/VT187/120]
01 p0053 N88-10341
Robotic sensors and actuators for a service manipulator system. Volume 2: Service Manipulator System (SMS) handbook
[MATRA-EPT/DT/VT187/227]
01 p0053 N88-10342
Robotic sensors and actuators for a service manipulator system. Volume 3, phase A report and program plan
[MATRA-EPT/DT/VT187/228]
01 p0054 N88-10343
Teleoperation and control study --- orbital servicing
[BAE-TP-8268] 01 p0076 N88-10489
Orbital Spacecraft Consumables Resupply System (OSCRS). Volume 4: Extended study results Part 1: Executive Summary
[NASA-CR-172012] 03 p0268 N88-11686
Orbital Spacecraft Consumables Resupply System (OSCRS): Monopropellant application to space station and OMV automatic refueling impacts of an ELV launch, volume 4
[NASA-CR-172029] 03 p0276 N88-11741
Payload configurations and serviceability --- Columbus Polar Platforms 03 p0339 N88-12133
Space station resistojet system requirements and interface definition study
[NASA-CR-180832] 04 p0409 N88-12541
Orbital Spacecraft Consumables Resupply System (OSCRS). Volume 1: Executive summary
[NASA-CR-172010] 05 p0553 N88-13368
In-orbit calibration adjustment of the Nimbus-7 SMMR
[NASA-TM-100678] 05 p0614 N88-13773
Servicer system demonstration plan and capability development
[NASA-CR-179246] 08 p0975 N88-15895
Proceedings of the 1st European In-Orbit Operations Technology Symposium
[ESA-SP-272] 12 p1585 N88-19484
Man-Tended Free Flyer operational design features
12 p1585 N88-19485
Cost-effective orbit transfer modes for satellite retrieval and servicing --- Space Station
12 p1586 N88-19489
Assembly of user systems at Space Station
12 p1586 N88-19490
Assembly and servicing of a European Space Station
12 p1586 N88-19492
NASA Office of Space Flight (OSF) in-orbit servicing program 12 p1587 N88-19498
In-orbit and laboratory exchange of ORUs designed/not designed for servicing 12 p1587 N88-19499
Utilization of SMS and EVA for the servicing of European Space Station 12 p1587 N88-19500
Multimission Modular Spacecraft (MMS). A serviceable design spacecraft 12 p1587 N88-19501
The ESA/Fokker service end-effector subsystem. A robotic/man-compatible servicing approach
12 p1587 N88-19502
Customer concerns regarding satellite servicing
12 p1587 N88-19503
Remote manipulation in orbital construction, servicing and repair missions: Is one arm enough? A comparative evaluation of the performance features of robots with one or more arms 12 p1588 N88-19509
Remote repair demonstration of Solar Maximum main electronics box 12 p1588 N88-19510
Treatment of unforeseen situations by online knowledge-based diagnostic systems --- spacecraft maintenance 12 p1589 N88-19511
EPOS: European Proximity Operations Simulation
12 p1589 N88-19515
EUROSIM: A design concept for an in-orbit operations simulator 12 p1589 N88-19517
Explorer Platform on-orbit servicing operations
12 p1591 N88-19526
Utilization of robotics and teleoperation for future in-orbit operations 12 p1591 N88-19527
Review of commercial spacecraft: Recovery and repair experiences. Implications for future spacecraft designs and operations 12 p1591 N88-19528
Robotics servicing experiment --- European space programs 12 p1591 N88-19529

Technology requirements for telerobotic satellite servicing in space 12 p1592 N88-19536
A teleoperated manipulator system concept for unmanned platforms — Columbus
12 p1593 N88-19537
External payload servicing: Operational requirements and technology 12 p1593 N88-19541
Turnaround operations analysis for OTV. Volume 1: Executive summary
[NASA-CR-179316] 13 p1729 N88-20340
Turnaround operations analysis for OTV. Volume 3: Technology development plan
[NASA-CR-179318] 13 p1729 N88-20342
Turnaround operations analysis for OTV. Volume 4: WBS and dictionary and cost methodology
[NASA-CR-179319] 13 p1729 N88-20343
Space station heavy lift launch vehicle utilization
[NASA-TM-100604] 14 p1873 N88-21188
Space station mobile transporter
14 p1927 N88-21488
Operational experience and design recommendations for teleoperated flight hardware
14 p1927 N88-21489
Design guidelines for robotically serviceable hardware
[NASA-TM-100700] 19 p2606 N88-25472
Man versus machine: The role of astronauts in extravehicular activity 19 p2699 N88-26045
Temperature rise in superfluid helium pumps
[NASA-TM-100997] 21 p2948 N88-27507
Ariane 5, HERMES and European vehicles for space station servicing
[SNIAS-881-422-102] 23 p3183 N88-28943
Remote servicing of space systems
23 p3260 N88-29409
A teleoperated robotic manipulator system for materials processing experiment servicing
23 p3260 N88-29410
Centaur operations at the space station: Cost and transportation analysis
[NASA-CR-182128] 24 p3332 N88-29835
Study of robotics spacecraft servicing and assembly in space. Volume 1: Executive summary
[ESA-CR(P)-2612-VOL-1] 24 p3333 N88-29839
Technology requirements for an orbiting fuel depot: A necessary element of a space infrastructure
[NASA-TM-101370] 24 p3334 N88-29845
Design and development of a refueling test bed
[FTMS-RP-ER-011] 24 p3357 N88-29986
ORBITAL SIMULATORS
U SPACE SIMULATORS
ORBITAL TRANSFER
U TRANSFER ORBITS
ORBITAL VELOCITY
Universal procedures for conversion of orbital elements to and from position and velocity (unperturbed orbits)
[RAE-TR-87043] 14 p1872 N88-21184
ORBITAL WORKERS
Implications of shiftwork in space for human physiology experiments 12 p1659 N88-19942
ORBITALS
NT ELECTRON ORBITALS
NT MOLECULAR ORBITALS
Symmetry and equivalence restrictions in electronic structure calculations
[NASA-TM-89252] 11 p1557 N88-19320
ORBITS
NT CIRCULAR ORBITS
NT EARTH ORBITS
NT ECCENTRIC ORBITS
NT ELLIPTICAL ORBITS
NT GEOSYNCHRONOUS ORBITS
NT PLANETARY ORBITS
NT POLAR ORBITS
NT SATELLITE ORBITS
NT SOLAR ORBITS
NT SPACECRAFT ORBITS
NT STATIONARY ORBITS
NT STELLAR ORBITS
NT TRANSFER ORBITS
Local and global techniques for the tracking of periodic solutions of parameter-dependent functional differential equations
[AD-A185756] 06 p0766 N88-14704
A quadratic-form analysis of the collisionless tearing mode
[AD-A188886] 12 p1695 N88-20144
Periodic orbits around a satellite modelled as a triaxial ellipsoid
[AD-A190592] 15 p2022 N88-22051
Distortion functions
[DE88-752634] 21 p3015 N88-27896
A limiting viscosity approach to the Riemann problem for materials exhibiting change of phase
[AD-A193477] 23 p3210 N88-29103
Monotone recurrence relations, their Birkhoff orbits and topological entropy
[AD-A193481] 23 p3276 N88-29504
ORCHARDS
Preliminary study on the application of digital processing of TM-LANDSAT data in the mapping of apple orchards in Fraiburgo (SC) 17 p2367 N88-24093
ORDER-DISORDER TRANSFORMATIONS
Vibrational properties of disordered solids. Far infrared studies: Performance report
[DE88-001474] 06 p0786 N88-14821
Dispersive hole transport in SiO2
[AD-A187077] 09 p1254 N88-17513
Positron-annihilation 2D-ACAR studies of disordered and defected alloys
[DE88-003118] 10 p1416 N88-18454
Theoretical studies of the interface electronic properties of tetrahedrally coordinated semiconductors
[AD-A187216] 11 p1555 N88-19306
Morphological studies of conductive polymers
[AD-A188456] 12 p1610 N88-19629
Ordered polymers for space applications
[AD-A188460] 12 p1610 N88-19630
Fast protonic conducting solid electrolytes
[AD-A188524] 12 p1698 N88-20160
A calorimetric determination of the enthalpy of formation and a description of the defect structure of the ordered beta-phase /Ni, Cu/ /1-x/ Al/x/
[NASA-TT-20157] 13 p1745 N88-20434
Optical studies of dynamical processes in disordered system
[DE88-005965] 13 p1837 N88-20993
Ordered structures in YBa2Cu3O/sub 7-y/, La2Cu3O/sub 7-y/, La/sub 2-x/Sr/sub x/CuO/sub 4-par. delta/ and related perovskites
[DE88-006461] 14 p1967 N88-21851
Renormalized Fermi liquid theory for disordered electron systems and the metal-insulator transition
[NOTA-INTERNA-900] 14 p1968 N88-21862
The theory of random alloys
[DE88-006408] 18 p2487 N88-24756
Structure and refinement of ordered aromatic heterocyclic polymers by diffraction methods: Application of results to electro-optic phenomena
[AD-A191859] 19 p2619 N88-25537
The structure and properties of grain boundaries in B2 ordered alloys
[DE88-009890] 20 p2773 N88-26447
Ordering transitions of ternary alloys A(1-x)B(x)C
20 p2873 N88-27054
Defects and disorder in amorphous and damaged silicon
[AD-A192277] 20 p2879 N88-27089
ORDNANCE
Compatibility of explosives: A data base system
[PB87-234464] 06 p0687 N88-14208
Texture profile in thermomechanically processed 2-inch-thick 5 Ni-steel armor plate
[AD-A189275] 13 p1741 N88-20410
Timing control system
[NASA-CASE-NPO-16882-1-CU]
18 p2506 N88-24863
ORES
U MINERALS
ORGANIC CHARGE TRANSFER SALTS
Organic metal (ET)4Hg3Br8A quasi-two-dimensional superconductor 14 p1974 N88-21778
ORGANIC CHEMISTRY
Super hydrides
[AD-A193710] 23 p3192 N88-28995
ORGANIC COMPOUNDS
NT ACETIC ACID
NT ACETYL COMPOUNDS
NT ACETYLENE
NT ACRYLIC ACID
NT ADENOSINE TRIPHOSPHATE
NT ADENOSINES
NT ALDOSTERONE
NT ALKANES
NT ALKENES
NT AMINO ACIDS
NT ANTHRACENE
NT ATROPINE
NT AZOLES
NT AZULENE
NT BENZENE
NT BUTADIENE
NT BUTANES
NT BUTENES
NT CAFFEINE
NT CARBAZOLES
NT CARBOHYDRATES
NT CARBONIC ANHYDRASE
NT CARBOXYLIC ACIDS
NT CAROTENE
NT CATALASE
NT CELLULOSE
NT CETANE
NT CHOLINESTERASE
NT CORTICOSTEROIDS
NT CUBANE
NT CYCLIC COMPOUNDS
NT CYCLIC HYDROCARBONS
NT CYCLOBUTANE
NT CYCLOHEXANE
NT CYTOCHROMES
NT DEOXYRIBONUCLEIC ACID
NT DICARBOXYLIC ACIDS
NT ENZYMES
NT ERGOTAMINE
NT ETHANE
NT ETHYLENE
NT FIBRINOGEN
NT FLUORINE ORGANIC COMPOUNDS
NT FLUOROCARBONS
NT FLUOROHYDROCARBONS
NT FLUOROPOLYMERS
NT FURANS
NT GLUCOSE
NT GLUTAMIC ACID
NT GLUTAMINE
NT GLUTATHIONE
NT GLYCOGENS
NT HEMOGLOBIN
NT HETEROCYCLIC COMPOUNDS
NT HMX
NT HYDROCARBONS
NT LIPIDS
NT LIQUEFIED NATURAL GAS
NT METHANE
NT METHYLENE
NT MORPHINE
NT NAPHTHALENE
NT NAPHTHENES
NT NATURAL GAS
NT NICOTINIC ACID
NT NUCLEIC ACIDS
NT NUCLEOSIDES
NT NUCLEOTIDES
NT ORGANIC CHARGE TRANSFER SALTS
NT ORGANIC LIQUIDS
NT ORGANIC LITHIUM COMPOUNDS
NT ORGANIC PHOSPHORUS COMPOUNDS
NT ORGANIC SILICON COMPOUNDS
NT OXYACETYLENE
NT PARAFFINS
NT PEPTIDES
NT PHOSPHAZENE
NT PHTHALOCYANIN
NT POLYBUTADIENE
NT POLYPEPTIDES
NT POLYTETRAFLUOROETHYLENE
NT POLYVINYL FLUORIDE
NT PROPANE
NT PROPYLENE
NT PROTEINS
NT PYRENES
NT PYRIDINES
NT PYRROLES
NT QUINOLINE
NT RDX
NT RIBONUCLEIC ACIDS
NT SEROTONIN
NT STARCHES
NT TEFLON (TRADEMARK)
NT THYMINE
NT TOLUENE
NT URACIL
NT VINYLIDENE
NT XANTHINES
Surface chemistry of transition metal carbides: A theoretical analysis
[AD-A184237] 03 p0291 N88-11829
Specific organic compounds in excreta
07 p0695 N88-15422
The Coupled Cluster Single and Double excitation (CCSD) method in quantum chemistry: An efficient formulation of the theory and application to closed shell molecular systems
[DE88-000475] 07 p0930 N88-15650
Estimation of aerial deposition and foliar uptake of xenobiotics: Assessment of current models
[DE88-000993] 09 p1188 N88-17117
Supercritical fluid extraction-gas chromatography of Volatile Organic Compounds (VOC) from tenax devices
[PB88-124300] 10 p1298 N88-17759
Evaluation and prediction of Henry's law constants and aqueous solubilities for solvents and hydrocarbon fuel components. Volume 1: Technical discussion
[AD-A188571] 12 p1613 N88-19643

Electrosorptive detection of simple organic compounds in liquid chromatography
[AD-A188757] 13 p1736 N88-20376
Mechanisms of photoinduced electron transfer
[DE88-004917] 13 p1836 N88-20983
The thermodynamic properties of organic oxygen compounds
[DE88-001208] 13 p1849 N88-21065
Properties of superconductors with strong electron-phonon interaction 14 p1974 N88-21779
Direct determination of part-per-billion levels of volatile organics in water and soil samples using glow discharge mass spectrometry
[DE88-011389] 21 p2910 N88-27272
National ambient Volatile Organic Compounds (VOCs) data base update, documentation
[PB88-195631] 21 p2971 N88-27646
Electron impact ionization cross-section of some organic compounds
[DE88-702044] 23 p3280 N88-29525
Band electronic structures and crystal packing forces
[DE88-010247] 23 p3289 N88-29585

ORGANIC FLUORINE COMPOUNDS
U FLUORINE ORGANIC COMPOUNDS

ORGANIC LASERS
NT DYE LASERS

ORGANIC LIQUIDS
Detection of vapors of flammable liquids in air by atmospheric sampling mass spectrometry/mass spectrometry
[DE88-000030] 02 p0196 N88-11227

ORGANIC LITHIUM COMPOUNDS
Tetrahedral carbon and interstitial electrons in Li cluster: CLi4 and (LiCH3)4
[AD-A184277] 04 p0496 N88-13055

ORGANIC MATERIALS
Consortium for Materials Development in Space. Technical section
[NASA-CR-181508] 03 p0296 N88-11859
Highly Non-Linear Optical (NLO) organic crystals
03 p0297 N88-11865
Highly Non-Linear Optical (NLO) organic crystals and films. Electrooptical organic materials
03 p0297 N88-11866
Theory of atomic additivity in molecular hyperpolizabilities 03 p0297 N88-11867
Proton abstraction as a route to conductive polymers
[AD-A184019] 04 p0421 N88-12612
Cellular solidification in a monotectic system
[NASA-TM-100317] 07 p0829 N88-15027
Exobiology and life science 07 p0883 N88-15356
Effects of energy, distance and orientation on electron transfer rates studied by pulse radiolysis in organic media
[DE88-002906] 08 p1082 N88-16521
Trace analysis by MS/MS on a double focussing mass spectrometer
[AD-A187954] 10 p1334 N88-17973
North Carolina Biomolecular Engineering and Materials Applications Center (NC-BEMAC)
[AD-A190923] 16 p2237 N88-23364
The evolution of cometary activity
18 p2594 N88-25416
Corrosion control through a better understanding of the metallic substrate/organic coating/interface
[AD-A193981] 22 p3056 N88-28132
Hydrogen storage by molecular polyhydrides
[AD-A194207] 23 p3191 N88-28989
Transport of organic vapors in multiphase polymer system
[AD-A194097] 23 p3198 N88-29033
Evaluation of organic coating deterioration and substrate corrosion in seawater using electrochemical impedance measurements 24 p3355 N88-29976

ORGANIC NITRATES
NT PETN

ORGANIC PHOSPHORUS COMPOUNDS
NT PHOSPHAZENE
FTIR (Fourier Transform Infrared) and FTNMR (Fourier Transform Nuclear Magnetic Resonance) study of organophosphorus surface reactions
[AD-A188337] 12 p1609 N88-19625
Determination of the partition coefficients of organophosphorus compounds using high-performance liquid chromatography
[AD-A189276] 13 p1737 N88-20385

ORGANIC SEMICONDUCTORS
Pyrolyzed organic polymer nitrogen dioxide sensor
19 p2669 N88-25868

ORGANIC SILICON COMPOUNDS
Boron-containing organosilane polymers and ceramic materials thereof
[NASA-CASE-ARC-11649-1-SB]
23 p3199 N88-29040

ORGANIZATIONS
NT EUROPEAN SPACE AGENCY
NT NORTH ATLANTIC TREATY ORGANIZATION (NATO)
NT WORLD METEOROLOGICAL ORGANIZATION
Source header list. Volume 2: L through Z
[AD-A184001] 03 p0385 N88-12419
National Center for Atmospheric Research
[PB87-228391] 04 p0470 N88-12901
Source header list. Volume 1: A through K
[AD-A184000] 04 p0501 N88-13086
Organizations of intermediation in technology transfer: Its role in technological innovation
[INPE-4354-TDL/297] 08 p1094 N88-16581
Hydrogen Energy Coordinating Committee: Summary of DOE hydrogen programs for FY 1987
[DE88-003960] 10 p1306 N88-17811
Soviet high-technology restructuring drive: the MNTK network
[AD-A188136] 11 p1565 N88-19370
Conditions and mechanisms of the process of technological innovation in Brazil: The role of research institutes
[INPE-4175-TDL/274] 11 p1567 N88-19383
Task allocation for efficient performance of a decentralized organization
[AD-A188699] 12 p1705 N88-20204
Implementing information systems/office automation in an Air Force environment
[AD-A188956] 12 p1707 N88-20218
NASA and the challenge of ISDN: The role of satellites in an ISDN world
[NASA-CR-182749] 15 p2126 N88-22676
Analysis and synthesis of decision-making organizations
[AD-A191948] 19 p2738 N88-26258
Decision aiding and coordination in decision-making organizations
[AD-A191950] 19 p2738 N88-26259
Modeling and evaluation of expert systems in decisionmaking organizations
[AD-A191951] 19 p2739 N88-26260
Coordination in decision-making organizations
[AD-A191952] 19 p2739 N88-26261
Anatomy of an organizational change effort at the Lewis Research Center
[NASA-CR-4146] 19 p2739 N88-26264
Strategic, organizational and standardization aspects of integrated information systems, volume 6
[AD-A195855] 24 p3437 N88-30457
Technical change needs organizational change
24 p3438 N88-30466

ORGANOMETALLIC COMPOUNDS
NT CHLOROPHYLLS
NT FERROCENES
NT HEMOGLOBIN
NT ORGANIC LITHIUM COMPOUNDS
United States - Japan Workshop on Dielectric and Piezoelectric Ceramics (3rd) held in Toyama, Japan on November 9-12, 1986
[AD-A185113] 05 p0568 N88-13460
Effects of hydrolysis on metallo-organic solution deposition of PZT films
[ATR-86(8443)-1] 06 p0679 N88-14160
Heteroepitaxial growth of 3-5 semiconductor compounds by metal-organic chemical vapor deposition for device applications
[NASA-CR-182346] 06 p0788 N88-14832
Superlattice photodetectors
[AD-A186956] 09 p1253 N88-17511
Molecular beam epitaxy for research on quantum well structures
[AD-A186791] 09 p1255 N88-17522
Chemical activation of molecules by metals: Experimental studies of electron distributions and bonding
[DE88-004465] 10 p1407 N88-18393
Feasibility studies of the growth of 3-5 compounds of boron by MOCVD
[NASA-CR-181622] 11 p1561 N88-19343
Preparation and characterization of thin films of alumina by metalorganic chemical vapor deposition
[AD-A188366] 12 p1608 N88-19614
The spectroscopy and reaction kinetics of coordinatively unsaturated metal carbonyls
[AD-A190533] 15 p2035 N88-22124
Molecular orbital studies of the bonding in heavy element organometallics: Progress report
[DE88-007765] 19 p2723 N88-26168
Metal grid base heterojunction transistor operating at 60 and 94 GHz
[AD-A194763] 23 p3207 N88-29087

ORGANOMETALLIC POLYMERS
Soluble metal chelate polymers of coordination numbers six, seven and eight
[AD-A185094] 05 p0568 N88-13459
Silicon containing photoresists
[AD-A188666] 12 p1605 N88-19601
Ceramic materials from preceramic organometallic copolymers
[DE88-006067] 14 p1892 N88-21301

ORIFICES
Dilution jet mixing program, phase 3
02 p0165 N88-11153
Drop formation from an orifice in an electric field
[DE87-014405] 03 p0322 N88-12034
The acoustic source created by turbulent flow over orifices and louvers
[REPT-97674] 06 p0776 N88-14764
Describing the source created by turbulent flow over orifices and louvers
[AD-A190254] 15 p2130 N88-22706

ORIGINS
Statistical fine structure in the inhomogeneously broadened electronic origin of pentacene in p-terphenyl
[AD-A191211] 16 p2176 N88-22968

ORION AIRCRAFT
U P-3 AIRCRAFT

ORION NEBULA
The Einstein survey of the young stars in the Orion Nebula 04 p0516 N88-13182
The velocity structure and turbulence at the center of the Orion Nebula 04 p0521 N88-13201
Models of recombination lines in radio H2 regions
[INPE-4302-TDL/277] 12 p1710 N88-20232
First detection of HCN J = 9 to 8 (797 GHz) line emission: Very high densities in the Orion core
[MPE-PREPRINT-110] 22 p3165 N88-28847

ORIONID METEOROIDS
Results of observations of the Eta Aquarid and Orionid meteor showers in 1980-1984 06 p0740 N88-14548
The structure of the Halley meteor stream and the orbital history of the comet 14 p2008 N88-21975

ORNITHOPTER AIRCRAFT
U RESEARCH AIRCRAFT

OROGRAPHY
The air flow on hills from models and experiments
[BMFT-FB-T-86-175] 02 p0198 N88-11236
The 54-hours continuous post-frontal precipitation north of the Alpine mountain barrier, 22-25 August 1975
02 p0203 N88-11268
Longer-duration post-frontal precipitation at Vancouver International Airport, 1953-1983
02 p0203 N88-11269
Observational analysis of the interaction between fronts and the orography in Taiwan during the late winter monsoon season 02 p0203 N88-11270
Detailed analysis of a mesoscale convective complex situation in the Carpathian Basin (Europe)
02 p0207 N88-11296
Cumulus and thunderstorm initiation by mountains
02 p0207 N88-11301
A real-data numerical study and four-dimensional data assimilation application for mesobeta-scale flow in complex terrain 02 p0212 N88-11329
Research work at the Meteorological Institute of the University of Munich (Federal Republic of Germany)
[MITT-56] 08 p1013 N88-16141
Model calculations of the behavior of orographically influenced cold fronts 08 p1015 N88-16155
Spectral analysis of an orographically structured area in the forefield of mesoscale flow simulations
08 p1016 N88-16160
Orographically influenced cold fronts in a spectral approach 08 p1016 N88-16161
Statistics of two-dimensional structure elements of mountainous ranges (mosaic model) for calculating three-dimensional reflection functions
[DFVLR-FB-87-33] 09 p1185 N88-17099
Numerical simulation of thermally generated mountain-foreland circulation
[DFVLR-FB-87-30] 09 p1190 N88-17132
The retardation of cold fronts at high mesoscale mountains 09 p1241 N88-17437
Systematic errors of the FSU global spectral model
10 p1356 N88-18103
Cloud physics studies in SCPP (Sierra Cooperative Pilot Project) from 1977-87
[PB88-136924] 11 p1516 N88-19054
The German Front Experiment 1987: Experimental design
[DFVLR-MITT-87-24] 16 p2234 N88-23343

ORR-SOMMERFELD EQUATIONS
Solution of the Orr-Sommerfeld equation for the Blausius boundary-layer documentation of program ORRBL and a test case
[NASA-CR-4169] 20 p2841 N88-26858

ORRERIES
U ASTRONOMICAL MODELS

ORTHOGONAL FUNCTIONS
NT WALSH FUNCTION

Errors in retrieving hydrological fields and fields of their differential characteristics by method of approximation by orthogonal functions 06 p0727 N88-14475

Spectral iterative technique with Gram-Schmidt orthoganalization
[PB88-127451] 10 p1399 N88-18338

The inverse problem and the pseudo-empirical orthogonal function method of solution. Part 1: Theory; Part 2: Application
[AD-A188894] 12 p1684 N88-20069

Space-time analysis of oceanographic fields by modified empirical orthogonal functions method
13 p1786 N88-20687

Group theoretic interpretations of Askey's scheme of hypergeometric orthogonal polynomials
[CWI-PM-R8703] 13 p1831 N88-20954

Identification of nonlinear output-affine systems using an orthogonal least squares algorithm
[RR-313] 14 p1958 N88-21678

A Gram-Schmidt space-time adaptive canceller using adaptive lattice filters
[AD-A189684] 14 p1959 N88-21684

New stable, vectorisable Kalman filter algorithms based on orthogonal transformations
[DFVLR-FB-87-52] 16 p2258 N88-23494

Orthogonal polynomials with respect to a symmetric inner product involving derivates
[REPT-87-59] 16 p2259 N88-23504

Solving singular systems using orthogonal functions
[AD-A190881] 16 p2260 N88-23512

Minimal parameter solution of the orthogonal matrix differential equation
[NASA-TM-4043] 17 p2383 N88-24165

Optimal a priori covariance selection for the solution of ill-conditioned nonlinear inverse problems
18 p2564 N88-25222

On a biorthogonal system associated with uniform asymptotic expansions
[CWI-AM-R8709] 18 p2566 N88-25240

Numerical simulations of flow around shuttle orbiter
19 p2635 N88-25633

Nonlinear conformal transformations and Clifford algebras
[PB87-225942] 19 p2719 N88-26147

Coherent structures in the axisymmetric turbulent jet mixing layer 21 p2947 N88-27504

Complex EOF analysis of intraseasonal tropical wind fluctuations 22 p3121 N88-28544

Sub-Saharan rainfall anomalies and global sea-surface temperature relationships for the recent fifteen year (1970-1984) period 22 p3122 N88-28552

The predictability of low frequency patterns in the NMC MRF 22 p3127 N88-28587

Determination of most probable predicted 50 kPa pattern by empirical orthogonal functions
22 p3128 N88-28593

Determining the spatial structure of fields of precipitation from space radar images in two orthogonal polarizations
24 p3450 N88-30531

ORTHOGONALITY

A computational examination of orthogonal distance regression
[AD-A184374] 03 p0371 N88-12337

Eigenvectors of distance-regular graphs
[AD-A185375] 05 p0641 N88-13919

Separable orthogonal coordinates and particle creation for an accelerating observer
[DE87-703358] 05 p0657 N88-14029

An orthogonal oriented quadrature hexagonal image pyramid
[NASA-TM-100054] 06 p0755 N88-14630

Optimal repeated measurements designs for comparing test treatments with a control
[AD-A185999] 07 p0917 N88-15569

Mechanism of change of vortex structure orientation in type-2 superconductors 09 p1239 N88-17425

Orthogonal patterns in binary neural networks
[NASA-TM-100060] 10 p1396 N88-18320

The parameterization of orthogonal matrices: A review mainly for statisticians
[AD-A189144] 13 p1829 N88-20936

An orthogonal parameter estimation algorithm for nonlinear stochastic systems
[RR-307] 14 p1966 N88-21736

Solving singular systems using orthogonal functions
[AD-A190881] 16 p2260 N88-23512

Development of adaptive grid schemes based on Poisson grid generators
[AD-A190983] 16 p2262 N88-23526

ORTHONORMAL FUNCTIONS

Estimation of multivariate binary density using orthonormal functions
[AD-A186386] 07 p0912 N88-15526

ORTHOPHOTOGRAPHY

Automatic production of orthophoto using SPOT images 22 p3112 N88-28487

High resolution orthoimage quadrangle maps using SPOT satellite data 22 p3112 N88-28488

ORTHOSTATIC TOLERANCE

Daily dynamics of some physiological indicators of man under desert condition 06 p0750 N88-14605

Human metabolism and peripheral circulation during antiorthostatic hypokinesia 07 p0891 N88-15398

Biorhythmological analysis of dynamics of pulmonary ventilation parameters during orthostatic tests
07 p0891 N88-15400

Circulatory response of males 45-52 years of age to antiorthostatic hypokinesia 07 p0894 N88-15416

Comparative evaluation of orthostatic stability following immersion in horizontal and vertical positions
10 p1363 N88-18143

Effect of antiorthostatic position and different illumination on sensitivity of skin in upper half of the body to ultraviolet radiation 10 p1363 N88-18145

Effect of exogenous cardiosynchronized counterpulsation on human regional and central hemodynamics 10 p1366 N88-18163

Changes in the status of the human tibia during antiorthostatic hypokinesia
[NASA-TT-20221] 13 p1810 N88-20813

Propranolol and the compensatory circulatory responses to orthostasis at high altitude
[AD-A192675] 22 p3131 N88-28618

ORTHOTROPIC PLATES

Spatial strength variation and statistical size effect of laminated orthotropic composite materials
04 p0427 N88-12646

A generalized variational method for solving stress intensity factors at cracks on the edge of holes in orthotropic plates
[IC-AERO-87-02] 17 p2348 N88-23992

The surface crack problem in an orthotropic plate under bending and tension
[NASA-CR-178281] 18 p2531 N88-25014

ORTHOTROPIC SHELLS

Nonsteady-state vibrations in acoustic medium of elastic elliptical shell subjected to instantaneously applied uniform pressure 02 p0160 N88-11000

ORTHOTROPISM

Numerical solution methods for viscoelastic orthotropic materials
[NASA-CR-182381] 08 p0971 N88-15874

An analytical study of the effects of transverse shear deformation and anisotropy on natural vibration frequencies of laminated cylinders
[NASA-TM-100554] 10 p1295 N88-17739

A simplified orthotropic formulation of the viscoplasticity theory based on overstress 14 p1929 N88-21505

OSCILLATING CYLINDERS

Experimental comparison of lightning simulation techniques to CV-580 airborne lightning strike measurements
[AD-A190576] 15 p2098 N88-22496

OSCILLATING FLOW

The phenomenology of Karman vortex streets via sound in oscillatory flow
[MPIS-MITT-84-1987] 02 p0122 N88-10775

A supersonic potential gradient method for the calculation of unsteady aerodynamic pressures on harmonically oscillating wings
[ESA-TT-930] 03 p0259 N88-11631

Unsteady aerodynamics of an oscillating cascade in a compressible flow field
[NASA-TM-100219] 05 p0549 N88-13346

Microcomputer analysis of regenerative heat exchangers for oscillating flow
[DE88-001773] 10 p1329 N88-17945

Oscillating airfoils: Achievements and conjectures
[AD-A190490] 15 p2014 N88-22006

A survey of oscillating flow in Stirling engine heat exchangers
[NASA-CR-182108] 15 p2067 N88-22322

Description of an oscillating flow pressure drop test rig
[NASA-TM-100905] 16 p2170 N88-22933

Oscillating flow over bluff bodies in a U-shaped water tunnel 16 p2201 N88-23131

Tests on oscillating flows in a pipe nozzle with an abrupt diameter variation
[MPIS-2/1987] 17 p2337 N88-23947

Surface tension and viscosity with Lagrangian hydrodynamics on a triangular mesh
[AD-A194120] 22 p3075 N88-28256

OSCILLATION DAMPERS

Variation of wave action: Modulations of the phase shift for strongly nonlinear dispersive waves with weak dissipation. A new adiabatic invariant involving the modulated phase shift for strongly nonlinear, slowly varying, and weakly damped oscillators. The modulated phase shift for weakly dissipated nonlinear oscillatory waves of the Korteweg-de vries type
[AD-A185630] 06 p0765 N88-14702

Characterizing particle combustion in a Rijke burner
[AD-A186157] 08 p0966 N88-15847

Response of a sequential damper to shock inputs
08 p0998 N88-16042

Survey of impact damper performance
16 p2217 N88-23227

Experimental study of unsteady separating turbulent boundary layers
[AD-A192997] 21 p2943 N88-27477

OSCILLATIONS

NT AIRFOIL OSCILLATIONS
NT ELECTRON OSCILLATIONS
NT H WAVES
NT HARMONIC OSCILLATION
NT MOLECULAR OSCILLATIONS
NT NONOSCILLATORY ACTION
NT PLASMA OSCILLATIONS
NT PRESSURE OSCILLATIONS
NT SOLAR OSCILLATIONS
NT SOUTHERN OSCILLATION
NT STABLE OSCILLATIONS
NT STELLAR OSCILLATIONS
NT TRANSIENT OSCILLATIONS
NT WING OSCILLATIONS

On oscillation of a kind of integro-differential equation with delay
[DE87-703059] 02 p0225 N88-11417

Oscillatory and nonoscillatory properties of first order differential equations with piecewise constant deviating arguments
[DE87-703061] 02 p0225 N88-11418

Theory of interstitial solutions
[BLL-M-37314-(5828.4)] 02 p0233 N88-11469

Physical design of parameters of Nd:YAG disk laser
03 p0302 N88-11904

Excitation of natural oscillations of a boundary layer by an external acoustic field 04 p0425 N88-12634

Dynamics of reverse flows at pump inlet
04 p0425 N88-12636

Oscillation theory for linear second-order differential systems
[DE87-011393] 04 p0484 N88-12980

Boundary effects on the drag of an oscillating sphere. Applications to the magnetic sphere rheometer. Attenuation and dispersion of acoustic waves in nematic liquid crystals 04 p0488 N88-13007

The dynamics of solar magnetic flux tubes subjected to resonant foot point shaking 04 p0507 N88-13118

An experimental investigation of the aerodynamics of a NACA 64A010 airfoil-flap combination with and without flap oscillations. Part 1: Steady-state characteristics
[NASA-TM-88217] 05 p0542 N88-13305

Interpretation of our present terrestrial climatic record
[DE88-000223] 06 p0744 N88-14573

Dimensional analysis of nonlinear oscillations in brain, heart and muscle
[DE87-014749] 06 p0751 N88-14614

Observation of instabilities in time during dynamic self-diffraction of light in anisotropic nonhomogeneous medium 06 p0769 N88-14730

A possible accelerator experiment to solve the solar neutrino puzzle
[PREPRINT-556] 06 p0776 N88-14778

The TITAN oscillating-field current-drive system
[DE88-001823] 06 p0782 N88-14798

Solar Dynamics and G-modes
[NASA-CR-180737] 06 p0805 N88-14911

Sliding charge density waves and related problems
[AD-A186720] 09 p1157 N88-16934

The dynamics of an oscillating four-bar linkage
09 p1181 N88-17074

Lifting-surface theory of oscillating propellers in compressible flow
[NAL-TR-943] 10 p1273 N88-17613

Betatron oscillations in a free electron laser
[DE88-004859] 10 p1337 N88-17990

Modal testing the EOLE
[DE88-003795] 10 p1350 N88-18066

Modal testing of a very flexible 110 m wind turbine structure
[DE88-003796] 10 p1351 N88-18072

Statistical studies of low frequency oscillations in satellite-observed stratospheric temperatures
10 p1353 N88-18086

Probability bounds for M-Skorohod oscillations
[AD-A187981] 10 p1404 N88-18371

Conditions at infinity for theories of oscillating wings and propellers in subsonic flow
[NAL-TR-937] 11 p1434 N88-18556

Modeling of limit cycle stall flutter oscillations
12 p1583 N88-19472

Predicting oscillatory finite difference solutions to the heat equation: A comparative study of the coefficient and matrix methods
[AD-A189591] 13 p1825 N88-20911

Stochastic and chaotic oscillations
[CWI-AM-R8704] 13 p1829 N88-20940
Bloch oscillations in small Josephson junctions: Their manifestation in switching effects
14 p1969 N88-21756
Hydrodynamical regimes in molten metals under a horizontal temperature gradient
14 p1988 N88-21859
Oscillation damped movement of suspended objects
[DE88-00[illegible]] 15 p2086 N88-22433
Discussion of two-mode two-photon CW laser oscillation 16 p2187 N88-23042
Low frequency ocean ambient noise: Measurements and theory
[AD-A191188] 16 p2237 N88-23362
Efficient implementation of essentially non-oscillatory shock capturing schemes, 2
[NASA-CR-181656] 17 p2392 N88-24217
Development of a computerized analysis for solid propellant combustion instability with turbulence
[NASA-CR-182351] 19 p2611 N88-25497
Control of combustion instabilities in ramjet motors
19 p2625 N88-25574
One person's view of velocity-coupled instability
19 p2629 N88-25595
The importance of steady and dynamic inflow on the stability of rotor-body systems 21 p2890 N88-27156
Periodic oscillations in nonlinear mechanical systems
21 p2963 N88-27599
Investigation of oscillating cascade aerodynamics by an experimental influence coefficient technique
[NASA-TM-101313] 22 p3039 N88-28041
Nonlinear oscillations of an inviscid liquid column under zero-gravity
[LRT-WE-9-FB-8(1987)] 22 p3063 N88-28173
Nonlinear oscillations of axially independent liquid column under zero-gravity environment
[LRT-WE-9-FB-12(1987)] 22 p3063 N88-28174
Nonlinear oscillations in paraboloidal containers
[LRT-WE-9-FB-3(1988)] 22 p3078 N88-28275
Steady and unsteady transonic pressure measurements on a clipped delta wing for pitching and control-surface oscillations
[NASA-TP-2594] 23 p3173 N88-28895
Prediction of dynamic derivatives
24 p3318 N88-29761
Theories of comparative analysis
[AD-A196328] 24 p3427 N88-30395
Intermediate polars observed in Brazil in the last eight years
[INPE-4567-PRE/1308] 24 p3454 N88-30559

OSCILLATOR STRENGTHS
The 2D Rydberg series in Al I
[NASA-TM-101189] 22 p3150 N88-28740
On selection rules and inelastic electron scattering at intermediate energies
[DE88-701833] 23 p3280 N88-29526

OSCILLATORS
NT CRYSTAL OSCILLATORS
NT HARMONIC OSCILLATORS
NT MAGNETRONS
NT MECHANICAL OSCILLATORS
NT MICROWAVE OSCILLATORS
NT PENDULUMS
NT PIEZOELECTRIC CRYSTALS
NT SYNCHRONIZED OSCILLATORS
NT VOLTAGE CONTROLLED OSCILLATORS
Induction linac-driven free-electron lasers: Status and future prospects
[DE87-012914] 01 p0051 N88-10329
Diode pumped solid-state laser oscillators for spectroscopic applications
[NASA-CR-180576] 01 p0052 N88-10331
Sideband suppression by an intracavity optical filter in the Los Alamos free-electron laser oscillator
[DE87-011740] 02 p0177 N88-11103
Dynamics and routes to chaos from quasiperiodicity
03 p0312 N88-11974
The impact of varves on solar physics
[NASA-CR-181519] 03 p0390 N88-12448
Measurement and analysis of cryogenic sapphire dielectric resonators and DROs
04 p0433 N88-12686
The 8.4-GHz low-noise maser pump source assembly
04 p0436 N88-12705
An analytical and experimental study of injection-locked two-port oscillators
[NASA-TM-100119] 04 p0439 N88-12727
Spectral evolution equation for the sideband instability in a free-electron laser oscillator
[DE88-000510] 04 p0447 N88-12771
Development of symbolic computation methods for nonlinear dynamics
[AD-A185562] 06 p0758 N88-14653
Production-process CO2 laser with amplified pulse-repetition operation 06 p0771 N88-14739
Periodically pulsed excimer master oscillator-regenerative amplifier laser set
06 p0772 N88-14741
Fundamental cyclotron frequency generation from a cusptron oscillator
[AD-A188187] 10 p1321 N88-17898
Conceptual designs of a 50 NM FEL (Free-Electron Laser) oscillator and a 20-40 NM SASE (Self-Amplified Spontaneous Emission) amplifier
[DE88-003150] 10 p1334 N88-17974
Explicit approximations for strictly nonlinear oscillators with slowly varying parameters with applications to free electron lasers
[DE88-004116] 10 p1336 N88-17984
Tapered wiggler analysis of high gain free electron laser oscillators
[AD-A187997] 10 p1338 N88-17997
Research and development of surface skimming bulk wave devices for sensor applications
[AD-A187504] 11 p1470 N88-18766
Polarization effects in laser-pumped Nd:YAG lasers
[DE88-004019] 11 p1492 N88-18904
Quenched-laser operation of a Littman dye oscillator
[DE88-004020] 11 p1493 N88-18915
Solid-state travelling wave amplifiers based on multi-stream instability
[AD-A189566] 12 p1624 N88-19718
Time-dependent Slow-Time-Scale theory of free-running and phase-locked gyrotron oscillators
[AD-A188910] 12 p1629 N88-19752
Quartz oscillator analysis
[DE88-005886] 13 p1764 N88-20550
Direct solar-pumped iodine laser amplifier
[NASA-CR-182674] 13 p1777 N88-20630
Quantum statistics of parametric oscillators above threshold 14 p1979 N88-21811
Survey of impact damper performance
16 p2217 N88-23227
Periodic response of nonlinear systems
16 p2217 N88-23228
Integral equation for the laser field: Multimode description of a free-electron laser oscillator
[DE88-007050] 18 p2521 N88-24956
Microwave and millimeter-wave resonant tunneling diodes 19 p2659 N88-25809
Thin-membrane Lamb-mode acoustic oscillators for chemical detection 19 p2673 N88-25895
Focused ion beam fabrication of graded channel FETs in GaAs and Si
[AD-A193098] 21 p2936 N88-27439
Long-pulse, high-power vircator experiments
[DE88-011787] 21 p2940 N88-27458
The design of a digital Eprom oscillator for electrical impedance tomography
[DE88-012243] 21 p2940 N88-27462
Efficiency optimization for FEL oscillators
[AD-A192541] 21 p2952 N88-27536
An electronically tuned, stable 8415-MHz dielectric resonator FET oscillator for space applications
22 p3068 N88-28205
Liquid oscillations in a prolate spheroidal container
[LRT-WE-9-FB-4(1988)] 22 p3078 N88-28276
Distortions in processed signals and their application in electronic design. Part 2: A new variable signal generator
[DE88-702732] 23 p3205 N88-29071
An OKQPSK modem incorporating numerically controlled carrier synthesis
[DE88-009536] 23 p3244 N88-29304
Nonlinear dynamics of coupled oscillator arrays
[AD-A194888] 24 p3367 N88-30053
Research on a two-stage free electron laser oscillator
[AD-A195991] 24 p3377 N88-30115

OSCILLOSCOPES
Online monitoring of laserpulses using the GPIB-interface of a Tektronix 2430 Digital Storage Oscilloscope
[DE88-002836] 07 p0856 N88-15201
Comparison of sampling oscilloscopes with less than 35 ps transition durations 19 p2658 N88-25793

OSMIUM
Johnson noise thermometer for high radiation and high temperature environments
[DE88-003770] 10 p1323 N88-17911
Johnson noise thermometer for high-radiation and high-temperature environments
17 p2434 N88-24480

OSMIUM COMPOUNDS
Improved cathode life testing
[REPT-3189-T] 02 p0168 N88-11056

OSMOSIS
NT REVERSE OSMOSIS
Investigations of Paramecium cells analyzed under microgravity conditions 07 p0884 N88-15367
Use of hydrophilic polymer coatings for control of electroosmosis and protein adsorption
07 p0925 N88-15620

OSMOTIC PRESSURE
U OSMOSIS

OSTEOPOROSIS
Prevention of disuse osteoporosis: Effect of sodium fluoride during five weeks of bed rest
[NASA-CR-172018] 01 p0075 N88-10483
Disuse condition stimulates bone resorption in organ culture 12 p1658 N88-19926
Effect of different doses of alpha-hydroxydimethyl-gamma-aminopropylidene phonate on rat bones 19 p2704 N88-26078

OTF
U OPTICAL TRANSFER FUNCTION

OTOLITH ORGANS
Long-term adaptation of the otolith organs
07 p0886 N88-15375
Morphology and development of the inner ear of Anurans 07 p0886 N88-15378
Two-dimensional static otolith model
10 p1367 N88-18167

OTV
U ORBIT TRANSFER VEHICLES

OUTCROPS
A comparison between SPOT and LANDSAT TM for mapping of vegetation and bedrock outcrops
22 p3100 N88-28409

OUTGASSING
Outgassing data for selecting spacecraft materials
[NASA-RP-1124] 01 p0019 N88-10117
An investigation of the behavior of outgassed molecules in thermal vacuums 02 p0133 N88-10836
Mass spectroscopic facility 03 p0296 N88-11651
Gas coma of Comet Giacobini-Zinner: Emission from grains 14 p2000 N88-21923
Anisotropic emission from comets: Fans versus jets. 1: Concept and modeling 14 p2001 N88-21927
Comet P/Halley: Visual magnitude estimates and gas production 14 p2007 N88-21968
Neutral environment for space station
18 p2590 N88-25391
Space station neutral external environment
18 p2590 N88-25392
The evolution of cometary activity
18 p2594 N88-25416

OUTLETS
NT VENTS
Optimization of outlet channel of plasma ion source
[DE88-700471] 10 p1410 N88-18415

OUTLETS (GEOLOGY)
U ESTUARIES

OUTLIERS (STATISTICS)
Identification of multivariate outliers and leverage points by means of robust covariance matrices
[REPT-87-15] 01 p0088 N88-10575
PROGRESS: A program for robust regression analysis on the IBM PC
[REPT-85-14] 01 p0088 N88-10576
Robust statistical methods for automated outlier detection 04 p0433 N88-12681
Robust prediction operations for stationary processes
[AD-A185408] 05 p0641 N88-13924
Simulated performance of an order statistic threshold strategy for detection of narrowband signals
11 p1474 N88-18796
Outliner resistant filtering and smoothing: 2D version
[AD-A193319] 21 p3012 N88-27874

OUTPUT
NT LASER OUTPUTS
Output power enhancement of AC Raman free-electron laser
[DE88-000503] 04 p0449 N88-12786
Equivalence of input-output stability and exponential stability for infinite dimensional systems
[TW-276] 05 p0638 N88-13903
Outlier resistant predictive source encoding for a Gaussian stationary nominal source
[AD-A186725] 09 p1232 N88-17387
Research on output feedback control
[NASA-CR-182543] 11 p1534 N88-19167
Output formatting in Apple-soft BASIC
[DE88-701413] 15 p2108 N88-22559
Near optimal blind deconvolution
[REPT-87-016] 15 p2123 N88-22655
Electrochemical hydrogen concentrator for phosphoric acid fuel cells
[AD-A191355] 16 p2229 N88-23317
Simulation methodology
[AD-A192548] 21 p2995 N88-27764
Linearized model matching for single-imput nonlinear systems
[AD-A193642] 23 p3256 N88-29445

OV-1 AIRCRAFT
Flaps-up takoff performance of the OV-1D aircraft with YT53-L-704 engine installed
[AD-A185960] 07 p0819 N88-14979

OVER-THE-HORIZON RADAR
The effect of equatorial ionospheric irregularities on the performance of a south-looking OTH-B (Over-The-Horizon-Backscatter) radar
[AD-A195090] 24 p3362 N88-30018
Modeling and performance of HF/OTH (High-Frequency/Over-the-Horizon) radar target identification systems
[AD-A196287] 24 p3365 N88-30038

OVERCAST
U CLOUD COVER

OVERPRESSURE
Modeling of the non-auditory response to blast overpressure
[AD-A187397] 10 p1369 N88-18184

OVERTONES
U HARMONICS

OVERVOLTAGE
The influence of current stressing on the structure of Ag contacts to GaAs
[DE88-005988] 15 p2140 N88-22771

OXALATES
Manufacturing of a barium titanate with high dielectric coefficient by decomposition of precipitates of double oxalates
[ISAL-IDI1-88-02] 21 p2911 N88-27278

OXIDATION
NT ELECTROCHEMICAL OXIDATION
NT PHOTOOXIDATION
NT RUSTING
Oxidation of TSX graphite over the temperature range 450 to 1200°C
[DE87-012230] 01 p0020 N88-10127
Si - SiO2 interfaces: A High Resolution Transmission Electron Microscopy (HRTEM) study
[DE87-012255] 01 p0028 N88-10181
The effect of sulfur and zirconium Co-doping on the oxidation of NiCrAl
[NASA-TM-100209] 02 p0150 N88-10940
Silicon oxidation photoassisted with a continuous wave CO2 laser beam and contribution to the study of silica layers obtained
[LAAS-87-158] 02 p0179 N88-11115
Thermal expansion mismatch and oxidation in thermal barrier coatings 02 p0189 N88-11182
Detailed mechanism of benzene oxidation
[NASA-TM-100202] 03 p0282 N88-11775
Detailed kinetic modeling of autoignition chemistry
[DE87-013226] 03 p0283 N88-11782
Quantitative electron probe microanalysis investigation of the oxidation of high temperature alloys at low oxygen partial pressures
[JUEL-2120] 03 p0288 N88-11811
The applicability of the catalytic wet-oxidation to CELSS 03 p0360 N88-12264
The effect of organic inhibitors on the atmospheric corrosion and solderability of copper
[DE88-000261] 04 p0414 N88-12565
Detailed mechanism of toluene oxidation and comparison with benzene
[NASA-TM-100261] 05 p0563 N88-13428
Occurance and growth of fatigue cracks in corrosion environment 05 p0604 N88-13704
High energy molecules of high symmetry
[AD-A185385] 05 p0647 N88-13965
Fatigue oxidation interaction in low cycle fatigue
06 p0719 N88-14420
Partial analysis of experiment LDEF A-0114
[NASA-CR-179236] 06 p0760 N88-14787
Investigation of fuel additive effects on sooting flames
[AD-A186403] 07 p0829 N88-15026
Sliding-wear properties of retained austenite in carburized layer
[PB87-149092] 07 p0833 N88-15054
Atomic oxygen effects on metals
07 p0924 N88-15617
Low temperature reactivity of chars towards oxygen, appendix E2
[DE88-004088] 10 p1298 N88-17760
The influence of the heating procedure on the oxidation behaviour of NiAl studied by XPS
[AERE-R-12496] 10 p1300 N88-17776
Lipid peroxidation in rat tissues with exposure to antiorthostatic hypokinesia, exercise and immobilization stress 10 p1365 N88-18159
Oxidative enzyme activity in healthy subjects and individuals with neurocirculatory dystonia during graded exercise 10 p1367 N88-18170
Optical measurements of surface oxide layer formation on metal films
[DE88-003163] 10 p1409 N88-18405
Formation of optical waveguides by ion implantation
[DE88-003894] 10 p1409 N88-18407
Effects of X irradiation and high field electron injection on the electrical properties of rapid thermal oxides
[DE88-002642] 10 p1417 N88-18461
A viscoelastic BEM (Boundary Element Method) for modeling oxidation
[AD-A187490] 11 p1452 N88-18653
Fuels combustion research
[AD-A187688] 11 p1453 N88-18657
Cost 501 Project U.K.10. Part 4: The oxidation of fecralloy steel co-extruded onto strong steel substrates
[AERE-R-12432-PT-4] 11 p1456 N88-18679
High temperature oxidation studies on alloys containing dispersed phase particles and clarification of the mechanism of growth of SiO2
[AD-A188158] 11 p1457 N88-18688
Studies of the electron spectrum with reference to the clean surfaces of iron, cobalt and nickel and their subsequent exposure to oxygen
11 p1459 N88-18700
Oxidation and protection of fiberglass-epoxy composite masts for photovoltaic arrays in the low Earth orbital environment
[NASA-TM-100839] 11 p1465 N88-18734
Dynamics of production and oxidation of boranes
[AD-A188988] 12 p1606 N88-19605
Thermal oxide growth on silicon: Intrinsic stress and silicon cleaning effects
[AD-A188790] 13 p1736 N88-20377
Novel catalysts for methane activation
[DE88-003637] 13 p1738 N88-20390
High-temperature thermosets derived from the Diels-Alder polymerization of bisbenzocyclobutenes and bimaleimides
[AD-A188800] 13 p1747 N88-20449
Oxidation/sulfidation of materials in an SO3/SO2/O2 thermochemical-transport, distributed-receiver, solar-energy system
[DE88-005875] 13 p1795 N88-20739
Oxide-bound transition metal complexes for methane activation
[PB88-169719] 14 p1867 N88-21277
Copper peroxide
[NASA-TT-20245] 14 p1888 N88-21282
Corrosion Research Center, University of Minnesota
[DE88-006681] 15 p2041 N88-22160
High temperature corrosion of ceramics
[DE88-006567] 15 p2046 N88-22193
Evaluation of direct methane conversion to higher hydrocarbons and oxygenates
[DE88-003612] 15 p2049 N88-22204
The analysis of fatigue crack growth mechanism and oxidation and fatigue life at elevated temperatures
[NASA-CR-182129] 16 p2179 N88-22987
Development of a laboratory test for multiport fuel injector deposits - evaluation of the Jet Fuel Thermal Oxidation Test apparatus (JFTOT)
[AD-A191313] 16 p2183 N88-23015
Enhanced emittance of oxidized 304 stainless steel
17 p2423 N88-24408
Surface composition-reactivity relationships in heterogeneous catalysis
[DE88-006679] 18 p2480 N88-24714
Calculation of oxidation rates for iron in CO-CO2
[DE88-007313] 18 p2487 N88-24757
Effect of carbohydrate oxidation on the tropospheric HOx-system 18 p2539 N88-25067
Kinetics of CO oxidation over a deactivated Rh(111) single crystal catalyst
[DE88-003000] 19 p2613 N88-25504
Oxidation behavior and microstructural studies of melt-spun glassy Fe-Al-Zr metal
[DE88-009964] 19 p2617 N88-25526
Liquid-phase oxidation of acetone with hydrogen peroxide on oxide catalysts 19 p2706 N88-26091
The adherence of nickel oxide on nickel during high temperature oxidation
[DE88-011194] 20 p2774 N88-26450
Research in energetic compounds
[AD-A192953] 20 p2781 N88-26494
Oxidation-erosion of metals and alloys: Models, verification, and prediction
[DE88-010016] 21 p2915 N88-27300
Kinetic of oxidation to air of a Fe-Al-Mn alloy system at 600-800(sup 0)C temperature range
[DE88-702309] 21 p2920 N88-27330
Methods of quantifying and enhancing reactive oxygen species production 21 p2924 N88-27357
Silicon oxidation studies: A review of recent studies on thin film silicon dioxide formation in the physics and chemistry of SiO2 and the Si-SiO2 interface
[AD-A193176] 21 p3021 N88-27932
Study of the erosion corrosion of alloys and coatings
[AD-A194337] 22 p3055 N88-28128
Development of a test method to determine potential peroxide content in turbine fuels. Part 2
[AD-A192244] 23 p3199 N88-29042
Preparation and testing of Nb-Zr and Nb-ZrO2 single crystals for deformation studies
[DE88-702788] 23 p3293 N88-29613
Modelling of CO oxidation in dilution jet flows
24 p3351 N88-29847

OXIDATION RESISTANCE
Research and development on high strength ceramic heaters discussed 04 p0404 N88-12506
Improved perfluoroalkylether fluid development
[NASA-CR-180872] 08 p0967 N88-15651
Oxidation resistance of CVD coatings
[AD-A178337] 09 p1147 N88-16875
Correlations of norbornenyl crosslinked polyimide resin structures with resin thermo-oxidative stability, resin glass transition temperature and composite initial mechanical properties
[NASA-TM-100791] 09 p1147 N88-16877
Reaction mechanism of sulfur dioxide with single crystal cobalt and chromium and CoCrAlY coatings
[AD-A185989] 09 p1253 N88-17509
Beneficial and detrimental effects of silica in the high temperature oxidation of 20Cr/25Ni/Nb stainless steel
[AERE-R-12667] 10 p1301 N88-17779
Study of adherent oxide scales
[AD-A187368] 11 p1456 N88-18680
High temperature oxidation studies on alloys containing dispersed phase particles and clarification of the mechanism of growth of SiO2
[AD-A188158] 11 p1457 N88-18688
Nondestructive evaluation of carbon-carbon coatings
[AD-A189524] 13 p1748 N88-20453
Effect of oxidation on strength and thermal stability of material based on Si3N4 14 p1896 N88-21319
Secondary electron emission characteristics improved by ion implantation 14 p1903 N88-21370
Strength and failure rate of composite materials with carbon in ceramic matrix 16 p2180 N88-22995
Recent advances in metallic/ceramic coatings for corrosion control in military applications
17 p2320 N88-23858
Design and demonstration of a system for the deposition of atomic-oxygen durable coatings for reflective solar dynamic power system concentrators
[NASA-CR-4158] 19 p2606 N88-25474
A thermally modified polymer matrix composite material with structural integrity to 371 C
[NASA-TM-100922] 19 p2609 N88-25483
Studies in support of oxidation-resistant composite materials
[AD-A193320] 21 p2905 N88-27238
Processing technology research in composites
[AD-A195693] 24 p3341 N88-29890

OXIDATION-REDUCTION REACTIONS
Electronic and ionic transport in polymers
[AD-A187253] 11 p1452 N88-18651
Dynamics of production and oxidation of boranes
[AD-A188988] 12 p1606 N88-19605
The redox chemistry of some peroxo and superoxo metal ion complexes
[AD-A189159] 12 p1606 N88-19606
Advanced B and Al combustion kinetics over wide temperature ranges
[AD-A190752] 15 p2036 N88-22128
Electronic and ionic transport in polymers
[AD-A190434] 15 p2045 N88-22185
Oxidation and reduction rates for organic carbon in the Amazon mainstream tributary and floodplain, inferred from distributions of dissolved gases
[NASA-CR-182943] 18 p2538 N88-25062
Photochemical and thermal modeling in the early atmosphere of the earth
[NASA-CR-183029] 18 p2543 N88-25083
Carbon analysis in natural olivine crystals of deep origin
[NASA-TT-20311] 19 p2734 N88-26239
Oxygen reduction in fuel cell electrolytes
[DE88-008240] 20 p2819 N88-26723
Defect characterization of the redox behavior and stability of conducting oxides
[DE88-010799] 20 p2878 N88-27086
High power storage system based on thin film solid ionics
[AD-A193623] 23 p3291 N88-29589
Electrocatalytic reduction of oxygen on modified oxide surfaces
[NASA-TM-101333] 24 p3352 N88-29852

OXIDE FILMS
Use of sol-gels in the application of ceramic oxide thin films
[DE87-013610] 01 p0028 N88-10176
Progress toward a superconducting opening switch
[DE87-014170] 02 p0167 N88-11051

The effects of thin anodic films on the cyclic microstrain/macrostrain behavior of tungsten
05 p0597 N88-13650

On 1064 nm and 350 nm laser damage thresholds of high index oxide films deposited from organic solutions and sols
[DE88-001636] 07 p0859 N88-15217

Fabrication and packaging of discontinuous MIM (Metal-Insulator-Metal) film arrays for efficient MM wave and IR detection and mixing
[AD-A186809] 09 p1146 N88-16869

New scientific findings on the morphology of aluminum oxide layers, serving as an adhesive basis
[MBB-Z-137/86] 10 p1312 N88-17640

Effect of the gate oxide thickness on the speed of MOS integrated circuits
[PB88-155783] 10 p1323 N88-17910

Optical measurements of surface oxide layer formation on metal films
[DE88-003163] 10 p1409 N88-18405

Effects of X irradiation and high field electron injection on the electrical properties of rapid thermal oxides
[DE88-002642] 10 p1417 N88-18461

Freestanding films of YBa2Cu3O/sub 6.9/
[DE88-003995] 10 p1419 N88-18471

SiO2 film stress distribution during thermal oxidation of Si
[AD-A189552] 12 p1612 N88-19637

Thermal oxide growth on silicon: Intrinsic stress and silicon cleaning effects
[AD-A188790] 13 p1736 N88-20377

Superconducting electronic film structures
[AD-A192907] 20 p2879 N88-27091

Low temperature film growth of the oxides of zinc, aluminum and vanadium (and related systems, oxides of gold and germanium, nitrides of aluminum and tungsten) by reactive sputter deposition
[AD-A193497] 23 p3191 N88-28966

OXIDES
NT ALKALINE EARTH OXIDES
NT ALUMINUM OXIDES
NT ANHYDRIDES
NT BARIUM OXIDES
NT BERYLLIUM OXIDES
NT BISMUTH OXIDES
NT BORON OXIDES
NT CALCIUM OXIDES
NT CARBON DIOXIDE
NT CARBON MONOXIDE
NT CERIUM OXIDES
NT CHROMIUM OXIDES
NT COBALT OXIDES
NT COPPER OXIDES
NT DIOXIDES
NT HAFNIUM OXIDES
NT HEMATITE
NT HYDROGEN PEROXIDE
NT IRON OXIDES
NT LANTHANUM OXIDES
NT LEAD OXIDES
NT LITHIUM OXIDES
NT MAGNESIUM OXIDES
NT MANGANESE OXIDES
NT METAL OXIDES
NT MOLYBDENUM OXIDES
NT NICKEL OXIDES
NT NIOBIUM OXIDES
NT NITROGEN DIOXIDE
NT NITROGEN OXIDES
NT NITROUS OXIDES
NT PEROXIDES
NT QUARTZ
NT RUTILE
NT SAPPHIRE
NT SILICON DIOXIDE
NT SILICON OXIDES
NT SULFUR DIOXIDES
NT TANTALUM OXIDES
NT TIN OXIDES
NT TITANIUM OXIDES
NT VANADIUM OXIDES
NT YTTRIUM OXIDES
NT ZINC OXIDES
NT ZIRCONIUM OXIDES

Preparation of oxide glasses from metal alkoxides by sol-gel method
[NASA-TT-20124] 02 p0154 N88-10965

The wear process during the RUNNING-IN of steel in lubricated sliding
[NAL-TR-922T] 02 p0181 N88-11130

Theory of the one- and two-dimensional electron gas
[DE87-012864] 02 p0244 N88-11540

High temperature low cycle fatigue of oxide dispersion strengthened and single crystal nickel base superalloys
06 p0720 N88-14422

High temperature low cycle fatigue behavior and creep-fatigue interation of MA 6000 ODS alloy
06 p0720 N88-14425

Non-phonon mechanisms of superconductivity in high T/sub c/ superconducting oxides and other materials and their manifestation
[DE88-002708] 07 p0939 N88-15709

Properties of lanthanide oxides as supports for transition metal catalysts
[DE88-004520] 11 p1456 N88-18678

High temperature oxidation studies on alloys containing dispersed phase particles and clarification of the mechanism of growth of SiO2
[AD-A188158] 11 p1457 N88-18688

An investigation of metal complexes of some 2-substituted and 2,6-disubstituted pyridine N-oxides
11 p1460 N88-18701

An electron spectroscopic investigation of high-temperature superconducting oxides
[DE88-003807] 11 p1558 N88-19325

An overview of recent developments in high-temperature superconductivity
[DE88-005477] 12 p1697 N88-20155

Discussion of radiation effects and high-temperature oxide superconductors
[DE88-001427] 13 p1846 N88-21046

Thermal conductivity of oxide ceramics
[DE88-005842] 15 p2042 N88-22169

Effects of 67.5 MeV electron irradiation on Y-Ba-Cu-O and Gd-Ba-Cu-O high-temperature superconductors
[AD-A191271] 16 p2283 N88-23669

Thermal and power availability transient responses for the Argonne monolithic solid oxide fuel cell
17 p2419 N88-24384

Development of protective coatings for ceramic tubular components
[PB88-197165] 20 p2776 N88-26463

Preparation of oxide superconductors
[DE88-009136] 20 p2875 N88-27063

Phenomenological approach to high T/sub c/ oxide superconductors
[DE88-701668] 20 p2876 N88-27074

Preparation and properties of new inorganic glasses and gel-derived solids
[AD-A192922] 21 p2917 N88-27315

Monolithic fuel cells
[DE88-012004] 21 p2969 N88-27636

Development of planar geometry solid oxide fuel cell technology, phase 1
[PB88-210356] 23 p3229 N88-29215

OXIDIZERS
NT LIQUID OXIDIZERS
NT LIQUID OXYGEN
NT ROCKET OXIDIZERS

Physiological and biochemical aspects of toxic effects of oxidants in man's environment (air, water)
07 p0890 N88-15391

A continuous oxidizer regression model for the combustion of composite solid propellants
[AD-A186742] 08 p0974 N88-15894

Thermal oxide growth on silicon: Intrinsic stress and silicon cleaning effects
[AD-A188790] 13 p1736 N88-20377

Basic research in supersonic combustion
19 p2634 N88-25623

Oxidizer heat exchanger component test
[NASA-CR-182159] 24 p3339 N88-29876

OXYACETYLENE

Blast waves generated by planar detonations
[DE88-002219] 09 p1164 N88-16979

OXYALKYLATION
U ALKYLATION

OXYGEN
NT LIQUID OXYGEN
NT OXYGEN ISOTOPES

Mechanisms of polymer degradation using an oxygen plasma generator
[NASA-TM-100681] 01 p0018 N88-10110

High intensity 5 eV O-atom exposure facility for material degradation studies 02 p0135 N88-10847

Spacecraft surface exposure to atomic oxygen in low Earth orbit 03 p0273 N88-11715

Scotopic sensitivity with 10 percent oxygen
[AD-A183973] 03 p0356 N88-12243

Inerting and atmospheres 04 p0406 N88-12524

Fire-related medical science 04 p0406 N88-12525

Ignition and combustion of metals in oxygen
04 p0407 N88-12530

High efficiency generation of 130-nm radiation from sum-frequency mixing in Hg
[DE87-013714] 04 p0431 N88-12674

Oxygen enriched combustion system performance study
[DE88-001500] 05 p0562 N88-13424

Anti-Stokes generation of 226 nm light
[DE88-001612] 05 p0589 N88-13590

Controlled ecological life support systems: Development of a plant growth module 06 p0630 N88-13854

Progress in the measurement of salinity and oxygen at the Woods Hole Oceanographic Institution
[PB88-106089] 06 p0748 N88-14598

High temperature stability of superconducting YBa2Cu3O subx as characterized by X-ray diffraction
[DE88-001856] 06 p0787 N88-14824

L2,3 XANES of the high T sub c superconductor YBa2Cu3O7 with variable oxygen content
[NOTA-INTERNA-888] 06 p0788 N88-14837

The carbon dioxide chaperon efficiency for the reaction H + O2 + M yields HO2 + M from ignition delay times behind reflected shock waves
[NASA-TM-100125] 07 p0830 N88-15036

Atomic oxygen effects on metals
07 p0924 N88-15617

Coulomb interactions and effective strong coupling Hamiltonians in Cu-O superconductors
[DE88-002942] 08 p1090 N88-16561

Oxygen diffusion in high T/sub c/-superconductors
[DE88-002965] 08 p1090 N88-16562

Determination of the melting and decomposition points of different materials in an oxygen stream
[INFORME-I-158/86] 09 p1142 N88-16844

The photons payload, G-494: A learning experience
10 p1288 N88-17701

Development and application of oxygen flow tagging for velocity measurements and flow visualization in turbulent three-dimensional supersonic flows
[AD-A187982] 10 p1289 N88-17714

Materials development for JPL oxygen plant
[DE88-003067] 10 p1297 N88-17752

Low temperature reactivity of chars towards oxygen, appendix E2
[DE88-004068] 10 p1298 N88-17760

Theoretical and observational problems with Holes in the far UV dayglow
[AD-A188190] 10 p1355 N88-18100

Effect of oxygen inhalation on respiratory function during exercise and exposure to added resistance to respiration
10 p1366 N88-18164

Study of the vibrational modes of subsurface oxygen on Al (111) using diode laser infrared reflection-absorption spectroscopy
[AD-A188322] 12 p1632 N88-19769

Closed system physiology: Role of oxygen in the development of wheat 12 p1655 N88-19916

Nitrogen's biological effect on oxygen transport through hematoparenchymal barrier 12 p1662 N88-19967

Resonance energy transfer between carbon monoxide and oxygen molecules using dye laser intracavity absorption spectroscopy
[AD-A188488] 12 p1689 N88-20104

Optimization of oxygen cutting process for titanium alloys 14 p1897 N88-21323

Solar generation and storage of O2 (a 1 delta g)
[NASA-CR-4127] 14 p1913 N88-21431

Spatial distribution of O(supra 1D) from Comet Halley
14 p1999 N88-21913

Total photoionization cross sections of atomic oxygen from threshold to 44.3A
[NASA-CR-182992] 17 p2397 N88-24252

The role of oxygen on the mechanical behavior of molybdenum alloys 17 p2401 N88-24278

Catalytic ignition of hydrogen and oxygen propellants
[NASA-TM-100957] 18 p2476 N88-24689

Effect of hydrogen, deuterium and oxygen on the anelastic properties of refractory alloys
[DE88-007349] 18 p2484 N88-24736

Design and demonstration of a system for the deposition of atomic-oxygen durable coatings for reflective solar dynamic power system concentrators
[NASA-CR-4158] 19 p2606 N88-25474

Paramagnetic spins in oxygen-loaded ceramic La2CuO4/sub 4 + delta/
[DE88-007114] 19 p2619 N88-25539

Theory of oxygen content, atomic ordering and oxygen diffusion in 1,2,3 superconducting oxides as a function of temperature and oxygen pressure
[DE88-007961] 19 p2735 N88-26248

In situ spectroscopic studies of transition metal macrocycles as catalysts for the electrochemical reduction of oxygen
[PB88-203195] 20 p2769 N88-26416

Electrocatalysts for oxygen electrodes
[DE88-008397] 20 p2819 N88-26724

The superconducting transition in oxygen deficient YBa2Cu3O(sub 7-Delta)
[DE88-009957] 20 p2877 N88-27079

Oxygen vacancy ordering and superconductivity in YBa2Cu3O(sub 7-x)
[DE88-010005] 20 p2877 N88-27083

Carbon deposition model for oxygen-hydrocarbon combustion, volume 1
[NASA-CR-179375] 21 p2908 N88-27254

Mechanism of the nitric oxide-carbon monoxide-oxygen reaction over a single crystal rhodium catalyst
[DE88-006274] 21 p2910 N88-27268
Breakdown of molecular oxygen by brief pulses of laser radiation
[DE88-702687] 23 p3220 N88-29168
Aeronomic problems of the molecular oxygen photodissociation. Part 3: Solar spectral irradiances in the region of the O2 Herzberg continuum, Schumann-Runge bands and continuum
[AERONOMICA-ACTA-A-332-1988]
24 p3343 N88-29897
Aeronomic problems of molecular oxygen photodissociation. Part 2: Theoretical absorption cross sections of the Schumann-Runge bands at 79 K
[AERONOMICA-ACTA-A-331-1988]
24 p3344 N88-29907
Aeronomic problems of molecular oxygen photodissociation. Part 4: The various parameters for the Herzberg continuum
[AERONOMICA-ACTA-A-333-1988]
24 p3352 N88-29955

OXYGEN ANALYZERS
The study of excited oxygen molecule gas species production and quenching on thermal protection system materials
[NASA-CR-172027] 02 p0233 N88-11470
A simplified CARS measurement system for rapid determination of temperature and oxygen concentration
[NASA-TM-100498] 03 p0374 N88-12353
Ultrasonic oxygen sensor
[AD-A189723] 15 p2105 N88-22537
Steady state and transient behavior of the Pd-SnO(sub x) MIS oxygen sensors 19 p2672 N88-25890

OXYGEN ATOMS
Degradation mechanisms of materials for large space systems in low Earth orbit
[NASA-CR-181472] 02 p0143 N88-10896
Partial analysis of experiment LDEF A-0114
[NASA-CR-179236] 06 p0780 N88-14787
Mast material test program (MAMATEP)
[NASA-TM-100821] 12 p1604 N88-19592
Measurement of rate constants of elementary gas reactions of importance to upper atmosphere and combustion systems
[AD-A189432] 13 p1737 N88-20386
Laboratory experiments of relevance to the space station environment 18 p2592 N88-25402

OXYGEN BREATHING
Scotopic sensitivity with 10 percent oxygen
[AD-A183973] 03 p0356 N88-12243
Man rating the b-1B molecular sieve oxygen generation system
[AD-A186275] 07 p0899 N88-15447
Experimental study of protective effect of antioxidant enzymes-superoxide dismutase and catalase-when using intermittent toxic modes of hyperbaric oxygenation
19 p2707 N88-26094
Human performance and acute hypoxia, chapter 12
[AD-A192604] 23 p3238 N88-29270

OXYGEN CONSUMPTION
Detection of hyperventilation of parachutists
[DFVLR-FB-87-11] 01 p0075 N88-10482
A device and methodology for measuring repetitive lifting VO2max (oxygen consumption rate)
[AD-A185195] 05 p0630 N88-13850
Oxygen transport during exercise at extreme simulated altitude: Operation Everest 2
[AD-A185720] 06 p0752 N88-14620
Maximal cardiorespiratory responses to one- and two-legged cycling during acute and long-term exposure to 4300m
[AD-A185730] 06 p0752 N88-14621
Role of hemoglobin affinity for oxygen in efficiency of blood respiratory function 07 p0892 N88-15406
Respiratory and cardiovascular responses to cold stress following repeated cold water immersion
[AD-A186460] 08 p1050 N88-16340
Increase in influence of oxygen on the body in the presence of helium 13 p1810 N88-20816
Hypothalamic-pituitary-adrenal responses to short duration high intensity cycle exercise
[AD-A192597] 21 p2985 N88-27727
Human acclimatization and physical performance at high altitude
[AD-A192651] 22 p3130 N88-28611
Alterations in upper extremity motor function in soldiers during acute high altitude exposure
[AD-A192676] 23 p3238 N88-29272
Effect of hypoxia on speech recognition in noise
[AD-A193943] 23 p3240 N88-29280

OXYGEN DEFICIENCY
U HYPOXIA

OXYGEN DETECTORS
U OXYGEN ANALYZERS

OXYGEN IONS
The tail lobe ion spectrometer: Theory and observations
[IFSI-86-12] 05 p0585 N88-13569
Total and partial cross sections for electron capture for C(q+) (q=6-2) and O(q+) (q=8-2) ions in collisions with H, H2 and He atoms
[IPPJ-AM-56] 09 p1252 N88-17501
Determination of the content of CO(+) and H2O(+) ions in the tail of Comet Giacobini-Zinner and Comet Halley 14 p2006 N88-21964
Polymeric electrolytes
[AD-A193766] 23 p3198 N88-29031
La2CuO(sub 4 + delta): A superconducting superoxide
[DE88-010325] 23 p3288 N88-29578

OXYGEN ISOTOPES
Relativisitic heavy ion collisions
[DE87-014292] 02 p0232 N88-11462
The atomic weight and isotopic composition of oxygen and their variation in nature
[DE87-014397] 04 p0413 N88-12558
Preparation and characterization of isotopic oxygen-enriched yttrium barium copper oxide
[DE88-010939] 22 p3154 N88-28766

OXYGEN MASKS
Miniature respiratory sensor
[AD-A193430] 23 p3243 N88-29300

OXYGEN METABOLISM
Operation Everest 2: Comparison of four instruments for measuring blood oxygen saturation
[AD-A186456] 08 p1049 N88-16337
Nitrogen's biological effect on oxygen transport through hematoparenchymal barrier 12 p1662 N88-19967
Increase in influence of oxygen on the body in the presence of helium 13 p1810 N88-20816

OXYGEN PLASMA
Photochemical ignition studies. 3: Ignition by efficient and resonant multiphoton photochemical formation of microplasmas
[AD-A184644] 03 p0283 N88-11780
Silicon containing photoresists
[AD-A188666] 12 p1605 N88-19601
Advanced diagnostics for reacting flows
[AD-A190485] 15 p2035 N88-22122

OXYGEN PRODUCTION
A review of recent activities in the NASA CELSS program 03 p0359 N88-12259
Man rating the b-1B molecular sieve oxygen generation system
[AD-A186275] 07 p0899 N88-15447
Photosynthetic water splitting
[DE88-007809] 20 p2830 N88-26791
Advancements in oxygen generation and humidity control by water vapor electrolysis
[NASA-CR-172073] 22 p3134 N88-28633

OXYGEN RECOMBINATION
The study of excited oxygen molecule gas species production and quenching on thermal protection system materials
[NASA-CR-172027] 02 p0233 N88-11470
Molecular sources of ionospheric holes
[AD-A191857] 18 p2541 N88-25082

OXYGEN SPECTRA
On the forbidden red lines of oxygen in comets
14 p2006 N88-21963
Rotational structure and absorption cross sections from 300 to 190 K of the Schumann-Runge bands
[AERONOMICA-ACTA-A-318-1987]
15 p2036 N88-22131
Structural studies on La/sub 2/CuO/sub 4+delta/
[DE88-006828] 18 p2561 N88-25330

OXYGEN SUPPLY EQUIPMENT
NT OXYGEN MASKS

OXYGEN TENSION
Quantitative electron probe microanalysis investigation of the oxidation of high temperature alloys at low oxygen partial pressures
[JUEL-2120] 03 p0288 N88-11811
Respiration and oxygen tension in the blood of animals exposed to high pressures 20 p2830 N88-26790

OXYGEN TOXICITY
U HYPEROXIA

OXYGENATION
Acid-base equilibrium and some rat blood parameters following exposure to hyperbaric oxygenation
07 p0894 N88-15420

OXYNITRIDES
Aluminum oxynitride spinel (ALON): A review
[AD-A184753] 03 p0294 N88-11845
Phosphorus oxynitride glass for laser applications
[DE88-005413] 12 p1632 N88-19768
Fracture toughness of silicon nitride-silicon nitride joints bonded with oxynitride glass
[DE88-005548] 15 p2043 N88-22172

OZONE
Diagnostics of atmospheric chemistry through ozone measurement
[INPE-4230-PRE/1105] 01 p0068 N88-10437
ECC (Electrochemical Concentration Cell) ozonesonde observations at South Pole, Antarctica during 1986
[PB87-207502] 02 p0197 N88-11228
The study of excited oxygen molecule gas species production and quenching on thermal protection system materials
[NASA-CR-172027] 02 p0233 N88-11470
Global environmental change research
[S-HRG-100-301] 03 p0348 N88-12199
Photochemical ozone overburden correction
05 p0615 N88-13778
Analysis of the breakdown of the Antarctic circumpolar vortex using TOMS ozone data
05 p0615 N88-13779
Insights into the general circulation of the lower stratosphere from TOMS 05 p0616 N88-13780
Ozone, jet streaks and severe weather
05 p0616 N88-13781
Lower-stratospheric/upper-tropospheric exchange processes associated with tropical cyclones as observed by TOMS 05 p0616 N88-13782
Tropical easterly jet located using TOMS data
05 p0616 N88-13783
The use of TOMS data for tropospheric ozone studies
05 p0616 N88-13784
Northwest Airlines flight experiments
05 p0617 N88-13786
An analysis of tropopause pressure and total ozone correlations 05 p0617 N88-13789
TOMS ozone data compared at mesoscale resolution to tropopause heights from the AVE radiosonde network and to VAS radiances over the south-central United States 05 p0617 N88-13790
Dobson-stations performance assessment using TOMS data 05 p0618 N88-13792
Comparison of ground based and TOMS measurements of SO2 from volcanic emissions
05 p0618 N88-13795
Selection of optimum wavelengths for ozone mapping from satellites 05 p0619 N88-13798
Determination of total ozone from HIRS2/MSU sounding data 05 p0619 N88-13799
Complementary information between UV and IR for remote sensing of total ozone 05 p0619 N88-13800
Observation guidelines for a Total Ozone Mapping Spectrometer (TOMS) in geosynchronous orbit
05 p0619 N88-13801
A geostationary imaging spectrometer TOMS instrument 05 p0619 N88-13802
A review of atmospheric ozone and current thinking on the Antarctic ozone hole
[AD-A185606] 06 p0732 N88-14501
Long-term variation of total ozone
[INPE-4307-PRE/1173] 08 p1023 N88-16182
Literature survey relating to the absorption properties of ozone in the near ultraviolet
[ESRO-SM-81] 09 p1190 N88-17129
Tropospheric ultraviolet radiation: Assessment of existing data and effect on ozone formation
[PB88-130133] 10 p1354 N88-18095
Experimental measurements of the uptake of ozone in rats and human subjects
[PB88-125422] 10 p1364 N88-18148
Ozone sonde and Dobson spectrometer data obtained during the MAP/GLOBUS 1983 campaign over Western Europe
[BPT-5/87] 13 p1802 N88-20771
Assessment of crop loss from air pollutants. Meteorology-atmospheric chemistry and long range transport
[PB88-146857] 15 p2089 N88-22448
Surface ozone and ozonesounding results from the ABLE-2B expedition to Amazonia
[INPE-4523-PRE/1275] 15 p2095 N88-22484
Ozonesonde observations at Lauder, New Zealand during the Spring and early Summer of 1986
[PB88-173273] 16 p2232 N88-23328
Study of polyatomic dynamics in the atmosphere
[AD-A190964] 16 p2233 N88-23334
Near-real-time TOMS, telecommunications and meteorological support for the 1987 Airborne Antarctic Ozone Experiment
[NASA-CR-4133] 16 p2233 N88-23336
The gamma 1 and gamma 3 bands of (16)O3: Line positions and intensities
[NASA-TM-101162] 17 p2445 N88-24541
Line positions and intensities for the gamma 1 + gamma 2 and gamma 2 + gamma 3 bands of (16)O3
[NASA-TM-101161] 17 p2446 N88-24542
Air pollution: Ozone attainment requires long-term solutions to solve complex problems
[PB88-167275] 18 p2538 N88-25060

Workshop on Atmospheric OH
[BPT-7/87] 18 p2538 N88-25063
Ozone in the atmosphere 18 p2539 N88-25064
Ultraviolet measurements: Measurements of photolysis rates 18 p2539 N88-25065
Motor vehicles as sources of compounds important to tropospheric and stratospheric ozone
[PB88-195219] 18 p2540 N88-25076
ECC (Electrochemical Concentration Cell) ozonesonde observations at South Pole, Antarctica during 1987
[PB88-202015] 21 p2970 N88-27644
Photochemical oxidant formation: Overview of current knowledge and emerging issues
[PB88-195235] 21 p2971 N88-27647
The detection and interpretation of long-term changes in ozone from space
[NASA-TM-101135] 21 p2971 N88-27650
Filling of the atmospheric transmission window due to emission from very high rotational levels of NO and O3
[AD-A194670] 23 p3233 N88-29239
European validation of SAGE-2 aerosol profiles
[AERONOMICA-ACTA-A-327-1988]
23 p3234 N88-29243
Recent measurements of ozone in the Amazon forests
[INPE-4494-PRE/1258] 24 p3389 N88-30185
Changes in stratospheric ozone: Observations and theories
[AERONOMICA-ACTA-A-334-1988]
24 p3390 N88-30188

OZONE DEPLETION
Scientific and Operational Requirements for TOMS Data
[NASA-CP-2497] 05 p0615 N88-13774
TOMS: The Antarctic ozone hole and ozone trends
05 p0615 N88-13775
October lower stratospheric Antarctic temperature and total ozone from 1979-1985 05 p0615 N88-13776
A review of atmospheric ozone and current thinking on the Antarctic ozone hole
[AD-A185608] 06 p0732 N88-14501
Ozone formation due to interaction of meteoroids with Earth's atmosphere 06 p0736 N88-14536
The 1987 Airborne Antarctic Ozone Experiment: The Nimbus-7 TOMS data atlas
[NASA-RP-1201] 13 p1791 N88-20714
An automated ozone photometer
[NASA-TM-100064] 14 p1906 N88-21404
Geochemistry of the middle and lower atmosphere: Environmental impact through the deterioration of the ozone layer
[INPE-4477-PRE/1241] 16 p2230 N88-23321
The potential impact on atmospheric ozone and temperature of increasing trace gas concentrations
[NASA-CR-182965] 17 p2373 N88-24112
Changes in the Antarctic atmosphere due to the reduction of stratospheric ozone
[ETN-88-92565] 18 p2540 N88-25074
Timing regulations to prevent stratospheric-ozone depletion
[R-3495-JMO/RC] 19 p2690 N88-25987
Impact on ozone attainment of CFC (chlorofluorocarbon) controls used to prevent future depletion of stratospheric ozone
[PB88-195177] 19 p2690 N88-25989
Meteorological atlas of the Southern Hemisphere lower stratosphere for August and September 1987
[NASA-TM-4049] 20 p2825 N88-26763
Radiative heat transfer to chemically reacting flow between concentric rotating spheres
[DE88-702538] 22 p3118 N88-28525
Present state of knowledge of the upper atmosphere 1988: An assessment report
[NASA-RP-1208] 23 p3232 N88-29233
Changes in stratospheric ozone: Observations and theories
[AERONOMICA-ACTA-A-334-1988]
24 p3390 N88-30188

OZONE HOLE
U OZONE DEPLETION

OZONE LAYER
U OZONOSPHERE

OZONOMETRY
Scientific and Operational Requirements for TOMS Data
[NASA-CP-2497] 05 p0615 N88-13774
TOMS: The Antarctic ozone hole and ozone trends
05 p0615 N88-13775
Analysis of the breakdown of the Antarctic circumpolar vortex using TOMS ozone data
05 p0615 N88-13779
The use of TOMS data for tropospheric ozone studies
05 p0616 N88-13784
Laboratory measurements of the ozone absorption coefficient in the wavelength region 339 to 362 nm at different temperatures
[NOTA-INTERNA-982] 07 p0878 N88-15324
ROCOZ-A (improved rocket launched ozone sensor) for middle atmosphere ozone measurements
08 p1029 N88-16233
Surface ozone measurements at a Swedish mountain site
[CM-72] 09 p1191 N88-17138
Ozone sonde and Dobson spectrometer data obtained during the MAP/GLOBUS 1983 campaign over Western Europe
[BPT-5/87] 13 p1802 N88-20771
Corrections for differential scattering by aerosols in the measurement of ozone by DIAL --- differential absorption lidar (DIAL)
[NPL-QU-78] 14 p1945 N88-21603
Workshop on Atmospheric OH
[BPT-7/87] 18 p2538 N88-25063
Ozone in the atmosphere 18 p2539 N88-25064
Ultraviolet measurements: Measurements of photolysis rates 18 p2539 N88-25065
Changes in the Antarctic atmosphere due to the reduction of stratospheric ozone
[ETN-88-92565] 18 p2540 N88-25074
Changes in stratospheric ozone: Observations and theories
[AERONOMICA-ACTA-A-334-1988]
24 p3390 N88-30188

OZONOSPHERE
The potential impact on atmospheric ozone and temperature of increasing trace gas concentrations
[NASA-CR-182965] 17 p2373 N88-24112

P

P WAVES
Multichannel deconvolution of P waves at seismic arrays and three component stations
[AD-A184450] 04 p0467 N88-12888
Earthquakes from peninsular India: Data from the Gauribidanur seismic array
[DE88-701232] 15 p2093 N88-22471
Acousto-ultrasonic input-output characterization of unidirectional fiber composite plate by P waves
[NASA-CR-4162] 19 p2678 N88-25923
Maximum-likelihood multichannel deconvolution of P waves at seismic arrays
[AD-A194990] 24 p3391 N88-30191
Discrimination studies using short-period P waves at upper mantle distances
[AD-A195468] 24 p3401 N88-30257

P-I-N DIODES
U DIODES
U P-I-N JUNCTIONS

P-I-N JUNCTIONS
Computer calculations of PIN diode limiter characteristics
[AD-A185563] 06 p0697 N88-14277
The qualitative determination of high injection effects in flux-loaded P-I-N diodes using the recombination radiation measuring method
[ETN-88-91475] 11 p1560 N88-19336
Research on high-efficiency, stacked, multijunction, amorphous silicon alloy thin-film solar cells
[DE88-001108] 13 p1793 N88-20723
Development program for 1.93-micron lasers
[NASA-CR-4148] 16 p2212 N88-23198
InP/GaInAs/InP PIN photodiode with FWHM less than 18 ps 19 p2658 N88-25799
Study of Staebler-Wronsky degradation effect in a Si:H based P-I-N solar cells
[NASA-CR-182564] 19 p2687 N88-25970
Silicon-on-insulator pin diodes
[AD-A193359] 21 p2937 N88-27445

P-N JUNCTIONS
An investigation of the equivalent circuit and carrier lifetimes of Si/SiGe heterostructure p-n diodes for frequencies between 0.5 and 18.5 MHz
[FOA-C-30469-3.2] 09 p1256 N88-17529
Photocurrent modeling of modern microcircuit PN junctions
[DE88-007037] 19 p2662 N88-25832

P-N-P JUNCTIONS
Joint services electronics program research in electronics
[AD-A192206] 18 p2504 N88-24857

P-N-P-N JUNCTIONS
Electric design rules related to latch-up and radiation --- simulation
[FOA-E-30006-3.1] 08 p0979 N88-15917
High density CMOS technology
11 p1561 N88-19342

P-TYPE SEMICONDUCTORS
Integrated fiber-optic coupler
[AD-A184494] 03 p0377 N88-12369
Preparation and characterization of Cu2Zn1-xMnxGeS4
[AD-A188113] 11 p1556 N88-19315
Point defect structure of Cr2O3
[AD-A187620] 11 p1556 N88-19317
Characterization of enhanced Schottky-barrier InGaAs/Al(1-x) \s strained channel modulation-doped field-effect transistors
[AD-A188820] 12 p1698 N88-20162
Fundamental studies and device development in beta silicon carbide
[AD-A189540] 12 p1699 N88-20165
Electrical properties of p-type and n-type ZnSe-ZnTe strained-layer superlattices 20 p2868 N88-27029

P-3 AIRCRAFT
Taiwan area mesoscale experiment: P-3 aircraft operations summary
[PB88-169073] 18 p2544 N88-25098

PACE
U PHYSICS AND CHEMISTRY EXPERIMENT IN SPACE

PACIFIC ISLANDS
NT JAPAN
NT NEW ZEALAND

PACIFIC OCEAN
V/STOL aircraft configurations and opportunities in the Pacific Basin
[NASA-TM-100005] 03 p0261 N88-11644
Tropical cyclone intensity prediction based on empirical orthogonal function representation of wind and shear fields
[AD-A184699] 03 p0353 N88-12229
On the interannual variability of South American climate and the Southern Oscillation 04 p0470 N88-12905
Interactions between the Asian monsoons, the tropical Pacific and the southern hemisphere extratropics
04 p0470 N88-12907
Tectonics of the Caroline Oceanic Step (southwestern Pacific Ocean) 06 p0725 N88-14462
Statistical structure of temperature field over South Pacific Ocean 06 p0726 N88-14465
Ferromanganese nodules of Antarctic sector in Pacific Ocean 06 p0727 N88-14472
Modes of surface circulation and climate over the tropical Atlantic, Eastern Pacific, and Indian Oceans
06 p0742 N88-14564
CTD/02 measurements during 1984 and 1985 as part of the Equatorial Pacific Ocean Climate Studies (EPOCS)
[PB88-102082] 06 p0746 N88-14600
Geosat crossover analysis in the tropical Pacific. Part 1: Constrained sinusoidal crossover adjustment
[NASA-CR-182391] 07 p0871 N88-15285
Biogeochemical cycling in the ocean. Part 1: Introduction to the effects of upwelling along the west coast of North America
[NASA-TM-88230] 07 p0882 N88-15349
Nature of Western Pacific transition zone
08 p1010 N88-16122
Neogene paleoclimate in Pacific Ocean subarctic region determined from study of diatoms
08 p1010 N88-16125
North Pacific Ocean. Subtropical front north of Hawaii, R/V Thomas G. Thompson: 7 January - 10 February 1974. CTD data report
[AD-A186565] 08 p1044 N88-16310
North Pacific Ocean. Tradewind region east of Hawaii, R/V Thomas G Thompson: 25 September - 1 November 1972. STD data report
[AD-A186566] 08 p1044 N88-16311
North Pacific Ocean. Subarctic front central Pacific, R/V Thomas G. Thompson: 8 September - 9 October 1975. CTD data report
[AD-A186567] 08 p1044 N88-16312
North Pacific Ocean. Northwest Pacific Transition Zone, R/V Thomas G. Thompson: 19 March - 1 May 1971. STD data report
[AD-A186568] 08 p1044 N88-16313
North Pacific Ocean. Gulf of Alaska, R/V Thomas G. Thompson: 1 February - 8 March 1967. STD data report
[AD-A186569] 08 p1045 N88-16314
North Pacific Ocean. Central Pacific Transition Zone, R/V Thomas G. Thompson: 25 March - 3 May 1968. STD data report
[AD-A186570] 09 p1195 N88-17160
North Pacific Ocean. Northeast Pacific Transition Zone, R/V Thomas G. Thompson: 1 November - 6 December 1969. STD data report
[AD-A186574] 09 p1195 N88-17161
Materials of the World Data Center B. Deep Seismic Sounding (DSS): Pacific data 09 p1196 N88-17167

Geological evolution and analysis of confirmed or suspected gas hydrate localities. Volume 9: Formation and stability of gas hydrates of the Middle America Trench
[DE88-001007] 10 p1347 N88-18050

CTD observations in the coastal transition zone off northern California, 16-25 February 1987
[AD-A187263] 10 p1357 N88-18111

JEDA (Joint Environmental Data Analysis) Center report on tropical Pacific subsurface thermal data management, 1986
[PB88-140090] 12 p1649 N88-19875

Tidal estimation in the Pacific with application to SEASAT altimetry
[NASA-TM-100694] 13 p1803 N88-20780

Dynamics of the Oceanic Surface Mixed Layer
[AD-A188348] 13 p1804 N88-20785

Equatorial turbulence: Mixed layer and thermocline
13 p1804 N88-20787

The mixed layer of the western equatorial Pacific Ocean
[HIG-1861] 13 p1805 N88-20789

Mixed-layer shear related to wind stress in the central equatorial Pacific 13 p1805 N88-20793

Monitoring ocean surface layer processes
13 p1806 N88-20801

CTD/O2 data collected in 1985 and 1986 for EPOCS (Equatorial Pacific Ocean Climate Studies)
[PB88-160775] 14 p1951 N88-21629

Physical, chemical and CTD (Conductivity/Temperature/Depth) data from the Marathon 2 expedition
[AD-A189930] 15 p2099 N88-22507

Diagnostic studies of the HxOy-NzOy-O3 photochemical system using data from NASA GTE field expeditions
[NASA-CR-183038] 19 p2689 N88-25984

MIZPAC (marginal ice zone Pacific) .84-86 CTD (Conductivity, Temperature, Depth) data report
[AD-A192478] 21 p2976 N88-27679

RB211 developments
[PNR90444] 22 p3045 N88-28069

The 1986-87 Pacific warm episode: Oceanic and Atmospheric features 22 p3120 N88-28535

Zonal wind observations at Christmas Island (2 deg N, 157 deg W) during the 1986-1987 El-Nino
22 p3120 N88-28539

Climatology of various synoptic systems over the tropical North Pacific 22 p3121 N88-28542

Some evidence for a Northern Hemispheric extratropic trigger mechanism of ENSO events
22 p3123 N88-28558

Persistence of North Pacific Sea surface temperature and atmospheric flow patterns 22 p3123 N88-28559

The impact of the El Nino event on the ECMWF model performance 22 p3125 N88-28576

PACKAGES
NT EREP
NT INSTRUMENT PACKAGES

PACKAGING
NT ELECTRONIC PACKAGING

The effect of different packagings on the vibration behavior and the coupling factors of steam turbine blading
[ETN-87-90425] 01 p0056 N88-10357

RADC/NBS (Rome Air Development Center/National Bureau of Standards) Workshop. Moisture Measurement and Control for Microelectronics (4)
[PB87-224614] 03 p0309 N88-11947

Fabrication and packaging of discontinuous MIM (Metal-Insulator-Metal) film arrays for efficient MM wave and IR detection and mixing
[AD-A186809] 09 p1146 N88-16869

Electrophoretically deposited styrene-acrylate coatings for suppression of internal electromagnetic pulse effects
[DE88-003620] 12 p1609 N88-19621

Response characteristics of dual MOSFET gamma-ray sensors produced by Mitel Corporation
[AD-A189026] 12 p1630 N88-19756

Utilization of dense packed planar acoustic echosounders to identify turbulence structure in the lowest levels of the atmosphere
[AD-A191006] 16 p2233 N88-23335

Procedures for identification and handling of Printed Circuit Boards (PCBs)
[AD-A191177] 23 p3206 N88-29078

PACKET SWITCHING

Modeling and performance evaluation of the DPS25 packet switching multiprocessor system --- communication networks
[ENST-87E009] 02 p0162 N88-11016

A packet-switched wide-area communication network simulator
[FUB-3-1986] 14 p1905 N88-21361

Alpha structure based B-HIVE multicomputer
[AD-A188706] 16 p2244 N88-23405

PACKET TRANSMISSION
NT ALOHA SYSTEM

The role of spread spectrum in packet radio networks
[AD-A184511] 03 p0306 N88-11929

Packet error probabilities in frequency-hopped spread spectrum packet radio networks. Markov frequency hopping patterns considered
[AD-A186071] 07 p0841 N88-15104

On the approximation of the output process of multi-user random access communication networks
[AD-A186197] 07 p0842 N88-15108

Adaptive spread spectrum networks
[AD-A187154] 09 p1152 N88-16900

The high speed local area network
19 p2717 N88-26133

PACKETS (COMMUNICATION)

Packet error probabilities in frequency-hopped spread spectrum packet radio networks. Markov frequency hopping patterns considered
[AD-A186071] 07 p0841 N88-15104

Channel access protocols for multihop packet radio networks
[AD-A186074] 07 p0842 N88-15105

Packet telecommand. System performance assessment study --- onboard data handling
[PTC/TNOT/0015/SAAB] 07 p0843 N88-15113

Exact analyses of slotted ring protocols for local area networks with one transmitting station
[MEMO-650] 14 p1967 N88-21737

Multiple address facility for packet radio: An investigation of performance/complexity trade off
[AD-A191043] 16 p2190 N88-23064

PACKINGS (SEALS)

Study on shaft seals for potassium turbine
[EL-891] 15 p2074 N88-22364

PADE APPROXIMATION

The matrix exponential in transient structural analysis
05 p0593 N88-13619

PAINTS

Paints required for aeronautical construction
[SNIAS-872-551-102] 05 p0569 N88-13470

Development of microencapsulated DNBM quaternary ammonium inhibitors for paints
17 p2319 N88-23851

Predictive corrosion modeling, volume 1
[AD-A191229] 18 p2485 N88-24739

Cleanability of aircraft polyurethane topcoats
[AD-A193456] 23 p3170 N88-28878

Prediction of degradation of polymeric coating materials 24 p3354 N88-29970

Electrochemical evaluation of the long term corrosion resistance of polymer coated steel
24 p3355 N88-29074

Reduced time frame for predicting coating performance 24 p3356 N88-29979

PAIR PRODUCTION

Single leptons from heavy quark production
[DE87-014917] 04 p0488 N88-13009

Vector boson pair production in e(+)e(-) collisions
[PREPRINT-549] 06 p0778 N88-14774

Study of tau pairs and search for new particles
[B8680488] 07 p0931 N88-15655

Two-photon exclusive meson production at large angles
[NIKHEF-H/87-4] 08 p1081 N88-16515

Electronic factors for K-shell-electron conversion probability and electron-positron pair formation probability in electric monopole transitions
[DE87-753040] 08 p1089 N88-16551

Characteristics of multimuon events from fourth generation quarks at the SSC (Superconducting Super Collider)
[DE88-002954] 09 p1257 N88-17535

Diffraction theory in QCD and beyond
[DE88-005958] 13 p1837 N88-20992

Model-independent requirements to the source of positrons in the galactic centre
[DE88-700968] 14 p1992 N88-21874

A new approach to generating negative ion beams
[AD-A191119] 18 p2572 N88-25276

Gamma rays from Cygnus X-1: Modeling and nonthermal pair production
[DE88-006830] 18 p2596 N88-25426

Cascade model of gamma-ray bursts: Power-law and annihilation-line components
[NASA-TM-101176] 21 p3032 N88-27998

Influence of pairing correlations on the probability and dynamics of tunneling through the barrier in fission and fusion of complex nuclei
[DE88-701500] 23 p3286 N88-29570

PALEOCLIMATOLOGY

Neogene paleoclimate in Pacific Ocean subarctic region determined from study of diatoms
08 p1010 N88-16125

Model validation research: Comparison of simulated and observed climate patterns for the past 18,000 years
[DE88-004945] 13 p1800 N88-20759

PALEOMAGNETISM

Statistics of the geomagnetic secular variation for the past 5Ma
[NASA-CR-181558] 04 p0467 N88-12880

PALEONTOLOGY

Use of space photographs for paleoseismogeological studies (on the example of Mongolian Altay)
08 p1008 N88-16110

PALLADIUM

A surface science investigation of potential intermediates, catalysts, and promoters in the synthesis of higher alcohols by metals
[DE87-014188] 02 p0144 N88-10906

The effect of additives on the reactivity of palladium surfaces for the chemisorption and hydrogenation of carbon monoxide: A surface science and catalytic study
[DE87-014685] 02 p0145 N88-10909

Characterization of catalysts with metal-support effects and of the species adsorbed on their surfaces
[DE87-014636] 04 p0414 N88-12564

Determination, by X-ray fluorescence, of platinum, palladium, ruthenium, iron and chromium in special steels
[PB87-132114] 06 p0683 N88-14183

Electron scattering off palladium isotopes. An investigation of the equivalence of the anharmonic vibrator model and the interacting boson model
[B8671274] 07 p0931 N88-15654

The response of ultrathin palladium gate sensors to hydrogen and carbon monoxide
19 p2672 N88-25885

Electronic and geometric structure of silver and palladium on aluminum (111) in monoatomic surface layers
[ETN-88-92120] 20 p2879 N88-27093

PALLADIUM COMPOUNDS

Steady state and transient behavior of the Pd-SnO(sub x) MIS oxygen sensors 19 p2672 N88-25880

The catalytic reactivity of thin film crystal surfaces
[DE88-006387] 19 p2732 N88-26228

PAM (MODULATION)
U PULSE AMPLITUDE MODULATION

PANEL METHOD (FLUID DYNAMICS)

ARSPNS: A method to calculate steady and unsteady potential flow about fixed and rotational lifting and nonlifting bodies
[NLR-TR-85114-U] 01 p0044 N88-10282

Integration of a supersonic unsteady aerodynamic code into the NASA FASTEX system
[NASA-CR-182329] 06 p0663 N88-14068

A direct calculation method for perturbation fields of moving bodies in compressible media at subsonic Mach numbers
[ETN-88-90808] 06 p0701 N88-14305

ARSPNSC: A method to calculate subsonic steady and unsteady potential flow about complex configurations
[NLR-TR-86122-U] 13 p1717 N88-20265

A panel method based on velocity potential to compute harmonically oscillating lift surface systems
[ETN-88-91886] 15 p2061 N88-22290

On the dynamic behavior of balloon during its launch; application of panel method and extension to unsteady problem
[ISAS-RN-622] 20 p2751 N88-26330

VSAERO analysis of tip planforms for the free-tip rotor
[NASA-CR-177487] 22 p3038 N88-28036

PANELS
NT CURVED PANELS
NT RECTANGULAR PANELS
NT WING PANELS

Interactive buckling effects in stiffened FRP panels
[ARE-TM(UMS)-87204] 01 p0059 N88-10378

Fabrication and testing of fire resistant graphite composite panels
[NASA-CR-177397] 04 p0397 N88-12472

Theoretical and practical aspects of the functional absorber method of arranging sound absorbing panels
[BBC-RD-1987/15] 05 p0646 N88-13955

Postbuckling of laminated anisotropic panels
[NASA-TM-100509] 08 p0994 N88-16011

Excimer plasma displays
[AD-A186731] 09 p1250 N88-17480

Detecting serial correlation in the error structure of a cross-lagged panel model
[AD-A189070] 12 p1685 N88-20077

Postbuckling delamination of a stiffened composite panel using finite element methods
[NASA-CR-182803] 15 p2030 N88-22098

The effective fracture toughness of aluminum at rapid heating rates
[AD-A189745] 15 p2038 N88-22146

Operational considerations for laminar flow aircraft
17 p2298 N88-23748

Stiffened titanium panels
[NASA-CASE-LAR-13814-1] 18 p2497 N88-24816

Nonlinear interaction between overall and local buckling of stiffened panels with symmetric cross-sections
[PB88-104054] 21 p2960 N88-27580
Two-dimensional sequential and concurrent finite element analysis of unstiffened and stiffened aluminum and composite panels with hole
[NASA-CR-183083] 22 p3086 N88-28325

PANORAMIC SCANNING
System for detecting objects that represent a threat
[NASA-TT-20244] 13 p1760 N88-20528
Atmospheric autorotating imaging device
[NASA-CASE-NPO-17390-1-CU]
18 p2519 N88-24944

PAPER (MATERIAL)
Fiber-reinforced composite hot-gas filters
[DE87-012257] 01 p0033 N88-10208
Observations on electrostatic effects in a filter test system
[AD-A188797] 13 p1736 N88-20378
Reference filters for electrostatic charging tendency measurements of fuels
[AD-A191717] 18 p2495 N88-24803
Effect of thickness on downward flame spread over paper
[NASA-TT-20282] 19 p2612 N88-25501
New duplicating paper with high resolution for aerial photography
[PB87-228706] 19 p2665 N88-25962
Absorption heat pumps
[DE88-752820] 23 p3229 N88-29218

PAPERS
FY 1985 scientific and technical reports, articles, papers and presentations
[NASA-TM-86521] 04 p0501 N88-13083

PARABOLAS
Spectral methods: Analysis and applications to flow problems
[AD-A186265] 07 p0850 N88-15156
Adaptive finite element methods for parabolic systems in one- and two-space dimensions
[AD-A186534] 08 p1073 N88-16475
Fitting a generalized parabola to data
[NPL-DITC-96/87] 09 p1229 N88-17364
Inversion of parabolic and paraboloidal projections
[AD-A187538] 10 p1405 N88-18380
An adaptive overlapping local grid refinement method for two-dimensional parabolic systems
[AD-A193560] 23 p3271 N88-29464
Reflection and scattering of acoustic rays computed for parabolic ice keel models
[AD-A193898] 23 p3278 N88-29517
Large displacement and rotational formulation for laminated cylindrical shells including parabolic transverse shear
[AD-A194871] 24 p3384 N88-30158

PARABOLIC ANTENNAS
New main reflector, subreflector and dual chamber concepts for compact range applications
[NASA-CR-181506] 04 p0402 N88-12498
Modification of parabolic dish antenna pattern using two symmetrically placed circular flat plates
[AD-A189543] 13 p1758 N88-20517
An improved method for calculating power density in the Fresnel region of circular parabolic reflector antennas
[AD-A190569] 15 p2060 N88-22284
The focal plane reception pattern calculation for a paraboloidal antenna with a nearby fence
[NASA-TM-100691] 24 p3365 N88-30039

PARABOLIC BODIES
Fundamentals and techniques of nonimaging optics research
[DE87-014544] 02 p0236 N88-11486
Mass transport in a parabolic conduit
[LRT-WE-9-FB-1(1988)] 22 p3077 N88-28273
Heat transport in a parabolic tube of circular cross-section
[LRT-WE-9-FB-2(1988)] 22 p3078 N88-28274
Nonlinear oscillations in paraboloidal containers
[LRT-WE-9-FB-3(1988)] 22 p3078 N88-28275

PARABOLIC DIFFERENTIAL EQUATIONS
Accurate, stable, explicit solution of the parabolized Navier-Stokes equations 01 p0043 N88-10276
Error estimates for finite element approximations of parabolic variational equations
[BONNER-MATHE-SCHR-179]
01 p0087 N88-10569
Computation of free boundaries
[PB87-226023] 06 p0763 N88-14680
Propagation of radiation along a constricting optical waveguide 07 p0920 N88-15590
Comparisons of Monte-Carlo and PNS (Parabolized Navier-Stokes) calculations for rarefied flow over reentry vehicle configurations
[DE88-004937] 11 p1435 N88-18560
A signal processing approach to the numerical solution of parabolic differential equations
11 p1539 N88-19197
A new parabolized Navier-Stokes code for chemically reacting flow fields 12 p1625 N88-19721
Boundary stabilization of the reaction-diffusion equation with unilateral conditions
[RR-315] 14 p1964 N88-21720
Almost-periodic solutions of nonlinear parabolic equations
[DE88-006423] 15 p2118 N88-22618
A posterior error estimation in a finite element method for parabolic partial differential equations
[AD-A190296] 15 p2120 N88-22636
Optimal discrete-time LQR problems for parabolic systems with unbounded input: Approximation and convergence
[NASA-CR-181673] 18 p2567 N88-25247
Accurate solution of parabolic equations by expansion in ultraspherical polynomials
[DE88-701829] 20 p2845 N88-26880
Numerical computation of space shuttle orbiter flow field
[NASA-CR-183193] 22 p3040 N88-28048
Numerical modeling results for mode propagation in a wedge
[AD-A193998] 22 p3147 N88-28718
Lessons learned in the mesh generation for PN/S calculations 23 p3245 N88-29314

PARABOLIC FLIGHT
Access to microgravity: A technical description of the NAE T-33 microgravity facility
[NAE-AN-47] 04 p0405 N88-12518
Respiratory parameters aboard an aircraft performing parabolic flights 12 p1653 N88-19902
The Marshall Space Flight Center KC-135 microgravity test program for FY84-86
[NASA-TM-4059] 22 p3056 N88-28136

PARABOLIC REFLECTORS
Wavefront error sensing
[NASA-CR-181504] 03 p0321 N88-12030
The formation of optical membrane reflector surfaces using uniform pressure loading
[DE87-012275] 03 p0376 N88-12367
New main reflector, subreflector and dual chamber concepts for compact range applications
[NASA-CR-181506] 04 p0402 N88-12498
MBA payload testing by Compact Antenna Test Range (CATR)
[ESA-CR(P)-2473] 08 p0977 N88-15906
The integration of a mesh reflector to a 15-foot box truss structure. Task 3: Box truss analysis and technology development
[NASA-CR-178228] 11 p1497 N88-18941
Modification of parabolic dish antenna pattern using two symmetrically placed circular flat plates
[AD-A189543] 13 p1758 N88-20517
Point-focus concentrator reflector assembly, phase 1
[DE88-003616] 13 p1792 N88-20720
Thermophotovoltaic space power system, phase 3
[NASA-CR-179327] 14 p1942 N88-21585
Reflux heat-pipe solar receivers for dish-electric systems
[DE88-008671] 21 p2968 N88-27631

PARABOLOIDS
U PARABOLIC BODIES

PARACHUTE DESCENT
Detection of hyperventilation of parachutists
[DFVLR-FB-87-11] 01 p0075 N88-10482
Parachute characteristics of Titan descent modules --- planetary probe
[BF-3/86-B] 02 p0122 N88-10774
Regulation of energy metabolism during parachute jumps 07 p0896 N88-15428
Galileo probe parachute test program: Wake properties of the Galileo probe at Mach numbers from 0.25 to 0.95
[NASA-RP-1130] 11 p1488 N88-18884
Parachute for in-flight training on parachute ejection
[REPT-87-11] 18 p2458 N88-24593

PARACHUTE FABRICS
Parachute materials
[DE87-014845] 04 p0411 N88-12550

PARACHUTES
NT DRAG CHUTES
NT RIBBON PARACHUTES
Developmental airdrop testing techniques and devices
[AGARD-AG-300-VOL-6] 04 p0398 N88-12481
Parachute materials
[DE87-014845] 04 p0411 N88-12550
An investigation of cruciform parachutes and towed targets
[BU-360] 14 p1862 N88-21122
Measurements of aerodynamic forces on unsteadily moving bluff parachute canopies
16 p2202 N88-23137
Parachute for in-flight training on parachute ejection
[REPT-87-11] 18 p2458 N88-24593

PARACHUTING
U PARACHUTE DESCENT

PARADOXES
Solar oscillations, gravitational multipole field of the Sun and the solar neutrino paradox
[DE88-002100] 07 p0946 N88-15752

PARAFFINS
High output paraffin actuators: Utilization in aerospace mechanisms 14 p1924 N88-21470

PARALLEL COMPUTERS
NT MIMD (COMPUTERS)
NT SIMD (COMPUTERS)
Report from the MPP Working Group to the NASA Associate Administrator for Space Science and Applications
[NASA-TM-87819] 02 p0223 N88-11402
Parallel algorithms for computer vision on the connection machine
[AD-A185842] 07 p0901 N88-15456
Research in progress at the Institute for Computer Applications in Science and Engineering
[NASA-CR-181607] 08 p1053 N88-16354
Implementing clips on a parallel computer
09 p1211 N88-17259
Massive fine-grain parallelism in array computation: A data flow solution 10 p1382 N88-18254
Finely grained parallelism in an applicative architecture
10 p1383 N88-18256
Implementation and analysis of a Navier-Stokes algorithm on parallel computers
[NASA-CR-181614] 10 p1390 N88-18301
The roll back chip: Hardware support for distributed simulation using time warp
[AD-A187823] 11 p1529 N88-19132
An analysis of multiple grain CHiP architectures
[AD-A189942] 15 p2110 N88-22570
Implementation and performance analysis of parallel assignment algorithms on a hypercube computer
[AD-A190678] 15 p2115 N88-22600
Design and implementation of a parallel computer for expert system applications
[DE88-005288] 15 p2115 N88-22601
Piecewise linear approach for timing simulation of VLSI (Very-Large-Scale-Integrated) circuits on serial and parallel computers
[AD-A191328] 16 p2252 N88-23462
Factorization of large integers on a massively parallel computer
[DE88-011625] 21 p2999 N88-27786
Optimisation algorithms for highly parallel computer architectures. The performance of the truncated Newton, conjugate gradient algorithm in FORTRAN and Ada
[AD-A193940] 23 p3265 N88-29435

PARALLEL FLOW
NT PIPE FLOW
NT THREE DIMENSIONAL FLOW
Some asymptotic modes of transonic vortex flow
04 p0425 N88-12632

PARALLEL PLATES
Quantum electrodynamics based on self-energy: Spontaneous emission in cavities
[DE87-703071] 02 p0232 N88-11461
A note on the aerodynamic design of thin parallel-sided aerofoil sections
[ARL-AERO-TM-388] 09 p1114 N88-16677
Changes in the turbulent boundary layer structure associated with net drag reduction by outer layer manipulators
[NASA-CR-178152] 11 p1483 N88-18853

PARALLEL PROCESSING (COMPUTERS)
NBS (National Bureau of Standards) research reports (April 1987)
[PB87-210258] 01 p0018 N88-10111
A graphical tool for observing the behavior of parallel logic programs
[DE87-011467] 01 p0080 N88-10516
A look at the evolution of mathematical software for dense matrix problems over the past fifteen years
[DE87-011485] 01 p0081 N88-10517
Measurement of fault-tolerant parallel processors
[PB87-208328] 01 p0084 N88-10539
A unified approach to parallel computation: Performance evaluation and architecturally independent parallel programming
[DE87-012519] 01 p0084 N88-10540
Solution methods for bidiagonal and tridiagonal linear systems for parallel and vector computers
[REPT-87-04] 01 p0085 N88-10552
Parallel computation of a domain decomposition method
[DE87-011444] 01 p0086 N88-10560
Locating parallel numerical tasks in the solution of viscous fluid flows
[DE87-013510] 02 p0169 N88-11064

Benchmarking the Connection Machine
[DE87-013500] 02 p0218 N88-11374

Implementation of preconditioned s-step conjugate gradient methods on a multiprocessor system with memory hierarchy
[DE87-014401] 02 p0222 N88-11400

Hardware-assisted multiprocessor performance measurements
[PB87-226906] 03 p0363 N88-12282

Mapping a battlefield simulation onto message-passing parallel architectures
[NASA-CR-178396] 03 p0363 N88-12287

Algorithms and hardware for efficient image smoothing
[TR-149] 03 p0365 N88-12296

Delft parallel processor 84/16
[PB87-226254] 03 p0366 N88-12305

Implementation of the Runge-Kutta-Fehlberg method for solution of ordinary differential equations on a parallel processor
[AD-A184660] 03 p0370 N88-12331

Programmable real-time digital video image processing
[PB87-104162] 04 p0430 N88-12661

Center for Supercomputing Research and Development (CEDAR)
[DE88-000807] 04 p0475 N88-12930

Principles for problem aggregation and assignment in medium scale multiprocessors
[NASA-CR-178379] 04 p0476 N88-12935

A tight upper bound for the speed-up of parallel best-first branch-and-bound algorithms
[AD-A184246] 04 p0477 N88-12939

Methods for design and evaluation of integrated hardware/software systems for concurrent computation
[NASA-CR-181522] 04 p0479 N88-12953

A review and analysis of Fortran 8x
[DE88-001320] 04 p0479 N88-12955

QR factorization of a dense matrix on a shared-memory multiprocessor
[DE88-001506] 04 p0480 N88-12956

Parallel superconvergent multigrid
[DE87-013153] 04 p0480 N88-12960

An approach to implementing state space searches on heterogeneous systems of multiprocessors
[DE88-001321] 04 p0482 N88-12967

Computational methods for problems in aerodynamics and large space structure using parallel and vector architectures
[AD-A185401] 05 p0541 N88-13294

Arrays for discrete Fourier transform
[REPT-87-019] 05 p0632 N88-13861

Storing and retrieving data in a parallel distributed memory system
[AD-A185177] 05 p0637 N88-13897

Research and development of finite elements and iterative algorithms for elliptic partial differential equations
[DE88-001381] 05 p0643 N88-13934

A zonal approach for the solution of coupled Euler and potential solutions of flows with complex geometries
[AD-A185465] 06 p0702 N88-14310

Methods for reducing computational costs of typical finite element unsteady hydrodynamic models
[AD-A185499] 06 p0702 N88-14312

Fast algorithms for structural optimization and least squares
[AD-A185766] 06 p0724 N88-14452

Optimal pre-scheduling of problem remappings
[NASA-CR-178378] 06 p0756 N88-14633

Parallel algorithms for polynomials
[PB87-226304] 06 p0756 N88-14635

Set of multi-process primitives for stack based machines
[PB87-234381] 06 p0756 N88-14636

Algorithms and programming tools for image processing on the MPP:3
[NASA-CR-182349] 06 p0757 N88-14641

Parallel pivoting combined with parallel reduction
[NASA-CR-178422] 06 p0760 N88-14662

Fault-tolerant computer architecture based on INMOS transputer processor 06 p0797 N88-14880

Reliability modelling for fault-tolerant parallel processor
[AD-A185667] 07 p0900 N88-15451

Massively parallel implementations of theories for apparent motion
[AD-A185641] 07 p0901 N88-15455

Monte Carlo photon transport on vector and parallel supercomputers
[DE88-002503] 07 p0905 N88-15486

AFL-1: A programming language for massively concurrent computers
[AD-A186422] 07 p0906 N88-15489

Local uniform mesh refinement for partial differential equations
[AD-A186312] 07 p0910 N88-15519

Application of parallel distributed processing to space based systems 08 p1059 N88-16393

Neural network based speech synthesizer: A preliminary report 08 p1064 N88-16429

A parallel algorithm for the general LU-factorization
[DE88-002177] 08 p1066 N88-16444

Numerical experiments with a parallel conjugate gradient method
[DE88-002178] 08 p1066 N88-16445

Media independent interface
[NASA-CR-172033] 08 p1066 N88-16446

Applicative parallelism: Potential and challenge
[DE87-011885] 08 p1068 N88-16459

ESA Bulletin No. 25
[ISSN-0376-4265] 09 p1128 N88-16767

Parallel-processing computer systems and their possible applications in the agency 09 p1128 N88-16774

Image chunking: Defining spatial building blocks for scene analysis
[AD-A187072] 09 p1200 N88-17191

First Annual Workshop on Space Operations Automation and Robotics (SOAR 87)
[NASA-CP-2491] 09 p1203 N88-17206

Performance analysis of parallel branch and bound search with the hypercube architecture
09 p1206 N88-17229

Algorithm design for scientific computation for highly parallel multiprocessor systems
[AD-A186713] 09 p1217 N88-17299

Occam/Ada parallel programming system
[ISAL-IDI1-87-11] 09 p1219 N88-17312

A parallel block cyclic reduction algorithm for the fast solution of elliptic equations
[DE88-003595] 09 p1221 N88-17324

A multithreaded processor architecture for parallel symbolic computation
[AD-A187034] 09 p1222 N88-17327

The effectiveness of caches and data prefetch buffers in large-scale shared memory multiprocessors
[DE88-003594] 09 p1223 N88-17334

Nonpreemptive run-time scheduling issues on a multitasked, multiprogrammed multiprocessor with dependencies, bidimensional tasks, folding and dynamic graphs
[DE88-003596] 09 p1223 N88-17335

The design of ultra high-speed numeric intensive systems (having fault tolerant and load balancing capabilities) 10 p1374 N88-18196

Hardware implementation for special functions. An application for combat simulation
10 p1374 N88-18197

On parallelism in software/hardware design tools
10 p1374 N88-18200

Role of broadcasting in multiprocessor systems
10 p1374 N88-18201

Image texture classification with an optical crossbar interconnected processor 10 p1375 N88-18202

A large-grain dataflow architecture
10 p1375 N88-18207

The mapping of parallel algorithms to reconfigurable parallel architectures 10 p1376 N88-18209

A distributed system architecture based on macro dataflow model 10 p1376 N88-18210

Distributed control of large parallel computers
10 p1376 N88-18215

Experiments with parallel program execution on a network of workstations 10 p1377 N88-18217

Predicate analysis for parallel program generation
10 p1377 N88-18222

An investigation of parallelism in rule based systems
10 p1377 N88-18223

The next generation of hypercube computers
10 p1378 N88-18226

A parallel computer based on cube connected cycles
10 p1378 N88-18227

Investigations on the usefulness of the Massively Parallel Processor for study of electronic properties of atomic and condensed matter systems
[NASA-CR-182514] 10 p1383 N88-18259

A measurement-based study of concurrency in a multiprocessor
[DE88-003536] 10 p1383 N88-18260

Features of a TeraFlop supercomputer
[DE88-003540] 10 p1384 N88-18263

The impact of hierarchical memory systems on linear algebra algorithm design
[DE88-003574] 10 p1385 N88-18274

PSolve: A concurrent algorithm for solving sparse systems of linear equations
[DE88-003584] 10 p1386 N88-18275

Introduction to a system for implementing neural net connections on SIMD architectures
[NASA-CR-181612] 10 p1386 N88-18279

Programming methodology and performance issues for advanced computer architectures
[DE88-003098] 10 p1387 N88-18287

A multiprocessor scheme for the singular value decomposition
[DE88-003591] 10 p1388 N88-18298

Parallel access to synchronization variables
[DE88-003570] 10 p1392 N88-18306

Loop coalescing: A compiler transformation for parallel machines
[DE88-003571] 10 p1392 N88-18307

The performance of software-managed multiprocessor caches on parallel numerical programs
[DE88-003590] 10 p1393 N88-18308

A parallel quasi-Newton method for partially separable large scale minimization
[DE88-003592] 10 p1393 N88-18309

Performance studies of a parallel processor for large linear programming problems
[PB88-121611] 10 p1393 N88-18310

Dynamic processor self-scheduling for general parallel nested loops
[DE88-003572] 10 p1393 N88-18311

Parallel discrete event simulation: A shared memory approach
[NASA-CR-182521] 10 p1393 N88-18312

Deadlock prevention in processor self-scheduling for parallel nested loops
[DE88-003573] 10 p1393 N88-18313

Parallel garbage collection on a virtual memory system
[DE88-003567] 10 p1396 N88-18317

Fast and practical parallel polynomial interpolation
[DE88-003530] 10 p1397 N88-18328

Center for Supercomputing Research and Development
[DE88-003564] 10 p1418 N88-18466

Automated radar target recognition based on models of neural nets 11 p1476 N88-18604

Optimal performance of distributed simulation programs
[AD-A187822] 11 p1529 N88-19131

Performance measurements of distributed simulation strategies
[AD-A187824] 11 p1529 N88-19133

Distributed computation of graphics primitives on a transputer network
[NASA-TM-100814] 11 p1531 N88-19147

A shared memory algorithm and proof for the alternative construct in CSP (Communicating Sequential Processes)
[AD-A187820] 11 p1533 N88-19156

Implementing dynamic arrays: A challenge for high-performance machines
[AD-A188142] 11 p1533 N88-19157

Parallel processing in nonlinear programming
[INPE-4298-PRE/1169] 11 p1533 N88-19158

Object recognition on a systolic array
[AD-A187726] 11 p1534 N88-19164

Performance of a multigrid method on parallel architecture 11 p1539 N88-19200

Allocation of database files across parallel stores for efficient processing of partial-match queries
[AD-A188196] 11 p1565 N88-19371

Architecture with parallel processing for incremental computation
[INPE-4326-PRE/1178] 12 p1675 N88-20012

An intelligent allocation algorithm for parallel processing
[NASA-CR-182648] 12 p1675 N88-20014

Efficient parallel architecture for highly coupled real-time linear system applications
[NASA-CR-182649] 12 p1675 N88-20015

Computer architecture for efficient algorithmic executions in real-time systems: New technology for avionics systems and advanced space vehicles
[NASA-CR-182650] 12 p1675 N88-20016

Automatic restructuring of FORTRAN programs for parallel execution
[DE88-003585] 12 p1676 N88-20018

BLITZ: Blitzen's micron-code assembly language design document, version 1.0
[TR88-14] 12 p1676 N88-20019

A laboratory facility for research in parallel computation
[AD-A188499] 12 p1680 N88-20044

Primal-dual parallel solution of very large sparse linear programs
[AD-A188500] 12 p1680 N88-20045

MultiRPC: A parallel remote procedure call mechanism
[AD-A188613] 12 p1680 N88-20046

ARCTIC: Programmer's manual and tutorial
[AD-A188619] 12 p1680 N88-20047

Analysis for architecture for image processing
[INPE-4294-PRE/1165] 13 p1791 N88-20715

The physical structure of concurrent problems and concurrent computers
[DE88-005812] 13 p1814 N88-20835

Parallel image compression
[NASA-CR-180758] 13 p1814 N88-20837

Implementation of a 3-D nonlinear MHD (magnetohydrodynamics) calculation on the Intel hypercube
[DE88-000625] 13 p1816 N88-20848

Gaussian techniques on shared memory multiprocessor computers
[DE88-005426] 13 p1817 N88-20855

Approximation algorithms for scheduling unrelated parallel machines
[CWI-OS-R8714] 13 p1817 N88-20861

Computing with structured connections networks
[AD-A189244] 13 p1821 N88-20886

A simulation study of a parallel processor with unbalanced loads
[AD-A189573] 13 p1822 N88-20887

On the design of parallel numerical methods in message passing and shared memory environments
[DE88-003566] 13 p1822 N88-20888

Perspectives on parallel computing
[CWI-OS-R8709] 13 p1822 N88-20889

Locality, communication and interconnect length in multicomputers
[CWI-CS-R8708] 13 p1822 N88-20890

Utilization of parallel processing in solving the inviscid form of the average-passage equation system for multistage turbomachinery
[NASA-TM-89845] 14 p1868 N88-21160

A parallel algorithm for computing the singular value decomposition of a matrix
[DE88-007059] 14 p1958 N88-21673

Evaluation of a parallel chart parser
[AD-A189172] 14 p1959 N88-21685

Parallel algorithms for mapping pipelined and parallel computations
[NASA-CR-181655] 14 p1960 N88-21687

Parallel processes in the knowledge based system HYDRA
[REPT-87-36] 14 p1960 N88-21689

Using a parallel computer system for statistical resampling methods
[REPT-87-47] 14 p1960 N88-21690

Proposal for a parallel system with image processing applications
[INPE-4293-PRE/1164] 14 p1961 N88-21696

Lewis Structures Technology, 1988. Volume 3: Structural Integrity Fatigue and Fracture Wind Turbines HOST
[NASA-CP-3003-VOL-3] 15 p2081 N88-22408

Parallel memory addressing using coincident optical pulses
[AD-A189767] 15 p2106 N88-22547

Applications of optical computing to problems with symbolic computations
[AD-A189772] 15 p2106 N88-22548

SimPL: A simulator for parallel LISP
[AD-A189831] 15 p2109 N88-22566

Transformations of concurrent algorithms for highly parallel systems: A one year project summary report
[AD-A190236] 15 p2111 N88-22576

Two-dimensional graphics tools for a transputer based display board
[NASA-TM-100820] 15 p2113 N88-22591

Logarithmically connected, repetitive computer networks and numerical applications
[DE88-006632] 15 p2114 N88-22592

Modeling a parallel architecture for image processing
[RR-646-I] 15 p2114 N88-22593

Simulation of fault tolerance in a hypercube arrangement of discrete processors
[AD-A189682] 15 p2114 N88-22594

The modeling, simulation and comparison of interconnection networks for parallel processing
[AD-A190571] 15 p2115 N88-22599

Implementation and performance analysis of parallel assignment algorithms on a hypercube computer
[AD-A190678] 15 p2115 N88-22600

Design and implementation of a parallel computer for expert system applications
[DE88-005288] 15 p2115 N88-22601

A direct-execution parallel architecture for the Advanced Continuous Simulation Language (ACSL)
[NASA-CR-182800] 15 p2115 N88-22602

Synapses that compute motion
[AD-A190389] 15 p2116 N88-22607

Study of microcomputer-based real-time programmable optical signal processor and application
[AD-A190076] 15 p2133 N88-22726

A methodolgy, based on analytical modeling, for the design of parallel and distributed architectures for relational database query processors
[AD-A189844] 15 p2149 N88-22825

Fast algorithms for Euler and Navier-Stokes simulations
[AD-A190697] 16 p2208 N88-23175

Lewis Structures Technology, 1988. Volume 1: Structural Dynamics
[NASA-CP-3003-VOL-1] 16 p2217 N88-23226

Parallel computer methods for eigenvalue extraction
16 p2218 N88-23233

Adapting high-level language programs for parallel processing using data flow 16 p2218 N88-23234

Iterative finite element solver on transputer networks
16 p2218 N88-23235

Multiprocessor graphics computation and display using transputers 16 p2218 N88-23236

Parafrase restructuring of FORTRAN code for parallel processing 16 p2221 N88-23258

Synthesis and simulation of systolic algorithms
[ETN-88-92183] 16 p2247 N88-23423

The PROMISE simulation system: Software for the simulation of parallel processes
[NLR-MP-86077-U] 16 p2247 N88-23427

A queueing network model for analyzing a class of branch and bound algorithms on a master-slave architecture
[CWI-OS-R8717] 16 p2249 N88-23441

VPC: A proposal for a vector parallel C programming language
[AD-A190885] 16 p2251 N88-23451

Simulation of FELIN logics. Polynomials roots simultaneous computation algorithms
[ETN-88-92182] 16 p2253 N88-23464

Locality, communication and interconnect length in multicomputers
[CWI-CS-R8743] 16 p2254 N88-23466

Parallel computing in combinatorial optimization
[CWI-OS-R8720] 16 p2254 N88-23468

Domain decomposition in parallel reservoir simulation
[REPT-87-63] 16 p2254 N88-23469

Power series for stationary distributions of coupled processor models
[REPT-87-70] 16 p2254 N88-23470

Parallelization of Gauss-Seidel algorithms as an example of parallel iterative equation solving
[REPT-87-76] 16 p2254 N88-23471

Parallel artificial intelligence search techniques for real time applications
[AD-A190683] 16 p2255 N88-23473

Parallelism in a Prolog knowledge base machine
[ETN-88-92187] 16 p2255 N88-23477

An efficient parallel algorithm for the simulation of three-dimensional compressible transition on a 20 processor Flex/32 multicomputer
[NASA-CR-178340] 17 p2337 N88-23943

Evolution of a family of image processing systems at INPE 17 p2361 N88-24065

Parallel processors and nonlinear structural dynamics algorithms and software
[NASA-CR-182925] 17 p2387 N88-24187

Parallel discrete-event simulation of FCFS stochastic queueing networks
[NASA-CR-181669] 17 p2389 N88-24203

Decomposition of linear programs using parallel computation
[AD-A191718] 18 p2556 N88-25173

An improved simulated annealing algorithm for standard cell placement
[NASA-CR-182952] 18 p2558 N88-25183

Algorithms and software for solving finite element equations on serial and parallel architectures
[NASA-CR-183027] 18 p2559 N88-25191

Network architecture for OPS5
[DE88-002602] 18 p2560 N88-25194

Cellular Array Processor (CAP) and its application to computer graphics 19 p2641 N88-25667

Signal processing computational needs
[AD-A191756] 19 p2642 N88-25674

Multidimensional nodal transport methods for multiple-instruction multiple-data distributed memory machines
[DE88-004732] 19 p2713 N88-26108

Intermediate level computer vision processing algorithm development for the content addressable array parallel processor
[AD-A192086] 19 p2714 N88-26111

Graphical Multiprocessing Analysis Tool (GMAT)
[DE88-008019] 19 p2715 N88-26116

Efficient parallel algorithm for the connected component problem and its implementation on the DPP84 (Delft Parallel Processor)
[PB87-225959] 19 p2715 N88-26118

On the implementation of applicative on shared-memory, MIMD multiprocessors
[DE88-005367] 19 p2718 N88-26136

SLAPP: A special multiprocessor array for signal processing and linear algebra
[AD-A191587] 19 p2719 N88-26146

Parallelization on a multiprocessor system of a solution method for the unsteady Navier-Stokes equations at high Reynolds numbers
[ONERA-NT-1987-8] 20 p2803 N88-26632

Computer science research, 1987: Computation Directorate
[DE88-008637] 20 p2834 N88-26812

The performance of the NEC SX-2 and Cray X-MP supercomputers
[DE88-009177] 20 p2835 N88-26813

Efficient bit-level, word-level and block-level systolic arrays for matrix-matrix multiplication
[DE88-011331] 20 p2841 N88-26856

Extensible networks. Part 1: Principles and constructions
[REPT-87-91-PT-1] 20 p2842 N88-26864

The scaled-sized model: A revision of Amdahl's law
[DE88-008114] 20 p2844 N88-26875

Computational fluid dynamics on parallel processors
[AD-A192397] 21 p2941 N88-27469

Supercomputer for parallel data analysis
[DE88-702148] 21 p2995 N88-27759

Linguistic semantics for parallel computation
[PB88-105960] 21 p2995 N88-27761

Bisimulation can't be traced
[AD-A192725] 21 p2996 N88-27766

Research into the architecture of CAD based robot vision systems
[AD-A193330] 21 p2997 N88-27776

The sub-implicit method: New multiprocessor algorithms for old implicit codes
[DE88-011345] 21 p2999 N88-27785

Implementing direct, spatially isolated problems on transputer networks
[NASA-TM-101297] 21 p3000 N88-27796

User's manual for the two-dimensional transputer graphics toolkit
[NASA-TM-100974] 21 p3001 N88-27799

Image processing using a parallel architecture
[AD-A192833] 21 p3002 N88-27803

Basic database operations on the butterfly parallel processor: Experiment results
[AD-A193199] 21 p3002 N88-27804

Parallel solutions to geometric problems on the scan model of computation
[AD-A192321] 21 p3004 N88-27819

A review of parallel methods for solving sets of linear equations and their application within optimisation algorithms
[AD-A193137] 21 p3006 N88-27830

Matrix substructuring, domain decomposition and particle methods: Current trends for solving PDEs in parallel
[DE88-009826] 21 p3007 N88-27836

Parallel implementation of the boundary element method
[DE88-011846] 21 p3007 N88-27839

Two-dimensional sequential and concurrent finite element analysis of unstiffened and stiffened aluminum and composite panels with hole
[NASA-CR-183083] 22 p3086 N88-28325

What have we learnt from using real parallel machines to solve real problems
[DE88-011227] 22 p3135 N88-28636

Partitioning of regular computation on multiprocessor systems
[NASA-CR-183176] 22 p3141 N88-28676

Queueing network models for parallel processing of task systems: An operational approach
[NASA-CR-183174] 22 p3141 N88-28677

Using Petri nets for real-time development environments
[REPT-88-005] 22 p3141 N88-28679

Parallel real-time expert systems
[AD-A193673] 23 p3264 N88-29434

Adaptive identification by systolic arrays
[AD-A193532] 23 p3266 N88-29444

Performance analysis of k-ary n-cube interconnection networks
[AD-A195542] 24 p3361 N88-30010

Reducing the parallel solution time of sparse circuit matrices using reordered Gaussian elimination and relaxation
[AD-A195152] 24 p3366 N88-30045

Performance prediction of concurrent systems
[NASA-CR-183175] 24 p3412 N88-30312

Parallel and distributed computation for fault-tolerant object recognition 24 p3419 N88-30350

PARALLEL PROGRAMMING

Report from the MPP Working Group to the NASA Associate Administrator for Space Science and Applications
[NASA-TM-87819] 02 p0223 N88-11402

Parallel algorithms for unconstrained and constrained nonlinear optimization
[PB87-230454] 06 p0756 N88-14634

Algorithms and programming tools for image processing on the MPP:3
[NASA-CR-182349] 06 p0757 N88-14641

Parallel logic programming and ZMOB and parallel systems software and hardware
[AD-A186300] 07 p0903 N88-15470
UNITY: A framework for study of parallel programming problem-solving
[AD-A185616] 07 p0906 N88-15490
Teaching artificial neural systems to drive: Manual training techniques for autonomous systems
09 p1207 N88-17238
Implementing clips on a parallel computer
09 p1211 N88-17259
Communications patterns in a symbolic multiprocessor
[AD-A186896] 09 p1215 N88-17282
Preconditioned iterative methods for partial differential equations
[DE88-003071] 09 p1230 N88-17372
Experimenting with parallel programing in logic
10 p1380 N88-18240
Parallel architectures for logic programming
10 p1380 N88-18241
Programming language translation for multicomputers
10 p1381 N88-18244
Parallelism at the microlevel: Cooperative microcontrollers with real time considerations
10 p1381 N88-18246
FX-87 reference manual, edition 1.0
[AD-A187031] 10 p1385 N88-18273
Experiences with serial and parallel algorithms for channel routing using simulated annealing
[NASA-CR-182530] 10 p1388 N88-18289
Theory and practice of fault tolerance in distributed systems
[AD-A187559] 11 p1540 N88-19204
Automatic restructuring of FORTRAN programs for parallel execution
[DE88-003585] 12 p1676 N88-20018
Design of the CONSUL programming language
[AD-A189202] 13 p1815 N88-20841
An interface between object-oriented systems
[AD-A189245] 13 p1815 N88-20844
Designing equivalent semantic models for process creation
[CWI-CS-R8732] 13 p1819 N88-20872
Activities and operations of the Advanced Computing Research Facility, October 1986-October 1987
[DE88-006223] 14 p1955 N88-21653
On the productivity of recursive list definitions
[CS-8707] 14 p1960 N88-21692
Supercomputer environment
[AD-A190633] 15 p2107 N88-22551
MultiScheme: A parallel processing system based on MIT (Massachusetts Institute of Technology) scheme
[AD-A190383] 15 p2114 N88-22597
VPC: A proposal for a vector parallel C programming language
[AD-A190885] 16 p2251 N88-23451
Beyond Ada: Generating Ada code from equational specifications
[AD-A191866] 18 p2557 N88-25176
The FORCE
[AD-A193463] 23 p3264 N88-29429

PARALLEL STRIP LINES
U MICROSTRIP TRANSMISSION LINES

PARALLELOGRAMS
NT RHOMBOIDS

PARAMAGNETIC AMPLIFIERS
U MASERS

PARAMAGNETIC RESONANCE
NT ELECTRON PARAMAGNETIC RESONANCE
Paramagnetic spins in oxygen-loaded ceramic La2CuO4/sub 4+delta/
[DE88-007114] 19 p2619 N88-25539
Paramagnetic point defects in boron-implanted HgO.7CdO.3Te
[AD-A193276] 21 p3021 N88-27934

PARAMAGNETISM
Electron Spin Resonance (ESR) measurements on intermediate-valence Ce compounds doped with paramagnetic ions: CeOs2:Gd ion and CePd3:Mn-ion
[ETN-88-91081] 09 p1256 N88-17526
Superconducting and magnetic properties of Fe-doped oxide superconductors
[DE88-003024] 10 p1416 N88-18451
Nuclear magnetic ordering and paramagnetic relaxation of diatomic molecules in Ca (OH)2
[B8881469] 23 p3281 N88-29532

PARAMECIA
Investigations of Paramecium cells analyzed under microgravity conditions 07 p0884 N88-15367
Experiments concerning gravisensitivity of protozoa
12 p1660 N88-19949
The Paramecium experiment --- Spacelab D1 mission
22 p3060 N88-28161

PARAMETER IDENTIFICATION
Maximum likelihood estimates of parameters in linear systems with process and measurement noise
[DFVLR-FB-87-20] 01 p0063 N88-10532
Breakdown points of affine equivariant estimators of multivariate location and covariance matrices
[REPT-87-14] 01 p0068 N88-10574
Modeling XV-15 tilt-rotor aircraft dynamics by frequency and time-domain identification techniques
03 p0263 N88-11657
Integrated 3-parameter diagram for determining thermodynamic properties of fluids
03 p0298 N88-11874
Full-envelope aerodynamic modeling of the Harrier aircraft
[NASA-TM-88376] 05 p0552 N88-13363
Non-linear maximum likelihood estimation of stability derivatives from range data
[NAL-TM-SE-8608] 05 p0552 N88-13365
Robot accuracy improvement through kinematic parameter identification 06 p0712 N88-14363
A new method of boundary parameter estimation for a two-dimensional diffusion system under noisy observations
[NASA-CR-178405] 06 p0767 N88-14714
Lie algebraic method in filtering and identification
[CWI-PM-R8606] 08 p1072 N88-16467
Contribution to the design of flexible manufacturing systems: Modeling, simulation, and evaluation of parameters
[ISAL-IDI1-87-04] 09 p1151 N88-16894
Parameter identification and sensitivity analysis for a robotic manipulator arm
[NASA-CR-181608] 10 p1385 N88-18272
The estimation of target trajectory parameters from Closest Point of Approach (CPA) time measurements in a field of acoustic sensors
[FB-3-87] 11 p1439 N88-18586
Fixed and adaptive interframe image prediction for remote piloting application
[AD-A187967] 11 p1471 N88-18771
Using ridge regression in systematic pointing error corrections 11 p1472 N88-18777
Overview of multi-input frequency domain modal testing methods with an emphasis on sine testing
11 p1499 N88-18949
Application of the estimation method to parameter performance date of solar water heating systems
[INPE-4266-PRE/1141] 11 p1508 N88-19007
A maximum likelihood parameter estimation program for general non-linear systems
[ARL-AERO-TM-392] 11 p1532 N88-19154
Realtime pilot model parameter identification
[AD-A188873] 12 p1584 N88-19476
Aircraft flight flutter testing at the NASA Ames-Dryden Flight Research Facility
[NASA-TM-100417] 13 p1723 N88-20301
Material parameter measurements at high temperatures
[NASA-CR-182707] 13 p1739 N88-20397
On error equations for determining Earth rotation parameters with VLBI network 13 p1756 N88-20500
An automated procedure for material parameter evaluation for viscoplastic constitutive models
14 p1932 N88-21520
Identification of nonlinear rational systems using a prediction-error estimation algorithm
[RR-317] 14 p1959 N88-21660
Application of the NARMAX method to nonlinear frequency response estimation
[RR-319] 14 p1964 N88-21721
Deterministic approximations of probability inequalities
[REPT-87-43] 14 p1966 N88-21732
An orthogonal parameter estimation algorithm for nonlinear stochastic systems
[RR-307] 14 p1966 N88-21736
Parametric methods of analysing linear and nonlinear systems
[RR-318] 14 p1967 N88-21741
Optimal control and identification of space structures
[AD-A190033] 15 p2025 N88-22065
A survey of oscillating flow in Stirling engine heat exchangers
[NASA-CR-182108] 15 p2067 N88-22322
Boundary shape identification problems in two-dimensional domains related to thermal testing of materials
[NASA-CR-181654] 15 p2105 N88-22541
Consistent estimates of autoregressive parameters for autoregressive moving average models
[RR-663-I] 15 p2109 N88-22564
Parametric study of supersonic STOVL flight characteristics
[NASA-CR-177330] 16 p2161 N88-22893
Analysis and design of gain scheduled control systems
[NASA-CR-182867] 16 p2163 N88-22904
Maximum likelihood parameter identification of flexible spacecraft
[LR-508] 16 p2168 N88-22924
Studies in reliability and inference
[AD-A191389] 16 p2217 N88-23223
Optimal control, estimation compensation of linear discrete-time systems with stochastic parameters
[REPT-87-56] 16 p2255 N88-23478
An algebraic construction of a class of one-dependent processes
[REPT-87-65] 16 p2259 N88-23507
Control law parameterization for an aeroelastic wind-tunnel model equipped with an active roll control system and comparison with experiment
[NASA-TM-100593] 17 p2306 N88-23807
Parameter estimation for boundary value problems by integral equations of the second kind
[NASA-CR-181660] 17 p2332 N88-23918
Parameter identification methods for improving structural dynamic models
[NASA-TM-100812] 17 p2349 N88-23994
Estimation of time- and state-dependent delays and other parameters in functional differential equations
[NASA-CR-181663] 17 p2383 N88-24164
Minimal parameter solution of the orthogonal matrix differential equation
[NASA-TM-4043] 17 p2383 N88-24165
Application of spline functions to digital image processing
[ETN-88-92194] 17 p2392 N88-24218
A recursive prediction error parameter estimator for nonlinear models
[RR-326] 17 p2392 N88-24222
TVC (Thrust Vector Control) jet vane thermal modeling using parametric system identification
[AD-A191516] 18 p2474 N88-24678
A fast and efficient procedure for generalized cross-validation with large data sets. Application to image reconstruction
[RR-669-M] 18 p2563 N88-25220
Single-mode projection filters for modal parameter identification for flexible structures
[NASA-CR-182680] 18 p2566 N88-25244
Recursive maximum likelihood identification of a nonlinear output-affine model
[RR-322] 18 p2569 N88-25257
System identification in vehicle dynamics
[DFVLR-MITT-87-22] 20 p2785 N88-26518
Parameter estimation of dynamical systems
20 p2785 N88-26519
Flight vehicle system identification: Status and prospects 20 p2785 N88-26520
Modeling and parameter identification of motor vehicles 20 p2785 N88-26521
Parametric estimation of aerodynamic nonlinearities in rolling moment due to sideslip using maximum likelihood method 20 p2736 N88-26528
Flight test preparation and measuring data validation for parameter identification 20 p2786 N88-26529
Application of complementary parameter identification techniques to flight test data of a transport aircraft
20 p2787 N88-26533
Parameter identification of the passenger simulation model MADYMO: Methods and experience
20 p2786 N88-26536
Parameter identification of material constants in a composite shell structure
[DE88-008115] 22 p3086 N88-28326
Parametric identification of mechanical structures
[ETN-88-92881] 22 p3088 N88-28339
Estimation of aircraft parameters using filter error methods and extended Kalman filter
[DFVLR-FB-88-15] 23 p3176 N88-28911
Identification and control of time-varying flexible structures: An artificial intelligence approach
23 p3265 N88-29437
Procedures for updating dynamic mathematical models, test phase --- spacecraft hardware
[MEBS-38/87] 24 p3335 N88-29852

PARAMETERIZATION
NT PARAMETER IDENTIFICATION
Moisture determinations in and under vegetation canopies. Part 2: Results after parameterization of the CLOUD model
[FEL-1986-63] 01 p0064 N88-10410
Description of NCAR (National Center for Atmospheric Research) Community Climate Model (CCM1)
[PB87-203782] 01 p0072 N88-10482
Statistically determined nickel cadmium performance relationships 02 p0165 N88-11039
Parametrization in scattering models
03 p0304 N88-11916

Nonlinear parametric least-squares adjustment
[AD-A184039] 03 p0371 N88-12336
Simulation studies for surfaces and materials strength
[NASA-CR-181535] 04 p0412 N88-12557
Local-optimal control in systems with delay
04 p0424 N88-12627
A review of parameterizations of microphysical processes in clouds for application in models of regional atmospheric deposition
[DE88-000451] 04 p0471 N88-12909
Estimation of a multivariate continuous variable panel model
[AD-A184472] 04 p0484 N88-12982
A system identification technique based on the random decrement signatures. Part 1: Theory and simulation
05 p0594 N88-13625
Fatigue crack growth: Statistical considerations
05 p0606 N88-13718
Nitrogen scale-up
[AD-A185702] 06 p0709 N88-14351
Report of the second session of the CAS/JSC working group on numerical experimentation — weather forecasting
[WMO/TD-168] 06 p0745 N88-14579
Balanced realizations: Canonical form, parametrization, model reduction
[PB87-123360] 06 p0757 N88-14642
Development of symbolic computation methods for nonlinear dynamics
[AD-A185562] 06 p0758 N88-14653
Asymptotically stable all-pass transfer functions: Canonical form, parametrization and realization
[PB87-123972] 06 p0763 N88-14684
A three-parameter generalisation of the beta-binomial distribution with applications
[AD-A185733] 06 p0766 N88-14720
Plasma parameters for alternate operating modes of TIBER-2
[DE88-001890] 06 p0783 N88-14802
TIBER 2 (Tokamak Ignition/Burn Experimental Reactor) parameters with neutral beams at high energies
[DE88-001891] 06 p0783 N88-14803
Parameter estimation for the Dirichlet-Multinomial Distribution (DMD) using supplementary beta-binomial data
[AD-A186335] 07 p0911 N88-15524
Energetics and dynamics of simple impulsive solar flares
[NASA-TM-87816] 07 p0947 N88-15755
Effect of extraneous factors on optical one-phonon transitions in impurity centers with cubic symmetry
08 p1077 N88-16496
Relativistic Calogero-Moser systems and solutions
[CWI-PM-R8702] 08 p1092 N88-16570
The accuracy of the radiation parameterization in mesoscale models
[DFVLR-IB-553-85/11] 09 p1190 N88-17133
Development of a physically-based general circulation model parameterization of clouds and their radiative interactions
[DE88-004060] 09 p1194 N88-17154
Fitting a generalized parabola to data
[NPL-DITC-96/87] 09 p1229 N88-17364
The TITAN Reversed-Field Pinch Reactor: Design-point determination and parametric studies
[DE88-001824] 09 p1251 N88-17498
Parametric study of choke flutter with a linear theory
10 p1283 N88-17673
Parameterization of radiative transfer in the Earth's atmosphere with specific applications to clouds
10 p1353 N88-18087
Effect of hypercapnic-hypoxic test on cariorespiratory parameters of individuals with neurocirculatory dystonia
10 p1367 N88-18169
Unidimensional Rasch model and multidimensional data: An analytic approach
[PB88-105861] 10 p1372 N88-18187
Hierachical object recognition using libraries of parameterized model sub-parts
[AD-A187476] 10 p1396 N88-18322
Semiempirical studies of atomic structure
[DE88-004086] 10 p1407 N88-18392
Analysis of learning curve fitting techniques
[AD-A187680] 11 p1535 N88-19173
Stochastic heuristics in network design: Parameter tuning and performance evaluation
[REPT-87-017] 11 p1541 N88-19210
Development savings through parametric modeling of program costs 12 p1700 N88-20175
Picking winners: Parametric cost estimating and project management 12 p1700 N88-20176
Parametric study of acceleration-induced stresses and frequency changes in doubly-rotated crystal resonators
[AD-A189261] 13 p1761 N88-20532
Generalized expression for radio navigation parameter error
13 p1787 N88-20691
Algebraic specifications for parameterized data types: The case of minimal computable algebras and parameters with equality
[CWI-CS-R8714] 13 p1826 N88-20916
Model structure selection for multivariable systems by cross-validation methods
[EUT-87-E-176] 13 p1827 N88-20926
The parameterization of orthogonal matrices: A review mainly for statisticians
[AD-A189144] 13 p1829 N88-20936
Non- and semi-parametric maximum likelihood estimators and the von Misis Method, part 1
[CWI-MS-R8709] 13 p1829 N88-20941
Representation of physical processes in global atmospheric models 14 p1935 N88-21542
Parameterization of radiation in a general circulation model 14 p1935 N88-21543
The role of radiation transfer in climate modification
14 p1936 N88-21549
An introduction to the parameterization of land-surface processes 14 p1937 N88-21554
Concentration inequalities for Gauss Markov estimators
[CWI-MS-R8706] 14 p1965 N88-21726
On a consistent estimate of the index of an extreme value distribution
[CWI-MS-R8710] 14 p1966 N88-21729
A robust scale estimator based on the shortest half
[REPT-87-36] 14 p1966 N88-21731
Modeling failures of intermittently used machines
[AD-A190298] 15 p2074 N88-22367
Parameterization of horizontal wind velocity variability
[AD-A190107] 15 p2097 N88-22493
Computer program for parameterization of nucleus-nucleus electromagnetic dissociation cross sections
[NASA-TM-4038] 16 p2270 N88-23584
Digital monoplotting, part 2
[B8735122-PT-2] 17 p2369 N88-24107
The liquid droplet radiator in space: A parametric approach 17 p2427 N88-24437
Analysis of lightning field changes during active thunderstorms in Florida 18 p2545 N88-25103
Making progress during a stall in the simplex algorithm
[DE88-007120] 18 p2558 N88-25182
Fast parametrization procedure for solar cells
[PB88-186416] 19 p2666 N88-25966
Scaling laws for geomagnetic tail current sheet acceleration
[AD-A193379] 19 p2691 N88-25998
Structural properties of multivariable linear systems
[PB88-181375] 19 p2717 N88-26134
Calculating the self-intersections of Bezier curves
[AD-A192371] 19 p2721 N88-26156
The Potts model in a random field
19 p2721 N88-26158
Parametric methodologies of cloud vertical transport for acid deposition models
[PB88-191374] 20 p2825 N88-26762
Lattice strain in heteroepitaxial films
20 p2868 N88-27032
An aspect graph-based control strategy for 3-D object recognition 21 p2927 N88-27377
Development of radiation and cloud parameterization programs for AFGL (Air Force Geophysics Laboratory) global models
[AD-A193369] 21 p2973 N88-27658
Design of multirate control systems via parameter optimization
[REPT-87-013] 22 p3142 N88-28686
Boundary layer manipulation 23 p3170 N88-28877
Human auditory and visual continuous evoked potentials 23 p3238 N88-29269
A fast parametric maximum flow algorithm, revision
[AD-A194026] 23 p3250 N88-29345
Properties of strong coupled superconductors
[DE88-702050] 23 p3287 N88-29574

PARAMETERS
U INDEPENDENT VARIABLES

PARAMETRIC AMPLIFIERS
Phase phenomena in parametric generators and amplifiers of ultrashort light pulses
07 p0918 N88-15576

PARAMETRIC OSCILLATORS
U PARAMETRIC AMPLIFIERS

PARASITIC DISEASES
TOMS as a monitor of the ultraviolet radiation environment: Applications to photobiology
05 p0617 N88-13785

PARITY
Coupled even-parity superconducting states: Square lattice
[AD-A193432] 21 p3022 N88-27938

PARKS
Comparative utilization of analog and digital processes in the treatment of MSS-LANDSAT data for studying the national parks of Brazil
[INPE-4011-TDL/240] 15 p2090 N88-22456
Temporal analysis of the changes in Parque Estadual de Jacupiranga vegetation through digital treatment of LANDSAT imagery 17 p2367 N88-24094

PARSING ALGORITHMS
Automated program recognition
[AD-A186421] 07 p0903 N88-15472
Semi-applicative programming
10 p1380 N88-18239
A parser generator for finitely ambiguous context-free grammars
[CWI-CS-R8712] 13 p1818 N88-20864
Evaluation of a parallel chart parser
[AD-A189172] 14 p1959 N88-21665
Programmer-friendly LL(1) parser generator
[PB88-126933] 20 p2841 N88-26857
A cockpit natural language study: Vocabulary and grammar analyses
[AD-A193289] 21 p2993 N88-27753

PARTIAL DIFFERENTIAL EQUATIONS
NT BIHARMONIC EQUATIONS
NT BURGER EQUATION
NT CAUCHY-RIEMANN EQUATIONS
NT ELLIPTIC DIFFERENTIAL EQUATIONS
NT EULER-CAUCHY EQUATIONS
NT FOKKER-PLANCK EQUATION
NT GAUSS EQUATION
NT HELMHOLTZ VORTICITY EQUATION
NT PARABOLIC DIFFERENTIAL EQUATIONS
NT POISSON EQUATION
NT VLASOV EQUATIONS
On the relational modeling of discrete PDE problems
[DE87-013336] 02 p0224 N88-11409
Determination of fractal dimension, connection of space and temporal chaos and application to experimental results 03 p0313 N88-11977
Numerical solution of partial differential equations on irregular grids
[DE87-014760] 03 p0369 N88-12324
Application of the finite difference method to the solution of mixed partial differential equations for the case of transonic flow
[ETN-87-90760] 03 p0370 N88-12327
Optimization of explicit time-stepping algorithms and Stream-Function-Coordinate (SFC) concept for fluid dynamics problems 04 p0445 N88-12762
A comparison of adaptive refinement techniques for elliptic problems
[DE88-000805] 04 p0485 N88-12987
Two classes of preconditioners computed using block matrix factorization techniques
[DE88-001313] 04 p0485 N88-12988
Numerical and analytical methods in nonlinear partial differential equations
[AD-A185210] 05 p0641 N88-13918
The Eckhaus Partial Differential Equation (PDE) I psi t + psi xx + 2(psi/sq)x psi +2(/psi/) to the 4th power psi = 0
[PREPRINT-546] 06 p0763 N88-14686
Equations of nonlinear Schroedinger type in 1 + 1 and 2 + 1 dimensions, obtained from integrable Partial Differential Equations (PDEs)
[PREPRINT-548] 06 p0764 N88-14687
Nonisospectral deformations and Darboux transformations for the 3rd order spectral problem
[PREPRINT-556] 06 p0764 N88-14690
Nonlinear evolution equations, rescalings, model partial differential equations (PDES) and their integrability, 2
[PREPRINT-560] 06 p0764 N88-14691
New methods for numerical solution of one class of strongly nonlinear partial differential equations with applications
[AD-A186166] 07 p0899 N88-15445
Local uniform mesh refinement for partial differential equations
[AD-A186312] 07 p0910 N88-15519
The paradoxical asymptotic status of massless springs
[AD-A185625] 07 p0928 N88-15637
Numerical experiments with a parallel conjugate gradient method
[DE88-002178] 08 p1066 N88-16445
Some stability results for the hopscotch difference method when applied to convection-diffusion equations
[CWI-NM-R8711] 08 p1072 N88-16465
Supercomputers for solving PDE (Partial Differential Equations) problems
[AD-A186583] 09 p1215 N88-17283
Feedback stabilization of distributed systems
[AD-A187111] 09 p1222 N88-17328
Techniques in linear and nonlinear partial differential equations
[AD-A187109] 09 p1227 N88-17347

Explicit-implicit methods for time-dependent partial differential equations
[CWI-NM-R8703] 09 p1228 N88-17355
Preconditioned iterative methods for partial differential equations
[DE88-003071] 09 p1230 N88-17372
Programming methodology and performance issues for advanced computer architectures
[DE88-003098] 10 p1387 N88-18287
Nonlinear filtering and large deviations: A PDE-Control theoretic approach
[AD-A187436] 10 p1396 N88-18321
A multigrid preconditioner applied to a two-dimensional convection-diffusion problem
[DE88-004765] 10 p1397 N88-18329
Parallels between control PDE's (Partial Differential Equations) and systems of ODE's (Ordinary Differential Equations)
[NASA-CR-182487] 10 p1398 N88-18331
On observer problems for systems governed by partial differential equations
[AD-A187430] 10 p1400 N88-18351
Applications of Lie group methods to the equations of magnetohydrodynamics 10 p1411 N88-18422
Canonical coordinates for partial differential equations
[NASA-CR-182486] 11 p1535 N88-19170
Conference on Maximum Principles and Eigenvalue Problems in Partial Differential Equations
[AD-A187870] 11 p1536 N88-19175
Multigrid methods in convex optimization
11 p1538 N88-19190
The Euler-Bernoulli beam equation with boundary energy dissipation
[AD-A189517] 13 p1765 N88-20560
Propagator solutions of partial differential equations applied to plasma transport
[DE88-006432] 13 p1816 N88-20852
Spectral element methods: Algorithms and architectures
[NASA-CR-182701] 13 p1820 N88-20878
Numerical solution of ill posed problems in partial differential equations
[AD-A189383] 13 p1825 N88-20909
A Lagrangian moving grid scheme for one-dimensional evolutionary partial differential equations
[CWI-NM-R8713] 13 p1827 N88-20922
Stabilization of explicit difference schemes by smoothing techniques
[CWI-NM-R8714] 13 p1827 N88-20923
Nonlinear differential equations
[DE88-006047] 13 p1828 N88-20933
Lie groups in prolongation theory
[B8721781] 14 p1967 N88-21743
New methods for numerical solution of one class of strongly nonlinear partial differential equations with applications
[AD-A189945] 15 p2119 N88-22630
Research in nonlinear partial differential equations and bifurcation theory
[AD-A190986] 16 p2260 N88-23514
Similarity solutions of nonlinear partial differential equations invariant to a family of affine groups
[DE88-003404] 18 p2567 N88-25245
Computer science research, 1987: Computation Directorate
[DE88-008637] 20 p2834 N88-26812
Nontrivial critical points for asymptotically quadratic function
[DE88-101851] 20 p2845 N88-26881
Feedback control of a hyperbolic partial-differential equation with viscoelastic damping
[AD-A192896] 21 p3003 N88-27810
Numerical optimization
[AD-A193032] 21 p3005 N88-27827
Unified multilevel adaptive finite element methods for elliptic problems
[DE88-011938] 21 p3007 N88-27840
Application of differential quadrature to the analysis of structural components 22 p3087 N88-28331
Why are certain nonlinear Partial Differential Equations (PDE) both widely applicable and integrable
[PREPRINT-582] 22 p3144 N88-28698
The construction of implicit and explicit solitary wave solutions of nonlinear partial differential equations
[AD-A193475] 23 p3269 N88-29452
MACSYMA program for the painleve test of nonlinear ordinary and partial differential equations
[AD-A194293] 23 p3270 N88-29458
Laser sensing for identification and control of distributed parameter systems
[AD-A195886] 24 p3379 N88-30124
Multiple solutions and bifurcation for a class of nonlinear Sturm-Liouville eigenvalue problems on an unbounded domain
[AD-A195954] 24 p3426 N88-30389

PARTIAL PRESSURE
NT OXYGEN TENSION
Inerting and atmospheres 04 p0406 N88-12524
Nitrogen's biological effect on oxygen transport through hematoparenchymal barrier 12 p1662 N88-19967
Phase transformations and thermodynamic behavior of the YBa2Cu3O(sub)x system via EMF measurements
[DE88-010054] 20 p2878 N88-27086

PARTICLE ACCELERATION
Channeled particle acceleration by plasma waves in metals
[DE87-010541] 01 p0093 N88-10604
Particle injection and cosmic ray acceleration at collisionless parallel shocks
[DE88-000507] 04 p0430 N88-12365
Prompt simultaneous acceleration of protons and electrons to relativistic energies by shock waves in solar flares
[IPPJ-851] 04 p0493 N88-13037
Optimization of charged particle acceleration rate over wave parameters in the scheme with acceleration by surface electromagnetic waves
[DE88-700320] 07 p0846 N88-15134
Experimental evaluation for efficiency of excitation slow plasma and cyclotron waves in collective accelerators
[DE88-700566] 07 p0938 N88-15687
Solar event of 27 April 1981 08 p1004 N88-16084
Characteristics of particle acceleration at high latitude
08 p1026 N88-16210
First results from the Viking associated Aureld-VIP rocket and EISCAT campaign --- auroras; Swedish satellite
08 p1026 N88-16211
Acceleration of auroral particles by magnetic field-aligned electric fields 08 p1031 N88-16246
Low frequency waves and small scale solitary structures observed by Viking --- Swedish satellite; auroras
08 p1099 N88-16611
On the potential role of concentrated field-aligned currents in solar physics 08 p1099 N88-16614
Acceleration of auroral particles by magnetic field-aligned electric fields
[TRITA-EPP-87-08] 09 p1190 N88-17131
Determination of molecular-ion structures through the use of accelerated beams
[DE88-002960] 09 p1246 N88-17467
Advanced nonlinear theory: Long-term stability at the SSC
[CEBAF-PR-87-027] 11 p1546 N88-19246
Waves and static electric fields in the auroral acceleration region 12 p1646 N88-19[illegible]56
The lattice nonlinearities and the long term stability of the SSC
[CEBAF-PR-87-009] 12 p1690 N88-20108
On the acceleration of electrons and positive ions in the same direction along magnetic field lines by parallel electric fields
[IRF-PREPRINT-103] 15 p2096 N88-22488
A chemical method for achieving acceleration of macroparticles to ultrahigh velocities
[DE88-006377] 15 p2128 N88-22695
Particle acceleration to high energies and amplification of coherent radiation by electromagnetic interactions in plasmas
[DE88-701020] 15 p2135 N88-22737
Simultaneous observation of upward moving field aligned energetic electrons and ions on auroral zone field lines
[IRF-PREPRINT-102] 16 p2231 N88-23326
Numerical simulation for particle acceleration and trapping by an electromagnetic wave
16 p2277 N88-23626
Scaling laws for geomagnetic tail current sheet acceleration
[AD-A193379] 19 p2691 N88-25998
Mechanisms for particle acceleration: Possibilities and constraints
[PB88-102538] 19 p2725 N88-26184
Accelerator research studies
[DE88-008236] 19 p2726 N88-26187

PARTICLE ACCELERATOR TARGETS
Development of nuclear models for higher energy calculations
[DE88-010919] 20 p2852 N88-26932

PARTICLE ACCELERATORS
NT BETATRONS
NT CYCLIC ACCELERATORS
NT ELECTRON ACCELERATORS
NT ION ACCELERATORS
NT LINEAR ACCELERATORS
NT MICROTRONS
NT STORAGE RINGS (PARTICLE ACCELERATORS)
NT SUPERCONDUCTING SUPER COLLIDER
NT SYNCHROTRONS
NT VAN DE GRAAFF ACCELERATORS
Investigations into the design of multi-terawatt magnetic switches
[DE87-012014] 01 p0040 N88-10254
Recording multiple signals on a single waveform recorder
[DE87-011632] 01 p0049 N88-10313
Open accelerating structures
[DE87-010540] 01 p0092 N88-10603
Current experiments in elementary particle physics
[DE87-013961] 02 p0231 N88-11456
Experimental nuclear physics
[DE87-014586] 02 p0231 N88-11459
Electron interactions with nuclei
[DE87-014587] 02 p0232 N88-11460
Saturn: A large area X-ray simulation accelerator
[DE87-012021] 02 p0233 N88-11472
Volume produced H(-),D(-) ion source for proton accelerator and thermo-nuclear fusion research by sheet plasma (III)
[IPPJ-838] 02 p0242 N88-115[illegible]1
The LPX (Long Pulse Experiment) facility
[DE87-010493] 03 p0311 N88-11964
A scientific workstation operator-interface for accelerator control
[DE87-014689] 03 p0362 N88-12278
Energy cascading in the beat-wave accelerator
[DE87-014727] 03 p0377 N88-12374
The role of basic research in society
[DE88-000459] 04 p0502 N88-13090
Experimental studies of elementary particle interactions at high energies
[DE88-000604] 05 p0648 N88-13971
The standard theory group: Summary and conclusions
[PREPRINT-551] 06 p0778 N88-14776
A possible accelerator experiment to solve the solar neutrino puzzle
[PREPRINT-556] 06 p0778 N88-14778
Collider constraints in the choices for wavelength and gradient scaling
[PB87-123691] 06 p0779 N88-14783
Simulation of effect on biological systems of impact wave from heavy charged particle track
07 p0896 N88-15429
Accelerators and Superconductivity: A Marriage of Convenience. Second John Adams Memorial Lecture
[DE88-700005] 07 p0931 N88-15656
High midplane accessibility stellarator windings for high current toroidal accelerators
[AD-A186235] 07 p0933 N88-15665
Design considerations for a negative ion source for DC operation of high-power, multi-megaelectron-volt neutral beams
[DE88-002692] 08 p1083 N88-16525
Solid antimatter
[PB87-166146] 09 p1259 N88-17549
The implementation of artificial intelligence in control systems
[DE88-003497] 10 p1396 N88-18318
The numerical simulation of accelerator components
[DE87-011597] 10 p1412 N88-18423
Incorporation of multigrid in accelerator software -- particle accelerators 11 p1539 N88-19199
Theory of elementary particle studies in weak iteration and grand unification and studies in accelerator design
[DE88-004261] 11 p1545 N88-19238
ZAP user's manual
[LBL-21270] 11 p1546 N88-19248
Initial operation of the Tevatron collider
[FNAL-TM-1449] 11 p1547 N88-19252
The CEBAF project and its few-body research program
[CEBAF-PR-87-014] 11 p1547 N88-19253
Mechanical design and construction of a 200 mA, 100 keV, dc, negative ion accelerator
[DE88-003855] 11 p1548 N88-19257
A practical guide to modern high energy particle accelerators
[DE88-004035] 11 p1548 N88-19260
Time-dependent Slow-Time-Scale theory of free-running and phase-locked gyrotron oscillators
[AD-A188910] 12 p1629 N88-19752
Development of electrostatic-accelerator free-electron lasers
[AD-A189507] 13 p1774 N88-20614
Collective acceleration of electrons and ions in a high relativistic electron beam
[DE88-005261] 13 p1838 N88-20896
Space experiments with particle accelerators (SEPAC): Description of instrumentation
[NASA-TM-89728] 14 p1945 N88-21606
Tutorial on computer control
[DE88-006185] 18 p2554 N88-25157
Computer programs for high-current beam transport in accelerators
[AD-A192356] 20 p2838 N88-26835

Superconducting rf and beam-cavity interactions
[DE88-008598] 20 p2852 N88-26936
Activities report of the Werner-Heisenberg Institute of Physics
[ETN-88-92946] 21 p3015 N88-27893

PARTICLE BEAMS
NT ATOMIC BEAMS
NT ELECTRON BEAMS
NT ION BEAMS
NT MOLECULAR BEAMS
NT NEUTRAL BEAMS
NT NEUTRINO BEAMS
NT NEUTRON BEAMS
NT PROTON BEAMS
NT RELATIVISTIC ELECTRON BEAMS
Status of inertial fusion
[DE87-010988] 01 p0099 N88-10654
Frozen-field, rigid-beam, uniform-conductivity-channel tracking force calculation
[DE87-012510] 02 p0190 N88-11190
Saturn: A large area X-ray simulation accelerator
[DE87-012021] 02 p0233 N88-11472
The LPX (Long Pulse Experiment) facility
[DE87-010493] 03 p0311 N88-11964
Single wire drift chamber design
[DE87-011002] 07 p0857 N88-15205
Physics and chemistry 07 p0883 N88-15359
Determination of beam orientation of optical diagnostics of excited 200-MeV hydrogen atoms resulting from photodetachment of H(-)ions
[AD-A189976] 14 p1981 N88-21823
Particle beam alignment system for single event upset-Van de Graaf experiments
[AD-A189695] 15 p2132 N88-22721
Utilization of dense packed planar acoustic echosounders to identify turbulence structure in the lowest levels of the atmosphere
[AD-A191006] 16 p2233 N88-23335
Bevalac external beamline optics
[LBL-23240] 19 p2727 N88-26194
Electron-impact-ionization and electron-attachment cross sections of radicals important in transient gaseous discharges
[AD-A192248] 20 p2770 N88-26424
Computer programs for high-current beam transport in accelerators
[AD-A192356] 20 p2836 N88-26835
Propagation of charged particle beams in the atmosphere
[AD-A193185] 21 p3014 N88-27887
Effects of charge distribution within a particle beam on the sub-Cerenkov radiation
[AD-A193992] 22 p3150 N88-28742
Beam optics test stand
[AD-A193901] 23 p3216 N88-29144
Moment invariants for particle beams
[DE88-011052] 23 p3281 N88-29537
Nonlinear analysis of non-neutral plasmas
[AD-A192506] 23 p3284 N88-29556
Cluster beam studies
[AD-A195182] 24 p3434 N88-30443

ARTICLE CHARGING
Combined aerodynamic size, charge-to-mass, and velocity measurements of aerosol particles
[ST-REPT-VOL-5-NO-4] 14 p1944 N88-21599

ARTICLE COLLISIONS
Relativistic heavy ion collisions
[DE87-014292] 02 p0232 N88-11462
A conceptual design of Final Focus Systems for linear colliders
[DE87-012840] 02 p0234 N88-11475
A relativistic Monte Carlo binary collision model for use in plasma particle simulation codes
[DE87-013287] 02 p0237 N88-11494
Nonequilibrium characteristics of nitrogen plasmas appropriate to an AOTV flight 03 p0319 N88-12019
Light scattering by oriented and randomly dispersed chiral particles
[DE87-014758] 03 p0376 N88-12368
W decays
[NOTA-INTERNA-877] 05 p0648 N88-13966
The kinetics and dynamics of iodine monofluoride formation in gas-phase collisions
[AD-A185715] 06 p0709 N88-14352
On the meteor trail spectra 06 p0737 N88-14533
Vector boson pair production in e(+)e(-) collisions
[PREPRINT-549] 06 p0778 N88-14774
Single weak gauge boson production at CLIC
[PREPRINT-550] 06 p0778 N88-14775
The standard theory group: Summary and conclusions
[PREPRINT-551] 06 p0778 N88-14776
Collider constraints in the choices for wavelength and gradient scaling
[PB87-123691] 06 p0779 N88-14783
Interaction of intense electromagnetic fields with SF/sub 6/ molecules and clusters in supersonic expansion
[DE88-700310] 07 p0846 N88-15132
Planetary science 07 p0883 N88-15356
Analysis of relativistic nucleus-nucleus interactions in emulsion chambers 07 p0926 N88-15624
Parton densities from deep inelastic scattering to hadronic processes at super collider energies
[NOTA-INTERNA-885] 07 p0930 N88-15646
Correlation effects on double electron capture in highly-charged, low-energy ion-atom collisions
[DE87-013179] 07 p0930 N88-15651
Study of tau pairs and search for new particles
[B8680488] 07 p0931 N88-15655
Resonance excitation in gamma gamma collisions at LEP200
[NIKHEF-H/87-3] 08 p1081 N88-16514
Status of cross section data for photon scattering by atoms
[DE87-011281] 08 p1081 N88-16517
Event classification in (anti)neutrino experiments using an Internal Picket Fence-External Muon Identifier (IPF-EMI) detector system
[NIKHEF-H/87-6] 09 p1245 N88-17457
Initial operation of the Tevatron collider
[FNAL-TM-1449] 11 p1547 N88-19252
Simulation of nuclear collisions at high energies in the frames of quark-gluon string model
[DE88-700914] 12 p1690 N88-20113
Fragmentation and flow in central collisions
[DE88-005386] 13 p1837 N88-20991
Hadronic overlap and total multiplicity distributions in high energy physics collisions
[NIKHEF-H/87-10] 13 p1838 N88-21001
The astrophysics of nebulae and active galactic nuclear emission-line regions: New methods and applications
13 p1858 N88-21111
Ground-state correlations in C12 and the mechanism of the (e,e'p) reaction
[B8729349] 14 p1980 N88-21816
Summary of supersymmetric particle search with the CELLO detector at Petra (Italy)
[NOTA-INTERNA-898] 14 p1980 N88-21818
Analysis of hadron production in deep inelastic muon-proton collisions through the fire-string model
[PREPRINT-578] 14 p1981 N88-21822
The silicon microstrip detector --- particle position measurement
[ETN-88-92235] 16 p2210 N88-23189
Ion generator and ion application system
[NASA-CASE-MFS-28122-1] 17 p2397 N88-24253
A new approach to generating negative ion beams
[AD-A191119] 18 p2572 N88-25276
Calorimetry applied to nucleus-nucleus collisions at ultrarelativistic energies
[DE88-006173] 18 p2573 N88-25282
Theoretical investigations of drift waves in a magnetic quadrupole 18 p2578 N88-25312
Heavy ion collisions with A = 10(sup 57): Aspects of nuclear stability and the nuclear equation of state in coalescing neutron-star binary systems
[DE88-008029] 19 p2741 N88-26277
Charged pion production and projectile breakup in 85A MeV(sup)12C induced heavy ion reactions
[LUIP-8802] 20 p2850 N88-26920

PARTICLE COUNTERS
U RADIATION COUNTERS

PARTICLE DECAY
U RADIOACTIVE DECAY

PARTICLE DENSITY (CONCENTRATION)
NT CARRIER DENSITY (SOLID STATE)
NT ELECTRON DENSITY (CONCENTRATION)
NT ELECTRON DENSITY PROFILES
NT ELECTRON DISTRIBUTION
NT ION DENSITY (CONCENTRATION)
NT IONOSPHERIC ELECTRON DENSITY
NT IONOSPHERIC ION DENSITY
NT MAGNETOSPHERIC ELECTRON DENSITY
NT MAGNETOSPHERIC ION DENSITY
NT PLASMA DENSITY
NT PROTON DENSITY (CONCENTRATION)
Design study for measurement of neutral hydrogen atom density by laser induced fluorescence method
[DE87-752964] 02 p0179 N88-11114
Performance and operating envelope of imaging and scattering particle sizing instruments
[NASA-CR-180859] 03 p0323 N88-12042
Restoration of particle pitch angle distribution functions by a maximum entropy algorithm
[ATR-86(7098)-3] 05 p0648 N88-13969
Parton densities from deep inelastic scattering to hadronic processes at super collider energies
[NOTA-INTERNA-885] 07 p0930 N88-15646
CAESAR investigations --- Coordinated Auroral Experiment using Scatter And Rockets (CAESAR)
08 p1031 N88-16249
Fluidization mechanisms in slurry flows
[DE88-005191] 13 p1766 N88-20563
Velocity and concentration measurements in flowing suspensions by nuclear magnetic resonance
[DE88-006225] 13 p1770 N88-20569
Dense-spray structure and phenomena. Part 1. Turbulence/dispersed-phase interactions
[AD-A190606] 15 p2065 N88-22315
Quantitative particle characterization by scattered ultrasound 20 p2848 N88-26908
The influence of ionization within a plasma opening switch
[AD-A193147] 21 p3017 N88-27906
Optical measurements of soot in premixed flames
[NASA-TM-101305] 24 p3373 N88-30090

PARTICLE DETECTORS
U RADIATION COUNTERS

PARTICLE DIFFUSION
NT IONIC DIFFUSION
Influence of a magnetic field on the diffusion of small particles in a turbulent flow
[DE87-702877] 01 p0046 N88-10291
Solar cosmic ray propagation in high-velocity solar wind stream 08 p1002 N88-16073
Investigations of the influence of chemical reactions of the vertical flow of gaseous and particulate compounds
08 p1017 N88-16165
Observation of injected silicon in heliotron E
17 p2441 N88-24524

PARTICLE EMISSION
NT ELECTRON EMISSION
NT FIELD EMISSION
NT ION EMISSION
NT NEUTRON EMISSION
NT PHOTOELECTRIC EMISSION
NT SECONDARY EMISSION
NT THERMIONIC EMISSION
Research in particles and fields
[NASA-CR-180412] 01 p0119 N88-10763
Single leptons from heavy quark production
[DE87-014917] 04 p0488 N88-13009
On the spatial structure of the Perseids meteor stream
06 p0740 N88-14550
WIPP (Wave Induced Particle Precipitation) experiment logistic support
[AD-A191184] 18 p2499 N88-24824
A theoretical determination of the density at a traveling source that emitts particles
[ISAS-RN-351] 21 p3013 N88-27883
Positron emission tomography: A new technique for observing fluid behavior in engineering systems
[PNR90471] 24 p3374 N88-30091

PARTICLE ENERGY
NT ELECTRON ENERGY
NT ELECTRON STATES
NT PROTON ENERGY
Cosmic-ray nuclear event with an anomalously strong concentration of energy and particles in the central region
[DE87-703376] 04 p0526 N88-13213
Inelastic two composite particle systems scattering at high energy
[DE88-701841] 20 p2851 N88-26928
The low-latitude auroral boundary: Steady-state and time-dependent representations
[AD-A193200] 21 p2972 N88-27656
Solar flares and magnetospheric particles: Investigations based upon the ONR-602 and ONR-604 experiments
[AD-A193396] 21 p3031 N88-27994

PARTICLE FLUX
U FLUX (RATE)

PARTICLE FLUX DENSITY
NT ELECTRON FLUX DENSITY
NT NEUTRON FLUX DENSITY
A processing method and results of meteor shower radar observations 06 p0738 N88-14539
Photographic fireball networks
06 p0738 N88-14540
A method of long-term radar shower data analysis
06 p0738 N88-14541
Incident meteoroid flux density
06 p0739 N88-14542
Models of sporadic meteor body distributions
06 p0739 N88-14543
On meteor stream spatial structure theory
06 p0739 N88-14544
Results of observations of the Eta Aquarid and Orionid meteor showers in 1980-1984 06 p0740 N88-14548
Structural peculiarities of the Quadrantid meteor shower 06 p0740 N88-14552

PARTICLE IN CELL TECHNIQUE
Trajectory versus PIC methods in diode design
[DE87-012135] 02 p0166 N88-11043
Numerical simulation of Tollmien-Schlichting waves by use of a modified vortex particle-in-cell method
[IC-AERO-85-02] 02 p0171 N88-11079

QUICKSILVER: A 3D, electromagnetic, PIC code
[DE87-013013] 02 p0245 N88-11547
FLIP (Fluid-Implicit-Particle): A low-dissipation, particle-in-cell method for fluid flow
[DE87-014745] 03 p0313 N88-11981
Performance and optimization of direct implicit time integration schemes for use in electrostatic particle simulation codes
[DE88-003254] 10 p1406 N88-18381
Development of Electromagnetic PIC code for LIB diode 16 p2276 N88-23622
Numerical simulation for particle acceleration and trapping by an electromagnetic wave
16 p2277 N88-23626
Two-dimensional focusing of self-magnetically insulated plasma focus diode 16 p2278 N88-23639
QN3D: A 3-dimensional quasi-neutral hybrid particle-in-cell code with applications to the tilt mode instability in field reversed configurations
18 p2580 N88-25325
Hybrid simulations
[DE88-009125] 19 p2715 N88-26123
Computer programs for high-current beam transport in accelerators
[AD-A192356] 20 p2838 N88-26835

PARTICLE INTERACTIONS
NT ELECTRON CAPTURE
NT ELEMENTARY PARTICLE INTERACTIONS
NT HIGH ENERGY INTERACTIONS
NT MOLECULAR COLLISIONS
NT MOLECULAR INTERACTIONS
NT NUCLEAR CAPTURE
NT NUCLEAR INTERACTIONS
NT NUCLEON-NUCLEON INTERACTIONS
NT PLASMA-PARTICLE INTERACTIONS
NT STRONG INTERACTIONS (FIELD THEORY)
NT WEAK ENERGY INTERACTIONS
NT WEAK INTERACTIONS (FIELD THEORY)
Relativisitic heavy ion collisions
[DE87-014292] 02 p0232 N88-11462
Superfluid He4 as a solar neutrino detector
[DE87-014477] 02 p0257 N88-11625
Momentum transport and particle dynamics in turbulent shear flows 03 p0317 N88-12002
On charm decays: Present status and future goals
[DE87-013586] 03 p0375 N88-12356
Particle physics and cosmology
[DE87-005400] 03 p0387 N88-12432
Future directions in interplays between particle and nuclear physics: Summary session
[DE87-011791] 04 p0489 N88-13013
The formation and thermochemical properties of multiligand complexes
[AD-A184935] 05 p0561 N88-13416
Feasibility study for gas-grain simulation facility
[NASA-CR-177488] 05 p0646 N88-13954
Mechanistic studies of polymeric samples exposed aboard STS 8
[NASA-CR-182364] 06 p0686 N88-14202
Analysis of relativistic nucleus-nucleus interactions in emulsion chambers 07 p0926 N88-15624
Nuclear structure at intermediate energies
[DE88-002796] 10 p1407 N88-18390
Kinetic and turbulence models for granular and two-phase flows 11 p1484 N88-18862
Channeling and dechanneling at high energy
[DE88-003989] 11 p1548 N88-19259
Big Bang Nucleosynthesis: Accelerator tests and can (UC OMEGA)(sub B) really be large
[DE88-003405] 11 p1570 N88-19396
Theoretical studies in few-body intermediate energy physics
[DE88-004101] 12 p1689 N88-20106
On (e,e'N) reactions
[CEBAF-PR-87-028] 12 p1690 N88-20109
Research in high energy elementary particle physics
[DE88-006065] 13 p1837 N88-20994
Quark core stars, quark stars and strange stars
[DE88-006991] 17 p2450 N88-24555
Calorimetry applied to nucleus-nucleus collisions at ultrarelativistic energies
[DE88-006173] 18 p2573 N88-25282
Atomic processes in matter-antimatter interactions
[DE88-008911] 19 p2723 N88-26172
Electron-positron physics at 1 TeV
[DE88-009019] 19 p2725 N88-26180
Mechanisms for particle acceleration: Possibilities and constraints
[PB88-102538] 19 p2725 N88-26184
Ion and electron interactions of atmospheric importance
[AD-A192255] 20 p2824 N88-26751
Charged pion production and projectile breakup in 85A MeV(sup)12C induced heavy ion reactions
[LUIP-8802] 20 p2850 N88-26920
Comparison of exclusive reactions at large momentum transfer
[DE88-007544] 20 p2851 N88-26922
Inelastic two composite particle systems scattering at high energy
[DE88-701841] 20 p2851 N88-26928
Recoil saturation of the self-energy in atomic systems
[DE88-010450] 20 p2851 N88-26930
Self-energies and the interactions of particles with surfaces
[DE88-010451] 21 p3014 N88-27885
Quark nuclear model: Classification groups and two and three body correlations
[NOTA-INTERNA-896] 21 p3014 N88-27891
Study of the production of Ko mesons in proton antiproton interactions at 630 GeV
[NOTA-INTERNA-908] 21 p3015 N88-27892
Study of superconducting properties in some many valley semiconductors
[DE88-702325] 23 p3291 N88-29583

PARTICLE LADEN JETS
On the periodic southward jets of Comet Halley before perihelion passage 14 p2008 N88-21978

PARTICLE MASS
Performance and operating envelope of imaging and scattering particle sizing instruments
[NASA-CR-180859] 03 p0323 N88-12042
On the spatial structure of the Perseids meteor stream
06 p0740 N88-14550
Scalar densities and baryon mass differences in lattice QCD with Wilson fermions
[PREPRINT-544] 06 p0778 N88-14773
A theoretical model for neutrino masses and mixing
[PREPRINT-553] 06 p0778 N88-14777
The paradoxical asymptotic status of massless springs
[AD-A185625] 07 p0928 N88-15637
Properties of nuclei and elementary particles at low and intermediate energies
[DE88-001913] 09 p1244 N88-17456
Measurements of gas turbine combustor and engine augmentor tube sooting characteristics
[AD-A187831] 11 p1440 N88-18592
The origin of low mass particles within and beyond the dust coma envelopes of Comet Halley
14 p2002 N88-21938
Theory of quark mixing matrix and invariant functions of mass matrices
[USIP-87-14] 22 p3159 N88-28800

PARTICLE MOTION
New directions in Vlasov plasma turbulence and anomalous transport
[DE87-014425] 02 p0238 N88-11500
Elements of plasma physics 03 p0271 N88-11703
A simplified approach to the dynamics of charged particles in the magnetosphere
03 p0273 N88-11718
Stochastic model of the motion of suspended particles in turbulent flow
[HSBW-MITT-21/1987] 03 p0315 N88-11990
Wave functions for bound states of relativistic electrons in a crystal at electron movement along crystallographic planes
[DE88-700563] 07 p0939 N88-15708
Nonlinear diffusion in the presence of a time-dependent external electric field
[INPE-4378-PRE/1198] 08 p1085 N88-16533
Introductory review: Physics of electron slowing-down processes
[DE88-002918] 09 p1248 N88-17466
Dynamics of coupled electron-nucleon motion in a laser field
[DE88-005063] 10 p1337 N88-17994
Energetic particle drift motions in the outer dayside magnetosphere
[DE88-005097] 11 p1512 N88-19034
Theory of laser cooling and spectroscopy of harmonically trapped single atoms
[AD-A189576] 13 p1775 N88-20617
Fragmentation and flow in central collisions
[DE88-005386] 13 p1837 N88-20991
Comparison of analytic and full guiding center behavior at a trapped-passing interface in stellarators
[DE88-004174] 13 p1842 N88-21025
Free Laplacian with attractive boundary conditions
[DE87-702971] 16 p2256 N88-23482
Electrical resistivity as quantum chaos
[DE88-007026] 16 p2284 N88-23675
Muon motion in titanium hydride
17 p2396 N88-24247
Optical guiding in the separable beam limit
[AD-A192452] 21 p2952 N88-27534
Regular and chaotic motion of fluid particles in a two dimensional fluid
[PREPRINT-591] 22 p3078 N88-28278
Application of optical correlation techniques to particle imaging velocimetry
[NASA-TM-101306] 23 p3218 N88-29152

PARTICLE PRECIPITATION
NT ELECTRON PRECIPITATION
Electrodynamics of midnight sector of auroral oval in period of slight disturbance 08 p1003 N88-16077
Formation of nuclei during precipitation in metallic mixed crystals
[NASA-TT-20248] 13 p1745 N88-20437
Stimulated Emission of Energetic Particles (SEEP)
[AD-A188724] 13 p1853 N88-21094
The precipitation of energetic heavy ions into the upper atmosphere of Jupiter
[NASA-TM-101155] 17 p2452 N88-24565
WIPP (Wave Induced Particle Precipitation) experiment logistic support
[AD-A191184] 18 p2499 N88-24824
The low-latitude auroral boundary: Steady-state and time-dependent representations
[AD-A193200] 21 p2972 N88-27656
Solar flares and magnetospheric particles: Investigations based upon the ONR-602 and ONR-604 experiments
[AD-A193396] 21 p3031 N88-27094

PARTICLE PRODUCTION
NT PAIR PRODUCTION
Single weak gauge boson production at CLIC
[PREPRINT-550] 06 p0778 N88-14775
The standard theory group: Summary and conclusions
[PREPRINT-551] 06 p0778 N88-14776
Production by pyrolysis of diffusion particles for velocimetry in shock tubes
[ISL-R-119/86] 11 p1456 N88-18671
Theoretical studies in few-body intermediate energy physics
[DE88-004101] 12 p1689 N88-20106
Simulation of nuclear collisions at high energies in the frames of quark-gluon string model
[DE88-700914] 12 p1690 N88-20113
Physics at large transverse momenta
[DE88-005758] 13 p1836 N88-20986
New limits on charged Higgs boson mass with CELLO at Petra (Italy) and status of the neutral Higgs boson search
[NOTA-INTERNA-897] 14 p1980 N88-21817
Analysis of hadron production in deep inelastic muon-proton collisions through the fire-string model
[PREPRINT-578] 14 p1981 N88-21822
The dust tail of Comet Halley
14 p2008 N88-21974
The role of electron-ion recombination in bulk antimatter production 16 p2268 N88-23567
Electromagnetic manipulation of atomic hydrogen
16 p2268 N88-23568
Production of heavy antinuclei: Review of experimental results 16 p2269 N88-23574
Subthreshold pion production in proton induced reactions at 180 to 201 MeV and He3 at 283 MeV
[ETN-88-92303] 17 p2397 N88-24250
Experimental elementary particle physics
[DE88-007510] 18 p2572 N88-25274
Charged pion production and projectile breakup in 85A MeV(sup)12C induced heavy ion reactions
[LUIP-8802] 20 p2850 N88-26920
Hadrons produced in atmospheric interactions
[DE88-702492] 23 p3309 N88-29712

PARTICLE SIZE DISTRIBUTION
Optical sizing of soot in gas turbine combustors and exhaust augmentor tubes
[AD-A183785] 01 p0006 N88-10034
The effect of RDX particle size on the shock sensitivity of cast PBX formulations. 2: Bimodal compositions
[DE87-009581] 01 p0031 N88-10198
Performance and operating envelope of imaging and scattering particle sizing instruments
[NASA-CR-180859] 03 p0323 N88-12042
Experimental and theoretical study of condensation in multicomponent mixtures
[DE88-000897] 04 p0413 N88-12563
Experiments on densely-loaded non-Newtonian slurries in laminar and turbulent pipe flows
[DE88-000719] 04 p0442 N88-12746
Operating envelopes of particle sizing instrumentation used for icing research
[NASA-CR-180870] 05 p0586 N88-13573
The application of doubly-truncated hydrometeor distributions to numerical cloud models
[AD-A185273] 05 p0627 N88-13636
Measurement of particle size distribution in a solid propellant rocket motor using light scattering
[AD-A184875] 06 p0673 N88-14124
An analysis of the effect of system variables on the quality of thin films and powders produced by laser-breakdown chemical vapor deposition
[DE88-001793] 06 p0708 N88-14342

Results of observations of the Eta Aquarid and Orionid meteor showers in 1980-1984 06 p0740 N88-14548

Radar observations of changes in precipitation size spectra associated with lightning
06 p0744 N88-14576

An aureolar radiometer for the determination of aerosol size distribution 08 p1018 N88-16174

Aerosol size distribution from measurements of the radiance in the solar aureole 08 p1019 N88-16176

Mechanisms of wear in single- and two-phase materials
[DE88-003846] 10 p1305 N88-17806

Turbulence interactions in single- and multi-phase turbulent mixing and combustion processes
[AD-A187505] 10 p1332 N88-17960

Measurements of gas turbine combustor and engine augmentor tube sooting characteristics
[AD-A187831] 11 p1440 N88-18592

Measurements of particulates in solid propellant rocket motors
[AD-A187777] 11 p1446 N88-18621

Measurement of combustion aerosol size distributions with multistage inertial impactors
[DE88-751101] 11 p1454 N88-18669

Diagnostics for research in atomization and turbulent two-phase flows
[AD-A187338] 11 p1482 N88-18843

Vertical structure of Venusian cloud layer at landing sites of Vega-1 and Vega-2 vehicles
13 p1725 N88-20317

Erosion in dual-phase microstructures
[DE88-004507] 13 p1743 N88-20421

Characterization and fundamental studies on CuO sorbent materials to determine attrition mechanisms on substrate gamma alumina
[DE88-003674] 13 p1749 N88-20456

Processing of nanophase ceramics
[DE88-005985] 13 p1752 N88-20475

Combined aerodynamic size, charge-to-mass, and velocity measurements of aerosol particles
[ST-REPT-VOL-5-NO-4] 14 p1944 N88-21599

Optical and hydrodynamic implications of Comet Halley dust size distribution 14 p2003 N88-21939

The evolution of the mass distribution of cometary particles 14 p2004 N88-21946

Transient compressible flow in porous materials
[DE88-006685] 15 p2067 N88-22324

Research on certain aspects of laser diffraction particle sizing relevant to autonomous self-diagnosing instrumentation
[AD-A190220] 15 p2071 N88-22348

The interaction of small particles with laser beams
[AD-A190716] 15 p2072 N88-22354

Obtaining information on cloud particles by a commercial miniature camera
[DFVLR-MITT-87-19] 16 p2234 N88-23342

Fog, rain and aerosol attenuation in the atmosphere
[AD-A190867] 16 p2235 N88-23350

Method of evaporation
[NASA-CASE-NPO-15609-2] 17 p2318 N88-23846

Transient particle deposition in a boundary layer of impulsive flow over a flat plate
[AD-A191537] 18 p2508 N88-24880

The 24th JANNAF Combustion Meeting, volume 1
[AD-A190163] 19 p2627 N88-25585

A review of particle sizing methods in rocket propulsion 19 p2630 N88-25597

Measurement of particulate size in solid propellant rocket motors 19 p2630 N88-25599

Instantaneous two-dimensional multiple particle sizing diagnostic 19 p2630 N88-25600

The preparation of mechanically alloyed powders for TEM (Transmission Electron Microscopy) examination
[DE88-008043] 20 p2775 N88-26460

Numerical modeling of the effect of particle size of explosives on shock initiation properties
[DE88-010479] 20 p2780 N88-26491

Preparation and properties of high Q microwave dielectrics in the (CA, SR, BA) zirconate system
[AD-A193127] 21 p2918 N88-27317

Real-time measurements of the size fractionation of ambient black carbon aerosols at elevated humidities
[DE88-010870] 23 p3215 N88-29138

Automatic data retrieval from rocket motor holograms
[AD-A195586] 24 p3337 N88-29864

Simulation study of spraying, streaming and vaporization phenomena associated with fuel injection
24 p3345 N88-29914

Turbulence effects on the droplet distribution behind airblast atomizers 24 p3346 N88-29915

Multiple scattering effects in drop sizing of dense fuel sprays by laser diffraction 24 p3346 N88-29917

Influence of operating conditions on the atomization and distribution of fuel by air blast atomizers
24 p3346 N88-29918

Particle size measurements in sooting combustion systems 24 p3348 N88-29931

Particle sizing in combustion systems, using scattered laser light
[AD-A196231] 24 p3352 N88-29953

Optical measurements of soot and temperature profiles in premixed propane-oxygen flames
[NASA-TM-101343] 24 p3358 N88-29997

Optical measurements of soot in premixed flames
[NASA-TM-101305] 24 p3373 N88-30090

Evaluation of the potential health hazards associated with the machining of carbon fiber composites
[AD-A194835] 24 p3408 N88-30286

PARTICLE SPIN
NT ISOTOPIC SPIN
NT NUCLEAR SPIN

Developments related to scattering eigen elements in Schroedinger operators for particles with spin
[ETN-88-91077] 09 p1229 N88-17361

PARTICLE TELESCOPES

Design, fabricate, calibrate, test and deliver two satellite electron flux detectors
[AD-A190799] 16 p2169 N88-22930

PARTICLE THEORY

Research program in elementary particle theory
[DE88-000159] 02 p0233 N88-11468

On charm decays: Present status and future goals
[DE87-013586] 03 p0375 N88-12356

Plasma theory and simulation
[AD-A187100] 09 p1249 N88-17486

Laser fluorescence velocimeter
[AD-A189010] 12 p1630 N88-19753

Theory of laser cooling and spectroscopy of harmonically trapped single atoms
[AD-A189576] 13 p1775 N88-20617

Particle physics and cosmology
[DE88-004944] 13 p1854 N88-21096

Summary of supersymmetric particle search with the CELLO detector at Petra (Italy)
[NOTA-INTERNA-898] 14 p1980 N88-21818

Renormalized Fermi liquid theory for disordered electron systems and the metal-insulator transition
[NOTA-INTERNA-900] 14 p1988 N88-21862

Particle cosmology comes of age
[DE88-006998] 15 p2151 N88-22844

Material void opening computation using particle method
[DE88-010950] 19 p2680 N88-25936

Analysis of transverse strength of composites using percolation theory
[AD-A193204] 21 p2904 N88-27234

Quark nuclear model: Classification groups and two and three body correlations
[NOTA-INTERNA-896] 21 p3014 N88-27891

PARTICLE TRACKS

Some new ideas in liquid detectors
[DE88-000732] 04 p0446 N88-12768

Dynamics of meteor streams
06 p0732 N88-14503

Scanning and measuring peculiarities with high-space resolution objects recorded at the Gabor holograms
[DE88-700373] 07 p0857 N88-15203

Algorithm and program for recognition of compactly positioned vertices of events for the HPD minimum guidance system
[DE88-700542] 07 p0905 N88-15482

An analytic model for ionization distributions produced in nanometer sites by protons
[DE88-003943] 10 p1406 N88-18385

Measuring accuracy of 3-dimensional bodies by the GOMER-1 device
[DE87-703230] 12 p1626 N88-19744

HNC: A detector to study ultraheavy cosmic rays
12 p1713 N88-20252

MIG-1 on-line measuring holographic microscope
[DE88-701103] 15 p2068 N88-22332

Flow velocity measurements by image processing of optically modulated traces 16 p2203 N88-23147

Optical system of laser illuminated streamer chamber
[DE88-702127] 18 p2577 N88-25306

Application of optical correlation techniques to particle imaging velocimetry
[NASA-TM-101306] 23 p3218 N88-29152

PARTICLE TRAJECTORIES
NT ELECTRON TRAJECTORIES

Influence of a magnetic field on the diffusion of small particles in a turbulent flow
[DE87-702877] 01 p0046 N88-10291

Use of back air trajectories in interpreting atmospheric chemistry data: A review and bibliography
[PB88-102108] 07 p0876 N88-15312

Particle transport in microdetonations — inertial confinement fusion pellets
[OEFZS-4402] 09 p1164 N88-16976

Particle-dynamics calculations of gravity flow of inelastic, frictional spheres
[DE88-005224] 13 p1770 N88-20586

Studies of heat and mass transfer during chemical vapor deposition 17 p2338 N88-23953

Centrifugal acceleration of ions in the polar magnetosphere
[NASA-TM-101148] 17 p2374 N88-24120

Gone with the solar wind: A study of protons accelerated by interplanetary shocks 19 p2743 N88-26263

Particle trajectories and potentials in a plane sheath moving in a magnetoplasma
[AD-A196228] 24 p3390 N88-30190

PARTICLES
NT AEROSOLS
NT ALPHA PARTICLES
NT ANTINEUTRINOS
NT ANTINUCLEONS
NT ANTIPARTICLES
NT ANTIPROTONS
NT ARGON PLASMA
NT BARYONS
NT BETA PARTICLES
NT BOSONS
NT BOUNDARY LAYER PLASMAS
NT CESIUM PLASMA
NT CHARGED PARTICLES
NT COLD PLASMAS
NT COLLISIONAL PLASMAS
NT COLLISIONLESS PLASMAS
NT CONDUCTION ELECTRONS
NT CORPUSCULAR RADIATION
NT COSMIC DUST
NT COSMIC PLASMA
NT CYLINDRICAL PLASMAS
NT DENSE PLASMAS
NT DEUTERIUM PLASMA
NT DEUTERONS
NT DROPS (LIQUIDS)
NT DUST
NT ELECTRON BEAMS
NT ELECTRON PLASMA
NT ELECTRON PRECIPITATION
NT ELECTRON-POSITRON PAIRS
NT ELECTRONS
NT ELEMENTARY PARTICLES
NT ENERGETIC PARTICLES
NT EVEN-EVEN NUCLEI
NT FAST NEUTRONS
NT FERMIONS
NT FINES
NT FOG
NT FREE ELECTRONS
NT GLUONS
NT GRAVITONS
NT HADRONS
NT HEAVY NUCLEI
NT HELIUM PLASMA
NT HIGH ENERGY ELECTRONS
NT HIGH TEMPERATURE PLASMAS
NT HOT ELECTRONS
NT HYDROGEN PLASMA
NT HYPERNUCLEI
NT INNER RADIATION BELT
NT INTERPLANETARY DUST
NT IONIZED GASES
NT KAONS
NT LASER PLASMAS
NT LEPTONS
NT MAGNETIC CLOUDS
NT MAGNETICALLY TRAPPED PARTICLES
NT MESON RESONANCE
NT MESONS
NT METAL PARTICLES
NT METAL POWDER
NT METALLIC PLASMAS
NT MICROPARTICLES
NT MIST
NT MUONS
NT NEUTRAL PARTICLES
NT NEUTRINOS
NT NEUTRONS
NT NITROGEN PLASMA
NT NONEQUILIBRIUM PLASMAS
NT NONUNIFORM PLASMAS
NT NUCLEAR PARTICLES
NT NUCLEI (NUCLEAR PHYSICS)
NT NUCLEONS
NT ODD-ODD NUCLEI
NT OXYGEN PLASMA
NT PARTICULATES
NT PARTONS
NT PHOTOELECTRONS
NT PHOTONS
NT PIONS
NT PLASMA CLOUDS

NT PLASMA FOCUS
NT PLASMA JETS
NT PLASMA LAYERS
NT PLASMA SHEATHS
NT PLASMAS (PHYSICS)
NT POLARONS
NT POLLEN
NT POSITRONS
NT POWDER (PARTICLES)
NT POWDERED ALUMINUM
NT PRIMARY COSMIC RAYS
NT PROTONS
NT QUARKS
NT RADIATION BELTS
NT RADIO JETS (ASTRONOMY)
NT RAINDROPS
NT RELATIVISTIC ELECTRON BEAMS
NT RELATIVISTIC PARTICLES
NT RELATIVISTIC PLASMAS
NT ROTATING PLASMAS
NT SEMICONDUCTOR PLASMAS
NT SINTERED ALUMINUM POWDER
NT SOLAR COSMIC RAYS
NT SOLAR ELECTRONS
NT SOLAR NEUTRINOS
NT SOLAR NEUTRONS
NT SOLAR PROTONS
NT SOLAR WIND
NT SOOT
NT SPACE PLASMAS
NT SPHERICAL PLASMAS
NT STELLAR WINDS
NT STRONGLY COUPLED PLASMAS
NT TERRESTHIAL DUST BELT
NT THERMAL NEUTRONS
NT THERMAL PLASMAS
NT TOROIDAL PLASMAS
NT TRAPPED PARTICLES
NT TRITONS
NT ZODIACAL DUST

Redistribution of particulates in shuttle bay during launch 02 p0133 N88-10837
Shear stress cleaning for surface departiculation
02 p0134 N88-10838
Particle velocity and stress gage measurements in spherical diverging flow
[DE87-007333] 03 p0321 N88-12033
Particle physics and cosmology
[DE87-005400] 03 p0387 N88-12432
Activities at government research laboratories reported 04 p0403 N88-12503
Use of a thermodynamic analog for pneumatic transport in horizontal pipes
[AD-A184076] 04 p0441 N88-12740
Plume mechanics and aerosol growth processes
[AD-A184467] 04 p0442 N88-12742
Experimental and analytic studies of the triggered lightning environment of the F106B
[NASA-CR-4104] 04 p0469 N88-12897
Separable orthogonal coordinates and particle creation for an accelerating observer
[DE87-703358] 05 p0657 N88-14029
Theoretical and numerical analysis of shock wave propagation through different dusty-gas mixture layers
06 p0699 N88-14292
Nature and the nonlinear evolution of electrostatic waves associated with the AMPTE (Active Magnetosphere Particle Tracer Explorers) solar wind releases
[AD-A185471] 06 p0806 N88-14920
Microgravity Particle Research on the Space Station
[NASA-CP-2496] 07 p0883 N88-15354
Astrophysics and the solar nebula
07 p0883 N88-15355
Planetary science 07 p0883 N88-15356
Physics and chemistry 07 p0883 N88-15359
Characterizing particle combustion in a Rijke burner
[AD-A186157] 08 p0966 N88-15847
Spray deposition: A fundamental study of droplet impingement, spreading and consolidation
[AD-A186627] 08 p0970 N88-15869
The morphology of emulsion polymerized latex particles
[DE88-002672] 08 p0972 N88-15879
Christiansen effect in infrared spectra of soil-derived atmospheric dusts
[AD-A187071] 09 p1248 N88-17479
Optimization of volume produced H(-) ions in a low-pressure hydrogen plasma
[IPPJ-853] 09 p1252 N88-17505
Ice-shelf response to ice-stream discharge fluctuation. Part 1: Unconfined ice tongues
[AD-A188147] 10 p1358 N88-18117
Dynamical and photometric studies of Saturn's rings
12 p1711 N88-20241
Global mixed-layer natural and anthropogenic fluxes
13 p1807 N88-20803
Double layer polarization of nonconducting spheroidal particles and its application to Kerr effect
[ISSN-0208-5658] 13 p1832 N88-20960
Mechanical behaviour of particle filled thermoplastics
[PB88-169297] 15 p2047 N88-22196
The interaction of small particles with laser beams
[AD-A190716] 15 p2072 N88-22354
Hybrid particle simulation for focusing of rotating and propagating LIB 16 p2276 N88-23624
On the efficient implementation of the fast multipole algorithm
[AD-A191167] 17 p2385 N88-24173
Particle-laden weakly swirling free jets: Measurements and predictions
[NASA-TM-100920] 18 p2466 N88-24639
Application of particle simulations to the NRL laser experiment
[AD-A191641] 18 p2520 N88-24953
Modelling of thermal plasma systems
18 p2576 N88-25314
Aerodynamic focusing of particles and heavy molecules
[DE88-007145] 19 p2596 N88-25440
Laser measurement of particle velocities in vacuum plasma spray deposition
[DE88-007111] 19 p2728 N88-26196
The influence of foreign particles on bearing metals
[NASA-TT-20155] 20 p2775 N88-26454
Reducing adhesion and agglomeration within a cloud of combustible particles
[NASA-TM-100902] 20 p2788 N88-26539
Research in theoretical particle physics
[DE88-008230] 20 p2851 N88-26927
On linear relationship between shock velocity and particle velocity
[DE88-701827] 20 p2880 N88-27099
Matrix substructuring, domain decomposition and particle methods: Current trends for solving PDEs in parallel
[DE88-009826] 21 p3007 N88-27836
Theoretical and experimental investigations on the structure of stationary shock waves in gas particle dispersions
[ETN-88-92983] 23 p3213 N88-29122
Theoretical particle physics
[DE88-011499] 23 p3295 N88-29621

PARTICULATE FILTERS
U FLUID FILTERS

PARTICULATE SAMPLING
Comparison of three aerosol sampling techniques and the differences in the nitrate determined by each
[DE87-011456] 03 p0348 N88-12200
Results from a questionnaire on particulate metrology in the UK
[NPL-MOM-81] 09 p1141 N88-16841
Measurement of combustion aerosol size distributions with multistage inertial impactors
[DE88-751101] 11 p1454 N88-18669

PARTICULATES
NT SOOT
Thermoplastic elastomers as LOVA binders
[AD-A185864] 07 p0835 N88-15067
Non-steady group combustion of a cloud of char particles
[DE87-010773] 08 p0966 N88-15849
A holographic investigation of particulates in metallized solid fuel ramjet combustion
[AD-A186687] 09 p1140 N88-16831
Surface acoustic wave deposition sensor
[DE87-006527] 09 p1243 N88-17452
Numerical simulation of near-surface environments and particulate clouds generated by large-area fires
[AD-A188375] 12 p1641 N88-19828
Interaction of particulate and transformation toughening
[AD-A189321] 13 p1741 N88-20412
Cavitation inception
[AD-A189220] 13 p1765 N88-20557
Production and turnover of suspended organic detritus in the coastal water of the southeastern continental shelf
[DE88-005118] 14 p1951 N88-21631
Theoretical prediction of single phase turbulent flow distribution in particulate bed reactors
17 p2419 N88-24386
Space station particulate contamination environment
18 p2591 N88-25397
The particulate environment surrounding the space station: Estimates from the PACS data
18 p2591 N88-25398
Effects of meteoroids and space debris on the particulate environment for space station 18 p2591 N88-25399
Analysis of debris from accelerated life test of the Hughes five-year Vuilleumier cryocooler
[AD-A193101] 21 p2931 N88-27400
The distribution of some chemical elements between dissolved and particulate phases in the ocean
[DE88-010181] 21 p2977 N88-27682

PARTITIONS (MATHEMATICS)
A multiple-time-scale turbulence model based on variable partitioning of turbulent kinetic energy spectrum
[NASA-CR-179222] 04 p0444 N88-12754
An emulation tool for simulating matrix operations on an SIMD (Single Instruction Multiple Data stream) multiprocessor
[AD-A188654] 12 p1678 N88-20030
Multiextremal optimization via adaptive partition algorithms
[REPT-87-44] 14 p1957 N88-21664
Graph labelings
[AD-A189649] 14 p1964 N88-21722
The global convergence of partitioned BFGS on problems with convex decompositions and Lipschitzian gradients
[DE88-006249] 14 p1968 N88-21744
Life prediction modeling based on strainrange partitioning 15 p2084 N88-22425
Some properties of modular equations and the partition function 18 p2564 N88-25224
Partitioning of regular computation on multiprocessor systems
[NASA-CR-183176] 22 p3141 N88-28676

PARTONS
Parton densities from deep inelastic scattering to hadronic processes at super collider energies
[NOTA-INTERNA-885] 07 p0930 N88-15646

PARTS
U COMPONENTS

PASCAL (PROGRAMMING LANGUAGE)
Comparison of pascal and the dBASE 3 PLUS language in programming an inventory management system
[AD-A184027] 03 p0365 N88-12300
Validation tests for standard PASCAL and extented PASCAL
[NPL-DITC-108/88] 22 p3139 N88-28863
Modularity in the PASCAL model compiler
[NPL-DITC-111/88] 22 p3139 N88-28864
Appraisal of prototype PASCAL program validation suite
[NPL-DITC-112/88] 22 p3139 N88-28865

PASSAGEWAYS
NT TRANSFER TUNNELS
Personnel occupied woven envelope robot power
[NASA-CR-182367] 07 p0856 N88-15196

PASSENGER AIRCRAFT
NT A-300 AIRCRAFT
NT A-320 AIRCRAFT
NT BO-105 HELICOPTER
NT BOEING 737 AIRCRAFT
NT BOEING 747 AIRCRAFT
NT CH-46 HELICOPTER
NT DO-28 AIRCRAFT
NT EUROPEAN AIRBUS
NT F-27 AIRCRAFT
NT VC-10 AIRCRAFT
Summary report of the history and events pertinent to the Civil Aeromedical Institute's evaluation of providing smoke/fume protective breathing equipment for airline passenger use
[AD-A184499] 03 p0261 N88-11645
Contribution to the improvement of the guidance accuracy of automatic pilots
[ETN-88-90607] 05 p0551 N88-13380
The intelligent wing. Aerodynamic development direction for future passenger aircraft
[MBB-UT-006/87] 10 p1313 N88-17848
Presentation of Class 1 designs for a family of commuter airplanes
[NASA-CR-182563] 11 p1439 N88-18587
Presentation of structural component designs for the family of commuter airplanes
[NASA-CR-182568] 12 p1581 N88-19463
A class 2 weight assessment for the implementation of commonality and preliminary structural designs for the family of commuter airplanes
[NASA-CR-182565] 12 p1581 N88-19464
Advanced proplan analysis for the family of commuter airplanes
[NASA-CR-182566] 12 p1582 N88-19468
Presentation of flight control design and handling quality commonality by separate surface stability augmentation for the family of commuter airplanes
[NASA-CR-182567] 12 p1583 N88-19471
A cost analysis for the implementation of commonality in the family of commuter airplanes, revised
[NASA-CR-182569] 12 p1706 N88-20221
In-service measurements of SAAB SF-340 landing gear loads
[FFA-TN-1987-48] 15 p2018 N88-22032

Class 2 design update for the family of commuter airplanes
[NASA-CR-182681] 18 p2464 N88-24629
Enhanced emergency smoke venting
[DOT/FAA/CT-88/22] 20 p2756 N88-26350
A contribution to the quantitative analysis of the influence of design parameters on the optimal design of passenger aircraft
[ETN-88-02979] 23 p3176 N88-28912

PASSENGERS
Aviation security: FAA (Federal Aviation Administration) needs preboard passenger screening performance standards
[PB87-216800] 02 p0124 N88-10783
Summary report of the history and events pertinent to the Civil Aeromedical Institute's evaluation of providing smoke/fume protective breathing equipment for airline passenger use
[AD-A184499] 03 p0261 N88-11645
Design, development and trials of an airline passenger telephone system 19 p2646 N88-25704

PASSIVATION
U PASSIVITY

PASSIVE SATELLITES
NT LAGEOS (SATELLITE)
Comparative analysis of passive communications satellites employing the SHF and HF spectrum for use in a strategic role
[AD-A194682] 24 p3362 N88-30019

PASSIVITY
Wide bandgap passivation layers on silicon
[DE87-014307] 02 p0244 N88-11543
A review of pitting corrosion in high temperature aqueous solutions
[DE88-003547] 10 p1302 N88-17787
Corrosion, passivity and breakdown of alloys used in high energy density batteries
[DE88-004891] 13 p1743 N88-20422
Experimental and theoretical investigation of passive damping concepts for member forced and free vibration
[NASA-CR-183082] 20 p2814 N88-26693

PASTES
Cement paste matrix composite materials center
[AD-A188657] 15 p2028 N88-22083

PATENT APPLICATIONS
Navigation system for land vehicles
[NASA-CASE-LAR-13322-1] 18 p2462 N88-24620
Airplane runway performance monitoring system
[NASA-CASE-LAR-13854-1-CU]
18 p2462 N88-24621
Nozzle fabrication technique
[NASA-CASE-MSC-21299-1] 18 p2475 N88-24684
Dual-fuel, dual-mode rocket engine
[NASA-CASE-LAR-13773-1] 18 p2475 N88-24685
Energy efficient continuous flow ash lockhopper
[NASA-CASE-NPO-16985-1-CU]
18 p2497 N88-24814
Low temperature storage container for transporting perishables to space station
[NASA-CASE-MFS-28248-1] 18 p2498 N88-24817
Noncontact temperature pattern measuring device
[NASA-CASE-NPO-17024-1-CU]
18 p2519 N88-24943
Atmospheric autorotating imaging device
[NASA-CASE-NPO-17390-1-CU]
18 p2519 N88-24944
Universal precision sine bar attachment
[NASA-CASE-MFS-28253-1] 18 p2523 N88-24971
Trailer shield assembly for a welding torch
[NASA-CASE-MFS-29260-1] 18 p2524 N88-24972
Radio Frequency (RF) strain monitor
[NASA-CASE-LAR-13705-1] 18 p2530 N88-25011
Optical pressure sealing couping (light joint)
[NASA-CASE-MFS-29348-1] 18 p2576 N88-25303
Crystal growth apparatus
[NASA-CASE-MFS-28182-1] 18 p2585 N88-25357
Ultrasonic method and apparatus for determining crack opening load
[NASA-CASE-LAR-13889-1] 24 p3385 N88-30160

PATENT POLICY
Identifying areas of leading edge Japanese science and technology: Activity analysis using SIC (Standard Industrial Classes) categories and scientific subfields
[PB87-204087] 02 p0249 N88-11574
Identifying areas of leading edge Japanese science and technology: Patent activity and citation analysis using US POC (Patent Office Classification) classification
[PB87-204095] 02 p0249 N88-11575
Thixotropic surface composition for phenolaldehyde resin laminates
[GB-PATENT-2-180-251-A] 04 p0410 N88-12545
Thermoplastic elastomer compositions --- cable jackets
[EP-PATENT-0-204-453-A1] 04 p0418 N88-12593
Detection of defects on structures
[EP-PATENT-0-210-794-A2] 04 p0453 N88-12807
Core material --- honeycombs
[EP-PATENT-0-196-926-A2] 05 p0558 N88-13393
Antistatic coating compositions
[GB-PATENT-2-177-413-A] 05 p0568 N88-13463
Flame retardant phenolic foams
[EP-PATENT-0-223-489-A2] 05 p0568 N88-13464
Process for the production of a thermoplastic elastomer composition
[EP-PATENT-0-202-782-A2] 05 p0569 N88-13465
Optical probe
[EP-PATENT-0-210-869-A1] 05 p0650 N88-13984
Preparation of amorphous silicon semiconductors
[GB-PATENT-2-176-054-A] 05 p0656 N88-14022
NASA patent abstracts bibliography: A continuing bibliography. Section 1: Abstracts (supplement 32)
[NASA-SP-7039(32)-SECT-1-ABST]
07 p0943 N88-15732
NASA patent abstracts bibliography: A continuing bibliography. Section 2: Indexes (supplement 32)
[NASA-SP-7039(32)-SECT-2] 10 p1425 N88-18511
NASA patent abstracts bibliography: A continuing bibliography. Section 1: Abstracts
[NASA-SP-7039(33)] 18 p2590 N88-25388
Argonne National Laboratory technology transfer report, FY87
[DE88-010091] 23 p3298 N88-29639

PATENTS
Identifying areas of leading edge Japanese science and technology: Activity analysis using SIC (Standard Industrial Classes) categories and scientific subfields
[PB87-204087] 02 p0249 N88-11574
Identifying areas of leading edge Japanese science and technology: Patent activity and citation analysis using US POC (Patent Office Classification) classification
[PB87-204095] 02 p0249 N88-11575
Magnetically switched power supply system for lasers
[NASA-CASE-NPO-16402-2] 18 p2505 N88-24862
Linear force device
[NASA-CASE-MSC-20549-2] 18 p2516 N88-24927
Range and range rate system
[NASA-CASE-MSC-20867-1] 18 p2521 N88-24956

PATHOGENESIS
Development of methods for the study of space motion sickness 07 p0892 N88-15408

PATHOLOGICAL EFFECTS
Questions on the evolution of the development program of the vertebrate inner ear under long term zero-g conditions 07 p0886 N88-15379
Neuropeptides in experimental head injury
[AD-A188067] 11 p1520 N88-19077

PATHOLOGY
NT HUMAN PATHOLOGY
Diagnostic value of some load tests in evaluation of nonspecific electrocardiographic changes
07 p0895 N88-15426
Squid instrumentation for neuromagnetic study of complex brain activity 21 p2978 N88-27691

PATHS
Two dimensional path planning with obstacles and shadows
[AD-A184075] 04 p0397 N88-12474
Task path planning, scheduling and learning for free-ranging robot systems 08 p1058 N88-16386

PATTERN DISTRIBUTION
U DISTRIBUTION (PROPERTY)

PATTERN RECOGNITION
NT CHARACTER RECOGNITION
Estimation of the position and orientation of objects using associative memories
[ESA-TT-1034] 01 p0079 N88-10507
Recognizing rigid objects by aligning them with an image
[AD-A184253] 03 p0368 N88-12316
On the recognition of curved objects
[AD-A184441] 04 p0478 N88-12945
An approach to object recognition: Aligning pictorial descriptions
[AD-A184462] 04 p0482 N88-12972
Intelligent signal analysis and recognition
[NASA-CR-181531] 04 p0501 N88-13084
Towards building a team of intelligent robots
[NASA-CR-181538] 05 p0589 N88-13595
A rudimentary database for three-dimensional objects using structural representation
[CSE-87-00004] 05 p0590 N88-13597
Supercomputing at Florida State University (FSU)
[DE87-013900] 05 p0654 N88-14009
Artificial intelligence systems
06 p0761 N88-14670
Transient classifier systems and man-machine interface research
[AD-A186213] 07 p0899 N88-15446
Automated program recognition
[AD-A186421] 07 p0903 N88-15472
Algorithm and program for recognition of compactly positioned vertices of events for the HPD minimum guidance system
[DE88-700542] 07 p0905 N88-15482
Pattern recognition techniques for failure trend detection in SSME ground tests 07 p0924 N88-15614
Recognition of polyhedral objects under structured illumination
[PB88-106703] 07 p0932 N88-15661
A knowledge-based object recognition system for applications in the space station
[NASA-CR-182411] 08 p0989 N88-15991
Research on visual information processing with special reference to oculomotor behavior in the areas of exploration, recognition and search
[AD-A186598] 08 p1051 N88-16346
Stability, reliability and cross-mode correlations of tests in a recommended 8-minute performance assessment battery
[NASA-CR-172039] 08 p1052 N88-16351
Embedded expert system for space shuttle main engine maintenance 08 p1056 N88-16382
Pattern-recognition software detecting the onset of failures in complex systems
[DE88-002861] 09 p1220 N88-17318
A comparison of algorithms for the analysis of images generated by two-dimensional electrophoresis
[DE88-003730] 09 p1220 N88-17319
Hierachical object recognition using libraries of parameterized model sub-parts
[AD-A187476] 10 p1396 N88-18322
Visual evoked potentials
[AD-A187942] 11 p1519 N88-19071
Learning functions from examples
[AD-A187725] 11 p1534 N88-19163
Object recognition on a systolic array
[AD-A187726] 11 p1534 N88-19164
Multiaperture optical system research
[AD-A188211] 11 p1549 N88-19267
Automated stereophotogrammetry
[AD-A189617] 12 p1630 N88-19757
An automatic system for extraction of information from a Computer Aided Design (CAD), selection, sequencing, and execution of turning processes
[INPE-4350-TDL/294] 12 p1676 N88-20020
A procedure for automatic classification of crop areas
[INPE-4467-PRE/1240] 13 p1790 N88-20708
Measures of similarity between fuzzy concepts: A comparative analysis
[AD-A189430] 13 p1825 N88-20910
Generalised threshold selection for edge detection
[RAE-TR-87035] 14 p1941 N88-21581
Range image segmentation and surface parameter extraction for a mobile robot
[DE87-013877] 15 p2073 N88-22360
Motion sickness: Quantitative, algorithmic malaise indication in real time
[AD-A189674] 15 p2101 N88-22518
Perception of complex auditory patterns
[AD-A190218] 15 p2102 N88-22524
Auditory perception of complex sounds
[AD-A190528] 15 p2103 N88-22529
Auditory pattern memory: Mechanisms of tonal sequence discrimination by human observers
[AD-A190337] 15 p2104 N88-22534
Rapid feature extraction via the radon transform
[AD-A190032] 15 p2110 N88-22573
Multi-disciplinary techniques for understanding time-varying space-based imagery
[AD-A190711] 15 p2117 N88-22610
Concurrent algorithms for a mobile robot vision system
[DE88-005850] 15 p2117 N88-22614
Multivariate analysis and its application
[AD-A189983] 15 p2124 N88-22661
Method and device for the detection and identification of a helicopter
[NASA-TT-20251] 15 p2129 N88-22698
Study of microcomputer-based real-time programmable optical signal processor and application
[AD-A190076] 15 p2133 N88-22726
OCR vision system, an alternative to bar code
[DE88-003761] 15 p2149 N88-22828
Activities report of the Department of Systems and Communications
[ENST-87D004] 16 p2189 N88-23053
Extraction of texts and symbols from unstructured vector data --- mapping 16 p2225 N88-23287
Generic cueing in image understanding
[RSRE-MEMO-4109] 17 p2386 N88-24181
Nonparametric discriminant analysis applied to the extraction and selection of radar target signature features
[AD-A191849] 18 p2501 N88-24833
Tests for the automatic pattern recognition of building surfaces by the TK 50 18 p2533 N88-25030

Feature extraction using the Hough transform [AD-A190679] 18 p2555 N88-25165
Real-time optical multiple object recognition and tracking system and method [NASA-CASE-NPO-17139-1-CU] 18 p2576 N88-25301
Cluster analysis of multiple planetary flow regimes [NASA-CR-182931] 18 p2594 N88-25418
A high dynamic range acousto-optic image correlator for real-time pattern recognition [DE88-007933] 19 p2726 N88-26191
Treatment of systematic errors in the processing of wide angle sonar sensor data for robotic navigation [DE88-008961] 20 p2756 N88-26352
Synoptic patterns related to tropical cyclone recurvature [AD-A192338] 20 p2827 N88-26771
Optical data processing [AD-A193024] 20 p2839 N88-26841
Optical correlation using the magneto-optic device [AD-A192342] 20 p2854 N88-26950
Applications of differential geometry to the shape analysis of gray-value images 21 p2924 N88-27358
An aspect graph-based control strategy for 3-D object recognition 21 p2927 N88-27377
Creating aspect graphs for use in object recognition 21 p2928 N88-27379
Linear feature extraction from radar imagery. Phase 2: Base contract report [AD-A192626] 21 p2931 N88-27404
Analysis of remotely sensed imagery using digital morphology [AD-A192738] 21 p2965 N88-27614
Fourth generation neurocognitive pattern analysis system 21 p2977 N88-27686
Texture perception and shape from texture [AD-A192923] 21 p2996 N88-27771
Simulation of real time problem solving [AD-A193436] 21 p2997 N88-27778
An optical 2-dimensional correlator for pattern recognition in embedded computing [DE88-007198] 21 p2998 N88-27780
Application of pattern recognition techniques to the identification of aerospace acoustic sources [NASA-CR-183116] 21 p3013 N88-27877
Pattern information processing and multimedia database system: Current research on multimedia information system [PB88-131917] 21 p3028 N88-27973
Research for reducing the labor intensive nature of high-resolution terrain analysis feature extraction [AD-A192661] 22 p3089 N88-28345
Natural object categorization [AD-A194103] 22 p3139 N88-28662
Survey of neural net paradigms for specification of discrete networks [AD-A192682] 22 p3141 N88-28674
Determining vehicle motion from stereo image sequences [AD-A194371] 23 p3216 N88-29140
Automatic line network extraction from aerial imagery of urban areas through knowledge-based image analysis [AD-A192399] 23 p3227 N88-29206
Limits of pattern discrimination in human vision [AD-A193449] 23 p3239 N88-29273
Analysis of the hopfield neural networks and their application to pattern recognition [AD-A193827] 23 p3239 N88-29279
Automatic object recognition 23 p3254 N88-29368
Two dimensional convolute integers for machine vision and image recognition 23 p3254 N88-29369
A generic expert system for materials processing in space 23 p3255 N88-29376
Corner extraction from radar images [AD-A194857] 24 p3362 N88-30020
Path planning and path following for the Amsterdam autonomous cart [FVI-86-22] 24 p3380 N88-30133
Eye movements and spatial pattern vision [AD-A195496] 24 p3408 N88-30290
An interactive testbed for development of expert tools for pattern recognition 24 p3419 N88-30349
Parallel and distributed computation for fault-tolerant object recognition 24 p3419 N88-30350
Nested neural networks [NASA-TM-101032] 24 p3423 N88-30373

PATTERN REGISTRATION
A smart, mapping, charting and geodesy control generator, phase 1 [AD-A188184] 10 p1347 N88-18055
Autocorrelation of control points on 11-band multispectral imagery [AD-A188185] 10 p1348 N88-18056
The modeling of error budget analysis and tolerance specifications for BRESEX multiband linear array CCD camera 17 p2355 N88-24029
Automatic registration of satellite imagery 17 p2364 N88-24080
Application of dynamic programming to image registration [ENST-87E022] 18 p2557 N88-25180
Method for combined image interpolation-restoration through a fir filter design technique [INPE-4561-PRE/1302] 24 p3413 N88-30315

PATTERNS
Orthogonal patterns in binary neural networks [NASA-TM-100060] 10 p1396 N88-18320

PAULI EXCLUSION PRINCIPLE
Theory of two-photon emission from atomic inner shells [AD-A187742] 11 p1543 N88-19223

PAVEMENTS
Polymer modified binders for bituminous or asphaltic paving layers [PC-5] 02 p0153 N88-10958
The ability of modified pavement quality concrete to resist ground erosion caused by VTOL aircraft [BAE-ARG-238] 03 p0267 N88-11683
Open-graded bases for airfield pavements [AD-A184461] 04 p0402 N88-12500
A laboratory study of asphalt concrete mix designs for high-contact pressure aircraft traffic [AD-A185753] 06 p0670 N88-14106
Comparative study of nondestructive pavement testing, MacDill Air Force Base, Florida [AD-A186082] 07 p0822 N88-14993
Evaluation of bituminous materials used in pavement recycling projects at Tyndall, MacDill, and Hurlburt Air Force Bases [AD-A188068] 10 p1317 N88-17871
Micro PAVER concept and development airport pavement management system [AD-A187360] 11 p1441 N88-18596
Probabilistic and reliability design procedures for flexible airfield pavements: Elastic layered method [AD-A187533] 11 p1442 N88-18600
Profilometer for bomb-damage-repaired airfield pavements and measurement of pavement upheaval. Report 1: Technology evaluation [AD-A187985] 11 p1442 N88-18601
Applications and limitations of the spectral-analysis-of-surface-waves method [PB88-136619] 11 p1513 N88-19038
Investigation of the inter-relationship between base pavement stiffness and asphalt overlay compaction [DOT/FAA/ES-88/1] 14 p1869 N88-21170
Design of overlays for rigid airport pavements [DOT/FAA/PM-87/19] 18 p2468 N88-24652

PAYLOAD ASSIST MODULE
An intelligent training system for payload-assist module deploys 09 p1204 N88-17214

PAYLOAD CONTROL
Test of the Hipparcos payload in the Liege vacuum facility focal 02 p0135 N88-10850
Hemispherical pointing mechanism drive unit --- satellite payloads antennas 14 p1874 N88-21193
Deployment, hold down and release mechanisms for Wind Scatterometer Antenna (WSA) --- ERS-1 wind scatterometer antenna (WSA) 14 p1876 N88-21207
A spin and deployment mechanism 14 p1926 N88-21479
Aerospace payload support systems [AFGL-TR-87-0241] 24 p3334 N88-29843

PAYLOAD DELIVERY (STS)
Payload deployment system --- STS 14 p1875 N88-21199
Noncryogenic propellants for a nuclear orbit transfer vehicle 17 p2428 N88-24444

PAYLOAD DEPLOYMENT & RETRIEVAL SYSTEM
NT REMOTE MANIPULATOR SYSTEM
Payload deployment method and system [NASA-CASE-MSC-21330-1] 18 p2470 N88-24660

PAYLOAD INTEGRATION
A monograph of the National Space Transportation System Office (NSTSO) integration activities conducted at the NASA Lyndon B. Johnson Space Center for the EASE/ACCESS payload flown on STS 61-B 02 p0139 N88-10876
EASE/ACCESS ground processing at Kennedy Space Center 02 p0139 N88-10877
RETE experiment Assembly, Integration, and Verification (AIV) activities [IFSI-87-6] 05 p0555 N88-13380
An AI approach for scheduling space-station payloads at Kennedy Space Center 08 p1064 N88-16425
Scheduling spacecraft operations 08 p1064 N88-16426
SYLDA: A dual-launch system for Ariane 09 p1125 N88-16745
Coorbiting Platform Utilization Study (CPLUS), executive summary --- Columbus [SN-WP-4000-DOC-6609/85/F] 09 p1133 N88-16796
Expert mission planning and replanning scheduling system for NASA KSC payload operations 09 p1209 N88-17247
Laser investigations for payload G-652 prior to filing pre-flight accommodation requirements 10 p1286 N88-17694
Modification of integrated partial payload lifting assembly [NASA-CR-182573] 11 p1443 N88-18607
The German Spacelab mission D1: Payload integration [ETN-88-91507] 14 p1871 N88-21179
Space nuclear reactor shielding optimization studies 17 p2408 N88-24320
Turbomachinery in space 17 p2408 N88-24321

PAYLOAD MASS RATIO
Ariane launch performance 09 p1125 N88-16743
Increased performance for Ariane 09 p1125 N88-16744

PAYLOAD RETRIEVAL (STS)
Cost-effective orbit transfer modes for satellite retrieval and servicing --- Space Station 12 p1586 N88-19489
Review of commercial spacecraft: Recovery and repair experiences. Implications for future spacecraft designs and operations 12 p1591 N88-19528

PAYLOAD TRANSFER
A spin and deployment mechanism 14 p1926 N88-21479

PAYLOADS
NT ASTRO MISSIONS (STS)
NT EARTH RADIATION BUDGET EXPERIMENT
NT GET AWAY SPECIALS (STS)
NT PHYSICS AND CHEMISTRY EXPERIMENT IN SPACE
NT SEPAC (PAYLOAD)
NT SHUTTLE IMAGING RADAR
NT SPACE SHUTTLE PAYLOADS
NT SPACE STATION PAYLOADS
NT SPACELAB
NT SPACELAB PAYLOADS
NT X RAY ASTROPHYSICS FACILITY
Redistribution of particulates in shuttle bay during launch 02 p0133 N88-10837
Test of the Hipparcos payload in the Liege vacuum facility focal 02 p0135 N88-10850
Estimating payload internal temperatures and radiator size for multimegawatt space platforms [DE88-000244] 03 p0275 N88-11738
The effect of maximum-allowable payload temperature on the mass of a multimegawatt space-based platform [DE88-001921] 05 p0555 N88-13381
Carbon Dioxide observational platform system (CO-OPS) Feasibility Study [NASA-CR-179225] 06 p0671 N88-14113
Performance considerations for the astrometric telescope facility on the phase 1 space station [NASA-TM-100040] 06 p0800 N88-14898
Orbital Replaceable Unit (ORU)/cold plate thermal interface study. Volume 1: Executive Summary [BAE-TP-8430] 07 p0855 N88-15195
Evaluate the application of modal test and analysis processes to structural fault detection in MSFC - STS project elements 07 p0927 N88-15630
Rapid prototyping and AI programming environments applied to payload modeling 08 p1061 N88-16405
Mechanical in-flight environment of Ariane payloads 09 p1126 N88-16748
Coorbiting Platform Utilization Study (CPLUS), executive summary --- Columbus [SN-WP-4000-DOC-6609/85/F] 09 p1133 N88-16796
Apollo Lightcraft project [NASA-CR-182575] 11 p1445 N88-18615
A lunar transportation system [NASA-CR-182561] 11 p1567 N88-19379
Mars Lander/Rover vehicle development: An advanced space design project for USRA and NASA/OAST [NASA-CR-182570] 11 p1567 N88-19380
Preliminary analysis of an integrated logistics system for OSSA payloads [NASA-CR-4114] 12 p1584 N88-19477
Preliminary analysis of an integrated logistics system for OSSA payloads. Volume 1: Executive summary 12 p1584 N88-19478
Preliminary analysis of an integrated logistics system for OSSA payloads. Volume 2: OSSA integrated logistics support strategy 12 p1584 N88-19479
Preliminary analysis of an integrated logistics system for OSSA payloads. Volume 3: OSSA integrated logistics support planning document 12 p1584 N88-19480

Automatic in-orbit payload deployment mechanisms, logistic operations and transport vehicle design compatibilities 12 p1586 N88-19493
Vehicle glow observed on the SONDA 3
[INPE-4297-PRE/1168] 12 p1600 N88-19581
Mars Lander/Rover vehicle development: An advanced space design project for USRA and NASA/OAST
[NASA-CR-182562] 12 p1709 N88-20226
Mars Lander/Rover vehicle development: An advanced space design project for USRA and NASA/OAST
[NASA-CR-182571] 12 p1709 N88-20227
The Joint NASA/Goddard-University of Maryland Research Program in Charged Particle and High Energy Photon Detector Technology
[NASA-CR-182612] 12 p1712 N88-20247
Expected value analysis for an unmanned expendable launch vehicle payload escape system
[AD-A189494] 13 p1728 N88-20337
Orbital transfer vehicle concept definition and system analysis study. Volume 2: OTV concept definition and evaluation. Book 1: Mission and system requirements
[NASA-CR-179321] 13 p1729 N88-20339
ERS-1 data products and services and their value for tropical countries 17 p2357 N88-24040
The effect of maximum allowable payload temperature on the mass of a multimegawatt space based platform
17 p2424 N88-24416
Lunar base surface mission operations. Lunar Base Systems Study (LBSS) task 4.1
[NASA-CR-172050] 18 p2594 N88-25415

PBRE (REACTORS)
U PEBBLE BED REACTORS

PCM (MATERIALS)
U PHASE CHANGE MATERIALS

PCM (MODULATION)
U PULSE CODE MODULATION

PCM TELEMETRY
Rivista Tecnica Selenia, volume 10, number 2
[ETN-87-90763] 01 p0011 N88-10064
Telemetry conditioning units for the European launcher Ariane 01 p0012 N88-10068
PCM telemetry standard
[ESA-PSS-46(TTC.A.02)ISSUE-1]
09 p1132 N88-16790

PDM (MODULATION)
U PULSE DURATION MODULATION

PEACETIME
The military techniques of tomorrow. A contribution to active peace assurance
[MBB-UA-1049/87] 10 p1315 N88-17860

PEBBLE BED REACTORS
Thermal-hydraulic considerations for particle bed reactors 17 p2400 N88-24266
Particle bed reactor scaling relationships
17 p2400 N88-24267
Direct nuclear propulsion for Earth-to-orbit vehicles
17 p2400 N88-24271
Nuclear propulsion systems for orbit transfer based on the particle bed reactor 17 p2401 N88-24272
Ultra high temperature direct propulsion
17 p2401 N88-24275
Small particle bed reactors: Sensitivity to Brayton cycle parameters 17 p2435 N88-24487
The closed Brayton cycle: An energy conversion system for near-term military space missions
17 p2435 N88-24488
Energy conversion system optimization study for multimegawatt space nuclear power application
17 p2436 N88-24492

PECLET NUMBER
Review of numerical methods for radionuclide transport in three-dimensional porous media, at high Peclet numbers
[CFDU/87/10] 18 p2538 N88-25061

PEDIMENTS
U PIEDMONTS

PEDIPLAINS
U PIEDMONTS

PEDOLOGY
U SOIL SCIENCE

PEEK
Electron beam irradiation effects on carbon fiber reinforced PEEK composite
[DE87-753001] 02 p0142 N88-10890
Effects of solvent exposures on poly(etheretherketone) (PEEK) and PEEK-fiberglass composites
[MLM-3405] 03 p0261 N88-11766
Molecular composites: Processing, post-treatment and mechanics
[AD-A184458] 04 p0410 N88-12547
Characterization of Mode 1 and Mode 2 delamination growth and thresholds in graphite/peek composites
[NASA-TM-100577] 16 p2172 N88-22947
The crystallization of tough thermoplastic resins in the presence of carbon fibers
[NASA-CR-182984] 20 p2776 N88-26464
Compression creep of filamentary composites
[NASA-CR-182550] 20 p2798 N88-26601

PEELING
Effect of peel angle on peel force
[AD-A186117] 08 p0972 N88-15878
Effect of post-cure heat-treatment on static and fatigue behaviour of XAS-914C carbon fibre composite
[AD-A186943] 10 p1294 N88-17735

PEGASUS SATELLITES
Orbit determination of 1965-09A for analysis of the eccentricity at 15th-order resonance
[RAE-TR-87059] 22 p3047 N88-28081

PELLETS
Microstructural effects in shock initiation of granular explosives
[DE87-011282] 01 p0031 N88-10200
CIT (Compact Ignition Tokamak) fueling
[DE88-002709] 12 p1692 N88-20125
Application of railgun principle to high-velocity hydrogen pellet injection for magnetic fusion reactor refueling
[DE88-005830] 13 p1728 N88-20334
Improvements to Raney copper zinc methanol synthesis catalysts 17 p2318 N88-23844
The JET (Joint European Torus) multipellet launcher and fueling of JET plasmas by multipellet injection
[DE88-008367] 19 p2729 N88-26206

PENALTY FUNCTION
An exact penalization viewpoint of constrained optimization
[DE88-001477] 04 p0486 N88-12995
Velocity-pressure integrated versus penalty finite element methods for high Reynolds number flows
[NASA-CR-179357] 20 p2803 N88-26635

PENDULUMS
Allowance for influence of gravity field nonuniformity
08 p1012 N88-16137
Evaluation of a miniature horizontal pendulum tilt transducer 12 p1577 N88-19435

PENETRATING PARTICLES
U CORPUSCULAR RADIATION

PENETRATION
Space station integrated wall design and penetration damage control
[NASA-CR-179169] 01 p0013 N88-10070
Analysis of compressible flow on high-velocity jet penetration 03 p0302 N88-11898
Models for penetration of thin plates
[DE87-013727] 03 p0332 N88-12090
Mechanical property evaluation of a series of commercial tungsten alloys
[AD-A185440] 05 p0565 N88-13446
Structural frequency functions for an impulsive, distributed forcing function 05 p0594 N88-13627
Study of extended least-square iterative techniques in electromagnetic scattering by penetrable objects
[PB88-105879] 06 p0694 N88-14262
Unsteady stall penetration experiments at high Reynolds number
[AD-A186120] 07 p0814 N88-14958
Earth penetrator strain gage applications
[DE88-002260] 09 p1166 N88-16993
New model to estimate the perforation power of kinetic energy projectiles
[PB87-166757] 09 p1175 N88-17040
Mechanism of change of vortex structure orientation in type-2 superconductors 09 p1239 N88-17425
Space station integrated wall damage and penetration damage control. Task 5: Space debris measurement, mapping and characterization system
[NASA-CR-179281] 10 p1285 N88-17688
Penetration theory for inclined and moving shaped charges
[MBB-UA-940/86] 10 p1315 N88-17861
An analysis of penetration and ricochet phenomena in oblique hypervelocity impact
[NASA-TM-100319] 10 p1339 N88-18004
Penetration depth measurements of YBa2Cu3O/sub 7-delta/ at 4 MHz
[DE88-003493] 10 p1420 N88-18478
Fracture toughness of steel weldments containing lack of penetration defects 11 p1501 N88-18965
Observations on electrostatic effects in a filter test system
[AD-A188797] 13 p1736 N88-20378
A direct correlation of strength with impact velocity
[AD-A189251] 13 p1741 N88-20409
Numerical analysis of critical penetration velocity for jet perpendicular penetration 16 p2186 N88-23037
Subsurface morphology and geoarchaeology revealed by spaceborne and airborne radar
17 p2353 N88-24022
Ballistic evaluation of applique armours: Presentation and interpretation of ballistic data
[MRL-TN-527] 19 p2635 N88-25629
Instrumentation for the measurement of penetrator dynamic response to permit force estimation
[DE88-010608] 20 p2809 N88-26666
GTAW characterization for weld penetration on 304L stainless steel
[DE88-010611] 20 p2810 N88-26672
Study of comet nucleus gamma-ray spectrometer penetration system
[NASA-CR-177393] 20 p2883 N88-27120
Investigation of hydrogen isotope penetration through stainless steels Kh18N10T and Kh3M2BFR
[DE88-702189] 21 p2915 N88-27297
Signal processing software for ground penetrating radar, user's manual
[AD-A194286] 23 p3203 N88-29059

PENETRATION BALLISTICS
U TERMINAL BALLISTICS

PENNING EFFECT
Ion traps for large storage capacity
16 p2268 N88-23570
Examination of the termalization of confined ions
[PB87-227815] 19 p2723 N88-26171
Theoretical atomic and molecular physics
[DE88-007122] 19 p2724 N88-26175

PENTACHLORIDES
U CHLORIDES

PENTAERYTHRITOL TETRANITRATE
U PETN

PENUMBRAS
Exploiting the IR: Solar and stellar spectroscopy in the IR 04 p0504 N88-13102

PEPTIDES
NT GLUTATHIONE
NT POLYPEPTIDES
Synthesis of high molecular weight peptide polymers and copolymers containing L-dope residues
[AD-A186462] 08 p0973 N88-15887
Neuropeptides in experimental head injury
[AD-A188067] 11 p1520 N88-19077
Protection from stress 12 p1664 N88-19978
Development of polymeric films with piezoelectrical properties from polypeptides; low, odd nylons; or polyureas
[AD-A190301] 15 p2044 N88-22181
Studies of model ion channels in defect-free multibilayers of phospholipids
[AD-A188740] 16 p2238 N88-23365
Role of opioid peptides in pathogenesis of vestibulovegetative disorders 19 p2704 N88-26079

PERCENTAGE
U RATIOS

PERCEPTION
NT AUDITORY PERCEPTION
NT CONSCIOUSNESS
NT MOTION PERCEPTION
NT PROPRIOCEPTION
NT SENSORY PERCEPTION
NT SOUND LOCALIZATION
NT SPACE PERCEPTION
NT TACTILE DISCRIMINATION
NT TOUCH
NT VISUAL DISCRIMINATION
NT VISUAL PERCEPTION
Studies of the processing of single words using positron tomographic measures of cerebral blood flow change
[AD-A184058] 03 p0356 N88-12244
An evaluation of perceptions of form, fit, function (F3) standardization on the Standard Inertial Navigation Unit (STD INU) program
[AD-A188955] 12 p1579 N88-19446
Relationship of encoding speed and memory tests to flight training performance
[AD-A190670] 15 p2105 N88-22539
The N2-P3 complex of the evoked potential and human performance 16 p2241 N88-23388
Problem solving in a natural task as a function of experience
[AD-A191160] 16 p2243 N88-23399
The interaction of sensory and perceptual variables: Spatial, temporal and orientation response to figure and ground
[AD-A192897] 20 p2832 N88-26798
Cognitive and neural bases of skilled performance
[AD-A193392] 21 p2992 N88-27747
Texture perception and shape from texture
[AD-A192923] 21 p2996 N88-27771
Issues in computer-assisted interpretation of graphs and quantitative information
[PB88-116280] 21 p2998 N88-27783
Advancement of latent trait theory
[AD-A194302] 24 p3408 N88-30289

PERCEPTRONS
U SELF ORGANIZING SYSTEMS

PERCEPTUAL ERRORS
Ejection situations in the U-2/TR-1: An analysis of emotions and events
[AD-A192872] 21 p2893 N88-27175
PERCHLORATES
NT AMMONIUM PERCHLORATES
NT LITHIUM PERCHLORATES
PERCOLATION
De-alloying
[DE87-012488] 01 p0022 N88-10139
Surface free energy of laser-produced bond percolators
[PB88-130865] 11 p1493 N88-18913
The percolation approach as a basis for experimental research on the mechanical properties of composite materials 14 p1886 N88-21271
Analysis of transverse strength of composites using percolation theory
[AD-A193204] 21 p2904 N88-27234
PERFECT GAS
U IDEAL GAS
PERFLUORO COMPOUNDS
Polyvinyl esters of omega-H-perfluoroacids and polyvinyl alcohol obtained from them
[AD-A184633] 03 p0279 N88-11755
Surface catalytic degradation study of two linear perfluoropolyalkylethers at 345 C
[NASA-TP-2774] 04 p0410 N88-12543
Electrochemical characteristics of acid electrolytes for fuel cells
[PB88-104641] 06 p0731 N88-14497
Improved perfluoroalkylether fluid development
[NASA-CR-180872] 08 p0967 N88-15851
The performance of perfluoropolyalkylether oils under boundary lubrication conditions
[AD-A191057] 17 p2323 N88-23869
Theoretical studies of solar lasers and converters
[NASA-CR-182927] 17 p2344 N88-23972
PERFORATED PLATES
Computational studies of wave-shaping in a blast simulator by perforated plates in the driver
[AD-A188200] 11 p1483 N88-18850
Stress-strain behaviour of a bolt hole in carbon fibre composite plates
[BU-354] 14 p1923 N88-21460
Finite element simulation of perforation of aluminum plates
[DE88-002092] 15 p2073 N88-22362
Operational considerations for laminar flow aircraft
17 p2298 N88-23748
Dynamical stress concentration problems, from every side, bordered and perforated plates
[ETN-88-92126] 20 p2815 N88-26703
PERFORATING
New model to estimate the perforation power of kinetic energy projectiles
[PB87-166757] 09 p1175 N88-17040
Optical Fourier transformation by lensless method with perforated mask and with modified Talbot interferometer for analysis of interferograms 09 p1236 N88-17408
Numerical simulation of the perforation of thin plates
[ISL-R-122/86] 11 p1495 N88-18926
PERFORATION
Analysis of the perforation of monolithic and simple laminate aluminium targets as a test of analytical deformation models
[MRL-R-1111] 20 p2813 N88-26686
PERFORMANCE
Post-test analyses of aqueous batteries developed for electric propulsion
[DE88-000655] 03 p0311 N88-11965
Nonconformity testing for the Graphical Kernel System (GKS)
[GMD/VAL-86-104] 06 p0757 N88-14644
Preliminary analysis of helium generation and its effects on the SP-100 system performance
17 p2422 N88-24406
PERFORMANCE PREDICTION
Propulsion Working Group report
01 p0016 N88-10098
Endurance testing of a natural gas-fueled rotary engine
[PB87-215703] 01 p0055 N88-10356
Global positioning satellite-based automatic landing system and wind estimated feedback for the AH-64 helicopter 02 p0124 N88-10784
Modeling and performance evaluation of the DPS25 packet switching multiprocessor system --- communication networks
[ENST-87E009] 02 p0162 N88-11016
Flight experience of solar mesosphere explorer's power system over high temperatures ranges
02 p0165 N88-11037
Real time charge efficiency monitoring for nickel electrodes in NICD and NIH2 cells
02 p0165 N88-11038
Methodology of performance evaluation of real time distributed systems
[ENST-87D003] 02 p0228 N88-11440
Stability of mechanical joints in launching vehicles: Local and global stationary values of energy density
03 p0270 N88-11696
The impact of environmental factors on the performance of millimeter wave seekers in smart munitions
[DE87-014277] 03 p0270 N88-11697
A hybrid numerical technique for predicting the aerodynamic and acoustic fields of advanced turboprops
[NASA-CR-174926] 03 p0374 N88-12352
Numerical prediction of propeller performance by vortex lattice method
[UTIAS-TN-265] 04 p0400 N88-12489
Applications of the hybrid automated reliability predictor
[NASA-TP-2760] 04 p0475 N88-12928
Predictions of F-111 TACT aircraft buffet response and correlations of fluctuating pressures measured on aluminum and steel models and the aircraft
[NASA-CR-4069] 05 p0529 N88-13218
The off-design performance of hypersonic waveriders
05 p0533 N88-13244
Numerical optimization of conical flow waveriders including detailed viscous effects
05 p0533 N88-13245
Dynamic stability of hypersonic conical lifting vehicles according to Newton-Busemann theory
05 p0534 N88-13247
Experiences using the Mark IV supersonic hypersonic arbitrary body program 05 p0534 N88-13249
The RAE experimental data-base for missiles at high Mach number and its use in assessing CFD methods
05 p0534 N88-13250
Damage considerations in sizing aircraft cells. Life predictions
[SNIAS-872-111-116] 05 p0546 N88-13330
Model helicopter rotor rig and associated strain gauge balance for performance studies
[NAL-TM-AE-8704] 05 p0552 N88-13364
Performability modeling based on real data: A casestudy
[NASA-CR-181563] 05 p0633 N88-13870
Mainline performance prediction for radial inflow turbines 06 p0712 N88-14366
Analysis and performance prediction of scramjet inlets utilizing a three-dimensional Navier-Stokes code
07 p0811 N88-14936
Flow in Centrifugal Compressors --- conference
[VKI-LS-1987-01] 07 p0850 N88-15160
Overview of NASA PTA propfan flight test program
08 p0957 N88-15805
Failure modes of laminate structures
[DE88-002579] 08 p0996 N88-16033
A validity study of a selection procedure for student airline pilots
[DFVLR-FB-87-34] 09 p1201 N88-17196
Method for predicting performance limits of centrifugal compressors 10 p1283 N88-17677
A strategy for failure prediction
10 p1380 N88-18243
Damage mechanisms and fatigue life prediction of graphite/epoxy laminates 11 p1449 N88-18637
Seventy-meter antenna performance predictions: GTD analysis compared with traditional ray-tracing methods
11 p1474 N88-18793
Test results of a 40-kW Stirling engine and comparison with the NASA Lewis computer code predictions
[NASA-TM-87050] 11 p1508 N88-19013
OMV man/system simulation integration: A preliminary analysis and recommendation
[NASA-CR-182602] 12 p1671 N88-20005
Robustifying the Kalman filter
[AD-A189240] 13 p1825 N88-20907
Analysis of induction motors based on the numerical solution of the magnetic field and circuit equations
[EL-59] 14 p1907 N88-21398
Stall flutter analysis of propfans
16 p2221 N88-23256
A correlational approach to predicting operator status
16 p2242 N88-23393
The performance of the VKI longshot hypersonic wind tunnel
[VKI-TN-161] 18 p2468 N88-24650
Propagation management for no-acknowledge HF communications links 18 p2502 N88-24843
Performance estimates for operations conducted while wearing individual protective equipment: User manual
[AD-A191871] 18 p2553 N88-25154
Armoured vehicle track elastomers: Research and development at MRL
[MRL-GD-0012] 19 p2620 N88-25541
A computer program for performance prediction of tripropellant rocket engines with tangential slot injection
19 p2627 N88-25581
Boundary layer simulator (BLIMPJ) improvement
19 p2627 N88-25582
Motor test data comparisons with laboratory data and stability predictions 19 p2629 N88-25594
A multiple chamber volume-filling model for prediction of transient solid rocket motor ballistic performance
19 p2633 N88-25618
Failure rate prediction of electronic components
[PB87-228953] 19 p2678 N88-25925
Predicting Air Combat Maneuvering (ACM) performance: Fleet fighter ACM readiness program grades as performance criteria
[AD-A191605] 19 p2710 N88-26089
Prediction of fatigue growth
[NLR-MP-87052-U] 20 p2816 N88-26707
A comparison of the various helicopter mathematical models used in the methodology assessment
21 p2869 N88-27149
A comparison of theory and experiment for aeroelastic stability of a hingeless rotor model in hover
21 p2889 N88-27150
A comparison of theory and flight test of the BO 105/BMR in hover and forward flight
21 p2890 N88-27155
Failure analysis of laminated composite angles
21 p2959 N88-27578
Recent advances in engine health management
22 p3033 N88-28005
Onboard Life Monitoring System (OLMOS): Engine life cycle calculation and trending 22 p3034 N88-28010
Goldstone solar system radar performance analysis
22 p3068 N88-28206
High-aspect-ratio wings 23 p3167 N88-28859
Measured and predicted responses of the Nord 260 aircraft to the low altitude atmospheric turbulence
24 p3312 N88-29723
Semi-empirical methods for conventional and unconventional missiles 24 p3318 N88-29758
Space marching Euler solvers
24 p3318 N88-29759
Numerical models for analytical predictions of combustor aerothermal performance characteristics
24 p3349 N88-29935
Three-dimensional gas turbine combustor modelling
24 p3349 N88-29937
Numerical modeling of combustion processes in gas turbines 24 p3350 N88-29939
Performance Prediction for Coatings. Proceedings of a Workshop
[AD-A188973] 24 p3354 N88-29966
Ultrasonic detection of diffusion and adhesion loss
24 p3354 N88-29967
Performance prediction of concurrent systems
[NASA-CR-183175] 24 p3412 N88-30312
Theories of comparative analysis
[AD-A196329] 24 p3427 N88-30395
PERFORMANCE TESTS
Numerical predictions of EML system performance
[DE87-011727] 01 p0011 N88-10061
Space station propulsion technology: Space station propulsion system test bed test plan
[NASA-CR-179201] 01 p0017 N88-10104
Fiber-reinforced composite hot-gas filters
[DE87-012257] 01 p0033 N88-10208
Test results and predictions for the response of near-ceiling sprinkler links in a full-scale compartment fire
[NBSIR-87/3633] 01 p0033 N88-10209
Analysis of the electromagnetic performance characteristics of stripline transformers
[DE87-012515] 01 p0042 N88-10264
Endurance testing of a natural gas-fueled rotary engine
[PB87-215703] 01 p0055 N88-10356
Hardware fault insertion and instrumentation system: Mechanization and validation
[NASA-CR-181445] 01 p0078 N88-10497
Analysis and synthesis of abstract data types through generalization from examples
[NASA-CR-178369] 01 p0081 N88-10519
Infra-red lamp panel study and assessment application to thermal vacuum testing of sigma telescope
02 p0132 N88-10830
Rocket nozzle thermal shock tests in an arc heater facility 02 p0133 N88-10832
Surveillance systems test and evaluation facilities
02 p0134 N88-10845
Characteristics and performance of the ESTEC large space simulator cryogenic system
02 p0135 N88-10849
Design, construction, activation, and operation of a high intensity acoustic test chamber
02 p0137 N88-10864
Operating experiences and test results of six cold helium compressors
[DE87-012115] 02 p0157 N88-10982

Battery development and testing at ESA
02 p0164 N88-11027
Nickel hydrogen low Earth orbit test program update and status 02 p0164 N88-11028
Grace DAKASEP alkaline battery separator
02 p0164 N88-11031
BRASILSAT A2: Ground and in-orbit anomalies
02 p0164 N88-11032
Qualification testing of General Electric 50 Ah nickel-cadmium cells with Pellon 2536 separator and passivated positive plates 02 p0165 N88-11036
Statistically determined nickel cadmium performance relationships 02 p0165 N88-11039
Test summary for advanced H2 cycle Ni-CD cell
02 p0165 N88-11040
Performance of high power S-band klystrons focused with permanent magnet
[DE87-753024] 02 p0167 N88-11053
The four spot time-of-flight laser anemometer
02 p0184 N88-11145
Constitutive modeling for isotropic materials
02 p0188 N88-11172
Lewis' enhanced laboratory for research into the fatigue and constitutive behavior of high temperature materials
02 p0189 N88-11177
Performance evaluation of a half-wave resonant slot antenna over perfect ground using NEC (Numerical Electromagnetic Code)
[AD-A184004] 03 p0308 N88-11942
Study of aeropropulsion laboratory pressure dropping and recommended test procedure
[AD-A184333] 03 p0322 N88-12038
Advanced natural gas fueled engine development. Part 1: Design and analyses
[PB87-224804] 03 p0331 N88-12087
Performance evaluation of artificial intelligence systems
[AD-A184054] 03 p0368 N88-12316
General-Purpose Heat Source Safety Verification Test Program: Edge-on flyer plate tests
[DE87-006309] 03 p0376 N88-12362
The aerodynamics of supersonic parachutes
[DE87-014846] 04 p0395 N88-12464
Performance and combustion characteristics of direct-injection stratified-charge rotary engines
[NASA-TM-100134] 04 p0400 N88-12490
Programmable Logic Arrays (PLA's) design for testability
[PB87-102935] 04 p0438 N88-12718
Long-range pulselength scaling of 351nm laser damage thresholds
[DE87-014754] 04 p0448 N88-12777
Calculation of the tribological properties of surfaces by semi-empirical methods
[AD-A184283] 04 p0450 N88-12791
Performance analysis of solar thermal power systems
[DE88-000563] 04 p0465 N88-12874
Performance monitoring and analysis of electric van fleet vehicles
[DE88-900066] 04 p0502 N88-13091
Application of modified loss and deviation correlations to transonic axial compressors
[AGARD-R-745] 05 p0549 N88-13344
Error control techniques for satellite and space communications
[NASA-CR-181581] 05 p0576 N88-13516
Establishment of complete minimum test sets for digital circuits with safety engineering significance
[ETN-88-90599] 05 p0578 N88-13526
Seal technology for liquid oxygen (LOX) turbopumps
[NASA-CR-1, 4866] 05 p0591 N88-13603
Trajectory control of robot manipulators with closed-kinematic chain mechanism
[NASA-TM-89305] 05 p0591 N88-13605
Test and evaluation of the transputer in a multi-transputer system
[AD-A184969] 05 p0631 N88-13859
High speed propeller performance and noise predictions at takeoff/landing conditions
[NASA-TM-100267] 05 p0646 N88-13960
Performance measurements of the Kolibrie and FACT rotor blades without tip vanes on the full-scale experimental wind turbine
[IW-R518] 06 p0665 N88-14077
Rendezvous and Docking Verification (RVDV) and in-orbit demonstration, executive summary
[RVD-RVDV-FR-AS-01] 06 p0673 N88-14120
Aerodynamic testing of small turbines
06 p0713 N88-14371
Aerodynamic design and test performance of supersonic turbines for the Vulcain rocket engine
06 p0713 N88-14373
Development of a supersonic steam turbine with a single stage pressure ratio of 200 for generator and mechanical drive
06 p0713 N88-14374
A 1,000-watt solar power unit for Far North
06 p0728 N88-14481
ATF (Advanced Toroidal Facility) ECH (Electron Cyclotron Heating) waveguide component development and testing
[DE88-001432] 06 p0782 N88-14797
Data acquisition, reduction and analysis of shock and vibration testing using a super microcomputer
[AD-A186123] 07 p0867 N88-15260
Realization and demonstration of a wind turbine of 200 kW demonstration project
[DE88-900207] 07 p0874 N88-15302
Feasibility of software built-in test for SDI (Strategic Defense Initiative) applications
[AD-A185750] 07 p0917 N88-15572
Pattern recognition techniques for failure trend detection in SSME ground tests 07 p0924 N88-15614
The development of test methodology for testing glassy materials 07 p0927 N88-15633
Determining structural performance
08 p0954 N88-15787
Analysis, design, construction and testing of a reaction wheel model for space applications
[INPE-4358-TDL/299] 08 p0963 N88-15834
The ESTEC Mini Compact Antenna Test Range
[ESA-CR(P)-2475] 08 p0977 N88-15907
Comparison of a thermoelectric cooling system and a groundwater heat pump
[DE88-001753] 08 p0984 N88-15950
Solid mechanics research for quantitative non-destructive evaluation
[AD-A186599] 08 p0993 N88-16010
Preliminary evaluation of a micro-based repeated measures testing system
[NASA-CR-172038] 08 p1048 N88-16331
Ada (trade name) compiler validation summary report. Systems designers' PLC SD Ada-plus VAX/VMS x MC68020. Version 2B.00. Host: VAX 8600. Target: Motorola MC68020. Completion of on-site testing
[AD-A186571] 08 p1053 N88-16356
Short pseudorandom test sequences
[AD-A185883] 08 p1054 N88-16357
Development of a menu of performance tests self-administered on a portable microcomputer
[NASA-CR-172040] 08 p1067 N88-16452
Helicopters as test carriers for avionics systems (HETAS)
[DFVLR-IB-112-85/18] 09 p1116 N88-16692
Integration testing of the propulsion system of Ariane's first stage 09 p1126 N88-16751
Testing a very good microwave interferometer
[TRITA-EPP-86-09] 09 p1167 N88-16996
The 5-GHz operation of the ITT and RCA streak tubes with a 7.5-ns time window
[DE88-003342] 09 p1169 N88-17008
An integration test for accelerometer evaluation
09 p1178 N88-17054
Development of a facility using robotics for testing automation of inertial instruments
09 p1213 N88-17271
A performance comparison of the Cray-2 and the Cray X-MP
[NASA-CR-177461] 09 p1216 N88-17288
Design and test of a high blade speed, high work capacity transonic turbine 10 p1281 N88-17658
Design and testing of a front stage for an advanced high pressure compressor 10 p1283 N88-17679
Simulation test beds for the space station electrical power system
[NASA-TM-100786] 10 p1290 N88-17715
Development of vertical takeoff aircraft with turbojet engines in Germany 10 p1309 N88-17822
Flight testing of fighter aircraft
[MBB/LKE-62/S/PUB/292] 10 p1312 N88-17844
Testing of a tail rotor system in a fiber composite type of construction
[MBB-UD-472/86] 10 p1314 N88-17854
Solid-state voltage standard performance and design guidelines
[PB88-123757] 10 p1322 N88-17905
Analysis of the performance of an air-water heat pump: Regulation of intrinsic performances
[DE88-900241] 10 p1349 N88-18061
Wake effects in a Fayette 95-IIS wind turbine array
[DE88-001103] 10 p1349 N88-18063
Modal testing the EOLE
[DE88-003795] 10 p1350 N88-18066
Preliminary results from the dynamic response testing of the Westinghouse 600-kW wind turbine
[DE88-001123] 10 p1350 N88-18070
Signal and data processing for IR sensors
10 p1374 N88-18199
A performance analysis of architectural scalability
[DE88-003537] 10 p1383 N88-18261
Factors causing unexpected variations in Ada benchmarks
[AD-A187231] 10 p1388 N88-18291
On the maneuvering of vehicles
[AD-A187632] 10 p1427 N88-18521
A performance index approach to aerodynamic design with the use of analysis codes only
[NASA-TP-2805] 11 p1433 N88-18552
Performance survey of airfoil profiles
[ETN-88-91093] 11 p1436 N88-18568
Columbus feasibility studies. Volume 4: Integration, test, and operations
[ETN-88-90576] 11 p1445 N88-18614
UHV (Ultra-High Vacuum) double crystal monochromator design
[DE88-003904] 11 p1456 N88-18676
Procedures for quantitative sensitivity and performance validation studies of a deterministic fire safety model
[NBS/GCR-88/544] 11 p1469 N88-18762
Conception and realization of components for a microchannel-plate detector, and testing of the detector system in the laboratory and in astronomical use
[ETN-88-91495] 11 p1491 N88-18899
Testing of a one-bladed 30-meter-diameter rotor on the DOE/NASA Mod-O wind turbine
[NASA-TM-100274] 11 p1509 N88-19014
Results of the 1987 NASA/JPL balloon flight solar cell calibration program
[NASA-CR-182617] 12 p1574 N88-19413
Simultaneous estimation and detection of bias shifts for inertial navigation systems 12 p1576 N88-19429
Reference position vector 12 p1577 N88-19432
Control test and validation for a large diameter high stability centrifuge 12 p1577 N88-19437
Rate and dynamic tests on the Canadian Strapdown Gyroscope (CSG-2) 12 p1578 N88-19439
The German Honeywell ring laser gyro: Development and test results 12 p1578 N88-19440
Simulation and tests of a satellite attitude and orbit control system. General considerations concerning an example case (INPE) and design of a servo rate table
[INPE-4282-PRE/1154] 12 p1599 N88-19572
Performance test results for the Eaton dc development power train in an electric test bed vehicle
[DE88-005458] 12 p1622 N88-19699
Planning, construction, and commissioning of a vacuum apparatus with a cold surface for the measurement of transistor functions at 20 K
[JUEL-SPEZ-397] 12 p1622 N88-19703
The effects of two Carlucci initiatives concurrency and streamlining, on the test and evaluation phase of system acquisitions 12 p1704 N88-20198
An investigation of classical dynamic scaling techniques applied to an oleo-pneumatic landing gear strut
[AD-A187664] 13 p1721 N88-20292
Combustion theory and related questions
[AD-A189160] 13 p1737 N88-20382
Materials Research Laboratory at Brown University
[AD-A188006] 13 p1739 N88-20396
Optimization of binary pigment coatings
[AD-A189103] 13 p1748 N88-20450
Improve the lifetime of the hollow fiber sodium sulfur cell
[DE88-004881] 13 p1751 N88-20469
Aluminum-air battery development
[DE88-006618] 13 p1762 N88-20543
Testing and development of electric vehicle batteries for EPRI Electric Transportation Program
[DE88-005894] 13 p1764 N88-20551
The evaluation of automatic barometers, illustrated by the Nakaasa barometer
[KNMI-TR-95] 13 p1774 N88-20610
Stable, high-efficiency, CuInSe2-based, polycrystalline, thin-film tandem solar cells
[DE88-001116] 13 p1793 N88-20726
Cadmium sulfide/copper ternary heterojunction cell research
[DE88-001122] 13 p1793 N88-20727
Pursuit tracking performance decrements associated with decreasing ambient illumination
[AD-A189336] 13 p1809 N88-20809
Electron emission from conductors subjected to intense, short-pulse electric fields
[DE88-005412] 13 p1836 N88-20985
Space infrared telescope facility wide field and diffraction limited array camera (IRAC)
[NASA-CR-182704] 13 p1853 N88-21092
Equipment test methods for externally produced electromagnetic transients
[RAE-TM-FS(F)-457] 14 p1865 N88-21140
Recommended test specification for the electromagnetic compatibility of aircraft equipment
[RAE-TM-FS(F)-510] 14 p1867 N88-21155
Qualification of the OLYMPUS reaction wheel
14 p1878 N88-21226

Qualification testing of the EUROSTAR Solar Array Drive Mechanism (SADM) 14 p1879 N88-21229

Determination of the modulus of elasticity of structural silicone sealants
[PB88-157458] 14 p1893 N88-21307

Industrial electric motors and controllers
[PB88-139569] 14 p1907 N88-21394

Performance of elastomeric bearings
[PB88-159470] 14 p1918 N88-21450

Combustion and performance characteristics of methanol plus higher alcohols in a spark ignition engine
[PB88-147962] 14 p1918 N88-21451

Space station full-scale docking/berthing mechanisms development 14 p1927 N88-21491

Development of a laboratory test for multiport injector deposits: Approaches 1 and 2
[AD-A190697] 15 p2048 N88-22203

Performance of single and multiple system AM stereo decoder receivers
[PB88-168307] 15 p2057 N88-22265

Performance test results: AXIAL-GAP, permanent magnet compressor motor
[DE88-006857] 15 p2061 N88-22289

UARS spacecraft recorder
[NASA-CR-180768] 15 p2068 N88-22331

Performance evaluation of molten salt thermal storage systems
[DE87-014645] 15 p2091 N88-22461

Prediction of physical fitness: Estimated percent body fat using body circumferences versus weight-height measures
[AD-A190233] 15 p2103 N88-22526

Exhaustive and pseudo-exhaustive testing
[AD-A190140] 15 p2111 N88-22574

Model-scale sound propagation experiment
[NASA-TM-100602] 15 p2130 N88-22709

Design and test of a new coaxial air joints
[DE88-751808] 16 p2164 N88-22908

Small-scale cleavage test of polymer products
[PB88-165360] 16 p2181 N88-23001

Development of a laboratory test for multiport fuel injector deposits - evaluation of the Jet Fuel Thermal Oxidation Test apparatus (JFTOT)
[AD-A191313] 16 p2183 N88-23015

Instrumentation for ultrafast electronics
[AD-A191379] 16 p2193 N88-23060

Use of water towing tanks for aerodynamics and hydrodynamics 16 p2204 N88-23149

The new UCSB (University of California, Santa Barbara) compact far-infrared FEL
[AD-A190664] 16 p2212 N88-23203

Roller drive materials performance
16 p2219 N88-23241

Microgravity manipulator demonstration
16 p2219 N88-23242

Spectroradiometry in the industrial test laboratory
16 p2272 N88-23598

Method of digital surface photometry of galaxies and its application to the edge-on galaxy NGC 5907
16 p2287 N88-23695

Test philosophy of the EH101 integrated avionic
17 p2303 N88-23775

Testing complex avionics software: A practical experience 17 p2306 N88-23794

Error control techniques for satellite and space communications
[NASA-CR-182686] 17 p2332 N88-23922

Botany Facility. Thermal Control (TC) subsystem test report on experiment container of laboratory model and breadboard centrifuge
[BF-TN-ER-061/86] 17 p2378 N88-24135

Botany Facility: Test report on breadboard tests for the determination of the heat transfer at the glass disk and of the temperature distribution in the fluorescent tube
[BF-TN-ER-053] 17 p2378 N88-24136

SP-100 GES test site 17 p2417 N88-24375

Development of refractory thermocouples for space nuclear power tests 17 p2434 N88-24478

SNAP fuel performance 17 p2435 N88-24484

Performance and long duration test of a 30 kw thermal arcjet engine
[AD-A190962] 18 p2474 N88-24677

An extended life and performance test of a low-power arcjet
[NASA-TM-100942] 18 p2476 N88-24687

Laboratory tests of laser gyroscopes for future utilization in multifunction systems for precision navigation and flight guidance 18 p2517 N88-24932

SRM propellant and polymer materials structural test program
[NASA-TP-2821] 18 p2530 N88-25013

Small scale bipolar nickel-hydrogen testing
[NASA-TM-100936] 18 p2536 N88-25059

The scaling of the threshold conditions for solid propellant erosive burning 19 p2630 N88-25601

Propagation effects by roadside trees measured at UHF and L-band for mobile satellite systems
19 p2644 N88-25693

Land mobile satellite propagation results
19 p2645 N88-25698

System architecture for the Canadian interim mobile satellite system 19 p2646 N88-25703

Design, development and trials of an airline passenger telephone system 19 p2646 N88-25704

Land mobile satellite demonstration system
19 p2646 N88-25706

Mobilestar field test program
19 p2646 N88-25707

Test results of the Electric Vehicle Field-Laboratory Correspondence Program, phase 1 report
[DE88-007706] 19 p2661 N88-25827

Pulsatile fluidic pump performance at elevated temperatures
[DE88-008046] 19 p2677 N88-25919

Solar assisted absorption or motor driven heat pump with earth seasonal storage. Part 2: Tables and figures
[DE88-900226] 19 p2686 N88-25964

Performance evaluation for multiprocessors programmed using monitors
[DE88-010056] 19 p2718 N88-26138

X-ray and optical analysis of surface properties of metal optics
[DE88-004033] 19 p2727 N88-26195

Hover performance tests of baseline metal and Advanced Technology Blade (ATB) rotor systems for the XV-15 tilt rotor aircraft
[NASA-CR-177436] 20 p2759 N88-26367

Digital communication transmitter and receiver test procedures
[AD-A191218] 20 p2788 N88-26540

Computer controlled procedures for traction battery power performance tests
[ETN-88-92352] 20 p2796 N88-26589

Evaluation of thermophosphor temperature technique
[DE88-007654] 20 p2805 N88-26638

Testing of a gravimeter LCR G 785
[B8735061] 20 p2806 N88-26643

Automated system for mathematical processing of the data from a hybrid spectrometer
[DE87-702995] 20 p2836 N88-26820

The evaluation of a deformable diffraction grating for a stigmatic EUV spectroheliometer
[NASA-CR-183064] 20 p2653 N88-26941

Plasma armature formation in high-pressure, high-velocity hydrogen
[DE88-008347] 20 p2857 N88-26967

A comparison of theory and experiment for aeroelastic stability of a hingeless rotor model in hover
21 p2889 N88-27150

A comparison of theory and experiment for coupled rotor-body stability of a hingeless rotor model in hover under simulated vacuum conditions
21 p2889 N88-27151

A comparison of theory and experiment for the aeroelastic stability of a bearingless model rotor in hover
21 p2890 N88-27153

Assembly Test Article (ATA)
[NASA-CR-179361] 21 p2903 N88-27226

Alkaline fuel cell performance investigation
[NASA-TM-100937] 21 p2909 N88-27267

Thermomechanical processing of Al alloy 2090 for grain refinement and superplasticity
[AD-A192333] 21 p2912 N88-27281

Sodium/sulfur cell evaluation results
[DE88-011488] 21 p2938 N88-27451

Post-test observations on CSPL (Chloride Silent Power Limited) cells
[DE88-011975] 21 p2940 N88-27461

The 210-HP diesel engine endurance and performance testing with fire resistant diesel fuel
[AD-A193153] 21 p2956 N88-27558

Basic mechanisms of diesel lubrication correlation of bench and engine tests
[AD-A193380] 21 p2956 N88-27561

Performance sensitivities for point-focus dish systems with secondary concentrators
[DE88-001152] 21 p2968 N88-27629

Photovoltaic Measurements and Performance Branch
[DE88-001142] 21 p2968 N88-27633

Performance evaluation of large-area glass-mirror heliostats
[DE88-011883] 21 p2969 N88-27636

Vapor Compression Distillation Subsystem (VCDS) component enhancement, testing and expert fault diagnostics development, volume 2
[NASA-CR-172076] 21 p2994 N88-27755

On-board data processing of navigation data at high latitudes in Antarctica 22 p3036 N88-28027

Performance of 10-kW class xenon ion thrusters
[NASA-TM-101282] 22 p3049 N88-28088

X-band resonant ring operation at 450 kW
22 p3064 N88-28181

Performance analysis of a noncoherently combined large aperture optical heterodyne receiver
22 p3065 N88-28189

An electronically tuned, stable 8415-MHz dielectric resonator FET oscillator for space applications
22 p3068 N88-28205

Goldstone solar system radar performance analysis
22 p3068 N88-28206

Development of 30 micrometers extrinsic silicon multiplexed infrared deterctor array
[NASA-CR-177446] 22 p3082 N88-28301

Acoustic detection of helicopters: Experiments
22 p3148 N88-28727

Performance of the Los Alamos expanding telescope
[DE88-010924] 22 p3151 N88-28751

Verification and tests --- space projects
22 p3160 N88-28814

Reliability assessment of Surface Mount Technology (SMT)
[AD-A193759] 23 p3208 N88-29089

Construction of a laser Doppler anemometer and its use for the testing of a novel probe for the measurement of the variations of the lateral component of the vortex vector
[MPIS-13/1987] 23 p3217 N88-29147

Two phase flow in a rotating screw tube (screw tube pump). Investigation of the function and efficiency of the screw tube pump
[MPIS-16/1987] 23 p3222 N88-29178

Effects of precipitation on wind turbine performance
[DE88-001144] 23 p3228 N88-29211

Systolic array fault tolerance performance analysis
[AD-A193521] 23 p3244 N88-29306

A performance study of the hypercube architecture
[AD-A194361] 23 p3264 N88-29433

On the design and optimization of distributed signal detection and parameter estimation systems
[AD-A193934] 23 p3266 N88-29446

SSTS (Space Surveillance and Tracking System): The importance of early test and evaluation organizational participation
[AD-A193745] 23 p3276 N88-29499

Controlled degradation of resolution of high-quality flight simulator images for training effectiveness evaluation
[AD-A196189] 24 p3330 N88-29823

Performance and lifetime assessment of MPD arc thruster technology
[NASA-TM-101293] 24 p3336 N88-29860

A small annular combustor of high power density, wide operating range and low manufacturing cost
24 p3351 N88-29951

Additional fracture and strength test results for A723 steel and 38644 titanium
[AD-A196329] 24 p3353 N88-29960

EMPTAC (Electromagnetic Pulse Test Aircraft) user's guide
[AD-A195072] 24 p3360 N88-30006

Qualification test levels for units to be derived from mechanical test data analysis --- ESA
[REPT-87-158-EI/ET/AG] 24 p3381 N88-30139

PERFUSION

U DIFFUSION

PERIDOTITE

An integrated study of the Alto Paranaiba Kimberlite Province, Minas Gerais, Brazil: A possible tool for diamond exploration 17 p2355 N88-24031

The petrogenesis of oceanic kimberlites and included mantle megacrysts: The Malaitan alnoite
24 p3397 N88-30232

PERIGEES

Study of a safe attitude for the Infrared Space Observatory (ISO) during perigee pass
[SNIAS-881-440-113] 23 p3185 N88-28954

PERIHELIONS

On the possible origin of meteoroid generating asteroid orbits 06 p0740 N88-14553

Comparative analysis of ultraviolet observations of Halley's comet on ASTRON astrophysical station before and after perihelion 08 p1004 N88-16096

Mars earth-based radar: 1986 results and 1988-1990 opportunities 23 p3306 N88-29697

PERIOD DOUBLING

Fully developed turbulence via Feigenbaum's period-doubling bifurcations
[DE88-000242] 04 p0441 N88-12739

Period-doubling universality in multidimensional dissipative and conservative systems
[PB88-148812] 13 p1832 N88-20961

PERIOD EQUATIONS

U PERIODIC FUNCTIONS

PERIODIC FUNCTIONS

NT COSINE SERIES
NT TANGENTS
NT TRIGONOMETRIC FUNCTIONS

Efficient computation of periodic Green's functions with application to grating structures
[AD-A184853] 05 p0640 N88-13912
Global bifurcation of periodic solutions with symmetry
[AD-A185881] 07 p0908 N88-15501
Almost-periodic solutions of nonlinear parabolic equations
[DE88-006423] 15 p2118 N88-22618
Periodically correlated processes and their stationary dilations
[NASA-CR-182904] 16 p2263 N88-23530
On a class of functionals invariant under a Z(sup n) action
[AD-A193474] 23 p3269 N88-29451
Periodic solutions of perturbed superquadratic Hamiltonian systems
[AD-A194292] 23 p3270 N88-29457
On the periodic nonlinearity and the multiplicity of solutions
[AD-A194295] 23 p3270 N88-29459

PERIODIC ORBITS
U ORBITS

PERIODIC PROCESSES
U CYCLES

PERIODIC VARIATIONS
NT ANNUAL VARIATIONS
NT DIURNAL VARIATIONS
NT NOCTURNAL VARIATIONS
NT SECULAR VARIATIONS
Basic properties and variability
02 p0252 N88-11593
On the interannual variability of South American climate and the Southern Oscillation 04 p0470 N88-12905
Long-period variations of wind parameters in the mesopause region and the solar cycle dependence
06 p0733 N88-14509
Short-term temporal variations of Nimbus-7 measurements of the solar UV spectral irradiance
[PB88-102132] 07 p0946 N88-15753
Quasiperiodic variations in manifestations of solar activity 08 p1004 N88-16083
Analysis of low frequency current fluctuations in the North-East Atlantic Ocean
[REPT-170] 09 p1196 N88-17165
A note on a diagonally implicit Runge-Kutta-Nystrom method
[CWI-NM-R8706] 09 p1228 N88-17358
Analysis of the spectral vanishing viscosity method for periodic conservation laws
[NASA-CR-181613] 09 p1231 N88-17378
An adaptive filtering technique for removing periodic noise from modal response data
[DE88-002347] 10 p1322 N88-17903
The absolute total magnitudes of periodic comets and their variations 14 p1994 N88-21887
The comet flux and the 15 Myr galactic cycle
14 p1995 N88-21889
Recent observations of the OH radio lines in comets
14 p1999 N88-21917
Color fluctuations in the inner coma of Comet Halley as measured from VEGA-2 14 p2000 N88-21925
Variation of grain properties at the dust outbursts --- Halley's comet 14 p2003 N88-21943
Dynamic characteristics of a vibrating beam with periodic variation in bending stiffness
[NASA-TP-2697] 17 p2348 N88-23988
Nonlinear vibrations of periodically stiffened plates
21 p2963 N88-27598
Periodic oscillations in nonlinear mechanical systems
21 p2963 N88-27599
Asymptotic giant branch stars in the Infrared Astronomical Satellite (IRAS) catalogs: Selection and analysis of the population characteristics
[MPE-PREPRINT-116] 22 p3163 N88-28840
Regular orbital variations in the ultraviolet resonance lines of YZ Cnc
[MPE-PREPRINT-117] 22 p3165 N88-28850
Time periodic control of a multi-blade helicopter
[AD-A194435] 23 p3180 N88-28931
Plane periodic satellite motions relative to center of mass in neighborhood of collinear libration point
24 p3445 N88-30507

PERIODICALS
Solar-geophysical data number 515, July 1987. Supplement (explanation of data reports)
[PB87-233169] 06 p0805 N88-14914
Wind Energy Technology: Generating power from the wind, a current awareness bulletin
[DE88-008292] 20 p2620 N88-26729

PERIODICITY
U PERIODIC VARIATIONS

PERIODICITY (BIOLOGY)
U RHYTHM (BIOLOGY)

PERIPHERAL CIRCULATION
Cardiac and peripheral circulation assessment by ultrasound on 3 astronauts during two 7-day space flights (1982 Salyut-7 - 1985 STS 51G)
12 p1656 N88-19921
Leg volume change under Lower Body Negative Pressure (LBNP) in dependence on stratification
[DFVLR-FB-87-47] 16 p2238 N88-23367
Physiological responses to acute exercise-heat stress
[AD-A192606] 21 p2986 N88-27732
The effects of acute cold exposure on exercise performance
[AD-A192650] 22 p3130 N88-28610
Alterations in cutaneous vasomotor regulation during acute and chronic hypoxia
[AD-A192653] 22 p3131 N88-28612

PERIPHERAL EQUIPMENT (COMPUTERS)
NT PRINTERS (DATA PROCESSING)
NT REMOTE CONSOLES
Computer architecture for research in meteorology and atmospheric chemistry
[PB88-145313] 11 p1510 N88-19020
Microvax networked computer system
[AD-A190308] 15 p2114 N88-22596
Definition of an auxiliary processor dedicated to real-time operating system kernels
[NASA-CR-183070] 20 p2841 N88-26860

PERIPHERIES
U BOUNDARIES

PERISCOPES
Welding monitoring system
[NASA-CASE-MFS-29177-1] 06 p0712 N88-14362

PERMANENT MAGNETS
Study of free-piston Stirling engine driven linear alternators
[NASA-CR-181425] 01 p0055 N88-10355
Process support compressor motor electromagnetic design summary
[DE87-014359] 02 p0167 N88-11048
Design verification tests for an axial gap permanent magnet compressor motor
[DE87-014360] 02 p0167 N88-11049
Performance of high power S-band klystrons focused with permanent magnet
[DE87-753024] 02 p0167 N88-11053
A long electromagnetic wiggler for the paladin free-electron laser experiments
[DE88-000970] 05 p0588 N88-13589
Development of a laced electromagnetic wiggler
[DE88-000972] 05 p0646 N88-13953
Dynamic high pressure process for fabricating superconducting and permanent magnetic materials
[DE88-000848] 06 p0785 N88-14817
Metallurgical processes in multi-component rare earth-transition metal permanent magnet alloys
[AD-A186401] 07 p0832 N88-15045
Modeling the behavior of oriented permanent magnet material using current double theory
[DE88-004446] 13 p1833 N88-20963
ONR Far East Scientific Bulletin, volume 12, number 3, July-September 1987
[AD-A188554] 13 p1851 N88-21081
A high performance inverter-fed drive system of an interior permanent magnet synchronous machine
[DE88-006753] 15 p2061 N88-22288
Performance test results: AXIAL-GAP, permanent magnet compressor motor
[DE88-006857] 15 p2061 N88-22289
A microcomputer-based control and simulation of an advanced IPM (Interior Permanent Magnet) synchronous machine drive system for electric vehicle propulsion
[DE88-006735] 18 p2505 N88-24859

PERMEABILITY
The water permeability of multi-layer coatings
[BLL-M-37252-(5828.4)] 02 p0148 N88-10927
Investigation of structure-permeability relationships of silicone polymer membranes
[PB87-230181] 03 p0293 N88-11839
Geological characterization and statistical comparison of outcrop and subsurface facies: Shannon Shelf sand ridges
[DE87-001243] 03 p0348 N88-12202
Novel macrocyclic carriers for proton-coupled liquid membrane transport
[DE88-000636] 04 p0413 N88-12560
A study of mechanisms of hydrogen diffusion in separation devices
[DE88-000328] 04 p0416 N88-12584
Programs for calculating transient Darcian flow through non-uniform materials
[DE88-001924] 07 p0852 N88-15177
Physics of immiscible flow in porous media
[PB88-131008] 11 p1487 N88-18873
The effect of Ca(OH)2-treated ceramic microspheres on the mechanical properties of high-temperature lightweight cement composites
[DE88-004590] 13 p1749 N88-20457
Molecular and electronic mechanism in the control of Na+ and K+ permeability of excitable cell membrane by ligand binding on receptor sites
[AD-A188725] 13 p1808 N88-20805
Use of nonporous metals membranes for the separation of hydrogen from gas mixtures
[BMFT-FB-T-86-206] 14 p1888 N88-21280
Synthesis and analysis of novel polymers with potential for providing both high permselectivity and permeability in gas separation applications
[DE88-006533] 15 p2043 N88-22174
Study of fracturing for groundwater research in the Sergipe state with remote sensing products
17 p2359 N88-24052
Interaction of vinylidene fluoride: Tetrafluoroethylene copolymer with ammonia
[NASA-TT-20292] 19 p2620 N88-25542
Characteristics of pressure loss during filtration using a porous ceramic filter
[DE88-752547] 20 p2798 N88-26604
Investigation of hydrogen isotope penetration through stainless steels Kh18N10T and Kh3M2BFR
[DE88-702189] 21 p2915 N88-27297
Optimal rheological characteristics in dynamic stability of polymer flow through porous media
[DE88-001225] 21 p2918 N88-27322
Hyperthermia: New thoughts on an old problem
[AD-A192602] 21 p2986 N88-27731

PERMEATING
Physics of immiscible flow in porous media
[PB88-131008] 11 p1487 N88-18873
The effect of H2S concentration and pH on hydrogen permeation in AISI 410 stainless steel in 5 percent NaCl
[NPL-DMA(A)-148] 14 p1890 N88-21293
Mechanisms of gas permeation through polymer membranes: Renewal proposal for period December 1, 1986 - November 30, 1989
[DE88-007436] 18 p2494 N88-24796
Hydrogen permeation through metallic foils
[DE88-702600] 23 p3193 N88-29000
Design criteria for extraction with chemical reaction and liquid membrane permeation
[NASA-TT-20352] 24 p3343 N88-29899

PERMITTIVITY
Automated microwave dielectric constant measurement
[AD-A184182] 04 p0431 N88-12667
Electromagnetic wave probing of Earth's environment
[NASA-CR-182358] 06 p0690 N88-14232
Mars: High resolution VLA observations at wavelengths of 2 and 6 cm and derived properties
06 p0804 N88-14909
Investigation of surface wave blindness in microstrip phased array antennas
[AD-A189326] 12 p1621 N88-19696
Characterization of 6 soils in the X-band, through measurements of complex permittivity
[INPE-4376-TDL/302] 12 p1639 N88-19814
Method for characterizing end-plate surface resistance of dielectric resonator 14 p1903 N88-21371
Processing and additive effects of ZrO2 on microstructure and dielectric porperties of BaTiO3 ceramics
[AD-A193126] 21 p2917 N88-27316
Active and passive remote sensing of ice
[AD-A193307] 21 p2966 N88-27617
Viking Landers and remote sensing
23 p3304 N88-29685

PERMUTATIONS
The Lambda network: A new permutation network
[DE88-003568] 10 p1392 N88-18305
Graphs related to Held's simple group
[CWI-PM-28707] 16 p2264 N88-23536

PEROVSKITES
Structural relationships in high temperature superconductors
[DE88-002924] 09 p1257 N88-17534
Ordered structures in YBa2Cu3O/sub 7-y/, La2Cu3O/sub 7-y/, La/sub 2-x/Sr/sub x/CuO/sub 4-par delta/ and related perovskites
[DE88-006461] 14 p1987 N88-21851
Probing the electronic and defect structure of perovskite superconductors
[DE88-008349] 21 p3022 N88-27939

PEROXIDES
NT HYDROGEN PEROXIDE
The redox chemistry of some peroxo and superoxo metal ion complexes
[AD-A189159] 12 p1606 N88-19606
Copper peroxide
[NASA-TT-20245] 14 p1888 N88-21282

Solar generation and storage of O2 (a 1 delta g)
[NASA-CR-4127] 14 p1913 N88-21431
Development of a test method to determine potential peroxide content in turbine fuels. Part 2
[AD-A192244] 23 p3199 N88-29042
Electrocatalytic reduction of oxygen on modified oxide surfaces
[NASA-TM-101333] 24 p3352 N88-29952
Determination of the hydroperoxide potential of jet fuels
[AD-A195975] 24 p3357 N88-29991

PERSEID METEOROIDS
On the spatial structure of the Perseids meteor stream
06 p0740 N88-14550

PERSONAL COMPUTERS
A work station for EXELFS data acquisition and analysis
[USIP-87-10] 01 p0078 N88-10498
A CAMAC system controlled by an IBM AT computer for time-resolved spectroscopy
[DE87-010111] 01 p0080 N88-10514
An evaluation of WPS-Plus word processing software for the IBM PC and compatibles
[DE87-011972] 01 p0081 N88-10518
Personal Computer (PC) based image processing applied to fluid mechanics
[NASA-TM-100024] 02 p0172 N88-11087
A mini system for nowcasting
02 p0204 N88-11278
Personal computers: A powerful tool for project management
[DE87-013381] 02 p0219 N88-11377
Electronic authoring tools
[DE87-011797] 02 p0248 N88-11567
The Macintosh computer as a tool for rapid data analysis and for producing camera ready viewgraphs/publications
[DE87-014350] 03 p0362 N88-12280
FORTRAN compiler performance benchmarks for the IBM personal computer
[LA-10883-MS] 03 p0363 N88-12284
BASIC desk-top computer program for the three-dimensional static configuration of an extensible flexible cable in a uniform stream
[AD-A184852] 05 p0609 N88-13737
Mixing Microsoft C and Microsoft FORTRAN program modules on the IBM Personal Computer
[DE88-001947] 05 p0637 N88-13895
Compilation and development of K-6 aerospace materials for implementation in NASA spacelink electronic information system 07 p0922 N88-15605
Satellite interference analysis and simulation using personal computers
[NASA-CR-182522] 10 p1319 N88-17890
Personal computers and All-In-1: Document transfer and translation
[DE88-003760] 10 p1384 N88-18264
TABLET: The personal computer of the year 2000
[NASA-CR-182528] 10 p1384 N88-18267
An IBM PC version of ASENT
[DE88-004244] 11 p1532 N88-19150
The global positioning system as an aid to the testing of inertial navigation units (volume 1, addendum 1)
[AD-A185783] 12 p1578 N88-19443
Output formatting in Apple-soft BASIC
[DE88-701413] 15 p2108 N88-22559
Implementation of a distributed adaptive routing algorithm on the Intel iPSC (Intel Personal Super-Computer)
[AD-A189849] 15 p2109 N88-22567
Measurement data processing system based on personal computer. For scramjet combustion test
[DE88-751807] 16 p2174 N88-22959
Practical image analysis using personal computers: The Canadian experience 17 p2356 N88-24037
Personal computer as a workstation in a cartographic automation system? 18 p2535 N88-25039
Advances in personal computers for scientific applications
[DE88-009824] 19 p2713 N88-26107
Synopsis of a computer program designed to interface a personal computer with the fast data acquisition system of a time-of-flight mass spectrometer
[NASA-CR-177474] 21 p3001 N88-27798
Waveform analysis on the IBM PC
[AD-A194243] 23 p3248 N88-29330
Aircraft noise prediction program propeller analysis system IBM-PC version user's manual version 2.0
[NASA-CR-181689] 24 p3428 N88-30399

PERSONALITY
Brain potentials and personality: A new look at stress susceptibility
[AD-A186931] 09 p1199 N88-17189
Brainstem response and state-trait variables
16 p2242 N88-23394
Research on piloting under conditions of breakdown in flight
[PB87-217980] 19 p2710 N88-26102

PERSONALITY TESTS
Computer response time measurements of mood, fatigue and symptom scale items: Implications for scale response time uses
[AD-A186093] 07 p0888 N88-15384
Temperament Structure Scales (TSS). Test manual
[ESA-TT-1069] 09 p1201 N88-17197

PERSONNEL
NT AIR TRAFFIC CONTROLLERS (PERSONNEL)
NT AIRCRAFT PILOTS
NT ASTRONAUTS
NT COSMONAUTS
NT CREWS
NT FLIGHT CREWS
NT GROUND CREWS
NT INSTRUCTORS
NT MEDICAL PERSONNEL
NT NAVIGATORS
NT OPERATORS (PERSONNEL)
NT ORBITAL WORKERS
NT PILOTS (PERSONNEL)
NT PROGRAMMERS
NT SCIENTISTS
NT SPACECREWS
Antarctic field tests of SARSAT personal locater beacons
[NASA-TM-4008] 01 p0063 N88-10403
A review of computer-assisted photo interpretation research at USAETL (US Army Engineer Topographic Laboratories)
[AD-A184034] 03 p0346 N88-12186
On computing environments in data analysis
[DE88-000078] 04 p0480 N88-12961
Group adaptation and individual adjustment in antarctica: A summary of recent research
[AD-A186605] 08 p1051 N88-16347
Lewis materials research and technology: An overview
09 p1119 N88-16699
Brain potentials and personality: A new look at stress susceptibility
[AD-A186931] 09 p1199 N88-17189
Information needs analysis for the Aeronautical Systems Division Executive Information System
[AD-A186912] 09 p1261 N88-17556
Relationships between coronary heart disease risk factors and serum ionized calcium in Kennedy Space Center Cohort
[NASA-TM-100979] 10 p1368 N88-18177
The accommodative status in the dark of US Navy fighter pilots
[AD-A188188] 10 p1370 N88-18186
Report of the participation in the International Training Course: Remote Sensing in Village Forestry
[INPE-4476-NTE/278] 12 p1637 N88-19802
A comparison of terrain association and resection as methods of position location
[AD-A189480] 13 p1790 N88-20710
Napping and human functioning during prolonged work
[AD-A190228] 15 p2102 N88-22525
Prediction of physical fitness: Estimated percent body fat using body circumferences versus weight-height measures
[AD-A190233] 15 p2103 N88-22526
An evaluation of the effects of high visual taskload on the separate behaviors involved in complex monitoring performance
[AD-A190641] 15 p2105 N88-22538
Relationship of encoding speed and memory tests to flight training performance
[AD-A190670] 15 p2105 N88-22539
Problem solving in a natural task as a function of experience
[AD-A191180] 16 p2243 N88-23399
US civil airmen statistics, 1987
[AD-A191714] 18 p2455 N88-24577
Development of inductive storage pulsed power generators
[AD-A193878] 22 p3117 N88-28521
Computer-aided decision making
[AD-A194210] 22 p3137 N88-28651
Flight information publication (FLIP) feedback
[AD-A194462] 23 p3174 N88-28897
Reliability and construct validity of reaction time, inspection time and machine-paced tests of cognitive speed
[AD-A193779] 23 p3241 N88-29289

PERSONNEL DEVELOPMENT
Field evaluation of interactive simulation for maintenance training: SH-3 helicopter electro-mechanical bladefold system
[AD-A185923] 07 p0821 N88-14991
Tutoring electronic troubleshooting in a simulated maintenance work environment
09 p1204 N88-17215
Anatomy of an organizational change effort at the Lewis Research Center
[NASA-CR-4146] 19 p2739 N88-26264

PERSONNEL MANAGEMENT
Development of a prototype H-46 helicopter diagnostic expert system
[AD-A186077] 07 p0809 N88-14924
Meta-analysis of leadership differences between males and females and the effect on performance
[AD-A187769] 11 p1564 N88-19361
People, procedures, performance: The keys to improving the development environment 12 p1704 N88-20197
Management and the executive
[AD-A190778] 18 p2587 N88-25374
The time of leaders 22 p3160 N88-28809

PERSONNEL PROPULSION SYSTEMS
U SELF MANEUVERING UNITS

PERSONNEL SELECTION
NT PILOT SELECTION
Antarctica as a model for the human exploration of Mars
[AD-A185835] 08 p1051 N88-16342
Temperament Structure Scales (TSS). Test manual
[ESA-TT-1069] 09 p1201 N88-17197
Human factor in engineering work
12 p1663 N88-19970
Field dependence-independence and its relationship to flight training performance
[AD-A188888] 12 p1670 N88-20003
The program Kennedy Approach as an experimental design of a dynamic computerized air traffic control test
[DFVLR-FB-87-50] 16 p2159 N88-22881
Utility NDE personnel qualification/certification: Enhanced personnel qualification requirements for ASME (American Society for Mechanical Engineers) Code Section 11 examinations
[DE88-006748] 16 p2216 N88-23222
Stress in relation to the physical and social environment 19 p2695 N88-26020
Selecting the right crew for future space stations: An analysis of selection research on offshore divers, aviation pilots and other high risk groups in Scandinavia
19 p2696 N88-26021
Selection and training of subjects to live and work in hostile and unusual environments
19 p2696 N88-26026
Selection of isolated space crews
19 p2697 N88-26028
USAF flying screening: First step on the road to wings
[AD-A192613] 20 p2833 N88-26804
Proposed improvements to the USAF flight screening program
[AD-A194506] 23 p3240 N88-29285
Validity of the academic aptitude composite of the Air Force Officer Qualifying Test (AFOQT)
[AD-A194753] 23 p3240 N88-29286
Literature review: Validity and potential usefulness of psychomotor ability tests for personnel selection and classification
[AD-A193558] 23 p3241 N88-29287

PERSPIRATION
Physiological and hematological responses of matched older and younger men during dry-heat acclimation
[AD-A186450] 18 p2550 N88-25139
Physiological responses to acute exercise-heat stress
[AD-A192606] 21 p2986 N88-27732
The role of textile material in clothing on thermoregulatory responses to intermittent exercise
[AD-A192599] 22 p3130 N88-28608
Depressed sweating during exercise at altitude
[AD-A192603] 22 p3130 N88-28609

PERT
Project Monitoring Package (PMP): A package for project activity monitoring
[DE88-701234] 15 p2107 N88-22554

PERTURBATION
NT ORBIT PERTURBATION
NT SATELLITE PERTURBATION
On the role of snow in the redistribution of precipitation by small scale topography 02 p0203 N88-11267
Magnetohydrodynamic stability of spheromak plasma in toroidal flux conserver with rectangular cross section 3. Stability for symmetric modes
[IPPJ-845] 02 p0241 N88-11524
Long wavelength vortices of low frequency interchange modes
[IPPJ-844] 02 p0241 N88-11525
Numerical study of the entrance flow and its transition in a circular pipe (2) 03 p0318 N88-12011
Hardware-assisted multiprocessor performance measurements
[PB87-226908] 03 p0363 N88-12282

Perturbation and characterization of nonlinear processes
[DE87-014580] 03 p0369 N88-12322

Identification of perturbations in turbomachines by the analysis of pressure signals, vibrations and wavelike motions
[ETN-88-90602] 05 p0590 N88-13600

Improvement of modal scaling factors using mass additive technique 05 p0593 N88-13620

Development of a data analysis system for the detection of lower level atmospheric turbulence with an acoustic sounder
[AD-A184972] 05 p0624 N88-13821

A direct calculation method for perturbation fields of moving bodies in compressible media at subsonic Mach numbers
[ETN-88-90608] 06 p0701 N88-14305

Evolution of perturbations in expanding universe
06 p0775 N88-14759

Analytical investigations of bulk wave resonators in the piezoelectric thin film on gallium-arsenide configuration
[AD-A185716] 06 p0789 N88-14840

Analysis and interpretation of satellite fragmentation data 06 p0798 N88-14885

Low-disturbance wind tunnels
07 p0811 N88-14937

An additional study and implementation of tone calibrated technique of modulation
[NASA-CR-182377] 07 p0844 N88-15117

Infrared emission and tidal interactions of spiral galaxies 07 p0923 N88-15611

Perturbations of the Sun's gravitational field due to solar oscillations
[DE88-002099] 07 p0946 N88-15751

Large-angle slewing maneuvers for flexible spacecraft
[NASA-CR-4123] 08 p1000 N88-16060

Dynamic modeling of the middle atmosphere
08 p1028 N88-16227

Adaptive proximate time-optimal servomechanisms
09 p1175 N88-17043

Convective wind fields as investigated with doppler lidar
[PB88-115472] 09 p1193 N88-17151

Perturbation theory for dual semigroups 2. Time-dependent perturbations in the sun-reflexive case
[PB88-113097] 09 p1230 N88-17369

Microgravity experiments in space: Compatibility with dynamic perturbing effects 09 p1241 N88-17435

Waves and static electric fields in the auroral acceleration region 12 p1646 N88-19856

On the theory of electromagnetic scattering from a raindrop splash
[AD-A188720] 14 p1906 N88-21393

Solutions for direct and indirect problems in free surface flows
[REPT-87-35] 14 p1909 N88-21409

Spacecraft trajectories
[ISBN-2-85-428166-7] 15 p2023 N88-22054

Comparative analysis
[AD-A190556] 15 p2065 N88-22313

Effect of vibrational excitation on rate parameters of atmospheric reactions
[AD-A190464] 15 p2094 N88-22477

Numerical methods for singularly perturbed differential equations with applications
[AD-A189786] 15 p2119 N88-22628

Density perturbations in a rotating universe
[DE87-703036] 15 p2151 N88-22840

Development and improvement of a code to calculate small, three dimensional, unsteady transonic perturbations
[ONERA-RTS-31/3064-RY-062-R]
17 p2338 N88-23951

Finite element simulation of the atmosphere's electromagnetic response to charge perturbations associated with lightning 17 p2375 N88-24124

On the propagating speed in difference approximations for conservation laws 19 p2639 N88-25658

The propagation of pressure perturbations in bubbly air/water flows 19 p2664 N88-25843

Peturbational analysis of the curved anisotropic optical fiber for the birefringence due to the geometry
[PB88-171848] 19 p2726 N88-26189

An initial investigation into methods of computing transonic aerodynamic sensitivity coefficients
[NASA-CR-183061] 20 p2752 N88-26332

The feasibility of the disturbance accommodating controller for precision antenna pointing
22 p3064 N88-28182

Asymptotic orders of reachability in perturbed linear systems
[AD-A192718] 22 p3143 N88-28688

A singular perturbation analysis of the weakly nonlinear evolution of long and short water waves and waves in boundary layers 23 p3209 N88-29102

Computation of the eigenvalues for perturbations of Poiseuille flow using a two-point boundary value method
[AD-A193479] 23 p3210 N88-29104

An exponential decay estimate for the stationary perturbation of Poiseuille flow
[AD-A193480] 23 p3210 N88-29105

Periodic solutions of perturbed superquadratic Hamiltonian systems
[AD-A194292] 23 p3270 N88-29457

Chaotic behaviour in quantum dynamics
[AD-A193936] 23 p3295 N88-29623

Theories of comparative analysis
[AD-A196328] 24 p3427 N88-30395

PERTURBATION THEORY

A study of a satellite-to-satellite tracking configuration by application of linear perturbation theory
[REPT-86.3] 01 p0011 N88-10059

Estimability of potential coefficients from orbit perturbations --- satellite geodesy
[REPT-86.1] 01 p0064 N88-10408

Development of many-body methods for flame chemistry and large molecule applications
[AD-A184451] 03 p0284 N88-11789

Theory of atomic additivity in molecular hyperpolizabilities 03 p0297 N88-11867

Analytical studies of axially symmetric motion of an incompressible viscous fluid between two concentric rotating spheres 04 p0444 N88-12757

The free electron laser sideband instability reconsidered
[AD-A184269] 04 p0447 N88-12773

Vibration and parametric excitation in rotating asymmetric circular plates 04 p0456 N88-12823

Model of solar-wind magnetosphere coupling
04 p0525 N88-13211

Design of low order controllers for robust disturbance rejection in large space structures
[AD-A185202] 05 p0555 N88-13376

Robustness of linear systems
[PB87-220042] 05 p0639 N88-13909

Molecular dynamics studies of aromatic hydrocarbon liquids
[DE88-001473] 05 p0648 N88-13973

Dynamics of meteor streams
06 p0732 N88-14503

Perturbative coherence in field theory
[DE88-700366] 07 p0941 N88-1571

Study on orbits near the triangular libration points in the perturbed restricted three body problem
[ESA-CR(P)-2440] 07 p0944 N88-15741

Synoptic perturbations and climate
08 p1016 N88-16158

Effect of extraneous factors on optical one-phonon transitions in impurity centers with cubic symmetry
08 p1077 N88-16496

An initial investigation into methods of computing transonic aerodynamics sensitivity coefficients
[NASA-CR-182444] 09 p1112 N88-16663

A dynamical system/coherent structure approach to the fully developed turbulent wall layer
10 p1267 N88-17578

Application of state-multipole Heisenberg equations to Raman excitation dynamics
[DE88-003828] 10 p1335 N88-17977

Theoretical studies of atomic transitions
[DE88-004719] 10 p1407 N88-18389

Nuclear structure at intermediate energies
[DE88-002796] 10 p1407 N88-18390

Theoretical and experimental analysis of pressure pulse transmission in non-Newtonian pipe flow
11 p1485 N88-18863

Domain perturbation method in the static equilibrium of masses in rotation
[INPE-4217-PRE/1098] 12 p1686 N88-20085

Horizontal scales of wind forced inertial motions
13 p1806 N88-20795

Unfoldings of quasi-periodic tori
[ZW-8706] 13 p1828 N88-20928

Finite width corrections to the Nambu action for the Nielsen-Olesen string
[DE88-006996] 15 p2147 N88-22812

Multicontinuations method and strong regular perturbations of linear operators
[DE88-701375] 16 p2263 N88-23533

Perturbation theory for dual semigroups. Part 3: Nonlinear Lipschitz continuous perturbations in the Sun-reflexive case
[CWI-AM-R8706-PT-3] 16 p2263 N88-23535

Stark effect in intense field. Perturbation theory and 1/n-expansion
[DE87-702947] 16 p2266 N88-23550

Electromagnetic scattering from nonlinear anisotropic cylinders 17 p2333 N88-23930

An experimental study of the coherent under-ice reflectivity of sound in the Greenland Sea Marginal Ice Zone 18 p2548 N88-25125

Perturbation theory for dual semigroups. Part 4: The intertwining formula and the canonical pairing
[CWI-AM-R8802-PT-4] 18 p2569 N88-25258

Magnetohydrodynamic squeeze film
[DE88-701876] 20 p2810 N88-26669

Recoil saturation of the self-energy in atomic systems
[DE88-010450] 20 p2851 N88-26930

Perturbation expansions generated by an approximate propagator
[DE88-702435] 21 p3011 N88-27866

Reminimization of energy integral and stability limit for non-ideal MHD (magnetohydrodynamic) plasma
[DE88-008422] 21 p3018 N88-27911

Self energy corrections to the ab initio band structures: Chromium
[DE88-701825] 21 p3020 N88-27927

Vortices on the world sheet and string's critical dynamics
[DE88-702116] 21 p3026 N88-27961

Multiphoton transitions in semiconductors in the non-perturbative approach
[DE88-702664] 22 p3157 N88-28786

Calculations in perturbative string field theory
[DE88-011616] 22 p3158 N88-28798

Unfoldings of quasi-periodic tori
[B8611118] 23 p3278 N88-29513

On the meaning of perturbation expansions in quantum field theory
[DE88-702138] 23 p3294 N88-29620

Free vibration of rectangular plates with a small initial curvature
[NASA-CR-179370] 24 p3383 N88-30148

PETN

Shock measurements on explosives in the supra compressive region
[DE87-008423] 01 p0031 N88-10196

The equation of state of PETN detonation products
[DE87-013796] 02 p0155 N88-10971

Thermal decomposition studies of explosives for component applications
[DE88-007201] 18 p2495 N88-24805

Freely expanding detonation products: Scaling of rate processes
[DE88-007827] 20 p2799 N88-26606

PETRI NETS

Strategies for concurrent processing of complex algorithms in data driven architectures
[NASA-CR-181435] 01 p0082 N88-10527

Petri nets as a support to symbolic execution of concurrent Ada programs
[REPT-87-007] 01 p0082 N88-10529

Methodology of performance evaluation of real time distributed systems
[ENST-87D003] 02 p0228 N88-11440

Computer aided design for Petri Nets
[AD-A186109] 07 p0902 N88-15465

Strategies for concurrent processing of complex algorithms 10 p1379 N88-18236

Conception of a knowledge-based system for designing distributed systems
[DFVLR-MITT-87-16] 14 p1961 N88-21694

Using Colored Stochastic Petri Net (CS-PN) software for protocol specification, validation, and evaluation
[ENST-87C004] 15 p2113 N88-22588

The Colored Stochastic Petri Net (CS-PN) software: Application to the validation and the performance evaluation of distributed systems
[ENST-87D005] 15 p2113 N88-22589

Simultaneous use of artificial intelligence and Petri nets: Application to the monitoring of a fabrication plan
[LAAS-87-354] 17 p2390 N88-24207

Some unsolved problems in modelling self-timed circuits using Petri Nets, series B, number 2
[PB86-181466] 18 p2507 N88-24872

Colored stochastic Petri nets. Application to real time distributed systems
[ENST-87E017] 20 p2839 N88-26843

On eclecticism in specifications: A case study centered around Petri nets --- software engineering
[REPT-87-008] 22 p3140 N88-28671

Using Petri nets for real-time development environments
[REPT-88-005] 22 p3141 N88-28679

PETROGRAPHY

A sedimentological and mineralogical study of the Koogah Formation, New South Wales
18 p2542 N88-25087

PETROLEUM
U CRUDE OIL

PETROLEUM PRODUCTS
NT ASPHALT
NT DIESEL FUELS
NT GASOLINE

Evaluation of the acute toxicity of a synthetic polyalphaolefin-based hydraulic fluid
[AD-A190412] 15 p2045 N88-22184

PETROLOGY
NT PETROGRAPHY
Geological characterization and statistical comparison of outcrop and subsurface facies: Shannon Shelf sand ridges
[DE87-001243] 03 p0348 N88-12202
Petrogenesis of basalts from the Archean Matachewan Dike Swarm Superior Province of Canada
06 p0796 N88-14878
Nature and origin of mineral coatings on volcanic rocks of the Black Mountain, Stonewall Mountain, and Kane Springs Wash volcanic centers, Southern Nevada
[NASA-CR-181437] 09 p1191 N88-17140
Aqueous alteration in S-N-C meteorites and implications for weathering products on Mars
23 p3303 N88-29673
Evidence for crustal recycling during the Archean: The parental magmas of the stillwater complex
24 p3396 N88-30226
The tectonic setting of Archean anorthosites
24 p3397 N88-30231
The petrogenesis of oceanic kimberlites and included mantle megacrysts: The Malaitan alnoite
24 p3397 N88-30232
Growth of the continental crust: A planetary-mantle perspective 24 p3400 N88-30251
Crustal underplating in the North American Craton: Evidence from the Petrogenesis of anorthositic rocks in the Middle Proterozoic Midcontinent Rift System
24 p3400 N88-30252

PH
Microstructural evolution and response to double-loop reactivation testing of heat-treated pH 13-8 Mo martensitic stainless steel
[DE87-009058] 02 p0146 N88-10915
The effect of H2S concentration and pH on hydrogen permeation in AISI 410 stainless steel in 5 percent NaCl
[NPL-DMA(A)-148] 14 p1890 N88-21293
The effect of H2S concentration and pH on the cracking resistance of AISI 410 stainless steel in 5 percent brine
[NPL-DMA(A)-149] 14 p1890 N88-21294
Complexation and hydrolysis reactions of iron(III)
17 p2322 N88-23867
Effect of process conditions on aluminum oxide thin film used in pH ISFET 19 p2673 N88-25892

PH FACTOR
Monitoring corrosion and process physical-chemical parameters in electric power plants
[CISE-3708] 06 p0682 N88-14182

PHANTOM AIRCRAFT
NT F-4 AIRCRAFT

PHARMACOLOGY
JPRS report: Science and technology. USSR: Life sciences
[JPRS-ULS-87-012] 03 p0355 N88-12238
JPRS report: Science and technology. USSR: Life sciences
[JPRS-ULS-87-009] 04 p0473 N88-12915
JPRS report: Science and technology. USSR: Life sciences
[JPRS-ULS-87-013] 06 p0750 N88-14608
Pharmacological resetting of the Circadian sleep-wake cycle
[AD-A186194] 07 p0889 N88-15385
Scaling physiological pharmacokinetic models by physiological time
[DE88-000335] 10 p1368 N88-18173
Changes in hemostasis system of animals under conditions of granulocytopoiesis inhibition under effect of decreased barometric pressure
12 p1651 N88-19890
JPRS report: Science and technology. USSR: Life sciences
[JPRS-ULS-88-002] 12 p1665 N88-19982
Changes in the status of the human tibia during antiorthostatic hypokinesia
[NASA-TT-20221] 13 p1810 N88-20813
Development of a C3 generic workstation: System overview 16 p2242 N88-23396
JPRS report: Science and technology. USSR: Life sciences
[JPRS-ULS-88-009] 20 p2829 N88-26785
Does dihydroergotamine used in therapeutical doses influence the physical and psychomotor performance of young pilots or other traffic drivers subjected to hypotonia?
[ETN-88-92136] 20 p2832 N88-26799

PHASE ANGLE
U PHASE SHIFT

PHASE CHANGE MATERIALS
Performance analysis of advanced spacecraft TPS
[NASA-CR-181532] 04 p0399 N88-12484
A study of the optimal transition temperatue of PCM (Phase Change Material) wallboard for solar energy storage
[DE88-001522] 04 p0466 N88-12882
Nickel hydroxide active material densities
[AD-A191411] 16 p2230 N88-23319
Magnetic studies of iron-rare-earth-metalloid alloys
[DE88-006801] 16 p2282 N88-23660
The morphological stability of continuous intergranular phases: Thermodynamic considerations
[DE88-006328] 18 p2584 N88-25350
Beam combining by phase transition nonlinear media
[AD-A194116] 23 p3283 N88-29547

PHASE COHERENCE
Optimized tracking of RF carriers with phase noise, including Pioneer 10 results 04 p0434 N88-12694
Coherent vortex structures in the wake of a stationary disk and of a disk excited to vibration
[ESA-TT-994] 09 p1163 N88-16968
Holographic phase correction
[RSRE-MEMO-4036] 09 p1167 N88-17000
Reduced tolerance imaging 2, volume 2
[AD-A189604] 13 p1829 N88-20939
Use of a coherent square wave reference to demodulate BPSK (Binary Phase Shift Keying) carriers and a visual indicator of the quality of received QPSK (Quadrature Phase Shift Keying) carriers
[AD-A193528] 23 p3204 N88-29065
Cooperative effects and intrinsic optical bistability in collections of atoms
[AD-A193993] 23 p3280 N88-29530

PHASE CONJUGATION
New physical explanation of phase-conjugate waves produced in backward stimulated scattering
03 p0302 N88-11900
Determination of the origin of self-pumped phase conjugation in barium titanate
[AD-A184697] 03 p0377 N88-12372
Research on acoustical scattering, diffraction catastrophes, optics of bubbles, photoacoustics, and acoustical phase conjugation
[AD-A185785] 06 p0776 N88-14761
Acoustical phase conjugation
[PREPRINT-561] 06 p0777 N88-14768
Self-pumped phase conjugation in a supersonically flowing medium
[AD-A188281] 10 p1338 N88-17998
Subpicosecond optical digital computation using phase conjugate parametric generators
[AD-A188279] 10 p1410 N88-18411
Nonlinear optical principles and the photorefractive effect applied to optical phase conjugation
[AD-A188856] 12 p1691 N88-20119
Analytical description of noise in phase-conjugate resonators
[PB88-171947] 19 p2726 N88-26188
Laser CO2/TEA frequency-stabilized by phase conjugation 22 p3082 N88-28303
Beam combining by phase transition nonlinear media
[AD-A194116] 23 p3283 N88-29547
Nonlinear optical phase conjugation techniques to reduce the physical size of lasers
[AD-A196170] 24 p3379 N88-30122

PHASE CONTROL
Phase control of the microwave radiation in free electron laser two-beam accelerator
[DE88-001460] 07 p0859 N88-15219
Determination of the commutation and angle and load response for a continuous-current, single phase controlled rectifier
[AD-A190602] 15 p2060 N88-22285
Active phase compensation system for fiber optic holography
[NASA-TM-101295] 20 p2805 N88-26641

PHASE DEMODULATORS
Use of a coherent square wave reference to demodulate BPSK (Binary Phase Shift Keying) carriers and a visual indicator of the quality of received QPSK (Quadrature Phase Shift Keying) carriers
[AD-A193528] 23 p3204 N88-29065

PHASE DETECTORS
Optimum filters and smoothers design for carrier phase and frequency tracking
[NASA-CR-182654] 12 p1618 N88-19679

PHASE DIAGRAMS
Contribution to the study of the Ti-Al phase diagram by conventional and high resolution electron microscopy
[ESA-TT-1021] 01 p0023 N88-10143
Theory of the carbon phase diagram at high pressures and temperatures
[DE87-012245] 01 p0028 N88-10180
Analysis of phase equilibria in NiTi-C system in high nickel regions
[BLL-M-37304-(5828.4)] 02 p0149 N88-10932
DTA/DSC studies of phase equilibria in binary mixtures of barium carbonate with alkali carbonates
[DE87-001195] 02 p0194 N88-11213
On the search for experimentally observed grain boundary phase transitions
[DE87-012747] 02 p0244 N88-11539
The mechanism by which sigma-phase forms in Fe-Cr-Ni system alloys
[BLL-M-37380-(5828.4)] 05 p0564 N88-13437
Phase diagram and thermochemical properties of the Al-Cu system
[ETN-88-91015] 05 p0566 N88-13447
Phase behavior in the Li-Al-O-H system at intermediate temperatures
[AD-A185732] 06 p0697 N88-14280
Theoretical studies of multicomponent mixtures: Phase equilibrium and transport
[DE88-002717] 07 p0831 N88-15040
Microstructural observations of the Sn-Pb solder/Cu system and thermal fatigue of the solder joint
[DE88-001392] 07 p0832 N88-15048
The generalized van der Waals theory of pure fluids and mixtures
[DE88-002380] 07 p0855 N88-15192
Determination of thermodynamic function of minerals at high temperatures
[DE88-001911] 07 p0940 N88-15713
Determination of thermodynamic function of minerals at high temperatures
[DE88-002311] 07 p0940 N88-15714
Copper oxidation states, vacancy ordering and their effect on high temperature superconductivity
[DE88-003079] 09 p1258 N88-17542
Metal hydrides
[DE88-005083] 10 p1299 N88-17766
Electronic structure of random alloys and the theory of ordering processes
[DE88-004476] 10 p1407 N88-18394
Transport and relaxation processes in supercritical fluids
[DE88-004804] 10 p1419 N88-18474
Joining of dissimilar materials with the pulsed Nd-YAG laser
[DE88-003757] 11 p1458 N88-18693
Electronic structure and phase stability of alloys
[DE88-004574] 11 p1562 N88-19350
Transformation, metallurgical response and behavior of the weld fusion zone and heat affected zone in Cr-Mo steels for fossil energy application
[DE88-006037] 13 p1744 N88-20430
Titanium powder frit made during the transformation alpha-beta
[ETN-88-91999] 16 p2177 N88-22976
The Time-Temperature-Transformation (TTT) diagram as a basis for relating the formation and properties of reactive coatings
[AD-A190872] 16 p2182 N88-23006
Vacancy ordering in the basal plane of YBa2Cu3O(sub)z
[DE88-004572] 18 p2583 N88-25348
Non-equilibrium phases and phase diagrams
[DE88-008896] 20 p2880 N88-27098
Migration and stability of HgCdTe lattice defects
[AD-A193293] 21 p3021 N88-27935
Raman spectroscopy on simple molecular systems at very high density
[DE88-010947] 23 p3191 N88-28987

PHASE ERROR
Effects on electromagnetic wave propagation at frequencies over 10 GHz due to inhomogeneities of the complex refraction index
[REPT-86-025] 01 p0036 N88-10228
Digital method for correction of the phase error in the discrete generation of periodic signals in real time
[INPE-4327-RPE/552] 12 p1618 N88-19676
Reduced tolerance imaging 2, volume 2
[AD-A189604] 13 p1829 N88-20939
Coherent RF error statistics
[AD-A193002] 20 p2792 N88-26560
Approximation problems of the Hilbert transform to identify minimum phase linear systems
[FUB-42-1986] 21 p2999 N88-27790
Direct bit detection receiver performance analyses for 8-DPSK (Differential Phase Shift Keyed) modulated signals operating with improper carrier phase synchronization
[AD-A193839] 22 p3070 N88-28220
Effect of phase errors in stepped-frequency radar systems
[AD-A194476] 23 p3203 N88-29061

PHASE LOCKED SYSTEMS
A compact digital communications system. Part 3: Generalising the phase locked loop
[RSRE-MEMO-4027-PT-3] 01 p0035 N88-10222
Detection of signals by weighted integrate-and-dump filter 04 p0435 N88-12696
Phase-locked semiconductor quantum well laser arrays
[AD-A185155] 05 p0588 N88-13583
Time-dependent Slow-Time-Scale theory of free-running and phase-locked gyrotron oscillators
[AD-A188910] 12 p1629 N88-19752

Resonator coupling of two ring cavity, argon-ion lasers
[AD-A189558] 13 p1775 N88-20616

An investigation of a distributed clock for local area networks with ring topology 18 p2516 N88-24924

Phase length optical phase-locked-loop sensor
[NASA-CASE-LAR-13387-1] 18 p2576 N88-25302

Contribution to speed regulation of small motors with phase-locked loops
[ETN-88-92373] 20 p2796 N88-26590

Spectral estimation of received phase in the presence of amplitude scintillation 22 p3064 N88-28180

Telemetry SNR improvement using the DSN Advanced Receiver with results for Pioneer 10
22 p3064 N88-28184

A digitally implemented phase-locked loop detection scheme for analysis of the phase and power stability of a calibration tone 22 p3066 N88-28196

Digital phase-lock loop having an estimator and predictor of error
[NASA-CASE-NPO-17196-1-CU]
23 p3205 N88-29076

Human auditory and visual continuous evoked potentials 23 p3238 N88-29269

Tolerances for phase locking of semiconductor laser arrays
[AD-A195974] 24 p3378 N88-30120

PHASE MATCHING

Frequency doubling conversion efficiencies for deep space optical communications 04 p0434 N88-12691

Significance of sensory signal phase mismatch in mechanisms of motion sickness development
20 p2830 N88-26787

PHASE MODULATION

NT PHASE SHIFT KEYING

HF sidebands in the ionosphere
05 p0574 N88-13497

Error control techniques for satellite and space communications
[NASA-CR-181581] 05 p0576 N88-13516

Adaptive digital phase modulation
[PB87-134607] 06 p0693 N88-14253

Variation of wave action: Modulations of the phase shift for strongly nonlinear dispersive waves with weak dissipation. A new adiabatic invariant involving the modulated phase shift for strongly nonlinear, slowly varying, and weakly damped oscillators. The modulated phase shift for weakly dissipated nonlinear oscillatory waves of the Korteweg-de vries type
[AD-A185630] 06 p0765 N88-14702

Modem for digital phase modulation: Results and summary
[PB87-149233] 07 p0845 N88-15129

Modulation of an intense beam by an external microwave source: Theory and simulation
[AD-A185683] 07 p0848 N88-15145

A fiber optic gyro strapdown reference system for guided weapons 12 p1597 N88-19560

Magnet strength fluctuations in the SSC (Superconducting Super Collider) lattice. Part 2: Frequency modulation
[DE88-006491] 15 p2141 N88-22774

Influence of alternating magnetic fields on Zn-67 Moessbauer resonance in ZnO
[PB88-186432] 18 p2584 N88-25352

Trellis-coded CPM for satellite-based mobile communications 19 p2648 N88-25718

Fiber optic sensors 19 p2670 N88-25870

Phase modulation of recoilless gamma radiation in Mossbauer spectroscopy
[ETN-88-92648] 24 p3428 N88-30403

PHASE RESPONSE

U FREQUENCY RESPONSE

U PHASE SHIFT

PHASE SHIFT

A compact digital communications system. Part 3: Generalising the phase locked loop
[RSRE-MEMO-4027-PT-3] 01 p0035 N88-10222

Basic properties and variability
02 p0252 N88-11593

Measurement of solid propellant combustion velocity by means of microwaves
[CERT-1/1316-MO] 03 p0283 N88-11778

Short baseline phase delay interferometry
04 p0433 N88-12683

Compensation of small-scale phase distortions by means of a Fourier phase corrector
06 p0708 N88-14345

Variation of wave action: Modulations of the phase shift for strongly nonlinear dispersive waves with weak dissipation. A new adiabatic invariant involving the modulated phase shift for strongly nonlinear, slowly varying, and weakly damped oscillators. The modulated phase shift for weakly dissipated nonlinear oscillatory waves of the Korteweg-de vries type
[AD-A185630] 06 p0765 N88-14702

Study of vibration relaxation in active medium of CO2-laser using phase-absorption method
07 p0919 N88-15582

Pressure and tension dependence of phase shift of polarization modes in birefringent single-mode fiber-optic waveguide 08 p1078 N88-16501

Magnetic rare earth superlattices
[DE88-003483] 10 p1418 N88-18465

Optics for large telescope 13 p1840 N88-21014

Considerations in GaAs standard cell design
[DE88-003310] 14 p1985 N88-21840

Determination of the commutation and angle and load response for a continuous-current, single phase controlled rectifier
[AD-A190602] 15 p2060 N88-22285

Near optimal blind deconvolution
[REPT-87-016] 15 p2123 N88-22655

A new fiber-optic-based phase-resolved phosphorescence spectrometer
[AD-A191325] 16 p2275 N88-23613

Doppler radar with multiphase modulation of transmitted and reflected signal
[NASA-CASE-MSC-18808-1] 17 p2332 N88-23923

Picosecond response of an optically controlled millimeter wave phase shifter 19 p2660 N88-25820

Phase comparator for range imaging laser radar
[DE88-008109] 21 p2954 N88-27545

Direct bit detection receiver performance analyses for 8-DPSK (Differential Phase Shift Keyed) modulated signals operating with improper carrier phase synchronization
[AD-A193839] 22 p3070 N88-28220

Experimental investigations for the generation of phase modes for adaptive antennas
[REPT-10-87] 23 p3205 N88-29074

PHASE SHIFT CIRCUITS

RELIC: A reliability simulator for integrated circuits
[AD-A187493] 11 p1477 N88-18811

Intergrated circuit design, phase 2
[AD-A189060] 13 p1760 N88-20530

Monolithic phase shifter study
[AD-A190213] 15 p2059 N88-22278

The superconducting phase shifter in the development of a terahertz imaging radar system
[AD-A190666] 16 p2188 N88-23046

Development of 20 GHz monolithic transmit modules
[NASA-CR-182134] 17 p2445 N88-24539

PHASE SHIFT KEYING

Bandwidth efficient block codes for M-ary PSK modulation
[NASA-CR-181543] 04 p0437 N88-12712

High data rate modem simulation for the space station multiple-access communications system
06 p0795 N88-14870

Envelope and phase statistics for non-Gaussian noise and resulting error probabilities for digital communications systems 12 p1617 N88-19672

Direct bit detection receiver noise performance analysis for 32-PSK and 64-PSK modulated signals
[AD-A190009] 15 p2056 N88-22256

The 2 FSK/QPSK (Frequency Shift Keying/Quadrature Phase Shift Keying) transmitter and receiver: Design and performance
[AD-A190028] 15 p2056 N88-22258

A Differential Phase Shift Keying (DPSK) modulator for a frequency hopping short wave system
[FOA-C-30460-3.3] 18 p2501 N88-24840

Codes for QPSK modulation with invariance under 90 degrees rotation 19 p2648 N88-25720

Trellis-coded MPSK modulation techniques for MSAT-X(sup)1 19 p2648 N88-25721

Modulation and coding for fast fading mobile satellite communication channels 19 p2648 N88-25722

Performance of the ICAO standard core service modulation and coding techniques
19 p2648 N88-25723

An 8-DPSK TCM modem for MSAT-X
19 p2649 N88-25725

Development of a coded 16-ary CPFSK coherent demodulator 19 p2649 N88-25726

Modem for the land mobile satellite channel
19 p2649 N88-25727

Error performance of voice band data signals with an overloaded delta modulator
[FEL-1987-05] 20 p2792 N88-26562

Digital carrier demodulation for the DSN Advanced Receiver 22 p3064 N88-28183

Automatic classification of digitally modulated signals
[AD-A194623] 23 p3203 N88-29064

Use of a coherent square wave reference to demodulate BPSK (Binary Phase Shift Keying) carriers and a visual indicator of the quality of received QPSK (Quadrature Phase Shift Keying) carriers
[AD-A193528] 23 p3204 N88-29065

Doppler-corrected differential detection system
[NASA-CASE-NPO-16987-1-CU]
24 p3359 N88-30001

PHASE SWITCHING INTERFEROMETERS

Imaging interferometry with non-redundant arrays
02 p0257 N88-11624

PHASE TRANSFORMATIONS

NT ARC MELTING
NT BOILING
NT COAL LIQUEFACTION
NT EVAPORATION
NT EVAPOTRANSPIRATION
NT FILM BOILING
NT FLASHING (VAPORIZING)
NT FREEZING
NT FUSION (MELTING)
NT LIQUEFACTION
NT MARTENSITIC TRANSFORMATION
NT MELTING
NT NUCLEATE BOILING
NT SUBLIMATION
NT TRANSPIRATION
NT VACUUM MELTING
NT VAPORIZING
NT ZONE MELTING

Nitrogen at high pressure
[DE87-013797] 01 p0021 N88-10130

Structure of rapidly solidified Ni-Ti
[DE87-012252] 02 p0147 N88-10921

Analysis of phase equilibria in NiTi-C system in high nickel regions
[BLL-M-37304-(5828.4)] 02 p0149 N88-10932

Shock-induced cooling in dense fluids
[DE87-014343] 02 p0170 N88-11067

Anelastic behaviour of materials under multiaxial strains. Part 3: Order-disorder transition, Shoek effect and Poisson's ratio in AISI-1080 steel
[DE87-703087] 02 p0191 N88-11193

Iterative solution of a nonlinear system arising in phase change problems
[DE87-014672] 02 p0226 N88-11426

Solute segregation to phase interfaces and grain boundaries: Studies by analytical electron microscopy and profile deconvolution
[DE87-012129] 02 p0243 N88-11537

On the search for experimentally observed grain boundary phase transitions
[DE87-012747] 02 p0244 N88-11539

Cure and properties of thermosetting polymers
[AD-A184669] 03 p0293 N88-11843

Wittig synthesis of conductive segmented block polymer compositions
[AD-A184018] 03 p0295 N88-11850

Determination of the origin of self-pumped phase conjugation in barium titanate
[AD-A184697] 03 p0377 N88-12372

Improper ferroelectricity: A theoretical and experimental study
[AD-A184614] 03 p0381 N88-12397

Phase equilibrium and crystal growth studies on AgGaSe2 and related nonlinear optical materials
[AD-A184768] 03 p0382 N88-12400

Phase transition of multifractals
[DE87-014344] 03 p0383 N88-12409

Experimental perspectives on heavy electron metals
[DE87-014766] 04 p0416 N88-12583

Synthesis of the monoclinic yttria by thermal plasma processing
[DE88-000496] 04 p0421 N88-12608

Nonlinear acoustics
[AD-A184271] 04 p0488 N88-13004

The Moessbauer effect of SnI4 at high pressure
[DE87-014771] 04 p0495 N88-13048

Guest-host interactions in thermotropic and lyotropic liquid crystals
[AD-A184402] 04 p0496 N88-13057

Radiation induced collapse of the crystalline structure
[DE87-014407] 04 p0498 N88-13064

The mechanism by which sigma-phase forms in Fe-Cr-Ni system alloys
[BLL-M-37380-(5828.4)] 05 p0564 N88-13437

Coupling effects between the ferrite and austenite phases during corrosion fatigue of a ferrite/austenite duplex stainless steel 05 p0605 N88-13706

Pressure induced phase transitions, superconductivity of phosphorus described 06 p0675 N88-14134

Precipitation in alumina-rich spinel: A transformation-toughened ceramic single crys.
[DE87-012380] 06 p0785 N88-14815

Atmospheric science 07 p0883 N88-15357

Embedded cluster models for electronic structure and energetics of complex oxides
[DE88-003097] 07 p0938 N88-15702

Change of europium crystallographic symmetry at helicoidal magnetic ordering
[DE88-700559] 07 p0939 N88-15707

Evolution from pure states into mixed states in de Sitter space
[DE88-750316] 07 p0945 N88-15745

Metal-oxide superconductor BaPbsub1-xBisubxO3: Unusual properties and new applications
08 p1077 N88-16494

Characterization of duplex stainless steel by TEM (Transmission Electron Microscopy), SANS (Small-Angle Neutron Scattering) and APFIM (Atom-Probe Field Ion Microscopy) techniques
[DE88-002916] 09 p1145 N88-16865

Superconductivity and crystal structure of high-pressure phases in V-Ru-H system 09 p1239 N88-17426

Theory of the tetragonal-to-orthorhombic structural phase transition in La2CuO4
[AD-A187141] 09 p1254 N88-17514

High temperature superconductivity research at Argonne National Laboratory
[DE88-003055] 09 p1258 N88-17541

Copper oxidation states, vacancy ordering and their effect on high temperature superconductivity
[DE88-003079] 09 p1258 N88-17542

Application of inverse gas chromatography to fluidity studies
[DE88-002896] 10 p1296 N88-17750

Influence of convection on microstructure
[NASA-CR-182489] 10 p1302 N88-17784

Irradiation effects in metals
[DE88-004272] 10 p1303 N88-17789

The role of composition and microstructure gradients on weld metal properties and behavior
[DE88-004956] 10 p1303 N88-17791

Fabrication, phase transformation studies and characterization of SiC-AIN-Al2OC ceramics
[DE88-004053] 10 p1306 N88-17807

Advanced materials for solid oxide fuel cells
[DE88-002338] 10 p1350 N88-18071

Application of Onsager's reciprocity relations to interface motion
[DE88-003288] 10 p1397 N88-18327

Electronic structure of random alloys and the theory of ordering processes
[DE88-004476] 10 p1407 N88-18394

High temperature processing of superconducting Y1Ba2Cu3O6.9
[DE88-003002] 10 p1416 N88-18449

Magnetic rare earth superlattices
[DE88-003483] 10 p1418 N88-18465

Order-disorder transition of Au and Pt (110) surfaces: The significance of relaxations and vibrations
[DE88-004651] 10 p1419 N88-18473

Superconductivity and phase stability in the heavy rare earth quaternary compounds RBa2Cu3O7 (R = Ho, Er, Tm, Yb, Lu)
[DE88-003478] 10 p1419 N88-18476

Superconducting properties and structural characterization of high T/sub c/ oxides
[DE88-003479] 10 p1420 N88-18477

Hadron-quark phase transition in dense stars
[DE88-003412] 10 p1429 N88-18532

Deactivation of alumina based catalysts
11 p1455 N88-18673

Crystallization and glass formation in electron and laser beam irradiated Cu-Zr alloys
[DE88-003390] 11 p1464 N88-18729

Perturbed angular correlations in zirconia ceramics
[DE88-004117] 11 p1464 N88-18731

Development of encapsulated lithium hydride thermal energy storage for space power systems
[DE88-004762] 11 p1507 N88-19001

An interdisciplinary approach to predictive modeling of structural adhesive bonding: Factors affecting the durability of titanium/epoxy bonds
[AD-A189503] 12 p1611 N88-19636

The role of point defects on structural phase transitions
[DE88-005209] 12 p1696 N88-20152

Phase transitions in two-dimensional superconducting arrays in a transverse magnetic field
[INPE-4457-RPE/559] 12 p1697 N88-20157

Interaction of particulate and transformation toughening
[AD-A189321] 13 p1741 N88-20412

Transformation, metallurgical response and behavior of the weld fusion zone and heat affected zone in Cr-Mo steels for fossil energy application
[DE88-006037] 13 p1744 N88-20430

Diffraction theory in QCD and beyond
[DE88-005958] 13 p1837 N88-20992

Rapid e-beam heating for measuring thermodynamics of metastable materials
[DE88-003565] 13 p1849 N88-21066

Experimental studies of elastic properties of crystals by Brillouin scattering
[DE88-005923] 14 p1986 N88-21848

Stability limits in the monoclinic-tetragonal transformations of zirconia
[DE88-005924] 14 p1986 N88-21849

Thermal analysis of heat storage canisters for a solar dynamic, space power system
[DE88-004199] 15 p2027 N88-22075

Directed-energy electron-beam processing of a hypoeutectic Cr90Ta10 alloy
[DE88-005621] 15 p2040 N88-22157

Transformation toughening of ceramics
[AD-A190399] 15 p2045 N88-22183

Synthesis of metastable superconductors by high dynamic pressure
[DE88-005620] 15 p2139 N88-22764

Superconductivity and the tailoring of lattice parameters of the compound YBa2Cu3O(sub x)
[DE88-005904] 15 p2140 N88-22769

An investigation of the crystalchemistry and thermochemistry of selected mineral systems
[AD-A189758] 15 p2142 N88-22781

Remarks on solid state amorphizing transformations
[DE88-006452] 15 p2145 N88-22803

Peculiarities of non-stationary heat transfer to superfluid helium
[DE88-701174] 16 p2200 N88-23124

The thermodynamic properties of quinoline and isoquinoline
[DE88-001218] 18 p2484 N88-24735

Dynamic consolidation of metal powders
[AD-A192126] 18 p2485 N88-24744

On the abnormal phenomena observed in the electrical resistivity measurement during the decomposition process of saturated Cu-Fe alloys
[NASA-TT-20183] 18 p2507 N88-24869

The Potts model in a random field
19 p2721 N88-26158

Refractory Materials of Zirconate. Part 2: Synthesis and some properties of strontium, zirconate, calcium zirconate and barium zirconate
[NASA-TT-20186] 20 p2779 N88-26483

Fluid dynamical model of ultrarelativistic heavy ion collisions
[DE88-007905] 20 p2850 N88-26921

The electronic structure of condensed molecular systems
[DE88-007823] 20 p2851 N88-26923

Shock wave compression and metallization of simple molecules
[DE88-008031] 20 p2851 N88-26925

Phase transformations and thermodynamic behavior of the YBa2Cu3O(sub)x system via EMF measurements
[DE88-010054] 20 p2878 N88-27086

Survey of the literature on fractals with possible applications to phase change processes
[DE88-012240] 21 p2911 N88-27277

On the systematics of phase transformation in metallic alloys
[DE88-008041] 21 p2913 N88-27288

Twin boundaries and heterophase interfaces in ferroelastic martensites
[DE88-011694] 21 p2916 N88-27304

Energy migration, motion and order in synthetic polymers
[AD-A193334] 21 p2918 N88-27320

Component stress during freeze/thaw cycling
[DE88-011204] 21 p2938 N88-27449

New synthetic approaches to boron hydride transformations
[AD-A193872] 22 p3052 N88-28108

Superconducting properties of oxygen deficient YBa2Cu3O(sub 7-delta)
[DE88-009969] 22 p3155 N88-28774

Band electronic structures and crystal packing forces
[DE88-010247] 23 p3289 N88-29585

Magnetic phase transitions in 90-K superconductors Ho1Ba2Cu3O(7-delta) and Gd1Ba2Cu3O(7-delta) observed by ZF-muon(+)SR
[DE88-752611] 23 p3290 N88-29588

Thermodynamical, optical and X-rays studies of some thermotropic liquid crystals
[DE88-702301] 23 p3290 N88-29590

Crustal evolution and the eclogite to granulite phase transition in xenoliths from the West African Craton
24 p3395 N88-30217

A method for the quantitative determination of crystalline phases by X-ray
[NASA-TT-20324] 24 p3434 N88-30444

PHASE VELOCITY

A spectral method for computing complete synthetic seismograms
[AD-A187663] 11 p1510 N88-19024

Phase velocity and attenuation of plane elastic waves in a particle-reinforced composite medium
[AD-A189414] 13 p1734 N88-20366

Two-phase flows in the wake of in-cylinder projectiles
[AD-A189422] 13 p1765 N88-20559

The superconducting phase shifter in the development of a terahertz imaging radar system
[AD-A190666] 16 p2188 N88-23046

PHASE-SPACE INTEGRAL

Fundamentals and techniques of nonimaging optics research
[DE87-014544] 02 p0236 N88-11488

Introduction to classical mechanics of systems with constraints, part 3
[DE88-701057] 13 p1850 N88-21073

PHASED ARRAYS

COSMIC --- Coherent Optical System of Modular Image Collectors (COSMIC); spaceborne telescope
01 p0095 N88-10623

A conformal aircraft phased array antenna for airplane-satellite communication in the L band
[ESA-TT-1057] 03 p0305 N88-11926

High power phased array and tailored gain semiconductor lasers 03 p0329 N88-12078

Multichannel deconvolution of P waves at seismic arrays and three component stations
[AD-A184450] 04 p0467 N88-12886

Theory of displaced phase center antenna for space based radar applications
[PB87-229837] 06 p0690 N88-14227

An analysis of simplified feed architectures for MMIC (Monolithic Microwave Integrated Circuit) T/R (Transmit/Receive) module arrays
[AD-A185474] 06 p0697 N88-14275

NORSAR detection processing system
[AD-A185968] 07 p0877 N88-15318

Optically controlled phased-array antenna technology for space communication systems
[NASA-TM-100852] 11 p1476 N88-18809

Investigation of surface wave blindness in microstrip phased array antennas
[AD-A189326] 12 p1621 N88-19696

Optical RF distribution links for MMIC phased array antennas
[NASA-TM-100841] 13 p1764 N88-20555

Optically interconnected phased arrays
[NASA-TM-100855] 14 p1908 N88-21400

Automated test device for FASR (Fixed Array Surveillance Radar) beam steering componentry
[AD-A191650] 18 p2500 N88-24829

MSAT mobile electronically steered phased array antenna development 19 p2647 N88-25711

MSAT-X electronically steered phased array antenna system 19 p2647 N88-25712

Proceedings of the Array Signal Processing Symposium: Treaty Verification Program
[DE88-008346] 20 p2790 N88-26548

A novel method to correct radiation pattern distortion of conformal antennas
[AD-A193675] 23 p3204 N88-29066

High frequency GaAlAs modulator and photodetector for phased array antenna applications
[NASA-TM-101328] 24 p3367 N88-30048

Maximum-likelihood multichannel deconvolution of P waves at seismic arrays
[AD-A194990] 24 p3391 N88-30191

PHENOL FORMALDEHYDE

A process for producing phenolic foams
[EP-PATENT-0-170-357-A1] 01 p0026 N88-10162

PHENOLIC RESINS

Thixotropic surface composition for phenolaldehyde resin laminates
[GB-PATENT-2-180-251-A] 04 p0410 N88-12545

PHENOLOGY

Pilot study of rice culture in sub-tropical high population density region (Madagascar) with SPOT 1 multispectral data 22 p3097 N88-28392

PHENOLS

Flame retardant phenolic foams
[EP-PATENT-0-223-489-A2] 05 p0568 N88-13464

Production of jet fuels from coal derived liquids. Volume 1: Market assessment for liquid by-products from the Great Plains gasification plant
[AD-A184846] 05 p0570 N88-13475

PHENOMENOLOGY

Phenomenological implications of the blown-up orbifolds
[DE87-014608] 03 p0373 N88-12347

Breaking of supersymmetry degeneracy and phenomenological conditions
[PREPRINT-559] 06 p0790 N88-14843

Phenomenological model of superconductivity of heavy fermions in U(sub 1-x)ThsubxBesub13
09 p1238 N88-17423

A viscoplastic theory applied to copper
[NASA-TM-100831] 14 p1926 N88-21497

State variable approach to deformation phenomena in Face Centered Cubic (FCC) metals
[VTT-44] 24 p3354 N88-29964

PHENYLS

NT POLYPHENYLS

Thermally stable aromatic structures from acyclic precursors. 1. Para polyphenylene model compounds from 3-Dimethyl amino hex-5-EN-1-YNES
[AD-A185300] 05 p0568 N88-13462
Boundary layer flow visualization for flight testing
17 p2297 N88-23742

PHILOSOPHY
NT PARADOXES
Resonance, information, and the primacy of process: Ancient light on modern information and communication theory and technology 10 p1424 N88-18506
Induction instrument for logic conclusion
[LRT-WE-9-FB-5(1987)] 22 p3144 N88-28697

PHOBOS
Periodic orbits around a satellite modelled as a triaxial ellipsoid
[AD-A190592] 15 p2022 N88-22051
Power requirements for mining and microwave processing of extraterrestrial resources
17 p2420 N88-24389

PHONETICS
Speech recognition: Acoustic-phonetic knowledge acquisition and representation
[AD-A185897] 07 p0840 N88-15097
Speech recognition: Acoustic-phonetic knowledge acquisition and representation
[AD-A187293] 10 p1320 N88-17893
Time-frequency representations for speech signals
[AD-A188661] 18 p2498 N88-24819

PHONOCARDIOGRAPHY
NT ECHOCARDIOGRAPHY

PHONON BEAMS
Effect of extraneous factors on optical one-phonon transitions in impurity centers with cubic symmetry
08 p1077 N88-16496

PHONONS
NT PHONON BEAMS
Anomalous phonon behavior of superconductor Y-Ba-Cu-O
[DE87-703401] 05 p0654 N88-14010
Phonon dispersion for several surfaces with ordered overlayers: A lattice dynamical study
07 p0876 N88-15315
On the coexistence of phonon and non-phonon (plasmon) mechanisms in new high T/sub c/ superconductors
[DE88-003188] 07 p0938 N88-15703
Non-phonon mechanisms of superconductivity in high T/sub c/ superconducting oxides and other materials and their manifestation
[DE88-002708] 07 p0939 N88-15709
Memory effects on infrared adsorbate spectra
[AD-A186976] 09 p1253 N88-17512
Dynamical properties of aluminium from experimental dispersion relations
[DE88-700240] 11 p1459 N88-18697
Raman scattering in mixed crystal semiconductors
12 p1696 N88-20149
Acoustic phonons, surface plasmons and surface acoustic plasmons in a superlattice and their nonreciprocal device applications
[AD-A188918] 12 p1698 N88-20163
Studies of transverse phonon modes in premartensitic indium-thallium alloys
[DE88-003481] 13 p1744 N88-20428
Nonequilibrium phonons and disorder in Al sub x Ga sub 1-x As 19 p2657 N88-25788
Phonons in semiconductor superlattices
20 p2869 N88-27035
Monte Carlo simulations of femtosecond relaxation of photoexcited electrons in AlGaAs/GaAs quantum wells
20 p2869 N88-27036

PHOSPHATES
NT ADENOSINE TRIPHOSPHATE
NT DIPHOSPHATES
NT INDIUM PHOSPHATES
Adhesion properties of polyelectrolyte-chemisorbed zinc phosphate conversion coatings
[DE87-012489] 01 p0029 N88-10186
Recent advances in metallic/ceramic coatings for corrosion control in military applications
17 p2320 N88-23858
Growth and characterization of thin films of ZnSnP(sub)2
[DE88-001164] 20 p2874 N88-27060

PHOSPHAZENE
Effect of sidechain length and crosslinking on ionic conductivity in polyphosphazene solid electrolytes
[AD-A184419] 04 p0497 N88-13058
Aromatic cyclotriphosphazenes
[NASA-CASE-ARC-11428-3] 18 p2477 N88-24692
Synthesis and characterization of new phosphazene polymers
[AD-A191508] 18 p2490 N88-24771

PHOSPHIDES
NT BORON PHOSPHIDES
NT GALLIUM PHOSPHIDES
NT INDIUM PHOSPHIDES
Cohesive energies of transition metal silicides and phosphides --- Knudsen effusion
[AD-A186691] 09 p1254 N88-17519

PHOSPHONIUM COMPOUNDS
Use of diphosphonates to correct disorders in calcium metabolism and mineral composition of bone tissue with 60-day hypokinesia in rats
[NASA-TT-20220] 13 p1809 N88-20807
Corrosion and corrosion inhibition of metals/alloys in methyphosphonic difluoride 17 p2319 N88-23850

PHOSPHORESCENCE
Canadian activities and goals in remote sensing of ocean colour and fluorescence from space
08 p1043 N88-16300
Federal Republic of Germany's interests, activities and goals in remote sensing of ocean colour/fluorescence from space 08 p1043 N88-16302
A new fiber-optic-based phase-resolved phosphorescence spectrometer
[AD-A191325] 16 p2275 N88-23613

PHOSPHORIC ACID
Electrochemical characteristics of acid electrolytes for fuel cells
[PB88-104641] 06 p0731 N88-14497
Factors governing light driven electron and proton translocation in proteins across membranes
[DE88-002716] 08 p1082 N88-16519
The effect on initial bond strength and durability of a Phosphoric Acid Dip (PAD) following chromic acid anodising of aluminum
[ARE-TM(UMM)-87402] 10 p1300 N88-17772
Studies of model ion channels in defect-free multibilayers of phospholipids
[AD-A188740] 16 p2238 N88-23365
Characterization of proton conducting polymer blends
19 p2669 N88-25867

PHOSPHORIC ACID FUEL CELLS
Synthesis of novel acid electrolytes for phosphoric acid fuel cells
[PB87-221305] 01 p0066 N88-10426
Electrochemical hydrogen concentrator for phosphoric acid fuel cells
[AD-A191355] 16 p2229 N88-23317
Compact regenerable sulfur scrubber for phosphoric acid fuel cells
[AD-A191356] 16 p2230 N88-23318
Phosphoric acid electric utility fuel cell technology development
[DE88-010187] 20 p2795 N88-26582

PHOSPHORS
Evaluating and testing thermographic phosphors for turbine-engine temperature measurements
[DE87-011772] 02 p0174 N88-11090
Calibration of a laser-pumped, thermographic phosphor remote thermometry system
[DE88-000452] 04 p0449 N88-12781
Performance and preference with various VDT (Video Display Terminal) phosphors
[AD-A184085] 04 p0475 N88-12925
Generation of specific chromaticities on CRT monitors
[AD-A187739] 11 p1440 N88-18590
Noncontact thermometry via laser pumped, thermographic phosphors: Characterization of systematic errors and industrial applications
[DE88-005599] 13 p1777 N88-20628
Remote temperature-measurement instrumentation for a heated rotating turbine disk
[DE88-006456] 18 p2516 N88-24925

PHOSPHORUS
Pressure induced phase transitions, superconductivity of phosphorus described 06 p0675 N88-14134
The influence of phosphorus on the solid state reaction between copper and silicon or germanium
[ETN-88-91361] 06 p0789 N88-14838
Influence of grain boundary phosphorus segregation on hydrogen embrittlement in steel
[DE88-700176] 11 p1459 N88-18696
Phosphorus oxynitride glass for laser applications
[DE88-005413] 12 p1632 N88-19768
Evaluation of thermophosphor temperature technique
[DE88-007654] 20 p2805 N88-26638
PECVD of amorphous nickel--phosphorus films
[DE88-011088] 21 p2915 N88-27299

PHOSPHORUS COMPOUNDS
NT ADENOSINE TRIPHOSPHATE
NT BORON PHOSPHIDES
NT DIPHOSPHATES
NT GALLIUM PHOSPHIDES
NT INDIUM PHOSPHATES
NT INDIUM PHOSPHIDES
NT ORGANIC PHOSPHORUS COMPOUNDS
NT PHOSPHATES
NT PHOSPHAZENE
NT PHOSPHIDES
NT PHOSPHONIUM COMPOUNDS
NT PHOSPHORIC ACID
NT PHOSPHORUS POLYMERS
Electrodeposition of amorphous Ni-Cr-P alloys
[DE88-006868] 19 p2616 N88-25521

PHOSPHORUS METABOLISM
Effects of extreme hypoxia on phospholipid metabolism in subcellular structures of rat brain
08 p1046 N88-16323
Effect of different doses of alpha-hydroxydimethyl-gamma-aminopropylidene phonate on rat bones 19 p2704 N88-26078

PHOSPHORUS POLYMERS
High-molecular compounds (selected articles)
[AD-A184668] 03 p0293 N88-11842
Effects of extreme hypoxia on phospholipid metabolism in subcellular structures of rat brain
08 p1046 N88-16323
New phosphorus based polymer systems
[AD-A190457] 15 p2045 N88-22166

PHOSPHORYLATION
Muscle preservation in the study of bioenergetic effects of hypokinesia 10 p1362 N88-18139

PHOTOABSORPTION
Intramolecular energy transfer reactions as a method for metal complex assisted production of hydrogen
[DE88-001621] 05 p0562 N88-13425
Nonuniformity of electromagnetic field at Lambda = 10.6 micron wavelength inside atmospheric aerosol particles
06 p0772 N88-14743
Experimental observation of photoresonance of electrons localized above surface of solid hydrogen
06 p0774 N88-14755
Photoabsorption and phototdissociation of molecules important in the interstellar medium
[NASA-CR-182435] 08 p1100 N88-16617
Memory effects on infrared adsorbate spectra
[AD-A186976] 09 p1253 N88-17512
Light absorption by an atom moving inside a spherical box
[AD-A187241] 10 p1407 N88-18395
Optical absorption in doped CdxHg1-xTe
[AD-A187434] 11 p1560 N88-19338

PHOTOACOUSTIC MICROSCOPY
Nondestructive evaluation of structural ceramics by photoacoustic microscopy
[NASA-CR-180858] 09 p1146 N88-16868
Nondestructive Evaluation (NDE) of structural ceramics by photoacoustic microscopy 17 p2325 N88-23884

PHOTOACOUSTIC SPECTROSCOPY
DSA RuO2/TiO2 electrode modeled by ion implantation: An in situ characterization by photoacoustic and photocurrent spectroscopy
[DE87-009129] 02 p0245 N88-11545
Study of IR laser photoacoustic spectra of organic molecules adsorbed on metal surface
03 p0301 N88-11891
A critical review of measurements of water vapor absorption in the 840 to 1100 cm(-1) spectral region
[NASA-CR-182361] 06 p0742 N88-14565
Photoacoustic infrared laser spectroscopy for analyzing gaseous contaminants
[ETN-88-90805] 07 p0831 N88-15041
Photoacoustic measurements of atmospheric aerosol absorption coefficients at ultraviolet, visible and infrared wavelengths 11 p1512 N88-19036
A laser-based photoacoustic spectrometer for direct breath C-13O2/C-12O2 measurement
[DE88-004915] 15 p2101 N88-22516
Photoacoustic Fourier transform infrared spectroscopy. An early detection technique for coatings degradation
24 p3354 N88-29968

PHOTOCATHODES
A focussed MCP (microchannel plate) image intensifier type for high speed gating
[DE88-000480] 05 p0583 N88-13555
Streak camera dynamic range optimization
[DE88-001632] 05 p0586 N88-13571
Stellar scintillometer atmospheric optical turbulence profiling experiment: A qualitative comparison of two identical instruments at AMOS (Air Force Maui Optical Station), 1985
[AD-A190589] 15 p2094 N88-22479

PHOTOCELLS
U PHOTOELECTRIC CELLS

PHOTOCHEMICAL REACTIONS
NT PHOTOCHROMISM
NT PHOTODECOMPOSITION
NT PHOTOLYSIS
NT PHOTOSYNTHESIS
NT RADIOLYSIS
The photophysics and chemistry of PAH (Polycyclic Aromatic Hydrocarbons) compounds
[DE87-014455] 02 p0153 N88-10954

Photochemical ignition studies. 3: Ignition by efficient and resonant multiphoton photochemical formation of microplasmas
[AD-A184644] 03 p0283 N88-11780
Proceedings of the Eleventh DOE Solar Photochemistry Research Conference
[DE88-000678] 04 p0466 N88-12883
Intramolecular energy transfer reactions as a method for metal complex assisted production of hydrogen
[DE88-001621] 05 p0562 N88-13425
Scientific and Operational Requirements for TOMS Data
[NASA-CP-2497] 05 p0615 N88-13774
Photochemical ozone overburden correction
05 p0615 N88-13778
Practical photochemistry: General considerations
[PB87-123396] 06 p0730 N88-14491
Laser action from syn-(methyl,methyl) bimane
[AD-A186314] 07 p0858 N88-15211
Effect of the band-gap characteristics on laser-induced dry etching of semiconductors
[DE88-001853] 07 p0937 N88-15695
Short-term temporal variations of Nimbus-7 measurements of the solar UV spectral irradiance
[PB88-102132] 07 p0946 N88-15753
Mechanisms of cloud layer formation in Venusian atmosphere 08 p1004 N88-16067
Variable band gap materials for thermophotovoltaic generators
[AD-A186858] 09 p1186 N88-17104
Control of solid-excitation-based photochemical dry etching of semiconductors by ion-bombardment-induced damage
[DE88-003214] 09 p1257 N88-17537
Energy transfer and photochemistry in biomimetic solar conversion
[PB88-130026] 10 p1348 N88-18057
Photochemical solar energy conversion utilizing semiconductors localized in membrane mimetic systems
[DE88-002887] 10 p1349 N88-18065
Photophysics and photochemistry of poly(di-n-hexylsilane) in room temperature solution
[AD-A187890] 11 p1462 N88-18714
Photochemical energy storage: Studies of inorganic photoassistance agents
[DE88-002596] 11 p1508 N88-19010
Initial results with the LLNL 2-D chemical-radiative-transport model of the troposphere and stratosphere
[DE88-004355] 11 p1512 N88-19033
The influence of atmospheric thermal tides on diurnal variations in chemical constituents in the mesosphere
11 p1512 N88-19035
Surface mediated photocatalysis
[AD-A188882] 12 p1603 N88-19589
Ultraviolet (180 to 300 nm) action spectra for inactivation and DNA photoproduct formation of Bacillus subtilis spores under ultrahigh vacuum 12 p1657 N88-19931
Photochemistry at structured surfaces: A classical electromagnetic approach
[AD-A189519] 13 p1737 N88-20387
Mechanisms of photoinduced electron transfer
[DE88-004917] 13 p1836 N88-20983
The photochemistry of some possible cometary CN parent species 14 p1997 N88-21905
The role of hydrogen thermalization in shaping the Lyman-alpha coma --- comets 14 p2007 N88-21971
Hard ceramic film by laser PVD
15 p2051 N88-22216
UV-Laser reactions of molecular adsorbates
[AD-A190796] 16 p2212 N88-23201
Nanosecond laser photolysis of opaque heterogeneous photosensitizers
[AD-A191424] 16 p2213 N88-23209
Time-resolved studies of free radicals and laser-initiated chain reactions
[DE88-006569] 16 p2266 N88-23553
Modification of polymers by photografting processes
17 p2323 N88-23871
Chemical kinetics and photochemical data for use in stratospheric modeling evaluation Number 8
[NASA-CR-182919] 17 p2351 N88-24012
Photochemical and thermal modeling in the early atmosphere of the earth
[NASA-CR-183029] 18 p2543 N88-25093
Recent advances in photochemical techniques for ignition and combustion enhancement
19 p2625 N88-25570
The solar flare of 18 August 1979: Incoherent scatter radar data and photochemical model comparisons
[DE88-007616] 19 p2743 N88-26286
Ultraviolet geometric albedo of Uranus
[NASA-CR-183099] 20 p2885 N88-27136
Photochemical oxidant formation: Overview of current knowledge and emerging issues
[PB88-195235] 21 p2971 N88-27647
Low-band-gap, amorphous-silicon-based alloys by photochemical vapor deposition
[DE88-001165] 21 p3023 N88-27944
Chemical interactions between the present-day Martian atmosphere and surface minerals
23 p3305 N88-29689
Photochemistry of ionospheric D-region with injection of nitrogen oxides 24 p3444 N88-30499

PHOTOCHEMISTRY
U PHOTOCHEMICAL REACTIONS

PHOTOCHROMISM
Anisotropy of light absorption by color centers in waveguides produced on photochromic glasses by diffusion 14 p1896 N88-21320
Quasi-liquid crystalline materials with special electro-optic properties
[AD-A194579] 23 p3282 N88-29544

PHOTOCLINOMETRY
U PHOTOGRAMMETRY

PHOTOCONDUCTIVITY
Construction and characterization of amorphous-silicon test structures
[DE87-013595] 01 p0029 N88-10182
Toward pulsed power uses for photoconductive semiconductor switches: Closing switches
[DE87-012020] 01 p0041 N88-10262
Recent developments in opening photoconductive semiconductor switches
[DE87-012130] 01 p0041 N88-10263
The application of photoconductive detectors to the measurement of X-ray production in laser produced plasmas
[DE88-001630] 07 p0934 N88-15671
Dispersive hole transport in SiO2
[AD-A187077] 09 p1254 N88-17513
High density CMOS technology
11 p1561 N88-19342
Pressure-dependent DLTS (Deep Level Transient Spectroscopy) experiments on Si-doped AlGaAs
[DE88-003842] 13 p1846 N88-21047
Liquid carbon
[AD-A191707] 18 p2491 N88-24776
Photoconductivity in carbon fibers
[AD-A191728] 18 p2492 N88-24782
Picosecond electrical pulses for VLSI electronics characterization 19 p2655 N88-25768
Picosecond photoconductive transceivers
19 p2656 N88-25777
Photoconductive generation of sub-picosecond electrical pulses and their measurement applications
19 p2656 N88-25778
Generation and forming of ultrashort high voltage pulses 19 p2657 N88-25782
Investigation of photoconductive picosecond microstripline switches on self-implanted Silicon On Sapphire (SOS) 19 p2657 N88-25789
Fast GaAs photoconductive detectors with high sensitivity integrated in coplaner systems onto GaAs substrates 19 p2658 N88-25790
Characteristics, packaging and physics of ultra high speed diode lasers and detectors
19 p2658 N88-25797
Picosecond optoelectronic study of a thin film transmission line structure 19 p2661 N88-25823
Photoconducting X-ray detectors for Z-pinch experiments
[DE88-007118] 19 p2728 N88-26199
Control of carrier lifetime in PbTe nipi superlattices by external photoinjection 20 p2863 N88-27006
Pressure-dependent measurement on n+GaAs (Si, Sn): The effect of deep donor (DX) states on the electrical properties and presistent photoconductivity effects
20 p2866 N88-27020
Magneto-optical studies of GaInAs-InP quantum wells
20 p2870 N88-27039

PHOTOCONDUCTORS
An optically strobed sample and hold circuit
[DE87-011877] 01 p0038 N88-10245
Ultrafast photoconductor detector-laser-diode transmitter
[DE87-013803] 03 p0329 N88-12082
Photoconductor switch and circuit analysis
[AD-A188168] 11 p1478 N88-18821
Microwave response of an HEMT photoconductor
[NASA-TM-100819] 11 p1480 N88-18835
Optical absorption in doped CdxHg1-xTe
[AD-A187434] 11 p1560 N88-19338
Silicon containing photoresists
[AD-A188666] 12 p1605 N88-19601
Infrared-sensitive spatial light modulator
[AD-A190391] 15 p2134 N88-22729
An optically strobed sample and hold circuit
19 p2656 N88-25772
High speed, high repetition rate, high voltage photoconductive switching 19 p2657 N88-25781
Graphite as a picosecond laser activated opening switch 19 p2657 N88-25783
A new optoelectronic CW microwave source
19 p2660 N88-25818
Electrical pulse compression by traveling-wave photoconductivity 19 p2661 N88-25822
Characterization of new FPS (Focus Projection and Scale) vidicons for scientific imaging applications
[DE88-011213] 22 p3080 N88-28280

PHOTOCURRENTS
U ELECTRIC CURRENT
U PHOTOELECTRIC EMISSION

PHOTODECOMPOSITION
Vectorial electron transfer on designed surfaces
[PB87-232229] 03 p0381 N88-12394
Theoretical bases of polymer photodegradation and photooxidation
[AD-A186533] 08 p0974 N88-15886
Instrumentation for collisional energy transfer studies
[AD-A188495] 12 p1689 N88-20105

PHOTODETACHMENT
Photodetachment neutralizer development. Laser window design study. Volume 2: Window design details
[DE88-000783] 09 p1170 N88-17014
Determination of beam orientation of optical diagnostics of excited 200-MeV hydrogen atoms resulting from photodetachment of H(-)ions
[AD-A189976] 14 p1981 N88-21823

PHOTODETECTORS
U PHOTOMETERS

PHOTODIODES
Photodiode matrix for the analysis of two-beam interferences
[PTB-OPT-23] 01 p0048 N88-10310
The use of splines in the modelling of a photodiode response
[NPL-DITC-88/87] 01 p0085 N88-10560
Optical communication with semiconductor laser diodes
[NASA-CR-182464] 09 p1154 N88-16918
Superlattice photodetectors
[AD-A186956] 09 p1253 N88-17511
Measurement of the gamma-ray response of some commercial silicon detectors
[AD-A187431] 11 p1543 N88-19221
Development of integrated detectors for attitude sensors
[INPE-4409-PRE/1222] 12 p1602 N88-19586
Characterization of integrated photovoltaic detectors for MECB solar sensors
[INPE-4408-PRE/1221] 12 p1630 N88-19754
A method to detect and digitize small plant movements 12 p1654 N88-19912
A 104-km unrepeatered bidirectional fiber optic demonstration link
[AD-A190282] 15 p2134 N88-22728
Hybrid PV HgCdTe IR detectors technology reliability and failure program: Environmental stress testing plan
[AD-A191165] 16 p2211 N88-23195
Spectral radiation measurement using a photodiode array as receiver 16 p2271 N88-23591
Application of chaos theory to 1/f noise
[AD-A191150] 17 p2334 N88-23935
Studies of boron implantation through photochemically deposited SiO2 films on Hg(sub 1-x)Cd(sub x)Te
[SD-TR-87-26] 19 p2621 N88-25548
High speed opto-isolator for radar applications
19 p2658 N88-25795
InP/GaInAs/InP PIN photodiode with FWHM less than 18 ps 19 p2658 N88-25799
MESFET compatible IMSM detectors
19 p2659 N88-25801
X-ray response of GaAlAs/GaAs radiation hardened double: Heterostructure photodiode compared to Si:PIN photodiodes
[DE88-007425] 19 p2733 N88-26231
Photodiodes for optical communication in the near infrared
[ETN-88-92379] 21 p3016 N88-27900
Array detectors for plasma spectrochemistry
[AD-A194220] 22 p3052 N88-28105
Effect of detector dead time on the performance of optical direct-detection communication links
22 p3065 N88-28190
Tunnelling currents in reverse biased CMT photodiodes
[RSRE-MEMO-4137] 23 p3209 N88-29097

PHOTODISSOCIATION
OH(A-X) fluorescence from photodissociative excitation of HO2 at 157.5 nm
[NASA-CR-181580] 05 p0563 N88-13429
Photoabsorption and photodissociation of molecules important in the interstellar medium
[NASA-CR-182435] 08 p1100 N88-16617
Energy disposal in ion-molecule reactions
[AD-A186772] 09 p1171 N88-17019

The photochemistry of some possible cometary CN parent species 14 p1997 N88-21905
Photodissociation lifetimes of CH and CD radicals in comets 14 p1998 N88-21906
Aeronomic problems of the molecular oxygen photodissociation. Part 3: Solar spectral irradiances in the region of the O2 Herzberg continuum, Schumann-Runge bands and continuum
[AERONOMICA-ACTA-A-332-1988] 24 p3343 N88-29897
Aeronomic problems of molecular oxygen photodissociation. Part 2: Theoretical absorption cross sections of the Schumann-Runge bands at 79 K
[AERONOMICA-ACTA-A-331-1988] 24 p3344 N88-29907
Aeronomic problems of molecular oxygen photodissociation. Part 4: The various parameters for the Herzberg continuum
[AERONOMICA-ACTA-A-333-1988] 24 p3352 N88-29955

PHOTOELASTIC ANALYSIS
Optical analysis of stress and strain in photoelastic particle assemblies
[ETN-88-91591] 09 p1182 N88-17082
Photoelastic model tests of the Dornier linear actuator --- far IR telescope 14 p1877 N88-21218
The use of photoelastic methods to study the stressed states of spot-welded joints 14 p1898 N88-21335
The mechanical properties of card measured by photographic Moire
[NPL-DMOM-87] 14 p1923 N88-21463

PHOTOELASTIC MATERIALS
Optical analysis of stress and strain in photoelastic particle assemblies
[ETN-88-91591] 09 p1182 N88-17082

PHOTOELASTIC STRESS MEASUREMENT
U PHOTOELASTIC ANALYSIS

PHOTOELASTICITY
Vibrational, mechanical and thermal properties of 3-5 semiconductors
[AD-A187569] 11 p1556 N88-19316

PHOTOELECTRIC CELLS
NT PHOTOVOLTAIC CELLS
NT SOLAR CELLS
NT VERTICAL JUNCTION SOLAR CELLS
Photovoltaic cells with n-silicon and conductive polymers
[ETN-88-92133] 20 p2821 N88-26734
Space photovoltaic generators: State of the art, trends
[REPT-881-440-106] 21 p2970 N88-27640

PHOTOELECTRIC EFFECT
NT PHOTOCONDUCTIVITY
NT PHOTOELECTRIC EMISSION
NT PHOTOIONIZATION
NT PHOTOVOLTAIC EFFECT
Metal intercalation characteristics of n-HfS2 photoelectrodes in non-aqueous electrolytes
[AD-A184381] 03 p0383 N88-12407
An experimental and theoretical investigation of optogalvanic effects
[AD-A189618] 12 p1625 N88-19720
NBS (National Bureau of Standards) measurement services: The NBS photodetector spectral response calibration transfer program
[PB88-201505] 24 p3376 N88-30109

PHOTOELECTRIC EMISSION
The photophysics and chemistry of PAH (Polycyclic Aromatic Hydrocarbons) compounds
[DE87-014455] 02 p0153 N88-10954
DSA RuO2/TiO2 electrode modeled by ion implantation: An in situ characterization by photoacoustic and photocurrent spectroscopy
[DE87-009129] 02 p0245 N88-11545
Short-pulse high-current-density photoemission in high electric fields
[DE87-014909] 03 p0310 N88-11951
Atomic and electronic structure of surfaces and chemisorbed layers
[DE87-014987] 04 p0498 N88-1306
Photocurrent generation from basic metals, utilizing a short pulsed ArF excimer laser
[AD-A184828] 05 p0587 N88-13579
Electronic band structure and photoemission: A review and projection
[DE88-002236] 06 p0787 N88-14829
Differential spectral radiometry 16 p2272 N88-23594
Physical properties of f electron systems
[DE88-006886] 18 p2581 N88-25331
Studies of metal-silicon, silicon-metal and silicide based interfaces: Synchrotron radiation photo emission and inverse photoemission investigations of interface formation and compound nucleation
[AD-A191808] 19 p2619 N88-25536
Photocurrent modeling of modern microcircuit PN junctions
[DE88-007037] 19 p2662 N88-25832
Investigation of electronic band structure of semiconductors by photoemission
[ETN-88-92370] 21 p3025 N88-27957
An undulator radiation source for spin-polarized photoemission studies of novel magnetic materials
[AD-A193756] 22 p3083 N88-28307
Bulk plasmon enhanced photoemission from Nb(100) surface resonances
[AD-A192711] 22 p3154 N88-28767

PHOTOELECTRIC GENERATORS
NT PHOTOVOLTAIC CELLS
NT SOLAR CELLS
NT VERTICAL JUNCTION SOLAR CELLS
Application of pulse compression and shaping to the FEL photoelectric injector
[DE88-007906] 19 p2675 N88-25910

PHOTOELECTRIC PHOTOMETERS
U ELECTROPHOTOMETERS

PHOTOELECTRICITY
NT PHOTOCONDUCTIVITY
NT PHOTOELECTRIC EFFECT
NT PHOTOELECTRIC EMISSION
NT PHOTOIONIZATION
NT PHOTOVOLTAIC EFFECT
Detective quantum efficiency and design of a parallel data recording system for EXELFS-measurements --- electron microscopy
[USIP-87-06] 01 p0050 N88-10318
New method of examining micrononhomogeneity of local centers in high-resistivity semiconductor materials under scanning electron microscope 14 p1969 N88-21754
Defects in high-mobility semiconductor systems
[AD-A192296] 20 p2879 N88-27090

PHOTOELECTROCHEMISTRY
Corrosion Research Center, University of Minnesota
[DE88-006681] 15 p2041 N88-22160

PHOTOELECTROMAGNETIC DETECTORS
U RADIATION MEASURING INSTRUMENTS

PHOTOELECTRON SPECTROSCOPY
Localization of Cu 3d levels in the high Tc superconductor YBa2Cu3O approximately 7 by Cu2p X-ray photoelectron spectroscopy
[NOTA-INTERNA-887] 07 p0939 N88-15710
High-temperature photoelectron spectroscopy: An increased sensitivity spectrometer for studying vapor-phase species produced at furnace temperatures greater than 2000K
[AD-A186542] 09 p1140 N88-16835
Gas-phase photoelectron spectroscopy of metals and metal oxides of importance in the upper atmosphere
[AD-A187771] 11 p1511 N88-19027
Laser photoelectron spectroscopy of ions
[DE88-006860] 15 p2033 N88-22113
Differential spectral radiometry 16 p2272 N88-23594
Electronic and geometric structure of silver and palladium on aluminum (111) in monoatomic surface layers
[ETN-88-92120] 20 p2879 N88-27093

PHOTOELECTRONICS
U ELECTRONICS
U PHOTOELECTRICITY

PHOTOELECTRONS
Near threshold behavior of photoelectron satellite intensities
[DE88-002231] 08 p1061 N88-16512
A simple interpretation of the Fe2(-) photoelectron spectrum
[NASA-CR-182553] 11 p1543 N88-19225
Photoenhanced attachment for optical control of diffuse discharges
[AD-A188989] 12 p1696 N88-20147

PHOTOEMISSION
U PHOTOELECTRIC EMISSION

PHOTOEMISSIVITY
U EMISSIVITY
U PHOTOELECTRIC EMISSION

PHOTOGEOLOGY
MEVTV Workshop on Nature and Composition of Surface Units on Mars
[NASA-CR-183075] 23 p3300 N88-29654
Surface composition of Mars: A Viking multispectral view 23 p3300 N88-29655
Mapping of volcanic units at Alba Patera, Mars 23 p3301 N88-29663
Small Martian volcanoes 23 p3302 N88-29668
Photogeological inferences of Martian surface composition 23 p3303 N88-29675

PHOTOGRAMMETRY
The program DSMME: Digital Situation Model, Measurement --- mapping 01 p0065 N88-10418
A review of computer-assisted photo interpretation research at USAETL (US Army Engineer Topographic Laboratories)
[AD-A184034] 03 p0346 N88-12186
Accuracy potential of non-metric cameras in close-range photogrammetry 04 p0463 N88-12862
The determination of exhaust cloud dimensions from films of space shuttle launches
[NASA-CR-4103] 06 p0732 N88-14500
The aerophotogrammetric determination of Earth surface deformations
[SER-C-321] 07 p0872 N88-15288
Optimization of photogrammetric image adjustment
[SER-C-323] 07 p0872 N88-15289
Theory and research on the disjunction of cross passage errors and systematic image errors in photogrammetric point determination
[SER-C-324] 07 p0872 N88-15290
Photogrammetric principles for combining remote sounding and three-dimensional mapping 08 p1012 N88-16135
Earth resources: A continuing bibliography with indexes (supplement 56)
[NASA-SP-7041(56)] 10 p1347 N88-18051
Dynamics of high-speed mechanisms with elastic members 13 p1779 N88-20643
Classification of small image areas by digital correlation for the connection of different images in photogrammetry and long-range reconnaissance
[ETN-88-91506] 14 p1940 N88-21578
Relative orientation
[AD-A190385] 15 p2089 N88-22449
Stereoscopic photographs, ground and aerial, of trees used in the arborization of Curitiba (PR) 17 p2366 N88-24091
Adjustment in photogrammetry: Methods, programs and applications
[B8735130] 17 p2369 N88-24105
Development in data structures in PHOCUS for digital mapping 18 p2534 N88-25034
The use of SPOT imagery on analytical photogrammetric instruments 22 p3110 N88-28471
Evaluation of SPOT cartographic capabilities over the Aix Marseille area (France) 22 p3110 N88-28476
Rigorous stereophotogrammetric treatment of SPOT images 22 p3111 N88-28482

PHOTOGRAPH INTERPRETATION
U PHOTOINTERPRETATION

PHOTOGRAPHIC DEVELOPERS
The calibration of photographic and spectroscopic films: Reciprocity failure and thermal responses of IIaO film at liquid nitrogen temperatures
[NASA-CR-181094] 13 p1773 N88-20606

PHOTOGRAPHIC EQUIPMENT
NT CAMERAS
NT DIFFRACTION LIMITED CAMERAS
NT FAINT OBJECT CAMERA
NT FRAMING CAMERAS
NT HIGH SPEED CAMERAS
NT MULTISPECTRAL BAND CAMERAS
NT PINHOLE CAMERAS
NT STREAK CAMERAS
NT TELEVISION CAMERAS
Trajectory measurement of the Fokker 100 aircraft during autoland testing
[NLR-MP-86010-U] 20 p2758 N88-26366

PHOTOGRAPHIC FILM
Use of a 35mm camera for remote surface cleanliness verification 02 p0133 N88-10835
The calibration of photographic and spectroscopic films: Reciprocity failure and thermal responses of IIaO film at liquid nitrogen temperatures
[NASA-CR-181094] 13 p1773 N88-20606
The calibration of photographic and spectroscopic films: The response of 2aO film to small dosages of alpha particles from 3/10th's rad to 8 rads at energy levels 153 MeV, 79 MeV and 47 MeV
[NASA-CR-177830] 13 p1773 N88-20608
New duplicating paper with high resolution for aerial photography
[PB87-228706] 19 p2685 N88-25962

PHOTOGRAPHIC MEASUREMENT
NT PHOTOGRAMMETRY

PHOTOGRAPHIC PLATES
The effects of humidity on the profile of photographic plates
[NPL-DMOM-88] 14 p1913 N88-21429
Method of digital surface photometry of galaxies and its application to the edge-on galaxy NGC 5907 16 p2287 N88-23695

PHOTOGRAPHIC PROCESSING
Improving coherent visualization by means of film optical filtering --- projectile visualization
[ISL-R-116/86] 02 p0176 N88-11097
Digital enhancement of flow field images
[NASA-TP-2770] 13 p1813 N88-20833

PHOTOGRAPHS
NT MICROPHOTOGRAPHS
NT MOTION PICTURES
NT PHOTOMICROGRAPHS
Academic course Space Methods for Studying Modern Landscapes of Continents 08 p1012 N88-16133
Automated stereophotogrammetry
[AD-A189617] 12 p1630 N88-19757
PLZT (Lead-Lathanium-Zirconium-Titanium) electro-optic photographic system
[AD-A193473] 23 p3215 N88-29137

PHOTOGRAPHY
NT AERIAL PHOTOGRAPHY
NT ASTRONOMICAL PHOTOGRAPHY
NT AUTORADIOGRAPHY
NT BLACK AND WHITE PHOTOGRAPHY
NT CINEMATOGRAPHY
NT CLOUD PHOTOGRAPHY
NT COLOR PHOTOGRAPHY
NT ELECTRO-OPTICAL PHOTOGRAPHY
NT FRACTOGRAPHY
NT HIGH SPEED PHOTOGRAPHY
NT HOLOGRAPHY
NT INFRARED IMAGERY
NT INFRARED PHOTOGRAPHY
NT METRIC PHOTOGRAPHY
NT MULTISPECTRAL PHOTOGRAPHY
NT ORTHOPHOTOGRAPHY
NT PHOTOMICROGRAPHY
NT RADAR PHOTOGRAPHY
NT SATELLITE-BORNE PHOTOGRAPHY
NT SCHLIEREN PHOTOGRAPHY
NT SHADOWGRAPH PHOTOGRAPHY
NT SPACEBORNE PHOTOGRAPHY
NT SPECKLE HOLOGRAPHY
NT SPECTROPHOTOGRAPHY
NT STEREOPHOTOGRAPHY
NT STEREOSCOPY
NT STREAK PHOTOGRAPHY
NT ULTRAVIOLET PHOTOGRAPHY
NT ULTRAVIOLET PHOTOMETRY
NT WHITE LIGHT HOLOGRAPHY
Use of a 35mm camera for remote surface cleanliness verification 02 p0133 N88-10835
Identifying areas of leading edge Japanese science and technology: Patent activity and citation analysis using US POC (Patent Office Classification) classification
[PB87-204095] 02 p0249 N88-11575
Tracking through turbulence at the Tonopah Test Range
[DE88-001448] 04 p0446 N88-12766
MAXIE 1 (Magnetospheric Atmospheric X-ray Imaging Experiment) Program
[AD-A185878] 07 p0877 N88-15317
A directed method for locating the focus of expansion
[AD-A185840] 07 p0906 N88-15491
Study on cineradiography
[ISL-R-120/86] 08 p0990 N88-15994
Pulsed laser stereophotography of plasmas and dynamically moving surfaces
[DE88-003170] 09 p1173 N88-17031
Description of MSFC engineering photographic analysis
[NASA-TM-4035] 11 p1491 N88-18900
Photographic filters
[INPE-4448-RPE/558] 12 p1692 N88-20124
The use of a water towing tank for aerodynamic testing and methods for quantitative evaluation of photographs
16 p2202 N88-23140
The USSR space systems for remote sensing of earth resources and the environment (sensor systems, processing techniques, applications)
17 p2356 N88-24035

PHOTOINTERPRETATION
Vegetation studies in the national Park of Comoe (Ivory Coast) using SPOT 1 satellite data
03 p0343 N88-12166
A review of computer-assisted photo interpretation research at USAETL (US Army Engineer Topographic Laboratories)
[AD-A184034] 03 p0346 N88-12186
Model-based building verification in aerial photographs
[AD-A186010] 07 p0870 N88-15276
Study of relief of ore regions using space images (on the example of Eastern Yakutia)
08 p1006 N88-16111
Automatic knowledge acquisition for aerial image interpretation
[AD-A188616] 12 p1636 N88-19810
Northeast Artificial Intelligence Consortium (NAIC) administrative matters and ancillary functions, volume 1
[AD-A189466] 12 p1682 N88-20055
Utilization of space color transformation, linear contrast and filtration for enhancement of colored digital images
[INPE-4310-PRE/1176] 14 p1983 N88-21831
Comparative utilization of analog and digital processes in the treatment of MSS-LANDSAT data for studying the national parks of Brazil
[INPE-4011-TDL/240] 15 p2090 N88-22456
Updating land-use of the Sao Jose dos Campos municipality through remote sensing data
[INPE-4479-RPE/562] 16 p2287 N88-23693
An integrated study of the Alto Paranaiba Kimberlite Province, Minas Gerais, Brazil: A possible tool for diamond exploration 17 p2355 N88-24031
Anomalies in the vegetation in the Alto Xingu - MT
17 p2357 N88-24043
Remote sensing and structural rupture: Application examples in the study of tectonics
17 p2359 N88-24050
Analysis and interpretation of image lithostructure: An application of the multiconcept in the metamorphic belt of Sul de Santana da Boa Vista (RS)
17 p2359 N88-24051
Application of its transformation in color enhancement of LANDSAT imagery 17 p2365 N88-24082
The 35 mm vertical aerial photographs for mapping stands of bracatinga in different age classes
17 p2366 N88-24087
Stereoscopic photographs, ground and aerial, of trees used in the arborization of Curitiba (PR)
17 p2366 N88-24091
Characteristics of drainage determinations in aerial photographs and relief determination on different scales planialtimetric charts for three soils in the state of Sao Paulo 17 p2367 N88-24095
Lithostructural interpretation of Chapda do Cachimbo (Pa-Am-Mt), based on radar and LANDSAT imagery
17 p2368 N88-24100
National Meeting on Remote Sensing Applied to Municipal Planning 19 p2681 N88-25939
Photointerpretation with instrumentation for evaluation of environmental impact: Mata Atlantica in Cubatao
19 p2683 N88-25946
Application of interactive graphic system (CAD/CAM) in the determination of process evolution in land use in the Ribeirao Preto municipality 19 p2684 N88-25956
PHOTODIGITIZE: A software/hardware system
[DE88-009575] 19 p2716 N88-26125
Methods of determining playa surface conditions using remote sensing
[AD-A192663] 21 p2965 N88-27612
An objective technique for Arctic cloud analysis using multispectral AVHRR (Advanced Very High Resolution Radiometer) satellite imagery
[AD-A194732] 23 p3235 N88-29250
High resolution Viking Orbiter images: A useful data source for testing the viability of geomorphic processes attributed to Martian landforms
23 p3307 N88-29703
The use of orbital remote sensing data for low cost ground-water survey
[INPE-4587-PRE/1318] 24 p3386 N88-30170
Reflectance pattern and the physical and chemical characteristics of three Brazilian Oxisols
[INPE-4590-PRE/1320] 24 p3387 N88-30172

PHOTOIONIZATION
A physico-chemical study of some areas of fundamental significance to biophysics
[DE87-013457] 02 p0217 N88-11365
Third-harmonic generation and multiphoton ionization spectroscopy
[DE87-013545] 03 p0281 N88-11769
Two-laser resonance enhanced photoionization spectrum of gas phase benzene
03 p0300 N88-11889
Theory of multiphoton ionization of atoms by strong, short pulsed lasers
[DE88-000963] 05 p0588 N88-13588
Photoinduced charge separation by polymer-bound chromophores
[DE88-002101] 06 p0685 N88-14198
Photoionization of atoms and ions: Application of time-dependent response method within the density functional theory
[AD-A185686] 07 p0930 N88-15649
Laser post-ionization secondary neutral mass spectroscopy
[DE88-002979] 09 p1172 N88-17027
Photoionization dynamics of excited molecular states
[DE88-002982] 09 p1246 N88-17468
Two-photon (VUV and visible) resonant ionization spectroscopy of atoms and molecules
[DE88-004332] 10 p1407 N88-18388
Theoretical studies of atomic transitions
[DE88-004719] 10 p1407 N88-18389
Resonantly-enhanced, four-photon ionization of krypton at laser intensities exceeding 10(12) W/sq cm
[DE88-005038] 11 p1544 N88-19229
Fast switching of far infrared radiation by refractive index change in semiconductors using photoionization
[ETN-88-91490] 11 p1551 N88-19279
A global model for planetary nebulae, taking into account central stellar evolution and influence on halo ionization
[ETN-88-91491] 11 p1568 N88-19389
Photoenhanced attachment for optical control of diffuse discharges
[AD-A188989] 12 p1696 N88-20147
To what extent is mass loading responsible for the Venus bowshock precursor?
[NASA-TM-89307] 12 p1711 N88-20230
The astrophysics of nebulae and active galactic nuclear emission-line regions: New methods and applications
13 p1858 N88-21111
Measurement of species concentrations in flames by laser-induced fluorescence
[DE88-007096] 14 p1869 N88-21286
Total photoionization cross sections of atomic oxygen from threshold to 44.3A
[NASA-CR-182992] 17 p2397 N88-24252
Selective detection in gas chromatography
[AD-A191499] 18 p2481 N88-24718
Photoionization dynamics and abundance patterns in laser vaporized tin and lead clusters
[AD-A191604] 18 p2482 N88-24722
High-order multiphoton ionization of the noble gases
[DE88-007489] 18 p2571 N88-25273
XUV source for ultra-high resolution photoionization spectroscopy
[DE88-007531] 19 p2614 N88-25510
Target designs for plasma-implosion-driven, photoionization-pumped soft X-ray lasers
[DE88-011278] 21 p2954 N88-27547
Multiphoton ionization of alkaline earth atoms in an intense laser field
[DE88-008078] 21 p3014 N88-27884

PHOTOLITHOGRAPHY
The production of ultrasmall and superfine holographic diffraction gratings using synchrotron radiation and lithographic techniques
[AD-A185395] 05 p0585 N88-13562
X-ray lithographic research: A collection of NRL contributions
[AD-A188313] 12 p1695 N88-20140

PHOTOLUMINESCENCE
NT X RAY FLUORESCENCE
Blue-green laser diode research program
[AD-A183517] 01 p0051 N88-10323
Photoluminescence studies of GaAs/AlAs superlattices
[DE87-013817] 02 p0245 N88-11548
400-nm photoluminescence of a color center in undoped YAG grown under reducing atmosphere
[DE88-001760] 07 p0858 N88-15213
Photoluminescence study of InP surfaces and InP-insulator interfaces
[ECL-87-13] 08 p1089 N88-16555
Optical characterization of GaAs/sub 1-x/Sb/sub x/ and GaAs/sub 1-x/Sb/sub x/GaAs strained layer superlattices
[DE88-003393] 10 p1418 N88-18464
Pulsed laser photothermal spectroscopy of liquids and solids
[DE88-003839] 11 p1455 N88-18675
Structural characterization of undoped and doped GaAs: A comparative study of four techniques
[DE88-004552] 11 p1555 N88-19304
Optical study of germanium, germanium plus arsenic, and germanium plus gallium implants in gallium arsenide
[AD-A189600] 13 p1845 N88-21045
Optical properties of quantum well structures with electric field: Life time free switching of luminescence intensity and virtual charge-induced ultrafast optical nonlinearity 14 p1976 N88-21794
Singlet oxygen behavior in solid polymer matrices
[DE88-005171] 15 p2043 N88-22171
Raman, photoluminescence and modulation spectroscopy of semiconductor heterostructures
20 p2861 N88-26997
Magneto-optical studies of GaInAs-InP quantum wells
20 p2870 N88-27039
Photoluminescence studies of InGaAlAs quaternary alloys
[DE88-007197] 20 p2874 N88-27062
Picosecond transient reflectivity of unpinned gallium arsenide (100) surfaces
[AD-A193242] 21 p3021 N88-27933
Ultrafast physics in semiconductor microstructures
[AD-A193300] 21 p3022 N88-27936
Intrinsic and extrinsic energy states of semiconductors and heterostructures using novel techniques
[DE88-008560] 23 p3269 N88-29582

PHOTOLYSIS

Photolytic processes for measurement of combustion heats of formation and reaction rates
[DE87-014047] 02 p0144 N88-10905

Energy transformation in molecular electronic systems
[DE87-013916] 03 p0282 N88-11771

Photochemical conversion of nucleic acid components catalyzed by lunar soil 06 p0750 N88-14604

Low-power photolytically pumped lasers
[DE88-002448] 08 p0991 N88-15998

Investigation of OH reaction products. Excimer laser photolysis/slab laser fluorescence under tropospheric conditions
[REPT-8] 09 p1191 N88-17137

Laser studies of the dynamics of free radical reactions
[DE88-004431] 10 p1337 N88-17989

Photolytic formation of free radicals and their effect on hydrocarbon pyrolysis chemistry in a concentrated solar environment
[DE88-004129] 13 p1794 N88-20730

Excimer laser photolysis studies of T-V (Translation-to-Vibration) energy transfer
[AD-A189613] 13 p1837 N88-20989

Photon-controlled growth of multilayered structures
[DE88-005061] 13 p1847 N88-21054

Techniques for studying fast reactions in liquids
[DE88-005917] 14 p1888 N88-21285

Nanosecond laser photolysis of opaque heterogeneous photosensitizers
[AD-A191424] 16 p2213 N88-23209

Ultraviolet measurements: Measurements of photolysis rates 18 p2539 N88-25065

An investigation of 2-6 superlattice deposition by laser photochemical techniques
[AD-A191547] 18 p2581 N88-25336

Photosynthetic water splitting
[DE88-007809] 20 p2830 N88-26791

Studies of photochemically and electrochemically driven electron transport in zeolites
[DE88-008644] 22 p3155 N88-28769

PHOTOMAGNETIC EFFECTS

Recording materials for optical disk memory discussed
06 p0684 N88-14193

PHOTOMAPPING

Evaluation of SPOT stereoscopic possibilities for cartography 03 p0342 N88-12156

Cartography and topography with SPOT
03 p0342 N88-12159

Use of SPOT panchromatic imagery to update forest maps of northern Quebec, Canada
03 p0344 N88-12172

Use of space photographs for geomorphological studies in southwestern Tajikistan 08 p1008 N88-16109

The use of LANDSAT-TM pictures for the detection of space-limiting elements for the benefit of landscape photomapping
[BCRS-87-02] 16 p2228 N88-23305

Cartographic applications of SPOT imagery
22 p3110 N88-28472

Larger scale image mapping with SPOT
22 p3111 N88-28481

High resolution orthoimage quadrangle maps using SPOT satellite data 22 p3112 N88-28488

Integrating multispectral imagery and ground level hyperspectral signature data
[AD-A195976] 24 p3386 N88-30166

PHOTOMETERS

NT ELECTROPHOTOMETERS
NT TOTAL OZONE MAPPING SPECTROMETER
NT ULTRAVIOLET SPECTROMETERS
NT ULTRAVIOLET SPECTROPHOTOMETERS

Direct detection of optical radiation through a sampling orifice for inductively coupled plasma atomic emission spectroscopy
[DE87-013609] 01 p0101 N88-10662

Comet West: A view from the HELIOS zodiacal light photometers 01 p0117 N88-10749

Optical probe
[EP-PATENT-0-210-869-A1] 05 p0650 N88-13984

Optical photometer for the Tirgo telescope
[IFSI-87-5] 05 p0650 N88-13985

Optical communication with semiconductor laser diodes
[NASA-CR-182464] 09 p1154 N88-16918

Growth of HgZnTe layers by LPE technique
[AD-A186723] 09 p1255 N88-17520

The photons payload, G-494: A learning experience
10 p1288 N88-17701

Remote sensing of atmospheric optical thickness and sea-water attenuation when submerged: Wavelength selection and anticipated errors
[AD-A187609] 11 p1548 N88-19262

Development of a high speed InGaAs/InP Schottky barrier photodetector for millimeter-wave fiber optical links
[AD-A188504] 12 p1629 N88-19750

Analysis of contamination data recorded by the IECM camera/photometer
[NASA-TM-100324] 14 p1882 N88-21246

An automated ozone photometer
[NASA-TM-100064] 14 p1908 N88-21404

Open questions in closed-loop photodetection
14 p1979 N88-21812

Thomson scattering for determining electron concentrations and temperatures in an inductively coupled plasma. 2: Description and evaluation of a multichannel instrument
[AD-A191324] 16 p2280 N88-23652

Characteristics, packaging and physics of ultra high speed diode lasers and detectors
19 p2658 N88-25797

Picosecond optical autocorrelation experiments on fast photodetectors 19 p2659 N88-25802

A survey of the Ap stars for rapid variability
20 p2884 N88-27127

Effect of interfacial phenomena on contact line heat Transfer-3
[AD-A194941] 24 p3343 N88-29901

High frequency GaAlAs modulator and photodetector for phased array antenna applications
[NASA-TM-101328] 24 p3367 N88-30048

PHOTOMETRY

NT ASTRONOMICAL PHOTOMETRY
NT ELECTROPHOTOMETRY
NT INFRARED PHOTOMETRY
NT SPECTROPHOTOMETRY
NT STELLAR SPECTROPHOTOMETRY
NT ULTRAVIOLET PHOTOMETRY
NT VISUAL PHOTOMETRY

Spectral analysis of APT RS CVn binary light curves
04 p0508 N88-13122

Starspots on the short-period RS CVn system SV Cam: 45 years of activity 04 p0508 N88-13123

The short-period RS CVn stars: Starspots and fundamental properties 04 p0508 N88-13124

Doppler snapshots 04 p0508 N88-13125

Titanium oxide absorption and spot sizes in II Peg, HR 1099 and UX Ari 04 p0508 N88-13126

Stellar cycle variability of solar-like stars: A sneak preview 04 p0510 N88-13136

Contemporaneous B,V,R,I photometry and H alpha spectroscopy of YY Gem 04 p0513 N88-13155

Brightness contrast and character height of five flat panel computer displays
[AD-A187743] 11 p1524 N88-19096

Zoom versus full-field sensitivity at the ETS (Experimental Test System)
[AD-A188162] 12 p1628 N88-19742

Photometry of P/Halley (1982i): Is what we have learned useful for other comets? 14 p1998 N88-21909

Narrow-band photometry of Comet P/Giacobini-Zinner at the time of ICE encounter 14 p1998 N88-21911

Dust photometry in the near nucleus region of Comet Halley from VEGA-2 observations
14 p2001 N88-21930

Speckle interferometry of asteroids
[NASA-CR-180438] 15 p2151 N88-22843

PHOTOMICROGRAPHS

Storing photomicrographs on optical laser disks
[DE37-013747] 04 p0449 N88-12785

PHOTOMICROGRAPHY

Study of stainless steel time-temperature sensitization diagrams, part 1
[ETN-87-90762] 03 p0289 N88-11815

Improving knowledge of the corrosion behavior of aluminum alloys of the 7XXX series
[REPT-48-451/F] 18 p2436 N88-24750

Microstructural effects in static and dynamic numerical experiments
[DE88-004289] 20 p2813 N88-26690

PHOTOMULTIPLIER TUBES

Study of solid state photomultiplier
[NASA-CR-177465] 05 p0583 N88-13556

Streak camera dynamic range optimization
[DE88-001632] 05 p0586 N88-13571

Signal processing studies program optical signal amplification, volume 1
[AD-A188055] 10 p1321 N88-17897

The off-axis channel macroplate
[NASA-CR-182938] 18 p2505 N88-24861

Array detectors for plasma spectrochemistry
[AD-A194220] 22 p3052 N88-28105

PHOTON BEAMS

National Synchrotron Light Source users manual: Guide to the VUV and X-ray beam lines
[DE88-001464] 04 p0490 N88-13020

Theory of two-photon emission from atomic inner shells
[AD-A187742] 11 p1543 N88-19223

Experimental set-up for measurements of Compton scattering cross section on light nuclei
[DE88-700161] 12 p1688 N88-20097

Correlations between photons in resonance fluorescence emitted by an atom near a metal surface
[AD-A188365] 12 p1689 N88-20102

Synchronous measurements of effective photon path length in visible and near-IR spectral regions in real cloud systems 13 p1790 N88-20706

PHOTONIC PROPULSION

NT LASER PROPULSION

PHOTONIC SWITCHING

U OPTICAL SWITCHING

PHOTONICS

Image sharpening observations of active galactic nuclei 01 p0098 N88-10643

A new technique for rocket and space-borne investigations of time-dependant auroral morphology
08 p1030 N88-16241

Multichannel anisotropic single-mode fiber optics for transducers 09 p1240 N88-17429

PHOTONS

Theoretical atomic and molecular photophysics
[DE87-014249] 02 p0231 N88-11458

Families of Bose rays in quantum optics
[DE87-014584] 02 p0236 N88-11489

XeCl excimer laser induced multiphoton ionization of ammonia molecule 03 p0299 N88-11883

High energy experimental physics
[DE87-013516] 03 p0376 N88-12363

Gamma ray lines from novae
04 p0526 N88-13214

Study of solid state photomultiplier
[NASA-CR-177465] 05 p0583 N88-13556

Photon counting image sensor development for astronomical applications
[NASA-CR-181507] 05 p0660 N88-14049

Photon stimulated desorption from oxidized Al(110)
[DE88-002209] 06 p0787 N88-14828

Monte Carlo photon transport on vector and parallel supercomputers
[DE88-002503] 07 p0905 N88-15486

Time characteristics of travelling wave lasing with two-photon picosecond optical pumping
07 p0918 N88-15578

Relativistic corrections for one- and two-photon matrix elements of weakly-bound systems
[NOTA-INTERNA-884] 07 p0929 N88-15645

Two-photon exclusive meson production at large angles
[NIKHEF-H/87-4] 08 p1081 N88-16515

Status of cross section data for photon scattering by atoms
[DE87-011281] 08 p1081 N88-16517

Memory effects on infrared adsorbate spectra
[AD-A186976] 09 p1253 N88-17512

Performance of a photon counting microchannel plate intensifier with wedge and strip image readout
[DE88-003831] 10 p1334 N88-17970

Application of state-multipole Heisenberg equations to Raman excitation dynamics
[DE88-003828] 10 p1335 N88-17977

The development of emission tomography for the nuclear industry
[AERE-R-12319] 10 p1341 N88-18014

Photonic temperature and pressure sensors for biosystems/pulsed microwave. Part 1: Interaction studies
[AD-A188867] 12 p1629 N88-19751

Proof of the feasibility of coherent and incoherent schemes for pumping a gamma-ray laser
[AD-A189238] 13 p1774 N88-20613

The use of four-photon Raman spectroscopy for the remote sensing of natural objects
[NASA-TT-20257] 13 p1791 N88-20716

The magnitude of secondary electron contributions in photon stimulated desorption
[AD-A189094] 13 p1835 N88-20980

Diffraction theory in QCD and beyond
[DE88-005958] 13 p1837 N88-20992

The response of a small liquid scintillation counter for low energy (gamma, p) experiments
[NOTA-INTERNA-901] 14 p1980 N88-21819

Measurement of the sup 4He(gamma, p)sup 3H total cross section and charge symmetry
[NOTA-INTERNA-902] 14 p1981 N88-21820

Cosmology for high energy physicists
[DE88-005705] 15 p2151 N88-22842

The position-sensitive counting of photons
16 p2271 N88-23590

Bimolecular reactions and energy-transfer processes of highly vibrationally excited molecules related to energetic materials
[AD-A189013] 18 p2571 N88-25270

Prospects for large dynamic range isotope analysis using photon burst mass spectrometry
[DE88-009110] 19 p2613 N88-25505

Third International Conference on Superlattices, Microstructures and Microdevices
[AD-A191416] 20 p2861 N88-26995

Infrared detectors based on the photon drag effect and intersubband absorption by a two-dimensional electron gas 20 p2867 N88-27024

Investigation of non-classical effects in two-photon interference processes 23 p3282 N88-29541

Intramolecular dynamics: A study of molecules at high levels of vibrational excitation
[AD-A195285] 24 p3428 N88-30400

PHOTONUCLEAR REACTIONS

Photon-assisted formation and cooling of molecular hydrogen
[MP-87-102] 16 p2267 N88-23563

PHOTOOXIDATION

Theoretical bases of polymer photodegradation and photooxidation
[AD-A186533] 08 p0974 N88-15889

Structure and function of the manganese complex involved in photosynthetic oxygen evolution determined by X-ray adsorption spectroscopy and electron paramagnetic resonance spectroscopy
[DE88-010360] 21 p2985 N88-27725

PHOTORECEPTORS

Laboratory equipment update
[AD-A189781] 15 p2102 N88-22522

Regulatory biochemical and metabolic responses in photoreceptors
[AD-A192898] 20 p2831 N88-26794

Limits of pattern discrimination in human vision
[AD-A193449] 23 p3239 N88-29273

PHOTORECONNAISSANCE

A review of computer-assisted photo interpretation research at USAETL (US Army Engineer Topographic Laboratories)
[AD-A184034] 03 p0346 N88-12186

Space applications in geography
08 p1007 N88-16104

Classification of small image areas by digital correlation for the connection of different images in photogrammetry and long-range reconnaissance
[ETN-88-91506] 14 p1940 N88-21578

PHOTOREDUCTION
U PHOTOCHEMICAL REACTIONS

PHOTORESISTIVITY
U PHOTOCONDUCTIVITY

PHOTORESISTORS
U PHOTOCONDUCTORS

PHOTOSENSITIVITY
NT LIGHT ADAPTATION
NT PHOTOTROPISM

Develop techniques for ion implantation of (lead-lanthanum-zirconate-titanate) for adaptive optics
[DE88-000642] 05 p0650 N88-13986

Nanosecond laser photolysis of opaque heterogeneous photosensitizers
[AD-A191424] 16 p2213 N88-23209

Dynamic range compression/expansion of light beams by photorefractive crystals
[NASA-CASE-NPO-17140-1-CU]
17 p2438 N88-24508

PHOTOSENSORS
U PHOTOELECTRICITY
U RADIATION MEASURING INSTRUMENTS

PHOTOSPHERE
NT SOLAR GRANULATION

Magnetic field twist driven by remote convective motions: Characteristics and twist rates 01 p0113 N88-10724

Spectroscopy and nonthermal processes
02 p0252 N88-11594

Thermal atmospheric models
02 p0253 N88-11599

Quasi-thermal models 02 p0253 N88-11600

Active region flows 02 p0255 N88-11611

Coronal magnetic fields produced by photospheric shear
[NASA-CR-181514] 03 p0390 N88-12447

Empirical relations between photospheric magnetic fields and atmospheric radiative losses for cool dwarf stars 04 p0511 N88-13145

An analysis of the photospheric line profiles in F, G, and K supergiants 04 p0513 N88-13157

New results from high angular resolution observations of alpha Ori 04 p0514 N88-13161

Emission features in IRAS LRS spectra of MS, S and CS stars 04 p0514 N88-13163

IUE observations of the hybrid K3 II star Iota Aurigae and constraints on the outer atmospheric structure
04 p0516 N88-13171

Solar flares and magnetic topology
[AD-A188692] 12 p1712 N88-20244

More than a solar cycle of synoptic solar and coronal data: A video presentation
[NASA-CR-181459] 23 p3308 N88-29708

PHOTOSYNTHESIS

Photocatalytic electrochemistry at a biological-membrane metal-colloid interface
[DE87-009122] 02 p0166 N88-11041

Operation of an experimental algal gas exchanger for use in a CELSS 03 p0358 N88-12255

Application of photosynthetic N(2)-fixing cyanobacteria to the CELSS program 03 p0358 N88-12257

A review of recent activities in the NASA CELSS program 03 p0359 N88-12259

Fundamental study on gas monitoring in CELSS
03 p0359 N88-12263

Study of the relationship between photosynthesis, respiration, transpiration, and mineral nutrition in wheat
03 p0360 N88-12268

Utilization of potatoes in bioregenerative life support systems 03 p0360 N88-12269

Wheat production in controlled environments
[UAES-PAPER-3324] 03 p0361 N88-12270

Artificial photosynthesis using chlorophyll based carotenoid-quinone triads
[DE88-001660] 07 p0884 N88-15362

Factors governing light driven electron and proton translocation in proteins across membranes
[DE88-002716] 08 p1082 N88-16519

Picosecond laser spectroscopy of charge-separation in photosynthetic model systems
[DE88-003122] 09 p1172 N88-17028

Energy transfer and photochemistry in biomimetic solar conversion
[PB88-130026] 10 p1348 N88-18057

Research on a solar biotechnology based on the culture of photosynthetic cells
[DE88-900129] 10 p1359 N88-18120

Spectroscopic studies of energy transfer in photosynthetic reaction centers of higher plants
[DE88-003850] 10 p1359 N88-18121

The evolution of glutathione metabolism in phototrophic microorganisms
[NASA-CR-182902] 19 p2695 N88-26015

Mechanisms of photochemical energy conversion by chlorophyll
[DE88-008763] 20 p2819 N88-26725

Photosynthetic water splitting
[DE88-007809] 20 p2830 N88-26791

Modeling the primary events of photosynthesis using chlorophyll containing fixed distance donor-acceptor molecules
[DE88-010033] 20 p2831 N88-26793

Factors governing light driven electron and proton translocation in proteins across membranes
[DE88-011120] 21 p2984 N88-27724

Structure and function of the manganese complex involved in photosynthetic oxygen evolution determined by X-ray adsorption spectroscopy and electron paramagnetic resonance spectroscopy
[DE88-010360] 21 p2985 N88-27725

Electrochemical and optical studies of model photosynthetic systems
[DE88-009291] 23 p3237 N88-29264

PHOTOTHERMAL CONVERSION

Pulsed laser photothermal spectroscopy of liquids and solids
[DE88-003839] 11 p1455 N88-18675

Thermophotovoltaic space power system, phase 3
[NASA-CR-179327] 14 p1942 N88-21585

Photochemical and thermal modeling in the early atmosphere of the earth
[NASA-CR-183029] 18 p2543 N88-25093

Noncontact photo-thermal sensing
[AD-A195450] 24 p3344 N88-29905

PHOTOTHERMOTROPISM
U ANISOTROPY
U PHOTOTROPISM
U TEMPERATURE EFFECTS

PHOTOTROPISM

The evolution of glutathione metabolism in phototrophic microorganisms
[NASA-CR-182902] 19 p2695 N88-26015

PHOTOTUBES
NT PHOTOMULTIPLIER TUBES

PHOTOVOLTAIC CELLS
NT SOLAR CELLS
NT VERTICAL JUNCTION SOLAR CELLS

The fundamentals of photovoltaic system electrical design
[DE87-009061] 02 p0194 N88-11214

Photovoltaic power modules for NASA's manned space station
[NASA-TM-100229] 03 p0277 N88-11745

Polymers in solar technologies
[DE88-001102] 03 p0294 N88-11849

Recent progress in space photovoltaic systems
[NASA-TM-100208] 03 p0311 N88-11966

Electricity from photovoltaic solar cells. Flat-Plate Solar Array Project of the US Department of Energy's National Photovoltaics Program: 10 years of progress
[NASA-TM-89653] 03 p0346 N88-12188

Low Earth orbit environmental effects on the space station photovoltaic power generation systems
[NASA-TM-100230] 03 p0387 N88-12429

Light funnel concentrator panel for solar power
[NASA-CR-179223] 04 p0464 N88-12870

Design description report for a photovoltaic power system for a remote satellite earth terminal
[NASA-CR-179586] 04 p0465 N88-12875

Radiation performance of AlGaAs concentrator cells and expected performance of cascade structures
[NASA-TM-100145] 04 p0465 N88-12878

Oxidation and protection of fiberglass-epoxy composite masts for photovoltaic arrays in the low Earth orbital environment
[NASA-TM-100839] 11 p1465 N88-18734

PbSnTe photovoltaic detectors for operation in the 2-14 micron band
[INPE-4252-PRE/1125] 11 p1508 N88-19008

Proceedings of the 1987 High-Efficiency Photovoltaic Subcontractors' Review Meeting
[DE88-003354] 11 p1508 N88-19011

Development of integrated detectors for attitude sensors
[INPE-4409-PRE/1222] 12 p1602 N88-19586

Mast material test program (MAMATEP)
[NASA-TM-100821] 12 p1604 N88-19592

Characterization of integrated photovoltaic detectors for MECB solar sensors
[INPE-4408-PRE/1221] 12 p1630 N88-19754

Concentrating photovoltaic collectors: Fabrication design
[PB88-148051] 12 p1640 N88-19821

SERI's Photovoltaic R and D Project: Recent progress and future directions
[DE88-001129] 13 p1794 N88-20728

Control strategies and hardware used in solar thermal applications
[DE88-004631] 13 p1794 N88-20731

Progress of amorphous silicon based solar cells and modules
[DE88-004666] 13 p1794 N88-20733

Crystalline photovoltaic cell technology: Present and future
[DE88-004684] 13 p1795 N88-20734

Power systems for production, construction, life support and operations in space
[NASA-TM-100838] 14 p1883 N88-21254

Recent advances in photovoltaic concentrator technology
[DE88-003948] 15 p2091 N88-22462

An integrated and modular digital modeling approach for the space station electrical power system development
[NASA-TM-100904] 16 p2170 N88-22935

Power source selection for neutral particle beam systems 17 p2407 N88-24314

Photovoltaic Advanced Research and Development Project, solar radiation research
[DE88-001143] 18 p2537 N88-25056

Advanced photovoltaic power system technology for lunar base applications
[NASA-TM-100965] 20 p2766 N88-26402

Photovoltaic concentrator technology: Recent results
[DE88-009588] 20 p2819 N88-26726

Photovoltaic cells with n-silicon and conductive polymers
[ETN-88-92133] 20 p2821 N88-26734

Growth and characterization of thin films of ZnSnP(sub)2
[DE88-001164] 20 p2874 N88-27080

Photovoltaic Energy. Electricity from Sunlight: A current awareness bulletin
[DE88-008289] 21 p2969 N88-27634

Reduced order modeling of grid-connected photovoltaic inverter systems
[DE88-010603] 21 p2969 N88-27635

SERI's photovoltaic research project: A foundation for tomorrow's utility-scale electricity
[DE88-001161] 23 p3230 N88-29220

Solar dynamic power systems
[ETN-88-92969] 23 p3230 N88-29224

PHOTOVOLTAIC CONVERSION

The preparation of thin films for photovoltaic conversion by novel MOCVD techniques
[DE87-001165] 02 p0194 N88-11212

SERI's Photovoltaic R and D Project: Recent progress and future directions
[DE88-001129] 13 p1794 N88-20728

Progress of amorphous silicon based solar cells and modules
[DE88-004666] 13 p1794 N88-20733

Thermophotovoltaic space power system, phase 3
[NASA-CR-179327] 14 p1942 N88-21585
Today's photovoltaic systems: An evaluation of their performance
[DE88-006926] 15 p2090 N88-22457
Three-dimensional models of conventional and vertical junction laser-photovoltaic energy converters
[NASA-TM-4039] 17 p2370 N88-24111
Photovoltaic Measurements and Performance Branch
[DE88-001142] 21 p2968 N88-27633
PHOTOVOLTAIC EFFECT
Photovoltaic energy systems
[DE88-007504] 19 p2687 N88-25968
PHTHALOCYANIN
Electrochromic cells with lutetium diphthalocyanine and semisolid polymer electrolytes
[AD-A188031] 10 p1352 N88-18078
PHUGOID OSCILLATIONS
U OSCILLATIONS
U OSCILLATORS
U PITCH (INCLINATION)
PHYSICAL CHEMISTRY
NT QUANTUM CHEMISTRY
A physico-chemical study of some areas of fundamental significance to biophysics
[DE87-013457] 02 p0217 N88-11365
Physico-chemical studies on copper sulfide behavior in the CdS-Cu2S solar cell
[ETN-88-91068] 09 p1187 N88-17109
Dry adhesive friction of elastomers: A study of the fundamental mechanical aspects
[ETN-88-92903] 23 p3198 N88-29036
PHYSICAL CONSTANTS TESTING REACTOR
U NUCLEAR RESEARCH AND TEST REACTORS
PHYSICAL ENDURANCE
U PHYSICAL FITNESS
PHYSICAL EXAMINATIONS
US civil airmen statistics, 1987
[AD-A191714] 18 p2455 N88-24577
PHYSICAL EXERCISE
Oxygen transport during exercise at extreme simulated altitude: Operation Everest 2
[AD-A185720] 06 p0752 N88-14620
Exercise in the heat: Effects of dinitrophenol administration
[AD-A185731] 06 p0752 N88-14622
Exercise thermoregulation after prolonged wakefulness
[AD-A186224] 08 p1048 N88-16327
Temperature regulation at rest and exercise during the human menstrual cycle
[AD-A186461] 08 p1050 N88-16341
Lipid peroxidation in rat tissues with exposure to antiorthostatic hypokinesia, exercise and immobilization stress 10 p1365 N88-18159
Effect of oxygen inhalation on respiratory function during exercise and exposure to added resistance to respiration
10 p1366 N88-18164
Oxidative enzyme activity in healthy subjects and individuals with neurocirculatory dystonia during graded exercise 10 p1367 N88-18170
Carbamates, atropine, and diazepam: Effects on performance in the running rat
[AD-A188009] 11 p1517 N88-19062
Manipulation of muscle glycogen concentrations using high and low carbohydrate diets and exercise
[AD-A187732] 11 p1519 N88-19069
Gastric emptying during exercise: Effects of acute heat stress, acclimation and hypohydration
[AD-A188008] 11 p1519 N88-19073
Heat acclimatization under controlled hyperthermia
12 p1665 N88-19981
Endocrine responses to resistance exercise
[AD-A188681] 12 p1667 N88-19993
Hypothalamic-pituitary-adrenal responses to short duration high intensity cycle exercise
[AD-A192597] 21 p2985 N88-27727
Metabolic and cardiorespiratory parameters during three consecutive days of exhaustive running
[AD-A192598] 21 p2985 N88-27728
Validation of a modified one-step rebreathing technique for measuring exercise cardiac output
[AD-A192600] 21 p2986 N88-27729
A resistive-film based force transducer for the study of exercise
[AD-A192601] 21 p2986 N88-27730
The role of textile material in clothing on thermoregulatory responses to intermittent exercise
[AD-A192599] 22 p3130 N88-28608
Depressed sweating during exercise at altitude
[AD-A192603] 22 p3130 N88-28609
The effects of acute cold exposure on exercise performance
[AD-A192650] 22 p3130 N88-28610
Influence of altitude and caffeine during rest and exercisé on plasma levels of proenkephalin peptide F
[AD-A192659] 22 p3131 N88-28616
Effects of air polution on human exercise performance
[AD-A192660] 22 p3131 N88-28617
PHYSICAL FITNESS
Physiological determinants of load bearing capacity
[AD-A184977] 05 p0629 N88-13848
The use of heart rate in the prescription and evaluation of exercise programs
[AD-A186454] 08 p1049 N88-16336
Development of a coping strategies questionnaire to assess endurance performance
[AD-A188010] 11 p1520 N88-19074
Fish as a tool for testing fitness in space
12 p1662 N88-19963
Lifting and carrying capacities relative to physical fitness measures
[AD-A189305] 13 p1809 N88-20808
Prediction of physical fitness: Estimated percent body fat using body circumferences versus weight-height measures
[AD-A190233] 15 p2103 N88-22526
Dietary factors related to physical fitness
[AD-A190272] 15 p2103 N88-22527
Behavioral, psychological and demographic predictors of physical fitness
[AD-A192697] 21 p2986 N88-27733
PHYSICAL OPTICS
Theoretical Aspects of Target Classification
[AGARD-LS-152] 03 p0303 N88-11909
Physical optics method: Prediction of radar signatures
03 p0304 N88-11914
Theoretical aspects of target classification: Physical optics and radon transform methods
03 p0304 N88-11915
Large bandwidth ground scattering model --- radar scattering
[FOA-C-30458-3.2] 05 p0576 N88-13511
Scattering and depolarization by random rough terrain and vegetation covered terrain-unified full wave approach 12 p1615 N88-19657
Coherence effects in optical physics with special reference to spectroscopy
[AD-A189520] 13 p1840 N88-21007
Curvature of blended rolled edge reflectors at the shadow boundary contour
[NASA-CR-182974] 18 p2576 N88-25300
PHYSICAL WORK
Nystagmometric distinctions of individuals regularly exposed to vibration 07 p0891 N88-15401
Lifting and carrying capacities relative to physical fitness measures
[AD-A189305] 13 p1809 N88-20808
Simultaneous multiple control force exertion capabilities of males and females versus helicopter control force design limits
[AD-A191653] 18 p2553 N88-25153
PHYSICS
JPRS report: Science and technology. China
[JPRS-CST-88-003] 13 p1755 N88-20495
JPRS report: Science and technology. USSR: Physics and mathematics
[JPRS-UPM-88-001] 14 p1968 N88-21751
PHYSICS AND CHEMISTRY EXPERIMENT IN SPACE
The challenge of G-376 10 p1288 N88-17705
PHYSIOCHEMISTRY
A geometrical model for determining the physicochemical properties of ternary metallic systems
[BLL-M-37303-(5828.4)] 02 p0149 N88-10931
Physicochemical correlates of human adaptation to extreme environments 06 p0750 N88-14607
Controlled Ecological Life Support Systems (CELSS) physiochemical waste management systems evaluation
[NASA-CR-177422] 06 p0754 N88-14626
PHYSIOGRAPHY
U GEOMORPHOLOGY
PHYSIOLOGICAL DEFENSES
NT IMMUNE SYSTEMS
PHYSIOLOGICAL EFFECTS
NT HEMODYNAMIC RESPONSES
NT PHYSIOLOGICAL RESPONSES
Eyesight trainer for pilots 03 p0355 N88-12239
Human adaptation to isolated and confined environments
[NASA-CR-181502] 03 p0357 N88-12248
Change in functional activity of cortical brain structures and their blood supply in alert rabbits in response to rocking 04 p0473 N88-12916
Human respiratory responses during high performance flight
[AGARD-AG-312] 04 p0474 N88-12923
Effect of night watches and intermittent sleep on state of circadian rhythms of physiological functions of fishermen 06 p0750 N88-14610
Exercise in the heat: Effects of dinitrophenol administration
[AD-A185731] 06 p0752 N88-14622
Proceedings and program draft in Gravitational Biology in the Federal Republic of Germany --- Effects of Weightlessness on the Human Organism
[ESA-TT-988] 07 p0884 N88-15363
JPRS report: Science and technology. USSR: Space Biology and Aerospace Medicine, volume 21, no. 4, July - August 1987
[JPRS-USB-88-002] 07 p0893 N88-15412
Morphometric analysis of rat aorta endothelium during long-term hypokinesia 07 p0894 N88-15417
Changes in functional parameters of animals during long-term inhalation of acetic acid
07 p0895 N88-15423
Physiological and immunological aspects of human adaptation to temperature elevation in a closed environment 07 p0895 N88-15424
Results of research with biological satellites
08 p1006 N88-16097
Research on cotton plants grown in space
08 p1006 N88-16098
Scientific objectives and functional requirements of life sciences in the Space Station 08 p1033 N88-16264
Operation Everest 2: Comparison of four instruments for measuring blood oxygen saturation
[AD-A186456] 08 p1049 N88-16337
Ultra-low frequency vibration data acquisition concerns in operating flight simulators
[DE88-004795] 10 p1285 N88-17687
JPRS Report: Science and Technology. USSR: Space Biology and Aerospace Medicine, volume 21, no. 5, September - October 1987
[JPRS-USB-88-003] 10 p1359 N88-18122
Effect of spaceflight factors on primate's blood circulation 10 p1359 N88-18124
Inflight simian circadian rhythms and temperature homeostasis aboard Cosmos-1514 biosatellite
10 p1359 N88-18125
Effect of spaceflight factors on primate hydration homeostasis 10 p1360 N88-18126
Investigation of effects of short-term exposure to high concentrations of carbon monoxide on operator's psychophysiological functions 10 p1361 N88-18133
Results of long-term electrocardiographic monitoring of cosmonauts 10 p1364 N88-18152
Effect of spaceflight factors on biological material flown aboard Cosmos-1514 biosatellite
10 p1364 N88-18154
Lipid peroxidation in rat tissues with exposure to antiorthostatic hypokinesia, exercise and immobilization stress 10 p1365 N88-18159
Certain aspects of human metabolism during spaceflights of varying duration
[NASA-TT-20215] 10 p1369 N88-18181
Basic results of medical studies during prolonged manned flights on-board the Salyut-7/Soyuz-T orbital complex
[NASA-TT-20217] 10 p1369 N88-18182
Modeling of the non-auditory response to blast overpressure
[AD-A187397] 10 p1369 N88-18184
Effects of breathing air containing contaminants such as CO2, CO and hydrocarbons at 1 and 5 atmospheres
[PB88-132915] 11 p1521 N88-19084
Implications of shiftwork in space for human physiology experiments 12 p1659 N88-19942
Renal effects of anti-gravity suit inflation in man in relation to cardiovascular and hormonal changes
12 p1661 N88-19959
The suspended Japanese quail as an animal model for experiments related to microgravity
12 p1662 N88-19960
Facilitory effects of voluntary movements on vestibulomotor reaction 12 p1664 N88-19976
Air quality and human performance, chapter 16
[AD-A188335] 12 p1666 N88-19988
Medical problems related to altitude in: Human performance physiology and environmental medicine at terrestrial extremes, chapter 14
[AD-A188340] 12 p1666 N88-19989
Motion sickness: A study of its effects on human physiology
[AD-A188821] 12 p1667 N88-19995
Protection against laser damage to human body reviewed 15 p2053 N88-22237
A comparison of visual evoked potential and behavioral measures of flashblindness in humans
[AD-A189757] 15 p2101 N88-22519
Age, alcohol, and simulated altitude: Effects on performance and breathalyzer scores
[AD-A190642] 15 p2103 N88-22531
Behavior, physiology and energy deposition in rats chronically exposed to 2450 MHz radiation
[PB88-171418] 16 p2237 N88-23363

Effects of moderate cold and heat stress on the potential work performance of industrial workers. Part 6: The effects of increasing vapour pressure at four air temperatures on the performance and physiology of white females
[PB88-124854] 18 p2550 N88-25137

Physiological and hematological responses of matched older and younger men during dry-heat acclimation
[AD-A186450] 18 p2550 N88-25139

Physiological effects on men of long duration confinement in a carbon dioxide enriched environment
19 p2695 N88-26017

Experience in occupational medicine, derived from 16 operational deep saturation trimix 5 dives in GUSI from 150 to 600 m 19 p2695 N88-26018

Effect of low-frequency whole-body vertical vibration on the serotoninergic system of the brain and spinal cord
19 p2704 N88-26081

Effect of long-term inhalation of acetic acid vapor on some functional parameters of man
19 p2705 N88-26084

Physiological monitoring methodology in the USAFSAM centrifuge 21 p2924 N88-27356

Hyperthermia: New thoughts on an old problem
[AD-A192602] 21 p2986 N88-27731

Simulator sickness in the AH-64 Apache combat mission simulator
[AD-A193419] 21 p2988 N88-27739

Human acclimatization and physical performance at high altitude
[AD-A192651] 22 p3130 N88-28611

Physiological effects of extremely low frequency electric and magnetic fields
[DE88-752814] 22 p3132 N88-28620

USAF hyperbaric animal transfer chamber system
[AD-A193633] 23 p3237 N88-29265

Effect of hypoxia on speech recognition in noise
[AD-A193943] 23 p3240 N88-29280

Nutrient requirements for high stress environments
[AD-A194595] 23 p3243 N88-29301

PHYSIOLOGICAL RESPONSES
NT HEMODYNAMIC RESPONSES

Determination of the individual state of acclimatization
[IZF-1986-27] 01 p0075 N88-10478

Human thermoregulatory model for whole body immersion in water at 20 and 28 C
[AD-A185052] 05 p0629 N88-13849

Maximal cardiorespiratory responses to one- and two-legged cycling during acute and long-term exposure to 4300m
[AD-A185730] 06 p0752 N88-14621

Measurement and modification of sensorimotor system function during visual-motor performance
[AD-A186351] 07 p0889 N88-15387

Mother-fetus system as object for investigation of mechanisms of physiological effect of weightlessness
07 p0891 N88-15402

Combined effect of microwaves and ionizing radiation
07 p0893 N88-15413

Circulatory response of males 45-52 years of age to antiorthostatic hypokinesia 07 p0894 N88-15416

Nucleic acid content of skeletal muscles during hypokinesia and in the recovery period
07 p0894 N88-15418

Changes in regional and central hemodynamics during seven-day water immersion 07 p0895 N88-15421

Effect of intermittent hypercapnia on visual analyzer function 07 p0896 N88-15431

Mononuclear phagocytes during adaptation of essentially healthy people to high altitudes
07 p0896 N88-15432

Prediction of human thermoregulatory responses and endurance time in water at 20 and 24C
[AD-A186223] 08 p1048 N88-16326

Exercise thermoregulation after prolonged wakefulness
[AD-A186224] 08 p1048 N88-16327

Influence of skeletal muscle glycogen on passive rewarming after hypothermia
[AD-A186451] 08 p1049 N88-16334

Determination of the effect of walking on the forced convective heat transfer coefficient using an articulated manikin
[AD-A186452] 08 p1049 N88-16335

The use of heart rate in the prescription and evaluation of exercise programs
[AD-A186454] 08 p1049 N88-16336

Portable, ambient air microclimate cooling in simulated desert and tropic conditions
[AD-A186457] 08 p1050 N88-16338

Rapid hypothermia subsequent to oral nicotinic acid and immersion in warm (30C) water
[AD-A186458] 08 p1050 N88-16339

Respiratory and cardiovascular responses to cold stress following repeated cold water immersion
[AD-A186460] 08 p1050 N88-16340

Temperature regulation at rest and exercise during the human menstrual cycle
[AD-A186461] 08 p1050 N88-16341

A-scan ultrasound measurement of ocular changes during accommodation
[AD-A186818] 09 p1198 N88-17181

Role of body fat in the prediction of the metabolic response for immersion in cold water
[AD-A186914] 09 p1198 N88-17182

Physiological and ecological implications of coupled heat- and water-transport mechanisms of endotherms and vegetation
[DE88-004170] 10 p1352 N88-18081

Membrane model of cupula or vestibular semicircular canals 10 p1361 N88-18132

Comparative evaluation of stress reponse of rats to different methods of simulating some effects of weightlessness 10 p1363 N88-18144

Second All-Union Conference on Physiology of Extreme States and Individual Protection of Man
10 p1363 N88-18147

JPRS Report: Science and Technology. USSR: Space Biology and Aerospace Medicine, volume 21, no. 6, November - December 1987
[JPRS-USB-88-004] 10 p1364 N88-18150

Polar worker adaptability to Antarctic high altitudes
10 p1366 N88-18165

Effect of hypercapnic-hypoxic test on cardiorespiratory parameters of individuals with neurocirculatory dystonia
10 p1367 N88-18169

Hemodynamic effects of beta-adrenergic blocking with obsidan in clinostatic and orthostatic positions
10 p1367 N88-18171

Supersonic and subsonic aircraft noise effects on animals: A literature survey
[AD-A186922] 10 p1404 N88-18373

Role of adenosine analogs and growth hormone in waking and sleep
[AD-A187897] 11 p1519 N88-19070

Operation Everest 2: Alterations in the immune system at high altitude
[AD-A188011] 11 p1520 N88-19075

Regulation of calcium metabolism during prolonged antiorthostatic hypokinesia
[NASA-TT-20219] 11 p1521 N88-19085

Changes in hemostasis system of animals under conditions of granulocytopoiesis inhibition under effect of decreased barometric pressure
12 p1651 N88-19890

Acute mountain sickness at 4500 m is not altered by repeated eight-hour exposures to 3200-3550 m normobaric hypoxic equivalent
[AD-A188358] 12 p1666 N88-19990

Neurohumoral aspects of sleep
[AD-A188653] 12 p1667 N88-19992

Endocrine responses to resistance exercise
[AD-A188681] 12 p1667 N88-19993

Plasma cortisol, renin and aldosterone during an intense heat acclimation program
[AD-A189387] 13 p1809 N88-20810

A program for the study of skeletal muscle catabolism following physical trauma
[AD-A189771] 15 p2102 N88-22521

Complex sound processing: An interdisciplinary approach
[AD-A189782] 15 p2102 N88-22523

Behavioral response of rats exposed to high-power microwave radiation
[AD-A192199] 18 p2548 N88-25128

A systems engineering based methodology for analyzing human electrocortical responses
[AD-A190809] 18 p2550 N88-25135

Extremely Low Frequency (ELF) communications program: Non-ionizing electromagnetic radiation literature evaluation and assessment, 1986-1987 literature review
[AD-A192024] 19 p2642 N88-25677

Method of assessing changes in biorhythmological structure of human physiological functions
19 p2706 N88-26088

Contra- and ipsilateral auditory stimuli produce different activation patterns at the human auditory cortex: A neuromagnetic study
[PB88-181490] 19 p2708 N88-26098

Regulatory biochemical and metabolic responses in photoreceptors
[AD-A192898] 20 p2831 N88-26794

Human response to prolonged motionless suspension in four types of full body harnesses
21 p2929 N88-27387

Electric and Magnetic Activity of the Central Nervous System: Research and Clinical Applications in Aerospace Medicine
[AGARD-CP-432] 21 p2977 N88-27683

The interaction of thalamo-cortical systems in the 40 Hz following response 21 p2979 N88-27694

A study of sources in the human brain associated with stereopsis 21 p2979 N88-27695

Cognitive task demands as reflected in physiological measures 21 p2980 N88-27699

Hypothalamic-pituitary-adrenal responses to short duration high intensity cycle exercise
[AD-A192597] 21 p2985 N88-27727

Physiological responses to acute exercise-heat stress
[AD-A192606] 21 p2986 N88-27732

Behavioral effects of exposure to the tempo high-power microwave system
[AD-A193305] 21 p2987 N88-27738

Plasma volume expansion in rats: Effects on thermoregulation and exercise
[AD-A192656] 22 p3130 N88-28606

Physiology of prolonged bed rest
[NASA-TM-101010] 22 p3130 N88-28607

The role of textile material in clothing on thermoregulatory responses to intermittent exercise
[AD-A192599] 22 p3130 N88-28608

Hierarchical structure in polymeric solids and its influence on properties
[AD-A194720] 23 p3197 N88-29029

Low doses of atropine sulfate impair retention of a well-learned spatial task
[AD-A194065] 23 p3237 N88-29266

Central adrenergic receptors as mediators of central response to stress: Study with Positron Emission Tomography (PET)
[AD-A194947] 24 p3407 N88-30284

PHYSIOLOGICAL TELEMETRY
U BIOTELEMETRY

PHYSIOLOGICAL TESTS
NT BODY SWAY TEST
NT VESTIBULAR TESTS

Determination of the individual state of acclimatization
[IZF-1986-27] 01 p0075 N88-10478

Measuring functional feasibility of human visual system 12 p1665 N88-19983

Literature review: Validity and potential usefulness of psychomotor ability tests for personnel selection and classification
[AD-A193558] 23 p3241 N88-29287

PHYSIOLOGY
NT AUDIOLOGY
NT ELECTROPHYSIOLOGY
NT EXERCISE PHYSIOLOGY
NT GRAVITATIONAL PHYSIOLOGY
NT MENSTRUATION
NT NEUROPHYSIOLOGY
NT PSYCHOPHYSIOLOGY
NT RESPIRATORY PHYSIOLOGY
NT UNDERWATER PHYSIOLOGY
NT WORKLOADS (PSYCHOPHYSIOLOGY)

JPRS report: Science and technology. USSR: Life sciences
[JPRS-ULS-87-012] 03 p0355 N88-12238

JPRS report: Science and technology. USSR: Life sciences
[JPRS-ULS-87-009] 04 p0473 N88-12915

JPRS report: Science and technology. USSR: Life sciences
[JPRS-ULS-87-011] 06 p0749 N88-14601

JPRS report: Science and technology. USSR: Life sciences
[JPRS-ULS-87-013] 06 p0750 N88-14606

USSR report: Life sciences. Biomedical and behavioral sciences
[JPRS-UBB-86-022] 08 p1046 N88-16318

Ultra-low frequency vibration data acquisition concerns in operating flight simulators
[DE88-004795] 10 p1285 N88-17687

Evaluation of spare room in cerebrospinal system using noninvasive methods 10 p1361 N88-18137

Scaling physiological pharmacokinetic models by physiological time
[DE88-000335] 10 p1368 N88-18173

USSR report: Life sciences. Biomedical and behavioral sciences
[JPRS-UBB-87-008] 12 p1662 N88-19986

JPRS report: Science and technology. USSR: Life sciences
[JPRS-ULS-88-009] 20 p2829 N88-26785

Squid instrumentation for neuromagnetic study of complex brain activity 21 p2978 N88-27691

Using IMSL mathematical and statistical computer subroutines in physiological and biomechanical research
[AD-A192594] 21 p2995 N88-27765

Vision and visual protection in fast jet aircraft
23 p3241 N88-29292

Comparison of morning with afternoon nitrogen elimination in resting subjects breathing 100 percent oxygen
[AD-A196191] 24 p3407 N88-30282

PHYTOPLANKTON
Thematic mapper research in the earth sciences: Small scale patches of suspended matter and phytoplankton in the Elbe River Estuary, German Bight and Tidal Flats [NASA-CR-182378] 08 p1019 N88-16180
Research on influence of individual sea water components on spectral brightness coefficient of outgoing radiation 13 p1785 N88-20682
Biological processes in the water column of the South Atlantic bight: Zooplankton responses [DE88-004811] 14 p1951 N88-21630
PICKOFFS
U SENSORS
PICKUPS
U SENSORS
PICOSECOND PULSES
Powerful picosecond ultraviolet laser output at 354.7 nanometers 03 p0327 N88-12063
Phase phenomena in parametric generators and amplifiers of ultrashort light pulses 07 p0918 N88-15576
Time characteristics of travelling wave lasing with two-photon picosecond optical pumping 07 p0918 N88-15578
Increasing time resolution of picosecond absorption spectrometer by selection of length of laser light pulses 07 p0919 N88-15579
Stimulated Raman scattering of picosecond light pulses in long dispersive medium 08 p1078 N88-16498
Kinetics and spectrum of light pulse used in picosecond holography 09 p1236 N88-17409
Subpicosecond optical digital computation using phase conjugate parametric generators [AD-A188279] 10 p1410 N88-18411
Time characteristics of ultrashort light pulses from dye lasers with distributed feedback 14 p1970 N88-21759
Nonlinear stage of ultrashort-pulse formation in solid-state laser 14 p1971 N88-21765
Investigation of ultrashort traveling-wave amplified spontaneous emission 16 p2187 N88-23040
Picosecond sampling of integrated circuits 19 p2655 N88-25767
Picosecond electrical pulses for VLSI electronics characterization 19 p2655 N88-25768
Picosecond photoconductive transceivers 19 p2656 N88-25777
Photoconductive generation of sub-picosecond electrical pulses and their measurement applications 19 p2656 N88-25778
Picosecond switching in Josephson tunnel junctions 19 p2657 N88-25780
High speed, high repetition rate, high voltage photoconductive switching 19 p2657 N88-25781
Generation and forming of ultrashort high voltage pulses 19 p2657 N88-25782
A simple technique to generate or gate microwave pulses with picosecond speeds 19 p2657 N88-25784
Investigation of photoconductive picosecond microstripline switches on self-implanted Silicon On Sapphire (SOS) 19 p2657 N88-25789
Picosecond optoelectronic switches using composite electronic materials 19 p2658 N88-25792
Comparison of sampling oscilloscopes with less than 35 ps transition durations 19 p2658 N88-25793
A technique for wing suppressed IR sampling 19 p2658 N88-25794
Picosecond measurements of gain-switching in a semiconductor laser driven by ultrashort electrical pulses 19 p2658 N88-25800
Picosecond optical autocorrelation experiments on fast photodetectors 19 p2659 N88-25802
Picosecond carrier transport in GaAs quantum wells 19 p2660 N88-25813
A new optoelectronic CW microwave source 19 p2660 N88-25818
Picosecond response of an optically controlled millimeter wave phase shifter 19 p2660 N88-25820
Electron device probing in the femtosecond time scale 19 p2660 N88-25821
Electrical pulse compression by traveling-wave photoconductivity 19 p2661 N88-25822
Picosecond optoelectronic study of a thin film transmission line structure 19 p2661 N88-25823
Radial compression of picosecond electrical pulses [DE88-008440] 21 p2953 N88-27544
A deconvolution technique using least-squares model-fitting and its application to optical pulse measurement [NPL-DES-87] 22 p3144 N88-28694
PICTURE ELEMENTS
U PIXELS
PIEDMONTS
Delineation of ephemeral fluvial networks on low-relief Piedmont surfaces, Plutonium Valley, Nevada, USA 22 p3093 N88-28367
PIERCING
Numerical simulation of the perforation of thin plates [ISL-R-122/86] 11 p1495 N88-18926
Phenomenological piercing characteristics of composite materials 14 p1895 N88-21315
PIERS
U WHARVES
PIEZOELECTRIC CERAMICS
NT LEAD ZIRCONATE TITANATES
United States - Japan Workshop on Dielectric and Piezoelectric Ceramics (3rd) held in Toyama, Japan on November 9-12, 1986 [AD-A185113] 05 p0568 N88-13460
Waves and vibrations in elastic superlattice composites 06 p0776 N88-14765
Contemporary ceramics and the new technological revolution 14 p1902 N88-21363
Effect of uniaxial compression on physical and mechanical properties of ferroelectric ceramic material 16 p2180 N88-22993
Piezoelectric and electrostrictive materials for transducer applications, volume 3 [AD-A194949] 24 p3377 N88-30112
PIEZOELECTRIC CRYSTALS
Defect characterization in quartz and related materials [AD-A184754] 03 p0294 N88-11846
A dynamic analysis of piezoelectric strained elements [AD-A191478] 18 p2503 N88-24851
A dynamic analysis of piezoelectric strained elements [AD-A196079] 24 p3432 N88-30430
PIEZOELECTRIC GAGES
Polymer materials for pressure sensors 06 p0676 N88-14141
Zeroshift of piezoelectric accelerometers in pyroshock measurements 08 p0997 N88-16039
PIEZOELECTRIC TRANSDUCERS
NT PIEZOELECTRIC GAGES
Active control of flexural vibrations in beams 06 p0794 N88-14866
User manual for ATILA, a finite-element code for modeling piezoelectric transducers [AD-A185948] 07 p0847 N88-15141
Ferroelectric properties and impact behavior of the PVF2 polymer and the VF2/C2F3H polarized copolymers --- vinylidene polyfluorides [ISL-CO-245/86] 08 p0971 N88-15876
New wide-band transducer developed 14 p1901 N88-21353
PIEZOELECTRICITY
Fabrication of standardized piezoelectric polymer shock gauges by the Bauer method [DE87-012738] 01 p0049 N88-10315
Developments in electronics ceramics reported 06 p0684 N88-14192
Analytical investigations of bulk wave resonators in the piezoelectric thin film on gallium-arsenide configuration [AD-A185716] 06 p0789 N88-14840
Piezoelectric laminates for torsional and bending model control: Theory and experiment 10 p1343 N88-18029
Recent progress in the dynamic applications of piezoelectric crystals 10 p1417 N88-18460
Piezoelectric polymer tactile sensor arrays for robotics [AD-A188852] 12 p1634 N88-19780
Development of polymeric films with piezoelectrical properties from polypeptides; low, odd nylons; or polyureas [AD-A190301] 15 p2044 N88-22181
A compact high resolution piezoresistive digital tactile sensor [DE88-000430] 16 p2210 N88-23188
Piezoelectric pushers for active vibration control of rotating machinery 16 p2218 N88-23229
Characterization of noncontact piezoelectric transducer with conically shaped piezoelement [NASA-CR-4151] 17 p2347 N88-23987
Dynamic consolidation of metal powders [AD-A192126] 18 p2485 N88-24744
Zinc-oxide thin films for integrated-sensor applications 19 p2673 N88-25896
Piezoelectric effects in strained layer superlattices 20 p2863 N88-27002
Piezoelectric and electrostrictive materials for transducer applications, volume 1 [AD-A194957] 24 p3374 N88-30096
Piezoelectric and electrostrictive materials for transducer applications, volume 2 [AD-A194956] 24 p3376 N88-30104
Piezoelectric and electrostrictive materials for transducer applications, volume 3 [AD-A194949] 24 p3377 N88-30112
PIEZORESISTIVE TRANSDUCERS
NT PIEZOELECTRIC GAGES
Characteristics of polysilicon layers and their application in sensors 19 p2669 N88-25861
Design and construction techniques for planar polysilicon pressure transducers with piezoresistive read-out 19 p2669 N88-25862
Integrated polysilicon tactile sensor 19 p2669 N88-25863
Noise in piezoresistive and capacitive sensors 19 p2670 N88-25874
Simulation of diaphragm-type IC pressure sensors 19 p2672 N88-25887
PIGMENTS
NT CAROTENE
NT CHLOROPHYLLS
NT CYTOCHROMES
Artificial photosynthesis using chlorophyll based carotenoid-quinone triads [DE88-001660] 07 p0884 N88-15362
Optimization of binary pigment coatings [AD-A189103] 13 p1748 N88-20450
PILE FOUNDATIONS
Breaking wave forces on vertical cylinders [RR-CE71] 03 p0338 N88-12126
PILOT ERROR
Brain activity during tactical decision-making. Part 2: Probe-evoked potentials and workload [AD-A188688] 12 p1667 N88-19994
Aircraft accident report: Northwest Airlines, Inc., McDonnell Douglas DC-9-82, N312RC, Detroit Metropolitan Wayne County Airport, Romulus, Michigan, August 16, 1987 [PB88-910406] 19 p2601 N88-25449
Research on piloting under conditions of breakdown in flight [PB87-217980] 19 p2710 N88-26102
PILOT PERFORMANCE
Investigation of interactions between limb-manipulator dynamics and effective vehicle roll control characteristics [NASA-CR-3983] 01 p0007 N88-10039
Report of safety survey: Human integration of approach charts [DOT/FAA/PM-87/15] 01 p0076 N88-10488
A research on pilot performance in the case of aircraft malfunction [ETN-87-90652] 02 p0217 N88-11369
A research on pilot performance in a flight incident situation [ETN-87-90653] 02 p0217 N88-11370
An aerodynamic performance evaluation of the NASA/Ames Research Center advanced concepts flight simulator [NASA-TM-89659] 03 p0268 N88-11685
Eyesight trainer for pilots 03 p0355 N88-12239
Investigation of pilot behavior in a training program for assessing handling qualities using a ground simulator [ESA-TT-999] 03 p0357 N88-12247
Effect of motion cues during complex curved approach and landing tasks: A piloted simulation study [NASA-TP-2773] 04 p0398 N88-12480
Some data processing requirements for precision Nap-Of-the-Earth (NOE) guidance and control of rotorcraft [NASA-CR-177453] 04 p0401 N88-12493
CGI delay compensation [NASA-TM-86703] 04 p0476 N88-12932
New US book on aviation psychology reviewed 07 p0896 N88-15433
Rotorcraft flight-propulsion control integration 09 p1108 N88-16643
Helicopter human factors research 09 p1109 N88-16644
Status of NASA/Army rotorcraft research and development piloted flight simulation 09 p1110 N88-16651
An integrated approach to rotorcraft human factors research 09 p1110 N88-16653
Refinement of eye-point-of-regard measurement with helicopter pilots in a flight experiment [ESA-TT-1073] 09 p1200 N88-17195
A validity study of a selection procedure for student airline pilots [DFVLR-FB-87-34] 09 p1201 N88-17196
A situation-response model for intelligent pilot aiding 09 p1208 N88-17241
Autonomous control procedures for shuttle rendezvous proximity operations 09 p1208 N88-17244
Are windshear training aid recommendations appropriate for other than large jet transports? Pilot procedures: Shear models 10 p1275 N88-17635
Trends in the distribution of tasks between commercial pilots and flight control systems [MBB-UT-008/87] 10 p1314 N88-17851
Cardiovascular and subjective measures of task demand in a low workload monitoring task [REPT-8804] 10 p1368 N88-18176
Cockpit data management [NASA-CR-178407] 11 p1438 N88-18579

Selected aspects of triazolam in relation to aviator performance in naval flight operations
[AD-A189322] 12 p1667 N88-19996

Field dependence-independence and its relationship to flight training performance
[AD-A188888] 12 p1670 N88-20003

The integration of artificial intelligence techniques to improve the effectiveness of electronic countermeasure strategies in a tactical environment
[AD-A189483] 12 p1682 N88-20056

Flight simulator experiments concerning take-off visibility minima
[NLR-TR-86050-U] 13 p1719 N88-20281

Psychophysical load of glider pilots on long-duration flights
[DFVLR-FB-87-38] 14 p1953 N88-21642

Aircraft accident report: North Star Aviation, Inc., PA-32 RT-300, N39614 and Alameda Aero Club Cessna 172, N75584, Oakland, California, March 31, 1987
[PB87-910412] 15 p2016 N88-22021

Relationship of encoding speed and memory tests to flight training performance
[AD-A190670] 15 p2105 N88-22539

Challenges of physiological monitoring in a Navy operational setting 16 p2239 N88-23374

Predicting operator workload during system design
16 p2239 N88-23375

Chronic stress as a factor in aircraft mishaps
16 p2239 N88-23376

Acute stress 16 p2239 N88-23377

Probe-evoked event-related potential techniques for evaluating aspects of attention and information processing 16 p2240 N88-23379

Defining and measuring pilot mental workload
16 p2240 N88-23383

Neurophysiological predictors of quality of performance 16 p2242 N88-23391

A correlational approach to predicting operator status
16 p2242 N88-23393

Aircraft accident/incident, Copperhill, Tennessee, February 22, 1986
[PB88-910407] 18 p2461 N88-24612

Analysis procedures and subjective flight results of a simulator validation and cue fidelity experiment
[NASA-TM-88270] 18 p2465 N88-24634

An evaluation of three linear scale radar altimeter displays
[AD-A192173] 18 p2465 N88-24636

Predicting Air Combat Maneuvering (ACM) performance: Fleet fighter ACM readiness program grades as performance criteria
[AD-A191605] 19 p2710 N88-26099

Research on piloting under conditions of breakdown in flight
[PB87-217980] 19 p2710 N88-26102

Aircraft accident report: Joe Foster Excavating, Inc., Bell 206B, N49606, in-flight collision with trees, Alamo, California, August 3, 1986
[PB88-910405] 20 p2755 N88-26345

Aircraft accident report: Midair collision of SkyWest Airlines Swearingen METRO 2, N163SW, and Mooney M20, N6485U, Kearns, Utah, January 15, 1987
[PB88-910404] 20 p2755 N88-26346

Checklist interruption and resumption: A linguistic study
[NASA-CR-177460] 20 p2756 N88-26348

Control of flight through microburst wind shear using deterministic trajectory optimization
20 p2761 N88-26375

Computer simulation of a single pilot flying a modern high-performance helicopter
[NASA-TM-100182] 20 p2761 N88-26376

Computer simulation of multiple pilots flying a modern high performance helicopter
[NASA-TM-100183] 20 p2761 N88-26377

Flight simulator: Field of view utilized in performing tactical maneuvers
[AD-A192412] 20 p2762 N88-26379

Does dihydroergotamine used in therapeutical doses influence the physical and psychomotor performance of young pilots or other traffic drivers subjected to hypotonia?
[ETN-88-92136] 20 p2832 N88-26799

Preliminary study within a project for the development of intelligent assistance to piloting: Formal description of combat pilot expertise and implementation of an interactive system to represent operations
[CERMA-87-31] 20 p2833 N88-26806

Microesotropia patients performa well as military jet pilots 21 p2925 N88-27363

Event-related brain potentials as indices of mental workload and attentional allocation
21 p2979 N88-27696

Fighter pilot performance during airborne and simulator missions. Physiological comparisons
21 p2981 N88-27704

The neuroelectric selection of Naval aviation personnel: An evaluation 21 p2981 N88-27707

Electroencephalographic correlates of pilot performance: Simulation and in-flight studies
21 p2982 N88-27711

Correlation between EEG abnormal activity and aircraft accidents: A long term observation
21 p2984 N88-27719

The auditory evoked response in military pilots
21 p2984 N88-27721

Personality, attitudes, and pilot training performance: Preliminary analysis
[AD-A193102] 21 p2991 N88-27746

Stress and the military pilot
[AD-A194313] 22 p3133 N88-28626

Proposed improvements to the USAF flight screening program
[AD-A194506] 23 p3240 N88-29285

Visual Effects in the High Performance Aircraft Cockpit
[AGARD-LS-156] 23 p3241 N88-29291

Vision and visual protection in fast jet aircraft
23 p3241 N88-29292

Visual related accidents/incidents
23 p3242 N88-29293

Advances in Flying Qualities
[AGARD-LS-157] 24 p3314 N88-29735

Pilot modeling 24 p3314 N88-29736

Pilot modeling applications 24 p3314 N88-29737

Low-speed longitudinal flying qualities of modern transport aircraft 24 p3314 N88-29738

The optimal control pilot model and applications
24 p3315 N88-29741

Threat expert system technology advisor
[NASA-CR-177479] 24 p3328 N88-29816

Prediction and measurement of human pilot dynamic characteristics in a manned rotorcraft simulation
[NASA-CR-183246] 24 p3410 N88-30297

PILOT PLANTS

Development of a pilot plant for the production of rapidly solidified aluminum alloy powders
[BMFT-FB-T-86-153] 02 p0146 N88-10914

Aviation turbine fuels from tar sands bitumen and heavy oils. Part 3: Laboratory sample production
[AD-A189278] 13 p1753 N88-20484

Turbine fuels from tar sands bitumen and heavy oil. Volume 2, phase 3: Process design specifications for a turbine fuel refinery charging San Ardo heavy crude oil
[AD-A190120] 16 p2183 N88-23011

An outdoor test facility for the large-scale production of microalgae
[DE88-001146] 21 p2984 N88-27723

PILOT SELECTION

Some aspects of sociopsychological screening of flying school applicants 07 p0890 N88-15392

A validity study of a selection procedure for student airline pilots
[DFVLR-FB-87-34] 09 p1201 N88-17196

The accommodative status in the dark of US Navy fighter pilots
[AD-A188188] 10 p1370 N88-18186

Personality, attitudes, and pilot training performance: Preliminary analysis
[AD-A193102] 21 p2991 N88-27746

PILOT TRAINING

A research on pilot performance in a flight incident situation
[ETN-87-90653] 02 p0217 N88-11370

New US book on aviation psychology reviewed
07 p0896 N88-15433

A prototype of pilot knowledge evaluation by an intelligent CAI (Computer-Aided Instruction) system using a Bayesian diagnostic model
[AD-A186060] 08 p1054 N88-16358

Are windshear training aid recommendations appropriate for other than large jet transports? Pilot procedures: Shear models 10 p1275 N88-17635

Windshear training aid. Volume 1: Overview, pilot guide, training program
[PB88-127196] 10 p1276 N88-17637

The accommodative status in the dark of US Navy fighter pilots
[AD-A188188] 10 p1370 N88-18186

MOAOPS and BOOM-MAP computer programs for sonic boom research, volume 1
[AD-A189548] 12 p1574 N88-19414

Field dependence-independence and its relationship to flight training performance
[AD-A188888] 12 p1670 N88-20003

Relationship of encoding speed and memory tests to flight training performance
[AD-A190670] 15 p2105 N88-22539

Task listing: Visually assisted and visually dependent tasks for fighter aircraft
[AD-A191041] 16 p2244 N88-23404

A look toward the future of complex avionics systems development using the USAF Test Pilot School's avionics systems test training aircraft 17 p2306 N88-23797

An enumeration of research to determine the optimal design and use of Army flight training simulators
[AD-A191242] 18 p2468 N88-24649

Development of training implying man-machine interface: From the aircraft to the spacecraft
19 p2700 N88-26052

Intelligent guidance and control for wind shear encounter
[NASA-CR-183060] 20 p2755 N88-26347

USAF flying screening: First step on the road to wings
[AD-A192613] 20 p2833 N88-26804

Preliminary study within a project for the development of intelligent assistance to piloting: Formal description of combat pilot expertise and implementation of an interactive system to represent operations
[CERMA-87-31] 20 p2833 N88-26806

Personality, attitudes, and pilot training performance: Preliminary analysis
[AD-A193102] 21 p2991 N88-27746

Cockpit and cabin crew coordination
[AD-A192445] 21 p2993 N88-27752

Flight information publication (FLIP) feedback
[AD-A194462] 23 p3174 N88-28697

Future air-to-air training for the RF-4
[AD-A194363] 23 p3240 N88-29284

General operational and training visual concerns
23 p3242 N88-29295

Controlled degradation of resolution of high-quality flight simulator images for training effectiveness evaluation
[AD-A196189] 24 p3330 N88-29823

PILOTED CENTRIFUGES

U HUMAN CENTRIFUGES

PILOTLESS AIRCRAFT

NT DRONE AIRCRAFT

The aerodynamic performance of propellers suitable for unmanned aircraft (UMAs)
[RAE-TM-AERO-2094] 09 p1112 N88-16667

Robotic air vehicle. Blending artificial intelligence with conventional software 09 p1210 N88-17252

PILOTS

Pilot-aided modulation for narrow-band satellite communications 19 p2649 N88-25728

An error floor in tone calibrated transmission
19 p2649 N88-25729

PILOTS (PERSONNEL)

NT AIRCRAFT PILOTS

Aircraft accident report: Grand Canyon Airlines, Inc., and Helitech, Inc., midair collision over Grand Canyon National Park, June 18, 1986
[PB87-910403] 06 p0666 N88-14087

US civil airmen statistics, 1987
[AD-A191714] 18 p2455 N88-24577

USAF flying screening: First step on the road to wings
[AD-A192613] 20 p2833 N88-26804

PINCH EFFECT

NT PLASMA PINCH
NT REVERSE FIELD PINCH
NT SCREW PINCH
NT THETA PINCH
NT ZETA PINCH

Transverse focussing using plasma wake fields
[DE87-011503] 01 p0099 N88-10652

Improvement of plasma confinement due to electron Landau damping in tokamaks
[DE88-752339] 15 p2136 N88-22747

Kinetic theoretical analysis for propagation of rotating ion beam in ICF 16 p2276 N88-23623

On selfsimilar thermonuclear ignition of a plasma in necks of zeta devices
[DE88-701640] 16 p2280 N88-23647

PINHOLE CAMERAS

A multi-frame ion pinhole camera for intense ion beam transport and focusing experiments
[DE88-007263] 18 p2516 N88-24926

Intense ion beam diagnostics for particle beam fusion experiments on PBFA 2
[DE88-007279] 18 p2577 N88-25308

PINHOLE OCCULTER FACILITY

Pinhole occulter experiment
[NASA-CR-179206] 02 p0235 N88-11481

PINHOLES

Particle beam alignment system for single event upset-Van de Graaf experiments
[AD-A189695] 15 p2132 N88-22721

PINNING

NT FLUX PINNING

Schottky-barrier formation on a covalent semiconductor without Fermi-level pinning: The Metal-MoS2(0001) interface
[AD-A193044] 21 p3021 N88-27931

Picosecond transient reflectivity of unpinned gallium arsenide (100) surfaces
[AD-A193242] 21 p3021 N88-27933

PINS
Review of diffusion barrier technology for application in SP-100 fuel pins
[DE88-000021] 02 p0234 N88-11480
Pin joints, gears, springs, cranks and other novel micromechanical structures
[DE88-002504] 07 p0864 N88-15245
Computed stress and strain distributions under interference fit and after coldworking
[AD-A186950] 10 p1342 N88-18024

PIONEER VENUS SPACECRAFT
Vertical structure of Venusian cloud layer at landing sites of Vega-1 and Vega-2 vehicles
13 p1725 N88-20317

PIONEER 12 SPACE PROBE
U PIONEER VENUS SPACECRAFT

PIONS
Electrical behavior of layers implanted with low energy pions in Si
[INPE-4199-PRE/1051] 01 p0102 N88-10670
Conceptual design of a high-resolution pion (0) spectrometer
[DE87-014757] 03 p0324 N88-12047
Experimental studies of elementary particle interactions at high energies
[DE88-000804] 05 p0648 N88-13971
Research in experimental nuclear physics
[DE88-004100] 10 p1408 N88-18397
Pion nucleus single charge exchange reactions above the delta(1232) resonance
[LA-11004-T] 11 p1544 N88-19231
Pion elastic and inelastic scattering near N = 28
[LA-10968-T] 11 p1544 N88-19232
Pion absorption in nuclei: The pion(+ or -),proton reactions
[LA-10997-T] 12 p1688 N88-20098
Theoretical studies in few-body intermediate energy physics
[DE88-004101] 12 p1689 N88-20106
Subthreshold pion production in proton induced reactions at 180 to 201 MeV and He3 at 283 MeV
[ETN-88-92303] 17 p2397 N88-24250
Charged pion production and projectile breakup in 85A MeV(sup)12C induced heavy ion reactions
[LUIP-8802] 20 p2850 N88-26920

PIPE FLOW
Large scale structures in turbulent pipe flow
[MPIS-MITT-83-1987] 02 p0172 N88-11085
Carbon dioxide treatment for scale removal and control in potable water systems
[AD-A184346] 04 p0412 N88-12556
Dynamics of reverse flows at pump inlet
04 p0425 N88-12636
Use of a thermodynamic analog for pneumatic transport in horizontal pipes
[AD-A184076] 04 p0441 N88-12740
Experiments on densely-loaded non-Newtonian slurries in laminar and turbulent pipe flows
[DE88-000719] 04 p0442 N88-12746
Flow induced pulsations in pipe systems
[ETN-88-91367] 06 p0702 N88-14307
The effect of eddy distribution on momentum and heat transfer near the wall in turbulent pipe flow
[NASA-TM-100257] 08 p0988 N88-15984
Investigation of critical heating in narrow flow channels with R12 refrigerant as model fluid
[GKSS-87/E/25] 09 p1163 N88-16972
The dynamics of heat transfer at a turbulent pipe flow
[OEFZS-4400] 09 p1164 N88-16975
On some asymptotics of laminar flow in a coiled pipe
10 p1328 N88-17936
Operating loading of piping systems
[ETN-88-91057] 11 p1484 N88-18856
Theoretical and experimental analysis of pressure pulse transmission in non-Newtonian pipe flow
11 p1485 N88-18863
Experiments on densely-loaded non-Newtonian slurries in laminar and turbulent pipe flows
[DE88-006209] 15 p2067 N88-22323
Piston-driven, unsteady separation at a sudden expansion in a tube: Flow visualization and Laser Doppler Anemometer (LDA) measurements
[ETN-88-92104] 15 p2068 N88-22329
Tests on oscillating flows in a pipe nozzle with an abrupt diameter variation
[MPIS-2/1987] 17 p2337 N88-23947
Modeling of cavitation phenomena in homogeneous flow in transitory regimes in pipes
[ISAL-IDI1-87-15] 17 p2337 N88-23948
Energy efficient continuous flow ash lockhopper
[NASA-CASE-NPO-16985-1-CU]
18 p2497 N88-24814
Hydroacoustic pulsating jet generator
[MPIS-7/1987] 18 p2510 N88-24891
Turbulent heat transfer and fluid flow measurements downstream of abrupt expansions and in a cavity of a circular tube at a uniform wall temperaturo
18 p2515 N88-24920
Pressure drop and heat transfer in turbulent non-Newtonian pipe flow of advanced energy transmission fluids
[DE88-010021] 19 p2666 N88-25853
Ammonia boiling in long tubes: Heat transfer and charge loss in vertical and horizontal tubes
[NASA-TT-20313] 19 p2667 N88-25858
Turbulence transition in a circular pipe
20 p2782 N88-26503
Characteristics of long size thermosyphons made of corrugated tube 20 p2784 N88-26511
Experiments on densely-loaded non-Newtonian slurries in laminar and turbulent pipe flows
[DE88-010579] 20 p2800 N88-26612
Investigation on refrigerant R12 critical boiling point in narrow flow pipes considered as model fluid
[ETN-88-92374] 20 p2802 N88-26626
Characterization of accelerating pipe flow
[AD-A193065] 21 p2943 N88-27481
Computational boundary conditions for the incompressible Navier-Stokes equations in channels and pipes
[AD-A193356] 21 p2944 N88-27487
Numerical computation of three-dimensional turbulent flow in tightly curved ducts and spiral turbine casings
[ETN-88-92362] 21 p2948 N88-27511
Investigations on drag reduction in turbulent pipe flows by addition of ionic and nonionic high polymers
[ETN-88-92380] 21 p2949 N88-27515
Investigations of rough surface effects on friction factors in turbulent pipe flow
[AD-A193774] 22 p3075 N88-28255
Application of rectangular co-ordinates to the problem of laminar combined convection in a straight horizontal tube whose circumference is heated nonuniformly
[PDR/CFDU/IC/33] 22 p3076 N88-28263
Mass transport in sector and annular sector tubes
[LRT-WE-9-FB-9(1987)] 22 p3077 N88-28269
Mass transport in a parabolic conduit
[LRT-WE-9-FB-1(1988)] 22 p3077 N88-28273
Heat transport in a parabolic tube of circular cross-section
[LRT-WE-9-FB-2(1988)] 22 p3078 N88-28274
Development of a hot-wire measurement technique for moderate intensity three-dimensional flows
22 p3080 N88-28289
Rotation symmetric inside flow with diametric expansion resolution
[ILR-MITT-193] 23 p3213 N88-29123
Laser Doppler Velocimeter (LDV) and pressure measurements of gas particle flows in bends
[VKI-TN-163] 24 p3372 N88-30083

PIPELINES
Electrical heating method --- pipelines, metal tanks
[GB-PATENT-2-137-059-A] 01 p0043 N88-10274
Investigation on ductile fracture behavior of 3-inch diameter Type 304 stainless steel pipe with a circumferential through-wall crack
[DE87-753016] 02 p0191 N88-11196
Dynamics of propellant feedline systems
[AD-A184865] 05 p0580 N88-13537
Dynamic modelling by finite element method of an elasto-acoustic beam with due consideration of flow and viscosity
[PB87-178166] 09 p1164 N88-16978
Chemical/hydrogen energy systems
[DE88-007013] 19 p2687 N88-25969

PIPELINING (COMPUTERS)
On the VLSI design of a pipeline Reed-Solomon decoder using systolic arrays 04 p0436 N88-12700
Arrays for discrete Fourier transform
[REPT-87-019] 05 p0632 N88-13861
Parallel algorithms for polynomials
[PB87-226304] 06 p0756 N88-14635
A multithreaded processor architecture for parallel symbolic computation
[AD-A187034] 09 p1222 N88-17327
Massive fine-grain parallelism in array computation: A data flow solution 10 p1382 N88-18254
A serial input pipelined multiplier
[REPT-87-030] 11 p1530 N88-19141
Parallel algorithms for mapping pipelined and parallel computations
[NASA-CR-181655] 14 p1960 N88-21687
Multiple-transform pipelines for image coding
[REPT-87-038] 15 p2108 N88-22561
Real time pipelined system for forming the sum of products in the processing of video data
[NASA-CASE-NPO-16462-1-CU]
17 p2384 N88-24169
The performance of the NEC SX-2 and Cray X-MP supercomputers
[DE88-009177] 20 p2835 N88-26813
Large-grain pipelining on distributed-memory multiprocessors
[DE88-009974] 23 p3264 N88-29432

PIPES (TUBES)
NT GAS PIPES
NT U BENDS
Blowdown of two-component gas mixtures in branching systems
[DE87-011392] 01 p0045 N88-10287
Damping characteristics of a composite-reinforced stainless-steel tube
[DE87-012455] 02 p0191 N88-11192
Numerical study of the entrance flow and its transition in a circular pipe (2) 03 p0318 N88-12011
Dynamics of reverse flows at pump inlet
04 p0425 N88-12636
Pipe and bend erosion by pneumatic transport of solids at high temperature
[DE88-001345] 04 p0429 N88-12658
Pulsed eddy-current inspection of thin-walled stainless steel tubing
[DE88-001492] 04 p0457 N88-12830
Development on thin wall tubes of dispersion type
[DE87-703384] 05 p0571 N88-13483
Design and test of high performance composite tubes for use in deep water drilling and production systems
[SNIAS-872-430-107] 05 p0572 N88-13487
High performance composite tubes for offshore applications
[SNIAS-872-430-116] 05 p0572 N88-13488
Qualification of expansion and joint welding procedures of tube-to-tubesheet joints for heat exchangers in nuclear power plants
[DE87-703526] 05 p0589 N88-13592
Finite element model for the stress and flexibility analysis of curved pipes
[DE87-703632] 05 p0592 N88-13608
Analysis of photopole data reduction models
05 p0593 N88-13616
Computation of turbulent flow of air through smooth and rough pipes using a two-equation turbulence model
06 p0700 N88-14298
Flow induced pulsations in pipe systems
[ETN-88-91367] 06 p0702 N88-14307
Tool and process for miniature explosive joining of tubes
[NASA-CASE-LAR-13662-1] 06 p0711 N88-14359
Creep test of Hastelloy X for use as the components of OGL-1 in helium environment
[DE88-750289] 07 p0834 N88-15059
The effect of asymmetric heating on flow stability and heat transfer for flow in a vertical tube
[DE88-003242] 07 p0855 N88-15193
A pulsed eddy current method for examining thin-walled stainless steel tubing
[DE88-002294] 07 p0866 N88-15255
Fully turbulent internal flow excitation of pipe systems
08 p1000 N88-16056
Indirect measurement of local condensing heat-transfer coefficient around horizontal finned tubes
[AD-A186929] 09 p1160 N88-16950
TOPP: A post-processor for TOPAZ, the one dimensional pipe flow analysis code
[DE88-003711] 09 p1164 N88-16981
Accuracies of southwell and force/stiffness methods in the prediction of buckling strength of hypersonic aircraft wing tubular panels
[NASA-TM-88295] 09 p1183 N88-17090
The dishomogeneity of the degree of sensitization in large recirculation pipes in Boiling Water Reactor (BWR) power plants
[CISE-3955] 09 p1247 N88-17473
Magneto-Inertia Confinement Approach (MICA) to fusion in dynamic Z-pinch formed from a frozen deuterium-tritium tube
[IPPJ-856] 09 p1252 N88-17504
Cost 501 Project UK10 part 3: Thermal fatigue damage of Fecralloy steel-sprayed and co-extruded tubing
[AERE-R-12230] 10 p1343 N88-18026
An experimental investigation of the hydrodynamic and heat-transfer behavior of aqueous foam in laminar tube flow
[DE88-004954] 11 p1483 N88-18855
Reduction of erosion in elbows due to flow modifications, phase 1
[DE88-001028] 13 p1769 N88-20584
The CTM program of masts and the CTM engineering model --- spacecraft mechanism
14 p1874 N88-21196
Statistical analysis of feasibility of non-destructive inspection of mechanical properties of hot worked pipes of alloy steels
[BLL-M-37598-(5828.4)] 14 p1922 N88-21455

Experiments on the creep behavior of semifinished X10NiCrAlTi 32 20 (Nicrofer 32 20) tubes under multiaxial loading --- nuclear reactors
[JUEL-2127] 14 p1923 N88-21464
Applications research studies of microtubules
[AD-A190855] 16 p2182 N88-23005
A reflux tube fabric radiator 17 p2421 N88-24394
Theoretical and experimental damping values of piping systems at high ductilities
[DE88-006717] 18 p2526 N88-24986
Numerical analysis of duct flow using three-dimensional parabolized Navier-Stokes equation
19 p2638 N88-25652
Statistical evaluation of light water reactor piping damping data for use in PRA (Probabilistic Risk Assessment) analyses
[DE88-007708] 19 p2661 N88-25828
Acoustic wave dispersion in a viscous, compressible, liquid-filled cylindrical elastic tube
19 p2722 N88-26164
Forced-convective boiling in small diameter tube
20 p2783 N88-26510
Evaluation of engineering leak before break assessment methods by piping tests
[PB88-126982] 20 p2788 N88-26538
Experimental investigation of turbulent flow in smooth and longitudinal grooved tubes
[NASA-TM-77480] 20 p2800 N88-26615
Cross flow induced vibrations in tube bundle by displaced and misaligned tube configurations
[ETN-88-92132] 20 p2801 N88-26621
Thermal and mechanical analysis of the Faraday shield for the compact ignition tokamak
[DE88-007855] 20 p2856 N88-26962
Characterization of accelerating pipe flow
[AD-A193065] 21 p2943 N88-27481
Distribution of weld quality in thin section stainless steel tube attachment welds
[PB88-109632] 21 p2955 N88-27555
Computation of failure probability of fatigue loaded cracked structures
[ETN-88-92360] 21 p2964 N88-27607
Mass transport in sector and annular sector tubes
[LRT-WE-9-FB-9(1987)] 22 p3077 N88-28269
Passive damping concepts for free and forced member and grillage vibration
[NASA-CR-183114] 23 p3225 N88-29196
Elastic-plastic analysis of part-through crack propagation in piping and pressure vessels
[DE88-701619] 23 p3225 N88-29198
Analytical study of graphite-epoxy tube response to thermal loads
[NASA-CR-183215] 24 p3341 N88-29884

PISTON ENGINES
NT DIESEL ENGINES
NT FREE-PISTON ENGINES
NT STIRLING ENGINES
Free-piston Stirling engine diaphragm-coupled heat-actuated heat pump component technology program, phase 1C
[DE88-003654] 10 p1330 N88-17949
Comparison between computed and measured swirl and turbulence in reciprocating engines
[PDR/CFDU/IC/32] 13 p1779 N88-20647
Investigation of the misfueling of reciprocating piston aircraft engines
[NASA-TP-2803] 14 p1865 N88-21144
Two-fluid turbulence models and reciprocating engines
[CFD/87/6] 14 p1918 N88-21449
Computer simulation of turbulent combustion in reciprocating engines
[CFDU/87/11] 18 p2482 N88-24725
Analytical and experimental investigation of ringless piston concept
[AD-A193213] 21 p2956 N88-27559
The application of the two-fluid model of turbulence to the 3-D simulation of turbulent combustion in reciprocating engines
[PDR/CFDU/IC/37] 22 p3052 N88-28110

PISTON THEORY
The performance of the VKI longshot hypersonic wind tunnel
[VKI-TN-161] 18 p2468 N88-24650

PISTONS
Piston ring friction and vehicle fuel economy
[DE87-014536] 02 p0181 N88-11127
Microcomputer control of a hydraulically actuated piston
[AD-A184130] 03 p0368 N88-12317
Overview of free-piston Stirling engine technology for space power application
[NASA-TM-88886] 03 p0386 N88-12427
Ideal-viscoplastic extrusion model with application to deforming pistons in light-gas guns
[UTIAS-TN-266] 04 p0429 N88-12657
Hot piston ring tests
[NASA-TM-100256] 06 p0729 N88-14486
Hot piston ring/cylinder liner materials: Selection and evaluation
[NASA-TM-100276] 08 p0971 N88-15872
Free-piston Stirling engine diaphragm-coupled heat-actuated heat pump component technology program, phase 1C
[DE88-003654] 10 p1330 N88-17949
Calibration of a Harwood DWT-1000 controlled-clearance piston gauge
[DE88-004496] 11 p1489 N88-18888
Piston-driven, unsteady separation at a sudden expansion in a tube: Flow visualization and Laser Doppler Anemometer (LDA) measurements
[ETN-88-92104] 15 p2068 N88-22329
Pump rod forces due to hydrodynamic effects in piston pumps
[PB88-164850] 16 p2214 N88-23212
Composite piston
[NASA-CASE-LAR-13435-1] 17 p2346 N88-23981
Analytical and experimental investigation of ringless piston concept
[AD-A192835] 20 p2810 N88-26673
Variable-compression-ratio pistons for high power output diesel engines 22 p3084 N88-28316
Static and dynamic metal-metal friction at plastic stress levels
[DE88-011261] 23 p3222 N88-29176

PITCH
Pilot-aided modulation for narrow-band satellite communications 19 p2649 N88-25728
An error floor in tone calibrated transmission
19 p2649 N88-25729

PITCH (INCLINATION)
Measurement of velocity and vorticity fields in the wake of an airfoil in periodic pitching motion
[NASA-TP-2780] 04 p0487 N88-13002
Restoration of particle pitch angle distribution functions by a maximum entropy algorithm
[ATR-86(7098)-3] 05 p0646 N88-13969
Handling qualities of a wide-body transport airplane utilizing Pitch Active Control Systems (PACS) for relaxed static stability application
[NASA-TP-2482] 07 p0821 N88-14967
Degradation of downlink distance measurement indexes by the addition of a third tone --- tone ranging
[CNES-CT/DRT/TIT/TR-122-T]
15 p2056 N88-22268
Hybrid procedure for dynamic measurements in transonic wind tunnels: Demonstrated by pitch oscillation
[DFVLR-FB-88-19] 21 p2900 N88-27211
Time periodic control of a multi-blade helicopter
[AD-A194435] 23 p3180 N88-28931

PITCH (MATERIAL)
Interfacial shear strength of pitch and high strain pan fibers in an epoxy matrix
[AD-A185966] 07 p0826 N88-15011
Electrical dc conductivity of pitch
[AD-A191266] 16 p2182 N88-23006
Electronic and structural studies of carbon/carbon composites
[AD-A191729] 19 p2609 N88-25481

PITCH ANGLES
U PITCH (INCLINATION)

PITCH ATTITUDE CONTROL
U LONGITUDINAL CONTROL

PITCHING MOMENTS
An experimental evaluation of advanced rotorcraft airfoils in the NASA Ames eleven-foot transonic wind tunnel
[NASA-CR-166587] 03 p0261 N88-11640
Dynamic stability of hypersonic conical lifting vehicles according to Newton-Busemann theory
05 p0534 N88-13247
Prediction of wing aeroelastic effects on aircraft life and pitching moment characteristics
05 p0551 N88-13356
Unsteady stall penetration experiments at high Reynolds number
[AD-A186120] 07 p0814 N88-14958
An experimental study of the effect of pitch rate on delta wing aerodynamics and stability
[NASA-CR-183159] 21 p2893 N88-27173
Control and use of unsteady flows: Insect use of various wing kinematics and related pressure measurements using a pitching airfoil 21 p2926 N88-27366
Forces and moments on a slender, cavitating body
[DE88-007208] 21 p2945 N88-27491

PITOT TUBES
Heterogeneous diffusion flame stabilization
[AD-A193014] 20 p2771 N88-26429

PITTING
Evaluation of load tracks and wear of two sets of bearings from space shuttle main engine high pressure oxygen turbopumps
[NASA-CR-178969] 07 p0861 N88-15223
Studies of the initiation of pitting corrosion on stainless steels
[AERE-M-3615] 10 p1301 N88-17778
A review of pitting corrosion in high temperature aqueous solutions
[DE88-003547] 10 p1302 N88-17787
Corrosion behavior of sputter-deposited aluminum-based alloys exposed to chloride solutions
[AD-A187262] 10 p1303 N88-17794
Significance of the local electrode potential within pits, crevices and cracks
[AD-A192482] 21 p2935 N88-27432
Corrosion problems associated with computer disk packs 22 p3054 N88-28121

PITUITARY GLAND
Morphological and functional state of the hypothalamo-hypophyseal neurosecretory system of rats flown aboard Cosmos-1667 10 p1365 N88-18156
Hypothalamic-pituitary-adrenal responses to short duration high intensity cycle exercise
[AD-A192597] 21 p2985 N88-27727

PITUITARY HORMONES
Role of adenosine analogs and growth hormone in waking and sleep
[AD-A187897] 11 p1519 N88-19070

PIVOTS
A new pivoting rule for the dual network simplex method
[REPT-87-17] 01 p0080 N88-10511
An examination of coating failure on wing pivot fittings of f111 aircraft
[AD-A185028] 05 p0546 N88-13328
Parallel pivoting combined with parallel reduction
[NASA-CR-178422] 06 p0760 N88-14862
Balloon-borne three-meter telescope for far-infrared and submillimeter astronomy
[NASA-CR-182310] 09 p1262 N88-17565
An extension of the MS pivoting rule to capacitated network flow problems
[REPT-87-33] 14 p1963 N88-21711

PIXELS
Textural features for image classification in remote sensing
[INPE-4169-PRE/1066] 08 p1020 N88-16181
Textural features for image classification in remote sensing 17 p2354 N88-24027
Study of methods of post-processing applied to a problem of standard classification
17 p2362 N88-24067
SEGMERGE: A scanline visible surface algorithm with adaptive span selection and inexpensive antialiasing
[DE88-009186] 20 p2836 N88-26826
Image focusing in space and time
[AD-A195839] 24 p3429 N88-30410

PLAGES (FACULAE)
U FACULAE

PLAINS
NT COASTAL PLAINS
NT FLOOD PLAINS
NT PLAYAS
NT TUNDRA
Analysis of winter season precipitation bands over the Southern Plains 14 p1947 N88-21609
Intercrater plains deposits and the origin of Martian valleys 23 p3301 N88-29661
Distribution and timing of thick transient air-fall deposits in Electris: Implications for the nature of the upland plains 23 p3303 N88-29674
Constraints on the origin of fractured terrane, Northern Martian plains 23 p3304 N88-29684
Origin of northern lowland plains: Constraints from boundary morphology 23 p3305 N88-29687
Early cratering rates and the nature of the Martian cratered uplands 23 p3306 N88-29694

PLANAR STRUCTURES
A study of scattering from E-plane circuit elements
[AD-A184473] 04 p0431 N88-12673
An adaptive subdivision method with crack prevention for rendering beta-spline objects
[AD-A184249] 04 p0477 N88-12940
Computation of natural frequencies of planar lattice structure
[AD-A185387] 05 p0641 N88-13920
The effect of collision angle on mach reflection
[AD-A185798] 06 p0704 N88-14318
The dynamics of coupled planar rigid bodies. Part 1: Reduction, equilibria and stability
[AD-A187467] 10 p1345 N88-18042
Technology development of a planer BiPolar transistor
[AD-A188761] 12 p1623 N88-19708

Nonaxisymmetric body supersonic, aerodynamic prediction
[AD-A189338] 13 p1716 N88-20259
On effectively labeling planar projections of polyhedra
[CWI-CS-R8715] 13 p1826 N88-20917
Quantitative use of exciplex-based vapor/liquid visualization systems, users' manual
[AD-A191649] 19 p2610 N88-25491
Large planar maneuvers for articulated flexible manipulators
[NASA-CR-183079] 19 p2711 N88-26104
Radiative heat transfer and selective emission in planar slab coatings on hot emissive substrates
[AD-A193133] 21 p2918 N88-27319
Guided wave interactions in millimeter-wave integrated circuits
[AD-A193017] 21 p2936 N88-27437
Development of planar geometry solid oxide fuel cell technology, phase 1
[PB88-210356] 23 p3229 N88-29215
Development of a general software package for the analysis and synthesis of planar antenna arrays for space applications
[S-247-02] 24 p3359 N88-30000
Advanced planar array development for space station
[NASA-CR-179373] 24 p3389 N88-30181
Particle trajectories and potentials in a plane sheath moving in a magnetoplasma
[AD-A196228] 24 p3390 N88-30190
Computer-Aided Structural Engineering (CASE) project. Computer program for analysis of planar grid structures (CGRID), user's guide
[AD-A195977] 24 p3413 N88-30317

PLANE STRAIN
Theoretical investigation of stress concentrations in damaged carbon fibre reinforced plastic plate structures. Volume 2: Tables, figures and plates
[BR99873-VOL-2] 03 p0280 N88-11762
Closure and propagation behavior of short fatigue cracks at different R-ratios 05 p0601 N88-13679
Analysis of crack closure under plane strain conditions
[NASA-CR-182369] 06 p0722 N88-14439
Fully plastic analysis of mixed mode plane-strain crack problems
[PB87-144929] 08 p0994 N88-16015
Fracture mechanics 17 p2324 N88-23877
Dynamic shear band development in plane strain
[AD-A190915] 18 p2526 N88-24988

PLANE STRESS
Theoretical investigation of stress concentrations in damaged carbon fibre reinforced plastic plate structures. Volume 2: Tables, figures and plates
[BR99873-VOL-2] 03 p0280 N88-11762
Analysis of crack closure under plane strain conditions
[NASA-CR-182369] 06 p0722 N88-14439
Elastic-plastic fracture investigation on stable crack growth for plane stress
[PB87-144820] 08 p0995 N88-16022
Static analysis of thin plates using the finite strip-element method 19 p2679 N88-25931

PLANE WAVES
New main reflector, subreflector and dual chamber concepts for compact range applications
[NASA-CR-181506] 04 p0402 N88-12498
Pulse-mode expansions and refractive indices in plane-wave propagation
[DE88-001328] 04 p0437 N88-12714
Dispersion equation for plane capillary-gravity wave on free surface of viscous incompressible fluid
04 p0459 N88-12842
Boundary effects on the drag of an oscillating sphere: Applications to the magnetic sphere rheometer. Attenuation and dispersion of acoustic waves in nematic liquid crystals 04 p0488 N88-13007
Plane longitudinal waves in solutions of Maxwell equations
[DE88-700347] 07 p0846 N88-15135
Interior impedance wedge diffraction with surface waves
[NASA-CR-182405] 07 p0854 N88-15186
Plane wave diffraction by a thin dielectric wedge
[RSRE-MEMO-4045] 09 p1153 N88-16912
Wave curves for simple isotropic elastic solids
[AD-A188665] 12 p1636 N88-19798
Phase velocity and attenuation of plane elastic waves in a particle-reinforced composite medium
[AD-A189414] 13 p1734 N88-20366
Detection and angle estimation of coherent plane waves 13 p1759 N88-20522
Research in nonlinear partial differential equations and bifurcation theory
[AD-A190986] 16 p2260 N88-23514
Saturation and the limit of jet mixing enhancement by single frequency plane wave excitation: Experiment and theory
[NASA-TM-100882] 17 p2295 N88-23732
Electromagnetic scattering from nonlinear anisotropic cylinders 17 p2333 N88-23930
Experimental investigation of the reflection of a planar shock wave over a double wedge
[AD-A193078] 21 p2943 N88-27482
On the degenerate Ferran-Ibanez solution for colliding plane gravitational waves
[MATH-REPT-209] 23 p3296 N88-29630
Time-domain far-field scattering of plane electromagnetic waves by a penetrable object in the Born approximation
[PB87-176129] 24 p3365 N88-30040
Mathematical problems of nonlinear wave propagation and of waves in heterogeneous media
[AD-A195970] 24 p3368 N88-30057

PLANET ORIGINS
U PLANETARY EVOLUTION

PLANETARY ATMOSPHERES
NT JUPITER ATMOSPHERE
NT MARS ATMOSPHERE
NT NEPTUNE ATMOSPHERE
NT PLANETARY IONOSPHERES
NT SATURN ATMOSPHERE
NT URANUS ATMOSPHERE
NT VENUS ATMOSPHERE
NT VENUS CLOUDS
Laboratory evaluation and application of microwave absorption properties under simulated conditions for planetary atmospheres
[NASA-CR-181466] 02 p0254 N88-11606
Planetary science 07 p0883 N88-15356
Atmospheric science 07 p0883 N88-15357
Extended atmospheres of outer planet satellites and comets
[NASA-CR-181449] 10 p1430 N88-18540
Gamma-ray and neutron spectroscopy of planetary surfaces and atmospheres
[DE88-004287] 10 p1430 N88-18541
A modeling analysis program for the JPL table mountain Io sodium cloud data
[NASA-CR-182555] 11 p1570 N88-19400
Negative viscosity in global circulations
13 p1786 N88-20685
A design study of onboard navigation and guidance during aerocapture at Mars
[NASA-CR-172053] 18 p2469 N88-24654
Investigation of Rossby-number similarity in the neutral boundary layer using large-eddy simulation
[DE88-008910] 19 p2666 N88-25851
The rate of volcanism on Venus
[NASA-CR-183039] 19 p2742 N88-26281
Experimental study of planetary gases with applications to planetary interior models
[NASA-CR-183098] 20 p2886 N88-27137
Interpretation of the polarimetric observations of Jupiter
[DE88-702414] 21 p3031 N88-27991
Polarization of light reflected by vertically inhomogeneous planetary atmosphere
[DE88-702416] 21 p3031 N88-27992
Workshop on the Origins of Solar Systems
[NASA-CR-183025] 24 p3451 N88-30536
The atmospheres of the earth and the other planets: Origin, evolution and composition
24 p3452 N88-30544

PLANETARY BOUNDARY LAYER
Effects of rainfall on the seasonal thermocline
[AD-A184432] 04 p0472 N88-12912
A bulk model for the unstable planetary boundary layer over the sea. A sensitivity investigation
[DM-51] 22 p3129 N88-28600

PLANETARY COMPOSITION
Growth of continental crust: Clues from Nd isotopes and Nb-Th relationships in mantle-derived magmas
24 p3393 N88-30205
The Kerala Khondalite Belt (KKB) of Southern India: An ensialic mobile belt 24 p3393 N88-30208
Does subduction zone magmatism produce average continental crust 24 p3394 N88-30214

PLANETARY CORES
NT EARTH CORE

PLANETARY CRUSTS
NT EARTH CRUST
Kinetics of thermochemical gas-solid reactions important in the Venus sulfur cycle
[NASA-CR-182963] 19 p2742 N88-26280
Morphologic contrasts between Nirgal and Auqakuh Valles, Mars: Evidence of different crustal properties
23 p3304 N88-29681
Stratigraphy of the Kasei Valles region, Mars
23 p3305 N88-29690
Growth of planetary crusts 24 p3400 N88-30247
Debris flows of the Simud-Tiu outflow system of Mars
24 p3442 N88-30485

PLANETARY ENTRY
U ATMOSPHERIC ENTRY

PLANETARY ENVIRONMENTS
NT JUPITER ATMOSPHERE
NT MARS ATMOSPHERE
NT MARS ENVIRONMENT
NT NEPTUNE ATMOSPHERE
NT PLANETARY ATMOSPHERES
NT PLANETARY IONOSPHERES
NT SATURN ATMOSPHERE
NT URANUS ATMOSPHERE
NT VENUS ATMOSPHERE
NT VENUS CLOUDS
Model of Jovian F region ionosphere
[NASA-CR-182587] 13 p1855 N88-21105

PLANETARY EVOLUTION
Remote sensing of planets and cartographic results
[HSBW-HEFT-14] 03 p0389 N88-12444
Studies in Aeolian geology
[NASA-CR-182328] 05 p0625 N88-13828
Impact-induced devolatilization and hydrogen isotopic fractionation of serpentine: Implications for planetary accretion
[NASA-CR-182877] 16 p2175 N88-22966
Reports of planetary geology and geophysics program, 1987
[NASA-TM-4041] 20 p2885 N88-27133
Mars: Spectral signatures seen and unseen
23 p3301 N88-29659
Workshop on the Growth of Continental Crust
[NASA-CR-183073] 24 p3392 N88-30201
Nd isotopes and crustal growth rate
24 p3392 N88-30203
An illustration of the complexity of continent formation
24 p3393 N88-30207
The Kerala Khondalite Belt (KKB) of Southern India: An ensialic mobile belt 24 p3393 N88-30208
The timing and mechanism of depletion in Lewisian granulites 24 p3394 N88-30209
Construction of mass-age curves for the continental crust: An empirical model and an example from the western US 24 p3394 N88-30213
Pb isotope constaints on the extent of crustal recycling into a steady state mantle 24 p3394 N88-30215
Decoupled Rb-Sr and Sm-Nd isotopic evolution of the continental crust 24 p3395 N88-30216
Early intense cratering: Effects on growth of earth's crust 24 p3395 N88-30219
The growth of continents and some consequences since 1.5 Ga 24 p3395 N88-30220
Growth of early archaean crust in the ancient Gneiss complex of Swaziland and adjacent Barberton Greenstone Belt, Southern Africa 24 p3396 N88-30223
Diapirs of the Mediterranean ridge: The tectonic regime of an incipient accreted terrane
24 p3396 N88-30224
Changing styles of crustal growth in Southern Africa: Constraints from geochemical and Sr-Nd isotope studies in Archaean to Pan African terrains
24 p3396 N88-30227
Growth of the continental crust: A planetary-mantle perspective 24 p3400 N88-30251
Exotic minerals in 3,500 million year old rocks: Evidence for large meteorite impacts 24 p3440 N88-30475
Lewis Cliff 86010, a unique Antarctic meteorite: Possible new clues to the early history of the solar system
24 p3442 N88-30482
Workshop on the Origins of Solar Systems
[NASA-CR-183025] 24 p3451 N88-30536
Physical processes and timescales in planet and small-body accretion 24 p3451 N88-30540
Terrestrial versus giant planet formation
24 p3451 N88-30543
The atmospheres of the earth and the other planets: Origin, evolution and composition
24 p3452 N88-30544

PLANETARY EXPLORATION
U SPACE EXPLORATION

PLANETARY GEOLOGY
NT MARS VOLCANOES
Remote sensing of planets and cartographic results
[HSBW-HEFT-14] 03 p0389 N88-12444
Planetary Geology: Goals, Future Directions, and Recommendations
[NASA-CP-3005] 19 p2742 N88-26279
Reports of planetary geology and geophysics program, 1987
[NASA-TM-4041] 20 p2885 N88-27133

PLANETARY GRAVITATION
Simulation and analysis of a geopotential research mission
[NASA-CR-182354] 06 p0670 N88-14109

PLANETARY IONOSPHERES
Relativistic electron precipitations in a pulsating aurora
04 p0468 N88-12894
Peculiarities of daytime ionosphere of Venus during years of low and high solar activity
08 p1005 N88-16091

Distribution of electron concentration in nightime atmosphere of Venus based on radio transmission data
08 p1005 N88-16092
Applicability of extremely low frequency global resonances for study of Venusian storm activity
08 p1005 N88-16093
Model of Jovian F region ionosphere
[NASA-CR-182587] 13 p1855 N88-21105
Tethered diagnostic package for use from the space station
[DE88-006264] 16 p2167 N88-22921

PLANETARY LANDING
Lunar base launch and landing facility conceptual design, 2nd edition
[NASA-CR-172049] 20 p2885 N88-27135

PLANETARY MAGNETIC FIELDS
Interplanetary magnetic field effects on the interaction of the solar wind with Venus 06 p0805 N88-14910
Magnetic field of planet Uranus: Predictions, measurements, interpretations 08 p1005 N88-16094

PLANETARY MANTLES
NT EARTH MANTLE
Astrophysics and the solar nebula
07 p0883 N88-15355

PLANETARY MAPPING
Remote sensing of planets and cartographic results
[HSBW-HEFT-14] 03 p0369 N88-12444

PLANETARY MASS
Construction of mass-age curves for the continental crust: An empirical model and an example from the western US 24 p3394 N88-30213
The growth of continents and some consequences since 1.5 Ga 24 p3395 N88-30220

PLANETARY MOTION
U SOLAR ORBITS

PLANETARY NEBULAE
The nucleus of LT-5: An unusual triple system? --- planetary nebula
[PUBL-SER-C-FASC-11] 03 p0366 N88-12436
Winds and shells around low-mass supergiants
04 p0514 N88-13164
High spatial resolution observations of dust and gas in NGC 7027 and the M8 Hourglass
06 p0801 N88-14903
A global model for planetary nebulae, taking into account central stellar evolution and influence on halo ionization
[ETN-88-91491] 11 p1568 N88-19389
Radiation transport in planetary nebulae
[ETN-88-91500] 14 p1993 N88-21880
The observability of carbon monoxide in planetary nebulae
[ETN-88-91498] 14 p2011 N88-21994
International ultraviolet explorer spectral atlas of planetary nebulae, central stars, and related objects
[NASA-RP-1203] 22 p3164 N88-28843

PLANETARY ORBITS
Discovery by Voyager-2 of predicted satellites which determine resonance nature of Uranian rings
08 p1006 N88-16095
The 1985 mutual phenomena of Jupiter's satellites observed in Brazil
[INPE-4526-PRE/1276] 15 p2152 N88-22848

PLANETARY RADIATION
Ray tracing of Jovian low frequency radiation
[NASA-CR-179262] 08 p1101 N88-16620
Research in particle and gamma-ray astrophysics
[NASA-CR-183111] 20 p2887 N88-27146

PLANETARY RINGS
NT SATURN RINGS
NT URANUS RINGS
Toward a comprehensive theory for the sweeping of trapped radiation by inert orbiting matter
[NASA-CR-182584] 11 p1569 N88-19395

PLANETARY SATELLITES
U NATURAL SATELLITES

PLANETARY SPACE FLIGHT
U INTERPLANETARY FLIGHT

PLANETARY SPACECRAFT
U INTERPLANETARY SPACECRAFT

PLANETARY STRUCTURE
Experimental study of planetary gases with applications to planetary interior models
[NASA-CR-183098] 20 p2886 N88-27137

PLANETARY SURFACES
NT MARS SURFACE
NT VENUS SURFACE
Shock-chemistry in natural materials and evolution of planetary surfaces
[DE87-012737] 02 p0254 N88-11604
Small reactor power systems for manned planetary surface bases
[NASA-TM-100223] 04 p0524 N88-13209
Studies in Aeolian geology
[NASA-CR-182328] 05 p0625 N88-13828
Running head: What color is it
[NASA-CR-182600] 11 p1551 N88-19260

Electromagnetic powered vehicles (EMPV) for Mars exploration 17 p2419 N88-24388

PLANETARY SYSTEMS
NT SOLAR SYSTEM
Reports of planetary astronomy, 1988
[NASA-TM-4063] 22 p3163 N88-28835

PLANETARY WAVES
A baroclinic wavy basic state model: Description and preliminary experiments
[KNMI-WR-87-1] 01 p0068 N88-10436
Dynamics of isolated intrathermocline eddy
04 p0460 N88-12845
Dynamic modeling of the middle atmosphere
08 p1028 N88-16227
Seasonal variations and excitation mechanisms of the equatorially trapped waves 13 p1798 N88-20751
Nonlinear normal mode initialization of a limited area model using nonstationary Rossby modes --- numerical weather forecasting
[KNMI-WR-87-10] 14 p1947 N88-21614
Interactions between synoptic and planatery scales of motion
[AD-A192328] 23 p3234 N88-29246
Rossby waves in mid-latitude oceans
24 p3405 N88-30273

PLANETESIMALS
U PROTOPLANETS

PLANETOLOGY
Laser simulation of light and plasma action on comets and planets 09 p1237 N88-17413
Reflectance spectroscopy in planetary science: Review and strategy for the future
[NASA-SP-493] 17 p2451 N88-24564
Research and Technology, 1987, Goddard Space Flight Center
[NAS 1.15:101097] 17 p2453 N88-24572
Planetary Geology: Goals, Future Directions, and Recommendations
[NASA-CP-3005] 19 p2742 N88-26279

PLANETS
NT EARTH (PLANET)
NT GAS GIANT PLANETS
NT JUPITER (PLANET)
NT MARS (PLANET)
NT NEPTUNE (PLANET)
NT TERRESTRIAL PLANETS
NT URANUS (PLANET)
NT VENUS (PLANET)

PLANFORMS
NT ARROW WINGS
NT DELTA WINGS
NT RECTANGULAR PANELS
NT RECTANGULAR PLANFORMS
NT RECTANGULAR PLATES
NT SWEPT FORWARD WINGS
NT SWEPTBACK WINGS
NT VARIABLE SWEEP WINGS
NT WING PLANFORMS
Planform effects on the supersonic aerodynamics of multibody configurations
[NASA-TP-2762] 04 p0393 N88-12454
Inflow measurements made with a laser velocimeter on a helicopter model in forward flight. Volume 4: Tapered planform blades at an advance ratio of 0.15
[NASA-TM-100544] 16 p2156 N88-22863

PLANIGRAPHY
U TOMOGRAPHY

PLANKTON
NT PHYTOPLANKTON
Varifront 3 expedition data report (USNS DE STEIGUER CRUISE 1202-82). Bioluminescence, hydrographic, nutrient, and satellite data from the Gulf of California (November-December 1981)
[AD-A185011] 05 p0620 N88-13805
The use of chlorophyll fluorescence measurements from space for separating constituents of sea water. Volume 2: Appendices
[ESA-CR(P)-2444-VOL-2] 07 p0873 N88-15295
Biological processes in the water column of the South Atlantic bight: Zooplankton responses
[DE88-004811] 14 p1951 N88-21630

PLANKTON BLOOM
U PLANKTON

PLANNING
NT AIRPORT PLANNING
NT MANAGEMENT PLANNING
NT MISSION PLANNING
NT PRODUCTION PLANNING
NT PROJECT PLANNING
NT REGIONAL PLANNING
NT URBAN PLANNING
CNET (Chief of Naval Education and Training) Program Automated Tracking System (CPATS): A comprehensive study
[AD-A184694] 03 p0385 N88-12418

Federal plan for meteorological services and supporting research, fiscal year 1988
[PB88-118716] 07 p0880 N88-15336
Task path planning, scheduling and learning for free-ranging robot systems 08 p1058 N88-16386
Qualitative models for planning: A gentle introduction
08 p1062 N88-16414
Operational aspects of a spacecraft planning/scheduling expert system
08 p1062 N88-16415
Prototype resupply scheduler
08 p1064 N88-16428
Loads and aeroelasticity division research and technology accomplishments for FY 1987 and plans for FY 1988
[NASA-TM-100534] 09 p1114 N88-16680
Trimodal interpretation of constraints for planning
09 p1209 N88-17248
Computer assisted instruction: Two decades in perspective
[AD-A186813] 09 p1216 N88-17289
Motion planning and control of robot manipulators via application of a computer graphics animated display
11 p1496 N88-18932
Preliminary analysis of an integrated logistics system for OSSA payloads
[NASA-CR-4114] 12 p1584 N88-19477
Preliminary analysis of an integrated logistics system for OSSA payloads. Volume 3: OSSA integrated logistics support planning document 12 p1584 N88-19480
Preliminary analysis on plasma equilibrium control. Conceptual design study of FY86 FER
[DE88-751441] 14 p1984 N88-21834
Hybrid PV HgCdTe IR detectors technology reliability and failure program: Environmental stress testing plan
[AD-A191165] 16 p2211 N88-23195
Identification of areas cultivated with soybeans in the cerrados regions through digital processingof satellite images: A methodological approach
17 p2358 N88-24048
Sensitivity analysis for the system reliability function
[AD-A191648] 18 p2525 N88-24979
Management and the executive
[AD-A190778] 18 p2587 N88-25374
Department of Defense statement on defense agency research and development to the Subcommittee on Defense of the Committee on Appropriations, United States House of Representatives, 100th Congress, second session
[AD-A191840] 18 p2588 N88-25377
Department of Defense Statement on the Balanced Technology Initiative to the Committee on Armed Services, United States Senate, 100th Congress, second session
[AD-A191841] 18 p2588 N88-25378
Centre for International Co-Operation and Appropriate Technology (CICAT)
[PB88-165501] 18 p2590 N88-25389
Plans for discourse
[AD-A192242] 20 p2832 N88-26802
Vision research. A national plan: 1983-1987, 1987 evaluation and update
[PB88-192604] 21 p2985 N88-27728
Motion planning for legged locomotion systems on uneven terrain 23 p3221 N88-29170
Motion planning with obstacles and dynamic constraints 23 p3222 N88-29175
Lisp Object State Saver (LOSS): A facility used to save partial schedules of the Hubble Space Telescope
24 p3421 N88-30360
Research on problem-solving systems
[AD-A195154] 24 p3423 N88-30370

PLANT DESIGN
Facility design validation of the information systems laboratory
[AD-A186309] 07 p0906 N88-15488
Lunar fiberglass: Properties and process design
[NASA-CR-182580] 11 p1466 N88-18740
Design of nuclear heat, power co-generation plant detailed 16 p2186 N88-23033
More on exact state reconstruction in deterministic digital control systems
[NASA-TP-2847] 22 p3063 N88-28177

PLANT ROOTS
Cytomorphology and ultrastructure of corn root meristem in weightlessness 12 p1651 N88-19891
Gravisensing in lentil seedling roots grown in space (Spacelab D-1 mission) 12 p1654 N88-19011
Graviperception of lentil seedling roots grown in space
22 p3061 N88-28165

PLANT STRESS
Overview of Austrian Airborne Imaging Spectrometer (AIS) programme and first results
05 p0612 N88-13762
Measuring near infrared spectral reflectance changes from water stressed conifer stands with AIS-2
05 p0613 N88-13765

PLANTING

Controlled ecological life support systems: Development of a plant growth module 05 p0630 N88-13854

PLANTS (BOTANY)

NT ALGAE
NT BLUE GREEN ALGAE
NT BRYOPHYTES
NT CHLORELLA
NT CONIFERS
NT CORN
NT COTTON
NT GRASSES
NT LEGUMINOUS PLANTS
NT MICROCYSTIS
NT PHYTOPLANKTON
NT POTATOES
NT RICE
NT SEA GRASSES
NT SOYBEANS
NT SUGAR CANE
NT TRADESCANTIA
NT TREES (PLANTS)
NT YEAST

Compilation of 1986 annual reports of the Navy ELF (Extremely Low Frequency) communications system ecological monitoring program, volume 1
[AD-A184561] 03 p0306 N88-11930

Controlled Ecological Life Support System. Design, Development, and Use of a Ground-Based Plant Growth Module
[NASA-CP-2479] 05 p0630 N88-13852

Uses of airborne laser Chayka-1 for probing water, land surfaces 06 p0725 N88-14461

A process study of the biothermal conversion of water hyacinths to methane
[DE88-000554] 06 p0730 N88-14488

Comparative anatomic analysis of seedling organs of pisum sativum (fabaceae) cultivated under space flight conditions 06 p0749 N88-14603

Investigation of effect of silver compounds on microflora in water reclaimed from atmospheric moisture condensate in a closed environment 07 p0892 N88-15407

Space station accommodations for life sciences research facilities. Phase 1: Conceptual design and programmatics studies for Missions SAAX0307, SAAX0302 and the transition from SAAX0307 to SAAX0302. Volume 2: Study results
[NASA-CR-179244] 08 p0962 N88-15829

Neogene paleoclimate in Pacific Ocean subarctic region determined from study of diatoms
08 p1010 N88-16125

Plant cell technologies in space: Background, strategies and prospects 09 p1198 N88-17177

Spectroscopic studies of energy transfer in photosynthetic reaction centers of higher plants
[DE88-003850] 10 p1359 N88-18121

Species biology and potential for controlling four exotic plants (Ammophila arenaria, Carpobrotus edulis, Cortaderia jubata and Gasoul crystallinum) on Vandenberg Air Force Base, California
[NASA-TM-100980] 10 p1363 N88-18148

Five New South Wales barrier lagoons: Their macrobenthic fauna and seagrass communities
11 p1517 N88-19059

Space station accommodations for life sciences research facilities: Phase A conceptual design and programmatics studies for Missions SAAX0307, SAAX0302 and the transition from SAAX0307 to SAAX0302. Volume 1: Executive summary
[NASA-CR-179267] 12 p1599 N88-19571

Plant biology in space 12 p1654 N88-19910

A method to detect and digitize small plant movements 12 p1654 N88-19912

Plant cell cultures in space biology studies
12 p1654 N88-19913

The use of plant protoplasts in biotechnological space research 12 p1655 N88-19914

Effects of cosmic heavy ion radiation and space microgravity on plant systems 12 p1658 N88-19936

The 35 mm vertical aerial photographs for mapping stands of bracatinga in different age classes
17 p2366 N88-24087

Mapping of plant associations and the variation of surface water in the Pantanal Mato-Grossense National Park, through remote sensing techniques
17 p2366 N88-24092

Botany Facility: The problems of plant fixation
[SIRA-A/7373/WP220/RJS/001]
17 p2379 N88-24140

Botany Facility: Problems of water supply, plant nutrients and soil in the Botany Facility
[SIRA-A/7373/WP220/RJS/003]
17 p2379 N88-24141

Supply and distribution of plant nutrients in the Botany Facility
[SIRA-A/7373/WP220/RJS/004]
17 p2379 N88-24142

Photochrome from green plants: Assay, purification and characterization
[DE88-007511] 19 p2702 N88-26067

PLANTS (INDUSTRIES)

U INDUSTRIAL PLANTS

PLASMA ACCELERATION

Hot plasmas in the Earth's magnetosphere
03 p0272 N88-11710

Particle injection and cosmic ray acceleration at collisionless parallel shocks
[DE88-000507] 04 p0430 N88-12665

Microphysics of the auroral acceleration region of other regions of the magnetosphere 08 p1096 N88-15592

Acceleration/heating processes on auroral field lines as observed by the Viking spacecraft
08 p1096 N88-16596

Stochastic acceleration of cometary ions: The effects of composition and source strength distributions
14 p1997 N88-21902

Nonlinear effects in plasma wake field acceleration
[DE88-700972] 15 p2134 N88-22734

PLASMA ANTENNAS

Analysis of plasma coupling with the prototype DIII-D ICRF antenna
[DE88-006085] 19 p2729 N88-26204

PLASMA ARC SPRAYING

U ARC SPRAYING

PLASMA ARC WELDING

Plasma joining of metal matrix composites
[AD-A184828] 05 p0557 N88-13390

The interaction of DC plasma jet with a melting metal: Experimental measurements and mathematical description
[AD-A185173] 05 p0651 N88-13993

Pulsed plasma arc welding process with double closed-loop adaptive penetration control system
[PB87-143780] 07 p0863 N88-15236

Study on arc sound in TIG and plasma welding processes and the possibility of its application in practice
[PB87-143947] 07 p0863 N88-15238

Study on the square wave alternating plasma arc welding for aluminum alloys
[PB87-143772] 07 p0863 N88-15239

Examination of the physical processes associated with the keyhole region of variable polarity plasma arc welds in aluminum alloy 2219 07 p0927 N88-15634

Plasma joining of metal matrix composites
[AD-A188559] 12 p1604 N88-19593

Plasma joining of metal matrix composites
[AD-A193939] 22 p3051 N88-28100

ARC length control for plasma welding
[NASA-CASE-MSC-20900-1] 24 p3380 N88-30131

PLASMA ARCS

U PLASMA JETS

PLASMA BUBBLES

In-situ plasma bubble observations associated with equatorial spread-F over Natal
[INPE-4488-PRE/1252] 15 p2095 N88-22482

PLASMA CHEMISTRY

Plasma deposition of silicon carbide thin films
[AD-A188093] 11 p1556 N88-19314

PLASMA CLOUDS

NT MAGNETIC CLOUDS

The expansion of magnetic clouds
01 p0115 N88-10737

CRRES chemical release mechanisms
14 p1874 N88-21192

A plasma wave instrument on the AMPTE/IRM (Active Magnetospheric Particle Tracing Explorers/Ion Release Module) spacecraft
[AD-A191216] 16 p2233 N88-23336

Application of particle simulations to the NRL laser experiment
[AD-A191641] 18 p2520 N88-24953

PLASMA COMPRESSION

System studies of compact ignition tokamaks
[DE87-014976] 02 p0239 N88-11508

Factors which affect operation of a plasma focus in various gases
[DE88-701882] 20 p2858 N88-26975

PLASMA CONDUCTIVITY

Current generation and induced conductivity of a plasma under common action of constant electric field and lower-hybrid or ECR waves
[DE88-700345] 07 p0935 N88-15680

Transport properties of conductive polymers
[AD-A188411] 12 p1610 N88-19628

Characterization of PEOS (Plasma Erosion Opening Switch) plasma parameters and conduction phase properties
[AD-A189024] 12 p1624 N88-19714

PLASMA CONFINEMENT

U PLASMA CONTROL

PLASMA CONTROL

Steady state theta pinch concept for slow formation of FRC
[ISSN-0469-4732] 01 p0098 N88-10648

Massachusetts Institute of Technology Plasma Fusion Center: 1986-1987 Report to the President
[DE87-013518] 01 p0101 N88-10661

Numerical simulation of laser filamentation experiments
[ETN-87-90959] 02 p0179 N88-11118

Computer models for kinetic equations of magnetically confined plasmas
[DE87-011571] 02 p0236 N88-11492

Field-reversing electron and ion rings for the confinement and heating of plasmas
[DE87-014669] 02 p0238 N88-11505

Improvement of energy confinement of neutral beam heated plasma by lower hybrid current drive in JT-60
[DE87-752983] 02 p0239 N88-11509

Two dimensional neutral transport analysis in tokamak plasma
[DE87-752984] 02 p0239 N88-11510

Analysis of energy confinement of slideaway discharges
[DE87-753008] 02 p0240 N88-11515

Reactivity for DT plasma with beam-induced tail in magnetic confinement system
[DE87-753017] 02 p0240 N88-11517

Feasibility of alpha particle measurement in a magnetically confined plasma by CO2 laser Thomson scattering
[DE88-000039] 02 p0241 N88-11522

Potential formation in the plasma confinement region of a radio-frequency plugged linear device
[IPPJ-843] 02 p0242 N88-11526

Application of a two fluid theoretical plasma transport model on current Tokamak reactor designs
[DE87-013511] 03 p0377 N88-12373

Measurement of parallel ion energy distribution function in PISCES plasma
[DE88-000108] 03 p0378 N88-12380

Interchange stability of noncircular reversed field pinches
[DE88-000177] 03 p0378 N88-12381

The role of stellarators in the advanced toroidal program
[DE87-014815] 04 p0491 N88-13025

Data base on the high heat flux behaviour of metals and carbon materials for plasma facing components: Experiments at the 10 MW neutral beam injection test stand of the IPP Nagoya
[IPPJ-AM-53] 04 p0492 N88-13031

Confinement time of electrons and H(-)/D(-) ions in the Uramoto type sheet plasma
[IPPJ-852] 04 p0492 N88-13032

Monte Carlo analysis of neoclassical transport for a compact helical system
[IPPJ-850] 04 p0492 N88-13033

MHD stability and control for mirror machines
04 p0493 N88-13036

ALT-1 pump limiter experiments
[DE88-000822] 05 p0651 N88-13989

A review of the experimental and theoretical status of the reversed-field pinch
[DE88-000529] 05 p0652 N88-14000

Confinement of energy in tokamak-10 plasma during electron-cyclotron-resonance heating
06 p0773 N88-14750

Reversed field pinch experiments: Summary of progress report
[DE88-002367] 07 p0934 N88-15673

Recent results of plasma research activities at the Instituto de Pesquisas Espaciais
[INPE-4383-PRE/1203] 08 p1085 N88-16538

Particle transport in microdetonations — inertial confinement fusion pellets
[OEFZS-4402] 09 p1164 N88-16976

Experimental study of the initial plasma formation stage in a linear theta pinch of inverted field
[DE88-700010] 09 p1249 N88-17485

Plasma theory and simulation
[AD-A187100] 09 p1249 N88-17486

Influence of fast alpha diffusion and thermal alpha buildup on Tokamak reactor performance
[DE88-003661] 09 p1251 N88-17496

Observation of enhanced electric field in an RF-plugged sheet plasma in the RFC-XX-M open-ended machine
[IPPJ-857] 09 p1252 N88-17503

Pump limiter experiments and analyses in the TEXTOR tokamak 09 p1252 N88-17506

D-3He fuels in a field-reversed configuration
[IPPJ-855] 10 p1411 N88-18419

Plasma confinement calculations for TIBER-2
[DE88-004044] 10 p1412 N88-18425

First and second harmonic ECRH experience at gyrotron frequencies at LLNL
[DE88-003998] 10 p1413 N88-18430

Stability of an RFP (Reversed-Field Pinch) with resistive and distant boundaries
[DE88-004155] 10 p1413 N88-18431

Toroidal confinement research concepts evaluation and tradeoff studies
[DE88-004277] 11 p1551 N88-19282

Toroidal confinement research concepts evaluation and tradeoff studies
[DE88-004841] 11 p1552 N88-19285

Diagnostics for intelligent control of MPD (Magneto-Plasma Dynamic) engines
[AD-A189619] 12 p1603 N88-19587

CIT (Compact Ignition Tokamak) fueling
[DE88-002709] 12 p1692 N88-20125

FOM contributions to the 14th European Conference on Controlled Fusion and Plasma Physics
[REPT-87-174] 12 p1693 N88-20129

Simulation of electron cyclotron heating in TFR
12 p1693 N88-20130

Formation of high-Beta plasmas in various modes of operation in TPE-2 12 p1693 N88-20132

SOAR: Space orbiting advanced fusion power reactor
[AD-A189234] 13 p1732 N88-20356

Reversed field pinch operation with a thin shell
[DE88-005521] 13 p1843 N88-21027

Preliminary analysis on plasma equilibrium control. Conceptual design study of FY86 FER
[DE88-751441] 14 p1984 N88-21834

New methods of confinement and heating of plasma in magnetic fields
[DE88-701021] 15 p2135 N88-22738

Long-time impurity confinement as a precursor to disruptions in ohmically heated tokamaks
[DE88-006183] 15 p2136 N88-22742

Improvement of plasma confinement due to electron Landau damping in tokamaks
[DE88-752339] 15 p2136 N88-22747

Transport simulations of ohmic ignition experiment: IGNITEX
[DE88-006055] 15 p2138 N88-22757

Ion traps for large storage capacity
16 p2268 N88-23570

A fusion based plasma propulsion system
17 p2401 N88-24274

Fluid dynamics of spherical cavity reactors
17 p2403 N88-24291

Stability of spheromak against current driven modes: Effects of flux hole on stability
[IPPJ-868] 19 p2730 N88-26211

Zero-dimensional calculation for ZT-H
[DE88-009175] 19 p2731 N88-26217

Symmetrized magnetic field configuration of low aspect ratio helical system
[IPPJ-869] 20 p2855 N88-26956

Neoclassical diffusion due to trapping/detrapping orbits in stellarators
[DE88-008566] 20 p2857 N88-26968

The effect of ICRF on the Alcator C Scrape-Off Layer plasma
[DE88-009821] 20 p2858 N88-26972

Tokamak magnetic turbulence over the safety factor range 0.6 less than q less than 3
[DE88-008421] 21 p3017 N88-27904

Optical imaging diagnostics for fusion plasmas
[DE88-997572] 21 p3018 N88-27910

A survey of the current experimental database for lower hybrid current-drive and heating
[DE88-009830] 23 p3283 N88-29552

Vortex formation and particle transport in a cross-field plasma sheath
[DE88-008931] 23 p3284 N88-29553

PLASMA COOLING

Methods and first results of plasma non-isothermal parameters measurements in meteor trails
06 p0737 N88-14531

Modeling and transport in semiconductor devices
[AD-A188760] 13 p1844 N88-21037

PLASMA CORE REACTORS

Fluid dynamics of spherical cavity reactors
17 p2403 N88-24291

PLASMA CURRENTS

Fast wave injection into high temperature tokamak plasmas in the lower-hybrid-density regime of JIPP T-IIU
[ISSN-0469-4732] 01 p0099 N88-10649

Use of polarimetry to measure the current profile in MTX
[DE87-013835] 02 p0237 N88-11495

Stability of spheroidal spheromak plasma by use of force-free approximation
[IPPJ-846] 02 p0241 N88-11523

Current-driven lower hybrid waves at the inner edge of the ring current --- magnetosphere
[MPE-PREPRINT-94] 02 p0243 N88-11534

Application of a two fluid theoretical plasma transport model on current Tokamak reactor designs
[DE87-013511] 03 p0377 N88-12373

Magnetic fluctuation behaviour of current termination in reversed field pinch
[IPPJ-849] 04 p0492 N88-13034

Observations of propagating double layers in a high current discharge
[TRITA-EPP-87-10] 05 p0652 N88-13997

Conceptual design of a radio-frequency driven compact tokamak
[INPE-4364-PRE/1190] 08 p1085 N88-16535

Shape of the plasma boundary in TBR
[INPE-4388-PRE/1208] 08 p1086 N88-16540

Tokamak with highly elongated cross-section of a plasma
[DE88-700356] 10 p1410 N88-18412

Structural consequences of railgun augmentation
[DE88-007036] 15 p2023 N88-22058

Interpretation of the northward B sub z (NBZ) Birkeland current system and polar cap convection patterns in terms of the impulsive penetration model
[AERONOMICA-ACTA-A-321-1987]
18 p2595 N88-25422

ECRH current drive in tokamak plasmas
[IPPJ-864] 19 p2729 N88-26209

Cosmic electric currents and the generalized Bennett pinch
[TRITA-EPP-87-14] 22 p3154 N88-28764

The interaction of Io with the plasma torus
23 p3308 N88-29704

RFP (Revised Field Pinch) plasma experiment at INPE
[INPE-4613-PRE/1336] 24 p3431 N88-30420

PLASMA CYLINDERS

NT CYLINDRICAL PLASMAS

PLASMA DECAY

Observation of nonlinear wave decay processes in the solar wind by the AMPTE IRM plasma wave experiment
[AD-A191409] 16 p2290 N88-23713

PLASMA DENSITY

Study of ionization equilibrium of high temperature and low density plasma
[DE87-703070] 02 p0238 N88-11502

X-ray pulsars: Accretion flow deceleration
03 p0390 N88-12451

ALT-1 pump limiter experiments
[DE88-000822] 05 p0651 N88-13989

State parameters of pulse-discharge plasma in xenon-filled closed tube 06 p0773 N88-14747

Unusually strong density decrease in near-Earth interplanetary plasma and magnetically quiet day as effects of isolated solar flare 08 p1002 N88-16072

Small scale plasma density structures observed by the Viking double probe instrument --- Swedish satellite
08 p1098 N88-16604

Pump limiter experiments and analysis in the TEXTOR tokamak 09 p1252 N88-17506

A study of single and binary ion plasma expansion into laboratory-generated plasma wakes
[NASA-CR-4125] 10 p1412 N88-18427

Large scale plasma irregularities observed in the nighttime ionosphere over Natal using a rocket-borne Langmuir probe
[INPE-4422-PRE/1226] 12 p1694 N88-20139

Ionization equilibrium and radiative energy losses in a stationary plasma
[DE88-700856] 14 p1984 N88-21832

Correlation between magnetic and electric field fluctuations observed during flyby near Halley's comet
14 p1996 N88-21897

Magnetic cavity formation at Comet Halley and at the AMPTE Li release 14 p1996 N88-21898

Long-time impurity confinement as a precursor to disruptions in ohmically heated tokamaks
[DE88-006183] 15 p2136 N88-22742

Application of magnetic barrier for increasing the efficiency of laser ion source
[DE88-701669] 16 p2212 N88-23200

Summary report on the Japan-US Workshop on the Assessment of Spectroscopic Data for Temperature and Density Measurements --- plasma diagnostics
[IPPJ-861] 17 p2439 N88-24512

Tokamak studies of density sensitive line ratios
17 p2441 N88-24521

Density diagnostics by hydrogen line intensity ratios: Excitation cross section between excited states
17 p2441 N88-24522

Spectral diagnostics for temperature and density measurements on ATF 17 p2442 N88-24525

Measurements of Z(sub eff) profile with a visible bremsstrahlung continuum detector array
17 p2443 N88-24529

Low frequency electrostatic turbulence in the polar cap E-region
[DRI-3-88] 18 p2540 N88-25077

Plasma neutralizer work at BNL (Brookhaven National Laboratory)
[DE88-007046] 18 p2579 N88-25317

Infrared and far-infrared laser development for plasma diagnostics at Oak Ridge National Laboratory
[DE88-007262] 19 p2674 N88-25604

Calculation of the line shapes of radiators immersed in plasma 19 p2729 N88-26210

Poloidal field measurements using laser enhanced attenuation of an energetic lithium beam
[DE88-008360] 20 p2856 N88-26963

A plasma ultraviolet source for short wavelength lasers
[AD-A192844] 21 p2952 N88-27537

Heating efficiency of beat wave excitation in a density gradient
[AD-A193066] 21 p3017 N88-27905

Density fluctuations in currentless high beta plasmas in Heliotr[illegible] E
[DE88-752310] 23 p3283 N88-29550

Consideration of plasma opening switches from a wave propagation perspective
[AD-A195681] 24 p3431 N88-30421

PLASMA DIAGNOSTICS

Diagnostic technique for monitoring high temperature plasma dynamics
[DE87-011786] 01 p0099 N88-10853

Nonlinear fluid equations for a low collisionality toroidal plasma
[DE87-013006] 01 p0100 N88-10855

Direct detection of optical radiation through a sampling orifice for inductively coupled plasma atomic emission spectroscopy
[DE87-013609] 01 p0101 N88-10862

Use of polarimetry to measure the current profile in MTX
[DE87-013835] 02 p0237 N88-11495

Thermally driven convective cells and tokamak edge turbulence
[DE87-014424] 02 p0238 N88-11499

Spectrograms of the visible region in the JT-60 tokamak (wavelength range from 2210 A to 5250 A)
[DE87-753002] 02 p0240 N88-11513

Laser blow-off experiments on ASDEX --- tokamak
[IPP-III/119] 02 p0243 N88-11535

Production of atom flows at materials evaporation by laser radiation
[DE87-703327] 03 p0328 N88-12074

Review of X-ray spectroscopy from laser-produced plasmas
[DE88-000755] 04 p0494 N88-13043

Proceedings of the 17th International Conference on Phenomena in Ionized Gases held in Budapest, Hungary, July 8-12, 1985: Invited papers
[DE87-703562] 05 p0651 N88-13987

Intracavity spectrum analyzer with NaF:F2(+):F3(-) crystal laser for long-wave IR wave band
07 p0919 N88-15584

Activities report of the Institute of Plasma Physics
[ETN-88-91020] 07 p0933 N88-15668

Method of plasma diagnostics by a heavy ion beam for the T-15 tokamak
[DE88-700342] 07 p0935 N88-15678

Relativistic plasma concentration measuring by Bremsstrahlung
[DE88-700560] 07 p0936 N88-15685

Diagnostic concept of the resonance cone technique and its application in ground and space experiments
08 p1027 N88-16222

Resonance cones in nonthermal plasmas: Laboratory experiments 08 p1027 N88-16223

MAIMIK: A high current electron beam experiment on a sounding rocket from Andoya rocket range (Norway)
08 p1030 N88-16243

Effect of neutral wind on the latitudinal variation of nighttime F-layer vertical movements
08 p1030 N88-16244

Remote and in-situ plasma measurements during the Coordinated Auroral Experiment using Scatter And Rockets (CAESAR) flight 08 p1032 N88-16252

Shape of the plasma boundary in TBR
[INPE-4388-PRE/1208] 08 p1086 N88-16540

Tangential Thomson scattering --- plasma diagnostics
[REPT-87-173] 08 p1087 N88-16548

Conditional sampling in plasma turbulence
08 p1097 N88-16603

Testing a very good microwave interferometer
[TRITA-EPP-86-09] 09 p1167 N88-16996

Microwave system for the microwave Tokamak experiment (MTX)
[DE88-002391] 09 p1250 N88-17487

Investigation of the evolution of the fusion processes in the plasma focus using time-resolved neutron spectroscopy
[IPF-87-4] 09 p1251 N88-17493

Overview of applications of Laser-Induced Breakdown Spectroscopy (LIBS) [DE88-004314] 10 p1336 N88-17987

Diagnostics for ATF [DE88-004175] 10 p1414 N88-18438

Ion energy diagnostics for voltage determinations in plasma-erosion-opening-switch experiments [DE88-004822] 11 p1479 N88-18827

ICF research at Los Alamos [DE88-005394] 11 p1493 N88-18916

Summaries of FY86 research in the Applied Plasma Physics Fusion Theory Program [DE88-004242] 11 p1554 N88-19298

A neutral-beam diagnostic for fast confined alpha particles in a burning plasma: Applicatoin on CIT (Compact Ignition Tokamak) [DE88-004890] 11 p1554 N88-19301

Diagnostics for intelligent control of MPD (Magneto-Plasma Dynamic) engines [AD-A189619] 12 p1603 N88-19587

An experimental and theoretical investigation of optogalvanic effects [AD-A189618] 12 p1625 N88-19720

Measurements of optically thin electron cyclotron emission from relativistic electrons [DE88-004713] 12 p1688 N88-20096

FOM contributions to the 14th European Conference on Controlled Fusion and Plasma Physics [REPT-87-174] 12 p1693 N88-20129

X-ray source model for Z-pinch aluminum plasmas [AD-A189509] 12 p1696 N88-20148

Laser pulse detection with infrared range semiconductor detectors [DE88-700657] 14 p1914 N88-21432

Variability of Comet Halley's coma: VEGA-1 and VEGA-2 magnetic field observations 14 p1995 N88-21891

Physical processes in the vicinity of the cometopause interpreted on the basis of plasma, magnetic field and plasma wave data measured on board VEGA-2 spacecraft --- Halley's comet 14 p1996 N88-21894

Some new features of plasma wave phenomena at Halley: APV-N observations --- VEGA 14 p1996 N88-21895

Plasma phenomena in the vicinity of the closest approach of VEGA-1, 2 spacecraft to the Comet Halley nucleus 14 p1996 N88-21899

Halley's environments by the Japanese Suisei spacecraft 14 p1999 N88-21915

Plasma tail of Comet Halley in January 1986 14 p2006 N88-21960

Advanced diagnostics for reacting flows [AD-A190485] 15 p2035 N88-22122

High-voltage inverse-square function generator [DE88-701109] 15 p2058 N88-22270

The development of high power KrF laser systems for plasma research by the application of stimulated Raman scattering [ETN-88-92220] 15 p2073 N88-22358

Corpuscular plasma diagnostics complex on a tokamak with a strong field [DE88-701576] 16 p2279 N88-23646

Measurement of time evolution of plasma electron component parameters on the Ogra-4 device by the Thomson scattering method [DE88-701575] 16 p2282 N88-23662

Summary report on the Japan-US Workshop on the Assessment of Spectroscopic Data for Temperature and Density Measurements --- plasma diagnostics [IPPJ-861] 17 p2439 N88-24512

Ion temperature measurement with spectroscopy in JT-60 17 p2439 N88-24513

X-ray emission from tokamaks 17 p2439 N88-24514

X-ray spectroscopic diagnostics on JIPPT-IIU and HELIOTRON-E 17 p2440 N88-24515

Helium-like titanium spectra from tokamak plasmas 17 p2440 N88-24516

Spectroscopic results from JET: Some examples of data comparison and data needs 17 p2440 N88-24517

Ion temperature profile measurement using charge exchange recombination spectroscopy on JIPP T-IIU 17 p2440 N88-24518

Spectroscopic measurements of ion temperature, rotation speed and beam deposition profile on DIII-D 17 p2440 N88-24519

Forbidden transitions as ion-temperature sensitive lines 17 p2441 N88-24520

Tokamak studies of density sensitive line ratios 17 p2441 N88-24521

Density diagnostics by hydrogen line intensity ratios: Excitation cross section between excited states 17 p2441 N88-24522

Spectroscopic study of heliotron E plasmas: Stark profile, CXR, poloidal rotation and carbon coating 17 p2441 N88-24523

Observation of injected silicon in heliotron E 17 p2441 N88-24524

Spectral diagnostics for temperature and density measurements on ATF 17 p2442 N88-24525

Cascade fluorescences from laser-excited lithium atom for plasma diagnostics 17 p2442 N88-24526

Spectroscopic data relevant to alpha particle diagnostics 17 p2442 N88-24527

Flux density measurements of neutral iron in TEXTOR with laser induced fluorescence 17 p2442 N88-24528

Measurements of Z(sub eff) profile with a visible bremsstrahlung continuum detector array 17 p2443 N88-24529

Hot electron diagnostics using X-ray imaging on GAMMA10 17 p2443 N88-24530

Polarization spectroscopy: Prospect and data needs 17 p2443 N88-24531

Intensity calibration of a VUV system by branching line pairs 17 p2443 N88-24533

Availability and quality of spectroscopic data and standards for tokamak studies 17 p2443 N88-24534

Trochoidal analysis of scattered electrons in a merged electron-ion beam [NASA-CASE-NPO-16789-1-CU] 18 p2573 N88-25281

Intense ion beam diagnostics for particle beam fusion experiments on PBFA 2 [DE88-007279] 18 p2577 N88-25308

A two-wavelength infrared interferometer/polarimeter system for CIT (Compact Ignition Tokamak) [DE88-007661] 18 p2579 N88-25321

Optical diagnostics for a high power, rf-inductively coupled plasma [DE88-007822] 18 p2579 N88-25322

Activities report in plasma physics [ETN-88-92221] 18 p25[illegible] N88-25324

Infrared and far-infrared laser develop[illegible] plasma diagnostics at Oak Ridge National Laboratory [DE88-007262] 19 p2674 N88-25904

The XRD (X-Ray Diode) array, the grazing incidence spectrometer and the X-ray imaging camera on PBFA 2 [DE88-007282] 19 p2728 N88-26200

Design and calibration of a two-channel low-noise heterodyne receiver for use in a CO2 laser Thomson scattering alpha particle diagnostic [DE88-007866] 19 p2728 N88-26201

Simultaneously time- and space-resolved spectroscopic characterization of laser-produced plasmas [DE88-008038] 19 p2728 N88-26202

A low divergence, high brightness lithium ion source for plasma diagnostics [DE88-008063] 19 p2729 N88-26203

Calculation of the line shapes of radiators immersed in plasma 19 p2729 N88-26210

An elliptical spectrograph/gated microchannel plate detector for time-resolved spectral measurements in the X-ray region [DE88-007590] 20 p2856 N88-26961

Poloidal field measurements using laser enhanced attenuation of an energetic lithium beam [DE88-008360] 20 p2856 N88-26963

Fusion programs in applied plasma physics and development and technology at GA Technologies, Inc. [DE88-008406] 20 p2856 N88-26964

A CO2 laser Thomson scattering diagnostic for fusion product alpha particle measurement [DE88-007683] 20 p2857 N88-26965

Multipoint Thomson scattering diagnostic for DIII-D [DE88-008737] 20 p2857 N88-26969

Developing diagnostic methods for plasma-particle interaction [DE88-007726] 20 p2858 N88-26973

Vertical viewing ECE diagnostic for the D3-D tokamak [DE88-010586] 20 p2860 N88-26987

MTX (Microwave Tokamak Experiment) plasma diagnostic system [DE88-011326] 20 p2861 N88-26993

Dynamics of a plasma produced under effect of the XeCl-laser radiation on metallic surface [DE88-701983] 21 p3017 N88-27902

Optical imaging diagnostics for fusion plasmas [DE88-997572] 21 p3018 N88-27910

Four-frame gated optical imager with 120-ps resolution [DE88-011735] 22 p3080 N88-28288

Introduction to laser plasma diagnostics [DE88-011056] 23 p3285 N88-29560

Apparatus for submillimeter laser diagnostics of high-temperature plasma [DE88-702464] 23 p3285 N88-29563

Ionospheric radio and propagation: Waves in plasmas 24 p3364 N88-30030

PLASMA DIFFUSION

Relation of wave energy and momentum with the plasma dispersion relation in an inhomogeneous plasma [DE88-002305] 08 p1084 N88-16530

Nonlinear diffusion in the presence of a time-dependent external electric field [INPE-4378-PRE/1198] 08 p1085 N88-16533

Chaotic diffusion across magnetic field in a model of electrostatic turbulent plasma [PREPRINT-566] 14 p1985 N88-21839

Consideration of plasma opening switches from a wave propagation perspective [AD-A195681] 24 p3431 N88-30421

PLASMA DIODES

Electron temperature measurements in an argon/cesium plasma diode [AD-A188835] 12 p1695 N88-20141

Development of inductive storage pulsed power generators [AD-A193878] 22 p3117 N88-28521

PLASMA DISCHARGES

U PLASMA JETS

PLASMA DISPERSION

U PLASMA DIFFUSION

PLASMA DISPLAY DEVICES

Excimer plasma displays [AD-A186731] 09 p1250 N88-17489

Brightness contrast and character height of five flat panel computer displays [AD-A187743] 11 p1524 N88-19096

PLASMA DRIFT

Curvature driven drift mirror instability in the magnetosphere [IFSI-86-14] 06 p0742 N88-14568

Effect of neutral wind on the latitudinal variation of nighttime F-layer vertical movements 08 p1030 N88-16244

A study of single and binary ion plasma expansion into laboratory-generated plasma wakes [NASA-CR-4125] 10 p1412 N88-18427

Plasma rotation in a tokamak [DE88-700855] 12 p1693 N88-20128

Large scale plasma irregularities observed in the nighttime ionosphere over Natal using a rocket-borne Langmuir probe [INPE-4422-PRE/1226] 12 p1694 N88-20139

The effects of a dc electric field on the current driven ion cyclotron instability [AD-A188877] 12 p1695 N88-20142

Improvement of plasma confinement due to electron Landau damping in tokamaks [DE88-752339] 15 p2136 N88-22747

Application of particle simulations to the NRL laser experiment [AD-A191641] 18 p2520 N88-24953

Plasma theory and simulation [AD-A194674] 23 p3286 N88-29565

Vortex formation and particle transport in a cross-field plasma sheath [AD-A194838] 24 p3432 N88-30425

PLASMA DYNAMICS

Diagnostic technique for monitoring high temperature plasma dynamics [DE87-011786] 01 p0099 N88-10653

Study of the mechanism for solar wind formation 01 p0118 N88-10756

A high-power RF linear accelerator for FELs (Free-Electron Lasers) [DE87-011795] 02 p0177 N88-11104

Laboratory and near-earth space plasma as a key to the plasma universe [TRITA-EPP-87-09] 05 p0652 N88-13996

Numerical models for high beta magnetohydrodynamic flow [DE88-001850] 05 p0654 N88-14008

A fluid simulation of the AMPTE lithium gas releases in the solar wind [TRITA-EPP-87-06] 05 p0661 N88-14056

State parameters of pulse-discharge plasma in xenon-filled closed tube 06 p0773 N88-14747

Experimental evidence of micro-nonequilibrium on the magnetopause and further predictions 08 p1098 N88-16606

Dynamical aspects of electrostatic double layers [TRITA-EPP-87-13] 09 p1250 N88-17492

Diagnostics for intelligent control of MPD (Magneto-Plasma Dynamic) engines [AD-A189619] 12 p1603 N88-19587

Electric fields in Earth orbital space. Magnetospheric structural dynamic response to external variables [AD-A188592] 12 p1643 N88-19836

Waves and static electric fields in the auroral acceleration region 12 p1646 N88-19856

Effects of toroidal forces in current loops embedded in a background plasma [AD-A188878] 12 p1695 N88-20143

Studies of ionosphere/magnetosphere dynamics using SABRE and HILAT [AD-A190947] 16 p2232 N88-23333

Spectroscopic measurements of ion temperature, rotation speed and beam deposition profile on DIII-D
17 p2440 N88-24519
Finite element methodology for integrated flow-thermal-structural analysis
[NASA-CR-183144] 21 p2964 N88-27606
Plasma theory and simulation
[AD-A194674] 23 p3286 N88-29565
Characteristics of solitary waves and weak double layers in the magnetospheric plasma
[IRF-PREPRINT-105] 24 p3431 N88-30418
Consideration of plasma opening switches from a wave propagation perspective
[AD-A195681] 24 p3431 N88-30421

PLASMA ELECTRODES
Behavior and structure of metal vapor arc plasma between molten electrodes
[DE88-001854] 06 p0782 N88-14801
Continuously frequency-tunable high-pressure CO2-laser with plasmatic cathode
09 p1238 N88-17418
Fundamental studies on MPD thrusters
[AD-A190307] 15 p2137 N88-22753
Basic processes of plasma propulsion
[AD-A192117] 18 p2577 N88-25310
Pierce diode with external circuit. Part 3: Chaotic behavior
[AD-A194837] 24 p3365 N88-30041

PLASMA ENGINES
Multi-stage plasma thruster
[AD-A183635] 01 p0017 N88-10105
Study of Plasma Motor Generator (PMG) tether system for orbit reboost
[NASA-CR-172016] 04 p0403 N88-12501
Completely magnetically contained electrothermal thrusters
[AD-A185674] 06 p0674 N88-14129
Diagnostics for intelligent control of MPD (Magneto-Plasma Dynamic) engines
[AD-A189619] 12 p1603 N88-19587
Fundamental studies on MPD thrusters
[AD-A190307] 15 p2137 N88-22753
Physical fluid mechanics in MPD thrusters
[AD-A190309] 15 p2138 N88-22754
Plasma-gas interaction studies in a hybrid plume plasma rocket
[AD-A190310] 15 p2138 N88-22755
MPD (magnetoplasmadynamic) thruster advanced pumping system concepts
[AD-A190513] 15 p2138 N88-22756
Megawatt level electric propulsion perspectives
17 p2404 N88-24294
Unified study of plasma/surface interactions for space power and propulsion
[AD-A195971] 24 p3338 N88-29870

PLASMA EQUILIBRIUM
On tokamak equilibrium
[DE87-014811] 02 p0239 N88-11507
Computational study of three-dimensional magnetohydrodynamic .equilibria in toroidal helical systems
[DE87-753007] 02 p0240 N88-11514
Elements of plasma physics 03 p0271 N88-11703
Simulation an experiment on plasma instability investigation in a tokamak with a divertor
[DE88-700352] 07 p0935 N88-15683
Model for plasma equilibrium configuration evolution in a tokamak with adiabatic compression
[DE88-700354] 07 p0936 N88-15684
Possibility of calculation of magnetic surface function gradient and related quantities
[DE88-700561] 07 p0936 N88-15686
Beta limitation of matter-antimatter boundary layers
[TRITA-EPP-87-11] 09 p1250 N88-17490
Tokamak with highly elongated cross-section of a plasma
[DE88-700356] 10 p1410 N88-18412
The Pierce diode with an external circuit. 2: Non-uniform equilibria
[AD-A188027] 11 p1478 N88-18818
Diagnostics for intelligent control of MPD (Magneto-Plasma Dynamic) engines
[AD-A189619] 12 p1603 N88-19587
Shear Alfven spectrum of analytic high-Beta equilibria
12 p1694 N88-20136
Effects of toroidal forces in current loops embedded in a background plasma
[AD-A188878] 12 p1695 N88-20143
Nonlinear resonance of two-dimensional ion layers
[AD-A188890] 12 p1695 N88-20145
Fully implicit three-dimensional MHD (magnetohydrodynamics) stability and evolution in toroidal geometry
[DE88-000624] 13 p1842 N88-21023
Nonlinear effects in plasma wake field acceleration
[DE88-700972] 15 p2134 N88-22734
Moment approach to neoclassical flows, currents and transport in auxiliary heated tokamaks
[DE88-008024] 21 p3016 N88-27901
ITER plasma equilibrium and poloidal field system design
[DE88-011005] 21 p3018 N88-27912
Theory and simulation of relaxed plasmoids
[AD-A192884] 21 p3032 N88-27997
Vortex formation and particle transport in a cross-field plasma sheath
[DE88-008931] 23 p3284 N88-29553
Plasmoid propagation
[AD-A192378] 23 p3284 N88-29555

PLASMA ETCHING
Silicon containing photoresists
[AD-A188666] 12 p1605 N88-19601
Fundamental studies and device development in beta silicon carbide
[AD-A189540] 12 p1699 N88-20165

PLASMA FLOW
U MAGNETOHYDRODYNAMIC FLOW

PLASMA FLUX MEASUREMENT
MHD energy fluxes for late type dwarfs
04 p0512 N88-13148
Array detectors for plasma spectrochemistry
[AD-A194220] 22 p3052 N88-28105

PLASMA FOCUS
Activities report of the Institute of Plasma Physics
[ETN-88-91020] 07 p0933 N88-15668
Investigation of the evolution of the fusion processes in the plasma focus using time-resolved neutron spectroscopy
[IPF-87-4] 09 p1251 N88-17493
The effects of optical smoothing techniques on filamentation in laser plasmas
[AD-A188719] 16 p2275 N88-23614
On the self-focusing of electric helicons
[DE88-701870] 20 p2848 N88-26905
Factors which affect operation of a plasma focus in various gases
[DE88-701882] 20 p2858 N88-26975
A plasma ultraviolet source for short wavelength lasers
[AD-A192844] 21 p2952 N88-27537

PLASMA FREQUENCIES
Elements of plasma physics 03 p0271 N88-11703
Laser thermal propulsion
[AD-A186407] 07 p0933 N88-15666
Microwave radiation from rotating, annular electron beams 11 p1475 N88-18801
The effects of a dc electric field on the current driven ion cyclotron instability
[AD-A188877] 12 p1695 N88-20142

PLASMA GENERATION
U PLASMA GENERATORS

PLASMA GENERATORS
NT JOINT EUROPEAN TORUS
NT PLASMA GUNS
NT TOKAMAK DEVICES
Mechanisms of polymer degradation using an oxygen plasma generator
[NASA-TM-100681] 01 p0018 N88-10110
Analysis of a series of electromagnetic launcher firings
[AR-005-131] 04 p0405 N88-12516
ICRF launcher studies
[DE88-001710] 04 p0495 N88-13046
Preparation of qualification tests of a plasma generator for the feeding of a hypersonic wind tunnel
05 p0530 N88-13222
High peak power ka-band gyrotron oscillator experiment
[AD-A185424] 05 p0585 N88-13563
A synthetic plasma source
[TRITA-EPP-86-15] 05 p0652 N88-13995
Plasma contactors for use with electodynamic tethers for power generation
[NASA-CR-182424] 08 p1087 N88-16547
Vacuum-arc plasma centrifuge experiment
[INPE-4509-PRE/1263] 15 p2138 N88-22758
Multiply stripped ion generation in the metal vapor vacuum arc
[DE88-008418] 19 p2725 N88-26179
Study of Plasma Motor Generator (PMG) tether system for orbit reboost
[NASA-CR-172074] 23 p3184 N88-28949
Bibliography of Soviet laser developments, number 88, March - April 1987
[AD-A195978] 24 p3378 N88-30116

PLASMA GUNS
Analytical solution of the equations for a coaxial plasma gun operating in the snowplow mode. 1. Weak coupling limit
[AD-A185370] 05 p0652 N88-13994
Antistokes coherent Raman diffusion of a nitriding plasma
[ONERA-RF-6/3644-PY] 16 p2175 N88-22962
Evaluation of the chromium oxide arc spraying treatment on solar energy collectors
[ETN-88-92564] 18 p2537 N88-25053
Refractory fibers surface treatment
[REPT-47-803/F] 21 p2922 N88-27339

PLASMA HEATING
NT ELECTRON CYCLOTRON HEATING
Mode purity measurements on gyrotrons for plasma heating at the stellarator W 7-AS
[IPF-87-3] 01 p0101 N88-10660
Massachusetts Institute of Technology Plasma Fusion Center: 1986-1987 Report to the President
[DE87-013518] 01 p0101 N88-10661
Field-reversing electron and ion rings for the confinement and heating of plasmas
[DE87-014669] 02 p0238 N88-11505
Transport analysis of OH and NBI heated discharges in JT-60
[DE87-752985] 02 p0239 N88-11511
Spectrograms of the visible region in the JT-60 tokamak (wavelength range from 2210 A to 5250 A)
[DE87-753002] 02 p0240 N88-11513
Reactivity for DT plasma with beam-induced tail in magnetic confinement system
[DE87-753017] 02 p0240 N88-11517
Fusion reactivity enhancement due to ion tail formation by beam and ion cyclotron heating
[DE87-753018] 02 p0240 N88-11518
Effect of electrostatic field on behaviour of peripheric plasma at high-frequency heating
[DE87-703328] 03 p0378 N88-12378
Negative ion beams for heating and current-drive in NET
[AD-A184390] 04 p0489 N88-13012
ALT-1 pump limiter experiments
[DE88-000822] 05 p0651 N88-13989
Atlas of atomic spectral lines of neptunium emitted by an inductively coupled plasma
[DE88-000640] 06 p0782 N88-14796
Techniques for ceramic sintering using microwave energy
[DE88-001416] 07 p0837 N88-15080
Electron acceleration by wave processes in the earth's ionosphere
[AD-A186110] 07 p0877 N88-15320
Studies on parametric instabilities in high-frequency wave heating of fusion plasmas
[PH-156] 07 p0933 N88-15667
Gyrotron development at the Instituto de Pesquisas Espaciais
[INPE-4240-PRE/1115] 08 p0990 N88-15992
A ray-tracing study of electron cyclotron resonance heating in tokamak plasmas with a superthermal electron tail
[INPE-4381-PRE/1201] 08 p1085 N88-16536
Absorption of electron cyclotron radiation in tokamak plasmas with a superthermal tail in the electron velocity distribution
[INPE-4391-PRE/1211] 08 p1086 N88-16541
Acceleration/heating processes on auroral field lines as observed by the Viking spacecraft
08 p1096 N88-16596
Theoretical studies of mass loss and shock phenomena in cool star envelopes
[NASA-CR-182433] 08 p1099 N88-16616
Experimental study of the initial plasma formation stage in a linear theta pinch of inverted field
[DE88-700010] 09 p1249 N88-17485
Microwave system for the microwave Tokamak experiment (MTX)
[DE88-002391] 09 p1250 N88-17487
D-3He fuels in a field-reversed configuration
[IPPJ-855] 10 p1411 N88-18419
New mode conversion process and overdense plasma heating in the electron cyclotron range of frequencies
[IPPJ-854] 10 p1411 N88-18420
ATF experimental plans
[DE88-004177] 10 p1414 N88-18439
Laser production and heating of plasma for MHD application
[NASA-TP-2798] 10 p1415 N88-18443
Induction linacs: A technology come of age for international cooperation
[DE88-003953] 11 p1548 N88-19258
Magnetic and inertial fusion status and development plans
[DE88-004405] 11 p1552 N88-19288
Microturbulent fluctuations in the TORTUR tokamak
12 p1693 N88-20131
The stability of a screw-pinch plasma to global MHD modes 12 p1694 N88-20133
Effects of toroidal forces in current loops embedded in a background plasma
[AD-A188878] 12 p1695 N88-20143

Experimental studies of plasma heating due to the parametric decay of a large amplitude pump into lower hybrid waves 13 p1841 N88-21017
Particle simulation research by plasma parametric heating caused by strong laser 14 p1903 N88-21368
Consistency between current ramp-up/recharging scenario by non-inductive current drive and dense and cold divertor plasma. Conceptual design study of FY86 FER [DE88-751438] 14 p1984 N88-21833
Preliminary analysis on plasma equilibrium control. Conceptual design study of FY86 FER [DE88-751441] 14 p1984 N88-21834
New methods of confinement and heating of plasma in magnetic fields [DE88-701021] 15 p2135 N88-22738
Heating and confinement studies of electron cyclotron resonance heated plasmas in Heliotron E [DE88-752312] 15 p2136 N88-22746
Theoretical studies of the heating of toroidal plasmas with radiofrequency electromagnetic radiation [DE88-006913] 15 p2137 N88-22749
Plasma-gas interaction studies in a hybrid plume plasma rocket [AD-A190310] 15 p2138 N88-22755
Measurements of Z(sub eff) profile with a visible bremsstrahlung continuum detector array 17 p2443 N88-24529
Activities report in plasma physics [ETN-88-92221] 18 p2560 N88-25324
A mode-transforming polarization-rotatable launcher for the ATF (Advanced Toroidal Facility) fusion experiment [DE88-005070] 19 p2730 N88-26213
Parallel gradient effects on ICRH (Ion Cyclotron Resonance Heating) in tokamaks [DE88-009038] 19 p2730 N88-26216
The effect of ICRF on the Alcator C Scrape-Off Layer plasma [DE88-009821] 20 p2858 N88-26972
Moment approach to neoclassical flows, currents and transport in auxiliary heated tokamaks [DE88-008024] 21 p3016 N88-27901
Heating efficiency of beat wave excitation in a density gradient [AD-A193066] 21 p3017 N88-27905
Plasma technology: Preliminary studies 2 [DE88-752815] 22 p3154 N88-28763
Initial operation and edge plasma studies in ATF (Advanced Toroidal Facility) [DE88-011400] 23 p3285 N88-29562
Apperatus for submillimeter laser diagnostics of high-temperature plasma [DE88-702464] 23 p3285 N88-29563
Theoretical modeling of accelerating arc plasmas [AD-A195606] 24 p3432 N88-30426

PLASMA INSTABILITY
U MAGNETOHYDRODYNAMIC STABILITY

PLASMA INTERACTIONS
NT LASER PLASMA INTERACTIONS
NT PLASMA-ELECTROMAGNETIC INTERACTION
NT PLASMA-PARTICLE INTERACTIONS
Evolution of the solar wind structure in the outer heliosphere 01 p0112 N88-10721
Solar wind-cometary interaction at the ionopause and associated phenomena 01 p0117 N88-10748
The solar wind interaction with comets: A post encounter view 01 p0118 N88-10751
Plasma-tail activity and the interplanetary medium at Halley's Comet during Armada Week: 6-14 March 1986 01 p0118 N88-10752
Coherent emission from relativistic beam-plasma interactions 04 p0493 N88-13039
Analysis of geophysical data bases and models for spacecraft interactions [AD-A184809] 05 p0555 N88-13375
Laboratory and near-earth space plasma as a key to the plasma universe [TRITA-EPP-87-09] 05 p0652 N88-13996
Unified study of plasma-surface interactions for space power and propulsion [AD-A186211] 07 p0825 N88-15007
Plasma theory and simulation [DE88-000412] 07 p0934 N88-15670
CAESAR investigations --- Coordinated Auroral Experiment using Scatter And Rockets (CAESAR) 08 p1031 N88-16249
Field-aligned fluxes of energetic electrons related to the onset of magnetospheric substorms 08 p1096 N88-16595
Critical Ionization Velocity (CIV) interaction: Some unsolved questions [TRITA-EPP-87-12] 09 p1250 N88-17491
On the role of the ionization frequency to gyrofrequency ratio in the critical ionization velocity interaction [TRITA-EPP-86-10] 10 p1410 N88-18414
A study of single and binary ion plasma expansion into laboratory-generated plasma wakes [NASA-CR-4125] 10 p1412 N88-18427
USU (Utah State University) Center of Excellence in Theory and Analysis of the Geo-Plasma Environment [AD-A187687] 11 p1511 N88-19026
Simulation of the plasma interaction with thin dust clouds 11 p1552 N88-19291
Improved confinement of screw pinch plasmas in SPICA 2 12 p1694 N88-20137
Hydrogen pumping and release by graphite under high flux plasma bombardment [DE88-005880] 13 p1842 N88-21021
Reversed field pinch operation with a thin shell [DE88-005521] 13 p1843 N88-21027
Modeling and transport in semiconductor devices [AD-A186760] 13 p1844 N88-21037
A comparison between wave observations performed in the environments of Comets Halley and Giacobini-Zinner 14 p1996 N88-21896
High power, high frequency radiation from beam-plasma interactions [AD-A190207] 15 p2137 N88-22752
Fundamental studies on MPD thrusters [AD-A190307] 15 p2137 N88-22753
A plasma wave instrument on the AMPTE/IRM (Active Magnetospheric Particle Tracing Explorers/Ion Release Module) spacecraft [AD-A191216] 16 p2233 N88-23336
The effects of optical smoothing techniques on filamentation in laser plasmas [AD-A188719] 16 p2275 N88-23614
Theoretical plasma physics research of active space experiments [AD-A192075] 18 p2577 N88-25309
Fluid dynamical model of ultrarelativistic heavy ion collisions [DE88-007905] 20 p2850 N88-26921
The effect of ICRF on the Alcator C Scrape-Off Layer plasma [DE88-009821] 20 p2858 N88-26972
Coupling between radiation and gas dynamics [AD-A194593] 23 p3211 N88-29113
Tokamak plasma interaction with limiters [UTIAS-325] 23 p3286 N88-29566

PLASMA JETS
NT RADIO JETS (ASTRONOMY)
NBS (National Bureau of Standards) measurement services: Radiometric standards in the vacuum ultraviolet [PB87-227625] 03 p0325 N88-12055
Mathematical models of plasma discharge control in a tokamak [DE87-702891] 03 p0378 N88-12377
Design study for asteroidal exploitation 03 p0389 N88-12445
Pulsed plasma jet igniters: Species measurements in methane combustion [DE88-001389] 05 p0562 N88-13422
The interaction of DC plasma jet with a melting metal: Experimental measurements and mathematical description [AD-A185173] 05 p0651 N88-13993
Observations of propagating double layers in a high current discharge [TRITA-EPP-87-10] 05 p0652 N88-13997
The effect of propane on atomic spectrometric signals in the direct current plasma [DE88-002457] 07 p0934 N88-15676
Analysis of the decomposition of transparent polymer materials (blocks) under the action of laser beams in free generation mode [AD-A187090] 09 p1147 N88-16873
Simulation of electron cyclotron heating in TFR 12 p1693 N88-20130
Improved confinement of screw pinch plasmas in SPICA 2 12 p1694 N88-20137
On the structure of pulsed plasma jets 13 p1843 N88-21030
Relativistic jet models for the BL Lacertae object Mrk 421 during three epochs of observation [NASA-TM-89727] 13 p1853 N88-21090
Structural consequences of railgun augmentation [DE88-007036] 15 p2023 N88-22058
Vacuum-arc plasma centrifuge experiment [INPE-4509-PRE/1263] 15 p2138 N88-22758
The thermal evolution of the jets in SS433 --- galactic object [MPE-PREPRINT-107] 16 p2289 N88-23705
Optical investigations of the thermal boundary layer in arc plasmas 18 p2578 N88-25313
Modelling of thermal plasma systems 18 p2578 N88-25314
Plasma neutralizer work at BNL (Brookhaven National Laboratory) [DE88-007046] 18 p2579 N88-25317
STARFIRE: Hypervelocity railgun development for high-pressure research [DE88-008348] 19 p2605 N88-25469
Plasma deposition: Investigations on a new approach [ETN-88-92619] 20 p2861 N88-26992
A study of mechanisms producing astrophysical jets [AD-A194100] 23 p3300 N88-29649
Theoretical modeling of accelerating arc plasmas [AD-A195606] 24 p3432 N88-30426

PLASMA LAYERS
NT PLASMA SHEATHS
Observations of propagating double layers in a high current discharge [TRITA-EPP-87-10] 05 p0652 N88-13997
Double layer formed by beam driven ion-acoustic turbulence [INPE-4292-PRE/1163] 08 p1086 N88-16543
Experimental investigation of double layers formed by ion-acoustic turbulence [INPE-4296-PRE/1167] 08 p1086 N88-16544
Plasma theory and simulation [AD-A187100] 09 p1249 N88-17486
Dynamical aspects of electrostatic double layers [TRITA-EPP-87-13] 09 p1250 N88-17492
Silicon containing photoresists [AD-A188666] 12 p1605 N88-19601
The effects of a dc electric field on the current driven ion cyclotron instability [AD-A188677] 12 p1695 N88-20142
Nonlinear resonance of two-dimensional ion layers [AD-A188890] 12 p1695 N88-20145
A proposal for the establishment of a center of excellence in theoretical geoplasma research [AD-A189742] 16 p2231 N88-23327
Absorption characteristics of Si3N4 ablation layer plasma 20 p2783 N88-26504
The effect of ICRF on the Alcator C Scrape-Off Layer plasma [DE88-009821] 20 p2858 N88-26972
The influence of ionization within a plasma opening switch [AD-A193147] 21 p3017 N88-27906
Characteristics of solitary waves and weak double layers in the magnetospheric plasma [IRF-PREPRINT-105] 24 p3431 N88-30418

PLASMA LOSS
Analysis of energy confinement of sideaway discharges [DE87-753008] 02 p0240 N88-11515
Potential formation in the plasma confinement region of a radio-frequency plugged linear device [IPPJ-843] 02 p0242 N88-11526
Characteristics of laser-plasma X-radiation source (review) 09 p1239 N88-17428

PLASMA OSCILLATIONS
Low-frequency oscillations in nonideal plasma 06 p0774 N88-14751
Particle simulation research by plasma parametric heating caused by strong laser 14 p1903 N88-21368
Nonlinear dynamics of interaction between charged particles modulated beam and bounded plasma regular oscillations [DE88-701681] 16 p2280 N88-23648

PLASMA PERTURBATION
U PLASMA OSCILLATIONS

PLASMA PHYSICS
Compact torus studies [DE87-014254] 02 p0237 N88-11496
Pressure structure of solar coronal loops 02 p0256 N88-11618
Space Environment Technology --- conference [ISBN-2-85428-170-5] 03 p0271 N88-11702
Elements of plasma physics 03 p0271 N88-11703
The solar wind 03 p0271 N88-11705
Ionosphere and plasmasphere 03 p0272 N88-11709
Three-dimensional charging effects --- spacecraft 03 p0273 N88-11720
Theoretical plasma physics [DE88-001475] 04 p0492 N88-13029
Activities report of the Ionospheric Observatory [UIO-SR-87-01] 05 p0625 N88-13827
Energy dependence of ion-induced sputtering yields of monatomic solids in the low energy region [IPPJ-AM-52] 05 p0651 N88-13988
Laboratory and near-earth space plasma as a key to the plasma universe [TRITA-EPP-87-09] 05 p0652 N88-13996
Comments on H. Arp The persistent problem of spiral galaxies [TRITA-EPP-87-05] 05 p0660 N88-14052
Cosmology in the plasma universe [TRITA-EPP-87-07] 05 p0660 N88-14053

JPRS report: Science and technology. USSR: Physics and mathematics
[JPRS-UPM-87-006] 06 p0769 N88-14727
Theoretical studies of kinetic mechanisms of negative ion formation in plasmas
[AD-A185735] 06 p0784 N88-14812
USSR report: Physics and mathematics
[JPRS-UPM-87-002] 07 p0918 N88-15575
Activities report of the Institute of Plasma Physics
[ETN-88-91020] 07 p0933 N88-15668
Plasma theory and simulation
[DE88-000412] 07 p0934 N88-15670
Electrodynamics of midnight sector of auroral oval in period of slight disturbance 08 p1003 N88-16077
JPRS report: Science and technology. USSR: Physics and mathematics
[JPRS-UPM-87-010] 08 p1075 N88-16485
Recent results of plasma research activities at the Instituto de Pesquisas Espaciais
[INPE-4383-PRE/1203] 08 p1085 N88-16538
Plasma centrifuge development at INPE
[INPE-4243-PRE/1117] 08 p1087 N88-16546
Solar corona and solar wind 08 p1094 N88-16584
Plasma theory and simulation
[AD-A187100] 09 p1249 N88-17486
Critical Ionization Velocity (CIV) interaction: Some unsolved questions
[TRITA-EPP-87-12] 09 p1250 N88-17491
Proceedings of the Energy Independence Conference: Fusion Energy and Plasma Physics
[DE88-700657] 09 p1253 N88-17507
Physics modeling support contract
[DE88-004039] 10 p1335 N88-17980
Plasma physics design and major specifications of candidate reactors for FER design studies. Conceptual design study of FY86 FER
[DE88-751066] 10 p1411 N88-18416
New mode conversion process and overdense plasma heating in the electron cyclotron range of frequencies
[IPPJ-854] 10 p1411 N88-18420
Plasma theory and simulation
[DE88-003620] 10 p1414 N88-18437
Toroidal confinement research concepts evaluation and tradeoff studies
[DE88-004841] 11 p1552 N88-19285
Sixteenth AINSE Plasma Physics Conference. Conference handbook
[DE88-700625] 11 p1552 N88-19290
Summaries of FY86 research in the Applied Plasma Physics Fusion Theory Program
[DE88-004242] 11 p1554 N88-19298
Basic physics of laser-plasma interactions
[ETN-88-92055] 14 p1984 N88-21838
Magic light high-power laser passes state certification
15 p2053 N88-22236
Theoretical model of the cathode spot on a unipolar arc
[AD-A190109] 15 p2059 N88-22277
Plasmapause formation
[AERONOMICA-ACTA-A-319-1987]
15 p2138 N88-22759
A proposal for the establishment of a center of excellence in theoretical geoplasma research
[AD-A189742] 16 p2231 N88-23327
Soviet magnetic confinement fusion research
[PB88-182316] 16 p2279 N88-23644
Theoretical plasma physics research of active space experiments
[AD-A192075] 18 p2577 N88-25309
Activities report in plasma physics
[ETN-88-92221] 18 p2580 N88-25324
Fusion programs in applied plasma physics and development and technology at GA Technologies, Inc.
[DE88-008406] 20 p2856 N88-26964
Plasma technology: Preliminary studies 2
[DE88-752815] 22 p3154 N88-28763
Plasma theory and simulation
[AD-A194674] 23 p3286 N88-29565
Pierce diode with external circuit. Part 3: Chaotic behavior
[AD-A194837] 24 p3365 N88-30041
Bibliography of Soviet laser developments, number 88, March - April 1987
[AD-A195978] 24 p3378 N88-30116

PLASMA PINCH
NT SCREW PINCH
NT THETA PINCH
NT ZETA PINCH
Transverse focussing using plasma wake fields
[DE87-011503] 01 p0099 N88-10652
Numerical simulation of the Reversed Field Pinch
[AD-A184353] 04 p0491 N88-13023
Advanced concepts theory annual report 1986
[AD-A184986] 05 p0651 N88-13991
Potential benefits of a broad magnetic fusion R and D program
[DE88-003288] 11 p1553 N88-19297
X-rays from z-pinches
[AD-A188911] 12 p1696 N88-20146
X-ray source model for Z-pinch aluminum plasmas
[AD-A189509] 12 p1696 N88-20148
Activities report in plasma physics
[ETN-88-92221] 18 p2580 N88-25324
Photoconducting X-ray detectors for Z-pinch experiments
[DE88-007118] 19 p2726 N88-26199
Factors which affect operation of a plasma focus in various gases
[DE88-701882] 20 p2858 N88-26975
Theory and simulation of relaxed plasmoids
[AD-A192884] 21 p3032 N88-27997
Cosmic electric currents and the generalized Bennett pinch
[TRITA-EPP-87-14] 22 p3154 N88-28764

PLASMA POTENTIALS
Potential formation in the plasma confinement region of a radio-frequency plugged linear device
[IPPJ-843] 02 p0242 N88-11526
Confinement time of electrons and H(-)/D(-) ions in the Uramoto type sheet plasma
[IPPJ-852] 04 p0492 N88-13032
Experimental investigation of double layers formed by ion-acoustic turbulence
[INPE-4296-PRE/1167] 08 p1086 N88-16544

PLASMA POWER SOURCES
NT PLASMA ENGINES
Advanced electric propulsion and space plasma contactor research
[NASA-CR-180862] 06 p0674 N88-14126

PLASMA PROBES
NT ELECTROSTATIC PROBES
Preparation of qualification tests of a plasma generator for the feeding of a hypersonic wind tunnel
05 p0530 N88-13222
Diagnostic concept of the resonance cone technique and its application in ground and space experiments
08 p1027 N88-16222
Resonance cones in nonthermal plasmas: Laboratory experiments 08 p1027 N88-16223

PLASMA PROPULSION
Study of Plasma Motor Generator (PMG) tether system for orbit reboost
[NASA-CR-172016] 04 p0403 N88-12501
Plasma thruster development
[AD-A184173] 04 p0408 N88-12536
Interplanetary propulsion using inertial fusion
[NASA-TM-89661] 04 p0409 N88-12540
Unified study of plasma-surface interactions for space power and propulsion
[AD-A186211] 07 p0825 N88-15007
Fundamental studies on MPD thrusters
[AD-A190307] 15 p2137 N88-22753
Physical fluid mechanics in MPD thrusters
[AD-A190309] 15 p2138 N88-22754
Plasma-gas interaction studies in a hybrid plume plasma rocket
[AD-A190310] 15 p2138 N88-22755
Interplanetary propulsion using inertial fusion
17 p2401 N88-24273
A fusion based plasma propulsion system
17 p2401 N88-24274
Basic processes of plasma propulsion
[AD-A192117] 18 p2577 N88-25310
The effects of magnetic nozzle configurations on plasma thrusters
[NASA-CR-183096] 19 p2732 N88-26223
Performance and lifetime assessment of MPD arc thruster technology
[NASA-TM-101293] 24 p3336 N88-29860

PLASMA PUMPING
Pump limiter experiments and analysis in the TEXTOR tokamak 09 p1252 N88-17506
A plasma ultraviolet source for short wavelength lasers
[AD-A192844] 21 p2952 N88-27537

PLASMA RADIATION
Direct detection of optical radiation through a sampling orifice for inductively coupled plasma atomic emission spectroscopy
[DE87-013609] 01 p0101 N88-10662
Radio studies of large scale structures of the Sun's corona and transient activity 01 p0114 N88-10728
Advanced concepts theory annual report 1986
[AD-A184986] 05 p0651 N88-13991
Electrostatic VLF emission determined from rocket and satellite experiments 08 p1002 N88-16068
X-rays from z-pinches
[AD-A188911] 12 p1696 N88-20146
X-ray source model for Z-pinch aluminum plasmas
[AD-A189509] 12 p1696 N88-20148
High power, high frequency radiation from beam-plasma interactions
[AD-A190207] 15 p2137 N88-22752
X-ray emission from tokamaks
17 p2439 N88-24514
Polarization spectroscopy: Prospect and data needs
17 p2443 N88-24531
Studies of spectral line ratio fluctuations using Inductively Coupled Plasma (ICP) light
[IRF-PREPRINT-100] 18 p2578 N88-25311
Dynamics of a plasma produced under effect of the XeCl-laser radiation on metallic surface
[DE88-701983] 21 p3017 N88-27902

PLASMA RENIN ACTIVITY
U IMMUNOASSAY

PLASMA RESONANCE
Self-consistent modification of a fast tail distribution by resonant fields in nonuniform plasmas
[AD-A183790] 01 p0099 N88-10650
Effect of plasma resonance on properties of surface waves 06 p0773 N88-14749
Electron acceleration by wave processes in the earth's ionosphere
[AD-A186110] 07 p0877 N88-15320
Diagnostic concept of the resonance cone technique and its application in ground and space experiments
08 p1027 N88-16222
A generalized description of the anomalous Doppler resonance and the stabilizing role of ion dynamics
[INPE-4384-PRE/1204] 08 p1081 N88-16513
Nonlinear resonance of two-dimensional ion layers
[AD-A188890] 12 p1695 N88-20145
Parametric instabilities of inhomogeneous plasma near the lower-hybrid resonance
[DE88-701201] 15 p2137 N88-22748
Electrostatic whistler mode conversion at plasma resonance
[AD-A192951] 20 p2860 N88-26989
Role of ordinary to extraordinary mode wave coupling in ionospheric heating experiments
[AD-A195335] 24 p3362 N88-30017

PLASMA RINGS
U TOROIDAL PLASMAS

PLASMA SHEATHS
Vortex dynamics and transport to the wall in a crossed-field plasma sheath
[DE87-013286] 01 p0100 N88-10657
Three-dimensional charging effects --- spacecraft
03 p0273 N88-11720
Analytical solution of the equations for a coaxial plasma gun operating in the snowplow mode. 1. Weak coupling limit
[AD-A185370] 05 p0652 N88-13994
Observations of an ion acoustic oscillation near a pulsed sheath
[INPE-4386-PRE/1206] 08 p0979 N88-15915
Plasma theory and simulation
[DE88-003620] 10 p1414 N88-18437
Effects of secondary electron emission on the collector and source sheaths of a finite ion temperature plasma
[DE88-008930] 20 p2858 N88-26971
The influence of ionization within a plasma opening switch
[AD-A193147] 21 p3017 N88-27906
Vortex formation and particle transport in a cross-field plasma sheath
[DE88-008931] 23 p3284 N88-29553
Plasma theory and simulation
[AD-A194674] 23 p3286 N88-29565
Vortex formation and particle transport in a cross-field plasma sheath
[AD-A194838] 24 p3432 N88-30425

PLASMA SOUND WAVES
U MAGNETOHYDRODYNAMIC WAVES
U PLASMA WAVES

PLASMA SPECTRA
Transport properties of conductive polymers
[AD-A188411] 12 p1610 N88-19628
Flux coordinate studies of elongated plasmas at high Beta 12 p1694 N88-20134
Shear Alfven spectrum of analytic high-Beta equilibria
12 p1694 N88-20136
Experimental study of the role of plasma polarization on line shape in dense laboratory plasmas
[ETN-88-92001] 13 p1844 N88-21033
Stimulated Emission of Energetic Particles (SEEP)
[AD-A188724] 13 p1853 N88-21094
Some new features of plasma wave phenomena at Halley: APV-N observations --- VEGA
14 p1996 N88-21895
Energy spectra of pick-up ions recorded during the encounter of Giotto with Comet Halley
14 p1997 N88-21901

Thomson scattering for determining electron concentrations and temperatures in an inductively coupled plasma. 2: Description and evaluation of a multichannel instrument
[AD-A191324] 16 p2280 N88-23652

Ion temperature measurement with spectroscopy in JT-60 17 p2439 N88-24513

X-ray emission from tokamaks
17 p2439 N88-24514

X-ray spectroscopic diagnostics on JIPPT-IIU and HELIOTRON-E 17 p2440 N88-24515

Helium-like titanium spectra from tokamak plasmas
17 p2440 N88-24516

Spectroscopic results from JET: Some examples of data comparison and data needs 17 p2440 N88-24517

Ion temperature profile measurement using charge exchange recombination spectroscopy on JIPP T-IIU
17 p2440 N88-24518

Spectroscopic measurements of ion temperature, rotation speed and beam deposition profile on DIII-D
17 p2440 N88-24519

Forbidden transitions as ion-temperature sensitive lines 17 p2441 N88-24520

Tokamak studies of density sensitive line ratios
17 p2441 N88-24521

Density diagnostics by hydrogen line intensity ratios: Excitation cross section between excited states
17 p2441 N88-24522

Observation of injected silicon in heliotron E
17 p2441 N88-24524

Spectral diagnostics for temperature and density measurements on ATF 17 p2442 N88-24525

Intensity calibration of a VUV system by branching line pairs 17 p2443 N88-24533

Availability and quality of spectroscopic data and standards for tokamak studies 17 p2443 N88-24534

Time-resolved doubly bent crystal X-ray spectrometer
[DE88-007899] 20 p2805 N88-26637

PLASMA SPRAYING

Thermal expansion mismatch and oxidation in thermal barrier coatings 02 p0189 N88-11182

Thermal barrier coating life prediction model development 02 p0190 N88-11183

Thermal barrier coating life prediction model development 02 p0190 N88-11184

Self-lubricating coatings for high-temperature applications 09 p1119 N88-16703

Corrosion Research Center, University of Minnesota
[DE88-006681] 15 p2041 N88-22160

Protective coatings on metals, volume 10
[PB88-174461] 16 p2181 N88-23000

Government research on ceramics coating technology
16 p2184 N88-23019

Microlaminate composite structures by low pressure plasma spray deposition
[DE88-006453] 19 p2610 N88-25488

Plasma deposition: Investigations on a new approach
[ETN-88-92619] 20 p2861 N88-26992

Thermal barrier coating life-prediction model development
[NASA-CR-179507] 22 p3058 N88-28142

PLASMA STABILITY

U MAGNETOHYDRODYNAMIC STABILITY

PLASMA TEMPERATURE

State parameters of pulse-discharge plasma in xenon-filled closed tube 06 p0773 N88-14747

Laser thermal propulsion
[AD-A186407] 07 p0933 N88-15666

Asymmetric double Langmuir probe for fast and automatic measurements of plasma temperature
[DE88-004773] 10 p1414 N88-18436

Electron temperature measurements in an argon/cesium plasma diode
[AD-A188835] 12 p1695 N88-20141

Temperature estimates for a free flowing railgun plasma
[MRL-R-1054] 13 p1843 N88-21032

Summary report on the Japan-US Workshop on the Assessment of Spectroscopic Data for Temperature and Density Measurements --- plasma diagnostics
[IPPJ-861] 17 p2439 N88-24512

Spectroscopic study of heliotron E plasmas: Stark profile, CXR, poloidal rotation and carbon coating
17 p2441 N88-24523

Spectral diagnostics for temperature and density measurements on ATF 17 p2442 N88-24525

Calculation of the line shapes of radiators immersed in plasma 19 p2729 N88-26210

Energy conversion measurements in laser-sustained argon plasmas for application to rocket propulsion
[AD-A194931] 24 p3337 N88-29861

PLASMA THEORY

U PLASMA PHYSICS

PLASMA TORCHES

Plasma and ion etching for failure analysis. Part 2. The etching of plastic encapsulant and other semiconductor device materials, using the Technics Giga Etch 100-E plasma etch system
[AERE-R-12212] 09 p1177 N88-17050

Waste destruction by plasma
[SNIAS-881-430-113] 21 p2971 N88-27651

Plasma torch design codes package
[SNIAS-881-430-115] 23 p3286 N88-29569

PLASMA TURBULENCE

New directions in Vlasov plasma turbulence and anomalous transport
[DE87-014425] 02 p0238 N88-11500

Theoretical plasma physics
[DE88-001475] 04 p0492 N88-13029

Observations of turbulence and fluctuations in the solar wind 04 p0525 N88-13212

Evolution of mean square magnetic vector potential in compressible, two-dimensional, magnetofluid turbulence
[AD-A184985] 05 p0651 N88-13990

Fluctuations in frequency of coherent radio signals in solar plasma according to Venera-15 and Venera-16 data 08 p1003 N88-16079

Dynamics and turbulence of solar wind in area of its formation based on radio transmission data measured with Venera-15 and Venera-16 spacecraft
08 p1003 N88-16080

Recent results of plasma research activities at the Instituto de Pesquisas Espaciais
[INPE-4383-PRE/1203] 08 p1085 N88-16538

Double layer formed by beam driven ion-acoustic turbulence
[INPE-4292-PRE/1163] 08 p1086 N88-16543

Experimental investigation of double layers formed by ion-acoustic turbulence
[INPE-4296-PRE/1167] 08 p1086 N88-16544

Design, construction and operation of a small RFP for turbulent plasma studies
[INPE-4241-PRE/1116] 08 p1087 N88-16545

Emerging flux, magnetic reconnection, plasma turbulence and waves in the transition zone of the solar atmosphere 08 p1096 N88-16597

Conditional sampling in plasma turbulence
08 p1097 N88-16603

Microturbulent fluctuations in the TORTUR tokamak
12 p1693 N88-20131

Chaotic diffusion across magnetic field in a model of electrostatic turbulent plasma
[PREPRINT-566] 14 p1985 N88-21839

PLASMA WAVES

NT ELECTROSTATIC WAVES

Channeled particle acceleration by plasma waves in metals
[DE87-010541] 01 p0093 N88-10604

Local spectra and wave distribution functions --- space plasma
[KGI-PREPRINT-099] 01 p0100 N88-10659

The duskside plasmapause/ring current interface: Convection and plasma wave observations
[MPE-PREPRINT-93] 02 p0243 N88-11533

Current-driven lower hybrid waves at the inner edge of the ring current --- magnetosphere
[MPE-PREPRINT-94] 02 p0243 N88-11534

Energy cascading in the beat-wave accelerator
[DE87-014727] 03 p0377 N88-12374

Output power enhancement of AC Raman free-electron laser
[DE88-000503] 04 p0449 N88-12786

Ballooning modes or Fourier modes in a toroidal plasma?
[AD-A184299] 04 p0491 N88-13022

Nature and the nonlinear evolution of electrostatic waves associated with the AMPTE (Active Magnetosphere Particle Tracer Explorers) solar wind releases
[AD-A185471] 06 p0806 N88-14920

Experimental research of electron beam instability on the Doppler anomalous effect
[DE88-700565] 07 p0932 N88-15658

Current generation and induced conductivity of a plasma under common action of constant electric field and lower-hybrid or ECR waves
[DE88-700345] 07 p0935 N88-15680

Experimental evaluation for efficiency of excitation slow plasma and cyclotron waves in collective accelerators
[DE88-700566] 07 p0936 N88-15687

Observations of an ion acoustic oscillation near a pulsed sheath
[INPE-4386-PRE/1206] 08 p0979 N88-15915

Wave acceleration of auroral electrons
08 p1031 N88-16245

Experiments on ion-acoustic rarefactive solitons in a multi-component plasma with negative ions
[INPE-4393-PRE/1213] 08 p1086 N88-16542

AMPTE-UKS ion observations at a quasi-parallel bow shock 08 p1095 N88-16589

Emerging flux, magnetic reconnection, plasma turbulence and waves in the transition zone of the solar atmosphere 08 p1096 N88-16597

Small scale MHD wave processes in the solar atmosphere and solar wind 08 p1098 N88-16606

An analysis of whistler-mode radiation from the Spacelab-2 electron beam, revision
[AD-A188228] 11 p1552 N88-19287

Experimental study of scattered waves and cylindrical antenna sheaths in a microwave driven plasma
11 p1553 N88-19293

Basic physics of laser-plasma interactions
[ETN-88-92055] 14 p1984 N88-21838

The foreshock region upstream from the Comet Halley bow shock 14 p1995 N88-21893

Physical processes in the vicinity of the cometopause interpreted on the basis of plasma, magnetic field and plasma wave data measured on board VEGA-2 spacecraft --- Halley's comet 14 p1996 N88-21894

Some new features of plasma wave phenomena at Halley: APV-N observations --- VEGA
14 p1996 N88-21895

A comparison between wave observations performed in the environments of Comets Halley and Giacobini-Zinner 14 p1996 N88-21896

Wave energy flow conservation for propagation in inhomogeneous Vlasov-Maxwell equilibria
[DE88-006705] 15 p2055 N88-22251

Nonlinear effects in plasma wake field acceleration
[DE88-700972] 15 p2134 N88-22734

Plasma wave radiative damping of a new type in a relativistic one-dimensional plasma
[DE88-701191] 15 p2135 N88-22739

Parametric instabilities of inhomogeneous plasma near the lower-hybrid resonance
[DE88-701201] 15 p2137 N88-22748

Survey of the Air Force P78-2 (SCATHA) satellite plasma wave data during electron gun operations
[AD-A191014] 16 p2168 N88-22926

A plasma wave instrument on the AMPTE/IRM (Active Magnetospheric Particle Tracing Explorers/Ion Release Module) spacecraft
[AD-A191216] 16 p2233 N88-23336

Numerical research of dispersion properties of plasma cylindrical waveguides located in magnetic field
[DE87-703009] 16 p2275 N88-23615

Observation of nonlinear wave decay processes in the solar wind by the AMPTE IRM plasma wave experiment
[AD-A191409] 16 p2290 N88-23713

Activities report in plasma physics
[ETN-88-92221] 18 p2580 N88-25324

Contaminant ions and waves in the space station environment 18 p2590 N88-25393

Observations of electron cyclotron harmonic emissions associated with field-aligned electron beams
[SD-TR-87-33] 19 p2724 N88-26173

Alternative analysis of CO2-laser-produced plasma waves
[DE88-008434] 19 p2730 N88-26215

On the self-focusing of electric helicons
[DE88-701870] 20 p2848 N88-26905

Kinetic modulational instability of electron cyclotron waves in plasmas
[DE88-701893] 20 p2859 N88-26978

Drift wave vortices and anomalous transport
[DE88-009562] 20 p2859 N88-26982

Generation of Adlam-Allen waves by plasma release experiments in the solar wind
[PB88-106000] 20 p2886 N88-27140

Plasmoid propagation
[AD-A192378] 23 p3284 N88-29555

Ionospheric radio and propagation: Waves in plasmas
24 p3364 N88-30030

Characteristics of solitary waves and weak double layers in the magnetospheric plasma
[IRF-PREPRINT-105] 24 p3431 N88-30418

Reconstruction of wave distribution functions in warm plasmas
[IRF-PREPRINT-104] 24 p3431 N88-30422

PLASMA-ELECTROMAGNETIC INTERACTION

NT LASER PLASMA INTERACTIONS

Environmental interactions of solar generators in space 03 p0274 N88-11730

Laboratory simulation of the electrodynamic interactions of a tethered satellite with an ionospheric plasma
[IFSI-86-3] 08 p0961 N88-15822

Absorption of cyclotron radiation in skin layer in Araks experiment 08 p1003 N88-16076

Fluctuations in frequency of coherent radio signals in solar plasma according to Venera-15 and Venera-16 data 08 p1003 N88-16079

MAIMIK: A high current electron beam experiment on a sounding rocket from Andoya rocket range (Norway)
08 p1030 N88-16243

Wave acceleration of auroral electrons
08 p1031 N88-16245

Absorption of electron cyclotron radiation in tokamak plasmas with a superthermal tail in the electron velocity distribution [INPE-4391-PRE/1211] 08 p1086 N88-16541

Coordinated Auroral Experiments using Scatter And Rocket investigations (CAESAR investigations) [MPAE-W-47-87-13] 15 p2096 N88-22487

Influence of plasma parameters on VLF radiation in near-rocket region 24 p3448 N88-30518

PLASMA-PARTICLE INTERACTIONS

Planetary science 07 p0883 N88-15356

Electrostatic VLF emission determined from rocket and satellite experiments 08 p1002 N88-16068

Analytically modeling the carbothermic reduction of alumina in a thermal plasma [DE88-005535] 13 p1841 N88-21020

Kinetics of electrons and molecules at plasma-beam discharge in molecular gases [DE88-701196] 16 p2275 N88-23616

Developing diagnostic methods for plasma-particle interaction [DE88-007726] 20 p2858 N88-26973

Equilibrium distribution functions for limited plasma-molecular systems [DE88-702412] 21 p3018 N88-27916

PLASMAGUIDES

Numerical research of dispersion properties of plasma cylindrical waveguides located in magnetic field [DE87-703009] 16 p2275 N88-23615

PLASMAPAUSE

The duskside plasmapause/ring current interface: Convection and plasma wave observations [MPE-PREPRINT-93] 02 p0243 N88-11533

Plasmapause formation [AERONOMICA-ACTA-A-319-1987] 15 p2138 N88-22759

PLASMAS (PHYSICS)

NT ARGON PLASMA
NT BETA PARTICLES
NT BOUNDARY LAYER PLASMAS
NT CESIUM PLASMA
NT COLD PLASMAS
NT COLLISIONAL PLASMAS
NT COLLISIONLESS PLASMAS
NT COSMIC PLASMA
NT CYLINDRICAL PLASMAS
NT DENSE PLASMAS
NT DEUTERIUM PLASMA
NT ELECTRON PLASMA
NT HELIUM PLASMA
NT HIGH TEMPERATURE PLASMAS
NT HYDROGEN PLASMA
NT LASER PLASMAS
NT METALLIC PLASMAS
NT NITROGEN PLASMA
NT NONEQUILIBRIUM PLASMAS
NT NONUNIFORM PLASMAS
NT OXYGEN PLASMA
NT PLASMA FOCUS
NT RELATIVISTIC PLASMAS
NT ROTATING PLASMAS
NT SEMICONDUCTOR PLASMAS
NT SOLAR WIND
NT SPACE PLASMAS
NT SPHERICAL PLASMAS
NT STELLAR WINDS
NT STRONGLY COUPLED PLASMAS
NT THERMAL PLASMAS
NT TOROIDAL PLASMAS

Exact solutions to the governing dynamic equations of plasma armature electromagnetic railguns [DE87-014442] 01 p0011 N88-10063

Plasma properties [DE87-013662] 01 p0101 N88-10663

Heavy-particle collisions in the plasma edge [DE87-012928] 02 p0237 N88-11493

Time-resolved temperature and density measurements in ionizing, uniformly irradiated UV-laser-produced plasmas [DE87-014649] 02 p0238 N88-11504

Two dimensional neutral transport analysis in tokamak plasma [DE87-752984] 02 p0239 N88-11510

Progress in stellarator/heliotron research, 1981-1986: Executive summary [DE88-000017] 02 p0241 N88-11519

Wavepacket propagation and current startup near the lower hybrid frequency in the torus [IPPJ-840] 02 p0242 N88-11529

Volume produced H(-),D(-) ion source for proton accelerator and thermo-nuclear fusion research by sheet plasma (III) [IPPJ-838] 02 p0242 N88-11531

Hollow cathode plasma coupling study, 1986 [NASA-CR-171985] 03 p0309 N88-11949

Helicity dissipation in the plasma edge [DE87-014762] 03 p0378 N88-12376

Analytic model of an imploding Z-pinch plasma colliding inelastically with a thin-shelled cylindrical target [DE88-000051] 03 p0378 N88-12379

Confinement time of electrons and H(-)/D(-) ions in the Uramoto type sheet plasma [IPPJ-852] 04 p0492 N88-13032

Monte Carlo analysis of neoclassical transport for a compact helical system [IPPJ-850] 04 p0492 N88-13033

Proceedings of the Japan-US Workshop P-92 on Plasma Material Interaction/High Heat Flux Data Needs for the Next Step Ignition and Steady State Devices [DE87-013568] 04 p0494 N88-13042

Review of X-ray spectroscopy from laser-produced plasmas [DE88-000755] 04 p0494 N88-13043

PISCES: Plasma-surface interactions and materials research [DE88-001323] 04 p0494 N88-13044

Radio continuum emission from the ionized stellar winds of the cool supergiants in zeta Aurigae-like systems 04 p0514 N88-13160

Theoretical atomic and molecular physics [DE88-001625] 05 p0649 N88-13974

Reversed field pinch plasmas with various boundary conditions [DE88-000832] 05 p0653 N88-14004

Flight model discharge system [AD-A185657] 06 p0673 N88-14122

Global convection patterns in the high latitude [AD-A185794] 06 p0743 N88-14571

State parameters of pulse-discharge plasma in xenon-filled closed tube 06 p0773 N88-14747

Self-alignment of ions drifting in plasma 06 p0774 N88-14752

Atlas of atomic spectral lines of neptunium emitted by an inductively coupled plasma [DE88-000640] 06 p0782 N88-14796

Edge plasmas and plasma/wall interactions in an ignition-class reversed field pinch [DE88-001825] 06 p0782 N88-14799

Plasma parameters for alternate operating modes of TIBER-2 [DE88-001890] 06 p0783 N88-14802

Modeling of thermal effects on TIBER 2 (Thermal Ignition/Burn Experimental Reactor) divertor during plasma disruptions [DE88-001893] 06 p0783 N88-14805

Comments on the theory of absolute and convective instabilities [PB87-124624] 06 p0783 N88-14808

Free-boundary equilibrium problem for helically symmetric plasmas [DE88-700101] 07 p0934 N88-15674

Interaction between a module cluster and a plasma in a magnetic field [PB87-148276] 07 p0934 N88-15675

The effect of propane on atomic spectrometric signals in the direct current plasma [DE88-002457] 07 p0934 N88-15676

TiN coatings on M2 steel produced by plasma assisted chemical vapor deposition [DE88-003189] 08 p0970 N88-15867

Relation of wave energy and momentum with the plasma dispersion relation in an inhomogeneous plasma [DE88-002305] 08 p1084 N88-16530

Magnetically insulated ion diode with a gas-breakdown plasma anode [INPE-4382-PRE/1202] 08 p1085 N88-16537

Advanced studies of integrable systems [AD-A186792] 09 p1151 N88-16895

Two-dimensional analysis for a scrapeoff and divertor regions with an MHD model. Conceptual design study of FY86 FER [DE88-751069] 09 p1251 N88-17497

The approach to equilibrium in a quark-gluon plasma [DE88-002117] 09 p1251 N88-17499

Total and partial cross sections for electron capture for C(q+) (q=6-2) and O(q+) (q=8-2) ions in collisions with H, H2 and He atoms [IPPJ-AM-56] 09 p1252 N88-17501

Optimization of volume produced H(-) ions in a low-pressure hydrogen plasma [IPPJ-853] 09 p1252 N88-17505

Optimization of outlet channel of plasma ion source [DE88-700471] 10 p1410 N88-18415

Investigations of stimulated Raman scattering from high density underdense plasmas irradiated by a 0.35 micron laser 10 p1411 N88-18421

The numerical simulation of accelerator components [DE87-011597] 10 p1412 N88-18423

The deposition rate dependence of plasma polymerization on the radius of curvature of the substrate [DE88-003811] 10 p1412 N88-18429

Zero temperature quark matter equation of state [DE88-003408] 10 p1422 N88-18496

Spectral line-broadening codes for hydrogen-, helium- and lithium-like ions in plasmas [DE88-005238] 11 p1552 N88-19289

Plasma deposition of silicon carbide thin films [AD-A188093] 11 p1556 N88-19314

Gas phase reactions of electrons, negative ions and free-radicals with transition metal complexes 11 p1560 N88-19339

Characterization of PEOS (Plasma Erosion Opening Switch) plasma parameters and conduction phase properties [AD-A189024] 12 p1624 N88-19714

Proceedings of US-Japan Heliotron-Stellarator Workshop, volume 4 [DE88-004787] 12 p1693 N88-20126

Plasma rotation in a tokamak [DE88-700855] 12 p1693 N88-20128

Acoustic phonons, surface plasmons and surface acoustic plasmons in a superlattice and their nonreciprocal device applications [AD-A188918] 12 p1698 N88-20163

Propagator solutions of partial differential equations applied to plasma transport [DE88-006432] 13 p1816 N88-20852

Interaction of a strong vortex with decaying turbulence [DE88-007102] 14 p1911 N88-21420

Alfven waves in plasma with finite ion temperatures 14 p1972 N88-21769

Three-wave parametric resonance in plasma of relativistic electron flux 14 p1972 N88-21772

Pulse duration control of XeCl*-laser by means of plasma shutter 14 p1973 N88-21774

Analytic solutions to dynamic equations of plasma armature railguns [DE88-006842] 15 p2023 N88-22057

Analysis of anomalous resistivity during the conduction phase of the plasma erosion opening switch [DE88-006382] 15 p2061 N88-22286

Magnetic fusion energy plasma interactive and high heat flux components. Volume 5: Technical assessment of critical issues in the steady state operation of fusion confinement devices [DE88-006920] 15 p2136 N88-22744

Measurements of edge turbulence with Langmuir probes in currentless Heliotron E plasmas [DE88-752313] 16 p2275 N88-23617

Some aspects of the unified model of non-ideal high-parameter plasmas: Electron EOS and conduction coefficients 16 p2277 N88-23632

Coronal fluid-dynamics in laser fusion 16 p2278 N88-23634

Self-similar expansions in ion beam fusion 16 p2278 N88-23635

Finite ion-relaxation and nonequilibrium radiation effects on laser-driven implosions 16 p2278 N88-23636

Research on anode plasma behavior of flashover pulsed ion sources 16 p2279 N88-23640

Time-resolved spectroscopic measurement of anode plasma in magnetically-insulated diode 16 p2279 N88-23641

On selfsimilar thermonuclear ignition of a plasma in necks of zeta devices [DE88-701640] 16 p2280 N88-23647

Space plasma contactor research, 1987 [NASA-CR-182148] 16 p2280 N88-23649

Thomson scattering for determining electron concentrations and temperatures in an inductively coupled plasma. 1: Assessment of the technique for a low-flow, low-power plasma [AD-A191323] 16 p2280 N88-23651

Thomson scattering for determining electron concentrations and temperatures in an inductively coupled plasma. 2: Description and evaluation of a multichannel instrument [AD-A191324] 16 p2280 N88-23652

On the magnetic structure and energy balance of EUV-emitting plasma in the quiet Sun 17 p2452 N88-24567

Theoretical plasma physics research of active space experiments [AD-A192075] 18 p2577 N88-25309

Theoretical investigations of drift waves in a magnetic quadrupole 18 p2578 N88-25312

Stochasticity in a Q-machine plasma 18 p2578 N88-25315

Plasma neutralizer work at BNL (Brookhaven National Laboratory) [DE88-007046] 18 p2579 N88-25317

Self shielding of surfaces irradiated by intense energy fluxes
[DE88-007094] 18 p2579 N88-25318

Optical diagnostics for a high power, rf-inductively coupled plasma
[DE88-007822] 18 p2579 N88-25322

Microlaminate composite structures by low pressure plasma spray deposition
[DE88-006453] 19 p2610 N88-25488

Accelerator research studies
[DE88-008236] 19 p2726 N88-26187

Simultaneously time- and space-resolved spectroscopic characterization of laser-produced plasmas
[DE88-008038] 19 p2728 N88-26202

Electron-acoustic waves in a beam-plasma system
[DE88-702053] 19 p2729 N88-26207

Inner-shell X-ray line spectra of highly ionized titanium, chromium, iron and nickel and their appliation to laboratory plasmas
[PB87-225181] 19 p2730 N88-26212

Vaporization studies of plasma interactive materials in simulated plasma disruption events
[DE88-010100] 19 p2731 N88-26222

Why plasma armature railguns don't work (and what can be done about it)
[DE88-007900] 20 p2763 N88-26384

Proceedings of the 2nd US-Japan Workshop on Advanced Plasma Modeling, volume 3
[IPPJ-867] 20 p2855 N88-26957

A Vlasov ion zero mass electron model for plasma simulations 20 p2855 N88-26958

Modeling of subtle kinetic processes in plasma simulation 20 p2856 N88-26959

Effects of secondary electron emission on the collector and source sheaths of a finite ion temperature plasma
[DE88-008930] 20 p2858 N88-26971

On the self-trapping of an electromagnetic wave in magnetized plasma
[DE88-701872] 20 p2858 N88-26974

Plasma separation process. Betacell (BCELL) code, user's manual
[DE88-006955] 20 p2859 N88-26981

Impurity transport calculations for a drift-dependent tokamak scrape-off plasma
[DE88-010053] 20 p2859 N88-26984

MACH2: A two-dimensional magnetohydrodynamic simulation code for complex experimental configurations
[AD-A192285] 20 p2860 N88-26988

Electrostatic whistler mode conversion at plasma resonance
[AD-A192951] 20 p2860 N88-26989

Plasma treatment of polymers for improved adhesion
[DE88-011623] 21 p2921 N88-27334

Ion Bernstein modes in current-carrying plasmas
21 p3017 N88-27903

Tokamak magnetic turbulence over the safety factor range 0.6 less than q less than 3
[DE88-008421] 21 p3017 N88-27904

The influence of ionization within a plasma opening switch
[AD-A193147] 21 p3017 N88-27906

Effects of low reflection on the collector and source sheaths of a finite ion temperature plasma
[DE88-008929] 21 p3017 N88-27908

Reminimization of energy integral and stability limit for non-ideal MHD (magnetohydrodynamic) plasma
[DE88-008422] 21 p3018 N88-27911

Global and local magnetohydrodynamic relaxations
[DE88-752602] 21 p3018 N88-27913

Design of divertor plate and measurements of double-null open divertor plasma in the JFT-2M tokamak
[DE88-753130] 21 p3018 N88-27914

Design of divertor plate and measurements of double-null open divertor plasma in the JFT-2M tokamak
[DE88-753130] 21 p3018 N88-27914

Analysis of lower hybrid current drive and rampup experiments on the JT-60 tokamak
[DE88-753136] 21 p3018 N88-27915

Electromagnetic wave incoherent reflection by a half-space of weakly-ionized plasma with an absorbing boundary
[DE88-702413] 21 p3019 N88-27917

Energy distribution and transfer in flowing hydrogen microwave plasmas 21 p3019 N88-27919

Activities report of the Institute for Extraterrestrial Physics
[MPE-206] 21 p3029 N88-27981

Measurement of macroscopic electric fields in solar plasma structures
[AD-A193291] 21 p3031 N88-27993

Theory and simulation of relaxed plasmoids
[AD-A192884] 21 p3032 N88-27997

Effect of a laser field in the electron inelastic scattering into plasma fields
[DE88-702295] 23 p3218 N88-29157

Waves and instabilities in an electron-positron plasma in an ultra-strong magnetic field
23 p3283 N88-29551

Fusion product spectra
[DE88-010912] 23 p3284 N88-29554

Nonlinear analysis of non-neutral plasmas
[AD-A192506] 23 p3284 N88-29556

Bootstrap currents in radio-frequency-driven tokamak equilibria
[DE88-011136] 23 p3285 N88-29561

Collector and source sheaths of a finite ion temperature plasma
[DE88-008934] 23 p3286 N88-29564

Millimeter wave generation by relativistic electron beams
[AD-A195683] 24 p3362 N88-30016

Autoionization for lower level detrapping in X-ray lasers
[AD-A195845] 24 p3379 N88-30123

Particle trajectories and potentials in a plane sheath moving in a magnetoplasma
[AD-A196226] 24 p3390 N88-30190

Ion kinetics in silane plasmas
[AD-A196202] 24 p3431 N88-30423

Ring current role in dynamics of fluctuating electron and ion fluxes in low-latitude magnetosphere
24 p3447 N88-30514

Plasma of earth's magnetosphere ring currents. Model compared with results of AMPTE/CCE experiment
24 p3447 N88-30515

PLASMASPHERE

Ionosphere and plasmasphere
03 p0272 N88-11709

Area of reduced electron concentration in terrestrial plasmasphere 08 p1003 N88-16078

Application of correlation method of reception of direct and reflected cosmic radiation to study of plasmaspheres of planet and distribution of radiation brightness
08 p1004 N88-16085

USU (Utah State University) Center of Excellence in Theory and Analysis of the Geo-Plasma Environment
[AD-A187687] 11 p1511 N88-19026

Observation of nonlinear wave decay processes in the solar wind by the AMPTE IRM plasma wave experiment
[AD-A191409] 16 p2290 N88-23713

Field-aligned structure of the storm time Pc 5 wave of November 14-15, 1979
[AD-A193022] 21 p2972 N88-27653

PLASMOIDS

U PLASMAS (PHYSICS)

PLASMONS

Plasmon resonance absorption in layered structures of silver with periodic corrugation
[DE87-013183] 02 p0231 N88-11453

A theoretical study of enhanced Smith-Purcell radiation from a bigrating
[AD-A184530] 03 p0329 N88-12080

A surface plasmon waveguide sensor: A new type of chemical transducer based on optical phenomena
[ETN-88-91322] 06 p0780 N88-14792

On the coexistence of phonon and non-phonon (plasmon) mechanisms in new high T/sub c/ superconductors
[DE88-003188] 07 p0938 N88-15703

Photoacoustic studies of surface plasmons in metallic microstructures
[DE88-004423] 11 p1460 N88-18703

Acoustic phonons, surface plasmons and surface acoustic plasmons in a superlattice and their nonreciprocal device applications
[AD-A188918] 12 p1698 N88-20163

Enhancement of second harmonic generation on silver gratings by resonant excitation of surface plasmon
[ETN-88-92304] 17 p2439 N88-24509

Extended and local plasmons in a lateral superlattice
20 p2870 N88-27041

Fundamental optical studies of competitive adsorption and thin film phenomena
[DE88-006780] 20 p2875 N88-27068

Solar energy conversion through the interaction of plasmons with tunnel junctions. Part A: Solar cell analysis. Part B: Photoconductor analysis
[NASA-CR-183044] 21 p2967 N88-27621

Bulk plasmon enhanced photoemission from Nb(100) surface resonances
[AD-A192711] 22 p3154 N88-28767

Optical emission from surface waves supported in thin metal films 23 p3282 N88-29540

System suitable for observing surface plasmon in a semi-infinite semiconductor superlattice
[DE88-702686] 23 p3293 N88-29606

PLASTIC AIRCRAFT STRUCTURES

Advanced organic composite materials for aircraft structures: Future program
[NASA-CR-181467] 06 p0678 N88-14155

Investigations on the modification of structural reliability by substitution of aluminum by carbon fiber reinforced plastics in aircraft construction
[ILR-MITT-195] 24 p3339 N88-29877

PLASTIC ANISOTROPY

NT ELASTIC ANISOTROPY

PLASTIC COATINGS

Vibration-absorbing characteristics of metal-polymer shells 02 p0158 N88-10991

Water disbondment characterization of organic Coating/metal substrate systems
[AD-A184847] 05 p0567 N88-13454

Plasma and ion etching for failure analysis. Part 2. The etching of plastic encapsulant and other semiconductor device materials, using the Technics Giga Etch 100-E plasma etch system
[AERE-R-12212] 09 p1177 N88-17050

Cleanability of aircraft polyurethane topcoats
[AD-A193456] 23 p3170 N88-28878

PLASTIC DEFORMATION

Superplastic deformation and post forming tensile properties of Ti-6Al-4V sheet
[RAE-TR-86015] 01 p0023 N88-10144

Large-strain softening of aluminum at elevated temperature
[DE87-011559] 01 p0024 N88-10153

Applications of dislocation theory to crack growth problems 02 p0190 N88-11188

Spread of plastic deformation in notched and cracked plates 03 p0337 N88-12122

Plastic strain localization between voids in shear deformation fields 04 p0427 N88-12648

Plasticity of aluminum and iron at high shear strain rate and high pressure 05 p0563 N88-13430

Tribology of thin film systems
[ETN-88-91365] 05 p0590 N88-13601

Surface deformation and fatigue crack initiation of alpha-iron 05 p0598 N88-13651

X-ray fatigue failure prediction based on plasticity response to microcracks 05 p0607 N88-13725

Thermometrical investigations on the near threshold fatigue crack propagation behavior
06 p0717 N88-14400

A critical review of the development of several viscoplastic constitutive theories
[AD-A185652] 07 p0867 N88-15262

On the relations between cyclic contraction ratio flowstress and deformation mechanisms in bainitic CrMoV steels
[DE87-753043] 08 p0968 N88-15856

The relationship of tensile specimen size and geometry effects to unique constitutive parameters for ductile materials
[AD-A186020] 08 p0994 N88-16012

Stability and metastability in semiconductor strained-layer structures
[DE88-003308] 09 p1258 N88-17544

Institute for Materials Science and Engineering, Fracture and Deformation Division: Technical activities, 1987
[PB88-153622] 10 p1345 N88-18039

Stress corrosion cracking and metal-induced embrittlement: Comparative studies of local chemistries
[DE88-003235] 13 p1742 N88-20419

Influence of hydrogen on crack formation tendency in heat-affected zone with stress concentrator
14 p1887 N88-21276

An internal variable constitutive model for the large deformation of metals at high temperatures
14 p1929 N88-21503

On the global/local time incrementing for viscoplastic analysis 14 p1932 N88-21519

Finite element (MARC) solution technologies for viscoplastic analyses 15 p2078 N88-22389

Phenomenological modelling of rate-dependent plasticity for high strain rate problems
[DE88-006647] 15 p2087 N88-22440

The mechanical behavior of particle filled thermoplastics
[ETN-88-92234] 16 p2181 N88-22999

The influence of the chemical nature of resins on their reticulation kinetics and the consequences for their nonelastic mechanical properties
[ETN-88-92539] 18 p2493 N88-24788

On the abnormal phenomena observed in the electrical resistivity measurement during the decomposition process of saturated Cu-Fe alloys
[NASA-TT-20183] 18 p2507 N88-24869

Dynamic shear band development in plane strain
[AD-A190915] 18 p2526 N88-24988

Plastic deformation and roughness of free metal surfaces
[PB88-196621] 20 p2772 N88-26439

Shape memory alloys: New materials for future engineering
[NASA-TT-20193] 20 p2775 N88-26455

Fatigue of lithium-aluminum alloys: An example of localization of the plastic deformation
[ETN-88-92309] 20 p2775 N88-26456
On the possibility of the soliton description of acoustic emission during plastic deformation of crystals
[DE88-701878] 20 p2876 N88-27075
Ultrasonic studies of stresses and plastic deformation in steel during tension and compression
[AD-A192306] 21 p2912 N88-27280
Analysis of grain refinement and superplasticity in aluminum-magnesium alloys
[AD-A193029] 21 p2912 N88-27283
Plastic yielding at crack tips
[AD-A192549] 21 p2960 N88-27582
Results on the influence of crack tip plasticity during dynamic crack growth
[AD-A193460] 23 p3225 N88-29194
Anisotropic constitutive modeling for nickel-base single crystal superalloys
[NASA-CR-182157] 24 p3353 N88-29961
State variable approach to deformation phenomena in Face Centered Cubic (FCC) metals
[VTT-44] 24 p3354 N88-29964
Response of SMA (Shielded Metal Arc) and narrow gap HY80 weldments to explosive shock loading
[AD-A195994] 24 p3385 N88-30162

PLASTIC FILMS
U POLYMERIC FILMS

PLASTIC FLOW
Relaxation of metastable semiconductor strained-layer structures by plastic flow
[DE88-002729] 08 p1090 N88-16560
On stress collapse in adiabatic shear bands
[AD-A187185] 11 p1498 N88-18942
Elasto-plastic analysis using a stress-based finite element method and an endochronic theory of plasticity
[DE88-003001] 15 p2075 N88-22372
Plastic flow and failure modeling under high strain rate loading
[AD-A194223] 23 p3226 N88-29199

PLASTIC MEMORY
Shape memory alloys: New materials for future engineering
[NASA-TT-20193] 20 p2775 N88-26455

PLASTIC PLATES
The nonlinear dynamic response of an elastic-plastic thin plate under impulse loading
[AD-A182147] 08 p0994 N88-16013

PLASTIC PROPELLANTS
Effect of moisture level in PBXW-109(E) (plastic-bonded explosive) mixes on the aging of the cured explosive
[AD-A190200] 15 p2048 N88-22202

PLASTIC PROPERTIES
NT ELASTOPLASTICITY
NT SUPERPLASTICITY
NT THERMOPLASTICITY
NT VISCOPLASTICITY
NT YIELD POINT
Relation between shock strength and strain-rate plasticity at maximum deviatoric stress
[DE87-011736] 01 p0061 N88-10390
Functional plasticity of the nervous system of vertebrates 01 p0074 N88-10474
3D inelastic analysis methods for hot section components 02 p0187 N88-11164
Plasticity of fibrous composites
[AD-A184637] 03 p0280 N88-11765
The behavior of plastic, ceramic masses in compression tests
[ETN-87-90603] 03 p0292 N88-11836
Surface deformation and fatigue crack initiation of alpha-iron 05 p0598 N88-13651
Embrittling effect of the plastic zone
05 p0607 N88-13721
A comparison of plastic work energy and external input for fatigue crack propagation 05 p0607 N88-13722
An overview of metal plasticity
[DE88-001658] 06 p0681 N88-14175
Absolute fatigue thresholds in metallic materials
06 p0717 N88-14399
The effects of loading history on fatigue crack growth threshold 06 p0718 N88-14406
Crack closure phenomena in modes 1 and 2 interactions 06 p0719 N88-14417
Dependence of strainrange partitioned fatigue life at elevated temperature on monotonic stress-strain properties 06 p0721 N88-14428
Axial creep-fatigue damage assessment in type 316 SS material 06 p0721 N88-14430
Function-dependent plasticity in the nervous system
07 p0886 N88-15377
Interrelation and measurement of formability, strengthening, and thermomechanical processing under metalworking conditions
[DE88-002485] 08 p0967 N88-15850
Fully plastic analysis of mixed mode plane-strain crack problems
[PB87-144929] 08 p0994 N88-16015
Application of inverse gas chromatography to fluidity studies
[DE88-002896] 10 p1296 N88-17750
Applications of energy density theory in cyclic plasticity
[AD-A186947] 10 p1342 N88-18023
Computed stress and strain distributions under interference fit and after coldworking
[AD-A186950] 10 p1342 N88-18024
Materials Research Laboratory at Brown University
[AD-A188006] 13 p1739 N88-20396
Microplasticity phenomena in graphite/magnesium metal matrix composites
[DE88-006772] 15 p2029 N88-22086
Elasto-plastic analysis using a stress-based finite element method and an endochronic theory of plasticity
[DE88-003001] 15 p2075 N88-22372
Measurement of the elastic-plastic surface flaw back surface topology and its relation to constraint
[DE88-006765] 15 p2087 N88-22437
Fatigue crack growth under full-scale cyclic plasticity
[DFVLR-FB-87-48] 16 p2222 N88-23263
Characterization of elastic-plastic properties of AS4/APC-2 thermoplastic composite
[NASA-CR-183145] 21 p2906 N88-27242
Thermomechanical processing of Al alloy 2090 for grain refinement and superplasticity
[AD-A192333] 21 p2912 N88-27281
An endochronic rate-sensitive constitutive equation for metals, application to generalized creep and large deformations
[AD-A194167] 22 p3055 N88-28125
Theory of acoustoplasticity and ultrasonic measurements of residual stresses
22 p3087 N88-28328

PLASTIC YIELDING
U PLASTIC DEFORMATION

PLASTICITY
U PLASTIC PROPERTIES

PLASTICIZERS
NMR (Nuclear Magnetic Resonance) imaging for detecting binder/plasticizers in green-state structural ceramics
[DE88-003111] 10 p1304 N88-17800
Reactive plasticizers in negative E-beam resists
[AD-A195161] 24 p3368 N88-30056

PLASTICS
NT ACRYLIC RESINS
NT CARBON FIBER REINFORCED PLASTICS
NT EPOXY RESINS
NT GLASS FIBER REINFORCED PLASTICS
NT KEVLAR (TRADEMARK)
NT NYLON (TRADEMARK)
NT PEEK
NT PHENOLIC RESINS
NT POLYAMIDE RESINS
NT POLYBUTADIENE
NT POLYETHER RESINS
NT POLYETHYLENES
NT POLYMETHYL METHACRYLATE
NT POLYPROPYLENE
NT POLYSTYRENE
NT POLYTETRAFLUOROETHYLENE
NT POLYVINYL ALCOHOL
NT POLYVINYL CHLORIDE
NT POLYVINYL FLUORIDE
NT REINFORCED PLASTICS
NT SYNTHETIC RESINS
NT TEFLON (TRADEMARK)
NT THERMOPLASTIC FILMS
NT THERMOPLASTIC RESINS
NT THERMOSETTING RESINS
NT VINYL COPOLYMERS
Requirements for a test stand for plastic rollers for the verification of nonequilibrium force laws
[ILR-MITT-176] 01 p0008 N88-10040
Anti-abrasion protection with highly organized materials
[DE87-014238] 01 p0029 N88-10187
Cure and properties of thermosetting polymers
[AD-A184669] 03 p0293 N88-11843
Polymer material for heat sensors
06 p0676 N88-14142
TMA-microrheological testing of polymers (thermomechanical analysis)
[PB87-228805] 06 p0683 N88-14187
Waves and vibrations in elastic superlattice composites 06 p0776 N88-14765
Selection of polymer materials for manufacturing optical parts
[AD-A185898] 07 p0836 N88-15069
Correlation between flammability and heat of combustion of polymers
[NASA-TT-20116] 08 p0973 N88-15884
Lithium/polymer electrolyte interfacial instability
[AD-A187164] 09 p1147 N88-16874
Flame retardants
[NASA-TT-20250] 13 p1739 N88-20400
Kinetics of polymer decomposition
[DE88-005500] 13 p1749 N88-20460
Solid hosts for dye laser rods. Part 1: Criteria for choosing a host material
[DE88-006478] 15 p2072 N88-22355
Soft-ground aircraft arresting systems
[AD-A190838] 16 p2165 N88-22912
Small-scale cleavage test of polymer products
[PB88-165360] 16 p2181 N88-23001
Differential technology in plastics industries differentiation in combination technology nonflammability technology
[NASA-TT-20256] 18 p2494 N88-24797
Statistical mechanics of polymer systems
[DE88-011172] 20 p2778 N88-26477

PLASTISOLS
NT SMOKE

PLATE (METAL)
U METAL PLATES

PLATE THEORY
An exact theory of elastic plates
[ETN-87-90675] 01 p0062 N88-10396
Correction to a single higher order theory of elastic plates
[ETN-87-90676] 01 p0062 N88-10397
The nonlinear dynamic response of an elastic-plastic thin plate under impulse loading
[AD-A182147] 08 p0994 N88-16013
Transient sound radiation from infinite thin plate
[ARE-TM(UHA)-87508] 09 p1243 N88-17449
An efficient Mindlin finite strip plate element based on assumed strain distribution 15 p2081 N88-22407
A generalized variational method for solving stress intensity factors at cracks on the edge of holes in orthotropic plates
[IC-AERO-87-02] 17 p2348 N88-23992
Improved finite strip Mindlin plate bending element using assumed shear strain distributions
[NASA-TM-100928] 23 p3225 N88-29

PLATEAUS
NT GREAT BASIN (US)
NT PIEDMONTS
The tectonic setting of the Seychelles, Mascarene and Amirante Plateaus in the Western Equatorial Indian Ocean 24 p3396 N88-30225

PLATES
Analysis of compressible flow on high-velocity jet penetration 03 p0302 N88-11898
Spread of plastic deformation in notched and cracked plates 03 p0337 N88-12122
Damping characteristics of a composite-reinforced stainless-steel plate
[DE88-000303] 04 p0457 N88-12828
Fracture-resistant characteristics of medium-strength plates with regard to the initiation, stable and unstable propagation of surface cracks
[PB87-144804] 08 p0996 N88-16025
Optimum design of geodesically stiffened composite plates
[NASA-CR-182499] 10 p1344 N88-18035
Transient dynamics of fibre reinforced composite plates
[IIT-B/CE/RR/87-1] 13 p1734 N88-20370
An experimental investigation of decelerating flow about two-dimensional cambered plates
[DE88-006598] 13 p1766 N88-20567
Finite element methodology for nonlinear free and harmonic forced vibrations of beam and plate structures
13 p1782 N88-20663
The analysis of non-linear dynamic behavior (including snap-through) of postbuckled plates by simple analytical solution
[NASA-TM-89165] 15 p2087 N88-22439
Stress-intensity factors for small surface and corner cracks in plates
[NASA-TM-100599] 15 p2088 N88-22445
Nonlinear vibrations of periodically stiffened plates
21 p2963 N88-27596

PLATES (STRUCTURAL MEMBERS)
NT ANISOTROPIC PLATES
NT ANNULAR PLATES
NT CIRCULAR PLATES
NT CORRUGATED PLATES
NT ELASTIC PLATES
NT END PLATES
NT METAL PLATES
NT ORTHOTROPIC PLATES
NT PERFORATED PLATES
NT PLASTIC PLATES

NT POROUS PLATES
NT RECTANGULAR PLATES
NT REINFORCED PLATES
Theoretical investigation of stress concentrations in damaged carbon fibre reinforced plastic plate structures. Volume 1: Main text
[BR99872-VOL-1] 03 p0280 N88-11761
Compactness of quasi-conforming element spaces, convergence of quasi-conforming element method
03 p0301 N88-11896
Damping analysis of flexural waves in fluid-loaded single and constrained plates
[AD-A185116] 05 p0609 N88-13739
Viscous drag reduction of horizontal plates
[VKI-TN-159] 07 p0851 N88-15171
A method for the approximate calculation of the skin friction coefficient of horizontal wavy plates
[VKI-TN-160] 07 p0851 N88-15172
Experimental investigation of damping characteristics of bolted structural connections for plates and shells
[AD-A186075] 07 p0867 N88-15259
Numerical solution methods for viscoelastic orthotropic materials
[NASA-CR-182381] 08 p0971 N88-15874
Stress strain fields at crack tip and stress intensity factors in Reissner's plate
[PB87-144945] 08 p0994 N88-16014
A nonlinear computational model for the strength and failure of composite plates and shells
11 p1501 N88-18964
Discrete vortex analysis of unsteady flow about two-dimensional cambered plates
[DE88-006597] 14 p1909 N88-21407
Transient analysis of a plate on an elastic foundation under a moving load 19 p2680 N88-25933
Hole diameters in plates impacted by projectiles
21 p2929 N88-27386
Power flow analysis of two coupled plates with arbitrary characteristics
[NASA-CR-183165] 22 p3075 N88-28251
Tripping of stiffened plates using a refined beam theory
[AD-A193989] 22 p3087 N88-28333

PLATES (TECTONICS)
The interpretation of crustal dynamics data in terms of plate motions and regional deformation near plate boundaries
[NASA-CR-181475] 03 p0349 N88-12205
Earthquake source mechanisms and transform fault tectonics in the Gulf of California
03 p0349 N88-12206
RRS DISCOVERY Cruise 161, 15 August (227)-19 September (262) 1986. Portuguese Ocean-continent boundary, plate boundaries west of Iberia and seismic structure of sediments off Madeira
[PB87-222006] 06 p0747 N88-14596
State-of-the-art for assessing earthquake hazards in the United States. Report 26: Parameters for specifying magnitude-related earthquake ground motions
[AD-A185997] 07 p0877 N88-15319
Relationship between oceanic geological formations and tectonic structures 13 p1785 N88-20683
The interpretation of crustal dynamics data in terms of plate interactions and active tectonics of the Anatolian Plate and surrounding regions in the Middle East
[NASA-CR-183024] 18 p2543 N88-25092
Geologic results obtained from the use of SPOT imagery along plate boundaries: Examples in the East African rift and of the northern-Caribbean collision
22 p3105 N88-28437
Intraplate deformation, stress in the lithosphere and the driving mechanism for plate motions
[NASA-CR-183121] 23 p3231 N88-29231
The tectonic setting of the Seychelles, Mascarene and Amirante Plateaus in the Western Equatorial Indian Ocean 24 p3396 N88-30225
Ridge-trench collision in Archean and Post-Archean crustal growth: Evidence from southern Chile
24 p3397 N88-30233
Continental growth through time by underplating of subducted oceanic crust: Evidence from kimberlites in South Africa and SW Pacific 24 p3399 N88-30244
Gravity anomalies, plate tectonics and the lateral growth of Precambrian North America 24 p3400 N88-30248
Solid earth as a recycling systems and the lateral growth of Precambrian North America 24 p3400 N88-30249
Crustal underplating in the North American Craton: Evidence from the Petrogenesis of anorthositic rocks in the Middle Proterozoic Midcontinent Rift System
24 p3400 N88-30252

PLATING
NT ELECTROPLATING
NT ION PLATING
NT NICKEL PLATE
Equations for determining CVD tungsten-rhenium alloy composition and plating rate
[DE87-008831] 01 p0024 N88-10152
Corrosion resistance of silver-plated carbon-aluminum composite 03 p0285 N88-11793
The analysis of metal finishing solutions by ion chromatography
[AD-A184812] 05 p0561 N88-13414
Analysis of nickel sulphamate bath using charging current compensated D.C. polarography
[NAL-TM-MT-8705] 05 p0564 N88-13433
Hydrogen embrittlement of gun steel
[AD-A188972] 13 p1740 N88-20407
Durability testing of an iridium-plated storable rocket engine injector
[AD-A190707] 15 p2027 N88-22078
Determination of aquo-complexes of chromium and iron in chromium plating and polishing solutions by ion chromatography
[AD-A190168] 15 p2039 N88-22148
Technical feasibility study of applying auto-control methods to plating process solutions
[DE88-008014] 19 p2641 N88-25670
Fabrication of a flexible conductor by vapor deposition
[DE88-007500] 19 p2661 N88-25826
A rapid electrochemical technique for determining the current efficiency for cadmium plating
[AD-A193679] 22 p3056 N88-28130

PLATINUM
NT PLATINUM ISOTOPES
Compatability of dispersion-strengthened platinum with resistojet propellants
[NASA-TP-2765] 04 p0409 N88-12538
Characterization of catalysts with metal-support effects and of the species adsorbed on their surfaces
[DE87-014636] 04 p0414 N88-12564
Determination, by X-ray fluorescence, of platinum, palladium, ruthenium, iron and chromium in special steels
[PB87-132114] 06 p0683 N88-14183
NBS (National Bureau of Standards) measurement services: Platinum resistance thermometer calibrations
[PB88-138367] 10 p1333 N88-17967
Order-disorder transition of Au and Pt (110) surfaces: The significance of relaxations and vibrations
[DE88-004651] 10 p1419 N88-18473
The effect of oriented defects on long-range ordering of hydrocarbon films: Azulene on Pt(111)
[AD-A196089] 24 p3344 N88-29904

PLATINUM ISOTOPES
Experimental and theoretical investigations of isotope shift and hyperfine structure on 5d elements (especially platinum, iridium and rhenium)
[ETN-88-93121] 24 p3353 N88-29957

PLAYAS
Methods of determining playa surface conditions using remote sensing
[AD-A192663] 21 p2965 N88-27612

PLENUM CHAMBERS
Advanced Technology for Aero Gas Turbine Components
[AGARD-CP-421] 10 p1279 N88-17647
Development of a plenum chamber burner system for an advanced VTOL engine 10 p1281 N88-17664

PLETHYSMOGRAPHY
A plethysmograph for measuring pulmonary ventilation in small animals
[AD-A184978] 05 p0629 N88-13846

PLEXIGLASS (TRADEMARK)
U POLYMETHYL METHACRYLATE

PLIES
U LAYERS

PLOTTERS
Use of modern scanner techniques in cartography
18 p2535 N88-25040

PLOTTING
Satellite orbits: Plot routines
[UIO-SR-87-02] 01 p0011 N88-10060
A computer code to process and plot laser altimetry data interactively on a microcomputer
[NASA-TM-100687] 05 p0554 N88-13371
Boeing 727 MLS (Microwave Landing System) terminal instrument procedures (TERPS) approach data collection and processing, data report
[AD-A185523] 06 p0667 N88-14090
On the influence of false plots on tracking relaibility: Simulations and preliminary analyses
[FOA-C-30443-3.2] 06 p0692 N88-14245
The effects of data structure on total time on test plots
[AD-A187628] 10 p1389 N88-18296
Physical, chemical and CTD (Conductivity/Temperature/Depth) data from the Marathon 2 expedition
[AD-A189930] 15 p2099 N88-22507
PLOT300: A Tektronics PLOT10 emulator for HP 9000 series 200/300 computers
[NASA-TM-100606] 16 p2250 N88-23447
Digital SPOT stereoplotting: An original approach to the formation of epipolar images and matching
22 p3113 N88-28493
Interactive plotting of NASTRAN aerodynamic models using NPLOT and DISSPLA
[AD-A194115] 23 p3226 N88-29204
A computer program package for introductory one-dimensional digital signal processing applications
[AD-A194656] 23 p3249 N88-29338
Implementation of the NCAR (National Centre for Atmospheric Research) graphics package at ARL (Aeronautical Research Laboratory)
[AD-A195163] 24 p3391 N88-30193

PLOTTING INSTRUMENTS
U PLOTTERS

PLOWED FIELDS
U FARMLANDS

PLUGS
Rotor self-lubricating axial stop
[NASA-CASE-MFS-28273-1] 17 p2344 N88-23974

PLUMBANE
U METAL HYDRIDES

PLUMES
NT ROCKET EXHAUST
Development and application of computational aerothermodynamics flowfield computer codes
[NASA-CR-181534] 04 p0395 N88-12465
Aircraft engine exhaust plume dynamics
[AD-A184238] 04 p0400 N88-12488
Plume mechanics and aerosol growth processes
[AD-A184467] 04 p0442 N88-12742
Active and passive plume distribution models in the convective boundary layer using a large eddy simulation model
[KNMI-TR-90] 05 p0581 N88-13546
High resolution ultraviolet filter development
[AD-A184183] 05 p0649 N88-13979
On the correlation of plume centerline velocity decay of turbulent acoustically excited jets
[NASA-TM-100193] 09 p1114 N88-16681
Measurement of velocity and temperature profiles in low-speed, turbulent non-isothermal flows
[PB88-155833] 11 p1486 N88-18872
Numerical simulation of near-surface environments and particulate clouds generated by large-area fires
[AD-A188375] 12 p1641 N88-19828
Kinetic mecnanisms for ionization and afterburning suppression
[AD-A189219] 13 p1737 N88-20383
Split-coefficient matrix solution and experimental study of axisymmetric underexpanded exhaust plumes
15 p2054 N88-22242
Plasma-gas interaction studies in a hybrid plume plasma rocket
[AD-A190310] 15 p2138 N88-22755
Detection of biomass burning and smoke plumes in the Amazon region through NOAA satellite imagery
17 p2365 N88-24085
Research study: Space shuttle main engine plume flowfield model
[NASA-CR-179336] 18 p2474 N88-24676
Evaluation of the communications impact of a low power arcjet thruster
[NASA-TM-100926] 18 p2475 N88-24682
Variable Mach number wall jets for control/propulsion on hypervelocity projectiles/interceptors: Tests with an existing model
[AD-A192845] 21 p2892 N88-27167
A computational analysis of under-expanded jets in the hypersonic regime
[NASA-TM-101319] 21 p2893 N88-27174
Nozzle lip effects on gas expansion into the plume backflow region
[AD-A192806] 21 p2942 N88-27475
Application of laser diffraction techniques to particle sizing in solid propellant rocket motors
[AD-A193841] 22 p3049 N88-28089
Project wind, phase 4 (smoke test), Meadow Brook Valley, Red Bluff, California
[AD-A194742] 22 p3128 N88-28596
Automatic data retrieval from rocket motor holograms
[AD-A195586] 24 p3337 N88-29864
Experimental evaluation of resistojet thruster plume shields
[NASA-TM-101363] 24 p3338 N88-29868

PLUNGERS
Influence of shock wave and gas pressure on the behavior of a pyrotechnical device
[SNIAS-872-430-111] 05 p0570 N88-13477
Advantages of internal thermal protection in a pyrotechnical plunger
[SNIAS-872-430-114] 05 p0571 N88-13478

Numerical simulation applied to the development of a pyrotechnical system [SNIAS-872-430-115] 05 p0571 N88-13479

PLUTONIUM

NT PLUTONIUM ISOTOPES

NT PLUTONIUM 238

PLUTONIUM ISOTOPES

NT PLUTONIUM 238

A long term radiological risk model for plutonium-fueled and fission reactor space nuclear system [DE87-010466] 06 p0779 N88-14782

Milliwatt generator project [DE88-011261] 20 p2853 N88-26939

PLUTONIUM 238

BIFOLD: A dual-mode nuclear space power system 17 p2404 N88-24292

PLUVIOGRAPHS

U RAIN GAGES

U RECORDING INSTRUMENTS

PLY ORIENTATION

Investigation of instability, dynamic forces, and effect of dynamic loading on strength of cages for the bearings in the high pressure oxygen turbopumps for the space shuttle main engine [NASA-CR-178970] 06 p0714 N88-14378

A study of the mechanical behavior of a 2-D carbon-carbon composite 11 p1449 N88-18638

Ply-level failure analysis of a graphite/epoxy laminate under bearing-bypass loading [NASA-TM-100578] 13 p1735 N88-20372

A preliminary investigation of finite-element modeling for composite rotor blades [NASA-TM-100559] 13 p1781 N88-20656

Delamination analysis in crossed layer composites [REPT-48-447/F] 16 p2171 N88-22942

Harmfulness of defects: Behaviour in service of a delamination in a composite containing many differently oriented layers [PB88-124714] 18 p2479 N88-24705

PNEUMATIC CONTROL

Space station resistojet system requirements and interface definition study [NASA-CR-180832] 04 p0409 N88-12541

Use of a thermodynamic analog for pneumatic transport in horizontal pipes [AD-A184076] 04 p0441 N88-12740

PNEUMATIC EQUIPMENT

A three-barrel repeating pneumatic pellet injector for plasma fueling of the Joint European Torus [DE88-000330] 04 p0491 N88-13026

A device and methodology for measuring repetitive lifting VO2max (oxygen consumption rate) [AD-A185195] 05 p0630 N88-13850

Electrical/pneudraulic design considerations [AD-A188097] 12 p1581 N88-19462

Reduction of erosion in elbows due to flow modifications, phase 1 [DE88-001028] 13 p1769 N88-20584

The pneumatic wind shear sensor: A tool for meteorological investigations and flight management 22 p3036 N88-28024

JUH-1H redesigned pneumatic boot deicing system flight test evaluation [AD-A194918] 24 p3322 N88-29785

Analysis of a feed device for the pneumatic transport of noncohesive particles [VKI-TM-44] 24 p3369 N88-30062

PNEUMATIC PROBES

Formulation of a general technique for predicting pneumatic attenuation errors in airborne pressure sensing devices [NASA-TM-100430] 13 p1723 N88-20302

PNEUMATIC RESET

U PNEUMATIC CONTROL

PNEUMATICS

Pipe and bend erosion by pneumatic transport of solids at high temperature [DE88-001345] 04 p0429 N88-12658

Analysis of a feed device for the pneumatic transport of noncohesive particles [VKI-TM-44] 24 p3369 N88-30062

Laser Doppler Velocimeter (LDV) and pressure measurements of gas particle flows in bends [VKI-TN-163] 24 p3372 N88-30083

POCKELS EFFECT

U BIREFRINGENCE

POGO EFFECTS

ESA Bulletin No. 8 [ETN-87-90513] 09 p1122 N88-16718

Launch vehicle vibration: Measures taken to avoid pogo on ESA's Ariane launch vehicle 09 p1123 N88-16727

POINCARE PROBLEM

Compactness of quasi-conforming element spaces, convergence of quasi-conforming element method 03 p0301 N88-11896

POINT DEFECTS

NT VACANCIES (CRYSTAL DEFECTS)

Hot spots: Subnanometer femtosecond energy localization [DE87-010276] 02 p0155 N88-10968

Effect of point defects on graphite lattice parameters [DE88-700340] 07 p0827 N88-15019

Effect of extraneous factors on optical one-phonon transitions in impurity centers with cubic symmetry 08 p1077 N88-16496

Diffusion studies in amorphous NiZr alloys [DE88-003009] 10 p1301 N88-17781

Silicon and indium doping of GaAs: Measurements of the effect of doping on mechanical behavior and relation with dislocation formation [DE88-003862] 11 p1554 N88-19303

Point defect structure of Cr2O3 [AD-A187620] 11 p1556 N88-19317

The role of point defects on structural phase transitions [DE88-005209] 12 p1696 N88-20152

Study of activationless reactions of point defects with impurities and impurity-defect complexes in alpha-iron [DE88-701028] 13 p1745 N88-20433

Point defects in irradiated silicates 17 p2408 N88-24319

A general qualitative study of point and extended defects and their interactions in non-metallic systems [AD-A191687] 19 p2618 N88-25532

Paramagnetic point defects in boron-implanted HgO.7CdO.3Te [AD-A193276] 21 p3021 N88-27934

Prediction of deep levels and equilibrium concentrations of defects in semiconductors 21 p3023 N88-27945

POINT IMPACT

The numerical solution of the elastohydrodynamically lubricated line and point contact problem, using multigrid techniques [ISBN-90-9001583-3] 06 p0714 N88-14377

POINT MATCHING METHOD (MATHEMATICS)

U BOUNDARY VALUE PROBLEMS

POINT SOURCES

Multipath time-delay estimation via the EM algorithm [PB88-106851] 07 p0845 N88-15124

Bistable cellular flames [DE88-003074] 09 p1142 N88-16848

Space-time processing of field produced by moving source 09 p1234 N88-17399

Bearing detection in the presence of two sources of varying coherence using the complex cepstrum [NASA-CR-181605] 09 p1243 N88-17451

Observation of a point source in Cygnus constellation with the underground detector at Frejus (France) [PITHA-87/02] 20 p2884 N88-27122

POINT SPREAD FUNCTIONS

Three dimensional reconstruction of optical microscope pictures using the three dimensional microscopic inverse point spread function [ETN-87-90420] 01 p0098 N88-10646

Vision of details in space and time [B8711402] 06 p0753 N88-14624

POINTING CONTROL SYSTEMS

NT ANNULAR SUSPENSION AND POINTING SYSTEM

An autonomous, closed-loop pointing system for use with satellite optics [DE87-012011] 02 p0235 N88-11483

Wavefront error sensing [NASA-CR-181504] 03 p0321 N88-12030

A new state space model for the NASA/JPL 70-meter antenna servo controls 04 p0436 N88-12702

A modern control theory based algorithm for control of the NASA/JPL 70-meter antenna axis servos 04 p0436 N88-12706

Knowledge-based monitoring of the pointing control system on the Hubble space telescope 08 p1057 N88-16378

Balloon-borne three-meter telescope for far-infrared and submillimeter astronomy [NASA-CR-182310] 09 p1262 N88-17565

Using ridge regression in systematic pointing error corrections 11 p1472 N88-18777

Optical links in the angle-data assembly of the 70-meter antennas 11 p1474 N88-18792

Progress toward a cosmic dust collection facility on space station [NASA-CR-182427] 12 p1598 N88-19566

Continued design of a Pointing, Acquisition, and Tracking (PAT) subsystem for InterSatellite Laser links (ISL2) [TELDIX-15-093-178] 14 p1905 N88-21384

Development of a magnetically suspended, tetrahedron-shaped antenna pointing system 14 p1926 N88-21478

Utilization of the IR telescope gimbaling system as a stabilized pointing platform for balloon payloads. Volume 1: Technical results [NASA-CR-179339] 18 p2522 N88-24962

Time-Optimal Adaptive Shaped Torque (TOAST) technical note [AD-A192719] 20 p2843 N88-26869

IPS guidestar selection for stellar mode (ASTRO) [NASA-TM-100336] 21 p2894 N88-27181

Slew-induced deformations in a space-based electromagnetic rail gun 21 p2929 N88-27385

The feasibility of the disturbance accommodating controller for precision antenna pointing 22 p3064 N88-28182

DSS 14 antenna calibrations for GSSR/VLA Saturn radar experiments 22 p3068 N88-28207

Modeling, designing and simulating a pointing control system for balloon-borne solar experiments [NASA-TM-100337] 22 p3082 N88-28300

POINTS (MATHEMATICS)

NT FIXED POINTS (MATHEMATICS)

NT INFLECTION POINTS

Point vortex dynamics: Recent results and open problems [DE87-014759] 03 p0314 N88-11982

Point processes [AD-A185398] 05 p0641 N88-13921

Errors in retrieving hydrological fields and fields of their differential characteristics by method of approximation by orthogonal functions 06 p0727 N88-14475

Testing and interval estimation in a change-point model allowing at most one change [AD-A185525] 06 p0767 N88-14716

Local likelihood method in the problems related to change points [AD-A185604] 06 p0768 N88-14718

Point processes in the plane [AD-A186017] 07 p0913 N88-15542

On the characterization of certain point processes [AD-A186427] 07 p0916 N88-15560

Automatic registration of satellite imagery 17 p2364 N88-24080

Procedure for converting a Wilson-Fowler spline to a cubic B-spline with double knots [DE88-008971] 20 p2844 N88-26878

Evaluation of a multi-point method for determining acoustic impedance [NASA-TM-100637] 20 p2849 N88-26913

An algorithm for determining the location of points in computer simulations [AD-A193713] 23 p3250 N88-29343

On the Nash point equilibria in the calculus of variations [AD-A194959] 24 p3424 N88-30381

POISEUILLE FLOW

U LAMINAR FLOW

POISONS

NT CARBAMATES (TRADENAME)

NT URETHANES

POISSON DENSITY FUNCTIONS

Explicit formulate for the distributions of stopping variables under Wald's truncated SPRT (Sequential Probability Radio Tests) for a poisson process [AD-A185053] 05 p0640 N88-13914

Decoupling identities and predictable transformations in exchangeability [AD-A186013] 07 p0913 N88-15540

A Prohorov bound for a Poisson process and a Bernoulli process [CWI-MS-R8701] 09 p1232 N88-17388

A code development system for computational fluid dynamics [AD-A188050] 11 p1482 N88-18848

Tests for uniformity arising from a series of events [AD-A189069] 13 p1828 N88-20935

Bias reduction when there is no unbiased estimate [AD-A189407] 13 p1829 N88-20937

Open questions in closed-loop photodetection 14 p1979 N88-21812

Extreme value for dependent sequences via the Stein-Chen method of poisson approximation [AD-A190325] 15 p2125 N88-22668

Development of adaptive grid schemes based on Poisson grid generators [AD-A190953] 16 p2262 N88-23528

Poisson functionals of Markov processes and queueing networks [AD-A191217] 18 p2568 N88-25252

On path properties of certain infinitely divisible processes [AD-A192016] 18 p2568 N88-25255

Full analysis of a powerful window random access algorithm [AD-A192437] 21 p2995 N88-27763

Multiple integration with respect to Poisson and Levy processes
[AD-A192895] 21 p3009 N88-27851
Poisson functionals of Markov processes and queueing networks
[AD-A194289] 22 p3145 N88-28705

POISSON EQUATION
Generation of body-fitted grids for two dimensional interior domains by the solution of a system of Poisson equations using multigrid techniques
[GMD-246] 01 p0044 N88-10281
The finite element method for electronic structure
[DE88-001706] 04 p0485 N88-12989
Point processes in the plane
[AD-A186017] 07 p0913 N88-15542
A vectorized Poisson solver over a spherical shell and its application to the quasi-geostrophic omega-equation
[NASA-CR-4116] 08 p1039 N88-16285
Fast Poisson solver on irregular regions by boundary integral-based domain decomposition methods
[DE88-003583] 10 p1399 N88-18340
Propagator solutions of partial differential equations applied to plasma transport
[DE88-006432] 13 p1816 N88-20852
Heating efficiency of beat wave excitation in a density gradient
[AD-A193066] 21 p3017 N88-27905
Three-dimensional zonal grids about arbitrary shapes by Poisson's equation
[NASA-TM-101018] 22 p3039 N88-28042
Poisson functionals of Markov processes and queueing networks
[AD-A194289] 22 p3145 N88-28705
An asymptotic evaluation of the tail of a multiple symmetric alpha-stable integral
[AD-A194570] 23 p3270 N88-29460

POISSON PROCESS
U POISSON DENSITY FUNCTIONS
U STOCHASTIC PROCESSES

POISSON RATIO
Anelastic behaviour of materials under multiaxial strains. Part 3: Order-disorder transition, Shoek effect and Poisson's ratio in AISI-1080 steel
[DE87-703087] 02 p0191 N88-11193

POLAR AURORAS
U AURORAS

POLAR CAPS
Configurations of the quiet polar cap and its response to a sudden increase of the energy input rate epsilon
[DMI-GEOPHYS-PAPERS-R-74]
03 p0350 N88-12210
Characteristics of particle acceleration at high latitude
08 p1026 N88-16210
F-layer polar cap arcs
[AD-A186592] 09 p1190 N88-17127
Collaborative studies of polar cap ionospheric dynamics
[AD-A187888] 10 p1355 N88-18098
The role of remote sensing in the study of polar ice sheets 14 p1939 N88-21570
Elements of sea ice dynamics and thermodynamics
14 p1939 N88-21571
High latitude ionospheric radio studies
[AD-A192270] 20 p2824 N88-26753
Rocket measurements within a polar cap arc: Ionospheric modelling
[AD-A192381] 20 p2824 N88-26754
On the conjugacy of the aurora: High and low latitudes
[AD-A193008] 20 p2824 N88-26755
Ionospheric convection and structure using ground-based digital ionosondes
[AD-A194246] 23 p3233 N88-29237
How dirty is Mars' North Polar cap, and why isn't it black 23 p3303 N88-29677

POLAR CUSPS
Polar cusp electrodynamics 08 p1030 N88-16242

POLAR METEOROLOGY
Large ice masses: Characteristics, behaviour and relation to climate 14 p1939 N88-21569

POLAR ORBITS
Study of mobile communications payload for Columbus Polar Platforms
[ITS-TR-056A/86] 01 p0034 N88-10220
Satellite environment: Polar orbits
03 p0272 N88-11713
Planning for future operational sensors and other priorities
[PB87-220802] 03 p0325 N88-12056
Viking quick look plots: A short description --- Swedish satellite 06 p0692 N88-14243
Polar platform element of Space Station: Mission objectives, European priorities, candidate instrumentation and selection procedure 09 p1129 N88-16779
Frozen orbit analysis in the Martian system
[AD-A189574] 13 p1856 N88-21106

POLAR PLATFORMS (SPACE STATIONS)
U SPACE STATION POLAR PLATFORMS

POLAR REGIONS
NT ANTARCTIC REGIONS
NT ARCTIC REGIONS
NT ROSS ICE SHELF
Forecasting polar lows using a numerical mesoscale model 02 p0210 N88-11321
Possible dynamical mechanisms for the Martian polar warming phenomenon
[NASA-CR-181454] 02 p0254 N88-11605
High latitude problems to be studied by incoherent scatter radars
[DMI-GEOPHYS-PAPERS-R-77]
03 p0350 N88-12211
Eastern - western Arctic Sea ice analysis 1986
[AD-A184016] 03 p0355 N88-12235
USSR report: Earth sciences
[JPRS-UES-86-006] 04 p0458 N88-12831
Huurre expedition to the North Pole in 1984
[PB87-220935] 04 p0462 N88-12858
Cloud cover determination in polar regions from satellite imagery
[NASA-CR-181544] 04 p0471 N88-12908
The polar ionosphere and interplanetary field
[AD-A185386] 05 p0624 N88-13822
Electric field measurements on Viking: First results
[TRITA-EPP-87-04] 05 p0625 N88-13826
Activities report of the Ionospheric Observatory
[UIO-SR-87-01] 05 p0625 N88-13827
Axial anisotropy of the intensity of the cosmic ray nuclear component
[IFSI-87-7] 05 p0662 N88-14061
Global convection patterns in the high latitude
[AD-A185794] 06 p0743 N88-14571
Atmosphere of Venus in southern polar area
08 p1005 N88-16088
Atmosphere of Venus in south polar area based on radio transmission data 08 p1005 N88-16089
Atmosphere of Venus in north polar area based on radio transmission data from Venera-15 and Venera-16 spacecraft 08 p1005 N88-16090
Instantaneous pictures of the high-latitude electrodynamics using Viking and DMSP/F7 observations --- Swedish satellite
08 p1025 N88-16209
Characteristics of particle acceleration at high latitude
08 p1026 N88-16210
The sodium layer at 69 N latitude in wintertime
08 p1027 N88-16218
Electrodynamics of the high latitude middle atmosphere 08 p1028 N88-16225
Comparison of simultaneous MST radar and electron density probe measurements in the polar mesosphere --- Mesospheric, Stratospheric, Tropospheric (MST)
08 p1028 N88-16226
Predictability of ice concentration in the high-latitude North Atlantic from statistical analysis of SST (Sea Surface Temperature) and ice concentration data
[AD-A186621] 08 p1045 N88-16315
Collaborative studies of polar cap ionospheric dynamics
[AD-A187888] 10 p1355 N88-18098
Upper-thermospheric observations and neutral-gas dynamics at high latitudes during solar maximum
[AD-A188058] 11 p1512 N88-19031
Polar mesospheric cloud experiment
[AD-A188936] 12 p1648 N88-19872
The 1987 Airborne Antarctic Ozone Experiment: The Nimbus-7 TOMS data atlas
[NASA-RP-1201] 13 p1791 N88-20714
Sea ice observations and models
14 p1939 N88-21572
The Greenland Sea Project: The Arctemiz project
14 p1939 N88-21573
Centrifugal acceleration of ions in the polar magnetosphere
[NASA-TM-101148] 17 p2374 N88-24120
Cloud cover determination in polar regions from satellite imagery
[NASA-CR-182906] 17 p2375 N88-24123
Low frequency electrostatic turbulence in the polar cap E-region
[DRI-3-88] 18 p2540 N88-25077
SAM 2 data user's guide
[NASA-RP-1200] 18 p2543 N88-25094
TE/TM (Transverse Electric/Transverse Magnetic) height profile measurements of transpolar VLF (Very Low Frequency) signals
[AD-A194503] 22 p3069 N88-28216
The influence of conductivities consistent with field-aligned currents on high-latitude convection patterns
[TRITA-EPP-88-02] 22 p3119 N88-28533
Intraseasonal variability in atmospheric surface pressure and relationship to polar motion
22 p3120 N88-28540
Variations in the atmosphere associated with the 11-year solar cycle 22 p3122 N88-28557
The relationship between polar sea ice and the position of the near equatorial convergence zone
22 p3123 N88-28563
Sea ice processes
[AD-A193980] 23 p3237 N88-29262
The effect of equatorial ionospheric irregularities on the performance of a south-looking OTH-B (Over-The-Horizon-Backscatter) radar
[AD-A195090] 24 p3362 N88-30018
MIZEX (marginal ice zone experiment) 1987 SAR (Synthetic Aperture Radar) data summary
[AD-A195560] 24 p3364 N88-30035

POLARIMETERS
Lyman alpha SMM/UVSP absolute calibration and geocoronal correction
[NASA-TM-100314] 03 p0389 N88-12446
A polarimetric rain backscatter model developed for coherent polarization diversity radar applications
13 p1759 N88-20520
A two-wavelength infrared interferometer/polarimeter system for CIT (Compact Ignition Tokamak)
[DE88-007681] 18 p2579 N88-25321
Investigations on multiport antennas for polarimetric and modal field scanning
[REPT-5-87] 23 p3205 N88-29073
Development of a multiport-hybrid-mode exciter for use in antennas for polarimetric field measurements
[REPT-12-87] 23 p3205 N88-29075

POLARIMETRY
Use of polarimetry to measure the current profile in MTX
[DE87-013835] 02 p0237 N88-11495
Signal-filter design and system performance for polarimetric radar
[AD-A189257] 13 p1758 N88-20514
Similarity and diversity of the polarization of comets
14 p2003 N88-21940
Cometary grains and interplanetary dust: A polarimetric sensing --- Halley 14 p2003 N88-21941
The dust around the nucleus of Comet Halley
14 p2003 N88-21942
Data volume reduction for imaging radar polarimetry
[NASA-CASE-NPO-17184-1-CU]
20 p2788 N88-26541
Interpretation of the polarimetric observations of Jupiter
[DE88-702414] 21 p3031 N88-27991

POLARITONS
NT PLASMONS
Surface polariton resonances and reflectance on a bigrating
[AD-A184663] 03 p0377 N88-12370
Nonlinear surface polaritons
[AD-A191046] 18 p2499 N88-24822

POLARITY
Examination of the physical processes associated with the keyhole region of variable polarity plasma arc welds in aluminum alloy 2219 07 p0927 N88-15634
The mechanism of stereo regulation during anionic polymerization of polar monomers
[AD-A186530] 08 p0973 N88-15888

POLARIZATION
Broadband linear polarization and chromospheric CaII H and K line emission in late-type main sequence stars
04 p0511 N88-13140
The effect of microgravity on mammalian cell polarization at the ultrastructural level --- Spacelab D1 mission
22 p3061 N88-28164
Determining the spatial structure of fields of precipitation from space radar images in two orthogonal polarizations
24 p3450 N88-30531

POLARIZATION (CHARGE SEPARATION)
NT DIELECTRIC POLARIZATION
The physics of charge separation preceding lightning strokes in thunderclouds
[NASA-CR-178371] 01 p0071 N88-10452
Photoinduced charge separation by polymer-bound chromophores
[DE88-002101] 06 p0685 N88-14198
Atmospheric science 07 p0883 N88-15357
Ferroelectric properties and impact behavior of the PVF2 polymer and the VF2/C2F3H polarized copolymers --- vinylidene polyfluorides
[ISL-CO-245/86] 08 p0971 N88-15876
Picosecond laser spectroscopy of charge-separation in photosynthetic model systems
[DE88-003122] 09 p1172 N88-17028
Preparation of thin film polyvinylidene fluoride shock wave pressure transducers
[PB88-156070] 11 p1490 N88-18893

Spontaneous decay and atomic fluorescence near a metal surface of an absorbing dielectric
[AD-A187506] 13 p1835 N88-20975
Determination of Tafel constants in nonlinear polarization curves
[AD-A192335] 21 p2912 N88-27282
Techniques and instrumentation for transient characterization of metal-insulator-semiconductor diodes. Applications to metal-insulator InP system
[ECL-87-17] 21 p3025 N88-27959
Electron impact ionization cross-section of some organic compounds
[DE88-702044] 23 p3280 N88-29525
An electrochemical impedance spectroscopy study of reactions at the metal/coating interface
24 p3355 N88-29975
POLARIZATION (SPIN ALIGNMENT)
Application of spin-sensitive electron spectroscopies to investigations of electronic and magnetic properties of solid surfaces and epitaxial systems
[DE87-014235] 02 p0245 N88-11550
High energy polarized electron beams
[CEBAF-R-87-002] 11 p1546 N88-19244
Recent progress in optical bistability and tristability
14 p1979 N88-21809
Magnetic traps for an anti-hydrogen gas
16 p2269 N88-23572
Observation of ferromagnetism in ultrathin f.c.c. films by spin polarised neutron reflection
20 p2865 N88-27015
An undulator radiation source for spin-polarized photoemission studies of novel magnetic materials
[AD-A193756] 22 p3083 N88-28307
Fluctuation and relaxation phenomena studied by means of nuclear orientation
[B8679671] 23 p3281 N88-29534
POLARIZATION (WAVES)
NT CIRCULAR POLARIZATION
NT ELLIPTICAL POLARIZATION
NT LINEAR POLARIZATION
Study of advanced satellite concept using a multifeed reconfigurable antenna. Detailed report on Polarization Sensitive Reflector (PSR) and offset parabolic antennas, Appendix 1
[ESA-CR(P)-2406-VOL-3] 01 p0013 N88-10075
Theory of atomic additivity in molecular hyperpolizabilities 03 p0297 N88-11867
Development of optical modulators for measurements of solar magnetic fields
[NASA-TM-100315] 04 p0490 N88-13016
A polarization diversity meteorological radar system
[AD-A189291] 13 p1758 N88-20515
Polarization spectroscopy: Prospect and data needs
17 p2443 N88-24531
POLARIZATION CHARACTERISTICS
Polarization effects in laser-pumped Nd:YAG lasers
[DE88-004019] 11 p1492 N88-18904
Effect of double layer structure on the determination of corrosion rates from polarization measurements
[DE88-010097] 20 p2774 N88-26448
POLARIZATION CHARTS
U GRAPHS (CHARTS)
U POLARIZATION (WAVES)
POLARIZED ELASTIC WAVES
Anomalies in electromagnetic absorption of circularly polarized ultrasonic waves by tungsten within Doppler-shifted cyclotron resonance range
06 p0775 N88-14756
POLARIZED ELECTROMAGNETIC RADIATION
NT POLARIZED LIGHT
NT SYNCHROTRON RADIATION
Optimization of charged particle acceleration rate over wave parameters in the scheme with acceleration by surface electromagnetic waves
[DE88-700320] 07 p0846 N88-15134
Polarization of electrons in an electromagnetic wave field in the presence of magnetic field
[DE88-700169] 13 p1757 N88-20509
Mode priming in an overmoded gyrotron oscillator
[AD-A189151] 13 p1772 N88-20602
POLARIZED LIGHT
Use of a 35mm camera for remote surface cleanliness verification 02 p0133 N88-10835
Multiple scattering of polarized light in cirrus clouds
13 p1801 N88-20768
Continuous collective molecule rotation of a nematic liquid crystal induced from light angular momentum
[FUB-17-1986] 14 p1986 N88-21845
Polarization of light reflected by vertically inhomogeneous planetary atmosphere
[DE88-702416] 21 p3031 N88-27992
POLARIZED RADIATION
NT POLARIZED ELASTIC WAVES
NT POLARIZED ELECTROMAGNETIC RADIATION
NT POLARIZED LIGHT
NT SYNCHROTRON RADIATION
POLAROGRAPHS
U POLAROGRAPHY
POLAROGRAPHY
Analysis of nickel sulphamate bath using charging current compensated D.C. polarography
[NAL-TM-MT-8705] 05 p0564 N88-13433
Water tunnel measurements by an electrochemical method 16 p2203 N88-23146
POLARONS
Soliton and polaron dynamics in conducting polymers
[DE88-702539] 23 p3198 N88-29035
POLICIES
NT ENERGY POLICY
NT PATENT POLICY
NT PROCUREMENT POLICY
Global environmental change research
[S-HRG-100-301] 03 p0348 N88-12199
National Science Foundation
[PB87-228375] 03 p0384 N88-12410
The attitudes of science policy, environmental, and utility leaders on US energy issues and fusion
[DE88-000784] 04 p0494 N88-13041
A study of the Department of Defense configuration management policies and procedures as applied to the FA-18 Strike/Fighter program
[AD-A184872] 05 p0657 N88-14034
National Aeronautics and Space Administration space station proposal, fiscal year 1988
[S-HRG-100-328] 05 p0659 N88-14043
On stochastic optimality of policies in first passage problems
[AD-A186293] 07 p0915 N88-15554
Relating service doctrine to space system requirements
[AD-A186620] 08 p1074 N88-16483
Organizations of intermediation in technology transfer: Its role in technological innovation
[INPE-4354-TDL/297] 08 p1094 N88-16581
Committee on Interagency Radiation Research and Policy Coordination
[DE88-003358] 09 p1188 N88-17121
Alternative Energy in the Midwest: Research and Applications. Conference Proceedings, Rosemont, Illinois, March 19-20, 1987
[PB88-142278] 11 p1509 N88-19015
Science and technology in India
[PB88-134747] 11 p1564 N88-19362
Conditions and mechanisms of the process of technological innovation in Brazil: The role of research institutes
[INPE-4175-TDL/274] 11 p1567 N88-19383
JPRS report. Science and technology: Europe and Latin America
[JPRS-ELS-87-054] 12 p1573 N88-19406
Communication satellites: Guidelines for a strategic plan
[NASA-TM-89306] 12 p1599 N88-19569
JPRS report: Science and technology. Europe and Latin America
[JPRS-ELS-88-001] 12 p1614 N88-19649
Systems approach to energy quality and efficiency
[PB88-139506] 12 p1640 N88-19823
JPRS report. Science and technology: Europe and Latin America
[JPRS-ELS-87-055] 12 p1686 N88-20086
Selling to NASA
[NASA-TM-89724] 12 p1705 N88-20208
Defending secrets, sharing data: New locks and keys for electronic information
[PB88-143185] 12 p1706 N88-20210
Implementing information systems/office automation in an Air Force environment
[AD-A188956] 12 p1707 N88-20218
Science, technology and the Constitution: Background paper
[PB88-142534] 12 p1708 N88-20222
JPRS report: Science and technology. Japan
[JPRS-JST-87-029] 15 p2052 N88-22228
A proposed national policy concerning the reentry of space reactors 17 p2415 N88-24359
Sensitivity analysis for the system reliability function
[AD-A191648] 18 p2525 N88-24979
Centre for International Co-Operation and Approriate Technology (CICAT)
[PB88-165501] 18 p2590 N88-25389
Timing regulations to prevent stratospheric-ozone depletion
[R-3495-JMO/RC] 19 p2690 N88-25987
An agenda for the strategic defense initiative
[RAND-P-7404] 20 p2847 N88-26898
SDI and/or arms control
[RAND-P-7357] 20 p2848 N88-26903
Space policy of common sense and moderation
[REPT-49/87] 20 p2883 N88-27118
Stress/fatigue and the ARNG (Army National Guard) aviator
[AD-A194184] 22 p3132 N88-28621
Quality control in microbiology: CDC lab manual
[PB88-179890] 23 p3237 N88-29263
SDI (Strategic Defense Initiative): A policy analysis
[AD-A194240] 23 p3275 N88-29493
The principles of mass and maneuver applied to space operations
[AD-A194037] 23 p3276 N88-29500
The problem of space in Soviet operational art
[AD-A194150] 23 p3278 N88-29502
POLISHING
Some speculations on the mechanisms of abrasive grinding and polishing
[DE87-014242] 02 p0181 N88-11126
A rapid polishing method for KBr and NaCl infrared windows
[DE88-002480] 07 p0862 N88-15229
Determination of aquo-complexes of chromium and iron in chromium plating and polishing solutions by ion chromatography
[AD-A190168] 15 p2039 N88-22148
Center for thin film studies
[AD-A191996] 19 p2732 N88-26226
POLITICS
Technology transfer to China
[PB87-223418] 04 p0502 N88-13087
German space policy on the threshold of the century. Analysis and proposals for the future
[ETN-88-90573] 07 p0943 N88-15734
Book analysis. Challenger: A major malfunction
[AD-A192458] 20 p2764 N88-26388
Political and economic barriers to information transfer
24 p3437 N88-30460
POLLEN
Examination of methods for pollen storage and dispersal
[TN-RB524-097/86] 17 p2378 N88-24134
POLLUTANTS
U CONTAMINANTS
POLLUTION
NT AIR POLLUTION
NT ENVIRONMENT POLLUTION
NT GLOBAL AIR POLLUTION
NT INDOOR AIR POLLUTION
NT NOISE POLLUTION
NT OIL POLLUTION
NT WATER POLLUTION
Withstand voltage of slightly polluted insulator chains in humid weather conditions
[DE88-752818] 22 p3072 N88-28237
POLLUTION CONTROL
Contamination control concepts for space station customer servicing 02 p0137 N88-10860
Emerging environmental constraints on the use of gasoline and diesel fuel and tradeoffs associated with the use of alternative fuels
[DE87-011504] 04 p0422 N88-12614
Innovative and alternative technology projects
[PB87-230165] 05 p0623 N88-13818
AN-30M cloud-seeding airplane in international exhibition 06 p0725 N88-14456
Integrated Global Background Monitoring Network
[DE88-001503] 06 p0731 N88-14499
The role of repowering in America's power generation future
[DOE/FE-0096] 10 p1351 N88-18076
Acid Precipitation: A current awareness bulletin
[DE88-007987] 20 p2821 N88-26738
POLLUTION MONITORING
Remote sensing of environmental pollution
[DFVLR-MITT-87-04] 01 p0067 N88-10428
An instrument for the quasi-continuous determination of atmospheric soot content
[DFVLR-FB-87-04] 01 p0068 N88-10433
Influence of surfactants on damping of gravity-capillary waves. 1: Frequency dependence
04 p0459 N88-12843
Hydrogen chloride measurements in launch-vehicle exhaust clouds
[DE87-011552] 08 p0964 N88-15837
Feasibility study for a 2nd generation system for airborne maritime pollution surveillance
[ETN-88-92108] 15 p2092 N88-22486
Application of SPOT imagery for oil spill contingency planning 22 p3108 N88-28460
POLLUTION TRANSPORT
Investigations of the dispersion of spontaneously released heavy gases
[WA-81] 01 p0066 N88-10427
A study of carbon monoxide distribution determinations for a global transport model
[NASA-CR-181423] 01 p0067 N88-10432

Opportunities for nowcasting air pollution episodes and accidental toxic and radioactive releases
02 p0210 N88-11317

Real-time evaluation and prediction of coastal dispersion near the SW tip of Africa --- effluents
02 p0210 N88-11318

Use of back air trajectories in interpreting atmospheric chemistry data: A review and bibliography
[PB88-102108] 07 p0876 N88-15312

Simulation of a typical flow in a broad valley
08 p1015 N88-16154

Simulation of global wet and dry deposition of nitric acid in a three-dimensional chemistry-transport model
[DE87-009847] 09 p1188 N88-17116

A comparison of multi-layer meso-alpha MLAM model results with surface and aircraft observations from CAPTEX
[DE88-000549] 09 p1188 N88-17118

Assessment of crop loss from air pollutants: Meteorology-atmospheric chemistry and long range transport
[PB88-146857] 15 p2089 N88-22448

Detection, monitoring and analysis of some environmental effects of fires in the Amazon region through utilization of NOAA and LANDSAT satellite imagery and aircraft data
[INPE-4503-TDL/326] 16 p2230 N88-23322

Review of numerical methods for radionuclide transport in three-dimensional porous media, at high Peclet numbers
[CFDU/87/10] 18 p2538 N88-25061

Prediction of regional pollutant dispersion using a nested-grid, three-dimensional numerical model
21 p2971 N88-27649

Development of an adjustable buoyancy balloon tracer of atmospheric motion. Phase 3: Refinement of the operational prototype system
[PB88-190764] 23 p3231 N88-29230

POLOIDAL FLUX

On tokamak equilibrium
[DE87-014811] 02 p0239 N88-11507

Poloidal magnetics of compact ignition tokamaks
[DE88-001774] 07 p0934 N88-15672

Evolution of poloidal variation of impurity density and ambipolar potential in rotating tokamak plasma, part 1
[DE88-006263] 13 p1842 N88-21022

An introduction to poloidal and toroidal fields
[MITT-54] 17 p2394 N88-24232

The 2-D magnetohydrostatic configurations leading to flares or quiescent filament eruptions
[NASA-TM-101147] 18 p2595 N88-25423

Toroidal and poloidal soft X-ray imaging system on the D3-D tokamak
[DE88-010585] 20 p2860 N88-26986

ITER plasma equilibrium and poloidal field system design
[DE88-011005] 21 p3018 N88-27912

Density fluctuations in currentless high beta plasmas in Heliotron E
[DE88-752310] 23 p3283 N88-29550

POLYACETYLENE

Novel polymers and copolymers and production of poly(acetylene)
[EP-PATENT-0-173-473-A2] 01 p0026 N88-10161

Ionically conductive polymers: Application to solid state batteries
[AD-A183733] 01 p0037 N88-10239

Molecular and supramolecular orientation in conducting polymers
[DE88-000533] 05 p0569 N88-13472

Time resolved spectroscopy facility for the study of nonlinear optical properties of semiconducting polymers
[AD-A191221] 18 p2490 N88-24768

POLYACRYLATES

U ACRYLIC RESINS

POLYAMIDE RESINS

NT KEVLAR (TRADEMARK)
NT NYLON (TRADEMARK)

Determination of the melting and decomposition points of different materials in an oxygen stream
[INFORME-I-158/86] 09 p1142 N88-16844

Development of polymeric films with piezoelectrical properties from polypeptides; low, odd nylons; or polyureas
[AD-A190301] 15 p2044 N88-22181

The adhesive bonding of thermoplastic composites
[AD-A190994] 16 p2173 N88-22953

Initial adhesive screening of novel polyamide-imides and their copolymers
[NASA-TM-100641] 20 p2779 N88-26481

Resistance of polyamide-6 against long time effects of various media at various temperatures
[NASA-TT-20297] 20 p2779 N88-26484

POLYATOMIC GASES

NT DIATOMIC GASES

POLYATOMIC MOLECULES

NT DIATOMIC MOLECULES

Picosecond CO2 laser interactions with polyatomic molecules
[DE87-012072] 01 p0051 N88-10327

A physico-chemical study of some areas of fundamental significance to biophysics
[DE87-013457] 02 p0217 N88-11365

Systematic studies of molecular vibrational anharmonicity and vibration-rotation interaction by self-consistent-field higher derivative methods: Applications to asymmetric and symmetric top and linear polyatomic molecules
[DE87-014691] 02 p0232 N88-11465

Study of polyatomic dynamics in the atmosphere
[AD-A190964] 16 p2233 N88-23334

Time-resolved studies of free radicals and laser-initiated chain reactions
[DE88-006569] 16 p2266 N88-23553

Proceedings of the Cooling, Condensation, and Storage of Hydrogen Cluster Ions Workshop
[AD-A189857] 16 p2266 N88-23555

Overview of hydrogen clusters
16 p2267 N88-23557

Large hydrogen cluster ions 16 p2267 N88-23558

Formation and reactivity of small hydrogen cluster ions 16 p2267 N88-23560

Electronic structure and stability of small cation and anion hydrogen clusters 16 p2267 N88-23562

Photon-assisted formation and cooling of molecular hydrogen
[MP-87-102] 16 p2267 N88-23563

Infrared spectroscopy of H3(+)
16 p2268 N88-23565

Vibrational spectroscopy of the hydrogen and hydrated hydronium cluster ions 16 p2268 N88-23566

The role of electron-ion recombination in bulk antimatter production 16 p2268 N88-23567

Electromagnetic manipulation of atomic hydrogen
16 p2268 N88-23568

Key problems and hydrogen atom formation
16 p2269 N88-23573

Production of heavy antinuclei: Review of experimental results 16 p2269 N88-23574

The cluster ion approach to the condensation and storage of antihydrogen 16 p2269 N88-23575

Analysis of containerless condensation of polyatomic hydrogen ions, with emphasis on H3(+,-) association channels and a future workshop to study related topics
16 p2269 N88-23576

Small molecule and small cluster ion formation in a low-density containerless mixture of electrons, protons and hydrogen atoms 16 p2269 N88-23577

POLYBENZIMIDAZOLE

Improved structural polymer alloys and composites
[AD-A192092] 19 p2619 N88-25538

POLYBUTADIENE

Distribution of chain ends inside the polybutadiene microspheres of SB diblock copolymers
[AD-A191257] 16 p2182 N88-23007

Environmental integrity of coating/metal interface
[AD-A192184] 18 p2492 N88-24786

Spatial organization of homopolymer chains inside spherical polybutadiene domains of SB diblock copolymers
[AD-A193390] 21 p2918 N88-27321

Blends of crystallizable polybutadienes
[AD-A194536] 23 p3197 N88-29026

POLYCARBONATES

The effect of heat treatment on fatigue crack growth in polycarbonate 05 p0606 N88-13714

Reinforcing of thermoplastic polycarbonate and polysulfone with carbon fibers: Production and characteristics of UD-compound objects
[NASA-TT-20158] 13 p1735 N88-20374

Interactions in miscible polymer blends
[AD-A193824] 22 p3058 N88-28144

POLYCRYSTALS

Understanding the transport properties of silicon grain boundaries and how they relate to I.C. applications of polysilicon
[DE87-013809] 01 p0104 N88-10677

Electrical properties of high T/sub c/ superconductors under high pressures
[DE87-012818] 02 p0245 N88-11546

Surface chemistry of transition metal carbides: A theoretical analysis
[AD-A184237] 03 p0291 N88-11829

X-ray analysis of polycrystalline aluminium subjected to fatigue cycling
[NAL-TM-MT-8706] 05 p0564 N88-13434

An overview of metal plasticity
[DE88-001658] 06 p0681 N88-14175

Observing effect of laser radiation of low-frequency Raman scattering of light 06 p0772 N88-14742

Magnetic investigations of superconductive, polycrystalline (RE)1Ba2Cu3O(7-x) compounds (RE = Y, Gd, Ho, Dy)
[DE88-002537] 08 p1090 N88-16558

X-ray diffraction study of thermotropic liquid crystalline polyesters and diester model compounds
[AD-A186788] 09 p1255 N88-17521

Adhesion of vapour phase deposited ultra-thin polyimide films on polycrystalline silver
[AD-A187930] 10 p1306 N88-17810

Proceedings of the Polycrystalline Thin Film Program Meeting
[DE87-001169] 11 p1557 N88-19321

Recommendations on developing polycrystalline alumina fiber 13 p1756 N88-20502

Photon-controlled growth of multilayered structures
[DE88-005061] 13 p1847 N88-21054

Strength and microstructure of ceramics
[AD-A190712] 15 p2046 N88-22191

Role of cracks in the creep of structural polycrystalline ceramics
[AD-A191485] 18 p2490 N88-24770

Characteristics of polysilicon layers and their application in sensors 19 p2669 N88-25861

The effects of thin compressive films on indentation fracture toughness measurements
[AD-A192243] 20 p2779 N88-26480

Pure metallic bridge and point-contact tunneling into single- and polycrystal YBa2Cu3O(sub 7-y)
[DE88-010030] 20 p2878 N88-27084

Microchemical analysis of polycrystalline Ni3Al and other ordered alloys using the field-ion microscope atom probe
[DE88-011519] 21 p2914 N88-27294

Superconducting thin films, composites and junctions
[AD-A193123] 21 p2937 N88-27440

POLYCYTHEMIA

Polycythemia and hydration status: Effects on blood volume and thermoregulation during exercise-heat stress
[AD-A185946] 07 p0888 N88-15383

POLYESTERS

Structure of thermotropic polyesters with large substituents
[AD-A184086] 04 p0418 N88-12595

X-ray diffraction study of thermotropic liquid crystalline polyesters and diester model compounds
[AD-A186788] 09 p1255 N88-17521

Polyether-polyester graft copolymer
[NASA-CASE-LAR-13447-1] 11 p1463 N88-18725

Combustion of PMMA, PE and PS in a ramjet
[VTH-LR-514] 18 p2484 N88-24733

Polyacrylic acid electrolyte-modified zinc phosphate conversion coatings for corrosion protection of steel
[DE88-004878] 19 p2617 N88-25527

POLYETHER RESINS

NT PEEK
NT POLYMETHYL METHACRYLATE

Polyether-polyester graft copolymer
[NASA-CASE-LAR-13447-1] 11 p1463 N88-18725

POLYETHERETHERKETONES

U PEEK

POLYETHYLENES

High ionic conductivity in PEO.PPG block polymer and salt solutions
[AD-A183502] 01 p0026 N88-10168

Ionically conductive polymers: Application to solid state batteries
[AD-A183733] 01 p0037 N88-10239

Physical properties of immiscible polymers
03 p0297 N88-11868

Polymer composition --- cable insulation
[EP-PATENT-0-199-444-A1] 04 p0418 N88-12594

Effects of additives on fire properties of polyethylene
[AD-A187064] 09 p1146 N88-16871

Nucleation and growth of calcium carbonate crystals on surface-modified polyethylene and polystyrene
[DE88-005126] 11 p1465 N88-18733

Fracture characteristics of a viscoelastic polymer under constant load: Experiments and analysis
11 p1501 N88-18963

Partial discharges and the electrical aging of cross linked polyethene (XLPE) cable insulation
[EUT-86-E-160] 14 p1892 N88-21300

Combustion of PMMA, PE and PS in a ramjet
[VTH-LR-514] 18 p2484 N88-24733

Combustion of PMMA (polymethylmethacrylate), PE (polyethylene) and PS (polystyrene) in a ramjet
[PB88-186572] 20 p2769 N88-26417

Morphological changes in polymer electrolyte cells
[AD-A195821] 24 p3368 N88-30054

POLYGONS

NT RECTANGLES
NT RHOMBOIDS
NT TRIANGLES

Two low-order mixed methods for the elasticity problem
[PB87-225272] 05 p0610 N88-13749

An application of digital cartography updating middle and small scale thematic maps using orbital data
[INPE-4460-TDL/317] 12 p1637 N88-19805
Investigation into the use of texturing for real-time computer animation
[AD-A191008] 16 p2251 N88-23454
Linear programming in R sup 3 and the skeleton and largest incircle of a convex polygon
[PB88-124664] 20 p2846 N88-26892

POLYHEDRONS
NT CUBES (MATHEMATICS)
NT ICOSAHEDRONS
NT PYRAMIDS
Two low-order mixed methods for the elasticity problem
[PB87-225272] 05 p0610 N88-13749
Adaptive grid for polyhedral visibility in object space: An implementation
[PB88-100938] 06 p0760 N88-14663
Recognition of polyhedral objects under structured illumination
[PB88-106703] 07 p0932 N88-15661
Polyhedral combinatorics
[CWI-OS-R8701] 08 p1072 N88-16466
On effectively labeling planar projections of polyhedra
[CWI-CS-R8715] 13 p1826 N88-20917

POLYIMIDE RESINS
Development of a polyimide matrix for filament winding with improved extensibility and fracture toughness for permanent use at 200 C
[BMFT-FB-T-86-118] 01 p0030 N88-10190
Addition polyimide composition
[EP-PATENT-0-167-304-A1] 01 p0053 N88-10337
Synthesis and characterization of block copolymers
[AD-A184406] 03 p0296 N88-11856
In-situ characterization of the interface of glass reinforced composites
[AD-A185136] 05 p0557 N88-13391
High temperature adhesive
[PB87-109229] 06 p0683 N88-14186
Correlations of norbornenyl crosslinked polyimide resin structures with resin thermo-oxidative stability, resin glass transition temperature and composite initial mechanical properties
[NASA-TM-100791] 09 p1147 N88-16877
Fabrication and electrical characterization of multilevel aluminum interconnects used to achieve silicon-hybrid wafer-scale integration
[AD-A190519] 15 p2060 N88-22282
New polyisoimides: An approach to in situ rigid-rod polyimide formation
[AD-A191665] 18 p2490 N88-24773
High temperature resins for injection. High temperature pre-impregnated
[RC-648676] 20 p2780 N88-26486

POLYIMIDES
Synthesis and characterization of processable polyimides with enhanced thermal stability
[NASA-CR-181447] 01 p0030 N88-10191
A quantum theoretical study of polyimides
[NASA-CR-181495] 03 p0292 N88-11831
Flexibilized copolyimide adhesives
[NASA-TM-89303] 05 p0570 N88-13474
Development of an impact- and solvent-resistant thermoplastic composite matrix, phase 4
[NASA-CR-178413] 06 p0677 N88-14145
An investigation of physical properties of thermoplastic polyimides
[NASA-TM-100530] 06 p0678 N88-14151
Space environmental effects on polymeric materials
[NASA-CR-182454] 09 p1148 N88-16879
Adhesion of vapour phase deposited ultra-thin polyimide films on polycrystalline silver
[AD-A187930] 10 p1306 N88-17810
Vapor phase deposition and growth of polyimide films on copper
[AD-A189969] 15 p2044 N88-22178
Evaluation of a thermoplastic polyimide (422) for bonding GR/PI composite
[NASA-TM-100584] 16 p2182 N88-23003
Carboxylate formation at the interface between a polyimide coating and cobalt 17 p2320 N88-23859
Improved structural polymer alloys and composites
[AD-A192092] 19 p2619 N88-25538
A monolithic gas flow sensor with polyimide as thermal insulator 19 p2669 N88-25864
Substituted 1,1,1-Triaryl-2,2,2-Trifluoroethanes and processes for their synthesis
[NASA-CASE-LEW-14345-1] 20 p2767 N88-26404
Initial adhesive screening of novel polyamide-imides and their copolymers
[NASA-TM-100641] 20 p2779 N88-26481

POLYMER CHEMISTRY
Novel polymers and copolymers and production of poly(acetylene)
[EP-PATENT-0-173-473-A2] 01 p0026 N88-10161
Novel conductive polymers
[EP-PATENT-0-182-548-A2] 01 p0026 N88-10163
Crosslinkable elastomeric materials
[EP-PATENT-0-181-735-A1] 01 p0026 N88-10165
Boronium complexes as polymer catalysts
[GB-PATENT-2-161-475-A] 01 p0026 N88-10166
Adhesion properties of polyelectrolyte-chemisorbed zinc phosphate conversion coatings
[DE87-012489] 01 p0029 N88-10186
Preparation of polymer polyols
[EP-PATENT-0-162-589-A1] 01 p0102 N88-10665
Experiments of the selection of a method evaluating the fire resistance of some materials based on macromolecular compounds
[NASA-TT-20129] 02 p0154 N88-10966
Physical properties of immiscible polymers
03 p0297 N88-11868
Estimations of gravitational effects on thermal denaturation process in a biopolymer
03 p0318 N88-12013
Simultaneous TG/DSC (thermogravimetry/Differential Scanning Calorimetry) and TG/MS (thermogravimetry/Mass Spectrometry) analyses of polymeric and energetic materials
[DE88-000727] 04 p0413 N88-12561
Effect of sidechain length and crosslinking on ionic conductivity in polyphosphazene solid electrolytes
[AD-A184419] 04 p0497 N88-13058
Characterization of the microstructures of various materials
[AD-A184961] 05 p0655 N88-14017
Correlation between flammability and heat of combustion of polymers
[NASA-TT-20116] 08 p0973 N88-15884
Theoretical bases of polymer photodegradation and photooxidation
[AD-A186533] 08 p0974 N88-15889
Contrasting conductance/viscosity relations in liquid states of vitreous and polymer solid electrolytes
[AD-A189378] 13 p1748 N88-20452
Examination of polysulfide sealants by scanning electron microscopy
[MRL-R-1096] 13 p1752 N88-20478
Aging properties of cable polmers (2)
[NASA-TT-20228] 13 p1752 N88-20479
Evidence for first polymer in Comet Halley: Polyoxymethylene 14 p1997 N88-21906
Molecular dynamics of materials possessing high energy content
[AD-A190034] 15 p2034 N88-22116
Donor acceptor polymerization chemistry as a vehicle to low energy cure matrix resins
[AD-A190119] 15 p2044 N88-22179
Research on stable processible conducting polymers for electronic applications
[AD-A190246] 15 p2044 N88-22180
Structural Ceramics
[NASA-CP-2427] 17 p2323 N88-23872
Synthesis and characterization of new phosphazene polymers
[AD-A191508] 18 p2490 N88-24771
Electronic and ionic transport in polymers
[AD-A191642] 18 p2490 N88-24772
Next-generation fire extinguishing agent. Phase 1: Suppression concepts
[AD-A192279] 19 p2614 N88-25514
Substituted 1,1,1-Triaryl-2,2,2-Trifluoroethanes and processes for their synthesis
[NASA-CASE-LEW-14345-1] 20 p2767 N88-26404
Fundamental studies of elastomers
[DE88-009679] 20 p2778 N88-26471
Statistical mechanics of polymer systems
[DE88-011172] 20 p2778 N88-26477
Initial adhesive screening of novel polyamide-imides and their copolymers
[NASA-TM-100641] 20 p2779 N88-26481
Energy migration, motion and order in synthetic polymers
[AD-A193334] 21 p2918 N88-27320
Optimization and scale-up performance of polymer electrolyte batteries
[AD-A193987] 22 p3073 N88-28243
The overcharge behavior of polymer electrolyte cells
[AD-A193984] 22 p3117 N88-28522
Polyazidoesters as energetic polymers and copolymer components with fluoro derivatives
[AD-A194236] 23 p3199 N88-29039
Prediction of degradation of polymeric coating materials 24 p3354 N88-29970
Novel ladder polymers for use as high temperature stable resins or coatings
[NASA-CASE-LEW-14203-1] 24 p3356 N88-29984

POLYMER MATRIX COMPOSITES
NT BORON-EPOXY COMPOSITES
NT CARBON FIBER REINFORCED PLASTICS
NT EPOXY MATRIX COMPOSITES
NT GLASS FIBER REINFORCED PLASTICS
NT GRAPHITE-POLYIMIDE COMPOSITES
NT REINFORCED PLASTICS
Ultrasonic examination of high performance polymer composites
[DRIC-T-7862] 01 p0027 N88-10170
Development and application of composites
03 p0286 N88-11795
Time-temperature-stress capabilities of composite materials for advanced supersonic technology application
[NASA-CR-178272] 06 p0677 N88-14144
Space environmental effects on polymeric materials
[NASA-CR-182418] 07 p0838 N88-15082
Aeropropulsion '87. Session 1: Aeropropulsion Materials Research
[NASA-CP-10003-SESS-1] 09 p1118 N88-16697
High temperature polymer matrix composites
09 p1119 N88-16700
Thermal deformation and strength of composite materials at high temperatures 14 p1885 N88-21263
Singlet oxygen behavior in solid polymer matrices
[DE88-005171] 15 p2043 N88-22171
Nondestructive evaluation by acousto-ultrasonics
15 p2082 N88-22412
Homogenization study of matrix behavior in a composite material
[ONERA-RT-1/7256-RY-060-R]
16 p2172 N88-22943
A thermally modified polymer matrix composite material with structural integrity to 371 C
[NASA-TM-100922] 19 p2609 N88-25483
Thermoplastic coating of carbon fibers
[NASA-CR-183067] 20 p2767 N88-26407
Irreversible deformations during fracture in polymers
[W-7/86] 20 p2780 N88-26485
Microwave polymerization of composite structures
[REPT-881-430-116] 21 p2922 N88-27343
The effects of moisture loss and elevated temperature upon the material damping of fibre reinforced polymer matrix composites
[UTIAS-324] 23 p3188 N88-28970

POLYMER PHYSICS
Mechanisms of polymer degradation using an oxygen plasma generator
[NASA-TM-100681] 01 p0018 N88-10110
Fluid mechanical issues in polymer processing
[DE88-002767] 08 p0972 N88-15880
Study of molecular mobility of noncrystaline polymer alloys of different compatibility using mechanical spectrometry
[ISAL-87-0032] 09 p1149 N88-16883
Integral equation theory of homopolymer melts
[DE88-005304] 13 p1751 N88-20470
Integral equation theory of polymer blends
[DE88-005305] 13 p1751 N88-20471
Next-generation fire extinguishing agent. Phase 1: Suppression concepts
[AD-A192279] 19 p2614 N88-25514
Storing bits on a DNA polymer chain
[AD-A195701] 24 p3356 N88-29981

POLYMERIC FILMS
Optical damage in polymers by millisecond light pulses
[DE87-013106] 02 p0151 N88-10943
Molecular composites: Processing, post-treatment and mechanics
[AD-A184458] 04 p0410 N88-12547
Elementary fluorination of polymers
[ETN-88-90812] 07 p0836 N88-15075
Use of hydrophilic polymer coatings for control of electroosmosis and protein adsorption
07 p0925 N88-15620
Interfacial effects in thin Li/PEO cells at room temperature
[AD-A186974] 09 p1157 N88-16931
Electrically conducting polymer-copper sulphide composite films, preparation by treatment of polymer-copper (2) acetate composites with hydrogen sulfide
[NASA-TT-20204] 10 p1305 N88-17803
Interactions of cultured human endothelial cells with polymeric surfaces
[PB88-112255] 10 p1369 N88-18178
Electronic and ionic transport in polymers
[AD-A187253] 11 p1452 N88-18651
Polymer reflectors research during FY86
[DE88-001101] 11 p1508 N88-19009
Transport properties of conductive polymers
[AD-A188411] 12 p1610 N88-19628
Morphological studies of conductive polymers
[AD-A188456] 12 p1610 N88-19629
The effects of thin polymeric surface films in reducing fretting corrosion and wear
[AD-A188633] 12 p1611 N88-19634

Molecular dynamics of laser ablation of a polymer coating
[DE88-004337] 13 p1750 N88-20466
Safety research of insulating materials of cable for nuclear power generating station
[NASA-TT-20202] 13 p1752 N88-20477
Measuring thin film properties using SAW (Surface Acoustic Wave) devices: Diffusivity and surface area
[DE88-002216] 13 p1834 N88-20970
Research on stable processible conducting polymers for electronic applications
[AD-A190246] 15 p2044 N88-22180
Development of polymeric films with piezoelectrical properties from polypeptides; low, odd nylons; or polyureas
[AD-A190301] 15 p2044 N88-22181
Polymer fuel cell as an energy storage component for space power applications 17 p2429 N88-24452
Mechanisms of gas permeation through polymer membranes: Renewal proposal for period December 1, 1986 - November 30, 1989
[DE88-007436] 18 p2494 N88-24796
Fabrication of a flexible conductor by vapor deposition
[DE88-007500] 19 p2661 N88-25826
Characterization of proton conducting polymer blends
19 p2669 N88-25867
Pyrolyzed organic polymer nitrogen dioxide sensor
19 p2669 N88-25868
Thermodynamic study of hygroscopic polymers using surface acoustic waves 19 p2672 N88-25882
Thin-membrane Lamb-mode acoustic oscillators for chemical detection 19 p2673 N88-25895
Refractory films from spin-cast carbon
[DE88-011251] 21 p2919 N88-27327
A resistive-film based force transducer for the study of exercise
[AD-A192601] 21 p2986 N88-27730
Chemistry of adhesion at the polyimide-metal interface
[AD-A194647] 22 p3058 N88-28143
SRM (Solid Rocket Motor) propellant and polymer materials structural modeling
[NASA-TP-2824] 22 p3089 N88-28343
Optical bistable behavior of a planar quasi-waveguide interferometer made with a conjugated organic polymer film
[AD-A194349] 22 p3152 N88-28756
The radiation sensitivity of select metal chelate polymers: Mechanistic changes at higher energies
[AD-A193467] 23 p3196 N88-29019
Polymeric heat pipe wick
[NASA-CASE-GSC-13019-1] 23 p3214 N88-29133
Performance Prediction for Coatings. Proceedings of a Workshop
[AD-A188973] 24 p3354 N88-29966
Electrochemical evaluation of the long term corrosion resistance of polymer coated steel
24 p3355 N88-29974
An electrochemical impedance spectroscopy study of reactions at the metal/coating interface
24 p3355 N88-29975
A review of melt and vapor growth techniques for polydiacetylene thin films for nonlinear optical applications
[NASA-TM-100340] 24 p3430 N88-30412

POLYMERIZATION
NT COPOLYMERIZATION
NT DIMERIZATION
Synthesis and characterization of processable polyimides with enhanced thermal stability
[NASA-CR-181447] 01 p0030 N88-10191
Applications and limitations of deuterium labeling methods to neutron scattering studies of polymers
[DE87-012936] 02 p0151 N88-10945
The influence of polymer structure on triplet luminescence
[DE87-014431] 02 p0152 N88-10952
Migration and transfer of triplet energy in selected polymer systems
[DE87-014432] 02 p0152 N88-10953
Polyvinyl esters of omega-H-perfluoroacids and polyvinyl alcohol obtained from them
[AD-A184633] 03 p0279 N88-11755
High-molecular compounds (selected articles)
[AD-A184668] 03 p0293 N88-11842
Cure and properties of thermosetting polymers
[AD-A184669] 03 p0293 N88-11843
Polymers in solar technologies
[DE88-001102] 03 p0294 N88-11849
Wittig synthesis of conductive segmented block polymer compositions
[AD-A184018] 03 p0295 N88-11850
Highly Non-Linear Optical (NLO) organic crystals and films. Electrooptical organic materials
03 p0297 N88-11866
Conductive polymers via reactive aligomer
[AD-A184270] 04 p0419 N88-12597
Conducting hybrid polymeric systems
[DE88-000527] 04 p0421 N88-12611
Proton abstraction as a route to conductive polymers
[AD-A184019] 04 p0421 N88-12612
Molecular-level synthesis and characterization of metal-polymer interfaces
[AD-A184956] 05 p0567 N88-13455
Molecular and supramolecular orientation in conducting polymers
[DE88-000533] 05 p0569 N88-13472
Effects of hydrolysis on metallo-organic solution deposition of PZT films
[ATR-86(8443)-1] 06 p0679 N88-14160
TMA-microrheological testing of polymers (thermomechanical analysis)
[PB87-228805] 06 p0683 N88-14187
Ionically conducting polymers: Principles and properties of solid electrolytes
[DE88-001552] 06 p0684 N88-14190
The morphology of emulsion polymerized latex particles
[DE88-002672] 08 p0972 N88-15879
Processing, fabrication, applications and limitations of inherently conducting polymers
[DE88-003210] 08 p0973 N88-15883
Synthesis of high molecular weight peptide polymers and copolymers containing L-dope residues
[AD-A186462] 08 p0973 N88-15887
The mechanism of stereo regulation during anionic polymerization of polar monomers
[AD-A186530] 08 p0973 N88-15888
A 13C and 15N solid state NMR characterization of aramid-containing nylon-6 polymers synthesized by in situ polymerization of caprolactam with benzoyl caprolactam derivatives
[AD-A187067] 09 p1147 N88-16872
Thermogravimetric analysis of polymeric materials for an intermediate temperature solid electrolyte
[DE88-004854] 10 p1306 N88-17809
The deposition rate dependence of plasma polymerization on the radius of curvature of the substrate
[DE88-003811] 10 p1412 N88-18429
Polymerization of fluorinated diacetylenes
[AD-A188051] 11 p1462 N88-18716
Polymeric materials for electro-optic testing
[AD-A188382] 12 p1610 N88-19627
Reinforcing of thermoplastic polycarbonate and polysulfone with carbon fibers: Production and characteristics of UD-compound objects
[NASA-TT-20158] 13 p1735 N88-20374
High-temperature thermosets derived from the Diels-Alder polymerization of bisbenzocyclobutenes and bismaleimides
[AD-A188800] 13 p1747 N88-20449
Donor acceptor polymerization chemistry as a vehicle to low energy cure matrix resins
[AD-A190119] 15 p2044 N88-22179
High-performance polymeric materials
[AD-A190708] 15 p2046 N88-22190
Elementary characterization of Fibredux 913 CTS 5 34 percent preimpregnated carbon-epoxy from Ciba Geigy
[M-484300] 16 p2171 N88-22941
Electrochemistry in near-critical and supercritical fluids. 5: The dimerization of quinoline and acridine radical anions and dianions in ammonia from -70 C to 150 C
[AD-A190858] 16 p2175 N88-22967
Complexation and hydrolysis reactions of iron(III)
17 p2322 N88-23867
Polymer precursors for SiC ceramic materials
17 p2326 N88-23889
Polymer precursors for ceramic composites
17 p2326 N88-23890
Aromatic cyclotriphosphazenes
[NASA-CASE-ARC-11428-3] 18 p2477 N88-24692
Current and future molecular structures of aerospace organic matrix resins 18 p2477 N88-24695
Synthesis and characterization of new phosphazene polymers
[AD-A191508] 18 p2490 N88-24771
Electronic and ionic transport in polymers
[AD-A191642] 18 p2490 N88-24772
Demixing of aqueous polymer two-phase systems in low gravity
[NASA-TM-101141] 18 p2496 N88-24809
Fundamental studies of elastomers
[DE88-009679] 20 p2778 N88-26471
Polymerization of epoxy matrix composites using pulsed microwaves
[CERT-3/1324-MO] 20 p2780 N88-26487
Structural study of impregnating resins of TGMDA/DDS type
[ETN-88-92167] 20 p2780 N88-26488
The electronic structure of condensed molecular systems
[DE88-007823] 20 p2851 N88-26923
Soluble metal chelate polymers of coordination numbers six, seven and eight
[AD-A192485] 21 p2917 N88-27314
Precursor chemistry and the structure of silica aerogels
[DE88-011253] 21 p2920 N88-27328
Study of crosslinking and nonelastic mechanical properties of epoxy and PSP networks --- epoxy resins; polystyrylpyridine resins (psp)
[ETN-88-92740] 21 p2921 N88-27337
Microwave polymerization of composite structures
[REPT-881-430-116] 21 p2922 N88-27343
Polymerization of azaethylenes (imines) and aza-1,3-dienes: Potential reactive monomers
[AD-A194717] 23 p3197 N88-29028
Novel ladder polymers for use as high temperature stable resins or coatings
[NASA-CASE-LEW-14203-1] 24 p3356 N88-29984
A review of melt and vapor growth techniques for polydiacetylene thin films for nonlinear optical applications
[NASA-TM-100340] 24 p3430 N88-30412

POLYMERS
Structure of sol-gel-derived inorganic polymers. 2: Silicates and borates
[DE87-013068] 01 p0027 N88-10172
Space environmental effects on polymeric materials
[NASA-CR-182454] 09 p1148 N88-16879
Modification of polymers by photografting processes
17 p2323 N88-23871
A computer model for the flow of a molten polymer in a narrow cavity
[NPL-DMA(A)-157] 22 p3058 N88-28146
Design analysis in polymeric materials
[NPL-DMA(A)-159] 22 p3058 N88-28147

POLYMETHYL METHACRYLATE
High-molecular compounds (selected articles)
[AD-A184668] 03 p0293 N88-11842
Development of crack under periodically pulsed laser radiation 06 p0774 N88-14754
Some aspects of the mechanics and mechanisms of dynamic brittle fracture 10 p1343 N88-18028
Combustion of PMMA, PE and PS in a ramjet
[VTH-LR-514] 18 p2484 N88-24733
Adhesion between polystyrene and polymethylmethacrylate
[AD-A192050] 18 p2492 N88-24785
Flame spread mechanisms over PMMA surfaces
[NASA-TT-20284] 19 p2612 N88-25500
Combustion of PMMA (polymethylmethacrylate), PE (polyethylene) and PS (polystyrene) in a ramjet
[PB88-186572] 20 p2769 N88-26417
Ignition and flame spread of PMMA
[NASA-TT-20290] 20 p2771 N88-26431
Irreversible deformations during fracture in polymers
[W-7/86] 20 p2780 N88-26485
Interactions in miscible polymer blends
[AD-A193824] 22 p3058 N88-28144

POLYNOMIALS
NT BINOMIALS
NT DYADICS
NT HERMITIAN POLYNOMIAL
Approximate polynomial preconditioning applied to biharmonic equations on vector supercomputers
[NASA-TM-100217] 01 p0087 N88-10563
Polynomial compensation, inversion, and approximation of discrete time linear systems
[NASA-TM-100027] 03 p0372 N88-12344
A simplified procedure for correcting both errors and erasures of a Reed-Solomon code using the Euclidean algorithm 04 p0435 N88-12698
On color polynomials of Fibonacci graphs
[AD-A184133] 04 p0486 N88-12996
Parallel algorithms for polynomials
[PB87-226304] 06 p0756 N88-14635
Progress in mathematical programming
[AD-A185729] 06 p0759 N88-14658
Diagonalisation methods in polynomial setting
[PB87-138616] 06 p0769 N88-14726
An O(n3L) interior point algorithm for convex quadratic programming
[AD-A186001] 07 p0909 N88-15504
Single-layer wire routing
[AD-A186990] 09 p1157 N88-16932
Acceleration techniques for decoupling algorithms in semiconductor simulation
[DE88-003593] 09 p1221 N88-17323
On exact solutions of multidimensional Schroedinger equation with polynomial potentials
[DE88-700460] 09 p1230 N88-17373
Fast and practical parallel polynomial interpolation
[DE88-003530] 10 p1397 N88-18328
Polynomial preconditioning for conjugate gradient methods
[DE88-005214] 10 p1399 N88-18342

Small degree solutions for the polynomial Bezout equation
[AD-A187630] 10 p1401 N88-18355
An exact pseudo polynomial algorithm for the 0-1 linear diophantine equation
[INPE-4289-PRE/1160] 11 p1531 N88-19148
Elimination of quantifiers of linear variables and corresponding transfer principles
[DE88-005692] 13 p1826 N88-20912
Group theoretic interpretations of Askey's scheme of hypergeometric orthogonal polynomials
[CWI-PM-R8703] 13 p1831 N88-20954
A polynomial approach to the H sub infinity control design method
[MEMO-662] 14 p1962 N88-21701
Generalizations of Laguerre (type) polynomials
[REPT-87-58] 14 p1963 N88-21714
Solution of the compressible Navier-Stokes equations of motion by Chebyshev polynomials for laminar shock-boundary layer flow
[AD-A191033] 16 p2208 N88-23176
Simulation of FELIN logics. Polynomials roots simultaneous computation algorithms
[ETN-88-92182] 16 p2253 N88-23464
Jacobi polynomials as generalized Faber polynomials
[CWI-PM-R8706] 16 p2258 N88-23498
Orthogonal polynomials with respect to a symmetric inner product involving derivates
[REPT-87-59] 16 p2259 N88-23504
On a classification of problems on sets of bilinear forms by formal polynomials
[RR-642-I-IMAG-53-LIFIA] 17 p2392 N88-24219
Sensitivity analysis for the system reliability function
[AD-A191648] 18 p2525 N88-24979
Null steering applications of polynomials with unimodular coefficients
[AD-A191087] 18 p2562 N88-25211
On a biorthogonal system associated with uniform asymptotic expansions
[CWI-AM-R8709] 18 p2566 N88-25240
High degree interpolation polynomial in Newton form
[NASA-CR-181677] 18 p2567 N88-25249
A new trajectory following polynomial-time algorithm for the linear programming problem
[REPT-87-87] 20 p2840 N88-26848
Accurate solution of parabolic equations by expansion in ultraspherical polynomials
[DE88-701829] 20 p2845 N88-26880
Finding minimum-cost circulations by canceling negative cycles
[AD-A192727] 21 p3005 N88-27825
Structure of bound states in polynomial potentials
[DE88-702437] 21 p3007 N88-27837
Evaluation of quantum mechanics path integrals by the approximations exact on a class of polynomial functionals
[DE88-702434] 21 p3011 N88-27865
Optimum-Path-to-Go guidance of command adjusted trajectory projectiles
[AD-A193377] 22 p3040 N88-28051
Solution to the compressible Navier-Stokes equations of motion by Chebyshev polynomials with implicit time stepping
[AD-A194119] 22 p3075 N88-28257
Random pseudo-polynomial algorithms and exact problems
[REPT-87-014] 22 p3140 N88-28672
Polynomials with restricted coefficients and their applications
[AD-A192589] 23 p3202 N88-29055
Polynomial definition of discrete field points of map of diffusion equation, part 1
[AD-A193697] 23 p3271 N88-29467
On matrix pencil equivalents of a general polynomial matrix
[MATH-REPT-207] 23 p3273 N88-29479

POLYPEPTIDES
NT GLUTATHIONE
Estimations of gravitational effects on thermal denaturation process in a biopolymer
03 p0318 N88-12013
Development of polymeric films with piezoelectrical properties from polypeptides; low, odd nylons; or polyureas
[AD-A190301] 15 p2044 N88-22181
Influence of altitude and caffeine during rest and exercise on plasma levels of proenkephalin peptide F
[AD-A192659] 22 p3131 N88-28616

POLYPHENYLS
Carbon residue studies of polyphenyl ethers and ester-based lubricants using a microcarbon residue tester
[AD-A188585] 12 p1611 N88-19632
The synthesis of polyphenylene from a CIS-dihydrocatechol biologically produced monomer
18 p2478 N88-24699

The crystallization of tough thermoplastic resins in the presence of carbon fibers
[NASA-CR-182984] 20 p2776 N88-26464

POLYPROPYLENE
High ionic conductivity in PEO.PPG block polymer and salt solutions
[AD-A183502] 01 p0026 N88-10168
Prediction of long-term creep in polypropylene from short-term tests
[NPL-DMA(A)-156] 22 p3088 N88-28337

POLYSACCHARIDES
NT CELLULOSE
NT GLYCOGENS
NT STARCHES

POLYSTATION DOPPLER TRACKING SYSTEM
A preliminary assessment of thunderstorm outflow wind measurement with airport surveillance radars
[AD-A189064] 13 p1799 N88-20757

POLYSTYRENE
Polymer chain segment orientation during stress relaxation
[DE87-013392] 01 p0027 N88-10174
Metal containing polymers as fuel cell catalysts
[AD-A184605] 03 p0347 N88-12194
Group contribution analysis of the damping behavior of homopolymers, statistical copolymers and interpenetrating polymer networks based on acrylic, vinyl and styrenic mers
[AD-A185904] 07 p0836 N88-15070
Study on the correlation of polystyrene (PS) film craze to its fracture behaviour by TEM (Transmission Electron Microscopy)
[PB87-143343] 08 p0970 N88-15870
Nucleation and growth of calcium carbonate crystals on surface-modified polyethylene and polystyrene
[DE88-005126] 11 p1465 N88-18733
A new polymer-based hydrogen getter
[DE88-004538] 13 p1751 N88-20467
Preferential surface adsorption in miscible blends of polystyrene and poly(vinyl methyl ether)
[AD-A191451] 18 p2490 N88-24769
Adhesion between polystyrene and polymethylmethacrylate
[AD-A192050] 18 p2492 N88-24785
Diffusion of homopolymers into nonequilibrum diblock copolymer structures
[DE88-005306] 18 p2494 N88-24794
Combustion of PMMA (polymethylmethacrylate), PE (polyethylene) and PS (polystyrene) in a ramjet
[PB88-186572] 20 p2769 N88-26417

POLYSULFIDES
Examination of polysulfide sealants by scanning electron microscopy
[MRL-R-1096] 13 p1752 N88-20478

POLYTETRAFLUOROETHYLENE
NT TEFLON (TRADEMARK)
An evaluation of effectiveness of PTFE (polytetrafluoroethylene) type friction reducers on reducing friction and wear
[AD-A187440] 10 p1340 N88-18010
Evaluation of transfer films of Salox M on 440C for HPOTP bearing cage applications, task 119
[NASA-CR-179020] 23 p3223 N88-29184

POLYTOPES
The perfectly matchable subgraph polytope of an arbitrary graph
[AD-A185993] 07 p0913 N88-15539
The clique polytope of a graph
[MEMO-663] 14 p1963 N88-21710

POLYURETHANE FOAM
Evaluation of the thermal effectiveness of urethane foam and fiberglass as insulation systems for tank cars
[PB88-100797] 06 p0686 N88-14207
Investigations of the stability of the cell opening of soft polyurethane foams
[ETN-88-91481] 11 p1463 N88-18724
Thermal conductivity of selected foams and systems from 100 to 300 K
[PB88-201553] 20 p2777 N88-26466

POLYURETHANE RESINS
Urea-polyurethane and polydimethylsiloxane mixtures. Morphology control using a block copolymer
[ISAL-IDI1-87-05] 02 p0153 N88-10959
Synthesis and characterization of block copolymers
[AD-A184405] 03 p0295 N88-11855
Study of aeropropulsion laboratory pressure drop rig and recommended test procedure
[AD-A184333] 03 p0322 N88-12038
High explosive moulding powders from RDX and aqueous polyurethane dispersions
[AD-A185026] 05 p0568 N88-13458
Structure-property relationships in thermoplastic elastomers 4. Dynamic mechanical relaxations in poly(dioxolane), poly(butyltrioxocane) and poly(propylene oxide) polyurethanes
[AD-A186278] 07 p0836 N88-15073
Optimization of binary pigment coatings
[AD-A189103] 13 p1748 N88-20450
Polyacrylic acid electrolyte-modified zinc phosphate conversion coatings for corrosion protection of steel
[DE88-004878] 19 p2617 N88-25527
Cleanability of aircraft polyurethane topcoats
[AD-A193456] 23 p3170 N88-28878

POLYVINYL ALCOHOL
Polyvinyl esters of omega-H-perfluoroacids and polyvinyl alcohol obtained from them
[AD-A184633] 03 p0279 N88-11755
High-molecular compounds (selected articles)
[AD-A184668] 03 p0293 N88-11842
Characterization of proton conducting polymer blends
19 p2669 N88-25867

POLYVINYL CHLORIDE
Effect of test temperature and frequency on fatigue crack propagation in PVC 05 p0606 N88-13715
Evaluation of flammability for cable-like polymers
[NASA-TT-20225] 13 p1752 N88-20476
Burning characteristics and flammability of PVC cables in groups
[NASA-TT-20226] 14 p1893 N88-21303

POLYVINYL FLUORIDE
Polymer materials for pressure sensors
06 p0676 N88-14141
Polymer material for heat sensors
06 p0676 N88-14142
Piezoelectric laminates for torsional and bending model control: Theory and experiment
10 p1343 N88-18029
Statistical-mechanical study of polyvinylidene fluoride
[AD-A188310] 12 p1609 N88-19624
Piezoelectric polymer tactile sensor arrays for robotics
[AD-A188852] 12 p1634 N88-19780

PONDEROMOTIVE FORCES
Numerical simulation of laser filamentation experiments
[ETN-87-90959] 02 p0179 N88-11118
HF sidebands in the ionosphere
05 p0574 N88-13497

PONTRYAGIN PRINCIPLE
Optimal control theory of load-following and parameter-tracking of nonlinear systems: An application of Pontryagin Maximum Principle to reactor dynamics
[DE88-004770] 11 p1532 N88-19152

POPULATION INVERSION
Active medium formation in lasers using mixtures of inert gases and optical breakdown pumping
06 p0709 N88-14347
Population inversion in gapless semiconductors as result of interband pumping 06 p0770 N88-14732
Further study of inversion layer MOS solar cells
07 p0925 N88-15621

POPULATION THEORY
A tight upper bound for the speed-up of parallel best-first branch-and-bound algorithms
[AD-A184246] 04 p0477 N88-12939
An urn model for the multi-sample capture/recapture sequential tagging process
[AD-A184470] 04 p0486 N88-12998
A comparison of the basket method and the stratified random sampling for contract change order negotiations
[AD-A184170] 04 p0500 N88-13080
A functional interpretation of the logistic equation
[REPT-87-037] 05 p0645 N88-13946
An elimination type two-stage procedure for selecting the population with the largest mean from k logistic populations
[AD-A185614] 07 p0916 N88-15566
On selecting the best of k lognormal distributions
[AD-A185628] 07 p0916 N88-15567
Perturbation theory for dual semigroups 2. Time-dependent perturbations in the sun-reflexive case
[PB86-113097] 09 p1230 N88-17369
Empirical and hierarchical Bayes competitors of preliminary test estimators in two sample problems
[AD-A190327] 15 p2125 N88-22670
Selecting the best binomial population: Parametric empirical Bayes approach
[AD-A193341] 23 p3269 N88-29450

POPULATIONS
Galaxy evolution in dense clusters
13 p1855 N88-21101
On two-stage allocation procedures for selection problems
[AD-A190766] 15 p2126 N88-22675
Thailand in maps. Application of the mapping system THEMAK2 for specific purpose atlas preparation
16 p2226 N88-23295
Burn-in with mixed populations
[AD-A194651] 22 p3085 N88-28321

PORES
U POROSITY

POROSITY
NT MICROPOROSITY

Influence of boron on porosity in nickel-base superalloy castings
03 p0299 N88-11877

Geological characterization and statistical comparison of outcrop and subsurface facies: Shannon Shelf sand ridges
[DE87-001243] 03 p0348 N88-12202

Porosity influence on the strength and elasticity of first-year sea ice
[AD-A184493] 03 p0354 N88-12233

Crack propagation properties of sintered steel
05 p0604 N88-13698

The use of NMR imaging to measure porosity and binder distributions in green-state and partially sintered ceramics
[DE88-003099] 08 p0972 N88-15881

Quantitative non-destructive evaluation of porous composite materials based on ultrasonic wave propagation
[NASA-CR-182544] 11 p1447 N88-18627

Porosity and fractality of a cometary nucleus
14 p2004 N88-21951

Effects of irradiation on thermal coalescence of pores in real crystals
[DE88-701683] 16 p2282 N88-23663

Krypton based adsorption type cryogenic refrigerator
[NASA-CASE-NPO-17334-1-CU]
17 p2331 N88-23917

Electrode films of porous agarose: The effects of physical structure on electron transport processes
[DE88-007366] 19 p2611 N88-25493

Employment of porous polytetrafluoroethylene Membrane with a hydrophilic and hydrophobic stratal structure for construction of an enzyme electrode
[NASA-TT-20296] 19 p2620 N88-25543

A model for insulated wires in the method of moments code NEC (Numerical Electromagnetics Code)
[DE88-008920] 20 p2794 N88-26577

Characterization of the surface area and porosity of sol-gel films using saw devices
[DE88-008794] 20 p2875 N88-27069

Gaseous tracer techniques for pore structure characterization of granular materials
[DE88-011542] 21 p2911 N88-27274

Application of controlled interfacial pore structures to kinetic studies in alumina
[DE88-010884] 21 p2919 N88-27326

Computer modeling for surface properties of carbon fibers 21 p2928 N88-27383

Method for maintaining precise suction strip porosities
[NASA-CASE-LAR-13638-1] 23 p3201 N88-29051

POROUS MATERIALS

Studies of transport processes in porous and ion exchange membranes
[ISBN-951-99847-0-4] 01 p0021 N88-10133

Optical characterization of silica aerogel glass
[DE87-014617] 02 p0153 N88-10956

Voltammetric investigation of porous silicon for integrated circuit applications
[DE87-009287] 02 p0166 N88-11042

The correlation between microstructure and thermomechanical properties of two-phase materials and porous sintered materials
[KFK-4205] 03 p0292 N88-11835

Development of a new method of measuring the characteristic impedance and complex wave number of a porous acoustic material
[AD-A185038] 05 p0646 N88-13957

Fundamental studies of surfaces processes and trace analysis using solid electrodes
[AD-A186156] 07 p0828 N88-15024

Programs for calculating transient Darcian flow through non-uniform materials
[DE88-001924] 07 p0852 N88-15177

Physics of immiscible flow in porous media
[PB88-131008] 11 p1487 N88-18873

Development, manufacturing and testing of a gas loaded variable conductance methanol heat pipe
[NLR-MP-87010-U] 13 p1767 N88-20571

Abrasion resistant porous silica antireflective coatings
[DE88-006230] 14 p1894 N88-21308

Molecular dynamics of materials possessing high energy content
[AD-A190034] 15 p2034 N88-22118

Transient compressible flow in porous materials
[DE88-006685] 15 p2067 N88-22324

Review of numerical methods for radionuclide transport in three-dimensional porous media, at high Peclet numbers
[CFDU/87/10] 18 p2538 N88-25061

POROUS PLATES

Fatigue failure of thin porous strips
04 p0426 N88-12640

POROUS WALLS

Heterogeneous diffusion flame stabilization
[AD-A193014] 20 p2771 N88-26429

Radiative heat transfer to steady flow of a chemically reacting fluid in a horizontal porous channel with variable wall temperature
[DE88-702704] 24 p3372 N88-30081

PORPHYRINS

NT CHLOROPHYLLS

Reactions of porphyrins in surfactant assemblies, microemulsions and in solutions
[AD-A184797] 05 p0560 N88-13412

Artificial photosynthesis using chlorophyll based carotenoid-quinone triads
[DE88-001660] 07 p0884 N88-15362

Novel catalysts for methane activation
[DE88-003637] 13 p1738 N88-20390

The design of methane activation catalysts
[DE88-002265] 23 p3199 N88-29043

PORTABLE EQUIPMENT

Loss of performance due to military clothing and equipment
[IZF-1986-13] 01 p0077 N88-10490

A portable hypercube simulator
[DE87-013369] 04 p0478 N88-12947

The Portable Instant Display and Analysis Spectrometer (PIDAS) 05 p0611 N88-13756

A comparison of measurements from the A/E35U-3 and PWMA (Portable Wear Metal Analyzer) spectrometers
[AD-A186855] 09 p1177 N88-17047

TABLET: The personal computer of the year 2000
[NASA-CR-182528] 10 p1384 N88-18267

A hybrid transform/DPCM encoder for data compression
[DE87-014852] 13 p1758 N88-20518

Ultrasonic inspection of irregular surfaces
[AERE-R-12465] 13 p1780 N88-20648

Portability of software. The use of software in the hardware mixture
[MBB/LWD-11/S/PUB/253] 16 p2246 N88-23416

An investigation of conformable antennas for the astronaut backpack communication system
[NASA-CR-182908] 17 p2333 N88-23929

PORTS (OPENINGS)

An analytical and experimental study of injection-locked two-port oscillators
[NASA-TM-100119] 04 p0439 N88-12727

Dimensions of ignition zones in blow-outs of combustible gases from rectangular and circular ports
07 p0918 N88-15577

POSITION (LOCATION)

NT SOLAR POSITION

Accurate position measuring spacecraft package
[ESA-CR(P)-2398-VOL-1] 01 p0004 N88-10022

Accurate position measuring spacecraft package, executive summary
[ESA-CR(P)-2398-VOL-2] 01 p0004 N88-10023

Antarctic field tests of SARSAT personal locater beacons
[NASA-TM-4008] 01 p0063 N88-10403

Energy-selected electron diffraction experiments using the rocking-crystal method in the raster microscope for the investigation of localization effects in single crystals
[ETN-87-90409] 01 p0104 N88-10682

Quantum mechanics with spontaneous localization and the quantum theory of measurement
[DE87-703072] 02 p0247 N88-11559

GPS vertical axis performance enhancement for helicopter precision landing approach
[NASA-CR-177443] 04 p0397 N88-12477

Effect of permissible variations of center-of-gravity locations of cargo airplane on its mass
04 p0424 N88-12625

Knot selection for least squares thin plate splines
[AD-A185681] 06 p0759 N88-14657

Recursive m-estimators of location and scale for dependent sequences
[AD-A186292] 07 p0903 N88-15469

A directed method for locating the focus of expansion
[AD-A185840] 07 p0906 N88-15491

Localization of Cu 3d levels in the high Tc superconductor YBa2Cu3O approximately 7 by Cu2p X-ray photoelectron spectroscopy
[NOTA-INTERNA-887] 07 p0939 N88-15710

Ariane localization technique by Data Relay Satellite (DRS)
[SES/ENG/TN-548/86] 08 p0961 N88-15821

Effects of uniform target density on random search
[AD-A186468] 08 p1073 N88-16473

Dynamic stress at critical locations of a structure as a criterion for mathematical model modification
09 p1180 N88-17066

Strategic placement of accelerometers to measure forces by the sum of weighted accelerations
[DE88-002262] 10 p1333 N88-17968

Reference position vector 12 p1577 N88-19432

Optimal selection of global positioning system set to minimize emitter location errors
[AD-A189559] 12 p1579 N88-19447

Cramer-Rao bounds on the accuracy of location and velocity estimations using CCD optical sensors
[AD-A188481] 12 p1629 N88-19748

The evaluation and selection of a 5th ground antenna site for the global positioning system
[AD-A189495] 13 p1720 N88-20286

A comparison of terrain association and resection as methods of position location
[AD-A189480] 13 p1790 N88-20710

Method for determining artillery position
[NASA-TT-20236] 14 p1979 N88-21813

Real-time environmental Arctic monitoring (R-TEAM)
[AD-A189948] 15 p2099 N88-22508

Target localization in an inhomogeneous medium
[AD-A190008] 15 p2130 N88-22703

Path following robot
[AD-A190960] 16 p2215 N88-23217

Algorithms and intuition
[NASA-CR-182900] 16 p2252 N88-23459

Point accessibility and primary workspace of simple six-link robots 17 p2345 N88-23976

Angular position measurements at high temperatures and high radiation environments
17 p2434 N88-24479

Search and rescue satellite system (SERES), phase A0
[ETN-88-92335] 18 p2472 N88-24669

Geometric rectangular data file (GERD): An aid to the rapid access to position data 18 p2534 N88-25037

Estimation of balloon position from wind data
[DE88-008968] 19 p2597 N88-25434

Tropical cyclone report
[AD-A191883] 19 p2693 N88-26009

NAVSTAR global positioning system
[AD-A192609] 20 p2757 N88-26354

Automatic omega station and LOP (Line Of Position) selection
[AD-A193302] 21 p2894 N88-27179

Radar information from the partial derivatives of the echo signal phase from a point scatterer
[AD-A193402] 21 p2933 N88-27415

Constructing a highly-available location service for a distributed environment
[AD-A192723] 21 p3001 N88-27801

An algorithm for determining the location of points in computer simulations
[AD-A193713] 23 p3250 N88-29343

DATATRAN: Datum transformation software
[AD-A195723] 24 p3387 N88-30175

Passive microwave measurements of water vapor fields and rain for locating fronts in cyclonic storms
[AD-A195632] 24 p3404 N88-30267

Adaptive control in positioning a rigid-flexible robot arm
[AD-A195194] 24 p3422 N88-30367

Utilizing dynamic stability of orient parts
[AD-A195730] 24 p3427 N88-30397

Study of modern instrumentation and methods for astronomic positioning in the field
[AD-A196173] 24 p3452 N88-30548

POSITION ERRORS

Effect of installation and calibration errors of sensors on system identification results of an aircraft
[ESA-TT-1059] 03 p0266 N88-11678

Determination of TRANET (tracking station coordinates for tracking network) and SMTP (Special Mission Tracking Program) tracking station coordinates for use in the WGS (World Geodetic System) 84
[AD-A185863] 07 p0817 N88-14972

A method and measures to evaluate trackers for air traffic control
[NLR-TR-86072-U] 13 p1720 N88-20287

A comparison of terrain association and resection as methods of position location
[AD-A189480] 13 p1790 N88-20710

A positioning system based on NAVSAT
[NLR-MP-87018-U] 20 p2757 N88-26358

Implementation of a flexible link model in a designed robot system, using the finite element method
[ETN-88-92902] 23 p3243 N88-29303

POSITION INDICATORS

Calibration of attitude control sensors
02 p0159 N88-10995

Effects of combining vertical and horizontal information into a primary flight display
[NASA-TP-2783] 04 p0399 N88-12487

Procedure for detection and identification of a helicopter
[NASA-TT-20234] 13 p1722 N88-20297

Development of an interactive real-time graphics system for the display of vehicle space positioning
[NASA-TM-100429] 13 p1730 N88-20344

Electronics and communications in air traffic control: The Presidential Address
[ETN-88-92057] 14 p1865 N88-21146

Accurate positioning of long, flexible ARM's (Articulated Robotic Manipulator) 16 p2219 N88-23243

Integrated multisensor navigation systems 17 p2294 N88-23722

Technical characteristics of the OmniTRACS: The first operation mobile Ku-band satellite communications system 19 p2647 N88-25709

POSITION SENSING

Error detection and recovery for robot motion planning with uncertainty [AD-A187746] 11 p1534 N88-19165

Long range sensor for rendezvous and docking missions 12 p1587 N88-19497

Procedure for detection and identification of a helicopter [NASA-TT-20234] 13 p1722 N88-20297

The silicon microstrip detector --- particle position measurement [ETN-88-92235] 16 p2210 N88-23189

Accurate positioning of long, flexible ARM's (Articulated Robotic Manipulator) 16 p2219 N88-23243

The position-sensitive counting of photons 16 p2271 N88-23590

Motion planning for a free-flying robot 23 p3255 N88-29378

Path planning and path following for the Amsterdam autonomous cart [FVI-86-22] 24 p3380 N88-30133

POSITIONING

Theoretical and practical aspects of the functional absorber method of arranging sound absorbing panels [BBC-RD-1987/15] 05 p0646 N88-13955

Errors in retrieving hydrological fields and fields of their differential characteristics by method of approximation by orthogonal functions 06 p0727 N88-14475

Improvement in robot positioning accuracy by a kinematic identification model 11 p1496 N88-18931

Geodetic positioning by employment of the GPS-NAVSTAR satellites applying the techniques of VLBI and sequential recursive optimal estimation [INPE-4438-TDL/311] 12 p1594 N88-19547

Method for determining artillery position [NASA-TT-20237] 13 p1834 N88-20974

A control technique for improved robot performance 17 p2391 N88-24212

Position and velocity determination using a Global Positioning System: An outline [B8735052] 20 p2757 N88-26355

Research project Loran-C of the Geometric Service of the Ministry of Public Works [B8735055] 20 p2757 N88-26356

The Sercel TR5S Global Positioning System (GPS) receiver [ETN-88-92473] 20 p2757 N88-26357

Acoustic helicopter positioning 22 p3148 N88-28726

Implementation of a flexible link model in a designed robot system, using the finite element method [ETN-88-92902] 23 p3243 N88-29303

Study of modern instrumentation and methods for astronomic positioning in the field [AD-A196173] 24 p3452 N88-30548

POSITIONING DEVICES (MACHINERY)

NT BOOMS (EQUIPMENT)
NT CAMS

Contributions to fast-reacting and high-precision three-phase positioning systems --- machinery [ETN-87-90427] 01 p0056 N88-10358

AVIRIS scan drive design and performance 06 p0706 N88-14330

Hemispherical pointing mechanism drive unit --- satellite payloads antennas 14 p1874 N88-21193

A pointing mechanism for intersatellite link system 14 p1874 N88-21194

Deployment, hold down and release mechanisms for Wind Scatterometer Antenna (WSA) --- ERS-1 wind scatterometer antenna (WSA) 14 p1876 N88-21207

Development and qualification of the OLYMPUS antenna pointing mechanism 14 p1879 N88-21227

POSITIVE IONS

NT CATIONS
NT HYDRONIUM IONS

On the acceleration of electrons and positive ions in the same direction along magnetic field lines by parallel electric fields [IRF-PREPRINT-103] 15 p2096 N88-22488

Stratospheric positive ion composition measurements and acetonitrile detection: A consistent picture [AERONOMICA-ACTA-A-326-1987] 18 p2542 N88-25084

POSITRON ANNIHILATION

Vector boson pair production in e(+)e(-) collisions [PREPRINT-549] 06 p0778 N88-14774

Single weak gauge boson production at CLIC [PREPRINT-550] 06 p0778 N88-14775

Positron annihilation spectroscopy of AlGaAs/GaAs interfaces in MOCVD-grown GaAs heterojunction solar cells [DE88-003903] 11 p1508 N88-19012

Study of defects in metals by positron annihilation [DE88-701042] 13 p1745 N88-20432

Cascade model of gamma-ray bursts: Power-law and annihilation-line components [NASA-TM-101176] 21 p3032 N88-27998

POSITRONIUM

Electron capture from solids by positrons [DE87-014355] 02 p0232 N88-11463

POSITRONS

Electron capture from solids by positrons [DE87-014355] 02 p0232 N88-11463

Studies of the processing of single words using positron tomographic measures of cerebral blood flow change [AD-A184058] 03 p0356 N88-12244

Gamma radiation at the 970 MeV plane positron channeling in diamond crystals [DE88-700557] 07 p0939 N88-15705

Three-dimensional image reconstruction in object space [DE88-900279] 12 p1712 N88-20246

Model-independent requirements to the source of positrons in the galactic centre [DE88-700968] 14 p1992 N88-21874

Variable-energy positron studies on liquids and liquid-solid interfaces [DE88-006356] 15 p2033 N88-22109

Annihilation momentum density of positrons trapped at vacancy-type defects in metals and alloys [DE88-005936] 15 p2144 N88-22797

The cluster ion approach to the condensation and storage of antihydrogen 16 p2269 N88-23575

Electron-positron physics at 1 TeV [DE88-009019] 19 p2725 N88-26180

Inelastic mean free paths of electrons and positrons in matter [DE88-008086] 20 p2851 N88-26929

Positron emission tomography: A new technique for observing fluid behavior in engineering systems [PNR90471] 24 p3374 N88-30091

POSTFLIGHT ANALYSIS

Propulsion estimation techniques 07 p0927 N88-15632

GAS 450: A space payload for the People Central Coast Student Experimenters 10 p1289 N88-17709

Space shuttle natural environment analysis [NASA-CR-179337] 21 p2976 N88-27676

POSTULATES

U AXIOMS

POSTURE

Sitting posture of helicopter pilots of the Royal Netherlands Air Force; preliminary recommendations [IZF-1986-16] 05 p0631 N88-13857

Sitting posture of pilots in the Boelkow 105c helicopter [IZF-1986-22] 09 p1202 N88-17202

Effect of antiorthostatic position and different illumination on sensitivity of skin in upper half of the body to ultraviolet radiation 10 p1363 N88-18145

Morphological manifestations of primate adaptation to orthograde statics and walking erect 10 p1366 N88-18162

The effect of orthostatic changes in central blood volume on the heart rate response to graded Valsalva maneuvers 12 p1653 N88-19904

Estimation of body fluid shift by electrical impedance in various postures 12 p1661 N88-19956

Ergonomy and interior furnishing of the cabins of deep diving manned submarines: The Nautile example --- couch 19 p2697 N88-26032

POTABLE LIQUIDS

NT POTABLE WATER

POTABLE WATER

Carbon dioxide treatment for scale removal and control in potable water systems [AD-A184346] 04 p0412 N88-12556

Cardiac rhythm of animals consuming reclaimed water differing in concentration of sodium and potassium ions 19 p2705 N88-26085

Validation of maximum permissible concentration of urea in reclaimed potable water and evaluation of its biological effect 19 p2705 N88-26086

POTASSIUM

NT LIQUID POTASSIUM

K-CO on transition metals: A local ionic interaction [AD-A184342] 04 p0496 N88-13056

Alkali metal diffuse band lasers [AD-A190244] 15 p2071 N88-22350

Study on shaft seals for potassium turbine [EL-891] 15 p2074 N88-22364

Cardiac rhythm of animals consuming reclaimed water differing in concentration of sodium and potassium ions 19 p2705 N88-26085

POTASSIUM BROMIDES

A rapid polishing method for KBr and NaCl infrared windows [DE88-002480] 07 p0862 N88-15229

POTASSIUM COMPOUNDS

NT POTASSIUM BROMIDES

Potassium cuprate (3) [NASA-TT-20246] 13 p1739 N88-20401

POTATOES

Utilization of potatoes in bioregenerative life support systems 03 p0360 N88-12269

Food Irradiation Newsletter, Vol. 11, No. 1 [DE88-700808] 12 p1671 N88-20004

POTENTIAL ENERGY

NT BIOELECTRIC POTENTIAL
NT COULOMB POTENTIAL
NT ELECTRIC POTENTIAL
NT GEOPOTENTIAL HEIGHT
NT IONIZATION POTENTIALS
NT LOW VOLTAGE
NT PLASMA POTENTIALS
NT QUANTUM WELLS
NT THRESHOLD VOLTAGE

Variational and nonvariational theory of frictionless adhesive contact between bodies [REPT-87-11] 01 p0054 N88-10345

Monte Carlo simulation of primitive atom-transfer reactions in solution [AD-A183977] 03 p0375 N88-12380

Simulation studies for surfaces and materials strength [NASA-CR-181535] 04 p0412 N88-12557

Coupling of vibrational modes of adsorbates: Application to field induced shifts for CO and CN on Cu(100) [AD-A187891] 11 p1453 N88-18659

Theoretical studies of the potential surface for the F + H2 greater than HF + H reaction [NASA-CR-182551] 11 p1557 N88-19319

Quantum Monte Carlo study of the MIES associated with H2 (X 1 sigma sub g (+)) and H2 (B 1 sigma sub u (+)) [AD-A189063] 13 p1835 N88-20977

Molecular reaction and energy transfer rate estimation for chemical-laser analysis [AD-A190664] 15 p2035 N88-22126

The H5(+) potential energy hypersurface: Characterization of ten distinct energetically low-lying stationary points 16 p2267 N88-23561

Theoretical calculations of XeF ground state kinetics [AD-A191398] 16 p2270 N88-23580

Computed potential energy surfaces for chemical reactions [NASA-CR-183168] 24 p3342 N88-29893

POTENTIAL FIELDS

Equation of gravitational-gyroscopic waves: Angular potential and its applications 08 p1079 N88-16504

Realistic conductivity geometry model of the human head for interpretation of neuromagnetic data [PB88-112230] 10 p1369 N88-18179

Motion planning for a free-flying robot 23 p3255 N88-29378

POTENTIAL FLOW

ARSPNS: A method to calculate steady and unsteady potential flow about fixed and rotational lifting and nonlifting bodies [NLR-TR-85114-U] 01 p0044 N88-10282

Perfine: Personal finite elements on a microcomputer [ETN-87-90678] 01 p0082 N88-10528

A full potential flow analysis with realistic wake influence for helicopter rotor airload prediction [NASA-CR-4007] 04 p0393 N88-12452

Calculation of aerodynamic characteristics of three-dimensional finite span wings in potential incompressible flow 04 p0425 N88-12631

Numerical analysis of supersonic flows using panel method 05 p0537 N88-13266

Computation of transonic flows with nacelle simulation [SNIAS-872-111-117] 05 p0542 N88-13300

Potential flow around two-dimensional airfoils using a singular integral method [NASA-CR-182345] 06 p0664 N88-14070

Finite-volume scheme for transonic potential flow about airfoils and bodies in an arbitrarily shaped channel 07 p0809 N88-14928

Breakdown of the conservative potential equation 07 p0809 N88-14929

Application of a full potential method for analysis of complex aircraft geometries 07 p0809 N88-14930

Finite element fundamentals, part 2 08 p0985 N88-15962

Inviscid flows, part 2 08 p0985 N88-15966

Wall jet analysis for circulation control aerodynamics. Part 2: Zonal modeling concepts for wall jet/potential flow coupling 10 p1269 N88-17593

A numerical procedure for conformal mapping of the exterior of a circle onto the exterior of a wing profile with a spoiler
[ISL-R-110/86] 11 p1536 N88-19180

A multigrid solver for two-dimensional transonic full potential flow calculations 11 p1538 N88-19189

A multigrid full potential transonic code for arbitrary configurations --- aircraft 11 p1539 N88-19195

A discretization of the integral equation for the time dependent linearized subsonic potential flow over a wing
[AD-A188534] 12 p1574 N88-19411

ARSPNSC: A method to calculate subsonic steady and unsteady potential flow about complex configurations
[NLR-TR-86122-U] 13 p1717 N88-20265

A physically consistent model for artificial dissipation in transonic potential flow computations
[NASA-TM-100846] 15 p2122 N88-22652

La Recherche Aerospatiale, bimonthly bulletin, number 1987-3, 238/May-June
[ESA-TT-1075] 16 p2206 N88-23161

The 2-D and 3-D time marching transonic potential flow method for propfans 16 p2220 N88-23245

Reduced order models for nonlinear aerodynamics
16 p2220 N88-23248

Improved potential flow computational methods with Euler corrections for airfoil and wing/body design
[AD-A192303] 20 p2752 N88-26334

Calculation of 2-D unsteady transonic full potential flow about oscillating airfoils by two complementary approaches
[PB88-127519] 20 p2753 N88-26341

An improved version of NCOREL: A computer program for 3-D nonlinear supersonic potential flow computations
[NASA-CR-4165] 22 p3038 N88-28039

Accurate solutions, parameter studies and comparisons for the Euler and potential flow equations
[NASA-TM-100664] 23 p3173 N88-28892

POTENTIAL GRADIENTS

A supersonic potential gradient method for the calculation of unsteady aerodynamic pressures on harmonically oscillating wings
[ESA-TT-930] 03 p0259 N88-11631

POTENTIAL THEORY

Resonant level lifetime in GaAs/ AlGaAs double-barrier structures
[AD-A185376] 05 p0655 N88-14020

Nacelle-wing interactions (studies 1986) development of a finite element code in a multi-domain version
[ONERA-RTS-10/3417-AY-308A]
08 p0950 N88-15764

Application of a nonisentropic full potential method to AGARD standard airfoils
[NASA-TM-100560] 13 p1716 N88-20263

Numerical solution of ill posed problems in partial differential equations
[AD-A189383] 13 p1825 N88-20909

A note on the analyticity of the Neumann Kernel and an associated quadrature problem in two-dimensional boundary element methods
[ETN-88-92054] 14 p1964 N88-21719

Use of long-distance pair potentials in calculations of defect characteristics in metals
[DE88-701039] 15 p2037 N88-22138

A panel method based on velocity potential to compute harmonically oscillating lift surface systems
[ETN-88-91886] 15 p2061 N88-22290

Full potential methods for analysis/design of complex aerospace configurations
[NASA-CR-3982] 17 p2296 N88-23736

On the efficient implementation of the fast multipole algorithm
[AD-A191167] 17 p2385 N88-24173

POTENTIOMETERS (RESISTORS)

Low cost corrosion sensors 22 p3054 N88-28123

POTENTIOMETRIC ANALYSIS

High energy molecules of high symmetry
[AD-A185385] 05 p0647 N88-13965

Shelf life degradation of selected anaerobic threadlocking adhesives at various storage temperatures
[AD-A187712] 11 p1461 N88-18711

POTENTIOMETRY

U POTENTIOMETRIC ANALYSIS

POWDER (PARTICLES)

NT FINES
NT METAL POWDER
NT POWDERED ALUMINUM
NT SINTERED ALUMINUM POWDER

Physics and chemistry of packing fine ceramic powders
[DE87-013709] 01 p0029 N88-10183

Measurement of agglomerate strength distributions in agglomerated powders
[DE87-013605] 01 p0090 N88-10591

Colloidal stability of oxidized silicon particles in ethanolic and aqueous media
[DE87-014783] 05 p0562 N88-13421

High explosive moulding powders from RDX and aqueous polyurethane dispersions
[AD-A185026] 05 p0568 N88-13458

Extinguishing diffusion flames with dry powder and halon at low Froude numbers
[PB87-111365] 06 p0679 N88-14159

An analysis of the effect of system variables on the quality of thin films and powders produced by laser-breakdown chemical vapor deposition
[DE88-001793] 06 p0708 N88-14342

Composite ceramic superconducting filaments for superconducting cable
[AD-A187833] 11 p1556 N88-19312

Effect of rigid inclusions on sintering
[DE88-005745] 12 p1609 N88-19623

Creep behavior of consolidated rapidly solidified Type 304 stainless steel powder containing helium
[DE88-005536] 13 p1743 N88-20424

A new process for synthesis of silicon nitride powders for advanced ceramics
[AD-A189354] 13 p1748 N88-20451

Processing of nanophase ceramics
[DE88-005985] 13 p1752 N88-20475

Scale-up of a batch-type chemical powder preparation process for high field varistor fabrication
[DE88-006601] 13 p1762 N88-20541

A hydroxycarbonate route to superconductor precursor powders
[DE88-003638] 13 p1846 N88-21052

Analysis of explosives. 1: Computer programs for processing of X-ray powder deffraction data
[PB88-156898] 14 p1894 N88-21309

The weldability of consolidated rapidly solidified Type 304 SS powders
[DE88-006738] 16 p2178 N88-22978

Colloidal characterization of silicon nitride and silicon carbide 17 p2325 N88-23883

Production of powdered sodium hydride with large specific surface by the catalyzed reaction of molten sodium with hydrogen-1
[NASA-TT-20185] 20 p2776 N88-26462

A study of solvent effects on the synthesis of pure component and composite ceramic powders by metal alkoxide hydrolysis
[DE88-008381] 20 p2777 N88-26470

Ceramic processing of high-T(sub)c superconductors
[DE88-010090] 20 p2878 N88-27087

Preparation and properties of high Q microwave dielectrics in the (CA, SR, BA) zirconate system
[AD-A193127] 21 p2918 N88-27317

Relative flow rates of explosive powders
[DE88-010767] 21 p2923 N88-27350

The first synthesis of chem-prep varistor LAC (Lightning Arrestor Connector) granules
[DE88-008005] 21 p2936 N88-27438

Sinterable ceramic powders from laser-heated gases
[AD-A194162] 23 p3197 N88-29024

POWDER METALLURGY

Isothermal forging and its effect on the microstructure of powder route nickel alloy AP1
[RAE-TM-P-1094] 01 p0022 N88-10138

Development and production of new and modified powders for sprayed coatings and components for saving important raw materials
[BMFT-FB-T-86-129] 01 p0025 N88-10159

GSSR powder metallurgy research, production expanding 03 p0286 N88-11797

Powder-metallurgical preparation of A15 superconductors
[ETN-87-90584] 03 p0380 N88-12392

Durability of powdered aluminum structures
04 p0429 N88-12655

A fundamental study of P/M processed elavated temperature aluminum alloys
[AD-A185393] 05 p0565 N88-13445

Tensile properties of extrusion consolidated Type 304 SS rapidly solidified powders
[DE87-014875] 05 p0566 N88-13450

Development on thin wall tubes of dispersion type
[DE87-703384] 05 p0571 N88-13483

Behavior of long and short fatigue cracks in a powder metallurgy superalloy at room and at high temperature
05 p0601 N88-13677

Undercooling and nucleation in iron nickel alloys
[AD-A185500] 06 p0683 N88-14184

Dynamic high pressure process for fabricating superconducting and permanent magnetic materials
[DE88-000848] 06 p0785 N88-14817

Methods of improving compacting quality of intricately shaped powder components
[BLL-M-37412-(5828.4)] 08 p0968 N88-15859

Powder metallurgical preparation of A15 superconductors
[ETN-88-91072] 09 p1144 N88-16858

Materials development for JPL oxygen plant
[DE88-003067] 10 p1297 N88-17752

Evaluation of centrifugal barrel tumbling process for impregnation of molybdenum disulfide powder lubricant
[BDX-613-3696] 11 p1464 N88-18727

Microdesigning of lightweight/high strength ceramic materials
[AD-A188526] 12 p1610 N88-19631

Activities report of the Materials Department
[ETN-88-91984] 13 p1745 N88-20436

A case study of the development of a military specification - zirconium powder for thermal batteries
[AD-A188751] 13 p1792 N88-20717

Processing, physical metallurgy and creep of NiAl + Ta and NiAl + Nb alloys
[NASA-CR-182113] 14 p1890 N88-21295

Processing, microstructure, and mechanical properties of silicon carbide particulate reinforced aluminum alloys
[AD-A188981] 15 p2037 N88-22136

Characterization of an explosively consolidated rapidly solidified Fe-16Ni-9Cr-5Mo-2Cu alloy powder
[DE88-006733] 15 p2041 N88-22162

Gamma-ray densitometry: Nondestructive analysis of density evolution during ceramic powder processing
[DE88-006671] 15 p2047 N88-22198

Titanium powder frit made during the transformation alpha-beta
[ETN-88-91999] 16 p2177 N88-22976

Fabrication of reactor shields at the Y-12 plant
17 p2402 N88-24283

Characterization of 7090 and 7091 profiles made with Cegedur powder --- powder metallurgy, aircraft construction materials
[REPT-48-441/F] 18 p2487 N88-24752

Laboratory scale inert gas atomizer for producing rapidly solidified powders
[DE88-006734] 18 p2497 N88-24812

Hot isostatic pressing of nickel aluminide powders
[DE88-009677] 19 p2617 N88-25525

The preparation of mechanically alloyed powders for TEM (Transmission Electron Microscopy) examination
[DE88-008043] 20 p2775 N88-26460

Stress corrosion evaluation of powder metallurgy aluminum alloy 7091 with the breaking load test method
22 p3053 N88-28115

Hot isostatic pressing of tungsten-nickel-iron composites
[FOA-C-20698-2.1] 22 p3056 N88-28135

An investigation into the metallurgical aspects of joining rapidly-solidified aluminum alloys
[AD-A194677] 23 p3194 N88-29009

POWDERED ALUMINUM

NT SINTERED ALUMINUM POWDER

Development of a pilot plant for the production of rapidly solidified aluminum alloy powders
[BMFT-FB-T-86-153] 02 p0146 N88-10914

Durability of powdered aluminum structures
04 p0429 N88-12655

Organic coatings to improve the storageability and safety of pyrotechnic compositions
[AD-A187158] 09 p1150 N88-16889

Plasma joining of metal matrix composites
[AD-A188559] 12 p1604 N88-19593

Advanced B and Al combustion kinetics over wide temperature ranges
[AD-A190752] 15 p2036 N88-22128

Dynamic consolidation of metal powders
[AD-A192126] 18 p2485 N88-24744

Mechanical testing and microscopic analysis of structure of extruded powder aluminum
[DE88-007193] 19 p2617 N88-25528

POWDERED METALS

U METAL POWDER

POWER AMPLIFIERS

V-band IMPATT power amplifier
[NASA-CR-180711] 01 p0042 N88-10267

Theoretical and experimental investigation of electron beam acceleration and sub-millimeter wave generation in cyclotron resonant cavities
[AD-A184806] 05 p0649 N88-13975

Design of a velocity and position control laboratory servo system
[AD-A186596] 08 p0990 N88-15997

RF pulse compression development
[DE88-004818] 11 p1479 N88-18826

Application of copper-carbon fiber composites to power semiconductor devices
[NASA-TT-20171] 15 p2031 N88-22101

Development of 20 GHz monolithic transmit modules
[NASA-CR-182134] 17 p2445 N88-24539

POWER CONDITIONING

Evaluation of stand-alone inverters for remote applications
[DE87-010957] 01 p0040 N88-10257

Estimating payload internal temperatures and radiator size for multimegawatt space platforms
[DE88-000244] 03 p0275 N88-11738

High average power solid state laser power conditioning system
[DE87-013558] 03 p0328 N88-12071
High energy density rechargeable batteries for aerospace power requirements
[AD-A184883] 05 p0577 N88-13519
Solar pumped, alkali vapor laser
[AD-A187156] 09 p1170 N88-17016
Laboratory evaluation and analysis of advanced lead-acid load-leveling batteries
[DE88-002851] 10 p1349 N88-18064
Microwave semiconductor research-materials, devices and circuits
[AD-A187121] 10 p1415 N88-18444
Lead-acid load-leveling battery testing at Argonne National Laboratory
[DE88-002853] 11 p1480 N88-18837
Evaluation of advanced lead-acid batteries developed for load-leveling applications
[DE88-002871] 11 p1481 N88-18838
Power systems for production, construction, life support and operations in space
[NASA-TM-100838] 14 p1883 N88-21254
Test results of high-voltage, high-power, solid-state remote power controllers
[NASA-TM-100322] 16 p2194 N88-23085
Application of the reactivity constraint approach to the transient control of spacecraft reactors
17 p2406 N88-24305
Reactor instrumentation and control design and performance simulation for SP-100
17 p2406 N88-24306
Nuclear reactor magnetohydrodynamic power generator for directed energy weapons 17 p2411 N88-24336
Parametric analyses of the TE SP-100 system performance 17 p2415 N88-24358
Energy storage evaluation for burst power applications
17 p2426 N88-24430
Multimegawatt power conditioning requirements study
17 p2438 N88-24504
A role for high frequency superconducting devices in free space power transmission systems
[NASA-TM-100971] 19 p2662 N88-25830
Determination of satcom access power levels within the ground segment
[RSRE-MEMO-4097] 22 p3070 N88-28226
Development of inductive storage pulsed power generators
[AD-A193878] 22 p3117 N88-28521
Power supply conditioning circuit
[NASA-CASE-NPO-17233-1-CU]
23 p3208 N88-29095
Utilization of artificial intelligence techniques for the Space Station power system 23 p3261 N88-29412
The dc power control for a liquid-fed resistojet
[NASA-TM-101326] 24 p3338 N88-29869

POWER CONVERTERS
Overview of free-piston Stirling engine technology for space power application
[NASA-TM-88886] 03 p0386 N88-12427
A comparative study of various electric propulsion systems and their impact on a nominal ship design
[AD-A187800] 11 p1477 N88-18816
SNAP-DYN: Concepts for multikilowatt space power applications 17 p2435 N88-24486
Alkali metal thermoelectric converter design for space power systems applications 17 p2437 N88-24499

POWER DENSITY (ELECTROMAGNETIC)
U RADIANT FLUX DENSITY

POWER EFFICIENCY
Development of a light duty gas engine for cogeneration service
[PB87-221297] 02 p0180 N88-11119
A new method for measuring waveguide propagation losses
[DE87-011305] 03 p0307 N88-11938
Adiabatic diesel engine component development: Reference engine for on-highway applications
[NASA-CR-179531] 03 p0386 N88-12428
Efficiency testing of a helicopter transmission planetary reduction stage
[NASA-TP-2795] 07 p0861 N88-15224
Solar pumped, alkali vapor laser
[AD-A187156] 09 p1170 N88-17016
High-efficiency GaAs semiconductor laser with longitudinal excitation by scanning electron beam
09 p1238 N88-17421
A comparative study of various electric propulsion systems and their impact on a nominal ship design
[AD-A187800] 11 p1477 N88-18816
Microwave generation from a cusptron oscillator with a six-vane circuit
[AD-A188377] 12 p1619 N88-19680
Hercules: A power analyzer for MOS VLSI circuits
[AD-A188702] 12 p1623 N88-19706
High power, high efficiency 770 nm laser diode array
[DE88-004043] 12 p1631 N88-19762
Low power consumption current transducer
[NASA-CASE-NPO-16888-1-CU]
17 p2335 N88-23937
High performance quarter-micron-gate MODFETs
19 p2656 N88-25776
Computer controlled procedures for traction battery power performance tests
[ETN-88-92352] 20 p2796 N88-26589

POWER GAIN
An experimental study of CW HF chemical laser amplifier performance and zero power gain
[AD-A185241] 05 p0588 N88-13584
Effect of electron beam divergence on the gain of free electron lasers 14 p1902 N88-21358

POWER GENERATORS
U ELECTRIC GENERATORS

POWER LINES
An asymptotic theory for a class of initial-boundary value problems for weakly nonlinear wave equations with an application to a model of the galloping oscillations of overhead transmission lines
[REPT-87-12] 01 p0086 N88-10556
Optical power line voltage and current measurement systems. Volume 1: Limits to the precision of electro-optic and magneto-optic sensors
[DE87-014558] 02 p0175 N88-11092
Thermoplastic elastomer compositions -- cable jackets
[EP-PATENT-0-204-453-A1] 04 p0418 N88-12593
Cape Blanco wind farm feasibility study
[DE88-003749] 10 p1349 N88-18060
Derivation of strength factors related to the coordination of the strength of transmission line components --- electric power lines
[S/T-REPT-VOL-5-NO-2] 11 p1500 N88-18959
Safety research of insulating materials of cable for nuclear power generating station
[NASA-TT-20202] 13 p1752 N88-20477
Partial discharges and the electrical aging of cross linked polyethene (XLPE) cable insulation
[EUT-86-E-160] 14 p1892 N88-21300
Asymptotics for a system of nonlinearly coupled wave equations with an application to the galloping oscillations of overhead transmission lines
[REPT-87-78] 17 p2348 N88-23991
Technologies applicable to space tethers
[NASA-CR-183055] 19 p2606 N88-25471
Voltages induced by lightning on electric power distribution lines: Field data and analysis results for the period July 1984-1986
[DE88-007841] 19 p2693 N88-26006
Development of external cooling cryo-resistive cable systems. Part 2: Insulation characteristics on 66 kV rated cryo-resistive testing cable
[DE88-770191] 20 p2793 N88-26571
Current induced by high-altitude electromagnetic pulse (HEMP) on wire above ground
[FOA-C-30485-4.2] 22 p3072 N88-28235

POWER MODULES (STS)
Photovoltaic power modules for NASA's manned space station
[NASA-TM-100229] 03 p0277 N88-11745

POWER PROCESSING SYSTEMS
U POWER CONDITIONING

POWER REACTORS
Low power consumption current transducer
[NASA-CASE-NPO-16888-1-CU]
17 p2335 N88-23937

POWER SERIES
NT TAYLOR SERIES
Power series for stationary distributions of coupled processor models
[REPT-87-70] 16 p2254 N88-23470
An improved spherical earth diffraction algorithm for SEKE
[AD-A195847] 24 p3360 N88-30005

POWER SPECTRA
Local spectra and wave distribution functions --- space plasma
[KGI-PREPRINT-099] 01 p0100 N88-10659
Multichannel deconvolution of P waves at seismic arrays and three component stations
[AD-A184450] 04 p0467 N88-12888
An examination of chaotic motion for the buckled beam 05 p0597 N88-13644
The acoustic source created by turbulent flow over orifices and louvers
[REPT-97674] 06 p0776 N88-14764
Evolution of spectral densities in weakly inhomogeneous plasmas
[PB87-137402] 06 p0784 N88-14811
Parametric and experimental analysis using a power flow approach
[NASA-CR-182460] 09 p1116 N88-16693
Spectral density estimates of coarsely quantized random vibration data 09 p1178 N88-17055
Universal power spectra for wave turbulence: Applications to wind waves, flicker noise, solar wind spectrum and classical second sound
10 p1318 N88-17879
How to generate equal probability design load conditions --- aircraft design
[NLR-TR-86060-U] 13 p1722 N88-20295
European approaches in standard spectrum development --- aircraft load spectra
[NLR-MP-87007-U] 13 p1782 N88-20661
Power spectral density analysis of wind-shear turbulence for related flight simulations
[NASA-CR-182721] 13 p1802 N88-20773
Analysis, suppression of land clutter characteristics reported 14 p1903 N88-21369
Spectral estimation of received phase in the presence of amplitude scintillation 22 p3064 N88-28180
Matching P.S.D.: Design loads
24 p3312 N88-29720
Performance of DS/SSMA communications in impulsive channels. Part 1: Correlation receivers
[AD-A195712] 24 p3362 N88-30021
Vibrational power flow analysis of rods and beams
[NASA-CR-183166] 24 p3383 N88-30151

POWER SUPPLIES
Pulsed current transformer for low inductive loads
[AD-A187224] 10 p1324 N88-17913

POWER SUPPLY CIRCUITS
Evaluation of high-voltage, high-power, solid-state remote power controllers for amps
07 p0924 N88-15612
A technique for low level, wide range CW microwave power meter calibrations
[DE88-004147] 10 p1333 N88-17966
Multi-hundred kilowatt roll ring assembly evaluation results
[NASA-TM-100865] 14 p1904 N88-21375
Arc lamp power supply using a voltage multiplier
[NASA-CASE-LAR-13202-1] 17 p2335 N88-23942

POWER TRANSMISSION
Power flow in terms of Poynting vector for Extremely Low Frequency (ELF) dipole sources in seawater
[ARE-TM(UTM)-87102] 01 p0035 N88-10221
Power systems for production, construction, life support and operations in space
[NASA-TM-100838] 14 p1883 N88-21254
Power components for the space station 20-kHz power distribution system
[NASA-TM-100866] 14 p1904 N88-21374
A role for high frequency superconducting devices in free space power transmission systems
[NASA-TM-100971] 19 p2662 N88-25830
HPM (High Power Microwave) simulation fidelity studies
[DE88-012229] 22 p3068 N88-28209

POWER TRANSMISSION (LASERS)
Thrust and specific impulse of repetitively-pulsed-laser propulsion rocket 03 p0318 N88-12012
Overview and future direction for blackbody solar-pumped lasers
[NASA-TM-100621] 21 p2955 N88-27553

POWERED LIFT AIRCRAFT
Civil applications of high-speed rotorcraft and powered-lift aircraft configurations
[NASA-TM-100035] 03 p0261 N88-11643
Application of empirical and linear methods to VSTOL powered-lift aerodynamics
[NASA-TM-100048] 10 p1267 N88-17581
Development of circulation control technology for powered-lift STOL aircraft 10 p1272 N88-17608
A potential flight evaluation of an upper-surface-blowing/circulation-control-wing concept
10 p1272 N88-17609
A perspective on 15 years of proof-of-concept aircraft development and flight research at Ames-Moffett by the Rotorcraft and Powered-Lift Flight Projects Division, 1970-1985
[NASA-RP-1187] 12 p1582 N88-19467
Takeoff predictions for powered-lift aircraft
[NASA-CR-177491] 19 p2597 N88-25431

POYNTING THEOREM
Power flow in terms of Poynting vector for Extremely Low Frequency (ELF) dipole sources in seawater
[ARE-TM(UTM)-87102] 01 p0035 N88-10221
SSVCO feed characteristics
[DE88-011322] 22 p3068 N88-28208

PPM (MODULATION)
U PULSE POSITION MODULATION

PRACTICES
U PROCEDURES

PRAIRIES
U GRASSLANDS

PRANDTL NUMBER

Ludwig Prandtl collected treatises on applied mechanics, hydro- and aerodynamics, part 1 [NASA-TT-20316] 20 p2752 N88-26337

Ludwig Prandtl collected treatises on applied mechanics, hydro- and aerodynamics, part 2, IV interfaces and resistance [NASA-TT-20315] 20 p2752 N88-26338

PRE-MAIN SEQUENCE STARS

NT T TAURI STARS

Soft X-ray observations of pre-main sequence stars in the chamaeleon dark cloud [NASA-CR-181457] 02 p0250 N88-11579

Fifth Cambridge Workshop on Cool Stars, Stellar Systems and the Sun 04 p0502 N88-13092

Disk accretion during the early stages of stellar evolution 04 p0505 N88-13106

Microwave observations of nonthermal phenomena in pre-main sequence stars 04 p0505 N88-13107

Pre-main sequence activity: How far is magnetism involved 04 p0517 N88-13179

Chromospheric variability mechanisms affecting pre-main sequence stars 04 p0517 N88-13180

A spherical, non-LTE, blanketed model stellar atmosphere for Phi Cas (FOIa) 10 p1428 N88-18528

Radio and infrared properties of young stars [NASA-CR-183252] 24 p3459 N88-30579

PREAMPLIFIERS

On the choice of a element low-noise preamplifier on bipolar transistors [DE88-700639] 10 p1322 N88-17904

Design of a charge sensitive preamplifier on high resistivity silicon [DE88-003491] 10 p1323 N88-17907

Low-noise cryogenically cooled broad-band microwave preamplifiers [DE88-004561] 10 p1324 N88-17912

An optical preamplifier for detection of CO2 laser radiation [AD-A190790] 18 p2520 N88-24949

PREBURNERS

Duct flow nonuniformities for Space Shuttle Main Engine (SSME) [NASA-CR-179338] 18 p2511 N88-24899

Evaluation and improvement of liquid propellant rocket chugging analysis techniques. Part 2: A study of low frequency combustion instability in rocket engine preburners using a heterogeneous stirred tank reactor model [NASA-CR-182724] 21 p2903 N88-27225

PRECAMBRIAN PERIOD

Metamorphic P-T paths and Precambrian crustal growth in East Antarctica 24 p3395 N88-30218

PRECAUTIONS

U ACCIDENT PREVENTION

PRECESSION

NT QUENCHING (ATOMIC PHYSICS)

Spin precession in stationary gravitational fields [DE88-701107] 15 p2093 N88-22470

Resonant spin-flavor precession of solar and supernova neutrinos [DE88-752604] 23 p3308 N88-29707

PRECIOUS METALS

U NOBLE METALS

PRECIPITATES

Modified 14Cr-16Ni stainless steels with improved creep resistance at 700 C due to tailored precipitate microstructures [DE87-014788] 03 p0290 N88-11825

Microstructural characterization of irradiated PWR steels using the atom probe field-ion microscope [DE88-000341] 03 p0291 N88-11828

The accommodation of precipitate plates modelled as a tensile test [DE88-000207] 04 p0454 N88-12814

Characterization of precipitates in a niobium-zirconium-carbon alloy [NASA-TM-100848] 16 p2178 N88-22981

Theoretical predictions of precipitate shapes in cubic alloys [DE88-010856] 21 p2914 N88-27291

PRECIPITATION

Digital processing of infrared and visible images from the GOES satellite and its integration with meteorological radar data 17 p2360 N88-24057

PRECIPITATION (CHEMISTRY)

Factors determining the morphology of precipitation in aluminum-germanium and aluminum-silicon alloys [DE87-014682] 03 p0287 N88-11806

Influence of creep on the precipitate structure under conditions of long-term creep. 4: Experiments on 10 CrMo 9 10 steel [BLL-CE-TRANS-8256-(9022.09)] 04 p0417 N88-12589

Precipitation of surfactants and surfactant mixtures in aqueous solutions [DE88-003333] 10 p1298 N88-17763

Temperature dependence of Kr precipitation in Ni [DE88-005953] 13 p1744 N88-20429

A hydroxycarbonate route to superconductor precursor powders [DE88-003638] 13 p1846 N88-21052

Effect of size of precipitates on recrystallization temperatures in Cu-Cr, Cu-Zr, and Cu-Zr-Cr alloys [NASA-TT-20166] 18 p2489 N88-24763

A study on the precipitation and reversion behaviors of Cu-0.3 percent Cr alloy by the step annealing method [NASA-TT-20169] 18 p2489 N88-24764

Dual mechanism bifunctional polymers: Design, synthesis and application of a new category of metal ion complexing agents [DE88-008233] 20 p2777 N88-26468

PRECIPITATION (METEOROLOGY)

NT ACID RAIN
NT RAIN
NT SNOW
NT SNOW COVER

Aqueous-phase reactions in clouds [DE86-005249] 01 p0069 N88-10445

Enhancement of surface-atmosphere fluxes by desert-fringe vegetation through reduction of surface albedo and of soil heat flux [NASA-CR-181442] 02 p0197 N88-11231

Forecasting the kind of precipitation in winter 02 p0202 N88-11266

Longer-duration post-frontal precipitation at Vancouver International Airport, 1953-1983 02 p0203 N88-11269

The importance of mesoscale waves in the upper troposphere for formation of cloud and precipitation areas 02 p0203 N88-11273

FRONTIERS: An operational system for nowcasting precipitation 02 p0204 N88-11279

Operational experiment in very short range forecast of precipitation 02 p0204 N88-11280

The impact on short-term precipitation forecast skill of time-dependent lateral and lower boundary conditions within a meso-beta numerical cloud prediction model 02 p0211 N88-11327

Use of four-dimensional data assimilation to improve a mesoscale-model precipitation forecast: A case study 02 p0213 N88-11340

Impact of a direct assimilation of satellite-inferred precipitation rates into a regional meteorological model 02 p0213 N88-11342

Initialization experiments with the NMC nested grid model --- National Meteorological Center (NMC) 02 p0213 N88-11343

The effect of enhanced conventional and VAS moisture analysis on RAFS short-range precipitation forecasts --- Regional Analysis and Forecasting System (RAFS) 02 p0215 N88-11352

A method for remote sensing of precipitable water vapor and liquid in the atmosphere using a 22-ghz radiometer [AD-A184204] 03 p0354 N88-12232

Computer modeling aids studies of precipitation formation 04 p0458 N88-12832

New precipitation map of world ocean 04 p0458 N88-12834

Measurements of vapor flux, liquid water contents, precipitation rates and riming in a Utah mountain cloud system [PB87-224945] 04 p0469 N88-12900

Radar observations of changes in precipitation size spectra associated with lightning 06 p0744 N88-14576

Report of the first session of the International Working Group on Data Management for the Global Precipitation Climatology project [WCP-132] 06 p0745 N88-14582

The global climate system: Autumn 1984 to spring 1986 [CSM-R84/86] 06 p0745 N88-14583

Moscow USSR. Limited surface observations climatic summary (LISOCS), parts A-F [AD-A188080] 11 p1514 N88-19046

Determination of atmospheric moisture structure from high resolution MAMS radiance data 11 p1515 N88-19049

Research and development to acquire and reduce melting layer cloud physics and evaluate a prototype M-meter [AD-A188390] 12 p1648 N88-19873

The mixed layer of the western equatorial Pacific Ocean [HIG-1861] 13 p1805 N88-20789

Spatial and temporal distribution of precipitation chemistry across Maryland in 1984, volume 1 [PB88-148929] 14 p1943 N88-21595

Spatial and temporal distribution of precipitation chemistry across Maryland in 1984, volume 2 [PB88-148937] 14 p1944 N88-21596

Satellite rainfall retrieval by logistic regression [NASA-CR-180485] 14 p1946 N88-21607

Analysis of winter season precipitation bands over the Southern Plains 14 p1947 N88-21609

Tropical circulations and the associated rainfall anomalies during two contrasting years [INPE-4506-PRE/1261-REV] 15 p2098 N88-22502

A drought watch system [WCP-134] 16 p2234 N88-23345

Taiwan area mesoscale experiment: Daily operations summary [PB88-169081] 16 p2235 N88-23348

Satellite observed Mesoscale Convective System (MCS) propagation characteristics and a 3-12 hour heavy precipitation forecast index [PB88-180161] 19 p2692 N88-26004

Meteorological aspects of wet deposition in Southern Finland [FMI-3] 19 p2693 N88-26007

A radar study of the interaction between lightning and precipitation [DE88-009120] 20 p2827 N88-26770

Factors influencing summer temperatures and precipitation in the southwest 22 p3124 N88-28565

On the modes of growing-season precipitation over central North America 22 p3124 N88-28567

On climate prediction for India 22 p3127 N88-28590

Characteristics of regression equations for specifying monthly precipitation amounts over the United States from the field of concurrent mean 700 mb heights 22 p3127 N88-28591

Determining the spatial structure of fields of precipitation from space radar images in two orthogonal polarizations 24 p3450 N88-30531

PRECIPITATION HARDENING

Investigation of rapidly-solidified dispersion strengthened titanium alloys [AD-A183882] 01 p0022 N88-10140

Microstructural evolution and response to double-loop reactivation testing of heat-treated pH 13-8 Mo martensitic stainless steel [DE87-009058] 02 p0146 N88-10915

Compatability of dispersion-strengthened platinum with resistojet propellants [NASA-TP-2765] 04 p0409 N88-12538

Role of interstitials and precipitates in initiation and propagation of L.C.F. cracks in austenitic stainless steels 06 p0718 N88-14411

Precipitation in alumina-rich spinel: A transformation-toughened ceramic single crystal [DE87-012380] 06 p0785 N88-14815

Long-term-aging embrittlement of cast duplex stainless steels: Mechanism and kinetics [DE88-002929] 09 p1145 N88-16861

Characterization of duplex stainless steel by TEM (Transmission Electron Microscopy), SANS (Small-Angle Neutron Scattering) and APFIM (Atom-Probe Field Ion Microscopy) techniques [DE88-002916] 09 p1145 N88-16865

Micro-mechanisms of deformation in SiC/Al composites [AD-A188282] 10 p1296 N88-17749

Dependence of hydrogen embrittlement of austenitic stainless steels on structural state of grain boundaries 14 p1896 N88-21316

The age hardening response of thermomechanically processed Al-Mg-Li alloys [AD-A189870] 15 p2039 N88-22147

Effects of cold working on precipitation in age hardenable alloys: On the copper alloys [NASA-TT-20164] 16 p2177 N88-22973

Deformation of rapidly solidified dispersion strengthened titanium alloys [AD-A190793] 16 p2179 N88-22984

The precipitation processes of Cu-Zr-Cr alloys [NASA-TT-20168] 18 p2488 N88-24758

Critical cooling rates on solution treatment of Cu-Cr and Cu-Be alloys [NASA-TT-20163] 18 p2488 N88-24760

Precipitation study by electrical resistivity measurement in Ni-Al alloys [DE88-701877] 20 p2773 N88-26440

PRECISION

Contributions to fast-reacting and high-precision three-phase positioning systems --- machinery [ETN-87-90427] 01 p0056 N88-10358

Limits to the precision of electro-optic and magneto-optic sensors [PB87-212536] 03 p0323 N88-12040

GPS vertical axis performance enhancement for helicopter precision landing approach [NASA-CR-177443] 04 p0397 N88-12477

Interactions between science and precision engineering
[DE87-010873] 04 p0426 N88-12643
A demonstration of high precision GPS orbit determination for geodetic applications
04 p0432 N88-12680
Precise near-earth navigation with GPS: A survey of techniques 04 p0433 N88-12682
Short baseline phase delay interferometry
04 p0433 N88-12683
Precision analysis of regular networks
[B8709808] 05 p0620 N88-13806
Faraday cup characterization of electron beam welding parameters
[DE88-001896] 07 p0864 N88-15241
CARS measurements of combustion. 1: Precision of thermometry
[NAL-TR-939] 10 p1299 N88-17769
On precision and accuracy (bias) statements for measurement procedures
[DE88-004434] 10 p1402 N88-18359
Development of mirrors for high-precision laser gyroscopes 18 p2517 N88-24931
Fabrication technology
[DE88-010598] 20 p2855 N88-26955
Aerodynamic data accuracy and quality: Requirements and capabilities in wind tunnel testing
[AGARD-AR-254] 23 p3173 N88-28893
High definition television: Evaluation for remote task performance
[DE88-011573] 23 p3202 N88-29057

PRECONDITIONING
Approximate polynomial preconditioning applied to biharmonic equations on vector supercomputers
[NASA-TM-100217] 01 p0087 N88-10563
Preconditioned iterative methods for partial differential equations
[DE88-003071] 09 p1230 N88-17372
Polynomial preconditioning for conjugate gradient methods
[DE88-005214] 10 p1399 N88-18342
Domain decomposition preconditioners for the spectral collocation method
[NASA-CR-181620] 10 p1400 N88-18345

PREDICTION ANALYSIS TECHNIQUES
Modelling of crack-tip deformation and transient electrochemical processes in relation to corrosion fatigue of steels cathodically protected in marine environments
[NPL-DMA(A)-145] 01 p0059 N88-10379
Dugdale solutions for strain hardening materials
[FD-6/1985] 01 p0059 N88-10380
Fatigue life evaluation according to local strain concept
[FF-14/1985] 01 p0059 N88-10381
The use of Hencky's equations for the estimation of multiaxial elastic-plastic notch stresses and strains
[FB-3/1986] 01 p0060 N88-10383
Stress-strain analysis and life predictions of a notched shaft under multiaxial loading
[FB-5/1986] 01 p0060 N88-10384
Crack initiation life estimations for notched specimens with residual stresses based on local strains
[FF-17/1986] 01 p0060 N88-10385
Criteria for determination of significant load cycles in variable amplitude load sequences
[NLR-MP-86013-U] 01 p0060 N88-10386
Prediction and spectral decomposition of wide sense stationary processes on Z squared
[ENST-87C001] 01 p0087 N88-10564
Predictive momentum management for a space station measurement and computation requirements
[NASA-CR-172026] 02 p0138 N88-10866
Cumulative fatigue and life prediction of fibre composites. Part 1: Literature reviews
[BR101013] 02 p0142 N88-10893
Cumulative fatigue and life prediction of fibre composites. Part 2: Experimental techniques and results
[BR101014] 02 p0142 N88-10894
Personal Computer (PC) based image processing applied to fluid mechanics
[NASA-TM-100024] 02 p0172 N88-11087
Component specific modeling
02 p0187 N88-11166
Prediction of fatigue cracking and rupture of large structures
[ONERA-RT-31/7169-RY-055-R]
02 p0192 N88-11199
Combustion in turbulent jets and buoyant flames
[PB87-232674] 03 p0283 N88-11779
Advanced natural gas fueled engine development. Part 2: Materials investigation
[PB87-223160] 03 p0331 N88-12088
Bearing loads in slider crank mechanisms
[PB87-216495] 03 p0332 N88-12089
Investigation of reliability of strength values measured on CFRP test bars by statistical methods. Part 1: Probability distributions for strength analysis
[ESA-TT-1036] 03 p0336 N88-12115
An algorithmic approach to crustal deformation analysis
[NASA-CR-181497] 03 p0349 N88-12203
Kinds of bootstraps and kinds of jackknives, discussed in terms of a year of weather-related data
[AD-A184495] 03 p0353 N88-12227
Tropical cyclone intensity prediction based on empirical orthogonal function representation of wind and shear fields
[AD-A184699] 03 p0353 N88-12229
A heteroscedastic hierarchical model
[AD-A184256] 03 p0372 N88-12340
Numerical prediction of propeller performance by vortex lattice method
[UTIAS-TN-265] 04 p0400 N88-12489
A study of two-phase flow in a reduced gravity environment
[NASA-CR-172035] 04 p0422 N88-12617
Creep life prediction based on stochastic model of microstructurally short crack growth
[NASA-TM-100245] 04 p0456 N88-12825
Results of the 1986 NASA/FAA/DFVLR main rotor test entry in the German-Dutch wind tunnel (DNW)
[NASA-TM-100507] 04 p0487 N88-13003
Hypersonic static and dynamic stability of axisymmetric shapes: A comparison of prediction methods and experiment 05 p0534 N88-13246
Experiences using the Mark IV supersonic hypersonic arbitrary body program 05 p0534 N88-13249
Application of modified loss and deviation correlations to transonic axial compressors
[AGARD-R-745] 05 p0549 N88-13344
An analytical study of the effects of transverse shear deformation and anisotropy on buckling loads of laminated cylinders
[NASA-TM-100508] 05 p0557 N88-13387
The simulation of the viscous flow around a cylinder by the random vortex method 05 p0579 N88-13534
Low thrust viscous nozzle flow fields prediction
[NASA-CR-182334] 05 p0582 N88-13551
An examination of chaotic motion for the buckled beam 05 p0597 N88-13644
Fatigue crack growth: Statistical considerations
05 p0606 N88-13718
Comparing hard and soft prior bounds in geophysical inverse problems
[NASA-CR-181557] 05 p0624 N88-13820
Specification of predictors necessary for the determination of over or underestimation of radar derived total rainfall
[AD-A185363] 05 p0628 N88-13838
Post stall behavior in axial-flow compressors
[AD-A185712] 06 p0665 N88-14081
Measurement of mechanical parameters to define damage criteria in delamination of crossed stratified layers
[DCQ/L-47-361/F] 06 p0678 N88-14154
Fatigue life prediction modeling for turbine hot section materials
[NASA-TM-100291] 06 p0724 N88-14453
Sound propagation over uneven ground and irregular topography
[NASA-CR-182352] 06 p0776 N88-14763
Prediction of physical workload in reduced gravity environments 06 p0794 N88-14867
Fracture study of windshield glass panes
06 p0799 N88-14891
Spherical models of QSO/AGN emission line clouds
06 p0806 N88-14921
Aeropropulsion '87. Session 3: Internal Fluid Mechanics Research
[NASA-CP-10003-SESS-3] 08 p0954 N88-15790
The dynamics and control of large-flexible space structures, part 10
[NASA-CR-182426] 08 p0963 N88-15830
Validation of a stochastic model to determine failure rates for communication-electronic systems
[AD-A186536] 08 p0980 N88-15920
A computationally efficient modelling of laminar separation bubbles
[NASA-CR-182417] 08 p0984 N88-15949
On free decay damping tests
08 p0997 N88-16041
Comprehensive inflight vibration and acoustic testing
08 p0999 N88-16052
A study of finite difference and finite element vertical discretization schemes for baroclinic prediction equations
[AD-A186617] 08 p1040 N88-16291
FOR3D: A computer model for solving the LSS (Lee-Saad-Schultz) three-dimensional, wide angle wave equation
[AD-A186649] 08 p1080 N88-16511
A review of research in rotor loads
09 p1106 N88-16629
Comprehensive rotorcraft analysis methods
09 p1106 N88-16630
Helicopter crashworthiness research program
09 p1107 N88-16635
Recent Langley helicopter acoustics contributions
09 p1109 N88-16646
A decade of aeroacoustic research at NASA Ames Research Center 09 p1109 N88-16648
Aeroacoustic research programs at the Army Aviation Research and Technology Activity
09 p1109 N88-16649
Optimized approach to damage tolerance ... spacecraft
[FOK-FSS-R-87-024] 09 p1134 N88-16806
Sublaminate damage mechanisms in composite structures
[AD-A186807] 09 p1137 N88-16815
A quasi-three-dimensional calculation procedure for the prediction of flow and heat transfer in heat exchanger passages 09 p1165 N88-16985
The failure and fracture analysis of adhesive bonds
[ETN-87-90713] 09 p1181 N88-17077
Fracture mechanics characterization of crack growth under creep and fatigue conditions
[W-2/87] 09 p1183 N88-17087
Improving the stability of predictor corrector methods by residue smoothing
[CWI-NM-R8707] 09 p1228 N88-17359
Modification of a successive corrections objective analysis for improved higher order calculations
[NASA-CR-182467] 09 p1230 N88-17370
Prediction of polytomous events: Model description, algorithm development and methodological aspects, with an application
[AD-A186549] 09 p1232 N88-17384
An experimental investigation of pressure driven three-dimensional turbulent boundary layers
10 p1327 N88-17934
Forecasting complications of cardiovascular disease in flight personnel 10 p1361 N88-18136
Radial mixing in turbomachines
[AD-A188028] 11 p1482 N88-18847
Kinetic and turbulence models for granular and two-phase flows 11 p1484 N88-18862
A posteriori error estimates in computational fluid mechanics 11 p1486 N88-18869
Fracture characteristics of a viscoelastic polymer under constant load: Experiments and analysis
11 p1501 N88-18963
Stochastic heuristics in network design: Parameter tuning and performance evaluation
[REPT-87-017] 11 p1541 N88-19210
Predictive wall adjustment strategy for two-dimensional flexible walled adaptive wind tunnel: A detailed description of the first one-step method
[NASA-CR-181635] 12 p1573 N88-19409
An interdisciplinary approach to predictive modeling of structural adhesive bonding: Factors affecting the durability of titanium/epoxy bonds
[AD-A189503] 12 p1611 N88-19636
Active vibration control of a cantilevered beam with three elastic coordinates
[AD-A188824] 12 p1636 N88-19797
Comparison of simulation modeling and satellite techniques for monitoring ecological processes
[NASA-CR-182592] 12 p1641 N88-19825
A study of combustion and flow behaviour in solid-propellant rocket motors
[UTIAS-280] 13 p1732 N88-20357
Ply-level failure analysis of a graphite/epoxy laminate under bearing-bypass loading
[NASA-TM-100578] 13 p1735 N88-20372
Detection and angle estimation of coherent plane waves 13 p1759 N88-20522
Pseudo-stationary oblique-shock-wave reflections in low gamma gases: Isobutane and sulphur hexafluoride
[UTIAS-TN-267] 13 p1768 N88-20576
Predictions and studies with a one-dimensional ice/ocean model
[AD-A189158] 13 p1803 N88-20776
Aberrations: Their effect on off-axis beam steering
[AD-A189601] 13 p1840 N88-21008
Strength and failure analysis of composite laminate containing a circular hole with reinforcement
[AD-A189629] 14 p1884 N88-21260
On the theory of electromagnetic scattering from a raindrop splash
[AD-A188720] 14 p1906 N88-21393

Experiments on the creep behavior of semifinished X10NiCrAlTi 32 20 (Nicrofer 32 20) tubes under multiaxial loading --- nuclear reactors
[JUEL-2127] 14 p1923 N88-21464
Probabilistic analysis of crack containing structures with the PARIS code
[KFK-4286] 14 p1924 N88-21465
Evaluation of structural analysis methods for life prediction 14 p1930 N88-21511
The 25 m horizontal-axis turbine as a test case for standard Dutch aerodynamic calculation methods for high-speed rotors
[R-762-D] 14 p1942 N88-21589
A prediction-error estimation algorithm for nonlinear output-affine systems
[RR-314] 14 p1959 N88-21679
Identification of nonlinear rational systems using a prediction-error estimation algorithm
[RR-317] 14 p1959 N88-21680
Admissibility in fair Bayes prediction problems. Part 1: General theory
[CWI-MS-R8703] 14 p1965 N88-21725
Large quantile estimation under extreme-value conditions
[CWI-MS-R8711] 14 p1966 N88-21730
Investigation of boundary layer disturbances caused by periodic heating of a thin ribbon
[AD-A190572] 15 p2065 N88-22314
Whisker-reinforced ceramic composites for heat engine components 15 p2082 N88-22410
Fracture technology for brittle materials
15 p2083 N88-22417
Grain boundary oxidation and low-cycle fatigue at elevated temperatures 15 p2083 N88-22420
Cumulative fatigue damage models
15 p2084 N88-22422
Life prediction modeling based on strainrange partitioning 15 p2084 N88-22425
Life prediction modeling based on cyclic damage accumulation 15 p2085 N88-22426
Fatigue damage modeling for coated single crystal superalloys 15 p2085 N88-22427
Life and reliability of rotating disks
15 p2085 N88-22428
Review and assessment of the HOST turbine heat transfer program 15 p2086 N88-22431
The existence of smooth densities for the prediction filtering and smoothing problems
[AD-A189865] 15 p2119 N88-22629
A numerical model of unsteady, subsonic aeroelastic behavior
[NASA-TM-101126] 16 p2156 N88-22862
Thermoviscoelastic characterization and predictions of Kevlar/epoxy composite laminates
[NASA-CR-182878] 16 p2172 N88-22946
Reynolds stress models of homogeneous turbulence
16 p2197 N88-23106
Application of the ONERA model to the life estimation under fatigue cracking of a Al-Li alloy. Parameter identification and test-experiment comparison under FALSTAFF loading
[ONERA-RT-32/7169-RY-063-R]
16 p2222 N88-23264
Modeling and estimation of a low degree geopotential model from terrestrial gravity data
[NASA-CR-182808] 16 p2232 N88-23330
Very short range statistical forecasting of automated weather observations
[AD-A190803] 16 p2235 N88-23349
Space plasma contactor research, 1987
[NASA-CR-182148] 16 p2280 N88-23649
PAN AIR analysis of the NASA/MCAIR 279-3: An advanced supersonic V/STOL fighter/attack aircraft
[NASA-TM-86836] 17 p2298 N88-23750
The prediction of satellite lifetimes
[RAE-TR-87030] 17 p2310 N88-23818
Ceramics for turbine engines
17 p2323 N88-23873
Some design considerations for ceramic components in heat engine applications 17 p2323 N88-23875
Generalized predictive control of multivariable systems
[OUEL-1640/86] 17 p2391 N88-24209
A recursive prediction error parameter estimator for nonlinear models
[RR-326] 17 p2392 N88-24222
Particle-laden weakly swirling free jets: Measurements and predictions
[NASA-TM-100920] 18 p2466 N88-24639
Design of overlays for rigid airport pavements
[DOT/FAA/PM-87/19] 18 p2468 N88-24652
Research study: Space shuttle main engine plume flowfield model
[NASA-CR-179336] 18 p2474 N88-24676
Predictive corrosion modeling, volume 1
[AD-A191229] 18 p2485 N88-24739
Environment assisted degradation mechanisms in advanced light metals
[NASA-CR-182907] 18 p2486 N88-24746
Investigation of the effect of minimum loads and compression of load spectra on the prediction capacities of the ONERA crack model --- wings
[ONERA-RTS-33/7169-RY-064-R]
18 p2527 N88-24994
Some stress intensity factor equations
[FFA-TN-1987-07] 18 p2527 N88-24995
Automated analysis of crack growth rate for obtaining da/dN versus delta K relation
[FFA-TN-1987-70] 18 p2527 N88-24996
Adaptive grid refinement for numerical weather prediction
[AD-A192172] 18 p2544 N88-25101
Adaptive time series analysis using predictive inference and entropy
[AD-A191858] 18 p2560 N88-25199
A multiple chamber volume-filling model for prediction of transient solid rocket motor ballistic performance
19 p2633 N88-25618
Propagation modeling for land mobile satellite systems
19 p2645 N88-25694
Picosecond response of an optically controlled millimeter wave phase shifter 19 p2660 N88-25820
A simple unified method for predicting the deflections of reinforced concrete structures
19 p2679 N88-25930
Changes in seismic velocity and apparent attenuation due to isotropic and anisotropic scattering: Results from physical modeling 19 p2691 N88-25997
BOLETIM: An expert system for weather forecasting
[INPE-4538-TDL/329] 19 p2693 N88-26011
Experimental and theoretical analysis of the radiative transfer within a sooty pool fire
[DE88-007099] 20 p2769 N88-26419
Interpreting forest biome productivity and cover utilizing nested scales of image resolution and biogeographical analysis
[NASA-CR-183036] 20 p2817 N88-26711
Synoptic patterns related to tropical cyclone recurvature
[AD-A192338] 20 p2827 N88-26771
Computation of ECM (Electronic Counter-Measures) war reserve materiel spare requirements
[AD-A193301] 21 p2897 N88-27195
Approximations of stochastic equations driven by predictable processes
[AD-A192714] 21 p3005 N88-27823
Robust prediction for stationary processes: 2D enriched version
[AD-A193318] 21 p3006 N88-27833
Method to predict external store carriage characteristics at transonic speeds
[NASA-CR-4170] 22 p3037 N88-28034
Applications of fatigue analyses: Aircraft engines
[PNR90439] 22 p3044 N88-28066
Analyses and correlations of environment assisted fatigue crack propagation for attachment lugs
22 p3053 N88-28116
Thermal barrier coating life-prediction model development
[NASA-CR-179507] 22 p3058 N88-28142
An application of the Bayesian method to the estimation and forecast of system hardware components MTBF
22 p3068 N88-28211
Prediction of long-term creep in polypropylene from short-term tests
[NPL-DMA(A)-156] 22 p3088 N88-28337
The relative utility of persistence and medium-range dynamical forecasts of monthly mean 700 mb heights
22 p3127 N88-28588
Computational tools for simulation methodologies
23 p3168 N88-28865
Critical conditions for failure in materials subjected to high rates of loading
[AD-A194697] 23 p3226 N88-29201
Atmospheric deposition of nitrate to the ocean surface
23 p3231 N88-29227
On Wiener-Masani's algorithm for finding the generating function of multivariate stochastic processes
[NASA-CR-182905] 23 p3273 N88-29481
Investigation of non-classical effects in two-photon interference processes 23 p3282 N88-29541
Special Course on Missile Aerodynamics
[AGARD-R-754] 24 p3317 N88-29755
Accuracy criteria for evaluating supersonic aerodynamic coefficient predictions 24 p3317 N88-29756
Survey on nonlinear effects 24 p3317 N88-29757
Prediction of base-flows 24 p3319 N88-29765
Next generation missile design
24 p3319 N88-29766
A new computational capability for ramjet projectiles
[AD-A196061] 24 p3327 N88-29812
Three-dimensional combustor predictors: A comparison of equilibrium and laminar flamelet chemistry models
24 p3350 N88-29940
Preliminary investigation of flow modeling during solid propellant processing
[AD-A196168] 24 p3357 N88-29987

PREDICTIONS
NT FLOOD PREDICTIONS
NT IMPACT PREDICTION
NT LINEAR PREDICTION
NT NOISE PREDICTION
NT NOISE PREDICTION (AIRCRAFT)
NT PERFORMANCE PREDICTION
Structural reliability and damage tolerance of ceramic composites for high-temperature applications
[PB87-208310] 01 p0019 N88-10119
HF (High Frequency) broadcasting planning model: A comparison of two versions
[PB87-210282] 01 p0036 N88-10230
Cooling effect of a single evaporating droplet on a hot semi-infinite metal body
[PB87-201802] 01 p0046 N88-10294
The development of a friction model predicting the sliding behavior of materials pairs, especially at low temperatures: Progress report and renewal proposal
[DE87-013941] 01 p0055 N88-10354
Life prediction and constitutive models for engine hot section anisotropic materials program
02 p0188 N88-11175
Coating life prediction 02 p0189 N88-11181
Thermal barrier coating life prediction model development 02 p0190 N88-11184
Thermal barrier coating life prediction model development 02 p0190 N88-11185
Applications of dislocation theory to crack growth problems 02 p0190 N88-11188
Severe weather potential (SPOT) plotfile generator
[PB87-217717] 02 p0216 N88-11360
Software reliability models for fault-tolerant avionics computers and related topics
[NASA-CR-181440] 02 p0220 N88-11382
Physical optics method: Prediction of radar signatures
03 p0304 N88-11914
A statistical rain attenuation prediction model with application to the advanced communication technology satellite project. Part 2: Theoretical development of a dynamic model and application to rain fade durations and tolerable control delays for fade countermeasures
[NASA-TM-100242] 03 p0308 N88-11945
Application of prediction of equilibrium to servo-controlled calorimetry measurements
[DE87-013745] 03 p0324 N88-12046
Laser sources today and tomorrow
[DE87-014247] 03 p0330 N88-12083
Comparison of measured temperatures, thermal stresses and creep residues with predictions on a built-up titanium structure
[NASA-TM-86814] 03 p0337 N88-12125
Vibration and parametric excitation in rotating asymmetric circular plates 04 p0456 N88-12823
Reevaluating the worst-case radiation response of MOS transistors
[DE87-014157] 04 p0497 N88-13059
The velocity structure and turbulence at the center of the Orion Nebula 04 p0521 N88-13201
Numerical prediction of turbulent flows in dump diffusers 05 p0537 N88-13265
Prediction of wing aeroelastic effects on aircraft life and pitching moment characteristics
05 p0551 N88-13356
Fiber composite structural durability and damage tolerance: Simplified predictive methods
[NASA-TM-100179] 05 p0560 N88-13409
Master plots for predicting the case-depth in laser surface treatments
[PB87-221875] 05 p0586 N88-13574
Significance of fatigue crack closure under spectrum loading 05 p0599 N88-13662
Low cycle fatigue life predictions of a 1CrMoV steel in terms of a J-controlled short crack growth model
05 p0599 N88-13665
Crack growth prediction in 3D structures under aeronautical-type spectrum loadings
05 p0602 N88-13688
Accurate rotor loads prediction using the FLAP (Force and Loads Analysis Program) dynamics code
[DE88-001109] 05 p0623 N88-13815
File usage analysis and resource usage prediction: A measurement-based study
[NASA-CR-181553] 05 p0633 N88-13867
Predictability of process resource usage: A measurement-based study of UNIX
[NASA-CR-181562] 05 p0633 N88-13869
Robust prediction operations for stationary processes
[AD-A185408] 05 p0641 N88-13924

A numerical model of unsteady, subsonic aeroelastic behavior
[NASA-TM-100487] 06 p0663 N88-14064

Life prediction of steel cords
06 p0715 N88-14386

Verification of severe local storm forecasts issued by the National Severe Storms Forecast Center, 1986
[PB88-101407] 06 p0747 N88-14594

Investigations on the crack growth retardation behavior and fatigue life prediction in structural materials
[PB87-143756] 07 p0827 N88-15016

Life prediction of thermomechanical fatigue using total strain version of strainrange partitioning (SRP): A proposal
[NASA-TP-2779] 07 p0867 N88-15263

On two methods of identifying influential sets of observations
[AD-A186270] 07 p0910 N88-15518

On rate of convergence of equivariation linear prediction estimates of the number of signals and frequencies of multiple sinusoids
[AD-A186034] 07 p0914 N88-15549

Computational prediction of propellant reorientation
08 p0982 N88-15940

A comparison of experimental and theoretical results for labyrinth gas seals with honeycomb stators
[NASA-CR-182441] 08 p0993 N88-16006

Statistical measures of clipped random signals
08 p1000 N88-16055

The effects of rotor unbalance on the vertical response of a soft-mounted block 08 p1000 N88-16057

Satellite monitoring of earthquake precursor effects in magnetosphere 08 p1007 N88-16103

Effectiveness of oceanographic method in earthquake prediction 08 p1010 N88-16124

Prediction of the next solar activity cycle
08 p1035 N88-16276

Predictability of ice concentration in the high-latitude North Atlantic from statistical analysis of SST (Sea Surface Temperature) and ice concentration data
[AD-A186621] 08 p1045 N88-16315

Experimental evidence of micro-nonequilibrium on the magnetopause and further predictions
08 p1098 N88-16606

Primordial nucleosynthesis during the keV era
[DE88-002233] 08 p1104 N88-16623

Dynamic stress at critical locations of a structure as a criterion for mathematical model modification
09 p1180 N88-17066

Accuracies of southwell and force/stiffness methods in the prediction of buckling strength of hypersonic aircraft wing tubular panels
[NASA-TM-88295] 09 p1183 N88-17090

A comparison of the predicted and measured gravitational stresses in VAWT (Vertical Axis Wind Turbine) blades
[DE88-002113] 09 p1187 N88-17111

Outlier resistant predictive source encoding for a Gaussian stationary nominal source
[AD-A186725] 09 p1232 N88-17387

Studies of the initiation of pitting corrosion on stainless steels
[AERE-M-3615] 10 p1301 N88-17778

A three-dimensional dual potential procedure for rotational flows 10 p1329 N88-17942

On the dynamic estimation of relative weights for observation and forecast in numerical weather prediction
[NASA-CR-182531] 10 p1356 N88-18106

Future directions in computer architecture
10 p1383 N88-18257

Application of a multigrid method to a buoyancy-induced flow problem
[DE88-003961] 10 p1397 N88-18326

Linear prediction of stationary vector sequences
[NASA-TM-100069] 10 p1403 N88-18366

Wing flutter calculations with the CAP-TSD unsteady transonic small disturbance program
[NASA-TM-100580] 12 p1575 N88-19419

Validation of GEMACS (General Electromagnetic Model for the Analysis of Complex Systems) for modeling lightning-induced electromagnetic fields
[AD-A188822] 12 p1620 N88-19687

Crop forecasting in Brazil: A short history of productivity models
[INPE-4150-PRE/1056] 12 p1637 N88-19801

Avionics acquisition, trends and future approaches
12 p1702 N88-20184

Structural materials: The changing scene
12 p1703 N88-20190

Formulation of a general technique for predicting pneumatic attenuation errors in airborne pressure sensing devices
[NASA-TM-100430] 13 p1723 N88-20302

Predictive monitoring research: Summary of the PREMON system
[NASA-CR-182687] 13 p1824 N88-20905

MOSFET performance degradation due to hot carriers
13 p1848 N88-21063

Millimeter-wave properties of the atmosphere: Laboratory studies and propagation modeling
[PB88-164215] 14 p1905 N88-21387

The atmosphere as a component of the climate system: Structure and variability 14 p1935 N88-21540

Carbon dioxide and climate 14 p1936 N88-21545

Flexiwall 3 SO: A second order predictive strategy for rapid wall adjustment in two-dimensional compressible flow
[NASA-CR-181662] 15 p2015 N88-22018

Forecast of Atlantic seasonal hurricane activity for 1988 15 p2098 N88-22500

The existence of smooth densities for the prediction filtering and smoothing problems
[AD-A189865] 15 p2119 N88-22629

The analysis of fatigue crack growth mechanism and oxidation and fatigue life at elevated temperatures
[NASA-CR-182129] 16 p2179 N88-22987

On the prediction of equilibrium states in homogeneous turbulence
[NASA-CR-181659] 16 p2207 N88-23174

The 2-D and 3-D time marching transonic potential flow method for propfans 16 p2220 N88-23245

Aeroelastic forced response analysis of turbomachinery 16 p2220 N88-23247

Predicting operator workload during system design
16 p2239 N88-23375

Neurophysiological predictors of quality of performance 16 p2242 N88-23391

Development and testing of a predictive methodology for optimization of man-machine interface in future avionics systems 17 p2304 N88-23780

Progress and future directions in computational fluid dynamics
[NASA-TM-100091] 18 p2456 N88-24579

Prediction of laminar and turbulent flows past single and twin airfoils 18 p2457 N88-24589

Simulating futures in extended common LISP
[NASA-TM-101000] 18 p2559 N88-25192

Automatic discovery of optimal classes
[NASA-TM-101174] 18 p2566 N88-25238

Single-mode projection filters for modal parameter identification for flexible structures
[NASA-CR-182680] 18 p2566 N88-25244

Energy measurements in oxygen-induced reactions at 60 A GeV and 200 A GeV
[DE88-006420] 18 p2573 N88-25283

Takeoff predictions for powered-lift aircraft
[NASA-CR-177491] 19 p2597 N88-25431

An assessment of the state of the art in predicting the failure of ceramics
[DE88-008998] 19 p2621 N88-25551

Mixing and thermodynamic critical phenomena of combusting monopropellant sprays
19 p2623 N88-25558

Velocity coupling 19 p2629 N88-25596

Modeling and experimental measurements of solid propellant flame structure 19 p2631 N88-25605

Pressure differential scanning calorimetry (DSC) evaluation of solid rocket propellant burn rate mod
19 p2631 N88-25606

Numerical analysis of three dimensional cascade flow by solving Navier-Stokes equations
19 p2638 N88-25650

Prediction of fatigue life of notched specimens under aircraft loading and importance of the relative method in the case of local strain approach, part 2
[TAE-595-PT-2] 19 p2680 N88-25934

Canopy reflectance modeling in a tropical wooded grassland
[NASA-CR-182981] 19 p2685 N88-25961

Health and environmental consequences of the Chernobyl nuclear power plant accident
[DOE/ER-0332] 19 p2689 N88-25985

RCL model for the development of hysteresis in superconductors
[DE88-702061] 19 p2733 N88-26234

Intelligent guidance and control for wind shear encounter
[NASA-CR-183060] 20 p2755 N88-26347

Prediction of continental shelf sediment transport using a theoretical model of the wave-current boundary layer
[AD-A192272] 20 p2829 N88-26783

Hot electrons in silicon dioxide: Ballistic to steady-state transport 20 p2871 N88-27042

Oxidation-erosion of metals and alloys: Models, verification, and prediction
[DE88-010016] 21 p2915 N88-27300

Prediction of velocity and temperature profiles in thermally driven gravity currents applied to stratified thermal storage tanks
[DE88-004452] 21 p2946 N88-27496

NDE performance in predicting failure strength of spherical composite specimens with implanted flaws
[DE88-008223] 21 p2959 N88-27575

Size effects in linear elastic fracture mechanics
21 p2964 N88-27609

Behavioral, psychological and demographic predictors of physical fitness
[AD-A192697] 21 p2986 N88-27733

Empirical tools for simulation methodologies
23 p3168 N88-28866

Digital phase-lock loop having an estimator and predictor of error
[NASA-CASE-NPO-17196-1-CU]
23 p3205 N88-29076

A statistical rain attenuation prediction model with application to the advanced communication technology satellite project. 1: Theoretical development and application to yearly predictions for selected cities in the United States
[NASA-CR-179498] 23 p3205 N88-29077

Prediction of degradation of polymeric coating materials 24 p3354 N88-29970

A reliability-based program for predicting the service life of organic coating systems 24 p3355 N88-29971

Predicting the durability of adhesives and coatings by remote detection of hidden defects and coating-thickness irregularities: A theoretical and numerical study
24 p3355 N88-29972

Contributions to engineering models of human-computer interaction, volume 1
[AD-A195590] 24 p3409 N88-30295

PREDICTORS
U PREDICTIONS

PREFLIGHT ANALYSIS

Laser investigations for payload G-652 prior to filing pre-flight accommodation requirements
10 p1286 N88-17694

Two implementations of the Expert System for the Flight Analysis System (ESFAS) project
23 p3259 N88-29400

PREFLIGHT OPERATIONS

Aviation security: FAA (Federal Aviation Administration) needs preboard passenger screening performance standards
[PB87-216800] 02 p0124 N88-10783

PREFORMS

Novel fiber preforms: Rare earth doping
[AD-A191549] 18 p2575 N88-25294

PREGNANCY

Mother-fetus system as object for investigation of mechanisms of physiological effect of weightlessness
07 p0891 N88-15402

Spleen lymphocyte nucleic acids in pregnant rats flown in space and their offspring 07 p0892 N88-15403

PREHEATERS
U HEATING EQUIPMENT

PREHEATING
U HEATING

PREIMPREGNATION

Elementary characterization of Fibredux 913 CTS 5 34 percent preimpregnated carbon-epoxy from Ciba Geigy
[M-484300] 16 p2171 N88-22941

Elementary characterization of preimpregnated carbon epoxy T400H/DA0506 from STRUCTIL. Test report M6-577100
[CEAT-047426] 18 p2478 N88-24703

PRELAUNCH TESTS
NT STATIC FIRING

Altitude simulation testing of Ariane's second-stage engine 09 p1126 N88-16747

Stage separation testing of Ariane
09 p1126 N88-16752

Pre-launch calibration of channels 1 and 2 of the advanced very high resolution radiometer
[PB88-157169] 14 p1913 N88-21427

PRELOADING
U PRESTRESSING

PREMIXED FLAMES

Turbulence generation in combustion
[AD-A184810] 05 p0561 N88-13413

Analysis of a turbulent premixed V-flame (influence of flame-thickening)
[NAL-TR-941] 10 p1299 N88-17770

Premixed turbulent flame calculation
16 p2196 N88-23096

On the structure, propagation, extinction and stability of laminar premixed flames in dissociation equilibrium
18 p2483 N88-24728

Driving of axial acoustic fields by side-wall stabilized premixed flames 19 p2629 N88-25592

Structure of laminar, premixed flames of CH2O/NO2/O2 mixtures 19 p2632 N88-25613

Modelling of premixed combustion using a thin flame sheet and the effect of the hydrodynamic instability
[DE88-009467] 20 p2770 N88-26423

Premixed turbulent flame propagation
[AD-A192955] 21 p2909 N88-27265
Theoretical study and numerical simulation of flame fronts
[PB88-122932] 22 p3051 N88-28104
The influence of pressure on soot formation
24 p3349 N88-29934
Flamelet modeling of turbulent premixed flames
24 p3350 N88-29942
Modeling the stability of a turbulent premixed flame, downstream from a step by a Lagrangian method
24 p3350 N88-29943
Numerical modelling of premixed flames in gaseous media 24 p3350 N88-29944
Gaseous premixed flames in non-uniform flows
24 p3351 N88-29945
Optical measurements of soot and temperature profiles in premixed propane-oxygen flames
[NASA-TM-101343] 24 p3358 N88-29997
Optical measurements of soot in premixed flames
[NASA-TM-101305] 24 p3373 N88-30090

PREMIXING
Numerical simulation of turbulent premixed combustion and decay of turbulent swirling flow
[DE87-014253] 03 p0284 N88-11787
Formation and destruction of nitrous oxide in lean, premixed combustion
[DE88-001390] 05 p0562 N88-13423
Mixing fuel particles for space combustion research using acoustics
[NASA-TM-100295] 14 p1872 N88-21186
Numerical simulation of turbulent premixed combustion and decay of turbulent swirling flow
[DE88-006588] 14 p1888 N88-21284

PREPARATION
NT PRECONDITIONING
NT PRESTRESSING
NT PRETREATMENT
Specimen preparation techniques for the examination of ceramic and metal-matrix composites
[DE88-005157] 15 p2030 N88-22094
Preparation of the operational phase of the European Remote Sensing Satellite ERS-1
[BCRS-87-06] 16 p2228 N88-23307

PREPOLYMERS
NT DIMERS
Conductive polymers via reactive aligomer
[AD-A184270] 04 p0419 N88-12597

PREPREGS
Damage initiation and growth in sateen laminates under static and cyclic loading 11 p1449 N88-18634
Fatigue damage development of various CFRP-laminates
[NASA-TT-20247] 16 p2172 N88-22945

PREPROCESSING
Measurements in the functional mock up test of the NAL QSTOL aircraft control system
[NAL-TR-928] 02 p0126 N88-10793
Integration of geometric modeling and advanced finite element preprocessing 11 p1526 N88-19114

PRESELECTORS
U PREAMPLIFIERS

PRESERVING
A shape preserving interpolant which has tension controls
[DE87-014615] 02 p0229 N88-11443
Irradiation preservation of seafood: Literature review
[DE88-001691] 05 p0631 N88-13858

PRESIDENTIAL REPORTS
Space shuttle accident: NASA's actions to address the Presidential Commission report
[PB88-135306] 15 p2024 N88-22059

PRESINTERING
U SINTERING

PRESSING (FORMING)
NT STAMPING
Selection of polymer materials for manufacturing optical parts
[AD-A185898] 07 p0836 N88-15069
Fabrication of YBa2Cu3O7 superconducting ceramics
[DE88-003012] 07 p0938 N88-15701

PRESSURE
NT ATMOSPHERIC PRESSURE
NT BASE PRESSURE
NT BLOOD PRESSURE
NT DENSIFICATION
NT DYNAMIC PRESSURE
NT FLUID PRESSURE
NT GAS PRESSURE
NT GEOPRESSURE
NT HIGH PRESSURE
NT HIGH VACUUM
NT HYDROSTATIC PRESSURE
NT HYPERTENSION
NT ILLUMINANCE
NT INLET PRESSURE
NT INTERNAL PRESSURE
NT INTRACRANIAL PRESSURE
NT ISOSTATIC PRESSURE
NT LOW PRESSURE
NT LOW VACUUM
NT LOWER BODY NEGATIVE PRESSURE
NT LUMINANCE
NT LUMINOUS INTENSITY
NT OVERPRESSURE
NT OXYGEN TENSION
NT PARTIAL PRESSURE
NT RADIATION PRESSURE
NT SOUND PRESSURE
NT STAGNATION PRESSURE
NT STATIC PRESSURE
NT THRUST CHAMBER PRESSURE
NT ULTRAHIGH VACUUM
NT VACUUM
NT VAPOR PRESSURE
NT WALL PRESSURE
NT WIND PRESSURE
Effects of pressure fluctuations on nickel electrodes
[AD-A184293] 03 p0311 N88-11967
Studies of pressure-velocity coupling schemes for analysis of incompressible and compressible flows
[NASA-CR-181526] 04 p0443 N88-12748
Spectral methods. Analysis and applications to flow problems
[AD-A186265] 07 p0850 N88-15156
Pressure and mass velocity measurements in solids subjected to dynamic loadings 07 p0921 N88-15595
A simplified computer code for reduction to burning rates of closed bomb pressure-time data (MINICB)
[AD-A189112] 13 p1736 N88-20380
Lattice relaxation of the DX centers in Ga/sub 1-x/Al/sub x/As and of the pressure-induced deep donors in GaAs
[DE88-005452] 13 p1848 N88-21061
Calibration of a hot-wire/hot-film anemometer over a range of temperatures, velocities and pressures
[AD-A189717] 14 p1913 N88-21430
Monthly mean global climatology of temperature, wind, geopotential height, and pressure for 0 - 120 km
[NASA-TM-100697] 15 p2099 N88-22503
Absolute pressure derivatives of deep level defects in 3-5 semiconductors
[DE88-006318] 15 p2140 N88-22772
Theory of oxygen content, atomic ordering and oxygen diffusion in 1,2,3 superconducting oxides as a function of temperature and oxygen pressure
[DE88-007961] 19 p2735 N88-26248
The acoustic field scattered from some approximate pressure release materials
[AD-A194768] 23 p3278 N88-29515
Determination of the specific area of liquid gas and the velocity of weak pressure waves in aqueous foams
[NASA-TT-20347] 24 p3373 N88-30087

PRESSURE CABINS
U PRESSURIZED CABINS

PRESSURE CHAMBERS
NT HYPERBARIC CHAMBERS
NT VACUUM CHAMBERS
Columbus pressurized module verification
02 p0134 N88-10842
Cooling electronic equipment at simulated high altitude in hypobaric chambers
[AD-A185196] 05 p0584 N88-13560

PRESSURE DEPENDENCE
Nitrogen at very high pressure
[DE87-013800] 01 p0021 N88-10131
Ignition and combustion of metals in oxygen
04 p0407 N88-12530
Retention processes in supercritical fluid chromatography
[DE88-000079] 04 p0413 N88-12559
Experimental perspectives on heavy electron metals
[DE87-014766] 04 p0416 N88-12583
Pressure and tension dependence of phase shift of polarization modes in birefringent single-mode fiber-optic waveguide 08 p1078 N88-16501
Pressure-dependent DLTS (Deep Level Transient Spectroscopy) experiments on Si-doped AlGaAs
[DE88-003842] 13 p1846 N88-21047
Kinetic measurements of thermal decomposition of energetic materials at high pressures
[AD-A191612] 19 p2622 N88-25552

PRESSURE DISTRIBUTION
Advanced turboprop wing installation effects measured by unsteady blade pressure and noise
[NASA-TM-100200] 01 p0002 N88-10008
Transonic analysis and design of axisymmetric bodies in nonuniform flow
[NASA-CR-4101] 01 p0003 N88-10013
Time-resolved measurements of shock-induced vapor-pressure profiles
[DE87-012972] 01 p0045 N88-10289
Regime dependent analysis experiments --- sea level pressure field 02 p0209 N88-11314
Mesoscale surface field analysis from routine observations --- pressure, wind fields
02 p0209 N88-11315
High resolution determination of true surface winds at sea from wind and pressure data
02 p0210 N88-11316
An improved method of analyzing surface geostrophic winds and pressure 02 p0212 N88-11334
Investigations on a transonic airfoil with a 30 mm wide perforation/cavity arrangement
[ESA-TT-1072] 03 p0260 N88-11634
Mechanical and flow excited vibrations of elastic plates and cylindrical shells in dense fluids
03 p0316 N88-11996
An experimental investigation of unsteadiness in swept shock wave/turbulent boundary layer interactions
04 p0445 N88-12760
Application of discrete vortex method to analysis of separated flow around aerofoils
05 p0537 N88-13268
Low speed wind tunnel investigation of propeller slipstream aerodynamic effects on different nacelle/wing combinations. Part 1: Total forces and moments and pressure distributions on nacelle/wing at different angles of attack and yaw and at different thrust coefficients
[FFA-TN-1987-22] 05 p0542 N88-13302
Plasticity of aluminum and iron at high shear strain rate and high pressure 05 p0563 N88-13430
Identification of perturbations in turbomachines by the analysis of pressure signals, vibrations and wavelike motions
[ETN-88-90602] 05 p0590 N88-13600
Gas diffusion studies in steady and nonsteady cavities
[AD-A185795] 06 p0704 N88-14318
Influence of gas exchange between ocean and atmosphere on formation of atmospheric pressure field
06 p0726 N88-14467
Mean pressure distribution and geostrophic circulation in the meteor zone 06 p0734 N88-14513
Circulation in the mesosphere and lower thermosphere during the MAP (Middle Atmosphere Program)/WINE (Winter in the Northern Europe) period
06 p0734 N88-14514
A study of the mechanism of internal gravity wave generation by quasigeostrophic meteorological motions
06 p0735 N88-14520
Observations of a midlatitude squall line boundary layer wake
[AD-A185609] 06 p0746 N88-14589
Laminar flow control leading edge glove flight test article development
[NASA-CR-172137] 07 p0815 N88-14960
Numerical study of a centrifugal impeller response to a downstream static pressure perturbation
07 p0851 N88-15170
The global balance of dynamic vorticity in relation to heat sources and sinks 07 p0876 N88-15316
Sound pressure distribution in front of a serrated boundary: Standing wave suppression and diffusion
07 p0928 N88-15639
Full scale and wind tunnel surface pressure measurements on the T.R.R.L. spray dispersion programme vehicles
[REPT-8623] 09 p1114 N88-16676
Ariane 4, long version: Pressure distribution measurements on two models of different scale of the Ariane 4 nose fairings in the transonic tunnel of F+W Emmen (Switzerland) with varying tunnel configurations. Comparison with measurements taken at Modane (France) and with calculations after the Euler method
[F+W-TF-1878] 09 p1122 N88-16716
Beta limitation of matter-antimatter boundary layers
[TRITA-EPP-87-11] 09 p1250 N88-17490
The further development of circulation control airfoils
10 p1270 N88-17594
Pressure distributions and oil-flow patterns for a swept circulation-control wing 10 p1270 N88-17596
Leeside crossflow modeling in Euler space-marching computations
[NASA-TM-89710] 10 p1325 N88-17924
Spatial pressure variations and three-dimensional effects on liquid sloshing loads
[PB88-120134] 10 p1326 N88-17926
A component synthesis method using Lanczos vectors
[DE88-002263] 10 p1403 N88-18368
Pressure distributions from high Reynolds number transonic tests of an NACA 0012 airfoil in the Langley 0.3-meter transonic cryogenic tunnel
[NASA-TM-100526] 11 p1435 N88-18565
A velocity-pressure integrated, mixed interpolation, Galerkin finite element method for high Reynolds number laminar flows
[NASA-CR-179264] 11 p1486 N88-18868

Application of the multigrid technique to the pressure-correction equation for the SIMPLE algorithm --- Semi-Implicit Method for Pressure Linked Equations (SIMPLE) 11 p1539 N88-19196

Compressible friction coefficients in a simulated heat pipe
[AD-A188818] 12 p1627 N88-19735

Pressure distributions and losses in a waterjet propulsion system
[AD-A188423] 12 p1633 N88-19777

Nonaxisymmetric body supersonic, aerodynamic prediction
[AD-A189338] 13 p1716 N88-20259

New definition of pressure-center coefficient of reentry craft with asymmetrical configuration
14 p1864 N88-21138

Comparison of pressure distributions on model and full-scale NACA 64-621 airfoils with ailerons for wind turbine application
[NASA-TM-100802] 14 p1943 N88-21593

High Reynolds number, low Mach number, steady flow field calculations over a NACA 0012 airfoil using Navier-Stokes and interactive boundary layer theory
[AD-A189671] 15 p2013 N88-22005

Contraction design for small low-speed wind tunnels
[NASA-CR-182747] 15 p2021 N88-22045

Structural consequences of railgun augmentation
[DE88-007036] 15 p2023 N88-22058

Investigation of side-wall effects in wind tunnel with supercritical airfoil testing 15 p2054 N88-22241

Aerothermal tests of quilted dome models on a flat plate at a Mach number of 6.5
[NASA-TP-2804] 15 p2067 N88-22325

Big whorls carry little whorls 16 p2195 N88-23094

Supersonic axial-flow fan flutter
16 p2221 N88-23255

Methodology for matching experimental and computational aerodynamic data
[NASA-TM-100592] 17 p2295 N88-23728

Pressure distributions from subsonic tests of an advanced laminar-flow-control wing with leading- and trailing-edge flaps
[NASA-TM-4040-PT-1] 17 p2300 N88-23758

Coal particle behaviour in a counter-current combustor
[TAE-606] 19 p2612 N88-25498

The pressure field generated in a cold-flow side-dump ramjet combustor 19 p2625 N88-25572

The propagation of pressure perturbations in bubbly air/water flows 19 p2664 N88-25843

Turbulence structure of mixing swirling flows
[AD-A193063] 21 p2943 N88-27478

Study of three-dimensional transonic flow separations
[AD-A193018] 22 p3037 N88-28032

Development of direct-inverse 3-D methods for applied transonic aerodynamic wing design and analysis
[NASA-CR-183127] 22 p3037 N88-28033

Prediction of the pressure distribution for radial inflow between co-rotating discs
[PNR90464] 22 p3076 N88-28261

Rotation symmetric inside flow with diametric expansion resolution
[ILR-MITT-193] 23 p3213 N88-29123

Acoustic pressure distribution on the bottom of a wedge-shaped ocean
[AD-A193961] 23 p3278 N88-29518

Pressure distributions from subsonic tests of an advanced laminar-flow-control wing with leading- and trailing-edge flaps
[NASA-TM-4040-PT-2] 24 p3321 N88-29776

An experimental study of an adaptive-wall wind tunnel
[NASA-CR-183152] 24 p3329 N88-29821

The effects of incoming boundary layer thickness on unsteady shock-induced turbulent separations induced by cylinders
[AD-A196190] 24 p3368 N88-30060

Studies on pressure response of gas bubbles contributions of condensed droplets in bubbles generated by a uniform nucleation
[NASA-TT-20343] 24 p3370 N88-30068

PRESSURE DRAG
NT INTERFERENCE DRAG
NT SUPERSONIC DRAG

The pressure drag and momentum flux during a cold frontal passage over the Alps 13 p1800 N88-20763

Multi-body aircraft with an all-movable center fuselage actively controlling fuselage pressure drag
[NASA-CASE-LAR-13511-1] 17 p2301 N88-23765

PRESSURE EFFECTS

Pressure effects on the thermal stability of SiC fibers
[NASA-TM-100146] 01 p0019 N88-10120

Apparatus for storing kinetic energy
[EP-PATENT-0-181-736-A1] 01 p0066 N88-10422

A numerical and analytical investigation of Rayleigh-Taylor instability in a solid tungsten plate
[DE87-013593] 01 p0087 N88-10562

Elastic moduli of copper under compression
[DE87-013137] 02 p0147 N88-10922

Nonsteady-state vibrations in acoustic medium of elastic elliptical shell subjected to instantaneously applied uniform pressure 02 p0160 N88-11000

Shock-induced cooling in dense fluids
[DE87-014343] 02 p0170 N88-11067

Pressure structure of solar coronal loops
02 p0256 N88-11618

Processing and properties of SiC/Nicalon composites
[DE87-013885] 03 p0279 N88-11757

Effects of cure pressure on resin flow, voids, and mechanical properties
[AD-A184267] 03 p0295 N88-11853

Millimeter-wave studies of moist air
[AD-A184681] 03 p0306 N88-11935

Effects of pressure fluctuations on nickel electrodes
[AD-A184293] 03 p0311 N88-11967

The Moessbauer effect of SnI4 at high pressure
[DE87-014771] 04 p0495 N88-13048

Fluid mass and thermal loading effects on the modal characteristics of space shuttle main engine liquid oxygen inlet splitter vanes 05 p0594 N88-13628

JPRS report: Science and technology. Japan
[JPRS-JST-87-028] 06 p0675 N88-14130

Pressure induced phase transitions, superconductivity of phosphorus described 06 p0675 N88-14134

Study of some superconducting and magnetic materials on high T sub c oxide superconductors
[NASA-CR-182330] 06 p0785 N88-14813

Effect of high pressure oxygen loading on the superconductivity of La2CuO4
[DE88-002108] 06 p0787 N88-14827

Model for plasma equilibrium configuration evolution in a tokamak with adiabatic compression
[DE88-700354] 07 p0936 N88-15684

Effects of commercial cladding on the fracture behavior of pressure vessel steel plates
[DE88-004333] 10 p1303 N88-17790

Evaluation of spare room in cerebrospinal system using noninvasive methods 10 p1361 N88-18137

Quick actuating closure and handling system
14 p1925 N88-21476

Pressure induced ageing of polymers
14 p1929 N88-21504

Modifications to the Langley 8-foot transonic pressure tunnel for the laminar flow control experiment
[NASA-TM-4032] 15 p2021 N88-22047

Oil flow patterns on a series of capsule-type re-entry vehicles at hypersonic speeds
[DE88-751805] 16 p2155 N88-22858

Electronic structure of matter at high compression: Isostructural transitions and approach of the Fermi-gas limit
[MPO-124] 16 p2266 N88-23551

Unsteady flow in a supercritical supersonic inlet
18 p2460 N88-24605

Structure/property/reactivity relations among nitramine and other energetic materials
[AD-A190878] 18 p2481 N88-24716

Optical pressure sealing couping (light joint)
[NASA-CASE-MFS-29348-1] 18 p2576 N88-25303

Pressure/temperature sensitive inorganic phosphors
19 p2627 N88-25563

Nonlinear mechanisms of solid propellant combustion instability 19 p2628 N88-25588

Life in a hyperbaric environment. A new O2-H2 breathing mixture for industrial diving 19 p2695 N88-26019

Contribution of ultrasonic Doppler detection of circulating bubbles to human interventions under the sea and in space 19 p2697 N88-26029

Deep level defects in semiconductors: Stress and pressure studies
[DE88-010855] 21 p3024 N88-27948

Influence of peak pressure on the substructure evolution and shock wave profiles of Ti-6Al-4V
[DE88-006458] 23 p3225 N88-29197

Mechanics of thrust fault formation
23 p3231 N88-29229

Origin of SNC kaersutitic amphibole: Experimental data 23 p3306 N88-29693

Comparison of the performance of a reverse flow annular combustion chamber under low and high pressure conditions 24 p3347 N88-29923

PRESSURE FIELDS
U PRESSURE DISTRIBUTION

PRESSURE GAGES
NT BAROMETERS
NT IONIZATION GAGES
NT PIEZOELECTRIC GAGES
NT VACUUM GAGES

Calibration of a Harwood DWT-1000 controlled-clearance piston gauge
[DE88-004496] 11 p1489 N88-18888

PRESSURE GRADIENTS

Local heat/mass transfer and pressure drop in a two-pass rib-roughened channel for turbine airfoil cooling
[NASA-CR-179635] 03 p0322 N88-12039

The formation of optical membrane reflector surfaces using uniform pressure loading
[DE87-012275] 03 p0376 N88-12367

NCSU code: Validation and extension on NAL's UNIVAC 1100/60 system
[PD-FM-8716] 04 p0476 N88-12931

Statistical theory of turbulent incompressible multimaterial flow
[DE88-000435] 05 p0579 N88-13535

Asymptotic analysis of a turbulent boundary layer in a strong adverse pressure gradient
[AD-A185406] 05 p0581 N88-13543

Mean velocities and Reynolds stresses in the juncture flow and in the shear layer downstream of an appendage
[AD-A185819] 08 p0980 N88-15923

Study of resistive pressure-gradient driven turbulence
[DE88-005062] 10 p1414 N88-18441

Shock wave/turbulent boundary layer interaction in high-Reynolds-number hypersonic flows
[AD-A188029] 11 p1434 N88-18555

Numerical model of the time independent mean flow in a rotating rocket motor 13 p1733 N88-20360

The turbulent heat flux in low Mach number flows with large density variations
[DE88-006445] 14 p1911 N88-21419

An experimental investigation of rocket ramjet nozzle assembly base pressures
[AD-A189714] 15 p2027 N88-22076

ALEX results: A comparison of measurements from a round and a rectangular duct with 3-D code predictions
[DE88-005947] 15 p2135 N88-22741

On local approximations of the pressure-strain term in turbulence models 16 p2197 N88-23102

Computational wing design studies relating to natural laminar flow 17 p2297 N88-23740

Surface curvature and pressure gradient effects on turbulent flow: An assessment based on numerical solution of the Reynolds equations 17 p2338 N88-23954

HeFlow: A program for calculating pressure and temperature of helium in forced-flow superconductors. Part 1: Numerical solutions. Part 2: HeFlow user's manual
[DE88-008941] 20 p2876 N88-27071

Experimental and analytical study of two-phase flow in zero gravity
[AD-A195223] 24 p3358 N88-29993

PRESSURE ICE

Underwater acoustic backscatter from a model of arctic ice open leads and pressure ridges
[AD-A184693] 03 p0354 N88-12234

Physical and structural characteristics of Weddell Sea pack ice
[AD-A188189] 10 p1356 N88-18119

MIZEX (marginal ice zone experiment) 1987 SAR (Synthetic Aperture Radar) data summary
[AD-A195560] 24 p3364 N88-30035

PRESSURE MEASUREMENT

Base pressure measurements on a missile body with cruciform tail
[ESA-TT-1062] 03 p0270 N88-11695

Study of aeropropulsion laboratory pressure drop ng and recommended test procedure
[AD-A184333] 03 p0322 N88-12038

Fluctuating pressure loads under high speed boundary layers
[NASA-TM-100517] 05 p0647 N88-13862

Performance of low upper-shelf material under pressurized-thermal-shock loading (PTSE-2)
[DE88-002297] 07 p0832 N88-15049

Multi-component stress history measurements and analysis
[DE88-000977] 09 p1168 N88-17004

A reliable data collection/control system
10 p1289 N88-17708

Development and application of oxygen flow tagging for velocity measurements and flow visualization in turbulent three-dimensional supersonic flows
[AD-A187982] 10 p1289 N88-17714

The use of optical fibers for shock pressure and timing measurements at high pressures
[DE88-004012] 10 p1334 N88-17971

Flash threshold of shocked aluminum silicofluoride
[DE88-003978] 10 p1339 N88-18005

Verification of the momemtum theory for rotors using measurements on a model helicopter
[R-840-S] 13 p1718 N88-20275

Formulation of a general technique for predicting pneumatic attenuation errors in airborne pressure sensing devices
[NASA-TM-100430] 13 p1723 N88-20302

Exhaust-gas pressure and temperature survey of F404-GE-400 turbofan engine
[NASA-TM-88273] 13 p1724 N88-20307
Remote fiber fluorimetry techniques for pressure measurements
[DE88-004486] 13 p1773 N88-20604
Evaluation of a theory for pressure-strain rate
16 p2198 N88-23108
Relations between two-point correlations and pressure strain terms 16 p2196 N88-23109
Initial condition effect on pressure waves in an axisymmetric jet
[NASA-TM-100915] 16 p2209 N88-23184
Unsteady pressure and structural response measurements of an elastic supercritical wing
[NASA-TM-100591] 17 p2299 N88-23756
Pressure measuring probe
[NASA-CASE-LAR-13853-1] 17 p2341 N88-23961
Calibration of averaging total pressure flight wake rake and natural-laminar-flow airfoil drag certification
[NASA-CR-181630] 19 p2599 N88-25443
Velocity-pressure integrated versus penalty finite element methods for high Reynolds number flows
[NASA-CR-179357] 20 p2803 N88-26635
Evaluation of a multi-point method for determining acoustic impedance
[NASA-TM-100637] 20 p2849 N88-26913
Shock initiation studies on heterogeneous explosives
[DE88-008681] 21 p2923 N88-27351
Control and use of unsteady flows: Insect use of various wing kinematics and related pressure measurements using a pitching airfoil 21 p2926 N88-27366
Measurement of pressure fluctuations in a resonant chamber with laser-induced iodine fluorescence
[DFVLR-FB-87-53] 21 p2955 N88-27551
A resistive-film based force transducer for the study of exercise
[AD-A192601] 21 p2986 N88-27730
Energy distribution and transfer in flowing hydrogen microwave plasmas 21 p3019 N88-27919
Steady and unsteady transonic pressure measurements on a clipped delta wing for pitching and control-surface oscillations
[NASA-TP-2594] 23 p3173 N88-28895
Intrinsic and extrinsic energy states of semiconductors and heterostructures using novel techniques
[DE88-008560] 23 p3289 N88-29582
Laser Doppler Velocimeter (LDV) and pressure measurements of gas particle flows in bends
[VKI-TN-163] 24 p3372 N88-30083

PRESSURE OSCILLATIONS
Predictions of F-111 TACT aircraft buffet response and correlations of fluctuating pressures measured on aluminum and steel models and the aircraft
[NASA-CR-4069] 05 p0529 N88-13216
Longitudinal mode combustion instabilities in air breathing engines 06 p0680 N88-14166
Gas diffusion studies in steady and nonsteady cavities
[AD-A185795] 06 p0704 N88-14318
Investigation of instability, dynamic forces, and effect of dynamic loading on strength of cages for the bearings in the high pressure oxygen turbopumps for the space shuttle main engine
[NASA-CR-178970] 06 p0714 N88-14378
Pressure measurements of impinging jet with asymmetric nozzle
[NASA-CR-182759] 15 p2014 N88-22011
Low frequency pressure oscillations in a model ramjet combustor 19 p2625 N88-25571
The pressure field generated in a cold-flow side-dump ramjet combustor 19 p2625 N88-25572
Dynamics and stability of combustion driven self oscillations in presence of various frequencies. Extensive stability criteria
[ETN-88-92123] 20 p2771 N88-26432
Observed normal mode structure of low frequency oscillations 22 p3126 N88-28595

PRESSURE PROBES
U PRESSURE SENSORS

PRESSURE PULSES
Operating loading of piping systems
[ETN-88-91057] 11 p1484 N88-18856
Theoretical and experimental analysis of pressure pulse transmission in non-Newtonian pipe flow
11 p1485 N88-18863
Transient interaction of electromagnetic pulses in dielectrics and microwave biophysics
[AD-A195687] 24 p3360 N88-30008

PRESSURE RATIO
Performance characteristics of magnesium-sodium nitrate flares in oxygen-nitrogen atmospheres
[AD-A185274] 05 p0570 N88-13476
Small High Pressure Ratio Turbines --- conference
[VKI-LS-1987-07] 06 p0712 N88-14364
Development of a supersonic steam turbine with a single stage pressure ratio of 200 for generator and mechanical drive 06 p0713 N88-14374
Improvement of the Reynolds-stress model by a new pressure-strain correlation
[NASA-CR-182699] 13 p1783 N88-20667

PRESSURE RECORDERS
A resistive-film based force transducer for the study of exercise
[AD-A192601] 21 p2986 N88-27730

PRESSURE RECOVERY
Compressible friction coefficients in a simulated heat pipe
[AD-A188818] 12 p1627 N88-19735

PRESSURE REDUCTION
A study of two-phase flow in a reduced gravity environment
[NASA-CR-172035] 04 p0422 N88-12617
Two-phase flow forms and pressure drop in horizontal T tube joints with vertical branch
[GKSS-87/E/12] 09 p1163 N88-16969
Composite reduced Navier-Stokes procedures for flow problems with strong pressure interactions
[AD-A191127] 18 p2508 N88-24875
Pressure drop and heat transfer in turbulent non-Newtonian pipe flow of advanced energy transmission fluids
[DE88-010021] 19 p2666 N88-25853
Decompression procedures and accidents in space and sea 19 p2698 N88-26035
Characteristics of pressure loss during filtration using a porous ceramic filter
[DE88-752547] 20 p2798 N88-26604
The use of fins to reduce the pressure drop in a rotating cavity with a radial flow
[PNR90465] 22 p3079 N88-28282

PRESSURE REGULATORS
Zero-G thermodynamic vent system for shuttle/Centaur 08 p0983 N88-15943
A control system for maintaining high stability in gas pressure
[DE88-003712] 09 p1175 N88-17042

PRESSURE RIDGES
U PRESSURE ICE

PRESSURE SENSORS
Calibration of a five hole probe and testing of an evaluation method for flow field measurements
[ESA-TT-1051] 03 p0325 N88-12051
Polymer materials for pressure sensors
06 p0676 N88-14141
Thin film electret boundary layer transition detector: A feasibility study
[AD-A185675] 07 p0856 N88-15199
An integrated pressure sensor for in-vivo use
10 p1333 N88-17965
Preparation of thin film polyvinylidene fluoride shock wave pressure transducers
[PB88-156070] 11 p1490 N88-18893
Photonic temperature and pressure sensors for biosystems/pulsed microwave. Part 1: Interaction studies
[AD-A188887] 12 p1629 N88-19751
Formulation of a general technique for predicting pneumatic attenuation errors in airborne pressure sensing devices
[NASA-TM-100430] 13 p1723 N88-20302
High Reynolds number pump facility for cavitation research
[AD-A189310] 13 p1765 N88-20558
A 150,000 pounds per square inch dynamic pressure calibrator
[AD-A190659] 15 p2069 N88-22335
Boundary layer measurements using hot-film sensors
17 p2297 N88-23743
Pressure measuring probe
[NASA-CASE-LAR-13853-1] 17 p2341 N88-23961
The 1986 IEEE Solid-State Sensor Workshop
[AD-A190922] 19 p2668 N88-25860
Characteristics of polysilicon layers and their application in sensors 19 p2669 N88-25861
Design and construction techniques for planar polysilicon pressure transducers with piezoresistive read-out 19 p2669 N88-25862
Stress modeling of microdiaphragm pressure sensors
19 p2670 N88-25873
Noise in piezoresistive and capacitive sensors
19 p2670 N88-25874
An integrated on-chip pressure sensor for accurate control applications 19 p2671 N88-25880
Simulation of diaphragm-type IC pressure sensors
19 p2672 N88-25887
Resonant structures for integrated sensors
19 p2673 N88-25893
Deposition techniques and properties of strain compensated LPCVD silicon nitride films
19 p2673 N88-25896
A resistive-film based force transducer for the study of exercise
[AD-A192601] 21 p2986 N88-27730
The pneumatic wind shear sensor: A tool for meteorological investigations and flight management
22 p3036 N88-28024
Further improvements relating to the temperature compensation of semiconductor strain gauge pressure transducers
[RAE-TR-87061] 22 p3081 N88-28298

PRESSURE SUITS
NT EXTRAVEHICULAR MOBILITY UNITS
NT SPACE SUITS
Research and development of anti-G life support systems. Part 1: Development and evaluation of uniform-pressure anti-G suits
[AD-A185658] 06 p0754 N88-14628
Effects of anti-g suit inflation on renin and aldosterone response physical exercise 12 p1659 N88-19944
Renal effects of anti-gravity suit inflation in man in relation to cardiovasculer and hormonal changes
12 p1661 N88-19959
Design, development and evaluation of Stanford/Ames EVA prehensors
[NASA-CR-182688] 15 p2105 N88-22540

PRESSURE TRANSDUCERS
U PRESSURE SENSORS

PRESSURE VESSEL DESIGN
The structures of large wound propulsion shells --- carbon fiber composites filament winding
[SNIAS-872-430-118] 05 p0559 N88-13406

PRESSURE VESSELS
NT PREBURNERS
Nondestructive inspection of the pressure vessel in Stuttgart. ALOK part. Phase 1: ALOK combined with conventional probes
[REPT-860113-TW] 01 p0057 N88-10367
Microstructural characterization of irradiated PWR steels using the atom probe field-ion microscope
[DE88-000341] 03 p0291 N88-11828
Making space nickel/hydrogen batteries lighter and less expensive
[DE88-000168] 05 p0578 N88-13530
Geometrically nonlinear analysis of stiffened panels
06 p0722 N88-14440
An automated flow calorimeter for heat capacity and enthalpy measuremunts at elevated temperatures and pressures
[DE88-002357] 07 p0857 N88-15206
Summary of HSST wide-plate crack-arrest tests and analyses
[DE88-002601] 08 p1000 N88-16061
Proceedings of the International Workshop on Engineering Design of Next Step Reversed Field Pinch Devices
[DE88-001915] 09 p1251 N88-17494
Effects of commercial cladding on the fracture behavior of pressure vessel steel plates
[DE88-004333] 10 p1303 N88-17790
Acoustic emission measurements of PWR weld materials with inserted defects
[AERE-R-12386] 10 p1341 N88-18016
Fracture mechanics and creep crack growth of 1 percent Cr 1/2 percent Mo steel with and without prior exposure to creep conditions
[NLR-TR-86051-U] 13 p1743 N88-20426
Fracture toughness characterization of SA508 and Sa533B RPB steels
[CISE-3908] 14 p1883 N88-21292
Remote maintenance design activities and research and development accomplishments for the compact ignition tokamak
[DE88-006980] 16 p2279 N88-23645
Cellular thermosetting fluoropolymers and process for making them
[NASA-CASE-GSC-13008-1] 17 p2326 N88-23894
Stress corrosion cracking of A723 steel pressure vessels: Two case studies
[AD-A191741] 18 p2527 N88-24990
Investigation of leaks in fiberglass-reinforced pressure vessels by direct observation of hollow fibers in glass cloth
[DE88-006936] 19 p2609 N88-25485
The effect of compression on individual pressure vessel nickel/hydrogen components
[NASA-TM-101312] 22 p3052 N88-28109
Elastic-plastic analysis of part-through crack propagation in piping and pressure vessels
[DE88-701619] 23 p3225 N88-29198

PRESSURE WAVES
U ELASTIC WAVES

PRESSURE WELDING
NT DIFFUSION WELDING
NT EXPLOSIVE WELDING
NT ULTRASONIC WELDING

best copy available

Inertia welding with variable magnitude of impact load
14 p1897 N88-21326
Apparatus for pressure welding of titanium structures with a controlled rate of deformation
[RAE-TRANS-2161] 19 p2677 N88-25915
Equipment for the pressure welding of metals and alloys utilising the effects of superplasticity
[RAE-TRANS-2162] 22 p3055 N88-28129

PRESSURIZED CABINS
The SAGA highly autonomous assistance submarine
19 p2696 N88-26034

PRESSURIZED WATER REACTORS
Two-phase flow forms and pressure drop in horizontal T tube joints with vertical branch
[GKSS-87/E/12] 09 p1163 N88-16969

PRESSURIZING
Research and development of anti-G life support systems. Part 1: Development and evaluation of uniform-pressure anti-G suits
[AD-A185658] 06 p0754 N88-14626
Pressurizing systems and air conditioning systems
[MBB/LKE-312/S/PUB/246] 13 p1812 N88-20628
Evaluation of fracture models through pressurized-thermal-shock testing
[DE88-011834] 21 p2963 N88-27603
A study of flame spreading and combustion phenomena of stick propellants
[AD-A193596] 22 p3052 N88-28106

PRESTON TUBES
U PITOT TUBES

PRESTRAINING
U PRESTRESSING

PRESTRESSING
Reinforced flexural elements for TEMP-STRESS Program
[DE87-012961] 01 p0061 N88-10391
Buckling and breakdown problems in structural mechanics. Failure of prestressed double-walled containers or rings
[MBB-UR-E-956/87] 13 p1783 N88-20671
Forced motion of initially stressed shells and plates
18 p2529 N88-25005
A simple unified method for predicting the deflections of reinforced concrete structures
19 p2679 N88-25930
Preloaded brake disc
[NASA-CASE-MSC-21132-1] 23 p3223 N88-29181
Free vibration of rectangular plates with a small initial curvature
[NASA-CR-179370] 24 p3383 N88-30148

PRETESTS
U TESTS

PRETREATMENT
NT PRESTRESSING
Method for preparing hydride configurations and reactive metal surfaces
[DE88-000845] 06 p0679 N88-14161
Growth and characteristics of materials for tunable lasers in the near infrared spectral region
[NASA-CR-182501] 11 p1491 N88-18901
A modified sulphuric acid anodising process used as a pretreatment for the adhesive bonding of aluminum alloys
[ARE-TM(UMM)-87410] 16 p2177 N88-22974
Colloidal characterization of silicon nitride and silicon carbide 17 p2325 N88-23683

PRETWISTING
U PRESTRESSING
U TWISTING

PREVENTION
NT ACCIDENT PREVENTION
NT CORROSION PREVENTION
NT FIRE PREVENTION
NT ICE PREVENTION
An adaptive subdivision method with crack prevention for rendering beta-spline objects
[AD-A184249] 04 p0477 N88-12940
Summary of Payload Integration Plan (PIP) for Starlab-1 flight experiment, enclosure 3
[NASA-TM-89713] 11 p1522 N88-19086

PRIMARY BATTERIES
NT ALKALINE BATTERIES
NT METAL AIR BATTERIES
NT NICKEL ZINC BATTERIES
NT SODIUM SULFUR BATTERIES
NT THERMAL BATTERIES
NT ZINC-OXYGEN BATTERIES
Development of standard cells in NMOS technology for the design of digital integrated circuits
[FI-82-TB-6] 03 p0310 N88-11953
The kinetics of charge-transfer reactions on passive lithium electrodes
[DE88-008256] 21 p2938 N88-27454

PRIMARY COSMIC RAYS
NT SOLAR COSMIC RAYS
Heavy element compositions and energy spectra of galactic and solar cosmic rays 03 p0272 N88-11714
Multiply charged particles in primary cosmic rays with energy less than or equal to 2 TeV
07 p0921 N88-15596
Charge composition of primary cosmic ray nuclei with z greater than or equal to 2 in energy region greater than or equal to 2 TeV 24 p3448 N88-30519

PRIMATES
NT HUMAN BEINGS
NT MONKEYS
Morphological manifestations of primate adaptation to orthograde statics and walking erect
10 p1366 N88-18162
Psychophysical, biochemical and histological studies of spectrally selective photic damage to primate retina
[AD-A188115] 11 p1517 N88-19063

PRIMERS (COATINGS)
Polyitaconic acid macromolecule primer for adhesive bonding and corrosion control of aluminum
17 p2319 N88-23849
Water based primers for structural adhesive bonding of aircraft 17 p2321 N88-23862
Primerless RTV silicones
[BDX-613-3807] 24 p3356 N88-29980

PRIMERS (EXPLOSIVES)
Stability of the high-temperature G-16 primer composition
[DE88-006201] 15 p2049 N88-22206

PRIMITIVE EARTH ATMOSPHERE
Exobiology and life science 07 p0883 N88-15358
Photochemical and thermal modeling in the early atmosphere of the earth
[NASA-CR-183029] 18 p2543 N88-25093

PRIMITIVE EQUATIONS
Implicit solution of the incompressible Navier-Stokes equations in primitive variables on non-staggered grids
10 p1326 N88-17930

PRINCIPAL COMPONENTS ANALYSIS
Effective use of principal component analysis with high resolution remote sensing data to delineate hydrothermal alteration and carbonate rocks 05 p0612 N88-13758
Illustrative examples of principal component analysis using GENSTAT/PCP
[AD-A185085] 05 p0644 N88-13941
Multistep component analysis of correlations
08 p1009 N88-16115
Environmental gradient analysis, ordination, and classification in environmental impact assessments
[AD-A187294] 11 p1509 N88-19016
Use of principal component method for analysis of multidimensional quantitative data in biomedical investigations 19 p2706 N88-26089

PRINTED CIRCUITS
The 8.4-GHz low-noise maser pump source assembly
04 p0436 N88-12705
Single-layer wire routing
[AD-A186990] 09 p1157 N88-16932
Random vibration (stress screening) of printed wiring assemblies 11 p1499 N88-18953
VAXELN experimentation: Programming a real-time clock and interrupt handling using VAXELN Ada 1.1
[AD-A188100] 11 p1525 N88-19107
Fabrication and electrical characterization of multilevel aluminum interconnects used to achieve silicon-hybrid wafer-scale integration
[AD-A190519] 15 p2060 N88-22282
The use of rule induction to assist in the diagnosis of avionic circuit board defects
[ETN-88-92077] 16 p2162 N88-22899
The inspection of electronic metallurgical bonds
[AD-A192197] 18 p2486 N88-24745
Thermal cycling tests on surface-mount assemblies
[DE88-007695] 21 p2939 N88-27453
Procedures for identification and handling of Printed Circuit Boards (PCBs)
[AD-A191177] 23 p3206 N88-29078

PRINTERS
NT PRINTERS (DATA PROCESSING)
The Quick Response Multicolor Printer (QRMP) system
[AD-A188140] 11 p1504 N88-18982
Report on desktop publishing
[AD-A187698] 11 p1528 N88-19128

PRINTERS (DATA PROCESSING)
Microvax networked computer system
[AD-A190308] 15 p2114 N88-22596

PRINTING
NT LITHOGRAPHY
NT PHOTOLITHOGRAPHY
The Quick Response Multicolor Printer (QRMP) system
[AD-A188140] 11 p1504 N88-18982
Synthesis and characterization of high-T(sub c) screen-printed Y-Ba-Cu-O films on alumina
[NASA-TM-100860] 15 p2146 N88-22905
Maps for the blind and methods of their production
16 p2227 N88-23298

PRIORITIES
A multi user random access communication system for users with different priorities
[AD-A186041] 07 p0841 N88-15102
Physics rationale for the engineering specifications for ZTH
[DE88-000938] 07 p0836 N88-15080
A note on the effect of preemptive policies on the stability of a priority queue
[AD-A186871] 09 p1227 N88-17345

PRISMS
Optical alignment of Centaur's inertial guidance system
[NASA-TM-88844] 04 p0405 N88-12515

PRIVACY
Incorporation of privacy elements in space station design
[NASA-CR-182748] 14 p1881 N88-21242
Computer resourcemanagement technology program (PE 64740F). Task no. 9: Advanced user authentication
[PB88-183066] 18 p2555 N88-25163

PRIVATE AIRCRAFT
U GENERAL AVIATION AIRCRAFT

PROBABILITY
U PROBABILITY THEORY

PROBABILITY DENSITY FUNCTIONS
NT NORMAL DENSITY FUNCTIONS
NT RAYLEIGH DISTRIBUTION
NT WEIBULL DENSITY FUNCTIONS
Analyses and assessments of span wise gust gradient data from NASA B-57B aircraft
[NASA-CR-178288] 01 p0002 N88-10007
Conditional second order closure for turbulent shear flows
[AD-A185369] 05 p0581 N88-13542
Dual cylindrical wave Laser-Doppler method for measurement of skin friction in fluid flow
06 p0700 N88-14207
HOC spectral analysis of an almost periodic random sequence in noise
[AD-A185526] 06 p0765 N88-14687
Estimation of multivariate binary density using orthonormal functions
[AD-A186386] 07 p0912 N88-15528
Necessary and sufficient conditions for the convergence of integrated and mean-integrated r-th order error of histogram density estimates
[AD-A186037] 07 p0914 N88-15550
Photoionization of atoms and ions: Application of time-dependent response method within the density functional theory
[AD-A185686] 07 p0830 N88-15048
An APL function for bivariate normal probabilities
[AD-A186535] 09 p1232 N88-17382
Some majorization inequalities for functions of exchangeable random variables
[AD-A188207] 11 p1536 N88-19178
Envelope and phase statistics for non-Gaussian noise and resulting error probabilities for digital communications systems 12 p1617 N88-19872
Bragg-cell receiver study
[NASA-CR-182684] 13 p1761 N88-20535
Electromagnetic shadowing by an exponentially distributed rough surface
[AD-A189677] 14 p1906 N88-21391
Electromagnetic scattering by an exponentially distributed rough surface with the introduction of a rough surface generation technique
[AD-A189678] 14 p1906 N88-21392
Filtering of jump processes
[AD-A189701] 15 p2123 N88-22696
Almost sure L(gamma)-norm convergence for data-based histogram density estimates
[AD-A189944] 17 p2383 N88-24228
Probabilistic finite element methods
18 p2564 N88-25220
Direct numerical simulations of the PDF's (Probability Density Functions) of a passive scalar in a forced mixing layer
[AD-A192134] 18 p2566 N88-25256
Cluster analysis of multiple planetary flow regimes
[NASA-CR-182931] 18 p2584 N88-25418

PROBABILITY DISTRIBUTION FUNCTIONS
Analyses and assessments of span wise gust gradient data from NASA B-57B aircraft
[NASA-CR-178288] 01 p0002 N88-10007
Investigation of reliability of strength values measured on CFRP test bars by statistical methods. Part 1: Probability distributions for strength analysis
[ESA-TT-1036] 03 p0336 N88-12115
Propagation of random initial conditions in time
04 p0486 N88-12960

An urn model for the multi-sample capture/recapture sequential tagging process
[AD-A184470] 04 p0486 N88-12998
Comparing hard and soft prior bounds in geophysical inverse problems
[NASA-CR-181557] 05 p0624 N88-13820
Explicit formulate for the distributions of stopping variables under Wald's truncated SPRT (Sequential Probability Radio Tests) for a poisson process
[AD-A185053] 05 p0640 N88-13914
A three-parameter generalisation of the beta-binomial distribution with applications
[AD-A185733] 06 p0768 N88-14720
On the extreme points of the set of all 2xn bivariate positive quadrant dependent distributions with fixed marginals and some applications
[AD-A186316] 07 p0911 N88-15521
The information metric for univariate linear elliptic models
[AD-A186385] 07 p0911 N88-15527
Some new approaches to multivariate probability distributions
[AD-A186038] 07 p0914 N88-15551
Strong representation of weak convergence
[AD-A186433] 07 p0916 N88-15563
Contributions to selection and ranking theory with special reference to logistic populations
[AD-A185629] 07 p0917 N88-15568
Measuring the dependence between two point processes through confidence intervals for the second order distribution
[AD-A186735] 08 p1074 N88-16481
Dependence of the expectancy of hitting on the number of spread shots. Determination of the expectancy of hitting using a spread salvo
[REPT-FM6] 10 p1310 N88-17829
The convergence rate for the strong law of large numbers: General lattice distributions
[AD-A187560] 10 p1402 N88-18362
Extrema of Gaussian process by simulation
11 p1541 N88-19211
Bragg-cell receiver study
[NASA-CR-182684] 13 p1761 N88-20535
Hadronic overlap and total multiplicity distributions in high energy physics collisions
[NIKHEF-H/87-10] 13 p1838 N88-21001
Advanced probabilistic methods for quantifying the effects of various uncertainties in structural response
15 p2080 N88-22401
Memory efficient evaluations of nonlinear stochastic equations and C3 applications
[AD-A189872] 15 p2110 N88-22569
Some comments on quadrant dependence in higher dimensions
[AD-A190329] 15 p2121 N88-22639
Structural decomposition of multiple time scale Markov processes
[AD-A189739] 15 p2123 N88-22657
A note on phase-type, almost phase-type, generalized hyperexponential and Coxian distribution, revision
[AD-A191236] 16 p2261 N88-23517
On solvability of an equation arising in the theory of M-estimates
[AD-A193059] 21 p3006 N88-27828
Polynomial definition of discrete field points of map of diffusion equation, part 1
[AD-A193697] 23 p3271 N88-29467

PROBABILITY THEORY

A problem in quantum probability --- statistical invariants problem
[REPT-87-06] 01 p0068 N88-10573
Components and cycles of a random function
[DE87-014155] 02 p0228 N88-11437
An empirical investigation of the use of ranks in pps sampling
[DE87-010609] 02 p0228 N88-11438
A probabilistic model of brittle crack formation
[AD-A184423] 03 p0338 N88-12129
More on the decoder error probability for Reed-Solomon codes 04 p0435 N88-12693
Foundations of O-theory 2: Measurements and relation to fuzzy set theory
[DE88-000013] 04 p0485 N88-12986
Lower bounds on bearing accuracy for closely spaced sources
[AD-A184258] 04 p0486 N88-12997
Subjective probability, combination of expert opinion and probabilistic approaches to information retrieval
04 p0501 N88-13085
Approximating multivariate normal orthant probabilities using the Clark algorithm
[AD-A184855] 05 p0634 N88-13873
Point processes
[AD-A185398] 05 p0641 N88-13921
Isotropic probability measures in infinite dimensional spaces: Inverse problems/prior information/stochastic inversion
[NASA-CR-181555] 05 p0643 N88-13936
The adaption and use of research codes for performance assessment
[DE88-000552] 06 p0756 N88-14639
Subcritical branching processes in a two state random environment, and a percolation problem on trees
[PB87-230439] 06 p0762 N88-14677
Packet error probabilities in frequency-hopped spread spectrum packet radio networks. Markov frequency hopping patterns considered
[AD-A186071] 07 p0841 N88-15104
Reliability and survivability of communication networks
[AD-A186248] 07 p0842 N88-15109
An elementary approach to the Daniell-Kolmogorov theorem and some related results
[AD-A186011] 07 p0909 N88-15505
Spectral representation of infinitely divisible processes
[AD-A186210] 07 p0910 N88-15515
On determining the weight for obtaining a large number of items
[AD-A186181] 07 p0915 N88-15553
Monte Carlo simulation of triangulated random surfaces in grand canonical ensemble
[DE88-700378] 07 p0941 N88-15718
A flux analysis of the solar cells
[INPE-4247-PRE/1120] 08 p1022 N88-16186
Short pseudorandom test sequences
[AD-A185883] 08 p1054 N88-16357
Electronic factors for K-shell-electron conversion probability and electron-positron pair formation probability in electric monopole transitions
[DE87-753040] 08 p1089 N88-16551
Probabilistic neural networks: In or out of equilibrium
[DE88-002907] 09 p1201 N88-17198
An application of fuzzy set theory to statistical hypothesis testing
[AD-A186705] 09 p1232 N88-17386
The evolution of naval warfare technology and the impact of space systems
[AD-A186900] 09 p1233 N88-17392
The impact of deployment rates on the effectiveness of strategic defenses
[AD-A186907] 09 p1233 N88-17393
Response of wind shear warning systems to turbulence with implication of nuisance alerts
10 p1274 N88-17618
Development of a graphics based two-attribute utility assessment program with application to mission planning
[AD-A187276] 10 p1388 N88-18292
Explicit solutions of moment problems, 1
[AD-A188018] 10 p1397 N88-18325
Asymptotic expansions for large deviation probabilities in the strong law of large numbers
[AD-A187432] 10 p1402 N88-18361
Probabilistic and reliability design procedures for flexible airfield pavements: Elastic layered method
[AD-A187533] 11 p1442 N88-18600
A lower bound for the decoder error probability of the linear MDS code 11 p1472 N88-18780
Frame synchronization performance and analysis
11 p1473 N88-18787
Derivation of strength factors related to the coordination of the strength of transmission line components --- electric power lines
[S/T-REPT-VOL-5-NO-2] 11 p1500 N88-18759
Generating the states of a probabilistic system
[AD-A187896] 11 p1540 N88-19208
Joint moments of the maximum in a critical branching process
[AD-A188157] 11 p1541 N88-19209
A computer code for the solution of large scale network reliability analysis problems
[AD-A188455] 12 p1660 N88-20042
Estimation of the probability of a long time to the first entrance to a state in a semi-Markov model
[AD-A188960] 12 p1685 N88-20074
Uncertain knowledge in distributed systems
[AD-A189017] 12 p1685 N88-20076
Convolution metrics and rates of convergence in the CLT (Central Limit Theorem)
[AD-A189341] 12 p1686 N88-20084
Characteristics of the positive lighting flash
[DE88-005854] 13 p1800 N88-20760
On the theory of the conversion of metallic mixed phases. 5: Fluctuations and nucleation in sub-cooled phases
[NASA-TT-20249] 14 p1890 N88-21296
Deterministic approximations of probability inequalities
[REPT-87-43] 14 p1966 N88-21732
Macroscopic quantum jumps in a single atom
14 p1975 N88-21784
Multiple model parameter adaptive control for in-flight simulation
[AD-A190568] 15 p2021 N88-22044
Probabilistic structural analysis computer code (NESSUS) 15 p2079 N88-22397
A probabilistic approach to low-level vision
[AD-A189041] 15 p2107 N88-22553
Mathematics clinic probabilistic position-fixing
[NASA-CR-182753] 15 p2125 N88-22672
Coordinate-momentum probability operator for point particles in a stationary electromagnetic field
[DE88-701165] 16 p2168 N88-23044
Applicability and limitations of probability models in connection with the reliability of large-scale technical installations
[W-3/87] 16 p2261 N88-23520
Restrictions in activity monitoring through remote sensing 17 p2365 N88-24084
Induction of models under uncertainty
[NASA-TM-101173] 17 p2394 N88-24230
Additive prophet inequalities for transforms of uniformly bounded pairwise independent random variables
[PB88-173513] 16 p2568 N88-25250
A perspective of PC-based probabilistic risk assessment
[DE88-006715] 18 p2568 N88-25251
Transition probabilities in OH A 2 sigma + - X 2 pi i: Bands with v prime = 0 and 1, v double prime = 0 to 4
[NASA-CR-182946] 18 p2584 N88-25353
Narrative compression coding for a channel with errors
[AD-A191577] 19 p2642 N88-25673
Study of probabilistic fatigue crack growth and associated scatter under constant-and-variable amplitude loading spectrum
[AD-A192027] 19 p2679 N88-25929
Timing regulations to prevent stratospheric-ozone depletion
[R-3495-JMO/RC] 19 p2690 N88-25987
Antenna heights for the optimum utilization of the oceanic evaporation duct. Part 3: Results from the Mediterranean measurements, volume 2
[AD-A192311] 20 p2791 N88-26554
Improved procedure for impact probability computation of aircraft crash based on Balfanz model
[JUEL-SPEZ-425] 21 p2894 N88-27176
Probabilistic anisotropic failure criteria for composite materials
[AD-A193046] 21 p2904 N88-27232
Computation of failure probability of fatigue loaded cracked structures
[ETN-88-92360] 21 p2964 N88-27607
Distributed algorithms for probabilistic solution of computational vision problems
[AD-A193150] 21 p2997 N88-27773
The computation of stationary distributions on Markov chains through perturbations
[AD-A193191] 21 p3009 N88-27855
Comparison of results based on a deterministic versus a statistical uncertainty analysis
[DE88-010751] 21 p3010 N88-27858
Probabilistic structural analysis to quantify uncertainties associated with turbopump blades
[NASA-TM-100278] 22 p3050 N88-28094
A probabilistic model of the apparent radiance of a rough sea
[AD-A193867] 22 p3129 N88-28602
Extremal two-correlations of two-valued stationary one-dependent processes
[REPT-88-01] 22 p3145 N88-28704
Use of Markov probability and reliability model generation methods in the analysis of reliability of a fault tolerant hardware and software based system with flexible repair policies
[PNR90467] 22 p3145 N88-28706
Analysis of the effect of faulty spares on the performance of diagnostic algorithms in reliable systems
[AD-A193526] 23 p3223 N88-29186
Mathematical algorithms for approximate reasoning
23 p3262 N88-29418
Minimizing escape probabilities: A large deviations approach
[AD-A194534] 23 p3275 N88-29496
Sequential approach to Colombeau's theory of generalized functions
[DE88-701869] 23 p3276 N88-29503
Influence of pairing correlations on the probability and dynamics of tunneling through the barrier in fission and fusion of complex nuclei
[DE88-701500] 23 p3286 N88-29570
Fatigue crack propagation: Probabilistic modeling and statistical analysis
[AD-A195885] 24 p3384 N88-30155
Venture theory: A model of decision weights
[AD-A194809] 24 p3426 N88-30391

PROBLEM SOLVING
NT ALTERNATING DIRECTION IMPLICIT METHODS
NT ASYMPTOTIC METHODS
NT ITERATIVE SOLUTION
NT THEOREM PROVING

Problem specifications and collated solutions of the two-phase numerical-benchmark exercise 1986-7 — two phase flow
[CFDU/87/1] 01 p0047 N88-10300

A study of carbon monoxide distribution determinations for a global transport model
[NASA-CR-181423] 01 p0067 N88-10432

A look at the evolution of mathematical software for dense matrix problems over the past fifteen years
[DE87-011485] 01 p0081 N88-10517

The reliability of numerical solutions of ordinary differential equations, obtained by implicit calculation schemes
[PTB-W-30] 01 p0085 N88-10549

On the maximum of solutions for a semilinear elliptic problem
[REPT-87-08] 01 p0086 N88-10554

Synthesizing controllers for uncertain systems by a quantitative pole-placement
[PB87-195590] 02 p0223 N88-11403

Oscillatory and nonoscillatory properties of first order differential equations with piecewise constant deviating arguments
[DE87-703061] 02 p0225 N88-11418

Technology applications branch graphics projects
[AD-A184621] 03 p0364 N88-12291

Performance evaluation of artificial intelligence systems
[AD-A184054] 03 p0368 N88-12316

Analogical inference and analogical access
[AD-A184345] 03 p0369 N88-12321

Implementation of the Runge-Kutta-Fehlberg method for solution of ordinary differential equations on a parallel processor
[AD-A184660] 03 p0370 N88-12331

Numerical solution of bound constrained problems
[DE88-000653] 03 p0371 N88-12334

Solution of nonlinear least-squares problems
[AD-A184010] 03 p0371 N88-12335

Design of digital filters for electronic instrumentation
[PB87-100418] 04 p0438 N88-12716

Principles for problem aggregation and assignment in medium scale multiprocessors
[NASA-CR-178379] 04 p0476 N88-12935

A model of functional knowledge and insight
[AD-A184113] 04 p0483 N88-12975

Back-of-the-envelope problems
[AD-A184105] 04 p0484 N88-12980

A 3-D Euler solution for hypersonic Mach numbers
05 p0533 N88-13240

Two low-order mixed methods for the elasticity problem
[PB87-225272] 05 p0610 N88-13749

Indirect solution of static problems using concurrent vector processing computers
[DE87-012105] 05 p0636 N88-13889

Application of the Von Karman equation to the bifurcation theory
[NOTA-INTERNA-891] 05 p0642 N88-13927

The solution of large linear inverse problems
06 p0691 N88-14238

Artificial intelligence systems
06 p0761 N88-14670

Tools and technologies for expert systems: A human factors perspective 06 p0797 N88-14882

Development of a prototype H-46 helicopter diagnostic expert system
[AD-A186077] 07 p0809 N88-14924

New methods for numerical solution of one class of strongly nonlinear partial differential equations with applications
[AD-A186166] 07 p0899 N88-15445

Investigation and implementation of an algorithm for computing optimal search paths
[AD-A185927] 07 p0902 N88-15461

UNITY: A framework for study of parallel programming problem-solving
[AD-A185616] 07 p0906 N88-15490

Optimal repeated measurements designs for comparing test treatments with a control
[AD-A185999] 07 p0917 N88-15569

Finite element fundamentals, part 1
08 p0985 N88-15961

Comparative performance of the conjugate gradient and SOR (Successive Over Relaxation) methods for computational thermal hydraulics
[DE88-002553] 08 p0988 N88-15986

Solution in vibration problems of rectangular plates with spline function
[PB87-143459] 08 p0996 N88-16029

Cirrus: An automated protocol analysis tool
[AD-A186646] 08 p1052 N88-16348

Deriving descriptions of the mind
[AD-A186647] 08 p1052 N88-16349

Problem solving as intelligent retrieval from distributed knowledge sources 08 p1059 N88-16392

Discovery and problem solving: Triangulation as a weak heuristic 08 p1062 N88-16412

Commonality analysis as a knowledge acquisition problem 08 p1062 N88-16413

Qualitative models for planning: A gentle introduction
08 p1062 N88-16414

Interfacing the expert: Characteristics and requirements for the user interface in expert systems
08 p1063 N88-16419

Case-based reasoning for space applications: Utilization of prior experience in knowledge-based systems
08 p1065 N88-16433

Application of artificial intelligence to impulsive orbital transfers 08 p1066 N88-16439

FOR3D: A computer model for solving the LSS (Lee-Saad-Schultz) three-dimensional, wide angle wave equation
[AD-A186649] 08 p1080 N88-16511

An initial investigation into methods of computing transonic aerodynamics sensitivity coefficients
[NASA-CR-182444] 09 p1112 N88-16663

Team problem solving: Effects of communication and function overlap
[AD-A187010] 09 p1152 N88-16896

Tutoring electronic troubleshooting in a simulated maintenance work environment
09 p1204 N88-17215

Performance analysis of parallel branch and bound search with the hypercube architecture
09 p1206 N88-17229

The empirical accuracy of uncertain inference models
09 p1208 N88-17243

Trimodal interpretation of constraints for planning
09 p1209 N88-17248

Advanced decision aiding techniques applicable to space 09 p1209 N88-17250

Explicit-implicit methods for time-dependent partial differential equations
[CWI-NM-R8703] 09 p1228 N88-17355

On exact solutions of multidimensional Schroedinger equation with polynomial potentials
[DE86-700460] 09 p1230 N88-17373

A fast Riemann solver with constant covolume applied to the random choice method
[CAR-[illegible]] 09 p1231 N88-17375

Continuous deformation algorithm on the product space of unit simplices, revised version
[PB88-114210] 10 p1387 N88-18281

A visual programming environment for the Navier-Stokes computer
[NASA-CR-181615] 10 p1390 N88-18299

Knowledge base refinement by monitoring abstract control knowledge, revision 1
[AD-A187502] 10 p1397 N88-18323

Applications of Lie group methods to the equations of magnetohydrodynamics 10 p1411 N88-18422

Finite element methods of analysis for high speed viscous flows
[NASA-CR-182529] 11 p1483 N88-18852

Modeling incorrect responses to multiple-choice items with multilinear formula score theory
[AD-A187667] 11 p1522 N88-19090

Effects of stress on judgement and decision making in dynamic tasks
[AD-A188203] 11 p1523 N88-19092

EqL: The language and its implementation
[AD-A188161] 11 p1530 N88-19137

Subroutines for solving the equation of diffusion in media with anisotropic properties
[DE88-700743] 11 p1536 N88-19179

A signal processing approach to the numerical solution of parabolic differential equations
11 p1539 N88-19197

Extrema of Gaussian process by simulation
11 p1541 N88-19211

The construction of a pedagogy to promote meaningful learning of strategies and tactics for solving problems of elementary combinatorics
[AD-A187928] 11 p1542 N88-19216

Learning by experimentation
[AD-A188912] 12 p1681 N88-20053

Northeast Artificial Intelligence Consortium (NAIC) administrative matters and ancillary functions, volume 1
[AD-A189466] 12 p1682 N88-20055

The inverse problem and the pseudo-empirical orthogonal function method of solution. Part 1: Theory; Part 2: Application
[AD-A188894] 12 p1684 N88-20069

Management information systems design implications: The effect of cognitive style and information presentation on problem solving
[AD-A188850] 12 p1705 N88-20205

Text organization and comprehensibility in technical writing
[AD-A188913] 12 p1707 N88-20217

NASA/UK TAP
[NASA-CR-180350] 12 p1708 N88-20223

Finite element methods for quasi-prismatic bodies with application to gears 13 p1779 N88-20644

A personalized and prescriptive decision aid for choice from a database of options
[AD-A188726] 13 p1811 N88-20820

An implementation of the OPS5 language for computers compatible with IBM-PC
[INPE-4291-PRE/1162] 13 p1821 N88-20882

New way to solve Volterra equations of the second kind
[PB88-148820] 13 p1828 N88-20931

Parallel algorithms for mapping pipelined and parallel computations
[NASA-CR-181655] 14 p1960 N88-21687

Comparative analysis
[AD-A190556] 15 p2065 N88-22313

A zonal approach for the solution of coupled Euler and potential solutions of flows with complex geometries
[AD-A189752] 15 p2114 N88-22595

Numerical solution of nonlinear algebraic equations in stiff ODE solving
[DE88-008634] 15 p2118 N88-22622

About disequations simplification
[RR-645-I-IMAG-55-LIFIA] 15 p2119 N88-22624

Admissible Bayes tests for structural relationship
[AD-A190326] 15 p2125 N88-22669

Water facilities in retrospect and prospect: An illuminating tool for vehicle design
16 p2200 N88-23126

Iterative finite element solver on transputer networks
16 p2218 N88-23235

Problem solving in a natural task as a function of experience
[AD-A191180] 16 p2243 N88-23399

Extending problem solver capabilities through case-based inference
[AD-A191332] 16 p2243 N88-23401

Vectorization of the odd-even hopscotch scheme and the alternating direction implicit scheme for the two-dimensional Burgers' equations
[CWI-NM-R8720] 16 p2249 N88-23440

On the trajectory of a linear programming problem
[REPT-87-53] 16 p2250 N88-23442

Capitalizing on failure through case-based inference
[AD-A190927] 16 p2255 N88-23480

Generalizing the structure of explanations in explanation-based learning
[AD-A191327] 16 p2256 N88-23481

A new block solver for large, full, unsymmetric, complex systems of linear algebraic equations
[AD-A190590] 16 p2256 N88-23483

Continuous decoupling transformations for linear boundary value problems
[ETN-88-92248] 16 p2258 N88-23493

Extracting information from problem solving experience
[AD-A191331] 16 p2286 N88-23688

Numerical modelling of flows using phoenics
17 p2339 N88-23955

A proposal of adaptation of a knowledge-based scene analysis model to some remote sensing problems
17 p2354 N88-24026

Navigation system from AVHRR data from NOAA series satellites 17 p2359 N88-24054

A proposal of adaptation of a knowledge-based scene analysis model to some remote sensing problems
17 p2362 N88-24068

Human problem solving in complex dynamic environments
[AD-A190786] 18 p2551 N88-25142

A mixed-integer linear programming problem which is efficiently solvable
[AD-A191028] 18 p2556 N88-25168

Algorithms and software for solving finite element equations on serial and parallel architectures
[NASA-CR-183027] 18 p2559 N88-25191

Optimal a priori covariance selection for the solution of ill-conditioned nonlinear inverse problems
18 p2564 N88-25222

Mixed min-max optimization problem with restrictions
18 p2565 N88-25232

Multigrid methods for elliptic Partial Differential Equations (PDEs)
[CWI-NM-R8722] 18 p2566 N88-25242

Similarity solutions of nonlinear partial differential equations invariant to a family of affine groups
[DE88-003404] 18 p2567 N88-25245

Numerical calculation of three dimensional flow by TVD scheme 19 p2638 N88-25649
La Recherche Aerospatiale, bimonthly bulletin, no. 1986-5, 234/September-October [ESA-TT-1032] 19 p2641 N88-25671
Scaling laws for geomagnetic tail current sheet acceleration [AD-A193379] 19 p2691 N88-25998
Accurate, productive aerodynamic simulation on patched mesh systems [AD-A192040] 19 p2714 N88-26110
Accurate, productive aerodynamic simulation on patched mesh systems [AD-A192040] 19 p2714 N88-26110
Engineering research centers and their evaluation [PB88-180054] 19 p2739 N88-26262
An initial investigation into methods of computing transonic aerodynamic sensitivity coefficients [NASA-CR-183061] 20 p2752 N88-26332
Use of direct solvers for multidimensional fluid flow computations [DE88-010063] 20 p2799 N88-26611
Vibration frequencies of tapered bars with nonclassical boundary conditions [NASA-CR-183059] 20 p2813 N88-26688
Inference and discovery in an exploratory laboratory [AD-A192231] 20 p2832 N88-26801
Challenge problems focusing on equality and combinatory logic: Evaluating automated theorem-proving programs [DE88-010057] 20 p2844 N88-26879
Combining expert opinions: An optimization framework [REPT-87-84] 20 p2846 N88-26895
Boundary layer solutions for the free-edge problem in composite laminates 21 p2904 N88-27229
The integration of decision support problems into feature modeling based design 21 p2927 N88-27372
Effects of numerical dissipation on finite-volume solutions of compressible flow problems [AD-A193173] 21 p2944 N88-27485
An investigation of techniques for determination of optimum/self-optimizing systems 21 p2963 N88-27600
Inspection methods in programming: Cliches and plans [AD-A192782] 21 p2996 N88-27767
Simulation of real time problem solving [AD-A193436] 21 p2997 N88-27776
Implementing direct, spatially isolated problems on transputer networks [NASA-TM-101297] 21 p3000 N88-27796
Intelligent Mobile Autonomous System (IMAS) [AD-A193181] 21 p3003 N88-27811
Transonic blade-vortex interactions 22 p3037 N88-28035
Heat exchanger demonstration expert system 22 p3066 N88-28193
On the pseudo-linearization problem for nonlinear systems [AD-A194021] 22 p3142 N88-28683
General analytic solution of certain functional equations of addition type [PREPRINT-583] 22 p3144 N88-28699
On recognizing ignorance 23 p3254 N88-29372
AI tools in computer based problem solving 23 p3263 N88-29424
Distributed knowledge base systems for diagnosis and information retrieval [AD-A193107] 23 p3296 N88-29633
Resonance excitation of linear and non-linear spiral density waves in a gaseous disk 23 p3299 N88-29643
Reducing the parallel solution time of sparse circuit matrices using reordered Gaussian elimination and relaxation [AD-A195152] 24 p3366 N88-30045
MOORE: A prototype expert system for diagnosing spacecraft problems 24 p3418 N88-30343
Research on problem-solving systems [AD-A195154] 24 p3423 N88-30370
Multiple solutions and bifurcation for a class of nonlinear Sturm-Liouville eigenvalue problems on an unbounded domain [AD-A195954] 24 p3426 N88-30389
Barriers to Information Transfer and Approaches Toward Their Reduction [AGARD-CP-430] 24 p3437 N88-30458
Linguistic barriers: Translation problems 24 p3438 N88-30465
Formulation and solution of economic equilibrium problems [AD-A196034] 24 p3439 N88-30470

PROCEDURES
NT BOUNDARY INTEGRAL METHOD
NT CREW PROCEDURES (INFLIGHT)
NT CREW PROCEDURES (PREFLIGHT)
NT FINITE ELEMENT METHOD
NT FINITE VOLUME METHOD
NT OPTICAL CORRECTION PROCEDURE
NT PANEL METHOD (FLUID DYNAMICS)
Study of aeropropulsion laboratory pressure drop rig and recommended test procedure [AD-A184333] 03 p0322 N88-12038
Implementation of a new shock testing procedure using nonstationary random excitation [DE87-014643] 04 p0456 N88-12827
The how and why of variable amplitude testing 05 p0603 N88-13690
The use of alloy 117 as a liquid metal current collector [AD-A185740] 06 p0698 N88-14281
AVHRR/HIRS (Advanced Very High Resolution Radiometer/High Resolution Infra-Red Sounder) operational method for satellite based sea surface temperature determination [PB88-107594] 06 p0706 N88-14340
A re-evaluation of fatigue threshold test methods 06 p0717 N88-14401
Practical photochemistry: General considerations [PB87-123386] 06 p0730 N88-14491
Development and testing of an interactive procedure for the improvement of objective analyses [AD-A186595] 08 p1040 N88-16290
Using output to evaluate and refine rules in rule-based expert systems 08 p1055 N88-16362
Are windshear training aid recommendations appropriate for other than large jet transports? Pilot procedures: Shear models 10 p1275 N88-17635
Supercritical fluid extraction-gas chromatography of Volatile Organic Compounds (VOC) from tenax devices [PB88-124300] 10 p1298 N88-17759
Research on a solar biotechnology based on the culture of photosynthetic cells [DE88-900129] 10 p1359 N88-18120
Air traffic control [FAA-ORDER-7110.65E] 12 p1576 N88-19426
A procedure for estimating the crystal densities of organic explosives [AD-A189023] 12 p1613 N88-19646
A simplified streamline swallowing procedure for the windward meridian of axisymmetric blunt bodies [AD-A188413] 12 p1626 N88-19732
Selling to NASA [NASA-TM-89724] 12 p1705 N88-20208
Software verification using partition analysis [AD-A190570] 15 p2112 N88-22562
Test procedures and standards for mechanical property measurements on metal matrix composites [NPL-DMA(A)-153] 16 p2172 N88-22944
Benefits of an object approach in a computer aided design environment [SNIAS-881-440-102] 21 p3000 N88-27791

PROCEEDINGS
U CONFERENCES
U CONGRESSIONAL REPORTS

PROCESS CONTROL (INDUSTRY)
Optimization of a controlled two-server maintenance system [INPE-4202-PRE/1083] 01 p0107 N88-10694
Needs assessment for NDT and characterization of ceramics: Assessment of inspection technology for green state and sintered ceramics [DE87-013550] 02 p0151 N88-10947
A fundamental study of the mechanical and microstructural response of elevated temperature PM aluminum-titanium alloys 03 p0289 N88-11819
Avionics and corrosion 05 p0547 N88-13336
Advances in processing techniques for nickel aluminides [DE87-014571] 05 p0566 N88-13449
Statistical process control applied to the liquid-fed ceramic melter process [DE88-000271] 05 p0569 N88-13471
Master plots for predicting the case-depth in laser surface treatments [PB87-221875] 05 p0586 N88-13574
Using hierarchically structured problem-solving knowledge in a rule-based process planning system [DE87-011639] 05 p0639 N88-13906
A study of the Department of Defense configuration management policies and procedures as applied to the FA-18 Strike/Fighter program [AD-A184872] 05 p0657 N88-14034
High temperature adhesive [PB87-109229] 06 p0683 N88-14186
Glassy GeO2 obtained by the gel process [NASA-TT-20125] 06 p0685 N88-14201
Knowledge acquisition for a simple expert controller [NASA-TT-20118] 06 p0761 N88-14672
Fluid mechanical issues in polymer processing [DE88-002767] 08 p0972 N88-15880
Improved silicon nitride for advanced heat engines [NASA-CR-175006] 08 p0973 N88-15886
Innovating systems and techniques for the diagnosis of materials and industrial plants [CISE-3856] 08 p0976 N88-15901
Intelligent process development of foam molding for the Thermal Protection System (TPS) of the space shuttle external tank 08 p1060 N88-16397
A problem of machine repair with a variable number of heterogeneous servers [INPE-4245-PRE/1116] 08 p1074 N88-16482
Experience of developing an integrated nondestructive assay system [DE88-003149] 09 p1184 N88-17092
Some process control/design considerations in the development of a microgravity mammalian cell bioreactor 09 p1197 N88-17174
Fabrication and materials evaluation of high performance aligned ceramic fibre reinforced glass matrix composite [AERE-R-12517] 10 p1294 N88-17736
Measurements as a process [DE88-005275] 11 p1497 N88-18938
The influence of processing variables on physical properties of sol-gel derived TiO2 films [DE88-005155] 11 p1539 N88-19331
Development of metastable processing paths for high temperature alloys [AD-A188682] 12 p1608 N88-19617
Reducing time required for the development of avionic systems 12 p1702 N88-20185
Prototype manufacturing techniques for reducing cost, schedule, and technical risk 12 p1702 N88-20189
Recommended replacements for tetryl in Australian production fuzes and related ordnance [MRL-R-1089] 13 p1754 N88-20489
EDF's studies and first choices regarding the design of electrical equipment [NASA-TT-20222] 13 p1764 N88-20553
Improvements in end point detection — semiconductor fabrication [RSRE-MEMO-4035/A] 14 p1899 N88-21336
Measurement of emissivity of industrial surfaces using a simple method [NASA-TT-20165] 15 p2036 N88-22130
Application and technology requirements for heat pumps at the process industries [DE88-006740] 15 p2062 N88-22293
A fault tolerant supervision system [INPE-4419-TDL/307] 15 p2148 N88-22819
Information systems for quality. Experience at the Nerviano Aeritalia plant. Avionic systems and equipment group [ETN-88-92274] 15 p2148 N88-22821
Automatic control of an industrial process and computer aided process control by means of an expert system [LAAS-88-004] 16 p2255 N88-23476
Simultaneous use of artificial intelligence and Petri nets: Application to the monitoring of a fabrication plan [LAAS-87-354] 17 p2390 N88-24207
Sensors for process control requirements for design and test 19 p2671 N88-25877
Effect of process conditions on aluminum oxide thin film used in pH ISFET 19 p2673 N88-25892
Granulation of pyrotechnic tracer composition R284T [MRL-TN-526] 20 p2780 N88-26490
Industrial processes influenced by gravity [NASA-CR-182140] 20 p2782 N88-26497
The knowledge based automatic extraction of the machinable surfaces for automatic CAD-CAM system [INPE-4542-PRE/1266] 20 p2836 N88-26824
The hole of a blanket tritium system on the fusion fuel cycle [DE88-010007] 20 p2859 N88-26983
Ceramic processing of high-T(sub)c superconductors [DE88-010090] 20 p2878 N88-27087
Processing and properties of advanced aluminum alloys [AD-A193224] 21 p2912 N88-27284
Optical diagnostics for metallurgical processes [DE88-009255] 21 p2913 N88-27289
Use of microwave measuring systems for the nondestructive control of resins and composites [REPT-881-430-123] 21 p2959 N88-27576
Nondestructive tests and high performance composite structures [SNIAS-881-430-119] 23 p3188 N88-28969
Molecular composites processing and properties, 1 [AD-A194113] 23 p3189 N88-28974
Advanced processing and properties of high performance alloys [AD-A193767] 23 p3194 N88-29010
Material and process selection and quality control for ESA space systems and associated equipment [ESA-PSS-01-70-ISSUE-3] 23 p3224 N88-29190
Preliminary investigation of flow modeling during solid propellant processing [AD-A196168] 24 p3357 N88-29987

PROCESSORS (COMPUTERS)
U CENTRAL PROCESSING UNITS

PROCUREMENT
NT GOVERNMENT PROCUREMENT
Specialized instrumentation for computational fluid dynamics research
[AD-A188160] 11 p1482 N88-18849
Electric vehicle demonstration project
[DE88-004076] 11 p1566 N88-19376
Commonality in the design and production of the H-423 (F3) and H-770 (F-15) RLG inertial navigation systems
12 p1577 N88-19431
Selling to NASA
[NASA-TM-89724] 12 p1705 N88-20208
Developing systems using state-of-the-art CAD/CAM technology 17 p2306 N88-23795

PROCUREMENT POLICY
Generic specifications for hybrid microcircuits
[ESA-PSS-01-608-ISSUE-2] 06 p0696 N88-14273
Promotion of European components for ESA projects
09 p1126 N88-16764
The technical reporting and approval procedure for materials and processes
[ESA-PSS-01-700-ISSUE-1] 22 p3162 N88-28833
The cost and performance implications of reliability improvements in the F-16A/B
[AD-A195096] 24 p3324 N88-29796

PRODUCT DEVELOPMENT
Development of a polyimide matrix for filament winding with improved extensibility and fracture toughness for permanent use at 200 C
[BMFT-FB-T-86-118] 01 p0030 N88-10190
Robotic sensors and actuators for a service manipulator system. Volume 3, phase A report and program plan
[MATRA-EPT/DT/VT167/228]
01 p0054 N88-10343
ESA technological research activities on lightweight mirrors — spaceborne interferometry
01 p0096 N88-10629
Development of a pilot plant for the production of rapidly solidified aluminum alloy powders
[BMFT-FB-T-86-153] 02 p0146 N88-10914
Development of highly porous calcium silicate hydrate materials with extremely low thermal conductivity
[BMFT-FB-T-86-164] 02 p0150 N88-10941
A 1987 progress report of manufacturing techniques for Gravity Probe B gyroscope rotors
[NASA-TM-100312] 02 p0176 N88-11101
Commercial perspective of an imaging spectrometer development program 03 p0340 N88-12138
Production of flows for aeroballistic investigation in the shock tubes of the Franco-German Research Institute (ISL), Saint-Louis (France)
[ISL-R-113/86] 05 p0541 N88-13295
Carbon-carbon composites and Aerospatiale. State of the art and prospects
[SNIAS-872-430-108] 05 p0559 N88-13401
A contribution to the realization of active filters for high frequency applications
[ETN-88-90811] 06 p0696 N88-14272
Design, production, and characterization of broadband optical waveguides
[DFVLR-FB-85-52] 06 p0780 N88-14791
Past, present and future role of Black Brant rocket systems to support international space science programs 08 p1034 N88-16272
The appropriate use of contract types in development contracts (a systems approach with emphasis on the European space sector)
[ESA-STR-222] 08 p1092 N88-16573
Specialist support for projects: Activities, methods and infrastructure 09 p1124 N88-16729
The objectives and methods of the technological research program 09 p1124 N88-16730
Technology developments to meet tomorrow's need for higher satellite frequencies 09 p1124 N88-16732
The Ariane launcher and its progress
09 p1125 N88-16742
The new approach to the definition of the ESA technological research program
09 p1127 N88-16763
The Ariane-3 program 09 p1128 N88-16771
Solid fuel combustion chamber
[VTH-LR-515] 09 p1141 N88-16842
Study for history of technology developments in European space projects
[REPT-8518-1] 10 p1286 N88-17690
The intelligent wing. Aerodynamic development direction for future passenger aircraft
[MBB-UT-008/87] 10 p1313 N88-17848
Trends in the development of space transportation systems
[MBB-UR-911/86] 10 p1315 N88-17857
Microgravity and Materials Processing Facility study (MMPF): Requirements and Analyses of Commercial Operations (RACO) preliminary data release
[NASA-CR-179309] 11 p1468 N88-18742
Splinter generator
[MBB-UA-1048/87] 11 p1491 N88-18897
The light pulse generator 869 for high speed investigations
[MPIS-9/1987] 11 p1491 N88-18898
Conception and realization of components for a microchannel-plate detector, and testing of the detector system in the laboratory and in astronomical use
[ETN-88-91495] 11 p1491 N88-18899
Automatic riveting machine for spherically-formed airframe structures
[ETN-88-91024] 11 p1495 N88-18924
Status of emerging technologies: An economic/technological assessment to the year 2000
[PB88-155775] 11 p1567 N88-19381
Assessment, development and application of combustor aerothermal models
[NASA-TM-100290] 12 p1582 N88-19469
EVA, the technological challenge
12 p1592 N88-19535
Multi-axis control of telemanipulators
12 p1593 N88-19539
Planning, construction, and commissioning of a vacuum apparatus with a cold surface for the measurement of transistor functions at 20 K
[JUEL-SPEZ-397] 12 p1622 N88-19703
Flight Vehicle Development Time and Cost Reduction
[AGARD-CP-424] 12 p1700 N88-20173
Risk reduction cost avoidance for full scale development begins with concept formulation
12 p1700 N88-20174
Picking winners: Parametric cost estimating and project management 12 p1700 N88-20176
Parametric study of the total cost of aircraft modernization in terms of development and equipment series costs 12 p1700 N88-20177
The increased time and cost of development: Causes and (some) remedies 12 p1701 N88-20178
Reasons for increasing development cost of rotary wing aircraft and ideas to reverse the trend
12 p1701 N88-20179
What can be done to face growing development costs
12 p1701 N88-20181
Optimizing powerplant design and development cycles
12 p1701 N88-20183
Reducing rotary wing aircraft development time/cost through the use of simulation 12 p1702 N88-20186
The use of simulation in the development of the Airbus 12 p1702 N88-20188
Use of demonstration/validation prototypes: Impact on total development costs and times
12 p1703 N88-20194
Engineering management for validation prototype phase 12 p1703 N88-20195
People, procedures, performance: The keys to improving the development environment 12 p1704 N88-20197
Organization of helicopter development activities with a view toward reduction of costs and cycles
12 p1704 N88-20200
Advanced Gas Turbine (AGT) technology development project
[NASA-CR-180891] 12 p1709 N88-20230
Pressurizing systems and air conditioning systems
[MBB/LKE-312/S/PUB/246] 13 p1812 N88-20828
Principles of a low-cost laser gyro for rotating vehicles and platforms
[DFVLR-MITT-87-15] 14 p1912 N88-21425
Further development of a stellar camera following the rotation-modulation-collimator principle for balloon-borne observations in the X-ray range
[ETN-88-91496] 14 p1913 N88-21428
French Multiproject Chip (MPC) activity report, 1986
[RR-650-I] 15 p2058 N88-22273
Development and qualification of an Augmented Electro-Thermal Hydrazine-Thruster (AEHT) with 0.1 to 0.2 N vacuum thrust
[BMFT-FB-W-86-012] 16 p2169 N88-22931
International commercialization of remote sensing
[BCRS-87-14] 16 p2228 N88-23310
Summary of the activities performed during the Botany Facility (BF) predevelopment phase for the Life Support S/S (LSS)
[TB-RB524-002/87] 17 p2378 N88-24133
P-Plus: Polar Platform utilization study, executive summary
[BAE-TP-8391] 18 p2469 N88-24653
Development of mirrors for high-precision laser gyroscopes 18 p2517 N88-24931
Navigation using the Teldix fiber-optic gyroscope
18 p2517 N88-24933
New semiconductor laser structure for an optical communication system
[ETN-88-92353] 20 p2807 N88-26654
Design of high performance microcomputers for numerical data processing
[ETN-88-92371] 20 p2835 N88-26818
Delfi-3 as a development environment for expert systems
[REPT-8767] 20 p2839 N88-26845
Investigation of expert system design approaches for electronic design environments
21 p2926 N88-27365
Planning for AIMS on the next generation 7J7 aircraft
22 p3035 N88-28017
Reaching for the skies: The Ariane family story and beyond. An introduction to Europe's successful series of space transportation systems
[ESA-BR-42] 22 p3046 N88-28076
Sensors adapted for acoustic detection
22 p3148 N88-28731
Starting point of a project: Decision mechanisms — space projects 22 p3159 N88-28806
The development phases of a project — space projects 22 p3159 N88-28807
Development of a glass fiber wing following the construction regulation FAR Part 23
[ETN-88-92966] 23 p3189 N88-28979
Development of a multiport-hybrid-mode exciter for use in antennas for polarimetric field measurements
[REPT-12-87] 23 p3205 N88-29075
Next-generation space manipulator
23 p3263 N88-29428

PRODUCTION COSTS
NT AIRCRAFT PRODUCTION COSTS
Making space nickel/hydrogen batteries lighter and less expensive
[DE88-000168] 05 p0578 N88-13630
A problem of machine repair with a variable number of heterogeneous servers
[INPE-4245-PRE/1118] 08 p1074 N88-16482
Production costs of hydrocarbon fuels from biomass
[DE88-006667] 18 p2495 N88-24914

PRODUCTION ENGINEERING
NT PRODUCTION PLANNING
Development and production of new and modified powders for sprayed coatings and components for saving important raw materials
[BMFT-FB-T-86-129] 01 p0025 N88-10159
Fabrication of microstructures with extreme structural heights by vacuum reaction injection molding and electroforming
[KFK-4267] 01 p0033 N88-10210
Development of a pilot plant for the production of rapidly solidified aluminum alloy powders
[BMFT-FB-T-86-153] 02 p0146 N88-10914
Selected aspects of microelectronics technology and applications: Numerically controlled machine tools. Technology trends series no. 2
[PB87-132973] 06 p0696 N88-14268
Effects of processing variables on the behavior of E-glass/913 and XAS carbon fibre/913 laminates subjected to hot/wet environmental conditions
[BR101940] 09 p1138 N88-16820
Advanced manufacturing management current and forthcoming technologies
[PNR90445] 22 p3158 N88-28802

PRODUCTION METHODS
U PRODUCTION ENGINEERING

PRODUCTION PLANNING
XCUT: A rule-based expert system for the automated process planning of machined parts
[DE87-011638] 05 p0639 N88-13865
Using hierarchically structured problem-solving knowledge in a rule-based process planning system
[DE87-011639] 05 p0639 N88-13866
An extended Cobb-Douglas form for use in production economics
[AD-A186372] 07 p0943 N88-15730
Product planning in civil aircraft construction
[MBB-UT-002/87] 10 p1313 N88-17849
Viscosity methods in optimal control of distributed systems
[AD-A188086] 10 p1401 N88-18237

PRODUCTIVITY
NBS (National Bureau of Standards) calibration services users guide: Fee schedule
[PB87-210654] 01 p0090 N88-10586
Implementing and managing change: A guide for assessing information technology
[DE88-000035] 02 p0249 N88-11571
Spinoff, 1987
[NASA-TM-89652] 02 p0250 N88-11577
The effect of radiation on the long term productivity of a plant based CELSS 03 p0361 N88-12271

Report on phase 1 of the project estimate development of a model for yield estimation of sugar cane based on LANDSAT and agromet data
[INPE-4466-RPE/560] 12 p1638 N88-19807
JPRS report: Science and technology. USSR: Life sciences
[JPRS-ULS-88-002] 12 p1665 N88-19982
Efficiency of human workers and means to increase it
12 p1666 N88-19986
Time and cost reduction through computer integrated manufacture 12 p1703 N88-20191
Improved flight test productivity using advanced on line data systems 12 p1703 N88-20193
People, procedures, performance: The keys to improving the development environment 12 p1704 N88-20197
Practical image analysis using personal computers: The Canadian experience 17 p2356 N88-24037
Interpretation of MSS/LANDSAT data for evaluation of physical distribution of mangroves in Cananeia-Iguape (SP) 17 p2363 N88-24072
Research on enhancing the utilization of digital multispectral data and geographic information systems in global habitability studies
[NASA-CR-182799] 17 p2368 N88-24101
Quality and productivity drive innovation and improvement at United Technologies Aerospace Operations, Inc.
[NASA-CR-182944] 18 p2525 N88-24983
The assessment of human/computer performance using human productivity measures: MIPS and BIPS are MEGAFLOPS
[DE87-013491] 21 p2993 N88-27750

PRODUCTS
NT ASPHALT
NT DIESEL FUELS
NT GASOLINE
NT GREASES
NT PETROLEUM PRODUCTS
NT REACTION PRODUCTS
An introduction to the GOES I-M imager and sounder instruments and the GVAR retransmission format
[NOAA-TR-NESDIS-33] 02 p0140 N88-10884
A note on compactifications of products of semigroups
[CWI-PM-R8701] 08 p1072 N88-16469
Fast serial input-serial output pipelined inner product units
[REPT-87-031] 11 p1530 N88-19142

PROFICIENCY
U ABILITIES

PROFILES
Possibilities of determining vertical profiles of microphysical characteristics of stratospheric aerosol using space measurements of transparency and solar halo 24 p3449 N88-30526
Estimation of soil temperature profile from remote microwave and IR measurements
24 p3450 N88-30532

PROFILOMETERS
Profilometer for bomb-damage-repaired airfield pavements and measurement of pavement upheaval. Report 1: Technology evaluation
[AD-A187985] 11 p1442 N88-18601
Space shuttle solid rocket motor Profile Measuring Device (PMD) 14 p1928 N88-21495

PROGNOZ SATELLITES
Intershock observations during STIP intervals 17 and 18 01 p0119 N88-10759
Measurement of galactic radio emission at frequency 37 GHz from aboard spacecraft
24 p3448 N88-30520

PROGRAM EVALUATION REVIEW TECHNIQUE
U PERT

PROGRAM MANAGEMENT
U PROJECT MANAGEMENT

PROGRAM VERIFICATION (COMPUTERS)
Design and implementation of a debugger for an abstract machine
[AD-A184891] 03 p0363 N88-12283
ADAMEASURE: An implementation of the Halstead and Henry metrics
[AD-A184005] 03 p0365 N88-12299
SDVS (State Delta Verification System): Program verification system development fiscal year 1986
[AD-A184338] 03 p0366 N88-12302
Experimental aerothermodynamic research of hypersonic aircraft
[NASA-CR-181533] 04 p0399 N88-12483
Digital-flight-control-system software written in automated-engineering-design language: A user's guide of verification and validation tools
[NASA-TM-88313] 04 p0401 N88-12494
SDVS (State Delta Verification System) 5 users' manual
[AD-A184339] 04 p0478 N88-12943
Aircraft interior noise reduction by alternate resonance tuning
[NASA-CR-181530] 04 p0488 N88-13005
Effectiveness of back-to-back testing
[TR-87-08] 05 p0632 N88-13865
RSDIMU acceptance testing system: Overview of acceptance software and procedures
05 p0632 N88-13866
An extension to the multilevel logic simulator for microcomputers
[AD-A185032] 05 p0634 N88-13879
The adaption and use of research codes for performance assessment
[DE88-000552] 06 p0756 N88-14639
Space station software reliability analysis based on failures observed during testing at the multisystem integration facility 06 p0798 N88-14884
Version description document for the Ada compiler validation capability (version 1.9) (for microcomputer)
[AD-A186390] 07 p0903 N88-15471
The NASA aircraft icing research program
08 p0957 N88-15803
An approach to the hierarchical specification, design and verification of software
[RSRE-MEMO-4063] 09 p1223 N88-17332
An expert system to support the verification/validation of flight-critical software
[MBB-UT-102/87] 10 p1314 N88-17852
A generalized method for automatic downhand and wirefeed control of a welding robot and positioner
[NASA-TP-2807] 10 p1316 N88-17869
AEV local verification for aviation, precipitation and temperature programs: AV, REL, TEM (September 1987 revision)
[PB88-115662] 10 p1355 N88-19101
Feasibility study of generating plans and strategies for software testing by knowledge based system
[AD-A187834] 11 p1529 N88-19134
A theory of program correctness, and algorithms for proofs
[ANL-87-4] 11 p1531 N88-19146
EqL's user's guide
[AD-A188351] 12 p1677 N88-20025
Research on automatic verification of finite-state concurrent systems
[AD-A188618] 12 p1677 N88-20029
Modification, implementation, and evaluation of a remote terminal emulator as a software validation and stress testing tool
[AD-A188833] 12 p1678 N88-20034
Dynamic run-time graphics
[DE87-008997] 13 p1820 N88-20879
Sensitivity of control-augmented structure obtained by a system decomposition method
[NASA-TM-100535] 14 p1954 N88-21647
Ada (Trademark) compiler validation summary report. ALSYS: AlsyCOMP-013, V2.0 HOST: IBM PC AT. Target: IBM 370 3084Q
[AD-A189640] 15 p2106 N88-22546
Software verification using partition analysis
[AD-A190570] 15 p2112 N88-22582
The Colored Stochastic Petri Net (CS-PN) software: Application to the validation and the performance evaluation of distributed systems
[ENST-87D005] 15 p2113 N88-22589
An approximation technique for solving a system of Fredholm integral equations for asymmetric detector response functions
[AD-A190577] 15 p2121 N88-22645
Program profiling in Cedar
[AD-A190883] 16 p2250 N88-23449
Supercomputer programming environments
[AD-A190887] 16 p2251 N88-23452
Testing complex avionics software: A practical experience 17 p2306 N88-23794
A benchmark for galactic cosmic ray transport codes
[NASA-TM-101157] 17 p2453 N88-24571
Automated test device for FASR (Fixed Array Surveillance Radar) beam steering componentry
[AD-A191650] 18 p2500 N88-24829
Advanced development of the boundary element method for elastic and inelastic thermal stress analysis
18 p2529 N88-25002
A general approach for automating source code verification
[AD-A191461] 18 p2556 N88-25170
Checkout system software for INPE satellites
[INPE-4554-PRE/1297] 19 p2715 N88-26120
Inspection methods in programming: Cliches and plans
[AD-A192782] 21 p2996 N88-27767
Verification of flight software written in C using ACSL
[DE88-006100] 21 p2998 N88-27779
A modular proof of correctness for a network synchronizer
[AD-A192726] 21 p3002 N88-27802
Loading and linking in a modular language, an exercise in verification by unification
[INF-87-30] 22 p3136 N88-28642
Air Force Systems Command software independent verification and validation implementation analysis and guidance
[AD-A194309] 22 p3137 N88-28653
Validation tests for standard PASCAL and extented PASCAL
[NPL-DITC-108/88] 22 p3139 N88-28663
Validation code for the Whetstone Benchmark
[NPL-DITC-107/88] 22 p3140 N88-28667
Validation of expert systems 23 p3262 N88-29416
Verification and validation of rulebased systems for Hubble Space Telescope ground support
24 p3421 N88-30351

PROGRAMMED INSTRUCTION
NT COMPUTER ASSISTED INSTRUCTION
KA-PROLOG. KAP-computer: Computer model and instructions set
[ETN-88-91948] 18 p2558 N88-25186

PROGRAMMERS
NOSTRADAMUS programmable translator user's manual and programmer's manual
[DE87-013414] 01 p0083 N88-10533
On computing environments in data analysis
[DE88-000078] 04 p0480 N88-12961
Programmer-friendly LL(1) parser generator
[PB88-126933] 20 p2841 N88-26857
The programmer's apprentice project: A research overview
[AD-A192784] 21 p2996 N88-27769

PROGRAMMING (SCHEDULING)
NT THRUST PROGRAMMING

PROGRAMMING LANGUAGES
NT ADA (PROGRAMMING LANGUAGE)
NT APL (PROGRAMMING LANGUAGE)
NT ASSEMBLY LANGUAGE
NT BASIC (PROGRAMMING LANGUAGE)
NT C (PROGRAMMING LANGUAGE)
NT COBOL
NT CONTEXT FREE LANGUAGES
NT FORTRAN
NT HIGH LEVEL LANGUAGES
NT LISP (PROGRAMMING LANGUAGE)
NT NATURAL LANGUAGE (COMPUTERS)
NT PASCAL (PROGRAMMING LANGUAGE)
NT PROLOG (PROGRAMMING LANGUAGE)
Naval Aviation Integrated Logistics: Technical users guide version 1.0
[DE87-013368] 01 p0001 N88-10001
EVA reference manual
[DE87-014073] 01 p0082 N88-10526
NOSTRADAMUS programmable translator user's manual and programmer's manual
[DE87-013414] 01 p0083 N88-10533
An embedded multiprocessor computer for proof-of-principle testing of exploratory systems concepts
[DE87-012735] 02 p0218 N88-11372
Praxis: The programming language: An advanced overview
[DE87-014319] 02 p0220 N88-11388
Integrating syntax, semantics, and discourse DARPA (Defense Advanced Research Projects Agency) Natural Language Understanding Program
[AD-A184505] 03 p0364 N88-12289
ERIC: An object-oriented simulation language
[AD-A184757] 03 p0364 N88-12293
Low-level vision on warp and the apply programming model
[AD-A184330] 03 p0369 N88-12320
A network definition and solution of simulation problems
[DE88-000675] 04 p0481 N88-12962
Mixing Microsoft C and Microsoft FORTRAN program modules on the IBM Personal Computer
[DE88-001947] 05 p0637 N88-13895
A requirements specification for a software design support system
[NASA-CR-182333] 05 p0637 N88-13896
Learning to program methodically. 3: The newly designed course of the elementary programming
[PB87-119871] 06 p0757 N88-14643
Benchmarking and evaluation of hardware description languages for design of VLSI systems
[PB87-134557] 06 p0758 N88-14648
Computer architectures for artificial intelligence
[PB87-123824] 06 p0761 N88-14671
Using multiple dialog modes in a user-system interface to accomodate different levels of user experience: An experimental study
[AD-A186115] 07 p0899 N88-15444
Formalizing reusable software components in the programmer's apprentice
[AD-A185843] 07 p0901 N88-15457

Image processing language development
[AD-A186251] 07 p0903 N88-15467
DoD Gateway Information System (DGIS) common command language: The first prototyping and the decision for artificial intelligence
[AD-A185950] 07 p0942 N88-15725
DoD Gateway Information System (DGIS): Common command language mapping
[AD-A185951] 07 p0942 N88-15726
Clips as a knowledge based language
08 p1055 N88-16365
CLIPS: An expert system tool for delivery and training
08 p1056 N88-16368
ESSAA: Embedded system safety analysis assistant
08 p1060 N88-16396
LISP based simulation generators for modeling complex space processes 08 p1061 N88-16403
Applicative parallelism: Potential and challenge
[DE87-011885] 08 p1068 N88-16459
Interchange of electronic design through VHDL and EIS 09 p1205 N88-17222
The IDEAL (Integrated Design and Engineering Analysis Languages) modeling methodology: Capabilities and Applications 09 p1206 N88-17227
Implementing clips on a parallel computer
09 p1211 N88-17259
ESL batteries and multi-segment applications — ESA Simulation Language (ESL)
[CS-1029/00-QFIN4] 10 p1322 N88-17901
SISAL: Initial MIMD performance results
10 p1375 N88-18208
Predicate analysis for parallel program generation
10 p1377 N88-18222
Software support for heterogeneous machines
10 p1378 N88-18224
Portable (and disposable) interpreters
10 p1380 N88-18237
Programming language translation for multicomputers
10 p1381 N88-18244
Finely grained parallelism in an applicative architecture
10 p1383 N88-18256
FX-87 reference manual, edition 1.0
[AD-A187031] 10 p1385 N88-18273
Graph transformation algorithms for array memory optimization in applicative languages
[DE88-004727] 10 p1387 N88-18283
Semantics of EqL
[AD-A188151] 10 p1389 N88-18297
A worked example of an application of the SAINT simulation program
[AD-A188198] 11 p1524 N88-19097
EqL: The language and its implementation
[AD-A188161] 11 p1530 N88-19137
A theory of program correctness, and algorithms for proofs
[ANL-87-4] 11 p1531 N88-19146
The SAS (Statistical Analysis System) by forms: Putting statistical power into the hands of an end-user
[DE88-002217] 11 p1541 N88-19212
Accessing hierarchical databases via SQL transactions in a multi-model database system
[AD-A187878] 11 p1565 N88-19369
A production-quality UNIX Very High Speed Integrated Circuit (VHSIC) Hardware Description Language (VHDL) subset analyzer
[AD-A188832] 12 p1623 N88-19710
EqL's user's guide
[AD-A188351] 12 p1677 N88-20025
Building software systems economically with mechanized logic: Initial design proposal
[AD-A188791] 12 p1678 N88-20031
A prototype for remotely shared textual workspaces
[AD-A188352] 12 p1679 N88-20040
Experience with Berkeley UNIX interprocess communications
[AD-A188353] 12 p1680 N88-20041
MultiRPC: A parallel remote procedure call mechanism
[AD-A188613] 12 p1680 N88-20046
ARCTIC: Programmer's manual and tutorial
[AD-A188619] 12 p1680 N88-20047
Design of the CONSUL programming language
[AD-A189202] 13 p1815 N88-20841
An interface between object-oriented systems
[AD-A189245] 13 p1815 N88-20844
Algebra of Communicating Processes (ACP)tau: A universal axiom system for process specification
[CWI-CS-R8725] 13 p1819 N88-20869
Designing equivalent semantic models for process creation
[CWI-CS-R8732] 13 p1819 N88-20872
Two normal form theorems for Communicating Sequential Processes (CSP) program
[CWI-CS-R8735] 13 p1819 N88-20874
Predicate-transformer semantics of general recursion
[CS-8709] 13 p1820 N88-20876
An implementation of the OPS5 language for computers compatible with IBM-PC
[INPE-4291-PRE/1162] 13 p1821 N88-20882
A proof rule process creation
[CWI-CS-R8710] 13 p1822 N88-20891
Type-checking Mini-ML: An algebraic specification with user-defined syntax
[CWI-CS-R8737] 13 p1827 N88-20921
Activities and operations of the Advanced Computing Research Facility, October 1986-October 1987
[DE88-006223] 14 p1955 N88-21653
Geometric modeling of flight information for graphical cockpit display
[AD-A190484] 15 p2021 N88-22043
Output formatting in Apple-soft BASIC
[DE88-701413] 15 p2108 N88-22559
A UNIX-based interactive VHDL (hardware description language) simulator
[AD-A189749] 15 p2109 N88-22565
Tutorial on GAMS (Generalized Algebraic Modeling System): A modeling language for optimization
[AD-A189867] 15 p2109 N88-22568
Argus reference manual
[AD-A190382] 15 p2111 N88-22578
Software structuring principles for VLSI CAD
[AD-A190386] 15 p2112 N88-22579
A direct-execution parallel architecture for the Advanced Continuous Simulation Language (ACSL)
[NASA-CR-182909] 15 p2115 N88-22602
The synthesizer generator, a useful tool?
[REPT-87-77] 16 p2250 N88-23443
Data management and language enhancement for generalized set theory computer language for operation of large relational databases
[NASA-CR-182868] 16 p2250 N88-23446
Supercomputer programming environments
[AD-A190887] 16 p2251 N88-23452
Editfont an interactive font editing system
[AD-A191007] 16 p2251 N88-23453
Parallelism in a Prolog knowledge base machine
[ETN-88-92187] 16 p2255 N88-23477
Linguistic definition of generic models in computer vision
[RSRE-MEMO-4110] 17 p2386 N88-24182
KA-PROLOG. KAP-computer: Computer model and instructions set
[ETN-88-91948] 18 p2558 N88-25186
The Sizing and Optimization Language, (SOL): Computer language for design problems
[NASA-TM-100565] 18 p2559 N88-25190
Design, implementation and evaluation of an operating system for a network of transputers
[AD-A186583] 18 p2559 N88-25193
The new MININEC (version 3): A mini-numerical electromagnetic code
[AD-A191778] 19 p2642 N88-25675
MVS (Multiple Virtual Storage) batch computing and data management at ANL
[DE88-007342] 19 p2718 N88-26137
FASTRUN phase sequencer descriptor language (PDL)
[DE88-007966] 20 p2837 N88-26828
Why is it difficult to program in von Neumann languages
[AD-A192830] 20 p2838 N88-26839
Contractions in comparing concurrency semantics
[CWI-CS-R8755] 20 p2840 N88-26850
A semantic approach to fairness
[CWI-CS-R8759] 20 p2840 N88-26853
Implementation of an OPS5 derivative on the Novix RISC processor
[DE88-011392] 21 p2994 N88-27756
Linguistic semantics for parallel computation
[PB88-105960] 21 p2995 N88-27761
Bisimulation can't be traced
[AD-A192725] 21 p2996 N88-27766
The SAS System by forms: Putting statistical power into the hands of an end-user
[DE88-010512] 21 p3010 N88-27857
Software development without languages
23 p3257 N88-29392
Programming language concepts for multiprocessors
[AD-A193465] 23 p3264 N88-29430
Conversion of productions in OPS5 to their equivalent English
[ORNL/TM-10246] 24 p3411 N88-30306
Syntactic closures
[AD-A195921] 24 p3412 N88-30311
Scheme86: A system for interpreting SCHEME
[AD-A195931] 24 p3413 N88-30319
Reification without evaluation
[AD-A195928] 24 p3414 N88-30326

PROGRAMS
NT ACEE PROGRAM
NT AGRISTARS PROJECT
NT BRAZILIAN SPACE PROGRAM
NT CANADIAN SPACE PROGRAM
NT CHINESE SPACE PROGRAM
NT DEFENSE PROGRAM
NT EARTH RESOURCES PROGRAM
NT EUROPEAN SPACE PROGRAMS
NT FRENCH SPACE PROGRAMS
NT GALILEO PROJECT
NT GLOBAL ATMOSPHERIC RESEARCH PROGRAM
NT INTERNATIONAL GEOSPHERE-BIOSPHERE PROGRAM
NT JAPANESE SPACE PROGRAM
NT NASA PROGRAMS
NT NASA SPACE PROGRAMS
NT NATIONAL AEROSPACE PLANE PROGRAM
NT PROJECT SETI
NT PROJECTS
NT QUIET ENGINE PROGRAM
NT ROVER PROJECT
NT SKYLAB PROGRAM
NT SPACE PROGRAMS
NT SUPERSONIC CRUISE AIRCRAFT RESEARCH
NT SWEDISH SPACE PROGRAM
NT TILT ROTOR RESEARCH AIRCRAFT PROGRAM
NT U.S.S.R. SPACE PROGRAM
NT UK SPACE PROGRAM
NT UNIVERSITY PROGRAM
Alternative fuels: Information on DOE's (Department of Energy's) methanol vehicle demonstration program
[PB88-118203] 13 p1753 N88-20481
The World Climate Research Program
14 p1935 N88-21538
Acid rain: Delays and management changes in the Federal research program
[GAO/RCED-87-89] 19 p2690 N88-25866

PROGRESS
Progress in the development of niobium alloyed high speed steel
[DE87-703549] 04 p0415 N88-12576
Recent progress in the p and h-p version on the finite element method
[AD-A187254] 10 p1400 N88-18347
Progress and future directions in computational fluid dynamics
[NASA-TM-100091] 18 p2456 N88-24579

PROJECT MANAGEMENT
Middle Atmosphere Program: Handbook for MAP, volume 24
[NASA-CR-181451] 01 p0069 N88-10444
Analysis and synthesis of abstract data types through generalization from examples
[NASA-CR-178369] 01 p0081 N88-10519
The microcomputer as an engineering management tool
[DE87-014882] 02 p0219 N88-11378
A review of hypertext in a NASA project management context 06 p0793 N88-14859
Research and technology objectives and plans. Summary, Fiscal Year 1986
[NASA-TM-87504] 06 p0800 N88-14884
The role of the DFVLR project management life sciences in the space program of the Federal Republic of Germany 07 p0884 N88-15344
Program draft for a special field: Gravitational biology
07 p0887 N88-15381
Risk analysis methodology survey
07 p0922 N88-15604
Design and management of research projects
[PB88-106380] 07 p0941 N88-15721
Aeropropulsion structures 08 p0954 N88-15786
Realization of the immediate objectives of the Aero-Gas Dynamics and Vibration Laboratory (LAGG) at the National Center for Research, Science and Technology (PUSPIPTEK) at Serpong, Java (Indonesia), Project TTA-79
[GG/QPR-10] 08 p1092 N88-16572
The ESA centralized management system for satellite electronic test and checkout instrumentation
09 p1124 N88-16731
Columbus feasibility studies. Volume 5: Programmatics
[ETN-88-91076] 09 p1134 N88-16802
Recommendations for a US ice coring program
[PB88-115043] 09 p1185 N88-17102
Study for history of technology developments in European space projects
[REPT-8518-1] 10 p1296 N88-17680
System analysis study of space platform and station accommodations for life sciences research facilities. Volume 2: Study results. Appendix E: Work breakdown structure and dictionary
[NASA-CR-179274] 10 p1292 N88-17723
Project management in astronautics: From Spacelab to Columbus
[MBB-URE-943/87] 10 p1315 N88-17858
Coordination: Southeast continental shelf studies
[DE88-003880] 10 p1357 N88-18110

What can be done to face growing development costs
12 p1701 N88-20181
Post-Challenger evaluation of space shuttle risk assessment and management
[NASA-CR-182461] 12 p1705 N88-20202
Application of expert systems in project management decision aiding
[NASA-CR-180762] 13 p1850 N88-21074
Engineering support of space shuttle experiment integration
[AD-A190135] 15 p2024 N88-22061
Project Monitoring Package (PMP): A package for project activity monitoring
[DE88-701234] 15 p2107 N88-22554
The multiannual National Remote Sensing Program (NRSP)
[BCRS-87-16] 16 p2229 N88-23311
Two decades of achievement in the ocean, 1968-1988
[PB88-167077] 16 p2236 N88-23356
The integration, characterisation and trialling of a modern complex airborne radar 17 p2305 N88-23791
Outline of the GPCP strategy
17 p2351 N88-24007
Acid rain: Delays and management changes in the Federal research program
[GAO/RCED-87-89] 19 p2690 N88-25988
Procedures for peer review assessments
[DE88-007749] 19 p2739 N88-26263
Management of large space projects --- conference
[ISBN-2-85-428192-6] 22 p3159 N88-28803
Management 22 p3159 N88-28804
Large space projects --- management
22 p3159 N88-28805
Starting point of a project: Decision mechanisms --- space projects 22 p3159 N88-28806
The development phases of a project --- space projects 22 p3159 N88-28807
Human organization --- space projects
22 p3160 N88-28808
The time of leaders 22 p3160 N88-28809
Contracts 22 p3160 N88-28810
Carrying out space projects 22 p3160 N88-28811
System configuration management --- space systems
22 p3160 N88-28813
Timetable control in a management system (space program) 22 p3160 N88-28815
Costs --- space projects 22 p3160 N88-28816
Value engineering --- space projects
22 p3160 N88-28817
Value analysis 22 p3161 N88-28819
Decision making aids: Methods and risks
22 p3161 N88-28820
Project management software
22 p3161 N88-28821
Management of large space projects. Financial means. Part 1: Financing of constructors
22 p3161 N88-28822
The role and the place of insurance of large space projects 22 p3161 N88-28826
Organization of the TDF1/TDF2 program
22 p3161 N88-28827
The Ariane line 22 p3161 N88-28828
The Ariane 5 program management specifications
22 p3162 N88-28829
Management of large space projects. Case study: The Hermes program 22 p3162 N88-28830
Case study: The Hermes program product assurance
22 p3162 N88-28831
Activities report of the World Meteorological Organization
[WMO-689] 24 p3404 N88-30265
PROJECT PLANNING
NAL news updated: FY87 business plan, developments 06 p0675 N88-14135
Supersonic STOVL propulsion technology program: An overview 08 p0957 N88-15808
Knowledge-based simulation
08 p1061 N88-16404
Planning and scheduling for robotic assembly
08 p1062 N88-16416
Planning activities in space 08 p1063 N88-16417
An AI approach for scheduling space-station payloads at Kennedy Space Center 08 p1064 N88-16425
Basic physics program for a low energy antiproton source in North America
[DE88-003148] 08 p1082 N88-16522
Critical issues in NASA information systems
[NASA-CR-182380] 08 p1093 N88-16577
Columbus feasibility studies. Volume 5: Programmatics
[ETN-88-91076] 09 p1134 N88-16802
The 1987 Get Away Special Experimenter's Symposium
[NASA-CP-2500] 10 p1286 N88-17691
Planet X probe: A fresh new look at an old familiar place 10 p1287 N88-17699
GAS 450: A space payload for the People Central Coast Student Experimenters 10 p1289 N88-17709
The NORSTAR Program: Space shuttle to space station 10 p1289 N88-17710
System analysis study of space platform and station accommodations for life sciences research facilities. Volume 2: Study results. Appendix E: Work breakdown structure and dictionary
[NASA-CR-179274] 10 p1292 N88-17723
Coordination: Southeast continental shelf studies
[DE88-003680] 10 p1357 N88-18110
Development of a graphics based two-attribute utility assessment program with application to mission planning
[AD-A187276] 10 p1388 N88-18292
Alternative Energy in the Midwest: Research and Applications. Conference Proceedings, Rosemont, Illinois, March 19-20, 1987
[PB88-142278] 11 p1509 N88-19015
AFAL (Air Force Astronautics Laboratory) technical objective document FY89
[AD-A187861] 11 p1567 N88-19378
Communication satellites: Guidelines for a strategic plan
[NASA-TM-89306] 12 p1599 N88-19569
European Progress on Space (EPOS): Participation in the creation of long term European space programs
[ILR-MITT-189] 14 p1671 N88-21180
Engineering support of space shuttle experiment integration
[AD-A190135] 15 p2024 N88-22061
Proposals for the pre-operational use of data from the European Remote Sensing Satellite ERS-1
[BCRS-86-02] 16 p2227 N88-23300
Preparation of the operational phase of the European Remote Sensing Satellite ERS-1
[BCRS-87-06] 16 p2228 N88-23307
Study of the plan for a national data center for the European Remote Sensing Satellite ERS-1
[BCRS-87-11] 16 p2228 N88-23309
The Engineer Studies Center guide to research and data collection
[AD-A189971] 16 p2285 N88-23680
Fuel cell systems program plan: Fiscal year 1988
[DE88-011080] 20 p2620 N88-26731
European transonic wind tunnel project: Assistance to the design group
[ONERA-RSF-11/0694-GY-010-G]
21 p2900 N88-27208
Studies concerning the European transonic wind tunnel
[ONERA-RSF-10/0694-GY-010-G]
21 p2900 N88-27209
Linear goal programming as a military decision aid
[AD-A194276] 22 p3137 N88-28652
Management 22 p3159 N88-28804
SDI (Strategic Defense Initiative) battle management/C3 (Command, Control and Communications) algorithms technology program plan
[AD-A194357] 23 p3275 N88-29495
PROJECT SETI
Intelligent signal analysis and recognition
[NASA-CR-181531] 04 p0501 N88-13084
SETI data controllers 11 p1474 N88-18795
The Telecommunications and Data Acquisition Report
[NASA-CR-183131] 22 p3063 N88-28178
DSS 13 microprocessor antenna controller
22 p3066 N88-28192
New CCIR report on SETI 22 p3067 N88-28204
PROJECTILE CRATERING
Hole diameters in plates impacted by projectiles
21 p2929 N88-27386
PROJECTILE PENETRATION
U TERMINAL BALLISTICS
PROJECTILES
NT HYPERVELOCITY PROJECTILES
NT SABOT PROJECTILES
Shock-wave studies using plastic flyers driven by an electric gun for hypervelocity impact on selected materials
[DE87-012631] 01 p0008 N88-10046
Switching devices used in the Lethality Test System
[DE87-011734] 01 p0011 N88-10062
Exact solutions to the governing dynamic equations of plasma armature electromagnetic railguns
[DE87-014442] 01 p0011 N88-10063
Laminar flow over a spinning projectile at an angle of attack 02 p0121 N88-10766
Jet formation and characterization of a conical shaped charge
[DE87-012102] 02 p0156 N88-10969
Improving coherent visualization by means of film optical filtering --- projectile visualization
[ISL-R-116/86] 02 p0176 N88-11097
Fin gaps and body slots of guided projectiles: Effects, data correlation and modeling
[AD-A184440] 03 p0270 N88-11698
The LLNL 150-mm equation-of-state gun system
[DE88-000423] 04 p0405 N88-12519
Mechanical property evaluation of a series of commercial tungsten alloys
[AD-A185440] 05 p0565 N88-13446
Optoelectronic measurement methods for ballistic experiments
[PB87-110706] 05 p0583 N88-13554
Computer simulations of ballistic experiments
[DE87-005835] 07 p0862 N88-15226
An investigation of oblique hypervelocity impact
07 p0927 N88-15629
New model to estimate the perforation power of kinetic energy projectiles
[PB87-166757] 09 p1175 N88-17040
Investigation of several spread shot conditions
[REPT-TR-164] 10 p1310 N88-17830
Splinter generator
[MBB-UA-1048/87] 11 p1491 N88-18897
Sub-scaling of projectile/target system damaged by hypervelocity
[AD-A188683] 12 p1634 N88-19779
What is the maximum length of a spin stabilized projectile
[PB88-130919] 13 p1728 N88-20336
Simulated impact damage in a thick graphite/epoxy laminate using spherical indenters
[NASA-TM-100539] 13 p1733 N88-20363
Two-phase flows in the wake of in-cylinder projectiles
[AD-A189422] 13 p1765 N88-20559
Mechanical design of a ultrahigh gravity UHV facility to launch and recover a low-speed projectile tested on board KC 135 14 p1877 N88-21216
Continuous measurements of in-bore projectile velocity
[DE88-006841] 15 p2023 N88-22056
Fluid motion in a spinning, coning cylinder via spatial eigenfunction expansion
[AD-A190758] 15 p2066 N88-22319
Efficient, high resolution computations of projectile and missile flow fields
[AD-A191086] 16 p2158 N88-22873
Power and energy requirements for electromagnetic launchers 17 p2420 N88-24391
Use of a two-stage light-gas gun as an injector for electromagnetic railguns
[DE88-007200] 18 p2469 N88-24657
Contact force history and dynamic response due to the impact of a soft projectile
[NASA-TM-100961] 20 p2611 N88-26679
Analysis of the perforation of monolithic and simple laminate aluminium targets as a test of analytical deformation models
[MRL-R-1111] 20 p2613 N88-26686
Charged pion production and projectile breakup in 85A MeV(sup)12C induced heavy ion reactions
[LUIP-8802] 20 p2650 N88-26920
Optimum-Path-to-Go guidance of command adjusted trajectory projectiles
[AD-A193377] 22 p3040 N88-28051
Computational fluid dynamics methods for low Reynolds number precessing/spinning incompressible flows
[AD-A193891] 23 p3212 N88-29119
Computational aerodynamic analysis for a range-limited 25mm training round
[AD-A185270] 24 p3320 N88-29772
A new computational capability for ramjet projectiles
[AD-A196061] 24 p3327 N88-29812
Numerical calculations of the response of a spinning spheroidal payload to coning motion
[AD-A195890] 24 p3368 N88-30058
PROJECTIVE GEOMETRY
On effectively labeling planar projections of polyhedra
[CWI-CS-R8715] 13 p1826 N88-20917
PROJECTS
NT AGRISTARS PROJECT
NT GALILEO PROJECT
NT PROJECT SETI
NT ROVER PROJECT
The International Satellite Land-Surface Climatology Project (ISLSCP) 14 p1937 N88-21558
Defense Small Business Innovation Research Program (SBIR). Volume 3: Air Force abstracts of phase 1 awards, 1987 17 p2448 N88-24548
PROKARYOTES
Biorack experiments in Spacelab D-1 and TML-1: Further developments in gravitational biology
12 p1661 N88-19953
PROLATE SPHEROIDS
The application of the hybrid iterative method to scattering by perfectly conducting bodies of revolution
11 p1475 N88-18802

Steady conduction of heat in prolate spheroidal systems
[LRT-WE-9-FB-16(1987)] 22 p3077 N88-28272
Liquid oscillations in a prolate spheroidal container
[LRT-WE-9-FB-4(1988)] 22 p3078 N88-28276

PROLOG (PROGRAMMING LANGUAGE)
How to use PROLOG for expert system programming
02 p0129 N88-10816
Near-horn prolog
[AD-A185172] 05 p0634 N88-13880
Automatic program generation from specifications using Prolog 08 p1065 N88-16437
DOD Gateway Information System (DGIS) common command language: Prolog knowledge base profile. Common command language report no. 3
[AD-A186150] 08 p1092 N88-16574
Experimenting with parallel programing in logic
10 p1380 N88-18240
KA-Prolog: Language definition
[GMD-249] 11 p1532 N88-19155
Implementing embedded artificial intelligence rules within algorithmic programming languages
[NASA-CR-178393] 14 p1959 N88-21686
Conversion of productions in OPS5 to their equivalent English
[ORNL/TM-10246] 24 p3411 N88-30306

PROMINENCES
NT SOLAR PROMINENCES
On the association of erupting magnetic fields with eruptive prominences and coronal mass ejections
01 p0113 N88-10727
Solar-geophysical data number 521, January 1988. Part 2: (Comprehensive reports). Data for July 1987 and miscellanea
[PB88-179221] 19 p2743 N88-26285

PRONE POSITION
Ergonomy and interior furnishing of the cabins of deep diving manned submarines: The Nautile example --- couch 19 p2697 N88-26032

PROOFS
U PROVING

PROP-FAN TECHNOLOGY
Aerodynamic and propeller performance characteristics of a propfan-powered, semispan model
[NASA-TM-86705] 06 p0667 N88-14092
Analysis and test evaluation of the dynamic stability of three advanced turboprop models at zero forward speed
[NASA-CR-175025] 06 p0668 N88-14095
Analysis and test evaluation of the dynamic response and stability of three advanced turboprop models at low forward speed
[NASA-CR-175026] 06 p0668 N88-14096
Large-Scale Advanced Prop-Fan (LAP) blade design
[NASA-CR-174790] 06 p0668 N88-14097
Aeropropulsion '87. Session 5: Subsonic Propulsion Technology
[NASA-CP-10003-SESS-5] 08 p0956 N88-15800
Overview of NASA PTA propfan flight test program
08 p0957 N88-15805
Analysis of possible transmission arrangements applicable for driving single or twin counterrotating fans on propfan engines 10 p1282 N88-17670
Vibration and flutter characteristics of the SR7L large-scale propfan
[NASA-TM-100272] 10 p1344 N88-18036
Technical-economical evaluation of a novel propfan concept in comparison with the turbofan for the nineties
[ETN-88-91022] 11 p1441 N88-18596
Counter-Rotating Integrated Shrouded Propfan (CRISP): The MTU propfan program --- Motoren und Turbinen Union (MTU)
[ETN-88-91023] 11 p1441 N88-18597
Advanced propfan analysis for the family of commuter airplanes
[NASA-CR-182598] 12 p1582 N88-19468
Large-Scale Advanced Prop-Fan (LAP)
[NASA-CR-182112] 13 p1723 N88-20306
Development of aeroelastic analysis methods for turborotors and propfans, including mistuning
16 p2219 N88-23244
The 2-D and 3-D time marching transonic potential flow method for propfans 16 p2220 N88-23245
Propfan model wind tunnel aeroelastic research results 16 p2220 N88-23246
A computational procedure for automated flutter analysis 16 p2220 N88-23250
Model forced response of propfans in yawed flow
16 p2221 N88-23253
Vibration and flutter analysis of the SR-7L large-scale propfan 16 p2221 N88-23254
Propfan test assessment testbed aircraft stability and control/performance 1/9-scale wind tunnel tests
[NASA-CR-182121] 20 p2757 N88-26360
Structural Tailoring of Advanced Turboprops (STAT)
[NASA-CR-180861] 22 p3045 N88-28074
Experimental investigation of propfan aeroelastic response in off-axis flow with mistuning
[NASA-TM-101320] 22 p3089 N88-28344
Multiple-Purpose Subsonic Naval Aircraft (MPSNA): Multiple Application Propfan Study (MAPS)
[NASA-CR-175104] 23 p3177 N88-28917
Test results at transonic speeds on a contoured over-the-wing propfan model
[NASA-TM-88206] 23 p3177 N88-28918
SR-7A aeroelastic model design report
[NASA-CR-174791] 23 p3179 N88-28928
Optical measurement of unducted fan blade deflections
[NASA-TM-100966] 23 p3216 N88-29142
Euler analysis of a swirl recovery vane design for use with an advanced single-rotation propfan
[NASA-TM-101357] 24 p3320 N88-29771

PROPAGATION
Propagation of random initial conditions in time
04 p0486 N88-12993
Space communication link propagation data for selected cities within the multiple beam and steerable antenna coverage areas of the advanced communications technology satellite
[NASA-TM-100861] 16 p2191 N88-23070
Kinetic theoretical analysis for propagation of rotating ion beam in ICF 16 p2276 N88-23623
The propagation of pressure perturbations in bubbly air/water flows 19 p2664 N88-25843
Satellite observed Mesoscale Convective System (MCS) propagation characteristics and a 3-12 hour heavy precipitation forecast index
[PB88-180161] 19 p2692 N88-26004
Perturbation expansions generated by an approximate propagator
[DE88-702435] 21 p3011 N88-27866

PROPAGATION (EXTENSION)
NT CRACK PROPAGATION
NT FLAME PROPAGATION
Error propagation in a digital avionic mini processor
[NASA-CR-181565] 05 p0633 N88-13872

PROPAGATION MODES
The wavenumber: An alternative to the directional coupler for multimode analysis in oversized waveguides
[IPF-87-2] 01 p0037 N88-10237
Optimization of mode converters for generating the fundamental TE(06) gyrotron output at 140 GHz
[IPF-87-1] 01 p0043 N88-10273

PROPAGATION VELOCITY
Coherent structure-reflective turbulent viscous flow modeling
[AD-A188339] 13 p1765 N88-20556
Detonation velocity of the hydrazinum nitrate-hydrazine water system
[NASA-TT-20213] 13 p1770 N88-20590
Numerical and experimental research on propagation of elastic stress waves in conical shell under axial impulsive loading 15 p2053 N88-22238
The determination of gravity and topography from seismic velocities, accounting for dynamic behavior of the Earth's mantle
[ETN-88-92420] 17 p2374 N88-24117
Determination of the specific area of liquid gas and the velocity of weak pressure waves in aqueous foams
[NASA-TT-20347] 24 p3373 N88-30087

PROPAGATORS
U PROPAGATION

PROPANE
Molecular dynamics studies of aromatic hydrocarbon liquids
[DE88-001473] 05 p0648 N88-13973
The effect of propane on atomic spectrometric signals in the direct current plasma
[DE88-002457] 07 p0934 N88-15676
Gas hydrate model development and validation
[DE88-001004] 10 p1298 N88-17762
Geological evolution and analysis of confirmed or suspected gas hydrate localities. Volume 9: Formation and stability of gas hydrates of the Middle America Trench
[DE88-001007] 10 p1347 N88-18050

PROPELLANT ADDITIVES
NT PROPELLANT BINDERS
NT SOLID ROCKET BINDERS
A holographic investigation of particulates in metallized solid fuel ramjet combustion
[AD-A186887] 09 p1140 N88-16831

PROPELLANT BINDERS
NT SOLID ROCKET BINDERS
High pressure strand burn rate tests of polyvinylnitrate/nitramine propellants
[AD-A184178] 04 p0422 N88-12615
Thermoplastic elastomers as LOVA binders
[AD-A185864] 07 p0835 N88-15067
Thermoplastic elastomers as LOVA binders
[AD-A185865] 07 p0835 N88-15068
Thermomechanical computations for GAP, a high energy binder for composite propellants
[FOA-C-20718-2.1] 24 p3357 N88-2998

PROPELLANT CHEMISTRY
Reaction products of solid propellants after burning at pressures up to 1000 MPa: Comparison between theoretical and experimental results
[ISL-CO-227/87] 22 p3059 N88-28153

PROPELLANT COMBUSTION
NT SOLID PROPELLANT COMBUSTION
NT SOLID PROPELLANT IGNITION
KR+ laser excitation of NH2 in atmospheric pressure flames
[AD-A183421] 01 p0050 N88-10022
High pressure strand burn rate tests of polyvinylnitrate/nitramine propellants
[AD-A184178] 04 p0422 N88-12615
Laser probes of propellant combustion chemistry
[AD-A184854] 05 p0561 N88-13415
Holographic investigation of metallized solid propellant combustion in two-dimensional and three-dimensional rocket motors
[AD-A187000] 09 p1140 N88-16832
Shuttle rocket booster computational fluid dynamics
[NASA-CR-182518] 10 p1293 N88-17733
Continued studies of programmed-splitting stick propellant
[AD-A188987] 12 p1613 N88-19644
On the possibility of high velocity deflagration front propagation by radiative energy transfer
[AD-A189022] 12 p1613 N88-19645
Bipropellant combustion in a liquid rocket combustion chamber 13 p1733 N88-20359
Mixing fuel particles for space combustion research using acoustics
[NASA-TM-100295] 14 p1872 N88-21186
Finite area combustor theoretical rocket performance
[NASA-TM-100785] 14 p1883 N88-21252
Catalytic ignition of hydrogen and oxygen propellants
[NASA-TM-100957] 18 p2476 N88-2469
The burning of HAN-based (hydroxylammonium nitrate) liquid propellants
[DE88-006863] 18 p2494 N88-24800
Electrical ignition of HAN-based liquid propellants
[AD-A191349] 18 p2495 N88-24801
Chemical kinetics of nitramine propellant combustion
[AD-A191556] 18 p2495 N88-24802
The 24th JANNAF Combustion Meeting, volume 2
[AD-A190164] 19 p2622 N88-25554
The combustion of hydroxylammonium nitrate based liquid propellants 19 p2622 N88-25555
A dynamic model of liquid propellant combustion
19 p2622 N88-25556
Droplet formation for liquid monopropellant jets
19 p2623 N88-25557
Mixing and thermodynamic critical phenomena of combusting monopropellant sprays
19 p2623 N88-25558
The development of a user friendly thermodynamic code for the personal computer 19 p2623 N88-25559
Measurement of burning rates of NOSOL-363 propellants under cross-flow and strand burner conditions using real-time X-ray radiography
19 p2623 N88-25560
Burning rate measurements of Non-Newtonian Liquid Propellant (NNLP) 19 p2623 N88-25561
Dynamical properties of a collapsing spherical cavity
19 p2623 N88-25562
Propellant combustion response to oscillatory radiant heat flux 19 p2626 N88-25589
Dynamics of propellant ignition
19 p2626 N88-25590
New instability phenomena in solid propellant combustion 19 p2626 N88-25591
Analysis of microwave burner measurement system using a microwave network analysis computer program
19 p2631 N88-25604
Modeling and experimental measurements of solid propellant flame structure 19 p2631 N88-25605
Solid rocket motor performance: A workshop report
19 p2631 N88-25607
How much do edges affect the ignition of a homogeneous reactive solid: Summary to date
19 p2631 N88-25608
Evaluation of techniques for direct measurement of burning rates in nozzleless motors
19 p2631 N88-25609
Deuterium isotope effects in the combustion of formulated nitramine propellants
19 p2632 N88-25611
Simultaneous thermogravimetric modulated beam mass spectrometry and time-of-flight velocity spectra measurements: Thermal decomposition mechanisms of RDX and HMX 19 p2632 N88-25612
Structure of laminar, premixed flames of CH2O/NO2/O2 mixtures 19 p2632 N88-25613

Temperature and species profiles in propellant ignition and combustion
19 p2633 N88-25616
Chemical kinetics modeling of HMX combustion
19 p2633 N88-25617
Rocket-propellant burn tests of silicide-coated niobium and tantalum
[DE88-010729] 20 p2781 N88-26496
Some properties of ignition gases. Review of measuring results in the years 1981-1986)
[PB88-106968] 21 p2908 N88-27259
Ignition and extinguishing of a Solid Fuel Ramjet (SOFRAM)
[FOA-C-20713-2.1] 24 p3337 N88-29865
Combustion diagnostics of propellant with new grain geometries
[AD-A194944] 24 p3342 N88-29895
Gas phase combustion chemistry of nitramine propellants
[AD-A195082] 24 p3344 N88-29902

PROPELLANT DECOMPOSITION
Free radical detection and reactions in the decomposition of energetic materials
[AD-A184677] 03 p0296 N88-11858
Test number 2 of propellant for rocket motor MK52
[PB87-226155] 05 p0571 N88-13480
The chemistry of the hypochlorite neutralization of hydrazine fuels
[DE88-002971] 10 p1307 N88-17812
Novel analytical X-ray Non-Destructive Evaluation (NDE) tool for quality control of energetic materials
[AD-A187737] 11 p1497 N88-18935
Chemical kinetics of nitramine propellant combustion
[AD-A191556] 18 p2495 N88-24802
Theoretical investigations of nitrocubane decomposition
[AD-A194556] 23 p3200 N88-29047
Gas phase combustion chemistry of nitramine propellants
[AD-A195082] 24 p3344 N88-29902

PROPELLANT EXPLOSIONS
Semiconductor bridge (SCB) igniter studies. 1: Comparison of SCB and hot-wire pyrotechnic actuators
[DE88-008802] 23 p3200 N88-29046

PROPELLANT GRAINS
Measurements of particulates in solid propellant rocket motors
[AD-A187777] 11 p1446 N88-18621
Mixing fuel particles for space combustion research using acoustics
[NASA-TM-100295] 14 p1872 N88-21186
Crack opening and extension in inert solid propellant. An experimental study
[AD-A189808] 15 p2048 N88-22201
Some properties of ignition gases. Review of measuring results in the years 1981-1986)
[PB88-106968] 21 p2908 N88-27259
A study of flame spreading and combustion phenomena of stick propellants
[AD-A192598] 22 p3052 N88-28106
Combustion diagnostics of propellant with new grain geometries
[AD-A194944] 24 p3342 N88-29895
Flamespreading processes in obliquely loaded stick propellant beds
[AD-A195081] 24 p3352 N88-29956
Descriptive characterization of propellant particles
[AD-A195176] 24 p3356 N88-29985

PROPELLANT MASS RATIO
The initial calculation of range and mission fuel during conceptual design --- aircraft design
[LR-525] 16 p2161 N88-22889

PROPELLANT OXIDIZERS
U ROCKET OXIDIZERS

PROPELLANT PROPERTIES
NT PROPELLANT SENSITIVITY
NT PROPELLANT STORABILITY
Modal survey of the space shuttle solid rocket motor using multiple input methods 05 p0593 N88-13617
Fuel property effects on the US Navy's TF30 engine
24 p3345 N88-29911
Alternative fuel spray behavior
24 p3345 N88-29912
The characterizatin of combustion by fuel composition: Measurements in a small conventional combustor
24 p3346 N88-29920

PROPELLANT SENSITIVITY
An infra-red investigation of HAN (Hydroxylammonium Nitrate)-based liquid propellants
[AD-A187226] 10 p1307 N88-17815
On the possibility of high velocity deflagration front propagation by radiative energy transfer
[AD-A189022] 12 p1613 N88-19645
Structure/property/reactivity relations among nitramine and other energetic materials
[AD-A190878] 18 p2481 N88-24716

PROPELLANT STORABILITY
Uranium nitride fuel swelling and thermal conductivity correlations 17 p2409 N88-24327

PROPELLANT STORAGE
Orbital Spacecraft Consumables Resupply System (OSCRS). Volume 2: Study results
[NASA-CR-172011] 03 p0268 N88-11667
DOE explosives safety manual
[DE88-000831] 04 p0422 N88-12616
Test number 2 of propellant for rocket motor MK52
[PB87-226155] 05 p0571 N88-13480
Turbomachinery in space 17 p2408 N88-24321
Weight savings in aerospace vehicles through propellant scavenging
[NASA-TM-100900] 19 p2605 N88-25470
Pressure/temperature sensitive inorganic phosphors
19 p2627 N88-25583

PROPELLANT TANKS
Orbital transfer vehicle studies overview
08 p0981 N88-15931
Low-g propellant gaging 08 p0982 N88-15937
Computational prediction of propellant reorientation
08 p0982 N88-15940
Low gravity liquid motions in spacecraft
08 p0982 N88-15941
Peacekeeper tank slosh model
08 p0983 N88-15942
Zero-G thermodynamic vent system for shuttle/Centaur 08 p0983 N88-15943
Orbital Propulsion Module (OPM). Study on coni-spherical surface tension tanks (COSTA)
[MBB-URV-170/87] 23 p3187 N88-28963

PROPELLANT TRANSFER
Orbital Spacecraft Consumables Resupply System (OSCRS). Volume 1: Executive summary
[NASA-CR-172010] 05 p0553 N88-13368
Servicer system demonstration plan and capability development
[NASA-CR-179246] 08 p0975 N88-15895
Design and development of a refueling test bed
[FTMS-RP-ER-011] 24 p3357 N88-29986

PROPELLANTS
NT COMPOSITE PROPELLANTS
NT CRYOGENIC ROCKET PROPELLANTS
NT DOUBLE BASE PROPELLANTS
NT DOUBLE BASE ROCKET PROPELLANTS
NT GELLED PROPELLANTS
NT GELLED ROCKET PROPELLANTS
NT GUN PROPELLANTS
NT HIGH TEMPERATURE PROPELLANTS
NT HMX
NT HTPB PROPELLANTS
NT LIQUID ROCKET PROPELLANTS
NT METAL PROPELLANTS
NT MONOPROPELLANTS
NT NITRAMINE PROPELLANTS
NT PLASTIC PROPELLANTS
NT RDX
NT ROCKET PROPELLANTS
NT RP-1 ROCKET PROPELLANTS
NT SLURRY PROPELLANTS
NT SOLID PROPELLANTS
NT SOLID ROCKET PROPELLANTS
NT TETRYL
Strategic Defense Initiative Organization/DARPA (Defense Advanced Research Projects Agency) workshop on laser propulsion. Volume 1: Executive summary
[DE87-003254] 06 p0768 N88-14722
SAMSS: An in-progress review of the Spacecraft Assembly, Maintenance, and Servicing Study
08 p0981 N88-15930
DSC (Differential Scanning Calorimeter) stability test for liquid propellants: A preliminary report
[AD-A187115] 09 p1150 N88-16868
Laser induced ignition of propellants
[AD-A191100] 16 p2168 N88-22927
Laser induced ignition of propellants
[AD-A191099] 16 p2213 N88-23206
An extinguisher to quench propellant fires
[AD-A190785] 18 p2497 N88-24813
SRM (Solid Rocket Motor) propellant and polymer materials structural modeling
[NASA-TP-2824] 22 p3089 N88-28343
Lunar lander conceptual design: Lunar base systems study task 2.2
[NASA-CR-172051] 24 p3335 N88-29854
Energy conversion measurements in laser-sustained argon plasmas for application to rocket propulsion
[AD-A194931] 24 p3337 N88-29861
Titrimetric analysis of HAN-based liquid propellants
[AD-A196225] 24 p3357 N88-29990

PROPELLER BLADES
Numerical prediction of propeller performance by vortex lattice method
[UTIAS-TN-265] 04 p0400 N88-12489
High speed propeller performance and noise predictions at takeoff/landing conditions
[NASA-TM-100267] 05 p0646 N88-13960
Large-Scale Advanced Prop-Fan (LAP) blade design
[NASA-CR-174790] 06 p0668 N88-14097
Aerodynamic and acoustic characteristics of an advanced propeller under take-off and landing conditions
[NAL-TR-935] 09 p1243 N88-17453
Numerical methods for propeller aerodynamics and acoustics at DFVLR 10 p1282 N88-17668
Numerical simulation of subsonic and transonic propeller flow
[NASA-TM-100163] 13 p1716 N88-20262
Calculation of the distributed loads on the blades of individual multiblade propellers in axial flow using linear and nonlinear lifting surface theories
[NASA-TT-20173] 13 p1719 N88-20276
Large-Scale Advanced Prop-Fan (LAP)
[NASA-CR-182112] 13 p1723 N88-20306
Development of aeroelastic analysis methods for turborotors and propfans, including mistuning
16 p2219 N88-23244
Modal forced response of propfans in yawed flow
16 p2221 N88-23253
Vibration and flutter analysis of the SR-7L large-scale propfan 16 p2221 N88-23254
Advanced turboprop aircraft flyover noise: Annoyance to counter-rotating-propeller configurations with an equal number of blades on each rotor, preliminary results
[NASA-TM-100612] 16 p2265 N88-23547
Optical measurement of propeller blade deflections
[NASA-TP-2841] 22 p3079 N88-28286

PROPELLER DRIVE
Noise levels from propeller-driven aircraft measured at ground level and at 1.2 m above the ground
[NPL-AC-110] 01 p0091 N88-10594

PROPELLER EFFICIENCY
The aerodynamic performance of propellers suitable for unmanned aircraft (UMAs)
[RAE-TM-AERO-2094] 09 p1112 N88-16667
Numerical methods for propeller aerodynamics and acoustics at DFVLR 10 p1282 N88-17668
Summary of low-speed wind tunnel results of several high-speed counterrotation propeller configurations
[NASA-TM-100945] 18 p2458 N88-24597
Finite element solution of 3-D turbulent Navier-Stokes equations for propeller-driven slender bodies
18 p2515 N88-24919
Aircraft noise prediction program propeller analysis system IBM-PC version user's manual version 2.0
[NASA-CR-181689] 24 p3428 N88-30399

PROPELLER FANS
Transonic analysis and design of axisymmetric bodies in nonuniform flow
[NASA-CR-4101] 01 p0003 N88-10013
Annoyance caused by advanced turboprop aircraft flyover noise: Single-rotating propeller configuration
[NASA-TP-2782] 09 p1242 N88-17441
Analysis of possible transmission arrangements applicable for driving single or twin counterrotating fans on propfan engines 10 p1282 N88-17670
The effects of rotational flow, viscosity, thickness, and shape on transonic flutter dip phenomena
[NASA-TM-100811] 11 p1502 N88-18969
Aeroelastic response of metallic and composite propfan models in yawed flow
[NASA-TM-100964] 24 p3326 N88-29807

PROPELLER SLIPSTREAMS
Low speed wind tunnel investigation of propeller slipstream aerodynamic effects on different nacelle/wing combinations. Part 1: Total forces and moments and pressure distributions on nacelle/wing at different angles of attack and yaw and at different thrust coefficients
[FFA-TN-1987-22] 05 p0542 N88-13302
Numerical simulation of subsonic and transonic propeller flow
[NASA-TM-100163] 13 p1716 N88-20262

PROPELLERS
NT CONTRAROTATING PROPELLERS
NT PROPELLER FANS
NT SHROUDED PROPELLERS
NT VARIABLE PITCH PROPELLERS
Advanced turboprop wing installation effects measured by unsteady blade pressure and noise
[NASA-TM-100200] 01 p0002 N88-10006
Numerical calculations of the flowfield around propellers 05 p0536 N88-13261
Aerodynamic and propeller performance characteristics of a propfan-powered, semispan model
[NASA-TM-86705] 06 p0667 N88-14092
An investigation of the effects of the propeller slipstream on a wing boundary layer 06 p0700 N88-14293
Advanced propeller research
08 p0957 N88-15806

The aerodynamic performance of propellers suitable for unmanned aircraft (UMAs)
[RAE-TM-AERO-2094] 09 p1112 N88-16667
Lifting-surface theory of oscillating propellers in compressible flow
[NAL-TR-943] 10 p1273 N88-17613
Aerodynamic performance of a scale-model, counter-rotating unducted fan 10 p1282 N88-17666
Numerical methods for propeller aerodynamics and acoustics at DFVLR 10 p1282 N88-17668
Analysis of highspeed propellers aerodynamics
10 p1282 N88-17669
Conditions at infinity for theories of oscillating wings and propellers in subsonic flow
[NAL-TR-937] 11 p1434 N88-18556
Analysis of in-flight acoustic data for a twin-engined turboprop airplane
[NASA-CR-178389] 11 p1543 N88-19220
Comparison of two transonic noise prediction formulations using the aircraft noise prediction program
[NASA-CR-181609] 12 p1688 N88-20095
Cavitation inception
[AD-A189220] 13 p1765 N88-20557
Porous wind tunnel corrections for counterrotation propeller testing
[NASA-TM-100873] 15 p2015 N88-22019
NASA advanced turboprop research and concept validation program
[NASA-TM-100891] 16 p2183 N88-22902
Measurements of the time dependent velocity field surrounding a model propeller in uniform water flow
16 p2205 N88-23155
NASA/industry advanced turboprop technology program
[NASA-TM-100929] 18 p2466 N88-24641
Numerical solutions of the Euler equations for the flow field around counter-rotating propellers
19 p2606 N88-25638
Optical measurement of unducted fan blade deflections
[NASA-TM-100966] 23 p3216 N88-29142
Analysis of the transmission of sound into the passenger compartment of a propeller aircraft using the finite element method
[FFA-TN-1988-15] 23 p3279 N88-29520
A comparison of simple analytical models for representing propeller aircraft structural and acoustic responses
[ISVR-TR-153] 23 p3279 N88-29523
Euler analysis of a swirl recovery vane design for use with an advanced single-rotation propfan
[NASA-TM-101357] 24 p3320 N88-29771

PROPORTIONAL COUNTERS
Electronics for the External Muon Detector (EMD) of ICARUS
[NOTA-INTERNA-880] 07 p0847 N88-15143
Single wire drift chamber design
[DE87-011002] 07 p0857 N88-15205
The position-sensitive counting of photons
16 p2271 N88-23590

PROPORTIONAL LIMIT
Carbon fiber reinforced glass matrix composites for space based applications
[AD-A184355] 04 p0410 N88-12546
Fastening high resistance bolts in real assemblies
[CRIF-MT-171] 07 p0861 N88-15221

PROPRIOCEPTION
Some remarks on gravitational biology
07 p0884 N88-15366
Perception and control of simulated self motion
[AD-A187444] 10 p1372 N88-18188
Covariant control of bilateral servos for in-orbit manipulation 12 p1580 N88-19520

PROPRIOCEPTORS
Functional development of gravity receptors in insects and amphibians 07 p0886 N88-15376
Role of optokinetic stimulation in vestibulospinal reflexes 10 p1360 N88-18131

PROPULSION
NT ASCENT PROPULSION SYSTEMS
NT AUXILIARY PROPULSION
NT CHEMICAL PROPULSION
NT ELECTRIC PROPULSION
NT ELECTROMAGNETIC PROPULSION
NT ELECTROSTATIC PROPULSION
NT HYBRID PROPULSION
NT ION PROPULSION
NT JET PROPULSION
NT LASER PROPULSION
NT LOW THRUST PROPULSION
NT MARINE PROPULSION
NT MASS DRIVERS (PAYLOAD DELIVERY)
NT NUCLEAR ELECTRIC PROPULSION
NT NUCLEAR PROPULSION
NT PLASMA PROPULSION
NT SOLAR THERMAL PROPULSION
NT SPACE STATION PROPULSION
NT SPACECRAFT PROPULSION
Calendar of selected aeronautical and space meetings
[AGARD-CAL-87/1] 05 p0657 N88-14033
Propulsion-induced effects caused by out-of-ground effects
[NASA-TM-100032] 06 p0666 N88-14088
Recent advances in high temperature instrumentation for hot section applications
[NASA-TM-100282] 06 p0707 N88-14339
Aeropropulsion '87. Session 3: Internal Fluid Mechanics Research
[NASA-CP-10003-SESS-3] 08 p0954 N88-15790
Chemical reacting flows 08 p0955 N88-15793
Aeropropulsion '87. Session 4: Instrumentation and Controls Research
[NASA-CP-10003-SESS-4] 08 p0955 N88-15794
Directions in propulsion control
08 p0956 N88-15799
Aeropropulsion '87. Session 5: Subsonic Propulsion Technology
[NASA-CP-10003-SESS-5] 08 p0956 N88-15800
Rotorcraft transmission 08 p0956 N88-15802
Rotorcraft flight-propulsion control integration
09 p1108 N88-16643
Impact and promise of NASA aeropropulsion technology 09 p1118 N88-16698
Institute for Computational Mechanics in Propulsion (ICOMP)
[NASA-TM-100790] 11 p1540 N88-19202
Activities report of the Energetics Department
[ETN-88-91981] 14 p1888 N88-21281
Research as part of the Air Force in aero propulsion technology (AFRAPT) program
[AD-A190336] 15 p2019 N88-22036
AFRAPT (Air Force Research in Aero Propulsion Technology) trainee program
[AD-A190525] 15 p2035 N88-22123
Costs and benefits of AC propulsion
[PB88-173380] 16 p2287 N88-23601
Gravitation electromagnetic theory
22 p3158 N88-28790
Special Course on Missile Aerodynamics
[AGARD-R-754] 24 p3317 N88-29755
Energy conversion measurements in laser-sustained argon plasmas for application to rocket propulsion
[AD-A194931] 24 p3337 N88-29861

PROPULSION SYSTEM CONFIGURATIONS
NT ASCENT PROPULSION SYSTEMS
Multi-stage plasma thruster
[AD-A183635] 01 p0017 N88-10105
An 8-cm ion thruster characterization
[NASA-CR-180819] 01 p0017 N88-10106
Flight propulsion control integration for V/STOL aircraft
[NASA-TM-100226] 03 p0267 N88-11680
Configuration evaluation and criteria plan. Volume 2: Evaluation criteria plan (update). Space Transportation Main Engine (STME) configuration study
[NASA-CR-181429] 03 p0270 N88-11699
Institute for Computational Mechanics in Propulsion (ICOMP) first year summary
[NASA-TM-100225] 03 p0370 N88-12330
Integrated control and display research for transition and vertical flight on the NASA V/STOL Research Aircraft (VSRA)
[NASA-TM-100029] 05 p0551 N88-13359
Hermes propulsion system
[SNIAS-872-422-109] 05 p0556 N88-13383
Space station onboard propulsion system: Technology study
[NASA-CR-179233] 07 p0825 N88-15006
Internal fluid mechanics research on supercomputers for aerospace propulsion systems
[NASA-TM-100289] 07 p0854 N88-15188
Equilibrium retention in the nozzle of oxygen hydrogen propulsion systems 07 p0924 N88-15616
Advanced fusion power: A preliminary assessment
[AD-A185903] 07 p0933 N88-15664
Aeropropulsion '87. Session 2: Aeropropulsion Structures Research
[NASA-CP-10003-SESS-2] 08 p0954 N88-15785
Aeropropulsion structures 08 p0954 N88-15786
Determining structural performance
08 p0954 N88-15787
Life prediction technologies for aeronautical propulsion systems 08 p0954 N88-15788
Integrated analysis and applications
08 p0954 N88-15789
Aeropropulsion '87. Session 6: High-Speed Propulsion Technology
[NASA-CP-10003-SESS-6] 08 p0957 N88-15807
Supersonic STOVL propulsion technology program: An overview 08 p0957 N88-15808
Propulsion challenges and opportunities for high-speed transport aircraft 08 p0958 N88-15809
Supersonic throughflow fans for high-speed aircraft
08 p0958 N88-15810
High-speed inlet research program and supporting analyses 08 p0958 N88-15811
Hypersonic propulsion research
08 p0958 N88-15812
CFD validation experiments for internal flows
[NASA-TM-100797] 09 p1114 N88-16679
Lewis materials research and technology: An overview
09 p1119 N88-16699
Calculation and design of a ramjet missile
[REPT-TR-500] 10 p1311 N88-17832
The MBB propulsion concepts for magnetic suspension railways: Retrospective view and prospects
[MBB-Z-141/87] 10 p1316 N88-17865
Technical-economical evaluation of a novel propfan concept in comparison with the turbofan for the nineties
[ETN-88-91022] 11 p1441 N88-18586
Counter-Rotating Integrated Shrouded Propfan (CRISP): The MTU propfan program --- Motoren und Turbinen Union (MTU)
[ETN-88-91023] 11 p1441 N88-18587
A comparative study of various electric propulsion systems and their impact on a nominal ship design
[AD-A187800] 11 p1477 N88-18816
Application of advanced computational technology to propulsion CFD
[NASA-TM-100843] 11 p1525 N88-19102
Advanced propfan analysis for the family of commuter airplanes
[NASA-CR-182586] 12 p1582 N88-19488
Electromagnetic propagation in PEC and absorbing curved S-ducts
[NASA-TM-100833] 12 p1621 N88-19808
A comparison of propulsion systems for potential space mission applications
[DE88-005637] 14 p1882 N88-21248
Advanced transmission studies
[NASA-TM-100867] 14 p1919 N88-21454
Activities report in flight and space travel
[ISSN-0070-3966] 14 p2012 N88-22000
Research and technology
[NASA-TM-100172] 15 p2153 N88-22851
The challenges and opportunities of supersonic transport propulsion technology
[NASA-TM-100921] 17 p2307 N88-23808
Heat transfer in aerospace propulsion
[NASA-TM-100874] 17 p2339 N88-23857
Nuclear propulsion systems for orbit transfer based on the particle bed reactor 17 p2401 N88-24272
Recent advances in low-thrust propulsion technology
[NASA-TM-100959] 18 p2569 N88-25280
A reusable rocket engine intelligen control
[NASA-TM-100963] 20 p2786 N88-26401
Variable Mach number wall jets for control/propulsion on hypervelocity projectiles/interceptors: Tests with an existing model
[AD-A192845] 21 p2882 N88-27167
Development of sensors for ceramic components in advanced propulsion systems: Survey and evaluation of measurement techniques for temperature, strain and heat flux for ceramic components in advanced propulsion systems
[NASA-CR-182111] 22 p3081 N88-28209
Experimental and analytical evaluation of the effects of simulated engine inlets on the blade vibratory stresses of the SR-3 model prop-fan
[NASA-CR-174959] 23 p3179 N88-28867
Orbital Propulsion Module (OPM). Study on coni-spherical surface tension tanks (COSTA)
[MBB-URV-170/87] 23 p3187 N88-28883
Evaluation of the advanced air breathing propulsion concepts, executive summary
[ESA-CR(P)-2540] 24 p3325 N88-29802
Evaluation of advanced air breathing concepts. Volume 1: Executive summary
[ESA-CR(P)-2539] 24 p3326 N88-29806
Spacecraft mass estimation, relationships and engine data: Task 1.1 of the lunar base systems study
[NASA-CR-172061] 24 p3332 N88-29838
The NASA Electric Propulsion Program
[NASA-TM-101324] 24 p3336 N88-29859
Hermes: Study of propulsion system for reusable man-rated spacecraft
[PSRM-TN-0000-00-04A] 24 p3337 N88-29860
Unified study of plasma/surface interactions for space power and propulsion
[AD-A195971] 24 p3338 N88-29870

PROPULSION SYSTEM PERFORMANCE
Propulsion Working Group report
01 p0016 N88-10098
Multi-stage plasma thruster
[AD-A183635] 01 p0017 N88-10105

An 8-cm ion thruster characterization
[NASA-CR-180818] 01 p0017 N88-10106
Flight propulsion control integration for V/STOL aircraft
[NASA-TM-100226] 03 p0267 N88-11680
Configuration evaluation and criteria plan. Volume 2: Evaluation criteria plan (update). Space Transportation Main Engine (STME) configuration study
[NASA-CR-181429] 03 p0270 N88-11699
Space station propulsion
[NASA-TM-100218] 03 p0277 N88-11746
NASA supersonic STOVL propulsion technology program
[NASA-TM-100227] 06 p0668 N88-14093
Propulsion estimation techniques
07 p0927 N88-15632
An investigation into the feasibility of using a dual-combustion mode ramjet in a high Mach number tactical missile
[AD-A186906] 09 p1119 N88-16705
Integration testing of the propulsion system of Ariane's first stage 09 p1126 N88-16751
A comparison of propulsion systems for potential space mission applications
[DE88-005637] 14 p1882 N88-21248
Activities report of the Energetics Department
[ETN-88-91981] 14 p1888 N88-21281
Nuclear propulsion systems for orbit transfer based on the particle bed reactor 17 p2401 N88-24272
High power ion thruster performance
17 p2404 N88-24295
Gas core reactors for direct nuclear propulsion
17 p2428 N88-24442
Status of high power electric propulsion technology
17 p2428 N88-24443
Noncryogenic propellants for a nuclear orbit transfer vehicle 17 p2428 N88-24444
Propulsion analysis and application potential of air breathing combined propulsion for ballistic space transporter
[ETN-88-92369] 21 p2903 N88-27227
COMPASS ground based engine monitoring program for general application --- Condition Monitoring and Performance Analysis Software System (COMPASS)
[PNR90420] 22 p3044 N88-28064
Evaluation of the advanced air breathing propulsion concepts, executive summary
[ESA-CR(P)-2540] 24 p3325 N88-29802
Evaluation of advanced air breathing concepts. Volume 1: Executive summary
[ESA-CR(P)-2539] 24 p3326 N88-29806
Hermes: Study of propulsion system for reusable man-rated spacecraft
[PSRM-TN-0000-00-04A] 24 p3337 N88-29866
Unified study of plasma/surface interactions for space power and propulsion
[AD-A195871] 24 p3338 N88-29870
Simulation of Vulcain engine operation at low inlet pressure
[ETN-88-93083] 24 p3339 N88-29875

PROPULSIVE EFFICIENCY
NT PROPELLER EFFICIENCY
Propulsion challenges and opportunities for high-speed transport aircraft 08 p0958 N88-15809
Gear systems for advanced turboprops
10 p1262 N88-17667
Rotorcraft flight-propulsion control integration: An eclectic design concept
[NASA-TP-2815] 12 p1584 N88-19475
China constructing high-altitude test cell
14 p1901 N88-21351
The 1988 overview of free-piston Stirling technology for space power at the NASA Lewis Research Center
[NASA-TM-100795] 16 p2170 N88-22934
Propfan model wind tunnel aeroelastic research results 16 p2220 N88-23246
Propulsive performance of a lifting flapping wing
17 p2295 N88-23733
Benefits of 20 kHz PMAD in a nuclear space station
17 p2398 N88-24256
High power ion thruster performance
17 p2404 N88-24295
Analytical and experimental investigation of ringless piston concept
[AD-A193213] 21 p2956 N88-27559

PROPYL COMPOUNDS
Identification of hydroxypropyl starch hydrolysate components 17 p2315 N88-23832

PROPYLENE
Studies on the use of propylene carbonate as a high-voltage insulator
[DE88-011788] 22 p3057 N88-28141

PROPYLENE OXIDE
Performance of polymer electrolyte cells at +25 to +100 C
[AD-A193969] 22 p3073 N88-28244

PROSPECTING
U EXPLORATION

PROSTHETIC DEVICES
The stress analysis of ceramic, polymeric, and metallic composite systems by the finite element method
18 p2529 N88-25004

PROTECTION
NT CIRCUIT PROTECTION
NT CORROSION PREVENTION
NT ENVIRONMENT PROTECTION
NT EYE PROTECTION
NT METEOROID PROTECTION
NT RADIATION PROTECTION
NT RADIATION SHIELDING
NT SOLAR RADIATION SHIELDING
NT THERMAL PROTECTION
Anti-abrasion protection with highly organized materials
[DE87-014238] 01 p0029 N88-10187
Lightning discharge protection rod
[NASA-CASE-LAR-13470-1] 06 p0666 N88-14093
A paper about electromagnetic pulse and principles of EMP protection
[FOA-C-30455-4.2] 06 p0692 N88-14246
Insect contamination protection for laminar flow surfaces 07 p0814 N88-14954
Solar cell cover glasses for satellites
15 p2052 N88-22225
Study of lightning and lightning protection (selected pages)
[AD-A190623] 15 p2098 N88-22498
Proposed quality assurance/quality control plan
[AD-A191490] 18 p2525 N88-24978
Vibration protection of inelastic structures by means of active and passive control 18 p2528 N88-25001
The use of liquid films for spacecraft survivability to laser radiation
[AD-A192954] 20 p2765 N88-26395
Future visual environment and concerns
23 p3242 N88-29299

PROTECTIVE CLOTHING
NT EXTRAVEHICULAR MOBILITY UNITS
NT PRESSURE SUITS
NT SPACE SUITS
Research and development of anti-G life support systems. Part 1: Development and evaluation of uniform-pressure anti-G suits
[AD-A185658] 06 p0754 N88-14628
Improvement of the construction of protective clothing for better wearability and comfort --- rainwear
[IZF-1986-26] 07 p0899 N88-15448
Portable, ambient air microclimate cooling in simulated desert and tropic conditions
[AD-A186457] 08 p1050 N88-16338
Perspectives in microclimate cooling involving protective clothing in hot environments
[AD-A188370] 12 p1671 N88-20007
Fit evaluation of female body armor
[AD-A188721] 14 p1953 N88-21638
Further development of a mathematical model for the specification of immersion clothing insulation
[IAM-653] 14 p1954 N88-21644
Study of benefits of passenger protective breathing equipment from analysis of past accidents
[DOT/FAA/CT-88/03] 18 p2461 N88-24610
The effects of different combinations of inlet air conditions used for cooling as measured on a heated manikin
[AD-A191116] 18 p2552 N88-25151
Performance estimates for operations conducted while wearing individual protective equipment: User manual
[AD-A191871] 18 p2553 N88-25154
The role of textile material in clothing on thermoregulatory responses to intermittent exercise
[AD-A192590] 22 p3130 N88-28608
Four-axis side-arm flight control simulator investigation
[AD-A196026] 24 p3409 N88-30294

PROTECTIVE COATINGS
NT ANODIC COATINGS
NT CERAMIC COATINGS
NT PRIMERS (COATINGS)
NT REFRACTORY COATINGS
Optimizing the application of high temperature corrosion resistant aluminium-silicon-base coatings
[BLL-M-37222-(5828.4)] 01 p0018 N88-10112
Development and production of new and modified powders for sprayed coatings and components for saving important raw materials
[BMFT-FB-T-86-129] 01 p0025 N88-10159
The water permeability of multi-layer coatings
[BLL-M-37252-(5828.4)] 02 p0148 N88-10927
Investigation of the structure of coatings of self fluxing alloys fused by laser energy
[BLL-M-37301-(5828.4)] 02 p0148 N88-10930
Comparison of high purity fine grain graphites from different suppliers with regard to physical, mechanical, and thermal properties --- Joint European Torus wall protection
[JUEL-SPEZ-401] 02 p0154 N88-10963
Coatings for Advanced Heat Engines Workshop: Book of abstracts
[DE87-012623] 02 p0180 N88-11121
Life prediction and constitutive models for engine hot section anisotropic materials program
02 p0188 N88-11175
Creep-fatigue behavior of NiCoCrAlY coated PWA 1480 02 p0189 N88-11176
Coating life prediction 02 p0189 N88-11181
Corrosion-resistant amorphous metallic coatings: Engineering development
[NASA-CR-181487] 03 p0287 N88-11802
Ion plating: Fundamental processing studies and synthesis of high performance coatings
[AD-A184766] 03 p0303 N88-11908
Carbon-fiber reinforced aluminum
04 p0403 N88-12507
Effect of long-term thermal aging on coated Celion/LARC-160 composites
[NASA-TM-100495] 04 p0410 N88-12544
Ceramic technology for advanced heat engines project
[DE88-001520] 04 p0420 N88-12605
Tribological properties of rf-sputtered MoS2 coatings
[DE88-000266] 04 p0452 N88-12802
An examination of coating failure on wing pivot fittings of f111 aircraft
[AD-A185029] 05 p0546 N88-13328
Simulated service test behavior of various internal and external coatings applied on CF6-50 first stage turbine blades
[NLR-MP-86018-U] 05 p0549 N88-13343
Coatings for high-temperature bearings and seals
[NASA-TM-100249] 05 p0567 N88-13453
Water disbondment characterization of organic Coating/metal substrate systems
[AD-A184847] 05 p0567 N88-13454
Antistatic coating compositions
[GB-PATENT-2-177-413-A] 05 p0568 N88-13463
Stress rupture behavior of silicon carbide coated, low modulus carbon/carbon composites
[NASA-CR-180863] 06 p0678 N88-14150
Life modeling of thermal barrier coatings for aircraft gas turbine engines
[NASA-TM-100283] 07 p0834 N88-15060
Chromic acid anodizing of aluminum foil
[NASA-CR-178417] 07 p0837 N88-15077
Use of hydrophilic polymer coatings for control of electroosmosis and protein adsorption
07 p0925 N88-15620
Hot piston ring/cylinder liner materials: Selection and evaluation
[NASA-TM-100276] 08 p0971 N88-15872
Effects of additives on fire properties of polyethylene
[AD-A187064] 09 p1146 N88-16871
Oxidation resistance of CVD coatings
[AD-A178337] 09 p1147 N88-16875
The effect of varying sputtering parameters on the microstructure and mechanical properties of 10 percent Ni + TiB2 thin films
[DE88-002600] 09 p1254 N88-17517
Bias, internal stress and substrate effects on the microstructure and properties of PVD-wear resistant coatings
[AERE-R-12360] 10 p1304 N88-17798
The soft/hard wet anodization of aluminum oxide and its use in a thin film multilayered capacitor
[AD-A187575] 10 p1325 N88-17919
High temperature oxidation studies on alloys containing dispersed phase particles and clarification of the mechanism of growth of SiO2
[AD-A188158] 11 p1457 N88-18688
Adhesion of PVD titanium coatings to beryllium substrates
[DE88-005147] 11 p1463 N88-18721
Oxidation and protection of fiberglass-epoxy composite masts for photovoltaic arrays in the low Earth orbital environment
[NASA-TM-100839] 11 p1465 N88-18734
Ion beam modification of film stress and the effectiveness of thin film encapsulants on GaAs
[DE88-004458] 11 p1558 N88-19328
Factors affecting the sticking of insects on modified aircraft wings
[NASA-CR-182615] 12 p1575 N88-19421
Mast material test program (MAMATEP)
[NASA-TM-100821] 12 p1604 N88-19592
Nondestructive evaluation of carbon-carbon coatings
[AD-A189524] 13 p1748 N88-20453
Abrasion and impact resistant coatings
[DE88-003562] 13 p1750 N88-20464

Safety research of insulating materials of cable for nuclear power generating station
[NASA-TT-20202] 13 p1752 N88-20477
Aging properties of cable polmers (2)
[NASA-TT-20228] 13 p1752 N88-20479
Measurement of the properties of lossy materials inside a finite conducting cylinder
[NASA-CR-182664] 13 p1832 N88-20962
JPRS report: Science and technology. USSR: Materials science
[JPRS-UMS-87-009] 14 p1884 N88-21261
Chemical vapor deposited silica coatings for solar mirror protection
[NASA-TM-100834] 14 p1893 N88-21306
Effect of protective coatings on high-temperature fatigue of heat-resistant alloys 14 p1895 N88-21314
Secondary electron emission characteristics improved by ion implantation 14 p1903 N88-21370
Laser surface melting
[BMFT-FB-T-86-072] 14 p1914 N88-21435
A constitutive model for an overlay coating
14 p1933 N88-21525
Development of a manufacturing unit for selective coating of solar absorbers made out of aluminum
[BMFT-FB-T-86-204] 14 p1942 N88-21590
Structure and properties of titanium nitride and zirconium nitride thin films prepared by reactive ion plating --- cutting tools
[ETN-88-92218] 15 p2042 N88-22167
Investigation of laser diagnostics of PACVD processes for depositing hard face coatings
[DE88-007083] 15 p2043 N88-22176
The corrosion resistance of an aluminum alloy coated with polysilazane derived ceramics
[AD-A190703] 15 p2046 N88-22189
JPRS report: Science and technology. USSR: Materials science
[JPRS-UMS-88-006] 16 p2179 N88-22966
Model study of thermal stresses in gas-turbine blades with protective coating 16 p2179 N88-22969
Protective coatings on metals, volume 10
[PB88-174461] 16 p2181 N88-23000
Development of a high-temperature resistant (700 F), corrosion-preventive organic coating
[AD-A191407] 16 p2182 N88-23009
Government research on ceramics coating technology
16 p2184 N88-23019
Inadequacies of EMI-seal material: A corrosion study
17 p2319 N88-23852
Surface conditioning products as tools for corrosion removal and corrosion prevention
17 p2320 N88-23856
Carboxylate formation at the interface between a polyimide coating and cobalt 17 p2320 N88-23859
Thrust chamber thermal barrier coating techniques
[NASA-TM-100933] 18 p2476 N88-24690
Isothermal and bithermal thermomechanical fatigue behavior of a NiCoCrAlY-coated single crystal superalloy
[NASA-TM-100907] 18 p2489 N88-24766
An investigation of ceramic coatings for protection of SiC from high-temperature corrosion
[DE88-007873] 18 p2493 N88-24790
A thermally modified polymer matrix composite material with structural integrity to 371 C
[NASA-TM-100922] 19 p2609 N88-25483
Corrosion prevention in gas turbines
[NLR-MP-87029-U] 20 p2760 N88-26373
Electrophoretic coatings. Part 1: Sandia applications
[DE88-006666] 20 p2776 N88-26465
The effects of thin compressive films on indentation fracture toughness measurements
[AD-A192243] 20 p2779 N88-26480
Rocket-propellant burn tests of silicide-coated niobium and tantalum
[DE88-010729] 20 p2781 N88-26496
Studies in support of oxidation-resistant composite materials
[AD-A193320] 21 p2905 N88-27238
Refractory fibers surface treatment
[REPT-47-803/F] 21 p2922 N88-27339
Proceedings of the 1987 Tri-Service Conference on Corrosion, volume 1
[AD-A191295] 22 p3053 N88-28114
Corrosion and stress corrosion of metals in decontamination solutions 22 p3054 N88-28118
Design guidelines for prevention of corrosion in combat and tactical vehicles
[AD-A194172] 22 p3055 N88-28126
Study of the erosion corrosion of alloys and coatings
[AD-A194337] 22 p3055 N88-28128
Corrosion control through a better understanding of the metallic substrate/organic coating/interface
[AD-A193961] 22 p3056 N88-28132
Optimization of fatigue and friction properties of titanium by means of surface treatments
[ECL-87-22] 22 p3056 N88-28133
Thermal barrier coating life-prediction model development
[NASA-CR-179507] 22 p3058 N88-28142
The effect of coatings on fatigue in aerospace materials --- gas turbine engines
[PNR90460] 22 p3059 N88-28150
Ultrafine microstructure composites prepared by chemical vapor deposition
[AD-A193849] 23 p3169 N88-28973
Processing technology research in composites
[AD-A195693] 24 p3341 N88-29890
Performance Prediction for Coatings. Proceedings of a Workshop
[AD-A188973] 24 p3354 N88-29966
Degradation of protective coatings on steel in corrosive environments 24 p3354 N88-29969
Prediction of degradation of polymeric coating materials 24 p3354 N88-29970
A reliability-based program for predicting the service life of organic coating systems 24 p3355 N88-29971
Electrical detection of coating deterioration
24 p3355 N88-29973
Electrochemical evaluation of the long term corrosion resistance of polymer coated steel
24 p3355 N88-29974
Evaluation of organic coating deterioration and substrate corrosion in seawater using electrochemical impedance measurements 24 p3355 N88-29976
Alternative immersion accelerated testing of coating systems for Naval shoreline facilities
24 p3355 N88-29977
Stressed fabric abrasion test procedure for urethane coated fabric fuel tanks
[AD-A196327] 24 p3356 N88-29982

PROTECTORS
Performance estimates for operations conducted while wearing individual protuctive equipment: User manual
[AD-A191871] 18 p2553 N88-25154

PROTEIN DENATURATION
U BIOPOLYMER DENATURATION

PROTEINS
NT CARBONIC ANHYDRASE
NT CATALASE
NT CHOLINESTERASE
NT CYTOCHROMES
NT ENZYMES
NT FIBRINOGEN
NT HEMOGLOBIN
Non-conventional approaches to food processing in CELSS, 1. Algal proteins: Characterization and process optimization 03 p0358 N88-12256
Biopolymers: Protein and nucleic acids
[AD-A185837] 07 p0835 N88-15066
Use of hydrophilic polymer coatings for control of electroosmosis and protein adsorption
07 p0925 N88-15620
Synthesis of high molecular weight peptide polymers and copolymers containing L-dope residues
[AD-A186462] 08 p0973 N88-15887
Evidence for human adaptive response to dehydration: Increase of circulating protein mass
[AD-A186225] 08 p1048 N88-16328
A comparison of algorithms for the analysis of images generated by two-dimensional electrophoresis
[DE88-003730] 09 p1220 N88-17319
Protein-crystal growth experiment (planned)
10 p1287 N88-17700
Response of coronary blood flow to step changes in plasma protein concentration in the isolated rat heart
12 p1651 N88-19892
Studies of molecular biology
[DE88-005906] 15 p2101 N88-22514
North Carolina Biomolecular Engineering and Materials Applications Center (NC-BEMAC)
[AD-A190923] 16 p2237 N88-23364
Optical monitoring of protein crystal growth
[NASA-CR-182869] 18 p2484 N88-24738
The electrokinetic behavior of calcium oxalate monohydrate in macromolecular solutions
[NASA-TM-101144] 18 p2493 N88-24791
A cardiostimulant protein from the Australian Red Waratah Sea anemone, Actinia tenebrosa
18 p2550 N88-25138
Two puzzling aspects of protein crystal growth
18 p2580 N88-25329
Hanging drop crystal growth apparatus and method
[NASA-CASE-MFS-28206-1-SB]
18 p2585 N88-25356
Crystal growth apparatus
[NASA-CASE-MFS-28182-1] 18 p2585 N88-25357
Experiments in microgravity environment: Protein crystallization
[REPT-881-430-101] 21 p2924 N88-27354

PROTOCOL (COMPUTERS)
Data Management Working Group report
01 p0016 N88-10097
The varieties of capabilities in Flex
[RSRE-MEMO-4042] 01 p0078 N88-10500
Space lab system analysis
[NASA-CR-179207] 02 p0138 N88-10869
Network reconstitution protocol
[AD-A184755] 03 p0367 N88-12309
An evaluation plan of bus architectures and protocols using the NASA Ames intelligent redundant actuation system
[NASA-CR-177458] 04 p0398 N88-12482
Distribution of records on a ring of processors
[PB87-235784] 06 p0758 N88-14649
Study of communication options in a distributed data handling system and survey of advanced man machine communications schemes. Work package 1: Interprocess communication
[ESA-CR(P)-2447] 07 p0843 N88-15114
A software planning and development methodology with resource allocation capability
[AD-A186088] 07 p0902 N88-15482
Cirrus: An automated protocol analysis tool
[AD-A186646] 08 p1052 N88-16346
AITI Test Report 87-002: Pratt and Whitney technical order transfer tests
[DE88-004045] 11 p1564 N88-19363
AITI Report 87-003: Honeywell technical order transfer tests
[DE88-004046] 11 p1564 N88-19364
Performance analysis of slotted ring protocols in High Speed Local Area Networks (HSLANS)
[INF-87-31] 14 p1955 N88-21652
Exact analyses of slotted ring protocols for local area networks with one transmitting station
[MEMO-650] 14 p1967 N88-21737
Using Colored Stochastic Petri Net (CS-PN) software for protocol specification, validation, and evaluation
[ENST-87C004] 15 p2113 N88-22588
A very simple construction for atomic multiwriter register
[CWI-CS-R8751] 16 p2249 N88-23436
A five-layer Open Systems Interconnection (OSI) implementation 17 p2390 N88-24204
An operational open-end file transfer protocol for mobile satellite communications 19 p2651 N88-25738
Integrated voice/data protocols for satellite channels
19 p2651 N88-25739
Minimum disclosure proofs of knowledge
[CWI-PM-R8710] 20 p2840 N88-26854
Markov chain computations to a solution of the mutual-exclusion problem in concurrency
[REPT-87-89] 20 p2847 N88-26896
A modular proof of correctness for a network synchronizer
[AD-A192726] 21 p3002 N88-27802
Performance analysis of FDDI
[NASA-CR-183206] 24 p3413 N88-30321

PROTON BEAMS
Performance of GaAs and silicon concentrator cells under 37 MeV proton irradiation
[NASA-TM-100144] 04 p0465 N88-12877
South African Association of Physicists in Medicine and Biology: 26th Annual Congress
[DE88-700624] 11 p1521 N88-19082
Initial operation of the Tevatron collider
[FNAL-TM-1449] 11 p1547 N88-19252
Microinstabilities in ion beam propagation
16 p2277 N88-23631
A multi-frame ion pinhole camera for intense ion beam transport and focusing experiments
[DE88-007283] 18 p2516 N88-24926
Intense ion beam diagnostics for particle beam fusion experiments on PBFA 2
[DE88-007279] 18 p2577 N88-25306
The XRD (X-Ray Diode) array, the grazing incidence spectrometer and the X-ray imaging camera on PBFA 2
[DE88-007282] 19 p2728 N88-26200

PROTON DENSITY (CONCENTRATION)
Calculation methods of atomic number density for various nuclear materials
[DE87-753006] 02 p0233 N88-11487

PROTON ENERGY
Study of the production of Ko mesons in proton antiproton interactions at 630 GeV
[NOTA-INTERNA-908] 21 p3015 N88-27892

PROTON IRRADIATION
Heavy ion and proton tests for subsystem upset
[AD-A195267] 24 p3434 N88-30442

PROTON SCATTERING
On the spin structure of the elastic ppbar scattering amplitude
[NOTA-INTERNA-892] 06 p0778 N88-14772

PROTON TELESCOPES
U PARTICLE TELESCOPES

PROTON-PROTON REACTIONS
Initial operation of the Tevatron collider
[FNAL-TM-1449] 11 p1547 N88-19252

PROTONS
NT SOLAR PROTONS
Effects of electron and proton irradiations on n/p and p/n GaAs cells grown by MOCVD
[NASA-TM-100199] 01 p0042 N88-10266
The elastic scattering of intermediate energy protons from (40)Ca and (208)Pb 01 p0092 N88-10599
Low altitude flux and dose measurements during two solar flare events 01 p0111 N88-10713
Volume produced H(-),D(-) ion source for proton accelerator and thermo-nuclear fusion research by sheet plasma (III)
[IPPJ-838] 02 p0242 N88-11531
Proton abstraction as a route to conductive polymers
[AD-A184019] 04 p0421 N88-12612
Prompt simultaneous acceleration of protons and electrons to relativistic energies by shock waves in solar flares
[IPPJ-851] 04 p0493 N88-13037
Experimental studies of elementary particle interactions at high energies
[DE88-000804] 05 p0648 N88-13971
An analytic model for ionization distributions produced in nanometer sites by protons
[DE88-003943] 10 p1406 N88-18385
Ion energy diagnostics for voltage determinations in plasma-erosion-opening-switch experiments
[DE88-004822] 11 p1479 N88-18827
Ground-state correlations in C12 and the mechanism of the (e,e'p) reaction
[B8729349] 14 p1980 N88-21816
The response of a small liquid scintillation counter for low energy (gamma, p) experiments
[NOTA-INTERNA-901] 14 p1980 N88-21819
Measurement of the sup 4He(gamma, p)sup 3H total cross section and charge symmetry
[NOTA-INTERNA-902] 14 p1981 N88-21820
Analysis of hadron production in deep inelastic muon-proton collisions through the fire-string model
[PREPRINT-578] 14 p1981 N88-21822
Photon-assisted formation and cooling of molecular hydrogen
[MP-87-102] 16 p2267 N88-23563
Small molecule and small cluster ion formation in a low-density containerless mixture of electrons, protons and hydrogen atoms 16 p2269 N88-23577
X-ray production in low energy proton stopping
[NASA-TM-100619] 16 p2270 N88-23582
Reference nuclear data for space applications
[DE88-007041] 16 p2270 N88-23583
Characterization of proton conducting polymer blends
19 p2669 N88-25867
Scaling laws for geomagnetic tail current sheet acceleration
[AD-A193379] 19 p2691 N88-25996
The protonic Beta double prime aluminas: Preparation, stability, conductivity and structure
[DE88-008442] 20 p2768 N88-26415
Rf cavity primer for cyclic proton accelerators
[DE88-010655] 20 p2853 N88-26938
PROTOPLANETS
Astrophysics and the solar nebula
07 p0883 N88-15355
Exobiology and life science 07 p0883 N88-15358
Cometary nucleus as aggregate of planetesimals
[ISAS-RN-364] 19 p2741 N88-26275
PROTOPLASTS
Plant cell cultures in space biology studies
12 p1654 N88-19913
The use of plant protoplasts in biotechnological space research 12 p1655 N88-19914
PROTOSTARS
NT PRE-MAIN SEQUENCE STARS
NT T TAURI STARS
Star formation and molecular clouds
24 p3451 N88-30537
PROTOTYPES
Double-effect absorption heat pump, phase 3
[PB87-232195] 03 p0317 N88-12005
A prototype expert system for separation science
[DE87-013542] 03 p0371 N88-12333
Renewed interest in airships for industry use discussed 04 p0424 N88-12628
Light funnel concentrator panel for solar power
[NASA-CR-179223] 04 p0464 N88-12870
A single-station weather forecasting expert system
[AD-A184889] 05 p0627 N88-13832
A prototype ray tracer
[AD-A184863] 05 p0634 N88-13874
A 1,000-watt solar power unit for Far North
06 p0728 N88-14481
Prototype space station automation system delivered and demonstrated at NASA 08 p1066 N88-16442
High-resolution Real-Time Radiography (RTR) system design
[AD-A187107] 09 p1166 N88-16992
Shared workspaces for real-time collaboration in distributed networks: Concepts, techniques, problems
[AD-A188150] 10 p1394 N88-18315
Prototype thin-film thermocouple/heat-flux sensor for a ceramic-insulated diesel engine
[NASA-TM-100798] 11 p1490 N88-18892
A new isodynamically-braked arm ergometer including the demonstration of a prototype
12 p1661 N88-19957
Reducing time required for the development of avionic systems 12 p1702 N88-20185
Prototype manufacturing techniques for reducing cost, schedule, and technical risk 12 p1702 N88-20189
Use of demonstration/validation prototypes: Impact on total development costs and times
12 p1703 N88-20194
Engineering management for validation prototype phase 12 p1703 N88-20195
Acceleration of prototype development and reduction of cost by multidisciplinary integration
12 p1704 N88-20199
The use of an automated flight test management system in the development of a rapid-prototyping flight research facility
[NASA-TM-100435] 13 p1823 N88-20896
Towards a tribology information system: The results of a Planning Workshop held at the National Bureau of Standards, July-August 1985
[PB88-168604] 14 p1918 N88-21448
STRUTEX: A prototype knowledge-based system for initially configuring a structure to support point loads in two dimensions
NASA-TM-100613] 16 p2250 N88-23448
Rapid prototyping of complex avionic system architectures 17 p2302 N88-23771
The integration, characterisation and trialling of a modern complex airborne radar 17 p2305 N88-23791
Coherent functional development: Key to successful future system integration 17 p2307 N88-23803
SP-100 GES test site 17 p2417 N88-24375
Analysis of plasma coupling with the prototype DIII-D ICRF antenna
[DE88-008085] 19 p2729 N88-26204
Analytical and experimental investigation of ringless piston concept
[AD-A192835] 20 p2810 N88-26673
Expert system application education project
[NASA-CR-183089] 20 p2843 N88-26867
Optical evaluation of prototype stretched-membrane mirror modules for solar central receivers
[DE88-011664] 21 p2969 N88-27637
SP-100 Ground Engineering Systems: Test facility control systems
[DE88-009195] 21 p3015 N88-27895
Study of Plasma Motor Generator (PMG) tether system for orbit reboost
[NASA-CR-172074] 23 p3184 N88-28949
PLZT (Lead-Lathanium-Zirconium-Titanium) electro-optic photographic system
[AD-A193473] 23 p3215 N88-29137
ADP (Automated Data Processing) requirements definition and documentation through user-developed prototypes
[AD-A194407] 23 p3248 N88-29332
Contingency rescheduling of spacecraft operations
24 p3416 N88-30337
Achieving real-time performance in FIESTA
24 p3418 N88-30344
PROTOZOA
NT AMOEBA
NT PARAMECIA
PROVING
NT THEOREM PROVING
Generating diagnostic knowledge from a structural and functional description 02 p0129 N88-10813
Use of a 35mm camera for remote surface cleanliness verification 02 p0133 N88-10835
Columbus pressurized module verification
02 p0134 N88-10842
Fin gaps and body slots of guided projectiles: Effects, data correlation and modeling
[AD-A184440] 03 p0270 N88-11698
East coast gravity validation study
[AD-A184292] 03 p0351 N88-12217
SDVS (State Delta Verification System): Program verification system development fiscal year 1986
[AD-A184338] 03 p0366 N88-12302
High resolution satellite imagery simulation --- treaty verification
[FOA-C-30462-3.3,9.3] 05 p0620 N88-13810
Design verification and fabrication of active control systems for the DAST ARW-2 high aspect ratio wing, part 1
[NASA-CR-177959-PT-1] 06 p0669 N88-14101
Design verification and fabrication of active control systems for the DAST ARW-2 high aspect ratio wing. Part 2: Appendices
[NASA-CR-177959-PT-2] 06 p0669 N88-14102
A flow visualization study of the leading edge separation bubble on a NACA 0012 airfoil with simulated glaze ice
[NASA-CR-180846] 07 p0816 N88-14966
An approach to validation and verification of the communications load model with supporting user's guide
[AD-A185926] 07 p0840 N88-15096
Correctness proofs for systolic algorithms: Palindromes and sorting
[PB88-106075] 07 p0912 N88-15534
Feasibility of software built-in test for SDI (Strategic Defense Initiative) applications
[AD-A185750] 07 p0917 N88-15572
Verification of FANTASTIC integrated code
07 p0924 N88-15613
Verification issues for rule-based expert systems
08 p1055 N88-16361
Temporal and contextual knowledge in model-based expert systems 08 p1055 N88-16363
Methodology for testing and validating knowledge bases 08 p1055 N88-16364
KBS V and V as related to automation of space station subsystems: Rationale for a KBS lifecycle
08 p1057 N88-16375
CFD validation experiments for internal flows
[NASA-TM-100797] 09 p1114 N88-16679
Approaches to the verification of rule-based expert systems 09 p1206 N88-17232
A formal approach to validation and verification for knowledge-based control systems
09 p1207 N88-17233
Expert system verification concerns in an operations environment 09 p1207 N88-17234
Building validation tools for knowledge-based systems
09 p1207 N88-17235
Methods for evaluating the quality and reliability of aerodynamic software programs
[PB87-169793] 09 p1219 N88-17314
Software program validity: A survey
[PB87-170593] 09 p1219 N88-17315
Simulation test beds for the space station electrical power system
[NASA-TM-100786] 10 p1290 N88-17715
Formal multilevel hierarchical verification of synchronous MOS VLSI circuits
[AD-A187532] 10 p1324 N88-17918
Navigation recovery block design description
[NASA-CR-182473] 10 p1342 N88-18022
Benchmark computation and finite element performance evaluation for a rhombic plate bending problem
[AD-A187402] 10 p1345 N88-18041
Automated data flow diagram verification
10 p1382 N88-18255
Procedures for quantitative sensitivity and performance validation studies of a deterministic fire safety model
[NBS/GCR-88/544] 11 p1469 N88-18762
A perspective on 15 years of proof-of-concept aircraft development and flight research at Ames-Moffett by the Rotorcraft and Powered-Lift Flight Projects Division, 1970-1985
[NASA-RP-1187] 12 p1582 N88-19467
The Hermes robot arm, its design and verification
12 p1588 N88-19508
Robotics servicing experiment --- European space programs 12 p1591 N88-19529
Rendezvous and docking (RVD) verification and demonstration in-orbit 12 p1592 N88-19531
Use of demonstration/validation prototypes: Impact on total development costs and times
12 p1703 N88-20194
Engineering management for validation prototype phase 12 p1703 N88-20195
A correlation study of X-29A aircraft and associated analytical development
[NASA-CR-183103] 13 p1722 N88-20296
Experimental verification of a finite-difference time-domain thin slot algorithm
[DE88-005572] 13 p1817 N88-20859
Software verification using partition analysis
[AD-A190570] 15 p2112 N88-22582
On the validation of a code and a turbulence model appropriate to circulation control airfoils
[NASA-TM-100090] 16 p2156 N88-22864
Knowledge based system verification and validation as related to automation of space station subsystems: Rationale for a knowledge based system lifecycle
17 p2387 N88-24192
Analysis procedures and subjective flight results of a simulator validation and cue fidelity experiment
[NASA-TM-88270] 18 p2465 N88-24634
Structural margins assessment approach
[NASA-TM-100332] 18 p2473 N88-24672

Computer resource management technology program (PE 64740F). Task no. 9: Advanced user authentication
[PB88-183066] 18 p2555 N88-25163

Application of flight systems methodologies to the validation of knowledge-based systems
[NASA-TM-100442] 18 p2561 N88-25207

The experimental verification of wall movement influence coefficients for an adaptive walled test section
[NASA-CR-181681] 19 p2598 N88-25439

Verification of regional climates of GISS GCM. Part 1: Winter
[NASA-TM-100695] 19 p2694 N88-26012

Minimum disclosure proofs of knowledge
[CWI-PM-R8710] 20 p2840 N88-26854

Oxidation-erosion of metals and alloys: Models, verification, and prediction
[DE88-010016] 21 p2915 N88-27300

Ada (trade name) compiler validation summary report: Verdix Corporation VAda-010-03315, version 5.5 MicroVAX 2 host ISBC 386/20P Intel target
[AD-A193226] 21 p2997 N88-27774

Ada (trade name) compiler validation summary report: Verdix corporation VAda-010-13125, version 5.41 Sun Microsystems Sun-3/160 host microbar GPC68020 target
[AD-A193415] 21 p2997 N88-27777

Ada (trade name) compiler validation summary report: Verdix Corporation VAda-010-0101, version 5.41 VAX-11/750
[AD-A193414] 22 p3136 N88-28645

Air Force Systems Command software independent verification and validation implementation analysis and guidance
[AD-A194309] 22 p3137 N88-28653

LO-CO-GRAF (low cost graphics): Generating maps to support command and control/crisis management using small computers
[AD-A193964] 22 p3139 N88-28661

Induction instrument for logic conclusion
[LRT-WE-9-FB-5(1987)] 22 p3144 N88-28697

Verification and tests --- space projects
22 p3160 N88-28814

Validity of the academic aptitude composite of the Air Force Officer Qualifying Test (AFOQT)
[AD-A194753] 23 p3240 N88-29286

Ada (trade name) compiler validation summary report: Verdix Corporation VAda-010-03205, version 5.42 MicroVAX 2 host and national DB32000 (NS32032 target
[AD-A193485] 23 p3247 N88-29326

Confirmation of slow-waves in a crosstie overlay coplanar waveguide and its application to band-reject gratings and reflectors
[AD-A194981] 24 p3361 N88-30011

PROVISIONING

Inventory behavior at remote sites
06 p0796 N88-14873

PROXIMITY EFFECT (ELECTRICITY)

Modeling of proximity coupling between superconducting filaments in superconducting dipole magnets
[DE87-014684] 03 p0382 N88-12403

The effect of magnetic impurities and barriers on the magnetization and critical current of fine filament NbTi composites
[DE88-004443] 10 p1419 N88-18472

PSEUDOMONAS

Study of certain biological characteristics of bacteria during the French-Soviet CYTOS-2 space experiment
04 p0473 N88-12917

PSEUDOPOTENTIALS

The pseudopotential density functional method applied to semiconducting crystals
[ETN-88-91362] 05 p0656 N88-14024

PSEUDORANDOM SEQUENCES

Short pseudorandom test sequences
[AD-A185883] 08 p1054 N88-16357

A comparison of generators for pseudo-random normal deviates
[DE88-011711] 21 p3010 N88-27859

Random number generation
[USIP-87-15] 22 p3145 N88-28707

PSYCHIATRY

NT NEUROPSYCHIATRY

Normative developmental equations for the EEG and their sensitivity to neurological and psychiatric disorders
21 p2977 N88-27687

PSYCHOACOUSTICS

Transient classifier systems and man-machine interface research
[AD-A186213] 07 p0899 N88-15446

Mechanisms mediating perception of complex acoustic patterns
[AD-A189765] 15 p2102 N88-22520

On categorizing sounds
[AD-A189784] 15 p2129 N88-22700

PSYCHOLOGICAL EFFECTS

NT DESYNCHRONIZATION (BIOLOGY)
NT ILLUSIONS
NT JET LAG

Human adaptation to isolated and confined environments
[NASA-CR-181502] 03 p0357 N88-12248

JPRS report: Science and technology. USSR: Space Biology and Aerospace Medicine, volume 21, no. 4, July - August 1987
[JPRS-USB-88-002] 07 p0893 N88-15412

New US book on aviation psychology reviewed
07 p0896 N88-15433

Medical and psychological problems of assuring flight safety under present conditions
10 p1359 N88-18123

Investigation of effects of short-term exposure to high concentrations of carbon monoxide on operator's psychophysiological functions 10 p1361 N88-18133

Incorporation of privacy elements in space station design
[NASA-CR-182748] 14 p1881 N88-21242

Ejection situations in the U-2/TR-1: An analysis of emotions and events
[AD-A192872] 21 p2893 N88-27175

CEEG dynamic brain mapping: A new method to evaluate brain function in different psychological and drug conditions 21 p2977 N88-27685

Using ERPS to study human information processing
21 p2980 N88-27698

Behavioral, psychological and demographic predictors of physical fitness
[AD-A192697] 21 p2986 N88-27733

Attitudes towards the cold: Effects on psychological mood and subjective reports of illness during cold weather training
[AD-A194777] 23 p3239 N88-29274

PSYCHOLOGICAL FACTORS

Some aspects of sociopsychological screening of flying school applicants 07 p0890 N88-15392

Antarctica as a model for the human exploration of Mars
[AD-A185835] 08 p1051 N88-16342

Temperament Structure Scales (TSS). Test manual
[ESA-TT-1069] 09 p1201 N88-17197

Effects of stress on judgement and decision making in dynamic tasks
[AD-A188203] 11 p1523 N88-19092

Protection from stress 12 p1664 N88-19978

On categorizing sounds
[AD-A189784] 15 p2129 N88-22700

Chronic stress as a factor in aircraft mishaps
16 p2239 N88-23376

A framework for a theory of mapping
[AD-A191071] 18 p2551 N88-25144

Selection and training of subjects to live and work in hostile and unusual environments
19 p2696 N88-26026

Rules, schema and decision making
[AD-A193389] 21 p3027 N88-27967

PSYCHOLOGICAL INDEXES

U PSYCHOLOGICAL TESTS

PSYCHOLOGICAL TESTS

Exploiting auxiliary information about items in the estimation of Rasch item difficulty parameters
[AD-A184383] 03 p0372 N88-12341

Development of a menu of performance tests self-administered on a portable microcomputer
[NASA-CR-172040] 08 p1067 N88-16452

Temperament Structure Scales (TSS). Test manual
[ESA-TT-1069] 09 p1201 N88-17197

Surrogate measures: A proposed alternative in human factors assessment of operational measures of performance 09 p1215 N88-17281

Modeling incorrect responses to multiple-choice items with multilinear formula score theory
[AD-A187887] 11 p1522 N88-19090

Field dependence-independence and its relationship to flight training performance
[AD-A188888] 12 p1670 N88-20003

Quasi-loglinear models for test and item analysis --- psychometrics
[B8716249] 14 p1952 N88-21636

Construction of a multidimensional questionnaire to determine interindividual differences in controlling attention
[DFVLR-FB-87-45] 14 p1952 N88-21637

Properties of some Bayesian scoring procedures for computerized adaptive tests
[AD-A189925] 15 p2124 N88-22660

The program Kennedy Approach as an experimental design of a dynamic computerized air traffic control test
[DFVLR-FB-87-50] 16 p2159 N88-22881

NASA-Ames workload research program
17 p2380 N88-24151

Selecting the right crew for future space stations: An analysis of selection research on offshore divers, aviation pilots and other high risk groups in Scandinavia
19 p2696 N88-26021

Reliability and construct validity of reaction time, inspection time and machine-paced tests of cognitive speed
[AD-A193779] 23 p3241 N88-29289

PSYCHOLOGY

NT AVIATION PSYCHOLOGY
NT COGNITIVE PSYCHOLOGY
NT MILITARY PSYCHOLOGY
NT PSYCHOACOUSTICS
NT PSYCHOPHYSICS
NT SPACE PSYCHOLOGY

Assessment of fatigue in aviation crews
[AD-A184129] 03 p0356 N88-12245

The attitudes of science policy, environmental, and utility leaders on US energy issues and fusion
[DE88-000784] 04 p0494 N88-13041

JPRS report: Science and technology. USSR: Life sciences
[JPRS-ULS-87-013] 06 p0750 N88-14606

Innovation and creativity: A critical linkage
[DE88-003309] 10 p1426 N88-18515

USSR report: Life sciences. Biomedical and behavioral sciences
[JPRS-UBB-87-008] 12 p1662 N88-19966

Management information systems design implications: The effect of cognitive style and information presentation on problem solving
[AD-A188850] 12 p1705 N88-20205

Problem solving in a natural task as a function of experience
[AD-A191180] 16 p2243 N88-23399

The representational code of the internal model of dynamic systems: An individual differences and dual task approach
[AD-A190876] 16 p2244 N88-23403

Models of incremental concept formation
[AD-A191597] 18 p2552 N88-25147

Attitudes towards the cold: Effects on psychological mood and subjective reports of illness during cold weather training
[AD-A194777] 23 p3239 N88-29274

Transformations of short-term visual memory
[AD-A193873] 23 p3241 N88-29290

Comparison of morning with afternoon nitrogen elimination in resting subjects breathing 100 percent oxygen
[AD-A196191] 24 p3407 N88-30282

Advancement of latent trait theory
[AD-A194302] 24 p3408 N88-30288

PSYCHOMETRICS

Computer response time measurements of mood, fatigue and symptom scale items: Implications for scale response time uses
[AD-A186093] 07 p0888 N88-15384

Tutoring electronic troubleshooting in a simulated maintenance work environment
09 p1204 N88-17215

Intelligent tutoring systems as tools for investigating individual differences in learning
09 p1204 N88-17216

Modeling incorrect responses to multiple-choice items with multilinear formula score theory
[AD-A187887] 11 p1522 N88-19090

Quasi-loglinear models for test and item analysis --- psychometrics
[B8716249] 14 p1952 N88-21636

Construction of a multidimensional questionnaire to determine interindividual differences in controlling attention
[DFVLR-FB-87-45] 14 p1952 N88-21637

Conjunctive measurement theory: Cognitive research prospects
[AD-A193627] 23 p3239 N88-29277

PSYCHOMOTOR PERFORMANCE

A comparison of the Army's Project A: Cognitive and psychomotor tests to analogous Air Force and Navy tests
[AD-A188636] 12 p1670 N88-20002

Mental-State Estimation, 1987
[NASA-CP-2504] 16 p2239 N88-23370

The biomorphic model of the human operator controlling a single or a double integrator
[LR-505] 16 p2243 N88-23402

Teleoperator human factors study
[NASA-CR-178930] 17 p2382 N88-24162

Research on piloting under conditions of breakdown in flight
[PB87-217980] 19 p2710 N88-26102

Does dihydroergotamine used in therapeutical doses influence the physical and psychomotor performance of young pilots or other traffic drivers subjected to hypotonia?
[ETN-88-92136] 20 p2832 N88-26799
Cognitive and neural bases of skilled performance
[AD-A193392] 21 p2992 N88-27747
Determinants of dual-task interference and resource theories in cognitive psychology
[DFVLR-FB-88-14] 21 p2992 N88-27748
Literature review: Validity and potential usefulness of psychomotor ability 'ests for personnel selection and classification
[AD-A193558] 23 p3241 N88-29287

PSYCHOPHYSICS
NT PSYCHOACOUSTICS
Psychophysical considerations in measuring MRTD with staring arrays -- minimum resolvable temperature difference (MRTD)
[RSRE-MEMO-4031] 01 p0076 N88-10487
Computing support for basic research in perception and cognition
[AD-A186192] 07 p0897 N88-15437
Vision algorithms and psychophysics
[AD-A186773] 09 p1200 N88-17193
Perception and control of simulated self motion
[AD-A187444] 10 p1372 N88-18186
Complex sound processing: An interdisciplinary approach
[AD-A189782] 15 p2102 N88-22523
Finding texture boundaries in images
[AD-A190554] 15 p2117 N88-22609
Does dihydroergotamine used in therapeutical doses influence the physical and psychomotor performance of young pilots or other traffic drivers subjected to hypotonia?
[ETN-88-92136] 20 p2832 N88-26799
Perception of motion in statistically-defined displays
[AD-A193076] 21 p2991 N88-27745
Models for motion perception
22 p3133 N88-28629
Effects of psychophysical lifting training on maximal repetitive lifting capacity
[AD-A192605] 23 p3238 N88-29271

PSYCHOPHYSIOLOGY
NT WORKLOADS (PSYCHOPHYSIOLOGY)
Evoked brain activity and personnel performance
[AD-A185922] 07 p0897 N88-15436
Considerations concerning the basic bandwidth reduction of high definition television systems (HDTV) component signals, based on psychophysiological properties of the eye
[IRT-B-83/87] 09 p1153 N88-16909
Neurocognitive predictions of performance
[AD-A188323] 12 p1669 N88-19998
An overview of current approaches and future challenges in physiological monitoring
16 p2239 N88-23371
Vagal tone as an index of mental state
16 p2239 N88-23373
Challenges of physiological monitoring in a Navy operational setting 16 p2239 N88-23374
Attention, effort, and fatigue: Neuropsychological perspectives 16 p2241 N88-23387
Physiological measures and mental-state assessment
16 p2242 N88-23392
Brainstem response and state-trait variables
16 p2242 N88-23394
The event-related brain potential as an index of information processing and cognitive activity: A program of basic research
[AD-A191244] 16 p2243 N88-23400
Psychophysiological measures of drowsiness as estimators of mental fatigue and performance degradation during sleep deprivation 21 p2980 N88-27702
Comparative aspects of multiple processes of attention
[AD-A195605] 24 p3408 N88-30291

PSYCHOSES
NT SCHIZOPHRENIA

PSYCHOTROPIC DRUGS
CEEG dynamic brain mapping: A new method to evaluate brain function in different psychological and drug conditions 21 p2977 N88-27685

PUBLIC HEALTH
JPRS report: Science and technology. USSR: Life sciences
[JPRS-ULS-87-012] 03 p0355 N88-12238
JPRS report: Science and technology. USSR: Life sciences
[JPRS-ULS-87-009] 04 p0473 N88-12915
JPRS report: Science and technology. USSR: Life sciences
[JPRS-ULS-87-013] 06 p0750 N88-14608
Food irradiation seminar: Asia and the Pacific
[DE88-700432] 09 p1202 N88-17203
USSR report: Life sciences. Biomedical and behavioral sciences
[JPRS-UBB-87-010] 12 p1651 N88-19889
Health and environmental consequences of the Chernobyl nuclear power plant accident
[DOE/ER-0332] 19 p2689 N88-25985

PUBLIC LAW
NT LEGAL LIABILITY

PUBLIC RELATIONS
Procedure and program used for data processing in a poll on nuclear energy utilization
[IFSI-87-3] 05 p0649 N88-13977
Datacast: The transmission system
[BBC-RD-1988/1] 14 p1905 N88-21385
Nuclear safety as applied to space power reactor systems 17 p2415 NBP-24360

PUBLICATIONS
U DOCUMENTS

PULMONARY CIRCULATION
Validation of a modified one-step rebreathing technique for non-invasive measurement of submaximal cardiac output
[AD-A192852] 21 p2987 N88-27735

PULMONARY FUNCTIONS
A plethysmograph for measuring pulmonary ventilation in small animals
[AD-A184976] 05 p0625 N88-13846
Load carriage induced alterations of pulmonary function
[AD-A186227] 07 p0889 N88-15386
Biorhythmological analysis of dynamics of pulmonary ventilation parameters during orthostatic tests
07 p0891 N88-15400

PULSARS
On the (lack of) proper motion of the Vela pulsar
01 p0097 N88-10635
X-ray pulsars: Accretion flow deceleration
03 p0390 N88-12451
Neutron stars observations as astrophysical probes
06 p0800 N88-14896
Self-modulational formation of pulsar microstructures
[NASA-CR-182420] 08 p1104 N88-16622
The formation of single millisecond pulsars in globular clusters
[MPE-PREPRINT-97] 10 p1428 N88-18525
A search for medium energy gamma ray pulsars
11 p1568 N88-19385
Topics in curved and flat space electromagnetism
13 p1854 N88-21100
Range determination of pulsars, taking into account H2 regions
[ETN-88-91492] 14 p1993 N88-21877
A 23 hour EXOSAT observation of the X-ray pulsar 1E2259+586 and the associated supernova remnant G109.1-1.0
[MPE-PREPRINT-99] 14 p1994 N88-21882
Strange, quark and metastable neutron stars
[DE88-702404] 21 p3030 N88-27984
Cascade model of gamma-ray bursts: Power-law and annihilation-line components
[NASA-TM-101176] 21 p3032 N88-27998
Very high energy cosmic gamma rays from radio and X-ray pulsars 23 p3309 N88-29711

PULSATING FLOW
U UNSTEADY FLOW

PULSE (CARDIOVASCULAR)
U HEART RATE

PULSE AMPLITUDE
Four-wave mixing used in optical amplitude encoding
03 p0376 N88-12366
Flow induced pulsations in pipe systems
[ETN-88-91367] 06 p0702 N88-14307
VAXGAP: A code for the routine analysis of gamma-ray pulse-height spectra on a VAX computer
[DE88-011702] 22 p3137 N88-28648

PULSE AMPLITUDE MODULATION
Telemetry applications handbook
[AD-A186825] 09 p1132 N88-16789
Bragg-cell receiver study
[NASA-CR-182684] 13 p1761 N88-20535
Polymerization of epoxy matrix composites using pulsed microwaves
[CERT-3/1324-MO] 20 p2760 N88-26487
Currents induced in a human being for electromagnetic fields to 10 kHz-50 MHz
[AD-A191977] 23 p3238 N88-29268

PULSE CODE MODULATION
NT DELTA MODULATION
NT DIFFERENTIAL PULSE CODE MODULATION
Telemetry applications handbook
[AD-A186825] 09 p1132 N88-16789

PULSE COMMUNICATION
A compact digital communications system. Part 3: Generalising the phase locked loop
[RSRE-MEMO-4027-PT-3] 01 p0035 N88-10222
Digital receiver structures and methods for the determination of the scanning frequency in modems for fast data transmission via telephone channels
[ETN-87-90429] 01 p0037 N88-10235
A digital audio link to the Channel Islands in the UHF television band: Preliminary experimental results
[BBC-RD-1987/9] 02 p0161 N88-11011
Theory and methods for design of pulse shapes for broadcast teletext
[CRC-1405] 02 p0162 N88-11013
Ultra-low power digital filter
[AD-A184485] 03 p0310 N88-11959
Cross-correlation of uniform cyclic difference set sequences
[AD-A184879] 05 p0640 N88-13913
A generalization of order statistic filters: The alpha-trimmed linear filter
[AD-A186125] 07 p0842 N88-15107
Requirements and options for communications services in support of the Systems Autonomy Demonstration Project 08 p1057 N88-16374
Digital bit error rate estimator for telemetry links
[INPE-4351-TDL/295] 12 p1598 N88-19563
High speed, bandpass sampling of digital communications waveforms
[AD-A189842] 15 p2056 N88-22254
Design for interoperability (interchangeability)
17 p2305 N88-23789
Direct bit detection receiver performance analyses for 8-DPSK (Differential Phase Shift Keyed) modulated signals operating with improper carrier phase synchronization
[AD-A193839] 22 p3070 N88-28220
The 44/20 GHz ground terminal
[AD-A194002] 23 p3204 N88-29069
Signals and systems 24 p3363 N88-30026

PULSE COMPRESSION
Generation of light pulses in semiconductor laser upon excitation by several electron beams
07 p0920 N88-15589
The design and implementation of surface acoustic wave devices for linear FM and a new non-linear FM pulse compression technique for radar applications
[AD-A186741] 08 p0980 N88-15922
RF pulse compression development
[DE88-004816] 11 p1479 N88-18826
Space-time structure of ultrashort light pulses formed during stimulated backscattering of laser beam
14 p1972 N88-21767
Time-domain frequency-selective optical memories: A study of the basic mechanisms and potential systems
[AD-A190854] 16 p2274 N88-23607
Application of pulse compression and shaping to the FEL photoelectric injector
[DE88-007908] 19 p2675 N88-25910
Development of inductive storage pulsed power generators
[AD-A193878] 22 p3117 N88-28521

PULSE DIFFRACTION
Diffraction moire: The dynamic regime
[DE87-014883] 03 p0335 N88-12111
Short pulse X-ray diffraction studies of shocked and annealed crystals using the JANUS research laser
[DE88-011329] 23 p3288 N88-29579

PULSE DOPPLER RADAR
NT MONOPULSE RADAR

PULSE DURATION
Picosecond CO2 laser interactions with polyatomic molecules
[DE87-012072] 01 p0051 N88-10327
Saturable absorbers for colliding pulse-locked Nd:YAG lasers 03 p0302 N88-11902
Thrust and specific impulse of repetitively-pulsed-laser propulsion rocket 03 p0318 N88-12012
Long-range pulselength scaling of 351nm laser damage thresholds
[DE87-014754] 04 p0448 N88-12777
Optimization of field emission electron beam sources for high-power lasers
[PB87-218814] 06 p0708 N88-14341
Laser pulse width dependent surface ripples on silicon
[PB88-127311] 10 p1336 N88-17982
Efficiency of fusion during periodic-pulse laser-beam welding 14 p1897 N88-21324
The technical feasibility of using spiked-radiation lasers to cut out and weld metals 14 p1898 N88-21332
Folded long-pulse XeCl excimer laser described
14 p1901 N88-21357
XeCl laser-pumped nanosecond dye lasers
14 p1902 N88-21359
Theoretical study of colliding pulse mode-locking in dye lasers 14 p1903 N88-21366
Laser pulse detection with infrared range semiconductor detectors
[DE88-700857] 14 p1914 N88-21432

Time characteristics of ultrashort light pulses from dye lasers with distributed feedback
14 p1970 N88-21759
Nonlinear stage of ultrashort-pulse formation in solid-state laser 14 p1971 N88-21765
Pulse duration control of XeCl*-laser by means of plasma shutter 14 p1973 N88-21774
Timing for subnanosecond pulses
[DE88-701390] 16 p2192 N88-23074
Monolithic fuel cell based power source for sprint power generation 17 p2407 N88-24313
Fundamental analysis of space nuclear-MHD generator for gigawatt-level power 17 p2411 N88-24337
Burst power gas core reactor with MHD power generation 17 p2433 N88-24472

PULSE DURATION MODULATION
Digital to analog and analog to digital conversion using pulse duration modulation
[ETN-87-90415] 01 p0078 N88-10499
Digital control of a direct current converter for a hybrid vehicle
[LAAS-87-266] 05 p0578 N88-13527
Digital control of high frequency pulse-width modulated inverters
[ETN-87-90711] 09 p1157 N88-16936
The theory and implementation of a high quality pulse width modulated waveform synthesiser applicable to voltage FED inverters
[ETN-87-90712] 09 p1157 N88-16937

PULSE GENERATORS
Operation of the TEMPO machine
[DE87-011285] 01 p0038 N88-10241
Development of a repetitive 1-MV, 22-kJ Marx generator
[DE87-011286] 01 p0038 N88-10242
Response of helical structures to high speed pulses or when can a helix be called an inductor
[DE87-014347] 01 p0090 N88-10587
Progress toward a superconducting opening switch
[DE87-014170] 02 p0167 N88-11051
A tutorial on Rogowski coil theory and operation
[DE88-000006] 02 p0230 N88-11449
The LPX (Long Pulse Experiment) facility
[DE87-010493] 03 p0311 N88-11964
RIIM two-pulse injector experiments
[DE88-000926] 05 p0653 N88-14005
Super-short yttrium aluminate pulse generator with controlled resonator Q-factor 06 p0772 N88-14740
Pulsed power sources based on MHD generators (a state-of-art review)
[DE88-700296] 07 p0935 N88-15677
A unified model for the WTS and the generation on Pi 2 pulsations — Westward Traveling Surge (WTS)
08 p1096 N88-16593
The railgun and its power source
[MRL-R-1058] 09 p1130 N88-16786
Periodic-pulse semiconductor laser with electron-beam pumping 09 p1238 N88-17422
Proposal for construction of an Energetic Particle Injector (EPI)
[INPE-4242-RPE/548] 12 p1690 N88-20112
Optimum transformer design for a pulsed power system
[DE88-006054] 13 p1760 N88-20525
High-voltage inverse-square function generator
[DE88-701109] 15 p2058 N88-22270
Pulsed power simulation problems in magic
[AD-A191110] 16 p2191 N88-23065
Photoconductive generation of sub-picosecond electrical pulses and their measurement applications
19 p2656 N88-25778
Generation and forming of ultrashort high voltage pulses 19 p2657 N88-25782
A simple technique to generate or gate microwave pulses with picosecond speeds 19 p2657 N88-25784
Energy variations in optical pulses from gain-switched AlGaAs diode lasers 19 p2658 N88-25796
Research in electromagnetic shielding theory. Part 2: EMP (electromagnetic pulse) simulation using small loops
[AD-A192882] 20 p2791 N88-26558
Radial compression of picosecond electrical pulses
[DE88-006440] 21 p2953 N88-27544
Production of intensive electron beam impulsions by setup of pseudoglare discharges
[ISL-CO-210/87] 21 p3019 N88-27920
Electromagnetic characterization and acceptance test of the electromagnetic pulse (EMP) simulator SPERANS
[FOA-C-30476-4.2] 22 p3071 N88-28230
The far field from a hybrid electromagnetic pulse (HPD) simulator
[FOA-C-30480-4.2] 22 p3071 N88-28231
Development of inductive storage pulsed power generators
[AD-A193878] 22 p3117 N88-28521
Distortions in processed signals and their application in electronic design. Part 2: A new variable signal generator
[DE88-702732] 23 p3205 N88-29071
Distortions in processed signals and their application in electronic design. Part 3: An automated generator of communication jamming signals
[DE88-702733] 23 p3205 N88-29072

PULSE HEATING
Stress intensity factors for cracked metallic structures under rapid thermal loading
[AD-A191219] 23 p3193 N88-29004

PULSE HEIGHT
U PULSE AMPLITUDE

PULSE MODULATION
NT DELTA MODULATION
NT DIFFERENTIAL PULSE CODE MODULATION
NT PULSE AMPLITUDE MODULATION
NT PULSE CODE MODULATION
NT PULSE DURATION MODULATION
NT PULSE POSITION MODULATION
Collection and analysis of specific ELINT Signal Parameters
[NASA-CR-181419] 01 p0033 N88-10213
Correction method for Barker-coded modulation
06 p0691 N88-14240
Pulse width modulator controller design for a brushless DC motor position servo
[AD-A186618] 08 p0980 N88-15921
Self-modulational formation of pulsar microstructures
[NASA-CR-182420] 08 p1104 N88-16622
Modulatable thin film field emission space gun
[AD-A189279] 13 p1845 N88-21043
Laser pulse detection with infrared range semiconductor detectors
[DE88-700857] 14 p1914 N88-21432
Error reduction in two-dimensional pulse-area modulation, with application to computer-generated transparencies — optical field synthesis
[EUT-87-E-172] 14 p1982 N88-21825
Frequency chirping in pulse modulated gain and real index guided single quantum well lasers
19 p2658 N88-25798
Effect of detector dead time on the performance of optical direct-detection communication links
22 p3065 N88-28190

PULSE POSITION MODULATION
Optical communication with semiconductor laser diodes
[NASA-CR-182464] 09 p1154 N88-15918
Effect of atmospheric turbulence on the bit error probability of a space to ground near infrared laser communications link using binary pulse position modulation and an avalanche photodiode detector
[NASA-TM-100699] 14 p1873 N88-21189

PULSE RADAR
NT MONOPULSE RADAR
A very wide frequency band pulsed/IF radar system
[NASA-CR-182889] 16 p2190 N88-23059
TDWR (Terminal Doppler Weather Radar) PRF (Pulse Repetition Frequency) selection criteria
[AD-A193089] 21 p2932 N88-27407

PULSE RATE
NT PULSE REPETITION RATE

PULSE RECORDERS
U COUNTERS

PULSE REPETITION RATE
Operation of the TEMPO machine
[DE87-011285] 01 p0038 N88-10241
Development of a repetitive 1-MV, 22-kJ Marx generator
[DE87-011286] 01 p0038 N88-10242
An optically strobed sample and hold circuit
[DE87-011877] 01 p0038 N88-10245

PULSE TIME MODULATION
NT PULSE DURATION MODULATION
NT PULSE POSITION MODULATION

PULSE WIDTH
U PULSE DURATION

PULSE WIDTH MODULATION
U PULSE DURATION MODULATION

PULSED LASERS
NT Q SWITCHED LASERS
NT ULTRASHORT PULSED LASERS
NT ULTRAVIOLET LASERS
Saturable absorbers for colliding pulse-locked Nd:YAG lasers 03 p0302 N88-11902
Thrust and specific impulse of repetitively-pulsed-laser propulsion rocket 03 p0318 N88-12012
Distributed feedback effects in lasers and high gain laser instabilities in optically pumped CH3F
03 p0329 N88-12079
The generation and suppression of synchrotron sidebands
[DE88-000532] 04 p0449 N88-12787
All-optical beam control by forced Rayleigh scattering
[AD-A184315] 04 p0490 N88-13018
Determination of a flow velocity field using four-exposure laser holography
[IMFL-3114-85/32] 05 p0585 N88-13565
Transient processes in the interaction between pulsed laser radiation and matter
[ISL-R-115/86] 05 p0588 N88-13586
Raman microprobe characterization of dielectric films following high-energy pulsed laser irradiation
[DE88-000559] 05 p0588 N88-13587
Theory of multiphoton ionization of atoms by strong, short pulsed lasers
[DE88-000963] 05 p0588 N88-13588
Production-process CO2 laser with amplified pulse-repetition operation 06 p0771 N88-14739
Super-short yttrium aluminate pulse generator with controlled resonator Q-factor 06 p0772 N88-14740
Periodically pulsed excimer master oscillator-regenerative amplifier laser set
06 p0772 N88-14741
Development of crack under periodically pulsed laser radiation 06 p0774 N88-14754
Study of kinetics of intracavity absorption in pulsed dye lasers 07 p0919 N88-15585
Effect of multiplication of spectral components of multi-frequency lasing of pulsed tunable laser
07 p0920 N88-15586
Generation of light pulses in semiconductor laser upon excitation by several electron beams
07 p0920 N88-15589
Formation of high-coherence radiation in free-running mode ruby laser for pulse holography
08 p1077 N88-16497
High-power periodic-pulse YAG:Nd3 + -laser system with telescopic unstable resonator and two-stage amplifier
09 p1237 N88-17414
Calculation of the spatial-temporal deformation of laser pulses in multiple scattering
[MBB-Z-111/87] 10 p1311 N88-17837
Monitoring interfacial dynamics by pulsed laser techniques
[DE88-003362] 10 p1335 N88-17976
Laser pulse width dependent surface ripples on silicon
[PB88-127311] 10 p1336 N88-17982
Overview of applications of Laser-Induced Breakdown Spectroscopy (LIBS)
[DE88-004314] 10 p1336 N88-17987
Optically controlled devices and ultrafast laser sources for signal processing
[AD-A187417] 10 p1338 N88-17995
Pulsed laser photothermal spectroscopy of liquids and solids
[DE88-003839] 11 p1455 N88-18675
Joining of dissimilar materials with the pulsed Nd-YAG laser
[DE88-003757] 11 p1458 N88-18693
Photoconductor switch and circuit analysis
[AD-A188166] 11 p1478 N88-18821
Picosecond laser studies of excited state processes
[AD-A189606] 12 p1607 N88-19607
Pulse-train amplification of subnanosecond near-transform-limited KrF laser pulses
[DE88-004460] 12 p1631 N88-19764
Microstructure characterization with a pulsed laser ultrasonic source
[DE88-005207] 12 p1632 N88-19766
Modeling and transport in semiconductor devices
[AD-A188760] 13 p1844 N88-21037
Efficiency of fusion during periodic-pulse laser-beam welding 14 p1897 N88-21324
The technical feasibility of using spiked-radiation lasers to cut out and weld metals 14 p1898 N88-21332
Folded long-pulse XeCl excimer laser described
14 p1901 N88-21357
XeCl laser-pumped nanosecond dye lasers
14 p1902 N88-21359
Laser pulse detection with infrared range semiconductor detectors
[DE88-700857] 14 p1914 N88-21432
Radiation absorption in neodymium glasses during passage of strong laser pulse 14 p1969 N88-21757
Time characteristics of ultrashort light pulses from dye lasers with distributed feedback
14 p1970 N88-21759
Effects of emission energy transient in periodic-pulse XeCl excimer laser of approximately 400 W average power 14 p1971 N88-21763
Nonlinear stage of ultrashort-pulse formation in solid-state laser 14 p1971 N88-21765
High-efficiency Y-Sc-Ga:Cr (sup)3+,Tu (sup)3+,Ho (sup)3+ garnet laser (gl= 2.088 gmm at room temperature 14 p1971 N88-21766
Space-time structure of ultrashort light pulses formed during stimulated backscattering of laser beam
14 p1972 N88-21767

Pulse duration control of XeCl*-laser by means of plasma shutter
14 p1973 N88-21774
A preliminary comparison of the transient effects of single versus multiple q-switched doubled-neodymium laser pulses
[AD-A189655] 15 p2071 N88-22347
Program to research laser-driven thermionic electron sources for free electron lasers
[AD-A190473] 15 p2072 N88-22353
Investigation of ultrashort traveling-wave amplified spontaneous emission 16 p2187 N88-23040
Observation of synchronously transient pumped mode-locking dye laser under negative cavity detuning
16 p2187 N88-23041
Time-resolved studies of free radicals and laser-initiated chain reactions
[DE88-006569] 16 p2266 N88-23553
Determination of tropospheric H concentrations by a double-pulsed UV laser method
18 p2539 N88-25070
The chirped-pulse free-electron laser
[DE88-009289] 20 p2807 N88-26651
Model for pulse amplification by a gaseous laser amplifier
[DE88-011729] 20 p2808 N88-26657
Process control improvements in pulsed Nd:YAG laser closure welding of electromechanical relays
[DE88-006275] 21 p2957 N88-27564
MIDIR (Mid-Infrared) laser, phase 1
[AD-A193935] 23 p3220 N88-29166
Breakdown of molecular oxygen by brief pulses of laser radiation
[DE88-702687] 23 p3220 N88-29168

PULSED RADIATION
NT ELECTROMAGNETIC PULSES
The Hermes-3 program
[DE87-012132] 02 p0234 N88-11473
The pulsation modes of CO Aur
[PUBL-SER-C-FASC-10] 03 p0387 N88 12430
Materials for acceleration by surface electromagnetic waves
[DE88-700312] 07 p0646 N88-15133
Advanced energy conversion concept for beamed-energy propulsion
[AD-A187336] 10 p1324 N88-17914
Emission of gamma rays from various materials pulsed with 14-MeV neutrons
[DE88-003837] 11 p1544 N88-19227
Response characteristics of dual MOSFET gamma-ray sensors produced by Mitel Corporation
[AD-A189026] 12 p1630 N88-19755
X-rays from z-pinches
[AD-A188911] 12 p1696 N88-20146
Practical constraints on sources for pulsed beam lithographies
[DE88-006594] 13 p1776 N88-20623
Fundamental analysis of space nuclear-MHD generator for gigawatt-level power 17 p2411 N88-24337

PULSES
NT ELECTRIC PULSES
NT ELECTROMAGNETIC PULSES
NT GEOMAGNETIC MICROPULSATIONS
NT GEOMAGNETIC PULSATIONS
NT PICOSECOND PULSES
NT PRESSURE PULSES
Toward pulsed power uses for photoconductive semiconductor switches: Closing switches
[DE87-012020] 01 p0041 N88-102[illegible]2
Short-pulse high-current-density photoemission in high electric fields
[DE87-014909] 03 p0310 N88-11951
Alternating current circuit theory and pulsed NMR (Nuclear Magnetic Resonance)
[DE88-000641] 04 p0440 N88-12732
High-power RF-pulsed modulators for the Los Alamos free-electron laser
[DE88-000514] 04 p0448 N88-12775
Increased gain of channel intensifier tubes by pulsed biasing
[DE88-000512] 04 p0490 N88-13016
Cerenkov radiation field analysis due to a passing electron beam
[AD-A184870] 05 p0649 N88-13976
Mixing and combustion of pulsed gas jets
[PB88-112834] 06 p0680 N88-14169
Mixing and combustion of pulsed gas jets
[PB88-108014] 06 p0680 N88-14170
The history and development of nonlinear stellar pulsation codes
[DE88-001828] 06 p0801 N88-14899
Gas phase pulse radiolysis
[DE88-002981] 10 p1296 N88-17751
The 80 fsec soliton-like pulses from an optical-nonlinear fiber resonator
[PB88-127303] 10 p1409 N88-18403
Ballistic deficits in pulse shaping amplifiers
[DE88-003908] 11 p1481 N88-18840
The optimum solution to instrument quantization effects 12 p1577 N88-19434
Pulse-train amplification of subnanosecond near-transform-limited KrF laser pulses
[DE88-004480] 12 p1631 N88-19764
Millimeter-wave pulse distortion by a single adsorption line simulating the terrestrial atmosphere
[PB88-161237] 14 p1906 N88-21388
Laser-heterodyne interferometry with streak camera detection
[DE88-003292] 14 p1914 N88-21437
Timing for subnanosecond pulses
[DE88-701390] 16 p2192 N88-23074
Optical sensors for the measurement of electric current and voltage
[PB88-172945] 16 p2193 N88-23077
Rotating-hoop, pulsed-energy converter
17 p2426 N88-24433
Silicon pulse sharpening diodes-switching kilovolts in 10's of picoseconds 19 p2661 N88-25824
Long-pulse, high-power vircator experiments
[DE88-011787] 21 p2940 N88-27458
An investigation of acoustic cavitation produced by pulsed ultrasound
[AD-A193523] 23 p3278 N88-29516

PULTRUSION
Potential for on-orbit manufacture of large space structures using the pultrusion process
[NASA-TM-4016] 05 p0557 N88-13386

PUMP IMPELLERS
Rotor dynamic behavior of centrifugal pumps
08 p0975 N88-15898

PUMP SEALS
Disk pumping test
[AD-A187199] 11 p1440 N88-18591

PUMPING
An advanced extruder-feeder biomass liquefaction reactor system 18 p2535 N88-25042

PUMPS
NT AXIAL FLOW PUMPS
NT CENTRIFUGAL PUMPS
NT ELECTROMAGNETIC PUMPS
NT FUEL PUMPS
NT TURBINE PUMPS
NT VACUUM PUMPS
NT WINDPOWERED PUMPS
Stirling engines and irrigation pumping
[DE88-000020] 02 p0181 N88-11125
Build, install and demonstrate a variable stroke pump control and windmill system
[DE87-014656] 03 p0347 N88-12191
Dynamics of reverse flows at pump inlet
04 p0425 N88-12636
The 8.4-GHz low-noise maser pump source assembly
04 p0436 N88-12705
Modular pump limiter systems for large tokamaks
[DE88-001487] 04 p0494 N88-13045
Utilization of FEP energetics
[NASA-CR-182373] 06 p0714 N88-14379
Materials development for JPL oxygen plant
[DE88-003067] 10 p1297 N88-17752
Vibration characteristics of pumped fluid systems (VCPFS) --- microgravity payloads
[ESA-CR(P)-2499] 14 p1895 N88-21310
Computer simulation of a motor pump unit to aid in interpreting vibration data
[DE88-004481] 16 p2223 N88-23270
Pumped two-phase heat transfer loop
[NASA-CASE-MSC-20841-2] 17 p2339 N88-23958
Pulsatile fluidic pump performance at elevated temperatures
[DE88-008046] 19 p2677 N88-25915
Temperature rise in superfluid helium pumps
[NASA-TM-100997] 21 p2948 N88-27507
Hydraulic pumps and hydraulic equipment at low temperatures
[DE88-752871] 21 p2958 N88-27570
Polymeric heat pipe wick
[NASA-CASE-GSC-13019-1] 23 p3214 N88-29133
Preliminary studies of NF3+H2 production of N2(A3 sigma(+)u) in a supersonic flow
[AD-A194479] 23 p3219 N88-29162

PUNCTURING
U PIERCING

PUPIL SIZE
A human factors evaluation of the Advanced Visual Technology System (AVTS) eye tracking oculometer
21 p2925 N88-27361

PUPILS
Pupil measures of alertness and mental load
16 p2239 N88-23378
Probe-evoked event-related potential techniques for evaluating aspects of attention and information processing 16 p2240 N88-23379

PURGING
Evaluation and improvement of liquid propellant rocket chugging analysis techniques. Part 1: A one-dimensional analysis of low frequency combustion instability in the fuel preburner of the space shuttle main engine
[NASA-CR-183106] 21 p2903 N88-27224

PURIFICATION
NT AIR PURIFICATION
Gas separation using solid electrolytes described
06 p0675 N88-14131
Gas cleaning at high temperatures and pressures for gas turbines
[DE88-751171] 11 p1440 N88-18593
Growth and characteristics of materials for tunable lasers in the near infrared spectral region
[NASA-CR-182501] 11 p1491 N88-18901

PURIFIERS
U PURIFICATION

PURINES
NT CAFFEINE
NT XANTHINES

PURITY
Carbon monoxide (CO) concentraiion in the air as a purity parameter
[INPE-4232-PRE/1107] 01 p0067 N88-10429
Production of metallic monocrystals described
03 p0286 N88-11796
Conductive polymers via reactive aligomer
[AD-A184270] 04 p0419 N88-12597
Electrochemical hydrogen concentrator for phosphoric acid fuel cells
[AD-A191355] 16 p2229 N88-23317
The variation of torsional ductility of high-purity aluminum with temperature and strain rate
[DE88-005618] 18 p2487 N88-24755

PURSUIT TRACKING
Estimation filters with adaptive scanning time for flying target tracking
[ETN-87-90401] 01 p0036 N88-10232
The isotropic rocket: A surveillance evasion game
[REPT-87-21] 05 p0645 N88-13949
Pursuit tracking performance decrements associated with decreasing ambient illumination
[AD-A189336] 13 p1809 N88-20809
Eye and head response to an attention cue in a dual task paradigm
[AD-A191052] 18 p2551 N88-25143

PUSHBROOM SENSOR MODES
HIRIS (High-Resolution Imaging Spectrometer: Science opportunities for the 1990s. Earth observing system. Volume 2C: Instrument panel report
[NASA-TM-89703] 07 p0871 N88-15282
Mid infrared multichannel focal plane breadboard --- pushbroom sensors
[RT-87/014] 14 p1982 N88-21827
Imaging instrument of the vegetation payload (SPOT 4)
[SNIAS-881-440-107] 24 p3386 N88-30169

PUSHING
Pusherless implosion, pulse tailoring and ignition scaling law for laser fusion 16 p2277 N88-23629

PWM (MODULATION)
U PULSE DURATION MODULATION

PYLONS
Compression pylon
[NASA-CASE-LAR-13777-1] 24 p3323 N88-29789

PYRAMIDS
An orthogonal oriented quadrature hexagonal image pyramid
[NASA-TM-100054] 06 p0755 N88-14630

PYRENES
Measurement of species concentrations in flames by laser-induced fluorescence
[DE88-007096] 14 p1889 N88-21286

PYREX (TRADEMARK)
U BOROSILICATE GLASS

PYRIDINES
An investigation of metal complexes of some 2-substituted and 2,6-disubstituted pyridine N-oxides
11 p1460 N88-18701
Study of crosslinking and nonelastic mechanical properties of epoxy and PSP networks --- epoxy resins, polystyrylpyridine resins (psp)
[ETN-88-92740] 21 p2921 N88-27337

PYRIMIDINES
NT THYMINE
NT URACIL

PYRITES
Reactions of some thiol collectors at noble-metal and pyrite electrodes
[PB88-138318] 11 p1455 N88-18674
Some equivalent circuit models for AC impedance analysis of pyrite/solution interface
[DE88-010574] 21 p2939 N88-27452

PYROELECTRICITY
Polymer material for heat sensors
06 p0676 N88-14142
Statistical-mechanical study of polyvinylidene fluoride
[AD-A188310] 12 p1609 N88-19624
Fast acting optical beam detection and deflection system
[AD-A192161] 18 p2521 N88-24954
Zinc-oxide thin films for integrated-sensor applications
19 p2673 N88-25896
PYROGRAPHALLOY
U COMPOSITE MATERIALS
U PYROLYTIC GRAPHITE
U REFRACTORY MATERIALS
PYROHYDROLYSIS
Effect of process conditions on aluminum oxide thin film used in pH ISFET 19 p2673 N88-25892
PYROLYSIS
Laser probes of propellant combustion chemistry
[AD-A184854] 05 p0561 N88-13415
Detailed mechanism of toluene oxidation and comparison with benzene
[NASA-TM-100261] 05 p0563 N88-13428
A study of the interaction of laser light with liquid propellant drops
[AD-A185117] 05 p0587 N88-13582
Process for preparing transition metal nitrides and transition metal carbonitrides and their reaction intermediates
[DE88-000849] 06 p0679 N88-14162
Production by pyrolysis of diffusion particles for velocimetry in shock tubes
[ISL-R-119/86] 11 p1455 N88-18671
The preparation of titanium nitride and titanium carbonitride by the preceramic polymer route
[AD-A188357] 12 p1610 N88-19626
Photolytic formation of free radicals and their effect on hydrocarbon pyrolysis chemistry in a concentrated solar environment
[DE88-004129] 13 p1794 N88-20730
Proceedings of the 1987 Biomass Thermochemical Conversion Contractors' Review Meeting
[DE88-006730] 18 p2535 N88-25041
Low pressure entrained flow pyrolysis of biomass to produce liquid fuels 18 p2535 N88-25043
Molecular-beam, mass-spectrometric studies of wood vapor and model compounds over HZSM-5 catalyst
18 p2535 N88-25044
Upgrading pyrolysis vapors to aromatic gasoline with zeolite catalysis at atmospheric pressure
18 p2536 N88-25045
Technical and economic evaluation of emerging biomass pyrolysis processes for gasoline production
18 p2536 N88-25048
Bench-scale studies on fluid-bed pyrolysis of wood using different contact gases 18 p2536 N88-25049
Evaluation of the toxicity of products from the thermal degradation of materials
[ETN-88-91995] 18 p2549 N88-25130
Flame spread mechanisms over PMMA surfaces
[NASA-TT-20284] 19 p2612 N88-25500
New instability phenomena in solid propellant combustion 19 p2628 N88-25591
Simultaneous thermogravimetric modulated beam mass spectrometry and time-of-flight velocity spectra measurements: Thermal decomposition mechanisms of RDX and HMX 19 p2632 N88-25612
Laser-RDX aerosol pyrolysis with matrix isolation of unstable intermediates 19 p2632 N88-25614
Refractory films from spin-cast carbon
[DE88-011251] 21 p2919 N88-27327
Determination of relative flammability of materials by pyrolysis and gas-chromatographic light hydrocarbon analysis
[DE88-012449] 24 p3343 N88-29896
The influence of pressure on soot formation
24 p3349 N88-29934
PYROLYTIC GRAPHITE
Data base on the high heat flux behaviour of metals and carbon materials for plasma facing components: Experiments at the 10 MW neutral beam injection test stand of the IPP Nagoya
[IPPJ-AM-53] 04 p0492 N88-13031
PYROLYTIC MATERIALS
NT PYROLYTIC GRAPHITE
Disclination structures in carbon and graphite
[AD-A191056] 17 p2322 N88-23868
Pyrolyzed organic polymer nitrogen dioxide sensor
19 p2669 N88-25866
PYROMETALLURGY
The nature of metallurgical reactions in underwater welding
[AD-A184464] 04 p0414 N88-12568
PYROMETERS
NT RADIATION PYROMETERS
Noncontact temperature pattern measuring device
[NASA-CASE-NPO-17024-1-CU]
18 p2519 N88-24943
Principles of the optical differential thermal analysis
[AD-A195951] 24 p3429 N88-30408
PYROMETRY
U TEMPERATURE MEASUREMENT
PYROPHORIC MATERIALS
Chemical analysis of charged Li/SO(sub)2 cells
02 p0163 N88-11026
PYROTECHNICS
NT HMX
Pyrotechnic component development at Sandia National Laboratory
[DE87-006899] 02 p0154 N88-10967
A nondissipative Pyrotechnic Arming and Firing Unit (PAFU)
[CRA/REPO/8019] 02 p0155 N88-10974
Performance characteristics of magnesium-sodium nitrate flares in oxygen-nitrogen atmospheres
[AD-A185274] 05 p0570 N88-13476
Advantages of internal thermal protection in a pyrotechnical plunger
[SNIAS-872-430-114] 05 p0571 N88-13478
Numerical simulation applied to the development of a pyrotechnical system
[SNIAS-872-430-115] 05 p0571 N88-13479
The TV-SAT/TDF/TELE-X pyrotechnical system
[CNES-87/CT/DRT/TVE/IL/358]
08 p0974 N88-15891
The Shock and Vibration Bulletin. Part 1: Welcome, Keynote Address, Invited Papers, Nondevelopment Items Workshop and Pyrotechnic Shock Workshop
[AD-A186748] 08 p0997 N88-16034
Designing electronics for pyrotechnic shock
08 p0997 N88-16038
Zeroshift of piezoelectric accelerometers in pyroshock measurements 08 p0997 N88-16039
Organic coatings to improve the storageability and safety of pyrotechnic compositions
[AD-A187158] 09 p1150 N88-16889
Measurement, data analysis and prediction of pyrotechnic shock from pin-pullers and separation joints
09 p1179 N88-17061
A pyrotechnic delay ignition system for a submarine launched marine signal
[MRL-R-1079] 13 p1754 N88-20487
A defect investigation of Thunderflash MK N5 (Navy)
[MRL-TN-522] 13 p1754 N88-20488
Stability of the high-temperature G-16 primer composition
[DE88-006201] 15 p2049 N88-22206
A pyrotechnical opening valve
[SNIAS-MU/TYS-NT-2-06(0)] 16 p2167 N88-22922
Ariane 4 pyrotechnics system: Definition of the chains and pyrotechnic devices
[CNES-88/CT/DRT/TVE/IL/25]
17 p2310 N88-23816
Pyrotechnic system failures: Causes and prevention
[NASA-TM-100633] 20 p2765 N88-26394
Granulation of pyrotechnic tracer composition R284T
[MRL-TN-528] 20 p2780 N88-26490
Diode laser ignition of high explosives and pyrotechnics
[DE88-008771] 21 p2923 N88-27352
Development and verification of NASA Standard Initiator-2 (NSI-2)
[NASA-CR-172069] 23 p3200 N88-29044
Development and verification of NASA Standard Initiator-2 (NSI-2): Appendix
[NASA-CR-172070] 23 p3200 N88-29045
Semiconductor bridge (SCB) igniter studies. 1: Comparison of SCB and hot-wire pyrotechnic actuators
[DE88-008802] 23 p3200 N88-29046
PYRROLES
NT CARBAZOLES
Transport properties of conductive polymers
[AD-A188411] 12 p1610 N88-19628
Morphological studies of conductive polymers
[AD-A188456] 12 p1610 N88-19629
P3V AIRCRAFT
U P-3 AIRCRAFT
P78-2 SATELLITE
U SCATHA SATELLITE

Q

Q FACTORS
Super-short yttrium aluminate pulse generator with controlled resonator Q-factor 06 p0772 N88-14740
Q SWITCHED LASERS
An investigation of unipolar arcing at atmospheric pressure in aluminum 2024 and aluminum coated glass slides
[AD-A184903] 05 p0577 N88-13521
Diode pumped fiber laser
[AD-A187694] 11 p1491 N88-18802
Development of high efficiency q-switched glass laser via sol-gel processing
[AD-A192301] 23 p3218 N88-29154
QCD
U QUANTUM CHROMODYNAMICS
QSO (RADIO SOURCES)
U QUASARS
QUADRANTID METEOROIDS
Structural peculiarities of the Quadrantid meteor shower 06 p0740 N88-14552
QUADRANTS
On the extreme points of the set of all 2xn bivariate positive quadrant dependent distributions with fixed marginals and some applications
[AD-A186316] 07 p0911 N88-15521
Some comments on quadrant dependence in higher dimensions
[AD-A190329] 15 p2121 N88-22639
QUADRATIC EQUATIONS
Analytical treatment of the spatial trilateration problem (4, 6, 0, 0)
[SER-A-104] 01 p0085 N88-10548
Quantization of quadratic friction revisited
[DE88-700839] 12 p1686 N88-20081
Distributions of quadratic forms
[AD-A190224] 15 p2124 N88-22663
A piecewise quadratic strength tensor theory for composites
[AD-A190929] 16 p2173 N88-22952
A feasibility study in path planning using optimization techniques
[AD-A193030] 21 p2894 N88-27177
Application of differential quadrature to the analysis of structural components 22 p3087 N88-28331
Periodic solutions of perturbed superquadratic Hamiltonian systems
[AD-A194292] 23 p3270 N88-29457
QUADRATIC PROGRAMMING
A Schur-complement method for sparse quadratic programming
[DE88-002520] 07 p0904 N88-15479
An O(n3L) interior point algorithm for convex quadratic programming
[AD-A186001] 07 p0909 N88-15504
Active vibration control of a cantilevered beam with three elastic coordinates
[AD-A188824] 12 p1636 N88-19797
Sufficient matrices and the linear complementarity problem
[AD-A190429] 15 p2128 N88-22690
QUADRATURE APPROXIMATION
U QUADRATURES
QUADRATURES
A quadrature formula for a double-pole singular integral
[PD-FM-8725] 04 p0485 N88-12990
An orthogonal oriented quadrature hexagonal image pyramid
[NASA-TM-100054] 06 p0755 N88-14630
A quadratic-form analysis of the collisionless tearing mode
[AD-A188886] 12 p1695 N88-20144
A note on the analyticity of the Neumann Kernel and an associated quadrature problem in two-dimensional boundary element methods
[ETN-88-92054] 14 p1964 N88-21719
Asymptotic of Peanokernels of finite fixed order
[ETN-88-92361] 21 p3008 N88-27843
Application of differential quadrature to the analysis of structural components 22 p3087 N88-28331
Use of a coherent square wave reference to demodulate BPSK (Binary Phase Shift Keying) carriers and a visual indicator of the quality of received QPSK (Quadrature Phase Shift Keying) carriers
[AD-A193528] 23 p3204 N88-29065
Generating semi-Gaussian two dimensional quadrature rules
[REPT-205] 23 p3272 N88-29476
QUADRUPOLE LENSES
U MAGNETIC LENSES
QUADRUPOLES
Research relative to an advanced rod control system for quadrupole mass spectrometry applications
[NASA-CR-181458] 02 p0167 N88-11050
Present status of the high resolution spectrometers
[CEBAF-PR-87-029] 02 p0234 N88-11476
High gradient superconducting quadrupoles
[DE87-013590] 02 p0244 N88-11541
Modeling the behavior of oriented permanent magnet material using current double theory
[DE88-004446] 13 p1833 N88-20963
The exact calculation of quadrupole sources for some incompressible flows
[NASA-TM-100623] 17 p2395 N88-24240

Theoretical investigations of drift waves in a magnetic quadrupole 18 p2578 N88-25312

QUALIFICATIONS

Qualification by analysis of IUS plume deflectors
09 p1179 N88-17063

Qualification of frequency response functions using the rigid-body response
[DE88-000745] 10 p1344 N88-18033

SP-100 flight qualification testing assessment
17 p2424 N88-24414

QUALITATIVE ANALYSIS

Solid state C-13 NMR characterization of textiles: Qualitative and quantitative analysis
[AD-A184349] 04 p0419 N88-12598

A low volume insert for solid state magic angle spinning NMR of small samples
[AD-A184359] 04 p0419 N88-12601

Predictive monitoring research: Summary of the PREMON system
[NASA-CR-182687] 13 p1824 N88-20905

Qualitative reasoning for physicists
[PB88-116298] 20 p2848 N88-26906

High hot-hardness gear lubricant evaluations, phase 2
[AD-A192309] 23 p3196 N88-29017

QUALITY

NT AIR QUALITY
NT ENVIRONMENTAL QUALITY
NT RIDING QUALITY
NT WATER QUALITY

Assessment of software quality for the AIRBUS A310 automatic pilot 02 p0128 N88-10804

The criterion of equal integrated quality: An improved method of planning DBS systems
[BBC-RD-1987/10] 02 p0161 N88-11012

Software quality measurement demonstration project (1)
[AD-A193429] 22 p3136 N88-28646

Aerodynamic data accuracy and quality: Requirements and capabilities in wind tunnel testing
[AGARD-AR-254] 23 p3173 N88-28893

High definition television: Evaluation for remote task performance
[DE88-011573] 23 p3202 N88-29057

An analysis of lateral-directional handling qualities and Eigenstructure of high performance aircraft
[AD-A194874] 24 p3328 N88-29814

QUALITY CONTROL

Wet deposition and snowpack monitoring operations and quality assurance manual
[PB87-212817] 01 p0064 N88-10413

Investment foundry melting stock. Rolls Royce requirements and demands in terms of quality and the relationship to end product performance
[PNR90397] 02 p0160 N88-11003

Implementation of finite element quality assurance in a commercial industrial organisation
[PNR90393] 02 p0183 N88-11137

Softwarr reliability models for fault-tolerant avionics computers and related topics
[NASA-CR-181440] 02 p0220 N88-11362

RADC/NBS (Rome Air Development Center/National Bureau of Standards) Workshop. Moisture Measurement and Control for Microelectronics (4)
[PB87-224614] 03 p0309 N88-11947

NBS (National Bureau of Standards) measurement services: Radiometric standards in the vacuum ultraviolet
[PB87-227625] 03 p0325 N88-12055

Software maintenance in scientific and engineering environments: An introduction and guide
[NASA-CR-177409] 04 p0479 N88-12954

Avionics and corrosion 05 p0547 N88-13336

Philosophy and practice of nondestructive tests of composite material structures at Aerospatiale Aquitaine
[SNIAS-872-430-105] 05 p0559 N88-13400

Chemical analysis for excimer laser systems
[DE88-001941] 05 p0589 N88-13591

Sandia software guidelines: Software quality planning
[DE88-001931] 05 p0636 N88-13894

Flammability, smoke and toxicity test on fire barrier fabric from the Porcher company --- Airbus aircraft
[ETN-88-91168] 06 p0666 N88-14085

AVHRR/HIRS (Advanced Very High Resolution Radiometer/High Resolution Infra-Red Sounder) operational method for satellite based sea surface temperature determination
[PB88-107594] 06 p0708 N88-14340

On-site meteorological program guidance for regulatory modeling applications
[PB87-227542] 06 p0731 N88-14498

Reliability modelling for fault-tolerant parallel processor
[AD-A185867] 07 p0900 N88-15451

Solid mechanics research for quantitative non-destructive evaluation
[AD-A186599] 08 p0993 N88-16010

Spacelab Data Processing Facility (SLDPF) quality assurance expert systems development
08 p1059 N88-16394

Photoluminescence study of InP surfaces and InP-insulator interfaces
[ECL-87-13] 08 p1089 N88-16555

ESTEC's product assurance activities
09 p1125 N88-16739

Training guidelines in non-destructive testing techniques
[DE88-700613] 10 p1342 N88-18019

Analysis and application of the constant tensile load test for polyethylene gas pipe materials
[DE88-002868] 10 p1345 N88-18037

A method for assessing the software engineering capability of contractors: Preliminary version
[AD-A187230] 10 p1388 N88-18290

Quality assurance of ceramic materials and gas turbine components
[IZFP-850303-TW] 11 p1465 N88-18735

Novel analytical X-ray Non-Destructive Evaluation (NDE) tool for quality control of energetic materials
[AD-A187737] 11 p1497 N88-18935

Random vibration (stress screening) of printed wiring assemblies 11 p1499 N88-18953

Quality control of upper air conventional data (TEMP and PILOT)
[INPE-4223-RPE/546] 12 p1647 N88-19862

Critical comparison of moving average and cumulative summation control charts for trace analysis data
[AD-A188312] 12 p1705 N88-20203

Quality enhancement with machine intelligence
[DE88-005639] 13 p1824 N88-20901

Electron beam sensitive devices for controllability
[RR-658-I] 14 p1906 N88-21403

Software quality assurance workstation
[P-1124/RT-14791] 14 p1957 N88-21670

Information systems for quality. Experience at the Nerviano Aeritalia plant. Avionic systems and equipment group
[ETN-88-92274] 15 p2148 N88-22821

Systems engineering technique
17 p2303 N88-23776

A quality philosophy for research and development
[DE88-006512] 18 p2524 N88-24977

Proposed quality assurance/quality control plan
[AD-A191490] 18 p2525 N88-24978

Quality and productivity drive innovation and improvement at United Technologies Aerospace Operations, Inc.
[NASA-CR-182944] 18 p2525 N88-24983

Study of Staebler-Wronsky degradation effect in a Si:H based P-I-N solar cells
[NASA-CR-182564] 19 p2687 N88-25970

Analytical determination of critical crack size in solar cells
[NASA-CR-183128] 20 p2821 N88-26736

Milliwatt generator project
[DE88-011261] 20 p2853 N88-26939

Optical characterization of silica aerogel
[DE88-008916] 20 p2854 N88-26946

Measuring dispersion effects of factors in factorial experiments
[AD-A193216] 21 p3006 N88-27831

Direct and inverse diffraction problems for QNDE (Quantitative Non-Destructive Evaluation) applications
[AD-A194721] 22 p3085 N88-28322

Quality of SPOT images 22 p3115 N88-28506

Effect of fiber diameter on the reliability of composites - automated laser diffraction implementation
[AD-A193524] 23 p3188 N88-28972

Qualification of expansion and welding procedures of tube-to-tubesheet joints for heat exchangers in nuclear power plants
[DE88-701621] 23 p3221 N88-29174

Material and process selection and quality control for ESA space systems and associated equipment
[ESA-PSS-01-70-ISSUE-3] 23 p3224 N88-29190

Quality control in microbiology: CDC lab manual
[PB88-179890] 23 p3237 N88-29263

Topics in adaptive control and inference
[AD-A194718] 23 p3266 N88-29443

Quality measures and assurance for AI (Artificial intelligence) software
[NASA-CR-4187] 24 p3411 N88-30304

QUALITY FACTORS

U Q FACTORS

QUANTILES

Quantile based unified distribution of extreme values and order statistics
[AD-A185171] 05 p0644 N88-13942

Quantile statistical data analysis
[AD-A185181] 05 p0644 N88-13943

A modified kernel quantile estimator under censoring
[AD-A186364] 07 p0911 N88-15525

A smooth nonparametric quantile estimator from right-censored data
[AD-A186180] 07 p0915 N88-15552

A generalized quantile estimator under censoring
[AD-A188260] 10 p1402 N88-18364

Large quantile estimation under extreme-value conditions
[CWI-MS-R8711] 14 p1966 N88-21730

Use of principal component method for analysis of multidimensional quantitative data in biomedical investigations 19 p2706 N88-26089

Joint asymptotic distribution of marginal quantiles and quantile functions in samples from a multivariate population
[AD-A193385] 21 p3010 N88-27856

QUANTITATIVE ANALYSIS

Auger electron spectroscopy of oxidized titanium overlayers: Speciation of homogeneous and heterogeneous samples
[KFK-4221] 02 p0146 N88-10913

Cooperative analysis of zirconium and zirconium alloys by fluorescent X-ray method
[DE87-753011] 02 p0148 N88-10926

Small-Angle Neutron Scattering (SANS) from polymers and colloids
[DE87-013548] 02 p0151 N88-10946

Design of an elemental analysis system for CELSS research 03 p0360 N88-12266

Studies on estimation of nickel in zinc base die casting by D.C. polarography
[PD-MT-8729] 04 p0417 N88-12588

Solid state C-13 NMR characterization of textiles: Qualitative and quantitative analysis
[AD-A184349] 04 p0419 N88-12598

Abundance and distribution of ultramafic microbreccia in Moses Rock Dike: Quantitative application of AIS data
05 p0613 N88-13766

Characterization of microstructure in metallic and composite materials
[AD-A186193] 07 p0826 N88-15012

Studies of supported metal catalysts
[DE88-002546] 07 p0831 N88-15036

Quantitative non-destructive evaluation of porous composite materials based on ultrasonic wave propagation
[NASA-CR-182544] 11 p1447 N88-18627

Procedures for quantitative sensitivity and performance validation studies of a deterministic fire safety model
[NBS/GCR-88/544] 11 p1469 N88-18762

Multicomponent analysis using synchronous-excitation phase-resolved fluorescence spectroscopy
[AD-A188663] 12 p1606 N88-19604

Quantitative determination of a hydrogen impurity in a sodium coolant by hydride thermal dissociation
[NASA-TT-20239] 13 p1740 N88-20402

Computer program in BASIC language for computation of spectrochemical analytical data
[DE88-701229] 15 p2032 N88-22106

Clinical measurements using fiber optic sensors
[DE88-005624] 15 p2134 N88-22731

The use of a water towing tank for aerodynamic testing and methods for quantitative evaluation of photographs
16 p2202 N88-23140

Development of an automated X-ray gauge for nondestructive quantitative analysis
[DE88-008633] 20 p2812 N88-26681

Direct determination of part-per-billion levels of volatile organics in water and soil samples using glow discharge mass spectrometry
[DE88-011389] 21 p2910 N88-27272

The electromagnetic spectrum: The information mine
[AD-A194316] 22 p3069 N88-28215

A method for the quantitative determination of crystalline phases by X-ray
[NASA-TT-20324] 24 p3434 N88-30444

QUANTIZATION

U MEASUREMENT

QUANTIZER

U COUNTERS

QUANTUM CHEMISTRY

A quantum theoretical study of polyimides
[NASA-CR-181495] 03 p0292 N88-11831

The Coupled Cluster Single and Double excitation (CCSD) method in quantum chemistry: An efficient formulation of the theory and application to closed shell molecular systems
[DE88-000475] 07 p0930 N88-15650

Clusters: Link between molecules and solids
[AD-A188170] 11 p1543 N88-19224

Quantum Monte Carlo study of the MIES associated with H2(X 1 sigma g +) and H2(B 1 sigma u +)
16 p2268 N88-23564

Gas phase combustion chemistry of nitramine propellants
[AD-A195082] 24 p3344 N88-29902

QUANTUM CHROMODYNAMICS
NT INSTANTONS
An introduction to charm and heavy quark physics
[DE87-013589] 02 p0231 N88-11455
Research program in elementary particle theory
[DE88-000159] 02 p0233 N88-11486
Scalar densities and baryon mass differences in lattice QCD with Wilson fermions
[PREPRINT-544] 06 p0778 N88-14773
The approach to equilibrium in a quark-gluon plasma
[DE88-002117] 09 p1251 N88-17499
Status of the electroweak theory
[DE88-002342] 10 p1422 N88-18494
Negative-energy quanta
[DE88-700904] 12 p1689 N88-20101
Diffraction theory in QCD and beyond
[DE88-005958] 13 p1837 N88-20992
Lattice QCD calculation of K yields pi nonleptonic weak transition and other hadronic weak parameters
[PREPRINT-580] 15 p2132 N88-22717
Computational quantum field theory
[DE88-700918] 16 p2284 N88-23672
Color charge motion in non-Abelian fields
[DE88-701306] 19 p2642 N88-25672
Comparison of exclusive reactions at large momentum transfer
[DE88-007544] 20 p2851 N88-26922
Theoretical studies in elementary particle physics
[DE88-006929] 20 p2851 N88-26926
An overview of lattice QCD
[DE88-010867] 21 p3026 N88-27963
Theoretical studies in high energy physics
[DE88-011606] 23 p3281 N88-29538
Theoretical particle physics
[DE88-011499] 23 p3295 N88-29621
Resonant spin-flavor precession of solar and supernova neutrinos
[DE88-752604] 23 p3308 N88-29707
QUANTUM EFFICIENCY
Detective quantum efficiency and design of a parallel data recording system for EXELFS-measurements --- electron microscopy
[USIP-87-06] 01 p0050 N88-10318
Study of solid state photomultiplier
[NASA-CR-177465] 05 p0583 N88-13556
Area detectors for X-ray spectroscopy
[DE88-001429] 06 p0679 N88-14163
Performance of a photon counting microchannel plate intensifier with wedge and strip image readout
[DE88-003831] 10 p1334 N88-17970
Low threshold ridge waveguide single quantum well lasers 13 p1777 N88-20631
Quantum nondemolition detection and squeezing in optical fibers 14 p1976 N88-21793
Results from the SLAC lasertron
[DE88-007816] 20 p2806 N88-26647
High performance charge transfer device detectors
[AD-A194409] 23 p3192 N88-28993
QUANTUM ELECTRODYNAMICS
LLE review
[DE87-014468] 02 p0178 N88-11110
Proceedings of the Workshop on Opportunities for Atomic Physics Using Slow, Highly-Charged Ions
[DE87-013991] 02 p0231 N88-11457
Quantum electrodynamics based on self-energy: Spontaneous emission in cavities
[DE87-703071] 02 p0232 N88-11461
QED description of relativistic Coulomb excitation in heavy ion collisions
[DE88-700834] 12 p1689 N88-20100
Negative-energy quanta
[DE88-700904] 12 p1689 N88-20101
Solid state research
[AD-A188388] 12 p1699 N88-20166
Chiral symmetry breaking in finite quantum electrodynamics
[DE88-700860] 12 p1699 N88-20169
Quantization of axial electrodynamics
[DE88-701498] 15 p2147 N88-22813
Research in the optical sciences
[AD-A192175] 18 p2575 N88-25297
Nonlinear dynamics of the electron self-field interaction
[DE88-010597] 21 p2934 N88-27420
Infrared detection using Rydberg atoms
[AD-A194308] 23 p3191 N88-28990
Relativistic theory of the Lamb shift based on self energy
[DE88-702658] 23 p3295 N88-29626
QUANTUM ELECTRONICS
Numerical studies of the dual HEMT/algorithm development and numerical studies of Schrodinger's equation
[AD-A184471] 04 p0478 N88-12946
Development and study of fibre-optic link lines on the basis of the KEM-8-4PD, KEM-8-4PR quantum-electronic modules
[DE88-700372] 07 p0932 N88-15663
Nanoelectronics
[AD-A186969] 09 p1156 N88-16930
Solid state research
[AD-A185987] 09 p1253 N88-17508
Molecular beam epitaxy for research on quantum well structures
[AD-A186791] 09 p1255 N88-17522
Microwave semiconductor research-materials, devices and circuits
[AD-A187121] 10 p1415 N88-18444
Joint services electronics program
[AD-A189262] 13 p1761 N88-20533
Theory of interactions of intense light with nonlinear, inhomogeneous and periodic structures and its applications to optical bistability, optic gyroscopes, nonlinear spectroscopy, radiation protection, X-ray emission and related fields
[AD-A190040] 15 p2133 N88-22725
Fluxons and order in long Josephson junctions
[AD-A190879] 16 p2282 N88-23665
Joint services electronics program
[AD-A192076] 18 p2504 N88-24856
Joint services electronics program research in electronics
[AD-A192206] 18 p2504 N88-24857
Random quantum interference in microdevices
20 p2866 N88-27021
Defects and disorder in amorphous and damaged silicon
[AD-A192277] 20 p2879 N88-27089
Solid state research
[AD-A192837] 21 p3020 N88-27929
Spectroscopic studies with multiple quantum well materials with applications to optical signal processing at room temperature
[AD-A194171] 24 p3429 N88-30409
QUANTUM GENERATORS
U STIMULATED EMISSION DEVICES
QUANTUM MECHANICS
NT PAULI EXCLUSION PRINCIPLE
NT QUANTUM ELECTRODYNAMICS
Quantum-mechanical aspects of classically chaotic driven systems
[DE87-013152] 02 p0178 N88-11106
Quantum mechanics with spontaneous localization and the quantum theory of measurement
[DE87-703072] 02 p0247 N88-11559
A study of mechanisms of hydrogen diffusion in separation devices
[DE88-000328] 04 p0416 N88-12584
Final (n,l) state-resolved electron capture by multiply charged ions from neutral atoms
[IPPJ-AM-54] 04 p0492 N88-13030
Theory of neutron scattering experiments on momentum distributions in quantum fluids
[DE87-01369] 05 p0648 N88-13968
Resonant level lifetime in GaAs/ AlGaAs double-barrier structures
[AD-A185376] 05 p0655 N88-14020
Example of correlation between space and spin coordinates
[DE87-703366] 05 p0657 N88-14030
A mechanism for symmetry breaking in antiferromagnetic Heisenberg systems
[ETN-88-91320] 05 p0657 N88-14031
Macroscopic quantum effects in a Josephson tunnel junction
[DE88-002239] 06 p0787 N88-14830
Group quantization of constrained systems
[PREPRINT-564] 06 p0790 N88-14844
Modified quantum mechanics of small composite systems
[NIKHEF-H/87-1] 06 p0790 N88-14845
Coherent states for the damped harmonic oscillator
[AD-A186111] 07 p0922 N88-15599
Core spline method for solution of quantum-mechanical systems of differential equations for bound states
[DE88-700492] 09 p1259 N88-17551
An overview of the transactional interpretation of quantum mechanics
[DE88-004236] 10 p1423 N88-18497
Fundamental properties of spin-polarized quantum systems
[DE88-004425] 10 p1423 N88-18499
SUSY anomaly in quantum-mechanical systems
[DE88-700890] 12 p1699 N88-20170
Gordon Conference on Intermetallic Compounds held at Tilton, New Hampshire on 20-24 July 1987
[AD-A188502] 13 p1745 N88-20435
Algebraic structure of linear and nonlinear models of open quantum systems
[PREPRINT-573] 14 p1968 N88-21747
Optical cooling and trapping 14 p1974 N88-21782
Dynamic and spectral properties of semiconductor lasers with quantum well, quantum wire, and quantum box structures 14 p1975 N88-21788
Squeezed state in degenerate parametric amplification discussed by H. Takahasi in 1963
14 p1976 N88-21790
Quantum nondemolition detection and squeezing in optical fibers 14 p1976 N88-21793
Berry's phase in fiber optics 14 p1977 N88-21797
Generation of number-phase minimum uncertainty states 14 p1978 N88-21803
Singular Lagrangians. Classical dynamics and quantization. Lectures for young scientists
[DE88-701158] 15 p2146 N88-22806
On the Hilbert space of supersymmetric quantum systems
[DE88-701648] 16 p2284 N88-23677
Modulation efficiency limited high frequency performance of the MODFET 19 p2657 N88-25786
Electron device probing in the femtosecond time scale
19 p2660 N88-25821
High resolution spectroscopy of dissociating molecules
[DE88-007959] 20 p2851 N88-26924
Quantum transport theory of resonant-tunneling heterostructure devices 20 p2865 N88-27017
Quantum interference and transport in microstructures
20 p2866 N88-27022
Combining relativity and quantum mechanics: Schroedinger's interpretation of psi
[DE88-701899] 20 p2880 N88-27102
Determination of quantum corrections for electrical conductivity mechanism of three dimensional, perturbed copper coatings. Weak localization and electron-electron interaction
[ETN-88-92378] 21 p2941 N88-27466
Evaluation of quantum mechanics path integrals by the approximations exact on a class of polynomial functionals
[DE88-702434] 21 p3011 N88-27865
Wigner distribution function: Relation to short-term spectral estimation, smoothing and performance in noise
[AD-A193865] 23 p3275 N88-29492
Investigation of non-classical effects in two-photon interference processes 23 p3282 N88-29541
QUANTUM OPTICS
Families of Bose rays in quantum optics
[DE87-014584] 02 p0236 N88-11489
Experimental observation of photoresonance of electrons localized above surface of solid hydrogen
06 p0774 N88-14755
Activities report in quantum optics
[ISSN-0177-0101] 09 p1248 N88-17482
QUANTUM STATISTICS
A problem in quantum probability --- statistical invariants problem
[REPT-87-06] 01 p0088 N88-10573
Families of Bose rays in quantum optics
[DE87-014584] 02 p0236 N88-11489
Regular effective action of gauge field theory and quantum gravity
[DE87-703076] 02 p0247 N88-11560
Electronic structure and phase stability of alloys
[DE88-004574] 11 p1562 N88-19350
Macroscopic quantum jumps in a single atom
14 p1975 N88-21784
Quantum statistics of parametric oscillators above threshold 14 p1979 N88-21811
QUANTUM THEORY
NT BOHR THEORY
Inequivalent quantizations and fundamentally perfect spaces
[DE87-014225] 02 p0229 N88-11446
Quantum mechanics with spontaneous localization and the quantum theory of measurement
[DE87-703072] 02 p0247 N88-11559
Regular effective action of gauge field theory and quantum gravity
[DE87-703076] 02 p0247 N88-11560
Program to development an optical transistor and switch
[AD-A185666] 06 p0697 N88-14278
Theoretical studies of kinetic mechanisms of negative ion formation in plasmas
[AD-A185735] 06 p0784 N88-14812
A simplified model of elementary particles
[NOTA-INTERNA-890] 07 p0930 N88-15647
Superstrings on quantum spacetime
[DE88-700106] 07 p0940 N88-15715
Instanton in supersymmetric theory with static disorder
[DE88-700357] 07 p0940 N88-15716
Activities report in quantum optics
[ISSN-0177-0101] 09 p1248 N88-17482
Research in theoretical physics
[DE88-003201] 09 p1259 N88-17546

Study of quantum mechanical effects in deep submicron, grating-gate field effect transistors
[AD-A188283] 10 p1325 N88-17923

Antimatter: Its history and its properties
[DE88-004306] 10 p1423 N88-18498

Quantum limits of superconducting heterodyne receivers
[AD-A188014] 11 p1478 N88-18817

Semileptonic weak interactions in nuclei: A relativistic analysis
[CEBAF-PR-87-024] 11 p1547 N88-19249

Generalised scattering model for the quantum modulation of electrons 11 p1563 N88-19357

On exterior variational calculus
[DE88-700861] 12 p1683 N88-20062

Topics in string theory: Task D
[DE88-004532] 12 p1699 N88-20167

Generalized Levinson's theorem and quantum sticking coefficients at O K
[AD-A189371] 12 p1699 N88-20171

Spontaneous decay and atomic fluorescence near a metal surface of an absorbing dielectric
[AD-A187508] 13 p1835 N88-20975

Quantum Monte Carlo study of the MIES associated with H2 (X 1 sigma sub g (+)) and H2 (B 1 sigma sub u (+))
[AD-A189063] 13 p1835 N88-20977

Algebraic structure of linear and nonlinear models of open quantum systems
[PREPRINT-573] 14 p1968 N88-21747

Super Virasoro algebra and solvable supersymmetric quantum field theories
[DE88-752299] 15 p2127 N88-22681

To the field theory with a fundamental mass
[DE88-701159] 15 p2146 N88-22807

Free Laplacian with attractive boundary conditions
[DE87-702971] 16 p2256 N88-23482

On a generalization of renormalization group equations to quantum field theories of an arbitrary type
[DE88-701143] 16 p2263 N88-23531

Fluxons and order in long Josephson junctions
[AD-A190879] 16 p2282 N88-23665

Electrical resistivity as quantum chaos
[DE88-007026] 16 p2284 N88-23675

Joint services electronics program
[AD-A190239] 18 p2503 N88-24848

Quantum gravity and new forces
[DE88-007829] 19 p2737 N88-26250

Transcending Newton's legacy
[DE88-010784] 19 p2738 N88-26254

Cosmic wavefunction with induced gravity
[DE88-701873] 20 p2884 N88-27129

Superalgebras with Grassmann algebra-valued structure constants from superfields
[DE88-702239] 21 p3011 N88-27862

Quark nuclear model: Classification groups and two and three body correlations
[NOTA-INTERNA-896] 21 p3014 N88-27891

Gravitation and electromagnetism
22 p3158 N88-28792

Infrared detection using Rydberg atoms
[AD-A194308] 23 p3191 N88-28990

CryoSQUID: A SQUID-based magnetic field sensor
[AD-A194237] 23 p3239 N88-29275

On nonlinear equations admitting soliton solutions with a deBroglie phase
[DE88-702694] 23 p3277 N88-29508

Towards a finite quantum gravity
[DE88-701497] 23 p3294 N88-29619

On the meaning of perturbation expansions in quantum field theory
[DE88-702138] 23 p3294 N88-29620

Chaotic behaviour in quantum dynamics
[AD-A193936] 23 p3295 N88-29623

QUANTUM WELLS

Quantum well laser diodes: Modeling and realization of GaAs/GaAlAs
[LAAS-87-165] 02 p0179 N88-11116

Phase-locked semiconductor quantum well laser arrays
[AD-A185155] 05 p0588 N88-13583

Impurity bands in quantum wells
[INPE-4250-PRE/1123] 08 p1089 N88-16552

Diagonal and off-diagonal disorder in doped quantum wells
[INPE-4255-PRE/1128] 08 p1089 N88-16556

Density of states of electrons bound to impurities in quantum wells of GaAlAs/GaAs
[INPE-4257-PRE/1130] 08 p1089 N88-16557

Low threshold ridge waveguide single quantum well lasers 13 p1777 N88-20631

Energy loss rates for light holes in InGaAs/GaAs strained layer single quantum wells
[DE88-005744] 13 p1848 N88-21062

Measurements of optical nonlinearities in MOCVD-grown GaAs/GaAlAs multiple quantum wells
14 p1975 N88-21787

Dynamic and spectral properties of semiconductor lasers with quantum well, quantum wire, and quantum box structures 14 p1975 N88-21788

Optical properties of quantum well structures with electric field: Life time free switching of luminescence intensity and virtual charge-induced ultrafast optical nonlinearity 14 p1976 N88-21794

High density femtosecond excitation of nonthermal carrier distributions in intrinsic and modulation doped GaAs quantum wells 14 p1977 N88-21798

Research on materials and components for opto-electronic signal processing and computing
[AD-A190130] 15 p2143 N88-22788

Local density of states in double-barrier resonant tunneling structures
[AD-A190673] 16 p2281 N88-23656

Optical properties of heterostructures and superlattices
[AD-A191542] 18 p2581 N88-25335

Optical nonlinearities in GaAs/GaAlAs multiple quantum wells fabricated by metalorganic chemical vapor deposition for use in optical signal processing
[AD-A191558] 18 p2582 N88-25337

Molecular Beam Epitaxy (MBE) for high speed devices
19 p2656 N88-25770

A proposed Quantum Well Injection Transit Time device (QWITT) 19 p2657 N88-25785

Frequency chirping in pulse modulated gain and real index guided single quantum well lasers
19 p2658 N88-25798

High-speed phenomena in GaAs multiple-quantum-wells 19 p2660 N88-25812

Picosecond carrier transport in GaAs quantum wells
19 p2660 N88-25813

Quantum-confined stark effect in InGaAs/InP quantum wells grown by metal-organic chemical vapor deposition
19 p2660 N88-25814

Dynamics of below-gap photoexcitation in GaAs quantum wells 19 p2660 N88-25815

Nonlinear optical properties and subpicosecond dynamics of excitons and electron-hole plasmas in multiple quantum well structures
[AD-A191926] 19 p2727 N88-26196

Far-infrared studies of doped AlGaAs/GaAs multiple-quantum-well structures
20 p2862 N88-26998

Electro-optical studies of Al(x)Ga(1-x)As/GaAs coupled quantum wells 20 p2862 N88-26999

Quantum wells and bulk AlGaAs under hydrostatic pressure 20 p2862 N88-27000

Auger recombination in GaSb/AlSb-multi quantum well heterostructures 20 p2862 N88-27001

Ultrafast optical nonlinearity in quantum well structures with electric field 20 p2863 N88-27003

Strained layer and lattice matched transverse junction stripe quantum well lasers for continuous room temperature operation 20 p2863 N88-27004

Quantum transport theory of resonant-tunneling heterostructure devices 20 p2865 N88-27017

Superlattice doping interfaces
20 p2866 N88-27019

Excitonic properties of GaAs-AlGaAs nanostructures
20 p2867 N88-27023

A 10 microns photoexcited avalanche gain due to electron impact ionization from GaAs quantum well superlattices 20 p2867 N88-27026

Novel quantum well optical devices
20 p2868 N88-27028

Direct imaging of the columnar structure of GaAs quantum wells 20 p2868 N88-27030

Monte Carlo simulations of femtosecond relaxation of photoexcited electrons in AlGaAs/GaAs quantum wells
20 p2869 N88-27036

Electron-phonon interactions in In(0.53)Ga(0.47)As and in In(0.53)Ga(0.47)As/InP quantum wells
20 p2869 N88-27037

Electronic structure of quantum-well states revealed under high pressures 20 p2870 N88-27038

Magneto-optical studies of GaInAs-InP quantum wells
20 p2870 N88-27039

On a-Si:H/a-SiN(x):H superlattices: Confinement or contamination 20 p2870 N88-27040

Direct measurement of ultrafast electron-hole plasma expansion at high density at an asymmetric GaAs quantum well 20 p2871 N88-27044

Solar energy conversion through the interaction of plasmons with tunnel junctions. Part A: Solar cell analysis. Part B: Photoconductor analysis
[NASA-CR-183044] 21 p2967 N88-27621

Ultrafast physics in semiconductor microstructures
[AD-A193300] 21 p3022 N88-27936

Laser spectroscopy of quantum well and superlattice structures
[AD-A193336] 21 p3022 N88-27937

A study of tunneling phenomena in gallium arsenide-aluminum gallium arsenide heterostructures
21 p3023 N88-27946

Infrared devices using semiconductor quantum wells
[RSRE-MEMO-4016] 22 p3157 N88-28788

Studies on strained (In,Ga)As/GaAs semiconductors and optical devices 23 p3287 N88-29575

Spectroscopic studies with multiple quantum well materials with applications to optical signal processing at room temperature
[AD-A194171] 24 p3429 N88-30409

QUARK MODELS

Quark nuclear model: Classification groups and two and three body correlations
[NOTA-INTERNA-896] 21 p3014 N88-27891

QUARKS

An introduction to charm and heavy quark physics
[DE87-013589] 02 p0231 N88-11455

Single leptons from heavy quark production
[DE87-014917] 04 p0488 N88-13009

The approach to equilibrium in a quark-gluon plasma
[DE88-002117] 09 p1251 N88-17499

Zero temperature quark matter equation of state
[DE88-003408] 10 p1422 N88-18496

Hadron-quark phase transition in dense stars
[DE88-003412] 10 p1429 N88-18532

Quark matter in astrophysics and cosmology
[DE88-003406] 10 p1429 N88-18534

Proton/antiproton yields $W_{(+/-)}$boson gamma X as a test of the quark charges
[NIKHEF-H/87-11] 13 p1836 N88-20987

Quark core stars, quark stars and strange stars
[DE88-006991] 17 p2450 N88-24555

Accuracy of analytic energy level formulas applied to hadronic spectroscopy of heavy mesons
[NASA-TM-4042] 19 p2725 N88-26185

Theoretical studies in elementary particle physics
[DE88-006929] 20 p2851 N88-26926

Strange, quark and metastable neutron stars
[DE88-702404] 21 p3030 N88-27984

Theory of quark mixing matrix and invariant functions of mass matrices
[USIP-87-14] 22 p3159 N88-28800

QUARRIES

U MINES (EXCAVATIONS)

QUARTZ

The use of optical fibers for shock pressure and timing measurements at high pressures
[DE88-004012] 10 p1334 N88-17971

Quartz oscillator analysis
[DE88-005886] 13 p1764 N88-20550

QUARTZ CRYSTALS

Aerosol sensor: Real time determination of aerosol mass size distributors using filtering quartz oscillators
[ETN-87-90397] 01 p0049 N88-10311

Defect characterization in quartz and related materials
[AD-A184754] 03 p0294 N88-11846

Quartz crystal resonators and oscillators for frequency control and timing applications
[AD-A193310] 21 p2937 N88-27443

Acoustic-optical detector of gravitational waves based on high-quality crystals
[DE88-702459] 23 p3232 N88-29232

QUARTZ LAMPS

Evaluation and certification of heater assemblies developed for thermal vacuum acceptance testing
02 p0136 N88-10853

A new type of lamp and reflector for I.R. simulation
02 p0136 N88-10855

QUARTZ TRANSDUCERS

Calibration of quartz load cells: An in-situ procedure for instrumented falling weight impact machines
[NPL-DMA(A)-155] 22 p3081 N88-28297

QUASARS

Extragalactic VLBI objects: Candidates for optical interferometry? 01 p0094 N88-10616

Galactic nuclei and quasars at high angular resolution
01 p0098 N88-10644

Spherical models of QSO/AGN emission line clouds
06 p0806 N88-14921

Finnish-Soviet Symposium on Radio Astronomy (1st) held at Otaniemi on August 26-27, 1985
[PB87-140661] 07 p0944 N88-15736

Prediction and analysis of basic gravitational microlensing phenomena 11 p1550 N88-19272

Data analysis of an observation of the quasar 3C 273 in the high-energy X-ray range, and the significance for astrophysical models
[ETN-88-91493] 14 p1993 N88-21878

Is the 3C273 quasar Mach nearer
[DE88-702235] 21 p3030 N88-27988

Detection of abundant molecular gas in the UV-excess quasar Mrk 1014 22 p3164 N88-28842

QUASI-PARTICLES
U ELEMENTARY EXCITATIONS

QUASI-STEADY STATES
Investigation of the quasi-steady approach used in transient two-phase flow analysis
[DE88-004303] 21 p2944 N88-27489

QUASI-STELLAR RADIO SOURCES
U QUASARS

QUASILINEARITY
U NONLINEARITY

QUATERNARY ALLOYS
Cadmium sulfide/copper ternary heterojunction cell research
[DE88-001122] 13 p1793 N88-20727
Development of microencapsulated DNBM quaternary ammonium inhibitors for paints
17 p2319 N88-23851
Photoluminescence studies of InGaAlAs quaternary alloys
[DE88-007197] 20 p2874 N88-27062

QUENCHING
On quench sensitivity of Cu-Cr alloys
[NASA-TT-20174] 18 p2489 N88-24765

QUENCHING (ATOMIC PHYSICS)
Quenched-laser operation of a Littman dye oscillator
[DE88-004020] 11 p1493 N88-18915
A new fiber-optic-based ion sensor
[AD-A191322] 16 p2274 N88-23612

QUENCHING (COOLING)
Investigation of rapidly-solidified dispersion strengthened titanium alloys
[AD-A183882] 01 p0022 N88-10140
Strain rate effects in fast-gas-cooled uranium-titanium and uranium-niobium alloys
[OUEL-1683/87] 02 p0149 N88-10937
Simulation of thermo-mechanical forming processes: A mixed Eulerian-Langrangian finite element method
[PB88-155247] 14 p1933 N88-21530
Critical cooling rates on solution treatment of Cu-Cr and Cu-Be alloys
[NASA-TT-20163] 18 p2488 N88-24760
The T-T-T curve in Cu-Cr alloy
[NASA-TT-20167] 20 p2774 N88-26453
Estimation of transient heat transfer coefficients in multidimensional problems by using inverse heat transfer methods 23 p3210 N88-29108

QUERY LANGUAGES
Distributed query processing: Present status and future direction 10 p1377 N88-18219
Reference model for DBMS (database management system) user facility
[PB88-169446] 13 p1851 N88-21080
The SAGE geographic analysis system
17 p2361 N88-24063
Using common subexpressions to optimize multiple queries
[DE88-008210] 20 p2844 N88-26877
Optimization techniques for relational database systems 22 p3137 N88-28650
Level 1 Ada/SQL (Structured Query Language) database language interface user's guide
[AD-A194480] 23 p3249 N88-29335

QUEUEING THEORY
Efficiency analysis of airborne Electronic CounterMeasures (ECM) systems
[AD-A184606] 03 p0306 N88-11934
The network queueing system
[NASA-CR-177433] 03 p0365 N88-12297
Heterogeneous multi-trunking queueing systems
[AD-A184255] 04 p0431 N88-12668
Waiting times in discrete-time cyclic-service systems — communication networks
[CWI-OS-R8707] 08 p0977 N88-15909
Sojourn times in the M/G/1 queue with deterministic feedback
[CWI-OS-R8708] 08 p1074 N88-16479
A note on the effect of preemptive policies on the stability of a priority queue
[AD-A186671] 09 p1227 N88-17345
A queueing system with independent Markov input streams
[AD-A187601] 10 p1402 N88-18363
Sojourn times in feedback queues
[CWI-OS-R8710] 13 p1830 N88-20947
Two queues with alternating service and switching times
[CWI-OS-R8712] 13 p1831 N88-20949
Impact of blocking policies in closed, exponential and symmetrical ring networks
[FUB-8-1986] 14 p1960 N88-21693
Tape versus queue and stacks: The lower bounds
[CWI-CS-R87[illegible]2] 16 p2249 N88-23437
A queueing network model for analyzing a class of branch and bound algorithms on a master-slave architecture
[CWI-OS-R8717] 16 p2249 N88-23441
Power series for stationary distributions of coupled processor models
[REPT-87-70] 16 p2254 N88-23470
Parallel discrete-event simulation of FCFS stochastic queueing networks
[NASA-CR-181669] 17 p2389 N88-24203
Poisson functionals of Markov processes and queueing networks
[AD-A191217] 18 p2568 N88-25252
Three-dimensional scene analysis using stero based imaging
[AD-A193120] 21 p2894 N88-271/8
Queueing network models for parallel processing of task systems: An operational approach
[NASA-CR-183174] 22 p3141 N88-28677
Poisson functionals of Markov processes and queueing networks
[AD-A194289] 22 p3145 N88-28705
Relaxed heaps: An alternative to fibonacci heaps
[AD-A194030] 23 p3272 N88-29470
Performance prediction of concurrent systems
[NASA-CR-183175] 24 p3412 N88-30312

QUIET ENGINE PROGRAM
Flight researh at NASA Ames Research Center: A test pilot's perspective
[NASA-TM-100025] 02 p0125 N88-10788

QUINOLINE
Electrochemistry in near-critical and supercritical fluids. 5: The dimerization of quinoline and acridine radical anions and dianions in ammonia from -70 C to 150 C
[AD-A190858] 16 p2175 N88-22967
The thermodynamic properties of quinoline and isoquinoline
[DE88-001218] 18 p2484 N88-24735

R

RACE FACTORS
A national model at Howard University demonstrating private sector interrelationships that facilitate research in predominantly Black colleges and universities
[DE88-000160] 04 p0502 N88-13089

RACON BEACONS
U RADAR BEACONS

RADAR
NT AIRBORNE SURVEILLANCE RADAR
NT COHERENT RADAR
NT CONTINUOUS WAVE RADAR
NT DOPPLER RADAR
NT EISCAT RADAR SYSTEM (EUROPE)
NT IMAGING RADAR
NT INCOHERENT SCATTER RADAR
NT INFRARED RADAR
NT METEOROLOGICAL RADAR
NT MONOPULSE RADAR
NT MOVING TARGET INDICATORS
NT MULTISTATIC RADAR
NT OPTICAL RADAR
NT OVER-THE-HORIZON RADAR
NT PULSE RADAR
NT RADAR MEASUREMENT
NT RANGE AND RANGE RATE TRACKING
NT SATELLITE-BORNE RADAR
NT SEARCH RADAR
NT SECONDARY RADAR
NT SIDE-LOOKING RADAR
NT SPACE BASED RADAR
NT SURVEILLANCE RADAR
NT SYNTHETIC APERTURE RADAR
Collection and analysis of specific ELINT Signal Parameters
[NASA-CR-181419] 01 p0033 N88-10213
JPRS report: Science and technology. China
[JPRS-CST-87-031] 03 p0299 N88-11880
Radar ECCM's new area: Anti-STEALTH and anti-ARM 03 p0299 N88-11881
On M-ARY sequential hypotheses testing for the classification of radar signals
[AD-A184094] 04 p0430 N88-12666
Correlation between refraction over sea and nature of radar reflections from sea surface
06 p0728 N88-14477
FAA air traffic control operations concepts. Volume 1: ATC background and analysis methodology
[AD-A185979] 07 p0818 N88-14973
TRACKER: A 3-D radio ray tracing code
[DE88-003267] 07 p0847 N88-15137
The design and implementation of surface acoustic wave devices for linear FM and a new non-linear FM pulse compression technique for radar applications
[AD-A186741] 08 p0980 N88-15922
Active and passive remote sensing of ice
[AD-A186685] 09 p1195 N88-17162
Wind shear radar simulation 10 p1274 N88-17625
Terrestrial Propagation Characteristics in Modern Systems of Communications, Surveillance, Guidance and Control
[AGARD-CP-407] 12 p1614 N88-19653
Radio and radar holes and multipath zones: The global and local influences on atmospheric refractive structure and resulting adverse radio and radar performance
12 p1617 N88-19667
Aircrew training devices: Utility and utilization of advanced instructional features, phase 4
[AD-A188418] 12 p1670 N88-20000
Simulation of effect of anti-radar stealth principle
13 p1755 N88-20496
Signal-filter design and system performance for polarimetric radar
[AD-A189257] 13 p1758 N88-20514
Modification of the BLUEMAX 2 terrain following model to incorporate radar detection
[AD-A190594] 15 p2017 N88-22028
High speed transcendental elementary function architecture in support of the Vector Wave Equation (VWE)
[AD-A189746] 15 p2119 N88-22627
The integration, characterisation and trialling of a modern complex airborne radar 17 p2305 N88-23791
High resolution radar techniques: Five contributions to MILINF 86
[PB88-172721] 18 p2498 N88-24821
Radio-wave scintillations and ionospheric irregularities at high latitudes
[AD-A192140] 18 p2501 N88-24837
The effects of better environmental inputs in estimating sea clutter
[AD-A192058] 19 p2643 N88-25678
Radar and EW applications of multi-gigahertz optical components and systems 19 p2660 N88-25816
Activities report of the Division of Reconnaissance and Seeker Systems
[FOA-C-30479-3.1/3.2/3.3/3.4]
22 p3116 N88-28513
Signal processing software for ground penetrating radar, user's manual
[AD-A194286] 23 p3203 N88-29059
Basic research in electronics (JSEP) Joint Services Electronics Program
[AD-A193072] 23 p3206 N88-29079
Scattering impulse response synthesis using random noise illumination: Initial concept evaluation
[AD-A195086] 24 p3364 N88-30034
Microwave remote sensing at INPE (Institute for Space Research) Brazil: Concepts and future prospects of soil moisture studies
[INPE-4569-PRE/1310] 24 p3388 N88-30178
The surface evaporative duct height product: An evaluation
[AD-A195918] 24 p3392 N88-30199
Validate algorithms for the determination of rainfall rates from SSM/I microwave satellite imagery
[AD-A195428] 24 p3404 N88-30270

RADAR ABSORBERS
NT ANTIRADAR COATINGS
The Soviet Stealth fighter: Check or checkmate
[AD-A195200] 24 p3323 N88-29791

RADAR ALTIMETERS
U RADIO ALTIMETERS

RADAR BEACONS
Analysis of ATCRBS (Air Traffic Control Radar Beacon System), mode select (Mode S) in combat operations
[AD-A193140] 22 p3040 N88-28050

RADAR BEAMS
Validate algorithms for the determination of rainfall rates from SSM/I microwave satellite imagery
[AD-A191337] 16 p2236 N88-23353
Automated test device for FASR (Fixed Array Surveillance Radar) beam steering componentry
[AD-A191650] 18 p2500 N88-24829
Utilization of a single clear-air Doppler radar beam to measure vertical divergence
[AD-A195543] 24 p3405 N88-30271

RADAR CLUTTER MAPS
TDWR (Terminal Doppler Weather Radar) clutter residue map generation and usage
[AD-A191148] 16 p2235 N98-23352

RADAR CORNER REFLECTORS
Scattering patterns of dihedral corner reflectors with impedance surface impedances
[NASA-CR-183078] 20 p2789 N88-26545

RADAR CROSS SECTIONS
Backscatter from a periodic rough surface at near grazing incidence
[NASA-CR-182397] 07 p0845 N88-15128
A study of Radar Cross Section (RCS) characteristics and their application in future weapon systems
[ETN-88-92081] 14 p1906 N88-21390

Modification of the BLUEMAX 2 terrain following model to incorporate radar detection
[AD-A190594] 15 p2017 N88-22028

High speed transcendental elementary function architecture in support of the Vector Wave Equation (VWE)
[AD-A189745] 15 p2119 N88-22627

The radar cross section of some simple reflectors at short wavelengths
[FOA-C-30472-3.3] 18 p2501 N88-24839

Almond test body --- for microwave anechoic chambers
[NASA-CASE-LAR-13747-1] 18 p2502 N88-24845

Microwave image understanding and its application to radar cross section management
20 p2788 N88-26542

Scattering patterns of dihedral corner reflectors with impedance surface impedances
[NASA-CR-183078] 20 p2789 N88-26545

Radar cross section studies/compact range research
[NASA-CR-183124] 20 p2792 N88-26565

Definition of long ocean wave slope for radar applications
[AD-A193198] 21 p2933 N88-27412

Effect of phase errors in stepped-frequency radar systems
[AD-A194476] 23 p3203 N88-29061

Comparative analysis of passive communications satellites employing the SHF and HF spectrum for use in a strategic role
[AD-A194682] 24 p3362 N88-30019

Measurement and interpretation of North Atlantic Ocean marine radar sea scatter
[AD-A196239] 24 p3364 N88-30036

Analysis of environmental parameters from the Panama City tower radar experiment
[AD-A194994] 24 p3404 N88-30264

RADAR DATA

Data analysis at the Oulu (Finland) EISCAT laboratory
06 p0691 N88-14241

Study of synthetic aperture radar data compression and encoding. Part 3: Performance evaluation of speckle suppression and data compression algorithms
[NLR-TR-85085-L-PT-3] 06 p0692 N88-14248

Study of synthetic aperture radar data compression and encoding. Part 4: Algorithm implementation aspects
[NLR-TR-85085-L-PT-4] 06 p0692 N88-14249

Flightpath reconstruction and systematic radar error estimation from multiradar range-azimuth measurements
[NLR-MP-85064-U] 06 p0693 N88-14251

Study of synthetic aperture radar data compression and encoding. Part 1: SAR image data analysis
[NLR-TR-85085-L-PT-1] 07 p0843 N88-15115

Study of synthetic aperture radar data compression and encoding. Part 2: SAR image speckle suppression and data compression algorithms
[NLR-TR-85085-L-PT-2] 07 p0843 N88-15116

Improved resolution atmospheric density measurements based on simulations 08 p1027 N88-16221

Proposals for the pre-operational use of data from the European Remote Sensing Satellite ERS-1
[BCRS-86-02] 16 p2227 N88-23300

Preparation and execution of calibration measurements for handling of airborne SAR data (AGRISAR)
[ETN-88-92338] 17 p2333 N88-23926

The CERSAT archiving and processing center --- ERS-1 19 p2701 N88-26059

Ocean satellite data and the needs of designers and operators of marine units 19 p2701 N88-26061

Non-Gaussian models for surface clutter
22 p3066 N88-28212

Some characteristics in synthetic aperture radar (SAR) raw data and SAR images
[FOA-C-30483-3.2] 22 p3071 N88-28232

A study of the feasibility of using sea and wind information from the ERS-1 satellite. Part 1: Wind scatterometer data
[NASA-CR-182833] 24 p3386 N88-30167

A study of the feasibility of using sea and wind information from the ERS-1 satellite. Part 2: Use of scatterometer and altimeter data in wave modeling and assimilation
[ESA-CR(P)-2604-PT-2] 24 p3387 N88-30176

RADAR DETECTION

The importance sampling and its application to radar simulation 01 p0012 N88-10065

Meteor detection on ST (MST) radars
06 p0740 N88-14554

Backscattering signal analysis concerning a three-dimensional object configuration on the basis of object motion
[ESA-TT-1044] 09 p1154 N88-16915

Airborne Doppler radar technology for wind shear detection 10 p1274 N88-17622

Experiments for the high resolution detection of moving targets using a CO2 laser radar
[MBB-UA-1044/87] 10 p1316 N88-17884

Aircraft accident report: Midair collision of Cessna-340A, N8716K, and North American SNJ-4N, N711SQ, Orlando, Florida, May 1, 1987
[PB88-910402] 13 p1720 N88-20262

Influence of hydrometeorological factors on visibility of objects detected by radar 13 p1790 N88-20707

Modification of the BLUEMAX 2 terrain following model to incorporate radar detection
[AD-A190594] 15 p2017 N88-22028

Acta aeronautica et astronautica sinica (selected articles)
[AD-A191552] 18 p2455 N88-24575

The VHF experimental radar LARA. A long-wavelength radar for helicopter detection 22 p3149 N88-28738

The radar detection of hovering helicopters
22 p3150 N88-28739

On adaptive cell-averaging CFAR (Constant False-Alarm Rate) radar signal detection
[AD-A196286] 24 p3360 N88-30009

Modeling and performance of HF/OTH (High-Frequency/Over-the-Horizon) radar target identification systems
[AD-A196287] 24 p3365 N88-30038

The surface evaporative duct height product: An evaluation
[AD-A195918] 24 p3392 N88-30199

RADAR ECHOES

NT CLUTTER
NT VENUS RADAR ECHOES

The hybrid wavefront resonance method
03 p0303 N88-11913

Photographic fireball networks
06 p0738 N88-14540

Meteor detection on ST (MST) radars
06 p0740 N88-14554

The Newcastle meteor radar
06 p0741 N88-14556

Waveform for short-dwell-time meteorological Doppler radars
[PB88-102199] 07 p0845 N88-15126

Radar echo signatures versus relative precipitation
[AD-A186162] 08 p0976 N88-15903

SAR (Synthetic Aperture Radar) imaging of ship wakes in the Gulf of Alaska
[AD-A186554] 10 p1317 N88-17872

On the theory of electromagnetic scattering from a raindrop splash
[AD-A188720] 14 p1906 N88-21393

TDWR (Terminal Doppler Weather Radar) PRF (Pulse Repetition Frequency) selection criteria
[AD-A193089] 21 p2932 N88-27407

Definition of long ocean wave slope for radar applications
[AD-A193198] 21 p2933 N88-27412

Radar information from the partial derivatives of the echo signal phase from a point scatterer
[AD-A193402] 21 p2933 N88-27415

The maximum entropy method for the analysis of short-time radar echoes from hovering helicopters
22 p3149 N88-28737

Measurement and interpretation of North Atlantic Ocean marine radar sea scatter
[AD-A196239] 24 p3364 N88-30036

RADAR EQUIPMENT

NT RADAR BEACONS
NT RADAR CORNER REFLECTORS
NT RADAR FILTERS
NT RADAR RECEIVERS
NT RADAR TRANSMITTERS

A preliminary assessment of thunderstorm outflow wind measurement with airport surveillance radars
[AD-A189064] 13 p1799 N88-20757

Considerations in GaAs standard cell design
[DE88-003310] 14 p1985 N88-21840

RADAR FILTERS

Multi-sensory tracking mount control
[AD-A194675] 23 p3249 N88-29339

RADAR IMAGERY

Venusian surface and crust 01 p0010 N88-10054

Dike zones on Venus
[NASA-TT-20111] 02 p0254 N88-11607

Delay-Doppler radar imaging
[AD-A184165] 03 p0308 N88-11943

Correction of inertial navigation system drift errors for an autonomous land vehicle using optical radar terrain data
[AD-A184973] 05 p0544 N88-13311

Study of synthetic aperture radar data compression and encoding. Part 3: Performance evaluation of speckle suppression and data compression algorithms
[NLR-TR-85085-L-PT-3] 06 p0692 N88-14248

Study of synthetic aperture radar data compression and encoding. Part 4: Algorithm implementation aspects
[NLR-TR-85085-L-PT-4] 06 p0692 N88-14249

Texture study of Synthetic Aperture Radar (SAR) images of ocean surfaces
[AD-A186021] 07 p0841 N88-15101

Study of synthetic aperture radar data compression and encoding. Part 1: SAR image data analysis
[NLR-TR-85085-L-PT-1] 07 p0843 N88-15115

Study of synthetic aperture radar data compression and encoding. Part 2: SAR image speckle suppression and data compression algorithms
[NLR-TR-85085-L-PT-2] 07 p0843 N88-15116

Processing of radar images of Venus on the Magiscan-2 analyzer 08 p1009 N88-16117

Earthnet's experience with Seasat SAR image processing 09 p1127 N88-16760

SAR (Synthetic Aperture Radar) imaging of ship wakes in the Gulf of Alaska
[AD-A186554] 10 p1317 N88-17872

Radar reflectivity and attenuation of radio waves in the melting layer of precipitation
[PB88-121553] 10 p1318 N88-17882

Integrated optical synthetic aperture radar processor
[AD-A188019] 11 p1471 N88-18772

The complex point spread function of the RSRE SAR (Synthetic Aperture Radar)
[AD-A189011] 12 p1621 N88-19693

Position, scale, and rotation invariant target recognition using range imagery
[AD-A188826] 12 p1633 N88-19772

A polarimetric rain backscatter model developed for coherent polarization diversity radar applications
13 p1759 N88-20520

Results of the testing of the segmentation program on RESEDA
[BCRS-87-01] 16 p2226 N88-23304

Validate algorithms for the determination of rainfall rates from SSM/I microwave satellite imagery
[AD-A188769] 16 p2233 N88-23337

Investigation of the imaging of ocean surface waves using a synthetic aperture radar
[SER-A-WISS-ABHANDL-84] 16 p2236 N88-23357

Preparation and execution of calibration measurements for handling of airborne SAR data (AGRISAR)
[ETN-88-92338] 17 p2333 N88-23926

The Shuttle Imaging Radar B (SIR-B) experiment report
[NASA-CR-182923] 17 p2334 N88-23932

Radar penetration in the Amazonian rain forest
17 p2352 N88-24015

Airborne and spaceborne radar images for geologic and environmental mapping in the Amazon rain forest, Brazil
17 p2353 N88-24021

Subsurface morphology and geoarchaeology revealed by spaceborne and airborne radar
17 p2353 N88-24022

The use of SLAR and SIRA imagenes for the classification of forest typen in tropical rain forests
17 p2356 N88-24036

Radar penetration in the Amazonian rain forest
17 p2358 N88-24044

Analysis and interpretation of image lithostructure: An application of the multiconcept in the metamorphic belt of Sul de Santana da Boa Vista (RS)
17 p2359 N88-24051

Digital processing of infrared and visible images from the GOES satellite and its integration with meteorological radar data 17 p2360 N88-24057

Interpretation of MSS/LANDSAT data for evaluation of physical distribution of mangroves in Cananeia-Iguape (SP) 17 p2363 N88-24072

Some geological aspects of the Pirapemas Lineament Belt 17 p2368 N88-24099

Lithostructural interpretation of Chapda do Cachimbo (Pa-Am-Mt), based on radar and LANDSAT imagery
17 p2368 N88-24100

Delay-doppler radar imaging
[AD-A191509] 18 p2499 N88-24826

Observation of stratiform rain with 94 GHz and s-b and Doppler radar
[AD-A192013] 18 p2544 N88-25100

Sources of scattering in vegetarian and other surfaces and objects
[NASA-CR-182975] 20 p2816 N88-26710

Image pyramid motion detection applied to sea ice
20 p2817 N88-26713

Linear feature extraction from radar imagery. Phase 2: Base contract report
[AD-A192828] 21 p2931 N88-27404

Some characteristics in synthetic aperture radar (SAR) raw data and SAR images
[FOA-C-30483-3.2] 22 p3071 N88-28232

Mars earth-based radar: 1986 results and 1988-1990 opportunities 23 p3306 N88-29697

Acoustooptic processing of two-dimensional signals using temporal and spatial integration
[AD-A194803] 24 p3359 N88-29999

Corner extraction from radar images
[AD-A194657] 24 p3362 N88-30020
MIZEX (marginal ice zone experiment) 1987 SAR (Synthetic Aperture Radar) data summary
[AD-A195560] 24 p3364 N88-30035
Range data description based on multiple characteristics 24 p3419 N88-30351
High-resolution (30 m) lunar radar images
24 p3442 N88-30486
Determining the spatial structure of fields of precipitation from space radar images in two orthogonal polarizations
24 p3450 N88-30531

RADAR MAPS
Inverse scattering analysis of diffraction limited SAR
[FOA-C-30459-3.2] 05 p0576 N88-13512
Preliminary airworthiness evaluation of a UH-1 equipped with a terrain mapping receiver antenna
[AD-A186274] 07 p0819 N88-14980
Marginal Ice Zone Experiment (MIZEX) 1984 VARAN-S data set
[ETN-88-92032] 14 p1950 N88-21625
Geometric restoration of satellite image data
[AD-A190462] 15 p2089 N88-22450
Digital monoplotting, part 1
[B8735122-PT-1] 17 p2369 N88-24106
Digital monoplotting, part 2
[B8735122-PT-2] 17 p2369 N88-24107

RADAR MEASUREMENT
Collection and analysis of specific ELINT Signal Parameters
[NASA-CR-181419] 01 p0033 N88-10213
Moisture determinations in and under vegetation canopies. Part 2: Results after parameterization of the CLOUD model
[FEL-1986-63] 01 p0064 N88-10410
Theoretical and lidar studies of the seasonal and nocturnal variations of the mesospheric sodium layer at Urbana, Illinois 01 p0068 N88-10435
A real-time system for automatic single-Doppler wind field analysis 02 p0200 N88-11249
Radar measurement methods for the observation of convective clouds, and comparison of measurements and numerical simulation
[ESA-TT-1049] 03 p0352 N88-12223
Contributions of lidar measurements to the study of long term variations of the middle atmosphere
[ETN-88-91237] 05 p0625 N88-13824
Electromagnetic wave probing of Earth's environment
[NASA-CR-182358] 06 p0690 N88-14232
The Cyclone meteor radar system for routine wind measurements in the lower thermosphere
06 p0741 N88-14555
Middle atmospheric wind measurements using a medium frequency radar
[AD-A185931] 07 p0879 N88-15330
Development of a Doppler wind lidar system for atmospheric wind measurements
08 p1027 N88-16217
The sodium layer at 69 N latitude in wintertime
08 p1027 N88-16218
Lidar metal density measurements in the upper atmosphere 08 p1027 N88-16219
Improved resolution atmospheric density measurements based on simulations 08 p1027 N88-16221
Comparison of simultaneous MST radar and electron density probe measurements in the polar mesosphere — Mesospheric, Stratospheric, Tropospheric (MST)
08 p1028 N88-16226
Project CONDOR: Middle atmosphere wind structure obtained with lightweight inflatable spheres near the equatorial electrojet 08 p1028 N88-16230
EISCAT measurements of ion velocities during Coordinated Auroral Experiment using Scatter And Rockets (CAESAR) campaign 08 p1031 N88-16251
Remote and in-situ plasma measurements during the Coordinated Auroral Experiment using Scatter And Rockets (CAESAR) flight 08 p1032 N88-16252
Future developments of auroral D-region research using the EISCAT VHF incoherent scatter radar
08 p1035 N88-16278
Investigation of the quantitative determination of two dimensional sea surface wave spectra from shipborne radar measurements
[GKSS-87/E/10] 09 p1195 N88-17163
Lower bounds on acceleration estimation accuracy
[AD-A188383] 12 p1619 N88-19681
Atmospheric backscatter at 10.6 microns; a compendium of measurements made outside the United Kingdom by the airborne LATAS coherent laser radar velocimeter
[RSRE-87002] 12 p1631 N88-19763
Applications of the differential reflectivity radar technique: Focus on estimation of rainfall parameters and microwave attenuation prediction
13 p1759 N88-20521
A preliminary assessment of thunderstorm outflow wind measurement with airport surveillance radars
[AD-A189064] 13 p1799 N88-20757
Inversion algorithms for geophysical problems
[AD-A189252] 13 p1815 N88-20845
Nonparametric discriminant analysis applied to the extraction and selection of radar target signature features
[AD-A191849] 18 p2501 N88-24833

RADAR NETWORKS
Study of microburst detection performance during 1985 in Memphis, Tennessee
[AD-A184013] 03 p0354 N88-12231
Description of data handling system installed December 11, 1986 — EISCAT 06 p0692 N88-14242

RADAR OBSERVATION
U RADAR TRACKING

RADAR PHOTOGRAPHY
Inverse scattering analysis of diffraction limited SAR
[FOA-C-30459-3.2] 05 p0576 N88-13512

RADAR RANGE
TDWR (Terminal Doppler Weather Radar) PRF (Pulse Repetition Frequency) selection criteria
[AD-A193069] 21 p2932 N88-27407
Effect of phase errors in stepped-frequency radar systems
[AD-A194476] 23 p3203 N88-29061

RADAR RECEIVERS
Goldstone solar system radar performance analysis
22 p3066 N88-28206

RADAR REFLECTIONS
U RADAR ECHOES

RADAR REFLECTORS
NT RADAR CORNER REFLECTORS

RADAR RESOLUTION
Distortion of wideband carbon dioxide laser radar waveforms due to atmospheric dispersion and absorption
[AD-A188687] 12 p1632 N88-19771
Retrieval of three-dimensional wind and temperature fields from single-Doppler radar data
12 p1646 N88-19858
High resolution radar techniques: Five contributions to MILINF 86
[PB88-172721] 18 p2498 N88-24821
Sources of scattering in vegetarian and other surfaces and objects
[NASA-CR-182975] 20 p2816 N88-26710

RADAR SCANNING
Study on propagation and inverse scattering — sea studies
[ESA-CR(P)-2394] 01 p0063 N88-10405
High latitude problems to be studied by incoherent scatter radars
[DMI-GEOPHYS-PAPERS-R-77]
03 p0350 N88-12211
Radar information from the partial derivatives of the echo signal phase from a point scatterer
[AD-A193402] 21 p2933 N88-27415

RADAR SCATTERING
Target strength: An overview of some recent theoretical developments 03 p0303 N88-11910
The hybrid wavefront resonance method
03 p0303 N88-11913
Physical optics method: Prediction of radar signatures
03 p0304 N88-11914
Input signal shaping: K-pulse
03 p0304 N88-11917
New main reflector, subreflector and dual chamber concepts for compact range applications
[NASA-CR-181506] 04 p0402 N88-12498
Large bandwidth ground scattering model — radar scattering
[FOA-C-30458-3.2] 05 p0576 N88-13511
Inverse scattering analysis of diffraction limited SAR
[FOA-C-30459-3.2] 05 p0576 N88-13512
The rocket and scatter experiment ROSE: Presentation of the scientific payload 08 p1034 N88-16269
Radar returns from ground clutter in vicinity of airports
10 p1274 N88-17624
The radar scattering coefficient as a function of forest stand parameters and viewing angle. An empirical study of the Pinus sylvestris L. in the Kootwijk forest (The Netherlands), extended with observations in the Speulder and Sprielder forest (The Netherlands)
[ETN-88-91348] 13 p1760 N88-20527
Radial track of moving objects determined by HF backscatter technique 14 p1901 N88-21354
Scattering patterns of dihedral corner reflectors with impedance surface impedances
[NASA-CR-183078] 20 p2789 N88-26545
South Pole lidar: Brief description of the instrument
[NOTA-INTERNA-907] 22 p3083 N88-28308
Measurement and interpretation of North Atlantic Ocean marine radar sea scatter
[AD-A196239] 24 p3364 N88-30036

RADAR SIGNATURES
An investigation on Faraday rotators and quarter-wave plates of a 35 GHz radar signature system
[DFVLR-FB-87-14] 01 p0037 N88-10236
Physical optics method: Prediction of radar signatures
03 p0304 N88-11914
Numerical modeling: Integral equation method
03 p0304 N88-11919
Radar echo signatures versus relative precipitation
[AD-A186162] 08 p0976 N88-15903
Radar descriptors for the classification of terrain features
[AD-A188145] 11 p1504 N88-16983
A polarimetric rain backscatter model developed for coherent polarization diversity radar applications
13 p1759 N88-20520
A study of Radar Cross Section (RCS) characteristics and their application in future weapon systems
[ETN-88-92081] 14 p1906 N88-21390
Research on Faraday rotators and quarter-wave plates of a 35-GHz radar signature system
[ESA-TT-1081] 16 p2169 N88-23052
Nonparametric discriminant analysis applied to the extraction and selection of radar target signature features
[AD-A191849] 18 p2501 N88-24833
Autoregressive moving average modeling of radar target signatures
[AD-A194612] 22 p3069 N88-28218
Viking Landers and remote sensing
23 p3304 N88-29885
The Soviet Stealth fighter: Check or checkmate
[AD-A195200] 24 p3323 N88-29791

RADAR TARGETS
Feature selection applied to radar target identification
[AD-A183880] 01 p0034 N88-10215
Theoretical Aspects of Target Classification
[AGARD-LS-152] 03 p0303 N88-11909
Target strength: An overview of some recent theoretical developments 03 p0303 N88-11910
The hybrid wavefront resonance method
03 p0303 N88-11913
Theoretical aspects of target classification: Physical optics and radon transform methods
03 p0304 N88-11915
Parametrization in scattering models
03 p0304 N88-11916
Input signal shaping: K-pulse
03 p0304 N88-11917
Numerical modeling: Integral equation method
03 p0304 N88-11919
Experiments: Test range facilities, part 1
03 p0304 N88-11920
Delay-Doppler radar imaging
[AD-A184165] 03 p0306 N88-11943
New main reflector, subreflector and dual chamber concepts for compact range applications
[NASA-CR-181506] 04 p0402 N88-12498
Detection of signals in non-Gaussian correlated noise derived from Cauchy processes
[AD-A187488] 10 p1320 N88-17894
Mono- and bistatic radar coverage diagrams including diffractive wave propagation 12 p1616 N88-19660
A method for discrimination of radar targets using complex natural resonances
[AD-A191848] 18 p2500 N88-24832
Nonparametric discriminant analysis applied to the extraction and selection of radar target signature features
[AD-A191849] 18 p2501 N88-24833
Evaluation of LISBON TAR SSR radar
[EEC/NOTE-5/87] 24 p3362 N88-30015
Modeling and performance of HF/OTH (High-Frequency/Over-the-Horizon) radar target identification systems
[AD-A196267] 24 p3365 N88-30038

RADAR TRACKING
Balloon track data analysis
[AD-A184750] 03 p0350 N88-12213
Media calibrations of the Doppler signal for a gravitational wave experiment — interplanetary medium
[IFSI-86-13] 05 p0625 N88-13825
Middle Atmosphere Program. Handbook for MAP, volume 25
[NASA-CR-181571] 06 p0732 N88-14502
The climatic wind regime in the lower thermosphere from meteor radar observations 06 p0733 N88-14506
Meteor observation by the Kyoto meteor radar
06 p0733 N88-14507
Hard- and software problems of spaced meteor observations by optical electronics
06 p0741 N88-14580
The correlation between methodological and low-level angle-of-arrival measurements 12 p1617 N88-19668

Aircraft accident report: Midair collision of Cessna-340A, N8716K, and North American SNJ-4N, N711SQ, Orlando, Florida, May 1, 1987
[PB88-910402] 13 p1720 N88-20282
A method and measures to evaluate trackers for air traffic control
[NLR-TR-86072-U] 13 p1720 N88-20287
Modification of the BLUEMAX 2 terrain following model to incorporate radar detection
[AD-A190594] 15 p2017 N88-22028
Polarimetric ISAR imaging using either measured or calculated transient signatures
[AD-A190077] 15 p2056 N88-22259
Studies of ionosphere/magnetosphere dynamics using SABRE and HILAT
[AD-A190947] 16 p2232 N88-23333
Space based radar application to air traffic control
17 p2399 N88-24262
A method for discrimination of radar targets using complex natural resonances
[AD-A191848] 18 p2500 N88-24832
Track performance considerations for monopulse radars
[AD-A196232] 24 p3360 N88-30007
MIZEX (marginal ice zone experiment) 1987 SAR (Synthetic Aperture Radar) data summary
[AD-A195560] 24 p3364 N88-30035
Modeling and performance of HF/OTH (High-Frequency/Over-the-Horizon) radar target identification systems
[AD-A196287] 24 p3365 N88-30038

RADAR TRANSMISSION
Inversion of simulated satellite signals
08 p1017 N88-16168
Electromagnetic interference to radar and radio link systems caused by large scale wind turbines
[FOA-C-30486-3.2] 22 p3071 N88-28234

RADAR TRANSMITTERS
Evaluation of LISBON TAR SSR radar
[EEC/NOTE-5/87] 24 p3362 N88-30015

RADIAL DISTRIBUTION
Fiber-optic accelerometer investigation
[AD-A185359] 05 p0584 N88-13561
Nonuniformity of electromagnetic field at Lambda = 10.6 micron wavelength inside atmospheric aerosol particles
06 p0772 N88-14743

RADIAL DRAINAGE PATTERNS
U DRAINAGE PATTERNS

RADIAL FLOW
Continuation finite element analysis of viscoelastic fluids 04 p0445 N88-12761
High pressure ratio turbine design constraints
[TRR-0279] 06 p0712 N88-14365
Mainline performance prediction for radial inflow turbines 06 p0712 N88-14366
Performance of supersonic impingement radial turbines 06 p0712 N88-14367
Conclusions from a research program on mixed flow gas generator turbines 06 p0713 N88-14368
Experimental and theoretical study of the dynamic operational behavior of a three stage radial compressor
[ETN-88-92129] 20 p2811 N88-26676
The use of fins to reduce the pressure drop in a rotating cavity with a radial flow
[PNR90485] 22 p3079 N88-28282

RADIAL VELOCITY
An application of L1 to astronomy — stellar velocity
[REPT-87-10] 01 p0108 N88-10702
Retrieval of three-dimensional wind and temperature fields from single-Doppler radar data
12 p1646 N88-19658
A preliminary assessment of thunderstorm outflow wind measurement with airport surveillance radars
[AD-A189064] 13 p1799 N88-20757
New measurements of radial velocities in clusters of galaxies
[INPE-4527-PRE/1277] 15 p2152 N88-22845
Radial velocities monitoring of a sample of barium and S stars using CORAVEL: Towards an evolutionary link between barium and S stars?
[SER-C-PREPUBL-FASC-19] 18 p2593 N88-25410
Radial velocity measurements of a sample of northern metal-deficient stars
[SER-C-PREPUBL-FASC-25] 24 p3455 N88-30564

RADIANCE
The use of satellite IR data in the enhancement of surface thermal fields 02 p0202 N88-11260
Use of simulated satellite radiances from a mesoscale numerical model to understand kinematic and dynamic processes 02 p0202 N88-11261
Quantum electrodynamics based on self-energy: Spontaneous emission in cavities
[DE87-703071] 02 p0232 N88-11461
The absolute radiometric calibration of space-based sensors 03 p0277 N88-11744
Calibrating AIS images using the surface as a reference 05 p0612 N88-13760
The influence of yellow substances on remote sensing of sea water constituents from space. Volume 1: Summary
[ESA-CR(P)-2443-VOL-1] 07 p0872 N88-15292
The influence of yellow substances on remote sensing of sea water constituents from space. Volume 2: Appendices
[ESA-CR(P)-2443-VOL-2] 07 p0873 N88-15293
Determination of cloud base height and emissivity from downwelling angular radiances
[AD-A185985] 07 p0879 N88-15331
Monte Carlo method calculation of spectral brightness coefficient of vegetation cover as function of illumination conditions 08 p1008 N88-16113
Aerosol size distribution from measurements of the radiance in the solar aureole 08 p1019 N88-16176
The iterative radiance model of the Meteorological Institute of the University of Munich (West Germany)
08 p1019 N88-16178
Vertical atmospheric sounding
[INPE-4370-PRE/1195] 08 p1036 N88-16283
Depolarized infrared reflectance from dry and wetted surfaces
[AD-A188213] 11 p1492 N88-18903
Determination of atmospheric moisture structure from high resolution MAMS radiance data
11 p1515 N88-19049
Remote sensing of atmospheric optical thickness and sea-water attenuation when submerged: Wavelength selection and anticipated errors
[AD-A187609] 11 p1548 N88-19262
Enhancements to the atmospheric transmittance/radiance program FASCODE
[AD-A188863] 12 p1643 N88-19839
Progress in X-ray laser experiments
[ETN-88-92004] 14 p1915 N88-21442
Relationship between optical transfer function and natural light field in sea or atmosphere
15 p2054 N88-22247
Calibration and processing of AVHRR data for temperature estimation
[INPE-4493-PRE/1257] 15 p2095 N88-22485
The NBS scale of radiance temperature
17 p2328 N88-23897
Estimation of total Outgoing Longwave Radiation (OLR) flux from geostationary meteorological satellite infrared window radiance 17 p2351 N88-24006
Spectral measurements for correcting LANDSAT data for atmospheric effects 17 p2362 N88-24066
Sky radiance distributions for thermal imaging backgrounds
[AD-A191135] 17 p2373 N88-24115
Effects of atmospheric model layering on LOWTRAN 6 calculations of 8-12 micrometers near-horizon sky radiances
[AD-A192969] 20 p2791 N88-26559
Numerical model for the computation of radiance distributions in natural waters with wind-roughened surfaces
[PB88-192703] 20 p2826 N88-26765
Eigenmatrix representations of radiance distributions in layered natural waters with wind-roughened surfaces
[PB88-188701] 20 p2828 N88-26780
IR (infrared) sky radiance distributions in the marine boundary layer
[AD-A193683] 22 p3119 N88-28531
A probabilistic model of the apparent radiance of a rough sea
[AD-A193867] 22 p3129 N88-28602
Filling of the atmospheric transmission window due to emission from very high rotational levels of NO and O3
[AD-A194670] 23 p3233 N88-29239

RADIANT COOLING
Thermal radiation from neutron stars
[MPE-203] 11 p1571 N88-19404

RADIANT FLUX DENSITY
NT ELECTRON FLUX DENSITY
NT ILLUMINANCE
NT IRRADIANCE
NT LUMINANCE
NT LUMINOUS INTENSITY
NT NEUTRON FLUX DENSITY
NT PARTICLE FLUX DENSITY
NT RADIANCE
NT SOLAR CONSTANT
NT SOLAR FLUX DENSITY
Monitored background radiometer
02 p0133 N88-10631
Instrument for radiation testing/screening electronic devices over an extended temperature range
[AD-A184245] 03 p0326 N88-12060
Report of the Joint Scientific Commitee Ad Hoc Working Group on Radiative Flux Measurements — Earth radiation budget
[WCP-136] 06 p0742 N88-14567
Nonuniformity of electromagnetic field at Lambda = 10.6 micron wavelength inside atmospheric aerosol particles
06 p0772 N88-14743
Overestimation of on-axis power density by the Fraunhofer (far-field) approximation
[AD-A186399] 07 p0843 N88-15111
The role of anisotropy in the long range reconnaissance of the albedo of land surfaces 08 p1017 N88-16169
High energy and high intensity laser effects on aerosols: Changes in droplet morphology, surrounding temperature and vapor concentration
[AD-A193825] 23 p3220 N88-29164

RADIANT HEATING
An approximate solution to the problem of heating massive bodies by both radiation and convection
[BLL-M-37315-(5828.4)] 02 p0170 N88-11068
Test methodology for infrared tubular heaters
[PB88-160916] 12 p1626 N88-19726

RADIANT INTENSITY
U RADIANT FLUX DENSITY

RADIATION ABSORPTION
NT ELECTROMAGNETIC ABSORPTION
NT GAMMA RAY ABSORPTION
NT INFRARED ABSORPTION
NT MOLECULAR ABSORPTION
NT MULTIPHOTON ABSORPTION
NT PHOTOABSORPTION
NT ULTRAVIOLET ABSORPTION
NT X RAY ABSORPTION
Transient absorption behavior of metals at the onset of the laser welding process
[DFVLR-FB-87-12] 01 p0025 N88-10160
Estimating scattered and absorbed radiation in plant canopies by remote sensing
[NASA-CR-181390] 02 p0193 N88-11205
Theoretical atomic and molecular photophysics
[DE87-014249] 02 p0231 N88-11458
Laboratory evaluation and application of microwave absorption properties under simulated conditions for planetary atmospheres
[NASA-CR-181466] 02 p0254 N88-11606
Millimeter-wave studies of moist air
[AD-A184681] 03 p0306 N88-11935
Study of kinetics of intracavity absorption in pulsed dye lasers 07 p0919 N88-15585
Explosive absorption of laser beam of finite diameter
07 p0921 N88-15597
The application of vector diffraction to the scalar anomalous diffraction approximation of Van de Hulst
[AD-A185930] 07 p0929 N88-15643
Absorption of cyclotron radiation in skin layer in Araks experiment 08 p1003 N88-16076
Nonlinear absorption of CO2 laser radiation in p-type InSb
[DE88-004055] 11 p1492 N88-18906
The YAlO(sub 3):Er laser
[PB88-130677] 11 p1493 N88-18911
Remote sensing of atmospheric optical thickness and sea-water attenuation when submerged: Wavelength selection and anticipated errors
[AD-A187609] 11 p1548 N88-19262
Laser fluorescence velocimeter
[AD-A189010] 12 p1630 N88-19753
Distortion of wideband carbon dioxide laser radar waveforms due to atmospheric dispersion and absorption
[AD-A188687] 12 p1632 N88-19771
Research on absorption of UV radiation in Venusian atmosphere from Vega-1 and Vega-2 landing modules
13 p1725 N88-20316
Spontaneous decay and atomic fluorescence near a metal surface of an absorbing dielectric
[AD-A187506] 13 p1835 N88-20975
Dependence of formation of radiative color centers in optical glass fibers on technological factors
14 p1896 N88-21321
Radiation absorption in neodymium glasses during passage of strong laser pulse 14 p1969 N88-21757
Dissipative relativistic radiation hydrodynamics
[DE88-702092] 19 p2665 N88-25846
Absorption characteristics of Si3N4 ablation layer plasma 20 p2783 N88-26504
Assessment of cochlear damage after microwave irradiation
[AD-A193237] 21 p2987 N88-27737
Differences in radiation budget parameters over Asia in relation to contrasting Indian monsoons
22 p3125 N88-28574
Coupling between radiation and gas dynamics
[AD-A194583] 23 p3211 N88-29113

RADIATION BELTS
NT INNER RADIATION BELT

Radiation effects in space
[DE87-012529] 01 p0075 N88-10479
Radiation belts 03 p0272 N88-11707
Analysis of geophysical data bases and models for spacecraft interactions
[AD-A184809] 06 p0555 N88-13375
Toward a comprehensive theory for the sweeping of trapped radiation by inert orbiting matter
[NASA-CR-182584] 11 p1569 N88-19395
Stimulated Emission of Energetic Particles (SEEP)
[AD-A188724] 13 p1853 N88-21094
Solar flares and magnetospheric particles: investigations based upon the ONR-602 and ONR-604 experiments
[AD-A193396] 21 p3031 N88-27994

RADIATION CHEMISTRY
NT PHOTODECOMPOSITION
NT PHOTODISSOCIATION
NT PHOTOLYSIS
NT RADIOLYSIS
Astromag: A particle spectrometer for the Space Station
[PREPRINT-557] 06 p0707 N88-14336
Effects of energy, distance and orientation on electron transfer rates studied by pulse radiolysis in organic media
[DE88-002906] 08 p1062 N88-16521
Diversity of comets, synergic temperature effects and the stability of organic compounds in icy nuclei
14 p2005 N88-21955
The radiation sensitivity of select metal chelate polymers: Mechanistic changes at higher energies
[AD-A193467] 23 p3196 N88-29019

RADIATION COUNTERS
NT CERENKOV COUNTERS
NT ELECTRON COUNTERS
NT NEUTRON COUNTERS
NT NEUTRON SPECTROMETERS
NT PARTICLE TELESCOPES
NT PROPORTIONAL COUNTERS
NT SCINTILLATION COUNTERS
NT SPARK CHAMBERS
Calibration constants for the 1986 BGO crystals matrix
[NOTA-INTERNA-886] 07 p0856 N88-15197
Ionization losses in BGO
[NOTA-INTERNA-889] 07 p0856 N88-15198
Characteristics of multimuon events from fourth generation quarks at the SSC (Superconducting Super Collider)
[DE88-002954] 09 p1257 N88-17535
Nonequilibrium superconductivity for particle detectors
[DE88-002876] 09 p1257 N88-17539
High energy cosmic muons and the calibration of the L3 electromagnetic calorimeter
[NOTA-INTERNA-895] 14 p2011 N88-21999
Large area nuclear particle detectors using ET materials
[NASA-CR-180777] 23 p3215 N88-29136

RADIATION DAMAGE
NT LASER DAMAGE
Effects of electron and proton irradiations on n/p and p/n GaAs cells grown by MOCVD
[NASA-TM-100199] 01 p0042 N88-10266
Optical damage in polymers by millisecond light pulses
[DE87-013106] 02 p0151 N88-10943
Effects of radiation damage in optical fibers: A tutoral
[PB87-210308] 02 p0235 N88-11482
Prevention of radiation induced degradations and of electrostatic perturbations on the Arabsat spacecraft in flight results 03 p0275 N88-11734
DNA damage and repair in human skin in situ
[DE87-014288] 03 p0356 N88-12241
Performance of GaAs and silicon concentrator cells under 37 MeV proton irradiation
[NASA-TM-100144] 04 p0465 N88-12877
Radiation performance of AlGaAs concentrator cells and expected performance of cascade structures
[NASA-TM-100145] 04 p0465 N88-12878
Reevaluating the worst-case radiation response of MOS transistors
[DE87-014157] 04 p0497 N88-13059
Swelling behavior of ferritic/martensitic steels
[DE88-001757] 06 p0682 N88-14177
UV radiation: Human exposure to ultraviolet radiation
[PB87-137410] 06 p0752 N88-14619
Evolution of radiation-induced voids and dislocations at low temperature
[DE88-700350] 07 p0939 N88-15704
Space environmental considerations for a long-term cryogenic storage vessel 08 p0981 N88-15933
Forward-biased current annealing of radiation damaged gallium arsenide and silicon solar cells
[AD-A186904] 09 p1186 N88-17105
Irradiation effects in metals
[DE88-004272] 10 p1303 N88-17769
Suppression of X-rays generated by runaway electrons in ATF
[DE88-004179] 10 p1414 N88-18440
The effects of low doses of 14 MeV neutrons on the tensile properties of three binary copper alloys
[DE88-003400] 11 p1456 N88-18691
Measurement of the gamma-ray response of some commercial silicon detectors
[AD-A187431] 11 p1543 N88-19221
JPRS report: Science and technology. USSR: Life sciences
[JPRS-ULS-88-002] 12 p1665 N88-19982
Study of defects in metals by positron annihilation
[DE88-701042] 13 p1745 N88-20432
In situ TEM observations of heavy ion damage in gallium arsenide
[DE88-005984] 14 p1986 N88-21843
X-ray production in low energy proton stopping
[NASA TM-100619] 16 p2270 N88-23582
Effects of 67.5 MeV electron irradiation on Y-Ba-Cu-O and Gd-Ba-Cu-O high-temperature superconductors
[AD-A191271] 16 p2283 N88-23669
Space nuclear reactor shielding optimization studies
17 p2408 N88-24320
Molecular characterization of structure and bonding in thin film materials
[DE88-006811] 18 p2584 N88-25351
An optically strobed sample and hold circuit
19 p2656 N88-25772
JFET/SOS (Junction Field-Effect Transistor/Silicon-on-Sapphire) devices: Gamma-radiation-induced effects
[AD-A193001] 20 p2795 N88-26586
Acute radiation syndrones and their management
[DE88-009839] 20 p2831 N88-26797
The Oak Ridge National Laboratory strategic defense initiative shield optimization program: Executive summary
[DE88-008016] 20 p2847 N88-26899
Electron irradiation effects in YBa2Cu3O7-Delta single crystals
[DE88-010050] 20 p2878 N88-27065
Data compilation for radiation damage on ceramic insulators. Revised with updated data and reviews
[DE88-753426] 21 p2920 N88-27329
Heavy ion and proton tests for subsystem upset
[AD-A195267] 24 p3434 N88-30442

RADIATION DETECTORS
NT DOSIMETERS
NT SILICON RADIATION DETECTORS
NT THRESHOLD DETECTORS (DOSIMETERS)
Construction and characterization of amorphous-silicon test structures
[DE87-013595] 01 p0029 N88-10182
Superfluid He4 as a solar neutrino detector
[DE87-014477] 02 p0257 N88-11625
Instrument for radiation testing/screening electronic devices over an extended temperature range
[AD-A184245] 03 p0326 N88-12060
Ultrafast photoconductor detector-laser-diode transmitter
[DE87-013803] 03 p0329 N88-12062
Design of source coders and joint source/channel coders for noisy channels
[NASA-CR-181547] 04 p0432 N88-12678
Low-cost teleoperator-controlled vehicle for damage assessment and dose measurement
[DE88-000713] 04 p0451 N88-12794
Study of solid state photomultiplier
[NASA-CR-177465] 05 p0583 N88-13556
Evaluation of surface energy and radiation balance systems on the Konza Prairie
[NASA-CR-182534] 10 p1355 N88-18097
PbSnTe photovoltaic detectors for operation in the 2-14 micron band
[INPE-4252-PRE/1125] 11 p1508 N88-19008
Advances in X-ray optics, 1987
[DE88-003298] 11 p1549 N88-19268
An attempt to measure the diffuse brightness of the sky at submillimeter wavelengths
12 p1710 N88-20233
HNC: A detector to study ultraheavy cosmic rays
12 p1713 N88-20252
An approximation technique for solving a system of Fredholm integral equations for asymmetric detector response functions
[AD-A190577] 15 p2121 N88-22645
A new fiber-optic-based phase-resolved phosphorescence spectrometer
[AD-A191325] 16 p2275 N88-23613
Superconducting thin film vertex detector for SSC (Superconducting Super Collider) applications
[DE88-005951] 17 p2445 N88-24535
Photoconducting X-ray detectors for Z-pinch experiments
[DE88-007118] 19 p2728 N88-26199

RADIATION DISTRIBUTION
NT ANTENNA RADIATION PATTERNS
NT DIFFRACTION PATTERNS
NT SIDELOBES
Radiation belts 03 p0272 N88-11707
Performance evaluation of a half-wave resonant slot antenna over perfect ground using NEC (Numerical Electromagnetic Code)
[AD-A184004] 03 p0308 N88-11942
Gamma-ray optics of multi-beam Borrmann modes with possible application to nuclear lasing
04 p0449 N88-12784
Statistical distribution of solar radiation (hourly sums): Cumulative frequency curves preparation of a European data set and direction for use
[PB87-107454] 04 p0467 N88-12886
RADSPHERE: A computer program for calculating the steady-state, axially symmetric, forced response and radiation field of a submerged spherical shell
[AD-A185025] 05 p0609 N88-13736
Cerenkov radiation field analysis due to a passing electron beam
[AD-A184870] 05 p0649 N88-13976
Nonequilibrium ionization of pregalactic plasma and lessening of relic radiation anisotropy
08 p1002 N88-16071
The role of anisotropy in the long range reconnaissance of the albedo of land surfaces 08 p1017 N88-16169
The iterative radiance model of the Meteorological Institute of the University of Munich (West Germany)
08 p1019 N88-16178
Acoustic field in waveguide with sloping bed
08 p1076 N88-16490
Diffraction of sound at junction of two waveguides
08 p1076 N88-16491
Optimizing HF antenna systems on the Dolphin and Sea Hawk helicopters
[AD-A186552] 09 p1152 N88-16901
Time domain wave propagation in multilayered integrated circuits
[AD-A187462] 10 p1324 N88-17916
A computer model investigation of a half square log-periodic array
[AD-A190955] 16 p2190 N88-23062
A diagnostic technique used to obtain cross range radiation centers from antenna patterns
[NASA-CR-182903] 16 p2192 N88-23071
Sky radiance distributions for thermal imaging backgrounds
[AD-A191135] 17 p2373 N88-24115
The new MININEC (version 3): A mini-numerical electromagnetic code
[AD-A191778] 19 p2642 N88-25675
Automated spectrometric unit for the study of radiation characteristics of cosmic radiation aboard Prognoz-9 space stations 19 p2706 N88-26090
Development of radiation and cloud parameterization programs for AFGL (Air Force Geophysics Laboratory) global models
[AD-A193369] 21 p2973 N88-27658
Stratocumulus and cloud-free reflectance from multi-spectral satellite measurements
[AD-A193899] 22 p3128 N88-28599
A novel method to correct radiation pattern distortion of conformal antennas
[AD-A193675] 23 p3204 N88-29066

RADIATION DOSAGE
Effects of radiation damage in optical fibers: A tutoral
[PB87-210308] 02 p0235 N88-11482
Variations in semiconductor device response in a medium-energy x-ray dose-enhancing environment
[DE87-012400] 02 p0243 N88-11536
Irradiations. Accumulated doses. Heavy ions -- space environment 03 p0272 N88-11708
The effect of radiation on the long term productivity of a plant based CELSS 03 p0361 N88-12271
Fabricate, calibrate and test a dosimeter for integration into the CRRES (Combined Release and Radiation Effects Satellite) satellite
[AD-A185439] 05 p0585 N88-13564
Research for electric energy systems
[DE88-001733] 06 p0695 N88-14265
UV radiation: Human exposure to ultraviolet radiation
[PB87-137410] 06 p0752 N88-14619
Effect of irradiation on the diffusion evolution of void ensemble in crystals
[DE88-700558] 07 p0939 N88-15706
Late radiation damage in bone, bone marrow and brain vasculature, with particular emphasis upon fractionation models
[DE87-753039] 08 p1048 N88-16330
The ISO narrow spectrum series of filtered X-radiations at NPL
[NPL-RS(EXT)-92] 09 p1245 N88-17462

Effects of the neutron spectrum on mechanical property changes in low dose irradiations
[DE88-003429] 10 p1302 N88-17786
International cooperative effort to establish ASTM (American Society for Testing and Materials) standards for the measurement of radiation dose for food processing
[DE88-002702] 10 p1372 N88-18190
South African Association of Physicists in Medicine and Biology: 26th Annual Congress
[DE88-700824] 11 p1521 N88-19082
Measurement of the gamma-ray response of some commercial silicon detectors
[AD-A187431] 11 p1543 N88-19221
Nuclear health and safety: Radiation exposures for some cloud-sampling personnel need to be reexamined
[PB88-130497] 12 p1662 N88-19965
Effects of whole-body irradiation with low-intensity microwaves on morphological, functional and cytochemical characteristics of leukocytes 12 p1663 N88-19971
The calibration of photographic and spectroscopic films: The response of 2aO film to small dosages of alpha particles from 3/10th's rad to 8 rads at energy levels 153 MeV, 79 MeV and 47 MeV
[NASA-CR-177830] 13 p1773 N88-20608
Anthropomorphic phantom radiation dosimetry at the NATO standard reference point at Aberdeen Proving Ground
[AD-A190506] 15 p2103 N88-22528
Modeling of radiation dose dependence of MOSFETs
17 p2416 N88-24370
Analysis of a nuclear orbital transfer vehicle reentry accident 17 p2425 N88-24426
Preliminary estimates of radiation exposures for manned interplanetary missions from anomalously large solar flare events
[NASA-TM-100620] 18 p2596 N88-25427
Radiation safety in commercial air traffic
[NASA-TM-101156] 19 p2600 N88-25447
Health and environmental consequences of the Chernobyl nuclear power plant accident
[DOE/ER-0332] 19 p2689 N88-25965
Hemorrhages and hemostasis in guinea pigs exposed to radiation at high altitude 19 p2705 N88-26083
Acute radiation syndrones and their management
[DE88-009639] 20 p2831 N88-26797
Behavioral effects of exposure to the tempo high-power microwave system
[AD-A193305] 21 p2987 N88-27736
Emetic mechanism in acute radiation sickness
[AD-A194102] 23 p3236 N88-29267
Study of biological effects and radiation protection to future European manned space flights
[DGT-33061] 23 p3281 N88-29535

RADIATION EFFECTS
NT LASER DAMAGE
NT RADIATION DAMAGE
NT RADIATION INJURIES
NT RADIOLYSIS
NT SINGLE EVENT UPSETS
An optically strobed sample and hold circuit
[DE87-011877] 01 p0038 N88-10245
Radiation effects in space
[DE87-012529] 01 p0075 N88-10479
The combined release and radiation effects satellite, a joint NASA/DOD program 02 p0135 N88-10851
Electron beam irradiation effects on carbon fiber reinforced PEEK composite
[DE87-753001] 02 p0142 N88-10890
Degradation mechanisms of materials for large space systems in low Earth orbit
[NASA-CR-181472] 02 p0143 N88-10896
The numerical simulation of the mesoscale characteristics associated with Baiu front. Part 1: Structure, low-level jet and radiation characteristics
02 p0203 N88-11272
Interaction between defects and the formation of dissipative structures in irradiated impure crystals
[DE87-703125] 02 p0246 N88-11552
Irradiation testing 03 p0274 N88-11727
Temperature hysteresis and magnetic transitions in amorphous Fe-Ni-Zr alloys
[DE88-000228] 03 p0294 ' N88-11848
Compilation of 1986 annual reports of the Navy ELF (Extremely Low Frequency) communications system ecological monitoring program, volume 1
[AD-A184561] 03 p0306 N88-11930
Compilation of 1986 annual reports of the Navy ELF (Extremely Low Frequency) communications system ecological monitoring program, volume 2
[AD-A184562] 03 p0306 N88-11931
Compilation of 1986 annual reports of the Navy ELF (Extremely Low Frequency) communications system ecological monitoring program, volume 3
[AD-A184563] 03 p0306 N88-11932
Health hazards of video display terminals. A comprehensive, annotated bibliography on a critical issue of workplace health and safety with sources for obtaining items and list of terminal suppliers
[RSI-IAS-4] 03 p0355 N88-12240
The effect of radiation on the long term productivity of a plant based CELSS 03 p0361 N88-12271
Low Earth orbit environmental effects on the space station photovoltaic power generation systems
[NASA-TM-100230] 03 p0387 N88-12429
Microgravity nucleation and particle coagulation experiments support
[NASA-CR-181540] 04 p0423 N88-12618
JPRS report: Science and technology. USSR: Life sciences
[JPRS-ULS-87-009] 04 p0473 N88-12915
Radiation induced collapse of the crystalline structure
[DE87-014407] 04 p0498 N88-13064
A study of charged particles/radiation damage to VLSI device materials
[NASA-CR-172036] 05 p0577 N88-13518
Fabricate, calibrate and test a dosimeter for integration into the CRRES (Combined Release and Radiation Effects Satellite) satellite
[AD-A185439] 05 p0585 N88-13564
TOMS as a monitor of the ultraviolet radiation environment: Applications to photobiology
05 p0617 N88-13785
Irradiation preservation of seafood: Literature review
[DE88-001691] 05 p0631 N88-13858
Basic energy sciences research in the Metals and Ceramics Division of Oak Ridge National Laboratory
[DE87-013538] 06 p0681 N88-14171
Program description of FIBRAM: A radiation attenuation model for optical fibers
[PB87-230686] 06 p0690 N88-14229
Observing effect of laser radiation of low-frequency Raman scattering of light 06 p0772 N88-14742
The role of hydrogen in radiation-induced defect formation in polysilicon gate MOS devices
[DE87-012374] 06 p0785 N88-14814
Theoretical aspects of channeling, damage, and range distributions for low (keV) and high (MeV) energy implantation
[DE88-000949] 06 p0786 N88-14818
Effect of point defects on graphite lattice parameters
[DE88-700340] 07 p0827 N88-15019
Karyometric evaluation of neuronal reactions of rat cerebral cortex to the combined effect of ionizing radiation, longitudinal accelerations and vibration
07 p0890 N88-15396
JPRS report: Science and technology. USSR: Space Biology and Aerospace Medicine, volume 21, no. 4, July - August 1987
[JPRS-USB-88-002] 07 p0893 N88-15412
Combined effect of microwaves and ionizing radiation
07 p0893 N88-15413
Effect of pyrocetam on mouse resistance to hypoxic hypoxia 2-3 months after exposure to X-radiation
07 p0895 N88-15425
Effect of irradiation on the diffusion evolution of void ensemble in crystals
[DE88-700558] 07 p0939 N88-15706
Experimental method for investigating helium effects in irradiated vanadium
[DE88-002891] 08 p0969 N88-15865
Electric design rules related to latch-up and radiation — simulation
[FOA-E-30006-3.1] 08 p0979 N88-15917
Results of research with biological satellites
08 p1006 N88-16097
Life sciences experiments on stratospheric balloons and sounding rockets 08 p1033 N88-16262
Contribution of stratospheric balloon flights in space biology 08 p1033 N88-16266
Late radiation damage in bone, bone marrow and brain vasculature, with particular emphasis upon fractionation models
[DE87-753039] 08 p1048 N88-16330
Photoabsorption and photodissociation of molecules important in the interstellar medium
[NASA-CR-182435] 08 p1100 N88-16617
Radon Research Program, FY-1987
[DE88-002633] 09 p1188 N88-17120
Laser simulation of light and plasma action on comets and planets 09 p1237 N88-17413
Dispersive hole transport in SiO2
[AD-A187077] 09 p1254 N88-17513
JPRS Report: Science and Technology. USSR: Space Biology and Aerospace Medicine, volume 21, no. 5, September - October 1987
[JPRS-USB-88-003] 10 p1359 N88-18122
Short- and long-term effects of nonlethal levels of fast high-energy helium ions on retention of developed and formation of new behavioral patterns in rats
10 p1362 N88-18140
Effect of antiorthostatic position and different illumination on sensitivity of skin in upper half of the body to ultraviolet radiation 10 p1363 N88-18145
Effect of spaceflight factors on biological material flown aboard Cosmos-1514 biosatellite
10 p1364 N88-18154
Combined effect of ionizing radiation and altered gas atmosphere on central nervous system
10 p1367 N88-18168
Radiation and temperature effects on the time-dependent response of T300/934 graphite/epoxy
[NASA-CR-182603] 11 p1451 N88-18646
Soluble polysilane derivatives: Chemistry and spectroscopy
[AD-A187889] 11 p1461 N88-18713
Photophysics and photochemistry of poly(di-n-hexylsilane) in room temperature solution
[AD-A187890] 11 p1462 N88-18714
Ceramic decomposition under irradiation
[DE88-004327] 11 p1464 N88-18732
Laser flash effects on chromatic discrimination in monkeys
[AD-A187703] 11 p1517 N88-19061
Radiation effects on gallium arsenide integrated optical devices
[DE88-004107] 11 p1551 N88-19277
Simulation of the plasma interaction with thin dust clouds 11 p1552 N88-19291
Radiation response of thin oxides grown by rapid thermal oxidation and rapid thermal annealing techniques
[DE88-003632] 11 p1561 N88-19347
Photohydrodynamical processes near compact objects
11 p1569 N88-19390
Photonic temperature and pressure sensors for biosystems/pulsed microwave. Part 1: Interaction studies
[AD-A188687] 12 p1629 N88-19751
Ultraviolet (180 to 300 nm) action spectra for inactivation and DNA photoproduct formation of Bacillus subtilis spores under ultrahigh vacuum 12 p1657 N88-19931
Survival and mutation induction of dehydrated yeast cells after UV exposure 12 p1657 N88-19932
Cellular effects of heavy ions: Experimental results and theoretical approaches — space radiation
12 p1658 N88-19933
Radiation problems in manned space flight with a view to the Space Station 12 p1658 N88-19934
Effects of heavy ions on egg-developing systems
12 p1658 N88-19935
Effects of cosmic heavy ion radiation and space microgravity on plant systems 12 p1658 N88-19936
Antibiotic activity in space, results and hypothesis
12 p1660 N88-19952
Nuclear health and safety: Radiation exposures for some cloud-sampling personnel need to be reexamined
[PB88-130497] 12 p1662 N88-19965
Effects of whole-body irradiation with low-intensity microwaves on morphological, functional and cytochemical characteristics of leukocytes 12 p1663 N88-19971
Food Irradiation Newsletter, Vol. 11, No. 1
[DE88-700808] 12 p1671 N88-20004
Effects of high temperature neutron irradiation on the physical, chemical and mechanical properties of fine-grained isotropic graphite 13 p1747 N88-20444
Degradations of thermal shock resistance and the fracture toughness of reactor graphite subjected to neutron irradiation 13 p1747 N88-20445
Computer simulation of tropospheric chemistry
[JUEL-2144] 13 p1798 N88-20756
Discussion of radiation effects and high-temperature oxide superconductors
[DE88-001427] 13 p1846 N88-21046
Effect of off-axis radiation in amplified spontaneous emission
[DE88-007001] 14 p1915 N88-21440
Laser enhanced adhesion of copper films to sapphire substrates
[DE88-006802] 15 p2038 N88-22144
The effective fracture toughness of aluminum at rapid heating rates
[AD-A189745] 15 p2038 N88-22146
Oxide optical coatings prepared by metal-organic vapor deposition
[DE88-006809] 15 p2043 N88-22175
A preliminary comparison of the transient effects of single versus multiple q-switched doubled-neodymium laser pulses
[AD-A189855] 15 p2071 N88-22347
High-efficiency thin-film silicon-on-GaP solar cell for improved radiation resistance
[AD-A190268] 15 p2091 N88-22460
Characterization of space radiation environment in terms of the energy deposition in functionally important volumes
[DE88-005627] 15 p2100 N88-22513

A comparison of visual evoked potential and behavioral measures of flashblindness in humans
[AD-A189757] 15 p2101 N88-22519
Computing X-ray effects in optics
[DE88-006722] 15 p2134 N88-22732
Behavior, physiology and energy deposition in rats chronically exposed to 2450 MHz radiation
[PB88-171418] 16 p2237 N88-23363
Numerical analysis for effects of irradiation nonuniformities on target implosion
16 p2276 N88-23621
Radiation effects in silicon
[DE88-006642] 16 p2282 N88-23659
The response of a power MOSFET (N-channel) and a dielectric isolated operational amplifier to the combined environmental effects of high temperature and total dose gamma radiation 17 p2406 N88-24309
Radiation hardening design of nuclear powered spacecraft 17 p2407 N88-24315
Defects in cubic silicon carbide on silicon
17 p2408 N88-24317
Analysis of thermal and radiation effects in materials using the GEMAT process 17 p2408 N88-24318
Radiation effects testing capabilities of the Texas A and M Nuclear Science Center 17 p2416 N88-24368
Silicon-on-insulator electronics for a space nuclear power system 17 p2431 N88-24461
The response of selected semiconductor technologies to the combined environmental effects of high temperature and total dose gamma radiation
17 p2431 N88-24462
Neutron effects on the electrical and switching characteristics of NPN bipolar power transistors
17 p2431 N88-24463
Development of refractory thermocouples for space nuclear power tests 17 p2434 N88-24476
Irradiation effects on tungsten stabilized martensitic steels
[DE88-007074] 18 p2486 N88-24748
Behavioral response of rats exposed to high-power microwave radiation
[AD-A192199] 18 p2548 N88-25126
Selective radiation absorption in aluminized composite propellant combustion 19 p2630 N88-25596
Extremely Low Frequency (ELF) communications system ecological monitoring program: Summary of 1986 progress
[AD-A192014] 19 p2642 N88-25676
Health and environmental consequences of the Chernobyl nuclear power plant accident
[DOE/ER-0332] 19 p2669 N88-25985
Noise and chaos in driven Josephson junctions
19 p2734 N88-26238
Abnormal diffusion of vacancies in metals
[DE88-701880] 20 p2773 N88-26441
Helium induced degradation in the weldability of an austenitic stainless steel
[DE88-009062] 20 p2773 N88-26443
Effects of cosmic rays on single event upsets
[NASA-CR-183053] 20 p2793 N88-26569
A method for estimating the susceptibility of electronic systems to HPM (High Power Microwave)
[DE88-012246] 21 p2934 N88-27422
Genetic effects of low level microwave radiation
[AD-A192687] 21 p2984 N88-27722
Effects of pulsed and CW (Continuous Wave) 2450 MHz radiation on transformation and chromosomes of human lymphocytes in vitro
[AD-A193104] 21 p2987 N88-27736
Assessment of cochlear damage after microwave irradiation
[AD-A193237] 21 p2987 N88-27737
Behavioral effects of exposure to the tempo high-power microwave system
[AD-A193305] 21 p2987 N88-27738
Dynamics of a plasma produced under effect of the XeCl-laser radiation on metallic surface
[DE88-701983] 21 p3017 N88-27902
Dose-enhancement effects in TaSi/Al- and Al-gate MOS devices
[DE88-005483] 21 p3020 N88-27926
Embryogenesis and organogenesis of Carausius morosus under spaceflight conditions
22 p3061 N88-28167
Dosimetric mapping inside Biorack --- Spacelab D1 mission 22 p3062 N88-28169
Avionics system design for high energy fields: A guide for the designer and airworthiness specialist
[NASA-CR-181590] 23 p3178 N88-28919
The radiation sensitivity of select metal chelate polymers: Mechanistic changes at higher energies
[AD-A193487] 23 p3196 N88-29019
Currents induced in a human being for electromagnetic fields to 10 kHz-50 MHz
[AD-A191977] 23 p3238 N88-29268
Vision and visual protection in fast jet aircraft
23 p3241 N88-29292
Study of biological effects and radiation protection to future European manned space flights
[DGT-33061] 23 p3261 N88-29535
An HVEM study of displacement cascade damage in Nb3Sn at 13 K
[DE88-009997] 23 p3289 N88-29584

RADIATION EXPOSURE
U RADIATION DOSAGE

RADIATION FIELDS
U RADIATION DISTRIBUTION

RADIATION HARDENING
Variations in semiconductor device response in a medium-energy x-ray dose-enhancing environment
[DE87-012400] 02 p0243 N88-11538
Effect of irradiation on the tensile properties of niobium-base alloys
[DE87-002409] 03 p0285 N88-11790
Dramatically improved radiation hardness for CMOS silicon gate integrated circuits even down to cryogenic temperatures
[AD-A184672] 03 p0381 N88-12398
Radiation hardness evaluation of thin film ferroelectric capacitors
[DE88-001357] 07 p0848 N88-15147
A report on the effects of neutron irradiation of GaAs semiconductors
[AD-A186816] 09 p1253 N88-17510
Dispersive hole transport in SiO2
[AD-A187077] 09 p1254 N88-17513
Radiation effects testing capabilities of the Texas A and M Nuclear Science Center 17 p2416 N88-24368
Development of the field-induced electron injection and impact ionization (F4I) technique for radiation hardness testing of MOS (Metal-Oxide-Semiconductor) gate insulators
[AD-A192114] 18 p2583 N88-25345
The postirradiation tensile properties and microstructure of several vanadium alloys
[DE88-007140] 19 p2615 N88-25515
Thermionic integrated circuit program
[DE88-010119] 19 p2662 N88-25833
X-ray response of GaAlAs/GaAs radiation hardened double: Heterostructure photodiode compared to Si:PIN photodiodes
[DE88-007425] 19 p2733 N88-26231
Electrophoretic coatings. Part 1: Sandia applications
[DE88-006686] 20 p2776 N88-26465
High bandwidth optoelectronic signal link for use in an EMP (electromagnetic pulse) plus radiation environment
[DE88-009254] 20 p2790 N88-26549
The p-well or n-well CMOS technology for advanced SEU-hard SRAMs
[DE88-006845] 22 p3156 N88-28777
EMPTAC (Electromagnetic Pulse Test Aircraft) user's guide
[AD-A195072] 24 p3360 N88-30006

RADIATION HAZARDS
Preliminary estimates of galactic cosmic ray exposures for manned interplanetary missions
[NASA-TM-100519] 05 p0661 N88-14058
South African Association of Physicists in Medicine and Biology: 26th Annual Congress
[DE88-700824] 11 p1521 N88-19082
Operational concerns involving a shadow-shielded nuclear reactor for space station applications
17 p2398 N88-24257
Radiation hardening design of nuclear powered spacecraft 17 p2407 N88-24315
Nuclear safety as applied to space power reactor systems 17 p2415 N88-24360
Radiation safety in commercial air traffic
[NASA-TM-101156] 19 p2600 N88-25447
Health and environmental consequences of the Chernobyl nuclear power plant accident
[DOE/ER-0332] 19 p2669 N88-25985
Products from cosmic-ray interactions in extraterrestrial matter: What they tell us about radiation backgrounds in space
[DE88-009143] 19 p2743 N88-26288
Studies of HZE particle interactions and transport for space radiation protection purposes
[NASA-TM-101159] 20 p2886 N88-27142

RADIATION HEATING
U RADIANT HEATING

RADIATION INJURIES
Assessment of cochlear damage after microwave irradiation
[AD-A193237] 21 p2987 N88-27737

RADIATION INTENSITY
U RADIANT FLUX DENSITY

RADIATION LAWS
NT KIRCHHOFF LAW OF RADIATION

RADIATION MEASUREMENT
Direct detection of optical radiation through a sampling orifice for inductively coupled plasma atomic emission spectroscopy
[DE87-013609] 01 p0101 N88-10692
Evaluation of the infrared test method for the olympus thermal balance tests 02 p0136 N88-10656
The development of diagnostic fuses
[SAND-86-0395] 03 p0311 N88-11963
Empirical relations between photospheric magnetic fields and atmospheric radiative losses for cool dwarf stars 04 p0511 N88-13145
Radio frequency electromagnetic interference fields. A study in Swedish industry
[FOA-E-30007-3.3] 06 p0692 N88-14247
NBS (National Bureau of Standards) measurement services: Fricke dosimetry in high-energy electron beams
[PB88-110374] 06 p0781 N88-14795
The use of the direct measurement of solar radiation for the determination of Pasquill Stability Parameter
[AD-A188084] 07 p0946 N88-15750
Method of determining atmospheric moisture content by measurement of upward radiation intensity in near IR
08 p1007 N88-16106
International cooperative effort to establish ASTM (American Society for Testing and Materials) standards for the measurement of radiation dose for food processing
[DE88-002702] 10 p1372 N88-18190
The inverse problem and the pseudo-empirical orthogonal function method of solution. Part 1: Theory. Part 2: Application
[AD-A188894] 12 p1664 N88-20069
Measurements of the cosmic background radiation
[NASA-CR-182637] 12 p1712 N88-20248
Global solar oscillations observed in the visible to near infrared continuum 13 p1858 N88-21110
A low-frequency measurement of the spectrum of the cosmic microwave background radiation
13 p1858 N88-21112
An approximation technique for solving a system of Fredholm integral equations for asymmetric detector response functions
[AD-A190577] 15 p2121 N88-22645
Radiation standards 16 p2272 N88-23582
Requirements for radiation receivers
16 p2272 N88-23583
Sky radiance distributions for thermal imaging backgrounds
[AD-A191135] 17 p2373 N88-24115
Results of radiation measurements in West Germany and from special measurement series in the Meteorological Observatory of Hamburg
[REPT-11] 18 p2542 N88-25086
Measurement of the radiative properties of gas and oil flames
[NASA-TT-20299] 19 p2612 N88-25802
Evaluation of surface energy and radiation balance systems for FIFE
[NASA-CR-183118] 20 p2828 N88-26778
Angular radiation models for Earth-atmosphere system. Volume 1: Shortwave radiation
[NASA-RP-1184] 21 p2976 N88-27677
Use of penetrating radiations for the dynamic examination of aero gas turbines
[PNR90470] 22 p3045 N88-28073
Stratocumulus and cloud-free reflectance from multi-spectral satellite measurements
[AD-A193899] 22 p3126 N88-28598

RADIATION MEASURING INSTRUMENTS
NT ADVANCED VERY HIGH RESOLUTION RADIOMETER
NT BOLOMETERS
NT CERENKOV COUNTERS
NT DICKE RADIOMETERS
NT DOSIMETERS
NT EBERT SPECTROMETERS
NT ELECTRON COUNTERS
NT ELECTROPHOTOMETERS
NT ELECTROSTATIC PROBES
NT FABRY-PEROT SPECTROMETERS
NT FLIR DETECTORS
NT INFRARED DETECTORS
NT INFRARED INSTRUMENTS
NT INFRARED RADIOMETERS
NT INFRARED SCANNERS
NT INFRARED SPECTROMETERS
NT INFRARED SPECTROPHOTOMETERS
NT MICROWAVE RADIOMETERS
NT NEUTRON COUNTERS
NT NEUTRON SPECTROMETERS
NT PARTICLE TELESCOPES
NT PHOTOMETERS
NT PROPORTIONAL COUNTERS
NT RADIATION COUNTERS
NT RADIATION DETECTORS

NT RADIOMETERS
NT SCINTILLATION COUNTERS
NT SILICON RADIATION DETECTORS
NT SOLAR SPECTROMETERS
NT SPARK CHAMBERS
NT SPECTROHELIOGRAPHS
NT SPECTROPHOTOMETERS
NT SPECTRORADIOMETERS
NT THRESHOLD DETECTORS (DOSIMETERS)
NT TOTAL OZONE MAPPING SPECTROMETER
NT ULTRAVIOLET SPECTROMETERS
NT ULTRAVIOLET SPECTROPHOTOMETERS
Development of response models for the Earth Radiation Budget Experiment (ERBE) sensors. Part 2: Analysis of the ERBE integrating sphere ground calibration
[NASA-CR-178293] 01 p0049 N88-10316
Ultraviolet measurements: Measurements of photolysis rates 18 p2539 N88-25065

RADIATION MEDICINE
U NUCLEAR MEDICINE

RADIATION METERS
U RADIATION MEASURING INSTRUMENTS

RADIATION NOISE
U ELECTROMAGNETIC NOISE

RADIATION PRESSURE
NT ILLUMINANCE
NT LUMINANCE
NT LUMINOUS INTENSITY
NT SOUND PRESSURE
Acoustic radiation from line- and point-loaded plates: Uniformly asymptotic solutions
[AD-A189367] 13 p1834 N88-20969
Optical trapping of neutral atoms and dielectric particles by radiation pressure 14 p1974 N88-21783
Doppler distortion of solar Fraunhofer lines in zodiacal light by reflection from interplanetary dust
19 p2740 N88-26270
Time-dependent mass loss from hot stars with and without radiative driving
[DE88-006899] 20 p2884 N88-27128

RADIATION PROTECTION
NT RADIATION SHIELDING
NT SOLAR RADIATION SHIELDING
Radiation effects in space
[DE87-012529] 01 p0075 N88-10479
Committee on Interagency Radiation Research and Policy Coordination
[DE88-003358] 09 p1188 N88-17121
Technical activities 1987, Center for Radiation Research
[PB88-129325] 09 p1245 N88-17464
South African Association of Physicists in Medicine and Biology: 28th Annual Congress
[DE88-700824] 11 p1521 N88-19082
Vega-1 and Vega-2 automatic stations: Functioning of flyby vehicles during encounter with Halley's comet
13 p1725 N88-20314
Theory of interactions of intense light with nonlinear, inhomogeneous and periodic structures and its applications to optical bistability, optic gyroscopes, nonlinear spectroscopy, radiation protection, X-ray emission and related fields
[AD-A190040] 15 p2133 N88-22725
Nuclear safety as applied to space power reactor systems 17 p2415 N88-24360
The use of liquid films for spacecraft survivability to laser radiation
[AD-A192954] 20 p2765 N88-26395
Mobile robot survival
[DE88-009108] 20 p2809 N88-26665
Studies of HZE particle interactions and transport for space radiation protection purposes
[NASA-TM-101159] 20 p2886 N88-27142
Study of biological effects and radiation protection to future European manned space flights
[DGT-33061] 23 p3281 N88-29535

RADIATION PYROMETERS
Noncontact Temperature Measurement
[NASA-CP-2503] 17 p2327 N88-23895
Radiation thermometry: The measurement problem
17 p2328 N88-23895
Noncontact temperature measurement in glass and other transparent materials 17 p2328 N88-23900
Multi-color pyrometer for materials processing in space
17 p2329 N88-23905
Direct emissivity measurements on liquids and corrections to multi-color pyrometers
17 p2329 N88-23906
Common but unappreciated sources of error in one, two, and multiple-color pyrometry 17 p2329 N88-23907
Fast optical pyrometry 17 p2329 N88-23908
The role of fiberoptics in remote temperature measurement 17 p2329 N88-23909
Laser pyrometry 17 p2330 N88-23910
Noncontact true temperature measurement, 2
17 p2330 N88-23911

RADIATION RESISTANCE
U RADIATION TOLERANCE

RADIATION SHIELDING
NT SOLAR RADIATION SHIELDING
A comparison of open and closed multimegawatt space power and weapon systems
[DE87-012975] 01 p0089 N88-10579
A paper about electromagnetic pulse and principles of EMP protection
[FOA-C-30455-4.2] 06 p0682 N88-14246
Shielding analysis of a small compact space nuclear reactor
[AD-A185566] 06 p0779 N88-14784
Suppression of X-rays generated by runaway electrons in ATF
[DE88-004179] 10 p1414 N88-18440
Project SKYLITE: A design exploration
[AD-A187906] 11 p1511 N88-19030
Radiation problems in manned space flight with a view to the Space Station 12 p1658 N88-19934
SOAR: Space orbiting advanced fusion power reactor
[AD-A189234] 13 p1732 N88-20356
Anthropomorphic phantom radiation dosimetry at the NATO standard reference point at Aberdeen Proving Ground
[AD-A190508] 15 p2103 N88-22528
X-ray production in low energy proton stopping
[NASA-TM-100619] 16 p2270 N88-23582
Operational concerns involving a shadow-shielded nuclear reactor for space station applications
17 p2398 N88-24257
Material tradeoffs to minimize flooding reactivity
17 p2399 N88-24265
Magnet shielding analysis for SOAR: A space fusion reactor 17 p2400 N88-24269
Fabrication of lithium hydride shields for space nuclear power systems 17 p2402 N88-24282
Fabrication of reactor shields at the Y-12 plant
17 p2402 N88-24283
Radiation hardening design of nuclear powered spacecraft 17 p2407 N88-24315
Space nuclear reactor shielding optimization studies
17 p2408 N88-24320
Comparison of open and closed multimegawatt space power systems 17 p2414 N88-24353
RSMASS: A simple model for estimating reactor/shield masses 17 p2414 N88-24355
MMW shielding design and analysis
17 p2430 N88-24457
Neutron effects on the electrical and switching characteristics of NPN bipolar power transistors
17 p2431 N88-24463
The Oak Ridge National Laboratory strategic defense initiative shield optimization program
[DE88-008946] 19 p2721 N88-26160
A method for estimating the susceptibility of electronic systems to HPM (High Power Microwave)
[DE88-012246] 21 p2934 N88-27422

RADIATION SICKNESS
Emetic mechanism in acute radiation sickness
[AD-A194102] 23 p3238 N88-29267

RADIATION SOURCES
NT MONOCHROMATORS
NT POINT SOURCES
The Hermes-3 program
[DE87-012132] 02 p0234 N88-11473
Center for X-Ray Optics, 1986
[DE88-000715] 04 p0449 N88-12783
Technical activities 1987, Center for Radiation Research
[PB88-129325] 09 p1245 N88-17464
On the time delay of the ultrahigh-energy radiation signal from the source Cygnus X-3
[DE88-700649] 10 p1431 N88-18547
Induction linacs: A technology come of age for international cooperation
[DE88-003953] 11 p1548 N88-19258
Coherent VUV source at 130 nm: Theory and modeling
[DE88-003874] 11 p1549 N88-19269
Microwave generation from a cusptron oscillator with a six-vane circuit
[AD-A188377] 12 p1619 N88-19680
X-ray source model for Z-pinch aluminum plasmas
[AD-A189509] 12 p1696 N88-20148
Long duration coherent Lyman-alpha sources
16 p2268 N88-23571
Ultraviolet radiometry: Radiation sources and measuring methods 16 p2272 N88-23596
Spectroradiometry in the industrial test laboratory
16 p2272 N88-23598
SNAP-DYN: Proven technology for wear-term, higher power in space 17 p2425 N88-24422
A plasma ultraviolet source for short wavelength lasers
[AD-A192844] 21 p2952 N88-27537
Guided radiation beams in free electron lasers
[AD-A194525] 22 p3082 N88-28305
An undulator radiation source for spin-polarized photoemission studies of novel magnetic materials
[AD-A193756] 22 p3083 N88-28307

RADIATION SPECTRA
NT ABSORPTION SPECTRA
NT BALMER SERIES
NT ELECTROMAGNETIC SPECTRA
NT ELECTRONIC SPECTRA
NT EMISSION SPECTRA
NT FRAUNHOFER LINES
NT GAMMA RAY SPECTRA
NT H ALPHA LINE
NT H BETA LINE
NT H LINES
NT HERZBERG BANDS
NT INFRARED SPECTRA
NT K LINES
NT LINE SPECTRA
NT LYMAN SPECTRA
NT MICROWAVE SPECTRA
NT RADIO SPECTRA
NT RAMAN SPECTRA
NT RYDBERG SERIES
NT SOLAR SPECTRA
NT STELLAR SPECTRA
NT ULTRAVIOLET SPECTRA
NT VIBRATIONAL SPECTRA
NT VISIBLE SPECTRUM
NT X RAY SPECTRA
Mathematics applied to nuclear geophysics
[INPE-4234-PRE/1109] 01 p0086 N88-10561
Cloud cover determination in polar regions from satellite imagery
[NASA-CR-181544] 04 p0471 N88-12908
Elementary process and meteor train spectra
06 p0732 N88-14504
On the meteor trail spectra 06 p0737 N88-14533
Fog, rain and aerosol attenuation in the atmosphere
[AD-A190867] 16 p2235 N88-23350
Spectral radiation measurement using a photodiode array as receiver 16 p2271 N88-23591

RADIATION THERAPY
Biology and Medicine Division
[DE87-009280] 14 p1952 N88-21632

RADIATION TOLERANCE
Nuclear health and safety: Radiation exposures for some cloud-sampling personnel need to be reexamined
[PB88-130497] 12 p1662 N88-19965
High-efficiency thin-film silicon-on-GaP solar cell for improved radiation resistance
[AD-A190268] 15 p2091 N88-22460
Neutron radiation tolerance of Au-activated silicon
17 p2408 N88-24316
Development of a GaAs solid state device model for high power applications
[DE88-009048] 19 p2734 N88-26242
A comparison of the radiation tolerance characteristics of multijunction solar cells with series and voltage-matched configurations
[NASA-TM-101177] 21 p2967 N88-27624
The p-well or n-well CMOS technology for advanced SEU-hard SRAMs
[DE88-006845] 22 p3156 N88-28777
Optical emission behavior and radiation resistance of epoxy resins
[DE88-752629] 23 p3196 N88-29023
Emetic mechanism in acute radiation sickness
[AD-A194102] 23 p3238 N88-29267

RADIATION TRANSPORT
Status of the solar and infrared radiation submodels in the LLNL 1-D and 2-D chemical-transport models
[DE87-014320] 01 p0069 N88-10441
The iterative radiance model of the Meteorological Institute of the University of Munich (West Germany)
08 p1019 N88-16178
Radiation transport in planetary nebulae
[ETN-88-91500] 14 p1993 N88-21880
Multigroup flux-limited asymptotic diffusion Fokker-Planck equation
[DE88-700958] 15 p2118 N88-22615
High-energy laser-assisted imaging through vaporizing aerosols
[DE88-007911] 18 p2521 N88-24957

RADIATIVE HEAT TRANSFER
Radiative and free-convective heat transfer from a finite horizontal plate inside an enclosure
02 p0133 N88-10833
Conjugated heat transfer from a radiating fluid in a rectangular channel 03 p0317 N88-12003
Nonequilibrium characteristics of nitrogen plasmas appropriate to an AOTV flight 03 p0319 N88-12019
The effects of minor trace gases on the transfer of thermal infrared radiation through the Earth's atmosphere 04 p0466 N88-12893

Heating of stellar chromospheres and coronae: Evidence for non-magnetic basal heating
04 p0503 N88-13098

A hybrid fibreglass-CFRP cloth for new furnishings — aircraft cabins
[SNIAS-872-111-109] 05 p0558 N88-13396

The ocean heat budget
[AD-A186130] 07 p0881 N88-15346

Radiative heat transfer solutions in plane-parallel participating media: Application to multilayer insulations for space vehicles
[INPE-4221-PRE/1101] 08 p0962 N88-15824

Three dimensional Monte Carlo simulation of molecular movement and heat radiation in vacuum devices: Computer code MOVAK3D — fusion reactors
[KFK-4292] 09 p1246 N88-17471

Studies on homogeneous and heterogeneous reactive flows 11 p1484 N88-18861

Transient radiative energy transfer in incompressible laminar flows
[NASA-CR-182605] 11 p1488 N88-18863

Investigation of supersonic chemically reacting and radiating channel flow
[NASA-CR-182726] 14 p1862 N88-21125

Climatology and space observations
[ISBN-2-85-428179-9] 14 p1935 N88-21536

The role of radiation transfer in climate modification
14 p1936 N88-21549

Net radiative flux at the Earth surface: Estimation from satellite observations 14 p1936 N88-21550

The thermal radiative properties of metals at high temperature
[DE88-006625] 15 p2038 N88-22141

Liquid-metal MHD power conversion for space electric systems 17 p2411 N88-24338

Transient thermohydraulic heat pipe modeling
17 p2413 N88-24347

Development of materials for fabric radiators
17 p2429 N88-24448

Moving belt radiator development status
[NASA-TM-100909] 19 p2607 N88-25477

Anomalous emissivity from periodic micro-machined silicon surfaces 19 p2670 N88-25872

Experimental and theoretical analysis of the radiative transfer within a sooty pool fire
[DE88-007099] 20 p2769 N88-26419

Ignition and flame spread of PMMA
[NASA-TT-20290] 20 p2771 N88-26431

Radiative heat transfer and selective emission in planar slab coatings on hot emissive substrates
[AD-A193133] 21 p2918 N88-27319

Radiative heat transfer to chemically reacting flow between concentric rotating spheres
[DE88-702538] 22 p3118 N88-28525

Flamelet chemistry modelling of soot formation for radiation 24 p3348 N88-29928

Radiation transfer in gas turbine combustors
24 p3348 N88-29929

The effect of particle properties on radiative heat transfer 24 p3350 N88-29941

Radiative heat transfer to steady flow of a chemically reacting fluid in a horizontal porous channel with variable wall temperature
[DE88-702704] 24 p3372 N88-30061

RADIATIVE LIFETIME

Computed potential energy surfaces for chemical reactions
[NASA-CR-183168] 24 p3342 N88-29893

RADIATIVE RECOMBINATION

The qualitative determination of high injection effects in flux-loaded P-I-N diodes using the recombination radiation measuring method
[ETN-88-91475] 11 p1560 N88-19336

The role of electron-ion recombination in bulk antimatter production 16 p2268 N88-23567

RADIATIVE TRANSFER

NT RADIATIVE HEAT TRANSFER

Circumstellar radio molecular lines
02 p0252 N88-11595

Circumstellar shells, the formation of grains, and radiation transfer 02 p0252 N88-11596

Observations and analysis of the photospheric magnetic fields on dwarf G, K and M stars
04 p0520 N88-13196

MODTRAN: A moderate resolution model for LOWTRAN
[AD-A185384] 05 p0574 N88-13503

Automated satellite cloud analysis: A multispectral approach to the problem of snow/cloud discrimination
[AD-A185672] 06 p0748 N88-14591

Observation and interpretation of solar S-component radiation at millimetre waves
[PB87-225207] 06 p0805 N88-14916

Estimation of broadband planetary albedo from operational narrowband satellite measurements
[PB88-107644] 07 p0945 N88-15748

Thematic mapper research in the earth sciences: Small scale patches of suspended matter and phytoplankton in the Elbe River Estuary, German Bight and Tidal Flats
[NASA-CR-182378] 08 p1019 N88-16180

Application of satellite data in variational analysis for global cyclonic systems
[NASA-CR-182468] 09 p1193 N88-17152

Parameterization of radiative transfer in the Earth's atmosphere with specific applications to clouds
10 p1353 N88-18087

Light absorption by an atom moving inside a spherical box
[AD-A187241] 10 p1407 N88-18395

On the possibility of high velocity deflagration front propagation by radiative energy transfer
[AD-A189022] 12 p1613 N88-19645

Models of recombination lines in radio H2 regions
[INPE-4302-TDL/277] 12 p1710 N88-20232

Dynamical and photometric studies of Saturn's rings
12 p1711 N88-20241

Multiple scattering of polarized light in cirrus clouds
13 p1801 N88-20768

Tabulation of Mie scattering calculation results for microwave radiative transfer modeling
[NASA-CR-4130] 14 p1947 N88-21612

Analytic and numerical modeling of heat and material transport in electrical hypervelocity guns
[AD-A192178] 18 p2469 N88-24655

Voyager imaging photometry and radiative transfer modeling of the spoke-like features in Saturn's outer B-ring 19 p2742 N88-26278

Validate algorithms for the determination of rainfall rates from SSM/I microwave satellite imagery
[AD-A192299] 21 p2974 N88-27664

Infrared detection using Rydberg atoms
[AD-A194308] 23 p3191 N88-28990

An analysis of heat transfer after loss of primary coolant in the SP-100 reactor system
[AD-A194619] 23 p3281 N88-29539

RADICALS

NT FREE RADICALS

NT HYDROXYL RADICALS

Photoabsorption and photodissociation of molecules important in the interstellar medium
[NASA-CR-182435] 08 p1100 N88-16617

On the interpretation of the CH cometary spectrum
14 p2007 N88-21969

Probing the possibility of a (12)C/(13)C abundance gradient from observations of interstellar CH+
[DE88-008908] 20 p2884 N88-27125

RADII

The deposition rate dependence of plasma polymerization on the radius of curvature of the substrate
[DE88-003811] 10 p1412 N88-18429

Fitting a circle to radially suppressed data
[NPL-DITC-103/87] 17 p2392 N88-24223

RADIO ALTIMETERS

An evaluation of three linear scale radar altimeter displays
[AD-A192173] 18 p2465 N88-24636

Determination of the ocean circulation by spaceborne radar altimeter 19 p2701 N88-26060

Ocean satellite data and the needs of designers and operators of marine units 19 p2701 N88-26061

Development of procedures for performing end-to-end tests on the ERS-1 radar altimeter and AMI using a compact antenna test range — Active Microwave Instrument (AMI)
[ESA-CR(P)-2558] 24 p3363 N88-30022

RADIO ANTENNAS

NT MICROWAVE ANTENNAS

A new state space model for the NASA/JPL 70-meter antenna servo controls 04 p0436 N88-12702

Analysis of the ICE combiner for multiple antenna arraying 04 p0436 N88-12704

A modern control theory based algorithm for control of the NASA/JPL 70-meter antenna axis servos
04 p0436 N88-12706

Power density measurements in the near field of the DSS 13 26-meter antenna 04 p0437 N88-12711

A dynamic simulation and feedback control scheme for the U.S. Marine Corps' Airborne Remotely Operated Device (AROD)
[AD-A186597] 08 p0953 N88-15784

Capacitor analysis for RF antennas
[DE88-004178] 10 p1318 N88-17663

Space-diversity effects on line-of-sight propagation paths 12 p1617 N88-19670

Some measurements of height gain at V.H.F.
12 p1617 N88-19671

Environmental projects. Volume 6: Environmental assessment. New 34-meter antenna at Venus site
[NASA-CR-182922] 17 p2332 N88-23919

Evaluation of vertical monopole antennas with elevated radials
[DE88-008339] 19 p2654 N88-25760

Radio astronomy 24 p3364 N88-30031

RADIO ASSISTED DETECTION AND RANGING

U RADAR

RADIO ASTRONOMY

Venusian surface and crust 01 p0010 N88-10064

Imaging at radio wavelengths
01 p0094 N88-10616

Circumstellar radio molecular lines
02 p0252 N88-11595

The Telecommunications and Data Acquisition Report
[NASA-CR-181546] 04 p0432 N88-12679

Intelligent signal analysis and recognition
[NASA-CR-181531] 04 p0501 N88-13084

Nonthermal phenomena in stellar coronae: Evidence from radio observations 04 p0503 N88-13096

A re-examination of the corona-wind dividing line: Diagnostics of non-coronal atmospheres
04 p0504 N88-13101

VLA observations of rapid 6 cm flux variations in alpha Ori 04 p0515 N88-13169

EVN (European VLBI network) and MERLIN observations of 5 superluminal radio sources
[PB87-110730] 04 p0520 N88-13193

Finnish-Soviet Symposium on Radio Astronomy (1st) held at Otaniemi on August 26-27, 1985
[PB87-140661] 07 p0944 N88-15736

Source and event selection for radio-planetary frame-tie measurements using the Phobos Landers
11 p1471 N88-18775

Solar radioimage restoration
[INPE-4312-TDL/279] 11 p1571 N88-19402

The Deep Space Network
[NASA-CR-182700] 13 p1759 N88-20524

Recent observations of the OH radio lines in comets
14 p1999 N88-21917

Thermal-nonthermal relationships in active galactic nuclei
[B8681482] 16 p2289 N88-23707

The polarization of radio galaxies: Its structure at low frequencies
[B8681611] 20 p2884 N88-27123

Laboratory evaluation and application of microwave absorption properties under simulated conditions for planetary atmospheres
[NASA-CR-182443] 23 p3300 N88-29653

Review of Radio Science, 1984-1986
24 p3363 N88-30023

Radio astronomy 24 p3364 N88-30031

The Deep Space Network: An instrument for radio astronomy research
[NASA-CR-183219] 24 p3453 N88-30554

RADIO ATTENUATION

The 6 GHz propagation measurements over a 51 km path in the UK 12 p1617 N88-19673

An EHF telecommunication system engineering model
12 p1618 N88-19674

A propagation campaign in a marine environment utilizing a digital system at 36 GHz 12 p1618 N88-19675

RADIO BEACONS

Antarctic field tests of SARSAT personal locator beacons
[NASA-TM-4008] 01 p0063 N88-10403

RADIO BROADCASTING

U BROADCASTING

RADIO BURSTS

NT SOLAR RADIO BURSTS

NT TYPE 3 BURSTS

Data recorded by the Rome room temperature gravitational wave antenna, during the supernova SN 1987 A in the Large Magellanic Cloud
[NOTA-INTERNA-879] 06 p0806 N88-14922

Solar-geophysical data number 521, January 1988. Part 2: (Comprehensive reports). Data for July 1987 and miscellanea
[PB88-179221] 19 p2743 N88-26285

RADIO COMMUNICATION

NT CODE DIVISION MULTIPLE ACCESS

NT RADIO RELAY SYSTEMS

NT RADIO TELEMETRY

NT TELEPHONY

NT TIME DIVISION MULTIPLE ACCESS

Two-signal cross modulation effects, half-IF effects and interference criteria in land mobile sharing with UHF (Ultra High Frequency) television
[PB87-228037] 05 p0576 N88-13514

MM-wave propagation and application in military communication systems 12 p1617 N88-19669

An investigation of conformable antennas for the astronaut backpack communication system
[NASA-CR-182908] 17 p2333 N88-23929

Development of the network architecture of the Canadian MSAT system 19 p2646 N88-25702

Wave propagation and remote sensing
24 p3364 N88-30029

RADIO CONTROL
Timing control system
[NASA-CASE-NPO-16882-1-CU]
18 p2506 N88-24863
Frequency domain identification of the dynamics of a scaled remotely-piloted helicopter
20 p2786 N88-26524

RADIO ECHOES
JPRS report: Science and technology. China
[JPRS-CST-87-031] 03 p0299 N88-11880
Height profile inversion of ionospheric movement from observed parameters of HF radio echoes
03 p0299 N88-11884
Terrestrial Propagation Characteristics in Modern Systems of Communications, Surveillance, Guidance and Control
[AGARD-CP-407] 12 p1614 N88-19653

RADIO EMISSION
NT CN EMISSION
NT HYDROXYL EMISSION
NT RADIO BURSTS
NT SOLAR RADIO BURSTS
NT SOLAR RADIO EMISSION
NT TYPE 3 BURSTS
Coronal and interplanetary Type 2 radio emission
01 p0114 N88-10731
A VLA survey of dMe flare stars
04 p0513 N88-13154
Radio continuum emission from the ionized stellar winds of the cool supergiants in zeta Aurigae-like systems
04 p0514 N88-13160
Radio emission from RS CVn binaries: A 5 GHz VLA survey of 93 systems 04 p0519 N88-13191
Ray tracing of Jovian low frequency radiation
[NASA-CR-179262] 08 p1101 N88-16620
Self-modulational formation of pulsar microstructures
[NASA-CR-182420] 08 p1104 N88-16622
The radio structure of active nuclei in edge-on spiral and Seyfert galaxies 09 p1264 N88-17576

RADIO EQUIPMENT
NT IONOSONDES
NT MICROWAVE ANTENNAS
NT RADIO ANTENNAS
NT RADIO BEACONS
NT RADIO FILTERS
NT RADIO RECEIVERS
NT RADIO TELESCOPES
NT RADIO TRANSMITTERS
NT RADIOSONDES
NT RADIOTELEPHONES
NT RAWINSONDES
NT RECEPTION DIVERSITY
NT SPACECRAFT ANTENNAS
NT SUPERHETERODYNE RECEIVERS
NT TRANSMITTER RECEIVERS
NT TRANSPONDERS
NT VERY LARGE ARRAY (VLA)
X-band uplink ground systems development: Part 2
04 p0436 N88-12703
MARCE data evaluation 10 p1286 N88-17693
Spread spectrum mobile radio communications
[AD-A187487] 11 p1470 N88-18765
Spread spectrum radio networks
[AD-A188914] 12 p1620 N88-19689
Static and dynamic jamming of networks
[AD-A188921] 12 p1620 N88-19690
Multiple address facility for packet radio: An investigation of performance/complexity trade off
[AD-A191043] 16 p2190 N88-23064
Practical VLF/LF radio test system
[AD-A191768] 18 p2500 N88-24831
A random access algorithm for environments with capture and limited feedback capabilities
[AD-A192233] 20 p2790 N88-26552
Random-access algorithms for environments with capture
[AD-A194303] 23 p3203 N88-29060

RADIO FILTERS
Extending the impulse response in order to reduce errors due to impulse noise and signal fading
19 p2649 N88-25730

RADIO FREQUENCIES
NT EXTREMELY HIGH FREQUENCIES
NT EXTREMELY LOW RADIO FREQUENCIES
NT HIGH FREQUENCIES
NT LOW FREQUENCIES
NT MICROWAVE FREQUENCIES
NT SUPERHIGH FREQUENCIES
NT ULTRAHIGH FREQUENCIES
NT VERY HIGH FREQUENCIES
NT VERY LOW FREQUENCIES
On adaptive signal processing of RF signals
[DE87-014192] 02 p0161 N88-11007
Potential formation in the plasma confinement region of a radio-frequency plugged linear device
[IPPJ-843] 02 p0242 N88-11526
Applications of neutral beam and rf technologies
[DE87-014936] 03 p0379 N88-12382
High-power RF-pulsed modulators for the Los Alamos free-electron laser
[DE88-000514] 04 p0448 N88-12775
Tribological properties of rf-sputtered MoS2 coatings
[DE88-000266] 04 p0452 N88-12802
Fluctuations in frequency of coherent radio signals in solar plasma according to Venera-15 and Venera-16 data 08 p1003 N88-16079
Conceptual design of a radio-frequency driven compact tokamak
[INPE-4364-PRE/1190] 08 p1085 N88-16535
Telemetry applications handbook
[AD-A186825] 09 p1132 N88-16789
F-layer polar cap arcs
[AD-A186592] 09 p1190 N88-17127
Observation of enhanced electric field in an RF-plugged sheet plasma in the RFC-XX-M open-ended machine
[IPPJ-857] 09 p1252 N88-17503
The radio structure of active nuclei in edge-on spiral and Seyfert galaxies 09 p1264 N88-17576
Photoconductor switch and circuit analysis
[AD-A188166] 11 p1478 N88-18821
RF steering in the CEBAF CW superconducting linac
[CEBAF-PR-87-013] 11 p1547 N88-19251
Identification of microwave line-of-sight multipath components 12 p1616 N88-19665
Application of radio frequency superconductivity to recirculating linacs
[CEBAF-PR-88-002] 12 p1690 N88-20107
The preparation, assembly and mounting of RF coaxial cables
[ESA-PSS-01-718-ISSUE-1] 13 p1756 N88-20504
Optical RF distribution links for MMIC phased array antennas
[NASA-TM-100841] 13 p1764 N88-20555
Progress in diagnostic techniques for SC cavities
[CEBAF-PR-88-003] 13 p1772 N88-20600
Theoretical studies of the heating of toroidal plasmas with radiofrequency electromagnetic radiation
[DE88-006913] 15 p2137 N88-22749
RF properties of superconducting Pb electroplated onto Cu
[DE88-005918] 15 p2139 N88-22765
Experimental radio frequency link for Ka-band communications applications
[NASA-TM-100824] 18 p2470 N88-24659
Arcing and rf signal generation during target irradiation by a high-energy, pulsed neutral particle beam
[DE88-007169] 18 p2471 N88-24664
Radio Frequency (RF) strain monitor
[NASA-CASE-LAR-13705-1] 18 p2530 N88-25011
Optical diagnostics for a high power, rf-inductively coupled plasma
[DE88-007822] 18 p2570 N88-25322
Large antenna experiments aboard the space shuttle: Application of nonuniform sampling techniques
19 p2652 N88-25745
Anomalous RF magnetoresistance in copper at 4 K
[DE88-010232] 19 p2722 N88-26162
Coherent RF error statistics
[AD-A193002] 20 p2792 N88-26560
Microwave calibration system 2
[AD-A192976] 20 p2805 N88-26639
Superconducting rf and beam-cavity interactions
[DE88-008598] 20 p2852 N88-26936
Rf cavity primer for cyclic proton accelerators
[DE88-010655] 20 p2853 N88-26938
Bootstrap currents in radio-frequency-driven tokamak equilibria
[DE88-011136] 23 p3265 N88-29561
Study of secondary emission properties of materials used for high power RF components in space
[ESA-CR(P)-2587] 24 p3361 N88-30012
Electromagnetic noise and interference
24 p3363 N88-30028
Radio and infrared properties of young stars
[NASA-CR-183252] 24 p3459 N88-30579

RADIO FREQUENCY HEATING
Fast wave injection into high temperature tokamak plasmas in the lower-hybrid-density regime of JIPP T-IIU
[ISSN-0469-4732] 01 p0099 N88-10649
Microwave superheaters for fusion
[DE88-001656] 05 p0653 N88-14007
A ray-tracing study of electron cyclotron resonance heating in tokamak plasmas with a superthermal electron tail
[INPE-4381-PRE/1201] 08 p1085 N88-16536
Absorption of electron cyclotron radiation in tokamak plasmas with a superthermal tail in the electron velocity distribution
[INPE-4391-PRE/1211] 08 p1086 N88-16541
Modeling considerations for selected rf-plasma edge effects
[DE88-003285] 09 p1252 N88-17500
Ionosonde studies of field-aligned irregularities during high-power HF heating at Arecibo
[AD-A195848] 24 p3401 N88-30256
The study of hydromagnetic waves and RF heating using the TORTUS tokamak, the development of diagnostic techniques based on submillimeter lasers and the gyrotron, and gas discharge 24 p3431 N88-30419

RADIO FREQUENCY INTERFERENCE
NT CHIRP
NT ELECTROMAGNETIC NOISE
NT IONOSPHERIC NOISE
NT SHOT NOISE
NT THERMAL NOISE
NT WHISTLERS
NT WHITE NOISE
Monitoring of harmful interference to the HF (High Frequency) broadcasting service. 3: Results of the June 1986 coordinated monitoring period
[PB87-210274] 01 p0036 N88-10229
A comparative analysis of equatorial and auroral-zone phase scintillation data
[AD-A184509] 03 p0350 N88-12212
An analysis of whistler-mode radiation from the Spacelab-2 electron beam, revision
[AD-A188226] 11 p1552 N88-19287
Analysis, suppression of land clutter characteristics reported 14 p1903 N88-21369
Radio frequency compatibility between IRS and SPOT 3: Preliminary study
[CNES-86/CT/DRT/TIT/TR/011]
14 p1905 N88-21383
Evaluation of the communications impact of a low power arcjet thruster
[NASA-TM-100926] 18 p2475 N88-24682
Propagation management for no-acknowledge HF communications links 18 p2502 N88-24843
Aircraft field degradation and electromagnetic compatibility
[PB88-183975] 19 p2602 N88-25456
Method and apparatus for measuring distance
[NASA-CASE-MSC-20912-1] 20 p2793 N88-26568
Airborne measurement of low frequency atmospheric noise ALFAN 1
[AD-A193056] 21 p2931 N88-27405
A notch filter instrument for measuring ELF (Extremely Low Frequency) MSK (Minimum Shift Keying) signals
[AD-A193324] 21 p2933 N88-27414
New CCIR report on SETI 22 p3067 N88-28204

RADIO FREQUENCY NOISE
U ELECTROMAGNETIC NOISE

RADIO FREQUENCY RADIATION
U RADIO WAVES

RADIO GALAXIES
Long-baseline astrometric interferometers
[AD-A188474] 12 p1713 N88-20250
Infrared astronomy at extremely faint light levels in support of the LAIRTS program
[AD-A191497] 18 p2592 N88-25404
The polarization of radio galaxies: Its structure at low frequencies
[B8681611] 20 p2884 N88-27123

RADIO INTERFERENCE
U RADIO FREQUENCY INTERFERENCE

RADIO INTERFEROMETERS
Long-baseline astrometric interferometers
[AD-A188474] 12 p1713 N88-20250

RADIO JETS (ASTRONOMY)
Long-baseline astrometric interferometers
[AD-A188474] 12 p1713 N88-20250

RADIO METEOROLOGY
Review of recent developments in evaporation ducting assessment 12 p1616 N88-19664

RADIO NAVIGATION
NT LORAN C
The Telecommunications and Data Acquisition Report
[NASA-CR-181546] 04 p0432 N88-12679
Generalized expression for radio navigation parameter error 13 p1787 N88-20691
NAVSTAR global positioning system
[AD-A192609] 20 p2757 N88-26354

RADIO OBSERVATION
Research in geodesy based upon radio interferometric observations of GPS (Global Positioning System) satellites
[AD-A184040] 03 p0346 N88-12187
New approaches to some methodological problems of meteor science 06 p0741 N88-14557

RADIO OCCULTATION
Laboratory evaluation and application of microwave absorption properties under simulated conditions for planetary atmospheres
[NASA-CR-181466] 02 p0254 N88-11606

Laboratory evaluation and application of microwave absorption properties under simulated conditions for planetary atmospheres
[NASA-CR-182443] 23 p3300 N88-29653
RADIO PROPAGATION
U RADIO TRANSMISSION
RADIO RANGE
Correlation between refraction over sea and nature of radar reflections from sea surface
06 p0728 N88-14477
RADIO RANGES
U RADIO BEACONS
RADIO RECEIVERS
NT SUPERHETERODYNE RECEIVERS
NT TRANSMITTER RECEIVERS
X-band uplink ground systems development: Part 2
04 p0436 N88-12703
Construction of a satellite simulator for the frequency range between 11.7 and 12.5 GHz
[IRT-TB-B-84/87] 16 p2166 N88-22917
An outdoor unit for Direct Broadcast Satellite (DBS) digital sound reception
[BMFT-FB-W-86-018] 16 p2189 N88-23050
The Sercel TRSS Global Positioning System (GPS) receiver
[ETN-88-92473] 20 p2757 N88-26357
RADIO REFLECTION
U RADIO ECHOES
RADIO RELAY SYSTEMS
NT CODE DIVISION MULTIPLE ACCESS
NT TIME DIVISION MULTIPLE ACCESS
Improvements to a UHF rebroadcast television link suffering tidal fading: Countisbury UHF relay station
[BBC-RD-1987/14] 05 p0573 N88-13495
Study of a Radio Relay Link (RRL). Cassini mission. Data package for final presentation
[ESA-CR(P)-2472] 07 p0847 N88-15138
A review of the role of surface reflection in multipath propagation over terrestrial microwave links
12 p1615 N88-19655
Space-diversity effects on line-of-sight propagation paths 12 p1617 N88-19670
RADIO SCATTERING
New approaches to some methodological problems of meteor science 06 p0741 N88-14557
Scattering and depolarization by random rough terrain and vegetation covered terrain-unified full wave approach 12 p1615 N88-19657
RADIO SIGNAL ATTENUATION
U RADIO ATTENUATION
RADIO SIGNAL PROPAGATION
U RADIO TRANSMISSION
RADIO SIGNALS
Implications of a simplified signal structure for Navsat
[REPT-83/1439] 01 p0005 N88-10024
Meteor-burst communications: Is this what the Navy needs?
[AD-A184433] 04 p0431 N88-12672
Two-signal cross modulation effects, half-IF effects and interference criteria in land mobile sharing with UHF (Ultra High Frequency) television
[PB87-226037] 05 p0576 N88-13514
Fluctuations in frequency of coherent radio signals in solar plasma according to Venera-15 and Venera-16 data 08 p1003 N88-16079
Indian Ocean validation
[AD-A194458] 23 p3175 N88-28902
RADIO SOURCES (ASTRONOMY)
NT EXTRAGALACTIC RADIO SOURCES
NT PULSARS
NT QUASARS
NT RADIO GALAXIES
NT RADIO JETS (ASTRONOMY)
NT RADIO STARS
USSR report: Space
[JPRS-USP-87-003] 01 p0009 N88-10050
Occultation of compact radio sources by the ion tail of Halley's Comet 01 p0118 N88-10753
Microwave observations of nonthermal phenomena in pre-main sequence stars 04 p0505 N88-13107
EVN (European VLBI network) and MERLIN observations of 5 superluminal radio sources
[PB87-110730] 04 p0520 N88-13193
The Spring 1985 high precision baseline test of the JPL GPS-based geodetic system
[NASA-CR-182886] 14 p1940 N88-21577
RADIO SPECTRA
NT MICROWAVE SPECTRA
Thermal-nonthermal relationships in active galactic nuclei
[B8891482] 16 p2269 N88-23707
RADIO STARS
NT PULSARS
The Parkes radio survey of active chromosphere stars
04 p0511 N88-13141
Infrared astronomy at extremely faint light levels in support of the LAIRTS program
[AD-A191497] 18 p2592 N88-25404
Radio astronomy 24 p3364 N88-30031
RADIO TELEMETRY
Spectral density estimates of coarsely quantized random vibration data 09 p1178 N88-17055
A deep-water OBS (Ocean Bottom Seismometer) array with real-time telemetry
[AD-A187404] 10 p1357 N88-18112
RADIO TELESCOPES
NT VERY LARGE ARRAY (VLA)
Radio astronomy 24 p3364 N88-30031
RADIO TRANSMISSION
NT IONOSPHERIC PROPAGATION
NT MICROWAVE ATTENUATION
NT MICROWAVE TRANSMISSION
NT MULTIPATH TRANSMISSION
NT SHORT WAVE RADIO TRANSMISSION
NT SPREAD SPECTRUM TRANSMISSION
NT TRANSEQUATORIAL PROPAGATION
Meteor-burst communications: Is this what the Navy needs?
[AD-A184433] 04 p0431 N88-12672
A raytrace method for a laterally heterogeneous environment
[AD-A186525] 08 p0978 N88-15912
Experimental Radio Data System (RDS): A survey of reception reliability in the UK
[BBC-RD-1987/17] 09 p1155 N88-16922
MARCE data evaluation 10 p1286 N88-17693
User's guide for the HF (High Frequency) broadcast antenna design and validation summary programs
[PB88-116124] 10 p1317 N88-17875
Source and event selection for radio-planetary frame-tie measurements using the Phobos Landers
11 p1471 N88-18775
Development of a ground-conductivity map for the area of the Federal Republic of Germany from measured field-strength contours 12 p1615 N88-19656
Scattering and depolarization by random rough terrain and vegetation covered terrain-unified full wave approach 12 p1615 N88-19657
VHF/UHF propagation by diffraction: Calculation by numerical integration 12 p1615 N88-19659
A diffraction based theoretical model for prediction of UHF path loss in cities 12 p1616 N88-19661
A program for the calculation of radio-wave transmission loss over the spherical earth and over obstacles
12 p1616 N88-19662
Review of recent developments in evaporation ducting assessment 12 p1616 N88-19664
Refractive index, meteorology and fading in line-of-sight transmission paths 12 p1616 N88-19666
The correlation between methodological and low-level angle-of-arrival measurements 12 p1617 N88-19668
Space-diversity effects on line-of-sight propagation paths 12 p1617 N88-19670
Some measurements of height gain at V.H.F.
12 p1617 N88-19671
An EHF telecommunication system engineering model
12 p1618 N88-19674
A propagation campaign in a marine environment utilizing a digital system at 36 GHz 12 p1618 N88-19675
Construction of a satellite simulator for the frequency range between 11.7 and 12.5 GHz
[IRT-TB-B-84/87] 16 p2166 N88-22917
WAVFLD: A program to compute ionospheric height gain functions and field strengths at VLF
[AD-A191159] 16 p2191 N88-23066
Environmental projects. Volume 6: Environmental assessment. New 34-meter antenna at Venus site
[NASA-CR-182922] 17 p2332 N88-23919
WIPP (Wave Induced Particle Precipitation) experiment logistic support
[AD-A191184] 18 p2499 N88-24824
An evaluation of two millimeter wave propagation models for horizontal atmospheric attenuation at 70-115 GHZ
[AD-A192699] 21 p2931 N88-27403
Rapid-scanning Fourier transform spectrometer for studies of propagation of near-millimeter-wave radiation through clear air and fog
[AD-A193752] 22 p3070 N88-28219
Activities report of the Electromagnetic Environment Division
[FOA-C-30484-3.2/3.3/4.1/4.2]
22 p3071 N88-28233
Electromagnetic interference to radar and radio link systems caused by large scale wind turbines
[FOA-C-30486-3.2] 22 p3071 N88-28234
RADIO TRANSMITTERS
NT IONOSONDES
NT RADIO BEACONS
NT RADIOSONDES
NT RADIOTELEPHONES
NT RAWINSONDES
NT TRANSMITTER RECEIVERS
Analysis of the ICE combiner for multiple antenna arraying 04 p0436 N88-12704
Power density measurements in the near field of the DSS 13 26-meter antenna 04 p0437 N88-12711
KOSPAS-SARSAT satellites used for ocean current study 24 p3450 N88-30534
RADIO WAVE REFRACTION
Terrestrial Propagation Characteristics in Modern Systems of Communications, Surveillance, Guidance and Control
[AGARD-CP-407] 12 p1614 N88-19653
Radio and radar holes and multipath zones: The global and local influences on atmospheric refractive structure and resulting adverse radio and radar performance
12 p1617 N88-19667
MM-wave propagation and application in military communication systems 12 p1617 N88-19669
RADIO WAVES
NT CENTIMETER WAVES
NT CN EMISSION
NT DECAMETRIC WAVES
NT DECIMETER WAVES
NT EXTRATERRESTRIAL RADIO WAVES
NT GALACTIC RADIO WAVES
NT HYDROXYL EMISSION
NT LONG WAVE RADIATION
NT MICROWAVE EMISSION
NT MICROWAVES
NT MILLIMETER WAVES
NT RADIO BURSTS
NT RADIO EMISSION
NT SHORT WAVE RADIATION
NT SOLAR RADIO BURSTS
NT SOLAR RADIO EMISSION
NT SUBMILLIMETER WAVES
NT TYPE 3 BURSTS
NT WHISTLERS
General theory of radio propagation through a stratified atmosphere
[PB87-226197] 04 p0430 N88-12682
Measured characteristics of 800/900 MHz mobile radio channels with high-angle propagation through moderately dense foliage
[CRC-1398] 05 p0573 N88-13493
Correlation between refraction over sea and nature of radar reflections from sea surface
06 p0728 N88-14477
Polar Geophysical Institute's studies of magnetosphere, ionosphere 06 p0728 N88-14480
A Jupiter Data Analysis Program (JDAP) research grant on wave accessibility and attributes
[NASA-CR-182348] 06 p0804 N88-14906
Solar-geophysical data number 515, July 1987. Part 1: (Prompt reports). Data for June 1987, May 1987 and late data
[PB87-233177] 06 p0805 N88-14912
Radar reflectivity and attenuation of radio waves in the melting layer of precipitation
[PB88-121553] 10 p1318 N88-17892
An assessment of the application of in situ ion-density data from DMSP to modeling of transionospheric scintillation
[AD-A188919] 12 p1643 N88-19840
Generalized expression for radio navigation parameter error 13 p1787 N88-20691
Trajectory synthesis of ionograms in presence of artificial ionospheric inhomogeneities 13 p1789 N88-20703
Power source selection for neutral particle beam systems 17 p2407 N88-24314
RADIOACTIVE CONTAMINANTS
The distribution of some chemical elements between dissolved and particulate phases in the ocean
[DE88-010181] 21 p2977 N88-27682
RADIOACTIVE DECAY
NT ALPHA DECAY
NT NEUTRON EMISSION
Summary and conclusions of the 6th Moriond workshop — standard electroweak model
[USIP-87-11] 01 p0092 N88-10902
Few body hypernuclear systems: Weak decays
[DE87-014920] 04 p0488 N88-13010
Nuclear beta decay after Les Houches
[DE87-014921] 04 p0489 N88-13011
Influences of the astrophysical environment on nuclear decay rates
[DE88-001461] 04 p0522 N88-13208
W decays
[NOTA-INTERNA-877] 05 p0648 N88-13968
Double beta decay and nuclear structure
[DE88-001966] 07 p0931 N88-15652
Theory of double beta decay
[DE88-002285] 07 p0931 N88-15653

Properties of nuclei and elementary particles at low and intermediate energies
[DE88-001913] 09 p1244 N88-17456
Calculated late time spectra of supernovae
[DE88-003296] 10 p1428 N88-18530
A look at Supernova 1987A
[DE88-003411] 10 p1429 N88-18531
Spontaneous decay and atomic fluorescence near a metal surface of an absorbing dielectric
[AD-A187508] 13 p1835 N88-20975
Gluino branching ratio effects on the search for supersymmetry
[PREPRINT-572] 14 p1981 N88-21821
A proposed national policy concerning the reentry of space reactors 17 p2415 N88-24359
A method for the analysis of heavy flavor decays
[NOTA-INTERNA-909] 22 p3150 N88-28744
Evidence of the in situ decay of Al-26 in a Semarkona chondrule 24 p3441 N88-30479
Lewis Cliff 86010, a unique Antarctic meteorite: Possible new clues to the early history of the solar system
24 p3442 N88-30482

RADIOACTIVE ELEMENTS
U RADIOACTIVE ISOTOPES

RADIOACTIVE ISOTOPES
NT COBALT 60
NT LAWRENCIUM
NT NEPTUNIUM
NT PLUTONIUM ISOTOPES
NT PLUTONIUM 238
NT TRITIUM
NT URANIUM 238
Content of natural radioactive elements in Venusian rocks determined using data from Vega-1 and Vega-2 stations 13 p1726 N88-20323
The Light-Weight Radioisotope Heater Unit (LWRHU): Development and application 17 p2405 N88-24299
MHW RTG performance during LES 8/9 and Voyager missions 17 p2405 N88-24300
Pioneer 10 and 11 RTG performance update
17 p2405 N88-24301
The radiation sensitivity of select metal chelate polymers: Mechanistic changes at higher energies
[AD-A193467] 23 p3196 N88-29019
The dynamics of transuranics and other radionuclides in natural environments, December 1985
[DE87-014456] 24 p3390 N88-30189

RADIOACTIVE MATERIALS
Airborne lidar experiments at the Savannah River Plant
[NASA-TM-4007] 02 p0194 N88-11209
The dynamic isotope power system: Technology status and demonstration program 17 p2422 N88-24400
RRSAS (Robotic Radiation Survey and Analysis System) Project: A real time sensor driven robotic system
[DE88-006825] 20 p2808 N88-26661

RADIOACTIVE NUCLIDES
U RADIOACTIVE ISOTOPES

RADIOACTIVE WASTES
A comparison of open and closed multimegawatt space power and weapon systems
[DE87-012975] 01 p0089 N88-10579
Highlights of the Chemical Technology Division's research activities
[DE88-000233] 03 p0282 N88-11773
The adaption and use of research codes for performance assessment
[DE88-000552] 06 p0756 N88-14639
JPRS report: Science and technology. Japan
[JPRS-JST-87-030] 16 p2185 N88-23026
Comparison of open and closed multimegawatt space power systems 17 p2414 N88-24353
Space reactor end of life issues
17 p2424 N88-24413
Review of numerical methods for radionuclide transport in three-dimensional porous media, at high Peclet numbers
[CFDU/87/10] 18 p2538 N88-25061
Optimization of mechanical/corrosion properties of TI-CODE 12 plate and sheet. Part 2: Thermomechanical processing effects
[DE88-007493] 19 p2616 N88-25517

RADIOACTIVITY
Radon Research Program, FY-1987
[DE88-002633] 09 p1188 N88-17120
Measurements of astrophysical reaction rates for radioactive samples
[DE88-004309] 10 p1429 N88-18537
Radioactivity as a means of nondestructive testing
[DE88-702778] 23 p3224 N88-29188

RADIOBIOLOGY
Critical phenomena and electromagnetic effects in biological membranes
[AD-A188156] 11 p1518 N88-19064
Biology and Medicine Division
[DE87-009280] 14 p1952 N88-21632

RADIOGENIC MATERIALS
The distribution of some chemical elements between dissolved and particulate phases in the ocean
[DE88-010181] 21 p2977 N88-27682

RADIOGRAPHY
NT AUTORADIOGRAPHY
NT COMPUTER AIDED TOMOGRAPHY
NT NEUTRON RADIOGRAPHY
NT TOMOGRAPHY
Cineradiography
[DE87-013158] 03 p0324 N88-12045
Flaw imaging and ultrasonic techniques for characterizing sintered silicon carbide
[NASA-TM-100177] 03 p0334 N88-12106
Measurement and control of damage in composite materials: Nondestructive controls by thermography, holography, and radiography
[SNIAS-872-430-110] 05 p0559 N88-13403
X-ray imaging: Status and trends
[DE88-000756] 05 p0649 N88-13980
Study on cineradiography
[ISL-R-120/86] 08 p0990 N88-15994
High-resolution Real-Time Radiography (RTR) system design
[AD-A187107] 09 p1166 N88-16992
Performance of a digital real time radiographic imaging system
[MRL-R-1068] 09 p1169 N88-17011
Durability and damage tolerance of aluminum castings
[AD-A186444] 10 p1341 N88-18013
Institute for Materials Science and Engineering, nondestructive evaluation: Technical activities 1987
[PB88-153655] 10 p1342 N88-18020
Characterization of sintered SiC by using NDE
15 p2082 N88-22413
Method of radiographic inspection of wooden members
[NASA-CASE-LAR-13724-1] 17 p2346 N88-23983
Rendering of surfaces from volume data
[AD-A193649] 22 p3143 N88-28689
Analysis of edge detection techniques for radiographic image measurement
[AD-A193650] 23 p3186 N88-28961
Comparison of 2-D Fourier and spatial techniques for removing noise in real-time X-ray radiography
[AD-A193700] 23 p3187 N88-28962
Development of graded reference radiographs for aluminum welds, phase 1
[AD-A195594] 24 p3381 N88-30140

RADIOISOTOPE BATTERIES
NT SNAP 19
Transactions of the Fourth Symposium on Space Nuclear Power Systems
[DE88-006164] 17 p2398 N88-24254
The Light-Weight Radioisotope Heater Unit (LWRHU): Development and application 17 p2405 N88-24299
Foil gas bearing system endurance testing dynamic isotope power system 17 p2405 N88-24302
Two-phase fluid management for a Rankine cycle isotope power system 17 p2405 N88-24303
Innovative methodology and developments in US space radioisotope power safety risk assessments
17 p2415 N88-24362
Status of modular RTG technology
17 p2422 N88-24403
Plasma separation process. Betacell (BCELL) code, user's manual
[DE88-006955] 20 p2859 N88-26981

RADIOLYSIS
Organic molecules on meteoritic solid substrates
[NASA-CR-181570] 05 p0560 N88-13411
Effects of energy, distance and orientation on electron transfer rates studied by pulse radiolysis in organic media
[DE88-002906] 08 p1082 N88-16521
Gas phase pulse radiolysis
[DE88-002981] 10 p1296 N88-17751
Electron transfer to iron(3) oxide colloids
[DE88-002885] 10 p1416 N88-18448

RADIOMETERS
NT ADVANCED VERY HIGH RESOLUTION RADIOMETER
NT DICKE RADIOMETERS
NT INFRARED DETECTORS
NT INFRARED RADIOMETERS
NT INFRARED SCANNERS
NT MICROWAVE RADIOMETERS
NT SPECTRORADIOMETERS
Development of response models for the Earth Radiation Budget Experiment (ERBE) sensors. Part 4: Preliminary nonscanner models and count conversion algorithms
[NASA-CR-178295] 01 p0050 N88-10317
Study on propagation and inverse scattering --- sea studies
[ESA-CR(P)-2394] 01 p0063 N88-10405
The use of fiber optics in the determination of temperature and extent of reaction in detonating explosives
[DE87-012632] 01 p0094 N88-10612
A VAS-numerical model impact study using the Gal-Chen variational approach — Visible Infrared Spin-Scan Radiometer Atmospheric Sounder (VAS)
02 p0213 N88-11339
NBS (National Bureau of Standards) measurement services: Radiometric standards in the vacuum ultraviolet
[PB87-227625] 03 p0325 N88-12055
Planning for future operational sensors and other priorities
[PB87-220802] 03 p0325 N88-12056
A method for remote sensing of precipitable water vapor and liquid in the atmosphere using a 22-ghz radiometer
[AD-A184204] 03 p0354 N88-12232
Lidar-radiometric method for determining liquid-water content of cirrus clouds 04 p0461 N88-12854
Development of response models for the Earth Radiation Budget Experiment (ERBE) sensors. Part 3: ERBE scanner measurement accuracy analysis due to reduced housekeeping data
[NASA-CR-178294] 05 p0583 N88-13553
Spectral and radiometric calibration of the Airborne Visible/Infrared Imaging Spectrometer
06 p0707 N88-14334
AVHRR/HIRS (Advanced Very High Resolution Radiometer/High Resolution Infra-Red Sounder) operational method for satellite based sea surface temperature determination
[PB88-107594] 06 p0708 N88-14340
An aureolar radiometer for the determination of aerosol size distribution 08 p1018 N88-16174
Design feasibility report on investigation of magnetic bearings for the ocean colour monitor radiometer scanner
[BAE-TP-7849] 09 p1174 N88-17036
A noise-adding radiometer for the Parkes antenna
11 p1473 N88-18788
PbSnTe photovoltaic detectors for operation in the 2-14 micron band
[INPE-4252-PRE/1125] 11 p1508 N88-19006
Remote sensing of atmospheric optical thickness and sea-water attenuation when submerged: Wavelength selection and anticipated errors
[AD-A187609] 11 p1548 N88-19262
Roentgenoradiometric analysis of aerosol in Venusian clouds by Vega-1 and Vega-2 automatic interplanetary stations 13 p1726 N88-20319
Coherence effects in optical physics with special reference to spectroscopy
[AD-A189520] 13 p1840 N88-21007
Activities report of the Toulouse Research Center
[ETN-88-91988] 13 p1850 N88-21077
Investigation into the development of computer aided design software for space based sensors
[NASA-CR-180772] 15 p2107 N88-22552
Description of the MPTR system: Multi Path Transmissometer Radiometer
[FEL-1987-14] 20 p2855 N88-26954
Microwave frequency nondestructive control
[CERT-2/1355-MO] 23 p3189 N88-28976
Improvements in techniques of microwave thermography
[AD-A194613] 23 p3203 N88-29062
NBS (National Bureau of Standards) measurement services: The NBS photodetector spectral response calibration transfer program
[PB88-201595] 24 p3376 N88-30109
Atmospheric corrections for in-flight satellite radiometric calibration
[AD-A196124] 24 p3391 N88-30194
Principles of the optical differential thermal analysis
[AD-A195951] 24 p3429 N88-30408

RADIOMETRIC CORRECTION
Object-dependent atmospheric influence on LANDSAT recordings 01 p0065 N88-10420
First assessment of processing and use of SPOT images by the Institut Geographique Nationale --- French National Geographic Institute 03 p0341 N88-12148
The radiometric processing of SLAR measuring values using the PARES program
[BCRS-86-04] 16 p2227 N88-23301
Some characteristics in synthetic aperture radar (SAR) raw data and SAR images
[FOA-C-30483-3.2] 22 p3071 N88-28232

RADIOMETRIC RECTIFICATION
U RADIOMETRIC CORRECTION

RADIOMETRIC RESOLUTION
The absolute radiometric calibration of space-based sensors 03 p0277 N88-11744
Restoration techniques for redisplay of LANDSAT-5 satellite imagery
[INPE-4189-PRE/1076] 13 p1791 N88-20712

Method for restoration and resampling of TM sensor imagery
[INPE-4491-PRE/1255] 15 p2090 N88-22454

RADIONUCLIDES
U RADIOACTIVE ISOTOPES

RADIOSENSITIVITY
U RADIATION TOLERANCE

RADIOSONDES
NT IONOSONDES
NT RAWINSONDES
VAS products as indices of thunderstorms and severe local storm potential --- Visible and Infrared Spin Scan Radiometer Atmospheric Sounder (VAS)
02 p0201 N88-11253
Forecasting and nowcasting cumulus convection with soundings released from a storm-intercept vehicle
02 p0202 N88-11262
Correlations of TOMS total ozone data (Nimbus-7 satellite) with tropopause height
05 p0617 N88-13788
Middle atmospheric wind measurements using a medium frequency radar
[AD-A185931] 07 p0879 N88-15330
Roys and radiosondes in the region
[INPE-4362-PRE/1188] 13 p1796 N88-20743
Tiros operational vertical sounder (TOVS) and radiosonding in the region 17 p2360 N88-24059

RADIOTELEPHONES
Adaptive digital phase modulation
[PB87-134607] 06 p0693 N88-14253
A diffraction based theoretical model for prediction of UHF path loss in cities 12 p1616 N88-19661
Design mobile satellite system architecture as an integral part of the cellular access digital network
19 p2650 N88-25736

RADIOTHERAPY
U RADIATION THERAPY

RADIUS
U RADII

RADOME MATERIALS
Dielectric behavior of electromagnetic (EM) windows materials irradiated by a CW CO2 high-power laser --- hypersonic/reentry vehicles
[ISL-CO-239/86] 09 p1154 N88-16913

RADON
NT RADON ISOTOPES
Rapid feature extraction via the radon transform
[AD-A190032] 15 p2110 N88-22573

RADON ISOTOPES
Radon-222 in the Antarctic Peninsula
[INPE-4486-PRE/1251] 15 p2092 N88-22468

RAIL TRANSPORTATION
Nowcasting for the national economy needs
02 p0199 N88-11241
Evaluation of the thermal effectiveness of urethane foam and fiberglass as insulation systems for tank cars
[PB88-100797] 06 p0686 N88-14207
TECOM's research efforts in the dynamic environments 08 p0999 N88-16048
Composite materials for rail transit systems
[NASA-CR-178401] 10 p1294 N88-17738
The MBB propulsion concepts for magnetic suspension railways: Retrospective view and prospects
[MBB-Z-141/87] 10 p1316 N88-17865
Identification of lateral operation dynamics of rail vehicles using roll test stand tests
20 p2787 N88-26534

RAILGUN ACCELERATORS
A feasibility study of a hypersonic real-gas facility
[NASA-CR-180423] 01 p0006 N88-10043
Numerical predictions of EML system performance
[DE87-011727] 01 p0011 N88-10061
Switching devices used in the Lethality Test System
[DE87-011734] 01 p0011 N88-10062
Exact solutions to the governing dynamic equations of plasma armature electromagnetic railguns
[DE87-014442] 01 p0011 N88-10063
Effects of barrel joints on hypervelocity projectiles
[DE87-013447] 02 p0157 N88-10983
Current-filamentation instability in railgun arcs
[AD-A184618] 03 p0269 N88-11693
Ultimate velocities for induction launchers
[DE87-012360] 04 p0404 N88-12513
Thermal analysis of electromagnetic launcher rails
[DE88-000166] 04 p0405 N88-12514
Analysis of a series of electromagnetic launcher firings
[AR-005-131] 04 p0405 N88-12516
Efficiency aspects of short, low velocity railguns
[AR-004-847] 04 p0405 N88-12517
Experimental investigation of a three-stage railgun incorporating puff-switching
[MRL-R-1056] 09 p1130 N88-16785
The railgun and its power source
[MRL-R-1058] 09 p1130 N88-16786
Pulsed current transformer for low inductive loads
[AD-A187224] 10 p1324 N88-17913
Structural integrity of metallic armature rail guns
[AD-A188735] 13 p1728 N88-20333
Application of railgun principle to high-velocity hydrogen pellet injection for magnetic fusion reactor refueling
[DE88-005830] 13 p1728 N88-20334
Temperature estimates for a free flowing railgun plasma
[MRL-R-1054] 13 p1843 N88-21032
Analytic solutions to dynamic equations of plasma armature railguns
[DE88-006842] 15 p2023 N88-22057
Structural consequences of railgun augmentation
[DE88-007036] 15 p2023 N88-22058
Railgun rail gouging by hypervelocity sliding contact
[DE88-006866] 16 p2166 N88-22916
Experimental investigation of a three-stage railgun incorporating puff-switching
[AD-A191044] 16 p2166 N88-22918
Fundamental limits to the velocity of solid armatures in railguns 18 p2469 N88-24656
The SRS (Segmented Rail Surface) railgun: A new approach to restrike control
[DE88-007907] 19 p2605 N88-25468
STARFIRE: Hypervelocity railgun development for high-pressure research
[DE88-008348] 19 p2605 N88-25469
Reaming experiments for the lethality test system
[DE88-007902] 20 p2763 N88-26383
Why plasma armature railguns don't work (and what can be done about it)
[DE88-007900] 20 p2763 N88-26384
Application of superconducting technology to earth-to-orbit electromagnetic launch systems
[DE88-010022] 20 p2763 N88-26386
Plasma armature formation in high-pressure, high-velocity hydrogen
[DE88-008347] 20 p2857 N88-26967
An interferometric measurement technique for railgun structures
[AD-A192851] 21 p2901 N88-27217
Slew-induced deformations in a space-based electromagnetic rail gun 21 p2929 N88-27385
Plasma behavior in the boundary layer near a railgun surface
[DE88-008889] 21 p3017 N88-27909
Theoretical modeling of accelerating arc plasmas
[AD-A195606] 24 p3432 N88-30426

RAILROADS
U RAIL TRANSPORTATION

RAILS
Application of Kalker's rolling contact theory to the simulation of rail vehicles
[DFVLR-FB-87-07] 01 p0057 N88-10363
On cleavage in fatigue for rail steels
06 p0716 N88-14388
Composite materials for rail transit systems
[NASA-CR-178401] 10 p1294 N88-17738
Structural integrity of metallic armature rail guns
[AD-A188735] 13 p1728 N88-20333

RAIN
NT ACID RAIN
Estimation from satellite imagery of summertime rainfall over varied space and time scales
[PB87-203246] 01 p0071 N88-10454
The 54-hours continuous post-frontal precipitation north of the Alpine mountain barrier, 22-25 August 1975
02 p0203 N88-11268
Conceptual models of Baiu front and Baiu frontal disturbances in multiscale characteristics --- East Asia
02 p0203 N88-11271
Evaluation of the Rainsat precipitation analysis system in real-time use 02 p0205 N88-11283
Convective scale interaction: Arc cloud lines and the development and evolution of deep convection
[NASA-CR-181469] 02 p0215 N88-11357
Development of a climatic map of rainfall attenuation for Europe
[REPT-372] 02 p0216 N88-11359
Estimates of satellite EHF communication outages due to attenuation by rain
[AD-A183969] 03 p0307 N88-11941
A statistical rain attenuation prediction model with application to the advanced communication technology satellite project. Part 2: Theoretical development of a dynamic model and application to rain fade durations and tolerable control delays for fade countermeasures
[NASA-TM-100242] 03 p0308 N88-11945
On the interannual variability of South American climate and the Southern Oscillation 04 p0470 N88-12905
Effects of rainfall on the seasonal thermocline
[AD-A184432] 04 p0472 N88-12912
Specification of predictors necessary for the determination of over or underestimation of radar derived total rainfall
[AD-A185363] 05 p0626 N88-13838
BARS-1M meteorological complex carried on IL-18 airplane 06 p0725 N88-14458
Estimation of rainfall rates in tropical cyclones by passive microwave radiometry 06 p0744 N88-14577
Improvement of the construction of protective clothing for better wearability and comfort --- rainwear
[IZF-1986-26] 07 p0890 N88-15448
The potential influence of rain on airfoil performance
08 p0952 N88-15774
Radar echo signatures versus relative precipitation
[AD-A186162] 08 p0976 N88-15903
Variations of tropical circulation and associated rainfall anomalies, during 2 years of contrast
[INPE-4359-TDL/300] 08 p1039 N88-16286
Full scale and wind tunnel surface pressure measurements on the T.R.R.L. spray dispersion programme vehicles
[REPT-8623] 09 p1114 N88-16676
Calibration of the ARL (Aeronautical Research Laboratories) rain and icing facility
[AD-A186776] 09 p1121 N88-16710
The structure and dynamics of monsoon depressions
10 p1355 N88-18102
Optimal sampling to provide user-specific climate information 11 p1515 N88-19051
A propagation campaign in a marine environment utilizing a digital system at 36 GHz 12 p1618 N88-19675
Study of cations in the precipation of Estacao Antartica Comandante Ferraz
[INPE-4377-PRE/1197] 12 p1644 N88-19843
Design of the primary pre-TRMM and TRMM ground truth site
[NASA-CR-182609] 12 p1647 N88-19865
A polarimetric rain backscatter model developed for coherent polarization diversity radar applications
13 p1759 N88-20520
Applications of the differential reflectivity radar technique: Focus on estimation of rainfall parameters and microwave attenuation prediction
13 p1759 N88-20521
Numerical simulation of medium scale disturbance on meiyu front 14 p1900 N88-21346
Satellite rainfall retrieval by logistic regression
[NASA-CR-180465] 14 p1946 N88-21607
Some models for rain and cloud attenuation of millimeter waves
[PB88-160809] 14 p1948 N88-21616
The growth potential of corona discharges from aircraft flying in precipitation
[AD-A190507] 15 p2094 N88-22478
Space communication link propagation data for selected cities within the multiple beam and steerable antenna coverage areas of the advanced communications technology satellite
[NASA-TM-100861] 16 p2191 N88-23070
Validate algorithms for the determination of rainfall rates from SSM/I microwave satellite imagery
[AD-A188769] 16 p2233 N88-23327
Fog, rain and aerosol attenuation in the atmosphere
[AD-A190867] 16 p2235 N88-23350
Validate algorithms for the determination of rainfall rates from SSM/I microwave satellite imagery
[AD-A191337] 16 p2236 N88-23353
Rainfall rates and drop-size distributions for environmental testing
[AD-A191342] 16 p2236 N88-23354
Partial likelihood analysis of time series models with application to rainfall-runoff data
[AD-A191157] 16 p2261 N88-23516
Airborne and spaceborne radar images for geologic and environmental mapping in the Amazon rain forest, Brazil
17 p2353 N88-24021
Observation of stratiform rain with 94 GHz and s-b and Doppler radar
[AD-A192013] 18 p2544 N88-25100
Meteorological satellite product support and research for project GALE
[NASA-CR-180969] 19 p2727 N88-26193
Present status of artificial rain making
[DE88-701823] 20 p2826 N88-26769
Rain attenuation at 35 GHz over an 18 km path
[AD-A194504] 22 p3069 N88-28217
Indian monsoon rainfall, 1986-1987
22 p3120 N88-28536
Modes of interannual climate variability and Sahel rainfall anomalies 22 p3121 N88-28547
ENSO, sea-surface temperatures and African rainfall
22 p3122 N88-28550
Sub-Saharan rainfall anomalies and global sea-surface temperature relationships for the recent fifteen year (1970-1984) period 22 p3122 N88-28552
Simulation studies of the influence of sea-surface temperature anomalies on the Sahelian circulation and rainfall 22 p3122 N88-28553

A statistical rain attenuation prediction model with application to the advanced communication technology satellite project. 1: Theoretical development and application to yearly predictions for selected cities in the United States
[NASA-CR-179498] 23 p3205 N88-29077

Effects of precipitation on wind turbine performance
[DE88-001144] 23 p3226 N88-29211

Validate algorithms for the determination of rainfall rates from SSM/I microwave satellite imagery
[AD-A195428] 24 p3404 N88-30270

RAIN FORESTS

Mapping of the mangroves of the Guanabarra Bay through the utilization of remote sensing techniques
[INPE-3942-TDL/229] 12 p1637 N88-19804

Photointerpretation with instrumentation for evaluation of environmental impact: Mata Atlantica in Cubatao
19 p2683 N88-25946

Bibliography on tropical rain forests and the global carbon cycle. Volume 1: An introduction to the literature
[DE88-010761] 22 p3118 N88-28523

RAIN GAGES

Wet deposition and snowpack monitoring operations and quality assurance manual
[PB87-212817] 01 p0064 N88-10413

RAIN IMPACT DAMAGE

In-flight rain damage tests of the shuttle thermal protection system
[NASA-TM-100438] 14 p1881 N88-21241

RAINDROPS

Anthropogenic effects on the droplet formation process, and ion concentrations in droplets --- clouds
08 p1018 N88-16175

On the theory of electromagnetic scattering from a raindrop splash
[AD-A186720] 14 p1906 N88-21393

A theoretical model of the washout of trace gases by raindrops in the atmosphere 17 p2375 N88-24125

RAINMAKING

Present status of artificial rain making
[DE88-701823] 20 p2826 N88-26769

RAINSTORMS

NT THUNDERSTORMS

Nowcasting rain/snow transitions and freezing rain
02 p0202 N88-11265

The application of divergence equation in the analysis of heavy rainfall 02 p0207 N88-11299

The mesoscale numerical model for heavy rainfall forecasting in Yangtze River Valley, China
02 p0211 N88-11326

Interactions between the Asian monsoons, the tropical Pacific and the southern hemisphere extratropics
04 p0470 N88-12907

Validate algorithms for the determination of rainfall rates from SSM/I microwave satellite imagery
[AD-A192299] 21 p2974 N88-27664

Passive microwave measurements of water vapor fields and rain for locating fronts in cyclonic storms
[AD-A195632] 24 p3404 N88-30267

RAKES

Calibration of averaging total pressure flight wake rake and natural-laminar-flow airfoil drag certification
[NASA-CR-181630] 19 p2599 N88-25443

RAMAN EFFECT

U RAMAN SPECTRA

RAMAN LASERS

Output power enhancement of AC Raman free-electron laser
[DE88-000503] 04 p0449 N88-12788

Raman microprobe characterization of dielectric films following high-energy pulsed laser irradiation
[DE88-000559] 05 p0588 N88-13587

Studies on nonlinear mechanisms of excimer laser propagation in fused silica fibers
[AD-A186822] 09 p1156 N88-16929

Laser raman studies related to liquid propellants: Structural characteristics inferred from the nitrate anion spectra
[AD-A188462] 12 p1612 N88-19641

Phase preservation cleanup in a double-pass Raman amplifier SBS (Stimulated Brillouin Scattering) conjugator
[AD-A189428] 13 p1761 N88-20536

Theoretical studies of Resonance Enhanced Stimulated Raman Scattering (RESRS) of frequency-doubled Alexandrite laser wavelength in cesium vapor
[NASA-CR-182870] 15 p2036 N88-22133

Unstable behavior of lasers and other optical systems
[AD-A190875] 16 p2213 N88-23204

Laser spectoscopy of plasmas
[AD-A193009] 20 p2881 N88-26991

RAMAN SCATTERING

U RAMAN SPECTRA

RAMAN SPECTRA

The polarization field for pulsed Raman transitions
[DE87-013118] 01 p0035 N88-10227

Large-scale stimulated rotational Raman scattering experiments using the LLNL Nova laser
[DE87-012661] 01 p0051 N88-10328

Spectroscopic studies of shocked and detonating explosives
[DE87-014216] 02 p0155 N88-10972

Theoretical atomic and molecular photophysics
[DE87-014249] 02 p0231 N88-11458

Enhanced noise and Raman scattering in plasma
[DE87-014466] 02 p0238 N88-11501

Enhanced Thomson scattering from laser plasmas
[DE87-014463] 02 p0238 N88-11503

Vibrational spectroscopy of shock-compressed fluid N2 and O2
[DE87-013138] 03 p0313 N88-11979

Raman scattering spectrum along a bevel etched GaAs on Si, TEM (Transmission Electron Microscope) study and GaAs P-I-N photodetector on Si
[DE88-000210] 04 p0498 N88-13066

High energy molecules of high symmetry
[AD-A185385] 05 p0647 N88-13965

Solitons in stimulated Raman scattering: Generation and control of ultrashort optical pulses
[AD-A185141] 05 p0650 N88-13983

Observing effect of laser radiation of low-frequency Raman scattering of light 06 p0772 N88-14742

Raman spectra of adsorbed layers on space shuttle and AOTV thermal protection system surface
06 p0799 N88-14890

Chapter 2: Threshold for Raman conversion of FEL laser pulses in the atmosphere
[DE88-002470] 07 p0859 N88-15215

Cross section of resonant Raman scattering of light by polyenes 07 p0920 N88-15591

Raman spectroscopic investigations of Hg-Cd-Te melts 07 p0926 N88-15625

Stimulated Raman scattering of picosecond light pulses in long dispersive medium 08 p1078 N88-16498

The suppression of stimulated hyper-Raman emission in Na due to parametric four-wave mixing
[DE88-003290] 09 p1172 N88-17030

Concept, construction, and experimental testing of a polychromator for a Raman lidar for the simultaneous telemetering of carbon dioxide and water vapor, relative to oxygen
[GKSS-87/E/20] 09 p1191 N88-17134

Application of state-multipole Heisenberg equations to Raman excitation dynamics
[DE88-003626] 10 p1335 N88-17977

Investigations of stimulated Raman scattering from high density underdense plasmas irradiated by a 0.35 micron laser 10 p1411 N88-18421

Vibrational, mechanical and thermal properties of 3-5 semiconductors
[AD-A187569] 11 p1556 N88-19316

Raman enhancement methods for molecular structure characterization of optical thin films
[DE88-003421] 11 p1558 N88-19324

Laser raman studies related to liquid propellants: Structural characteristics inferred from the nitrate anion spectra
[AD-A188462] 12 p1612 N88-19641

Raman scattering in mixed crystal semiconductors
12 p1696 N88-20149

Phase preservation cleanup in a double-pass Raman amplifier SBS (Stimulated Brillouin Scattering) conjugator
[AD-A189428] 13 p1761 N88-20536

Observation of anomalous low J-value Stokes and anti-Stokes lines in stimulated rotational Raman scattering over long air paths
[DE88-003756] 14 p1911 N88-21418

Three-wave parametric resonance in plasma of relativistic electron flux 14 p1972 N88-21772

Theoretical studies of Resonance Enhanced Stimulated Raman Scattering (RESRS) of frequency-doubled Alexandrite laser wavelength in cesium vapor
[NASA-CR-182870] 15 p2036 N88-22133

The development of high power KrF laser systems for plasma research by the application of stimulated Raman scattering
[ETN-88-92220] 15 p2073 N88-22356

Amplification of signals in fiber optics using the stimulated Raman effect
[AD-A190281] 15 p2133 N88-22727

Surface enhanced Raman scattering applied to surface chemical kinetics
[AD-A191275] 16 p2176 N88-22969

Experimental investigation on stimulated Raman scattering in high-pressure hydrogen by ruby laser
16 p2186 N88-23034

Theoretical studies of Resonance Enhanced Stimulated Raman Scattering (RESRS) of frequency doubled Alexandrite laser wavelength in cesium vapor
[NASA-CR-182871] 17 p2317 N88-23841

Effect of uniaxial stress on the Raman spectra of graphite fibers
[AD-A191730] 18 p2492 N88-24783

Atmospheric propagation of laser beams
[AD-A191447] 18 p2520 N88-24952

Alternative analysis of CO2-laser-produced plasma waves
[DE88-008434] 19 p2730 N88-26215

Raman and absorption spectrophotometric studies of selected lanthanide, californium-doped lanthanide, and actinide trihalides in the solid state
[DE88-008234] 20 p2874 N88-27061

Refractory films from spin-cast carbon
[DE88-011251] 21 p2919 N88-27327

Soliton and polaron dynamics in conducting polymers
[DE88-702539] 23 p3198 N88-29035

Molecular fluorescence measurements with a charge-coupled device detector
[AD-A194437] 23 p3216 N88-29141

RAMAN SPECTROSCOPY

High temperature CO2 study: Anti-Stokes coherent Raman diffusion and infrared spectroscopy
[ESA-TT-1048] 03 p0282 N88-11777

A simplified CARS measurement system for rapid determination of temperature and oxygen concentration
[NASA-TM-100496] 03 p0374 N88-12353

Real-time Raman detection of molecular changes in ceramics undergoing sliding friction
[DE88-000558] 04 p0421 N88-12609

Raman scattering as a diagnostic technique for cathode characterization
[AD-A184434] 04 p0439 N88-12726

Spectroscopic investigations and measurements of certain ARC jet parameters 06 p0796 N88-14877

Raman spectra of adsorbed layers on space shuttle and AOTV thermal protection system surface
06 p0799 N88-14890

Studies of supported metal catalysts
[DE88-002546] 07 p0831 N88-15038

CARS measurements of combustion. 1: Precision of thermometry
[NAL-TR-939] 10 p1299 N88-17769

CARS measurements of combustion. 2: Gas species concentration measurements
[NAL-TR-940] 11 p1453 N88-18663

Some applications of surface Raman and infrared spectroscopies to mechanistic electrochemistry involved adsorbed species
[AD-A188777] 12 p1606 N88-19602

Measurement of detonation temperature of hydrogen-oxygen mixture by CARS (Coherent Anti-Stokes Raman Spectroscopy)
[NASA-TT-20227] 13 p1739 N88-20398

Characterization of redox states of nickel hydroxide film electrodes by in-situ Raman spectroscopy
[AD-A189288] 13 p1741 N88-20411

The use of four-photon Raman spectroscopy for the remote sensing of natural objects
[NASA-TT-20257] 13 p1791 N88-20716

Antistokes coherent Raman diffusion of a nitriding plasma
[ONERA-RF-6/3644-PY] 16 p2175 N88-22962

Requirements for temperature and species concentration measurements in microgravity combustion experiments 17 p2329 N88-23903

Laser Diagnostics for combustion temperature and species measurements 17 p2330 N88-23912

Micro-Raman analysis of dielectric optical thin films
[AD-A191228] 17 p2445 N88-24537

Molecular characterization of structure and bonding in thin film materials
[DE88-006811] 18 p2584 N88-25351

Dual Stokes cars measurements in supersonic combusting flow 19 p2625 N88-25569

Raman, photoluminescence and modulation spectroscopy of semiconductor heterostructures
20 p2861 N88-26997

Mitsubishi Electric Advance (R and D Edition), Volume 41
[PB88-194162] 21 p2929 N88-27388

Polarization selective Raman microspectroscopy
21 p2930 N88-27397

Steady-state approximations in Raman excitation equations
[DE88-011759] 21 p3014 N88-27889

Characterization of crystalline silicon by electrochemical and Raman spectroscopy at the frontier semiconductor/electrolyte
[ETN-88-92354] 21 p3025 N88-27956

Raman spectroscopy on simple molecular systems at very high density
[DE88-010947] 23 p3191 N88-28987

RAMJET ENGINES

NT SUPERSONIC COMBUSTION RAMJET ENGINES

Flame driving of longitudinal instabilities in liquid fueled dump combustors
[AD-A185536] 01 p0006 N88-10033
An experimental investigation of the ignition and flammability limits of various hydrocarbon fuels in a two-dimensional solid fuel ramjet
[AD-A184968] 05 p0549 N88-13342
High-speed inlet research program and supporting analyses 08 p0958 N88-15811
A holographic investigation of particulates in metallized solid fuel ramjet combustion
[AD-A186887] 09 p1140 N88-16831
Military jet fuels, 1944-1987
[AD-A186752] 09 p1150 N88-16890
Application of similarity techniques between reduced and natural scale models of Ramjet engines
[INPE-4269-PRE/1142] 11 p1441 N88-18595
An experimental investigation of rocket ramjet nozzle assembly base pressures
[AD-A189714] 15 p2027 N88-22076
Water flow visualisation of a ramrocket combustion chamber 16 p2202 N88-23138
Aeropropulsive characteristics of isolated combined turbojet/ramjet nozzles at Mach numbers from 0 to 1.20
[NASA-TP-2814] 17 p2299 N88-23757
The 24th JANNAF Combustion Meeting, volume 2
[AD-A190164] 19 p2622 N88-25554
Characteristic time correlations to liquid fuel ramjet combustion efficiency 19 p2624 N88-25566
Low frequency pressure oscillations in a model ramjet combustor 19 p2625 N88-25571
The pressure field generated in a cold-flow side-dump ramjet combustor 19 p2625 N88-25572
Effects of Mach number on acoustic-vortex interactions in a ramjet 19 p2625 N88-25573
Control of combustion instabilities in ramjet motors
19 p2625 N88-25574
Ignition and flammability characteristics of solid fuel ramjets 19 p2626 N88-25575
An efficient computational tool for ramjet combustor research
[DE88-010034] 20 p2760 N88-26369
Combustion of PMMA (polymethylmethacrylate), PE (polyetnylane) and PS (polystyrene) in a ramjet
[PB88-186572] 20 p2769 N88-26417
Heterogeneous diffusion flame stabilization
[AD-A193014] 20 p2771 N88-26429
Air intake aerodynamics 24 p3318 N88-29762
Semiempirical methods for airbreathing missiles
24 p3318 N88-29763
Evaluation of the advanced air breathing propulsion concepts, executive summary
[ESA-CR(P)-2540] 24 p3325 N88-29802
Evaluation of advanced air breathing concepts. Volume 1: Executive summary
[ESA-CR(P)-2539] 24 p3326 N88-29806
A new computational capability for ramjet projectiles
[AD-A196061] 24 p3327 N88-29812
Review of research concerning Solid Fuel Ramjet (SOFRAM) at the Research Institute of National Defence (FOA) 2
[FOA-C-20714-2.1] 24 p3327 N88-29813
Ignition and extinguishing of a Solid Fuel Ramjet (SOFRAM)
[FOA-C-20713-2.1] 24 p3337 N88-29865
RAMJET MISSILES
An investigation into the feasibility of using a dual-combustion mode ramjet in a high Mach number tactical missile
[AD-A186906] 09 p1119 N88-16705
Calculation and design of a ramjet missile
[REPT-TR-500] 10 p1311 N88-17832
An experimental investigation of rocket ramjet nozzle assembly base pressures
[AD-A189714] 15 p2027 N88-22076
RANDOM ACCESS
A multi user random access communication system for users with different priorities
[AD-A186041] 07 p0841 N88-15102
On the approximation of the output process of multi-user random access communication networks
[AD-A186197] 07 p0842 N88-15108
An algorithm for random access communication over a noisy channel
[AD-A191315] 16 p2252 N88-23461
An access alternative for mobile satellite networks
19 p2651 N88-25737
Full analysis of a powerful window random access algorithm
[AD-A192437] 21 p2995 N88-27763
RANDOM ACCESS MEMORY
A study of charged particles/radiation damage to VLSI device materials
[NASA-CR-172036] 05 p0577 N88-13518
Comparison of 2D memory SEU transport simulation with experiments
[ATR-86(8139)-2-REV-A] 05 p0656 N88-14025
Fuzzy logic inference processor for real time control: A second generation full custom design
[AD-A188155] 11 p1471 N88-18773
A methodology for hardware verification based on logic simulation
[AD-A188553] 12 p1622 N88-19704
Random access memory testing: Theory and practice. The gains of fault modeling
[EUT-86-E-161] 14 p1955 N88-21649
Self-checking logic arrays
[RR-656-I] 15 p2106 N88-22545
A random access algorithm for environments with capture and limited feedback capabilities
[AD-A192233] 20 p2790 N88-26552
Research on wide area workstations
[AD-A192529] 22 p3136 N88-28643
Random-access algorithms for environments with capture
[AD-A194303] 23 p3203 N88-29060
The effects of total dose on the SEU sensitivity of CMOS static RAMS — single event upset (SEU), satellite components
[AERE-R-12779] 24 p3428 N88-30401
RANDOM DISTRIBUTIONS
U STATISTICAL DISTRIBUTIONS
RANDOM LOADS
NT GUST LOADS
The effect of fretting corrosion on the fatigue strength of steel and cast iron under sinusoidal and random loading
[LBF-FB-177] 01 p0023 N88-10142
Fatigue under nonnormal random stresses using Monte Carlo method 05 p0607 N88-13723
Random loading fatigue crack growth: Crack closure considerations 06 p0797 N88-14881
Fatigue crack growth due to random loading
[DE88-004641] 10 p1345 N88-18038
Fatigue crack growth due to random loading
18 p2531 N88-25017
Prediction of fatigue life of notched specimens under aircraft loading and importance of the relative method in the case of local strain approach, part 2
[TAE-595-PT-2] 19 p2680 N88-25934
RANDOM NOISE
NT RANDOM SIGNALS
Reception of pseudo noise-modulated signals using digital correlators for satellite navigation tasks
[ETN-87-90426] 01 p0037 N88-10234
Evaluation of a satellite laser ranging technique using pseudonoise code modulated laser diodes
[NASA-CR-182347] 06 p0708 N88-14343
HOC spectral analysis of an almost periodic random sequence in noise
[AD-A185528] 06 p0765 N88-14697
Adaptive detection in non-stationary interference, part 3
[AD-A185622] 07 p0844 N88-15118
Series representations of infinitely divisible random vectors and a generalized shot noise in Banach spaces
[AD-A186429] 07 p0918 N88-15574
Predicting transforms of stable noise and other Gaussian mixtures
[AD-A189280] 12 p1684 N88-20071
Optimal and conventional space-time processing in flow noise
[AD-A189104] 13 p1833 N88-20965
Information and coding capacities of mismatched Gaussian channels
[AD-A190321] 15 p2124 N88-22665
Conditions for information capacity of the discrete-time Gaussian channel to be increased by feedback
[AD-A190317] 15 p2127 N88-22687
Coding capacity of discrete-time Gaussian and nonGaussian channels
[AD-A190318] 15 p2127 N88-22688
Scattering impulse response synthesis using random noise illumination: Initial concept evaluation
[AD-A195086] 24 p3364 N88-30034
RANDOM NUMBERS
RANDOM NUMBER: A syntax-directed package to produce random numbers in user-specified, univariate distributions. User's guide
[DE87-014278] 02 p0228 N88-11436
Components and cycles of a random function
[DE87-014155] 02 p0228 N88-11437
A study of data compactation using numerical methods
[INPE-4317-TDL/284] 13 p1828 N88-20929
A comparison of generators for pseudo-random normal deviates
[DE88-011711] 21 p3010 N88-27859
Random number generation
[USIP-87-15] 22 p3145 N88-28707
A study of the effect of random input motion on low Reynolds number flows
[AD-A195559] 24 p3316 N88-29747
RANDOM PROCESSES
NT RANDOM WALK
Mechanical shock test specification using nonstationary random excitation models
[DE87-013650] 04 p0454 N88-12812
Implementation of a new shock testing procedure using nonstationary random excitation
[DE87-014643] 04 p0456 N88-12827
Propagation of random initial conditions in time
04 p0486 N88-12993
Subcritical branching processes in a two state random environment, and a percolation problem on trees
[PB87-230439] 06 p0762 N88-14677
Von Mises' definition of random sequences reconsidered
[PB87-230512] 06 p0767 N88-14715
Random loading fatigue crack growth: Crack closure considerations 06 p0797 N88-14881
A fast Riemann solver with constant covolume applied to the random choice method
[CAR-87-19] 09 p1231 N88-17375
Nonlinear and diffraction effects in sound beams with random transverse structure 09 p1235 N88-17402
Electronic structure of random alloys and the theory of ordering processes
[DE88-004476] 10 p1407 N88-18394
Random-choice based hybrid methods for one and two dimensional gas dynamics
[CAR-88-01] 14 p1910 N88-21415
Thermal expansion behavior of randomly oriented short carbon fiber reinforced copper composites
[NASA-TT-20175] 15 p2031 N88-22099
Random processes, turbulence and disordering fields
[AD-A190123] 15 p2063 N88-22303
Random Process Simulation for stochastic fatigue analysis
[NASA-TM-100464] 15 p2123 N88-22654
Random processes, turbulence and disordering fields
[AD-A191399] 16 p2209 N88-23181
Periodically correlated processes and their stationary dilations
[NASA-CR-182904] 16 p2263 N88-23530
Computational sciences
[AD-A190826] 18 p2564 N88-25226
Numerical solution of a system of random Volterra integral equations. 1: Successive approximation method
18 p2564 N88-25227
Numerical solutions to stochastic difference equations
18 p2564 N88-25229
Numerical solution to a system of random Volterra integral equations 18 p2565 N88-25230
Approximate solution of random differential equation
18 p2565 N88-25233
A method for the numerical solution of random Cauchy singular integral equation 18 p2565 N88-25234
Numerical solution of random Love's integral equation
18 p2565 N88-25235
On the exceedance random measures for stationary processes
[AD-A192838] 21 p3009 N88-27848
Maximum dynamic responses using matched filter theory and random process theory
[NASA-TM-100653] 22 p3042 N88-28059
Random pseudo-polynomial algorithms and exact problems
[REPT-87-014] 22 p3140 N88-28672
RANDOM SAMPLING
Large antenna experiments aboard the space shuttle: Application of nonuniform sampling techniques
19 p2652 N88-25745
RANDOM SIGNALS
Statistical measures of clipped random signals
08 p1000 N88-16055
RANDOM VARIABLES
On the least squares estimator in moving average models of order one
[AD-A186028] 07 p0909 N88-15508
A new method of estimation in a moving average model of order one
[AD-A186039] 07 p0909 N88-15510
Bounding the expectation of convex functions with limited distribution information
[AD-A186147] 07 p0910 N88-15512
Strong laws of large numbers for arrays of orthogonal random variables
[AD-A186159] 07 p0910 N88-15513
On the asymptotic joint distributions of the eigenvalues of random matrices which arise under components of covariance model
[AD-A186387] 07 p0915 N88-15558
On hypercontractivity of alpha-stable random variables, 0 less than alpha less than 2
[AD-A186425] 07 p0915 N88-15559

An elimination type two-stage procedure for selecting the population with the largest mean from k logistic populations
[AD-A185614] 07 p0916 N88-15566
On selecting the best of k lognormal distributions
[AD-A185628] 07 p0916 N88-15567
Practical applicability of exact and approximate forms of the randomization test for two independent samples
[AD-A186815] 09 p1231 N88-17381
Explicit solutions of moment problems, 1
[AD-A186018] 10 p1397 N88-18325
Some majorization inequalities for functions of exchangeable random variables
[AD-A188207] 11 p1536 N88-19178
Motion in a random gyrotropic environment in D dimensions
[PB87-170650] 12 p1685 N88-20079
Convolution metrics and rates of convergence in the CLT (Central Limit Theorem)
[AD-A189341] 12 p1686 N88-20084
On the expectation of the product of four matrix-valued Gaussian random variables
[EUT-87-E-178] 13 p1828 N88-20927
Effects of state recovery on creep buckling under variable loading 14 p1933 N88-21527
Deterministic approximations of probability inequalities
[REPT-87-43] 14 p1966 N88-21732
Stopping rules and observed significance levels
[AD-A190320] 15 p2124 N88-22664
Effects of randomness of parameters on mean wave propagation in a viscoelastic medium
[REPT-87-60] 16 p2206 N88-23166
Mahler's method in transcendence theory
17 p2393 N88-24227
Additive prophet inequalities for transforms of uniformly bounded pairwise independent random variables
[PB88-173513] 18 p2568 N88-25250
Exact tests for variance component models with unequal cell frequencies in the last stage
[AD-A191645] 18 p2568 N88-25253
Strong law for mixing sequence
[AD-A193615] 23 p3274 N88-29490

RANDOM VIBRATION
The analysis of nonstationary vibration data
05 p0592 N88-13610
Analysis of shock and vibration environments for cargo on C9B transport aircraft 08 p0999 N88-16051
Evaluation of vibration specifications for acoustic environments 08 p0999 N88-16053
Spectral density estimates of coarsely quantized random vibration data 09 p1178 N88-17055
System characterization in nonlinear random vibration
09 p1180 N88-17071
Random vibration (stress screening) of printed wiring assemblies 11 p1499 N88-18953
Nonstationary solution in random vibration theory
[PB88-163746] 14 p1933 N88-21529
The concept of an impact resonance diagram for characterizing the nonlinear response of impact vibration
[DE88-005475] 15 p2086 N88-22432
Random vibration analysis of rattling structures
[DE88-007196] 20 p2813 N88-26691
Diffusion models of crack growth due to random overloads
[DE88-006811] 21 p2962 N88-27595
Analytical and experimental studies of beam waveguide absorbers for structural damping
[AD-A195085] 24 p3382 N88-30144

RANDOM WALK
Dynamic stress at critical locations of a structure as a criterion for mathematical model modification
09 p1180 N88-17066
Mixing properties for random walk in random scenery
[REPT-87-48] 14 p1966 N88-21734
Eigenmodes of a random walk on a 2-D lattice torus with one trap
[DE88-007830] 20 p2844 N88-26874
Range of a constrained random walk
[PB88-126867] 20 p2847 N88-26897

RANGE (EXTREMES)
NT PROPORTIONAL LIMIT
NT RADIO RANGE
Extrema of skewed stable processes
[AD-A185422] 05 p0642 N88-13925
On the characterization of certain point processes
[AD-A186427] 07 p0916 N88-15560
On the extreme order statistics for a stationary sequence
[AD-A186428] 07 p0916 N88-15561
Physics of condensed matter at extreme conditions
[DE88-006232] 13 p1832 N88-20958
Calibration of a hot-wire/hot-film anemometer over a range of temperatures, velocities and pressures
[AD-A189717] 14 p1913 N88-21430
MultiScheme: A parallel processing system based on MIT (Massachusetts Institute of Technology) scheme
[AD-A190383] 15 p2114 N88-22597
Extrema principles of entrophy production and energy dissipation in fluid mechanics
[NASA-TM-100992] 18 p2519 N88-24946

RANGE AND RANGE RATE TRACKING
Range and range rate system
[NASA-CASE-MSC-20867-1] 18 p2521 N88-24958

RANGE CONTROL
U TRAJECTORY CONTROL

RANGE FINDERS
NT LASER RANGE FINDERS
Long range sensor for rendezvous and docking missions 12 p1587 N88-19497
Degradation of downlink distance measurement indexes by the addition of a third tone --- tone ranging
[CNES-CT/DRT/TIT/TR-122-T]
15 p2056 N88-22268
Analysis of a range estimator which uses MLS angle measurements
[NASA-CR-182896] 16 p2160 N88-22884

RANGE INDICATORS
U RANGE FINDERS

RANGE MEASUREMENT
U RANGEFINDING

RANGEFINDING
JPRS report: Science and technology. China
[JPRS-CST-87-025] 03 p0300 N88-11866
GPS vertical axis performance enhancement for helicopter precision landing approach
[NASA-CR-177443] 04 p0397 N88-12477
Tau ranging revisited 04 p0437 N88-12710
Range imagery algorithms for the detection of obstacles by autonomous vehicles
[AD-A185421] 05 p0659 N88-14045
The analysis of recent crustal movements in static and kinematic models
[SER-B-279] 09 p1191 N88-17136
The Telecommunications and Data Acquisition Report
[NASA-CR-182545] 11 p1471 N88-18774
Source and event selection for radio-planetary frame-tie measurements using the Phobos Landers
11 p1471 N88-18775
A simplified, general-purpose deep-space ranging correlator design 11 p1473 N88-18786
The effects of atmospheric and thermohaline variability on the validation of the GEOSAT altimeter oceanographic signal between Scotland and Iceland
[AD-A189324] 12 p1650 N88-19882
Range determination of pulsars, taking into account H2 regions
[ETN-88-91492] 14 p1993 N88-21877
Baseline estimation from simultaneous satellite laser tracking
[NASA-CR-182750] 15 p2022 N88-22052
An optical preamplifier for detection of CO2 laser radiation
[AD-A190790] 18 p2520 N88-24949
Range data description based on multiple characteristics 24 p3419 N88-30351

RANGES (FACILITIES)
NT BALLISTIC RANGES
NT TEST RANGES

RANGING
U RANGEFINDING

RANKINE CYCLE
Organic Rankine-cycle power systems working fluids study. Topical report No. 1: Fluorinol 85
[DE87-014604] 02 p0195 N88-11217
Application of Organic Rankine Cycles (ORCs) to decentralized power generation, preliminary study
[DE87-753331] 03 p0347 N88-12197
Design of a condenser-boiler for a binary mercury-organic Rankine cycle solar dynamic space power system
[AD-A184188] 03 p0348 N88-12198
Microwave superheaters for fusion
[DE88-001656] 05 p0653 N88-14007
Supersonic turbines for organic fluid Rankine cycles from 3 to 1300 kW 06 p0713 N88-14375
An experiment to investigate Rankine cycle two-phase microgravity issues
[DE88-004197] 10 p1308 N88-17818
Study on shaft seals for potassium turbine
[EL-891] 15 p2074 N88-22364
Development of an integrated heat pipe-thermal storage system for a solar receiver
[NASA-TM-101099] 15 p2091 N88-22458
Two-phase fluid management for a Rankine cycle isotope power system 17 p2405 N88-24303
An experiment to investigate Rankine cycle two-phase microgravity issues 17 p2409 N88-24322
Design of a high-power-density Ljungstroem turbine using potassium as a working fluid
17 p2409 N88-24323
Nuclear Rankine/flywheel MMW space power concept
17 p2413 N88-24349
Status of the organic Rankine cycle for space applications 17 p2422 N88-24402
Optimization of organic Rankine cycles for space station applications 17 p2423 N88-24407
Dynamic isotope power system critical component verification 17 p2425 N88-24421
SNAP-DYN: Proven technology for wear-term, higher power in space 17 p2425 N88-24422
Energy storage for nuclear burst power systems
17 p2426 N88-24431
Review of alkali metal and refractory alloy compatibility for Rankine cycle applications 17 p2428 N88-24447
Trade study for kWe class space reactors
17 p2430 N88-24454
A high power density radial-in-flow reactor split core design for space power systems
17 p2430 N88-24455
Experimental demonstrations of organic Rankine cycle waste heat rejection systems 17 p2432 N88-24469
Potassium Rankine power system for space power
17 p2433 N88-24476
A combined Rankine/Brayton pulse power cycle
17 p2435 N88-24490
Energy conversion system optimization study for multimegawatt space nuclear power application
17 p2436 N88-24492
C-CAMP: A closed cycle alkali metal power system
[DE88-009715] 19 p2688 N88-25975
Analytical and experimental investigation of ringless piston concept
[AD-A192835] 20 p2810 N88-26673
Reactor applications of the Compact Fusion Advanced Rankine (CFAR) cycle for a D-T tokamak fusion reactor
[DE88-011351] 22 p3153 N88-28762
Study of toluene stability for an Organic Rankine Cycle (ORC) space-based power system
[NASA-CR-180884] 24 p3337 N88-29863
Study of toluene rotary fluid management device and shear flow condenser performance for a space-based organic Rankine power system
[NASA-CR-180885] 24 p3338 N88-29872

RANKING
Contributions to selection and ranking theory with special reference to logistic populations
[AD-A185629] 07 p0917 N88-15568
The r-rank of the groups of exceptional Lie type
[CWI-PM-R8607] 08 p1072 N88-16468
An application of fuzzy set theory to statistical hypothesis testing
[AD-A186705] 09 p1232 N88-17386
Verification of an algorithm for log-time sorting by square comparison
[CWI-CS-R8729] 14 p1956 N88-21656
An assessment of index term ranking
21 p3028 N88-27974

RAOULT LAW
Certain questions of thermodynamic theory of weak solutions 18 p2586 N88-25368

RAPID EYE MOVEMENT STATE
Model based monitoring of human sleep stages
[ISBN-90-9001448-9] 06 p0752 N88-14618

RAPID QUENCHING (METALLURGY)
Investigation of rapidly-solidified dispersion strengthened titanium alloys
[AD-A183882] 01 p0022 N88-10140
Structure of rapidly solidified Ni-Ti
[DE87-012252] 02 p0147 N88-10921
Shock-induced melting and rapid solidification
[DE88-000226] 03 p0288 N88-11810
Effect of rapid solidification on short-range order: A magnetic study
[AD-A185216] 05 p0565 N88-13444
Tensile properties of extrusion consolidated Type 304 SS rapidly solidified powders
[DE87-014875] 05 p0566 N88-13450
Development of iron aluminides
[AD-A185190] 05 p0568 N88-13461
Microstructural modification during laser welding
[DE88-002344] 09 p1144 N88-16860
Remarks on solid state amorphizing transformations
[DE88-006452] 15 p2145 N88-22803
The weldability of consolidated rapidly solidified Type 304 SS powders
[DE88-006738] 16 p2178 N88-22978
Effect of alloying, rapid solidification, and surface kinetics on the high temperature environmental resistance of niobium
[AD-A192093] 18 p2485 N88-24743
Laboratory scale inert gas atomizer for producing rapidly solidified powders
[DE88-006734] 18 p2497 N88-24812
Rapid thermal annealing of silicon layers amorphized by ion implantation
[DE88-702307] 23 p3290 N88-29591

RAPID SOLIDIFICATION
U RAPID QUENCHING (METALLURGY)
U SOLIDIFICATION
RAPID TRANSIT SYSTEMS
Costs and benefits of AC propulsion
[PB88-173380] 16 p2287 N88-23691
Simulation models for the dynamics of tracked vehicle systems: State-of-the-art and open problems
20 p2785 N88-26522
RARE EARTH ALLOYS
Exploratory development in the system Al-Sc-X
[DE88-006242] 19 p2618 N88-25529
RARE EARTH COMPOUNDS
NT CERIUM COMPOUNDS
NT CERIUM OXIDES
NT EUROPIUM COMPOUNDS
NT LANTHANUM TELLURIDES
NT LUTETIUM COMPOUNDS
NT NEODYMIUM COMPOUNDS
Gaining control over rare earth valence fluctuations
[DE87-010116] 01 p0103 N88-10671
Metallurgical processes in multi-component rare earth-transition metal permanent magnet alloys
[AD-A186401] 07 p0832 N88-15045
Superconductivity and phase stability in the heavy rare earth quaternary compounds RBa2Cu3O7 (R = Ho, Er, Tm, Yb, Lu)
[DE88-003478] 10 p1419 N88-18476
Large momentum pairing in one-dimensional systems
[AD-A189226] 13 p1835 N88-20981
Magnetic studies of iron-rare-earth-metalloid alloys
[DE88-006601] 16 p2282 N88-23660
Novel fiber preforms: Rare earth doping
[AD-A191549] 18 p2575 N88-25294
Magnetic phase transitions in 90-K superconductors Ho1Ba2Cu3O(7-delta) and Gd1Ba2Cu3O(7-delta) observed by ZF-muon(+)SR
[DE88-752611] 23 p3290 N88-29588
RARE EARTH ELEMENTS
NT CERIUM
NT DYSPROSIUM
NT ERBIUM
NT EUROPIUM
NT GADOLINIUM
NT HOLMIUM
NT LANTHANUM
NT NEODYMIUM
NT NEODYMIUM ISOTOPES
NT SAMARIUM ISOTOPES
NT YTTERBIUM
NT YTTRIUM
Some electronic factors influencing superconductivity in some rare-Earth-like elements and the beginning of rare-Earth series
[DE87-702582] 01 p0102 N88-10668
Study on substructures of martensite in steels containing rare earth metals
[PB87-143996] 07 p0833 N88-15050
Effect of rare earth elements on the hydrogen-induced cracking in high strength low alloy steel
[PB87-143806] 07 p0833 N88-15052
The synthesis and characterization of some rare earth arsenides
[AD-A186445] 08 p0965 N88-15839
Rare earth elements in heat treatable steels
[PB87-144002] 08 p0968 N88-15858
Energy transfer and non-linear optical properties at near ultraviolet wavelengths: Rare earth 4f yields 5d transitions in crystals and glasses
[DE88-005403] 13 p1840 N88-21012
Thermochemistry and high temperature thermodynamic properties of rare earth-alkaline earth-copper oxide superconductors
[DE88-005976] 15 p2140 N88-22770
Absorption spectra and energy levels of Gd(3+), Nd(3+) and Cr(3+) in the garnet Gd3Sc2Ga3O12
[AD-A193634] 23 p3292 N88-29599
RARE GAS-HALIDE LASERS
NT KRYPTON FLUORIDE LASERS
NT XENON CHLORIDE LASERS
NT XENON FLUORIDE LASERS
Efficiency of ionic noble gas and alkali metal molecules as ultraviolet and far-ultraviolet lasers
09 p1238 N88-17419
RARE GASES
NT ARGON
NT ARGON ISOTOPES
NT HELIUM
NT HELIUM ISOTOPES
NT KRYPTON
NT KRYPTON ISOTOPES
NT LIQUID HELIUM
NT LIQUID HELIUM 2
NT NEON
NT RADON
NT RADON ISOTOPES
NT XENON
Microgravity nucleation and particle coagulation experiments support
[NASA-CR-181541] 04 p0423 N88-12619
Active medium formation in lasers using mixtures of inert gases and optical breakdown pumping
06 p0709 N88-14347
Combustion of a double base fuel in the presence of inert gases
[INPE-4516-RPE/564] 16 p2170 N88-22936
High-order multiphoton ionization of the noble gases
[DE88-007489] 18 p2571 N88-25273
Alternate techniques for noble-gas detection
[DE88-009471] 19 p2613 N88-25507
Method for the isotopically selective detection of inert gases
[DE88-008370] 20 p2769 N88-26421
Rare Gas Halide (RGH) kinetics
[AD-A192352] 20 p2770 N88-26425
The electronic structure of condensed molecular systems
[DE88-007823] 20 p2851 N88-26323
Non-atmospheric noble gases from CO(sub 2) well ga
24 p3441 N88-30476
Noble gases, C,N, and Si isotopes in interstellar SiC form the Murchison carbonaceous chondrite
24 p3442 N88-30483
RAREFACTION
Rarefaction velocities in shocked lead
[DE87-013141] 02 p0146 N88-10917
Low Reynolds number influence on aerodynamic performance of hypersonic lifting vehicles
05 p0531 N88-13230
Experiments on ion-acoustic rarefactive solitons in a multi-component plasma with negative ions
[INPE-4393-PRE/1213] 08 p1086 N88-16542
RAREFACTION WAVES
U ELASTIC WAVES
RAREFIED GAS DYNAMICS
Rarefied gas numerical wind tunnel. 2: Two-dimensional and axially symmetric bodies 05 p0536 N88-13273
Comparisons of Monte-Carlo and PNS (Parabolized Navier-Stokes) calculations for rarefied flow over reentry vehicle configurations
[DE88-004937] 11 p1435 N88-18560
Rarefied gas numerical wind tunnel 3. Universal code for three dimensional bodies 19 p2637 N88-25644
RAREFIED GASES
NT INTERPLANETARY GAS
NT INTERSTELLAR GAS
NT NEUTRAL GASES
Rotational flow of rarefied gas between two coaxial cylinders with slip conditions
[INPE-4277-PRE/1149] 12 p1627 N88-19738
Nozzle lip effects on gas expansion into the plume backflow region
[AD-A192806] 21 p2942 N88-27475
RASERS
U MASERS
RASTER SCANNING
A raster scan algorithm for generating visible parametric surfaces
[DE88-003222] 09 p1220 N88-17321
The US Army Electronic Map Data (EMD) initiative
[AD-A188209] 11 p1565 N88-19372
RATE METERS
U MEASURING INSTRUMENTS
RATES (PER TIME)
NT ACCELERATION (PHYSICS)
NT ACOUSTIC VELOCITY
NT AIRSPEED
NT ANGULAR ACCELERATION
NT ANGULAR VELOCITY
NT ARRHYTHMIA
NT BIT ERROR RATE
NT BURNING RATE
NT COLLISION PARAMETERS
NT COLLISION RATES
NT CRITICAL VELOCITY
NT CURRENT DENSITY
NT DECAY RATES
NT DECELERATION
NT DRIFT RATE
NT ELECTRON ACCELERATION
NT ELECTRON FLUX DENSITY
NT EVAPORATION RATE
NT FLOW VELOCITY
NT FLUX (RATE)
NT FLUX DENSITY
NT GROUP VELOCITY
NT HEART RATE
NT HEAT FLUX
NT HIGH GRAVITY ENVIRONMENTS
NT HIGH SPEED
NT HYPERSONIC SPEED
NT ILLUMINANCE
NT IMPACT ACCELERATION
NT ION PRODUCTION RATES
NT IRRADIANCE
NT LIGHT SPEED
NT LOADING RATE
NT LOW SPEED
NT LUMINANCE
NT LUMINOUS INTENSITY
NT MAGNETIC FLUX
NT MASS FLOW RATE
NT NEUTRON FLUX DENSITY
NT ORBITAL VELOCITY
NT PARTICLE ACCELERATION
NT PARTICLE FLUX DENSITY
NT PHASE VELOCITY
NT PLASMA ACCELERATION
NT PROPAGATION VELOCITY
NT PULSE REPETITION RATE
NT RADIAL VELOCITY
NT RADIANCE
NT RADIANT FLUX DENSITY
NT RECOMBINATION COEFFICIENT
NT RELATIVISTIC VELOCITY
NT RESPIRATORY RATE
NT ROTOR SPEED
NT SOLAR CONSTANT
NT SOLAR FLUX
NT SOLAR FLUX DENSITY
NT SOLAR WIND VELOCITY
NT SOUND INTENSITY
NT SPIN REDUCTION
NT STRAIN ENERGY RELEASE RATE
NT STRAIN RATE
NT SUBSONIC SPEED
NT SUPERSONIC SPEED
NT TACHYCARDIA
NT TERMINAL VELOCITY
NT TIP SPEED
NT TRANSONIC SPEED
NT TRANSVERSE ACCELERATION
NT WIND VELOCITY
Asynchronous rotation in close binary systems with circular orbits 04 p0506 N88-13131
Estimation of rainfall rates in tropical cyclones by passive microwave radiometry 06 p0744 N88-14577
Vapor condensation on a turbulent liquid interface
08 p0982 N88-15[illegible]
The effects of data structure on total time on test plots
[AD-A187628] 10 p1389 N88-18296
The convergence rate for the strong law of large numbers: General lattice distributions
[AD-A187560] 10 p1402 N88-18362
Mass loss from evolved stars
11 p1569 N88-19394
Measurement of rate constants of elementary gas reactions of importance to upper atmosphere and combustion systems
[AD-A189432] 13 p1737 N88-20386
Increasing the rate at which ceramic castings undergo preliminary heat-treatment in an ultra-high frequency magnetic field 14 p1886 N88-21275
Two puzzling aspects of protein crystal growth
18 p2580 N88-25329
Kinetics of thermochemical gas-solid reactions important in the Venus sulfur cycle
[NASA-CR-182963] 19 p2742 N88-26280
The rate of volcanism on Venus
[NASA-CR-183039] 19 p2742 N88-26281
A simulation analysis of errors in the measurement of standard electrochemical rate constants from phase-selective impedance data
[AD-A192739] 20 p2770 N88-26426
Effect of double layer structure on the determination of corrosion rates from polarization measurements
[DE88-010097] 20 p2774 N88-26448
Rain attenuation at 35 GHz over an 18 km path
[AD-A194504] 22 p3069 N88-28217
Systolic array fault tolerance performance analysis
[AD-A193521] 23 p3244 N88-29306
Validate algorithms for the determination of rainfall rates from SSM/I microwave satellite imagery
[AD-A195426] 24 p3404 N88-30270
RATINGS
Cetane scale evaluation and possible modification
[AD-A189730] 15 p2048 N88-22200
RATIONS
NT SPACE RATIONS
RATIOS
NT ASPECT RATIO
NT COMPRESSION RATIO
NT DIMENSIONLESS NUMBERS
NT FINENESS RATIO
NT FROUDE NUMBER

NT HIGH ASPECT RATIO
NT HIGH REYNOLDS NUMBER
NT INDEXES (RATIOS)
NT LEAF AREA INDEX
NT LIFT DRAG RATIO
NT LOW ASPECT RATIO
NT LOW REYNOLDS NUMBER
NT MACH NUMBER
NT MASS RATIOS
NT NUSSELT NUMBER
NT PAYLOAD MASS RATIO
NT PECLET NUMBER
NT POISSON RATIO
NT PRANDTL NUMBER
NT PRESSURE RATIO
NT PROPELLANT MASS RATIO
NT RAYLEIGH NUMBER
NT REYNOLDS NUMBER
NT RICHARDSON NUMBER
NT SCALE (RATIO)
NT SIGNAL TO NOISE RATIOS
NT THICKNESS RATIO
NT VOID RATIO
Microgravity nucleation and particle coagulation experiments support
[NASA-CR-181541] 04 p0423 N88-12619
Carbon abundances and C12/C13 ratios in M giants
04 p0515 N88-13167
Hydrogen and deuterium in the local interstellar medium 04 p0521 N88-13204
Determination of the fiber ratio in carbon fiber/resin composites by means of image analysis
[SNIAS-872-422-101] 05 p0558 N88-13398
On the role of the ionization frequency to gyrofrequency ratio in the critical ionization velocity interaction
[TRITA-EPP-86-10] 10 p1410 N88-18414
Isotopic composition of Halley dust
14 p2002 N88-21933
High-fidelity in isotope ratio measurements for resonance ionization mass spectrometry
[DE88-009129] 19 p2613 N88-25506
The ratio of microwaves to X-rays in solar flares: The case for the thick target model
[NASA-CR-183102] 19 p2743 N88-26287
On the estimation of a variance ratio
[AD-A193190] 21 p3009 N88-27854
RATS
The toxicology and metabolism of nickel compounds
[DE87-014801] 04 p0474 N88-12921
Combined effect of microwaves and ionizing radiation
07 p0893 N88-15413
Experiments with rats flown aboard Cosmos-1667 biosatellite (main objectives, conditions and results)
07 p0893 N88-15414
Brain morphogenesis in rats developing in weightlessness 07 p0894 N88-15415
Morphometric analysis of rat aorta endothelium during long-term hypokinesia 07 p0894 N88-15417
Nucleic acid content of skeletal muscles during hypokinesia and in the recovery period
07 p0894 N88-15418
Acid-base equilibrium and some rat blood parameters following exposure to hyperbaric oxygenation
07 p0894 N88-15420
Changes in functional parameters of animals during long-term inhalation of acetic acid
07 p0895 N88-15423
Effect of steroid hormones on biogenic amine levels in lungs during development of pulmonary hypertension in rats submitted to chronic hypobaric hypoxia
07 p0896 N88-15430
Histomorphometric analysis of rat bones after spaceflight aboard Cosmos-1667 biosatellite
10 p1360 N88-18128
Effect of weightlessness on replicative function of rat hepatocyte DNA 10 p1360 N88-18129
RNA-synthesizing activity in rat liver following flight aboard Cosmos-1667 10 p1360 N88-18130
Short- and long-term effects of nonlethal levels of fast high-energy helium ions on retention of developed and formation of new behavioral patterns in rats
10 p1362 N88-18140
Myosin Ca sup (2+), Mg sup (2+)-adenosine triphosphatase activity in ray myocardium following 30-day expose to 1.1 and 2.0 G 10 p1362 N88-18141
Kinetic toxic aspect of potential use of sulfur hexafluoride in closed environments 10 p1362 N88-18142
Comparative evaluation of stress response of rats to different methods of simulating some effects of weightlessness 10 p1363 N88-18144
Experimental measurements of the uptake of ozone in rats and human subjects
[PB88-125422] 10 p1364 N88-18149
Investigation of genetic structures of rat germ cells following flight aboard Cosmos-1514 biosatellite during their prenatal development 10 p1364 N88-18155
Morphological and functional state of the hypothalamo-hypophyseal neurosecretory system of rats flown aboard Cosmos-1667 10 p1365 N88-18156
Investigation of rat skeletal muscles following short-term spaceflight aboard Cosmos-1667 biosatellite
10 p1365 N88-18157
Morphological study of early changes in rat bones in simulated weightlessness 10 p1365 N88-18158
Lipid peroxidation in rat tissues with exposure to antiorthostatic hypokinesia, exercise and immobilization stress 10 p1365 N88-18159
Effect of cardioactive compounds on rat myocardium actomyosin following exposure to accelerations
10 p1365 N88-18161
Effect of external electrostatic field on catecholamine secretion by rat adrenals 10 p1366 N88-18166
New book on metabolic aspects of spaceflight stress
10 p1367 N88-18172
Scaling physiological pharmacokinetic models by physiological time
[DE88-000335] 10 p1368 N88-18173
Response of coronary blood flow to step changes in plasma protein concentration in the isolated rat heart
12 p1651 N88-19892
Life sciences research in space: The requirement for animal models 12 p1654 N88-19909
Does 7-day hindquarters unloading simulate 7 days of weightlessness exposure in rat trabecular bone?
12 p1657 N88-19928
The influence of space flight on water-salt homeostasis in man and animals 12 p1659 N88-19943
Cyropreservation of isolated rat hepathocytes for future use in Spacelab experiments: Preliminary results
12 p1660 N88-19950
Behavior, physiology and energy deposition in rats chronically exposed to 2450 MHz radiation
[PB88-171418] 16 p2237 N88-23363
Behavioral response of rats exposed to high-power microwave radiation
[AD-A192199] 18 p2548 N88-25128
Dexamethasone regulates glutamine synthetase expression in rat skeletal muscles
[NASA-CR-182935] 18 p2549 N88-25129
RAWINSONDES
The use of TOMS-modified VAS data for large-scale NWP 05 p0618 N88-13791
Minimum Energy Routing through Interactive Techniques (MERIT) modeling
[NASA-CR-182535] 10 p1356 N88-18105
RAY ACOUSTICS
U GEOMETRICAL ACOUSTICS
RAY OPTICS
U GEOMETRICAL OPTICS
RAY TRACING
Present status of the high resolution spectrometers
[CEBAF-PR-87-029] 02 p0234 N88-11478
A FORTRAN code for the calculation of probe volume geometry changes in a laser anemometry system caused by window refraction
[NASA-TM-100210] 03 p0364 N88-12288
Coupled acoustic and ocean thermodynamic model
[AD-A184357] 04 p0472 N88-12911
A prototype ray tracer
[AD-A184863] 05 p0634 N88-13874
TRACKER: A 3-D radio ray tracing code
[DE88-003267] 07 p0847 N88-15137
A raytrace method for a laterally heterogeneous environment
[AD-A186525] 08 p0978 N88-15912
A ray-tracing study of electron cyclotron resonance heating in tokamak plasmas with a superthermal electron tail
[INPE-4381-PRE/1201] 08 p1085 N88-16536
Absorption of electron cyclotron waves by superthermal electron velocity distributions in tokamak plasmas
[INPE-4385-PRE/1205] 08 p1086 N88-16539
The effect of asymmetric current-supporting electron velocity distributions on second harmonic electron cyclotron resonance heating: A ray-tracing treatment for the compass tokamak
[INPE-4389-PRE/1209] 08 p1087 N88-16549
Seventy-meter antenna performance predictions: GTD analysis compared with traditional ray-tracing methods
11 p1474 N88-18793
Ray tracing optical analysis of offset solar collector for space station solar dynamic system
[NASA-TM-100853] 15 p2027 N88-22080
Simulation and analysis of wave propagation through random media 21 p2947 N88-27503
A probabilistic model of the apparent radiance of a rough sea
[AD-A193867] 22 p3129 N88-28602
Ionosonde studies of field-aligned irregularities during high-power HF heating at Arecibo
[AD-A195848] 24 p3401 N88-30256
RAYLEIGH DISTRIBUTION
Rayleigh-Taylor instability in compressible fluids
[DE88-002473] 07 p0852 N88-15179
Analytical and numerical analysis of finite amplitude Rayleigh-Taylor instability
[DE88-004056] 11 p1474 N88-18797
Rayleigh-Taylor instability in inertial confinement fusion
[DE88-701411] 15 p2137 N88-22750
Resonant structures for integrated sensors
19 p2673 N88-25893
A multiple-scales partial solution of the pulse-forced Rayleigh-Plesset equation of cavitation bubble dynamics
[AD-A193733] 23 p3212 N88-29118
RAYLEIGH EQUATIONS
The Rayleigh-Taylor instability in ablatively accelerated targets with 1, 1/2 and 1/4 micrometers laser light
[AD-A185945] 07 p0858 N88-15208
Reynold stress closure in jet flows using wave models
[NASA-CR-182662] 12 p1628 N88-19741
RAYLEIGH NUMBER
The numerical and analytical study of bifurcation and multicellular flow instability due to natural convection between narrow horizontal isothermal cylindrical annuli at high Rayleigh numbers
[AD-A186113] 07 p0849 N88-15151
Experimental study of local natural convection heat transfer in inclined and rotating enclosures
09 p1165 N88-16986
Periodic natural convection in a rectangular enclosure of low aspect ratio 10 p1329 N88-17941
High Rayleigh number convection in rectangular enclosures with differentially heated vertical walls and aspect ratios between zero and unity
[NASA-TM-100277] 12 p1628 N88-19739
RAYLEIGH SCATTERING
Optical characterization of silica aerogel glass
[DE87-014617] 02 p0153 N88-10956
Rayleigh scattering measurements of a freejet with homogeneous condensation 03 p0319 N88-12020
All-optical beam control by forced Rayleigh scattering
[AD-A184315] 04 p0490 N88-13018
Chemical reactions in turbulent mixing flows
[AD-A186141] 07 p0849 N88-15153
Mixing in variable density, isothermal turbulent flows and implications for chemically reacting turbulent flows
[PB88-110044] 07 p0852 N88-15176
Rayleigh lidar observations of gravity wave activity in the stratosphere and lower mesosphere
[NASA-CR-182384] 09 p1189 N88-17123
Thermodynamic theory of fluctuations and Rayleigh light scattering in solutions 13 p1785 N88-20681
Laser Diagnostics for combustion temperature and species measurements 17 p2330 N88-23912
Application of Rayleigh scattering to turbulent flow with heat transfer and combustion
[AD-A191565] 18 p2481 N88-24720
Instrumentation for turbulent reacting flows
[AD-A191671] 18 p2515 N88-24923
Developing diagnostic methods for plasma-particle interaction
[DE88-007726] 20 p2856 N88-26973
Investigations on Mie and Rayleigh scattering as basis for the development of Rayleigh temperature lidars with aid of Michelson interferometry
[GKSS-87/E/62] 21 p2976 N88-27675
RAYLEIGH WAVES
A numerical and analytical investigation of Rayleigh-Taylor instability in a solid tungsten plate
[DE87-013593] 01 p0087 N88-10562
Numerical model of Rayleigh instability and spin-off eddies on fronts 13 p1788 N88-20696
Electron-Rayleigh wave interaction in thin film carbons
[AD-A191727] 18 p2492 N88-24781
A comparison of analytical techniques for modeling the Rayleigh-Taylor response of elastic-plastic solids
[DE88-010372] 21 p2962 N88-27596
Finite-difference simulations of Rayleigh-wave scattering by shallow heterogeneity
[AD-A194961] 24 p3402 N88-30259
RAYLEIGH-BENARD CONVECTION
Rayleigh-Benard convection in a Hele-Shaw cell: A numerical study
[KFK-4212] 01 p0044 N88-10280
Special Course on Modern Theoretical and Experimental Approaches to Turbulent Flow Structure and its Modelling
[AGARD-R-755] 03 p0312 N88-11970
Dynamics and routes to chaos from quasiperiodicity
03 p0312 N88-11974
A deterministic approach to turbulence: Chaos in Rayleigh-Benard convection 03 p0313 N88-11975
Determination of fractal dimension, connection of space and temporal chaos and application to experimental results 03 p0313 N88-11977

A dissipation principle and its consequences for structured shock waves in thermoelastic materials
[DE87-013723] 04 p0454 N88-12813
Investigation of surface tension driven convection as a feasibility study for a micro-gravity experiment
[NASA-CR-182504] 11 p1466 N88-18739
RAYLEIGH-RITZ METHOD
Postbuckling of laminated anisotropic panels
[NASA-TM-100509] 08 p0994 N88-16011
RB-57 AIRCRAFT
U B-57 AIRCRAFT
RC CIRCUITS
Realization of active high pass filters for group velocity correction
[MPE-IN-REPT-47] 08 p0979 N88-15918
RC NETWORKS
U RC CIRCUITS
RDX
The effect of RDX particle size on the shock sensitivity of cast PBX formulations. 2: Bimodal compositions
[DE87-009581] 01 p0031 N88-10196
High pressure strand burn rate tests of polyvinylnitrate/nitramine propellants
[AD-A184178] 04 p0422 N88-12615
High explosive moulding powders from RDX and aqueous polyurethane dispersions
[AD-A185026] 05 p0568 N88-13456
Mechanism of and particle size effects on shock sensitivity of heterogeneous pressed explosives: Preliminary assessment of binderless RDX in fuze trains
[MRL-R-1077] 09 p1150 N88-16892
Laser ignition of nitramine composite propellants and crack propagation and branching in burning solid propellants
[AD-A189260] 13 p1753 N88-20483
Laser-RDX aerosol pyrolysis with matrix isolation of unstable intermediates 19 p2632 N88-25614
Theoretical studies of the chemical reactions involved in the ignition of nitramines 19 p2632 N88-25615
Discovery of a low temperature form of TAGN (Triaminoguanidinium Nitrate)
[AD-A196059] 24 p3357 N88-29989
REACTION BONDING
Development of a statistically proven injection molding method for reaction bonded silicon nitride, sintering reaction bonded silicon nitride, and sintered silicon nitride
[ETN-87-90575] 02 p0160 N88-11002
Investigation on diffusion reaction brazing of aluminium
[PB87-143368] 08 p0992 N88-16001
Development, high temperature properties, and microanalysis of nonoxide ceramics
[ETN-88-92103] 14 p1893 N88-21304
Carboxylate formation at the interface between a polyimide coating and cobalt 17 p2320 N88-23859
REACTION JET BACKPACKS
U SELF MANEUVERING UNITS
REACTION JETS
U JET FLOW
U JET THRUST
REACTION KINETICS
Hot-spot reaction in unsustained shocks
[DE87-011781] 01 p0044 N88-10277
Research on one-dimensional two-phase flow. Theory on hydrodynamic balance in two fluid model and its application
[DE87-702615] 01 p0045 N88-10290
Theoretical approaches to chemical dynamics in highly compressed fluids
[DE87-012242] 01 p0046 N88-10296
Kinetics investigations of atmospheric chemical reactions
[PB87-213351] 01 p0069 N88-10439
Aqueous-phase reactions in clouds
[DE86-005249] 01 p0069 N88-10445
Numerical simulation of a supersonic chemically reacting mixing layer 02 p0143 N88-10900
Photolytic processes for measurement of combustion heats of formation and reaction rates
[DE87-014047] 02 p0144 N88-10905
On the modelling of non-reactive and reactive turbulent combustor flows 02 p0169 N88-11061
Some speculations on the mechanisms of abrasive grinding and polishing
[DE87-014242] 02 p0181 N88-11126
Experimental nuclear physics
[DE87-014586] 02 p0231 N88-11459
Solute segregation to phase interfaces and grain boundaries: Studies by analytical electron microscopy and profile deconvolution
[DE87-012129] 02 p0243 N88-11537
Laser spectroscopy and gas-phase chemistry in CVD
[DE87-013715] 03 p0281 N88-11770
Detailed mechanism of benzene oxidation
[NASA-TM-100202] 03 p0282 N88-11775
Detailed kinetic modeling of autoignition chemistry
[DE87-013226] 03 p0283 N88-11782
The calculation of thermal rate constants for gas-phase and heterogeneous reactions in combustion processes
[AD-A184435] 03 p0284 N88-11788
Kinetics of CO adsorption on nickel using time resolved vibration spectroscopy
[ETN-87-90615] 03 p0289 N88-11814
Perturbation and characterization of nonlinear processes
[DE87-014580] 03 p0369 N88-12322
Computer simulations of fragmentation
[DE87-900985] 03 p0375 N88-12358
Development of the non-equilibrium reactive chemical transport code CHMTRNS
[DE88-000682] 04 p0481 N88-12964
Guest-host interactions in thermotropic and lyotropic liquid crystals
[AD-A184402] 04 p0496 N88-13057
Numerical analysis of axisymmetric flow with H2-O2 reactions 05 p0538 N88-13272
Laser probes of propellant combustion chemistry
[AD-A184854] 05 p0561 N88-13415
Detailed mechanism of toluene oxidation and comparison with benzene
[NASA-TM-100261] 05 p0563 N88-13428
Effect of rapid solidification on stainless steel weld metal microstructures and its implications on the Schaeffler diagram
[DE88-001489] 05 p0566 N88-13451
Reactive sticking coefficients of silane on silicon
[DE88-000601] 05 p0570 N88-13473
Theoretical studies of solar lasers and converters
[NASA-CR-181569] 05 p0587 N88-13577
Fracture kinetics of corrosion fatigue
05 p0605 N88-13708
Numerical methods for reaction-diffusion problems with non-differentiable kinetics
[AD-A185405] 05 p0641 N88-13923
Exploitation of the sol-gel route in processing of ceramics and composites
[AD-A185482] 06 p0686 N88-14204
The kinetics and dynamics of iodine monofluoride formation in gas-phase collisions
[AD-A185715] 06 p0709 N88-14352
Quick measurement of individual stress reaction level: Development of the Emotional Stress Reaction Questionnaire (ESRQ)
[FOA-C-50050-5.3] 06 p0752 N88-14617
Theoretical studies of kinetic mechanisms of negative ion formation in plasmas
[AD-A185735] 06 p0784 N88-14812
European reacting flow research: A final assessment
[AD-A185833] 07 p0828 N88-15022
Carbon monoxide and turbulence-chemistry interactions: Blowoff and extinction of turbulent diffusion flames
[AD-A186276] 07 p0828 N88-15025
SRB combustion dynamics analysis computer program (CDA-1)
[NASA-CR-182404] 07 p0830 N88-15032
The carbon dioxide chaperon efficiency for the reaction H + O2 + M yields HO2 + M from ignition delay times behind reflected shock waves
[NASA-TM-100125] 07 p0830 N88-15036
Lyman-alfa/OH-resonance-absorbtion measurements and simulation calculations for the investigation of the induction behavior of methane/ethane/oxygen mixtures in reflected shock waves
[ETN-88-90806] 07 p0831 N88-15042
Chemical reactions in turbulent mixing flows
[AD-A186141] 07 p0849 N88-15153
Feasibility of a complex compound heat pump
[PB88-113022] 07 p0853 N88-15183
Atomic oxygen effects on metals
07 p0924 N88-15617
Non-phonon mechanisms of superconductivity in high T/sub c/ superconducting oxides and other materials and their manifestation
[DE88-002708] 07 p0939 N88-15709
An analytical study of the hydrogen-air reaction mechanism with application to scramjet combustion
[NASA-TP-2791] 08 p0966 N88-15846
Ionic mechanisms of soot formation in flames
[AD-A186195] 08 p0966 N88-15848
Non-steady group combustion of a cloud of char particles
[DE87-010773] 08 p0966 N88-15849
Nb3Al formation in sputter-deposited Nb/Al multi-layer samples
[DE88-003192] 08 p0970 N88-15868
Tin activated reactive ion plating and its application
[PB87-144036] 08 p0970 N88-15871
Nonequilibrium reacting flows
08 p0985 N88-15959
The effects of fuel composition on ignition delay in homogeneous charge and direct injection compression ignition engines
[DE88-003691] 09 p1143 N88-16848
Long-term-aging embrittlement of cast duplex stainless steels: Mechanism and kinetics
[DE88-002929] 09 p1145 N88-16861
Lithium/polymer electrolyte interfacial instability
[AD-A187164] 09 p1147 N88-16874
Morphology control and reinforcing mechanisms using an elastomer in an epoxy network based on diamine menthane
[ISAL-IDI1-87-09] 09 p1148 N88-16881
DSC (Differential Scanning Calorimeter) stability test for liquid propellants: A preliminary report
[AD-A187115] 09 p1150 N88-16888
Computational fluid dynamics and aerothermodynamics
[NASA-CR-182490] 09 p1166 N88-16989
Insights into the mechanisms of chemical reactions: Reaction paths for chemical reactions
[DE88-003041] 10 p1297 N88-17755
Flame propagation in the approximation of straight-line trajectories of burning products
[DE88-700675] 10 p1297 N88-17756
Diffusion description of flame propagation due to the translational motion of burning reaction products
[DE88-700676] 10 p1297 N88-17757
Low temperature reactivity of chars towards oxygen, appendix E2
[DE88-004088] 10 p1298 N88-17760
Kinetic studies following state-selective laser excitation
[DE88-004094] 10 p1335 N88-17981
Chemical activation of molecules by metals: Experimental studies of electron distributions and bonding
[DE88-004465] 10 p1407 N88-18393
Measurements of astrophysical reaction rates for radioactive samples
[DE88-004309] 10 p1429 N88-18537
Combustion of hydrogen and hydrocarbons in fluorine
[AD-A188018] 11 p1453 N88-18662
Voltammetric investigation of porous silicon for integrated circuit applications
[DE88-004024] 11 p1456 N88-18677
Fundamental studies of corrosion of nonoxide structural ceramics
[PB88-141536] 11 p1461 N88-18709
Crystallization and glass formation in electron and laser beam irradiated Cu-Zr alloys
[DE88-003390] 11 p1464 N88-18729
Picosecond laser studies of excited state processes
[AD-A189606] 12 p1607 N88-19607
Instrumentation for collisional energy transfer studies
[AD-A188495] 12 p1689 N88-20105
Kinetic mechanisms for ionization and afterburning suppression
[AD-A189219] 13 p1737 N88-20383
Measurement of rate constants of elementary gas reactions of importance to upper atmosphere and combustion systems
[AD-A189432] 13 p1737 N88-20386
Kinetics of polymer decomposition
[DE88-005500] 13 p1749 N88-20460
Experimental and theoretical constraints on the origin of mid-ocean ridge geothermal fluids
13 p1804 N88-20784
Analytically modeling the carbothermic reduction of alumina in a thermal plasma
[DE88-005535] 13 p1841 N88-21020
Basic research on natural gas combustion phenomena
[PB88-168380] 14 p1887 N88-21278
Infrared absorption spectroscopy and chemical kinetics of free radicals
[DE88-006536] 15 p2033 N88-22112
Molecular dynamics of materials possessing high energy content
[AD-A190034] 15 p2034 N88-22118
The spectroscopy and reaction kinetics of coordinatively unsaturated metal carbonyls
[AD-A190533] 15 p2035 N88-22124
Molecular reaction and energy transfer rate estimation for chemical-laser analysis
[AD-A190664] 15 p2035 N88-22126
Advanced B and Al combustion kinetics over wide temperature ranges
[AD-A190752] 15 p2036 N88-22128
High temperature oxidation and electrochemical studies related to hot corrosion
[AD-A190699] 15 p2040 N88-22156
Effect of vibrational excitation on rate parameters of atmospheric reactions
[AD-A190464] 15 p2094 N88-22477

Lumped model generation and evaluation: Sensitivity and Lie algebraic techniques with applications to combustion
[AD-A190402] 15 p2127 N88-22689

Surface enhanced Raman scattering applied to surface chemical kinetics
[AD-A191275] 16 p2176 N88-22969

Kinetics of electrons and molecules at plasma-beam discharge in molecular gases
[DE88-701196] 16 p2275 N88-23616

Chemical kinetics and photochemical data for use in stratospheric modeling evaluation Number 8
[NASA-CR-182919] 17 p2351 N88-24012

Experiments on reactions of the electronically excited molecule nitron NH (a sup 1 delta) and carbon CH2 (a bar sup 1 A(1)) in gas phase
[MPIS-3/1987] 17 p2397 N88-24249

Calculation of oxidation rates for iron in CO-CO2
[DE88-007313] 18 p2487 N88-24757

The influence of the chemical nature of resins on their reticulation kinetics and the consequences for their nonelastic mechanical properties
[ETN-88-92539] 18 p2493 N88-24788

The burning of HAN-based (hydroxylammonium nitrate) liquid propellants
[DE88-006863] 18 p2494 N88-24800

Chemical kinetics of nitramine propellant combustion
[AD-A191556] 18 p2495 N88-24802

Laboratory experiments on atmospheric OH reactions
18 p2539 N88-25066

Bimolecular reactions and energy-transfer processes of highly vibrationally excited molecules related to energetic materials
[AD-A189013] 18 p2571 N88-25270

A new approach to generating negative ion beams
[AD-A191119] 18 p2572 N88-25276

Spectroscopy and energy transfer kinetics of the interhalogens
[AD-A192103] 18 p2583 N88-25344

An improved external recycle reactor for determining gas-solid reaction kinetics
[NASA-TM-101160] 19 p2611 N88-25492

Next-generation fire extinguishing agent. Phase 1: Suppression concepts
[AD-A192279] 19 p2614 N88-25514

Kinetic measurements of thermal decomposition of energetic materials at high pressures
[AD-A191612] 19 p2622 N88-25552

Chemical kinetics modeling of HMX combustion
19 p2633 N88-25617

Simulation of axisymmetric flow with H2O2 reactions
19 p2638 N88-25651

Kinetics of thermochemical gas-solid reactions important in the Venus sulfur cycle
[NASA-CR-182963] 19 p2742 N88-26280

Rare Gas Halide (RGH) kinetics
[AD-A192352] 20 p2770 N88-26425

The influence of uncompensated solution resistance on the determination and standard electrochemical rate constants using cyclic voltammetry and some comparisons with AC voltammetry
[AD-A192825] 20 p2770 N88-26427

Oxygen reduction in fuel cell electrolytes
[DE88-008240] 20 p2819 N88-26723

Defect characterization of the redox behavior and stability of conducting oxides
[DE88-010799] 20 p2878 N88-27088

Laser probes of natural gas ignition chemistry
[PB88-212568] 21 p2910 N88-27271

Laser probes and numerical modeling as process diagnostics in chemical vapor deposition
[DE88-011622] 21 p2911 N88-27275

Study of crosslinking and nonelastic mechanical properties of epoxy and PSP networks --- epoxy resins; polystyrylpyridine resins (psp)
[ETN-88-92740] 21 p2921 N88-27337

Shock initiation studies on heterogeneous explosives
[DE88-008681] 21 p2923 N88-27351

Methods of quantifying and enhancing reactive oxygen species production 21 p2924 N88-2735

The kinetics of charge-transfer reactions on passive lithium electrodes
[DE88-009256] 21 p2939 N88-27454

Studies of photochemically and electrochemically driven electron transport in zeolites
[DE88-008644] 22 p3155 N88-28769

Reaction dynamics on semiconductor surfaces
[AD-A194305] 22 p3156 N88-28781

Thermodynamic data bases for multivalent elements: An example for ruthenium
[DE88-004395] 23 p3190 N88-28984

Theoretical investigations of nitrocubane decomposition
[AD-A194556] 23 p3200 N88-29047

N2(A3epsilon u+) by reaction of N2F4+H2 in a supersonic flow
[AD-A194493] 23 p3219 N88-29163

Chemical kinetics of hydrogen and P(sub b) centers
[DE88-010528] 23 p3291 N88-29594

Experiments and modeling of multi-component fuel behavior in combustion
[AD-A195011] 24 p3343 N88-29896

Flamelet modeling of turbulent premixed flames
24 p3350 N88-29942

Cosmochemical trends of volatile elements in the solar system 24 p3451 N88-30542

REACTION PRODUCTS

Development of strength in cements
[PB87-232971] 06 p0684 N88-14189

The influence of phosphorus on the solid state reaction between copper and silicon or germanium
[ETN-88-91361] 06 p0789 N88-14838

Investigation of OH reaction products. Excimer laser photolysis/slab laser fluorescence under tropospheric conditions
[REPT-8] 09 p1191 N88-17137

Solar-assisted hydrogen generation by photoelectrocatalysis
[PB88-160932] 12 p1605 N88-19597

Ultraviolet (180 to 300 nm) action spectra for inactivation and DNA photoproduct formation of Bacillus subtilis spores under ultrahigh vacuum 12 p1657 N88-19931

Proton/antiproton yields W(+/-)boson gamma X as a test of the quark charges
[NIKHEF-H/87-11] 13 p1836 N88-20987

New limits on charged Higgs boson mass with CELLO at Petra (Italy) and status of the neutral Higgs boson search
[NOTA-INTERNA-897] 14 p1960 N88-21817

The synthesis of polyphenylene from a CIS-dihydrocatechol biologically produced monomer
18 p2478 N88-24699

Laser-RDX aerosol pyrolysis with matrix isolation of unstable intermediates 19 p2632 N88-25614

Theoretical studies of the chemical reactions involved in the ignition of nitramines 19 p2632 N88-25615

Reaction products of solid propellants after burning at pressures up to 1000 MPa: Comparison between theoretical and experimental results
[ISL-CO-227/87] 22 p3059 N88-28153

REACTION RATE

U REACTION KINETICS

REACTION TIME

Contributions to fast-reacting and high-precision three-phase positioning systems --- machinery
[ETN-87-90427] 01 p0056 N88-10358

Computer response time measurements of mood, fatigue and symptom scale items: Implications for scale response time uses
[AD-A186093] 07 p0888 N88-15384

A deep-water OBS (Ocean Bottom Seismometer) array with real-time telemetry
[AD-A187404] 10 p1357 N88-18112

A comparison of keyboard designs for cockpit applications
[AD-A187775] 12 p1581 N88-19460

Picosecond laser studies of excited state processes
[AD-A189606] 12 p1607 N88-19607

Training in time interval discrimination using verbal feedback 12 p1665 N88-19985

The effects of hypoxia on P300 and reaction time
[DCIEM-87-RR-12] 21 p2979 N88-27697

REACTION WHEELS

Analysis, design, construction and testing of a reaction wheel model for space applications
[INPE-4358-TDL/299] 08 p0963 N88-15834

Reaction wheel experimental model of artificial satellite attitude control: Construction, simulation, and tests
[INPE-4274-PRE/1146] 11 p1490 N88-18896

Spacecraft redesign to reduce microphonic response of a VCO component 11 p1499 N88-18955

Reaction wheel control through digital technique using reference models
[INPE-4220-PRE/1100] 12 p1599 N88-19570

Nutational stability of a satellite equipped with an active magnetic momentum wheel 20 p2784 N88-26513

SIRTF nod maneuvers
[NASA-TM-101007] 22 p3048 N88-28085

REACTIVITY

The effect of additives on the reactivity of palladium surfaces for the chemisorption and hydrogenation of carbon monoxide: A surface science and catalytic study
[DE87-014685] 02 p0145 N88-10909

Reactivity for DT plasma with beam-induced tail in magnetic confinement system
[DE87-753017] 02 p0240 N88-11517

Conductive polymers via reactive aligomer
[AD-A184270] 04 p0419 N88-12597

Reactions of porphyrins in surfactant assemblies, microemulsions and in solutions
[AD-A184797] 05 p0560 N88-13412

Method for preparing hydride configurations and reactive metal surfaces
[DE88-000845] 06 p0679 N88-14161

The use of alloy 117 as a liquid metal current collector
[AD-A185740] 06 p0698 N88-14281

Organic coatings to improve the storageability and safety of pyrotechnic compositions
[AD-A187158] 09 p1150 N88-16889

Low temperature reactivity of chars towards oxygen, appendix E2
[DE88-004088] 10 p1298 N88-17760

Local stoichiometry and atomic interdiffusion during reactive metal/mercury-cadmium-telluride junction formation
[AD-A187554] 10 p1421 N88-18488

Nonmonotonic evolution and thermodynamic trends at metal/(Hg,Cd)Te interfaces: Yb/Hg0.78Cd0.22Te
[AD-A187591] 10 p1422 N88-18490

Metal contacts to cadmium telluride (CdTe)
[AD-A188306] 12 p1698 N88-20159

Properties of reactively sputtered WNx films Zhao, X.-A.
[AD-A188711] 13 p1835 N88-20976

Molecular collision processes in gases and at surfaces
[AD-A189518] 13 p1836 N88-20982

Molecular dynamics of materials possessing high energy content
[AD-A190034] 15 p2034 N88-22118

The Time-Temperature-Transformation (TTT) diagram as a basis for relating the formation and properties of reactive coatings
[AD-A190872] 16 p2182 N88-23006

Agenda for advancing electrochemical science and technology 17 p2321 N88-23861

Effects of space-dependent cross sections on core physics parameters for compact fast spectrum space power reactors 17 p2399 N88-24263

Application of the reactivity constraint approach to the transient control of spacecraft reactors
17 p2406 N88-24305

A review of diffusion barrier technology for application in SP-100 fuel pins 17 p2410 N88-24328

Surface composition-reactivity relationships in heterogeneous catalysis
[DE88-006679] 18 p2480 N88-24714

Structure/property/reactivity relations among nitramine and other energetic materials
[AD-A190878] 18 p2481 N88-24716

The catalytic reactivity of thin film crystal surfaces
[DE88-006387] 19 p2732 N88-26228

In-situ reactive of X-ray optics by glow discharge
[DE88-009840] 20 p2854 N88-26947

Deformation, fracture and explosive properties of reactive materials
[AD-A193080] 21 p2923 N88-27348

Effect of fuel burnup and cross sections on modular HTGR (High-Temperature Gas-cooled Reactor) reactivity coefficients
[DE88-006656] 22 p3151 N88-28748

Active sites and roles of solid acid base catalysts
[NASA-TT-20333] 24 p3345 N88-29909

Reactive plasticizers in negative E-beam resists
[AD-A195161] 24 p3368 N88-30056

REACTOR CORES

Mechanistic model for void distribution in flashing flow
[DE88-002948] 10 p1326 N88-17928

Gas-cooled reactor power systems for space
[DE88-005220] 11 p1545 N88-19240

Transactions of the Fourth Symposium on Space Nuclear Power Systems
[DE88-006164] 17 p2398 N88-24254

Effects of space-dependent cross sections on core physics parameters for compact fast spectrum space power reactors 17 p2399 N88-24263

Considerations pertinent to the Doppler effect for space reactors 17 p2399 N88-24264

Material tradeoffs to minimize flooding reactivity
17 p2399 N88-24265

Thermal-hydraulic considerations for particle bed reactors 17 p2400 N88-24266

Fully passive space reactor conceptual design
17 p2403 N88-24288

Acoustical gas core reactor with MHD power generation for burst power in a bimodal system
17 p2403 N88-24290

Interaction of the control system with core nuclear design for fast spectrum space power reactors
17 p2405 N88-24304

Advanced thermionic converter technology for inductive output coupling 17 p2407 N88-24311

Cermet fuel thermal conductivity
17 p2410 N88-24329

Transient analysis of heat pipe vapor dynamics
17 p2412 N88-24341

Fabrication of a niobium 1 percent zirconium containment for SP-100 primary lithium system materials mass transfer studies 17 p2417 N88-24373

Reactor core coolability with reduced power levels
17 p2425 N88-24425

Benchmark physics experiments for SP-100
17 p2429 N88-24453

A high power density radial-in-flow reactor split core design for space power systems
17 p2430 N88-24455

Effect of fuel burnup and cross sections on modular HTGR (High-Temperature Gas-cooled Reactor) reactivity coefficients
[DE88-006656] 22 p3151 N88-28748

REACTOR DESIGN

Transient modeling of the thermohydraulic behavior of high temperature heat pipes for space reactor applications 02 p0136 N88-10857

Gas-cooled reactor for space power systems
[DE87-011549] 02 p0233 N88-11471

Technical evaluation of major candidate blanket systems for fusion power reactor
[DE87-752989] 02 p0239 N88-11512

Application of a two fluid theoretical plasma transport model on current Tokamak reactor designs
[DE87-013511] 03 p0377 N88-12373

Modular pump limiter systems for large tokamaks
[DE88-001487] 04 p0494 N88-13045

Effect of plasma rotation in tokamak on stabilizing action of electrically conducting wall 06 p0773 N88-14748

Main physics features driving design concept and physics design constraints. Conceptual design study of FY86 FER
[DE88-750309] 07 p0936 N88-15689

Some process control/design considerations in the development of a microgravity mammalian cell bioreactor 09 p1197 N88-17174

A solar receiver-reactor with specularly reflecting walls for high-temperature thermoelectrochemical and thermochemical processes
[AD-A187612] 10 p1351 N88-18077

Plasma physics design and major specifications of candidate reactors for FER design studies. Conceptual design study of FY86 FER
[DE88-751066] 10 p1411 N88-18416

Development of tokamak reactor system analysis code NEW-TORSAC
[DE88-751067] 10 p1411 N88-18417

Conceptual design study of Fusion Experimental Reactor (FY86 FER): Safety
[DE88-751071] 10 p1411 N88-18418

Design issues for a laboratory high gain fusion facility
[DE88-004406] 10 p1413 N88-18434

The 1988 failure rate screening data for fusion reliability and risk analysis
[DE88-006798] 14 p1984 N88-21837

Incorporating reliability into the design of experimental fusion facilities
[DE88-006767] 16 p2275 N88-23618

Transactions of the Fourth Symposium on Space Nuclear Power Systems
[DE88-006164] 17 p2398 N88-24254

Status of CEA design and simulation studies of a 200 KWe turboelectric space power system
17 p2400 N88-24268

Safety constraints and considerations in the development of nuclear powered propulsion
17 p2401 N88-24276

Fully passive space reactor conceptual design
17 p2403 N88-24288

Space based nuclear-pumped laser/reactor concepts
17 p2403 N88-24289

The role of integral experiments and nuclear cross section evaluations in space nuclear reactor design
17 p2404 N88-24293

Sodium heat engine/AMTEC system experiments
17 p2409 N88-24325

Gas-cooled reactor power systems for space
17 p2413 N88-24350

Development and implementation of a space nuclear safety program 17 p2415 N88-24361

Innovative methodology and developments in US space radioisotope power safety risk assessments
17 p2415 N88-24362

Advanced LMMHD space power generation concept
17 p2415 N88-24364

Expert systems approach to modeling systems with the ATHENA thermal-hydraulics code
17 p2416 N88-24365

SOAR: Space orbiting advanced fusion power reactor
17 p2416 N88-24366

Multimegawatt nuclear power system for lunar base applications 17 p2416 N88-24367

Neutronics conceptual design of a UF6-fueled gaseous laser system 17 p2422 N88-24405

The application of high-rate biaxial testing to the design of containment vessels for radioisotope heat sources
17 p2426 N88-24428

Research and development of electrical insulators for thermionic applications 17 p2429 N88-24449

MMW shielding design and analysis
17 p2430 N88-24457

Ceramic electrical insulator development for thermoelectric SACE power system
17 p2430 N88-24459

Comparison of 20-kWe space nuclear power systems: Impact of reactor temperature and technology upon system design and performances 17 p2433 N88-24475

Small particle bed reactors: Sensitivity to Brayton cycle parameters 17 p2435 N88-24487

SP-100 ground engineering systems test facility control systems 17 p2436 N88-24496

TRICE design, evaluation and feasibility tests
17 p2437 N88-24498

Lightweight power bus for a baseload nuclear reactor in space 17 p2438 N88-24505

The safety designs for the TITAN reversed-field pinch reactor study
[DE88-008169] 19 p2729 N88-26205

Fusion programs in applied plasma physics and development and technology at GA Technologies, Inc.
[DE88-008406] 20 p2856 N88-26964

REACTOR FUELS

U NUCLEAR FUELS

REACTOR MATERIALS

Behavior of graphites under intense heat loads
[DE87-012128] 01 p0028 N88-10179

Comparative tests of high temperature creep-rupture behavior of the austenitic CrNi steel DIN W.NR.1.4970 in argon and steam
[KFK-4261] 01 p0063 N88-10402

Development and testing of a system for the partially automated evaluation of holographic interferograms in the experimental stress analysis of reactor components
[ETN-87-90574] 02 p0175 N88-11095

Highlights of the Chemical Technology Division's research activities
[DE88-000233] 03 p0282 N88-11773

Effect of irradiation on the tensile properties of niobium-base alloys
[DE87-002409] 03 p0285 N88-11790

Low activation ferritic alloys for nuclear fusion reactors
[DE87-010711] 03 p0286 N88-11801

Reduced-activation ferritic steels: A comparison with Cr-Mo steels
[DE88-000332] 03 p0290 N88-11826

Data base on the high heat flux behaviour of metals and carbon materials for plasma facing components: Experiments at the 10 MW neutral beam injection test stand of the IPP Nagoya
[IPPJ-AM-53] 04 p0492 N88-13031

Kinetics and mechanism of thermal aging embrittlement of duplex stainless steels
[DE88-002987] 06 p0969 N88-15866

The dishomogeneity of the degree of sensitization in large recirculation pipes in Boiling Water Reactor (BWR) power plants
[CISE-3955] 09 p1247 N88-17473

Mechanisms of intergranular attack and stress corrosion cracking of alloy 600 by high-temperature caustic solutions containing impurities
[DE87-012820] 10 p1300 N88-17773

Weldability of tritium-charged 304L stainless steel
[DP-1740] 12 p1607 N88-19611

IAEA Specialists' Meeting on Graphite Component Structural Design
[DE88-780006] 13 p1746 N88-20439

Fracture criterion of reactor graphite under multiaxial stresses 13 p1746 N88-20442

High temperature Young's modulus of IG-110 graphite
13 p1746 N88-20443

Effects of high temperature neutron irradiation on the physical, chemical and mechanical properties of fine-grained isotropic graphite 13 p1747 N88-20444

Degradations of thermal shock resistance and the fracture toughness of reactor graphite subjected to neutron irradiation 13 p1747 N88-20445

Application of ISRM testing methods to fracture toughness testing of graphite 13 p1747 N88-20446

Notch sensitivity of graphite materials for VHTR
13 p1747 N88-20447

Nondestructive testings of HTGR graphites
13 p1747 N88-20448

Fracture toughness characterization of SA508 and Sa533B RPB steels
[CISE-3908] 14 p1889 N88-21292

The Nordic J-R curve round robin test program --- reactor steel
[VTT-RR-510] 14 p1923 N88-21459

Experiments on the creep behavior of semifinished X10NiCrAlTi 32 20 (Nicrofer 32 20) tubes under multiaxial loading --- nuclear reactors
[JUEL-2127] 14 p1923 N88-21464

The 1988 failure rate screening data for fusion reliability and risk analysis
[DE88-006798] 14 p1984 N88-21837

Development of a computer code CRACK for elastic and elastoplastic fracture mechanics analysis of 2-D structures by finite element technique
[DE88-701231] 15 p2075 N88-22370

Material tradeoffs to minimize flooding reactivity
17 p2399 N88-24265

Thermal-hydraulic considerations for particle bed reactors 17 p2400 N88-24266

Particle bed reactor scaling relationships
17 p2400 N88-24267

Fabrication of reactor shields at the Y-12 plant
17 p2402 N88-24283

Ammonia cleanup of lithium containing components
17 p2403 N88-24287

The role of integral experiments and nuclear cross section evaluations in space nuclear reactor design
17 p2404 N88-24293

Innovative methodology and developments in US space radioisotope power safety risk assessments
17 p2415 N88-24362

Creep behavior of tungsten/niobium and tungsten/niobium-1 percent zirconium composites
17 p2425 N88-24427

Liquid metal testing at ETEC for the SP-100 program
17 p2428 N88-24446

Irradiation effects on tungsten stabilized martensitic steels
[DE88-007074] 18 p2496 N88-24748

The safety designs for the TITAN reversed-field pinch reactor study
[DE88-008169] 19 p2729 N88-26205

Helium induced degradation in the weldability of an austenitic stainless steel
[DE88-009062] 20 p2773 N88-26443

Creep behavior for Hastelloy-XR
[DE88-753428] 21 p2914 N88-27295

REACTOR PHYSICS

Fusion reactor physics and technology studies
[DE87-013691] 01 p0101 N88-10864

Effects of space-dependent cross sections on core physics parameters for compact fast spectrum space power reactors 17 p2399 N88-24263

Fast critical experiment data for space reactors
17 p2403 N88-24286

The role of integral experiments and nuclear cross section evaluations in space nuclear reactor design
17 p2404 N88-24293

ATHENA heat pipe transient model
17 p2412 N88-24344

Neutronics conceptual design of a UF6-fueled gaseous laser system 17 p2422 N88-24405

Benchmark physics experiments for SP-100
17 p2429 N88-24453

REACTOR SAFETY

Research on one-dimensional two-phase flow. Theory on hydrodynamic balance in two fluid model and its application
[DE87-702615] 01 p0045 N88-10290

Development and testing of a system for the partially automated evaluation of holographic interferograms in the experimental stress analysis of reactor components
[ETN-87-90574] 02 p0175 N88-11095

Gas-cooled reactor for space power systems
[DE87-011549] 02 p0233 N88-11471

A long term radiological risk model for plutonium-fueled and fission reactor space nuclear system
[DE87-010466] 06 p0779 N88-14782

Design issues for a laboratory high gain fusion facility
[DE88-004406] 10 p1413 N88-18434

Uncertainties in hydrogen combustion
[DE88-005354] 13 p1739 N88-20395

Potential off-normal events and associated radiological source terms for the compact ignition tokamak: Fusion Safety Program
[DE88-004112] 13 p1842 N88-21024

The 1988 failure rate screening data for fusion reliability and risk analysis
[DE88-006798] 14 p1984 N88-21837

Transactions of the Fourth Symposium on Space Nuclear Power Systems
[DE88-006164] 17 p2398 N88-24254

Operational concerns involving a shadow-shielded nuclear reactor for space station applications
17 p2398 N88-24257

Considerations pertinent to the Doppler effect for space reactors 17 p2399 N88-24264

Material tradeoffs to minimize flooding reactivity
17 p2399 N88-24265

Safety constraints and considerations in the development of nuclear powered propulsion
17 p2401 N88-24276
Fast critical experiment data for space reactors
17 p2403 N88-24286
The role of integral experiments and nuclear cross section evaluations in space nuclear reactor design
17 p2404 N88-24293
Reactor instrumentation and control design and performance simulation for SP-100
17 p2406 N88-24306
Development and implementation of a space nuclear safety program 17 p2415 N88-24361
Innovative methodology and developments in US space radioisotope power safety risk assessments
17 p2415 N88-24362
Inherently safe space reactors
17 p2415 N88-24363
A novel plant protection strategy for transient reactors
17 p2425 N88-24423
Evaluation of UN fuel pin failure modes and motion of fuel during severe accidents for reactors in space
17 p2425 N88-24424
Reactor core coolability with reduced power levels
17 p2425 N88-24425
The application of high-rate biaxial testing to the design of containment vessels for radioisotope heat sources
17 p2426 N88-24428
The NERVA derivative reactor and a systematic approach to multiple space power requirements
17 p2430 N88-24458
Automatic reactor control system for transient operation 17 p2436 N88-24493
An optimal disturbance rejection control system for multimegawatt space nuclear power systems
17 p2436 N88-24495
SP-100 ground engineering systems test facility control systems 17 p2436 N88-24496
Analysis and developments of failure concepts in fracture mechanics based on research results in the field of component safety topics: J-integral concept; crack resistance curves; dynamic criterion
[V-19/86] 18 p2530 N88-25009
Statistical evaluation of light water reactor piping damping data for use in PRA (Probabilistic Risk Assessment) analyses
[DE88-007706] 19 p2661 N88-25828
Health and environmental consequences of the Chernobyl nuclear power plant accident
[DOE/ER-0332] 19 p2689 N88-25985
The safety designs for the TITAN reversed-field pinch reactor study
[DE88-008169] 19 p2729 N88-26205
Overview of the TITAN-2 reversed-field pinch aqueous fusion power core design
[DE88-008170] 20 p2857 N88-26966
An analysis of heat transfer after loss of primary coolant in the SP-100 reactor system
[AD-A194619] 23 p3281 N88-29539

REACTOR TECHNOLOGY
Some new fatigue tests in high temperature water and liquid sodium environment
[DE87-753019] 02 p0192 N88-11197
Gas-cooled reactor for space power systems
[DE87-011549] 02 p0233 N88-11471
Creep test of Hastelloy X for use as the components of OGL-1 in helium environment
[DE88-750289] 07 p0834 N88-15059
Comparative performance of the conjugate gradient and SOR (Successive Over Relaxation) methods for computational thermal hydraulics
[DE88-002553] 08 p0986 N88-15986
Two-phase reduced gravity experiments for a space reactor design
[DE86-015530] 09 p1247 N88-17475
The TITAN Reversed-Field Pinch Reactor: Design-point determination and parametric studies
[DE88-001624] 09 p1251 N88-17498
IAEA Specialists' Meeting on Graphite Component Structural Design
[DE88-780006] 13 p1746 N88-20439
Government research on ceramics coating technology
16 p2184 N88-23019
Transactions of the Fourth Symposium on Space Nuclear Power Systems
[DE88-006164] 17 p2398 N88-24254
Status of CEA design and simulation studies of a 200 KWe turboelectric space power system
17 p2400 N88-24268
Comparison of 20-kWe space nuclear power systems: Impact of reactor temperature and technology upon system design and performances 17 p2433 N88-24475
Potassium Rankine power system for space power
17 p2433 N88-24476
Small particle bed reactors: Sensitivity to Brayton cycle parameters 17 p2435 N88-24487
Systems analysis of INTOR-like designs
[DE88-004422] 18 p2578 N88-25316
The safety designs for the TITAN reversed-field pinch reactor study
[DE88-008169] 19 p2729 N88-26205
Fusion product spectra
[DE88-010912] 23 p3284 N88-29554

READ-ONLY MEMORY DEVICES
Optical laser technology, specifically CD-ROM (Compact Disc - Read Only Memory) and its application to the storage and retrieval of information
[AD-A184111] 03 p0330 N88-12086
Self-checking logic arrays
[RR-656-I] 15 p2106 N88-22545

READING
Data acquisition and processing for surface plate calibration
[AD-A187264] 11 p1564 N88-19366
Working memory capacity: An individual differences approach
[AD-A192359] 20 p2833 N88-26803
The role of working memory in language comprehension
[AD-A192721] 20 p2833 N88-26805

READJUSTMENT
U ADJUSTING

READOUT
Low noise-low power monolithic multiplexing readout electronics for silicon strip detectors
[MPI-PAE/EXP.EL.178] 02 p0168 N88-11057
Performance of a photon counting microchannel plate intensifier with wedge and strip image readout
[DE88-003831] 10 p1334 N88-17970
Comparison of five readout techniques for an integrated magnetometer 19 p2671 N88-25876

REAGENTS
Proposed quality assurance/quality control plan
[AD-A191490] 18 p2525 N88-24978
Method of dispensing reagent chemicals in space
[NASA-CASE-LAR-13607-1-CU]
23 p3200 N88-29048

REAL GASES
PRMIXn: A computer program for thermophysical properties of real gases and gas mixtures
[GKSS-86/E/59] 01 p0020 N88-10125
Hypersonic laminar boundary layer: Parametric study for the representation of real gas effects
05 p0532 N88-13236
On the numerical simulation of three-dimensional hypersonic flow 05 p0532 N88-13237
Hypersonic blunt body computations including real gas effects
[NASA-TM-100074] 10 p1400 N88-18344
Splitting of inviscid fluxes for real gases
[NASA-TM-100856] 14 p1964 N88-21717
High speed inlet calculations with real gas effects
[NASA-CR-182167] 20 p2752 N88-26336
Low density real gas flows about hypersonic vehicles
[AD-A194251] 22 p3075 N88-28253

REAL NUMBERS
NT INTEGERS
Explicit solutions of moment problems, 1
[AD-A186016] 10 p1397 N88-18325
Flexible valued algebras of four-dimensions
[ETN-88-92382] 21 p3006 N88-27844

REAL TIME OPERATION
Real time analysis of detonation products
[DE87-007453] 01 p0031 N88-10195
Aerosol sensor: Real time determination of aerosol mass size distributors using filtering quartz oscillators
[ETN-87-90397] 01 p0049 N88-10311
File management using balanced trees
[ENST-87D001] 01 p0106 N88-10693
Measurements in the functional mock up test of the NAL QSTOL aircraft control system
[NAL-TR-928] 02 p0126 N88-10793
Real-time expert systems: A status report
02 p0129 N88-10817
Rapid toxicity detection in water quality control utilizing automated multispecies biomonitoring for permanent space stations 02 p0135 N88-10848
Use of a 5 cm Doppler radar to detect and forecast severe thunderstorms in a real time forecast operation
02 p0200 N88-11247
A real-time system for automatic single-Doppler wind field analysis 02 p0200 N88-11249
Evaluation of the Rainsat precipitation analysis system in real-time use 02 p0205 N88-11283
Real-time evaluation and prediction of coastal dispersion near the SW tip of Africa --- effluents
02 p0210 N88-11318
Short range forecasting of sea breeze generated thunderstorms at the Kennedy Space Center: A real-time experiment using a primitive equation mesoscale numerical model 02 p0211 N88-11324
Methodology of performance evaluation of real time distributed systems
[ENST-87D003] 02 p0228 N88-11440
The Avionics Flight Evaluation System (AFES) of the DFVLR
[ESA-TT-1037] 03 p0266 N88-11677
On the control of a compliant robot arm
03 p0332 N88-12095
Real time analysis of the results from mechanized ultrasonic testing
[DE87-752511] 03 p0334 N88-12107
Concepts and techniques for support of real time distributed operating systems
[AD-A184491] 03 p0367 N88-12307
An inexpensive real-time interactive three-dimensional flight simulation system
[AD-A184340] 04 p0402 N88-12499
Real-time Raman detection of molecular changes in ceramics undergoing sliding friction
[DE88-000558] 04 p0421 N88-12609
Performability modeling based on real data: A casestudy
[NASA-CR-181563] 05 p0633 N88-13870
Presentation of SIGMA (Interactive Assisted Geometry System). A computer assisted shape design program developed at the Aerospatiale Aircraft Division
[SNIAS-872-111-110] 05 p0635 N88-13884
Conceptual issues in measuring the behavior of a distributed real-time process-control computer system
[DE87-009748] 05 p0638 N88-13898
Conceptual issues in measuring the behavior of a distributed real-time process-control computer system
[DE87-014251] 05 p0638 N88-13899
On real-time systems using local area networks
[AD-A185475] 06 p0694 N88-14256
Atmospheric electricity
[NASA-CR-179239] 06 p0744 N88-14575
Objects architecture: A comprehensive design approach for real-time, distributed, fault-tolerant, reactive operating systems
[AD-A185476] 06 p0755 N88-14631
A Multipurpose Adaptive Controller (MAC) for real time digital regulation
[REPT-87-028] 06 p0762 N88-14673
Dynamics formulations for the real-time simulation of constrained motion 06 p0795 N88-14872
A multiple node software development environment
[DE87-010995] 07 p0905 N88-15484
A distributed architecture for intelligent monitoring and anomaly diagnosis of the Hubble Space Telescope
08 p1057 N88-16379
A multiprocessing architecture for real-time monitoring
08 p1059 N88-16390
A framework for real-time distributed expert systems: On-orbit spacecraft fault diagnosis, monitoring and control 08 p1066 N88-16440
TES: A modular systems approach to expert system development for real time space applications
08 p1066 N88-16441
Performance of a digital real time radiographic imaging system
[MRL-R-1068] 09 p1169 N88-17011
Beyond rules: The next generation of expert systems
09 p1210 N88-17256
A conceptual framework for intelligent real-time information processing 09 p1211 N88-17257
TDAS: The Thermal Expert System (TEXSYS) data acquisition system 09 p1211 N88-17258
Real-time artificial intelligence issues in the development of the adaptive tactical navigator
09 p1211 N88-17260
Communication and control in an integrated manufacturing system 09 p1212 N88-17263
Occam/Ada parallel programming system
[ISAL-IDI1-87-11] 09 p1219 N88-17312
Reduction of time delays in Runge-Kutta integration methods --- systems simulation
[MBB/LKE-132/S/PUB/241/A]
09 p1229 N88-17363
Investigation of real-time two-dimensional visualization of fuel spray liquid/vapor distribution via exciplex fluorescence
[AD-A188268] 10 p1307 N88-17816
A smart, mapping, charting and geodesy control generator, phase 1
[AD-A188184] 10 p1347 N88-18055
A deep-water OBS (Ocean Bottom Seismometer) array with real-time telemetry
[AD-A187404] 10 p1357 N88-18112
Real time artificial intelligence architecture
10 p1380 N88-18242
Parallelism at the microlevel: Cooperative microcontrollers with real time considerations
10 p1381 N88-18246
Future directions in computer architecture
10 p1383 N88-18257

Shared workspaces for real-time collaboration in distributed networks: Concepts, techniques, problems
[AD-A188150] 10 p1394 N88-18315

Integrated optical synthetic aperture radar processor
[AD-A188019] 11 p1471 N88-18772

Fuzzy logic inference processor for real time control: A second generation full custom design
[AD-A188155] 11 p1471 N88-18773

A microspectrofluorometer system based on real time digital techniques
[REPT-86-014] 11 p1490 N88-18891

Real-time kinematic and dynamic analysis and adaptive model following control of manipulator arms
11 p1495 N88-18927

VAXELN experimentation: Programming a real-time clock and interrupt handling using VAXELN Ada 1.1
[AD-A188100] 11 p1525 N88-19107

Applicability of Ada (trademark) tasking for avionics executives
[AD-A188827] 12 p1578 N88-19445

The use of hardware-in-the-loop-techniques in the development of a modern air-to-surface missile system
12 p1597 N88-19562

Digital method for correction of the phase error in the discrete generation of periodic signals in real time
[INPE-4327-RPE/552] 12 p1618 N88-19676

An intelligent allocation algorithm for parallel processing
[NASA-CR-182648] 12 p1675 N88-20014

Efficient parallel architecture for highly coupled real-time linear system applications
[NASA-CR-182649] 12 p1675 N88-20015

Computer architecture for efficient algorithmic executions in real-time systems: New technology for avionics systems and advanced space vehicles
[NASA-CR-182650] 12 p1675 N88-20016

A prototype for remotely shared textual workspaces
[AD-A188352] 12 p1679 N88-20040

ARCTIC: Programmer's manual and tutorial
[AD-A188619] 12 p1680 N88-20047

Improved flight test productivity using advanced on line data systems 12 p1703 N88-20193

Development of an interactive real-time graphics system for the display of vehicle space positioning
[NASA-TM-100429] 13 p1730 N88-20344

Western aeronautical test range real-time graphics software package MAGIC
[NASA-TM-100425] 13 p1757 N88-20506

The 1987 Airborne Antarctic Ozone Experiment: The Nimbus-7 TOMS data atlas
[NASA-RP-1201] 13 p1791 N88-20714

Configuration management issues and objectives for a real-time research flight test support facility
[NASA-TM-100437] 13 p1813 N88-20832

Dynamic run-time graphics
[DE87-008997] 13 p1820 N88-20879

Development of a real-time aeroperformance analysis technique for the X-29A advanced technology demonstrator
[NASA-TM-100432] 14 p1866 N88-21151

A microprocessor-based real-time simulator of a turbofan engine
[NASA-TM-100889] 14 p1868 N88-21163

Global meteorological data facility for real-time field experiments support and guidance
[NASA-TM-4023] 14 p1947 N88-21608

Real-time flight test data distribution and display
[NASA-TM-100424] 15 p2022 N88-22050

Real-time stressed channel simulator
[AD-A190223] 15 p2025 N88-22067

A review on holography, its principles and applications
[ISL-CO-242/86] 15 p2069 N88-22338

Support for FY87 midlatitude electron-density calibration campaign
[AD-A190174] 15 p2094 N88-22476

Real-time environmental Arctic monitoring (R-TEAM)
[AD-A189946] 15 p2099 N88-22508

Motion sickness: Quantitative, algorithmic malaise indication in real time
[AD-A189674] 15 p2101 N88-22518

Conflict resolution in cooperative systems
[AD-A190351] 15 p2104 N88-22535

Optical switching and control techniques using nonlinear optical wave mixing
[AD-A190467] 15 p2134 N88-22730

A fault tolerant supervision system
[INPE-4419-TDL/307] 15 p2148 N88-22819

Near-real-time TOMS, telecommunications and meteorological support for the 1987 Airborne Antarctic Ozone Experiment
[NASA-CR-4133] 16 p2233 N88-23338

Parallel artificial intelligence search techniques for real time applications
[AD-A190883] 16 p2255 N88-23473

Real time thermal imaging of high temperature semiconductor melts 17 p2330 N88-23914

A timing evaluator for C programs generated by the model system
[AD-A191204] 17 p2385 N88-24174

Genetic algorithms for adaptive real-time control in space systems 17 p2388 N88-24195

TES: A modular systems approach to expert system development for real-time space applications
17 p2388 N88-24197

Evaluating evaporation with satellite thermal data
[AD-A192042] 18 p2531 N88-25019

Beyond Ada: Generating Ada code from equational specifications
[AD-A191866] 18 p2557 N88-25176

Representation and decision mechanisms in artificial intelligence
[AD-A191083] 18 p2560 N88-25197

Real-time optical multiple object recognition and tracking system and method
[NASA-CASE-NPO-17139-1-CU]
18 p2576 N88-25301

Real-time image difference detection using a polarization rotation spacial light modulator
[NASA-CASE-NPO-17144-1-CU]
18 p2576 N88-25305

An intelligent processing environment for real-time simulation
[NASA-CR-183056] 19 p2715 N88-26119

Automation tools for demonstration of goal directed and self-repairing flight control systems
[NASA-CR-179433] 19 p2715 N88-26121

RAGS (Realtime Acquisition and Graphics System): An off-the-shelf hardware and system software small data acquisition computer
[DE88-008399] 19 p2716 N88-26128

An instrument control and data analysis program for NMR imaging and spectroscopy
[DE88-007377] 19 p2717 N88-26132

A high dynamic range acousto-optic image correlator for real-time pattern recognition
[DE88-007933] 19 p2726 N88-26191

A high fidelity real-time simulation of a small turboshaft engine
[NASA-TM-100991] 20 p2761 N88-26378

Environmental monitoring of a titan 34D 5 1/2 segment solid rocket motor static firing
[AD-A192975] 20 p2766 N88-26400

Laser ranging data analysis
[NASA-CR-183115] 20 p2792 N88-26567

RRSAS (Robotic Radiation Survey and Analysis System) Project: A real time sensor driven robotic system
[DE88-006825] 20 p2808 N88-26661

Colored stochastic Petri nets. Application to real time distributed systems
[ENST-87E017] 20 p2839 N88-26843

Definition of an auxiliary processor dedicated to real-time operating system kernels
[NASA-CR-183070] 20 p2841 N88-26860

An investigation of performance improvement in knowledge-based control systems
21 p2928 N88-27382

TDWR (Terminal Doppler Weather Radar) PRF (Pulse Repetition Frequency) selection criteria
[AD-A193089] 21 p2932 N88-27407

FTMP data acquisition environment
[NASA-TM-100636] 21 p2938 N88-27447

Development of a hybrid simulator for robotic manipulators
[AD-A193119] 21 p2956 N88-27557

Army space systems for terrestrial applications
[AD-A192735] 21 p2965 N88-27613

Implementation of an OPS5 derivative on the Novix RISC processor
[DE88-011392] 21 p2994 N88-27756

Simulation of real time problem solving
[AD-A193436] 21 p2997 N88-27776

Notes on operating system requirements for the next millennium
[DE88-010712] 21 p3002 N88-27805

Satellite attitude determination using a CCD (Charge-Coupled-Device) star camera
[AD-A192662] 22 p3046 N88-28080

Using Petri nets for real-time development environments
[REPT-88-005] 22 p3141 N88-28679

Comparison of 2-D Fourier and spatial techniques for removing noise in real-time X-ray radiography
[AD-A193700] 23 p3187 N88-28962

Real-time measurements of the size fractionation of ambient black carbon aerosols at elevated humidities
[DE88-010870] 23 p3215 N88-29138

Machine vision for real time orbital operations
23 p3253 N88-29367

Intelligent test integration system
23 p3254 N88-29371

Distributed cooperating processes in a mobile robot control system 23 p3256 N88-29386

An expert system for a distributed real-time trainer
23 p3261 N88-29411

Real-time space system control with expert systems
23 p3262 N88-29418

Semantic based man-machine interface for real-time communication 23 p3262 N88-29421

Parallel real-time expert systems
[AD-A193673] 23 p3264 N88-29434

Intelligent fault diagnosis and failure management of flight control actuation systems
[NASA-CR-177481] 24 p3323 N88-29790

MIZEX (marginal ice zone experiment) 1987 SAR (Synthetic Aperture Radar) data summary
[AD-A195560] 24 p3364 N88-30035

Geometric modeling for computer aided design
[NASA-CR-183161] 24 p3413 N88-30320

A static scheduler for the computer aided prototyping system: An implementation guide
[AD-A194340] 24 p3414 N88-30322

Achieving real-time performance in FIESTA
24 p3418 N88-30344

Mission telemetry system monitor: A real-time knowledge-based system 24 p3418 N88-30345

Autonomous image data reduction by analysis and interpretation 24 p3418 N88-30347

Automatic mathematical modeling for real time simulation system 24 p3420 N88-30356

A standard architecture for controlling robots
[AD-A195929] 24 p3423 N88-30371

Applications of synchrotron radiation to materials science: Diffraction imaging (topography) and microradiography
[NASA-CR-183265] 24 p3434 N88-30440

REAL VARIABLES
- NT ABEL FUNCTION
- NT ASYMPTOTES
- NT ASYMPTOTIC SERIES
- NT BESSEL FUNCTIONS
- NT BIHARMONIC EQUATIONS
- NT BINARY INTEGRATION
- NT BOREL SETS
- NT BURGER EQUATION
- NT CALCULUS OF VARIATIONS
- NT CAUCHY-RIEMANN EQUATIONS
- NT COLLINEARITY
- NT COPLANARITY
- NT COSINE SERIES
- NT CUBIC EQUATIONS
- NT DELTA FUNCTION
- NT DIFFERENTIAL EQUATIONS
- NT EINSTEIN EQUATIONS
- NT ELLIPTIC DIFFERENTIAL EQUATIONS
- NT EULER-CAUCHY EQUATIONS
- NT EXISTENCE THEOREMS
- NT EXTREMUM VALUES
- NT FOKKER-PLANCK EQUATION
- NT FOURIER-BESSEL TRANSFORMATIONS
- NT GAUSS EQUATION
- NT GREEN'S FUNCTIONS
- NT HANKEL FUNCTIONS
- NT HELMHOLTZ VORTICITY EQUATION
- NT HYPERBOLIC DIFFERENTIAL EQUATIONS
- NT HYPERBOLIC FUNCTIONS
- NT HYPERPLANES
- NT INTEGRAL CALCULUS
- NT J INTEGRAL
- NT JACOBI MATRIX METHOD
- NT KERNEL FUNCTIONS
- NT LEBESGUE THEOREM
- NT LIAPUNOV FUNCTIONS
- NT LIMITS (MATHEMATICS)
- NT LINEAR EQUATIONS
- NT LIPSCHITZ CONDITION
- NT MAXIMA
- NT MEASURE AND INTEGRATION
- NT MINIMA
- NT NEUMANN PROBLEM
- NT NONLINEAR EQUATIONS
- NT NONLINEAR EVOLUTION EQUATIONS
- NT NUMERICAL INTEGRATION
- NT PADE APPROXIMATION
- NT PARABOLIC DIFFERENTIAL EQUATIONS
- NT PARTIAL DIFFERENTIAL EQUATIONS
- NT PERIODIC FUNCTIONS
- NT POISSON EQUATION
- NT POWER SERIES
- NT QUADRATIC EQUATIONS
- NT RICCATI EQUATION
- NT RUNGE-KUTTA METHOD
- NT SERIES (MATHEMATICS)
- NT STURM-LIOUVILLE THEORY
- NT TANGENTS
- NT TAYLOR SERIES
- NT TRIGONOMETRIC FUNCTIONS
- NT VECTOR ANALYSIS
- NT VLASOV EQUATIONS

NT VORTICITY
NT VORTICITY EQUATIONS
NT WEIERSTRASS FUNCTIONS
NT WEIGHTING FUNCTIONS
Unique normal forms for lambda calculus with surjective pairing
[PB88-173539] 16 p2260 N88-23508
REARWARD FACING STEPS
U BACKWARD FACING STEPS
REATTACHED FLOW
Calculation of the flow through a single-sided sudden expansion with the Computer Program for Parabolic and Elliptic Flows (COPPEF) computer program
[VTH-LR-523] 09 p1163 N88-16973
Surface flow visualization of separated flows on the forebody of an F-18 aircraft and wind-tunnel model
[NASA-TM-100436] 14 p1863 N88-21127
Wave interactions in a three-dimensional attachment line boundary layer
[NASA-CR-181653] 14 p1910 N88-21414
Method and apparatus for detecting laminar flow separation and reattachment
[NASA-CASE-LAR-13952-1-SB]
16 p2513 N88-24910
REB
U RELATIVISTIC ELECTRON BEAMS
REBREATHING
Validation of a modified one-step rebreathing technique for measuring exercise cardiac output
[AD-A192600] 21 p2966 N88-27729
Validation of a modified one-step rebreathing technique for non-invasive measurement of submaximal cardiac output
[AD-A192652] 21 p2967 N88-27735
RECEIVERS
NT RADAR RECEIVERS
NT RADIO RECEIVERS
NT RADIOTELEPHONES
NT SUPERHETERODYNE RECEIVERS
NT TELEVISION RECEIVERS
NT TRANSMITTER RECEIVERS
Reception of pseudo noise-modulated signals using digital correlators for satellite navigation tasks
[ETN-87-90426] 01 p0037 N88-10234
Direct Absorption Receiver (DAR) systems assessment
[DE87-012277] 02 p0196 N88-11222
Tau ranging revisited 04 p0437 N88-12710
Remote sensing of atmospheric crosswinds by utilizing speckle-turbulence interaction and optical heterodyne detection
[AD-A187580] 10 p1347 N88-18052
A solar receiver-reactor with specularly reflecting walls for high-temperature thermoelectrochemical and thermochemical processes
[AD-A187612] 10 p1351 N88-18077
A deep-water OBS (Ocean Bottom Seismometer) array with real-time telemetry
[AD-A187404] 10 p1357 N88-18112
A simplified, general-purpose deep-space ranging correlator design 11 p1473 N88-18786
Quantum limits of superconducting heterodyne receivers
[AD-A188014] 11 p1478 N88-18817
Signal-filter design and system performance for polarimetric radar
[AD-A189257] 13 p1758 N88-20514
System for detecting objects that represent a threat
[NASA-TT-20244] 13 p1760 N88-20528
Bragg-cell receiver study
[NASA-CR-182684] 13 p1761 N88-20535
Performance of single and multiple system AM stereo decoder receivers
[PB88-168307] 15 p2057 N88-22265
A 30 GHz monolithic receive module technology assessment
[NASA-CR-180825] 16 p2194 N88-23084
Requirements for radiation receivers
16 p2272 N88-23593
Mini-station for VHF reception: Argos system simplified description
[INPE-4551-NTE/279] 19 p2655 N88-2576
Design and calibration of a two-channel low-noise heterodyne receiver for use in a CO2 laser Thomson scattering alpha particle diagnostic
[DE88-007866] 19 p2728 N88-26201
Digital communication transmitter and receiver test procedures
[AD-A191216] 20 p2788 N88-26540
SIS (Superconductor-Insulator-Superconductor) mixer research
[AD-A192908] 20 p2879 N88-27092
Airborne measurement of low frequency atmospheric noise ALFAN 1
[AD-A193058] 21 p2931 N88-27405
Multifilter spectrometer (FEB) for microwave atmospheric sounder
[AD-A192312] 21 p2935 N88-27426
Digital carrier demodulation for the DSN Advanced Receiver 22 p3064 N88-28183
Telemetry SNR improvement using the DSN Advanced Receiver with results for Pioneer 10
22 p3064 N88-28184
Advanced Receiver tracking of Voyager 2 near solar conjunction 22 p3065 N88-28185
Performance analysis of a noncoherently combined large aperture optical heterodyne receiver
22 p3065 N88-28189
Direct bit detection receiver performance analyses for 8-DPSK (Differential Phase Shift Keyed) modulated signals operating with improper carrier phase synchronization
[AD-A193639] 22 p3070 N88-28220
Solar energy absorption efficiency of an ellipsoidal receiver-reactor with specularly reflecting walls
[AD-A193726] 22 p3117 N88-28520
On adaptive cell-averaging CFAR (Constant False-Alarm Rate) radar signal detection
[AD-A196286] 24 p3360 N88-30009
Performance of DS/SSMA communications in impulsive channels. Part 1: Correlation receivers
[AD-A195712] 24 p3362 N88-30021
RECEIVING SYSTEMS
U RECEIVERS
RECEPTACLES (CONTAINERS)
U CONTAINERS
RECEPTION DIVERSITY
Space-diversity effects on line-of-sight propagation paths 12 p1617 N88-19670
A polarization diversity meteorological radar system
[AD-A189291] 13 p1756 N88-20515
RECEPTORS (PHYSIOLOGY)
NT CHEMORECEPTORS
NT GRAVIRECEPTORS
NT OTOLITH ORGANS
NT PHOTORECEPTORS
NT PROPRIOCEPTORS
RECHARGING
The MOLICEL(R) rechargeable lithium system: Multicell battery aspects 02 p0163 N88-11024
A new concept in an electrically rechargeable zinc-air alkaline battery
[DE88-003858] 13 p1762 N88-20539
RECIPROCAL THEOREMS
A periodic small-cluster approach to many-body problems
[DE88-002235] 06 p0763 N88-14683
RECIPROCATING ENGINES
U PISTON ENGINES
RECIPROCATION
Reciprocating sliding wear characteristics of copper-carbon fiber composites
[NASA-TT-20176] 15 p2031 N88-22100
RECIPROCITY THEOREM
Time-domain reciprocity theorems for electromagnetic fields in dispersive media
[PB88-126925] 10 p1319 N88-17886
The calibration of photographic and spectroscopic films: Reciprocity failure and thermal responses of IIaO film at liquid nitrogen temperatures
[NASA-CR-181094] 13 p1773 N88-20606
RECIRCULATION
U CIRCULATION
RECIRCULATIVE FLUID FLOW
Improved numerical methods for turbulent viscous recirculating flows 02 p0185 N88-11148
Aerothermal modeling program, phase 2
02 p0185 N88-11149
Efficient numerical techniques for complex fluid flows
02 p0185 N88-11151
Numerical implementation and performance of Reynolds stress closures in finite volume computations of recirculating and strongly swirling flows
08 p0967 N88-15976
Numerical calculation of turbulent recirculating flows
[TUM-LSM-84/29] 09 p1161 N88-16959
Sea duct: A deep-sea computer-controlled recirculating flume for the study of sea floor stability
[AD-A187734] 11 p1516 N88-19056
Improved numerical methods for turbulent viscous recirculating flows
[NASA-CR-180852] 19 p2599 N88-25445
RECLAMATION
NT GAS RECOVERY
NT MATERIALS RECOVERY
NT SOLVOLYSIS
NT WATER RECLAMATION
RECOGNITION
NT CHARACTER RECOGNITION
NT PATTERN RECOGNITION
NT SPEECH RECOGNITION
NT TARGET RECOGNITION
Recognition of isolated non-speech sounds
[AD-A184600] 03 p0306 N88-11933
Windshear training aid. Volume 1: Overview, pilot guide, training program
[PB88-127196] 10 p1276 N88-17637
Applications of matnematical morphology to range imagery
[AD-A189316] 12 p1584 N88-20072
A probabilistic approach to low-level vision
[AD-A189041] 15 p2107 N88-22553
Models of incremental concept formation
[AD-A191597] 18 p2552 N88-25147
Rules, schema and decision making
[AD-A193389] 21 p3027 N88-27967
Visual motion perception and visual attentive processes
[AD-A193640] 23 p3241 N88-29288
Multilevel computational theory of stereoscopic visual image processing
[AD-A195331] 24 p3408 N88-30288
The combinatorics of object recognition in cluttered environments using constrained search
[AD-A196224] 24 p3422 N88-30364
Symbolic construction of a 2D scale-space image
[AD-A195926] 24 p3423 N88-30374
RECOIL IONS
Inelastic ion-surface collisions
[AFGL-TR-87-0206] 19 p2724 N88-26174
RECOMBINATION COEFFICIENT
Nascent vibrational/rotational distribution produced by hydrogen atom recombination
[AD-A193005] 20 p2852 N88-26933
RECOMBINATION REACTIONS
NT ATOMIC RECOMBINATION
NT ELECTRON-ION RECOMBINATION
NT HYDROGEN RECOMBINATIONS
NT ION RECOMBINATION
NT OXYGEN RECOMBINATION
NT RADIATIVE RECOMBINATION
High-efficiency silicon solar cells: Numerical modeling, transient measurements, efficiency goals, and v-shaped grooves
[DE87-012842] 01 p0066 N88-10423
Failure analysis of a 3.5 inch, 50 ampere-hour nickel-hydrogen cell 02 p0164 N88-11030
OH(A-X) fluorescence from photodissociative excitation of HO2 at 157.5 nm
[NASA-CR-181580] 05 p0563 N88-13429
Helium-ion-induced release of hydrogen from graphite
[DE88-002599] 09 p1142 N88-16846
Calculations of rate constants for the three-body recombination of H2 in the presence of H2
[NASA-CR-182548] 11 p1454 N88-18664
Models of recombination lines in radio H2 regions
[INPE-4302-TDL/277] 12 p1710 N88-20232
Study of activationless reactions of point defects with impurities and impurity-defect complexes in alpha-iron
[DE88-701028] 13 p1745 N88-20433
The astrophysics of nebulae and active galactic nuclear emission-line regions: New methods and applications
13 p1858 N88-21111
Studies of molecular biology
[DE88-005906] 15 p2101 N88-22514
A model for nitrogen atom recombination on a silicon dioxide surface
[AD-A189843] 15 p2142 N88-22784
Theoretical studies of dynamics combustion
[DE88-007565] 19 p2611 N88-25495
Auger recombination in GaSb/AlSb-multi quantum well heterostructures 20 p2862 N88-27001
Control of carrier lifetime in PbTe nipi superlattices by external photoinjection 20 p2863 N88-27006
Influence of the temperature-dependence of recombination life-time of free carriers in amorphous semiconductors on thermostimulated photocurrent spectra
[DE88-702728] 23 p3293 N88-29609
Computed potential energy surfaces for chemical reactions
[NASA-CR-183168] 24 p3342 N88-29893
On formulating a simple D-region model
[AD-A195841] 24 p3392 N88-30197
RECOMMENDATIONS
NT SUGGESTION
Observation guidelines for a Total Ozone Mapping Spectrometer (TOMS) in geosynchronous orbit
05 p0619 N88-13801
Space shuttle accident: NASA's actions to address the Presidential Commission report
[PB88-135306] 15 p2024 N88-22059
Engineering research centers and their evaluation
[PB88-180054] 19 p2739 N88-26262
Flight information publication (FLIP) feedback
[AD-A194462] 23 p3174 N88-28897
RECOMPRESSION
U COMPRESSING

RECONNAISSANCE
NT AERIAL RECONNAISSANCE
NT PHOTORECONNAISSANCE
NT SPECTRAL RECONNAISSANCE
Interim review of the possibilities and opportunities for the ONR tropical cyclone motion research initiative
[AD-A185679] 06 p0746 N88-14592
Cooperative analysis expert situation assessment research 09 p1206 N88-17228
Feasibility report: Operation of light air cushion vehicle at McMurdo Sound, Antarctica
[AD-A189057] 13 p1755 N88-20494
Activities report of the Division of Reconnaissance and Seeker Systems
[FOA-C-30479-3.1/3.2/3.3/3.4]
22 p3116 N88-28513
RECONNAISSANCE AIRCRAFT
NT MIRAGE AIRCRAFT
NT U-2 AIRCRAFT
Aquila remotely piloted vehicle: Its potential battlefield contribution still in doubt
[PB88-120241] 13 p1721 N88-20289
The specification and design of a future maritime reconnaissance aircraft 17 p2303 N88-23772
RECONNAISSANCE SPACECRAFT
Specification for an infrared satellite surveillance system for the detection of aircraft
[AD-A189592] 13 p1797 N88-20746
RECONSTRUCTION
NT WAVE FRONT RECONSTRUCTION
Propulsion estimation techniques
07 p0827 N88-15632
Further developments in exact state reconstruction in deterministic digital control systems
[NASA-TP-2812] 11 p1466 N88-18751
More on exact state reconstruction in deterministic digital control systems
[NASA-TP-2847] 22 p3063 N88-28177
RECORDING
NT DATA RECORDING
NT DATA SMOOTHING
NT MAGNETIC RECORDING
Recording multiple signals on a single waveform recorder
[DE87-011632] 01 p0049 N88-10313
Digital imaging techniques for single- and multi-phase reacting flowfields 10 p1327 N88-17933
Development of fiber optic systems for recording and transmitting holographic information
[AD-A189406] 13 p1773 N88-20603
Computer controlled data acquisition system for the NASA 1986 Rocket Triggered Lightning Program
[DE88-008335] 20 p2826 N88-26786
A 1/2-inch high-definition baseband VCR
21 p2930 N88-27393
Maximum-likelihood multichannel deconvolution of P waves at seismic arrays
[AD-A194990] 24 p3391 N88-30191
RECORDING INSTRUMENTS
NT BATHYTHERMOGRAPHS
NT FLIGHT RECORDERS
NT PLOTTERS
NT PRESSURE RECORDERS
NT SEISMOGRAPHS
Recording materials for optical disk memory discussed
06 p0684 N88-14193
RECORDS
Electronic Records Administration at the Savannah River Plant
[DE87-014842] 03 p0384 N88-12415
Quantifying some information processing aspects of the pilot's instrument crosscheck
[AD-A186114] 07 p0898 N88-15443
An introduction to the historical records of China about Mars 23 p3301 N88-29664
RECOVERABILITY
Communications satellite systems operations with the space station. Volume 3: Supplementary technical report
[NASA-CR-180875] 09 p1133 N88-16794
Navigation recovery block design description
[NASA-CR-182473] 10 p1342 N88-18022
RECOVERABLE LAUNCH VEHICLES
A two stage launch vehicle for use as an advanced space transportation system for logistics support of the space station
[NASA-CR-182572] 11 p1443 N88-18606
Space shuttle phase B wind tunnel model and test information. Volume 3: Launch configuration
[NASA-CR-178416-VOL-3-PT-2]
24 p3315 N88-29744
Space shuttle phase B wind tunnel model and test information. Volume 1: Booster configuration
[NASA-CR-178414-VOL-1-PT-1]
24 p3315 N88-29745
Space shuttle phase B wind tunnel model and test information. Volume 1: Booster configuration
[NASA-CR-178414-VOL-1-PT-2]
24 p3320 N88-29770
RECOVERABLE SPACECRAFT
NT AEROSPACE PLANES
NT CHALLENGER (ORBITER)
NT DISCOVERY (ORBITER)
NT HERMES MANNED SPACEPLANE
NT HOTOL LAUNCH VEHICLE
NT REUSABLE SPACECRAFT
NT SPACE SHUTTLE ORBITERS
NT SPACE SHUTTLES
NT X-30 VEHICLE
RECREATION
Spinoff, 1987
[NASA-TM-89652] 02 p0250 N88-11577
RECRYSTALLIZATION
Elimination of subboundaries in 0.5-micron-thick Si-on-insulation films produced by ZMR
[AD-A184590] 03 p0361 N88-12396
Cyclic deformation of an extruded AlMgSi alloy
05 p0598 N88-13654
Dynamic recrystallization during high temperature low cycle fatigue of nickel
[DE88-003224] 10 p1302 N88-17788
Grain refinement during primary breakdown of alloy 718
[DE88-005193] 13 p1743 N88-20423
Fundamental studies on high temperature deformation recrystallization, and grain growth of two-phase materials
[AD-A189725] 15 p2036 N88-22145
Analysis of grain refinement and superplasticity in aluminum-magnesium alloys
[AD-A193029] 21 p2912 N88-27283
Study of feasibility and optimization conditions of laser treatments: Application of the local recrystallization of aluminum
[ISAL-87-0048] 21 p2916 N88-27309
Rapid thermal annealing of silicon layers amorphized by ion implantation
[DE88-702307] 23 p3290 N88-29591
RECTANGLES
An experimental and numerical investigation of swirling flows in a rectangular nozzle 06 p0700 N88-14295
Thermosolutal convection in high-aspect-ratio enclosures
[NASA-TM-100803] 11 p1486 N88-18871
Minimum weight design of rectangular and tapered helicopter rotor blades with frequency constraints
[NASA-TM-100561] 12 p1582 N88 19465
Fingering flow patterns of thermosolutal convection in rectangular enclosures
[NASA-TM-100854] 14 p1911 N88-21417
ALEX results: A comparison of measurements from a round and a rectangular duct with 3-D code predictions
[DE88-005947] 15 p2135 N88-22741
Nonlinear hydroelastic vibrations in rectangular containers
[LRT-WE-9-FB-7(1987)] 22 p3088 N88-28340
RECTANGULAR COORDINATES
U CARTESIAN COORDINATES
RECTANGULAR DRAINAGE
U DRAINAGE PATTERNS
RECTANGULAR PANELS
Advanced radiator concepts utilizing honeycomb panel heat pipes
[NASA-CR-172017] 04 p0443 N88-12747
Geometrically nonlinear analysis of stiffened panels
06 p0722 N88-14440
A summary of experimental results on square plates and stiffened panels subjected to air-blast loading
09 p1178 N88-17057
Predicted and measured strain responses of isotropic panels to base excitation
[NASA-TM-4054] 19 p2679 N88-25928
RECTANGULAR PLANFORMS
NT RECTANGULAR PANELS
NT RECTANGULAR PLATES
The determination of the topological structure of skin friction lines on a rectangular wing-body combination
[NASA-CR-4168] 20 p2753 N88-26343
RECTANGULAR PLATES
Experiments: Test range facilities, part 2
03 p0305 N88-11921
On free decay damping tests
08 p0997 N88-16041
Free vibration of rectangular plates with a small initial curvature
[NASA-CR-179370] 24 p3383 N88-30148
RECTANGULAR WAVEGUIDES
Two-dimensional electron fluid computer calculations of nanosecond pulse, low pressure microwave air breakdown in a rectangular waveguide and their verification by experimental measurement
[DE88-004407] 12 p1618 N88-19678
Calculations of high-frequency parameters of disc-loaded waveguides
[DE88-702178] 21 p2933 N88-27417
RECTANGULAR WIND TUNNELS
Flow visualization on a small scale
[AD-A194728] 23 p3181 N88-28935
RECTIFICATION
NT GEOMETRIC RECTIFICATION (IMAGERY)
RECTIFIERS
NT AVALANCHE DIODES
NT CRYSTAL RECTIFIERS
NT GERMANIUM DIODES
NT THYRATRONS
NT THYRISTORS
Operation of multistage power supplies for electron beam welding installations 03 p0286 N88-11800
Determination of the commutation and angle and load response for a continuous-current, single phase controlled rectifier
[AD-A190602] 15 p2060 N88-22285
RECUPERATORS
U REGENERATORS
RECURSION FORMULAS
U RECURSIVE FUNCTIONS
RECURSIVE FUNCTIONS
Solution methods for bidiagonal and tridiagonal linear systems for parallel and vector computers
[REPT-87-04] 01 p0085 N88-10552
Irreducible *-representations of the Lie superalgebra osp(1,4) with finite-degenerated vacuum
[DE87-703069] 02 p0225 N88-11420
Design of digital filters for electronic instrumentation
[PB87-100418] 04 p0438 N88-12716
Analysis of a parallel solution method for tridiagonal systems
[PB87-230538] 06 p0762 N88-14678
Recursion operator and bihamiltonian structure for integrable multi-dimensional lattices
[PREPRINT-552] 06 p0764 N88-14688
Round-off error propagation in four generally applicable, recursive, least-squares-estimation schemes
[NASA-TM-100055] 06 p0766 N88-14708
Recursive m-estimators of location and scale for dependent sequences
[AD-A186292] 07 p0903 N88-15489
Recursive forward dynamics for multiple robot arms moving a common task object
[NASA-CR-182526] 10 p1340 N88-18008
Dynamic observers as asymptotic limits of recursive filters: Special cases
[AD-A187578] 10 p1397 N88-18324
Recursive inversion of externally defined linear systems
[NASA-TM-100070] 11 p1541 N88-19215
Predicate-transformer semantics of general recursion
[CS-8709] 13 p1820 N88-20876
On the productivity of recursive list definitions
[CS-8707] 14 p1960 N88-21692
The biHamiltonian formulations of integrable evolution equations in multidimensions
[PREPRINT-568] 14 p1966 N88-21745
Recursion operator and Backlund Transformation for the Ruijsenaars-Toda lattice
[PREPRINT-577] 14 p1968 N88-21750
A recursive prediction error parameter estimator for nonlinear models
[RR-326] 17 p2392 N88-24222
Recursive maximum likelihood identification of a nonlinear output-affine model
[RR-322] 18 p2569 N88-25257
Parallel solutions to geometric problems on the scan model of computation
[AD-A192321] 21 p3004 N88-27819
Recursive mass matrix factorization and inversion: An operator approach to open- and closed-chain multibody dynamics
[NASA-CR-182516] 23 p3247 N88-29328
Adaptive identification by systolic arrays
[AD-A193532] 23 p3266 N88-29444
RECYCLING
Biomass recycle as a means to improve the energy efficiency of CELSS algal culture systems
03 p0358 N88-12254
Preliminary experimental results of gas recycling subsystems except carbon dioxide concentration
03 p0359 N88-12261
An overview of Japanese CELSS research activities
03 p0360 N88-12267
Evaluation of bituminous materials used in pavement recycling projects at Tyndall, MacDill, and Hurlburt Air Force Bases
[AD-A188068] 10 p1317 N88-17871
An improved external recycle reactor for determining gas-solid reaction kinetics
[NASA-TM-101160] 19 p2611 N88-25492

Evidence for crustal recycling during the Archean: The parental magmas of the stillwater complex 24 p3396 N88-30226
Continental crustal formation and recycling: Evidence from oceanic basalts 24 p3396 N88-30238
Solid earth as a recycling systems and the lateral growth of Precambrian North America 24 p3400 N88-30249

RED BLOOD CELLS
U ERYTHROCYTES

RED DWARF STARS
The M-type stars
[NASA-SP-492] 02 p0252 N88-11592
Microwave observations of red dwarf flare stars 04 p0513 N88-13153
An astrometric search for a stellar companion to the sun 04 p0520 N88-13195

RED GIANT STARS
NT CARBON STARS
Basic properties and variability 02 p0252 N88-11593
Thermal atmospheric models 02 p0253 N88-11599
Fifth Cambridge Workshop on Cool Stars, Stellar Systems and the Sun 04 p0502 N88-13092
Exploiting the IR: Solar and stellar spectroscopy in the IR 04 p0504 N88-13102
VLA observations of rapid 6 cm flux variations in alpha Ori 04 p0515 N88-13169
Infrared excesses of barium stars 04 p0516 N88-13174
Membership of Cepheids and red giants in 8 open clusters: NGC 129, 6067, 6649, 6664, IC 4725, Ly 6, Ru 79
[PUBL-SER-C-FASC-13] 07 p0944 N88-15739

RED SHIFT
Ultraviolet observations of cataclysmic variables: The IUE archive
[MPE-PREPRINT-91] 02 p0250 N88-11580
Magnitude-redshift relation in a perturbed Friedmann universe
[DE87-753020] 02 p0252 N88-11590
Number count-redshift relation in universe models with nonzero cosmological constant
[DE87-703043] 03 p0388 N88-12435
Flux tube dynamics and solar/stellar redshift measurements 04 p0503 N88-13095
Finnish-Soviet Symposium on Radio Astronomy (1st) held at Otaniemi on August 26-27, 1985
[PB87-140661] 07 p0944 N88-15736
Coherence effects in optical physics with special reference to spectroscopy
[AD-A189520] 13 p1840 N88-21007
Galaxy evolution in dense clusters 13 p1855 N88-21101
Multiple object redshift determinations in clusters of galaxies using OCTOPUS
[INPE-4528-PRE/1278] 15 p2150 N88-22835
New measurements of radial velocities in clusters of galaxies
[INPE-4527-PRE/1277] 15 p2152 N88-22845
Is the 3C273 quasar Mach nearer
[DE88-702235] 21 p3030 N88-27988
Gravitational redshift of self-gravitating systems of dark matter in the universe
[DE88-702688] 23 p3300 N88-29650
A deep redshift survey of field galaxies. Comments on the reality of the Butcher-Oemler effect
[NASA-CR-183255] 24 p3454 N88-30558

REDOX CELLS
Zinc-redox battery: A technology update
[DE87-010737] 01 p0040 N88-10256

REDUCED GRAVITY
Preliminary study of a containerless processing facility for Columbus, executive summary
[ESA-ITT/AO/1-1834/85F] 01 p0032 N88-10203
Preliminary study of a biotechnology research facility for microgravity, executive summary
[MATRA-EPT/AS/VT209/246/NT] 01 p0032 N88-10204
Preliminary study of a gravitational biology facility for Columbus, executive summary
[MATRA-EPT/AS/VT209/255/NT] 01 p0032 N88-10205
Calculation of the eigenvibrations of axisymmetric fluid configurations with a singularity method, taking into account surface tension effects under reduced gravity
[ETN-87-90438] 01 p0048 N88-10304
Aquarack: Aims and Possible Research Projects
[DFVLR-MITT-87-01] 01 p0073 N88-10469
Investigations of the survey of the reproductive biology of Xiphophorus in an Aquarack 01 p0074 N88-10471
Xiphophorus as an experimental system for genetic and biological development studies under microgravity conditions 01 p0074 N88-10472
Research and development at the Marshall Space Flight Center Neutral Buoyancy Simulator 02 p0139 N88-10878
A preliminary study of a fluid science laboratory for space station (Columbus). Part 4: Executive summary
[NLR-TR-87023-L-PT-4] 02 p0170 N88-11072
Consortium for Materials Development in Space. Technical section
[NASA-CR-181508] 03 p0296 N88-11859
Physical vapor transport crystal growth 03 p0296 N88-11860
Highly Non-Linear Optical (NLO) organic crystals 03 p0297 N88-11865
Physical properties of immiscible polymers 03 p0297 N88-11868
High temperature superconductors 03 p0297 N88-11869
Cast iron freezing mechanisms 03 p0298 N88-11870
Access to microgravity: A technical description of the NAE T-33 microgravity facility
[NAE-AN-47] 04 p0405 N88-12518
Microgravity combustion fundamentals 04 p0407 N88-12528
A study of two-phase flow in a reduced gravity environment
[NASA-CR-172035] 04 p0422 N88-12617
Microgravity nucleation and particle coagulation experiments support
[NASA-CR-181540] 04 p0423 N88-12618
Microgravity nucleation and particle coagulation experiments support
[NASA-CR-181541] 04 p0423 N88-12619
Low gravity fluid-thermal experiments
[DE88-000553] 04 p0423 N88-12620
Results from the melting of tungsten composites under microgravity (TEXUS 10 flight)
[FOA-C-20676-2.1] 05 p0571 N88-13482
Feasibility study for gas-grain simulation facility
[NASA-CR-177468] 05 p0646 N88-13954
Electron cytochemical detection of Ca(2)+-ATPase in protonema of moss funaria hygrometrica (H e d w.) under hypogravitation 06 p0749 N88-14602
Prediction of physical workload in reduced gravity environments 06 p0794 N88-14867
Allowable gravity-levels for Spacelab, Columbus and EURECA --- materials science
[BF-R-66.525-2] 07 p0838 N88-15084
Microgravity Particle Research on the Space Station
[NASA-CP-2496] 07 p0883 N88-15354
Astrophysics and the solar nebula 07 p0883 N88-15355
Planetary science 07 p0883 N88-15356
Atmospheric science 07 p0883 N88-15357
Exobiology and life science 07 p0883 N88-15358
Physics and chemistry 07 p0883 N88-15359
Distinctive changes in arterial pressure and blood flow in common carotid artery of monkeys flown aboard Cosmos-1514 biosatellite 07 p0892 N88-15404
Resolution of holograms produced by the fluid experiment system and the holography ground system 07 p0923 N88-15609
Tether Elevator Crawler Systems (TECS) 07 p0927 N88-15631
The effect of microgravity on flame spread over a thin fuel
[NASA-TM-100195] 08 p0967 N88-15853
Cryogenic Fluid Management Technology Workshop. Volume 1: Presentation material and discussion
[NASA-CP-10001] 08 p0980 N88-15924
Low-g propellant gaging 08 p0982 N88-15937
Low gravity liquid motions in spacecraft 08 p0982 N88-15941
Proceedings of the 8th ESA Symposium on European Rocket and Balloon Programs and Related Research
[ESA-SP-270] 08 p1024 N88-16201
The Swedish sounding rocket and balloon program 08 p1025 N88-16205
Preliminary Material Science Experiment Rocket (MASER) 1 results and the evolution of the MASER program 08 p1033 N88-16260
Flight results of the ESA experiment modules in Materials Science Experiment Rocket (MASER) 1 08 p1033 N88-16261
Life sciences experiments on stratospheric balloons and sounding rockets 08 p1033 N88-16262
The D-1 Biorack results: A base for further space biological investigations 08 p1033 N88-16263
Scientific objectives and functional requirements of life sciences in the Space Station 08 p1033 N88-16264
The ESA Anthrorack project: Integrated research in human physiology 08 p1033 N88-16265
Contribution of stratospheric balloon flights in space biology 08 p1033 N88-16266
Skylark sounding rocket development-Skylark 8 08 p1035 N88-16274
Sounding rockets/microgravity products and service 08 p1035 N88-16277
Zero gravity and living organism 08 p1046 N88-16320
Realization of an instrument to measure temperature and concentration gradients in fluids --- microgravity
[CISE-3128] 09 p1168 N88-17003
Space Bioreactor Science Workshop
[NASA-CP-2485] 09 p1196 N88-17168
Suspension cell culture in microgravity and development of a space bioreactor 09 p1196 N88-17169
Space bioreactor: Design/process flow 09 p1197 N88-17170
Computer control of a microgravity mammalian cell bioreactor 09 p1197 N88-17172
Potential use of the bioreactor to determine effects of microgravity and other environmental parameters on growth of hybridoma cells 09 p1198 N88-17178
Cell culture experiments planned for the space bioreactor 09 p1198 N88-17180
Scientific Colloquium in Honor of Prof. Dr. Rer. Nat. Hermann L. Jordan
[DFVLR-MITT-87-11] 09 p1240 N88-17432
Microgravity experiments in space: Compatibility with dynamic perturbing effects 09 p1241 N88-17435
Two-phase reduced gravity experiments for a space reactor design
[DE86-015530] 09 p1247 N88-17475
Microgravity research at the University of Mexico: Experiments in payload G-006 10 p1286 N88-17692
Ten past and ten future GAS/MAUS-payloads 10 p1287 N88-17696
An update to the MITRE/WPI Space Shuttle Program GASCAN G-408 10 p1287 N88-17697
Electrochemical growth of linear conducting crystals in microgravity 10 p1287 N88-17698
Protein-crystal growth experiment (planned) 10 p1287 N88-17700
A payload for investigating the influence of convection on GaAs crystal growth 10 p1288 N88-17702
Application of Hoffman modulation contrast microscopy coupled with three-wavelength two-beam interferometry to the in situ direct observation of the growth process of a crystal in microgravity 10 p1288 N88-17704
The challenge of G-376 10 p1288 N88-17705
A reliable data collection/control system 10 p1289 N88-17708
GAS 450: A space payload for the People Central Coast Student Experimenters 10 p1289 N88-17709
An experiment to investigate Rankine cycle two-phase microgravity issues
[DE88-004197] 10 p1308 N88-17818
NASA Workshop on Biological Adaptation
[NASA-TM-89468] 10 p1368 N88-18174
Non-proprietary research projects of the Center for the Space Processing of Engineering Materials
[AR-2] 10 p1426 N88-18516
Microgravity isolation mount
[ESA-CR(P)-2480] 11 p1443 N88-18604
Mass transport phenomena between bubbles and dissolved gases in liquids under reduced gravity conditions
[NASA-TM-100273] 11 p1455 N88-18672
Investigation of surface tension driven convection as a feasibility study for a micro-gravity experiment
[NASA-CR-182504] 11 p1466 N88-18739
Experimental investigation of low gravity two-phase flow behavior
[DE88-003779] 11 p1466 N88-18741
Microgravity and Materials Processing Facility study (MMPF). Requirements and Analyses of Commercial Operations (RACO) preliminary data release
[NASA-CR-179309] 11 p1466 N88-18742
Study of industry requirements that can be fulfilled by combustion experimentation aboard space station
[NASA-CR-180854] 11 p1566 N88-19377
Computational aspects of robotic experiment manipulation in a microgravity environment 12 p1589 N88-19512
Proceedings of the 3rd European Symposium on Life Sciences Research in Space
[ESA-SP-271] 12 p1652 N88-19893
Life sciences in the framework of the ESA microgravity program and future flight opportunities 12 p1652 N88-19895
ESA's facility for research in human physiology in space: Anthrorack 12 p1652 N88-19896
Second-generation respiratory monitoring system for microgravity studies in man 12 p1653 N88-19906
Plant biology in space 12 p1654 N88-19910
Ecological algal system in microgravity conditions: Preliminary results 12 p1655 N88-19915
Fluid volume changes in astronauts: How they fit our understanding of physiology 12 p1655 N88-19919

Cardiovascular adaptation to zero-g during a long term flight (237 days) on board the Salyut 7 Soviet space station (1984) 12 p1655 N88-19920

Cardiac and peripheral circulation assessment by ultrasound on 3 astronauts during two 7-day space flights (1982 Salyut-7 - 1985 STS 51G)
12 p1656 N88-19921

Physiological reactions upon controlled changes of blood distribution in humans 12 p1656 N88-19924

Effects of cosmic heavy ion radiation and space microgravity on plant systems 12 p1658 N88-19936

Vestibular integrated function and microgravity
12 p1658 N88-19937

Microgravity User Support Center (MUSC) for EURECA, Spacelab and Columbus missions
12 p1660 N88-19947

Biorack experiments in Spacelab D-1 and TML-1: Further developments in gravitational biology
12 p1661 N88-19953

Why life science in space? The next step to go beyond 12 p1661 N88-19954

The suspended Japanese quail as an animal model for experiments related to microgravity
12 p1662 N88-19960

Animal research on the Space Station
12 p1662 N88-19964

Development of an optical diagnostic instrument. Part 2: Instrument development --- space laboratories
[NLR-TR-87079-L-PT-2] 13 p1841 N88-21016

Mixing fuel particles for space combustion research using accoustics
[NASA-TM-100295] 14 p1872 N88-21186

Mechanical design of a ultrahigh gravity UHV facility to launch and recover a low-speed projectile tested on board KC 135 14 p1877 N88-21216

Towards a practical microgravity environment --- isolation mount 14 p1878 N88-21223

Vibration characteristics of pumped fluid systems (VCPFS) --- microgravity payloads
[ESA-CR(P)-2499] 14 p1895 N88-21310

Generation and coalescence of bubbles and stability of foams under microgravity conditions
[BMFT-FB-W-86-020] 16 p2184 N88-23017

Microgravity robotics technology program
[NASA-TM-100698] 16 p2215 N88-23219

Microgravity mechanisms and robotics program
16 p2219 N88-23237

Base reaction optimization of manipulators with redundant kinematics 16 p2219 N88-23238

Microgravity manipulator demonstration
16 p2219 N88-23242

Noncontact temperature measurements in the microgravity fluids and transport phenomena discipline
17 p2328 N88-23901

Microgravity combustion discipline working group summary of requirements for noncontact temperature measurements 17 p2328 N88-23902

Requirements for temperature and species concentration measurements in microgravity combustion experiments 17 p2329 N88-23903

Separation of biological materials in microgravity
[NASA-TM-101142] 17 p2331 N88-23916

An experiment to investigate Rankine cycle two-phase microgravity issues 17 p2409 N88-24322

Theoretical and experimental investigation of swirl flow phase separators for microgravity applications
17 p2411 N88-24335

Microgravity thaw experiment (MITEX)
17 p2427 N88-24439

Reduced-gravity two-phase flow experiments in the NASA KC-135 17 p2431 N88-24465

Analysis and interpretation of low gravity boiling experiments in the KC-135 17 p2432 N88-24466

Microgravity two-phase fluid flow pattern modeling
17 p2432 N88-24467

Experimental investigation of a microgravity separator for two phase mixtures containing small volumes of gas/vapor 17 p2432 N88-24468

Low gravity thermal management using dielectrophoretic forces 17 p2432 N88-24470

Thermodynamic modeling of the no-vent fill methodology for transferring cryogens in low gravity
[NASA-TM-100932] 18 p2476 N88-24686

Operational facilities of EURECA A1 mission
[ETN-88-91939] 18 p2496 N88-24810

Acoustic convective system
[NASA-CASE-NPO-17278-1-CU]
18 p2498 N88-24818

Moving belt radiator development status
[NASA-TM-100909] 19 p2607 N88-25477

Solid-state combustion synthesis of ceramics and alloys in reduced gravity
[NASA-CR-4163] 19 p2608 N88-25479

Industrial processes influenced by gravity
[NASA-CR-182140] 20 p2782 N88-26497

Experiments in microgravity environment: Protein crystallization
[REPT-881-430-101] 21 p2924 N88-27354

The Marshall Space Flight Center KC-135 microgravity test program for FY84-86
[NASA-TM-4059] 22 p3056 N88-28136

Biorack on Spacelab D1: An overview of the first flight of Biorack, an ESA facility for life sciences research in microgravity
[ESA-SP-1091] 22 p3059 N88-28154

A brief overview of the results of the experiments using the ESA Biorack Facility on the German Spacelab D1 mission 22 p3060 N88-28155

The Biorack facility and its performance during the D1 Spacelab mission 22 p3060 N88-28156

The effects of microgravity on genetic recombination in Escherichia coli --- Spacelab D1 mission
22 p3060 N88-28157

Growth and differentiation of Bacillus subtilis under microgravity conditions 22 p3060 N88-28158

The Antibio experiment --- Spacelab D1 mission
22 p3060 N88-28159

Contraction behavior and protoplasmic streaming in the slime mold Physarum polycephalum (Physarum kinetics) --- Spacelab D1 mission 22 p3060 N88-28160

The Paramecium experiment --- Spacelab D1 mission
22 p3060 N88-28161

The biological clock of Chlamydomonas reinhardii in space 22 p3061 N88-28162

Effect of microgravity on lymphocyte activation --- Spacelab D1 mission 22 p3061 N88-28163

The effect of microgravity on mammalian cell polarization at the ultrastructural level --- Spacelab D1 mission
22 p3061 N88-28164

Graviperception of lentil seedling roots grown in space
22 p3061 N88-28165

Effects of short spaceflights on Drosophila melanogaster embryogenesis and life span 22 p3061 N88-28166

Embryogenesis and organogenesis of Carausius morosus under spaceflight conditions
22 p3061 N88-28167

The role of gravity in the establishment of the dorso/ventral axis in the amphibian embryo --- Spacelab D1 mission 22 p3062 N88-28168

Microgravity science and applications bibliography, 1987 revision
[NASA-TM-4067] 22 p3062 N88-28171

Experimental and analytical study of two-phase flow in zero gravity
[AD-A195223] 24 p3358 N88-29993

Containment of a silicone fluid free surface in reduced gravity using barrier coatings
[NASA-TM-101314] 24 p3371 N88-30072

REDUCTION

Balanced realizations: Canonical form, parametrization, model reduction
[PB87-123360] 06 p0757 N88-14642

Parallel pivoting combined with parallel reduction
[NASA-CR-178422] 06 p0760 N88-14662

Reducing adhesion and agglomeration within a cloud of combustible particles
[NASA-TM-100902] 20 p2788 N88-26539

REDUCTION (CHEMISTRY)

NT HYDROGENATION

Activated metal oxide surfaces as highly basic and reducing environments
[AD-A184958] 05 p0561 N88-13417

Properties of lanthanide oxides as supports for transition metal catalysts
[DE88-004520] 11 p1456 N88-18678

Solar-assisted hydrogen generation by photoelectrocatalysis
[PB88-160932] 12 p1605 N88-19597

Analytically modeling the carbothermic reduction of alumina in a thermal plasma
[DE88-005535] 13 p1841 N88-21020

The evolution of glutathione metabolism in phototrophic microorganisms
[NASA-CR-182902] 19 p2695 N88-26015

In situ spectroscopic studies of transition metal macrocycles as catalysts for the electrochemical reduction of oxygen
[PB88-203195] 20 p2769 N88-26416

Nickel hydrogen cell positive-electrode studies: Cobalt segregation in reducing environments
[AD-A193025] 20 p2796 N88-26587

Super hydrides
[AD-A193710] 23 p3192 N88-28995

Breakdown of molecular oxygen by brief pulses of laser radiation
[DE88-702687] 23 p3220 N88-29168

REDUCTION (MATHEMATICS)

U OPTIMIZATION

REDUNDANCY

Measurement of fault-tolerant parallel processors
[PB87-208328] 01 p0084 N88-10539

Flight test of a resident backup software system
02 p0128 N88-10605

An evaluation plan of bus architectures and protocols using the NASA Ames intelligent redundant actuation system
[NASA-CR-177458] 04 p0398 N88-12482

Fault-tolerant computer architecture based on INMOS transputer processor 06 p0797 N88-14880

Inadequacy of conventional dynamic recovery mechanisms in the presence of temporary failures
[AD-A186311] 07 p0866 N88-15251

Directions in propulsion control
08 p0956 N88-15799

Construction of control systems with diversified redundancy for electrical machines
[BIA-5/86] 11 p1481 N88-18842

On the danger of redundancies in some aerospace mechanisms 14 p1925 N88-21475

Analytical sensor redundancy assessment
[NASA-CR-182892] 16 p2163 N88-22901

Dynamic modelling and estimation of the error due to asynchronism in a redundant asynchronous multiprocessor system
[NASA-CR-177427] 21 p2898 N88-27205

Investigations on the modification of structural reliability by substitution of aluminum by carbon fiber reinforced plastics in aircraft construction
[ILR-MITT-195] 24 p3339 N88-29877

REDUNDANCY ENCODING

Robust control system design
02 p0127 N88-10600

REDUNDANT COMPONENTS

PRAAGE: An interactive IBM-PC code for unreliability/aging analysis
[DE87-012124] 04 p0453 N88-12803

On the danger of redundancies in some aerospace mechanisms 14 p1925 N88-21475

REDUNDANT STRUCTURES

U REDUNDANT COMPONENTS

REELS

Tethered diagnostic package for use from the space station
[DE88-006264] 16 p2167 N88-22921

REENTRY

NT HYPERSONIC REENTRY
NT SPACECRAFT REENTRY

Thermal stress analysis of space shuttle orbiter subjected to reentry aerodynamic heating
[NASA-TM-88286] 01 p0061 N88-10389

Analysis of a nuclear orbital transfer vehicle reentry accident 17 p2425 N88-24426

REENTRY BODIES

U REENTRY VEHICLES

REENTRY EFFECTS

Hypersonic aerodynamics: Applications for HOTOL
05 p0535 N88-13252

REENTRY GLIDERS

U LIFTING REENTRY VEHICLES

REENTRY PHYSICS

Compressible boundary layers --- atmospheric reentry
[CERT-OA-13/5005-AYD] 20 p2801 N88-26823

REENTRY SHIELDING

Ceramic-ceramic shell tile thermal protection system and method thereof
[NASA-CASE-ARC-11641-1] 11 p1448 N88-18628

A model for nitrogen atom recombination on a silicon dioxide surface
[AD-A189843] 15 p2142 N88-22784

REENTRY TRAJECTORIES

Maneuverable reentry vehicle trajectory footprints: Calculation and properties
[DE88-004726] 10 p1292 N88-17726

REENTRY VEHICLES

NT AEROSPACE PLANES
NT CHALLENGER (ORBITER)
NT DISCOVERY (ORBITER)
NT HERMES MANNED SPACEPLANE
NT HOTOL LAUNCH VEHICLE
NT LIFTING REENTRY VEHICLES
NT MANEUVERABLE REENTRY BODIES
NT REUSABLE SPACECRAFT
NT SPACE SHUTTLE ORBITERS
NT SPACE SHUTTLES
NT X-30 VEHICLE

The aerothermodynamic environment for holes in hypersonic configurations
[DE87-014651] 02 p0121 N88-10787

Aerodynamic design and performance of a bent-axis geometry vehicle
[DE87-013726] 02 p0124 N88-10788

Scene simulation for passive IR systems
02 p0137 N88-10861

Dual S/X-band RV antenna
[DE87-014853] 03 p0305 N88-11923

Proceedings: SDIO/DARPA Workshop on Laser Propulsion. Volume 3: Viewgraphs
[DE88-000964] 04 p0450 N88-12790
High-velocity reverse ballistic rocket sled testing at Sandia National Laboratories 09 p1179 N88-17059
Comparisons of Monte-Carlo and PNS (Parabolized Navier-Stokes) calculations for rarefied flow over reentry vehicle configurations
[DE88-004937] 11 p1435 N88-18560
Three-dimensional flow fields past reentry vehicles
11 p1484 N88-18858
A simplified streamline swallowing procedure for the windward meridian of axisymmetric blunt bodies
[AD-A188413] 12 p1626 N88-19732
Features of Soyuz TM spacecraft
13 p1727 N88-20329
New definition of pressure-center coefficient of reentry craft with asymmetrical configuration
14 p1864 N88-21136
Oil flow patterns on a series of capsule-type re-entry vehicles at hypersonic speeds
[DE88-751805] 16 p2155 N88-22858
Experimental investigation of hypersonic aerodynamics
[NASA-CR-182973] 18 p2458 N88-24591
A simulation of post boost vehicle deployment of multiple reentry vehicles
[DE88-009537] 20 p2764 N88-26391
In-flight motor torque estimates for the second-stage Strypi 9 launch vehicle
[DE88-010633] 21 p2902 N88-27222
Study of hypersonic boundary layers
[CERT-RSF-OA-17/5005-AYD]
23 p3213 N88-29121

REFERENCE ATMOSPHERES
Monthly mean global climatology of temperature, wind, geopotential height, and pressure for 0 - 120 km
[NASA-TM-100697] 15 p2099 N88-22503

REFERENCE STARS
Rigorous compilation of the Northern International Reference Stars (NIRS) 03 p0387 N88-12431
IPS guidestar selection for stellar mode (ASTRO)
[NASA-TM-100336] 21 p2894 N88-27181
Astron observations of supernova 1987A in large magellanic cloud 24 p3445 N88-30504
The guide star catalog
[NASA-CR-183253] 24 p3452 N88-30547

REFERENCES (STANDARDS)
U STANDARDS

REFINING
High-density jet fuels from coal syncrudes, appendix 4
[DE88-003132] 10 p1307 N88-17813
Knowledge base refinement by monitoring abstract control knowledge, revision 1
[AD-A187502] 10 p1397 N88-18323
Aviation turbine fuels from tar sands bitumen and heavy oils. Part 3: Laboratory sample production
[AD-A189278] 13 p1753 N88-20484
Activities of As, Sb, Bi and Pb in copper mattes and their effects on impurity elimination
[TKK-V-A10(1988)] 15 p2041 N88-22165
Turbine fuels from tar sands bitumen and heavy oil. Volume 2, phase 3: Process design specifications for a turbine fuel refinery charging San Ardo heavy crude oil
[AD-A190120] 16 p2183 N88-23011
Feasibility of producing jet fuel from GPGP (Great Plains Gasification Plant) by-products
[DE88-010233] 20 p2781 N88-26492
An adaptive overlapping local grid refinement method for two-dimensional parabolic systems
[AD-A193560] 23 p3271 N88-29464

REFLECTANCE
NT BIDIRECTIONAL REFLECTANCE
NT SPECTRAL REFLECTANCE
Estimating regional evapotranspiration from remotely sensed data by surface energy balance models
[NASA-CR-181400] 01 p0064 N88-10411
Unified Sun and sky illumination for shadows under trees
[DE87-014232] 01 p0083 N88-10535
Estimating scattered and absorbed radiation in plant canopies by remote sensing
[NASA-CR-181390] 02 p0193 N88-11205
Understanding passive cooling systems
[PB87-210464] 02 p0194 N88-11211
Deformation effects on microwave reflectivity
[AD-A185684] 07 p0844 N88-15120
The anisotropy of reflected solar radiation over several types of land surface 08 p1018 N88-16171
High-sensitivity recording of weak reflected or scattered radiation by method of coherent intracavity reception with YAG:Nd(3+) laser 08 p1078 N88-16502
Experimental aspects of high-T/sub c/ superconductors
[DE88-003019] 08 p1090 N88-16564
Statistics of two-dimensional structure elements of mountainous ranges (mosaic model) for calculating three-dimensional reflection functions
[DFVLR-FB-87-33] 09 p1185 N88-17099
Variable band gap materials for thermophotovoltaic generators
[AD-A186858] 09 p1186 N88-17104
Radar reflectivity and attenuation of radio waves in the melting layer of precipitation
[PB88-121553] 10 p1318 N88-17882
Improved canopy reflectance modeling and scene inference through improved understanding of scene pattern
[NASA-CR-182488] 10 p1347 N88-18049
Optical measurements of surface oxide layer formation on metal films
[DE88-003163] 10 p1409 N88-18405
Depolarized infrared reflectance from dry and wetted surfaces
[AD-A188213] 11 p1492 N88-18903
The angular reflectance signature of the canopy hot spot in the optical regime
[DE88-005385] 11 p1505 N88-18991
Target-reflectivity models for various terrain types
[DE88-005510] 11 p1505 N88-18992
An experimental measurement of metal multilayer X-ray reflectivity degradation due to intense X-ray flux
[LA-10989-T] 11 p1547 N88-19255
Running head: What color is it
[NASA-CR-182600] 11 p1551 N88-19280
Measuring and modeling near surface reflected and emitted radiation fluxes at the FIFE site
[NASA-CR-182660] 12 p1640 N88-19818
Applications of the differential reflectivity radar technique: Focus on estimation of rainfall parameters and microwave attenuation prediction
13 p1759 N88-20521
Pseudo-stationary oblique-shock-wave reflections in low gamma gases: Isobutane and sulphur hexafluoride
[UTIAS-TN-267] 13 p1768 N88-20576
Research relative to angular distribution of snow reflectance/snow cover characterization and microwave emission
[NASA-CR-182733] 14 p1941 N88-21582
Experimental research on skin reflection, transmission, absorption of light rays 16 p2187 N88-23039
Spectral measurements for correcting LANDSAT data for atmospheric effects 17 p2353 N88-24020
The use of SLAR and SIRA imagenes for the classification of forest typen in tropical rain forests
17 p2356 N88-24036
Analysis of the parameters responsible for the variations of the illumination conditions in the LANSAT data
17 p2362 N88-24070
An experimental study of the coherent under-ice reflectivity of sound in the Greenland Sea Marginal Ice Zone 18 p2548 N88-25125
Remote sensing of acoustic properties of shallow water sediments: A review
[AD-A192107] 18 p2570 N88-25267
A disposable liquid microcell for near-infrared reflectance analysis
[AD-A192190] 18 p2575 N88-25298
Design and demonstration of a system for the deposition of atomic-oxygen durable coatings for reflective solar dynamic power system concentrators
[NASA-CR-4158] 19 p2606 N88-25474
Canopy reflectance modeling in a tropical wooded grassland
[NASA-CR-182981] 19 p2665 N88-25961
Numerical model for the computation of radiance distributions in natural waters with wind-roughened surfaces
[PB88-192703] 20 p2826 N88-26765
Observation of ferromagnetism in ultrathin f.c.c. films by spin polarised neutron reflection
20 p2865 N88-27015
Picosecond transient reflectivity of unpinned gallium arsenide (100) surfaces
[AD-A193242] 21 p3021 N88-27933
Stratocumulus and cloud-free reflectance from multi-spectral satellite measurements
[AD-A193899] 22 p3128 N88-28599
Seismic reflection experiments imaging the physical nature of crustal structures in southern California
23 p3232 N88-29235
Mars: Spectral signatures seen and unseen
23 p3301 N88-29659
Spectral reflectance of SNC meteorites: Relationships to Martian surface composition
23 p3304 N88-29683
The surface composition of Mars from earthbased observations 23 p3306 N88-29696
Martian surface analogs: Laboratory spectral studies in the mid infrared 23 p3307 N88-29699
The effect of the near earth micrometeoroid environment on a highly reflective mirror surface
[NASA-TM-101307] 24 p3332 N88-29833
Electromagnetic metrology 24 p3363 N88-30024
TM/LANDSAT-5 data to evaluate wheat and bean percent soil cover and leaf area index
[INPE-4609-PRE/1332] 24 p3385 N88-30165
Reflectance pattern and the physical and chemical characteristics of three Brazilian Oxisols
[INPE-4590-PRE/1320] 24 p3387 N88-30172
Study of the spectral response of soybeans
[INPE-4592-PRE/1322] 24 p3387 N88-30174
Deep seismic reflection profiling and continental growth curves 24 p3396 N88-30222
Physical properties of surface materials on Martian volcanoes: Dust-covered lava and ash
24 p3443 N88-30493

REFLECTED RADIATION
U REFLECTED WAVES

REFLECTED RAYS
U REFLECTED WAVES

REFLECTED WAVES
Analytical investigation of reflection of a regular or mach reflection over a secondary wedge
[AD-A185690] 06 p0703 N88-14316
The carbon dioxide chaperon efficiency for the reaction H + O2 + M yields HO2 + M from ignition delay times behind reflected shock waves
[NASA-TM-100125] 07 p0830 N88-15036
Application of correlation method of reception of direct and reflected cosmic radiation to study of plasmaspheres of planet and distribution of radiation brightness
08 p1004 N88-16085
Method of determining atmospheric moisture content by measurement of upward radiation intensity in near IR
08 p1007 N88-16106
Radiation balance components above the tropical evergreen Amazon forests (3rd campaign of data collection)
[INPE-4195-PRE/1079] 11 p1513 N88-19039
Flow/acoustic interaction in duct inflow
[AD-A189264] 13 p1833 N88-20967

REFLECTION
NT INFRARED REFLECTION
NT MACH REFLECTION
NT OPTICAL REFLECTION
NT SIGNAL REFLECTION
NT SPECULAR REFLECTION
NT WAVE REFLECTION
A new approach to modeling and interpreting electromagnetic sounding data
[DE88-000460] 04 p0438 N88-12715
Horn design equations for the NBS (National Bureau of Standards) horn-type noise standards
[PB88-110226] 07 p0844 N88-15122
Accurate boundary conditions for exterior problems in gas dynamics
[NASA-TM-100807] 11 p1537 N88-19182
Electrochromic thin films
[DE88-751099] 11 p1559 N88-19334
Solving reflexive domain equations in a category of complete metric spaces
[CWI-CS-R8709] 13 p1832 N88-20956
Vegetation mapping using high resolution MSS (multispectral scanner) data: Canopy reflectance and shadow problems encountered and possible solutions
[DE88-004273] 14 p1939 N88-21574
Infrared reflection-absorption spectroscopy of hyperfine layers on surfaces of semiconductors and dielectrics
14 p1969 N88-21755
Millimeter and submillimeter waves and frequency selective surfaces
[AD-A191511] 18 p2500 N88-24827
Identification of cascaded microwave circuits with moderate reflections using reflections and transmission measurements
[PB88-171921] 18 p2503 N88-24849
Dielectric compound parabolic concentrating solar collector with frustrated total internal reflection absorber
[DE88-009986] 19 p2688 N88-25976
The use of liquid films for spacecraft survivability to laser radiation
[AD-A192954] 20 p2765 N88-26395
Experimental investigation of the reflection of a planar shock wave over a double wedge
[AD-A193078] 21 p2943 N88-27482
Attachable interferometric strain gages
[AD-A192390] 21 p2950 N88-27522
Effects of low reflection on the collector and source sheaths of a finite ion temperature plasma
[DE88-008929] 21 p3017 N88-27908
Electromagnetic wave incoherent reflection by a half-space of weakly-ionized plasma with an absorbing boundary
[DE88-702413] 21 p3019 N88-27917

Polarization of light reflected by vertically inhomogeneous planetary atmosphere
[DE88-702416] 21 p3031 N88-27992
Arctic ice attenuation model study
[AD-A193382] 22 p3146 N88-28715
Reflection and scattering of acoustic rays computed for parabolic ice keel models
[AD-A193698] 23 p3278 N88-29517

REFLECTION COEFFICIENT
U REFLECTANCE

REFLECTIVITY
U REFLECTANCE

REFLECTOR ANTENNAS
NT PARABOLIC ANTENNAS
NT TWO REFLECTOR ANTENNAS
Physical optics method: Prediction of radar signatures
03 p0304 N88-11914
A simplified approach to axisymmetric dual-reflector antenna design
[NASA-TP-2797] 09 p1111 N88-16662
Compensation of relector antenna surface distortion using an array feed
[NASA-TM-100286] 11 p1476 N88-18805
Multiple-beam ground station reflector antenna system: A preliminary study
[EUT-87-E-171] 14 p1904 N88-21379
An improved method for calculating power density in the Fresnel region of circular parabolic reflector antennas
[AD-A190569] 15 p2060 N88-22264
Analysis and experiments concerning the performance and calibration of compact antenna-test ranges
[PB88-169263] 16 p2188 N88-23047
Analysis and experiments concerning the performance and calibration of compact antenna-test ranges
[ISBN-9-09-001727-5] 16 p2188 N88-23048
Case study of active array feed compensation with sidelobe control for reflector surface distortion
[NASA-TM-100287] 16 p2192 N88-23073
A microstrip array feed for MSAT spacecraft reflector antenna 19 p2652 N88-25747
Active feed array compensation for reflector antenna surface distortions
[NASA-TM-100826] 19 p2654 N88-25762
Analytical approximation of a distorted reflector surface defined by a discrete set of points
[NASA-TM-101323] 21 p2934 N88-27424

REFLECTOR SATELLITES
U PASSIVE SATELLITES

REFLECTORS
NT PARABOLIC REFLECTORS
NT RADAR CORNER REFLECTORS
NT SOLAR COLLECTORS
NT SOLAR REFLECTORS
NT WIGGLER MAGNETS
A new type of lamp and reflector for I.R. simulation
02 p0136 N88-10655
A multibody dynamic analysis of the N-ROSS (Navy Remote Ocean Sensing System) satellite rotating flexible reflector using Kane's method
[AD-A184452] 04 p0462 N88-12860
A simplified approach to axisymmetric dual-reflector antenna design
[NASA-TP-2797] 09 p1111 N88-16662
Study on a double reflector compact range --- satellite antennas
[S-201-05] 09 p1153 N88-16908
A new approach for shaping of dual-reflector antennas
[NASA-CR-182581] 11 p1476 N88-18806
Polymer reflectors research during FY86
[DE88-001101] 11 p1508 N88-19009
Workshop on Technology Development Issues for the Large Deployable Reflector (LDR)
[NASA-CP-2407] 12 p1710 N88-20235
Features and applications of the integrated composites analyzer (ICAN) code 15 p2078 N88-22391
LDR structural experiment definition
[NASA-TM-100618] 17 p2312 N88-23826
The radar cross section of some simple reflectors at short wavelengths
[FOA-C-30472-3.3] 18 p2501 N88-24839
Joint services electronics program
[AD-A191749] 18 p2504 N88-24853
Confirmation of slow-waves in a crosstie overlay coplanar waveguide and its application to band-reject gratings and reflectors
[AD-A194981] 24 p3361 N88-30011

REFLEXES
NT VESTIBULAR NYSTAGMUS

REFRACTED RADIATION
U REFRACTED WAVES

REFRACTED RAYS
U REFRACTED WAVES

REFRACTED WAVES
Refraction of shear wave into nonlinearly elastic or elastoplastic half-space 02 p0159 N88-10999
AFAR (Azores Fixed Acoustic Range) measurements of intensity and intensity moments
[AD-A184431] 03 p0355 N88-12237
Mathematical models of sound waves in fluids
[AD-A189270] 13 p1834 N88-20968

REFRACTION
NT ATMOSPHERIC REFRACTION
NT BIREFRINGENCE
NT KERR ELECTROOPTICAL EFFECT
NT RADIO WAVE REFRACTION
Optical characterization of silica aerogel glass
[DE87-014617] 02 p0153 N88-10956
A FORTRAN code for the calculation of probe volume geometry changes in a laser anemometry system caused by window refraction
[NASA-TM-100210] 03 p0364 N88-12288
Low-frequency VLBI in space and interstellar refraction
[PB87-127643] 06 p0696 N88-14267
Correlation between refraction over sea and nature of radar reflections from sea surface
06 p0728 N88-14477
A-scan ultrasound measurement of ocular changes during accommodation
[AD-A186818] 09 p1198 N88-17181
Crystalline sulfur dioxide: Crystal field splittings, absolute band intensities and complex refractive indices derived from infrared spectra
[NASA-CR-182502] 09 p1258 N88-17547
Research on materials and components for opto-electronic signal processing and computing
[AD-A190130] 15 p2143 N88-22788
Refraction in underwater acoustics --- navigation systems
[B8735053] 17 p2395 N88-24236
Ray scattering from a collection of ice keels
[AD-A191757] 19 p2722 N88-26163

REFRACTIVE INDEX
U REFRACTIVITY

REFRACTIVITY
A 15 cm aperture LED scintillometer for C(n) squared and crosswind measurements
[KNMI-WR-87-3] 01 p0070 N88-10448
Precise measurement of refractive index and absorption coefficient of near millimeter wave and far infrared materials
[AD-A184536] 03 p0293 N88-11840
Aluminum oxynitride spinel (ALON): A review
[AD-A184753] 03 p0294 N88-11845
Microwave refractive index structure function profiles (Cn2) measured from a small aircraft
[AD-A184343] 04 p0431 N88-12670
Pulse-mode expansions and refractive indices in plane-wave propagation
[DE88-001328] 04 p0437 N88-12714
The application of vector diffraction to the scalar anomalous diffraction approximation of Van de Hulst
[AD-A185930] 07 p0929 N88-15643
A raytrace method for a laterally heterogeneous environment
[AD-A186525] 08 p0978 N88-15912
Christiansen effect in infrared spectra of soil-derived atmospheric dusts
[AD-A187071] 09 p1248 N88-17479
The stability of free-electron lasers against filamentation
[DE88-004712] 10 p1414 N88-18435
An evaluation of the impact of variable temporal and spatial data resolution upon IREPS (Integrated Refractive Effects Prediction System)
[AD-A187764] 11 p1470 N88-18769
Fast switching of far infrared radiation by refractive index change in semiconductors using photoionization
[ETN-88-91490] 11 p1551 N88-19279
Correcting ray field failures caused by focusing in an inhomogeneous duct: A critical look at the Gaussian beam method 12 p1616 N88-19663
Refractive index, meteorology and fading in line-of-sight transmission paths 12 p1616 N88-19666
Optical properties of compressible inhomogeneous shear layers relevant to high power lasers
[AD-A189299] 12 p1633 N88-19774
Analysis of the inter-layer independence of stellar scintillometer profiles of Cn2
[AD-A189372] 12 p1645 N88-19854
Nonlinear optical principles and the photorefractive effect applied to optical phase conjugation
[AD-A188856] 12 p1691 N88-20119
Refractive index gradients in nuclear-reactor-pumped lasers: Gasdynamic effects
[DE88-006099] 13 p1776 N88-20621
Nonlinear refractive index measurements of glasses and crystals
[DE88-005673] 13 p1840 N88-21009
Stellar scintillometer atmospheric optical turbulence profiling experiment: A qualitative comparison of two identical instruments at AMOS (Air Force Maui Optical Station), 1985
[AD-A190589] 15 p2094 N88-22479
Spectral measurements in a disturbed boundary layer over snow
[AD-A190217] 15 p2097 N88-22494
Dispersion measurements of microcrystals in the near ultraviolet and infrared
[DE88-006234] 15 p2145 N88-22800
The optical properties of aerosols
[AD-A191420] 16 p2176 N88-22972
IREPS (Integrated Refractive Effects Prediction System) 3.0, user's manual
[AD-A190398] 16 p2188 N88-23045
Dynamic range compression/expansion of light beams by photorefractive crystals
[NASA-CASE-NPO-17140-1-CU]
17 p2438 N88-24506
Silicon-sapphire waveguides
[AD-A191754] 18 p2504 N88-24854
Construction of approximations to acoustic Green's functions for nonhomogeneous oceans using transmutation
[PB88-185384] 18 p2548 N88-25126
Determination of doping profiles in silicon from resistivity measurements via the four-point probe in combination with layer strippings via anodic oxidation
18 p2583 N88-25347
Numerical investigation of acoustic energy exchange through flow turning 19 p2629 N88-25593
Influence of refractive index and solar concentration on optical power absorption in slabs
[NASA-TM-4056] 19 p2726 N88-26190
Optical characterization of silica aerogel
[DE88-008916] 20 p2854 N88-26946
Predicting optical degradation of a laser beam through a turbulent shear layer 21 p2927 N88-27376
Monte-Carlo estimation of the influence of plant architecture parameters on spectral brightness
24 p3450 N88-30533

REFRACTOMETERS
Fiber optics refractometer for absorption machines
[DE88-002296] 07 p0932 N88-15662
A refractometer for the interferometric determination of the helium abundance in the Jupiter atmosphere
[BONN-IR-86-23] 07 p0946 N88-15749

REFRACTORY COATINGS
Thermal barrier coating life prediction model development 02 p0190 N88-11183
Thermal barrier coating life prediction model development 02 p0190 N88-11184
Thermal barrier coating life prediction model development 02 p0190 N88-11185
Reaction mechanism of sulfur dioxide with single crystal cobalt and chromium and CoCrAlY coatings
[AD-A185989] 09 p1253 N88-17509
Hermetic coating of optical fibers
[AD-A189686] 15 p2044 N88-22177

REFRACTORY MATERIALS
NT CHROMIUM
NT IRIDIUM
NT IRIDIUM ISOTOPES
NT MOLYBDENUM
NT MOLYBDENUM ALLOYS
NT NIOBIUM
NT NIOBIUM ALLOYS
NT NIOBIUM ISOTOPES
NT OSMIUM
NT REFRACTORY METAL ALLOYS
NT REFRACTORY METALS
NT RHENIUM
NT RHENIUM ALLOYS
NT RHENIUM ISOTOPES
NT TANTALUM
NT TANTALUM ALLOYS
NT TUNGSTEN
NT TUNGSTEN ALLOYS
High temperature metal matrix composites for future aerospace systems
[NASA-TM-100212] 02 p0149 N88-10936
Coatings for Advanced Heat Engines Workshop: Book of abstracts
[DE87-012623] 02 p0180 N88-11121
High temperature characterization of ceramic materials
[REPT-NT-3403] 03 p0292 N88-11837
Cu-2 mechanical properties and microstructural stability of advanced steam cycle materials
[DE88-001519] 05 p0566 N88-13452
Material design of high-purpose glass discussed
06 p0675 N88-14133
Projects within the Center for Advanced Materials
[PB88-123054] 06 p0677 N88-14143

Astrophysics and the solar nebula
07 p0863 N88-15355

The synthesis and characterization of some rare earth arsenides
[AD-A186445] 08 p0965 N88-15839

Ethynylated aromatics as high temperature matrix resins
[NASA-TM-89829] 11 p1450 N88-18640

Hot corrosion in gas turbines: A new, unique and informative technique is EASE (Electronic Absorption Spectroscopy Experiments)
[AD-A188508] 12 p1583 N88-19470

Development of metastable processing paths for high temperature alloys
[AD-A188682] 12 p1608 N88-19617

Basic research in ceramic and semiconductor science at selected Japanese laboratories, based on a September 1986 visit: Highlights, summary and overview and detailed notes from selected Japanese laboratories
[DOE/ER-0314] 12 p1696 N88-20150

High-temperature metal matrix composites
[AD-A189516] 13 p1734 N88-20367

Statistical considerations of graphite strength for assessing design allowable stresses
13 p1746 N88-20441

Fracture criterion of reactor graphite under multiaxial stresses 13 p1746 N88-20442

High temperature Young's modulus of IG-110 graphite
13 p1746 N88-20443

Effects of high temperature neutron irradiation on the physical, chemical and mechanical properties of fine-grained isotropic graphite 13 p1747 N88-20444

Degradations of thermal shock resistance and the fracture toughness of reactor graphite subjected to neutron irradiation 13 p1747 N88-20445

JPRS report: Science and technology. China
[JPRS-CST-87-023] 14 p1863 N88-21130

Contemporary ceramics and the new technological revolution 14 p1902 N88-21363

Nonlinear Constitutive Relations for High Temperature Applications, 1986
[NASA-CP-10010] 14 p1926 N88-21498

High temperature materials: What's available
[AERE-R-12632] 15 p2028 N88-22081

Fundamental studies on high temperature deformation recrystallization, and grain growth of two-phase materials
[AD-A189725] 15 p2038 N88-22145

Biaxial experiments supporting the development of constitutive theories for advanced high-temperature materials 15 p2078 N88-22386

Refractory Materials of Zirconate. Part 2: Synthesis and some properties of strontium, zirconate, calcium zirconate and barium zirconate
[NASA-TT-20136] 20 p2779 N88-26483

Radiative heat transfer and selective emission in planar slab coatings on hot emissive substrates
[AD-A193133] 21 p2918 N88-27319

Refractory fibers surface treatment
[REPT-47-803/F] 21 p2922 N88-27339

The High Temperature Materials Laboratory: A new research and user facility at the Oak Ridge National Laboratory
[DE88-010792] 22 p3057 N88-28138

Very high temperature materials for mechanical application
[SNIAS-881-430-106] 23 p3189 N88-28978

REFRACTORY METAL ALLOYS
NT MOLYBDENUM ALLOYS
NT NIOBIUM ALLOYS
NT RHENIUM ALLOYS
NT TANTALUM ALLOYS
NT TUNGSTEN ALLOYS

Properties of refractory metals processed by enhanced sintering treatments
[AD-A184944] 05 p0565 N88-13440

Characterization of precipitates in a niobium-zirconium-carbon alloy
[NASA-TM-100848] 16 p2178 N88-22981

Review of alkali metal and refractory alloy compatibility for Rankine cycle applications 17 p2428 N88-24447

Effect of hydrogen, deuterium and oxygen on the anelastic properties of refractory alloys
[DE88-007349] 18 p2484 N88-24736

REFRACTORY METALS
NT CHROMIUM
NT IRIDIUM
NT IRIDIUM ISOTOPES
NT MOLYBDENUM
NT NIOBIUM
NT NIOBIUM ISOTOPES
NT OSMIUM
NT RHENIUM
NT RHENIUM ISOTOPES
NT TANTALUM
NT TUNGSTEN

Properties of refractory metals processed by enhanced sintering treatments
[AD-A184944] 05 p0565 N88-13440

Development of reliable fuel pins for space reactor applications 17 p2409 N88-24326

Refractory metal alloys and composites for space power systems
[NASA-TM-100946] 21 p2916 N88-27310

REFRASIL (TRADEMARK)
U FIBERS
U SILICON DIOXIDE

REFRIGERANTS

Optimized ground coupled heat pump mechanical package
[DE87-014899] 04 p0441 N88-12738

Development of a low noise 10 K J-T refrigeration system
[AD-A185258] 05 p0571 N88-13484

Investigation of critical heating in narrow flow channels with R12 refrigerant as model fluid
[GKSS-87/E/25] 09 p1163 N88-16972

Investigation on refrigerant R12 critical boiling point in narrow flow pipes considered as model fluid
[ETN-88-92374] 20 p2802 N88-26626

Thermal conductivity of pure fluids in a large region around the critical point
[ETN-88-92135] 20 p2881 N88-27103

REFRIGERATING

Development of a low noise 10 K J-T refrigeration system
[AD-A186004] 07 p0838 N88-15085

Large capacity cryopropellant orbital storage facility
08 p0961 N88-15932

REFRIGERATING MACHINERY
NT REFRIGERATORS

Oxygen chemisorption cryogenic refrigerator
[NASA-CASE-NPO-16734-1-CU]
06 p0689 N88-14223

Air Force cryocooler development for spacecraft
08 p0963 N88-15945

Study of a magnetic refrigerator for space applications for temperatures under 20 K
[NASA-TT-20283] 19 p2641 N88-25668

REFRIGERATORS

A 2.3-GHz cryogenically cooled HEMT amplifier for DSS 13 04 p0434 N88-12689

A cold ejector for closed-cycle helium refrigerators
04 p0434 N88-12690

Traveling-wave maser closed-cycle refrigerator data acquisition and display system 04 p0437 N88-12708

Two-watt, 4-Kelvin closed cycle refrigerator performance 04 p0437 N88-12709

Development of a low noise 10 K J-T refrigeration system
[AD-A185258] 05 p0571 N88-13484

Evaluation of a cryogenic refrigerator for cooling focal plane instrumentation — satellite instruments
[BAE-TP-8095-VOL-1] 05 p0572 N88-13485

Evaluation of a cryogenic refrigerator for cooling focal plane instrumentation. Appendix B: Accommodation study — satellite instruments
[BAE-TP-8095-VOL-2] 05 p0572 N88-13486

Self operating absorption cooling system using solar energy: Small power experimental plant
[DE88-900194] 07 p0874 N88-15299

Cryogenics program overview
08 p0981 N88-15926

Ames Research Center cryogenics program
08 p0981 N88-15927

Cryocooler systems demonstration
[AD-A188025] 11 p1467 N88-18745

Dilution refrigerator with non-valve adsorption system of sup 3/He circulation
[DE88-700974] 15 p2050 N88-22209

Thin superconducting film characterization by surface acoustic waves
[AD-A190417] 15 p2143 N88-22791

Krypton based adsorption type cryogenic refrigerator
[NASA-CASE-NPO-17334-1-CU]
17 p2331 N88-23917

Cryogenic regenerator including saran-carbon heat conduction matrix
[NASA-CASE-NPO-17291-1-CU]
17 p2337 N88-23946

Electrodynamic driver for the space thermoacoustic refrigerator (STAR)
[AD-A192337] 20 p2785 N88-26517

Magnetic heat pumps
[DE88-012058] 21 p2969 N88-27639

CryoSQUID: A SQUID-based magnetic field sensor
[AD-A194237] 23 p3239 N88-29275

REFUELING
NT AIR TO AIR REFUELING

Orbital Spacecraft Consumables Resupply System (OSCRS). Volume 4: Extended study results Part 1: Executive Summary
[NASA-CR-172012] 03 p0268 N88-11686

Orbital Spacecraft Consumables Resupply System (OSCRS): Monopropellant application to space station and OMV automatic refueling impacts of an ELV launch, volume 4
[NASA-CR-172029] 03 p0276 N88-11741

Refueling and density control in the ZT-40M reversed field pinch
[DE88-000504] 04 p0493 N88-13040

Orbital Spacecraft Consumables Resupply System (OSCRS). Volume 1: Executive summary
[NASA-CR-172010] 05 p0553 N88-13368

Safety implications of onboard refueling vapor recovery systems
[PB88-102603] 07 p0839 N88-15088

Investigation of the need for in-use dispensing rate limits and fuel nozzle geometry standardization
[PB88-102611] 07 p0839 N88-15089

Summary and analysis of comments on the recommended practice for the measurement of refueling emissions
[PB88-101530] 07 p0876 N88-15313

SAMSS: An in-progress review of the Spacecraft Assembly, Maintenance, and Servicing Study
08 p0981 N88-15930

Application of railgun principle to high-velocity hydrogen pellet injection for magnetic fusion reactor refueling
[DE88-005830] 13 p1728 N88-20334

Investigation of the misfueling of reciprocating piston aircraft engines
[NASA-TP-2803] 14 p1865 N88-21144

Implementation of a visual servoing system for evaluation of robotic refueling applications
[AD-A189676] 14 p1954 N88-21645

Development and evaluation of an airplane fuel tank ullage composition model. Volume 2: Experimental determination of airplane fuel tank ullage compositions
[AD-A190408] 15 p2017 N88-22025

Fault diagnosis in orbital refueling operations
17 p2381 N88-24154

Thermodynamic modeling of the no-vent fill methodology for transferring cryogens in low gravity
[NASA-TM-100932] 18 p2476 N88-24686

Temperature rise in superfluid helium pumps
[NASA-TM-100997] 21 p2948 N88-27507

Inflight rearming
[AD-A193564] 23 p3176 N88-28909

Technology requirements for an orbiting fuel depot: A necessary element of a space infrastructure
[NASA-TM-101370] 24 p3334 N88-29845

Design and development of a refueling test bed
[FTMS-RP-ER-011] 24 p3357 N88-29986

REGENERATION (ENGINEERING)

Performance of rotary regenerative heat exchanger: A numerical simulation 01 p0046 N88-10292

Heat engine regenerators: Research status and needs
[DE87-013581] 01 p0054 N88-10348

Effects of a regenerating heat treatment on the creep behavior and the lifetime during creep test loading
[ETN-88-91063] 09 p1144 N88-16855

Cryogenic regenerator including saran-carbon heat conduction matrix
[NASA-CASE-NPO-17291-1-CU]
17 p2337 N88-23946

Advanced life support control/monitor instrumentation concepts for flight application
[NASA-CR-177378] 20 p2833 N88-26807

Full analysis of a powerful window random access algorithm
[AD-A192437] 21 p2995 N88-27763

Advancements in oxygen generation and humidity control by water vapor electrolysis
[NASA-CR-172073] 22 p3134 N88-28633

REGENERATION (PHYSIOLOGY)

Limb regeneration in amphibians, a suitable model for investigations of the effects of weightlessness as regards evolution and modifications 07 p0885 N88-15369

Nucleic acid content of skeletal muscles during hypokinesia and in the recovery period
07 p0894 N88-15418

Plant cell cultures in space biology studies
12 p1654 N88-19913

Aspects of bioregenerative life support systems
12 p1655 N88-19917

Organs and tissues regeneration in amphibia under the space flight conditions 12 p1660 N88-19951

Regenerative life support system research
[NASA-CR-182606] 12 p1671 N88-20006

Evaluation of a burned area and the vegetation regeneration affected by the burning in the Parque Nacional de Brazilia through TM/LANDSAT data
17 p2363 N88-24073

REGENERATIVE COOLING
Review of convectively cooled structures for hypersonic flight
[NASA-TM-87740] 17 p2310 N88-23817
REGENERATIVE CYCLES
U REGENERATION (ENGINEERING)
REGENERATIVE FUEL CELLS
Candidate advanced energy storage concepts for multimegawatt burst power systems
17 p2426 N88-24434
Monolithic fuel cell based power source for burst power generation 17 p2429 N88-24450
High power density alkaline fuel cell technology for MMW space burst power 17 p2429 N88-24451
All inorganic ambient temperature rechargeable lithium battery
[DE88-008425] 19 p2662 N88-25834
Regenerative fuel cell energy storage system for a low earth orbit space station
[NASA-CR-174802] 24 p3389 N88-30184
REGENERATORS
NT THERMOSIPHONS
Assessment of energy storage concepts for use in sprint power 17 p2407 N88-24312
Fatigue failure of regenerator screens in a high frequency Stirling engine 17 p2436 N88-24491
Advanced EMU electrochemically regenerable CO2 and moisture absorber module breadboard
[NASA-CR-172054] 21 p2993 N88-27754
REGIMES
On regime selection in global atmospheric flow
17 p2374 N88-24119
REGIONAL PLANNING
NT URBAN PLANNING
Remote sensing with LANDSAT 5 Thematic Mapper (TM) and its application to various planning levels: A case study from the Wuerzburg area, West Germany
[DFVLR-FB-86-62] 01 p0065 N88-10421
The atlas of regional development
16 p2226 N88-23291
Analyses of heliport system plans
[DOT/FAA/PM-87/31] 17 p2308 N88-23510
Topographic data processing for environmental planning 18 p2534 N88-25032
Remote sensing techniques applied to the study of metropolitan regions: The west sector of the Sao Paulo metropolitan area 19 p2681 N88-25941
Territorial management program
19 p2682 N88-25942
Aerial photography as an instrument of municipal and regional planning: Metropolitan area of Sao Paulo (SP)
19 p2684 N88-25957
Remote sensing applied to integrated regional development programs 19 p2685 N88-25958
Utilization of a satellite communication system to protect the national communication network
[FUB-33-1986] 21 p2934 N88-27423
REGIONS
NT AMAZON REGION (SOUTH AMERICA)
NT ANTARCTIC REGIONS
NT ARCTIC REGIONS
NT AURORAL ZONES
NT BRILLOUIN ZONES
NT D REGION
NT E REGION
NT EQUATORIAL REGIONS
NT F REGION
NT F 2 REGION
NT FRESNEL REGION
NT HABITATS
NT NEW ENGLAND (US)
NT NULL ZONES
NT POLAR REGIONS
NT REMOTE REGIONS
NT ROSS ICE SHELF
NT SPORADIC E LAYER
NT SUBARCTIC REGIONS
NT TEMPERATE REGIONS
NT TROPICAL REGIONS
A physical metallurgical basis for heat-affected zone and base-plate properties of a microalloyed HSLA steel
[AD-A180200] 01 p0022 N88-10137
Computation of transonic separated wing flows using an Euler/Navier-Stokes zonal approach
[NASA-TM-88311] 02 p0173 N88-11089
V/STOL aircraft configurations and opportunities in the Pacific Basin
[NASA-TM-100005] 03 p0261 N88-11644
Regional intercomparisons of General Circulation Model predictions and historical climate data: CO2
[DE88-010416] 23 p3235 N88-29248
REGISTERS
Vector performance of register-to-register vector computers
[DE88-004013] 10 p1384 N88-18265
REGISTERS (COMPUTERS)
On proving register atomicity
[CWI-CS-R8707] 13 p1818 N88-20862
Atomic multireader register --- computer storage
[CWI-CS-R8722] 14 p1954 N88-21648
Simple multireader registers using time-stamp schemes
[CWI-CS-R8758] 20 p2835 N88-26819
REGOLITH
Energy requirements for HE-3 mining operations on the Moon 17 p2420 N88-24390
Sub-kilometer rampart craters in the equatorial region of Mars: Possible implications for the state and distribution of regolith H2O 23 p3302 N88-29666
Some probable characteristics of the Martian regolith
23 p3303 N88-29678
REGRESSION (STATISTICS)
U REGRESSION ANALYSIS
REGRESSION ANALYSIS
NT REGRESSION COEFFICIENTS
Identification of multivariate outliers and leverage points by means of robust covariance matrices
[REPT-87-15] 01 p0088 N88-10575
PROGRESS: A program for robust regression analysis on the IBM PC
[REPT-85-14] 01 p0088 N88-10576
Tropical cyclone intensity prediction based on empirical orthogonal function representation of wind and shear fields
[AD-A184699] 03 p0353 N88-12229
A computational examination of orthogonal distance regression
[AD-A184374] 03 p0371 N88-12337
Regressed relations for forced convection heat transfer in a direct injection stratified charge rotary engine
[NASA-TM-100124] 05 p0549 N88-13345
An APL workspace for conducting nonparametric statistical inference
[AD-A184971] 05 p0634 N88-13877
Least squares for fuzzy vector data regression
[AD-A185156] 05 p0640 N88-13917
Interactive nonlinear least squares program
[PB88-109855] 06 p0760 N88-14661
Asymptotic normality of poly-t densities with Bayesian applications
[AD-A185718] 06 p0768 N88-14719
Discrete reliability growth models using failure discounting
[AD-A186380] 07 p0866 N88-15252
Objective prediction of monthly mean surface temperature and climatological relationships to mid-tropospheric heights
[DE88-000908] 07 p0880 N88-15340
Estimation and testing in truncated and nontruncated linear median-regression models
[AD-A186317] 07 p0911 N88-15522
Variable selection in logistic regression
[AD-A188032] 07 p0914 N88-15547
Conditionally unbiased bounded influence robust regression with applications to generalized linear models
[AD-A186319] 07 p0915 N88-15556
A continuous oxidizer regression model for the combustion of composite solid propellants
[AD-A186742] 08 p0974 N88-15894
Short data length effects in an asymptotically efficient ARMA (AutoRegressive Moving Average) spectral estimator
[AD-A186561] 08 p1068 N88-16458
Test of linearity in general regression models
[AD-A186036] 08 p1073 N88-16477
Tensorial calibration. Part 1: First order tensorial calibration
[AD-A186708] 09 p1167 N88-16995
Detection of soil erosion with Thematic Mapper (TM) satellite data within Pinyon-Juniper woodlands
[NASA-CR-182476] 09 p1185 N88-17103
A note on computing robust regression estimates via iteratively reweighted least squares
[AD-A186709] 09 p1227 N88-17352
Prediction of polytomous events: Model description, algorithm development and methodological aspects, with an application
[AD-A186549] 09 p1232 N88-17384
Using ridge regression in systematic pointing error corrections 11 p1472 N88-18777
Improving battery reliability by using regression trees
[DE88-004539] 11 p1481 N88-18841
Estimation in linear models with censored data
[AD-A187209] 11 p1540 N88-19203
Department of Defense World Geodetic System 1984: Its definition and relationships with local geodetic systems
[AD-A188815] 12 p1639 N88-19811
Survival analysis using additive risk models
[AD-A189053] 13 p1825 N88-20906
Spatial and temporal distribution of precipitation chemistry across Maryland in 1984, volume 1
[PB88-148929] 14 p1943 N88-21595
Concentration inequalities for Gauss Markov estimators
[CWI-MS-R8706] 14 p1965 N88-21726
Modeling failures of intermittently used machines
[AD-A190298] 15 p2074 N88-22367
Inference for a nonlinear semimartingale regression model
[AD-A190857] 16 p2262 N88-23527
Spectral measurements for correcting LANDSAT data for atmospheric effects 17 p2353 N88-24020
Estimation of an area cultivated with wheat from LANDSAT data through a two-phase sampling method
17 p2357 N88-24041
Evaluation of an estimation system for an irrigated area in a tropical region through TM-LANDSAT imagery
17 p2363 N88-24075
On Hotelling's approach to testing for a nonlinear parameter in regression
[AD-A191189] 17 p2393 N88-24229
Automated analysis of crack growth rate for obtaining da/dN versus delta K relation
[FFA-TN-1987-70] 18 p2527 N88-24996
Asymptotic theory for weighted least squares estimators in Aalen's additive risk model
[AD-A191065] 18 p2562 N88-25210
Symmetrized nearest neighbor regression estimates
[AD-A191998] 18 p2568 N88-25254
A statistical treatment of accelerated life test data for copper-water heat pipes 20 p2783 N88-26509
Asymptotic normality of minimum L1-norm estimates in linear models
[AD-A193399] 21 p3006 N88-27835
On climate prediction for India
22 p3127 N88-28590
Characteristics of regression equations for specifying monthly precipitation amounts over the United States from the field of concurrent mean 700 mb heights
22 p3127 N88-28591
Two biased estimation techniques in linear regression: Application to aircraft
[NASA-TM-100649] 23 p3274 N88-29489
REGRESSION COEFFICIENTS
Estimation of a multivariate continuous variable panel model
[AD-A184472] 04 p0484 N88-12982
Strong consistency of estimation of number of regression variables when the errors are independent and their expectations are not equal to each other
[AD-A186025] 07 p0909 N88-15507
Estimating the solar irradiance of an intermountain region using GOES (Geostationary Operational Environmental Satellite) satellite data: A test of two statistical models
[AD-A188414] 12 p1642 N88-19834
Leave-K-Out diagnostics for time series
[AD-A191343] 16 p2261 N88-23518
Min-max bias robust regression
[AD-A191345] 16 p2263 N88-23529
REGULARITY
Regularity properties of a doubly degenerate equation in hydrology
[REPT-87-07] 01 p0064 N88-10409
Regularity of the Albanese map for nonoriented surfaces
[DE88-006428] 15 p2126 N88-22679
Pairwise complete regularity as a separation axiom
[REPT-87-57] 16 p2264 N88-23539
Regularity of solutions for nonlinear degenerate elliptic boundary value problems
[DE88-702646] 22 p3146 N88-28710
Regularity and numerical solution of eigenvalue problems with piecewise analytic data
[AD-A194993] 24 p3425 N88-30387
REGULATION
U CONTROL
REGULATIONS
Airworthiness of long-life jet transport structures
03 p0265 N88-11674
DOE explosives safety manual
[DE88-000831] 04 p0422 N88-12616
Deterministic uncertainty analysis
[DE88-006139] 13 p1829 N88-20942
The impact of independent research and development regulations on companies not required to negotiate advanced independent research and development agreements
[AD-A190007] 15 p2147 N88-22818
Advisory circular: Noise certification handbook
[FAA-AC-36-4B] 17 p2394 N88-24234
Discussions and agreements in the United Nations on important issues associated with nuclear power in space
17 p2423 N88-24411

International and domestic mobile satellite regulatory proceedings: A comparison of outcomes and discussion of implications 19 p2644 N88-25690
International and domestic regulator issues facing the Canadian MSAT system 19 p2644 N88-25692
Timing regulations to prevent stratospheric-ozone depletion
[R-3495-JMO/RC] 19 p2690 N88-25987
New CCIR report on SETI 22 p3067 N88-28204
The OFP (Operational Flight Program) update cycle needs you
[AD-A194910] 24 p3325 N88-29798

REGULATORS
NT AUTOMATIC FREQUENCY CONTROL
NT FLOW REGULATORS
NT FREQUENCY CONTROL
NT PRESSURE REGULATORS
NT SPEED REGULATORS
NT VOLTAGE REGULATORS
A feasibility study in path planning using optimization techniques
[AD-A193030] 21 p2894 N88-27177

REGULATORY MECHANISMS (BIOLOGY)
Daily dynamics of some physiological indicators of man under desert condition 06 p0750 N88-14605
Physicochemical correlates of human adaptation to extreme environments 06 p0750 N88-14607
Neurophysiological analysis of hypothalamic regulation mechanisms of primary sleep and hypobiosis
06 p0751 N88-14611
Distinctive changes in arterial pressure and blood flow in common carotid artery of monkeys flown aboard Cosmos-1514 biosatellite 07 p0892 N88-15404
Biofeedback control of alveolar carbon dioxide tension to eliminate hypocapnia in man in the presence of hypoxia 07 p0892 N88-15405
NASA Workshop on Biological Adaptation
[NASA-TM-89468] 10 p1368 N88-18174
Regulation of calcium metabolism during prolonged antiorthostatic hypokinesia
[NASA-TT-20219] 11 p1521 N88-19085
Dexamethasone regulates glutamine synthetase expression in rat skeletal muscles
[NASA-CR-182935] 18 p2549 N88-25129

REHEATING
U HEATING

REIGNITION
U IGNITION

REINFORCED PLASTICS
NT CARBON FIBER REINFORCED PLASTICS
NT GLASS FIBER REINFORCED PLASTICS
Short fiber reinforced thermoplastic composites for armor applications: Interfacial bonding
[DE88-004007] 10 p1295 N88-17742
Fiber-reinforced plastic composites. Possibilities and limitations of applications as machine-construction materials
[NASA-TT-20159] 15 p2031 N88-22102
Injection compression for short fiber reinforced plastics
[SNIAS-881-430-118] 21 p2922 N88-27344

REINFORCED PLATES
Optimal ribbing of long plate made of composite material 04 p0426 N88-12641
Interaction of ultrasonic waves with composite plates
[AD-A191879] 18 p2478 N88-24702
Plasma joining of metal matrix composites
[AD-A193939] 22 p3051 N88-28100

REINFORCED SHELLS
Solution of geometrically nonlinear problem for reinforced shell of revolution having arbitrary shape
04 p0426 N88-12637
Rational reinforcement of cylindrical shells with variable stiffness frames subjected to external pressure
04 p0426 N88-12638
Experimental studies on the tripping behavior of narrow T-stiffened flat plates subjected to hydrostatic pressure and underwater shock 05 p0592 N88-13613
Monolithic nature of transversely reinforced composites 14 p1885 N88-21267

REINFORCEMENT (PSYCHOLOGY)
Training in time interval discrimination using verbal feedback 12 p1665 N88-19965

REINFORCEMENT (STRUCTURES)
Reinforced flexural elements for TEMP-STRESS Program
[DE87-012961] 01 p0061 N88-10391
Optimal ribbing of long plate made of composite material 04 p0426 N88-12641
Geometrically nonlinear analysis of stiffened panels
06 p0722 N88-14440
Buckling of braced monosymmetric cantilevers: Timoshenko energy approach
[PB87-133849] 06 p0723 N88-14445
The Shock and Vibration Bulletin. Part 4: Structural Dynamics and Modal Test and Analysis
[AD-A186751] 09 p1179 N88-17062
Analysis of reinforced concrete structures under the effects of localized detonations
09 p1179 N88-17064
Reinforced cocnrete arches under blast and shock environments 09 p1180 N88-17065
Woven frameworks for three-dimensional reinforcement 14 p1884 N88-21262
Stiffened titanium panels
[NASA-CASE-LAR-13814-1] 18 p2497 N88-24816
A simple unified method for predicting the deflections of reinforced concrete structures
19 p2679 N88-25930
An assessment of modelling techniques for the finite element analysis of reinforced concrete plate and shell structures
[AD-A192263] 20 p2814 N88-26697
Cold worked reinforcing bars in tensile test under high loading rate and low temperatures
[DE88-752983] 21 p2964 N88-27610

REINFORCEMENT RINGS
Redesign of solid rocket booster/external tank attachment ring for the space transportation system
[NASA-TM-100476] 01 p0017 N88-10101
Structural analysis of the space shuttle solid rocket booster/external tank attach ring
[NASA-TM-100510] 11 p1446 N88-18618

REINFORCING FIBERS
NT BORON FIBERS
NT CARBON FIBERS
Pressure effects on the thermal stability of SiC fibers
[NASA-TM-100146] 01 p0019 N88-10120
Interfacial shear strength of pitch and high strain pan fibers in an epoxy matrix
[AD-A185966] 07 p0826 N88-15011
Short fiber reinforced thermoplastic composites for armor applications: Interfacial bonding
[DE88-004007] 10 p1295 N88-17742
Use of reinforced inorganic cement materials for spark wire and drift chamber wire frames
[NASA-CR-180759] 13 p1746 N88-20438
PNL-1 improved ceramic composites through controlled fiber matrix interaction
[DE88-005660] 13 p1750 N88-20462
Creep behavior of tungsten/niobium and tungsten/niobium-1 percent zirconium composites
17 p2425 N88-24427
Properties of two composite materials made of toughened epoxy resin and high-strain graphite fiber
[NASA-TP-2826] 19 p2609 N88-25480
The two isotropic asymptotes of fiber composites
[AD-A192305] 21 p2904 N88-27231
Theoretical and experimental analysis of the toughening behavior of whisker reinforcement in ceramic matrix composites
[DE88-011841] 21 p2906 N88-27241
Wave propagation and vibration of fibre reinforced laminates
[AD-A194144] 22 p3051 N88-28101
Thermoplastic composite with continuous fibers
[FOA-C-20707-2.6] 22 p3051 N88-28103
Elastic wave dispersion in laminated composite plate
[AD-A192289] 23 p3188 N88-28967
A study of the critical factors controlling the synthesis of ceramic matrix composites from preceramic polymers
[AD-A195405] 24 p3340 N88-29881
Some theoretical considerations of the surface tension of liquid metals for metal matrix composites
[AD-A195999] 24 p3340 N88-29882

REINFORCING MATERIALS
Bibliography of textbooks on fibre reinforced plastics (212 books)
[PB87-146080] 07 p0827 N88-15017
Fabrication and materials evaluation of high performance aligned ceramic fibre reinforced glass matrix composite
[AERE-R-12517] 10 p1294 N88-17736
Viscoelastic behavior of a polyetheretherketone (PEEK) composite
[AD-A189545] 13 p1734 N88-20368
Fracture criteria for discontinuously reinforced metal matrix composites
[NASA-CR-182665] 13 p1782 N88-20662
Strength and failure analysis of composite laminate containing a circular hole with reinforcement
[AD-A189629] 14 p1884 N88-21260
Woven frameworks for three-dimensional reinforcement 14 p1884 N88-21262
Monolithic nature of transversely reinforced composites 14 p1885 N88-21267
The two isotropic asymptotes of fiber composites
[AD-A192305] 21 p2904 N88-27231

REISSNER THEORY
Stress strain fields at crack tip and stress intensity factors in Reissner's plate
[PB87-144945] 08 p0994 N88-16014

RELATIVISTIC EFFECTS
Relativistic stochastic mechanics
[PREPRINT-543] 06 p0790 N88-14842
Relativistic corrections for one- and two-photon matrix elements of weakly-bound systems
[NOTA-INTERNA-884] 07 p0929 N88-15645
A note on Fujikawa's method of determining the critical dimension of the relativistic string
[NIKHEF-H/87-5] 08 p1092 N88-16571
Considerations of acceleration effects in relativistic kinematics 09 p1260 N88-17553
Can the causal pathologies of Goedel-type universes be avoided in higher-derivative gravity
[DE88-700185] 11 p1568 N88-19387
Relativistic jet models for the BL Lacertae object Mrk 421 during three epochs of observation
[NASA-TM-89727] 13 p1853 N88-21090
Topics in curved and flat space electromagnetism
13 p1854 N88-21100

RELATIVISTIC ELECTRON BEAMS
A simple self-breaking 2 MV gas switch
[DE87-014346] 02 p0166 N88-11047
Laser induced fluorescent study of relativistic electron beams
[AD-A184456] 04 p0447 N88-12774
Relativistic electron precipitations in a pulsating aurora
04 p0468 N88-12894
Variable collision frequency effects on hose and sausage instabilities in relativistic electron beams
[AD-A184206] 04 p0490 N88-13021
Coherent emission from relativistic beam-plasma interactions 04 p0493 N88-13039
Modulation of an intense beam by an external microwave source: Theory and simulation
[AD-A185683] 07 p0848 N88-15145
Relativistic plasma concentration measuring by Bremsstrahlung
[DE88-700560] 07 p0936 N88-15685
Wave functions for bound states of relativistic electrons in a crystal at electron movement along crystallographic planes
[DE88-700563] 07 p0939 N88-15708
Collective acceleration of electrons and ions in a high relativistic electron beam
[DE88-005261] 13 p1838 N88-20998
Design of electron beam accelerator for microwave application
[DE88-005252] 13 p1838 N88-20999
XeF excimer laser pumped by high-intensity relativistic electron beam 14 p1901 N88-21355
Three-wave parametric resonance in plasma of relativistic electron flux 14 p1972 N88-21772
High pressure operation of beam diodes for generating relativistic electron beams 16 p2279 N88-23643
Deep dielectric charging effects due to high energy electrons in earth's outer magnetosphere
[AD-A192154] 18 p2541 N88-25083
SARLAC: A relativistic electron beam code
[AD-A193134] 21 p2932 N88-27411
Propagation of charged particle beams in the atmosphere
[AD-A193185] 21 p3014 N88-27887
Millimeter wave generation by relativistic electron beams
[AD-A195683] 24 p3362 N88-30016
Research on a two-stage free electron laser oscillator
[AD-A195991] 24 p3377 N88-30115

RELATIVISTIC PARTICLES
NT RELATIVISTIC ELECTRON BEAMS
Analysis of relativistic nucleus-nucleus interactions in emulsion chambers 07 p0926 N88-15624
On a possibility of ion acceleration up to high energies in a high-current electron beam
[DE88-700532] 07 p0931 N88-15657
Relativistic Calogero-Moser systems and solutions
[CWI-PM-R8702] 08 p1092 N88-16570
Single nucleon coincidence cross sections in a relativistic mean field theory
[CEBAF-PR-87-016] 11 p1546 N88-19243
Action-angle maps and scattering theory for some finite-dimensional integrable systems. The pure solution case
[CWI-PM-R8704] 13 p1831 N88-20955
The multistring model VENUS for ultrarelativistic heavy ion collisions
[DE88-007666] 18 p2573 N88-25284
Experiments with high energy nuclear beams at Brookhaven: From AGS to RHIC (Relativistic Heavy Ion Collider)
[DE88-007042] 18 p2574 N88-25287

Experiments on insulation of relativistic electron flows in oblique and tapered magnetic fields
[DE88-007199] 19 p2724 N88-26176
Passage of relativistic magnetic dipole moments through magnetic fields
[DE88-702640] 23 p3295 N88-29624

RELATIVISTIC PLASMAS
A relativistic Monte Carlo binary collision model for use in plasma particle simulation codes
[DE87-013287] 02 p0237 N88-11494
Plasma wave radiative damping of a new type in a relativistic one-dimensional plasma
[DE88-701191] 15 p2135 N88-22739
ECRH current drive in tokamak plasmas
[IPPJ-864] 19 p2729 N88-26209

RELATIVISTIC THEORY
Superluminal velocities within relativity theory
[ETN-87-90958] 02 p0247 N88-11563
Nonlinear, relativistic Langmuir waves in astrophysical magnetospheres
[NASA-CR-182422] 08 p1024 N88-16197
Relativistic electromagnetic waves in an electron-ion plasma
[NASA-CR-182421] 08 p1085 N88-16532
Relativistic Calogero-Moser systems and solutions
[CWI-PM-R8702] 08 p1092 N88-16570
Relativistic theory of gravitation and new concepts about space-time 09 p1240 N88-17431
Hamiltonian approach to relativistic theory of gravity and to general relativity theory
[DE88-700404] 10 p1422 N88-18492
Semileptonic weak interactions in nuclei: A relativistic analysis
[CEBAF-PR-87-024] 11 p1547 N88-19249
Hamiltonian formalism in the model of the relativistic string with rigidity
[DE88-701503] 15 p2147 N88-22815
Bogolyubov transformation in relativistic theory of gravitation
[DE88-701592] 16 p2232 N88-23329
Relativistic theory of gravitation and criticism of General Relativity Theory (GRT)
[DE88-701304] 16 p2284 N88-23673
On the self-trapping of an electromagnetic wave in magnetized plasma
[DE88-701872] 20 p2858 N88-26974
Relativistic theory of the Lamb shift based on self energy
[DE88-702658] 23 p3295 N88-29626

RELATIVISTIC VELOCITY
Superluminal velocities within relativity theory
[ETN-87-90958] 02 p0247 N88-11563
On a possibility of ion acceleration up to high energies in a high-current electron beam
[DE88-700532] 07 p0931 N88-15657
Collective acceleration of electrons and ions in a high relativistic electron beam
[DE88-005261] 13 p1838 N88-20998
The multistring model VENUS for ultrarelativistic heavy ion collisions
[DE88-007666] 18 p2573 N88-25284
A study of mechanisms producing astrophysical jets
[AD-A194100] 23 p3300 N88-29649

RELATIVITY
Volume functions in the general theory of relativity
[ETN-87-90408] 01 p0069 N88-10582
On the theory of the Michelson-Morley experiment in the Earth's gravitational field
[DE87-703077] 02 p0198 N88-11233
Superluminal velocities within relativity theory
[ETN-87-90958] 02 p0247 N88-11563
New notions about space-time and gravitation
[DE87-703259] 03 p0383 N88-12406
Analysis of absolute space-time Lorentz theories
[DE87-703371] 04 p0500 N88-13076
Homogeneous space-time of Goedel type in higher-derivate gravity
[DE87-703690] 04 p0500 N88-13077
Gravity from symmetry breakdown of a gauge affine theory
[DE88-001671] 04 p0500 N88-13079
Cosmological applications of singular hypersurfaces in general relativity 04 p0521 N88-13202
Relativistic stellar pulsations 06 p0801 N88-14902
A simplified model of elementary particles
[NOTA-INTERNA-890] 07 p0930 N88-15647
Criterion of singularity in general theory of relativity
09 p1240 N88-17430
On higher derivative gravity
[DE88-700619] 10 p1354 N88-18090
Hamiltonian approach to relativistic theory of gravity and to general relativity theory
[DE88-700404] 10 p1422 N88-18492
Antimatter: Its history and its properties
[DE88-004306] 10 p1423 N88-18498
Velocity reversal and the arrows of time
[DE88-004237] 10 p1429 N88-18536
Notes on a class of homogeneous space-times
[DE88-700138] 11 p1562 N88-19353
Experimental analysis of absolute space-time Lorentz theories
[DE88-700140] 11 p1563 N88-19355
Seventy years of the general theory of relativity
[DE88-700764] 11 p1563 N88-19356
Relative chaos in stellar systems
[DE88-700148] 12 p1710 N88-20234
Topics in curved and flat space electromagnetism
13 p1854 N88-21100
Galilei relativity principle in classical electrodynamics
[DE87-703203] 14 p1904 N88-21376
Special relativity theory (one-dimensional case) without the postulate on the equality of directions
[DE88-701366] 16 p2284 N88-23674
From general relativity to the theory of superstrings
18 p2587 N88-25369
Dissipative relativistic radiation hydrodynamics
[DE88-702092] 19 p2665 N88-25846
Deviation equation as an equation of motion
[DE88-702134] 19 p2722 N88-26161
General relativity invariance and string field theory
[DE88-702045] 19 p2737 N88-26252
Transcending Newton's legacy
[DE88-010764] 19 p2738 N88-26254
On microphysical principles of thermofluid dynamics
[ETN-88-92095] 20 p2801 N88-26620
Theory of relativity and super-light-speeds-I: Kinematical part
[DE88-701832] 20 p2880 N88-27100
Combining relativity and quantum mechanics: Schroedinger's interpretation of psi
[DE88-701899] 20 p2880 N88-27102
Gravitation electromagnetic theory
22 p3158 N88-28790
On the GKP and BS constructions of C-boundary
[DE88-702643] 22 p3159 N88-28799
Time travel in the homogeneous Som-Raychaudhuri universe
[DE88-702220] 23 p3295 N88-29622
On neutrino fields in Einstein-Cartan theory
[MATH-REPT-208] 23 p3295 N88-29629

RELAXATION (MECHANICS)
NT SPIN-LATTICE RELAXATION
NT STRESS RELAXATION
Pure dephasing of a vibrational adbond
[AD-A185222] 05 p0609 N88-13740
Structure-property relationships in thermoplastic elastomers 4. Dynamic mechanical relaxations in poly(dioxolane), poly(butyltrioxocane) and poly(propylene oxide) polyurethanes
[AD-A186278] 07 p0836 N88-15073
Structural relaxation and mechanical properties of amorphous Fe-Zr alloys 07 p0840 N88-15094
Structural relaxation in strained-layer heterostructures
[DE88-002326] 07 p0868 N88-15264
Lattice relaxation of the DX centers in Ga/sub 1-x/Al/sub x/As and of the pressure-induced deep donors in GaAs
[DE88-005452] 13 p1848 N88-21061

RELAXATION METHOD (MATHEMATICS)
Theoretical and practical aspects of multigrid methods in boundary element calculations
[NLR-MP-85021-U] 03 p0370 N88-12328
An application of a gradient relaxation method to noisy infrared images
[AD-A184666] 03 p0377 N88-12371
A note on the use of symmetric line Gauss-Seidel for the steady upwind differenced Euler equations
[AD-A185223] 05 p0580 N88-13540
Matching segments from a map and an aerial image using relaxation techniques
[SNIAS-872-422-103] 05 p0620 N88-13809
Upwind relaxation algorithms for Euler/Navier-Stokes equations 07 p0810 N88-14931
Choice of implicit and explicit operators for the upwind differencing method
[NASA-TM-100857] 14 p1964 N88-21718
Relaxation scheme for compressible flows
19 p2640 N88-25663
Numerical integration of Navier-Stokes equations by application of multigrid concept
[ETN-88-92365] 21 p2949 N88-27513
Relaxed heaps: An alternative to fibonacci heaps
[AD-A194030] 23 p3272 N88-29470

RELAXATION TIME
Ion-matrix coupling in polymer electrolytes from relaxation time studies
[AD-A184632] 03 p0293 N88-11841
Theoretical studies of Resonance Enhanced Stimulated Raman Scattering (RESRS) of frequency-doubled Alexandrite laser wavelength in cesium vapor
[NASA-CR-182870] 15 p2036 N88-22133

RELEASING
Hydrogen retention and release from uranium dioxide
[DE88-002042] 07 p0829 N88-15030
Deployable booms and antennas on AMPTE-IRM
14 p1874 N88-21198
Modification and development of the external tank hydrogen vent umbilical system for the space shuttle vehicle 14 p1928 N88-21496
A plasma wave instrument on the AMPTE/IRM (Active Magnetospheric Particle Tracing Explorers/Ion Release Module) spacecraft
[AD-A191216] 16 p2233 N88-23336
Design, development, fabrication and launch support for a high altitude release of neodymium vapor
[AD-A194196] 22 p3118 N88-28527
Effects of tectonic release on broadband regional distance bodywaves
[AD-A194247] 22 p3119 N88-28529

RELIABILITY
NT AIRCRAFT RELIABILITY
NT CIRCUIT RELIABILITY
NT COMPONENT RELIABILITY
NT SPACECRAFT RELIABILITY
NT STRUCTURAL RELIABILITY
Wire interconnection reliability and moisture levels in hybrid microcircuits with epoxy-attached components
[DE87-012987] 01 p0039 N88-10247
Computing systems dependability and fault tolerance: Basic concepts and terminology
02 p0127 N88-10797
Needs assessment for nondestructive testing and materials characterization for improved reliability in structural ceramics for heat engines
[DE88-000040] 02 p0153 N88-10957
Software reliability models for fault-tolerant avionics computers and related topics
[NASA-CR-181440] 02 p0220 N88-11382
Electronic system reliability and effectiveness
[AD-A184522] 03 p0311 N88-11961
Programmable Logic Arrays (PLA's) design for testability
[PB87-102935] 04 p0438 N88-12718
Reliability of Li/SO2 cells for long-life applications
[DE88-001360] 04 p0440 N88-12735
Software reliability perspectives
[NASA-CR-181523] 04 p0479 N88-12952
Development of an interface for an ultrareliable fault-tolerant control system and an electronic servo-control unit
[NASA-TM-88236] 05 p0553 N88-13367
Electromagnetics and electrothermal approach to evaluate failures in microelectronic devices caused by electrostatic discharges: Stochastical aspects of the device reliability
[AD-A184906] 05 p0577 N88-13522
Composite reliability enhancement via preloading
[AD-A185938] 07 p0826 N88-15010
Reliability and survivability of communication networks
[AD-A186248] 07 p0842 N88-15109
How errors in component reliability affect system reliability
[AD-A186264] 07 p0865 N88-15249
Supportability in aircraft systems through technology and acquisition strategy applications
[AD-A186465] 08 p0949 N88-15759
Reliability issues in distributed operating systems
[PB88-100870] 08 p0993 N88-16009
Experimental Radio Data System (RDS): A survey of reception reliability in the UK
[BBC-RD-1987/17] 09 p1155 N88-16922
Analysis of the reliability of Royal Australian Air force non-destructive inspection
[AD-A186979] 09 p1177 N88-17049
Methods for evaluating the quality and reliability of aerodynamic software programs
[PB87-169793] 09 p1219 N88-17314
Johnson noise thermometer for high radiation and high temperature environments
[DE88-003770] 10 p1323 N88-17911
Analysis and application of the constant tensile load test for polyethylene gas pipe materials
[DE88-002868] 10 p1345 N88-18037
Improving battery reliability by using regression trees
[DE88-004539] 11 p1481 N88-18841
Specialized instrumentation for computational fluid dynamics research
[AD-A188160] 11 p1482 N88-18849
A procedure for estimating the crystal densities of organic explosives
[AD-A189023] 12 p1613 N88-19646
Reliability analyses of a surface mounted package using finite element simulation
[AD-A189488] 12 p1624 N88-19717
Statistical aspects of reliability, maintainability and availability
[AD-A188491] 12 p1634 N88-19763

Estimating system and component reliabilities under partial information on cause of failure
[AD-A189107] 13 p1780 N88-20653

Stochastic comparisons of order statistics, with applications in reliability
[AD-A189408] 13 p1829 N88-20938

Advanced capacitor development
[AD-A189985] 15 p2059 N88-22276

Present, future of automotive hybrid IC applications discussed 16 p2185 N88-23024

Hybrid PV HgCdTe IR detectors technology reliability and failure program: Environmental stress testing plan
[AD-A191165] 16 p2211 N88-23195

Laser comparison study of Nd:BEL and Nd:YAG
[AD-A191084] 16 p2213 N88-23205

Computerized life and reliability modelling for turboprop transmissions
[NASA-TM-100918] 16 p2215 N88-23220

Studies in reliability and inference
[AD-A191309] 16 p2217 N88-23223

Relating design and environmental variables to reliability 17 p2418 N88-24383

Preliminary analysis of helium generation and its effects on the SP-100 system performance
17 p2422 N88-24406

Johnson noise thermometer for high-radiation and high-temperature environments
17 p2434 N88-24480

Descriptions of HF and VHF Loran-C buoys and evaluations as potential datum marker buoys
[AD-A192069] 18 p2462 N88-24618

An extended life and performance test of a low-power arcjet
[NASA-TM-100942] 18 p2476 N88-24687

Sensitivity analysis for the system reliability function
[AD-A191646] 18 p2525 N88-24979

Pyrotechnic system failures: Causes and prevention
[NASA-TM-100633] 20 p2765 N88-26394

An evaluation methodology for dependable multiprocessors
[AD-A192799] 20 p2842 N88-26863

Probabilistic anisotropic failure criteria for composite materials
[AD-A193046] 21 p2904 N88-27232

Test and calibration system for monitoring the Advanced Technologies Testing Aircraft System (ATTAS) data acquisition system 22 p3037 N88-28029

The impact of increased aircraft reliability on maintenance facility design
[AD-A194395] 22 p3042 N88-28057

Another approach for forecasting forecast skill
22 p3126 N88-28580

Estimating reliability with discrete growth models
[AD-A193845] 22 p3143 N88-28692

Use of Markov probability and reliability model generation methods in the analysis of reliability of a fault tolerant hardware and software based system with flexible repair policies
[PNR90467] 22 p3145 N88-28706

Effect of fiber diameter on the reliability of composites - automated laser diffraction implementation
[AD-A193524] 23 p3188 N88-28972

Reliability assessment of Surface Mount Technology (SMT)
[AD-A193759] 23 p3208 N88-29089

Remotely Operated Vehicle (ROV) reliability study, phase 1
[AD-A194367] 23 p3222 N88-29177

Analysis of the effect of faulty spares on the performance of diagnostic algorithms in reliable systems
[AD-A193526] 23 p3223 N88-29186

Reliability and Maintainability (R and M)
[AD-A193857] 23 p3224 N88-29187

Literature review: Validity and potential usefulness of psychomotor ability tests for personnel selection and classification
[AD-A193558] 23 p3241 N88-29287

Reliability and construct validity of reaction time, inspection time and machine-paced tests of cognitive speed
[AD-A193779] 23 p3241 N88-29289

A minitab macro for the Kaplan-Meier product limit estimator and the Tarone-Ware class of tests
[AD-A194298] 23 p3248 N88-29331

An expert system for reliability modeling
23 p3252 N88-29355

Exact lower confidence limits for the reliability of k of n systems for zero failures and nonconservativeness of the maximus method
[AD-A194299] 23 p3274 N88-29485

The cost and performance implications of reliability improvements in the F-16A/B
[AD-A195096] 24 p3324 N88-29796

A reliability-based program for predicting the service life of organic coating systems 24 p3355 N88-29971

RELIABILITY ANALYSIS

Wet deposition and snowpack monitoring operations and quality assurance manual
[PB87-212817] 01 p0064 N88-10413

The reliability of numerical solutions of ordinary differential equations, obtained by implicit calculation schemes
[PTB-W-30] 01 p0085 N88-10549

Application of fracture mechanics theory in the reliability analysis of structural ceramics in multiaxial loading
03 p0335 N88-12113

Investigation of reliability of strength values measured on CFRP test bars by statistical methods. Part 1: Probability distributions for strength analysis
[ESA-TT-1036] 03 p0336 N88-12115

A reliability concept for optimizing aircraft design
04 p0423 N88-12622

Applications of the hybrid automated reliability predictor
[NASA-TP-2760] 04 p0475 N88-12928

On the next generation of reliability analysis tools
[NASA-CR-178380] 04 p0487 N88-13000

Space station software reliability analysis based on failures observed during testing at the multisystem integration facility 06 p0798 N88-14884

An independent evaluation of the CH-46 Safety Reliability and Maintainability Program (SR and M)
[AD-A186310] 07 p0817 N88-14971

Estimating system reliability: Monte Carlo methods, sensitivity and errors in input parameters
[AD-A186182] 07 p0865 N88-15248

Fault tree reliability analysis of the Naval Postgraduate School mini-satellite (ORION)
[AD-A186283] 07 p0866 N88-15250

Discrete reliability growth models using failure discounting
[AD-A186380] 07 p0866 N88-15252

Reliability modelling for fault-tolerant parallel processor
[AD-A185867] 07 p0900 N88-15451

Causes and distribution of failures in semiconductor lasers (a review) 07 p0919 N88-15581

Integrated analysis and applications
08 p0954 N88-15789

Rotor dynamic behavior of centrifugal pumps
08 p0975 N88-15898

SURE reliability analysis: Program and mathematics
[NASA-TP-2764] 09 p1231 N88-17380

An anlysis of the reliability of tree-structured interconnection networks 10 p1378 N88-18228

Derivation of strength factors related to the coordination of the strength of transmission line components --- electric power lines
[S/T-REPT-VOL-5-NO-2] 11 p1500 N88-18959

Reliability based analysis of contact problems
[NASA-CR-182117] 11 p1503 N88-18975

Reliability analyses of a surface mounted package using finite element simulation
[AD-A189488] 12 p1624 N88-19717

An experiment in software reliability: Additional analyses using data from automated replications
[NASA-CR-178395] 12 p1676 N88-20017

A computer code for the solution of large scale network reliability analysis problems
[AD-A188455] 12 p1680 N88-20042

A fault injection experiment using the AIRLAB Diagnostic Emulation Facility
[NASA-CR-178390] 13 p1823 N88-20895

CARE 3 User's Workshop
[NASA-CP-10011] 14 p1954 N88-21646

The 1988 failure rate screening data for fusion reliability and risk analysis
[DE88-006798] 14 p1984 N88-21837

Monte Carlo reliability analysis
[AD-A189972] 15 p2074 N88-22366

Reliability analysis within a Computer Aided Engineering (CAE) infrastructure
[NLR-MP-86059-U] 15 p2074 N88-22369

Whisker-reinforced ceramic composites for heat engine components 15 p2082 N88-22410

Methodology for software reliability prediction, volume 1
[AD-A190018] 15 p2110 N88-22571

Methodology for software reliability prediction, volume 3
[AD-A190019] 15 p2110 N88-22572

Analysis and testing of the SURE program
[NASA-TP-2817] 15 p2123 N88-22653

Digital avionics design and reliability analyzer
[NASA-CR-181641] 16 p2254 N88-23472

The PAWS and STEM reliability analysis programs
[NASA-TM-100572] 16 p2262 N88-23526

Automatically generated acceptance test: A software reliability experiment
[NASA-CR-181667] 17 p2347 N88-23984

Reliability of stochastically forced systems (extended version)
[CWI-AM-R8801] 18 p2526 N88-24985

Semi-Markov adjunction to the Computer-Aided Markov Evaluator (CAME)
[NASA-CR-181645] 19 p2678 N88-25924

Estimating reliability with discrete growth models
[AD-A193845] 22 p3143 N88-28692

Use of Markov probability and reliability model generation methods in the analysis of reliability of a fault tolerant hardware and software based system with flexible repair policies
[PNR90467] 22 p3145 N88-28706

Approximate evaluation of semi-Markov chain reliability models
[AD-A194669] 23 p3223 N88-29185

Investigations on the modification of structural reliability by substitution of aluminum by carbon fiber reinforced plastics in aircraft construction
[ILR-MITT-195] 24 p3339 N88-29877

RELIABILITY CONTROL

U QUALITY CONTROL

U RELIABILITY ENGINEERING

RELIABILITY ENGINEERING

The application of emulation techniques in the analysis of highly reliable, guidance and control computer systems 02 p0127 N88-10798

Some approaches to the design of high integrity software 02 p0127 N88-10799

Reliability modeling of fault-tolerant computer based systems 02 p0127 N88-10801

Software reliability models for fault-tolerant avionics computers and related topics
[NASA-CR-181440] 02 p0220 N88-11382

Reliability-based optimal structural and mechanical design 03 p0335 N88-12109

Reliability of voting in fault-tolerant software systems for small output spaces
[TR-87-16] 05 p0632 N88-13864

Effectiveness of back-to-back testing
[TR-87-08] 05 p0632 N88-13865

A software reliability model with variable fault exposure coefficient
[REPT-87-029] 06 p0757 N88-14646

Evaluate the application of modal test and analysis processes to structural fault detection in MSFC - STS project elements 07 p0927 N88-15630

Innovating systems and techniques for the diagnosis of materials and industrial plants
[CISE-3856] 08 p0976 N88-15901

Hardware/software reliability study --- space programs
[REPT-65.5686] 09 p1218 N88-17307

Probabilistic and reliability design procedures for flexible airfield pavements: Elastic layered method
[AD-A187533] 11 p1442 N88-18600

Modification, implementation, and evaluation of a remote terminal emulator as a software validation and stress testing tool
[AD-A188833] 12 p1678 N88-20034

Comparative analysis of multistage interconnection networks
[AD-A190436] 15 p2115 N88-22598

Information systems for quality. Experience at the Nerviano Aeritalia plant. Avionic systems and equipment group
[ETN-88-92274] 15 p2148 N88-22821

Incorporating reliability into the design of experimental fusion facilities
[DE88-006767] 16 p2275 N88-23618

Integrated avionics reliability 17 p2294 N88-23723

Advanced LMMHD space power generation concept
17 p2415 N88-24364

The VIPER microprocessor
[RSRE-87014] 22 p3135 N88-28640

Reliable onboard computing for critical space systems
[RR-670-I] 22 p3135 N88-28641

Expert systems for MSFC power systems
23 p3255 N88-29375

Blackboard architectures and their relationship to autonomous space systems 23 p3261 N88-29414

A nonlinear filtering process diagnostic system for the Space Station 23 p3262 N88-29417

Intelligent fault diagnosis and failure management of flight control actuation systems
[NASA-CR-177481] 24 p3323 N88-29790

RELIC RADIATION

Dipole component of relict radiation determined from Relikt experiment data 08 p1002 N88-16070

Nonequilibrium ionization of pregalactic plasma and lessening of relic radiation anisotropy
08 p1002 N88-16071

Measurements of the cosmic background radiation
[NASA-CR-182637] 12 p1712 N88-20248

A map of the cosmic background radiaton at 3 millimeters
[INPE-4529-PRE/1279] 15 p2152 N88-22850

RELIEF MAPS

Study of relief of ore regions using space images (on the example of Eastern Yakutia)
06 p1006 N88-16111

Photogrammetric principles for combining remote sounding and three-dimensional mapping
06 p1012 N88-16135

Naval weapons center active fault map series
[AD-A188425] 12 p1643 N88-19835

Topographic data processing for environmental planning 18 p2534 N88-25032

REMAGNETIZATION

U MAGNETIZATION

REMELTING

U MELTING

REMOTE CONSOLES

Modification, implementation, and evaluation of a remote terminal emulator as a software validation and stress testing tool
[AD-A188833] 12 p1678 N88-20034

REMOTE CONTROL

NT RADIO CONTROL

Robotic sensors and actuators for a service manipulator system. Volume 1: Executive summary
[MATRA-EPT/DT/VT187/120]
01 p0053 N88-10341

Robotic sensors and actuators for a service manipulator system. Volume 2: Service Manipulator System (SMS) handbook
[MATRA-EPT/DT/VT187/227]
01 p0053 N88-10342

Robotic sensors and actuators for a service manipulator system. Volume 3, phase A report and program plan
[MATRA-EPT/DT/VT187/228]
01 p0054 N88-10343

Technology survey for a robot which will investigate the condition of underground pipe
[PB87-209979] 01 p0055 N88-10351

Teleoperation and control study --- orbital servicing
[BAE-TP-8268] 01 p0076 N88-10489

An autonomous, closed-loop pointing system for use with satellite optics
[DE87-012011] 02 p0235 N88-11483

Low-cost teleoperator-controlled vehicle for damage assessment and dose measurement
[DE88-000713] 04 p0451 N88-12794

Experiences in teleoperation of land vehicles
[DE88-000429] 06 p0711 N88-14355

Experiences in teleoperation of land vehicles
[DE88-001695] 06 p0711 N88-14357

Packet telecommand. System performance assessment study --- onboard data handling
[PTC/TNOT/0015/SAAB] 07 p0843 N88-15113

Evaluation of high-voltage, high-power, solid-state remote power controllers for amps
07 p0924 N88-15612

Software simulation of time delay in teleoperation
08 p1056 N88-16371

Promising concepts for ground-to-orbit experiment teleoperation --- Columbus 12 p1590 N88-19518

Teleoperation for a Spacelab technology experiment
12 p1590 N88-19521

Utilization of robotics and teleoperation for future in-orbit operations 12 p1591 N88-19527

Human interfaces in remote driving
[DE88-006843] 14 p1953 N88-21643

Test results of high-voltage, high-power, solid-state remote power controllers
[NASA-TM-100322] 16 p2194 N88-23085

Teleoperator human factors study
[NASA-CR-178930] 17 p2382 N88-24162

A control technique for improved robot performance
17 p2391 N88-24212

Computer aided remote control: A general concept for intervention in the nuclear, underwater, and space domains 19 p2699 N88-26046

Airborne remote operated device
[DE88-010324] 21 p2895 N88-27188

Development of remote control welding system of large structures
[PB87-219653] 22 p3083 N88-28309

Remotely Operated Vehicle (ROV) reliability study, phase 1
[AD-A194367] 23 p3222 N88-29177

REMOTE HANDLING

A hydrogen/nickel oxide battery for remote applications
[DE87-009048] 04 p0464 N88-12872

Experiences in teleoperation of land vehicles
[DE88-001695] 06 p0711 N88-14357

Heuristic control of the Utah/MIT dextrous robot hand
06 p0793 N88-14858

Dynamics, control and sensor issues pertinent to robotic hands for the EVA retriever system
06 p0796 N88-14876

Operational experience and design recommendations for teleoperated flight hardware
14 p1927 N88-21489

Space spider crane
[NASA-CASE-LAR-13411-1-SB]
17 p2312 N88-23826

Design study. Manipulator systems for model handling in European transonic wind tunnels
[ETN-88-91944] 18 p2468 N88-24651

Mobile remote manipulator system for a tetrahedral truss
[NASA-CASE-MSC-20985-1] 20 p2765 N88-26398

REMOTE MANIPULATOR SYSTEM

Robotic sensors and actuators for a service manipulator system. Volume 1: Executive summary
[MATRA-EPT/DT/VT187/120]
01 p0053 N88-10341

Robotic sensors and actuators for a service manipulator system. Volume 2: Service Manipulator System (SMS) handbook
[MATRA-EPT/DT/VT187/227]
01 p0053 N88-10342

Teleoperation and control study --- orbital servicing
[BAE-TP-8268] 01 p0076 N88-10489

Evaluation of vision systems for teleoperated land vehicles
[DE87-013066] 03 p0333 N88-12100

Telerobotic controller development
08 p1056 N88-16370

Utilization of SMS and EVA for the servicing of European Space Station 12 p1587 N88-19500

Robotic intelligence issues for space manipulator monitoring, control programming
12 p1588 N88-19504

On a knowledge based assisted system for highly autonomous control of experiment-manipulators in the Man-Tended Free Flyer 12 p1588 N88-19505

The Hermes robot arm, its design and verification
12 p1588 N88-19508

Remote manipulation in orbital construction, servicing and repair missions: Is one arm enough? A comparative evaluation of the performance features of robots with one or more arms 12 p1588 N88-19509

Computational aspects of robotic experiment manipulation in a microgravity environment
12 p1589 N88-19512

Covariant control of bilateral servos for in-orbit manipulation 12 p1590 N88-19520

Teleoperation for a Spacelab technology experiment
12 p1590 N88-19521

The Hermes manipulation system (HERA) simulation facility development 12 p1591 N88-19524

A comparative survey of mathematical models for dynamic simulation of in-orbit manipulation operations
12 p1592 N88-19533

Dynamics modeling, simulation, and control of a spacecraft/manipulator system
12 p1592 N88-19534

A teleoperated manipulator system concept for unmanned platforms --- Columbus
12 p1593 N88-19537

Multi-axis control of telemanipulators
12 p1593 N88-19539

System and concept design of the SSRMS latching end effector --- Space Station 14 p1875 N88-21204

Operational experience and design recommendations for teleoperated flight hardware
14 p1927 N88-21489

Robotic joint experiments under ultravacuum
14 p1927 N88-21490

Design study. Manipulator systems for model handling in European transonic wind tunnels
[ETN-88-91944] 18 p2468 N88-24651

Dynamics of a flexible orbiting platform with MRMS
[ISSN-0265-6808] 18 p2473 N88-24673

Remote servicing of space systems
23 p3260 N88-29409

A teleoperated robotic manipulator system for materials processing experiment servicing
23 p3260 N88-29410

Study of software requirements and artificial intelligence techniques for robotics
[TL-3333] 24 p3422 N88-30365

REMOTE REGIONS

NT ANTARCTIC REGIONS

NT ARCTIC REGIONS

Evaluation of the Shasta Waterless System as a remote site sanitation facility
[AD-A186000] 07 p0898 N88-15442

REMOTE SENSING

Study of Earth from space and strengthening of economy 01 p0010 N88-10055

Study on propagation and inverse scattering --- sea studies
[ESA-CR(P)-2394] 01 p0063 N88-10405

Study on the suitability of a European data relay satellite to support a system of remote sensing satellites
[ESA-CR(P)-2400] 01 p0063 N88-10406

Remote Sensing-Arid Lands Workshop, Page, Arizona, June 10-12, 1986
[DE87-012368] 01 p0064 N88-10412

Remote sensing with LANDSAT 5 Thematic Mapper (TM) and its application to various planning levels: A case study from the Wuerzburg area, West Germany
[DFVLR-FB-86-62] 01 p0065 N88-10421

Remote sensing of environmental pollution
[DFVLR-MITT-87-04] 01 p0067 N88-10429

Fiber optic engineering sensor system. Preliminary program management plan, phase 3 revision
[AD-A183663] 01 p0093 N88-10605

Correlation between aircraft MSS and LIDAR remotely sensed data on a forested wetland in South Carolina
[NASA-TM-89643] 02 p0193 N88-11204

Estimating scattered and absorbed radiation in plant canopies by remote sensing
[NASA-CR-181390] 02 p0193 N88-11205

Airborne lidar experiments at the Savannah River Plant
[NASA-TM-4007] 02 p0194 N88-11209

Horizontal shape matching applied to VAS data --- Visible and Infrared Spin Scan Radiometer Atmospheric Sounder (VAS) 02 p0201 N88-11254

Statistical remote sensing algorithm development: A complementary process to mesoscale numerical models
02 p0206 N88-11292

Evaluation of one-sided nuclear magnetic resonance for remote detection of explosives
[AD-A184490] 03 p0296 N88-11857

Planning for future operational sensors and other priorities
[PB87-220602] 03 p0325 N88-12056

Commercial Opportunities for Remote Sensing with Polar Platforms
[ESA-SP-269] 03 p0339 N88-12131

Legal protection of the Polar Platform's users
03 p0339 N88-12135

Confidentiality of data --- Columbus Polar Platforms
03 p0339 N88-12136

Market potential for commercial remote sensing
03 p0339 N88-12137

An overview of remote sensing users' requirements
03 p0340 N88-12139

MBB-ERNO view of remote sensing commercialization
03 p0340 N88-12140

The CNR/PSN Advanced Microwave Imaging Radiometer (AMIR) --- satellite-borne
03 p0340 N88-12141

X-band SAR for a European remote sensing payload
03 p0340 N88-12142

Evolution of remote sensing utilization in geological mapping and ore exploration: Example in Zimbabwe
03 p0343 N88-12165

Vegetation studies in the national Park of Comoe (Ivory Coast) using SPOT 1 satellite data
03 p0343 N88-12166

A comparative thematic mapping analysis of SPOT data: The Vientiane Plain (Laos) 03 p0343 N88-12168

The distinction between different water masses using optical remote sensing applied to data from the Alboran Sea Experiment 1982
[DFVLR-FB-86-46] 03 p0345 N88-12181

The correspondence of surface climate parameters with satellite and terrain data
[NASA-CR-181515] 03 p0346 N88-12185

A method for remote sensing of precipitable water vapor and liquid in the atmosphere using a 22-ghz radiometer
[AD-A184204] 03 p0354 N88-12232

Remote sensing of planets and cartographic results
[HSBW-HEFT-14] 03 p0389 N88-12444

Calibration of a laser-pumped, thermographic phosphor remote thermometry system
[DE88-000452] 04 p0449 N88-12781

The Portable Instant Display and Analysis Spectrometer (PIDAS) 05 p0611 N88-13756

Effective use of principal component analysis with high resolution remote sensing data to delineate hydrothermal alteration and carbonate rocks 05 p0612 N88-13758

Land cover/use classification of Cairns, Queensland, Australia: A remote sensing study involving the conjunctive use of the airborne imaging spectrometer, the large format camera and the thematic mapper simulator
05 p0612 N88-13759

In-orbit calibration adjustment of the Nimbus-7 SMMR
[NASA-TM-100678] 05 p0614 N88-13773

Study on data compression systems for operational remote sensing --- meteosat imagery
[NLR-TR-86029-L] 05 p0620 N88-13806

A system overview of the Airborne Visible/Infrared Imaging Spectrometer (AVIRIS)
06 p0705 N88-14325

Airborne Visible/Infrared Imaging Spectrometer (AVIRIS) spectrometer design and performance
06 p0706 N88-14327

AVIRIS foreoptics, fiber optics and on-board calibrator
06 p0706 N88-14328

Evaluation of a satellite laser ranging technique using pseudonoise code modulated laser diodes
[NASA-CR-182347] 06 p0708 N88-14343

Uses of airborne laser Chayka-1 for probing water, land surfaces 06 p0725 N88-14461

Remote acoustic sounding of ferromanganese nodules
06 p0727 N88-14471

Application of remote sensing to agricultural field trials
[ISBN-90-6754-089-7] 06 p0729 N88-14483

Remote sensing in mineral exploration
[PB87-138558] 06 p0729 N88-14484

On-site meteorological program guidance for regulatory modeling applications
[PB87-227542] 06 p0731 N88-14498

Wind shear detection. Forward-looking sensor technology
[NASA-CP-10004] 07 p0817 N88-14970

Review of the potential of satellite remote sensing for marine flood protection
[IOS-237] 07 p0870 N88-15280

Remote sensing of the biosphere
[NASA-CR-182382] 07 p0871 N88-15281

From pattern to process: The strategy of the Earth Observing System: Volume 2: EOS Science Steering Committee report
[NASA-TM-89702] 07 p0871 N88-15283

SAR (Synthetic Aperture Radar). Earth observing system. Volume 2F: Instrument panel report
[NASA-TM-89701] 07 p0871 N88-15284

The influence of yellow substances on remote sensing of sea water constituents from space. Volume 1: Summary
[ESA-CR(P)-2443-VOL-1] 07 p0872 N88-15292

The influence of yellow substances on remote sensing of sea water constituents from space. Volume 2: Appendices
[ESA-CR(P)-2443-VOL-2] 07 p0873 N88-15293

Multistep component analysis of correlations
08 p1009 N88-16115

Commercial applications and scientific research requirements for thermal-infrared observations of terrestrial surfaces
[NASA-TM-89704] 08 p1019 N88-16179

Ocean Colour Workshop --- conference
[ESA-SP-1083] 08 p1042 N88-16292

Overview of ESA's activities in ocean colour remote sensing 08 p1042 N88-16294

Remote sensing of ocean colour for studies of biological productivity and biochemical cycles
08 p1042 N88-16296

Technical aspects of future ocean colour remote sensing 08 p1042 N88-16298

Status and prospects of the Joint Research Commitee (JRC) work on the application of ocean colour monitoring from space 08 p1043 N88-16299

Canadian activities and goals in remote sensing of ocean colour and fluorescence from space
08 p1043 N88-16300

Federal Republic of Germany's interests, activities and goals in remote sensing of ocean colour/fluorescence from space 08 p1043 N88-16302

Italian activities in ocean colour remote sensing
08 p1043 N88-16304

National Remote Sensing Program (NRSP) of the Netherlands 08 p1043 N88-16305

The use of chlorophyll fluorescence measurements from space for separating constituents of sea water
08 p1043 N88-16307

The influence of yellow substances on remote sensing of sea-water constituents from space
08 p1044 N88-16308

Remote measurement of aerosol stream velocity with continuous-wave CO2-laser 08 p1079 N88-16506

Trends in research and development in the Netherlands. The influence of national science policy between 1973 and 1986
[B8701588] 08 p1094 N88-16530

Parallel-processing computer systems and their possible applications in the agency 09 p1128 N88-16774

Tethers: An outline of a new concept for Earth observation 09 p1129 N88-16781

Construction of airborne radars for remote sensing
[PB88-113063] 09 p1154 N88-16916

Fundamental aspects of the physics of remote sensing
[ESA-TT-1045] 09 p1185 N88-17100

Report of the Workshop on Space Systems Possibilities for a Global Energy and Water Cycle Experiment
[WCP-137] 09 p1193 N88-17147

Infrared low-level wind shear work
10 p1275 N88-17628

NROSS (Navy Remote Ocean Sensing System). A force multiplier
[AD-A186653] 10 p1346 N88-18045

Space-based remote sensing of the Earth: A report to the Congress
[NASA-TM-89709] 10 p1346 N88-18046

Earth resources: A continuing bibliography with indexes (supplement 56)
[NASA-SP-7041(56)] 10 p1347 N88-18051

Remote sensing of atmospheric crosswinds by utilizing speckle-turbulence interaction and optical heterodyne detection
[AD-A187580] 10 p1347 N88-18052

Evaluation of a temperature remote sensing technique
[AD-A187885] 10 p1347 N88-18053

Analysis of quasi-geostrophic forcing during the AIMCS (Airborne Investigations of Mesoscale Convective Systems) Project. Volume 2: Results for June 14 through July 16, 1984
[PB88-123807] 10 p1354 N88-18092

Coordination: Southeast continental shelf studies
[DE88-003680] 10 p1357 N88-18110

Multisource context classification methods in remote sensing 11 p1504 N88-18985

General determination of Earth surface type and cloud amount using multispectral AVHRR data
[NOAA-TR-NESDIS-39] 11 p1506 N88-18997

Low cost telemetry and telecommand system for remote measurement of magnitude character
[INPE-4273-PRE/1145] 12 p1598 N88-19564

Principal space programs in the area of microwaves
[INPE-4164-PRE/1064] 12 p1618 N88-19677

Report of the participation in the International Training Course: Remote Sensing in Village Forestry
[INPE-4476-NTE/278] 12 p1637 N88-19802

Mapping of the mangroves of the Guanabarra Bay through the utilization of remote sensing techniques
[INPE-3942-TDL/229] 12 p1637 N88-19804

Research in remote sensing of vegetation
[NASA-CR-182663] 12 p1639 N88-19817

Spectrophotometric remote sensing of the diffuse aurora
[AD-A188599] 12 p1643 N88-19837

National Severe Storms Laboratory, fiscal year 1987
[PB88-140108] 12 p1647 N88-19863

Remote sensing of meteorological parameters with the aid of a clear-air Doppler radar
[PB88-142518] 12 p1647 N88-19864

Relationships between remotely-sensed surface properties and subsurface structure in the ocean
[AD-A189317] 12 p1650 N88-19881

Photographic filters
[INPE-4448-RPE/558] 12 p1692 N88-20124

The radar scattering coefficient as a function of forest stand parameters and viewing angle. An empirical study of the Pinus sylvestris L. in the Kootwijk forest (The Netherlands), extended with observations in the Speulder and Spnelder forest (The Netherlands)
[ETN-88-91348] 13 p1760 N88-20527

Remote fiber fluorimetry techniques for pressure measurements
[DE88-004486] 13 p1773 N88-20604

Remote sensing of earth terrain
[NASA-CR-182677] 13 p1790 N88-20711

Determination of Earth rotation by the combination of data from different space geodetic systems
[NASA-CR-181388] 13 p1791 N88-20713

The use of four-photon Raman spectroscopy for the remote sensing of natural objects
[NASA-TT-20257] 13 p1791 N88-20716

Activities and objectives of the Polar Research Board
[DE88-004543] 13 p1797 N88-20747

Summary of along-track data from the Earth radiation budget satellite for several major desert regions
[NASA-RP-1197] 13 p1802 N88-20772

Activities report in aeronautics and astronautics
[ETN-88-91332] 13 p1859 N88-21115

Lidar active remote sensing. Applications to the atmosphere 14 p1936 N88-21547

The role of remote sensing in the study of polar ice sheets 14 p1939 N88-21570

Vegetation mapping using high resolution MSS (multispectral scanner) data: Canopy reflectance and shadow problems encountered and possible solutions
[DE88-004273] 14 p1939 N88-21574

Investigation of European remote sensing user needs in accessing MOS-1 payload
[ESA-CR(P)-2535] 14 p1940 N88-21580

Research relative to angular distribution of snow reflectance/snow cover characterization and microwave emission
[NASA-CR-182733] 14 p1941 N88-21582

Optical properties of Southern Hemisphere aerosols: Report of the joint CSIRO/NASA study
[NASA-CR-179287] 14 p1945 N88-21605

Satellite rainfall retrieval by logistic regression
[NASA-CR-180485] 14 p1946 N88-21607

Activities report in flight and space travel
[ISSN-0070-3966] 14 p2012 N88-22000

Development of remote sensing techniques capable of delineating soils as an aid to soil survey
[NASA-CR-182610] 15 p2089 N88-22452

Orbital remote sensing: An instrument for monitoring urban growth
[INPE-4456-PRE/1267] 15 p2150 N88-22833

A PC-based receiver-decoder for remote sensor monitoring
[DE88-004733] 16 p2192 N88-23075

Users guide to CAESAR
[BCRS-87-04] 16 p2228 N88-23306

Preparation of the operational phase of the European Remote Sensing Satellite ERS-1
[BCRS-87-06] 16 p2228 N88-23307

Study of the plan for a national data center for the European Remote Sensing Satellite ERS-1
[BCRS-87-11] 16 p2228 N88-23309

International commercialization of remote sensing
[BCRS-87-14] 16 p2228 N88-23310

The multiannual National Remote Sensing Program (NRSP)
[BCRS-87-16] 16 p2229 N88-23311

Earth resources: A continuing bibliography with indexes (issue 57)
[NASA-SP-7041(57)] 16 p2229 N88-23314

Use of energy emission for detecting the necessity of irrigation in wheat in field conditions
[INPE-4461-TDL/318] 16 p2229 N88-23315

Detection, monitoring and analysis of some environmental effects of fires in the Amazon region through utilization of NOAA and LANDSAT satellite imagery and aircraft data
[INPE-4503-TDL/326] 16 p2230 N88-23322

Applications of multitemporal compositions obtained from LANDSAT data in the study of urban growth
[INPE-4480-PRE/1246] 16 p2287 N88-23692

Thermal remote anemometer system
[NASA-CASE-LAR-13508-1] 17 p2342 N88-23962

Prospects of satellite wind sensing systems in the years 1995-2000 17 p2350 N88-24004

The geometric workstation, a new approach for geometric corrections of remotely sensed data
17 p2352 N88-24017

A proposal of adaptation of a knowledge-based scene analysis model to some remote sensing problems
17 p2354 N88-24026

Shape detection in remote sensing through graph isomorphism 17 p2354 N88-24028

Satellite remote sensing of turbidity and sediment concentration in Lagoa dos Patos
17 p2355 N88-24032

Practical image analysis using personal computers: The Canadian experience 17 p2356 N88-24037

International cooperation in remote sensing: The ESA experience 17 p2356 N88-24038

ERS-1 data products and services and their value for tropical countries 17 p2357 N88-24040

Estimation of an area cultivated with wheat from LANDSAT data through a two-phase sampling method
17 p2357 N88-24041

Remote sensing techniques in the estimation of the area cultivated with beans, corn, and castor beans in the Irece County (Bahia State) 17 p2358 N88-24045

A proposal of adaptation of a knowledge-based scene analysis model to some remote sensing problems
17 p2362 N88-24068

Terrain classification using SPOT images and the computer system GOP-300
[FOA-C-20677-2.7] 17 p2368 N88-24102

Soviet remote sensing research and technology
[FASAC-TAR-3130] 17 p2369 N88-24108

An update on remote measurement of soil moisture over vegetation using infrared temperature measurements: A FIFE perspective
[NASA-CR-182926] 17 p2370 N88-24109

Review of power requirements for satellite remote sensing systems 17 p2419 N88-24387

The gamma 1 and gamma 3 bands of (16)O3: Line positions and intensities
[NASA-TM-101162] 17 p2445 N88-24541

Reflectance spectroscopy in planetary science: Review and strategy for the future
[NASA-SP-493] 17 p2451 N88-24564

Evaluating evaporation with satellite thermal data
[AD-A192042] 18 p2531 N88-25019

The application of satellites in connection with the environment
[ETN-88-92474] 18 p2532 N88-25020

Information analysis of integral equations in remote sensing of atmospheric aerosols
18 p2532 N88-25022

DMSP-SSM/1 NASA algorithm validation using primarily LANDSAT and secondarily DMSP and/or AVHRR visible and thermal infrared satellite imagery
[NASA-CR-182979] 18 p2532 N88-25024

Aircraft/lidar turbulence comparison
18 p2546 N88-25111

Remote sensing of acoustic properties of shallow water sediments: A review
[AD-A192107] 18 p2570 N88-25267

Activities report of the Division of Optical Technology
[FOA-C-30477-3] 18 p2576 N88-25299

National Meeting on Remote Sensing Applied to Municipal Planning 19 p2661 N88-25939

Suggested hurricane operational scenario for GOES I-M
[NASA-TM-89729] 19 p2692 N88-26002

Remote determination of chlorophyll concentration in the ocean using an optical pulse radar
[NASA-TT-20301] 19 p2694 N88-26014

Overview of space missions and techniques for ocean monitoring 19 p2700 N88-26053

The contribution of space to maritime activities
19 p2700 N88-26055

Sensors in spaceborne oceanography
19 p2700 N88-26056

Contribution of space to marine activities
19 p2700 N88-26057

The role of space borne imaging radars in environmental monitoring: Some shuttle imaging radar results in Asia
[NASA-TM-101175] 20 p2789 N88-26544

Remote sensing and satellite applications to the needs of the gas and pipeline industry
[PB88-202668] 20 p2817 N88-26714

Surface hydrology, sediment transport dynamics and remote sensing of disturbed watersheds in a humid temperate region
[DE88-008719] 20 p2817 N88-26715

Satellite remote sensing of the wet bulb globe temperature heat stress index, phase 2
[AD-A192798] 20 p2818 N88-26717

Review of methods for remote sensing of atmospheric emissions from stationary sources
[PB88-190483] 20 p2821 N88-26739

Remote sensing of temperature profiles. Performance test of PASS
[DE88-753108] 20 p2826 N88-26768

Methods of determining playa surface conditions using remote sensing
[AD-A192663] 21 p2965 N88-27612

Analysis of remotely sensed imagery using digital morphology
[AD-A192738] 21 p2965 N88-27614

Active and passive remote sensing of ice
[AD-A193307] 21 p2966 N88-27617

Remote sensing of wetlands: Applications overview
[DE88-010695] 21 p2966 N88-27618

The detection and interpretation of long-term changes in ozone from space
[NASA-TM-101135] 21 p2971 N88-27650

Computer simulation procedure for designing airborne aerometric monitoring programs
[DE88-011696] 21 p2975 N88-27674

Fiber optic sensing systems using high frequency resonant sensing heads with intensity sensors
[NASA-TM-101318] 22 p3080 N88-28293

SPOT 1 Image Utilization, Assessment, Results
[ISBN-2-85-428188-8] 22 p3089 N88-28346

The contribution of remote sensing to hydrology and hydrogeology 22 p3090 N88-28347

Mapping of streamflow and soil infiltration of a Sahelian catchment area by SPOT image interpretation: The Oursi pond catchment area in Burkino Faso
22 p3090 N88-28348

The use of SPOT images for water resources surveys in the Kasserine Basin (Tunisia)
22 p3090 N88-28349

SPOT image exploitation for glacial mass balance fluctuation monitoring in the French Alps
22 p3090 N88-28350

SPOT on land and lakes in the Hubei Province (China)
22 p3090 N88-28351

Evaluation of SPOT imagery for monitoring irrigated lands 22 p3090 N88-28352

An evaluation of SPOT imagery for wetland monitoring
22 p3091 N88-28353

Comparative study of crop and soil mapping using multitemporal and multispectral SPOT and LANDSAT data 22 p3091 N88-28354

Water resources and agricultural land use investigations in northeastern Gujerat (India) 22 p3091 N88-28355

Study of the forests on the banks of the Gambia and criteria for detecting mortality 22 p3091 N88-28356

Use of SPOT satellite in agrohydrology: Detection of spring water excess in a grassland region
22 p3091 N88-28357

Review of the studies of geography and environment and studies on spectral characteristics of SPOT HRV data 22 p3091 N88-28358

Evaluation of the grassy biomass in the Sahelian zone in the South Tamesna region (Niger): Prospects and limits of use of SPOT data 22 p3092 N88-28359

Changes in species composition of heathland, monitored by means of remote sensing and field mapping: The results of the HEISPOT project 22 p3092 N88-28360

Topography of an Antartic ice stream
22 p3092 N88-28361

Spatial and spectral registration of Javanese landscape units with SPOT 22 p3092 N88-28362

Comparison between the respective contributions of the TM LANDSAT-4 and HRV SPOT-1 data to the land use mapping of Mediterranean coastal zone
22 p3092 N88-28363

Land use systems and rural landscapes in the center of Veracruz State (Mexico): First results
22 p3092 N88-28364

SPOT for earthquake hazard zoning in southern Italy
22 p3093 N88-28365

Discrimination of sand transport rates and environmental consequences in central Egypt from SPOT data
22 p3093 N88-28366

Delineation of ephemeral fluvial networks on low-relief Piedmont surfaces, Plutonium Valley, Nevada, USA
22 p3093 N88-28367

Following the seasonal evolution of a natural environment in a humid tropical region. Preliminary Evaluation of SPOT (PEPS) number 186: Bangui, Central Africa 22 p3093 N88-28368

Application of SPOT to agricultural information systems in temperate regions 22 p3093 N88-28369

Potential use of SPOT satellite data for the national resources inventory 22 p3093 N88-28370

Methodological developments on crop inventories using SPOT and ground surveys 22 p3094 N88-28371

Evaluation of annual crop surfaces and territorial inventory in the Paris basin by combining classic statistical inquiries and SPOT data (Preliminary Evaluation Program for SPOT 127) 22 p3094 N88-28372

Evaluation of automatic texture analysis for increased crop identification accuracy with SPOT data
22 p3094 N88-28373

Application of SPOT multidate data to wheat yield estimation in Beauce (France) 22 p3094 N88-28374

An evaluation of multidate SPOT data for agriculture and land use mapping in the United Kingdom
22 p3094 N88-28375

The suitability of SPOT imagery for monitoring landscape patterns 22 p3094 N88-28376

Characterization, topology, and cartography of grasslands for the development of fodder resources. (Preliminary Evaluation Program for SPOT number 26)
22 p3095 N88-28377

HRV data for the applications on renewable resources in Canada --- SPOT 22 p3095 N88-28378

SPOT-1 HRV data and vegetation amount
22 p3095 N88-28379

Attempt to inventory vines using oblique SPOT images
22 p3095 N88-28380

Analysis of soils using remote sensing information at the scale of the parcel 22 p3095 N88-28381

Comparative variations of spectral signatures in a cultivated area of the Paris Basin (27 May, 26 June, 1 July 1986) 22 p3095 N88-28382

Monitoring of agricultural production in West Africa. The need to integrate different satellite platforms
22 p3096 N88-28383

Use of SPOT imagery for vegetation/biomass mapping, geotechnical mapping, catchment area determination, and settlement location in the Turkana district, northern Kenya 22 p3096 N88-28384

Digital and visual analysis of SPOT and TM data for crop discrimination in southern Brazil
22 p3096 N88-28385

A comparative thematic mapping analysis of SPOT data: The Vientiane Plain (Lao PDR)
22 p3096 N88-28386

Evaluation of SPOT data for crop inventory and monitoring in Sudanian Africa. Example of Bane area (Burkina Faso) 22 p3096 N88-28388

Identification of farming systems in the cotton area of West Burkina Faso from SPOT-1 data
22 p3097 N88-28389

Monitoring Tunisia's steppes with SPOT
22 p3097 N88-28390

Study of savannah formation in the Sudanian zone. Northwest sector of the La Comoe park, Ivory Coast
22 p3097 N88-28391

Pilot study of rice culture in sub-tropical high population density region (Madagascar) with SPOT 1 multispectral data 22 p3097 N88-28392

Using SPOT HRV data to update the distribution of the paddy field in Taiwan 22 p3097 N88-28393

Agro-ecological mapping from SPOT 1 data in southern Thailand: New questions for an analysis of the farming-systems 22 p3097 N88-28394

SPOT applications on Columbia's coffee zone
22 p3097 N88-28395

Use of SPOT data in preliminary steps of road project studies especially suited for developing countries
22 p3098 N88-28396

SPOT imagery for detecting residential expansion on the rural-urban fringe of Toronto, Canada
22 p3098 N88-28397

Spread of large tropical conurbations
22 p3098 N88-28398

Utilization of remote sensing for the observation of urban populations. Ongoing research in Quito (Ecuador)
22 p3098 N88-28399

Integration of SPOT data into a geocoded information system 22 p3098 N88-28400

Utilizing SPOT data for seismic shot-line mapping and environmental monitoring in oil and gas exploration
22 p3098 N88-28401

Preliminary comparative analysis of LANDSAT and SPOT data for the study of the sanding phenomenon: Zaafrane region (Algeria) 22 p3099 N88-28402

An evaluation of the applicability of SPOT stereoscopic imagery to the Canada Land Use Monitoring Program (CLUMP) 22 p3099 N88-28403

Topographic suppression and advances in classification for land cover mapping using SPOT-1 HRV imagery
22 p3099 N88-28404

Monitoring Moneragala (Sri Lanka) with SPOT imagery
22 p3099 N88-28405

Monitoring urban land cover changes at the urban fringe from SPOT HRV imagery in south-east England
22 p3099 N88-28406

Thematic mapping of central Java (Indonesia)
22 p3100 N88-28412

Utilization of SPOT-1 multispectral data for mapping land cover and phytohygiene monitoring in the central zone of the Mercantour National Park (France)
22 p3100 N88-28413

Applications of SPOT data for urban real estate investment information systems
22 p3101 N88-28414

Mapping and urban multi-experimental assessment of SPOT: Urban results 22 p3101 N88-28415

SPOT-1 over New Zealand: Analysis of SPOT imagery for land use investigations 22 p3101 N88-28416

Comparison of SPOT, LANDSAT TM and combined data for urban studies 22 p3101 N88-28417

Utilization of SPOT multispectral data for urban planning 22 p3101 N88-28418

First results of international investigations of the applications of SPOT-1 data to geologic problems, mineral and energy exploration 22 p3101 N88-28419

Rate of slip on the Altin Dagh Fault (North Tibet, China) 22 p3102 N88-28420

Karst and submarine fresh water discharge in the Antalya area, southern Turkey 22 p3102 N88-28421

Results of the Geosat program to evaluate SPOT data for petroleum and mineral exploration
22 p3102 N88-28422

The application of SPOT data to the structural geology of western Nevada 22 p3102 N88-28423

Application SPOT-1 data to mining activity: Example of the Imiter Silver Mine, Morocco
22 p3102 N88-28424

Evaluation of SPOT imagery contribution to petroleum exploration: The Suez Rift (Egypt)
22 p3102 N88-28425

Evaluation of SPOT imagery for discriminating vegetation communities associated with surficial and bedrock geology and identifying anomalous and stressed vegetation associated with mineralization
22 p3103 N88-28426

SPOT imagery as an aid to understanding volcanism and tectonics: Examples from the Chilean Andes and the Tibetan Plateau 22 p3103 N88-28427

Role of SPOT in geological application of remote sensing 22 p3103 N88-28428

SPOT imagery preliminary contribution to cartography and geodynamics in the Benue trough (Nigeria)
22 p3103 N88-28429

An evaluation of SPOT imagery for Earth science studies in the Antarctic. Preliminary Evaluation Program (PEPS) 269 for SPOT 22 p3103 N88-28430

Structural analysis of the Jura mountains-Rhine Graben intersection (Switzerland) for petroleum exploration using SPOT stereoscopic data 22 p3103 N88-28431

Methodology for the use of SPOT imagery in petroleum exploration. Example of the Bas-Languedoc area (France) 22 p3104 N88-28432

Analyzing the stratigraphy, tectonism, and mineralization at the Spanish side of the pyrite belt, Huelva province, Spain, using SPOT imagery 22 p3104 N88-28433

Geologic applications of SPOT-1, TM, and NOAA-7 data: Finding and defining unmapped structural features
22 p3104 N88-28434
Comparing different images for ground water survey based on lineament analysis 22 p3104 N88-28435
Spectral and spatial attribute evaluation of SPOT data in geological mapping of precambrian terrains in semiarid environment of Brazil 22 p3104 N88-28436
Geologic results obtained from the use of SPOT imagery along plate boundaries: Examples in the East African rift and of the northern-Caribbean collision
22 p3105 N88-28437
SPOT images and geochemical mapping of lateritic covers in southern Mali 22 p3105 N88-28438
Analysis of the multispectral content and of SPOT subscenes in two regions of Burundi. Lithologic and tectonic interpretations 22 p3105 N88-28439
SPOT imagery for landslide cartography in mountainous areas. Example of the French Maritime Alps
22 p3105 N88-28440
SPOT for slope instability survey in Nepal
22 p3105 N88-28441
Detailed geological mapping of the massif of Sainte Victoire (Provence, France) using SPOT imagery. Comparison with other multisource data. New tectonic interpretation of this region 22 p3105 N88-28442
Satellite remote sensing for forest management. A review illustrated with research results on SPOT 1 data
22 p3106 N88-28443
An evaluation of the utility of SPOT and Thematic Mapper data for providing forest inventory information
22 p3106 N88-28444
Forest mapping by visual interpretation of SPOT images 22 p3106 N88-28446
Forest management applications of SPOT data in Australia 22 p3106 N88-28447
SPOT multispectral data and maritime pine stands in southwest of France 22 p3106 N88-28448
Stand-based forestry inventory from SPOT image
22 p3106 N88-28449
Potential of SPOT imagery as a tool for forest mapping in Quebec 22 p3107 N88-28450
Assessment of large area forest disturbances caused by biotic and abiotic factors on the basis of SPOT images 22 p3107 N88-28451
Study of deforestation in the Vosges (France) by remote sensing 22 p3107 N88-28452
Contribution to the mapping of forests in an intensively divided area, with the help of SPOT image data
22 p3107 N88-28453
SPOT 1: Image utilization, assessment, results. A study of the Elburgon Forest area (Kenya) showing the spectral responses of different forest tree species
22 p3107 N88-28454
SPOT investigations of estuaries and coastal zones: An overview 22 p3107 N88-28455
SPOT: A tool to aid preselection of sites favorable for aquiculture. Evaluation and perspectives of the Preliminary Evaluation Program for SPOT (PEPS) ALIAS Caledonie
22 p3108 N88-28456
The monitoring of sediment transport, water circulation and mixing in estuaries and coastal waters
22 p3108 N88-28457
Evaluation of SPOT data for remote sensing of physical and biological properties of estuaries and coastal zones
22 p3108 N88-28458
Utilization of SPOT in hydrography
22 p3108 N88-28459
Application of SPOT imagery for oil spill contingency planning 22 p3108 N88-28460
The use of SPOT data in mapping coastal areas
22 p3108 N88-28461
SPOT: A satellite for oceanography
22 p3108 N88-28462
Contribution of SPOT satellite to qualitative and quantitative mapping of marine vegetation in the English Channel, North Atlantic, western Mediterranean, and South Pacific 22 p3109 N88-28464
Physiography and kinematics of the western coast of the province of Huelva (Andalousia, Spain)
22 p3109 N88-28465
Use of SPOT HRV data in the US Army Corps of Engineers dredging program 22 p3109 N88-28466
Contributions of SPOT imagery to the study of the littoral environments of Saloum (Senegal)
22 p3109 N88-28467
Relevance of a thematic map (SPOT data) with regards to the real flora and structure of the vegetation covering of salt marshes (Mont Saint Michel Bay, France)
22 p3109 N88-28468
Application of SPOT data to renewable resources in the Maldives 22 p3109 N88-28469
The prospects for topographic mapping using SPOT data 22 p3110 N88-28470
The use of SPOT imagery on analytical photogrammetric instruments 22 p3110 N88-28471
Cartographic applications of SPOT imagery
22 p3110 N88-28472
The use of SPOT imagery for topographic mapping
22 p3110 N88-28473
Digital terrain modelling with SPOT data and geological applications 22 p3110 N88-28474
The use of SPOT data for mapping and DEM production --- digital elevation model (DEM)
22 p3110 N88-28475
Evaluation of SPOT cartographic capabilities over the Aix Marseille area (France) 22 p3110 N88-28476
Assessment of SPOT imagery for topographic revision and vegetation mapping 22 p3111 N88-28477
A geometrical analysis of SPOT data
22 p3111 N88-28478
Topographic mapping with SPOT 1 data. A practical approach by the Ordnance Survey
22 p3111 N88-28479
Metric applications of SPOT's lateral stereoscopy
22 p3111 N88-28480
Larger scale image mapping with SPOT
22 p3111 N88-28481
Rigorous stereophotogrammetric treatment of SPOT images 22 p3111 N88-28482
Mapping and urban multi-experimental assessment of SPOT: Mapping results 22 p3112 N88-28483
Study of stereoradiometry on SPOT images
22 p3112 N88-28484
Studies on system performance of SPOT (space and ground segments) 22 p3112 N88-28485
Radiometric analysis and potential of SPOT HRV imagery for applications in urban environments and geology 22 p3112 N88-28486
Automatic production of orthophoto using SPOT images 22 p3112 N88-28487
High resolution orthoimage quadrangle maps using SPOT satellite data 22 p3112 N88-28488
Automatic extraction of high resolution elevation data from SPOT stereo images 22 p3113 N88-28489
Automatic creation of digital terrain models from SPOT image pairs 22 p3113 N88-28490
Production of satellite image maps based on SPOT data 22 p3113 N88-28491
Surface reflectance factors derived from SPOT-1 HRV data at two view angles 22 p3113 N88-28492
Digital SPOT stereoplotting: An original approach to the formation of epipolar images and matching
22 p3113 N88-28493
From the extraction of linear networks towards following of them on SPOT images with the help of a knowledge-based interpretation system
22 p3113 N88-28494
Extraction of thin networks by an oriented following of ridges and valleys 22 p3113 N88-28495
SPOT images features extraction
22 p3114 N88-28496
SPOT: A data capture and data updating tool for the French National Geographic Institute's (IGN's) cartographic data base 22 p3114 N88-28497
Use of SPOT imagery in a geographic information system 22 p3114 N88-28498
SEP/VIPS 32 geographic information system. Processing and thematic analysis of images, maps, and associated data 22 p3114 N88-28499
Training of the Group for the Development of Aerospace Remote sensing 22 p3114 N88-28501
Contribution of SPOT to geographic information systems 22 p3114 N88-28502
Summary of analysis and processing techniques used on SPOT imagery 22 p3115 N88-28503
The SPOT program 22 p3115 N88-28504
SPOT data acquisition and distribution
22 p3115 N88-28505
Quality of SPOT images 22 p3115 N88-28506
Survey of SPOT-1 operation 22 p3115 N88-28507
Perspectives for the SPOT program
22 p3115 N88-28508
Closing of the Preliminary Evaluation Program for SPOT (PEPS): Assessment of the acquisition, production, and monitoring of PEPS 22 p3115 N88-28509
The world's water resources: A major neglect. A study in remote sensing in hydrology and water management
[ESA-BR-40] 22 p3116 N88-28511
Activities report of the Division of Reconnaissance and Seeker Systems
[FOA-C-30479-3.1/3.2/3.3/3.4]
22 p3116 N88-28513
Investigations into the properties, conditions and effects of the ionosphere
[AD-A194245] 22 p3118 N88-28528
Genesis of Atlantic lows experiment NASA electra boundary layer flights data report
[NASA-TM-100703] 22 p3128 N88-28597
Spectral characteristics and the extent of paleosols of the Palouse formation
[NASA-CR-180947] 23 p3228 N88-29210
Activities report in remote sensing
[ETN-88-92905] 23 p3309 N88-29714
Wave propagation and remote sensing
24 p3364 N88-30029
Microwave remote sensing in the French industries
[ETN-88-93081] 24 p3387 N88-30171
Structure of eastern Turkestan Ridge based on space photographs 24 p3450 N88-30530
Estimation of soil temperature profile from remote microwave and IR measurements
24 p3450 N88-30532

REMOTE SENSORS
NT THEMATIC MAPPERS (LANDSAT)
Efficient placement of structural dynamics sensors on the space station
[NASA-CR-172015] 01 p0017 N88-10103
Robotic sensors and actuators for a service manipulator system. Volume 1: Executive summary
[MATRA-EPT/DT/VT187/120]
01 p0053 N88-10341
Robotic sensors and actuators for a service manipulator system. Volume 2: Service Manipulator System (SMS) handbook
[MATRA-EPT/DT/VT187/227]
01 p0053 N88-10342
Robotic sensors and actuators for a service manipulator system. Volume 3, phase A report and program plan
[MATRA-EPT/DT/VT187/228]
01 p0054 N88-10343
Earth resources: A continuing bibliography with indexes (issue 55)
[NASA-SP-7041(55)] 01 p0065 N88-10415
The absolute radiometric calibration of space-based sensors 03 p0277 N88-11744
Detector normalization --- SPOT remote sensors
03 p0341 N88-12151
Absolute and interband calibration --- SPOT
03 p0341 N88-12152
Spectroscopic and retrieval studies in support of SCRIBE (Stratospheric Cryogenic Interferometer Balloon Experiment)
[AD-A184037] 03 p0351 N88-12216
A multibody dynamic analysis of the N-ROSS (Navy Remote Ocean Sensing System) satellite rotating flexible reflector using Kane's method
[AD-A184452] 04 p0462 N88-12860
In-situ characterization of the interface of glass reinforced composites
[AD-A185136] 05 p0557 N88-13391
Italy's Institute of Research on Electromagnetic Waves--the Istituto di Ricerca sulle Onde Elettromagnetiche
[AD-A185020] 05 p0574 N88-13501
Development of response models for the Earth Radiation Budget Experiment (ERBE) sensors. Part 3: ERBE scanner measurement accuracy analysis due to reduced housekeeping data
[NASA-CR-178294] 05 p0583 N88-13553
Estimation of marine boundary layer depth and relative humidity with multispectral satellite measurements
[AD-A184881] 05 p0620 N88-13804
Software design for an airborne gravity measurement system
[AD-A185000] 05 p0634 N88-13878
HIRIS (High-Resolution Imaging Spectrometer: Science opportunities for the 1990s. Earth observing system. Volume 2C: Instrument panel report
[NASA-TM-89703] 07 p0871 N88-15282
SAR (Synthetic Aperture Radar). Earth observing system. Volume 2F: Instrument panel report
[NASA-TM-89701] 07 p0871 N88-15284
Technical aspects of future ocean colour remote sensing 08 p1042 N88-16298
Developments in ocean colour research in the United Kingdom 08 p1043 N88-16306
Sea surface current estimates off central California as derived from enhanced AVHRR (Advanced Very High Resolution Radiometer) infrared images
[AD-A186867] 09 p1194 N88-17155
Remote sensing of atmospheric optical thickness and sea-water attenuation when submerged: Wavelength selection and anticipated errors
[AD-A187609] 11 p1548 N88-19262
Long range sensor for rendezvous and docking missions 12 p1587 N88-19497
Airborne electromagnetic sounding of sea ice thickness and sub-ice bathymetry
[AD-A188939] 12 p1649 N88-19879
The application of thermal imaging sensors and image processing techniques to a short range surface-to-air missile system
[ETN-88-92080] 14 p1982 N88-21829
Instrumentation to provide an active control capability for distributed parameter systems
[AD-A190043] 15 p2076 N88-22375

Feasibility study for a 2nd generation system for airborne maritime pollution surveillance
[ETN-88-92108] 15 p2092 N88-22486
Support for FY87 midlatitude electron-density calibration campaign
[AD-A190174] 15 p2094 N88-22476
The multiannual National Remote Sensing Program (NRSP)
[BCRS-87-16] 16 p2229 N88-23311
A new fiber-optic-based ion sensor
[AD-A191322] 16 p2274 N88-23612
Remote sensing of acoustic properties of shallow water sediments: A review
[AD-A192107] 18 p2570 N88-25267
Fiber optic sensors 19 p2670 N88-25870
Satellite remote sensing of the wet bulb globe temperature heat stress index, phase 2
[AD-A192796] 20 p2818 N88-26717
Development of procedures for performing end-to-end tests on the ERS-1 radar altimeter and AMI using a compact antenna test range — Active Microwave Instrument (AMI)
[ESA-CR(P)-2558] 24 p3363 N88-30022

REMOTELY PILOTED VEHICLES
Full-scale transport controlled impact demonstration program
[NASA-TM-89642] 01 p0004 N88-10021
HiMAT flight program: Test results and program assessment overview
[NASA-TM-86725] 01 p0005 N88-10026
Evaluation of vision systems for teleoperated land vehicles
[DE87-013066] 03 p0333 N88-12100
Operator multiple-tasking study for remotely operated platforms
[AD-A184487] 03 p0362 N88-12276
Experiences in teleoperation of land vehicles
[DE88-001695] 06 p0711 N88-14357
An autopilot design for the United States Marine Corps' airborne remotely operated device
[AD-A186379] 07 p0820 N88-14963
A dynamic simulation and feedback control scheme for the U.S. Marine Corps' Airborne Remotely Operated Device (AROD)
[AD-A186597] 08 p0953 N88-15784
Robotic air vehicle. Blending artificial intelligence with conventional software 09 p1210 N88-17252
Search problems in mission planning and navigation of autonomous aircraft
[NASA-CR-182666] 12 p1579 N88-19448
Aquila remotely piloted vehicle: Its potential battlefield contribution still in doubt
[PB88-120241] 13 p1721 N88-20289
A demonstration of retro-traverse using a semi-autonomous land vehicle
[DE88-009851] 21 p2957 N88-27568
Development and design of windtunnel and test facility for RPV (Remote Piloted Vehicle) enhancement devices
[AD-A194842] 24 p3329 N88-29822

REMOVAL
Geometry and reproducibility of a plasma-supported removal of material by laser radiation
[ETN-87-90436] 01 p0052 N88-10335
A new compression method with fast searching on large databases
[DE87-010966] 01 p0106 N88-10691
Cleanliness tests with the Omega Meter: A comparative study for solder flux removal
[DE88-004634] 11 p1460 N88-18704

REMS
U RAPID EYE MOVEMENT STATE

RENAL FUNCTION
Regulation of calcium metabolism during prolonged antiorthostatic hypokinesia
[NASA-TT-20219] 11 p1521 N88-19085
Is ANF implied in the night attenuated renal response to central hypervolemia? 12 p1659 N88-19945
Human adaptation to various hypercapnic conditions in relation to salivary electrolyte dynamics and renal function 12 p1664 N88-19977

RENDEZVOUS
NT ORBITAL RENDEZVOUS
NT SPACE RENDEZVOUS

RENDEZVOUS GUIDANCE
Autonomous control procedures for shuttle rendezvous proximity operations 09 p1206 N88-17244
Space vehicle approach velocity judgments under simulated visual space conditions
[NASA-TM-89437] 11 p1523 N88-19094

RENDEZVOUS TRAJECTORIES
Safe and fuel minimum reference trajectories for closed loop controlled approaches — space stations
12 p1585 N88-19488

REPAIRING
U MAINTENANCE

REPEATERS
The software repeater (an exercise in Z specification)
[RSRE-MEMO-4090] 14 p1958 N88-21677
A 104-km unrepeatered bidirectional fiber optic demonstration link
[AD-A190282] 15 p2134 N88-22726
Spectral modelling of the soft gamma ray repeater
[DE88-007027] 17 p2453 N88-24570

REPETITION
Preliminary evaluation of a micro-based repeated measures testing system
[NASA-CR-172038] 08 p1048 N88-16331

REPLACING
Commonality analysis as a knowledge acquisition problem 08 p1062 N88-16413
A comparative assessment of US and UK explosives qualified as replacements for tetryl
[MRL-R-1094] 13 p1754 N88-20486
Recommended replacements for tetryl in Australian production fuzes and related ordnance
[MRL-R-1089] 13 p1754 N88-20489
Proposal for a new aggressor aircraft
[AD-A194311] 22 p3041 N88-28056

REPLENISHMENT
Study of helium transfer technology for STICCR: Fluid management
[NASA-CR-177463] 10 p1291 N88-17720
Kinetics of thermochemical gas-solid reactions important in the Venus sulfur cycle
[NASA-CR-182963] 19 p2742 N88-26280
The rate of volcanism on Venus
[NASA-CR-183039] 19 p2742 N88-26281

REPORTS
NT CONGRESSIONAL REPORTS
NT PRESIDENTIAL REPORTS
Aircraft accidents
[JB-84] 01 p0004 N88-10020
NASA's new technology reporting system: A review and future prospects
[NASA-CR-180954] 01 p0105 N88-10686
Electronics engineering thrust area report, FY86
[DE87-014616] 03 p0309 N88-11950
National Center for Atmospheric Research
[PB87-228391] 04 p0470 N88-12901
FY 1985 scientific and technical reports, articles, papers and presentations
[NASA-TM-86521] 04 p0501 N88-13063
Workshop on Avionics Corrosion Control
[AGARD-R-733] 05 p0547 N88-13331
Role of technical information in innovation
[PB87-235368] 05 p0658 N88-14039
Role of the technical report in technological innovation
[PB87-232500] 05 p0658 N88-14040
Eddy Current Seminar, 24-26 March 1986
[PB87-124988] 06 p0696 N88-14269
International workshop on two-phase flow fundamentals
[DE88-001478] 06 p0699 N88-14287
Airborne Visible/Infrared Imaging Spectrometer (AVIRIS). A description of the sensor, ground data processing facility, laboratory calibration, and first results
[NASA-CR-182365] 06 p0705 N88-14325
Research reports: 1987 NASA/ASEE Summer Faculty Fellowship Program
[NASA-CR-179219] 07 p0922 N88-15601
Aircraft accident reports: Brief format, US Civil and Foreign Aviation, Issue Number 7 of 1986 accidents
[PB87-916909] 08 p0952 N88-15781
FY87 scientific and technical reports, articles, papers, and presentations
[NASA-TM-100318] 08 p1093 N88-16578
Aircraft accident/incident summary reports, Des Moines, Iowa, November 25, 1985; Chicago, Illinois, August 10, 1986
[PB88-910411] 09 p1115 N88-16685
JPRS report: Science and technology. USSR: Physics and mathematics
[JPRS-UPM-87-009] 09 p1233 N88-17395
Cumulative reports and publications through December 31, 1987
[NASA-CR-181624] 11 p1524 N88-19099
Activities report of Lufthansa
[ISSN-0176-5085] 16 p2155 N88-22855
Aircraft accident/incident summary reports: Modena, Pennsylvania, March 17, 1986; Redwater, Texas, April 4, 1986
[PB88-910403] 16 p2159 N88-22878
Naval research reviews, volume 39, number 3
[AD-A191392] 16 p2264 N88-23543
Acid Precipitation: A current awareness bulletin
[DE88-007987] 20 p2821 N88-26738
RLE progress report, January 1 to December 31, 1987
[RLE-PR-130] 21 p3011 N88-27869
International ultraviolet explorer observatory operations
[NASA-CR-180775] 22 p3145 N88-28708
Activities report in remote sensing
[ETN-88-92905] 23 p3309 N88-29714

REPRESENTATIONS
The total interval of a graph
[AD-A189648] 15 p2119 N88-22625
Approximation and representation of explicit surfaces in the presence of singularities
[ETN-88-92191] 16 p2258 N88-23496
Knowledge representation in geographic information systems
[ETN-88-92470] 20 p2882 N88-27112
An introduction to the nested sequence of tuples data model and algebra
[REPT-87-049] 22 p3145 N88-28702

REPRODUCTION (BIOLOGY)
Investigations of the survey of the reproductive biology of Xiphophorus in an Aquarack
01 p0074 N88-10471
Xiphophorus as an experimental system for genetic and biological development studies under microgravity conditions 01 p0074 N88-10472
Long term investigations of the growth, metabolism, and reproduction of fish under conditions close to weightlessness 01 p0074 N88-10473
Investigations of the reproductive physiology of the rainbow trout (Salmo gairdneri Richardson)
07 p0885 N88-15370
Changes in the morphological and molecular biological processes during early embryo development in amphibians under micro-g conditions 07 p0885 N88-15371
Long duration confinement of aquatic organisms in weightlessness (aquaspace) 07 p0887 N88-15380
Mother-fetus system as object for investigation of mechanisms of physiological effect of weightlessness
07 p0891 N88-15402

REPRODUCTION (COPYING)
NT XEROGRAPHY
The Quick Response Multicolor Printer (QRMP) system
[AD-A188140] 11 p1504 N88-18982
Data acquisition and processing for surface plate calibration
[AD-A187264] 11 p1564 N88-19366
New duplicating paper with high resolution for aerial photography
[PB87-228706] 19 p2685 N88-25962
The transition from traditional to modern map reproduction
[B8735128] 20 p2816 N88-26718

REPRODUCTIVE SYSTEMS
NT TESTES

REPUBLIC MILITARY AIRCRAFT
U MILITARY AIRCRAFT

REPUBLIC OF CHINA
U TAIWAN

REPULSION
U FORCE

REQUIREMENTS
Space Station Mission Planning System (MPS) development study. Volume 1: Executive summary
[NASA-CR-179202] 01 p0009 N88-10047
Space Station Mission Planning System (MPS) development study. Volume 2
[NASA-CR-179200] 01 p0009 N88-10048
Space Station Mission Planning Study (MPS) development study. Volume 3: Software development plan
[NASA-CR-179203] 01 p0009 N88-10049
Telepresence work station system definition study, part 2
[NASA-CR-172006] 01 p0013 N88-10071
Space Assembly, Maintenance, and Servicing Study (SAMSS) 01 p0015 N88-10089
System Development Working Group report
01 p0016 N88-10092
Structures and Materials Working Group report
01 p0016 N88-10093
Space station contamination considerations
02 p0137 N88-10859
The MOLICEL(R) rechargeable lithium system: Multicell battery aspects 02 p0163 N88-11024
Fault tree safety analysis of a large Li/SOCl(sub)2 spacecraft battery 02 p0163 N88-11025
Rotorcraft Design for Operations
[AGARD-CP-423] 03 p0262 N88-11649
The influence of operational requirements on LHX concept formulation 03 p0262 N88-11650
Apache for the battlefield of today and the 21st century 03 p0265 N88-11670
The EH-101 integrated project: A naval, utility and commercial helicopter system 03 p0265 N88-11672
How space, the fourth operational medium, supports operational maneuver
[AD-A184742] 03 p0373 N88-12346

Advanced Information Processing System (AIPS) proof-of-concept system functional requirements I/O network system services
[NASA-CR-181481] 03 p0384 N88-12412
Fire-related standards and testing
04 p0406 N88-12522
MHD stability and control for mirror machines
04 p0493 N88-13036
Design and assembly sequence analysis of option 3 for CETF reference space station
[NASA-TM-100503] 05 p0553 N88-13369
Roughness and waviness requirements for laminar flow surfaces 07 p0613 N88-14953
Documentation in a software maintenance environment
[AD-A185892] 07 p0901 N88-15459
Derivation of equipment vibration requirements for AV-8B 08 p0997 N88-16037
Requirements and options for communications services in support of the Systems Autonomy Demonstration Project 08 p1057 N88-16374
The role of photodetectors in optical signal processing
[AD-A186804] 09 p1247 N88-17476
Crew interface with windshear systems
10 p1275 N88-17631
Helicopter external vision requirements and visual display characteristics: A report/bibliography, revision A
[AD-A187075] 10 p1276 N88-17641
Specification of an engine and its components starting from a consideration of aircraft missions
10 p1279 N88-17651
An integrated aero/mechanical performance approach to high technology turbine design
10 p1280 N88-17657
A framework for evaluating computer architectures to support systems with security requirements, with applications
[AD-A187062] 10 p1392 N88-18303
Design loads for Swedish military aircraft in a twenty years' perspective 12 p1580 N88-19456
Orbital analysis of a STS (Space Transportation System) external tank in low earth orbit
[AD-A188629] 12 p1593 N88-19542
Low cost mobile robot
[AD-A188507] 12 p1633 N88-19778
Turnaround operations analysis for OTV. Volume 1: Executive summary
[NASA-CR-179316] 13 p1729 N88-20340
Turnaround operations analysis for OTV. Volume 2: Detailed technical report
[NASA-CR-179317] 13 p1729 N88-20341
Intergrated circuit design, phase 2
[AD-A189060] 13 p1760 N88-20530
Space station power system requirements
[NASA-TM-100886] 14 p1881 N88-21245
Large-scale wind turbine structures
15 p2085 N88-22429
Monitoring the usage of a computer system
[DE88-004310] 15 p2106 N88-22542
The modeling, simulation and comparison of interconnection networks for parallel processing
[AD-A190571] 15 p2115 N88-22599
Tactical Rubidium Frequency Standard (TRFS)
[AD-A191049] 16 p2193 N88-23078
Manned Mars mission accommodation: Sprint mission
[NASA-TM-100596] 16 p2290 N88-23711
A structured approach to weapon system design
17 p2303 N88-23773
Advanced EVA system design requirements study
17 p2380 N88-24147
Advisory circular: Noise certification handbook
[FAA-AC-36-4B] 17 p2394 N88-24234
Potassium Rankine power system for space power
17 p2433 N88-24476
Automatic reactor control system for transient operation 17 p2436 N88-24493
Required operational capacity for a 7-1/2 ton capacity, Air Mobile Crane (AMC)
[AD-A192023] 19 p2601 N88-25451
On 3-5 transistors for MM-wave applications
[AD-A191580] 19 p2661 N88-25825
Checkout system software for INPE satellites
[INPE-4554-PRE/1297] 19 p2715 N88-26120
SLAPP: A special multiprocessor array for signal processing and linear algebra
[AD-A191587] 19 p2719 N88-26146
Real time data base management
[AD-A191756] 19 p2739 N88-26265
The free-electron laser: Theoretical innovations and gas-loaded experiment 20 p2806 N88-26646
Electrical load and power source capacity report for the C-130 aircraft Self Contained Navigation System (SCNS): LSI model 6216A, 6216B, 6216C, revision
[AD-A193079] 21 p2895 N88-27186
Sources and nature of cost analysis data base reference manual
[AD-A193099] 21 p3028 N88-27976
A 2.3-GHz low-noise cryo-FET amplifier
22 p3066 N88-28195
Model test of air-exchange efficiency
[DE88-752862] 23 p3201 N88-29049
An overview of technology for spoken interaction with machines
[AD-A194153] 23 p3202 N88-29058
Remotely Operated Vehicle (ROV) reliability study, phase 1
[AD-A194367] 23 p3222 N88-29177
Night lighting and night vision goggle compatibility
23 p3242 N88-29297
Centralized class A flight mishap investigation
[AD-A194397] 24 p3322 N88-29786
Long haul communications in the HF spectrum utilizing high speed modems
[AD-A194683] 24 p3360 N88-30003
Achieving real-time performance in FIESTA
24 p3418 N88-30344

RESCUE OPERATIONS
System for SAR missions 03 p0265 N88-11671
An evaluation of the methods for rescuing EVA (Extravehicular Activities) crewmembers and recovering equipment detached and adrift from the space station
[AD-A189683] 14 p1871 N88-21181
Design and development of an avionics system adapted to helicopter missions 17 p2305 N88-23786
KOSPAS-SARSAT satellites used for ocean current study 24 p3450 N88-30534

RESEARCH
NT DYNAMIC PROGRAMMING
NT LINEAR PROGRAMMING
NT MARKET RESEARCH
NT NONLINEAR PROGRAMMING
NT NUCLEAR RESEARCH
NT QUADRATIC PROGRAMMING
Transactions of the 4th Army Conference on Applied Mathematics and Computing
[AD-A183544] 01 p0085 N88-10547
Research in particles and fields
[NASA-CR-180412] 01 p0119 N88-10763
Crystalline cell research status and direction
[DE87-014214] 03 p0382 N88-12402
The impact of information technology on research in science and engineering
[DE88-000342] 03 p0385 N88-12417
Procedure and program used for data processing in a poll on nuclear energy utilization
[IFSI-87-3] 05 p0649 N88-13977
Budget and programs for 1986 research
[IFSI-86-16] 05 p0660 N88-14048
EISCAT research in Finland in 1986
06 p0691 N88-14234
EISCAT research programs for 1987
06 p0692 N88-14244
Program draft for a special field: Gravitational biology
07 p0887 N88-15381
Index of USA-CERL publications for October 1984 - June 1987
[AD-A186375] 07 p0942 N88-15728
Earth materials research: Report of a Workshop on Physics and Chemistry of Earth Materials
[NASA-CR-182519] 10 p1298 N88-17761
Interdisciplinary research in mathematics, science and technology education
[PB88-131446] 10 p1398 N88-18333
Genetic research in space
[NASA-TT-20216] 11 p1518 N88-19066
Research on algorithms for nonlinear programming
[AD-A188326] 12 p1677 N88-20024
Data base design and implementation
[AD-A190414] 15 p2149 N88-22827
NASA scientific and technical publications: A catalog of Special Publications, Reference Publications, Conference Publications, and Technical Papers, 1987
[NASA-SP-7063(02)] 15 p2149 N88-22830
JPRS report: Science and technology. China
[JPRS-CST-88-009] 16 p2186 N88-23030
Aircraft flight dynamics research in past decade reviewed 16 p2186 N88-23031
JPRS report: Science and technology. China
[JPRS-CST-88-001] 16 p2186 N88-23036
Atmospheric Science and Remote Sensing Laboratory
[NASA-CR-179290] 16 p2236 N88-23355
Fast Algorithm Simulation and Test (FAST) facility
[AD-A191183] 16 p2252 N88-23457
The Engineer Studies Center guide to research and data collection
[AD-A189971] 16 p2285 N88-23680
Soviet combustion research
[PB88-182324] 18 p2483 N88-24730
Activities report of the Communications Department
[ENST-88D003] 21 p2931 N88-27401
Vanderbilt free electron laser project in biomedical and materials research
[AD-A195961] 24 p3378 N88-30121
Center for opto-electronic systems research
[AD-A195159] 24 p3429 N88-30411

RESEARCH AIRCRAFT
NT B-70 AIRCRAFT
NT ROTOR SYSTEMS RESEARCH AIRCRAFT
NT U-2 AIRCRAFT
An integrated study of structures, aerodynamics and controls on the forward swept wing X-29A and the oblique wing research aircraft
[NASA-CR-181548] 04 p0399 N88-12486
First results from the Airborne Visible/Infrared Imaging Spectrometer (AVIRIS) 06 p0707 N88-14335
A perspective on 15 years of proof-of-concept aircraft development and flight research at Ames-Moffett by the Rotorcraft and Powered-Lift Flight Projects Division, 1970-1985
[NASA-RP-1187] 12 p1582 N88-19467
A correlation study of X-29A aircraft and associated analytical development
[NASA-CR-183103] 13 p1722 N88-20296
Development of a real-time aeroperformance analysis technique for the X-29A advanced technology demonstrator
[NASA-TM-100432] 14 p1866 N88-21151
Performance improvements of an F-15 airplane with an integrated engine-flight control system
[NASA-TM-100431] 14 p1867 N88-21159
Development of an integrated set of research facilities for the support of research flight test
[NASA-TM-100427] 14 p1869 N88-21169
The NASA integrated test facility and its impact on flight research
[NASA-TM-100418] 14 p1870 N88-21177
First flight simulator test of the head-up display for NAL QSTOL experimental aircraft (ASUKA)
[DE88-751804] 16 p2162 N88-22896
Development of an airborne facility for advanced avionics research 17 p2307 N88-23801
Taiwan area mesoscale experiment: P-3 aircraft operations summary
[PB88-169073] 18 p2544 N88-25098
The identification of the direct lift control flap system of the research aircraft ATTAS
20 p2786 N88-26527
Investigations into the triggered lightning response of the F106B thunderstorm research aircraft
[NASA-CR-3902] 23 p3236 N88-29258
The NAE atmospheric research aircraft
24 p3313 N88-29730

RESEARCH AND DEVELOPMENT
Blagov commentary on Mir station, first manning
01 p0009 N88-10051
Lithium/iron sulfide batteries: Development and demonstration
[DE87-014222] 01 p0042 N88-10265
Budget reimbursements: The National Aeronautics and Space Administration's reimbursable work
[PB87-207296] 01 p0107 N88-10696
Space technology to meet future needs
[NASA-CR-181473] 02 p0130 N88-10819
Battery development and testing at ESA
02 p0164 N88-11027
Stirling engine research at national and university laboratories in Japan
[DE87-014622] 02 p0180 N88-11123
Planning for US ion cyclotron heating research relevant to the compact ignition tokamak and Alcator C-Mod
[DE88-000022] 02 p0241 N88-11520
JPRS report: Science and technology. China
[JPRS-CST-87-032] 03 p0376 N88-12365
A role for national laboratories in enhancing economic competitiveness. The example of high-temperature superconductors: CNSS papers, No. 1
[DE87-013633] 03 p0379 N88-12386
Materials studies for magnetic fusion energy applications at low temperatures-X
[PB87-232575] 03 p0381 N88-12395
National Science Foundation
[PB87-228375] 03 p0384 N88-12410
National Aeronautics and Space Administration Authorization Act, 1988
[PUB-LAW-100-147] 03 p0385 N88-12422
Solar energy: European research and development
[PB87-107645] 04 p0463 N88-12866
Aerothermodynamics research at NASA Ames
05 p0533 N88-13242
Innovative and alternative technology projects
[PB87-230165] 05 p0623 N88-13818
CELSS Program Meeting 05 p0630 N88-13853
The birth of big science: Nuclear physics as advanced technology source
[NOTA-INTERNA-881] 05 p0648 N88-13967

Role of technical information in innovation
[PB87-235388] 05 p0658 N88-14039

Role of the technical report in technological innovation
[PB87-232500] 05 p0658 N88-14040

AGARD: The NATO Advisory Group for Aerospace Research and Development
[AD-A185062] 05 p0662 N88-14063

Tethers in space handbook
[NASA-CR-181371] 06 p0673 N88-14123

Material design of high-purpose glass discussed
06 p0675 N88-14133

NAL news updated: FY87 business plan, developments 06 p0675 N88-14135

Recent trends in superconductor development discussed 06 p0688 N88-14215

Laser development, evolution of applied technologies described 06 p0689 N88-14221

Strategic management of research and development: A literature search
[NASA-CR-182337] 06 p0790 N88-14847

National Aeronautics and Space Administration (NASA)/American Society for Engineering Education (ASEE) Summer Faculty Fellowship Program, 1987. Volume 1
[NASA-CR-172009-VOL-1] 06 p0792 N88-14855

Federal plan for meteorological services and supporting research, fiscal year 1988
[PB88-118716] 07 p0880 N88-15336

Design and management of research projects
[PB88-106380] 07 p0941 N88-15721

Life prediction technologies for aeronautical propulsion systems 08 p0954 N88-15788

Supersonic STOVL propulsion technology program: An overview 08 p0957 N88-15808

Safety guidelines and procedures for bioscience-based industry and other applied microbiology
[PB87-140521] 08 p1045 N88-16316

Trends in research and development in the Netherlands. The influence of national science policy between 1973 and 1986
[B8701588] 08 p1094 N88-16580

Organizations of intermediation in technology transfer: Its role in technological innovation
[INPE-4354-TDL/297] 08 p1094 N88-16581

Loads and aeroelasticity division research and technology accomplishments for FY 1987 and plans for FY 1988
[NASA-TM-100534] 09 p1114 N88-16680

Impact and promise of NASA aeropropulsion technology 09 p1118 N88-16698

Lewis materials research and technology: An overview
09 p1119 N88-16699

The objectives and methods of the technological research program 09 p1124 N88-16730

Research and technology 1987
[NASA-TM-4021] 09 p1265 N88-17577

Director of R and D institutions (Government of India)
[PB88-127162] 10 p1285 N88-17685

Research and development. Technical-scientific publications (1956-1987): Retrospective view and prospects. Jubilee edition on the occasion of the 75th birthday of Dipl.-Engr. Dr.-Engr. E. H. Ludwig Boelkow
[ISSN-0931-9751] 10 p1309 N88-17819

Research, development, and growth strategy
10 p1309 N88-17820

Research and technology 1987 annual report of the Kennedy Space Center
[NASA-TM-100303] 10 p1431 N88-18548

Lithium/disulfide battery R and D
[DE88-003032] 11 p1481 N88-18839

Research briefing on high-temperature superconductivity
[PB88-133004] 11 p1561 N88-19344

Science and technology in India
[PB88-134747] 11 p1564 N88-19362

Communication satellites: Guidelines for a strategic plan
[NASA-TM-89306] 12 p1599 N88-19569

Technology development of a planar BiPolar transistor
[AD-A188761] 12 p1623 N88-19708

Research and technology, 1987
[NASA-TM-100323] 12 p1713 N88-20253

AGARD Highlights 88/1 14 p2012 N88-22001

The impact of independent research and development regulations on companies not required to negotiate advanced independent research and development agreements
[AD-A190007] 15 p2147 N88-22818

Marshall Space Flight Center 1960-1985: 25th anniversary report
[NASA-TM-100326] 15 p2153 N88-22852

Langley aerospace test highlights, 1987
[NASA-TM-100595] 15 p2153 N88-22853

Space directorate research and technology accomplishments for fiscal year 1987
[NASA-TM-100607] 15 p2153 N88-22854

Government research on ceramics coating technology
16 p2184 N88-23019

Sunshine project for FY 1987 outlined
16 p2184 N88-23021

Activities report of the Department of Systems and Communications
[ENST-87D004] 16 p2189 N88-23053

Computer-assisted cartography research and development report of the Federal Republic of Germany 1984 - 1986 16 p2226 N88-23289

The multiannual National Remote Sensing Program (NRSP)
[BCRS-87-16] 16 p2229 N88-23311

Activities report of the Imagery Department
[ENST-87D008] 16 p2273 N88-23604

DOE (Department of Energy) national laboratories and the semiconductor industry: Continuing the joint planning
[PB88-170295] 16 p2281 N88-23657

Department of Housing and Urban Development independent agencies appropriations for 1989. Part 7: National Aeronautics and Space Administration
[GPO-85-166] 16 p2286 N88-23689

Preparing for the new programs. The ESA technological research and development program 1988-1990
[ESA-SP-1095] 17 p2309 N88-23814

Structural ceramics research
17 p2324 N88-23876

Soviet remote sensing research and technology
[FASAC-TAR-3130] 17 p2369 N88-24108

Research and Technology, 1987, Goddard Space Flight Center
[NAS 1.15:100097] 17 p2453 N88-24572

The application of hydrocarbon bioconversion technology to aerospace materials production
18 p2478 N88-24698

A quality philosophy for research and development
[DE88-006512] 18 p2524 N88-24977

Department of Defense statement on defense agency research and development to the Subcommittee on Defense of the Committee on Appropriations, United States House of Representatives, 100th Congress, second session
[AD-A191840] 18 p2588 N88-25377

The FY 1989 Department of Defense statement on the Science and Technology Program to 100th Congress, second session
[AD-A191843] 18 p2588 N88-25380

Centre for International Co-Operation and Approriate Technology (CICAT)
[PB88-165501] 18 p2590 N88-25389

Electrical and chemical sensors for biological cell research 19 p2669 N88-25866

Procedures for peer review assessments
[DE88-007749] 19 p2739 N88-26263

Exploratory battery technology development and testing report for 1986
[DE88-009670] 20 p2794 N88-26578

Space policy of common sense and moderation
[REPT-49/87] 20 p2883 N88-27118

United States Air Force Graduate Student Summer Support Program, volume 2
[AD-A191122] 21 p2924 N88-27355

Vision research. A national plan: 1983-1987, 1987 evaluation and update
[PB88-192604] 21 p2985 N88-27726

Engineering data compendium. Human perception and performance. User's guide
[LC-87-19560] 21 p2993 N88-27749

Materials research, superconductor and thin layer technology
[REPT-50/87] 21 p3025 N88-27955

High technology space flight orientation program: Overview and recommendations
[ETN-88-92332] 21 p3029 N88-27979

Engineering data compendium. Human perception and performance, volume 1
[LC-87-19560] 22 p3134 N88-28630

Engineering data compendium. Human perception and performance, volume 2
[LC-87-19560] 22 p3134 N88-28631

Engineering data compendium. Human perception and performance, volume 3
[LC-87-19560] 22 p3134 N88-28632

A study of the National Physics Laboratory microdosimetry research programme in collaboration with the University of Leeds (United Kingdom)
[NPL-RS(EXT)-93] 23 p3217 N88-29148

Competition: Issued on establishing and using Federally funded research and development centers
[PB88-178884] 23 p3296 N88-29632

History of aeroelasticity in Germany from the beginning to 1945
[ESA-TT-1082] 24 p3319 N88-29767

With an eye to the future: ESA general studies program 1988
[ESA-SP-1100] 24 p3435 N88-30447

RESEARCH FACILITIES

Aquarack: Aims and Possible Research Projects
[DFVLR-MITT-87-01] 01 p0073 N88-10469

The Aquarack as a potential instrument for basic research work in space biology: Inventory and scientific dispositions 01 p0073 N88-10470

Surveillance systems test and evaluation facilities
02 p0134 N88-10845

Lewis' enhanced laboratory for research into the fatigue and constitutive behavior of high temperature materials
02 p0189 N88-11177

MBB simulation facilities applied for rotorcraft research 03 p0263 N88-11655

Research simulators for helicopters
03 p0263 N88-11656

Experiments. Test range facilities, part 1
03 p0304 N88-11920

FY 1985 scientific and technical reports, articles, papers and presentations
[NASA-TM-86521] 04 p0501 N88-13083

Aerothermodynamics research at NASA Ames
05 p0533 N88-13242

Metrology and calibrating laboratories
[ETN-88-90761] * 06 p0670 N88-14104

Polar Geophysical Institute's studies of magnetosphere, ionosphere 06 p0728 N88-14480

Design of the Backscatter Spectroscopy System for the Nova Laser Facility
[DE88-001880] 07 p0859 N88-15214

Research reports: 1987 NASA/ASEE Summer Faculty Fellowship Program
[NASA-CR-179219] 07 p0922 N88-15601

Physics rationale for the engineering specifications for ZTH
[DE88-000938] 07 p0936 N88-15690

Life prediction technologies for aeronautical propulsion systems 08 p0954 N88-15788

CEBAF design overview and project status
[CEBAF-PR-88-001] 09 p1246 N88-17470

Director of R and D institutions (Government of India)
[PB88-127162] 10 p1285 N88-17685

System analysis study of space platform and station accommodations for life sciences research facilities. Volume 1: Executive summary. Phase A: Conceptual design and programmatics
[NASA-CR-179268] 10 p1291 N88-17721

System analysis study of space platform and station accommodations for life sciences research facilities. Volume 2: Study results, attachment 2. Phase A: Conceptual design and programmatics
[NASA-CR-179272] 10 p1291 N88-17722

Relationships between coronary heart disease risk factors and serum ionized calcium in Kennedy Space Center Cohort
[NASA-TM-100979] 10 p1366 N88-18177

Design issues for a laboratory high gain fusion facility
[DE88-004406] 10 p1413 N88-18434

Research and technology 1987 annual report of the Kennedy Space Center
[NASA-TM-100303] 10 p1431 N88-18548

Engineering thrust areas, 1988
[DE88-005103] 11 p1466 N88-18753

Institute for Computational Mechanics in Propulsion (ICOMP)
[NASA-TM-100790] 11 p1540 N88-19202

A perspective on 15 years of proof-of-concept aircraft development and flight research at Ames-Moffett by the Rotorcraft and Powered-Lift Flight Projects Division, 1970-1985
[NASA-RP-1187] 12 p1582 N88-19467

Conceptualization and design of a variable-gravity research facility
[NASA-CR-182574] 12 p1595 N88-19550

Conceptual design and programmatics studies of space station accommodations for Life Sciences Research Facilities (LSRF)
[NASA-CR-179270] 12 p1598 N88-19567

Space station accommodations for life sciences research facilities: Phase A conceptual design and programmatics studies for Missions SAAX0307, SAAX0302 and the transition from SAAX0307 to SAAX0302. Volume 1: Executive summary
[NASA-CR-179267] 12 p1599 N88-19571

Photonic temperature and pressure sensors for biosystems/pulsed microwave. Part 1: Interaction studies
[AD-A188887] 12 p1629 N88-19751

A laboratory facility for research in parallel computation
[AD-A188499] 12 p1680 N88-20044

Basic research in ceramic and semiconductor science at selected Japanese laboratories, based on a September 1986 visit: Highlights, summary and overview and detailed notes from selected Japanese laboratories
[DOE/ER-0314] 12 p1696 N88-20150

A review of technologies applicable to low-speed flight of high-performance aircraft investigated in the Langley 14- x 22-foot subsonic tunnel
[NASA-TP-2796] 13 p1717 N88-20264
Aircraft flight flutter testing at the NASA Ames-Dryden Flight Research Facility
[NASA-TM-100417] 13 p1723 N88-20301
High Reynolds number pump facility for cavitation research
[AD-A189310] 13 p1765 N88-20558
The use of an automated flight test management system in the development of a rapid-prototyping flight research facility
[NASA-TM-100435] 13 p1823 N88-20896
The continuous electron beam accelerator facility
[CEBAF-PR-87-017] 13 p1838 N88-20996
Development of an integrated set of research facilities for the support of research flight test
[NASA-TM-100427] 14 p1869 N88-21169
The NASA integrated test facility and its impact on flight research
[NASA-TM-100418] 14 p1870 N88-21177
Test facilities of the structural dynamics branch of NASA Lewis Research Center
[NASA-TM-100800] 14 p1934 N88-21534
Laboratory Information Management System (LIMS): A case study
[NASA-TM-100835] 14 p1961 N88-21697
Chronology of KSC and KSC related events for 1987
[NASA-CR-182754] 14 p2012 N88-22002
Procedures and requirements for testing in the Langley Research Center unitary plan wind tunnel
[NASA-TM-100529] 15 p2015 N88-22016
Function of Japan Fine Ceramics Center described
15 p2052 N88-22227
Structural dynamics branch research and accomplishments for fiscal year 1987
[NASA-TM-100279] 15 p2088 N88-22446
Marshall Space Flight Center 1960-1985: 25th anniversary report
[NASA-TM-100328] 15 p2153 N88-22852
Development of a mobile research flight test support capability
[NASA-TM-100428] 16 p2159 N88-22883
Development of an airborne facility for advanced avionics research 17 p2307 N88-23801
Structures and Dynamics Division research and technology plans for FY 1988 and accomplishments for FY 1987
[NASA-TM-100585] 17 p2350 N88-24000
Aerospace energy systems laboratory: Requirements and design approach
[NASA-TM-100423] 17 p2380 N88-24206
Analysis procedures and subjective flight results of a simulator validation and cue fidelity experiment
[NASA-TM-88270] 18 p2465 N88-24634
SHaRE: Collaborative materials science research
[DE88-007175] 18 p2467 N88-24646
Preparation for microgravity: The role of the microgravity materials science laboratory
[NASA-TM-100906] 18 p2497 N88-24811
Metals and Ceramics Division
[DE88-008955] 19 p2618 N88-25530
A detailed description of the uncertainty analysis for high area ratio rocket nozzle tests at the NASA Lewis Research Center 19 p2626 N88-25580
Engineering research centers and their evaluation
[PB88-180054] 19 p2739 N88-26262
Solar microwave radiation maps measured at Metsaehovi Radio Research Station in 1980-1981
[PB88-193453] 19 p2741 N88-26276
Building an artificial intelligence capability at Los Alamos
[DE88-009155] 20 p2842 N88-26866
Photovoltaic Measurements and Performance Branch
[DE88-001142] 21 p2968 N88-27633
Publications on acoustics research at the Langley Research Center during 1980-1986
[NASA-TM-100590] 21 p3013 N88-27801
The High Temperature Materials Laboratory: A new research and user facility at the Oak Ridge National Laboratory
[DE88-010782] 22 p3057 N88-28138
Langley Research Center Metrology Program status for fiscal year 1987
[NASA-TM-100651] 22 p3086 N88-28324
Software modifications to total data reporting accessory for metabolic measurement cart
[AD-A193641] 22 p3132 N88-28623
Bibliography of Lewis Research Center technical publications announced in 1987
[NASA-TM-100910] 22 p3162 N88-28832
The NBS/NRL (National Bureau of Standards/Naval Research Laboratory) free electron laser facility
[AD-A194214] 23 p3219 N88-29159
Center for opto-electronic systems research instrumentation grant
[AD-A193711] 23 p3262 N88-29545
Helicopter transmission research at NASA Lewis Research Center
[NASA-TM-100962] 24 p3379 N88-30128
An improvement in the numerical integration procedure used in the NASA Marshall engineering thermosphere model
[NASA-CR-179389] 24 p3392 N88-30200
Science at NASA field centers: Findings and recommendations on the scope, strength and interactions of science and science-related technology programs
[NASA-TM-101188] 24 p3459 N88-30581
Research and technology of the Lyndon B. Johnson Space Center
[NASA-TM-100463] 24 p3460 N88-30583

RESEARCH MANAGEMENT

Documentation as a management strategy for reaching goals in high-risk research-oriented projects
[DE87-012394] 01 p0105 N88-10685
Alternative fuels: Information on DOD's (Department of Defense's) methanol vehicle program
[PB87-213328] 02 p0156 N88-10976
Gallium arsenide and multibandgap solar cell research
[DE87-012260] 02 p0194 N88-11215
Siting and Geotechnical Program Fucus and Directions. Report upon the deliberations of a workshop held at the Illinois Institute of Technology, Chicago, Illinois on August 4-5, 1986
[PB87-206272] 02 p0198 N88-11238
Report from the MPP Working Group to the NASA Associate Administrator for Space Science and Applications
[NASA-TM-87819] 02 p0223 N88-11402
Electronics engineering thrust area report, FY86
[DE87-014616] 03 p0309 N88-11950
Materials sciences programs: Fiscal Year 1987
[DE88-000672] 04 p0429 N88-12659
National Center for Atmospheric Research
[PB87-228391] 04 p0470 N88-12901
COLA2: A computer program for the structural synthesis of two components using general modal coordinates
[DE88-001457] 04 p0481 N88-12963
Nuclear techniques in studies of condensed matter
[NASA-RP-1195] 04 p0489 N88-13015
A national model at Howard University demonstrating private sector interrelationships that facilitate research in predominantly Black colleges and universities
[DE88-000160] 04 p0502 N88-13089
The role of basic research in society
[DE88-000459] 04 p0502 N88-13090
The birth of big science: Nuclear physics as advanced technology source
[NOTA-INTERNA-881] 05 p0648 N88-13967
A short introduction to the status and motivation for reversed field pinch and compact toroid research
[DE88-000487] 05 p0652 N88-13999
University research initiative research program summaries
[AD-A184876] 05 p0658 N88-14035
Research for electric energy systems
[DE88-001733] 06 p0695 N88-14265
HOST turbine heat transfer program summary
[NASA-TM-100280] 06 p0704 N88-14320
Research in elementary particle physics
[DE88-002130] 06 p0777 N88-14771
Research and technology objectives and plans. Summary, Fiscal Year 1986
[NASA-TM-87504] 06 p0800 N88-14894
Summaries of FY 1987 engineering research
[DE88-002572] 07 p0840 N88-15096
WOCE Core Project 2 Planning Meeting: The Southern Ocean
[WCP-138] 07 p0882 N88-15348
Research reports: 1987 NASA/ASEE Summer Faculty Fellowship Program
[NASA-CR-179219] 07 p0922 N88-15601
Physics rationale for the engineering specifications for ZTH
[DE88-000938] 07 p0936 N88-15690
Design and management of research projects
[PB88-106380] 07 p0941 N88-15721
German space policy on the threshold of the century. Analysis and proposals for the future
[ETN-88-90573] 07 p0943 N88-15734
Past, present and future role of Black Brant rocket systems to support international space science programs 08 p1034 N88-16272
Research in progress at the Institute for Computer Applications in Science and Engineering
[NASA-CR-181607] 08 p1053 N88-16354
The objectives and methods of the technological research program 09 p1124 N88-16730
The new approach to the definition of the ESA technological research program
09 p1127 N88-16763
Recommendations for a US ice coring program
[PB88-115043] 09 p1185 N88-17102
Performance analysis of parallel branch and bound search with the hypercube architecture
09 p1206 N88-17229
Technical activities 1987, Center for Radiation Research
[PB88-129325] 09 p1245 N88-17464
X-29A forward-swept-wing flight research program status
[NASA-TM-100413] 10 p1277 N88-17644
Study for history of technology developments in European space projects
[REPT-8518-1] 10 p1286 N88-17690
Research, development, and growth strategy
10 p1309 N88-17820
Research studies on extreme ultraviolet and soft X-ray lasers
[AD-A187506] 10 p1336 N88-17996
Features of a TeraFlop supercomputer
[DE88-003540] 10 p1384 N88-18263
Research in experimental nuclear physics
[DE88-004100] 10 p1408 N88-18397
Innovative arrangements for industry/DOE laboratory collaboration in high temperature superconductivity
[DE88-004320] 10 p1420 N88-18482
Journal of Research of the National Bureau of Standards, volume 92, number 5, September-October 1987
[PB88-124409] 10 p1426 N88-18518
Journal of Research of the National Bureau of Standards, volume 92, number 6, November-December 1987
[PB88-136516] 10 p1426 N88-18519
High performance composites research at NASA-Langley
[NASA-TM-100518] 11 p1450 N88-18542
Engineering thrust areas, 1988
[DE88-005103] 11 p1468 N88-18753
AFGL (Air Force Geophysics Laboratory) fiscal year 1988 Air Force technical objectives document
[AD-A187701] 11 p1503 N88-18977
Cumulative reports and publications through December 31, 1987
[NASA-CR-181624] 11 p1524 N88-19099
Institute for Computational Mechanics in Propulsion (ICOMP)
[NASA-TM-100790] 11 p1540 N88-19202
Experimental elementary particle physics at the University of Pittsburgh
[DE88-003542] 11 p1545 N88-19234
Study of industry requirements that can be fulfilled by combustion experimentation aboard space station
[NASA-CR-180854] 11 p1566 N88-19377
Alternative program approaches for the advanced satellite technology program
[AD-A188917] 12 p1600 N88-19576
Research on flow control
[AD-A189014] 12 p1627 N88-19736
Advanced Gas Turbine (AGT) technology development project
[NASA-CR-180891] 12 p1709 N88-20230
Mission directed goals for electric vehicle battery research and development: The Task Force on electric vehicle battery goals
[DE88-005601] 13 p1763 N88-20548
The use of an automated flight test management system in the development of a rapid-prototyping flight research facility
[NASA-TM-100435] 13 p1823 N88-20896
Computation and graphics in mathematical research
[DE88-005796] 13 p1831 N88-20953
Aeronautics and space report of the President: 1986 activities 13 p1852 N88-21087
Development of an integrated set of research facilities for the support of research flight test
[NASA-TM-100427] 14 p1869 N88-21169
Metals. Preliminary study for an Innovation-Oriented research Program (IOP)
[ETN-88-91317] 14 p1889 N88-21290
Innovation-Oriented research Program (IOP) metals. Annexes
[ETN-88-91318] 14 p1889 N88-21231
CTD/O2 data collected in 1985 and 1986 for EPOCS (Equatorial Pacific Ocean Climate Studies)
[PB88-160775] 14 p1951 N88-21629
Activities report in aerospace
[ETN-88-91976] 14 p1991 N88-21866
Engineering support of space shuttle experiment integration
[AD-A190135] 15 p2024 N88-22061
Summary of the 1987 Gordon Research Conference on Corrosion
[AD-A189737] 15 p2041 N88-22161

Structural dynamics branch research and accomplishments for fiscal year 1987
[NASA-TM-100279] 15 p2088 N88-22446
The Department of Defense Superconductivity Research and Development (DSRD) options. A study of possible directions for exploitation of superconductivity in military applications
[AD-A189747] 15 p2142 N88-22780
Space directorate research and technology accomplishments for fiscal year 1987
[NASA-TM-100607] 15 p2153 N88-22854
Advanced electric propulsion research
[NASA-CR-182130] 16 p2170 N88-22937
Ionospheric research in Antarctica
[INPE-4521-PRE/1273] 16 p2232 N88-23331
Naval research reviews, volume 39, number 3
[AD-A191392] 16 p2264 N88-23543
Advice for astronomical research
[ISBN-9-03-460977-4] 16 p2289 N88-23703
Fiber waveguide sensors for intelligent materials
[NASA-CR-183028] 17 p2343 N88-23968
Structures and Dynamics Division research and technology plans for FY 1988 and accomplishments for FY 1987
[NASA-TM-100585] 17 p2350 N88-24000
An overview of advanced battery development at Sandia National Laboratories
[DE88-006823] 18 p2506 N88-24867
Space station architectural elements and issues definition study
[NASA-CR-3941] 18 p2587 N88-25371
The Department of Defense report on the merit review process for competitive selection of university research projects and an analysis of the potential for expanding the geographic distribution of research for the Committees on Appropriations, United States Congress
[AD-A191842] 18 p2588 N88-25379
NASA history data book. Volume 1: NASA resources 1958-1968
[NASA-SP-4012-VOL-1] 18 p2596 N88-25428
NASA historical data book. Volume 2: Programs and projects 1958-1968
[NASA-SP-4012-VOL-2] 18 p2596 N88-25429
NASA historical data book. Volume 3: Programs and projects 1969-1978
[NASA-SP-4012-VOL-3] 18 p2596 N88-25430
Acid rain: Delays and management changes in the Federal research program
[GAO/RCED-87-89] 19 p2690 N88-25988
Computer-aided research
[DE88-007771] 19 p2714 N88-26114
Anatomy of an organizational change effort at the Lewis Research Center
[NASA-CR-4146] 19 p2739 N88-26264
Flight research and testing
[NASA-TM-100439] 20 p2758 N88-26361
Plastic deformation and roughness of free metal surfaces
[PB88-196621] 20 p2772 N88-26439
Novel magnetic materials research using free electron lasers
[DE88-009969] 20 p2807 N88-26652
Building an artificial intelligence capability at Los Alamos
[DE88-009155] 20 p2842 N88-26866
Issues and recommendations associated with distributed computation and data management systems for the space sciences
[NASA-CR-183026] 20 p2881 N88-27108
Aerospace applications studies, 1971-1987
[AGARD-R-759] 21 p2889 N88-27147
Air Force technical objective document, FY89
[AD-A193110] 21 p2896 N88-27194
Soviet dynamic fracture mechanics research
[FASAC-TAR-3140] 21 p2962 N88-27597
Finite element methodology for integrated flow-thermal-structural analysis
[NASA-CR-183144] 21 p2964 N88-27606
Atmospheric turbulence research at DFVLR
[AGARD-R-752] 21 p2975 N88-27669
Federal Council on Science, Engineering and Technology: Committee on Computer Research and Applications, Subcommittee on Science and Engineering Computing: The US Supercomputer Industry
[DE88-011262] 21 p2994 N88-27756
RLE progress report, January 1 to December 31, 1987
[RLE-PR-130] 21 p3011 N88-27869
Publications on acoustics research at the Langley Research Center during 1980-1986
[NASA-TM-100590] 21 p3013 N88-27881
The High Temperature Materials Laboratory: A new research and user facility at the Oak Ridge National Laboratory
[DE88-010792] 22 p3057 N88-28138
Development and verification of NASA Standard Initiator-2 (NSI-2)
[NASA-CR-172069] 23 p3200 N88-29044
Development and verification of NASA Standard Initiator-2 (NSI-2): Appendix
[NASA-CR-172070] 23 p3200 N88-29045
SERI's photovoltaic research project: A foundation for tomorrow's utility-scale electricity
[DE88-001161] 23 p3230 N88-29220
Competition: Issued on establishing and using Federally funded research and development centers
[PB88-178884] 23 p3296 N88-29632
Argonne National Laboratory technology transfer report, FY87
[DE88-010091] 23 p3298 N88-29639
Activities report in remote sensing
[ETN-88-92905] 23 p3309 N88-29714
Space shuttle phase B wind tunnel model and test information. Volume 1: Booster configuration
[NASA-CR-178414-VOL-1-PT-2]
24 p3320 N88-29770
Noncontact photo-thermal sensing
[AD-A195450] 24 p3344 N88-29905
Helicopter transmission research at NASA Lewis Research Center
[NASA-TM-100962] 24 p3379 N88-30128
Science at NASA field centers: Findings and recommendations on the scope, strength and interactions of science and science-related technology programs
[NASA-TM-101188] 24 p3459 N88-30581
Research and technology of the Lyndon B. Johnson Space Center
[NASA-TM-100463] 24 p3460 N88-30583

RESEARCH PROJECTS
University program management information system, fiscal year 1985
[NASA-TM-88361] 06 p0790 N88-14846
Acid rain: Delays and management changes in the Federal research program
[GAO/RCED-87-89] 19 p2690 N88-25988

RESEARCH VEHICLES
NT X-30 VEHICLE
A multiprocessor avionics system for an unmanned research vehicle
[AD-A194606] 24 p3325 N88-29800

RESERVOIRS
Observations of wind waves on a reservoir
[IOS-234] 02 p0193 N88-11206
Understanding passive cooling systems
[PB87-210464] 02 p0194 N88-11211
Study of reservoir water quality utilizing remote sensing techniques: Methodological concepts
17 p2364 N88-24076
Utilization of LANDSAT-TM imagery in the hydroenergetic inventory of the Paraiba de Sul River Basin 17 p2364 N88-24077
Unstable heat pipes
[DE88-010780] 23 p3229 N88-29217

RESIDENTIAL AREAS
Remote sensing techniques applied to the study of metropolitan regions: The west sector of the Sao Paulo metropolitan area 19 p2681 N88-25941
SPOT imagery for detecting residential expansion on the rural-urban fringe of Toronto, Canada
22 p3098 N88-28397
Applications of SPOT data for urban real estate investment information systems
22 p3101 N88-28414
Mapping and urban multi-experimental assessment of SPOT: Urban results 22 p3101 N88-28415

RESIDENTIAL ENERGY
Transient development of stratification in a partially divided enclosure
[DE87-011742] 05 p0572 N88-13490
Heat pump and appliance research
[PB88-102462] 07 p0853 N88-15184
Short Reference Years: Short weather data sets for faster simulations of solar energy systems and energy consumption in buildings
[DE88-900198] 07 p0881 N88-15343
Actual performance and economic feasibility of residential solar water heaters
[INPE-4399-RPE/555] 08 p1023 N88-16191
Effect of storage thermal behavior in seasonal storage solar heating systems
[PB88-114236] 10 p1350 N88-18067

RESIDUAL STRENGTH
Fiber composite structural durability and damage tolerance: Simplified predictive methods
[NASA-TM-100179] 05 p0560 N88-13409
Investigation of low velocity impact damage on filamentary composite materials
07 p0923 N88-15607
Residual stiffness and strength of Kevlar/epoxy laminated impulsively loaded to 7.9 ktaps
[DE88-003724] 09 p1149 N88-16886
Effects of moisture, elevated temperature, and fatigue loading on the behavior of graphite/epoxy buffer strip panels with center cracks
[NASA-TM-100558] 12 p1603 N88-19590

RESIDUAL STRESS
Stress-strain behavior of components subject to residual stresses taking the example of an orifice plate
[FF-10/1986] 01 p0059 N88-10375
Crack initiation life estimations for notched specimens with residual stresses based on local strains
[FF-17/1986] 01 p0060 N88-10385
Stress measurements in sol-gel films
[DE87-014487] 02 p0153 N88-10955
On the stressing of annealed NITINOL: The electrical resistance and calorimetric effects
[AD-A184465] 04 p0414 N88-12569
The evolution of local mechanical properties of Al 2219-T851 during fatigue 05 p0598 N88-13653
The influence of microstructure and residual stresses on the initiation and propagation of short surface cracks on AlMgSi1 05 p0601 N88-13674
Observations on the effect of overloads on fatigue crack growth 05 p0602 N88-13684
The effect of heat treatment on fatigue crack growth in polycarbonate 05 p0606 N88-13714
Analysis of end stresses in glass-metal bimaterial strips
[DE87-007848] 05 p0610 N88-13750
Threshold stress intensity for stable crack growth in high strength steel at ambient temperature and below
06 p0718 N88-14407
Interface characteristics and the mechanical properties of metal matrix composites
[AD-A186441] 08 p0966 N88-15845
Residual stress effect on stability of axially loaded columns
[PB87-143889] 08 p0996 N88-16032
Bias, internal stress and substrate effects on the microstructure and properties of PVD-wear resistant coatings
[AERE-R-12360] 10 p1304 N88-17798
Mechanical response of unidirectional boron/aluminum under combined loading
[NASA-CR-182595] 12 p1604 N88-19591
Evolution of hardening and damage during viscoplastic deformation
[AD-A190714] 15 p2077 N88-22381
Stress corrosion cracking of A723 steel pressure vessels: Two case studies
[AD-A191741] 18 p2527 N88-24990
The stress analysis of ceramic, polymeric, and metallic composite systems by the finite element method
18 p2529 N88-25004
The use of micromachined structures for the management of mechanical properties and adhesion of thin films 19 p2674 N88-25899
Observations on residual stresses in ceramic composites by neutron diffraction techniques
[DE88-009937] 20 p2778 N88-26472
Lattice strain in heteroepitaxial films
20 p2868 N88-27032
Thermo-viscoelastic analysis of composite materials, volume 1
[NASA-CR-183048-VOL-1] 21 p2904 N88-27230
Studies of internal stresses and surface roughness of sputtered Be and BeB films
[DE88-011737] 22 p3086 N88-28327
Theory of acoustoplasticity and ultrasonic measurements of residual stresses
22 p3087 N88-28329
Determination of the residual stresses in welded structures using the elastoplastodynamic method
[ETN-88-92745] 22 p3087 N88-28330
Thin film-residual stress assessment
[AD-A193205] 23 p3196 N88-29018
The mechanical behavior of surface modified ceramics
[DE88-010564] 23 p3196 N88-29022
A dynamic analysis of piezoelectric strained elements
[AD-A196079] 24 p3432 N88-30430

RESIDUES
Implementation of a digital optical matrix-vector multiplier using a holographic look-up table and residue arithmetic
[NASA-CR-180431] 01 p0078 N88-10496
Low extractable wipers for cleaning space flight hardware 02 p0137 N88-10863
Synthesis of high molecular weight peptide polymers and copolymers containing L-dope residues
[AD-A186462] 08 p0973 N88-15887
A programmable global system for the manipulation of residue numbers
[ETN-88-91476] 11 p1530 N88-18139
Carbon residue studies of polyphenyl ethers and ester-based lubricants using a microcarbon residue tester
[AD-A188585] 12 p1611 N88-19632

TDWR (Terminal Doppler Weather Radar) clutter residue map generation and usage
[AD-A191148] 16 p2235 N88-23352
Residual smoothing for accelerating the Alternating Direction Implicit (ADI) iteration method for elliptic difference equations
[CWI-NM-R8721] 16 p2259 N88-23500

RESIN BONDING
Interfacial shear strength of pitch and high strain pan fibers in an epoxy matrix
[AD-A185966] 07 p0826 N88-15011
Adhesion between polystyrene and polymethylmethacrylate
[AD-A192050] 18 p2492 N88-24785

RESIN MATRIX COMPOSITES
NT BORON-EPOXY COMPOSITES
NT GRAPHITE-EPOXY COMPOSITES
Composite structural materials
[NASA-CR-181416] 02 p0190 N88-11186
Time-temperature-stress capabilities of composite materials for advanced supersonic technology application
[NASA-CR-178272] 06 p0677 N88-14144
Fatigue behaviour of hybrid composites
[BR102236] 09 p1138 N88-16819
Mechanics of composite materials: Past, present and future
[NASA-TM-100793] 10 p1295 N88-17744
Ethynylated aromatics as high temperature matrix resins
[NASA-TM-89829] 11 p1450 N88-18640
Interlaminar fracture toughness of thermoplastic composites
[NASA-TM-100532] 15 p2030 N88-22097
Donor acceptor polymerization chemistry as a vehicle to low energy cure matrix resins
[AD-A190119] 15 p2044 N88-22179
Characterization of Mode 1 and Mode 2 delamination growth and thresholds in graphite/peek composites
[NASA-TM-100577] 16 p2172 N88-22947
Influence of fiber reinforcement on the vitreous transition temperature of M 10 matrix composites
[ONERA-RT-44/7086-M] 17 p2316 N88-23835
Proceedings of the American Society for Composites
[AD-A189861] 18 p2477 N88-24693
Current and future molecular structures of aerospace organic matrix resins 18 p2477 N88-24695
Industrial perspective on current and future needs in aerospace matrix resin chemistry
18 p2477 N88-24696
Applications of biotechnology to synthetic chemistry for aerospace matrix resins development
18 p2478 N88-24697
The 700 F properties of autoclave cured PMR-2 composites
[NASA-TM-100923] 18 p2480 N88-24712
The composite aeroengine
[PNR90451] 22 p3045 N88-28070
New acousto-ultrasonic techniques applied to aerospace materials
[NASA-TM-101299] 22 p3066 N88-28323
Novel ladder polymers for use as high temperature stable resins or coatings
[NASA-CASE-LEW-14203-1] 24 p3356 N88-29984

RESINS
NT ACRYLIC RESINS
NT EPOXY RESINS
NT KEVLAR (TRADEMARK)
NT NYLON (TRADEMARK)
NT PEEK
NT PHENOLIC RESINS
NT POLYAMIDE RESINS
NT POLYETHER RESINS
NT POLYIMIDE RESINS
NT POLYMETHYL METHACRYLATE
NT POLYURETHANE RESINS
NT SYNTHETIC RESINS
NT THERMOPLASTIC FILMS
NT THERMOPLASTIC RESINS
NT THERMOSETTING RESINS
NT VINYL COPOLYMERS
Effects of cure pressure on resin flow, voids, and mechanical properties
[AD-A184267] 03 p0295 N88-11853
Influence of carbon fiber surface treatment
[ETN-88-92536] 18 p2492 N88-24787
Electrophoretic coatings. Part 1: Sandia applications
[DE88-008866] 20 p2776 N88-26465

RESISTANCE
Experimental determination of the coefficients of the hydraulic resistance of apertures in the rotary disks
[AD-A190627] 15 p2066 N88-22317

RESISTANCE COEFFICIENTS
U RESISTANCE

RESISTANCE THERMOMETERS
A device for measuring fast temperature fluctuations --- atmospheric temperature
[KNMI-TR-92] 01 p0070 N88-10449
NBS (National Bureau of Standards) measurement services: Platinum resistance thermometer calibrations
[PB88-138367] 10 p1333 N88-17967

RESISTIVITY
U ELECTRICAL RESISTIVITY

RESISTOJET ENGINES
Space station propulsion
[NASA-TM-100216] 03 p0277 N88-11746
Slip casting and extruding shapes of rhemium with metal oxide additives. Part 2: Development of grain stabilized rhenium parts for resistojets
[NASA-CR-180851] 03 p0278 N88-11749
Compatability of dispersion-strengthened platinum with resistojet propellants
[NASA-TP-2765] 04 p0409 N88-12538
Space station resistojet system requirements and interface definition study
[NASA-CR-180832] 04 p0409 N88-12541
Magnetic emissions testing of the space station engineering model resistojet
[NASA-TM-100788] 10 p1292 N88-17728
Component data base for space station resistojet auxiliary propulsion
[NASA-CR-180834] 10 p1293 N88-17731
Electric propulsion options for the SP-100 reference mission 17 p2404 N88-24296
Development of a liquid-fed water resistojet
[NASA-TM-100927] 18 p2523 N88-24968
Experimental evaluation of resistojet thruster plume shields
[NASA-TM-101363] 24 p3338 N88-29868
The dc power control for a liquid-fed resistojet
[NASA-TM-101326] 24 p3338 N88-29869

RESISTOJETS
U RESISTOJET ENGINES

RESISTORS
NT POTENTIOMETERS (RESISTORS)
NT THERMISTORS
Resistor cooling in a vacuum
[DE88-000696] 04 p0440 N88-12733

RESOLUTION
NT ANGULAR RESOLUTION
NT HIGH RESOLUTION
NT IMAGE RESOLUTION
NT RADAR RESOLUTION
NT RADIOMETRIC RESOLUTION
NT SPATIAL RESOLUTION
NT SPECTRAL RESOLUTION
NT TEMPORAL RESOLUTION
Geometric analysis of ensemble of solutions in two-phase flow and complete resolution of problem of choking
[DE88-001687] 04 p0445 N88-12764
Improvement of deep resolution in ultrasonic echographic nondestructive evaluation using signal processing methods
[PB87-147658] 07 p0866 N88-15256
Conflict resolution in cooperative systems
[AD-A190351] 15 p2104 N88-22535
Television monitor field shifter and an opto-electronic method for obtaining a stereo image of optimal depth resolution and reduced depth distrotion on a single screen
[NASA-CASE-NPO-17249-1-CU]
17 p2332 N88-23024
The complexity of AI algorithms
[AD-A193494] 23 p3265 N88-29438
An analysis of results of a high-resolution world ocean circulation model
[AD-A195760] 24 p3405 N88-30272

RESOLVING POWER
U RESOLUTION

RESONANCE
NT CYCLOTRON RESONANCE
NT ELECTRON PARAMAGNETIC RESONANCE
NT MAGNETIC RESONANCE
NT MESON RESONANCE
NT NUCLEAR MAGNETIC RESONANCE
NT OPTICAL RESONANCE
NT ORBITAL RESONANCES (CELESTIAL MECHANICS)
NT PARAMAGNETIC RESONANCE
NT PLASMA RESONANCE
NT RESONANT VIBRATION
NT SPIN RESONANCE
Direct detection of optical radiation through a sampling orifice for inductively coupled plasma atomic emission spectroscopy
[DE87-013609] 01 p0101 N88-10662
Assessment of structural integrity from forced vibration testing
[DE87-014642] 02 p0191 N88-11195
Plasmon resonance absorption in layered structures of silver with periodic corrugation
[DE87-013183] 02 p0231 N88-11453
Singularity expansion method: Target Resonances
03 p0303 N88-11912
The hybrid wavefront resonance method
03 p0303 N88-11913
Surface polariton resonances and reflectance on a bigrating
[AD-A184663] 03 p0377 N88-12370
The itinerant resonating-valence-bond model for superconductivity
[DE87-014794] 03 p0380 N88-12391
The dynamics of solar magnetic flux tubes subjected to resonant foot point shaking 04 p0507 N88-13118
Resonant level lifetime in GaAs/ AlGaAs double-barrier structures
[AD-A185376] 05 p0655 N88-14020
Parametric and resonance interaction of ultrashort light pulses in nonlinear multilevel medium
06 p0773 N88-14746
Modal analyses of the Kernville diagnostic canister
[DE88-003268] 07 p0870 N88-15277
The single particle and collective descriptions of the anomalous Doppler resonance and the role of ion dynamics
[INPE-4390-PRE/1210] 08 p0976 N88-15904
Discovery by Voyager-2 of predicted satellites which determine resonance nature of Uranian rings
08 p1006 N88-16095
Geometric structure, pseudoband gaps, and surface vibrational resonances on metal surfaces
[AD-A187001] 09 p1143 N88-16851
The early years of string theory: The dual resonance model
[DE88-003521] 11 p1563 N88-19359
Resonance energy transfer between carbon monoxide and oxygen molecules using dye laser intracavity absorption spectroscopy
[AD-A188488] 12 p1689 N88-20104
Electromagnetic scattering from and natural resonances of the circular strip 13 p1759 N88-20523
Design, optimization and construction of a dc-SQUID with complete flux transformer circuits
[PB88-160742] 14 p1907 N88-21399
Tunable condensed-media laser with antiresonant ring cavity 14 p1971 N88-21764
Three-wave parametric resonance in plasma of relativistic electron flux 14 p1972 N88-21772
Theoretical studies of Resonance Enhanced Stimulated Raman Scattering (RESRS) of frequency-doubled Alexandrite laser wavelength in cesium vapor
[NASA-CR-182870] 15 p2036 N88-22133
The concept of an impact resonance diagram for characterizing the nonlinear response of impact vibration
[DE88-005475] 15 p2086 N88-22432
Low frequency ocean ambient noise: Measurements and theory
[AD-A191188] 16 p2237 N88-23362
Theoretical studies of Resonance Enhanced Stimulated Raman Scattering (RESRS) of frequency doubled Alexandrite laser wavelength in cesium vapor
[NASA-CR-182871] 17 p2317 N88-23841
Harmonic considerations for electrical distribution feeders
[DE88-007649] 18 p2505 N88-24860
Contributions of autoionizing resonances to the electron collisional excitation rates for Be-like ions
[AD-A190924] 18 p2572 N88-25275
High-fidelity in isotope ratio measurements for resonance ionization mass spectrometry
[DE88-009129] 19 p2613 N88-25506
A proposed Quantum Well Injection Transit Time device (QWITT) 19 p2657 N88-25785
Microwave and millimeter-wave resonant tunneling diodes 19 p2659 N88-25809
Quantum transport calculation of resonant-tunneling response time 19 p2659 N88-25810
Aircraft interior noise reduction by alternate resonance tuning
[NASA-CR-182540] 20 p2849 N88-26909
Resonant tunneling in InGaAs-InP double-barrier structures and superlattices 20 p2871 N88-27047
Excellent negative differential resistance of InGaAs/InAlAs resonant tunneling barrier structures and applications to a new functional device, RHET
20 p2872 N88-27048
Aeromechanical stability analysis of COPTER
21 p2891 N88-27161
Nonlinear stochastic interaction in aeroelastic structures
[AD-A193427] 21 p2961 N88-27589
Orbit determination of 1965-09A for analysis of the eccentricity at 15th-order resonance
[RAE-TR-87059] 22 p3047 N88-28081

Bulk plasmon enhanced photoemission from Nb(100) surface resonances
[AD-A192711] 22 p3154 N88-28767

Resonance excitation of linear and non-linear spiral density waves in a gaseous disk
23 p3299 N88-29643

Storing bits on a DNA polymer chain
[AD-A195701] 24 p3356 N88-29981

Impurity analysis in SIMOX samples by high-efficiency resonance ionization time-of-flight mass spectrometry
[DE88-012061] 24 p3367 N88-30051

Resonance effects accompanying motion with low thrust in earth-moon system 24 p3446 N88-30510

RESONANCE CHARGE EXCHANGE

Charge exchange in low energy (keV) and hyperthermal energy (10-100 eV) ion scattering
[AD-A187643] 11 p1543 N88-19222

RESONANCE FLUORESCENCE

Millimeter-wave studies of moist air
[AD-A184681] 03 p0306 N88-11935

Solitons in stimulated Raman scattering: Generation and control of ultrashort optical pulses
[AD-A185141] 05 p0650 N88-13983

Correlations between photons in resonance fluorescence emitted by an atom near a metal surface
[AD-A188365] 12 p1689 N88-20102

RESONANCE LINES

Formation and passivation of new paramagnetic defects associated with thermal oxides on silicon
[DE88-002720] 07 p0938 N88-15699

Low-power photolytically pumped lasers
[DE88-002448] 08 p0991 N88-15998

Inner-shell X-ray line spectra of highly ionized titanium, chromium, iron and nickel and their appliation to laboratory plasmas
[PB87-225181] 19 p2730 N88-26212

RESONANCE RADIATION

U RESONANCE FLUORESCENCE

RESONANCE SCATTERING

Resonance excitation in gamma gamma collisions at LEP200
[NIKHEF-H/87-3] 08 p1081 N88-16514

Nucleon resonances and nuclei: Experimental aspects
[CEBAF-PR-87-025] 11 p1545 N88-19233

RESONANT CAVITIES

U CAVITY RESONATORS

RESONANT FREQUENCIES

Accurate ab initio calculations which demonstrate a 3 Pi u ground state for Al2
[NASA-TM-89302] 01 p0102 N88-10666

Vibration-absorbing characteristics of metal-polymer shells 02 p0158 N88-10991

Systematic studies of molecular vibrational anharmonicity and vibration-rotation interaction by self-consistent-field higher derivative methods: Applications to asymmetric and symmetric top and linear polyatomic molecules
[DE87-014691] 02 p0232 N88-11465

Two-laser resonance enhanced photoionization spectrum of gas phase benzene
03 p0300 N88-11889

A new method to real-normalize measured complex modes 05 p0593 N88-13618

Initial dynamic load estimates during configuration design 05 p0593 N88-13621

Dynamic behavior of dissymmetric rotor bearings modelled with a periodic coefficient large system
05 p0596 N88-13640

Computation of natural frequencies of planar lattice structure
[AD-A185387] 05 p0641 N88-13920

Finite element method with continuous mass elements
[PB87-143384] 08 p0995 N88-16019

The dynamics of an oscillating four-bar linkage
09 p1181 N88-17074

Centaur G Prime modal test 09 p1181 N88-17075

Using frequency-domain methods to identify XV-15 aeroelastic modes
[NASA-TM-100033] 10 p1277 N88-17646

Time domain wave propagation in multilayered integrated circuits
[AD-A187462] 10 p1324 N88-17916

Electro-mechanical vibratory system
11 p1500 N88-18958

Study of inhomogeneously filled cylindrical resonant cavities by the finite integration technique
[PB88-133707] 12 p1697 N88-20156

Time-domain system for identification of the natural resonant frequencies of aircraft relevant to electromagnetic compatibility testing
[PB88-164520] 13 p1759 N88-20519

The concept of an impact resonance diagram for characterizing the nonlinear response of impact vibration
[DE88-005475] 15 p2086 N88-22432

Single mode levitation and translation
[NASA-CASE-NPO-16675-1-CU]
17 p2395 N88-24241

Open channel flow near the resonance speed
18 p2514 N88-24918

Resonant structures for integrated sensors
19 p2673 N88-25893

FEB structural analysis, revision H
[AD-A192302] 20 p2814 N88-26698

Vibration response of constrained viscoelastically damped plates: Analyses and experiments
[AD-A192329] 20 p2815 N88-26699

Prediction of the aeroelastic behavior of tuned blades. Application to aircraft engines
[ISAL-87-0046] 21 p2897 N88-27199

Natural frequencies and stability of immiscible cylindrical z-independent liquid systems
[LRT-WE-9-FB-1(1987)] 22 p3053 N88-28112

Natural frequencies and stability of immiscible spherical liquid systems
[LRT-WE-9-FB-2(1987)] 22 p3053 N88-28113

Natural frequencies and stability of circular cylindrical immiscible liquid systems
[LRT-WE-9-FB-3(1987)] 22 p3062 N88-28172

Nonlinear oscillations of axially independent liquid column under zero-gravity environment
[LRT-WE-9-FB-12(1987)] 22 p3063 N88-28174

Measure of hydrogen concentration profile in materials by resonant nuclear reactions
[DE88-702599] 23 p3193 N88-28999

Effects on the resonant frequencies caused by loading a spherical cavity with a dielectric sphere
[AD-A193864] 23 p3277 N88-29511

Laser sensing for identification and control of distributed parameter systems
[AD-A195886] 24 p3379 N88-30124

RESONANT VIBRATION

The effect of different packagings on the vibration behavior and the coupling factors of steam turbine blading
[ETN-87-90425] 01 p0056 N88-10357

Equivalent circuit consideration on the rotation of resonant modes of double resonant vibrators
07 p0839 N88-15092

Analyses by equivalent mechanical circuits of bending vibration bars with load-impedance at one end
07 p0840 N88-15093

Sea resonance vibrational source of seismic waves
08 p1010 N88-16126

Theoretical and experimental damping values of piping systems at high ductilities
[DE88-006717] 18 p2526 N88-24986

The role of acoustic resonances in unsteady turbomachinery aerodynamics
[PNR90455] 22 p3147 N88-28720

RESONATORS

NT CAVITY RESONATORS
NT OPTICAL RESONATORS

Measurement and analysis of cryogenic sapphire dielectric resonators and DROs
04 p0433 N88-12686

Equivalent circuit consideration on the rotation of resonant modes of double resonant vibrators
07 p0839 N88-15092

Analyses by equivalent mechanical circuits of bending vibration bars with load-impedance at one end
07 p0840 N88-15093

GERA computer code for calculation of two-dimensional electromagnetic fields in resonators and electron-optical systems by the finite element method
[DE88-700678] 11 p1480 N88-18631

Parametric study of acceleration-induced stresses and frequency changes in doubly-rotated crystal resonators
[AD-A189261] 13 p1761 N88-20532

Quartz oscillator analysis
[DE88-005886] 13 p1764 N88-20550

Semiclassical theory of injected lasers with arbitrary stable and unstable resonators
[AD-A189514] 13 p1775 N88-20615

Resonator coupling of two ring cavity, argon-ion lasers
[AD-A189558] 13 p1775 N88-20616

Method for characterizing end-plate surface resistance of dielectric resonator 14 p1903 N88-21371

Efficient narrow linewidth waveguide dye laser pumped by CuCl laser 16 p2187 N88-23038

Surface wave accelerometer
[ETN-88-92000] 16 p2210 N88-23192

Electrothermal instability in superconducting resonators
[DE88-701684] 16 p2262 N88-23664

Low noise cryogenic dielectric resonator oscillator
[NASA-CASE-NPO-17157-1-CU]
20 p2797 N88-26596

Quartz crystal resonators and oscillators for frequency control and timing applications
[AD-A193310] 21 p2937 N88-27443

X-band resonant ring operation at 450 kW
22 p3064 N88-28181

RESOURCE ALLOCATION

Semi-arid ecosystem development as a function of resource processing and allocation
[DE88-000690] 07 p0875 N88-15309

A software planning and development methodology with resource allocation capability
[AD-A186088] 07 p0902 N88-15462

Physics rationale for the engineering specifications for ZTH
[DE88-000936] 07 p0936 N88-15690

Iterative-deepening heuristic search for optimal and semi-optimal resource allocation
08 p1062 N88-16410

Planning activities in space 08 p1063 N88-16417

An AI approach for scheduling space-station payloads at Kennedy Space Center 08 p1064 N88-16425

Scheduling spacecraft operations
08 p1064 N88-16426

The resource envelope as a basis for space station management system scheduling
08 p1064 N88-16427

Preliminary analysis of an integrated logistics system for OSSA payloads. Volume 2: OSSA integrated logistics support strategy 12 p1584 N88-19479

Dynamic resource allocation in a hierarchical multiprocessor system: A preliminary study
[NASA-CR-183177] 22 p3141 N88-28675

RESOURCES

NT AQUIFERS
NT COAL
NT CRUDE OIL
NT EARTH RESOURCES
NT FORESTS
NT FOSSIL FUELS
NT GEOTHERMAL RESOURCES
NT GLACIERS
NT ICEBERGS
NT LAND ICE
NT MARINE RESOURCES
NT NATURAL GAS
NT OIL FIELDS
NT RAIN FORESTS
NT TAR SANDS
NT UNDERWATER RESOURCES
NT WATER RESOURCES

RESOURCES MANAGEMENT

NT FOREST MANAGEMENT
NT LAND MANAGEMENT

Study of Earth from space and strengthening of economy 01 p0010 N88-10055

Optimum dimensioning of field service centers: Analysis of the problem and solutions thereof
01 p0012 N88-10066

A unified approach to parallel computation: Performance evaluation and architecturally independent parallel programming
[DE87-012519] 01 p0084 N88-10540

Knowledge acquisition issues encountered during the development of an estimating expert system
[DE87-013320] 02 p0248 N88-11568

Spinoff, 1987
[NASA-TM-89652] 02 p0250 N88-11577

Desertification in the Sahelian and Sudanian Zones of West Africa
[PB87-217063] 03 p0345 N88-12183

University research initiative research program summaries
[AD-A184876] 05 p0658 N88-14035

Detection of soil erosion with Thematic Mapper (TM) satellite data within Pinyon-Juniper woodlands
[NASA-CR-182476] 09 p1185 N88-17103

Air Force geographic information and analysis system
[DE88-001420] 10 p1424 N88-18505

Computer-Aided Design Information System (CADIS): User's manual
[DE88-004365] 10 p1424 N88-18509

Wind energy resource survey of New Zealand: National resource assessment
[PB88-139365] 12 p1640 N88-19822

Systems approach to energy quality and efficiency
[PB88-139506] 12 p1640 N88-19823

Orbital remote sensing: An instrument for monitoring urban growth
[INPE-4456-PRE/1287] 15 p2150 N88-22833

Resource management in dialog cell specification (DICE) method
[CWI-CS-R8746] 16 p2246 N88-23433

A proposal for a project entitled assessment of forest resources in Uruguay submitted to the United Nations Industrial Development Organization (UNIDO)
17 p2352 N88-24016

Remote sensing and data integration: Practical solutions for resource managers 17 p2356 N88-24034

Identification of areas cultivated with soybeans in the cerrados regions, through digital processingof satellite images: A methodological approach
17 p2358 N88-24048
Research on enhancing the utilization of digital multispectral data and geographic information systems in global habitability studies
[NASA-CR-182799] 17 p2368 N88-24101
Department of Defense Statement on the Technology Base to the Subcommittee on Defense Industry and Technology of the Committee on Armed Services, United States Senate, 100th Congress, second session
[AD-A191639] 18 p2566 N88-25376
Application of remote sensing in the conservation of natural areas: Ribeira Valley 19 p2683 N88-25949
Remote sensing technique applied to vegetation as an aid to municipal planning 19 p2683 N88-25951
Remote sensing applied to the monitoring of mineral extraction in the proximity of urban areas: Pros and cons
19 p2684 N88-25954
Remote sensing applied to integrated regional development programs 19 p2685 N88-25958
Application of SPOT data to renewable resources in the Maldives 22 p3109 N88-28469
LRS-2: A specialized knowledge system for launch resource scheduling
[AD-A194625] 23 p3182 N88-28941
A scheduling and resource management system for space applications 23 p3256 N88-29383
Intelligent resource management for local area networks: Approach and evolution
23 p3256 N88-29385
Study of the spectral response of soybeans
[INPE-4592-PRE/1322] 24 p3387 N88-30174

RESPIRATION
NT HIGH ALTITUDE BREATHING
Fundamental study on gas monitoring in CELSS
03 p0359 N88-12263
Study of the relationship between photosynthesis, respiration, transpiration, and mineral nutrition in wheat
03 p0360 N88-12266
Human respiratory responses during high performance flight
[AGARD-AG-312] 04 p0474 N88-12923
Short-term in vitro screening studies related to the inhalation toxicology of potentially toxic aerosols
[AD-A184815] 05 p0629 N88-13845
A plethysmograph for measuring pulmonary ventilation in small animals
[AD-A184978] 05 p0629 N88-13846
Maximal cardiorespiratory responses to one- and two-legged cycling during acute and long-term exposure to 4300m
[AD-A185730] 06 p0752 N88-14621
Biorhythmological analysis of dynamics of pulmonary ventilation parameters during orthostatic tests
07 p0891 N88-15400
Role of hemoglobin affinity for oxygen in efficiency of blood respiratory function 07 p0892 N88-15406
Changes in functional parameters of animals during long-term inhalation of acetic acid
07 p0895 N88-15423
Exercise thermoregulation after prolonged wakefulness
[AD-A186224] 08 p1048 N88-16327
Experimental measurements of the uptake of ozone in rats and human subjects
[PB88-125422] 10 p1364 N88-18149
Effect of oxygen inhalation on respiratory function during exercise and exposure to added resistance to respiration
10 p1366 N88-18164
Toxic effects of man-made mineral fibers with particular reference to ceramic fibers
[AD-A187949] 11 p1519 N88-19072
Electromagnetic metrics of mental workload
[AD-A188205] 11 p1523 N88-19093
Respiratory parameters aboard an aircraft performing parabolic flights 12 p1653 N88-19902
Breath-by-breath measurement of alveolar gas exchange 12 p1653 N88-19905
Nitrogen's biological effect on oxygen transport through hematoparenchymal barrier 12 p1662 N88-19967
Human adaptation to various hypercapnic conditions in relation to salivary electrolyte dynamics and renal function 12 p1664 N88-19977
Air quality and human performance, chapter 16
[AD-A188335] 12 p1666 N88-19988
Fibrous glass aerosols: A literature review
[AD-A188420] 12 p1672 N88-20008
Increase in influence of oxygen on the body in the presence of helium 13 p1810 N88-20816
A laser-based photoacoustic spectrometer for direct breath C-13O2/C-12O2 measurement
[DE88-004915] 15 p2101 N88-22516
Vagal tone as an index of mental state
16 p2239 N88-23373
Mathematical modelling of the heat and water vapour transport in the human respiratory tract
17 p2382 N88-24160
Effect of long-term inhalation of acetic acid vapor on some functional parameters of man
19 p2705 N88-26084
Respiration and oxygen tension in the blood of animals exposed to high pressures 20 p2830 N88-26790
Metabolic and cardiorespiratory parameters during three consecutive days of exhaustive running
[AD-A192596] 21 p2985 N88-27728

RESPIRATORY DISEASES
NT ASTHMA

RESPIRATORY PHYSIOLOGY
Load carriage induced alterations of pulmonary function
[AD-A186227] 07 p0889 N88-15386
The respiratory system under weightlessness
12 p1653 N88-19901
Respiratory parameters aboard an aircraft performing parabolic flights 12 p1653 N88-19902
The effect of orthostatic changes in central blood volume on the heart rate response to graded Valsalva maneuvers 12 p1653 N88-19904
Breath-by-breath measurement of alveolar gas exchange 12 p1653 N88-19905
Second-generation respiratory monitoring system for microgravity studies in man 12 p1653 N88-19906
Lung function in simulated microgravity
12 p1654 N88-19907
Closed system physiology: Role of oxygen in the development of wheat 12 p1655 N88-19916

RESPIRATORY RATE
Vital signs rate meter
[AD-A187015] 09 p1198 N88-17183
Desynchronization of heart rate and breathing frequency after transmeridional flight across three time zones
12 p1663 N88-19968

RESPIRATORY SYSTEM
NT ALVEOLI
NT GLOTTIS
NT LARYNX
NT LUNGS
Radon Research Program, FY-1987
[DE88-002633] 09 p1188 N88-17120
JPRS Report: Science and Technology. USSR: Space Biology and Aerospace Medicine, volume 21, no. 6, November - December 1987
[JPRS-USB-88-004] 10 p1364 N88-18150
Effect of hypercapnic-hypoxic test on cariorespiratory parameters of individuals with neurocirculatory dystonia
10 p1367 N88-18169
Modeling of the non-auditory response to blast overpressure
[AD-A187397] 10 p1369 N88-18184
The respiratory system under weightlessness
12 p1653 N88-19901
Mathematical modelling of the heat and water vapour transport in the human respiratory tract
17 p2382 N88-24160
Accidental hypothermia
[AD-A194967] 24 p3406 N88-30278
Models of cerebral-body perfusion and cerebral chemical transport
[AD-A194945] 24 p3407 N88-30283

RESPONDERS
U TRANSPONDERS

RESPONSE BIAS
Response characteristics of dual MOSFET gamma-ray sensors produced by Mitel Corporation
[AD-A189026] 12 p1630 N88-19755
Picosecond optical autocorrelation experiments on fast photodetectors 19 p2659 N88-25802
A nonparametric multidimensional IRT approach with applications to ability estimation and test bias
[AD-A194212] 23 p3273 N88-29483

RESPONSE TIME (COMPUTERS)
Adaptive line of sight algorithms
[DE87-014275] 01 p0061 N88-10523
High performance clause indexing
[DE87-011399] 01 p0106 N88-10688
Indirect solution of static problems using concurrent vector processing computers
[DE87-012105] 05 p0636 N88-13889
An empirical investigation of load indices for load balancing applications
[AD-A185763] 06 p0724 N88-14451
A comparison of the Cray-2 performance before and after the installation of memory pseudo-banking
[NASA-CR-177462] 09 p1215 N88-17287
Graph transformation algorithms for array memory optimization in applicative languages
[DE88-004727] 10 p1387 N88-18283
Modules of nanosecond logic electronics system with computer control
[DE88-700190] 11 p1479 N88-18828
Object recognition on a systolic array
[AD-A187726] 11 p1534 N88-19164
Computer aided fast turnaround laboratory for research in VLSI (Very Large Scale Integration)
[AD-A189451] 12 p1624 N88-19715
Computer program in BASIC language for computation of spectrochemical analytical data
[DE88-701229] 15 p2032 N88-22106
COMESH: A corner mesh finite difference code to solve multigroup diffusion equations in multidimensions
[DE88-701248] 15 p2108 N88-22555
Concepts for robot motion primitives required for space station teleoperations 23 p3257 N88-29387

RESPONSES
NT DYNAMIC RESPONSE
NT HEMODYNAMIC RESPONSES
NT MODAL RESPONSE
NT PHYSIOLOGICAL RESPONSES
NT TRANSIENT RESPONSE
Engine/airframe response evaluation of the HH-60A helicopter equipped with the T700-GE-701 transient droop improvement electronic control unit
[AD-A184443] 04 p0401 N88-12492
Shadow systems and attractors in reaction-diffusion equations
[AD-A185804] 06 p0766 N88-14706
Computer response time measurements of mood, fatigue and symptom scale items: Implications for scale response time uses
[AD-A186093] 07 p0888 N88-15384
Corrosion behavior of sputter-deposited aluminum-based alloys exposed to chloride solutions
[AD-A187262] 10 p1303 N88-17794
Computer aided fast turnaround laboratory for research in VLSI (Very Large Scale Integration)
[AD-A189451] 12 p1624 N88-19715
Distraction and inhibition in continuous CRT performance: A replication and some new findings
[PB88-150941] 13 p1811 N88-20821
The interaction of sensory and perceptual variables: Spatial, temporal and orientation response to figure and ground
[AD-A192897] 20 p2832 N88-26798
Synchronous response modelling and control of an annular momentum control device
[NASA-CR-4166] 24 p3358 N88-29995
Numerical simulation of the function of scientific instrumentation for measuring the speed of electron devices
[AD-A194969] 24 p3376 N88-30103
Dirichlet prior in Bayesian estimation of item response curves
[AD-A195311] 24 p3426 N88-30392

REST
NT BED REST
Influence of altitude and caffeine during rest and exercise on plasma levels of proenkephalin peptide F
[AD-A192659] 22 p3131 N88-28616

RESTORATION
Method for combined image interpolation-restoration through a fir filter design technique
[INPE-4561-PRE/1302] 24 p3413 N88-30315

RESTRAINTS
U CONSTRAINTS

RESTRICTIONS
U CONSTRICTIONS

RESUSCITATION
Accidental hypothermia
[AD-A194967] 24 p3406 N88-30278

RETAINING
Hydrogen retention and release from uranium dioxide
[DE88-002042] 07 p0829 N88-15030

RETARDANTS
NT FLAME RETARDANTS

RETARDING
The generation and suppression of synchrotron sidebands
[DE88-000532] 04 p0449 N88-12787
Fatigue crack retardation in aluminum alloys
05 p0602 N88-13681
Effect of overload ratios on fatigue crack growth behavior in Ti-6Al-4V alloy
[PB87-147062] 07 p0833 N88-15055
The retardation of cold fronts at high mesoscale mountains 09 p1241 N88-17437

RETARDING ION MASS SPECTROMETERS
U MASS SPECTROMETERS

RETENTION (PSYCHOLOGY)
Short- and long-term effects of nonlethal levels of fast high-energy helium ions on retention of developed and formation of new behavioral patterns in rats
10 p1362 N88-18140
Working memory capacity: An individual differences approach
[AD-A192359] 20 p2833 N88-26803

Skilled memory and expertise: Mechanisms of exceptional performance
[AD-A193829] 22 p3133 N88-28628
Low doses of atropine sulfate impair retention of a well-learned spatial task
[AD-A194065] 23 p3237 N88-29266

RETINA
NT FOVEA
Psychophysical, biochemical and histological studies of spectrally selective photic damage to primate retina
[AD-A188115] 11 p1517 N88-19063
Functional assessment of laser irradiation
[AD-A195735] 24 p3408 N88-30287

RETINAL ADAPTATION
NT DARK ADAPTATION
NT LIGHT ADAPTATION

RETIREMENT FOR CAUSE
Engine component retirement for cause. Volume 1: Executive summary
[AD-A192730] 20 p2760 N88-26371

RETORC (TORPEDOES)
U TORPEDOES

RETRACTABLE EQUIPMENT
Development of the Extendable and Retractable Mast (ERM), Design phase 2. Volume 1 — spacecraft payloads
[RP-2010-0000-DS/09] 11 p1467 N88-18750
DARM: A new deployment and retraction mechanism which does not need electric power
14 p1876 N88-21206
The EURECA antenna deployment and retraction mechanisms 14 p1878 N88-21225
The X-beam as a deployable boom for the space station 14 p1925 N88-21473
Motion synchronization of a mechanism to deploy and restow a truss beam 14 p1925 N88-21474

RETRACTABLE LANDING GEAR
U LANDING GEAR
U RETRACTABLE EQUIPMENT

RETRIEVAL
NT DATA RETRIEVAL
NT INFORMATION RETRIEVAL
NT PAYLOAD RETRIEVAL (STS)
Mechanical design of a ultrahigh gravity UHV facility to launch and recover a low-speed projectile tested on board KC 135 14 p1877 N88-21216

RETROFITTING
Computer-aided design analysis of 57-mm, angular-contact, cryogenic turbopump bearings
[NASA-TP-2816] 11 p1496 N88-18933
Servojet retrofit
[AD-A191075] 18 p2522 N88-24964
Aircraft avionics and missile system installation cost study. Volume 1: Technical report and appendices A through E
[AD-A194605] 23 p3178 N88-28923

RETURN TO EARTH SPACE FLIGHT
The comet rendezvous asteroid flyby mission
14 p2005 N88-21956
Retrieving samples from comet nuclei
14 p2006 N88-21959

REUSABLE LAUNCH VEHICLES
NT HOTOL LAUNCH VEHICLE
Ballistic Single Stage Carrier Vehicle (BETA): A single stage reusable ballistic space shuttle concept
[MBB-UR-949/70] 10 p1310 N88-17828
Space shuttle phase B wind tunnel model and test information. Volume 3: Launch configuration
[NASA-CR-178416-VOL-3-PT-2]
24 p3315 N88-29744
Evaluation of the advanced air breathing propulsion concepts, executive summary
[ESA-CR(P)-2540] 24 p3325 N88-29802
Evaluation of advanced air breathing concepts. Volume 1: Executive summary
[ESA-CR(P)-2539] 24 p3326 N88-29806

REUSABLE ROCKET ENGINES
A reusable rocket engine intelligen control
[NASA-TM-100963] 20 p2766 N88-26401

REUSABLE SPACECRAFT
NT AEROSPACE PLANES
NT CHALLENGER (ORBITER)
NT DISCOVERY (ORBITER)
NT HERMES MANNED SPACEPLANE
NT HOTOL LAUNCH VEHICLE
NT SPACE SHUTTLE ORBITERS
NT SPACE SHUTTLES
NT X-30 VEHICLE
Ballistic Single Stage Carrier Vehicle (BETA): A single stage reusable ballistic space shuttle concept
[MBB-UR-949/70] 10 p1310 N88-17828
Trends in the development of space transportation systems
[MBB-UR-911/86] 10 p1315 N88-17857
Three-dimensional Euler solutions for hypersonic Mach numbers
[MBB-UR-944/87] 10 p1315 N88-17859
Space shuttle phase B wind tunnel model and test information. Volume 1: Booster configuration
[NASA-CR-178414-VOL-1-PT-1]
24 p3315 N88-29745
Space shuttle phase B wind tunnel model and test information. Volume 1: Booster configuration
[NASA-CR-178414-VOL-1-PT-2]
24 p3320 N88-29770
Lunar lander conceptual design: Lunar base systems study task 2.2
[NASA-CR-172051] 24 p3335 N88-29854

REUSE
Automated software development workstation
23 p3263 N88-29423

REVERBERATION
The effect of reverberation on active sonar performance
[ARE-TM(UJS)-87104] 03 p0374 N88-12350
Signal, noise, and reverberation in bistatic sonar systems
[FOA-C-20703-2.7] 22 p3147 N88-28721

REVERBERATION CHAMBERS
Measurement of shielding effectiveness of different cable and shielding configurations by mode-stirred techniques
[PB88-155791] 10 p1319 N88-17885
EMR (Electromagnetic Radiation) test facilities evaluation of reverberating chamber located at RADC (Rome Air Development Center), Griffiss AFB (Air Force Base), Rome, New York
[PB88-178827] 15 p2022 N88-22048

REVERSE FIELD PINCH
Steady state theta pinch concept for slow formation of FRC
[ISSN-0469-4732] 01 p0098 N88-10648
A tapered poloidal gap for the reduction of field errors
[DE87-014750] 03 p0377 N88-12375
Interchange stability of noncircular reversed field pinches
[DE88-000177] 03 p0378 N88-12381
Numerical simulation of the Reversed Field Pinch
[AD-A184353] 04 p0491 N88-13023
Transport simulations of the oscillating field current drive experiment in the ZT-40M reversed field pinch
[DE88-000538] 04 p0491 N88-13027
Magnetic fluctuation behaviour of current termination in reversed field pinch
[IPPJ-849] 04 p0492 N88-13034
Refueling and density control in the ZT-40M reversed field pinch
[DE88-000504] 04 p0493 N88-13040
Dynamic processes in field-reversed-configuration compact toroids
[DE87-014756] 05 p0652 N88-13998
A short introduction to the status and motivation for reversed field pinch and compact toroid research
[DE88-000487] 05 p0652 N88-13999
A review of the experimental and theoretical status of the reversed-field pinch
[DE88-000529] 05 p0652 N88-14000
Reversed field pinch plasmas with various boundary conditions
[DE88-000832] 05 p0653 N88-14004
The TITAN oscillating-field current-drive system
[DE88-001823] 06 p0782 N88-14798
Edge plasmas and plasma/wall interactions in an ignition-class reversed field pinch
[DE88-001825] 06 p0782 N88-14799
The TITAN magnet configuration
[DE88-001826] 06 p0782 N88-14800
Reversed field pinch experiments: Summary of progress report
[DE88-002367] 07 p0934 N88-15673
Experimental model of halo plasma observed in small-aspect FRC plasma
[INPE-4159-PRE/1061] 08 p1085 N88-16534
Design, construction and operation of a small RFP for turbulent plasma studies
[INPE-4241-PRE/1116] 08 p1087 N88-16545
Experimental study of the initial plasma formation stage in a linear theta pinch of inverted field
[DE88-700010] 09 p1249 N88-17485
Proceedings of the International Workshop on Engineering Design of Next Step Reversed Field Pinch Devices
[DE88-001915] 09 p1251 N88-17494
The TITAN Reversed-Field Pinch Reactor: Design-point determination and parametric studies
[DE88-001824] 09 p1251 N88-17498
D-3He fuels in a field-reversed configuration
[IPPJ-855] 10 p1411 N88-18419
Stability of an RFP (Reversed-Field Pinch) with resistive and distant boundaries
[DE88-004155] 10 p1413 N88-18431
Zero-dimensional model of a reversed field pinch fusion reactor
[DE88-005213] 10 p1414 N88-18442
Improved zero dimensional model of a reversed field pinch fusion device
[DE88-005212] 12 p1693 N88-20127
Reversed field pinch operation with a thin shell
[DE88-005521] 13 p1843 N88-21027
Electrical circuit modeling of reversed field pinches
[DE88-006942] 15 p2136 N88-22745
QN3D: A 3-dimensional quasi-neutral hybrid particle-in-cell code with applications to the tilt mode instability in field reversed configurations
18 p2580 N88-25325
The safety designs for the TITAN reversed-field pinch reactor study
[DE88-008169] 19 p2729 N88-26205
Overview of the TITAN-2 reversed-field pinch aqueous fusion power core design
[DE88-008170] 20 p2857 N88-26966
RFP (Revised Field Pinch) plasma experiment at INPE
[INPE-4613-PRE/1336] 24 p3431 N88-30420

REVERSE OSMOSIS
Reverse osmosis treatment to remove inorganic contaminants from drinking water
[PB88-147780] 12 p1605 N88-19598

REVERSE TIME
U REACTION TIME

REVERSED FLOW
Dynamics of reverse flows at pump inlet
04 p0425 N88-12636
Comparison of the performance of a reverse flow annular combustion chamber under low and high pressure conditions 24 p3347 N88-29923

REVERSING
A flash spectrum of Cl I, C I, N I, and Ni II absorption in 31 Cygni: A direct observation of the reversing layer
04 p0513 N88-13158
Dislocation free zone model of fracture under reverse loading
[DE88-002676] 07 p0869 N88-15276
Analysis of reversible and irreversible hydrogen trapping in metals
[NPL-DMA(A)-154] 16 p2177 N88-22977
A study on the precipitation and reversion behaviors of Cu-0.3 percent Cr alloy by the step annealing method
[NASA-TT-20169] 18 p2489 N88-24764

REVIEWING
Procedures for peer review assessments
[DE88-007749] 19 p2739 N88-26263

REVISIONS
Revision of the information standards for flight mechanics
[DFVLR-MITT-87-06] 03 p0265 N88-11675
Uniform laws and regulations as adopted by the National Conference on Weights and Measures (72nd), 1987
[PB88-123724] 06 p0689 N88-14225
Model-based building verification in aerial photographs
[AD-A186010] 07 p0870 N88-15278
Influence of base modifications on in-flight base drag in the presence of jet exhaust for Mach numbers from 0.7 to 1.5
[NASA-TP-2802] 11 p1488 N88-18881
Computer-aided design analysis of 57-mm, angular-contact, cryogenic turbopump bearings
[NASA-TP-2816] 11 p1496 N88-18933
HELIOS modeling of point-focusing solar concentrators
[DE88-004933] 12 p1640 N88-19820
Modified theory of gravity
[DE88-700835] 12 p1642 N88-19830
Parametric study of the total cost of aircraft modernization in terms of development and equipment series costs 12 p1700 N88-20177
Systematic behavior of NMC medium range forecasts and the effect of model changes 1985-87
22 p3125 N88-28575

REVOLUTION (MOTION)
U REVOLVING

REVOLVING
Incipient fault detection study for advanced spacecraft systems
[NASA-CR-172014] 02 p0183 N88-11138
The application of the hybrid iterative method to scattering by perfectly conducting bodies of revolution
11 p1475 N88-18802

REYNOLDS EQUATION
Calculations of viscous flows with a multigrid method
13 p1769 N88-20580
High-speed flow calculations past 3-D configurations based on the Reynolds averaged Navier-Stokes equations
[NASA-TM-100062] 14 p1911 N88-21421

REYNOLDS LAW
U REYNOLDS EQUATION
REYNOLDS NUMBER
NT HIGH REYNOLDS NUMBER
NT LOW REYNOLDS NUMBER
Reynolds number effects on the small scale structure of a turbulent channel flow 01 p0001 N88-10004
The structure of separated flow regions occurring near the leading edge of airfoils including transition
[NASA-CR-181434] 01 p0002 N88-10011
Numerical study of the entrance flow and its transition in a circular pipe (2) 03 p0318 N88-12011
The drag of slender axisymmetric cones in rarefied hypersonic flow 05 p0531 N88-13229
Computational study of three-dimensional wake structures
[REPT-2] 05 p0539 N88-13281
Effects of free stream turbulence, Reynolds number and incidence angle on axial turbine cascade performance
05 p0548 N88-13339
Regressed relations for forced convection heat transfer in a direct injection stratified charge rotary engine
[NASA-TM-100124] 05 p0549 N88-13345
Instability and transition in curved channel flow
10 p1328 N88-17938
A low speed wind tunnel investigation of Reynolds number effects on a 60-deg swept wing configuration with leading and trailing edge flaps
[NASA-CR-181684] 19 p2598 N88-25441
Investigation of the validity of Reynolds averaged turbulence models at the frequencies that occur in turbomachinery
[NASA-CR-182162] 22 p3048 N88-28087
Reynolds number effects and the wind tunnel environment 23 p3168 N88-28862
Experimental tools: The tunnel and the model
23 p3168 N88-28864
REYNOLDS STRESS
Turbulence modelling through one point closures-applications-enlightening by large eddy simulation 03 p0312 N88-11972
Reynolds-stress and dissipation rate budgets in a turbulent channel flow
[NASA-TM-89451] 07 p0852 N88-15174
Turbulence models for practical applications
08 p0986 N88-15974
Numerical implementation and performance of Reynolds stress closures in finite volume computations of recirculating and strongly swirling flows
08 p0987 N88-15976
Improvement of the Reynolds-stress model by a new pressure-strain correlation
[NASA-CR-182699] 13 p1783 N88-20667
Development of subminiature multi-sensor hot-wire probes
[NASA-TM-100052] 15 p2069 N88-22336
Studying Turbulence Using Numerical Simulation Databases. Proceedings of the 1987 Summer Program
[NASA-CR-182692] 16 p2194 N88-23086
Study of one-dimensional spectral dynamic equations of the Reynolds stresses in homogeneous anisotropic turbulence: Application to split-spectrum modeling
16 p2196 N88-23095
On local approximations of the pressure-strain term in turbulence models 16 p2197 N88-23102
Local structure of intercomponent energy transfer in homogeneous turbulent shear flow
16 p2197 N88-23103
Test code for the assessment and improvement of Reynolds stress models 16 p2197 N88-23105
Reynolds stress models of homogeneous turbulence
16 p2197 N88-23106
The decay of isotropic turbulence in a rapidly rotating frame 16 p2197 N88-23107
Evaluation of a theory for pressure-strain rate
16 p2198 N88-23108
The simulation of coherent structures in a laminar boundary layer 16 p2198 N88-23111
Active layer model for wall-bounded turbulence
16 p2199 N88-23115
Coherent structures in the axisymmetric turbulent jet mixing layer 21 p2947 N88-27504
Development of a hot-wire measurement technique for moderate intensity three-dimensional flows
22 p3080 N88-28289
Analysis method for the production of Reynolds stresses in compressible turbulent flow (fluid mechanics)
[NASA-TT-20330] 24 p3373 N88-30088
Development of a more general Reynolds stress closure for swirling flow
[AD-A195121] 24 p3374 N88-30092
RF-4 AIRCRAFT
Future air-to-air training for the RF-4
[AD-A194363] 23 p3240 N88-29284
RH-2 HELICOPTER
U UH-1 HELICOPTER
RHENIUM
NT RHENIUM ISOTOPES
Slip casting and extruding shapes of rhenium with metal oxide additives. Part 2: Development of grain stabilized rhenium parts for resistojets
[NASA-CR-180851] 03 p0278 N88-11749
Johnson noise thermometer for high radiation and high temperature environments
[DE88-003770] 10 p1323 N88-17911
Compatibility in space reactor fuel systems
[DE88-005698] 13 p1839 N88-21004
Johnson noise thermometer for high-radiation and high-temperature environments
17 p2434 N88-24480
Iridium-coated rhenium thrusters by CVD
[NASA-TM-101309] 24 p3339 N88-29874
RHENIUM ALLOYS
Equations for determining CVD tungsten-rhenium alloy composition and plating rate
[DE87-008831] 01 p0024 N88-10152
RHENIUM ISOTOPES
A nuclear structure study of the proposed gamma-ray laser candidate nucleus Re-186
[DE88-004299] 10 p1336 N88-17986
Experimental and theoretical investigations of isotope shift and hyperfine structure on 5d elements (especially platinum, iridium and rhenium)
[ETN-88-93121] 24 p3353 N88-29957
RHEOLOGY
Rheological behaviors of an elastomeric membrane
[DE87-013105] 01 p0061 N88-10392
Colloidal structure of bitumens. Relationship between composition-structure behavior
[PC-4] 02 p0146 N88-10912
Rheological and aging characterization of elastomers
[DE87-009598] 02 p0151 N88-10944
Experiments on densely-loaded non-Newtonian slurries in laminar and turbulent pipe flows
[DE88-000719] 04 p0442 N88-12746
TMA-microrheological testing of polymers (thermomechanical analysis)
[PB87-228805] 06 p0683 N88-14187
The effective elastic properties of low-density foams
[DE87-014629] 06 p0684 N88-14194
Physics and chemistry 07 p0883 N88-15359
Thermoplastic elastomers as LOVA binders
[AD-A186563] 10 p1304 N88-17797
Continual capillary viscosimetry using extrusiograph techniques
[PB88-166293] 15 p2046 N88-22195
Experiments on densely-loaded non-Newtonian slurries in laminar and turbulent pipe flows
[DE88-006209] 15 p2067 N88-22323
Electrical dc conductivity of pitch
[AD-A191266] 16 p2182 N88-23008
Characterization of aluminum/RP-1 gel propellant properties
[NASA-TM-100951] 18 p2496 N88-24808
Experiments on densely-loaded non-Newtonian slurries in laminar and turbulent pipe flows
[DE88-010579] 20 p2800 N88-26612
Effects of a temperature-dependent rheology on large scale continental extension
[NASA-CR-183117] 20 p2825 N88-26759
Optimal rheological characteristics in dynamic stability of polymer flow through porous media
[DE88-001225] 21 p2918 N88-27322
A review: Quantitative models for lava flows on Mars
23 p3301 N88-29656
Photogeological inferences of Martian surface composition 23 p3303 N88-29675
Lava flow-field morphology: A case study from Mount Etna, Sicily 23 p3303 N88-29676
Ultrasonic detection of diffusion and adhesion loss
24 p3354 N88-29967
Lava thicknesses: Implications for rheological and crustal development 24 p3443 N88-30490
Small-scale volcanic landforms indicative of distributary tube systems 24 p3444 N88-30496
RHODESIA
U ZIMBABWE
RHODIUM
Laser-induced desorption determinations of surface diffusion on Rh(111)
[DE88-005159] 11 p1454 N88-18667
Model catalyst studies of SMSI (Strong Metal/Support Interactions) and the role of D-electrons in chemisorption and catalysis
[DE88-004518] 13 p1738 N88-20393
The relationship of the chemical bonding topology of high critical temperature copper oxide superconductors to that of the chevrel phases and the ternary lanthanide rhodium borides
[AD-A189255] 13 p1845 N88-21042
Oxide-bound transition metal complexes for methane activation
[PB88-169719] 14 p1887 N88-21277
Mechanism of the nitric oxide-carbon monoxide-oxygen reaction over a single crystal rhodium catalyst
[DE88-006274] 21 p2910 N88-27268
RHODIUM COMPOUNDS
Catalytic activation of carbon dioxide by metal complexes
[AD-A192310] 21 p2909 N88-27262
RHOMBOIDS
Benchmark computation and finite element performance evaluation for a rhombic plate bending problem
[AD-A187402] 10 p1345 N88-18041
RHYTHM (BIOLOGY)
NT CIRCADIAN RHYTHMS
Infradian biorhythms of human vital signs
06 p0750 N88-14606
Biorhythmological analysis of dynamics of pulmonary ventilation parameters during orthostatic tests
07 p0891 N88-15400
New book on space ecology reviewed
07 p0897 N88-15434
Center for the study of rhythmic processes
[AD-A188204] 11 p1520 N88-19078
Interrelationship of heart rhythm indicators and resistance to hypoxia in Antarctic polar workers
12 p1664 N88-19974
Method of assessing changes in biorhythmological structure of human physiological functions
19 p2706 N88-26088
RIBBON PARACHUTES
Parachute characteristics of Titan descent modules --- planetary probe
[BF-3/86-B] 02 p0122 N88-10774
The aerodynamics of supersonic parachutes
[DE87-014846] 04 p0395 N88-12464
RIBBONS
Tape wrapping apparatus and method
[EP-PATENT-0-181-747-A2] 01 p0053 N88-10336
Investigation of boundary layer disturbances caused by periodic heating of a thin ribbon
[AD-A190572] 15 p2065 N88-22314
RIBONUCLEIC ACIDS
RNA-synthesizing activity in rat liver following flight aboard Cosmos-1667 10 p1360 N88-18130
RIBS (SUPPORTS)
Local heat/mass transfer and pressure drop in a two-pass rib-roughened channel for turbine airfoil cooling
[NASA-CR-179635] 03 p0322 N88-12039
Optimal ribbing of long plate made of composite material 04 p0426 N88-12641
The viscous flow on surfaces with streamwise riblets
[DFVLR-FB-87-21] 09 p1162 N88-16961
The viscous flow on surfaces with streamline riblets
[ESA-TT-1091] 24 p3370 N88-30067
RICCATI EQUATION
Oscillation theory for linear second-order differential systems
[DE87-011393] 04 p0484 N88-12983
Strong convergence and convergence rates of approximating solutions for algebraic Riccati equations in Hilbert spaces
[AD-A186190] 08 p1072 N88-16464
A LQG regulator for the angular motion of the rotor at a tuned gyroscope
[INPE-4280-PRE/1152] 12 p1631 N88-19759
Control, stability and filter for a discrete linear stochastic system with correlated noise
[PB88-109525] 21 p3004 N88-27818
Convergence of Galerkin approximations for operator Riccati equations: A nonlinear evolution equation approach
[NASA-CR-181706] 24 p3425 N88-30386
RICE
Pilot study of rice culture in sub-tropical high population density region (Madagascar) with SPOT 1 multispectral data 22 p3097 N88-28392
Using SPOT HRV data to update the distribution of the paddy field in Taiwan 22 p3097 N88-28393
RICHARDSON NUMBER
Some results from the Amazon Forest micrometeorological experiment
[INPE-4631-PRE/1346] 24 p3403 N88-30263
RICHARDSON-DUSHMAN EQUATION
U TEMPERATURE EFFECTS
U THERMIONIC EMISSION
RIDGES
Experimental and theoretical constraints on the origin of mid-ocean ridge geothermal fluids
13 p1804 N88-20784
RIDING QUALITY
Measurement of suspension and ride characteristics of the M1 main battle tank 05 p0596 N88-13637
RIEMANN INTEGRAL
U MEASURE AND INTEGRATION

RIEMANN MANIFOLD
On the cosmological constant in the heterotic string theory
[DE87-703099] 02 p0247 N88-11562
Computer-aided study of a class of Riemannian space-times
[DE87-703367] 05 p0645 N88-13950
A fast Riemann solver with constant covolume applied to the random choice method
[CAR-87-19] 09 p1231 N88-17375
Path integration on the upper half-plane
[DE88-751050] 12 p1682 N88-20057
String theory and algebraic geometry of moduli spaces
[CWI-PM-R8705] 13 p1849 N88-21070
Markov processes applied to control, replacement and signal analysis
[AD-A190563] 15 p2126 N88-22674
Regularity of the Albanese map for nonoriented surfaces
[DE88-006428] 15 p2126 N88-22679
Vortices on the world sheet and string's critical dynamics
[DE88-702116] 21 p3026 N88-27961

RIEMANN PROBLEM
U CAUCHY PROBLEM

RIEMANN SPACE
U RIEMANN MANIFOLD

RIEMANN SPHERE
U RIEMANN MANIFOLD

RIFT VALLEYS
U VALLEYS

RIFTS
U GEOLOGICAL FAULTS

RIGID BODIES
U RIGID STRUCTURES

RIGID ROTOR HELICOPTERS
Time periodic control of a multi-blade helicopter
[AD-A194435] 23 p3180 N88-28931

RIGID ROTORS
An experimental investigation of the flap-lag-torsion aeroelastic stability of a small-scale hingeless helicopter rotor in hover
[NASA-TP-2546] 13 p1715 N88-20257
A comparison of theory and experiment for coupled rotor-body stability of a hingeless rotor model in hover under simulated vacuum conditions
21 p2889 N88-27151
A comparison of theory and experiment for coupled rotor-body stability of a hingeless rotor model in hover
21 p2889 N88-27152
Aeroelastic modeling of rotor blades with spanwise variable elastic axis offset: Classic issues revisited and new formulations 21 p2890 N88-27158
Aeromechanical stability analysis of COPTER
21 p2891 N88-27161

RIGID ROTORS (PLASMA PHYSICS)
NT PLASMA PHYSICS

RIGID STRUCTURES
NT RIGID ROTORS
Flap-lag equations of motion of rigid, articulated rotor blades with three hinge sequences
[NASA-TM-100023] 04 p0401 N88-12495
Numerical simulations of impact tests on a rigid wall --- armor steel
[SNIAS-872-320-102] 05 p0610 N88-13744
Stability analysis of a rigid body with a flexible attachment using the energy-casimir method
[AD-A185646] 06 p0723 N88-14449
Formulation methods of rigid multibody systems for large space structures and some results of computer simulation
[NAL-TR-942] 10 p1293 N88-17730
The dynamics of two coupled rigid bodies
[AD-A187592] 10 p1341 N88-18012
Qualification of frequency response functions using the rigid-body response
[DE88-000745] 10 p1344 N88-18033
The dynamics of coupled planar rigid bodies. Part 1: Reduction, equilibria and stability
[AD-A187467] 10 p1345 N88-18042
Parametric dependence in the equilibrium dynamics of rotating structures
[AD-A187817] 11 p1498 N88-18945
Automatic feedback control of a rigid body for finite displacements 18 p2473 N88-24674
Recursive mass matrix factorization and inversion: An operator approach to open- and closed-chain multibody dynamics
[NASA-CR-182516] 23 p3247 N88-29328
Clevis joint for deployable space structures
[NASA-CASE-LAR-13898-1] 24 p3380 N88-30130

RILLS
U VALLEYS

RING CURRENTS
The duskside plasmapause/ring current interface: Convection and plasma wave observations
[MPE-PREPRINT-93] 02 p0243 N88-11533
Current-driven lower hybrid waves at the inner edge of the ring current --- magnetosphere
[MPE-PREPRINT-94] 02 p0243 N88-11534
Ring current role in dynamics of fluctuating electron and ion fluxes in low-latitude magnetosphere
24 p3447 N88-30514
Plasma of earth's magnetosphere ring currents. Model compared with results of AMPTE/CCE experiment
24 p3447 N88-30515

RING LASERS
Distributed feedback effects in lasers and high gain laser instabilities in optically pumped CH3F
03 p0329 N88-12079
Study on a unidirectional ring laser gyro. Part 1: Proposition of the principle and studies on the components
[NAL-TR-933] 09 p1169 N88-17010
Studies of fluorine combustion
[AD-A187646] 11 p1452 N88-18656
Thirteenth Biennial Guidance Test Symposium, volume 1
[AD-A185782] 12 p1576 N88-19427
Calibration of a ring laser gyro inertial navigation system 12 p1576 N88-19428
The optimum solution to instrument quantization effects 12 p1577 N88-19434
The German Honeywell ring laser gyro: Development and test results 12 p1578 N88-19440
Laser gyro attitude control system feasibility
[AD-A189368] 13 p1720 N88-20285
Resonator coupling of two ring cavity, argon-ion lasers
[AD-A189558] 13 p1775 N88-20616
Solid-state ring laser with acoustooptical phase nonreciprocity of opposing waves
14 p1970 N88-21761
Monolithic integration on a GaAs substrate of a quarter ring laser and an optical guide coupled by an evanescent wave
[ETN-88-92308] 17 p2344 N88-23969
Precision measurement of the Fresnel drag coefficient using a ring laser
[AD-A196025] 24 p3366 N88-30043

RING STRUCTURES
NT REINFORCEMENT RINGS
An experimental and theoretical study of the bending behavior of Kevlar 49/epoxy beams and rings
[DE87-010430] 01 p0061 N88-10394
Investigations of the equilibrium and stability of thin-walled double rings. A contribution to the solution of single-sided contact problems
[ETN-87-90044] 09 p1181 N88-17076
Buckling and breakdown problems in structural mechanics. Failure of prestressed double-walled containers or rings
[MBB-UR-E-956/87] 13 p1783 N88-20671
New wide-band transducer developed
14 p1901 N88-21353
Unrestrained out-of-plane buckling of monosymmetric rings
[PB88-155213] 14 p1923 N88-21458
Tunable condensed-media laser with antiresonant ring cavity 14 p1971 N88-21764
Vibrations of rotating thick or thin rings
18 p2529 N88-25003
Analytical and experimental investigation of ringless piston concept
[AD-A192835] 20 p2810 N88-26673
Transport in GaAs heterojunction ring structures
20 p2864 N88-27011

RINGS
Hot piston ring tests
[NASA-TM-100256] 06 p0729 N88-14486
Hot piston ring/cylinder liner materials: Selection and evaluation
[NASA-TM-100276] 08 p0971 N88-15872
Multi-hundred kilowatt roll ring assembly evaluation results
[NASA-TM-100865] 14 p1904 N88-21375
On the bending response of Kevlar 49/epoxy beams and rings
[DE88-006824] 18 p2530 N88-25012

RINGS (MATHEMATICS)
Class of N-associative rings
[PB87-230421] 06 p0769 N88-14724
The classification problem of finite rings by computable means
[AD-A185869] 07 p0908 N88-15500

RIPPLES
Laser pulse width dependent surface ripples on silicon
[PB88-127311] 10 p1336 N88-17982
Recording a surface acoustic wave on the surface of silicon
[PB88-130372] 11 p1490 N88-18694
Problems in modeling TF ripple loss of fast alphas from a tokamak reactor
[DE88-000612] 11 p1553 N88-19296
Superconductors with structured surfaces: Fields and currents
[AD-A189353] 12 p1699 N88-20164
Helical ripple transport in stellarators at low collision frequency
[DE88-006431] 13 p1843 N88-21031

RISK
Hypersonic aerodynamics: Applications for HOTOL
05 p0535 N88-13252
A long term radiological risk model for plutonium-fueled and fission reactor space nuclear system
[DE87-010466] 06 p0779 N88-14782
Risk analysis methodology survey
07 p0922 N88-15604
Instrumentation utilisation for risk control in safety operations --- balloons and rockets
08 p1030 N88-16240
Group adaptation and individual adjustment in antarctica: A summary of recent research
[AD-A186605] 08 p1051 N88-16347
Sudden in-flight incapacitation in general aviation
[AD-A187044] 09 p1115 N88-16682
Committee on Interagency Radiation Research and Policy Coordination
[DE88-003358] 09 p1188 N88-17121
Medical and psychological problems of assuring flight safety under present conditions
10 p1359 N88-18123
Modeling of the non-auditory response to blast overpressure
[AD-A187397] 10 p1369 N88-18184
Risk reduction cost avoidance for full scale development begins with concept formulation
12 p1700 N88-20174
Post-Challenger evaluation of space shuttle risk assessment and management
[NASA-CR-182461] 12 p1705 N88-20202
The space station assembly phase: Flight telerobotic servicer feasibility, volume 1
[NASA-CR-182689] 13 p1731 N88-20351
Survival analysis using additive risk models
[AD-A189053] 13 p1825 N88-20906
A systems analysis of fire suppression alternatives for the US space station
[AD-A189847] 15 p2025 N88-22064
Asymptotic theory for weighted least squares estimators in Aalen's additive risk model
[AD-A191085] 18 p2562 N88-25210
A perspective of PC-based probabilistic risk assessment
[DE88-006715] 18 p2568 N88-25251
Decision making aids: Methods and risks
22 p3161 N88-28820
Risk analysis in space system safety
22 p3161 N88-28825
Venture theory: A model of decision weights
[AD-A194809] 24 p3426 N88-30391

RITZ AVERAGING METHOD
Predicted and measured strain responses of isotropic panels to base excitation
[NASA-TM-4054] 19 p2679 N88-25928

RIVER BASINS
NT DELAWARE RIVER BASIN (US)
Analysis of squall line based on conventional data
02 p0207 N88-11295
The mesoscale numerical model for heavy rainfall forecasting in Yangtze River Valley, China
02 p0211 N88-11326
Oxidation and reduction rates for organic carbon in the Amazon mainstream tributary and floodplain, inferred from distributions of dissolved gases
[NASA-CR-182943] 18 p2538 N88-25062
Photointerpretation with instrumentation for evaluation of environmental impact: Mata Atlantica in Cubatao
19 p2683 N88-25946
Use of remote sensing in the study of superficial formation certifying the development of integrated economy-case example: Rio Claro (SP) region
19 p2683 N88-25950

RIVERS
NT OHIO RIVER (US)
Evaluation of the magnetic induction conductivity method for detecting frazil ice deposits
[AD-A186940] 09 p1194 N88-17157
Landuse and landform studies of the Mahanadi River Delta with the help of satellite MSS band
17 p2355 N88-24033
Geomorphologic sector maps of Niquizanga-Mayares, province of San Juan, Argentina
17 p2368 N88-24098

Influence of the Yukon River on the Bering Sea
[NASA-CR-182802] 17 p2376 N88-24126
The impact of disorganized occupation of urban sub-basins: Sub-basin of the Cabucu River, metropolitan area of Sao Paulo (SP) 19 p2682 N88-25945
Delineation of ephemeral fluvial networks on low-relief Piedmont surfaces, Plutonium Valley, Nevada, USA
22 p3093 N88-28367

RIVETED JOINTS
Experimental and theoretical investigation of mechanically fastened composites
[AD-A185896] 07 p0826 N88-15008
Damage mechanisms of CFRP riveted joints
11 p1449 N88-18636
On the calculation of stresses in pin-loaded anisotropic plates
[ETN-88-92239] 16 p2222 N88-23261

RIVETING
Automatic riveting machine for spherically-formed airframe structures
[ETN-88-91024] 11 p1495 N88-18924

RIVETS
Crack distribution and growth rates for critical fastener holes in Mirage wing RH79
[AD-A189080] 13 p1722 N88-20293

RNA
U RIBONUCLEIC ACIDS

ROADS
NT HIGHWAYS
Nowcasting for the national economy needs
02 p0199 N88-11241
Feasibility study of a range of products drawn from SPOT satellite imagery and specific to road-laying studies
03 p0342 N88-12157
A texture analysis approach to computer vision for identification of roads in aerial photographs
[AD-A189340] 12 p1639 N88-19815
Computer aided cartographic representation of traffic data: The traffic intensity maps of Baden-Wuerttemberg (Federal Republic of Germany)
16 p2225 N88-23282
Digitizing the traffic network of JOG 250 by scanning -- JOG 250 map 18 p2533 N88-25029
Propagation effects by roadside trees measured at UHF and L-band for mobile satellite systems
19 p2644 N88-25693
Use of SPOT data in preliminary steps of road project studies especially suited for developing countries
22 p3098 N88-28396
Automatic line network extraction from aerial imagery of urban areas through knowledge-based image analysis
[AD-A192399] 23 p3227 N88-29208

ROADWAY POWERED VEHICLES
Simulation models for the dynamics of tracked vehicle systems: State-of-the-art and open problems
20 p2785 N88-26522

ROBOTICS
Telepresence work station system definition study, part 2
[NASA-CR-172006] 01 p0013 N88-10071
Space station platforms 01 p0015 N88-10086
Telerobotics 01 p0015 N88-10090
Robotic sensors and actuators for a service manipulator system. Volume 1: Executive summary
[MATRA-EPT/DT/VT187/120]
01 p0053 N88-10341
Robotic sensors and actuators for a service manipulator system. Volume 2: Service Manipulator System (SMS) handbook
[MATRA-EPT/DT/VT187/227]
01 p0053 N88-10342
Robotic sensors and actuators for a service manipulator system. Volume 3, phase A report and program plan
[MATRA-EPT/DT/VT187/228]
01 p0054 N88-10343
Augmenting the control of a flexible manipulator with passive mechanical damping 01 p0055 N88-10350
Multimedia sensory systems for the solution of the error recovery problem --- robots
[REPT-87-010] 01 p0084 N88-10545
Digital algorithms for the control and dynamic decoupling of industrial robot axes
[ETN-87-90441] 01 p0084 N88-10546
Object-oriented data base management for robot programming
[ETN-87-90367] 01 p0105 N88-10687
Optimization of a controlled two-server maintenance system
[INPE-4202-PRE/1083] 01 p0107 N88-10694
USSR Report: Engineering and Equipment
[JPRS-UEQ-87-007] 02 p0157 N88-10985
Human factors in robotic system design discussed
02 p0158 N88-10988
Robotics and Intelligent Systems Program
[DE87-014561] 02 p0223 N88-11404
Components for measuring robots
[KFK-PFT-126] 03 p0332 N88-12092
On the control of a compliant robot arm
03 p0332 N88-12095
Dynamics and stability of bipedal locomotion robots
03 p0333 N88-12096
A theory for the articulation of robot manipulators
03 p0333 N88-12097
Teleoperator and robotics system analysis
[NASA-CR-179220] 03 p0334 N88-12105
Operator multiple-tasking study for remotely operated platforms
[AD-A184487] 03 p0362 N88-12276
Architecture for dynamic task allocation in a man-robot symbiotic system
[DE87-013872] 03 p0362 N88-12277
Two dimensional path planning with obstacles and shadows
[AD-A184075] 04 p0397 N88-12474
Autonomous Land Vehicle (ALV) planning and navigation system
[AD-A184243] 04 p0397 N88-12475
Correction of inertial navigation system drift errors for an autonomous land vehicle using optical radar terrain data
[AD-A184973] 05 p0544 N88-13311
Towards building a team of intelligent robots
[NASA-CR-181538] 05 p0589 N88-13595
Collision-free motion of two robot arms in a common workspace
[CSE-87-00002] 05 p0589 N88-13596
Behavioral Architecture Robot Control System (BARCS): A new way of building robots
[REPT-87-036] 05 p0638 N88-13902
National Aeronautics and Space Administration (NASA)/American Society for Engineering Education (ASEE) Summer Faculty Fellowship Program, 1987. Volume 1
[NASA-CR-172009-VOL-1] 06 p0792 N88-14855
Heuristic control of the Utah/MIT dextrous robot hand
06 p0793 N88-14858
National Aeronautics and Space Administration (NASA)/American Society for Engineering Education (ASEE) Summer Faculty Fellowship Program, 1987. Volume 2
[NASA-CR-172009-VOL-2] 06 p0796 N88-14874
Dynamics, control and sensor issues pertinent to robotic hands for the EVA retriever system
06 p0796 N88-14876
Time-domain robotic vision application
06 p0798 N88-14886
Proceedings of Image Understanding Workshop, volume 2
[AD-A186104] 07 p0902 N88-15464
Advancing automation and robotics technology for the space station and for the US economy: Submitted to the United States Congress October 1, 1987
[NASA-TM-100777] 08 p0959 N88-15816
Advancing automation and robotics technology for the space station and for the US economy: Submitted to the United States Congress May 15, 1987
[NASA-TM-89811] 08 p0959 N88-15817
Advancing automation and robotics technology for the space station and for the US economy: Submitted to the United States Congress October 1, 1986
[NASA-TM-89190] 08 p0960 N88-15818
Third Conference on Artificial Intelligence for Space Applications, part 1
[NASA-CP-2492-Pt-1] 08 p1055 N88-16360
Issues associated with telerobotic systems in space
08 p1056 N88-16369
Telerobotic controller development
08 p1056 N88-16370
Software simulation of time delay in teleoperation
08 p1056 N88-16371
Task path planning, scheduling and learning for free-ranging robot systems 08 p1058 N88-16386
Goal driven kinematic simulation of flexible arm robot for space station missions 08 p1059 N88-16388
Heuristic search in robot configuration space using variable metric 08 p1059 N88-16389
The power of neural nets 08 p1064 N88-16430
First Annual Workshop on Space Operations Automation and Robotics (SOAR 87)
[NASA-CP-2491] 09 p1203 N88-17206
Robotic planner expert system (RPLANES)
09 p1209 N88-17246
Robotic air vehicle. Blending artificial intelligence with conventional software 09 p1210 N88-17252
Communication and control in an integrated manufacturing system 09 p1212 N88-17263
Development of Moire machine vision
09 p1212 N88-17264
Implementation of a robotic flexible assembly system
09 p1212 N88-17265
System integration of a Telerobotic Demonstration System (TDS) testbed 09 p1212 N88-17266
Vision technology/algorithms for space robotics applications 09 p1212 N88-17267
The use of computer graphic simulation in the development of robotic systems
09 p1214 N88-17275
Intelligent robotic tracker 09 p1214 N88-17276
An efficient representation of spatial information for expert reasoning in robotic vehicles
09 p1214 N88-17278
A generalized method for automatic downhand and wirefeed control of a welding robot and positioner
[NASA-TP-2807] 10 p1316 N88-17869
NASA/NBS (National Aeronautics and Space Administration/National Bureau of Standards) standard reference model for Telerobot Control System Architecture (NASREM)
[PB88-124773] 10 p1338 N88-17999
Design conditions and workspace for the generally-proportioned 3-hinge spherical wrist for robots
10 p1339 N88-18003
Recursive forward dynamics for multiple robot arms moving a common task object
[NASA-CR-182526] 10 p1340 N88-18008
Parameter identification and sensitivity analysis for a robotic manipulator arm
[NASA-CR-181608] 10 p1385 N88-18272
A computer simulation study of an expert system for walking machine motion planning
[AD-A187907] 11 p1438 N88-18577
Robotic assembly and testing of rotary solenoids
[BDX-613-3663] 11 p1480 N88-18834
Voice/natural language interfacing for robotic control
[AD-A187765] 11 p1494 N88-18917
Improvement in robot positioning accuracy by a kinematic identification model 11 p1496 N88-18931
Motion planning and control of robot manipulators via application of a computer graphics animated display
11 p1496 N88-18932
Visual integration and detection of discontinuities: The key role of intensity edges
[AD-A188012] 11 p1520 N88-19076
Research in knowledge representation for natural language communication and planning assistance
[AD-A187355] 11 p1522 N88-19087
Error detection and recovery for robot motion planning with uncertainty
[AD-A187746] 11 p1534 N88-19165
Optically coupled tactile sensor array for robotics
11 p1550 N88-19273
JPRS report. Science and technology: Europe and Latin America
[JPRS-ELS-87-054] 12 p1573 N88-19406
Output aiming control
[AD-A188463] 12 p1583 N88-19473
Robotic intelligence issues for space manipulator monitoring, control programming
12 p1588 N88-19504
On a knowledge based assisted system for highly autonomous control of experiment-manipulators in the Man-Tended Free Flyer 12 p1588 N88-19505
A knowledge-based approach for sensory-controlled assembly operations 12 p1588 N88-19506
Mobile robot activity model for autonomous free flying platforms 12 p1588 N88-19507
Computational aspects of robotic experiment manipulation in a microgravity environment
12 p1589 N88-19512
EPOS: European Proximity Operations Simulation
12 p1589 N88-19515
Ground based supervisory and programming system for automatic experiment execution in orbit
12 p1590 N88-19519
Teleoperation for a Spacelab technology experiment
12 p1590 N88-19521
EUROSIM: A concept of total system support
12 p1590 N88-19523
Utilization of robotics and teleoperation for future in-orbit operations 12 p1591 N88-19527
Robotics servicing experiment --- European space programs 12 p1591 N88-19529
ROTEX: The Robotic Technology Experiment on Spacelab D-2 mission 12 p1592 N88-19530
Definition of the EUROSIM simulation subsystem
12 p1592 N88-19532
A comparative survey of mathematical models for dynamic simulation of in-orbit manipulation operations
12 p1592 N88-19533
Technology requirements for telerobotic satellite servicing in space 12 p1592 N88-19536
Man-tended options for European space robotics
12 p1593 N88-19538
Piezoelectric polymer tactile sensor arrays for robotics
[AD-A188852] 12 p1634 N88-19780

Terrain classification from digital elevation data using slope and curvature information
[AD-A188940] 12 p1639 N88-19812
A representation for serial robotic tasks
12 p1681 N88-20048
Physics for robots
[AD-A189056] 12 p1682 N88-20054
JPRS report. Science and technology: Europe and Latin America
[JPRS-ELS-87-055] 12 p1686 N88-20086
The space station assembly phase: Flight telerobotic servicer feasibility, volume 1
[NASA-CR-182689] 13 p1731 N88-20351
The space station assembly phase: Flight telerobotic servicer feasibility. Volume 2: Methodology and case study
[NASA-CR-182690] 13 p1731 N88-20352
Modelling and simulation of a rate controlled manipulator arm — Hermes
[NLR-TR-87010-U] 13 p1778 N88-20639
The dynamic control of robotic manipulators in space
[NASA-CR-182710] 13 p1779 N88-20646
Ultrasonic inspection of irregular surfaces
[AERE-R-12465] 13 p1780 N88-20648
Geometry and graphics applied to robotics
[CWI-CS-R8727] 13 p1824 N88-20903
ONR Far East Scientific Bulletin, volume 12, number 3, July-September 1987
[AD-A188554] 13 p1851 N88-21081
Robotic joint experiments under ultravacuum
14 p1927 N88-21490
Improving the man-machine interface to robotic systems
[NPL-DITC-100/87] 14 p1953 N88-21641
Implementation of a visual servoing system for evaluation of robotic refueling applications
[AD-A189676] 14 p1954 N88-21645
Electromagnetic sensor arrays for nondestructive evaluation and robot control
[AD-A190210] 15 p2056 N88-22260
Range image segmentation and surface parameter extraction for a mobile robot
[DE87-013877] 15 p2073 N88-22360
Telerobotic operation of conventional robot manipulators
[DE88-005718] 15 p2073 N88-22363
A probabilistic approach to low-level vision
[AD-A189041] 15 p2107 N88-22553
Microgravity mechanisms and robotics program
16 p2219 N88-23237
Recognizing and locating partially occluded planar objects for assembly routines
[LAAS-87-360] 16 p2247 N88-23422
Contribution to the automatic generation of floor plan placing --- integrated circuit design
[ETN-88-92193] 16 p2247 N88-23426
Contribution to the adaptive dynamic control of a robot manipulator
[LAAS-87-350] 16 p2255 N88-23475
Technology Reports of Kyushu University, volume 61, no. 2
[ISSN-0023-2718] 16 p2256 N88-23485
Realization of natural language style robot task instruction by using the object oriented concept
16 p2257 N88-23487
A design analysis for an automated robotic workpiece manipulator 17 p2344 N88-23975
A software design tool for the analysis of robot dynamics properties
[NLR-MP-86064-U] 17 p2385 N88-24171
A robotic language for cooperative multi-robots
17 p2387 N88-24186
A control technique for improved robot performance
17 p2391 N88-24212
Precise computer controlled positioning of robot end effectors using force sensors
[NASA-CR-182887] 17 p2391 N88-24213
Energy optimal trajectory planning for robot manipulators and autonomous vehicles 17 p2437 N88-24497
A universal computer control system for motors
[NASA-CASE-NPO-17134-1-CU]
18 p2506 N88-24864
The coordination of multiple robotic manipulators
[AD-A190869] 18 p2522 N88-24963
The efficacy of using human myoelectric signals to control the limbs of robots in space
[NASA-CR-182901] 18 p2553 N88-25155
Introduction to compliance in programming of robots
[ETN-88-92189] 18 p2561 N88-25201
Modeling of geometric reasoning for robot programming
[ETN-88-92290] 18 p2561 N88-25202
Analysis of a closed-kinematic chain robot manipulator
[NASA-CR-183031] 18 p2561 N88-25206
Lunar base surface mission operations. Lunar Base Systems Study (LBSS) task 4.1
[NASA-CR-172050] 18 p2594 N88-25415
Design guidelines for robotically serviceable hardware
[NASA-TM-100700] 19 p2606 N88-25472
Flexible tactile sensing arrays for robotics: Architectural robustness and yield considerations
19 p2671 N88-25878
Automatic calibration of space based manipulators and mechanisms
[NASA-CR-182804] 19 p2676 N88-25912
Computer aided remote control: A general concept for intervention in the nuclear, underwater, and space domains 19 p2699 N88-26046
Treatment of systematic errors in the processing of wide angle sonar sensor data for robotic navigation
[DE88-008961] 20 p2756 N88-26352
Design of a controller to reduce residual vibration in the positioning control of flexible robotic manipulators
20 p2808 N88-26658
RRSAS (Robotic Radiation Survey and Analysis System) Project: A real time sensor driven robotic system
[DE88-006825] 20 p2808 N88-26661
An introduction to robot joint control methods
[NLR-TR-86080-U] 20 p2811 N88-26677
Simulation of space manipulator operations (EUROSIM)
[NLR-MP-87017-U] 20 p2811 N88-26678
Experiments in adaptive control of a very flexible one link manipulator 20 p2842 N88-26865
Kinematics of Hooke universal joint robot wrists
[NASA-TM-100567] 20 p2843 N88-26870
Aircraft refueling demonstrator using a microbot alpha 2 robot 21 p2926 N88-27367
Compliant robotic structures, part 3
[AD-A192426] 21 p2955 N88-27556
Development of a hybrid simulator for robotic manipulators
[AD-A193119] 21 p2956 N88-27557
Dexterous hands: Optimizing grasp by design and planning 21 p2958 N88-27572
The VITE model: A neutral command circuit for a generating arm and articulator trajectories
[AD-A192715] 21 p2987 N88-27734
The robust tracking control of nonlinear systems with uncertain dynamics 21 p2999 N88-27788
Intelligent Mobile Autonomous System (IMAS)
[AD-A193181] 21 p3003 N88-27811
Mobile robotics R and D at the Savannah River Laboratory
[DE88-011665] 22 p3083 N88-28310
The analysis and control of robotic manipulators operating at or near kinematically singular configurations
22 p3084 N88-28315
Uncertainty analysis in automatic robot programming
[RR-695-I-IMAG-68-LIFIA] 22 p3142 N88-28685
Motion planning with obstacles and dynamic constraints 23 p3222 N88-29175
Study on design and control of torque-controlled manipulators
[NASA-TT-20197] 23 p3223 N88-29183
Implementation of a flexible link model in a designed robot system, using the finite element method
[ETN-88-92902] 23 p3243 N88-29303
Second Conference on Artificial Intelligence for Space Applications
[NASA-CP-3007] 23 p3251 N88-29351
Space station as a vital focus for advancing the technologies of automation and robotics
[IAF-86-62] 23 p3251 N88-29352
Machine vision for real time orbital operations
23 p3253 N88-29367
A plan for time-phased incorporation of automation and robotics on the US space station
23 p3255 N88-29377
The use of computer graphic simulation in the development of robotic systems
23 p3257 N88-29388
A robotic system for automation of logistics functions on the Space Station 23 p3260 N88-29407
A teleoperated robotic manipulator system for materials processing experiment servicing
23 p3260 N88-29410
Next-generation space manipulator
23 p3263 N88-29428
Study of robotics spacecraft servicing and assembly in space. Volume 1: Executive summary
[ESA-CR(P)-2612-VOL-1] 24 p3333 N88-29839
Low level image processing techniques using the pipeline image processing engine in the flight telerobotic servicer 24 p3418 N88-30346
An automated computerized vision technique for determination of three-dimensional object geometry
24 p3419 N88-30348
Study of software requirements and artificial intelligence techniques for robotics
[TL-3333] 24 p3422 N88-30365
Adaptive control in positioning a rigid-flexible robot arm
[AD-A195194] 24 p3422 N88-30367
Research on problem-solving systems
[AD-A195154] 24 p3423 N88-30370
A standard architecture for controlling robots
[AD-A195929] 24 p3423 N88-30371
Kalman filter-based algorithms for estimating depth from image sequences
[AD-A195818] 24 p3424 N88-30380
Utilizing dynamic stability of orient parts
[AD-A195730] 24 p3427 N88-30397

ROBOTS

Robotic sensors and actuators for a service manipulator system. Volume 1: Executive summary
[MATRA-EPT/DT/VT187/120]
01 p0053 N88-10341
Robotic sensors and actuators for a service manipulator system. Volume 2: Service Manipulator System (SMS) handbook
[MATRA-EPT/DT/VT187/227]
01 p0053 N88-10342
Robotic sensors and actuators for a service manipulator system. Volume 3, phase A report and program plan
[MATRA-EPT/DT/VT187/228]
01 p0054 N88-10343
Traction-drive seven degrees-of-freedom telerobot arm: A concept for manipulation in space
[DE87-010895] 01 p0054 N88-10346
Technology survey for a robot which will investigate the condition of underground pipe
[PB87-209979] 01 p0055 N88-10351
Teleoperation and control study --- orbital servicing
[BAE-TP-8268] 01 p0076 N88-10489
Digital algorithms for the control and dynamic decoupling of industrial robot axes
[ETN-87-90441] 01 p0084 N88-10546
Robotics and Intelligent Systems Program
[DE87-014561] 02 p0223 N88-11404
Components for measuring robots
[KFK-PFT-126] 03 p0332 N88-12092
On the control of a compliant robot arm
03 p0332 N88-12095
A theory for the articulation of robot manipulators
03 p0333 N88-12097
The 3-D world modeling for an autonomous robot
[DE87-013878] 03 p0333 N88-12102
Human motor reactions to dangerous motions in robot operations
[PB87-222196] 03 p0361 N88-12275
Low-cost teleoperator-controlled vehicle for damage assessment and dose measurement
[DE88-000713] 04 p0451 N88-12794
Static standing and dynamic walking of a practical biped robot
[DE88-001367] 04 p0451 N88-12795
Expert robots in nuclear plants
[DE87-014839] 04 p0452 N88-12800
Controlling robots with spoken commands
[DE88-000537] 04 p0452 N88-12801
Ground vehicle convoying
[DE88-000360] 04 p0502 N88-13088
Towards building a team of intelligent robots
[NASA-CR-181538] 05 p0589 N88-13595
Collision-free motion of two robot arms in a common workspace
[CSE-87-00002] 05 p0589 N88-13596
Dealing with unanticipated events in autonomous navigation
[DE88-000590] 05 p0590 N88-13602
Trajectory control of robot manipulators with closed-kinematic chain mechanism
[NASA-TM-89305] 05 p0591 N88-13605
Cartesian path control of a two-degree-of-freedom robot manipulator
[NASA-CR-182331] 05 p0639 N88-13908
Range imagery algorithms for the detection of obstacles by autonomous vehicles
[AD-A185421] 05 p0659 N88-14045
Robot accuracy improvement through kinematic parameter identification 06 p0712 N88-14363
Optical seam tracking in robotic arc welding
[VTT-RR-463] 06 p0713 N88-14376
Self calibration of motion and stereo vision for mobile robot navigation
[AD-A185602] 06 p0781 N88-14794
A demonstration of autonomous navigation and machine vision using the HERMIES-2B robot
[DE88-002298] 07 p0862 N88-15228
Roles of knowledge in motor learning
[AD-A186420] 07 p0897 N88-15438
Software simulation of time delay in teleoperation
08 p1056 N88-16371

Task path planning, scheduling and learning for free-ranging robot systems 08 p1058 N88-16386

Development of a task-level robot programming and simulation system 08 p1058 N88-16387

Goal driven kinematic simulation of flexible arm robot for space station missions 08 p1059 N88-16388

Heuristic search in robot configuration space using variable metric 08 p1059 N88-16389

Real time AI expert system for robotic applications 08 p1061 N88-16408

Solid modeling for the manipulative robot arm (power) and adaptive vision control for space station missions 08 p1061 N88-16409

Planning and scheduling for robotic assembly 08 p1062 N88-16416

Substructure discovery in executed action sequences [AD-A186446] 08 p1069 N88-16462

An optimal resolved rate law for kinematically redundant manipulators 09 p1212 N88-17268

Telerobotic research at NASA Langley Research Center 09 p1213 N88-17269

Manipulator arm design for the Extravehicular Teleoperator Assist Robot (ETAR): Applications on the space station 09 p1213 N88-17270

Development of a facility using robotics for testing automation of inertial instruments 09 p1213 N88-17271

Telerobotic truss assembly 09 p1213 N88-17272

Crew interface with a telerobotic control station 09 p1213 N88-17273

Telerobot for space station 09 p1213 N88-17274

Task-level robot programming: Integral part of evolution from teleoperation to autonomy 09 p1214 N88-17279

Navigation planning using quadtrees [DE88-003706] 09 p1225 N88-17343

A generalized method for automatic downhand and wireless control of a welding robot and positioner [NASA-TP-2807] 10 p1316 N88-17869

Design conditions and workspace for the generally-proportioned 3-hinge spherical wrist for robots 10 p1339 N88-18003

Parameter identification and sensitivity analysis for a robotic manipulator arm [NASA-CR-181608] 10 p1385 N88-18272

A computer simulation study of an expert system for walking machine motion planning [AD-A187907] 11 p1438 N88-18577

Fuzzy logic inference processor for real time control: A second generation full custom design [AD-A188155] 11 p1471 N88-18773

Adaptive control of a manipulator with a flexible link [NASA-CR-181637] 11 p1476 N88-18807

Time varying controller design for robot manipulator control [AD-A188094] 11 p1494 N88-18919

Kinematic and dynamic analyses of the Stanford/JPL robot hand [DE88-004637] 11 p1495 N88-18923

Robotics applications in the testing of inertial sensors 12 p1577 N88-19433

In-orbit automatic assembly of reticular structures 12 p1586 N88-19491

Mobile robot activity model for autonomous free flying platforms 12 p1588 N88-19507

The Hermes robot arm, its design and verification 12 p1588 N88-19508

Remote manipulation in orbital construction, servicing and repair missions: Is one arm enough? A comparative evaluation of the performance features of robots with one or more arms 12 p1588 N88-19509

Covariant control of bilateral servos for in-orbit manipulation 12 p1590 N88-19520

The Hermes manipulation system (HERA) simulation facility development 12 p1591 N88-19524

ROTEX: The Robotic Technology Experiment on Spacelab D-2 mission 12 p1592 N88-19530

User's guide: Lower neck transducer for the Hybrid 3 dummy [PB88-133319] 12 p1628 N88-19743

Evaluation tests of lower neck transducer for the Hybrid II Dummy [PB88-133327] 12 p1628 N88-19745

Low cost mobile robot [AD-A188507] 12 p1633 N88-19778

Free boundary problems arising in the control of a flexible robot arm [AD-A189124] 12 p1634 N88-19781

Intelligent control of robot manipulators in hazardous environments [DE88-003305] 13 p1778 N88-20638

Force distribution and trajectory control for closed kinematic chains with applications to walking machines 13 p1779 N88-20642

Ultrasonic inspection of irregular surfaces [AERE-R-12465] 13 p1780 N88-20648

Robotic joint prototype for space applications 14 p1878 N88-21222

A joint actuator design for a robotic manipulator 14 p1879 N88-21232

An efficient gradient projection optimization scheme for a seven-degree-of-freedom redundant robot with spherical wrist [DE88-005440] 14 p1919 N88-21453

Implementation of a visual servoing system for evaluation of robotic refueling applications [AD-A189676] 14 p1954 N88-21645

Range image segmentation and surface parameter extraction for a mobile robot [DE87-013877] 15 p2073 N88-22360

Telerobotic operation of conventional robot manipulators [DE88-005718] 15 p2073 N88-22363

The visit problem: Visibility graph-based solution [DE88-000343] 15 p2108 N88-22556

Insertions using geometric analysis and hybrid force-position control: Method and analysis [DE87-013652] 15 p2117 N88-22611

Concurrent algorithms for a mobile robot vision system [DE88-005850] 15 p2117 N88-22614

Path following robot [AD-A190960] 16 p2215 N88-23217

Automatic control of robot motion [AD-A191012] 16 p2215 N88-23218

Microgravity robotics technology program [NASA-TM-100898] 16 p2215 N88-23219

Microgravity mechanisms and robotics program 16 p2219 N88-23237

Accurate positioning of long, flexible ARM's (Articulated Robotic Manipulator) 16 p2219 N88-23243

Point accessibility and primary workspace of simple six-link robots 17 p2345 N88-23976

A control technique for improved robot performance 17 p2391 N88-24212

Induction of models under uncertainty [NASA-TM-101173] 17 p2394 N88-24230

Energy optimal trajectory planning for robot manipulators and autonomous vehicles 17 p2437 N88-24497

Kinematics, dynamics and control of a closed chain mechanism manipulator 18 p2523 N88-24967

Real-time implementation of a kinematic optimization scheme for seven-degree-of-freedom redundant robots with spherical wrists [DE88-006785] 18 p2524 N88-24974

Robot navigation using simple sensor fusion [DE88-006184] 18 p2561 N88-25203

A concurrent on-board vision system for a mobile robot [DE88-007475] 19 p2676 N88-25914

Proceedings of the Colloquium on Space and Sea [ESA-SP-280] 19 p2695 N88-26016

Tasks foreseen for space robots and an example of an associated orbital infrastructure 19 p2699 N88-26044

ELIT: An autonomous underwater observation robot 19 p2699 N88-26048

Underwater robotics in the service of oil field exploitation: The Running and Interconnecting Tool (RIT) in the East Frigg field (North Sea) 19 p2699 N88-26049

Simple 2-D navigation for wheeled vehicles [DE88-007115] 20 p2756 N88-26351

Force servo control of a commercial gantry robot [DE88-006649] 20 p2808 N88-26660

Sensor fusion for robot navigation [DE88-008383] 20 p2809 N88-26663

Mobile robot survival [DE88-009108] 20 p2809 N88-26665

Optimization of performance criteria with bounded joint velocities for robots with one degree of redundancy [DE88-003915] 20 p2810 N88-26670

Local free-space mapping and path guidance for mobile robots [AD-A192970] 20 p2810 N88-26674

Diagnosing faults in autonomous robot plan execution [NASA-CR-182480] 20 p2841 N88-26859

Three-dimensional scene analysis using stero based imaging [AD-A193120] 21 p2894 N88-27178

In-flight load measurements of the Robot-X canards [AD-A193428] 21 p2895 N88-27187

Aircraft refueling demonstrator using a microbot alpha 2 robot 21 p2926 N88-27367

Motor-response learning at a process control panel by an autonomous robot [DE88-005055] 21 p2955 N88-27554

Compliant robotic structures, part 3 [AD-A192426] 21 p2955 N88-27556

Development of a hybrid simulator for robotic manipulators [AD-A193119] 21 p2956 N88-27557

Control of free-flying space robot manipulator systems [NASA-CR-183017] 21 p2956 N88-27562

Control of free-flying space robot manipulator systems [NASA-CR-183104] 21 p2957 N88-27563

Research into the architecture of CAD based robot vision systems [AD-A193330] 21 p2997 N88-27776

Mobile robotics R and D at the Savannah River Laboratory [DE88-011665] 22 p3083 N88-28310

Energy storage considerations for a robotic Mars surface sampler [NASA-TM-100969] 22 p3166 N88-28853

Motion planning for legged locomotion systems on uneven terrain 23 p3221 N88-29170

Implementation of a flexible link model in a designed robot system, using the finite element method [ETN-88-92902] 23 p3243 N88-29303

Motion planning for a free-flying robot 23 p3255 N88-29378

Distributed cooperating processes in a mobile robot control system 23 p3256 N88-29386

Concepts for robot motion primitives required for space station teleoperations 23 p3257 N88-29387

Personnel occupied woven envelope robot 23 p3260 N88-29408

Remote servicing of space systems 23 p3260 N88-29409

Modeling robot flexibility for endpoint force control [AD-A195923] 24 p3380 N88-30132

Haptic exploration in humans and machines: Attribute integration and machine recognition/implementation [AD-A193692] 24 p3410 N88-30299

Simulation of a two link robot manipulator with elastic members [AD-A196014] 24 p3422 N88-30368

ROBUSTNESS (MATHEMATICS)

Identification of multivariate outliers and leverage points by means of robust covariance matrices [REPT-87-15] 01 p0088 N88-10575

Extensions of the small mu test for robust stability [OUEL-1666/87-REV] 02 p0223 N88-11406

New feedback design methodologies for large space structures: A multi-criterion optimization approach 04 p0408 N88-12535

Robust statistical methods for automated outlier detection 04 p0433 N88-12681

Solution of some 3-D viscous and inviscid supersonic flow problems by finite-volume space-marching schemes 05 p0532 N88-13235

Robustness of linear systems [PB87-220042] 05 p0639 N88-13909

Robust prediction operations for stationary processes [AD-A185408] 05 p0641 N88-13924

Maximum entropy/optimal projection design synthesis for decentralized control of large space structures [AD-A186359] 07 p0824 N88-15003

Robust prediction and interpolation for vector stationary processes, 2d enriched version [AD-A185875] 07 p0865 N88-15247

Conditionally unbiased bounded influence robust regression with applications to generalized linear models [AD-A186319] 07 p0915 N88-15556

A methodology for the synthesis of robust feedback systems [NASA-CR-182455] 09 p1225 N88-17342

A note on computing robust regression estimates via iteratively reweighted least squares [AD-A186709] 09 p1227 N88-17352

An integrated pressure sensor for in-vivo use 10 p1333 N88-17965

Stable, robust tracking by sliding mode control [AD-A188278] 10 p1401 N88-18358

Automated radar target recognition based on models of neural nets 11 p1476 N88-18804

Robustness in cost performance models [AD-A187183] 11 p1566 N88-19374

Choice of implicit and explicit operators for the upwind differencing method [NASA-TM-100857] 14 p1964 N88-21718

A robust scale estimator based on the shortest half [REPT-87-36] 14 p1966 N88-21731

Development and application of the p-version of the finite element method [AD-A190036] 15 p2120 N88-22633

Robust adaptive regulation without persistent excitation [NASA-TM-100571] 18 p2561 N88-25204

The robust tracking control of nonlinear systems with uncertain dynamics 21 p2999 N88-27788

Robust prediction for stationary processes: 2D enriched version [AD-A193318] 21 p3006 N88-27833

Robust design of cascade control [REPT-88-006] 22 p3142 N88-28687

Robust control of multivariable and large scale systems
[AD-A194250] 23 p3266 N88-29441

ROCK INTRUSIONS
NT BATHOLITHS
Dike zones on Venus
[NASA-TT-20111] 02 p0254 N88-11607
Drilling investigation of a young magmatic intrusion beneath the Inyo Domes, Long Valley, California: Structural and textural studies
[DE88-006613] 18 p2541 N88-25078
Recycling of lower continental crust through foundering of cumulates from contaminated mafic intrusions
24 p3393 N88-30204
Crustal evolution and the eclogite to granulite phase transition in xenoliths from the West African Craton
24 p3395 N88-30217
Evidence for crustal recycling during the Archean: The parental magmas of the stillwater complex
24 p3396 N88-30226

ROCK MECHANICS
Research needs for hydrocarbon fuels
[DE87-014555] 06 p0687 N88-14209

ROCKET BOOSTERS
U BOOSTER ROCKET ENGINES

ROCKET CHAMBERS
U THRUST CHAMBERS

ROCKET ENGINE CASES
Slip casting and extruding shapes of rhemium with metal oxide additives. Part 2: Development of grain stabilized rhenium parts for resistojets
[NASA-CR-180851] 03 p0278 N88-11749
The structures of large wound propulsion shells --- carbon fiber composites filament winding
[SNIAS-872-430-118] 05 p0559 N88-13406
STA-2A NDT testing
[NASA-CR-179301] 11 p1497 N88-18937
Rocket motor case materials. An evaluation of new fibers for composites
[FOA-C-20696-2.1] 21 p2906 N88-27245

ROCKET ENGINE CONTROL
Selection of efficient correcting motor for an artificial Earth satellite 08 p1007 N88-16102
Intelligent on board control for field emission electric propulsion system 12 p1589 N88-19513

ROCKET ENGINE DESIGN
Hermes propulsion system
[SNIAS-872-422-109] 05 p0556 N88-13383
Skylark sounding rocket development-Skylark 8
08 p1035 N88-16274
Arcjet thruster research and technology
[NASA-CR-180865] 10 p1293 N88-17732
Arcjet thruster research and technology, phase 1
[NASA-CR-182107] 17 p2314 N88-23830
Dual-fuel, dual-mode rocket engine
[NASA-CASE-LAR-13773-1] 18 p2475 N88-24685

ROCKET ENGINES
NT APOGEE BOOST MOTORS
NT ARC JET ENGINES
NT BOOSTER ROCKET ENGINES
NT DUCTED ROCKET ENGINES
NT ELECTRIC ROCKET ENGINES
NT ELECTROSTATIC ENGINES
NT ELECTROTHERMAL ENGINES
NT HYDRAZINE ENGINES
NT HYDROGEN OXYGEN ENGINES
NT ION ENGINES
NT LIQUID AIR CYCLE ENGINES
NT LIQUID PROPELLANT ROCKET ENGINES
NT MERCURY ION ENGINES
NT NOZZLELESS ROCKET ENGINES
NT NUCLEAR ENGINE FOR ROCKET VEHICLES
NT NUCLEAR ROCKET ENGINES
NT RESISTOJET ENGINES
NT REUSABLE ROCKET ENGINES
NT SOLID PROPELLANT ROCKET ENGINES
NT SPACE SHUTTLE BOOSTERS
NT SPACE SHUTTLE MAIN ENGINE
NT UPPER STAGE ROCKET ENGINES
The numerical simulation of an idealised one-dimensional, steady monopropellant rocket
[PDR/CFDU/IC/31] 01 p0018 N88-10107
A life test of a 22-Newton (5-lbf) hydrazine rocket
[NASA-TM-100232] 03 p0278 N88-11750
Plasma thruster development
[AD-A184173] 04 p0408 N88-12536
A two-dimensional finite difference program for thermal analysis of rocket thrust chambers
[NASA-TM-100191] 04 p0409 N88-12539
The VISTA spacecraft: Advantages of ICF (Inertial Confinement Fusion) for interplanetary fusions propulsion applications
[NASA-CR-181549] 04 p0491 N88-13024
Numerical model of the time independent mean flow in a rotating rocket motor 13 p1733 N88-20360
Crack opening and extension in inert solid propellant. An experimental study
[AD-A189808] 15 p2048 N88-22201
Test plan and facilities for qualifying nuclear rocket fuel elements 17 p2434 N88-24482
Thrust chamber thermal barrier coating techniques
[NASA-TM-100933] 18 p2476 N88-24690
The 24th JANNAF Combustion Meeting, volume 2
[AD-A190164] 19 p2622 N88-25554
Numerical grid generation and flow simulation in SSME thrust chamber 19 p2626 N88-25577
A computer program for performance prediction of tripropellant rocket engines with tangential slot injection
19 p2627 N88-25581
Analysis of flow through pump of large rocket engine
19 p2637 N88-25646
Energy conversion measurements in laser-sustained argon plasmas for application to rocket propulsion
[AD-A194931] 24 p3337 N88-29861
Automatic data retrieval from rocket motor holograms
[AD-A195586] 24 p3337 N88-29864
Iridium-coated rhenium thrusters by CVD
[NASA-TM-101309] 24 p3339 N88-29874

ROCKET EXHAUST
The Shock and Vibration Bulletin. Part 4: Structural Dynamics and Modal Test and Analysis
[AD-A186751] 09 p1179 N88-17062
Qualification by analysis of IUS plume deflectors
09 p1179 N88-17063
Kinetic mechanisms for ionization and afterburning suppression
[AD-A189219] 13 p1737 N88-20383
Environmental monitoring of a titan 34D 5 1/2 segment solid rocket motor static firing
[AD-A192975] 20 p2766 N88-26400
Variable Mach number wall jets for control/propulsion on hypervelocity projectiles/interceptors: Tests with an existing model
[AD-A192845] 21 p2892 N88-27167
SRB/SLEEC (Solid Rocket Booster/Shingle Lap Extendible Exit Cone) feasibility study, volume 2. Appendix A: Design study for a SLEEC actuation system
[NASA-CR-178974] 23 p3187 N88-28965
Studies on rocket exhaust plumes and impingement effects related to the Columbus Space Station program: Executive summary
[DFVLR-IB-222-88-A-12] 24 p3337 N88-29862

ROCKET FIRING
Orbital transfer vehicle 3000 LBF thrust chamber assembly hot fire test program
[NASA-CR-182145] 24 p3336 N88-29858

ROCKET FLIGHT
Instrumentation utilisation for risk control in safety operations --- balloons and rockets
08 p1030 N88-16240
Flight results of the ESA experiment modules in Materials Science Experiment Rocket (MASER) 1
08 p1033 N88-16261
Guidance of high-altitude sounding rockets using the S19 and Spinning Rocket Altitude Control (SPINRAC) systems 08 p1034 N88-16273
Zone crystallization experiments in mirror heating facilities
[BMFT-FB-W-86-023] 16 p2184 N88-23016
Wind tunnel investigation of wing and control panel loads at transonic and supersonic speeds on some schematic cruciform missile configurations
[FFA-TN-1986-43] 18 p2457 N88-24585

ROCKET LAUNCHING
NT ORBITAL LAUNCHING
Hydrogen chloride measurements in launch-vehicle exhaust clouds
[DE87-011552] 06 p0964 N88-15837
Esrange (Sweden): New installations, future plans and investments --- rocket range 08 p1029 N88-16235
Facilities and plans for improvements at Andoya (Norway) rocket range 08 p1029 N88-16236
The DFVLR-German Space Operations Center (GSOC) mobile rocket base 08 p1029 N88-16237
High altitude chemical release systems for project BIME (Brazilian Ionospheric Modification Experiments) project IMS (Ionospheric Modification Studies) project PIIE (Polar Ionospheric Irregularities Experiment) project polar arcs
[AD-A188299] 12 p1642 N88-19833

ROCKET MOTOR CASES
U ROCKET ENGINE CASES

ROCKET NOSE CONES
SRB/SLEEC (Solid Rocket Booster/Shingle Lap Extendible Exit Cone) feasibility study, volume 2. Appendix A: Design study for a SLEEC actuation system
[NASA-CR-178974] 23 p3187 N88-28965

ROCKET NOZZLES
Rocket nozzle thermal shock tests in an arc heater facility 02 p0133 N88-10832
Thrust and specific impulse of repetitively-pulsed-laser propulsion rocket 03 p0318 N88-12012
High performance Solid Rocket Motor (SRM) submerged nozzle/combustion cavity flowfield assessment
[NASA-CR-179307] 11 p1446 N88-18822
An experimental investigation of rocket ramjet nozzle assembly base pressures
[AD-A189714] 15 p2027 N88-22076
Aeropropulsive characteristics of isolated combined turbojet/ramjet nozzles at Mach numbers from 0 to 1.20
[NASA-TP-2814] 17 p2299 N88-23757
Arcjet thruster research and technology, phase 1
[NASA-CR-182107] 17 p2314 N88-23830
Nozzle fabrication technique
[NASA-CASE-MSC-21299-1] 18 p2475 N88-24684
A detailed description of the uncertainty analysis for high area ratio rocket nozzle tests at the NASA Lewis Research Center 19 p2626 N88-25580
Boundary layer development as a function of chamber pressure in the NASA Lewis 1030:1 area ratio rocket nozzle
[NASA-TM-100917] 19 p2664 N88-25841
Analysis of edge detection techniques for radiographic image measurement
[AD-A193650] 23 p3186 N88-28961

ROCKET OXIDIZERS*
The chemistry of the hypochlorite neutralization of hydrazine fuels
[DE88-002971] 10 p1307 N88-17812

ROCKET PROPELLANT TANKS
U PROPELLANT TANKS

ROCKET PROPELLANTS
NT CRYOGENIC ROCKET PROPELLANTS
NT DOUBLE BASE ROCKET PROPELLANTS
NT GELLED ROCKET PROPELLANTS
NT LIQUID ROCKET PROPELLANTS
NT METAL PROPELLANTS
NT MONOPROPELLANTS
NT NITRAMINE PROPELLANTS
NT RP-1 ROCKET PROPELLANTS
NT SLURRY PROPELLANTS
NT SOLID ROCKET PROPELLANTS
Orbital Spacecraft Consumables Resupply System (OSCRS). Volume 2: Study results
[NASA-CR-172011] 03 p0268 N88-11667
A life test of a 22-Newton (5-lbf) hydrazine rocket
[NASA-TM-100232] 03 p0278 N88-11750
Compatability of dispersion-strengthened platinum with resistojet propellants
[NASA-TP-2765] 04 p0409 N88-12538
Test number 2 of propellant for rocket motor MK52
[PB87-226155] 05 p0571 N88-13480
Space station onboard propulsion system: Technology study
[NASA-CR-179233] 07 p0825 N88-15006
Evidences for distributed combustion
19 p2628 N88-25586
Possibilities of economical improvements for Moon based rocket propulsion using lunar propellants
[ILR-MITT-196] 24 p3338 N88-29871

ROCKET PROPELLED SLEDS
Static force and moment test of the Holloman narrow-gage rocket sled at Mach numbers from 3.5 to 5.5
[AD-A186291] 07 p0822 N88-14995
High-velocity reverse ballistic rocket sled testing at Sandia National Laboratories 09 p1179 N88-17059
Reference position vector 12 p1577 N88-19432

ROCKET SONDES
U SOUNDING ROCKETS

ROCKET SOUNDING
The German scientific balloon and sounding rocket program 08 p1024 N88-16202
The Norwegian scientific balloon and sounding rocket program 1987-1990 08 p1025 N88-16204
The Swedish sounding rocket and balloon program
08 p1025 N88-16205
Swiss scientific balloon and sounding rocket experiments 1985-1987 08 p1025 N88-16206
First results from the Viking associated Aureld-VIP rocket and EISCAT campaign --- auroras; Swedish satellite
08 p1026 N88-16211
Report on ground-based activity at Andoya (Norway) in relation to the Aureld-VIP high rocket and to the Viking satellite --- Swedish satellite 08 p1026 N88-16212
How ground-based observations contribute to rocket, balloon and space shuttle experiments: Experience from the past and outlook for the future
08 p1026 N88-16216
New techniques for rocket and balloon-borne instrumentation for investigations of the structure, dynamics and electrodynamics of the middle atmosphere 08 p1027 N88-16220
ROCOZ-A (improved rocket launched ozone sensor) for middle atmosphere ozone measurements
08 p1029 N88-16233

MAIMIK: A high current electron beam experiment on a sounding rocket from Andoya rocket range (Norway)
08 p1030 N88-16243
CAESAR investigations --- Coordinated Auroral Experiment using Scatter And Rockets (CAESAR)
08 p1031 N88-16249
Observations of field-aligned current structures during the Coordinated Auroral Experiment using Scatter And Radar (CAESAR) flight 2 08 p1031 N88-16250
EISCAT measurements of ion velocities during Coordinated Auroral Experiment using Scatter And Rockets (CAESAR) campaign 08 p1031 N88-16251
Remote and in-situ plasma measurements during the Coordinated Auroral Experiment using Scatter And Rockets (CAESAR) flight 08 p1032 N88-16252
Low frequency electrostatic waves observed on board the Coordinated Auroral Experiment using Scatter And Rockets (CAESAR) 2 payload 08 p1032 N88-16253
The rocket and scatter experiment ROSE: Presentation of the scientific payload 08 p1034 N88-16269
Rocket experiments and payloads for Super CAMP --- Cold Arctic Mesopause Project (CAMP)
08 p1034 N88-16271
Coordinated Auroral Experiments using Scatter And Rocket investigations (CAESAR investigations)
[MPAE-W-47-87-13] 15 p2096 N88-22487
Rocket measurements within a polar cap arc: Ionospheric modelling
[AD-A192381] 20 p2824 N88-26754

ROCKET TEST FACILITIES
Ground shock profiles for an accidental explosion at the proposed Large Rocket Test Facility at Arnold Engineering Development Center
[DE88-002652] 07 p0853 N88-15180
Test plan and facilities for qualifying nuclear rocket fuel elements 17 p2434 N88-24482

ROCKET THRUST
Thrust and specific impulse of repetitively-pulsed-laser propulsion rocket 03 p0318 N88-12012
A two-dimensional finite difference program for thermal analysis of rocket thrust chambers
[NASA-TM-100191] 04 p0409 N88-12539
Space station propulsion technology
[NASA-CP-179260] 08 p0964 N88-15835

ROCKET VEHICLES
NT ARIANE LAUNCH VEHICLE
NT BLACK BRANT SOUNDING ROCKETS
NT CENTAUR LAUNCH VEHICLE
NT MULTISTAGE ROCKET VEHICLES
NT PAYLOAD ASSIST MODULE
NT SINGLE STAGE ROCKET VEHICLES
NT SKYLARK ROCKET VEHICLE
NT SOUNDING ROCKETS
NT TITAN LAUNCH VEHICLES
Instrumentation package for a shrouded SWERVE/EPW rocket sled test
[DE87-014267] 01 p0008 N88-10045
Effect of rotation on the lateral stability of a free-flying column subjected to an axial thrust with directional control
[AD-A188690] 13 p1728 N88-20338

ROCKET-BORNE INSTRUMENTS
ROCOZ-A (improved rocket launched ozone sensor) for middle atmosphere ozone measurements
08 p1029 N88-16233
A new technique for rocket and space-borne investigations of time-dependant auroral morphology
08 p1030 N88-16241
Ultraviolet rocket-spectra of a sunspot
08 p1032 N88-16257
Preliminary Material Science Experiment Rocket (MASER) 1 results and the evolution of the MASER program 08 p1033 N88-16260
The rocket and scatter experiment ROSE: Presentation of the scientific payload 08 p1034 N88-16269
MRS-3000 meteorological rocket probe for the MMR-06 dart integrated meteorological rocket system
[NASA-TT-20303] 19 p2693 N88-26010

ROCKETS
Vehicle glow observed on the SONDA 3
[INPE-4297-PRE/1168] 12 p1600 N88-19581

ROCKS
NT ANDESITE
NT ANORTHOSITE
NT BASALT
NT BATHOLITHS
NT BEDROCK
NT BRECCIA
NT CARBONACEOUS ROCKS
NT COAL
NT ECLOGITE
NT GNEISS
NT GRANITE
NT IGNEOUS ROCKS
NT LUNAR ROCKS
NT PERIDOTITE
NT REGOLITH
NT SANDSTONES
NT SEDIMENTARY ROCKS
A mineral reconnaissance sampling manual for Costa Rica: Cenual American energy and resource project
[DE87-014997] 04 p0462 N88-12859
Analysis of airborne imaging spectrometer data for the Ruby Mountains, Montana, by use of absorption-band-depth images 05 p0614 N88-13771
Mapping hydrothermally altered rocks in the Northern Grapevine Mountains, Nevada and California with the airborne imaging spectrometer 05 p0614 N88-13772
X-ray microfluorescence analysis of thin- and thick-sectioned geologic materials
[DE87-009803] 09 p1189 N88-17126
Nature and origin of mineral coatings on volcanic rocks of the Black Mountain, Stonewall Mountain, and Kane Springs Wash volcanic centers, Southern Nevada
[NASA-CR-181437] 09 p1191 N88-17140
Microwave dielectric spectrum of rocks
[NASA-TM-89719] 12 p1642 N88-19831
Elemental composition of Venusian rocks in northeastern part of Terra Aphrodite (determined using data from Vega-2 landing module)
13 p1726 N88-20322
Content of natural radioactive elements in Venusian rocks determined using data from Vega-1 and Vega-2 stations 13 p1726 N88-20323
P/Halley dust coma: Grains or rocks?
14 p2002 N88-21936
Carbon analysis in natural olivine crystals of deep origin
[NASA-TT-20311] 19 p2734 N88-26239
Prospects for hot dry rock in the future
[DE88-010909] 20 p2820 N88-26730
Fine-scale traverses in cumulate rocks, Stillwater Complex: A lunar analogue study
[NASA-CR-183066] 20 p2823 N88-26747
Relationships among earth's gravity field, magnetic field, crustal structure and the magnetic character of crustal rocks
[AD-A195539] 24 p3392 N88-30198
Mid to late proterozoic magmatism within Northeastern North America and its iplications for the growth of the continental crust 24 p3397 N88-30229
Growth of the lower continental crust
24 p3398 N88-30236
Geochronological and lead-isotope evidences for rapid crust formation in middle-proterozoic time: The Labrador example 24 p3398 N88-30239
Trace element differences between Archean, Proterozoic and Phanerozoic crustal components: Implications for crustal growth processes
24 p3399 N88-30243
Exotic minerals in 3,500 million year old rocks: Evidence for large meteorite impacts 24 p3440 N88-30475

RODENTS
NT MICE
NT RATS

RODS
NT CONTROL RODS
Geometrically nonlinear rod mechanism analogy of axisymmetrically loaded spherical shells based on a comprehensive approach to the stability of circular arches
[ETN-87-90419] 01 p0062 N88-10398
A creep measurement of unidirectional epoxy-fiberglass rod
[DE87-014812] 04 p0411 N88-12553
Lightning discharge protection rod
[NASA-CASE-LAR-13470-1] 06 p0666 N88-14083
A direct correlation of strength with impact velocity
[AD-A189251] 13 p1741 N88-20409
Solid hosts for dye laser rods. Part 1: Criteria for choosing a host material
[DE88-006478] 15 p2072 N88-22355
Vibrational power flow analysis of rods and beams
[NASA-CR-183166] 24 p3383 N88-30151

ROENTGEN SATELLITE
U ROSAT MISSION

ROGALLO WINGS
U FOLDING STRUCTURES

ROLL
Investigation of interactions between limb-manipulator dynamics and effective vehicle roll control characteristics
[NASA-CR-3983] 01 p0007 N88-10039
Multi-hundred kilowatt roll ring assembly evaluation results
[NASA-TM-100865] 14 p1904 N88-21375
Aerodynamics in ground effect and predicted landing ground roll of a fighter configuration with a secondary-nozzle thrust reverser
[NASA-TP-2834] 24 p3317 N88-29752
Computer programs for calculation of sting pitch and roll angles required to obtain angles of attack and sideslip on wind tunnel models
[NASA-TM-100659] 24 p3329 N88-29820

ROLL CONTROL
U LATERAL CONTROL

ROLL FORMING
Hardening of metal during production of bent shapes
[BLL-M-37250-(5828.4)] 02 p0148 N88-10928
Interrelation and measurement of formability, strengthening, and thermomechanical processing under metalworking conditions
[DE88-002485] 08 p0967 N88-15850

ROLLER BEARINGS
Improved oil-off survivability of tapered roller bearings
[NASA-CR-180804] 02 p0182 N88-11135
Ceramic bearings for use in gas turbine engines
[NASA-TM-100288] 10 p1340 N88-18007
Corrosion-wear process under rolling-sliding motion
[AD-A189603] 13 p1778 N88-20635
High temperature solid lubrication by catalytically generated carbon
[AD-A190804] 16 p2182 N88-23004

ROLLERS
Requirements for a test stand for plastic rollers for the verification of nonequilibrium force laws
[ILR-MITT-176] 01 p0008 N88-10040
Development, features of roller rocker arm reported
06 p0689 N88-14219
Evaluation of a high-torque backlash-free roller actuator 16 p2219 N88-23239
Roller drive materials performance
16 p2219 N88-23241
Brief evaluation of the alloy 17-4-PH (Z5 CNU 17-04). Semifinished product: 205 mm dia forged roller, test reports
[DF/NH-3616/84] 17 p2322 N88-23866
A study of the floating roller peel test for adhesives
[AD-A194114] 23 p3198 N88-29034

ROLLING
Mode 2 fracture mechanics 15 p2083 N88-22418

ROLLING CONTACT LOADS
Requirements for a test stand for plastic rollers for the verification of nonequilibrium force laws
[ILR-MITT-176] 01 p0008 N88-10040
Application of Kalker's rolling contact theory to the simulation of rail vehicles
[DFVLR-FB-87-07] 01 p0057 N88-10363
Wear of hard steel in rolling lubricated contact
[RP-699] 03 p0332 N88-12094
The numerical solution of the elastohydrodynamically lubricated line and point contact problem, using multigrid techniques
[ISBN-90-9001583-3] 06 p0714 N88-14377
Mechanisms of rolling contact spalling
[NASA-CR-179243] 06 p0714 N88-14380
The quasi-static contact problem with friction for three dimensional elastic bodies
[REPT-87-51] 14 p1918 N88-21447
Calculation of rolling contact of two viscoelastic cylinders with application to the steady state normal contact problem
[ILR-MITT-188] 18 p2530 N88-25008
Energy dissipation in a rolling aircraft tire
[NASA-CR-182978] 19 p2676 N88-25913
Investigation of rolling contact fatigue of ball bearings
[NASA-TT-20196] 19 p2678 N88-25922
Frequency dependent sliding coefficients for general three-dimensional rolling contact in high frequency range
[ILR-MITT-192] 22 p3085 N88-28318

ROLLING MOMENTS
Mechanisms of rolling contact spalling
[NASA-CR-179243] 06 p0714 N88-14380
Parametric estimation of aerodynamic nonlinearities in rolling moment due to sideslip using maximum likelihood method 20 p2786 N88-26528

ROLLUP SOLAR ARRAYS
U SOLAR ARRAYS

ROM DEVICES
U READ-ONLY MEMORY DEVICES

ROOM TEMPERATURE
Behavior of long and short fatigue cracks in a powder metallurgy superalloy at room and at high temperature
05 p0601 N88-13677
Data recorded by the Rome room temperature gravitational wave antenna, during the supernova SN 1987 A in the Large Magellanic Cloud
[NOTA-INTERNA-879] 06 p0806 N88-14922
Lithium fast-ion conductors: Polymer based materials
[AD-A187879] 11 p1461 N88-18712
Photophysics and photochemistry of poly(di-n-hexylsilane) in room temperature solution
[AD-A187890] 11 p1462 N88-18714
High-efficiency Y-Sc-Ga:Cr (sup)3+,Tu (sup)3+,Ho (sup)3+ garnet laser (gl= 2.088 gmm at room temperature 14 p1971 N88-21766

Chemical vapor deposition of TiO2 thin films at room temperature
[DE88-008892] 21 p2953 N88-27542
A new near-infrared tunable-room temperature solid state laser La3Ga5SiO14:Cr(3+)
[DE88-011341] 21 p2953 N88-27543
Relation between strength, creep and relaxation behavior in Cu and Al at room temperature
[ETN-88-92982] 23 p3195 N88-29015
Alternative immersion accelerated testing of coating systems for Naval shoreline facilities
24 p3355 N88-29977

ROOMS
NT CLEAN ROOMS

ROOT-MEAN-SQUARE ERRORS
Detection of signals by weighted integrate-and-dump filter 04 p0435 N88-12696
Spectral- and spatial-domain filtering and sampling approach to the numerical solution of electromagnetic scattering problems
[PB88-106711] 06 p0694 N88-14261
Study of extended least-square iterative techniques in electromagnetic scattering by penetrable objects
[PB88-105879] 06 p0694 N88-14262
Response of wind shear warning systems to turbulence with implication of nuisance alerts
10 p1274 N88-17618
Seismic inversion by a RMS (Root-Mean-Square) Born approximation in the space-time domain
[PB88-165402] 15 p2131 N88-22711
Calculation of root-mean-square loads
[BLL-M-37776-(5828.4)] 16 p2531 N88-25015

ROOTS OF EQUATIONS
Detection of critical points: The first step to automatic line generalization 05 p0619 N88-13803
General solution of certain functional equations
[PREPRINT-554] 06 p0764 N88-14689
Simulation of FELIN logics. Polynomials roots simultaneous computation algorithms
[ETN-88-92182] 16 p2253 N88-23464
A primal-dual algorithm for the computation of the minimum of a convex function on the intersection of convex functions, and its application in data analysis
[RR-638-M] 18 p2563 N88-25217
A full but elementary treatment of systems of homogeneous ordinary linear differential equations with constant coefficients
[REPT-87-82] 20 p2845 N88-26887

ROSAT MISSION
Some highlights on ROSAT mechanisms
14 p1874 N88-21195
Design, construction and performance of the ROSAT high resolution X-ray mirror assembly
[MPE-PREPRINT-101] 15 p2150 N88-22836

ROSS ICE SHELF
Ice-shelf response to ice-stream discharge fluctuation. Part 1: Unconfined ice tongues
[AD-A188147] 10 p1358 N88-18117

ROSSBY REGIMES
Radio emission from RS CVn binaries: A 5 GHz VLA survey of 93 systems 04 p0519 N88-13191
Nonlinear normal mode initialization of a limited area model using nonstationary Rossby modes --- numerical weather forecasting
[KNMI-WR 87-10] 14 p1947 N88-21614

ROSSBY WAVES
U PLANETARY WAVES

ROTARY DRIVES
U MECHANICAL DRIVES

ROTARY ENGINES
NT WANKEL ENGINES
Endurance testing of a natural gas-fueled rotary engine
[PB87-215703] 01 p0055 N88-10356
Performance and combustion characteristics of direct-injection stratified-charge rotary engines
[NASA-TM-100134] 04 p0400 N88-12490
Regressed relations for forced convection heat transfer in a direct injection stratified charge rotary engine
[NASA-TM-100124] 05 p0549 N88-13345

ROTARY STABILITY
NT GYROSCOPIC STABILITY
Control and stabilization mechanisms of submunitions
[DFVLR-IB-111-86/9] 03 p0259 N88-11630
Numerical and analytical study of fluid dynamic forces in seals and bearings
[NASA-TM-100268] 11 p1485 N88-18867
Parametric dependence in the equilibrium dynamics of rotating structures
[AD-A187817] 11 p1498 N88-18945

ROTARY WING AIRCRAFT
NT AH-64 HELICOPTER
NT BO-105 HELICOPTER
NT CH-46 HELICOPTER
NT COMPOUND HELICOPTERS
NT HEAVY LIFT HELICOPTERS
NT HELICOPTERS
NT MILITARY HELICOPTERS
NT OH-58 HELICOPTER
NT RIGID ROTOR HELICOPTERS
NT ROTOR SYSTEMS RESEARCH AIRCRAFT
NT TANDEM ROTOR HELICOPTERS
NT TILT ROTOR AIRCRAFT
NT UH-1 HELICOPTER
NT UH-60A HELICOPTER
NT XV-15 AIRCRAFT
Civil applications of high-speed rotorcraft and powered-lift aircraft configurations
[NASA-TM-100035] 03 p0261 N88-11643
Operational load measurements on service helicopters
03 p0263 N88-11658
Test stand performance of a convertible engine for advanced V/STOL and rotorcraft propulsion
[NASA-TM-100211] 03 p0266 N88-11679
NASA/Army Rotorcraft Technology. Volume 3: Systems Integration, Research Aircraft, and Industry
[NASA-CP-2495-VOL-3] 09 p1110 N88-16650
McDonnell Douglas Helicopter Company independent research and development: Preparing for the future
09 p1111 N88-16660
General Rotorcraft Aeromechanical Stability Program (GRASP) version 1.03: User's manual
[NASA-TM-100043] 09 p1219 N88-17313
Helicopter external vision requirements and visual display characteristics: A report/bibliography, revision A
[AD-A187075] 10 p1276 N88-17641
Rotorcraft weight trends in light of structural material characteristics
[AD-A186576] 10 p1276 N88-17642
A perspective on 15 years of proof-of-concept aircraft development and flight research at Ames-Moffett by the Rotorcraft and Powered-Lift Flight Projects Division, 1970-1985
[NASA-RP-1187] 12 p1582 N88-19467
Rotorcraft flight-propulsion control integration: An eclectic design concept
[NASA-TP-2815] 12 p1584 N88-19475
Reasons for increasing development cost of rotary wing aircraft and ideas to reverse the trend
12 p1701 N88-20179
Reducing rotary wing aircraft development time/cost through the use of simulation 12 p1702 N88-20186
Some rotorcraft applications of computational fluid dynamics
[NASA-TM-100066] 18 p2459 N88-24601
Rotorcraft TCAS (traffic alert and collision avoidance system) evaluation: Group 3 results
[AD-A191719] 18 p2461 N88-24614
Zero/zero rotorcraft certification issues. Volume 1: Executive summary
[NASA-CR-177483-VOL-1] 19 p2602 N88-25453
Zero/zero rotorcraft certification issues. Volume 2: Plenary session presentations
[NASA-CR-177483-VOL-2] 19 p2602 N88-25454
Zero/zero rotorcraft certification issues. Volume 3: Working group results
[NASA-CR-177483-VOL-3] 19 p2602 N88-25455
Hover performance tests of baseline metal and Advanced Technology Blade (ATB) rotor systems for the XV-15 tilt rotor aircraft
[NASA-CR-177436] 20 p2759 N88-26367
A general-purpose approach to computer-aided dynamic analysis of a flexible helicopter
[NASA-TM-101002] 20 p2816 N88-26709
Prediction and measurement of human pilot dynamic characteristics in a manned rotorcraft simulation
[NASA-CR-183246] 24 p3410 N88-30297

ROTARY WINGS
NT BEARINGLESS ROTORS
NT CIRCULATION CONTROL ROTORS
NT RIGID ROTORS
NT TILTING ROTORS
NT X WING ROTORS
Analytical modeling of helicopter static and dynamic induced velocity in GRASP
[NASA-TM-100026] 02 p0123 N88-10777
An experimental evaluation of advanced rotorcraft airfoils in the NASA Ames eleven-foot transonic wind tunnel
[NASA-CR-166587] 03 p0261 N88-11640
Analytic investigation of helicopter rotor blade appended aeroelastic devices
[NASA-CR-166525] 03 p0266 N88-11676
Velocity scaled aeroelastic testing of an unducted fan
[GTL-191] 05 p0548 N88-13337
Artificial and natural icing tests of AH-64, phase 2
[AD-A188231] 11 p1439 N88-18585
A code development system for computational fluid dynamics
[AD-A188050] 11 p1482 N88-18848
Verification of the momentum theory for rotors using measurements on a model helicopter
[R-840-S] 13 p1718 N88-2[illegible]75
Measurements on a helicopter rotor
[R-764-S] 14 p1861 N88-21119
Investigations on higher harmonic blade pitch control at helicopters
[DFVLR-FB-87-36] 14 p1868 N88-21165
Tip vortices of isolated wings and helicopter rotor blades
[AD-A191336] 16 p2158 N88-22874
Structurally tailorable non-linear snap-through spring system
[NASA-CASE-LAR-13729-1] 18 p2523 N88-24970
Limits of design feasibility of multiwing wind turbines with individual articulated wing structure
[ILR-MITT-180] 18 p2537 N88-25052
Grid generation of a helicopter rotary-wing
19 p2640 N88-25665
Helicopter main-rotor noise: Determination of source contributions using scaled model data
[NASA-TP-2825] 20 p2848 N88-26907
An unsteady helicopter rotor: Fuselage interaction analysis
[NASA-CR-4178] 23 p3171 N88-28880
JUH-1H redesigned pneumatic boot deicing system flight test evaluation
[AD-A194918] 24 p3322 N88-29785

ROTATING
U ROTATION

ROTATING BODIES
NT BEARINGLESS ROTORS
NT CIRCULATION CONTROL ROTORS
NT COMPRESSOR ROTORS
NT FLYWHEELS
NT HELICOPTER TAIL ROTORS
NT IMPELLERS
NT PUMP IMPELLERS
NT RIGID ROTORS
NT ROTARY WINGS
NT ROTATING CYLINDERS
NT ROTATING DISKS
NT ROTATING SPHERES
NT ROTORS
NT TAIL ROTORS
NT TILTING ROTORS
NT TURBINE WHEELS
NT X WING ROTORS
Control and stabilization mechanisms of submunitions
[DFVLR-IB-111-86/9] 03 p0259 N88-11630
Semiempirical method for prediction of aerodynamic forces and moments on a steadily spinning light airplane
[NASA-TM-4009] 04 p0393 N88-12456
Airborne tracking sunphotometer apparatus and system
[NASA-CASE-ARC-11622-1] 06 p0730 N88-14492
Parametric dependence in the equilibrium dynamics of rotating structures
[AD-A187817] 11 p1498 N88-18945
An L-U implicit multigrid algorithm to solve the Euler equations for transonic flow in rotating turbomachinery passages 13 p1718 N88-20270
Topics in curved and flat space electromagnetism
13 p1854 N88-21100
The calculation of transonic flow over the shuttle orbiter using slender body theory 18 p2460 N88-24606
Effects of Coriolis acceleration on the vibrations of spinning structures 18 p2522 N88-24966
Drag measurements on a laminar flow body of revolution in Langley's 13 inch magnetic suspension and balance system
[NASA-CR-182909] 19 p2597 N88-25432

ROTATING CYLINDERS
Experiments on the flow of viscoelastic fluids between eccentric rotating cylinders 12 p1625 N88-19723
Compressible flow in a pie-shaped cylinder rotating about the vertex 18 p2460 N88-24604
Moving belt radiator development status
[NASA-TM-100909] 19 p2607 N88-25477
Numerical simulation of unsteady incompressible flow in a partially-filled rotating cylinder
[AD-A196001] 24 p3371 N88-30073

ROTATING DISKS
Coherent vortex structures in the wake of a stationary disk and of a disk excited to vibration
[ESA-TT-994] 09 p1163 N88-16968
Solution of a rotating Navier-Stokes problem by a nonlinear multigrid algorithm 11 p1538 N88-19194
Life and reliability of rotating disks
15 p2085 N88-22428
Remote temperature-measurement instrumentation for a heated rotating turbine disk
[DE88-006456] 18 p2516 N88-24925
Prediction of the pressure distribution for radial inflow between co-rotating discs
[PNR90464] 22 p3076 N88-28261

Numerical predictions for the flow induced by an enclosed rotating disc
[PNR90463] 22 p3078 N88-26281

ROTATING ENVIRONMENTS

Gastric emptying assessment by echography after a stress (rotating chair) 12 p1661 N88-19955

ROTATING FLUIDS

NT ROTATING LIQUIDS

Linear and nonlinear theories of flow through an actuator disk --- windpowered pumps
[R-803-A] 03 p0316 N88-11995

Turbulent mixing in a rotating, stratified fluid
04 p0445 N88-12759

Compressor large bandwidth noise emission mechanisms
[ETN-88-91177] 05 p0646 N88-13959

Rotational flow of rarefied gas between two coaxial cylinders with slip conditions
[INPE-4277-PRE/1149] 12 p1627 N88-19738

Mushroom-shaped currents (eddy dipoles) under rotation and stratification conditions
13 p1764 N88-20678

Development of a rotary fluid transfer coupling and support mechanism for space station
14 p1928 N88-21493

Experimental demonstrations of organic Rankine cycle waste heat rejection systems 17 p2432 N88-24469

Simulations of a missile with liquid payload under launch conditions
[AD-A191479] 18 p2463 N88-24625

Study of toluene rotary fluid management device and shear flow condenser performance for a space-based organic Rankine power system
[NASA-CR-180885] 24 p3338 N88-29872

ROTATING GENERATORS

NT AC GENERATORS
NT DYNAMOMETERS
NT TURBOGENERATORS

Finnish-Soviet Symposium on Radio Astronomy (1st) held at Otaniemi on August 26-27, 1985
[PB87-140661] 07 p0944 N88-15736

ROTATING LIQUIDS

On rotating sphere-on-a-plate experiments and the questions of whether high angle grain boundaries melt below bulk melting temperatures
[DE88-006627] 15 p2038 N88-22142

Fluid motion in a spinning, coning cylinder via spatial eigenfunction expansion
[AD-A190758] 15 p2066 N88-22319

Computational fluid dynamics methods for low Reynolds number precessing/spinning incompressible flows
[AD-A193891] 23 p3212 N88-29119

Numerical calculations of the response of a spinning spheroidal payload to coning motion
[AD-A195890] 24 p3368 N88-30059

Numerical simulation of unsteady incompressible flow in a partially-filled rotating cylinder
[AD-A196001] 24 p3371 N88-30073

ROTATING MATTER

Can the causal pathologies of Goedel-type universes be avoided in higher-derivative gravity
[DE88-700185] 11 p1568 N88-19387

Plasma rotation in a tokamak
[DE88-700855] 12 p1693 N88-20128

ROTATING PLASMAS

Effect of plasma rotation in tokamak on stabilizing action of electrically conducting wall 06 p0773 N88-14748

Evolution of poloidal variation of impurity density and ambipolar potential in rotating tokamak plasma, part 1
[DE88-006263] 13 p1842 N88-21022

Evolution of poloidal variation of impurity density and ambipolar potential in rotating tokamak plasma, part 2
[DE88-009882] 19 p2731 N88-26218

ROTATING SHAFTS

NT TURBOSHAFTS

Dynamic response of a geared train of rotors subjected to random support excitations 09 p1181 N88-17073

Dynamic stability of elastic rotor-bearing systems via Liapunov's direct method 21 p2958 N88-2757[illegible]

Development of high temperature, high pressure rotating shaft seals
[DE88-001029] 23 p3221 N88-29172

ROTATING SPHERES

Analytical studies of axially symmetric motion of an incompressible viscous fluid between two concentric rotating spheres 04 p0444 N88-12757

Rotation of magnetized particle in electrically conducting viscous medium 06 p0770 N88-14733

Radiative heat transfer to chemically reacting flow between concentric rotating spheres
[DE88-702538] 22 p3118 N88-28525

ROTATING STALLS

Investigation of the excitation of turbine blade vibration in axial compressors in rotating stall
[ETN-87-90377] 01 p0007 N88-10035

A Navier-Stokes study of cascade flow fields including inlet distortion and rotating stall
[AD-A193109] 21 p2943 N88-27483

A mapping of the viscous flow behavior in a controlled diffusion compressor cascade using laser Doppler velocimetry and preliminary evaluation of codes for the prediction of stall
[AD-A194490] 23 p3211 N88-29112

Modeling of large stall in axial compressors
[VKI-TN-164] 23 p3213 N88-29124

ROTATING VEHICLES

U ROTATING BODIES
U VEHICLES

ROTATION

NT COROTATION
NT COUNTER ROTATION
NT EARTH ROTATION
NT MOLECULAR ROTATION
NT MUON SPIN ROTATION
NT SATELLITE ROTATION
NT SOLAR ROTATION
NT STELLAR ROTATION

The corrosion of iron rotating hemispheres in 1 M sulfuric acid: An electrochemical impedance study
[DE87-014679] 02 p0148 N88-10925

Coolant passage heat transfer with rotation
02 p0186 N88-11160

Filamentation instability of rotating light ion beams in fusion target chambers
[IPPJ-839] 02 p0242 N88-11530

Development, construction and testing of a novel internal combustion engine with conical rotating slide valve
[DE88-900071] 05 p0589 N88-13593

The Jeffcott equations in nonlinear rotordynamics
07 p0928 N88-15636

Application of a simple rotational spherical grating mounting to high resolution soft X-ray spectroscopy
[PB87-164836] 09 p1142 N88-16845

Experimental study of local natural convection heat transfer in inclined and rotating enclosures
09 p1165 N88-16986

Design conditions and workspace for the generally-proportioned 3-hinge spherical wrist for robots
10 p1339 N88-18003

Mathematical modeling of the postbuckling behavior of structural elements 11 p1500 N88-18960

Analysis of a rotating advanced-technology space station for the year 2025
[NASA-CR-178345] 12 p1600 N88-19580

Domain perturbation method in the static equilibrium of masses in rotation
[INPE-4217-PRE/1098] 12 p1686 N88-20085

The effect of combustion gas flow on the rotational dynamics of a spinning solid fuel rocket
13 p1732 N88-20358

Numerical model of the time independent mean flow in a rotating rocket motor 13 p1733 N88-20360

Parametric study of acceleration-induced stresses and frequency changes in doubly-rotated crystal resonators
[AD-A189261] 13 p1761 N88-20532

Eddy current losses induced by rotation of magnetisation
[BLL-M-37634-(5828.4)] 14 p1890 N88-21298

New representation for kinematics of manipulator
[DE88-751446] 14 p1917 N88-21445

Rotation of universe --- metagalaxies
14 p1974 N88-21780

Comparison of active regions on the nucleus of Comet Halley 14 p2004 N88-21948

P/Halley activity in November 1985
14 p2006 N88-21966

Dust tail streamers and Halley's nucleus rotation
14 p2008 N88-21979

The light curve of P/Halley and the rotation of its nucleus 14 p2009 N88-21984

Experimental investigation of a spanwise forced mixing layer
[AD-A190136] 15 p2013 N88-22007

Coupled bending-torsion steady-state response of pretwisted, nonuniform rotating beams using a transfer-matrix method
[NASA-TM-100596] 15 p2086 N88-22435

Density perturbations in a rotating universe
[DE87-703036] 15 p2151 N88-22840

Effects of translational and rotational nonequilibrium on CW (Continuous Wave) chemical laser performance
[AD-A191425] 16 p2214 N88-23210

Kinetic theoretical analysis for propagation of rotating ion beam in ICF 16 p2276 N88-23623

Hybrid particle simulation for focusing of rotating and propagating LIB 16 p2276 N88-23624

Microinstabilities in ion beam propagation
16 p2277 N88-23631

Studies of heat and mass transfer during chemical vapor deposition 17 p2338 N88-23953

The effects of inlet turbulence and rotor/stator interactions on the aerodynamics and heat transfer of a large-scale rotating turbine model. Part 4: Aerodynamic data tabulation
[NASA-CR-179469] 17 p2339 N88-23956

A generic multibody simulation
[NASA-CR-182949] 17 p2388 N88-24198

Spectroscopic measurements of ion temperature, rotation speed and beam deposition profile on DIII-D
17 p2440 N88-24519

Atmospheric autorotating imaging device
[NASA-CASE-NPO-17390-1-CU]
18 p2519 N88-24944

Para-ortho abundance ratio of molecular hydrogen in NGC2023
[ISAS-RN-352] 18 p2573 N88-25286

Some operational aspects of a rotating advanced-technology space station for the year 2025
[NASA-CR-181617] 20 p2765 N88-26397

Rotation symmetric vortex in axiparallel flow
[ETN-88-92364] 21 p2948 N88-27512

Development of high temperature, high pressure rotating shaft seals
[DE88-001029] 23 p3221 N88-29172

The aspect ratio dependence of the attractor dimension in Taylor-Couette flow
[AD-A196297] 24 p3369 N88-30065

ROTATIONAL FLOW

U FLUID FLOW
U VORTICES

ROTOR AERODYNAMICS

A full potential flow analysis with realistic wake influence for helicopter rotor airload prediction
[NASA-CR-4007] 04 p0393 N88-12452

A comparison of experimental and theoretical results for labyrinth gas seals with honeycomb stators
[NASA-CR-182441] 08 p0993 N88-16006

Experimental rotordynamic coefficient results for honeycomb seals
[NASA-CR-182440] 08 p0993 N88-16007

NASA/Army Rotorcraft Technology. Volume 1: Aerodynamics, and Dynamics and Aeroelasticity
[NASA-CP-2495-VOL-1] 09 p1105 N88-16625

Accomplishments at NASA Langley Research Center in rotorcraft aerodynamics technology
09 p1105 N88-16626

The development of CFD methods for rotor applications 09 p1105 N88-16627

A summary of recent NASA/Army contributions to rotorcraft vibrations and structural dynamics technology
09 p1105 N88-16628

A review of research in rotor loads
09 p1106 N88-16629

Comprehensive rotorcraft analysis methods
09 p1106 N88-16630

Rotorcraft aeroelastic stability
09 p1106 N88-16631

NASA/Army Rotorcraft Technology. Volume 2: Materials and Structures, Propulsion and Drive Systems, Flight Dynamics and Control, and Acoustics
[NASA-CP-2495-VOL-2] 09 p1106 N88-16632

Numerical modeling of multidimensional flow in seals and bearings used in rotating machinery
[NASA-TM-100779] 09 p1165 N88-16988

Frequency-response identification of XV-15 tilt-rotor aircraft dynamics 10 p1277 N88-17643

Special flight mechanical features of the bearingless helicopter rotor
[MBB-FM-315/O] 10 p1309 N88-17825

La Recherche Aerospatiale, bimonthly bulletin, number 1987-1, 236/January-February
[ESA-TT-1055] 11 p1433 N88-18549

Verification of the momemtum theory for rotors using measurements on a model helicopter
[R-840-S] 13 p1718 N88-20275

Measurements on a helicopter rotor
[R-764-S] 14 p1861 N88-21119

The 25 m horizontal-axis turbine as a test case for standard Dutch aerodynamic calculation methods for high-speed rotors
[R-762-D] 14 p1942 N88-21589

Advancing-side directivity and retreating-side interactions of model rotor blade-vortex interaction noise
[NASA-TP-2784] 15 p2131 N88-22710

Piezoelectric pushers for active vibration control of rotating machinery 16 p2218 N88-23229

Active control and system identification of rotordynamic structure 16 p2218 N88-23230

Research investigation of helicopter main rotor/tail rotor interaction noise
[NASA-CR-4143] 19 p2722 N88-26165

A review of gear housing dynamics and acoustics literature
[NASA-CR-183110] 20 p2811 N88-26675

Integrated Technology Rotor Methodology Assessment Workshop
[NASA-CP-10007] 21 p2889 N88-27148
Comparison of experimental rotor damping data-reduction techniques 21 p2891 N88-27159
Comparison of experimental coupled helicopter rotor/body stability results with a simple analytical model
21 p2891 N88-27160

ROTOR BLADES
Active control of helicopter vibration using multiloop self-adaptive control 03 p0264 N88-11660
Minimisation of helicopter vibration through active control of structural response 03 p0264 N88-11662
Impacts of rotor hub design criteria on the operational capabilities of rotorcraft systems
03 p0264 N88-11663
Performance measurements of the Kolibrie and FACT rotor blades without tip vanes on the full-scale experimental wind turbine
[IW-R518] 06 p0665 N88-14077
Design and test of a high blade speed, high work capacity transonic turbine 10 p1281 N88-17658
Experimental investigation of a supercritical compressor rotor blade section 10 p1284 N88-17680
A preliminary investigation of finite-element modeling for composite rotor blades
[NASA-TM-100558] 13 p1781 N88-20656
Optimal placement of tuning masses for vibration reduction in helicopter rotor blades
[NASA-TM-100562] 13 p1782 N88-20665
FLAP (Force and Loads Analysis Program) code development and validation
[DE88-001131] 15 p2075 N88-22371
Inflow measurements made with a laser velocimeter on a helicopter model in forward flight. Volume 4: Tapered planform blades at an advance ratio of 0.15
[NASA-TM-100544] 16 p2156 N88-22863
Minimum weight design of rotorcraft blades with multiple frequency and stress constraints
[NASA-TM-100569] 16 p2161 N88-22892
Supersonic axial-flow fan flutter
16 p2221 N88-23255
Hover performance tests of baseline metal and Advanced Technology Blade (ATB) rotor systems for the XV-15 tilt rotor aircraft
[NASA-CR-177436] 20 p2759 N88-26367

ROTOR BLADES (TURBOMACHINERY)
Integration of dynamic, aerodynamic and structural optimization of helicopter rotor blades
[NASA-CR-181441] 01 p0002 N88-10012
ARSPNS: A method to calculate steady and unsteady potential flow about fixed and rotational lifting and nonlifting bodies
[NLR-TR-85114-U] 01 p0044 N88-10282
A method for the efficient calculation of elastic rotor blade dynamic response in forward flight
04 p0394 N88-12460
Measurements and calculations of aerodynamic torques for a vertical-axis wind turbine
[DE88-001783] 04 p0465 N88-12876
Results of the 1986 NASA/FAA/DFVLR main rotor test entry in the German-Dutch wind tunnel (DNW)
[NASA-TM-100507] 04 p0487 N88-13003
Solution procedure for the Navier-Stokes equations applied to rotors 05 p0579 N88-13533
Noise of a model counterrotation propeller with reduced aft rotor diameter at simulated takeoff/approach conditions (F7/A3)
[NASA-TM-100254] 05 p0647 N88-13961
An explicit Runge-Kutta method for unsteady rotor/stator interaction
[NASA-TM-100787] 07 p0816 N88-14967
Blade vibration problems in centrifugal compressors. Fundamental considerations 07 p0851 N88-15165
Blade vibration due to different flow excitation
07 p0851 N88-15166
Blade excitation due to unsteady flow phenomena
07 p0851 N88-15167
Accomplishments at NASA Langley Research Center in rotorcraft aerodynamics technology
09 p1105 N88-16626
A review of research in rotor loads
09 p1106 N88-16629
NASA's rotorcraft icing research program
09 p1108 N88-16641
Three-dimensional incompressible flowfield analysis for establishing rotor designs which optimize power extraction 10 p1329 N88-17943
Design graphs for the first two bending Eigenvibration forms of rotating beams consisting of two beam points
[IW-86006R] 13 p1783 N88-20670
Measurement and analysis of the noise radiated by low Mach numbers centrifugal blowers
[AD-A189226] 13 p1833 N88-20966
Visualisation of the flow at the tip of a high speed axial flow turbine rotor
[AD-A189928] 15 p2063 N88-22300
Visualisation of the flow at the tip of a high speed axial flow turbine rotor: An assessment of flow visualisation techniques and the requirement of the experimental turbine
[AD-A189929] 15 p2063 N88-22301
Improvements to tilt rotor performance through passive blade twist control
[NASA-TM-100583] 15 p2086 N88-22434
Experimental vibration damping characteristics of the third-stage rotor of a three-stage transonic axial-flow compressor
[NASA-TM-100948] 18 p2466 N88-24642
Extensive verification of blade-to-blade flow code based on Denton scheme 19 p2638 N88-25654
The MOD-2 wind turbine: Aeroacoustical noise sources, emissions, and potential impact
[DE88-001132] 19 p2687 N88-25971
Effects of static equilibrium and higher-order nonlinearities on rotor blade stability in hover
21 p2890 N88-27157
A review of non-contacting displacement measurement techniques used to monitor the movement of rotor blades in gas turbine aero engines
[PNR90457] 22 p3045 N88-28071
SR-7A aeroelastic model design report
[NASA-CR-174791] 23 p3179 N88-28928

ROTOR BODY INTERACTIONS
A 0.15-scale study of configuration effects on the aerodynamic interaction between main rotor and fuselage
[NASA-CR-166577] 04 p0395 N88-12462
Integrated Technology Rotor Methodology Assessment Workshop
[NASA-CP-10007] 21 p2889 N88-27148
A comparison of theory and experiment for coupled rotor-body stability of a hingeless rotor model in hover under simulated vacuum conditions
21 p2889 N88-27151
A comparison of theory and experiment for coupled rotor-body stability of a hingeless rotor model in hover
21 p2889 N88-27152
A comparison of theory and experiment for coupled rotor body stability of a bearingless rotor model in hover and forward flight 21 p2890 N88-27154
The importance of steady and dynamic inflow on the stability of rotor-body systems 21 p2890 N88-27156
Comparison of experimental coupled helicopter rotor/body stability results with a simple analytical model
21 p2891 N88-27160
Program user's manual for an unsteady helicopter rotor-fuselage aerodynamic analysis
[NASA-CR-181701] 22 p3039 N88-28047

ROTOR DISKS
U TURBINE WHEELS

ROTOR HUBS
U HUBS
U ROTORS

ROTOR SPEED
Helicopter main-rotor speed effects on far-field acoustic levels
[NASA-TM-100512] 02 p0230 N88-11451
Study on a rotor speed control system for a horizontal axis windmill
[NAL-TR-931] 10 p1349 N88-18062
A LQG regulator for the angular motion of the rotor at a tuned gyroscope
[INPE-4280-PRE/1152] 12 p1631 N88-19759

ROTOR SYSTEMS RESEARCH AIRCRAFT
Flight researh at NASA Ames Research Center: A test pilot's perspective
[NASA-TM-100025] 02 p0125 N88-10788

ROTORCRAFT
U ROTARY WING AIRCRAFT

ROTORCRAFT AIRCRAFT
Development of rotorcraft interior noise control concepts. Phase 2: Full scale testing, revision 1
[NASA-CR-172594-REV-1] 06 p0777 N88-14769
Delamination durability of composite materials for rotorcraft 09 p1107 N88-16634
The role of aviation technology in the Caribbean Basin
[NASA-CR-183069] 20 p2745 N88-26289

ROTORS
NT BEARINGLESS ROTORS
NT CIRCULATION CONTROL ROTORS
NT COMPRESSOR ROTORS
NT FLYWHEELS
NT HELICOPTER TAIL ROTORS
NT IMPELLERS
NT PUMP IMPELLERS
NT RIGID ROTORS
NT ROTARY WINGS
NT TAIL ROTORS
NT TILTING ROTORS
NT TURBINE WHEELS
NT X WING ROTORS
Turbines with counterrotating runners for aircraft power plants 02 p0158 N88-10992
A 1987 progress report of manufacturing techniques for Gravity Probe B gyroscope rotors
[NASA-TM-100312] 02 p0176 N88-11101
Measurement of airfoil heat transfer coefficients on a turbine stage 02 p0186 N88-11158
Controlling the dynamic environment during NOE flight
03 p0264 N88-11661
A full potential flow analysis with realistic wake influence for helicopter rotor airload prediction
[NASA-CR-4007] 04 p0393 N88-12452
Flap-lag equations of motion of rigid, articulated rotor blades with three hinge sequences
[NASA-TM-100023] 04 p0401 N88-12495
Calculation of helicopter rotor blade/vortex interaction by Navier-Stokes procedures
[NASA-CR-177441] 05 p0540 N88-13291
Model helicopter rotor rig and associated strain gauge balance for performance studies
[NAL-TM-AE-8704] 05 p0552 N88-13364
Dynamic behavior of dissymmetric rotor bearings modelled with a periodic coefficient large system
05 p0596 N88-13640
Coupled elastic rotor/body vibrations with inplane degrees of freedom 05 p0596 N88-13643
Development of an unsteady wake theory appropriate for aeroelastic analyses of rotors in hover and forward flight
[NASA-CR-182357] 06 p0664 N88-14075
Euler solution of multiblade rotor flow
[NASA-TM-100014] 06 p0704 N88-14322
Creep-fatigue cracking in high temperature turbine rotors 06 p0720 N88-14426
Lift distribution and velocity field measurements for a three-dimensional, steady blade/vortex interaction
[NASA-TM-100013] 07 p0815 N88-14962
Measurement in a wind tunnel of the modification of mean wind and turbulence characteristics due to induction effects near wind turbine rotors
[DE88-000249] 07 p0815 N88-14963
The effects of rotor unbalance on the vertical response of a soft-mounted block 08 p1000 N88-16057
Rotorcraft flight research with emphasis on rotor systems 09 p1111 N88-16656
Dynamic response of a geared train of rotors subjected to random support excitations 09 p1181 N88-17073
The further development of circulation control airfoils
10 p1270 N88-17594
A research program on the aerodynamics of a highly loaded turbine stage 10 p1280 N88-17655
The unsteady gas flow through stator and rotor of a turbomachine 10 p1281 N88-17660
Optimal design and parameter identification of flexible rotor-bearing systems 10 p1339 N88-18002
Electro-mechanical vibratory system
11 p1500 N88-18958
Site effects on wind characteristics at a turbine rotor
[DE88-005135] 11 p1507 N88-19003
Testing of a one-bladed 30-meter-diameter rotor on the DOE/NASA Mod-O wind turbine
[NASA-TM-100274] 11 p1509 N88-19014
Acoustic measurements from a rotor blade-vortex interaction noise experiment in the German-Dutch Wind Tunnel (DNW)
[NASA-TM-4024] 11 p1542 N88-19218
Minimum weight design of rectangular and tapered helicopter rotor blades with frequency constraints
[NASA-TM-100561] 12 p1582 N88-19465
Dynamic modelling of flexible rotor shafts mounted on hydrodynamic bearings 13 p1779 N88-20641
Inflow measurement made with a laser velocimeter on a helicopter model in forward flight. Volume 2: Rectangular planform blades at an advance ratio of 0.23
[NASA-TM-100542] 14 p1864 N88-21139
Inflow measurement made with a laser velocimeter on a helicopter model in forward flight. Volume 3: Rectangular planform blades at an advance ratio of 0.30
[NASA-TM-100543] 15 p2015 N88-22015
Visualisation of the flow at the tip of a high speed axial flow turbine rotor
[AD-A189928] 15 p2063 N88-22300
On the computation of stationary deterministic behavior of nonlinear dynamic systems with applications to rotor-bearing structures
[ETN-88-92241] 16 p2214 N88-23213
Active control and system identification of rotordynamic structure 16 p2218 N88-23230
Development of aeroelastic analysis methods for turborotors and propfans, including mistuning
16 p2219 N88-23244
The 2-D and 3-D time marching transonic potential flow method for propfans 16 p2220 N88-23245

Acoustic characteristics of 1/20-scale model helicopter rotors
[NASA-CR-177355] 16 p2265 N88-23548
Vibration and control of flexible rotor supported by magnetic bearings
[NASA-TM-100888] 17 p2345 N88-23977
Inflow measurements made with a laser velocimeter on a helicopter model in forward flight. Volume 1: Rectangular planform blades at an advance ration of 0.15
[NASA-TM-100541] 18 p2460 N88-24607
Entrance and exit region friction factor models for annular seal analysis
[NASA-CR-183084] 19 p2678 N88-25921
Improved method for stress and compatibility analysis of multicomponent rotating systems
[NASA-TM-100884] 19 p2680 N88-25935
Dynamic stability of elastic rotor-bearing systems via Liapunov's direct method 21 p2958 N88-27571
Euler equation computations for the flow over a hovering helicopter rotor
[NASA-CR-177493] 22 p3038 N88-28037
An analytical investigation of geared system dynamics containing spur and helical gears
22 p3085 N88-28317
Investigation of helicopter rotor blade/wake interactive impulsive noise
[NASA-CR-177435] 23 p3171 N88-28882
The effects of inlet turbulence and rotor/stator interactions on the aerodynamics and heat transfer of a large-scale rotating turbine model. Volume 3: Heat transfer data tabulation 65 percent axial spacing
[NASA-CR-179468] 23 p3180 N88-28930
Three-dimensional Navier-Stokes simulations of turbine rotor-stator interaction
[NASA-TM-100081] 24 p3316 N88-29750
An unconditionally stable Runge-Kutta method for unsteady flows
[NASA-TM-101347] 24 p3321 N88-29780
The effects of inlet turbulence and rotor/stator interactions on the aerodynamics and heat transfer of a large-scale rotating turbine model. Volume 2: Heat transfer data tabulation. 15 percent axial spacing
[NASA-CR-179467] 24 p3326 N88-29804
Spray automated balancing of rotors: Methods and materials
[NASA-CR-182151] 24 p3330 N88-29825

ROUGHNESS
NT SEA ROUGHNESS
NT SURFACE ROUGHNESS
X-ray studies of strain, interface and impurity in semiconductors
[DE87-013856] 01 p0104 N88-10678
Precision metrology comparing ultrasonic and other techniques for the determination of steel thickness
[DE87-011051] 02 p0230 N88-11452
Studies on high-speed electroforming
[DE88-001395] 04 p0429 N88-12656
Computation of turbulent flow of air through smooth and rough pipes using a two-equation turbulence model
06 p0700 N88-14298
Fractal surface finish
[DE88-007972] 22 p3057 N88-28137
Green's function approach to roughening transition of one-dimensional restricted solid on solid model
[DE88-702723] 23 p3278 N88-29512

ROUND TRIP TRAJECTORIES
Mission profiles of the MTFF co-orbiting with the US Space Station 12 p1585 N88-19487

ROUTES
Two dimensional path planning with obstacles and shadows
[AD-A184075] 04 p0397 N88-12474
Single-layer wire routing
[AD-A186990] 09 p1157 N88-16932
Automatic routing module 09 p1210 N88-17251
Minimum Energy Routing through Interactive Techniques (MERIT) modeling
[NASA-CR-182535] 10 p1356 N88-18105
Deadlock-free message routing in processor networks
[CS-8706] 14 p1960 N88-21691
Implementation of a distributed adaptive routing algorithm on the Intel iPSC (Intel Personal Super-Computer)
[AD-A189849] 15 p2109 N88-22567
Contribution of space to marine activities
19 p2700 N88-26057
Indian Ocean validation
[AD-A194458] 23 p3175 N88-28902

ROVER PROJECT
History of some direct nuclear propulsion developments since 1946 17 p2400 N88-24270
A critique of NERVA based nuclear reactor design and performance for MMW space propulsion applications
17 p2404 N88-24297
Nuclear propulsion: Past, present and future
17 p2427 N88-24441
The NERVA derivative reactor and a systematic approach to multiple space power requirements
17 p2430 N88-24458

ROVING VEHICLES
Aerosols in Martian Atmosphere and Natural Dust Observation (AMANDO). Proposal for the Mars orbiter balloon and rover to study the Martian atmosphere, its thermal content, and its interaction with the soil
[IFSI-87-9] 08 p1100 N88-16619
Mars Lander/Rover vehicle development: An advanced space design project for USRA and NASA/OAST
[NASA-CR-182562] 12 p1709 N88-20226
Electromagnetic powered vehicles (EMPV) for Mars exploration 17 p2419 N88-24388
Energy storage considerations for a robotic Mars surface sampler
[NASA-TM-100969] 22 p3166 N88-28853

RP-1 ROCKET PROPELLANTS
Characterization of aluminum/RP-1 gel prupellant properties
[NASA-TM-100951] 18 p2496 N88-24808

RPV
U REMOTELY PILOTED VEHICLES

RUANDA-URUNDI
U BURUNDI

RUBBER
NT BUNA (TRADEMARK)
NT ELASTOMERS
NT LATEX
NT SYNTHETIC RUBBERS
NT VULCANIZED ELASTOMERS
Basic research on macromolecular dynamics
[PB88-141643] 10 p1305 N88-17805
Numerical-experimental investigation of singularity at a crack in nonlinear rubber elasticity
11 p1500 N88-18961
Rubber-modified epoxies: Interfacial tension and morphology
[AD-A192464] 21 p2917 N88-27313
Elastic behavior of a rubber layer bonded between two rigid spheres
[AD-A193698] 23 p3198 N88-29030
Determination of the hydroperoxide potential of jet fuels
[AD-A195975] 24 p3357 N88-29991

RUBIDIUM
NT RUBIDIUM ISOTOPES
On-orbit frequency stability analysis of the GPS NAVSTAR 6 rubidium clock and NAVSTARs 9 and 10 cesium clocks
[AD-A184984] 05 p0544 N88-13312
A rubidium-stabilised laser diode for interferometry
[NPL-MOM-85] 14 p1914 N88-21433
Ultrahigh coherent semiconductor lasers and their applications to Rb atomic clock
14 p1976 N88-21789
Tactical Rubidium Frequency Standard (TRFS)
[AD-A191049] 16 p2193 N88-23078
Tactical Rubidium Frequency Standard (TRFS), volume 2
[AD-A191190] 18 p2503 N88-24850
Tactical Rubidium Frequency Standard (TRFS), volume 1
[AD-A192981] 20 p2805 N88-26640

RUBIDIUM ISOTOPES
Development and applications of new technical advances to problems of fluid/electrolyte/mineral imbalance in military personnel
[AD-A186437] 07 p0889 N88-15388

RUBY LASERS
A mode-locked ruby laser with chlorophyll d as saturable absorber 03 p0327 N88-12064
Noncontact temperature measurements of hot steel bodies using an electromagnetic acoustic transducer (EMAT)
[DE88-000560] 04 p0446 N88-12765
Formation of high-coherence radiation in free-running mode ruby laser for pulse holography
08 p1077 N88-16497
Multipoint Thomson scattering diagnostic for DIII-D
[DE88-008737] 20 p2857 N88-26969

RUDDERS
The use of aeroelastic wind tunnel models to prove structural design 05 p0551 N88-13355

RULES
NT FLIGHT RULES
NT INSTRUMENT FLIGHT RULES
NT SELECTION RULES (NUCLEAR PHYSICS)
NT VISUAL FLIGHT RULES
A rule-based system for arrival sequencing and scheduling in air traffic control 02 p0129 N88-10815
Genie inference engine rule writer's guide
[AD-A185709] 06 p0762 N88-14675
FORTRAN 77 programming guidelines
[DFVLR-MITT-87-10] 07 p0905 N88-15487
Using output to evaluate and refine rules in rule-based expert systems 08 p1055 N88-16362
Approaches to the verification of rule-based expert systems 09 p1206 N88-17232
A rule-based Lisp dialect translator using paramodulation 10 p1380 N88-18238
Directions for programming in FORTRAN 77
[NASA-TT-20317] 20 p2839 N88-26842
Towards knowledge bases-semantics, rules and object-oriented programming
[PB88-108154] 20 p2882 N88-27110
Rules, schema and decision making
[AD-A193389] 21 p3027 N88-27967
Generating semi-Gaussian two dimensional quadrature rules
[REPT-205] 23 p3272 N88-29476

RUN TIME (COMPUTERS)
File usage analysis and resource usage prediction: A measurement-based study
[NASA-CR-181553] 05 p0633 N88-13867
Predictability of process resource usage: A measurement-based study of UNIX
[NASA-CR-181562] 05 p0633 N88-13869
Nonpreemptive run-time scheduling issues on a multitasked, multiprogrammed multiprocessor with dependencies, bidimensional tasks, folding and dynamic graphs
[DE88-003598] 09 p1223 N88-17335
A digital logic simulator with concurrent programming considerations
[AD-A188823] 12 p1678 N88-20032
Modeling and optimum time performance for concurrent processing
[NASA-CR-4167] 20 p2797 N88-26595
Matrix substructuring, domain decomposition and particle methods: Current trends for solving PDEs in parallel
[DE88-009826] 21 p3007 N88-27836

RUNGE-KUTTA METHOD
Navier-Stokes cascade analysis with a stiff Kappa-Epsilon turbulence solver
[NASA-TM-100218] 02 p0123 N88-10778
Implementation and evaluation of several continuously imbedded methods of Sarafyan
[DE88-000025] 02 p0221 N88-11393
Implementation of the Runge-Kutta-Fehlberg method for solution of ordinary differential equations on a parallel processor
[AD-A184660] 03 p0370 N88-12331
Application of Runge Kutta time marching scheme for the computation of transonic flows in turbomachines
[NASA-TM-86997] 04 p0394 N88-12461
An explicit Runge-Kutta method for unsteady rotor/stator interaction
[NASA-TM-100787] 07 p0816 N88-14967
Diagonally implicit Runge-Kutta-Nystrom methods for oscillatory problems
[CWI-NM-R8704] 09 p1228 N88-17356
A note on a diagonally implicit Runge-Kutta-Nystrom method
[CWI-NM-R8706] 09 p1228 N88-17358
Reduction of time delays in Runge-Kutta integration methods --- systems simulation
[MBB/LKE-132/S/PUB/241/A]
09 p1229 N88-17363
Applications of a multigrid finite volume method with Runge-Kutta time integrations for solving the Euler and Navier-Stokes equations 11 p1539 N88-19201
Numerical methods in the resolution of control electrovalve model
[INPE-4154-RPE/540] 13 p1764 N88-20554
An adaptive grid technique for solution of the Euler equations 13 p1768 N88-20579
Convergence of Runge-Kutta methods on classes of stiff initial value problems
[CWI-NM-R8717] 13 p1827 N88-20924
Effects of numerical dissipation on finite-volume solutions of compressible flow problems
[AD-A193173] 21 p2944 N88-27485
KRYSI, an ODE solver combining a semi-implicit Runge-Kutta method and a preconditioned Krylov method
[DE88-012245] 21 p3008 N88-27841
Runge-Kutta finite-volume simulation of laminar transonic flow over the ONERA M6 wing using the Navier-Stokes equations
[FFA-TN-1987-06] 22 p3039 N88-28045
An unconditionally stable Runge-Kutta method for unsteady flows
[NASA-TM-101347] 24 p3321 N88-29780

RUNNING
Metabolic and cardiorespiratory parameters during three consecutive days of exhaustive running
[AD-A192598] 21 p2985 N88-27728

Gastric emptying during walking and running: Effects of varied exercise intensity
[AD-A194025] 23 p3240 N88-29281

RUNOFFS
U DRAINAGE

RUNWAY CONDITIONS
A new look at the use of linear methods to predict aircraft dynamic response to taxi over bomb damaged and repaired airfields 09 p1180 N88-17069
Aircraft and ground vehicle friction correlation test results obtained under winter runway conditions during joint FAA/NASA Runway Friction Program
[NASA-TM-100506] 11 p1438 N88-18582
An investigation of the spray produced by a yawed wheel, including measurement of impact forces - aircraft wheels
[BU-363] 14 p1866 N88-21150
Airplane runway performance monitoring system
[NASA-CASE-LAR-13854-1-CU] 18 p2462 N88-24621

RUNWAYS
The ability of modified pavement quality concrete to resist ground erosion caused by VTOL aircraft
[BAE-ARG-238] 03 p0267 N88-11683
Optimum take-off run of aircraft on ground airfields 04 p0423 N88-12623
A laboratory study of asphalt concrete mix designs for high-contact pressure aircraft traffic
[AD-A185753] 06 p0670 N88-14106
Chicago's O'Hare Runway Configuration Management System (RCMS). Volume 1: Description of the operational software
[AD-A185886] 07 p0821 N88-14990
Comparative study of nondestructive pavement testing, MacDill Air Force Base, Florida
[AD-A186082] 07 p0822 N88-14993
Chicago's O'Hare Runway Configuration Management System (RCMS). Volume 2: Users guide
[AD-A186222] 08 p0953 N88-15783
A new look at the use of linear methods to predict aircraft dynamic response to taxi over bomb damaged and repaired airfields 09 p1180 N88-17069
Evaluation of bituminous materials used in pavement recycling projects at Tyndall, MacDill, and Hurlburt Air Force Bases
[AD-A188068] 10 p1317 N88-17871
Micro PAVER concept and development airport pavement management system
[AD-A187360] 11 p1441 N88-18598
Probabilistic and reliability design procedures for flexible airfield pavements: Elastic layered method
[AD-A187533] 11 p1442 N88-18600
Profilometer for bomb-damage-repaired airfield pavements and measurement of pavement upheaval. Report 1: Technology evaluation
[AD-A187985] 11 p1442 N88-18601
Soft-ground aircraft arresting systems
[AD-A190838] 16 p2165 N88-22912
Microwave landing system mathematical modeling study for Midway Airport Runway 22L, Chicago, Illinois
[AD-A191721] 18 p2462 N88-24616
Airplane runway performance monitoring system
[NASA-CASE-LAR-13854-1-CU] 18 p2462 N88-24621
Takeoff predictions for powered-lift aircraft
[NASA-CR-177491] 19 p2597 N88-25431
Alternate/modified binders for airfield pavements
[AD-A192781] 21 p2899 N88-27206
Improvement of head-up display standards. Volume 5: Head up display ILS (instrument Landing System) accuracy flight tests
[AD-A194602] 23 p3178 N88-28922
Airport surface traffic automation study
[AD-A194553] 23 p3181 N88-28934
An analysis of time and space requirements for aircraft turnrounds
[TT-8705] 24 p3322 N88-29783

RUPTURING
Stress rupture behavior of silicon carbide coated, low modulus carbon/carbon composites
[NASA-CR-180863] 06 p0678 N88-14150
Ductile failure
[AD-A189429] 13 p1781 N88-20654
Internal fluid dynamics within a nonspinning partially liquid-filled shell due to burster rupture
[AD-A191055] 18 p2507 N88-24874
Critical conditions for failure in materials subjected to high rates of loading
[AD-A194607] 23 p3226 N88-29201

RURAL AREAS
Land-use classification in a region north-west of Wuerzburg (Federal Republic of Germany) using digital, multispectral LANDSAT 5 Thematic Mapper data
[DFVLR-FB-87-37] 14 p1940 N88-21579

RURAL LAND USE
The contribution of satellite data in drawing up maps used in rural development 03 p0343 N88-12167
A comparative thematic mapping analysis of SPOT data: The Vientiane Plain (Laos) 03 p0343 N88-12168
Water resources and agricultural land use investigations in northeastern Gujarat (India) 22 p3091 N88-28355
Spatial and spectral registration of Javanese landscape units with SPOT 22 p3092 N88-28362
Land use systems and rural landscapes in the center of Veracruz State (Mexico): First results 22 p3092 N88-28364
An evaluation of multidate SPOT data for agriculture and land use mapping in the United Kingdom 22 p3094 N88-28375
Discrimination methods of traditional fields in a humid tropical region (Shaba, Zaire) using digital classification on SPOT data 22 p3096 N88-28387
Monitoring Tunisia's steppes with SPOT 22 p3097 N88-28390
Agro-ecological mapping from SPOT 1 data in southern Thailand: New questions for an analysis of the farming-systems 22 p3097 N88-28394
SPOT-1 over New Zealand: Analysis of SPOT imagery for land use investigations 22 p3101 N88-28416

RUSTING
Reduced time frame for predicting coating performance 24 p3356 N88-29979

RUTHENIUM
Ruthenium catalysts and their use in ammonia production
[GB-PATENT-2-136-704-A] 01 p0020 N88-10123
Determination, by X-ray fluorescence, of platinum, palladium, ruthenium, iron and chromium in special steels
[PB87-132114] 06 p0683 N88-14183
Contrast between the chemical, structural and electronic properties of thin films of Cu and Ni on the Ru(0001) surface
[DE88-002360] 07 p0938 N88-15698
Superconductivity and crystal structure of high-pressure phases in V-Ru-H system 09 p1239 N88-17426
Growth and electronic properties of strained metal overlayers
[DE87-010956] 10 p1417 N88-18463
Thermodynamic data bases for multivalent elements: An example for ruthenium
[DE88-004395] 23 p3190 N88-28984

RUTHENIUM COMPOUNDS
Intramolecular energy transfer reactions as a method for metal complex assisted production of hydrogen
[DE88-001621] 05 p0562 N88-13425

RUTILE
Electrochemical and optical investigations on ion-implanted TiO2 samples
[ETN-88-91485] 11 p1455 N88-18670

RYDBERG SERIES
Two-laser resonance enhanced photoionization spectrum of gas phase benzene 03 p0300 N88-11889
Study of energy levels and decay mechanisms for singlet Rydberg states of molecular nitrogen
[AD-A192505] 21 p3014 N88-27886
The 2D Rydberg series in Al I
[NASA-TM-101189] 22 p3150 N88-28740

S

S BAND
U SUPERHIGH FREQUENCIES
U ULTRAHIGH FREQUENCIES

S CURVES
Electromagnetic fields backscattered from an s-shaped inlet cavity with an absorber coating on its inner walls
[NASA-CR-182401] 07 p0845 N88-15130
Electromagnetic propagation in PEC and absorbing curved S-ducts
[NASA-TM-100833] 12 p1621 N88-19698

S GLASS
S-glass analysis by X-ray spectroscopy
[DE88-004636] 11 p1454 N88-18666

S MATRIX THEORY
Integrable quantum systems and classical Lie algebras
[DE88-700872] 12 p1683 N88-20063
Action-angle maps and scattering theory for some finite-dimensional integrable systems. The pure solution case
[CWI-PM-R8704] 13 p1831 N88-20955
Analysis of networks with parameters S: Generalization of junction matrix
[INPE-4535-PRE/1282] 20 p2793 N88-26570
Polarization of light reflected by vertically inhomogeneous planetary atmosphere
[DE88-702416] 21 p3031 N88-27992
Theory of quark mixing matrix and invariant functions of mass matrices
[USIP-87-14] 22 p3159 N88-28800

S STARS
Emission features in IRAS LRS spectra of MS, S and CS stars 04 p0514 N88-13163
Radial velocities monitoring of a sample of barium and S stars using CORAVEL: Towards an evolutionary link between barium and S stars?
[SER-C-PREPUBL-FASC-19] 18 p2593 N88-25410

S WAVES
Refraction of shear wave into nonlinearly elastic or elastoplastic half-space 02 p0159 N88-10999
Lg wave excitation and propagation in the presence of one-, two-, and three-dimensional heterogeneities
[AD-A187364] 11 p1510 N88-19022
Investigation of the use of horizontally polarised shear waves for TOFD studies on austenitic steel
[AERE-R-12145] 13 p1780 N88-20649
Earthquakes from peninsular India: Data from the Gauribidanur seismic array
[DE88-701232] 15 p2093 N88-22471
Input-output characterization of fiber composites by SH waves
[NASA-CR-4153] 17 p2347 N88-23986

S-A-W DEVICES
U SURFACE ACOUSTIC WAVE DEVICES

S-N DIAGRAMS
Cyclic fatigue damage characteristics observed for simple loadings extended to multiaxial life prediction
[NASA-CR-182126] 18 p2531 N88-25016

SABOT PROJECTILES
A feasibility study of a hypersonic real-gas facility
[NASA-CR-180423] 01 p0008 N88-10043
Combined calculation of deformation and stress for the body and sabot of an APFSDS 03 p0302 N88-11899
Launchability of base-driven electromagnetic projectiles
[AD-A189635] 15 p2023 N88-22055

SACCADIC EYE MOVEMENTS
Influence of moving visual environment on saccadic eye movements and fixation 21 p2926 N88-27368

SACCHARIDES
U CARBOHYDRATES

SADDLE POINTS
Transient periodic behavior related to a saddle-node bifurcation
[ETN-88-91321] 05 p0642 N88-13928

SAFETY
NT AEROSPACE SAFETY
NT AIRCRAFT SAFETY
NT FLIGHT SAFETY
NT INDUSTRIAL SAFETY
NT REACTOR SAFETY
Human motor reactions to dangerous motions in robot operations
[PB87-222196] 03 p0361 N88-12275
General-Purpose Heat Source Safety Verification Test Program: Edge-on flyer plate tests
[DE87-006309] 03 p0376 N88-12362
DOE explosives safety manual
[DE88-000831] 04 p0422 N88-12616
Comparison of fire resistance of metallic and nonmetallic structures
[SNIAS-872-551-101] 05 p0572 N88-13489
Establishment of complete minimum test sets for digital circuits with safety engineering significance
[ETN-88-90599] 05 p0578 N88-13526
An independent evaluation of the CH-46 Safety Reliability and Maintainability Program (SR and M)
[AD-A186310] 07 p0817 N88-14971
Fault tree reliability analysis of the Naval Postgraduate School mini-satellite (ORION)
[AD-A186283] 07 p0866 N88-15250
Summary of the report of the Senior Committee on Environmental, Safety and Economic Aspects of Magnetic Fusion Energy
[DE88-003270] 07 p0937 N88-15692
Solid mechanics research for quantitative non-destructive evaluation
[AD-A186599] 08 p0993 N88-16010
ESSAA: Embedded system safety analysis assistant 08 p1060 N88-16396
Helicopter human factors research 09 p1109 N88-16644
Organic coatings to improve the storageability and safety of pyrotechnic compositions
[AD-A187158] 09 p1150 N88-16889
The TITAN Reversed-Field Pinch Reactor: Design-point determination and parametric studies
[DE88-001824] 09 p1251 N88-17498
Minimizing development flight test time and cost in the US Air Force 12 p1703 N88-20192
Characteristics of the positive lighting flash
[DE88-005854] 13 p1800 N88-20760

Burning characteristics and flammability of PVC cables in groups
[NASA-TT-20226] 14 p1893 N88-21303
Orbital transfer vehicle: Concept definition and system analysis study
[NASA-CR-179315] 15 p2024 N88-22060
United Nations deliberations of the use of nuclear power sources in space: 1978-1987 17 p2423 N88-24410
Discussions and agreements in the United Nations on important issues associated with nuclear power in space
17 p2423 N88-24411
Critical nuclear launch issues: A perspective from the State of Florida 17 p2423 N88-24412
Space reactor end of life issues
17 p2424 N88-24413
Designing to safe power limits in hybrid circuits
[DE88-005533] 18 p2506 N88-24865
Quality and productivity drive innovation and improvement at United Technologies Aerospace Operations, Inc.
[NASA-CR-182944] 18 p2525 N88-24983
Radiation safety in commercial air traffic
[NASA-TM-101156] 19 p2600 N88-25447
Pressure/temperature sensitive inorganic phosphors
19 p2627 N88-25583
Risk analysis in space system safety
22 p3161 N88-28825
Avionics system design for high energy fields: A guide for the designer and airworthiness specialist
[NASA-CR-181590] 23 p3178 N88-28919
Numerical field model simulation of full scale fire tests in a closed spherical/cylindrical vessel
[AD-A195067] 24 p3359 N88-29998
Improvement of head-up display standards. Volume 3: An evaluation of head-up display safety
[AD-A195787] 24 p3410 N88-30300

SAFETY DEVICES
NT ARRESTING GEAR
NT ESCAPE CAPSULES
The use of Kevlar on aero-engine fan containment casings
[PNR90410] 02 p0182 N88-11134
Spinoff, 1987
[NASA-TM-89652] 02 p0250 N88-11577
Experimental and mathematical investigation of response characteristics and aging phenomena in safety fuse elements
[ETN-88-91478] 11 p1480 N88-18832
Variable response load limiting device
[NASA-CASE-LAR-12801-1] 17 p2346 N88-23982
Timing control system
[NASA-CASE-NPO-16882-1-CU]
18 p2506 N88-24863

SAFETY FACTORS
Computer simulation of thermal modeling of primary lithium cells 02 p0163 N88-11022
Chemical analysis of charged Li/SO(sub)2 cells
02 p0163 N88-11026
Small space reactor power systems for unmanned solar system exploration missions
[NASA-TM-100228] 05 p0660 N88-14054
Safety implications of onboard refueling vapor recovery systems
[PB88-102603] 07 p0839 N88-15088
Safety philosophy, policy, and requirements for manned spaceflight. Volume 1: Executive summary
[HEG-0886/1036-VOL-1] 08 p0962 N88-15826
Post-Challenger evaluation of space shuttle risk assessment and management
[NASA-CR-182461] 12 p1705 N88-20202
Technical challenges in the development of a European space suit system and comparison with underwater suits
19 p2696 N88-26024
Safety aspects in design and operation practice of GKSS underwater simulation plant GUSI
19 p2698 N88-26037
Safety of extravehicular space activities
19 p2698 N88-26038
Reducing risks inherent in operating underwater craft: The contribution of classification, the example of the SAGA highly autonomous support submarine
19 p2699 N88-26042
Control of flight through microburst wind shear using deterministic trajectory optimization
20 p2761 N88-26375
The VIPER microprocessor
[RSRE-87014] 22 p3135 N88-28640
Study on long-term evolution towards European manned spaceflight. Volume 1: Executive summary
[ERNO-OX1-002/88-VOL-1] 24 p3330 N88-29827

SAFETY MANAGEMENT
Aircraft accident/incident summary reports: Unalaska, Alaska, September 25, 1985; Jenkinsburg, Georgia, September 29, 1985; Boston, Massachusetts, December 15, 1985; Dekalb, Texas, December 31, 1985; and Erie, Pennsylvania, February 21, 1986
[PB87-910408] 02 p0123 N88-10780
UV radiation: Human exposure to ultraviolet radiation
[PB87-137410] 06 p0752 N88-14619
Risk analysis methodology survey
07 p0922 N88-15604
Evaluate the application of modal test and analysis processes to structural fault detection in MSFC - STS project elements 07 p0927 N88-15630
Safety guidelines and procedures for bioscience-based industry and other applied microbiology
[PB87-140521] 08 p1045 N88-16316
Environmental projects. Volume 4: Asbestos survey
[NASA-CR-182527] 10 p1353 N88-18083
Conceptual design study of Fusion Experimental Reactor (FY86 FER). Safety
[DE88-751071] 10 p1411 N88-18418
Research field of fire technology in Finland
[DE88-751094] 11 p1467 N88-18747
Procedures for quantitative sensitivity and performance validation studies of a deterministic fire safety model
[NBS/GCR-88/544] 11 p1469 N88-18762
Spacecraft fire-safety experiments for space station: Technology development mission
[NASA-CR-182114] 13 p1731 N88-20353
Flame retardants
[NASA-TT-20250] 13 p1739 N88-20400
Safety research of insulating materials of cable for nuclear power generating station
[NASA-TT-20202] 13 p1752 N88-20477
EDF's studies and first choices regarding the design of electrical equipment
[NASA-TT-20222] 13 p1764 N88-20553
Environmental projects. Volume 5, part 1: Study of subsurface contamination. Part 2: Guide to implement environmental compliance programs
[NASA-CR-182691] 13 p1796 N88-20741
Nuclear safety as applied to space power reactor systems 17 p2415 N88-24360

SAGE SATELLITE
European validation of SAGE-2 aerosol profiles
[AERONOMICA-ACTA-A-327-1988]
23 p3234 N88-29243

SAHARA DESERT (AFRICA)
Discrimination of sand transport rates and environmental consequences in central Egypt from SPOT data
22 p3093 N88-28366

SAILPLANES
U GLIDERS

SALICYLATES
Method for sampling of methyl salicylate vapor in air using passivated stainless steel syringes and analysis by gas chromatography
[AD-A187838] 11 p1447 N88-18624

SALINITY
Porosity influence on the strength and elasticity of first-year sea ice
[AD-A184493] 03 p0354 N88-12233
Effects of rainfall on the seasonal thermocline
[AD-A184432] 04 p0472 N88-12912
Progress in the measurement of salinity and oxygen at the Woods Hole Oceanographic Institution
[PB88-108089] 06 p0748 N88-14598
Seasonal cycling of sulfur and iron in porewaters of a Delaware salt marsh
[NASA-CR-182385] 07 p0876 N88-15311
Multipurpose corrosion inhibitors for aerospace materials in Naval environments
[AD-A186728] 09 p1143 N88-16853
Physical properties of summer sea ice in the Fram Strait, June-July 1984
[AD-A186937] 09 p1194 N88-17156
Editing master oceanographic observation data set 4
[AD-A188405] 12 p1649 N88-19876
Determination of mean thermohaline characteristics of the ocean 13 p1784 N88-20675
Estimates of ocean-atmosphere thermal interaction in Gulf Stream energy-active test range in winter of 1984
13 p1785 N88-20679
Propagation of subsurface salinity maximum in tropical Atlantic 13 p1786 N88-20686
Space-time analysis of oceanographic fields by modified empirical orthogonal functions method
13 p1786 N88-20687
Intrathermocline lens of Mediterranean water in tropical North Atlantic 13 p1786 N88-20688
Model of hydrodynamic adjustment of temperature, salinity and current fields 13 p1789 N88-20700
Microwave and structural properties of saline ice
[AD-A189307] 13 p1803 N88-20779
YABLED cruises part 2: Data from YABLED-17 through YABLED-26, January-October 1985
[PB88-163597] 14 p1950 N88-21627
Physical, chemical and CTD (Conductivity/Temperature/Depth) data from the Marathon 2 expedition
[AD-A189930] 15 p2099 N88-22507
Hydrographic observations in the northwestern Weddell Sea Marginal Ice Zone during March 1986
[PB88-173240] 16 p2237 N88-23359
Influence of the Yukon River on the Bering Sea
[NASA-CR-182802] 17 p2376 N88-24126
Expendable conductivity, temperature and depth system (XCTD) development program
[AD-A192182] 18 p2547 N88-25121

SALIVA
Human adaptation to various hypercapnic conditions in relation to salivary electrolyte dynamics and renal function 12 p1664 N88-19977

SALT SPRAY TESTS
Corrosion behavior of sputter-deposited aluminum-based alloys exposed to chloride solutions
[AD-A187262] 10 p1303 N88-17794
Stress corrosion of C ring specimen in salt spray tests
[I-186/87] 21 p2916 N88-27307

SALTS
Turbine airfoil deposition models and their hot corrosion implications 02 p0189 N88-11178

SALYUT SPACE STATION
Basic results of medical studies during prolonged manned flights on-board the Salyut-7/Soyuz-T orbital complex
[NASA-TT-20217] 10 p1369 N88-18182
The USSR space systems for remote sensing of earth resources and the environment (sensor systems, processing techniques, applications)
17 p2356 N88-24035
The Soviet MIR space station
[AD-A194040] 23 p3184 N88-28951

SAMARIUM
NT SAMARIUM ISOTOPES

SAMARIUM ISOTOPES
Nd isotopes and crustal growth rate
24 p3392 N88-30203
Changing styles of crustal growth in Southern Africa: Constraints from geochemical and Sr-Nd isotope studies in Archaean to Pan African terrains
24 p3396 N88-30227

SAMPLED DATA
U DATA SAMPLING

SAMPLED DATA SYSTEMS
U DATA SAMPLING

SAMPLERS
Wet deposition and snowpack monitoring operations and quality assurance manual
[PB87-212817] 01 p0064 N88-10413

SAMPLES
Rosetta: A mission to sample the nucleus of a comet
14 p2005 N88-21958

SAMPLING
NT AIR SAMPLING
NT CORE SAMPLING
NT DATA SAMPLING
NT PARTICULATE SAMPLING
NT RANDOM SAMPLING
Fast dynamic studies with PC384-7B; system improvements and development of an automated blood sampling system --- tomography
[USIP-87-05] 01 p0075 N88-10481
Measurements in the functional mock up test of the NAL QSTOL aircraft control system
[NAL-TR-928] 02 p0126 N88-10793
The correspondence of surface climate parameters with satellite and terrain data
[NASA-CR-181515] 03 p0346 N88-12185
Superoxide dismutase assays
[AD-A183972] 03 p0356 N88-12242
Microcomputer control of a hydraulically actuated piston
[AD-A184130] 03 p0368 N88-12317
A mineral reconnaissance sampling manual for Costa Rica: Central American energy and resource project
[DE87-014997] 04 p0462 N88-12859
RRS DISCOVERY cruise 160, 30 June-25 July, 1986. Geochemical sampling over the Madeira and Porcupine Abyssal Plains
[PB87-222030] 04 p0471 N88-12910
An urn model for the multi-sample capture/recapture sequential tagging process
[AD-A184470] 04 p0486 N88-12998
Sample reuse in statistical remodeling
[AD-A184916] 05 p0643 N88-13938
Aviation turbine fuels from tar sands bitumen and heavy oils. Part 2. Laboratory sample production
[AD-A185744] 06 p0687 N88-14211

On determining the weight for obtaining a large number of items
[AD-A186181] 07 p0915 N88-15553
Regulation of nonlinear and generalized linear systems
[AD-A186706] 09 p1224 N88-17338
Practical applicability of exact and approximate forms of the randomization test for two independent samples
[AD-A186815] 09 p1231 N88-17381
The accommodative status in the dark of US Navy fighter pilots
[AD-A188188] 10 p1370 N88-18186
Using SIR (Scientific Information Retrival) system for data management during a field program
[DE88-001555] 10 p1424 N88-18508
Frequency-sampling design of two-dimensional FIR digital filters with nonuniform samples
[AD-A187773] 11 p1477 N88-18815
Ideal shrinking and expansion of discrete sequences
[NASA-TM-88202] 11 p1524 N88-19100
Sampling intervals
[AD-A189445] 12 p1573 N88-19408
Isotopic and chemical studies of early crustal metasedimentary rocks
[NASA-CR-182711] 14 p1944 N88-21601
Analysis of meteorological conditions and haze distribution for the Second Arctic Gas and Aerosol Sampling Program (AGASP 2), March-April 1986
[PB88-164140] 14 p1948 N88-21618
High speed, bandpass sampling of digital communications waveforms
[AD-A189842] 15 p2056 N88-22254
Empirical and hierarchical Bayes competitors of preliminary test estimators in two sample problems
[AD-A190327] 15 p2125 N88-22670
Instrumentation for ultrafast electronics
[AD-A191379] 16 p2193 N88-23080
Evaluation of an estimation system for an irrigated area in a tropical region through TM-LANDSAT imagery
17 p2363 N88-24075
A disposable liquid microcell for near-infrared reflectance analysis
[AD-A192190] 18 p2575 N88-25298
A non-contact picosecond prober for integrated circuit testing 19 p2655 N88-25766
Picosecond sampling of integrated circuits
19 p2655 N88-25767
Electro-optic sampling of high-speed, InP-based integrated circuits 19 p2655 N88-25769
An optically strobed sample and hold circuit
19 p2656 N88-25772
Comparison of sampling oscilloscopes with less than 35 ps transition durations 19 p2658 N88-25793
Asynchronous optical sampling for laser-based combustion diagnostics in high pressure flames
[AD-A192920] 20 p2770 N88-26428
Analysis of debris from accelerated life test of the Hughes five-year Vuilleumier cryocooler
[AD-A193101] 21 p2931 N88-27400
Sampling strategies for Monte-Carlo forecasting methods 22 p3126 N88-28583
Importance sampling for stochastic simulations
[AD-A193585] 22 p3138 N88-28654
Elemental composition of the Martian surface
23 p3302 N88-29665
Viking Landers and remote sensing
23 p3304 N88-29685
Recent observations of carbon monoxide in the Amazon Rain Forest
[INPE-4478-PRE/1245] 24 p3390 N88-30186
The dynamics of transuranics and other radionuclides in natural environments, December 1985
[DE87-014456] 24 p3390 N88-30189
New type of primitive meteorite found in Antarcitca
24 p3441 N88-30478

SAMPLING DEVICES
U SAMPLERS

SAN ANDREAS FAULT
Correlation of data on strain accumulation adjacent to the San Andreas Fault with available models
[NASA-CR-180757] 13 p1796 N88-20742
Geodetic measurement of deformation east of the San Andreas fault in Central California
[NASA-CR-182709] 13 p1798 N88-20754

SAND DUNES
U DUNES

SANDS
NT TAR SANDS
Environmental processes and spectral reflectance characteristics associated with soil erosion in desert fringe regions
[NASA-CR-182332] 05 p0620 N88-13811

SANDSTONES
Geological characterization and statistical comparison of outcrop and subsurface facies: Shannon Shelf sand ridges
[DE87-001243] 03 p0348 N88-12202
Abundance and distribution of ultramafic microbreccia in Moses Rock Dike: Quantitative application of AIS data
05 p0613 N88-13766

SANDWICH CONSTRUCTION
U SANDWICH STRUCTURES

SANDWICH STRUCTURES
Mechanical properties characterization of composite sandwich materials intended for space antenna applications
[NASA-TM-88893] 01 p0020 N88-10121
Process for producing sandwich mouldings
[EP-PATENT-0-191-623-A2] 04 p0426 N88-12642
Analysis of the voltage-current characteristics of metal-isolator-tin-telluride sandwich structures
[ETN-88-91089] 09 p1256 N88-17528

SANITATION
Evaluation of the Shasta Waterless System as a remote site sanitation facility
[AD-A186000] 07 p0898 N88-15442

SAPPHIRE
Measurement and analysis of cryogenic sapphire dielectric resonators and DROs
04 p0433 N88-12686
Laser enhanced adhesion of copper films to sapphire substrates
[DE88-006802] 15 p2038 N88-22144

SARCOMA
U CANCER

SARSAT
Antarctic field tests of SARSAT personal locater beacons
[NASA-TM-4008] 01 p0063 N88-10403
Search and rescue satellite system (SERES), phase A0
[ETN-88-92335] 18 p2472 N88-24669
COSPAS/SARSAT 406-MHz emergency beacon digital controller
[NASA-TM-100859] 20 p2792 N88-26566
KOSPAS-SARSAT satellites used for ocean current study 24 p3450 N88-30534

SAS
Annotated computer output for illustrative examples of clustering using the mixture method and two comparable methods from SAS
[AD-A184687] 03 p0364 N88-12292

SAS-D
U IUE

SATAN (SENSOR)
U TERRAIN ANALYSIS

SATELLITE ALTIMETRY
Precise orbit computation, gravity model adjustment and altimeter data processing for the ERS-1 altimetry mission
[ESA-CR(P)-2436] 02 p0130 N88-10820
An exploratory study of inland water and land altimetry using Seasat data
[ESA-CR(P)-2433] 02 p0193 N88-11208
GEOSAT altimeter geophysical data record user handbook
[PB87-213336] 03 p0276 N88-11743
Radial orbit error reduction and sea surface topography determination using satellite altimetry
04 p0462 N88-12861
Error assessments of widely-used orbit error approximations in satellite altimetry
[NASA-CR-182390] 07 p0823 N88-14998
An efficient algorithm for computing the crossovers in satellite altimetry
[NASA-CR-18[illegible]9] 07 p0871 N88-15286
On estimating the basin-scale ocean circulation from satellite altimetry. Part 1: Straightforward spherical harmonic expansion
[NASA-CR-182387] 07 p0882 N88-15352
The effects of atmospheric and thermohaline variability on the validation of the GEOSAT altimeter oceanographic signal between Scotland and Iceland
[AD-A189324] 12 p1650 N88-19882
Seasat orbit determination experiments in preparation for the ERS-1 altimetry mission
[ETN-88-91842] 14 p1871 N88-21182
Study of the dynamic topography of oceans by means of satellite altimetry 14 p1938 N88-21567
From satellite altimetry to ocean topography, a survey of data processing techniques
[ETN-88-91841] 14 p1939 N88-21575
Determination of the ocean circulation by spaceborne radar altimeter 19 p2701 N88-26060
FORTRAN programs for computation of time dependent sea levels and trajectory errors from satellite altimeter data
[BONN-MITT-73] 21 p2901 N88-27216
Microwave instrument for planetary mission (Titan/CASSINI mission orbiter spacecraft)
[BAE-CS/TP-8359] 24 p3375 N88-30102
A study of the feasibility of using sea and wind information from the ERS-1 satel[illegible]. Part 1: Wind scatterometer data
[NASA-CR-182833] 24 p3386 N88-30167
A study of the feasibility of using sea and wind information from the ERS-1 satellite. Part 2: Use of scatterometer and altimeter data in wave modeling and assimilation
[ESA-CR(P)-2604-PT-2] 24 p3387 N88-30176

SATELLITE ANTENNAS
Study of advanced satellite concept using a multifeed reconfigurable antenna
[ESA-CR(P)-2406-VOL-1] 01 p0013 N88-10073
Study of advanced satellite concept using a multifeed reconfigurable antenna. Detailed report on mission definition, coverage analysis and performance requirements, antenna geometry
[ITS-TR-014.C/85] 01 p0013 N88-10074
Study of advanced satellite concept using a multifeed reconfigurable antenna. Detailed report on Polarization Sensitive Reflector (PSR) and offset parabolic antennas, Appendix 1
[ESA-CR(P)-2406-VOL-3] 01 p0013 N88-10075
Study of advanced satellite concept using a multifeed reconfigurable antenna. Appendix 3 : Feeding network, final performance analysis, study of reconfiguration possibilities
[ITS-TR-032/85] 01 p0014 N88-10076
Data Relay Satellite antenna subsystem study
[ESA-CR(P)-2435-VOL-2] 02 p0162 N88-11014
Study of antenna configuration for Data Relay Satellite (DRS) user spacecraft
[A5/516/86] 02 p0162 N88-11018
DRS (Data Relay Satellite) antenna subsystem study
[ESA-CR(P)-2435-VOL-1] 02 p0162 N88-11019
Studies of the structural dynamic behavior of satellite antenna system
[AD-A185526] 06 p0673 N88-14121
Space environmental effects on polymeric materials
[NASA-CR-182418] 07 p0838 N88-15082
ESA Bulletin No. 8
[ETN-87-90513] 09 p1122 N88-16718
European developments in antenna technology
09 p1123 N88-16725
Study of dual beam antenna systems for the data relay satellite, volume 1
[S-272-02-VOL-1] 09 p1152 N88-16905
Study of dual beam antenna systems for the data relay satellite. Volume 2: Executive summary
[S-272-03-VOL-2] 09 p1153 N88-16906
Study on a double reflector compact range --- satellite antennas
[S-201-05] 09 p1153 N88-16908
Hemispherical pointing mechanism drive unit --- satellite payloads antennas 14 p1874 N88-21193
A pointing mechanism for intersatellite link system
14 p1874 N88-21194
Some highlights on ROSAT mechanisms
14 p1874 N88-21195
Deployable booms and antennas on AMPTE-IRM
14 p1874 N88-21198
Aerospatiale unfurlable reflector and associated mechanisms 14 p1875 N88-21203
Design of a linear actuator and breadboard test result --- far IR telescope 14 p1877 N88-21217
Photoelastic model tests of the Dornier linear actuator --- far IR telescope 14 p1877 N88-21218
Fine adjustment mechanism for FIRST
14 p1878 N88-21219
The EURECA antenna deployment and retraction mechanisms 14 p1878 N88-21225
Development and qualification of the OLYMPUS antenna pointing mechanism 14 p1879 N88-21227
Antenna system for MSAT mission
19 p2651 N88-25742
Antenna technology for advanced mobile communication systems 19 p2651 N88-25743
Large antenna experiments aboard the space shuttle: Application of nonuniform sampling techniques
19 p2652 N88-25745
The 15-meter antenna performance optimization using an interdisciplinary approach 19 p2652 N88-25746
A microstrip array feed for MSAT spacecraft reflector antenna 19 p2652 N88-25747
Technologies for antenna shape and vibration control
19 p2652 N88-25748
Dynamics of satellites with radial wire antennas
20 p2784 N88-26514
Development of procedures for performing end-to-end tests on the ERS-1 radar altimeter and AMI using a compact antenna test range --- Active Microwave Instrument (AMI)
[ESA-CR(P)-2558] 24 p3383 N88-30022

A 30/20 GHz multibeam array antenna suitable for future high rate TDMA European satellite networks
[ETN-88-93079] 24 p3365 N88-30037

SATELLITE ATMOSPHERES
Microwave instrument for planetary mission (Titan/CASSINI mission orbiter spacecraft)
[BAE-CS/TP-8359] 24 p3375 N88-30102

SATELLITE ATTITUDE CONTROL
Aerospace research at the National Aerospace Laboratory (NLR)
[ETN-87-90821] 01 p0107 N88-10697
The mechanical properties of solid state diffusion bonds between Ti-6Al-4V and 304L stainless steel
[BAJ-TR-113-1987] 03 p0332 N88-12093
Advanced gyros in spacecraft control. Digital capture loops for dry tuned gyros
[UTEF-120046] 08 p0962 N88-15827
Exploring hypotheses in attitude control fault diagnosis
08 p1058 N88-16384
Control and stabilization of ESA satellites
09 p1124 N88-16734
Fine attitude measurement system study. Volume 1: Executive summary
[BAE-TP-7831-VOL-1] 09 p1133 N88-16795
Fine attitude measurement system study, volume 2
[BAE-TP-7831-VOL-2] 09 p1133 N88-16796
Fine attitude measurement system study. Volume 3: Appendices
[BAE-TP-7831-VOL-3] 09 p1133 N88-16797
Preliminary design of the ORION attitude control system
[AD-A187179] 10 p1292 N88-17729
Investigation of the spin stability of the NPS (Naval Postgraduate School) mini-satellite (Orion)
[AD-A187781] 11 p1445 N88-18613
Construction aspects of testbeds for attitude control systems simulation of artificial satellites
[INPE-4283-PRE/1155] 11 p1445 N88-18616
Table with aerostatic bearings for simulation in one degree of freedom of Attitude Control Systems of artificial satellites
[INPE-4320-TDL/287] 11 p1445 N88-18617
Reaction wheel experimental model of artificial satellite attitude control: Construction, simulation, and tests
[INPE-4274-PRE/1146] 11 p1490 N88-18896
Design of a spherical air bearing simulator for tests of the attitude control system of artificial satellites
[INPE-4284-PRE/1156] 12 p1595 N88-19551
Table with aerostatic bearings for simulation in one degree of freedom attitude control systems of artificial satellites
[INPE-4272-PRE/1144] 12 p1595 N88-19552
Reaction wheel control through digital technique using reference models
[INPE-4220-PRE/1100] 12 p1599 N88-19570
Simulation and tests of a satellite attitude and orbit control system. General considerations concerning an example case (INPE) and design of a servo rate table
[INPE-4282-PRE/1154] 12 p1599 N88-19572
Attitude control of an artificial satellite through the extension of the linear quadratic regulator theory
[INPE-4407-TDL/304] 12 p1600 N88-19577
Cold gas jet system for satellite attitude control-modeling and simulation
[INPE-4279-PRE/1150] 12 p1601 N88-19583
Modeling of a nutation damper for satellite stabilization through rotation
[INPE-4275-PRE/1147] 12 p1601 N88-19584
Development of integrated detectors for attitude sensors
[INPE-4409-PRE/1222] 12 p1602 N88-19586
Gas consumption estimation of an attitude control system of an artificial satellite (utilizing DRF) in limit cycle phase
[INPE-4338-RPE/553] 13 p1731 N88-20350
An advanced low-cost 2-axis active magnetic bearing flywheel --- satellite attitude control
14 p1877 N88-21213
High lifetime mechanisms implemented in infrared horizon scanning sensors --- SPOT
14 p1877 N88-21214
Evolution of large momentum and reaction wheels
14 p1879 N88-21230
Nutational stability of a satellite equipped with an active magnetic momentum wheel 20 p2784 N88-26513
Dynamics of satellites with radial wire antennas
20 p2784 N88-26514
Study of a safe attitude for the Infrared Space Observatory (ISO) during perigee pass
[SNIAS-881-440-113] 23 p3185 N88-28954
SCARES: A Spacecraft Control Anomaly Resolution Expert System 23 p3256 N88-29381

SATELLITE ATTITUDE DISTURBANCE
U SPACECRAFT STABILITY

SATELLITE CAPTURE
U SPACECRAFT RECOVERY

SATELLITE COMMUNICATION
The criterion of equal integrated quality: An improved method of planning DBS systems
[BBC-RD-1987/10] 02 p0161 N88-11012
Estimates of satellite EHF communication outages due to attenuation by rain
[AD-A183969] 03 p0307 N88-11941
An allotment planning concept and related computer software for planning the fixed satellite service at the 1988 space WARC
[NASA-TM-100244] 03 p0308 N88-11944
A statistical rain attenuation prediction model with application to the advanced communication technology satellite project. Part 2: Theoretical development of a dynamic model and application to rain fade durations and tolerable control delays for fade countermeasures
[NASA-TM-100242] 03 p0308 N88-11945
Design description report for a photovoltaic power system for a remote satellite earth terminal
[NASA-CR-179586] 04 p0465 N88-12875
Error control techniques for satellite and space communications
[NASA-CR-181581] 05 p0576 N88-13516
Round table on the future of satellite communications and broadcasting in Europe
[ESA-STR-221] 07 p0843 N88-15112
Transient electromagnetic scattering from heterogeneous lossy spheres
[AD-A186669] 09 p1152 N88-16903
Comparison of direct and heterodyne detection optical intersatellite communication links
09 p1169 N88-17013
Complementary satellite sound broadcasting systems: A NASA assessment for the Voice of America
[NASA-TM-100300] 10 p1321 N88-17899
Digital bit error rate estimator for telemetry links
[INPE-4351-TDL/295] 12 p1598 N88-19563
Alternative force structuring strategies for military satellite communication systems
[AD-A189492] 13 p1758 N88-20516
Effect of atmospheric turbulence on the bit error probability of a space to ground near infrared laser communications link using binary pulse position modulation and an avalanche photodiode detector
[NASA-TM-100699] 14 p1873 N88-21189
Real-time environmental Arctic monitoring (R-TEAM)
[AD-A189948] 15 p2099 N88-22508
Error control techniques for satellite and space communications
[NASA-CR-182886] 17 p2332 N88-23922
Experiments applications guide: Advanced Communications Technology Satellite (ACTS)
[NASA-TM-100265] 22 p3048 N88-28082
A statistical rain attenuation prediction model with application to the advanced communication technology satellite project. 1: Theoretical development and application to yearly predictions for selected cities in the United States
[NASA-CR-179498] 23 p3205 N88-29077
Comparative analysis of passive communications satellites employing the SHF and HF spectrum for use in a strategic role
[AD-A194682] 24 p3362 N88-30019
Signals and systems 24 p3363 N88-30026

SATELLITE CONFIGURATIONS
Evaluation of a cryogenic refrigerator for cooling focal plane instrumentation. Appendix B: Accommodation study --- satellite instruments
[BAE-TP-8095-VOL-2] 05 p0572 N88-13486
Study of reconfigurable payloads for direct broadcast satellites, summary
[DBS87-0004] 09 p1135 N88-16808
System configuration management --- space systems
22 p3160 N88-28813
PSDE/SAT 2: Preliminary spacecraft configuration study, executive summary
[ESA-CR(P)-2618] 24 p3333 N88-29840

SATELLITE CONTROL
NT SATELLITE ATTITUDE CONTROL
ESA Bulletin No. 10
[ETN-87-90514] 09 p1123 N88-16728
Range and mission scheduling automation using combined AI and operations research techniques
09 p1209 N88-17249
Attitude and orbit control for the AMPTE-UKS (Active Magnetospheric Particle Tracer Explores-UK Subsatellite): Evaluation of the in-flight performance
[PB87-225199] 19 p2604 N88-25467

SATELLITE DEFENSE
U SPACECRAFT DEFENSE

SATELLITE DESIGN
The new generation of SPOT satellites
03 p0345 N88-12178
Mechanical design of the ac bracket package for the RETE experiment
[IFSI-87-4] 05 p0555 N88-13379
A geostationary imaging spectrometer TOMS instrument 05 p0619 N88-13802
Fault tree reliability analysis of the Naval Postgraduate School mini-satellite (ORION)
[AD-A186283] 07 p0856 N88-15250
Specialist support for projects: Activities, methods and infrastructure 09 p1124 N88-16729
Lightsats and their attraction to budget oriented Federal agencies 10 p1289 N88-17711
Into the thermosphere: The atmosphere explorers
[NASA-SP-490] 10 p1353 N88-18084
Investigation of the spin stability of the NPS (Naval Postgraduate School) mini-satellite (Orion)
[AD-A187781] 11 p1445 N88-18613
A logical structuration for an administration of space projects
[INPE-4435-TDL/310] 12 p1585 N88-19482
Study of the optimization of satellite system design for transfer orbit
[MBB-URV-135] 13 p1727 N88-20332
CRRES chemical release mechanisms
14 p1874 N88-21192
Definition and implementation study for the Varan-S radar
[CNES-CT/DRT/TIT/RL-143-T]
15 p2058 N88-22267
Structural acoustics design manual
[ESA-PSS-03-1201-ISSUE-1] 17 p2311 N88-23821
MSAT-X: A technical introduction and status report
[NASA-CR-182921] 17 p2334 N88-23933
The high-throughput X-ray spectroscopy mission E6889478 MN513835 --- ESA program
[ESA-SP-1092] 17 p2450 N88-24554
Starting point of a project: Decision mechanisms --- space projects 22 p3159 N88-28806
PSDE/SAT 2: Preliminary spacecraft configuration study, executive summary
[ESA-CR(P)-2618] 24 p3333 N88-29840
Low cost satellite
[ESA-CR(P)-2560] 24 p3334 N88-29844

SATELLITE DOPPLER POSITIONING
The sequential evaluation of Doppler satellite observations
[REPT-141] 01 p0010 N88-10057
Solid Earth mission end-to-end data system study
[C04825.08/FR] 17 p2309 N88-23811
Specifications and performance of ultrastable oscillators in the DORIS orbitography and positioning system
[ETN-88-92761] 24 p3331 N88-29831

SATELLITE DRAG
Gradiometer accommodation on board a drag-free satellite 12 p1645 N88-19850
Using nonstationary models of the atmosphere to describe satellite drag 24 p3445 N88-30502

SATELLITE GROUND SUPPORT
Training in satellite ground system operations
09 p1129 N88-16775

SATELLITE GROUND TRACKS
An intelligent tutor for the space domain
09 p1204 N88-17217

SATELLITE IMAGERY
Object-dependent atmospheric influence on LANDSAT recordings 01 p0065 N88-10420
GOES observations for the FIRE/SRB Wisconsin experiment region from October 11 through November 2, 1986
[NASA-TM-100485] 01 p0071 N88-10453
Estimation from satellite imagery of summertime rainfall over varied space and time scales
[PB87-203246] 01 p0071 N88-10454
Tropical cyclone center locations from enhanced infrared satellite imagery
[PB87-213450] 01 p0071 N88-10455
Study, design, and evaluation of data reduction by encoding or information extraction. Part 1: Data generation analysis --- multispectral satellite imagery
[NLR-TR-85094-L-PT-1] 01 p0078 N88-10501
Study, design and evaluation of data reduction by encoding or information extraction. Part 2: Operational considerations --- multispectral satellite imagery
[NLR-TR-85094-L-PT-2] 01 p0079 N88-10502
Study, design and evaluation of data reduction by encoding or information extraction. Part 3: Algorithm design --- multispectral satellite imagery
[NLR-TR-85094-L-PT-3] 01 p0079 N88-10503
Study, design and evaluation of data reduction by encoding or information extraction. Part 4: Performance demonstration --- multispectral satellite imagery
[NLR-TR-85094-L-PT-4] 01 p0079 N88-10504
Study, design and evaluation of data reduction by encoding or information extraction. Part 5: Algorithm implementation aspects --- multispectral satellite imagery
[NLR-TR-85094-L-PT-5] 01 p0079 N88-10505
An introduction to the GOES I-M imager and sounder instruments and the GVAR retransmission format
[NOAA-TR-NESDIS-33] 02 p0140 N88-10884

Operational cloud-clearing techniques of VAS radiance data --- Visible and Infrared Spin Scan Radiometer Atmospheric Sounder (VAS) 02 p0201 N88-11256

Observation of the development of mesoscale systems by operational meteorological satellites 02 p0201 N88-11259

The use of satellite IR data in the enhancement of surface thermal fields 02 p0202 N88-11260

The importance of mesoscale waves in the upper troposphere for formation of cloud and precipitation areas 02 p0203 N88-11273

On the interaction between radar and satellite image nowcasting systems and mesoscale numerical models 02 p0204 N88-11277

Satellite imagery and conceptual models in mesoscale forecasting 02 p0205 N88-11282

Evaluation of the Rainsat precipitation analysis system in real-time use 02 p0205 N88-11283

The Pacific Weather Center Satellite Facility: An overview 02 p0205 N88-11286

Simulation of mesoscale satellite sounder data from a mesoscale numerical model 02 p0214 N88-11345

Mesoscale forecasting with satellite data: Challanges and opportunities for today and tomorrow 02 p0215 N88-11353

SPOT 1: First In-Flight Results --- conferences [ISBN-2-85428-177-2] 03 p0340 N88-12143

Development of the SPOT commercial service: Preliminary conclusions after six months of operations 03 p0340 N88-12144

Satimage and the Nordic SPOT market 03 p0340 N88-12145

SPOT Image Corporation: Early results 03 p0340 N88-12146

The Canadian SPOT program 03 p0340 N88-12147

First assessment of processing and use of SPOT images by the Institut Geographique Nationale --- French National Geographic Institute 03 p0341 N88-12148

Results of the satellite and the Toulouse (France) receiving station operator --- SPOT 03 p0341 N88-12149

Signal to noise ratios --- SPOT images 03 p0341 N88-12150

Modulation transfer function --- SPOT 03 p0341 N88-12153

Intrinsic and extrinsic geometric quality --- SPOT images 03 p0341 N88-12154

Registration of SPOT images 03 p0341 N88-12155

Evaluation of SPOT stereoscopic possibilities for cartography 03 p0342 N88-12156

Feasibility study of a range of products drawn from SPOT satellite imagery and specific to road-laying studies 03 p0342 N88-12157

Adaptation of numerical SPOT data to an urban environment 03 p0342 N88-12158

Cartography and topography with SPOT 03 p0342 N88-12159

Application of SPOT-1 data to mineral exploration in Nevada 03 p0343 N88-12163

Geological interpretation of a SPOT image over Kenya: The Gregory rift network of faults 03 p0343 N88-12164

Vegetation studies in the national Park of Comoe (Ivory Coast) using SPOT 1 satellite data 03 p0343 N88-12166

The contribution of satellite data in drawing up maps used in rural development 03 p0343 N88-12167

SPOT data for crop discrimination in southern Brazil 03 p0343 N88-12169

SPOT: A tool for agricultural statistics 03 p0344 N88-12170

Stand based forest inventory from SPOT IMAGE. First experiments 03 p0344 N88-12173

Use of SPOT images for coastal development and inventory of aquacultural sites in New Caledonia (ALIAS project). First results 03 p0344 N88-12175

Contribution of SPOT data to the physiographic study of coastal environment: La Pointe d'Arcay and l'Anse de l'Aiguillon (France) 03 p0344 N88-12176

The use of SPOT images for water resources surveys. The examples of the Kasserine area (Tunisia) and the Jebel Amour (Algeria) 03 p0345 N88-12179

Eastern - western Arctic Sea ice analysis 1986 [AD-A184016] 03 p0355 N88-12235

Cloud cover determination in polar regions from satellite imagery [NASA-CR-181544] 04 p0471 N88-12908

Tropical easterly jet located using TOMS data 05 p0616 N88-13783

Application of TOMS data to weather analysis models 05 p0617 N88-13787

National Point Of Contact (NPOC)-SPOT inquiry 1986 [NLR-MP-86055-U] 05 p0620 N88-13807

Study on data compression systems for operational remote sensing --- meteosat imagery [NLR-TR-86029-L] 05 p0620 N88-13808

High resolution satellite imagery simulation --- treaty verification [FOA-C-30462-3.3,9.3] 05 p0620 N88-13810

Mesoscale applications of high resolution imagery [AD-A185039] 05 p0627 N88-13833

AVHRR/HIRS (Advanced Very High Resolution Radiometer/High Resolution Infra-Red Sounder) operational method for satellite based sea surface temperature determination [PB88-107594] 06 p0708 N88-14340

Remote sensing in mineral exploration [PB87-138558] 06 p0729 N88-14484

Automated satellite cloud analysis: A multispectral approach to the problem of snow/cloud discrimination [AD-A185672] 06 p0746 N88-14591

Solar-geophysical activity reports for STIP (Study of Travelling Interplanetary Phenomena) Interval 15, 12-21 February 1984 ground level event and STIP Interval 16, 20 April-4 May 1984 Forbush decrease [PB87-232658] 06 p0805 N88-14915

Review of the potential of satellite remote sensing for marine flood protection [IOS-237] 07 p0870 N88-15280

An investigation of offshore circulation using satellite data and feature tracking techniques [AD-A186271] 07 p0881 N88-15347

Space photographs of the Onega-Ladoga isthmus and prediction of useful minerals 08 p1006 N88-16108

French activities in ocean colour observations 08 p1043 N88-16303

Earthnet's experience with Seasat SAR image processing 09 p1127 N88-16760

Technical assessment of the joint CSIRO/Bureau of Meteorology proposal for a geostationary imager/sounder over the Australian region [RTP-15] 09 p1135 N88-16811

Detection of soil erosion with Thematic Mapper (TM) satellite data within Pinyon-Juniper woodlands [NASA-CR-182476] 09 p1185 N88-17103

A multiple-satellite observation of the high-latitude auroral activity on 11 January 1983 [AD-A175170] 09 p1189 N88-17122

Nature and origin of mineral coatings on volcanic rocks of the Black Mountain, Stonewall Mountain, and Kane Springs Wash volcanic centers, Southern Nevada [NASA-CR-181437] 09 p1191 N88-17140

Meteorological Information Extraction Center (MIEC) processing --- Meteosat imagery [ESA-STR-224] 09 p1192 N88-17143

Introduction to the Meteosat system [ESA-SP-1041] 09 p1193 N88-17146

Application of satellite data in variational analysis for global cyclonic systems [NASA-CR-182468] 09 p1193 N88-17152

Handbook of the GEMS image processing system [RAE-TR-86062] 09 p1219 N88-17310

Inexpensive solution for the mass distribution of satellite images [PB88-114038] 10 p1317 N88-17873

Analysis of quasi-geostrophic forcing during the AIMCS (Airborne Investigations of Mesoscale Convective Systems) Project. Volume 2: Results for June 14 through July 16, 1984 [PB88-123807] 10 p1354 N88-18092

Character of five selected LANDSAT lineaments in southwestern Pennsylvania: Report of investigations, 1987 [PB88-133517] 11 p1505 N88-18988

An application of digital cartography updating middle and small scale thematic maps using orbital data [INPE-4460-TDL/317] 12 p1637 N88-19805

Influence of solar illumination conditions on TM/Landsat data [INPE-4463-TDL/320] 12 p1638 N88-19806

Comparison of simulation modeling and satellite techniques for monitoring ecological processes [NASA-CR-182592] 12 p1641 N88-19825

Mesoscale monitoring of the soil freeze/thaw boundary from orbital microwave radiometry [NASA-CR-182659] 12 p1645 N88-19855

Dynamical and photometric studies of Saturn's rings 12 p1711 N88-20241

An investigation of Doppler satellite positioning multi-station adjustment software 13 p1730 N88-20345

Restoration techniques for redisplay of LANDSAT-5 satellite imagery [INPE-4189-PRE/1076] 13 p1791 N88-20712

Analysis for architecture for image processing [INPE-4294-PRE/1165] 13 p1791 N88-20715

Aspects and applications of primary processing of visual information [INPE-4290-PRE/1161] 13 p1841 N88-21015

IUE program SUGSD: Varability time scale of H Ly-alpha from Uranus [NASA-CR-182706] 13 p1856 N88-21107

Optical properties of Southern Hemisphere aerosols: Report of the joint CSIRO/NASA study [NASA-CR-179287] 14 p1945 N88-21605

Image processing on VEGA pictures 14 p2009 N88-21983

Geometric restoration of satellite image data [AD-A190462] 15 p2089 N88-22450

Satellite UV image processing [AD-A190466] 15 p2089 N88-22451

Project CODEAMA/FUNCATE (test-area of Barreirinha-AM): Field report [INPE-4500-RPE/563] 15 p2090 N88-22455

Comparative utilization of analog and digital processes in the treatment of MSS-LANDSAT data for studying the national parks of Brazil [INPE-4011-TDL/240] 15 p2090 N88-22456

Calibration and processing of AVHRR data for temperature estimation [INPE-4493-PRE/1257] 15 p2095 N88-22485

Detection, monitoring and analysis of some environmental effects of fires in the Amazon region through utilization of NOAA and LANDSAT satellite imagery and aircraft data [INPE-4503-TDL/326] 16 p2230 N88-23322

Validate algorithms for the determination of rainfall rates from SSM/I microwave satellite imagery [AD-A188769] 16 p2233 N88-23337

NOAA-ERL-ARL (National Oceanic and Atmospheric Administration-Environmental Research Laboratories-Air Resources Laboratory) solar UV radiation and climate research project: Program description [PB88-169396] 16 p2233 N88-23339

Validate algorithms for the determination of rainfall rates from SSM/I microwave satellite imagery [AD-A191337] 16 p2236 N88-23353

Updating land-use of the Sao Jose dos Campos municipality through remote sensing data [INPE-4479-RPE/562] 16 p2287 N88-23693

A low cost automatic Earth observation satellite tracking ground receiving station 17 p2309 N88-23815

Meteorological Satellite Center Technical Note No. 16 [ISSN-0388-9653] 17 p2350 N88-24003

Latitudinal and seasonal variation of the cloud characteristic parameters and their effects on the cloud classification 17 p2351 N88-24005

Some problems with regard to the TOVS processing detected by using NOAA-HRPT data check program 17 p2351 N88-24009

Enhanced infra-red picture of LR-FAX for spring and autumn seasons 17 p2351 N88-24011

Latin American Symposium on Remote Sensing. 4th Brazilian Remote Sensing Symposium and 6th SELPER Plenary Meeting, volume 1 17 p2352 N88-24013

A comparison of supervised maximum likelihood and decision tree classification for crop cover estimation from multitemporal LANDSAT MSS data 17 p2352 N88-24014

Mapping from LANDSAT and SPOT satellite imagery 17 p2352 N88-24018

Spectral measurements for correcting LANDSAT data for atmospheric effects 17 p2353 N88-24020

Mapping soil and rock variation from satellite images in the Sahel 17 p2354 N88-24023

An integrated study of the Alto Paranaiba Kimberlite Province, Minas Gerais, Brazil: A possible tool for diamond exploration 17 p2355 N88-24031

Satellite remote sensing of turbidity and sediment concentration in Lagoa dos Patos 17 p2355 N88-24032

Practical image analysis using personal computers: The Canadian experience 17 p2356 N88-24037

Presentation of the METEOSAT system and the roles of EUMETSAT within the meteorological community 17 p2357 N88-24039

ERS-1 data products and services and their value for tropical countries 17 p2357 N88-24040

Estimation of an area cultivated with wheat from LANDSAT data through a two-phase sampling method 17 p2357 N88-24041

Utilization of TM/LANDSAT images in the implanted forests mapping in the Mogi-Guacu Region (SP-Brazil) 17 p2357 N88-24042

Anomalies in the vegetation in the Alto Xingu - MT 17 p2357 N88-24043

Remote sensing techniques in the estimation of the area cultivated with beans, corn, and castor beans in the Irece County (Bahia State) 17 p2358 N88-24045

CANASATE: Sugar cane mapping by satellite 17 p2358 N88-24046

Spectral behavior of crops through analysis of LANDSAT-TM data 17 p2358 N88-24047

Identification of areas cultivated with soybeans in the cerrados regions, through digital processingof satellite images: A methodological approach 17 p2358 N88-24048

Structure and dynamics of vegetation in the middle semi-arid tropics. Quixaba's Caatinga (PE): Terrain analysis of MSS/LANDSAT data 17 p2358 N88-24049

Study of fracturing for groundwater research in the Sergipe state with remote sensing products 17 p2359 N88-24052

A system for determination of wind fields using geostationary meterological satellites 17 p2360 N88-24056

Digital processing of infrared and visible images from the GOES satellite and its integration with meteorological rader data 17 p2360 N88-24057

Thematic mapping utilizing data from the Thematic Mapper sensor of the LANDSAT satellite 17 p2361 N88-24060

Geometric image correction: An approach for the registration of LANDSAT-TM digital images supported by topographical maps of medium and great scales 17 p2361 N88-24061

Generation of thematic maps for updating aeronautical pilot charts utilizing LANDSAT-TM images 17 p2361 N88-24062

Evolution of a family of image processing systems at INPE 17 p2361 N88-24065

Spectral measurements for correcting LANDSAT data for atmospheric effects 17 p2362 N88-24066

Analysis of the parameters responsible for the variations of the illumination conditions in the LANSAT data 17 p2362 N88-24070

Tornado tracks in Southwestern Brazil, Eastern Paraguay, and Northwestern Argentina 17 p2362 N88-24071

Interpretation of MSS/LANDSAT data for evaluation of physical distribution of mangroves in Cananeia-Iguape (SP) 17 p2363 N88-24072

Evaluation of an estimation system for an irrigated area in a tropical region through TM-LANDSAT imagery 17 p2363 N88-24075

Study of reservoir water quality utilizing remote sensing techniques: Methodological concepts 17 p2364 N88-24076

Utilization of LANDSAT-TM imagery in the hydroenergetic inventory of the Paraiba de Sul River Basin 17 p2364 N88-24077

Evaluation of the floodable area of the canal of Sao Goncalo through TM-LANDSAT 5 imagery 17 p2364 N88-24078

Automatic registration of satellite imagery 17 p2364 N88-24080

Visualization of digital terrain models 17 p2364 N88-24081

Application of its transformation in color enhancement of LANDSAT imagery 17 p2365 N88-24082

Evaluation of a flood period (June, 1984) in the southern region of Laguna dos Patos, through remote sensing data, meteorological and oceanographic 17 p2365 N88-24083

Detection of biomass burning and smoke plumes in the Amazon region through NOAA satellite imagery 17 p2365 N88-24085

Evaluation of the mangrove area at the Piaui River (SE) through remote sensing 17 p2365 N88-24086

Dune fields in central Western Argentina 17 p2366 N88-24088

The breaked anticlines, cuesta and crest homoclines, ortoclinal valleys, and other forms of relief outcrops delineated with the help of remote sensing imagery 17 p2366 N88-24089

Mapping of plant associations and the variation of surface water in the Pantanal Mato-Grossense National Park, through remote sensing techniques 17 p2366 N88-24092

Temporal analysis of the changes in Parque Estadual de Jacupiranga vegetation through digital treatment of LANDSAT imagery 17 p2367 N88-24094

Evaluation of TM false color composites for crop discrimination 17 p2367 N88-24096

Some geological aspects of the Pirapemas Lineament Belt 17 p2368 N88-24099

Lithostructural interpretation of Chapda do Cachimbo (Pa-Am-Mt), based on radar and LANDSAT imagery 17 p2368 N88-24100

Research on enhancing the utilization of digital multispectral data and geographic information systems in global habitability studies [NASA-CR-182799] 17 p2368 N88-24101

Terrain classification using SPOT images and the computer system GOP-300 [FOA-C-20677-2.7] 17 p2368 N88-24102

Coupling of satellite remote sensing to digitized topographic map to detect changes in land use [B8735129] 17 p2369 N88-24104

Influence of the Yukon River on the Bering Sea [NASA-CR-182802] 17 p2376 N88-24126

Ice conditions along the Ohio River as observed on LANDSAT images, 1972-1985 [AD-A191172] 18 p2531 N88-25018

DMSP-SSM/1 NASA algorithm validation using primarily LANDSAT and secondarily DMSP and/or AVHRR visible and thermal infrared satellite imagery [NASA-CR-182979] 18 p2532 N88-25024

Monitoring biological impacts of space shuttle launches from Vandenberg Air Force Base: Establishment of baseline conditions [NASA-TM-100982] 18 p2549 N88-25133

Application of dynamic programming to image registration [ENST-87E022] 18 p2557 N88-25180

The Io sulfur torus in 1981 [NASA-TM-101139] 18 p2595 N88-25419

National Meeting on Remote Sensing Applied to Municipal Planning 19 p2681 N88-25939

Mapping of land use in Sao Jose dos Campos municipality by remote sensing, an aid for the elaboration of its PDDI 19 p2681 N88-25940

Technique to obtain the agricultural ownership limits by satellite imagery, to approve control, and to accompany agricultural activity 19 p2682 N88-25943

The use of satellite imagery for municipal conditions in rural recording in Pereira Barreto (SP) 19 p2682 N88-25944

The impact of hemp production on the development of the municipalities of Araras, Leme, Santa Cruz da Conceicao and Pirassununga 19 p2683 N88-25948

Application of remote sensing in the conservation of natural areas: Ribeira Valley 19 p2683 N88-25949

Use of remote sensing in the study of superficial formation certifying the development of integrated economy-case example: Rio Claro (SP) region 19 p2683 N88-25950

Canopy reflectance modeling in a tropical wooded grassland [NASA-CR-182981] 19 p2685 N88-25961

Separability of cultivation through digital analysis of SPOT and TM data [INPE-4541-PRE/1287] 19 p2685 N88-25963

Suggested hurricane operational scenario for GOES I-M [NASA-TM-89729] 19 p2692 N88-26002

Bathymetry estimation by analyzing swell on SPOT images 19 p2701 N88-26062

Image processing applied to quantitative numerical cartography of ocean circulation 19 p2702 N88-26065

Methods for processing satellite images and their application to underwater operations 19 p2702 N88-26066

Checkout system software for INPE satellites [INPE-4554-PRE/1297] 19 p2715 N88-26120

Meteorological satellite product support and research for project GALE [NASA-CR-180989] 19 p2727 N88-26193

Voyager imaging photometry and radiative transfer modeling of the spoke-like features in Saturn's outer B-ring 19 p2742 N88-26278

Interpreting forest biome productivity and cover utilizing nested scales of image resolution and biogeographical analysis [NASA-CR-183036] 20 p2817 N88-26711

Hydrologic models for land-atmosphere retrospective studies of the use of LANDSAT and AVHRR data [NASA-CR-182861] 20 p2817 N88-26712

Hydrologic models for land-atmosphere retrospective studies of the use of LANDSAT and AVHRR data [NASA-CR-182862] 20 p2818 N88-26716

Validate algorithms for the determination of rainfall rates from SSM/I microwave satellite imagery [AD-A192299] 21 p2974 N88-27664

SPOT 1 Image Utilization, Assessment, Results [ISBN-2-85-428188-8] 22 p3089 N88-28346

The contribution of remote sensing to hydrology and hydrogeology 22 p3090 N88-28347

Mapping of streamflow and soil infiltration of a Sahelian catchment area by SPOT image interpretation: The Oursi pond catchment area in Burkino Faso 22 p3090 N88-28348

The use of SPOT images for water resources surveys in the Kasserine Basin (Tunisia) 22 p3090 N88-28349

SPOT image exploitation for glacial mass balance fluctuation monitoring in the French Alps 22 p3090 N88-28350

SPOT on land and lakes in the Hubei Province (China) 22 p3090 N88-28351

Evaluation of SPOT imagery for monitoring irrigated lands 22 p3090 N88-28352

An evaluation of SPOT imagery for wetland monitoring 22 p3091 N88-28353

Comparative study of crop and soil mapping using multitemporal and multispectral SPOT and LANDSAT data 22 p3091 N88-28354

Water resources and agricultural land use investigations in northeastern Gujarat (India) 22 p3091 N88-28355

Study of the forests on the banks of the Gambia and criteria for detecting mortality 22 p3091 N88-28356

Use of SPOT satellite in agrohydrology: Detection of spring water excess in a grassland region 22 p3091 N88-28357

Review of the studies of geography and environment and studies on spectral characteristics of SPOT HRV data 22 p3091 N88-28358

Evaluation of the grassy biomass in the Sahelian zone in the South Tamesna region (Niger): Prospects and limits of use of SPOT data 22 p3092 N88-28359

Changes in species composition of heathland, monitored by means of remote sensing and field mapping: The results of the HEISPOT project 22 p3092 N88-28360

Topography of an Antartic ice stream 22 p3092 N88-28361

Spatial and spectral registration of Javanese landscape units with SPOT 22 p3092 N88-28362

Comparison between the respective contributions of the TM LANDSAT-4 and HRV SPOT-1 data to the land use mapping of Mediterranean coastal zone 22 p3092 N88-28363

Land use systems and rural landscapes in the center of Veracruz State (Mexico): First results 22 p3092 N88-28364

SPOT for earthquake hazard zoning in southern Italy 22 p3093 N88-28365

Discrimination of sand transport rates and environmental consequences in central Egypt from SPOT data 22 p3093 N88-28366

Delineation of ephemeral fluvial networks on low-relief Piedmont surfaces, Plutonium Valley, Nevada, USA 22 p3093 N88-28367

Following the seasonal evolution of a natural environment in a humid tropical region. Preliminary Evaluation of SPOT (PEPS) number 186: Bangui, Central Africa 22 p3093 N88-28368

Application of SPOT to agricultural information systems in temperate regions 22 p3093 N88-28369

Potential use of SPOT satellite data for the national resources inventory 22 p3093 N88-28370

Methodological developments on crop inventories using SPOT and ground surveys 22 p3094 N88-28371

Evaluation of annual crop surfaces and territorial inventory in the Paris basin by combining classic statistical inquiries and SPOT data (Preliminary Evaluation Program for SPOT 127) 22 p3094 N88-28372

Evaluation of automatic texture analysis for increased crop identification accuracy with SPOT data 22 p3094 N88-28373

Application of SPOT multidate data to wheat yield estimation in Beauce (France) 22 p3094 N88-28374

An evaluation of multidate SPOT data for agriculture and land use mapping in the United Kingdom 22 p3094 N88-28375

The suitability of SPOT imagery for monitoring landscape patterns 22 p3094 N88-28376

Characterization, topology, and cartography of grasslands for the development of fodder resources. (Preliminary Evaluation Program for SPOT number 26) 22 p3095 N88-28377

HRV data for the applications on reneweable resources in Canada --- SPOT 22 p3095 N88-28378

SPOT-1 HRV data and vegetation amount 22 p3095 N88-28379

Attempt to inventory vines using oblique SPOT images 22 p3095 N88-28380

Analysis of soils using remote sensing information at the scale of the parcel 22 p3095 N88-28381

Comparative variations of spectral signatures in a cultivated area of the Paris Basin (27 May, 26 June, 1 July 1986) 22 p3095 N88-28382

Monitoring of agricultural production in West Africa. The need to integrate different satellite platforms 22 p3096 N88-28383

Use of SPOT imagery for vegetation/biomass mapping, geotechnical mapping, catchment area determination, and settlement location in the Turkana district, northern Kenya 22 p3096 N88-28384

Digital and visual analysis of SPOT and TM data for crop discrimination in southern Brazil 22 p3096 N88-28385

A comparative thematic mapping analysis of SPOT data: The Vientiane Plain (Lao PDR) 22 p3096 N88-28386

Discrimination methods of traditional fields in a humid tropical region (Shaba, Zaire) using digital classification on SPOT data 22 p3096 N88-28387

Evaluation of SPOT data for crop inventory and monitoring in Sudanian Africa. Example of Bane area (Burkina Faso) 22 p3096 N88-28388

Identification of farming systems in the cotton area of West Burkina Faso from SPOT-1 data
22 p3097 N88-28389

Monitoring Tunisia's steppes with SPOT
22 p3097 N88-28390

Study of savannah formation in the Sudanian zone. Northwest sector of the La Comoe park, Ivory Coast
22 p3097 N88-28391

Pilot study of rice culture in sub-tropical high population density region (Madagascar) with SPOT 1 multispectral data 22 p3097 N88-28392

Using SPOT HRV data to update the distribution of the paddy field in Taiwan 22 p3097 N88-28393

Agro-ecological mapping from SPOT 1 data in southern Thailand: New questions for an analysis of the farming-systems 22 p3097 N88-28394

SPOT applications on Columbia's coffee zone
22 p3097 N88-28395

Use of SPOT data in preliminary steps of road project studies especially suited for developing countries
22 p3098 N88-28396

SPOT imagery for detecting residential expansion on the rural-urban fringe of Toronto, Canada
22 p3098 N88-28397

Spread of large tropical conurbations
22 p3098 N88-28398

Utilization of remote sensing for the observation of urban populations. Ongoing research in Quito (Ecuador)
22 p3098 N88-28399

Integration of SPOT data into a geocoded information system 22 p3098 N88-28400

Utilizing SPOT data for seismic shot-line mapping and environmental monitoring in oil and gas exploration
22 p3098 N88-28401

Preliminary comparative analysis of LANDSAT and SPOT data for the study of the sanding phenomenon: Zaafrane region (Algeria) 22 p3099 N88-28402

An evaluation of the applicability of SPOT stereoscopic imagery to the Canada Land Use Monitoring Program (CLUMP) 22 p3099 N88-28403

Topographic suppression and advances in classification for land cover mapping using SPOT-1 HRV imagery
22 p3099 N88-28404

Monitoring Moneragala (Sri Lanka) with SPOT imagery
22 p3099 N88-28405

Monitoring urban land cover changes at the urban fringe from SPOT HRV imagery in south-east England
22 p3099 N88-28406

Preliminary analyses of SPOT HRV multispectral products for arid and temperate environments
22 p3099 N88-28407

Assessment of SPOT satellite based system in humid tropical vegetation identification, classification and monitoring 22 p3100 N88-28408

A comparison between SPOT and LANDSAT TM for mapping of vegetation and bedrock outcrops
22 p3100 N88-28409

Accuracy of land use classification for SPOT image data 22 p3100 N88-28410

Analysis of SPOT multispectral data concerning a border zone between two geographical regions in southern Belgium 22 p3100 N88-28411

Thematic mapping of central Java (Indonesia)
22 p3100 N88-28412

Utilization of SPOT-1 multispectral data for mapping land cover and phytohygiene monitoring in the central zone of the Mercantour National Park (France)
22 p3100 N88-28413

Applications of SPOT data for urban real estate investment information systems
22 p3101 N88-28414

Mapping and urban muiti-experimental assessment of SPOT: Urban results · 22 p3101 N88-28415

SPOT-1 over New Zealand: Analysis of SPOT imagery for land use investigations 22 p3101 N88-28416

Comparison of SPOT, LANDSAT TM and combined data for urban studies 22 p3101 N88-28417

Utilization of SPOT multispectral data for urban planning 22 p3101 N88-28418

First results of international investigations of the applications of SPOT-1 data to geologic problems, mineral and energy exploration 22 p3101 N88-28419

Rate of slip on the Altin Dagh Fault (North Tibet, China) 22 p3102 N88-28420

Karst and submarine fresh water discharge in the Antalya area, southern Turkey 22 p3102 N88-28421

Results of the Geosat program to evaluate SPOT data for petroleum and mineral exploration
22 p3102 N88-28422

The application of SPOT data to the structural geology of western Nevada 22 p3102 N88-28423

Application SPOT-1 data to mining activity: Example of the Imiter Silver Mine, Morocco
22 p3102 N88-28424

Evaluation of SPOT imagery contribution to petroleum exploration: The Suez Rift (Egypt)
22 p3102 N88-28425

Evaluation of SPOT imagery for discriminating vegetation communities associated with surficial and bedbrock geology and identifying anomalous and stressed vegetation associated with mineralization
22 p3103 N88-28426

SPOT imagery as an aid to understanding volcanism and tectonics: Examples from the Chilean Andes and the Tibetan Plateau 22 p3103 N88-28427

Role of SPOT in geological application of remote sensing 22 p3103 N88-28428

SPOT imagery preliminary contribution to cartography and geodynamics in the Benue trough (Nigeria)
22 p3103 N88-28429

An evaluation of SPOT imagery for Earth science studies in the Antarctic. Preliminary Evaluation Program (PEPS) 289 for SPOT 22 p3103 N88-28430

Structural analysis of the Jura mountains-Rhine Graben intersection (Switzerland) for petroleum exploration using SPOT stereoscopic data 22 p3103 N88-28431

Methodology for the use of SPOT imagery in petroleum exploration. Example of the Bas-Languedoc area (France) 22 p3104 N88-28432

Analyzing the stratigraphy, tectonism, and mineralization at the Spanish side of the pyrite belt, Huelva province, Spain, using SPOT imagery 22 p3104 N88-28433

Geologic applications of SPOT-1, TM, and NOAA-7 data: Finding and defining unmapped structural features
22 p3104 N88-28434

Comparing different images for ground water survey based on lineament analysis 22 p3104 N88-28435

Spectral and spatial attribute evaluation of SPOT data in geological mapping of precambrian terrains in semiarid environment of Brazil 22 p3104 N88-28436

Geologic results obtained from the use of SPOT imagery along plate boundaries: Examples in the East African rift and of the northern-Caribbean collision
22 p3105 N88-28437

SPOT images and geochemical mapping of lateritic covers in southern Mali 22 p3105 N88-28438

Analysis of the multispectral content and of SPOT subscenes in two regions of Burundi. Lithologic and tectonic interpretations 22 p3105 N88-28439

SPOT imagery for landslide cartography in mountainous areas. Example of the French Maritime Alps
22 p3105 N88-28440

SPOT for slope instability survey in Nepal
22 p3105 N88-28441

Detailed geological mapping of the massif of Sainte Victoire (Provence, France) using SPOT imagery. Comparison with other multisource data. New tectonic interpretation of this region 22 p3105 N88-28442

Satellite remote sensing for forest management. A review illustrated with research results on SPOT 1 data
22 p3106 N88-28443

An evaluation of the utility of SPOT and Thematic Mapper data for providing forest inventory information
22 p3106 N88-28444

SPOT-1 satellite imagery for forest inventory in Sweden 22 p3106 N88-28445

Forest mapping by visual interpretation of SPOT images 22 p3106 N88-28446

Forest management applications of SPOT data in Australia 22 p3106 N88-28447

SPOT multispectral data and maritime pine stands in southwest of France 22 p3106 N88-28448

Stand-based forestry inventory from SPOT image
22 p3106 N88-28449

Potential of SPOT imagery as a tool for forest mapping in Quebec 22 p3107 N88-28450

Assessment of large area forest disturbances caused by biotic and abiotic factors on the basis of SPOT images 22 p3107 N88-28451

Study of deforestation in the Vosges (France) by remote sensing 22 p3107 N88-28452

Contribution to the mapping of forests in an intensively divided area, with the help of SPOT image data
22 p3107 N88-28453

SPOT 1: Image utilization, assessment, results. A study of the Elburgon Forest area (Kenya) showing the spectral responses of different forest tree species
22 p3107 N88-28454

SPOT investigations of estuaries and coastal zones: An overview 22 p3107 N88-28455

SPOT: A tool to aid preselection of sites favorable for aquiculture. Evaluation and perspectives of the Preliminary Evaluation Program for SPOT (PEPS) ALIAS Caledonie
22 p3108 N88-28456

The monitoring of sediment transport, water circulation and mixing in estuaries and coastal waters
22 p3108 N88-28457

Evaluation of SPOT data for remote sensing of physical and biological properties of estuaries and coastal zones
22 p3108 N88-28458

Utilization of SPOT in hydrography
22 p3108 N88-28459

Application of SPOT imagery for oil spill contingency planning 22 p3108 N88-28460

The use of SPOT data in mapping coastal areas
22 p3108 N88-28461

SPOT: A satellite for oceanography
22 p3108 N88-28462

Contribution of SPOT satellite to qualitative and quantitative mapping of marine vegetation in the English Channel, North Altantic, western Mediterranean, and South Pacific 22 p3109 N88-28464

Physiography and kinematics of the western coast of the province of Huelva (Andalousia, Spain)
22 p3109 N88-28465

Use of SPOT HRV data in the US Army Corps of Engineers dredging program 22 p3109 N88-28466

Contributions of SPOT imagery to the study of the littoral environments of Saloum (Senegal)
22 p3109 N88-28467

Relevance of a thematic map (SPOT data) with regards to the real flora and structure of the vegetation covering of salt marshes (Mont Saint Michel Bay, France)
22 p3109 N88-28468

Application of SPOT data to renewable resources in the Maldives 22 p3109 N88-28469

The prospects for topographic mapping using SPOT data 22 p3110 N88-28470

The use of SPOT imagery on analytical photogrammetric instruments 22 p3110 N88-28471

Cartographic applications of SPOT imagery
22 p3110 N88-28472

The use of SPOT imagery for topographic mapping
22 p3110 N88-28473

Digital terrain modelling with SPOT data and geological applications 22 p3110 N88-28474

The use of SPOT data for mapping and DEM production --- digital elevation model (DEM)
22 p3110 N88-28475

Evaluation of SPOT cartographic capabilities over the Aix Marseille area (France) 22 p3110 N88-28476

Assessment of SPOT imagery for topographic revision and vegetation mapping 22 p3111 N88-28477

Topographic mapping with SPOT 1 data. A practical approach by the Ordnance Survey
22 p3111 N88-28479

Metric applications of SPOT's lateral stereoscopy
22 p3111 N88-28480

Larger scale image mapping with SPOT
22 p3111 N88-28481

Rigorous stereophotogrammetric treatment of SPOT images 22 p3111 N88-28482

Mapping and urban multi-experimental assessment of SPOT: Mapping results 22 p3112 N88-28483

Study of stereoradiometry on SPOT images
22 p3112 N88-28484

Studies on system performance of SPOT (space and ground segments) 22 p3112 N88-28485

Radiometric analysis and potential of SPOT HRV imagery for applications in urban environments and geology 22 p3112 N88-28486

Automatic production of orthophoto using SPOT images 22 p3112 N88-28487

High resolution orthoimage quadrangle maps using SPOT satellite data 22 p3112 N88-28488

Automatic extraction of high resolution elevation data from SPOT stereo images 22 p3113 N88-28489

Automatic creation of digital terrain models from SPOT image pairs 22 p3113 N88-28490

Production of satellite image maps based on SPOT data 22 p3113 N88-28491

Surface reflectance factors derived from SPOT-1 HRV data at two view angles 22 p3113 N88-28492

Digital SPOT stereoplotting: An original approach to the formation of epipolar images and matching
22 p3113 N88-28493

From the extraction of linear networks towards following of them on SPOT images with the help of a knowledge-based interpretation system
22 p3113 N88-28494

Extraction of thin networks by an oriented following of ridges and valleys 22 p3113 N88-28495

SPOT images features extraction
22 p3114 N88-28496

SPOT: A data capture and data updating tool for the French National Geographic Institute's (IGN's) cartographic data base 22 p3114 N88-28497

Use of SPOT imagery in a geographic information system 22 p3114 N88-28498

SEP/VIPS 32 geographic information system. Processing and thematic analysis of images, maps, and associated data 22 p3114 N88-28499

Space imagery as a teaching aid in secondary education 22 p3114 N88-28500

Training of the Group for the Development of Aerospace Remote sensing 22 p3114 N88-28501

Contribution of SPOT to geographic information systems 22 p3114 N88-28502

Summary of analysis and processing techniques used on SPOT imagery 22 p3115 N88-28503

The SPOT program 22 p3115 N88-28504

SPOT data acquisition and distribution 22 p3115 N88-28505

Quality of SPOT images 22 p3115 N88-28506

Survey of SPOT-1 operation 22 p3115 N88-28507

Perspectives for the SPOT program 22 p3115 N88-28508

Closing of the Preliminary Evaluation Program for SPOT (PEPS): Assessment of the acquisition, production, and monitoring of PEPS 22 p3115 N88-28509

Use of LANDSAT images of vegetation cover to estimate effective hydraulic properties of soils [NASA-CR-183185] 22 p3116 N88-28514

The patterns of tropical convection during the 1986-87 ENSO 22 p3120 N88-28537

An objective technique for Arctic cloud analysis using multispectral AVHRR (Advanced Very High Resolution Radiometer) satellite imagery [AD-A194732] 23 p3235 N88-29250

Surface composition of Mars: A Viking multispectral view 23 p3300 N88-29655

The history of Martian volcanism determined from a revised relative chronology 23 p3301 N88-29657

High resolution Viking Orbiter images: A useful data source for testing the viability of geomorphic processes attributed to Martian landforms 23 p3307 N88-29703

Microwave instrument for planetary mission (Titan/CASSINI mission orbiter spacecraft) [BAE-CS/TP-8359] 24 p3375 N88-30102

TM/LANDSAT-5 data to evaluate wheat and bean percent soil cover and leaf area index [INPE-4609-PRE/1332] 24 p3385 N88-30165

Evaluation of LANDSAT-TM data for geomorphological mapping [INPE-4593-PRE/1324] 24 p3386 N88-30168

Imaging instrument of the vegetation payload (SPOT 4) [SNIAS-881-440-107] 24 p3386 N88-30169

The use of orbital remote sensing data for low cost ground-water survey [INPE-4587-PRE/1318] 24 p3386 N88-30170

Reflectance pattern and the physical and chemical characteristics of three Brazilian Oxisols [INPE-4590-PRE/1320] 24 p3387 N88-30172

Use of digital images as a mineral prospecting tool in the tin province of Goias, Brazil [INPE-4537-PRE/1284] 24 p3387 N88-30173

Relief effect correction on LANDSAT imagery for forest applications using digital terrain models [INPE-4611-PRE/1334] 24 p3388 N88-30179

LANDSAT TM and agrometeorological data for wheat yield estimation at the farm level [INPE-4591-PRE/1321] 24 p3388 N88-30180

Volcanic contribution to crustal growth in the Central Andes: A new estimate and a discussion of uncertainties 24 p3401 N88-30255

Validate algorithms for the determination of rainfall rates from SSM/I microwave satellite imagery [AD-A195426] 24 p3404 N88-30270

Compression and decompression of imaging sensor signals (CADISS): A multiprocessor system for image compression/decompression on board scientific satellites [NLR-TR-87076-L] 24 p3414 N88-30323

Analytical method for approximate geodetic referencing of scanner images of meteorological artificial earth satellites using control points 24 p3449 N88-30527

Determining the spatial structure of fields of precipitation from space radar images in two orthogonal polarizations 24 p3450 N88-30531

SATELLITE INSTRUMENTS

Evaluation of a satellite laser ranging technique using pseudonoise code modulated laser diodes [NASA-CR-182347] 06 p0708 N88-14343

Into the thermosphere: The atmosphere explorers [NASA-SP-490] 10 p1353 N88-18064

Investigation of the diffuse ultraviolet background with DE data [NASA-CR-182863] 19 p2741 N88-26271

Research and development objectives: Installation, startup, and test operation of a remote and program controlled measuring table for the calibration of EGRET experiment [ETN-88-92105] 22 p3152 N88-28752

SATELLITE LAUNCHING

U SPACECRAFT LAUNCHING

SATELLITE LIFETIME

Forward-biased current annealing of radiation damaged gallium arsenide and silicon solar cells [AD-A186904] 09 p1186 N88-17105

SATELLITE MANEUVERS

U SPACECRAFT MANEUVERS

SATELLITE NAVIGATION SYSTEMS

Reception of pseudo noise-modulated signals using digital correlators for satellite navigation tasks [ETN-87-90426] 01 p0037 N88-10234

GPS vertical axis performance enhancement for helicopter precision landing approach [NASA-CR-177443] 04 p0397 N88-12477

A demonstration of high precision GPS orbit determination for geodetic applications 04 p0432 N88-12680

Precise near-earth navigation with GPS: A survey of techniques 04 p0433 N88-12682

A positioning system based on NAVSAT [NLR-MP-87018-U] 20 p2757 N88-26358

Study on NAVSAT system evaluation, phase 2. Part 1: Study results [NLR-TR-87061-L-PT-1] 22 p3041 N88-28054

Study on NAVSAT system evaluation, phase 2. Part 2: Detailed simulation results [NLR-TR-87061-L-PT-2] 22 p3041 N88-28055

Accuracy of satellite data navigation [AD-A195877] 24 p3322 N88-29787

Low cost satellite [ESA-CR(P)-2560] 24 p3334 N88-29844

SATELLITE NETWORKS

NT ARGOS SYSTEM

Accurate position measuring spacecraft package [ESA-CR(P)-2398-VOL-1] 01 p0004 N88-10022

Accurate position measuring spacecraft package, executive summary [ESA-CR(P)-2398-VOL-2] 01 p0004 N88-10023

Study of mobile communications payload for Columbus Polar Platforms [ITS-TR-056A/86] 01 p0034 N88-10220

Study on the suitability of a European data relay satellite to support a system of remote sensing satellites [ESA-CR(P)-2400] 01 p0063 N88-10406

Study into a data relay satellite mission analysis tool [ESA-CR(P)-2422] 02 p0220 N88-11384

The Black College satellite telecommunications network planning in support of energy-related collaborative research [DE88-000182] 03 p0307 N88-11940

Interoperability and integration of data relay satellite systems 03 p0339 N88-12134

Study of the feasiblity of a satellite communication system for road transportation home office to vehicle communication. Volume 1: Conceptual analysis [SC/87-E/6-VOL-1] 05 p0575 N88-13505

Study of the feasibility of a satellite communication system for road transportation home office to vehicle communication. Volume 2: Market study [SC/87-E/6-VOL-2] 05 p0575 N88-13506

Low frequency VLBI in space using GAS-Can satellites: Report on the May 1987 JPL Workshop [NASA-CR-182362] 06 p0801 N88-14904

Round table on the future of satellite communications and broadcasting in Europe [ESA-STR-221] 07 p0843 N88-15112

Method for joint adjustment of satellite and surface geodetic networks 08 p1007 N88-16105

Study of reconfigurable payloads for direct broadcast satellites, summary [DBS87-0004] 09 p1135 N88-16808

An introduction to military satellite communications [RSRE-MEMO-3976] 09 p1153 N88-16911

Introduction to the Meteosat system [ESA-SP-1041] 09 p1193 N88-17146

The orientation of global satellite networks 11 p1506 N88-18996

On-board processing for mobile satellite communications [ESA-CR(P)-2519] 14 p1905 N88-21382

Activities report in flight and space travel [ISSN-0070-3966] 14 p2012 N88-22000

Degradation of downlink distance measurement indexes by the addition of a third tone --- tone ranging [CNES-CT/DRT/TIT/TR-122-T] 15 p2058 N88-22268

MSAT-X: A technical introduction and status report [NASA-CR-182921] 17 p2334 N88-23933

Satellites at sea --- INMARSAT 19 p2700 N88-26054

Document transfer by a digital satellite link [NLR-MP-86071-U] 20 p2792 N88-26564

The Frequency Division Multiple Access/Time Domain Multiplex (FDMA/TDM) system reviewed 22 p3069 N88-28214

Business telecommunications using satellite microterminals: Gaining the competitive edge [ESA-BR-49] 22 p3070 N88-28225

Determination of satcom access power levels within the ground segment [RSRE-MEMO-4097] 22 p3070 N88-28226

Performance of a rapid carrier acquisition circuit for satellite ground terminal modems [RSRE-TEST-REPORT-87/CC3/2] 22 p3071 N88-28227

NOA: A Network Operator Assistant for scheduling Tracking and Data Relay Satellite System (TDRSS) 23 p3259 N88-29403

Optical multiple access intersatellite links [BAE-TP-8502] 24 p3361 N88-30013

SATELLITE OBSERVATION

USSR report: Space [JPRS-USP-87-003] 01 p0009 N88-10050

The sequential evaluation of Doppler satellite observations [REPT-141] 01 p0010 N88-10057

Study on the suitability of a European data relay satellite to support a system of remote sensing satellites [ESA-CR(P)-2400] 01 p0063 N88-10406

How we get pictures from space, revised edition [NF-151/7-87-REV] 02 p0193 N88-11203

Observation of the development of mesoscale systems by operational meteorological satellites 02 p0201 N88-11259

Use of simulated satellite radiances from a mesoscale numerical model to understand kinematic and dynamic processes 02 p0202 N88-11261

Research in geodesy based upon radio interferometric observations of GPS (Global Positioning System) satellites [AD-A184040] 03 p0346 N88-12187

IRAS and near IR observations of active binaries 04 p0518 N88-13186

Budget and programs for 1986 research [IFSI-86-16] 05 p0660 N88-14048

Satellite observations of extreme ultraviolet radiation [AD-A185043] 05 p0661 N88-14059

Report of the International Satellite Cloud Climatology Project (ISCCP) workshop on cloud algorithms in the polar regions [WCP-131] 06 p0745 N88-14581

Review of the potential of satellite remote sensing for marine flood protection [IOS-237] 07 p0870 N88-15280

The influence of yellow substances on remote sensing of sea water constituents from space. Volume 1: Summary [ESA-CR(P)-2443-VOL-1] 07 p0872 N88-15292

The influence of yellow substances on remote sensing of sea water constituents from space. Volume 2: Appendices [ESA-CR(P)-2443-VOL-2] 07 p0873 N88-15293

The use of chlorophyll fluorescence measurements from space for separating constituents of sea water. Volume 1: Summary [ESA-CR(P)-2444-VOL-1] 07 p0873 N88-15294

The use of chlorophyll fluorescence measurements from space for separating constituents of sea water. Volume 2: Appendices [ESA-CR(P)-2444-VOL-2] 07 p0873 N88-15295

Feasibility studies of optical processing of image bandwidth compression schemes [AD-A186073] 07 p0932 N88-15660

Longitudinal variations of equatorial ionosphere determined from Intercosmos-19 artificial Earth satellite data 08 p1003 N88-16074

Satellite monitoring of earthquake precursor effects in magnetosphere 08 p1007 N88-16103

Research work at the Meteorological Institute of the University of Munich (Federal Republic of Germany) [MITT-56] 08 p1013 N88-16141

Inversion of simulated satellite signals 08 p1017 N88-16168

Commercial applications and scientific research requirements for thermal-infrared observations of terrestrial surfaces [NASA-TM-89704] 08 p1019 N88-16179

Global views of the aurora from the Viking satellite --- Swedish satellite 08 p1025 N88-16208

Instantaneous pictures of the high-latitude electrodynamics using Viking and DMSP/F7 observations --- Swedish satellite 08 p1025 N88-16209

The Meteosat operational program 09 p1127 N88-16759

Fine attitude measurement system study. Volume 1: Executive summary [BAE-TP-7831-VOL-1] 09 p1133 N88-16795

Fine attitude measurement system study, volume 2 [BAE-TP-7831-VOL-2] 09 p1133 N83-16796

Fine attitude measurement system study. Volume 3: Appendices [BAE-TP-7831-VOL-3] 09 p1133 N88-16797

A multiple-satellite observation of the high-latitude auroral activity on 11 January 1983 [AD-A175170] 09 p1189 N88-17122

NROSS (Navy Remote Ocean Sensing System): A force multiplier
[AD-A186853] 10 p1346 N88-18045
Earth resources: A continuing bibliography with indexes (supplement 56)
[NASA-SP-7041(56)] 10 p1347 N88-18051
Application of satellite data in observational and theoretical studies of the evolving structure of baroclinic waves
[NASA-CR-179277] 10 p1354 N88-18091
Proceedings of an ESA-NASA Workshop on a Joint Solid Earth Program
[NASA-CR-182642] 12 p1644 N88-19844
Spaceborne magnetometry 12 p1644 N88-19846
Terrestrial gravity data and comparisons with satellite data 12 p1644 N88-19848
Calibration of the solar radiation estimation method by satellites
[INPE-4349-PRE/1185] 12 p1646 N88-19861
An investigation of Doppler satellite positioning multi-station adjustment software
13 p1730 N88-20345
Analysis of spectral reflectance characteristics of targets under satellites and automatic cloud recognition
13 p1755 N88-20498
Radiative processes affecting ocean mixed-layer heat content and their monitoring from satellite
13 p1806 N88-20800
Climatology and space observations
[ISBN-2-85-428179-9] 14 p1935 N88-21536
The Earth radiation budget and its spatial and temporal variations 14 p1936 N88-21548
Net radiative flux at the Earth surface: Estimation from satellite observations 14 p1936 N88-21550
Satellite estimations of the solar radiation flux at the surface 14 p1936 N88-21551
Satellite retrieval of cloud cover parameters and the International Satellite Cloud Climatology Program (ISCCP) 14 p1937 N88-21552
Measurement from satellites of land surface parameters and fluxes in the thermal infrared bands: Problems and methods 14 p1937 N88-21557
The role of remote sensing in the study of polar ice sheets 14 p1939 N88-21570
Elements of sea ice dynamics and thermodynamics
14 p1939 N88-21571
Extension of the vegetation mission to thermal infrared spectral bands
[CNES-T-86/224-CT/DRT/TIT/IO]
16 p2227 N88-23299
Turbidity patterns in the delta waters of southwest Netherlands on Thematic Mapper (TM) and multispectral scanner (MSS) satellite images
[BCRS-86-06] 16 p2227 N88-23303
Near-real-time TOMS, telecommunications and meteorological support for the 1987 Airborne Antarctic Ozone Experiment
[NASA-CR-4133] 16 p2233 N88-23338
Prospects of satellite wind sensing systems in the years 1995-2000 17 p2350 N88-24004
Latitudinal and seasonal variation of the cloud characteristic parameters and their effects on the cloud classification 17 p2351 N88-24005
Estimation of total Outgoing Longwave Radiation (OLR) flux from geostationary meteorological satellite infrared window radiance 17 p2351 N88-24006
The application of satellites in connection with the environment
[ETN-88-92474] 18 p2532 N88-25020
Satellite observed Mesoscale Convective System (MCS) propagation characteristics and a 3-12 hour heavy precipitation forecast index
[PB88-180161] 19 p2692 N88-26004
Sensors in spaceborne oceanography
19 p2700 N88-26056
Remote sensing and satellite applications to the needs of the gas and pipeline industry
[PB88-202668] 20 p2817 N88-26714
Diffusion of slight solar induced disturbances in the middle atmosphere
[MITT-53] 20 p2825 N88-26758
Cyrogenic test facilities for an optical cryomechanism qualification
[REPT-881-440-116] 21 p2901 N88-27219
Optimized observation periods required to achieve geodetic accuracies using the global positioning system
[AD-A193644] 22 p3041 N88-28052
The world's water resources: A major neglect. A study in remote sensing in hydrology and water management
[ESA-BR-40] 22 p3116 N88-28511
Stratocumulus and cloud-free reflectance from multi-spectral satellite measurements
[AD-A193899] 22 p3128 N88-28599
Obligue metallogenic zones recognized by interpreting space photographs of southern Tien Shan
24 p3450 N88-30529

SATELLITE ORBIT CALCULATION
U ORBIT CALCULATION
SATELLITE ORBITS
NT GEOSYNCHRONOUS ORBITS
NT POLAR ORBITS
NT STATIONARY ORBITS
The contraction of satellite orbits under the influence of air drag. Part 8: Orbital lifetime in an oblate atmosphere, when perigee distance is perturbed by odd zonal harmonics in the geopotential
[RAE-TR-86069-PT-8] 01 p0010 N88-10058
Satellite orbits: Plot routines
[UIO-SR-87-02] 01 p0011 N88-10060
Precise orbit computation, gravity model adjustment and altimeter data processing for the ERS-1 altimetry mission
[ESA-CR(P)-2436] 02 p0130 N88-10820
On air-drag perturbation of transit satellite and selection of parameters in orbit improvement
03 p0269 N88-11691
Advanced simulation and analysis of a geopotential research mission
[NASA-CR-182355] 06 p0670 N88-14108
Simulation and analysis of a geopotential research mission
[NASA-CR-182354] 06 p0670 N88-14109
An orbit simulation study of a geopotential research mission including satellite-to-satellite tracking and disturbance compensation systems
[NASA-CR-182353] 07 p0823 N88-14997
Investigation of the feasibility of an analytical method of accounting for the effects of atmospheric drag on satellite motion 07 p0923 N88-15608
An evaluation of semianalytical satellite theory against long arcs of real data for highly eccentric orbits
[AD-A185825] 08 p0960 N88-15819
An intelligent tutor for the space domain
09 p1204 N88-17217
Relative motion of two satellites in close-elliptical orbits
[AD-A188851] 12 p1594 N88-19543
Analysis of orbital geometry and orbit maintenance of an Earth observation satellite
[INPE-4276-PRE/1148] 12 p1594 N88-19549
NAVARES: A prototype expert system for NAVSTAR anomaly resolution
[AD-A189491] 12 p1600 N88-19579
The evaluation and selection of a 5th ground antenna site for the global positioning system
[AD-A189495] 13 p1720 N88-20286
Orbit accuracy requirement of GPS for precise positioning and orbit determination within local area
13 p1756 N88-20499
Analysis of the orbit of Cosmos 1335 (1982-07A) at 3:12 resonance
[RAE-TR-87041] 14 p1872 N88-21185
Baseline estimation from simultaneous satellite laser tracking
[NASA-CR-182750] 15 p2022 N88-22052
The prediction of satellite lifetimes
[RAE-TR-87030] 17 p2310 N88-23818
Orbit determination of 1965-09A for analysis of the eccentricity at 15th-order resonance
[RAE-TR-87059] 22 p3047 N88-28081
A standard library for modeling satellite orbits on a microcomputer
[AD-A195759] 24 p3331 N88-29830
Experimental and analytical study of two-phase flow in zero gravity
[AD-A195223] 24 p3358 N88-29993
Plane periodic satellite motions relative to center of mass in neighborhood of collinear libration point
24 p3445 N88-30507
Resonance effects accompanying motion with low thrust in earth-moon system 24 p3446 N88-30510
SATELLITE ORIENTATION
Analysis of free molecular effects on the attitude of satellites in geostationary transfer orbit. Part 1: Theoretical analysis
[DFVLR-IB-222-86-A/08] 01 p0014 N88-10077
Analysis of free molecular effects on the attitude of satellites in geostationary transfer orbit. Part 2: Force and torque measurement in free molecular wind tunnel tests
[DFVLR-IB-222-86-A/07] 01 p0014 N88-10078
An autonomous, closed-loop pointing system for use with satellite optics
[DE87-012011] 02 p0235 N88-11483
Fine attitude measurement system study. Volume 1: Executive summary
[BAE-TP-7831-VOL-1] 09 p1133 N88-16795
Fine attitude measurement system study, volume 2
[BAE-TP-7831-VOL-2] 09 p1133 N88-16796
Fine attitude measurement system study. Volume 3: Appendices
[BAE-TP-7831-VOL-3] 09 p1133 N88-16797

SATELLITE PERTURBATION
The contraction of satellite orbits under the influence of air drag. Part 8: Orbital lifetime in an oblate atmosphere, when perigee distance is perturbed by odd zonal harmonics in the geopotential
[RAE-TR-86069-PT-8] 01 p0010 N88-10058
A study of a satellite-to-satellite tracking configuration by application of linear perturbation theory
[REPT-86.3] 01 p0011 N88-10059
Analysis of free molecular effects on the attitude of satellites in geostationary transfer orbit. Part 1: Theoretical analysis
[DFVLR-IB-222-86-A/08] 01 p0014 N88-10077
Analysis of free molecular effects on the attitude of satellites in geostationary transfer orbit. Part 2: Force and torque measurement in free molecular wind tunnel tests
[DFVLR-IB-222-86-A/07] 01 p0014 N88-10078
Estimability of potential coefficients from orbit perturbations --- satellite geodesy
[REPT-86.1] 01 p0064 N88-10408
Prevention of radiation induced degradations and of electrostatic perturbations on the Arabsat spacecraft in flight results 03 p0275 N88-11734
Simulation and analysis of a geopotential research mission
[NASA-CR-182354] 06 p0670 N88-14109
Orbit correction requirements for a natural resources satellite
[INPE-4286-PRE/1158] 12 p1594 N88-19548
Analysis of orbital geometry and orbit maintenance of an Earth observation satellite
[INPE-4276-PRE/1148] 12 p1594 N88-19549
SATELLITE POWER TRANSMISSION (TO EARTH)
ESA Bulletin No. 25
[ISSN-0376-4265] 09 p1128 N88-16767
Satellite power systems under consideration by the United Nations 09 p1128 N88-16773
SATELLITE RENDEZVOUS
U ORBITAL RENDEZVOUS
SATELLITE REPAIR
U ORBITAL SERVICING
SATELLITE ROTATION
A multibody dynamic analysis of the N-ROSS (Navy Remote Ocean Sensing System) satellite rotating flexible reflector using Kane's method
[AD-A184452] 04 p0462 N88-12860
Preliminary design of the ORION attitude control system
[AD-A187179] 10 p1292 N88-17729
A spin and deployment mechanism
14 p1926 N88-21479
Rotational evolution of dynamically symmetric gyrostat with internal friction 24 p3446 N88-30509
SATELLITE SOUNDING
An introduction to the GOES I-M imager and sounder instruments and the GVAR retransmission format
[NOAA-TR-NESDIS-33] 02 p0140 N88-10884
Improved geostationary satellite soundings for the mesoscale weather analysis/forecast operation
02 p0200 N88-11252
Horizontal shape matching applied to VAS data --- Visible and Infrared Spin Scan Radiometer Atmospheric Sounder (VAS) 02 p0201 N88-11254
Automated detection of severe thunderstorms using geosynchronous infrared data 02 p0201 N88-11257
Mesoscale analysis and nowcasting via a numerical model coupled with satellite sounder data
02 p0211 N88-11328
Methods of incorporating satellite data into mesoscale numerical forecast models 02 p0212 N88-11336
Simulation of mesoscale satellite sounder data from a mesoscale numerical model 02 p0214 N88-11345
The effect of enhanced conventional and VAS moisture analysis on RAFS short-range precipitation forecasts --- Regional Analysis and Forecasting System (RAFS)
02 p0215 N88-11352
Scientific and Operational Requirements for TOMS Data
[NASA-CP-2497] 05 p0615 N88-13774
Dobson-stations performance assessment using TOMS data 05 p0618 N88-13792
Volcanic eruption detection with TOMS
05 p0618 N88-13793
Analysis of SO2 signals in SBUV/TOMS data
05 p0618 N88-13794
Comparison of ground based and TOMS measurements of SO2 from volcanic emissions
05 p0618 N88-13795
Use of satellite data in volcano monitoring
05 p0618 N88-13797
Selection of optimum wavelengths for ozone mapping from satellites 05 p0619 N88-13798
Determination of total ozone from HIRS2/MSU sounding data 05 p0619 N88-13799
Complementary information between UV and IR for remote sensing of total ozone 05 p0619 N88-13800

Observation guidelines for a Total Ozone Mapping Spectrometer (TOMS) in geosynchronous orbit 05 p0619 N88-13801
Electric field measurements on Viking: First results [TRITA-EPP-87-04] 05 p0625 N88-13826
High Resolution Picture Transmission (HRPT) data processing from NOAA series satellites [INPE-4372-PRE/1195] 08 p0963 N88-15831
Limiting accuracy of scatterometer determination of wind speed over ocean from satellite 08 p1007 N88-16107
The German scientific balloon and sounding rocket program 08 p1024 N88-16202
Viking: The first Swedish satellite 08 p1025 N88-16207
Report on ground-based activity at Andoya (Norway) in relation to the Aureld-VIP high rocket and to the Viking satellite --- Swedish satellite 08 p1026 N88-16212
Vertical atmospheric sounding [INPE-4370-PRE/1195] 08 p1036 N88-16283
Microphysics of the auroral acceleration region of other regions of the magnetosphere 08 p1096 N88-16592
Preliminary results from the dc electric field experiment on Viking --- Swedish satellite [TRITA-EPP-87-03] 09 p1190 N88-17130
Roys and radiosondes in the region [INPE-4362-PRE/1188] 13 p1796 N88-20743
Satellite gradiometry [B8735057] 16 p2229 N88-23313
Simultaneous observation of upward moving field aligned energetic electrons and ions on auroral zone field lines [IRF-PREPRINT-102] 16 p2231 N88-23326
Some problems with regard to the TOVS processing detected by using NOAA-HRPT data check program 17 p2351 N88-24009
Processing of HRPT data from the NOAA series satellites 17 p2359 N88-24053
Tiros operational vertical sounder (TOVS) and radiosonding in the region 17 p2360 N88-24059
Suggested hurricane operational scenario for GOES I-M [NASA-TM-89729] 19 p2692 N88-26002
Field-aligned structure of the storm time Pc 5 wave of November 14-15, 1979 [AD-A193022] 21 p2972 N88-27653
Snapshots of high-latitude electrodynamics using Viking and DMSP/F7 observations [TRITA-EPP-88-01] 23 p3234 N88-29244
Possibilities of determining vertical profiles of microphysical characteristics of stratospheric aerosol using space measurements of transparency and solar halo 24 p3449 N88-30526

SATELLITE SURFACES
NT LUNAR SURFACE

SATELLITE TELEVISION
The role of the L-Sat program in the evolution of European communications satellites 09 p1127 N88-16758
Image processing on VEGA pictures 14 p2009 N88-21983

SATELLITE TEMPERATURE
COS-B in-orbit study [ESA-CR(P)-2420] 01 p0017 N88-10102
Thermal analysis in steady state conditions for satellites [INPE-4429-TDL/309] 12 p1599 N88-19574
A study of satellite emission computed tomography [AD-A189567] 13 p1797 N88-20745
Far infrared spectroscopy telescope (FIRST) inflatable thermal shield, phase 1 [SR/FIS/108(87)CZ] 24 p3453 N88-30552

SATELLITE TRACKING
NT SATELLITE-TO-SATELLITE TRACKING
Precise orbit computation, gravity model adjustment and altimeter data processing for the ERS-1 altimetry mission [ESA-CR(P)-2436] 02 p0130 N88-10820
Research in geodesy based upon radio interferometric observations of GPS (Global Positioning System) satellites [AD-A184040] 03 p0346 N88-12187
Optimized tracking of RF carriers with phase noise, including Pioneer 10 results 04 p0434 N88-12694
An intelligent tutor for the space domain 09 p1204 N88-17217
Estimation of geopotential from satellite-to-satellite range rate data: Numerical results [NASA-CR-180771] 14 p1941 N88-21583
Baseline estimation from simultaneous satellite laser tracking [NASA-CR-182750] 15 p2022 N88-22052
A low cost automatic Earth observation satellite tracking ground receiving station 17 p2309 N88-23815
The Telecommunications and Data Acquisition Report [NASA-CR-183131] 22 p3063 N88-28178
The limits of direct satellite tracking with the Global Positioning System (GPS) 22 p3064 N88-28179
Approximation of atmospheric density by Chebyshev polynomials in predicting motion of low artificial earth satellites 24 p3445 N88-30503

SATELLITE TRANSMISSION
Implications of a simplified signal structure for Navsat [REPT-63/1439] 01 p0005 N88-10024
The Black College satellite telecommunications network planning in support of energy-related collaborative research [DE88-000182] 03 p0307 N88-11940
Propagation effects on satellite systems at frequencies below 10 GHz: A handbook for satellite systems design [NASA-RP-1108/2] 06 p0690 N88-14226
The role of the L-Sat program in the evolution of European communications satellites 09 p1127 N88-16758
MARCE data evaluation 10 p1286 N88-17693
Construction of a satellite simulator for the frequency range between 11.7 and 12.5 GHz [IRT-TB-B-84/87] 16 p2166 N88-22917
Atmospheric corrections for in-flight satellite radiometric calibration [AD-A196124] 24 p3391 N88-30194

SATELLITE-BORNE INSTRUMENTS
NT ADVANCED VERY HIGH RESOLUTION RADIOMETER
NT TOTAL OZONE MAPPING SPECTROMETER
A VAS-numerical model impact study using the Gal-Chen variational approach --- Visible Infrared Spin-Scan Radiometer Atmospheric Sounder (VAS) 02 p0213 N88-11339
Planning for future operational sensors and other priorities [PB87-220802] 03 p0325 N88-12056
The CNR/PSN Advanced Microwave Imaging Radiometer (AMIR) --- satellite-borne 03 p0340 N88-12141
Absolute and interband calibration --- SPOT 03 p0341 N88-12152
The new generation of SPOT satellites 03 p0345 N88-12178
Evaluation of a cryogenic refrigerator for cooling focal plane instrumentation --- satellite instruments [BAE-TP-8095-VOL-1] 05 p0572 N88-13485
Evaluation of a cryogenic refrigerator for cooling focal plane instrumentation. Appendix B: Accommodation study --- satellite instruments [BAE-TP-8095-VOL-2] 05 p0572 N88-13486
Development of response models for the Earth Radiation Budget Experiment (ERBE) sensors. Part 3: ERBE scanner measurement accuracy analysis due to reduced housekeeping data [NASA-CR-178294] 05 p0583 N88-13553
HIRIS (High-Resolution Imaging Spectrometer: Science opportunities for the 1990s. Earth observing system. Volume 2C: Instrument panel report [NASA-TM-89703] 07 p0871 N88-15282
LANDSAT thematic mapper radiometric calibration study [NASA-CR-182410] 07 p0872 N88-15287
Alouette-ISIS program summary [NASA-CR-180747] 08 p1023 N88-16195
Contribution of stratospheric balloon flights in space biology 08 p1033 N88-16266
Design feasibility report on investigation of magnetic bearings for the ocean colour monitor radiometer scanner [BAE-TP-7849] 09 p1174 N88-17036
Statistical studies of low frequency oscillations in satellite-observed stratospheric temperatures 10 p1353 N88-18086
High efficiency, long life traveling wave tubes for future communications satellites [NASA-TM-100837] 12 p1598 N88-19565
Spaceborne gravity gradiometry characterizing the data type 12 p1644 N88-19847
GRADIO three-axis electrostatic accelerometers 12 p1645 N88-19849
Gradiometer accommodation on board a drag-free satellite 12 p1645 N88-19850
Concept of an Opto-electronic Accelerometer System (OAS) 12 p1645 N88-19852
Polar mesospheric cloud experiment [AD-A188936] 12 p1648 N88-19872
The bit-error rate performance of a satellite microwave matrix switch [NASA-TM-100285] 16 p2167 N88-22920
Prospects of satellite wind sensing systems in the years 1995-2000 17 p2350 N88-24004
The high-throughput X-ray spectroscopy mission E6889478 MN513835 --- ESA program [ESA-SP-1092] 17 p2450 N88-24554
The French spaceborne oceanography program 19 p2701 N88-26058
The Oak Ridge National Laboratory strategic defense initiative shield optimization program: Executive summary [DE88-008016] 20 p2847 N88-26899
Basic research for the geodynamics program [NASA-CR-183149] 21 p2973 N88-27662

SATELLITE-BORNE PHOTOGRAPHY
Evaluation of digital, multitemporal LANDSAT 5 thematic mapper data for the determination of the aerial snowcover extent and spectral separation of various surface types in the inner Oetztal (West Germany) with special regard to the significance of aerial snowcover information for water resources management [DFVLR-FB-86-46] 03 p0345 N88-12180
Varifront 3 expedition data report (USNS DE STEIGUER CRUISE 1202-82). Bioluminescence, hydrographic, nutrient, and satellite data from the Gulf of California (November-December 1981) [AD-A185011] 05 p0620 N88-13805
Modeling cloudy and clear interval length probabilities using space shuttle imagery [AD-A185290] 05 p0627 N88-13837
Investigations on the application of space photographs (Spacelab metric camera) for routine inventories of extensively managed forest areas [DFVLR-FB-87-22] 09 p1185 N88-17098
Oceanographic features of the east and southeast Indian Ocean for June 1983 [AD-A186948] 09 p1195 N88-17158
An objective technique for Arctic cloud analysis using multispectral AVHRR (Advanced Very High Resolution Radiometer) satellite imagery [AD-A194732] 23 p3235 N88-29250
Structure of eastern Turkestan Ridge based on space photographs 24 p3450 N88-30530

SATELLITE-BORNE RADAR
Review of inversion techniques for spaceborne lidar systems [AD-A184164] 04 p0447 N88-12772
The role of space borne imaging radars in environmental monitoring: Some shuttle imaging radar results in Asia [NASA-TM-101175] 20 p2789 N88-26544

SATELLITE-TO-SATELLITE TRACKING
A study of a satellite-to-satellite tracking configuration by application of linear perturbation theory [REPT-86.3] 01 p0011 N88-10059
Study of a satellite-to-satellite tracking gravity mission [ESA-CR(P)-2419] 02 p0198 N88-11237
An orbit simulation study of a geopotential research mission including satellite-to-satellite tracking and disturbance compensation systems [NASA-CR-182353] 07 p0823 N88-14997
Continued design of a Pointing, Acquisition, and Tracking (PAT) subsystem for InterSatellite Laser links (ISL2) [TELDIX-15-093-178] 14 p1905 N88-21384

SATELLITES
Toward a comprehensive theory for the sweeping of trapped radiation by inert orbiting matter [NASA-CR-182584] 11 p1569 N88-19395

SATURABLE REACTORS
Low power consumption current transducer [NASA-CASE-NPO-16888-1-CU] 17 p2335 N88-23937

SATURATED HYDROCARBONS
U ALKANES

SATURATION
Design for performance enhancement in feedback control systems with multiple saturating nonlinearities [NASA-CR-182614] 11 p1535 N88-19168
Design of feedback control systems for stable plants with saturating actuators [NASA-CR-182613] 12 p1681 N88-20050
Measurements of optical nonlinearities in MOCVD-grown GaAs/GaAlAs multiple quantum wells 14 p1975 N88-21787
Saturation and the limit of jet mixing enhancement by single frequency plane wave excitation: Experiment and theory [NASA-TM-100882] 17 p2295 N88-23732

SATURATION (CHEMISTRY)
Optimizing the application of high temperature corrosion resistant aluminium-silicon-base coatings [BLL-M-37222-(5828.4)] 01 p0018 N88-10112

SATURN
Astron observations of supernova 1987A in large magellanic cloud 24 p3445 N88-30504

SATURN ATMOSPHERE
An analysis of longitude variations in the equatorial spectrum of Saturn 10 p1430 N88-18539
Extended atmospheres of outer planet satellites and comets [NASA-CR-181449] 10 p1430 N88-18540
Extended atmospheres of outer planet satellites and comets [NASA-CR-183157] 24 p3457 N88-30572

SATURN RINGS
Study of a Radio Relay Link (RRL). Cassini mission. Data package for final presentation
[ESA-CR(P)-2472] 07 p0847 N88-15138
Simulation of the plasma interaction with thin dust clouds 11 p1552 N88-19291
Dynamical and photometric studies of Saturn's rings
12 p1711 N88-20241
Voyager imaging photometry and radiative transfer modeling of the spoke-like features in Saturn's outer B-ring 19 p2742 N88-26278
SATURN SATELLITES
NT TITAN
Extended atmospheres of outer planet satellites and comets
[NASA-CR-181449] 10 p1430 N88-18540
SAVANNAHS
U GRASSLANDS
SCALARS
Scalar densities and baryon mass differences in lattice QCD with Wilson fermions
[PREPRINT-544] 06 p0778 N88-14773
The application of vector diffraction to the scalar anomalous diffraction approximation of Van de Hulst
[AD-A185930] 07 p0929 N88-15643
On the expectation of the product of four matrix-valued Gaussian random variables
[EUT-87-E-178] 13 p1828 N88-20927
Direct numerical simulation of buoyantly driven turbulence 16 p2196 N88-23097
Existence of periodic solutions in n-dimensional retarded functional differential equations
[RR-325] 17 p2392 N88-24221
Direct numerical simulations of the PDF's (Probability Density Functions) of a passive scalar in a forced mixing layer
[AD-A192134] 18 p2568 N88-25256
The covariance of scalar fields scattered by pressure-release randomly rough surfaces
[AD-A192489] 22 p3146 N88-28714
SCALE (CORROSION)
Carbon dioxide treatment for scale removal and control in potable water systems
[AD-A184346] 04 p0412 N88-12556
Beneficial and detrimental effects of silica in the high temperature oxidation of 20Cr/25Ni/Nb stainless steel
[AERE-R-12667] 10 p1301 N88-17779
Point defect structure of Cr2O3
[AD-A187620] 11 p1556 N88-19317
SCALE (RATIO)
Detection of critical points: The first step to automatic line generalization 05 p0619 N88-13803
SCALE EFFECT
Cavitation inception scale effects. 1. Nuclei distributions in natural waters. 2. Cavitation inception in a turbulent shear flow
[AD-A186553] 08 p0988 N88-15987
Dynamic interaction of convective cumulus with large-scale environment
[MITT-55] 20 p2827 N88-26773
Size effects in linear elastic fracture mechanics
21 p2964 N88-27609
SCALE HEIGHT
An analysis of apparent-motion vectors in, and the structure of, A mid-latitude sporadic E layer using a 2.66 MHz radar
[AD-A186126] 07 p0877 N88-15321
SCALE MODELS
Evaluation of a scale-model experiment to investigate long-range acoustic propagation
[NASA-TP-2748] 02 p0230 N88-11450
Underwater acoustic backscatter from a model of arctic ice open leads and pressure ridges
[AD-A184693] 03 p0354 N88-12234
A 0.15-scale study of configuration effects on the aerodynamic interaction between main rotor and fuselage
[NASA-CR-166577] 04 p0395 N88-12462
Analytical investigation of the dynamics of tethered constellations in Earth orbit (phase 2)
[NASA-CR-179218] 04 p0408 N88-12533
Measurement of model deformation in wind tunnels
05 p0551 N88-13358
A system identification technique based on the random decrement signatures. Part 2: Experimental results
05 p0594 N88-13626
On the subgrid-scale modeling of compressible turbulence
[NASA-CR-178420] 06 p0702 N88-14309
ASSESS-2: An aircraft simulation of Spacelab
09 p1123 N88-16723
Aerodynamic performance of a scale-model, counter-rotating unducted fan 10 p1282 N88-17666
The assessment of the sound insulation requirements for a large broadcasting studio, using a scale model: Practical details
[BBC-RD-1987/21] 10 p1318 N88-17878
Application of similarity techniques between reduced and natural scale models of Ramjet engines
[INPE-4269-PRE/1142] 11 p1441 N88-18595
Sub-scaling of projectile/target system damaged by hypervelocity
[AD-A188683] 12 p1634 N88-19779
An investigation of classical dynamic scaling techniques applied to an oleo-pneumatic landing gear strut
[AD-A187664] 13 p1721 N88-20292
Scale model development for aeroelasticity studies
[ETN-88-91887] 14 p1868 N88-21164
Space station full-scale docking/berthing mechanisms development 14 p1927 N88-21491
Visualization of the air flowing through a dynamic model of the vocal folds
[ISVR-TR-154] 14 p1952 N88-21634
Model-scale sound propagation experiment
[NASA-TM-100602] 15 p2130 N88-22709
MPD (magnetoplasmadynamic) thruster advanced pumping system concepts
[AD-A190513] 15 p2138 N88-22756
Limits of design feasibility of multiwing wind turbines with individual articulated wing structure
[ILR-MITT-180] 18 p2537 N88-25052
Frequency domain identification of the dynamics of a scaled remotely-piloted helicopter
20 p2786 N88-26524
Flow visualization on a small scale
[AD-A194728] 23 p3181 N88-28935
Model test of air-exchange efficiency
[DE88-752862] 23 p3201 N88-29049
Test of an 0.8-scale model of the AH-64 Apache in the NASA Langley full-scale wind tunnel
[AD-A196129] 24 p3319 N88-29768
SCALERS
Multichannel scaling analyzer
[DE88-700541] 07 p0905 N88-15481
SCALING
A multiple-time-scale turbulence model based on variable partitioning of turbulent kinetic energy spectrum
[NASA-CR-179222] 04 p0444 N88-12754
Transport scaling in the collisionless-detrapping regime in stellarators
[DE88-001511] 05 p0653 N88-14006
Collider constraints in the choices for wavelength and gradient scaling
[PB87-123691] 06 p0779 N88-14783
On the smallest scale for the incompressible Navier-Stokes equations
[NASA-CR-181628] 11 p1434 N88-18558
The scaling of the threshold conditions for solid propellant erosive burning 19 p2630 N88-25601
SCALING LAWS
Reynolds number effects on the small scale structure of a turbulent channel flow 01 p0001 N88-10004
An analysis of an available set of linear programming test problems
[DE87-014578] 02 p0221 N88-11392
Relative merits of size, field, and current on ignited Tokamak performance: A comparison of CITs and Super-JETs
[DE88-000038] 02 p0241 N88-11521
Finite size scaling and lattice gauge theory
[DE87-014139] 02 p0245 N88-11549
An experimental investigation of unsteadiness in swept shock wave/turbulent boundary layer interactions
04 p0445 N88-12760
Improvement of modal scaling factors using mass additive technique 05 p0593 N88-13620
Nonlinear evolution equations, rescalings, model partial differential equations (PDES) and their integrability, 2
[PREPRINT-560] 06 p0764 N88-14691
The effect of response scaling on the detection of singularities in multiresponse estimation
[AD-A185964] 07 p0908 N88-15503
Anomalous scaling laws in multifractal objects
[NOTA-INTERNA-883] 07 p0916 N88-15565
A crude scaling law for lasertrons
[DE88-003880] 09 p1173 N88-17032
Plasma physics design and major specifications of candidate reactors for FER design studies. Conceptual design study of FY86 FER
[DE88-751066] 10 p1411 N88-18416
Atomic-scale simulation in materials science
[DE88-005204] 11 p1544 N88-19230
Cavitation inception
[AD-A189220] 13 p1765 N88-20557
Similarity theories and microturbulence in the atmospheric mixed layer 13 p1806 N88-20802
Scale model development for aeroelasticity studies
[ETN-88-91887] 14 p1868 N88-21164
Transport processes during directional solidification and crystal growth: Scaling and experimental study
14 p1988 N88-21857
Pusherless implosion, pulse tailoring and ignition scaling law for laser fusion 16 p2277 N88-23629
Scaling laws for homogeneous turbulent shear flows in a rotating frame
[NASA-CR-181672] 19 p2665 N88-25847
Scaling laws for geomagnetic tail current sheet acceleration
[AD-A193379] 19 p2691 N88-25998
The scaled-sized model: A revision of Amdahl's law
[DE88-008114] 20 p2844 N88-26875
Optimization and scale-up performance of polymer electrolyte batteries
[AD-A193987] 22 p3073 N88-28243
Faster scaling algorithms for network problems
[AD-A194032] 23 p3251 N88-29348
SCANNERS
NT COASTAL ZONE COLOR SCANNER
NT HORIZON SCANNERS
NT INFRARED SCANNERS
NT MULTISPECTRAL BAND SCANNERS
NT OCEAN COLOR SCANNER
NT OPTICAL SCANNERS
NT THEMATIC MAPPERS (LANDSAT)
NT ULTRASONIC SCANNERS
Fast dynamic studies with PC384-7B; system improvements and development of an automated blood sampling system --- tomography
[USIP-87-05] 01 p0075 N88-10481
Scene simulation for passive IR systems
02 p0137 N88-10861
Development of response models for the Earth Radiation Budget Experiment (ERBE) sensors. Part 3: ERBE scanner measurement accuracy analysis due to reduced housekeeping data
[NASA-CR-178294] 05 p0583 N88-13553
ISTP SBIR phase 1 Full-Sky Scanner. A feasibility study
[NASA-CR-180749] 10 p1333 N88-17964
Multidimensional system analysis of electro-optic sensors with sampled deterministic output
[AD-A187083] 10 p1408 N88-18399
Report on desktop publishing
[AD-A187698] 11 p1528 N88-19128
OCR vision system, an alternative to bar code
[DE88-003761] 15 p2149 N88-22828
Orbital navigation, docking and obstacle avoidance as a form of three dimensional model-based image understanding 17 p2388 N88-24194
Atmospheric autorotating imaging device
[NASA-CASE-NPO-17390-1-CU]
18 p2519 N88-24944
Use of modern scanner techniques in cartography
18 p2535 N88-25040
Fracture physics of delamination of composite materials
[AD-A192021] 19 p2609 N88-25482
Equipment for an advanced electron beam lithography system
[AD-A192956] 21 p2936 N88-27435
Parallel solutions to geometric problems on the scan model of computation
[AD-A192321] 21 p3004 N88-27819
Rapid-scanning Fourier transform spectrometer for studies of propagation of near-millimeter-wave radiation through clear air and fog
[AD-A193752] 22 p3070 N88-28219
SCANNING
NT CONICAL SCANNING
NT PANORAMIC SCANNING
NT RADAR SCANNING
NT RASTER SCANNING
Estimation filters with adaptive scanning time for flying target tracking
[ETN-87-90401] 01 p0036 N88-10232
Digital receiver structures and methods for the determination of the scanning frequency in modems for fast data transmission via telephone channels
[ETN-87-90429] 01 p0037 N88-10235
In-orbit calibration adjustment of the Nimbus-7 SMMR
[NASA-TM-100678] 05 p0614 N88-13773
AVIRIS scan drive design and performance
06 p0706 N88-14330
Quantifying some information processing aspects of the pilot's instrument crosscheck
[AD-A186114] 07 p0898 N88-15443
Scanning finite element calculation method
[PB87-143442] 08 p0995 N88-16017
High-speed assembly language (80386/80387) programming for laser spectra scan control and data acquisition providing improved resolution water vapor spectroscopy
[NASA-CR-4117] 08 p1053 N88-16355

Orbital navigation, docking and obstacle avoidance as a form of three dimensional model-based image understanding
08 p1061 N88-16406
Future television systems: Comparison of sequent ial and interlaced scanning
[BBC-RD-1987/18] 09 p1155 N88-16923
Soft maps for US Army electronic map background applications
[AD-A188427] 12 p1638 N88-19809
Systems for ultrasonic scanning, analysis and imagery
15 p2082 N88-22414
Flaw characterization in structural ceramics using scanning laser acoustic microscopy
15 p2082 N88-22415
Nondestructive evaluation of sintered ceramics
15 p2083 N88-22416
Three-dimensional flow visualization using laser-sheet scanning
16 p2203 N88-23143
Digitizing the traffic network of JOG 250 by scanning -- JOG 250 map
18 p2533 N88-25029
SEGMERGE: A scanline visible surface algorithm with adaptive span selection and inexpensive antialiasing
[DE88-009186] 20 p2836 N88-26826
Scanning tunneling microscopy as a surface chemical probe
[AD-A192710] 21 p2909 N88-27263
Investigations on multiport antennas for polarimetric and modal field scanning
[REPT-5-87] 23 p3205 N88-29073
Scanning electron microscopy study of adhesion in sea urchin blastulae
[NASA-CR-183136] 24 p3406 N88-30275

SCANNING DEVICES
U SCANNERS

SCANNING LASER ACOUSTIC MICROSCOPE (SLAM)
U ACOUSTIC MICROSCOPES

SCAR PROGRAM
U SUPERSONIC CRUISE AIRCRAFT RESEARCH

SCARS (GEOLOGY)
U EROSION

SCATHA SATELLITE
Survey of the Air Force P78-2 (SCATHA) satellite plasma wave data during electron gun operations
[AD-A191014] 16 p2168 N88-22926
A severe spacecraft-charging event on SCATHA in September 1982
[AD-A193007] 20 p2765 N88-26396
Ion gun generated electromagnetic interference on the SCATHA satellite
[AD-A195179] 24 p3335 N88-29853

SCATTER PROPAGATION
Active and passive remote sensing of ice
[AD-A186685] 09 p1195 N88-17162
Multiple scattering of waves in discrete random media
[AD-A191068] 18 p2499 N88-24823

SCATTERERS
U SCATTERING

SCATTERING
NT ACOUSTIC SCATTERING
NT ATMOSPHERIC SCATTERING
NT BACKSCATTERING
NT COHERENT SCATTERING
NT COMPTON EFFECT
NT ELASTIC SCATTERING
NT ELECTROMAGNETIC SCATTERING
NT ELECTRON SCATTERING
NT FORWARD SCATTERING
NT HALOS
NT INCOHERENT SCATTERING
NT INELASTIC SCATTERING
NT INVERSE SCATTERING
NT ION SCATTERING
NT LIGHT SCATTERING
NT MICROWAVE SCATTERING
NT MIE SCATTERING
NT NEUTRON SCATTERING
NT NUCLEAR SCATTERING
NT PROTON SCATTERING
NT RADAR SCATTERING
NT RAMAN SPECTRA
NT RAYLEIGH SCATTERING
NT RESONANCE SCATTERING
NT REVERBERATION
NT THOMSON SCATTERING
NT TROPOSPHERIC SCATTERING
NT WAVE SCATTERING
NT X RAY SCATTERING
Surface scattering characteristics and the measurement of particulate contamination
02 p0137 N88-10862
Theoretical atomic and molecular photophysics
[DE87-014249] 02 p0231 N88-11456
JPRS report: Science and technology. China
[JPRS-CST-87-034] 03 p0301 N88-11897
New physical explanation of phase-conjugate waves produced in backward stimulated scattering
03 p0302 N88-11900
Uniform geometrical theory of diffraction
03 p0303 N88-11911
Singularity expansion method: Target Resonances
03 p0303 N88-11912
Numerical modeling: Integral equation method
03 p0304 N88-11919
Experiments: Test range facilities, part 2
03 p0305 N88-11921
Anti-Stokes generation of 226 nm light
[DE88-001612] 05 p0589 N88-13590
Atomic beam studies of the interaction of hydrogen with transition metal surfaces
[DE88-000208] 05 p0648 N88-13970
Energy dependence of ion-induced sputtering yields of monatomic solids in the low energy region
[IPPJ-AM-52] 05 p0651 N88-13988
Helium atom surface scattering apparatus for studies of crystalline surface dynamics
[DE88-002104] 06 p0787 N88-14826
Raman spectroscopic investigations of Hg-Cd-Te melts
07 p0926 N88-15625
Scattering of optical radiation by bursting water particles in fog
09 p1236 N88-17410
High-temperature charge-density studies of CeO/sub 2-x/ using X-ray and neutron diffraction techniques
[DE88-002988] 09 p1257 N88-17536
Investigation of a ray-mode representation of the Green's function in a rectangular cavity
[PB88-131677] 11 p1469 N88-18763
Electromagnetic scattering by an exponentially distributed rough surface with the introduction of a rough surface generation technique
[AD-A189678] 14 p1906 N88-21392
Observation of anomalous low J-value Stokes and anti-Stokes lines in stimulated rotational Raman scattering over long air paths
[DE88-003756] 14 p1911 N88-21418
Exciton relaxation phenomena in a disordered system
14 p1978 N88-21802
The elastic properties of monoclinic ZrO2
[DE88-005920] 14 p1986 N88-21847
Experimental studies of elastic properties of crystals by Brillouin scattering
[DE88-005923] 14 p1986 N88-21848
Brillouin scattering and transmission electron microscopy studies of radiation-induced elastic softening, disordering and amorphization of intermetallic compounds
[DE88-005927] 14 p1987 N88-21850
Theory of the dissociation dynamics of small molecules on metal surfaces: Finite temperature studies
[DE88-006495] 15 p2132 N88-22716
The optical properties of aerosols
[AD-A191420] 16 p2176 N88-22972
K-pulse estimation from incomplete multiple-frequency scattering data and target identification
[AD-A190827] 16 p2190 N88-23061
Enhanced backscattering from rough surfaces
[AD-A190995] 16 p2190 N88-23063
An experimental study of the coherent under-ice reflectivity of sound in the Greenland Sea Marginal Ice Zone
18 p2548 N88-25125
Changes in seismic velocity and apparent attenuation due to isotropic and anisotropic scattering: Results from physical modeling
19 p2691 N88-25997
Solution of Faddeev-Yakubovsky differential equations by the finite-dimensional approximation method for four spinless particles in the 1 + 3 scattering problem
[DE87-702983] 19 p2719 N88-26145
Ray scattering from a collection of ice keels
[AD-A191757] 19 p2722 N88-26163
Microwave image understanding and its application to radar cross section management
20 p2788 N88-26542
The theory of electron-polar phonon scattering rates in semiconductor micro-structures
20 p2871 N88-27043
Radar information from the partial derivatives of the echo signal phase from a point scatterer
[AD-A193402] 21 p2933 N88-27415
The effect of particle properties on radiative heat transfer
24 p3350 N88-29941
Scattering impulse response synthesis using random noise illumination: Initial concept evaluation
[AD-A195086] 24 p3364 N88-30034
Finite-difference simulations of Rayleigh-wave scattering by shallow heterogeneity
[AD-A194961] 24 p3402 N88-30259

SCATTERING AMPLITUDE
On the spin structure of the elastic ppbar scattering amplitude
[NOTA-INTERNA-892] 06 p0778 N88-14772
Absorption, scattering, and thermal radiation by conductive fibers
[AD-A186105] 07 p0842 N88-15106
Eikonal solutions to optical model coupled-channel equations
[NASA-TP-2830] 24 p3428 N88-30402

SCATTERING COEFFICIENTS
High-sensitivity recording of weak reflected or scattered radiation by method of coherent intracavity reception with YAG:Nd(3+) laser
08 p1078 N88-16502
Active and passive remote sensing of ice
[AD-A186685] 09 p1195 N88-17162
Acoustic backscattering from bottom sediment at normal incidence in the laboratory
[AD-A186905] 09 p1242 N88-17443
Effect of translucence of engineering ceramics on heat transfer in diesel engines
[DE88-003732] 10 p1305 N88-17804
Atmospheric backscatter at 10.6 microns; a compendium of measurements made outside the United Kingdom by the airborne LATAS coherent laser radar velocimeter
[RSRE-87002] 12 p1631 N88-19763
The radar scattering coefficient as a function of forest stand parameters and viewing angle. An empirical study of the Pinus sylvestris L. in the Kootwijk forest (The Netherlands), extended with observations in the Speulder and Sprielder forest (The Netherlands)
[ETN-88-91348] 13 p1760 N88-20527
Ray scattering from a collection of ice keels
[AD-A191757] 19 p2722 N88-26163

SCATTERING CROSS SECTIONS
Ab initio methods for electron-molecule collisions
[DE87-011728] 01 p0092 N88-10598
Heavy-particle collisions in the plasma edge
[DE87-012928] 02 p0237 N88-11493
Applied nuclear science research and development
[LA-10915-PR] 03 p0374 N88-12355
Magnetic diffuse scattering
[DE87-013539] 04 p0489 N88-13014
Electromagnetic wave probing of Earth's environment
[NASA-CR-182358] 06 p0690 N88-14232
On the spin structure of the elastic ppbar scattering amplitude
[NOTA-INTERNA-892] 06 p0778 N88-14772
Cross section of resonant Raman scattering of light by polyenes
07 p0920 N88-15591
The application of vector diffraction to the scalar anomalous diffraction approximation of Van de Hulst
[AD-A185930] 07 p0929 N88-15643
Hyperspherical coordinate theory of two-electron processes: Future plans
[DE87-010653] 08 p1081 N88-16516
Status of cross section data for photon scattering by atoms
[DE87-011281] 08 p1081 N88-16517
Introductory review: Physics of electron slowing-down processes
[DE88-002918] 09 p1246 N88-17466
The application of the hybrid iterative method to scattering by perfectly conducting bodies of revolution
11 p1475 N88-18802
Single nucleon coincidence cross sections in a relativistic mean field theory
[CEBAF-PR-87-016] 11 p1546 N88-19243
An efficient numerical algorithm for solving scattering and inverse scattering problems of electromagnetic waves
[AD-A188479] 12 p1619 N88-19684
Experimental set-up for measurements of Compton scattering cross section on light nuclei
[DE88-700161] 12 p1688 N88-20097
Vibration spectra of oxygen and vanadium atoms in vanadium-oxygen disordered interstitial alloys
[DE87-703166] 13 p1740 N88-20404
Measurement of the sup 4He(gamma, p)sup 3H total cross section and charge symmetry
[NOTA-INTERNA-902] 14 p1981 N88-21820
Inelastic two composite particle systems scattering at high energy
[DE88-701841] 20 p2851 N88-26928
Effect of a laser field in the electron inelastic scattering into plasma fields
[DE88-702295] 23 p3218 N88-29157
Neutrino detection primer
[AD-A193805] 23 p3280 N88-29529

SCATTERING FUNCTIONS
Developments related to scattering eigen elements in Schroedinger operators for particles with spin
[ETN-88-91077] 09 p1229 N88-17361
Synchronous measurements of effective photon path length in visible and near-IR spectral regions in real cloud systems
13 p1790 N88-20706

SCATTERING MATRIX
U S MATRIX THEORY

SCATTEROMETERS
Study of a payload for Columbus Polar Platform Earth observation demonstration mission, executive summary
[ESA-CR(P)-2412] 01 p0014 N88-10079

Deployment, hold down and release mechanisms for Wind Scatterometer Antenna (WSA) --- ERS-1 wind scatterometer antenna (WSA) 14 p1876 N88-21207
Preparation and execution of calibration measurements for handling of airborne SAR data (AGRISAR)
[ETN-88-92338] 17 p2333 N88-23926
A study of the feasibility of using sea and wind information from the ERS-1 satellite. Part 1: Wind scatterometer data
[NASA-CR-182833] 24 p3386 N88-30167
A study of the feasibility of using sea and wind information from the ERS-1 satellite. Part 2: Use of scatterometer and altimeter data in wave modeling and assimilation
[ESA-CR(P)-2604-PT-2] 24 p3387 N88-30176

SCAVENGING
Auxiliary propulsion technology for advanced Earth-to-orbit vehicles
[NASA-TM-100237] 06 p0674 N88-14127
Atmospheric science 07 p0883 N88-15357
STS propellant scavenging systems study. Part 2, volume 1: Executive summary and study results
[NASA-CR-179275] 10 p1290 N88-17716
STS propellant scavenging systems study. Part 2, volume 2: Cost and WBS/dictionary
[NASA-CR-179276] 10 p1290 N88-17717
Weight savings in aerospace vehicles through propellant scavenging
[NASA-TM-100900] 19 p2605 N88-25470

SCENE ANALYSIS
The 3-D world modeling for an autonomous robot
[DE87-013878] 03 p0333 N88-12102
Methods for design and evaluation of integrated hardware/software systems for concurrent computation
[NASA-CR-181522] 04 p0479 N88-12953
Television motion measurement for DATV and other applications
[BBC-RD-1987/11] 05 p0573 N88-13496
Some vision algorithms 06 p0795 N88-14871
Proceedings of Image Understanding Workshop, volume 1
[AD-A186103] 07 p0902 N88-15463
Recognition of polyhedral objects under structured illumination
[PB88-106703] 07 p0932 N88-15661
Estimation of broadband planetary albedo from operational narrowband satellite measurements
[PB88-107644] 07 p0945 N88-15748
Thematic mapper research in the earth sciences: Small scale patches of suspended matter and phytoplankton in the Elbe River Estuary, German Bight and Tidal Flats
[NASA-CR-182378] 08 p1019 N88-16180
Image chunking: Defining spatial building blocks for scene analysis
[AD-A187072] 09 p1200 N88-17191
Development of Moire machine vision
09 p1212 N88-17264
General determination of Earth surface type and cloud amount using multispectral AVHRR data
[NOAA-TR-NESDIS-39] 11 p1506 N88-18997
Three-dimensional scene analysis using stero based imaging
[AD-A193120] 21 p2894 N88-27178

SCF
U SELF CONSISTENT FIELDS

SCHEDULES
The development of laboratory vibration test schedules: Philosophies and techniques 08 p0999 N88-16049
Laboratory vibration test schedules development beyond MIL-STD-810D 08 p0999 N88-16050
Operational aspects of a spacecraft planning/scheduling expert system
08 p1062 N88-16415
Timetable control in a management system (space program) 22 p3160 N88-28815
Inflight rearming
[AD-A193564] 23 p3176 N88-28909

SCHEDULING
NT PREDICTION ANALYSIS TECHNIQUES
A rule-based system for arrival sequencing and scheduling in air traffic control 02 p0129 N88-10815
Optimal pre-scheduling of problem remappings
[NASA-CR-178378] 06 p0756 N88-14633
On stochastic optimality of policies in first passage problems
[AD-A186293] 07 p0915 N88-15554
Third Conference on Artificial Intelligence for Space Applications, part 1
[NASA-CP-2492-Pt-1] 08 p1055 N88-16360
Intelligent process development of foam molding for the Thermal Protection System (TPS) of the space shuttle external tank 08 p1060 N88-16397
Knowledge-based simulation
08 p1061 N88-16404
Planning and scheduling for robotic assembly
08 p1062 N88-16416
An AI approach for scheduling space-station payloads at Kennedy Space Center 08 p1064 N88-16425
Scheduling spacecraft operations
08 p1064 N88-16426
The resource envelope as a basis for space station management system scheduling
08 p1064 N88-16427
Prototype resupply scheduler
08 p1064 N88-16428
Performance analysis of parallel branch and bound search with the hypercube architecture
09 p1206 N88-17229
Expert mission planning and replanning scheduling system for NASA KSC payload operations
09 p1209 N88-17247
Range and mission scheduling automation using combined AI and operations research techniques
09 p1209 N88-17249
Nonpreemptive run-time scheduling issues on a multitasked, multiprogrammed multiprocessor with dependencies, bidimensional tasks, folding and dynamic graphs
[DE88-003598] 09 p1223 N88-17335
A note on the effect of preemptive policies on the stability of a priority queue
[AD-A186871] 09 p1227 N88-17345
An evaluation of project scheduling techniques in a dynamic environment
[AD-A187057] 09 p1260 N88-17554
Dynamic processor self-scheduling for general parallel nested loops
[DE88-003572] 10 p1393 N88-18311
Deadlock prevention in processor self-scheduling for parallel nested loops
[DE88-003573] 10 p1393 N88-18313
A traveling-salesman-based approach to aircraft scheduling in the terminal area
[NASA-TM-100062] 12 p1576 N88-19424
Schedule and cost control of development
12 p1704 N88-20196
Approximation algorithms for scheduling unrelated parallel machines
[CWI-OS-R8714] 13 p1817 N88-20861
Satellite acquisition: Global positioning system acquisition changes after Challenger's accident
[PB88-155536] 14 p1880 N88-21236
Discrete generalized networks: Application to integer constrained flow problems
[AD-A190823] 16 p2190 N88-23060
Elementary and middle school science improvement project
[NASA-CR-179328] 16 p2285 N88-23679
Performance effectiveness and the work/rest cycle
[AD-A191448] 18 p2551 N88-25145
A mixed-integer linear programming problem which is efficiently solvable
[AD-A191028] 18 p2556 N88-25168
LRS-2: A specialized knowledge system for launch resource scheduling
[AD-A194625] 23 p3182 N88-28941
A knowledge-based decision support system for payload scheduling 23 p3252 N88-29358
A scheduling and resource management system for space applications 23 p3255 N88-29383
A space station onboard scheduling assistant
23 p3259 N88-29402
NOA: A Network Operator Assistant for scheduling Tracking and Data Relay Satellite System (TDRSS)
23 p3259 N88-29403
Experiment scheduling for Spacelab missions
23 p3259 N88-29404
A static scheduler for the computer aided prototyping system: An implementation guide
[AD-A194340] 24 p3414 N88-30322
Contingency rescheduling of spacecraft operations
24 p3416 N88-30337
Knowledge based tools for Hubble Space Telescope planning and scheduling: Constraints and strategies
24 p3417 N88-30338
The proposal entry processor: Telescience applications for Hubble Space Telescope science operations
24 p3417 N88-30339
Candidate functions for advanced technology implementation in the Columbus mission planning environment 24 p3417 N88-30340
Integrated resource scheduling in a distributed scheduling environment 24 p3417 N88-30342
Lisp Object State Saver (LOSS): A facility used to save partial schedules of the Hubble Space Telescope
24 p3421 N88-30360
The P-3 Scheduling Support System (P-3 S3)
[AD-A194824] 24 p3436 N88-30450

SCHEMATICS
U CIRCUIT DIAGRAMS

SCHIFF BASES
U IMINES

SCHIZOPHRENIA
Information processing deficits in psychiatric populations: Implications for normal workload assessment 16 p2241 N88-23390

SCHLIEREN PHOTOGRAPHY
Development of flow visualization techniques for use in the Hot Gas Laboratory
[BAE-ARG-233] 03 p0325 N88-12052
Development of an optical diagnostic instrument. Part 2: Instrument development --- space laboratories
[NLR-TR-87079-L-PT-2] 13 p1841 N88-21016

SCHOOLS
A summary of the Naval Postgraduate School research program
[AD-A186362] 07 p0942 N88-15727
Elementary and middle school science improvement project
[NASA-CR-179328] 16 p2285 N88-23679

SCHOTTKY BARRIER DIODES
U SCHOTTKY DIODES

SCHOTTKY DIODES
Study and realization of Schottky diodes for forthcoming integrated hyperfrequency devices
[LAAS-87-062] 02 p0167 N88-11054
Comparative investigation of heterodyne mixers at 1000 GHz
[FTL-068627] 09 p1158 N88-16940
Development of a high speed InGaAs/InP Schottky barrier photodetector for millimeter-wave fiber optical links
[AD-A188594] 12 p1629 N88-19750
Characterization of enhanced Schottky-barrier InGaAs/Al(1-x)As strained channel modulation-doped field-effect transistors
[AD-A188820] 12 p1698 N88-20162
The influence of current stressing on the structure of Ag contacts to GaAs
[DE88-005988] 15 p2140 N88-22771
Research investigation directed toward extending the useful range of the electromagnetic spectrum
[AD-A190198] 17 p2332 N88-23920
Research investigation directed toward extending the useful range of the electromagnetic spectrum, appendix
[AD-A190199] 17 p2332 N88-23921
Novel silicon Schottky barrier infrared imaging arrays
17 p2439 N88-24510
Schottky-barrier formation on a covalent semiconductor without Fermi-level pinning: The Metal-MoS2(0001) interface
[AD-A193044] 21 p3021 N88-27931
Blue-green laser diode research program
[AD-A191980] 23 p3218 N88-29153

SCHOTTKY EFFECT
U WORK FUNCTIONS

SCHROEDINGER EQUATION
Numerical studies of the dual HEMT/algorithm development and numerical studies of Schrodinger's equation
[AD-A184471] 04 p0478 N88-12946
Darboux and Baecklund transformations for the Schroedinger equation
[PREPRINT-545] 06 p0763 N88-14685
Equations of nonlinear Schroedinger type in 1 + 1 and 2 + 1 dimensions, obtained from integrable Partial Differential Equations (PDEs)
[PREPRINT-548] 06 p0764 N88-14687
Nonisospectral deformations and Darboux transformations for the 3rd order spectral problem
[PREPRINT-558] 06 p0764 N88-14690
The inverse back scattering problem for the Schroedinger equation in two space dimensions
[AD-A185603] 06 p0765 N88-14701
Modified quantum mechanics of small composite systems
[NIKHEF-H/87-1] 06 p0790 N88-14845
Developments related to scattering eigen elements in Schroedinger operators for particles with spin
[ETN-88-91077] 09 p1229 N88-17361
On exact solutions of multidimensional Schroedinger equation with polynomial potentials
[DE88-700460] 09 p1230 N88-17373
Further study of relation of von Karman equation for elastic large deflection problem and Schrodinger equation for quantum eigenvalues problem
14 p1899 N88-21341
Geometric methods and the gauge structure of Berry's phase
[DE88-006538] 15 p2127 N88-22682
Free Laplacian with attractive boundary conditions
[DE87-702971] 16 p2256 N88-23482
Combining relativity and quantum mechanics: Schroedinger's interpretation of psi
[DE88-701899] 20 p2880 N88-27102
Cauchy problem for the nonlinear Schroedinger equation
[DE88-702454] 21 p3011 N88-27867

SCHUMANN-RUNGE BANDS

Aeronomic problems of the molecular oxygen photodissociation. Part 3: Solar spectral irradiances in the region of the O2 Herzberg continuum, Schumann-Runge bands and continuum
[AERONOMICA-ACTA-A-332-1988] 24 p3343 N88-29897

Aeronomic problems of molecular oxygen photodissociation. Part 2: Theoretical absorption cross sections of the Schumann-Runge bands at 79 K
[AERONOMICA-ACTA-A-331-1988] 24 p3344 N88-29907

SCHWARTZ INEQUALITY

Baecklund transformation and the Schwarzian derivative
[AD-A190277] 15 p2127 N88-22684

SCHWARZSCHILD METRIC

Criterion of singularity in general theory of relativity
09 p1240 N88-17430

SCIENCE

Interdisciplinary research in mathematics, science and technology education
[PB88-131446] 10 p1398 N88-18333

SCIENTIFIC SATELLITES

NT AMPTE (SATELLITES)
NT ASTRONOMICAL SATELLITES
NT AZUR SATELLITE
NT COSMIC BACKGROUND EXPLORER SATELLITE
NT DYNAMICS EXPLORER 1 SATELLITE
NT EXOSAT SATELLITE
NT EXPLORER SATELLITES
NT EXPLORER 47 SATELLITE
NT EXPLORER 51 SATELLITE
NT EXPLORER 54 SATELLITE
NT EXPLORER 55 SATELLITE
NT GAMMA RAY OBSERVATORY
NT GEOPOTENTIAL RESEARCH MISSION
NT HUBBLE SPACE TELESCOPE
NT INTERNATIONAL SUN EARTH EXPLORER 3
NT INTERNATIONAL SUN EARTH EXPLORERS
NT MAGSAT SATELLITES
NT SOLAR MESOSPHERE EXPLORER
NT SPACE INFRARED TELESCOPE FACILITY
NT UK SATELLITES
NT X RAY ASTROPHYSICS FACILITY

Report on the scientific satellites of the European Space Agency
[ESA-SP-1090] 01 p0014 N88-10081

Viking quick look plots: A short description --- Swedish satellite 06 p0692 N88-14243

Analysis and interpretation of satellite fragmentation data 06 p0798 N88-14885

Viking: The first Swedish satellite
08 p1025 N88-16207

MAXIE 1
[AD-A189688] 14 p1882 N88-21247

Evaluating evaporation with satellite thermal data
[AD-A192042] 18 p2531 N88-25019

MAXIE-1 (Magnetospheric Atmospheric X-ray Imaging Experiment)
[AD-A192846] 21 p2902 N88-27221

SCIENTISTS

Report from the MPP Working Group to the NASA Associate Administrator for Space Science and Applications
[NASA-TM-87819] 02 p0223 N88-11402

On the occasion of the 50th anniversary of the death of Professor Hugo Junkers
[MBB/LW-3016/S/PUB/201] 02 p0257 N88-11627

National Center for Atmospheric Research
[PB87-228391] 04 p0470 N88-12901

A study of the minority college programs at the NASA Johnson Space Center 06 p0798 N88-14887

Research reports: 1987 NASA/ASEE Summer Faculty Fellowship Program
[NASA-CR-179219] 07 p0922 N88-15601

Networking requirements and future alternatives
[NASA-TM-89711] 10 p1426 N88-18517

SCINTILLATION

A comparative analysis of equatorial and auroral-zone phase scintillation data
[AD-A184509] 03 p0350 N88-12212

Study on cineradiography
[ISL-R-120/86] 08 p0990 N88-15994

F-layer polar cap arcs
[AD-A186592] 09 p1190 N88-17127

An assessment of the application of in situ ion-density data from DMSP to modeling of transionospheric scintillation
[AD-A188919] 12 p1643 N88-19840

Analysis of the inter-layer independence of stellar scintillometer profiles of Cn2
[AD-A189372] 12 p1645 N88-19854

Measurements of the scintillation time constants of inorganic crystals for the development of a triple-Phoswich detector for high-energy X-ray quanta
[ETN-88-91501] 14 p1993 N88-21875

Stellar scintillometer atmospheric optical turbulence profiling experiment: A qualitative comparison of two identical instruments at AMOS (Air Force Maui Optical Station), 1985
[AD-A190589] 15 p2094 N88-22479

Design, fabricate, calibrate, test and deliver two satellite electron flux detectors
[AD-A190799] 16 p2169 N88-22930

Radio-wave scintillations and ionospheric irregularities at high latitudes
[AD-A192140] 18 p2501 N88-24837

Spectral estimation of received phase in the presence of amplitude scintillation 22 p3064 N88-28180

SCINTILLATION COUNTERS

A layered scintillation detector for solar neutron observations
[DE87-011354] 01 p0049 N88-10314

A 15 cm aperture LED scintillometer for C(n) squared and crosswind measurements
[KNMI-WR-87-3] 01 p0070 N88-10448

A program to study antiprotons in the cosmic rays: Arizona collaboration
[NASA-CR-180702] 01 p0120 N88-10764

Multichannel electron counter with high space resolution
[DE88-700564] 07 p0857 N88-15204

The response of a small liquid scintillation counter for low energy (gamma, p) experiments
[NOTA-INTERNA-901] 14 p1980 N88-21819

Measurements of the scintillation time constants of inorganic crystals for the development of a triple-Phoswich detector for high-energy X-ray quanta
[ETN-88-91501] 14 p1993 N88-21875

Stellar scintillometer atmospheric optical turbulence profiling experiment: A qualitative comparison of two identical instruments at AMOS (Air Force Maui Optical Station), 1985
[AD-A190589] 15 p2094 N88-22479

Study of light transmission methods from scintillators to optical fiber with wave length shifter
[DE88-701587] 18 p2574 N88-25292

SCINTILLATORS

U SCINTILLATION COUNTERS

SCINTILLOMETERS

U SCINTILLATION COUNTERS

SCISSION

U CLEAVAGE

SCORPIO CONSTELLATION

U SCORPIUS CONSTELLATION

SCORPIUS CONSTELLATION

The angular diameter of alpha Scorpii in the near-infrared Ca II triplet 04 p0514 N88-13162

SCOTLAND

SeaSoar profiles in the Iceland-Scotland area, May 1987
[IOS-253] 18 p2548 N88-25124

SCPC TRANSMISSION

U SINGLE CHANNEL PER CARRIER TRANSMISSION

SCRAMJET ENGINES

U SUPERSONIC COMBUSTION RAMJET ENGINES

SCRAMJETS

U SUPERSONIC COMBUSTION RAMJET ENGINES

SCREEN EFFECT

Sensitivity of F-106B leading-edge-vortex images to flight and vapor-screen parameters
[NASA-TP-2818] 17 p2300 N88-23760

SCREW DISLOCATIONS

The effects of thin anodic films on the cyclic microstrain/macrostrain behavior of tungsten
05 p0597 N88-13650

SCREW PINCH

FOM contributions to the 14th European Conference on Controlled Fusion and Plasma Physics
[REPT-87-174] 12 p1693 N88-20129

Formation of high-Beta plasmas in various modes of operation in TPE-2 12 p1693 N88-20132

The stability of a screw-pinch plasma to global MHD modes 12 p1694 N88-20133

Improved confinement of screw pinch plasmas in SPICA 2 12 p1694 N88-20137

SCREWS

An advanced extruder-feeder biomass liquefaction reactor system 18 p2535 N88-25042

Empirical fatigue crack growth data for a tension loaded threaded fastener
[AD-A194112] 22 p3088 N88-28334

SCRUBBERS

Compact regenerable sulfur scrubber for phosphoric acid fuel cells
[AD-A191356] 16 p2230 N88-23318

SCRUBBING

U WASHING

SEA BREEZE

Short range forecasting of sea breeze generated thunderstorms at the Kennedy Space Center: A real-time experiment using a primitive equation mesoscale numerical model 02 p0211 N88-11324

Validation of a three dimensional numerical model of the sea breeze in complex terrain
02 p0211 N88-11325

Mesoscale analysis and forecasting for the 1987 America's Cup, Fremantle, Western Australia
02 p0214 N88-11350

Atmospheric diffusion at coastal site in presence of sea-breeze
[DE88-700038] 07 p0876 N88-15314

SEA GRASSES

Five New South Wales barrier lagoons: Their macrobenthic fauna and seagrass communities
11 p1517 N88-19059

SEA ICE

NT ICE FLOES
NT ICEBERGS
NT PRESSURE ICE

Porosity influence on the strength and elasticity of first-year sea ice
[AD-A184493] 03 p0354 N88-12233

Eastern - western Arctic Sea ice analysis 1986
[AD-A184016] 03 p0355 N88-12235

The ice conditions in the Greenland waters, 1981
[ISBN-87-7478-276-2] 05 p0629 N88-13844

Electromagnetic wave probing of Earth's environment
[NASA-CR-182358] 06 p0690 N88-14232

Report of the second session of the working group on sea ice and climate
[WCP-128] 06 p0745 N88-14580

Navarin Basin Ice Drift Program
[PB88-104021] 06 p0748 N88-14599

Predictability of ice concentration in the high-latitude North Atlantic from statistical analysis of SST (Sea Surface Temperature) and ice concentration data
[AD-A186621] 08 p1045 N88-16315

Physical properties of summer sea ice in the Fram Strait, June-July 1984
[AD-A186937] 09 p1194 N88-17156

Active and passive remote sensing of ice
[AD-A186685] 09 p1195 N88-17162

NASA Oceanic Processes Program
[NASA-TM-4025] 10 p1357 N88-18109

Physical and structural characteristics of Weddell Sea pack ice
[AD-A188189] 10 p1358 N88-18119

Airborne electromagnetic sounding of sea ice thickness and sub-ice bathymetry
[AD-A188939] 12 p1649 N88-19879

Predictions and studies with a one-dimensional ice/ocean model
[AD-A189158] 13 p1803 N88-20776

Microwave and structural properties of saline ice
[AD-A189307] 13 p1803 N88-20779

Mechanical properties of sea ice and sea ice deformation in the near-shore zone
[PB88-147889] 13 p1804 N88-20782

Elements of sea ice dynamics and thermodynamics
14 p1939 N88-21571

Sea ice observations and models
14 p1939 N88-21572

The Greenland Sea Project: The Arctemiz project
14 p1939 N88-21573

The effects of time-dependent winds and ocean eddies on ice motion in a marginal ice zone
[AD-A190105] 15 p2100 N88-22511

Hydrographic observations in the northwestern Weddell Sea Marginal Ice Zone during March 1986
[PB88-173240] 16 p2237 N88-23359

An investigation of Soviet capabilities in extended range arctic ice forecasting
[AD-A191082] 17 p2376 N88-24127

Sea ice kinematics: Space and time scales
[AD-A191162] 17 p2376 N88-24128

Examples of ice pack rigidity and mobility characteristics determined from ice motion
[AD-A191163] 17 p2377 N88-24129

DMSP-SSM/1 NASA algorithm validation using primarily LANDSAT and secondarily DMSP and/or AVHRR visible and thermal infrared satellite imagery
[NASA-CR-182979] 18 p2532 N88-25024

Higher frequency ambient noise in the arctic ocean
[AD-A192203] 18 p2547 N88-25122

Ray scattering from a collection of ice keels
[AD-A191757] 19 p2722 N88-26163

Active and passive remote sensing of ice
[AD-A193307] 21 p2966 N88-27617

The relationship between polar sea ice and the position of the near equatorial convergence zone
22 p3123 N88-28563

Arctic ice attenuation model study
[AD-A193382] 22 p3146 N88-28715

An objective technique for Arctic cloud analysis using multispectral AVHRR (Advanced Very High Resolution Radiometer) satellite imagery
[AD-A194732] 23 p3235 N88-29250
Meteorological features during the marginal ice zone experiment from 20 March to 10 April 1987
[AD-A193960] 23 p3235 N88-29251
Sea ice processes
[AD-A193980] 23 p3237 N88-29262
Reflection and scattering of acoustic rays computed for parabolic ice keel models
[AD-A193898] 23 p3278 N88-29517
MIZEX (marginal ice zone experiment) 1987 SAR (Synthetic Aperture Radar) data summary
[AD-A195560] 24 p3364 N88-30035

SEA KNIGHT HELICOPTER
U CH-46 HELICOPTER

SEA LAUNCHING
The effect of a turbulent airstream on a vertically-launched missile at high angles of attack
[AD-A192408] 20 p2758 N88-26363

SEA LEVEL
Regime dependent analysis experiments --- sea level pressure field 02 p0209 N88-11314
Mesoscale surface field analysis from routine observations --- pressure, wind fields
02 p0209 N88-11315
Sea level changes
[DE87-014357] 04 p0472 N88-12913
Expectations for water level deviations at the delta works: Zierikzee (Netherlands), November 1981-February 1986
[KNMI-TR-93] 05 p0628 N88-13840
FORTRAN programs for computation of time dependent sea levels and trajectory errors from satellite altimeter data
[BONN-MITT-73] 21 p2901 N88-27216
Reduce uncertainty in projection of future sea-level changes due to ice wastage
[DE88-009883] 22 p3129 N88-28601

SEA ROUGHNESS
Studies of thin surface films aim at seeing deep ocean processes 04 p0460 N88-12847
Impact force as a part of the total breaking wave force on a vertical cylinder
[RR-CE78] 24 p3384 N88-30154

SEA STATES
Cavitation inception scale effects. 1. Nuclei distributions in natural waters. 2. Cavitation inception in a turbulent shear flow
[AD-A186553] 08 p0988 N88-15987
A propagation campaign in a marine environment utilizing a digital system at 36 GHz 12 p1618 N88-19675
Low frequency ocean ambient noise: Measurements and theory
[AD-A191188] 16 p2237 N88-23362
A probabilistic model of the apparent radiance of a rough sea
[AD-A193867] 22 p3129 N88-28602

SEA SURFACE TEMPERATURE
The distinction between different water masses using optical remote sensing applied to data from the Alboran Sea Experiment 1982
[DFVLR-FB-86-48] 03 p0345 N88-12181
A multibody dynamic analysis of the N-ROSS (Navy Remote Ocean Sensing System) satellite rotating flexible reflector using Kane's method
[AD-A184452] 04 p0462 N88-12860
On the interannual variability of South American climate and the Southern Oscillation 04 p0470 N88-12905
AVHRR/HIRS (Advanced Very High Resolution Radiometer/High Resolution Infra-Red Sounder) operational method for satellite based sea surface temperature determination
[PB88-107594] 06 p0708 N88-14340
The effect of latitude on the development of tropical cyclones
[AD-A185670] 06 p0746 N88-14590
Predictability of ice concentration in the high-latitude North Atlantic from statistical analysis of SST (Sea Surface Temperature) and ice concentration data
[AD-A186621] 08 p1045 N88-16315
NASA Oceanic Processes Program
[NASA-TM-4025] 10 p1357 N88-18109
Spatial-temporal variability of North Pacific sea surface temperature anomaly patterns 11 p1516 N88-19058
Tropic heat MR (Meteorological Recorder) meteorological data (April 1984 - June 1985)
[PB88-161286] 14 p1948 N88-21620
Influence of the Yukon River on the Bering Sea
[NASA-CR-182802] 17 p2376 N88-24126
Determination of mesoscale variability of sea surface temperature and attenuation in the North Atlantic from satellite measurement
[REPT-162] 18 p2548 N88-25127
The active layer of the upper Atlantic Ocean
22. p3124 N88-28566

SEA URCHINS
Scanning electron microscopy study of adhesion in sea urchin blastulae
[NASA-CR-183136] 24 p3406 N88-30275
Immunofluorescence localization of dissociation supernatant and extracellular matrix components in Lytechinus pictus sectioned embryos
[NASA-CR-183137] 24 p3406 N88-30276

SEA WALLS
U BREAKWATERS

SEA WATER
Power flow in terms of Poynting vector for Extremely Low Frequency (ELF) dipole sources in seawater
[ARE-TM(UTM)-87102] 01 p0035 N88-10221
Hydrochemical structure of Gulf Stream frontal zone waters 06 p0727 N88-14476
Foam generation and air entrainment near a free surface
[AD-A185986] 07 p0848 N88-15149
The influence of yellow substances on remote sensing of sea water constituents from space. Volume 1: Summary
[ESA-CR(P)-2443-VOL-1] 07 p0872 N88-15292
The influence of yellow substances on remote sensing of sea water constituents from space. Volume 2: Appendices
[ESA-CR(P)-2443-VOL-2] 07 p0873 N88-15293
The use of chlorophyll fluorescence measurements from space for seperating constituents of sea water. Volume 1: Summary
[ESA-CR(P)-2444-VOL-1] 07 p0873 N88-15294
The use of chlorophyll fluorescence measurements from space for separating constituents of sea water. Volume 2: Appendices
[ESA-CR(P)-2444-VOL-2] 07 p0873 N88-15295
Cavitation inception scale effects. 1. Nuclei distributions in natural waters. 2. Cavitation inception in a turbulent shear flow
[AD-A186553] 08 p0988 N88-15987
The use of chlorophyll fluorescence measurements from space for separating constituents of sea water
08 p1043 N88-16307
The influence of yellow substances on remote sensing of sea-water constituents from space
08 p1044 N88-16308
Sea surface current estimates off central California as derived from enhanced AVHRR (Advanced Very High Resolution Radiometer) infrared images
[AD-A186667] 09 p1194 N88-17155
The analytical exponential decay coefficient of the submarine light field
[AD-A187215] 11 p1548 N88-19261
Remote sensing of atmospheric optical thickness and sea-water attenuation when submerged: Wavelength selection and anticipated errors
[AD-A187609] 11 p1548 N88-19262
Editing master oceanographic observation data set 4
[AD-A188405] 12 p1649 N88-19876
Cavitation inception
[AD-A189220] 13 p1765 N88-20557
Determination of mean thermohaline characteristics of the ocean 13 p1784 N88-20675
Research on influence of individual sea water components on spectral brightness coefficient of outgoing radiation 13 p1785 N88-20682
Predictions and studies with a one-dimensional ice/ocean model
[AD-A189158] 13 p1803 N88-20776
Experimental and theoretical constraints on the origin of mid-ocean ridge geothermal fluids
13 p1804 N88-20784
Relationship between optical transfer function and natural light field in sea or atmosphere
15 p2054 N88-22247
Physical, chemical and CTD (Conductivity/Temperature/Depth) data from the Marathon 2 expedition
[AD-A189930] 15 p2099 N88-22507
MIZPAC (marginal ice zone Pacific) 84-86 CTD (Conductivity, Temperature, Depth) data report
[AD-A192478] 21 p2976 N88-27679
Evaluation of organic coating deterioration and substrate corrosion in seawater using electrochemical impedance measurements 24 p3355 N88-29976

SEALANTS
U SEALERS

SEALERS
Process for the production of a thermoplastic elastomer composition
[EP-PATENT-0-202-782-A2] 05 p0569 N88-13465
Examination of polysulfide sealants by scanning electron microscopy
[MRL-R-1096] 13 p1752 N88-20478
Determination of the modulus of elasticity of structural silicone sealants
[PB88-157458] 14 p1893 N88-21307
Inadequacies of EMI-seal material: A corrosion study
17 p2319 N88-23852
Primerless RTV silicones
[BDX-613-3807] 24 p3356 N88-29980

SEALING
The axisymmetric sealing gap with variable viscosity. A variable hydraulic resistance
[ETN-87-90604] 03 p0314 N88-11867
Metal modification for improved glass-ceramic to metal seals: 1. Auger results on ion implantation and vapor deposition films
[DE88-005244] 10 p1339 N88-18006
Processing of glass to aluminum (low melting metals) seals via an injection molding technique
[DE88-004689] 13 p1751 N88-20466
Composite repair of cracked aluminum alloy aircraft structure
[AD-A190514] 18 p2455 N88-24573
Sample decomposition in sealed teflon vessels
[NASA-TT-20189] 18 p2494 N88-24798
Optical pressure sealing couping (light joint)
[NASA-CASE-MFS-29348-1] 18 p2576 N88-25303

SEALS (STOPPERS)
NT HERMETIC SEALS
NT LABYRINTH SEALS
NT O RING SEALS
NT PACKINGS (SEALS)
NT PLUGS
NT PUMP SEALS
Coatings for high-temperature bearings and seals
[NASA-TM-100249] 05 p0587 N88-13453
Three-dimensional dynamic labyrinth seal analysis
[AD-A185353] 05 p0590 N88-13599
Seal technology for liquid oxygen (LOX) turbopumps
[NASA-CR-174866] 05 p0591 N88-13603
Processing and interfacial analysis of glass-ceramic to metal seals
[DE88-002999] 08 p0971 N88-15873
Numerical modeling of multidimensional flow in seals and bearings used in rotating machinery
[NASA-TM-100779] 09 p1165 N88-16986
Tribological properties of alumina-boria-silicate fabric from 25 to 850 C
[NASA-TM-100806] 11 p1464 N88-18726
Numerical and analytical study of fluid dynamic forces in seals and bearings
[NASA-TM-100268] 11 p1485 N88-18867
Properties fo seals made with Li2O-Al2O3-SiO2-glass ceramics and aluminum-containing austenitic stainless steels
[DE88-004688] 12 p1633 N88-19776
Thermal stress minimized, two component, turbine shroud seal
[NASA-CASE-LEW-14212-1] 17 p2345 N88-23978
Botany Facility: Magnetic fluid seal considerations for the centrifuge
[SIRA-A/7373/WP110/MAC004]
17 p2378 N88-24138
Entrance and exit region friction factor models for annular seal analysis
[NASA-CR-183084] 19 p2678 N88-25821
Development of high temperature, high pressure rotating shaft seals
[DE88-001029] 23 p3221 N88-29172

SEAMOUNTS
Bathymetric hazard survey test
[AD-A189150] 13 p1803 N88-20775
Identification and acoustic characterization of seamounts
[AD-A192204] 18 p2548 N88-25123

SEAMS (JOINTS)
Automatic seam welding with infrared sensor feedback
[DE87-013556] 01 p0055 N88-10352

SEARCH AND RESCUE SATELLITE
U SARSAT

SEARCH FOR EXTRATERRESTRIAL INTELLIGENCE
U PROJECT SETI

SEARCH PROFILES
Parallel artificial intelligence search techniques for real time applications
[AD-A190683] 16 p2255 N88-23473
A flexible search strategy for production systems
23 p3262 N88-29420

SEARCH RADAR
NT OVER-THE-HORIZON RADAR
A preliminary assessment of thunderstorm outflow wind measurement with airport surveillance radars
[AD-A189064] 13 p1799 N88-20757
Automated test device for FASR (Fixed Array Surveillance Radar) beam steering componentry
[AD-A191650] 18 p2500 N88-24829

Analysis of ATCRBS (Air Traffic Control Radar Beacon System), mode select (Mode S) in combat operations
[AD-A193140] 22 p3040 N88-28050

SEARCHING
NT SEARCH PROFILES
A new compression method with fast searching on large databases
[DE87-010986] 01 p0106 N88-10691
System for SAR missions 03 p0265 N88-11671
An astrometric search for a stellar companion to the sun 04 p0520 N88-13195
An automated supernova search and the design strategy
[DE88-001827] 05 p0660 N88-14051
Investigation and implementation of an algorithm for computing optimal search paths
[AD-A185627] 07 p0902 N88-15461
Investigation of candidate data structures and search algorithms to support a knowledge based fault diagnosis system 07 p0923 N88-15606
Research on visual information processing with special reference to oculomotor behavior in the areas of exploration, recognition and search
[AD-A186598] 08 p1051 N88-16346
Effects of uniform target density on random search
[AD-A186468] 08 p1073 N88-16473
Visual attention effects on discrimination of line orientation and line arrangement
[AD-A187013] 09 p1200 N88-17190
Hierachical object recognition using libraries of parameterized model sub-parts
[AD-A187476] 10 p1396 N88-18322
Search problems in mission planning and navigation of autonomous aircraft
[NASA-CR-182666] 12 p1579 N88-19448

SEAS
NT ADRIATIC SEA
NT BEAUFORT SEA (NORTH AMERICA)
NT BERING SEA
NT BLACK SEA
NT CARIBBEAN SEA
NT MEDITERRANEAN SEA
NT NORTH SEA
Hydrographic observations in the northwestern Weddell Sea Marginal Ice Zone during March 1986
[PB88-173240] 16 p2237 N88-23359
Eigenmatrix representations of radiance distributions in layered natural waters with wind-roughened surfaces
[PB88-188701] 20 p2828 N88-26780

SEASAT SATELLITES
An exploratory study of inland water and land altimetry using Seasat data
[ESA-CR(P)-2433] 02 p0193 N88-11208
Earthnet's experience with Seasat SAR image processing 09 p1127 N88-16760
Tidal estimation in the Pacific with application to SEASAT altimetry
[NASA-TM-100694] 13 p1803 N88-20780
Seasat orbit determination experiments in preparation for the ERS-1 altimetry mission
[ETN-88-91842] 14 p1871 N88-21182

SEASONAL VARIATIONS
U ANNUAL VARIATIONS

SEASONS
NT SPRING (SEASON)
NT SUMMER
NT WINTER
Modes of surface circulation and climate over the tropical Atlantic, Eastern Pacific, and Indian Oceans
06 p0742 N88-14564
Effect of storage thermal behavior in seasonal storage solar heating systems
[PB88-114236] 10 p1350 N88-18067
Northern Hemisphere 700 mb teleconnections based on half-monthly mean anomaly data stratified by season and by sign 22 p3123 N88-28561
On the modes of growing-season precipitation over central North America 22 p3124 N88-28567
Differences in radiation budget parameters over Asia in relation to contrasting Indian monsoons
22 p3125 N88-28574
Typical weather months in the past (1973-1983) in Central Europe
[AD-A194701] 23 p3235 N88-29249

SEATS
NT BARANY CHAIR
Variable response load limiting device
[NASA-CASE-LAR-12801-1] 17 p2346 N88-23982

SEAWEEDS
Contribution of SPOT satellite to qualitative and quantitative mapping of marine vegetation in the English Channel, North Altantic, western Mediterranean, and South Pacific
22 p3109 N88-28464

SECONDARY BATTERIES
U STORAGE BATTERIES

SECONDARY EMISSION
External surface charging mechanisms --- spacecraft
03 p0273 N88-11719
Analysis of relativistic nucleus-nucleus interactions in emulsion chambers 07 p0926 N88-15624
The magnitude of secondary electron contributions in photon stimulated desorption
[AD-A189094] 13 p1835 N88-20980
Secondary electron emission characteristics improved by ion implantation 14 p1903 N88-21370
Question on the measurement of the metal work function in an electron spectrometer by the secondary-electron emission threshold method
[NASA-TT-20190] 16 p2178 N88-22979
Effects of secondary electron emission on the collector and source sheaths of a finite ion temperature plasma
[DE88-008930] 20 p2858 N88-26971
Plasma theory and simulation
[AD-A194674] 23 p3286 N88-29565
Study of secondary emission properties of materials used for high power RF components in space
[ESA-CR(P)-2587] 24 p3361 N88-30012

SECONDARY FLOW
Flow field measurements in a 90 degree turning duct
02 p0186 N88-11157
Secondary subharmonic instability of boundary layers with pressure gradient and suction
[NASA-CR-4112] 07 p0848 N88-15148
Mean velocities and Reynolds stresses in the juncture flow and in the shear layer downstream of an appendage
[AD-A185819] 08 p0980 N88-15923
Experimental study of secondary flow in the presence of two jet arrays on the wall of a turbine blade
[ECL-87-11] 08 p0987 N88-15981
Investigation of dihedral effects in compressor cascades 10 p1282 N88-17672
Secondary flow measurements with L2F-technique in centrifugal compressors 10 p1283 N88-17676
Design and testing of a front stage for an advanced high pressure compressor 10 p1283 N88-17679
Computation of secondary flows in an axial multistage compressor 10 p1284 N88-17681
Flow patterns induced by vortices
[NAL-TR-932] 10 p1332 N88-17963
Disk pumping test
[AD-A187199] 11 p1440 N88-18591
A review of approaches to the study of turbulence modification by means of non-Newtonian additives
[AD-A188799] 12 p1627 N88-19734
Secondary instability of compressible boundary layer to subharmonic three-dimensional disturbances
[NASA-CR-4144] 16 p2200 N88-23122
The aspect ratio dependence of the attractor dimension in Taylor-Couette flow
[AD-A196297] 24 p3369 N88-30065

SECONDARY RADAR
Validate algorithms for the determination of rainfall rates from SSM/I microwave satellite imagery
[AD-A191337] 16 p2236 N88-23353
Fine resolution errors in secondary surveillance radar altitude reporting
[RSRE-87019] 23 p3175 N88-28906

SECONDARY WAVES
U S WAVES

SECRETIONS
NT ALDOSTERONE
NT CORTICOSTEROIDS
NT HORMONES
NT PITUITARY HORMONES
Effect of external electrostatic field on catecholamine secretion by rat adrenals 10 p1366 N88-18166
Gastric emptying during walking and running: Effects of varied exercise intensity
[AD-A194025] 23 p3240 N88-29281

SECULAR PERTURBATION
U LONG TERM EFFECTS

SECULAR VARIATIONS
Statistics of the geomagnetic secular variation for the past 5Ma
[NASA-CR-181558] 04 p0467 N88-12890

SECURITY
NT AIRPORT SECURITY
NT COMPUTER INFORMATION SECURITY
Assessment of the impacts of transferring certain nuclear reactor technologies to the Soviet Union and Eastern Europe
[DE87-014388] 02 p0249 N88-11576
Bar code document accountability system performance update
[DE88-002256] 06 p0791 N88-14849
Application of a database system for inventory management of classified material
[AD-A186986] 09 p1261 N88-17558
Use of fiber optic equipment for security
[DE88-007898] 20 p2853 N88-26943
Technology security, volume 1
[DE88-008612] 21 p3029 N88-27978
Report to Congress on the effectiveness of the Civil Aviation Security Program
[AD-A195282] 24 p3322 N88-29784
Antisatellite weapons and satellite deployment strategies
[AD-A195014] 24 p3427 N88-30396

SEDATIVES
Pharmacological resetting of the Circadian sleep-wake cycle
[AD-A186194] 07 p0889 N88-15385
Selected aspects of triazolam in relation to aviator performance in naval flight operations
[AD-A189322] 12 p1667 N88-19996
Role of opioid peptides in pathogenesis of vestibulovegetative disorders 19 p2704 N88-26079

SEDIMENT TRANSPORT
Sea duct: A deep-sea computer-controlled recirculating flume for the study of sea floor stability
[AD-A187734] 11 p1516 N88-19056
Surface hydrology, sediment transport dynamics and remote sensing of disturbed watersheds in a humid temperate region
[DE88-008719] 20 p2817 N88-26715
Prediction of continental shelf sediment transport using a theoretical model of the wave-current boundary layer
[AD-A192272] 20 p2829 N88-26783

SEDIMENTARY ROCKS
NT CARBONACEOUS ROCKS
NT COAL
NT SANDSTONES
Preliminary results from an investigation of AIS-1 data over an area of epithermal alteration: Plateau, Northern Queensland, Australia 05 p0613 N88-13768
Isotopic and chemical studies of early crustal metasedimentary rocks
[NASA-CR-182711] 14 p1944 N88-21601

SEDIMENTS
NT SANDS
NT TAR SANDS
Geoacoustic models of the Hudson Canyon area
[AD-A183535] 01 p0073 N88-10465
A mineral reconnaissance sampling manual for Costa Rica: Central American energy and resource project
[DE87-014997] 04 p0462 N88-12859
Two-layer stratified flow analysis of gravity currents and turbidity currents in lakes, reservoirs and the ocean
04 p0463 N88-12864
RRS DISCOVERY cruise 160, 30 June-25 July, 1986. Geochemical sampling over the Madeira and Porcupine Abyssal Plains
[PB87-222030] 04 p0471 N88-12910
Colloidal stability of oxidized silicon particles in ethanolic and aqueous media
[DE87-014783] 05 p0562 N88-13421
Concentration coefficients of elements in ferromanganese nodules relative to ocean sediments
06 p0726 N88-14464
Tectonics of sedimentary cover and basement of Labrador Sea 06 p0726 N88-14468
Modern concept concerning transport of bottom sediments in abyssal regions of world ocean
06 p0728 N88-14478
Formation of sediments in fuels containing added sulphonic acids --- marine diesel fuels
[RAE-TM-NAV-ENG-1163] 09 p1150 N88-16891
Acoustic backscattering from bottom sediment at normal incidence in the laboratory
[AD-A186905] 09 p1242 N88-17443
Geological evolution and analysis of confirmed or suspected gas hydrate localities. Volume 10: Basin analysis, formation and stability of gas hydrates of the Aleutian Trench and the Bering Sea
[DE88-001008] 10 p1346 N88-18048
Data-base of Antarctic pre-Pleistocene sediment cores
[PB88-124151] 10 p1354 N88-18094
Rapid underway sediment classification by electrical methods
[AD-A187477] 10 p1357 N88-18114
Resolution of the magnetotelluric method for determining local inhomogeneities in the sedimentary cover 13 p1789 N88-20701
Satellite remote sensing of turbidity and sediment concentration in Lagoa dos Patos
17 p2355 N88-24032
Geological evolution and analysis of confirmed or suspected gas hydrate localities. Volume 2: Basin analysis, formation and stability of gas hydrates in the Black Sea
[DE88-001052] 18 p2532 N88-25023
Evaluation of the biot coefficients
[AD-A191643] 18 p2570 N88-25265
Remote sensing of acoustic properties of shallow water sediments: A review
[AD-A192107] 18 p2570 N88-25267

best copy available

The Martian sedimentary record
23 p3302 N88-29669
Surface units on Mars: The assemblage in the Valles Marineris 23 p3304 N88-29680
Early cratering rates and the nature of the Martian cratered uplands 23 p3306 N88-29694
Constraints on continental accretion from sedimentation 24 p3392 N88-30202
The growth of continents and some consequences since 1.5 Ga 24 p3395 N88-30220
Solid earth as a recycling systems and the lateral growth of Precambrian North America 24 p3400 N88-30249
Spectral analysis of the Elatina varve series
[NASA-CR-183085] 24 p3402 N88-30260

SEEBECK COEFFICIENT
U SEEBECK EFFECT

SEEBECK EFFECT
Optimisation of the thermoelectric figure of merit of modified silicon germanium alloys
[AD-A191347] 16 p2283 N88-23670

SEEDS
Simulation of effect on biological systems of impact wave from heavy charged particle track
07 p0896 N88-15429
Research on cotton plants grown in space
08 p1006 N88-16098
Effect of spaceflight factors on biological material flown aboard Cosmos-1514 biosatellite
10 p1364 N88-18154

SEEKERS
U HOMING DEVICES

SEEPAGE
Nonseismic, surface geophysical and geochemical prospecting technology
[PB88-196613] 23 p3227 N88-29207

SEGMENTS
Segmented hollow cathode discharges for copper ion lasers
[ETN-87-90403] 01 p0052 N88-10333
Numerical arc segmentation algorithm for a radio conference-NASARC (version 2.0) technical manual
[NASA-TM-100160] 08 p0977 N88-15910
Image segmentation via fractal dimension
[AD-A188825] 12 p1678 N88-20033
Results of the testing of the segmentation program on RESEDA
[BCRS-87-01] 16 p2228 N88-23304
Adaptive segmentation evaluation
[AD-A190965] 16 p2274 N88-23609
Automatic registration of satellite imagery
17 p2364 N88-24080
The SRS (Segmented Rail Surface) railgun: A new approach to restrike control
[DE88-007907] 19 p2605 N88-25466

SEGREGATION
U SEPARATION

SEISMIC WAVES
NT RAYLEIGH WAVES
Institute of Geophysics and Planetary Physics at Lawrence Livermore National Laboratory
[DE87-014618] 02 p0251 N88-11583
A new approach to modeling and interpreting electromagnetic sounding data
[DE88-000490] 04 p0438 N88-12715
Multichannel deconvolution of P waves at seismic arrays and three component stations
[AD-A184450] 04 p0467 N88-12888
NORSAR detection processing system
[AD-A185968] 07 p0877 N88-15318
Sea resonance vibrational source of seismic waves
08 p1010 N88-16126
Correlation between seismic activity and variations of microseismic oscillations 08 p1011 N88-16131
Determining trajectory of ground movement accompanying seismic phenomena
08 p1011 N88-16132
Materials of the World Data Center B. Deep Seismic Sounding (DSS): Pacific data 09 p1196 N88-17167
Regional wave attenuation and seismic moment from the inversion of NORESS spectra
[AD-A187399] 11 p1510 N88-19023
State-of-the-art for assessing earthquake hazards in the US. Parameters for specifying intensity-related earthquake ground motions
[AD-A188230] 11 p1512 N88-19032
Ultrasonic physical modeling of seismic wave propagation from graben-like structures
[AD-A188086] 13 p1796 N88-20744
Geodetic measurement of deformation east of the San Andreas fault in Central California
[NASA-CR-182709] 13 p1798 N88-20754
Earthquakes from peninsular India: Data from the Gauribidanur seismic array
[DE88-701232] 15 p2093 N88-22471
Characteristics of seismic sources of some Asian earthquakes and Soviet underground explosions from Gauribidanur array records
[DE88-701233] 15 p2093 N88-22472
Seismic inversion by a RMS (Root-Mean-Square) Born approximation in the space-time domain
[PB88-165402] 15 p2131 N88-22711
The determination of gravity and topography from seismic velocities, accounting for dynamic behavior of the Earth's mantle
[ETN-88-92420] 17 p2374 N88-24117
Remote sensing of acoustic properties of shallow water sediments: A review
[AD-A192107] 18 p2570 N88-25267
Statistical evaluation of light water reactor piping damping data for use in PRA (Probabilistic Risk Assessment) analyses
[DE88-007708] 19 p2661 N88-25828
Influence of scattering on seismic waves: Physical mechanisms contributing to attenuation in the crust
[AD-A191699] 19 p2690 N88-25992
Seismic body waves and the earth's inner core
[DE88-007395] 19 p2691 N88-25994
Changes in seismic velocity and apparent attenuation due to isotropic and anisotropic scattering: Results from physical modeling 19 p2691 N88-25997
Proceedings of the Array Signal Processing Symposium: Treaty Verification Program
[DE88-006346] 20 p2790 N88-26548
Stochastic geologic effects on near-field ground motions in alluvium
[AD-A192315] 21 p2972 N88-27652
Effects of tectonic release on broadband regional distance bodywaves
[AD-A194247] 22 p3119 N88-28529
Interactions between air and ground sound at the Earth surface 22 p3149 N88-28733
Acoustic-seismic helicopter detection
22 p3149 N88-28734
Seismic reflection experiments imaging the physical nature of crustal structures in southern California
23 p3232 N88-29235
Maximum-likelihood multichannel deconvolution of P waves at seismic arrays
[AD-A194990] 24 p3391 N88-30191
Deep seismic reflection profiling and continental growth curves 24 p3396 N88-30222
Discrimination studies using short-period P waves at upper mantle distances
[AD-A195468] 24 p3401 N88-30257

SEISMOGRAPHS
Research and development activities of the Seismology Section
[DE88-701235] 16 p2231 N88-23323

SEISMOLOGY
NT HELIOSEISMOLOGY
The interpretation of crustal dynamics data in terms of plate motions and regional deformation near plate boundaries
[NASA-CR-181475] 03 p0349 N88-12205
Earthquake source mechanisms and transform fault tectonics in the Gulf of California
03 p0349 N88-12206
Interseismic deformation for normal fault earthquakes
03 p0349 N88-12207
Transform fault earthquakes in the North Atlantic: Source mechanisms and depth of faulting
03 p0350 N88-12208
RRS DISCOVERY Cruise 161, 15 August (227)-19 September (262) 1986. Portuguese Ocean-continent boundary, plate boundaries west of Iberia and seismic structure of sediments off Madeira
[PB87-222006] 06 p0747 N88-14596
NORSAR detection processing system
[AD-A185968] 07 p0877 N88-15318
State-of-the-art for assessing earthquake hazards in the United States. Report 26: Parameters for specifying magnitude-related earthquake ground motions
[AD-A185997] 07 p0877 N88-15319
Use of space photographs for paleoseismogeological studies (on the example of Mongolian Altay)
08 p1008 N88-16110
New data on structure of earth's crust and seismicity of basins in Atlantic and Indian Oceans
08 p1010 N88-16123
Sea resonance vibrational source of seismic waves
08 p1010 N88-16126
Geomechanical model of seismofocal zone of active continental margin 08 p1011 N88-16128
Comprehensive method for defining seismogenic zones 08 p1011 N88-16129
A deep-water OBS (Ocean Bottom Seismometer) array with real-time telemetry
[AD-A187404] 10 p1357 N88-18112
Regional wave attenuation and seismic moment from the inversion of NORESS spectra
[AD-A187399] 11 p1510 N88-19023
Applications and limitations of the spectral-analysis-of-surface-waves method
[PB88-136619] 11 p1513 N88-19038
Numerical modeling of wave migration of seismic data
13 p1786 N88-20694
Interactive automated system for testing analog units of digital seismic stations 13 p1789 N88-20702
Correlation of data on strain accumulation adjacent to the San Andreas Fault with available models
[NASA-CR-180757] 13 p1796 N88-20742
Research and development activities of the Seismology Section
[DE88-701235] 16 p2231 N88-23323
The determination of gravity and topography from seismic velocities, accounting for dynamic behavior of the Earth's mantle
[ETN-88-92420] 17 p2374 N88-24117
Stochastic geologic effects on near-field ground motions in alluvium
[AD-A192315] 21 p2972 N88-27652
SPOT for earthquake hazard zoning in southern Italy
22 p3093 N88-28385
Utilizing SPOT data for seismic shot-line mapping and environmental monitoring in oil and gas exploration
22 p3098 N88-28401
Maximum-likelihood multichannel deconvolution of P waves at seismic arrays
[AD-A194990] 24 p3391 N88-30191

SEISMOMETERS
U SEISMOGRAPHS

SELECTION
NT PERSONNEL SELECTION
NT PILOT SELECTION
NT SITE SELECTION
On detection of change points using mean vectors
[AD-A185581] 06 p0767 N88-14717
Maximum likelihood principle and model selection when the true model is unspecified
[AD-A186027] 07 p0914 N88-15544
Variable selection in logistic regression
[AD-A186032] 07 p0914 N88-15547
Control variate selection for multiresponse simulation
[AD-A186637] 08 p1069 N88-16463
Advanced human factors engineering tool technologies
[AD-A189390] 13 p1812 N88-20825
Structure and surface characterizations of high strength carbon fibers
[AD-A189642] 15 p2029 N88-22087
On two-stage allocation procedures for selection problems
[AD-A190766] 15 p2126 N88-22675
Sensor and actuator selection for large space structure control
[AD-A194912] 24 p3333 N88-29842

SELECTION RULES (NUCLEAR PHYSICS)
On selection rules and inelastic electron scattering at intermediate energies
[DE88-701833] 23 p3280 N88-29526

SELECTIVE SURFACES
Millimeter and submillimeter waves and frequency selective surfaces
[AD-A191511] 18 p2500 N88-24827

SELECTIVITY
Selective growth velocity in needle crystals
14 p1966 N88-21858
Synthesis and analysis of novel polymers with potential for providing both high permselectivity and permeability in gas separation applications
[DE88-006533] 15 p2043 N88-22174

SELECTORS
Selection and effects of channels in distributed communication and decision making tasks: A theoretical review and a proposed research paradigm
[AD-A191807] 18 p2587 N88-25375

SELENIDES
NT CADMIUM SELENIDES
NT COPPER SELENIDES
NT ZINC SELENIDES
Tunable optical sources/growth and characterization of nonlinear optical materials
[AD-A190874] 16 p2274 N88-23608

SELENIUM
Phase equilibrium and crystal growth studies on AgGaSe2 and related nonlinear optical materials
[AD-A184768] 03 p0382 N88-12400
Thermal expansion of some Ge-Se-Te glasses
[PD-MT-8722] 04 p0420 N88-12606
Studies on some Ge-Se-Te glasses
[PD-MT-8721] 04 p0420 N88-12607
J = O Task Force
[DE88-001326] 04 p0450 N88-12786

SELENIUM COMPOUNDS
NT CADMIUM SELENIDES
NT COPPER SELENIDES
NT SELENIDES
NT ZINC SELENIDES
Review of selenium thermodynamic data
[DE88-006194] 13 p1849 N88-21068

SELF ADAPTIVE CONTROL SYSTEMS
Active control of helicopter vibration using multiloop self-adaptive control 03 p0264 N88-11660
Wavefront error sensing
[NASA-CR-181504] 03 p0321 N88-12030
Simplified self-tuning control algorithms
[OUEL-1657/86] 07 p0907 N88-15494
Self-adaptive data bases
[AD-A186414] 07 p0942 N88-15729

SELF ALIGNMENT
Self-alignment of ions drifting in plasma
06 p0774 N88-14752
Design, manufacture and spin test of high contact ratio helicopter transmission utilizing Self-Aligning Bearingless Planetary (SABP)
[NASA-CR-4155] 18 p2524 N88-24975

SELF CONSISTENT FIELDS
Self-consistent modification of a fast tail distribution by resonant fields in nonuniform plasmas
[AD-A183790] 01 p0099 N88-10650
The H5(+) potential energy hypersurface: Characterization of ten distinct energetically low-lying stationary points 16 p2237 N88-23561
Quantum Monte Carlo study of the MIES associated with H2(X 1 sigma g +) and H2(B 1 sigma u +)
16 p2268 N88-23564
Raychaudhuri equation in the self-consistent Einstein-Cartan theory with spin-density
[NASA-TM-101145] 17 p2447 N88-24546

SELF DEPLOYING SPACE STATIONS
U SELF ERECTING DEVICES
U SPACE STATIONS

SELF DIFFUSION (SOLID STATE)
Investigations of crystallization velocity and boron diffusion in glassy iron-boron alloys and of activity coefficients of boron in crystalline iron-boron alloys
[ETN-87-90613] 03 p0381 N88-12393
The influence of phosphorus on the solid state reaction between copper and silicon or germanium
[ETN-88-91381] 06 p0789 N88-14836
Heterogeneous isotope exchange between solid cesium iodide and gaseous methyl iodide
[ETN-88-91085] 09 p1141 N88-16840
Transport and relaxation processes in supercritical fluids
[DE88-004804] 10 p1419 N88-18474
A multigrid approach for the solution of a nonlinear diffusion equation in a time-dependent area using Cartesian coordinates
[GMD-STUDIEN-122] 16 p2257 N88-23491

SELF ERECTING DEVICES
The 15-meter antenna performance optimization using an interdisciplinary approach 19 p2652 N88-25746

SELF EXCITATION
Dynamics of reverse flows at pump inlet
04 p0425 N88-12636
Longitudinal mode combustion instabilities in air breathing engines 06 p0680 N88-14166
The design and performance of a real-time self excited vocoder 19 p2653 N88-25753

SELF FOCUSING
Numerical simulation of laser filamentation experiments
[ETN-87-90959] 02 p0179 N88-11116
Theory of transient thermal self-focusing of sound beams 09 p1234 N88-17401
On the self-focusing of electric helicons
[DE88-701870] 20 p2848 N88-26905

SELF INDUCED VIBRATION
NT SUPERSONIC FLUTTER
NT TRANSONIC FLUTTER
Investigations on higher harmonic blade pitch control of helicopters
[DFVLR-FB-87-36] 14 p1868 N88-21155

SELF LUBRICATION
Coatings for high-temperature bearings and seals
[NASA-TM-100249] 05 p0567 N88-13453
Self-lubricating coatings for high-temperature applications 09 p1119 N88-16703

SELF MANEUVERING UNITS
Personnel occupied woven envelope robot
23 p3260 N88-29408

SELF ORGANIZING SYSTEMS
Experiments in isolated digit recognition using the multilayer perceptron
[RSRE-MEMO-4073] 17 p2333 N88-23927
Hierarchical organization for large, dynamic radio networks
[AD-A193942] 23 p3204 N88-29067
Radial basis functions, multi-variable functional interpolation and adaptive networks
[RSRE-MEMO-4148] 23 p3265 N88-29436

SELF REGULATING
U AUTOMATIC CONTROL

SELF REPAIRING DEVICES
Automation tools for demonstration of goal directed and self-repairing flight control systems
[NASA-CR-179433] 19 p2715 N88-26121

SELF TESTS
Programmable Logic Arrays (PLA's) design for testability
[PB87-102935] 04 p0438 N88-12718

SELSYNS (TRADEMARK)
U SERVOMOTORS

SEMANTICS
Semantic network processing systems --- artificial intelligence
[OUEL-1677/87] 02 p0223 N88-11401
Integrating syntax, semantics, and discourse DARPA (Defense Advanced Research Projects Agency) Natural Language Understanding Program
[AD-A184505] 03 p0364 N88-12289
Near-horn prolog
[AD-A185172] 05 p0634 N88-13880
Annotated algebraic specification of the static semantics of pool
[PB88-106695] 07 p0912 N88-15533
Ada (trade name) compiler validation summary report: Systems designers' PLC SD Ada-plus VAX/VMS x MC68020. Version 26.00. Host: VAX 8600. Target: Motorola MC68020. Completion of on-site testing
[AD-A186571] 08 p1053 N88-16356
The use and generation of illustrative examples in computer-based instructional systems
08 p1060 N88-16400
Conceptual information processing: A robust approach to KBS-DBMS integration 08 p1063 N88-16422
Semantics of EqL
[AD-A188151] 10 p1389 N88-18297
Research in knowledge representation for natural language communication and planning assistance
[AD-A187355] 11 p1522 N88-19087
KR: An efficient knowledge representation system
[AD-A187705] 11 p1529 N88-19129
EqL: The language and its implementation
[AD-A188161] 11 p1530 N88-19137
An evaluation of historical algebras
[AD-A188350] 12 p1684 N88-20067
Using design axioms and topology to model database semantics
[CWI-CS-R8711] 13 p1818 N88-20863
Algebra of Communicating Processes (ACP)tau: A universal axiom system for process specification
[CWI-CS-R8725] 13 p1819 N88-20869
Designing equivalent semantic models for process creation
[CWI-CS-R8732] 13 p1819 N88-20872
Predicate-transformer semantics of general recursion
[CS-8709] 13 p1820 N88-20876
A fully abstract semantics for data flow nets
[CWI-CS-R8724] 13 p1822 N88-20893
A convergence theorem in process algebra
[CWI-CS-R8733] 13 p1827 N88-20920
A fully abstract semantics for event-based simulation
[AD-A190560] 15 p2080 N88-22283
Inference engine for expert systems
[INPE-4465-TDL/321] 15 p2113 N88-22590
Semantics for Prolog via term rewrite systems
[CWI-CS-R8739] 16 p2247 N88-23428
Semantics for logic programs without occur check
[CWI-CS-R8740] 16 p2248 N88-23429
Towards fully abstract semantics for local variables: Preliminary report
[AD-A191065] 16 p2251 N88-23456
Readiness and failures in the algebra of communicating processes
[CWI-CS-R8748] 16 p2258 N88-23499
Contractions in comparing concurrency semantics
[CWI-CS-R8755] 20 p2840 N88-26850
A semantic approach to fairness
[CWI-CS-R8759] 20 p2840 N88-26853
Towards knowledge bases-semantics, rules and object-oriented programming
[PB88-108154] 20 p2882 N88-27110
Hiding in stream semantics of uniform concurrency
[PB88-121579] 20 p2882 N88-27114
A cockpit natural language study: Vocabulary and grammar analyses
[AD-A193289] 21 p2993 N88-27753
Linguistic semantics for parallel computation
[PB88-105880] 21 p2995 N88-27761
Unification and set-valued functions for functional and logic programming
[AD-A193643] 23 p3250 N88-29341
Validation of expert systems 23 p3262 N88-29416
Semantic based man-machine interface for real-time communication 23 p3262 N88-29421
An expert system for natural language processing
23 p3263 N88-29426
Exploiting lexical regularities in designing natural language systems
[AD-A195922] 24 p3423 N88-30375

SEMICIRCULAR CANALS
Membrane model of cupula or vestibular semicircular canals 10 p1361 N88-18132

SEMICONDUCTING FILMS
Excimer laser-assisted deposition of GaAs, AlAs and (Al,Ga)As from Lewis acid-base adducts
[AD-A184586] 03 p0329 N88-12081
Some investigations of molecular beam epitaxial growth of 3-5 semiconductor films via Monte-Carlo computer simulations, carrier tunnelling and spectroscopic ellipsometry
[AD-A185520] 06 p0789 N88-14839
Neutron and X-ray scattering studies of layered solids
09 p1246 N88-17469
Gas source MBE (Molecular Beam Epitaxy)
[AD-A189763] 15 p2142 N88-22782
Beam assisted fabrication of 3-5/Si monolithic devices
[AD-A189979] 15 p2142 N88-22785
Fundamental properties and devices applications of Ge(x)Si(1-x)/Si superlattices
[AD-A190129] 15 p2143 N88-22787
Thin superconducting film characterization by surface acoustic waves
[AD-A190417] 15 p2143 N88-22791
Silicon-on-insulator pin diodes
[AD-A193359] 21 p2937 N88-27445
Molecular beam epitaxy of GaP films on Si substrates
[PB88-131974] 21 p3020 N88-27923
Laser induced chemical vapor epitaxial growth of gallium arsenide films
[AD-A194254] 23 p3291 N88-29595

SEMICONDUCTOR DEVICES
NT AVALANCHE DIODES
NT BIPOLAR TRANSISTORS
NT CHARGE COUPLED DEVICES
NT CHARGE TRANSFER DEVICES
NT CMOS
NT FIELD EFFECT TRANSISTORS
NT GALLIUM ARSENIDE LASERS
NT GERMANIUM DIODES
NT HETEROJUNCTION DEVICES
NT HIGH ELECTRON MOBILITY TRANSISTORS
NT JFET
NT JUNCTION DIODES
NT JUNCTION TRANSISTORS
NT LIGHT EMITTING DIODES
NT METAL OXIDE SEMICONDUCTORS
NT MIM (SEMICONDUCTORS)
NT MIM DIODES
NT MIS (SEMICONDUCTORS)
NT MODFETS
NT MSM (SEMICONDUCTORS)
NT PHOTODIODES
NT PHOTOVOLTAIC CELLS
NT SCHOTTKY DIODES
NT SEMICONDUCTOR LASERS
NT SILICON TRANSISTORS
NT SOI (SEMICONDUCTORS)
NT SOLAR CELLS
NT SOS (SEMICONDUCTORS)
NT THERMISTORS
NT THYRISTORS
NT TRANSFERRED ELECTRON DEVICES
NT TRANSISTOR AMPLIFIERS
NT TRANSISTORS
NT VARISTORS
NT VERTICAL JUNCTION SOLAR CELLS
Calorimetric Absorption Spectroscopy (CAS): A new method for the characterization of the optical properties of semiconductor systems
[ETN-87-90407] 01 p0098 N88-10645
Electrical behavior of layers implanted with low energy pions in Si
[INPE-4199-PRE/1051] 01 p0102 N88-10670
Variations in semiconductor device response in a medium-energy x-ray dose-enhancing environment
[DE87-012400] 02 p0243 N88-11538
Ohmic contacting schemes to gallium arsenide devices
[DE87-014627] 02 p0244 N88-11544
RADC/NBS (Rome Air Development Center/National Bureau of Standards) Workshop: Moisture Measurement and Control for Microelectronics (4)
[PB87-224614] 03 p0309 N88-11947
Vectorial electron transfer on designed surfaces
[PB87-232229] 03 p0381 N88-12394
Epitaxial reactor development for growth of silicon-on-insulator devices
[AD-A184758] 03 p0382 N88-12399

Molecular beam epitaxial growth and characterization of 3-5 compound semiconductor single and multiple interface structures
[AD-A185400] 05 p0656 N88-14021

Area detectors for X-ray spectroscopy
[DE88-001429] 06 p0679 N88-14163

High frequency periodic time domain waveform measurement system
[PB87-225256] 06 p0695 N88-14264

Structure of layered crystals studied by high energy ion beams
[DE88-001675] 06 p0786 N88-14822

Analytical investigations of bulk wave resonators in the piezoelectric thin film on gallium-arsenide configuration
[AD-A185716] 06 p0789 N88-14840

High-temperature electronics
08 p0956 N88-15797

Crystal diffraction lenses for imaging gamma-ray telescope
[DE88-003084] 08 p1083 N88-16529

Relaxation of metastable semiconductor strained-layer structures by plastic flow
[DE88-002729] 08 p1090 N88-16560

Nanoelectronics
[AD-A186969] 09 p1156 N88-16930

Acceleration techniques for decoupling algorithms in semiconductor simulation
[DE88-003593] 09 p1221 N88-17323

Study of quantum mechanical effects in deep submicron, grating-gate field effect transistors
[AD-A188283] 10 p1325 N88-17923

Microwave semiconductor research-materials, devices and circuits
[AD-A187121] 10 p1415 N88-18444

Corner compensation structures for (110) oriented silicon
[DE88-003300] 10 p1417 N88-18455

An electro-optic explosive igniter
[DE88-004728] 11 p1466 N88-18738

Microelectronic applications of the conductor-thin insulator-semiconductor (CIS) structure
11 p1560 N88-19341

Electronic properties of semiconductor inversion layers in sub-micron structures
[AD-A188635] 12 p1698 N88-20161

Electrical properties of medium field, chem-prep varistors
[DE88-006147] 13 p1762 N88-20540

Improvements in end point detection --- semiconductor fabrication
[RSRE-MEMO-4035/A] 14 p1899 N88-21336

JPRS report: Science and technology. China
[JPRS-CST-87-038] 14 p1901 N8[illegible]

Applications of lasers to semiconductor studies
14 p1901 N88-2135

Laser pulse detection with infrared range semiconductor detectors
[DE88-700657] 14 p1914 N88-21432

The Shubnikov de Haas effect in narrow-gap semimagnetic semiconductors
[ETN-88-92249] 14 p1988 N88-21861

Application of copper-carbon fiber composites to power semiconductor devices
[NASA-TT-20171] 15 p2031 N88-22101

Temperature-dependent conductivity of oxygen-depleted YBCO ceramics
[AD-A190340] 15 p2044 N88-22182

Growth of Pb/sub 1-x/Eu/sub x/Te epitaxial layers by the liquid phase epitaxy technique
[DE88-701022] 15 p2139 N88-22763

Development program for 1.93-micron lasers
[NASA-CR-4148] 16 p2212 N88-23198

Radiation effects in silicon
[DE88-006642] 16 p2282 N88-23659

Limited reaction processing for semiconductor device fabrication
[AD-A190913] 16 p2283 N88-23666

Development of 20 GHz monolithic transmit modules
[NASA-CR-182134] 17 p2445 N88-24539

Simple high speed camera with CCD-sensor
[MPIS-8/1987] 18 p2518 N88-24940

Advanced development of double-injection, deep-impurity semiconductor switches
[NASA-CR-182118] 18 p2583 N88-25346

Ceramic substrates for semiconductor applications reported: AIN substrates 19 p2633 N88-25621

Organization of a Topical Meeting on Picosecond Electronics and Optoelectronics
[AD-A187136] 19 p2655 N88-25765

Molecular Beam Epitaxy (MBE) for high speed devices
19 p2656 N88-25770

Multigigahertz logic based on InP-MISFET's exhibiting extremely high transconductance
19 p2656 N88-25771

Millimeter-wave integrated circuits
19 p2656 N88-25774

Fast GaAs photoconductive detectors with high sensitivity integrated in coplanar systems onto GaAs substrates 19 p2658 N88-25790

Non-stationary transport in MODFET's and heterojunction devices 19 p2659 N88-25804

Carrier transport in semiconductor magnetic sensors under nonuniform fields 19 p2672 N88-25888

Tin oxide microsensors on thin silicon membranes
19 p2673 N88-25897

Workshop report and presentations from the Semiconductor Research Corporation-DOE Semiconductor Task Force Workshop
[DE88-007690] 19 p2733 N88-26232

Ion implantation processing of 3-5 strained-layer semiconductors
[DE88-005270] 19 p2734 N88-26240

Plasma separation process. Betacell (BCELL) code, user's manual
[DE88-006955] 20 p2859 N88-26981

Raman, photoluminescence and modulation spectroscopy of semiconductor heterostructures
20 p2861 N88-26997

Energy levels and magneto-electric effects in some quasi uni-dimensional semiconductor heterostructures
20 p2864 N88-27009

Quantum transport in an electron waveguide
20 p2864 N88-27010

Random quantum interference in microdevices
20 p2866 N88-27021

Recent applications of Monte Carlo methods for semiconductor microdevice simulation
20 p2871 N88-27046

Excellent negative differential resistance of InGaAs/InAIAs resonant tunneling barrier structures and applications to a new functional device, RHET
20 p2872 N88-27048

Fermi level dependent native defect formation: Consequences for metal-semiconductor and semiconductor-semiconductor interfaces
[DE88-008247] 20 p2875 N88-27[illegible]96

Studying the physics and operation of multi-terminal near-micron and sub-micron length, hot electron semiconductor devices
[AD-A193380] 21 p2938 N88-27446

Solid state research
[AD-A192837] 21 p3020 N88-27929

Investigation of electronic band structure of semiconductors by photoemission
[ETN-88-92370] 21 p3025 N88-27957

Further improvements relating to the temperature compensation of semiconductor strain gauge pressure transducers
[RAE-TR-87061] 22 p3081 N88-28298

Semiconductor bridge (SCB) igniter studies. 1: Comparison of SCB and hot-wire pyrotechnic actuators
[DE88-008802] 23 p3200 N88-29046

Studies on strained (In,Ga)As/GaAs semiconductors and optical devices 23 p3287 N88-29575

Electronic and optical devices and applications
24 p3363 N88-30027

Automatic prober for the dc characterisation of gallium arsenide devices. Part 2: The data sorting and display facility
[AD-A195408] 24 p3377 N88-30111

Tolerances for phase locking of semiconductor laser arrays
[AD-A195974] 24 p3378 N88-30120

Application of nondestructive testing techniques to materials testing
[AD-A195716] 24 p3381 N88-30138

Light-millimeter wave interactions in semiconductor devices
[AD-A195898] 24 p3432 N88-30428

Waveform relaxation applied to transient device simulation
[AD-A194992] 24 p3432 N88-30429

SEMICONDUCTOR DIODES
NT AVALANCHE DIODES
NT GERMANIUM DIODES
NT GUNN DIODES
NT JUNCTION DIODES
NT LIGHT EMITTING DIODES
NT PHOTODIODES
NT SCHOTTKY DIODES
NT TUNNEL DIODES

Blue-green laser diode research program
[AD-A183517] 01 p0051 N88-10323

AlGaAs heterojunction lasers
[NASA-CR-4119] 09 p1171 N88-17020

Ultra-high speed integrated optical waveguide devices for optical computing
[AD-A188470] 12 p1691 N88-20118

Growth of Pb/sub 1-x/Eu/sub x/Te epitaxial layers by the liquid phase epitaxy technique
[DE88-701022] 15 p2139 N88-22763

Design and evaluation of single-lobed far-field pattern laser arrays: AlGaAs/GaAs and InGaAsP/InP systems --- optical communication
[LAAS-88-023] 16 p2214 N88-23211

Diode laser ignition of high explosives and pyrotechnics
[DE88-008771] 21 p2923 N88-27352

A GaAs solid state device model for high power applications
[DE88-011320] 21 p2939 N88-27457

Photodiodes for optical communication in the near infrared
[ETN-88-92379] 21 p3016 N88-27900

Blue-green laser diode research program
[AD-A191980] 23 p3218 N88-29153

SEMICONDUCTOR INSULATOR SEMICONDUCTORS
U SIS (SEMICONDUCTORS)

SEMICONDUCTOR JUNCTIONS
NT HETEROJUNCTIONS
NT N-P-N JUNCTIONS
NT P-I-N JUNCTIONS
NT P-N JUNCTIONS
NT P-N-P JUNCTIONS
NT P-N-P-N JUNCTIONS
NT SILICON JUNCTIONS

Optimization of SIS mixer elements
[NASA-CR-180710] 01 p0104 N88-10680

Investigation of silicon surface passivation by silicon nitride film deposition
[NASA-CR-182350] 06 p0729 N88-14487

Photoluminescence study of InP surfaces and InP-insulator interfaces
[ECL-87-13] 08 p1089 N88-16555

Electron tunneling in junctions doped with semiconductors and metals 19 p2734 N88-26236

A comparison of the radiation tolerance characteristics of multijunction solar cells with series and voltage-matched configurations
[NASA-TM-101177] 21 p2967 N88-27624

SEMICONDUCTOR LASERS
NT GALLIUM ARSENIDE LASERS

Blue-green laser diode research program
[AD-A183517] 01 p0051 N88-10323

Status, development of laser devices in China
03 p0303 N88-11907

High power phased array and tailored gain semiconductor lasers 03 p0329 N88-12078

Phase-locked semiconductor quantum well laser arrays
[AD-A185155] 05 p0588 N88-13583

Nonconventional optical techniques for optical wavefront processing
[AD-A185099] 05 p0650 N88-13982

Causes and distribution of failures in semiconductor lasers (a review) 07 p0919 N88-15581

Generation of light pulses in semiconductor laser upon excitation by several electron beams
07 p0920 N88-15589

Electro-optical studies of semiconductor compounds for electroluminescent and laser devices
[PH-155] 07 p0937 N88-15693

Semiconductor laser with electron-beam pumping and fiber-optic output waveguide 09 p1235 N88-17405

Dye lasers pumped by radiation from high-power semiconductor lasers 09 p1237 N88-17417

Periodic-pulse semiconductor laser with electron-beam pumping 09 p1238 N88-17422

Ultra-high speed integrated optical waveguide devices for optical computing
[AD-A188470] 12 p1691 N88-20118

Fiber-coupled external-cavity semiconductor high power laser
[AD-A188454] 13 p1774 N88-20611

High power, high efficiency, 2D laser diode arrays for pumping solid state lasers
[DE88-004042] 13 p1777 N88-20632

Dynamic and spectral properties of semiconductor lasers with quantum well, quantum wire, and quantum box structures 14 p1975 N88-21788

Ultrahigh coherent semiconductor lasers and their applications to Rb atomic clock
14 p1976 N88-21789

Generation of number-phase minimum uncertainty states 14 p1978 N88-21803

Fabrication and characterization of semiconductor lasers of Pb(1-x)Sn(x)Te
[INPE-4253-PRE/1126] 15 p2072 N88-22367

Generation of tunable coherent radiation in 3 micrometers-5 micrometers region using semiconductor lasers in external cavities
[AD-A190660] 16 p2212 N88-23202

Design and evaluation of single-lobed far-field pattern laser arrays: AlGaAs/GaAs and InGaAsP/InP systems --- optical communication
[LAAS-88-023] 16 p2214 N88-23211

Distributed feedback lasers
[NASA-CR-4154] 18 p2520 N88-24948

Characteristics, packaging and physics of ultra high speed diode lasers and detectors
19 p2658 N88-25797

Frequency chirping in pulse modulated gain and real index guided single quantum well lasers
19 p2658 N88-25798

Picosecond measurements of gain-switching in a semiconductor laser driven by ultrashort electrical pulses
19 p2658 N88-25800

New semiconductor laser structure for an optical communication system
[ETN-88-92353] 20 p2807 N88-26654

Blue-green laser diode research program
[AD-A191980] 23 p3218 N88-29153

Mode locking of semiconductor laser with external cavity
[AD-A196018] 24 p3378 N88-30117

SEMICONDUCTOR PLASMAS

Fundamental studies and device development in beta silicon carbide
[AD-A189540] 12 p1699 N88-20165

Modeling and transport in semiconductor devices
[AD-A188760] 13 p1844 N88-21037

SEMICONDUCTORS (MATERIALS)

NT ACCEPTOR MATERIALS
NT AMORPHOUS SEMICONDUCTORS
NT AMORPHOUS SILICON
NT CMOS
NT DONOR MATERIALS
NT METAL OXIDE SEMICONDUCTORS
NT MIM (SEMICONDUCTORS)
NT MIS (SEMICONDUCTORS)
NT N-TYPE SEMICONDUCTORS
NT ORGANIC SEMICONDUCTORS
NT P-TYPE SEMICONDUCTORS
NT PHOTOCONDUCTORS
NT SOS (SEMICONDUCTORS)
NT SUPERLATTICES

Construction and characterization of amorphous-silicon test structures
[DE87-013595] 01 p0029 N88-10182

Toward pulsed power uses for photoconductive semiconductor switches: Closing switches
[DE87-012020] 01 p0041 N88-10262

Recent developments in opening photoconductive semiconductor switches
[DE87-012130] 01 p0041 N88-10263

Metal-sensing layer-semiconductor and metal-sensing layer-metal heterostructure gas sensors
[DE87-011293] 01 p0103 N88-10674

X-ray studies of strain, interface and impurity in semiconductors
[DE87-013856] 01 p0104 N88-10678

Reduction of CO2 to methanol and methane by photo and dark reactions on semiconductor and metal electrodes
[PB87-226825] 02 p0156 N88-10975

Semiconductor detector performance for low-energy X-rays
[DE87-014132] 02 p0244 N88-11542

Coupling and absorption phenomena in semiconductor-clad dielectric optical waveguides
[DE87-013446] 03 p0307 N88-11939

Measurement of the electron density and the attachment rate coefficient in silane/helium discharges
[AD-A184266] 04 p0496 N88-13051

Valence bond cluster studies of alkali metal/semiconductor bonding
[AD-A184276] 04 p0496 N88-13054

Novel dynamical investigations of excitons and their structure in semiconductors
[DE87-014868] 04 p0499 N88-13070

Far infrared Fourier transform spectroscopy of semiconductors
[DE88-000158] 04 p0499 N88-13072

Supersonic beam observations of semiconductor clusters
[AD-A184991] 05 p0655 N88-14018

The pseudopotential density functional method applied to semiconducting crystals
[ETN-88-91362] 05 p0656 N88-14024

JPRS report: Science and technology. USSR: Physics and mathematics
[JPRS-UPM-87-008] 06 p0769 N88-14727

Population inversion in gapless semiconductors as result of interband pumping 06 p0770 N88-14732

Heteroepitaxial growth of 3-5 semiconductor compounds by metal-organic chemical vapor deposition for device applications
[NASA-CR-182346] 06 p0788 N88-14832

Some investigations of molecular beam epitaxial growth of 3-5 semiconductor films via Monte-Carlo computer simulations, carrier tunnelling and spectroscopic ellipsometry
[AD-A185520] 06 p0789 N88-14839

Improving the method of calculating electronic properties of narrow bandgap semiconductors
07 p0926 N88-15627

Electro-optical studies of semiconductor compounds for electroluminescent and laser devices
[PH-155] 07 p0937 N88-15693

Effect of the band-gap characteristics on laser-induced dry etching of semiconductors
[DE88-001853] 07 p0937 N88-15695

A flux analysis of the solar cells
[INPE-4247-PRE/1120] 08 p1022 N88-16186

JPRS report: Science and technology. USSR: Physics and mathematics
[JPRS-UPM-87-010] 08 p1075 N88-16485

Instability of strong-absorption domain in semiconductor 08 p1077 N88-16495

Photoluminescence study of InP surfaces and InP-insulator interfaces
[ECL-87-13] 08 p1089 N88-16555

Interpretation of the temperature dependence of conductivity in superconducting oxides
[DE88-003028] 08 p1091 N88-16565

Plasma and ion etching for failure analysis. Part 2. The etching of plastic encapsulant and other semiconductor device materials, using the Technics Giga Etch 100-E plasma etch system
[AERE-R-12212] 09 p1177 N88-17050

JPRS report: Science and technology. USSR: Physics and mathematics
[JPRS-UPM-87-009] 09 p1233 N88-17395

Linear theory of generation of longitudinal sound waves in semiconductors upon interband absorption of optical radiation 09 p1234 N88-17397

Visible InGaAsP/GaAsP lasers produced by epitaxial growth from liquid phase 09 p1237 N88-17416

A report on the effects of neutron irradiation of GaAs semiconductors
[AD-A186816] 09 p1253 N88-17510

Control of solid-excitation-based photochemical dry etching of semiconductors by ion-bombardment-induced damage
[DE88-003214] 09 p1257 N88-17537

Stability and metastability in semiconductor strained-layer structures
[DE88-003308] 09 p1258 N88-17544

An advanced microcomputer design for processing of semiconductor materials 10 p1288 N88-17703

Application of nondestructive testing techniques to materials testing
[AD-A187645] 10 p1342 N88-18021

Photochemical solar energy conversion utilizing semiconductors localized in membrane mimetic systems
[DE88-002887] 10 p1349 N88-18065

Microwave semiconductor research-materials, devices and circuits
[AD-A187121] 10 p1415 N88-18444

Tight binding theory of semiconductors
10 p1415 N88-18447

Microscopic control of metallization stability
[AD-A187553] 10 p1421 N88-18487

Local stoichiometry and atomic interdiffusion during reactive metal/mercury-cadmium-telluride junction formation
[AD-A187554] 10 p1421 N88-18488

Nonmonotonic evolution and thermodynamic trends at metal/(Hg,Cd)Te interfaces: Yb/Hg0.78Cd0.22Te
[AD-A187591] 10 p1422 N88-18490

CdTe(110)-Mn interface reaction and the formation of non-equilibrium ternary semimagnetic semiconductor alloys
[AD-A187593] 10 p1422 N88-18491

PbSnTe photovoltaic detectors for operation in the 2-14 micron band
[INPE-4252-PRE/1125] 11 p1508 N88-19006

Digital control of the Czochralski growth of Gallium arsenide-controller software reference manual
[AD-A187210] 11 p1526 N88-19127

Atomic-scale simulation in materials science
[DE88-005204] 11 p1544 N88-19230

Fast switching of far infrared radiation by refractive index change in semiconductors using photoionization
[ETN-88-91490] 11 p1551 N88-19279

Theoretical studies of the interface electronic properties of tetrahedrally coordinated semiconductors
[AD-A187216] 11 p1555 N88-19306

High pressure electronic transport in semiconductors
[AD-A187428] 11 p1555 N88-19305

Laser measurements of state-resolved Ga and in atom sticking and desorption on metal and semiconductor surfaces
[AD-A187644] 11 p1555 N88-19310

Vibrational, mechanical and thermal properties of 3-5 semiconductors
[AD-A187569] 11 p1556 N88-19316

Electron paramagnetic resonance studies of Mn(2+) in 2-6 semiconductor alloys 11 p1560 N88-19340

Feasibility studies of the growth of 3-5 compounds of boron by MOCVD
[NASA-CR-181622] 11 p1561 N88-19343

Raman scattering in mixed crystal semiconductors
12 p1696 N88-20149

Basic research in ceramic and semiconductor science at selected Japanese laboratories, based on a September 1986 visit: Highlights, summary and overview and detailed notes from selected Japanese laboratories
[DOE/ER-0314] 12 p1696 N88-20150

Metal contacts to cadmium telluride (CdTe)
[AD-A188306] 12 p1698 N88-20159

Thin-film diffusion barriers for metal-semiconductor contacts
[AD-A188712] 13 p1844 N88-21035

New method of examining micrononhomogeneity of local centers in high-resistivity semiconductor materials under scanning electron microscope 14 p1969 N88-21754

Infrared reflection-absorption spectroscopy of hyperfine layers on surfaces of semiconductors and dielectrics
14 p1969 N88-21755

United States - Japan Seminar on Quantum Mechanical Aspects of Quantum Electronics
[AD-A186938] 14 p1974 N88-21781

Enhanced excitonic optical nonlinearity and exciton dynamics in semiconductor microstructures
14 p1977 N88-21795

Free carrier nonlinear optics 14 p1977 N88-21796

High density femtosecond excitation of nonthermal carrier distributions in intrinsic and modulation doped GaAs quantum wells 14 p1977 N88-21798

Dynamical aspects of carrier tunneling in semiconductor superlattices 14 p1977 N88-21799

Experimental and theoretical studies of coherent and nonthermal processes in semiconductors probed by femtosecond laser techniques 14 p1977 N88-21800

Femtosecond studies in hot carrier relaxation in GaAs and AlGaAs 14 p1977 N88-21801

Amorphous semiconductors made in space
15 p2051 N88-22221

Pb(1-x)Sn(x)Te crystal growth in space
15 p2051 N88-22223

Absolute pressure derivatives of deep level defects in 3-5 semiconductors
[DE88-006318] 15 p2140 N88-22772

Examination of temperature effects on gate-to-drain avalanche breakdown in GaAs MESFETs (Metal-Semiconductor Field Effect Transistors) by measuring light emission under RF drive
[AD-A189634] 15 p2141 N88-22778

Repetitive opening switches using optically activated semiconductors
[AD-A190196] 15 p2143 N88-22790

Interface formation and precursory dynamics
[AD-A190741] 15 p2144 N88-22794

Fermi level stabilization in semiconductors: Implications for implant activation efficiency
[DE88-006332] 15 p2145 N88-22801

UV-Laser reactions of molecular adsorbates
[AD-A190796] 16 p2212 N88-23201

Investigation of non-linear optical behavior of semiconductors for optical switching, volume 1
[AD-A191297] 16 p2274 N88-23611

DOE (Department of Energy) national laboratories and the semiconductor industry: Continuing the joint planning
[PB88-170295] 16 p2281 N88-23657

Radiation effects in silicon
[DE88-006642] 16 p2282 N88-23659

Limited reaction processing for semiconductor device fabrication
[AD-A190913] 16 p2283 N88-23666

Microscopic control of semiconductor interface reactivity
[AD-A191193] 16 p2283 N88-23668

Optimisation of the thermoelectric figure of merit of modified silicon germanium alloys
[AD-A191347] 16 p2283 N88-23670

Non-contact temperature measurement requirements for electronic materials processing
17 p2326 N88-23898

Real time thermal imaging of high temperature semiconductor melts 17 p2330 N88-23914

Preparation of improved PbSnTe thermoelectric alloys and evaluation of their figure of merit
[AD-A191346] 17 p2445 N88-24536

Liquid encapsulated float zone process and apparatus
[NASA-CASE-MFS-28144-1] 17 p2446 N88-24545

Time resolved spectroscopy facility for the study of nonlinear optical properties of semiconducting polymers
[AD-A191221] 18 p2490 N88-24768

Stress measurements in graphite fibers by laser raman spectroscopy
[AD-A191710] 18 p2491 N88-24779

Joint services electronics program
[AD-A190239] 18 p2503 N88-24848

Mathematical models for VLSI device simulation
[AD-A191125] 18 p2562 N88-25212

Electronic structure, elementary excitations, optical and transport properties of semiconductor superlattices
[AD-A190795] 18 p2581 N88-25333

An investigation of 2-6 superlattice deposition by laser photochemical techniques
[AD-A191547] 18 p2581 N88-25336

Recent data on Si:As impurity band conduction multiplexed arrays
[AD-A191752] 18 p2582 N88-25340

Studies of metal-silicon, silicon-metal and silicide based interfaces: Synchrotron radiation photo emission and inverse photoemission investigations of interface formation and compound nucleation
[AD-A191808] 19 p2619 N88-25536

Nonequilibrium phonons and disorder in Al sub x Ga sub 1-x As 19 p2657 N88-25788

Direct subpicosecond measurement of carrier mobility of photoexcited electrons in GaAs
19 p2659 N88-25803

Longitudinally localized optical carrier injection for femtosecond transport studies 19 p2659 N88-25806

Optical sensing of magnetic fields
19 p2670 N88-25871

Digital control of the czochralski growth of gallium arsenide. System reference manual. Valid for Czochralski growth controller software version 2.4
[AD-A191997] 19 p2732 N88-26227

Workshop report and presentations from the Semiconductor Research Corporation-DOE Semiconductor Task Force Workshop
[DE88-007690] 19 p2733 N88-26232

Ion implantation processing of 3-5 strained-layer semiconductors
[DE88-005270] 19 p2734 N88-26240

Auger recombination in GaSb/AlSb-multi quantum well heterostructures 20 p2862 N88-27001

Piezoelectric effects in strained layer superlattices
20 p2863 N88-27002

Semiconductor microcrystallites in porous glass and their applications in optics 20 p2863 N88-27005

Ferromagnetic/semiconductor hybrid structures
20 p2865 N88-27013

Properties of synthetic magnetic superlattices
20 p2865 N88-27014

EXAFS studies of the microstructure of semiconductor alloys, defects and semiconductor-metal interfaces
20 p2868 N88-27031

Phonons in semiconductor superlattices
20 p2869 N88-27035

Electron-phonon interactions in In(0.53)Ga(0.47)As and in In(0.53)Ga(0.47)As/InP quantum wells
20 p2869 N88-27037

Electronic structure of quantum-well states revealed under high pressures 20 p2870 N88-27038

The theory of electron-polar phonon scattering rates in semiconductor micro-structures
20 p2871 N88-27043

Vertical electronic transport in novel semiconductor heterojunction structures 20 p2871 N88-27045

Influence of interfaces on electronic and magnetic properties of MnSe/ZnSe superlattices near monolayer limit 20 p2872 N88-27050

Atomistic simulation of stability, metastability and growth of strained layer structures 20 p2873 N88-27053

Electrical study of metal/group 3-5 semiconductor interfaces: Comparison with the atomic-level studies
20 p2874 N88-27059

Growth and characterization of thin films of ZnSnP(sub)2
[DE88-001164] 20 p2874 N88-27060

Defects in high-mobility semiconductor systems
[AD-A192298] 20 p2879 N88-27090

Epitaxy and properties of two dimensional GaInAs semiconductor structures
[ETN-88-92357] 20 p2879 N88-27094

Numerical calculations of dopent diffusion involving flashlamp heating of silicon 21 p2929 N88-27384

Polarization selective Raman microspectroscopy
21 p2930 N88-27397

NDP (Neutron Depth Profiling) evaluations of boron-implanted compound semiconductors
[AD-A192306] 21 p2934 N88-27425

Studying the physics and operation of multi-terminal near-micron and sub-micron length, hot electron semiconductor devices
[AD-A193380] 21 p2938 N88-27446

Solid state research
[AD-A192837] 21 p3020 N88-27929

Schottky-barrier formation on a covalent semiconductor without Fermi-level pinning: The Metal-MoS2(0001) interface
[AD-A193044] 21 p3021 N88-27931

Ultrafast physics in semiconductor microstructures
[AD-A193300] 21 p3022 N88-27936

Prediction of deep levels and equilibrium concentrations of defects in semiconductors 21 p3023 N88-27945

Deep level defects in semiconductors: Stress and pressure studies
[DE88-010855] 21 p3024 N88-27948

X-ray studies of strain, interface and impurities in semiconductors
[DE88-012460] 21 p3025 N88-27954

Techniques and instrumentation for transient characterization of metal-insulator-semiconductor diodes. Applications to metal-insulator InP system
[ECL-87-17] 21 p3025 N88-27959

The p-well or n-well CMOS technology for advanced SEU-hard SRAMs
[DE88-006845] 22 p3156 N88-28777

Reaction dynamics on semiconductor surfaces
[AD-A194305] 22 p3156 N88-28781

The VPE-hydride technique with alloy source: Equilibrium analysis
[AD-A194036] 22 p3157 N88-28784

Multiphoton transitions in semiconductors in the non-perturbative approach
[DE88-702664] 22 p3157 N88-28786

Infrared devices using semiconductor quantum wells
[RSRE-MEMO-4018] 22 p3157 N88-28788

DARPA-URI consortium meetings on submicron heterostructures of diluted magnetic semiconductors
[AD-A193499] 23 p3206 N88-29081

The diamond as a new electronic material
[NASA-TT-20354] 23 p3209 N88-29098

Local environment approach for deep-level defects in semiconductors: Application to the vacancy in silicon
[DE88-702017] 23 p3287 N88-29573

Intrinsic and extrinsic energy states of semiconductors and heterostructures using novel techniques
[DE88-008560] 23 p3289 N88-29582

Electronic states in tunneling semiconductor superlattices
[DE88-011571] 23 p3290 N88-29587

Study of superconducting properties in some many valley semiconductors
[DE88-702325] 23 p3291 N88-29593

Lattice-matched HgZnTe epitaxy development
[AD-A193677] 23 p3292 N88-29600

Hot electron emission in semiconductors
[AD-A194101] 23 p3292 N88-29601

System suitable for observing surface plasmon in a semi-infinite semiconductor superlattice
[DE88-702686] 23 p3293 N88-29606

Vibration spectra induced by impurities in 3-5-compounds semiconductors
[DE88-702730] 23 p3293 N88-29610

Power MISFETs on OnP
[AD-A195242] 24 p3433 N88-30436

Joint services electronics program
[AD-A195731] 24 p3434 N88-30439

SEMISOLIDS

Electrochromic cells with lutetium diphthalocyanine and semisolid polymer electrolytes
[AD-A188031] 10 p1352 N88-18078

SEMISPAN MODELS

Tip aerodynamics from wind tunnel test of semi-span wing
[NASA-TM-88253] 05 p0540 N88-13290

SENDERS
U TRANSMITTERS

SENSE ORGANS
NT CHEMORECEPTORS
NT COCHLEA
NT CORNEA
NT EAR
NT EYE (ANATOMY)
NT FOVEA
NT GRAVIRECEPTORS
NT MIDDLE EAR
NT OCULOMOTOR NERVES
NT OTOLITH ORGANS
NT PHOTORECEPTORS
NT PROPRIOCEPTORS
NT PUPILS
NT RETINA
NT SEMICIRCULAR CANALS
NT VESTIBULES

Functional development of gravity receptors in insects and amphibians 07 p0886 N88-15376

Regulatory biochemical and metabolic responses in photoreceptors
[AD-A192898] 20 p2831 N88-26794

SENSES
U SENSORY PERCEPTION

SENSIBILITY
U SENSITIVITY

SENSING
U DETECTION

SENSITIVITY
NT IMPACT RESISTANCE
NT LIGHT ADAPTATION
NT NOTCH SENSITIVITY
NT PHOTOSENSITIVITY
NT PHOTOTROPISM
NT PROPELLANT SENSITIVITY
NT RADIATION TOLERANCE
NT SPECTRAL SENSITIVITY

The effect of RDX particle size on the shock sensitivity of cast PBX formulations. 2: Bimodal compositions
[DE87-009581] 01 p0031 N88-10198

Microstructural effects in shock initiation of granular explosives
[DE87-011282] 01 p0031 N88-10200

Scotopic sensitivity with 10 percent oxygen
[AD-A183973] 03 p0356 N88-12243

Aerodynamic sensitivities from subsonic, sonic and supersonic unsteady, nonplanar lifting-surface theory
[NASA-TM-100502] 04 p0394 N88-12459

Investigation, development and application of optimal output feedback theory. Vol. 4: Measures of eigenvalue/eigenvector sensitivity to system parameters and unmodeled dynamics
[NASA-CR-4108] 04 p0482 N88-12960

Sensitivity of the H alpha line to expansion, geometrical extent and temperature gradient in the G and K supergiant chromospheres 04 p0514 N88-13159

Langlie Test Method Program for use with the HP-41CV/X calculator
[DE88-001935] 06 p0667 N88-14210

Tailorable infrared sensing device with strain layer superlattice structure
[NASA-CASE-NPO-16807-1-CU]
06 p0786 N88-14836

Estimating system reliability: Monte Carlo methods, sensitivity and errors in input parameters
[AD-A186182] 07 p0865 N88-15248

Comparison of sensitivity and precision of holographic and speckle-interferometry methods with Fourier-plane recording 08 p1078 N88-16500

Mechanism of and particle size effects on shock sensitivity of heterogeneous pressed explosives: Preliminary assessment of binderless RDX in fuze trains
[MRL-R-1077] 09 p1150 N88-16892

Design of a charge sensitive preamplifier on high resistivity silicon
[DE88-003491] 10 p1323 N88-17907

A semianalytical technique for sensitivity analysis of unsteady aerodynamic computations
[NASA-TM-100810] 11 p1503 N88-18976

Visual contrast sensitivity functions obtained from untrained observers using tracking and staircase procedures
[AD-A187715] 11 p1522 N88-19089

Analysis of the sensitivity of the attitude control system of an artificial satellite
[INPE-4285-PRE/1157] 12 p1599 N88-19573

Sensitivity reduction over a frequency band
[AD-A189123] 12 p1621 N88-19694

Computer aided fast turnaround laboratory for research in VLSI (Very Large Scale Integration)
[AD-A189451] 12 p1624 N88-19715

Metal contacts to cadmium telluride (CdTe)
[AD-A188306] 12 p1696 N88-20150

Anomalous shock sensitivity/density relationship for RDX-polyethylene wax and related formulations from MRL Small Scale Gap Test (SSGT) measurements
[MRL-R-1099] 13 p1739 N88-20390

Some properties of Australian produced explosive composition H-6
[MRL-TN-525] 13 p1754 N88-20480

Computational aspects of sensitivity calculations in transient structural analysis
[NASA-TM-100589] 14 p1924 N88-21487

Sensitivity of control-augmented structure obtained by a system decomposition method
[NASA-TM-100535] 14 p1954 N88-21647

Shape sensitivity analysis of wing static aeroelastic characteristics
[NASA-TP-2808] 15 p2018 N88-22031

Infrared-sensitive spatial light modulator
[AD-A190391] 15 p2134 N88-22720

French evaluation of Japanese biosensors
16 p2184 N88-23020

Sensitivity analysis and multidisciplinary optimization for aircraft design: Recent advances and results
[NASA-TM-100630] 17 p2302 N88-23766

On quench sensitivity of Cu-Cr alloys
[NASA-TT-20174] 18 p2489 N88-24785

A multi-frame ion pinhole camera for intense ion beam transport and focusing experiments
[DE88-007283] 18 p2516 N88-24926
Reducing sensitivity to errors in free electron laser amplifiers
[DE88-007017] 18 p2522 N88-24960
Sensitivity analysis for the system reliability function
[AD-A191648] 18 p2525 N88-24979
Simulation of diaphragm-type IC pressure sensors
19 p2672 N88-25887
A mixed-modem solution for sensitive data segregation on a broadband network
[DE88-001765] 19 p2718 N88-26139
The T-T-T curve in Cu-Cr alloy
[NASA-TT-20167] 20 p2774 N88-26453
Performance sensitivities for point-focus dish systems with secondary concentrators
[DE88-001152] 21 p2968 N88-27629
The radiation sensitivity of select metal chelate polymers: Mechanistic changes at higher energies
[AD-A193467] 23 p3196 N88-29019
Acoustic-optical detector of gravitational waves based on high-quality crystals
[DE88-702459] 23 p3232 N88-29232
Phase sensitive amplification with SIS (Superconductor-Insulator-Superconductor) quasiparticle mixers
[AD-A194594] 23 p3291 N88-29596

SENSITIZING
Study of stainless steel time-temperature sensitization diagrams, part 1
[ETN-87-90762] 03 p0289 N88-11815
The dishomogeneity of the degree of sensitization in large recirculation pipes in Boiling Water Reactor (BWR) power plants
[CISE-3955] 09 p1247 N88-17473

SENSORIMOTOR PERFORMANCE
NT PSYCHOMOTOR PERFORMANCE
Measurement and modification of sensorimotor system function during visual-motor performance
[AD-A186351] 07 p0889 N88-15387
Risk of hypertension and functional cerebral laterality in oil expedition works in far north
12 p1665 N88-19980
Neurophysiological precursors of accurate visuomotor performance 21 p2981 N88-27706
Alterations in upper extremity motor function in soldiers during acute high altitude exposure
[AD-A192676] 23 p3236 N88-29272

SENSORS
Metal-sensing layer-semiconductor and metal-sensing layer-metal heterostructure gas sensors
[DE87-011293] 01 p0103 N88-10674
Opimal detection of sensor failures in flight control systems using deterministic observers
02 p0128 N88-10803
Combustion control with smart sensors
[DE87-013688] 03 p0261 N88-11768
On the root locus method applied to flexural vibration control systems 03 p0320 N88-12022
Limits to the precision of electro-optic and magneto-optic sensors
[PB87-212536] 03 p0323 N88-12040
Turbine flow meter with optical fiber pick-up
[NAL-TR-923] 09 p1169 N88-17009
A quantitative method for evaluating sensor layouts
09 p1178 N88-17056
Multichannel anisotropic single-mode fiber optics for transducers 09 p1240 N88-17429
ISTP SBIR phase 1 Full-Sky Scanner: A feasibility study
[NASA-CR-180749] 10 p1333 N88-17964
Signal and data processing for IR sensors
10 p1374 N88-18199
Prototype thin-film thermocouple/heat-flux sensor for a ceramic-insulated diesel engine
[NASA-TM-100796] 11 p1490 N88-18892
Optically coupled tactile sensor array for robotics
11 p1550 N88-19273
Spectral contents readout of birefringent sensors
[NASA-CR-179430] 13 p1784 N88-20673
Electromagnetic sensor arrays for nondestructive evaluation and robot control
[AD-A190210] 15 p2056 N88-22260
Analytical sensor redundancy assessment
[NASA-CR-182892] 16 p2163 N88-22901
A comparison of integrated and separate systems for flight control and navigation 17 p2303 N88-23779
Fiber waveguide sensors for intelligent materials
[NASA-CR-183028] 17 p2343 N88-23968
Design considerations for the development of an implantable sensor for the continuous measurement of glucose in the diabetic patient 17 p2382 N88-24159
User's guide to the Fault Inferring Nonlinear Detection System (FINDS) computer program
[NASA-CR-178410] 18 p2462 N88-24619
Automatic calibration of space based manipulators and mechanisms
[NASA-CR-182804] 19 p2676 N88-25912
Fiber optic sensors with internal referencing
[NASA-TM-100893] 20 p2806 N88-26644
RRSAS (Robotic Radiation Survey and Analysis System) Project: A real time sensor driven robotic system
[DE88-006825] 20 p2808 N88-26661
Nuclear and ionic charge distribution experiment on ISEE-1 and ISEE-3
[NASA-CR-180776] 23 p3183 N88-28947
Sensor and actuator selection for large space structure control
[AD-A194912] 24 p3333 N88-29842

SENSORY DISCRIMINATION
NT BRIGHTNESS DISCRIMINATION
NT TACTILE DISCRIMINATION
NT VISUAL DISCRIMINATION

SENSORY FEEDBACK
Center for the study of rhythmic processes
[AD-A188204] 11 p1520 N88-19078
Steady-state evoked potentials possibilities for mental-state estimation 16 p2240 N88-23380

SENSORY PERCEPTION
NT AUDITORY PERCEPTION
NT CONSCIOUSNESS
NT PROPRIOCEPTION
NT SPACE PERCEPTION
NT TACTILE DISCRIMINATION
NT TOUCH
NT VISUAL DISCRIMINATION
NT VISUAL PERCEPTION
Brain potentials and personality: A new look at stress susceptibility
[AD-A186931] 09 p1199 N88-17189
Engineering data compendium. Human perception and performance. User's guide
[LC-87-19560] 21 p2993 N88-27749
Engineering data compendium. Human perception and performance, volume 1
[LC-87-19560] 22 p3134 N88-28630
Engineering data compendium. Human perception and performance, volume 2
[LC-87-19560] 22 p3134 N88-28631
Engineering data compendium. Human perception and performance, volume 3
[LC-87-19560] 22 p3134 N88-28632

SENSORY STIMULATION
Sleep induced in cat by electric stimulation of acoustic and motor areas in brain cortex
06 p0751 N88-14612
Vestibular response to caloric stimulation during orbital flight 12 p1658 N88-19939
Significance of sensory signal phase mismatch in mechanisms of motion sickness development
20 p2830 N88-26787

SENTENCES
NT SYLLABLES
NT WORDS (LANGUAGE)

SEO (INDIAN SPACECRAFT)
U INDIAN SPACECRAFT

SEPAC (PAYLOAD)
Space experiments with particle accelerators (SEPAC): Description of instrumentation
[NASA-TM-89726] 14 p1945 N88-21606

SEPARATED FLOW
NT BOUNDARY LAYER SEPARATION
The structure of separated flow regions occurring near the leading edge of airfoils including transition
[NASA-CR-181434] 01 p0002 N88-10011
Investigations of separated flow states on wings of medium aspect ratio taking into account the wind tunnel interference problem
[ETN-87-90437] 01 p0003 N88-10016
An inviscid model of planar, separated flows of finite extent
[RAE-TR-86070] 01 p0044 N88-10279
Intergration effects of D-shaped, underwing, aft-mounted, seperate-flow, flow-through nacelles on a high-wing transport
[NASA-TM-4016] 02 p0122 N88-10773
Computation of transonic separated wing flows using an Euler/Navier-Stokes zonal approach
[NASA-TM-88311] 02 p0173 N88-11089
Three-dimensional unsteady flow elicited by finite wings and complex configurations 04 p0395 N88-12468
Investigation of low-speed turbulent separated flow around airfoils
[NASA-CR-177450] 04 p0396 N88-12471
Numerical simulation of unsteady separated flows
[AD-A184132] 04 p0442 N88-12741
Driving mechanism of unsteady separation shock motion in hypersonic interactive flow 05 p0530 N88-13226
Application of discrete vortex method to analysis of separated flow around aerofoils
05 p0537 N88-13268
Characteristics of a separating confluent boundary layer and the downstream wake
[NASA-TM-100046] 06 p0704 N88-14323
A theory for the core flow of leading-edge vortices
07 p0810 N88-14935
Vortex dynamics 07 p0812 N88-14945
A flow visualization study of the leading edge separation bubble on a NACA 0012 airfoil with simulated glaze ice
[NASA-CR-180846] 07 p0816 N88-14966
Analysis of three-dimensional viscous internal flows
[AD-A186254] 07 p0849 N88-15155
Unsteady three-dimensional flow separation
[NASA-CR-182412] 08 p0949 N88-15761
Calculation of symmetric and asymmetric vortex seperation on cones and tangent ogives based on discrete vortex models
[NASA-CR-4122] 08 p0950 N88-15768
Three-dimensional unsteady flow elicited by finite wings and complex configurations
[AD-A186464] 08 p0951 N88-15770
Wind tunnel investigations of periodic vortex separation on rough-surface circular cylinders using acoustic measuring methods
[DFVLR-FB-87-24] 09 p1112 N88-16665
Solution of the three-dimensional Navier-Stokes equations for transonic flow using a multigrid method
10 p1267 N88-17579
Control of vortical separation on conical bodies
10 p1267 N88-17580
Fluctuations and massive separation in three-dimensional shock-wave/boundary-layer interactions
[NASA-TM-89224] 11 p1434 N88-18559
Some aspects of aircraft dynamic loads due to flow separation
[AGARD-R-750] 11 p1439 N88-18588
Numerical model of the time independent mean flow in a rotating rocket motor 13 p1733 N88-20360
Surface flow visualization of separated flows on the forebody of an F-18 aircraft and wind-tunnel model
[NASA-TM-100436] 14 p1863 N88-21127
A flight test investigation into flow separation and structural response for a transport aircraft at buffet onset
[RAE-TR-87006] 14 p1867 N88-21156
On the prediction of highly vortical flows using an Euler equation model, part 2
[AD-A190245] 15 p2064 N88-22305
Dense-spray structure and phenomena. Part 1. Turbulence/dispersed-phase interactions
[AD-A190606] 15 p2065 N88-22315
A new laminar water tunnel to study the transition process in a blasius layer and in a separation bubble and a new tool for industrial aerodynamics and hydrodynamic research 16 p2204 N88-23150
Propfan model wind tunnel aeroelastic research results 16 p2220 N88-23246
Stall flutter analysis of propfans
16 p2221 N88-23256
Unsteady flow about cambered plates
[AD-A191226] 17 p2337 N88-23945
Accounting for the effects of unsteady, separated boundary layers in transonic two dimensional calculations
[ONERA-RT-30/3064-RY-063-R]
17 p2338 N88-23952
Theoretical and experimental investigation of swirl flow phase separators for microgravity applications
17 p2411 N88-24335
Experimental investigation of a microgravity separator for two phase mixtures containing small volumes of gas/vapor 17 p2432 N88-24468
Unsteady flow in a supercritical supersonic inlet
18 p2460 N88-24605
Instability of laminar separation bubbles: Causes and effects
[AD-A191168] 18 p2508 N88-24876
Computation of the turbulent boundary layer downstream of vortex generators
[AD-A191544] 18 p2508 N88-24881
Improving the performance of a finite element method using vector analysis on CRAY 1
[ETN-88-92153] 18 p2513 N88-24907
Method and apparatus for detecting laminar flow separation and reattachment
[NASA-CASE-LAR-13952-1-SB]
18 p2513 N88-24910
Turbulent heat transfer and fluid flow measurements downstream of abrupt expansions and in a cavity of a circular tube at a uniform wall temperature
18 p2515 N88-24920
Method of forming a multiple layer dielectric and a hot film sensor therewith
[NASA-CASE-LAR-13678-1] 18 p2584 N88-25355

Development of a method of calculating unstable flows of cascades separated at the leading edge
[PB87-228714] 19 p2598 N88-25437
Vortex methods for separated flows
[NASA-TM-100068] 20 p2753 N88-26342
A study of flow separation in transonic flow using inviscid and viscous computational fluid dynamics (CFD) schemes
[NASA-CR-183119] 20 p2801 N88-26618
Treatment of the separated flow around profiles (nonviscous, incompressible, two dimensional flow) by the singularities method
[ISL-R-106/87] 20 p2803 N88-26633
Experimental study of unsteady separating turbulent boundary layers
[AD-A192997] 21 p2943 N88-27477
Physical mechanisms in shock-induced turbulent separated flow
[AD-A193165] 21 p2944 N88-27484
A documentation of two- and three-dimensional shock-separated turbulent boundary layers
[NASA-TM-101008] 21 p2949 N88-27519
Study of three-dimensional transonic flow separations
[AD-A193018] 22 p3037 N88-28032
The dynamic behavior of a turbulent boundary layer subjected to a shock-induced separation
[AD-A194164] 22 p3075 N88-28252
Development and analysis of turbulent non-equilibrium boundary layers 23 p3169 N88-28872
Shock boundary layer interaction
23 p3170 N88-28873
Classical separation, trailing-edge flows and buffeting
23 p3170 N88-28874
Vortex flows 23 p3170 N88-28875
Direct-solution techniques for viscous flows and their control
[AD-A194775] 23 p3211 N88-29114
Numerical methods: Euler time dependent solver
24 p3318 N88-29760
The effects of incoming boundary layer thickness on unsteady shock-induced turbulent separations induced by cylinders
[AD-A196190] 24 p3368 N88-30060
Numerical simulation of nozzle flows
[AD-A195144] 24 p3369 N88-30064

SEPARATION
Segregation effects in welded stainless steels
[DE88-701224] 15 p2037 N88-22139

SEPARATORS
NT AIR FILTERS
NT DUST COLLECTORS
NT EVAPORATORS
NT FLUID FILTERS
NT SIEVES
Grace DAKASEP alkaline battery separator
02 p0164 N88-11031
Qualification testing of General Electric 50 Ah nickel-cadmium cells with Pellon 2536 separator and passivated positive plates 02 p0165 N88-11036
Physical properties of immiscible polymers
03 p0297 N88-11888
Plasma centrifuge development at INPE
[INPE-4243-PRE/1117] 08 p1087 N88-16546
Research on fluid dynamic energy separation
[DE88-002776] 10 p1339 N88-18001
A graph separator theorem and its application to Gaussian elimination to optimize Boolean expressions for parallel evaluation
[AD-A188527] 14 p1962 N88-21706
Theoretical and experimental investigation of swirl flow phase seperators for microgravity applications
17 p2411 N88-24335
Experimental investigation of a microgravity separator for two phase mixtures containing small volumes of gas/vapor 17 p2432 N88-24468
Flotation processes
[PB88-180302] 18 p2540 N88-25075
Fundamental studies of separation processes
[DE88-007467] 19 p2611 N88-25494

SEQUENCING
Cross-correlation of uniform cyclic difference set sequences
[AD-A184679] 05 p0640 N88-13913
HOC spectral analysis of an almost periodic random sequence in noise
[AD-A185528] 06 p0765 N88-14697
Von Mises' definition of random sequences reconsidered
[PB87-230512] 06 p0767 N88-14715
Recursive m-estimators of location and scale for dependent sequences
[AD-A183292] 07 p0903 N88-15469
On the characterization of certain point processes
[AD-A186427] 07 p0916 N88-15560
On the extreme order statistics for a stationary sequence
[AD-A186428] 07 p0916 N88-15561
Future television systems: Comparison of sequent ial and interlaced scanning
[BBC-RD-1987/18] 09 p1155 N88-16923
Strongly sequential term rewriting systems
[PB88-126693] 10 p1398 N88-18334
Linear prediction of stationary vector sequences
[NASA-TM-100069] 10 p1403 N88-18366
Ideal shrinking and expansion of discrete sequences
[NASA-TM-88202] 11 p1524 N88-19100
The roll back chip: Hardware support for distributed simulation using time warp
[AD-A187823] 11 p1529 N88-19132
Computer aided fast turnaround laboratory for research in VLSI (Very Large Scale Integration)
[AD-A189451] 12 p1624 N88-19715
An automatic system for extraction of information from a Computer Aided Design (CAD), selection, sequencing, and execution of turning processes
[INPE-4350-TDL/294] 12 p1676 N88-20020
A graph separator theorem and its application to Gaussian elimination to optimize Boolean expressions for parallel evaluation
[AD-A188527] 14 p1962 N88-21706
SSME technology test bed fast shutdown assessment
[NASA-CR-179354] 17 p2314 N88-23831
Spatial organization of homopolymer chains inside spherical polybutadiene domains of SB diblock copolymers
[AD-A193390] 21 p2918 N88-27321
Robust prediction for stationary processes: 2D enriched version
[AD-A193318] 21 p3006 N88-27833
Strong law for mixing sequence
[AD-A193615] 23 p3274 N88-29490
Performance of DS/SSMA communications in impulsive channels. Part 1: Correlation receivers
[AD-A195712] 24 p3362 N88-30021

SEQUENTIAL ANALYSIS
The sequential evaluation of Doppler satellite observations
[REPT-141] 01 p0010 N88-10057
Explicit formulate for the distributions of stopping variables under Wald's truncated SPRT (Sequential Probability Radio Tests) for a poisson process
[AD-A185053] 05 p0640 N88-13914
Statistical selection procedures
[AD-A185868] 07 p0913 N88-15538
Strongly sequential term rewriting systems
[PB88-126693] 10 p1398 N88-18334
DASM: A tool for Decomposition and Analysis of Sequential Machines
[EUT-87-E-170] 14 p1956 N88-21660
Efficient monotone sequential design
[CWI-MS-R8705] 14 p1962 N88-21707
Sequential tests for the drift of a Wiener process with a smooth prior and the heat equation
[AD-A190322] 15 p2121 N88-22638

SEQUENTIAL COMPUTERS
A model for architectural comparison
[AD-A195993] 24 p3411 N88-30302

SEQUENTIAL CONTROL
Substructure discovery in executed action sequences
[AD-A186446] 08 p1069 N88-16462

SERIES (MATHEMATICS)
NT ASYMPTOTIC SERIES
NT COSINE SERIES
NT PADE APPROXIMATION
NT POWER SERIES
NT TAYLOR SERIES
Recursive m-estimators of location and scale for dependent sequences
[AD-A186292] 07 p0903 N88-15469
Series representations of infinitely divisible random vectors and a generalized shot noise in banach spaces
[AD-A186502] 08 p1073 N88-16474
A representation for serial robotic tasks
12 p1681 N88-20048
Detecting serial correlation in the error structure of a cross-lagged panel model
[AD-A189070] 12 p1685 N88-20077
Distributions of quadratic forms
[AD-A190224] 15 p2124 N88-22663

SERIES EXPANSION
Spherical harmonic expansion of the Levitus Sea surface topography
[NASA-CR-181448] 02 p0216 N88-11362
Asymptotic form of stationary solutions of the Navier-Stokes equations for large Reynolds numbers
04 p0459 N88-12838
The shifted Adams method for ordinary differential equations
[DE88 000810] 04 p0486 N88-12994
The simulation of the viscous flow around a cylinder by the random vortex method 05 p0579 N88-13534
Contributions to selection and ranking theory with special reference to logistic populations
[AD-A185629] 07 p0917 N88-15566
On the Edgeworth expansion and the bootstrap approximation for a Studentized U-statistic
[CWI-MS-R8708] 14 p1965 N88-21726
On a biorthogonal system associated with uniform asymptotic expansions
[CWI-AM-R8709] 18 p2566 N88-25240
Accurate solution of parabolic equations by expansion in ultraspherical polynomials
[DE88-701829] 20 p2845 N88-26880
Asymptotic orders of reachability in perturbed linear systems
[AD-A192718] 22 p3143 N88-28888
Why are certain nonlinear Partial Differential Equations (PDE) both widely applicable and integrable
[PREPRINT-582] 22 p3144 N88-28898
Solution of large order Fourier-Bessel equations
[ARE-TM(UHA)-88504] 23 p3272 N88-29475
On the meaning of perturbation expansions in quantum field theory
[DE88-702138] 23 p3294 N88-29620
An improved spherical earth diffraction algorithm for SEKE
[AD-A195847] 24 p3360 N88-30005

SEROTONIN
Effect of low-frequency whole-body vertical vibration on the serotoninergic system of the brain and spinal cord
19 p2704 N88-26081

SERPENTINE
Impact-induced devolatilization and hydrogen isotopic fractionation of serpentine: Implications for planetary accretion
[NASA-CR-182677] 16 p2175 N88-22966

SERVICE LIFE
Ensuring the service life of designs (experience in aircraft construction) 02 p0157 N88-10966
Improving repairability of gears
02 p0158 N88-10969
Space station propulsion
[NASA-TM-100216] 03 p0277 N88-11746
Ultra-fine grained alloy material
[AD-A184500] 03 p0290 N88-11880
Durability (lifetime) predictions adhesively bonded structures
[AD-A184069] 03 p0335 N88-12110
Investigation of instability, dynamic forces, and effect of dynamic loading on strength of cages for the bearings in the high pressure oxygen turbopumps for the space shuttle main engine
[NASA-CR-178970] 06 p0714 N88-14378
Turbine engine monitoring systems: Can they benefit component improvement program management?
[AD-A186992] 09 p1120 N88-16706
Evaluation of bituminous materials used in pavement recycling projects at Tyndall, MacDill, and Hurlburt Air Force Bases
[AD-A188068] 10 p1317 N88-17871
Computer-aided design analysis of 57-mm, angular-contact, cryogenic turbopump bearings
[NASA-TP-2816] 11 p1496 N88-18933
Sodium-sulfur technology evaluation at Argonne National Laboratory
[DE88-002852] 13 p1762 N88-20544
Failure mechanism of He-Ne lasers
14 p1902 N88-21382
Experience with duplex bearings in narrow angle oscillating applications 14 p1926 N88-21484
Titanium carbide coatings for aerospace ball bearings
14 p1927 N88-21486
Two gimbal bearing case studies: Some lessons learned 14 p1927 N88-21487
Robotic joint experiments under ultravacuum
14 p1927 N88-21490
Evaluation of structural analysis methods for life prediction 14 p1930 N88-21511
MPD (magnetoplasmadynamic) thruster advanced pumping system concepts
[AD-A190513] 15 p2138 N88-22756
Development of a flexible and economic helicopter engine monitoring system
[PB88-165147] 16 p2160 N88-22867
The effect of titanium reinforcement on the life of positive grids in lead-acid batteries 17 p2320 N88-23657
Pioneer 10 and 11 RTG performance update
17 p2405 N88-24301
Foil gas bearing system endurance testing dynamic isotope power system 17 p2405 N88-24302
AMTEC electrode development
17 p2409 N88-24324
Gas-cooled reactor power systems for space
17 p2413 N88-24330

Analysis of closed cycle megawatt class space power systems with nuclear reactor heat sources
17 p2413 N88-24351
Performance and long duration test of a 30 kw thermal arcjet engine
[AD-A190962] 18 p2474 N88-24677
An extended life and performance test of a low-power arcjet
[NASA-TM-100942] 18 p2476 N88-24687
Harmfulness of defects: Behaviour in service of a delamination in a composite containing many differently oriented layers
[PB88-124714] 18 p2479 N88-24705
Nickel hydrogen low earth orbit life testing
[AD-A191946] 18 p2504 N88-24855
Effect of LEO cycling at shallow depths of discharge on MANTECH IPV nickel-hydrogen cells
[NASA-TM-101300] 19 p2688 N88-25978
Engine component retirement for cause. Volume 1: Executive summary
[AD-A192730] 20 p2760 N88-26371
A statistical treatment of accelerated life test data for copper-water heat pipes 20 p2783 N88-26509
Results from life test in progress on eagle-picher nickel cadmium cells
[AD-A192816] 21 p2936 N88-27434
Sodium/sulfur cell evaluation results
[DE88-011488] 21 p2938 N88-27451
Background to the UK military requirements for engine usage, condition and maintenance management systems
22 p3033 N88-28004
Corrosion and stress corrosion of metals in decontamination solutions 22 p3054 N88-28118
Modeling discrete bathtub and upside down bathtub mean residual life functions
[AD-A192000] 22 p3085 N88-28320
Burn-in with mixed populations
[AD-A194651] 22 p3085 N88-28321
Life-span knowledge engineering for space operations
23 p3259 N88-29401
Fuel effects on flame radiation and hot-section durability 24 p3347 N88-29925
A reliability-based program for predicting the service life of organic coating systems 24 p3355 N88-29971
In-house capacitor technology program
[AD-A194804] 24 p3367 N88-30049

SERVICES
NT MEDICAL SERVICES
NT METEOROLOGICAL SERVICES
Freedom of Information Act: Fee waiver practices at the FBI (Federal Bureau of Investigation)
[PB87-216727] 02 p0249 N88-11573
Reuse: A Reliable Unified Service Environment for distributed systems 10 p1379 N88-18231

SERVOCONTROL
A new state space model for the NASA/JPL 70-meter antenna servo controls 04 p0436 N88-12702
A modern control theory based algorithm for control of the NASA/JPL 70-meter antenna axis servos
04 p0436 N88-12706
Development of an interface for an ultrareliable fault-tolerant control system and an electronic servo-control unit
[NASA-TM-88236] 05 p0553 N88-13367
Description and analysis of a cascade control of fluid flow
[PB87-112686] 06 p0698 N88-14282
Covariant control of bilateral servos for in-orbit manipulation 12 p1590 N88-19520
Servo-actuator control for sampled-data feedback disturbance rejection --- helicopters
[ESA-TT-1002] 16 p2163 N88-22903
Study on design and control of torque-controlled manipulators
[NASA-TT-20197] 23 p3223 N88-29183

SERVOMECHANISMS
NT SERVOMOTORS
Application of prediction of equilibrium to servo-controlled calorimetry measurements
[DE87-013745] 03 p0324 N88-12046
Design of a velocity and position control laboratory servo system
[AD-A186596] 08 p0990 N88-15997
Control system simulation for a single-link flexible arm
[AD-A187037] 09 p1174 N88-17035
Adaptive proximate time-optimal servomechanisms
09 p1175 N88-17043
Covariant control of bilateral servos for in-orbit manipulation 12 p1590 N88-19520
Implementation of a visual servoing system for evaluation of robotic refueling applications
[AD-A189678] 14 p1954 N88-21645
Photo-optical converter of angular displacements in digital servomechanisms
[DE87-703208] 14 p1961 N88-21686
Servo-actuator control for sampled-data feedback disturbance rejection --- helicopters
[ESA-TT-1002] 16 p2163 N88-22903
Path following robot
[AD-A190960] 16 p2215 N88-23217
Roller drive materials performance
16 p2219 N88-23241
Force servo control of a commercial gantry robot
[DE88-006649] 20 p2808 N88-26660
Study on design and control of torque-controlled manipulators
[NASA-TT-20197] 23 p3223 N88-29183
A standard architecture for controlling robots
[AD-A195929] 24 p3423 N88-30371

SERVOMOTORS
Modelling of a hydraulic motor and servo-valve to produce a desired system response using analogue and digital compensation techniques
[ETN-88-92079] 14 p1899 N88-21337

SERVOS
U SERVOMOTORS

SERVOSTABILITY CONTROL
U SERVOCONTROL

SET THEORY
NT BOREL SETS
NT EQUIVALENCE
Maintaining state constraints in relational databases: A proof theoretic basis
[DE87-014329] 02 p0248 N88-11559
A characterization of separating pairs and triplets in a graph
[AD-A184278] 04 p0477 N88-12941
On the number of minimum size separating vertex sets in a graph
[AD-A184279] 04 p0478 N88-12942
Foundations of O-theory 2: Measurements and relation to fuzzy set theory
[DE88-000013] 04 p0485 N88-12986
Diagonalisation methods in polynomial setting
[PB87-138616] 06 p0769 N88-14726
Theoretical investigations of chaotic dynamics
[AD-A186404] 07 p0867 N88-15261
An O(n3L) interior point algorithm for convex quadratic programming
[AD-A186001] 07 p0909 N88-15504
An elementary approach to the Daniell-Kolmogorov theorem and some related results
[AD-A186011] 07 p0909 N88-15505
On the extreme points of the set of all 2xn bivariate positive quadrant dependent distributions with fixed marginals and some applications
[AD-A186316] 07 p0911 N88-15521
Stationary regenerative sets and subordinators
[AD-A186298] 07 p0918 N88-15573
A fast bottom-up algorithm for computing the cut sets of noncoherent fault trees
[DE88-003741] 09 p1220 N88-17320
Norm inequalities for derivatives and differences
[DE88-002920] 09 p1230 N88-17371
An application of fuzzy set theory to statistical hypothesis testing
[AD-A186705] 09 p1232 N88-17386
A unified approach for digital image processing problems: Mathematical morphology
[INPE-4311-TDL/278] 11 p1537 N88-19183
Measures of similarity between fuzzy concepts: A comparative analysis
[AD-A189430] 13 p1825 N88-20910
Compact representation of the separating k-sets of a graph
[AD-A189650] 14 p1965 N88-21723
Data management and language enhancement for generalized set theory computer language for operation of large relational databases
[NASA-CR-182868] 16 p2250 N88-23446
Algorithms and data structures for an expanded family of matroid intersection problems
[AD-A191482] 18 p2562 N88-25213
A primal-dual algorithm for the computation of the minimum of a convex function on the intersection of convex functions, and its application in data analysis
[RR-638-M] 18 p2563 N88-25217
Multicriteria integer programming for problems involving linear and nonlinear utility functions
[AD-A194530] 23 p3249 N88-29336
Unification and set-valued functions for functional and logic programming
[AD-A193643] 23 p3250 N88-29341
A methodology for multiple rule system integration and resolution within a singular knowledge base
23 p3261 N88-29413
Mathematical algorithms for approximate reasoning
23 p3262 N88-29418
Practical higher-order functional and logic programming based on lambda-calculus and set-abstraction
[AD-A193645] 23 p3271 N88-29466

SETI
U PROJECT SETI

SEX FACTOR
Gender and cognitive style differences at the human-computer interface
[NPL-DITC-90/87] 01 p0077 N88-10493
Meta-analysis of leadership differences between males and females and the effect on performance
[AD-A187769] 11 p1564 N88-19361

SEX GLANDS
NT TESTES

SEYFERT GALAXIES
Comparison of global and nuclear properties of starburst and Seyfert 1 galaxies 03 p0388 N88-12438
The radio structure of active nuclei in edge-on spiral and Seyfert galaxies 09 p1264 N88-17576
IUE evidence on the nature of the innermost broad-line region in Seyfert 1 galaxies 17 p2450 N88-24552
AGN (OIII) emission line profiles: Dependencies on galaxy inclination and Balmer decrement
[INPE-4596-PRE/1324] 24 p3459 N88-30577

SFAR
U SOUND FIXING AND RANGING

SHADOWGRAPH PHOTOGRAPHY
NT SCHLIEREN PHOTOGRAPHY
Development of flow visualization techniques for use in the Hot Gas Laboratory
[BAE-ARG-233] 03 p0325 N88-12052

SHADOWGRAPHS
U SHADOWGRAPH PHOTOGRAPHY

SHADOWS
NT PENUMBRAS
Unified Sun and sky illumination for shadows under trees
[DE87-014232] 01 p0083 N88-10535
Shadow systems and attractors in reaction-diffusion equations
[AD-A185604] 06 p0766 N88-14706
Color shadow methods of analyzing reconstructed wave front 09 p1236 N88-17407
Manual for obscuration code with space station applications
[NASA-CR-178099] 17 p2334 N88-23931
Shape from shading, occlusion and texture
[AD-A184840] 18 p2571 N88-25269
Curvature of blended rolled edge reflectors at the shadow boundary contour
[NASA-CR-182974] 18 p2576 N88-25300

SHAFTS (MACHINE ELEMENTS)
NT ROTATING SHAFTS
NT TURBOSHAFTS
Digital algorithms for the control and dynamic decoupling of industrial robot axes
[ETN-87-90441] 01 p0084 N88-10546
Analysis of 7- X 10-foot high speed wind tunnel shaft loads in support of fan blade failure investigation
[NASA-TM-100504] 04 p0402 N88-12496
Exact finite element method analysis of viscoelastic tapered structures to transient loads
05 p0585 N88-13632
The Jeffcott equations in nonlinear rotordynamics
07 p0928 N88-15636
Dynamic modelling of flexible rotor shafts mounted on hydrodynamic bearings 13 p1779 N88-20641
Study on shaft seals for potassium turbine
[EL-891] 15 p2074 N88-22364
Angular position measurements at high temperatures and high radiation environments
17 p2434 N88-24479
SRB/SLEEC (Solid Rocket Booster/Shingle Lap Extendible Exit Cone) feasibility study, volume 2. Appendix A: Design study for a SLEEC actuation system
[NASA-CR-178974] 23 p3187 N88-28965

SHALLOW SHELL EQUATIONS
Effective treatment of membrane and shear locking phenomena in curved shear-deformable axisymmetric shell element 04 p0428 N88-12652
Forced motion of initially stressed shells and plates
18 p2529 N88-25005

SHALLOW SHELLS
Blade vibration problems in centrifugal compressors. Fundamental considerations 07 p0851 N88-15165
Nonlinear dynamic analysis and optimal control of shallow shells 23 p3224 N88-29191

SHALLOW WATER
Nearshore wave transformation study of sites near Port Canaveral Inlet, Florida
[AD-A186968] 09 p1195 N88-17159
Remote sensing of acoustic properties of shallow water sediments: A review
[AD-A192107] 18 p2570 N88-25267
Fully implicit splitting method for accurate tidal computations
[PB88-183637] 20 p2828 N88-26781

SHANKS
U JOINTS (JUNCTIONS)

SHANNON INFORMATION THEORY
U INFORMATION THEORY
SHAPE CONTROL
Multisurface control mechanism for a deployable antenna: Far Infrared and Submillimeter Space Telescope (FIRST) technology study
[RP-FA-D003] 09 p1135 N88-16807
Development of metastable processing paths for high temperature alloys
[AD-A188682] 12 p1608 N88-19617
The 15-meter diameter hoop/column antenna surface control actuator system 14 p1824 N88-21469
Technologies for antenna shape and vibration control
19 p2652 N88-25748
Robust design of distributed controllers for large flexible space structures
[NASA-CR-183202] 24 p3380 N88-30134
SHAPE MEMORY ALLOYS
NT NITINOL ALLOYS
A comparison of high damping shape memory alloys with Cu-Mn-based and Fe-Cr-based alloys
[AD-A184110] 04 p0414 N88-12566
Martensitic transformation and microstructures in sintered NiAl alloys
[NASA-TT-20192] 19 p2616 N88-25519
Shape memory alloys: New materials for future engineering
[NASA-TT-20193] 20 p2775 N88-26455
SHAPED CHARGES
Jet formation and characterization of a conical shaped charge
[DE87-012102] 02 p0155 N88-10969
Destruction test of small scaled solid propellant motors
[ISAS-R-620] 03 p0278 N88-11752
Jet initiation of PBX 9502
[DE88-000493] 05 p0571 N88-13481
Developments in instrumental techniques for observations of magnetospheric and ionospheric shaped charge releases 08 p1031 N88-16248
Penetration theory for inclined and moving shaped charges
[MBB-UA-940/86] 10 p1315 N88-17861
SHAPES
NT CONVEXITY
NT ELLIPTICITY
NT LINE SHAPE
NT T SHAPE
Shape optimization of linear antennas
[ETN-87-90413] 01 p0036 N88-10233
Theory and methods for design of pulse shapes for broadcast teletext
[CRC-1405] 02 p0162 N88-11013
A shape preserving interpolant which has tension controls
[DE87-014615] 02 p0229 N88-11443
Observations on the hydrodynamic flow visualization at ONERA
[PD-FM-8718] 04 p0444 N88-12753
An approach to object recognition: Aligning pictorial descriptions
[AD-A184462] 04 p0482 N88-12972
Shape optimization of damping layers
05 p0585 N88-13635
The statistics of the shape of small fatigue cracks
05 p0599 N88-13666
Electromagnetic fields backscattered from an s-shaped inlet cavity with an absorber coating on its inner walls
[NASA-CR-182401] 07 p0845 N88-15130
An experimental mapping of the flow field behind a glaze ice shape on a NACA 0012 airfoil
[NASA-CR-180847] 08 p0950 N88-15766
Shape isomers as candidates for the gamma ray laser storage state
[DE88-005226] 11 p1492 N88-18909
Design modeling for shape optimization
11 p1527 N88-19122
Shape optimization of three-dimensional stamped and solid automotive components
[GMR-5168] 11 p1528 N88-19123
An investigation of cruciform parachutes and towed targets
[BU-360] 14 p1862 N88-21122
Electrohydrodynamic migration of charged droplets in an insulating fluid
[NASA-TM-100849] 14 p1912 N88-21424
Study of mean free path effects on growth of ultrafine metallic aerosols
[AD-A190206] 15 p2039 N88-22149
Mixed finite element formulation applied to shape optimization 16 p2221 N88-23252
Implications of the trapping-desorption and direct inelastic scattering channels on Dicke-narrowed lineshapes
[AD-A191410] 16 p2270 N88-23581
Shape detection in remote sensing through graph isomorphism 17 p2354 N88-24028
An analytic model for aerodynamic shapes
[AD-A191573] 18 p2456 N88-24583
Shape stability in composites
18 p2479 N88-24706
Stiffened titanium panels
[NASA-CASE-LAR-13814-1] 18 p2497 N88-24816
Shape from shading, occlusion and texture
[AD-A184840] 18 p2571 N88-25269
Flexible tactile sensing arrays for robotics: Architectural robustness and yield considerations
19 p2671 N88-25878
Theoretical predictions of precipitate shapes in cubic alloys
[DE88-010856] 21 p2914 N88-27291
Texture perception and shape from texture
[AD-A192923] 21 p2996 N88-27771
Distortion functions
[DE88-752634] 21 p3015 N88-27896
Three-dimensional zonal grids about arbitrary shapes by Poisson's equation
[NASA-TM-101018] 22 p3039 N88-28042
Using primal sketch primitives as the basis for the Hough transform
[INPE-4564-PRE/1305] 24 p3412 N88-30310
Symbolic construction of a 2D scale-space image
[AD-A195926] 24 p3423 N88-30374
SHARP LEADING EDGES
Tests on the AFWAL 65 deg delta wing at NLR: A study of vortex flow development between Mach = 0.4 and 4
[NLR-MP-86058-U] 13 p1717 N88-20266
Development of a method of calculating unstable flows of cascades separated at the leading edge
[PB87-228714] 19 p2598 N88-25437
SHATTERING
U FRAGMENTATION
SHEAR
An analytical study of the effects of transverse shear deformation and anisotropy on buckling loads of laminated cylinders
[NASA-TM-100508] 05 p0557 N88-13387
Temperature-dependent tensile and shear response of graphite/aluminum
[NASA-CR-182914] 19 p2609 N88-25484
SHEAR CREEP
Viscoelastic properties of EA951 adhesive: A source of creep deformations of a strongback
[DE88-001581] 06 p0685 N88-14197
SHEAR DISTURBANCES
U S WAVES
SHEAR FATIGUE
U SHEAR STRESS
SHEAR FLOW
Two-dimensional shear flow turbulence: A statistical theory of vortex filaments
[DE87-012234] 01 p0046 N88-10295
Shearing flow over Stokes wave. Part one: General theory
[ETN-87-90957] 02 p0171 N88-11074
Analysis of the motions and effects of hairpin vortices
03 p0316 N88-11997
Nonequilibrium fluctuations and transport in sheared fluids 03 p0316 N88-11999
Heat and moisture transport in the atmospheric boundary layer
[AD-A184222] 04 p0470 N88-12904
Three-dimensional structure of boundary layers in transition to turbulence
[AD-A185466] 06 p0702 N88-14311
Turbulence in hypersonic flow
[AD-A185624] 07 p0815 N88-14961
Nonlinear and nonparallel stability problems
[AD-A186406] 07 p0850 N88-15159
Interpretation of equatorial current meter data as internal waves
[PB88-108113] 08 p1044 N88-16309
Investigation of the influence of wind shear on the aerodynamic characteristics of aircraft using a vortex-lattice method 10 p1274 N88-17619
Analysis of shear-layer probe data for holes in hypersonic configurations
[DE88-003992] 11 p1435 N88-18564
Structure of shear flow turbulence and its control
[AD-A187909] 11 p1482 N88-18846
Transport and stability properties of free shear flows
13 p1768 N88-20577
Research on turbulence in bottom boundary layer in ocean 13 p1788 N88-20697
Mixed-layer shear related to wind stress in the central equatorial Pacific 13 p1805 N88-20793
Mixed-layer fronts in the California current
13 p1805 N88-20794
Enhancement of data acquisition and numerical computation capabilities for unsteady fluid dynamics
[AD-A190115] 15 p2063 N88-22302
A new method of measuring multigrade oil shear elasticity and viscosity at high shear rates
[AD-A190145] 15 p2064 N88-22304
Instruments for use in experimental studies of complex turbulent shear flow: Three component LDVs
[AD-A190526] 15 p2065 N88-22312
Direct numerical simulation of buoyantly driven turbulence 16 p2196 N88-23097
Modeling of turbulent transport as a volume process
16 p2196 N88-23099
A statistical investigation of the single-point pdf of velocity and vorticity based on direct numerical simulations 16 p2196 N88-23101
Local structure of intercomponent energy transfer in homogeneous turbulent shear flow
16 p2197 N88-23103
A general form for the dissipation length scale in turbulent shear flows 16 p2197 N88-23104
Relations between two-point correlations and pressure strain terms 16 p2198 N88-23109
Conditionally-averaged structures in wall-bounded turbulent flows 16 p2198 N88-23112
Structure of turbulent shear flows
16 p2198 N88-23113
Inflectional instabilities in the wall region of bounded turbulent shear flows 16 p2199 N88-23114
An investigation of ducted propellers in axisymmetric shear flow 16 p2202 N88-23136
Experimental study of vortex sheets in plane flow
16 p2203 N88-23142
Dynamics and control of turbulent shear flows
[AD-A191527] 18 p2508 N88-24879
LLNL granular solids flow project
[DE88-007492] 18 p2513 N88-24906
A single streamwise vortical structure and its instability in shear flows 18 p2515 N88-24921
Atomization in a turbulent shear layer: Preliminary measurements 19 p2624 N88-25565
Scaling laws for homogeneous turbulent shear flows in a rotating frame
[NASA-CR-181672] 19 p2665 N88-25847
Influence of wind shear on the aerodynamic characteristics of airplanes
[NASA-TP-2827] 20 p2755 N88-26344
A numerical simulation of two-dimensional transient shear flow
[ISAS-RN-627] 20 p2797 N88-26600
Stability of a coastal upwelling front over topography
[AD-A192354] 20 p2829 N88-26784
Evolution of hairpin vortices in a shear flow
[NASA-TM-100858] 20 p2845 N88-26885
Cavitation inception in a turbulent shear flow
[DE88-011486] 21 p2946 N88-27497
Granular flow: Particle-dynamics simulations of steady flow
[DE88-011342] 21 p2948 N88-27506
Direct simulation of stable stratified homogeneous turbulent shear flows
[DFVLR-FB-88-04] 21 p2949 N88-27516
The Kelvin-Helmholtz instability in a stratified shear flow
[CFD/88/2] 22 p3076 N88-28265
Stability of parallel inviscid shear flow with mean spanwise variation
[FFA-TN-1987-57] 22 p3079 N88-28285
Nonlinear surface and internal waves on shear flow
[PREPRINT-584] 22 p3129 N88-28604
Study of toluene rotary fluid management device and shear flow condenser performance for a space-based organic Rankine power system
[NASA-CR-180885] 24 p3336 N88-29872
SHEAR LAYERS
A note on the instability of a vortex sheet leaving a semi-infinite plate
[DFVLR-FB-87-16] 01 p0004 N88-10019
On the instability of thin circular shear layers
04 p0395 N88-12467
Blowup for a nonlinear evolution equation and self-reproducing strained shear layers
04 p0444 N88-12755
Combustion related shear-flow dynamics in elliptic supersonic jets 05 p0531 N88-13232
Experimental investigation of heterogeneous compressible shear layers 06 p0700 N88-14284
Nonlinear and nonparallel stability problems
[AD-A186406] 07 p0850 N88-15159
Mean velocities and Reynolds stresses in the juncture flow and in the shear layer downstream of an appendage
[AD-A185619] 08 p0940 N88-15823
Cavitation inception scale effects. 1. Nuclei distributions in natural waters. 2. Cavitation inception in a turbulent shear flow
[AD-A186553] 08 p0966 N88-15987
Active feedback interaction with a shear layer
[AD-A188525] 12 p1573 N88-19410

Time-accurate simulations of a shear layer forced at a single frequency
[NASA-TM-100836] 12 p1628 N88-19740

Optical properties of compressible inhomogeneous shear layers relevant to high power lasers
[AD-A189299] 12 p1633 N88-19774

Three-dimensional shear layer experiments and their use as test cases for calculation methods
[NLR-MP-86036-U] 13 p1767 N88-20570

Numerical model of Rayleigh instability and spin-off eddies on fronts 13 p1788 N88-20696

Instruments for use in experimental studies of complex turbulent shear flow: Three component LDVs
[AD-A190526] 15 p2065 N88-22312

Shear-layer structures in near-wall turbulence
16 p2198 N88-23110

Dynamics and control of turbulent shear flows
[AD-A191527] 18 p2508 N88-24879

Characteristics of merging shear layers and turbulent wakes of a multi-element airfoil
[NASA-TM-100053] 18 p2511 N88-24900

Stability of a coastal upwelling front over topography
[AD-A192354] 20 p2829 N88-26784

Predicting optical degradation of a laser beam through a turbulent shear layer 21 p2927 N88-27376

An analysis of horizontal temperature gradients and heat content in the mixed layer and the surface forcing during PATCHEX
[AD-A192330] 21 p2976 N88-27678

Aerodynamics of seeing on large transport aircraft
[NASA-CR-183122] 23 p3174 N88-28896

SHEAR PROPERTIES

NT SHEAR STRENGTH

Two-dimensional shear flow turbulence: A statistical theory of vortex filaments
[DE87-012234] 01 p0046 N88-10295

Refraction of shear wave into nonlinearly elastic or elastoplastic half-space 02 p0159 N88-10999

Stability of low-shear Tokamaks
[DE88-000305] 03 p0379 N88-12383

Determination of through-plane shear moduli for glass-reinforced plastics
[PB87-106274] 04 p0418 N88-12592

Steady shearing in a viscoplastic solid
[AD-A184341] 04 p0454 N88-12810

The evolution of plastic strain in steady, plastic shock waves
[DE87-013812] 04 p0456 N88-12826

Studies of unsteadiness in boundary layers
[AD-A185662] 06 p0703 N88-14315

The effect of shear lips on fatigue crack growth in Al-2024 sheet material 06 p0718 N88-14408

Shear failure in round bar tensile tests of Al-Zn-Mg-Cu alloys
[PB87-143632] 07 p0869 N88-15271

Successful mixed formulation for axisymmetric shell analysis employing discontinuous stress fields of the same order as the displacement field
[DE88-700021] 09 p1178 N88-17052

Boundary stabilization of thin elastic plates
[AD-A187123] 10 p1343 N88-18025

On stress collapse in adiabatic shear bands
[AD-A187185] 11 p1498 N88-18942

High shear rate rheometry of low-viscosity liquids
[AD-A188447] 12 p1627 N88-19733

Parametric study of acceleration-induced stresses and frequency changes in doubly-rotated crystal resonators
[AD-A189261] 13 p1761 N88-20532

The buckling and vibration of composite plates using the Levy method considering shear deformation and rotary inertia
[AD-A189743] 15 p2076 N88-22374

The influence of cathodic protection on erosion-corrosion of metals and model alloys
[AD-A191613] 18 p2485 N88-24742

Pulsed spray structure and atomisation techniques
[AD-A192280] 20 p2800 N88-26614

An experimental and analytical evaluation of a biaxial test for determining shear properties of composite materials
[NASA-CR-182928] 21 p2962 N88-27593

Small scale mixing in the initial region of a jet
[AD-A193500] 23 p3192 N88-28964

Critical conditions for failure in materials subjected to high rates of loading
[AD-A194697] 23 p3226 N88-29201

Kinetic theory for electrostatic waves due to transverse velocity shears
[AD-A193404] 23 p3284 N88-29557

Large displacement and rotational formulation for laminated cylindrical shells including parabolic transverse shear
[AD-A194871] 24 p3384 N88-30158

SHEAR STRAIN

Plastic strain localization between voids in shear deformation fields 04 p0427 N88-12648

Effective treatment of membrane and shear locking phenomena in curved shear-deformable axisymmetric shell element 04 p0428 N88-12652

Vibration and buckling of geometrically imperfect laminated cylindrical shells 04 p0456 N88-12822

Plasticity of aluminum and iron at high shear strain rate and high pressure 05 p0563 N88-13430

The analysis of deformations and strains in composites by moire interferometry
[AD-A187482] 10 p1345 N88-18043

Geodetic measurement of deformation east of the San Andreas fault in Central California
[NASA-CR-182709] 13 p1798 N88-20754

An efficient Mindlin finite strip plate element based on assumed strain distribution 15 p2081 N88-22407

Dynamic shear band development in plane strain
[AD-A190915] 18 p2526 N88-24988

Improved finite strip Mindlin plate bending element using assumed shear strain distributions
[NASA-TM-100928] 23 p3225 N88-29195

SHEAR STRENGTH

Shear strength of the ASDEX upgrade Toroidal Field (TF) coil insulation: Rupture, fatigue and creep behavior --- tokamak
[IPP-1/230] 01 p0059 N88-10376

Spatial strength variation and statistical size effect of laminated orthotropic composite materials
04 p0427 N88-12646

Flexibilized copolyimide adhesives
[NASA-TM-89303] 05 p0570 N88-13474

Effect of interface on mechanical properties of graphite/201 aluminum composites
05 p0606 N88-13717

Interfacial shear strength of pitch and high strain pan fibers in an epoxy matrix
[AD-A185966] 07 p0826 N88-15011

Improving the interlaminar shear strength of carbon fiber-epoxy composites through carbon fiber bromination
[NASA-TM-100248] 07 p0827 N88-15018

A nonlinear computational model for the strength and failure of composite plates and shells
11 p1501 N88-18964

An investigation of the mechanical properties of improved carbon fibre composite materials
[RAE-TR-86021] 14 p1884 N88-21259

Evaluation of a thermoplastic polyimide (422) for bonding GR/PI composite
[NASA-TM-100584] 16 p2182 N88-23003

SHEAR STRESS

NT TORSIONAL STRESS

Free-edge delamination: Laminate width and loading conditions effects
[NASA-TM-100238] 04 p0411 N88-12551

A refined nonlinear analysis of laminated composite plates and shells
[AD-A184436] 04 p0454 N88-12811

Analysis of end stresses in glass-metal bimaterial strips
[DE87-007848] 05 p0610 N88-13750

A method for the approximate calculation of the skin friction coefficient of horizontal wavy plates
[VKI-TN-160] 07 p0851 N88-15172

The NASA aircraft icing research program
08 p0957 N88-15803

Shear and mixing effects on cells in agitated microcarrier tissue culture reactors 09 p1197 N88-17173

Strength and structure of Ga sub 1-xIn sub xAs alloys
[AD-A188092] 10 p1303 N88-17795

Ethynylated aromatics as high temperature matrix resins
[NASA-TM-89829] 11 p1450 N88-18640

On stress collapse in adiabatic shear bands
[AD-A187185] 11 p1498 N88-18942

Variation of the wind stress related to frontal passages during FASINEX (Frontal Air-Sea Interaction Experiment) 1986
[AD-A187180] 11 p1514 N88-19042

Sea duct: A deep-sea computer-controlled recirculating flume for the study of sea floor stability
[AD-A187734] 11 p1516 N88-19056

Mechanical response of unidirectional boron/aluminum under combined loading
[NASA-CR-182595] 12 p1604 N88-19591

Three-dimensional scattering of impulsive acoustic waves by a semi-infinite crack in the plane interface of a half space and a layer
[PB88-146966] 12 p1687 N88-20089

Bodies in unsteady flow
[AD-A190416] 15 p2064 N88-22306

Stochastic estimation of conditional eddies in turbulent channel flow 16 p2194 N88-23087

Coherent structure 16 p2199 N88-23117

Computation and characteristics of pulsatile multi-bifurcation flow 18 p2483 N88-24729

Method and apparatus for detecting laminar flow separation and reattachment
[NASA-CASE-LAR-13952-1-SB]
18 p2513 N88-24910

Resolved shear stress intensity coefficient and fatigue crack growth in large crystals
[NASA-CR-182137] 18 p2526 N88-24997

Characterization of accelerating pipe flow
[AD-A193065] 21 p2943 N88-27481

Liquid crystals for unsteady surface shear stress visualization
[DE88-010570] 21 p2951 N88-27527

Shear stress at a film-substrate interface due to mismatch strain
[AD-A193461] 23 p3288 N88-29577

Experimental determination of drag modifications due to elastic compliant surfaces using quantitative visual techniques
[AD-A194785] 24 p3372 N88-30082

Development of a more general Reynolds stress closure for swirling flow
[AD-A195121] 24 p3374 N88-30092

SHEAR WAVES

U S WAVES

SHEARING

Coronal magnetic fields produced by photospheric shear
[NASA-CR-181514] 03 p0390 N88-12447

Steady shearing in a viscoplastic solid
[AD-A184341] 04 p0454 N88-12810

An analytical study of the effects of transverse shear deformation and anisotropy on natural vibration frequencies of laminated cylinders
[NASA-TM-100554] 10 p1295 N88-17739

Applications of the lateral shearing interferometer in measurement of synchrotron radiation optical elements
[DE88-005184] 13 p1840 N88-21011

SHEARING STRESS

U SHEAR STRESS

SHEATHS

NT ION SHEATHS

NT PLASMA SHEATHS

Research and development of electrical insulators for thermionic applications 17 p2429 N88-24449

Effects of low reflection on the collector and source sheaths of a finite ion temperature plasma
[DE88-008929] 21 p3017 N88-27908

Collector and source sheaths of a finite ion temperature plasma
[DE88-008934] 23 p3286 N88-29564

SHEET METAL

U METAL SHEETS

SHELL STABILITY

Geometrically nonlinear rod mechanism analogy of axisymmetrically loaded spherical shells based on a comprehensive approach to the stability of circular arches
[ETN-87-90419] 01 p0062 N88-10398

Determination of the ultimate loads for corrugated-steel, barrel-type shell structures
[AD-A187716] 11 p1498 N88-18944

Tripping of stiffened plates using a refined beam theory
[AD-A193989] 22 p3087 N88-28333

Thickness effects on the stability of shell like structures 23 p3224 N88-29192

Computational aerodynamic analysis for a range-limited 25mm training round
[AD-A185270] 24 p3320 N88-29772

SHELL THEORY

Nonsteady state vibrations in acoustic medium of elastic elliptical shell subjected to instantaneously applied uniform pressure 02 p0160 N88-11000

An integral equation analysis of inelastic shells
03 p0336 N88-12118

Solution of geometrically nonlinear problem for reinforced shell of revolution having arbitrary shape
04 p0426 N88-12637

Rational reinforcement of cylindrical shells with variable stiffness frames subjected to external pressure
04 p0426 N88-12638

Finite deformations of shell with rigid inclusion
04 p0426 N88-12639

Effective treatment of membrane and shear locking phenomena in curved shear-deformable axisymmetric shell element 04 p0428 N88-12652

Calculation of displacement, constraints and eigenmodes of rotating blades
[ETN-88-92296] 16 p2224 N88-23277

An electron-scattering study of N-15
[ETN-88-92479] 16 p2266 N88-23552

SHELLFISH

Irradiation preservation of seafood: Literature review
[DE88-001601] 05 p0631 N88-13858

SHELLS (STRUCTURAL FORMS)
NT ANISOTROPIC SHELLS
NT CONICAL SHELLS
NT CYLINDRICAL SHELLS
NT DOMES (STRUCTURAL FORMS)
NT ELASTIC SHELLS
NT FLUID FILLED SHELLS
NT LIQUID FILLED SHELLS
NT METAL SHELLS
NT ORTHOTROPIC SHELLS
NT REINFORCED SHELLS
NT SHALLOW SHELLS
NT SPHERICAL SHELLS
NT THIN WALLED SHELLS
NT TOROIDAL SHELLS
Analysis of shell-type structures subjected to time-dependent mechanical and thermal loading
[NASA-CR-181409] 01 p0060 N88-10388
USSR report: Engineering and equipment
[JPRS-UEQ-87-008] 04 p0423 N88-12621
Finite deformations of shell with rigid inclusion
04 p0426 N88-12639
The structures of large wound propulsion shells --- carbon fiber composites filament winding
[SNIAS-872-430-118] 05 p0559 N88-13406
Optical deformation measurement on shells following the raster principle
[ETN-88-90608] 05 p0609 N88-13741
An element of a multilayer shell for the computation of composite structures
[ONERA-RT-14/3542-RY-051-R]
05 p0610 N88-13742
Development of a shell system for DS moulds at RR precision casting facility --- directional solidification (DS)
[PNR90400] 09 p1151 N88-16893
Consistent linearization of the element-independent corotational formulation for the structural analysis of general shells
[NASA-CR-178418] 09 p1181 N88-17078
A nonlinear computational model for the strength and failure of composite plates and shells
11 p1501 N88-18684
Optimal filament shells loaded with internal pressure in a centrifugal force field 14 p1885 N88-21286
Preliminary 2-D shell analysis of the space shuttle solid rocket boosters
[NASA-TM-100515] 17 p2348 N88-23989
Three-dimensional curved shell and solid-shell transition finite elements with temperature and temperature gradients as primary variables for steady state heat conduction
17 p2349 N88-23997
Adaptive finite element methods for shells
[AD-A193221] 21 p2960 N88-27585
Parameter identification of material constants in a composite shell structure
[DE88-008115] 22 p3086 N88-28326
Experimental investigation of the effects of underwater exposure on the damping characteristics of bolted structural connections for plates and shells
[AD-A194486] 23 p3226 N88-29200
SHIELDING
NT ELECTROMAGNETIC SHIELDING
NT HEAT SHIELDING
NT MAGNETIC SHIELDING
NT RADIATION SHIELDING
NT REENTRY SHIELDING
NT SOLAR RADIATION SHIELDING
NT SPACECRAFT SHIELDING
Review of diffusion barrier technology for application in SP-100 fuel pins
[DE88-000021] 02 p0234 N88-11480
On the role of crack tip shielding in influencing the behavior of long and small fatigue cracks in aluminum-lithium alloy 2090 05 p0600 N88-13671
Effect of plasma rotation in tokamak on stabilizing action of electrically conducting wall 06 p0773 N88-14748
Laminar flow control leading edge glove flight test article development
[NASA-CR-172137] 07 p0815 N88-14960
An estimate of the noise shielding on the fuselage resulting from installing a short duct around an advanced propeller
[NASA-TM-100262] 10 p1405 N88-18379
Laser countermeasure impacts and penalties
[DE88-006871] 18 p2520 N88-24947
Trailer shield assembly for a welding torch
[NASA-CASE-MFS-29260-1] 18 p2524 N88-24972
Systems analyses of INTOR-like designs
[DE88-004422] 18 p2578 N88-25316
Self shielding of surfaces irradiated by intense energy fluxes
[DE88-307094] 18 p2579 N88-25318
Experimental evaluation of resistojet thruster plume shields
[NASA-TM-101363] 24 p3336 N88-29868
SHIELDS (GEOLOGY)
U BEDROCK
SHIFT REGISTERS
A labeling procedure for linear finite-state codes
11 p1472 N88-18781
Novel silicon Schottky barrier infrared imaging arrays
17 p2439 N88-24510
SHIP HULLS
Experimental studies on the tripping behavior of narrow T-stiffened flat plates subjected to hydrostatic pressure and underwater shock 05 p0592 N88-13613
Validation of the Underwater Shock Analysis (USA) program. Part 1: Theoretical considerations --- ship design
[REPT-5073713-86-01] 06 p0702 N88-14308
Steady ship waves at low Froude numbers, part 2
[AD-A176805] 09 p1160 N88-16953
Mechanisms in thermal mechanical forming of plates
[AD-A187797] 11 p1466 N88-18744
An investigation of ducted propellers in axisymmetric shear flow 16 p2202 N88-23136
Revised Impact Dynamic Design-Analysis Method (RIDDAM)
[AD-A190479] 16 p2217 N88-23225
Tripping of stiffened plates using a refined beam theory
[AD-A193969] 22 p3087 N88-28333
Numerical field model simulation of full scale fire tests in a closed spherical/cylindrical vessel
[AD-A195067] 24 p3359 N88-29998
Response of SMA (Shielded Metal Arc) and narrow gap HY80 weldments to explosive shock loading
[AD-A195994] 24 p3385 N88-30162
SHIPS
NT AIRCRAFT CARRIERS
NT SUBMARINES
The EH-101 integrated project: A naval, utility and commercial helicopter system 03 p0265 N88-11672
Visualization of the flow field around a generic destroyer model in a simulated turbulent atmospheric boundary layer
[AD-A184658] 03 p0320 N88-12023
Integrated control and display research for transition and vertical flight on the NASA V/STOL Research Aircraft (VSRA)
[NASA-TM-100029] 05 p0551 N88-13359
A summary of experimental results on square plates and stiffened panels subjected to air-blast loading
09 p1176 N88-17057
The evolution of naval warfare technology and the impact of space systems
[AD-A186900] 09 p1233 N88-17392
Application of a database system for inventory management of classified material
[AD-A186986] 09 p1261 N88-17558
A pyrotechnic delay ignition system for a submarine launched marine signal
[MRL-R-1079] 13 p1754 N88-20487
CTD/O2 data collected in 1985 and 1986 for EPOCS (Equatorial Pacific Ocean Climate Studies)
[PB88-160775] 14 p1951 N88-21629
Measurements of the time dependent velocity field surrounding a model propeller in uniform water flow
16 p2205 N88-23155
Low frequency ocean ambient noise: Measurements and theory
[AD-A191186] 16 p2237 N88-23362
Satellites at sea --- INMARSAT
19 p2700 N88-26054
Contribution of space to marine activities
19 p2700 N88-26057
Vertical ship motions and sea loads considering nonlinear effects
[TAE-592] 20 p2784 N88-26515
SHIVERING
Influence of skeletal muscle glycogen on passive rewarming after hypothermia
[AD-A186451] 08 p1049 N88-16334
Manipulation of muscle glycogen concentrations using high and low carbohydrate diets and exercise
[AD-A187732] 11 p1519 N88-19069
SHOCK
The Shock and Vibration Digest, Volume 19, No. 11
03 p0265 N88-11673
The Shock and Vibration Digest, Volume 19, No. 10
03 p0336 N88-12112
Impact-induced devolatilization and hydrogen isotopic fractionation of serpentine: Implications for planetary accretion
[NASA-CR-182877] 16 p2175 N88-22966
SHOCK ABSORBERS
Steering mechanism --- vehicles
[EP-PATENT-0-181-700-A1] 01 p0053 N88-10338
Non-linear shipboard shock analysis of the Tomahawk missile shock isolation system 05 p0582 N88-13614
Liquid spring design methodology for shock isolation system applications 08 p0958 N88-16043
Design and test of a spacecraft instrument shock isolator 08 p0996 N88-16044
Suspension design for a satellite transport container
[INPE-4352-TDL/296] 12 p1600 N88-19578
Variable response load limiting device
[NASA-CASE-LAR-12801-1] 17 p2346 N88-23982
SHOCK DIFFUSERS
U DIFFUSERS
U SHOCK WAVE ATTENUATION
SHOCK FRONTS
Monitoring of Pc3 pulsations in solar wind and at Earth by interplanetary magnetic field
08 p1002 N88-16060
Vehicle glow observed on the SONDA 3
[INPE-4297-PRE/1168] 12 p1600 N88-19581
SHOCK HEATING
Theoretical studies of mass loss and shock phenomena in cool star envelopes
[NASA-CR-182433] 08 p1099 N88-16616
SHOCK LAYERS
Absorption characteristics of Si3N4 ablation layer plasma 20 p2783 N88-26504
Research in applied mathematics
[AD-A192385] 21 p3004 N88-27620
SHOCK LOADS
NT BLAST LOADS
Shock-chemistry in natural materials and evolution of planetary surfaces
[DE87-012737] 02 p0254 N88-11604
Shock-induced chemical synthesis of phases similar to the high temperature superconductor oxides
[DE87-013725] 03 p0380 N88-12387
Shock compression of solids as a physical-chemical-mechanical process
[DE88-001674] 05 p0563 N88-13427
Experimental studies on the tripping behavior of narrow T-stiffened flat plates subjected to hydrostatic pressure and underwater shock 05 p0582 N88-13613
On the simulation of ballistic shock loads
05 p0583 N88-13615
Response of a sequential damper to shock inputs
08 p0998 N88-16047
Liquid spring design methodology for shock isolation system applications 08 p0998 N88-16043
A modal control based limiting performance formulation for shock excited systems 08 p0998 N88-16046
Analysis of shock and vibration environments for cargo on C5B transport aircraft 08 p0999 N88-16051
The Shock and Vibration Bulletin. Part 2: Instrumentation, shock analysis, and shock testing
[AD-A186749] 09 p1178 N88-17053
Retarded potential technique applied for shock wave loading of doubly symmetric submerged structures
09 p1179 N88-17058
Measurement, data analysis and prediction of pyrotechnic shock from pin-pullers and separation joints
09 p1179 N88-17061
Suspension design for a satellite transport container
[INPE-4352-TDL/296] 12 p1600 N88-19578
Investigations into shock-induced enhancement of mixing and combustion in supersonic burners
[AD-A189609] 12 p1607 N88-19608
The effects of incoming boundary layer thickness on unsteady shock-induced turbulent separations induced by cylinders
[AD-A196190] 24 p3369 N88-30080
Response of SMA (Shielded Metal Arc) and narrow gap HY80 weldments to explosive shock loading
[AD-A195994] 24 p3385 N88-30162
SHOCK RESISTANCE
NT IMPACT RESISTANCE
SHOCK SIMULATORS
Scaling the electromagnetically driven explosive shock simulator 05 p0582 N88-13612
SHOCK SPECTRA
Conservatism implications of shock test tailoring for multiple design environments 05 p0582 N88-13611
Designing electronics for pyrotechnic shock
08 p0997 N88-16039
Dynamic substructuring for shock spectrum analysis using component mode synthesis
11 p1499 N88-18860
La Recherche Aerospatiale, bimonthly bulletin, no. 1986-5, 234/September-October
[ESA-TT-1032] 19 p2641 N88-25871
SHOCK TESTS
Conservatism implications of shock test tailoring for multiple design environments
[DE87-013927] 03 p0338 N88-12127
Mechanical shock test specification using nonstationary random excitation models
[DE87-013650] 04 p0464 N88-12812

Implementation of a new shock testing procedure using nonstationary random excitation
[DE87-014643] 04 p0456 N88-12827

The 58th Shock and Vibration Symposium, volume 1
[NASA-CP-2488-VOL-1] 05 p0592 N88-13609

Conservatism implications of shock test tailoring for multiple design environments 05 p0592 N88-13611

Scaling the electromagnetically driven explosive shock simulator 05 p0592 N88-13612

Non-linear shipboard shock analysis of the Tomahawk missile shock isolation system 05 p0592 N88-13614

Ground shock profiles for an accidental explosion at the proposed Large Rocket Test Facility at Arnold Engineering Development Center
[DE88-002652] 07 p0853 N88-15180

The Shock and Vibration Bulletin. Part 1: Welcome, Keynote Address, Invited Papers, Nondevelopment Items Workshop and Pyrotechnic Shock Workshop
[AD-A186748] 08 p0997 N88-16034

Guidelines for qualifying non-development equipment to shock and vibration 08 p0997 N88-16036

Designing electronics for pyrotechnic shock
08 p0997 N88-16038

The Shock and Vibration Bulletin. Part 3: Isolation and damping, vibration test criteria, and vibration analysis and test
[AD-A186750] 08 p0997 N88-16040

The Shock and Vibration Bulletin. Part 2: Instrumentation, shock analysis, and shock testing
[AD-A186749] 09 p1178 N88-17053

A quantitative method for evaluating sensor layouts
09 p1178 N88-17056

Measurement, data analysis and prediction of pyrotechnic shock from pin-pullers and separation joints
09 p1179 N88-17061

Design and dynamic testing of an instrumented spacecraft component 11 p1498 N88-18952

Experimental comparison of lightning simulation techniques to CV-580 airborne lightning strike measurements
[AD-A190576] 15 p2098 N88-22496

SHOCK TUBES
NT SHOCK TUNNELS

Fast shock tube assemblies
[DE87-011732] 01 p0008 N88-10042

Production of flows for aeroballistic investigation in the shock tubes of the Franco-German Research Institute (ISL), Saint-Louis (France)
[ISL-R-113/86] 05 p0541 N88-13295

Velocity interferometry in shock tubes and shock tunnels
[ISL-CO-203/87] 09 p1122 N88-16713

A review of some flow visualization experiments carried out at the Institut Franco-Allemand de Recherches (ISL) shock tubes
[ISL-CO-243/86] 09 p1163 N88-16974

Blast waves generated by planar detonations
[DE88-002219] 09 p1164 N88-16979

Production by pyrolysis of diffusion particles for velocimetry in shock tubes
[ISL-R-119/86] 11 p1455 N88-18671

Computational studies of wave-shaping in a blast simulator by perforated plates in the driver
[AD-A188200] 11 p1483 N88-18850

Investigation of heat transfer to a flat plate in a shock tube
[AD-A189538] 13 p1766 N88-20561

Plate response analysis using shock tube
[AD-A190826] 18 p2526 N88-24987

Test of a prototype gate with fast opening equipping the shock tube 0 2.40 m at CEG
[PB87-227664] 19 p2504 N88-25465

Numerical simulation of the shock tube flows by TVD scheme 19 p2638 N88-25648

Surface temperature thermal fluxmeters for shock tubes
[NASA-TT-20319] 20 p2762 N88-26381

A shock-tube experiment on gases mixing processes associated with CO2/N2 mixing gasdynamic laser
[ISAS-RN-350] 20 p2797 N88-26598

Navier-Stokes simulation of shock-tube flows over a wedge-type step by finite volume method
[ISAS-RN-628] 20 p2797 N88-26599

SHOCK TUNNELS

Shock tunnels for real gas hypersonics
05 p0530 N88-13223

Velocity interferometry in shock tubes and shock tunnels
[ISL-CO-203/87] 09 p1122 N88-16713

A numerical study of the test time in a hypersonic shock tunnel
[AD-A194057] 23 p3172 N88-28888

SHOCK WAVE ATTENUATION

Static magnetization and microwave loss in shock-modified ferrites
[DE87-012362] 02 p0146 N88-10916

SHOCK WAVE GENERATORS
NT SHOCK TUBES
NT SHOCK TUNNELS

SHOCK WAVE INTERACTION

Interaction of interplanetary shocks with nonuniform ambient solar wind 01 p0116 N88-10740

Large-scale interaction of the solar wind with comets Halley and Giacobini-Zinner 01 p0117 N88-10745

The global interaction of comets with the solar wind
01 p0117 N88-10746

Effect of dissipation on propagation of spherical detonation shock wave 02 p0159 N88-10898

Spectroscopy and nonthermal processes
02 p0252 N88-11594

The effects of sweep and bluntness on a glancing shock wave turbulent boundary layer interaction
05 p0531 N88-13227

Interferometric data for a shock-wave/boundary-layer interaction
[NASA-TM-89227] 05 p0543 N88-13306

The effect of collision angle on mach reflection
[AD-A185798] 06 p0704 N88-14319

Separated flow 07 p0812 N88-14944

Examination of the development of a compressible turbulent boundary layer on a rough and porous wall
[PB87-148266] 07 p0815 N88-14964

Experimental research on swept shock wave/boundary layer interactions
[AD-A187250] 10 p1331 N88-17957

Velocity measurements in a 3D (three dimensional) shock wave laminar boundary layer interaction
[AD-A187334] 10 p1332 N88-17959

The structure and control of three-dimensional shock wave turbulent boundary layer interactions
[AD-A187642] 10 p1332 N88-17961

Shock wave/turbulent boundary layer interaction in high-Reynolds-number hypersonic flows
[AD-A188029] 11 p1434 N88-18555

Fluctuations and massive separation in three-dimensional shock-wave/boundary-layer interactions
[NASA-TM-89224] 11 p1434 N88-18559

Resonant Alfven wave instabilities driven by streaming fast particles 13 p1855 N88-21104

An experimental-computational investigation of transonic shock wave-turbulent boundary layer interaction in a curved test section
[CWI-NM-R8716] 14 p1909 N88-21408

Numerical and experimental investigation of multiple shock wave/turbulent boundary layer interactions in a rectangular duct
[AD-A190772] 15 p2066 N88-22320

Numerical study of unsteady viscous hypersonic blunt body flows with an impinging shock
[NASA-TM-100096] 15 p2122 N88-22650

High-resolution shock-capturing schemes for inviscid and viscous hypersonic flows
[NASA-TM-100097] 15 p2122 N88-22651

La Recherche Aerospatiale, bimonthly bulletin, number 1987-3, 238/May-June
[ESA-TT-1075] 16 p2206 N88-23161

Technology Reports of Kyushu University, volume 61, no. 2
[ISSN-0023-2718] 16 p2256 N88-23485

Theoretical investigation of 3-D shock wave-turbulent boundary layer interactions, part 6
[AD-A191546] 18 p2509 N88-24882

Gone with the solar wind: A study of protons accelerated by interplanetary shocks 19 p2743 N88-26283

Compressible boundary layers --- atmospheric reentry
[CERT-OA-13/5005-AYD] 20 p2801 N88-26623

A documentation of two- and three-dimensional shock-separated turbulent boundary layers
[NASA-TM-101008] 21 p2949 N88-27519

The dynamic behavior of a turbulent boundary layer subjected to a shock-induced separation
[AD-A194184] 22 p3075 N88-28252

Shock boundary layer interaction
23 p3170 N88-28873

Noise generation and boundary layer effects in vortex-airfoil interaction and methods of digital hologram analysis for these flow fields
[AD-A194191] 23 p3171 N88-28883

Shock waves in unsteady flows
[NASA-TT-20329] 23 p3214 N88-29134

Numerical simulation of nozzle flows
[AD-A195144] 24 p3369 N88-30064

Experimental and numerical investigation of the effect of distributed suction on oblique shock wave/turbulent boundary layer interaction
[NASA-TM-101334] 24 p3372 N88-30084

SHOCK WAVE PROFILES

Effect of dissipation on propagation of spherical detonation shock wave 02 p0159 N88-10898

Theoretical and experimental investigations on the structure of stationary shock waves in gas particle dispersions
[ETN-88-92983] 23 p3213 N88-29122

Influence of peak pressure on the substructure evolution and shock wave profiles of Ti-6Al-4V
[DE88-006458] 23 p3225 N88-29197

SHOCK WAVE PROPAGATION

Change in interplanetary shock acceleration preceding STIP interval 17 01 p0112 N88-10719

Rarefaction velocities in shocked lead
[DE87-013141] 02 p0146 N88-10917

Explicit and implicit soil modelling for dynamic soil-structure interaction problems
04 p0428 N88-12650

Theoretical and numerical analysis of shock wave propagation through different dusty-gas mixture layers
06 p0699 N88-14292

Validation of the Underwater Shock Analysis (USA) program. Part 1: Theoretical considerations --- ship design
[REPT-5073713-86-01] 06 p0702 N88-14308

Steady waves in a nonlinear theory of viscoelasticity
[AD-A185548] 06 p0723 N88-14449

Misty picture weather-watch and microbarograph project: Experiments 9412-14-18
[DE88-003949] 11 p1514 N88-19047

On the possibility of high velocity deflagration front propagation by radiative energy transfer
[AD-A189022] 12 p1613 N88-19645

Research in applied mathematics
[AD-A192385] 21 p3004 N88-27820

SHOCK WAVES
NT DETONATION WAVES
NT OBLIQUE SHOCK WAVES
NT SONIC BOOMS

Shock-wave studies using plastic flyers driven by an electric gun for hypervelocity impact on selected materials
[DE87-012631] 01 p0008 N88-10046

Real time analysis of detonation products
[DE87-007453] 01 p0031 N88-10195

The effect of RDX particle size on the shock sensitivity of cast PBX formulations. 2: Bimodal compositions
[DE87-009581] 01 p0031 N88-10196

Hot-spot reaction in unsustained shocks
[DE87-011781] 01 p0044 N88-10277

Time-resolved measurements of shock-induced vapor-pressure profiles
[DE87-012972] 01 p0045 N88-10289

Rayleigh-Taylor instability in compressible fluids
[DE87-013494] 01 p0047 N88-10297

Relation between shock strength and strain-rate plasticity at maximum deviatoric stress
[DE87-011736] 01 p0061 N88-10390

Propagating shocks in the corona
01 p0112 N88-10716

Interactions of oblique interplanetary discontinuities and their manifestations during STIP intervals 15-19
01 p0119 N88-10758

Hot spots: Subnanometer femtosecond energy localization
[DE87-010276] 02 p0155 N88-10868

Visible emission from granular explosives during shock initiation
[DE87-012361] 02 p0155 N88-10870

Spectroscopic studies of shocked and detonating explosives
[DE87-014216] 02 p0155 N88-10872

Computations of hypervelocity impact using the CTH shock wave physics code
[DE87-013067] 02 p0169 N88-11062

Modeling shockwave deformation via molecular dynamics
[DE87-013157] 02 p0169 N88-11063

Shock-induced cooling in dense fluids
[DE87-014343] 02 p0170 N88-11067

Vibrational spectroscopy of shock-compressed fluid N2 and O2
[DE87-013136] 03 p0313 N88-11979

Numerical calculation of two dimensional fluid flow with strong shocks
[KFK-4191] 03 p0314 N88-11986

Steady tonation and flagration waves in reactive continua
[RARDE-2/73] 03 p0315 N88-11989

Application of an upwind algorithm to the parabolized Navier-Stokes equations 03 p0316 N88-12000

An experimental investigation of quasi-conical shock wave/turbulent boundary layer interactions
03 p0317 N88-12004

On the scheme dependency of the three-dimensional Euler solutions 03 p0318 N88-12010

Thrust and specific impulse of repetitively-pulsed-laser propulsion rocket 03 p0318 N88-12012

Nonequilibrium characteristics of nitrogen plasmas appropriate to an AOTV flight 03 p0319 N88-12019
A study of chaos and mixing in Rayleigh-Taylor and Richtmyer-Meshkov unstable interfaces
[AD-A184751] 03 p0320 N88-12026
Particle velocity and stress gage measurements in spherical diverging flow
[DE87-007333] 03 p0321 N88-12033
Models for penetration of thin plates
[DE87-013727] 03 p0332 N88-12090
Numerical experiments with a symmetric high-resolution shock-capturing scheme
[NASA-TM-88325] 03 p0370 N88-12332
Shock-induced chemical synthesis of phases similar to the high temperature superconductor oxides
[DE87-013725] 03 p0380 N88-12387
Adiabatic supernova expansion into the circumstellar medium
[DE87-014241] 03 p0387 N88-12433
Neutrinos in supernovae
[DE87-014295] 03 p0387 N88-12434
Particle injection and cosmic ray acceleration at collisionless parallel shocks
[DE88-000507] 04 p0430 N88-12665
Three-dimensional, free-Lagrange hydrodynamics
[DE88-000494] 04 p0443 N88-12749
An experimental investigation of unsteadiness in swept shock wave/turbulent boundary layer interactions
04 p0445 N88-12760
Numerical modeling of slow shocks
[DE87-014768] 04 p0454 N88-12806
A dissipation principle and its consequences for structured shock waves in thermoelastic materials
[DE87-013723] 04 p0454 N88-12813
The evolution of plastic strain in steady, plastic shock waves
[DE87-013812] 04 p0456 N88-12826
Slow-mode shocks in the earth's magnetosphere
[DE88-000483] 04 p0468 N88-12895
Prompt simultaneous acceleration of protons and electrons to relativistic energies by shock waves in solar flares
[IPPJ-851] 04 p0493 N88-13037
Core bounce supernovae
[DE87-014910] 04 p0520 N88-13197
Driving mechanism of unsteady separation shock motion in hypersonic interactive flow 05 p0530 N88-13226
On the numerical simulation of three-dimensional hypersonic flow 05 p0532 N88-13237
Numerical experiments with hypersonic flows beneath a cone-delta-wing combination 05 p0532 N88-13238
The off-design performance of hypersonic waveriders
05 p0533 N88-13244
Influence of shock wave and gas pressure on the behavior of a pyrotechnical device
[SNIAS-872-430-111] 05 p0570 N88-13477
On the simulation of ballistic shock loads
05 p0593 N88-13615
The Shock and Vibration Digest, Volume 19, No. 12
05 p0610 N88-13746
Analytical investigation of reflection of a regular or mach reflection over a secondary wedge
[AD-A185690] 06 p0703 N88-14316
Dynamic high pressure process for fabricating superconducting and permanent magnetic materials
[DE88-000846] 06 p0785 N88-14817
Breakdown of the conservative potential equation
07 p0809 N88-14929
Upwind relaxation algorithms for Euler/Navier-Stokes equations 07 p0810 N88-14931
The carbon dioxide chaperon efficiency for the reaction H + O2 + M yields HO2 + M from ignition delay times behind reflected shock waves
[NASA-TM-100125] 07 p0830 N88-15036
Lyman-alfa/OH-resonance-absorbtion measurements and simulation calculations for the investigation of the induction behavior of methane/ethane/oxygen mixtures in reflected shock waves
[ETN-88-90806] 07 p0831 N88-15042
The Shock and Vibration Bulletin. Part 3: Isolation and damping, vibration test criteria, and vibration analysis and test
[AD-A186750] 08 p0997 N88-16040
Analytical study of the effect of early warning on optimal shock isolation 08 p0998 N88-16047
Criteria of interplanetary parameters causing intense magnetic storms (Dst less than -100nT)
[NASA-CR-182423] 08 p1024 N88-16200
Shock structure and noise of supersonic jets in simulated flight to Mach 0.4
[NASA-TP-2785] 08 p1080 N88-16510
Bidirectional electron heat flux events in space
[DE88-001791] 08 p1084 N88-16531
AMPTE-UKS ion observations at a quasi-parallel bow shock 08 p1095 N88-16589
Experimental investigation of shock-induced disturbances on transonic airfoils
[DFVLR-FB-87-28] 09 p1112 N88-16666
Mechanism of and particle size effects on shock sensitivity of heterogeneous pressed explosives: Preliminary assessment of binderless RDX in fuze trains
[MRL-R-1077] 09 p1150 N88-16892
A guide to the transient three phase porous flow model implemented in the two-dimensional CRAY-TENSOR code: Physics, numerics, and code description
[DE88-003709] 09 p1165 N88-16963
Multi-component stress history measurements and analysis
[DE88-000977] 09 p1168 N88-17004
Reinforced cocnrete arches under blast and shock environments 09 p1180 N88-17065
Transverse flow deflections associated with fast coronal mass ejecta in interplanetary space
[DE88-003180] 09 p1263 N88-17566
NF85: A three-dimensional, air-dynamics computer code for analyzing explosions in structures
[DE88-005085] 10 p1331 N88-17953
The use of optical fibers for shock pressure and timing measurements at high pressures
[DE88-004012] 10 p1334 N88-17971
Supernova mechanisms: Before and after SN1987a
[DE88-003469] 10 p1429 N88-18533
Operating loading of piping systems
[ETN-88-91057] 11 p1484 N88-18856
A lecture on detonation-shock dynamics
[DE88-004313] 11 p1487 N88-18879
Preparation of thin film polyvinylidene fluoride shock wave pressure transducers
[PB88-156070] 11 p1490 N88-18893
Approximate method for predicting the permanent set in a beam in vacuo and in water subject to a shock wave 11 p1500 N88-18957
Reynold stress closure in jet flows using wave models
[NASA-CR-182662] 12 p1628 N88-19741
Wave curves for simple isotropic elastic solids
[AD-A188865] 12 p1636 N88-19798
To what extent is mass loading responsible for the Venus bowshock precursor?
[NASA-TM-89307] 12 p1711 N88-20239
Anomalous shock sensitivity/density relationship for RDX-polyethylene wax and related formulations from MRL Small Scale Gap Test (SSGT) measurements
[MRL-R-1099] 13 p1739 N88-20399
Use of the LLNL 40 kV electric gun to study the shock response of 21-6-9 stainless steel
[DE87-014550] 13 p1742 N88-20418
Investigation of heat transfer to a flat plate in a shock tube
[AD-A189538] 13 p1766 N88-20561
An interferometric investigation of the diffraction of planar shock waves over a half-diamond cylinder in air
[UTIAS-322] 13 p1768 N88-20575
Pseudo-stationary oblique-shock-wave reflections in low gamma gases: Isobutane and sulphur hexafluoride
[UTIAS-TN-267] 13 p1768 N88-20576
Theoretical investigation of the wave shaping process in a section of ladder fracture tape
[MRL-R-1081] 13 p1771 N88-20595
Impact shock generator from explosively driven plates
[DE88-003596] 14 p1918 N88-21452
Buckling of blast loaded cylinder
[AD-A190124] 15 p2076 N88-22376
The structure of sonic underexpanded turbulent air jets in still air
[AD-A190856] 16 p2157 N88-22870
Efficient implementation of essentially non-oscillatory shock capturing schemes, 2
[NASA-CR-181656] 17 p2392 N88-24217
Passive shock wave-boundary layer control for the Bell FX69-H-098 airfoil 18 p2457 N88-24588
On symmetric TVD schemes
19 p2639 N88-25659
Non-oscillatory spectral Fourier methods for shock wave calculations
[NASA-CR-181675] 19 p2720 N88-26148
Numerical modeling of the effect of particle size of explosives on shock initiation properties
[DE88-010479] 20 p2780 N88-26491
Australian structures response evaluation: Ground shock and air blast measurements for site investigation survey
[MRL-TN-526] 20 p2813 N88-26685
Shock wave compression and metalization of simple molecules
[DE88-008031] 20 p2851 N88-26925
On linear relationship between shock velocity and particle velocity
[DE88-701827] 20 p2880 N88-27099
Experimental investigation of the reflection of a planar shock wave over a double wedge
[AD-A193076] 21 p2943 N88-27482
A documentation of two- and three-dimensional shock-separated turbulent boundary layers
[NASA-TM-101008] 21 p2949 N88-27519
Solution to the compressible Navier-Stokes equations of motion by Chebyshev polynomials with implicit time stepping
[AD-A194119] 22 p3075 N88-28257
Influence of peak pressure on the substructure evolution and shock wave profiles of Ti-6Al-4V
[DE88-006458] 23 p3225 N88-29197

SHOOTING STAR AIRCRAFT
U T-33 AIRCRAFT

SHORELINES
Atmospheric diffusion at coastal site in presence of sea-breeze
[DE88-700036] 07 p0876 N88-15314
Trace element geochemistry of the South Atlantic Bight
[DE88-003515] 10 p1356 N88-18108
Meteorological features during the marginal ice zone experiment from 20 March to 10 April 1987
[AD-A193960] 23 p3235 N88-29251

SHORT CIRCUITS
The Pierce diode with an external circuit. 2: Non-uniform equilibria
[AD-A188027] 11 p1478 N88-18818
Shorts in self-checking circuits
[RR-657-I] 14 p1908 N88-21402
Pierce diode with external circuit. Part 3: Chaotic behavior
[AD-A194837] 24 p3365 N88-30041

SHORT CRACKS
Fracture mechanics analysis for short cracks
[AD-A192002] 18 p2527 N88-24992

SHORT HAUL AIRCRAFT
NT A-300 AIRCRAFT
NT A-320 AIRCRAFT
NT EUROPEAN AIRBUS
Flight researh at NASA Ames Research Center: A test pilot's perspective
[NASA-TM-100025] 02 p0125 N88-10788
Current fire safety design aspects of commuter aircraft
[DOT/FAA/CT-87/32] 19 p2600 N88-25448

SHORT TAKEOFF AIRCRAFT
Civil applications of high-speed rotorcraft and powered-lift aircraft configurations
[NASA-TM-100035] 03 p0261 N88-11643
V/STOL aircraft configurations and opportunities in the Pacific Basin
[NASA-TM-100005] 03 p0261 N88-11644
Flaps-up takoff performance of the OV-1D aircraft with YT53-L-704 engine installed
[AD-A185960] 07 p0819 N88-14979
Study on a unidirectional ring laser gyro. Part 1: Proposition of the principle and studies on the components
[NAL-TR-933] 09 p1169 N88-17010
Recommendations for ground effects research for V/STOL and STOL aircraft and associated equipment for large scale testing
[NASA-CR-177429] 10 p1268 N88-17585
An aerodynamic comparison of blown and mechanical high lift airfoils 10 p1272 N88-17606
Development of circulation control technology for powered-lift STOL aircraft 10 p1272 N88-17608
Circulation control STOL aircraft design aspects
10 p1272 N88-17610
A review of technologies applicable to low-speed flight of high-performance aircraft investigated in the Langley 14- x 22-foot subsonic tunnel
[NASA-TP-2796] 13 p1717 N88-20264
Parametric study of supersonic STOVL flight characteristics
[NASA-CR-177330] 16 p2161 N88-22893
A numerical study of the hot gas environment around a STOVL aircraft in ground proximity
[NASA-TM-100895] 17 p2295 N88-23729
Method for prediction and determination of takeoff performance for vectored thrust vehicles
[AD-A191809] 18 p2463 N88-24626
Takeoff predictions for powered-lift aircraft
[NASA-CR-177491] 19 p2597 N88-25431
Low-speed wind-tunnel test of a STOL supersonic-cruise fighter concept
[NASA-TM-4050] 20 p2761 N88-26374
Aerodynamics in ground effect and predicted landing ground roll of a fighter configuration with a secondary-nozzle thrust reverser
[NASA-TP-2834] 24 p3317 N88-29752

SHORT WAVE RADIATION
NT CENTIMETER WAVES
NT DECIMETER WAVES
NT MICROWAVE EMISSION
NT MICROWAVES
NT MILLIMETER WAVES
NT SUBMILLIMETER WAVES

Studies on nonlinear mechanisms of excimer laser propagation in fused silica fibers
[AD-A186822] 09 p1156 N88-16929
A MININEC model of the miniloop antenna
[AD-A191759] 18 p2500 N88-24830
Angular radiation models for Earth-atmosphere system. Volume 1: Shortwave radiation
[NASA-RP-1184] 21 p2976 N88-27677

SHORT WAVE RADIO TRANSMISSION
Meteor-burst communications: Is this what the Navy needs?
[AD-A184433] 04 p0431 N88-12672
Digital correlator for the portable channel prober measurement instrument
[AD-A189065] 14 p1904 N88-21377

SHORTENING
U REDUCTION

SHOT NOISE
Series representations of infinitely divisible random vectors and a generalized shot noise in Banach spaces
[AD-A186429] 07 p0918 N88-15574
Series representations of infinitely divisible random vectors and a generalized shot noise in banach spaces
[AD-A186502] 08 p1073 N88-16474

SHRINKAGE
Process for producing sandwich mouldings
[EP-PATENT-0-191-623-A2] 04 p0426 N88-12642

SHROUDED BODIES
U SHROUDS

SHROUDED PROPELLERS
Ducted propeller design and analysis
[DE88-001925] 06 p0664 N88-14069
An estimate of the noise shielding on the fuselage resulting from installing a short duct around an advanced propeller
[NASA-TM-100262] 10 p1405 N88-18379
An investigation of ducted propellers in axisymmetric shear flow 16 p2202 N88-23136

SHROUDED TURBINES
Thermal stress minimized, two component, turbine shroud seal
[NASA-CASE-LEW-14212-1] 17 p2345 N88-23978

SHROUDS
Instrumentation package for a shrouded SWERVE/EPW rocket sled test
[DE87-014267] 01 p0008 N88-10045
Degradation of beam brightness by field emission from a cathode shroud
[DE88-008345] 20 p2794 N88-26576

SHUNTS
U CIRCUITS

SHUTDOWNS
Failure control techniques for the SSME
[NASA-CR-179224] 04 p0409 N88-12537
SSME technology test bed fast shutdown assessment
[NASA-CR-179354] 17 p2314 N88-23831
Evaluation and improvement of liquid propellant rocket chugging analysis techniques. Part 1: A one-dimensional analysis of low frequency combustion instability in the fuel preburner of the space shuttle main engine
[NASA-CR-183106] 21 p2903 N88-27224
Evaluation and improvement of liquid propellant rocket chugging analysis techniques. Part 2: A study of low frequency combustion instability in rocket engine preburners using a heterogeneous stirred tank reactor model
[NASA-CR-182724] 21 p2903 N88-27225

SHUTTERS
Mode locking in Nd-laser by means of Gd-Sc-Ga-garnet shutter 09 p1237 N88-17412
Nonlinear stage of ultrashort-pulse formation in solid-state laser 14 p1971 N88-21765
Pulse duration control of XeCl*-laser by means of plasma shutter 14 p1973 N88-21774

SHUTTLE BOOSTERS
U SPACE SHUTTLE BOOSTERS

SHUTTLE GLOW
U SPACECRAFT GLOW

SHUTTLE IMAGING RADAR
The Shuttle Imaging Radar B (SIR-B) experiment report
[NASA-CR-182923] 17 p2334 N88-23932
Subsurface morphology and geoarchaeology revealed by spaceborne and airborne radar
17 p2353 N88-24022
The role of space borne imaging radars in environmental monitoring: Some shuttle imaging radar results in Asia
[NASA-TM-101178] 18 p2502 N88-24844
The role of space borne imaging radars in environmental monitoring: Some shuttle imaging radar results in Asia
[NASA-TM-101175] 20 p2789 N88-26544

SHUTTLE ORBITERS
U SPACE SHUTTLE ORBITERS

SHUTTLE PALLET SATELLITES
Testing of heat pipes on SPAS-01
[BMFT-FB-W-86-014] 06 p0672 N88-14119

The Cryogenic Infrared Spectrometer and Telescope for the Atmosphere (CRISTA) experiment on Astro-SPAS
08 p1034 N88-16270

SI
U INTERNATIONAL SYSTEM OF UNITS

SIALON
High temperature characterization of ceramic materials
[REPT-NT-3403] 03 p0292 N88-11837

SIC (COEFFICIENT)
U STRUCTURAL INFLUENCE COEFFICIENTS

SICKNESSES
NT ALTITUDE SICKNESS
NT DECOMPRESSION SICKNESS
Attitudes towards the cold: Effects on psychological mood and subjective reports of illness during cold weather training
[AD-A194777] 23 p3239 N88-29274

SID (IONOSPHERIC DISTURBANCES)
U SUDDEN IONOSPHERIC DISTURBANCES

SIDE INLETS
Hot-wire measurements of compressor blade wakes in a cascade wind tunnel
[AD-A194737] 23 p3181 N88-28936

SIDE-LOOKING RADAR
Construction of airborne radars for remote sensing
[PB88-113063] 09 p1154 N88-16916
Marginal Ice Zone Experiment (MIZEX) 1984 VARAN-S data set
[ETN-88-92032] 14 p1950 N88-21625
Definition and implementation study for the Varan-S radar
[CNES-CT/DRT/TIT/RL-143-T]
15 p2058 N88-22267
The radiometric processing of SLAR measuring values using the PARES program
[BCRS-86-04] 16 p2227 N88-23301
Investigation of the usefulness of speckle analysis in imaging radar systems
[BCRS-86-05] 16 p2227 N88-23302

SIDEBANDS
Sideband suppression by an intracavity optical filter in the Los Alamos free-electron laser oscillator
[DE87-011740] 02 p0177 N88-11103
Spectral evolution equation for the sideband instability in a free-electron laser oscillator
[DE88-000510] 04 p0447 N88-12771
The free electron laser sideband instability reconsidered
[AD-A184269] 04 p0447 N88-12773
Analysis of sideband spectra from untapered undulator using analytical technique
[DE87-014763] 04 p0448 N88-12778
The generation and suppression of synchrotron sidebands
[DE88-000532] 04 p0449 N88-12787
Comparison of sideband spectra obtained from analytical formula and from numerical simulation in free-electron laser
[DE88-000521] 04 p0450 N88-12789
HF sidebands in the ionosphere
05 p0574 N88-13497
The structure of the sideband spectrum in free electron lasers
[AD-A186952] 09 p1170 N88-17015

SIDELOBE REDUCTION
Adaptive interference techniques for mobile antennas
19 p2647 N88-25714

SIDELOBES
Adaptive detection in non-stationary interference, part 3
[AD-A185622] 07 p0844 N88-15116
Compensation of relector antenna surface distortion using an array feed
[NASA-TM-100286] 11 p1476 N88-18805
Conformal microstrip slot antenna and antenna array
[AD-A189623] 15 p2055 N88-22252
An improved method for calculating power density in the Fresnel region of circular parabolic reflector antennas
[AD-A190569] 15 p2060 N88-22284
Case study of active array feed compensation with sidelobe control for reflector surface distortion
[NASA-TM-100287] 16 p2192 N88-23073
TDWR (Terminal Doppler Weather Radar) clutter residue map generation and usage
[AD-A191148] 16 p2235 N88-23352
Sidelobe level of an adaptive array using the SMI (Sampled Matrix Inversion) algorithm
[AD-A193131] 21 p2932 N88-27409

SIDERITE METEORITES
U IRON METEORITES

SIDESLIP
Effects of winglets on a first-generation jet transport wing. 7: Sideslip effects on winglet loads and selected wing loads at subsonic speeds for a full-span model
[NASA-TP-2619] 11 p1436 N88-18567
Parametric estimation of aerodynamic nonlinearities in rolling moment due to sideslip using maximum likelihood method 20 p2786 N88-26528
Angle of attack and sideslip estimation using an inertial reference platform
[AD-A194876] 24 p3319 N88-29769
Computer programs for calculation of sting pitch and roll angles required to obtain angles of attack and sideslip on wind tunnel models
[NASA-TM-100659] 24 p3329 N88-29820

SIERRA LEONE
Global solar radiation in Sierra Leone (West Africa)
[DE88-702725] 23 p3235 N88-29252

SIERRA NEVADA MOUNTAINS (CA)
Structure and modification of winter mountain clouds in the Sierra Nevada: Nowcasting/forecasting the onset of supercooled liquid water 02 p0202 N88-11263

SIEVES
The flow downstream of screens and the formation of longitudinal vortices in the stagnation point flow
[DFVLR-FB-87-27] 09 p1162 N88-16963
Size-reduction and sorting behavior in sieve hammer mills
[ETN-88-91480] 11 p1467 N88-18749

SIGHT
U VISUAL PERCEPTION

SIGNAL ANALYSIS
NT CEPSTRAL ANALYSIS
Intelligent signal analysis and recognition
[NASA-CR-181531] 04 p0501 N88-13084
The Newcastle meteor radar
06 p0741 N88-14556
Flow diagnostics and visualization in wind tunnels and flight 07 p0811 N88-14940
Backscattering signal analysis concerning a three-dimensional object configuration on the basis of object motion
[ESA-TT-1044] 09 p1154 N88-16915
Markov processes applied to control, replacement and signal analysis
[AD-A190563] 15 p2126 N88-22674
Software development for the reconstruction of source parameters using research and development arrays
[REPT-840445-TW] 16 p2246 N88-23417
Acoustic emission frequency discrimination
[NASA-CASE-MSC-20467-1] 17 p2342 N88-23966
Evaluation of the communications impact of a low power arcjet thruster
[NASA-TM-100926] 18 p2475 N88-24682
Artificial intelligence applied to process signal analysis
23 p3252 N88-29359

SIGNAL ANALYZERS
Analysis of counting errors in the phase/Doppler particle analyzer
[NASA-TM-100231] 03 p0323 N88-12043
Lower bounds on bearing accuracy for closely spaced sources
[AD-A184258] 04 p0486 N88-12997
An interface for the connection of the SCP2160A pulse analyser to a Hewlett-Packard desk-top computer
[RSRE-MEMO-4030] 22 p3073 N88-28245

SIGNAL DETECTION
NT CORRELATION DETECTION
Nonlinear techniques for detection and filtering of discrete-time signals 02 p0160 N88-11004
Radar ECCM's new area: Anti-STEALTH and anti-ARM 03 p0299 N88-11881
Detection of signals by the digital integrate-and-dump filter with offset sampling 04 p0435 N88-12695
Detection of signals by weighted integrate-and-dump filter 04 p0435 N88-12696
Development of an acoustic echosounder for detection of lower level atmospheric turbulence
[AD-A184877] 05 p0626 N88-13831
Adaptive detection in non-stationary interference, part 3
[AD-A185622] 07 p0844 N88-15118
Transient classifier systems and man-machine interface research
[AD-A186213] 07 p0899 N88-15446
High frequency acoustic underwater communication with low probability of being traced
[REPT-4-87] 09 p1242 N88-17447
Detection of signals in non-Gaussian correlated noise derived from Cauchy processes
[AD-A187488] 10 p1320 N88-17894
A deep-water OBS (Ocean Bottom Seismometer) array with real-time telemetry
[AD-A187404] 10 p1357 N88-18112
The Telecommunications and Data Acquisition Report
[NASA-CR-182545] 11 p1471 N88-18774

Simulated performance of an order statistic threshold strategy for detection of narrowband signals
11 p1474 N88-18796

On the design of suboptimal matched filters for three-dimensional moving target detection
[AD-A188384] 12 p1619 N88-19882

Detection and angle estimation of coherent plane waves 13 p1759 N88-20522

Method for set-up for researching signal curve development
[NASA-TT-20235] 13 p1760 N88-20526

Masking of motion cues by random motion: Comparison of human performance with a signal detection model
[UTIAS-313] 14 p1953 N88-21639

Earthquakes from peninsular India: Data from the Gauribidanur seismic array
[DE88-701232] 15 p2093 N88-22471

Characteristics of seismic sources of some Asian earthquakes and Soviet underground explosions from Gauribidanur array records
[DE88-701233] 15 p2093 N88-22472

Study of microcomputer-based real-time programmable optical signal processor and application
[AD-A190076] 15 p2133 N88-22726

Research and development activities of the Seismology Section
[DE88-701235] 16 p2231 N88-23323

Utilization of dense packed planar acoustic echosounders to identify turbulence structure in the lowest levels of the atmosphere
[AD-A191006] 16 p2233 N88-23335

Information and stochastic systems
[AD-A192167] 18 p2501 N88-24838

Identification and acoustic characterization of seamounts
[AD-A192204] 18 p2548 N88-25123

An optically strobed sample and hold circuit
19 p2656 N88-25772

Comparison of sampling oscilloscopes with less than 35 ps transition durations 19 p2658 N88-25793

Noise in piezoresistive and capacitive sensors
19 p2670 N88-25874

Comparison of five readout techniques for an integrated magnetometer 19 p2671 N88-25876

Proceedings of the Array Signal Processing Symposium: Treaty Verification Program
[DE88-008346] 20 p2790 N88-26548

Surface disturbances produced by low-level, subsonic B-1 aircraft
[AD-A192257] 20 p2824 N88-26752

Direct bit detection receiver performance analyses for 8-DPSK (Differential Phase Shift Keyed) modulated signals operating with improper carrier phase synchronization
[AD-A193839] 22 p3070 N88-28220

Effects of tectonic release on broadband regional distance bodywaves
[AD-A194247] 22 p3119 N88-28529

Computer-controlled measurements of nonlinear standing waves
[AD-A193840] 22 p3147 N88-28717

SQUID (superconducting quantum interference device) arrays for simultaneous magnetic measurements: Calibration and source localization performance
[AD-A193815] 23 p3216 N88-29143

Evaluation of atmospheric effects for operational tactical decision aid
[AD-A194205] 23 p3232 N88-29236

Improvements in techniques of microwave thermography
[AD-A193620] 23 p3239 N88-29276

On the design and optimization of distributed signal detection and parameter estimation systems
[AD-A193934] 23 p3266 N88-29446

On adaptive cell-averaging CFAR (Constant False-Alarm Rate) radar signal detection
[AD-A196286] 24 p3360 N88-30009

A detection theory analysis of visual display performance
[AD-A196291] 24 p3409 N88-30292

SIGNAL DETECTORS

Icing detector with early warning capability
[AOA-4.1.0055] 03 p0325 N88-12050

Surface acoustic wave deposition sensor
[DE87-006527] 09 p1243 N88-17452

A deep-water OBS (Ocean Bottom Seismometer) array with real-time telemetry
[AD-A187404] 10 p1357 N88-18112

Computation of LMS (Least-Mean-Square) and matched digital filters for optical clutter suppression
[AD-A188885] 12 p1687 N88-20093

Preliminary comparison of some coincidence methods for gravitational wave detectors
[NOTA-INTERNA-903] 14 p1945 N88-21604

Applications research studies of microtubules
[AD-A190855] 16 p2182 N88-23005

Method and apparatus for detecting laminar flow separation and reattachment
[NASA-CASE-LAR-13952-1-SB]
18 p2513 N88-24910

Design and testing of a luminance and chrominance stabilization system for a computer-controlled color display
[AD-A191922] 18 p2554 N88-25159

Novel nonlinear signal processing principles
[AD-A191644] 19 p2707 N88-26097

Local free-space mapping and path guidance for mobile robots
[AD-A192970] 20 p2810 N88-26674

Laboratory feasibility study of a composite embedded fiber optic sensor for measurement of structural vibrations
[AD-A194270] 22 p3152 N88-28754

Analytical methods in stochastic control and nonlinear filtering
[AD-A194272] 24 p3426 N88-30388

SIGNAL DISCRIMINATORS

U SIGNAL DETECTORS

SIGNAL DISTORTION

A generalization of order statistic filters: The alpha-trimmed linear filter
[AD-A186125] 07 p0842 N88-15107

Solution of the Lloyd-Max quantizer parameters by the method of successive substitution
[AD-A187829] 11 p1540 N88-19207

The effects of solar cycle and latitude dependence on the formation of ionospheric C layer
[INPE-4342-TDL/293] 16 p2232 N88-23332

SIGNAL ENCODING

NT AMPLITUDE MODULATION
NT DELTA MODULATION
NT DIFFERENTIAL PULSE CODE MODULATION
NT FREQUENCY MODULATION
NT FREQUENCY SHIFT KEYING
NT PHASE MODULATION
NT PHASE SHIFT KEYING
NT PULSE AMPLITUDE MODULATION
NT PULSE CODE MODULATION
NT PULSE DURATION MODULATION
NT PULSE MODULATION
NT PULSE POSITION MODULATION

Study of a coding and modulation system for the V32 call of the CCITT
[ENST-87E007] 02 p0162 N88-11015

Bandwidth efficient block codes for M-ary PSK modulation
[NASA-CR-181543] 04 p0437 N88-12712

Study of synthetic aperture radar data compression and encoding. Part 3: Performance evaluation of speckle suppression and data compression algorithms
[NLR-TR-85085-L-PT-3] 06 p0692 N88-14248

Study of synthetic aperture radar data compression and encoding. Part 4: Algorithm implementation aspects
[NLR-TR-85085-L-PT-4] 06 p0692 N88-14249

Study of synthetic aperture radar data compression and encoding. Part 1: SAR image data analysis
[NLR-TR-85085-L-PT-1] 07 p0843 N88-15115

Study of synthetic aperture radar data compression and encoding. Part 2: SAR image speckle suppression and data compression algorithms
[NLR-TR-85085-L-PT-2] 07 p0843 N88-15116

Multichannel 2-D power spectral estimation and applications
[AD-A191273] 16 p2191 N88-23068

Coding for write-unidirectional memories and conflict resolution
[ENST-87C005] 16 p2245 N88-23408

A new code for Galileo 22 p3065 N88-28186

Direct bit detection receiver performance analyses for 8-DPSK (Differential Phase Shift Keyed) modulated signals operating with improper carrier phase synchronization
[AD-A193839] 22 p3070 N88-28220

SIGNAL FADEOUT

U SIGNAL FADING

SIGNAL FADING

Measured characteristics of 800/900 MHz mobile radio channels with high-angle propagation through moderately dense foliage
[CRC-1398] 05 p0573 N88-13493

Improvements to a UHF rebroadcast television link suffering tidal fading: Countisbury UHF relay station
[BBC-RD-1987/14] 05 p0573 N88-13495

An additional study and implementation of tone calibrated technique of modulation
[NASA-CR-182377] 07 p0844 N88-15117

The design of trellis codes for fading channels
[NASA-CR-182523] 10 p1320 N88-17891

Propagation effects by roadside trees measured at UHF and L-band for mobile satellite systems
19 p2644 N88-25693

Propagation modeling for land mobile satellite systems
19 p2645 N88-25694

Attenuated direct and scattered wave propagation on simulated land mobile satellite service paths in the presence of trees 19 p2645 N88-25695

Trellis-coded MPSK modulation techniques for MSAT-X(sup)1 19 p2648 N88-25721

Performance of the ICAO standard core service modulation and coding techniques
19 p2648 N88-25723

Extending the impulse response in order to reduce errors due to impulse noise and signal fading
19 p2649 N88-25730

SIGNAL GENERATORS

NT FREQUENCY SYNTHESIZERS
NT FUNCTION GENERATORS

Results of the use of an automated electrical measuring instrument calibration system
[SNIAS-881-430-107] 23 p3217 N88-29146

SIGNAL MEASUREMENT

NBS (National Bureau of Standards) wideband sampling wattmeter
[PB87-210324] 03 p0323 N88-12041

Wave propagation experiments on 22-bay lattice
[AD-A186140] 07 p0824 N88-15002

The optimum solution to instrument quantization effects 12 p1577 N88-19434

The effects of atmospheric and thermohaline variability on the validation of the GEOSAT altimeter oceanographic signal between Scotland and Iceland
[AD-A189324] 12 p1650 N88-19882

Alaska Loran C probe test results
[AD-A189131] 13 p1720 N88-20284

Bragg-cell receiver study
[NASA-CR-182684] 13 p1761 N88-20535

An analysis of the efficiency and directivity of the sound generated by a moving laser source
[AD-A192220] 20 p2849 N88-26914

A notch filter instrument for measuring ELF (Extremely Low Frequency) MSK (Minimum Shift Keying) signals
[AD-A193324] 21 p2933 N88-27414

SIGNAL MIXING

Four-wave mixing used in optical amplitude encoding
03 p0376 N88-12386

Self-pumped phase conjugation in a supersonically flowing medium
[AD-A188281] 10 p1338 N88-17906

Optical signal processing using nonlinear optics
[AD-A188461] 12 p1691 N88-20117

Studies of coherent beam processing concepts, phase 1
[AD-A194749] 22 p3083 N88-28306

SIGNAL PROCESSING

Monitoring of harmful interference to the HF (High Frequency) broadcasting service. 3: Results of the June 1986 coordinated monitoring period
[PB87-210274] 01 p0036 N88-10229

Independence in sonar observations
[ARE-TR-87102] 01 p0088 N88-10572

White noise calculus for two-parameter filtering
[ENST-87C003] 01 p0088 N88-10578

Measurements in the functional mock up test of the NAL QSTOL aircraft control system
[NAL-TR-928] 02 p0126 N88-10793

Nonlinear techniques for detection and filtering of discrete-time signals 02 p0160 N88-11004

On adaptive signal processing of RF signals
[DE87-014192] 02 p0161 N88-11007

A digital audio link to the Channel Islands in the UHF television band: Protection of television signals from digitally modulated interference
[BBC-RD-1987/7] 02 p0161 N88-11010

Experiments: Test range facilities, part 1
03 p0304 N88-11920

An antenna array processing system for multiple source bearing estimation 03 p0305 N88-11927

Research in monolithic signal-processing circuits
[AD-A184680] 03 p0311 N88-11962

SBNR (Signed Binary Number Representations) digital signal processor architecture
[AD-A184603] 03 p0364 N88-12290

End of year report for parallel vision algorithm design and implementation
[AD-A184327] 03 p0366 N88-12301

The effect of reverberation on active sonar performance
[ARE-TM(UJS)-87104] 03 p0374 N88-12350

Optical alignment of Centaur's inertial guidance system
[NASA-TM-88844] 04 p0405 N88-12515

On a circular correlation technique for filtering randomly noisy data
[AD-A184317] 04 p0431 N88-12669

Application of lattice filtering techniques to CW measured time domain data
[AD-A184351] 04 p0431 N88-12671

Accommodating the residue of processed or computed digital video signals within the 8 bit CCIR recommendation 601
[BBC-RD-1987/12] 04 p0432 N88-12676

Robust statistical methods for automated outlier detection 04 p0433 N88-12681

Frequency doubling conversion efficiencies for deep space optical communications 04 p0434 N88-12691

Design of digital filters for electronic instrumentation
[PB87-100418] 04 p0438 N88-12716

Interferometry theory for the block 2 processor
[NASA-CR-181551] 04 p0440 N88-12730

Measured characteristics of 800/900 MHz mobile radio channels with high-angle propagation through moderately dense foliage
[CRC-1398] 05 p0573 N88-13493

Italy's Institute of Research on Electromagnetic Waves--the Istituto di Ricerca sulle Onde Elettromagnetiche
[AD-A185020] 05 p0574 N88-13501

Analysis of SO2 signals in SBUV/TOMS data
05 p0618 N88-13794

Estimation of marine boundary layer depth and relative humidity with multispectral satellite measurements
[AD-A184881] 05 p0620 N88-13804

Cross-correlation of uniform cyclic difference set sequences
[AD-A184879] 05 p0640 N88-13913

Two digital X-ray imaging systems for applications in X-ray diffraction
[PB87-123683] 06 p0669 N88-14103

Theory of displaced phase center antenna for space based radar applications
[PB87-229837] 06 p0690 N88-14227

Discussion on the modelling and processing of signals from an acousto-optic spectrum analyzer
[AD-A185639] 06 p0694 N88-14257

Statistical techniques for signal processing
[AD-A185774] 06 p0694 N88-14259

Signal chain for the Airborne Visible/Infrared Imaging Spectrometer (AVIRIS) 06 p0706 N88-14331

Fast algorithms for structural optimization and least squares
[AD-A185766] 06 p0724 N88-14452

Fiber optic single mode sensors
[FOA-C-30453-3.1] 06 p0780 N88-14790

Digital signal processing algorithms for automatic voice recognition 06 p0793 N88-14862

Time-domain robotic vision application
06 p0798 N88-14886

A generalization of order statistic filters: The alpha-trimmed linear filter
[AD-A186125] 07 p0842 N88-15107

An additional study and implementation of tone calibrated technique of modulation
[NASA-CR-182377] 07 p0844 N88-15117

Improvement of deep resolution in ultrasonic echographic nondestructive evaluation using signal processing methods
[PB87-147658] 07 p0866 N88-15256

Strong consistency of maximum likelihood parameter estimation of superimposed exponential signals in noise
[AD-A186384] 07 p0911 N88-15526

On simultaneous estimation of the number of signals and frequencies under a model with multiple sinusoids
[AD-A186026] 07 p0913 N88-15543

On the direction of arrival estimation
[AD-A186031] 07 p0914 N88-15546

On rate of convergence of equivariation linear prediction estimates of the number of signals and frequencies of multiple sinusoids
[AD-A186034] 07 p0914 N88-15549

High Resolution Picture Transmission (HRPT) data processing from NOAA series satellites
[INPE-4372-PRE/1195] 08 p0963 N88-15831

A simultaneous M-ary channel hypothesis test with least-mean-square signal amplitude estimation
[AD-A186526] 08 p0978 N88-15913

Optical communication with semiconductor laser diodes
[NASA-CR-182464] 09 p1154 N88-16918

Limiting of YUV digital video signals
[BBC-RD-1987/22] 09 p1155 N88-16924

High performance VLSI algorithms and architectures for digital signal processing 09 p1155 N88-16926

Spectral density estimates of coarsely quantized random vibration data 09 p1178 N88-17055

Fractal images: Procedure and theory
[AD-A187014] 09 p1217 N88-17293

Space-time processing of field produced by moving source 09 p1234 N88-17399

The role of photodetectors in optical signal processing
[AD-A186804] 09 p1247 N88-17476

A report on the effects of neutron irradiation of GaAs semiconductors
[AD-A186818] 09 p1253 N88-17510

Response of wind shear warning systems to turbulence with implication of nuisance alerts
10 p1274 N88-17618

Signal processing for an optical wide band data transmission system
[DE88-003854] 10 p1319 N88-17888

Detection of signals in non-Gaussian correlated noise derived from Cauchy processes
[AD-A187486] 10 p1320 N88-17894

Signal processing studies program optical signal amplification, volume 2
[AD-A188054] 10 p1320 N88-17896

Signal processing studies program optical signal amplification, volume 1
[AD-A188055] 10 p1321 N88-17897

Signal processing studies program VLSI designs for unary functions
[AD-A188053] 10 p1325 N88-17922

An integrated pressure sensor for in-vivo use
10 p1333 N88-17965

Optically controlled devices and ultrafast laser sources for signal processing
[AD-A187417] 10 p1338 N88-17995

Signal and data processing for IR sensors
10 p1374 N88-18199

Wafer scale implementation of a GaAs systolic signal processor cell 10 p1381 N88-18247

Ground clutter processing for wind measurements with airport surveillance radars
[AD-A187708] 11 p1514 N88-19044

A signal processing approach to the numerical solution of parabolic differential equations
11 p1539 N88-19197

Digital method for correction of the phase error in the discrete generation of periodic signals in real time
[INPE-4327-RPE/552] 12 p1618 N88-19676

Optimum filters and smoothers design for carrier phase and frequency tracking
[NASA-CR-182654] 12 p1618 N88-19679

Mathematical foundations of signal processing. 2: The role of group theory
[AD-A188482] 12 p1620 N88-19685

VLSI implementations for digital signal processing
[AD-A189612] 12 p1624 N88-19719

Structural-acoustic interior noise modeling and analysis from experimental data
[PB88-141775] 12 p1687 N88-20088

Optical signal processing using nonlinear optics
[AD-A188461] 12 p1691 N88-20117

Architecture specification for PAVE PILLAR avionics
[AD-A188722] 13 p1723 N88-20303

The acoustic-modeling problem in automatic speech recognition
[AD-A188529] 13 p1757 N88-20510

Statistical signal processing using a class of iterative estimation algorithms
[AD-A189050] 13 p1757 N88-20511

System for detecting objects that represent a threat
[NASA-TT-20244] 13 p1760 N88-20528

Bragg-cell receiver study
[NASA-CR-182684] 13 p1761 N88-20535

Analysis for architecture for image processing
[INPE-4294-PRE/1165] 13 p1791 N88-20715

Study of photochromic materials for use in optical signal processing
[AD-A189068] 13 p1839 N88-21006

Digital correlator for the portable channel prober measurement instrument
[AD-A189065] 14 p1904 N88-21377

On-board processing for mobile satellite communications
[ESA-CR(P)-2519] 14 p1905 N88-21382

Squeezed state in degenerate parametric amplification discussed by H. Takahasi in 1963
14 p1976 N88-21790

Generating squeezed microwave radiation with a Josephson parametric amplifier
14 p1978 N88-21805

Merit of Hadamard transform active absorption spectrometer described 15 p2053 N88-22232

Optimum signal processing in distributed sensor systems
[AD-A189443] 15 p2055 N88-22250

Direct bit detection receiver noise performance analysis for 32-PSK and 64-PSK modulated signals
[AD-A190009] 15 p2056 N88-22256

A hardware/software system for implementing geophysical diffraction tomography
[DE88-006411] 15 p2094 N88-22480

Auditory perception of complex sounds
[AD-A190528] 15 p2103 N88-22529

Selective mechanisms in auditory and bimodal signal processing
[AD-A190529] 15 p2103 N88-22530

Auditory pattern memory: Mechanisms of tonal sequence discrimination by human observers
[AD-A190337] 15 p2104 N88-22534

Investigation into the development of computer aided design software for space based sensors
[NASA-CR-180772] 15 p2107 N88-22552

Memory efficient evaluations of nonlinear stochastic equations and C3 applications
[AD-A189872] 15 p2110 N88-22569

Design and implementation of VLSI prime factor algorithm processor
[AD-A190483] 15 p2112 N88-22580

Cholesky downdating on a hypercube
[DE88-006780] 15 p2113 N88-22586

The adjoint process in stochastic optimal control
[AD-A189720] 15 p2116 N88-22605

Nonlinear signal processing using neural networks: Prediction and system modelling
[DE88-006479] 15 p2118 N88-22621

Near optimal blind deconvolution
[REPT-87-016] 15 p2123 N88-22655

Filtering of jump processes
[AD-A189701] 15 p2123 N88-22656

The partially observed stochastic minimum principle
[AD-A189787] 15 p2124 N88-22658

Multivariate analysis and its application
[AD-A189983] 15 p2124 N88-22661

Spatial matched processing for multipath propagation
[AD-A189790] 15 p2129 N88-22701

Space time processing, environmental-acoustic effects
[AD-A190764] 15 p2130 N88-22708

Space-variant optical systems
[AD-A189967] 15 p2133 N88-22724

Infrared-sensitive spatial light modulator
[AD-A190391] 15 p2134 N88-22729

Autonomous control system for Czochralski growth of LEC GaAs
[AD-A189725] 15 p2141 N88-22779

Research on materials and components for opto-electronic signal processing and computing
[AD-A190130] 15 p2143 N88-22788

Analysis of a range estimator which uses MLS angle measurements
[NASA-CR-182896] 16 p2160 N88-22884

A compact high resolution piezoresistive digital tactile sensor
[DE88-000430] 16 p2210 N88-23188

The TMS32010 evaluation module controller --- signal processor
[EUT-86-E-162] 16 p2245 N88-23407

HIFI: A design method for implementing signal processing algorithms on VLSI processor arrays
[ETN-88-92238] 16 p2247 N88-23421

The PROMISE simulation system: Software for the simulation of parallel processes
[NLR-MP-86077-U] 16 p2247 N88-23427

Error control techniques for satellite and space communications
[NASA-CR-182886] 17 p2332 N88-23922

Doppler radar with multiphase modulation of transmitted and reflected signal
[NASA-CASE-MSC-18808-1] 17 p2332 N88-23923

Processing of HRPT data from the NOAA series satellites 17 p2359 N88-24053

Near surface current determined from INPE's satellite-tracked buoy, during 6-26 November, 1985
17 p2360 N88-24058

Angular position measurements at high temperatures and high radiation environments
17 p2434 N88-24479

Time-frequency representations for speech signals
[AD-A188661] 18 p2498 N88-24819

Signal processing with degenerate four-wave mixing
[AD-A191496] 18 p2499 N88-24825

A method for discrimination of radar targets using complex natural resonances
[AD-A191848] 18 p2500 N88-24832

Propagation management for no-acknowledge HF communications links 18 p2502 N88-24843

Optics: Perspectives for Measurement Techniques and Signal Processing for Flight Guidance --- conference
[DFVLR-MITT-87-21] 18 p2516 N88-24928

Investigations in electro-optical multistability for signal processing 18 p2518 N88-24938

Low frequency electrostatic turbulence in the polar cap E-region
[DRI-3-88] 18 p2540 N88-25077

An experimental study of the coherent under-ice reflectivity of sound in the Greenland Sea Marginal Ice Zone 18 p2548 N88-25125

Optical computing based on neuronal models
[AD-A191481] 18 p2575 N88-25293

Optical nonlinearities in GaAs/GaAlAs multiple quantum wells fabricated by metalorganic chemical vapor deposition for use in optical signal processing
[AD-A191558] 18 p2582 N88-25337

Signal processing computational needs
[AD-A191756] 19 p2642 N88-25674

Multipath measurements for land mobile satellite service using global positioning system signals
19 p2645 N88-25700

Adaptive interference techniques for mobile antennas
19 p2647 N88-25714

Interleaver design for trellis-coded differential 8-PSK modulation with non-coherent detection
19 p2648 N88-25719

Mini-station for VHF reception: Argos system simplified description
[INPE-4551-NTE/279] 19 p2655 N88-25764

Organization of a Topical Meeting on Picosecond Electronics and Optoelectronics
[AD-A187136] 19 p2655 N88-25765

A simple technique to generate or gate microwave pulses with picosecond speeds 19 p2657 N88-25784

Characteristics and application of wideband guided-wave devices 19 p2660 N88-25817

Active control of 2-D instability waves on an axisymmetric body
[AD-A191578] 19 p2663 N88-25835

Novel nonlinear signal processing principles
[AD-A191644] 19 p2707 N88-26097

SLAPP: A special multiprocessor array for signal processing and linear algebra
[AD-A191587] 19 p2719 N88-26146

Proceedings of the Array Signal Processing Symposium: Treaty Verification Program
[DE88-008346] 20 p2790 N88-26548

Signal processing in digital speech transmission systems
[ETN-88-92122] 20 p2792 N88-26561

A microcomputer based frequency-domain processor for laser Doppler anemometry
[NASA-TM-100998] 20 p2803 N88-26634

Display and processing of multidimensional signals with the aid of fractal image sequences
[ETN-88-92131] 20 p2806 N88-26642

MAXIE-1 (Magnetospheric Atmospheric X-ray Imaging Experiment)
[AD-A192646] 21 p2902 N88-27221

A numerically efficient digital matched filter for periodic and windowed periodic radar waveforms
[AD-A193132] 21 p2932 N88-27410

Fourth generation neurocognitive pattern analysis system 21 p2977 N88-27686

The application of non-stationary data analysis techniques in the identification of changes in the electroencephalogram associated with the onset of drowsiness 21 p2978 N88-27688

A statistical procedure for the evaluation of presence/non-presence of stimulus-related EEG activity
21 p2978 N88-27689

Demodulation processes in auditory perception
[AD-A193421] 21 p2988 N88-27740

Robust methods for array signal processing
[AD-A192854] 21 p3012 N88-27871

Solid state research
[AD-A192637] 21 p3020 N88-27929

Experiments applications guide: Advanced Communications Technology Satellite (ACTS)
[NASA-TM-100265] 22 p3048 N88-28082

The Telecommunications and Data Acquisition Report
[NASA-CR-183131] 22 p3063 N88-28178

Spectral estimation of received phase in the presence of amplitude scintillation 22 p3064 N88-28180

Telemetry SNR improvement using the DSN Advanced Receiver with results for Pioneer 10
22 p3064 N88-28184

Advanced Receiver tracking of Voyager 2 near solar conjunction 22 p3065 N88-28185

Strawman Optical Reception Development Antenna (SORDA) 22 p3065 N88-28187

Performance analysis of a noncoherently combined large aperture optical heterodyne receiver
22 p3065 N88-28189

Effect of detector dead time on the performance of optical direct-detection communication links
22 p3065 N88-28190

A wideband, high-resolution spectrum analyzer
22 p3066 N88-28194

A digitally implemented phase-locked loop detection scheme for analysis of the phase and power stability of a calibration tone 22 p3066 N88-28196

The behavior of a Costas loop in the presence of space telemetry signals 22 p3067 N88-28198

DSN very long baseline interferometry system Mark IV-88 22 p3067 N88-28199

Baseband assembly analog-to-digital converter board
22 p3067 N88-282[illegible]1

An evaluation of Interactive Laboratory System software, ILS-PC/DOS: A digital signal processing software package
[AD-A193838] 22 p3138 N88-28657

Application of the Hilbert transform to Doppler radar signals from a hypervelocity gun
[AD-A193690] 22 p3146 N88-28716

Method and apparatus for non-destructive testing of temper embrittlement in steels
[NASA-CASE-LAR-13817-1] 23 p3195 N88-29012

Signal processing software for ground penetrating radar, user's manual
[AD-A194286] 23 p3203 N88-29059

Automatic classification of digitally modulated signals
[AD-A194623] 23 p3203 N88-29064

Basic research in electronics (JSEP) Joint Services Electronics Program
[AD-A193072] 23 p3206 N88-29079

Anti-aliasing filters for dynamics and control experiments
[AD-A193758] 23 p3226 N88-29203

A computer program package for introductory one-dimensional digital signal processing applications
[AD-A194656] 23 p3249 N88-29338

Object discrimination via bulk temperature/velocity filtering, phase 1
[AD-A194533] 23 p3274 N88-29487

Acoustooptic processing of two-dimensional signals using temporal and spatial integration
[AD-A194803] 24 p3359 N88-29999

Doppler-corrected differential detection system
[NASA-CASE-NPO-16987-1-CU]
24 p3359 N88-30001

Review of Radio Science, 1984-1986
24 p3363 N88-30023

Signals and systems 24 p3363 N88-30026

Quantitative surface temperature measurement using two-color thermographic phosphors and video equipment
[NASA-CASE-LAR-13740-1] 24 p3376 N88-30105

Reconstruction of multidimensional signals from multiple level threshold crossings
[AD-A195561] 24 p3425 N88-30383

Spectroscopic studies with multiple quantum well materials with applications to optical signal processing at room temperature
[AD-A194171] 24 p3429 N88-30409

SIGNAL RECEPTION

NT SYLLABLES
NT SYMBOLS
NT TELEVISION RECEPTION

Optimized tracking of RF carriers with phase noise, including Pioneer 10 results 04 p0434 N88-12694

An analysis of simplified feed architectures for MMIC (Monolithic Microwave Integrated Circuit) T/R (Transmit/Receive) module arrays
[AD-A185474] 06 p0697 N88-14275

Automatic antenna switching design for Extra Vehicular Activity (EVA) communication system
06 p0797 N88-14883

Adaptive detection in non-stationary interference, part 3
[AD-A185622] 07 p0844 N88-15118

High-sensitivity recording of weak reflected or scattered radiation by method of coherent intracavity reception with YAG:Nd(3+) laser 08 p1078 N88-16502

Fabrication and packaging of discontinuous MIM (Metal-Insulator-Metal) film arrays for efficient MM wave and IR detection and mixing
[AD-A186809] 09 p1146 N88-16869

Spread spectrum mobile radio communications
[AD-A187487] 11 p1470 N88-18765

Phase calibration generator 11 p1473 N88-18785

Target localization in an inhomogeneous medium
[AD-A190008] 15 p2130 N88-22703

Digital communication transmitter and receiver test procedures
[AD-A191218] 20 p2788 N88-26540

The focal plane reception pattern calculation for a paraboloidal antenna with a nearby fence
[NASA-TM-100691] 24 p3365 N88-30039

SIGNAL REFLECTION

Delay-Doppler radar imaging
[AD-A184165] 03 p0308 N88-11943

Correlation between refraction over sea and nature of radar reflections from sea surface
06 p0728 N88-14477

Adaptive detection in non-stationary interference, part 3
[AD-A185622] 07 p0844 N88-15118

The characteristics of two broadband (2 MHz to 10 MHz) switched vee antennas
[AD-A187874] 11 p1471 N88-18770

Remote determination of chlorophyll concentration in the ocean using an optical pulse radar
[NASA-TT-20301] 19 p2694 N88-26014

SIGNAL STABILIZATION

Optimized tracking of RF carriers with phase noise, including Pioneer 10 results 04 p0434 N88-12694

X-band uplink ground systems development: Part 2
04 p0436 N88-12703

Some properties of the Hilbert transform
[DE88-002465] 09 p1227 N88-17350

Comparison of five readout techniques for an integrated magnetometer 19 p2671 N88-25876

SIGNAL TO NOISE RATIOS

Masking effects of fine and coarse grain pictorial noise
[IZF-1985-21] 01 p0076 N88-10485

Maximum likelihood estimates of parameters in linear systems with process and measurement noise
[DFVLR-FB-87-20] 01 p0083 N88-10532

ISIS: Image reconstruction methods and signal-to-noise ratio investigations --- spaceborne interferometry
01 p0094 N88-10619

Signal to noise ratios --- SPOT images
03 p0341 N88-12150

Detector normalization --- SPOT remote sensors
03 p0341 N88-12151

Optimized tracking of RF carriers with phase noise, including Pioneer 10 results 04 p0434 N88-12694

Detection of signals by the digital integrate-and-dump filter with offset sampling 04 p0435 N88-12695

Detection of signals by weighted integrate-and-dump filter 04 p0435 N88-12696

Lower bounds on bearing accuracy for closely spaced sources
[AD-A184258] 04 p0486 N88-12987

Measured noise performance of a direct-sequence spread-spectrum system and a comparison of single vice dual-channel delay-lock loops
[AD-A186288] 07 p0843 N88-15110

Adaptive detection in non-stationary interference, part 3
[AD-A185622] 07 p0844 N88-15118

A simultaneous M-ary channel hypothesis test with least-mean-square signal amplitude estimation
[AD-A186526] 08 p0978 N88-15913

High-sensitivity recording of weak reflected or scattered radiation by method of coherent intracavity reception with YAG:Nd(3+) laser 08 p1078 N88-16502

On the signal strength dependency on pressure in laser sub-Doppler saturation spectroscopy with special attention to gaseous diatonic molecules
[USIP-87-13] 09 p1171 N88-17023

The relationship between vision carrier-to-noise ratio and picture signal-to-noise ratio in a System I television receiver
[BBC-RD-1987/23] 10 p1318 N88-17877

New monostatic balanced Doppler velocimeter using a polarization preserving fiber
[PB88-130869] 11 p1490 N88-18895

Envelope and phase statistics for non-Gaussian noise and resulting error probabilities for digital communications systems 12 p1617 N88-19672

Signal-filter design and system performance for polarimetric radar
[AD-A189257] 13 p1758 N88-20514

Detection and angle estimation of coherent plane waves 13 p1759 N88-20522

A preliminary assessment of thunderstorm outflow wind measurement with airport surveillance radars
[AD-A189064] 13 p1799 N88-20757

Preliminary comparison of some coincidence methods for gravitational wave detectors
[NOTA-INTERNA-903] 14 p1945 N88-21604

Masking of motion cues by random motion: Comparison of human performance with a signal detection model
[UTIAS-313] 14 p1953 N88-21639

Direct bit detection receiver noise performance analysis for 32-PSK and 64-PSK modulated signals
[AD-A190009] 15 p2056 N88-22256

The 2 FSK/QPSK (Frequency Shift Keying/Quadrature Phase Shift Keying) transmitter and receiver: Design and performance
[AD-A190028] 15 p2056 N88-22258

Multiplex methods in infrared spectrometry
16 p2271 N88-23566

Loran-C monitor correlation over a 92-mile baseline in Ohio 17 p2293 N88-23720

Analysis of binarized Hartley phase-only filter performance with respect to stochastic noise
[DE88-007604] 18 p2519 N88-24945

Codes for QPSK modulation with invariance under 90 degrees rotation 19 p2648 N88-25720

Signal processing in digital speech transmission systems
[ETN-88-92122] 20 p2792 N88-26561

Detection of acceleration (+Gz) induced blackout by matched-filtering of visual evoked potentials
21 p2982 N88-27710

The behavior of a Costas loop in the presence of space telemetry signals 22 p3067 N88-28198

Direct bit detection receiver performance analyses for 8-DPSK (Differential Phase Shift Keyed) modulated signals operating with improper carrier phase synchronization
[AD-A193839] 22 p3070 N88-28220

Effect of phase errors in stepped-frequency radar systems
[AD-A194476] 23 p3203 N88-29061

Multi-sensory tracking mount control
[AD-A194675] 23 p3249 N88-29339

Analytical methods in stochastic control and nonlinear filtering
[AD-A194272] 24 p3426 N88-30388

SIGNAL TRANSMISSION
NT ALOHA SYSTEM
NT AUTOMATIC PICTURE TRANSMISSION
NT BIOTELEMETRY
NT CODE DIVISION MULTIPLE ACCESS
NT DATA TRANSMISSION
NT FREQUENCY DIVISION MULTIPLE ACCESS
NT IONOSPHERIC PROPAGATION
NT MICROWAVE ATTENUATION
NT MICROWAVE TRANSMISSION
NT MULTIPATH TRANSMISSION
NT MULTIPLE ACCESS
NT PACKET TRANSMISSION
NT PCM TELEMETRY
NT RADAR TRANSMISSION
NT RADIO TELEMETRY
NT RADIO TRANSMISSION
NT SATELLITE TRANSMISSION
NT SHORT WAVE RADIO TRANSMISSION
NT SINGLE CHANNEL PER CARRIER TRANSMISSION
NT TELEMETRY
NT TELEVISION TRANSMISSION
NT TRANSEQUATORIAL PROPAGATION

The absolute radiometric calibration of space-based sensors 03 p0277 N88-11744

Experiments: Test range facilities, part 2
03 p0305 N88-11921

Design of digital filters for electronic instrumentation
[PB87-100418] 04 p0438 N88-12716

Measured characteristics of 800/900 MHz mobile radio channels with high-angle propagation through moderately dense foliage
[CRC-1398] 05 p0573 N88-13493

Time domain electromagnetic waves in multilayered media
[AD-A185055] 05 p0574 N88-13502

Fiber optic video link
[FOA-C-30444-3.1] 06 p0780 N88-14789

An additional study and implementation of tone calibrated technique of modulation
[NASA-CR-182377] 07 p0844 N88-15117

Waveform for short-dwell-time meteorological Doppler radars
[PB88-102199] 07 p0845 N88-15126

High Resolution Picture Transmission (HRPT) data processing from NOAA series satellites
[INPE-4372-PRE/1195] 08 p0963 N88-15831

Method for set-up for researching signal curve development
[NASA-TT-20235] 13 p1760 N88-20526

Upward propagating electric fields from thunderstorms and VLF transmitters 13 p1801 N88-20767

Results of one way transit time measuring in navigation experiment NAVEX
[DFVLR-MITT-87-17] 14 p1865 N88-21145

Target localization in an inhomogeneous medium
[AD-A190008] 15 p2130 N88-22703

Trellis-coded CPM for satellite-based mobile communications 19 p2648 N88-25718

An error floor in tone calibrated transmission
19 p2649 N88-25729

Extending the impulse response in order to reduce errors due to impulse noise and signal fading
19 p2649 N88-25730

Non-stationary transport in MODFET's and heterojunction devices 19 p2659 N88-25804

Radar and EW applications of multi-gigahertz optical components and systems 19 p2660 N88-25816

A 1/2-inch high-definition baseband VCR
21 p2930 N88-27393

Dependence effects in unique signal transmission
[DE88-010331] 21 p2933 N88-27419

SIGNALS

Controlling XeCl-laser by means of external signal with less than 2 W/cm (sup)2 intensity
14 p1972 N88-21768

SIGNATURE ANALYSIS

Fundamental aspects of the physics of remote sensing
[ESA-TT-1045] 09 p1185 N88-17100

Open questions in closed-loop photodetection
14 p1979 N88-21812

Autoregressive moving average modeling of radar target signatures
[AD-A194612] 22 p3069 N88-28218

Variability in spectral signatures of terrestrial volcanic rocks and implications for volcanology on Mars
23 p3303 N88-29672

SIGNATURES
NT INFRARED SIGNATURES
NT MAGNETIC SIGNATURES
NT RADAR SIGNATURES
NT SPECTRAL SIGNATURES

A system identification technique based on the random decrement signatures. Part 1: Theory and simulation
05 p0594 N88-13625

A system identification technique based on the random decrement signatures. Part 2: Experimental results
05 p0594 N88-13626

Interaction of a vortex pair with a free surface
[AD-A186619] 08 p0988 N88-15988

The angular reflectance signature of the canopy hot spot in the optical regime
[DE88-005385] 11 p1505 N88-18991

Toward a comprehensive theory for the sweeping of trapped radiation by inert orbiting matter
[NASA-CR-182584] 11 p1569 N88-19395

Polarimetric ISAR imaging using either measured or calculated transient signatures
[AD-A190077] 15 p2056 N88-22259

Anomalies in the heat-capacity signatures of submonolayer adsorbates with attractive lateral interactions
[AD-A190736] 15 p2147 N88-22817

SIGNIFICANCE

Determining differences in rates corresponding to a given significance level
[AD-A185004] 05 p0644 N88-13940

SIGNS (SYMBOLS)
U SYMBOLS

SIGNS AND SYMPTOMS

Computer response time measurements of mood, fatigue and symptom scale items: Implications for scale response time uses
[AD-A186093] 07 p0888 N88-15384

Motion sickness: Quantitative, algorithmic malaise indication in real time
[AD-A189674] 15 p2101 N88-22518

Simulator sickness in the AH-64 Apache combat mission simulator
[AD-A193419] 21 p2988 N88-27739

Alterations in upper extremity motor function in soldiers during acute high altitude exposure
[AD-A192676] 23 p3238 N88-29272

SIKORSKY AIRCRAFT
NT UH-60A HELICOPTER

Recent Sikorsky R and D progress
09 p1111 N88-16659

SILANES

Laser spectroscopy and gas-phase chemistry in CVD
[DE87-013715] 03 p0281 N88-11770

Measurement of the electron density and the attachment rate coefficient in silane/helium discharges
[AD-A184268] 04 p0496 N88-13051

Reactive sticking coefficients of silane on silicon
[DE88-000601] 05 p0570 N88-13473

Soluble polysilane derivatives: Chemistry and spectroscopy
[AD-A187889] 11 p1461 N88-18713

Photophysics and photochemistry of poly(di-n-hexylsilane) in room temperature solution
[AD-A187890] 11 p1462 N88-18714

High-performance polymeric materials
[AD-A190708] 15 p2046 N88-22190

Polymer precursors for ceramic composites
17 p2326 N88-23890

Boron-containing organosilane polymers and ceramic materials thereof
[NASA-CASE-ARC-11649-1-SB]
23 p3199 N88-29040

Ion kinetics in silane plasmas
[AD-A196202] 24 p3431 N88-30423

SILENCERS

Silencium resonators (Silators) for the attenuation and elimination of sound
[MBB-Z-546/83] 10 p1312 N88-17841

SILICA
U SILICON DIOXIDE

SILICA GEL

Separation of anionic from nonionic alkoxy compounds using silica gel
[GB-PATENT-2-140-415-A] 01 p0020 N88-10122

Structure of sol-gel-derived inorganic polymers. 2: Silicates and borates
[DE87-013068] 01 p0027 N88-10172

Optical characterization of silica aerogel glass
[DE87-014617] 02 p0153 N88-10956

Mass transfer mechanisms for water adsorbed on silica gel
[DE88-005993] 15 p2032 N88-22107

Structure of sol-gel silica
[DE88-006870] 15 p2033 N88-22114

A model for insulated wires in the method of moments code NEC (Numerical Electromagnetics Code)
[DE88-008920] 20 p2794 N88-26577

Optical characterization of silica aerogel
[DE88-008916] 20 p2854 N88-26946

Precursor chemistry and the structure of silica aerogels
[DE88-011253] 21 p2920 N88-27328

SILICA GLASS

Optical characterization of silica aerogel glass
[DE87-014617] 02 p0153 N88-10956

Environmental fracture toughness and static fatigue crack propagation of silica glass
05 p0606 N88-13716

Novel fiber preforms: Rare earth doping
[AD-A191549] 18 p2575 N88-25294

Adhesion of hydrated silicate films
[DE88-011250] 21 p2920 N88-27333

Development of high efficiency q-switched glass laser via sol-gel processing
[AD-A192301] 23 p3218 N88-29154

SILICATES
NT ALUMINUM SILICATES
NT ANDESITE
NT CALCIUM SILICATES
NT GARNETS
NT YTTRIUM-ALUMINUM GARNET
NT ZEOLITES

Structure of sol-gel-derived inorganic polymers. 2: Silicates and borates
[DE87-013068] 01 p0027 N88-10172

Some speculations on the mechanisms of abrasive grinding and polishing
[DE87-014242] 02 p0181 N88-11126

The effect of temperature on fatigue crack initiation from aluminosilicate inclusions 06 p0720 N88-14427

Electron microscopy study of morphology and composition of a ferrisilicate catalyst
[DE88-005754] 11 p1562 N88-19352

High-performance polymeric materials
[AD-A190708] 15 p2046 N88-22190

Point defects in irradiated silicates
17 p2406 N88-24319

The evolution of cometary activity
18 p2594 N88-25416

Adhesion of hydrated silicate films
[DE88-011250] 21 p2920 N88-27333

Recycling of lower continental crust through foundering of cumulates from contaminated mafic intrusions
24 p3393 N88-30204

SILICIDES
NT DISILICIDES

Cohesive energies of transition metal silicides and phosphides --- Knudsen effusion
[AD-A186691] 09 p1254 N88-17519

Initial development of high-temperature titanium silicide alloys
[DE88-007860] 20 p2772 N88-26437

Rocket propellant burn tests of silicide-coated niobium and tantalum
[DE88-010729] 20 p2781 N88-26496

SILICON
NT AMORPHOUS SILICON

Si - SiO2 interfaces: A High Resolution Transmission Electron Microscopy (HRTEM) study
[DE87-012255] 01 p0028 N88-10181

Construction and characterization of amorphous-silicon test structures
[DE87-013595] 01 p0029 N88-10182

Effect of high-temperature annealing on the microstructure and thermoelectric properties of GaP doped SiGe
[NASA-TM-100164] 01 p0029 N88-10188

Monocrystalline silicon gradiometer for gravity experiments in space
[NASA-CR-181452] 01 p0050 N88-10321

Electrical behavior of layers implanted with low energy pions in Si
[INPE-4199-PRE/1051] 01 p0102 N88-10670

Chemical vapor deposition of B6P and B6As films
[DE87-009288] 02 p0151 N88-10942

Hydrogen annealing of P(sub) b and E prime defect centers in oxidized silicon wafers
[DE87-014293] 02 p0152 N88-10951

Preparation of oxide glasses from metal alkoxides by sol-gel method
[NASA-TT-20124] 02 p0154 N88-10965

Voltammetric investigation of porous silicon for integrated circuit applications
[DE87-009287] 02 p0166 N88-11042

Wide bandgap passivation layers on silicon
[DE87-014307] 02 p0244 N88-11543
Bond character at a silicon/copper surface
[AD-A184167] 03 p0295 N88-11851
Integrated fiber-optic coupler
[AD-A184494] 03 p0377 N88-12369
Elimination of subboundaries in 0.5-micron-thick Si-on-insulation films produced by ZMR
[AD-A184590] 03 p0381 N88-12396
Dramatically improved radiation hardness for CMOS silicon gate integrated circuits even down to cryogenic temperatures
[AD-A184672] 03 p0381 N88-12398
Epitaxial reactor development for growth of silicon-on-insulator devices
[AD-A184758] 03 p0382 N88-12399
Performance of GaAs and silicon concentrator cells under 37 MeV proton irradiation
[NASA-TM-100144] 04 p0465 N88-12877
Colloidal stability of oxidized silicon particles in ethanolic and aqueous media
[DE87-014783] 05 p0562 N88-13421
Reactive sticking coefficients of silane on silicon
[DE88-000601] 05 p0570 N88-13473
Technology upgrade of a silicon compiler
[AD-A184873] 05 p0655 N88-14016
Preparation of amorphous silicon semiconductors
[GB-PATENT-2-176-054-A] 05 p0656 N88-14022
Effects of hydrolysis on metallo-organic solution deposition of PZT films
[ATR-86(8443)-1] 06 p0679 N88-14160
Theoretical aspects of channeling, damage, and range distributions for low (keV) and high (MeV) energy implantation
[DE88-000949] 06 p0786 N88-14818
Silicon microscale mechanisms from (110) oriented wafers
[DE88-002096] 06 p0787 N88-14825
The influence of phosphorus on the solid state reaction between copper and silicon or germanium
[ETN-88-91361] 06 p0789 N88-14838
Diamond turning of silicon for optics applications
[DE88-002501] 07 p0840 N88-15095
Formation and passivation of new paramagnetic defects associated with thermal oxides on silicon
[DE88-002720] 07 p0938 N88-15699
Radiant power degradation of silicon-doped gallium arsenide and gallium aluminum arsenide infrared light-emitting diodes
[AD-A186726] 09 p1157 N88-16935
IRAC test report. Gallium doped silicon band 2: Read noise and dark current
[NASA-TM-87813] 09 p1159 N88-16945
Forward-biased current annealing of radiation damaged gallium arsenide and silicon solar cells
[AD-A186904] 09 p1186 N88-17105
The mechanism of anisotropic silicon etching and its relevance for micromachinings
[MBB-UA-1013/86] 10 p1311 N88-17838
Laser pulse width dependent surface ripples on silicon
[PB88-127311] 10 p1336 N88-17982
Optical measurements of surface oxide layer formation on metal films
[DE88-003163] 10 p1409 N88-18405
Corner compensation structures for (110) oriented silicon
[DE88-003300] 10 p1417 N88-18455
Recording a surface acoustic wave on the surface of silicon
[PB88-130372] 11 p1490 N88-18894
Measurement of the gamma-ray response of some commercial silicon detectors
[AD-A187431] 11 p1543 N88-19221
Atomistic simulation of low-energy beam deposition
[DE88-004344] 11 p1544 N88-19228
Development of VLSI optical data link
[AD-A187883] 11 p1549 N88-19265
Silicon and indium doping of GaAs: Measurements of the effect of doping on mechanical behavior and relation with dislocation formation
[DE88-003862] 11 p1554 N88-19303
Formation of buried nitride layers in (110) silicon
[DE88-003255] 11 p1557 N88-19323
Silicon containing photoresists
[AD-A188666] 12 p1605 N88-19601
Preparation and characterization of thin films of alumina by metalorganic chemical vapor deposition
[AD-A188366] 12 p1608 N88-19614
Polymeric materials for electro-optic testing
[AD-A188382] 12 p1610 N88-19627
Hydrodynamic simulation of forced convection in the Czochralski process
[INPE-4471-TDL/323] 12 p1697 N88-20158
Thermal oxide growth on silicon: Intrinsic stress and silicon cleaning effects
[AD-A188790] 13 p1736 N88-20377
Focused ion beam fabrication of graded channel FET's in GaAs and Si
[AD-A189166] 13 p1845 N88-21040
Pressure-dependent DLTS (Deep Level Transient Spectroscopy) experiments on Si-doped AlGaAs
[DE88-003842] 13 p1846 N88-21047
X-ray diffraction study of a thin GaAs film on Si(100)
[DE88-005290] 13 p1847 N88-21055
Initial stages of silicon growth on the (100) surface of silicon by localized laser CVD
[DE88-005420] 13 p1848 N88-21059
Modeling growth of interdendritic silicon ribbons
14 p1897 N88-21322
Breathing mode lattice relaxation associated with carrier emission and capture by deep electronic levels in silicon
[DE88-003844] 14 p1985 N88-21842
Fabrication and electrical characterization of multilevel aluminum interconnects used to achieve silicon-hybrid wafer-scale integration
[AD-A190519] 15 p2060 N88-22282
High-efficiency thin-film silicon-on-GaP solar cell for improved radiation resistance
[AD-A190268] 15 p2091 N88-22460
Fundamental properties and devices applications of Ge(x)Si(1-x)/Si superlattices
[AD-A190129] 15 p2143 N88-22787
The structure of the boron-hydrogen complex in silicon
[DE88-005433] 15 p2144 N88-22795
Neutron radiation tolerance of Au-activated silicon
17 p2408 N88-24316
Improved GaP doped SiGe thermoelectric material
17 p2437 N88-24503
Observation of injected silicon in heliotron E
17 p2441 N88-24524
Metastability in SiGe/Si strained-layer structures
[DE88-007603] 18 p2585 N88-25361
On the use of convergent beam electron diffraction for identification of antiphase boundaries in GaAs grown on Si
[DE88-008220] 18 p2585 N88-25362
Silicon pulse sharpening diodes-switching kilovolts in 10's of picoseconds 19 p2661 N88-25824
Microminiature fluidic amplifier
19 p2669 N88-25865
Anomalous emissivity from periodic micro-machined silicon surfaces 19 p2670 N88-25872
Stress modeling of microdiaphragm pressure sensors
19 p2670 N88-25873
Application-specific packaging for custom micromechanical structures 19 p2671 N88-25879
High dose uranium ion implantation into silicon
[LBL-23509] 19 p2725 N88-26182
Defects in high-mobility semiconductor systems
[AD-A191618] 19 p2732 N88-26224
X-ray response of GaAlAs/GaAs radiation hardened double: Heterostructure photodiode compared to Si:PIN photodiodes
[DE88-007425] 19 p2733 N88-26231
Ductile-brittle transition of cutting behavior in diamond turning of single crystal Si
[DE88-008690] 20 p2809 N88-26664
Kinetic of oxidation to air of a Fe-Al-Mn alloy system at 600-800(sup 0)C temperature range
[DE88-702309] 21 p2920 N88-27330
Studying the physics and operation of multi-terminal near-micron and sub-micron length, hot electron semiconductor devices
[AD-A193380] 21 p2938 N88-27446
Molecular beam epitaxy of GaP films on Si substrates
[PB88-131974] 21 p3020 N88-27923
Development of 30 micrometers extrinsic silicon multiplexed infrared deterctor array
[NASA-CR-177446] 22 p3082 N88-28301
Atomistic simulation of silicon grain boundaries
[DE88-009925] 22 p3155 N88-28771
Sol-gel processing of metal-oxide-semiconductor structures
[DE88-009853] 22 p3156 N88-28778
Sol-gel kinetics: Si(sup)29 NMR and a statistical reaction model
[DE88-011545] 23 p3191 N88-28988
Stress corrosion of ceramic materials
[AD-A191979] 23 p3195 N88-29016
Local environment approach for deep-level defects in semiconductors: Application to the vacancy in silicon
[DE88-702017] 23 p3287 N88-29573
Ultrafast processes and spectroscopy with free electron lasers
[AD-A195248] 24 p3379 N88-30126

SILICON ALLOYS
Factors determining the morphology of precipitation in aluminum-germanium and aluminum-silicon alloys
[DE87-014682] 03 p0287 N88-11606
Cyclic deformation of an extruded AlMgSi alloy
05 p0598 N88-13654
Stability diagrams for epitaxial strained layers
[DE88-003935] 10 p1418 N88-18470
Brittle to ductile transition to cleavage fracture
[DE88-004074] 10 p1420 N88-18481
Optimisation of the thermoelectric figure of merit of modified silicon germanium alloys
[AD-A191347] 16 p2283 N88-23670
Preparation of improved PbSnTe thermoelectric alloys and evaluation of their figure of merit
[AD-A191346] 17 p2445 N88-24538
Improved properties of SiGe/GaP alloys
[NASA-CASE-NPO-17259-1-CU]
18 p2585 N88-25358
Hydrogenated amorphous silicon-germanium alloys
[DE88-001147] 19 p2620 N88-25546
Low-band-gap, amorphous-silicon-based alloys by photochemical vapor deposition
[DE88-001165] 21 p3023 N88-27944
Calculation of the specific and volumetric enthalpies of Ge-Si alloys
[DE88-008949] 21 p3026 N88-27965

SILICON CARBIDES
Pressure effects on the thermal stability of SiC fibers
[NASA-TM-100146] 01 p0019 N88-10120
Physics and chemistry of packing fine ceramic powders
[DE87-013709] 01 p0029 N88-10183
Laser chemically vapor deposited silicon-carbide: Growth features, topography, microstructure, and composition
[DE87-013767] 01 p0029 N88-10184
Fiber-reinforced composite hot-gas filters
[DE87-012257] 01 p0033 N88-10208
An investigation of the high strain rate deformation of SiCw/2124 Al composite
[OUEL-1675/87] 02 p0142 N88-10695
Processing and properties of SiC/Nicalon composites
[DE87-013885] 03 p0279 N88-11757
The infiltration kinetics of aluminum in silicon carbide compacts
[AD-A184682] 03 p0290 N88-11823
Characterization and thermal conductivity of hot-pressed silicon carbide
[DKG-25] 03 p0292 N88-11834
Flaw imaging and ultrasonic techniques for characterizing sintered silicon carbide
[NASA-TM-100177] 03 p0334 N88-12106
Carbon-fiber reinforced aluminum
04 p0403 N88-12507
Composite materials with glass matrix
[SGR/PR-4305/86-SV/JC] 05 p0558 N88-13394
Fabrication of composites by chemical vapor deposition
[DE87-014565] 05 p0559 N88-13408
Structural characterization of ion implanted beta-SiC thin films
[DE87-014567] 05 p0656 N88-14027
Stress rupture behavior of silicon carbide coated, low modulus carbon/carbon composites
[NASA-CR-180863] 06 p0678 N88-14150
Sintering and densification of particulate composites: Inclusion size and clustering
[DE88-002230] 06 p0685 N88-14199
Cyclic fatigue of ceramics at high temperatures
[PB87-127700] 06 p0685 N88-14200
Micromechanisms of fatigue crack growth and fracture toughness in metal matrix composites
[AD-A186941] 09 p1137 N88-16816
Investigation of microstructural factors that cause low fracture toughness in silicon carbide whisker/Al alloy composites
[AD-A186443] 09 p1137 N88-16817
Microstructures and properties of SiC whisker-reinforced mullite composites
[DE88-002611] 09 p1139 N88-16826
Wire-cut electrical discharge machinability of ceramics
[AD-A186989] 09 p1146 N88-16870
Fabrication and materials evaluation of high performance aligned ceramic fibre reinforced glass matrix composite
[AERE-R-12517] 10 p1294 N88-17736
Micro-mechanisms of deformation in SiC/Al composites
[AD-A188282] 10 p1296 N88-17749
Friction and wear of monolithic and fiber reinforced silicon-ceramics sliding against IN-718 alloy at 25 to 800 C in atmospheric air at ambient pressure
[NASA-TM-100294] 10 p1304 N88-17796
NMR (Nuclear Magnetic Resonance) imaging for detecting binder/plasticizers in green-state structural ceramics
[DE88-003111] 10 p1304 N88-17800
Fabrication, phase transformation studies and characterization of SiC-AlN-Al2OC ceramics
[DE88-004053] 10 p1306 N88-17807

Plasma deposition of silicon carbide thin films
[AD-A188093] 11 p1556 N88-19314
Effect of rigid inclusions on sintering
[DE88-005745] 12 p1609 N88-19623
Fundamental studies and device development in beta silicon carbide
[AD-A189540] 12 p1699 N88-20165
Composites strengthening
[AD-A189258] 13 p1734 N88-20364
The influence of the fiber-matrix bond on the mechanical behavior of NICALON/SiC composites
[DE88-006155] 13 p1734 N88-20369
Nondestructive evaluation of carbon-carbon coatings
[AD-A189524] 13 p1748 N88-20453
Ultrasonic characterization of non-uniform porosity distributions in SiC ceramic
[DE88-004814] 13 p1749 N88-20459
Development, high temperature properties, and microanalysis of nonoxide ceramics
[ETN-88-92103] 14 p1893 N88-21304
Processing, texture and mechanical properties of sintered silicon carbide
[NASA-TT-20253] 14 p1893 N88-21305
Microwave sintering of alumina-SiC composites at 2.45 and 60 GHz
[DE88-006455] 15 p2030 N88-22095
Processing, microstructure, and mechanical properties of silicon carbide particulate reinforced aluminum alloys
[AD-A188981] 15 p2037 N88-22136
Characterization of sintered SiC by using NDE
15 p2082 N88-22413
Strength and cracking resistance of ceramics. Report 3: SiC ceramics 16 p2180 N88-22994
Structure and mechanical properties of metal matrix composites made using semi-solid processes: The case of the system Al-Si/SiC
[ETN-88-92299] 17 p2316 N88-23836
Nondestructive evaluation of structural ceramics
17 p2324 N88-23876
Improved silicon carbide for advanced heat engines
17 p2324 N88-23879
Strength optimization of alpha-SiC by improved processing 17 p2324 N88-23880
Colloidal characterization of silicon nitride and silicon carbide 17 p2325 N88-23883
Molten salt corrosion of SiC and Si3N4
17 p2325 N88-23885
Thermal cyclic durability testing of ceramic materials for turbine engines 17 p2325 N88-23886
Ceramic matrix composites 17 p2325 N88-23888
Polymer precursors for SiC ceramic materials
17 p2326 N88-23889
SiC fiber analysis 17 p2326 N88-23891
SiC fiber reinforced reaction-bonded Si3N4 composites 17 p2326 N88-23892
High frequency ultrasonic characterization of sintered SiC
[NASA-TM-100825] 17 p2347 N88-23985
Defects in cubic silicon carbide on silicon
17 p2408 N88-24317
An investigation of ceramic coatings for protection of SiC from high-temperature corrosion
[DE88-007873] 18 p2493 N88-24790
Auger analysis of a fiber/matrix interface in a ceramic matrix composite
[NASA-TM-100892] 19 p2610 N88-25487
Interface modification in Nicalon (trademark)/SiC composites
[DE88-009708] 20 p2767 N88-26409
Observations on residual stresses in ceramic composites by neutron diffraction techniques
[DE88-009937] 20 p2778 N88-26472
Factors influencing the toughening behavior of whisker reinforced ceramics
[DE88-011396] 20 p2779 N88-26479
As-received microstructure of a SiC/Ti-15-3 composite
[NASA-TM-100938] 22 p3050 N88-28095
Investigation of a SiC/Ti-24Al-11Nb composite
[NASA-TM-100956] 23 p3190 N88-28980
Determination of impurities in silicon carbide by ICP AES (inductively coupled plasma atomic emission spectrometry) after coprecipitation with lanthanum hydroxide
[NASA-TT-20332] 23 p3193 N88-29003
Sinterable ceramic powders from laser-heated gases
[AD-A194162] 23 p3197 N88-29024
Boron-containing organosilane polymers and ceramic materials thereof
[NASA-CASE-ARC-11649-1-SB]
23 p3199 N88-29040
Processing technology research in composites
[AD-A195693] 24 p3341 N88-29890
Electrical properties of materials for elevated temperature resistance strain gage application
[NASA-CR-182214] 24 p3376 N88-30106

SILICON COMPOUNDS
NT ALUMINUM SILICATES
NT ANDESITE
NT CALCIUM SILICATES
NT DISILICIDES
NT GARNETS
NT ORGANIC SILICON COMPOUNDS
NT QUARTZ
NT SILANES
NT SILICATES
NT SILICIDES
NT SILICON CARBIDES
NT SILICON DIOXIDE
NT SILICON NITRIDES
NT SILICON OXIDES
NT YTTRIUM-ALUMINUM GARNET
NT ZEOLITES
Flash threshold of shocked aluminum silicofluoride
[DE88-003978] 10 p1339 N88-18005
Silicon-germanium heterostructures
13 p1844 N88-21034
Recent data on Si:As impurity band conduction multiplexed arrays
[AD-A191752] 18 p2582 N88-25340
Photorefractive damage mechanism in electro-optic materials
[AD-A194560] 23 p3282 N88-29543

SILICON DIOXIDE
NT QUARTZ
Mechanism of mechanical fatigue of fused silica
[DE87-014199] 02 p0152 N88-10950
Formation and passivation of new paramagnetic defects associated with thermal oxides on silicon
[DE88-002720] 07 p0938 N88-15699
Studies on nonlinear mechanisms of excimer laser propagation in fused silica fibers
[AD-A186822] 09 p1156 N88-16929
Dispersive hole transport in SiO2
[AD-A187077] 09 p1254 N88-17513
Beneficial and detrimental effects of silica in the high temperature oxidation of 20Cr/25Ni/Nb stainless steel
[AERE-R-12667] 10 p1301 N88-17779
A viscoelastic BEM (Boundary Element Method) for modeling oxidation
[AD-A187490] 11 p1452 N88-18653
High temperature oxidation studies on alloys containing dispersed phase particles and clarification of the mechanism of growth of SiO2
[AD-A188158] 11 p1457 N88-18688
SiO2 film stress distribution during thermal oxidation of Si
[AD-A189552] 12 p1612 N88-19637
Oxide-bound transition metal complexes for methane activation
[PB88-169719] 14 p1887 N88-21277
Chemical vapor deposited silica coatings for solar mirror protection
[NASA-TM-100834] 14 p1893 N88-21306
Abrasion resistant porous silica antireflective coatings
[DE88-006230] 14 p1894 N88-21308
Infrared reflection-absorption spectroscopy of hyperfine layers on surfaces of semiconductors and dielectrics
14 p1969 N88-21755
A model for nitrogen atom recombination on a silicon dioxide surface
[AD-A189843] 15 p2142 N88-22784
Studies of boron implantation through photochemically deposited SiO2 films on Hg(sub 1-x)Cd(sub x)Te
[SD-TR-87-26] 19 p2621 N88-25548
Improved adhesion for SiO2 particles in silica substrates using helium-ion irradiation
[DE88-008915] 21 p2920 N88-27332
Silicon oxidation studies: A review of recent studies on thin film silicon dioxide formation in the physics and chemistry of SiO2 and the Si-SiO2 interface
[AD-A193176] 21 p3021 N88-27932

SILICON FILMS
Laser chemically vapor deposited silicon-carbide: Growth features, topography, microstructure, and composition
[DE87-013767] 01 p0029 N88-10184
Understanding the transport properties of silicon grain boundaries and how they relate to I.C. applications of polysilicon
[DE87-013809] 01 p0104 N88-10677
The soft/hard wet anodization of aluminum oxide and its use in a thin film multilayered capacitor
[AD-A187575] 10 p1325 N88-17919
Apparatus for the study of silicon film deposition and silicon etching
[AD-A187616] 10 p1334 N88-17972
Grazing incidence X-ray scattering study of defect structures in MBE GaAs/Si using synchrotron radiation
[DE88-004556] 10 p1420 N88-18483
Synthesis and characterization of thin films
[AD-A187335] 10 p1421 N88-18485
Development of VLSI optical data link
[AD-A187884] 11 p1549 N88-19266
Studies of boron implantation through photochemically deposited SiO2 films on Hg(sub 1-x)Cd(sub x)Te
[SD-TR-87-26] 19 p2621 N88-25548
Chemical multisensors with selective encapsulation of ion-selective membranes 19 p2670 N88-25869
Air loading effects on a capacitively sensed membrane supported silicon accelerometer
19 p2672 N88-25886
Tin oxide microsensors on thin silicon membranes
19 p2673 N88-25897
Deposition techniques and properties of strain compensated LPCVD silicon nitride films
19 p2673 N88-25898
The use of micromachined structures for the management of mechanical properties and adhesion of thin films 19 p2674 N88-25899
Stability of uncapsulated weight cells with thin film elongation measurement bands under influence of humidity, temperature and operation voltage
[ETN-88-92383] 21 p2951 N88-27531
Silicon oxidation studies: A review of recent studies on thin film silicon dioxide formation in the physics and chemistry of SiO2 and the Si-SiO2 interface
[AD-A193176] 21 p3021 N88-27932
Laser crystallized silicon films on alumina ceramic substrates and application to thin film c-Si solar cells
[PB88-131966] 22 p3116 N88-28515

SILICON JUNCTIONS
An investigation of the equivalent circuit and carrier lifetimes of Si/SiGe heterostructure p-n diodes for frequencies between 0.5 and 18.5 MHz
[FOA-C-30469-3.2] 09 p1256 N88-17529
Characterization of crystalline silicon by electrochemical and Raman spectroscopy at the frontier semiconductor/electrolyte
[ETN-88-92354] 21 p3025 N88-27956

SILICON NITRIDES
Development of a statistically proven injection molding method for reaction bonded silicon nitride, sintering reaction bonded silicon nitride, and sintered silicon nitride
[ETN-87-90575] 02 p0160 N88-11002
Electron microscopy studies of tensile cyclic fatigue-tested silicon nitride ceramics
[DE88-001438] 06 p0685 N88-14196
Investigation of silicon surface passivation by silicon nitride film deposition
[NASA-CR-182350] 06 p0729 N88-14487
Improved silicon nitride for advanced heat engines
[NASA-CR-175006] 08 p0973 N88-15886
Wire-cut electrical discharge machinability of ceramics
[AD-A186989] 09 p1146 N88-16870
Focused ultrasonic backscatter technique for near-surface flaw detection in structural ceramics
[DE88-003112] 09 p1183 N88-17091
NMR (Nuclear Magnetic Resonance) imaging for detecting binder/plasticizers in green-state structural ceramics
[DE88-003111] 10 p1304 N88-17800
A viscoelastic BEM (Boundary Element Method) for modeling oxidation
[AD-A187490] 11 p1452 N88-18653
Investigations of surface coatings based on silicon and nitrogen: From amorphous Si to silicon nitride
[DE88-004995] 12 p1609 N88-19622
A new process for synthesis of silicon nitride powders for advanced ceramics
[AD-A189354] 13 p1748 N88-20451
Dynamic tensile cyclic fatigue of Si3N4
[DE88-003919] 13 p1781 N88-20658
Optical study of germanium, germanium plus arsenic, and germanium plus gallium implants in gallium arsenide
[AD-A189600] 13 p1845 N88-21045
Photon-controlled growth of multilayered structures
[DE88-005061] 13 p1847 N88-21054
Development, high temperature properties, and microanalysis of nonoxide ceramics
[ETN-88-92103] 14 p1893 N88-21304
Effect of oxidation on strength and thermal stability of material based on Si3N4 14 p1896 N88-21319
Fracture toughness of silicon nitride-silicon nitride joints bonded with oxynitride glass
[DE88-005548] 15 p2043 N88-22172
Flaw characterization in structural ceramics using scanning laser acoustic microscopy
15 p2082 N88-22415
Nondestructive evaluation of structural ceramics
17 p2324 N88-23876
Improved silicon nitride for advanced heat engines
17 p2324 N88-23881
Improved processing of Si3N4
17 p2325 N88-23882
Colloidal characterization of silicon nitride and silicon carbide 17 p2325 N88-23883

Molten salt corrosion of SiC and Si3N4
17 p2325 N88-23885
Thermal cyclic durability testing of ceramic materials for turbine engines 17 p2325 N88-23886
SiC fiber reinforced reaction-bonded Si3N4 composites 17 p2326 N88-23892
Environmental effects on slow crack growth in silicon nitride
[DE88-007206] 18 p2494 N88-24795
Auger analysis of a fiber/matrix interface in a ceramic matrix composite
[NASA-TM-100892] 19 p2610 N88-25487
Deposition techniques and properties of strain compensated LPCVD silicon nitride films
19 p2673 N88-25898
Application of electron microscopy for the analysis of the mechanical behavior of advanced ceramics
[DE88-005049] 20 p2777 N88-26469
Application of magnification xeroradiography to advanced ceramics
[DE88-009965] 20 p2778 N88-26473
Absorption characteristics of Si3N4 ablation layer plasma 20 p2783 N88-26504
The high temperature creep deformation of Si3N4-6Y2O3-2Al2O3
[NASA-CR-183204] 23 p3190 N88-28981
Sinterable ceramic powders from laser-heated gases
[AD-A194162] 23 p3197 N88-29024

SILICON OXIDES
NT QUARTZ
NT SILICON DIOXIDE
Holographically correcting synthetic aperture aberrations
[AD-A189510] 12 p1692 N88-20123
Thermal oxide growth on silicon: Intrinsic stress and silicon cleaning effects
[AD-A188790] 13 p1736 N88-20377
Polarization properties of SiO masers
13 p1858 N88-21113
Hot electrons in silicon dioxide: Ballistic to steady-state transport 20 p2871 N88-27042

SILICON POLYMERS
NT SILICONES
NT SILOXANES
High yield synthesis of B4C/BN ceramic materials by pyrolysis of polymeric Lewis base adducts of decaborane(14)
[AD-A188154] 11 p1462 N88-18717
The 1986 IEEE Solid-State Sensor Workshop
[AD-A190922] 19 p2668 N88-25860
Characteristics of polysilicon layers and their application in sensors 19 p2669 N88-25861
Design and construction techniques for planar polysilicon pressure transducers with piezoresistive read-out 19 p2669 N88-25862
Integrated polysilicon tactile sensor
19 p2669 N88-25863
Thermal management of integrated microsensors
19 p2670 N88-25875
Deposition techniques and properties of strain compensated LPCVD silicon nitride films
19 p2673 N88-25898
Photovoltaic cells with n-silicon and conductive polymers
[ETN-88-92133] 20 p2821 N88-26734
Silicon-on-insulator pin diodes
[AD-A193359] 21 p2937 N88-27445
Boron-containing organosilane polymers and ceramic materials thereof
[NASA-CASE-ARC-11649-1-SB]
23 p3199 N88-29040

SILICON RADIATION DETECTORS
Low noise-low power monolithic multiplexing readout electronics for silicon strip detectors
[MPI-PAE/EXP.EL.178] 02 p0168 N88-11057
Design of a charge sensitive preamplifier on high resistivity silicon
[DE88-003491] 10 p1323 N88-17907
The silicon microstrip detector --- particle position measurement
[ETN-88-92235] 16 p2210 N88-23189

SILICON RECTIFIERS
U CRYSTAL RECTIFIERS

SILICON SOLAR CELLS
U SOLAR CELLS

SILICON TRANSISTORS
NT SOS (SEMICONDUCTORS)
Development of Si/SiGe heterostructures
[AD-A189527] 13 p1845 N88-21044
Thermal vacuum sensors based on integrated silicon thermopiles
[ETN-88-92237] 16 p2210 N88-23190
Integrated magnetic field sensor using high magnetotransistors
[ETN-88-92356] 21 p2941 N88-27465

SILICON-ON-INSULATOR SEMICONDUCTORS
U SOI (SEMICONDUCTORS)

SILICON-ON-SAPPHIRE JUNCTIONS
U SOS (SEMICONDUCTORS)

SILICON-ON-SAPPHIRE SEMICONDUCTORS
U SOS (SEMICONDUCTORS)

SILICON-ON-SAPPHIRE TRANSISTORS
U SOS (SEMICONDUCTORS)

SILICONES
NT SILOXANES
Investigation of structure-permeability relationships of silicone polymer membranes
[PB87-230181] 03 p0293 N88-11839
Determination of the modulus of elasticity of structural silicone sealants
[PB88-157456] 14 p1893 N88-21307
Primerless RTV silicones
[BDX-613-3807] 24 p3356 N88-29980
Containment of a silicone fluid free surface in reduced gravity using barrier coatings
[NASA-TM-101314] 24 p3371 N88-30072

SILOXANES
Synthesis, NMR characterization and electrical properties of siloxane-based polymer electrolytes
[AD-A184184] 04 p0418 N88-12596
Synthesis and structure property studies of toughened epoxy resins via functionalized polysiloxanes
[AD-A187984] 11 p1462 N88-18715
Ionic conductive polymers based on crosslinked elastic siloxane-ethylene oxide copolymers
[DE88-011243] 21 p2917 N88-27311
Functional study of the Si/SiO2 structures. Application to the implementation of an integrated ion sensor
[ECL-87-16] 22 p3073 N88-28246
Quasi-liquid crystalline materials with special electro-optic properties
[AD-A194579] 23 p3282 N88-29544

SILTS
U SEDIMENTS

SILVER
Plasmon resonance absorption in layered structures of silver with periodic corrugation
[DE87-013183] 02 p0231 N88-11453
Study of IR laser photoacoustic spectra of organic molecules adsorbed on metal surface
03 p0301 N88-11891
Simulation of the layer-growth dynamics in silver films: Dynamics of adatom clusters and vacancy clusters on Ag(100)
[DE87-014764] 03 p0380 N88-12390
Phase equilibrium and crystal growth studies on AgGaSe2 and related nonlinear optical materials
[AD-A184768] 03 p0382 N88-12400
Coverage dependence of adsorbate-substrate bond lengths: Chlorine and caesium adsorbed on silver single crystals
[PB87-125142] 06 p0788 N88-14833
Sputtered silver films to improve chromium carbide based solid lubricant coatings for use to 900 C
[NASA-TM-100783] 08 p0973 N88-15885
Adhesion of vapour phase deposited ultra-thin polyimide films on polycrystalline silver
[AD-A187930] 10 p1306 N88-17810
Photoacoustic studies of surface plasmons in metallic microstructures
[DE88-004423] 11 p1460 N88-18703
Optical waveguide formation by ion implantation of Ti or Ag
[DE88-004595] 11 p1551 N88-19278
Tunable optical sources/growth and characterization of nonlinear optical materials
[AD-A190874] 16 p2274 N88-23608
Interface characterization of Cu-Cu and Cu-Ag-Cu low temperature solid state bonds
[AD-A191015] 16 p2283 N88-23667
Electronic and geometric structure of silver and palladium on aluminum (111) in monoatomic surface layers
[ETN-88-92120] 20 p2879 N88-27093
Functional study of the Si/SiO2 structures. Application to the implementation of an integrated ion sensor
[ECL-87-16] 22 p3073 N88-28246

SILVER ALLOYS
In-situ vibrational spectroscopy of specifically adsorbed azide on silver electrodes
[AD-A188511] 12 p1605 N88-19600

SILVER CHLORIDES
Silver multi-layers for planar Ag/AgCl reference electrodes 19 p2672 N88-25883

SILVER COMPOUNDS
NT SILVER CHLORIDES
NT SILVER IODIDES
Investigation of effect of silver compounds on microflora in water reclaimed from atmospheric moisture condensate in a closed environment 07 p0632 N88-15407

SILVER HALIDES
NT SILVER CHLORIDES
NT SILVER IODIDES

SILVER IODIDES
Altered and enhanced iodargyrite with bismuth triiodide for use in precipitation enhancement operations
[AD-A185229] 05 p0561 N88-13419

SIMD (COMPUTERS)
A parallel computer based on cube connected cycles
10 p1378 N88-18227
Introduction to a system for implementing neural net connections on SIMD architectures
[NASA-CR-181612] 10 p1386 N88-18279
BLITZ: Blitzen's micron-code assembly language design document, version 1.0
[TR88-14] 12 p1676 N88-20019
An emulation tool for simulating matrix operations on an SIMD (Single Instruction Multiple Data stream) multiprocessor
[AD-A188654] 12 p1678 N88-20030
The physical structure of concurrent problems and concurrent computers
[DE88-005812] 13 p1814 N88-20835
An analysis of multiple grain CHiP architectures
[AD-A189942] 15 p2110 N88-22570
What have we learnt from using real parallel machines to solve real problems
[DE88-011227] 22 p3135 N88-28636

SIMICOR (IMAGE CORRELATOR)
U IMAGE CORRELATORS

SIMILARITIES
U ANALOGIES

SIMILARITY THEOREM
NT LAGRANGE SIMILARITY HYPOTHESIS
Clustering by means of medoids
[REPT-87-03] 01 p0085 N88-10551
Similar solutions for viscous hypersonic flow over a slender three-fourths-power body of revolution
[NASA-TM-100205] 04 p0443 N88-12752
Determining Langmuir circulation parameters on basis of similarity theory 13 p1765 N88-20680
On a class of similarity solutions of the equation u sub t = (absolute value of u sup m-1 u sub x) sub x with m greater than -1
[REPT-87-54] 14 p1963 N88-21713

SIMILITUDE LAW
Scale model development for aeroelasticity studies
[ETN-88-91887] 14 p1868 N88-21164

SIMPLEX METHOD
A new pivoting rule for the dual network simplex method
[REPT-87-17] 01 p0080 N88-10511
An exponential example for Terlaky's pivoting rule for the criss-cross simplex method
[REPT-87-18] 01 p0080 N88-10512
On the volume of a n-dimensional simplex
[REPT-87-16] 01 p0086 N88-10557
An analysis of an available set of linear programming test problems
[DE87-014578] 02 p0221 N88-11392
Progress in mathematical programming
[AD-A185729] 06 p0759 N88-14658
Eliminating columns in the simplex method for linear programming
[DE88-004191] 10 p1386 N88-18277
Continuous deformation algorithm on the product space of unit simplices, revised version
[PB88-114210] 10 p1387 N88-18281
Primal-dual parallel solution of very large sparse linear programs
[AD-A188500] 12 p1680 N88-20045
An extension of the MS pivoting rule to capacitated network flow problems
[REPT-87-33] 14 p1963 N88-21711
Making progress during a stall in the simplex algorithm
[DE88-007120] 18 p2558 N88-25182
Linear programming for Air Force decision aiding
21 p2928 N88-27378

SIMULATED ALTITUDE
U ALTITUDE SIMULATION

SIMULATION
NT ALTITUDE SIMULATION
NT ANALOG SIMULATION
NT COMPUTER SYSTEMS SIMULATION
NT COMPUTERIZED SIMULATION
NT CONTROL SIMULATION
NT DIGITAL SIMULATION
NT ENVIRONMENT SIMULATION
NT EXHAUST FLOW SIMULATION
NT FLIGHT SIMULATION
NT LANDING SIMULATION
NT MOTION SIMULATION
NT NEUTRAL BUOYANCY SIMULATION
NT SOLAR SIMULATION

NT SPACE ENVIRONMENT SIMULATION
NT SYSTEMS SIMULATION
NT WEIGHTLESSNESS SIMULATION

Simulations using the pseudo-current algorithm
[DE87-012403] 01 p0040 N88-10255

Multidimensional modeling of convective heat transfer with application to IC engines
[DE87-011046] 01 p0055 N88-10353

Description of the Mountain Cloud Chemistry Program version of the PLUVIUS MOD 5.0 reactive storm simulation model
[DE87-012846] 01 p0070 N88-10450

A simulation study of interfaces in Ni, Al and NiGAl with and without boron
[DE87-013156] 01 p0102 N88-10667

Comparison of MHD simulation for the February 1986 events with interplanetary observations by the spacecraft Sakigake 01 p0113 N88-10722

A simulation of the IPS variations from a magnetohydrodynamical simulation
01 p0118 N88-10755

Fourteenth Space Simulation Conference: Testing for a Permanent Presence in Space
[NASA-CP-2446] 02 p0132 N88-10829

Rocket nozzle thermal shock tests in an arc heater facility 02 p0133 N88-10832

Surveillance systems test and evaluation facilities
02 p0134 N88-10845

Thermal testing by internal IR heating of the FEP module 02 p0136 N88-10854

A new type of lamp and reflector for I.R. simulation
02 p0136 N88-10855

Scene simulation for passive IR systems
02 p0137 N88-10861

Numerical simulation of transient two-phase flow
[CFDU/87/4] 02 p0171 N88-11077

Impact of turbulence modeling on numerical accuracy and efficiency of compressible flow simulations
[NASA-TM-88333] 02 p0173 N88-11088

The numerical simulation of the mesoscale characteristics associated with Baiu front. Part 1: Structure, low-level jet and radiation characteristics
02 p0203 N88-11272

RANDOM NUMBER: A syntax-directed package to produce random numbers in user-specified, univariate distributions. User's guide
[DE87-014278] 02 p0228 N88-11436

Saturn: A large area X-ray simulation accelerator
[DE87-012021] 02 p0233 N88-11472

High explosive simulations of supernovae and the supernova shell fragmentation model of solar system formation
[DE87-014708] 02 p0251 N88-11584

Wake shield 03 p0296 N88-11871

Fundamentals of turbulence for turbulence modeling and simulation 03 p0312 N88-11971

Turbulence modelling through one point closures-applications-enlightening by large eddy simulation 03 p0312 N88-11972

Lattice gas hydrodynamics 03 p0313 N88-11978

A modular BLSS simulation model
03 p0359 N88-12260

Monte Carlo simulation of primitive atom-transfer reactions in solution
[AD-A183977] 03 p0375 N88-12360

Gravitational accretion of hot dark matter
03 p0388 N88-12439

Some experiences with the viscous-inviscid interaction approach
[NASA-TM-100015] 04 p0395 N88-12466

Analysis of sideband spectra from untapered undulator using analytical technique
[DE87-014763] 04 p0448 N88-12778

A network definition and solution of simulation problems
[DE88-000675] 04 p0481 N88-12962

Transport simulations of the oscillating field current drive experiment in the ZT-40M reversed field pinch
[DE88-000536] 04 p0491 N88-13027

A comparison of the basket method and the stratified random sampling for contract change order negotiations
[AD-A184170] 04 p0500 N88-13080

European hypersonic wind tunnels
05 p0530 N88-13221

The simulation of the viscous flow around a cylinder by the random vortex method 05 p0579 N88-13534

The statistics of the shape of small fatigue cracks
05 p0599 N88-13666

Numerical simulations of impact tests on a rigid wall — armor steel
[SNIAS-872-320-102] 05 p0610 N88-13744

Feasibility study for gas-grain simulation facility
[NASA-CR-177468] 05 p0646 N88-13954

Comparison of 2D memory SEU transport simulation with experiments
[ATR-86(8139)-2-REV-A] 05 p0656 N88-14025

On the influence of false plots on tracking relaibility: Simulations and preliminary analyses
[FOA-C-30443-3.2] 06 p0692 N88-14245

Satellite ground-terminal user simulation
[NASA-TM-100234] 06 p0694 N88-14260

Numerical simulation of boundary layers. Part 3: Turbulence and relaminarization in sink flows
[NASA-TM-88220] 06 p0698 N88-14283

A process study of the biothermal conversion of water hyacinths to methane
[DE88-000554] 06 p0730 N88-14488

Wind tunnel wall interference
07 p0811 N88-14938

Incompressible viscous flow simulations of the NFAC wind tunnel
[NASA-CR-177431] 07 p0816 N88-14969

European reacting flow research: A final assessment
[AD-A185833] 07 p0828 N88-15022

Developing an accelerated endurance test for greases: A status report
[AD-A185963] 07 p0836 N88-15072

An approach to validation and verification of the communications load model with supporting user's guide
[AD-A185926] 07 p0840 N88-15098

The determination of equivalent bearing loading for the BSMT that simulate SSME high pressure oxidizer turbopump conditions using the SHABERTH/SINDA computer programs 07 p0925 N88-15623

Plasma theory and simulation
[DE88-000412] 07 p0934 N88-15670

An experimental mapping of the flow field behind a glaze ice shape on a NACA 0012 airfoil
[NASA-CR-180847] 08 p0950 N88-15766

A multistage mesh generator for solving the average-passage equation system
[NASA-CR-179539] 08 p0951 N88-15769

Development of an emulation-simulation thermal control model for space station application
[NASA-CR-182409] 08 p0962 N88-15823

Vapor condensation on a turbulent liquid interface
08 p0982 N88-15939

Numerical simulation of turbulent spots in channel and boundary layer flows 08 p0983 N88-15948

Temporal and contextual knowledge in model-based expert systems 08 p1055 N88-16363

Rapid prototyping and AI programming environments applied to payload modeling 08 p1061 N88-16405

Numerical simulation of heat transfer turbulence, volume 4
[AD-A185132] 09 p1159 N88-16947

Proceedings of the Energy Independence Conference: Fusion Energy and Plasma Physics
[DE88-700657] 09 p1253 N88-17507

Numerical simulation of axisymmetric turbulent flow in combustors and diffusors
[NASA-CR-4115] 10 p1268 N88-17582

NASA wind shear model: Summary of model analyses
10 p1273 N88-17617

Satellite interference analysis and simulation using personal computers
[NASA-CR-182522] 10 p1319 N88-17890

Evaluation of regional-scale air quality models: Chairmen reports from four workshops
[DE88-001397] 10 p1352 N88-18080

Comparative evaluation of stress repsonse of rats to different methods of simulating some effects of weighlessness 10 p1363 N88-18144

Morphological study of early changes in rat bones in simulated weightlessness 10 p1365 N88-18158

Vector performance of register-to-register vector computers
[DE88-004013] 10 p1384 N88-18265

Parallel discrete event simulation: A shared memory approach
[NASA-CR-182521] 10 p1393 N88-18312

Performance and optimization of direct implicit time integration schemes for use in electrostatic particle simulation codes
[DE88-003254] 10 p1406 N88-18381

Supernova mechanisms: Before and after SN1987a
[DE88-003489] 10 p1429 N88-18533

Gamma-ray and neutron spectroscopy of planetary surfaces and atmospheres
[DE88-004287] 10 p1430 N88-18541

Simulated performance of an order statistic threshold strategy for detection of narrowband signals
11 p1474 N88-18796

Extrema of Gaussian process by simulation
11 p1541 N88-19211

Atomic-scale simulation in materials science
[DE88-005204] 11 p1544 N88-19230

Two dimensional simulations of multipass beam breakup
[CEBAF-PR-87-008] 11 p1547 N88-19254

Manned simulation: Helpful means to determine and improve structural load criteria 12 p1581 N88-19459

Table with aerostatic bearings for simulation in one degree of freedom attitude control systems of artificial satellites
[INPE-4272-PRE/1144] 12 p1595 N88-19552

Simulation and tests of a satellite attitude and orbit control system. General considerations concerning an example case (INPE) and design of a servo rate table
[INPE-4282-PRE/1154] 12 p1599 N88-19572

A methodology for hardware verification based on logic simulation
[AD-A188553] 12 p1622 N88-19704

Reliability analyses of a surface mounted package using finite element simulation
[AD-A189488] 12 p1624 N88-19717

Wavenumber - frequency structure of turbulent flow in a channel from a direct simulation
[AD-A189079] 12 p1627 N88-19737

Gradiometer mission spectral analysis and simulation studies: Past and future 12 p1645 N88-19851

Full scale architectural simulation techniques for space stations 12 p1651 N88-19887

OMV man/system simulation integration: A preliminary analysis and recommendation
[NASA-CR-182602] 12 p1671 N88-20005

Experimental analysis of algorithms
[AD-A188528] 12 p1677 N88-20028

Analysis of simulated annealing type algorithms
[AD-A189382] 12 p1679 N88-20037

Reducing rotary wing aircraft development time/cost through the use of simulation 12 p1702 N88-20186

The use of simulation in the development of the Airbus 12 p1702 N88-20188

Interaction between two-dimensional sonic jets and supersonic flow to model heat addition in a supersonic combustor
[AD-A189572] 13 p1716 N88-20261

Numerical simulation of subsonic and transonic propeller flow
[NASA-TM-100163] 13 p1716 N88-20262

The effect of combustion gas flow on the rotational dynamics of a spinning solid fuel rocket
13 p1732 N88-20358

Simulated impact damage in a thick graphite/epoxy laminate using spherical indenters
[NASA-TM-100539] 13 p1733 N88-20363

Model catalyst studies of SMSI (Strong Metal/Support Interactions) and the role of D-electrons in chemisorption and catalysis
[DE88-004518] 13 p1738 N88-20393

Applications of the differential reflectivity radar technique: Focus on estimation of rainfall parameters and microwave attenuation prediction
13 p1759 N88-20521

Center for Turbulence Research 1987 activities
[NASA-CR-182693] 13 p1769 N88-20583

Corrosion-wear process under rolling-sliding motion
[AD-A189603] 13 p1778 N88-20635

Structural clearances and internal friction: Simulation by Eigen distortions
[ISSN-0208-5658] 13 p1779 N88-20640

Two dimensional uncorrelated bias in fix algorithms
[NASA-CR-182683] 13 p1815 N88-20847

Predictive monitoring research: Summary of the PREMON system
[NASA-CR-182687] 13 p1824 N88-20905

Very high energy gamma ray astrophysics
[DE88-005821] 13 p1854 N88-21095

Potential applications of computational fluid dynamics to biofluid analysis
[NASA-TM-100089] 14 p1911 N88-21422

A general 2D electrical model for diagonally connected MHD generators
[DE88-004283] 14 p1984 N88-21835

Numerical simulation of turbulent flames using vortex methods
[AD-A189813] 15 p2034 N88-22116

A fully abstract semantics for event-based simulation
[AD-A190560] 15 p2060 N88-22283

Finite element simulation of perforation of aluminum plates
[DE88-002092] 15 p2073 N88-22362

Monte Carlo reliability analysis
[AD-A189972] 15 p2074 N88-22366

Experimental comparison of lightning simulation techniques to CV-580 airborne lightning strike measurements
[AD-A190576] 15 p2098 N88-22496

Exhaustive and pseudo-exhaustive testing
[AD-A190140] 15 p2111 N88-22574

A direct-execution parallel architecture for the Advanced Continuous Simulation Language (ACSL)
[NASA-CR-182809] 15 p2115 N88-22602

An approximation technique for solving a system of Fredholm integral equations for asymmetric detector response functions
[AD-A190577] 15 p2121 N88-22645

Random Process Simulation for stochastic fatigue analysis
[NASA-TM-100464] 15 p2123 N88-22654
The application of linear maximum likelihood estimation of aerodynamic derivatives for the Bell-205 and Bell-206
[AD-A191279] 16 p2161 N88-22694
Pulsed power simulation problems in magic
[AD-A191110] 16 p2191 N88-23065
Modeling scalar flux and the energy and dissipation equations 16 p2196 N88-23096
Direct numerical simulation of buoyantly driven turbulence 16 p2196 N88-23097
Premixed turbulent flame calculation
16 p2196 N88-23098
Coherent structure 16 p2199 N88-23117
Fast algorithms for Euler and Navier-Stokes simulations
[AD-A190897] 16 p2208 N88-23175
Calculation of displacement, constraints and eigenmodes of rotating blades
[ETN-88-92296] 16 p2224 N88-23277
Numerical simulation of coastal upwelling phenomena in Cabo Frio (RJ) through a two layer finite element model
[INPE-4502-RPE/561] 16 p2237 N88-23361
Fast Algorithm Simulation and Test (FAST) facility
[AD-A191183] 16 p2252 N88-23457
Hybrid particle simulation for focusing of rotating and propagating LIB 16 p2276 N88-23624
Single phase liquid immersion cooling of discrete heat sources in a vertical channel
[AD-A191224] 17 p2337 N88-23944
Finite element simulation of the atmosphere's electromagnetic response to charge perturbations associated with lightning 17 p2375 N88-24124
Simulating futures in extended common LISP
[NASA-TM-101000] 18 p2559 N88-25192
NAS: The first year
[NASA-TM-101006] 18 p2560 N88-25196
A constraint algorithm for maintaining rigid bonds in molecular dynamics simulations of large molecules
[AD-A191663] 18 p2572 N88-25277
Effects of Mach number on acoustic-vortex interactions in a ramjet 19 p2625 N88-25573
Numerical simulations of astrophysical jets
19 p2636 N88-25635
Numerical simulation of supersonic free-jets
19 p2636 N88-25639
Numerical calculation of three dimensional flow by TVD scheme 19 p2638 N88-25649
Simulation of axisymmetric flow with H2O2 reactions
19 p2638 N88-25651
Numerical simulation of turbulent flow using the exponential expression of k-Epsilon equation
19 p2640 N88-25662
Attenuated direct and scattered wave propagation on simulated land mobile satellite service paths in the presence of trees 19 p2645 N88-25695
Modulation efficiency limited high frequency performance of the MODFET 19 p2657 N88-25786
Accurate, productive aerodynamic simulation on patched mesh systems
[AD-A192040] 19 p2714 N88-26110
Simulated measurement of power flow in structures near to simple sources and simple boundaries
[NASA-TM-89124] 19 p2722 N88-26166
A simulation analysis of errors in the measurement of standard electrochemical rate constants from phase-selective impedance data
[AD-A192739] 20 p2770 N88-26426
Research in electromagnetic shielding theory. Part 2: EMP (electromagnetic pulse) simulation using small loops
[AD-A192882] 20 p2791 N88-26558
Navier-Stokes simulation of shock-tube flows over a wedge-type step by finite volume method
[ISAS-RN-626] 20 p2797 N88-26599
A numerical simulation of two-dimensional transient shear flow
[ISAS-RN-627] 20 p2797 N88-26600
Monte Carlo simulations of femtosecond relaxation of photoexcited electrons in AlGaAs/GaAs quantum wells
20 p2869 N88-27036
Atomistic simulation of stability, metastability and growth of strained layer structures 20 p2873 N88-27053
Documentation of the Benson Diesel Engine Simulation Program
[NASA-TM-100940] 21 p2898 N88-27201
Implicit finite-difference simulation of an internal flow in a nozzle: An example of a physical application on a hypercube
[AD-A192475] 21 p2942 N88-27472
Numerical experiments on turbulent mixing
[AD-A192572] 21 p2942 N88-27473
Granular flow: Particle-dynamics simulations of steady flow
[DE88-011342] 21 p2948 N88-27506
Direct simulation of stable stratified homogeneous turbulent shear flows
[DFVLR-FB-88-04] 21 p2949 N88-27516
Cloud simulation warm cloud experiments: Droplet growth and aerosol scavenging
[AD-A192944] 21 p2974 N88-27666
Electroencephalographic correlates of pilot performance: Simulation and in-flight studies
21 p2982 N88-27711
Analysis of lower hybrid current drive and rampup experiments on the JT-60 tokamak
[DE88-753136] 21 p3018 N88-27915
Method to predict external store carriage characteristics at transonic speeds
[NASA-CR-4170] 22 p3037 N88-28034
HPM (High Power Microwave) simulation fidelity studies
[DE88-012229] 22 p3068 N88-28209
Some screening experiments in objective prediction of monthly mean temperature over the United States during the winter season 22 p3127 N88-28589
Importance sampling for stochastic simulations
[AD-A193585] 22 p3138 N88-28654
Atomistic simulation of silicon grain boundaries
[DE88-009925] 22 p3155 N88-28771
Boundary layer simulation and control in wind tunnels
[AGARD-AR-224] 23 p3167 N88-28857
Missiles, fuselage and similar bodies
23 p3167 N88-28858
Empirical tools for simulation methodologies
23 p3168 N88-28866
Transport-type configurations
23 p3169 N88-28867
Introduction and critical flow phenomena
23 p3169 N88-28870
Shock boundary layer interaction
23 p3170 N88-28873
Classical separation, trailing-edge flows and buffeting
23 p3170 N88-28874
Vortex flows 23 p3170 N88-28875
Boundary layer manipulation 23 p3170 N88-28877
Natural convection immersion cooling of an array of simulated chips in an enclosure filled with dielectric liquid
[AD-A193594] 23 p3207 N88-29068
Typical weather months in the past (1973-1983) in Central Europe
[AD-A194701] 23 p3235 N88-29249
The gradient method for interface tracking
[AD-A194477] 23 p3248 N88-29334
Fusion product spectra
[DE88-010912] 23 p3284 N88-29554
Systematic properties of clusters of galaxies in different cosmological scenarios 23 p3299 N88-29646
Laboratory evaluation and application of microwave absorption properties under simulated conditions for planetary atmospheres
[NASA-CR-182443] 23 p3300 N88-29653
Variation in the thickness of ejecta cover on Mars with increasing crater density 23 p3307 N88-29701
Simulation of Vulcain engine operation at low inlet pressure
[ETN-88-93083] 24 p3339 N88-29875
Finite-difference simulations of Rayleigh-wave scattering by shallow heterogeneity
[AD-A194961] 24 p3402 N88-30259
Simulation of a two link robot manipulator with elastic members
[AD-A196014] 24 p3422 N88-30368
Waveform relaxation applied to transient device simulation
[AD-A194992] 24 p3432 N88-30429
Simulations of lava flows on Mars
24 p3443 N88-30495

SIMULATOR TRAINING
U TRAINING SIMULATORS

SIMULATORS
NT COCKPIT SIMULATORS
NT CONTROL SIMULATION
NT FLIGHT SIMULATORS
NT MOTION SIMULATORS
NT SHOCK SIMULATORS
NT SOLAR SIMULATORS
NT SPACE SIMULATORS
NT TRAINING SIMULATORS
NT VERTICAL MOTION SIMULATORS
NT VIBRATION SIMULATORS
Infra-red lamp panel study and assessment application to thermal vacuum testing of sigma telescope
02 p0132 N88-10830
The Hermes-3 program
[DE87-012132] 02 p0234 N88-11473
New main reflector, subreflector and dual chamber concepts for compact range applications
[NASA-CR-181506] 04 p0402 N88-12498
SCRAM JET (Supersonic Combustion Ramjet) combustion experiments 04 p0404 N88-12512
On the simulation of ballistic shock loads
05 p0593 N88-13615
Tutoring electronic troubleshooting in a simulated maintenance work environment
09 p1204 N88-17215
Design of a neural network simulator on a transputer array 09 p1205 N88-17221
Table with aerostatic bearings for simulation in one degree of freedom of Attitude Control Systems of artificial satellites
[INPE-4320-TDL/287] 11 p1445 N88-18617
A dynamic analysis of the parallel-plate EMP (electromagnetic pulse) simulator using a wire mesh approximation and the numerical electromagnetics code
[AD-A187535] 11 p1470 N88-18767
RELIC: A reliability simulator for integrated circuits
[AD-A187493] 11 p1477 N88-18811
Computational studies of wave-shaping in a blast simulator by perforated plates in the driver
[AD-A188200] 11 p1483 N88-18850
Reaction wheel experimental model of artificial satellite attitude control: Construction, simulation, and tests
[INPE-4274-PRE/1146] 11 p1490 N88-18896
The Hermes manipulation system (HERA) simulation facility development 12 p1591 N88-19524
A methodology for hardware verification based on logic simulation
[AD-A183553] 12 p1622 N88-19704
A digital circuit design environment
[AD-A188831] 12 p1623 N88-19709
Engine flow simulation for wind tunnel testing at NLR
[NLR-MP-87011-U] 13 p1723 N88-20305
A microprocessor-based real-time simulator of a turbofan engine
[NASA-TM-100889] 14 p1868 N88-21163
A packet-switched wide-area communication network simulator
[FUB-3-1986] 14 p1905 N88-21381
The effects of torque response and time delay on rotorcraft vertical axis handling qualities
[AD-A189873] 15 p2017 N88-22023
Development and evaluation of an airplane fuel tank ullage composition model. Volume 2: Experimental determination of airplane fuel tank ullage compositions
[AD-A190408] 15 p2017 N88-22025
Real-time stressed channel simulator
[AD-A190223] 15 p2025 N88-22067
A UNIX-based interactive VHDL (hardware description language) simulator
[AD-A189749] 15 p2109 N88-22565
Construction of a satellite simulator for the frequency range between 11.7 and 12.5 GHz
[IRT-TB-B-84/87] 16 p2166 N88-22917
Preliminary measurements of heat flux in a subsonic gun simulator
[AD-A191090] 16 p2208 N88-23178
Development of an airborne facility for advanced avionics research 17 p2307 N88-23801
Safety aspects in design and operation practice of GKSS underwater simulation plant GUSI
19 p2698 N88-26037
Research in electromagnetic shielding theory. Part 2: EMP (electromagnetic pulse) simulation using small loops
[AD-A192882] 20 p2791 N88-26558
The UMAC simulator 20 p2834 N88-26811
Can CNV amplitude predict ability to accomplish a demanding task? 21 p2980 N88-27700
Block Oriented Simulation System (BOSS)
[NASA-CR-182947] 21 p2995 N88-27760
Goldstone solar system radar performance analysis
22 p3068 N88-28208
The p-well or n-well CMOS technology for advanced SEU-hard SRAMs
[DE88-006845] 22 p3156 N88-28777

SIMULTANEOUS IMAGE CORRELATOR
U IMAGE CORRELATORS

SINE WAVES
On simultaneous estimation of the number of signals and frequencies under a model with multiple sinusoids
[AD-A186026] 07 p0913 N88-15543
On rate of convergence of equivariation linear prediction estimates of the number of signals and frequencies of multiple sinusoids
[AD-A186034] 07 p0914 N88-15549
Fatigue effects of a swept sine test
08 p0999 N88-16054
Overview of multi-input frequency domain modal testing methods with an emphasis on sine testing
11 p1499 N88-18949
Sinusoidal transform coding 19 p2653 N88-25752

SINGLE CHANNEL PER CARRIER TRANSMISSION

Ionospheric total electron content estimation for single-frequency global positioning system receivers
02 p0161 N88-11005

Measured noise performance of a direct-sequence spread-spectrum system and a comparison of single vice dual-channel delay-lock loops
[AD-A186288] 07 p0843 N88-15110

SINGLE CRYSTALS

Energy-selected electron diffraction experiments using the rocking-crystal method in the raster microscope for the investigation of localization effects in single crystals
[ETN-87-90409] 01 p0104 N88-10682

Constitutive modeling for single crystal superalloys
02 p0187 N88-11168

Constitutive modeling of superalloy single crystals with verification testing 02 p0188 N88-11169

Creep-fatigue behavior of NiCoCrAlY coated PWA 1480 02 p0189 N88-11176

Production of metallic monocrystals described
03 p0286 N88-11796

Consortium for Materials Development in Space. Technical section
[NASA-CR-181508] 03 p0296 N88-11859

Materials preparation and longevity in hyperthermal atomic oxygen 03 p0297 N88-11862

Investigation of two laser beam coupling and amplification in Ce-doped SBN single crystals
03 p0327 N88-12069

Determination of the origin of self-pumped phase conjugation in barium titanate
[AD-A184697] 03 p0377 N88-12372

Monocrystal sputtering by the computer simulation code ACOCT
[IPPJ-848] 04 p0493 N88-13035

Evaluation of the Mellen EDG furnace for growth of large diameter GaAs single crystals in a horizontal configuration
[DE88-000463] 04 p0498 N88-13068

The structure of adsorbed sulfur and carbon on molybdenum and rhenium single crystal surfaces, and their influence on carbon monoxide and hydrocarbon chemisorption
[DE88-001393] 04 p0499 N88-13073

Environmentally assisted cracking: Overview of evidence for an adsorption-induced localised-slip process
[AD-A185175] 05 p0565 N88-13443

Surface deformation and fatigue crack initiation of alpha-iron 05 p0598 N88-13651

Low cycle fatigue behaviour of notched specimens of nickel based superalloy single crystal
05 p0605 N88-13712

An overview of fatigue 05 p0608 N88-13729

Preparation and characterization of members of the system (Zn,Se)1-xGaPx
[AD-A185073] 05 p0655 N88-14019

New application of transition metal carbides detailed
06 p0675 N88-14132

Growth of solid solution single crystals
[NASA-TP-2787] 06 p0688 N88-14212

High temperature low cycle fatigue of oxide dispersion strengthened and single crystal nickel base superalloys
06 p0720 N88-14422

Orientation effects in copper single crystals fatigued at elevated temperatures 06 p0720 N88-14423

Coverage dependence of adsorbate-substrate bond lengths: Chlorine and caesium adsorbed on silver single crystals
[PB87-125142] 06 p0788 N88-14833

Grain boundary and surface diffusion in oxides
[DE88-002348] 07 p0938 N88-15697

Low field characterization of YBa2Cu3O sub 7-delta single crystals
[DE88-002695] 07 p0938 N88-15700

A laboratory study of tin whisker growth
[ESA-STR-223] 08 p1069 N88-16553

Epitaxial growth and new phase of single crystal Dy by molecular beam epitaxy
[DE88-002850] 09 p1256 N88-17531

CdTe(110)-Mn interface reaction and the formation of non-equilibrium ternary semimagnetic semiconductor alloys
[AD-A187593] 10 p1422 N88-18491

Single-crystal structural study of La2Cu/sub 0.95/Li/sub 0.05/O4
[DE88-003482] 11 p1554 N88-19302

Silicon and indium doping of GaAs: Measurements of the effect of doping on mechanical behavior and relation with dislocation formation
[DE88-003862] 11 p1554 N88-19303

Autonomous Liquid Encapsulated Czochralski (LEC) growth of single crystal GaAs by intelligent digital control
[AD-A187211] 11 p1555 N88-19305

Preparation and characterization of Cu2Zn1-xMnxGeS4
[AD-A188113] 11 p1556 N88-19315

An in situ annealing study of lead implanted single crystal calcium titanate
[DE88-005435] 11 p1562 N88-19351

The cyclic stress-strain behavior of a single crystal nickel-base superalloy
[NASA-TM-100269] 12 p1607 N88-19610

Contact and current noise in beta alumina and Nasicon ceramics
[AD-A189168] 12 p1611 N88-19635

The effects of temperature and strain rate on the yielding behavior of the single crystal superalloy PWA 1480
14 p1931 N88-21517

The elastic properties of monoclinic ZrO2
[DE88-005920] 14 p1986 N88-21847

Bithermal fatigue of a nickel-base superalloy single crystal
[NASA-TM-100885] 15 p2042 N88-22168

Single crystal growth by laser CVD
15 p2050 N88-22213

Unified constitutive model for single crystal deformation behavior with applications 15 p2078 N88-22366

The kinetics of contact noise in NaBeta alumina
[AD-A190651] 15 p2130 N88-22707

An investigation of the crystalchemistry and thermochemistry of selected mineral systems
[AD-A189758] 15 p2142 N88-22781

Dispersion measurements of microcrystals in the near ultraviolet and infrared
[DE88-006234] 15 p2145 N88-22800

Fatique crack growth behavior of a single crystal alloy as observed through an in situ fatigue loading stage
[NASA-TM-100863] 16 p2179 N88-22986

UV-Laser reactions of molecular adsorbates
[AD-A190796] 16 p2212 N88-23201

SSME single-crystal turbine blade dynamics
16 p2221 N88-23257

Defects in cubic silicon carbide on silicon
17 p2408 N88-24317

Interaction of slow neutrons with Ge74 single crystals
[DE87-703010] 17 p2445 N88-24536

Isothermal and bithermal thermomechanical fatigue behavior of a NiCoCrAlY-coated single crystal superalloy
[NASA-TM-100907] 18 p2489 N88-24766

Resolved shear stress intensity coefficient and fatigue crack growth in large crystals
[NASA-CR-182137] 18 p2528 N88-24997

Electronic controller for reciprocating rotary crystallizer
[NASA-TM-101140] 18 p2584 N88-25354

Stress modeling of microdiaphragm pressure sensors
19 p2670 N88-25873

Accelerated fatigue crack growth behavior of PWA 1480 single crystal alloy and its dependence on the deformation mode
[NASA-TM-100943] 20 p2772 N88-26436

Development of a model procedure for the determination of volume diffusion lengths by transient measurements on monocrystal silicon solar cells
[ETN-88-92119] 20 p2821 N88-26733

Anisotropic characteristic lengths in single crystal YBa2Cu3O(sub 7-Delta)
[DE88-009959] 20 p2877 N88-27080

Pure metallic bridge and point-contact tunneling into single- and polycrystal YBa2Cu3O(sub 7-y)
[DE88-010030] 20 p2878 N88-27084

Electron irradiation effects in YBa2Cu3O7-Delta single crystals
[DE88-010050] 20 p2878 N88-27085

Mechanism of the nitric oxide-carbon monoxide-oxygen reaction over a single crystal rhodium catalyst
[DE88-006274] 21 p2910 N88-27268

Energy migration, motion and order in synthetic polymers
[AD-A193334] 21 p2918 N88-27320

Silicon-on-insulator pin diodes
[AD-A193359] 21 p2937 N88-27445

Experimental fabrication of thin film single crystalline solar cells
[PB88-131958] 21 p2967 N88-27627

Growth and characterization of CuGaS2, CuAlS2 and CuGa0.9Al0.1S2 single crystals
[AD-A192963] 21 p3021 N88-27930

Experimental fabrication of thin film single crystalline solar cells
[PB88-131958] 22 p3116 N88-28516

Effect of neutron irradiation on critical magnetization current in single crystal YBa2Cu3O(sub 7-delta)
[DE88-009970] 22 p3156 N88-28775

Preparation and testing of Nb-Zr and Nb-ZrO2 single crystals for deformation studies
[DE88-702798] 23 p3293 N88-29613

Anisotropic constitutive modeling for nickel-base single crystal superalloys
[NASA-CR-182157] 24 p3353 N88-29961

Streaking images that appear only in the plane of diffraction in undoped GaAs single crystals: Diffraction imaging (topography) by monochromatic synchrotron radiation
[NASA-CR-183267] 24 p3433 N88-30437

SINGLE ENGINE AIRCRAFT

NT F-16 AIRCRAFT
NT F-106 AIRCRAFT
NT MIG AIRCRAFT
NT MIRAGE AIRCRAFT
NT T-33 AIRCRAFT

SINGLE EVENT UPSETS

MARECS-A case 03 p0274 N88-11729

Comparison of 2D memory SEU transport simulation with experiments
[ATR-86(8139)-2-REV-A] 05 p0656 N88-14025

Effects of cosmic rays on single event upsets
[NASA-CR-183053] 20 p2793 N88-26569

The effects of total dose on the SEU sensitivity of CMOS static RAMS — single event upset (SEU), satellite components
[AERE-R-12779] 24 p3428 N88-30401

The Single Event Upset (SEU) test facility on the Hardwell tandem generator for cosmic ray simulation
[AERE-R-12396] 24 p3459 N88-30580

SINGLE INSTRUCTION MULTIPLE DATA STREAM

U SIMD (COMPUTERS)

SINGLE STAGE ROCKET VEHICLES

NT BLACK BRANT SOUNDING ROCKETS

Ballistic Single Stage Carrier Vehicle (BETA): A single stage reusable ballistic space shuttle concept
[MBB-UR-949/70] 10 p1310 N88-17828

SINGLE STAGE TO ORBIT VEHICLES

NT HOTOL LAUNCH VEHICLE

SINGLE-PHASE FLOW

Theoretical prediction of single phase turbulent flow distribution in particulate bed reactors
17 p2419 N88-24366

SINGULAR INTEGRAL EQUATIONS

A quadrature formula for a double-pole singular integral
[PD-FM-8725] 04 p0485 N88-12990

Potential flow around two-dimensional airfoils using a singular integral method
[NASA-CR-182345] 06 p0664 N88-14070

A spline collocation method for integral equations of the first kind with logarithmic singularity --- boundary value problems
[REPT-87-39] 14 p1963 N88-21712

SINGULARITY (MATHEMATICS)

Breakdown of steady and unsteady interacting boundary layers
[NLR-MP-86047-U] 01 p0045 N88-10284

Study of closed loop control singularity in dynamic systems with a constraint on the final state
[LAAS-87-180] 02 p0223 N88-11405

Singularity expansion method: Target Resonances
03 p0303 N88-11912

The hybrid wavefront resonance method
03 p0303 N88-11913

Singularities in X-ray spectra of metals
[DE88-001440] 06 p0681 N88-14174

The effect of response scaling on the detection of singularities in multiresponse estimation
[AD-A185964] 07 p0908 N88-15503

Anomalous scaling laws in multifractal objects
[NOTA-INTERNA-883] 07 p0916 N88-15565

Boundary elements combined with singular fields for three-dimensional cracked solids
[RAE-TR-87038] 09 p1183 N88-17086

Criterion of singularity in general theory of relativity
09 p1240 N88-17430

Numerical-experimental investigation of singularity at a crack in nonlinear rubber elasticity
11 p1500 N88-18961

Singular Lagrangians. Classical dynamics and quantization. Lectures for young scientists
[DE88-701158] 15 p2146 N88-22806

Formal solution of differential linear systems in the proximity of a singularity
[ETN-88-92190] 16 p2258 N88-23495

Approximation and representation of explicit surfaces in the presence of singularities
[ETN-88-92191] 16 p2258 N88-23496

Analysis and modeling of complex non-stationary flows
[PB88-127188] 19 p2664 N88-25842

Linearization along invariant manifolds and a generalization of the Hartman-Grobman theorems for degenerate singularities of vector fields in R cubed
[REPT-87-80] 20 p2845 N88-26886

The analysis and control of robotic manipulators operating at or near kinematically singular configurations
22 p3084 N88-28315

A singular perturbation analysis of the weakly nonlinear evolution of long and short water waves and waves in boundary layers 23 p3209 N88-29102

A minimax method for a class of Hamiltonian systems with singular potentials
[AD-A193478] 23 p3270 N88-29453

SINKS
NT HEAT SINKS

SINKS (GEOLOGY)
U STRUCTURAL BASINS

SINTERED ALUMINUM POWDER

Microdesigning of lightweight/high strength ceramic materials
[AD-A188526] 12 p1610 N88-19631

Characterization of 7090 and 7091 profiles made with Cegedur powder — powder metallurgy, aircraft construction materials
[REPT-48-441/F] 18 p2467 N88-24752

SINTERING

Toughening of alpha-alumina: Preliminary results
[DE87-702776] 01 p0026 N88-10178

Analytical electron microscopy characterization of boron in sintered alpha-SiC
[DE87-012532] 02 p0142 N88-10889

Needs assessment for NDT and characterization of ceramics: Assessment of inspection technology for green state and sintered ceramics
[DE87-013550] 02 p0151 N88-10947

Structure and grain coarsening during the processing of engineering ceramics
[NASA-TM-100235] 03 p0293 N88-11838

Cast iron freezing mechanisms
03 p0298 N88-11870

Research and development on high strength ceramic heaters discussed 04 p0404 N88-12506

Sintered steels of high resistance alloyed to Nb, Mo, Mn and Si
[DE87-703546] 04 p0415 N88-12573

Studies of alumina additions in zirconia - magnesia
[DE87-703500] 04 p0419 N88-12602

Fatigue failure of thin porous strips
04 p0426 N88-12640

Corrosion resistance of sintered alloy steels
[BLL-M-37363-(5828.4)] 05 p0564 N88-13438

Properties of refractory metals processed by enhanced sintering treatments
[AD-A184944] 05 p0565 N88-13440

Results from the melting of tungsten composites under microgravity (TEXUS 10 flight)
[FOA-C-20676-2.1] 05 p0571 N88-13482

Crack propagation properties of sintered steel
05 p0604 N88-13698

Metallurgical processes in multi-component rare earth-transition metal permanent magnet alloys
[AD-A186401] 07 p0832 N88-15045

Techniques for ceramic sintering using microwave energy
[DE88-001416] 07 p0837 N88-15080

The use of NMR imaging to measure porosity and binder distributions in green-state and partially sintered ceramics
[DE88-003099] 08 p0972 N88-15881

Improved silicon nitride for advanced heat engines
[NASA-CR-175006] 08 p0973 N88-15886

The migration of grain boundaries in ceramic materials with particular reference to the sintering process
[DE88-004085] 10 p1306 N88-17808

High temperature processing of superconducting Y1Ba2Cu3O6.9
[DE88-003002] 10 p1416 N88-18449

Improved magnetization for YBa2Cu3O/sub 7-delta annealed in oxygen above 1000 C
[DE88-003934] 10 p1418 N88-18469

Freestanding films of YBa2Cu3O/sub 6.9/
[DE88-003995] 10 p1419 N88-18471

Deactivation of alumina based catalysts
11 p1455 N88-18673

Composite ceramic superconducting filaments for superconducting cable
[AD-A187833] 11 p1556 N88-19312

Effect of rigid inclusions on sintering
[DE88-005745] 12 p1609 N88-19623

Mass transport and chemical demixing of Y-Ba-Cu-O compounds during sintering in temperature gradients
[DE88-004887] 12 p1696 N88-20151

Processing of nanophase ceramics
[DE88-005985] 13 p1752 N88-20475

The unique characteristics of the structure of composite materials made on a base of sphalerite-analogous boron nitride 14 p1886 N88-21273

Development, high temperature properties, and microanalysis of nonoxide ceramics
[ETN-88-92103] 14 p1893 N88-21304

Processing, texture and mechanical properties of sintered silicon carbide
[NASA-TT-20253] 14 p1893 N88-21305

Microwave sintering of alumina-SiC composites at 2.45 and 60 GHz
[DE88-006455] 15 p2030 N88-22095

Titanium powder frit made during the transformation alpha-beta
[ETN-88-91999] 16 p2177 N88-22976

Improved silicon carbide for advanced heat engines
17 p2324 N88-23879

Strength optimization of alpha-SiC by improved processing 17 p2324 N88-23880

Improved silicon nitride for advanced heat engines
17 p2324 N88-23881

Improved processing of Si3N4
17 p2325 N88-23882

High frequency ultrasonic characterization of sintered SiC
[NASA-TM-100825] 17 p2347 N88-23985

Martensitic transformation and microstructures in sintered NiAl alloys
[NASA-TT-20178] 18 p2488 N88-24761

Martensitic transformation and microstructures in sintered NiAl alloys
[NASA-TT-20192] 19 p2616 N88-25519

Assessment of opportunities for gas-fired sintering in the advanced ceramics and powdered metals industries
[PB88-197157] 19 p2620 N88-25545

Sintering of the heterogeneous MgO compacts
[DE88-010357] 20 p2767 N88-26406

Manufacturing of a ceramic-ceramic composite matrix using the sol-gel procedure
[ETN-88-92157] 20 p2768 N88-26414

Preparation of oxide superconductors
[DE88-009136] 20 p2875 N88-27063

SINUSOIDS
U SINE WAVES

SIR-A
U SHUTTLE IMAGING RADAR

SIR-B
U SHUTTLE IMAGING RADAR

SIRTF
U SPACE INFRARED TELESCOPE FACILITY

SIS (SEMICONDUCTORS)

Optimization of SIS mixer elements
[NASA-CR-180710] 01 p0104 N88-10680

Quantum limits of superconducting heterodyne receivers
[AD-A188014] 11 p1476 N88-18817

SITE SELECTION

Siting and Geotechnical Program Focus and Directions. Report upon the deliberations of a workshop held at the Illinois Institute of Technology, Chicago, Illinois on August 4-5, 1986
[PB87-206272] 02 p0198 N88-11236

On the exact solution of large-scale simple plant location problems
[FI-032-TB-22E] 02 p0229 N88-11441

Use of SPOT images for coastal development and inventory of aquacultural sites in New Caledonia (ALIAS project). First results 03 p0344 N88-12175

Variability of wind power near Oklahoma City and implications for siting of wind turbines
[DE88-000444] 04 p0470 N88-12902

Cape Blanco wind farm feasibility study
[DE88-003748] 10 p1348 N88-18059

The evaluation and selection of a 5th ground antenna site for the global positioning system
[AD-A189495] 13 p1720 N88-20286

Environmental assessment for the compact ignition Tokamak
[DE88-005633] 15 p2135 N88-22740

Utilization of LANDSAT-TM , for aiding in the localization of archeological sites in the state of Sao Paulo
17 p2362 N88-24069

Review of numerical methods for radionuclide transport in three-dimensional porous media, at high Peclet numbers
[CFDU/87/10] 18 p2538 N88-25061

Extremely Low Frequency (ELF) communications system ecological monitoring program: Summary of 1986 progress
[AD-A192014] 19 p2642 N88-25676

Australian structures response evaluation: Ground shock and air blast measurements for site investigation survey
[MRL-TN-526] 20 p2813 N88-26665

Review of geographic processing techniques applicable to regional analysis
[DE88-010759] 21 p2970 N88-27643

SPOT: A tool to aid preselection of sites favorable for aquiculture. Evaluation and perspectives of the Preliminary Evaluation Program for SPOT (PEPS) ALIAS Caledonie
22 p3108 N88-28456

Geology of six possible Martian landing sites
23 p3304 N88-29682

SITES
NT LANDING SITES
NT LAUNCHING PADS
NT LAUNCHING SITES

Atmospheric diffusion at coastal site in presence of sea-breeze
[DE88-700038] 07 p0876 N88-15314

An analytic model for ionization distributions produced in nanometer sites by protons
[DE88-003943] 10 p1406 N88-18085

Lunar fiberglass: Properties and process design
[NASA-CR-182580] 11 p1466 N88-18740

Site effects on wind characteristics at a turbine rotor
[DE88-005135] 11 p1507 N88-19003

Crustal Dynamics Project: Catalogue of site information
[NASA-RP-1198] 11 p1513 N88-19037

Maps for tourists. A systematic approach to tourist cartography 16 p2227 N88-23296

SITTING POSITION

Sitting posture of helicopter pilots of the Royal Netherlands Air Force; preliminary recommendations
[IZF-1986-16] 05 p0631 N88-13857

Sitting posture of pilots in the Boelkow 105c helicopter
[IZF-1986-22] 09 p1202 N88-17202

SIZE (DIMENSIONS)
NT GRAIN SIZE

The effect of size and surface on the lifetime prediction of StE 460 notched bars
[FD-6/1986] 01 p0058 N88-10374

Estimating payload internal temperatures and radiator size for multimegawatt space platforms
[DE88-000244] 03 p0275 N88-11738

Rayleigh scattering measurements of a freejet with homogeneous condensation 03 p0319 N88-12020

Scaling of size/time/temperature associated with dilatation and distortion in uniaxial specimens
03 p0336 N88-12117

Titanium oxide absorption and spot sizes in II Peg, HR 1099 and UX Ari 04 p0508 N88-13126

The filtering problem for infinite dimensional stochastic processes
[AD-A186431] 07 p0916 N88-15662

Size effects in linear elastic fracture mechanics
21 p2964 N88-27809

SIZE DETERMINATION

Results from a questionnaire on particulate metrology in the UK
[NPL-MOM-81] 09 p1141 N88-16841

Electrohydrodynamic migration of charged droplets in an insulating fluid
[NASA-TM-100849] 14 p1912 N88-21424

Combined aerodynamic size, charge-to-mass, and velocity measurements of aerosol particles
[ST-REPT-VOL-5-NO-4] 14 p1944 N88-21598

Consequences of the size determination of P/Halley by space probes on the scale of sizes of cometary nuclei
14 p2009 N88-21986

Gas turbine smoke measurement: A smoke generator for the assessment of current and future techniques
24 p3348 N88-29830

Particle size measurements in sooting combustion systems 24 p3348 N88-29831

The effect of particle properties on radiative heat transfer 24 p3350 N88-29941

SIZE DISTRIBUTION
NT PARTICLE SIZE DISTRIBUTION

Cavitation inception scale effects. 1. Nuclei distributions in natural waters. 2. Cavitation inception in a turbulent shear flow
[AD-A186553] 08 p0988 N88-15987

Approximating the size of a dynamically growing asynchronous distributed network
[AD-A187011] 09 p1152 N88-16899

Cometary magnitude distribution: The tabulated data
14 p1995 N88-21888

Information analysis of integral equations in remote sensing of atmospheric aerosols
18 p2532 N88-25022

Small-droplet spray measurements with a scattered-light scanner
[NASA-TM-100973] 20 p2806 N88-25845

Holographic determination of droplet size distributions
[DFVLR-MITT-88-05] 22 p3074 N88-28250

SIZE SEPARATION

Size-reduction and sorting behavior in sieve hammer mills
[ETN-88-91480] 11 p1467 N88-18749

SIZING (SEPARATION)
U SIZE SEPARATION

SIZING (SHAPING)

Mission requirements and aircraft sizing
05 p0545 N88-13317

SKELETON
U MUSCULOSKELETAL SYSTEM

SKEWNESS
Extrema of skewed stable processes
[AD-A185422] 05 p0642 N88-13925
Dual cylindrical wave Laser-Doppler method for measurement of skin friction in fluid flow
06 p0700 N88-14297

SKILLS
U ABILITIES

SKIN (ANATOMY)
Local human skin potential: Spatial distribution, magnitude and origin
[DE87-012882] 01 p0075 N88-10480
DNA damage and repair in human skin in situ
[DE87-014288] 03 p0356 N88-12241
Effect of antiorthostatic position and different illumination on sensitivity of skin in upper half of the body to ultraviolet radiation 10 p1363 N88-18145
Experimental research on skin reflection, transmission, absorption of light rays 16 p2187 N88-23039

SKIN (STRUCTURAL MEMBER)
Damage tolerance of stiffened-skin structures: Prediction and experimental verification
[NLR-MP-86041-U] 06 p0667 N88-14091
Absorption of cyclotron radiation in skin layer in Araks experiment 08 p1003 N88-16076
Low frequency eddy current detection and evaluation of corrosion in aircraft skins
[ETN-88-91664] 09 p1144 N88-16859

SKIN FRICTION
NT AERODYNAMIC DRAG
NT FRICTION DRAG
NT SUPERSONIC DRAG
NT VISCOUS DRAG
Effect of viscosity on a vertical cylinder due to surface waves
[ETN-87-90960] 02 p0171 N88-11075
Dual cylindrical wave Laser-Doppler method for measurement of skin friction in fluid flow
06 p0700 N88-14297
Overview of the Langley viscous drag reduction program 07 p0812 N88-14946
Riblets for aircraft skin-friction reduction
07 p0814 N88-14955
Airfoil large eddy breakup devices for turbulent drag reduction 07 p0814 N88-14956
A method for the approximate calculation of the skin friction coefficient of horizontal wavy plates
[VKI-TN-160] 07 p0851 N88-15172
A review of approaches to the study of turbulence modification by means of non-Newtonian additives
[AD-A186799] 12 p1627 N88-19734
Enhanced viscous flow drag reduction using acoustic excitation
[NASA-CR-182734] 15 p2062 N88-22295
Boundary layer measurements using hot-film sensors
17 p2297 N88-23743
Manipulation of the structure of a turbulent boundary layer 18 p2512 N88-24901
The determination of the topological structure of skin friction lines on a rectangular wing-body combination
[NASA-CR-4168] 20 p2753 N88-26343
A new method of calculating the boundary layer characteristics downstream of manipulators. Part 2: Skin friction and net drag reduction
[PNR90456] 22 p3076 N88-28280
Skin friction balance
[NASA-CASE-LAR-13710-1] 23 p3216 N88-29145
Development and design of windtunnel and test facility for RPV (Remote Piloted Vehicle) enhancement devices
[AD-A194842] 24 p3329 N88-29822

SKIN RESISTANCE
Interaction of acoustic and electromagnetic waves involved in anomalous skin effect
08 p1079 N88-16503
Estimation of body fluid shift by electrical impedance in various postures 12 p1661 N88-19956

SKIN TEMPERATURE (BIOLOGY)
Temperature regulation at rest and exercise during the human menstrual cycle
[AD-A186461] 08 p1050 N88-16341
Analysis of annular microstrip antennas for hyperthermic applicators
[PB88-181508] 19 p2643 N88-25679
Physiological responses to acute exercise-heat stress
[AD-A192606] 21 p2986 N88-27732
Depressed sweating during exercise at altitude
[AD-A192603] 22 p3130 N88-28609

SKIN TEMPERATURE (NON-BIOLOGICAL)
Correlations of velocity and temperature fluctuations in the stagnation-point flow of circular cylinder in turbulent flow
[NASA-TM-100930] 19 p2597 N88-25435

SKIS
Airworthiness and flight characteristics test of a ski assembly for the UH-60A Black Hawk helicopter
[AD-A191414] 16 p2162 N88-22895

SKULL
Realistic conductivity geometry model of the human head for interpretation of neuromagnetic data
[PB88-112230] 10 p1369 N88-18179

SKY
NT NIGHT SKY
Unified Sun and sky illumination for shadows under trees
[DE87-014232] 01 p0063 N88-10535
ISTP SBIR phase 1 Full-Sky Scanner: A feasibility study
[NASA-CR-180749] 10 p1333 N88-17964
Analysis of deep sky sources found by the infrared astronomy satellite
[AD-A189605] 13 p1853 N88-21089
Effects of atmospheric model layering on LOWTRAN 6 calculations of 8-12 micrometers near-horizon sky radiances
[AD-A192969] 20 p2791 N88-26559

SKY BRIGHTNESS
IR (infrared) sky radiance distributions in the marine boundary layer
[AD-A193683] 22 p3119 N88-28531

SKY RADIATION
NT AIRGLOW
NT DAYGLOW
NT GEOCORONAL EMISSIONS
NT NIGHTGLOW
Sky radiance distributions for thermal imaging backgrounds
[AD-A191135] 17 p2373 N88-24115

SKY SURVEYS (ASTRONOMY)
A search for X-ray luminous late type stars in NIPSS data 04 p0511 N88-13143
A search for very low mass (brown dwarf) stars as wide binaries using a seven element infrared camera-photometer 04 p0512 N88-13150
A VLA survey of dMe flare stars
04 p0513 N88-13154
An automated supernova search and the design strategy
[DE88-001827] 05 p0660 N88-14051
A sky temperature survey at 19.2 GHz using a balloon borne Dicke radiometer for anisotropy tests of the cosmic microwave background 11 p1571 N88-19403
The imaging of extra-galactic low-energy gamma-ray sources prospects, techniques, and instrumentation
[NASA-CR-182536] 12 p1713 N88-20251
Survival analysis, or what to do with upper limits in astronomical surveys
[NASA-CR-182936] 17 p2449 N88-24551
Ultraviolet spectra of subluminous objects found in the Kiso Schmidt survey and systematic reanalysis of the archived ultraviolet spectra of white dwarfs observed with the IUE satellite under the Astrophysics Data Program (ADP)
[NASA-CR-182976] 18 p2592 N88-25406
Investigation of the diffuse ultraviolet background with DE data
[NASA-CR-182863] 19 p2741 N88-26271
A survey of the Ap stars for rapid variability
20 p2884 N88-27127

SKY WAVES
NT WHISTLERS

SKYLAB PROGRAM
Earth resources: A continuing bibliography with indexes (issue 55)
[NASA-SP-7041(55)] 01 p0065 N88-10415

SKYLARK
U SKYLARK ROCKET VEHICLE

SKYLARK ROCKET VEHICLE
Skylark sounding rocket development-Skylark 8
08 p1035 N88-16274

SLABS
Fracture mechanisms and strengthening of slab lasers
[DE88-004002] 11 p1493 N88-18914

SLANT
U SLOPES

SLANT PERCEPTION
U SPACE PERCEPTION

SLEDS
NT ROCKET PROPELLED SLEDS

SLEEP
NT HYPNOSIS
Sleep and wakefulness: Handbook for flight medical officers, second edition
[AGARD-AG-270(E)] 02 p0217 N88-11366
Neurophysiological analysis of hypothalamic regulation mechanisms of primary sleep and hypobiosis
06 p0751 N88-14611
Sleep induced in cat by electric stimulation of acoustic and motor areas in brain cortex
06 p0751 N88-14612
Model based monitoring of human sleep stages
[ISBN-90-9001448-9] 06 p0752 N88-14618
Pharmacological resetting of the Circadian sleep-wake cycle
[AD-A186194] 07 p0889 N88-15385
Discrete adaptation to sensory conflict
10 p1363 N88-18146
Neurohumoral aspects of sleep
[AD-A188653] 12 p1667 N88-19992
The application of non-stationary data analysis techniques in the identification of changes in the electroencephalogram associated with the onset of drowsiness 21 p2978 N88-27688
Psychophysiological measures of drowsiness as estimators of mental fatigue and performance degradation during sleep deprivation 21 p2980 N88-27702

SLEEP DEPRIVATION
Sleep and wakefulness: Handbook for flight medical officers, second edition
[AGARD-AG-270(E)] 02 p0217 N88-11366
Assessment of physical activity intensity by heart rate during sleep limited military operations
[AD-A185913] 07 p0888 N88-15382
Pharmacological resetting of the Circadian sleep-wake cycle
[AD-A186194] 07 p0889 N88-15385
Role of adenosine analogs and growth hormone in waking and sleep
[AD-A187897] 11 p1519 N88-19070
Napping and human functioning during prolonged work
[AD-A190226] 15 p2102 N88-22525
Psychophysiological measures of drowsiness as estimators of mental fatigue and performance degradation during sleep deprivation 21 p2980 N88-27702

SLENDER BODIES
NT SLENDER CONES
Computational study of three-dimensional wake structures
[REPT-2] 05 p0539 N88-13281
Calculations of the turbulent wake behind a slender self-propelled double-body and comparisons with experiment
[AD-A185661] 06 p0703 N88-14314
Centerplane source distribution for slender bodies
10 p1328 N88-17940
Experimental research on center of pressure of slender body with two pointed ends 14 p1864 N88-21137
The calculation of transonic flow over the shuttle orbiter using slender body theory 18 p2460 N88-24606
Finite element solution of 3-D turbulent Navier-Stokes equations for propeller-driven slender bodies
18 p2515 N88-24919
Forces and moments on a slender, cavitating body
[DE88-007208] 21 p2945 N88-27491
A calculation of the turbulent boundary layer on a slender ellipsoid at low incidence
[FFA-TN-1988-02] 23 p3213 N88-29126
Semi-empirical methods for conventional and unconventional missiles 24 p3318 N88-29758

SLENDER CONES
The drag of slender axisymmetric cones in rarefied hypersonic flow 05 p0531 N88-13229

SLENDER WINGS
A theory for the core flow of leading-edge vortices
07 p0810 N88-14935
Calculated unsteady aerodynamics of wings
[AD-A189608] 12 p1574 N88-19415
Optimal control of the wing rock phenomenon
21 p2927 N88-27373
High-aspect-ratio wings 23 p3167 N88-28859
Delta wing configurations 23 p3167 N88-28860

SLEWING
Dynamics of spacecraft control laboratory experiment (SCOLE) slew maneuvers
[NASA-CR-4098] 01 p0014 N88-10082
Recent advances in structural dynamics of large space structures
[NASA-TM-100513] 02 p0138 N88-10867
Combined problem of slew maneuver control and vibration suppression
[NASA-CR-181537] 04 p0455 N88-12817
The dynamics and control of large-flexible space structures, part 10
[NASA-CR-182426] 08 p0963 N88-15830
Large-angle slewing maneuvers for flexible spacecraft
[NASA-CR-4123] 08 p1000 N88-16060
Slew-induced deformations in a space-based electromagnetic rail gun 21 p2929 N88-27385

SLIDING
The wear process during the RUNNING-IN of steel in lubricated sliding
[NAL-TR-922T] 02 p0181 N88-11130
Dynamic analysis of a structure with sliding base
08 p0998 N88-16045
Sliding charge density waves and related problems
[AD-A186720] 09 p1157 N88-16934

Friction and wear of monolithic and fiber reinforced silicon-ceramics sliding against IN-718 alloy at 25 to 800 C in atmospheric air at ambient pressure
[NASA-TM-100294]. 10 p1304 N88-17796
Stable, robust tracking by sliding mode control
[AD-A188278] 10 p1401 N88-18358
The flying characteristics of the membrane slider bearing 18 p2522 N88-24965

SLIDING CONTACT
Traction model development
[AD-A188450] 15 p2073 N88-22359

SLIDING FRICTION
The development of a friction model predicting the sliding behavior of materials pairs, especially at low temperatures: Progress report and renewal proposal
[DE87-013941] 01 p0055 N88-10354
Application of Kalker's rolling contact theory to the simulation of rail vehicles
[DFVLR-FB-87-07] 01 p0057 N88-10363
The friction and wear of TPS fibers
[NASA-CR-181496] 03 p0291 N88-11830
Real-time Raman detection of molecular changes in ceramics undergoing sliding friction
[DE88-000558] 04 p0421 N88-12609
Literature review of solid lubrication mechanisms
[AD-A185010] 05 p0567 N88-13456
Surface gouging by hypervelocity sliding contact between metallic materials
[DE88-001937] 06 p0682 N88-14178
The use of alloy 117 as a liquid metal current collector
[AD-A185740] 06 p0698 N88-14281
Mechanisms of wear in single- and two-phase materials
[DE88-003846] 10 p1305 N88-17806
Reciprocating sliding wear characteristics of copper-carbon fiber composites
[NASA-TT-20176] 15 p2031 N88-22100
Railgun rail gouging by hypervelocity sliding contact
[DE88-006866] 16 p2166 N88-22916
Study of temperature and stress fields of two sliding cylinders
[ETN-88-92134] 20 p2815 N88-26704
Studies of dynamic contact of ceramics and alloys for advanced heat engines
[DE88-008996] 21 p2919 N88-27324
Frequency dependent sliding coefficients for general three-dimensional rolling contact in high frequency range
[ILR-MITT-192] 22 p3085 N88-28316
Static and dynamic metal-metal friction at plastic stress levels
[DE88-011261] 23 p3222 N88-29176
Stability of stick-slip phenomenon by using constitutive friction laws of Dietrich and Ruina
[ILR-MITT-197] 24 p3379 N88-30127

SLIP BANDS
U EDGE DISLOCATIONS

SLIP CASTING
Slip casting and extruding shapes of rhenium with metal oxide additives. Part 2: Development of grain stabilized rhenium parts for resistojets
[NASA-CR-180851] 03 p0278 N88-11749
Slip casting of advanced ceramics and composites
[DE88-003424] 11 p1467 N88-18746

SLIP FLOW
Rotational flow of rarefied gas between two coaxial cylinders with slip conditions
[INPE-4277-PRE/1149] 12 p1627 N88-19738
Slip velocity method for three-dimensional compressible turbulent boundary layers
[NASA-TM-100586] 13 p1771 N88-20592

SLIPSTREAMS
NT PROPELLER SLIPSTREAMS
An investigation of the effects of the propeller slipstream on a wing boundary layer 06 p0700 N88-14293

SLITS
Experimental investigation of simplest inhomogeneities in cylindrical slit line
[DE88-702388] 21 p2933 N88-27418

SLOPES
Computational study of three-dimensional wake structures
[REPT-2] 05 p0539 N88-13281
Wind and temperature structure on the slopes of a mountain valley
[DE88-000080] 07 p0880 N88-15338
Detecting and interval estimation about a slope change point
[AD-A186030] 07 p0909 N88-15509
Numerical modeling results for mode propagation in a wedge
[AD-A193998] 22 p3147 N88-28718
A preliminary investigation of drag reduction and mechanism for a blunt body of revolution with slanted base
[NASA-TT-20349] 24 p3317 N88-29753

SLOSHING
U LIQUID SLOSHING

SLOT ANTENNAS
Performance evaluation of a half-wave resonant slot antenna over perfect ground using NEC (Numerical Electromagnetic Code)
[AD-A184004] 03 p0308 N88-11942
Mutual admittance between slots in cylinders of arbitrary shape
[AD-A184254] 04 p0439 N88-12723
Conformal microstrip slot antenna and antenna array
[AD-A189623] 15 p2055 N88-22252
Current-drive on the Versator-2 tokamak with a slotted-waveguide fast-wave coupler
[DE88-006261] 15 p2136 N88-22743
Picosecond photoconductive transceivers
19 p2656 N88-25777

SLOTS
Fin gaps and body slots of guided projectiles: Effects, data correlation and modeling
[AD-A184440] 03 p0270 N88-11698
Mutual admittance between slots in cylinders of arbitrary shape
[AD-A184254] 04 p0439 N88-12723
Optical communication with semiconductor laser diodes
[NASA-CR-182464] 09 p1154 N88-16918
Experimental verification of a finite-difference time-domain thin slot algorithm
[DE88-005572] 13 p1817 N88-20859
Cavitation inception in rectangular two-dimensional slots
[AD-A190677] 15 p2066 N88-22318
Solid rocket motor aft field joint flow field analysis
[NASA-CR-179288] 18 p2474 N88-24675
Electromagnetic penetration into a conducting circular cylinder through a narrow slot, TE case
[AD-A191802] 18 p2500 N88-24828
Characteristics of merging shear layers and turbulent wakes of a multi-element airfoil
[NASA-TM-100053] 18 p2511 N88-24900

SLOTTED ANTENNAS
U SLOT ANTENNAS

SLOTTED WIND TUNNELS
Theoretical and experimental studies of the transonic flow field and associated boundary conditions near a longitudinally-slotted wind-tunnel wall
[NASA-CR-181169] 08 p0959 N88-15815
Wall interference assessment/correction of data from tests of a CAST 10-2/DOA 2 airfoil in the Langley 0.3-m transonic cryogenic tunnel 20 p2751 N88-26331

SLOW NEUTRONS
U THERMAL NEUTRONS

SLURRIES
Two-phase non-Newtonian hydrodynamic modeling of slurries
[DE87-011519] 01 p0047 N88-10298
Experiments on densely-loaded non-Newtonian slurries in laminar and turbulent pipe flows
[DE88-000719] 04 p0442 N88-12746
Heat transfer investigations in a slurry bubble column
[DE88-001445] 06 p0699 N88-14286
Laser velocimeter measurements of solids in multiphase flow
[DE88-000196] 11 p1487 N88-18876
Fluidization mechanisms in slurry flows
[DE88-005191] 13 p1766 N88-20563
Experiments on densely-loaded non-Newtonian slurries in laminar and turbulent pipe flows
[DE88-006209] 15 p2067 N88-22323
An advanced extruder-feeder biomass liquefaction reactor system 18 p2535 N88-25042
Experiments on densely-loaded non-Newtonian slurries in laminar and turbulent pipe flows
[DE88-010579] 20 p2800 N88-26612

SLURRY PROPELLANTS
Fuels combustion research
[AD-A187688] 11 p1453 N88-18657
Liquid phase decomposition in slurry fuels
19 p2624 N88-25564

SMALL ASTRONOMY SATELLITES
U SAS

SMALL PERTURBATION FLOW
A transonic-small-disturbance wing design methodology
[NASA-TP-2806] 10 p1273 N88-17614
Steady and unsteady transonic small disturbance analysis of realistic aircraft configurations
[NASA-TM-100557] 13 p1717 N88-20269
Transonic flow field analysis for real fuselage configurations 14 p1864 N88-21133

SMEAR
Extending the impulse response in order to reduce errors due to impulse noise and signal fading
19 p2649 N88-25730

SMELTING
LFCM (Liquid-Fed Ceramic Melter) vitrification technology
[DE88-003441] 09 p1149 N88-16887
Activities of As, Sb, Bi and Pb in copper mattes and their effects on impurity elimination
[TKK-V-A10(1988)] 15 p2041 N88-22165
Plasma technology: Preliminary studies 2
[DE88-752815] 22 p3154 N88-28763

SMOG
Ozone in the atmosphere 18 p2539 N88-25064

SMOKE
Summary report of the history and events pertinent to the Civil Aeromedical Institute's evaluation of providing smoke/fume protective breathing equipment for airline passenger use
[AD-A184499] 03 p0261 N88-11645
Structural characteristics of dean vortices in a curved channel
[AD-A184724] 03 p0320 N88-12024
The development of low level coastal flow fields when solar radiation is blocked by smoke
[DE87-014348] 03 p0354 N88-12230
Flammability, smoke and toxicity test on fire barrier fabric from the Porcher company --- Airbus aircraft
[ETN-88-91168] 06 p0666 N88-14085
A holographic investigation of particulates in metalized solid fuel ramjet combustion
[AD-A186887] 09 p1140 N88-18331
Effects of additives on fire properties of polyethylene
[AD-A187064] 09 p1146 N88-16871
The visioceilometer and its tactical applications
[AD-A188216] 12 p1647 N88-19866
Detection of biomass burning and smoke plumes in the Amazon region through NOAA satellite imagery
17 p2365 N88-24085
Enhanced emergency smoke venting
[DOT/FAA/CT-88/22] 20 p2756 N88-26350
A study relating to the fog oil replacement program
[AD-A192536] 21 p2923 N88-27347
Application of laser diffraction techniques to particle sizing in solid propellant rocket motors
[AD-A193841] 22 p3049 N88-28089
Project wind, phase 4 (smoke test), Meadow Brook Valley, Red Bluff, California
[AD-A194742] 22 p3128 N88-28596
Smoke hoods: Net safety benefit analysis --- aircraft accidents
[CAA-PAPER-87017] 23 p3174 N88-28898
Flow visualization on a small scale
[AD-A194728] 23 p3181 N88-28935
Flow visualization by laser sheet
[AD-A194481] 23 p3211 N88-29111
Gas turbine smoke measurement: A smoke generator for the assessment of current and future techniques
24 p3348 N88-29930
Numerical field model simulation of full scale fire tests in a closed spherical/cylindrical vessel
[AD-A195067] 24 p3359 N88-29998

SMOKE ABATEMENT
Military jet fuels, 1944-1987
[AD-A186752] 09 p1150 N88-16890

SMOKE TRAILS
Development of flow visualization techniques for use in the Hot Gas Laboratory
[BAE-ARG-233] 03 p0325 N88-12052

SMOOTHING
NT DATA SMOOTHING
Computation of turbulent flow of air through smooth and rough pipes using a two-equation turbulence model
06 p0700 N88-14298
Analysis of smoothing matrices for the preconditioning of elliptic difference equations
[CWI-NM-R8705] 09 p1228 N88-17357
Improving the stability of predictor-corrector methods by residue smoothing
[CWI-NM-R8707] 09 p1228 N88-17359
Optimal application of Morrison's iterative noise removal for deconvolution. Appendices
[NASA-CR-182477] 09 p1231 N88-17376
Optimum filters and smoothers design for carrier phase and frequency tracking
[NASA-CR-182654] 12 p1618 N88-19679
The existence of smooth densities for the prediction filtering and smoothing problems
[AD-A189665] 15 p2119 N88-22629
The effects of optical smoothing techniques on filamentation in laser plasmas
[AD-A188719] 16 p2275 N88-23614
A comparative study of Chebyshev acceleration and residue smoothing in the solution of nonlinear elliptic difference equations
[CWI-NM-R8723] 18 p2569 N88-25259

Distributive iteration for indefinite systems as smoothing method in multigrid process on example of Stokes and Navier-Stokes equations with emphasis on incomplete decompositions
[ETN-88-92127] 21 p2948 N88-27509
Outliner resistant filtering and smoothing: 2D version
[AD-A193319] 21 p3012 N88-27874

SMU (MANEUVERING UNITS)
U SELF MANEUVERING UNITS

SNAILS
The influence of weightlessness on the metabolism of the Biomphalaria glabrata 01 p0074 N88-10475

SNAP
NT FISSION ELECTRIC CELLS
NT SNAP 19
SNAP-DYN: Proven technology for wear-term, higher power in space 17 p2425 N88-24422
SNAP fuel performance 17 p2435 N88-24484
SNAP-DYN: Concepts for multikilowatt space power applications 17 p2435 N88-24486

SNAP 19
Pioneer 10 and 11 RTG performance update
17 p2405 N88-24301

SNATCHING
U SPACECRAFT RECOVERY

SNOW
On the role of snow in the redistribution of precipitation by small scale topography 02 p0203 N88-11267
Thunderstorms with snow: A comprehensive, empirical study of their occurrence, development and structure
[AD-A185929] 07 p0879 N88-15329
Active and passive remote sensing of ice
[AD-A186685] 09 p1195 N88-17162
Aircraft and ground vehicle friction correlation test results obtained under winter runway conditions during joint FAA/NASA Runway Friction Program
[NASA-TM-100506] 11 p1438 N88-18582
Determination of the ultimate loads for corrugated-steel, barrel-type shell structures
[AD-A187716] 11 p1498 N88-18944
Characteristics of coherent and incoherent waves in snow at microwave and millimeter wave frequencies
[AD-A188990] 12 p1620 N88-19592
Study of cations in the precipation of Estacao Antartica Comandante Ferraz
[INPE-4377-PRE/1197] 12 p1644 N88-19843
Reduce uncertainty in projection of future sea-level changes due to ice wastage
[DE88-009883] 22 p3129 N88-28601

SNOW COVER
Evaluation of digital, multitemporal LANDSAT 5 thematic mapper data for the determination of the aerial snowcover extent and spectral separation of various surface types in the inner Oetztal (West Germany) with special regard to the significance of aerial snowcover information for water resources management
[DFVLR-FB-86-46] 03 p0345 N88-12180
Remote sensing of earth terrain
[NASA-CR-182677] 13 p1790 N88-20711
Research relative to angular distribution of snow reflectance/snow cover characterization and microwave emission
[NASA-CR-182733] 14 p1941 N88-21582
Spectral measurements in a disturbed boundary layer over snow
[AD-A190217] 15 p2097 N88-22494
Ice conditions along the Ohio River as observed on LANDSAT images, 1972-1985
[AD-A191172] 18 p2531 N88-25018
Higher frequency ambient noise in the arctic ocean
[AD-A192203] 18 p2547 N88-25122
Active and passive remote sensing of ice
[AD-A193307] 21 p2966 N88-27617

SNOWPLOW EFFECT
U PLASMA DYNAMICS

SNOWSTORMS
Nowcasting rain/snow transitions and freezing rain
02 p0202 N88-11265

SOAPS
The elliptic Sinh-Gordon equation and the construction of toroidal soap bubbles
[DE88-006426] 15 p2113 N88-2258

SOCIAL FACTORS
Problems in integrating geographic data
[DE87-012880] 01 p0106 N88-10689
The role of basic research in society
[DE88-000459] 04 p0502 N88-13090
Activities report of the Technical University of Twente
[ETN-88-90620] 06 p0799 N88-14892
Some aspects of sociopsychological screening of flying school applicants 07 p0890 N88-15392
Antarctica as a model for the human exploration of Mars
[AD-A185835] 08 p1051 N88-16342
Social factors in space station interiors
12 p1651 N88-19888
Do we need a new cartography?
16 p2225 N88-23283
Stress in relation to the physical and social environment 19 p2695 N88-26020
Selection and training of subjects to live and work in hostile and unusual environments
19 p2696 N88-26026

SOCIAL ISOLATION
Stress in relation to the physical and social environment 19 p2695 N88-26020

SOCIOLOGY
NT SOCIAL FACTORS

SODIUM
NT LIQUID SODIUM
NT SODIUM VAPOR
Blue-green laser diode research program
[AD-A183517] 01 p0051 N88-10323
Theoretical and lidar studies of the seasonal and nocturnal variations of the mesospheric sodium layer at Urbana, Illinois 01 p0068 N88-10435
Lidar investigations of M-zone
06 p0741 N88-14558
The sodium layer at 69 N latitude in wintertime
08 p1027 N88-16218
Lidar metal density measurements in the upper atmosphere 08 p1027 N88-16219
The suppression of stimulated hyper-Raman emission in Na due to parametric four-wave mixing
[DE88-003290] 09 p1172 N88-17030
A modeling analysis program for the JPL table mountain Io sodium cloud data
[NASA-CR-182555] 11 p1570 N88-19400
Quantitative determination of a hydrogen impurity in a sodium coolant by hydride thermal dissociation
[NASA-TT-20239] 13 p1740 N88-20402
Use of long-distance pair potentials in calculations of defect characteristics in metals
[DE88-701039] 15 p2037 N88-22138
The kinetics of contact noise in NaBeta alumina
[AD-A190651] 15 p2130 N88-22707
Associative two-body condensation in laser-cooled sodium and hydrogen 16 p2267 N88-23559
Theoretical studies of solar-pumped lasers
[NASA-CR-182929] 17 p2344 N88-23971
Cardiac rhythm of animals consuming reclaimed water differing in concentration of sodium and potassium ions
19 p2705 N88-26085
Production of powdered sodium hydride with large specific surface by the catalyzed reaction of molten sodium with hydrogen-1
[NASA-TT-20185] 20 p2776 N88-26462
Spectral line shapes from highly ionized sodium plasmas
[AD-A193401] 21 p3017 N88-27907

SODIUM CHLORIDES
Electronic conduction in molten sodium chloride
[DE87-010063] 02 p0144 N88-10901
Experimental verification of vapor deposition rate theory in high velocity burner rigs 02 p0169 N88-11179
The role of inclusions in corrosion fatigue crack initiation in Q1N 05 p0604 N88-13699
Geochemistry of freezing brines, low-temperature properties of sodium chloride
[AD-A185751] 06 p0680 N88-14168
The factors which govern the acceleration of corrosion fatigue crack growth rate of a ferritic stainless steel
06 p0717 N88-14402
Fatigue thresholds of C.Mn steels in saline environments 06 p0717 N88-14403
A rapid polishing method for KBr and NaCl infrared windows
[DE88-002480] 07 p0862 N88-15229
The influence of strain on hydrogen entry, transport, and embrittlement of a high strength steel in aqueous sodium chloride solution
[AD-A189302] 12 p1608 N88-19619
The effect of H2S concentration and pH on hydrogen permeation in AISI 410 stainless steel in 5 percent NaCl
[NPL-DMA(A)-148] 14 p1890 N88-21293
Corrosion of tungsten alloys in marine environments
17 p2320 N88-23854
Nuclear magnetic resonance spectrometer
[AD-A192928] 21 p2950 N88-27523
Alternative immersion accelerated testing of coating systems for Naval shoreline facilities
24 p3355 N88-29977

SODIUM COMPOUNDS
NT SODIUM CHLORIDES
NT SODIUM FLUORIDES
NT SODIUM HYDRIDES
NT SODIUM HYDROXIDES
NT SODIUM NITRATES
Corrosion-wear process under rolling-sliding motion
[AD-A189603] 13 p1778 N88-20635

SODIUM FLUORIDES
Prevention of disuse osteoporosis: Effect of sodium fluoride during five weeks of bed rest
[NASA-CR-172018] 01 p0075 N88-10483
Interatomic Auger rates for the sodium fluoride crystal
[DE87-013012] 03 p0382 N88-12401
Intracavity spectrum analyzer with NaF:F2(+):F3(-) crystal laser for long-wave IR wave band
07 p0919 N88-15584
High temperature solar electrothermal processing-3. Zinc from zinc oxide at 1200-1675K using a non-consumable anode
[AD-A186600] 09 p1141 N88-16836

SODIUM HYDRIDES
Production of powdered sodium hydride with large specific surface by the catalyzed reaction of molten sodium with hydrogen-1
[NASA-TT-20185] 20 p2776 N88-26462

SODIUM HYDROXIDES
Improvements to Raney copper zinc methanol synthesis catalysts 17 p2318 N88-23844
Titrimetric analysis of HAN-based liquid propellants
[AD-A196225] 24 p3357 N88-29990

SODIUM NITRATES
Performance characteristics of magnesium-sodium nitrate flares in oxygen-nitrogen atmospheres
[AD-A185274] 05 p0570 N88-13476

SODIUM SULFUR BATTERIES
Extended abstracts: Eighth Battery and Electrochemical Contractors' Conference
[DE88-000960] 06 p0730 N88-14489
Improve the lifetime of the hollow fiber sodium sulfur cell
[DE88-004881] 13 p1751 N88-20469
Sodium-sulfur technology evaluation at Argonne National Laboratory
[DE88-002852] 13 p1762 N88-20544
A novel class of positive electrodes for rechargeable batteries
[DE88-004559] 13 p1763 N88-20545
Failure analysis of Chloride Silent Power, Ltd. PB cells
[DE88-010567] 21 p2938 N88-27448
Component stress during freeze/thaw cycling
[DE88-011204] 21 p2938 N88-27449
Sodium/sulfur cell evaluation results
[DE88-011488] 21 p2938 N88-27451
Effect of thermal cycling on CSPL (Chloride Silent Power Ltd.) sodium/sulfur cells
[DE88-011205] 21 p2939 N88-27455
Post-test observations on CSPL (Chloride Silent Power Limited) cells
[DE88-011975] 21 p2940 N88-27461
Considerations and measurements of latent-heat-storage salts for secondary thermal battery applications
[DE88-011091] 23 p3228 N88-29213

SODIUM VAPOR
Solar pumped, alkali vapor laser
[AD-A187156] 09 p1170 N88-17016
Alkali metal diffuse band lasers
[AD-A190244] 15 p2071 N88-22350

SOFAR
U SOUND FIXING AND RANGING

SOFT LANDING SPACECRAFT
NT AEROSPACE PLANES
NT HOTOL LAUNCH VEHICLE
NT LANDING MODULES
NT LUNAR LANDING MODULES
NT X-30 VEHICLE

SOFTENING
Large-strain softening of aluminum at elevated temperature
[DE87-011559] 01 p0024 N88-10153
Study of the characteristic curve of hardening and softening during low-cycle fatigue process
06 p0719 N88-14414
Brillouin scattering and transmission electron microscopy studies of radiation-induced elastic softening, disordering and amorphization of intermetallic compounds
[DE88-005927] 14 p1987 N88-21850

SOFTWARE (COMPUTERS)
U COMPUTER PROGRAMS
U COMPUTER SYSTEMS PROGRAMS

SOFTWARE ENGINEERING
NT COMPUTER PROGRAMMING
NT LANGUAGE PROGRAMMING
NT LOGIC PROGRAMMING
NT MICROPROGRAMMING
NT PARALLEL PROGRAMMING
NT SYMBOLIC PROGRAMMING
Color display programming for aviation
[DFVLR-MITT-87-03] 01 p0006 N88-10031
Space Station Mission Planning System (MPS) development study. Volume 1: Executive summary
[NASA-CR-179202] 01 p0009 N88-10047

Space Station Mission Planning System (MPS) development study. Volume 2
[NASA-CR-179200] 01 p0009 N88-10048
Space Station Mission Planning Study (MPS) development study. Volume 3: Software development plan
[NASA-CR-179203] 01 p0009 N88-10049
Attitude Control Working Group report
01 p0016 N88-10099
Collection and analysis of specific ELINT Signal Parameters
[NASA-CR-181419] 01 p0033 N88-10213
A brief discussion of formally based approaches to rapid prototyping
[BAE-WAA-RP-RES-SWE-440]
01 p0079 N88-10508
Analysis and synthesis of abstract data types through generalization from examples
[NASA-CR-178369] 01 p0081 N88-10519
Some approaches to the design of high integrity software 02 p0127 N88-10799
Assessment of software quality for the AIRBUS A310 automatic pilot 02 p0128 N88-10804
Software reliability models for fault-tolerant avionics computers and related topics
[NASA-CR-181440] 02 p0220 N88-11382
A design methodology for the utilization of metrics within various phases of software lifecycle models
[DE87-010519] 02 p0220 N88-11385
Prototype Rendezvous Onboard Software (PROBS)
[MATRA-EPT-DT-PRB-2A-00068]
02 p0222 N88-11396
Dynamic image interpretation for autonomous vehicle navigation
[AD-A184043] 03 p0262 N88-11647
JPRS report: Science and technology. China
[JPRS-CST-87-026] 03 p0269 N88-11688
An allotment planning concept and related computer software for planning the fixed satellite service at the 1988 space WARC
[NASA-TM-100244] 03 p0308 N88-11944
Technology applications branch graphics projects
[AD-A184621] 03 p0364 N88-12291
Issues in image processing software development for a multi-user, multi-programming environment
[DE88-000358] 03 p0365 N88-12298
National Science Foundation
[PB87-228375] 03 p0384 N88-12410
Programmable real-time digital video image processing
[PB87-104162] 04 p0430 N88-12661
Software reliability perspectives
[NASA-CR-181523] 04 p0479 N88-12952
Software maintenance in scientific and engineering environments: An introduction and guide
[NASA-CR-177409] 04 p0479 N88-12954
Managing distributed derived data: A preliminary proposal
[DE88-000714] 04 p0481 N88-12966
Intelligent signal analysis and recognition
[NASA-CR-181531] 04 p0501 N88-13084
Towards building a team of intelligent robots
[NASA-CR-181538] 05 p0589 N88-13595
A rudimentary database for three-dimensional objects using structural representation
[CSE-87-00004] 05 p0590 N88-13597
Experiments in fault tolerant software reliability
[NASA-CR-181554] 05 p0632 N88-13863
Reliability of voting in fault-tolerant software systems for small output spaces
[TR-87-16] 05 p0632 N88-13864
Effectiveness of back-to-back testing
[TR-87-08] 05 p0632 N88-13865
RSDIMU acceptance testing system: Overview of acceptance software and procedures
05 p0632 N88-13866
Software design for an airborne gravity measurement system
[AD-A185000] 05 p0634 N88-13878
An Ada graphical tool to support software development
[DE87-014854] 05 p0636 N88-13891
Sandia software guidelines: Software quality planning
[DE88-001931] 05 p0636 N88-13894
A requirements specification for a software design support system
[NASA-CR-182333] 05 p0637 N88-13896
Role of technical information in innovation
[PB87-235388] 05 p0658 N88-14039
Approaches and possible improvements in the area of multibody dynamics modeling
[NASA-CR-179227] 06 p0663 N88-14067
Atmospheric electricity
[NASA-CR-179239] 06 p0744 N88-14575
Window system: A toolbox for interactive computer graphics
[PB87-234282] 06 p0756 N88-14637
A software reliability model with variable fault exposure coefficient
[REPT-87-029] 06 p0757 N88-14646
How to estimate the total number of errors in a software system
[PB87-132130] 06 p0758 N88-14647
Virtual image processor: A prototype implementation
[AD-A185560] 06 p0758 N88-14652
National Aeronautics and Space Administration (NASA)/American Society for Engineering Education (ASEE) Summer Faculty Fellowship Program, 1987. Volume 2
[NASA-CR-172009-VOL-2] 06 p0796 N88-14874
Space station software reliability analysis based on failures observed during testing at the multisystem integration facility 06 p0798 N88-14884
A plan for collecting ada software development cost, schedule and environment data
[AD-A185905] 07 p0902 N88-15460
A software planning and development methodology with resource allocation capability
[AD-A186088] 07 p0902 N88-15462
Software enhancements and modifications to Program FDTD executable on the Cray X-MP computer
[DE88-001877] 07 p0904 N88-15476
Modelling of clustering effects in point processes: An application to failures in SPC-systems (stored program control-systems)
[PB87-149241] 07 p0904 N88-15480
A multiple node software development environment
[DE87-010995] 07 p0905 N88-15484
Enhancement of computer system for applications software branch 07 p0923 N88-15610
An easy-to-use diagnostic system development shell
08 p1055 N88-16366
Interactive knowledge acquisition tools
08 p1060 N88-16401
A learning apprentice for software parts composition
08 p1065 N88-16436
Automatic program generation from specifications using Prolog 08 p1065 N88-16437
On acquisition of programming knowledge
08 p1065 N88-16438
Information handling architecture and software for CIM (Computer Integrated Manufacturing)
[PB88-105820] 08 p1067 N88-16453
Standardization of software development
[INPE-4330-NTE/272] 08 p1068 N88-16455
Proposal of a methodology for the conceptual design of the Distributed Data Base
[INPE-4315-TDL/282] 08 p1093 N88-16576
Development of a comprehensive software engineering environment 09 p1203 N88-17211
Simplifying the construction of domain-specific automatic programming systems: The NASA automated software development workstation project
09 p1204 N88-17212
The knowledge-based software assistant
09 p1204 N88-17213
Algorithm design for scientific computation for highly parallel multiprocessor systems
[AD-A186713] 09 p1217 N88-17299
Design and implementation of elementary functions in Ada
[CWI-NM-R8710] 09 p1218 N88-17304
Hardware/software reliability study --- space programs
[REPT-65.5686] 09 p1218 N88-17307
Description of a limited VAX-Ada program support environment developed within UDP division version 1.0
[ARE-TM(UDP)-87103] 09 p1219 N88-17308
Software program validity: A survey
[PB87-170593] 09 p1219 N88-17315
A proposal for a feasibility study on the design of software interfaces in large systems
[NPL-DITC-89/87] 09 p1222 N88-17330
An approach to the hierarchical specification, design and verification of software
[RSRE-MEMO-4063] 09 p1223 N88-17332
Advances in reliable numerical computation: A summary --- conference
[NPL-DITC-102/87] 09 p1229 N88-17367
An expert system to support the verification/validation of flight-critical software
[MBB-UT-102/87] 10 p1314 N88-17852
Design sensitivity analysis of nonlinear structural systems and numerical implementation with established finite element codes 10 p1344 N88-18032
Why reusable software isn't 10 p1376 N88-18212
Towards reusable software designs and implementations 10 p1376 N88-18213
Archetyping: A knowledge-based reuse paradigm
10 p1376 N88-18214
Developing a standard taxonomy or software engineering standards 10 p1379 N88-18234
Future directions in computer architecture and software workshop 10 p1383 N88-18258
A method for assessing the software engineering capability of contractors: Preliminary version
[AD-A187230] 10 p1388 N88-18290
The design and implementation of pedagogical software for the multi-backend/multi-lingual database system
[AD-A188106] 11 p1530 N88-19135
Compact high order schemes for the Euler equations
[NASA-CR-181625] 11 p1530 N88-19138
KA-Prolog: Language definition
[GMD-249] 11 p1532 N88-19155
The SAS (Statistical Analysis System) by forms: Putting statistical power into the hands of an end-user
[DE88-002217] 11 p1541 N88-19212
Accessing hierarchical databases via SQL transactions in a multi-model database system
[AD-A187878] 11 p1565 N88-19369
Prototype on-board software for rendezvous and docking 12 p1586 N88-19496
Robotic intelligence issues for space manipulator monitoring, control programming
12 p1588 N88-19504
EUROSIM: A design concept for an in-orbit operations simulator 12 p1589 N88-19517
EUROSIM: A concept of total system support
12 p1590 N88-19523
Definition of the EUROSIM simulation subsystem
12 p1592 N88-19532
A production-quality UNIX Very High Speed Integrated Circuit (VHSIC) Hardware Description Language (VHDL) subset analyzer
[AD-A188832] 12 p1623 N88-19710
Computer architecture for efficient algorithmic executions in real-time systems: New technology for avionics systems and advanced space vehicles
[NASA-CR-182650] 12 p1675 N88-20016
An experiment in software reliability: Additional analyses using data from automated replications
[NASA-CR-178395] 12 p1676 N88-20017
Building software systems economically with mechanized logic: Initial design proposal
[AD-A188791] 12 p1678 N88-20031
Investigation of low energy space plasma
[NASA-CR-182611] 12 p1694 N88-20138
Martian Clouds Data Workshop
[NASA-CR-182431] 12 p1711 N88-20236
Theoretical investigation of EM wave generation and radiation in the ULF, ELF and VLF bands by the electrodynamic orbiting tether
[NASA-CR-182720] 13 p1760 N88-20529
Algebra of Communicating Processes (ACP)tau: A universal axiom system for process specification
[CWI-CS-R8725] 13 p1819 N88-20869
Two normal form theorems for Communicating Sequential Processes (CSP) program
[CWI-CS-R8735] 13 p1819 N88-20874
Type-checking Mini-ML: An algebraic specification with user-defined syntax
[CWI-CS-R8737] 13 p1827 N88-20921
On the design of some systolic algorithms
[CS-8705] 14 p1957 N88-21668
Software quality assurance workstation
[P-1124/RT-14791] 14 p1957 N88-21670
Design method for Ada programs
[ESA-CR(P)-2528] 14 p1958 N88-21671
Public tool interfaces for software development environments
[RSRE-87004] 14 p1958 N88-21674
Procedures for updating dynamic mathematical models
[EMSB-23/86] 14 p1964 N88-21716
Common database interface for heterogeneous software engineering tools
[AD-A189628] 14 p1991 N88-21870
Sigma system: Overview, prospects
15 p2052 N88-22230
Investigation into the development of computer aided design software for space based sensors
[NASA-CR-180772] 15 p2107 N88-22552
Using Colored Stochastic Petri Net (CS-PN) software for protocol specification, validation, and evaluation
[ENST-87C004] 15 p2113 N88-22586
Nonlinear normal mode initialization of the NCAR (National Center for Atmospheric Research) CCM (Community Climate Model)
[PB88-171814] 16 p2235 N88-23347
Portability of software. The use of software in the hardware mixture
[MBB/LWD-11/S/PUB/253] 16 p2246 N88-23416
Software development for the reconstruction of source parameters using research and development arrays
[REPT-840445-TW] 16 p2246 N88-23417
The official handbook of MASCOT, version 3.1, issue 1 — software tool
[BR103975] 16 p2246 N88-23419
The synthesizer generator, a useful tool?
[REPT-87-77] 16 p2250 N88-23443

The Design, Development and Testing of Complex Avionics Systems
[AGARD-CP-417] 17 p2302 N88-23767

The avionics software architecture impact on system architecture 17 p2303 N88-23778

Testing complex avionics software: A practical experience 17 p2306 N88-23794

Interfacing and integrating hardware and software design systems 17 p2306 N88-23796

Software engineering for the British Aerospace Experimental Aircraft Programme (EAP)
17 p2306 N88-23798

A software life cycle support environment
17 p2306 N88-23800

Implantation of a geo-cartographical information system through microcomputers 17 p2361 N88-24064

COMTAL vision one/20 programming processor system from the VAX 11/780 17 p2364 N88-24079

Protection and security mechanisms in the SMITE capability computer
[RSRE-MEMO-4117] 17 p2384 N88-24167

Development environment for secure software
[RSRE-87015] 17 p2386 N88-24179

Separability and security models --- software
[RSRE-87020] 17 p2386 N88-24180

The Environment for Application Software Integration and Execution (EASIE) version 1.0. Volume 4: System installation and maintenance guide
[NASA-TM-100576] 17 p2386 N88-24185

Knowledge based system verification and validation as related to automation of space station subsystems: Rationale for a knowledge based system lifecycle
17 p2387 N88-24192

TALOS: A distributed architecture for intelligent monitoring and anomaly diagnosis of the Hubble Space Telescope 17 p2388 N88-24193

Models and metrics for software management and engineering
[NASA-CR-182953] 17 p2389 N88-24200

An OOD (Object-Oriented Design) paradigm for flight simulators
[AD-A191097] 18 p2467 N88-24647

The Environment for Application Software Integration and Execution (EASIE), version 1.0. Volume 3: Program execution guide
[NASA-TM-100575] 18 p2558 N88-25184

Algorithms and software for solving finite element equations on serial and parallel architectures
[NASA-CR-183027] 18 p2559 N88-25191

Theory of numerical information environment and its applications 19 p2640 N88-25666

Checkout system software for INPE satellites
[INPE-4554-PRE/1297] 19 p2715 N88-26120

Position and velocity determination using a Global Positioning System: An outline
[B8735062] 20 p2757 N88-26355

Research in computer science 1985/6
[PB88-113840] 20 p2835 N88-26815

Script editor: An editor for the specification phase in the development of computer based learning
[REPT-87-68] 20 p2839 N88-26846

Fixpoint representations of characteristic sets of linear-time temporal formulas
[CWI-CS-R8754] 20 p2840 N88-26849

NEXT: An expert system development tool to support engineering design
[NLR-MP-86070-U] 20 p2843 N88-26871

Design and development of courseware for goniometry
[REPT-87-73] 20 p2881 N88-27106

Control of free-flying space robot manipulator systems
[NASA-CR-183104] 21 p2957 N88-27563

Space shuttle natural environment analysis
[NASA-CR-179337] 21 p2976 N88-27676

Block Oriented Simulation System (BOSS)
[NASA-CR-182947] 21 p2995 N88-27790

The programmer's apprentice project: A research overview
[AD-A192784] 21 p2996 N88-27769

Software engineering guidelines for RASP and ANDECS: Requirements and architectural design
[DFVLR-MITT-88-07] 21 p3000 N88-27793

FORTRAN 77 implementation of abstract datatype models
[DFVLR-MITT-88-08] 21 p3000 N88-27794

A PRELUDE (analysis and design of control systems-preliminary utilities depository). A data-based interactive system of control software, user's guide
[DFVLR-MITT-88-12] 21 p3000 N88-27795

The management of software in airborne recording systems 22 p3035 N88-28019

Software engineering for the EBR-2 data acquisition system conversion
[DE88-009850] 22 p3136 N88-28647

Appraisal of prototype PASCAL program validation suite
[NPL-DITC-112/88] 22 p3139 N88-28665

ALGRES: A system for the specification and prototyping of complex databases
[REPT-87-018] 22 p3140 N88-28668

On eclecticism in specifications: A case study centered around Petri nets --- software engineering
[REPT-87-008] 22 p3140 N88-28671

Using Petri nets for real-time development environments
[REPT-88-005] 22 p3141 N88-28679

Verification and tests --- space projects
22 p3160 N88-28814

The SMITE object oriented backing store
[RSRE-MEMO-4147] 23 p3244 N88-29308

Investigation of the use of High Order Languages (HOLs) for on-board software
[CRI/FR/HOL-C/1/87] 23 p3251 N88-29349

A software engineering approach to expert system design and verification 23 p3252 N88-29356

Automated software development workstation
23 p3263 N88-29423

An expert system for natural language processing
23 p3263 N88-29426

Advanced information processing system: Input/output network management software
[NASA-CR-181678] 23 p3264 N88-29431

Central user and browse service --- ERS-1 ground segment
CU-PG-MDA-SY-0005] 23 p3297 N88-29637

Improvements of DCAP 1, phase 2-3/A
[D2-RP-AI-106] 24 p3414 N88-30325

The need for a comprehensive expert system development methodology 24 p3421 N88-30362

Study of software requirements and artificial intelligence techniques for robotics
[TL-3333] 24 p3422 N88-30365

The P-3 Scheduling Support System (P-3 S3)
[AD-A194824] 24 p3436 N88-30450

SOFTWARE TOOLS

An evaluation of WPS-Plus word processing software for the IBM PC and compatibles
[DE87-011972] 01 p0081 N88-10518

Benchmarking the Connection Machine
[DE87-013500] 02 p0218 N88-11374

The VAXONLINE software system at Fermilab
[DE87-013565] 02 p0220 N88-11387

A general approach to error propagation
[DE87-014287] 02 p0224 N88-11412

Electronic authoring tools
[DE87-011797] 02 p0248 N88-11567

Microcomputer control of spectroscopic instruments
[ATR-86(8431)-4] 03 p0326 N88-12058

A scientific workstation operator-interface for accelerator control
[DE87-014689] 03 p0362 N88-12278

The structure-mapping engine: Algorithm and examples
[AD-A184042] 03 p0368 N88-12315

Image processing for optical engineering applications
[PB87-210035] 03 p0376 N88-12364

IDMS application documentation made easy
[DE88-000199] 03 p0384 N88-12416

Guidelines for preparing software user documentation
[NASA-CR-181550] 04 p0480 N88-12959

A network definition and solution of simulation problems
[DE88-000675] 04 p0481 N88-12962

On the next generation of reliability analysis tools
[NASA-CR-178380] 04 p0487 N88-13000

A requirements specification for a software design support system
[NASA-CR-182333] 05 p0637 N88-13896

Software-implemented fault insertion: An FTMP example
[NASA-CR-178423] 06 p0761 N88-14668

Documentation in a software maintenance environment
[AD-A185892] 07 p0901 N88-15459

After ten years of metafiles: Where does the Computer Graphics Metafile fit
[DE88-001840] 07 p0904 N88-15474

A multiple node software development environment
[DE87-010995] 07 p0905 N88-15484

Integration of symbolic and algorithmic hardware and software for the automation of space station subsystems
[NASA-TM-89705] 07 p0907 N88-15497

Research in progress at the Institute for Computer Applications in Science and Engineering
[NASA-CR-181607] 08 p1053 N88-16354

CLIPS: An expert system tool for delivery and training
08 p1056 N88-16368

Interactive knowledge acquisition tools
08 p1060 N88-16401

Standardization of software development
[INPE-4330-NTE/272] 08 p1068 N88-16455

Development of a comprehensive software engineering environment 09 p1203 N88-17211

Building validation tools for knowledge-based systems
09 p1207 N88-17235

Hardware/software reliability study --- space programs
[REPT-65.5686] 09 p1218 N88-17307

An approach to the hierarchical specification, design and verification of software
[RSRE-MEMO-4063] 09 p1223 N88-17332

Concept of a programmable maintenance processor applicable to multiprocessing systems
[NASA-TM-100406] 09 p1223 N88-17333

Nonpreemptive run-time scheduling issues on a multitasked, multiprogrammed multiprocessor with dependencies, bidimensional tasks, folding and dynamic graphs
[DE88-003598] 09 p1223 N88-17335

Navigation recovery block design description
[NASA-CR-182473] 10 p1342 N88-18022

On parallelism in software/hardware design tools
10 p1374 N88-18200

An applicative programmer's approach to matrix algebra, lessons for hardware and software
10 p1382 N88-18251

Factors causing unexpected variations in Ada benchmarks
[AD-A187231] 10 p1386 N88-18291

Chips: A tool for developing software interfaces interactively
[AD-A187499] 10 p1389 N88-18295

The performance of software-managed multiprocessor caches on parallel numerical programs
[DE88-003590] 10 p1393 N88-18308

EUROSIM: A concept of total system support
12 p1590 N88-19523

Quality control of upper air conventional data (TEMP and PILOT)
[INPE-4223-RPE/546] 12 p1647 N88-19862

A knowledge acquisition tool for the intelligent processing of materials
[AD-A186982] 12 p1679 N88-20036

Investigation of low energy space plasma
[NASA-CR-182611] 12 p1694 N88-20138

Development of a dependency theory toolbox for database design
[AD-A188872] 12 p1707 N88-20216

Western aeronautical test range real-time graphics software package MAGIC
[NASA-TM-100425] 13 p1757 N88-20506

Advanced human factors engineering tool technologies
[AD-A189390] 13 p1812 N88-20825

MacCAD (Macintosh Computer Aided Design), computer aided design tool for system analysis
[AD-A189241] 13 p1815 N88-20843

Steps into a geometer's workbench
[CWI-CS-R8726] 13 p1819 N88-20870

A packet-switched wide-area communication network simulator
[FUB-3-1986] 14 p1905 N88-21381

Public tool interfaces for software development environments
[RSRE-87004] 14 p1958 N88-21674

Ada tasking in Ten15
[RSRE-MEMO-4074] 14 p1958 N88-21676

The software repeater (an exercise in Z specification)
[RSRE-MEMO-4090] 14 p1958 N88-21677

Reliability analysis within a Computer Aided Engineering (CAE) infrastructure
[NLR-MP-86059-U] 15 p2074 N88-22369

Supercomputer environment
[AD-A190633] 15 p2107 N88-22551

A graphics editor for structured analysis with a data dictionary
[AD-A190618] 15 p2112 N88-22584

Using Colored Stochastic Petri Net (CS-PN) software for protocol specification, validation, and evaluation
[ENST-87C004] 15 p2113 N88-22588

The Colored Stochastic Petri Net (CS-PN) software: Application to the validation and the performance evaluation of distributed systems
[ENST-87D005] 15 p2113 N88-22589

Two-dimensional graphics tools for a transputer based display board
[NASA-TM-100820] 15 p2113 N88-22591

A fault tolerant supervision system
[INPE-4419-TDL/307] 15 p2148 N88-22819

An integrated and modular digital modeling approach for the space station electrical power system development
[NASA-TM-100904] 16 p2170 N88-22935

Integrated multidisciplinary analysis tool IMAT users' guide
[NASA-TM-100605] 16 p2223 N88-23273

The official handbook of MASCOT, version 3.1, issue 1 --- software tool
[BR103975] 16 p2246 N88-23419

HIFI: A design method for implementing signal processing algorithms on VLSI processor arrays
[ETN-88-92238] 16 p2247 N88-23421

The PROMISE simulation system: Software for the simulation of parallel processes
[NLR-MP-86077-U] 16 p2247 N88-23427

The synthesizer generator, a useful tool?
[REPT-87-77] 16 p2250 N88-23443

A description of an automated database comparison program
[NASA-TM-100609] 16 p2253 N88-23463

The Design, Development and Testing of Complex Avionics Systems
[AGARD-CP-417] 17 p2302 N88-23767

Managing advanced avionic system design
17 p2304 N88-23783

Advanced development of a cockpit automation design support system 17 p2304 N88-23785

Design and development of an avionics system adapted to helicopter missions 17 p2305 N88-23786

Testing complex avionics software: A practical experience 17 p2306 N88-23794

Developing systems using state-of-the-art CAD/CAM technology 17 p2306 N88-23795

Software engineering for the British Aerospace Experimental Aircraft Programme (EAP)
17 p2306 N88-23798

Avionics systems: Development method and computer tools 17 p2306 N88-23799

A software life cycle support environment
17 p2306 N88-23800

Workshops for the design of avionics systems and the development of onboard software
17 p2307 N88-23802

Coherent functional development: Key to successful future system integration 17 p2307 N88-23803

Automatically generated acceptance test: A software reliability experiment
[NASA-CR-181667] 17 p2347 N88-23984

A software design tool for the analysis of robot dynamics properties
[NLR-MP-86064-U] 17 p2385 N88-24171

The Environment for Application Software Integration and Execution (EASIE) version 1.0. Volume 4: System installation and maintenance guide
[NASA-TM-100576] 17 p2386 N88-24185

Parallel processors and nonlinear structural dynamics algorithms and software
[NASA-CR-182925] 17 p2387 N88-24187

Third Conference on Artificial Intelligence for Space Applications, part 2
[NASA-CP-2492-PT-2] 17 p2387 N88-24188

Integration of symbolic and algorithmic hardware and software for the automation of space station subsystems
17 p2387 N88-24190

Automatic program generation from specifications using PROLOG 17 p2388 N88-24196

Graphics software tool for VT terminals (VTGRAPH)
[NASA-TM-100331] 17 p2389 N88-24201

Description of graphics translation software between Intergraph and Tektronix systems
[NASA-TM-100335] 17 p2389 N88-24202

New York TRACON demonstration of program recoding requirements analysis document
[DOT/FAA/CT-87/34] 18 p2462 N88-24622

The Environment for Application Software Integration and Execution (EASIE), version 1.0. Volume 3: Program execution guide
[NASA-TM-100575] 18 p2558 N88-25184

The -mdoc macro package: A software tool to support computer documentation standards
[DE88-000500] 18 p2559 N88-25188

NFEARS: A nonlinear adaptive finite element solver, part 1
[AD-A191823] 18 p2563 N88-25215

PHOTODIGITIZE: A software/hardware system
[DE88-009575] 19 p2716 N88-26125

GRAPHICS MANAGER (GFXMGR): An interactive graphics software program for the Advanced Electronics Design (AED) graphics controller, Model 767
[DE88-010370] 19 p2717 N88-26131

The UMAC simulator 20 p2834 N88-26811

A multiprocess operating system for 16 bit microcomputers or porting Unix (trademark) to a NS32016 with enhancements 20 p2836 N88-26822

Numerical optimization, system theoretic and software tools for the integrated design of flexible structures and their control systems
[AD-A192927] 21 p2895 N88-27183

User's manual for the two-dimensional transputer graphics toolkit
[NASA-TM-100974] 21 p3001 N88-27799

Improving the performance of AI algorithms
[AD-A192848] 21 p3003 N88-27809

Software modifications to total data reporting accessory for metabolic measurement cart
[AD-A193641] 22 p3132 N88-28623

Software quality measurement demonstration project (1)
[AD-A193429] 22 p3136 N88-28646

Software engineering for the EBR-2 data acquisition system conversion
[DE88-009950] 22 p3136 N88-28647

Appraisal of prototype PASCAL program validation suite
[NPL-DITC-112/88] 22 p3139 N88-28665

Validation code for the Whetstone Benchmark
[NPL-DITC-107/88] 22 p3140 N88-28667

ALGRES: A system for the specification and prototyping of complex databases
[REPT-87-018] 22 p3140 N88-28668

Artificial intelligence software acquisition program, volume 2
[AD-A194239] 22 p3141 N88-28680

Signal processing software for ground penetrating radar, user's manual
[AD-A194286] 23 p3203 N88-29059

Software development without languages
23 p3257 N88-29392

Knowledge based programming environments: A perspective 23 p3258 N88-29393

Requirements for a tool to aid in the development of expert systems for space station applications
23 p3258 N88-29398

Benchmarking expert system tools
23 p3259 N88-29399

Two implementations of the Expert System for the Flight Analysis System (ESFAS) project
23 p3259 N88-29400

A flexible search strategy for production systems
23 p3262 N88-29420

AI tools in computer based problem solving
23 p3263 N88-29424

Networking and AI systems: Requirements and benefits 23 p3263 N88-29425

Expert system technology as a data processing tool
23 p3263 N88-29427

Artificial intelligence software acquisition program, volume 1
[AD-A194104] 23 p3267 N88-29447

Central user and browse service --- ERS-1 ground segment
[CU-PG-MDA-SY-0005] 23 p3287 N88-29637

Quality measures and assurance for AI (Artificial Intelligence) software
[NASA-CR-4187] 24 p3411 N88-30304

An operations manual for the digital data system
[NASA-CR-181688] 24 p3415 N88-30329

The proposal entry processor: Telescience applications for Hubble Space Telescope science operations
24 p3417 N88-30339

SOI (SEMICONDUCTORS)

Epitaxial reactor development for growth of silicon-on-insulator devices
[AD-A184758] 03 p0382 N88-12399

Silicon-on-insulator electronics for a space nuclear power system 17 p2431 N88-24461

JFET/SOS (Junction Field-Effect Transistor/Silicon-on-Sapphire) devices: Gamma-radiation-induced effects
[AD-A193001] 20 p2795 N88-26586

Silicon-on-insulator pin diodes
[AD-A193359] 21 p2937 N88-27445

Evaluation of silicon-on-insulator MOS (Metal-Oxide-Semiconductor) transistor response to 10-keV X-ray and cobalt-60 irradiation
[DE88-006102] 23 p3206 N88-29082

SOIL EROSION

Remote Sensing-Arid Lands Workshop, Page, Arizona, June 10-12, 1986
[DE87-012368] 01 p0064 N88-10412

Environmental processes and spectral reflectance characteristics associated with soil erosion in desert fringe regions
[NASA-CR-182332] 05 p0620 N88-13811

Soil erosion and causative factors at Vandenberg Air Force Base, California
[NASA-TM-100981] 17 p2381 N88-24156

SOIL MAPPING

The Earthnet Heat Capacity Mapping Mission (HCMM) data-processing system at Lannion (France)
09 p1127 N88-16761

Development of remote sensing techniques capable of delineating soils as an aid to soil survey
[NASA-CR-182610] 15 p2069 N88-22452

Comparative study of crop and soil mapping using multitemporal and multispectral SPOT and LANDSAT data 22 p3091 N88-28354

SPOT images and geochemical mapping of lateritic covers in southern Mali 22 p3105 N88-28438

SOIL MECHANICS

Enhancement of surface-atmosphere fluxes by desert-fringe vegetation through reduction of surface albedo and of soil heat flux
[NASA-CR-181442] 02 p0197 N88-11231

Explicit and implicit soil modelling for dynamic soil-structure interaction problems
04 p0428 N88-12650

Error analysis for geotechnical engineering
[AD-A186795] 09 p1189 N88-17124

Computer Applications in Geotechnical Engineering (CAGE) and Geotechnical aspects of the Computer-Aided Structural Engineering (G-CASE) projects. User's guide. UTEXAS2 slope-stability package. Volume 1: User's manual
[AD-A187674] 11 p1511 N88-19025

A parametric study of embedded cantilever retaining walls: The results of a finite element study
[RR-CE83] 24 p3383 N88-30152

Computer-Aided Structural Engineering (CASE) project. Development of design formulas for ribbed mat foundations on expansive soils
[AD-A194807] 24 p3412 N88-30307

SOIL MOISTURE

Moisture determinations in and under vegetation canopies. Part 2: Results after parameterization of the CLOUD model
[FEL-1986-63] 01 p0064 N88-10410

Characterization of 6 soils in the X-band, through measurements of complex permittivity
[INPE-4376-TDL/302] 12 p1639 N88-19814

An introduction to the parameterization of land-surface processes 14 p1937 N88-21554

Measurement of the water content of soil from space and application to the regional water balance
14 p1938 N88-21561

Theory of neutron moisture probes and interpretation of measurements in complex soil and water systems
17 p2342 N88-23965

An update on remote measurement of soil moisture over vegetation using infrared temperature measurements: A FIFE perspective
[NASA-CR-182926] 17 p2370 N88-24109

Microwave remote sensing at INPE (Institute for Space Research) Brazil: Concepts and future prospects of soil moisture studies
[INPE-4569-PRE/1310] 24 p3388 N88-30178

SOIL SCIENCE

Significance of foundation-soil separation in dynamic soil-structure interaction 05 p0596 N88-13641

The unsteady ground heat flow at the contact surface between a glacier run and the subsoil
08 p1014 N88-16147

A semianalytical solution of the heat conduction equation for several boundary conditions
08 p1014 N88-16148

Aerosols in Martian Atmosphere and Natural Dust Observation (AMANDO). Proposal for the Mars orbiter balloon and rover to study the Martian atmosphere, its thermal content, and its interaction with the soil
[IFSI-87-9] 08 p1100 N88-16619

Critical comparison of moving average and cumulative summation control charts for trace analysis data
[AD-A188312] 12 p1705 N88-20203

SOILS

NT ALLUVIUM
NT LATERITES
NT LUNAR SOIL
NT SANDS
NT TAR SANDS

Significance of foundation-soil separation in dynamic soil-structure interaction 05 p0596 N88-13641

Analysis of airborne imaging spectrometer data for the Ruby Mountains, Montana, by use of absorption-band-depth images 05 p0614 N88-13771

An analytical soil thermodynamic model for the diurnal variation of ground surface temperature
[AD-A185388] 05 p0625 N88-13823

Computer-aided analysis for the Mechanics of Granular Materials (MGM) experiment, part 2
07 p0926 N88-15626

Global digital data sets of soil type, soil texture, surface slope and other properties: Documentation of archived data tape
[NASA-TM-100685] 09 p1185 N88-17097

Detection of soil erosion with Thematic Mapper (TM) satellite data within Pinyon-Juniper woodlands
[NASA-CR-182476] 09 p1185 N88-17103

Thermal properties of soil: A case study
[INPE-4332-TDL/289] 12 p1637 N88-19803

Characterization of 6 soils in the X-band, through measurements of complex permittivity
[INPE-4376-TDL/302] 12 p1639 N88-19814

Modeling surface exchanges: The soil-vegetation-atmosphere continuum
14 p1937 N88-21553

Sensitivity of general circulation models to surface processes 14 p1937 N88-21556

Development of remote sensing techniques capable of delineating soils as an aid to soil survey
[NASA-CR-182610] 15 p2089 N88-22452

Mapping soil and rock variation from satellite images in the Sahel 17 p2354 N88-24023

Indentification of shallow groundwater regions in semi-arid Brazil by remote sensing methods
17 p2355 N88-24030

Characteristics of drainage determinations in aerial photographs and relief determination on different scales planialtimetric charts for three soils in the state of Sao Paulo 17 p2367 N88-24095

Botany Facility: Problems of water supply, plant nutrients and soil in the Botany Facility
[SIRA-A/7373/WP220/RJS/003]
17 p2379 N88-24141

Monitoring biological impacts of space shuttle launches from Vandenberg Air Force Base: Establishment of baseline conditions
[NASA-TM-100982] 18 p2549 N88-25133

The impact of hemp production on the development of the municipalities of Araras, Leme, Santa Cruz da Conceicao and Pirassununga 19 p2683 N88-25948

Vegetation studies on Vandenberg Air Force Base, California
[NASA-TM-100985] 20 p2831 N88-26795

Direct determination of part-per-billion levels of volatile organics in water and soil samples using glow discharge mass spectrometry
[DE88-011389] [illegible] p2910 N88-27272

Analysis of soils using remote sensing information at the scale of the parcel 22 p3095 N88-28361

Use of LANDSAT images of vegetation cover to estimate effective hydraulic properties of soils
[NASA-CR-183185] 22 p3116 N88-28514

Nonseismic, surface geophysical and geochemical prospecting technology
[PB88-196613] 23 p3227 N88-29207

Spectral characteristics and the extent of paleosols of the Palouse formation
[NASA-CR-180947] 23 p3228 N88-29210

Regional environmental studies using national data bases and GIS (Geographic Information System)
[DE88-008368] 23 p3230 N88-29225

Viking Landers and remote sensing
23 p3304 N88-29685

The surface composition of Mars from earthbased observations 23 p3306 N88-29696

Reflectance pattern and the physical and chemical characteristics of three Brazilian Oxisols
[INPE-4590-PRE/1320] 24 p3387 N88-30172

The dynamics of transuranics and other radionuclides in natural environments, December 1985
[DE87-014456] 24 p3390 N88-30189

Estimation of soil temperature profile from remote microwave and IR measurements
24 p3450 N88-30532

SOL-GEL PROCESSES

Stress measurements in sol-gel films
[DE87-014467] 02 p0153 N88-10955

Preparation of oxide glasses from metal alkoxides by sol-gel method
[NASA-TT-20124] 02 p0154 N88-10965

Study of ceramic-fiber/ceramic sol-gel based matrix composites
[SNIAS-872-430-120] 05 p0569 N88-13469

Exploitation of the sol-gel route in processing of ceramics and composites
[AD-A185482] 06 p0686 N88-14204

On 1064 nm and 350 nm laser damage thresholds of high index oxide films deposited from organic solutions and sols
[DE88-001636] 07 p0859 N88-15217

The influence of processing variables on physical properties of sol-gel derived TiO2 films
[DE88-005155] 11 p1559 N88-19331

Structure of sol-gel silica
[DE88-006870] 15 p2033 N88-22114

Sol/gel processing techniques for glass matrix composites
[AD-A191748] 18 p2478 N88-24701

Manufacturing of a ceramic-ceramic composite matrix using the sol-gel procedure
[ETN-88-92157] 20 p2768 N88-26414

Characterization of the surface area and porosity of sol-gel films using saw devices
[DE88-008794] 20 p2875 N88-27069

Preparation and properties of new inorganic glasses and gel-derived solids
[AD-A192922] 21 p2917 N88-27315

Ellipsometric imaging of drying sol-gel films
[DE88-011785] 21 p2921 N88-27335

Application of sol-gel procedures to ceramic composites
[ETN-88-92741] 21 p2921 N88-27336

Comparison of sol-gel procedures for zircon and alumina
[REPT-881-430-106] 21 p2922 N88-27342

Sol-gel processing of metal-oxide-semiconductor structures
[DE88-009853] 22 p3156 N88-28778

Electrical properties of metal-oxide-silicon structures with sol-gel oxides
[DE88-011791] 22 p3156 N88-28779

Sol-gel kinetics: Si(sup)29 NMR and a statistical reaction model
[DE88-011545] 23 p3191 N88-28988

The sol-gel synthesis of ceramics
[SNIAS-881-430-114] 23 p3199 N88-29037

Al2O3-TiO2 and Al2TiO5 ceramic materials
[SNIAS-881-430-122] 23 p3199 N88-29038

Development of high efficiency q-switched glass laser via sol-gel processing
[AD-A192301] 23 p3218 N88-29154

SOLAR ACTIVITY

NT FACULAE
NT SOLAR FLARES
NT SOLAR PROMINENCES
NT SPICULES
NT SUNSPOTS

Low altitude flux and dose measurements during two solar flare events 01 p0111 N88-10713

Probable detection of solar neutrons by ground-level neutron monitors during STIP interval 16
01 p0111 N88-10715

Solar energetic particles events observed by Prognoz-10 Intercosmos (May-October 1985)
01 p0111 N88-10716

The large Type 4 radio burst event of 24 April 1985 interpreted by dynamic spectral recordings and associated recordings 01 p0112 N88-10717

Propagating shocks in the corona
01 p0112 N88-10718

Solar origins of coronal mass ejections
01 p0113 N88-10726

Radio studies of large scale structures of the Sun's corona and transient activity 01 p0114 N88-10728

Solar events and their influence on the interplanetary medium 01 p0115 N88-10734

Solar activity, magnetic clouds, and geomagnetic storms 01 p0115 N88-10735

Quantification of the background signal to solar neutrino detection from cosmogenic activation of the atmosphere
[DE87-013830] 01 p0119 N88-10762

Magnetic fields in the overshoot zone: The great escape 02 p0256 N88-11616

A numerical study of the thermal stability of solar loops 02 p0256 N88-11619

The Sun and the solar activity
03 p0271 N88-11704

Irradiations. Accumulated doses. Heavy ions --- space environment 03 p0272 N88-11706

Solar magnetic and velocity fields
[AD-A184360] 03 p0390 N88-12449

Asymmetry and variations of solar limb darkening along the diameter defined by diurnal motion in April 1981
04 p0506 N88-13111

Calibration of the Ca II K line-core density and the magnetic flux density in stars using solar data
04 p0507 N88-13116

Three-halves law in sunspot cycle shape
[NASA-CR-181520] 04 p0525 N88-13210

The appearance and disappearance of magnetic flux on the quiet sun
[AD-A185432] 05 p0661 N88-14055

Solar-geophysical data number 515, July 1987. Part 1: (Prompt reports). Data for June 1987, May 1987 and late data
[PB87-233177] 06 p0805 N88-14912

Solar-geophysical data number 515, July 1987. Part 2: (Comprehensive reports). Data for January 1987 and miscellanea
[PB87-233185] 06 p0805 N88-14913

Solar-geophysical activity reports for STIP (Study of Travelling Interplanetary Phenomena) interval 15, 12-21 February 1984 ground level event and STIP interval 16, 20 April-4 May 1984 Forbush decrease
[PB87-232658] 06 p0805 N88-14915

Quasiperiodic variations in manifestations of solar activity 08 p1004 N88-16083

Prediction of the next solar activity cycle
08 p1035 N88-16276

Bern solar observations. Solar data for January-December 1986
[REPT-53] 09 p1263 N88-17569

Neutrino magnetic moment and time variation of solar neutrino flux
[DE88-700687] 10 p1430 N88-18542

Development of high stability fiber optic spectrophotometric systems for study of solar/stellar magnetic activity
[AD-A189327] 13 p1852 N88-21088

Sunspot frequency and solar activity
[PUBL-17/87] 14 p2011 N88-21996

Table of solar activity associated with coronal mass ejections observed by the SMM coronagraph/polarimeter in 1980
[PB88-170881] 14 p2011 N88-21998

Solar-geophysical data number 520, December 1987. Part 2: (Comprehensive reports). Data for June 1987 and miscellanea
[PB88-164207] 15 p2152 N88-22849

Development of a digital sun sensor for a spin-stabilized satellite
[INPE-4508-TDL/327] 16 p2169 N88-22929

The gamma-ray spectrometer experiment on the solar maximum mission satellite
[NASA-CR-182977] 17 p2452 N88-24569

The SAMEX vector magnetograph: A design study for a space-based solar vector magnetograph
[NASA-TM-4048] 18 p2596 N88-25424

Automated spectrometric unit for the study of radiation characteristics of cosmic radiation aboard Prognoz-9 space stations 19 p2706 N88-26090

Solar microwave radiation maps measured at Metsaehovi Radio Research Station in 1980-1981
[PB88-193453] 19 p2741 N88-26276

Solar-geophysical data number 521, January 1988. Part 1: (Prompt reports). Data for December 1987, November 1987 and late data
[PB88-179213] 19 p2743 N88-26284

Diffusion of slight solar induced disturbances in the middle atmosphere
[MITT-53] 20 p2825 N88-26758

Solar-geophysical data number 522, February 1988. Part 2: (Comprehensive reports). Data for August 1987 and miscellanea
[PB88-194741] 20 p2886 N88-27138

Solar-geophysical data number 522, February 1988. Part 1: (Prompt reports). Data for January 1988, December 1987 and late data
[PB88-194733] 20 p2886 N88-27139

Modeling, designing and simulating a pointing control system for balloon-borne solar experiments
[NASA-TM-100337] 22 p3082 N88-28300

SOLAR ACTIVITY EFFECTS

The Sun and the solar activity
03 p0271 N88-11704

Contributions of lidar measurements to the study of long term variations of the middle atmosphere
[ETN-88-91237] 05 p0625 N88-13824

Characteristics of atmospheric disturbances with a quasi-two day period 06 p0734 N88-14515

On the dependence of the lower thermospheric wind regime on the solar cycle 06 p0736 N88-14524

Radar observations of high-latitude lower-thermospheric and upper-mesospheric winds and their response to geomagnetic activity 06 p0742 N88-14563

Solar-geophysical data number 515, July 1987. Supplement (explanation of data reports)
[PB87-233169] 06 p0805 N88-14914

New book on space ecology reviewed
07 p0897 N88-15434

Dynamics and turbulence of solar wind in area of its formation based on radio transmission data measured with Venera-15 and Venera-16 spacecraft
08 p1003 N88-16080

Peculiarities of daytime ionosphere of Venus during years of low and high solar activity
08 p1005 N88-16091

Distribution of electron concentration in nighttime atmosphere of Venus based on radio transmission data
08 p1005 N88-16092

Interplanetary and geophysical effects of a coronal transient 08 p1095 N88-16587

Solar-geophysical data number 516, August 1987. Part 1: (Prompt reports). Data for July 1987, June 1987 and late data
[PB88-114368] 09 p1263 N88-17570

Solar-geophysical data number 516, August 1987. Part 2: (Comprehensive reports). Data for February 1987
[PB88-114376] 09 p1264 N88-17571

Upper-thermospheric observations and neutral-gas dynamics at high latitudes during solar maximum
[AD-A188058] 11 p1512 N88-19031

The effects of solar cycle and latitude dependence on the formation of ionospheric C layer
[INPE-4342-TDL/293] 16 p2232 N88-23332

Diffusion of slight solar induced disturbances in the middle atmosphere
[MITT-53] 20 p2825 N88-26758

Advanced Receiver tracking of Voyager 2 near solar conjunction 22 p3065 N88-26185
X-band noise temperature near the Sun at a 34-meter high efficiency antenna 22 p3067 N88-26200
Variations in the atmosphere associated with the 11-year solar cycle 22 p3122 N88-28557

SOLAR ARRAYS
Phase 3 study of selected tether applications in space. Volume 2: Study results
[NASA-CR-179186] 02 p0132 N88-10826
Imaging interferometry with non-redundant arrays
02 p0257 N88-11624
Environmental interactions of solar generators in space 03 p0274 N88-11730
Electricity from photovoltaic solar cells. Flat-Plate Solar Array Project of the US Department of Energy's National Photovoltaics Program: 10 years of progress
[NASA-TM-89653] 03 p0348 N88-12188
Characteristics of current solar central receiver projects
[DE88-001314] 04 p0466 N88-12880
The high performance solar array GSR3
[SNIAS-872-422-106] 05 p0622 N88-13814
Study of large solar arrays (SOLA), phase 2A
[BAE-SS/1109] 09 p1186 N88-17106
Study of Large Solar Arrays (SOLA). Phase 2A: Amplifying information to final report (SS/1109)
[BAE-SS/1110] 09 p1248 N88-17480
Oxidation and protection of fiberglass-epoxy composite masts for photovoltaic arrays in the low Earth orbital environment
[NASA-TM-100839] 11 p1465 N88-18734
Mast material test program (MAMATEP)
[NASA-TM-100821] 12 p1604 N88-19592
Vega-1 and Vega-2 automatic stations: Functioning of flyby vehicles during encounter with Halley's comet
13 p1725 N88-20314
Direct absorption receiver control studies
[DE87-013653] 13 p1795 N88-20737
The development status of the strongback array --- spacecraft structure 14 p1875 N88 21201
The SPOT solar array. Box opening mechanisms physical vapor deposition (PVD)-MoS2: Lubricated slides. Functional evaluation 14 p1876 N88-21211
Qualification testing of the EUROSTAR Solar Array Drive Mechanism (SADM) 14 p1879 N88-21229
Solar cell experiment on the first satellite of the Brazilian complete space mission
[INPE-4248-PRE/1121] 14 p1880 N88-21238
Contamination of optical surfaces --- Space Station
18 p2592 N88-25400
Assessment of the effects of space debris and meteoroids environment on the space station solar array assembly
[NASA-TM-101315] 23 p3185 N88-28959
Advanced planar array development for space station
[NASA-CR-179373] 24 p3389 N88-30181
Alternative module configurations for advanced solar arrays on low orbit and extended lifetime missions (AMOC 2)
[ESA-CR(P)-2581] 24 p3389 N88-30182

SOLAR ATMOSPHERE
What's needed in the UV and EUV
02 p0255 N88-11612
First results on quiet and magnetic granulation from SOUP 02 p0255 N88-11613
Solar ultraviolet spectrum obtained from a balloon gondola 08 p1032 N88-16258
Small scale MHD wave processes in the solar atmosphere and solar wind 08 p1096 N88-16608
MHD waves in the solar atmosphere
08 p1096 N88-16609
Negative viscosity in global circulations
13 p1786 N88-20665
On the magnetic structure and energy balance of EUV-emitting plasma in the quiet Sun
17 p2452 N88-24587
The SAMEX vector magnetograph: A design study for a space-based solar vector magnetograph
[NASA-TM-4048] 18 p2596 N88-25424

SOLAR AZIMUTH
U AZIMUTH
U SOLAR POSITION

SOLAR BACKSCATTER UV SPECTROMETER
Nimbus 7 Solar Backscatter Ultraviolet (SBUV) spectral scan solar irradiance and Earth radiance product user's guide
[NASA-RP-1199] 09 p1184 N88-17096

SOLAR CELLS
NT VERTICAL JUNCTION SOLAR CELLS
Effects of electron and proton irradiations on n/p and p/n GaAs cells grown by MOCVD
[NASA-TM-100199] 01 p0042 N88-10266
High-efficiency silicon solar cells: Numerical modeling, transient measurements, efficiency goals, and v-shaped grooves
[DE87-012842] 01 p0066 N88-10423
The fundamentals of photovoltaic system electrical design
[DE87-009061] 02 p0194 N88-11214
Gallium arsenide and multibandgap solar cell research
[DE87-012260] 02 p0194 N88-11215
CuInSe2 solar cell research by sputter deposition
[DE87-001184] 02 p0195 N88-11219
Wide bandgap passivation layers on silicon
[DE87-014307] 02 p0244 N88-11543
Recent progress in space photovoltaic systems
[NASA-TM-100206] 03 p0311 N88-11966
Mechanically stacked multijunction solar cells: An update on Sandia programs
[DE87-014641] 03 p0347 N88-12190
Crystalline cell research status and direction
[DE87-014214] 03 p0382 N88-12402
Performance of GaAs and silicon concentrator cells under 37 MeV proton irradiation
[NASA-TM-100144] 04 p0465 N88-12877
Radiation performance of AlGaAs concentrator cells and expected performance of cascade structures
[NASA-TM-100145] 04 p0465 N88-12878
Characteristics of current solar central receiver projects
[DE88-001314] 04 p0466 N88-12880
The high performance solar array GSR3
[SNIAS-872-422-106] 05 p0622 N88-13814
Development of mechanically stacked tandem concentrator cells
[DE88-001926] 06 p0730 N88-14490
Surface modification using ion beams: Recent developments at ORNL
[DE88-000951] 06 p0786 N88-14819
The results of the 1984/1985 Round-Robin Calibration of Reference Solar Cells for the Summit Working Group on Technology, Growth and Employment
[DE88-900215] 07 p0874 N88-15303
Further study of inversion layer MOS solar cells
07 p0925 N88-15621
A flux analysis of the solar cells
[INPE-4247-PRE/1120] 08 p1022 N88-16186
Variable band gap materials for thermophotovoltaic generators
[AD-A186858] 09 p1186 N88-17104
Forward-biased current annealing of radiation damaged gallium arsenide and silicon solar cells
[AD-A186904] 09 p1186 N88-17105
Physico-chemical studies on copper sulfide behavior in the CdS-Cu2S solar cell
[ETN-88-91068] 09 p1187 N88-17109
A comparison of different module configurations for multibandgap solar cells
[DE88-002718] 09 p1187 N88-17113
Investigation of the subsequent treatment and the stability of CuxS-CdS thin-film solar cells
[ETN-88-91488] 11 p1507 N88-19006
Proceedings of the 1987 High-Efficiency Photovoltaic Subcontractors' Review Meeting
[DE88-003354] 11 p1508 N88-19011
Positron annihilation spectroscopy of AlGaAs/GaAs interfaces in MOCVD-grown GaAs heterojunction solar cells
[DE88-003803] 11 p1508 N88-19012
Results of the 1987 NASA/JPL balloon flight solar cell calibration program
[NASA-CR-182617] 12 p1574 N88-19413
Acoustic phonons, surface plasmons and surface acoustic plasmons in a superlattice and their nonreciprocal device applications
[AD-A188918] 12 p1698 N88-20163
Research on multibandgap solar cells
[DE87-012261] 13 p1792 N88-20721
Research on high-efficiency, stacked, multijunction, amorphous silicon alloy thin-film solar cells
[DE88-001108] 13 p1793 N88-20723
CdZnTe as a wide-band-gap absorber for a tandem, thin-film solar cell
[DE88-001114] 13 p1793 N88-20724
Research on single-crystal CdTe solar cells
[DE88-001115] 13 p1793 N88-20725
Stable, high-efficiency, CuInSe2-based, polycrystalline, thin-film tandem solar cells
[DE88-001116] 13 p1793 N88-20726
Cadmium sulfide/copper ternary heterojunction cell research
[DE88-001122] 13 p1793 N88-20727
SERI's Photovoltaic R and D Project: Recent progress and future directions
[DE88-001129] 13 p1794 N88-20728
Progress of amorphous silicon based solar cells and modules
[DE88-004666] 13 p1794 N88-20733
Thin-film cadmium telluride solar cells
[DE88-001107] 13 p1846 N88-21050
Investigations of the origins of metastable, light-induced changes in hydrogenated amorphous silicon
[DE88-001117] 13 p1846 N88-21051
Solar cell experiment on the first satellite of the Brazilian complete space mission
[INPE-4248-PRE/1121] 14 p1880 N88-21238
Polysilicon-contacted p+ emitters for silicon solar cell applications
[DE88-005106] 14 p1942 N88-21586
Considerations in GaAs standard cell design
[DE88-003310] 14 p1985 N88-21840
Thermal analysis of heat storage canisters for a solar dynamic, space power system
[DE88-004199] 15 p2027 N88-22075
Solar cell cover glasses for satellites
15 p2052 N88-22225
High-efficiency thin-film silicon-on-GaP solar cell for improved radiation resistance
[AD-A190268] 15 p2091 N88-22460
Optimization of organic Rankine cycles for space station applications 17 p2423 N88-24407
Progress in InP solar cell research
[NASA-TM-100914] 18 p2507 N88-24870
Aging behavior of Au-based ohmic contacts to GaAs
[NASA-CR-182146] 19 p2662 N88-25831
Fast parametrization procedure for solar cells
[PB88-186416] 19 p2686 N88-25966
Photovoltaic energy systems
[DE88-007504] 19 p2687 N88-25968
Study of Staebler-Wronsky degradation effect in a Si:H based P-I-N solar cells
[NASA-CR-182564] 19 p2687 N88-25970
Electrophoretic coatings. Part 1: Sandia applications
[DE88-008666] 20 p2776 N88-26465
Photovoltaic concentrator technology: Recent results
[DE88-009588] 20 p2819 N88-26726
Development of a model procedure for the determination of volume diffusion lengths by transient measurements on monocrystal silicon solar cells
[ETN-88-92119] 20 p2821 N88-26733
Photovoltaic cells with n-silicon and conductive polymers
[ETN-88-92133] 20 p2821 N88-26734
Analytical determination of critical crack size in solar cells
[NASA-CR-183128] 20 p2821 N88-26736
Solar cell modeling and simulation
[AD-A193249] 21 p2966 N88-27620
Solar energy conversion through the interaction of plasmons with tunnel junctions. Part A: Solar cell analysis. Part B: Photoconductor analysis
[NASA-CR-183044] 21 p2967 N88-27621
Device physics related to the granular nature of CuInSe2 solar cells
[DE88-001159] 21 p2967 N88-27622
Laser-heated CVD process for depositing thin films for low-cost solar-cell applications
[DE88-001162] 21 p2967 N88-27623
A comparison of the radiation tolerance characteristics of multijunction solar cells with series and voltage-matched configurations
[NASA-TM-101177] 21 p2967 N88-27624
Experimental fabrication of thin film single crystalline solar cells
[PB88-131958] 21 p2967 N88-27627
Amorphous silicon solar cells using a metal substrate
[PB88-131941] 21 p2968 N88-27628
Space photovoltaic generators. State of the art, trends
[REPT-881-440-106] 21 p2970 N88-27640
Low-band-gap, amorphous-silicon-based alloys by photochemical vapor deposition
[DE88-001165] 21 p3023 N88-27944
Laser crystallized silicon films on alumina ceramic substrates and application to thin film c-Si solar cells
[PB88-131966] 22 p3116 N88-28515
Experimental fabrication of thin film single crystalline solar cells
[PB88-131958] 22 p3116 N88-28516
Theoretical investigation on heterojunction solar cell
[DE88-701837] 23 p3229 N88-29219
Construction of gallium arsenide solar concentrator for space use
[AD-A194658] 23 p3230 N88-29222
Long-term behavior of energy production systems with the example of HELIOS and SYMPHONIE
[ETN-88-92988] 23 p3230 N88-29223
Alternative module configurations for advanced solar arrays on low orbit and extended lifetime missions (AMOC 2)
[ESA-CR(P)-2581] 24 p3389 N88-30182

SOLAR COLLECTORS
Focusing solar energy collector
02 p0159 N88-10996

Development of an innovative, low-cost solar collector
[PB87-206819] 02 p0194 N88-11210

DTA/DSC studies of phase equilibria in binary mixtures of barium carbonate with alkali carbonates
[DE87-001195] 02 p0194 N88-11213

Proceedings of the Solar Thermal Technology Conference
[DE87-014441] 02 p0195 N88-11220

Direct Absorption Receiver flow experiments
[DE87-014655] 02 p0196 N88-11221

Direct Absorption Receiver (DAR) systems assessment
[DE87-012277] 02 p0196 N88-11222

An evaluation of the LEC-460 solar collector
[DE88-000052] 02 p0196 N88-11224

Polymers in solar technologies
[DE88-001102] 03 p0294 N88-11849

Numerical and experimental investigation of the unsteady temperature distribution in solar central receivers
[ESA-TT-1050] 03 p0347 N88-12193

Crystalline cell research status and direction
[DE87-014214] 03 p0382 N88-12402

Light funnel concentrator panel for solar power
[NASA-CR-179223] 04 p0464 N88-12870

Performance of GaAs and silicon concentrator cells under 37 MeV proton irradiation
[NASA-TM-100144] 04 p0465 N88-12877

International Energy Agency (IEA) Small Solar Power Systems (SSPS) sodium cavity and external receiver performance comparison
[DE88-001310] 04 p0465 N88-12879

Characteristics of current solar central receiver projects
[DE88-001314] 04 p0466 N88-12880

Design, fabrication and delivery of a miniature Cassegranian concentrator solar array system
[NASA-CR-179237] 06 p0730 N88-14493

Mean and peak wind load reduction on heliostats
[DE87-012281] 07 p0873 N88-15296

Satellite techniques of solar resource assessment for focusing and non-focusing solar collector systems
[DE88-001657] 07 p0874 N88-15298

Performance of highly concentrating mirror collectors and collector systems
[DFVLR-FB-87-29] 09 p1186 N88-17107

Side-by-side comparisons of evacuated compound parabolic concentrator and flat plate solar collector systems at temperatures of 90 to 100°C
[DE88-004717] 10 p1351 N88-18073

A solar receiver-reactor with specularly reflecting walls for high-temperature thermoelectrochemical and thermochemical processes
[AD-A187612] 10 p1351 N88-18077

Los Alamos optical materials reliability, maintainability, and exposure testing program
[DE88-001953] 10 p1409 N88-18404

HELIOS modelling of point-focusing solar concentrators
[DE88-004933] 12 p1640 N88-19820

Control strategies and hardware used in solar thermal applications
[DE88-004631] 13 p1794 N88-20731

Direct absorption receiver control studies
[DE87-013653] 13 p1795 N88-20737

A five year weathering experiment with solar collectors
[DE88-900369] 13 p1796 N88-20740

Advanced sensible heat solar receiver for space power
[NASA-TM-100847] 14 p1882 N88-21249

Space station solar concentrator materials research
[NASA-TM-100862] 14 p1882 N88-21250

Direct conversion of solar energy to thermal energy
[BMFT-FB-T-86-220] 14 p1943 N88-21592

Thermal modeling of solar central receiver cavities
[DE88-004940] 14 p1943 N88-21534

Ray tracing optical analysis of offset solar collector for space station solar dynamic system
[NASA-TM-100853] 15 p2027 N88-2208C

Development of an integrated heat pipe-thermal storage system for a solar receiver
[NASA-TM-101099] 15 p2091 N88-22458

Progress in InP solar cell research
[NASA-TM-100914] 18 p2507 N88-24870

Evaluation of the chromium oxide arc spraying treatment on solar energy collectors
[ETN-88-92584] 18 p2537 N88-25053

Design and demonstration of a system for the deposition of atomic-oxygen durable coatings for reflective solar dynamic power system concentrators
[NASA-CR-4158] 19 p2606 N88-25474

Thermal distortion analysis of the space station solar dynamic concentrator
[NASA-TM-100868] 19 p2606 N88-25475

Dielectric compound parabolic concentrating solar collector with frustrated total internal reflection absorber
[DE88-009986] 19 p2688 N88-25976

Advanced heat receiver conceptual design study
[NASA-CR-180901] 19 p2688 N88-25977

Influence of refractive index and solar concentration on optical power absorption in slabs
[NASA-TM-4056] 19 p2726 N88-26190

Performance sensitivities for point-focus dish systems with secondary concentrators
[DE88-001152] 21 p2968 N88-27629

Calculation of the specific and volumetric enthalpies of Ge-Si alloys
[DE88-008949] 21 p3026 N88-27965

Lewis Research Center space station electric power system test facilities
[NASA-TM-100924] 23 p3182 N88-28942

Construction of gallium arsenide solar concentrator for space use
[AD-A194658] 23 p3230 N88-29222

The effect of the near earth micrometeoroid environment on a highly reflective mirror surface
[NASA-TM-101307] 24 p3332 N88-29833

SOLAR COMPANION STAR
U NEMESIS (STAR)

SOLAR CONSTANT

Aerosol optical depth and ratios of diffuse-sky to total solar irradiance measured from aircraft following the eruption of El Chichon
[PB88-100789] 07 p0878 N88-15326

SOLAR CONVERTERS
U SOLAR GENERATORS

SOLAR CORONA
NT CORONAL HOLES
NT CORONAL LOOPS

Propagating shocks in the corona
01 p0112 N88-10718

Magnetic field twist driven by remote convective motions: Characteristics and twist rates 01 p0113 N88-10724

Solar origins of coronal mass ejections
01 p0113 N88-10726

On the association of erupting magnetic fields with eruptive prominences and coronal mass ejections
01 p0113 N88-10727

Radio studies of large scale structures of the Sun's corona and transient activity 01 p0114 N88-10728

Observations of the brightness temperature distribution of the quiet solar corona at decametric wavelengths
01 p0114 N88-10729

Meterwave observations of a coronal hole
01 p0114 N88-10730

Coronal and interplanetary Type 2 radio emission
01 p0114 N88-10731

Coronal mass ejections: The long-term variation of their occurrence rate and the solar wind mass flux
01 p0114 N88-10732

Was the eclipse comet of 1893 a disconnected coronal transient? 01 p0115 N88-10733

High-resolution continuum observations of the Sun
02 p0255 N88-11614

Statistical properties of small high-velocity events in the solar transition region 04 p0506 N88-13112

Magnetic field draping about coronal mass ejecta
[DE88-001805] 05 p0661 N88-14057

Astrophysics and the solar nebula
07 p0883 N88-15355

Exobiology and life science 07 p0883 N88-15358

Total light flux and colour of solar corona
[PB87-143335] 07 p0946 N88-15754

Proceedings of the 21st ESLAB Symposium on Small Scale Processes in the Chromosphere/Corona, Interplanetary Medium and Planetary Magnetospheres
[ESA-SP-275] 08 p1094 N88-16582

Solar corona and solar wind 08 p1094 N88-16584

Observations and modeling of the prominence/corona transition region 08 p1094 N88-16585

Gasflows in the transition region above sunspot
08 p1095 N88-16586

Interplanetary and geophysical effects of a coronal transient 08 p1095 N88-16587

Flux tubes and loops in the solar chromosphere and corona 08 p1095 N88-16591

Emerging flux, magnetic reconnection, plasma turbulence and waves in the transition zone of the solar atmosphere 08 p1096 N88-16597

The effects of viscosity on resistive ballooning modes in line-tied coronal magnetic fields
08 p1097 N88-16599

Coronal heating by means of helical magnetohydrodynamic turbulence
[AD-A187084] 10 p1410 N88-18413

Table of solar activity associated with coronal mass ejections observed by the SMM coronagraph/polarimeter in 1980
[PB88-170881] 14 p2011 N88-21998

The properties of solar coronal active regions deduced from X-ray line spectra
[AD-A193026] 20 p2886 N88-27141

More than a solar cycle of synoptic solar and coronal data: A video presentation
[NASA-CR-181459] 23 p3308 N88-29708

Corona-solar wind coupling review
[AFGL-TR-87-0203] 24 p3458 N88-30575

SOLAR CORPUSCULAR RADIATION
NT SOLAR ELECTRONS
NT SOLAR NEUTRINOS
NT SOLAR NEUTRONS
NT SOLAR PROTONS

SOLAR COSMIC RAYS

Solar cosmic ray propagation in high-velocity solar wind stream 08 p1002 N88-16073

Automated spectrometric unit for the study of radiation characteristics of cosmic radiation aboard Prognoz-9 space stations 19 p2706 N88-26090

Solar flares and magnetospheric particles: Investigations based upon the ONR-602 and ONR-604 experiments
[AD-A193396] 21 p3031 N88-27994

SOLAR CYCLES
NT SUNSPOT CYCLE

STIP Symposium on Physical Interpretation of Solar/Interplanetary and Cometary Intervals
[NASA-CR-181201] 01 p0110 N88-10709

Overview of STIP intervals 15-19
01 p0110 N88-10710

Quantification of the background signal to solar neutrino detection from cosmogenic activation of the atmosphere
[DE87-013830] 01 p0119 N88-10762

The impact of varves on solar physics
[NASA-CR-181519] 03 p0390 N88-12448

Drought, solar activity link established by Leningrad geophysicists 04 p0458 N88-12835

Spectral analysis of APT RS CVn binary light curves
04 p0508 N88-13122

Starspots on the short-period RS CVn system SV Cam: 45 years of activity 04 p0508 N88-13123

Stellar cycle variability of solar-like stars: A sneak preview 04 p0510 N88-13136

A comprehensive exploration of late-type stars in the far-ultraviolet 04 p0520 N88-13194

Long-period variations of wind parameters in the mesopause region and the solar cycle dependence
06 p0733 N88-14509

On the dependence of the lower thermospheric wind regime on the solar cycle 06 p0736 N88-14524

Max '91: Flare research at the next solar maximum
[NASA-TM-89700] 06 p0806 N88-14919

Prediction of the next solar activity cycle
08 p1035 N88-16276

Solar-geophysical data number 516, August 1987. Part 1: (Prompt reports). Data for July 1987, June 1987 and late data
[PB88-114368] 09 p1263 N88-17570

Variations in the atmosphere associated with the 11-year solar cycle 22 p3122 N88-28557

Basic causes of amplitude modulation in climatic/weather parameters
[DE88-702743] 23 p3236 N88-29254

Neutrino electrodynamics and possible effects for solar neutrinos
[DE88-701647] 23 p3308 N88-29705

More than a solar cycle of synoptic solar and coronal data: A video presentation
[NASA-CR-181459] 23 p3308 N88-29708

Spectral analysis of the Elatina varve series
[NASA-CR-183085] 24 p3402 N88-30260

SOLAR DISK
U SUN

SOLAR DYNAMIC POWER SYSTEMS

Electrical Power Working Group report
01 p0016 N88-10095

Photovoltaic power modules for NASA's manned space station
[NASA-TM-100229] 03 p0277 N88-11745

Design of a condenser-boiler for a binary mercury-organic Rankine cycle solar dynamic space power system
[AD-A184186] 03 p0348 N88-12198

Status of 20 kHz space station power distribution technology
[NASA-TM-100781] 08 p0964 N88-15838

Solar concentrator advanced development program, task 1
[NASA-CR-179489] 10 p1350 N88-18068

Computer-aided modeling and prediction of performance of the modified Lundell class of alternators in space station solar dynamic power systems
[NASA-CR-182538] 11 p1507 N88-19000

Solar dynamic power system definition study
[NASA-CR-180877] 13 p1733 N88-20361

Space station power system requirements
[NASA-TM-100886] 14 p1881 N88-21245

Advanced sensible heat solar receiver for space power
[NASA-TM-100847] 14 p1882 N88-21249
Space station solar concentrator materials research
[NASA-TM-100862] 14 p1882 N88-21250
Power systems for production, construction, life support and operations in space
[NASA-TM-100838] 14 p1883 N88-21254
Ray tracing optical analysis of offset solar collector for space station solar dynamic system
[NASA-TM-100853] 15 p2027 N88-22060
Structural assessment of a space station solar dynamic heat receiver thermal energy storage canister
15 p2081 N88-22406
Solar dynamic heat rejection technology. Task 2: Heat pipe radiator development
[NASA-CR-182141] 16 p2209 N88-23182
The multi-disciplinary design study: A life cycle cost algorithm
[NASA-CR-4156] 17 p2385 N88-24172
Speculations on future opportunities to evolve Brayton powerplants aboard the space station
17 p2398 N88-24258
Design and demonstration of a system for the deposition of atomic-oxygen durable coatings for reflective solar dynamic power system concentrators
[NASA-CR-4158] 19 p2606 N88-25474
Thermal distortion analysis of the space station solar dynamic concentrator
[NASA-TM-100868] 19 p2606 N88-25475
Liquid metal thermal electric converter theoretical and experimental studies
[DE88-008806] 19 p2688 N88-25974
Advanced heat receiver conceptual design study
[NASA-CR-180901] 19 p2688 N88-25977
Solar dynamic power systems
[ETN-88-92969] 23 p3230 N88-29224
Study of toluene stability for an Organic Rankine Cycle (ORC) space-based power system
[NASA-CR-180884] 24 p3337 N88-29863
Study of toluene rotary fluid management device and shear flow condenser performance for a space-based organic Rankine power system
[NASA-CR-180885] 24 p3338 N88-29872

SOLAR DYNAMICS
U HELIOSEISMOLOGY

SOLAR ECLIPSES
Observations of the solar chromosphere in Kunming
[PB87-143319] 07 p0944 N88-15737

SOLAR ELECTRONS
Structural dynamics of high-latitude magnetosphere determined from solar electron data
24 p3444 N88-30500

SOLAR ENERGY
Focusing solar energy collector
02 p0159 N88-10996
Proceedings of the Solar Thermal Technology Conference
[DE87-014441] 02 p0195 N88-11220
Application of solar technology to fuel production chemical processing, and thermochemical energy transport: Status and future
[DE87-014172] 03 p0346 N88-12189
Solar energy: European research and development
[PB87-107645] 04 p0463 N88-12866
Technical evaluation of a solar-powered absorption cooling system (LiBr-H2O)
[PB87-108254] 04 p0463 N88-12867
International Energy Agency (IEA) Small Solar Power Systems (SSPS) sodium cavity and external receiver performance comparison
[DE88-001310] 04 p0465 N88-12879
A study of the optimal transition temperatue of PCM (Phase Change Material) wallboard for solar energy storage
[DE88-001522] 04 p0466 N88-12882
Proceedings of the Eleventh DOE Solar Photochemistry Research Conference
[DE88-000678] 04 p0466 N88-12883
The developmental status of solar thermochemical hydrogen production
[DE88-001778] 04 p0466 N88-12884
Self operating absorption cooling system using solar energy: Small power experimental plant
[DE88-900194] 07 p0874 N88-15299
Definition and economic evaluation of Space Solar Power Systems (SSPS), part 1
[ILR-MITT-184-1(1987)] 08 p1022 N88-16189
Definition and economic evaluation of Space Solar Power Systems (SSPS), part 2
[ILR-MITT-184-2(1987)] 08 p1022 N88-16190
Solar assisted absorption or motor driven heat pump with earth seasonal storage, part 1
[DE88-900191] 09 p1187 N88-17114
Proceedings of the 12th Symposium of Japan Solar Energy Society
[DE88-770029] 11 p1507 N88-19005
Solar generation and storage of O2 (a 1 delta g)
[NASA-CR-4127] 14 p1913 N88-21431
Solar assisted absorption or motor driven heat pump with earth seasonal storage. Part 2: Tables and figures
[DE88-900226] 19 p2686 N88-25964
Integrated solar reforming for thermochemical energy transport
[DE88-005010] 19 p2686 N88-25967
Dielectric compound parabolic concentrating solar collector with frustrated total internal reflection absorber
[DE88-009986] 19 p2688 N88-25976
Photovoltaic Measurements and Performance Branch
[DE88-001142] 21 p2968 N88-27633

SOLAR ENERGY ABSORBERS
Development of an innovative, low-cost solar collector
[PB87-206819] 02 p0194 N88-11210
Characterization of transparent insulation materials --- solar energy absorbers
[ETN-88-91052] 09 p1163 N88-16970
Development of a manufacturing unit for selective coating of solar absorbers made out of aluminum
[BMFT-FB-T-86-204] 14 p1942 N88-21590
Technical applications of solar energy. Project: Selective coatings
[BMFT-FB-T-86-213] 14 p1943 N88-21591
Direct conversion of solar energy to thermal energy
[BMFT-FB-T-86-220] 14 p1943 N88-21592
Solar energy absorption efficiency of an ellipsoidal receiver-reactor with specularly reflecting walls
[AD-A193726] 22 p3117 N88-28520

SOLAR ENERGY CONVERSION
NT PHOTOTHERMAL CONVERSION
NT PHOTOVOLTAIC CONVERSION
Engineering principles and concepts for active solar systems
[DE87-001181] 01 p0066 N88-10425
The fundamentals of photovoltaic system electrical design
[DE87-009061] 02 p0194 N88-11214
Solar thermal technology
[DE87-001171] 02 p0195 N88-11218
Proceedings of the Solar Thermal Technology Conference
[DE87-014441] 02 p0195 N88-11220
An evaluation of the LEC-460 solar collector
[DE88-000052] 02 p0196 N88-11224
Polymers in solar technologies
[DE88-001102] 03 p0294 N88-11849
Energy transfer and photochemistry in biomimetic solar conversion
[PB88-130026] 10 p1348 N88-18057
Photochemical solar energy conversion utilizing semiconductors localized in membrane mimetic systems
[DE88-002887] 10 p1349 N88-18065
Design of the Sandia-Israel 20-kW reflux heat-pipe solar receiver/reactor
[DE88-001312] 13 p1794 N88-20729
Control strategies and hardware used in solar thermal applications
[DE88-004631] 13 p1794 N88-20731
Oxidation/sulfidation of materials in an SO3/SO2/O2 thermochemical-transport, distributed-receiver, solar-energy system
[DE88-005875] 13 p1795 N88-20739
Direct conversion of solar energy to thermal energy
[BMFT-FB-T-86-220] 14 p1943 N88-21592
Comparison of electrically driven lasers for space power transmission
[NASA-TM-4045] 16 p2212 N88-23197
Performance sensitivities for point-focus dish systems with secondary concentrators
[DE88-001152] 21 p2968 N88-27629
Reflux heat-pipe solar receivers for dish-electric systems
[DE88-008671] 21 p2968 N88-27631
SERI's photovoltaic research project: A foundation for tomorrow's utility-scale electricity
[DE88-001161] 23 p3230 N88-29220

SOLAR FACULAE
U FACULAE

SOLAR FLARES
A layered scintillation detector for solar neutron observations
[DE87-011354] 01 p0049 N88-10314
STIP Symposium on Physical Interpretation of Solar/Interplanetary and Cometary Intervals
[NASA-CR-181201] 01 p0110 N88-10709
Solar-terrestrial observations during STIP interval 15 (12-21 February 1984) 01 p0111 N88-10711
Overview of the MONSEE UAG report on STIP intervals No. 15 and 16: The 24-25 April 1984 Forbush decrease period 01 p0111 N88-10712
Low altitude flux and dose measurements during two solar flare events 01 p0111 N88-10713
The largest white light flare ever observed: 25 April 1984, 0001 UT 01 p0111 N88-10714
Probable detection of solar neutrons by ground-level neutron monitors during STIP interval 16
01 p0111 N88-10715
Solar energetic particles events observed by Prognoz-10 Intercosmos (May-October 1985)
01 p0111 N88-10716
Two dimensional imaging observations of meter-decameter bursts associated with the February 1986 flare activity 01 p0113 N88-10723
Solar origins of coronal mass ejections
01 p0113 N88-10726
Radio studies of large scale structures of the Sun's corona and transient activity 01 p0114 N88-10728
An account of a flare related shock event recorded by the energetic particle detector EPONA of the Giotto spacecraft during September 1985 (STIP interval 18)
01 p0118 N88-10757
Solar-geophysical data number 513, May 1987. Part 1: (Prompt reports). Data for April, March 1987 and late data
[PB87-204939] 01 p0119 N88-10760
Solar-geophysical data number 513, May 1987. Part 2: (Comprehensive reports). Data for November 1986 and miscellanea
[PB87-204974] 01 p0119 N88-10761
Loop interaction in the visible emission corona: Morphological details 02 p0256 N88-11622
Sunspot observations from the SOUP instrument on Spacelab 2 02 p0257 N88-11623
Solar-geophysical data number 514, June 1987. Part 2: (Comprehensive reports). Data for December 1986
[PB87-217279] 03 p0390 N88-12450
Prompt simultaneous acceleration of protons and electrons to relativistic energies by shock waves in solar flares
[IPPJ-851] 04 p0493 N88-13037
A large X-ray flare on Sigma 2 coronae borealis observed with exosat 04 p0508 N88-13121
The appearance and disappearance of magnetic flux on the quiet sun
[AD-A185432] 05 p0661 N88-14055
Flares: Solar and stellar
[PB87-124962] 06 p0806 N88-14917
Max '91: Flare research at the next solar maximum
[NASA-TM-89700] 06 p0806 N88-14919
Energetics and dynamics of simple impulsive solar flares
[NASA-TM-87816] 07 p0947 N88-15755
Flare doublet: Interplanetary and geomagnetic effects
08 p1001 N88-16066
Unusually strong density decrease in near-Earth interplanetary plasma and magnetically quiet day as effects of isolated solar flare 08 p1002 N88-16072
Solar event of 27 April 1981 08 p1004 N88-16084
Magnetic reconnection and solar flare loops
08 p1094 N88-16583
Interplanetary and geophysical effects of a coronal transient 08 p1095 N88-16587
Small-scale structure in solar flare radio emission
08 p1097 N88-16598
Dynamic evolution of the source volumes of gradual and impulsive solar flare emissions
[NASA-TM-87815] 08 p1102 N88-16621
Solar-geophysical data number 517, September 1987. Part 1: (Prompt reports). Data for August, July 1987 and late data
[PB88-128426] 10 p1430 N88-18544
Solar-geophysical data number 517, September 1987. Part 2: (Comprehensive reports). Data for March 1987 and miscellanea
[PB88-128434] 10 p1431 N88-18545
Solar flares and magnetic topology
[AD-A188692] 12 p1712 N88-20244
Solar-geophysical data number 519, November 1987. Part 2: (Comprehensive reports). Data for May 1987 and miscellanea
[PB88-158910] 14 p2011 N88-21997
Solar-geophysical data number 520, December 1987. Part 1: (Prompt reports). Data for November 1987, October 1987 and late data
[PB88-164199] 16 p2290 N88-23712
The gamma-ray spectrometer experiment on the solar maximum mission satellite
[NASA-CR-182977] 17 p2452 N88-24589
The 2-D magnetohydrostatic configurations leading to flares or quiescent filament eruptions
[NASA-TM-101147] 18 p2595 N88-25423
Preliminary estimates of radiation exposures for manned interplanetary missions from anomalously large solar flare events
[NASA-TM-100620] 18 p2596 N88-25427

Solar-geophysical data number 521, January 1988. Part 2: (Comprehensive reports). Data for July 1987 and miscellanea
[PB88-179221] 19 p2743 N88-26285
The solar flare of 18 August 1979: Incoherent scatter radar data and photochemical model comparisons
[DE88-007616] 19 p2743 N88-26286
The ratio of microwaves to X-rays in solar flares: The case for the thick target model
[NASA-CR-183102] 19 p2743 N88-26287
The properties of solar coronal active regions deduced from X-ray line spectra
[AD-A193026] 20 p2886 N88-27141
The hard X-ray burst spectrometer event listing 1980-1987
[NASA-TM-4036] 20 p2887 N88-27144
Measurement of macroscopic electric fields in solar plasma structures
[AD-A193291] 21 p3031 N88-27993
Solar flares and magnetospheric particles: Investigations based upon the ONR-602 and ONR-604 experiments
[AD-A193396] 21 p3031 N88-27994
Solar-geophysical data number 523, March 1988. Part 1: (Prompt reports). Data for February 1988, January 1988 and late data
[PB88-212766] 24 p3458 N88-30574
Solar-geophysical data number 523, March 1988. Part 2: (Comprehensive reports). Data for September 1987 and miscellanea
[PB88-212774] 24 p3458 N88-30576

SOLAR FLUX
High-resolution continuum observations of the Sun
02 p0255 N88-11614
Total light flux and colour of solar corona
[PB87-143335] 07 p0946 N88-15754
Solar event of 27 April 1981 08 p1004 N88-16084
Neutrino magnetic moment and time variation of solar neutrino flux
[DE88-700687] 10 p1430 N88-18542
Reflux heat-pipe solar receivers for dish-electric systems
[DE88-008671] 21 p2968 N88-27631

SOLAR FLUX DENSITY
NT SOLAR CONSTANT
Short term variability between 120 and 300 mm from Solar Mesosphere Explorer (SME) observations
[AERONOMICA-ACTA-A-328-1988]
23 p3306 N88-29709

SOLAR FURNACES
A solar receiver-reactor with specularly reflecting walls for high-temperature thermoelectrochemical and thermochemical processes
[AD-A187612] 10 p1351 N88-18077
Polymer reflectors research during FY86
[DE88-001101] 11 p1506 N88-19009
Photolytic formation of free radicals and their effect on hydrocarbon pyrolysis chemistry in a concentrated solar environment
[DE88-004129] 13 p1794 N88-20730
Solar energy absorption efficiency of an ellipsoidal receiver-reactor with specularly reflecting walls
[AD-A193726] 22 p3117 N88-28520

SOLAR GENERATORS
NT SOLAR CELLS
NT SOLAR DYNAMIC POWER SYSTEMS
NT VERTICAL JUNCTION SOLAR CELLS
Environmental interactions of solar generators in space 03 p0274 N88-11730
Recent progress in space photovoltaic systems
[NASA-TM-100208] 03 p0311 N88-11966
Solar converging method 04 p0403 N88-12504
Design description report for a photovoltaic power system for a remote satellite earth terminal
[NASA-CR-179586] 04 p0465 N88-12875
International Energy Agency (IEA) Small Solar Power Systems (SSPS) sodium cavity and external receiver performance comparison
[DE88-001310] 04 p0465 N88-12879
A 1,000-watt solar power unit for Far North
06 p0728 N88-14481
Short Reference Years: Short weather data sets for faster simulations of solar energy systems and energy consumption in buildings
[DE88-900198] 07 p0881 N88-15343
Definition and economic evaluation of Space Solar Power Systems (SSPS), part 1
[ILR-MITT-184-1(1987)] 08 p1022 N88-16189
Definition and economic evaluation of Space Solar Power Systems (SSPS), part 2
[ILR-MITT-184-2(1987)] 08 p1022 N88-16190
Oxidation/sulfidation of materials in an SO3/SO2/O2 thermochemical-transport, distributed-receiver, solar-energy system
[DE88-005875] 13 p1795 N88-20739
Thermal analysis of heat storage canisters for a solar dynamic, space power system
[DE88-004199] 15 p2027 N88-22075
Reflux heat-pipe solar receivers for dish-electric systems
[DE88-008671] 21 p2968 N88-27631
Photovoltaic Energy. Electricity from Sunlight: A current awareness bulletin
[DE88-008289] 21 p2969 N88-27634
Space photovoltaic generators. State of the art, trends
[REPT-881-440-106] 21 p2970 N88-27640
SERI's photovoltaic research project: A foundation for tomorrow's utility-scale electricity
[DE88-001161] 23 p3230 N88-29220

SOLAR GRANULATION
First results on quiet and magnetic granulation from SOUP 02 p0255 N88-11613
High-resolution continuum observations of the Sun
02 p0255 N88-11614
Large-scale horizontal flows from SOUP observations of solar granulation 02 p0256 N88-11621
Loop interaction in the visible emission corona: Morphological details 02 p0256 N88-11622
Sunspot observations from the SOUP instrument on Spacelab 2 02 p0257 N88-11623

SOLAR HEATING
Statistical distribution of solar radiation (hourly sums): Cumulative frequency curves preparation of a European data set and direction for use
[PB87-107454] 04 p0467 N88-12886
Transient development of stratification in a partially divided enclosure
[DE87-011742] 05 p0572 N88-13490
Evaluation of thermal storage for solar heating systems: Executive summary
[DE88-900219] 07 p0874 N88-15304
Short Reference Years: Short weather data sets for faster simulations of solar energy systems and energy consumption in buildings
[DE88-900198] 07 p0881 N88-15343
Actual performance and economic feasibility of residential solar water heaters
[INPE-4399-RPE/555] 08 p1023 N88-16191
Solar tides in the upper equatorial thermosphere: A comparison between AE-E data and the NCAR thermospheric general circulation model
[AD-A186160] 08 p1023 N88-16196
Solar assisted absorption or motor driven heat pump with earth seasonal storage, part 1
[DE88-900191] 09 p1187 N88-17114
Effect of storage thermal behavior in seasonal storage solar heating systems
[PB88-114236] 10 p1350 N88-18067
Application of the estimation method to parameter performance date of solar water heating systems
[INPE-4268-PRE/1141] 11 p1508 N88-19007
Advanced utilization of solar energy: Utilization for biotechnology
[DE88-770031] 12 p1640 N88-19819

SOLAR HOUSES
Advanced utilization of solar energy: Utilization for biotechnology
[DE88-770031] 12 p1640 N88-19819

SOLAR INSTRUMENTS
NT SPECTROHELIOGRAPHS

SOLAR INTERIOR
Oscillations of solar models with internal element diffusion
[DE88-003156] 09 p1264 N88-17573

SOLAR LASERS
U SOLAR-PUMPED LASERS

SOLAR LIMB
Small-scale energy storage and release as the cause of the stellar X-ray corona 02 p0255 N88-11615

SOLAR MAGNETIC FIELD
On the association of erupting magnetic fields with eruptive prominences and coronal mass ejections
01 p0113 N88-10727
Theoretical Problems in High Resolution Solar Physics, 2
[NASA-CP-2483] 02 p0254 N88-11609
First results on quiet and magnetic granulation from SOUP 02 p0255 N88-11613
Small-scale energy storage and release as the cause of the stellar X-ray corona 02 p0255 N88-11615
Magnetic fields in the overshoot zone: The great escape 02 p0256 N88-11616
Theoretical modelling of the fine structures in sunspots 02 p0256 N88-11617
Pressure structure of solar coronal loops
02 p0256 N88-11618
The Sun and the solar activity
03 p0271 N88-11704
The solar wind 03 p0271 N88-11705
Solar magnetic and velocity fields
[AD-A184360] 03 p0390 N88-12449
Development of optical modulators for measurements of solar magnetic fields
[NASA-TM-100315] 04 p0490 N88-13016
Large scale solar and stellar magnetic fields
04 p0507 N88-13117
The appearance and disappearance of magnetic flux on the quiet sun
[AD-A185432] 05 p0661 N88-14055
Magnetic reconnection and solar flare loops
08 p1094 N88-16583
Flux tubes and loops in the solar chromosphere and corona 08 p1095 N88-16591
Emerging flux, magnetic reconnection, plasma turbulence and waves in the transition zone of the solar atmosphere 08 p1096 N88-16597
The effects of viscosity on resistive ballooning modes in line-tied coronal magnetic fields
08 p1097 N88-16599
Solar-geophysical data number 517, September 1987. Part 1: (Prompt reports). Data for August, July 1987 and late data
[PB88-128426] 10 p1430 N88-18544
Development of high stability fiber optic spectrophotometric systems for study of solar/stellar magnetic activity
[AD-A189327] 13 p1852 N88-21088
Magnetic field hourly averages from the Rome-GSFC experiment aboard Helios 1 and Helio 2
[NASA-TM-89782] 14 p2011 N88-21995
The SAMEX vector magnetograph: A design study for a space-based solar vector magnetograph
[NASA-TM-4048] 18 p2596 N88-25424

SOLAR MAXIMUM MISSION
In-orbit and laboratory exchange of ORUs designed/not designed for servicing 12 p1587 N88-19499
Remote repair demonstration of Solar Maximum main electronics box 12 p1588 N88-19510

SOLAR MESOSPHERE EXPLORER
Short term variability between 120 and 300 mm from Solar Mesosphere Explorer (SME) observations
[AERONOMICA-ACTA-A-328-1988]
23 p3306 N88-29709

SOLAR NEBULA
U SOLAR CORONA

SOLAR NEIGHBORHOOD
A spectral survey of 26 G9-M6 flare stars in the solar neighborhood 04 p0512 N88-13149
A VLA survey of dMe flare stars
04 p0513 N88-13154
An astrometric search for a stellar companion to the sun 04 p0520 N88-13195
Hydrogen and deuterium in the local interstellar medium 04 p0521 N88-13204

SOLAR NEUTRINOS
Superfluid He4 as a solar neutrino detector
[DE87-014477] 02 p0257 N88-11625
A possible accelerator experiment to solve the solar neutrino puzzle
[PREPRINT-556] 06 p0778 N88-14778
Solar oscillations, gravitational multipole field of the Sun and the solar neutrino paradox
[DE88-002100] 07 p0946 N88-15752
Stable, heavy, neutral particles in the sun and in toponium decay 17 p2452 N88-24568
Cosmions and stars
[DE88-010886] 20 p2887 N88-27145
Neutrino electrodynamics and possible effects for solar neutrinos
[DE88-701647] 23 p3308 N88-29705
Resonant spin-flavor precession of solar and supernova neutrinos
[DE88-752604] 23 p3308 N88-29707

SOLAR NEUTRONS
A layered scintillation detector for solar neutron observations
[DE87-011354] 01 p0049 N88-10314
Probable detection of solar neutrons by ground-level neutron monitors during STIP interval 16
01 p0111 N88-10715

SOLAR NOISE
U SOLAR RADIO EMISSION

SOLAR OBSERVATORIES
NT PINHOLE OCCULTER FACILITY
Theoretical Problems in High Resolution Solar Physics, 2
[NASA-CP-2483] 02 p0254 N88-11609
Bern solar observations. Solar data for January-December 1986
[REPT-53] 09 p1263 N88-17569
NASA Marshall Space Flight Center solar observatory
[NASA-TM-100339] 24 p3332 N88-29832
Coordinated study of Solar-Terrestrial Observatory (STO) payloads on space station
[NASA-CR-183142] 24 p3334 N88-29848

SOLAR ORBITS

Single-burn transfer to nominally periodic orbit in the vicinity of point L2 of Earth-Sun system and related problems 08 p1006 N88-16100

Numerical evidence that the motion of Pluto is chaotic
[AD-A195920] 24 p3455 N88-30568

SOLAR OSCILLATIONS

First results on quiet and magnetic granulation from SOUP 02 p0255 N88-11613

Large-scale horizontal flows from SOUP observations of solar granulation 02 p0256 N88-11621

Sunspot observations from the SOUP instrument on Spacelab 2 02 p0257 N88-11623

Perturbations of the Sun's gravitational field due to solar oscillations
[DE88-002099] 07 p0946 N88-15751

Solar oscillations, gravitational multipole field of the Sun and the solar neutrino paradox
[DE88-002100] 07 p0946 N88-15752

Global solar oscillations observed in the visible to near infrared continuum 13 p1858 N88-21110

SOLAR PHYSICS

About the interest of solar interferometric observations
01 p0094 N88-10615

Solar-geophysical data number 513, May 1987. Part 1: (Prompt reports). Data for April, March 1987 and late data
[PB87-204939] 01 p0119 N88-10760

Solar-geophysical data number 513, May 1987. Part 2: (Comprehensive reports). Data for November 1986 and miscellanea
[PB87-204974] 01 p0119 N88-10761

Theoretical Problems in High Resolution Solar Physics, 2
[NASA-CP-2483] 02 p0254 N88-11609

High-resolution continuum observations of the Sun
02 p0255 N88-11614

Solar-geophysical data number 514, June 1987. Part 1: (Prompt reports). Data for May 1987, April 1987 and late data
[PB87-217261] 02 p0257 N88-11626

The impact of varves on solar physics
[NASA-CR-181519] 03 p0390 N88-12448

Solar-geophysical data number 514, June 1987. Part 2: (Comprehensive reports). Data for December 1986
[PB87-217279] 03 p0390 N88-12450

Exploiting the IR: Solar and stellar spectroscopy in the IR 04 p0504 N88-13102

Three-halves law in sunspot cycle shape
[NASA-CR-181520] 04 p0525 N88-13210

Solar-geophysical data number 515, July 1987. Part 1: (Prompt reports). Data for June 1987, May 1987 and late data
[PB87-233177] 06 p0805 N88-14912

Solar-geophysical data number 515, July 1987. Part 2: (Comprehensive reports). Data for January 1987 and miscellanea
[PB87-233185] 06 p0805 N88-14913

Solar-geophysical activity reports for STIP (Study of Travelling Interplanetary Phenomena) Interval 15, 12-21 February 1984 ground level event and STIP Interval 16, 20 April-4 May 1984 Forbush decrease
[PB87-232658] 06 p0805 N88-14915

On the potential role of concentrated field-aligned currents in solar physics 08 p1099 N88-16614

Solar-geophysical data number 516, August 1987. Part 2: (Comprehensive reports). Data for February 1987
[PB88-114376] 09 p1264 N88-17571

Solar-geophysical data number 518, October 1987. Part 2: (Comprehensive reports). Data for April 1987
[PB88-138060] 12 p1711 N88-20242

Solar-geophysical data number 518, October 1987. Part 1: (Prompt reports). Data for September 1987, August 1987 and late data
[PB88-138078] 12 p1712 N88-20243

Research and technology, 1987
[NASA-TM-100323] 12 p1713 N88-20253

Solar-geophysical data number 519, November 1987. Part 2: (Comprehensive reports). Data for May 1987 and miscellanea
[PB88-158910] 14 p2011 N88-21997

Solar-geophysical data number 520, December 1987. Part 1: (Prompt reports). Data for November 1987, October 1987 and late data
[PB88-164199] 16 p2290 N88-23712

Stable, heavy, neutral particles in the sun and in toponium decay 17 p2452 N88-24566

An image processing system for research in solar physics
[AD-A191673] 18 p2595 N88-25421

Solar-geophysical data number 521, January 1988. Part 1: (Prompt reports). Data for December 1987, November 1987 and late data
[PB88-179213] 19 p2743 N88-26284

Solar-geophysical data number 521, January 1988. Part 2: (Comprehensive reports). Data for July 1987 and miscellanea
[PB88-179221] 19 p2743 N88-26285

Solar-geophysical data number 523, March 1988. Part 1: (Prompt reports). Data for February 1988, January 1988 and late data
[PB88-212766] 24 p3458 N88-30574

Solar-geophysical data number 523, March 1988. Part 2: (Comprehensive reports). Data for September 1987 and miscellanea
[PB88-212774] 24 p3458 N88-30576

SOLAR PLANETARY INTERACTIONS

NT SOLAR TERRESTRIAL INTERACTIONS

Peculiarities of daytime ionosphere of Venus during years of low and high solar activity
08 p1005 N88-16091

Solar-geophysical data number 516, August 1987. Part 2: (Comprehensive reports). Data for February 1987
[PB88-114376] 09 p1264 N88-17571

SOLAR PLASMA (RADIATION)

U SOLAR WIND

SOLAR POSITION

Influence of solar illumination conditions on TM/Landsat data
[INPE-4463-TDL/320] 12 p1638 N88-19806

SOLAR POWER GENERATION

U SOLAR GENERATORS

SOLAR POWER SATELLITES

Technology for large space systems: A bibliography with indexes (supplement 18)
[NASA-SP-7046(18)] 21 p2901 N88-27214

SOLAR POWER SOURCES

U SOLAR GENERATORS

SOLAR PROBES

NT HELIOS 1
NT HELIOS 2

SOLAR PROMINENCES

STIP Symposium on Physical Interpretation of Solar/Interplanetary and Cometary Intervals
[NASA-CR-181201] 01 p0110 N88-10709

Solar-geophysical data number 513, May 1987. Part 2: (Comprehensive reports). Data for November 1986 and miscellanea
[PB87-204974] 01 p0119 N88-10761

Solar-geophysical data number 514, June 1987. Part 2: (Comprehensive reports). Data for December 1986
[PB87-217279] 03 p0390 N88-12450

Observations and modeling of the prominence/corona transition region 08 p1094 N88-16585

Emerging flux, magnetic reconnection, plasma turbulence and waves in the transition zone of the solar atmosphere 08 p1096 N88-16597

Solar-geophysical data number 517, September 1987. Part 2: (Comprehensive reports). Data for March 1987 and miscellanea
[PB88-128434] 10 p1431 N88-18545

Magnetohydrodynamic (MHD) simulation of solar prominence formation 13 p1858 N88-21109

Solar-geophysical data number 519, November 1987. Part 2: (Comprehensive reports). Data for May 1987 and miscellanea
[PB88-158910] 14 p2011 N88-21997

Measurement of macroscopic electric fields in solar plasma structures
[AD-A193291] 21 p3031 N88-27993

SOLAR PROPULSION

NT SOLAR THERMAL PROPULSION

SOLAR PROTONS

Automated spectrometric unit for the study of radiation characteristics of cosmic radiation aboard Prognoz-9 space stations 19 p2706 N88-26090

SOLAR RADIATION

NT SOLAR COSMIC RAYS
NT SOLAR ELECTRONS
NT SOLAR NEUTRINOS
NT SOLAR NEUTRONS
NT SOLAR PROTONS
NT SOLAR RADIO BURSTS
NT SOLAR RADIO EMISSION
NT SOLAR WIND
NT SOLAR X-RAYS
NT SUNLIGHT
NT TYPE 3 BURSTS

Balloon-based infrared solar occultation measurements of stratospheric O3, H2O, HNO3 and CFC-12
[NOAA-TR-NESDIS-34] 01 p0068 N88-10438

Solar Energy Meteorological Research and Training Site, Alaska
[DE87-013706] 01 p0069 N88-10440

Status of the solar and infrared radiation submodels in the LLNL 1-D and 2-D chemical-transport models
[DE87-014320] 01 p0069 N88-10441

Solar modulation of the cosmic radiation in the heliosphere 01 p0112 N88-10720

Mathematical modelling of solar ultraviolet radiation induced optical degradation in anodized aluminum
02 p0135 N88-10846

A quasi-physical model for converting hourly global horizontal to direct normal insolation
[DE87-012273] 03 p0349 N88-12204

Calendar year 1985 solar and weather data for Austin, Texas
[PB87-220174] 03 p0352 N88-12219

The development of low level coastal flow fields when solar radiation is blocked by smoke
[DE87-014348] 03 p0354 N88-12230

Statistical distribution of solar radiation (hourly sums): Cumulative frequency curves preparation of a European data set and direction for use
[PB87-107454] 04 p0467 N88-12886

A comprehensive exploration of late-type stars in the far-ultraviolet 04 p0520 N88-13194

Finnish contributions to EISCAT science in 1986
06 p0691 N88-14235

Latitude coverage of observations of the middle atmosphere by solar absorption spectrometry from a heliosynchronous orbit
[AERONOMICA-ACTA-A-316-1987]
06 p0742 N88-14566

Rome Neutron Monitor (NM) - 64 data for 5 solar particle ground-level events
[IFSI-86-7] 06 p0806 N88-14918

Satellite techniques of solar resource assessment for focusing and non-focusing solar collector systems
[DE88-001657] 07 p0874 N88-15298

The solar radiation incident at the top of the atmosphere of Uranus and Neptune
[AERONOMICA-ACTA-A-317-1987]
07 p0878 N88-15323

Short Reference Years: Short weather data sets for faster simulations of solar energy systems and energy consumption in buildings
[DE86-900198] 07 p0881 N88-15343

Finnish-Soviet Symposium on Radio Astronomy (1st) held at Otaniemi on August 26-27, 1985
[PB87-140661] 07 p0944 N88-15736

The use of the direct measurement of solar radiation for the determination of Pasquill Stability Parameter
[AD-A186084] 07 p0946 N88-15750

The anisotropy of reflected solar radiation over several types of land surface 08 p1018 N88-16171

An aureolar radiometer for the determination of aerosol size distribution 08 p1018 N88-16174

Aerosol size distribution from measurements of the radiance in the solar aureole 08 p1019 N88-16176

The iterative radiance model of the Meteorological Institute of the University of Munich (West Germany)
08 p1019 N88-16178

Solar ultraviolet spectrum obtained from a balloon gondola 08 p1032 N88-16256

Dynamic evolution of the source volumes of gradual and impulsive solar flare emissions
[NASA-TM-87815] 08 p1102 N88-16621

Nimbus 7 Solar Backscatter Ultraviolet (SBUV) spectral scan solar irradiance and Earth radiance product user's guide
[NASA-RP-1199] 09 p1184 N88-17096

Solar-geophysical data number 516, August 1987. Part 1: (Prompt reports). Data for July 1987, June 1987 and late data
[PB88-114368] 09 p1263 N88-17570

Solar-geophysical data number 516, August 1987. Part 2: (Comprehensive reports). Data for February 1987
[PB88-114376] 09 p1264 N88-17571

Parameterization of radiative transfer in the Earth's atmosphere with specific applications to clouds
10 p1353 N88-18087

Evaluation of surface energy and radiation balance systems on the Konza Prairie
[NASA-CR-182534] 10 p1355 N88-18097

Radiation balance components above the tropical evergreen Amazon forests (3rd campaign of data collection)
[INPE-4195-PRE/1079] 11 p1513 N88-19039

Influence of radiation and thermal conduction on temperature distribution in the thin wall of a hollow cylinder
[INPE-4428-TDL/308] 12 p1626 N88-19730

Calibration of the solar radiation estimation method by satellites
[INPE-4349-PRE/1185] 12 p1646 N88-19861

Vertical turbulent transfer of matter in thin ocean surface layer during daytime heating 13 p1767 N88-20693

Direct absorption receiver control studies
[DE87-013653] 13 p1795 N88-20737

Radiative processes affecting ocean mixed-layer heat content and their monitoring from satellite
13 p1806 N88-20800

Satellite estimations of the solar radiation flux at the surface 14 p1936 N88-21551

Solar-geophysical data number 520, December 1987. Part 2: (Comprehensive reports). Data for June 1987 and miscellanea
[PB88-164207] 15 p2152 N88-22849
NOAA-ERL-ARL (National Oceanic and Atmospheric Administration-Environmental Research Laboratories-Air Resources Laboratory) solar UV radiation and climate research project: Program description
[PB88-169396] 16 p2233 N88-23339
Comparison of the solar radiation estimation method by satellites 17 p2360 N88-24055
Photovoltaic Advanced Research and Development Project, solar radiation research
[DE88-001143] 18 p2537 N88-25056
Results of radiation measurements in West Germany and from special measurement series in the Meteorological Observatory of Hamburg
[REPT-11] 18 p2542 N88-25088
Observations of cosmic rays in the outer heliosphere
[NASA-CR-182942] 18 p2596 N88-25425
Preliminary estimates of radiation exposures for manned interplanetary missions from anomalously large solar flare events
[NASA-TM-100620] 18 p2596 N88-25427
The ratio of microwaves to X-rays in solar flares: The case for the thick target model
[NASA-CR-183102] 19 p2743 N88-26287
Determination and application of bidirectional solar-optical properties of fenestration systems
[DE88-010364] 20 p2620 N88-26727
On the global radiation incident variously orientated surfaces on the South Coast of Finland
[FMI-5] 20 p2623 N88-26746
Solar-geophysical data number 522, February 1988. Part 1: (Prompt reports). Data for January 1988, December 1987 and late data
[PB88-194733] 20 p2886 N88-27139
Overview and future direction for blackbody solar-pumped lasers
[NASA-TM-100621] 21 p2955 N88-27553
Development of radiation and cloud parameterization programs for AFGL (Air Force Geophysics Laboratory) global models
[AD-A193369] 21 p2973 N88-27658
SERI standard broadband format: A solar and meteorological data archival format
[DE88-001145] 21 p3028 N88-27975
IR (infrared) sky radiance distributions in the marine boundary layer
[AD-A193683] 22 p3119 N88-28531
Differences in radiation budget parameters over Asia in relation to contrasting Indian monsoons
22 p3125 N88-28574
A comparison of typical meteorological year solar radiation information with the SOLMET data base
[DE88-009242] 23 p3234 N88-29247
Global solar radiation in Sierra Leone (West Africa)
[DE88-702725] 23 p3235 N88-29252
Mathematical correlation between variations in solar radiation parameters. Part 1: Daily sums of global radiation and midday global radiation
[DE88-702742] 23 p3236 N88-29253
Basic causes of amplitude modulation in climatic/weather parameters
[DE88-702743] 23 p3236 N88-29254
Short term variability between 120 and 300 mm from Solar Mesosphere Explorer (SME) observations
[AERONOMICA-ACTA-A-328-1988]
23 p3308 N88-29709
Energy budget and ground temperatures in hot regions
[AD-A196298] 24 p3404 N88-30268

SOLAR RADIATION SHIELDING
A near-earth optical communications terminal with a corevolving planetary sun shield
04 p0434 N88-12693
Air temperature shield tests
[AD-A187459] 11 p1514 N88-19043
OLYMPUS shuttle specific radiator shield
14 p1879 N88-21234

SOLAR RADIO BURSTS
NT TYPE 3 BURSTS
The large Type 4 radio burst event of 24 April 1985 interpreted by dynamic spectral recordings and associated recordings 01 p0112 N88-10717
Two dimensional imaging observations of meter-decameter bursts associated with the February 1986 flare activity 01 p0113 N88-10723
Coronal and interplanetary Type 2 radio emission
01 p0114 N88-10731
Solar-geophysical data number 513, May 1987. Part 1: (Prompt reports). Data for April, March 1987 and late data
[PB87-204939] 01 p0119 N88-10760
Solar-geophysical data number 513, May 1987. Part 2: (Comprehensive reports). Data for November 1986 and miscellanea
[PB87-204974] 01 p0119 N88-10761
Solar-geophysical data number 514, June 1987. Part 2: (Comprehensive reports). Data for December 1986
[PB87-217279] 03 p0390 N88-12450
Solar-geophysical data number 517, September 1987. Part 2: (Comprehensive reports). Data for March 1987 and miscellanea
[PB88-128434] 10 p1431 N88-18545
Solar-geophysical data number 519, November 1987. Part 2: (Comprehensive reports). Data for May 1987 and miscellanea
[PB88-158910] 14 p2011 N88-21997
Solar-geophysical data number 523, March 1988. Part 2: (Comprehensive reports). Data for September 1987 and miscellanea
[PB88-212774] 24 p3458 N88-30576

SOLAR RADIO EMISSION
NT SOLAR RADIO BURSTS
NT TYPE 3 BURSTS
Variations of the semi-diurnal tidal wind in the meteor region with periods of about 27 and 13.5 days
06 p0734 N88-14516
Solar-geophysical activity reports for STIP (Study of Traveling Interplanetary Phenomena) interval 15, 12-21 February 1984 ground level event and STIP interval 16, 20 April-4 May 1984 Forbush decrease
[PB88-101274] 06 p0802 N88-14906
Observation and interpretation of solar S-component radiation at millimetre waves
[PB87-225207] 06 p0805 N88-14916
Finnish-Soviet Symposium on Radio Astronomy (1st) held at Otaniemi on August 26-27, 1985
[PB87-140661] 07 p0944 N88-15736
Solar-geophysical data number 517, September 1987. Part 1: (Prompt reports). Data for August, July 1987 and late data
[PB88-128426] 10 p1430 N88-18544
Solar-geophysical data number 520, December 1987. Part 1: (Prompt reports). Data for November 1987, October 1987 and late data
[PB88-164199] 16 p2290 N88-23712
Solar-geophysical data number 523, March 1988. Part 1: (Prompt reports). Data for February 1988, January 1988 and late data
[PB88-212766] 24 p3458 N88-30574

SOLAR RADIO WAVES
U SOLAR RADIO EMISSION

SOLAR RECEIVERS
U SOLAR COLLECTORS

SOLAR REFLECTORS
NT SOLAR COLLECTORS
Design concepts to improve high performance solar simulator 02 p0136 N88-10852
Solar thermal technology
[DE87-001171] 02 p0195 N88-11218
Solar converging method 04 p0403 N88-12504
Point-focus concentrator reflector assembly, phase 1
[DE88-003616] 13 p1792 N88-20720
Chemical vapor deposited silica coatings for solar mirror protection
[NASA-TM-100834] 14 p1893 N88-21306
Contamination of optical surfaces --- Space Station
18 p2592 N88-25400
Specular steel surfaces for solar mirror substrates
[DE88-001153] 21 p2968 N88-27630
Planarization of metal substrates for solar mirrors
[DE88-011492] 23 p3229 N88-29214

SOLAR ROTATION
Variations of the semi-diurnal tidal wind in the meteor region with periods of about 27 and 13.5 days
06 p0734 N88-14516

SOLAR SEISMOLOGY
U HELIOSEISMOLOGY

SOLAR SELECTIVE COATINGS
U SELECTIVE SURFACES

SOLAR SENSORS
Airborne tracking sunphotometer apparatus and system
[NASA-CASE-ARC-11622-1] 06 p0730 N88-14492
Development of integrated detectors for attitude sensors
[INPE-4409-PRE/1222] 12 p1602 N88-19586
Characterization of integrated photovoltaic detectors for MECB solar sensors
[INPE-4408-PRE/1221] 12 p1630 N88-19754

SOLAR SIMULATION
ESA Bulletin No. 25
[ISSN-0376-4265] 09 p1126 N88-16767
Development of infrared techniques for testing spacecraft 09 p1128 N88-16772

SOLAR SIMULATORS
Design concepts to improve high performance solar simulator 02 p0136 N88-10852
Development of infrared techniques for testing spacecraft 09 p1128 N88-16772

SOLAR SPECTRA
Loop interaction in the visible emission corona: Morphological details 02 p0256 N88-11622
Solar magnetic and velocity fields
[AD-A184360] 03 p0390 N88-12449
Calibrating AIS images using the surface as a reference 05 p0612 N88-13760
Short-term temporal variations of Nimbus-7 measurements of the solar UV spectral irradiance
[PB88-102132] 07 p0946 N88-15753
Measurement of macroscopic electric fields in solar plasma structures
[AD-A193291] 21 p3031 N88-27993
Aeronomic problems of the molecular oxygen photodissociation. Part 3: Solar spectral irradiances in the region of the O2 Herzberg continuum, Schumann-Runge bands and continuum
[AERONOMICA-ACTA-A-332-1988]
24 p3343 N88-29897
Atmospheric corrections for in-flight satellite radiometric calibration
[AD-A196124] 24 p3391 N88-30194
Spectral analysis of the Elatina varve series
[NASA-CR-183085] 24 p3402 N88-30260

SOLAR SPECTROMETERS
Small-scale structure in solar flare radio emission
08 p1097 N88-16598
The hard X-ray burst spectrometer event listing 1980-1987
[NASA-TM-4036] 20 p2887 N88-27144

SOLAR SYSTEM
High explosive simulations of supernovae and the supernova shell fragmentation model of solar system formation
[DE87-014708] 02 p0251 N88-11584
Royal Observatory, Edinburgh: Research and Facilities
[ISSN-0267-6281] 14 p1993 N88-21881
Space infrared telescope facility project
[NASA-CR-183058] 20 p2883 N88-27121
Activities report of the Institute for Extraterrestrial Physics
[MPE-206] 21 p3029 N88-27981
Lewis Cliff 86010, a unique Antarctic meteorite: Possible new clues to the early history of the solar system
24 p3442 N88-30482
Noble gases, C,N, and Si isotopes in interstellar SiC form the Murchison carbonaceous chondrite
24 p3442 N88-30483
Workshop on the Origins of Solar Systems
[NASA-CR-183025] 24 p3451 N88-30536
Star formation and molecular clouds
24 p3451 N88-30537
Observations of star formation
24 p3451 N88-30538
Cosmochemical trends of volatile elements in the solar system 24 p3451 N88-30542
Terrestrial versus giant planet formation
24 p3451 N88-30543

SOLAR TEMPERATURE
Observations and modeling of the prominence/corona transition region 08 p1094 N88-16585

SOLAR TERRESTRIAL INTERACTIONS
STIP Symposium on Physical Interpretation of Solar/Interplanetary and Cometary Intervals
[NASA-CR-181201] 01 p0110 N88-10709
Overview of STIP intervals 15-19
01 p0110 N88-10710
Solar-terrestrial observations during STIP interval 15 (12-21 February 1984) 01 p0111 N88-10711
Overview of the MONSEE UAG report on STIP intervals No. 15 and 16: The 24-25 April 1984 Forbush decrease period 01 p0111 N88-10712
The large Type 4 radio burst event of 24 April 1985 interpreted by dynamic spectral recordings and associated recordings 01 p0112 N88-10717
Solar-terrestrial research in the space station era
01 p0117 N88-10747
Space Environment Technology --- conference
[ISBN-2-85428-170-5] 03 p0271 N88-11702
The solar wind 03 p0271 N88-11705
Hot plasmas in the Earth's magnetosphere
03 p0272 N88-11710
Magnetospheric storms 03 p0272 N88-11711
Configurations of the quiet polar cap and its response to a sudden increase of the energy input rate epsilon
[DMI-GEOPHYS-PAPERS-R-74]
03 p0350 N88-12210
Drought, solar activity link established by Leningrad geophysicists 04 p0458 N88-12835
Solar-geophysical activity reports for STIP (Study of Travelling Interplanetary Phenomena) interval 15, 12-21 February 1984 ground level event and STIP interval 16, 20 April-4 May 1984 Forbush decrease
[PB88-101274] 06 p0802 N88-14906

Solar-geophysical activity reports for STIP (Study of Travelling Interplanetary Phenomena) Interval 15, 12-21 February 1984 ground level event and STIP Interval 16, 20 April-4 May 1984 Forbush decrease
[PB87-232658] 06 p0805 N88-14915

New book on space ecology reviewed
07 p0897 N88-15434

Flare doublet: Interplanetary and geomagnetic effects
08 p1001 N88-16066

Monitoring of Pc3 pulsations in solar wind and at Earth by interplanetary magnetic field
08 p1002 N88-16069

Unusually strong density decrease in near-Earth interplanetary plasma and magnetically quiet day as effects of isolated solar flare 08 p1002 N88-16072

Interplanetary and geophysical effects of a coronal transient 08 p1095 N88-16587

The formation of boundary layers by the entry of low-energy electrons and energetic ions into the Earth's magnetosphere 08 p1095 N88-16590

International geosphere-biosphere program: A study of global change
[PB88-142393] 11 p1510 N88-16321

Interpretation of the northward B sub z (NBZ) Birkeland current system and polar cap convection patterns in terms of the impulsive penetration model
[AERONOMICA-ACTA-A-321-1987]
18 p2595 N88-25422

Diffusion of slight solar induced disturbances in the middle atmosphere
[MITT-53] 20 p2825 N88-26758

Coordinated study of Solar-Terrestrial Observatory (STO) payloads on space station
[NASA-CR-183142] 24 p3334 N88-29848

Corona-solar wind coupling review
[AFGL-TR-87-0203] 24 p3458 N88-30575

SOLAR THERMAL ELECTRIC POWER PLANTS

Performance analysis of solar thermal power systems
[DE88-000563] 04 p0465 N88-12874

Definition and economic evaluation of Space Solar Power Systems (SSPS), part 1
[ILR-MITT-184-1(1987)] 08 p1022 N88-16189

Definition and economic evaluation of Space Solar Power Systems (SSPS), part 2
[ILR-MITT-184-2(1987)] 08 p1022 N88-16190

Power from the sun: Principles of high temperature solar thermal technology
[DE87-001104] 13 p1795 N88-20736

SOLAR THERMAL PROPULSION

Solar thermal propulsion for orbit transfer vehicles
17 p2428 N88-24445

SOLAR WIND

Change in interplanetary shock acceleration preceding STIP Interval 17 01 p0112 N88-10719

Evolution of the solar wind structure in the outer heliosphere 01 p0112 N88-10721

Study of pickup of cometary ions in turbulent solar winds 01 p0113 N88-10725

Coronal mass ejections: The long-term variation of their occurrence rate and the solar wind mass flux
01 p0114 N88-10732

Dynamics of magnetic clouds in interplanetary space
01 p0115 N88-10736

A numerical study of transient, thermally-conductive solar wind 01 p0115 N88-10738

A two-fluid model for solar wind fluid with higher order moments 01 p0116 N88-10739

Interaction of interplanetary shocks with nonuniform ambient solar wind 01 p0116 N88-10740

An overview of STIP interval 18: September 1985, the G-Z encounter 01 p0116 N88-10741

Comparative plasma tails of Venus and comets
01 p0116 N88-10742

Large-scale interaction of the solar wind with comets Halley and Giacobini-Zinner 01 p0117 N88-10745

The global interaction of comets with the solar wind
01 p0117 N88-10746

Solar wind-cometary interaction at the ionopause and associated phenomena 01 p0117 N88-10748

Solar wind effects on the outer ion coma of Comet Halley 01 p0117 N88-10750

The solar wind interaction with comets: A post encounter view 01 p0118 N88-10751

Plasma-tail activity and the interplanetary medium at Halley's Comet during Armada Week: 6-14 March 1986
01 p0118 N88-10752

Study of the mechanism for solar wind formation
01 p0118 N88-10756

A numerical study of the thermal stability of solar loops 02 p0256 N88-11619

Solar transition region and coronal response to heating rate perturbations 02 p0256 N88-11620

The solar wind 03 p0271 N88-11705

Hot plasmas in the Earth's magnetosphere
03 p0272 N88-11710

Magnetospheric storms 03 p0272 N88-11711

High latitude F-region drift studies
[AD-A184466] 04 p0467 N88-12889

Model of solar-wind magnetosphere coupling
04 p0525 N88-13211

Observations of turbulence and fluctuations in the solar wind 04 p0525 N88-13212

A fluid simulation of the AMPTE lithium gas releases in the solar wind
[TRITA-EPP-87-06] 05 p0661 N88-14056

Magnetic field draping about coronal mass ejecta
[DE88-001805] 05 p0661 N88-14057

Interplanetary magnetic field effects on the interaction of the solar wind with Venus 06 p0805 N88-14910

Monitoring of Pc3 pulsations in solar wind and at Earth by interplanetary magnetic field
08 p1002 N88-16069

Solar cosmic ray propagation in high-velocity solar wind stream 08 p1002 N88-16073

Fluctuations in frequency of coherent radio signals in solar plasma according to Venera-15 and Venera-16 data 08 p1003 N88-16079

Dynamics and turbulence of solar wind in area of its formation based on radio transmission data measured with Venera-15 and Venera-16 spacecraft
08 p1003 N88-16080

Bidirectional electron heat flux events in space
[DE88-001791] 08 p1094 N88-16531

Solar corona and solar wind 08 p1094 N88-16584

The formation of boundary layers by the entry of low-energy electrons and energetic ions into the Earth's magnetosphere 08 p1095 N88-16590

Numerical simulation of solar wind and magnetospheric phenomena 08 p1097 N88-16600

Small scale MHD wave processes in the solar atmosphere and solar wind 08 p1098 N88-16608

Observations of small scale structures using data from the wave experiment on the AMPTE-UKS spacecraft
08 p1099 N88-16612

Transverse flow deflections associated with fast coronal mass ejecta in interplanetary space
[DE88-003180] 09 p1263 N88-17566

Data reduction and analysis of HELIOS plasma wave data
[NASA-CR-182466] 09 p1264 N88-17572

Universal power spectra for wave turbulence: Applications to wind waves, flicker noise, solar wind spectrum and classical second sound
10 p1318 N88-17879

Personal overview of solar wind 6
[DE88-003147] 10 p1430 N88-18543

The relation of solar wind structure to hydromagnetic discontinuities
[DE88-004304] 10 p1431 N88-18546

Electric fields in Earth orbital space. Magnetospheric structural dynamic response to external variables
[AD-A188592] 12 p1643 N88-19836

To what extent is mass loading responsible for the Venus bowshock precursor?
[NASA-TM-89307] 12 p1711 N88-20239

Solar wind observation at the time of closest encounter with Comet Halley 14 p1995 N88-21890

Calculation of the shape of the contact surface at Comet Halley 14 p1995 N88-21892

A comparison between wave observations performed in the environments of Comets Halley and Giacobini-Zinner 14 p1996 N88-21896

Magnetic cavity formation at Comet Halley and at the AMPTE Li release 14 p1996 N88-21898

Plasmapause formation
[AERONOMICA-ACTA-A-319-1987]
15 p2138 N88-22759

Observation of nonlinear wave decay processes in the solar wind by the AMPTE IRM plasma wave experiment
[AD-A191409] 16 p2290 N88-23713

Interpretation of the northward B sub z (NBZ) Birkeland current system and polar cap convection patterns in terms of the impulsive penetration model
[AERONOMICA-ACTA-A-321-1987]
18 p2595 N88-25422

Spacecraft requirements for predictions of geomagnetic activity (a tutorial)
[AD-A191943] 19 p2685 N88-25959

Gone with the solar wind: A study of protons accelerated by interplanetary shocks 19 p2743 N88-26283

Generation of Adlam-Allen waves by plasma release experiments in the solar wind
[PB88-106000] 20 p2886 N88-27140

Magnetohydrodynamic wave propagation in the solar wind
[DE88-702411] 21 p3032 N88-27995

Stability of Venusian ionopause
24 p3448 N88-30523

Corona-solar wind coupling review
[AFGL-TR-87-0203] 24 p3458 N88-30575

SOLAR WIND VELOCITY

Nature and the nonlinear evolution of electrostatic waves associated with the AMPTE (Active Magnetosphere Particle Tracer Explorers) solar wind releases
[AD-A185471] 06 p0806 N88-14920

Dynamics and turbulence of solar wind in area of its formation based on radio transmission data measured with Venera-15 and Venera-16 spacecraft
08 p1003 N88-16080

SOLAR X-RAYS

Small-scale energy storage and release as the cause of the stellar X-ray corona 02 p0255 N88-11615

A large X-ray flare on Sigma 2 coronae borealis observed with exosat 04 p0508 N88-13121

Magnetic reconnection and solar flare loops
08 p1094 N88-16583

Dynamic evolution of the source volumes of gradual and impulsive solar flare emissions
[NASA-TM-87815] 08 p1102 N88-16621

Solar-geophysical data number 517, September 1987. Part 2: (Comprehensive reports). Data for March 1987 and miscellanea
[PB88-128434] 10 p1431 N88-18545

The properties of solar coronal active regions deduced from X-ray line spectra
[AD-A193026] 20 p2886 N88-27141

Solar-geophysical data number 523, March 1988. Part 2: (Comprehensive reports). Data for September 1987 and miscellanea
[PB88-212774] 24 p3458 N88-30576

SOLAR-PUMPED LASERS

Design studies for a solar pumped laser device
[DFVLR-FB-87-39] 13 p1777 N88-20629

Direct solar-pumped iodine laser amplifier
[NASA-CR-182674] 13 p1777 N88-20630

Theoretical studies of solar-pumped lasers
[NASA-CR-182929] 17 p2344 N88-23971

Theoretical studies of solar lasers and converters
[NASA-CR-182927] 17 p2344 N88-23972

SOLDERED JOINTS

Fatigue and thermal fatigue of Pb-Sn solder joints
[DE87-012881] 01 p0024 N88-10150

Microstructural observations of the Sn-Pb solder/Cu system and thermal fatigue of the solder joint
[DE88-001392] 07 p0832 N88-15048

The inspection of metallurgical bounds in electronic systems
[AD-A192064] 18 p2582 N88-25343

Thermal cycling tests on surface-mount assemblies
[DE88-007695] 21 p2939 N88-27453

SOLDERING

The effect of organic inhibitors on the atmospheric corrosion and solderability of copper
[DE88-000261] 04 p0414 N88-12565

Cleanliness tests with the Omega Meter: A comparative study for solder flux removal
[DE88-004634] 11 p1460 N88-18704

Comparison of isopropyl alcohol and trichloroethylene in removing solder flux
[DE88-005556] 14 p1889 N88-21288

The inspection of electronic metallurgical bonds
[AD-A192197] 18 p2486 N88-24745

Conductivity mechanism and operating behavior of electrically conductive adhesives on the example of a power transistor
[ETN-88-92355] 21 p2940 N88-27484

SOLDERS

Fatigue and thermal fatigue of Pb-Sn solder joints
[DE87-012881] 01 p0024 N88-10150

Effect of hold time on fatigue of lead rich PbSn solder
06 p0715 N88-14387

Thermomechanical fatigue of lead-base low tin solder
06 p0721 N88-14432

Evaluation of solder flux solvents in a vapor-degreasing application for hybrid microcircuits
[BDX-613-3636] 11 p1468 N88-18752

SOLENOIDS

High repetition rate electron beam RF-acceleration and sub-millimeter wave generation via a free electron laser
[AD-A186066] 07 p0858 N88-15209

Harmonic expansion for the magnetic field of the helical solenoid
[DE88-700100] 07 p0928 N88-15638

Robotic assembly and testing of rotary solenoids
[BDX-613-3663] 11 p1480 N88-18834

Use of magnetic materials in excimer laser circuits
[DE88-006449] 19 p2674 N88-25903

SOLID ELECTRODES

Fundamental studies of surfaces processes and trace analysis using solid electrodes
[AD-A186156] 07 p0828 N88-15024

The overcharge behavior of polymer electrolyte cells
[AD-A193984] 22 p3117 N88-29522

SOLID ELECTROLYTES

Nuclear magnetic resonance studies of ion motion in solid electrolytes
[DE87-014547] 02 p0232 N88-11464

Studies of alumina additions in zirconia - magnesia
[DE87-703500] 04 p0419 N88-12602

Effect of sidechain length and crosslinking on ionic conductivity in polyphosphazene solid electrolytes
[AD-A184419] 04 p0497 N88-13058

JPRS report: Science and technology. Japan
[JPRS-JST-87-028] 06 p0675 N88-14130

Gas separation using solid electrolytes described
06 p0675 N88-14131

Ionically conducting polymers: Principles and properties of solid electrolytes
[DE88-001552] 06 p0684 N88-14190

Lithium/polymer electrolyte interfacial instability
[AD-A187164] 09 p1147 N88-16874

Interfacial effects in thin Li/PEO cells at room temperature
[AD-A186974] 09 p1157 N88-16931

Thermogravimetric analysis of polymeric materials for an intermediate temperature solid electrolyte
[DE88-004854] 10 p1306 N88-17809

Electrochromic cells with lutetium diphthalocyanine and semisolid polymer electrolytes
[AD-A188031] 10 p1352 N88-18078

Electronic and ionic transport in polymers
[AD-A187253] 11 p1452 N88-18651

Lithium fast-ion conductors: Polymer based materials
[AD-A187879] 11 p1461 N88-18712

Fast protonic conducting solid electrolytes
[AD-A188524] 12 p1698 N88-20160

Contrasting conductance/viscosity relations in liquid states of vitreous and polymer solid electrolytes
[AD-A189378] 13 p1748 N88-20452

Recent advances in solid polymer electrolyte fuel cell technology
[DE88-005380] 15 p2092 N88-22464

The kinetics of contact noise in NaBeta alumina
[AD-A190651] 15 p2130 N88-22707

Preparation technology for thin film solid electrolyte fuel cells
[PB88-131925] 20 p2821 N88-26735

Failure analysis of Chloride Silent Power, Ltd. PB cells
[DE88-010567] 21 p2938 N88-27448

The overcharge behavior of polymer electrolyte cells
[AD-A193984] 22 p3117 N88-28522

Polymeric electrolytes
[AD-A193766] 23 p3198 N88-29031

SOLID LUBRICANTS

Composite bearing materials containing solid lubricant in filamentary form, stages 3 and 4
[IRD-87/2] 01 p0054 N88-10344

The wear process during the RUNNING-IN of steel in lubricated sliding
[NAL-TR-922T] 02 p0181 N88-11130

Calculation of the tribological properties of surfaces by semi-empirical methods
[AD-A184283] 04 p0450 N88-12791

Coatings for high-temperature bearings and seals
[NASA-TM-100249] 05 p0567 N88-13453

Literature review of solid lubrication mechanisms
[AD-A185010] 05 p0567 N88-13456

The tribological properties of MoS2 coatings in vacuum, low relative humidity and high relative humidity environments
[DE88-001611] 06 p0711 N88-14356

Sputtered silver films to improve chromium carbide based solid lubricant coatings for use to 900 C
[NASA-TM-100783] 08 p0973 N88-15885

Tribological properties of alumina-boria-silicate fabric from 25 to 850 C
[NASA-TM-100806] 11 p1464 N88-18726

The performance of thin solid films for satellite gears
14 p1876 N88-21209

A test facility for the in-vacuo assessment of dry lubricants and small mechanisms at cryogenic temperatures 14 p1878 N88-21224

High temperature solid lubrication by catalytically generated carbon
[AD-A190804] 16 p2182 N88-23004

Investigation of rolling contact fatigue of ball bearings
[NASA-TT-20196] 19 p2678 N88-25922

Status and directions of modified tribological surfaces by ion processes
[NASA-TM-101304] 22 p3063 N88-28176

Evaluation of transfer films of Salox M on 440C for HPOTP bearing cage applications, task 119
[NASA-CR-179020] 23 p3223 N88-29184

SOLID MECHANICS

Solid mechanics research for quantitative non-destructive evaluation
[AD-A188599] 08 p0993 N88-16010

A collaborative program of research in engineering sciences
[DE88-003383] 10 p1423 N88-18504

Symmetry and global bifurcation in nonlinear solid mechanics
[AD-A190521] 15 p2121 N88-22642

Probabilistic finite element methods
18 p2564 N88-25223

Analytical determination of critical crack size in solar cells
[NASA-CR-183129] 20 p2821 N88-26736

Finite element method for plate structures with inclined angles
[ILR-MITT-182] 21 p3008 N88-27842

Some stability criteria in fluid and solid mechanics
21 p3027 N88-27966

SOLID PHASES

Grain boundary phase equilibria in metallic systems
[DE87-014123] 01 p0104 N88-10679

Microgravity thaw experiment (MITEX)
17 p2427 N88-24439

SOLID PROPELLANT COMBUSTION

NT SOLID PROPELLANT IGNITION

Measurement of solid propellant combustion velocity by means of microwaves
[CERT-1/1316-MO] 03 p0283 N88-11778

Influence of shock wave and gas pressure on the behavior of a pyrotechnical device
[SNIAS-872-430-111] 05 p0570 N88-13477

Advantages of internal thermal protection in a pyrotechnical plunger
[SNIAS-872-430-114] 05 p0571 N88-13478

Numerical simulation applied to the development of a pyrotechnical system
[SNIAS-872-430-115] 05 p0571 N88-13479

A continuous oxidizer regression model for the combustion of composite solid propellants
[AD-A186742] 08 p0974 N88-15894

Holographic investigation of metalized solid propellant combustion in two-dimensional and three-dimensional rocket motors
[AD-A187000] 09 p1140 N88-16832

The correlation of HMX (cyclotetramethylenetetranitramine) particle characterization techniques to propellant burn rate
[AD-A187119] 09 p1140 N88-16833

Design of a solid fuel combustion chamber
[VTH-LR-447] 09 p1141 N88-16837

Investigation of the flow and combustion behavior in a solid fuel combustion chamber, including the measuring program
[VTH-LR-460] 09 p1141 N88-16838

Design of a gas mass flow control system for the gas inlet installation of a solid fuel combustion chamber
[VTH-LR-471] 09 p1141 N88-16839

Solid fuel combustion chamber
[VTH-LR-515] 09 p1141 N88-16842

Combustion mechanisms
[AD-A187979] 11 p1453 N88-18660

Speed control of a missile with throttleable ducted rocket propulsion 12 p1597 N88-19561

Combustion theory and related questions
[AD-A189160] 13 p1737 N88-20382

Laser ignition of nitramine composite propellants and crack propagation and branching in burning solid propellants
[AD-A189260] 13 p1753 N88-20483

Combustion behavior of the vitiator. Experimental results of a second test series
[VTH-LR-509] 18 p2484 N88-24734

Development of a computerized analysis for solid propellant combustion instability with turbulence
[NASA-CR-182351] 19 p2611 N88-25497

Combustion of PMMA (polymethylmethacrylate), PE (polyethylene) and PS (polystyrene) in a ramjet
[PB88-186572] 20 p2769 N88-26417

Reaction products of solid propellants after burning at pressures up to 1000 MPa. Comparison between theoretical and experimental results
[ISL-CO-227/87] 22 p3059 N88-28153

SOLID PROPELLANT IGNITION

Ignition studies in a two-stage closed vessel using various igniter materials
[ISL-CO-231/86] 09 p1142 N88-16843

Laser ignition of nitramine composite propellants and crack propagation and branching in burning solid propellants
[AD-A189260] 13 p1753 N88-20483

Some properties of ignition gases. Review of measuring results in the years 1981-1986)
[PB88-106968] 21 p2908 N88-27259

SOLID PROPELLANT ROCKET ENGINES

NT APOGEE BOOST MOTORS

NT SPACE SHUTTLE BOOSTERS

Results of the development motor 8 test firing
[GFO-78-692] 03 p0278 N88-11751

Destruction test of small scaled solid propellant motors
[ISAS-R-620] 03 p0278 N88-11752

Structural analysis of a bolted joint concept for the space shuttle's solid rocket motor casing
[NASA-TM-89092] 04 p0407 N88-12531

Modal survey of the space shuttle solid rocket motor using multiple input methods 05 p0593 N88-13817

Measurement of particle size distribution in a solid propellant rocket motor using light scattering
[AD-A184875] 06 p0673 N88-14124

Verification of FANTASTIC integrated code
07 p0924 N88-15613

A European apogee boost motor for GEOS
09 p1123 N88-16719

Holographic investigation of metalized solid propellant combustion in two-dimensional and three-dimensional rocket motors
[AD-A187000] 09 p1140 N88-16832

Measurements of particulates in solid propellant rocket motors
[AD-A187777] 11 p1446 N88-18621

NASA (National Aeronautics and Space Administration) procurement: The 1973 space shuttle solid rocket motor contractor selection
[PB88-135264] 11 p1447 N88-18623

Speed control of a missile with throttleable ducted rocket propulsion 12 p1597 N88-19561

Transient Pressure Test Article (TPTA) 1.1 and 1.1A, volume 1
[NASA-CR-179322-VOL-1] 12 p1603 N88-19588

A study of combustion and flow behaviour in solid-propellant rocket motors
[UTIAS-280] 13 p1732 N88-20357

The effect of combustion gas flow on the rotational dynamics of a spinning solid fuel rocket
13 p1732 N88-20358

Space shuttle solid rocket motor Profile Measuring Device (PMD) 14 p1928 N88-21495

Combustion of a double base fuel in the presence of inert gases
[INPE-4516-RPE/564] 16 p2170 N88-22936

Preliminary 2-D shell analysis of the space shuttle solid rocket boosters
[NASA-TM-100515] 17 p2348 N88-23989

Solid rocket motor aft field joint flow field analysis
[NASA-CR-179288] 18 p2474 N88-24675

SRM propellant and polymer materials structural test program
[NASA-TP-2821] 18 p2530 N88-25013

Driving of axial acoustic fields by side-wall stabilized premixed flames 19 p2629 N88-25592

Motor test data comparisons with laboratory data and stability predictions 19 p2629 N88-25594

One person's view of velocity-coupled instability
19 p2629 N88-25595

Measurement of particulate size in solid propellant rocket motors 19 p2630 N88-25599

An interactive computer code for preliminary design of solid propellant rocket motors
[AD-A192869] 20 p2766 N88-26399

Environmental monitoring of a titan 34D 5 1/2 segment solid rocket motor static firing
[AD-A192975] 20 p2766 N88-26400

Application of laser diffraction techniques to particle sizing in solid propellant rocket motors
[AD-A193841] 22 p3049 N88-28089

SRM (Solid Rocket Motor) propellant and polymer materials structural modeling
[NASA-TP-2824] 22 p3089 N88-28343

SRB/SLEEC (Solid Rocket Booster/Shingle Lap Extendible Exit Cone) feasibility study, volume 1
[NASA-CR-178973] 23 p3187 N88-28964

SOLID PROPELLANTS

NT COMPOSITE PROPELLANTS

NT DOUBLE BASE ROCKET PROPELLANTS

NT HMX

NT HTPB PROPELLANTS

NT METAL PROPELLANTS

NT NITRAMINE PROPELLANTS

NT PLASTIC PROPELLANTS

NT SOLID ROCKET PROPELLANTS

High pressure strand burn rate tests of polyvinylnitrate/nitramine propellants
[AD-A184178] 04 p0422 N88-12615

SRB combustion dynamics analysis computer program (CDA-1)
[NASA-CR-182404] 07 p0830 N88-15032

An investigation into the feasibility of using a dual-combustion mode ramjet in a high Mach number tactical missile
[AD-A186906] 09 p1119 N88-16705

Advanced B and Al combustion kinetics over wide temperature ranges
[AD-A190752] 15 p2036 N88-22128

Technical instructions for a control operating system of the gas flow installation for the solid fuel combustion chamber
[LR-507] 20 p2788 N88-26537

SOLID ROCKET BINDERS
Thermoplastic elastomers as LOVA binders
[AD-A185864] 07 p0835 N88-15067

SOLID ROCKET BOOSTERS (SPACE SHUTTLE)
U SPACE SHUTTLE BOOSTERS

SOLID ROCKET PROPELLANTS
NT DOUBLE BASE ROCKET PROPELLANTS
NT HMX
NT HTPB PROPELLANTS
NT METAL PROPELLANTS
Modal survey of the space shuttle solid rocket motor using multiple input methods 05 p0593 N88-13617
Measurements of particulates in solid propellant rocket motors
[AD-A187777] 11 p1446 N88-18621
LGM-30B stage 2 disected motor test report
[AD-A190771] 15 p2027 N88-22079
Advanced B and Al combustion kinetics over wide temperature ranges
[AD-A190752] 15 p2036 N88-22128
Crack opening and extension in inert solid propellant. An experimental study
[AD-A189808] 15 p2046 N88-22201
The 24th JANNAF Combustion Meeting, volume 1
[AD-A190163] 19 p2627 N88-25585
Characterization of a modified Rijke burner for measurement of distributed combustion
19 p2628 N88-25587
Propellant combustion response to oscillatory radiant heat flux 19 p2628 N88-25589
New instability phenomena in solid propellant combustion 19 p2628 N88-25591
A review of particle sizing methods in rocket propulsion 19 p2630 N88-25597
The scaling of the threshold conditions for solid propellant erosive burning 19 p2630 N88-25601
Dimensional analysis and experimental observation of the coupling phenomena between combustion and fracture of damaged propellant samples
19 p2630 N88-25603
Analysis of microwave burner measurement system using a microwave network analysis computer program
19 p2631 N88-25604
Pressure differential scanning calorimetry (DSC) evaluation of solid rocket propellant burn rate mod
19 p2631 N88-25606
Solid rocket motor performance: A workshop report
19 p2631 N88-25607
Structure of laminar, premixed flames of CH2O/NO2/O2 mixtures 19 p2632 N88-25613
Reaction products of solid propellants after burning at pressures up to 1000 MPa: Comparison between theoretical and experimental results
[ISL-CO-227/87] 22 p3059 N88-28153
Automatic data retrieval from rocket motor holograms
[AD-A195586] 24 p3337 N88-29864
Ignition and extinguishing of a Solid Fuel Ramjet (SOFRAM)
[FOA-C-20713-2.1] 24 p3337 N88-29865
Combustion diagnostics of propellant with new grain geometries
[AD-A194944] 24 p3342 N88-29895
Descriptive characterization of propellant particles
[AD-A195176] 24 p3356 N88-29985
Preliminary investigation of flow modeling during solid propellant processing
[AD-A196168] 24 p3357 N88-29987

SOLID ROTATION
U ROTATING BODIES

SOLID SOLUTIONS
Non-lattice matched metallic superlattices
[DE87-011512] 04 p0497 N88-13062
Growth of solid solution single crystals
[NASA-TP-2787] 06 p0688 N88-14212
The physics of metallic superlattices: An experimental point of view
[DE88-003080] 10 p1416 N88-18452
Positron-annihilation 2D-ACAR studies of disordered and defected alloys
[DE88-003118] 10 p1416 N88-18454
Irreversible dissolution of solid solutions: A kinetic and stoichiometric model
[DE88-009194] 19 p2614 N88-25513

SOLID STATE
Formation of amorphous alloys by solid state reactions
[DE87-013175] 02 p0146 N88-10918
Survey state of the art: Electrical load management techniques and equipment
[AD-A184083] 05 p0577 N88-13517
Study of solid state photomultiplier
[NASA-CR-177465] 05 p0583 N88-13556
New branch of solid-state physics
08 p1079 N88-16508
Solid state research
[AD-A185987] 09 p1253 N88-17508
Studies of nonlinear and chaotic phenomena in solid state systems
[DE88-002330] 09 p1254 N88-17515
Solid-state voltage standard performance and design guidelines
[PB88-123757] 10 p1322 N88-17[illegible]5
Studies in solid state ionics
[DE88-700830] 11 p1559 N88-19333
Test results of high-voltage, high-power, solid-state remote power controllers
[NASA-TM-100322] 16 p2194 N88-23085
Interface characterization of Cu-Cu and Cu-Ag-Cu low temperature solid state bonds
[AD-A191015] 16 p2263 N88-23667
Reactor instrumentation and control design and performance simulation for SP-100
17 p2406 N88-24306
Solid-state combustion synthesis of ceramics and alloys in reduced gravity
[NASA-CR-4163] 19 p2608 N88-25479
Raman and absorption spectrophotometric studies of selected lanthanide, californium-doped lanthanide, and actinide trihalides in the solid state
[DE88-008234] 20 p2874 N88-27061

SOLID STATE DEVICES
NT AVALANCHE DIODES
NT BIPOLAR TRANSISTORS
NT CHARGE COUPLED DEVICES
NT CHARGE TRANSFER DEVICES
NT CMOS
NT CRYSTAL RECTIFIERS
NT FIELD EFFECT TRANSISTORS
NT GALLIUM ARSENIDE LASERS
NT GERMANIUM DIODES
NT HETEROJUNCTION DEVICES
NT HIGH ELECTRON MOBILITY TRANSISTORS
NT JFET
NT JUNCTION DIODES
NT JUNCTION TRANSISTORS
NT LIGHT EMITTING DIODES
NT METAL OXIDE SEMICONDUCTORS
NT MIM (SEMICONDUCTORS)
NT MIM DIODES
NT MIS (SEMICONDUCTORS)
NT MODFETS
NT MSM (SEMICONDUCTORS)
NT PHOTODIODES
NT PHOTOVOLTAIC CELLS
NT RUBY LASERS
NT SCHOTTKY DIODES
NT SEMICONDUCTOR DEVICES
NT SEMICONDUCTOR LASERS
NT SILICON TRANSISTORS
NT SIS (SEMICONDUCTORS)
NT SOI (SEMICONDUCTORS)
NT SOLAR CELLS
NT SOLID STATE LASERS
NT SOS (SEMICONDUCTORS)
NT THERMISTORS
NT THYRISTORS
NT TRANSFERRED ELECTRON DEVICES
NT TRANSISTOR AMPLIFIERS
NT TRANSISTORS
NT VARISTORS
NT VERTICAL JUNCTION SOLAR CELLS
NT YAG LASERS
Chemically modified microelectrode arrays. New kinds of electronic devices
[AD-A184389] 04 p0439 N88-12724
Fabricate, calibrate and test a dosimeter for integration into the CRRES (Combined Release and Radiation Effects Satellite) satellite
[AD-A185439] 05 p0585 N88-13564
Evaluation of high-voltage, high-power, solid-state remote power controllers for amps
07 p0924 N88-15612
Joint services electronics program
[AD-A187587] 10 p1325 N88-17920
Electrochromic cells with lutetium diphthalocyanine and semisolid polymer electrolytes
[AD-A188031] 10 p1352 N88-18078
The physics of very small structures
[AD-A187672] 11 p1556 N88-19311
Solid state research
[AD-A188388] 12 p1699 N88-20166
Solid-state electrochemical processes in dye films
[AD-A188756] 13 p1844 N88-21036
Instrumentation for the characterization and development of millimeter wave components compatible with monolithic integration
[AD-A189724] 15 p2059 N88-22275
Hermetically sealable package for hybrid solid-state electronic devices and the like
[NASA-CASE-MSC-20181-1] 17 p2335 N88-23941
Characterization of a 30-GHz IMPATT solid state amplifier
[NASA-TM-100876] 18 p2503 N88-24847
Joint services electronics program
[AD-A192076] 18 p2504 N88-24856
Organization of a Topical Meeting on Picosecond Electronics and Optoelectronics
[AD-A187136] 19 p2655 N88-25785
On 3-5 transistors for MM-wave applications
[AD-A191580] 19 p2661 N88-25825
The 1986 IEEE Solid-State Sensor Workshop
[AD-A190922] 19 p2668 N88-25860
Development of a GaAs solid state device model for high power applications
[DE88-009048] 19 p2734 N88-26242
A GaAs solid state device model for high power applications
[DE88-011320] 21 p2939 N88-27457
Solid state research
[AD-A192837] 21 p3020 N88-27929
Space-charge-wave solid state microwave amplifier
[AD-A193792] 23 p3208 N88-29091
Phase sensitive amplification with SIS (Superconductor-Insulator-Superconductor) quasiparticle mixers
[AD-A194594] 23 p3291 N88-29596
High power storage system based on thin film solid ionics
[AD-A193623] 23 p3291 N88-29598

SOLID STATE LASERS
NT GALLIUM ARSENIDE LASERS
NT RUBY LASERS
NT YAG LASERS
Diode pumped solid-state laser oscillators for spectroscopic applications
[NASA-CR-180576] 01 p0052 N88-10331
High energy efficient solid state laser sources
[NASA-CR-181362] 01 p0052 N88-10332
High average power solid state laser power conditioning system
[DE87-013558] 03 p0328 N88-12071
Laser development, evolution of applied technologies described 06 p0689 N88-14221
Super-short yttrium aluminate pulse generator with controlled resonator Q-factor 06 p0772 N88-14740
Laser Program
[DE87-011009] 07 p0858 N88-15212
The YAlO(sub 3):Er laser
[PB88-130877] 11 p1493 N88-18911
Growth of Cr,Nd:Gd3Sc2Al3O12 (Cr,Nd:GSAG) crystals by the Heat Exchanger Method (HEM)(trademark)
[DE88-004041] 11 p1558 N88-19326
High power, high efficiency 770 nm laser diode array
[DE88-004043] 12 p1631 N88-19762
Direct solar-pumped iodine laser amplifier
[NASA-CR-182674] 13 p1777 N88-20630
High power, high efficiency, 2D laser diode arrays for pumping solid state lasers
[DE88-004042] 13 p1777 N88-20632
Energy transfer and non-linear optical properties at near ultraviolet wavelengths: Rare earth 4f yields 5d transitions in crystals and glasses
[DE88-005403] 13 p1840 N88-21012
Time characteristics of ultrashort light pulses from dye lasers with distributed feedback
14 p1970 N88-21759
Solid-state ring laser with acoustooptical phase nonreciprocity of opposing waves
14 p1970 N88-21761
Nonlinear stage of ultrashort-pulse formation in solid-state laser 14 p1971 N88-21765
Tunable optical sources/growth and characterization of nonlinear optical materials
[AD-A190874] 16 p2274 N88-23608
Fracture of solid state lasers
[DE88-007023] 18 p2522 N88-24961
Laser spectroscopy investigations of materials for solid state laser systems
[AD-A192514] 21 p2952 N88-27535
A new near-infrared tunable-room temperature solid state laser La3Ga5SiO14:Cr(3+)
[DE88-011341] 21 p2953 N88-27543
Solid-state laser research report: Energy transfer in non-uniform codoped crystals
[AD-A194358] 23 p3219 N88-29161
Spectral properties of semiconductor lasers with external resonators
[ETN-88-93119] 24 p3379 N88-30125

SOLID SURFACES
NT CRYSTAL SURFACES
An investigation of the behavior of outgassed molecules in thermal vacuums 02 p0133 N88-10806

Application of spin-sensitive electron spectroscopies to investigations of electronic and magnetic properties of solid surfaces and epitaxial systems
[DE87-014235] 02 p0245 N88-11550

Pure dephasing of a vibrational adbond
[AD-A185222] 05 p0609 N88-13740

Unified study of plasma-surface interactions for space power and propulsion
[AD-A186211] 07 p0825 N88-15007

A model for nitrogen atom recombination on a silicon dioxide surface
[AD-A189643] 15 p2142 N88-22784

SOLID SUSPENSIONS

Stochastic model of the motion of suspended particles in turbulent flow
[HSBW-MITT-21/1987] 03 p0315 N88-11990

The influence of yellow substances on remote sensing of sea-water constituents from space
08 p1044 N88-16308

A small concentration expansion for the effective heat conductivity of a random disperse two-component material; an assessment of Batchelor's renormalization method
[REPT-87-71] 16 p2207 N88-23168

SOLID-SOLID INTERFACES

Behavior of metal ceramic interfaces
[PB87-147500] 07 p0837 N88-15076

Formation and passivation of new paramagnetic defects associated with thermal oxides on silicon
[DE88-002720] 07 p0936 N88-15699

Interfacial effects in thin Li/PEO cells at room temperature
[AD-A186974] 09 p1157 N88-16931

Thermodynamics of wetting by liquid metals
[DE88-003634] 11 p1563 N88-19360

Friction and wear of ceramics
17 p2323 N88-23874

Studies of metal-silicon, silicon-metal and silicide based interfaces: Synchrotron radiation photo emission and inverse photoemission investigations of interface formation and compound nucleation
[AD-A191808] 19 p2619 N88-25536

Thermo-mechanical cracking in coated media with a cavity by a moving asperity friction
[AD-A193311] 21 p2961 N88-27586

Green's function approach to roughening transition of one-dimensional restricted solid on solid model
[DE88-702723] 23 p3278 N88-29512

SOLIDIFICATION

NT MELT SPINNING

Formation of amorphous alloys by solid state reactions
[DE87-013175] 02 p0146 N88-10918

Structure of rapidly solidified Ni-Ti
[DE87-012252] 02 p0147 N88-10921

On the role of convective motion during dendrite growth: Experiments under variable gravity, revised
[NASA-CR-179213] 02 p0156 N88-10979

Shock-induced melting and rapid solidification
[DE88-000226] 03 p0288 N88-11810

Influence of boron on porosity in nickel-base superalloy castings 03 p0299 N88-11877

Analytical treatment of the melting and solidification of latent heat store materials in finned tube geometries
[IKE-5-223] 03 p0314 N88-11985

Microstructure of amorphous and crystalline zirconium alloys rapidly solidified
[DE87-703700] 05 p0564 N88-13432

Effect of rapid solidification on short-range order: A magnetic study
[AD-A185216] 05 p0565 N88-13444

Tensile properties of extrusion consolidated Type 304 SS rapidly solidified powders
[DE87-014875] 05 p0566 N88-13450

Effect of rapid solidification on stainless steel weld metal microstructures and its implications on the Schaeffler diagram
[DE88-001489] 05 p0566 N88-13451

Development of iron aluminides
[AD-A185190] 05 p0568 N88-13461

Thermo-mechanical behavior of high temperature fiber composites 06 p0678 N88-14 49

Behavior and structure of metal vapor arc plasma between molten electrodes
[DE88-001854] 06 p0782 N88-14801

Cellular solidification in a monotectic system
[NASA-TM-100317] 07 p0829 N88-15027

A numerical thermal model of the rapid solidification parameters in the capacitor discharge welding process
[DE88-002206] 07 p0864 N88-15244

Investigations in field of surface forces in metallurgy
[BLL-M-47406-(5828.4)] 08 p0969 N88-15860

Transparent metal model study of the use of a cellular growth front to form aligned monotectic composite materials
[NASA-CR-182414] 08 p0969 N88-15861

Spray deposition: A fundamental study of droplet impingement, spreading and consolidation
[AD-A186627] 08 p0970 N88-15869

Microstructural modification during laser welding
[DE88-002344] 09 p1144 N88-16860

Microgravity research at the University of Mexico: Experiments in payload G-006 10 p1286 N88-17692

Application of Onsager's reciprocity relations to interface motion
[DE88-003286] 10 p1397 N88-18327

Void formation in solidification
[DE88-003895] 11 p1452 N88-18650

Effect of density change on rapid liquid-solid interface kinetics and heat flow
[DE88-004286] 11 p1487 N88-18878

Development of metastable processing paths for high temperature alloys
[AD-A188682] 12 p1608 N88-19617

A fundamental understanding of the effect of alloying elements on the corrosion resistance of rapidly solidified Mg alloys
[AD-A189385] 13 p1741 N88-20413

Experimental and theoretical methods for investigating helium effects in rapidly solidified metals
[DE88-005542] 13 p1743 N88-20425

Growth and deformation mechanisms of refractory alloy hybrid materials
[AD-A190492] 15 p2039 N88-22152

Characterization of an explosively consolidated rapidly solidified Fe-16Ni-9Cr-5Mo-2Cu alloy powder
[DE88-006733] 15 p2041 N88-22162

Remarks on solid state amorphizing transformations
[DE88-006452] 15 p2145 N88-22803

The weldability of consolidated rapidly solidified Type 304 SS powders
[DE88-006738] 16 p2178 N88-22978

Deformation of rapidly solidified dispersion strengthened titanium alloys
[AD-A190793] 16 p2179 N88-22984

Effect of alloying, rapid solidification, and surface kinetics on the high temperature environmental resistance of niobium
[AD-A192093] 18 p2485 N88-24743

Laboratory scale inert gas atomizer for producing rapidly solidified powders
[DE88-006734] 18 p2497 N88-24812

Survey of the literature on fractals with possible applications to phase change processes
[DE88-012240] 21 p2911 N88-27277

A computer model for the flow of a molten polymer in a narrow cavity
[NPL-DMA(A)-157] 22 p3058 N88-28146

Solidification with natural circulation
[DE88-011197] 22 p3074 N88-28248

A fundamental study of P/M processed elevated temperature aluminum alloys
[AD-A192958] 23 p3194 N88-29005

An investigation into the metallurgical aspects of joining rapidly-solidified aluminum alloys
[AD-A194677] 23 p3194 N88-29009

SOLIDS

TIPS-1 user's manual: Cray-1 version
[DE87-013297] 01 p0081 N88-10522

Theory of defects in non-metallic solids
[DE87-014068] 02 p0152 N88-10949

Electron capture from solids by positrons
[DE87-014355] 02 p0232 N88-11463

Optical instrumentation and study of gas-solid suspension flows
[DE88-000147] 04 p0442 N88-12744

Monocrystal sputtering by the computer simulation code ACOCT
[IPPJ-848] 04 p0493 N88-13035

Shock compression of solids as a physical-chemical-mechanical process
[DE88-001674] 05 p0563 N88-13427

Vibrational properties of disordered solids: Far infrared studies: Performance report
[DE88-001474] 06 p0786 N88-14821

Impact of solids on composite materials
[NASA-CR-182395] 07 p0827 N88-15015

Pressure and mass velocity measurements in solids subjected to dynamic loadings 07 p0921 N88-15595

Equation of state of condensed materials physical principles and applications
[NASA-TT-20007] 08 p0968 N88-15855

A guide to the transient three phase porous flow model implemented in the two-dimensional CRAY-TENSOR code: Physics, numerics, and code description
[DE88-003709] 09 p1165 N88-16983

A modified version of the phase sensitive technique for measurements of absolute sound velocity in solids
[DE88-002303] 10 p1405 N88-18378

Pulsed laser photothermal spectroscopy of liquids and solids
[DE88-003839] 11 p1455 N88-18675

Wave curves for simple isotropic elastic solids
[AD-A188865] 12 p1636 N88-19798

Stress analysis in elastic solids with many cracks
[AD-A189015] 12 p1635 N88-19799

Material instabilities in solids
[AD-A189525] 13 p1738 N88-20388

Properties of molecular solids and fluids at high pressure and temperature
[DE88-004195] 13 p1738 N88-20391

Innovative, counterflow gas/fine solids, direct contact heat exchanger
[DE88-004744] 13 p1770 N88-20585

Particle-dynamics calculations of gravity flow of inelastic, frictional spheres
[DE88-005224] 13 p1770 N88-20586

Kinetics of combustion of finely divided solid fuel in granules
[BLL-M-37626-(5828.4)] 14 p1888 N88-21283

Theory of Muon method for study of solid and liquid hydrogen 14 p1972 N88-21770

Density measurements on solids and liquids
[PB88-164934] 15 p2036 N88-22129

A 3-D solid rendering of NDT data
[DE88-006199] 15 p2076 N88-22373

Dynamical optimization techniques for the calculation of electronic structure in solids
[DE88-006010] 15 p2140 N88-22768

Thermal and power availability transient responses for the Argonne monolithic solid oxide fuel cell
17 p2419 N88-24384

Self-consistent model for the brittle response of solids
18 p2528 N88-24999

An evaluation of some thermodynamic and transport properties of solid and liquid lithium over the temperature range 200 to 1700 K
[DE88-008947] 19 p2614 N88-25512

A general qualitative study of point and extended defects and their interactions in non-metallic systems
[AD-A191687] 19 p2618 N88-25532

Equation of state of solid neon from X-ray diffraction measurements to 110 GPa
[DE88-008723] 19 p2734 N88-26241

Research on the kinetics of phase changes in solids
[AD-A192222] 20 p2814 N88-26696

Lattice theory of fracture of solids with layered structure
[DE88-701867] 20 p2876 N88-27073

A comparison of analytical techniques for modeling the Rayleigh-Taylor response of elastic plastic solids
[DE88-010372] 21 p2962 N88-27596

Monolithic fuel cells
[DE88-012004] 21 p2969 N88-27638

SOLIDS FLOW

Laser velocimeter measurements of solids in multiphase flow
[DE88-000196] 11 p1487 N88-18876

LLNL granular solids flow project
[DE88-007492] 18 p2513 N88-24906

LLNL Granular Solids Flow Project
[DE88-008023] 19 p2564 N88-25844

SOLITARY WAVES

Intensive synoptic eddies and quasigeostrophic approximation 04 p0460 N88-12844

Dynamics of isolated intrathermocline eddy
04 p0460 N88-12845

Soliton twin boundaries of the cubic-tetragonal martensitic transformations in ferroelastic materials
[DE87-014741] 04 p0495 N88-13047

Solitons in stimulated Raman scattering: Generation and control of ultrashort optical pulses
[AD-A185141] 05 p0650 N88-13983

The Eckhaus Partial Differential Equation (PDE) I psi t + psi xx + 2(psi/sq)x psi + 2(/psi/) to the 4th power psi = 0
[PREPRINT-546] 06 p0762 N88-14686

Soliton mode of propagation of light pulses through single-mode optical fibers and problems of its experimental realization 07 p0920 N88-15592

Experiments on ion-acoustic rarefactive solitons in a multi-component plasma with negative ions
[INPE-4393-PRE/1213] 08 p1086 N88-16542

Relativistic Calogero-Moser systems and solutions
[CWI-PM-R8702] 08 p1092 N88-16570

Low frequency waves and small scale solitary structures observed by Viking — Swedish satellite, auroras
08 p1099 N88-16611

Advanced studies of integrable systems
[AD-A186792] 09 p1151 N88-16895

The 80 fsec soliton-like pulses from an optical nonlinear fiber resonator
[PB88-127303] 10 p1403 N88-18403

Super Virasoro algebra and solvable supersymmetric quantum field theories
[DE88-752299] 15 p2127 N88-22681

Interaction of solitons in single model optical fibres
17 p2439 N88-24511

Nonlinear surface polaritons [AD-A191046] 18 p2499 N88-24822
Nonlinear surface and internal waves on shear flow [PREPRINT-584] 22 p3129 N88-28604
The construction of implicit and explicit solitary wave solutions of nonlinear partial differential equations [AD-A193475] 23 p3269 N88-29452
On nonlinear equations admitting soliton solutions with a deBroglie phase [DE88-702694] 23 p3277 N88-29508
Characteristics of solitary waves and weak double layers in the magnetospheric plasma [IRF-PREPRINT-105] 24 p3431 N88-30418

SOLITONS
U SOLITARY WAVES

SOLUBILITY
Aqueous-phase reactions in clouds [DE86-005249] 01 p0069 N88-10445
Thermodynamics of interaction between nitrogen and molten nickel alloys [BLL-M-37309-(5828.4)] 02 p0149 N88-10934
Near-infrared dichroism of a mesogenic transition metal complex and its solubility in nematic hosts [DE87-014471] 03 p0287 N88-11805
Investigation of structure-permeability relationships of silicone polymer membranes [PB87-230181] 03 p0293 N88-11839
Physical properties of immiscible polymers 03 p0297 N88-11868
High temperature superconductors 03 p0297 N88-11869
Conducting hybrid polymeric systems [DE88-000527] 04 p0421 N88-12611
Electrochemical characteristics of acid electrolytes for fuel cells [PB88-104641] 06 p0731 N88-14497
Soluble polysilane derivatives: Chemistry and spectroscopy [AD-A187889] 11 p1461 N88-18713
Physics of immiscible flow in porous media [PB88-131008] 11 p1487 N88-18873
Evaluation and prediction of Henry's law constants and aqueous solubilities for solvents and hydrocarbon fuel components. Volume 1: Technical discussion [AD-A188571] 12 p1613 N88-19643
Prediction of thermodynamic properties, including solubility equilibria and vapor pressures, for mixed aqueous electrolytes to high temperatures [DE88-006317] 14 p1990 N88-21863
Improved structural polymer alloys and composites [AD-A192092] 19 p2619 N88-25538
Synthesis of model polymers and related structures in support of vinyl monomer grafting studies [DE88-010245] 20 p2778 N88-26476
Critical point wetting drop tower experiment [NASA-CR-183062] 20 p2798 N88-26603
A method for determining the solubility of hydrogen in molten aluminum-lithium alloys [DE88-009807] 21 p2910 N88-27270
Interfacial tension of immiscible polymer blends: Temperature and molecular weight dependence [AD-A192463] 21 p2917 N88-27312
Soluble metal chelate polymers of coordination numbers six, seven and eight [AD-A192465] 21 p2917 N88-27314
Natural frequencies and stability of immiscible cylindrical z-independent liquid systems [LRT-WE-9-FB-1(1987)] 22 p3053 N88-28112

SOLUTES
Van der Waals clusters of aromatic molecules studied using supersonic molecular jet spectroscopy [AD-A186087] 07 p0929 N88-15644
Thermosolutal convection in high-aspect-ratio enclosures [NASA-TM-100803] 11 p1486 N88-18871
The coordination cluster theory for metallic solutions [DE88-005934] 13 p1738 N88-20389
High resolution detection of solute segregation to the cores of dislocations in grain boundaries [DE88-009168] 20 p2877 N88-27076

SOLUTION
Numerical solution of weak forms of conservation laws on optimal unstructured triangular grids 20 p2797 N88-26597
Solution of the Orr-Sommerfeld equation for the Blausius boundary-layer documentation of program ORRBL and a test case [NASA-CR-4169] 20 p2841 N88-26858
A systolic array for efficient execution of the Faddeev algorithm [DE88-011330] 22 p3135 N88-28635

SOLUTIONS
NT AIR
NT ALVEOLAR AIR
NT AQUEOUS SOLUTIONS
NT DETONABLE GAS MIXTURES
NT GAS MIXTURES
NT HIGH TEMPERATURE AIR
NT SOLID SOLUTIONS
Accurate, stable, explicit solution of the parabolized Navier-Stokes equations 01 p0043 N88-10276
Theory of interstitial solutions [BLL-M-37314-(5828.4)] 02 p0233 N88-11469
A 13C and 15N solid state NMR characterization of aramid-containing nylon-6 polymers synthesized by in situ polymerization of caprolactam with benzoyl caprolactam derivatives [AD-A187067] 09 p1147 N88-16872
On the barotropic model of the ocean circulation [AD-A188148] 10 p1358 N88-18118
The coordination cluster theory for metallic solutions [DE88-005934] 13 p1738 N88-20389
Prediction of high-temperature thermodynamic properties of mixed electrolyte solutions including solubility equilibria, vapor pressure depression and boiling point elevation [DE88-006344] 13 p1849 N88-21069
Fingering flow patterns of thermosolutal convection in rectangular enclosures [NASA-TM-100854] 14 p1911 N88-21417
Almost-periodic solutions of nonlinear parabolic equations [DE88-006423] 15 p2118 N88-22618
Bayesian solutions to a 2 x 2 decision matrix using interval scaled payoffs with an application to foreign policy decisions [AD-A190863] 16 p2260 N88-23511
Certain questions of thermodynamic theory of weak solutions 18 p2586 N88-25368
The influence of uncompensated solution resistance on the determination and standard electrochemical rate constants using cyclic voltammetry and some comparisons with AC voltammetry [AD-A192825] 20 p2770 N88-26427
A matroid algorithm and its application to the efficient solution of two optimization problems on graphs, revision [AD-A192709] 20 p2838 N88-26838
Ill-posed problems and integral equations [AD-A193709] 22 p3143 N88-28691
The construction of implicit and explicit solitary wave solutions of nonlinear partial differential equations [AD-A193475] 23 p3269 N88-29452
Weak solution of the Langevin equation on a generalized functional space [AD-A194290] 23 p3270 N88-29456
Structure and dynamics of solutions of lithium salts relevant to battery construction [AD-A195399] 24 p3366 N88-30044

SOLVENTS
Effects of solvent exposures on poly(etheretherketone) (PEEK) and PEEK-fiberglass composites [MLM-3405] 03 p0281 N88-11766
Saturable absorbers for colliding pulse-locked Nd:YAG lasers 03 p0302 N88-11902
Re-usable thin-layer spectroelectrochemical cell for non-aqueous solvent systems [AD-A186951] 09 p1248 N88-17478
Cleanliness tests with the Omega Meter: A comparative study for solder flux removal [DE88-004634] 11 p1460 N88-18704
Comparison of isopropyl alcohol and trichloroethylene in removing solder flux [DE88-005556] 14 p1889 N88-21288
A study of solvent effects on the synthesis of pure component and composite ceramic powders by metal alkoxide hydrolysis [DE88-008381] 20 p2777 N88-26470
Hydrogen storage by molecular polyhydrides [AD-A194207] 23 p3191 N88-28989

SOLVOLYSIS
Descriptive characterization of propellant particles [AD-A195176] 24 p3356 N88-29985

SONAR
Independence in sonar observations [ARE-TR-87102] 01 p0088 N88-10572
The effect of reverberation on active sonar performance [ARE-TM(UJS)-87104] 03 p0374 N88-12350
Correction of inertial navigation system drift errors for an autonomous land vehicle using optical radar terrain data [AD-A184973] 05 p0544 N88-13311
User manual for ATILA, a finite-element code for modeling piezoelectric transducers [AD-A185948] 07 p0847 N88-15141
Transient classifier systems and man-machine interface research [AD-A186213] 07 p0899 N88-15446
Observations of the upper ocean using a multi-beam Doppler sonar [AD-A188896] 12 p1649 N88-19878
Human efficiency for visual detection of targets on CRT displays using a two-level multiple channel time history format [AD-A188419] 12 p1670 N88-20001
Observations of waves and Langmuir circulation with Doppler sonars 13 p1805 N88-20790
Robot navigation using simple sensor fusion [DE88-006184] 18 p2561 N88-25203
Treatment of systematic errors in the processing of wide angle sonar sensor data for robotic navigation [DE88-008961] 20 p2756 N88-26352
Sensor fusion for robot navigation [DE88-008383] 20 p2809 N88-26663
Signal, noise, and reverberation in bistatic sonar systems [FOA-C-20703-2.7] 22 p3147 N88-28721
Basic research in electronics (JSEP) Joint Services Electronics Program [AD-A193072] 23 p3206 N88-29079

SONDES
NT IONOSONDES
NT RADIOSONDES
NT RAWINSONDES
Ozonesonde observations at Lauder, New Zealand during the Spring and early Summer of 1986 [PB88-173273] 16 p2232 N88-23328

SONIC BOOMS
MOAOPS and BOOM-MAP computer programs for sonic boom research, volume 1 [AD-A189548] 12 p1574 N88-19414

SONIC FATIGUE
U ACOUSTIC FATIGUE

SONIC FLOW
U TRANSONIC FLOW

SONIC SPEED
U ACOUSTIC VELOCITY

SOOT
An instrument for the quasi-continuous determination of atmospheric soot content [DFVLR-FB-87-04] 01 p0068 N88-10433
Investigation of fuel additive effects on sooting flames [AD-A186403] 07 p0829 N88-15026
Ionic mechanisms of soot formation in flames [AD-A186195] 08 p0966 N88-15848
Measurements of gas turbine combustor and engine augmentor tube sooting characteristics [AD-A187831] 11 p1440 N88-18592
Fuels combustion research [AD-A187688] 11 p1453 N88-18657
Experimental and theoretical analysis of the radiative transfer within a sooty pool fire [DE88-007099] 20 p2769 N88-26419
Real-time measurements of the size fractionation of ambient black carbon aerosols at elevated humidities [DE88-010870] 23 p3215 N88-29138
Combustion and fuels in gas turbine engines [AGARD-CP-422] 24 p3345 N88-29910
The performance of a surrogate blend in simulating JP-4 in a spray-fueled combustor 24 p3347 N88-29926
Radiation from soot-containing flames 24 p3347 N88-29927
Flamelet chemistry modelling of soot formation for radiation 24 p3348 N88-29928
Large ionic species in sooting acetylene and benzene flames 24 p3348 N88-29932
Rates of formation of soot from hydrocarbon flames and its destruction 24 p3349 N88-29933
The influence of pressure on soot formation 24 p3349 N88-29934
Particle sizing in combustion systems, using scattered laser light [AD-A196231] 24 p3352 N88-29953
Optical measurements of soot and temperature profiles in premixed propane-oxygen flames [NASA-TM-101343] 24 p3358 N88-29997
Optical measurements of soot in premixed flames [NASA-TM-101305] 24 p3373 N88-30090

SORBENTS
NT ADSORBENTS

SORPTION
NT ADSORPTION
NT CHEMISORPTION
Working fluids for sorption heat pumps [DE88-900203] 07 p0874 N88-15301
Synthesis and analysis of novel polymers with potential for providing both high permselectivity and permeability in gas separation applications [DE88-006533] 15 p2043 N88-22174

SORTING
U CLASSIFYING

SOS (SEMICONDUCTORS)
Silicon-sapphire waveguides [AD-A191754] 18 p2504 N88-24854
Investigation of photoconductive picosecond microstripline switches on self-implanted Silicon On Sapphire (SOS) 19 p2657 N88-25789

Carrier lifetime versus ion-implantation dose in Silicon On Sapphire 19 p2658 N88-25791
Picosecond optoelectronic switches using composite electronic materials 19 p2658 N88-25792
JFET/SOS (Junction Field-Effect Transistor/Silicon-on-Sapphire) devices: Gamma-radiation-induced effects
[AD-A193001] 20 p2795 N88-26586

SOUND
U ACOUSTICS

SOUND ABSORPTION
U SOUND TRANSMISSION

SOUND AMPLIFICATION
A continued study of optical sound generation and amplification
[AD-A188362] 12 p1691 N88-20116

SOUND BARRIER
U ACOUSTIC VELOCITY

SOUND DETECTING AND RANGING
A method of improving remote reproduction of a sound field by one-third-octave analysis and digital filtering
[RAE-TM-FS(F)-679] 22 p3147 N88-28722

SOUND DETECTORS
U SOUND TRANSDUCERS

SOUND FIELDS
Excitation of natural oscillations of a boundary layer by an external acoustic field 04 p0425 N88-12634
RADSPHERE: A computer program for calculating the steady-state, axially symmetric, forced response and radiation field of a submerged spherical shell
[AD-A185025] 05 p0609 N88-13738
Development of a new method of measuring the characteristic impedance and complex wave number of a porous acoustic material
[AD-A185038] 05 p0646 N88-13957
Mode pattern of field generated by parametric radiator in acoustic waveguide 08 p1076 N88-16488
Acoustic field in waveguide with sloping bed
08 p1076 N88-16490
Sound propagation through a turbulent atmosphere: Experimental techniques and data analysis
[AD-A188691] 12 p1688 N88-20094
Invariant characteristics of acoustic field in stratified ocean 13 p1788 N88-20698
Measurement and analysis of the noise radiated by low Mach numbers centrifugal blowers
[AD-A189226] 13 p1833 N88-20966
Flow/acoustic interaction in duct inflow
[AD-A189264] 13 p1833 N88-20967
Acoustic radiation from line- and point-loaded plates: Uniformly asymptotic solutions
[AD-A189367] 13 p1834 N88-20969
A computerized investigation using the method of images to predict the sound field in a fluid wedge overlying a slow fluid half-space
[AD-A190013] 15 p2130 N88-22704
Driving of axial acoustic fields by side-wall stabilized premixed flames 19 p2629 N88-25592
Numerical investigation of acoustic energy exchange through flow turning 19 p2629 N88-25593
Velocity coupling 19 p2629 N88-25596
Vertical directionality of ambient noise at 32 deg N as a function of longitude: Tape number 86180
[AD-A193226] 21 p3012 N88-27872
The covariance of scalar fields scattered by pressure-release randomly rough surfaces
[AD-A192489] 22 p3146 N88-28714
A method of improving remote reproduction of a sound field by one-third-octave analysis and digital filtering
[RAE-TM-FS(F)-679] 22 p3147 N88-28722
Acoustic pressure distribution on the bottom of a wedge-shaped ocean
[AD-A193961] 23 p3278 N88-29518

SOUND FIXING AND RANGING
Outdoor sound propagation, its implications for unattended ground sensors
[FEL-1986-64] 20 p2850 N88-26917

SOUND FREQUENCIES
U ACOUSTIC FREQUENCIES

SOUND GENERATORS
Flow induced pulsations in pipe systems
[ETN-88-91367] 06 p0702 N88-14307
Linear theory of generation of longitudinal sound waves in semiconductors upon interband absorption of optical radiation 09 p1234 N88-17397
A continued study of optical sound generation and amplification
[AD-A188362] 12 p1691 N88-20116
Design of a sound neck in connection with the model-support system of a transonic wind tunnel test section
[ILR-MITT-186(1987)] 14 p1869 N88-21171
Software development for the reconstruction of source parameters using research and development arrays
[REPT-840445-TW] 16 p2246 N88-23417

SOUND INTENSITY
Sound power measurements in situ using a reference sound source
[PB88-182571] 20 p2849 N88-26910

SOUND LOCALIZATION
Method for determining the coordinates of sound sources by means of a sound measurement system
[NASA-TT-20242] 13 p1834 N88-20972
Software development for the reconstruction of source parameters using research and development arrays
[REPT-840445-TW] 16 p2246 N88-23417
Proceedings of the French-German Colloquium on Helicopter Detection
[ISL-R-104/87] 22 p3147 N88-28723
Acoustic helicopter positioning
22 p3148 N88-28726
Acoustic detection of helicopters: Experiments
22 p3148 N88-28727
Acoustic direction finding of flying helicopters
22 p3148 N88-28728
Examples of the application of acoustics for the detection and classification of targets 22 p3148 N88-28729
Detection of helicopters using ground-controlled microphones 22 p3148 N88-28730

SOUND MEASUREMENT
U ACOUSTIC MEASUREMENT

SOUND PERCEPTION
U AUDITORY PERCEPTION

SOUND PRESSURE
Sound pressure distribution in front of a serrated boundary: Standing wave suppression and diffusion
07 p0928 N88-15639
Diffraction of sound at junction of two waveguides
08 p1076 N88-16491
Sound propagation through a turbulent atmosphere: Experimental techniques and data analysis
[AD-A188891] 12 p1688 N88-20094
Development of a computerized analysis for solid propellant combustion instability with turbulence
[NASA-CR-182351] 19 p2611 N88-25497
An analysis of the efficiency and directivity of the sound generated by a moving laser source
[AD-A192220] 20 p2849 N88-26914
Acoustic pressure distribution on the bottom of a wedge-shaped ocean
[AD-A193961] 23 p3278 N88-29518

SOUND PROPAGATION
NT VOICE
Sound propagation over uneven ground and irregular topography
[NASA-CR-182352] 06 p0776 N88-14763
The properties of sound propagation in liquid constrained viscoelastic and polymeric structures
[AD-A185944] 07 p0929 N88-15640
Use of boundary-layer method for problem of sound propagation through channel with variable cross-section containing stream of fluid 09 p1233 N88-17396
Comparison of the rough surface reflection coefficient with specularly scattered acoustic data
[AD-A187086] 09 p1242 N88-17444
Optically stimulated sound from gas bubbles in water
12 p1686 N88-20087
Sound propagation through a turbulent atmosphere: Experimental techniques and data analysis
[AD-A188891] 12 p1688 N88-20094
Construction of approximations to acoustic Green's functions for nonhomogeneous oceans using transmutation
[PB88-185384] 18 p2548 N88-25126
Linear and nonlinear acoustic wave propagation in the atmosphere
[NASA-CR-4157] 18 p2571 N88-25268
Outdoor sound propagation, its implications for unattended ground sensors
[FEL-1986-64] 20 p2850 N88-26917
Sound propagation at low altitude
22 p3148 N88-28725

SOUND TRANSDUCERS
NT ELECTROACOUSTIC TRANSDUCERS
NT HYDROPHONES
NT MICROPHONES
Noncontact temperature measurements of hot steel bodies using an electromagnetic acoustic transducer (EMAT)
[DE88-000560] 04 p0446 N88-12765
Mode pattern of field generated by parametric radiator in acoustic waveguide 08 p1076 N88-16488
Acoustic helicopter positioning
22 p3148 N88-28726
Sensors adapted for acoustic detection
22 p3148 N88-28731
Correlation method and sensors adapted to the environment 22 p3149 N88-28732

SOUND TRANSMISSION
Active minimisation of acoustic fields. A review of research into the active control of sound undertaken at ISVR from 1983 to 1986
[ISVR-TR-146] 01 p0091 N88-10593
The effect of ocean fluctuations on sound transmission in the ocean
[AD-A184382] 03 p0355 N88-12236
Nonlinear acoustics
[AD-A184271] 04 p0488 N88-13004
Aircraft interior noise reduction by alternate resonance tuning
[NASA-CR-181530] 04 p0488 N88-13005
An analysis of sound absorbing linings for the interior of the NASA Ames 80 x 120-foot wind tunnel
[NASA-CR-177396] 04 p0488 N88-13006
Theoretical and practical aspects of the functional absorber method of arranging sound absorbing panels
[BBC-RD-1987/15] 05 p0646 N88-13955
Multipath time-delay estimation via the EM algorithm
[PB88-106851] 07 p0845 N88-15124
The properties of sound propagation in liquid constrained viscoelastic and polymeric structures
[AD-A185944] 07 p0929 N88-15640
Identification and proposed control of helicopter transmission noise at the source
09 p1109 N88-16647
Comparison of the rough surface reflection coefficient with specularly scattered acoustic data
[AD-A187086] 09 p1242 N88-17444
Silencium resonators (Silators) for the attenuation and elimination of sound
[MBB-Z-546/83] 10 p1312 N88-17841
Sound transmission through the walls of light aircraft: An investigation of structure-borne noise in a Handley Page 137 Jetstream 3 aircraft
[NASA-CR-182509] 10 p1405 N88-18376
A study of methods to predict and measure the transmission of sound through the walls of light aircraft
[NASA-CR-182656] 12 p1687 N88-20090
Sound propagation through a turbulent atmosphere: Experimental techniques and data analysis
[AD-A188891] 12 p1688 N88-20094
A continued study of optical sound generation and amplification
[AD-A188362] 12 p1691 N88-20116
Spatial matched processing for multipath propagation
[AD-A189790] 15 p2129 N88-22701
Target localization in an inhomogeneous medium
[AD-A190008] 15 p2130 N88-22703
A computerized investigation using the method of images to predict the sound field in a fluid wedge overlying a slow fluid half-space
[AD-A190013] 15 p2130 N88-22704
An outdoor unit for Direct Broadcast Satellite (DBS) digital sound reception
[BMFT-FB-W-86-016] 16 p2189 N88-23050
Sources and levels of background noise in the NASA Ames 40- by 80-foot wind tunnel
[NASA-TM-100077] 17 p2395 N88-24239
Signal processing in digital speech transmission systems
[ETN-88-92122] 20 p2792 N88-26561
Aircraft interior noise reduction by alternate resonance tuning
[NASA-CR-182540] 20 p2849 N88-26909
Acoustic diffraction by an absorbing finite strip in a moving fluid
[PB88-191382] 20 p2849 N88-26912
Reflection and scattering of acoustic rays computed for parabolic ice keel models
[AD-A193898] 23 p3278 N88-29517
Acoustic pressure distribution on the bottom of a wedge-shaped ocean
[AD-A193961] 23 p3278 N88-29518
Analysis of the transmission of sound into the passenger compartment of a propeller aircraft using the finite element method
[FFA-TN-1988-15] 23 p3279 N88-29520

SOUND VELOCITY
U ACOUSTIC VELOCITY

SOUND WAVES
NT AERODYNAMIC NOISE
NT AIRCRAFT NOISE
NT BLADE SLAP NOISE
NT ENGINE NOISE
NT ION ACOUSTIC WAVES
NT JET AIRCRAFT NOISE
NT LAMB WAVES
NT NOISE (SOUND)
NT SONIC BOOMS
NT THERMAL NOISE
Geoacoustic models of the Hudson Canyon area
[AD-A183535] 01 p0073 N88-10465

Finite difference solution of a generic differential equation
[PB87-205878] 01 p0087 N88-10568
A new method for determining acoustic properties of the seabed from the ambient noise field in the ocean
[RAE-TR-86035] 01 p0090 N88-10590
The phenomenology of Karman vortex streets via sound in oscillatory flow
[MPIS-MITT-84-1987] 02 p0122 N88-10775
Boundary effects on the drag of an oscillating sphere: Applications to the magnetic sphere rheometer. Attenuation and dispersion of acoustic waves in nematic liquid crystals 04 p0488 N88-13007
Theoretical and practical aspects of the functional absorber method of arranging sound absorbing panels
[BBC-RD-1987/15] 05 p0646 N88-13955
Full field visualization of surface and bulk acoustic waves using heterodyne holographic interferometry
[AD-A185071] 05 p0646 N88-13958
Nonlinear reflection of sound wave in gas mixture
06 p0769 N88-14728
Dependence of acoustical characteristics of laser-induced breakdown in dielectric materials on shape of inelastic region 06 p0774 N88-14753
Waves and vibrations in elastic superlattice composites 06 p0776 N88-14765
The properties of sound propagation in liquid constrained viscoelastic and polymeric structures
[AD-A185944] 07 p0929 N88-15640
Characterizing particle combustion in a Rijke burner
[AD-A186157] 08 p0966 N88-15847
Approximation of noncorrelated reflections in problem of sound propagation through waveguide with rough boundary 08 p1076 N88-16487
Diffraction of sound at junction of two waveguides
08 p1076 N88-16491
Equation of acoustic and gravitational waves in stratified moving medium 08 p1077 N88-16493
Stimulated Mandelstam-Brillouin scattering during forward scattering of light 08 p1078 N88-16499
Interaction of acoustic and electromagnetic waves involved in anomalous skin effect
08 p1079 N88-16503
The assessment of the sound insulation requirements for a large broadcasting studio, using a scale model: Theoretical considerations
[BBC-RD-1987/20] 09 p1155 N88-16921
Linear theory of generation of longitudinal sound waves in semiconductors upon interband absorption of optical radiation 09 p1234 N88-17397
Theory of transient thermal self-focusing of sound beams 09 p1234 N88-17401
Nonlinear and diffraction effects in sound beams with random transverse structure 09 p1235 N88-17402
Transient sound radiation from infinite thin plate
[ARE-TM(UHA)-87506] 09 p1243 N88-17449
Surface acoustic wave deposition sensor
[DE87-006527] 09 p1243 N88-17452
Cryogenic acoustic microscopy
[AD-A187274] 10 p1299 N88-17767
The assessment of the sound insulation requirements for a large broadcasting studio, using a scale model: Practical details
[BBC-RD-1987/21] 10 p1318 N88-17878
Johnson noise thermometer for high radiation and high temperature environments
[DE88-003770] 10 p1323 N88-17911
Microscopic modeling of sound waves in granular material
[DE88-000348] 10 p1405 N88-18375
Scattering of impulsive acoustic waves by a semi-infinite crack in the plane interface of a half-space and a layer
[PB88-126396] 10 p1405 N88-18377
A modified version of the phase sensitive technique for measurements of absolute sound velocity in solids
[DE88-002303] 10 p1405 N88-18378
Evolution of acoustic gravity wave packet in spatially and temporally varying wind 11 p1469 N88-18760
Acoustic wave electroless deposition monitor
[DE88-004023] 11 p1489 N88-18887
Recording a surface acoustic wave on the surface of silicon
[PB88-130372] 11 p1490 N88-18894
The temporal and spatial acoustical response of a point-driven fluid-loaded plate
[AD-A188504] 12 p1636 N88-19794
Method for determination of the wind velocity and direction
[NASA-TT-20233] 13 p1802 N88-20769
Flow/acoustic interaction in duct inflow
[AD-A189264] 13 p1833 N88-20967
Mathematical models of sound waves in fluids
[AD-A189270] 13 p1834 N88-20968
Acoustic radiation from line- and point-loaded plates: Uniformly asymptotic solutions
[AD-A189367] 13 p1834 N88-20969
Modeling of laser ultrasound generation in a weld pool
[DE88-005546] 13 p1834 N88-20971
Method for determining artillery position
[NASA-TT-20238] 13 p1834 N88-20973
Perception of complex auditory patterns
[AD-A190218] 15 p2102 N88-22524
Mechanisms mediating the perception of complex acoustic patterns
[AD-A190112] 15 p2130 N88-22705
Generation and propagation of sound waves in a collapsing or anti-collapsing star with uniform density
[DE87-703034] 15 p2151 N88-22839
Propagation of acoustic gravity wave spectrum through vertical wind shear region 16 p2186 N88-23035
Study of the boundary layer of a flow pulsed by acoustic waves
[ETN-88-91998] 16 p2206 N88-23163
Refraction in underwater acoustics --- navigation systems
[B8735053] 17 p2395 N88-24236
Johnson noise thermometer for high-radiation and high-temperature environments
17 p2434 N88-24480
Evaluation of the biot coefficients
[AD-A191643] 18 p2570 N88-25265
Acoustic wave dispersion in a viscous, compressible, liquid-filled cylindrical elastic tube
19 p2722 N88-26164
Dynamics and stability of combustion driven self oscillations in presence of various frequencies. Extensive stability criteria
[ETN-88-92123] 20 p2771 N88-26432
Studying materials using acoustic waves
[AD-A192234] 20 p2850 N88-26915
On the possibility of the soliton description of acoustic emission during plastic deformation of crystals
[DE88-701878] 20 p2876 N88-27075
Reflection of sound in open ended ducts
[PB88-103478] 21 p3012 N88-27870
Propagation of acoustic disturbances in transonic flow fields of lifting wings
[DFVLR-FB-88-13] 21 p3013 N88-27880
Computer-controlled measurements of nonlinear standing waves
[AD-A193840] 22 p3147 N88-28717
The role of acoustic resonances in unsteady turbomachinery aerodynamics
[PNR90455] 22 p3147 N88-28720
Interactions between air and ground sound at the Earth surface 22 p3149 N88-28733
Acoustic-seismic helicopter detection
22 p3149 N88-28734
In situ fault detection by the hybrid ray mode method
[AD-A195226] 24 p3381 N88-30137

SOUNDERS
U SOUNDING

SOUNDING
NT ACOUSTIC SOUNDING
NT ATMOSPHERIC SOUNDING
NT BALLOON SOUNDING
NT ECHO SOUNDING
NT IONOSPHERIC SOUNDING
NT MICROWAVE SOUNDING
NT ROCKET SOUNDING
NT SATELLITE SOUNDING
A new approach to modeling and interpreting electromagnetic sounding data
[DE88-000460] 04 p0438 N88-12715
Materials of the World Data Center B. Deep Seismic Sounding (DSS): Pacific data 09 p1196 N88-17167
Airborne electromagnetic sounding of sea ice thickness and sub-ice bathymetry
[AD-A188939] 12 p1649 N88-19879
HF (High Frequency) Maximum Usable Frequency (MUF) model uncertainty assessment
[AD-A189132] 13 p1757 N88-20513

SOUNDING ROCKETS
NT BLACK BRANT SOUNDING ROCKETS
NT SKYLARK ROCKET VEHICLE
Proceedings of the 8th ESA Symposium on European Rocket and Balloon Programs and Related Research
[ESA-SP-270] 08 p1024 N88-16201
Esrange (Sweden): New installations, future plans and investments --- rocket range 08 p1029 N88-16235
Facilities and plans for improvements at Andoya (Norway) rocket range 08 p1029 N88-16236
Preliminary Material Science Experiment Rocket (MASER) 1 results and the evolution of the MASER program 08 p1033 N88-16260
Future plans for the NASA suborbital program
08 p1034 N88-16267
Guidance of high-altitude sounding rockets using the S19 and Spinning Rocket Altitude Control (SPINRAC) systems 08 p1034 N88-16273
Sounding rockets/microgravity products and service
08 p1035 N88-16277
In-situ plasma bubble observations associated with equatorial spread-F over Natal
[INPE-4488-PRE/1252] 15 p2095 N88-22482
Electric field measurement by S-520-9 sounding rocket using the time of flight technique of lithium ion beam
[ISAS-RN-367] 18 p2543 N88-25096
Rocket-borne low energy ion measurements in space
18 p2593 N88-25412
MRS-3000 meteorological rocket probe for the MMR-06 dart integrated meteorological rocket system
[NASA-TT-20303] 19 p2693 N88-26010
Design, development, fabrication and launch support for a high altitude release of neodymium vapor
[AD-A194196] 22 p3118 N88-28527
Aerospace payload support systems
[AFGL-TR-87-0241] 24 p3334 N88-29843

SOUNDS (TOPOGRAPHIC FEATURES)
The physical oceanography of the northern Baffin Bay-Nares Strait region
[AD-A190015] 15 p2100 N88-22509

SOUTH AMERICA
On the interannual variability of South American climate and the Southern Oscillation 04 p0470 N88-12905
A study on electric fields and conductivity associated with electrified clouds in the region of South America
[INPE-4487-TDL/325] 15 p2096 N88-22486

SOUTH WEST AFRICA
U NAMIBIA

SOUTHERN HEMISPHERE
NT ANTARCTIC REGIONS
NT ROSS ICE SHELF
October lower stratospheric Antarctic temperature and total ozone from 1979-1985 05 p0615 N88-13776
Atmosphere of Venus in south polar area based on radio transmission data 08 p1005 N88-16089
Meteorological atlas of the Southern Hemisphere lower stratosphere for August and September 1987
[NASA-TM-4049] 20 p2825 N88-26763
Recent secular changes in the wintertime circulation of the Southern Hemisphere 22 p3122 N88-28555

SOUTHERN OSCILLATION
On the interannual variability of South American climate and the Southern Oscillation 04 p0470 N88-12905
Variations of tropical circulation and associated rainfall anomalies, during 2 years of contrast
[INPE-4359-TDL/300] 08 p1039 N88-16286
Survey of acoustic techniques for monitoring El Nino
[PB88-157615] 13 p1804 N88-20783

SOVIET SATELLITES
NT COSMOS SATELLITES
NT INTERCOSMOS SATELLITES
NT PROGNOZ SATELLITES

SOVIET SPACECRAFT
NT MIR SPACE STATION
NT SALYUT SPACE STATION
NT SOYUZ SPACECRAFT
Soviet spacecraft engineering research
[FASAC-TAR-3090] 17 p2311 N88-23823
Soviet space program handbook
[AD-A194332] 22 p3046 N88-28077

SOVIET UNION
U U.S.S.R.

SOYBEANS
Estimating scattered and absorbed radiation in plant canopies by remote sensing
[NASA-CR-181390] 02 p0193 N88-11205
Spectral behavior of crops through analysis of LANDSAT-TM data 17 p2358 N88-24047
Identification of areas cultivated with soybeans in the cerrados regions, through digital processingof satellite images: A methodological approach
17 p2358 N88-24048
Evaluation of TM false color composites for crop discrimination 17 p2367 N88-24096
Study of the spectral response of soybeans
[INPE-4592-PRE/1322] 24 p3387 N88-30174

SOYUZ SPACECRAFT
USSR report: Space
[JPRS-USP-87-003] 01 p0009 N88-10050
Basic results of medical studies during prolonged manned flights on-board the Salyut-7/Soyuz-T orbital complex
[NASA-TT-20217] 10 p1369 N88-18162
Soviet space transport systems
13 p1727 N88-20328
Features of Soyuz TM spacecraft
13 p1727 N88-20329
The USSR space systems for remote sensing of earth resources and the environment (sensor systems, processing techniques, applications)
17 p2356 N88-24035

SPACE
State-of-the-art in true space-time finite element method 17 p2391 N88-24215

Space station as a vital focus for advancing the technologies of automation and robotics
[IAF-86-62] 23 p3251 N88-29352

SPACE ADAPTATION SYNDROME
Cosmonauts' hormonal responses after brief spaceflights 07 p0890 N88-15394
Experiments with rats flown aboard Cosmos-1667 biosatellite (main objectives, conditions and results)
07 p0893 N88-15414
JPRS Report: Science and Technology. USSR: Space Biology and Aerospace Medicine, volume 21, no. 5, September - October 1987
[JPRS-USB-88-003] 10 p1359 N88-18122
Inflight simian circadian rhythms and temperature homeostasis aboard Cosmos-1514 biosatellite
10 p1359 N88-18125
Discrete adaptation to sensory conflict
10 p1363 N88-18146
Genetic research in space
[NASA-TT-20216] 11 p1518 N88-19066
Cardiovascular adaptation to zero-g during a long term flight (237 days) on board the Salyut 7 Soviet space station (1984) 12 p1655 N88-19920
Cardiac and peripheral circulation assessment by ultrasound on 3 astronauts during two 7-day space flights (1982 Salyut-7 - 1985 STS 51G)
12 p1656 N88-19921
Load and control of the cardiocirculatory system in weightlessness 12 p1656 N88-19922
Neuro-reflex mechanisms of circulation regulation in simulated microgravity 12 p1656 N88-19923
The rate of adaptation to altered g in the human centrifuge: Implications for simulations of mass-discrimination in space flight
12 p1659 N88-19941
Gastric emptying assessment by echography after a stress (rotating chair) 12 p1661 N88-19955
The relationship between preflight underwater training and space motion sickness 19 p2696 N88-26025
Results of medical research conducted in 1985 during long-term spaceflights 19 p2702 N88-26070

SPACE BASED RADAR
Theory of displaced phase center antenna for space based radar applications
[PB87-229837] 06 p0690 N88-14227
Parametric analysis of power requirements for space-based radar 17 p2399 N88-24260
Space based radar application to air traffic control
17 p2399 N88-24262
The role of space borne imaging radars in environmental monitoring: Some shuttle imaging radar results in Asia
[NASA-TM-101178] 18 p2502 N88-24844

SPACE BASES
NT LUNAR BASES
NT SPACE COLONIES
Small reactor power systems for manned planetary surface bases
[NASA-TM-100223] 04 p0524 N88-13209

SPACE BIOLOGY
U EXOBIOLOGY

SPACE CAPSULES
NT ESCAPE CAPSULES

SPACE CHARGE
Filementation instability of rotating light ion beams in fusion target chambers
[PPJ-839] 02 p0242 N88-11530
Intense electron beams
[DE88-002456] 09 p1247 N88-17474
A ring model of the lasertron
[DE88-004656] 10 p1323 N88-17908
Generalized equations for emittance and field energy of high-current beams in periodic focusing
[DE88-004448] 10 p1404 N88-18372
Experimental results of a high-gain microwave FEL operating at 140 GHz
[DE88-004358] 11 p1492 N88-18907
Wiggler taper optimization for free-electron-laser amplifiers with moderate space-charge effects
[DE88-003756] 13 p1775 N88-20618
Theoretical model of the cathode spot on a unipolar arc
[AD-A190109] 15 p2059 N88-22277
Deep dielectric charging effects due to high energy electrons in earth's outer magnetosphere
[AD-A192154] 18 p2541 N88-25083
Accelerator research studies
[DE88-007124] 18 p2574 N88-25290
Spacecraft requirements for predictions of geomagnetic activity (a tutorial)
[AD-A191943] 19 p2685 N88-25959
Results from the SLAC lasertron
[DE88-007816] 20 p2806 N88-26647
Space-charge-wave solid state microwave amplifier
[AD-A193792] 23 p3208 N88-29091
Beam optics test stand
[AD-A193901] 23 p3216 N88-29144

SPACE COLONIES
Steps toward lunar settlement
[DE88-009141] 21 p2900 N88-27213

SPACE COMMERCIALIZATION
Space station: Leadership for the future
[NASA-PAM-509/8-87] 01 p0013 N88-10072
Moving the factory into orbit 02 p0134 N88-10844
Commercial Opportunities for Remote Sensing with Polar Platforms
[ESA-SP-269] 03 p0339 N88-12131
Possible commercial use of the polar platforms --- Columbus 03 p0339 N88-12132
Market potential for commercial remote sensing
03 p0339 N88-12137
Commercial perspective of an imaging spectrometer development program 03 p0340 N88-12138
MBB-ERNO view of remote sensing commercialization
03 p0340 N88-12140
SPOT 1: First In-Flight Results --- conferences
[ISBN-2-85428-177-2] 03 p0340 N88-12143
Development of the SPOT commercial service: Preliminary conclusions after six months of operations
03 p0340 N88-12144
Satimage and the Nordic SPOT market
03 p0340 N88-12145
SPOT Image Corporation: Early results
03 p0340 N88-12146
Definition and economic evaluation of Space Solar Power Systems (SSPS), part 2
[ILR-MITT-184-2(1987)] 08 p1022 N88-16190
The ILV: A new commercial expendable launch vehicle --- Industrial Launch Vehicle (ILV)
08 p1035 N88-16275
The prospects of space utilization
[MBB-UR-931/86] 10 p1314 N88-17856
Space-based remote sensing of the Earth: A report to the Congress
[NASA-TM-89709] 10 p1346 N88-18046
Preparation for microgravity: The role of the microgravity materials science laboratory
[NASA-TM-100906] 18 p2497 N88-24811
Business telecommunications using satellite microterminals: Gaining the competitive edge
[ESA-BR-49] 22 p3070 N88-28225
Applications of SPOT data for urban real estate investment information systems
22 p3101 N88-28414
SPOT data acquisition and distribution
22 p3115 N88-28505
Commercialization and export --- aerospace industry
22 p3161 N88-26824

SPACE COMMUNICATION
NT SATELLITE COMMUNICATION
NT SPACECRAFT COMMUNICATION
The Telecommunications and Data Acquisition Report
[NASA-CR-181546] 04 p0432 N88-12679
An evolutionary communications scenario for Mars exploration
[NASA-TM-100263] 05 p0576 N88-13515
High data rate modem simulation for the space station multiple-access communications system
06 p0795 N88-14870
Optically controlled phased-array antenna technology for space communication systems
[NASA-TM-100852] 11 p1476 N88-18809
Monolithic microwave integrated circuit technology for advanced space communication
[NASA-TM-100829] 14 p1906 N88-21389
Error control techniques for satellite and space communications
[NASA-CR-182886] 17 p2332 N88-23922
Service offerings and interfaces for the ACTS network of Earth stations
[NASA-TM-100809] 18 p2471 N88-24663
Telescience testbed pilot program
[NASA-CR-183207] 24 p3412 N88-30309
The Deep Space Network: An instrument for radio astronomy research
[NASA-CR-183219] 24 p3453 N88-30554

SPACE COOLING (BUILDINGS)
Engineering principles and concepts for active solar systems
[DE87-001181] 01 p0066 N88-10425
Understanding passive cooling systems
[PB87-210464] 02 p0194 N88-11211
Life-cycle cost analysis of residential heat pumps and alternative HVAC (Heating, Ventilating and Air-Conditioning) systems
[DE88-003701] 07 p0839 N88-15090
Heat pump and appliance research
[PB88-102462] 07 p0853 N88-15184
Water source heat pump: How to get home heating and cooling from your own back yard
[DE88-900180] 07 p0875 N88-15306
Short Reference Years: Short weather data sets for faster simulations of solar energy systems and energy consumption in buildings
[DE88-900198] 07 p0881 N88-15343
Field experience with aquifer thermal energy storage
[DE88-007075] 18 p2538 N88-25058

SPACE DEBRIS
Space environmental considerations for a long-term cryogenic storage vessel 08 p0981 N88-15933
Space station integrated wall damage and penetration damage control. Task 5: Space debris measurement, mapping and characterization system
[NASA-CR-179281] 10 p1265 N88-17688
Nuclear-powered space debris sweeper
17 p2418 N88-24380
Effects of meteoroids and space debris on the particulate environment for space station 18 p2591 N88-25399
Assessment of the effects of space debris and meteoroids environment on the space station solar array assembly
[NASA-TM-101315] 23 p3185 N88-28959

SPACE DENSITY
Galactic interstellar abundance surveys with IUE and IRAS 04 p0522 N88-13206

SPACE DIVERSITY
U RECEPTION DIVERSITY

SPACE ENVIRONMENT
U AEROSPACE ENVIRONMENTS

SPACE ENVIRONMENT SIMULATION
NT NEUTRAL BUOYANCY SIMULATION
NT WEIGHTLESSNESS SIMULATION
Irradiation testing 03 p0274 N88-11727
Laboratory simulation of the electrodynamic interactions of a tethered satellite with an ionospheric plasma
[IFSI-86-3] 08 p0961 N88-15822
Experimental evidence of micro-nonequilibrium on the magnetopause and further predictions
08 p1098 N88-16606
ASSESS-2: An aircraft simulation of Spacelab
09 p1123 N88-16723
Major spacecraft hardware testing in Europe
09 p1125 N88-16740
Development of infrared techniques for testing spacecraft 09 p1128 N88-16772
Seven year thermal vacuum real life test of a medium speed (despin) mechanism manufactured by Dornier System
[ESA-ESTL-64] 09 p1175 N88-17038
EUROSIM: A design concept for an in-orbit operations simulator 12 p1589 N88-19517
Ultraviolet (180 to 300 nm) action spectra for inactivation and DNA photoproduct formation of Bacillus subtilis spores under ultrahigh vacuum 12 p1657 N88-19931
Survival and mutation induction of dehydrated yeast cells after UV exposure 12 p1657 N88-19932
Cellular effects of heavy ions: Experimental results and theoretical approaches --- space radiation
12 p1658 N88-19933
Activities report of the Toulouse Research Center
[ETN-88-91988] 13 p1850 N88-21077
Simulation of cometary nuclei
14 p2005 N88-21954
Development of a slip-ring system for energy transfer in space conditions. Space flight qualification and extended life tests
[BMFT-FB-W-86-019] 16 p2169 N88-22932
Different techniques for intervening under the sea: Possible links with space applications
19 p2697 N88-26030
Contribution to the study of materials behavior in space environment
[SNIAS-881-430-104] 23 p3189 N88-28977
The effects of total dose on the SEU sensitivity of CMOS static RAMS --- single event upset (SEU), satellite components
[AERE-R-12779] 24 p3428 N88-30401
The Single Event Upset (SEU) test facility on the Hardwell tandem generator for cosmic ray simulation
[AERE-R-12896] 24 p3459 N88-30580

SPACE ENVIRONMENTAL LUBRICATION
U SPACECRAFT LUBRICATION

SPACE ERECTABLE STRUCTURES
Access flight hardware design and development
02 p0139 N88-10873
Planning and scheduling for robotic assembly
08 p1062 N88-16416
Satellite assembly in geostationary orbit: A plug-and-socket concept 09 p1128 N88-16769
Space station structures development
[NASA-CR-179261] 09 p1133 N88-16792
The integration of a mesh reflector to a 15-foot box truss structure. Task 3: Box truss analysis and technology development
[NASA-CR-178228] 11 p1497 N88-18941

A 60-meter erectable assembly concept for a control of flexible structures flight experiment
[NASA-TM-100497] 14 p1873 N88-21190
Bi-stem gripping apparatus
[NASA-CASE-MFS-28185-1] 17 p2345 N88-23979
Development of a space deployable radiator using heat pipes
[SNIAS-881-440-104] 23 p3214 N88-29128
Clevis joint for deployable space structures
[NASA-CASE-LAR-13898-1] 24 p3380 N88-30130
Far infrared spectroscopy telescope (FIRST) inflatable thermal shield, phase 1
[SR/FIS/108(87)CZ] 24 p3453 N88-30552

SPACE EXPER WITH PARTICLE ACCELERATORS
U SEPAC (PAYLOAD)

SPACE EXPLORATION
USSR report: Space
[JPRS-USP-87-003] 01 p0009 N88-10050
A matter-antimatter propulsion system for manned interstellar flight
[DE87-013311] 02 p0141 N88-10665
How we get pictures from space, revised edition
[NF-151/7-87-REV] 02 p0193 N88-11203
Small reactor power systems for manned planetary surface bases
[NASA-TM-100223] 04 p0524 N88-13209
An evolutionary communications scenario for Mars exploration
[NASA-TM-100263] 05 p0576 N88-13515
Small space reactor power systems for unmanned solar system exploration missions
[NASA-TM-100226] 05 p0660 N88-14054
Unispace 82 09 p1128 N88-16766
America plans for space
[AD-A187465] 10 p1289 N88-17713
Deep space target location with Hubble Space Telescope (HST) and Hipparcos data
[NASA-CR-182520] 10 p1427 N88-18524
Interplanetary mission design handbook. Volume 1, Part 5: Mars-to-Earth ballistic mission opportunities, 1992-2007
[NASA-CR-182525] 10 p1430 N88-18538
Soviet space transport systems
13 p1727 N88-20328
The Deep Space Network
[NASA-CR-182700] 13 p1759 N88-20524
Electromagnetic powered vehicles (EMPV) for Mars exploration 17 p2419 N88-24388
Reflectance spectroscopy in planetary science: Review and strategy for the future
[NASA-SP-493] 17 p2451 N88-24564
Planetary Geology: Goals, Future Directions, and Recommendations
[NASA-CP-3005] 19 p2742 N88-26279
Reports of planetary astronomy, 1988
[NASA-TM-4063] 22 p3163 N88-28835
The NASA Electric Propulsion Program
[NASA-TM-101324] 24 p3336 N88-29859
Volatiles on Mars
[NASA-CR-183113] 24 p3456 N88-30571

SPACE FLIGHT
NT INTERPLANETARY FLIGHT
NT INTERSTELLAR TRAVEL
NT LONG DURATION SPACE FLIGHT
NT MANNED SPACE FLIGHT
NT RETURN TO EARTH SPACE FLIGHT
NT SPACE SHUTTLE MISSION 31-A
NT SPACE SHUTTLE MISSION 31-B
NT SPACE SHUTTLE MISSION 41-C
NT SPACE SHUTTLE MISSION 51-L
NT SPACE SHUTTLE MISSION 61-B
NT SPACE SHUTTLE MISSIONS
Radiation effects in space
[DE87-012529] 01 p0075 N88-10479
The Proceedings of the Symposium on Mechanics for Space Flight
[ISAS-SP-5] 03 p0317 N88-12006
USSR Space Life Sciences Digest index to issues 10-14
[NASA-CR-3922(17)] 07 p0883 N88-15361
Development of methods for the study of space motion sickness 07 p0892 N88-15408
Research on cotton plants grown in space
08 p1006 N88-16098
Advantages of manned lunar base
08 p1009 N88-16118
Possible use of plasmids for study of effect of space flight factors on biological objects
08 p1046 N88-16319
Electrochemical carbon dioxide concentrator subsystem development
[NASA-CR-177411] 08 p1053 N88-16353
Organs and tissues regeneration in amphibia under the space flight conditions 12 p1660 N88-19951
Advanced space propulsion study - antiproton and beamed power propulsion
[AD-A189218] 13 p1732 N88-20355
Langley aerospace test highlights, 1987
[NASA-TM-100595] 15 p2153 N88-22853
Possibilities and limits for use of laser propulsion systems in interorbital space flight
[ILR-MITT-185] 18 p2475 N88-24683
Soviet space program handbook
[AD-A194332] 22 p3046 N88-28077

SPACE FLIGHT FEEDING
National Aeronautics and Space Administration (NASA)/American Society for Engineering Education (ASEE) Summer Faculty Fellowship Program, 1987. Volume 1
[NASA-CR-172009-VOL-1] 06 p0792 N88-14855
The determination of nutritional requirements for Safe Haven Food Supply System (emergency/survival foods)
06 p0792 N88-14856
Design concepts for bioreactors in space
09 p1198 N88-17179

SPACE FLIGHT STRESS
JPRS report: Science and technology. USSR: Space Biology and Aerospace Medicine, volume 21, no. 3, May - June 1987
[JPRS-USB-88-001] 07 p0889 N88-15389
Cosmonauts' hormonal responses after brief spaceflights 07 p0890 N88-15394
Third Soviet-French Symposium on Space Cytology
07 p0893 N88-15411
Effect of spaceflight factors on primate's blood circulation 10 p1359 N88-18124
Effect of weightlessness on replicative function of rat hepatocyte DNA 10 p1360 N88-18129
RNA-synthesizing activity in rat liver following flight aboard Cosmos-1667 10 p1360 N88-18130
Comparative evaluation of stress repsonse of rats to different methods of simulating some effects of weightlessness 10 p1363 N88-18144
JPRS Report: Science and Technology. USSR: Space Biology and Aerospace Medicine, volume 21, no. 6, November - December 1987
[JPRS-USB-88-004] 10 p1364 N88-18150
New book on metabolic aspects of spaceflight stress
10 p1367 N88-18172
Cytomorphology and ultrastructure of corn root meristem in weightlessness 12 p1651 N88-19891
Hypnosis: Possible applications for cosmonauts
12 p1665 N88-19984
JPRS report: Science and technology. USSR: Space Biology and Aerospace Medicine, volume 22, no. 1, January - February 1988
[JPRS-USB-88-005] 19 p2702 N88-26069
Growth and differentiation of cells in organotypical rat embryo cerebellar culture developing in weightlessness
19 p2703 N88-26076
Macaca rhesus tolerance to +Gz accelerations
19 p2704 N88-26080
Method for measuring absolute linear parameters of chromosomes 19 p2707 N88-26095
Effect of weightlessness on brain development (results of flight of pregnant rats on Kosmos-1514 biosatellite and study of subsequent development of their progeny on earth 20 p2829 N88-26786

SPACE FLIGHT TRAINING
Summary of Payload Integration Plan (PIP) for Starlab-1 flight experiment, enclosure 3
[NASA-TM-89713] 11 p1522 N88-19086
An expert system for a distributed real-time trainer
23 p3261 N88-29411
An intelligent training system for space shuttle flight controllers 24 p3415 N88-30331

SPACE GLIDERS
U LIFTING REENTRY VEHICLES

SPACE HABITATS
Design concepts for bioreactors in space
09 p1198 N88-17179

SPACE HEATING (BUILDINGS)
Engineering principles and concepts for active solar systems
[DE87-001181] 01 p0066 N88-10425
Life-cycle cost analysis of residential heat pumps and alternative HVAC (Heating, Ventilating and Air-Conditioning) systems
[DE88-003701] 07 p0839 N88-15090
Heat pump and appliance research
[PB88-102462] 07 p0853 N88-15184
Water source heat pump: How to get home heating and cooling from your own back yard
[DE88-900160] 07 p0875 N88-15306
Use of a general control simulation program to evaluate HVAC control stability
[DE88-000476] 08 p0975 N88-15896
Advanced utilization of solar energy: Utilization for biotechnology
[DE88-770031] 12 p1640 N88-19819
Field experience with aquifer thermal energy storage
[DE88-007075] 18 p2538 N88-25058

SPACE INDUSTRIALIZATION
NT SPACE MANUFACTURING
NT SPACE PROCESSING
Microgravity and Materials Processing Facility study (MMPF): Requirements and Analyses of Commercial Operations (RACO) preliminary data release
[NASA-CR-179309] 11 p1466 N88-18742
Economic impact of space flight activities in West Germany. Influence of allocations of Bundesministerium fuer Forschung und Technologie
[ETN-88-92106] 21 p2901 N88-27215

SPACE INFRARED TELESCOPE FACILITY
Space Infrared Telescope Facility (SIRTF) design and thermal analysis 08 p0982 N88-15934
Study of helium transfer technology for STICCR: Fluid management
[NASA-CR-177463] 10 p1291 N88-17720
Space infrared telescope facility project
[NASA-CR-183058] 20 p2883 N88-27121
SIRTF nod maneuvers
[NASA-TM-101007] 22 p3048 N88-28085
Survey of material for an infrared-opaque coating
[NASA-TM-88204] 22 p3153 N88-28757

SPACE LABORATORIES
NT MANNED ORBITAL LABORATORIES
NT SPACELAB
Preliminary study of a biotechnology research facility for microgravity, executive summary
[MATRA-EPT/AS/VT209/246/NT]
01 p0032 N88-10204
Preliminary study of a gravitational biology facility for Columbus, executive summary
[MATRA-EPT/AS/VT209/255/NT]
01 p0032 N88-10205
System analysis study of space platform and station accommodations for life sciences research facilities. Volume 2: Study results. Appendix E: Work breakdown structure and dictionary
[NASA-CR-179274] 10 p1292 N88-17723
System analysis study of space platform and station accommodations for life sciences research facilities. Volume 2: Study results. Appendix D: Life sciences research facility requirements
[NASA-CR-179273] 10 p1292 N88-17724
Development of an optical diagnostic instrument. Part 2: Instrument development --- space laboratories
[NLR-TR-87079-L-PT-2] 13 p1841 N88-21016
Microgravity mechanisms and robotics program
16 p2219 N88-23237
Botany Facility pre-phase C/D. Core payload for EURECA, volume 1
[BF-RP-ER-015-VOL-1] 17 p2379 N88-24144
Simulation of space manipulator operations (EUROSIM)
[NLR-MP-87017-U] 20 p2811 N88-26678

SPACE LAW
Legal protection of the Polar Platform's users
03 p0339 N88-12135
JPRS report: Science and technology. USSR: Space
[JPRS-USP-88-001] 24 p3444 N88-30498

SPACE LOGISTICS
Orbital Spacecraft Consumables Resupply System (OSCRS): Monopropellant application to space station and OMV automatic refueling impacts of an ELV launch, volume 4
[NASA-CR-172029] 03 p0276 N88-11741
Inventory behavior at remote sites
06 p0796 N88-14873
A robotic system for automation of logistics functions on the Space Station 23 p3260 N88-29407

SPACE MAINTENANCE
Expert system study for spacecraft management
[TL-2699-ISS-1] 07 p0824 N88-15004
Orbital Replaceable Unit (ORU)/cold plate thermal interface study. Volume 1: Executive Summary
[BAE-TP-8430] 07 p0855 N88-15195
SAMSS: An in-progress review of the Spacecraft Assembly, Maintenance, and Servicing Study
08 p0981 N88-15930
Man-Tended Free Flyer operational design features
12 p1585 N88-19485
Operational experience and design recommendations for teleoperated flight hardware
14 p1927 N88-21489
Remote servicing of space systems
23 p3260 N88-29409

SPACE MANUFACTURING
Moving the factory into orbit 02 p0134 N88-10844
Physical vapor transport crystal growth
03 p0296 N88-11880
Microgravity nucleation and particle coagulation experiments support
[NASA-CR-181540] 04 p0423 N88-12618

Potential for on-orbit manufacture of large space structures using the pultrusion process
[NASA-TM-4016] 05 p0557 N88-13388
LISP based simulation generators for modeling complex space processes 08 p1061 N88-16403
Lunar fiberglass: Properties and process design
[NASA-CR-182580] 11 p1466 N88-18740
Some operational aspects of a rotating advanced-technology space station for the year 2025
[NASA-CR-181617] 20 p2765 N88-26397
Steps toward lunar settlement
[DE88-009141] 21 p2900 N88-27213
Homogeneity of glasses: Experiment WL-IHF-05 in D1 mission --- Spacelab
[ETN-88-92339] 21 p2924 N88-27353
Experiments in microgravity environment: Protein crystallization
[REPT-881-430-101] 21 p2924 N88-27354

SPACE MECHANICS
NT ASTRODYNAMICS
NT CELESTIAL MECHANICS
NT KEPLER LAWS
NT ORBITAL MECHANICS

SPACE MISSIONS
NT ASTEROID MISSIONS
NT CASSINI MISSION
NT FLYBY MISSIONS
NT GIOTTO MISSION
NT MANNED MARS MISSIONS
NT SOLAR MAXIMUM MISSION
NT ULYSSES MISSION
Recent progress in space photovoltaic systems
[NASA-TM-100208] 03 p0311 N88-11966
Relating service doctrine to space system requirements
[AD-A186620] 08 p1074 N88-16483
Critical issues for establishment of a permanently-occupied lunar base
[AD-A187128] 09 p1263 N88-17567
America plans for space
[AD-A187465] 10 p1289 N88-17713
Rendezvous and docking verification and demonstration in orbit, executive summary
[MBB-303-16/86] 10 p1291 N88-17719
A technique for capture analysis of low thrust missions in a planetary system
[AD-A188934] 12 p1594 N88-19544
The German Spacelab mission D1: Payload integration
[ETN-88-91507] 14 p1871 N88-21179
A comparison of propulsion systems for potential space mission applications
[DE88-005637] 14 p1882 N88-21248
Retrieving samples from comet nuclei
14 p2006 N88-21959
Electric propulsion options for the SP-100 reference mission 17 p2404 N88-24296
Safety of extravehicular space activities
19 p2698 N88-26038
Launch operations to support future space forces
[AD-A192679] 20 p2881 N88-27107
LRS-2: A specialized knowledge system for launch resource scheduling
[AD-A194625] 23 p3182 N88-28941
The principles of mass and maneuver applied to space operations
[AD-A194037] 23 p3276 N88-29500

SPACE NAVIGATION
Calibration of attitude control sensors
02 p0159 N88-10995
The navigation experiment NAVEX: Experimental results of clock synchronization
[DFVLR-MITT-87-05] 03 p0271 N88-11701
Satellite autonomous navigation with SHAD (Stellar Horizon Atmospheric Dispersion)
[AD-A184988] 05 p0544 N88-13313
Orbital navigation, docking and obstacle avoidance as a form of three dimensional model-based image understanding 08 p1061 N88-16406
The navigation experiment NAVEX: Experimental results of clock synchronization
[ESA-TT-1084] 09 p1132 N88-16791
Space shuttle onboard navigation console expert/trainer system 09 p1203 N88-17208
Verifying shuttle onboard software using expert systems 09 p1207 N88-17237
Orbital navigation, docking and obstacle avoidance as a form of three dimensional model-based image understanding 17 p2388 N88-24194

SPACE OBSERVATIONS (FROM EARTH)
A comparison of interferometry from space and ground 01 p0094 N88-10614
Fiber-linked telescope arrays on the ground and in space 01 p0095 N88-10626
Ground-based optical interferometry
01 p0096 N88-10631
Ground-based interferometry with the European Very Large Telescope (VLT) 01 p0096 N88-10632
CERGA high angular resolution optical network --- astronomical interferometry 01 p0096 N88-10633
Practical limits to ground based interferometry and its impact on space interferometry
01 p0096 N88-10634
Milliarcsecond ground-based imaging with single telescopes 01 p0097 N88-10637
Activities report in astronomy
[ISSN-0531-4496] 01 p0108 N88-10701
How we get pictures from space, revised edition
[NF-151/7-87-REV] 02 p0193 N88-11203
An automated supernova search and the design strategy
[DE88-001827] 05 p0660 N88-14051
Max '91: Flare research at the next solar maximum
[NASA-TM-89700] 06 p0806 N88-14919
The French balloon and sounding rocket space program 08 p1025 N88-16203
The Swedish sounding rocket and balloon program
08 p1025 N88-16205
Swiss scientific balloon and sounding rocket experiments 1985-1987 08 p1025 N88-16206
How ground-based observations contribute to rocket, balloon and space shuttle experiments: Experience from the past and outlook for the future
08 p1026 N88-16216
Some ground-based optical observations of Comet Halley during its post-perihelion passage
08 p1033 N88-16259
Bern solar observations. Solar data for January-December 1986
[REPT-53] 09 p1263 N88-17569
Dust coma morphology of Comet Halley during the Giotto encounter 14 p2000 N88-21921
Investigation of the Sun-aligned F-region walls and related phenomena in the auroral latitude range
[AFGL-TR-87-0248] 19 p2692 N88-26000
Amateur astronomy in the space age
[RAE-TM-SS-4] 22 p3163 N88-28836
The surface composition of Mars from earthbased observations 23 p3306 N88-29696
Mars earth-based radar: 1986 results and 1988-1990 opportunities 23 p3306 N88-29697
Activities report in astronomy
[ISSN-0531-4496] 24 p3451 N88-30535

SPACE PERCEPTION
A parallel model of the kinetic depth effect using local computations
[AD-A181945] 01 p0083 N88-10536
Computer-controlled testing of visual-spatial ability
[AD-A183971] 03 p0357 N88-12249
Latency differences and effects of selective attention to gratings in the central and right visual fields: 2
[DE87-014730] 04 p0473 N88-12918
Interaction of different modules in depth perception. Stereo and shading
[AD-A185607] 06 p0759 N88-14655
Perception and control of simulated self motion
[AD-A187444] 10 p1372 N88-18188
Visual evoked potentials
[AD-A187942] 11 p1519 N88-19071
Position, scale, and rotation invariant target recognition using range imagery
[AD-A188828] 12 p1633 N88-19772
Spatial cognition 17 p2380 N88-24152
The interaction of sensory and perceptual variables: Spatial, temporal and orientation response to figure and ground
[AD-A192897] 20 p2832 N88-26798
A model for visual attention
[AD-A193061] 21 p2991 N88-27744
Visual motion perception and visual attentive processes
[AD-A193640] 23 p3241 N88-29288
Central serous chorioretinopathy in USAF aviators: A review
[AD-A195697] 24 p3407 N88-30280

SPACE PHOTOGRAPHY
U SPACEBORNE PHOTOGRAPHY

SPACE PLASMAS
NT SOLAR WIND
NT STELLAR WINDS
Local spectra and wave distribution functions --- space plasma
[KGI-PREPRINT-099] 01 p0100 N88-10659
Comparative plasma tails of Venus and comets
01 p0116 N88-10742
Overview of plasma observations during the Halley flybys 01 p0116 N88-10743
The geosynchronous plasma environment
03 p0273 N88-11716
Three-dimensional charging effects --- spacecraft
03 p0273 N88-11720
Flux tube dynamics and solar/stellar redshift measurements 04 p0503 N88-13095
Nonthermal phenomena in stellar coronae: Evidence from radio observations 04 p0503 N88-13096
Observational constraints and evidence for saturation
04 p0503 N88-13097
Observations of turbulence and fluctuations in the solar wind 04 p0525 N88-13212
Activities report of the Ionospheric Observatory
[UIO-SR-87-01] 05 p0625 N88-13827
Evolution of spectral densities in weakly inhomogeneous plasmas
[PB87-137402] 06 p0784 N88-14811
Neutron stars observations as astrophysical probes
06 p0800 N88-14896
Unusually strong density decrease in near-Earth interplanetary plasma and magnetically quiet day as effects of isolated solar flare 08 p1002 N88-16072
Viking: The first Swedish satellite
08 p1025 N88-16207
Bidirectional electron heat flux events in space
[DE88-001791] 08 p1084 N88-16531
Proceedings of the 21st ESLAB Symposium on Small Scale Processes in the Chromosphere/Corona, Interplanetary Medium and Planetary Magnetospheres
[ESA-SP-275] 08 p1094 N88-16582
Coupling of microscopic and macroscopic processes in the Earth's magnetotail 08 p1095 N88-16588
AMPTE-UKS ion observations at a quasi-parallel bow shock 08 p1095 N88-16589
Microphysics of the auroral acceleration region of other regions of the magnetosphere 08 p1096 N88-16592
Acceleration/heating processes on auroral field lines as observed by the Viking spacecraft
08 p1096 N88-16596
Small scale plasma density structures observed by the Viking double probe instrument --- Swedish satellite
08 p1098 N88-16604
Self-modulational formation of pulsar microstructures
[NASA-CR-182420] 08 p1104 N88-16622
Laser simulation of light and plasma action on comets and planets 09 p1237 N88-17413
Electric field measurement by S-520-9 sounding rocket using the time of flight technique of lithium ion beam
[ISAS-RN-367] 18 p2543 N88-25095
Contaminant ions and waves in the space station environment 18 p2590 N88-25393
Kinetic modulational instability of electron cyclotron waves in plasmas
[DE88-701893] 20 p2859 N88-26978
Generation of Adlam-Allen waves by plasma release experiments in the solar wind
[PB88-106000] 20 p2886 N88-27140

SPACE PLATFORMS
NT COLUMBUS SPACE STATION
NT EURECA (ESA)
NT SPACE STATION POLAR PLATFORMS
NT SYNCHRONOUS PLATFORMS
A test-bed for space interferometry: Space Platform Interferometer (SPI) 01 p0097 N88-10640
Moving the factory into orbit 02 p0134 N88-10844
Mission Peculiar Equipment Support Structure: A platform for space construction
02 p0139 N88-10874
Estimating payload internal temperatures and radiator size for multimegawatt space platforms
[DE88-000244] 03 p0275 N88-11738
Considerations concerning a thermal joint for a deployable or steerable battery radiator for the Columbus Polar Platform
[NLR-TR-86055-U] 03 p0276 N88-11739
Commercial Opportunities for Remote Sensing with Polar Platforms
[ESA-SP-269] 03 p0339 N88-12131
Possible commercial use of the polar platforms --- Columbus 03 p0339 N88-12132
Payload configurations and serviceability --- Columbus Polar Platforms 03 p0339 N88-12133
Legal protection of the Polar Platform's users
03 p0339 N88-12135
Confidentiality of data --- Columbus Polar Platforms
03 p0339 N88-12136
X-band SAR for a European remote sensing payload
03 p0340 N88-12142
The effect of maximum-allowable payload temperature on the mass of a multimegawatt space-based platform
[DE88-001921] 05 p0555 N88-13381
Communications payload concepts for geostationary facilities
[NASA-TM-100154] 05 p0576 N88-13513
Carbon Dioxide observational platform system (CO-OPS) Feasibility Study
[NASA-CR-179225] 06 p0671 N88-14113
Feasibility study of a carbon dioxide observational platform system. Volume 2: Programmatics
[NASA-CR-180404] 06 p0672 N88-14114

Polar platform element of Space Station: Mission objectives, European priorities, candidate instrumentation and selection procedure 09 p1129 N88-16779
Model of space platform electromagnetic (EMC) configuration
[ESA-CR(P)-2500] 09 p1135 N88-16809
System analysis study of space platform and station accommodations for life sciences research facilities. Volume 1: Executive summary. Phase A: Conceptual design and programmatics
[NASA-CR-179268] 10 p1291 N88-17721
System analysis study of space platform and station accommodations for life sciences research facilities. Volume 2: Study results, attachment 2. Phase A: Conceptual design and programmatics
[NASA-CR-179272] 10 p1291 N88-17722
Mobile robot activity model for autonomous free flying platforms 12 p1588 N88-19507
Explorer Platform on-orbit servicing operations
12 p1591 N88-19526
A thermal equilibrium model for multi-megawatt space platforms 17 p2410 N88-24332
Individual satellite power requirements calculated from specified constellation performance
17 p2420 N88-24392
The effect of maximum allowable payload temperature on the mass of a multimegawatt space based platform
17 p2424 N88-24416
Space Power Reference Source (SPRS): A user's guide to SDI Space Power Technology Programs
17 p2427 N88-24440
A nuclear powered space based multimegawatt MHD disc power system 17 p2432 N88-24471
Tasks foreseen for space robots and an example of an associated orbital infrastructure
19 p2699 N88-26044
Defensive platform size and survivability
[DE88-011634] 23 p3184 N88-28948
Analytical investigation of the dynamics of tethered constellations in earth orbit
[NASA-CR-179371] 23 p3184 N88-28950
Expandable pallet for space station interface attachments
[NASA-CASE-MSC-21117-1] 23 p3185 N88-28958
Technology requirements for an orbiting fuel depot: A necessary element of a space infrastructure
[NASA-TM-101370] 24 p3334 N88-29845
Interim Flight Opportunity (IFO). Volume 1: Executive summary --- space platform
[SE/LS/AP-36-818/CN-VOL-1]
24 p3334 N88-29849

SPACE POWER REACTORS
NT FISSION ELECTRIC CELLS
Fast critical experiment data for space reactors
[DE87-007005] 01 p0093 N88-10605
Gas-cooled reactor for space power systems
[DE87-011549] 02 p0233 N88-11471
Review of diffusion barrier technology for application in SP-100 fuel pins
[DE88-000021] 02 p0234 N88-11480
Low gravity fluid-thermal experiments
[DE88-000553] 04 p0423 N88-12620
Small space reactor power systems for unmanned solar system exploration missions
[NASA-TM-100228] 05 p0660 N88-14054
A long term radiological risk model for plutonium-fueled and fission reactor space nuclear system
[DE87-010466] 06 p0779 N88-14782
Value-assessment of energy storage concepts in burst power systems
[DE87-013756] 09 p1187 N88-17115
Two-phase reduced gravity experiments for a space reactor design
[DE86-015530] 09 p1247 N88-17475
Molybdenum-base cermet fuel development
[DE88-005529] 13 p1839 N88-21003
Power transmission studies for tethered SP-100
[NASA-TM-100864] 14 p1883 N88-21251
Requirements and cost considerations for a Combined Space Nuclear Reactor Test Facility
[DE88-006763] 15 p2132 N88-22719
Transactions of the Fourth Symposium on Space Nuclear Power Systems
[DE88-006164] 17 p2398 N88-24254
Overview of NASA Lewis Research Center free-piston Stirling engine technology activities applicable to space power systems 17 p2398 N88-24255
Speculations on future opportunities to evolve Brayton powerplants aboard the space station
17 p2399 N88-24258
The results of application studies for space nuclear power 17 p2398 N88-24259
Effects of space-dependent cross sections on core physics parameters for compact fast spectrum space power reactors 17 p2399 N88-24263
Considerations pertinent to the Doppler effect for space reactors 17 p2390 N88-24264
Status of CEA design and simulation studies of a 200 KWe turboelectric space power system
17 p2400 N88-24268
Magnet shielding analysis for SOAR: A space fusion reactor 17 p2400 N88-24269
A fusion based plasma propulsion system
17 p2401 N88-24274
Preliminary study of niobium alloy contamination by transport through helium 17 p2402 N88-24279
Fabrication of lithium hydride shields for space nuclear power systems 17 p2402 N88-24282
Conceptual design of the SP-100 GES test site
17 p2402 N88-24284
Fast critical experiment data for space reactors
17 p2403 N88-24286
Fully passive space reactor conceptual design
17 p2403 N88-24288
Space based nuclear-pumped laser/reactor concepts
17 p2403 N88-24289
Acoustical gas core reactor with MHD power generation for burst power in a bimodal system
17 p2403 N88-24290
Fluid dynamics of spherical cavity reactors
17 p2403 N88-24291
BIFOLD: A dual-mode nuclear space power system
17 p2404 N88-24292
Electric propulsion options for the SP-100 reference mission 17 p2404 N88-24296
Interaction of the control system with core nuclear design for fast spectrum space power reactors
17 p2405 N88-24304
Application of the reactivity constraint approach to the transient control of spacecraft reactors
17 p2406 N88-24305
An adaptive load-following control system for a space nuclear power system 17 p2406 N88-24307
The effect of elevated temperature on irradiated MOS devices 17 p2406 N88-24308
The response of a power MOSFET (N-channel) and a dielectric isolated operational amplifier to the combined environmental effects of high temperature and total dose gamma radiation 17 p2406 N88-24309
Advanced thermionic converter technology for inductive output coupling 17 p2407 N88-24311
Monolithic fuel cell based power source for sprint power generation 17 p2407 N88-24313
Power source selection for neutral particle beam systems 17 p2407 N88-24314
Radiation hardening design of nuclear powered spacecraft 17 p2407 N88-24315
Space nuclear reactor shielding optimization studies
17 p2408 N88-24320
Design of a high-power-density Ljungstroem turbine using potassium as a working fluid
17 p2409 N88-24323
Development of reliable fuel pins for space reactor applications 17 p2409 N88-24326
Helium-3 fusion fuel resources for space power
17 p2410 N88-24330
Thermal management for multi-modal nuclear power plants 17 p2410 N88-24331
A thermal equilibrium model for multi-megawatt space platforms 17 p2410 N88-24332
A review of impact design criteria for space power heat rejection systems 17 p2410 N88-24333
Fundamental analysis of space nuclear-MHD generator for gigawatt-level power 17 p2411 N88-24337
Liquid-metal MHD power conversion for space electric systems 17 p2411 N88-24338
Studies for the definition of a Faraday converter for space nuclear systems 17 p2411 N88-24339
Design of a superconducting alternator for space-based power generation 17 p2412 N88-24340
Progress in the computer modeling of the liquid phase behavior of a liquid metal heat pipe
17 p2412 N88-24342
A liquid metal MHD concept for multimegawatt space power application 17 p2413 N88-24348
Nuclear Rankine/flywheel MMW space power concept
17 p2413 N88-24349
Gas-cooled reactor power systems for space
17 p2413 N88-24350
Analysis of closed cycle megawatt class space power systems with nuclear reactor heat sources
17 p2413 N88-24351
A dynamic model for the aft accumulator in the TE SP-100 system 17 p2414 N88-24354
RSMASS: A simple model for estimating reactor/shield masses 17 p2414 N88-24355
SP-100 control system modeling
17 p2414 N88-24356
ATHENA simulation of the 300 kW SP-100
17 p2414 N88-24357
Parametric analyses of the TE SP-100 system performance 17 p2415 N88-24358
A proposed national policy concerning the reentry of space reactors 17 p2415 N88-24359
Nuclear safety as applied to space power reactor systems 17 p2415 N88-24360
Development and implementation of a space nuclear safety program 17 p2415 N88-24361
Innovative methodology and developments in US space radioisotope power safety risk assessments
17 p2415 N88-24362
Inherently safe space reactors
17 p2415 N88-24363
Advanced LMMHD space power generation concept
17 p2415 N88-24364
SOAR: Space orbiting advanced fusion power reactor
17 p2416 N88-24366
Multimegawatt nuclear power system for lunar base applications 17 p2416 N88-24367
Radiation effects testing capabilities of the Texas A and M Nuclear Science Center 17 p2416 N88-24368
A generalized method for optimizing the mass of space power systems 17 p2416 N88-24369
Fabrication of SP-100 fuel barrier structures by chemical vapor deposition 17 p2416 N88-24371
SP-100 system modeling: SNPSAM update
17 p2417 N88-24372
Fabrication of a niobium 1 percent zirconium containment for SP-100 primary lithium system materials mass transfer studies 17 p2417 N88-24373
Transactions of the Fifth Symposium on Space Nuclear Power Systems
[DE88-006165] 17 p2417 N88-24374
SP-100 GES test site 17 p2417 N88-24375
Civil missions applications study
17 p2417 N88-24376
Applications of nuclear power to lunar and Mars missions 17 p2417 N88-24377
Air Force space power requirements and nuclear power assessment methodology 17 p2418 N88-24378
Nuclear-powered space debris sweeper
17 p2418 N88-24380
EETAP (End-to-End Transient Analysis Program) for space nuclear power system simulation
17 p2418 N88-24381
Optimization of SP-100 thermoelectric electromagnetic pump 17 p2418 N88-24382
Relating design and environmental variables to reliability 17 p2418 N88-24383
Power requirements for mining and microwave processing of extraterrestrial resources
17 p2420 N88-24389
Power and energy requirements for electromagnetic launchers 17 p2420 N88-24391
Possible creep studies of lithium with a compact device 17 p2422 N88-24404
Neutronics conceptual design of a UF6-fueled gaseous laser system 17 p2422 N88-24405
Preliminary analysis of helium generation and its effects on the SP-100 system performance
17 p2422 N88-24406
Optimization of organic Rankine cycles for space station applications 17 p2423 N88-24407
Assessment of nuclear reactor concepts for low power space applications 17 p2423 N88-24409
United Nations deliberations of the use of nuclear power sources in space: 1978-1987 17 p2423 N88-24410
Discussions and agreements in the United Nations on important issues associated with nuclear power in space
17 p2423 N88-24411
Critical nuclear launch issues: A perspective from the State of Florida 17 p2423 N88-24412
Space reactor end of life issues
17 p2424 N88-24413
SP-100 flight qualification testing assessment
17 p2424 N88-24414
Liquid droplet radiator development
17 p2424 N88-24415
The effect of maximum allowable payload temperature on the mass of a multimegawatt space based platform
17 p2424 N88-24416
Space vehicle/nuclear reactor thermal radiation integration issues 17 p2424 N88-24417
MACRAD: A mass analysis code for radiators
17 p2424 N88-24418
The Curie point radiator 17 p2424 N88-24420
Dynamic isotope power system critical component verification 17 p2425 N88-24421
Evaluation of UN fuel pin failure modes and motion of fuel during severe accidents for reactors in space
17 p2425 N88-24424
Reactor core coolability with reduced power levels
17 p2425 N88-24425
Analysis of a nuclear orbital transfer vehicle reentry accident 17 p2425 N88-24426

Creep behavior of tungsten/niobium and tungsten/niobium-1 percent zirconium composites 17 p2425 N88-24427

The application of high-rate biaxial testing to the design of containment vessels for radioisotope heat sources 17 p2426 N88-24428

Value assessment of energy storage concepts in burst power systems 17 p2426 N88-24432

A multimegawatt space power source radiator design 17 p2427 N88-24436

An irradiation performance data base for nitride fuels 17 p2427 N88-24438

Liquid metal testing at ETEC for the SP-100 program 17 p2428 N88-24446

Review of alkali metal and refractory alloy compatibility for Rankine cycle applications 17 p2428 N88-24447

Development of materials for fabric radiators 17 p2429 N88-24448

Polymer fuel cell as an energy storage component for space power applications 17 p2429 N88-24452

Benchmark physics experiments for SP-100 17 p2429 N88-24453

Trade study for kWe class space reactors 17 p2430 N88-24454

A high power density radial-in-flow reactor split core design for space power systems 17 p2430 N88-24455

Transient analyses of multimegawatt space reactors 17 p2430 N88-24456

MMW shielding design and analysis 17 p2430 N88-24457

The NERVA derivative reactor and a systematic approach to multiple space power requirements 17 p2430 N88-24458

Ceramic electrical insulator development for thermoelectric SACE power system 17 p2430 N88-24459

Apparatus for the measurement of resistivity of glasses and ceramics 17 p2431 N88-24460

Silicon-on-insulator electronics for a space nuclear power system 17 p2431 N88-24461

Experimental demonstrations of organic Rankine cycle waste heat rejection systems 17 p2432 N88-24469

A nuclear powered space based multimegawatt MHD disc power system 17 p2432 N88-24471

Burst power gas core reactor with MHD power generation 17 p2433 N88-24472

Molybdenum-base cermet fuel development 17 p2434 N88-24481

Test plan and facilities for qualifying nuclear rocket fuel elements 17 p2434 N88-24482

A comparison of uranium nitride and mixed carbide fuels swelling 17 p2435 N88-24485

Energy conversion system optimization study for multimegawatt space nuclear power application 17 p2436 N88-24492

Automatic reactor control system for transient operation 17 p2436 N88-24493

Experimental evaluation of the MIT-SNL period-generated minimum time control laws for the rapid adjustment of reactor power 17 p2436 N88-24494

An optimal disturbance rejection control system for multimegawatt space nuclear power systems 17 p2436 N88-24495

SP-100 ground engineering systems test facility control systems 17 p2436 N88-24496

TRICE design, evaluation and feasibility tests 17 p2437 N88-24498

Multimegawatt power conditioning requirements study 17 p2438 N88-24504

Lightweight power bus for a baseload nuclear reactor in space 17 p2438 N88-24505

SP-100 Ground Engineering Systems: Test facility control systems
[DE88-009195] 21 p3015 N88-27895

Comparative analysis of the space power architecture studies
[NASA-TM-100977] 22 p3049 N88-28090

Customizing Space Nuclear Power System Analysis Model (SNPSAM): Introducing a secondary coolant loop
[AD-A194620] 22 p3151 N88-28750

Lewis Research Center space station electric power system test facilities
[NASA-TM-100924] 23 p3182 N88-28942

Transient thermal analysis of three fast-charging latent heat storage configurations for a space-based power system
[DE88-009714] 23 p3186 N88-28960

An analysis of heat transfer after loss of primary coolant in the SP-100 reactor system
[AD-A194619] 23 p3281 N88-29539

SPACE PROBES

NT GALILEO PROBE

NT GALILEO SPACECRAFT

NT GIOTTO MISSION

NT HELIOS 1

NT HELIOS 2

NT MARS OBSERVER

NT MARS PROBES

Parachute characteristics of Titan descent modules --- planetary probe
[BF-3/86-B] 02 p0122 N88-10774

Study of fault tolerant techniques for satellite data handling
[FTT/REP/0001/SAAB] 05 p0632 N88-13860

Study of descent of probes with high lift-drag ratio into the atmosphere of Jupiter 08 p1006 N88-16101

Applications of expert systems for satellite autonomy 08 p1066 N88-16443

Rocket and airjet propulsion for ballistic and aerodynamic space probes
[REPT-TR-527] 10 p1310 N88-17826

SPACE PROCESSING

Preliminary study of a containerless processing facility for Columbus, executive summary
[ESA-ITT/AO/1-1834/85F] 01 p0032 N88-10203

Prephase A study of a crystallization laboratory for Columbus, executive summary
[ESA-ITT/AO/1-1866/85F] 01 p0032 N88-10206

Consortium for Materials Development in Space. Technical section
[NASA-CR-181508] 03 p0296 N88-11859

Materials preparation and longevity in hyperthermal atomic oxygen 03 p0297 N88-11862

Physical properties of immiscible polymers 03 p0297 N88-11868

High temperature superconductors 03 p0297 N88-11869

Cast iron freezing mechanisms 03 p0298 N88-11870

Materials processing in space program support
[NASA-CR-179217] 03 p0298 N88-11872

Design study for asteroidal exploitation 03 p0389 N88-12445

Center for the Space Processing of Engineering Materials 07 p0838 N88-15083

Preliminary Material Science Experiment Rocket (MASER) 1 results and the evolution of the MASER program 08 p1033 N88-16260

Space Bioreactor Science Workshop
[NASA-CP-2485] 09 p1196 N88-17168

Suspension cell culture in microgravity and development of a space bioreactor 09 p1196 N88-17169

Space bioreactor: Design/process flow 09 p1197 N88-17170

Plant cell technologies in space: Background, strategies and prospects 09 p1198 N88-17177

Cell culture experiments planned for the space bioreactor 09 p1198 N88-17180

Materials processing in space: An introduction to the G-480 payload 10 p1287 N88-17695

Ten past and ten future GAS/MAUS-payloads 10 p1287 N88-17696

An update to the MITRE/WPI Space Shuttle Program GASCAN G-408 10 p1287 N88-17697

The challenge of G-376 10 p1288 N88-17705

Non-proprietary research projects of the Center for the Space Processing of Engineering Materials
[AR-2] 10 p1426 N88-18516

Microgravity and Materials Processing Facility study (MMPF). Requirements and Analyses of Commercial Operations (RACO) preliminary data release
[NASA-CR-179309] 11 p1466 N88-18742

Cell cultures in space: From basic research to biotechnology 2 12 p1660 N88-19948

Preliminary market analysis for large zeolite crystals
[NASA-CR-182882] 15 p2049 N88-22207

JPRS report: Science and technology. Japan
[JPRS-JST-88-001] 15 p2051 N88-22218

Space utilization plans 15 p2051 N88-22219

Space experiment plan FMPT 15 p2051 N88-22220

Amorphous semiconductors made in space 15 p2051 N88-22221

Pb(1-x)Sn(x)Te crystal growth in space 15 p2051 N88-22223

On-orbit technology experiment facility definition
[NASA-TM-100614] 17 p2311 N88-23824

Non-contact temperature measurement requirements for electronic materials processing 17 p2328 N88-23898

Noncontact temperature measurement: Requirements and applications for metals and alloys research 17 p2328 N88-23899

Multi-color pyrometer for materials processing in space 17 p2329 N88-23905

Separation of biological materials in microgravity
[NASA-TM-101142] 17 p2331 N88-23916

Power requirements for mining and microwave processing of extraterrestrial resources 17 p2420 N88-24389

Microgravity thaw experiment (MITEX) 17 p2427 N88-24439

Preparation for microgravity: The role of the microgravity materials science laboratory
[NASA-TM-100906] 18 p2497 N88-24811

Analysis of the performance of the space ultravacuum research facility in attached and free-flyer mode
[NASA-TM-100325] 20 p2763 N88-26387

Industrial processes influenced by gravity
[NASA-CR-182140] 20 p2782 N88-26497

Method of dispensing reagent chemicals in space
[NASA-CASE-LAR-13607-1-CU] 23 p3200 N88-29048

Optimization of low gravity materials processing experiments using expert systems 23 p3252 N88-29361

A generic expert system for materials processing in space 23 p3255 N88-29376

A teleoperated robotic manipulator system for materials processing experiment servicing 23 p3260 N88-29410

SPACE PROGRAMS

NT BRAZILIAN SPACE PROGRAM

NT CANADIAN SPACE PROGRAM

NT CHINESE SPACE PROGRAM

NT EARTH RESOURCES PROGRAM

NT EUROPEAN SPACE PROGRAMS

NT FRENCH SPACE PROGRAMS

NT GALILEO PROJECT

NT JAPANESE SPACE PROGRAM

NT NASA SPACE PROGRAMS

NT PROJECT SETI

NT ROVER PROJECT

NT SKYLAB PROGRAM

NT SWEDISH SPACE PROGRAM

NT U.S.S.R. SPACE PROGRAM

NT UK SPACE PROGRAM

National Aeronautics and Space Administration space station proposal, fiscal year 1988
[S-HRG-100-328] 05 p0659 N88-14043

Advantages of manned lunar base 08 p1009 N88-16118

Hardware/software reliability study --- space programs
[REPT-65.5686] 09 p1218 N88-17307

An update to the MITRE/WPI Space Shuttle Program GASCAN G-408 10 p1287 N88-17697

A logical structuration for an administration of space projects
[INPE-4435-TDL/310] 12 p1585 N88-19482

Principal space programs in the area of microwaves
[INPE-4164-PRE/1064] 12 p1618 N88-19677

Proceedings of the 3rd European Symposium on Life Sciences Research in Space
[ESA-SP-271] 12 p1652 N88-19893

Aeronautics and space report of the President: 1986 activities 13 p1852 N88-21087

Space projects for the 90's relevant to climatology 14 p1935 N88-21539

Space policy of common sense and moderation
[REPT-49/87] 20 p2883 N88-27118

High technology space flight orientation program: Overview and recommendations
[ETN-88-92332] 21 p3029 N88-27979

History of manned spaceflight
[CNES-NT-121] 21 p3032 N88-28000

Management of large space projects --- conference
[ISBN-2-85-428192-6] 22 p3159 N88-28803

Management 22 p3159 N88-28804

Large space projects --- management 22 p3159 N88-28805

The development phases of a project --- space projects 22 p3159 N88-28807

Human organization --- space projects 22 p3160 N88-28808

Carrying out space projects 22 p3160 N88-28811

Timetable control in a management system (space program) 22 p3160 N88-28815

Costs --- space projects 22 p3160 N88-28816

Value engineering --- space projects 22 p3160 N88-28817

Price estimates and analysis 22 p3161 N88-28818

Management of large space projects. Financial means. Part 1: Financing of constructors 22 p3161 N88-28822

Means of financing --- space projects 22 p3161 N88-28823

The role and the place of insurance of large space projects 22 p3161 N88-28826

SPACE PSYCHOLOGY

Selecting the right crew for future space stations: An analysis of selection research on offshore divers, aviation pilots and other high risk groups in Scandinavia 19 p2696 N88-26021

SPACE RADIATION

U EXTRATERRESTRIAL RADIATION

SPACE RADIATORS
U SPACECRAFT RADIATORS
SPACE RATIONS
Space and sea: Is there a place for ionization?
19 p2699 N88-26043
SPACE RENDEZVOUS
NT ORBITAL RENDEZVOUS
Prototype Rendezvous Onboard Software (PROBS)
[MATRA-EPT-DT-PRB-2A-00068]
02 p0222 N88-11396
Rendezvous and Docking Verification (RVDV) and in-orbit demonstration, executive summary
[RVD-RVDV-FR-AS-01] 06 p0673 N88-14120
Rendezvous and docking verification and demonstration in orbit, executive summary
[MBB-303-16/86] 10 p1291 N88-17719
The RVD mission: The on-board data processing requirements 12 p1586 N88-19495
Prototype on-board software for rendezvous and docking 12 p1586 N88-19496
Long range sensor for rendezvous and docking missions 12 p1587 N88-19497
Motion simulation for in-orbit operations
12 p1589 N88-19514
A software engineering approach to expert system design and verification 23 p3252 N88-29356
SPACE SCIENCES
U AEROSPACE SCIENCES
SPACE SELF MANEUVERING UNITS
U SELF MANEUVERING UNITS
SPACE SHUTTLE BOOSTERS
Redesign of solid rocket booster/external tank attachment ring for the space transportation system
[NASA-TM-100476] 01 p0017 N88-10101
Stability of mechanical joints in launching vehicles: Local and global stationary values of energy density
03 p0270 N88-11696
Results of the development motor 8 test firing
[GPO-78-692] 03 p0278 N88-11751
Shuttle rocket booster computational fluid dynamics
[NASA-CR-182518] 10 p1293 N88-17733
Structural analysis of the space shuttle solid rocket booster/external tank attach ring
[NASA-TM-100510] 11 p1446 N88-18618
High performance Solid Rocket Motor (SRM) submerged nozzle/combustion cavity flowfield assessment
[NASA-CR-179307] 11 p1446 N88-18622
NASA (National Aeronautics and Space Administration) procurement: The 1973 space shuttle solid rocket motor contractor selection
[PB88-135264] 11 p1447 N88-18623
STA-2A NDT testing
[NASA-CR-179301] 11 p1497 N88-18937
Calculation of flow about posts and powerhead model
[NASA-CR-179305] 12 p1625 N88-19722
Preliminary 2-D shell analysis of the space shuttle solid rocket boosters
[NASA-TM-100515] 17 p2348 N88-23989
Effects of natural environment on first generation solid rocket booster thermal protection system materials
[NASA-TM-100329] 17 p2373 N88-24113
Quality and productivity drive innovation and improvement at United Technologies Aerospace Operations, Inc.
[NASA-CR-182944] 18 p2525 N88-24983
SRM propellant and polymer materials structural test program
[NASA-TP-2821] 18 p2530 N88-25013
Assembly Test Article (ATA)
[NASA-CR-179361] 21 p2903 N88-27226
SPACE SHUTTLE MAIN ENGINE
Configuration evaluation and criteria plan. Volume 2: Evaluation criteria plan (update). Space Transportation Main Engine (STME) configuration study
[NASA-CR-181429] 03 p0270 N88-11699
Failure control techniques for the SSME
[NASA-CR-179224] 04 p0409 N88-12537
The 58th Shock and Vibration Symposium, volume 1
[NASA-CP-2488-VOL-1] 05 p0592 N88-13609
Fluid mass and thermal loading effects on the modal characteristics of space shuttle main engine liquid oxygen inlet splitter vanes 05 p0594 N88-13628
Incipient failure detection of space shuttle main engine turbopump bearings using vibration envelope detection
05 p0595 N88-13629
High frequency data acquisition system for space shuttle main engine testing 05 p0595 N88-13630
Space shuttle main engine vibration data base
05 p0595 N88-13631
Thermal finite-element analysis of space shuttle main engine turbine blade
[NASA-TM-100117] 05 p0610 N88-13745
Analysis of internal flows relative to the space shuttle main engine
[NASA-CR-179240] 06 p0674 N88-14125
Evaluation of load tracks and wear of two sets of bearings from space shuttle main engine high pressure oxygen turbopumps
[NASA-CR-178969] 07 p0661 N88-15223
Pattern recognition techniques for failure trend detection in SSME ground tests 07 p0924 N88-15614
Equilibrium retention in the nozzle of oxygen hydrogen propulsion systems 07 p0924 N88-15616
The determination of equivalent bearing loading for the BSMT that simulate SSME high pressure oxidizer turbopump conditions using the SHABERTH/SINDA computer programs 07 p0925 N88-15623
SSME environment database development
[NASA-CR-179245] 08 p0964 N88-15836
Embedded expert system for space shuttle main engine maintenance 08 p1058 N88-16382
Space shuttle main engine anomaly data and inductive knowledge based systems: Automated corporate expertise 08 p1060 N88-16398
An expert system to analyze high frequency dependent data for the space shuttle main engine turbopumps
08 p1060 N88-16399
Automatic mathematical modeling for space application 08 p1060 N88-16402
RB-ARD: A proof of concept rule-based abort
08 p1065 N88-16435
Computer-aided design analysis of 57-mm, angular-contact, cryogenic turbopump bearings
[NASA-TP-2816] 11 p1496 N88-18933
Rocketdyne automated dynamics data analysis and management system 11 p1499 N88-18954
Calculation of flow about posts and powerhead model
[NASA-CR-179305] 12 p1625 N88-19722
Duct flow nonuniformities: Effect of struts in SSME HGM II(+)
[NASA-CR-179285] 15 p2062 N88-22296
Advanced probabilistic methods for quantifying the effects of various uncertainties in structural response
15 p2080 N88-22401
Thermal-structural analyses of Space Shuttle Main Engine (SSME) hot section components
15 p2081 N88-22404
SSME single-crystal turbine blade dynamics
16 p2221 N88-23257
SSME technology test bed fast shutdown assessment
[NASA-CR-179354] 17 p2314 N88-23831
Research study: Space shuttle main engine plume flowfield model
[NASA-CR-179336] 18 p2474 N88-24676
Duct flow nonuniformities for Space Shuttle Main Engine (SSME)
[NASA-CR-179338] 18 p2511 N88-24899
Numerical grid generation and flow simulation in SSME thrust chamber 19 p2626 N88-25577
Evaluation and improvement of liquid propellant rocket chugging analysis techniques. Part 1: A one-dimensional analysis of low frequency combustion instability in the fuel preburner of the space shuttle main engine
[NASA-CR-183106] 21 p2903 N88-27224
Evaluation and improvement of liquid propellant rocket chugging analysis techniques. Part 2: A study of low frequency combustion instability in rocket engine preburners using a heterogeneous stirred tank reactor model
[NASA-CR-182724] 21 p2903 N88-27225
Evaluation of transfer films of Salox M on 440C for HPOTP bearing cage applications, task 119
[NASA-CR-179020] 23 p3223 N88-29184
Automatic mathematical modeling for real time simulation system 24 p3420 N88-30356
SPACE SHUTTLE MISSION 31-A
Comparison of flight-measured and calculated temperatures on the space shuttle orbiter
[NASA-TM-88278] 03 p0321 N88-12029
Studies of the vestibulo-ocular reflex on STS 4, 5 and 6
[NASA-TM-100461] 12 p1666 N88-19987
SPACE SHUTTLE MISSION 31-B
Studies of the vestibulo-ocular reflex on STS 4, 5 and 6
[NASA-TM-100461] 12 p1666 N88-19987
SPACE SHUTTLE MISSION 41-C
In-orbit and laboratory exchange of ORUs designed/not designed for servicing 12 p1587 N88-19499
SPACE SHUTTLE MISSION 51-L
Space shuttle accident: NASA's actions to address the Presidential Commission report
[PB88-135306] 15 p2024 N88-22059
SPACE SHUTTLE MISSION 61-B
A synopsis of the EVA training conducted on EASE/ACCESS for STS-61-B 02 p0140 N88-10879
Overview of crew member energy expenditure during Shuttle Flight 61-8 EASE/ACCESS task performance
02 p0140 N88-10882
SPACE SHUTTLE MISSIONS
NT SPACE SHUTTLE MISSION 31-A
NT SPACE SHUTTLE MISSION 31-B
NT SPACE SHUTTLE MISSION 41-C
NT SPACE SHUTTLE MISSION 51-L
NT SPACE SHUTTLE MISSION 61-B
Meteorological systems support to critical shuttle requirements on the Eastern Test Range --- STS
02 p0205 N88-11281
The 1987 Get Away Special Experimenter's Symposium
[NASA-CP-2500] 10 p1286 N88-17691
Spacelab: An international success story
[NASA-SP-487] 11 p1566 N88-19375
SPACE SHUTTLE ORBITAL FLIGHT TEST 4
U SPACE TRANSPORTATION SYSTEM 4 FLIGHT
SPACE SHUTTLE ORBITER 099
U CHALLENGER (ORBITER)
SPACE SHUTTLE ORBITER 103
U DISCOVERY (ORBITER)
SPACE SHUTTLE ORBITERS
NT CHALLENGER (ORBITER)
NT DISCOVERY (ORBITER)
The composition of the gas in the loading inlet of the Space Shuttle Orbiter
[ETN-87-90430] • 01 p0012 N88-10069
Effects of forced and free convections on structural temperatures of space shuttle orbiter during reentry flight
[NASA-TM-86800] 01 p0043 N88-10275
Thermal stress analysis of space shuttle orbiter subjected to reentry aerodynamic heating
[NASA-TM-88286] 01 p0061 N88-10389
Contamination control of the space shuttle Orbiter crew compartment 02 p0133 N88-10834
Pinhole occulter experiment
[NASA-CR-179206] 02 p0235 N88-11481
Comparison of flight-measured and calculated temperatures on the space shuttle orbiter
[NASA-TM-88278] 03 p0321 N88-12029
Numerical simulation of the hypersonic flow around lifting vehicles 05 p0532 N88-13234
The effects of RCS jet firing on the isolated Orbiter and mated coast phases of the glide return to launch site maneuver at Mach number 6 (IA302B)
[NASA-CR-180223] 20 p2766 N88-26403
SPACE SHUTTLE PAYLOADS
NT ASTRO MISSIONS (STS)
NT EARTH RADIATION BUDGET EXPERIMENT
NT GET AWAY SPECIALS (STS)
NT PHYSICS AND CHEMISTRY EXPERIMENT IN SPACE
NT SPACELAB
NT X RAY ASTROPHYSICS FACILITY
Phase 3 study of selected tether applications in space. Volume 2: Study results
[NASA-CR-179186] 02 p0132 N88-10828
An investigation of the behavior of outgassed molecules in thermal vacuums 02 p0133 N88-10836
Space Construction
[NASA-CP-2490] 02 p0138 N88-10870
The flight demonstration program and selection process 02 p0138 N88-10871
Mission Peculiar Equipment Support Structure: A platform for space construction
02 p0139 N88-10874
Marshall Space Flight Center's role in EASE/ACCESS mission management 02 p0139 N88-10875
A monograph of the National Space Transportation System Office (NSTSO) integration activities conducted at the NASA Lyndon B. Johnson Space Center for the EASE/ACCESS payload flown on STS 61-B
02 p0139 N88-10876
EASE/ACCESS ground processing at Kennedy Space Center 02 p0139 N88-10877
Overview of crew member energy expenditure during Shuttle Flight 61-8 EASE/ACCESS task performance
02 p0140 N88-10882
High power ion thruster performance
[NASA-TM-100127] 04 p0409 N88-12542
Potential for on-orbit manufacture of large space structures using the pultrusion process
[NASA-TM-4016] 05 p0557 N88-13388
Mechanistic studies of polymeric samples exposed aboard STS 8
[NASA-CR-182364] 06 p0686 N88-14202
NASA (National Aeronautics and Space Administration) ADP (Automated Data Processing) system: Information on the automated mission and the payload tracking system
[PB88-104969] 07 p0942 N88-15730
The dynamics and control of large-flexible space structures, part 10
[NASA-CR-182426] 08 p0963 N88-15830
Experiment control and data system for an infrared detector array with maximum sensitivity
[ETN-88-91497] 09 p1136 N88-16813

POCC capabilities document. Payload support capabilities description: MCC, JSC POCC, remote POCC interface
[NASA-TM-89708] 09 p1260 N88-17555
Payload bay atmospheric vent airflow testing at the Vibration and Acoustic Test Facility
[NASA-TM-100460] 11 p1437 N88-18572
Modification of integrated partial payload lifting assembly
[NASA-CR-182573] 11 p1443 N88-18607
Project SKYLITE: A design exploration
[AD-A187906] 11 p1511 N88-19030
Explorer Platform on-orbit servicing operations
12 p1591 N88-19526
Research and technology, 1987
[NASA-TM-100323] 12 p1713 N88-20253
Deployable/retrievable boom: One application to tethered satellite 14 p1874 N88-21197
Payload deployment system --- STS
14 p1875 N88-21199
OLYMPUS shuttle specific radiator shield
14 p1879 N88-21234
Space experiment plan FMPT
15 p2051 N88-22220
The Shuttle Imaging Radar B (SIR-B) experiment report
[NASA-CR-182923] 17 p2334 N88-23932
High power ion thruster performance
17 p2404 N88-24295
Payload deployment method and system
[NASA-CASE-MSC-21330-1] 18 p2470 N88-24660
The detection and interpretation of long-term changes in ozone from space
[NASA-TM-101135] 21 p2971 N88-27650
Design considerations for the ORION satellite: Structure, propulsion and attitude control subsystems for a small, general purpose spacecraft
[AD-A193837] 22 p3048 N88-26086
Aerospace payload support systems
[AFGL-TR-87-0241] 24 p3334 N88-29843
Containment of a silicone fluid free surface in reduced gravity using barrier coatings
[NASA-TM-101314] 24 p3371 N88-30072
Spacelab data processing facility (SLDPF) Quality Assurance (QA)/Data Accounting (DA) expert systems: Transition from prototypes to operational systems
24 p3420 N88-30353

SPACE SHUTTLE SOLID ROCKET MOTORS
U SPACE SHUTTLE BOOSTERS

SPACE SHUTTLES
NT HERMES MANNED SPACEPLANE
Fourteenth Space Simulation Conference: Testing for a Permanent Presence in Space
[NASA-CP-2446] 02 p0132 N88-10829
Redistribution of particulates in shuttle bay during launch 02 p0133 N88-10837
Moving the factory into orbit 02 p0134 N88-10844
Spacecraft material flammability testing and configurations 04 p0407 N88-12529
Structural analysis of a bolted joint concept for the space shuttle's solid rocket motor casing
[NASA-TM-89092] 04 p0407 N88-12531
Proceedings: SDIO/DARPA Workshop on Laser Propulsion. Volume 3: Viewgraphs
[DE88-000964] 04 p0450 N88-12790
The analysis of nonstationary vibration data
05 p0592 N88-13610
Model survey of the space shuttle solid rocket motor using multiple input methods 05 p0593 N88-13617
Modeling cloudy and clear interval length probabilities using space shuttle imagery
[AD-A185290] 05 p0627 N88-13837
An analytical method for ditching analysis of an airborne vehicle
[NASA-CR-4120] 07 p0816 N88-14968
Propulsion estimation techniques
07 p0927 N88-15632
The Jeffcott equations in nonlinear rotordynamics
07 p0928 N88-15636
SSME environment database development
[NASA-CR-179245] 08 p0964 N88-15836
Zero-G thermodynamic vent system for shuttle/Centaur 08 p0983 N88-15943
Third Conference on Artificial Intelligence for Space Applications, part 1
[NASA-CP-2492-Pt-1] 08 p1055 N88-16360
Telerobotic controller development
08 p1056 N88-16370
Space shuttle main engine anomaly data and inductive knowledge based systems: Automated corporate expertise 08 p1060 N88-16398
Prototype resupply scheduler
08 p1064 N88-16428
RB-ARD: A proof of concept rule-based abort
08 p1065 N88-16435
Lateral stability and control derivatives extracted from space shuttle Challenger flight data
[NASA-TM-100520] 09 p1132 N88-16786
Centaur G Prime modal test 09 p1181 N88-17075
Space shuttle onboard navigation console expert/trainer system 09 p1203 N88-17208
Expert system verification concerns in an operations environment 09 p1207 N88-17234
Verifying shuttle onboard software using expert systems 09 p1207 N88-17237
Analysis of shear-layer probe data for holes in hypersonic configurations
[DE88-003992] 11 p1435 N88-18564
Cornering characteristics of the main-gear tire of the space shuttle orbiter
[NASA-TP-2790] 11 p1438 N88-18583
Space shuttle phase B wind tunnel test database
[NASA-CR-4121] 11 p1444 N88-18611
Structural analysis of the space shuttle solid rocket booster/external tank attach ring
[NASA-TM-100510] 11 p1446 N88-18618
Effect of element size on the solution accuracies of finite-element heat transfer and thermal stress analyses of space shuttle orbiter
[NASA-TM-88292] 11 p1502 N88-18971
Orbital analysis of a STS (Space Transportation System) external tank in low earth orbit
[AD-A188829] 12 p1593 N88-19542
Transient Pressure Test Article (TPTA) 1.1 and 1.1A, volume 1
[NASA-CR-179322-VOL-1] 12 p1603 N88-19588
Lateral and longitudinal stability and control parameters for the space shuttle discovery as determined from flight test data
[NASA-TM-100555] 13 p1724 N88-20309
Soviet space transport systems
13 p1727 N88-20328
A 60-meter erectable assembly concept for a control of flexible structures flight experiment
[NASA-TM-100497] 14 p1873 N88-21190
In-flight rain damage tests of the shuttle thermal protection system
[NASA-TM-100438] 14 p1881 N88-21241
Analysis of contamination data recorded by the IECM camera/photometer
[NASA-TM-100324] 14 p1882 N88-21246
Chronology of KSC and KSC related events for 1987
[NASA-CR-182754] 14 p2012 N88-22002
Engineering support of space shuttle experiment integration
[AD-A190135] 15 p2024 N88-22061
A method of atmospheric density measurements during space shuttle entry using ultraviolet-laser Rayleigh scattering
[NASA-TM-100056] 15 p2069 N88-22337
Survey of the Air Force P78-2 (SCATHA) satellite plasma wave data during electron gun operations
[AD-A191014] 16 p2168 N88-22926
A decade of computer simulations for space shuttle aerodynamics
[NASA-TM-100990] 18 p2459 N88-24603
Structural margins assessment approach
[NASA-TM-100332] 18 p2473 N88-24672
Numerical simulations of flow around shuttle orbiter
19 p2635 N88-25633
Book analysis. Challenger: A major malfunction
[AD-A192458] 20 p2764 N88-26388
Space shuttle phase B wind tunnel model and test information. Volume 2: Orbiter configuration
[NASA-CR-178415-VOL-2-PT-2]
21 p2893 N88-27172
Space shuttle natural environment analysis
[NASA-CR-179337] 21 p2976 N88-27676
Space shuttle phase B wind tunnel model and test information. Volume 2: Orbiter configuration
[NASA-CR-178415-VOL-2-PT-1]
23 p3171 N88-28881
Progress on a Monte Carlo shuttle contamination model
[AD-A193694] 23 p3183 N88-28945
Preloaded brake disc
[NASA-CASE-MSC-21132-1] 23 p3223 N88-29181
Space shuttle phase B wind tunnel model and test information. Volume 3: Launch configuration
[NASA-CR-178416-VOL-3-PT-2]
24 p3315 N88-29744
Space shuttle phase B wind tunnel model and test information. Volume 1: Booster configuration
[NASA-CR-178414-VOL-1-PT-1]
24 p3315 N88-29745
Space shuttle phase B wind tunnel model and test information. Volume 1: Booster configuration
[NASA-CR-178414-VOL-1-PT-2]
24 p3320 N88-29770
Ascent guidance for a winged boost vehicle
[NASA-CR-172083] 24 p3334 N88-29846

SPACE SIMULATORS
A modern space simulation facility to accommodate high production acceptance testing 02 p0134 N88-10841
Characteristics and performance of the ESTEC large space simulator cryogenic system
02 p0135 N88-10849
Structural Assembly Demonstration Experiment (SADE)
[NASA-CR-179205] 02 p0138 N88-10868
Research and development at the Marshall Space Flight Center Neutral Buoyancy Simulator
02 p0139 N88-10878
Environment test laboratory
[ETN-88-91885] 14 p1869 N88-21166
Simulation of cometary nuclei
14 p2005 N88-21954

SPACE STATION PAYLOADS
Phase 3 study of selected tether applications in space. Volume 2: Study results
[NASA-CR-179186] 02 p0132 N88-10828
Communications payload concepts for geostationary facilities
[NASA-TM-100154] 05 p0576 N88-13513
Microgravity Particle Research on the Space Station
[NASA-CP-2496] 07 p0883 N88-15354
Astrophysics and the solar nebula
07 p0883 N88-15355
Planetary science 07 p0883 N88-15356
Atmospheric science 07 p0883 N88-15357
Exobiology and life science 07 p0883 N88-15358
Physics and chemistry 07 p0883 N88-15359
System analysis study of space platform and station accommodations for life sciences research facilities. Volume 2: Study results. Appendix E: Work breakdown structure and dictionary
[NASA-CR-179274] 10 p1292 N88-17723
System analysis study of space platform and station accommodations for life sciences research facilities. Volume 2: Study results. Appendix D: Life sciences research facility requirements
[NASA-CR-179273] 10 p1292 N88-17724
Progress toward a cosmic dust collection facility on space station
[NASA-CR-182427] 12 p1598 N88-19566
Conceptual design and programmatics studies of space station accommodations for Life Sciences Research Facilities (LSRF)
[NASA-CR-179270] 12 p1598 N88-19567
Space station accommodations for life sciences research facilities: Phase A conceptual design and programmatics studies for Missions SAAX0307, SAAX0302 and the transition from SAAX0307 to SAAX0302. Volume 1: Executive summary
[NASA-CR-179267] 12 p1599 N88-19571
Analysis of low gravity tolerance of model experiments for space station: Preliminary results for directional solidification
[NASA-CR-182657] 12 p1614 N88-19648
Research and technology, 1987
[NASA-TM-100323] 12 p1713 N88-20253
Requirements for temperature and species concentration measurements in microgravity combustion experiments 17 p2329 N88-23903
Mars rover/sample return mission requirements affecting space station
[NASA-CR-172048] 18 p2594 N88-25414
A knowledge-based decision support system for payload scheduling 23 p3252 N88-29358
Coordinated study of Solar-Terrestrial Observatory (STO) payloads on space station
[NASA-CR-183142] 24 p3334 N88-29848

SPACE STATION POLAR PLATFORMS
A teleoperated manipulator system concept for unmanned platforms --- Columbus
12 p1593 N88-19537
P-Plus: Polar Platform utilization study, executive summary
[BAE-TP-8391] 18 p2469 N88-24653

SPACE STATION POWER SUPPLIES
Space station assembly/servicing capabilities
01 p0016 N88-10100
Solar converging method 04 p0403 N88-12504
Space station systems: A bibliography with indexes
[NASA-SP-7056(05)] 05 p0556 N88-13382
Power components for the space station 20-kHz power distribution system
[NASA-TM-100866] 14 p1904 N88-21374
Structural assessment of a space station solar dynamic heat receiver thermal energy storage canister
15 p2081 N88-22406
Benefits of 20 kHz PMAD in a nuclear space station
17 p2398 N88-24256
Operational concerns involving a shadow-shielded nuclear reactor for space station applications
17 p2398 N88-24257

Speculations on future opportunities to evolve Brayton powerplants aboard the space station
17 p2398 N88-24258
Hydrogen turbines for space power systems: A simplified axial flow gas turbine model 17 p2419 N88-24385
AC power system breadboard
[NASA-CR-179369] 22 p3049 N88-28091
Lewis Research Center space station electric power system test facilities
[NASA-TM-100924] 23 p3182 N88-28942
Expert systems for MSFC power systems
23 p3255 N88-29375
Utilization of artificial intelligence techniques for the Space Station power system 23 p3261 N88-29412
Regenerative fuel cell energy storage system for a low earth orbit space station
[NASA-CR-174802] 24 p3389 N88-30184

SPACE STATION PROPULSION
Space station propulsion technology: Space station propulsion system test bed test plan
[NASA-CR-179201] 01 p0017 N88-10104
Space station integrated propulsion and fluid system study: Fluid systems configuration databook
[NASA-CR-179215] 03 p0278 N88-11753
Space station systems: A bibliography with indexes
[NASA-SP-7056(05)] 05 p0556 N88-13382

SPACE STATION STRUCTURES
Space station resistojet system requirements and interface definition study
[NASA-CR-180832] 04 p0409 N88-12541
Advanced radiator concepts utilizing honeycomb panel heat pipes
[NASA-CR-172017] 04 p0443 N88-12747
Space station systems: A bibliography with indexes
[NASA-SP-7056(05)] 05 p0556 N88-13382
Personnel occupied woven envelope robot power
[NASA-CR-182367] 07 p0856 N88-15196
Solar concentrator advanced development program, task 1
[NASA-CR-179489] 10 p1350 N88-18068
LDR structural experiment definition
[NASA-TM-100618] 17 p2312 N88-23826
Mobile remote manipulator system for a tetrahedral truss
[NASA-CASE-MSC-20985-1] 20 p2765 N88-26398

SPACE STATIONS
NT COLUMBUS SPACE STATION
NT MIR SPACE STATION
NT SALYUT SPACE STATION
NT SPACE STATION POLAR PLATFORMS
Space Station Mission Planning System (MPS) development study. Volume 1: Executive summary
[NASA-CR-179202] 01 p0009 N88-10047
Space Station Mission Planning System (MPS) development study. Volume 2
[NASA-CR-179200] 01 p0009 N88-10048
Space Station Mission Planning Study (MPS) development study. Volume 3: Software development plan
[NASA-CR-179203] 01 p0009 N88-10049
Space station integrated wall design and penetration damage control
[NASA-CR-179169] 01 p0013 N88-10070
Space station: Leadership for the future
[NASA-PAM-509/8-87] 01 p0013 N88-10072
Study of a payload for Columbus Polar Platform Earth observation demonstration mission, executive summary
[ESA-CR(P)-2412] 01 p0014 N88-10079
Columbus preparatory program. Payload element study on a technology demonstration mission, executive summary
[CS-RP-AI-016] 01 p0014 N88-10080
Spacecraft 2000
[NASA-CP-2473] 01 p0015 N88-10084
Space station platforms 01 p0015 N88-10086
Space station assembly/servicing capabilities
01 p0016 N88-10100
Efficient placement of structural dynamics sensors on the space station
[NASA-CR-172015] 01 p0017 N88-10103
Preliminary study of a containerless processing facility for Columbus, executive summary
[ESA-ITT/AO/1-1834/85F] 01 p0032 N88-10203
Prephase A study of a crystallization laboratory for Columbus, executive summary
[ESA-ITT/AO/1-1866/85F] 01 p0032 N88-10206
Study of mobile communications payload for Columbus Polar Platforms
[ITS-TR-056A/86] 01 p0034 N88-10220
Catalytic processes for space station waste conversion
[NASA-CR-177423] 01 p0077 N88-10491
Space station based interferometry
01 p0096 N88-10628
Solar-terrestrial research in the space station era
01 p0117 N88-10747
Fourteenth Space Simulation Conference: Testing for a Permanent Presence in Space
[NASA-CP-2446] 02 p0132 N88-10829
Columbus pressurized module verification
02 p0134 N88-10842
Moving the factory into orbit 02 p0134 N88-10844
Rapid toxicity detection in water quality control utilizing automated multispecies biomonitoring for permanent space stations 02 p0135 N88-10848
Space station contamination considerations
02 p0137 N88-10859
Contamination control concepts for space station customer servicing 02 p0137 N88-10860
Predictive momentum management for a space station measurement and computation requirements
[NASA-CR-172026] 02 p0138 N88-10866
Space Construction
[NASA-CP-2490] 02 p0138 N88-10870
Space station: National Aeronautics and Space Administration's 1987 cost estimate
[PB87-220760] 02 p0140 N88-10883
Pinhole occulter experiment
[NASA-CR-179206] 02 p0235 N88-11481
Orbital Spacecraft Consumables Resupply System (OSCRS). Volume 4: Extended study results Part 1: Executive Summary
[NASA-CR-172012] 03 p0268 N88-11686
Orbital Spacecraft Consumables Resupply System (OSCRS): Monopropellant application to space station and OMV automatic refueling impacts of an ELV launch, volume 4
[NASA-CR-172028] 03 p0276 N88-11741
Photovoltaic power modules for NASA's manned space station
[NASA-TM-100229] 03 p0277 N88-11745
Space station propulsion
[NASA-TM-100216] 03 p0277 N88-11746
Space station integrated propulsion and fluid system study: Fluid systems configuration databook
[NASA-CR-179215] 03 p0278 N88-11753
An allotment planning concept and related computer software for planning the fixed satellite service at the 1988 space WARC
[NASA-TM-100244] 03 p0308 N88-11944
Potential applications of expert systems and operations research to space station logistics functions
[NASA-CR-180473] 03 p0372 N88-12342
Department of Housing and Urban Development-Independent Agencies Appropriations for fiscal year 1988, Thursday, 9 April 1987: National Aeronautics and Space Administration
03 p0386 N88-12424
Department of Housing and Urban Development-Independent Agencies Appropriations for fiscal year 1988, Friday, 10 April 1987: National Aeronautics and Space Administration
03 p0386 N88-12425
Spacecraft Fire Safety
[NASA-CP-2476] 04 p0406 N88-12520
Space station internal environmental and safety concerns 04 p0407 N88-12527
Optimization techniques applied to passive measures for in-orbit spacecraft survivability
[NASA-CR-179216] 04 p0408 N88-12532
An assessment of clinical chemical sensing technology for potential use in space station health maintenance facility
[NASA-CR-172013] 04 p0475 N88-12926
Space suit extravehicular hazards protection development
[NASA-TM-100458] 04 p0475 N88-12927
Orbital Spacecraft Consumables Resupply System (OSCRS). Volume 1: Executive summary
[NASA-CR-172010] 05 p0553 N88-13368
Design and assembly sequence analysis of option 3 for CETF reference space station
[NASA-TM-100503] 05 p0553 N88-13369
Space station systems: A bibliography with indexes
[NASA-SP-7056(05)] 05 p0556 N88-13382
Feasibility study for gas-grain simulation facility
[NASA-CR-177468] 05 p0646 N88-13954
National Aeronautics and Space Administration space station proposal, fiscal year 1988
[S-HRG-100-328] 05 p0659 N88-14043
The 1988 NASA (National Aeronautics and Space Administration) authorization
[GPO-80-245] 05 p0659 N88-14044
Approaches and possible improvements in the area of multibody dynamics modeling
[NASA-CR-179227] 06 p0663 N88-14067
Controlled Ecological Life Support Systems (CELSS) conceptual design option study
[NASA-CR-177421] 06 p0754 N88-14625
Controlled Ecological Life Support Systems (CELSS) physiochemical waste management systems evaluation
[NASA-CR-177422] 06 p0754 N88-14626
National Aeronautics and Space Administration (NASA)/American Society for Engineering Education (ASEE) Summer Faculty Fellowship Program, 1987. Volume 2
[NASA-CR-172009-VOL-2] 06 p0796 N88-14874
Performance considerations for the astrometric telescope facility on the phase 1 space station
[NASA-TM-100040] 06 p0800 N88-14896
Space station accommodations for lunar base elements: A study
[NASA-TM-100501] 06 p0804 N88-14907
A space transportation system operations model
[NASA-TM-100481] 07 p0823 N88-14999
Space station onboard propulsion system: Technology study
[NASA-CR-179233] 07 p0825 N88-150
Chromic acid anodizing of aluminum foil
[NASA-CR-178417] 07 p0837 N88-1507
Space environmental effects on polymeric materia
[NASA-CR-182418] 07 p0838 N88-15082
Integration of symbolic and algorithmic hardware and software for the automation of space station subsystems
[NASA-TM-89705] 07 p0907 N88-15497
Some considerations on measuring the Newtonian gravitational constant G in an orbiting laboratory
07 p0922 N88-15603
The feasibility of using TAE as the UIL for the space station and for other internal NASA tasks and projects
07 p0925 N88-15618
Can space station software be specified through Ada?
07 p0925 N88-15622
Advancing automation and robotics technology for the space station and for the US economy: Submitted to the United States Congress October 1, 1987
[NASA-TM-100777] 08 p0959 N88-15816
Advancing automation and robotics technology for the space station and for the US economy: Submitted to the United States Congress May 15, 1987
[NASA-TM-89811] 08 p0959 N88-15817
Advancing automation and robotics technology for the space station and for the US economy: Submitted to the United States Congress October 1, 1986
[NASA-TM-89190] 08 p0960 N88-15818
Development of an emulation-simulation thermal control model for space station application
[NASA-CR-182409] 08 p0962 N88-15823
Space station accommodations for life sciences research facilities. Phase 1: Conceptual design and programmatics studies for Missions SAAX0307, SAAX0302 and the transition from SAAX0307 to SAAX0302. Volume 2: Study results
[NASA-CR-179244] 08 p0962 N88-15829
Space station propulsion technology
[NASA-CR-179260] 08 p0964 N88-15835
Status of 20 kHz space station power distribution technology
[NASA-TM-100781] 08 p0964 N88-15838
Third Conference on Artificial Intelligence for Space Applications, part 1
[NASA-CP-2492-Pt-1] 08 p1055 N88-16360
Telerobotic controller development
08 p1056 N88-16370
MTK: An AI tool for model-based reasoning
08 p1056 N88-16372
Integration of symbolic and algorithmic hardware and software for the automation of space station subsystems
08 p1056 N88-16373
KBS V and V as related to automation of space station subsystems: Rationale for a KBS lifecycle
08 p1057 N88-16375
Monitoring of space station life support systems with miniature mass spectrometry and artificial intelligence
08 p1057 N88-16376
Artificial intelligence and space power systems automation 08 p1058 N88-16381
Goal driven kinematic simulation of flexible arm robot for space station missions 08 p1059 N88-16388
FMEAssist: A knowledge-based approach to Failure Modes and Effects Analysis 08 p1060 N88-16395
Solid modelling for the manipulative robot arm (power) and adaptive vision control for space station missions
08 p1061 N88-16409
Planning and scheduling for robotic assembly
08 p1062 N88-16416
Planning activities in space 08 p1063 N88-16417
Intelligent man/machine interfaces on the space station 08 p1063 N88-16418
An AI approach for scheduling space-station payloads at Kennedy Space Center 08 p1064 N88-16425
The resource envelope as a basis for space station management system scheduling
08 p1064 N88-16427
Prototype resupply scheduler
08 p1064 N88-16428
Prototype space station automation system delivered and demonstrated at NASA 08 p1066 N88-16442

Applications of expert systems for satellite autonomy 08 p1066 N88-16443
Space station structures development [NASA-CR-179261] 09 p1133 N88-16792
Communications satellite systems operations with the space station. Volume 3: Supplementary technical report [NASA-CR-180875] 09 p1133 N88-16794
Development of a coupled expert system for the spacecraft attitude control problem 09 p1205 N88-17223
User interface devices for mission control 09 p1205 N88-17224
Design knowledge capture for the space station 09 p1208 N88-17239
Vision technology/algorithms for space robotics applications 09 p1212 N88-17267
Manipulator arm design for the Extravehicular Teleoperator Assist Robot (ETAR): Applications on the space station 09 p1213 N88-17270
Telerobot for space station 09 p1213 N88-17274
Space station integrated wall damage and penetration damage control. Task 5: Space debris measurement, mapping and characterization system [NASA-CR-179281] 10 p1265 N88-17688
The 1987 Get Away Special Experimenter's Symposium [NASA-CP-2500] 10 p1286 N88-17691
Simulation test beds for the space station electrical power system [NASA-TM-100786] 10 p1290 N88-17715
System analysis study of space platform and station accommodations for life sciences research facilities. Volume 1: Executive summary. Phase A: Conceptual design and programmatics [NASA-CR-179268] 10 p1291 N88-17721
System analysis study of space platform and station accommodations for life sciences research facilities. Volume 2: Study results, attachment 2. Phase A: Conceptual design and programmatics [NASA-CR-179272] 10 p1291 N88-17722
Report of the Committee on the Space Station of the National Research Council [NASA-CR-181602] 10 p1292 N88-17727
Magnetic emissions testing of the space station engineering model resistojet [NASA-TM-100785] 10 p1292 N88-17728
Component data base for space station resistojet auxiliary propulsion [NASA-CR-180834] 10 p1293 N88-17731
NASA/NBS (National Aeronautics and Space Administration/National Bureau of Standards) standard reference model for Telerobot Control System Architecture (NASREM) [PB88-124773] 10 p1338 N88-17999
Assessment of mixed fleet potential for space station launch and assembly [NASA-TM-100550] 11 p1443 N88-18608
Orbiter transfer vehicle concept definition and system analysis study. Volume 4: Space station accommodations. Revision 1 [NASA-CR-179293] 11 p1444 N88-18609
Orbital transfer vehicle concept definition and system analysis study. Volume 4, Appendix A: Space station accommodations. Revision 1 [NASA-CR-179294] 11 p1444 N88-18610
Space station operating system study [NASA-CR-179308] 11 p1446 N88-18619
Microgravity and Materials Processing Facility study (MMPF): Requirements and Analyses of Commercial Operations (RACO) preliminary data release [NASA-CR-179309] 11 p1466 N88-18742
Phase calibration generator 11 p1473 N88-18785
Computer-aided modeling and prediction of performance of the modified Lundell class of alternators in space station solar dynamic power systems [NASA-CR-182538] 11 p1507 N88-19000
Space vehicle approach velocity judgments under simulated visual space conditions [NASA-TM-89437] 11 p1523 N88-19094
Study of industry requirements that can be fulfilled by combustion experimentation aboard space station [NASA-CR-180854] 11 p1566 N88-19377
A lunar transportation system [NASA-CR-182561] 11 p1567 N88-19379
Preliminary analysis of an integrated logistics system for OSSA payloads [NASA-CR-4114] 12 p1584 N88-19477
Preliminary analysis of an integrated logistics system for OSSA payloads. Volume 1: Executive summary 12 p1584 N88-19478
Preliminary analysis of an integrated logistics system for OSSA payloads. Volume 2: OSSA integrated logistics support strategy 12 p1584 N88-19479
Preliminary analysis of an integrated logistics system for OSSA payloads. Volume 3: OSSA integrated logistics support planning document 12 p1584 N88-19480
Preliminary analysis of an integrated logistics system for OSSA payloads. Volume 4: Supportability analysis of the 1.8m centrifuge 12 p1584 N88-19481
State-of-the-art technologies for construction in space: A review [AD-A188412] 12 p1585 N88-19483
Proceedings of the 1st European In-Orbit Operations Technology Symposium [ESA-SP-272] 12 p1585 N88-19484
Safe rendezvous approach to a space station by impulsive transfers and continuous thrust arcs 12 p1585 N88-19486
Assembly and servicing of a European Space Station 12 p1586 N88-19492
Utilization of SMS and EVA for the servicing of European Space Station 12 p1587 N88-19500
Robotic intelligence issues for space manipulator monitoring, control programming 12 p1588 N88-19504
EUROSIM: A concept of total system support 12 p1590 N88-19523
Technology requirements for telerobotic satellite servicing in space 12 p1592 N88-19536
Analysis of a rotating advanced-technology space station for the year 2025 [NASA-CR-178345] 12 p1600 N88-19580
Space Station Human Factors Research Review. Volume 3: Space Station Habitability and Function: Architectural Research [NASA-CP-2426-VOL-3] 12 p1650 N88-19883
Space station architectural elements model study. Space station human factors research review 12 p1650 N88-19884
Space station architectural elements model study [REPT-31799] 12 p1650 N88-19885
Space station group activities habitability module study: A synopsis 12 p1651 N88-19886
Full scale architectural simulation techniques for space stations 12 p1651 N88-19887
Social factors in space station interiors 12 p1651 N88-19888
Vega-1 and Vega-2 automatic stations: Functioning of flyby vehicles during encounter with Halley's comet 13 p1725 N88-20314
Study on long term evolution Towards European Autonomous Manned Spaceflight (STEAMS) [SNIAS-SE/LS/AP-35-073] 13 p1727 N88-20330
Turnaround operations analysis for OTV. Volume 1: Executive summary [NASA-CR-179316] 13 p1729 N88-20340
Turnaround operations analysis for OTV. Volume 2: Detailed technical report [NASA-CR-179317] 13 p1729 N88-20341
The space station assembly phase: Flight telerobotic servicer feasibility, volume 1 [NASA-CR-182689] 13 p1731 N88-20351
The space station assembly phase: Flight telerobotic servicer feasibility. Volume 2: Methodology and case study [NASA-CR-182690] 13 p1731 N88-20352
Spacecraft fire-safety experiments for space station: Technology development mission [NASA-CR-182114] 13 p1731 N88-20353
Solar dynamic power system definition study [NASA-CR-180877] 13 p1733 N88-20361
The dynamic control of robotic manipulators in space [NASA-CR-182710] 13 p1779 N88-20646
An evaluation of the methods for rescuing EVA (Extravehicular Activities) crewmembers and recovering equipment detached and adrift from the space station [AD-A189683] 14 p1871 N88-21181
Space station heavy lift launch vehicle utilization [NASA-TM-100604] 14 p1873 N88-21188
Incorporation of privacy elements in space station design [NASA-CR-182748] 14 p1881 N88-21242
Space station power system requirements [NASA-TM-100886] 14 p1881 N88-21245
Multi-hundred kilowatt roll ring assembly evaluation results [NASA-TM-100865] 14 p1904 N88-21375
Space station mobile transporter 14 p1927 N88-21488
Superconducting magnet technique for ASTROMAG on the space station [DE88-004560] 15 p2025 N88-22063
A systems analysis of fire suppression alternatives for the US space station [AD-A189847] 15 p2025 N88-22064
Ray tracing optical analysis of offset solar collector for space station solar dynamic system [NASA-TM-100853] 15 p2027 N88-22080
Japanese space station module 15 p2052 N88-22224
Solar cell cover glasses for satellites 15 p2052 N88-22225
Vibrations of structures with parametric uncertainties [AD-A190400] 15 p2076 N88-22378
Research and technology [NASA-TM-100172] 15 p2153 N88-22851
Tethered diagnostic package for use from the space station [DE88-006264] 16 p2167 N88-22921
An integrated and modular digital modeling approach for the space station electrical power system development [NASA-TM-100904] 16 p2170 N88-22935
JPRS report: Science and technology. Japan [JPRS-JST-87-030] 16 p2185 N88-23026
Microgravity mechanisms and robotics program 16 p2219 N88-23237
Base reaction optimization of manipulators with redundant kinematics 16 p2219 N88-23238
Department of Housing and Urban Development independent agencies appropriations for 1989. Part 7: National Aeronautics and Space Administration [GPO-85-166] 16 p2286 N88-23689
Manned Mars mission accommodation: Sprint mission [NASA-TM-100598] 16 p2290 N88-23711
On-orbit technology experiment facility definition [NASA-TM-100614] 17 p2311 N88-23824
LDR structural experiment definition [NASA-TM-100618] 17 p2312 N88-23826
Locking hinge [NASA-CASE-MSC-21056-1] 17 p2312 N88-23827
Manual for obscuration code with space station applications [NASA-CR-178099] 17 p2334 N88-23931
Space Station Human Factors Research Review. Volume 1: EVA Research and Development [NASA-CP-2426-VOL-1] 17 p2379 N88-24145
Advanced EVA system design requirements study 17 p2380 N88-24147
Space Station Human Factors Research Review. Volume 4: Inhouse Advanced Development and Research [NASA-CP-2426-VOL-4] 17 p2380 N88-24148
Space station proximity operations and window design 17 p2380 N88-24149
Spatial cognition 17 p2380 N88-24152
Fault diagnosis in orbital refueling operations 17 p2381 N88-24154
Third Conference on Artificial Intelligence for Space Applications, part 2 [NASA-CP-2492-PT-2] 17 p2387 N88-24188
MTK: An AI tool for model-based reasoning 17 p2387 N88-24189
Integration of symbolic and algorithmic hardware and software for the automation of space station subsystems 17 p2387 N88-24190
Connecting remote systems for demonstration of automation technologies 17 p2387 N88-24191
Knowledge based system verification and validation as related to automation of space station subsystems: Rationale for a knowledge based system lifecycle 17 p2387 N88-24192
Status of the organic Rankine cycle for space applications 17 p2422 N88-24402
Optimization of organic Rankine cycles for space station applications 17 p2423 N88-24407
Research and Technology, 1987, Goddard Space Flight Center [NAS 1.15:101097] 17 p2453 N88-24572
Space station architectural elements model study [NASA-CR-4027] 18 p2464 N88-24632
Possibilities and limits for use of laser propulsion systems in interorbital space flight [ILR-MITT-185] 18 p2475 N88-24683
Human performance issues arising from manned space station missions [NASA-CR-3942] 18 p2553 N88-25156
Space station architectural elements and issues definition study [NASA-CR-3941] 18 p2587 N88-25371
Space station habitability recommendations based on a systematic comparative analysis of analogous conditions [NASA-CR-3943] 18 p2587 N88-25372
A Study of Space Station Contamination Effects — conference [NASA-CP-3002] 18 p2590 N88-25390
Neutral environment for space station 18 p2590 N88-25391
Space station neutral external environment 18 p2590 N88-25392
Contaminant ions and waves in the space station environment 18 p2590 N88-25393
Space station induced electromagnetic effects 18 p2591 N88-25394
Space station contamination study: Assessment of contaminant spectral brightness 18 p2591 N88-25395

Calculation of space station infrared irradiance from atmosphere-induced emissions
18 p2591 N88-25396
Space station particulate contamination environment
18 p2591 N88-25397
The particulate environment surrounding the space station: Estimates from the PACS data
18 p2591 N88-25398
Effects of meteoroids and space debris on the particulate environment for space station 18 p2591 N88-25399
Contamination of optical surfaces --- Space Station
18 p2592 N88-25400
Surface interactions relevant to space station contamination problems 18 p2592 N88-25401
Laboratory experiments of relevance to the space station environment 18 p2592 N88-25402
Contamination of the space station environment by vented chemicals 18 p2592 N88-25403
Centaur operations at the space station
[NASA-CR-179593] 19 p2606 N88-25473
Evaluation of the ion trap mass spectrometer for potential application in the space station
[DE88-008940] 19 p2674 N88-25902
Selecting the right crew for future space stations: An analysis of selection research on offshore divers, aviation pilots and other high risk groups in Scandinavia
19 p2696 N88-26021
The US space programme spacewalk/extravehicular activity experience: Past, present and future
19 p2697 N88-26031
Habitability of the Space Station: From vehicle to living space 19 p2697 N88-26033
Recent research on crew wardroom habitability for the Space Station 19 p2698 N88-26039
Tasks foreseen for space robots and an example of an associated orbital infrastructure
19 p2699 N88-26044
Some operational aspects of a rotating advanced-technology space station for the year 2025
[NASA-CR-181617] 20 p2765 N88-26397
Vapor Compression Distillation Subsystem (VCDS) component enhancement, testing and expert fault diagnostics development, volume 2
[NASA-CR-172076] 21 p2994 N88-27755
Block Oriented Simulation System (BOSS)
[NASA-CR-182947] 21 p2995 N88-27760
Vapor Compression Distillation Subsystem (VCDS) component enhancement, testing and expert fault diagnostics development, volume 1
[NASA-CR-172072] 22 p3134 N88-28634
Ariane 5, HERMES and European vehicles for space station servicing
[SNIAS-881-422-102] 23 p3183 N88-28943
Space transportation nodes assumptions and requirements: Lunar base systems study task 2.1
[NASA-CR-172052] 23 p3183 N88-28944
Expandable pallet for space station interface attachments
[NASA-CASE-MSC-21117-1] 23 p3185 N88-28958
Assessment of the effects of space debris and meteoroids environment on the space station solar array assembly
[NASA-TM-101315] 23 p3185 N88-28959
Collet lock joint for space station truss
[NASA-CASE-MSC-21207-1] 23 p3222 N88-29180
Second Conference on Artificial Intelligence for Space Applications
[NASA-CP-3007] 23 p3251 N88-29351
A plan for time-phased incorporation of automation and robotics on the US space station
23 p3255 N88-29377
A space station onboard scheduling assistant
23 p3259 N88-29402
A robotic system for automation of logistics functions on the Space Station 23 p3260 N88-29407
Definition of common support equipment and space station interface requirements for IOC model technology experiments
[NASA-TM-100656] 24 p3336 N88-29856
Study of toluene rotary fluid management device and shear flow condenser performance for a space-based organic Rankine power system
[NASA-CR-180885] 24 p3338 N88-29872
Advanced planar array development for space station
[NASA-CR-179373] 24 p3389 N88-30181
Space station proximity operations windows: Human factors design guidelines
[NASA-TM-88233] 24 p3410 N88-30301
A shared-world conceptual model for integrating space station life sciences telescience operations
24 p3416 N88-30333
Integrated resource scheduling in a distributed scheduling environment 24 p3417 N88-30342
The space station assembly phase: System design trade-offs for the flight telerobotic servicer
24 p3420 N88-30357

SPACE SUITS
NT EXTRAVEHICULAR MOBILITY UNITS
Space suit extravehicular hazards protection development
[NASA-TM-100458] 04 p0475 N88-12927
EVA, the technological challenge
12 p1592 N88-19535
Space cabin atmosphere and extracurricular sortie --- embolisms 19 p2696 N88-26023
Technical challenges in the development of a European space suit system and comparison with underwater suits
19 p2696 N88-26024

SPACE SURVEILLANCE (GROUND BASED)
Photographic observations of the large scale features of Comet Halley 16 p2288 N88-23698
SSTS (Space Surveillance and Tracking System): The importance of early test and evaluation organizational participation
[AD-A193745] 23 p3276 N88-29499

SPACE SURVEILLANCE (SPACEBORNE)
Surveillance systems test and evaluation facilities
02 p0134 N88-10845
Strategic Defense Initiative Program: Status of space surveillance and tracking system
[PB88-150438] 14 p1967 N88-21739

SPACE SYSTEMS ENGINEERING
U AEROSPACE ENGINEERING

SPACE TELESCOPE
U HUBBLE SPACE TELESCOPE

SPACE TOOLS
An introduction to robot joint control methods
[NLR-TR-86080-U] 20 p2811 N88-26677
Study of software requirements and artificial intelligence techniques for robotics
[TL-3333] 24 p3422 N88-30365

SPACE TRANSPORTATION
NT SPACE TRANSPORTATION SYSTEM
Soviet space transport systems
13 p1727 N88-20328

SPACE TRANSPORTATION SYSTEM
Space Construction
[NASA-CP-2490] 02 p0138 N88-10870
The flight demonstration program and selection process 02 p0138 N88-10871
A monograph of the National Space Transportation System Office (NSTSO) integration activities conducted at the NASA Lyndon B. Johnson Space Center for the EASE/ACCESS payload flown on STS 61-B
02 p0139 N88-10876
Pinhole occulter experiment
[NASA-CR-179206] 02 p0235 N88-11461
Results of the development motor 8 test firing
[GPO-78-692] 03 p0278 N88-11751
Department of Housing and Urban Development-Independent Agencies Appropriations for fiscal year 1988, Friday, 10 April 1987: National Aeronautics and Space Administration
03 p0386 N88-12425
The determination of exhaust cloud dimensions from films of space shuttle launches
[NASA-CR-4103] 06 p0732 N88-14500
A space transportation system operations model
[NASA-TM-100481] 07 p0823 N88-14999
Evaluate the application of modal test and analysis processes to structural fault detection in MSFC - STS project elements 07 p0927 N88-15630
NASA (National Aeronautics and Space Administration) ADP (Automated Data Processing) system: Information on the automated mission and the payload tracking system
[PB88-104989] 07 p0942 N88-15730
A study to evaluate STS heads-up ascent trajectory performance employing a minimum-Hamiltonian optimization strategy
[NASA-TP-2793] 08 p0960 N88-15820
Lateral stability and control derivatives extracted from space shuttle Challenger flight data
[NASA-TM-100520] 09 p1132 N88-16788
STS propellant scavenging systems study. Part 2, volume 1: Executive summary and study results
[NASA-CR-179275] 10 p1290 N88-17716
STS propellant scavenging systems study. Part 2, volume 2: Cost and WBS/dictionary
[NASA-CR-179276] 10 p1290 N88-17717
Ballistic Single Stage Carrier Vehicle (BETA): A single stage reusable ballistic space shuttle concept
[MBB-UR-949/70] 10 p1310 N88-17828
Trends in the development of space transportation systems
[MBB-UR-911/86] 10 p1315 N88-17857
Research and technology 1987 annual report of the Kennedy Space Center
[NASA-TM-100303] 10 p1431 N88-18546
A two stage launch vehicle for use as an advanced space transportation system for logistics support of the space station
[NASA-CR-182572] 11 p1443 N88-18606
Assessment of mixed fleet potential for space station launch and assembly
[NASA-TM-100550] 11 p1443 N88-18608
Orbital analysis of a STS (Space Transportation System) external tank in low earth orbit
[AD-A188829] 12 p1593 N88-19542
Post-Challenger evaluation of space shuttle risk assessment and management
[NASA-CR-182461] 12 p1705 N88-20202
Research and technology, 1987
[NASA-TM-100323] 12 p1713 N88-20253
Department of Housing and Urban Development independent agencies appropriations for 1989. Part 7: National Aeronautics and Space Administration
[GPO-85-166] 16 p2286 N88-23689
Technology development program for twenty-first century aerospace vehicles 17 p2302 N88-23768
Large antenna experiments aboard the space shuttle: Application of nonuniform sampling techniques
19 p2652 N88-25745
Mark IV-85 mission support planning and future mission set 22 p3067 N88-28202
Space transportation nodes assumptions and requirements: Lunar base systems study task 2.1
[NASA-CR-172052] 23 p3183 N88-28944
SRB/SLEEC (Solid Rocket Booster/Shingle Lap Extendible Exit Cone) feasibility study, volume 1
[NASA-CR-178973] 23 p3187 N88-28964

SPACE TRANSPORTATION SYSTEM FLIGHTS
NT SPACE TRANSPORTATION SYSTEM 4 FLIGHT

SPACE TRANSPORTATION SYSTEM 4 FLIGHT
Studies of the vestibulo-ocular reflex on STS 4, 5 and 6
[NASA-TM-100461] 12 p1666 N88-19987

SPACE VEHICLE CHECKOUT PROGRAM
RETE experiment Assembly, Integration, and Verification (AIV) activities
[IFSI-87-6] 05 p0555 N88-13380
The KATE shell: An implementation of model-based control, monitor and diagnosis 09 p1210 N88-17255
Study of the assembly, integration and verification programs of telecommunication satellites applicable to other satellite programs
[MATRA-100/CC/MLG/031/87]
24 p3334 N88-29847

SPACE VEHICLE CONTROL
U SPACECRAFT CONTROL

SPACE WEAPONS
A comparison of open and closed multimegawatt space power and weapon systems
[DE87-012975] 01 p0089 N88-10579
The impact of deployment rates on the effectiveness of strategic defenses
[AD-A186907] 09 p1233 N88-17383
A strategy for space warfare
[AD-A186658] 09 p1233 N88-17394
AFAL (Air Force Astronautics Laboratory) technical objective document FY89
[AD-A187861] 11 p1567 N88-19378
Vapor-mist for lightweight high voltage space insulation systems
[DE87-011704] 13 p1762 N88-20538
Constellation sizing for modest directed energy platforms
[DE88-007033] 15 p2070 N88-22343
Parametric analysis of power requirements for space-based radar 17 p2399 N88-24260
Monolithic fuel cell based power source for sprint power generation 17 p2407 N88-24313
Analysis of closed cycle megawatt class space power systems with nuclear reactor heat sources
17 p2413 N88-24351
The effect of operating temperature on open, multimegawatt space power systems
17 p2414 N88-24352
Comparison of open and closed multimegawatt space power systems 17 p2414 N88-24353
RSMASS: A simple model for estimating reactor/shield masses 17 p2414 N88-24355
Hydrogen turbines for space power systems: A simplified axial flow gas turbine model 17 p2419 N88-24385
Power and energy requirements for electromagnetic launchers 17 p2420 N88-24391
Individual satellite power requirements calculated from specified constellation performance
17 p2420 N88-24392
Candidate advanced energy storage concepts for multimegawatt burst power systems
17 p2426 N88-24434
Monitoring space weaponry: Detection and verification issues
[DE88-008726] 20 p2847 N88-26900
SDI and/or arms control
[RAND-P-7357] 20 p2848 N88-26903
Launch operations to support future space forces
[AD-A192679] 20 p2881 N88-27107

Slew-induced deformations in a space-based electromagnetic rail gun 21 p2929 N88-27385
Future SDI (Strategic Defense Initiative) decision making
[AD-A192794] 21 p3010 N88-27860
Overview of the SDI (Strategic Defense Initiative) Program in short wavelength chemical lasers
[DE88-007912] 21 p3010 N88-27861
Electronic combat roadmap for space
[AD-A194262] 22 p3146 N88-28709
SDI (Strategic Defense Initiative) battle management/C3 (Command, Control and Communications) algorithms technology program plan
[AD-A194357] 23 p3275 N88-29495
A submillimeter wavelength space-based imaging radar
[AD-A195846] 24 p3364 N88-30033
Looking beyond the strategic defense initiative
[AD-A195079] 24 p3427 N88-30394
Antisatellite weapons and satellite deployment strategies
[AD-A195014] 24 p3427 N88-30396

SPACE-TIME CONTINUUM
U RELATIVITY

SPACE-TIME FUNCTIONS
Volume functions in the general theory of relativity
[ETN-87-90408] 01 p0089 N88-10582
Inequivalent quantizations and fundamentally perfect spaces
[DE87-014225] 02 p0229 N88-11446
Superconformal invariance and superstring in background fields
[DE87-703097] 02 p0247 N88-11561
Our universe as an attractor in a superstring model
[DE87-703066] 02 p0251 N88-11585
New notions about space-time and gravitation
[DE87-703259] 03 p0383 N88-12408
Analysis of absolute space-time Lorentz theories
[DE87-703371] 04 p0500 N88-13076
Homogeneous space-time of Goedel type in higher-derivate gravity
[DE87-703690] 04 p0500 N88-13077
Computer-aided study of a class of Riemannian space-times
[DE87-703367] 05 p0645 N88-13950
Superstrings on quantum spacetime
[DE88-700106] 07 p0940 N88-15715
Space-time processing of field produced by moving source 09 p1234 N88-17399
Criterion of singularity in general theory of relativity
09 p1240 N88-17430
Relativistic theory of gravitation and new concepts about space-time 09 p1240 N88-17431
Machine models and simulations
[PB88-118690] 10 p1386 N88-18280
Spatial-temporal variability of North Pacific sea surface temperature anomaly patterns 11 p1516 N88-19058
Notes on a class of homogeneous space-times
[DE88-700136] 11 p1562 N88-19353
Experimental analysis of absolute space-time Lorentz theories
[DE88-700140] 11 p1563 N88-19355
Space-time analysis of oceanographic fields by modified empirical orthogonal functions method
13 p1786 N88-20687
Space-time structure of ultrashort light pulses formed during stimulated backscattering of laser beam
14 p1972 N88-21767
Strings in four dimensions
[DE88-006435] 14 p1990 N88-21864
Seismic inversion by a RMS (Root-Mean-Square) Born approximation in the space-time domain
[PB88-165402] 15 p2131 N88-22711
Einstein metrics and Brans-Dicke superfields
[DE88-006992] 15 p2146 N88-22809
Quantization of axial electrodynamics
[DE88-701498] 15 p2147 N88-22813
Cosmology for high energy physicists
[DE88-005705] 15 p2151 N88-22842
Big whorls carry little whorls 16 p2195 N88-23094
Local time displacement as a symmetry of nature in flat space-time
[NASA-TM-100610] 16 p2264 N88-23542
Raychaudhuri equation in the self-consistent Einstein-Cartan theory with spin-density
[NASA-TM-101145] 17 p2447 N88-24546
Photon limited image processing in the space-time domain
[AD-A193142] 21 p2972 N88-27655
Electromagnetic theory of the gravitation
22 p3158 N88-28793
Global gauge anomaly of classical groups in even dimension
[DE88-008572] 22 p3158 N88-28797
On the GKP and BS constructions of C-boundary
[DE88-702643] 22 p3159 N88-28799
Open bosonic string in background electromagnetic field
[DE88-702140] 23 p3201 N88-29053
Time travel in the homogeneous Som-Raychaudhuri universe
[DE88-702220] 23 p3295 N88-29622
Image focusing in space and time
[AD-A195839] 24 p3429 N88-30410

SPACE-TIME METRIC
U SPACE-TIME FUNCTIONS

SPACEBORNE ASTRONOMY
ESA Workshop on Optical Interferometry in Space
[ESA-SP-273] 01 p0094 N88-10613
A comparison of interferometry from space and ground 01 p0094 N88-10614
Imaging strategies for a spaceborne interferometer
01 p0094 N88-10617
ISIS: Image reconstruction methods and signal-to-noise ratio investigations --- spaceborne interferometry
01 p0094 N88-10619
ISIS: Image reconstruction experiments and comparison of various array configurations --- spaceborne interferometry 01 p0095 N88-10620
OASIS: A mission concept --- Optical Aperture Synthesis Space Interferometry (OASIS) 01 p0095 N88-10622
Binary Star Explorer 01 p0095 N88-10624
ISIS: Imaging Speckle Interfereometer in Space
01 p0095 N88-10625
Proposed studies of a 30 meter imaging interferometer concept --- spaceborne astronomy
01 p0096 N88-10627
Space station based interferometry
01 p0096 N88-10628
NASA/JPL study on optical imaging interferometry in space 01 p0096 N88-10630
Aperture synthesis in space: Technical problems
01 p0097 N88-10638
Solar interferometry with a 4-aperture nonredundant and stabilized network 01 p0097 N88-10639
A test-bed for space interferometry: Space Platform Interferometer (SPI) 01 p0097 N88-10640
Dike zones on Venus
[NASA-TT-20111] 02 p0254 N88-11607
The Swedish sounding rocket and balloon program
08 p1025 N88-16205
Swiss scientific balloon and sounding rocket experiments 1985-1987 08 p1025 N88-16206
Infrared astronomy: Why and how?
09 p1123 N88-16722
Use of Space Station for space science
09 p1129 N88-16782
Microgravity payloads and missions for Space Station: Some issues affecting compatibility with other payloads
09 p1129 N88-16783
Experiment control and data system for an infrared detector array with maximum sensitivity
[ETN-88-91497] 09 p1136 N88-16813
Preparation of photometric measurements on a million stars in the framework of the satellite project HIPPARCOS/TYCHO
[ETN-88-91502] 13 p1853 N88-21093
The X-ray properties of AM Her stars
[MPE-PREPRINT-106] 16 p2289 N88-23704
SW UMa and V426 Oph: EXOSAT surprises
19 p2740 N88-26269
International ultraviolet explorer observatory operations
[NASA-CR-180775] 22 p3145 N88-28708
EXOSAT observations of Hercules X-1
[MPE-PREPRINT-119] 22 p3164 N88-28841
Beyond the visible: A decade of observations with the International Ultraviolet Explorer (IUE)
[ESA-F09] 24 p3331 N88-29828
ESA report to the 27th COSPAR meeting
[ESA-SP-1098] 24 p3453 N88-30556
The high-throughput X-ray spectroscopy mission: The mission-science report
[ESA-SP-1097] 24 p3453 N88-30557

SPACEBORNE EXPERIMENTS
NT PHYSICS AND CHEMISTRY EXPERIMENT IN SPACE
Blagov commentary on Mir station, first manning
01 p0009 N88-10051
Final phase of Project Vega 01 p0009 N88-10053
The Aquarack as a potential instrument for basic research work in space biology: Inventory and scientific dispositions 01 p0073 N88-10470
Xiphophorus as an experimental system for genetic and biological development studies under microgravity conditions 01 p0074 N88-10472
Life support systems for biological experiments under weightlessness in the German and European space programs 01 p0074 N88-10477
Trickle water and feeding system in plant culture and light-dark cycle effects on plant growth
03 p0361 N88-12273
Microgravity nucleation and particle coagulation experiments support
[NASA-CR-181540] 04 p0423 N88-12618
Microgravity nucleation and particle coagulation experiments support
[NASA-CR-181541] 04 p0423 N88-12619
Study of certain biological characteristics of bacteria during the French-Soviet CYTOS-2 space experiment
04 p0473 N88-12917
Research on Electrodynamic Tether Effects (RETE) experiment Electrical Ground Support Equipment (EGSE) --- tethered satellite
[IFSI-87-2] 05 p0555 N88-13378
RETE experiment Assembly, Integration, and Verification (AIV) activities
[IFSI-87-6] 05 p0555 N88-13380
Partial analysis of experiment LDEF A-0114
[NASA-CR-179236] 06 p0780 N88-14787
Allowable gravity-levels for Spacelab, Columbus and EURECA --- materials science
[BF-R-66.525-2] 07 p0838 N88-15084
Microgravity Particle Research on the Space Station
[NASA-CP-2496] 07 p0883 N88-15354
Astrophysics and the solar nebula
07 p0883 N88-15355
Planetary science 07 p0883 N88-15356
Atmospheric science 07 p0883 N88-15357
Exobiology and life science 07 p0883 N88-15358
Physics and chemistry 07 p0883 N88-15359
Proceedings and program draft in Gravitational Biology in the Federal Republic of Germany --- Effects of Weightlessness on the Human Organism
[ESA-TT-988] 07 p0884 N88-15363
The role of the DFVLR project management life sciences in the space program of the Federal Republic of Germany 07 p0884 N88-15364
A theoretical concept for state changes and shape changes in weightlessness 07 p0884 N88-15365
Experiments with rats flown aboard Cosmos-1667 biosatellite (main objectives, conditions and results)
07 p0893 N88-15414
Multiply charged particles in primary cosmic rays with energy less than or equal to 2 TeV
07 p0921 N88-15596
Space station accommodations for life sciences research facilities. Phase 1: Conceptual design and programmatics studies for Missions SAAX0307, SAAX0302 and the transition from SAAX0307 to SAAX0302. Volume 2: Study results
[NASA-CR-179244] 08 p0962 N88-15829
LeRC cryogenic fluid management program overview
08 p0981 N88-15928
Cryogenic fluid management program flight concept definition 08 p0981 N88-15929
How ground-based observations contribute to rocket, balloon and space shuttle experiments: Experience from the past and outlook for the future
08 p1026 N88-16216
Scheduling spacecraft operations
08 p1064 N88-16426
Microgravity experiments in space: Compatibility with dynamic perturbing effects 09 p1241 N88-17435
Microgravity research at the University of Mexico: Experiments in payload G-006 10 p1286 N88-17692
An update to the MITRE/WPI Space Shuttle Program GASCAN G-408 10 p1287 N88-17697
The photons payload, G-494: A learning experience
10 p1288 N88-17701
The challenge of G-376 10 p1288 N88-17705
Project Explorer takes its second step: GAS-608 in engineering development 10 p1288 N88-17707
The NORSTAR Program: Space shuttle to space station 10 p1289 N88-17710
Into the thermosphere: The atmosphere explorers
[NASA-SP-490] 10 p1353 N88-18084
Preliminary analysis of an integrated logistics system for OSSA payloads
[NASA-CR-4114] 12 p1584 N88-19477
Preliminary analysis of an integrated logistics system for OSSA payloads. Volume 4: Supportability analysis of the 1.8m centrifuge 12 p1584 N88-19481
Promising concepts for ground-to-orbit experiment teleoperation --- Columbus 12 p1590 N88-19518
Ground based supervisory and programming system for automatic experiment execution in orbit
12 p1590 N88-19519
Robotics servicing experiment --- European space programs 12 p1591 N88-19529
Cytomorphology and ultrastructure of corn root meristem in weightlessness 12 p1651 N88-19891
The European Space Agency's role in life sciences and research in space 12 p1652 N88-19894
Exobiology and botany facilities for EURECA
12 p1652 N88-19898
Life sciences research in space: The requirement for animal models 12 p1654 N88-19909

Fish as a tool for testing fitness in space
12 p1662 N88-19963
Animal research on the Space Station
12 p1662 N88-19964
Thermal structure of Venusian Atmosphere determined from results of measurements from Vega-2 landing module 13 p1725 N88-20315
Vibration characteristics of pumped fluid systems (VCPFS) --- microgravity payloads
[ESA-CR(P)-2499] 14 p1895 N88-21310
Engineering support of space shuttle experiment integration
[AD-A190135] 15 p2024 N88-22061
Space utilization plans 15 p2051 N88-22219
Amorphous semiconductors made in space
15 p2051 N88-22221
Containerless glass melting 15 p2051 N88-22222
Pb(1-x)Sn(x)Te crystal growth in space
15 p2051 N88-22223
Solar cell cover glasses for satellites
15 p2052 N88-22225
Noncontact temperature measurements in the microgravity fluids and transport phenomena discipline
17 p2328 N88-23901
Microgravity combustion discipline working group summary of requirements for noncontact temperature measurements 17 p2328 N88-23902
Requirements for temperature and species concentration measurements in microgravity combustion experiments 17 p2329 N88-23903
Non-contact temperature measurements for biotechnology discipline working group
17 p2329 N88-23904
Airborne and spaceborne radar images for geologic and environmental mapping in the Amazon rain forest, Brazil
17 p2353 N88-24021
Botany Facility pre-phase C/D. Core payload for EURECA, volume 2
[BF-RP-ER-015-VOL-2] 17 p2377 N88-24130
Botany Facility: The problems of plant fixation
[SiRA-A/7373/WP220/RJS/001]
17 p2379 N88-24140
Theoretical plasma physics research of active space experiments
[AD-A192075] 18 p2577 N88-25309
Contamination of the space station environment by vented chemicals 18 p2592 N88-25403
Application of AI to space systems
19 p2634 N88-25626
Microgravity science and applications bibliography, 1987 revision
[NASA-TM-4067] 22 p3062 N88-28171
Experimental proof of quasilongitudinal propagation of low-frequency waves in middle latitudes in upper ionosphere 24 p3447 N88-30516
Influence of plasma parameters on VLF radiation in near-rocket region 24 p3448 N88-30518
Charge composition of primary cosmic ray nuclei with z greater than or equal to 2 in energy region greater than or equal to 2 TeV 24 p3448 N88-30519

SPACEBORNE LASERS
Atmospheric Lidar Experiment In Space (ALEXIS)
[DFVLR-MITT-88-10] 22 p3118 N88-28526
Spaceborne lidar: Development of a laboratory test system
[BF-R-66.090-1] 24 p3378 N88-30118

SPACEBORNE PHOTOGRAPHY
NT SATELLITE-BORNE PHOTOGRAPHY
Remote sensing of planets and cartographic results
[HSBW-HEFT-14] 03 p0389 N88-12444
Space applications in geography
08 p1007 N88-16104
Use of space photographs for geomorphological studies in southwestern Tajikistan 08 p1008 N88-16109
Academic course Space Methods for Studying Modern Landscapes of Continents 08 p1012 N88-16133
Photogrammetric principles for combining remote sounding and three-dimensional mapping
08 p1012 N88-16135
Using space photography of the Earth in the classroom: Drought in Africa
[NASA-CR-182948] 19 p2685 N88-25960

SPACEBORNE TELESCOPES
NT GERMAN INFRARED LABORATORY
NT HUBBLE SPACE TELESCOPE
NT INFRARED SPACE OBSERVATORY (ISO)
NT SPACE INFRARED TELESCOPE FACILITY
NT X RAY ASTROPHYSICS FACILITY
OASIS: A mission concept --- Optical Aperture Synthesis Space Interferometry (OASIS) 01 p0095 N88-10622
COSMIC --- Coherent Optical System of Modular Image Collectors (COSMIC); spaceborne telescope
01 p0095 N88-10623
Fiber-linked telescope arrays on the ground and in space 01 p0095 N88-10626
Wavefront error sensing
[NASA-CR-181504] 03 p0321 N88-12030
Study of solid state photomultiplier
[NASA-CR-177465] 05 p0583 N88-13556
Multisurface control mechanism for a deployable antenna: Far Infrared and Submillimeter Space Telescope (FIRST) technology study
[RP-FA-D003] 09 p1135 N88-16807
Design of a linear actuator and breadboard test result --- far IR telescope 14 p1877 N88-21217
Fine adjustment mechanism for FIRST
14 p1878 N88-21219
Design, construction and performance of the ROSAT high resolution X-ray mirror assembly
[MPE-PREPRINT-101] 15 p2150 N88-22836

SPACECRAFT ANTENNAS
Mechanical properties characterization of composite sandwich materials intended for space antenna applications
[NASA-TM-88893] 01 p0020 N88-10121
Thermal testing by internal IR heating of the FEP module 02 p0136 N88-10854
Dual S/X-band RV antenna
[DE87-014853] 03 p0305 N88-11923
MBA payload testing by Compact Antenna Test Range (CATR)
[ESA-CR(P)-2473] 08 p0977 N88-15906
The ESTEC Mini Compact Antenna Test Range
[ESA-CR(P)-2475] 08 p0977 N88-15907
Latching mechanisms for IOC --- EURECA
14 p1875 N88-21205
Features and applications of the integrated composites analyzer (ICAN) code 15 p2078 N88-22391
Development of a general software package for the analysis and synthesis of planar antenna arrays for space applications
[S-247-02] 24 p3359 N88-30000

SPACECRAFT CABIN ATMOSPHERES
Progress in European CELSS activities
03 p0358 N88-12252
Space cabin atmosphere and extracurricular sortie --- embolisms 19 p2696 N88-26023

SPACECRAFT CABINS
Contamination control of the space shuttle Orbiter crew compartment 02 p0133 N88-10834
Space station group activities habitability module study: A synopsis 12 p1651 N88-19886

SPACECRAFT CHARGING
Space Environment Technology --- conference
[ISBN-2-85428-170-5] 03 p0271 N88-11702
The geosynchronous plasma environment
03 p0273 N88-11716
Introduction to the problem of environmentally induced discharges 03 p0273 N88-11717
External surface charging mechanisms --- spacecraft
03 p0273 N88-11719
Three-dimensional charging effects --- spacecraft
03 p0273 N88-11720
Modeling of environmentally-induced effects within satellites. Part 1: NASCAP modeling of satellites
03 p0273 N88-11721
Modeling of environmentally-induced transients within satellites. Part 2: Discharge coupling transients
03 p0273 N88-11722
Discharge phenomena --- spacecraft
03 p0274 N88-11723
In-flight diagnosis: Analysis of spurious events --- spacecraft 03 p0274 N88-11724
Electromagnetic interaction between an electric discharge and cabling inside a satellite
03 p0274 N88-11725
Electromagnetic effects of a discharge on circuitry --- spacecraft 03 p0274 N88-11726
Charging calculations for the HIPPARCOS satellite
03 p0274 N88-11728
MARECS-A case 03 p0274 N88-11729
Electromagnetic compatibility (EMC) phenomena and prevention of the effects --- spacecraft
03 p0274 N88-11731
Electrostatic discharges in geostationary orbit: The case of Telecom 1 03 p0275 N88-11733
Flight model discharge system
[AD-A185657] 06 p0673 N88-14122
MAIMIK: A high current electron beam experiment on a sounding rocket from Andoya rocket range (Norway)
08 p1030 N88-16243
Spacecraft dielectric surface charging property determination
[NASA-CR-180879] 14 p1881 N88-21243
Simulations of the electrostatic charging of ESA communications satellites
[ESA-STM-239] 18 p2472 N88-24670
Deep dielectric charging effects due to high energy electrons in earth's outer magnetosphere
[AD-A192154] 18 p2541 N88-25083
Spacecraft requirements for predictions of geomagnetic activity (a tutorial)
[AD-A191943] 19 p2685 N88-25959
Ion gun generated electromagnetic interference on the SCATHA satellite
[AD-A195179] 24 p3335 N88-29853

SPACECRAFT COMMUNICATION
NT SATELLITE COMMUNICATION
Coherent infrared detection, volume B --- CO2 laser intersatellite data link
[ESA-CR(P)-2392-VOL-1] 01 p0034 N88-10218
Coherent infrared detection, volume D --- CC2 laser intersatellite data link
[ESA-CR(P)-2392-VOL-2] 01 p0034 N88-10219
A conformal aircraft phased array antenna for airplane-satellite communication in the L band
[ESA-TT-1057] 03 p0305 N88-11926
Error control techniques for satellite and space communications
[NASA-CR-181581] 05 p0576 N88-13516
Results on the low elevation angle propagation experiment, part 1
[TUD-R-328] 06 p0693 N88-14250
Satellite ground-terminal user simulation
[NASA-TM-100234] 06 p0694 N88-14260
Study of a Radio Relay Link (RRL). Cassini mission. Data package for final presentation
[ESA-CR(P)-2472] 07 p0847 N88-15138
The Telecommunications and Data Acquisition Report
[NASA-CR-182545] 11 p1471 N88-18774
Spacecraft telecommunications system mass estimates 11 p1473 N88-18784
The evaluation and selection of a 5th ground antenna site for the global positioning system
[AD-A189495] 13 p1720 N88-20286
A pointing mechanism for intersatellite link system
14 p1874 N88-21194
Continued design of a Pointing, Acquisition, and Tracking (PAT) subsystem for InterSatellite Laser links (ISL2)
[TELDIX-15-093-178] 14 p1905 N88-21384
Construction of a 60 GHz Traveling Wave Tube (TWT) for intersatellite link on geostationary orbit (ISL/TWT)
[BMFT-FB-W-86-015] 16 p2192 N88-23076
Environmental projects. Volume 6: Environmental assessment. New 34-meter antenna at Venus site
[NASA-CR-182922] 17 p2332 N88-23919
Connecting remote systems for demonstration of automation technologies 17 p2387 N88-24191
Assessment of optical communications systems for the Data Relay Satellite
[ESA-CR(P)-2488-VOL-2] 18 p2502 N88-24842
Document transfer by a digital satellite link
[NLR-MP-86071-U] 20 p2792 N88-26564
Optical multiple access intersatellite links
[BAE-TP-8502] 24 p3361 N88-30013
The LTPP communication processor --- Columbus and Hermes
[CL/CP/SES/FR/004] 24 p3415 N88-30328
A rule-based systems approach to spacecraft communications configuration optimization
24 p3417 N88-30341

SPACECRAFT COMPONENTS
NT COMMAND MODULES
NT LANDING MODULES
NT LUNAR LANDING MODULES
NT SPACECRAFT CABINS
NT SPACECRAFT MODULES
Telemetry conditioning units for the European launcher Ariane 01 p0012 N88-10068
Mobile test fixture system for use in a thermal vacuum facility 02 p0134 N88-10843
Mathematical modelling of solar ultraviolet radiation induced optical degradation in anodized aluminum
02 p0135 N88-10846
A nondissipative Pyrotechnic Arming and Firing Unit (PAFU)
[CRA/REPO/8019] 02 p0155 N88-10974
Incipient fault detection study for advanced spacecraft systems
[NASA-CR-172014] 02 p0183 N88-11138
Electromagnetic effects of a discharge on circuitry --- spacecraft 03 p0274 N88-11726
Fire-related standards and testing
04 p0406 N88-12522
Fire extinguishment and inhibition in spacecraft environments 04 p0406 N88-12523
High energy density rechargeable batteries for aerospace power requirements
[AD-A184883] 05 p0577 N88-13519
Natural frequencies and structural integrity assessment of large space structures
[AD-A186139] 07 p0824 N88-15001
Heat pipes for space use 09 p1124 N88-16736
Major spacecraft hardware testing in Europe
09 p1125 N88-16740

Promotion of European components for ESA projects
09 p1128 N88-16764
Space station structures development
[NASA-CR-179261] 09 p1133 N88-16792
Activities report in tribology
[ESA-ESTL-79] 09 p1174 N88-17037
The 58th Shock and Vibration Symposium, volume 2
[NASA-CP-2488-VOL-2] 11 p1499 N88-18948
Design and dynamic testing of an instrumented spacecraft component 11 p1499 N88-18952
SOAR: Space orbiting advanced fusion power reactor
[AD-A189234] 13 p1732 N88-20356
Proceedings of the 3rd European Space Mechanisms and Tribology Symposium
[ESA-SP-279] 14 p1874 N88-21191
Models for steady and nonsteady Coulomb torque in ball bearings 14 p1876 N88-21208
Towards a practical microgravity environment --- isolation mount 14 p1878 N88-21223
Cryogenic test facilities for an optical cryomechanism qualification 14 p1879 N88-21228
Structural latches for modular assembly of spacecraft and space mechanisms 14 p1925 N88-21471
A pyrotechnical opening valve
[SNIAS-MU/TYS-NT-2-06(0)] 16 p2167 N88-22922
TES: A modular systems approach to expert system development for real-time space applications
17 p2388 N88-24197
The use of liquid films for spacecraft survivability to laser radiation
[AD-A192954] 20 p2765 N88-26395
Study of secondary emission properties of materials used for high power RF components in space
[ESA-CR(P)-2587] 24 p3361 N88-30012
Heavy ion and proton tests for subsystem upset
[AD-A195267] 24 p3434 N88-30442

SPACECRAFT CONFIGURATIONS
NT SATELLITE CONFIGURATIONS
Adaptive control of Large Space Structure (LSS)
[ISAS-R-621] 03 p0276 N88-11740
Payload configurations and serviceability --- Columbus Polar Platforms 03 p0339 N88-12133
The 1988 NASA (National Aeronautics and Space Administration) authorization
[GPO-80-245] 05 p0659 N88-14044
Zero-G thermodynamic vent system for shuttle/Centaur 08 p0983 N88-15943
Space station overview 09 p1129 N88-16780
Space station structures development
[NASA-CR-179261] 09 p1133 N88-16792
Coorbiting Platform Utilization Study (CPLUS), executive summary --- Columbus
[SN-WP-4000-DOC-6609/85/F]
09 p1133 N88-16798
Analysis of a rotating advanced-technology space station for the year 2025
[NASA-CR-178345] 12 p1600 N88-19580
Ludwig Prandtl collected treatises on applied mechanics, hydro- and aerodynamics, part 1
[NASA-TT-20316] 20 p2752 N88-26337
EXSAT: Expert system to configure telecommunication satellites
[SNIAS-881-440-101] 21 p2902 N88-27223
Space shuttle phase B wind tunnel model and test information. Volume 2: Orbiter configuration
[NASA-CR-178415-VOL-2-PT-1]
23 p3171 N88-28881

SPACECRAFT CONSTRUCTION MATERIALS
Outgassing data for selecting spacecraft materials
[NASA-RP-1124] 01 p0019 N88-10117
High intensity 5 eV O-atom exposure facility for material degradation studies 02 p0135 N88-10847
Spacecraft surface exposure to atomic oxygen in low Earth orbit 03 p0273 N88-11715
Discharge phenomena --- spacecraft
03 p0274 N88-11723
Discharge prevention of geosynchronous orbit conductive thermal control materials and grounding systems 03 p0274 N88-11732
Fire-related standards and testing
04 p0406 N88-12522
Spacecraft material flammability testing and configurations 04 p0407 N88-12529
Carbon fiber reinforced glass matrix composites for space based applications
[AD-A184355] 04 p0410 N88-12546
Influence of bonding shop moisture on metal-honeycomb junctions bonded with ultra-thin adhesive films
[SNIAS-872-422-112] 05 p0558 N88-13399
First International Week of Adhesive Bonding and Assembling
[SNIAS-872-430-106] 05 p0569 N88-13468
Time-temperature-stress capabilities of composite materials for advanced supersonic technology application
[NASA-CR-178272] 06 p0677 N88-14144
Spectroscopic investigations and measurements of certain ARC jet parameters 06 p0796 N88-14877
Multipurpose corrosion inhibitors for aerospace materials in Naval environments
[AD-A186728] 09 p1143 N88-16853
Space environmental effects on polymeric materials
[NASA-CR-182454] 09 p1148 N88-16879
Soviet spacecraft engineering research
[FASAC-TAR-3090] 17 p2311 N88-23823
Aluminum alloy
[NASA-CASE-LAR-13924-1-CU]
18 p2487 N88-24753
Reinforced plastics: Winding and weaving technologies for space products
[SNIAS-881-430-103] 21 p2922 N88-27341
The technical reporting and approval procedure for materials and processes
[ESA-PSS-01-700-ISSUE-1] 22 p3162 N88-28833
Contribution to the study of materials behavior in space environment
[SNIAS-881-430-104] 23 p3189 N88-28977
Very high temperature materials for mechanical application
[SNIAS-881-430-106] 23 p3189 N88-28978
Material and process selection and quality control for ESA space systems and associated equipment
[ESA-PSS-01-70-ISSUE-3] 23 p3224 N88-29190
Study of secondary emission properties of materials used for high power RF components in space
[ESA-CR(P)-2587] 24 p3361 N88-30012

SPACECRAFT CONTAMINATION
Fourteenth Space Simulation Conference: Testing for a Permanent Presence in Space
[NASA-CP-2446] 02 p0132 N88-10829
Contamination control concepts for space station customer servicing 02 p0137 N88-10860
Surface scattering characteristics and the measurement of particulate contamination 02 p0137 N88-10862
Low extractable wipers for cleaning space flight hardware 02 p0137 N88-10863
Spacecraft surface exposure to atomic oxygen in low Earth orbit 03 p0273 N88-11715
Analysis of geophysical data bases and models for spacecraft interactions
[AD-A184809] 05 p0555 N88-13375
Analysis of contamination data recorded by the IECM camera/photometer
[NASA-TM-100324] 14 p1882 N88-21246
A Study of Space Station Contamination Effects --- conference
[NASA-CP-3002] 18 p2590 N88-25390
Neutral environment for space station
18 p2590 N88-25391
Space station neutral external environment
18 p2590 N88-25392
Contaminant ions and waves in the space station environment 18 p2590 N88-25393
Space station induced electromagnetic effects
18 p2591 N88-25394
Space station contamination study: Assessment of contaminant spectral brightness
18 p2591 N88-25395
Space station particulate contamination environment
18 p2591 N88-25397
The particulate environment surrounding the space station: Estimates from the PACS data
18 p2591 N88-25398
Effects of meteoroids and space debris on the particulate environment for space station 18 p2591 N88-25399
Contamination of optical surfaces --- Space Station
18 p2592 N88-25400
Surface interactions relevant to space station contamination problems 18 p2592 N88-25401
Laboratory experiments of relevance to the space station environment 18 p2592 N88-25402
Contamination of the space station environment by vented chemicals 18 p2592 N88-25403
Progress on a Monte Carlo shuttle contamination model
[AD-A193694] 23 p3183 N88-28945
Studies on rocket exhaust plumes and impingement effects related to the Columbus Space Station program: Executive summary
[DFVLR-IB-222-88-A-12] 24 p3337 N88-29862

SPACECRAFT CONTROL
NT SATELLITE ATTITUDE CONTROL
NT SATELLITE CONTROL
Dynamics of spacecraft control laboratory experiment (SCOLE) slew maneuvers
[NASA-CR-4098] 01 p0014 N88-10082
Telemetry, Tracking, and Control Working Group report 01 p0016 N88-10096
Attitude Control Working Group report
01 p0016 N88-10099
Predictive momentum management for a space station measurement and computation requirements
[NASA-CR-172026] 02 p0138 N88-10866
Equal-modulus vector programmed frequency control of minimally redundant structure of powered, single-degree-of-freedom gyroscopes for spacecraft attitude control system 02 p0159 N88-10994
A linear quadratic Gaussian with loop transfer recovery proximity operations autopilot for spacecraft
[NASA-CR-172028] 02 p0227 N88-11433
Adaptive control of Large Space Structure (LSS)
[ISAS-R-621] 03 p0276 N88-11740
New feedback design methodologies for large space structures: A multi-criterion optimization approach
04 p0408 N88-12535
Combined problem of slew maneuver control and vibration suppression
[NASA-CR-181537] 04 p0455 N88-12817
Modeling and control of large flexible vehicles in the atmosphere and space
[AD-A185368] 05 p0555 N88-13377
Optimal control of large space structures via generalized inverse matrix
[NASA-CR-182336] 05 p0639 N88-13907
Guidance and control strategies for aerospace vehicles
[NASA-CR-181579] 05 p0643 N88-13935
Expert system study for spacecraft management
[TL-2699-ISS-1] 07 p0824 N88-15004
The dynamics and control of large-flexible space structures, part 10
[NASA-CR-182426] 08 p0963 N88-15830
Large-angle slewing maneuvers for flexible spacecraft
[NASA-CR-4123] 08 p1000 N88-16060
Gyrostabilizer system of Kvant module
08 p1006 N88-16099
Study of descent of probes with high lift-drag ratio into the atmosphere of Jupiter 08 p1006 N88-16101
Third Conference on Artificial Intelligence for Space Applications, part 1
[NASA-CP-2492-Pt-1] 08 p1055 N88-16360
KBS V and V as related to automation of space station subsystems: Rationale for a KBS lifecycle
08 p1057 N88-16375
A distributed architecture for intelligent monitoring and anomaly diagnosis of the Hubble Space Telescope
08 p1057 N88-16379
Expert systems relations in space applications
08 p1059 N88-16391
Application of parallel distributed processing to space based systems 08 p1059 N88-16393
ESSAA: Embedded system safety analysis assistant
08 p1060 N88-16396
Similarity networks as a knowledge representation for space applications 08 p1062 N88-16411
A framework for real-time distributed expert systems: On-orbit spacecraft fault diagnosis, monitoring and control 08 p1066 N88-16440
TES: A modular systems approach to expert system development for real time space applications
08 p1066 N88-16441
Applications of expert systems for satellite autonomy
08 p1066 N88-16443
MPAD MCC workstation system: ADDAM and EEVE
09 p1203 N88-17209
Development of a coupled expert system for the spacecraft attitude control problem
09 p1205 N88-17223
Verifying shuttle onboard software using expert systems 09 p1207 N88-17237
Expert system applications in spacecraft subsystem controllers 09 p1210 N88-17254
Formulation methods of rigid multibody systems for large space structures and some results of computer simulation
[NAL-TR-942] 10 p1293 N88-17730
Intelligent on board control for field emission electric propulsion system 12 p1589 N88-19513
Activities report in aeronautics and astronautics
[ETN-88-91332] 13 p1859 N88-21115
A feedback double path compensating control structure for the attitude control of a flexible spacecraft
[INPE-4464-PRE/1239] 14 p1880 N88-21240
Technology development program for twenty-first century aerospace vehicles 17 p2302 N88-23768
Three axis attitude control system
[NASA-CASE-GSC-12970-1] 17 p2308 N88-23808
Travelling wave concepts for the modeling and control of space structures
[AD-A191235] 17 p2310 N88-23819
TALOS: A distributed architecture for intelligent monitoring and anomaly diagnosis of the Hubble Space Telescope 17 p2388 N88-24193

Genetic algorithms for adaptive real-time control in space systems 17 p2388 N88-24195
Guidance and control strategies for aerospace vehicles
[NASA-CR-183032] 18 p2467 N88-24644
Low authority control of large space structures using a constrained threshold control formulation
18 p2472 N88-24667
A feedback linearization approach to spacecraft control using momentum exchange devices
[NASA-CR-172057] 18 p2472 N88-24668
Spacecraft applications of advanced global positioning system technology
[NASA-CR-172063] 20 p2757 N88-26359
Simulation of attitude and maneuvers for the Brazilian spin-stabilized satellite
[INPE-4271-PRE/1143] 22 p3046 N88-28079
Study of standard generic approach for spacecraft (S/C) autonomy and automation (phase 3). Book A: Autonomy concept description
[ESA-CR(P)-2555-VOL-1] 23 p3185 N88-28955
Study of standard generic approach for spacecraft (S/C) autonomy and automation (phase 3). Book B: Autonomy concept application example
[ESA-CR(P)-2555-VOL-2] 23 p3185 N88-28956
Study of standard generic approach for spacecraft (S/C) autonomy and automation (phase 3). Book C: Autonomy concept summary
[ESA-CR(P)-2555-VOL-3] 23 p3185 N88-28957
Intelligent interfaces for expert systems
23 p3258 N88-29397
Theory of filtering and control with application to control of large space structures
[AD-A195500] 24 p3335 N88-29851
Synchronous response modelling and control of an annular momentum control device
[NASA-CR-4166] 24 p3358 N88-29995
Robust design of distributed controllers for large flexible space structures
[NASA-CR-183202] 24 p3380 N88-30134
Automated space vehicle control for rendezvous proximity operations 24 p3416 N88-30335
An approach to CMG steering using feedback linearization
[NASA-CR-183172] 24 p3422 N88-30369
Increasing accuracy in evaluating vector of state under conditions of incomplete observability of expanded system 24 p3446 N88-30511

SPACECRAFT DEFENSE
An examination of the Advanced Communications Technology Satellite (ACTS) and its application to the Defense Data Network (DDN)
[AD-A184003] 03 p0276 N88-11742
ADAM (Acquisition Deployment and Maneuvering): The space game
[AD-A189512] 12 p1685 N88-20078
Alternative force structuring strategies for military satellite communication systems
[AD-A189492] 13 p1758 N88-20516
Antisatellite weapons and satellite deployment strategies
[AD-A195014] 24 p3427 N88-30396

SPACECRAFT DESIGN
NT SATELLITE DESIGN
Spacecraft 2000 program overview
01 p0015 N88-10085
Space station platforms 01 p0015 N88-10086
Space Assembly, Maintenance, and Servicing Study (SAMSS) 01 p0015 N88-10089
Spacecraft Systems Working Group report
01 p0015 N88-10091
System Development Working Group report
01 p0016 N88-10092
Structures and Materials Working Group report
01 p0016 N88-10093
Thermal Control Working Group report
01 p0016 N88-10094
COSMIC --- Coherent Optical System of Modular Image Collectors (COSMIC); spaceborne telescope
01 p0095 N88-10623
Proposed studies of a 30 meter imaging interferometer concept --- spaceborne astronomy
01 p0096 N88-10627
NASA/JPL study on optical imaging interferometry in space 01 p0096 N88-10630
Aerospace research at the National Aerospace Laboratory (NLR)
[ETN-87-90821] 01 p0107 N88-10697
Determination of life cycle costs in astronautics
[MBB-UR-E-910/86-PUB] 02 p0249 N88-11572
Electromagnetic compatibility (EMC) phenomena and prevention of the effects --- spacecraft
03 p0274 N88-11731
Aeroassisted manned transfer vehicle (TAXi) for advanced Mars Transportation: NASA/USRA 1987 Senior Design Project
[NASA-CR-181478] 03 p0275 N88-11736
Adaptive control of Large Space Structure (LSS)
[ISAS-R-621] 03 p0276 N88-11740
Space station integrated propulsion and fluid system study: Fluid systems configuration databook
[NASA-CR-179215] 03 p0278 N88-11753
Design study for asteroidal exploitation
03 p0389 N88-12445
New feedback design methodologies for large space structures: A multi-criterion optimization approach
04 p0408 N88-12535
General aerodynamic-aerothermodynamic concepts for Hermes 05 p0535 N88-13251
Hermes propulsion system
[SNIAS-872-422-109] 05 p0556 N88-13383
Introduction to local area network design on Ariane 5 and future launchers
[SNIAS-872-422-102] 05 p0635 N88-13886
Auxiliary propulsion technology for advanced Earth-to-orbit vehicles
[NASA-TM-100237] 06 p0674 N88-14127
NAL news updated: FY87 business plan, developments 06 p0675 N88-14135
Airborne particulate matter in spacecraft
[NASA-CP-2499] 06 p0753 N88-14623
Safety philosophy, policy, and requirements for manned spaceflight. Volume 1: Executive summary
[HEG-0886/1036-VOL-1] 08 p0962 N88-15826
Space station accommodations for life sciences research facilities. Phase 1: Conceptual design and programmatics studies for Missions SAAX0307, SAAX0302 and the transition from SAAX0307 to SAAX0302. Volume 2: Study results
[NASA-CR-179244] 08 p0962 N88-15829
The TV-SAT/TDF/TELE-X pyrotechnical system
[CNES-87/CT/DRT/TVE/IL/358]
08 p0974 N88-15891
Space Infrared Telescope Facility (SIRTF) design and thermal analysis 08 p0982 N88-15934
FMEAssist: A knowledge-based approach to Failure Modes and Effects Analysis 08 p1060 N88-16395
Space station overview 09 p1129 N88-16780
The Columbus program, an overview
09 p1130 N88-16784
Columbus feasibility studies. Volume 1: Requirements and system concept
[ETN-88-91073] 09 p1134 N88-16799
Columbus feasibility studies. Volume 2: Element constituents, mechanical
[ETN-88-91074] 09 p1134 N88-16800
Columbus feasibility studies. Volume 3: Avionics, systems
[ETN-88-91075] 09 p1134 N88-16801
Model of space platform electromagnetic (EMC) configuration
[ESA-CR(P)-2500] 09 p1135 N88-16809
Kinetic isolation tether experiment
[NASA-CR-182458] 09 p1135 N88-16810
Design knowledge capture for the space station
09 p1208 N88-17239
Apollo Lightcraft project
[NASA-CR-182575] 11 p1445 N88-18615
Spacecraft telecommunications system mass estimates 11 p1473 N88-18784
The 58th Shock and Vibration Symposium, volume 2
[NASA-CP-2488-VOL-2] 11 p1499 N88-18948
Spacecraft redesign to reduce microphonic response of a VCO component 11 p1499 N88-18955
Man-Tended Free Flyer operational design features
12 p1585 N88-19485
Multimission Modular Spacecraft (MMS): A serviceable design spacecraft 12 p1587 N88-19501
Columbus Simulation Facility (CSF)
12 p1590 N88-19522
Alternative program approaches for the advanced satellite technology program
[AD-A188917] 12 p1600 N88-19576
Space Station Human Factors Research Review. Volume 3: Space Station Habitability and Function: Architectural Research
[NASA-CP-2426-VOL-3] 12 p1650 N88-19883
Space station architectural elements model study. Space station human factors research review
12 p1650 N88-19884
Radiation problems in manned space flight with a view to the Space Station 12 p1658 N88-19934
Flight Vehicle Development Time and Cost Reduction
[AGARD-CP-424] 12 p1700 N88-20173
Mars Lander/Rover vehicle development: An advanced space design project for USRA and NASA/OAST
[NASA-CR-182562] 12 p1709 N88-20226
Mars Lander/Rover vehicle development: An advanced space design project for USRA and NASA/OAST
[NASA-CR-182571] 12 p1709 N88-20227
Study on long term evolution Towards European Autonomous Manned Spaceflight (STEAMS)
[SNIAS-SE/LS/AP-35-073] 13 p1727 N88-20330
On the sensitivity of complex, internally coupled systems
[NASA-TM-100537] 13 p1813 N88-20829
Docking/berthing subsystem: Design and breadboard test 14 p1879 N88-21233
Nonlinear analysis and optimal design of dynamic mechanical systems for spacecraft application
[AD-A190644] 15 p2026 N88-22070
Study of surface discharges
[ONERA-12/7236-PY] 15 p2026 N88-22073
Japanese space station module
15 p2052 N88-22224
External tank gamma ray imaging telescope study. Final review, phase 2
[NASA-CR-179320] 15 p2150 N88-22634
A pyrotechnical opening valve
[SNIAS-MU/TYS-NT-2-06(0)] 16 p2167 N88-22922
Manned Mars mission accommodation: Sprint mission
[NASA-TM-100598] 16 p2290 N88-23711
Technology development program for twenty-first century aerospace vehicles 17 p2302 N88-23768
Colombus feasibility studies, executive summary
[ETN-88-92334] 17 p2311 N88-23820
Advanced EVA system design requirements study
17 p2380 N88-24147
Space Station Human Factors Research Review. Volume 4: Inhouse Advanced Development and Research
[NASA-CP-2426-VOL-4] 17 p2380 N88-24148
Space station proximity operations and window design
17 p2380 N88-24149
Radiation hardening design of nuclear powered spacecraft 17 p2407 N88-24315
A review of impact design criteria for space power heat rejection systems 17 p2410 N88-24333
Relating design and environmental variables to reliability 17 p2418 N88-24383
Progress and future directions in computational fluid dynamics
[NASA-TM-100091] 18 p2456 N88-24579
High speed and high angle of attack aerodynamic characteristics of winged space vehicle
[ISSN-0285-6808] 18 p2459 N88-24599
Attitude control laws for gas-jet spacecraft
18 p2467 N88-24643
Structural margins assessment approach
[NASA-TM-100332] 18 p2473 N88-24672
Mars rover/sample return mission requirements affecting space station
[NASA-CR-172048] 18 p2594 N88-25414
Weight savings in aerospace vehicles through propellant scavenging
[NASA-TM-100900] 19 p2605 N88-25470
Boundary layer simulator (BLIMPJ) improvement
19 p2627 N88-25582
Numerical simulations of aerodynamic contribution of flows about a space-plane-type configuration
19 p2635 N88-25632
Considerations for spacecraft design for MSAT
19 p2651 N88-25741
Recent research on crew wardroom habitability for the Space Station 19 p2698 N88-26039
Marine techniques: R and D axes, identification of areas of common interest with space techniques
19 p2699 N88-26047
Design and testing of a high power spacecraft thermal management system
[NASA-TM-4051] 20 p2764 N88-26389
EXSAT: Expert system to configure telecommunication satellites
[SNIAS-881-440-101] 21 p2902 N88-27223
Design of booster wound structures --- spacecraft structures
[SNIAS-881-430-102] 21 p2903 N88-27228
Literal dynamic modeling
[REPT-881-440-114] 22 p3048 N88-28083
Performance and technical tolerance --- space projects 22 p3160 N88-28812
Study of standard generic approach for spacecraft (S/C) autonomy and automation (phase 3). Book A: Autonomy concept description
[ESA-CR(P)-2555-VOL-1] 23 p3185 N88-28955
Study of standard generic approach for spacecraft (S/C) autonomy and automation (phase 3). Book B: Autonomy concept application example
[ESA-CR(P)-2555-VOL-2] 23 p3185 N88-28956
Study of standard generic approach for spacecraft (S/C) autonomy and automation (phase 3). Book C: Autonomy concept summary
[ESA-CR(P)-2555-VOL-3] 23 p3185 N88-28957

Space station as a vital focus for advancing the technologies of automation and robotics
[IAF-88-62] 23 p3251 N88-29352

Study on long-term evolution towards European manned spaceflight. Volume 1: Executive summary
[ERNO-OX1-002/88-VOL-1] 24 p3330 N88-29827

Spacecraft mass estimation, relationships and engine data: Task 1.1 of the lunar base systems study
[NASA-CR-172061] 24 p3332 N88-29836

Maintenance and supply options
[NASA-CR-172062] 24 p3332 N88-29837

Study on conceptual design of spacecraft using Computer Aided Engineering (CAE)
[SNIAS-820-CA/TS] 24 p3333 N88-29841

Interim Flight Opportunity (IFO). Volume 1: Executive summary --- space platform
[SE/LS/AP-36-818/CN-VOL-1]
24 p3334 N88-29849

MANIP --- spacecraft modeling program
[MANIP-217A] 24 p3335 N88-29855

SPACECRAFT DOCKING

Blagov commentary on Mir station, first manning
01 p0009 N88-10051

Rendezvous and Docking Verification (RVDV) and in-orbit demonstration, executive summary
[RVD-RVDV-FR-AS-01] 06 p0673 N88-14120

Docking/Berthing Subsystem (DBS). Development part 1: Latching analysis --- Columbus
[ESA-CR(P)-2479] 08 p0962 N88-15825

Orbital navigation, docking and obstacle avoidance as a form of three dimensional model-based image understanding 08 p1061 N88-16406

Rendezvous and docking verification and demonstration in orbit, executive summary
[MBB-303-16/86] 10 p1291 N88-17719

Space vehicle approach velocity judgments under simulated visual space conditions
[NASA-TM-89437] 11 p1523 N88-19094

Analysis of RVD operations in manned space missions
12 p1586 N88-19494

The RVD mission: The on-board data processing requirements 12 p1586 N88-19495

Prototype on-board software for rendezvous and docking 12 p1586 N88-19496

Long range sensor for rendezvous and docking missions 12 p1587 N88-19497

Motion simulation for in-orbit operations
12 p1589 N88-19514

EPOS: European Proximity Operations Simulation
12 p1589 N88-19515

Dynamic testing of a docking system --- ground-based simulator 12 p1589 N88-19516

Rendezvous and docking (RVD) verification and demonstration in-orbit 12 p1592 N88-19531

Development of an intermodule connector for serviceable spacecraft 14 p1877 N88-21212

Docking/berthing subsystem: Design and breadboard test 14 p1879 N88-21233

Space station full-scale docking/berthing mechanisms development 14 p1927 N88-21491

Orbital navigation, docking and obstacle avoidance as a form of three dimensional model-based image understanding 17 p2388 N88-24194

Range and range rate system
[NASA-CASE-MSC-20867-1] 18 p2521 N88-24958

OMV docking simulator 23 p3255 N88-29379

SPACECRAFT ELECTRONIC EQUIPMENT

Spacecraft 2000
[NASA-CP-2473] 01 p0015 N88-10084

The ESA centralized management system for satellite electronic test and checkout instrumentation
09 p1124 N88-16731

Multicarrier demodulator design, volume 1 --- communication satellites
[ESA-CR(P)-2468-VOL-1] 09 p1158 N88-16941

Multicarrier demodulator design. Volume 2: Executive summary --- communication satellites
[ESA-CR(P)-2468-VOL-2] 09 p1158 N88-16942

Development of a multiplexer module for use in a spaceborne cryogenic environment based on GaAs MESFET technology
[RPT/CRY/62463/BOP] 11 p1559 N88-19335

Specifications and performance of ultrastable oscillators in the DORIS orbitography and positioning system
[ETN-88-92761] 24 p3331 N88-29831

The effects of total dose on the SEU sensitivity of CMOS static RAMS --- single event upset (SEU), satellite components
[AERE-R-12779] 24 p3426 N88-30401

SPACECRAFT ENVIRONMENTS

Fourteenth Space Simulation Conference: Testing for a Permanent Presence in Space
[NASA-CP-2446] 02 p0132 N88-10829

Contamination control of the space shuttle Orbiter crew compartment 02 p0133 N88-10834

Space station contamination considerations
02 p0137 N88-10859

Contamination control concepts for space station customer servicing 02 p0137 N88-10860

Environmental life support system technology study --- space flight
[ESA-CR(P)-2432] 02 p0218 N88-11371

Spacecraft Fire Safety
[NASA-CP-2476] 04 p0406 N88-12520

Fire extinguishment and inhibition in spacecraft environments 04 p0406 N88-12523

Inerting and atmospheres 04 p0406 N88-12524

Fire-related medical science 04 p0406 N88-12525

Aircraft fire safety research 04 p0406 N88-12526

Space station internal environmental and safety concerns 04 p0407 N88-12527

Microgravity combustion fundamentals
04 p0407 N88-12528

Spacecraft material flammability testing and configurations 04 p0407 N88-12529

Analysis of geophysical data bases and models for spacecraft interactions
[AD-A184809] 05 p0555 N88-13375

Flight model discharge system
[AD-A185657] 06 p0673 N88-14122

Controlled Ecological Life Support Systems (CELSS) conceptual design option study
[NASA-CR-177421] 06 p0754 N88-14625

Controlled Ecological Life Support Systems (CELSS) physiochemical waste management systems evaluation
[NASA-CR-177422] 06 p0754 N88-14626

Physiological and immunological aspects of human adaptation to temperature elevation in a closed environment 07 p0895 N88-15424

Some considerations on measuring the Newtonian gravitational constant G in an orbiting laboratory
07 p0922 N88-15603

Goal driven kinematic simulation of flexible arm robot for space station missions 08 p1059 N88-16388

GAS eleven node thermal model (GEM)
10 p1289 N88-17712

Spacecraft fire detection and extinguishment: A bibliography
[NASA-CR-180880] 11 p1444 N88-18612

NASDA's new test facilities for satellites and rockets
11 p1490 N88-18951

Survey of the Air Force P78-2 (SCATHA) satellite plasma wave data during electron gun operations
[AD-A191014] 16 p2168 N88-22926

Advancements in oxygen generation and humidity control by water vapor electrolysis
[NASA-CR-172073] 22 p3134 N88-28633

SPACECRAFT EQUIPMENT

NT SPACECRAFT ELECTRONIC EQUIPMENT

A modern space simulation facility to accommodate high production acceptance testing 02 p0134 N88-10841

Transient modeling of the thermohydraulic behavior of high temperature heat pipes for space reactor applications 02 p0136 N88-10857

Microgravity nucleation and particle coagulation experiments support
[NASA-CR-181540] 04 p0423 N88-12618

Microgravity nucleation and particle coagulation experiments support
[NASA-CR-181541] 04 p0423 N88-12619

Space station accommodations for life sciences research facilities. Phase 1: Conceptual design and programmatics studies for Missions SAAX0307, SAAX0302 and the transition from SAAX0307 to SAAX0302. Volume 2: Study results
[NASA-CR-179244] 08 p0962 N88-15829

Air Force cryocooler development for spacecraft
08 p0983 N88-15945

Issues associated with telerobotic systems in space
08 p1056 N88-16369

Task path planning, scheduling and learning for free-ranging robot systems 08 p1058 N88-16386

Heuristic search in robot configuration space using variable metric 08 p1059 N88-16389

Development of a facility using robotics for testing automation of inertial instruments
09 p1213 N88-17271

Microgravity isolation mount
[ESA-CR(P)-2480] 11 p1443 N88-18604

Development of the Extendable and Retractable Mast (ERM). Design phase 2. Volume 1 --- spacecraft payloads
[RP-2010-0000-DS/09] 11 p1467 N88-18750

Covariant control of bilateral servos for in-orbit manipulation 12 p1590 N88-19520

A comparative survey of mathematical models for dynamic simulation of in-orbit manipulation operations
12 p1592 N88-19533

High efficiency, long life traveling wave tubes for future communications satellites
[NASA-TM-100837] 12 p1598 N88-19565

The preparation, assembly and mounting of RF coaxial cables
[ESA-PSS-01-718-ISSUE-1] 13 p1758 N88-20504

Proceedings of the 3rd European Space Mechanisms and Tribology Symposium
[ESA-SP-279] 14 p1874 N88-21191

The CTM program of masts and the CTM engineering model --- spacecraft mechanism
14 p1874 N88-21196

The development status of the strongback array --- spacecraft structure 14 p1875 N88-21201

DARM: A new deployment and retraction mechanism which does not need electric power
14 p1876 N88-21206

Robotic joint prototype for space applications
14 p1878 N88-21222

A joint actuator design for a robotic manipulator
14 p1879 N88-21232

Development of an engineering model dynamic cooler --- spacecraft payloads
[F+W-TF-B-1885] 14 p1895 N88-21311

Accurate positioning of long, flexible ARM's (Articulated Robotic Manipulator) 16 p2219 N88-23243

Acoustic convective system
[NASA-CASE-NPO-17278-1-CU]
18 p2498 N88-24818

Range and range rate system
[NASA-CASE-MSC-20867-1] 18 p2521 N88-24958

Study of a magnetic refrigerator for space applications for temperatures under 20 K
[NASA-TT-20283] 19 p2641 N88-25668

Automatic calibration of space based manipulators and mechanisms
[NASA-CR-182804] 19 p2676 N88-25912

Different techniques for intervening under the sea: Possible links with space applications
19 p2697 N88-26030

Computer aided remote control: A general concept for intervention in the nuclear, underwater, and space domains 19 p2699 N88-26046

Heat pump augmented radiator for low-temperature space applications
[DE88-008369] 20 p2765 N88-26393

Transient thermal analysis of three latent heat storage configurations for rapid thermal charging
[DE88-006943] 20 p2881 N88-27104

Surface Tension Confined Liquid Cryogen Cooler (STCLCC)
[NASA-CASE-GSC-13112-1] 23 p3201 N88-29050

Material and process selection and quality control for ESA space systems and associated equipment
[ESA-PSS-01-70-ISSUE-3] 23 p3224 N88-29190

Qualification test levels for units to be derived from mechanical test data analysis --- ESA
[REPT-87-158-EI/ET/AG] 24 p3381 N88-30139

SPACECRAFT GLOW

Mechanistic studies of polymeric samples exposed aboard STS 8
[NASA-CR-182364] 06 p0686 N88-14202

Vehicle glow observed on the SONDA 3
[INPE-4297-PRE/1168] 12 p1600 N88-19581

Space station contamination study: Assessment of contaminant spectral brightness
18 p2591 N88-25395

Calculation of space station infrared irradiance from atmosphere-induced emissions
18 p2591 N88-25396

SPACECRAFT GUIDANCE

Guidance and control strategies for aerospace vehicles
[NASA-CR-181579] 05 p0643 N88-13935

An analysis of the effect of aeroassist maneuvers on orbital transfer vehicle performance
[NASA-TM-89117] 06 p0672 N88-14116

Verifying shuttle onboard software using expert systems 09 p1207 N88-17237

Aeroassisted orbit transfer vehicle trajectory analysis
[NASA-TM-89138] 12 p1599 N88-19575

Computer architecture for efficient algorithmic executions in real-time systems: New technology for avionics systems and advanced space vehicles
[NASA-CR-182650] 12 p1675 N88-20016

Aeroassist flight experiment guidance Quiet Time
[NASA-TM-100556] 14 p1881 N88-21244

Identification of a star field from a spinning satellite
[CNES-NT-120] 15 p2026 N88-22074

Guidance and control strategies for aerospace vehicles
[NASA-CR-183032] 18 p2467 N88-24644

A design study of onboard navigation and guidance during aerocapture at Mars
[NASA-CR-172053] 18 p2469 N88-24654

Time minimal computation of feedback control schemes for optimal guidance problems used in space flight
[ETN-88-92989] 23 p3184 N88-28953

Ascent guidance for a winged boost vehicle
[NASA-CR-172083] 24 p3334 N88-29646

SPACECRAFT INSTRUMENTS
NT SATELLITE INSTRUMENTS
Calibration of attitude control sensors
02 p0159 N88-10995
Roentgenoradiometric analysis of aerosol in Venusian clouds by Vega-1 and Vega-2 automatic interplanetary stations 13 p1726 N88-20319
A method of atmospheric density measurements during space shuttle entry using ultraviolet-laser Rayleigh scattering
[NASA-TM-100056] 15 p2069 N88-22337
NIMBUS-7 CZCS. Coastal Zone Color Scanner imagery for selected coastal regions. North America - Europe. South America - Africa - Antarctica. Level 2 photographic product
[NASA-CR-180755] 15 p2089 N88-22447
A plasma wave instrument on the AMPTE/IRM (Active Magnetospheric Particle Tracing Explorers/Ion Release Module) spacecraft
[AD-A191216] 16 p2233 N88-23336
Measurement of galactic radio emission at frequency 37 GHz from aboard spacecraft
24 p3448 N88-30520

SPACECRAFT LANDING
NT MARS LANDING
NT PLANETARY LANDING
Applications of expert systems for satellite autonomy
08 p1066 N88-16443
Lunar base launch and landing facility conceptual design, 2nd edition
[NASA-CR-172049] 20 p2885 N88-27135

SPACECRAFT LAUNCHING
Analysis of the bivariate parameter wind differences between Jimsphere and Windsonde
[NASA-TM-4014] 01 p0072 N88-10461
Meteorological systems support to critical shuttle requirements on the Eastern Test Range --- STS
02 p0205 N88-11281
Department of Housing and Urban Development-Independent Agencies Appropriations for fiscal year 1988, Thursday, 9 April 1987: National Aeronautics and Space Administration
03 p0386 N88-12424
The determination of exhaust cloud dimensions from films of space shuttle launches
[NASA-CR-4103] 06 p0732 N88-14500
Ariane localization technique by Data Relay Satellite (DRS)
[SES/ENG/TN-548/86] 08 p0961 N88-15821
Ariane launch performance 09 p1125 N88-16743
SYLDA: A dual-launch system for Ariane
09 p1125 N88-16745
Preliminary orbit determination algorithms: Application to the Brazilian satellite
[INPE-4411-NTE/276] 12 p1594 N88-19546
Satellite acquisition: Global positioning system acquisition changes after Challenger's accident
[PB88-155536] 14 p1880 N88-21236
Radio frequency compatibility between IRS and SPOT 3: Preliminary study
[CNES-86/CT/DRT/TIT/TR/011]
14 p1905 N88-21383
JPRS report: Science and technology. China
[JPRS-CST-87-043] 15 p2053 N88-22233
Chronology of China's successful satellite launchings
15 p2053 N88-22234
Direct nuclear propulsion for Earth-to-orbit vehicles
17 p2400 N88-24271
Monitoring biological impacts of space shuttle launches from Vandenberg Air Force Base: Establishment of baseline conditions
[NASA-TM-100982] 18 p2549 N88-25133
Launch operations to support future space forces
[AD-A192679] 20 p2881 N88-27107
Design considerations for the ORION satellite: Structure, propulsion and attitude control subsystems for a small, general purpose spacecraft
[AD-A193837] 22 p3048 N88-28086
Reduced flexibility in processing Titan 4 space launch vehicles at Cape Canaveral Air Force Station
[AD-A194908] 24 p3332 N88-29834

SPACECRAFT LUBRICATION
The performance of thin solid films for satellite gears
14 p1876 N88-21209
The SPOT solar array. Box opening mechanisms physical vapor deposition (PVD)-MoS2: Lubricated slides. Functional evaluation 14 p1876 N88-21211
A test facility for the in-vacuo assessment of dry lubricants and small mechanisms at cryogenic temperatures 14 p1878 N88-21224

SPACECRAFT MAINTENANCE
A data structure and algorithm for fault diagnosis
08 p1065 N88-16432
Remote manipulation in orbital construction, servicing and repair missions: Is one arm enough? A comparative evaluation of the performance features of robots with one or more arms 12 p1586 N88-19509
Remote repair demonstration of Solar Maximum main electronics box 12 p1588 N88-19510
Treatment of unforeseen situations by online knowledge-based diagnostic systems --- spacecraft maintenance 12 p1589 N88-19511
Review of commercial spacecraft: Recovery and repair experiences. Implications for future spacecraft designs and operations 12 p1591 N88-19526

SPACECRAFT MANEUVERS
NT ORBITAL MANEUVERS
An analysis of the effect of aeroassist maneuvers on orbital transfer vehicle performance
[NASA-TM-89117] 06 p0672 N88-14116
Dynamics formulations for the real-time simulation of constrained motion 06 p0795 N88-14872
The dynamics and control of large-flexible space structures, part 10
[NASA-CR-182426] 08 p0963 N88-15830
Large-angle slewing maneuvers for flexible spacecraft
[NASA-CR-4123] 08 p1000 N88-16060
EPOS: European Proximity Operations Simulation
12 p1589 N88-19515
Aeroassist flight experiment guidance Quiet Time
[NASA-TM-100556] 14 p1881 N88-21244
Orbital navigation, docking and obstacle avoidance as a form of three dimensional model-based image understanding 17 p2388 N88-24194
SIRTF nod maneuvers
[NASA-TM-101007] 22 p3048 N88-28085

SPACECRAFT MODELS
Efficient placement of structural dynamics sensors on the space station
[NASA-CR-172015] 01 p0017 N88-10103
Evaluation of the infrared test method for the olympus thermal balance tests 02 p0136 N88-10856
Modeling of environmentally-induced effects within satellites. Part 1: NASCAP modeling of satellites
03 p0273 N88-11721
Modeling of environmentally-induced transients within satellites. Part 2: Discharge coupling transients
03 p0273 N88-11722
Flight model discharge system
[AD-A185657] 06 p0673 N88-14122
Thermal structural control modelling techniques --- spacecraft
[FOK-TR-R-86-030] 08 p0962 N88-15828
Dynamic tests of the Ariane launch vehicle
09 p1126 N88-16749
GAS eleven node thermal model (GEM)
10 p1289 N88-17712
Columbus Simulation Facility (CSF)
12 p1590 N88-19522
Dynamics modeling, simulation, and control of a spacecraft/manipulator system
12 p1592 N88-19534
Literal dynamic modeling
[REPT-881-440-114] 22 p3048 N88-28083
Procedures for updating dynamic mathematical models, test phase --- spacecraft hardware
[MEBS-38/87] 24 p3335 N88-29852
MANIP --- spacecraft modeling program
[MANIP-217A] 24 p3335 N88-29855

SPACECRAFT MODULES
NT COMMAND MODULES
NT LANDING MODULES
NT LUNAR LANDING MODULES
Space station internal environmental and safety concerns 04 p0407 N88-12527
Controlled Ecological Life Support Systems (CELSS) conceptual design option study
[NASA-CR-177421] 06 p0754 N88-14625
Columbus pressurized module utilization study, executive summary
[CS-RP-AI-027] 07 p0825 N88-15005
Flight results of the ESA experiment modules in Materials Science Experiment Rocket (MASER) 1
08 p1033 N88-16261
Satellite assembly in geostationary orbit: A plug-and-socket concept 09 p1128 N88-16769
Space station overview 09 p1129 N88-16780
Columbus feasibility studies. Volume 2: Element constituents, mechanical
[ETN-88-91074] 09 p1134 N88-16800
In-orbit and laboratory exchange of ORUs designed/not designed for servicing 12 p1587 N88-19499
Multimission Modular Spacecraft (MMS). A serviceable design spacecraft 12 p1587 N88-19501
CRRES chemical release mechanisms
14 p1874 N88-21192
Development of an intermodule connector for serviceable spacecraft 14 p1877 N88-21212
Docking/berthing subsystem: Design and breadboard test 14 p1879 N88-21233
Space station architectural elements model study
[NASA-CR-4027] 18 p2464 N88-24632
Habitability of the Space Station: From vehicle to living space 19 p2697 N88-26033
Recent research on crew wardroom habitability for the Space Station 19 p2698 N88-26039
Maintenance and supply options
[NASA-CR-172062] 24 p3332 N88-29837
Alternative module configurations for advanced solar arrays on low orbit and extended lifetime missions (AMOC 2)
[ESA-CR(P)-2581] 24 p3389 N88-30182

SPACECRAFT MOTION
Relative motion near the triangular libration points in the Earth-Moon system 01 p0097 N88-10636
Concept definition study for recovery of tumbling satellites. Volume 2: Supporting research and technology report
[NASA-CR-179229] 06 p0672 N88-14117
Concept definition study for recovery of tumbling satellites. Volume 1: Executive summary, study results
[NASA-CR-179228] 06 p0672 N88-14118
Low gravity liquid motions in spacecraft
08 p0982 N88-15941
Single-burn transfer to nominally periodic orbit in the vicinity of point L2 of Earth-Sun system and related problems 08 p1006 N88-16100
The nonlinear dynamics of a spacecraft coupled to the vibration of a contained fluid
[DE88-007035] 16 p2168 N88-22925
Contribution to the numerical solution of airplane spin motion
[ETN-88-92368] 21 p2896 N88-27190
Approximation of atmospheric density by Chebyshev polynomials in predicting motion of low artificial earth satellites 24 p3445 N88-30503

SPACECRAFT ORBITAL ASSEMBLY
U ORBITAL ASSEMBLY

SPACECRAFT ORBITS
NT GEOSYNCHRONOUS ORBITS
NT POLAR ORBITS
NT SATELLITE ORBITS
NT STATIONARY ORBITS
NT TRANSFER ORBITS
Thermal testing by internal IR heating of the FEP module 02 p0136 N88-10854
Limitation of spacecraft orbit near colinear libration center of limited elliptical three body problem
08 p1003 N88-16075
Orbital navigation, docking and obstacle avoidance as a form of three dimensional model-based image understanding 08 p1061 N88-16406
Optimal thrust vector control of coplanar orbital evasive maneuvers
[AD-A189544] 13 p1730 N88-20346
Canonical variables and canonical integrals for motion in near-circular orbits 24 p3446 N88-30512

SPACECRAFT PERFORMANCE
COS-B in-orbit study
[ESA-CR(P)-2420] 01 p0017 N88-10102
MARECS-A case 03 p0274 N88-11729
RETE experiment Assembly, Integration, and Verification (AIV) activities
[IFSI-87-6] 05 p0555 N88-13380
Why mechanisms are critical to spacecraft performance 09 p1125 N88-16737
Predictive monitoring research: Summary of the PREMON system
[NASA-CR-182687] 13 p1824 N88-20905
Design and testing of a high power spacecraft thermal management system
[NASA-TM-4051] 20 p2764 N88-26389
Survey of SPOT-1 operation 22 p3115 N88-28507
Verification and tests --- space projects
22 p3160 N88-28614
A scheduling and resource management system for space applications 23 p3256 N88-29383
Study of the assembly, integration and verification programs of telecommunication satellites applicable to other satellite programs
[MATRA-100/CC/MLG/031/87]
24 p3334 N88-29847

SPACECRAFT POWER SUPPLIES
Electrical Power Working Group report
01 p0016 N88-10065
A matter-antimatter propulsion system for manned interstellar flight
[DE87-013311] 02 p0141 N88-10885
BRASILSAT A2: Ground and in-orbit anomalies
02 p0164 N88-11032
International Ultraviolet Explorer (IUE) spacecraft battery performance update 02 p0164 N88-11033
Earth Radiation Budget Satellite (ERBS) orbiting profiles and Ni-Cd use 02 p0165 N88-11034

Flight experience of solar mesosphere explorer's power system over high temperatures ranges
02 p0165 N88-11037

Real time charge efficiency monitoring for nickel electrodes in NICD and NIH2 cells
02 p0165 N88-11038

Gas-cooled reactor for space power systems
[DE87-011549] 02 p0233 N88-11471

Environmental interactions of solar generators in space
03 p0274 N88-11730

Photovoltaic power modules for NASA's manned space station
[NASA-TM-100229] 03 p0277 N88-11745

SPRE 1 free-piston Stirling engine testing at NASA Lewis Research Center
[NASA-TM-100241] 03 p0277 N88-11747

The ac power system testbed
[NASA-CR-175068] 03 p0309 N88-11948

Recent progress in space photovoltaic systems
[NASA-TM-100208] 03 p0311 N88-11966

Overview of free-piston Stirling engine technology for space power application
[NASA-TM-88886] 03 p0386 N88-12427

Low Earth orbit environmental effects on the space station photovoltaic power generation systems
[NASA-TM-100230] 03 p0387 N88-12429

Study of Plasma Motor Generator (PMG) tether system for orbit reboost
[NASA-CR-172016] 04 p0403 N88-12501

Space station resistojet system requirements and interface definition study
[NASA-CR-180832] 04 p0409 N88-12541

Low gravity fluid-thermal experiments
[DE88-000553] 04 p0423 N88-12620

The effect of maximum-allowable payload temperature on the mass of a multimegawatt space-based platform
[DE88-001921] 05 p0555 N88-13381

Making space nickel/hydrogen batteries lighter and less expensive
[DE88-000168] 05 p0578 N88-13530

The high performance solar array GSR3
[SNIAS-872-422-108] 05 p0622 N88-13814

Progress toward the evolution of a Stirling space engine
[NASA-TM-100221] 05 p0659 N88-14046

Status of 20 kHz space station power distribution technology
[NASA-TM-100781] 08 p0964 N88-15838

A knowledge-based system for monitoring the electrical power system of the Hubble Space Telescope
08 p1058 N88-16380

Artificial intelligence and space power systems automation 08 p1058 N88-16381

The European space battery test center
09 p1125 N88-16738

Solar pumped, alkali vapor laser
[AD-A187156] 09 p1170 N88-17016

Study of large solar arrays (SOLA), phase 2A
[BAE-SS/1109] 09 p1186 N88-17106

Study of Large Solar Arrays (SOLA). Phase 2A. Amplifying information to final report (SS/1109)
[BAE-SS/1110] 09 p1248 N88-17480

Simulation test beds for the space station electrical power system
[NASA-TM-100786] 10 p1290 N88-17715

ESL batteries and multi-segment applications --- ESA Simulation Language (ESL)
[CS-1029/00-QFIN4] 10 p1322 N88-17901

Creep behavior of tungsten/niobium and tungsten/niobium-1 percent zirconium composites
[NASA-TM-100804] 11 p1460 N88-18707

Computer-aided modeling and prediction of performance of the modified Lundell class of alternators in space station solar dynamic power systems
[NASA-CR-182538] 11 p1507 N88-19000

Development of encapsulated lithium hydride thermal energy storage for space power systems
[DE88-004762] 11 p1507 N88-19001

Solar dynamic power system definition study
[NASA-CR-180877] 13 p1733 N88-20361

Advanced sensible heat solar receiver for space power
[NASA-TM-100847] 14 p1882 N88-21249

Power systems for production, construction, life support and operations in space
[NASA-TM-100838] 14 p1883 N88-21254

Test facilities of the structural dynamics branch of NASA Lewis Research Center
[NASA-TM-100800] 14 p1934 N88-21534

Thermophotovoltaic space power system, phase 3
[NASA-CR-179327] 14 p1942 N88-21585

Thermal analysis of heat storage canisters for a solar dynamic, space power system
[DE88-004199] 15 p2027 N88-22075

Development of an integrated heat pipe-thermal storage system for a solar receiver
[NASA-TM-101099] 15 p2091 N88-22458

Development of a slip-ring system for energy transfer in space conditions. Space flight qualification and extended life tests
[BMFT-FB-W-86-019] 16 p2169 N88-22932

The 1988 overview of free-piston Stirling technology for space power at the NASA Lewis Research Center
[NASA-TM-100795] 16 p2170 N88-22934

An integrated and modular digital modeling approach for the space station electrical power system development
[NASA-TM-100904] 16 p2170 N88-22935

Value of energy storage in pulsed space power systems
[AD-A191311] 16 p2170 N88-22938

The application of high temperature superconductors to space electrical power distribution components
[NASA-TM-100901] 16 p2171 N88-22939

Comparison of electrically driven lasers for space power transmission
[NASA-TM-4045] 16 p2212 N88-23197

Aerospace energy systems laboratory: Requirements and design approach
[NASA-TM-100423] 17 p2390 N88-24206

Parametric analysis of power requirements for space-based radar 17 p2399 N88-24260

Megawatt level electric propulsion perspectives
17 p2404 N88-24294

The Light-Weight Radioisotope Heater Unit (LWRHU): Development and application 17 p2405 N88-24299

MHW RTG performance during LES 8/9 and Voyager missions 17 p2405 N88-24300

Foil gas bearing system endurance testing dynamic isotope power system 17 p2405 N88-24302

Two-phase fluid management for a Rankine cycle isotope power system 17 p2405 N88-24303

Reactor instrumentation and control design and performance simulation for SP-100
17 p2406 N88-24306

A review of thermionic power conversion systems for SDI applications 17 p2407 N88-24310

Radiation hardening design of nuclear powered spacecraft 17 p2407 N88-24315

The effect of operating temperature on open, multimegawatt space power systems
17 p2414 N88-24352

Transactions of the Fifth Symposium on Space Nuclear Power Systems
[DE88-006165] 17 p2417 N88-24374

Air Force space power requirements and nuclear power assessment methodology 17 p2418 N88-24378

Thermal and power availability transient responses for the Argonne monolithic solid oxide fuel cell
17 p2419 N88-24384

Review of power requirements for satellite remote sensing systems 17 p2419 N88-24387

Individual satellite power requirements calculated from specified constellation performance
17 p2420 N88-24392

A transient model for liquid metal heat pipes
17 p2421 N88-24398

The dynamic isotope power system: Technology status and demonstration program 17 p2422 N88-24400

Characteristics of the closed Brayton cycle for dynamic isotope power systems 17 p2422 N88-24401

Status of the organic Rankine cycle for space applications 17 p2422 N88-24402

Status of modular RTG technology
17 p2422 N88-24403

Optimization of organic Rankine cycles for space station applications 17 p2423 N88-24407

Energy storage evaluation for burst power applications
17 p2426 N88-24430

Energy storage for nuclear burst power systems
17 p2426 N88-24431

Candidate advanced energy storage concepts for multimegawatt burst power systems
17 p2426 N88-24434

A multimegawatt space power source radiator design
17 p2427 N88-24436

The liquid droplet radiator in space: A parametric approach 17 p2427 N88-24437

Space Power Reference Source (SPRS). A user's guide to SDI Space Power Technology Programs
17 p2427 N88-24440

Gigawatt, closed cycle, vapor core-MHD space power system conceptual design study
17 p2433 N88-24473

Critical issues for SOAR: The space orbiting advanced fusion power reactor 17 p2433 N88-24474

Comparison of 20-kWe space nuclear power systems: Impact of reactor temperature and technology upon system design and performances 17 p2433 N88-24475

Potassium Rankine power system for space power
17 p2433 N88-24476

Low cross-section Mo-Nb thermocouples for nuclear application: The state-of-the-art
17 p2433 N88-24477

Material property and irradiation performance correlations for nitride fuels 17 p2434 N88-24483

SNAP fuel performance 17 p2435 N88-24484

SNAP-DYN: Concepts for multikilowatt space power applications 17 p2435 N88-24486

The closed Brayton cycle: An energy conversion system for near-term military space missions
17 p2435 N88-24488

The effect of operating temperature and turbine blade cooling on Brayton cycle space power systems
17 p2435 N88-24489

A combined Rankine/Brayton pulse power cycle
17 p2435 N88-24490

Energy conversion system optimization study for multimegawatt space nuclear power application
17 p2436 N88-24492

Automatic reactor control system for transient operation 17 p2436 N88-24493

Alkali metal thermoelectric converter design for space power systems applications 17 p2437 N88-24499

A capillary pumped SHE/AMTEC system
17 p2437 N88-24500

High power density electrodes for AMTEC
17 p2437 N88-24501

Multimegawatt power conditioning requirements study
17 p2438 N88-24504

Lightweight power bus for a baseload nuclear reactor in space 17 p2438 N88-24505

Component improvement of free-piston Stirling engine key technology for space power
[NASA-TM-100950] 19 p2607 N88-25476

Hydrogen turbines for space power systems: A simplified axial flow gas turbine model
[DE88-009585] 19 p2677 N88-25920

Effect of LEO cycling at shallow depths of discharge on MANTECH IPV nickel-hydrogen cells
[NASA-TM-101300] 19 p2688 N88-25978

The design and fabrication of a Stirling engine heat exchanger module with an integral heat pipe
[NASA-TM-101296] 20 p2820 N88-26732

Refractory metal alloys and composites for space power systems
[NASA-TM-100946] 21 p2916 N88-27310

Space photovoltaic generators. State of the art, trends
[REPT-881-440-106] 21 p2970 N88-27640

Arcjet power supply and start circuit
[NASA-CASE-LEW-14374-1] 23 p3181 N88-28939

Thin film coatings for space electrical power system applications
[NASA-TM-101325] 23 p3187 N88-28966

Solar dynamic power systems
[ETN-88-92969] 23 p3230 N88-29224

Possibilities of economical improvements for Moon based rocket propulsion using lunar propellants
[ILR-MITT-196] 24 p3338 N88-29871

Alternative module configurations for advanced solar arrays on low orbit and extended lifetime missions (AMOC 2)
[ESA-CR(P)-2581] 24 p3389 N88-30182

Fuel cells for space use
[FCP-TR-DOS-SY-026] 24 p3389 N88-30183

SPACECRAFT PRELAUNCH TESTS
U SPACE VEHICLE CHECKOUT PROGRAM

SPACECRAFT PROPULSION
NT ELECTROMAGNETIC PROPULSION
NT ELECTROSTATIC PROPULSION
NT ION PROPULSION
NT MASS DRIVERS (PAYLOAD DELIVERY)
NT PLASMA PROPULSION
NT SOLAR THERMAL PROPULSION

Spacecraft 2000
[NASA-CP-2473] 01 p0015 N88-10084

A matter-antimatter propulsion system for manned interstellar flight
[DE87-013311] 02 p0141 N88-10885

Auxiliary propulsion system flight package
[NASA-CR-180828] 02 p0141 N88-10886

High temperature metal matrix composites for future aerospace systems
[NASA-TM-100212] 02 p0149 N88-10938

Space station propulsion
[NASA-TM-100216] 03 p0277 N88-11746

A low-power arcjet cyclic lifetest
[NASA-TM-100233] 03 p0278 N88-11748

Thrust and specific impulse of repetitively-pulsed-laser propulsion rocket 03 p0318 N88-12012

Design study for asteroidal exploitation
03 p0389 N88-12445

Interplanetary propulsion using inertial fusion
[NASA-TM-89661] 04 p0409 N88-12540

The VISTA spacecraft: Advantages of ICF (Inertial Confinement Fusion) for interplanetary fusions propulsion applications
[NASA-CR-181549] 04 p0491 N88-13024

Space station onboard propulsion system: Technology study
[NASA-CR-179233] 07 p0825 N88-15006

Advanced fusion power: A preliminary assessment
[AD-A185903] 07 p0933 N88-15664

Space station propulsion technology
[NASA-CR-179260] 08 p0964 N88-15835

Selection of efficient correcting motor for an artificial Earth satellite 08 p1007 N88-16102

Electric propulsion: A controversial must for long-lived applications satellites 09 p1124 N88-16735

Rocket and airjet propulsion for ballistic and aerodynamic space probes
[REPT-TR-527] 10 p1310 N88-17826

Soviet space transport systems
13 p1727 N88-20328

Advanced space propulsion study - antiproton and beamed power propulsion
[AD-A189218] 13 p1732 N88-20355

Cermet-fueled reactors for advanced space applications
[DE88-005528] 13 p1839 N88-21002

Test facilities of the structural dynamics branch of NASA Lewis Research Center
[NASA-TM-100800] 14 p1934 N88-21534

Prospects for antiproton production and propulsion
16 p2267 N88-23556

Heat transfer in aerospace propulsion
[NASA-TM-100874] 17 p2339 N88-23957

The results of application studies for space nuclear power 17 p2396 N88-24259

History of some direct nuclear propulsion developments since 1946 17 p2400 N88-24270

Interplanetary propulsion using inertial fusion
17 p2401 N88-24273

A fusion based plasma propulsion system
17 p2401 N88-24274

Ultra high temperature direct propulsion
17 p2401 N88-24275

Safety constraints and considerations in the development of nuclear powered propulsion
17 p2401 N88-24276

A critique of NERVA based nuclear reactor design and performance for MMW space propulsion applications
17 p2404 N88-24297

Gas core reactors for direct nuclear propulsion
17 p2428 N88-24442

Status of high power electric propulsion technology
17 p2428 N88-24443

Performance and long duration test of a 30 kw thermal arcjet engine
[AD-A190962] 18 p2474 N88-24677

Development of a liquid-fed water resistojet
[NASA-TM-100927] 18 p2523 N88-24968

Propulsion analysis and application potential of air breathing combined propulsion for ballistic space transporter
[ETN-88-92369] 21 p2903 N88-27227

Performance of 10-kW class xenon ion thrusters
[NASA-TM-101292] 22 p3049 N88-28086

Gravitational propulsion 22 p3158 N88-28796

Orbital Propulsion Module (OPM). Study on coni-spherical surface tension tanks (COSTA)
[MBB-URV-170/87] 23 p3187 N88-28963

Spacecraft mass estimation, relationships and engine data: Task 1.1 of the lunar base systems study
[NASA-CR-172061] 24 p3332 N88-29836

Possibilities of economical improvements for Moon based rocket propulsion using lunar propellants
[ILR-MITT-196] 24 p3338 N88-29871

SPACECRAFT RADIATORS

Membrane heat pipe development for space radiator applications
[DE88-006015] 01 p0045 N88-10285

Considerations concerning a thermal joint for a deployable or steerable battery radiator for the Columbus Polar Platform
[NLR-TR-86055-U] 03 p0276 N88-11739

The effect of maximum-allowable payload temperature on the mass of a multimegawatt space-based platform
[DE88-001921] 05 p0555 N88-13361

Moveable thermal joints for deployable or steerable spacecraft radiator systems
[NLR-MP-87016-U] 13 p1730 N88-20347

OLYMPUS shuttle specific radiator shield
14 p1879 N88-21234

Fabric space radiators
[DE88-005569] 14 p1880 N88-21237

Development of a lightweight structure with load bearing capability and high thermal conductance
17 p2420 N88-24393

A reflux tube fabric radiator 17 p2421 N88-24394

Liquid droplet radiator development
17 p2424 N88-24415

Fabric radiators 17 p2427 N88-24435

A multimegawatt space power source radiator design
17 p2427 N88-24436

The liquid droplet radiator in space: A parametric approach 17 p2427 N88-24437

Space power radiation cooled dc transmission line analysis 17 p2438 N88-24506

Arc-textured metal surfaces for high thermal emittance space radiators
[NASA-TM-100894] 18 p2487 N88-24754

Moving belt radiator development status
[NASA-TM-100909] 19 p2607 N88-25477

Heat pump augmented radiators for spacecraft thermal management
[DE88-007890] 20 p2764 N88-26392

Development of a space deployable radiator using heat pipes
[SNIAS-881-440-104] 23 p3214 N88-29128

SPACECRAFT RECOVERY

Concept definition study for recovery of tumbling satellites. Volume 2: Supporting research and technology report
[NASA-CR-179229] 06 p0672 N88-14117

Concept definition study for recovery of tumbling satellites. Volume 1: Executive summary, study results
[NASA-CR-179228] 06 p0672 N88-14118

Rendezvous and Docking Verification (RVDV) and in-orbit demonstration, executive summary
[RVD-RVDV-FR-AS-01] 06 p0673 N88-14120

Review of commercial spacecraft: Recovery and repair experiences. Implications for future spacecraft designs and operations 12 p1591 N88-19528

SPACECRAFT REENTRY

Effects of forced and free convections on structural temperatures of space shuttle orbiter during reentry flight
[NASA-TM-86800] 01 p0043 N88-10275

Ceramic-ceramic shell tile thermal protection system and method thereof
[NASA-CASE-ARC-11641-1] 11 p1448 N88-18628

A method of atmospheric density measurements during space shuttle entry using ultraviolet-laser Rayleigh scattering
[NASA-TM-100056] 15 p2069 N88-22337

New concepts for atmospheric braking deceleration in planetary atmosphere entry
[SNIAS-CAS-DECE-P003-DPAA]
16 p2168 N88-22923

A proposed national policy concerning the reentry of space reactors 17 p2415 N88-24359

SPACECRAFT RELIABILITY

Configuration evaluation and criteria plan. Volume 2: Evaluation criteria plan (update). Space Transportation Main Engine (STME) configuration study
[NASA-CR-181429] 03 p0270 N88-11699

Natural frequencies and structural integrity assessment of large space structures
[AD-A186139] 07 p0824 N88-15001

Risk analysis in space system safety
22 p3161 N88-28825

Case study: The Hermes program product assurance
22 p3162 N88-28831

A scheduling and resource management system for space applications 23 p3256 N88-29383

Hermes: Study of propulsion system for reusable man-rated spacecraft
[PSRM-TN-0000-00-04A] 24 p3337 N88-29866

SPACECRAFT RENDEZVOUS

U SPACE RENDEZVOUS

SPACECRAFT SENSORS

U SPACECRAFT INSTRUMENTS

SPACECRAFT SHIELDING

Consortium for Materials Development in Space. Technical section
[NASA-CR-181508] 03 p0296 N88-11859

Wake shield 03 p0298 N88-11871

Optimization techniques applied to passive measures for in-orbit spacecraft survivability
[NASA-CR-179216] 04 p0408 N88-12532

SPACECRAFT STABILITY

Pinhole occulter experiment
[NASA-CR-179206] 02 p0235 N88-11461

Concept definition study for recovery of tumbling satellites. Volume 2: Supporting research and technology report
[NASA-CR-179229] 06 p0672 N88-14117

Concept definition study for recovery of tumbling satellites. Volume 1: Executive summary, study results
[NASA-CR-179228] 06 p0672 N88-14118

Modeling of a nutation damper for satellite stabilization through rotation
[INPE-4275-PRE/1147] 12 p1601 N88-19584

Vibrations of structures with parametric uncertainties
[AD-A190400] 15 p2076 N88-22378

The Proceedings of the Symposium on Mechanics for Space Flight 1987
[ISAS-SP-6] 20 p2762 N88-26499

Nutational stability of a satellite equipped with an active magnetic momentum wheel 20 p2784 N88-26513

SPACECRAFT STRUCTURES

Spacecraft surface exposure to atomic oxygen in low Earth orbit 03 p0273 N88-11715

Computational methods for problems in aerodynamics and large space structure using parallel and vector architectures
[AD-A185401] 05 p0541 N88-13294

Viscous damped space structure for reduced jitter
05 p0594 N88-13623

Evaluate the application of modal test and analysis processes to structural fault detection in MSFC - STS project elements 07 p0927 N88-15630

The development of test methodology for testing glassy materials 07 p0927 N88-15633

Thermal structural control modelling techniques --- spacecraft
[FOK-TR-R-86-030] 08 p0962 N88-15828

Mechanical in-flight environment of Ariane payloads
09 p1126 N88-16748

Analytical interactive approach for phenomena involving structures, thermal and control aspects. Volume 1: Theory --- spacecraft structures
[ESA-CR(P)-2503-VOL-1] 09 p1134 N88-16803

Analytical interactive approach for phenomena involving structures, thermal, and control aspects. Volume 2: Toward the solution --- spacecraft structures
[ESA-CR(P)-2503-VOL-2] 09 p1134 N88-16804

Analytical interactive approach for phenomena involving structures, thermal, and control aspects. Volume 3: Executive summary --- spacecraft structures
[ESA-CR(P)-2503-VOL-3] 09 p1134 N88-16805

Optimized approach to damage tolerance --- spacecraft
[FOK-FSS-R-87-024] 09 p1134 N88-16806

Integrity control of carbon fiber reinforced plastics (CFRP) structural elements. Conclusion with respect to the control methodology of CFRP primary structures in manned space flight and the implications to the design, analysis and testing of CFRP structural elements, executive summary
[MBB-TR-RB517-014/85] 09 p1139 N88-16824

Measurement, data analysis and prediction of pyrotechnic shock from pin-pullers and separation joints
09 p1179 N88-17061

In-orbit automatic assembly of reticular structures
12 p1586 N88-19491

Suspension design for a satellite transport container
[INPE-4352-TDL/296] 12 p1600 N88-19578

Development of isostatic mounts and associated guidelines --- spacecraft payloads
[CASA-IM-WP-301] 13 p1731 N88-20354

Numerical solution of multibody systems in space applications 14 p1875 N88-21200

The development status of the strongback array --- spacecraft structure 14 p1875 N88-21201

A sequentially deployable structure for space applications 14 p1875 N88-21202

Optimal control and identification of space structures
[AD-A190033] 15 p2025 N88-22065

Wave propagation and dynamics of lattice structures
[AD-A190037] 15 p2025 N88-22066

Vibration control of large structures
[AD-A191358] 16 p2168 N88-22926

Lewis Structures Technology, 1988. Volume 1: Structural Dynamics
[NASA-CP-3003-VOL-1] 16 p2217 N88-23226

Base reaction optimization of manipulators with redundant kinematics 16 p2219 N88-23236

Travelling wave concepts for the modeling and control of space structures
[AD-A191235] 17 p2310 N88-23819

Structural acoustics design manual
[ESA-PSS-03-1201-ISSUE-1] 17 p2311 N88-23821

Insert design handbook
[ESA-PSS-03-1202-ISSUE-1] 17 p2311 N88-23822

Progress and future directions in computational fluid dynamics
[NASA-TM-100091] 18 p2456 N88-24579

Study of the influence of metallurgical factors on fatigue and fracture of aerospace structural materials
[AD-A192909] 20 p2774 N88-26452

Design of booster wound structures --- spacecraft structures
[SNIAS-881-430-102] 21 p2903 N88-27226

Reinforced plastics: Winding and weaving technologies for space products
[SNIAS-881-430-103] 21 p2922 N88-27341

Vibration control of large structures
[AD-A193317] 21 p2961 N88-27587

Optical method to measure the deformations of structures loaded by hydraulic pressure
[SNIAS-881-430-111] 22 p3088 N88-28338
Nondestructive investigations for space use
[SNIAS-881-430-105] 23 p3224 N88-29189
Dynamics of articulated aerospace structures
[AD-A195685] 24 p3324 N88-29794
Sensor and actuator selection for large space structure control
[AD-A194912] 24 p3333 N88-29842
Laser sensing for identification and control of distributed parameter systems
[AD-A195886] 24 p3379 N88-30124

SPACECRAFT SURVIVABILITY
Spacecraft fire detection and extinguishment: A bibliography
[NASA-CR-180880] 11 p1444 N88-18612
The use of liquid films for spacecraft survivability to laser radiation
[AD-A192954] 20 p2765 N88-26395
SCARES: A Spacecraft Control Anomaly Resolution Expert System 23 p3256 N88-29381

SPACECRAFT TELEVISION
NT SATELLITE TELEVISION

SPACECRAFT TEMPERATURE
Effects of forced and free convections on structural temperatures of space shuttle orbiter during reentry flight
[NASA-TM-88800] 01 p3043 N88-10275
The effect of maximum-allowable payload temperature on the mass of a multimegawatt space-based platform
[DE88-001921] 05 p0555 N88-13381
EUREX D: An expert system for failure diagnosis and recovery in the TCS of the European retrievable carrier EURECA 08 p1058 N88-16365
Moveable thermal joints for deployable or steerable spacecraft radiator systems
[NLR-MP-87016-U] 13 p1730 N88-20347
Feasibility demonstration of a sensor for high-quality two-phase flow --- Space Station
[NLR-TR-87009-U] 13 p1767 N88-20569
MTK: An AI tool for model-based reasoning
17 p2387 N88-24189
Heat pump-augmented systems for spacecraft thermal management 17 p2424 N88-24419
The Curie point radiator 17 p2424 N88-24420
Design and testing of a high power spacecraft thermal management system
[NASA-TM-4051] 20 p2764 N88-26389
Biorack thermal performance during the D1 mission --- Spacelab 22 p3062 N88-28170
The heat pipe network of TDF-1/TV-SAT. Review of the development at completion
[SNIAS-881-440-103] 23 p3213 N88-29127
Reasoning about fault diagnosis for the space station common module thermal control system
23 p3258 N88-29395
MANIP --- spacecraft modeling program
[MANIP-217A] 24 p3335 N88-29855

SPACECRAFT TRACKING
NT SATELLITE TRACKING
NT SATELLITE-TO-SATELLITE TRACKING
Spacecraft 2000
[NASA-CP-2473] 01 p0015 N88-10084
Telemetry, Tracking, and Control Working Group report 01 p0016 N88-10096
Mode calibrations of the Doppler signal for a gravitational wave experiment --- interplanetary medium
[IFSI-86-13] 05 p0625 N88-13825
Investigation of design considerations for Telemetry, Tracking and Command (TT and C) antenna system on Naval Postgraduate School Orion mini-satellite
[AD-A187130] 10 p1291 N88-17718
Using ridge regression in systematic pointing error corrections 11 p1472 N88-18777
Spacecraft applications of advanced global positioning system technology
[NASA-CR-172055] 21 p2694 N88-27180
Advanced Receiver tracking of Voyager 2 near solar conjunction 22 p3065 N88-28185
Determination of the Venus flyby orbits of the Soviet Vega probes using VLBI techniques
22 p3067 N88-28203

SPACECRAFT TRAJECTORIES
NT INTERPLANETARY TRAJECTORIES
Safe and fuel minimum reference trajectories for closed loop controlled approaches --- space stations
12 p1585 N88-19488
A technique for capture analysis of low thrust missions in a planetary system
[AD-A188934] 12 p1594 N88-19544
Optimal thrust vector control of coplanar orbital evasive maneuvers
[AD-A189544] 13 p1730 N88-20346
IMP 7 (Explorer 47) trajectory, September 26, 1972 to September 25, 1978
[NASA-CR-182697] 14 p1871 N88-21183
Spacecraft trajectories
[ISBN-2-85-428166-7] 15 p2023 N88-22054

SPACECREWS
An assessment of clinical chemical sensing technology for potential use in space station health maintenance facility
[NASA-CR-172013] 04 p0475 N88-12926
Antarctica as a model for the human exploration of Mars
[AD-A185835] 08 p1051 N88-16342
Hemolysis in runners as evidenced by low serum haptoglobin: Implications for preflight monitoring of astronauts
[NASA-TM-100304] 11 p1518 N88-19067
Studies of the vestibulo-ocular reflex on STS 4, 5 and 6
[NASA-TM-100461] 12 p1686 N88-19987
An evaluation of the methods for rescuing EVA (Extravehicular Activities) crewmembers and recovering equipment detached and adrift from the space station
[AD-A189683] 14 p1871 N88-21181
Space station habitability recommendations based on a systematic comparative analysis of analogous conditions
[NASA-CR-3943] 18 p2587 N88-25372
Selecting the right crew for future space stations: An analysis of selection research on offshore divers, aviation pilots and other high risk groups in Scandinavia
19 p2696 N88-26021
Selection of isolated space crews
19 p2697 N88-26028
The US space programme spacewalk/extravehicular activity experience: Past, present and future
19 p2697 N88-26031
The human element in space: Lessons from Antarctica
[AD-A193440] 21 p2988 N88-27741
History of manned spaceflight
[CNES-NT-121] 21 p3032 N88-28000
An expert system for a distributed real-time trainer
23 p3261 N88-29411

SPACELAB
Space Station Mission Planning System (MPS) development study. Volume 1: Executive summary
[NASA-CR-179202] 01 p0009 N88-10047
Space lab system analysis
[NASA-CR-179207] 02 p0136 N88-10869
Allowable gravity-levels for Spacelab, Columbus and EURECA --- materials science
[BF-R-66.525-2] 07 p0838 N88-15084
Spacelab Data Processing Facility (SLDPF) quality assurance expert systems development
08 p1059 N88-16394
Rapid prototyping and AI programming environments applied to payload modeling 08 p1061 N88-16405
Project management in astronautics: From Spacelab to Columbus
[MBB-URE-943/87] 10 p1315 N88-17858
Spacelab: An international success story
[NASA-SP-487] 11 p1566 N88-19375
Second-generation respiratory monitoring system for microgravity studies in man 12 p1653 N88-19906
Implications of shiftwork in space for human physiology experiments 12 p1659 N88-19942
Microgravity User Support Center (MUSC) for EURECA, Spacelab and Columbus missions
12 p1660 N88-19947
The German Spacelab mission D1: Payload integration
[ETN-88-91507] 14 p1871 N88-21179
Space experiments with particle accelerators (SEPAC): Description of instrumentation
[NASA-TM-89728] 14 p1945 N88-21606
Space experiment plan FMPT
15 p2051 N88-22220
Amorphous semiconductors made in space
15 p2051 N88-22221
Containerless glass melting 15 p2051 N88-22222
Pb(1-x)Sn(x)Te crystal growth in space
15 p2051 N88-22223
Experiment scheduling for Spacelab missions
23 p3259 N88-29404
Spacelab data processing facility (SLDPF) Quality Assurance (QA)/Data Accounting (DA) expert systems: Transition from prototypes to operational systems
24 p3420 N88-30353

SPACELAB PAYLOADS
Space Station Mission Planning System (MPS) development study. Volume 2
[NASA-CR-179200] 01 p0009 N88-10046
Planning and execution of the NAVEX experiment in the Spacelab Mission D1
[DFVLR-FB-87-03] 01 p0010 N88-10056
The navigation experiment NAVEX: Experimental results of clock synchronization
[DFVLR-MITT-87-05] 03 p0271 N88-11701
First flight of the ATMOS instrument during the Spacelab 3 Mission, April 29 through May 6, 1985
[NASA-CR-182360] 06 p0726 N88-14482
Resolution of holograms produced by the fluid experiment system and the holography ground system
07 p0923 N88-15609
A backscatter lidar proposed for the second German Spacelab mission 08 p1018 N88-16173
The D-1 Biorack results: A base for further space biological investigations 08 p1033 N88-16263
The ESA Anthrorack project: Integrated research in human physiology 08 p1033 N88-16265
ESA Bulletin No. 8
[ETN-87-90513] 09 p1122 N88-16718
ASSESS-2: An aircraft simulation of Spacelab
09 p1123 N88-16723
White blood cells in space: An experiment for the first Spacelab mission 09 p1127 N88-16757
The navigation experiment NAVEX: Experimental results of clock synchronization
[ESA-TT-1084] 09 p1132 N88-16791
Investigations on the application of space photographs (Spacelab metric camera) for routine inventories of extensively managed forest areas
[DFVLR-FB-87-22] 09 p1185 N88-17098
Teleoperation for a Spacelab technology experiment
12 p1590 N88-19521
ROTEX: The Robotic Technology Experiment on Spacelab D-2 mission 12 p1592 N88-19530
ESA's facility for research in human physiology in space: Anthrorack 12 p1652 N88-19896
The ESA facility Biorack 12 p1652 N88-19897
BIOTEX, a project for biotechnological basic experiments under microgravity --- Spacelab
12 p1652 N88-19899
The respiratory system under weightlessness
12 p1653 N88-19901
Gravisensing in lentil seedling roots grown in space (Spacelab D-1 mission) 12 p1654 N88-19911
The use of plant protoplasts in biotechnological space research 12 p1655 N88-19914
Vestibular response to caloric stimulation during orbital flight 12 p1658 N88-19939
Synopsis of the Spacelab D-1 frog statolith experiment STATEX 12 p1659 N88-19940
Cyropreservation of isolated rat hepathocytes for future use in Spacelab experiments: Preliminary results
12 p1660 N88-19950
Biorack experiments in Spacelab D-1 and TML-1: Further developments in gravitational biology
12 p1661 N88-19953
Application of ARIADNE: A data bank-based information system for human physiology research --- Spacelab Anthrorack 12 p1662 N88-19962
Results of one way transit time measuring in navigation experiment NAVEX
[DFVLR-MITT-87-17] 14 p1865 N88-21145
The German Spacelab mission D1: Payload integration
[ETN-88-91507] 14 p1871 N88-21179
Securing the timescale of the NAVEX-reference clock and rate determinations by time comparisons with the help of the Global Positioning System (GPS) --- Spacelab D1 mission
[DFVLR-MITT-87-20] 16 p2159 N88-22879
Navigation experiment NAVEX. The reading differences between all ground station measuring clocks during each Spacelab pass of the D1 mission
[DFVLR-MITT-87-23] 16 p2159 N88-22880
The NAVEX experiment in the Spacelab D1 mission: Planning and execution
[ESA-TT-1078] 16 p2166 N88-22913
Zone crystallization experiments in mirror heating facilities
[BMFT-FB W-86-023] 16 p2184 N88-23016
Liquid motions in partially filled containers: Preliminary results of the D-1 mission --- Spacelab
[NLR-MP-86042-U] 20 p2802 N88-26629
Homogeneity of glasses: Experiment WL-IHF-05 in D1 mission --- Spacelab
[ETN-88-92339] 21 p2924 N88-27353
Biorack on Spacelab D1: An overview of the first flight of Biorack, an ESA facility for life sciences research in microgravity
[ESA-SP-1091] 22 p3059 N88-28154
A brief overview of the results of the experiments using the ESA Biorack Facility on the German Spacelab D1 mission 22 p3060 N88-28155
The Biorack facility and its performance during the D1 Spacelab mission 22 p3060 N88-28156
The effects of microgravity on genetic recombination in Escherichia coli --- Spacelab D1 mission
22 p3060 N88-28157

Growth and differentiation of Bacillus subtilis under microgravity conditions 22 p3060 N88-28158
The Antibio experiment --- Spacelab D1 mission 22 p3060 N88-28159
Contraction behavior and protoplasmic streaming in the slime mold Physarum polycephalum (Physarum kinetics) --- Spacelab D1 mission 22 p3060 N88-28160
The Paramecium experiment --- Spacelab D1 mission 22 p3060 N88-28161
The biological clock of Chlamydomonas reinhardii in space 22 p3061 N88-28162
Effect of microgravity on lymphocyte activation --- Spacelab D1 mission 22 p3061 N88-28163
The effect of microgravity on mammalian cell polarization at the ultrastructural level --- Spacelab D1 mission 22 p3061 N88-28164
Graviperception of lentil seedling roots grown in space 22 p3061 N88-28165
Effects of short spaceflights on Drosophila melanogaster embryogenesis and life span 22 p3061 N88-28166
Embryogenesis and organogenesis of Carausius morosus under spaceflight conditions 22 p3061 N88-28167
The role of gravity in the establishment of the dorso/ventral axis in the amphibian embryo --- Spacelab D1 mission 22 p3062 N88-28168
Dosimetric mapping inside Biorack --- Spacelab D1 mission 22 p3062 N88-28169
Biorack thermal performance during the D1 mission --- Spacelab 22 p3062 N88-28170
Biosample: Preservation, handling and observation system synthesis and breadboarding --- Spacelab [ESA-CR(P)-2609] 24 p3336 N88-29857
Fluid physics double rack --- Spacelab [SD-TN-AI-012] 24 p3358 N88-29992
Accommodation concept for fluid physics facilities, volume 2 --- Spacelab [SG-TN-AI-027-VOL-2] 24 p3358 N88-29994

SPAIN
Physiography and kinematics of the western coast of the province of Huelva (Andalousia, Spain) 22 p3109 N88-28465

SPALLATION
Experimental measurements and numerical simulations of metal spallation by detonating solid explosives [DE87-013227] 01 p0054 N88-10347
Study of adherent oxide scales [AD-A187368] 11 p1456 N88-18680
Impact shock generator from explosively driven plates [DE88-003596] 14 p1918 N88-21452
Spallation and dynamic fracture as an effect of laser induced shock-waves [AD-A193513] 23 p3188 N88-28971

SPALLING
Mechanisms of rolling contact spalling [NASA-CR-179243] 06 p0714 N88-14360

SPANWISE BLOWING
Numerical study of delta wing leading edge blowing [NASA-CR-183101] 20 p2752 N88-26335

SPARE PARTS
A problem of machine repair with a variable number of heterogeneous servers [INPE-4245-PRE/1118] 08 p1074 N88-16482
Systems integrated human engineering on the Navy's rapid acquisition of manufactured parts/test and integration facility 09 p1206 N88-17226
Computation of ECM (Electronic Counter-Measures) war reserve materiel spare requirements [AD-A193301] 21 p2897 N88-27195
Computers in weapons systems: A look at the F-15 [AD-A194498] 23 p3178 N88-28920

SPARK CHAMBERS
Use of reinforced inorganic cement materials for spark wire and drift chamber wire frames [NASA-CR-180759] 13 p1746 N88-20438

SPARK DISCHARGES
U ELECTRIC SPARKS

SPARK GAPS
Development of a repetitive 1-MV, 22-kJ Marx generator [DE87-011288] 01 p0038 N88-10242
Characterization of surface discharge switches and high performance applications [DE87-011763] 01 p0041 N88-10261
Development of a high-energy crowbar for the Los Alamos free-electron laser [DE87-014748] 02 p0179 N88-11113
A tapered poloidal gap for the reduction of field errors [DE87-014750] 03 p0377 N88-12375

SPARK IGNITION
Japanese industrial research on lean combustion: A case study: International Research Monitoring Program [DE87-013839] 02 p0144 N88-10904
The role of low temperature chemistry in the autoignition of n-butane [DE88-002385] 07 p0829 N88-15031
Fuel nitrogen conversion in a supercharged spark ignition engine [DE88-003739] 08 p0974 N88-15893
The effects of fuel composition on ignition delay in homogeneous charge and direct injection compression ignition engines [DE88-003691] 09 p1143 N88-16849
Status of alcohol fuels utilization technology for highway transportation: A 1986 perspective. Volume 2: Compression ignition engines [DE88-006059] 13 p1753 N88-20485
Combustion and performance characteristics of methanol plus higher alcohols in a spark ignition engine [PB88-147962] 14 p1918 N88-21451
Minimum ignition energy measurements using laser induced spark initiation 19 p2632 N88-25610
Summary of discussions at the Tenth Meeting of the Sandia Cooperative Group on the Aerothermochemistry of Turbulent Combustion [DE88-008467] 21 p2910 N88-27269
Experimental validation of a zero-dimensional computer model for spark-ignition engines [DE88-009034] 21 p2957 N88-27565

SPARK MACHINING
Wire-cut electrical discharge machinability of ceramics [AD-A186989] 09 p1146 N88-16870

SPARK SHADOWGRAPH PHOTOGRAPHY
U SHADOWGRAPH PHOTOGRAPHY

SPARKS
NT ELECTRIC SPARKS
Coupling of a spark source mass spectrograph and a ND-YAG laser [DE88-012116] 21 p2951 N88-27530

SPAS (ESA PLATFORMS)
U SHUTTLE PALLET SATELLITES

SPATIAL DEPENDENCIES
Spatial strength variation and statistical size effect of laminated orthotropic composite materials 04 p0427 N88-12646

SPATIAL DISTRIBUTION
NT STAR DISTRIBUTION
Method for single-shot measurement of picosecond laser pulse-lengths without electronic time dispersion [DE87-013171] 02 p0178 N88-11107
Forecasting stratus over the British Isles 02 p0209 N88-11310
Structural frequency functions for an impulsive, distributed forcing function [DE87-013811] 03 p0333 N88-12101
Illustrations of a density-equalizing map projection technique [DE87-013992] 03 p0339 N88-12130
Cloud cover determination in polar regions from satellite imagery [NASA-CR-181544] 04 p0471 N88-12908
The giant spot on II Peg in 1986 04 p0506 N88-13120
Structural frequency functions for an impulsive, distributed forcing function 05 p0594 N88-13627
Meteor velocity distribution and an optimum monitoring mathematical model 06 p0739 N88-14546
On the spatial structure of the Perseids meteor stream 06 p0740 N88-14550
The use of chlorophyll fluorescence measurements from space for separating constituents of sea water. Volume 1: Summary [ESA-CR(P)-2444-VOL-1] 07 p0873 N88-15294
The use of chlorophyll fluorescence measurements from space for separating constituents of sea water. Volume 2: Appendices [ESA-CR(P)-2444-VOL-2] 07 p0873 N88-15295
Acoustic scattering from composite wind-wave surfaces 3: Forward scatter intensities and spatial coherence at low and high frequencies and small grazing angles for Bubble-free regimes [AD-A185908] 07 p0881 N88-15345
A directed method for locating the focus of expansion [AD-A185840] 07 p0906 N88-15491
Study on the mechanical stresses in the elements of the model of a toroidal magnet of a tokamak with strong field [DE88-700343] 07 p0935 N88-15679
Longitudinal variations of equatorial ionosphere determined from Intercosmos-19 artificial Earth satellite data 08 p1003 N88-16074
Predictability of ice concentration in the high-latitude North Atlantic from statistical analysis of SST (Sea Surface Temperature) and ice concentration data [AD-A186621] 08 p1045 N88-16315
Convective wind fields as investigated with doppler lidar [PB88-115472] 09 p1193 N88-17151
Image chunking: Defining spatial building blocks for scene analysis [AD-A187072] 09 p1200 N88-17191
Study of quantum mechanical effects in deep submicron, grating-gate field effect transistors [AD-A188283] 10 p1325 N88-17923
Evolution of acoustic gravity wave packet in spatially and temporally varying wind 11 p1469 N88-18760
Visual contrast sensitivity functions obtained from untrained observers using tracking and staircase procedures [AD-A187715] 11 p1522 N88-19089
Spatial distribution of carbon and native defects in large-diameter bulk grown GaAs [DE88-003870] 11 p1562 N88-19348
To the problem of determining true volume steam content by measured values of mean density of a mixture in thermally unsteady two-phase flows [DE88-700840] 12 p1626 N88-19726
A segmented calorimeter for low-energy particle beams in space [DE88-001806] 13 p1838 N88-20997
Arcs in cesium seeded noble gases resulting from a magnetically induced electric field [EUT-87-E-177] 13 p1843 N88-21028
Spatial distribution of traffic in a cellular mobile data network [EUT-87-E-168] 14 p1904 N88-21378
Experimental and numerical study of liquid distribution in dispersive-annular flow [DE88-700844] 14 p1909 N88-21406
Spatial and temporal distribution of precipitation chemistry across Maryland in 1984, volume 1 [PB88-148929] 14 p1943 N88-21595
Spatial and temporal distribution of precipitation chemistry across Maryland in 1984, volume 2 [PB88-148937] 14 p1944 N88-21596
Spatial distribution of O(supra 1D) from Comet Halley 14 p1999 N88-21913
The representational code of the internal model of dynamic systems: An individual differences and dual task approach [AD-A190876] 16 p2244 N88-23403
Thomson scattering for determining electron concentrations and temperatures in an inductively coupled plasma. 1: Assessment of the technique for a low-flow, low-power plasma [AD-A191323] 16 p2260 N88-23651
Anomalies in the vegetation in the Alto Xingu - MT 17 p2357 N88-24043
An investigation of Soviet capabilities in extended range arctic ice forecasting [AD-A191082] 17 p2376 N88-24127
Sea ice kinematics: Space and time scales [AD-A191162] 17 p2376 N88-24128
Instantaneous two-dimensional multiple particle sizing diagnostic 19 p2630 N88-25600
Spatial organization of homopolymer chains inside spherical polybutadiene domains of SB diblock copolymers [AD-A193390] 21 p2918 N88-27321
Radar information from the partial derivatives of the echo signal phase from a point scatterer [AD-A193402] 21 p2933 N88-27415
A three-dimensional model of the gas-cell atomic frequency standard [AD-A193218] 21 p3011 N88-27868
Flow dynamics stimulated by hairpin-like vortices in initially laminar boundary layers [AD-A194253] 22 p3075 N88-28254
Distribution of hydroxyl clouds in the galaxy [DE88-702415] 22 p3164 N88-28844
The spatial and temporal variability of the arctic atmospheric boundary layer and its effect on electromagnetic (EM) propagation [AD-A193958] 23 p3204 N88-29068
HPM (High-Power Microwave) coupling into realistic targets [DE88-011788] 23 p3207 N88-29084
Low doses of atropine sulfate impair retention of a well-learned spatial task [AD-A194065] 23 p3237 N88-29266
Eye movements and spatial pattern vision [AD-A195496] 24 p3408 N88-30290
A detection theory analysis of visual display performance [AD-A196291] 24 p3409 N88-30292
Determining the spatial structure of fields of precipitation from space radar images in two orthogonal polarizations 24 p3450 N88-30531

SPATIAL FILTERING
Analysis of airborne imaging spectrometer data for the Ruby Mountains, Montana, by use of absorption-band-depth images 05 p0614 N88-13771
Spectral- and spatial-domain filtering and sampling approach to the numerical solution of electromagnetic scattering problems [PB88-106711] 06 p0694 N88-14261

Large-aperture sparse array antenna systems of moderate bandwidth for multiple emitter location
[AD-A188409] 12 p1619 N88-19683

Infrared-sensitive spatial light modulator
[AD-A190391] 15 p2134 N88-22729

Generation of thematic maps for updating aeronautical pilot charts utilizing LANDSAT-TM images
17 p2361 N88-24062

Real-time optical multiple object recognition and tracking system and method
[NASA-CASE-NPO-17139-1-CU]
18 p2576 N88-25301

Optical correlation using the magneto-optic device
[AD-A192342] 20 p2854 N88-26950

The predictability of low frequency patterns in the NMC MRF 22 p3127 N88-28587

Comparison of 2-D Fourier and spatial techniques for removing noise in real-time X-ray radiography
[AD-A193700] 23 p3187 N88-28962

SPATIAL ISOTROPY
U ISOTROPY
U SPATIAL DISTRIBUTION

SPATIAL MARCHING

A spatial marching technique for the inviscid blunt body problem 05 p0533 N88-13239

Leeside crossflow modeling in Euler space-marching computations
[NASA-TM-89710] 10 p1325 N88-17924

Split-coefficient matrix solution and experimental study of axisymmetric underexpanded exhaust plumes
15 p2054 N88-22242

SPATIAL ORIENTATION
U ATTITUDE (INCLINATION)

SPATIAL RESOLUTION

Estimation from satellite imagery of summertime rainfall over varied space and time scales
[PB87-203246] 01 p0071 N88-10454

What's needed in the UV and EUV
02 p0255 N88-11612

Visual evoked responses to sinusoidal gratings presented in central and right visual fields: 1
[DE87-014731] 04 p0473 N88-12919

Resolution limitations and optimization of the LLNL streak camera focus
[DE88-001633] 05 p0586 N88-13572

High-spatial-resolution TOVS observations for the FIRE/SRB Wisconsin experiment region from October 14 through November 2, 1986
[NASA-TM-100522] 06 p0747 N88-14593

High spatial resolution observations of dust and gas in NGC 7027 and the M8 Hourglass
06 p0801 N88-14903

Multichannel electron counter with high space resolution
[DE88-700564] 07 p0857 N88-15204

HIRIS (High-Resolution Imaging Spectrometer: Science opportunities for the 1990s. Earth observing system. Volume 2C: Instrument panel report
[NASA-TM-89703] 07 p0871 N88-15282

Method for restoration and resampling of TM sensor imagery
[INPE-4491-PRE/1255] 15 p2090 N88-22454

Sources of digital spatial data for geographic information systems
[AD-A189788] 15 p2148 N88-22824

A compact high resolution piezoresistive digital tactile sensor
[DE88-000430] 16 p2210 N88-23188

Spatial filtering on digital images
17 p2354 N88-24025

Effects of spatial resolution in CARS measurements
[PB88-121900] 18 p2482 N88-24727

Spatial stability of a compressible mixing layer
[NASA-CR-181671] 18 p2514 N88-24916

Investigation of the potential impact of new photonic materials on optical processing systems
21 p2924 N88-27359

Perception of motion in statistically-defined displays
[AD-A193076] 21 p2991 N88-27745

Research for reducing the labor intensive nature of high-resolution terrain analysis feature extraction
[AD-A192661] 22 p3089 N88-28345

Spectral and spatial attribute evaluation of SPOT data in geological mapping of precambrian terrains in semiarid environment of Brazil 22 p3104 N88-28436

Comparison of 2-D Fourier and spatial techniques for removing noise in real-time X-ray radiography
[AD-A193700] 23 p3187 N88-28962

SPECIES DIFFUSION

Species biology and potential for controlling four exotic plants (Ammophila arenaria, Carpobrotus edulis, Cortaderia jubata and Gasoul crystallinum) on Vandenberg Air Force Base, California
[NASA-TM-100980] 10 p1363 N88-18148

SPECIFIC GRAVITY
U DENSITY (MASS/VOLUME)

SPECIFIC HEAT

Specific heat of the high T/sub c superconductors (La,M)2CuO4 and YBa2Cu3O7 in magnetic fields
[DE87-014680] 03 p0380 N88-12388

Magnetic field dependence of the specific heat of some high-T/sub c/ superconductors
[DE87-014078] 04 p0497 N88-13063

Heavy Fermions and coherence in Kondo lattices: Specific heat of low energy excitation in Cer systems
[ETN-88-91080] 09 p1255 N88-17525

Specific heat of novel thin-film material systems
10 p1415 N88-18446

Research on high-specific-heat dielectrics
[AD-A187248] 11 p1461 N88-18710

Thermal conductivity, electrical conductivity and specific heat of copper-carbon fiber composite
[NASA-TT-20172] 16 p2172 N88-22948

Long-time tunneling in amorphous metals at helium temperatures
[DE88-701150] 16 p2281 N88-23654

Transient analysis of Li and LiH thermal storage spheres 17 p2411 N88-24334

The thermodynamic properties of quinoline and isoquinoline
[DE88-001218] 18 p2484 N88-24735

The precipitation processes of Cu-Zr-Cr alloys
[NASA-TT-20168] 18 p2488 N88-24758

Interactions between superconductivity and Kondo-grid properties in CeCu2Si2. Measurement results of specific heat under high pressure
[ETN-88-92377] 21 p3025 N88-27958

Discovery of a low temperature form of TAGN (Triaminoguanidinium Nitrate)
[AD-A196059] 24 p3357 N88-29989

SPECIFIC IMPULSE

Advanced energy conversion concept for beamed-energy propulsion
[AD-A187336] 10 p1324 N88-17914

Megawatt level electric propulsion perspectives
17 p2404 N88-24294

High power ion thruster performance
17 p2404 N88-24295

Nuclear electric propulsion system: Nuclear plant and thermomechanical conversion system
17 p2405 N88-24298

Solar thermal propulsion for orbit transfer vehicles
17 p2428 N88-24445

Performance of a hydrogen pulsed electrothermal thruster. Strategic defense initiative organization innovative science and technology. SBIR, phase 1
[AD-A191999] 18 p2475 N88-24679

Unified study of plasma/surface interactions for space power and propulsion
[AD-A195971] 24 p3338 N88-29870

SPECIFICATIONS
NT AIRCRAFT SPECIFICATIONS
NT EQUIPMENT SPECIFICATIONS
NT FUNCTIONAL DESIGN SPECIFICATIONS

Operating experiences and test results of six cold helium compressors
[DE87-012115] 02 p0157 N88-10982

Dual S/X-band RV antenna
[DE87-014853] 03 p0305 N88-11923

The aerodynamics of supersonic parachutes
[DE87-014846] 04 p0395 N88-12464

Mechanical shock test specification using nonstationary random excitation models
[DE87-013650] 04 p0454 N88-12812

Conservatism implications of shock test tailoring for multiple design environments 05 p0592 N88-13611

LISP: A language for stratified design
[AD-A185606] 06 p0759 N88-14654

FAA air traffic control operations concepts. Volume 5: ATCT/TCCC (Airport Traffic Control Tower/Tower Control Computer Complex) tower controllers
[AD-A185983] 07 p0818 N88-14977

DOE data exchange format specification, mechanical products/drafting: Version 1.2.2: CADCAM-045
[DE88-001923] 07 p0904 N88-15477

Annotated algebraic specification of the static semantics of pool
[PB88-106695] 07 p0912 N88-15533

Study on the model of a toroidal magnet for a tokamak with a strong field
[DE88-700346] 07 p0935 N88-15681

Main physics features driving design concept and physics design constraints. Conceptual design study of FY86 FER
[DE88-750309] 07 p0936 N88-15689

Evaluation of CWMS (Continuous-Wave Measurement System) single-wire dipole antenna
[DE88-003979] 09 p1155 N88-16920

Specification of an engine and its components starting from a consideration of aircraft missions
10 p1279 N88-17651

Plasma physics design and major specifications of candidate reactors for FER design studies. Conceptual design study of FY86 FER
[DE88-751066] 10 p1411 N88-18416

Conceptual design study of Fusion Experimental Reactor (FY86 FER): Safety
[DE88-751071] 10 p1411 N88-18418

Workshop on Design Loads for Advanced Fighters
[AGARD-R-746] 12 p1579 N88-19449

Changes in USAF structural loads requirements
12 p1580 N88-19452

A methodology for hardware verification based on logic simulation
[AD-A188553] 12 p1622 N88-19704

The formal specification of computer systems
[AD-A188947] 12 p1675 N88-20013

Engine testing for synfuel operation
[DE88-006044] 13 p1779 N88-20645

Algebraic specifications for parameterized data types. The case of minimal computable algebras and parameters with equality
[CWI-CS-R8714] 13 p1826 N88-20916

Type-checking Mini-ML: An algebraic specification with user-defined syntax
[CWI-CS-R8737] 13 p1827 N88-20921

Performance of elastomeric bearings
[PB88-159470] 14 p1918 N88-21450

The effects of torque response and time delay on rotorcraft vertical axis handling qualities
[AD-A189873] 15 p2017 N88-22023

Program profiling in Cedar
[AD-A190883] 16 p2250 N88-23449

The specification and design of a future maritime reconnaissance aircraft 17 p2303 N88-23772

Systems engineering technique
17 p2303 N88-23776

Modeling of functional specifications for onboard software: Experience with the Rafale avionics system
17 p2303 N88-23777

Interfacing and integrating hardware and software design systems 17 p2306 N88-23796

Development of complex avionics systems: Experience from French military programs 17 p2307 N88-23804

Specification for IBM/IBM compatible 3480 tape cartridge
[NASA-TM-100702] 17 p2384 N88-24168

Nonlinear flying quality parameters based on dynamic inversion
[AD-A192146] 18 p2464 N88-24627

Use of a two-stage light-gas gun as an injector for electromagnetic railguns
[DE88-007200] 18 p2469 N88-24657

The -mdoc macro package: A software tool to support computer documentation standards
[DE88-000500] 18 p2559 N88-25188

Multipath measurements for land mobile satellite service using global positioning system signals
19 p2645 N88-25700

Analytical determination of critical crack size in solar cells
[NASA-CR-183128] 20 p2821 N88-26736

Script editor: An editor for the specification phase in the development of computer based learning
[REPT-87-68] 20 p2839 N88-26846

The evaluation of a deformable diffraction grating for a stigmatic EUV spectroheliometer
[NASA-CR-183064] 20 p2853 N88-26941

Assembly Test Article (ATA)
[NASA-CR-179361] 21 p2903 N88-27226

The MELMUX MX-7100 series high-speed digital multiplexers 21 p2930 N88-27396

The Ariane 5 program management specifications
22 p3162 N88-28829

The technical reporting and approval procedure for materials and processes
[ESA-PSS-01-700-ISSUE-1] 22 p3162 N88-28833

High hot-hardness gear lubricant evaluations, phase 2
[AD-A192309] 23 p3196 N88-29017

Material and process selection and quality control for ESA space systems and associated equipment
[ESA-PSS-01-70-ISSUE-3] 23 p3224 N88-29190

Level 1 Ada/SQL (Structured Query Language) database language interface user's guide
[AD-A194480] 23 p3249 N88-29335

SPECIMEN GEOMETRY

A mixed finite element method for the computation of stress in a composite with loaded holes
[ONERA-RT-34/4242-RY-054-R]
01 p0062 N88-10395

Nondestructive control: Modeling of electromagnetic phenomena, defect characterization, and sensor optimization
[ECL-86-14] 08 p0993 N88-16008

The relationship of tensile specimen size and geometry effects to unique constitutive parameters for ductile materials
[AD-A186020] 08 p0994 N88-16012
Application of ISRM testing methods to fracture toughness testing of graphite 13 p1747 N88-20446
Damage in a perforated graphite-epoxy plate under monotonic, cyclic biaxial loading
[ONERA-NT-1987-5] 20 p2816 N88-26708
Stress corrosion of C ring specimen in salt spray tests
[I-186/87] 21 p2916 N88-27307
An experimental and analytical evaluation of a biaxial test for determining shear properties of composite materials
[NASA-CR-182928] 21 p2962 N88-27593
Mixed finite element methods to compute stress in a load composite specimen with holes: Numerical results
[ONERA-RT-37/4242-RY-062-R] 22 p3068 N88-28336

SPECIMENS
The influence of small defects on tensile specimen ductility and symmetry of deformation
[AD-A187983] 10 p1346 N88-18044
Cyropreservation of isolated rat hepathocytes for future use in Spacelab experiments: Preliminary results
12 p1660 N88-19950
Specimen preparation techniques for the examination of ceramic and metal-matrix composites
[DE88-005157] 15 p2030 N88-22094
Method of radiographic inspection of wooden members
[NASA-CASE-LAR-13724-1] 17 p2346 N88-23983
Sample decomposition in sealed teflon vessels
[NASA-TT-20189] 18 p2494 N88-24798
Low temperature storage container for transporting perishables to space station
[NASA-CASE-MFS-28248-1] 18 p2498 N88-24817

SPECKLE HOLOGRAPHY
Comparison of sensitivity and precision of holographic and speckle-interferometry methods with Fourier-plane recording 08 p1078 N88-16500

SPECKLE INTERFEROMETRY
New results from high angular resolution observations of alpha Ori 04 p0514 N88-13161
Comparison of sensitivity and precision of holographic and speckle-interferometry methods with Fourier-plane recording 08 p1078 N88-16500
Investigations of high resolution imaging through the Earth's atmosphere using speckle interferometry
[AD-A189295] 12 p1692 N88-20121
Speckle interferometry of asteroids
[NASA-CR-180438] 15 p2151 N88-22843
Speckle imaging of active galactic nuclei: NGC 1068 and NGC 4151 18 p2592 N88-25407
An upper limit on the primordial He4 abundance from speckle interferometric observations of muon Cassiopeiae 23 p3298 N88-29641
Binary star measurements using digital speckle interferometer of 6-m telescope
24 p3448 N88-30521

SPECKLE PATTERNS
ISIS: Imaging Speckle Interfereometer in Space
01 p0095 N88-10625
Study of synthetic aperture radar data compression and encoding. Part 3: Performance evaluation of speckle suppression and data compression algorithms
[NLR-TR-85085-L-PT-3] 06 p0692 N88-14248
Study of synthetic aperture radar data compression and encoding. Part 2: SAR image speckle suppression and data compression algorithms
[NLR-TR-85085-L-PT-2] 07 p0843 N88-15116
Calculation of noise in spatial speckle-field holograms under conditions of saturated photoresponse
09 p1235 N88-17403
Investigation of the usefulness of speckle analysis in imaging radar systems
[BCRS-86-05] 16 p2227 N88-23302
Speckle imaging of active galactic nuclei: NGC 1068 and NGC 4151 18 p2592 N88-25407
Digital image processing from speckle interferograms by correlation methods: Application in atmospheric optics, astronomy, and biology
[ETN-88-92125] 20 p2855 N88-26953
Methods for indirect imaging through the atmosphere
[ONERA-NT-1987-4] 20 p2884 N88-27124

SPECTRA
NT ABSORPTION SPECTRA
NT ATOMIC SPECTRA
NT BALMER SERIES
NT ELECTROMAGNETIC SPECTRA
NT ELECTRONIC SPECTRA
NT EMISSION SPECTRA
NT ENERGY SPECTRA
NT FRAUNHOFER LINES
NT GAMMA RAY SPECTRA
NT H ALPHA LINE
NT H BETA LINE
NT H LINES
NT HERZBERG BANDS
NT INFRARED SPECTRA
NT K LINES
NT LINE SPECTRA
NT LYMAN SPECTRA
NT MASS SPECTRA
NT MICROWAVE SPECTRA
NT MOLECULAR SPECTRA
NT NEUTRON SPECTRA
NT NOISE SPECTRA
NT OXYGEN SPECTRA
NT PLASMA SPECTRA
NT POWER SPECTRA
NT RADIATION SPECTRA
NT RADIO SPECTRA
NT RAMAN SPECTRA
NT RYDBERG SERIES
NT SCHUMANN-RUNGE BANDS
NT SHOCK SPECTRA
NT SOLAR SPECTRA
NT SPECTRAL BANDS
NT STELLAR SPECTRA
NT ULTRAVIOLET SPECTRA
NT VIBRATIONAL SPECTRA
NT VISIBLE SPECTRUM
NT X RAY SPECTRA
EVA reference manual
[DE87-014073] 01 p0082 N88-10526
Comparison of sideband spectra obtained from analytical formula and from numerical simulation in free-electron laser
[DE88-000521] 04 p0450 N88-12789
SUSIE reference manual
[DE88-001462] 05 p0636 N88-13893
The structure of the sideband spectrum in free electron lasers
[AD-A186952] 09 p1170 N88-17015
Scattering of optical radiation by bursting water particles in fog 09 p1236 N88-17410
Systematic errors of the FSU global spectral model
10 p1356 N88-18103
Well-posedness and spectral estimation for infinite dimensional systems
[AD-A187621] 10 p1401 N88-18354
Lg wave excitation and propagation in the presence of one-, two-, and three-dimensional heterogeneities
[AD-A187364] 11 p1510 N88-19022
Estimation of sea surface wave spectra using acoustic tomography
[AD-A187837] 11 p1516 N88-19057
Emission of gamma rays from various materials pulsed with 14-MeV neutrons
[DE88-003837] 11 p1544 N88-19227
Inversion algorithms for geophysical problems
[AD-A189252] 13 p1815 N88-20845
New method of examining micrononhomogeneity of local centers in high-resistivity semiconductor materials under scanning electron microscope 14 p1969 N88-21754
Multichannel 2-D power spectral estimation and applications
[AD-A191273] 16 p2191 N88-23068
Time-frequency representations for speech signals
[AD-A188661] 18 p2498 N88-24819
Molecular-beam, mass-spectrometric studies of wood vapor and model compounds over HZSM-5 catalyst
18 p2535 N88-25044
Wavenumber spectra from THIR 6.7 micron water vapor data 20 p2824 N88-26756
Qualitative characteristics of open waveguide resonator spectra
[DE88-702387] 23 p3202 N88-29056

SPECTRAL ABSORPTION
U ABSORPTION SPECTRA

SPECTRAL ANALYSIS
U SPECTRUM ANALYSIS

SPECTRAL BANDS
NT ABSORPTION SPECTRA
NT FRAUNHOFER LINES
NT HERZBERG BANDS
NT SCHUMANN-RUNGE BANDS
Analysis of SO2 signals in SBUV/TOMS data
05 p0618 N88-13794
Analysis of hydrocarbon band 3.35 in spectrum of Halley's Comet using data from infrared spectrometer on Vega-1 spacecraft 13 p1727 N88-20327
The gamma 1 and gamma 3 bands of (16)O3: Line positions and intensities
[NASA-TM-101162] 17 p2445 N88-24541
Line positions and intensities for the gamma 1 + gamma 2 and gamma 2 + gamma 3 bands of (16)O3
[NASA-TM-101161] 17 p2446 N88-24542
Spectral characteristics and the extent of paleosols of the Palouse formation
[NASA-CR-180947] 23 p3228 N88-29210
Atmospheric corrections for in-flight satellite radiometric calibration
[AD-A196124] 24 p3391 N88-30194

SPECTRAL CORRELATION
Multistep component analysis of correlations
08 p1009 N88-16115
Correlation and spectral density measurements by LDA --- flow measurement
[ISL-CO-244/86] 14 p1910 N88-21412
Spectrometry and spectral radiometry
16 p2271 N88-23566
Selective radiation absorption in aluminized composite propellant combustion 19 p2630 N88-25598

SPECTRAL EMISSION
PG 0308 + 096: A short-period white dwarf + dM binary with strongly modulated H-alpha emission
04 p0509 N88-13132
Evidence for expanding magnetic loops in coronae of cool stars 04 p0510 N88-13134
X-rays, color, and the Vaughan-Preston gap
04 p0510 N88-13135
Determination of cloud base height and emissivity from downwelling angular radiances
[AD-A185985] 07 p0879 N88-15331
NBS (National Bureau of Standards) measurement services: Spectral irradiance calibrations
[PB88-123781] 10 p1408 N88-18401
Research on influence of individual sea water components on spectral brightness coefficient of outgoing radiation 13 p1785 N88-20682
A spectroscopic study of absorption and emission features of interstellar dust components
[B8681462] 16 p2269 N88-23706
Space station contamination study: Assessment of contaminant spectral brightness
18 p2591 N88-25395
Calculation of space station infrared irradiance from atmosphere-induced emissions
18 p2591 N88-25396
Speckle imaging of active galactic nuclei: NGC 1068 and NGC 4151 18 p2592 N88-25407
Design, development, fabrication and launch support for a high altitude release of neodymium vapor
[AD-A194196] 22 p3116 N88-28527

SPECTRAL ENERGY DISTRIBUTION
Local spectra and wave distribution functions --- space plasma
[KGI-PREPRINT-099] 01 p0100 N88-10659
A spectral survey of 26 G9-M6 flare stars in the solar neighborhood 04 p0512 N88-13149
Evolution of spectral densities in weakly inhomogeneous plasmas
[PB87-137402] 06 p0784 N88-14811
Power spectral density analysis of wind-shear turbulence for related flight simulations
[NASA-CR-182721] 13 p1802 N88-20773
Inversion algorithms for geophysical problems
[AD-A189252] 13 p1815 N88-20845
Three dimensional spectral energy measurement on turbulence subjected to a high degree of plane deformation
[ETN-88-92537] 18 p2511 N88-24896
Study of the structure of turbulence in accelerating transitional boundary layers
[AD-A191698] 19 p2663 N88-25837
Statistical description of stochastic dynamics
[AD-A192924] 21 p3009 N88-27852

SPECTRAL LINE WIDTH
Statistical fine structure in inhomogeneously broadened absorption lines in solids
[AD-A190341] 16 p2174 N88-22957
Studies of spectral line ratio fluctuations using Inductively Coupled Plasma (ICP) light
[IRF-PREPRINT-100] 18 p2578 N88-25311
Spectral line shapes from highly ionized sodium plasmas
[AD-A193401] 21 p3017 N88-27907

SPECTRAL LINES
U LINE SPECTRA

SPECTRAL METHODS
An adaptive pseudo-spectral method for reaction diffusion problems
[NASA-CR-178394] 02 p0224 N88-11414
Airborne Visible/Infrared Imaging Spectrometer (AVIRIS) spectrometer design and performance
06 p0706 N88-14327
Spectral methods: Analysis and applications to flow problems
[AD-A186265] 07 p0850 N88-15156
Spectral representation of infinitely divisible processes
[AD-A186210] 07 p0910 N88-15515
Spectral dilation of L(B,H)-valued measures and its application to stationary dilation for Banach space valued processes
[NASA-CR-182388] 07 p0913 N88-15536

Prognosis using spectral embedding — weather forecasting 08 p1016 N88-16157

High-speed assembly language (80386/80387) programming for laser spectra scan control and data acquisition providing improved resolution water vapor spectroscopy
[NASA-CR-4117] 08 p1053 N88-16355

Short data length effects in an asymptotically efficient ARMA (AutoRegressive Moving Average) spectral estimator
[AD-A186561] 08 p1068 N88-16458

Analysis of the spectral vanishing viscosity method for periodic conservation laws
[NASA-CR-181613] 09 p1231 N88-17378

Coupling finite element and spectral methods: First results
[NASA-CR-181606] 09 p1231 N88-17379

Kinetics and spectrum of light pulse used in picosecond holography 09 p1236 N88-17409

Conjugate gradient spectral iterative technique
[PB88-126917] 10 p1398 N88-18337

Spectral iterative technique with Gram-Schmidt orthoganalization
[PB88-127451] 10 p1399 N88-18338

Domain decomposition preconditioners for the spectral collocation method
[NASA-CR-181620] 10 p1400 N88-18345

On the smallest scale for the incompressible Navier-Stokes equations
[NASA-CR-181628] 11 p1434 N88-18558

Recursive inversion of externally defined linear systems
[NASA-TM-100070] 11 p1541 N88-19215

How to generate equal probability design load conditions — aircraft design
[NLR-TR-86060-U] 13 p1722 N88-20295

Low-order spectral models of atmospheric circulation: A survey
[CWI-AM-R8705] 13 p1797 N88-20748

Spectral element methods: Algorithms and architectures
[NASA-CR-182701] 13 p1820 N88-20878

Spectrum fatigue testing for materials characterization
[VTT-RR-502] 15 p2088 N88-22443

Development of remote sensing techniques capable of delineating soils as an aid to soil survey
[NASA-CR-182610] 15 p2089 N88-22452

Propagation of acoustic gravity wave spectrum through vertical wind shear region 16 p2186 N88-23035

An efficient parallel algorithm for the simulation of three-dimensional compressible transition on a 20 processor Flex/32 multicomputer
[NASA-CR-178340] 17 p2337 N88-23943

Effects of spatial resolution in CARS measurements
[PB88-121900] 18 p2482 N88-24727

Analysis of a six-component barotropic spectral model: Chaotic motion, predictability and vacillation — atmospheric circulation
[CWI-AM-R8710] 18 p2542 N88-25090

La Recherche Aerospatiale, bimonthly bulletin, no. 1986-5, 234/September-October
[ESA-TT-1032] 19 p2641 N88-25671

Non-oscillatory spectral Fourier methods for shock wave calculations
[NASA-CR-181675] 19 p2720 N88-26148

Semi-discrete approximations to nonlinear systems of conservation laws; consistency and L(infinity)-stability imply convergence
[NASA-CR-181683] 19 p2721 N88-26157

Study and implementation of ultrahigh frequency coupling devices using the fin line technology — millimeter waves
[ETN-88-92307] 20 p2796 N88-26588

Spectral resolution of the Navier-Stokes equations in multi-domain curved complex geometries
[ONERA-NT-1987-2] 20 p2802 N88-26631

Solution of the Orr-Sommerfeld equation for the Blausius boundary-layer documentation of program ORRBL and a test case
[NASA-CR-4169] 20 p2841 N88-26858

SPECTRAL NOISE
U WHITE NOISE

SPECTRAL RECONNAISSANCE

The role of anisotropy in the long range reconnaissance of the albedo of land surfaces 08 p1017 N88-16169

Radiation absorption in the infrared spectral range: A comparison between laboratory measurements and theoretical calculation illustrated by a H2O 2.7 micrometer 08 p1018 N88-16170

Long range reconnaissance of trace gases: A special aspect of emission spectroscopy
08 p1018 N88-16172

Earth resources: A continuing bibliography with indexes (supplement 56)
[NASA-SP-7041(56)] 10 p1347 N88-18051

SPECTRAL REFLECTANCE

Development of response models for the Earth Radiation Budget Experiment (ERBE) sensors. Part 2: Analysis of the ERBE integrating sphere ground calibration
[NASA-CR-178293] 01 p0049 N88-10316

Surface polariton resonances and reflectance on a bigrating
[AD-A184663] 03 p0377 N88-12370

AIS-2 radiometry and a comparison of methods for the recovery of ground reflectance
05 p0611 N88-13757

Calibrating AIS images using the surface as a reference 05 p0612 N88-13760

AIS-2 spectra of California wetland vegetation
05 p0613 N88-13763

Toward detecting California shrubland canopy chemistry with AIS data 05 p0613 N88-13764

Measuring near infrared spectral reflectance changes from water stressed conifer stands with AIS-2
05 p0613 N88-13765

Preliminary results from an investigation of AIS-1 data over an area of epithermal alteration: Plateau, Northern Queensland, Australia 05 p0613 N88-13768

Causes of spurious features in spectral reflectance data 05 p0614 N88-13769

Automatic continuum analysis of reflectance spectra
05 p0614 N88-13770

Mapping hydrothermally altered rocks in the Northern Grapevine Mountains, Nevada and California with the airborne imaging spectrometer 05 p0614 N88-13772

Environmental processes and spectral reflectance characteristics associated with soil erosion in desert fringe regions
[NASA-CR-182332] 05 p0620 N88-13811

NBS (National Bureau of Standards) measurement services: Spectral reflectance
[PB88-109905] 06 p0779 N88-14785

Monte Carlo method calculation of spectral brightness coefficient of vegetation cover as function of illumination conditions 08 p1008 N88-16113

Transport properties of conductive polymers
[AD-A183411] 12 p1610 N88-19628

Influence of solar illumination conditions on TM/Landsat data
[INPE-4463-TDL/320] 12 p1638 N88-19606

Research in remote sensing of vegetation
[NASA-CR-182663] 12 p1639 N88-19817

Analysis of spectral reflectance characteristics of targets under satellites and automatic cloud recognition
13 p1755 N88-20498

Spectral reflective characteristics of sea surface
13 p1784 N88-20676

Space station solar concentrator materials research
[NASA-TM-100862] 14 p1882 N88-21250

Reflectance spectroscopy in planetary science: Review and strategy for the future
[NASA-SP-493] 17 p2451 N88-24564

Optical constants of minerals and other materials from the millimeter to the ultraviolet
[AD-A192210] 18 p2482 N88-24724

Methods of determining playa surface conditions using remote sensing
[AD-A192663] 21 p2965 N88-27612

SPOT 1: Image utilization, assessment, results. A study of the Elburgon Forest area (Kenya) showing the spectral responses of different forest tree species
22 p3107 N88-28454

Study of stereoradiometry on SPOT images
22 p3112 N88-28484

Surface reflectance factors derived from SPOT-1 HRV data at two view angles 22 p3113 N88-28492

Variations in spectral reflectance signature in healthy stands of pine and spruce
[FOA-C-30468-3.1] 22 p3116 N88-28512

Monte-Carlo estimation of the influence of plant architecture parameters on spectral brightness
24 p3450 N88-30533

SPECTRAL RESOLUTION

What's needed in the UV and EUV
02 p0255 N88-11612

Preliminary results from an investigation of AIS-1 data over an area of epithermal alteration: Plateau, Northern Queensland, Australia 05 p0613 N88-13768

HIRIS (High-Resolution Imaging Spectrometer: Science opportunities for the 1990s. Earth observing system. Volume 2C: Instrument panel report
[NASA-TM-89703] 07 p0871 N88-15282

Velocity resolved far-infrared spectroscopy of galactic sources 13 p1854 N88-21099

Merit of Hadamard transform active absorption spectrometer described 15 p2053 N88-22232

Dispersive spectral apparatus
16 p2271 N88-23587

Spectral resolution of the Navier-Stokes equations in multi-domain curved complex geometries
[ONERA-NT-1987-2] 20 p2802 N88-26631

Time-resolved doubly bent crystal X-ray spectrometer
[DE88-007899] 20 p2805 N88-26637

The collection of statistics on the frequency of cloud cover over North America
[AD-A193093] 21 p2974 N88-27667

Spectral and spatial attribute evaluation of SPOT data in geological mapping of precambrian terrains in semiarid environment of Brazil 22 p3104 N88-28436

On the multiple grating spectrometer resolving power
[PREPRINT-585] 22 p3153 N88-28761

SPECTRAL SENSITIVITY

Hard- and software problems of spaced meteor observations by optical electronics
06 p0741 N88-14560

Improvements in profiler wind estimates using smoothed data in the spectrum finder algorithm
[PB88-102181] 07 p0881 N88-15342

High-temperature photoelectron spectroscopy. An increased sensitivity spectrometer for studying vapor-phase species produced at furnace temperatures greater than 2000K
[AD-A186542] 09 p1140 N88-16835

Psychophysical, biochemical and histological studies of spectrally selective photic damage to primate retina
[AD-A188115] 11 p1517 N88-19063

Spectral properties of semiconductor lasers with external resonators
[ETN-88-93119] 24 p3379 N88-30125

SPECTRAL SIGNATURES

Solar-geophysical data number 514, June 1987. Part 1: (Prompt reports). Data for May 1987, April 1987 and late data
[PB87-217261] 02 p0257 N88-11626

Analysis of the parameters responsible for the variations of the illumination conditions in the LANSAT data
17 p2362 N88-24070

Comparative variations of spectral signatures in a cultivated area of the Paris Basin (27 May, 26 June, 1 July 1986) 22 p3095 N88-28382

Mars: Spectral signatures seen and unseen
23 p3301 N88-29659

Variability in spectral signatures of terrestrial volcanic rocks and implications for volcanology on Mars
23 p3303 N88-29672

Spectral reflectance of SNC meteorites: Relationships to Martian surface composition
23 p3304 N88-29683

Integrating multispectral imagery and ground level hyperspectral signature data
[AD-A195976] 24 p3386 N88-30166

SPECTROGRAMS

Spectrograms of the visible region in the JT-60 tokamak (wavelength range from 2210 A to 5250 A)
[DE87-753002] 02 p0240 N88-11513

Variations of the vertical and horizontal velocities of the small-scale structures and the physical problems related to overshoot layers 04 p0507 N88-13115

SPECTROGRAPHS

AURIO: A proposal for flying auroral imaging observatory on the Polar Platform in the Space Station/Columbus program 08 p1034 N88-16268

Mechanisms mediating perception of complex acoustic patterns
[AD-A189765] 15 p2102 N88-22520

Rutherford magnetic spectrograph for intense ion beam measurements on PBFA 2
[DE88-007281] 19 p2725 N88-26181

Coupling of a spark source mass spectrograph and a ND-YAG laser
[DE88-012116] 21 p2951 N88-27530

SPECTROHELIOGRAPHS

The evaluation of a deformable diffraction grating for a stigmatic EUV spectroheliometer
[NASA-CR-182371] 06 p0707 N88-14337

The evaluation of a deformable diffraction grating for a stigmatic EUV spectroheliometer
[NASA-CR-183064] 20 p2853 N88-26941

SPECTROHELIOSCOPES
U SPECTROHELIOGRAPHS

SPECTROMETERS
NT EBERT SPECTROMETERS
NT FABRY-PEROT SPECTROMETERS
NT GAMMA RAY SPECTROMETERS
NT IMAGING SPECTROMETERS
NT INFRARED SPECTROMETERS
NT LASER SPECTROMETERS
NT MASS SPECTROMETERS
NT MICROWAVE SPECTROMETERS
NT NEUTRON SPECTROMETERS
NT SOLAR BACKSCATTER UV SPECTROMETER
NT SOLAR SPECTROMETERS
NT SPECTROHELIOGRAPHS
NT TIME OF FLIGHT SPECTROMETERS
NT TOTAL OZONE MAPPING SPECTROMETER
NT ULTRAVIOLET SPECTROMETERS

The wavenumber: An alternative to the directional coupler for multimode analysis in oversized waveguides
[IPF-87-2] 01 p0037 N88-10237
Diode pumped solid-state laser oscillators for spectroscopic applications
[NASA-CR-180576] 01 p0052 N88-10331
Spectrometric test of a linear array sensor
[NASA-TM-100676] 01 p0064 N88-10414
Instrumental and operational aspects of an EXELFS system connected to JEOL 100C STEM
[USIP-87-09] 01 p0092 N88-10601
Present status of the high resolution spectrometers
[CEBAF-PR-87-029] 02 p0234 N88-11478
Conceptual design of a high-resolution pion (0) spectrometer
[DE87-014757] 03 p0324 N88-12047
Commercial perspective of an imaging spectrometer development program 03 p0340 N88-12138
Evidence for expanding magnetic loops in coronae of cool stars 04 p0510 N88-13134
Airborne Visible/Infrared Imaging Spectrometer (AVIRIS). A description of the sensor, ground data processing facility, laboratory calibration, and first results
[NASA-CR-182365] 06 p0705 N88-14325
A system overview of the Airborne Visible/Infrared Imaging Spectrometer (AVIRIS)
06 p0705 N88-14326
Astromag: A particle spectrometer for the Space Station
[PREPRINT-557] 06 p0707 N88-14336
Characteristics of an Ebert monochromator for an infrared spectrometer in the wavelength range 1 micrometer to 15 micrometers
[AD-A186945] 09 p1166 N88-16991
A comparison of measurements from the A/E35U-3 and PWMA (Portable Wear Metal Analyzer) spectrometers
[AD-A186855] 09 p1177 N88-17047
Error modeling and confidence interval estimation for inductively coupled plasma calibration curves
[AD-A186711] 09 p1250 N88-17488
A combined cosmic ray muon spectrometer and high energy air shower array
[DE88-003057] 09 p1264 N88-17574
Characterization of the arc/spark excitation sources used in the spectrometric oil analysis program
[AD-A187131] 10 p1297 N88-17758
Evaluation of a temperature remote sensing technique
[AD-A187885] 10 p1347 N88-18053
Atomic and molecular gas phase spectrometry
[AD-A187562] 11 p1452 N88-18655
A microspectrofluorometer system based on real time digital techniques
[REPT-86-014] 11 p1490 N88-18891
Interfacing of a microcomputer with a simultaneous atomic-emission spectrometer
[PB88-139571] 11 p1526 N88-19109
Development of a cryogenic stepping drive for ISO/LWS 14 p1878 N88-21220
Quantitative AES: The establishment of a standard reference spectrum for the accurate determination of spectrometer transmission functions
[NPL-DMA(A)-151] 14 p1887 N88-21279
Digital filter unit for selection of spectrometric information
[DE87-702990] 16 p2246 N88-23415
Spectral radiometry: Methods, measuring techniques, and applications --- conference
[PTB-OPT-24] 16 p2271 N88-23585
Spectrometry and spectral radiometry
16 p2271 N88-23586
Dispersive spectral apparatus
16 p2271 N88-23587
Heterodyne spectrometer for the very high frequency range between 300 and 3000 GHz (1 mm to 0.1 mm) using a mixer in open structure
16 p2271 N88-23589
Spectral radiation measurement using a photodiode array as receiver 16 p2271 N88-23591
A new fiber-optic-based phase-resolved phosphorescence spectrometer
[AD-A191325] 16 p2275 N88-23613
X-ray spectroscopic diagnostics on JIPPT-IIU and HELIOTRON-E 17 p2440 N88-24515
Automated spectrometric unit for the study of radiation characteristics of cosmic radiation aboard Prognoz-9 space stations 19 p2706 N88-26090
The XRD (X-Ray Diode) array, the grazing incidence spectrometer and the X-ray imaging camera on PBFA 2
[DE88-007282] 19 p2728 N88-26200
Scanning tunneling microscopy as a surface chemical probe
[AD-A192710] 21 p2909 N88-27263
Multifilter spectrometer (FEB) for microwave atmospheric sounder
[AD-A192312] 21 p2935 N88-27426
Nuclear magnetic resonance spectrometer
[AD-A192928] 21 p2950 N88-27523
Calibration of the portable wear metal analyzer
[AD-A192971] 21 p2950 N88-27524
Rapid-scanning Fourier transform spectrometer for studies of propagation of near-millimeter-wave radiation through clear air and fog
[AD-A193752] 22 p3070 N88-28219
Molecular fluorescence measurements with a charge-coupled device detector
[AD-A194437] 23 p3216 N88-29141

SPECTROMETRY
U SPECTROMETERS

SPECTROPHOTOGRAPHY
The calibration of photographic and spectroscopic films: Reciprocity failure and thermal responses of IIaO film at liquid nitrogen temperatures
[NASA-CR-181094] 13 p1773 N88-20606

SPECTROPHOTOMETERS
NT INFRARED SPECTROPHOTOMETERS
NT ULTRAVIOLET SPECTROPHOTOMETERS
Comparison of ground based and TOMS measurements of SO2 from volcanic emissions
05 p0618 N88-13795
NBS (National Bureau of Standards) measurement services: Spectral reflectance
[PB88-109905] 06 p0779 N88-14785
A new class of multiple dispersion grating spectrometers
[PREPRINT-569] 14 p1983 N88-21830
Ground-based facility for spectrophotometric studies of the airflow and aurora
[AP-29] 22 p3119 N88-28532
NBS (National Bureau of Standards) measurement services: The NBS photodetector spectral response calibration transfer program
[PB88-201595] 24 p3376 N88-30109

SPECTROPHOTOMETRY
NT STELLAR SPECTROPHOTOMETRY
High resolution electron and ion microscopy
[AERE-R-12502] 10 p1297 N88-17754
Electrochemical and optical investigations on ion-implanted TiO2 samples
[ETN-88-91485] 11 p1455 N88-18670
Spectrophotometric remote sensing of the diffuse aurora
[AD-A188599] 12 p1643 N88-19837
The type Ia supernova 1986G in NGC5128: Optical photometry and spectra
[INPE-4426-PRE/1230] 12 p1710 N88-20231
Development of high stability fiber optic spectrophotometric systems for study of solar/stellar magnetic activity
[AD-A189327] 13 p1852 N88-21088
Color fluctuations in the inner coma of Comet Halley as measured from VEGA-2 14 p2000 N88-21925
The evolution of CN emission in Halley's comet with heliocentric distance 14 p2006 N88-21961
Outburst of Halley's comet 14 p2007 N88-21967
Spectrophotometric observations of Comet Halley
14 p2007 N88-21972
Single-laboratory evaluation of SW-846 methods 7090/7091 determination of beryllium by flame and furnace atomic absorption spectrophotometry
[PB88-171434] 16 p2175 N88-22963
The dynamics of SBO galaxies. Part 1: The data
[SER-C-PREPUBL-FASC-22] 24 p3455 N88-30567

SPECTROPOLARIMETERS
U POLARIMETERS

SPECTRORADIOMETERS
Spectrometric test of a linear array sensor
[NASA-TM-100676] 01 p0064 N88-10414
AIS-2 radiometry and a comparison of methods for the recovery of ground reflectance
05 p0611 N88-13757
Characteristics of an Ebert monochromator for an infrared spectrometer in the wavelength range 1 micrometer to 15 micrometers
[AD-A186945] 09 p1166 N88-16991
Spectral radiometry: Methods, measuring techniques, and applications --- conference
[PTB-OPT-24] 16 p2271 N88-23585
Spectrometry and spectral radiometry
16 p2271 N88-23586
Differential spectral radiometry
16 p2272 N88-23594
Reflection standards for spectroradiometry. Realization and calibration 16 p2272 N88-23595
Ultraviolet radiometry: Radiation sources and measuring methods 16 p2272 N88-23596
Spectroradiometry in the industrial test laboratory
16 p2272 N88-23598
Spectroradiometry in meteorology
16 p2272 N88-23599
Spectroradiometry in industrial safety
16 p2272 N88-23600
Spectroradiometry in materials testing
16 p2273 N88-23601
Study of stereoradiometry on SPOT images
22 p3112 N88-28484

SPECTROSCOPES
U SPECTROMETERS

SPECTROSCOPIC ANALYSIS
Auger electron spectroscopy of oxidized titanium overlayers: Speciation of homoneneous and heterogeneous samples
[KFK-4221] 02 p0146 N88-10813
Chemical analysis for excimer laser systems
[DE88-001941] 05 p0580 N88-13591
Determination, by X-ray fluorescence, of platinum, palladium, ruthenium, iron and chromium in special steels
[PB87-132114] 06 p0683 N88-14183
Re-usable thin-layer spectroelectrochemical cell for non-aqueous solvent systems
[AD-A186951] 09 p1248 N88-17478
Method for sampling of methyl salicylate vapor in air using passivated stainless steel syringes and analysis by gas chromatography
[AD-A187838] 11 p1447 N88-18624
An experimental method for species concentration measurements in a welding arc using laser-induced fluorescence
[DE88-005638] 13 p1778 N88-20636
Computer program in BASIC language for computation of spectrochemical analytical data
[DE88-701229] 15 p2032 N88-22106
In situ spectroscopic studies of transition metal macrocycles as catalysts for the electrochemical reduction of oxygen
[PB88-203195] 20 p2769 N88-26416
Array detectors for plasma spectrochemistry
[AD-A194220] 22 p3052 N88-28105
Applications of charge transfer devices in spectroscopy
[AD-A194408] 23 p3192 N88-28992

SPECTROSCOPIC TELESCOPES
NT STRATOSCOPE TELESCOPES
Crystal diffraction lenses for imaging gamma-ray telescope
[DE88-003084] 08 p1083 N88-16529

SPECTROSCOPY
NT ABSORPTION SPECTROSCOPY
NT ASTRONOMICAL SPECTROSCOPY
NT AUGER SPECTROSCOPY
NT AURORAL SPECTROSCOPY
NT ELECTRON SPECTROSCOPY
NT FLAME SPECTROSCOPY
NT GAS SPECTROSCOPY
NT INFRARED SPECTROSCOPY
NT LASER SPECTROSCOPY
NT MAGNETIC SPECTROSCOPY
NT MASS SPECTROSCOPY
NT MOLECULAR SPECTROSCOPY
NT NUCLEAR RADIATION SPECTROSCOPY
NT OPTICAL EMISSION SPECTROSCOPY
NT PHOTOACOUSTIC SPECTROSCOPY
NT PHOTOELECTRON SPECTROSCOPY
NT RAMAN SPECTROSCOPY
NT SPECTROPHOTOGRAPHY
NT SPECTROPHOTOMETRY
NT SPECTROSCOPIC ANALYSIS
NT STELLAR SPECTROPHOTOMETRY
NT ULTRAVIOLET SPECTROSCOPY
NT X RAY SPECTROSCOPY
A CAMAC system controlled by an IBM AT computer for time-resolved spectroscopy
[DE87-010111] 01 p0080 N88-10514
Spectroscopic studies of shocked and detonating explosives
[DE87-014216] 02 p0155 N88-10972
Third-harmonic generation and multiphoton ionization spectroscopy
[DE87-013545] 03 p0281 N88-11769
Supercritical fluid chromatography/supersonic jet spectroscopy
[DE88-000297] 03 p0282 N88-11774
Spectroscopic and retrieval studies in support of SCRIBE (Stratospheric Cryogenic Interferometer Balloon Experiment)
[AD-A184037] 03 p0351 N88-12216
Interatomic Auger rates for the sodium fluoride crystal
[DE87-013012] 03 p0382 N88-12401
Doppler snapshots 04 p0508 N88-13125
Spectroscopic monitoring of RS CVn stars at Kitt Peak using the Penn State fiber optic echelle
04 p0509 N88-13127
H alpha and Ca II emission line variability of FK comae 04 p0509 N88-13128
Evidence for an additional source of opacity during the impulsive phase of stellar flares
04 p0510 N88-13133

Contemporaneous B,V,R,I photometry and H alpha spectroscopy of YY Gem 04 p0513 N88-13155

Applications of nonlinear hole burning spectroscopy
[AD-A184943] 05 p0587 N88-13580

Design of the Backscatter Spectroscopy System for the Nova Laser Facility
[DE88-001880] 07 p0859 N88-15214

USSR report: Physics and mathematics
[JPRS-UPM-87-002] 07 p0918 N88-15575

Raman spectroscopic investigations of Hg-Cd-Te melts 07 p0926 N88-15625

High-speed assembly language (80386/80387) programming for laser spectra scan control and data acquisition providing improved resolution water vapor spectroscopy
[NASA-CR-4117] 08 p1053 N88-16355

JPRS report: Science and technology. USSR: Physics and mathematics
[JPRS-UPM-87-009] 09 p1233 N88-17395

Product kinetic and internal energy distributions via velocity-aligned Doppler spectroscopy
[DE88-003510] 10 p1298 N88-17764

Overview of applications of Laser-Induced Breakdown Spectroscopy (LIBS)
[DE88-004314] 10 p1336 N88-17987

Spectroscopic studies of energy transfer in photosynthetic reaction centers of higher plants
[DE88-003850] 10 p1359 N88-18121

Rovibrational spectroscopy of ArCO van der Waals complex
[DE88-004291] 10 p1406 N88-18387

Soluble polysilane derivatives: Chemistry and spectroscopy
[AD-A187869] 11 p1461 N88-18713

Positron annihilation spectroscopy of AlGaAs/GaAs interfaces in MOCVD-grown GaAs heterojunction solar cells
[DE88-003903] 11 p1508 N88-19012

Multicomponent analysis using synchronous-excitation phase-resolved fluorescence spectroscopy
[AD-A188883] 12 p1606 N88-19604

Millimeter and submillimeter wave research: Spectroscopy, energy transfer, and techniques
[AD-A188952] 12 p1620 N88-19691

Advanced electron optics for vibrational spectroscopy
[AD-A188469] 12 p1629 N88-19747

An electrochemical and spectroscopic study of electrode systems
[AD-A189274] 13 p1737 N88-20384

Supercritical fluid chromatography/supersonic jet spectroscopy
[DE88-004438] 13 p1738 N88-20392

Coherence effects in optical physics with special reference to spectroscopy
[AD-A189520] 13 p1840 N88-21007

Development and evaluation of instrumentation and methods for multi-element analysis
[AD-A189345] 13 p1841 N88-21018

Measurement of species concentrations in flames by laser-induced fluorescence
[DE88-007096] 14 p1889 N88-21286

Optical cooling and trapping 14 p1974 N88-21782

Spectrographic detection of nitrogen impurity in helium
[DE88-752301] 15 p2033 N88-22111

Summary report on the Japan-US Workshop on the Assessment of Spectroscopic Data for Temperature and Density Measurements --- plasma diagnostics
[IPPJ-861] 17 p2439 N88-24512

Helium-like titanium spectra from tokamak plasmas
17 p2440 N88-24516

Spectroscopic study of heliotron E plasmas: Stark profile, CXR, poloidal rotation and carbon coating
17 p2441 N88-24523

Spectral diagnostics for temperature and density measurements on ATF 17 p2442 N88-24525

Spectroscopic data relevant to alpha particle diagnostics 17 p2442 N88-24527

Polarization spectroscopy: Prospect and data needs
17 p2443 N88-24531

Availability and quality of spectroscopic data and standards for tokamak studies 17 p2443 N88-24534

Reflectance spectroscopy in planetary science: Review and strategy for the future
[NASA-SP-493] 17 p2451 N88-24564

Optical diagnostics for a high power, rf-inductively coupled plasma
[DE88-007822] 18 p2579 N88-25322

Spectroscopy and energy transfer kinetics of the interhalogens
[AD-A192103] 18 p2583 N88-25344

XUV source for ultra-high resolution photoionization spectroscopy
[DE88-007531] 19 p2614 N88-25510

Supercritical fluid chromatography/supersonic jet spectroscopy
[DE88-007935] 19 p2614 N88-25511

Simultaneously time- and space-resolved spectroscopic characterization of laser-produced plasmas
[DE88-008038] 19 p2728 N88-26202

Velocity measurements and flow visualization in turbulent three-dimensional supersonic flows using oxygen flow tagging
[AD-A192551] 21 p2892 N88-27165

Optical diagnostics for metallurgical processes
[DE88-009255] 21 p2913 N88-27289

Calibration of the portable wear metal analyzer
[AD-A192971] 21 p2950 N88-27524

Use of Moessbauer spectroscopy to study implanted surfaces
[DE88-010452] 21 p3023 N88-27942

Recent advances in optical spectroscopy using high performance array detectors
[AD-A194219] 22 p3152 N88-28753

International ultraviolet explorer spectral atlas of planetary nebulae, central stars, and related objects
[NASA-RP-1203] 22 p3164 N88-28843

Determination of impurities in silicon carbide by ICP AES (inductively coupled plasma atomic emission spectrometry) after coprecipitation with lanthanum hydroxide
[NASA-TT-20332] 23 p3193 N88-29003

Electrochemical evaluation of the long term corrosion resistance of polymer coated steel
24 p3355 N88-29974

An electrochemical impedance spectroscopy study of reactions at the metal/coating interface
24 p3355 N88-29975

Ultrafast processes and spectroscopy with free electron lasers
[AD-A195248] 24 p3379 N88-30126

Observations of faint field galaxies
[NASA-CR-183251] 24 p3453 N88-30555

A deep redshift survey of field galaxies. Comments on the reality of the Butcher-Oemler effect
[NASA-CR-183255] 24 p3454 [illegible]0558

SPECTRUM ANALYSIS

NT CEPSTRAL ANALYSIS
NT FLAME SPECTROSCOPY
NT MAXIMUM ENTROPY METHOD

A work station for EXELFS data acquisition and analysis
[USIP-87-10] 01 p0078 N88-10498

Mathematics applied to nuclear geophysics
[INPE-4234-PRE/1109] 01 p0086 N88-10561

An application of L1 to astronomy --- stellar velocity
[REPT-87-10] 01 p0108 N88-10702

Design and development of a database for spectral data and analysis results
[DE87-011323] 02 p0247 N88-11564

Analysis of sideband spectra from untapered undulator using analytical technique
[DE87-014763] 04 p0448 N88-12778

Evidence for expanding magnetic loops in coronae of cool stars 04 p0510 N88-13134

Magnetic fields on K and M stars
04 p0510 N88-13137

A spectral survey of 26 G9-M6 flare stars in the solar neighborhood 04 p0512 N88-13149

Proceedings of the Third Airborne Imaging Spectrometer Data Analysis Workshop
[NASA-CR-181552] 05 p0611 N88-13755

Evaluation of AIS-2 (1986) data over hydrothermally altered granitoid rocks of the Singatse Range (Yerington) Nevada and comparison with 1985 AIS-1 data
05 p0613 N88-13767

Application of Vandermonde decomposition to directional and modal analysis of broadband transients
[AD-A185007] 05 p0646 N88-13956

Incoherent radar spectra 06 p0691 N88-14239

Discussion on the modelling and processing of signals from an acousto-optic spectrum analyzer
[AD-A185639] 06 p0694 N88-14257

Spectral and radiometric calibration of the Airborne Visible/Infrared Imaging Spectrometer
06 p0707 N88-14334

HOC spectral analysis of an almost periodic random sequence in noise
[AD-A185528] 06 p0765 N88-14697

Intracavity spectrum analyzer with NaF:F2(+):F3(-) crystal laser for long-wave IR wave band
07 p0919 N88-15584

Effect of multiplication of spectral components of multi-frequency lasing of pulsed tunable laser
07 p0920 N88-15586

HEAO-1 observations of gamma-ray bursts
07 p0947 N88-15756

Comparative analysis of ultraviolet observations of Halley's comet on ASTRON astrophysical station before and after perihelion 08 p1004 N88-16086

Spectral analysis of an orographically structured area in the forefield of mesoscale flow simulations
08 p1016 N88-16160

Orographically influenced cold fronts in a spectral approach 08 p1016 N88-16161

Mesospheric dynamics and chemistry from SME data
[NASA-CR-182465] 09 p1191 N88-17139

Nature and origin of mineral coatings on volcanic rocks of the Black Mountain, Stonewall Mountain, and Kane Springs Wash volcanic centers, Southern Nevada
[NASA-CR-181437] 09 p1191 N88-17140

Growth and characteristics of materials for tunable lasers in the near infrared spectral region
[NASA-CR-182501] 11 p1491 N88-18901

The 58th Shock and Vibration Symposium, volume 2
[NASA-CP-2488-VOL-2] 11 p1499 N88-18948

Dynamic substructuring for shock spectrum analysis using component mode synthesis
11 p1499 N88-18950

Regional wave attenuation and seismic moment from the inversion of NORESS spectra
[AD-A187399] 11 p1510 N88-19023

Applications and limitations of the spectral-analysis-of-surface-waves method
[PB88-136619] 11 p1513 N88-19038

Running head: What color is it
[NASA-CR-182600] 11 p1551 N88-19280

Spectral images and multi-component models of the chromospheres of AR Lacertae
11 p1568 N88-19384

High resolution infrared absorption spectra of various trace gases present in the upper atmosphere of the Earth
[NASA-CR-182590] 12 p1642 N88-19829

Microwave dielectric spectrum of rocks
[NASA-TM-89719] 12 p1642 N88-19831

Gradiometer mission spectral analysis and simulation studies: Past and future 12 p1645 N88-19851

Elemental composition of Venusian rocks in northeastern part of Terra Aphrodite (determined using data from Vega-2 landing module)
13 p1726 N88-20322

Analysis of hydrocarbon band 3.35 in spectrum of Halley's Comet using data from infrared spectrometer on Vega-1 spacecraft 13 p1727 N88-20327

Spectral contents readout of birefringent sensors
[NASA-CR-179430] 13 p1784 N88-20673

Stratospheric trace gas distributions from far infrared thermal emission spectroscopy
13 p1797 N88-20749

Planetary scale barotropic spectral model
13 p1801 N88-20766

Computer programs for calculating group cross-section covariances from uncertainty parameters in the ENDF/B-V format. UNC 32/33 --- neutron physics
[ECN-202] 13 p1837 N88-20995

Development and evaluation of instrumentation and methods for multi-element analysis
[AD-A189345] 13 p1841 N88-21018

On the interpretation of the 3 micron emission feature in the spectrum of Comet Halley: Abundances in Comet Halley and in interstellar matter
14 p2002 N88-21935

Optical and hydrodynamic implications of Comet Halley dust size distribution 14 p2003 N88-21939

Development of remote sensing techniques capable of delineating soils as an aid to soil survey
[NASA-CR-182610] 15 p2089 N88-22452

Spectral measurements in a disturbed boundary layer over snow
[AD-A190217] 15 p2097 N88-22494

Multiple object redshift determinations in clusters of galaxies using OCTOPUS
[INPE-4528-PRE/1278] 15 p2150 N88-22835

Multichannel 2-D power spectral estimation and applications
[AD-A191273] 16 p2191 N88-23068

Spectral analysis in the linear geodetic boundary value problem
[B8735056] 16 p2259 N88-23502

Spectral measurements for correcting LANDSAT data for atmospheric effects 17 p2353 N88-24020

Utilization of LANDSAT-TM , for aiding in the localization of archeological sites in the state of Sao Paulo
17 p2362 N88-24069

Study of reservoir water quality utilizing remote sensing techniques: Methodological concepts
17 p2364 N88-24076

Differential spectral synthesis of the stellar populations in the bulges of spiral galaxies 17 p2451 N88-24558

Studies of spectral line ratio fluctuations using Inductively Coupled Plasma (ICP) light
[IRF-PREPRINT-100] 18 p2578 N88-25311

Measurement of HO2 and other trace gases in the stratosphere using a high resolution far-infrared spectrometer at 28 KM
[NASA-CR-180400] 20 p2821 N88-26737

Multifilter spectrometer (FEB) for microwave atmospheric sounder
[AD-A192312] 21 p2935 N88-27426
Statistical analysis of dyadic stationary processes
[AD-A193057] 21 p3009 N88-27853
Array detectors for plasma spectrochemistry
[AD-A194220] 22 p3052 N88-28105
A wideband, high-resolution spectrum analyzer
22 p3066 N88-28194
ENSO, sea-surface temperatures and African rainfall
22 p3122 N88-28550
Backlund transformations associated with a Riemann-Hilbert spectral problem
[PREPRINT-596] 22 p3146 N88-28712
Qualitative characteristics of open waveguide resonator spectra
[DE88-702387] 23 p3202 N88-29056
Large aperture multi-dimensional laser radar testbed
[AD-A193447] 23 p3218 N88-29155
Surface composition of Mars: A Viking multispectral view 23 p3300 N88-29655
The optical spectroscopy of copper-blue luminescence in zinc sulfide crystals. Zero-phonon line spectra under the influence of magnetic field, temperature and excitation intensity
[ETN-88-93122] 24 p3344 N88-29903
Acoustooptic processing of two-dimensional signals using temporal and spatial integration
[AD-A194803] 24 p3359 N88-29999
Spectral analysis of the Elatina varve series
[NASA-CR-183085] 24 p3402 N88-30260

SPECULAR REFLECTION
Radiative heat transfer solutions in plane-parallel participating media: Application to multilayer insulations for space vehicles
[INPE-4221-PRE/1101] 08 p0962 N88-15824
Polymer reflectors research during FY86
[DE88-001101] 11 p1508 N88-19009
Deformation, fracture and explosive properties of reactive materials
[AD-A193080] 21 p2923 N88-27348
Solar energy absorption efficiency of an ellipsoidal receiver-reactor with specularly reflecting walls
[AD-A193726] 22 p3117 N88-28520

SPEECH
NT PHONETICS
NT SYLLABLES
NT WORDS (LANGUAGE)
Recognition of isolated non-speech sounds
[AD-A184600] 03 p0306 N88-11933
Studies of the processing of single words using positron tomographic measures of cerebral blood flow change
[AD-A184058] 03 p0356 N88-12244
Neural network based speech synthesizer: A preliminary report 08 p1064 N88-16429
Voice stress analysis 16 p2242 N88-23395
Time-frequency representations for speech signals
[AD-A188661] 18 p2498 N88-24819
Sinusoidal transform coding 19 p2653 N88-25752
Analysis and improvement of the vector quantization in SELP (Stochastically Excited Linear Prediction)
19 p2653 N88-25756
A cockpit natural language study: Vocabulary and grammar analyses
[AD-A193289] 21 p2993 N88-27753

SPEECH BASEBAND COMPRESSION
Speech coding at 4800 bps for mobile satellite communications 19 p2652 N88-25749

SPEECH DEFECTS
A study of the performance of automatic speech recognisers with speech impaired children
[RSRE-MEMO-4040] 01 p0076 N88-10486

SPEECH DISCRIMINATION
U SPEECH RECOGNITION

SPEECH RECOGNITION
A study of the performance of automatic speech recognisers with speech impaired children
[RSRE-MEMO-4040] 01 p0076 N88-10486
Language modelling for automatic speech recognition: A review
[RSRE-MEMO-4038] 01 p0084 N88-10544
Integrated voice and visual systems research topics
[NASA-CR-177417] 03 p0356 N88-12246
Controlling robots with spoken commands
[DE88-000537] 04 p0452 N88-12801
National Aeronautics and Space Administration (NASA)/American Society for Engineering Education (ASEE) Summer Faculty Fellowship Program, 1987. Volume 1
[NASA-CR-172009-VOL-1] 06 p0792 N88-14855
Digital signal processing algorithms for automatic voice recognition 06 p0793 N88-14862
Speech recognition: Acoustic-phonetic knowledge acquisition and representation
[AD-A185897] 07 p0840 N88-15097
Comparison of alphanumeric data entry methods for advanced helicopter cockpits
[AD-A186934] 09 p1201 N88-17201
Mathematical structures for speech recognition
[AD-A187063] 09 p1217 N88-17295
Voice technology using personal computers
[AD-A186743] 09 p1218 N88-17300
Speech recognition: Acoustic-phonetic knowledge acquisition and representation
[AD-A187293] 10 p1320 N88-17393
A two-stage isolated-word recognition system using discriminant analysis
[AD-A187425] 10 p1402 N88-18360
Voice/natural language interfacing for robotic control
[AD-A187765] 11 p1494 N88-18917
Evaluating the performance of the LPC (Linear Predictive Coding) 2.4 kbps (kilobits per second) processor with bit errors using a sentence verification task
[AD-A188573] 12 p1620 N88-19686
Spire based speaker-independent continuous speech recognition using mixed feature sets
[AD-A188834] 12 p1620 N88-19688
Northeast Artificial Intelligence Consortium (NAIC) administrative matters and ancillary functions, volume 1
[AD-A189466] 12 p1682 N88-20055
The acoustic-modeling problem in automatic speech recognition
[AD-A188529] 13 p1757 N88-20510
Perception of complex auditory patterns
[AD-A190218] 15 p2102 N88-22524
Auditory perception of complex sounds
[AD-A190528] 15 p2103 N88-22529
Algorithms and architectures for acoustic phonetical detection of continuous speech
[ENST-87E016] 16 p2189 N88-23054
Investigation of air transportation technology at Massachusetts Institute of Technology, 1986
17 p2293 N88-23716
Experiments in isolated digit recognition using the multilayer perceptron
[RSRE-MEMO-4073] 17 p2333 N88-23927
Experimental evaluation of algorithms for connected speech recognition using hidden Markov models
[RSRE-MEMO-4099] 17 p2333 N88-23928
ACSB: A minimum performance assessment
19 p2649 N88-25731
Novel nonlinear signal processing principles
[AD-A191644] 19 p2707 N88-26097
Signal processing in digital speech transmission systems
[ETN-88-92122] 20 p2792 N88-26561
A review of workload measurement in relation to verbal comprehension 21 p2925 N88-27360
Demodulation processes in auditory perception
[AD-A193421] 21 p2988 N88-27740
Survey of neural net paradigms for specification of discrete networks
[AD-A192682] 22 p3141 N88-28674
An overview of technology for spoken interaction with machines
[AD-A194153] 23 p3202 N88-29058
Effect of hypoxia on speech recognition in noise
[AD-A193943] 23 p3240 N88-29280
Hidden Markov models for automatic speech recognition: Theory and application
[RSRE-MEMO-4135] 23 p3251 N88-29350

SPEECHES
U LECTURES

SPEED
U VELOCITY

SPEED CONTROL
A simulation study of a speed control system for autonomous on-road operation of automotive vehicles
[AD-A184030] 03 p0362 N88-12279
The theory and implementation of a high quality pulse width modulated waveform synthesiser applicable to voltage FED inverters
[ETN-87-90712] 09 p1157 N88-16937
Speed control of a missile with throttleable ducted rocket propulsion 12 p1597 N88-19561
Contribution to speed regulation of small motors with phase-locked loops
[ETN-88-92373] 20 p2796 N88-26590
Reduction in mill air compressor power requirements through installation of a variable frequency speed control
[DE88-008493] 23 p3221 N88-29171

SPEED INDICATORS
NT TACHOMETERS

SPEED REGULATION
U SPEED CONTROL

SPEED REGULATORS
The design of a turboshaft speed governor using modern control techniques
[NASA-CR-175046] 01 p0053 N88-10339
Engine/airframe response evaluation of the HH-60A helicopter equipped with the T700-GE-701 transient droop improvement electronic control unit
[AD-A184443] 04 p0401 N88-12492
Contribution to speed regulation of small motors with phase-locked loops
[ETN-88-92373] 20 p2796 N88-26590

SPENT FUELS
Atlas of atomic spectral lines of neptunium emitted by an inductively coupled plasma
[DE88-000640] 06 p0782 N88-14796
Numerical computations of natural convection heat transfer in irregular geometries
[DE88-002358] 07 p0852 N88-15178

SPERMATOGENESIS
Investigations of the reproductive physiology of the rainbow trout (Salmo gairdneri Richardson)
07 p0885 N88-15370

SPHERES
NT CONCENTRIC SPHERES
NT FALLING SPHERES
NT ROTATING SPHERES
Development of response models for the Earth Radiation Budget Experiment (ERBE) sensors. Part 2: Analysis of the ERBE integrating sphere ground calibration
[NASA-CR-178293] 01 p0049 N88-10316
Division algebras and sphere fibrations
[ETN-87-90677] 01 p0087 N88-10566
Particle velocity and stress gage measurements in spherical diverging flow
[DE87-007333] 03 p0321 N88-12033
Dynamical analysis of molecular decay at spherical surfaces
[AD-A184908] 05 p0647 N88-13964
Nonuniformity of electromagnetic field at Lambda = 10.6 micron wavelength inside atmospheric aerosol particles
06 p0772 N88-14743
Assessment of anomalous gravitational field of elastic Earth 07 p0921 N88-15594
Application of a simple rotational spherical grating mounting to high resolution soft X-ray spectroscopy
[PB87-164836] 09 p1142 N88-16845
Light absorption by an atom moving inside a spherical box
[AD-A187241] 10 p1407 N88-18395
The application of the hybrid iterative method to scattering by perfectly conducting bodies of revolution
11 p1475 N88-18802
A program for the calculation of radio-wave transmission loss over the spherical earth and over obstacles
12 p1616 N88-19662
Simulated impact damage in a thick graphite/epoxy laminate using spherical indenters
[NASA-TM-100539] 13 p1733 N88-20363
Distribution of chain ends inside the polybutadiene microspheres of SB diblock copolymers
[AD-A191257] 16 p2182 N88-23007
The structure and stability of spherically expanding flames 17 p2318 N88-23842
Theoretical predictions of precipitate shapes in cubic alloys
[DE88-010856] 21 p2914 N88-27291
Light scattering by charged spheres
[AD-A193753] 22 p3153 N88-28759
Elastic behavior of a rubber layer bonded between two rigid spheres
[AD-A193698] 23 p3198 N88-29030
Effects on the resonant frequencies caused by loading a spherical cavity with a dielectric sphere
[AD-A193864] 23 p3277 N88-29511

SPHERICAL COORDINATES
Density variations of meteor flux along the Earth's orbit 06 p0739 N88-14545
Hyperspherical coordinate theory of two-electron processes: Future plans
[DE87-010653] 08 p1081 N88-16516
Generation of surface grids through elliptic partial differential equations for aircraft and missile configurations
[AD-A186631] 11 p1535 N88-19169
Adiabatic representation of three-body problem in hyperspherical coordinates. Statement of the problem
[DE88-701162] 15 p2126 N88-22678
A formulation for the boundary-layer equations in general coordinates
[NASA-TM-100079] 18 p2459 N88-24600
An improved spherical earth diffraction algorithm for SEKE
[AD-A195847] 24 p3360 N88-30005

SPHERICAL HARMONICS
Atlas of wide-field-of-view outgoing longwave radiation derived from Nimbus 7 Earth radiation budget data set - November 1978 to October 1985
[NASA-RP-1186] 01 p0070 N88-10451
Ab initio methods for electron-molecule collisions
[DE87-011728] 01 p0092 N88-10596

Spherical harmonic expansion of the Levitus Sea surface topography
[NASA-CR-181448] 02 p0216 N88-11362
Statistics of the geomagnetic secular variation for the past 5Ma
[NASA-CR-181558] 04 p0467 N88-12890
Rotation of magnetized particle in electrically conducting viscous medium 06 p0770 N88-14733
Modeling and estimation of a low degree geopotential model from terrestrial gravity data
[NASA-CR-182808] 16 p2232 N88-23330

SPHERICAL PLASMAS
Stability of spheroidal spheromak plasma by use of force-free approximation
[IPPJ-846] 02 p0241 N88-11523

SPHERICAL SHELLS
Geometrically nonlinear rod mechanism analogy of axisymmetrically loaded spherical shells based on a comprehensive approach to the stability of circular arches
[ETN-87-90419] 01 p0062 N88-10398
Microgravity nucleation and particle coagulation experiments support
[NASA-CR-181541] 04 p0423 N88-12619
RADSPHERE: A computer program for calculating the steady-state, axially symmetric, forced response and radiation field of a submerged spherical shell
[AD-A185025] 05 p0609 N88-13738
A vectorized Poisson solver over a spherical shell and its application to the quasi-geostrophic omega-equation
[NASA-CR-4116] 08 p1039 N88-16285
Retarded potential technique applied for shock wave loading of doubly symmetric submerged structures
09 p1179 N88-17058
Cubic spline solution of symmetric buckling problems of clamped shallow spherical shells
15 p2053 N88-22239
Method and apparatus for growing crystals
[NASA-CASE-MFS-28137-1] 17 p2446 N88-24544

SPHERICAL TANKS
Mass transport in annular spherical system
[LRT-WE-9-FB-11(1987)] 22 p3077 N88-28271
Orbital Propulsion Module (OPM) Study on coni-spherical surface tension tanks (COSTA)
[MBB-URV-170/87] 23 p3187 N88-28963

SPHEROIDS
NT OBLATE SPHEROIDS
NT PROLATE SPHEROIDS

SPHEROMAKS
Acceleration to hypervelocities using minimum energy concepts
[DE87-011796] 01 p0089 N88-10583
Stability of spheroidal spheromak plasma by use of force-free approximation
[IPPJ-846] 02 p0241 N88-11523
Magnetohydrodynamic stability of spheromak plasma in toroidal flux conserver with rectangular cross section 3. Stability for symmetric modes
[IPPJ-845] 02 p0241 N88-11524
Reversed field pinch experiments: Summary of progress report
[DE86-002367] 07 p0934 N88-15673
Stability of spheromak against current driven modes: Effects of flux hole on stability
[IPPJ-868] 19 p2730 N88-26211

SPICULES
Active region flows 02 p0255 N88-11611

SPIKE ANTENNAS
U MONOPOLE ANTENNAS

SPIKING
Distributed feedback effects in lasers and high gain laser instabilities in optically pumped CH3F
03 p0329 N88-12079

SPILLING
Products of the neutralization of hydrazine fuels with hypochlorite, 2
[DE87-011454] 01 p0030 N88-10193
Hydrocarbon fuel spill dispersion on water: Literature review
[AD-A192486] 21 p2922 N88-27346

SPIN
NT ELECTRON CAPTURE
NT ISOTOPIC SPIN
NT NUCLEAR SPIN
NT PARTICLE SPIN
NT SPIN-SPIN COUPLING
Gravitational interaction of massless fields with higher spins (s greater than 2) 06 p0775 N88-14760
ISTP SBIR phase 1 Full-Sky Scanner: A feasibility study
[NASA-CR-180749] 10 p1333 N88-17964
Spin precession in stationary gravitational fields
[DE88-701107] 15 p2093 N88-22470
Effective electron interactions due to virtual charge and spin excitations in an extended Hubbard model for Cu-O superconductors
[DE88-005971] 15 p2139 N88-22766
Refractory films from spin-cast carbon
[DE88-011251] 21 p2919 N88-27327

SPIN DYNAMICS
Laminar flow over a spinning projectile at an angle of attack 02 p0121 N88-10766
Plasmon resonance absorption in layered structures of silver with periodic corrugation
[DE87-013183] 02 p0231 N88-11453
Torsion as a source of expansion in a Bianchi type I universe in the self-consistent Einstein-Cartan theory of a perfect fluid with spin density
[AD-A184200] 03 p0322 N88-12037
Fundamental properties of spin-polarized quantum systems
[DE88-004425] 10 p1423 N88-18499
Investigation of the spin stability of the NPS (Naval Postgraduate School) mini-satellite (Orion)
[AD-A187781] 11 p1445 N88-18613
Laser measurements of state-resolved Ga and in atom sticking and desorption on metal and semiconductor surfaces
[AD-A187644] 11 p1555 N88-19310
Can the causal pathologies of Goedel-type universes be avoided in higher-derivative gravity
[DE88-700185] 11 p1568 N88-19387
The effect of combustion gas flow on the rotational dynamics of a spinning solid fuel rocket
13 p1732 N88-20358
Fluid motion in a spinning, coning cylinder via spatial eigenfunction expansion
[AD-A190758] 15 p2066 N88-22319
Energy transfer processes in free radicals: A collaborative experimental and theoretical investigation
[AD-A191264] 16 p2269 N88-23578
Raychaudhuri equation in the self-consistent Einstein-Cartan theory with spin-density
[NASA-TM-101145] 17 p2447 N88-24546
Inflation in Einstein-Cartan theory with energy-momentum tensor with spin
[NASA-TM-101164] 17 p2447 N88-24547
A scientific basis for an alternate cathode architecture
[AD-A191498] 18 p2481 N88-24717
Theoretical investigation of the development of the normal fluid and superfluid velocity distributions during spin-up for a He2-filled cylinder
[MPIS-6/1987] 18 p2510 N88-24892
Dynamics of satellites with radial wire antennas
20 p2784 N88-26514
Properties of synthetic magnetic superlattices
20 p2865 N88-27014
A method for reducing the coning of a spinning vehicle
[DE88-010971] 21 p2896 N88-27189
Contribution to the numerical solution of airplane spin motion
[ETN-88-92368] 21 p2896 N88-27190
Dissolution rates of polymers and copolymers based on methyl, ethyl and butyl methacrylate
[AD-A194713] 23 p3197 N88-29027
Passage of relativistic magnetic dipole moments through magnetic fields
[DE88-702640] 23 p3295 N88-29624
Resonant spin-flavor precession of solar and supernova neutrinos
[DE88-752604] 23 p3308 N88-29707

SPIN GLASS
Nonlinear relaxation and ergodicity breakdown in random anisotropy spin glasses
[PREPRINT-565] 06 p0764 N88-14693
Superconductive analogue of spin glasses
[DE88-702059] 19 p2733 N88-26233

SPIN REDUCTION
Seven year thermal vacuum real life test of a medium speed (despin) mechanism manufactured by Dornier System
[ESA-ESTL-64] 09 p1175 N88-17038

SPIN RESONANCE
Nuclear structure studies at intermediate energies
[DE88-006683] 18 p2571 N88-25271
Paramagnetic spins in oxygen-loaded ceramic La2CuO4/sub 4 + delta/
[DE88-007114] 19 p2619 N88-25539

SPIN STABILIZATION
Effect of void gas lying between fluid slugs in nutation dampers 03 p0319 N88-12015
Country plans three-axis weather satellite
06 p0688 N88-14218
Attitude dynamics for satellites stabilized through spin
[INPE-4403-NTE/275] 08 p0963 N88-15833
Control and stabilization of ESA satellites
09 p1124 N88-16734
Investigation of the spin stability of the NPS (Naval Postgraduate School) mini-satellite (Orion)
[AD-A187781] 11 p1445 N88-18613
Separation dynamics for the last stage of a launch vehicle and satellite
[INPE-4281-PRE/1153] 12 p1601 N88-19582
Modeling of a nutation damper for satellite stabilization through rotation
[INPE-4275-PRE/1147] 12 p1601 N88-19584
Identification of a star field from a spinning satellite
[CNES-NT-120] 15 p2026 N88-22074
Development of a digital sun sensor for a spin-stabilized satellite
[INPE-4508-TDL/327] 16 p2169 N88-22929
Dynamics of satellites with radial wire antennas
20 p2784 N88-26514
A method for reducing the coning of a spinning vehicle
[DE88-010971] 21 p2896 N88-27189
Simulation of attitude and maneuvers for the Brazilian spin-stabilized satellite
[INPE-4271-PRE/1143] 22 p3046 N88-28079
Computational aerodynamic analysis for a range-limited 25mm training round
[AD-A185270] 24 p3320 N88-29772

SPIN TEMPERATURE
Spin disorder resistivity and bare Curie temperature in the ferromagnetic superconductor ErRh4B4
[DE88-003016] 10 p1415 N88-18445

SPIN WAVES
U MAGNONS

SPIN-LATTICE RELAXATION
Nuclear magnetic resonance studies of ion motion in solid electrolytes
[DE87-014547] 02 p0232 N88-11464
Nonlinear relaxation and ergodicity breakdown in random anisotropy spin glasses
[PREPRINT-565] 06 p0764 N88-14693
Transport and relaxation processes in supercritical fluids
[DE88-004804] 10 p1419 N88-18474
Nuclear magnetic ordering and paramagnetic relaxation of diatomic molecules in Ca (OH)2
[B8681469] 23 p3281 N88-29532
Static and dynamic behavior of a quasi one-dimensional Heisenberg antiferromagnet in the long-range ordered state. A nuclear magnetic resonance study performed with a He3-He4 dilution refrigerator
[B8705564] 23 p3281 N88-29533
Fluctuation and relaxation phenomena studied by means of nuclear orientation
[B8679671] 23 p3281 N88-29534

SPIN-ORBIT INTERACTIONS
NT ELECTRON CAPTURE

SPIN-SPIN COUPLING
Example of correlation between space and spin coordinates
[DE87-703366] 05 p0657 N88-14030

SPINAL CORD
Neuropeptides in experimental head injury
[AD-A188067] 11 p1520 N88-19077
Effect of low-frequency whole-body vertical vibration on the serotoninergic system of the brain and spinal cord
19 p2704 N88-26081

SPINEL
Aluminum oxynitride spinel (ALON): A review
[AD-A184753] 03 p0294 N88-11845
Precipitation in alumina-rich spinel: A transformation-toughened ceramic single crystal
[DE87-012380] 06 p0785 N88-14815
The migration of grain boundaries in ceramic materials with particular reference to the sintering process
[DE88-004085] 10 p1306 N88-17808
Research on high-specific-heat dielectrics
[AD-A187248] 11 p1461 N88-18710

SPIRAL GALAXIES
NT ANDROMEDA GALAXY
NT BARRED GALAXIES
NT MILKY WAY GALAXY
Comments on H. Arp The persistent problem of spiral galaxies
[TRITA-EPP-87-05] 05 p0660 N88-14052
Infrared emission and tidal interactions of spiral galaxies 07 p0923 N88-15611
The radio structure of active nuclei in edge-on spiral and Seyfert galaxies 09 p1264 N88-17576
Global properties of star formation in spiral galaxies
14 p1994 N88-21883
Molecular gas in Virgo cluster spiral galaxies
17 p2450 N88-24557
Surface photometric investigations for spiral galaxies of large dimension structures in edge-on gemetry
[ETN-88-92126] 21 p3030 N88-27985
The dynamics of SBO galaxies. Part 1: The data
[SER-C-PREPUBL-FASC-22] 24 p3455 N88-30567

SPLASHING
Numerical simulation of splash of droplet at unit gravity 05 p0538 N88-13275
SPLEEN
Spleen lymphocyte nucleic acids in pregnant rats flown in space and their offspring 07 p0892 N88-15403
SPLINE FUNCTIONS
The use of splines in the modelling of a photodiode response
[NPL-DITC-88/87] 01 p0085 N88-10550
An adaptive subdivision method with crack prevention for rendering beta-spline objects
[AD-A184249] 04 p0477 N88-12940
Stability properties of spline approximations for retarded systems
[PB87-220919] 05 p0639 N88-13910
The Wilson-Fowler spline in a global IGES (Initial Graphics Exchange Specification) coordinate frame
[DE88-001942] 06 p0757 N88-14640
Solution in vibration problems of rectangular plates with spline function
[PB87-143459] 08 p0996 N88-16029
Strategies for knot placement in least squares data fitting by splines
[NPL-DITC-101/87] 09 p1229 N88-17366
The NPL data approximation subroutine library: Current and planned facilities
[NPL-DITC-104/87] 14 p1959 N88-21681
A spline collocation method for integral equations of the first kind with logarithmic singularity --- boundary value problems
[REPT-87-39] 14 p1963 N88-21712
Cubic spline solution of symmetric buckling problems of clamped shallow spherical shells
15 p2053 N88-22239
Application of spline functions to digital image processing
[ETN-88-92194] 17 p2392 N88-24218
Open or closed curves by regularized B-splines
[RR-652-M] 18 p2563 N88-25218
SPLINES
Knot selection for least squares thin plate splines
[AD-A185681] 06 p0759 N88-14657
Core spline method for solution of quantum-mechanical systems of differential equations for bound states
[DE88-700492] 09 p1259 N88-17551
Procedure for converting a Wilson-Fowler spline to a cubic B-spline with double knots
[DE88-008971] 20 p2844 N88-26878
SPLITS (GEOLOGY)
U GEOLOGICAL FAULTS
SPLITTING
A survey of upwind principles for the multidimensional Euler equations 08 p0984 N88-15953
Schwarz splitting and template operators
[AD-A187956] 10 p1404 N88-18370
The splitting of Comet Halley 1986
14 p2010 N88-21989
Fully implicit splitting method for accurate tidal computations
[PB88-183637] 20 p2828 N88-26781
SPOILERS
A numerical procedure for conformal mapping of the exterior of a circle onto the exterior of a wing profile with a spoiler
[ISL-R-110/86] 11 p1536 N88-19180
Air-jet spoiler
[BU-364] 13 p1722 N88-20299
Theoretical and experimental investigations of a vortex drag behind a wing profile with spoiler
[ISL-PU-309/87] 21 p2892 N88-27169
Investigations of aircraft control with jet spoilers
[ISL-R-112/87] 21 p2898 N88-27202
SPONGES (MATERIALS)
The origin of the spicule skeleton of fresh water sponges (Spongillides) 07 p0885 N88-15388
SPONTANEOUS COMBUSTION
Fire tests on loose-fill insulation materials
[DE88-751182] 11 p1467 N88-18748
SPONTANEOUS EMISSION
Effect of off-axis radiation in amplified spontaneous emission
[DE88-007001] 14 p1915 N88-21440
Investigation of ultrashort traveling-wave amplified spontaneous emission 16 p2187 N88-23040
SPORADIC E LAYER
An analysis of apparent-motion vectors in, and the structure of, A mid-latitude sporadic E layer using a 2.66 MHz radar
[AD-A186126] 07 p0877 N88-15321
SPORADIC METEOROIDS
Models of sporadic meteor body distributions
06 p0739 N88-14543
Lidar investigations of M-zone
06 p0741 N88-14558
Optical electronics for meteor observations
06 p0741 N88-14559
SPORES
NT MICROSPORES
SPOT (FRENCH SATELLITE)
SPOT 1: First In-Flight Results --- conferences
[ISBN-2-85428-177-2] 03 p0340 N88-12143
Development of the SPOT commercial service: Preliminary conclusions after six months of operations
03 p0340 N88-12144
Satimage and the Nordic SPOT market
03 p0340 N88-12145
SPOT Image Corporation: Early results
03 p0340 N88-12146
The Canadian SPOT program
03 p0340 N88-12147
First assessment of processing and use of SPOT images by the Institut Geographique Nationale --- French National Geographic Institute 03 p0341 N88-12148
Results of the satellite and the Toulouse (France) receiving station operator --- SPOT
03 p0341 N88-12149
Signal to noise ratios --- SPOT images
03 p0341 N88-12150
Detector normalization --- SPOT remote sensors
03 p0341 N88-12151
Absolute and interband calibration --- SPOT
03 p0341 N88-12152
Modulation transfer function --- SPOT
03 p0341 N88-12153
Intrinsic and extrinsic geometric quality --- SPOT images 03 p0341 N88-12154
Registration of SPOT images
03 p0341 N88-12155
Evaluation of SPOT stereoscopic possibilities for cartography 03 p0342 N88-12156
Feasibility study of a range of products drawn from SPOT satellite imagery and specific to road-laying studies
03 p0342 N88-12157
Adaptation of numerical SPOT data to an urban environment 03 p0342 N88-12158
Cartography and topography with SPOT
03 p0342 N88-12159
Vegetation classification, land systems and mapping using SPOT multispectral data: Preliminary results
03 p0342 N88-12160
SPOT for earthquake hazard zoning in southern Italy, a provisional report 03 p0342 N88-12161
Flood monitoring using SPOT
03 p0342 N88-12162
Application of SPOT-1 data to mineral exploration in Nevada 03 p0343 N88-12163
Geological interpretation of a SPOT image over Kenya: The Gregory rift network of faults
03 p0343 N88-12164
Evolution of remote sensing utilization in geological mapping and ore exploration: Example in Zimbabwe
03 p0343 N88-12165
Vegetation studies in the national Park of Comoe (Ivory Coast) using SPOT 1 satellite data
03 p0343 N88-12166
SPOT data for crop discrimination in southern Brazil
03 p0343 N88-12169
SPOT: A tool for agricultural statistics
03 p0344 N88-12170
Application of multitemporal SPOT data for crop monitoring: Effects of frost and drought
03 p0344 N88-12171
Use of SPOT panchromatic imagery to update forest maps of northern Quebec, Canada
03 p0344 N88-12172
Stand based forest inventory from SPOT IMAGE. First experiments 03 p0344 N88-12173
Applicability of SPOT for forest inventory, mapping and change monitoring 03 p0344 N88-12174
Use of SPOT images for coastal development and inventory of aquacultural sites in New Caledonia (ALIAS project). First results 03 p0344 N88-12175
Contribution of SPOT data to the physiographic study of coastal environment: La Pointe d'Arcay and l'Anse de l'Aiguillon (France) 03 p0344 N88-12176
Coastal dynamics of the mouth of the Saloum (Senegal) --- SPOT imagery 03 p0345 N88-12177
The new generation of SPOT satellites
03 p0345 N88-12178
The use of SPOT images for water resources surveys. The examples of the Kasserine area (Tunisia) and the Jebel Amour (Algeria) 03 p0345 N88-12179
National Point Of Contact (NPOC)-SPOT inquiry 1986
[NLR-MP-86055-U] 05 p0620 N88-13807
The SPOT solar array. Box opening mechanisms physical vapor deposition (PVD)-MoS2: Lubricated slides. Functional evaluation 14 p1876 N88-21211
High lifetime mechanisms implemented in infrared horizon scanning sensors --- SPOT
14 p1877 N88-21214
Radio frequency compatibility between IRS and SPOT 3: Preliminary study
[CNES-86/CT/DRT/TIT/TR/011]
14 p1905 N88-21380
Terrain classification using SPOT images and the computer system GOP-300
[FOA-C-20677-2.7] 17 p2368 N88-24102
Bathymetry estimation by analyzing swell on SPOT images 19 p2701 N88-26062
Contribution of spaceborne high resolution radiometers to mapping of precoastal depths
19 p2701 N88-26063
SPOT 1 Image Utilization, Assessment, Results
[ISBN-2-85-428188-8] 22 p3089 N88-28346
The contribution of remote sensing to hydrology and hydrogeology 22 p3090 N88-28347
Mapping of streamflow and soil infiltration of a Sahelian catchment area by SPOT image interpretation: The Oursi pond catchment area in Burkino Faso
22 p3090 N88-28348
The use of SPOT images for water resources surveys in the Kasserine Basin (Tunisia)
22 p3090 N88-28349
SPOT image exploitation for glacial mass balance fluctuation monitoring in the French Alps
22 p3090 N88-28350
SPOT on land and lakes in the Hubei Province (China)
22 p3090 N88-28351
Evaluation of SPOT imagery for monitoring irrigated lands 22 p3090 N88-28352
An evaluation of SPOT imagery for wetland monitoring
22 p3091 N88-28353
Comparative study of crop and soil mapping using multitemporal and multispectral SPOT and LANDSAT data 22 p3091 N88-28354
Water resources and agricultural land use investigations in northeastern Gujarat (India) 22 p3091 N88-28355
Study of the forests on the banks of the Gambia and criteria for detecting mortality 22 p3091 N88-28356
Use of SPOT satellite in agrohydrology: Detection of spring water excess in a grassland region
22 p3091 N88-28357
Review of the studies of geography and environment and studies on spectral characteristics of SPOT HRV data 22 p3091 N88-28358
Evaluation of the grassy biomass in the Sahelian zone in the South Tamesna region (Niger): Prospects and limits of use of SPOT data 22 p3092 N88-28359
Changes in species composition of heathland, monitored by means of remote sensing and field mapping: The results of the HEISPOT project 22 p3092 N88-28360
Topography of an Antartic ice stream
22 p3092 N88-28361
Spatial and spectral registration of Javanese landscape units with SPOT 22 p3092 N88-28362
Comparison between the respective contributions of the TM LANDSAT-4 and HRV SPOT-1 data to the land use mapping of Mediterranean coastal zone
22 p3092 N88-28363
Land use systems and rural landscapes in the center of Veracruz State (Mexico): First results
22 p3092 N88-28364
SPOT for earthquake hazard zoning in southern Italy
22 p3093 N88-28365
Discrimination of sand transport rates and environmental consequences in central Egypt from SPOT data
22 p3093 N88-28366
Delineation of ephemeral fluvial networks on low-relief Piedmont surfaces, Plutonium Valley, Nevada, USA
22 p3093 N88-28367
Following the seasonal evolution of a natural environment in a humid tropical region. Preliminary Evaluation of SPOT (PEPS) number 186: Bangui, Central Africa 22 p3093 N88-28368
Application of SPOT to agricultural information systems in temperate regions 22 p3093 N88-28369
Potential use of SPOT satellite data for the national resources inventory 22 p3093 N88-28370
Methodological developments on crop inventories using SPOT and ground surveys 22 p3094 N88-28371
Evaluation of annual crop surfaces and territorial inventory in the Paris basin by combining classic statistical inquiries and SPOT data (Preliminary Evaluation Program for SPOT 127) 22 p3094 N88-28372
Evaluation of automatic texture analysis for increased crop identification accuracy with SPOT data
22 p3094 N88-28373
Application of SPOT multidate data to wheat yield estimation in Beauce (France) 22 p3094 N88-28374
An evaluation of multidate SPOT data for agriculture and land use mapping in the United Kingdom
22 p3094 N88-28375
The suitability of SPOT imagery for monitoring landscape patterns 22 p3094 N88-28376

Characterization, topology, and cartography of grasslands for the development of fodder resources (Preliminary Evaluation Program for SPOT number 26) 22 p3095 N88-28377

HRV data for the applications on reneweable resources in Canada --- SPOT 22 p3095 N88-28378

SPOT-1 HRV data and vegetation amount 22 p3095 N88-28379

Attempt to inventory vines using oblique SPOT images 22 p3095 N88-28380

Analysis of soils using remote sensing information at the scale of the parcel 22 p3095 N88-28381

Comparative variations of spectral signatures in a cultivated area of the Paris Basin (27 May, 26 June, 1 July 1986) 22 p3095 N88-28382

Monitoring of agricultural production in West Africa. The need to integrate different satellite platforms 22 p3096 N88-28383

Use of SPOT imagery for vegetation/biomass mapping, geotechnical mapping, catchment area determination, and settlement location in the Turkana district, northern Kenya 22 p3096 N88-28384

Digital and visual analysis of SPOT and TM data for crop discrimination in southern Brazil 22 p3096 N88-28385

A comparative thematic mapping analyses of SPOT data: The Vientiane Plain (Lao PDR) 22 p3096 N88-28386

Discrimination methods of traditional fields in a humid tropical region (Shaba, Zaire) using digital classification on SPOT data 22 p3096 N88-28387

Evaluation of SPOT data for crop inventory and monitoring in Sudanian Africa. Example of Bane area (Burkina Faso) 22 p3096 N88-28388

Identification of farming systems in the cotton area of West Burkina Faso from SPOT-1 data 22 p3097 N88-28389

Monitoring Tunisia's steppes with SPOT 22 p3097 N88-28390

Study of savannah formation in the Sudanian zone. Northwest sector of the La Comoe park, Ivory Coast 22 p3097 N88-28391

Pilot study of rice culture in sub-tropical high population density region (Madagascar) with SPOT 1 multispectral data 22 p3097 N88-28392

Using SPOT HRV data to update the distribution of the paddy field in Taiwan 22 p3097 N88-28393

Agro-ecological mapping from SPOT 1 data in southern Thailand: New questions for an analysis of the farming-systems 22 p3097 N88-28394

SPOT applications on Columbia's coffee zone 22 p3097 N88-28395

Use of SPOT data in preliminary steps of road project studies especially suited for developing countries 22 p3098 N88-28396

SPOT imagery for detecting residential expansion on the rural-urban fringe of Toronto, Canada 22 p3098 N88-28397

Spread of large tropical conurbations 22 p3098 N88-28398

Utilization of remote sensing for the observation of urban populations. Ongoing research in Quito (Ecuador) 22 p3098 N88-28399

Integration of SPOT data into a geocoded information system 22 p3098 N88-28400

Utilizing SPOT data for seismic shot-line mapping and environmental monitoring in oil and gas exploration 22 p3098 N88-28401

Preliminary comparative analysis of LANDSAT and SPOT data for the study of the sanding phenomenon: Zaafrane region (Algeria) 22 p3099 N88-28402

An evaluation of the applicability of SPOT stereoscopic imagery to the Canada Land Use Monitoring Program (CLUMP) 22 p3099 N88-28403

Topographic suppression and advances in classification for land cover mapping using SPOT-1 HRV imagery 22 p3099 N88-28404

Monitoring Moneragala (Sri Lanka) with SPOT imagery 22 p3099 N88-28405

Monitoring urban land cover changes at the urban fringe from SPOT HRV imagery in south-east England 22 p3099 N88-28406

Preliminary analyses of SPOT HRV multispectral products for arid and temperate environments 22 p3099 N88-28407

Assessment of SPOT satellite based system in humid tropical vegetation identification, classification and monitoring 22 p3100 N88-28408

A comparison between SPOT and LANDSAT TM for mapping of vegetation and bedrock outcrops 22 p3100 N88-28409

Accuracy of land use classification for SPOT image data 22 p3100 N88-28410

Analysis of SPOT multispectral data concerning a border zone between two geographical regions in southern Belgium 22 p3100 N88-28411

Thematic mapping of central Java (Indonesia) 22 p3100 N88-28412

Utilization of SPOT-1 multispectral data for mapping land cover and phytohygiene monitoring in the central zone of the Mercantour National Park (France) 22 p3100 N88-28413

Applications of SPOT data for urban real estate investment information systems 22 p3101 N88-28414

Mapping and urban multi-experimental assessment of SPOT: Urban results 22 p3101 N88-28415

SPOT-1 over New Zealand: Analysis of SPOT imagery for land use investigations 22 p3101 N88-28416

Comparison of SPOT, LANDSAT TM and combined data for urban studies 22 p3101 N88-28417

Utilization of SPOT multispectral data for urban planning 22 p3101 N88-28418

First results of international investigations of the applications of SPOT-1 data to geologic problems, mineral and energy exploration 22 p3101 N88-28419

Rate of slip on the Altin Dagh Fault (North Tibet, China) 22 p3102 N88-28420

Karst and submarine fresh water discharge in the Antalya area, southern Turkey 22 p3102 N88-28421

Results of the Geosat program to evaluate SPOT data for petroleum and mineral exploration 22 p3102 N88-28422

The application of SPOT data to the structural geology of western Nevada 22 p3102 N88-28423

Application SPOT-1 data to mining activity: Example of the Imiter Silver Mine, Morocco 22 p3102 N88-28424

Evaluation of SPOT imagery contribution to petroleum exploration: The Suez Rift (Egypt) 22 p3102 N88-28425

Evaluation of SPOT imagery for discriminating vegetation communities associated with surficial and bedbrock geology and identifying anomalous and stressed vegetation associated with mineralization 22 p3103 N88-28426

SPOT imagery as an aid to understanding volcanism and tectonics: Examples from the Chilean Andes and the Tibetan Plateau 22 p3103 N88-28427

Role of SPOT in geological application of remote sensing 22 p3103 N88-28428

SPOT imagery preliminary contribution to cartography and geodynamics in the Benue trough (Nigeria) 22 p3103 N88-28429

An evaluation of SPOT imagery for Earth science studies in the Antarctic. Preliminary Evaluation Program (PEPS) 289 for SPOT 22 p3103 N88-28430

Structural analysis of the Jura mountains-Rhine Graben intersection (Switzerland) for petroleum exploration using SPOT stereoscopic data 22 p3103 N88-28431

Methodology for the use of SPOT imagery in petroleum exploration. Example of the Bas-Languedoc area (France) 22 p3104 N88-28432

Analyzing the stratigraphy, tectonism, and mineralization at the Spanish side of the pyrite belt, Huelva province, Spain, using SPOT imagery 22 p3104 N88-28433

Geologic applications of SPOT-1, TM, and NOAA-7 data: Finding and defining unmapped structural features 22 p3104 N88-28434

Comparing different images for ground water survey based on lineament analysis 22 p3104 N88-28435

Spectral and spatial attribute evaluation of SPOT data in geological mapping of precambrian terrains in semiarid environment of Brazil 22 p3104 N88-28436

Geologic results obtained from the use of SPOT imagery along plate boundaries: Examples in the East African rift and of the northern-Caribbean collision 22 p3105 N88-28437

SPOT images and geochemical mapping of lateritic covers in southern Mali 22 p3105 N88-28438

Analysis of the multispectral content and of SPOT subscenes in two regions of Burundi. Lithologic and tectonic interpretations 22 p3105 N88-28439

SPOT imagery for landslide cartography in mountainous areas. Example of the French Maritime Alps 22 p3105 N88-28440

SPOT for slope instability survey in Nepal 22 p3105 N88-28441

Detailed geological mapping of the massif of Sainte Victoire (Provence, France) using SPOT imagery. Comparison with other multisource data. New tectonic interpretation of this region 22 p3105 N88-28442

Satellite remote sensing for forest management. A review illustrated with research results on SPOT 1 data 22 p3106 N88-28443

An evaluation of the utility of SPOT and Thematic Mapper data for providing forest inventory information 22 p3106 N88-28444

SPOT-1 satellite imagery for forest inventory in Sweden 22 p3106 N88-28445

Forest mapping by visual interpretation of SPOT images 22 p3106 N88-28446

Forest management applications of SPOT data in Australia 22 p3106 N88-28447

SPOT multispectral data and maritime pine stands in southwest of France 22 p3106 N88-28448

Stand-based forestry inventory from SPOT image 22 p3106 N88-28449

Potential of SPOT imagery as a tool for forest mapping in Quebec 22 p3107 N88-28450

Assessment of large area forest disturbances caused by biotic and abiotic factors on the basis of SPOT images 22 p3107 N88-28451

Study of deforestation in the Vosges (France) by remote sensing 22 p3107 N88-28452

Contribution to the mapping of forests in an intensively divided area, with the help of SPOT image data 22 p3107 N88-28453

SPOT 1: Image utilization, assessment, results. A study of the Elburgon Forest area (Kenya) showing the spectral responses of different forest tree species 22 p3107 N88-28454

SPOT investigations of estuaries and coastal zones: An overview 22 p3107 N88-28455

SPOT: A tool to aid preselection of sites favorable for aquiculture. Evaluation and perspuctives of the Preliminary Evaluation Program for SPOT (PEPS) ALIAS Caledonie 22 p3108 N88-28456

The monitoring of sediment transport, water circulation and mixing in estuaries and coastal waters 22 p3108 N88-28457

Evaluation of SPOT data for remote sensing of physical and biological properties of estuaries and coastal zones 22 p3108 N88-28458

Utilization of SPOT in hydrography 22 p3108 N88-28459

Application of SPOT imagery for oil spill contingency planning 22 p3108 N88-28460

The use of SPOT data in mapping coastal areas 22 p3108 N88-28461

SPOT: A satellite for oceanography 22 p3108 N88-28462

Contribution of SPOT satellite to qualitative and quantitative mapping of marine vegetation in the English Channel, North Altantic, western Mediterranean, and South Pacific 22 p3109 N88-28464

Physiography and kinematics of the western coast of the province of Huelva (Andalousia, Spain) 22 p3109 N88-28465

Use of SPOT HRV data in the US Army Corps of Engineers dredging program 22 p3109 N88-28466

Contributions of SPOT imagery to the study of the littoral environments of Saloum (Senegal) 22 p3109 N88-28467

Relevance of a thematic map (SPOT data) with regards to the real flora and structure of the vegetation covering of salt marshes (Mont Saint Michel Bay, France) 22 p3109 N88-28468

Application of SPOT data to renewable resources in the Maldives 22 p3109 N88-28469

The prospects for topographic mapping using SPOT data 22 p3110 N88-28470

The use of SPOT imagery on analytical photogrammetric instruments 22 p3110 N88-28471

Cartographic applications of SPOT imagery 22 p3110 N88-28472

The use of SPOT imagery for topographic mapping 22 p3110 N88-28473

Digital terrain modelling with SPOT data and geological applications 22 p3110 N88-28474

The use of SPOT data for mapping and DEM production --- digital elevation model (DEM) 22 p3110 N88-28475

Evaluation of SPOT cartographic capabilities over the Aix Marseille area (France) 22 p3110 N88-28476

Assessment of SPOT imagery for topographic revision and vegetation mapping 22 p3111 N88-28477

A geometrical analysis of SPOT data 22 p3111 N88-28478

Topographic mapping with SPOT 1 data. A practical approach by the Ordnance Survey 22 p3111 N88-28479

Metric applications of SPOT's lateral stereoscopy 22 p3111 N88-28480

Larger scale image mapping with SPOT 22 p3111 N88-28481

Rigorous stereophotogrammetric treatment of SPOT images 22 p3111 N88-28482

Mapping and urban multi-experimental assessment of SPOT: Mapping results 22 p3112 N88-28483

Study of stereoradiometry on SPOT images 22 p3112 N88-28484

Studies on system performance of SPOT (space and ground segments) 22 p3112 N88-28485

Radiometric analysis and potential of SPOT HRV imagery for applications in urban environments and geology 22 p3112 N88-28486

Automatic production of orthophoto using SPOT images 22 p3112 N88-28487
High resolution orthoimage quadrangle maps using SPOT satellite data 22 p3112 N88-28488
Automatic extraction of high resolution elevation data from SPOT stereo images 22 p3113 N88-28489
Automatic creation of digital terrain models from SPOT image pairs 22 p3113 N88-28490
Production of satellite image maps based on SPOT data 22 p3113 N88-28491
Surface reflectance factors derived from SPOT-1 HRV data at two view angles 22 p3113 N88-28492
Digital SPOT stereoplotting: An original approach to the formation of epipolar images and matching
22 p3113 N88-28493
From the extraction of linear networks towards following of them on SPOT images with the help of a knowledge-based interpretation system
22 p3113 N88-28494
Extraction of thin networks by an oriented following of ridges and valleys 22 p3113 N88-28495
SPOT images features extraction
22 p3114 N88-28496
SPOT: A data capture and data updating tool for the French National Geographic Institute's (IGN's) cartographic data base 22 p3114 N88-28497
Use of SPOT imagery in a geographic information system 22 p3114 N88-28498
SEP/VIPS 32 geographic information system. Processing and thematic analysis of images, maps, and associated data 22 p3114 N88-28499
Space imagery as a teaching aid in secondary education 22 p3114 N88-28500
Training of the Group for the Development of Aerospace Remote sensing 22 p3114 N88-28501
Contribution of SPOT to geographic information systems 22 p3114 N88-28502
Summary of analysis and processing techniques used on SPOT imagery 22 p3115 N88-28503
The SPOT program 22 p3115 N88-28504
SPOT data acquisition and distribution
22 p3115 N88-28505
Quality of SPOT images 22 p3115 N88-28506
Survey of SPOT-1 operation 22 p3115 N88-28507
Perspectives for the SPOT program
22 p3115 N88-28508
Closing of the Preliminary Evaluation Program for SPOT (PEPS): Assessment of the acquisition, production, and monitoring of PEPS 22 p3115 N88-28509
Imaging instrument of the vegetation payload (SPOT 4)
[SNIAS-881-440-107] 24 p3386 N88-30169

SPOT WELDS
Development of research on fatigue of spot-weld in automobile structures in Japan
05 p0606 N88-13728
The use of photoelastic methods to study the stressed states of spot-welded joints 14 p1898 N88-21335

SPRAY CHARACTERISTICS
Fuel-injector/air-swirl characterization
[NASA-CR-180864] 07 p0820 N88-14985
Liquid sprays and flow studies in the direct-injection diesel engine under motored conditions
[NASA-TM-100135] 11 p1440 N88-18594
An investigation of the spray produced by a yawed wheel, including measurement of impact forces --- aircraft wheels
[BU-363] 14 p1866 N88-21150
Experimental research of combustion systems
21 p2927 N88-27371
Holographic determination of droplet size distributions
[DFVLR-MITT-88-05] 22 p3074 N88-28250
Turbulence effects on the droplet distribution behind airblast atomizers 24 p3346 N88-29915
Nozzle airflow influences on fuel patternation
24 p3346 N88-29916
Spray performance of a vaporizing fuel injector
24 p3346 N88-29919

SPRAYED COATINGS
Development and production of new and modified powders for sprayed coatings and components for saving important raw materials
[BMFT-FB-T-86-129] 01 p0025 N88-10159
Cost 501 Project UK10 part 3: Thermal fatigue damage of Fecralloy steel-sprayed and co-extruded tubing
[AERE-R-12230] 10 p1343 N88-18026
Stability of uncapsulated weight cells with thin film elongation measurement bands under influence of humidity, temperature and operation voltage
[ETN-88-92383] 21 p2951 N88-27531
Spray automated balancing of rotors: Methods and materials
[NASA-CR-182151] 24 p3330 N88-29825

SPRAYED PROTECTIVE COATINGS
U PROTECTIVE COATINGS
U SPRAYED COATINGS

SPRAYERS
Shear stress cleaning for surface departiculation
02 p0134 N88-10838
The TAB method for numerical calculation of spray droplet breakup
[DE87-011756] 04 p0442 N88-12743
The KIVA-2 computer program for transient multidimensional chemically reactive flows with sprays
[DE88-000502] 07 p0854 N88-15191
Spray deposition: A fundamental study of droplet impingement, spreading and consolidation
[AD-A186627] 08 p0970 N88-15869
Dense-spray structure and phenomena. Part 2: Pressure-atomized sprays
[AD-A190312] 15 p2064 N88-22307
Laser measurement of particle velocities in vacuum plasma spray deposition
[DE88-007111] 19 p2728 N88-26198
Pulsed spray structure and atomisation techniques
[AD-A192280] 20 p2800 N88-26614

SPRAYING
NT ARC SPRAYING
NT FLAME SPRAYING
NT PLASMA SPRAYING
Ceramics thin film 04 p0403 N88-12505
Fire extinguishment and inhibition in spacecraft environments 04 p0406 N88-12523
Comparison of UNL laser imaging and sizing system and a phase/Doppler system for analyzing sprays from a NASA nozzle
[NASA-CR-182437] 09 p1161 N88-16956
Dense-spray structure and phenomena. Part 1: Turbulence/dispersed-phase interactions
[AD-A190606] 15 p2065 N88-22315
Mixing and thermodynamic critical phenomena of combusting monopropellant sprays
19 p2623 N88-25558
Atomization in a turbulent shear layer: Preliminary measurements 19 p2624 N88-25565
Anatomy of group burning mode transitions in spray group combustion 19 p2626 N88-25578
Small-droplet spray measurements with a scattered-light scanner
[NASA-TM-100973] 20 p2806 N88-26645

SPRAYING APPARATUS
U SPRAYERS

SPRAYS
U SPRAYERS

SPREAD F
Large scale plasma irregularities observed in the nighttime ionosphere over Natal using a rocket-borne Langmuir probe
[INPE-4422-PRE/1226] 12 p1694 N88-20139
In-situ plasma bubble observations associated with equatorial spread-F over Natal
[INPE-4488-PRE/1252] 15 p2095 N88-22482

SPREAD SPECTRUM TRANSMISSION
The role of spread spectrum in packet radio networks
[AD-A184511] 03 p0306 N88-11929
SBNR (Signed Binary Number Representations) digital signal processor architecture
[AD-A184603] 03 p0364 N88-12290
Performance analysis of coded frequency-hopped spread-spectrum systems with unknown interference
[AD-A186069] 07 p0841 N88-15103
Packet error probabilities in frequency-hopped spread spectrum packet radio networks. Markov frequency hopping patterns considered
[AD-A186071] 07 p0841 N88-15104
Measured noise performance of a direct-sequence spread-spectrum system and a comparison of single vice dual-channel delay-lock loops
[AD-A186288] 07 p0843 N88-15110
Coding for spread-spectrum communications networks
[AD-A185667] 07 p0844 N88-15119
Adaptive spread spectrum networks
[AD-A187154] 09 p1152 N88-16900
Wideband HF (High Frequency) modeling and simulation
[PB88-116116] 10 p1317 N88-17874
Spread spectrum mobile radio communications
[AD-A187487] 11 p1470 N88-18765
Spread spectrum radio networks
[AD-A188914] 12 p1620 N88-19689
Propagation effects on spread-spectrum mobile satellite systems 19 p2645 N88-25699
Coding for meteor-burst communications channel and side information for channels with block-interference
23 p3202 N88-29054
Statistical analysis of the LMS (Last Mean Squares) and modified stochastic gradient
[AD-A195497] 24 p3424 N88-30376

SPREADING
Dependence of the expectancy of hitting on the number of spread shots. Determination of the expectancy of hitting using a spread salvo
[REPT-FM6] 10 p1310 N88-17829
Investigation of several spread shot conditions
[REPT-TR-164] 10 p1310 N88-17830
Tectonics and three-dimensional structure of spreading centers: Microearthquake studies and tomographic inversions
[PB88-163290] 14 p1945 N88-21602
The spreading and mixing of dense gas clouds in still air
[KNMI-WR-87-12] 16 p2230 N88-23320
A study of flame spreading and combustion phenomena of stick propellants
[AD-A193598] 22 p3052 N88-28106

SPRING (SEASON)
Insights into the general circulation of the lower stratosphere from TOMS 05 p0616 N88-13780
Use of SPOT satellite in agrohydrology. Detection of spring water excess in a grassland region
22 p3091 N88-28357

SPRINGS (ELASTIC)
Non-linear shipboard shock analysis of the Tomahawk missile shock isolation system 05 p0592 N88-13614
Pin joints, gears, springs, cranks and other novel micromechanical structures
[DE88-002504] 07 p0864 N88-15245
The paradoxical asymptotic status of massless springs
[AD-A185625] 07 p0928 N88-15637
Nonlinear line-spring model for surface crack analysis with particular reference to work hardening materials
[PB87-144838] 08 p0994 N88-16016
Liquid spring design methodology for shock isolation system applications 08 p0998 N88-16043
Payload deployment system --- STS
14 p1875 N88-21199
Locking hinge
[NASA-CASE-MSC-21056-1] 17 p2312 N88-23827
Structurally tailorable non-linear snap-through spring system
[NASA-CASE-LAR-13729-1] 18 p2523 N88-24970
Stability of dynamical systems supported by rubber springs 19 p2680 N88-25932
Leaf spring
[GB-PATENT-2-192-689-A] 23 p3222 N88-29179

SPRINKLING
Test results and predictions for the response of near-ceiling sprinkler links in a full-scale compartment fire
[NBSIR-87/3633] 01 p0033 N88-10209

SPUTTERING
NT MAGNETRON SPUTTERING
Metallic superlattices with monolayer modulation
[DE87-012724] 01 p0023 N88-10145
Synergism of electroplating and vacuum processes
[DE87-013496] 01 p0033 N88-10211
Electron sputtering in the analytical electron microscope: Calculations and experimental data
[DE87-011457] 01 p0049 N88-10312
CuInSe2 solar cell research by sputter deposition
[DE87-001184] 02 p0195 N88-11219
Corrosion-resistant amorphous metallic coatings: Engineering development
[NASA-CR-181487] 03 p0287 N88-11802
Tribological properties of rf-sputtered MoS2 coatings
[DE88-000266] 04 p0452 N88-12802
Monocrystal sputtering by the computer simulation code ACOCT
[IPPJ-848] 04 p0493 N88-13035
Non-lattice matched metallic superlattices
[DE87-011512] 04 p0497 N88-13062
An investigation of unipolar arcing at atmospheric pressure in aluminum 2024 and aluminum coated glass slides
[AD-A184903] 05 p0577 N88-13521
Energy dependence of ion-induced sputtering yields of monatomic solids in the low energy region
[IPPJ-AM-52] 05 p0651 N88-13988
The tribological properties of MoS2 coatings in vacuum, low relative humidity and high relative humidity environments
[DE88-001611] 06 p0711 N88-14356
Nb3Al formation in sputter-deposited Nb/Al multi-layer samples
[DE88-003192] 08 p0970 N88-15868
Sputtered silver films to improve chromium carbide based solid lubricant coatings for use to 900 C
[NASA-TM-100783] 08 p0973 N88-15885
Depth of origin of sputtered atoms: Experimental and theoretical study of Cu/Ru(0001)
[DE88-002848] 08 p1082 N88-16520

Calculated sputtering and atomic displacement cross-sections for applications to medium voltage analytical electron microscopy
[DE88-002904] 09 p1168 N88-17006
Modeling considerations for selected rf-plasma edge effects
[DE88-003285] 09 p1252 N88-17500
The effect of varying sputtering parameters on the microstructure and mechanical properties of 10 percent Ni + TiB2 thin films
[DE88-002600] 09 p1254 N88-17517
Corrosion behavior of sputter-deposited aluminum-based alloys exposed to chloride solutions
[AD-A187262] 10 p1303 N88-17794
Apperatus for the study of silicon film deposition and silicon etching
[AD-A187616] 10 p1334 N88-17972
Fabrication and evaluation of transmissive multilayer optics for 8 keV X-rays
[DE88-003999] 10 p1409 N88-18402
Synthesis and characterization of thin films
[AD-A187335] 10 p1421 N88-18485
Electrochromic thin films
[DE88-751099] 11 p1559 N88-19334
Properties of reactively sputtered WNx films Zhao, X. -A.
[AD-A188711] 13 p1835 N88-20976
Superconducting superlattice structures
[DE88-005346] 13 p1847 N88-21058
A novel method for sputter-deposition of high T(sub c) superconductor films via a computer-controlled mass analyzed ion beam
[DE88-006001] 13 p1848 N88-21064
Recent advances in solid polymer electrolyte fuel cell technology
[DE88-005380] 15 p2092 N88-22464
Preparation of large area NbN/AlN/NbN Josephson junctions
[DE88-006074] 15 p2145 N88-22799
Auger electron spectroscopy of contrast-forming layers on metals
[NASA-TT-20182] 16 p2178 N88-22980
The effects of thin compressive films on indentation fracture toughness measurements
[AD-A192243] 20 p2779 N88-26480
Laser desorption/ablation studies by resonance ionization mass spectrometry
[DE88-009124] 20 p2807 N88-26650
Formation of metastable structures and amorphous phases in Cu-W alloys using the triod sputtering technique
[DE88-009051] 21 p2915 N88-27298
Erosion/redeposition modeling and calculations for carbon
[DE88-010382] 22 p3057 N88-28139
Status and directions of modified tribological surfaces by ion processes
[NASA-TM-101304] 22 p3063 N88-28176
Preparation of superconducting YBa2Cu3O(sub 7-x) films by magnetron sputtering
[DE88-009977] 23 p3289 N88-29583

SQUALLS
The combined use of diagnosed mesoscale frontogenesis and satellite imagery in forecasting squall line formation 02 p0201 N88-11258
Analysis of squall line based on conventional data
02 p0207 N88-11295
Observations of a midlatitude squall line boundary layer wake
[AD-A185609] 06 p0746 N88-14589
Density flows at the mountain edge
08 p1016 N88-16156

SQUARE WAVES
Study on the square wave alternating plasma arc welding for aluminum alloys
[PB87-143772] 07 p0863 N88-15239
Use of a coherent square wave reference to demodulate BPSK (Binary Phase Shift Keying) carriers and a visual indicator of the quality of received QPSK (Quadrature Phase Shift Keying) carriers
[AD-A193528] 23 p3204 N88-29065

SQUEEZE FILMS
Magnetohydrodynamic squeeze film
[DE88-701676] 20 p2810 N88-26669

SQUEEZED STATES (QUANTUM THEORY)
United States - Japan Seminar on Quantum Mechanical Aspects of Quantum Electronics
[AD-A186938] 14 p1974 N88-21781
Squeezed state in degenerate parametric amplification discussed by H. Takahasi in 1963
14 p1976 N88-21790
Squeezed states of light 14 p1976 N88-21791
Pulsed squeezed light 14 p1976 N88-21792
Generation of number-phase minimum uncertainty states 14 p1978 N88-21803
Squeezing via travelling-wave forward four-wave mixing in atomic vapors: Comparison with nondegenerate theory 14 p1978 N88-21804
Generating squeezed microwave radiation with a Josephson parametric amplifier
14 p1978 N88-21805
Detecting squeezed states by cross-correlation
14 p1978 N88-21806
Nonclassical lights 14 p1979 N88-21810
Quantum statistics of parametric oscillators above threshold 14 p1979 N88-21811

SQUEEZING
U COMPRESSING

SQUID (DETECTORS)
Capacitive resonant transducer for the Frascati gravitational antenna
[IFSI-86-9] 05 p0576 N88-13528
Hitachi develops ceramic superconducting device
06 p0688 N88-14214
Design, optimization and construction of a dc-SQUID with complete flux transformer circuits
[PB88-160742] 14 p1907 N88-21399
Inductive spurious coupling of a dc-SQUID to resonant input circuit
[NOTA-INTERNA-894] 14 p1908 N88-21401
Squid instrumentation for neuromagnetic study of complex brain activity 21 p2978 N88-27691
CryoSQUID: A SQUID-based magnetic field sensor
[AD-A194237] 23 p3239 N88-29275
Planar thin film SQUID with integral flux concentrator
[NASA-CASE-MFS-28282-1] 23 p3292 N88-29602

SR (REACTORS)
U SATURABLE REACTORS

SRB (SOLID ROCKET BOOSTERS)
U SPACE SHUTTLE BOOSTERS

SRI LANKA
Monitoring Moneragala (Sri Lanka) with SPOT imagery
22 p3099 N88-28405

STABILITY
NT ACOUSTIC INSTABILITY
NT AERODYNAMIC STABILITY
NT AIRCRAFT STABILITY
NT BAROCLINIC INSTABILITY
NT BOUNDARY LAYER STABILITY
NT COMBUSTION STABILITY
NT CONTROL STABILITY
NT DIMENSIONAL STABILITY
NT DIRECTIONAL STABILITY
NT DYNAMIC STABILITY
NT FLAME STABILITY
NT FLOW STABILITY
NT FREQUENCY STABILITY
NT GOERTLER INSTABILITY
NT GYROSCOPIC STABILITY
NT LATERAL STABILITY
NT LONGITUDINAL STABILITY
NT LOW SPEED STABILITY
NT MAGNETOHYDRODYNAMIC STABILITY
NT MOTION STABILITY
NT ROTARY STABILITY
NT SHELL STABILITY
NT SPACECRAFT STABILITY
NT STATIC STABILITY
NT STORAGE STABILITY
NT STRUCTURAL STABILITY
NT SURFACE STABILITY
NT SYSTEMS STABILITY
NT THERMAL STABILITY
Rayleigh-Taylor instability in compressible fluids
[DE87-013494] 01 p0047 N88-10297
Models of high spatial frequency thermal blooming instabilities
[DE87-014280] 01 p0052 N88-10330
The atomic weight and isotopic composition of nitrogen and their variation in nature
[DE87-012867] 02 p0144 N88-10902
Organic Rankine-cycle power systems working fluids study. Topical report No. 1: Fluorinol 85
[DE87-014604] 02 p0195 N88-11217
Stability of semidiscrete approximations for hyperbolic initial-boundary-value problems: An eigenvalue analysis
[NASA-TM-88328] 02 p0227 N88-11434
Filamentation instability of rotating light ion beams in fusion target chambers
[IPPJ-839] 02 p0242 N88-11530
Dynamics and stability of bipedal locomotion robots
03 p0333 N88-12096
Interchange stability of noncircular reversed field pinches
[DE88-000177] 03 p0378 N88-12381
Atomic frequency standards for ultra-high-frequency stability 04 p0433 N88-12685
The shifted Adams method for ordinary differential equations
[DE88-000810] 04 p0486 N88-12994
Variable collision frequency effects on hose and sausage instabilities in relativistic electron beams
[AD-A184206] 04 p0490 N88-13021
Computational methods for problems in aerodynamics and large space structure using parallel and vector architectures
[AD-A185401] 05 p0541 N88-13294
Colloidal stability of oxidized silicon particles in ethanolic and aqueous media
[DE87-014783] 05 p0562 N88-13421
Stability properties of spline approximations for retarded systems
[PB87-220919] 05 p0639 N88-13910
Extrema of skewed stable processes
[AD-A185422] 05 p0642 N88-13925
Tutorial on elementary bifurcation theory
[DE87-014849] 05 p0642 N88-13932
Asymptotically stable all-pass transfer functions: Canonical form, parametrization and realization
[PB87-123972] 06 p0763 N88-14684
Existence and stability of transition layers
[AD-A185806] 06 p0766 N88-14707
High temperature stability of superconducting YBa2Cu3O subx as characterized by X-ray diffraction
[DE88-001856] 06 p0787 N88-14824
Nonlinear and nonparallel stability problems
[AD-A186406] 07 p0850 N88-15159
Structural relaxation in strained-layer heterostructures
[DE88-002326] 07 p0868 N88-15264
Analysis of stable crack growth with isotropic and kinematic hardening
[PB87-144911] 07 p0868 N88-15266
Weak convergence of sums of moving averages in the alpha-stable domain of attraction
[AD-A186430] 07 p0912 N88-15529
Local properties of index-alpha stable fields
[AD-A186432] 07 p0912 N88-15530
Some new approaches to multivariate probability distributions
[AD-A186038] 07 p0914 N88-15551
Admissible and singular translates of stable processes
[AD-A186426] 07 p0917 N88-15571
The use of the direct measurement of solar radiation for the determination of Pasquill Stability Parameter
[AD-A186084] 07 p0946 N88-15750
Elastic-plastic fracture investigation on stable crack growth for plane stress
[PB87-144820] 08 p0995 N88-16022
Matrix functions in the stability of higher-order numerical schemes
[INPE-4246-PRE/1119] 08 p1073 N88-16472
DSC (Differential Scanning Calorimeter) stability test for liquid propellants: A preliminary report
[AD-A187115] 09 p1150 N88-16888
A control system for maintaining high stability in gas pressure
[DE88-003712] 09 p1175 N88-17042
A note on the effect of preemptive policies on the stability of a priority queue
[AD-A186871] 09 p1227 N88-17345
Cohesive energies of transition metal silicides and phosphides --- Knudsen effusion
[AD-A186691] 09 p1254 N88-17519
Stability and metastability in semiconductor strained-layer structures
[DE68-003308] 09 p1258 N88-17544
Molecular dynamics study of high-temperature grain-boundary stability in a (100) sigma = 29 bicrystal model
[DE88-002955] 09 p1258 N88-17546
Diffusion studies in amorphous NiZr alloys
[DE88-003009] 10 p1301 N88-17781
One-dimensional leakage-flow vibration instabilities
[DE88-002875] 10 p1330 N88-17947
Instabilities and chaos in a multimode, standing-wave, CW dye laser
[DE88-005028] 10 p1337 N88-17993
Comparative evaluation of orthostatic stability following immersion in horizontal and vertical positions
10 p1363 N88-18143
Stable, robust tracking by sliding mode control
[AD-A188278] 10 p1401 N88-18358
Electronic structure of random alloys and the theory of ordering processes
[DE88-004476] 10 p1407 N88-18394
Electronic structure and phase stability of alloys
[DE88-004574] 11 p1562 N88-19350
Preliminary investigation of stability of a fin-stiffened slender strut
[NASA-TM-4034] 12 p1599 N88-19568
Design of feedback control systems for stable plants with saturating actuators
[NASA-CR-182613] 12 p1681 N88-20050
The lattice nonlinearities and the long term stability of the SSC
[CEBAF-PR-87-009] 12 p1690 N88-20108

Stability and uniqueness in nonlinear continuum mechanics
[AD-A189616] 12 p1699 N88-20172

An experimental investigation of the flap-lag-torsion aeroelastic stability of a small-scale hingeless helicopter rotor in hover
[NASA-TP-2546] 13 p1715 N88-20257

Some properties of Australian produced explosive composition H-6
[MRL-TN-525] 13 p1754 N88-20490

Numerical experiments on the stability of controlled boundary layers
[NASA-CR-181649] 13 p1771 N88-20591

Three-wave parametric resonance in plasma of relativistic electron flux 14 p1972 N88-21772

Comprehensive model for laser instability in a CO2 laser with gaseous saturable absorber
14 p1979 N88-21808

Recent progress in optical bistability and tristability
14 p1979 N88-21809

Stability limits in the monoclinic-tetragonal transformations of zirconia
[DE88-005924] 14 p1986 N88-21849

Convection effects on stability at the solidification front 14 p1988 N88-21860

Equilibrium stability of strained epitaxial layers on a rigid substrate
[INPE-4254-PRE/1127] 15 p2145 N88-22604

Stability and control methodology for conceptual aircraft design. Volume 1: Methodology manual
[AD-A191314] 16 p2164 N88-22906

Secondary instability of compressible boundary layer to subharmonic three-dimensional disturbances
[NASA-CR-4144] 16 p2200 N88-23122

Experimental study of vortex sheets in plane flow
16 p2203 N88-23142

Method and models for R-curve instability calculations
[NASA-TM-100935] 16 p2224 N88-23278

Microinstabilities in ion beam propagation
16 p2277 N88-23631

Stability requirement FOT ignition and high gain implosion = 2-D simulation for high neutron yield experiment = 16 p2278 N88-23633

Electrothermal instability in superconducting resonators
[DE88-701684] 16 p2282 N88-23664

Mechanics of instability-related delimination growth
[NASA-TM-100622] 17 p2349 N88-23998

Observations of frontal instabilities on an upwelling filament
[AD-A191051] 17 p2375 N88-24122

Shape stability in composites
18 p2479 N88-24706

Spatial stability of a compressible mixing layer
[NASA-CR-181671] 18 p2514 N88-24916

Investigations in electro-optical multistability for signal processing 18 p2518 N88-24938

Theoretical investigations of drift waves in a magnetic quadrupole 18 p2578 N88-25312

Stability of dynamical systems supported by rubber springs 19 p2680 N88-25932

Instability-related delamination growth of embedded and edge delaminations 20 p2767 N88-26406

The protonic Beta double prime aluminas: Preparation, stability, conductivity and structure
[DE88-008442] 20 p2768 N88-26415

Modelling of premixed combustion using a thin flame sheet and the effect of the hydrodynamic instability
[DE88-009467] 20 p2770 N88-26423

Phase stability and alloy design of ordered intermetallics
[DE88-007479] 20 p2772 N88-26435

The effects of gradients on boundary stability
[DE88-009592] 20 p2773 N88-26445

A numerical study of Rayleigh-Taylor instability in aluminum and steel plates
[DE88-010475] 20 p2774 N88-26449

Resistance of polyamide-6 against long time effects of various media at various temperatures
[NASA-TT-20297] 20 p2779 N88-26484

An experimental study of the effect of pitch rate on delta wing aerodynamics and stability
[NASA-CR-183159] 21 p2893 N88-27173

Research opportunities below 300 nm at the NBS Free-Electron Laser Facility
[AD-A193100] 21 p2953 N88-27538

Transverse resistive wall instability in a high-power, short-wavelength free-electron laser
[DE88-011730] 21 p2954 N88-27549

On plasma stability under anisotropic random electric field influence
[DE88-702422] 21 p3019 N88-27918

Migration and stability of HgCdTe lattice defects
[AD-A193293] 21 p3021 N88-27935

Some stability criteria in fluid and solid mechanics
21 p3027 N88-27966

Modification of YBa2Cu3O(7-x) ceramics by adsorbed water and other gases
[DE88-011518] 22 p3057 N88-28140

A digitally implemented phase-locked loop detection scheme for analysis of the phase and power stability of a calibration tone 22 p3066 N88-28196

Unstable heat pipes
[DE88-010780] 23 p3229 N88-29217

Stability of semidiscrete approximations for hyperbolic initial-boundary-value problems: Stationary modes
[NASA-TM-100994] 23 p3270 N88-29455

Stability experimental results of cable-in-conduit superconductor for fusion
[DE88-753424] 23 p3290 N88-29589

Study of toluene stability for an Organic Rankine Cycle (ORC) space-based power system
[NASA-CR-180884] 24 p3337 N88-29863

Circuit design criteria for stable lateral inhibition neural networks
[AD-A195066] 24 p3366 N88-30046

Recent insights into instability and transition to turbulence in open-flow systems
[NASA-CR-181693] 24 p3372 N88-30079

Stability of Venusian ionopause
24 p3448 N88-30523

The stability of disk galaxies and constraints on their mass-luminosity ratio
[SER-C-PREPUBL-FASC-27] 24 p3455 N88-30565

STABILITY AUGMENTATION

A wind tunnel model with dynamic control
[BU-352] 13 p1724 N88-20310

Conceptual final paper on the preliminary design of an oblique flying wing SST
[NASA-CR-182879] 16 p2161 N88-22891

STABILITY DERIVATIVES

NT PITCHING MOMENTS
NT ROLLING MOMENTS
NT YAWING MOMENTS

Controlling the dynamic environment during NOE flight
03 p0264 N88-11661

Low speed wind tunnel investigation of propeller slipstream aerodynamic effects on different nacelle/wing combinations. Part 1: Total forces and moments and pressure distributions on nacelle/wing at different angles of attack and yaw and at different thrust coefficients
[FFA-TN-1987-22] 05 p0542 N88-13302

STABILITY TESTS

NT FLIGHT STABILITY TESTS
NT WIND TUNNEL STABILITY TESTS

Stability analysis of a rigid body with a flexible attachment using the energy-casimir method
[AD-A185646] 06 p0723 N88-14449

DSC (Differential Scanning Calorimeter) stability test for liquid propellants: A preliminary report
[AD-A187115] 09 p1150 N88-16888

STABILIZATION

NT SIGNAL STABILIZATION
NT SPIN STABILIZATION
NT THREE AXIS STABILIZATION

Performances of an Actively Stabilized Stellar interferometer (ASSI): Faint magnitudes, low fringe contrast measurements and operationality
01 p0097 N88-10641

Control and stabilization mechanisms of submunitions
[DFVLR-IB-111-86/9] 03 p0259 N88-11630

Slip casting and extruding shapes of rhemium with metal oxide additives. Part 2: Development of grain stabilized rhenium parts for resistojets
[NASA-CR-180851] 03 p0278 N88-11749

Processing, fabrication, applications and limitations of inherently conducting polymers
[DE88-003210] 08 p0973 N88-15883

The structure of the sideband spectrum in free electron lasers
[AD-A186952] 09 p1170 N88-17015

Feedback stabilization of distributed systems
[AD-A187111] 09 p1222 N88-17328

Boundary stabilization of thin elastic plates
[AD-A187123] 10 p1343 N88-18025

Time delays and boundary feedback stabilization in one-dimensional viscoelasticity, appendices A through H
[AD-A187534] 10 p1401 N88-18353

Fermi level stabilization in semiconductors: Implications for implant activation efficiency
[DE88-006332] 15 p2145 N88-22801

Concepts for a laser gyroscope of the highest precision 18 p2517 N88-24929

Heterogeneous diffusion flame stabilization
[AD-A193014] 20 p2771 N88-26429

Feedback stabilization of du/dt=Au + bf in Hilbert space when the normalization function is less than or equal to r
[AD-A193510] 23 p3277 N88-29506

STABILIZED PLATFORMS

Vega-1 and Vega-2 automatic stations: Functioning of flyby vehicles during encounter with Halley's comet
13 p1725 N88-20314

STABILIZERS (FLUID DYNAMICS)

Pointwise stabilization for coupled quasilinear and linear wave equations
[AD-A190031] 15 p2120 N88-22632

STABLE OSCILLATIONS

Mode priming in an overmoded gyrotron oscillator
[AD-A189151] 13 p1772 N88-20602

Oscillating airfoils: Achievements and conjectures
[AD-A190490] 15 p2014 N88-22006

STACKING FAULTS

U CRYSTAL DEFECTS

STACKS

Mechanically stacked multijunction solar cells: An update on Sandia programs
[DE87-014641] 03 p0347 N88-12190

Development of mechanically stacked tandem concentrator cells
[DE88-001926] 06 p0730 N88-14490

Changing the layers of mind
[AD-A186648] 08 p1052 N88-16350

Portable (and disposable) interpreters
10 p1380 N88-18237

Phosphoric acid electric utility fuel cell technology development
[DE88-010187] 20 p2795 N88-26582

STAGE SEPARATION

The TV-SAT/TDF/TELE-X pyrotechnical system
[CNES-87/CT/DRT/TVE/IL/358]
08 p0974 N88-15891

Stage separation testing of Ariane
09 p1126 N88-16752

The Ariane fairing and its separation systems
09 p1128 N88-16754

Separation dynamics for the last stage of a launch vehicle and satellite
[INPE-4281-PRE/1153] 12 p1601 N88-19582

Investigation of Super*Zip separation joint
[NASA-TM-4031] 15 p2026 N88-22072

STAGING (ROCKETS)

U STAGE SEPARATION

STAGNATION FLOW

Efficient shell implosion and target design
16 p2277 N88-23630

Correlations of velocity and temperature fluctuations in the stagnation-point flow of circular cylinder in turbulent flow
[NASA-TM-100930] 19 p2597 N88-25435

A simple, analytic 3-dimensional downburst model based on boundary layer stagnation flow
[NASA-TM-100632] 22 p3042 N88-28058

STAGNATION POINT

The flow downstream of screens and the formation of longitudinal vortices in the stagnation point flow
[DFVLR-FB-87-27] 09 p1162 N88-16963

Computational fluid dynamics and aerothermodynamics
[NASA-CR-182490] 09 p1166 N88-16989

Stagnating turbulent reacting flows
[AD-A191449] 18 p2508 N88-24877

Correlations of velocity and temperature fluctuations in the stagnation-point flow of circular cylinder in turbulent flow
[NASA-TM-100930] 19 p2597 N88-25435

STAGNATION PRESSURE

Time-resolved measurements of shock-induced vapor-pressure profiles
[DE87-012972] 01 p0045 N88-10289

Low thrust viscous nozzle flow fields prediction
[NASA-CR-182334] 05 p0582 N88-13551

Pusherless implosion, pulse tailoring and ignition scaling law for laser fusion 16 p2277 N88-23629

STAGNATION REGION

U STAGNATION POINT

STAINING

Use of lasers with F sub A(II)-color center KCl:Li crystals in the intraresonator laser spectroscopy method
06 p0769 N88-14729

STAINLESS STEELS

NT AUSTENITIC STAINLESS STEELS
NT FERRITIC STAINLESS STEELS
NT MARTENSITIC STAINLESS STEELS

Studies on temporal field emission from stainless steel surfaces
[DE87-014237] 02 p0147 N88-10919

Experimental determination of flow potential surfaces supporting a multiaxial formulation of viscoplasticity
02 p0187 N88-11167

Damping characteristics of a composite-reinforced stainless-steel tube
[DE87-012455] 02 p0191 N88-11182

Investigation on ductile fracture behavior of 3-inch diameter Type 304 stainless steel pipe with a circumferential through-wall crack
[DE87-753016] 02 p0191 N88-11196
Precision metrology comparing ultrasonic and other techniques for the determination of steel thickness
[DE87-011051] 02 p0230 N88-11452
Investigations of creep cavitation in Type 304 stainless steel
[DE87-014198] 03 p0287 N88-11803
Crevice corrosion of stainless steels and related alloys. Part 2: Summary of experimental test data for input to mathematical model
[BR99871-PT-2] 03 p0289 N88-11816
Effect of helium on irradiation creep in an austenitic stainless steel
[DE87-013754] 03 p0290 N88-11824
The mechanical properties of solid state diffusion bonds between Ti-6Al-4V and 304L stainless steel
[BAJ-TR-113-1987] 03 p0332 N88-12093
Mechanical properties of a microalloyed steel with high niobium content
[DE87-703545] 04 p0415 N88-12572
Partial substitution of vanadium by niobium in AISI H13 steel
[DE87-703548] 04 p0415 N88-12575
The aging behavior of types 308 and 308CRE stainless steels and its effect on mechanical properties
[DE87-012541] 04 p0417 N88-12590
Creep life prediction based on stochastic model of microstructurally short crack growth
[NASA-TM-100245] 04 p0456 N88-12825
Damping characteristics of a composite-reinforced stainless-steel plate
[DE88-000303] 04 p0457 N88-12828
Pulsed eddy-current inspection of thin-walled stainless steel tubing
[DE88-001492] 04 p0457 N88-12830
Data base on the high heat flux behaviour of metals and carbon materials for plasma facing components: Experiments at the 10 MW neutral beam injection test stand of the IPP Nagoya
[IPPJ-AM-53] 04 p0492 N88-13031
Study of the influence of mechanical - thermal treatments on the creep behavior of a niobium stainless steel
[DE87-703506] 05 p0563 N88-13431
Tensile properties of extrusion consolidated Type 304 SS rapidly solidified powders
[DE87-014875] 05 p0566 N88-13450
Effect of rapid solidification on stainless steel weld metal microstructures and its implications on the Schaeffler diagram
[DE88-001489] 05 p0566 N88-13451
Cu-2 mechanical properties and microstructural stability of advanced steam cycle materials
[DE88-001519] 05 p0566 N88-13452
Coupling effects between the ferrite and austenite phases during corrosion fatigue of a ferrite/austenite duplex stainless steel 05 p0605 N88-13706
Fractographic and microstructural aspects of fracture toughness testing in irradiated 304 stainless steel
[DE88-000795] 06 p0681 N88-14172
Determination, by X-ray fluorescence, of platinum, palladium, ruthenium, iron and chromium in special steels
[PB87-132114] 06 p0683 N88-14183
The factors which govern the acceleration of corrosion fatigue crack growth rate of a ferritic stainless steel
06 p0717 N88-14402
Near-threshold fatigue crack growth behavior at cryogenic temperature 06 p0718 N88-14409
Mixed mode fatigue crack growth using the Brasilian disc 06 p0719 N88-14416
Axial creep-fatigue damage assessment in type 316 SS material 06 p0721 N88-14430
Study on the cryogenic toughness of stainless steel weld metals
[PB87-143830] 07 p0834 N88-15057
The effect of deformation rate on JBK-75 stainless steel forgings
[DE88-001696] 07 p0834 N88-15061
A pulsed eddy current method for examining thin-walled stainless steel tubing
[DE88-002294] 07 p0866 N88-15255
Kinetics and mechanism of thermal aging embrittlement of duplex stainless steels
[DE88-002987] 08 p0969 N88-15866
Study on the fracture behavior of 9 percent Ni steel welded joint
[PB87-143863] 08 p0995 N88-16023
Long-term-aging embrittlement of cast duplex stainless steels: Mechanism and kinetics
[DE88-002929] 09 p1145 N88-16861
Long-term aging of cast stainless steels: Mechanisms and resulting properties
[DE88-002888] 09 p1145 N88-16864
Characterization of duplex stainless steel by TEM (Transmission Electron Microscopy), SANS (Small-Angle Neutron Scattering) and APFIM (Atom-Probe Field Ion Microscopy) techniques
[DE88-002916] 09 p1145 N88-16865
Aging degradation of cast stainless steels: Effects on mechanical properties
[DE88-003053] 09 p1145 N88-16866
Application of ac-impedance method on determination of corrosion rate of metals
[DE88-750307] 10 p1300 N88-17771
Effect of low-temperature aging on the mechanical properties of cast stainless steels
[DE88-002872] 10 p1300 N88-17774
Studies of the initiation of pitting corrosion on stainless steels
[AERE-M-3615] 10 p1301 N88-17778
Beneficial and detrimental effects of silica in the high temperature oxidation of 20Cr/25Ni/Nb stainless steel
[AERE-R-12667] 10 p1301 N88-17779
Cost 501 Project UK10 part 3: Thermal fatigue damage of Fecralloy steel-sprayed and co-extruded tubing
[AERE-R-12230] 10 p1343 N88-18026
In situ ultrahigh vacuum friction measurement and wear track analysis of ion implanted 304 stainless steel
[DE88-004537] 11 p1494 N88-18922
Weldability of tritium-charged 304L stainless steel
[DP-1740] 12 p1607 N88-19611
Hydrogen induced cracks in armor steel weldments fabricated with austenitic filler alloys
[AD-A188733] 13 p1740 N88-20406
Use of the LLNL 40 kV electric gun to study the shock response of 21-6-9 stainless steel
[DE87-014550] 13 p1742 N88-20418
Creep behavior of consolidated rapidly solidified Type 304 stainless steel powder containing helium
[DE88-005536] 13 p1743 N88-20424
Study of defects in metals by positron annihilation
[DE88-701042] 13 p1745 N88-20432
The effect of H2S concentration and pH on hydrogen permeation in AISI 410 stainless steel in 5 percent NaCl
[NPL-DMA(A)-148] 14 p1890 N88-21293
The effect of H2S concentration and pH on the cracking resistance of AISI 410 stainless steel in 5 percent brine
[NPL-DMA(A)-149] 14 p1890 N88-21294
Statistical analysis of feasibility of non-destructive inspection of mechanical properties of hot worked pipes of alloy steels
[BLL-M-37598-(5828.4)] 14 p1922 N88-21455
Cyclic uniaxial and biaxial hardening of type 304 stainless steel modeled by the viscoplasticity theory based on overstress 14 p1931 N88-21514
Some implications for cyclic plastic and viscoplastic equations based on nonproportional loading experiments
14 p1931 N88-21515
Segregation effects in welded stainless steels
[DE88-701224] 15 p2037 N88-22139
Grain growth behavior of extrusion consolidated centrifugally atomized Type 304 stainless steel powder
[DE88-006788] 15 p2038 N88-22143
The weldability of consolidated rapidly solidified Type 304 SS powders
[DE88-006738] 16 p2178 N88-22978
Enhanced emittance of oxidized 304 stainless steel
17 p2423 N88-24408
The effects of Hertzian stress and test ambient on the friction coefficient of MsS2 coatings
[DE88-008118] 20 p2777 N88-26467
GTAW characterization for weld penetration on 304L stainless steel
[DE88-010611] 20 p2810 N88-26672
Investigation of hydrogen isotope penetration through stainless steels Kh18N10T and Kh3M2BFR
[DE88-702189] 21 p2915 N88-27297
Thermal conductivity and thermal expansion of stainless steels D9 and HT9
[DE88-011973] 21 p2916 N88-27306
Distribution of weld quality in thin section stainless steel tube attachment welds
[PB88-109632] 21 p2955 N88-27555
Method of forming dynamic membrane on stainless steel support
[NASA-CASE-MSC-18172-3] 23 p3201 N88-29052
State variable approach to deformation phenomena in Face Centered Cubic (FCC) metals
[VTT-44] 24 p3354 N88-29964
An experimental study of biaxial yield in modified 9Cr-1Mo steel at room temperature
[NASA-CR-175012] 24 p3385 N88-30164

STALLING
Post stall behavior in axial-flow compressors
[AD-A185712] 06 p0665 N88-14081
Possibilities for on-line surge suppression by fast guide vane adjustment in axial compressors
10 p1263 N88-17674

STAMPING
Contribution to the study of wrinkling in metal stamping
[ISAL-IDI1-87-08] 08 p0976 N88-15900
Shape optimization of three-dimensional stamped and solid automotive components
[GMR-5168] 11 p1528 N88-19123

STANDARD ATMOSPHERES
U REFERENCE ATMOSPHERES

STANDARD DEVIATION
Coherent RF error statistics
[AD-A193002] 20 p2792 N88-26560

STANDARDIZATION
NT COMMONALITY
Fabrication of standardized piezoelectric polymer shock gauges by the Bauer method
[DE87-012738] 01 p0049 N88-10315
Study of aeropropulsion laboratory pressure drop rig and recommended test procedure
[AD-A184333] 03 p0322 N88-12038
Formalizing reusable software components in the programmer's apprentice
[AD-A185843] 07 p0901 N88-15457
The use of heart rate in the prescription and evaluation of exercise programs
[AD-A186454] 08 p1049 N88-16336
Standardization of software development
[INPE-4330-NTE/272] 08 p1068 N88-16455
Effects of additives on fire properties of polyethylene
[AD-A187064] 09 p1146 N88-16871
Interfacing slave designs to Fastbus: Practical experience
[DE88-002807] 09 p1215 N88-17286
An evaluation of perceptions of form, fit, function (F3) standardization on the Standard Inertial Navigation Unit (STD INU) program
[AD-A188955] 12 p1579 N88-19446
Some reflections on the standardization of bed-rest procedures for weightlessness simulation (cardiovascular and endocrine apsects) 12 p1662 N88-19961
European approaches in standard spectrum development --- aircraft load spectra
[NLR-MP-87007-U] 13 p1782 N88-20661
Public tool interfaces for software development environments
[RSRE-87004] 14 p1958 N88-21674
Inventory of topographic mapping and standardization of geographic names as the basis of a Geographic Information System (GIS) 16 p2225 N88-23281
Interfacing and integrating hardware and software design systems 17 p2306 N88-23796
Characterization of lubricants in terms of transition diagram data
[AD-A194264] 23 p3197 N88-29025
Improvement of head-up display standards. Volume 3: An evaluation of head-up display safety
[AD-A195787] 24 p3410 N88-30300
Strategic, organizational and standardization aspects of integrated information systems, volume 6
[AD-A195855] 24 p3437 N88-30457

STANDARDS
NT FREQUENCY STANDARDS
NT REFERENCE ATMOSPHERES
Viscosity measurements at high temperatures on a standard reference material supplied by BCR --- Bureau Communite de Reference (BCR)
[NPL-DMA(A)-146] 01 p0020 N88-10126
Center for Electronics and Electrical Engineering Technical Progress Bulletin covering center programs, October to December 1986 with 1987 CEEE events calendar
[PB87-226890] 02 p0168 N88-11058
Center for Electronics and Electrical Engineering technical publication announcements covering center programs, July to September 1986 with 1987 CEEE events calendar
[PB87-223442] 02 p0168 N88-11059
AGARD standard aeroelastic configurations for dynamic response. Candidate configuration I.-wing 445.6
[NASA-TM-100492] 02 p0192 N88-11202
Evaluating computers and their performance: Perspectives, pitfalls, and paths
[DE87-014264] 02 p0218 N88-11375
Definitions as database records
[DE87-014057] 02 p0248 N88-11570
Revision of the information standards for flight mechanics
[DFVLR-MITT-87-06] 03 p0265 N88-11675
Center for Electronics and Electrical Engineering Technical Progress Bulletin covering center programs, January to March 1987 with 1987 CEEE events calendar
[PB87-224648] 03 p0309 N88-11946
Requirements for the calibration of mechanical shock transducers
[PB87-227591] 03 p0325 N88-12054

NBS (National Bureau of Standards) measurement services: Radiometric standards in the vacuum ultraviolet
[PB87-227625] 03 p0325 N88-12055
Calibration standard for metallographic microscopes
[RFP-3956-REV] 03 p0326 N88-12057
Balloon track data analysis
[AD-A184750] 03 p0350 N88-12213
FORTRAN compiler performance benchmarks for the IBM personal computer
[LA-10883-MS] 03 p0363 N88-12284
Los Alamos National Laboratory computer benchmarking 1986
[LA-10898-MS] 03 p0363 N88-12285
Fire-related standards and testing
04 p0406 N88-12522
The atomic weight and isotopic composition of oxygen and their variation in nature
[DE87-014397] 04 p0413 N88-12558
Atomic frequency standards for ultra-high-frequency stability 04 p0433 N88-12685
Optimization of dilatometer test procedures
[DE87-014998] 04 p0447 N88-12769
Standard fatigue test specimens for fastener evaluation
[AGARD-AG-304] 04 p0455 N88-12818
Metrology and calibrating laboratories
[ETN-88-90761] 06 p0670 N88-14104
Uniform laws and regulations as adopted by the National Conference on Weights and Measures (72nd), 1987
[PB88-123724] 06 p0689 N88-14225
Nonconformity testing for the Graphical Kernel System (GKS)
[GMD/VAL-86-104] 06 p0757 N88-14644
NBS (National Bureau of Standards) measurement services: Spectral reflectance
[PB88-109905] 06 p0779 N88-14785
Horn design equations for the NBS (National Bureau of Standards) horn-type noise standards
[PB88-110226] 07 p0844 N88-15122
Development of Soviet state ergonomic standards (GOST)
[AD-A185536] 07 p0899 N88-15449
Soviet state ergonomic standards (GOST)
[AD-A185537] 07 p0900 N88-15450
After ten years of metafiles: Where does the Computer Graphics Metafile fit
[DE88-001840] 07 p0904 N88-15474
Thermodynamic values from computer summation of group additivity data
[AD-A186131] 07 p0940 N88-15711
Summary record of presentations to the Federal Telecommunication Standards Committee/Fiber optics task group
[PB88-110853] 08 p0978 N88-15911
PCM telemetry standard
[ESA-PSS-46(TTC.A.02)ISSUE-1]
09 p1132 N88-16790
Results from a questionnaire on particulate metrology in the UK
[NPL-MOM-81] 09 p1141 N88-16841
The ISO narrow spectrum series of filtered X-radiations at NPL
[NPL-RS(EXT)-92] 09 p1245 N88-17462
Influence of non-metallic elements in the mechanical properties of 20 Mn Mo Ni 55 steel
[DE88-700412] 10 p1300 N88-17775
Solid-state voltage standard performance and design guidelines
[PB88-123757] 10 p1322 N88-17905
NBS (National Bureau of Standards) measurement services: Platinum resistance thermometer calibrations
[PB88-138367] 10 p1333 N88-17967
NASA/NBS (National Aeronautics and Space Administration/National Bureau of Standards) standard reference model for Telerobot Control System Architecture (NASREM)
[PB88-124773] 10 p1338 N88-17999
Developing a standard taxonomy or software engineering standards 10 p1379 N88-18234
NBS (National Bureau of Standards) measurement services: Spectral irradiance calibrations
[PB88-123781] 10 p1408 N88-18401
Journal of Research of the National Bureau of Standards, volume 92, number 5, September-October 1987
[PB88-124409] 10 p1426 N88-18518
Journal of Research of the National Bureau of Standards, volume 92, number 6, November-December 1987
[PB88-138516] 10 p1426 N88-18519
Running head: What color is it
[NASA-CR-182600] 11 p1551 N88-19260
Ultrasonic measurements research: Progress in 1987
[AD-A188508] 12 p1667 N88-20092
Standardized environmental fatigue sequence for the evaluation of composite components in combat aircraft (ENSTAFF = ENvironmental falSTAFF)
[LBF-FB-179] 13 p1722 N88-20300
Orbital transfer vehicle concept definition and system analysis study. Volume 2: OTV concept definition and evaluation. Book 1: Mission and system requirements
[NASA-CR-179321] 13 p1729 N88-20339
The preparation, assembly and mounting of RF coaxial cables
[ESA-PSS-01-718-ISSUE-1] 13 p1756 N88-20504
Quantitative AES: The establishment of a standard reference spectrum for the accurate determination of spectrometer transmission functions
[NPL-DMA(A)-151] 14 p1887 N88-21279
An overview of the army GIS (Geographic Information Systems) Research Program
[AD-A189711] 14 p1992 N88-21871
Computer grading of extensometers (BS 3846)
[NPL-DMA(A)-152] 15 p2108 N88-22560
NASA and the challenge of ISDN: The role of satellites in an ISDN world
[NASA-CR-182749] 15 p2126 N88-22676
COBOL Analysis System (CAS) users manual
[PB88-171442] 16 p2250 N88-23445
Radiation standards 16 p2272 N88-23592
Requirements for radiation receivers
16 p2272 N88-23593
Reflection standards for spectroradiometry. Realization and calibration 16 p2272 N88-23595
Unified interchange format for computer data (standard file format)
[ESA-STR-225] 17 p2386 N88-24183
Discussions and agreements in the United Nations on important issues associated with nuclear power in space
17 p2423 N88-24411
Mobile satellite services: International co-ordination, co-operation and competition 19 p2644 N88-25691
Reducing risks inherent in operating underwater craft: The contribution of classification, the example of the SAGA highly autonomous support submarine
19 p2699 N88-26042
Center for Electronics and Electrical Engineering technical publication announcements covering Center programs, July to September 1987
[PB88-196530] 20 p2793 N88-26572
Fiber optic sensors with internal referencing
[NASA-TM-100893] 20 p2806 N88-26644
Improvement of head-up display standards. Volume 1: Head-up display design guide, appendix
[AD-A192973] 20 p2834 N88-26809
Unified methods of accelerated laboratory tests of the preparations for temporary protection of cars
[NASA-TT-20298] 21 p2921 N88-27336
A 1/2-inch high-definition baseband VCR
21 p2930 N88-27393
Ada (trade name) compiler validation summary report: Verdix Corporation VAda-010-03315, version 5.5 MicroVAX 2 host ISBC 386/20P Intel target
[AD-A193226] 21 p2997 N88-27774
Ada (trade name) compiler validation summary report: Verdix corporation VAda-010-13125, version 5.41 Sun Microsystems Sun-3/160 host microbar GPC68020 target
[AD-A193415] 21 p2997 N88-27777
The exploitation of Aircraft Integrated Monitoring System (AIMS) data in height-keeping studies for aircraft operating above FL 290 22 p3036 N88-28026
A new code for Galileo 22 p3065 N88-28186
Langley Research Center Metrology Program status for fiscal year 1987
[NASA-TM-100651] 22 p3086 N88-28324
Validation code for the Whetstone Benchmark
[NPL-DITC-107/88] 22 p3140 N88-28667
High hot-hardness gear lubricant evaluations, phase 2
[AD-A192309] 23 p3196 N88-29017
Vision and visual protection in fast jet aircraft
23 p3241 N88-29292
Ada (trade name) compiler validation summary report: Verdix Corporation VAda-010-03205, version 5.42 MicroVAX 2 host and national DB32000 (NS32032 target
[AD-A193485] 23 p3247 N88-29326
Integration of LANTIRN (Low Altitude Navigation and Targeting Infrared for Night) into operational fighter training
[AD-A194906] 24 p3325 N88-29799
Using standards to break down information transfer barriers 24 p3439 N88-30467

STANDING WAVES
Sound pressure distribution in front of a serrated boundary: Standing wave suppression and diffusion
07 p0928 N88-15639
Instabilities and chaos in a multimode, standing-wave, CW dye laser
[DE88-005028] 10 p1337 N88-17993
Solid-state ring laser with acoustooptical phase nonreciprocity of opposing waves
14 p1970 N88-21761
Computer-controlled measurements of nonlinear standing waves
[AD-A193840] 22 p3147 N88-28717

STANDS
U SUPPORTS

STANNIDES
NT NIOBIUM STANNIDES

STAPHYLOCOCCUS
Study of certain biological characteristics of bacteria during the French-Soviet CYTOS-2 space experiment
04 p0473 N88-12917

STAR CLUSTERS
NT GLOBULAR CLUSTERS
Membership of Cepheids and red giants in 8 open clusters: NGC 129, 6067, 6649, 6664, IC 4725, Ly 6, Ru 79
[PUBL-SER-C-FASC-13] 07 p0944 N88-15739
Color-magnitude diagrams of star clusters in the Magellanic clouds from wide-field electronography. Part 3: NGC 1841
[PUBL-SER-C-FASC-14] 07 p0944 N88-15740
Clustering of galaxies and clusters of galaxies in a decaying-particle cosmological model with a massive decay product
[DE88-753434] 23 p3298 N88-29642

STAR DISTRIBUTION
Basic properties and variability
02 p0252 N88-11593

STAR FIELDS
U STAR DISTRIBUTION

STAR FORMATION
The Einstein survey of the young stars in the Orion Nebula 04 p0518 N88-13182
VLBI research on OH-maser IN W33
08 p1001 N88-16064
Global properties of star formation in spiral galaxies
14 p1994 N88-21883
Submillimeter and far infrared line observations of M17 SW: A clumpy molecular cloud penetrated by UV radiation
[NASA-CR-182866] 16 p2288 N88-23701
Infrared astronomy at extremely faint light levels in support of the LAIRTS program
[AD-A191497] 18 p2592 N88-25404
Star formation and molecular clouds
24 p3451 N88-30537
Observations of star formation
24 p3451 N88-30538
Starbursts and their dynamics
[NASA-CR-180227] 24 p3452 N88-30549

STAR TRACKERS
Satellite autonomous navigation with SHAD (Stellar Horizon Atmospheric Dispersion)
[AD-A184968] 05 p0544 N88-13313
Fine attitude measurement system study. Volume 1: Executive summary
[BAE-TP-7831-VOL-1] 09 p1133 N88-16795
Fine attitude measurement system study, volume 2
[BAE-TP-7831-VOL-2] 09 p1133 N88-16796
Fine attitude measurement system study. Volume 3: Appendices
[BAE-TP-7831-VOL-3] 09 p1133 N88-16797
Integrated focal plane star sensor
[OG-RT/86-0156] 09 p1262 N88-17562
Identification of a star field from a spinning satellite
[CNES-NT-120] 15 p2026 N88-22074
Satellite attitude determination using a CCD (Charge-Coupled-Device) star camera
[AD-A192662] 22 p3046 N88-28080

STAR TRACKING
U STAR TRACKERS

STARBURST GALAXIES
Comparison of global and nuclear properties of starburst and Seyfert 1 galaxies 03 p0388 N88-12438
Galaxy evolution in dense clusters
13 p1855 N88-21101
Starbursts and their dynamics
[NASA-CR-180227] 24 p3452 N88-30549

STARCHES
Identification of hydroxypropyl starch hydrolysate components 17 p2315 N88-23832

STARK EFFECT
Relaxation effect of stark split levels for two-level system interacting with symmetrical strong resonant bichromatic field 03 p0299 N88-11882
Experimental and theoretical studies of coherent and nonthermal processes in semiconductors probed by femtosecond laser techniques 14 p1977 N88-21800
Stark effect in intense field. Perturbation theory and 1/n-expansion
[DE87-702947] 16 p2266 N88-23550

Time-resolved spectroscopic measurement of anode plasma in magnetically-insulated diode
16 p2279 N88-23641
Spectroscopic study of heliotron E plasmas: Stark profile, CXR, poloidal rotation and carbon coating
17 p2441 N88-24523
High-order multiphoton ionization of the noble gases
[DE88-007489] 18 p2571 N88-25273
Quantum-confined stark effect in InGaAs/InP quantum wells grown by metal-organic chemical vapor deposition
19 p2660 N88-25814
Dynamics of below-gap photoexcitation in GaAs quantum wells 19 p2660 N88-25815
Novel quantum well optical devices
20 p2868 N88-27028

STARS
NT A STARS
NT ASYMPTOTIC GIANT BRANCH STARS
NT B STARS
NT BINARY STARS
NT BLACK HOLES (ASTRONOMY)
NT CARBON STARS
NT CATACLYSMIC VARIABLES
NT CEPHEID VARIABLES
NT COOL STARS
NT DOUBLE STARS
NT DWARF NOVAE
NT DWARF STARS
NT EARLY STARS
NT ECLIPSING BINARY STARS
NT F STARS
NT FLARE STARS
NT G STARS
NT GIANT STARS
NT HERCULES NOVA
NT HOT STARS
NT INFRARED STARS
NT K STARS
NT LATE STARS
NT M STARS
NT MAGNETIC STARS
NT MAIN SEQUENCE STARS
NT MIRA VARIABLES
NT NEMESIS (STAR)
NT NEUTRON STARS
NT NOVAE
NT O STARS
NT PRE-MAIN SEQUENCE STARS
NT PROTOSTARS
NT PULSARS
NT RADIO STARS
NT RED DWARF STARS
NT RED GIANT STARS
NT REFERENCE STARS
NT S STARS
NT SUBGIANT STARS
NT SUN
NT SUPERGIANT STARS
NT SUPERMASSIVE STARS
NT SUPERNOVA 1987A
NT SUPERNOVAE
NT T TAURI STARS
NT VARIABLE STARS
NT WHITE DWARF STARS
NT WOLF-RAYET STARS
NT X RAY BINARIES
NT X RAY STARS
Calibration of the Ca II K line-core density and the magnetic flux density in stars using solar data
04 p0507 N88-13116
Active phases on II Peg 04 p0507 N88-13119
The giant spot on II Peg in 1986
04 p0508 N88-13120
Spectral analysis of APT RS CVn binary light curves
04 p0508 N88-13122
Starspots on the short-period RS CVn system SV Cam: 45 years of activity 04 p0508 N88-13123
The short-period RS CVn stars: Starspots and fundamental properties 04 p0508 N88-13124
Doppler snapshots 04 p0508 N88-13125
Titanium oxide absorption and spot sizes in II Peg, HR 1099 and UX Ari 04 p0508 N88-13126
Spectroscopic monitoring of RS CVn stars at Kitt Peak using the Penn State fiber optic echelle
04 p0509 N88-13127
The X-ray orbital lightcurves of AR Lac and TY Pyx
04 p0509 N88-13129
X-rays, color, and the Vaughan-Preston gap
04 p0510 N88-13135
Stellar activity and the rotation of Hyades stars
04 p0510 N88-13139
Relativistic stellar pulsations 06 p0801 N88-14902
Galaxy evolution in dense clusters
13 p1855 N88-21101
Stars, gas and dust in the Andromeda galaxy
[B8679680] 16 p2289 N88-23708
Research and Technology, 1987, Goddard Space Flight Center
[NAS 1.15:101097] 17 p2453 N88-24572
Cosmions and stars
[DE88-010886] 20 p2887 N88-27145
Apparent brightness of stars and lasers
22 p3065 N88-28188
Study of modern instrumentation and methods for astronomic positioning in the field
[AD-A196173] 24 p3452 N88-30548

STARSPOTS
NT SUNSPOTS
The giant spot on II Peg in 1986
04 p0508 N88-13120
Spectral analysis of APT RS CVn binary light curves
04 p0508 N88-13122
Starspots on the short-period RS CVn system SV Cam: 45 years of activity 04 p0508 N88-13123
The short-period RS CVn stars: Starspots and fundamental properties 04 p0508 N88-13124
Titanium oxide absorption and spot sizes in II Peg, HR 1099 and UX Ari 04 p0508 N88-13126
Flares: Solar and stellar
[PB87-124962] 06 p0806 N88-14917
Mapping stellar surface features
09 p1262 N88-17564

STARTING
NT AIR START
Performance of supersonic impingement radial turbines 06 p0712 N88-14367
Experimental study of two-dimensional vortex patterns for impulsively started bodies in comparison with other configurations 11 p1435 N88-18562
On the start up of supersonic underexpanded jets --- Mach disks 11 p1435 N88-18563
Possible creep studies of lithium with a compact device 17 p2422 N88-24404
Arcjet power supply and start circuit
[NASA-CASE-LEW-14374-1] 23 p3181 N88-28939

STATE EQUATIONS
U EQUATIONS OF STATE

STATE ESTIMATION
Maximum likelihood estimates of parameters in linear systems with process and measurement noise
[DFVLR-FB-87-20] 01 p0083 N88-10532
Propulsion estimation techniques
07 p0927 N88-15632
Reduction of time delays in Runge-Kutta integration methods --- systems simulation
[MBB/LKE-132/S/PUB/241/A]
09 p1229 N88-17363
Further developments in exact state reconstruction in deterministic digital control systems
[NASA-TP-2812] 11 p1468 N88-18751
Control test and validation for a large diameter high stability centrifuge 12 p1577 N88-19437
A state-space approach to super-optimal H sup infinity control problems
[OUEL-1690/87] 14 p1962 N88-21702
Estimation of time- and state-dependent delays and other parameters in functional differential equations
[NASA-CR-181663] 17 p2383 N88-24164
Computer aided design for linear control State Variable System (SVS)
[AD-A193282] 21 p2997 N88-27775
More on exact state reconstruction in deterministic digital control systems
[NASA-TP-2847] 22 p3063 N88-28177
Increasing accuracy in evaluating vector of state under conditions of incomplete observability of expanded system 24 p3446 N88-30511

STATE VECTORS
Inequivalent quantizations and fundamentally perfect spaces
[DE87-014225] 02 p0229 N88-11446
Teleoperator and robotics system analysis
[NASA-CR-179220] 03 p0334 N88-12105
SDVS (State Delta Verification System): Program verification system development fiscal year 1986
[AD-A184338] 03 p0366 N88-12302
Optimal observers for ARMA models
[OUEL-1659/86] 07 p0907 N88-15495
Linear state space modeling of a turbofan engine
[AD-A190110] 15 p2019 N88-22035
A state-space approach to discrete-time super-optimal H sup inf control problems
[OUEL-1712/87] 17 p2391 N88-24211
A design study of onboard navigation and guidance during aerocapture at Mars
[NASA-CR-172053] 18 p2469 N88-24654
Increasing accuracy in evaluating vector of state under conditions of incomplete observability of expanded system 24 p3446 N88-30511

STATIC AERODYNAMIC CHARACTERISTICS
The physics and mathematical description of the Achilles heel of stationary wind turbine aerodynamics: The tip flow
[R-812-D] 03 p0260 N88-11635

STATIC CHARACTERISTICS
NT STATIC AERODYNAMIC CHARACTERISTICS
The Lewis Strain Gauge Laboratory: Status and plans
02 p0184 N88-11146
Attitude determination of artificial satellites through joint application of static and dynamic optimal estimation techniques
[INPE-4415-TDL/306] 08 p0963 N88-15832
Static and dynamic jamming of networks
[AD-A188921] 12 p1620 N88-19690
Domain perturbation method in the static equilibrium of masses in rotation
[INPE-4217-PRE/1098] 12 p1686 N88-20085
Experimental research on center of pressure of slender body with two pointed ends 14 p1864 N88-21137

STATIC DEFORMATION
Influence of the static deformation on a wing in the unsteady aerodynamic 05 p0551 N88-13357
Optical method to measure the deformations of structures loaded by hydraulic pressure
[SNIAS-881-430-111] 22 p3088 N88-28338

STATIC DISCHARGERS
Antistatic coating compositions
[GB-PATENT-2-177-413-A] 05 p0568 N88-13463

STATIC ELECTRICITY
Development of test methods for the electrostatic properties of nonhomogeneous fabrics, phase 2
[AD-A190853] 18 p2489 N88-24767
Light scattering by charged spheres
[AD-A193753] 22 p3153 N88-28759

STATIC FIRING
Altitude simulation testing of Ariane's second-stage engine 09 p1126 N88-16747
Integration testing of the propulsion system of Ariane's first stage 09 p1126 N88-16751
Transient Pressure Test Article (TPTA) 1.1 and 1.1A, volume 1
[NASA-CR-179322-VOL-1] 12 p1603 N88-19588
Environmental monitoring of a titan 34D 5 1/2 segment solid rocket motor static firing
[AD-A192975] 20 p2766 N88-26400

STATIC FRICTION
Further refinement and applications of the mixed computational algorithm for plane elastic contact problems
[AD-A188308] 12 p1683 N88-20065
Static and dynamic metal-metal friction at plastic stress levels
[DE88-011281] 23 p3222 N88-29176

STATIC LOADS
Reinforced flexural elements for TEMP-STRESS Program
[DE87-012961] 01 p0061 N88-10391
Investigation on ductile fracture behavior of 3-inch diameter Type 304 stainless steel pipe with a circumferential through-wall crack
[DE87-753016] 02 p0191 N88-11196
Static standing and dynamic walking of a practical biped robot
[DE88-001367] 04 p0451 N88-12795
Experimental studies on the tripping behavior of narrow T-stiffened flat plates subjected to hydrostatic pressure and underwater shock 05 p0592 N88-13613
Static force and moment test of the Holloman narrow-gage rocket sled at Mach numbers from 3.5 to 5.5
[AD-A186291] 07 p0822 N88-14995
A comparison of the predicted and measured gravitational stresses in VAWT (Vertical Axis Wind Turbine) blades
[DE88-002113] 09 p1187 N88-17111
Durability of compound cylinder under static internal-pressure repeat load of long duration
16 p2180 N88-22991
Diffusion models of crack growth due to random overloads
[DE88-008811] 21 p2962 N88-27595
Static and dynamic metal-metal friction at plastic stress levels
[DE88-011281] 23 p3222 N88-29176

STATIC MODELS
The analysis of recent crustal movements in static and kinematic models
[SER-B-279] 09 p1191 N88-17136

STATIC PRESSURE
NT HYDROSTATIC PRESSURE
Effect of empennage arrangement on single-engine nozzle/afterbody static pressures at transonic speeds
[NASA-TP-2753] 02 p0122 N88-10771

The structure of sonic underexpanded turbulent air jets in still air
[AD-A190856] 16 p2157 N88-22870
STATIC STABILITY
NT DIMENSIONAL STABILITY
NT SHELL STABILITY
NT STRUCTURAL STABILITY
Handling qualities of a wide-body transport airplane utilizing Pitch Active Control Systems (PACS) for relaxed static stability application
[NASA-TP-2482] 07 p0821 N88-14987
Material instabilities in solids
[AD-A189525] 13 p1738 N88-20388
An experimental study to determine the flow and the subsonic static and dynamic stability characteristics of aircraft operating at high angles-of-attack
16 p2201 N88-23129
Stability of stick-slip phenomenon by using constitutive friction laws of Dietrich and Ruina
[ILR-MITT-197] 24 p3379 N88-30127
STATIC TESTS
NT STATIC FIRING
Static force and moment test of the Holloman narrow-gage rocket sled at Mach numbers from 3.5 to 5.5
[AD-A186291] 07 p0822 N88-14995
Static performance of an axisymmetric nozzle with post-exit vanes for multiaxis thrust vectoring
[NASA-TP-2800] 13 p1719 N88-20280
Static performance of nonaxisymmetric nozzles with yaw thrust-vectoring vanes
[NASA-TP-2813] 14 p1861 N88-21118
Static mechanical properties of 30 x 11.5 - 14.5, type 8 aircraft tires of bias-ply and radial-belted design
[NASA-TP-2810] 14 p1867 N88-21157
STATIC THRUST
Static performance of nonaxisymmetric nozzles with yaw thrust-vectoring vanes
[NASA-TP-2813] 14 p1861 N88-21118
STATICS
NT AEROSTATICS
NT ELECTROSTATICS
NT HYDROSTATICS
Development of methods for the analysis of the frequency and voltage statics of electricity users and electrical networks
[ETN-87-90412] 01 p0043 N88-10271
Static aeroelastic considerations in the definition of design loads for fighter airplanes
05 p0550 N88-13351
Research in applied mathematics ralated to identification of noisy systems
[AD-A189355] 13 p1825 N88-20908
Static dielectric breakdown strength of condensed heterogeneous high explosives
[AD-A191035] 16 p2183 N88-23014
A static scheduler for the computer aided prototyping system: An implementation guide
[AD-A194340] 24 p3414 N88-30322
STATIONARY ORBITS
Numerical arc segmentation algorithm for a radio conference: A software tool for communication satellite systems planning
[NASA-TM-100789] 16 p2167 N88-22919
STATIONKEEPING
Phase 3 study of selected tether applications in space. Volume 2: Study results
[NASA-CR-179186] 02 p0132 N88-10828
A linear quadratic Gaussian with loop transfer recovery proximity operations autopilot for spacecraft
[NASA-CR-172028] 02 p0227 N88-11433
Development and qualification of an Augmented Electro-Thermal Hydrazine-Thruster (AEHT) with 0.1 to 0.2 N vacuum thrust
[BMFT-FB-W-86-012] 16 p2169 N88-22931
On the collision hazard of colocated geostationary satellites
[DFVLR-FB-88-02] 23 p3184 N88-28952
STATIONS
NT AUTOMATIC WEATHER STATIONS
NT COLUMBUS SPACE STATION
NT CREW WORKSTATIONS
NT GROUND STATIONS
NT HYDROELECTRIC POWER STATIONS
NT INTEGRATED MISSION CONTROL CENTER
NT MIR SPACE STATION
NT POLYSTATION DOPPLER TRACKING SYSTEM
NT SALYUT SPACE STATION
NT SPACE STATION POLAR PLATFORMS
NT SPACE STATIONS
NT TRACKING STATIONS
NT WEATHER STATIONS
NT WORKSTATIONS
The significance of orientation unknowns in station and net adjustments 11 p1506 N88-18994
STATISTICAL ANALYSIS
NT AMPLITUDE DISTRIBUTION ANALYSIS
NT ANALYSIS OF VARIANCE
NT BIVARIATE ANALYSIS
NT CORRELATION COEFFICIENTS
NT COVARIANCE
NT DISCRIMINANT ANALYSIS (STATISTICS)
NT FACTOR ANALYSIS
NT GOODNESS OF FIT
NT LIKELIHOOD RATIO
NT MAXWELL-BOLTZMANN DENSITY FUNCTION
NT MULTIVARIATE STATISTICAL ANALYSIS
NT NONPARAMETRIC STATISTICS
NT NORMAL DENSITY FUNCTIONS
NT ORTHOGONALITY
NT POISSON DENSITY FUNCTIONS
NT PROBABILITY DENSITY FUNCTIONS
NT PROBABILITY DISTRIBUTION FUNCTIONS
NT QUANTILES
NT RAYLEIGH DISTRIBUTION
NT REGRESSION ANALYSIS
NT REGRESSION COEFFICIENTS
NT SEQUENTIAL ANALYSIS
NT STANDARD DEVIATION
NT STATISTICAL CORRELATION
NT STATISTICAL DECISION THEORY
NT STATISTICAL TESTS
NT VARIANCE (STATISTICS)
NT WEIBULL DENSITY FUNCTIONS
Analyses and assessments of span wise gust gradient data from NASA B-57B aircraft
[NASA-CR-178268] 01 p0002 N88-10007
Low cycle fatigue on isotropic fine-grained graphite
[DE87-702627] 01 p0028 N88-10177
Two-dimensional shear flow turbulence: A statistical theory of vortex filaments
[DE87-012234] 01 p0046 N88-10295
Analysis of the bivariate parameter wind differences between Jimsphere and Windsonde
[NASA-TM-4014] 01 p0072 N88-10461
Statistically determined nickel cadmium performance relationships 02 p0165 N88-11039
Software reliability models for fault-tolerant avionics computers and related topics
[NASA-CR-181440] 02 p0220 N88-11382
An antenna array processing system for multiple source bearing estimation 03 p0305 N88-11927
Geological characterization and statistical comparison of outcrop and subsurface facies: Shannon Shelf sand ridges
[DE87-001243] 03 p0348 N88-12202
Spatial strength variation and statistical size effect of laminated orthotropic composite materials
04 p0427 N88-12646
Robust statistical methods for automated outlier detection 04 p0433 N88-12681
Statistics of the geomagnetic secular variation for the past 5Ma
[NASA-CR-181558] 04 p0467 N88-12890
Statistical inference: Computer oriented algorithmic approach
[DE87-013874] 04 p0478 N88-12948
An urn model for the multi-sample capture/recapture sequential tagging process
[AD-A184470] 04 p0486 N88-12998
Statistical properties of small high-velocity events in the solar transition region 04 p0506 N88-13112
Statistical process control applied to the liquid-fed ceramic melter process
[DE88-000271] 05 p0569 N88-13471
A system identification technique based on the random decrement signatures. Part 1: Theory and simulation
05 p0594 N88-13625
A system identification technique based on the random decrement signatures. Part 2: Experimental results
05 p0594 N88-13626
Fatigue crack growth: Statistical considerations
05 p0606 N88-13718
Global atmospheric circulation statistics: Four year averages
[NASA-TM-100690] 05 p0628 N88-13842
An APL workspace for conducting nonparametric statistical inference
[AD-A184971] 05 p0634 N88-13877
Sample reuse in statistical remodeling
[AD-A184916] 05 p0643 N88-13938
Quantile based unified distribution of extreme values and order statistics
[AD-A185171] 05 p0644 N88-13942
Quantile statistical data analysis
[AD-A185181] 05 p0644 N88-13943
Presentation of a computer program permitting the exploitation of tests designed to determine the sensitivity of one shot devices to a parameter. Application to a degenerate one shot sequence
[SNIAS-872-430-117] 05 p0644 N88-13945
Boeing 727 MLS (Microwave Landing System) terminal instrument procedures (TERPS) approach data collection and processing, data report
[AD-A185523] 06 p0667 N88-14090
Statistical techniques for signal processing
[AD-A185774] 06 p0694 N88-14259
Statistical structure of temperature field over South Pacific Ocean 06 p0728 N88-14465
Geophysical-geomorphological statistical regionalization of North Atlantic
06 p0726 N88-14466
A statistical study of variations of internal gravity wave energy characteristics in meteor zone
06 p0735 N88-14523
A unified mathematical approach to image analysis
[AD-A185719] 06 p0765 N88-14703
Adaptive detection in non-stationary interference, part 3
[AD-A185622] 07 p0844 N88-15118
Statistical analyses of measured directional wave and current data
[PB87-144523] 07 p0853 N88-15185
Robust prediction and interpolation for vector stationary processes, 2d enriched version
[AD-A185875] 07 p0865 N88-15247
How errors in component reliability affect system reliability
[AD-A186264] 07 p0865 N88-15249
On two methods of identifying influential sets of observations
[AD-A186270] 07 p0910 N88-15516
Statistical selection procedures
[AD-A185868] 07 p0913 N88-15538
Mathematical techniques for system realization and identification
[AD-A186352] 07 p0915 N88-15557
On the extreme order statistics for a stationary sequence
[AD-A186428] 07 p0916 N88-15561
Increasing time resolution of picosecond absorption spectrometer by selection of length of laser light pulses
07 p0919 N88-15579
Turbulence models for practical applications
08 p0986 N88-15974
Statistical measures of clipped random signals
08 p1000 N88-16055
Statistical model of interaction of electromagnetic waves with natural objects being sensed
08 p1008 N88-16112
Predictability of ice concentration in the high-latitude North Atlantic from statistical analysis of SST (Sea Surface Temperature) and ice concentration data
[AD-A186621] 08 p1045 N88-16315
Conditional sampling in plasma turbulence
08 p1097 N88-16603
Fracture-mechanical, statistics and fractographic investigations on the steel 20 MnMoNi 55 in the ductile-brittle transition domain
[ETN-88-91064] 09 p1144 N88-16856
Strength and toughness of a brittle material
[VTT-RR-479] 09 p1183 N88-17089
Statistics of two-dimensional structure elements of mountainous ranges (mosaic model) for calculating three-dimensional reflection functions
[DFVLR-FB-87-33] 09 p1185 N88-17099
Error analysis for geotechnical engineering
[AD-A186795] 09 p1189 N88-17124
An application of fuzzy set theory to statistical hypothesis testing
[AD-A186705] 09 p1232 N88-17386
Outlier resistant predictive source encoding for a Gaussian stationary nominal source
[AD-A186725] 09 p1232 N88-17387
Calculating measurement imprecision and uncertainty
[DE88-003981] 09 p1233 N88-17391
Statistics of breakdown centers appearing during propagation of laser radiation through turbulent atmosphere 09 p1236 N88-17411
Helicopter activities in Germany
[MBB-UD-487/86] 10 p1314 N88-17853
Radar reflectivity and attenuation of radio waves in the melting layer of precipitation
[PB88-121553] 10 p1318 N88-17882
Statistical studies of low frequency oscillations in satellite-observed stratospheric temperatures
10 p1353 N88-18086
On precision and accuracy (bias) statements for measurement procedures
[DE88-004434] 10 p1402 N88-18359
A generalized quantile estimator under censoring
[AD-A188280] 10 p1402 N88-18364
Los Alamos optical materials reliability, maintainability, and exposure testing program
[DE88-001953] 10 p1409 N88-18404
Advances in calculating macroionic solution structure
[DE88-003799] 10 p1409 N88-18406

A semianalytical technique for sensitivity analysis of unsteady aerodynamic computations
[NASA-TM-100810] 11 p1503 N88-18976

Causes and prevention of occupational Repetition Strain Injuries (RSI) 11 p1521 N88-19083

Joint moments of the maximum in a critical branching process
[AD-A188157] 11 p1541 N88-19209

The SAS (Statistical Analysis System) by forms: Putting statistical power into the hands of an end-user
[DE88-002217] 11 p1541 N88-19212

Optimal arrangement of components via pairwise rearrangements
[AD-A187633] 11 p1541 N88-19213

Robustness in cost performance models
[AD-A187183] 11 p1566 N88-19374

Sampling intervals
[AD-A189445] 12 p1573 N88-19408

Systems approach to energy quality and efficiency
[PB88-139506] 12 p1640 N88-19823

Comparison of simulation modeling and satellite techniques for monitoring ecological processes
[NASA-CR-182592] 12 p1641 N88-19825

Estimating the solar irradiance of an intermountain region using GOES (Geostationary Operational Environmental Satellite) satellite data: A test of two statistical models
[AD-A188414] 12 p1642 N88-19834

Pre-convective environmental conditions indicative of non-tornadic severe thunderstorm winds over Southeast Florida
[AD-A188679] 12 p1648 N88-19870

Worldwide distributions of shipboard surface meteorological observations for EM propagation analysis
[AD-A188771] 12 p1648 N88-19871

Experimental analysis of algorithms
[AD-A188528] 12 p1677 N88-20028

Predicting transforms of stable noise and other Gaussian mixtures
[AD-A189280] 12 p1684 N88-20071

Detecting serial correlation in the error structure of a cross-lagged panel model
[AD-A189070] 12 p1685 N88-20077

Pion absorption in nuclei: The pion(+ or -),proton reactions
[LA-10997-T] 12 p1688 N88-20098

Management information systems design implications: The effect of cognitive style and information presentation on problem solving
[AD-A188850] 12 p1705 N88-20205

Design methodology for allocating data in a distributed database
[AD-A188826] 12 p1706 N88-20215

Statistical considerations of graphite strength for assessing design allowable stresses
13 p1746 N88-20441

Statistical signal processing using a class of iterative estimation algorithms
[AD-A189050] 13 p1757 N88-20511

HF (High Frequency) Maximum Usable Frequency (MUF) model uncertainty assessment
[AD-A189132] 13 p1757 N88-20513

Tests for uniformity arising from a series of events
[AD-A189069] 13 p1828 N88-20935

Stochastic comparisons of order statistics, with applications in reliability
[AD-A189408] 13 p1829 N88-20938

Application of expert systems in project management decision aiding
[NASA-CR-180762] 13 p1850 N88-21074

Electromagnetic scattering by an exponentially distributed rough surface with the introduction of a rough surface generation technique
[AD-A189678] 14 p1906 N88-21392

Statistical analysis of feasibility of non-destructive inspection of mechanical properties of hot worked pipes of alloy steels
[BLL-M-37598-(5828.4)] 14 p1922 N88-21455

Assimilation of meteorological observations
14 p1936 N88-21544

Spatial and temporal distribution of precipitation chemistry across Maryland in 1984, volume 2
[PB88-148937] 14 p1944 N88-21596

Analysis of winter season precipitation bands over the Southern Plains 14 p1947 N88-21609

Quasi-loglinear models for test and item analysis --- psychometrics
[B8716249] 14 p1952 N88-21636

The NPL data approximation subroutine library: Current and planned facilities
[NPL-DITC-104/87] 14 p1959 N88-21681

Using a parallel computer system for statistical resampling methods
[REPT-87-47] 14 p1960 N88-21690

General aviation activity and avionics survey: 1986 data
[AD-A189986] 15 p2013 N88-22003

Results of the International Comparison of Absolute Gravimeters (2nd) held in Sevres, France in June-July 1985
[AD-A189869] 15 p2093 N88-22474

The collection of statistics on the frequency of cloud cover over North America
[AD-A190456] 15 p2097 N88-22495

Properties of some Bayesian scoring procedures for computerized adaptive tests
[AD-A189925] 15 p2124 N88-22660

Empirical and hierarchical Bayes competitors of preliminary test estimators in two sample problems
[AD-A190327] 15 p2125 N88-22670

Statistical fine structure in inhomogeneously broadened absorption lines in solids
[AD-A190341] 16 p2174 N88-22957

Statistical fine structure in the inhomogeneously broadened electronic origin of pentacene in p-terphenyl
[AD-A191211] 16 p2176 N88-22968

Modeling of turbulent transport as a volume process
16 p2196 N88-23099

A statistical investigation of the single-point pdf of velocity and vorticity based on direct numerical simulations 16 p2196 N88-23101

Seasonal variation for structural strength value
[PB88-169248] 16 p2222 N88-23260

Analysis of means in some nonstandard situations
[ETN-88-92247] 16 p2262 N88-23522

Remote sensing techniques in the estimation of the area cultivated with beans, corn, and castor beans in the Irece County (Bahia State) 17 p2358 N88-24045

Characteristics of drainage determinations in aerial photographs and relief determination on different scales planialtimetric charts for three soils in the state of Sao Paulo 17 p2367 N88-24095

An investigation of Soviet capabilities in extended range arctic ice forecasting
[AD-A191082] 17 p2376 N88-24127

Survival analysis, or what to do with upper limits in astronomical surveys
[NASA-CR-182936] 17 p2449 N88-24551

Performance estimates for operations conducted while wearing individual protective equipment: User manual
[AD-A191871] 18 p2553 N88-25154

Annotated computer output for split plot design: SAS GLM
[AD-A190800] 18 p2555 N88-25167

A method for the numerical solution of random Cauchy singular integral equation 18 p2565 N88-25234

Exact tests for variance component models with unequal cell frequencies in the last stage
[AD-A191645] 18 p2568 N88-25253

On path properties of certain infinitely divisible processes
[AD-A192016] 18 p2568 N88-25255

Statistical evaluation of light water reactor piping damping data for use in PRA (Probabilistic Risk Assessment) analyses
[DE88-007708] 19 p2661 N88-25828

Determining system maintainability as a probability
[DE88-007722] 19 p2679 N88-25927

Circulation statistics from seasonal and perpetual January and July simulations with the NCAR (National Center for Atmospheric Research) Community Climate Model (CCM1):R15
[PB88-192620] 20 p2823 N88-26748

Kinetic theory for plane flows of rough, inelastic, circular disks 21 p2946 N88-27499

The low-latitude auroral boundary: Steady-state and time-dependent representations
[AD-A193200] 21 p2972 N88-27656

The collection of statistics on the frequency of cloud cover over North America
[AD-A193093] 21 p2974 N88-27667

A statistical procedure for the evaluation of presence/non-presence of stimulus-related EEG activity
21 p2978 N88-27689

Computation of filters by sampling and quantization
[AD-A192839] 21 p3005 N88-27826

On the exceedance random measures for stationary processes
[AD-A192838] 21 p3009 N88-27848

Statistical analysis of dyadic stationary processes
[AD-A193057] 21 p3009 N88-27853

The SAS System by forms: Putting statistical power into the hands of an end-user
[DE88-010512] 21 p3010 N88-27857

Comparison of results based on a deterministic versus a statistical uncertainty analysis
[DE88-010751] 21 p3010 N88-27858

Analysis of lower hybrid current drive and rampup experiments on the JT 60 tokamak
[DE88-753136] 21 p3018 N88-27915

Modeling discrete bathtub and upside down bathtub mean residual life functions
[AD-A192000] 22 p3085 N88-28320

Evaluation of annual crop surfaces and territorial inventory in the Paris basin by combining classic statistical inquiries and SPOT data (Preliminary Evaluation Program for SPOT 127) 22 p3094 N88-28372

Complex EOF analysis of intraseasonal tropical wind fluctuations 22 p3121 N88-28544

Sub-Saharan rainfall anomalies and global sea-surface temperature relationships for the recent fifteen year (1970-1984) period 22 p3122 N88-28552

Northern Hemisphere 700 mb teleconnections based on half-monthly mean anomaly data stratified by season and by sign 22 p3123 N88-28561

On the modes of growing-season precipitation over central North America 22 p3124 N88-28567

Correction of systematic errors in NMC medium range forecasts 22 p3126 N88-28584

Theoretical and practical limits of predictability of the NMC medium-range model 22 p3127 N88-28586

A comparison of typical meteorological year solar radiation information with the SOLMET data base
[DE88-009242] 23 p3234 N88-29247

A minitab macro for the Kaplan-Meier product limit estimator and the Tarone-Ware class of tests
[AD-A194298] 23 p3248 N88-29331

Multi-sensory tracking mount control
[AD-A194675] 23 p3249 N88-29339

Commentary on Harold Hotelling's articles on the teaching of statistics
[AD-A194215] 23 p3273 N88-29484

Limiting distributions of non-linear vector functions of stationary Gaussian processes
[AD-A194569] 23 p3274 N88-29488

Asymptotic modal analysis and statistical energy analysis
[NASA-CR-183077] 23 p3278 N88-29514

Measurement and analysis of low altitude atmospheric turbulence obtained using a specially instrumented Gnat aircraft 24 p3313 N88-29728

Re-assessment of gust statistics using CAADRP data
24 p3313 N88-29732

Fatigue crack propagation: Probabilistic modeling and statistical analysis
[AD-A195885] 24 p3384 N88-30155

Statistical analysis of the LMS (Last Mean Squares) and modified stochastic gradient
[AD-A195497] 24 p3424 N88-30376

Instrumentation for computational statistical research
[AD-A195887] 24 p3426 N88-30390

STATISTICAL COMMUNICATION THEORY
U COMMUNICATION THEORY

STATISTICAL CORRELATION

Independence in sonar observations
[ARE-TR-87102] 01 p0088 N88-10572

An application of L1 to astronomy --- stellar velocity
[REPT-87-10] 01 p0108 N88-10702

The velocity structure and turbulence at the center of the Orion Nebula 04 p0521 N88-13201

Control charts when the observations are correlated
[AD-A186388] 07 p0866 N88-15253

STATISTICAL DECISION THEORY

Bayesian solutions to a 2 x 2 decision matrix using interval scaled payoffs with an application to foreign policy decisions
[AD-A190863] 16 p2260 N88-23511

STATISTICAL DISTRIBUTIONS
NT BRIGHTNESS DISTRIBUTION
NT PROBABILITY DISTRIBUTION FUNCTIONS
NT RAYLEIGH DISTRIBUTION

RANDOM NUMBER: A syntax-directed package to produce random numbers in user-specified, univariate distributions. User's guide
[DE87-014278] 02 p0228 N88-11436

Light scattering by oriented and randomly dispersed chiral particles
[DE87-014758] 03 p0376 N88-12368

On the geometrical description of fatigue crack surfaces 05 p0607 N88-13727

The application of doubly-truncated hydrometeor distributions to numerical cloud models
[AD-A185273] 05 p0627 N88-13836

Quantile based unified distribution of extreme values and order statistics
[AD-A185171] 05 p0644 N88-13942

Tracking procedure for non-normally distributed measurement errors
[AD-A186287] 07 p0903 N88-15468

Recursive m-estimators of location and scale for dependent sequences
[AD-A186292] 07 p0903 N88-15469

Detecting and interval estimation about a slope change point
[AD-A186030] 07 p0909 N88-15509

Additional investigations in landing process of aircraft: Test distributions
[DFVLR-MITT-87-13] 09 p1115 N88-16685

Analysis of gases in the earth's crust
[PB88-141619] 10 p1354 N88-18093

Five New South Wales barrier lagoons: Their macrobenthic fauna and seagrass communities
11 p1517 N88-19059

Position finding and tolerances
[AD-A187685] 11 p1540 N88-19205

Analysis of impact crater arrangement on the Venutian surface (from photographic materials of the Venera-15 and -16 spacecraft)
[NASA-TT-20211] 11 p1571 N88-19401

Design of the primary pre-TRMM and TRMM ground truth site
[NASA-CR-182609] 12 p1647 N88-19865

On the theory of electromagnetic scattering from a raindrop splash
[AD-A188720] 14 p1906 N88-21393

Grain boundary oxidation and low-cycle fatigue at elevated temperatures 15 p2083 N88-22420

Statistical inference for stochastic processes
[AD-A190491] 15 p2126 N88-22673

Evaluation of an estimation system for an irrigated area in a tropical region through TM-LANDSAT imagery
17 p2363 N88-24075

Evaluation of the floodable area of the canal of Sao Goncalo through TM-LANDSAT 5 imagery
17 p2364 N88-24078

Restrictions in activity monitoring through remote sensing 17 p2365 N88-24084

The 35 mm vertical aerial photographs for mapping stands of bracatinga in different age classes
17 p2366 N88-24087

Preliminary study on the application of digital processing of TM-LANDSAT data in the mapping of apple orchards in Fraiburgo (SC) 17 p2367 N88-24093

Some geological aspects of the Pirapemas Lineament Belt 17 p2368 N88-24099

The theory of random alloys
[DE88-006408] 18 p2487 N88-24756

Interpreting forest biome productivity and cover utilizing nested scales of image resolution and biogeographical analysis
[NASA-CR-183036] 20 p2817 N88-26711

Range of a constrained random walk
[PB88-126867] 20 p2847 N88-26897

Aperiodic superlattices: Structured randomness
20 p2873 N88-27055

The computation of stationary distributions on Markov chains through perturbations
[AD-A193191] 21 p3009 N88-27855

A probabilistic model of the apparent radiance of a rough sea
[AD-A193867] 22 p3129 N88-28602

Additional investigations into the aircraft landing process: Test distributions
[ESA-TT-1099] 23 p3177 N88-28913

Selecting the best binomial population: Parametric empirical Bayes approach
[AD-A193341] 23 p3269 N88-29450

Sequential approach to Colombeau's theory of generalized functions
[DE88-701869] 23 p3276 N88-29503

AGN (OIII) emission line profiles: Dependencies on galaxy inclination and Balmer decrement
[INPE-4596-PRE/1324] 24 p3459 N88-30577

STATISTICAL MECHANICS

Statistical mechanical theory of condensed explosives
[DE87-009137] 01 p0031 N88-10197

Chaos: Chto Delat? (What is to be done?)
[DE88-000513] 05 p0643 N88-13933

Relativistic stochastic mechanics
[PREPRINT-543] 06 p0790 N88-14842

A study of the free energy of the Lenz-Ising model using the cluster variation method of Morita
[AD-A186023] 08 p1073 N88-16476

Electronic structure and phase stability of alloys
[DE88-004574] 11 p1562 N88-19350

Integral equation theory of polymer blends
[DE88-005305] 13 p1751 N88-20471

Memory efficient evaluations of nonlinear stochastic equations and C3 applications
[AD-A189872] 15 p2110 N88-22569

A small concentration expansion for the effective heat conductivity of a random disperse two-component material; an assessment of Batchelor's renormalization method
[REPT-87-71] 16 p2207 N88-23168

The two-dimensional one component plasma in a doubly periodic background: Exact results
[AD-A191260] 16 p2280 N88-23650

Introduction to lattice gauge theory
[DE88-006073] 18 p2584 N88-25349

Thermo field dynamics and para statistical mechanics
[DE88-702057] 19 p2737 N88-26253

On microphysical principles of thermofluid dynamics
[ETN-88-92095] 20 p2801 N88-26620

Extension of Boltzmann's theory to a liquid
[DE88-009153] 20 p2880 N88-27097

Statistical description of stochastic dynamics
[AD-A192924] 21 p3009 N88-27852

A virtual statistical mechanical neural computer
[AD-A193962] 22 p3139 N88-28660

STATISTICAL MOMENTS
U DISTRIBUTION MOMENTS

STATISTICAL PROBABILITY
U PROBABILITY THEORY

STATISTICAL TESTS

Determining differences in rates corresponding to a given significance level
[AD-A185004] 05 p0644 N88-13940

Contributions to selection and ranking theory with special reference to logistic populations
[AD-A185629] 07 p0917 N88-15568

Asymptotic error bounds for power approximations to multinomial tests of fit
[MEMO-640] 08 p1072 N88-16470

An application of fuzzy set theory to statistical hypothesis testing
[AD-A186705] 09 p1232 N88-17386

Statistical aspects of reliability, maintainability and availability
[AD-A188491] 12 p1634 N88-19783

On the Edgeworth expansion and the bootstrap approximation for a Studentized U-statistic
[CWI-MS-R8708] 14 p1965 N88-21728

Distributions of quadratic forms
[AD-A190224] 15 p2124 N88-22663

Stopping rules and observed significance levels
[AD-A190320] 15 p2124 N88-22664

Admissible Bayes tests for structural relationship
[AD-A190326] 15 p2125 N88-22669

On Hotelling's approach to testing for a nonlinear parameter in regression
[AD-A191189] 17 p2393 N88-24229

A minitab macro for the Kaplan-Meier product limit estimator and the Tarone-Ware class of tests
[AD-A194298] 23 p3248 N88-29331

A nonparametric multidimensional IRT approach with applications to ability estimation and test bias
[AD-A194212] 23 p3273 N88-29483

Exact lower confidence limits for the reliability of k of n systems for zero failures and nonconservativeness of the maximus method
[AD-A194299] 23 p3274 N88-29485

Instrumentation for computational statistical research
[AD-A195687] 24 p3426 N88-30390

STATISTICAL WEATHER FORECASTING

Forecasting the kind of precipitation in winter
02 p0202 N88-11266

Statistical very short-range forecasting via analogues
02 p0206 N88-11290

Statistical remote sensing algorithm development: A complementary process to mesoscale numerical models
02 p0206 N88-11292

A severe weather forecast software package
02 p0206 N88-11294

Statistical relationships between the mesoscale organization of convection and the large-scale wind profiles during GATE --- GARP Atlantic Tropical Experiment (GATE) 02 p0208 N88-11302

Mesoscale MOS forecast support for 1988 winter Olympics ski events --- model output statistics (MOS)
02 p0209 N88-11312

Extrapolation of extremum values of the wind velocity
08 p1015 N88-16150

The bimodality of large scale averaged flow parameters --- statistical weather forecasting
08 p1016 N86-16159

A drought watch system
[WCP-134] 16 p2234 N88-23345

Comparative verification between GEM model and official aviation terminal forecasts
18 p2546 N88-25115

STATOR BLADES

Computational study on thermal efficiency of ceramic gas turbine
[DE88-753114] 20 p2809 N88-26667

Numerical solutions of unsteady inviscid transonic turbine cascade flows
[AD-A196111] 24 p3316 N88-29748

STATORS

Measurement of airfoil heat transfer coefficients on a turbine stage 02 p0186 N88-11158

Flow in a model turbine stator
02 p0187 N88-11163

Turbine airfoil deposition models and their hot corrosion implications 02 p0189 N88-11178

An explicit Runge-Kutta method for unsteady rotor/stator interaction
[NASA-TM-100787] 07 p0816 N88-14967

A comparison of experimental and theoretical results for labyrinth gas seals with honeycomb stators
[NASA-CR-182441] 08 p0993 N88-16006

Experimental rotordynamic coefficient results for honeycomb seals
[NASA-CR-182440] 08 p0993 N88-16007

The unsteady gas flow through stator and rotor of a turbomachine 10 p1281 N88-17660

Parametric study of choke flutter with a linear theory
10 p1283 N88-17673

Computer-aided modeling and prediction of performance of the modified Lundell class of alternators in space station solar dynamic power systems
[NASA-CR-182538] 11 p1507 N88-19000

Piezoelectric pushers for active vibration control of rotating machinery 16 p2218 N88-23229

Study on the heat resisting and cooling property of the ceramics-metal hybrid stator vanes
[DE88-753117] 20 p2810 N88-26668

The effects of inlet turbulence and rotor/stator interactions on the aerodynamics and heat transfer of a large-scale rotating turbine model. Volume 3: Heat transfer data tabulation 65 percent axial spacing
[NASA-CR-179468] 23 p3180 N88-28930

Three-dimensional Navier-Stokes simulations of turbine rotor-stator interaction
[NASA-TM-100081] 24 p3316 N88-29750

An unconditionally stable Runge-Kutta method for unsteady flows
[NASA-TM-101347] 24 p3321 N88-29780

The effects of inlet turbulence and rotor/stator interactions on the aerodynamics and heat transfer of a large-scale rotating turbine model. Volume 2: Heat transfer data tabulation. 15 percent axial spacing
[NASA-CR-179467] 24 p3326 N88-29804

STAYS
U GUY WIRES

STEADY FLOW
NT COUETTE FLOW

Calculation of stationary and low frequency unsteady flows in a steam turbine end stage
[MITT-23] 01 p0057 N88-10364

Instability of steady flow with constant vorticity in vessels with elliptical cross-section 02 p0159 N88-10997

SHARP simulation of discontinuities in highly convective steady flow
[NASA-TM-100240] 05 p0642 N88-13931

Measurements of the time dependent velocity field surrounding a model propeller in uniform water flow
16 p2205 N88-23155

A variational finite element method for three-dimensional, steady, compressible, viscous flows
18 p2512 N88-24904

An h-p adaptive finite element method for steady compressible flow 21 p2941 N88-27467

An efficient patched grid Navier-Stokes solution for multiple bodies, phase 1
[AD-A194166] 23 p3211 N88-29110

Contamination and distortion of steady flow field induced by discrete frequency disturbances in aircraft gas engines
[AD-A195440] 24 p3370 N88-30069

STEADY STATE

A baroclinic wavy basic state model: Description and preliminary experiments
[KNMI-WR-87-1] 01 p0068 N88-10436

A two-fluid model for solar wind fluid with higher order moments 01 p0116 N88-10739

Blade loss transient dynamics analysis, volume 1. Task 2: TETRA 2 theoretical development
[NASA-CR-179632] 02 p0125 N88-10791

Blade loss transient dynamics analysis, volume 2. Task 2: TETRA 2 user's manual
[NASA-CR-179633] 02 p0126 N88-10792

Proceedings of the Japan-US Workshop P-92 on Plasma Material Interaction/High Heat Flux Data Needs for the Next Step Ignition and Steady State Devices
[DE87-013568] 04 p0494 N88-13042

PISCES: Plasma-surface interactions and materials research
[DE88-001323] 04 p0494 N88-13044

An experimental investigation of the aerodynamics of a NACA 64A010 airfoil-flap combination with and without flap oscillations. Part 1: Steady-state characteristics
[NASA-TM-88217] 05 p0542 N88-13305

RADSPHERE: A computer program for calculating the steady-state, axially symmetric, forced response and radiation field of a submerged spherical shell
[AD-A185025] 05 p0609 N88-13738

Numerical methods for reaction-diffusion problems with non-differentiable kinetics
[AD-A185405] 05 p0641 N88-13923

Gas diffusion studies in steady and nonsteady cavities
[AD-A185795] 06 p0704 N88-14318

A loading system for creep testing under constant compressive stress
[NASA-TT-20119] 06 p0722 N88-14441

Steady-state deformation of some lithium ceramics
[DE88-003116] 08 p0972 N88-15882

Influence of viscosity on the structure of a magnetic neutral layer 08 p1096 N88-16605

Dynamic evolution of the source volumes of gradual and impulsive solar flare emissions
[NASA-TM-87815] 08 p1102 N88-16621

Optimization of volume produced H(-) ions in a low-pressure hydrogen plasma
[IPPJ-853] 09 p1252 N88-17505

On the barotropic model of the ocean circulation
[AD-A188148] 10 p1358 N88-18118

Thermal analysis in steady state conditions for satellites
[INPE-4429-TDL/309] 12 p1599 N88-19574

Accelerating the computation of steady state solutions for non-equilibrium, chemically reacting flow fields
12 p1625 N88-19724

Optimum duration of steady-state stage in friction welding of metals without artificial braking
14 p1898 N88-21330

Coupled bending-torsion steady-state response of pretwisted, nonuniform rotating beams using a transfer-matrix method
[NASA-TM-100596] 15 p2086 N88-22435

Magnetic fusion energy plasma interactive and high heat flux components. Volume 5: Technical assessment of critical issues in the steady state operation of fusion confinement devices
[DE88-006920] 15 p2136 N88-22744

Analysis of closed cycle megawatt class space power systems with nuclear reactor heat sources
17 p2413 N88-24351

EETAP (End-to-End Transient Analysis Program) for space nuclear power system simulation
17 p2418 N88-24381

HTPIPE: A steady state heat pipe analysis program
17 p2421 N88-24396

Periodic solutions in aircraft cruise-dash optimization
18 p2464 N88-24631

Steady state and transient behavior of the Pd-SnO(sub x) MIS oxygen sensors 19 p2672 N88-25890

Evolution of poloidal variation of impurity density and ambipolar potential in rotating tokamak plasma, part 2
[DE88-009882] 19 p2731 N88-26218

Periodic oscillations in nonlinear mechanical systems
21 p2963 N88-27599

The low-latitude auroral boundary: Steady-state and time-dependent representations
[AD-A193200] 21 p2972 N88-27656

Steady-state approximations in Raman excitation equations
[DE88-011759] 21 p3014 N88-27889

Steady and unsteady transonic pressure measurements on a clipped delta wing for pitching and control-surface oscillations
[NASA-TP-2594] 23 p3173 N88-28895

An exponential decay estimate for the stationary perturbation of Poiseuille flow
[AD-A193480] 23 p3210 N88-29105

Finite element analysis of steady and transiently moving/rolling nonlinear viscoelastic structure. Part 1: Theory
[NASA-CR-179886] 23 p3273 N88-29480

STEADY STATE FLOW
U EQUILIBRIUM FLOW

STEAM

Development of creep resistant austenitic stainless steels for advanced steam cycle superheater application
[DE87-012929] 01 p0023 N88-10147

Comparative tests of high temperature creep-rupture behavior of the austenitic CrNi steel DIN W.NR.1.4970 in argon and steam
[KFK-4261] 01 p0063 N88-10402

National Aerospace Laboratory experiment
04 p0404 N88-12509

Cu-2 mechanical properties and microstructural stability of advanced steam cycle materials
[DE88-001519] 05 p0566 N88-13452

To the problem of determining true volume steam content by measured values of mean density of a mixture in thermally unsteady two-phase flows
[DE88-700840] 12 p1626 N88-19726

STEAM FLOW

National Aerospace Laboratory experiment
04 p0404 N88-12509

Study of a water-steam two phase flow in a T-branch
[ETN-88-92306] 20 p2601 N88-26624

STEAM GENERATORS
U BOILERS

STEAM TURBINES

The effect of different packagings on the vibration behavior and the coupling factors of steam turbine blading
[ETN-87-90425] 01 p0056 N88-10357

Calculation of stationary and low frequency unsteady flows in a steam turbine end stage
[MITT-23] 01 p0057 N88-10364

Development of a supersonic steam turbine with a single stage pressure ratio of 200 for generator and mechanical drive 06 p0713 N88-14374

On line instrument systems for monitoring steam turbogenerators
[CISE-3860] 08 p0990 N88-15995

Open-cycle centrifugal vapor-compression heat pump
[PB88-157391] 11 p1488 N88-18885

Design of a high-power-density Ljungstroem turbine using potassium as a working fluid
17 p2409 N88-24323

STEEL STRUCTURES

The effect of fretting corrosion on the fatigue strength of steel and cast iron under sinusoidal and random loading
[LBF-FB-177] 01 p0023 N88-10142

Deformation induced cracking in steel girder bridges and retrofit guidelines
[PB88-102710] 07 p0868 N88-15265

A summary of experimental results on square plates and stiffened panels subjected to air-blast loading
09 p1178 N88-17057

Removal of out-of-plane distortion in mild steel panels using flame heating, volume 1
[AD-A187802] 11 p1457 N88-18684

Removal of out-of-plane distortion in mild steel panels using flame heating, volume 2
[AD-A187803] 11 p1457 N88-18685

Characteristics of welds joining parts of high-strength pipe steels and produced by beam of continuous-wave CO2-laser 14 p1897 N88-21325

STEELS
NT AUSTENITIC STAINLESS STEELS
NT BAINITIC STEEL
NT CARBON STEELS
NT CHROMIUM STEELS
NT FERRITIC STAINLESS STEELS
NT HIGH STRENGTH STEELS
NT LOW CARBON STEELS
NT MARAGING STEELS
NT MARTENSITIC STAINLESS STEELS
NT NICKEL STEELS
NT STAINLESS STEELS

Optimizing the application of high temperature corrosion resistant aluminium-silicon-base coatings
[BLL-M-37222-(5828.4)] 01 p0018 N88-10112

A physical metallurgical basis for heat-affected zone and base-plate properties of a microalloyed HSLA steel
[AD-A180200] 01 p0022 N88-10137

Development of ultrafine grains and related properties in Hadfield manganese steels
[DE87-011884] 01 p0024 N88-10154

Crack propagation behavior of the materials StE 460 and AlMg 4.5Mn
[FD-1/1986] 01 p0058 N88-10373

The effect of size and surface on the lifetime prediction of StE 460 notched bars
[FD-6/1986] 01 p0058 N88-10374

Fatigue crack propagation of low-alloy steel in a vacuum environment
[DE87-013770] 01 p0061 N88-10393

The water permeability of multi-layer coatings
[BLL-M-37252-(5828.4)] 02 p0148 N88-10927

Anelastic behaviour of materials under multiaxial strains. Part 3: Order-disorder transition, Shoek effect and Poisson's ratio in AISI-1080 steel
[DE87-703087] 02 p0191 N88-11193

Microstructural characterization of irradiated PWR steels using the atom probe field-ion microscope
[DE88-000341] 03 p0291 N88-11828

Sintered steels of high resistance alloyed to Nb, Mo, Mn and Si
[DE87-703546] 04 p0415 N88-12573

Progress in the development of niobium alloyed high speed steel
[DE87-703549] 04 p0415 N88-12576

Hadfield steels with Nb and Ti carbides
[DE87-703706] 04 p0416 N88-12579

Corrosion of ferritic steels by molten lithium: Influence of competing thermal gradient mass transfer and surface product reactions
[DE88-000334] 04 p0417 N88-12585

Effects of stress-relieving on the mechanical properties and the structure of specimens of high-temperature fine-grained structural steels heat-treated to simulate welding
[BLL-CE-TRANS-8258-(9022.09)]
04 p0417 N88-12586

Influence of creep on the precipitate structure under conditions of long-term creep. 4: Experiments on 10 CrMo 9 10 steel
[BLL-CE-TRANS-8256-(9022.09)]
04 p0417 N88-12589

Corrosion resistance of sintered alloy steels
[BLL-M-37363-(5828.4)] 05 p0564 N88-13438

Master plots for predicting the case-depth in laser surface treatments
[PB87-221875] 05 p0586 N88-13574

The mechanics of fatigue-crack nucleation in a low-alloy steel under fretting conditions 05 p0597 N88-13649

The influence of the topography of fracture surfaces on crack closure 05 p0598 N88-13657

Striations and the fatigue growth mechanism in a micro-alloyed steel 05 p0599 N88-13661

Fatigue of 30CrMnSiNi2A notched specimens under spectrum loading 05 p0602 N88-13689

Interaction of microstructure and fatigue in tool steels
05 p0603 N88-13693

Tensile mean stress effects on uniaxial fatigue behavior of 1045 HR steel 05 p0603 N88-13694

The initiation and growth of fatigue cracks in carburised 9Cr1Mo steel 05 p0603 N88-13696

Crack propagation properties of sintered steel
05 p0604 N88-13698

The role of inclusions in corrosion fatigue crack initiation in Q1N 05 p0604 N88-13699

The influence of crack conditions on hydrogen uptake by steels 05 p0604 N88-13702

Modeling the effect of sulfur on the threshold environmental cracking rate of steels in high temperature water 05 p0604 N88-13703

Fracture analysis of drawn composite dual-phase steel wire
[DE88-001396] 06 p0681 N88-14173

Ion-beam nitriding of steels
[NASA-CASE-LEW-14104-2] 06 p0682 N88-14179

An investigation of fatigue crack growth in a ductile material at high growth rates 06 p0715 N88-14383

Life prediction of steel cords
06 p0715 N88-14386

On cleavage in fatigue for rail steels
06 p0716 N88-14388

Fatigue crack growth behavior in hydrogen gas environment 06 p0716 N88-14391

The relationship between microstructural size and fatigue threshold in iron and steel
06 p0716 N88-14396

Threshold behaviour of semi-elliptic hydrogen-induced and fatigue-induced cracks 06 p0717 N88-14397

A model for ultra-low fatigue crack growth
06 p0717 N88-14404

The effects of loading history on fatigue crack growth threshold 06 p0718 N88-14406

Study of the characteristic curve of hardening and softening during low-cycle fatigue process
06 p0719 N88-14414

Fatigue oxidation interaction in low cycle fatigue
06 p0719 N88-14420

Thermal mechanical low cycle fatigue of 25CDV4-10 steel 06 p0721 N88-14429

Transients in elevated temperature crack growth
[DE87-013189] 06 p0724 N88-14454

Characterization of current steels. The 35 NCD 16 alloy in 30 mm diam laminated bars made by Aubert and Duval
[CEAT-41/N/76] 07 p0832 N88-15046

Study on substructures of martensite in steels containing rare earth metals
[PB87-143996] 07 p0833 N88-15050

Tribological studies on high speed steel cutting tools
[DE88-002550] 07 p0864 N88-15246

Study on characteristics of SCC propagation da/dt for welded joint
[PB87-143640] 07 p0869 N88-15270

Analysis of load-bearing capacity of nitrided layer
[PB87-144176] 08 p0968 N88-15857

Rare earth elements in heat treatable steels
[PB87-144002] 08 p0968 N88-15858

Investigations in field of surface forces in metallurgy
[BLL-M-47406-(5828.4)] 08 p0969 N88-15860

TiN coatings on M2 steel produced by plasma assisted chemical vapor deposition
[DE88-003189] 08 p0970 N88-15867

Mechanical properties of steel-to-steel adhesive bonds
[PB88-111299] 08 p0971 N88-15877

The relationship of tensile specimen size and geometry effects to unique constitutive parameters for ductile materials
[AD-A186020] 08 p0994 N88-16012

Fracture-resistant characteristics of medium-strength plates with regard to the initiation, stable and unstable propagation of surface cracks
[PB87-144804] 08 p0996 N88-16025

Study of the temperature dependence of the mechanical characteristics of the steels GX 5 CrNi 13 4 and GGG 40 in tensile and bending tests
[DE88-001469] 09 p1143 N88-16850
Influence of non-metallic elements in the mechanical properties of 20 Mn Mo Ni 55 steel
[DE88-700412] 10 p1300 N88-17775
A detailed microstructural examination of the cause of HAZ cracking in type 316 steel
[AERE-R-12428] 10 p1301 N88-17777
Effects of commercial cladding on the fracture behavior of pressure vessel steel plates
[DE88-004333] 10 p1303 N88-17790
Acoustic emission-microstructural relations in ferritic steels. Part 3: The effect of inclusion content
[AERE-R-12041] 10 p1341 N88-18015
Acoustic emission measurements of PWR weld materials with inserted defects
[AERE-R-12386] 10 p1341 N88-18016
The measurement of stress in steels of varying microstructure by Barkhausen and magneto-acoustic emission
[AERE-R-12387] 10 p1343 N88-18027
Effects of sulfur content on the plain strain fracture toughness of inertia welds in 4340 steel
[AD-A188192] 11 p1458 N88-18689
Influence of grain boundary phosphorus segregation on hydrogen embrittlement in steel
[DE88-700176] 11 p1459 N88-18696
Protecting old oil tanks made of steel against internal corrosion using organic coatings
[DE88-751089] 11 p1459 N88-18698
Hydrogen embrittlement of gun steel
[AD-A188972] 13 p1740 N88-20407
Non-destructive evaluation techniques applied to the study of fatigue microcrack growth in steel alloys
[DE88-004090] 13 p1742 N88-20420
Transformation, metallurgical response and behavior of the weld fusion zone and heat affected zone in Cr-Mo steels for fossil energy application
[DE88-006037] 13 p1744 N88-20430
Corrosion-wear process under rolling-sliding motion
[AD-A189603] 13 p1778 N88-20635
Influence of hydrogen on crack formation tendency in heat-affected zone with stress concentrator
14 p1887 N88-21276
Rust converters
[AD-A188757] 14 p1891 N88-21299
Some structural aspects of crack propagation in heat-resistant steels under cyclic thermal and mechanical load 14 p1896 N88-21317
Efficiency of fusion during periodic-pulse laser-beam welding 14 p1897 N88-21324
Simulation of thermo-mechanical forming processes: A mixed Eulerian-Langrangian finite element method
[PB88-155247] 14 p1933 N88-21530
Influence of temperature on the tensile strength and toughness characteristics. Material 35NCD16 ESR. Test report M5-521800
[M5-521800] 15 p2041 N88-22163
Characterization of HYTUF steel. Semifinished product: 160 mm dia forging block. Processor: C3f. Test Report M3-434600
[M3-434600] 15 p2041 N88-22164
Analysis of reversible and irreversible hydrogen trapping in metals
[NPL-DMA(A)-154] 16 p2177 N88-22977
Dynamic fracture toughness evaluation by measurement of CTOD
[WNS/ASD-88-02] 16 p2178 N88-22982
Corrosion of electroless nickel-coated steel
[AD-A191045] 16 p2179 N88-22985
Environment effects on crack propagation with tensile stress
[GKSS-87/E/46] 16 p2223 N88-23267
Technology Reports of Kyushu University, volume 61, no. 2
[ISSN-0023-2718] 16 p2256 N88-23485
Irradiation effects on tungsten stabilized martensitic steels
[DE88-007074] 18 p2486 N88-24748
Stress corrosion cracking of A723 steel pressure vessels: Two case studies
[AD-A191741] 18 p2527 N88-24990
Prediction of fatigue life of notched specimens under aircraft loading and importance of the relative method in the case of local strain approach, part 2
[TAE-595-PT-2] 19 p2680 N88-25934
A numerical study of Rayleigh-Taylor instability in aluminum and steel plates
[DE88-010475] 20 p2774 N88-26449
Ultrasonic studies of stresses and plastic deformation in steel during tension and compression
[AD-A192306] 21 p2912 N88-27280
Cold worked reinforcing bars in tensile test under high loading rate and low temperatures
[DE88-752993] 21 p2964 N88-27610
Specular steel surfaces for solar mirror substrates
[DE88-001153] 21 p2968 N88-27630
Influence of dispersed additives reinforcement on the wear reinforcement mechanisms of the alumina-steel couple. Macroscopic and structural aspects
[ECL-86-01] 22 p3059 N88-28148
Method and apparatus for non-destructive testing of temper embrittlement in steels
[NASA-CASE-LAR-13817-1] 23 p3195 N88-29012
High hot-hardness gear lubricant evaluations, phase 2
[AD-A192309] 23 p3196 N88-29017
Critical conditions for failure in materials subjected to high rates of loading
[AD-A194697] 23 p3226 N88-29201
Damage initiation in the short beam shear test of composite materials using stiffness reduction
[AD-A194880] 24 p3340 N88-29883
Crystal structures of ordered carbon metal alloys
[AD-A195597] 24 p3353 N88-29959
Performance Prediction for Coatings. Proceedings of a Workshop
[AD-A188973] 24 p3354 N88-29966
Degradation of protective coatings on steel in corrosive environments 24 p3354 N88-29969
Electrical detection of coating deterioration
24 p3355 N88-29973
Electrochemical evaluation of the long term corrosion resistance of polymer coated steel
24 p3355 N88-29974
An electrochemical impedance spectroscopy study of reactions at the metal/coating interface
24 p3355 N88-29975
Evaluation of organic coating deterioration and substrate corrosion in seawater using electrochemical impedance measurements 24 p3355 N88-29976
Alternative immersion accelerated testing of coating systems for Naval shoreline facilities
24 p3355 N88-29977
The effect of notch root radius on the determination of toughness in ultrahigh strength steel friction welds
[AD-A195952] 24 p3384 N88-30156
Response of SMA (Shielded Metal Arc) and narrow gap HY80 weldments to explosive shock loading
[AD-A195994] 24 p3385 N88-30162

STEEP GRADIENT AIRCRAFT
U V/STOL AIRCRAFT

STEEPEST ASCENT METHOD
U STEEPEST DESCENT METHOD

STEEPEST DESCENT METHOD
Dynamical optimization techniques for the calculation of electronic structure in solids
[DE88-006010] 15 p2140 N88-22768

STEEPNESS
U SLOPES

STEERABLE ANTENNAS
MSAT mobile electronically steered phased array antenna development 19 p2647 N88-25711
MSAT-X electronically steered phased array antenna system 19 p2647 N88-25712
The JPL mechanically steered antenna
19 p2647 N88-25715

STEERING
Steering mechanism --- vehicles
[EP-PATENT-0-181-700-A1] 01 p0053 N88-10338
GPS vertical axis performance enhancement for helicopter precision landing approach
[NASA-CR-177443] 04 p0397 N88-12477
RF steering in the CEBAF CW superconducting linac
[CEBAF-PR-87-013] 11 p1547 N88-19251
Aberrations: Their effect on off-axis beam steering
[AD-A189601] 13 p1840 N88-21008
Null steering applications of polynomials with unimodular coefficients
[AD-A191087] 18 p2562 N88-25211
Local free-space mapping and path guidance for mobile robots
[AD-A192970] 20 p2810 N88-26674
Time-Optimal Adaptive Shaped Torque (TOAST) technical note
[AD-A192719] 20 p2843 N88-26869
Guided radiation beams in free electron lasers
[AD-A194525] 22 p3082 N88-28305

STELLAR ACTIVITY
NT FACULAE
NT SOLAR ACTIVITY
NT SOLAR FLARES
NT SOLAR PROMINENCES
NT SPICULES
NT STARSPOTS
NT STELLAR FLARES
NT SUNSPOTS
Fifth Cambridge Workshop on Cool Stars, Stellar Systems and the Sun 04 p0502 N88-13092
The photospheric magnetic fields of cool stars: Recent results of survey and time-variability programs
04 p0503 N88-13094
Observational constraints and evidence for saturation
04 p0503 N88-13097
Heating of stellar chromospheres and coronae: Evidence for non-magnetic basal heating
04 p0503 N88-13098
Active phases on II Peg 04 p0507 N88-13119
Stellar activity and the rotation of Hyades stars
04 p0510 N88-13139
Activity in warm stars 04 p0511 N88-13142
Measurements of stellar magnetic fields: Empirical constraints on dynamo and rotational evolution theories
04 p0518 N88-13185
The EUV line flux variations and activity in Alpha Orionis 08 p1032 N88-16256
EXOSAT observations of Hercules X-1
[MPE-PREPRINT-119] 22 p3164 N88-28841
On the origin of gamma ray bursts
[MPE-PREPRINT-120] 22 p3166 N88-28855
Activity-rotation relations for lower main sequence stars 23 p3298 N88-29640
Starbursts and their dynamics
[NASA-CR-180227] 24 p3452 N88-30549

STELLAR ATMOSPHERES
NT CHROMOSPHERE
NT SOLAR ATMOSPHERE
Analysis of the carbon star G77-61
[ETN-87-90422] 01 p0109 N88-10707
The M-type stars
[NASA-SP-492] 02 p0252 N88-11592
Spectroscopy and nonthermal processes
02 p0252 N88-11594
Thermal atmospheric models
02 p0253 N88-11599
Quasi-thermal models 02 p0253 N88-11600
The atmospheres of M dwarfs: Observations
02 p0253 N88-11601
M dwarfs: Theoretical work 02 p0253 N88-11602
X-ray pulsars: Accretion flow deceleration
03 p0390 N88-12451
Atmospheres of stars in the limits of thin and thick convection zones: The M dwarfs
04 p0505 N88-13104
Atmospheres of stars in the limits of thick and thin convection zones: M giants 04 p0505 N88-13105
Spectroscopic monitoring of RS CVn stars at Kitt Peak using the Penn State fiber optic echelle
04 p0509 N88-13127
Magnetic fields on K and M stars
04 p0510 N88-13137
Activity in warm stars 04 p0511 N88-13142
Empirical relations between photospheric magnetic fields and atmospheric radiative losses for cool dwarf stars 04 p0511 N88-13145
A flash spectrum of Cl I, C I, N I, and Ni II absorption in 31 Cygni: A direct observation of the reversing layer
04 p0513 N88-13158
Application of dynamic atmosphere models to the analysis of angular diameter observations of Mira variables 04 p0515 N88-13168
IUE observations of the hybrid K3 II star Iota Aurigae and constraints on the outer atmospheric structure
04 p0516 N88-13171
Time series infrared spectroscopy of long period variables 04 p0516 N88-13172
Water masers associated with 2 carbon stars: EU Andromedae and V778 Cygni 04 p0517 N88-13176
Gamma ray lines from novae
04 p0526 N88-13214
Onset of type 2 supernova in circumstellar envelope created by the stellar wind from presupernova
[DE88-700448] 10 p1428 N88-18526
A spherical, non-LTE, blanketed model stellar atmosphere for Phi Cas (FOIa)
10 p1428 N88-18528
Consistent transport coefficients in astrophysics
[NASA-TM-101154] 17 p2451 N88-24560
Evolutionary helium and CNO anomalies in the atmospheres and winds of massive hot stars
[NASA-CR-183254] 24 p3452 N88-30550

STELLAR COLOR
Stellar activity and the rotation of Hyades stars
04 p0510 N88-13139
JHK photometry of CN-rich field giants
04 p0516 N88-13175
Radio emission from RS CVn binaries: A 5 GHz VLA survey of 93 systems 04 p0519 N88-13191
The type Ia supernova 1986G in NGC5128: Optical photometry and spectra
[INPE-4426-PRE/1230] 12 p1710 N88-20231
Differential spectral synthesis of the stellar populations in the bulges of spiral galaxies 17 p2451 N88-24558

Spectral classification of Low Mass X-ray Binaries (LMXB) energy spectra with color-color diagrams
[MPE-PREPRINT-111] 22 p3163 N88-28837

STELLAR COMPOSITION
The M-type stars
[NASA-SP-492] 02 p0252 N88-11592
Radial velocity measurements of a sample of northern metal-deficient stars
[SER-C-PREPUBL-FASC-25] 24 p3455 N88-30564

STELLAR CORES
Speckle imaging of active galactic nuclei: NGC 1068 and NGC 4151 18 p2592 N88-25407
Microwave spectroscopy and gravitational collapse 18 p2594 N88-25413

STELLAR CORONAS
NT CORONAL HOLES
NT CORONAL LOOPS
NT SOLAR CORONA
Small-scale energy storage and release as the cause of the stellar X-ray corona 02 p0255 N88-11615
A re-examination of the corona-wind dividing line: Diagnostics of non-coronal atmospheres 04 p0504 N88-13101
X-rays, color, and the Vaughan-Preston gap 04 p0510 N88-13135
Relations between chromospheric and coronal structure, flux-flux correlations and convective zone properties 04 p0510 N88-13138

STELLAR DOPPLER SHIFT
U DOPPLER EFFECT
U EXTRATERRESTRIAL RADIATION

STELLAR ENVELOPES
The M-type stars
[NASA-SP-492] 02 p0252 N88-11592
Spectroscopy and nonthermal processes 02 p0252 N88-11594
Circumstellar radio molecular lines 02 p0252 N88-11595
Circumstellar shells, the formation of grains, and radiation transfer 02 p0252 N88-11596
Mass loss 02 p0253 N88-11597
Circumstellar chemistry 02 p0253 N88-11598
Adiabatic supernova expansion into the circumstellar medium
[DE87-014241] 03 p0387 N88-12433
Emission features in IRAS LRS spectra of MS, S and CS stars 04 p0514 N88-13163
Winds and shells around low-mass supergiants 04 p0514 N88-13164
Far infrared circumstellar debris shells of red supergiant stars 04 p0515 N88-13165
Consistent spherical Nonlocal Thermal Equilibrium (NLTE) models for objects with B-star-like luminosities
[ETN-88-90601] 06 p0800 N88-14897
Low mass stars with mass loss and low-luminosity carbon star formation 06 p0801 N88-14900
Onset of type 2 supernova in circumstellar envelope created by the stellar wind from presupernova
[DE88-700448] 10 p1428 N88-18526
Mass loss from evolved stars 11 p1569 N88-19394
Polarization properties of SiO masers 13 p1858 N88-21113

STELLAR EVOLUTION
NT STAR FORMATION
NT STELLAR MASS ACCRETION
Soft X-ray observations of pre-main sequence stars in the chamaeleon dark cloud
[NASA-CR-181457] 02 p0250 N88-11579
Basic properties and variability 02 p0252 N88-11593
Grids of evolutionary models of massive stars with mass loss and overshooting. Properties of Wolf-Rayet stars sensitive to overshooting
[PUBL-SER-C-FASC-12] 03 p0388 N88-12437
Angular momentum evolution of young stars 04 p0504 N86-13099
Post-zero-age main sequence rotation 04 p0504 N88-13100
Atmospheres of stars in the limits of thick and thin convection zones: M giants 04 p0505 N88-13105
Disk accretion during the early stages of stellar evolution 04 p0505 N88-13106
The onset of chromospheric activity among the A- and F- type stars 04 p0511 N88-13144
Neutron capture nucleosynthesis in low mass AGB stars 04 p0517 N88-13178
Spin-up and spin-down on the way to the main sequence 04 p0518 N88-13181
The Einstein survey of the young stars in the Orion Nebula 04 p0518 N88-13182
Measurements of stellar magnetic fields: Empirical constraints on dynamo and rotational evolution theories 04 p0518 N88-13185
Stromgren photometry of RSCVn and HD108102 04 p0519 N88-13187
Influences of the astrophysical environment on nuclear decay rates
[DE88-001461] 04 p0522 N88-13208
The role of fragmentation in interaction of meteoroids with the Earth's atmosphere 06 p0737 N88-14532
Low mass stars with mass loss and low-luminosity carbon star formation 06 p0801 N88-14900
Physics and chemistry 07 p0883 N88-15359
AGB (Asymptotic Giant Branch): Star evolution
[DE88-001829] 07 p0945 N88-15742
HEAO-1 observations of gamma-ray bursts 07 p0947 N88-15756
An introduction to nuclear astrophysics
[DE88-002761] 08 p1100 N88-16618
The distances and absolute magnitudes of RR Lyrae variable stars 11 p1568 N88-19386
Intermixing processes in massive stars and their influence on stellar evolution and nucleosynthesis
[ETN-88-91484] 11 p1568 N88-19388
A global model for planetary nebulae, taking into account central stellar evolution and influence on halo ionization
[ETN-88-91491] 11 p1568 N88-19389
Pre-supernova evolution of SN 1987A
[SER-C-PREPUBL-FASC-15] 18 p2593 N88-25409
Radial velocities monitoring of a sample of barium and S stars using CORAVEL: Towards an evolutionary link between barium and S stars?
[SER-C-PREPUBL-FASC-19] 18 p2593 N88-25410
Review of the theoretical changes of surface chemistry during massive star evolution
[SER-C-PREPUBL-FASC-17] 18 p2593 N88-25411
Asymptotic giant branch stars in the Infrared Astronomical Satellite (IRAS) catalogs: Selection and analysis of the population characteristics
[MPE-PREPRINT-116] 22 p3163 N88-28840
The evolution of low-mass X-ray binaries
[MPE-PREPRINT-118] 22 p3165 N88-28851
Evolutionary helium and CNO anomalies in the atmospheres and winds of massive hot stars
[NASA-CR-183254] 24 p3452 N88-30550
Radio and infrared properties of young stars
[NASA-CR-183252] 24 p3459 N88-30579

STELLAR FIELDS
U STAR DISTRIBUTION

STELLAR FLARES
NT SOLAR FLARES
Atmospheres of stars in the limits of thin and thick convection zones: The M dwarfs 04 p0505 N88-13104
Evidence for an additional source of opacity during the impulsive phase of stellar flares 04 p0510 N88-13133
The Parkes radio survey of active chromosphere stars 04 p0511 N88-13141
Excess emission in the wings of the Hydrogen Balmer lines during a flare on the late-type dMe star YZ CMi 04 p0511 N88-13146
Exosat results on the dMe flare Star Wolf 630AB and on VB 8 04 p0512 N88-13151
IUE/Optical/VLA flares on AD Leo 04 p0512 N88-13152
A helium flare on the active G5 dwarf Kappa Ceti 04 p0519 N88-13189
Flares: Solar and stellar
[PB87-124962] 06 p0806 N88-14917

STELLAR GRAVITATION
Relativistic stellar pulsations 06 p0801 N88-14902
Spectroscopic determinations of surface gravities of giant stars, and ultraviolet observations of RR Lyrae and X Arietis 11 p1569 N88-19391

STELLAR INTERIORS
NT SOLAR INTERIOR
NT STELLAR CORES
Magnetic fields in the overshoot zone: The great escape 02 p0256 N88-11616

STELLAR LUMINOSITY
The atmospheres of M dwarfs: Observations 02 p0253 N88-11601
The closest solar analogs in the bright star catalogue 04 p0506 N88-13110
The Wilson-Bappu relationship: A barometric effect 04 p0516 N88-13170
Pre-main sequence activity: How far is magnetism involved 04 p0517 N88-13179
The contribution of accretion luminosity to the infrared spectra of T Tauri stars: A possible test 04 p0518 N88-13183
M dwarfs from the Einstein medium sensitivity survey 04 p0519 N88-13188
Radio emission from RS CVn binaries: A 5 GHz VLA survey of 93 systems 04 p0519 N88-13191
Consistent spherical Nonlocal Thermal Equilibrium (NLTE) models for objects with B-star-like luminosities
[ETN-88-90601] 06 p0800 N88-14897
Low mass stars with mass loss and low-luminosity carbon star formation 06 p0801 N88-14900
A survey study of energy distribution in component stars of Algol-type binary systems 06 p0801 N88-14901
Differential spectral synthesis of the stellar populations in the bulges of spiral galaxies 17 p2451 N88-24558
Ultraviolet spectra of subluminous objects found in the Kiso Schmidt survey and systematic reanalysis of the archived ultraviolet spectra of white dwarfs observed with the IUE satellite under the Astrophysics Data Program (ADP)
[NASA-CR-182976] 18 p2592 N88-25406

STELLAR MAGNETIC FIELDS
NT SOLAR MAGNETIC FIELD
Coronal magnetic fields produced by photospheric shear
[NASA-CR-181514] 03 p0390 N88-12447
Fifth Cambridge Workshop on Cool Stars, Stellar Systems and the Sun 04 p0502 N88-13092
Measurements of stellar magnetic fields 04 p0503 N88-13093
The photospheric magnetic fields of cool stars: Recent results of survey and time-variability programs 04 p0503 N88-13094
Nonthermal phenomena in stellar coronae: Evidence from radio observations 04 p0503 N88-13096
Calibration on the Sun for stellar magnetic fields 04 p0506 N88-13113
Large scale solar and stellar magnetic fields 04 p0507 N88-13117
The short-period RS CVn stars: Starspots and fundamental properties 04 p0508 N88-13124
Evidence for expanding magnetic loops in coronae of cool stars 04 p0510 N88-13134
Magnetic fields on K and M stars 04 p0510 N88-13137
Activity in warm stars 04 p0511 N88-13142
Empirical relations between photospheric magnetic fields and atmospheric radiative losses for cool dwarf stars 04 p0511 N88-13145
Pre-main sequence activity: How far is magnetism involved 04 p0517 N88-13179
Measurements of stellar magnetic fields: Empirical constraints on dynamo and rotational evolution theories 04 p0518 N88-13185
Observations and analysis of the photospheric magnetic fields on dwarf G, K and M stars 04 p0520 N88-13196
Polarization properties of SiO masers 13 p1858 N88-21113
EXO033319-2554.2: A 55-MG eclipsing AM Herculis binary
[MPE-PREPRINT-114] 22 p3163 N88-28838

STELLAR MAGNITUDE
The closest solar analogs in the bright star catalogue 04 p0506 N88-13110
The distances and absolute magnitudes of RR Lyrae variable stars 11 p1568 N88-19386

STELLAR MASS
Mass loss 02 p0253 N88-11597
Circumstellar chemistry 02 p0253 N88-11598
The atmospheres of M dwarfs: Observations 02 p0253 N88-11601
Flux tube dynamics and solar/stellar redshift measurements 04 p0503 N88-13095
Atmospheres of stars in the limits of thick and thin convection zones: M giants 04 p0505 N88-13105
Disk accretion during the early stages of stellar evolution 04 p0505 N88-13106
Microwave observations of nonthermal phenomena in pre-main sequence stars 04 p0505 N88-13107
The closest solar analogs in the bright star catalogue 04 p0506 N88-13110
Application of dynamic atmosphere models to the analysis of angular diameter observations of Mira variables 04 p0515 N88-13168
Neutron capture nucleosynthesis in low mass AGB stars 04 p0517 N88-13178
A survey study of energy distribution in component stars of Algol-type binary systems 06 p0801 N88-14901
EXOSAT guest observer program. Binary parameters of the X-ray Pulsar 4U1626-67
[NASA-CR-182374] 06 p0802 N88-14905
BE Ursae Majoris: A detached binary with a unique reprocessing spectrum
[NASA-CR-182419] 08 p1083 N88-16526
A spherical, non-LTE, blanketed model stellar atmosphere for Phi Cas (FOIa) 10 p1428 N88-18528
Spectroscopic determinations of surface gravities of giant stars, and ultraviolet observations of RR Lyrae and X Arietis 11 p1569 N88-19391
Hydrodynamical models of supernova SN 1987 A in the LMC
[DE88-701123] 15 p2151 N88-22837
A review of the Initial Mass Function (IMF) --- stellar mass
[MPE-PREPRINT-112] 22 p3165 N88-28848

Mass transfer instabilities due to angular momentum flows in close binaries --- stars
[MPE-PREPRINT-113] 22 p3165 N88-28849
The evolution of low-mass X-ray binaries
[MPE-PREPRINT-118] 22 p3165 N88-28851

STELLAR MASS ACCRETION
The contribution of accretion luminosity to the infrared spectra of T Tauri stars: A possible test
04 p0518 N88-13183

STELLAR MASS EJECTION
Solar origins of coronal mass ejections
01 p0113 N88-10726
On the association of erupting magnetic fields with eruptive prominences and coronal mass ejections
01 p0113 N88-10727
Coronal mass ejections: The long-term variation of their occurrence rate and the solar wind mass flux
01 p0114 N88-10732
The M-type stars
[NASA-SP-492] 02 p0252 N88-11592
IRAS and cool stellar mass loss
04 p0515 N88-13166
Magnetic field draping about coronal mass ejecta
[DE88-001805] 05 p0661 N88-14057
AGB (Asymptotic Giant Branch): Star evolution
[DE88-001829] 07 p0945 N88-15742
Numerical modelling of the classical nova outburst
[NASA-TM-89707] 07 p0945 N88-15746
Theoretical studies of mass loss and shock phenomena in cool star envelopes
[NASA-CR-182433] 08 p1099 N88-16616
Transverse flow deflections associated with fast coronal mass ejecta in interplanetary space
[DE88-003180] 09 p1263 N88-17566
Stellar energy loss and anomalous contributions to the (photon photon) (neutrino antineutrino) interaction
[DE88-700618] 10 p1428 N88-18529
Mass loss from evolved stars
11 p1569 N88-19394
Magnetohydrodynamic (MHD) simulation of solar prominence formation 13 p1858 N88-21109
Solar-geophysical data number 519, November 1987. Part 2: (Comprehensive reports). Data for May 1987 and miscellanea
[PB88-158910] 14 p2011 N88-21997
Table of solar activity associated with coronal mass ejections observed by the SMM coronagraph/polarimeter in 1980
[PB88-170881] 14 p2011 N88-21998

STELLAR MODELS
Dynamic effects of stellar winds and associated HII regions on the interstellar medium
[ETN-87-90421] 01 p0109 N88-10706
Analysis of the carbon star G77-61
[ETN-87-90422] 01 p0109 N88-10707
High explosive simulations of supernovae and the supernova shell fragmentation model of solar system formation
[DE87-014708] 02 p0251 N88-11584
The M-type stars
[NASA-SP-492] 02 p0252 N88-11592
Grids of evolutionary models of massive stars with mass loss and overshooting. Properties of Wolf-Rayet stars sensitive to overshooting
[PUBL-SER-C-FASC-12] 03 p0388 N88-12437
Relations between chromospheric and coronal structure, flux-flux correlations and convective zone properties
04 p0510 N88-13138
Theoretical studies of mass loss and shock phenomena in cool star envelopes
[NASA-CR-182433] 08 p1099 N88-16616
A spherical, non-LTE, blanketed model stellar atmosphere for Phi Cas (FOIa)
10 p1428 N88-18528
Intermixing processes in massive stars and their influence on stellar evolution and nucleosynthesis
[ETN-88-91484] 11 p1568 N88-19388
A global model for planetary nebulae, taking into account central stellar evolution and influence on halo ionization
[ETN-88-91491] 11 p1568 N88-19389
The effects of rotation on the winds from hot stars
11 p1569 N88-19393
Galaxy evolution in dense clusters
13 p1855 N88-21101
Hydrodynamical models of supernova SN 1987 A in the LMC
[DE88-701123] 15 p2151 N88-22837
Pre-supernova evolution of SN 1987A
[SER-C-PREPUBL-FASC-15] 18 p2593 N88-25409
On the origin of gamma ray bursts
[MPE-PREPRINT-120] 22 p3166 N88-28855

STELLAR MOTIONS
NT SOLAR OSCILLATIONS
NT SOLAR ROTATION
NT STELLAR ORBITS
NT STELLAR OSCILLATIONS
NT STELLAR ROTATION
On the (lack of) proper motion of the Vela pulsar
01 p0097 N88-10635
Basic properties and variability
02 p0252 N88-11593
The kinematics of late-type supergiants
[SER-C-PREPUBL-FASC-28] 24 p3454 N88-30560

STELLAR ORBITS
Asynchronous rotation in close binary systems with circular orbits 04 p0509 N88-13131
Regular orbital variations in the ultraviolet resonance lines of YZ Cnc
[MPE-PREPRINT-117] 22 p3165 N88-28850
Duplicity in the solar neighborhood: Part 4: Spectroscopic orbits for four dwarf M stars
[SER-C-PREPUBL-FASC-21] 24 p3454 N88-30561
Orbital stability in rotating triaxial stellar systems
[SER-C-PREPUBL-FASC-24] 24 p3455 N88-30569

STELLAR OSCILLATIONS
NT SOLAR OSCILLATIONS
The ultrashort period dwarf nova SW Ursae Majoris
24 p3453 N88-30553

STELLAR PHYSICS
NT SOLAR PHYSICS
The M-type stars
[NASA-SP-492] 02 p0252 N88-11592
The atmospheres of M dwarfs: Observations
02 p0253 N88-11601
Active phases on II Peg 04 p0507 N88-13119
The short-period RS CVn stars: Starspots and fundamental properties 04 p0508 N88-13124
Relativistic stellar pulsations 06 p0801 N88-14902
Activities in astrophysics
[INPE-4582-PRE/1316] 24 p3456 N88-30570

STELLAR RADIATION
NT STELLAR WINDS
Ultraviolet observations of AM Her --- cataclysmic variable
[MPE-PREPRINT-92] 02 p0250 N88-11581
The M-type stars
[NASA-SP-492] 02 p0252 N88-11592
Basic properties and variability
02 p0252 N88-11593
Spectroscopy and nonthermal processes
02 p0252 N88-11594
Circumstellar shells, the formation of grains, and radiation transfer 02 p0252 N88-11596
The pulsation modes of CO Aur
[PUBL-SER-C-FASC-10] 03 p0387 N88-12430
VLA observations of rapid 6 cm flux variations in alpha Ori 04 p0515 N88-13169
A comprehensive exploration of late-type stars in the far-ultraviolet 04 p0520 N88-13194
The history and development of nonlinear stellar pulsation codes
[DE88-001828] 06 p0801 N88-14899
Relativistic stellar pulsations 06 p0801 N88-14902
Observations of gamma bursts from GBS 0526-66
08 p1001 N88-16065
The EUV line flux variations and activity in Alpha Orionis 08 p1032 N88-16256
On the time delay of the ultrahigh-energy radiation signal from the source Cygnus X-3
[DE88-700649] 10 p1431 N88-18547
Thermal radiation from neutron stars
[MPE-203] 11 p1571 N88-19404
Analysis of the inter-layer independence of stellar scintillometer profiles of Cn2
[AD-A189372] 12 p1645 N88-19854
To the opportunities of cluster analysis of light curves of supernovae
[DE88-701642] 21 p3030 N88-27982
EXO033319-2554.2: A 55-MG eclipsing AM Herculis binary
[MPE-PREPRINT-114] 22 p3163 N88-28838
Radio and infrared properties of young stars
[NASA-CR-183252] 24 p3459 N88-30579

STELLAR ROTATION
NT SOLAR ROTATION
Angular momentum evolution of young stars
04 p0504 N88-13099
Post-zero-age main sequence rotation
04 p0504 N88-13100
Large scale solar and stellar magnetic fields
04 p0507 N88-13117
Asynchronous rotation in close binary systems with circular orbits 04 p0509 N88-13131
Relations between chromospheric and coronal structure, flux-flux correlations and convective zone properties
04 p0510 N88-13138
Stellar activity and the rotation of Hyades stars
04 p0510 N88-13139
Broadband linear polarization and chromospheric CaII H and K line emission in late-type main sequence stars
04 p0511 N88-13140
Spin-up and spin-down on the way to the main sequence 04 p0518 N88-13181
Observations and analysis of the photospheric magnetic fields on dwarf G, K and M stars
04 p0520 N88-13196
The effects of rotation on the winds from hot stars
11 p1569 N88-19393
Activity-rotation relations for lower main sequence stars 23 p3298 N88-29640
Orbital stability in rotating triaxial stellar systems
[SER-C-PREPUBL-FASC-24] 24 p3455 N88-30569

STELLAR SPECTRA
NT SOLAR SPECTRA
An application of L1 to astronomy --- stellar velocity
[REPT-87-10] 01 p0108 N88-10702
Ultraviolet observations of cataclysmic variables: The IUE archive
[MPE-PREPRINT-91] 02 p0250 N88-11580
The M-type stars
[NASA-SP-492] 02 p0252 N88-11592
Spectroscopy and nonthermal processes
02 p0252 N88-11594
Comparison of global and nuclear properties of starburst and Seyfert 1 galaxies 03 p0388 N88-12438
A large X-ray flare on Sigma 2 coronae borealis observed with exosat 04 p0508 N88-13121
Spectroscopic monitoring of RS CVn stars at Kitt Peak using the Penn State fiber optic echelle
04 p0509 N88-13127
H alpha and Ca II emission line variability of FK comae 04 p0509 N88-13128
PG 0308 + 096: A short-period white dwarf + dM binary with strongly modulated H-alpha emission
04 p0509 N88-13132
Evidence for an additional source of opacity during the impulsive phase of stellar flares
04 p0510 N88-13133
Magnetic fields on K and M stars
04 p0510 N88-13137
The Wilson-Bappu relationship: A barometric effect
04 p0516 N88-13170
IUE observations of the hybrid K3 II star Iota Aurigae and constraints on the outer atmospheric structure
04 p0516 N88-13171
Time series infrared spectroscopy of long period variables 04 p0516 N88-13172
Synthetic spectra for the N-type carbon star TX Psc
04 p0516 N88-13173
Water masers associated with 2 carbon stars: EU Andromedae and V778 Cygni 04 p0517 N88-13176
The delta upsilon = 1 fundamental bands of carbon monoxide in late-type stars 04 p0517 N88-13177
Pre-main sequence activity: How far is magnetism involved 04 p0517 N88-13179
Chromospheric variability mechanisms affecting pre-main sequence stars 04 p0517 N88-13180
Measurements of stellar magnetic fields: Empirical constraints on dynamo and rotational evolution theories
04 p0518 N88-13185
IRAS and near IR observations of active binaries
04 p0518 N88-13186
M dwarfs from the Einstein medium sensitivity survey
04 p0519 N88-13188
A helium flare on the active G5 dwarf Kappa Ceti
04 p0519 N88-13189
A comprehensive exploration of late-type stars in the far-ultraviolet 04 p0520 N88-13194
Observations of gamma bursts from GBS 0526-66
08 p1001 N88-16065
BE Ursae Majoris: A detached binary with a unique reprocessing spectrum
[NASA-CR-182419] 08 p1083 N88-16526
Theoretical studies of mass loss and shock phenomena in cool star envelopes
[NASA-CR-182433] 08 p1099 N88-16616
Gamma-ray imaging observations of the Crab and Cygnus regions 10 p1427 N88-18522
Calculated late time spectra of supernovae
[DE88-003296] 10 p1428 N88-18530
The type Ia supernova 1986G in NGC5128: Optical photometry and spectra
[INPE-4426-PRE/1230] 12 p1710 N88-20231
A 23 hour EXOSAT observation of the X-ray pulsar 1E2259 + 586 and the associated supernova remnant G109.1-1.0
[MPE-PREPRINT-99] 14 p1994 N88-21882
The X-ray properties of AM Her stars
[MPE-PREPRINT-106] 16 p2289 N88-23704
IUE evidence on the nature of the innermost broad-line region in Seyfert 1 galaxies 17 p2450 N88-24552

Duplicity in the solar neighborhood. Part 3: New spectroscopic elements for nine solar-type binary stars
[SER-C-PREPUBL-FASC-18-PT-3] 18 p2592 N88-25405
Analysis of emission features in IRAS LRS spectra
21 p2928 N88-27380
Spectral classification of Low Mass X-ray Binaries (LMXB) energy spectra with color-color diagrams
[MPE-PREPRINT-111] 22 p3163 N88-28837
International ultraviolet explorer spectral atlas of planetary nebulae, central stars, and related objects
[NASA-RP-1203] 22 p3164 N88-28843
The ultrashort period dwarf nova SW Ursae Majoris
24 p3453 N88-30553
Duplicity in the solar neighborhood: Part 5: Spectroscopic orbit for the nearby double-lined solar-type star HR 8581
[SER-C-PREPUBL-FASC-23] 24 p3455 N88-30562

STELLAR SPECTROPHOTOMETRY
The M-type stars
[NASA-SP-492] 02 p0252 N88-11592
Basic properties and variability
02 p0252 N88-11593
Infrared excesses of barium stars
04 p0516 N88-13174
JHK photometry of CN-rich field giants
04 p0516 N88-13175
Stromgren photometry of RSCVn and HD108102
04 p0519 N88-13187
Mapping stellar surface features
09 p1262 N88-17564
Preparation of photometric measurements on a million stars in the framework of the satellite project HIPPARCOS/TYCHO
[ETN-88-91502] 13 p1853 N88-21093
A new determination of the Geneva photometric passbands and their absolute calibration
[SER-C-PREPUBL-FASC-26] 24 p3452 N88-30546

STELLAR STRUCTURE
Pressure structure of solar coronal loops
02 p0256 N88-11618
The onset of chromospheric activity among the A- and F- type stars 04 p0511 N88-13144
Surface photometric investigations for spiral galaxies of large dimension structures in edge-on gemetry
[ETN-88-92126] 21 p3030 N88-27985

STELLAR SYSTEMS
Fifth Cambridge Workshop on Cool Stars, Stellar Systems and the Sun 04 p0502 N88-13092
Relative chaos in stellar systems
[DE88-700148] 12 p1710 N88-20234
Asymptotic giant branch populations in composite stellar systems 13 p1854 N88-21098
Orbital stability in rotating triaxial stellar systems
[SER-C-PREPUBL-FASC-24] 24 p3455 N88-30569

STELLAR TEMPERATURE
Application of dynamic atmosphere models to the analysis of angular diameter observations of Mira variables 04 p0515 N88-13168
Pre-main sequence activity: How far is magnetism involved 04 p0517 N88-13179
BE Ursae Majoris: A detached binary with a unique reprocessing spectrum
[NASA-CR-182419] 08 p1083 N88-16526
A spherical, non-LTE, blanketed model stellar atmosphere for Phi Cas (FOIa)
10 p1428 N88-18528
The astrophysics of nebulae and active galactic nuclear emission-line regions: New methods and applications
13 p1858 N88-21111

STELLAR WINDS
Dynamic effects of stellar winds and associated HII regions on the interstellar medium
[ETN-87-90421] 01 p0109 N88-10706
A re-examination of the corona-wind dividing line: Diagnostics of non-coronal atmospheres
04 p0504 N88-13101
The acceleration of winds by MHD waves in open magnetic structures 04 p0506 N88-13109
Radio continuum emission from the ionized stellar winds of the cool supergiants in zeta Aurigae-like systems
04 p0514 N88-13160
Winds and shells around low-mass supergiants
04 p0514 N88-13164
Theoretical studies of mass loss and shock phenomena in cool star envelopes
[NASA-CR-182433] 08 p1099 N88-16616
Onset of type 2 supernova in circumstellar envelope created by the stellar wind from presupernova
[DE88-700448] 10 p1428 N88-18526
The effects of rotation on the winds from hot stars
11 p1569 N88-19393
Colliding stellar winds in the eclipsing Wolf-Rayet binary V444 Cygni
[NASA-CR-182937] 17 p2451 N88-24563
Propagation of linear gravity waves in a relativistic atmosphere
[DE88-702062] 19 p2691 N88-25995
Time-dependent mass loss from hot stars with and without radiative driving
[DE88-008899] 20 p2884 N88-27128
Regular orbital variations in the ultraviolet resonance lines of YZ Cnc
[MPE-PREPRINT-117] 22 p3165 N88-28850
Evolutionary helium and CNO anomalies in the atmospheres and winds of massive hot stars
[NASA-CR-183254] 24 p3452 N88-30550

STELLARATORS
Mode purity measurements on gyrotrons for plasma heating at the stellarator W 7-AS
[IPF-87-3] 01 p0101 N88-10660
Computational study of three-dimensional magnetohydrodynamic equilibria in toroidal helical systems
[DE87-753007] 02 p0240 N88-11514
Progress in stellarator/heliotron research, 1981-1986: Executive summary
[DE88-000017] 02 p0241 N88-11519
The role of stellarators in the advanced toroidal program
[DE87-014815] 04 p0491 N88-13025
Transport scaling in the collisionless-detrapping regime in stellarators
[DE88-001511] 05 p0653 N88-14006
High midplane accessibility stellarator windings for high current toroidal accelerators
[AD-A186235] 07 p0933 N88-15665
Activities report of the Institute of Plasma Physics
[ETN-88-91020] 07 p0933 N88-15668
Benchmarks of neutral beam injection codes for stellarators
[DE88-003786] 10 p1412 N88-18428
Diagnostics for ATF
[DE88-004175] 10 p1414 N88-18438
ATF experimental plans
[DE88-004177] 10 p1414 N88-18439
Low aspect ratio torsatrons
[DE88-004173] 11 p1552 N88-19284
Summaries of FY86 research in the Applied Plasma Physics Fusion Theory Program
[DE88-004242] 11 p1554 N88-19298
Proceedings of US-Japan Heliotron-Stellarator Workshop, volume 3
[DE88-004788] 11 p1554 N88-19299
Proceedings of US-Japan Heliotron-Stellarator Workshop, volume 2
[DE88-004789] 11 p1554 N88-19300
Proceedings of US-Japan Heliotron-Stellarator Workshop, volume 4
[DE88-004787] 12 p1693 N88-20126
Comparison of analytic and full guiding center behavior at a trapped-passing interface in stellarators
[DE88-004174] 13 p1842 N88-21025
Helical ripple transport in stellarators at low collision frequency
[DE88-006431] 13 p1843 N88-21031
Spectral diagnostics for temperature and density measurements on ATF 17 p2442 N88-24525
Neoclassical diffusion due to trapping/detrapping orbits in stellarators
[DE88-008566] 20 p2857 N88-26968

STEP FAULTS
U GEOLOGICAL FAULTS

STEP FUNCTIONS
Effect of phase errors in stepped-frequency radar systems
[AD-A194476] 23 p3203 N88-29061

STEPPES
Monitoring Tunisia's stoppes with SPOT
22 p3097 N88-28390

STEPPING MOTORS
Theoretical and experimental investigations on a linear, permanently excited stepping motor
[ETN-88-91061] 09 p1158 N88-16939
Development of a cryogenic stepping drive for ISO/LWS 14 p1878 N88-21220

STEREOCHEMISTRY
The mechanism of stereo regulation during anionic polymerization of polar monomers
[AD-A186530] 08 p0973 N88-15888
New phosphorus based polymer systems
[AD-A190457] 15 p2045 N88-22186
Topological stereochemistry
[AD-A191867] 18 p2477 N88-24691

STEREOGRAPHY
U STEREOPHOTOGRAPHY

STEREOPHONICS
Performance of single and multiple system AM stereo decoder receivers
[PB88-168307] 15 p2057 N88-22265

STEREOPHOTOGRAPHY
Evaluation of SPOT stereoscopic possibilities for cartography 03 p0342 N88-12156
Pulsed laser stereophotography of plasmas and dynamically moving surfaces
[DE88-003170] 09 p1173 N88-17031
Automated stereophotogrammetry
[AD-A189617] 12 p1630 N88-19757
Relative orientation
[AD-A190385] 15 p2089 N88-22449
Stereoscopic photographs, ground and aerial, of trees used in the arborization of Curitiba (PR)
17 p2366 N88-24091
Finding wheels of vehicles in stereo images
[AD-A194372] 22 p3080 N88-28292
Metric applications of SPOT's lateral stereoscopy
22 p3111 N88-28480
Rigorous stereophotogrammetric treatment of SPOT images 22 p3111 N88-28482
Study of stereoradiometry on SPOT images
22 p3112 N88-28484
Automatic extraction of high resolution elevation data from SPOT stereo images 22 p3113 N88-28489
Automatic creation of digital terrain models from SPOT image pairs 22 p3113 N88-28490
Digital SPOT stereoplotting: An original approach to the formation of epipolar images and matching
22 p3113 N88-28493
Determining vehicle motion from stereo image sequences
[AD-A194371] 23 p3216 N88-29140

STEREOSCOPIC PHOTOGRAPHY
U STEREOPHOTOGRAPHY

STEREOSCOPIC VISION
Self calibration of motion and stereo vision for mobile robot navigation
[AD-A185602] 06 p0781 N88-14794
Computing 3-D structure of rigid objects using stereo and motion 08 p1061 N88-16407
Visual evoked potentials
[AD-A187942] 11 p1519 N88-19071
Three-dimensional information from stereovision process 12 p1593 N88-19540
Television monitor field shifter and an opto-electronic method for obtaining a stereo image of optimal depth resolution and reduced depth distrotion on a single screen
[NASA-CASE-NPO-17249-1-CU] 17 p2332 N88-23924
Multilevel computational theory of stereoscopic visual image processing
[AD-A195331] 24 p3408 N88-30288

STEREOSCOPY
NT STEREOPHOTOGRAPHY
Stereo and eye movement
[AD-A193588] 22 p3142 N88-28681

STERILIZATION
Controlled ecological life support systems: Development of a plant growth module 05 p0630 N88-13854

STERNS
U AFTERBODIES

STEROIDS
NT ALDOSTERONE
NT CORTICOSTEROIDS

STIFF STRUCTURES
U RIGID STRUCTURES

STIFFENING
Interactive buckling effects in stiffened FRP panels
[ARE-TM(UMS)-87204] 01 p0059 N88-10378
Vibration and buckling of geometrically imperfect laminated cylindrical shells 04 p0456 N88-12822
Experimental studies on the tripping behavior of narrow T-stiffened flat plates subjected to hydrostatic pressure and underwater shock 05 p0592 N88-13613
Geometrically nonlinear analysis of stiffened panels
06 p0722 N88-14440
Optimum design of geodesically stiffened composite plates
[NASA-CR-182499] 10 p1344 N88-18035
Preliminary investigation of stability of a fin-stiffened slender strut
[NASA-TM-4034] 12 p1599 N88-19568
Postbuckling delamination of a stiffened composite panel using finite element methods
[NASA-CR-182803] 15 p2030 N88-22098
Local buckling and crippling of composite stiffener sections
[NASA-TM-101133] 17 p2317 N88-23840
Stiffened titanium panels
[NASA-CASE-LAR-13814-1] 18 p2497 N88-24816
Nonlinear vibrations of periodically stiffened plates
21 p2963 N88-27598

STIFFNESS
Control of a flexible one-link manipulator
[AD-A185035] 05 p0590 N88-13598

A comparison of experimental and theoretical results for labyrinth gas seals with honeycomb stators
[NASA-CR-182441] 08 p0993 N88-16006
Development of a new generation of high-temperature composite materials 09 p1119 N88-16702
Reliability of structures with stiffness and strength degradation 09 p1180 N88-17068
A superelement component dynamic synthesis method 11 p1500 N88-18956
Wave propagation in laminated composite plates
[AD-A188999] 12 p1604 N88-19594
Investigation of the inter-relationship between base pavement stiffness and asphalt overlay compaction
[DOT/FAA/ES-88/1] 14 p1869 N88-21170
Investigation and synthesis of high temperature and increased stiffness RSP aluminum alloys
[AD-A190407] 15 p2039 N88-22151
Dynamic characteristics of a vibrating beam with periodic variation in bending stiffness
[NASA-TP-2697] 17 p2348 N88-23988
Stiffness degradation of composite laminates
20 p2767 N88-26405
A micromechanics model of the stiffness and strength of laminates with fiber waviness
[NASA-CR-181670] 20 p2768 N88-26413
Nonlinear interaction between overall and local buckling of stiffened panels with symmetric cross-sections
[PB88-104054] 21 p2960 N88-27580
Analysis of stiffness reduction, failure and stress concentration in fiber composite laminates
[AD-A193519] 22 p3050 N88-28096
Two-dimensional sequential and concurrent finite element analysis of unstiffened and stiffened aluminum and composite panels with hole
[NASA-CR-183083] 22 p3086 N88-28325
Damage initiation in the short beam shear test of composite materials using stiffness reduction
[AD-A194880] 24 p3340 N88-29883
Nonlinear stress-strain and inelastic rebound with exponential stiffness
[AD-A195667] 24 p3384 N88-30159

STIFFNESS MATRIX
Frequency domain identification of structural dynamic systems with general damping matrices
03 p0337 N88-12120
Identification of linear structural models
03 p0337 N88-12121
Hybrid FEM (Finite Element Method) approach to stress distribution in the vicinity of a notch in non-homogeneous materials
[PB87-143392] 07 p0868 N88-15268
An efficient Mindlin finite strip plate element based on assumed strain distribution 15 p2081 N88-22407
Improved finite strip Mindlin plate bending element using assumed shear strain distributions
[NASA-TM-100928] 23 p3225 N88-29195
Geometric and material nonlinear analysis of structures comprising rectangular hollow sections
[CE-79] 24 p3382 N88-30141

STIGMATISM
The evaluation of a deformable diffraction grating for a stigmatic EUV spectroheliometer
[NASA-CR-182371] 06 p0707 N88-14337

STIMULANTS
NT ATROPINE
NT CAFFEINE
NT NOREPINEPHRINE
Propranolol and the compensatory circulatory responses to orthostasis at high altitude
[AD-A192675] 22 p3131 N88-28618

STIMULATED EMISSION
A simplified approach to axisymmetric dual-reflector antenna design
[NASA-TP-2797] 09 p1111 N88-16662
Optically stimulated sound from gas bubbles in water
12 p1686 N88-20087
Stimulated Emission of Energetic Particles (SEEP)
[AD-A188724] 13 p1853 N88-21094
Survey of the Air Force P78-2 (SCATHA) satellite plasma wave data during electron gun operations
[AD-A191014] 16 p2168 N88-22926
Theoretical studies of solar-pumped lasers
[NASA-CR-182920] 17 p2344 N88-23971
Monolithic fuel cell based power source for sprint power generation 17 p2407 N88-24313

STIMULATED EMISSION DEVICES
NT AIRBORNE LASERS
NT ARGON LASERS
NT ATMOSPHERIC LASERS
NT CARBON DIOXIDE LASERS
NT CARBON MONOXIDE LASERS
NT CHEMICAL LASERS
NT CONTINUOUS WAVE LASERS
NT DISTRIBUTED FEEDBACK LASERS
NT DYE LASERS
NT EXCIMER LASERS
NT FREE ELECTRON LASERS
NT GALLIUM ARSENIDE LASERS
NT GAMMA RAY LASERS
NT GAS LASERS
NT GASDYNAMIC LASERS
NT GLASS LASERS
NT HCN LASERS
NT HELIUM-NEON LASERS
NT HF LASERS
NT HIGH POWER LASERS
NT HYDROGEN MASERS
NT INFRARED LASERS
NT INTERSTELLAR MASERS
NT IODINE LASERS
NT KRYPTON FLUORIDE LASERS
NT LASERS
NT LIQUID LASERS
NT MASERS
NT METAL VAPOR LASERS
NT NEODYMIUM LASERS
NT NITROGEN LASERS
NT NOVA LASER SYSTEM
NT NUCLEAR PUMPED LASERS
NT PULSED LASERS
NT Q SWITCHED LASERS
NT RAMAN LASERS
NT RARE GAS-HALIDE LASERS
NT RING LASERS
NT RUBY LASERS
NT SEMICONDUCTOR LASERS
NT SOLAR-PUMPED LASERS
NT SOLID STATE LASERS
NT SPACEBORNE LASERS
NT TEA LASERS
NT TRAVELING WAVE MASERS
NT TUNABLE LASERS
NT TWO-WAVELENGTH LASERS
NT ULTRASHORT PULSED LASERS
NT ULTRAVIOLET LASERS
NT WATER MASERS
NT WAVEGUIDE LASERS
NT X RAY LASERS
NT XENON CHLORIDE LASERS
NT XENON FLUORIDE LASERS
NT YAG LASERS
Laser countermeasure impacts and penalties
[DE88-006871] 18 p2520 N88-24947

STIMULATION
NT AUDITORY STIMULI
NT SENSORY STIMULATION
Advancing automation and robotics technology for the space station and for the US economy: Submitted to the United States Congress October 1, 1986
[NASA-TM-89190] 08 p0960 N88-15818
Role of optokinetic stimulation in vesibulospinal reflexes 10 p1360 N88-18131
Disuse condition stimulates bone resorption in organ culture 12 p1656 N88-19926
Neck receptor stimulation in 0 and 1 g
12 p1658 N88-19938
Phase preservation cleanup in a double-pass Raman amplifier SBS (Stimulated Brillouin Scattering) conjugator
[AD-A189428] 13 p1761 N88-20536
Amplification of signals in fiber optics using the stimulated Raman effect
[AD-A190281] 15 p2133 N88-22727
Unstable behavior of lasers and other optical systems
[AD-A190875] 16 p2213 N88-23204

STIMULI
Cognitive task demands as reflected in physiological measures 21 p2980 N88-27699

STIRLING CYCLE
Heat engine regenerators: Research status and needs
[DE87-013581] 01 p0054 N88-10348
RE-1000 free-piston Stirling engine hydraulic output system description
[NASA-TM-100185] 01 p0108 N88-10700
Overview of free-piston Stirling engine technology for space power application
[NASA-TM-88886] 03 p0386 N88-12427
Design concepts for the ASTROMAG cryogenic system
[NASA-CR-181505] 04 p0497 N88-13060
The Goddard Space Flight Center mechanical cooler program 08 p0963 N88-15944
Cryocooler systems demonstration
[AD-A188025] 11 p1467 N88-18745
Test results of a 40-kW Stirling engine and comparison with the NASA Lewis computer code predictions
[NASA-TM-87050] 11 p1508 N88-19013
Magnetic heat pump design
[DE88-007730] 20 p2798 N88-26605

STIRLING ENGINES
Study of free-piston Stirling engine driven linear alternators
[NASA-CR-181425] 01 p0055 N88-10355
RE-1000 free-piston Stirling engine hydraulic output system description
[NASA-TM-100185] 01 p0108 N88-10700
Stirling engine research at national and university laboratories in Japan
[DE87-014622] 02 p0180 N88-11123
Stirling engines and irrigation pumping
[DE88-000020] 02 p0181 N88-11125
Automotive Stirling engine: Mod 2 design report
[NASA-CR-175106] 02 p0250 N88-11578
SPRE 1 free-piston Stirling engine testing at NASA Lewis Research Center
[NASA-TM-100241] 03 p0277 N88-11747
Overview of free-piston Stirling engine technology for space power application
[NASA-TM-88886] 03 p0386 N88-12427
Progress toward the evolution of a Stirling space engine
[NASA-TM-100221] 05 p0659 N88-14046
Hot piston ring tests
[NASA-TM-100256] 06 p0729 N88-14486
Report to Congress on the Automotive Technology Development Program
[DE88-003742] 07 p0864 N88-15242
Hot piston ring/cylinder liner materials: Selection and evaluation
[NASA-TM-100276] 08 p0971 N88-15872
Overview of heat transfer and fluid flow problem areas encountered in Stirling engine modeling
[NASA-TM-100131] 09 p1262 N88-17561
Free-piston Stirling engine diaphragm-coupled heat-actuated heat pump component technology program, phase 1C
[DE88-003654] 10 p1330 N88-17949
Free-piston Stirling engine diaphragm-coupled heat-actuated heat pump component technology program, phase 1B
[DE88-003653] 11 p1483 N88-18854
Test results of a 40-kW Stirling engine and comparison with the NASA Lewis computer code predictions
[NASA-TM-87050] 11 p1508 N88-19013
Cast iron-base alloy for cylinder/regenerator housing
[NASA-CR-182116] 12 p1608 N88-19613
A survey of oscillating flow in Stirling engine heat exchangers
[NASA-CR-182108] 15 p2067 N88-22322
Description of an oscillating flow pressure drop test rig
[NASA-TM-100905] 16 p2170 N88-22933
The 1988 overview of free-piston Stirling technology for space power at the NASA Lewis Research Center
[NASA-TM-100795] 16 p2170 N88-22934
Overview of NASA Lewis Research Center free-piston Stirling engine technology activities applicable to space power systems 17 p2398 N88-24255
Fatigue failure of regenerator screens in a high frequency Stirling engine 17 p2436 N88-24491
Component improvement of free-piston Stirling engine key technology for space power
[NASA-TM-100950] 19 p2607 N88-25476
The design and fabrication of a Stirling engine heat exchanger module with an integral heat pipe
[NASA-TM-101296] 20 p2820 N88-26732
Phase 1 results from the Stirling-powered vehicle project
[NASA-TM-100978] 21 p3029 N88-27980
Testing of a variable-stroke Stirling engine
[NASA-TM-100899] 24 p3440 N88-30472

STIRRING
Coagulation in stirred tanks
[B8711373] 05 p0562 N88-13420

STOCHASTIC PROCESSES
NT MARKOV CHAINS
NT MARKOV PROCESSES
NT RANDOM PROCESSES
NT RANDOM WALK
Processing of fractal functions by linear and nonlinear operators
[RAE-TR-85079] 01 p0088 N88-10571
A problem in quantum probability --- statistical invariants problem
[REPT-87-06] 01 p0088 N88-10573
Stochastic integration for operator valued processes on Hilbert spaces and on nuclear spaces
[ENST-87D002] 01 p0089 N88-10580
A stochastic delamination growth model for fatigue loaded laminated composite materials
02 p0141 N88-10866
Stochastic model of the motion of suspended particles in turbulent flow
[HSBW-MITT-21/1987] 03 p0315 N88-11990
Operator multiple-tasking study for remotely operated platforms
[AD-A184487] 03 p0362 N88-12276

Stochastic model of the NASA/MSFC ground facility for large space structures with uncertain parameters: The maximum entropy approach
[NASA-CR-181489] 03 p0372 N88-12343

Some stochastic aspects of intergranular creep cavitation
[DE88-000065] 04 p0416 N88-12581

The TAB method for numerical calculation of spray droplet breakup
[DE87-011756] 04 p0442 N88-12743

Electromagnetics and electrothermal approach to evaluate failures in microelectronic devices caused by electrostatic discharges: Stochastical aspects of the device reliability
[AD-A184906] 05 p0577 N88-13522

Conditional second order closure for turbulent shear flows
[AD-A185369] 05 p0581 N88-13542

Fatigue crack growth under random overloads
05 p0602 N88-13682

Computer aided modeling and fatigue failure forecast under stochastic loading 05 p0607 N88-13720

On the geometrical description of fatigue crack surfaces 05 p0607 N88-13727

Comparing hard and soft prior bounds in geophysical inverse problems
[NASA-CR-181557] 05 p0624 N88-13820

Explicit formulate for the distributions of stopping variables under Wald's truncated SPRT (Sequential Probability Radio Tests) for a poisson process
[AD-A185053] 05 p0640 N88-13914

Point processes
[AD-A185398] 05 p0641 N88-13921

Robust prediction operations for stationary processes
[AD-A185408] 05 p0641 N88-13924

Isotropic probability measures in infinite dimensional spaces: Inverse problems/prior information/stochastic inversion
[NASA-CR-181555] 05 p0643 N88-13936

Freidlin-Wentzell type estimates and the law of the iterated logarithm for a class of stochastic processes related to symmetric statistics
[AD-A185366] 05 p0644 N88-13944

On the correlation free forms for nonlinear stochastic systems
[DE87-011169] 05 p0645 N88-13947

Computing block-angular Karmarker projections with applications to stochastic programming, revision
[AD-A185647] 06 p0759 N88-14656

On the relations between increasing functions associated with two-parameter continuous martingales
[AD-A185572] 06 p0765 N88-14699

Stochastic approximation and large deviations: General results for w.p.l. Convergence
[AD-A185818] 06 p0768 N88-14721

Relativistic stochastic mechanics
[PREPRINT-543] 06 p0790 N88-14842

A multicut algorithm for two-stage stochastic linear programs
[AD-A186148] 07 p0903 N88-15466

Stochastic filtering solutions for ill-posed linear problems and their extension to measurable transformations
[AD-A186016] 07 p0909 N88-15506

Strong laws of large numbers for arrays of orthogonal random variables
[AD-A186159] 07 p0910 N88-15513

Spectral representation of infinitely divisible processes
[AD-A186210] 07 p0910 N88-15515

Upper bounds on the expected value of a convex function using gradient and conjugate function information
[AD-A186246] 07 p0910 N88-15517

Remark on the multiple Wienor integral
[AD-A186015] 07 p0913 N88-15541

Point processes in the plane
[AD-A186017] 07 p0913 N88-15542

On stochastic optimality of policies in first passage problems
[AD-A186293] 07 p0915 N88-15554

On hypercontractivity of alpha-stable random variables, 0 less than alpha less than 2
[AD-A186425] 07 p0915 N88-15559

The filtering problem for infinite dimensional stochastic processes
[AD-A186431] 07 p0916 N88-15562

Sublinear upper bounds for stochastic programs with recourse, revision
[AD-A186436] 07 p0916 N88-15564

Validation of a stochastic model to determine failure rates for communication-electronic systems
[AD-A186536] 08 p0980 N88-15920

Optimal correction problem of a multidimensional stochastic system
[AD-A186727] 09 p1228 N88-17353

A Prohorov bound for a Poisson process and a Bernoulli process
[CWI-MS-R8701] 09 p1232 N88-17388

Persistence characteristics of 500 mb blocking and zonal flows in the mid-latitudes of the Northern and Southern Hemispheres 10 p1353 N88-18088

Explicit solutions of moment problems, 1
[AD-A186018] 10 p1397 N88-18325

Prediction of the response and optimal control of stochastic parametrically and externally excited nonlinear systems 11 p1496 N88-18930

Deterministic equivalent for a continuous linear-convex stochastic control problem
[AD-A187818] 11 p1540 N88-19206

Stochastic heuristics in network design: Parameter tuning and performance evaluation
[REPT-87-017] 11 p1541 N88-19210

Extrema of Gaussian process by simulation
11 p1541 N88-19211

Recursive inversion of externally defined linear systems
[NASA-TM-100070] 11 p1541 N88-19215

On relaxation algorithms based on Markov random fields
[AD-A189043] 13 p1814 N88-20840

Stochasticity in nonlinear Hamiltonian systems
[DE88-005499] 13 p1826 N88-20915

Stochastic comparisons of order statistics, with applications in reliability
[AD-A189408] 13 p1829 N88-20938

Stochastic and chaotic oscillations
[CWI-AM-R8704] 13 p1829 N88-20940

Nonstationary solution in random vibration theory
[PB88-163746] 14 p1933 N88-21529

Identification of nonlinear rational systems using a prediction-error estimation algorithm
[RR-317] 14 p1959 N88-21680

An orthogonal parameter estimation algorithm for nonlinear stochastic systems
[RR-307] 14 p1966 N88-21736

Open questions in closed-loop photodetection
14 p1979 N88-21812

Stochastic acceleration of cometary ions: The effects of composition and source strength distributions
14 p1997 N88-21902

Random processes, turbulence and disordering fields
[AD-A190123] 15 p2063 N88-22303

Vibrations of structures with parametric uncertainties
[AD-A190400] 15 p2076 N88-22378

Probabilistic structural analysis computer code (NESSUS) 15 p2079 N88-22397

Memory efficient evaluations of nonlinear stochastic equations and C3 applications
[AD-A189872] 15 p2110 N88-22569

Using Colored Stochastic Petri Net (CS-PN) software for protocol specification, validation, and evaluation
[ENST-87C004] 15 p2113 N88-22588

The Colored Stochastic Petri Net (CS-PN) software: Application to the validation and the performance evaluation of distributed systems
[ENST-87D005] 15 p2113 N88-22589

The adjoint process in stochastic optimal control
[AD-A189720] 15 p2116 N88-22605

Martingale representation and the Malliavin calculus
[AD-A189721] 15 p2119 N88-22626

The existence of smooth densities for the prediction filtering and smoothing problems
[AD-A189865] 15 p2119 N88-22629

Normed Bellman equation with degenerate diffusion coefficients and its application to differential equations
[AD-A190319] 15 p2120 N88-22637

Random Process Simulation for stochastic fatigue analysis
[NASA-TM-100464] 15 p2123 N88-22654

The partially observed stochastic minimum principle
[AD-A189787] 15 p2124 N88-22658

Approximations in extreme value theory
[AD-A189817] 15 p2124 N88-22659

Stopping rules and observed significance levels
[AD-A190320] 15 p2124 N88-22664

Estimation of convolution tails
[AD-A190323] 15 p2125 N88-22666

Continuity of symmetric stable processes
[AD-A190324] 15 p2125 N88-22667

Extreme value for dependent sequences via the Stein-Chen method of poisson approximation
[AD-A190325] 15 p2125 N88-22668

Detection of the number, locations and magnitudes of jumps
[AD-A190328] 15 p2125 N88-22671

Statistical inference for stochastic processes
[AD-A190491] 15 p2126 N88-22673

Stochastic evolution equations driven by nuclear space valued martingales
[AD-A189342] 15 p2126 N88-22677

Conditions for information capacity of the discrete-time Gaussian channel to be increased by feedback
[AD-A190317] 15 p2127 N88-22687

Studying Turbulence Using Numerical Simulation Databases. Proceedings of the 1987 Summer Program
[NASA-CR-182692] 16 p2194 N88-23086

Stochastic estimation of conditional eddies in turbulent channel flow 16 p2194 N88-23087

Optimal control, estimation compensation of linear discrete-time systems with stochastic parameters
[REPT-87-56] 16 p2255 N88-23478

An algebraic construction of a class of one-dependent processes
[REPT-87-65] 16 p2259 N88-23507

A note on phase-type, almost phase-type, generalized hyperexponential and Coxian distribution, revision
[AD-A191236] 16 p2261 N88-23517

Stochastic approach of image segmentation. A model of cooperation between region primitives and boundaries
[ETN-88-92192] 16 p2262 N88-23523

Modeling, filtering and control of stochastic processes --- communication networks
[ENST-87E021] 17 p2333 N88-23925

Parallel discrete-event simulation of FCFS stochastic queueing networks
[NASA-CR-181669] 17 p2389 N88-24203

Stochasticity in elliptical galaxies
[SER-C-PREPUBL-FASC-20] 17 p2450 N88-24556

Information and stochastic systems
[AD-A192167] 18 p2501 N88-24836

Analysis of binarized Hartley phase-only filter performance with respect to stochastic noise
[DE88-007604] 18 p2519 N88-24945

Reliability of stochastically forced systems (extended version)
[CWI-AM-R8801] 18 p2526 N88-24985

Computational sciences
[AD-A190826] 18 p2564 N88-25226

Numerical solutions to stochastic difference equations
18 p2564 N88-25229

On path properties of certain infinitely divisible processes
[AD-A192016] 18 p2568 N88-25255

Stochasticity in a Q-machine plasma
18 p2578 N88-25315

Study of probabilistic fatigue crack growth and associated scatter under constant-and-variable amplitude loading spectrum
[AD-A192027] 19 p2679 N88-25929

Stochastic modeling of EM scattering from foliage
[AD-A192258] 20 p2790 N88-26553

Two classes of self-similar stable processes with stationary increments
[AD-A192842] 20 p2846 N88-26894

Simulation and analysis of wave propagation through random media 21 p2947 N88-27503

Nonlinear stochastic interaction in aeroelastic structures
[AD-A193427] 21 p2961 N88-27589

Stochastic geologic effects on near-field ground motions in alluvium
[AD-A192315] 21 p2972 N88-27652

Simulation methodology
[AD-A192548] 21 p2995 N88-27764

Control, stability and filter for a discrete linear stochastic system with correlated noise
[PB88-109525] 21 p3004 N88-27818

A Wong-Zakai type theorem for certain discontinuous semimartingales
[AD-A192713] 21 p3005 N88-27822

Approximations of stochastic equations driven by predictable processes
[AD-A192714] 21 p3005 N88-27823

Computation of filters by sampling and quantization
[AD-A192839] 21 p3005 N88-27826

On the exceedance random measures for stationary processes
[AD-A192838] 21 p3009 N88-27848

A note on vector bimeasures
[AD-A192841] 21 p3009 N88-27849

A study on Lebesgue decomposition of measures induced by stable processes
[AD-A192893] 21 p3009 N88-27850

Multiple integration with respect to Poisson and Levy processes
[AD-A192895] 21 p3009 N88-27851

Statistical description of stochastic dynamics
[AD-A192924] 21 p3009 N88-27852

A virtual statistical mechanical neural computer
[AD-A193962] 22 p3139 N88-28660

Theory of Laplacian fractals: Diffusion limited aggregation and dielectric breakdown model
[PREPRINT-590] 22 p3144 N88-28701

Extremal two-correlations of two-valued stationary one-dependent processes
[REPT-88-01] 22 p3145 N88-28704

Dynamic analysis of computer and communications sytems: Semi-Markov approach
23 p3244 N88-29305
Weak solution of the Langevin equation on a generalized functional space
[AD-A194290] 23 p3270 N88-29456
An asymptotic evaluation of the tail of a multiple symmetric alpha-stable integral
[AD-A194570] 23 p3270 N88-29460
On Wiener-Masani's algorithm for finding the generating function of multivariate stochastic processes
[NASA-CR-182905] 23 p3273 N88-29481
Stochastic game approach to guidance design
[AD-A194574] 23 p3276 N88-29498
Theory of filtering and control with application to control of large space structures
[AD-A195500] 24 p3335 N88-29851
Statistical analysis of the LMS (Last Mean Squares) and modified stochastic gradient
[AD-A195497] 24 p3424 N88-30376
Stability, stochastic stationarity and generalized Lyapunov equations for two-point boundary-value descriptor systems
[AD-A195645] 24 p3425 N88-30385
Analytical methods in stochastic control and nonlinear filtering
[AD-A194272] 24 p3426 N88-30388

STOICHIOMETRY
Structural properties of high-T/sub c/ oxide super conductors
[DE88-002974] 08 p1090 N88-16563
Copper oxidation states, vacancy ordering and their effect on high temperature superconductivity
[DE88-003079] 09 p1258 N88-17542
Local stoichiometry and atomic interdiffusion during reactive metal/mercury-cadmium-telluride junction formation
[AD-A187554] 10 p1421 N88-18488
Processing relationships in YBa2Cu3O(7-x) superconductors
[DE88-005137] 11 p1559 N88-19330
Investigations of surface coatings based on silicon and nitrogen: From amorphous Si to silicon nitride
[DE88-004995] 12 p1609 N88-19622
Electron diffraction evidence for the ordering of excess nickel atoms by relation to stoichiometry in nickel-rich beta'-NiAl formation of a nickel-aluminum (Ni2Al) superlattices
[NASA-TT-20177] 14 p1890 N88-21297
Irreversible dissolution of solid solutions: A kinetic and stoichiometric model
[DE88-009194] 19 p2614 N88-25513
A study of the interaction of diffusion flames with a vortex pair flowfield 21 p2908 N88-27258
Premixed turbulent flame propagation
[AD-A192955] 21 p2909 N88-27265

STOKES FLOW
Shearing flow over Stokes wave. Part one: General theory
[ETN-87-90957] 02 p0171 N88-11074
Rotation of magnetized particle in electrically conducting viscous medium 06 p0770 N88-14733
Chaos, mappings and spatial complexity in fluids
11 p1484 N88-18860
New mixed finite element methods
18 p2567 N88-25248
High performance solutions of the Stokes problem using mini-elements, self-adaptive grids, and multigrid methods: Applications
[ECL-87-15] 22 p3077 N88-28266

STOKES LAW
Two domain decomposition techniques for Stokes problems
[DE88-008724] 19 p2720 N88-26149

STOKES LAW (FLUID MECHANICS)
La Recherche Aerospatiale, bimonthly bulletin, number 1987-1, 236/January-February
[ESA-TT-1055] 11 p1433 N88-18549
Boundary effects on the drag of a cylinder in axial motion at low Reynolds number 13 p1768 N88-20578
A simple explanation of the Stokes phenomenon
[AD-A193253] 21 p3006 N88-27832

STOL AIRCRAFT
U SHORT TAKEOFF AIRCRAFT

STOMACH
Gastric emptying during exercise: Effects of acute heat stress, acclimation and hypohydration
[AD-A188008] 11 p1519 N88-19073
Gastric emptying during walking and running: Effects of varied exercise intensity
[AD-A194025] 23 p3240 N88-29281

STONES (ROCKS)
U ROCKS

STONY METEORITES
NT ACHONDRITES
NT CARBONACEOUS CHONDRITES
NT CARBONACEOUS METEORITES
NT CHONDRITES

STOPPING
Algorithms with conic termination for nonlinear optimization
[DE88-005893] 13 p1816 N88-20851
Merge and termination in process algebra
[CWI-CS-R8716] 13 p1826 N88-20918
Stopping rules and observed significance levels
[AD-A190320] 15 p2124 N88-22664
Soft-ground aircraft arresting systems
[AD-A190838] 16 p2165 N88-22912

STOPPING POWER
Studies of HZE particle interactions and transport for space radiation protection purposes
[NASA-TM-101159] 20 p2886 N88-27142

STORAGE
Solar generation and storage of O2 (a 1 delta g)
[NASA-CR-4127] 14 p1913 N88-21431

STORAGE BATTERIES
NT LEAD ACID BATTERIES
NT NICKEL CADMIUM BATTERIES
NT NICKEL HYDROGEN BATTERIES
NT NICKEL ZINC BATTERIES
NT ZINC-BROMIDE BATTERIES
High energy density rechargeable batteries for aerospace power requirements
[AD-A184883] 05 p0577 N88-13519
Interfacial effects in thin Li/PEO cells at room temperature
[AD-A186974] 09 p1157 N88-16931
A novel class of positive electrodes for rechargeable batteries
[DE88-004559] 13 p1763 N88-20545
Candidate advanced energy storage concepts for multimegawatt burst power systems
17 p2426 N88-24434
Small scale bipolar nickel-hydrogen testing
[NASA-TM-100936] 18 p2538 N88-25059
All inorganic ambient temperature rechargeable lithium battery
[DE88-008425] 19 p2662 N88-25834
Ambient temperature secondary lithium batteries using LiAl lithium insertion anodes
[DE88-006394] 20 p2793 N88-26574
Exploratory battery technology development and testing report for 1986
[DE88-009870] 20 p2794 N88-26578
Considerations and measurements of latent-heat-storage salts for secondary thermal battery applications
[DE88-011091] 23 p3228 N88-29213
Structure and dynamics of solutions of lithium salts relevant to battery construction
[AD-A195399] 24 p3366 N88-30044

STORAGE RINGS (PARTICLE ACCELERATORS)
Brightness and coherence of radiation from undulators and high-gain free electron lasers
[DE87-011093] 02 p0177 N88-11102
Interactive Design of Accelerators (IDA)
[DE87-013298] 02 p0234 N88-11476
Compact electron storage rings
[DE87-013301] 02 p0234 N88-11477
High energy polarized electron beams
[CEBAF-R-87-002] 11 p1546 N88-19244
ZAP user's manual
[LBL-21270] 11 p1546 N88-19248
On bunch lengthening using the fourth harmonic cavity in the NSLS VUV ring
[DE88-007392] 18 p2574 N88-25288
Activities report of the Werner-Heisenberg Institute of Physics
[ETN-88-92946] 21 p3015 N88-27893
Distortion functions
[DE88-752634] 21 p3015 N88-27896

STORAGE STABILITY
Pyrotechnic component development at Sandia National Laboratory
[DE87-006899] 02 p0154 N88-10967
Effects of long term storage on aerospace nickel cadmium cell performance 02 p0165 N88-11035
Shelf life degradation of selected anaerobic threadlocking adhesives at various storage temperatures
[AD-A187712] 11 p1461 N88-18711
Cyropreservation of isolated rat hepathocytes for future use in Spacelab experiments: Preliminary results
12 p1660 N88-19950
Material degradation in a barium hydroxide latent heat storage pilot unit
[DFVLR-FB-87-46] 16 p2175 N88-22961
Aging of CFRP due to longterm storage in heated air
[DFVLR-FB-88-05] 21 p2922 N88-27345

STORAGE TANKS
Electrical heating method --- pipelines, metal tanks
[GB-PATENT-2-137-059-A] 01 p0043 N88-10274
Orbital Spacecraft Consumables Resupply System (OSCRS). Volume 2: Study results
[NASA-CR-172011] 03 p0268 N88-11687
Contribution of acoustic analysis to assess damage in fluid storage tanks under high pressure --- composite materials, filament winding
[SNIAS-872-430-119] 05 p0559 N88-13407
Space environmental considerations for a long-term cryogenic storage vessel 08 p0981 N88-15933
Space Infrared Telescope Facility (SIRTF) design and thermal analysis 08 p0982 N88-15934
Thermal analysis for the Cryogenic Fluid Management Flight Experiment (CFMFE) 08 p0982 N88-15935
Protecting old oil tanks made of steel against internal corrosion using organic coatings
[DE88-751089] 11 p1459 N88-18698
Examination of methods for pollen storage and dispersal
[TN-RB524-097/86] 17 p2378 N88-24134
Prediction of velocity and temperature profiles in thermally driven gravity currents applied to stratified thermal storage tanks
[DE88-004452] 21 p2946 N88-27496

STORE RELEASE
U EXTERNAL STORE SEPARATION

STORM DAMAGE
Forecast of Atlantic seasonal hurricane activity for 1988 15 p2098 N88-22500

STORM ENHANCEMENT
The effect of latitude on the development of tropical cyclones
[AD-A185670] 06 p0746 N88-14590
Tropical cyclones, 1987: Central North Pacific
[PB88-188081] 18 p2547 N88-25119

STORM SUPPRESSION
The studies of physical models on hailstorms and their applications in nowcasting 02 p0207 N88-11300

STORM SURGES
An hourly analysis, updating and short-range forecasting system --- numerical weather forecasting
02 p0206 N88-11288
Hurricane Elena storm surge data
[AD-A184573] 03 p0353 N88-12228
Hurricane Danny storm surge data, report 4
[AD-A186373] 07 p0879 N88-15334
Hurricane Kate storm surge data, report 5
[AD-A186374] 07 p0880 N88-15335
Hurricane climatology for the Atlantic and Gulf coasts of the United States
[PB88-114657] 08 p1039 N88-16288

STORMS
NT CYCLONES
NT HAILSTORMS
NT HURRICANES
NT MAGNETIC STORMS
NT MICROBURSTS (METEOROLOGY)
NT RAINSTORMS
NT SNOWSTORMS
NT STORMS (METEOROLOGY)
NT SUDDEN IONOSPHERIC DISTURBANCES
NT THUNDERSTORMS
NT TORNADOES
NT TROPICAL STORMS
NT TYPHOONS
NWS (National Weather Service) watch/warning verification flash flood, winter storm and high wind, January 1980 - June 1986
[PB87-223053] 04 p0469 N88-12898
Ozone, jet streaks and severe weather
05 p0616 N88-13781
Model investigations of atmospheric ammonia scavenging
[DE88-002337] 09 p1194 N88-17153
Using SIR (Scientific Information Retrival) system for data management during a field program
[DE88-001555] 10 p1424 N88-18508
Effects of stress on judgement and decision making in dynamic tasks
[AD-A188203] 11 p1523 N88-19092
National Severe Storms Laboratory, fiscal year 1987
[PB88-140108] 12 p1647 N88-19863
Research and development to acquire and reduce melting layer cloud physics and evaluate a prototype M-meter
[AD-A188390] 12 p1648 N88-19873
TDWR (Terminal Doppler Weather Radar) PRF (Pulse Repetition Frequency) selection criteria
[AD-A193089] 21 p2932 N88-27407
Passive microwave measurements of water vapor fields and rain for locating fronts in cyclonic storms
[AD-A195632] 24 p3404 N88-30267

STORMS (METEOROLOGY)
NT CYCLONES
NT HAILSTORMS
NT HURRICANES
NT MICROBURSTS (METEOROLOGY)
NT RAINSTORMS
NT SNOWSTORMS
NT THUNDERSTORMS
NT TORNADOES
NT TROPICAL STORMS
NT TYPHOONS
Description of the Mountain Cloud Chemistry Program version of the PLUVIUS MOD 5.0 reactive storm simulation model
[DE87-012846] 01 p0070 N88-10450
The use of McIDAS as a Mesoscale forecasting tool during the Canadian Atlantic storms programs --- Man-computer Interactive Data Access System (McIDAS) 02 p0205 N88-11284
A short-range forecasting experiment conducted during the Canadian Atlantic storms program
02 p0205 N88-11285
A severe weather forecast software package
02 p0206 N88-11294
A review of the analysis forecasting and research about severe local storms in Guangdong province (China)
02 p0207 N88-11298
Severe weather potential (SPOT) plotfile generator
[PB87-217717] 02 p0216 N88-11360
Theory of heat and moisture exchange between finely disperse storm-generated spray and turbulent air flow
04 p0461 N88-12851
Prediction of polytomous events: Model description, algorithm development and methodological aspects, with an application
[AD-A186549] 09 p1232 N88-17384
Pre-convective environmental conditions indicative of non-tornadic severe thunderstorm winds over Southeast Florida
[AD-A188679] 12 p1648 N88-19870
STOSS-AND-LEE TOPOGRAPHY
U GLACIAL DRIFT
STOWAGE (ONBOARD EQUIPMENT)
Locking hinge
[NASA-CASE-MSC-21056-1] 17 p2312 N88-23827
Expendable pallet for space station interface attachments
[NASA-CASE-MSC-21117-1] 23 p3185 N88-28958
STRAIN AGING
U PRECIPITATION HARDENING
STRAIN DISTRIBUTION
Experimental and theoretical investigation of mechanically fastened composites
[AD-A185896] 07 p0826 N88-15008
Structural relaxation in strained-layer heterostructures
[DE88-002326] 07 p0868 N38-15264
A summary of experimental results on square plates and stiffened panels subjected to air-blast loading
09 p1178 N88-17057
Computed stress and strain distributions under interference fit and after coldworking
[AD-A186950] 10 p1342 N88-18024
Development of reliable fuel pins for space reactor applications 17 p2409 N88-24326
Design and construction techniques for planar polysilicon pressure transducers with piezoresistive read-out 19 p2669 N88-25862
Compression creep of filamentary composites
[NASA-CR-182550] 20 p2798 N88-26601
STRAIN ENERGY METHODS
Fatigue life evaluation according to local strain concept
[FF-14/1985] 01 p0059 N88-10381
Estimation multiaxial elastic-plastic notch stresses and strains in combined loading
[FB-2/1986] 01 p0060 N88-10382
A comparison of plastic work energy and external input for fatigue crack propagation 05 p0607 N88-13722
Design and dynamic testing of an instrumented spacecraft component 11 p1499 N88-18952
Vibration response of constrained viscoelastically damped plates: Analyses and experiments
[AD-A192329] 20 p2815 N88-26699
STRAIN ENERGY RELEASE RATE
Strain-energy-release rate analysis of the end-notched flexure specimen using the finite-element method
[NASA-TM-100494] 05 p0608 N88-13735
Sublaminate damage mechanisms in composite structures
[AD-A186807] 09 p1137 N88-16815
Three-dimensional analysis of a postbuckled embedded delamination
[NASA-TP-2823] 20 p2812 N88-26684
STRAIN FATIGUE
U FATIGUE (MATERIALS)
STRAIN GAGE ACCELEROMETERS
Zeroshift of piezoelectric accelerometers in pyroshock measurements 08 p0997 N88-16039
STRAIN GAGES
Balancing strain gauge bridges
[GB-PATENT-2-129-567-A] 01 p0048 N88-10307
Strain gages in engineering geodesy
[SER-C-320] 01 p0048 N88-10309
Fabrication of standardized piezoelectric polymer shock gauges by the Bauer method
[DE87-012738] 01 p0049 N88-10315
Notes on transducer design based on resistance strain gages with applied temperature compensation
[FFA-MEMO-129] 01 p0050 N88-10319
The development of a high temperature static strain gage system 02 p0184 N88-11142
Elevated temperature strain gages
02 p0184 N88-11144
The Lewis Strain Gauge Laboratory: Status and plans
02 p0184 N88-11146
Model helicopter rotor rig and associated strain gauge balance for performance studies
[NAL-TM-AE-8704] 05 p0552 N88-13364
Earth penetrator strain gage applications
[DE88-002260] 09 p1166 N88-16993
Strain gage balance for half models 302-6. Calibration report --- wind tunnels
[F+W-FO-1803] 09 p1168 N88-17001
Strain gage sting balance 204-6. Calibration report --- wind tunnels
[F+W-FO-1838] 09 p1168 N88-17002
Multi-component stress history measurements and analysis
[DE88-000977] 09 p1168 N88-17004
Manoeuvres by default, by demand and by design
12 p1580 N88-19455
Determination of the toughness of a brittle material using strain gages
[ETN-88-92540] 18 p2527 N88-24993
Design and construction techniques for planar polysilicon pressure transducers with piezoresistive read-out 19 p2669 N88-25862
Deposition techniques and properties of strain compensated LPCVD silicon nitride films
19 p2673 N88-25898
In-flight load measurements of the Robot-X canards
[AD-A193428] 21 p2895 N88-27187
Attachable interferometric strain gages
[AD-A192390] 21 p2950 N88-27522
Further improvements relating to the temperature compensation of semiconductor strain gauge pressure transducers
[RAE-TR-87061] 22 p3081 N88-28298
Electrical properties of materials for elevated temperature resistance strain gage application
[NASA-CR-182214] 24 p3376 N88-30106
Method of attaching strain gauges to various materials
[NASA-CASE-LAR-13797-1] 24 p3376 N88-30108
STRAIN HARDENING
Dugdale solutions for strain hardening materials
[FD-6/1985] 01 p0059 N88-10380
Tensile behavior of superplastic Al-Cu-Li-Zr alloy 2090 at cryogenic temperatures
[DE87-014084] 02 p0147 N88-10923
Hadfield steels with Nb and Ti carbides
[DE87-703706] 04 p0416 N88-12579
Fatigue, fracture and strain hardening of high carbon hardened alloy steel
[AD-A186101] 07 p0831 N88-15043
Processing, structure and properties of heavily deformed in situ composites
[AD-A189611] 13 p1742 N88-20416
Response of aluminum alloys to erosive particle impacts
[DE88-005910] 15 p2041 N88-22159
Strain hardening at large strains in aluminum alloys
[DE88-007415] 18 p2484 N88-24737
STRAIN MEASUREMENT
The development of a high temperature static strain gage system 02 p0184 N88-11142
The Lewis Strain Gauge Laboratory: Status and plans
02 p0184 N88-11146
High temperature stress-strain analysis
02 p0188 N88-11170
Measurement of model deformation in wind tunnels
05 p0551 N88-13358
Application of finite element methods with cyclic elasto-plastic strain analysis to low cycle fatigue analysis of engine components
[AR-004-512] 05 p0596 N88-13642
Axial creep-fatigue damage assessment in type 316 SS material 06 p0721 N88-14430
Thermomechanical fatigue of lead-base low tin solder
06 p0721 N88-14432
A quantitative method for evaluating sensor layouts
09 p1178 N88-17056
Optical analysis of stress and strain in photoelastic particle assemblies
[ETN-88-91591] 09 p1182 N88-17082
The influence of strain on hydrogen entry, transport, and embrittlement of a high strength steel in aqueous sodium chloride solution
[AD-A189302] 12 p1608 N88-19619
Correlation of data on strain accumulation adjacent to the San Andreas Fault with available models
[NASA-CR-180757] 13 p1796 N88-20742
The mechanical properties of card measured by photographic Moire
[NPL-DMOM-87] 14 p1923 N88-21463
Research sensors 15 p2085 N88-22430
Strain intensity factor approach for predicting the strength of continuously reinforced metal matrix composites
[NASA-TM-100617] 17 p2317 N88-23838
Radio Frequency (RF) strain monitor
[NASA-CASE-LAR-13705-1] 18 p2530 N88-25011
Uniaxial tensile strain measurement for ceramic testing at elevated temperature: Requirements, problems and solutions
[DE88-008090] 19 p2621 N88-25550
Predicted and measured strain responses of isotropic panels to base excitation
[NASA-TM-4054] 19 p2679 N88-25928
Ion implantation processing of 3-5 strained-layer semiconductors
[DE88-005270] 19 p2734 N88-26240
Component stress during freeze/thaw cycling
[DE88-011204] 21 p2938 N88-27449
Optical method to measure the deformations of structures loaded by hydraulic pressure
[SNIAS-881-430-111] 22 p3088 N88-28338
Piezoelectric and electrostrictive materials for transducer applications, volume 2
[AD-A194956] 24 p3376 N88-30104
STRAIN RATE
An investigation of the high strain rate deformation of SiCw/2124 Al composite
[OUEL-1675/87] 02 p0142 N88-10895
Strain rate effects in fast-gas-cooled uranium-titanium and uranium-niobium alloys
[OUEL-1683/87] 02 p0149 N88-10937
Experimental determination of flow potential surfaces supporting a multiaxial formulation of viscoplasticity
02 p0187 N88-11167
Material behaviour at high rates of strain
[OUEL-1684/87] 02 p0192 N88-11200
Work-in-progress presented at the Army Symposium on Solid Mechanics, 1986: Lightening of the Force
[AD-A184791] 04 p0427 N88-12644
A direct method to obtain constitutive model constants from cylinder impact test results
04 p0427 N88-12647
Influence of strain rate and notch depth on tensile properties of HITCO 6250
[DE88-001324] 04 p0455 N88-12816
The evolution of plastic strain in steady, plastic shock waves
[DE87-013812] 04 p0456 N88-12826
Plasticity of aluminum and iron at high shear strain rate and high pressure 05 p0563 N88-13430
A critical review of the development of several viscoplastic constitutive theories
[AD-A185652] 07 p0867 N88-15262
Theory of deformation. Part 1: Kinematics
[DE88-003007] 08 p1001 N88-16062
The effect of strain rate on the strength and ductility of SiCw/2124 Al composite
[OUEL-1692/87] 14 p1924 N88-21466
An internal variable constitutive model for the large deformation of metals at high temperatures
14 p1929 N88-21503
Constitutive modeling and thermoviscoplasticity
14 p1930 N88-21506
Creep rupture analysis of a beam resting on high temperature foundation 14 p1930 N88-21509
Controlled-strain rate tests at very low strain rates of 2618 aluminum at 200 C 14 p1931 N88-21513
The effects of temperature and strain rate on the yielding behavior of the single crystal superalloy PWA 1480
14 p1931 N88-21517
Nonlinear structural analysis of a turbine airfoil using the Walker viscoplastic material model for B1900 + Hf
14 p1932 N88-21522
Unified constitutive models for high-temperature structural applications 14 p1932 N88-21523
Effect of strain rate on high-temperature low-cycle fatigue behavior of Hastelloy X and Hastelloy XR
[DE88-752302] 15 p2037 N88-22140
The CRREL (Cold Regions Research and Engineering Laboratory) Hopkinson bar apparatus
[AD-A190599] 15 p2077 N88-22380

Unified constitutive model development for metal matrix composites at high temperature
15 p2078 N88-22387

Unified constitutive model for single crystal deformation behavior with applications 15 p2078 N88-22388

Phenomenological modelling of rate-dependent plasticity for high strain rate problems
[DE88-006647] 15 p2087 N88-22440

Evaluation of a theory for pressure-strain rate
16 p2198 N88-23108

Relations between two-point correlations and pressure strain terms 16 p2198 N88-23109

Superplasticity: A fundamental investigation on deformation mechanism and cavitation phenomena
[AD-A191546] 18 p2485 N88-24741

The variation of torsional ductility of high-purity aluminum with temperature and strain rate
[DE88-005618] 18 p2487 N88-24755

Metastability in SiGe/Si strained-layer structures
[DE88-007603] 18 p2585 N88-25361

Influence of strain rate on the substructure evolution and yield behavior of Ti-6Al-4V
[DE88-006457] 19 p2616 N88-25520

Apparatus for pressure welding of titanium structures with a controlled rate of deformation
[RAE-TRANS-2161] 19 p2677 N88-25915

Temperature, moisture and strain rate effects on the compressive mechanical behavior of Nylon 6/6
[DE88-010734] 21 p2961 N88-27591

Environmental cracking of a superferritic stainless steel under slow strain rate conditions
22 p3053 N88-28117

Development of sensors for ceramic components in advanced propulsion systems: Survey and evaluation of measurement techniques for temperature, strain and heat flux for ceramic components in advanced propulsion systems
[NASA-CR-182111] 22 p3081 N88-28299

A transversely isotropic thermoelastic theory
[NASA-TM-101302] 22 p3087 N88-28332

Plastic flow and failure modeling under high strain rate loading
[AD-A194223] 23 p3226 N88-29199

STRAIN SOFTENING

U PLASTIC DEFORMATION

STRAKES

Transonic Navier-Stokes computations of strake-generated vortex interactions for a fighter-like configuration
[NASA-TM-100009] 15 p2014 N88-22010

Wind-tunnel investigation of actuated forebody strakes for yaw control at high angles of attack
17 p2299 N88-23754

Helicopter anti-torque system using fuselage strakes
[NASA-CASE-LAR-13630-1] 17 p2308 N88-23809

Actuated forebody strakes
[NASA-CASE-LAR-13983-1] 18 p2464 N88-24628

STRANGE ATTRACTORS

Dimension densities for turbulent systems with spatially decaying correlation functions
[DE87-010119] 02 p0169 N88-11066

Anomalous scaling laws in multifractal objects
[NOTA-INTERNA-883] 07 p0916 N88-15565

STRAPDOWN INERTIAL GUIDANCE

Test equipment with fiber optic data bus and laser gyro strapdown system LTN-90 for the helicopter BO-105
[ESA-TT-1038] 01 p0005 N88-10025

NAVSIM 2: A computer program for simulating aided-inertial navigation for aircraft
[NASA-CR-177438] 04 p0398 N88-12478

Advances in Air-Launched Weapon Guidance and Control
[AGARD-CP-431] 12 p1596 N88-19553

A prototype fibre optic gyroscope for missile guidance applications 12 p1596 N88-19554

A fiber optic gyro strapdown reference system for guided weapons 12 p1597 N88-19560

An analysis of DREO's (Defence Research Establishment Ottawa) analog rebalance loops for the CSG-2 (Canadian Strapdown Gyroscope) tuned-rotor gyroscope
[AD-A188577] 12 p1629 N88-19749

Utilization of strapdown inertial and non-inertial sensors in determination of satellite attitude by Kalman filters
[INPE-4313-TDL/280] 13 p1731 N88-20349

Design, simulation and laboratory testing of an inertial system for measuring the attitude and narrow-spaced motions
[DFVLR-FB-87-42] 14 p1912 N88-21426

The NAE atmospheric research aircraft
24 p3313 N88-29730

STRATA

NT SUBSTRATES

STRATEGIC MATERIALS

International role of US geoscience
[NASA-CR-182407] 08 p1035 N88-16281

STRATEGY

Technology transfer to China
[PB87-223418] 04 p0502 N88-13087

Strategic management of research and development: A literature search
[NASA-CR-182337] 06 p0790 N88-14847

Investigation of design concepts for large space structures to support military applications
[AD-A186098] 07 p0824 N88-15000

Performance analysis of coded frequency-hopped spread-spectrum systems with unknown interference
[AD-A186069] 07 p0841 N88-15103

Strategies of data analysis
[AD-A186033] 07 p0914 N88-15548

Cirrus: An automated protocol analysis tool
[AD-A186646] 08 p1052 N88-16348

Research, development, and growth strategy
10 p1309 N88-17820

State-of-the-art technologies for construction in space: A review
[AD-A188412] 12 p1585 N88-19483

Static and dynamic jamming of networks
[AD-A188921] 12 p1620 N88-19690

Alternative force structuring strategies for military satellite communication systems
[AD-A189492] 13 p1758 N88-20516

Parallel image compression
[NASA-CR-180758] 13 p1814 N88-20837

Johnson Space Center's strategic game plan: Charting a course to the year 2000 and beyond
[NASA-TM-89733] 13 p1850 N88-21076

Anatomy of an organizational change effort at the Lewis Research Center
[NASA-CR-4146] 19 p2739 N88-26264

SDI: Myth or reality
[DE88-009121] 20 p2847 N88-26901

The strategic defense initiative: Strategic implications
[AD-A192341] 20 p2847 N88-26902

Rules, schema and decision making
[AD-A193389] 21 p3027 N88-27967

Technology transfer for DOE's Office of Transportation Systems: Assessment and strategies
[DE88-010760] 21 p3029 N88-27977

Electronic combat roadmap for space
[AD-A194282] 22 p3146 N88-28709

Defensive platform size and survivability
[DE88-011634] 23 p3184 N88-28948

The advice taker/inquirer: A system for high-level acquisition of expert knowledge
24 p3421 N88-30359

Antisatellite weapons and satellite deployment strategies
[AD-A195014] 24 p3427 N88-30396

STRATIFICATION

NT ATMOSPHERIC STRATIFICATION

NT INTERCALATION

The correspondence of surface climate parameters with satellite and terrain data
[NASA-CR-181515] 03 p0346 N88-12185

Influence of stratification in near-surface water layer on intensity of gas exchange between atmosphere and water 04 p0459 N88-12841

Transient development of stratification in a partially divided enclosure
[DE87-011742] 05 p0572 N88-13490

Two-layer model of circulation in world ocean with detailed description of seasonal evolution of upper quasihomogeneous layer 06 p0727 N88-14470

North Pacific Ocean. Gulf of Alaska, R/V Thomas G. Thompson: 1 February - 8 March 1967. STD data report
[AD-A186569] 08 p1045 N88-16314

Dynamics of the Oceanic Surface Mixed Layer
[AD-A188348] 13 p1804 N88-20785

Structures and fluxes in a deep convecting mixed layer 13 p1804 N88-20786

Equatorial turbulence: Mixed layer and thermocline
13 p1804 N88-20787

On the zonal momentum balance at the equator
13 p1805 N88-20788

The mixed layer of the western equatorial Pacific Ocean
[HIG-1861] 13 p1805 N88-20789

Unsteady shallowing mixed layer
13 p1805 N88-20791

Horizontal scales of wind forced inertial motions
13 p1806 N88-20795

Subduction 13 p1806 N88-20796

Hamiltonian description of the interaction of surface waves with mixed-layer currents
13 p1806 N88-20799

Monitoring ocean surface layer processes
13 p1806 N88-20801

The main ocean thermocline
14 p1938 N88-21563

Role of ordinary to extraordinary mode wave coupling in ionospheric heating experiments
[AD-A195335] 24 p3362 N88-30017

Mathematical problems of nonlinear wave propagation and of waves in heterogeneous media
[AD-A195970] 24 p3368 N88-30057

STRATIFIED FLOW

Regressed relations for forced convection heat transfer in a direct injection stratified charge rotary engine
[NASA-TM-100124] 05 p0549 N88-13345

Far field of steady waves produced by local perturbation sources in stream of stratified fluid
06 p0771 N88-14736

Mushroom-shaped currents (eddy dipoles) under rotation and stratification conditions
13 p1784 N88-20678

Direct simulation of stable stratified homogeneous turbulent shear flows
[DFVLR-FB-88-04] 21 p2949 N88-27516

STRATIGRAPHY

Geoacoustic models of the Hudson Canyon area
[AD-A183535] 01 p0073 N88-10465

Research needs for hydrocarbon fuels
[DE87-014555] 06 p0687 N88-14209

Neogene paleoclimate in Pacific Ocean subarctic region determined from study of diatoms
08 p1010 N88-16125

Geological evolution and analysis of confirmed or suspected gas hydrate localities. Volume 10: Basin analysis, formation and stability of gas hydrates of the Aleutian Trench and the Bering Sea
[DE88-001008] 10 p1346 N88-18048

Geological evolution and analysis of confirmed or suspected gas hydrate localities. Volume 2: Basin analysis, formation and stability of gas hydrates in the Black Sea
[DE88-001052] 18 p2532 N88-25023

Analyzing the stratigraphy, tectonism, and mineralization at the Spanish side of the pyrite belt, Huelva province, Spain, using SPOT imagery 22 p3104 N88-28433

Stratigraphy of the Kasei Valles region, Mars
23 p3305 N88-29690

Documenting volcano-tectonic episodes in Mars' stratigraphic record 23 p3306 N88-29695

Ridged and gullied terrains in the Martian uplands
23 p3307 N88-29700

Variation in the thickness of ejecta cover on Mars with increasing crater density 23 p3307 N88-29701

Deep seismic reflection profiling and continental growth curves 24 p3396 N88-30222

STRATOCUMULUS CLOUDS

Mesoscale applications of high resolution imagery
[AD-A185039] 05 p0627 N88-13833

STRATOPAUSE

Ion composition measurements in the upper stratosphere --- parachute-borne mass spectrometer
[ETN-87-90423] 01 p0069 N88-10442

STRATOSCOPE TELESCOPES

Vibration isolation system for the Stratospheric Observatory For Infrared Astronomy (SOFIA)
14 p1926 N88-21483

STRATOSCOPE 1 TELESCOPE

U STRATOSCOPE TELESCOPES

STRATOSCOPE 2 TELESCOPE

U STRATOSCOPE TELESCOPES

STRATOSPHERE

NT OZONOSPHERE

NT STRATOPAUSE

Balloon-based infrared solar occultation measurements of stratospheric O3, H2O, HNO3 and CFC-12
[NOAA-TR-NESDIS-34] 01 p0068 N88-10436

Kinetics investigations of atmospheric chemical reactions
[PB87-213351] 01 p0069 N88-10439

Airborne lidar studies of Arctic polar stratospheric clouds 01 p0069 N88-10443

ECC (Electrochemical Concentration Cell) ozonesonde observations at South Pole, Antarctica during 1986
[PB87-207502] 02 p0197 N88-11228

Production of NO by galactic cosmic rays and lightning
[DE87-014613] 02 p0197 N88-11230

Stratospheric particles: Synchrotron X-ray fluorescence determination of trace element contents
[DE87-012482] 02 p0198 N88-11234

Spectroscopic and retrieval studies in support of SCRIBE (Stratospheric Cryogenic Interferometer Balloon Experiment)
[AD-A184037] 03 p0351 N88-12216

October lower stratospheric Antarctic temperature and total ozone from 1979-1985 05 p0615 N88-13776

Insights into the general circulation of the lower stratosphere from TOMS 05 p0616 N88-13780

Lower-stratospheric/upper-tropospheric exchange processes associated with tropical cyclones as observed by TOMS 05 p0616 N88-13782

Comparison of ground based and TOMS measurements of SO2 from volcanic emissions
05 p0618 N88-13795

Observations of inertial period waves and vertical velocities in the tropical middle atmosphere using the MST radar technique 06 p0742 N88-14562

Description of data on the Nimbus 7 LIMS map archive tape: Water vapor and nitrogen dioxide
[NASA-TP-2761] 06 p0744 N88-14572

Middle atmospheric wind measurements using a medium frequency radar
[AD-A185931] 07 p0879 N88-15330

Large-scale dynamics of the mean flow breakdown in the stratosphere and mesosphere during the winter 1983/84 08 p1028 N88-16228

In-situ stratospheric water vapor measurements on board long duration balloons 08 p1029 N88-16232

Rayleigh lidar observations of gravity wave activity in the stratosphere and lower mesosphere
[NASA-CR-182384] 09 p1189 N88-17123

Measurement of vertical distributions of halogenated hydrocarbons in the stratosphere
[ETN-88-91065] 09 p1191 N88-17135

Statistical studies of low frequency oscillations in satellite-observed stratospheric temperatures
10 p1353 N88-18086

An analysis of longitude variations in the equatorial spectrum of Saturn 10 p1430 N88-18539

Initial results with the LLNL 2-D chemical-radiative-transport model of the troposphere and stratosphere
[DE88-004355] 11 p1512 N88-19033

High altitude chemical release systems for project BIME (Brazilian Ionospheric Modification Experiments) project IMS (Ionospheric Modification Studies) project PIIE (Polar Ionospheric Irregularities Experiment) project polar arcs
[AD-A188299] 12 p1642 N88-19833

Stratospheric trace gas distributions from fair infrared thermal emission spectroscopy
13 p1797 N88-20749

Ultraviolet absorption cross sections of methylbromide at stratospheric temperatures
[AERONOMICA-ACTA-A-320-1987]
15 p2036 N88-22132

Stratospheric electric field and conductivity measurements over electrified convective clouds in the South American region, revised
[INPE-4046-PRE/1012-REV-3]
15 p2095 N88-22483

A study on electric fields and conductivity associated with electrified clouds in the region of South America
[INPE-4487-TDL/325] 15 p2096 N88-22486

Chemical kinetics and photochemical data for use in stratospheric modeling evaluation Number 8
[NASA-CR-182919] 17 p2351 N88-24012

Stratospheric positive ion composition measurements and acetonitrile detection: A consistent picture
[AERONOMICA-ACTA-A-326-1987]
18 p2542 N88-25084

Three-dimensional temperature fields in the atmosphere up to 50 km altitude
[ETN-88-92150] 18 p2542 N88-25089

SAM 2 data user's guide
[NASA-RP-1200] 18 p2543 N88-25094

Radiation safety in commercial air traffic
[NASA-TM-101156] 19 p2600 N88-25447

Theory on conductivity measurement technique for Langmuir probes in the stratosphere
[INPE-4514-PRE/1266] 19 p2692 N88-25999

Meteorological atlas of the Southern Hemisphere lower stratosphere for August and September 1987
[NASA-TM-4049] 20 p2825 N88-26763

Design, development, fabrication and launch support for a high altitude release of neodymium vapor
[AD-A194196] 22 p3116 N88-28527

Ultraviolet absorption cross sections of chloro- and chlorofluoromethanes at stratospheric temperatures
[AERONOMICA-ACTA-A-324-1988]
23 p3231 N88-29223

Present state of knowledge of the upper atmosphere 1988: An assessment report
[NASA-RP-1208] 23 p3232 N88-29233

Forty-eight-inch lidar aerosol measurements taken at the Langley Research Center, May 1974 to December 1987
[NASA-RP-1209] 23 p3232 N88-29234

Changes in stratospheric ozone: Observations and theories
[AERONOMICA-ACTA-A-334-1988]
24 p3390 N88-30188

Possibilities of determining vertical profiles of microphysical characteristics of stratospheric aerosol using space measurements of transparency and solar halo 24 p3449 N88-30526

STRATOSPHERE RADIATION

Long range reconnaissance of trace gases: A special aspect of emission spectroscopy
08 p1018 N88-16172

STRATOSPHERIC AEROSOL & GAS EXPERIMENT

U SAGE SATELLITE

STRATOTANKER AIRCRAFT

U C-135 AIRCRAFT

STRATUS CLOUDS

Forecasting stratus over the British Isles
02 p0209 N88-11310

Stratocumulus and cloud-free reflectance from multi-spectral satellite measurements
[AD-A193899] 22 p3128 N88-28599

STREAK CAMERAS

Progress toward a crystal streak camera using tungsten bronze crystals for the electrooptic material
[DE87-013110] 03 p0323 N88-12044

Evaluation system for crystal streak cameras
[DE88-000238] 03 p0324 N88-12048

Streak camera dynamic range optimization
[DE88-001632] 05 p0586 N88-13571

Resolution limitations and optimization of the LLNL streak camera focus
[DE88-001633] 05 p0586 N88-13572

Flat-field response and geometric distortion measurements of optical streak cameras
[DE88-002394] 09 p1168 N88-17005

Resolution limitations and optimization of the ITT F4157 streak tube focus for fast (10 ps) operation
[DE88-003727] 09 p1169 N88-17007

The 5-GHz operation of the ITT and RCA streak tubes with a 7.5-ns time window
[DE88-003342] 09 p1169 N88-17008

Zoom versus full-field sensitivity at the ETS (Experimental Test System)
[AD-A188162] 12 p1628 N88-19742

Laser-heterodyne interferometry with streak camera detection
[DE88-003292] 14 p1914 N88-21437

Summary and conclusions on electrooptical streak camera project
[DE88-006616] 15 p2069 N88-22334

STREAK PHOTOGRAPHY

Programmable 10 MHz optical fiducial system for hydrodiagnostic cameras
[DE87-013223] 02 p0175 N88-11091

Evaluation system for crystal streak cameras
[DE88-000238] 03 p0324 N88-12048

STREAM FUNCTIONS (FLUIDS)

Optimization of explicit time-stepping algorithms and Stream-Function-Coordinate (SFC) concept for fluid dynamics problems 04 p0445 N88-12762

Extensions of the control volume based finite element method for fluid flow problems 06 p0700 N88-14296

Inviscid flows, part 1: Formulation of inviscid rotational flow problems by velocity potential and stream function methods. Applications to turbomachines
08 p0985 N88-15964

Viscous flows. Part 3: Formulation of the Navier-Stokes equations by stream function vorticity methods
08 p0986 N88-15969

Resonant Alfven wave instabilities driven by streaming fast particles 13 p1855 N88-21104

STREAMLINE FLOW

U LAMINAR FLOW

STREAMLINED BODIES

NT FAIRINGS

STREAMLINING

Observations on the hydrodynamic flow visualization at ONERA
[PD-FM-8718] 04 p0444 N88-12753

Predictive wall adjustment strategy for two-dimensional flexible walled adaptive wind tunnel: A detailed description of the first one-step method
[NASA-CR-181635] 12 p1573 N88-19409

An evaluation in a modern wind tunnel of the transonic adaptive wall adjustment strategy developed by NPL in the 1940's
[NASA-CR-181623] 12 p1575 N88-19417

A simplified streamline swallowing procedure for the windward meridian of axisymmetric blunt bodies
[AD-A188413] 12 p1626 N88-19732

The effects of two Carlucci initiatives concurrency and streamlining, on the test and evaluation phase of system acquisitions 12 p1704 N88-20198

Streamlining invitation for bids
[AD-A188941] 12 p1705 N88-20206

Empty test section streamlining of the transonic self-streamlining wind tunnel fitted with new walls
[NASA-CR-181680] 19 p2598 N88-25442

The determination of the topological structure of skin friction lines on a rectangular wing-body combination
[NASA-CR-4168] 20 p2753 N88-26343

STREAMS

NT GAS STREAMS

Ice-shelf response to ice-stream discharge fluctuation. Part 1: Unconfined ice tongues
[AD-A188147] 10 p1358 N88-18117

A queueing system with independent Markov input streams
[AD-A187601] 10 p1402 N88-18363

Hiding in stream semantics of uniform concurrency
[PB88-121579] 20 p2882 N88-27114

Stream function-vorticity finite elements and the resolution of the Navier-Stokes equations
[DE88-702318] 21 p2945 N88-27494

STRENGTH OF MATERIALS

U MECHANICAL PROPERTIES

STRESS (PHYSIOLOGY)

NT ACCELERATION STRESSES (PHYSIOLOGY)

Assessment of the reliability of a correction procedure for WGT (Wet Globe Thermometer) (Botsball) measurements of heat stress
[AD-A185193] 05 p0584 N88-13559

Microwave challenges to the thermoregulatory system
[AD-A185391] 05 p0629 N88-13847

Physiological determinants of load bearing capacity
[AD-A184977] 05 p0629 N88-13848

A device and methodology for measuring repetitive lifting VO2max (oxygen consumption rate)
[AD-A185195] 05 p0630 N88-13850

Daily dynamics of some physiological indicators of man under desert condition 06 p0750 N88-14605

Quick measurement of individual stress reaction level: Development of the Emotional Stress Reaction Questionnaire (ESRQ)
[FOA-C-50050-5.3] 06 p0752 N88-14617

Exercise in the heat: Effects of dinitrophenol administration
[AD-A185731] 06 p0752 N88-14622

Polycythemia and hydration status: Effects on blood volume and thermoregulation during exercise-heat stress
[AD-A185946] 07 p0888 N88-15383

Load carriage induced alterations of pulmonary function
[AD-A186227] 07 p0889 N88-15386

General biological character of adaptive capacity of mammalian metabolism in response to diverse and extreme environmental factors 08 p1047 N88-16324

Prediction of human thermoregulatory responses and endurance time in water at 20 and 24C
[AD-A186223] 08 p1048 N88-16326

Portable, ambient air microclimate cooling in simulated desert and tropic conditions
[AD-A186457] 08 p1050 N88-16338

Brain potentials and personality: A new look at stress susceptibility
[AD-A186931] 09 p1199 N88-17189

Comparative evaluation of stress repsonse of rats to different methods of simulating some effects of weightlessness 10 p1363 N88-18144

Second All-Union Conference on Physiology of Extreme States and Individual Protection of Man
10 p1363 N88-18147

Manipulation of muscle glycogen concentrations using high and low carbohydrate diets and exercise
[AD-A187732] 11 p1519 N88-19069

Gastric emptying during exercise: Effects of acute heat stress, acclimation and hypohydration
[AD-A188008] 11 p1519 N88-19073

Development of a coping strategies questionnaire to assess endurance performance
[AD-A188010] 11 p1520 N88-19074

Operation Everest 2: Alterations in the immune system at high altitude
[AD-A188011] 11 p1520 N88-19075

Causes and prevention of occupational Repetition Strain Injuries (RSI) 11 p1521 N88-19083

Conceptualization and design of a variable-gravity research facility
[NASA-CR-182574] 12 p1595 N88-19550

Endocrine responses to resistance exercise
[AD-A188681] 12 p1667 N88-19993

Motion sickness: A study of its effects on human physiology
[AD-A188821] 12 p1667 N88-19995

Plasma cortisol, renin and aldosterone during an intense heat acclimation program
[AD-A189387] 13 p1809 N88-20810

Challenges of physiological monitoring in a Navy operational setting 16 p2239 N88-23374

Stress in relation to the physical and social environment 19 p2695 N88-26020

Ergonomy and interior furnishing of the cabins of deep diving manned submarines: The Nautile example --- couch 19 p2697 N88-26032

Significance of nutrition to change in human carbohydrate and lipid metabolism under emotional stress 19 p2703 N88-26073

Analysis of clinical symptoms of human decompression sickness during altitude chamber studies
19 p2703 N88-26074

Satellite remote sensing of the wet bulb globe temperature heat stress index, phase 2
[AD-A192798] 20 p2818 N88-26717

Effect of weightlessness on brain development (results of flight of pregnant rats on Kosmos-1514 biosatellite and study of subsequent development of their progeny on earth 20 p2829 N88-26786

Can CNV amplitude predict ability to accomplish a demanding task? 21 p2980 N88-27700

Hyperthermia: New thoughts on an old problem
[AD-A192602] 21 p2986 N88-27731

Variability in intake and dehydration in young men during a simulated desert walk
[AD-A192654] 22 p3131 N88-28613

Hormonal regulation of fluid and electrolytes: Effects of heat exposure and exercise in the heat
[AD-A192655] 22 p3131 N88-28614

The impact of hyperthermia and hypohydration on circulation, strength, endurance and health
[AD-A192657] 22 p3131 N88-28615

Stress/fatigue and the ARNG (Army National Guard) aviator
[AD-A194184] 22 p3132 N88-28621

Hierarchical structure in polymeric solids and its influence on properties
[AD-A194720] 23 p3197 N88-29029

Currents induced in a human being for electromagnetic fields to 10 kHz-50 MHz
[AD-A191977] 23 p3236 N88-29268

Visual related accidents/incidents
23 p3242 N88-29293

Nutrient requirements for high stress environments
[AD-A194595] 23 p3243 N88-29301

Accidental hypothermia
[AD-A194967] 24 p3406 N88-30278

STRESS (PSYCHOLOGY)

Antarctica as a model for the human exploration of Mars
[AD-A185835] 08 p1051 N88-16342

Overlearning and positive thinking alleviate negative effects of stress on performance
[FOA-C-50051-5.3] 08 p1051 N88-16344

Brain potentials and personality: A new look at stress susceptibility
[AD-A186931] 09 p1199 N88-17169

Second All-Union Conference on Physiology of Extreme States and Individual Protection of Man
10 p1363 N88-18147

Hemodynamic effects of beta-adrenergic blocking with obsidan in clinostatic and orthostatic positions
10 p1367 N88-18171

Development of a coping strategies questionnaire to assess endurance performance
[AD-A188010] 11 p1520 N88-19074

Conceptualization and design of a variable-gravity research facility
[NASA-CR-182574] 12 p1595 N88-19550

Protection from stress 12 p1664 N88-19978

Individual functional typology of sympathoadrenal system as indicator of physiological status in adverse environments 12 p1665 N88-19979

Mental-State Estimation, 1987
[NASA-CP-2504] 16 p2239 N88-23370

Chronic stress as a factor in aircraft mishaps
16 p2239 N88-23376

Acute stress 16 p2239 N88-23377

Voice-stress measure of mental workload
16 p2240 N88-23381

A correlational approach to predicting operator status
16 p2242 N88-23393

Voice stress analysis 16 p2242 N88-23395

Stress in relation to the physical and social environment 19 p2695 N88-26020

Significance of nutrition to change in human carbohydrate and lipid metabolism under emotional stress 19 p2703 N88-26073

Thermal stress and its effects on fine motor skill and decoding tasks 21 p2926 N88-27369

Stress and the military pilot
[AD-A194313] 22 p3133 N88-28626

Attitudes towards the cold: Effects on psychological mood and subjective reports of illness during cold weather training
[AD-A194777] 23 p3236 N88-29274

Nutrient requirements for high stress environments
[AD-A194595] 23 p3243 N88-29301

Central adrenergic receptors as mediators of central response to stress: Study with Positron Emission Tomography (PET)
[AD-A194947] 24 p3407 N88-30284

STRESS ANALYSIS

NT BOUNDARY ELEMENT METHOD

Compendium of post-failure analysis techniques for composite materials
[AD-A183783] 01 p0016 N88-10113

Polymer chain segment orientation during stress relaxation
[DE87-013392] 01 p0027 N88-10174

Ion-implantation-induced stress in glasses: Variation of damage mode efficiency with changes in glass structure
[DE87-013523] 01 p0028 N88-10175

Low cycle fatigue on isotropic fine-grained graphite
[DE87-702627] 01 p0028 N88-10177

A generalized least-squares determination of triaxial stress states by X-ray diffraction and the associated errors
[AD-A183851] 01 p0058 N88-10371

The use of Hencky's equations for the estimation of multiaxial elastic-plastic notch stresses and strains
[FB-3/1986] 01 p0060 N88-10383

Stress-strain analysis and life predictions of a notched shaft under multiaxial loading
[FB-5/1986] 01 p0060 N88-10384

Criteria for determination of significant load cycles in variable amplitude load sequences
[NLR-MP-86013-U] 01 p0060 N88-10386

Relation between shock strength and strain-rate plasticity at maximum deviatoric stress
[DE87-011736] 01 p0061 N88-10390

A user's guide for BIE3D: A boundary integral equation computer program for three-dimensional elastostatic analysis
[RAE-TM-MAT-STR-1078] 01 p0079 N88-10509

Shearing flow over Stokes wave. Part one: General theory
[ETN-87-90957] 02 p0171 N88-11074

Development and testing of a system for the partially automated evaluation of holographic interferograms in the experimental stress analysis of reactor components
[ETN-87-90574] 02 p0175 N88-11095

3D inelastic analysis methods for hot section components 02 p0187 N88-11164

Component specific modeling
02 p0187 N88-11166

Constitutive modeling of superalloy single crystals with verification testing 02 p0188 N88-11169

Constitutive modeling for isotropic materials
02 p0188 N88-11171

Applications of dislocation theory to crack growth problems 02 p0190 N88-11188

Energy changes in transforming solids
[DE87-011257] 02 p0191 N88-11194

Diffraction moire: The dynamic regime
[DE87-014883] 03 p0335 N88-12111

Nonlinear thermoviscoelastic analysis of metallic plane curved beams 03 p0336 N88-12119

Kinetics of crack growth: Thermal/mechanical interaction 03 p0337 N88-12124

Failure analysis of composite structure materials
[AD-A184468] 04 p0410 N88-12548

On the stressing of annealed NITINOL: The electrical resistance and calorimetric effects
[AD-A184465] 04 p0414 N88-12569

Effects of stress-relieving on the mechanical properties and the structure of specimens of high-temperature fine-grained structural steels heat-treated to simulate welding
[BLL-CE-TRANS-8258-(9022.09)]
04 p0417 N88-12586

Influence of creep on the precipitate structure under conditions of long-term creep. 4: Experiments on 10 CrMo 9 10 steel
[BLL-CE-TRANS-8256-(9022.09)]
04 p0417 N88-12589

Influence of strain rate and notch depth on tensile properties of HITCO 6250
[DE88-001324] 04 p0455 N88-12816

Higher order theory analysis of a modified free-edge delamination specimen 04 p0455 N88-12820

The evolution of plastic strain in steady, plastic shock waves
[DE87-013812] 04 p0456 N88-12826

A comparison of structural frequency response functions measured with forces from 500 to 250,000 lb
[DE88-000668] 04 p0457 N88-12829

Large change-of-curvature effects in quadratic finite elements for CAD of membrane structures
04 p0480 N88-12958

Development of an integrated BEM approach for hot fluid structure interaction
[NASA-CR-181577] 05 p0556 N88-13384

Micromechanics of the degradation of composite materials
[[illegible]IAS-872-430-113] 05 p0559 N88-13405

Finite element model for the stress and flexibility analysis of curved pipes
[DE87-703632] 05 p0592 N88-13608

Fatigue under nonnormal random stresses using Monte Carlo method 05 p0607 N88-13723

Analysis of end stresses in glass-metal bimaterial strips
[DE87-007846] 05 p0610 N88-13750

Stresses and displacements in two, three and four layered structures submitted to flexible or rigid loads
[AD-A185707] 06 p0723 N88-14450

Transient welding strain measurement by Moire technique: A comparison between experimental measurement and numerical analysis for strain-stress cycles during GTA spot-welding
[PB87-143871] 07 p0868 N88-15269

Thermal stress analysis of a cooled monochromator crystal
[DE86-002116] 07 p0937 N88-15596

Composite/metal jointing technology for vehicle weight reduction
[DE88-900228] 08 p0992 N88-16005

Generalized displacement method in the finite element analysis of incompressible material
[PB87-143434] 08 p0995 N88-16018

Study of the technique of stress determination by measuring magnetism
[PB87-143905] 08 p0996 N88-16026

Fatigue effects of a swept sine test
08 p0999 N88-16054

Review of fatigue and fracture research at NASA Langley Research Center 09 p1106 N88-16633

Optical analysis of stress and strain in photoelastic particle assemblies
[ETN-88-91591] 09 p1182 N88-17082

A comparison of the predicted and measured gravitational stresses in VAWT (Vertical Axis Wind Turbine) blades
[DE88-002113] 09 p1187 N88-17111

Finite element substructuring methods for composite mechanics
[NASA-TM-100297] 10 p1296 N88-17745

Analytical and experimental characterization of damage processes in composite laminates
[AD-A187221] 10 p1296 N88-17746

Basic research on macromolecular dynamics
[PB88-141643] 10 p1305 N88-17805

Flaw identification from forced vibration testing
[DE88-002641] 10 p1342 N88-18016

Computed stress and strain distributions under interference fit and after coldworking
[AD-A186950] 10 p1342 N88-18024

Frequency response function estimation at level
[DE88-002644] 10 p1344 N88-18034

On delamination of (+ or - theta sub n/90 sub n/2) sub s laminates subject to tensile loading
[AD-A188095] 11 p1447 N88-18626

Fracture mechanisms and strengthening of slab lasers
[DE88-004002] 11 p1493 N88-18914

Development of encapsulated lithium hydride thermal energy storage for space power systems
[DE88-004762] 11 p1507 N88-19001

SiO2 film stress distribution during thermal oxidation of Si
[AD-A189552] 12 p1612 N88-19637

A hybrid-stress finite element approach for stress and vibration analysis in linear anisotropic elasticity
[NASA-CR-179311] 12 p1634 N88-19794

Stress analysis in elastic solids with many cracks
[AD-A189015] 12 p1636 N88-19796

Modification, implementation, and evaluation of a remote terminal emulator as a software validation and stress testing tool
[AD-A188833] 12 p1678 N88-20034

Delamination stresses in semicircular laminated composite bars
[NASA-TM-4026] 13 p1735 N88-20375

The use of photoelastic methods to study the stressed states of spot-welded joints 14 p1898 N88-21335

JPRS report: Science and technology. China
[JPRS-CST-87-042] 14 p1899 N88-21338

Mathematical stress analysis of composite materials
14 p1900 N88-21349

Nonlinear Constitutive Relations for High Temperature Applications, 1986
[NASA-CP-10010] 14 p1928 N88-21486

A constitutive model with damage for high temperature superalloys 14 p1930 N88-21510

Cyclic uniaxial and biaxial hardening of type 304 stainless steel modeled by the viscoplasticity theory based on overstress 14 p1931 N88-21514

On 3-D inelastic analysis methods for hot section components. Volume 1: Special finite element models
[NASA-CR-180893] 14 p1934 N88-21535

Efficient method for structural optimization
15 p2054 N88-22240

Development of a computer code CRACK for elastic and elastoplastic fracture mechanics analysis of 2-D structures by finite element technique
[DE88-701231] 15 p2075 N88-22370

Lewis Structures Technology, 1988. Volume 2: Structural Mechanics
[NASA-CP-3003-VOL-2] 15 p2077 N88-22382

Finite element (MARC) solution technologies for viscoplastic analyses 15 p2078 N88-22389

Three-dimensional inelastic approximate analysis code (MOMM) 15 p2079 N88-22392

Specialty three-dimensional finite element analysis codes 15 p2079 N88-22393

Probabilistic structural analysis computer code (NESSUS) 15 p2079 N88-22397

Structural tailoring of advanced turboprops
15 p2080 N88-22400

Thermal-structural analyses of Space Shuttle Main Engine (SSME) hot section components
15 p2081 N88-22404

Structural assessment of a space station solar dynamic heat receiver thermal energy storage canister
15 p2081 N88-22406

Whisker-reinforced ceramic composites for heat engine components 15 p2082 N88-22410

Minimum weight design of rotorcraft blades with multiple frequency and stress constraints
[NASA-TM-100569] 16 p2161 N88-22892

Hybrid PV HgCdTe IR detectors technology reliability and failure program: Environmental stress testing plan
[AD-A191165] 16 p2211 N88-23195

On the calculation of stresses in pin-loaded anisotropic plates
[ETN-88-92239] 16 p2222 N88-23261

On the calculation of stresses in pin-loaded anisotropic plates
[LR-529] 16 p2223 N88-23268

A generalized variational method for solving stress intensity factors at cracks on the edge of holes in orthotropic plates
[IC-AERO-87-02] 17 p2348 N88-23992

Possible creep studies of lithium with a compact device 17 p2422 N88-24404

Analysis of notched metal matrix composites under tension loading
[NASA-TM-100629] 18 p2480 N88-24713

On the reversion phenomena of Cu-3 percent Ti alloys
[NASA-TT-20170] 18 p2488 N88-24762

Stress measurements in graphite fibers by laser raman spectroscopy
[AD-A191710] 18 p2491 N88-24779

Effect of uniaxial stress on the Raman spectra of graphite fibers
[AD-A191730] 18 p2492 N88-24783

Computational fluid dynamics applied to the prediction of the heat-transfer, mechanical and thermal-stress behavior of heat exchangers
[CFDU/87/7] 18 p2510 N88-24893

Plate response analysis using shock tube
[AD-A190828] 18 p2526 N88-24987

Advanced development of the boundary element method for elastic and inelastic thermal stress analysis
18 p2529 N88-25002

Forced motion of initially stressed shells and plates
18 p2529 N88-25005

Fatigue crack growth due to random loading
18 p2531 N88-25017

Influence of strain rate on the substructure evolution and yield behavior of Ti-6Al-4V
[DE88-006457] 19 p2616 N88-25520

Simulation of diaphragm-type IC pressure sensors
19 p2672 N88-25887

Static analysis of thin plates using the finite strip-element method 19 p2679 N88-25931

Improved method for stress and compatibility analysis of multicomponent rotating systems
[NASA-TM-100884] 19 p2680 N88-25935

A constitutive model with damage for high-temperature superalloys 20 p2771 N88-26434

Observations on residual stresses in ceramic composites by neutron diffraction techniques
[DE88-009937] 20 p2778 N88-26472

Vertical ship motions and sea loads considering nonlinear effects
[TAE-592] 20 p2784 N88-26515

Stress concentration around circular hole in a composite material specimen representative of the X-29A forward-swept wing aircraft
[NASA-CR-179435] 20 p2814 N88-26694

Dynamical stress concentration problems, from every side, bordered and perforated plates
[ETN-88-92128] 20 p2815 N88-26703

Study of temperature and stress fields of two sliding cylinders
[ETN-88-92134] 20 p2815 N88-26704

Stress analysis using infrared thermography
[ETN-88-92169] 20 p2816 N88-26705

Stress-related phenomena in transient radiation-induced absorption in optical fibers
[DE88-010956] 20 p2854 N88-26949

Lattice strain in heteroepitaxial films
20 p2868 N88-27032

Boundary layer solutions for the free-edge problem in composite laminates 21 p2904 N88-27229

Thermal stress and its effects on fine motor skill and decoding tasks 21 p2926 N88-27369

An experimental and analytical evaluation of a biaxial test for determining shear properties of composite materials
[NASA-CR-182928] 21 p2962 N88-27593

Verification of the ADINA finite element code for creep analysis: Problems from the open literature
[DE88-011826] 21 p2962 N88-27594

Analyses and correlations of environment assisted fatigue crack propagation for attachment lugs
22 p3053 N88-28116

Environmental cracking of a superferritic stainless steel under slow strain rate conditions
22 p3053 N88-28117

Studies of internal stresses and surface roughness of sputtered Be and BeB films
[DE88-011737] 22 p3086 N88-28327

Mixed finite element methods to compute stress in a load composite specimen with holes: Numerical results
[ONERA-RT-37/4242-RY-062-R]
22 p3088 N88-28336

Structural dynamics of maneuvering aircraft
[AD-A192376] 23 p3176 N88-28908

Thin film-residual stress assessment
[AD-A193205] 23 p3196 N88-29018

Aeroelastic response of metallic and composite propfan models in yawed flow
[NASA-TM-100964] 24 p3326 N88-29807

Thermal stress analysis in PMR-15 carbon fibre laminates
[ETN-88-93123] 24 p3341 N88-29986

Stresses in cylindrical shells with tangential nozzles submitted to external loads and internal pressure
[CRIF-MT-172] 24 p3382 N88-30146

Determination of multiaxial flow surfaces at elevated temperatures using the concept of dissipation potential
[ORNL/TM-10787] 24 p3383 N88-30149

STRESS CALCULATIONS

U STRESS ANALYSIS

STRESS CONCENTRATION

On the relations between cyclic contraction ratio, flow stress, and deformation mechanisms in bainitic CrMoV steels
[VTT-36] 01 p0025 N88-10158

Theoretical investigation of stress concentrations in damaged carbon fibre reinforced plastic plate structures. Volume 1: Main text
[BR99872-VOL-1] 03 p0280 N88-11761

Theoretical investigation of stress concentrations in damaged carbon fibre reinforced plastic plate structures. Volume 2: Tables, figures and plates
[BR99873-VOL-2] 03 p0280 N88-11762

Stress state of welded joints of dissimilar materials obtained by diffusion welding 03 p0286 N88-11799

Evaluation method of the brittle fracture strength in structurally stress-concentrated regions
[PB87-129490] 06 p0721 N88-14435

Effect of rare earth elements on the hydrogen-induced cracking in high strength low alloy steel
[PB87-143806] 07 p0833 N88-15052

Hybrid FEM (Finite Element Method) approach to stress distribution in the vicinity of a notch in non-homogeneous materials
[PB87-143392] 07 p0868 N88-15268

SiO2 film stress distribution during thermal oxidation of Si
[AD-A189552] 12 p1612 N88-19637

Influence of hydrogen on crack formation tendency in heat-affected zone with stress concentrator
14 p1887 N88-21276

Evolution of hardening and damage during viscoplastic deformation
[AD-A190714] 15 p2077 N88-22381

Stress concentration around circular hole in a composite material specimen representative of the X-29A forward-swept wing aircraft
[NASA-CR-179435] 20 p2814 N88-26694

Dynamical stress concentration problems, from every side, bordered and perforated plates
[ETN-88-92128] 20 p2815 N88-26703

Failure analysis of quasi-isotropic composite laminates with free edges under off-axis loading
22 p3049 N88-28092

Analysis of stiffness reduction, failure and stress concentration in fiber composite laminates
[AD-A193519] 22 p3050 N88-28096

Mixed finite element methods to compute stress in a load composite specimen with holes: Numerical results
[ONERA-RT-37/4242-RY-062-R]
22 p3088 N88-28336

A comprehensive study on damage tolerance properties of notched composite laminates
[AD-A192952] 23 p3188 N88-28968

Development and experimental verification of a two-dimensional numerical model of piezoelectrically induced threshold voltage shifts in GaAs MESFETs
[AD-A193462] 23 p3206 N88-29080

Shear stress at a film-substrate interface due to mismatch strain
[AD-A193461] 23 p3288 N88-29577

STRESS CORROSION

NT STRESS CORROSION CRACKING

The application of group radiators for the determination of tension crack corrosion
[BAM-06264] 01 p0022 N88-10141

Influence of some parameters on the stress corrosion of a ABNT 304 stainless steel in MgCl/sub 2/
[DE87-703707] 04 p0416 N88-12580

A study of corrosion fatigue crack initiation, growth and the threshold condition under variable amplitude loading
05 p0604 N88-13701

The influence of crack conditions on hydrogen uptake by steels 05 p0604 N88-13702

Occurance and growth of fatigue cracks in corrosion environment 05 p0604 N88-13704

The role of composition and microstructure gradients on weld metal properties and behavior
[DE88-004956] 10 p1303 N88-17791

Aircraft corrosion problems and research in the Netherlands
[NLR-MP-86066-U] 13 p1744 N88-20427

Stress corrosion of C ring specimen in salt spray tests
[I-186/87] 21 p2916 N88-27307

Phenomena of the ionic transport in the stress corrosion of metals
[DE88-702502] 23 p3195 N88-29013

Stress corrosion of ceramic materials
[AD-A191979] 23 p3195 N88-29016

STRESS CORROSION CRACKING

Stress corrosion cracking of high-strength steels in aqueous environments 03 p0289 N88-11818

Effects of stress-relieving on the mechanical properties and the structure of specimens of high-temperature fine-grained structural steels heat-treated to simulate welding
[BLL-CE-TRANS-8258-(9022.09)]
04 p0417 N88-12586

Environmentally assisted cracking: Overview of evidence for an adsorption-induced localised-slip process
[AD-A185175] 05 p0565 N88-13443

Fatigue crack propagation in Al-Zn-Mg bicrystals and its dependence on the environment
05 p0605 N88-13707

Fracture kinetics of corrosion fatigue
05 p0605 N88-13708

The influence of grain boundary chemistry and structure on the intergranular attack and intergranular stress corrosion cracking of austenitic alloys
[DE88-002436] 07 p0835 N88-15063

Study on characteristics of SCC propagation da/dt for welded joint
[PB87-143640] 07 p0869 N88-15270

Multipurpose corrosion inhibitors for aerospace materials in Naval environments
[AD-A186728] 09 p1143 N88-16853

Mechanisms of intergranular attack and stress corrosion cracking of alloy 600 by high-temperature caustic solutions containing impurities
[DE87-012820] 10 p1300 N88-17773

Computer aided testing procedure for stress corrosion cracking investigations
[GKSS-86/E/63] 11 p1460 N88-18706

Reduction of residual stresses and distortion in girth welded pipes
[AD-A187728] 11 p1494 N88-18920

Comparative investigations of indirect crack length measurement under fatigue loading in a corrosive environment
[GKSS-86/E/64] 11 p1502 N88-18971

Stress corrosion cracking and metal-induced embrittlement: Comparative studies of local chemistries
[DE88-003235] 13 p1742 N88-20419

Controlling stress corrosion cracking in mechanism components of ground support equipment
14 p1926 N88-21480

Effect of loading conditions on environment-sensitive fracture
[BR102697] 14 p1934 N88-21533

Stress corrosion of ceramic materials
[AD-A190501] 15 p2045 N88-22187

best copy available

Environmentally assisted crack growth in structural alloys: Perspectives and new directions
[AD-A190137] 15 p2076 N88-22377
Environment effects on crack propagation with tensile stress
[GKSS-87/E/46] 16 p2223 N88-23267
Stress corrosion cracking properties of Al-Li alloys
17 p2320 N88-23853
Stress corrosion cracking of A723 steel pressure vessels: Two case studies
[AD-A191741] 18 p2527 N88-24990
Stress corrosion evaluation of powder metallurgy aluminum alloy 7091 with the breaking load test method
22 p3053 N88-28115
Corrosion and stress corrosion of metals in decontamination solutions 22 p3054 N88-28118
Design guidelines for prevention of corrosion in combat and tactical vehicles
[AD-A194172] 22 p3055 N88-28126

STRESS CYCLES
Fracture morphologies of carbon-black-loaded SBR (Styrene-Butadiene Rubber) subjected to low-cycle, high-stress fatigue
[DE88-006808] 16 p2161 N88-23002
Theory of viscoplasticity based on overstress with applications 18 p2529 N88-25007

STRESS DISTRIBUTION
NT STRESS CONCENTRATION
The use of Hencky's equations for the estimation of multiaxial elastic-plastic notch stresses and strains
[FB-3/1986] 01 p0060 N88-10383
Stress-strain analysis and life predictions of a notched shaft under multiaxial loading
[FP-5/1986] 01 p0060 N88-10384
Crack initiation life estimations for notched specimens with residual stresses based on local strains
[FF-17/1986] 01 p0060 N88-10385
Three-dimensional finite element based, interative approach for analysis of laminated composites
03 p0280 N88-11763
Free-edge delamination: Laminate width and loading conditions effects
[NASA-TM-100238] 04 p0411 N88-12551
Plastic strain localization between voids in shear deformation fields 04 p0427 N88-12648
Constraint effects in fatigue crack growth
05 p0606 N88-13719
Telemetric laser extensometry technique for monitoring deflections in small cracks 05 p0607 N88-13724
On the geometrical description of fatigue crack surfaces 05 p0607 N88-13727
Profiles of self stress and of load stress at notches
06 p0719 N88-14419
Wave propagation experiments on 22-bay lattice
[AD-A186140] 07 p0824 N88-15002
Experimental and theoretical investigation of mechanically fastened composites
[AD-A185896] 07 p0826 N88-15008
A method for the approximate calculation of the skin friction coefficient of horizontal wavy plates
[VKI-TN-160] 07 p0851 N88-15172
Deformation induced cracking in steel girder bridges and retrofit guidelines
[PB88-102710] 07 p0868 N88-15265
Stress strain fields at crack tip and stress intensity factors in Reissner's plate
[PB87-144945] 08 p0994 N88-16014
Successful mixed formulation for axisymmetric shell analysis employing discontinuous stress fields of the same order as the displacement field
[DE88-700021] 09 p1178 N88-17052
To determine the stress distribution in the vicinity of GRP end pads where the specimen is held and loaded (CFC coupon specimens) --- glass reinforced plastic (GRP) carbon fiber composite (CFC)
[BAE-WST-R-RES-CFC-12023]
09 p1182 N88-17080
Further tests to determine the stress distribution in the vicinity of GRP end pads where the specimen is held and loaded (CFC coupon specimens) --- glass reinforced plastic (GRP) carbon fiber composite (CFC)
[BAE-WST-R-RES-CFC-12023-ADD-1]
09 p1182 N88-17081
Computed stress and strain distributions under interference fit and after coldworking
[AD-A186950] 10 p1342 N88-18024
A study of the mechanical behavior of a 2-D carbon-carbon composite 11 p1449 N88-18638
Matrix-fiber stress transfer in composite materials: Elasto-plastic model with an interphase layer
[PB88-136635] 11 p1450 N88-18643
Reduction of residual stresses and distortion in girth welded pipes
[AD-A187728] 11 p1494 N88-18920
The stress field surrounding the tip of a crack propagating in a finite body 11 p1500 N88-18962
Thermal-mechanical fatigue testing of a titanium-aluminide alloy
[AD-A189555] 12 p1609 N88-19620
SiO2 film stress distribution during thermal oxidation of Si
[AD-A189552] 12 p1612 N88-19637
A technique for local refinement of the stress field by finite element method
[INPE-4219-PRE/1099] 12 p1683 N88-20061
Cyclic crack growth emanating at a round notch considering viscoplasticity
[AD-A189577] 13 p1781 N88-20655
Local refinement of stress field by finite element method
[INPE-4321-TDL/288] 13 p1828 N88-20930
The use of photoelastic methods to study the stressed states of spot-welded joints 14 p1898 N88-21335
Mathematical stress analysis of composite materials
14 p1900 N88-21349
Data requirements to model creep in 9Cr-1Mo-V steel
14 p1931 N88-21512
A test for interfacial effects and stress transfer in ceramic matrix composites
[NASA-CR-182758] 15 p2046 N88-22194
Phenomenological modelling of rate-dependent plasticity for high strain rate problems
[DE88-006647] 15 p2087 N88-22440
Durability of compound cylinder under static internal-pressure repeat load of long duration
16 p2180 N88-22991
Stress modeling of microdiaphragm pressure sensors
19 p2670 N88-25873
Study of temperature and stress fields of two sliding cylinders
[ETN-88-92134] 20 p2815 N88-26704
Boundary layer solutions for the free-edge problem in composite laminates 21 p2904 N88-27229
The three-dimensional stress field around a cylindrical inclusion in a plate of arbitrary thickness
21 p2963 N88-27602
Mechanics of thrust fault formation
23 p3231 N88-29229
Shear stress at a film-substrate interface due to mismatch strain
[AD-A193461] 23 p3288 N88-29577
A test for interfacial effects and stress transfer in ceramic matrix composites
[NASA-CR-182873] 24 p3340 N88-29880
Particle size measurements in sooting combustion systems 24 p3348 N88-29931

STRESS FIELDS
U STRESS DISTRIBUTION

STRESS FUNCTIONS
Non- and semi-parametric maximum likelihood estimators and the von Mises Method, part 1
[CWI-MS-R8709] 13 p1829 N88-20941
A central limit theorem for M-estimators by the von Mises method
[CWI-MS-R8713] 16 p2262 N88-23525
Dynamic shear band development in plane strain
[AD-A190915] 18 p2526 N88-24988
Dynamical stress concentration problems, from every side, bordered and perforated plates
[ETN-88-92128] 20 p2815 N88-26703

STRESS INTENSITY FACTORS
Crack propagation behavior of the materials StE 460 and AlMg 4.5Mn
[FD-1/1986] 01 p0058 N88-10373
Crack behavior in ceramic materials under static, slowly increasing, and cyclic loading conditions
[KFK-4209] 02 p0154 N88-10964
Development and testing of a system for the partially automated evaluation of holographic interferograms in the experimental stress analysis of reactor components
[ETN-87-90574] 02 p0175 N88-11095
Large change-of-curvature effects in quadratic finite elements for CAD of membrane structures
04 p0480 N88-12958
Stress intensity factors for cracking metal structures under rapid thermal loading, phase 1
[AD-A184112] 05 p0591 N88-13606
Finite element model for the stress and flexibility analysis of curved pipes
[DE87-703632] 05 p0592 N88-13608
Closure behavior under constant effective stress intensity loading conditions 05 p0598 N88-13656
Fatigue crack propagation of short and long cracks: Phys. basis, prediction methods and engineering significance 05 p0599 N88-13664
Behavior of short cracks in a 2024 aluminum alloy sheet tested at several stress ratios 05 p0600 N88-13669
the influence of temper embrittlement on fatigue crack growth in hydrogen 05 p0605 N88-13709
Constraint effects in fatigue crack growth
05 p0606 N88-13719
Development of research on fatigue of spot-weld in automobile structures in Japan
05 p0608 N88-13728
Fatigue crack growth 05 p0608 N88-13734
Influence of crack closure on fatigue crack propagation and threshold 06 p0716 N88-14394
A re-evaluation of fatigue threshold test methods
06 p0717 N88-14401
Influence of stress ratio R on fatigue threshold delta K(th) for 40Cr steel 06 p0718 N88-14405
The effects of loading history on fatigue crack growth threshold 06 p0718 N88-14406
Threshold stress intensity for stable crack growth in high strength steel at ambient temperature and below
06 p0718 N88-14407
The effect of shear lips on fatigue crack growth in Al-2024 sheet material 06 p0718 N88-14408
Threshold and crack-growth tests on pre-cracked specimens produced in cyclic compression
06 p0718 N88-14412
Fracture study of windshield glass panes
06 p0790 N88-14801
Stress strain fields at crack tip and stress intensity factors in Reissner's plate
[PB87-144945] 08 p0994 N88-16014
Stress intensity and crack displacement for small edge cracks
[NASA-TP-2801] 09 p1184 N88-17085
Threshold fatigue crack growth in Ti-6Al-2Sn-4Zr-6Mo
[AD-A189560] 13 p1741 N88-20415
Growth of fatigue cracks in nickel alloys at high temperatures 14 p1896 N88-21318
Stress-intensity factors for small surface and corner cracks in plates
[NASA-TM-100599] 15 p2088 N88-22445
Strain intensity factor approach for predicting the strength of continuously reinforced metal matrix composites
[NASA-TM-100617] 17 p2317 N88-23838
Hydrogen embrittlement susceptibility of high strength ESR 4340 steel alloys for ballistically resistant/[illegible] components 17 p2319 N88-[illegible]
Fracture mechanics 17 p2324 N88-23877
A generalized variational method for solving stress intensity factors at cracks on the edge of holes in orthotropic plates
[IC-AERO-87-02] 17 p2348 N88-23982
Determination of the toughness of a brittle material using strain gages
[ETN-88-92540] 18 p2527 N88-24980
Some stress intensity factor equations
[FFA-TN-1987-07] 18 p2527 N88-24985
Automated analysis of crack growth rate for obtaining da/dN versus delta K relation
[FFA-TN-1987-70] 18 p2527 N88-24986
Resolved shear stress intensity coefficient and fatigue crack growth in large crystals
[NASA-CR-182137] 18 p2528 N88-24987
The surface crack problem in an orthotropic plate under bending and tension
[NASA-CR-178281] 18 p2531 N88-25014
A method for the numerical solution of random Cauchy singular integral equation 18 p2565 N88-25234
Dimensional analysis and experimental observation of the coupling phenomena between combustion and fracture of damaged propellant samples
19 p2630 N88-25603
Lattice theory of fracture of solids with layered structure
[DE88-701867] 20 p2876 N88-27073
Stress intensity factors for cracked metallic structures under rapid thermal loading
[AD-A191219] 23 p3193 N88-28004
The use of a surface acoustic wave technique to study the growth behavior of small cracks in a high strength steel alloy 23 p3225 N88-29193
Elastic-plastic analysis of part-through crack propagation in piping and pressure vessels
[DE88-701619] 23 p3225 N88-29198
Stress intensity factors for cracked metallic structures under rapid thermal loading
[AES-8609709F-1] 24 p3353 N88-29862
Wide range stress intensity factor expression for an edge-cracked round bar bend specimen
[AD-A196285] 24 p3382 N88-30147
Obtaining stress intensity factors on cracks, by means of fitting techniques on numerical results calculated with the finite element method 24 p3384 N88-30153

STRESS MEASUREMENT
Stress measurements in sol-gel films
[DE87-014467] 02 p0153 N88-10955
Particle velocity and stress gage measurements in spherical diverging flow
[DE87-007333] 03 p0321 N88-12033

Multi-component stress history measurements and analysis
[DE88-000977] 09 p1168 N88-17004
Optical analysis of stress and strain in photoelastic particle assemblies
[ETN-88-91591] 09 p1182 N88-17082
The measurement of stress in steels of varying microstructure by Barkhausen and magneto-acoustic emission
[AERE-R-12387] 10 p1343 N88-18027
SiO2 film stress distribution during thermal oxidation of Si
[AD-A189552] 12 p1612 N88-19637
Stress measurements in graphite fibers by laser raman spectroscopy
[AD-A191710] 18 p2491 N88-24779
In-flight load measurements of the Robot-X canards
[AD-A193428] 21 p2895 N88-27187
Polarization selective Raman microspectroscopy
21 p2930 N88-27397
Effects of applied stress and temperature on the nonlinear elastic properties of graphite fibers
[AD-A194469] 22 p3050 N88-28093
Report on an overseas visit to USA relating to the thermoelastic measurement of stresses, 16-21 August 1987
[AD-A195313] 24 p3365 N88-30161

STRESS PROPAGATION
Instability-related delamination growth of embedded and edge delaminations 20 p2767 N88-26406
User's manual for C-HEMP: A two-dimensional wave propagation code. Volume 1: Description and derivations of the code
[AD-A193197] 21 p2944 N88-27486

STRESS RELAXATION
Polymer chain segment orientation during stress relaxation
[DE87-013392] 01 p0027 N88-10174
Tensile mean stress effects on uniaxial fatigue behavior of 1045 HR steel 05 p0603 N88-13694
Relaxation of metastable semiconductor strained-layer structures by plastic flow
[DE88-002729] 08 p1090 N88-16560
Stability and metastability in semiconductor strained-layer structures
[DE88-003308] 09 p1258 N88-17544
SiO2 film stress distribution during thermal oxidation of Si
[AD-A189552] 12 p1612 N88-19637
Effects of state recovery on creep buckling under variable loading 14 p1933 N88-21527
Corrosion Research Center, University of Minnesota
[DE88-006681] 15 p2041 N88-22160
Effect of uniaxial compression on physical and mechanical properties of ferroelectric ceramic material
16 p2180 N88-22993
Stress relaxation of a titanium (Ti-6Al-4V) threaded joint
[DE88-010102] 21 p2961 N88-27590
The mechanical behavior of surface modified ceramics
[DE88-010564] 23 p3196 N88-29022

STRESS RUPTURE STRENGTH
U CREEP RUPTURE STRENGTH

STRESS TENSORS
Characteristics of thermooptical sound excitation in metals 08 p1076 N88-16486
Optical analysis of stress and strain in photoelastic particle assemblies
[ETN-88-91591] 09 p1182 N88-17082
A simplified orthotropic formulation of the viscoplasticity theory based on overstress 14 p1929 N88-21505
Investigation of the components of the energy-momentum tensor in the neighborhood of crack tips under special materials and loading conditions
[W-4/87] 14 p1934 N88-21531
Phenomenological modelling of rate-dependent plasticity for high strain rate problems
[DE88-008647] 15 p2087 N88-22440

STRESS WAVES
Shearing flow over Stokes wave. Part one: General theory
[ETN-87-90857] 02 p0171 N88-11074
Numerical and experimental research on propagation of elastic stress waves in conical shell under axial impulsive loading 15 p2053 N88-22238
Acousto-ultrasonic input-output characterization of unidirectional fiber composite plate by SV waves
[NASA-CR-4152] 16 p2217 N88-23224

STRESS-STRAIN DIAGRAMS
The relationship of tensile specimen size and geometry effects to unique constitutive parameters for ductile materials
[AD-A186020] 08 p0994 N88-16012
Development of a unified constitutive model for an isotropic nickel base superalloy Rene 80
14 p1929 N88-21501
A simplified key-curve approach for J-R-curve testing of CT specimens
[VTT-RR-503] 15 p2166 N88-22444

STRESS-STRAIN RELATIONSHIPS
On the relations between cyclic contraction ratio, flow stress, and deformation mechanisms in bainitic CrMoV steels
[VTT-36] 01 p0025 N88-10158
Stress-strain behavior of components subject to residual stresses taking the example of an orifice plate
[FF-10/1986] 01 p0059 N88-10375
Constitutive modeling of superalloy single crystals with verification testing 02 p0188 N88-11169
High temperature stress-strain analysis
02 p0188 N88-11170
Constitutive modeling for isotropic materials
02 p0188 N88-11172
Material behaviour at high rates of strain
[OUEL-1684/87] 02 p0192 N88-11200
Generalized hybrid variational principle, corresponding finite element model 03 p0301 N88-11895
Particle velocity and stress gage measurements in spherical diverging flow
[DE87-007333] 03 p0321 N88-12033
A direct method to obtain constitutive model constants from cylinder impact test results
04 p0427 N88-12647
The effect of temperature on the tensile properties of HSLA-100 steel
[AD-A184951] 05 p0565 N88-13441
Cyclic deformation and crack initiation
05 p0597 N88-13646
Fatigue of 30CrMnSiNi2A notched specimens under spectrum loading 05 p0602 N88-13689
Thermo-mechanical behavior of high temperature fiber composites 06 p0678 N88-14149
Near-threshold fatigue 06 p0716 N88-14392
Dependence of strainrange partitioned fatigue life at elevated temperature on monotonic stress-strain properties 06 p0721 N88-14428
Stresses and displacements in two, three and four layered structures submitted to flexible or rigid loads
[AD-A185707] 06 p0723 N88-14450
Composite reliability enhancement via preloading
[AD-A185938] 07 p0826 N88-15010
Study on the mechanical stresses in the elements of the model of a toroidal magnet of a tokamak with strong field
[DE88-700343] 07 p0935 N88-15679
On the relations between cyclic contraction ratio flowstress and deformation mechanisms in bainitic CrMoV steels
[DE87-753043] 08 p0968 N88-15856
Stress strain fields at crack tip and stress intensity factors in Reissner's plate
[PB87-144945] 08 p0994 N88-16014
Theory of deformation. Part 1: Kinematics
[DE88-003007] 08 p1001 N88-16062
Dynamic stress at critical locations of a structure as a criterion for mathematical model modification
09 p1180 N88-17066
Stability and metastability in semiconductor strained-layer structures
[DE88-003308] 09 p1258 N88-17544
Relationship between fatigue life in the creep-fatigue region and stress-strain response
[NASA-TM-100796] 10 p1345 N88-18040
On delamination of (+ or - theta sub m/90 sub n/2) sub s laminates subject to tensile loading
[AD-A188095] 11 p1447 N88-18626
The cyclic stress-strain behavior of a single crystal nickel-base superalloy
[NASA-TM-100269] 12 p1607 N88-19610
Development of a constitutive equation for HSLA (High-Strength Low-Alloy)-100 at cryogenic temperatures
[AD-A189243] 13 p1740 N88-20408
Parametric study of acceleration-induced stresses and frequency changes in doubly-rotated crystal resonators
[AD-A189261] 13 p1761 N88-20532
Body tensor formalism in finite deformation elasticity and application to the torsion of a circular cylinder
13 p1780 N88-20651
Improvement of the Reynolds-stress model by a new pressure-strain correlation
[NASA-CR-182699] 13 p1783 N88-20667
Stress-strain behaviour of a bolt hole in carbon fibre composite plates
[BU-354] 14 p1923 N88-21460
The effect of strain rate on the strength and ductility of SiCw/2124 Al composite
[OUEL-1682/87] 14 p1924 N88-21466
A simplified orthotropic formulation of the viscoplasticity theory based on overstress 14 p1929 N88-21505
Constitutive response of Rene 80 under thermal mechanical loads 14 p1932 N88-21524
The CRREL (Cold Regions Research and Engineering Laboratory) Hopkinson bar apparatus
[AD-A190599] 15 p2077 N88-22380
Biaxial experiments supporting the development of constitutive theories for advanced high-temperature materials 15 p2078 N88-22386
Fatigue damage mapping 15 p2084 N88-22423
Bithermal fatigue: A simplified alternative to thermomechanical fatigue 15 p2084 N88-22424
Behaviour of fibre-reinforced composites under dynamic loading
[AD-A191310] 16 p2174 N88-22955
Analysis of crack-tip fields in a viscoplastic material
17 p2349 N88-23996
Analysis of notched metal matrix composites under tension loading
[NASA-TM-100629] 18 p2480 N88-24713
Role of cracks in the creep of structural polycrystalline ceramics
[AD-A191485] 18 p2490 N88-24770
A transversely isotropic thermoelastic theory
[NASA-TM-101302] 22 p3087 N88-28332
Relation between strength, creep and relaxation behavior in Cu and Al at room temperature
[ETN-88-92982] 23 p3195 N88-29015
Plastic flow and failure modeling under high strain rate loading
[AD-A194223] 23 p3226 N88-29199
Intraplate deformation, stress in the lithosphere and the driving mechanism for plate motions
[NASA-CR-183121] 23 p3231 N88-29231
Shear stress at a film-substrate interface due to mismatch strain
[AD-A193461] 23 p3288 N88-29577
Anisotropic constitutive modeling for nickel-base single crystal superalloys
[NASA-CR-182157] 24 p3353 N88-29961
Nonlinear stress-strain and inelastic rebound with exponential stiffness
[AD-A195667] 24 p3384 N88-30159

STRESS-STRAIN-TIME RELATIONS
Analysis of crack-tip fields in a viscoplastic material
17 p2349 N88-23996

STRESSES
NT AXIAL STRESS
NT COMBINED STRESS
NT CRITICAL LOADING
NT PLANE STRESS
NT RESIDUAL STRESS
NT REYNOLDS STRESS
NT SHEAR STRESS
NT TENSILE STRESS
NT THERMAL STRESSES
NT TORSIONAL STRESS
NT TRIAXIAL STRESSES
Component specific modeling
02 p0187 N88-11166
Anelastic behaviour of materials under multiaxial strains. Part 3: Order-disorder transition, Shoek effect and Poisson's ratio in AISI-1080 steel
[DE87-703087] 02 p0191 N88-11193
Investigations of creep cavitation in Type 304 stainless steel
[DE87-014198] 03 p0287 N88-11803
Superoxide dismutase assays
[AD-A183972] 03 p0356 N88-12242
Initial dynamic load estimates during configuration design 05 p0593 N88-13621
A study of fatigue crack growth life under random stresses 05 p0602 N88-13685
Tensile mean stress effects on uniaxial fatigue behavior of 1045 HR steel 05 p0603 N88-13694
Stress effects and the optimum format of a scrolling seven-line VDT text window
[AD-A185559] 06 p0758 N88-14651
Assessment of anomalous gravitational field of elastic Earth 07 p0921 N88-15594
Study on the mechanical stresses in the elements of the model of a toroidal magnet of a tokamak with strong field
[DE88-700343] 07 p0935 N88-15679
Study on the model of a toroidal magnet for a tokamak with a strong field
[DE88-700346] 07 p0935 N88-15681
Failure modes of laminate structures
[DE88-002579] 08 p0996 N88-16033
Creep and fatigue research efforts on advanced materials 09 p1119 N88-16701
A large strain thermomechanical forming model for elastic-viscoplastic behavior in metals
10 p1301 N88-17780
Effects of the neutron spectrum on mechanical property changes in low dose irradiations
[DE88-003429] 10 p1302 N88-17786
A component synthesis method using Lanczos vectors
[DE88-002263] 10 p1403 N88-18368

Kinetic and turbulence models for granular and two-phase flows 11 p1484 N88-18862
Random vibration (stress screening) of printed wiring assemblies 11 p1499 N88-18953
Ion beam modification of film stress and the effectiveness of thin film encapsulants on GaAs
[DE88-004458] 11 p1558 N88-19328
Thermal oxide growth on silicon: Intrinsic stress and silicon cleaning effects
[AD-A188790] 13 p1736 N88-20377
Real-time stressed channel simulator
[AD-A190223] 15 p2025 N88-22067
Elasto-plastic analysis using a stress-based finite element method and an endochronic theory of plasticity
[DE88-003001] 15 p2075 N88-22372
Does the pipe diffusion of self-interstitials in crystals under stresses exist
[DE88-701027] 15 p2139 N88-22762
A dynamic analysis of piezoelectric strained elements
[AD-A191478] 18 p2503 N88-24851
Theory of viscoplasticity based on overstress with applications 18 p2529 N88-25007
A new boundary integral equation formulation for elastodynamic and elastostatic crack analysis
[AD-A192967] 20 p2815 N88-26702
Ultrasonic studies of stresses and plastic deformation in steel during tension and compression
[AD-A192308] 21 p2912 N88-27280
Granular flow: Particle-dynamics simulations of steady flow
[DE88-011342] 21 p2946 N88-27506
Fiber-optics used to record high-speed photographs inside a pressurized tank during lethality testing
[DE88-011283] 21 p2951 N88-27529
Deep level defects in semiconductors: Stress and pressure studies
[DE88-010855] 21 p3024 N88-27948
Stress related failures causing open metallization
[AD-A195061] 24 p3383 N88-30150

STRETCHING
Spectral dilation of L(B,H)-valued measures and its application to stationary dilation for Banach space valued processes
[NASA-CR-182388] 07 p0913 N88-15536
Optical evaluation of prototype stretched-membrane mirror modules for solar central receivers
[DE88-011884] 21 p2969 N88-27637

STRIATION
Surface gouging by hypervelocity sliding contact between metallic materials
[DE88-001937] 06 p0682 [illegible]4178
Interaction of a vortex pair with a free surface
[AD-A188619] 08 p0988 N88-1[illegible]
The striae in the dust tails of great comets: A formal comparison of the goodness of fit by various theories, and a new proposal 14 p2002 N88-21937

STRING THEORY
Research program in elementary particle theory
[DE88-000159] 02 p0233 N88-11468
Superconformal invariance and superstring in background fields
[DE87-703097] 02 p0247 N88-11561
On the cosmological constant in the heterotic string theory
[DE87-703099] 02 p0247 N88-11562
Our universe as an attractor in a superstring model
[DE87-703066] 02 p0251 N88-11585
Cosmological applications of singular hypersurfaces in general relativity 04 p0521 N88-13202
Introduction to string field theory
[DE87-014583] 05 p0657 N88-14032
Superstrings on quantum spacetime
[DE88-700106] 07 p0940 N88-15715
A note on Fujikawa's method of determining the critical dimension of the relativistic string
[NIKHEF-H/87-5] 08 p1092 N88-16571
Ambiguity in determining the effective action for string-corrected Einstein gravity
[PB87-166153] 09 p1259 N88-17550
Research in theoretical physics: Results from last year 1986/87
[DE88-004922] 10 p1423 N88-18502
Cosmic strings: A problem or a solution
[DE88-003410] 10 p1429 N88-18535
The early years of string theory: The dual resonance model
[DE88-003521] 11 p1563 N88-19359
Simulation of nuclear collisions at high energies in the frames of quark-gluon string model
[DE88-700914] 12 p1690 N88-20113
String theory and algebraic geometry of moduli spaces
[CWI-PM-R8705] 13 p1849 N88-21070
Introduction to classical mechanics of systems with constraints, part 3
[DE88-701057] 13 p1850 N88-21073
Early reheating and cosmic strings
13 p1855 N88-21103
Analysis of hadron production in deep inelastic muon-proton collisions through the fire-string model
[PREPRINT-578] 14 p1981 N88-21822
Strings in four dimensions
[DE88-006435] 14 p1990 N88-21864
Recent developments in the path integral approach to anomalies
[DE87-703032] 15 p2118 N88-22616
Path integral, BRS symmetry, and string and membrane theories
[DE88-752300] 15 p2146 N88-22810
Involution-dependent constants and the cancellation of divergences in the 1-loop open string amplitude
[DE88-006537] 15 p2146 N88-22811
Finite width corrections to the Nambu action for the Nielsen-Olesen string
[DE88-006996] 15 p2147 N88-22812
Cosmology for high energy physicists
[DE88-005705] 15 p2151 N88-22842
Hyperelliptic statsums in superstring theory
[DE88-701646] 16 p2284 N88-23676
Integrability of fermionic string in superfluid Hamiltonian approach
[DE88-701662] 16 p2284 N88-23678
Introduction to covariant formulation of superstring (field) theory
[DE87-703038] 18 p2586 N88-25363
The geometry of the Virasoro group for physicists
[DE88-007374] 18 p2586 N88-25366
Comment on non-renormalization theorem in the four dimensional superstrings
[DE88-752551] 18 p2586 N88-25367
From general relativity to the theory of superstrings
18 p2587 N88-25369
Superstrings
[DE87-702982] 19 p2737 N88-26249
General relativity invariance and string field theory
[DE88-702045] 19 p2737 N88-26252
Topics in gauge theories and the unification of elementary particle interactions
[DE88-008112] 19 p2738 N88-26256
Algebraic and arithmetic geometry in string theory
[CWI-PM-R8708] 20 p2848 N88-26904
Research in theoretical particle physics
[DE88-008230] 20 p2851 N88-26927
Geometry of superconformal manifolds, part 1
[DE88-702405] 21 p3011 N88-27863
Closed string fields as parameters of extra gauge symmetry of open string field theory
[DE88-702046] 21 p3026 N88-27960
Vortices on the world sheet and string's critical dynamics
[DE88-702116] 21 p3026 N88-27961
Dynamical evolution of cosmic strings
[DE88-011724] 21 p3030 N88-27989
The ground state of the bosonic string
[USIP-88-01] 22 p3151 N88-28746
The Hilbert space of the closed bosonic string
[USIP-88-04] 22 p3151 N88-28747
Calculations in perturbative string field theory
[DE88-011616] 22 p3158 N88-28798
Open bosonic string in background electromagnetic field
[DE88-702140] 23 p3201 N88-29053
Holomorphic geometry of interacting string
[DE88-702714] 23 p3295 N88-29627
The Hilbert space of the open bosonic string
[USIP-88-02] 23 p3295 N88-29628
Introduction to string theory
[DE88-702706] 24 p3435 N88-30445

STRINGS
Verification of a systolic algorithm for string comparison
[CWI-CS-R8734] 13 p1819 N88-20873
Hamiltonian formalism in the model of the relativistic string with rigidity
[DE88-701503] 15 p2147 N88-22815
String driven inflation
[DE88-006994] 15 p2151 N88-22841

STRIP TRANSMISSION LINES
NT MICROSTRIP TRANSMISSION LINES
Time domain electromagnetic waves in multilayered media
[AD-A185055] 05 p0574 N88-13502
Time domain wave propagation in multilayered integrated circuits
[AD-A187462] 10 p1324 N88-17916
Conformal microstrip slot antenna and antenna array
[AD-A189623] 15 p2055 N88-22252
Investigation of radiating and guiding structures in microstrip patch antennas
[AD-A191445] 16 p2193 N88-23082
Time domain wave propagation in multilayered integrated circuits
[AD-A193821] 22 p3073 N88-28241

STRONG INTERACTIONS (FIELD THEORY)
An introduction to charm and heavy quark physics
[DE87-013589] 02 p0231 N88-11455

STRONGLY COUPLED PLASMAS
Error modeling and confidence interval estimation for inductively coupled plasma calibration curves
[AD-A186711] 09 p1250 N88-17480
Development and evaluation of instrumentation and methods for multi-element analysis
[AD-A189345] 13 p1841 N88-21018
The two-dimensional one component plasma in a doubly periodic background: Exact results
[AD-A191260] 16 p2280 N88-23650
Thomson scattering for determining electron concentrations and temperatures in an inductively coupled plasma. 1: Assessment of the technique for a low-flow, low-power plasma
[AD-A191323] 16 p2280 N88-23651
Thomson scattering for determining electron concentrations and temperatures in an inductively coupled plasma. 2: Description and evaluation of a multichannel instrument
[AD-A191324] 16 p2280 N88-23652
MACH2: A two-dimensional magnetohydrodynamic simulation code for complex experimental configurations
[AD-A192265] 20 p2860 N88-26988
Role of ordinary to extraordinary mode wave coupling in ionospheric heating experiments
[AD-A195335] 24 p3362 N88-30017

STRONTIUM
Superconducting properties and structural characterization of high T/sub c/ oxides
[DE88-003479] 10 p1420 N88-18477
High temperature superconductivity
[AD-A190259] 16 p2281 N88-23655
Lewis Cliff 86010, a unique Antarctic meteorite: Possible new clues to the early history of the solar system
24 p3442 N88-30482

STRONTIUM COMPOUNDS
Superconductivity in La/sub 1.85-x/Nd/sub x/Sr/sub .15/CuO
[DE88-003014] 09 p1258 N88-17540

STRUCTURAL ANALYSIS
NT BERNSTEIN ENERGY PRINCIPLE
NT DYNAMIC STRUCTURAL ANALYSIS
NT ENERGY METHODS
NT EQUILIBRIUM METHODS
NT FLUTTER ANALYSIS
NT MATRIX METHODS
NT STRAIN ENERGY METHODS
Redesign of solid rocket booster/external tank attachment ring for the space transportation system
[NASA-TM-100476] 01 p0017 N88-10101
Structural reliability and damage tolerance of ceramic composites for high-temperature applications
[PB87-208310] 01 p0019 N88-10119
Mean flow structure of a turbulent junction vortex
[PB87-206231] 01 p0047 N88-10301
Assessment of the COFSI/MAST I project
[NASA-CR-181366] 01 p0053 N88-10340
Analysis of shell-type structures subjected to time-dependent mechanical and thermal loading
[NASA-CR-181409] 01 p0060 N88-10388
Reinforced flexural elements for TEMP-STRESS Program
[DE87-012961] 01 p0061 N88-10391
Dynamical simulation of structural multiplicity in grain boundaries
[DE87-012746] 01 p0103 N88-10676
Reliability of finite element methods in North America
[AGARD-R-748] 02 p0184 N88-11139
Turbine Engine Hot Section Technology, 1985
[NASA-CP-2405] 02 p0184 N88-11140
3D inelastic analysis methods for hot section components 02 p0187 N88-11164
3-D inelastic analysis methods for hot section components 02 p0187 N88-11165
High temperature stress-strain analysis
02 p0188 N88-11170
Constitutive modeling for isotropic materials
02 p0188 N88-11171
Combined calculation of deformation and stress for the body and sabot of an APFSDS
03 p0302 N88-11869
Reliability-based optimal structural and mechanical design 03 p0335 N88-12109
The Shock and Vibration Digest, Volume 19, No. 10
03 p0335 N88-12112
Reduced complexity structural modeling for automated airframe synthesis
[NASA-CR-177440] 04 p0393 N88-12453

An integrated study of structures, aerodynamics and controls on the forward swept wing X-29A and the oblique wing research aircraft
[NASA-CR-181548] 04 p0389 N88-12486

USSR report: Engineering and equipment
[JPRS-UEQ-87-008] 04 p0423 N88-12621

Work-in-progress presented at the Army Symposium on Solid Mechanics, 1986: Lightening of the Force
[AD-A184791] 04 p0427 N88-12644

Explicit and implicit soil modelling for dynamic soil-structure interaction problems
04 p0428 N88-12650

Corrosion control by composite material substitution with application to the M-939 5-ton truck
04 p0428 N88-12654

Detection of defects on structures
[EP-PATENT-0-210-794-A2] 04 p0453 N88-12807

A refined nonlinear analysis of laminated composite plates and shells
[AD-A184436] 04 p0454 N88-12811

Extremum methods of structural analysis for system reliability assessment 04 p0456 N88-12824

Light funnel concentrator panel for solar power
[NASA-CR-179223] 04 p0464 N88-12870

Methods for design and evaluation of integrated hardware/software systems for concurrent computation
[NASA-CR-181522] 04 p0479 N88-12953

Large change-of-curvature effects in quadratic finite elements for CAD of membrane structures
04 p0480 N88-12958

COLA2: A computer program for the structural synthesis of two components using general modal coordinates
[DE88-001457] 04 p0481 N88-12963

Nuclear techniques in studies of condensed matter
[NASA-RP-1195] 04 p0489 N88-13015

Novel dynamical investigations of excitons and their structure in semiconductors
[DE87-014868] 04 p0499 N88-13070

Static Aeroelastic Effects on High Performance Aircraft
[AGARD-CP-403] 05 p0550 N88-13348

Space station systems: A bibliography with indexes
[NASA-SP-7056(05)] 05 p0556 N88-13382

Micromechanics of the degradation of composite materials
[SNIAS-872-430-113] 05 p0559 N88-13405

Fiber composite structural durability and damage tolerance: Simplified predictive methods
[NASA-TM-100179] 05 p0560 N88-13409

Mechanical property evaluation of a series of commercial tungsten alloys
[AD-A185440] 05 p0565 N88-13446

The matrix exponential in transient structural analysis
05 p0593 N88-13619

Simultaneous structural and control optimization via linear quadratic regulator eigenstructure assignment
05 p0594 N88-13622

Structural frequency functions for an impulsive, distributed forcing function 05 p0594 N88-13627

Exact finite element method analysis of viscoelastic tapered structures to transient loads
05 p0595 N88-13632

Optimal shock isolation with minimum settling time
05 p0595 N88-13633

Significance of foundation-soil separation in dynamic soil-structure interaction 05 p0596 N88-13641

An element of a multilayer shell for the computation of composite structures
[ONERA-RT-14/3542-RY-051-R]
05 p0610 N88-13742

Experimental studies on acoustic emission monitoring of crack propagation in offshore structures: A literature survey 05 p0610 N88-13748

Structural tests and development of a laminar flow control wing surface composite chordwise joint
[NASA-CR-172462] 06 p0663 N88-14066

Design verification and fabrication of active control systems for the DAST ARW-2 high aspect ratio wing, part 1
[NASA-CR-177959-PT-1] 06 p0669 N88-14101

Continuum modeling of large lattice structures: Status and projections
[NASA-TP-2767] 06 p0672 N88-14115

Geometric nonlinear analysis of asymmetric thin-walled members
[PB87-133856] 06 p0723 N88-14446

Fundamental aspects of the structure of supersonic turbulent boundary
[AD-A186366] 07 p0815 N88-14959

Natural frequencies and structural integrity assessment of large space structures
[AD-A186139] 07 p0824 N88-15001

New mechanism of the high temperature (reversible) temper brittleness of alloy steels
[PB87-143954] 07 p0833 N88-15056

Experimental investigation of damping characteristics of bolted structural connections for plates and shells
[AD-A186075] 07 p0867 N88-15259

Structural relaxation in strained-layer heterostructures
[DE88-002326] 07 p0868 N88-15264

Typhoon structural evolution
[AD-A186090] 07 p0879 N88-15333

Contrast between the chemical, structural and electronic properties of thin films of Cu and Ni on the Ru(0001) surface
[DE88-002360] 07 p0938 N88-15698

Aeropropulsion '87. Session 2: Aeropropulsion Structures Research
[NASA-CP-10003-SESS-2] 08 p0954 N88-15785

Integrated analysis and applications
08 p0954 N88-15789

Overview of NASA PTA propfan flight test program
08 p0957 N88-15805

Mixed method of finite strip and finite element
[PB87-143467] 08 p0996 N88-16027

The Shock and Vibration Bulletin. Part 3: Isolation and damping, vibration test criteria, and vibration analysis and test
[AD-A186750] 08 p0997 N88-16040

Evaluation of vibration specifications for acoustic environments 08 p0999 N88-16053

North Pacific Ocean. Subtropical front north of Hawaii, R/V Thomas G. Thompson: 7 January - 10 February 1974. CTD data report
[AD-A186565] 08 p1044 N88-16310

Analytical interactive approach for phenomena involving structures, thermal and control aspects. Volume 1: Theory --- spacecraft structures
[ESA-CR(P)-2503-VOL-1] 09 p1134 N88-16803

Analytical interactive approach for phenomena involving structures, thermal, and control aspects. Volume 2: Toward the solution --- spacecraft structures
[ESA-CR(P)-2503-VOL-2] 09 p1134 N88-16804

Analytical interactive approach for phenomena involving structures, thermal, and control aspects. Volume 3: Executive summary --- spacecraft structures
[ESA-CR(P)-2503-VOL-3] 09 p1134 N88-16805

Gas erosion of impeller housing in the operation of a high-temperature, high-pressure helium circulator
[DE88-002807] 09 p1175 N88-17041

The Shock and Vibration Bulletin. Part 4: Structural Dynamics and Modal Test and Analysis
[AD-A186751] 09 p1179 N88-17062

Analysis of reinforced concrete structures under the effects of localized detonations
09 p1179 N88-17064

Reinforced cocnrete arches under blast and shock environments 09 p1180 N88-17065

Optimized structure design using reanalysis techniques 09 p1180 N88-17067

Consistent linearization of the element-independent corotational formulation for the structural analysis of general shells
[NASA-CR-178418] 09 p1181 N88-17076

FABSTRAN: A computer program for frame and beam static and transient response analysis (nonlinear)
[ARE-TR-86205] 09 p1182 N88-17079

Self-adaptive analysis of three-dimensional structures using a p-version of finite element method
[FFA-TN-1987-31] 09 p1182 N88-17084

Rotorcraft weight trends in light of structural material characteristics
[AD-A186576] 10 p1276 N88-17642

Structural analysis of the space shuttle solid rocket booster/external tank attach ring
[NASA-TM-100510] 11 p1446 N88-18618

Study of the mechanical behavior of a 2-D carbon-carbon composite
[NASA-CR-182594] 11 p1451 N88-18649

Structural analysis using X-ray scattering and neutron scattering on binary amorphous (Co,Cu)Ti alloys
[ETN-88-91487] 11 p1459 N88-18699

Study of the production of some superconducting and magnetic materials by solidification in the drop tube and drop tower
[NASA-CR-182494] 11 p1461 N88-18708

Experimental set-up and mathematical modeling of H-shaped beam type structure
[AD-A187196] 11 p1466 N88-18743

Structure of shear flow turbulence and its control
[AD-A187909] 11 p1482 N88-18846

Dynamic substructuring for shock spectrum analysis using component mode synthesis
11 p1499 N88-18950

Approximate method for predicting the permanent set in a beam in vacuo and in water subject to a shock wave 11 p1500 N88-18957

Mathematical modeling of the postbuckling behavior of structural elements 11 p1500 N88-18960

Structural analysis methods development for turbine hot section components
[NASA-TM-100298] 11 p1501 N88-18967

Deformations in VLBI antennas
[NASA-TM-100696] 11 p1502 N88-18970

Dynamic analysis of plane frames by microcomputer
11 p1531 N88-19143

An interdisciplinary approach to predictive modeling of structural adhesive bonding: Factors affecting the durability of titanium/epoxy bonds
[AD-A189503] 12 p1611 N88-19636

Structural shape optimization in multidisciplinary system synthesis
[NASA-TM-100538] 12 p1614 N88-19650

Advanced durability analysis. Volume 1: Analytical methods
[AD-A188341] 12 p1635 N88-19789

On analysis of viscoelastic structures
[AD-A188445] 12 p1636 N88-19793

Structural-acoustic interior noise modeling and analysis from experimental data
[PB88-141775] 12 p1687 N88-20086

Dynamical and photometric studies of Saturn's rings
12 p1711 N88-20241

A correlation study of X-29A aircraft and associated analytical development
[NASA-CR-183103] 13 p1722 N88-20296

Viscoelastic behavior of a polyetheretherketone (PEEK) composite
[AD-A189545] 13 p1734 N88-20368

Materials Research Laboratory at Brown University
[AD-A188006] 13 p1739 N88-20396

A fundamental understanding of the effect of alloying elements on the corrosion resistance of rapidly solidified Mg alloys
[AD-A189385] 13 p1741 N88-20413

Recent developments in nondestructive evaluation for structural ceramics
[DE88-005889] 13 p1751 N88-20473

Time-domain system for identification of the natural resonant frequencies of aircraft relevant to electromagnetic compatibility testing
[PB88-164520] 13 p1758 N88-20519

Control of structure in turbulent flows: Bifurcating and blooming jets
[AD-A189607] 13 p1766 N88-20562

Structural clearances and internal friction: Simulation by Eigen distortions
[ISSN-0208-5658] 13 p1779 N88-20640

Sixteenth NASTRAN (trademark) Users' Colloquium
[NASA-CP-2505] 13 p1780 N88-20652

A preliminary investigation of finite-element modeling for composite rotor blades
[NASA-TM-100559] 13 p1781 N88-20656

Component mode synthesis using experimental modes enhanced by mass loading
[DE88-006097] 13 p1781 N88-20657

Finite element methodology for nonlinear free and harmonic forced vibrations of beam and plate structures
13 p1782 N88-20663

Fluid-thermal-structural study of aerodynamically heated leading edges
[NASA-TM-100579] 13 p1783 N88-20666

Analysis of shell-type structures subjected to time-dependent mechanical and thermal loading
[NASA-CR-182705] 13 p1783 N88-20668

Activities report of the Structures Department
[ETN-88-91986] 13 p1783 N88-20672

Microwave and structural properties of saline ice
[AD-A189307] 13 p1803 N88-20779

Biophysical applications of solid state and tritium NMR
[DE88-005328] 13 p1808 N88-20806

Robustifying the Kalman filter
[AD-A189240] 13 p1825 N88-20907

The synthesis, characterization and structural studies of In(C5H4Me) by X-ray diffraction and electron diffraction techniques and a reinvestigation of the crystalline state of In(C5H5) by X-ray diffraction studies
[AD-A189110] 13 p1844 N88-21038

Exploring the relation between interface structure and mechanical properties in multilayer structures
[DE88-005428] 13 p1848 N88-21060

Spacecraft dielectric surface charging property determination
[NASA-CR-180879] 14 p1881 N88-21243

Unrestrained out-of-plane buckling of monosymmetric rings
[PB88-155213] 14 p1923 N88-21458

Structural and material testing of a composite microlite wing model
[BU-355] 14 p1923 N88-21461

Experiments on the creep behavior of semifinished X10NiCrAlTi 32 20 (Nicrofer 32 20) tubes under multiaxial loading --- nuclear reactors
[JUEL-2127] 14 p1923 N88-21464

Probabilistic analysis of crack containing structures with the PARIS code
[KFK-4286] 14 p1924 N88-21465

Nonlinear Constitutive Relations for High Temperature Applications, 1986
[NASA-CP-10010] 14 p1928 N88-21498

Evaluation of structural analysis methods for life prediction 14 p1930 N88-21511

On the global/local time incrementing for viscoplastic analysis 14 p1932 N88-21519

Nonlinear structural analysis of a turbine airfoil using the Walker viscoplastic material model for B1900 + Hf 14 p1932 N88-21522

Sensitivity of control-augmented structure obtained by a system decomposition method
[NASA-TM-100535] 14 p1954 N88-21647

Aero/structural tailoring of engine blades (AERO/STAEBL)
[NASA-CR-180805] 14 p1959 N88-21662

Implementing embedded artificial intelligence rules within algorithmic programming languages
[NASA-CR-178393] 14 p1959 N88-21686

Properties of the nucleus of P/Halley 14 p2004 N88-21952

Galvanic corrosion initiatives
[AD-A190658] 15 p2040 N88-22155

Transformation toughening of ceramics
[AD-A190399] 15 p2045 N88-22183

Developments in ceramic superconducting materials 15 p2052 N88-22229

JPRS report: Science and technology. China
[JPRS-CST-87-043] 15 p2053 N88-22233

Efficient method for structural optimization 15 p2054 N88-22240

UARS spacecraft recorder
[NASA-CR-180768] 15 p2068 N88-22331

Buckling of blast loaded cylinder
[AD-A190124] 15 p2076 N88-22376

Environmentally assisted crack growth in structural alloys: Perspectives and new directions
[AD-A190137] 15 p2076 N88-22377

Vibrations of structures with parametric uncertainties
[AD-A190400] 15 p2076 N88-22378

The composite blade structural analyzer (COBSTRAN) 15 p2078 N88-22390

Three-dimensional inelastic approximate analysis code (MOMM) 15 p2079 N88-22392

METCAN: The metal matrix composite analyzer 15 p2079 N88-22395

Probabilistic structural analysis computer code (NESSUS) 15 p2079 N88-22397

Structural tailoring of high-speed turbine blades (SSME/STAEBL) 15 p2080 N88-22398

Computational structural mechanics for engine structures 15 p2080 N88-22399

Structural tailoring of advanced turboprops 15 p2080 N88-22400

Advanced probabilistic methods for quantifying the effects of various uncertainties in structural response 15 p2080 N88-22401

Thermostructural analysis of simulated cowl lips 15 p2080 N88-22403

Thermal-structural analyses of Space Shuttle Main Engine (SSME) hot section components 15 p2081 N88-22404

Structural analyses of engine wall cooling concepts and materials 15 p2081 N88-22405

Structural assessment of a space station solar dynamic heat receiver thermal energy storage canister 15 p2081 N88-22406

Whisker-reinforced ceramic composites for heat engine components 15 p2082 N88-22410

Continuous fiber ceramic matrix composites for heat engine components 15 p2082 N88-22411

Flaw characterization in structural ceramics using scanning laser acoustic microscopy 15 p2082 N88-22415

Improvements to tilt rotor performance through passive blade twist control
[NASA-TM-100583] 15 p2086 N88-22434

Experimental design and structural optimization
[PB88-169255] 15 p2087 N88-22436

Bilateral symmetry elements of the Zhamanshin impact crater
[NASA-TT-20288] 15 p2096 N88-22490

Structural decomposition of multiple time scale Markov processes
[AD-A189739] 15 p2123 N88-22657

An investigation of the crystalchemistry and thermochemistry of selected mineral systems
[AD-A189758] 15 p2142 N88-22781

Path integral, BRS symmetry, and string and membrane theories
[DE88-752300] 15 p2146 N88-22810

Research and technology
[NASA-TM-100172] 15 p2153 N88-22851

Coherent structure 16 p2199 N88-23117

Coherent structures: Comments on mechanisms 16 p2199 N88-23118

Coherent structures and dynamical systems 16 p2199 N88-23119

Coherent structures and modeling: Some background comments 16 p2199 N88-23120

Multigrid for structures analysis 16 p2218 N88-23232

Vibration and flutter analysis of the SR-7L large-scale propfan 16 p2221 N88-23254

A nonlinear computation for composite structures
[ONERA-RT-15/3542-RY-062-R] 16 p2222 N88-23265

STRUTEX: A prototype knowledge-based system for initially configuring a structure to support point loads in two dimensions
[NASA-TM-100613] 16 p2250 N88-23448

Applicability and limitations of probability models in connection with the reliability of large-scale technical installations
[W-3/87] 16 p2261 N88-23520

Travelling wave concepts for the modeling and control of space structures
[AD-A191235] 17 p2310 N88-23819

Structural acoustics design manual
[ESA-PSS-03-1201-ISSUE-1] 17 p2311 N88-23821

Nondestructive Evaluation (NDE) of structural ceramics by photoacoustic microscopy 17 p2325 N88-23884

Remote sensing and structural rupture: Application examples in the study of tectonics 17 p2359 N88-24050

Analysis and interpretation of image lithostructure: An application of the multiconcept in the metamorphic belt of Sul de Santana os Boa Vista (RS) 17 p2359 N88-24051

Study of fracturing for groundwater research in the Sergipe state with remote sensing products 17 p2359 N88-24052

Lithostructural interpretation of Chapda do Cachimbo (Pa-Am-Mt), based on radar and LANDSAT imagery 17 p2368 N88-24100

The structural analysis of some crystalline and semi-crystalline substances using X-ray and neutron diffraction 17 p2445 N88-24540

Analysis of dust grain properties in two star forming regions through comparison of theoretical models to observations 17 p2451 N88-24559

Research on aero-thermodynamic distortion induced structural dynamic response of multi-stage compressor blading
[AD-A192169] 18 p2456 N88-24584

Electromagnetic damping and vibration isolation of space structures
[AD-A191492] 18 p2471 N88-24665

Fundamental studies of beta phase decomposition modes in titanium alloys
[AD-A191495] 18 p2485 N88-24740

Calculation of rolling contact of two viscoelastic cylinders with application to the steady state normal contact problem
[ILR-MITT-188] 18 p2530 N88-25006

Probabilistic finite element methods 18 p2564 N88-25223

Simulated measurement of power flow in structures near to simple sources and simple boundaries
[NASA-TM-89124] 19 p2722 N88-26166

Sensitivity to crack initiation in thick assemblies. Test report 48-444
[REPT-48-444] 20 p2758 N88-26365

Surface phases and their influence on metal-oxide interfaces
[DE88-007938] 20 p2769 N88-26420

Australian structures response evaluation: Ground shock and air blast measurements for site investigation survey
[MRL-TN-526] 20 p2813 N88-26685

FEB structural analyses, revision H
[AD-A192302] 20 p2814 N88-26696

Vibrational impacts of hush house operation
[DE88-006983] 21 p2899 N88-27207

Microchemical analysis of polycrystalline Ni3Al and other ordered alloys using the field-ion microscope atom probe
[DE88-011519] 21 p2914 N88-27294

Finite element method for plate structures with inclined angles
[ILR-MITT-182] 21 p3008 N88-27842

Structural Tailoring of Advanced Turboprops (STAT)
[NASA-CR-180861] 22 p3045 N88-28074

The effect of microgravity on mammalian cell polarization at the ultrastructural level --- Spacelab D1 mission 22 p3061 N88-28164

Application of differential quadrature to the analysis of structural components 22 p3087 N88-28331

Parametric identification of mechanical structures
[ETN-88-92891] 22 p3088 N88-28339

Modal synthesis by use of substructures with fixed or free coupling points
[ILR-MITT-191] 22 p3089 N88-28341

SRM (Solid Rocket Motor) propellant and polymer materials structural modeling
[NASA-TP-2824] 22 p3089 N88-28343

Structural analysis of the Jura mountains-Rhine Graben intersection (Switzerland) for petroleum exploration using SPOT stereoscopic data 22 p3103 N88-28431

Laboratory feasibility study of a composite embedded fiber optic sensor for measurement of structural vibrations
[AD-A194270] 22 p3152 N88-28754

A fundamental study of P/M processed elevated temperature aluminum alloys
[AD-A192958] 23 p3194 N88-29005

Structural relationship between icosahedral and Frank-Kasper phases of Al-Li-Cu
[AD-A193768] 23 p3195 N88-29011

Nondestructive investigations for space use
[SNIAS-881-430-105] 23 p3224 N88-29180

Experimental investigation of the effects of underwater exposure on the damping characteristics of bolted structural connections for plates and shells
[AD-A194486] 23 p3226 N88-29200

Interactive plotting of NASTRAN aerodynamic models using NPLOT and DISSPLA
[AD-A194115] 23 p3226 N88-29204

Computer programs for generation of NASTRAN and VIBRA-6 aircraft models
[AD-A195467] 24 p3323 N88-29792

Constitutive modeling for isotropic materials
[NASA-CR-182132] 24 p3327 N88-29811

Attenuated total reflectance FT-IR spectroscopy to measure interfacial reaction kinetics at silica surfaces
[AD-A196330] 24 p3344 N88-29908

Stress intensity factors for cracked metallic structures under rapid thermal loading
[AES-8609709F-1] 24 p3353 N88-29962

Analytical and experimental studies of beam waveguide absorbers for structural damping
[AD-A195085] 24 p3392 N88-30144

Computer-Aided Structural Engineering (CASE) project. Development of design formulas for ribbed mat foundations on expansive soils
[AD-A194807] 24 p3412 N88-30307

Computer-Aided Structural Engineering (CASE) project. Computer program for analysis of planar grid structures (CGRID), user's guide
[AD-A195977] 24 p3413 N88-30317

Structuring processes in expanding laser-produced plasmas
[AD-A195249] 24 p3431 N88-30424

Structural dynamics of high-latitude magnetosphere determined from solar electron data 24 p3444 N88-30500

STRUCTURAL BASINS
NT DELAWARE RIVER BASIN (US)
NT GREAT BASIN (US)
NT RIVER BASINS
NT WATERSHEDS

Typhoon structural evolution
[AD-A186090] 07 p0879 N88-15333

On estimating the basin-scale ocean circulation from satellite altimetry. Part 1: Straightforward spherical harmonic expansion
[NASA-CR-182387] 07 p0882 N88-15352

New data on structure of earth's crust and seismicity of basins in Atlantic and Indian Oceans 08 p1010 N88-16123

Bathymetric hazard survey test
[AD-A189150] 13 p1803 N88-20775

The impact of disorganized occupation of urban sub-basins: Sub-basin of the Cabucu River, metropolitan area of Sao Paulo (SP) 19 p2682 N88-25945

STRUCTURAL BEAMS
U BEAMS (SUPPORTS)

STRUCTURAL DESIGN
NT PRESSURE VESSEL DESIGN

Integration of dynamic, aerodynamic and structural optimization of helicopter rotor blades
[NASA-CR-181441] 01 p0002 N88-10012

A feasibility study of a hypersonic real-gas facility
[NASA-CR-180423] 01 p0008 N88-10043

Blagov commentary on Mir station, first manning 01 p0009 N88-10051

Space station integrated wall design and penetration damage control
[NASA-CR-179169] 01 p0013 N88-10070

Telepresence work station system definition study, part 2
[NASA-CR-172006] 01 p0013 N88-10071

Propulsion Working Group report 01 p0016 N88-10096

Space station propulsion technology: Space station propulsion system test bed test plan
[NASA-CR-179201] 01 p0017 N88-10104
Linear emittance damper with megagauss fields
[DE87-013562] 01 p0093 N88-10606
Phase 3 study of selected tether applications in space. Volume 2: Study results
[NASA-CR-179186] 02 p0132 N88-10826
Models of degradation of stratified composite structures
[ONERA-RT-13/3542-RY-061-R]
02 p0142 N88-10892
Advances in nickel hydrogen technology at Yardney Battery Division 02 p0164 N88-11029
International Ultraviolet Explorer (IUE) spacecraft battery performance update 02 p0164 N88-11033
Qualification testing of General Electric 50 Ah nickel-cadmium cells with Pellon 2536 separator and passivated positive plates 02 p0165 N88-11036
Test summary for advanced H2 cycle NI-CD cell
02 p0165 N88-11040
Prediction of fatigue cracking and rupture of large structures
[ONERA-RT-31/7169-RY-055-R]
02 p0192 N88-11199
The Shock and Vibration Digest, Volume 19, No. 11
03 p0265 N88-11673
Airworthiness of long-life jet transport structures
03 p0265 N88-11674
Pump assisted heat pipe 03 p0319 N88-12018
Structural characteristics of dean vortices in a curved channel
[AD-A184724] 03 p0320 N88-12024
Reliability-based optimal structural and mechanical design 03 p0335 N88-12109
The Shock and Vibration Digest, Volume 19, No. 10
03 p0335 N88-12112
Parachute materials
[DE87-014845] 04 p0411 N88-12550
Design of digital filters for electronic instrumentation
[PB87-100418] 04 p0438 N88-12716
Design of efficient FIR filters with minimal delay
[PB87-100434] 04 p0438 N88-12717
Lifting bodies: An attractive aerodynamic configuration choice for hypervelocity vehicles
05 p0534 N88-13248
Static aeroelastic considerations in the definition of design loads for fighter airplanes
05 p0550 N88-13351
The use of aeroelastic wind tunnel models to prove structural design 05 p0551 N88-13355
Design and assembly sequence analysis of option 3 for CETF reference space station
[NASA-TM-100503] 05 p0553 N88-13369
Space station systems: A bibliography with indexes
[NASA-SP-7056(05)] 05 p0556 N88-13382
Surface treatment problems found in new aircraft designed using structural composites
[SNIAS-872-111-113] 05 p0558 N88-13397
A complete linearized theory for the analysis and design of two-dimensional hydrofoils near a free surface
[UTIAS-TN-264] 05 p0579 N88-13531
Initial dynamic load estimates during configuration design 05 p0593 N88-13621
The high performance solar array GSR3
[SNIAS-872-422-108] 05 p0622 N88-13814
Structural optimization in the design process --- aircraft
[SNIAS-872-111-115] 05 p0635 N88-13885
Small space reactor power systems for unmanned solar system exploration missions
[NASA-TM-100226] 05 p0660 N88-14054
Design, fabrication and delivery of a miniature Cassegrainian concentrator solar array system
[NASA-CR-179237] 06 p0730 N88-14493
Aircraft engine hot section technology: An overview of the HOST Project 08 p0957 N88-15804
Design and test of a spacecraft instrument shock isolator
08 p0998 N88-16044
Comprehensive rotorcraft analysis methods
09 p1106 N88-16630
Advanced composite airframe program: Today's technology
09 p1107 N88-16636
Integrity control of carbon fiber reinforced plastics (CFRP) structural elements. Conclusion with respect to the control methodology of CFRP primary structures in manned space flight and the implications to the design, analysis and testing of CFRP structural elements, executive summary
[MBB-TR-RB517-014/85] 09 p1139 N88-16824
Three-dimensional incompressible flowfield analysis for establishing rotor designs which optimize power extraction
10 p1329 N88-17943
Optimal design and parameter identification of flexible rotor-bearing systems
10 p1339 N88-18002
Design conditions and workspace for the generally-proportioned 3-hinge spherical wrist for robots
10 p1339 N88-18003
Design sensitivity analysis of nonlinear structural systems and numerical implementation with established finite element codes 10 p1344 N88-18032
Physical and structural characteristics of Weddell Sea pack ice
[AD-A188189] 10 p1358 N88-18119
Apollo Lightcraft project
[NASA-CR-182575] 11 p1445 N88-18615
An optimal structure for a 34-meter millimeter-wave center-fed BWG antenna: The Cross-Box concept
11 p1472 N88-18778
Derivation of strength factors related to the coordination of the strength of transmission line components --- electric power lines
[S/T-REPT-VOL-5-NO-2] 11 p1500 N88-18959
Problems in modeling TF ripple loss of fast alphas from a tokamak reactor
[DE88-000612] 11 p1553 N88-19296
Interaction between structural considerations and system design in advanced flight controls
12 p1580 N88-19458
Manned simulation: Helpful means to determine and improve structural load criteria 12 p1581 N88-19459
Presentation of structural component designs for the family of commuter airplanes
[NASA-CR-182568] 12 p1581 N88-19463
A class 2 weight assessment for the implementation of commonality and preliminary structural designs for the family of commuter airplanes
[NASA-CR-182565] 12 p1581 N88-19464
Presentation of flight control design and handling quality commonality by separate surface stability augmentation for the family of commuter airplanes
[NASA-CR-182567] 12 p1583 N88-19471
Automatic in-orbit payload deployment mechanisms, logistic operations and transport vehicle design compatibilities 12 p1586 N88-19493
Conceptualization and design of a variable-gravity research facility
[NASA-CR-182574] 12 p1595 N88-19550
Progress toward a cosmic dust collection facility on space station
[NASA-CR-182427] 12 p1598 N88-19566
Conceptual design and programmatics studies of space station accommodations for Life Sciences Research Facilities (LSRF)
[NASA-CR-179270] 12 p1598 N88-19567
Space station accommodations for life sciences research facilities: Phase A conceptual design and programmatics studies for Missions SAAX0307, SAAX0302 and the transition from SAAX0307 to SAAX0302. Volume 1: Executive summary
[NASA-CR-179267] 12 p1599 N88-19571
Concentrating photovoltaic collectors: Fabrication design
[PB88-148051] 12 p1640 N88-19821
Optics of the CEBAF CW superconducting accelerator
[CEBAF-PR-87-012] 12 p1690 N88-20110
Orbital transfer vehicle concept definition and system analysis study. Volume 2: OTV concept definition and evaluation. Book 1: Mission and system requirements
[NASA-CR-179321] 13 p1729 N88-20339
Development of isostatic mounts and associated guidelines --- spacecraft payloads
[CASA-IM-WP-301] 13 p1731 N88-20354
X-ray computed tomography for structural ceramic applications: Beam hardening corrections
[DE88-005891] 13 p1752 N88-20474
Aluminum-air battery development
[DE88-006617] 13 p1762 N88-20542
Structural clearances and internal friction: Simulation by Eigen distortions
[ISSN-0208-5658] 13 p1779 N88-20640
Potential off-normal events and associated radiological source terms for the compact ignition tokamak: Fusion Safety Program
[DE88-004112] 13 p1842 N88-21024
Space infrared telescope facility wide field and diffraction limited array camera (IRAC)
[NASA-CR-182704] 13 p1853 N88-21092
A sequentially deployable structure for space applications 14 p1875 N88-21202
Thermophotovoltaic space power system, phase 3
[NASA-CR-179327] 14 p1942 N88-21585
Large-scale wind turbine structures
15 p2085 N88-22429
Design studies of primary aircraft structures in ARALL laminates
[LR-520] 16 p2160 N88-22888
Experimental design and structural optimization
[ETN-88-92232] 16 p2257 N88-23492
Insert design handbook
[ESA-PSS-03-1202-ISSUE-1] 17 p2311 N88-23822
LDR structural experiment definition
[NASA-TM-100618] 17 p2312 N88-23826
Ceramics for turbine engines
17 p2323 N88-23873
Gigawatt, closed cycle, vapor core-MHD space power system conceptual design study
17 p2433 N88-24473
Small particle bed reactors: Sensitivity to Brayton cycle parameters 17 p2435 N88-24487
A combined Rankine/Brayton pulse power cycle
17 p2435 N88-24490
Alkali metal thermoelectric converter design for space power systems applications 17 p2437 N88-24499
A capillary pumped SHE/AMTEC system
17 p2437 N88-24500
Performance of vapor-fed sodium heat engine/AMTEC systems 17 p2437 N88-24502
Multimegawatt power conditioning requirements study
17 p2438 N88-24504
Experimental vibration damping characteristics of the third-stage rotor of a three-stage transonic axial-flow compressor
[NASA-TM-100948] 18 p2466 N88-24642
Design of overlays for rigid airport pavements
[DOT/FAA/PM-87/19] 18 p2468 N88-24652
Fundamental limits to the velocity of solid armatures in railguns 18 p2469 N88-24656
Use of a two-stage light-gas gun as an injector for electromagnetic railguns
[DE88-007200] 18 p2469 N88-24657
Structural margins assessment approach
[NASA-TM-100332] 18 p2473 N88-24672
Dynamics of a flexible orbiting platform with MRMS
[ISSN-0285-6808] 18 p2473 N88-24673
Internal erosion rates of a 10-kW xenon ion thruster
[NASA-TM-100954] 18 p2476 N88-24688
Calculation of assemblies bonded with quasi-elastic adhesives
[REPT-47-632/F] 18 p2493 N88-24793
Space station architectural elements and issues definition study
[NASA-CR-3941] 18 p2587 N88-25371
Modulation efficiency limited high frequency performance of the MODFET 19 p2657 N88-25786
Advanced energy system program
[PB88-183025] 19 p2686 N88-25965
Accelerator research studies
[DE88-008236] 19 p2726 N88-26187
Computer-Aided Engineering (CAE) for engineering design 21 p2929 N88-27390
Optimal design of viscoelastic structures
21 p2959 N88-27579
A hidden-surface removal algorithm for structures defined by triangular and rectangular surface patches
[DFVLR-MITT-88-03] 21 p3000 N88-27792
Probabilistic structural analysis to quantify uncertainties associated with turbopump blades
[NASA-TM-100278] 22 p3050 N88-28094
Missiles, fuselages and similar bodies
23 p3169 N88-28869
Comparison of the influence of different gust models on structural design 24 p3312 N88-29722
Lunar lander conceptual design: Lunar base systems study task 2.2
[NASA-CR-172051] 24 p3335 N88-29854
Gas turbine combustion modeling
24 p3349 N88-29936
A small annular combustor of high power density, wide operating range and low manufacturing cost
24 p3351 N88-29951
Alternative module configurations for advanced solar arrays on low orbit and extended lifetime missions (AMOC 2)
[ESA-CR(P)-2581] 24 p3389 N88-30182
The space station assembly phase: System design trade-offs for the flight telerobotic servicer
24 p3420 N88-30357

STRUCTURAL DESIGN CRITERIA
Rational reinforcement of cylindrical shells with variable stiffness frames subjected to external pressure
04 p0426 N88-12638
Simultaneous structural and control optimization via linear quadratic regulator eigenstructure assignment
05 p0594 N88-13622
Evaluation of vibration specifications for acoustic environments 08 p0999 N88-16053
Rotorcraft handling-qualities design criteria development 09 p1109 N88-16645
Workshop on Design Loads for Advanced Fighters
[AGARD-R-746] 12 p1579 N88-19449
Structural design requirements for aircraft incorporating active control technology 12 p1580 N88-19453
Manoeuvres by default, by demand and by design
12 p1580 N88-19455

How to generate equal probability design load conditions --- aircraft design
[NLR-TR-86060-U] 13 p1722 N88-20295
Some design considerations for ceramic components in heat engine applications 17 p2323 N88-23875
Frequency dependent sliding coefficients for general three-dimensional rolling contact in high frequency range
[ILR-MITT-192] 22 p3085 N88-26318
SR-7A aeroelastic model design report
[NASA-CR-174791] 23 p3179 N88-26928

STRUCTURAL DYNAMICS
U DYNAMIC STRUCTURAL ANALYSIS

STRUCTURAL ENGINEERING
Efficient placement of structural dynamics sensors on the space station
[NASA-CR-172015] 01 p0017 N88-10103
Strain gages in engineering geodesy
[SER-C-320] 01 p0048 N88-10309
Activities report in metal manufacturing
[ISSN-0524-7705] 07 p0839 N88-15086
Index of USA-CERL publications for October 1984 - June 1987
[AD-A186375] 07 p0942 N88-15728
Aeropropulsion structures 08 p0954 N88-15786
Computer Applications in Geotechnical Engineering (CAGE) and Geotechnical aspects of the Computer-Aided Structural Engineering (G-CASE) projects. User's guide. UTEXAS2 slope-stability package. Volume 1: User's manual
[AD-A187674] 11 p1511 N88-19025
Stabilization and control problems in structural dynamics
[AD-A190197] 15 p2073 N88-22361
Travelling wave concepts for the modeling and control of space structures
[AD-A191235] 17 p2310 N88-23819
Probabilistic anisotropic failure criteria for composite materials
[AD-A193046] 21 p2904 N88-27232
An investigation of techniques for determination of optimum/self-optimizing systems
21 p2963 N88-27600
Development of remote control welding system of large structures
[PB87-219853] 22 p3083 N88-26309
Computer-Aided Structural Engineering (CASE) project. Development of design formulas for ribbed mat foundations on expansive soils
[AD-A194807] 24 p3412 N88-30307
Computer-Aided Structural Engineering (CASE) project. Computer program for analysis of planar grid structures (CGRID), user's guide
[AD-A195977] 24 p3413 N88-30317

STRUCTURAL FAILURE
Assessment of structural integrity from forced vibration testing
[DE87-014642] 02 p0191 N88-11195
Natural frequencies and structural integrity assessment of large space structures
[AD-A186139] 07 p0824 N88-15001
Postbuckling of laminated anisotropic panels
[NASA-TM-100509] 08 p0994 N88-16011
Damage mechanics of fiber reinforced plastics: A general view 11 p1448 N88-18631
Buckling and breakdown problems in structural mechanics. Failure of prestressed double-walled containers or rings
[MBB-UR-E-956/87] 13 p1783 N88-20671
Analysis and developments of failure concepts in fracture mechanics based on research results in the field of component safety topics: J-integral concept; crack resistance curves; dynamic criterion
[V-19/86] 18 p2530 N88-25009
Loading rate sensitivity of open hole composites in compression
[NASA-TM-100634] 19 p2610 N88-25490
Critical issues and directions for fracture mechanics and structural integrity
[AD-A193050] 21 p2960 N88-27584
Durability of continuous fiber reinforced metal matrix composites
[AD-A193868] 22 p3050 N88-28097
The development of acoustic emission for structural integrity monitoring of aircraft
[AD-A196264] 24 p3427 N88-30398

STRUCTURAL FATIGUE
U FATIGUE (MATERIALS)

STRUCTURAL FOUNDATIONS
U FOUNDATIONS

STRUCTURAL INFLUENCE COEFFICIENTS
The nonlinear dynamic response of an elastic-plastic thin plate under impulse loading
[AD-A182147] 08 p0994 N88-16013

STRUCTURAL MATERIALS
U CONSTRUCTION MATERIALS

STRUCTURAL MEMBERS
NT ANISOTROPIC PLATES
NT ANNULAR PLATES
NT BEAMS (SUPPORTS)
NT BOX BEAMS
NT CANTILEVER BEAMS
NT CIRCULAR PLATES
NT COLUMNS (SUPPORTS)
NT CORRUGATED PLATES
NT CURVED BEAMS
NT ELASTIC PLATES
NT END PLATES
NT FLAT PLATES
NT GIRDERS
NT I BEAMS
NT LONGERONS
NT MEMBRANE STRUCTURES
NT METAL PLATES
NT ORTHOTROPIC PLATES
NT PERFORATED PLATES
NT PLASTIC PLATES
NT PLATES (STRUCTURAL MEMBERS)
NT POROUS PLATES
NT RECTANGULAR PLATES
NT REINFORCED PLATES
NT SKIN (STRUCTURAL MEMBER)
NT STRAKES
NT STRUTS
NT TIMOSHENKO BEAMS
NT TRUSSES
NT WING PANELS
Possibilities for the modeling of dynamically loaded cylindrical structural parts in the wind tunnel
[KU-SFB-210/T/24] 01 p0001 N88-10005
NDE (Nondestructive Evaluation) of advanced structural ceramics
[DE87-014417] 03 p0292 N88-11832
Performance evaluation of a half-wave resonant slot antenna over perfect ground using NEC (Numerical Electromagnetic Code)
[AD-A184004] 03 p0308 N88-11942
Potential for on-orbit manufacture of large space structures using the pultrusion process
[NASA-TM-4016] 05 p0557 N88-13388
Distortional buckling formulae for thin-walled channel columns
[PB87-124012] 06 p0722 N88-14437
Geometric nonlinear analysis of asymmetric thin-walled members
[PB87-133856] 06 p0723 N88-14446
Chromic acid anodizing of aluminum foil
[NASA-CR-178417] 07 p0837 N88-15077
Fastening high resistance bolts in real assemblies
[CRIF-MT-171] 07 p0861 N88-15221
High-resolution Real-Time Radiography (RTR) system design
[AD-A187107] 09 p1166 N88-16992
Laboratory studies related to in-flight acoustic emission monitoring
[AD-A186714] 09 p1242 N88-17445
Environment assisted degradation mechanisms in aluminum-lithium alloys
[NASA-CR-182482] 10 p1301 N88-17782
Modern materials for light constructions --- aircraft
[MBB-Z-136/86] 10 p1312 N88-17839
Dynamic response of some structural elements fabricated from a non-linear elastic material
10 p1344 N88-18031
Optimum design of geodesically stiffened composite plates
[NASA-CR-182499] 10 p1344 N88-18035
Characterization of damped structural connections for multi-component systems
[NASA-TM-100801] 11 p1502 N88-18974
The place for thermoplastic composites in structural components
[AD-A189149] 12 p1604 N88-19596
A study of damage tolerance in curved composite panels
[AD-A190617] 15 p2029 N88-22092
Characterization of structural connections for multicomponent systems 16 p2220 N88-23251
Experimental and theoretical investigation of passive damping concepts for member forced and free vibration
[NASA-CR-183082] 20 p2814 N88-26693
Critical issues and directions for fracture mechanics and structural integrity
[AD-A193050] 21 p2960 N88-27584
Application of differential quadrature to the analysis of structural components 22 p3087 N88-28331
Dynamics of articulated aerospace structures
[AD-A195685] 24 p3324 N88-29794

STRUCTURAL PROPERTIES (GEOLOGY)
Interseismic deformation for normal fault earthquakes
03 p0349 N88-12207
Studies in Aeolian geology
[NASA-CR-182328] 05 p0625 N88-13828
Petrogenesis of basalts from the Archean Matachewan Dike Swarm Superior Province of Canada
06 p0796 N88-14875
New data on structure of earth's crust and seismicity of basins in Atlantic and Indian Oceans
08 p1010 N88-16123
Statistics of two-dimensional structure elements of mountainous ranges (mosaic model) for calculating three-dimensional reflection functions
[DFVLR-FB-87-33] 09 p1185 N88-17099
Character of five selected LANDSAT lineaments in southwestern Pennsylvania: Report of investigations, 1987
[PB88-133517] 11 p1505 N88-18989
New data on the formation conditions and age of the Kamensk and Gusev astroblemes
[NASA-TT-20212] 11 p1513 N88-19040
Synthesis of finite displacements and displacements in continental margins
[NASA-CR-1826[illegible]] 12 p1642 N88-19832
Geophysical study of the structure and processes of the continental convergence zones: Alpine-Himalayan Belt
[NASA-CR-182647] 12 p1644 N88-19842
Martian geomorphology and its relation to subsurface volatiles
[NASA-CR-182428] 12 p1711 N88-20237
Relationship between oceanic geological formations and tectonic structures 13 p1785 N88-20883
Bilateral symmetry elements of the Zhamanshin impact crater
[NASA-TT-20288] 15 p2096 N88-22490
A three-dimensional gravity model of the geologic structure of Long Valley caldera
[DE88-006331] 16 p2231 N88-23324
Subsurface morphology and geoarchaeology revealed by spaceborne and airborne radar
17 p2353 N88-24022
An integrated study of the Alto Paranaiba Kimberlite Province, Minas Gerais, Brazil: A possible tool for diamond exploration 17 p2355 N88-24031
Landuse and landform studies of the Mahanadi River Delta with the help of satellite MSS band
17 p2355 N88-24033
Remote sensing and structural rupture: Application examples in the study of tectonics
17 p2359 N88-24050
Analysis and interpretation of image lithostructure: An application of the multiconcept in the metamorphic belt of Sul de Santana da Boa Vista (RS)
17 p2359 N88-24051
Dune fields in central Western Argentina
17 p2366 N88-24088
The breaked anticlines, cuesta and crest homoclines, ortoclinal valleys, and other forms of relief outcrops delineated with the help of remote sensing imagery
17 p2366 N88-24089
Some geological aspects of the Pirapemas Lineament Belt 17 p2368 N88-24099
Lithostructural interpretation of Chapda do Cachimbo (Pa-Am-Mt), based on radar and LANDSAT imagery
17 p2368 N88-24100
A sedimentological and mineralogical study of the Koogah Formation, New South Wales
18 p2542 N88-25087
Use of remote sensing in the study of superficial formation certifying the development of integrated economy-case example: Rio Claro (SP) region
19 p2683 N88-25850
Stochastic geologic effects on near-field ground motions in alluvium
[AD-A192315] 21 p2972 N88-27652
Structural analysis of the Jura mountains-Rhine Graben intersection (Switzerland) for petroleum exploration using SPOT stereoscopic data 22 p3103 N88-28431
Analyzing the stratigraphy, tectonism, and mineralization at the Spanish side of the pyrite belt, Huelva province, Spain, using SPOT imagery 22 p3104 N88-28433
Geologic applications of SPOT-1, TM, and NOAA-7 data: Finding and defining unmapped structural features
22 p3104 N88-28434
Comparing different images for ground water survey based on lineament analysis 22 p3104 N88-28435
The Martian sedimentary record
23 p3302 N88-29660
Photogeological inferences of Martian surface composition 23 p3303 N88-29675
Some probable characteristics of the Martian regolith
23 p3303 N88-29679
Surface units on Mars: The assemblage in the Valles Marineris 23 p3304 N88-29680
Stratigraphy of the Kasei Valles region, Mars
23 p3305 N88-29690

Diapirs of the Mediterranean ridge: The tectonic regime of an incipient accreted terrane
24 p3396 N88-30224

The tectonic setting of the Seychelles, Mascarene and Amirante Plateaus in the Western Equatorial Indian Ocean 24 p3396 N88-30225

Ridge-trench collision in Archean and Post-Archean crustal growth: Evidence from southern Chile
24 p3397 N88-30233

Reappraisal of the geology of Kangimut Sammisoq, Ameralik Fjord, Southern West Greenland: Crustal structure and interpretation of isotopic data
24 p3398 N88-30234

Archean crustal evolution of the northern North China Craton 24 p3398 N88-30235

Evolution of the Dharwar Craton: A terrain of early Archean crustal stability, long term orogenic cycles and large scale palaeobiological activity
24 p3399 N88-30241

Spectral analysis of the Elatina varve series
[NASA-CR-183085] 24 p3402 N88-30260

Debris flows of the Simud-Tiu outflow system of Mars
24 p3442 N88-30485

High-resolution (30 m) lunar radar images
24 p3442 N88-30486

Mars: Volcanism in the Valles Marineris overlooked
24 p3443 N88-30491

The Martian highland paterae: Evidence for explosive volcanism on Mars 24 p3443 N88-30492

Physical properties of surface materials on Martian volcanoes: Dust-covered lava and ash
24 p3443 N88-30493

Rifts of deeply eroded Hawaiian basaltic shields: A structural analog for large Martian volcanoes
24 p3443 N88-30494

Small-scale volcanic landforms indicative of distributary tube systems 24 p3444 N88-30496

STRUCTURAL RELIABILITY

Ensuring the service life of designs (experience in aircraft construction) 02 p0157 N88-10986

A reliability concept for optimizing aircraft design
04 p0423 N88-12622

The strength of hybrid composites
[BR101991] 09 p1138 N88-16821

Integrity control of carbon fiber reinforced plastics (CFRP) structural elements. Conclusion with respect to the control methodology of CFRP primary structures in manned space flight and the implications to the design, analysis and testing of CFRP structural elements, executive summary
[MBB-TR-RB517-014/85] 09 p1139 N88-16824

The Shock and Vibration Bulletin. Part 4: Structural Dynamics and Modal Test and Analysis
[AD-A186751] 09 p1179 N88-17062

Reliability of structures with stiffness and strength degradation 09 p1180 N88-17068

Micro PAVER concept and development airport pavement management system
[AD-A187360] 11 p1441 N88-18598

Structural integrity of metallic armature rail guns
[AD-A186735] 13 p1728 N88-20333

Crack opening and extension in inert solid propellant. An experimental study
[AD-A189808] 15 p2048 N88-22201

Applicability and limitations of probability models in connection with the reliability of large-scale technical installations
[W-3/87] 16 p2261 N88-23520

Critical issues and directions for fracture mechanics and structural integrity
[AD-A193050] 21 p2960 N88-27584

Computation of failure probability of fatigue loaded cracked structures
[ETN-88-92360] 21 p2964 N88-27607

Durability of continuous fiber reinforced metal matrix composites
[AD-A193868] 22 p3050 N88-28097

Automated early fatigue damage sensing system
[AD-A195717] 24 p3382 N88-30143

STRUCTURAL RIGIDITY
U STRUCTURAL STABILITY

STRUCTURAL STABILITY
NT SHELL STABILITY

Models of degradation of stratified composite structures
[ONERA-RT-13/3542-RY-061-R]
02 p0142 N88-10892

Stability of mechanical joints in launching vehicles: Local and global stationary values of energy density
03 p0270 N88-11696

Vibration and buckling of geometrically imperfect laminated cylindrical shells 04 p0456 N88-12922

Three-dimensional structure of boundary layers in transition to turbulence
[AD-A185486] 06 p0702 N88-14311

Flow in labyrinth seals and its influence on rotor stability of turbocompressors 07 p0851 N88-15168

Analysis of reinforced concrete structures under the effects of localized detonations
09 p1179 N88-17064

Reinforced concrete arches under blast and shock environments 09 p1180 N88-17065

Investigations of the stability of the cell opening of soft polyurethane foams
[ETN-88-91481] 11 p1463 N88-18724

Vibrations of structures with parametric uncertainties
[AD-A190400] 15 p2076 N88-22378

Rigidity and smoothness of motion
[AD-A190555] 15 p2128 N88-22694

A thermally modified polymer matrix composite material with structural integrity to 371 C
[NASA-TM-100922] 19 p2609 N88-25483

Structure and refinement of ordered aromatic heterocyclic polymers by diffraction methods: Application of results to electro-optic phenomena
[AD-A191859] 19 p2619 N88-25537

Stability control of leakage flow channels
[DE88-009995] 23 p3210 N88-29107

STRUCTURAL STRAIN

Stresses and displacements in two, three and four layered structures submitted to flexible or rigid loads
[AD-A185707] 06 p0723 N88-14450

Predicted and measured strain responses of isotropic panels to base excitation
[NASA-TM-4054] 19 p2679 N88-25928

STRUCTURAL VIBRATION
NT BENDING VIBRATION
NT FLUTTER
NT LINEAR VIBRATION
NT SELF INDUCED VIBRATION
NT SUPERSONIC FLUTTER
NT TRANSONIC FLUTTER

Test of the Hipparcos payload in the Liege vacuum facility focal 02 p0135 N88-10850

Active control of helicopter vibration using multiloop self-adaptive control 03 p0264 N88-11660

Controlling the dynamic environment during NOE flight
03 p0264 N88-11661

Minimisation of helicopter vibration through active control of structural response 03 p0264 N88-11662

Identification of perturbations in turbomachines by the analysis of pressure signals, vibrations and wavelike motions
[ETN-88-90602] 05 p0590 N88-13600

The 58th Shock and Vibration Symposium, volume 1
[NASA-CP-2488-VOL-1] 05 p0592 N88-13609

The analysis of nonstationary vibration data
05 p0592 N88-13610

Simultaneous structural and control optimization via linear quadratic regulator eigenstructure assignment
05 p0594 N88-13622

Viscous damped space structure for reduced jitter
05 p0594 N88-13623

On the glitches in the force transmitted by an electrodynamic exciter to a structure
05 p0594 N88-13624

Fluid mass and thermal loading effects on the modal characteristics of space shuttle main engine liquid oxygen inlet splitter vanes 05 p0594 N88-13628

Incipient failure detection of space shuttle main engine turbopump bearings using vibration envelope detection
05 p0595 N88-13629

Space shuttle main engine vibration data base
05 p0595 N88-13631

Optimal shock isolation with minimum settling time
05 p0595 N88-13633

A passive vibration-cancelling isolation mount
05 p0595 N88-13636

Advanced joining concepts for passive vibration control 05 p0596 N88-13638

Dynamic response of laminated composite plates using a three-dimensional hybrid-stress finite-element formulation 05 p0596 N88-13639

Studies on fluid-structural vibration using boundary element method
[PB87-129508] 06 p0699 N88-14291

Flow in Centrifugal Compressors — conference
[VKI-LS-1987-01] 07 p0850 N88-15160

Blade vibration due to different flow excitation
07 p0851 N88-15166

Blade excitation due to unsteady flow phenomena
07 p0851 N88-15167

Data acquisition, reduction and analysis of shock and vibration testing using a super microcomputer
[AD-A186123] 07 p0867 N88-15260

Parametric and experimental analysis using a power flow approach
[NASA-CR-182460] 09 p1116 N88-16693

Mechanical in-flight environment of Ariane payloads
09 p1126 N88-16748

A review of two-phase flow-induced vibration
[DE88-001855] 09 p1160 N88-16955

The Shock and Vibration Bulletin. Part 4: Structural Dynamics and Modal Test and Analysis
[AD-A186751] 09 p1179 N88-17062

Optimized structure design using reanalysis techniques 09 p1180 N88-17067

Reliability of structures with stiffness and strength degradation 09 p1180 N88-17068

A new look at the use of linear methods to predict aircraft dynamic response to taxi over bomb damaged and repaired airfields 09 p1180 N88-17069

Frequency response functions of a nonlinear system
09 p1180 N88-17070

System characterization in nonlinear random vibration
09 p1180 N88-17071

A review of flow-induced vibration in two-phase flow
[DE88-002873] 10 p1329 N88-17946

Strategic placement of accelerometers to measure forces by the sum of weighted accelerations
[DE88-002262] 10 p1333 N88-17968

Dynamic response of some structural elements fabricated from a non-linear elastic material
10 p1344 N88-18031

The 58th Shock and Vibration Symposium, volume 2
[NASA-CP-2488-VOL-2] 11 p1499 N88-18948

Overview of multi-input frequency domain modal testing methods with an emphasis on sine testing
11 p1499 N88-18949

Spacecraft redesign to reduce microphonic response of a VCO component 11 p1499 N88-18955

Electro-mechanical vibratory system
11 p1500 N88-18958

The Shock and Vibration Digest, volume 20, no. 3
12 p1635 N88-19786

Wave propagation and dynamics of lattice structures
[AD-A190037] 15 p2025 N88-22066

Wave propagation and dynamics of lattice structures
[AD-A190611] 15 p2025 N88-22069

Stabilization and control problems in structural dynamics
[AD-A190197] 15 p2073 N88-22361

Instrumentation to provide an active control capability for distributed parameter systems
[AD-A190043] 15 p2076 N88-22375

Vibrations of structures with parametric uncertainties
[AD-A190400] 15 p2076 N88-22378

Vibration control of large structures
[AD-A191358] 16 p2168 N88-22928

Lewis Structures Technology, 1988. Volume 1: Structural Dynamics
[NASA-CP-3003-VOL-1] 16 p2217 N88-23226

Piezoelectric pushers for active vibration control of rotating machinery 16 p2218 N88-23229

Structural acoustics design manual
[ESA-PSS-03-1201-ISSUE-1] 17 p2311 N88-23821

Vibration testing of ACT fuselage
19 p2634 N88-25627

Predicted and measured strain responses of isotropic panels to base excitation
[NASA-TM-4054] 19 p2679 N88-25928

Modeling and parameter identification of motor vehicles 20 p2785 N88-26521

Vibration control of large structures
[AD-A193317] 21 p2961 N88-27587

Coupled thermal vibrations of beams with temperature-dependent properties
21 p2963 N88-27601

Laboratory feasibility study of a composite embedded fiber optic sensor for measurement of structural vibrations
[AD-A194270] 22 p3152 N88-28754

Nonlinear vibrations of imperfect thin walled cylindrical shells
[ETN-88-92904] 23 p3227 N88-29205

ASKA-acoustics: Theory and applications — vibro acoustics
[FFA-TN-1988-13] 23 p3279 N88-29519

STRUCTURAL WEIGHT

Assessment of energy storage concepts for use in sprint power 17 p2407 N88-24312

RSMASS: A simple model for estimating reactor/shield masses 17 p2414 N88-24355

A generalized method for optimizing the mass of space power systems 17 p2416 N88-24369

STRUCTURES

Comparison of measured temperatures, thermal stresses and creep residues with predictions on a built-up titanium structure
[NASA-TM-88814] 03 p0337 N88-12125

NFBS: A three-dimensional, air-dynamics computer code for analyzing explosions in structures
[DE88-005085] 10 p1331 N88-17953

Engine structures: A bibliography of Lewis Research Center's research for 1980-1987
[NASA-TM-100842] 17 p2350 N88-24002

STRUTS
Effect of a model support strut on measurement of aerodynamic longitudinal and lateral coefficients
[PB87-170288] 09 p1113 N88-16670
Preliminary investigation of stability of a fin-stiffened slender strut
[NASA-TM-4034] 12 p1599 N88-19568
An investigation of classical dynamic scaling techniques applied to an oleo-pneumatic landing gear strut
[AD-A187664] 13 p1721 N88-20292
The X-beam as a deployable boom for the space station 14 p1925 N88-21473
Duct flow nonuniformities: Effect of struts in SSME HGM II(+)
[NASA-CR-179285] 15 p2062 N88-22296
Test of an 0.8-scale model of the AH-64 Apache in the NASA Langley full-scale wind tunnel
[AD-A196129] 24 p3319 N88-29768
STS
U SPACE TRANSPORTATION SYSTEM
STS-4
U SPACE TRANSPORTATION SYSTEM 4 FLIGHT
STS-5
U SPACE SHUTTLE MISSION 31-A
STS-6
U SPACE SHUTTLE MISSION 31-B
STS-13
U SPACE SHUTTLE MISSION 41-C
STS-31
U SPACE SHUTTLE MISSION 61-B
STS-33
U SPACE SHUTTLE MISSION 51-L
STUDENTS
Field evaluation of interactive simulation for maintenance training: SH-3 helicopter electro-mechanical bladefold system
[AD-A185923] 07 p0821 N88-14991
The sine and cosine function for class 4-VWO. Exploration of possible bottlenecks
[REPT-87-72] 20 p2881 N88-27105
Computer-aided decision making
[AD-A194210] 22 p3137 N88-28651
STUDIES
U INVESTIGATION
STURM-LIOUVILLE OPERATOR
U STURM-LIOUVILLE THEORY
STURM-LIOUVILLE THEORY
Discontinuous inverse Sturm-Liouville problems with symmetric potentials
[DE88-009803] 19 p2720 N88-26152
STYRENES
NT POLYSTYRENE
SUBARCTIC REGIONS
North Pacific Ocean. Subarctic front central Pacific, R/V Thomas G. Thompson: 8 September - 9 October 1975. CTD data report
[AD-A186567] 08 p1044 N88-16312
North Pacific Ocean. Northwest Pacific Transition Zone, R/V Thomas G. Thompson: 19 March - 1 May 1971. STD data report
[AD-A186568] 08 p1044 N88-16313
North Pacific Ocean. Gulf of Alaska, R/V Thomas G. Thompson: 1 February - 8 March 1967. STD data report
[AD-A186569] 08 p1045 N88-16314
North Pacific Ocean. Central Pacific Transition Zone, R/V Thomas G. Thompson: 25 March - 3 May 1968. STD data report
[AD-A186570] 09 p1195 N88-17160
SUBASSEMBLIES
Components for measuring robots
[KFK-PFT-126] 03 p0332 N88-12092
SUBCARRIER WAVES
U CARRIER WAVES
SUBCIRCUITS
U CIRCUITS
U SUBASSEMBLIES
SUBDIVISIONS
Taper sectioning to magnify the interface thickness of a dissimilar metal joint
[RFP-3890-REV] 03 p0333 N88-12099
An adaptive subdivision method with crack prevention for rendering beta-spline objects
[AD-A184249] 04 p0477 N88-12940
SUBDUCTION (GEOLOGY)
Relationship between oceanic geological formations and tectonic structures 13 p1785 N88-20683
Recycling of lower continental crust through foundering of cumulates from contaminated mafic intrusions
24 p3393 N88-30204
Pluton emplacement and magmatic arc construction: A model from the Patagonian batholith
24 p3393 N88-30206
An illustration of the complexity of continent formation
24 p3393 N88-30207
Does subduction zone magmatism produce average continental crust 24 p3394 N88-30214
Decoupled Rb-Sr and Sm-Nd isotopic evolution of the continental crust 24 p3395 N88-30216
Continental crustal formation and recycling: Evidence from oceanic basalts 24 p3398 N88-30238
Continental growth through time by underplating of subducted oceanic crust: Evidence from kimberlites in South Africa and SW Pacific 24 p3399 N88-30244
SUBGIANT STARS
Infrared excesses of barium stars
04 p0516 N88-13174
SUBGRAVITY
U REDUCED GRAVITY
SUBHARMONIC GENERATORS
Secondary subharmonic instability of boundary layers with pressure gradient and suction
[NASA-CR-4112] 07 p0848 N88-15148
SUBLATTICES
U LATTICES (MATHEMATICS)
SUBLAYERS
U SUBSTRATES
SUBLIMATION
Sublimation characteristics of H2O comet nucleus with CO2 impurities 14 p2010 N88-21968
The evolution of cometary activity
18 p2594 N88-25416
SUBLIMINAL STIMULI
Two attentional models of classical conditioning: Variations in CS effectiveness revisited
[AD-A187697] 11 p1522 N88-19088
SUBMARINES
Experimental studies on the tripping behavior of narrow T-stiffened flat plates subjected to hydrostatic pressure and underwater shock 05 p0592 N88-13613
Interaction of a vortex pair with a free surface
[AD-A186619] 08 p0988 N88-15988
A pyrotechnic delay ignition system for a submarine launched marine signal
[MRL-R-1079] 13 p1754 N88-20487
Experiments to investigate the vortices shed from a submarine-like body of revolution
16 p2205 N88-23156
Revised Impact Dynamic Design-Analysis Method (RIDDAM)
[AD-A190479] 16 p2217 N88-23225
Ergonomy and interior furnishing of the cabins of deep diving manned submarines: The Nautile example --- couch 19 p2697 N88-26032
The SAGA highly autonomous assistance submarine
19 p2698 N88-26034
Reducing risks inherent in operating underwater craft: The contribution of classification, the example of the SAGA highly autonomous support submarine
19 p2699 N88-26042
ELIT: An autonomous underwater observation robot
19 p2699 N88-26048
Tripping of stiffened plates using a refined beam theory
[AD-A193989] 22 p3087 N88-28333
Numerical field model simulation of full scale fire tests in a closed spherical/cylindrical vessel
[AD-A195067] 24 p3359 N88-29996
Response of SMA (Shielded Metal Arc) and narrow gap HY80 weldments to explosive shock loading
[AD-A195994] 24 p3385 N88-30162
SUBMERGED BODIES
NT DIVING (UNDERWATER)
Breaking wave forces on vertical cylinders
[RR-CE71] 03 p0338 N88-12126
Validation of the Underwater Shock Analysis (USA) program. Part 1: Theoretical considerations — ship design
[REPT-5073713-86-01] 06 p0702 N88-14308
Retarded potential technique applied for shock wave loading of doubly symmetric submerged structures
09 p1179 N88-17058
The use of a water towing tank for aerodynamic testing and methods for quantitative evaluation of photographs
16 p2202 N88-23140
Computer aided remote control: A general concept for intervention in the nuclear, underwater, and space domains 19 p2699 N88-26046
Marine techniques: R and D axes, identification of areas of common interest with space techniques
19 p2699 N88-26047
Underwater robotics in the service of oil field exploitation: The Running and Interconnecting Tool (RIT) in the East Frigg field (North Sea) 19 p2699 N88-26049
SUBMERGING
Natural convection immersion cooling of an array of simulated chips in an enclosure filled with dielectric liquid
[AD-A193594] 23 p3207 N88-29088
Alternative immersion accelerated testing of coating systems for Naval shoreline facilities
24 p3355 N88-29977
SUBMILLIMETER WAVES
High repetition rate electron beam RF-acceleration and sub-millimeter wave generation via a free electron laser
[AD-A186066] 07 p0858 N88-15209
Holes in OI 130 nm emission fields of upper atmosphere during day 08 p1004 N88-16082
PRONAOS: A submillimeter facility --- astronomical balloon 08 p1032 N88-16256
Quantum limits of superconducting heterodyne receivers
[AD-A188014] 11 p1478 N88-18817
Millimeter and submillimeter wave research: Spectroscopy, energy transfer, and techniques
[AD-A188952] 12 p1620 N88-19601
An attempt to measure the diffuse brightness of the sky at submillimeter wavelengths
12 p1710 N88-20233
Development and applications of optical interferometric micrometrology in the angstrom and subangstrom range
[NASA-TM-100299] 16 p2211 N88-23196
Heterodyne spectrometer for the very high frequency range between 300 and 3000 GHz (1 mm to 0.1 mm) using a mixer in open structure
16 p2271 N88-23589
Telescope illumination and beam measurements for submillimeter astronomy
[MPE-PREPRINT-88] 16 p2288 N88-23699
The galactic nucleus at mm-, sub-mm and far-infrared wavelengths
[MPE-PREPRINT-102] 16 p2288 N88-23700
Balloon-borne three-meter telescope for far-infrared and submillimeter astronomy
[NASA-CR-182924] 17 p2449 N88-24550
Millimeter and submillimeter waves and frequency selective surfaces
[AD-A191511] 18 p2500 N88-24827
Apparatus for submillimeter laser diagnostics of high-temperature plasma
[DE88-702464] 23 p3285 N88-29563
A submillimeter wavelength space-based imaging radar
[AD-A195846] 24 p3364 N88-30033
The study of hydromagnetic waves and RF heating using the TORTUS tokamak, the development of diagnostic techniques based on submillimeter lasers and the gyrotron, and gas discharge 24 p3431 N88-30419
SUBMINIATURIZATION
Development of subminiature multi-sensor hot-wire probes
[NASA-TM-100052] 15 p2069 N88-22336
SUBROUTINE LIBRARIES (COMPUTERS)
The SUPRENUM communications subroutine library for grid-oriented problems
[DE88-000137] 04 p0479 N88-12950
A new library of CAMAC routines for the control of the system CRATE by a microVAX in the VAXELN environment
[NOTA-INTERNA-893] 06 p0761 N88-14667
Implementation of elementary functions in Ada
[CWI-NM-R8709] 09 p1218 N88-17300
Contributions to a numerical library in Ada
[NPL-DITC-98/87] 09 p1219 N88-17309
FORTRAN 77 error handling of the RASP library
[DFVLR-MITT-87-14] 14 p1957 N88-21669
The NPL data approximation subroutine library: Current and planned facilities
[NPL-DITC-104/87] 14 p1959 N88-21681
Ada user library
[FOA-C-20657-2.7] 16 p2246 N88-23418
Proposal for standard mathematical packages in Ada
[CWI-NM-R8718] 16 p2249 N88-23439
PLOT300: A Tektronics PLOT10 emulator for HP 9000 series 200/300 computers
[NASA-TM-100606] 16 p2250 N88-23447
TRANSL: A PATRAN translator subroutine library
[DE88-010976] 21 p2998 N88-27784
SUBROUTINES
Using MINOS (Modular In-core Nonlinear Optimization System) as a subroutine for decomposition
[DE87-013086] 02 p0221 N88-11390
The circular serial autocorrelation computer program
[AD-A184795] 03 p0365 N88-12295
MODTRAN: A moderate resolution model for LOWTRAN
[AD-A185384] 05 p0574 N88-13503
Mixing Microsoft C and Microsoft FORTRAN program modules on the IBM Personal Computer
[DE88-001947] 05 p0637 N88-13695
Rationale for the design of the Ada (tradename) programming language
[AD-A187106] 09 p1217 N88-17297
Wave group analysis based on Kimura's method
[AD-A187610] 11 p1516 N88-19055
Subroutines for solving the equation of diffusion in media with anisotropic properties
[DE88-700743] 11 p1536 N88-19179

Design of an aeroelastic composite wing wind tunnel model
[AD-A188855] 12 p1582 N88-19466
BLITZ: Blitzen's micron-code assembly language design document, version 1.0
[TR88-14] 12 p1676 N88-20019
Computer programs for calculating group cross-section covariances from uncertainty parameters in the ENDF/B-V format. UNC 32/33 — neutron physics
[ECN-202] 13 p1837 N88-20995
Finite area combustor theoretical rocket performance
[NASA-TM-100785] 14 p1883 N88-21252
Expressing mathematical subroutines constructively
[AD-A190559] 15 p2121 N88-22644
CIMAG2: The computer program to generate color images
[AD-A191847] 18 p2557 N88-25175
Photocurrent modeling of modern microcircuit PN junctions
[DE88-007037] 19 p2662 N88-25832
Effective communication between a microVAX and a specialized high-speed subprocessor
[DE88-007957] 19 p2714 N88-26115
Using IMSL mathematical and statistical computer subroutines in physiological and biomechanical research
[AD-A192594] 21 p2995 N88-27765

SUBSETS (MATHEMATICS)
U SET THEORY

SUBSONIC FLOW
Three-dimensional calculation in high subsonic axial compressor rotor and its comparison with L2F velocity measurement 03 p0300 N88-11886
Solution of the two-dimensional Euler equations on unstructured triangular meshes
04 p0396 N88-12469
Wakes of two dimensional bluff bodies in subsonic flow. Influence of a separating plate and of a pulsed injection of momentum
[IMFL-4200-86/75] 05 p0541 N88-13297
A numerical model of unsteady, subsonic aeroelastic behavior
[NASA-TM-100487] 06 p0663 N88-14064
A direct calculation method for perturbation fields of moving bodies in compressible media at subsonic Mach numbers
[ETN-88-90609] 06 p0701 N88-14305
Boundary layer transition 07 p0811 N88-14942
Experimental investigation of the subsonic high-altitude operation of the NASA Lewis 10- by 10-foot supersonic wind tunnel
[NASA-TM-100214] 08 p0959 N88-15814
Navier-Stokes computations for circulation control airfoils 10 p1269 N88-17592
A numerical study of unsteady two-dimensional subsonic compressible base flow 10 p1327 N88-17931
Conditions at infinity for theories of oscillating wings and propellers in subsonic flow
[NAL-TR-937] 11 p1434 N88-18556
A discretization of the integral equation for the time dependent linearized subsonic potential flow over a wing
[AD-A188534] 12 p1574 N88-19411
Numerical simulation of subsonic and transonic propeller flow
[NASA-TM-100163] 13 p1716 N88-20262
ARSPNSC: A method to calculate subsonic steady and unsteady potential flow about complex configurations
[NLR-TR-86122-U] 13 p1717 N88-20265
Finite element calculations for aerodynamic coefficients of a 3-dimensional body in subsonic flow using Green's function method
[NASA-TT-20208] 13 p1718 N88-20272
Effect of flow convergence on turbulence level in stream 14 p1973 N88-21773
Study of the boundary layer of a flow pulsed by acoustic waves
[ETN-88-91998] 16 p2206 N88-23163
Numerical simulations of the flat-plate laminar boundary layer in subsonic and supersonic flow
[PDR/CFDU/IC/36] 18 p2511 N88-24495
Influence of rear body geometry on the velocity characteristics of the near wake
[ISL-R-113/87] 20 p2753 N88-26339
Three-dimensional viscous flow computations of a circular jet in subsonic and supersonic cross flow
[NASA-CR-182153] 20 p2800 N88-26616
Navier-Stokes calculations of transonic flows past cavities
[NASA-CR-180484] 23 p3212 N88-29116

SUBSONIC SPEED
Aerodynamic sensitivities from subsonic, sonic and supersonic unsteady, nonplanar lifting-surface theory
[NASA-TM-100502] 04 p0394 N88-12459
Effects of winglets on a first-generation jet transport wing. 7: Sideslip effects on winglet loads and selected wing loads at subsonic speeds for a full-span model
[NASA-TP-2619] 11 p1436 N88-18567
Preliminary measurements of heat flux in a subsonic gun simulator
[AD-A191090] 16 p2208 N88-23178
Integrated Application of Active Controls (IAAC) technology to an advanced subsonic transport project: Program review
[NASA-CR-3880] 17 p2301 N88-23763
Theoretical-numerical study of feasibility of use of winglets on low aspect ration wings at subsonic and transonic Mach numbers at reduce drag
[NASA-CR-4174] 21 p2892 N88-27168
Pressure distributions from subsonic tests of an advanced laminar-flow-control wing with leading- and trailing-edge flaps
[NASA-TM-4040-PT-2] 24 p3321 N88-29776

SUBSONIC WIND TUNNELS
The vertical test section (VMK) of DFVLR in Cologne-Porz, Federal Republic of Germany (status 1986)
[ESA-TT-1053] 03 p0267 N88-11682
Effect of flow convergence on turbulence level in stream 14 p1973 N88-21773
A comparative study of vortex flows in wind and water tunnels 16 p2204 N88-23151

SUBSTITUTES
Concept and analysis of a direct-injection alcohol layer charge motor
[ETN-88-91482] 11 p1495 N88-18925
Solution of the Lloyd-Max quantizer parameters by the method of successive substitution
[AD-A187829] 11 p1540 N88-19207

SUBSTITUTION
U SUBSTITUTES

SUBSTRATES
Laser chemically vapor deposited silicon-carbide: Growth features, topography, microstructure, and composition
[DE87-013767] 01 p0029 N88-10184
The water permeability of multi-layer coatings
[BLL-M-37252-(5828.4)] 02 p0148 N88-10927
Epitaxial reactor development for growth of silicon-on-insulator devices
[AD-A184758] 03 p0382 N88-12[illegible]39
Effectiveness of electrodeposited coatings in reducing atmospheric corrosion of copper substrates
[DE87-013651] 05 p0566 N88-13448
Water disbondment characterization of organic Coating/metal substrate systems
[AD-A184847] 05 p0567 N88-13454
Reactive sticking coefficients of silane on silicon
[DE88-000601] 05 p0570 N88-13473
Raman microprobe characterization of dielectric films following high-energy pulsed laser irradiation
[DE88-000559] 05 p0588 N88-13587
Tribology of thin film systems
[ETN-88-91365] 05 p0590 N88-13601
Effects of hydrolysis on metallo-organic solution deposition of PZT films
[ATR-86(8443)-1] 06 p0679 N88-14180
Investigation of silicon surface passivation by silicon nitride film deposition
[NASA-CR-182350] 06 p0729 N88-14487
Coverage dependence of adsorbate-substrate bond lengths: Chlorine and caesium adsorbed on silver single crystals
[PB87-125142] 06 p0788 N88-14833
Monolayer films prepared by the spontaneous self-assembly of symmetrical and unsymmetrical dialkyl sulfides from solution onto gold substrates: Structure, properties, and reactivity of constituent functional groups
[AD-A186717] 09 p1137 N88-16814
Adhesion of vapour phase deposited ultra-thin polyimide films on polycrystalline silver
[AD-A187930] 10 p1306 N88-17810
The soft/hard wet anodization of aluminum oxide and its use in a thin film multilayered capacitor
[AD-A187575] 10 p1325 N88-17919
Interactions of cultured human endothelial cells with polymeric surfaces
[PB88-112255] 10 p1369 N88-18178
The deposition rate dependence of plasma polymerization on the radius of curvature of the substrate
[DE88-003811] 10 p1412 N88-18429
Optical characterization of GaAs/sub 1-x/Sb/sub x/ and GaAs/sub 1-x/Sb/sub x/GaAs strained layer superlattices
[DE88-003393] 10 p1418 N88-18464
Adhesion of PVD titanium coatings to beryllium substrates
[DE88-005147] 11 p1483 N88-18721
Surface mediated photocatalysis
[AD-A188882] 12 p1603 N88-19589
Preparation and characterization of thin films of alumina by metalorganic chemical vapor deposition
[AD-A188386] 12 p1608 N88-19614
Research on mercury cadmium telluride
[AD-A189155] 13 p1845 N88-21039
X-ray diffraction study of a thin GaAs film on Si(100)
[DE88-005290] 13 p1847 N88-21055
Vapor phase deposition and growth of polyimide films on copper
[AD-A189969] 15 p2044 N88-22178
Laser evaporation studies
[AD-A189815] 15 p2071 N88-22346
Processing defects and strength of alumina substrates
[W-10/87] 15 p2087 N88-22441
High-efficiency thin-film silicon-on-GaP solar cell for improved radiation resistance
[AD-A190268] 15 p2091 N88-22460
RF properties of superconducting Pb electroplated onto Cu
[DE88-005918] 15 p2139 N88-22765
A model for nitrogen atom recombination on a silicon dioxide surface
[AD-A189843] 15 p2142 N88-22784
Equilibrium stability of strained epitaxial layers on a rigid substrate
[INPE-4254-PRE/1127] 15 p2145 N88-22804
Synthesis and characterization of high-T(sub c) screen-printed Y-Ba-Cu-O films on alumina
[NASA-TM-100860] 15 p2146 N88-22805
Surface enhanced Raman scattering applied to surface chemical kinetics
[AD-A191275] 16 p2176 N88-22969
Monolithic integration on a GaAs substrate of a quarter ring laser and an optical guide coupled by an evanescent wave
[ETN-88-92308] 17 p2344 N88-23969
On the use of convergent beam electron diffraction for identification of antiphase boundaries in GaAs grown on Si
[DE88-008220] 18 p2585 N88-25362
JPRS report: Science and technology. Japan
[JPRS-JST-88-005] 19 p2633 N88-25619
Ceramic substrates for semiconductor applications reported: AlN substrates 19 p2633 N88-25621
AlN substrate applications 19 p2634 N88-25622
Plasma deposition: Investigations on a new approach
[ETN-88-92619] 20 p2861 N88-26092
MBE growth of HgTe/CdTe superlattices on Si(100) substrates 20 p2869 N88-27033
Preparation of high-T(sub)c Y1Ba2Cu3O(sub 7-Delta) superconducting thin films by MBE (Molecular-Beam-Epitaxy) techniques
[DE88-009999] 20 p2877 N88-27082
Improved adhesion for SiO2 particles in silica substrates using helium-ion irradiation
[DE88-008915] 21 p2920 N88-27332
Amorphous silicon solar cells using a metal substrate
[PB88-131941] 21 p2968 N88-27628
Specular steel surfaces for solar mirror substrates
[DE88-001153] 21 p2968 N88-27630
Chemistry of adhesion at the polyimide-metal interface
[AD-A194647] 22 p3058 N88-28143
Low temperature film growth of the oxides of zinc, aluminum and vanadium (and related systems, oxides of gold and germanium, nitrides of aluminum and tungsten) by reactive sputter deposition
[AD-A193497] 23 p3191 N88-28986
Planarization of metal substrates for solar mirrors
[DE88-011492] 23 p3229 N88-29214
Evaluation of organic coating deterioration and substrate corrosion in seawater using electrochemical impedance measurements 24 p3355 N88-29976
Ion exchange processes for fabrication of integrated optical waveguide structures into glass substrates
[VTT-46] 24 p3429 N88-30405

SUBSTRUCTURES
Mechanical strength and niobium and niobium-base alloys substructures
[DE87-703692] 04 p0415 N88-12577
Substructure discovery in executed action sequences
[AD-A186446] 08 p1069 N88-16462
Finite element substructuring methods for composite mechanics
[NASA-TM-100297] 10 p1296 N88-17745
Influence of strain rate on the substructure evolution and yield behavior of Ti-6Al-4V
[DE88-006457] 19 p2616 N88-25520

SUBTROPICAL REGIONS
U TEMPERATE REGIONS
U TROPICAL REGIONS

SUCTION
Investigation of viscous/inviscid interaction in transonic flow over airfoils with suction 06 p0664 N88-14074
Laminar flow control leading edge glove flight test article development
[NASA-CR-172137] 07 p0815 N88-14960
Control of laminar flow around of the wing in free-air conditions
[AD-A187479] 15 p2013 N88-22004

Flow quality of NAL two-dimensional transonic wind tunnel. Part 1: Mach number distributions, flow angularities and preliminary study of side wall boundary layer suction
[NASA-TT-20209] 16 p2165 N88-22911
Operational considerations for laminar flow aircraft
17 p2216 N88-23748
Investigation of viscous/inviscid interaction in transonic flow over airfoils with suction
[NASA-CR-183112] 21 p2945 N88-27490
Method for maintaining precise suction strip porosities
[NASA-CASE-LAR-13638-1] 23 p3201 N88-29051
Experimental and numerical investigation of the effect of distributed suction on oblique shock wave/turbulent boundary layer interaction
[NASA-TM-101334] 24 p3372 N88-30084

SUD AVIATION AIRCRAFT
NT CONCORDE AIRCRAFT

SUDDEN IONOSPHERIC DISTURBANCES
Solar-geophysical data number 513, May 1987. Part 1: (Prompt reports). Data for April, March 1987 and late data
[PB87-204939] 01 p0119 N88-10760
Solar-geophysical data number 515, July 1987. Part 1: (Prompt reports). Data for June 1987, May 1987 and late data
[PB87-233177] 06 p0805 N88-14912
Solar-geophysical data number 517, September 1987. Part 1: (Prompt reports). Data for August, July 1987 and late data
[PB88-128426] 10 p1430 N88-18544
Solar-geophysical data number 520, December 1987. Part 1: (Prompt reports). Data for November 1987, October 1987 and late data
[PB88-164199] 16 p2290 N88-23712
Solar-geophysical data number 521, January 1988. Part 1: (Prompt reports). Data for December 1987, November 1987 and late data
[PB88-179213] 19 p2743 N88-26284

SUDDEN STORM COMMENCEMENTS
A compilation of Sudden Storm Commencements (SSCs), associated interplanetary disturbances, and cosmic ray variations
[IFSI-86-11] 06 p0807 N88-14923
A possible role for ionospheric ions in triggering a geomagnetic substorm onset 08 p1096 N88-16594
National Severe Storms Laboratory, fiscal year 1987
[PB88-140108] 12 p1647 N88-19863

SUGAR CANE
Report on phase 1 of the project estimate development of a model for yield estimation of sugar cane based on LANDSAT and agromet data
[INPE-4486-RPE/560] 12 p1638 N88-19807
CANASATE: Sugar cane mapping by satellite
17 p2358 N88-24046
Spectral behavior of crops through analysis of LANDSAT-TM data 17 p2358 N88-24047
Evaluation of TM false color composites for crop discrimination 17 p2367 N88-24096
Application of interactive graphic system (CAD/CAM) in the determination of process evolution in land use in the Ribeirao Preto municipality 19 p2684 N88-25956

SUGARS
NT GLUCOSE

SUGGESTION
Hypnosis: Possible applications for cosmonauts
12 p1665 N88-19984

SUITS
NT EXTRAVEHICULAR MOBILITY UNITS
NT PRESSURE SUITS
NT SPACE SUITS

SULFATES
Copper electroforming from acid sulfate baths: Preliminary studies
[INPE-4375-RPE/554] 08 p0969 N88-15864
Meteorological aspects of wet deposition in Southern Finland
[FMI-3] 19 p2693 N88-26007
Kinetics of thermochemical gas-solid reactions important in the Venus sulfur cycle
[NASA-CR-182963] 19 p2742 N88-26280

SULFIDATION
Oxidation/sulfidation of materials in an SO3/SO2/O2 thermochemical-transport, distributed-receiver, solar-energy system
[DE88-005875] 13 p1795 N88-20739

SULFIDES
NT BISMUTH SULFIDES
NT CADMIUM SULFIDES
NT COPPER SULFIDES
NT DISULFIDES
NT HYDROGEN SULFIDE
NT LEAD SULFIDES
NT MOLYBDENUM DISULFIDES
NT MOLYBDENUM SULFIDES
NT POLYSULFIDES
NT PYRITES
NT ZINC SULFIDES
Lithium/iron sulfide batteries: Development and demonstration
[DE87-014222] 01 p0042 N88-10265
The effect of non-metallic inclusions on fatigue and fatigue thresholds of 25Mn-5Cr-1Ni steel
06 p0718 N88-14410
Monolayer films prepared by the spontaneous self-assembly of symmetrical and unsymmetrical dialkyl sulfides from solution onto gold substrates: Structure, properties, and reactivity of constituent functional groups
[AD-A186717] 09 p1137 N88-16814
The crystallization of tough thermoplastic resins in the presence of carbon fibers
[NASA-CR-182984] 20 p2776 N88-26464
Weathering of sulfides on Mars
23 p3301 N88-29662

SULFONATES
Thermogravimetric analysis of polymeric materials for an intermediate temperature solid electrolyte
[DE88-004854] 10 p1306 N88-17809

SULFONES
Reinforcing of thermoplastic polycarbonate and polysulfone with carbon fibers: Production and characteristics of UD-compound objects
[NASA-TT-20158] 13 p1735 N88-20374

SULFONIC ACID
Formation of sediments in fuels containing added sulphonic acids --- marine diesel fuels
[RAE-TM-NAV ENG-1163] 09 p1150 N88-16891
Molecular composites processing and properties, 1
[AD-A194113] 23 p3189 N88-28974

SULFUR
The effect of sulfur and zirconium Co-doping on the oxidation of NiCrAl
[NASA-TM-100209] 02 p0150 N88-10940
Modeling the effect of sulfur on the threshold environmental cracking rate of steels in high temperature water 05 p0604 N88-13703
Sulfur-induced ductility-dip cracking in weld metal of low-carbon steel
[PB87-143814] 07 p0833 N88-15051
Seasonal cycling of sulfur and iron in porewaters of a Delaware salt marsh
[NASA-CR-182385] 07 p0876 N88-15311
Acoustic emission-microstructural relations in ferritic steels. Part 3: The effect of inclusion content
[AERE-R-12041] 10 p1341 N88-18015
Study of adherent oxide scales
[AD-A187308] 11 p1456 N88-18680
Preparation and characterization of Cu2Zn1-xMnxGeS4
[AD-A188113] 11 p1556 N88-19315
The Io sulfur torus in 1981
[NASA-TM-101139] 18 p2595 N88-25419
Hydrogen embrittlement of iron-nickel alloys
[AD-A195909] 24 p3353 N88-29958

SULFUR COMPOUNDS
NT BISMUTH SULFIDES
NT CADMIUM SULFIDES
NT COPPER SULFIDES
NT DISULFIDES
NT HYDROGEN SULFIDE
NT LEAD SULFIDES
NT MOLYBDENUM DISULFIDES
NT MOLYBDENUM SULFIDES
NT POLYSULFIDES
NT PYRITES
NT SULFATES
NT SULFIDES
NT SULFONATES
NT SULFONES
NT SULFUR DIOXIDES
NT SULFUR FLUORIDES
NT SULFURIC ACID
NT THIOLS
NT ZINC SULFIDES
Investigations of the influence of chemical reactions of the vertical flow of gaseous and particulate compounds
08 p1017 N88-16165
Electronic and ionic transport in polymers
[AD-A191642] 18 p2490 N88-24772
Uses of lunar sulfur
[DE88-009119] 21 p3031 N88-27990

SULFUR DIOXIDES
Volcanic eruption detection with TOMS
05 p0618 N88-13793
Analysis of SO2 signals in SBUV/TOMS data
05 p0618 N88-13794
TOMS and the NOAA/FAA volcano support plan
05 p0618 N88-13796
Use of satellite data in volcano monitoring
05 p0618 N88-13797
Crystalline sulfur dioxide: Crystal field splittings, absolute band intensities and complex refractive indices derived from infrared spectra
[NASA-CR-182502] 09 p1256 N88-17547
The role of repowering in America's power generation future
[DOE/FE-0096] 10 p1351 N88-18076
The role of analytical chemistry in assessing atmospheric effects of combustion
[DE88-003909] 10 p1352 N88-18082
Assessment of crop loss from air pollutants: Meteorology-atmospheric chemistry and long range transport
[PB88-146857] 15 p2089 N88-22448
A theoretical model of the washout of trace gases by raindrops in the atmosphere 17 p2375 N88-24125
Kinetics of thermochemical gas-solid reactions important in the Venus sulfur cycle
[NASA-CR-182963] 19 p2742 N88-26280
Episodic vs. epochal release of SO2 on Mars
23 p3305 N88-29689

SULFUR FLUORIDES
Optical determination of the virial coefficients of the gases C2H4, C2H6 and SF6
[ETN-87-90610] 03 p0282 N88-11776
Interaction of intense electromagnetic fields with SF/sub 6/ molecules and clusters in supersonic expansion
[DE88-700310] 07 p0846 N88-15132
Kinetic toxic aspect of potential use of sulfur hexafluoride in closed environments 10 p1362 N88-18142
Pseudo-stationary oblique-shock-wave reflections in low gamma gases: Isobutane and sulphur hexafluoride
[UTIAS-TN-267] 13 p1768 N88-20576

SULFUR OXIDES
NT SULFUR DIOXIDES

SULFURIC ACID
The corrosion of iron rotating hemispheres in 1 M sulfuric acid: An electrochemical impedance study
[DE87-014679] 02 p0146 N88-10825
A modified sulphuric acid anodizing process used as a pretreatment for the adhesive bonding of aluminum alloys
[ARE-TM(UMM)-87410] 16 p2177 N88-22974
The rate of volcanism on Venus
[NASA-CR-183039] 19 p2742 N88-26281
Kinetic of martensitic transformations induced by hydrogen in the austenite
[DE88-701623] 23 p3194 N88-29007

SUMMARIES
NT ABSTRACTS
Summaries of physical research in the geosciences
[DE88-000833] 04 p0409 N88-12896
University research initiative research program summaries
[AD-A184876] 05 p0658 N88-14035
Summary of comparison between experimental and analytical (including empirical) results for initiation of crack growth for surface cracks
[DE88-001604] 06 p0721 N88-14433
Summaries of FY 1987 engineering research
[DE88-002572] 07 p0840 N88-15096
Summary of the report of the Senior Committee on Environmental, Safety and Economic Aspects of Magnetic Fusion Energy
[DE88-003270] 07 p0837 N88-15682
A summary of the Naval Postgraduate School research program
[AD-A186362] 07 p0942 N88-15727
Annual data summary and climatological evaluation CERC (Coastal Engineering Research Center) field research facility, 1985. Volume 1. Main text and appendixes A and B
[AD-A186442] 08 p1039 N88-16289
Aircraft accident/incident summary reports, Des Moines, Iowa, November 25, 1985; Chicago, Illinois, August 10, 1986
[PB88-910411] 09 p1115 N88-16665
Summaries of FY86 research in the Applied Plasma Physics Fusion Theory Program
[DE88-004242] 11 p1554 N88-19296
Whither many-body theory. A summary of the Oulu Conference
[DE88-003095] 11 p1563 N88-19358
Revised Uniform Summary of Surface Weather Observations, Loring AFB, Maine, Parts A - F
[AD-A188201] 14 p1947 N88-21810
Summary and conclusions on electrooptical streak camera project
[DE88-008616] 15 p2060 N88-22334
Narrative domain implementation
[AD-A192265] 20 p2843 N88-26889

SUMMER
The role of low-level cooling in a conceptual model of the Australian summertime cool change: Implications for very-short-range forecasting 02 p0204 N88-11275

Physical properties of summer sea ice in the Fram Strait, June-July 1984
[AD-A188937] 09 p1194 N88-17156

Report on project WIND: Preliminary experiments with the UK Meteorological Office mesoscale model, September 1987
[AD-A191621] 18 p2544 N88-25099

MIZPAC (marginal ice zone Pacific) 84-86 CTD (Conductivity, Temperature, Depth) data report
[AD-A192478] 21 p2976 N88-27679

Factors influencing summer temperatures and precipitation in the southwest 22 p3124 N88-28565

UMS

Weak convergence of sums of moving averages in the alpha-stable domain of attraction
[AD-A186430] 07 p0912 N88-15529

Fast serial input-serial output pipelined inner product units
[REPT-87-031] 11 p1530 N88-19142

UN

Unified Sun and sky illumination for shadows under trees
[DE87-014232] 01 p0083 N88-10535

About the interest of solar interferometric observations 01 p0094 N88-10615

Solar interferometry with a 4-aperture nonredundant and stabilized network 01 p0097 N88-10639

The Sun and the solar activity 03 p0271 N88-11704

Fifth Cambridge Workshop on Cool Stars, Stellar Systems and the Sun 04 p0502 N88-13092

Calibration on the Sun for stellar magnetic fields 04 p0506 N88-13113

Variations of the vertical and horizontal velocities of the small-scale structures and the physical problems related to overshoot layers 04 p0507 N88-13115

The dynamics of solar magnetic flux tubes subjected to resonant foot point shaking 04 p0507 N88-13118

The appearance and disappearance of magnetic flux on the quiet sun
[AD-A185432] 05 p0661 N88-14755

Perturbations of the Sun's gravitational field due to solar oscillations
[DE88-002090] 07 p0946 N88-15751

Oscillations of solar models with internal element diffusion
[DE88-003156] 09 p1264 N88-17573

Solar microwave radiation maps measured at Metsaehovi Radio Research Station in 1978-1979
[PB88-127543] 13 p1857 N88-21108

Stable, heavy, neutral particles in the sun and in toponium decay 17 p2452 N88-24588

MHD bending waves in a current sheet
[NASA-TM-101149] 18 p2579 N88-25323

UN SENSORS

U SOLAR SENSORS

UNLIGHT

Sunlight supply and gas exchange systems in microalgal bioreactor 03 p0359 N88-12258

Influence of solar illumination conditions on TM/Landsat data
[INPE-4463-TDL/320] 12 p1638 N88-19806

UNRISE

The lengthening and shortening of the day
[KNMI-TR-91] 05 p0628 N88-13839

Computing basic solar and lunar data from the Air Almanac
[AD-A190777] 16 p2290 N88-23710

UNSET

The lengthening and shortening of the day
[KNMI-TR-91] 05 p0628 N88-13839

Computing basic solar and lunar data from the Air Almanac
[AD-A190777] 16 p2290 N88-23710

UNSPOT CYCLE

Three-halves law in sunspot cycle shape
[NASA-CR-181520] 04 p0525 N88-13210

Development of high stability fiber optic spectrophotometric systems for study of solar/stellar magnetic activity
[AD-A189027] 13 p1852 N88-21098

Sunspot frequency and solar activity
[PUBL-17/87] 14 p2011 N88-21895

UNSPOTS

The large Type 4 radio burst event of 24 April 1985 interpreted by dynamic spectral recordings and associated recordings 01 p0112 N88-10717

Quantification of the background signal to solar neutrino detection from cosmogenic activation of the atmosphere
[DE87-013830] 01 p0119 N88-10762

Magnetic field morphology in the upper layers 02 p0255 N88-11610

Theoretical modelling of the fine structures in sunspots 02 p0256 N88-11617

Large-scale horizontal flows from SOUP observations of solar granulation 02 p0256 N88-11621

Sunspot observations from the SOUP instrument on Spacelab 2 02 p0257 N88-11623

Variations of the semi-diurnal tidal wind in the meteor region with periods of about 27 and 13.5 days 06 p0734 N88-14516

Solar Dynamics and G-modes
[NASA-CR-180737] 06 p0805 N88-14911

Flares: Solar and stellar
[PB87-124962] 06 p0806 N88-14917

Ultraviolet rocket-spectra of a sunspot 08 p1032 N88-16257

Gasflows in the transition region above sunspot 08 p1095 N88-16586

Solar-geophysical data number 516, August 1987. Part 1: (Prompt reports). Data for July 1987, June 1987 and late data
[PB88-114368] 09 p1263 N88-17570

Spectral analysis of the Elatina varve series
[NASA-CR-183085] 24 p3400 N88-30280

SUPERALLOYS

U HEAT RESISTANT ALLOYS

SUPERCHARGERS

Fuel nitrogen conversion in a supercharged spark ignition engine
[DE88-003739] 08 p0974 N88-15893

Technology developments for a compound cycle engine 09 p1107 N88-16637

Servojet retrofit
[AD-A191075] 18 p2522 N88-24964

New super alloys used in turbochargers 19 p2634 N88-25628

SUPERCHARGING

U SUPERCHARGERS

SUPERCOMPUTERS

NT CRAY COMPUTERS

NBS (National Bureau of Standards) research reports (April 1987)
[PB87-210258] 01 p0018 N88-10111

NOSTRADAMUS programmable translator user's manual and programmer's manual
[DE87-013414] 01 p0083 N88-10533

Approximate polynomial preconditioning applied to biharmonic equations on vector supercomputers
[NASA-TM-100217] 01 p0087 N88-10563

An embedded multiprocessor computer for proof-of-principle testing of exploratory systems concepts
[DE87-012735] 02 p0218 N88-11372

Implementation of preconditioned s-step conjugate gradient methods on a multiprocessor system with memory hierarchy
[DE87-014401] 02 p0222 N88-11400

Report from the MPP Working Group to the NASA Associate Administrator for Space Science and Applications
[NASA-TM-87819] 02 p0223 N88-11402

Energy transformation in molecular electronic systems
[DE87-013916] 03 p0282 N88-11771

Numerical simulation system 04 p0404 N88-12511

Center for Supercomputing Research and Development (CEDAR)
[DE88-000807] 04 p0475 N88-12930

The SUPRENUM communications subroutine library for grid-oriented problems
[DE88-000137] 04 p0479 N88-12950

Programming techniques for high-speed processing of large scale numerical simulation on supercomputers 05 p0537 N88-13269

Vectorizing the FFTs on supercomputer SX system 05 p0537 N88-13270

Tridiagonal approximate factorization method: A preconditioning technique for solving nonsymmetric linear systems suitable to supercomputers 05 p0537 N88-13271

Supercomputing at Florida State University (FSU)
[DE87-013800] 05 p0654 N88-14009

Some performance comparisons for a fluid dynamics code
[PB88-113709] 07 p0852 N88-15175

Internal fluid mechanics research on supercomputers for aerospace propulsion systems
[NASA-TM-100289] 07 p0844 N88-15186

Monte Carlo photon transport on vector and parallel supercomputers
[DE88-002503] 07 p0905 N88-15486

Applicative parallelism: Potential and challenge
[DE87-011885] 08 p1068 N88-16459

Supercomputers for solving PDE (Partial Differential Equations) problems
[AD-A186583] 09 p1215 N88-17283

A performance comparison of the Cray-2 and the Cray X-MP
[NASA-CR-177461] 09 p1216 N88-17286

Interdisciplinary research in applied mathematics
[AD-A186793] 09 p1226 N88-17344

Emerging supercomputer architectures
[DE88-003539] 10 p1384 N88-18262

Features of a TeraFlop supercomputer
[DE88-003540] 10 p1384 N88-18263

Supercomputer performance: The theory, practice, and results
[DE88-004697] 10 p1384 N88-18266

Using program structure to achieve prefetching for cache memories
[DE88-003598] 10 p1387 N88-18282

Dynamic processor self-scheduling for general parallel nested loops
[DE88-003572] 10 p1393 N88-18311

Performance and evaluation at the Center for Supercomputing Research and Development
[DE88-003563] 10 p1417 N88-18456

Center for Supercomputing Research and Development
[DE88-003564] 10 p1418 N88-18465

The Livermore FORTRAN Kernels: A computer test of the numerical performance range -- benchmark tests
[UCRL-53745] 11 p1531 N88-19144

Data flow graph optimization in IF1
[DE88-004396] 11 p1532 N88-19151

A report on the study of algorithms to enhance vector computer performance for the discretized one-dimensional time-dependent heat conduction equation: EPIC research, phase 1
[DE88-005642] 13 p1820 N88-20880

Activities report of the Toulouse Research Center
[ETN-88-91988] 13 p1850 N88-21077

Supercomputer-aided generalized mixer analysis and optimization
[FUB-15-1986] 14 p1957 N88-21688

Supercomputer environment
[AD-A190633] 15 p2107 N88-22551

Implementation of a distributed adaptive routing algorithm on the Intel iPSC (Intel Personal Super-Computer)
[AD-A189849] 15 p2109 N88-22567

The good, the bad and the ugly: Comparing high-speed computer systems
[DE88-007498] 16 p2245 N88-23412

Supercomputer programming environments
[AD-A190887] 16 p2251 N88-23452

Effective use of shared memory multiprocessors
[DE88-007019] 18 p2560 N88-25195

Computer science research, 1987: Computation Directorate
[DE88-008637] 20 p2834 N88-26812

The performance of the NEC SX-2 and Cray X-MP supercomputers
[DE88-008177] 20 p2835 N88-26813

Federal Council on Science, Engineering and Technology: Committee on Computer Research and Applications; Subcommittee on Science and Engineering Computing: The US Supercomputer Industry
[DE88-011262] 21 p2994 N88-27756

Supercomputer for parallel data analysis
[DE88-702148] 21 p2995 N88-27759

Hypervelocity impact analysis with supercomputers
[DE88-008907] 21 p3001 N88-27797

Notes on operating system requirements for the next millennium
[DE88-010712] 21 p3002 N88-27805

Microsupercomputers: Design and implementation
[AD-A194712] 22 p3135 N88-28638

Supermap for Cray FORTRAN: A user's guide
[NASA-CR-177410] 24 p3412 N88-30308

SUPERCONDUCTING MAGNETS

Modeling of proximity coupling between superconducting filaments in superconducting dipole magnets
[DE87-014684] 03 p0382 N88-12403

Design concepts for the ASTROMAG cryogenic system
[NASA-CR-181505] 04 p04[illegible] N88-13080

Completely magnetically contained electrothermal thrusters
[AD-A185674] 06 p0674 N88-14129

Astromag: A particle spectrometer for the Space Station
[PREPRINT-557] 06 p0707 N88-14336

The TITAN magnet configuration
[DE88-001826] 06 p0762 N88-14600

Study on the model of a toroidal magnet for a tokamak with a strong field
[DE88-700346] 07 p0935 N88-15681

The superconducting gravimeter: Application, calibration, and further development
[SER-C-329] 09 p1167 N88-16998

Development activities for a 21-T superconducting magnet and cryostat
[DE88-004370] 11 p1558 N88-19327

Advances in applied superconductivity: A preliminary evaluation of goals and impacts
[DE88-006441] 14 p1986 N88-21844
Superconducting magnet technique for ASTROMAG on the space station
[DE88-004560] 15 p2025 N88-22063
Fluids, gels and glasses under extreme conditions of pressure and temperature
[AD-A190655] 15 p2035 N88-22125
Magnet strength fluctuations in the SSC (Superconducting Super Collider) lattice. Part 2: Frequency modulation
[DE88-006491] 15 p2141 N88-22774
The Department of Defense Superconductivity Research and Development (DSRD) options. A study of possible directions for exploitation of superconductivity in military applications
[AD-A189747] 15 p2142 N88-22780
SSC (Superconducting Super Collider) magnet technology
[DE88-007386] 19 p2733 N88-26230
Magnetic heat pumps
[DE88-012058] 21 p2969 N88-27639
High-T(sub c) superconductor and its use in superconducting magnets
[DE88-008403] 23 p3289 N88-29581

SUPERCONDUCTING POWER TRANSMISSION
The status of R and D for superconducting power transmission systems
[DE88-003499] 11 p1561 N88-19346
Conductor loss in superconducting power transmission cables
[DE88-011414] 23 p3290 N88-29586

SUPERCONDUCTING QUANTUM INTERFEROMETERS
U SQUID (DETECTORS)

SUPERCONDUCTING SUPER COLLIDER
Characteristics of multimuon events from fourth generation quarks at the SSC (Superconducting Super Collider)
[DE88-002954] 09 p1257 N88-17535
Advanced nonlinear theory: Long-term stability at the SSC
[CEBAF-PR-87-027] 11 p1546 N88-19246
A practical guide to modern high energy particle accelerators
[DE88-004035] 11 p1548 N88-19260
The lattice nonlinearities and the long term stability of the SSC
[CEBAF-PR-87-009] 12 p1690 N88-20108
Optics of the CEBAF CW superconducting accelerator
[CEBAF-PR-87-012] 12 p1690 N88-20110
Physics at large transverse momenta
[DE88-005758] 13 p1836 N88-20986
Magnet strength fluctuations in the SSC (Superconducting Super Collider) lattice. Part 2: Frequency modulation
[DE88-006491] 15 p2141 N88-22774
SSC (Superconducting Super Collider) magnet technology
[DE88-007386] 19 p2733 N88-26230

SUPERCONDUCTIVITY
NT KONDO EFFECT
Superconducting properties of metallic superlattices
[DE87-012725] 01 p0023 N88-10146
Design and testing of electrical insulation for superconducting coils
[DE87-012256] 01 p0039 N88-10246
Some electronic factors influencing superconductivity in some rare-Earth-like elements and the beginning of rare-Earth series
[DE87-702582] 01 p0102 N88-10668
Simple instrumentation for testing of ceramic superconductors
[DE87-013849] 01 p0103 N88-10672
Grain boundary effects in processing high T/sub c/ superconductors
[DE87-009297] 01 p0103 N88-10673
Optimization of SIS mixer elements
[NASA-CR-180710] 01 p0104 N88-10680
Progress toward a superconducting opening switch
[DE87-014170] 02 p0167 N88-11051
Theory of the one- and two-dimensional electron gas
[DE87-012864] 02 p0244 N88-11540
High gradient superconducting quadrupoles
[DE87-013590] 02 p0244 N88-11541
Electrical properties of high T/sub c/ superconductors under high pressures
[DE87-012818] 02 p0245 N88-11546
Superconductivity of pseudobinary compounds A15 (V-Cr)3Si, (V-MO)3Si, Mo3(Si-Re), bombarded with fast neutrons 03 p0285 N88-11792
High temperature superconductors
03 p0297 N88-11869
A role for national laboratories in enhancing economic competitiveness. The example of high-temperature superconductors: CNSS papers, No. 1
[DE87-013633] 03 p0379 N88-12386
Superconductivity as a synchronous spatial alternation of valence bonds
[AD-A184208] 03 p0382 N88-12405
Experimental perspectives on heavy electron metals
[DE87-014766] 04 p0416 N88-12583
Valence bond theory and superconductivity
[AD-A184274] 04 p0496 N88-13052
The chemical bond and superconductivity
[AD-A184275] 04 p0496 N88-13053
Non-lattice matched metallic superlattices
[DE87-011512] 04 p0497 N88-13062
Pressure induced phase transitions, superconductivity of phosphorus described 06 p0675 N88-14134
Superconducting material development
06 p0689 N88-14217
The use of alloy 117 as a liquid metal current collector
[AD-A185740] 06 p0698 N88-14281
Studies of tunneling in metals under high pressure
06 p0775 N88-14757
High temperature stability of superconducting YBa2Cu3O subx as characterized by X-ray diffraction
[DE88-001656] 06 p0787 N88-14824
Effect of high pressure oxygen loading on the superconductivity of La2CuO4
[DE88-002108] 06 p0787 N88-14827
Atomic-level studies of superconducting YBa2Cu3O sub 7-x
[DE88-002522] 06 p0786 N88-14831
L2,3 XANES of the high T sub c superconductor YBa2Cu3O7 with variable oxygen content
[NOTA-INTERNA-886] 06 p0788 N88-14837
Accelerators and Superconductivity: A Marriage of Convenience. Second John Adams Memorial Lecture
[DE88-700005] 07 p0931 N88-15656
Low field characterization of YBa2Cu3O sub 7-delta single crystals
[DE88-002895] 07 p0936 N88-15700
On the coexistence of phonon and non-phonon (plasmon) mechanisms in new high T/sub c/ superconductors
[DE88-003188] 07 p0938 N88-15703
Metal-oxide superconductor BaPbsub1-xBisubxO3: Unusual properties and new applications
08 p1077 N88-16494
Magnetic investigations of superconductive, polycrystalline (RE)1Ba2Cu3O(7-x) compounds (RE = Y, Gd, Ho, Dy)
[DE88-002537] 08 p1090 N88-16558
Experimental aspects of high-T/sub c/ superconductors
[DE88-003019] 08 p1090 N88-16564
Microstructure modifications of micron thick NbN films to improve J/sub c/ and H/sub c2/
[DE88-003078] 08 p1091 N88-16567
JPRS report: Science and technology. USSR: Physics and mathematics
[JPRS-UPM-87-009] 09 p1233 N88-17395
Phenomenological model of superconductivity of heavy fermions in U(sub 1-x)ThsubxBesub13
09 p1236 N88-17423
Properties of superconducting tunnel structures in microwave radiation field 09 p1239 N88-17424
Superconductivity and crystal structure of high-pressure phases in V-Ru-H system 09 p1239 N88-17426
Bulk superconductivity in La2CuO4
[DE88-002509] 09 p1254 N88-17516
Nonequilibrium superconductivity for particle detectors
[DE88-002876] 09 p1257 N88-17539
Superconductivity in La/sub 1.85-x/Nd/sub x/Sr/sub .15/CuO
[DE88-003014] 09 p1258 N88-17540
High temperature superconductivity research at Argonne National Laboratory
[DE88-003055] 09 p1258 N88-17541
Copper oxidation states, vacancy ordering and their effect on high temperature superconductivity
[DE88-003079] 09 p1258 N88-17542
Electrochemical growth of linear conducting crystals in microgravity 10 p1287 N88-17698
Spin disorder resistivity and bare Curie temperature in the ferromagnetic superconductor ErRh4B4
[DE88-003016] 10 p1415 N88-18445
Normal and superconducting state properties of La2-xSr/sub x/CuO4
[DE88-003013] 10 p1416 N88-18450
Superconducting and magnetic properties of Fe-doped oxide superconductors
[DE88-003024] 10 p1416 N88-18451
The physics of metallic superlattices: An experimental point of view
[DE88-003080] 10 p1416 N88-18452
Electronic structure, charge transfer excitations and high temperature superconductivity
[DE88-003096] 10 p1416 N88-18453
Positron-annihilation 2D-ACAR studies of disordered and defected alloys
[DE88-003118] 10 p1416 N88-18454
Performance and evaluation at the Center for Supercomputing Research and Development
[DE88-003563] 10 p1417 N88-18456
Comparative evaluation of resistive and inductive techniques for measuring temperature of superconducting transition
[DE88-700603] 10 p1417 N88-18457
The structure and properties of twin boundaries in superconducting YBa2Cu3O7
[DE88-003884] 10 p1418 N88-18468
Freestanding films of YBa2Cu3O/sub 6.9/
[DE88-003995] 10 p1419 N88-18471
Grain boundaries, planar defects and superconducting properties of YBa2Cu3O7
[DE88-003477] 10 p1419 N88-18475
Superconductivity and phase stability in the heavy rare earth quaternary compounds RBa2Cu3O7 (R = Ho, Er, Tm, Yb, Lu)
[DE88-003478] 10 p1419 N88-18476
Superconducting properties and structural characterization of high T/sub c/ oxides
[DE88-003479] 10 p1420 N88-18477
Penetration depth measurements of YBa2Cu3O/sub 7-delta/ at 4 MHz
[DE88-003493] 10 p1420 N88-18478
The electronic structure of YBa2Cu3O/sub 7-delta/ above and below T/sub c/
[DE88-003495] 10 p1420 N88-18479
Simulation and processing of high resolution images of defects and interfaces in superconducting YBa2Cu3O7
[DE88-003856] 10 p1420 N88-18480
Innovative arrangements for industry/DOE laboratory collaboration in high temperature superconductivity
[DE88-704320] 10 p1420 N88-18482
Superconductivity of thin film intermetallic compounds
[AD-A187563] 10 p1421 N88-18489
The injector for the CEBAF CW superconducting linac
[CEBAF-PR-87-011] 11 p1546 N88-19241
RF steering in the CEBAF CW superconducting linac
[CEBAF-PR-87-013] 11 p1547 N88-19251
Single-crystal structural study of La2Cu/sub 0.95/Li/sub 0.05/O4
[DE88-003482] 11 p1554 N88-19302
Composite ceramic superconducting filaments for superconducting cable
[AD-A187833] 11 p1556 N88-19312
An electron spectroscopic investigation of high-temperature superconducting oxides
[DE88-003807] 11 p1558 N88-19325
Processing relationships in YBa2Cu3O(7-x) superconductors
[DE88-005137] 11 p1559 N88-19330
Research briefing on high-temperature superconductivity
[PB88-133004] 11 p1561 N88-19344
Mass transport and chemical demixing of Y-Ba-Cu-O compounds during sintering in temperature gradients
[DE88-004887] 12 p1696 N88-20151
An overview of recent developments in high-temperature superconductivity
[DE88-005477] 12 p1697 N88-20155
Progress in diagnostic techniques for SC cavities
[CEBAF-PR-88-003] 13 p1772 N88-20800
Large momentum pairing in one-dimensional systems
[AD-A189228] 13 p1835 N88-20981
Theoretical studies on the electronic structure and properties of complex ceramic crystals and glasses
[DE88-005837] 13 p1846 N88-21049
Competing interactions in metallic superlattices
[DE88-005344] 13 p1847 N88-21057
Superconducting superlattice structures
[DE88-005345] 13 p1847 N88-21058
Design, optimization and construction of a dc-SQUID with complete flux transformer circuits
[PB88-160742] 14 p1907 N88-21399
Superconducting transition temperature of Cu-Nb microcomposites 14 p1973 N88-21775
Thermal model describing development of normal region in superconductor film carrying electric current
14 p1973 N88-21776
Giant Josephson signal in wide superconducting films
14 p1973 N88-21777
Properties of superconductors with strong electron-phonon interaction 14 p1974 N88-21779
Advances in applied superconductivity: A preliminary evaluation of goals and impacts
[DE88-006441] 14 p1986 N88-21844
Magnetic impurities in superconductors
[DE88-006917] 14 p1986 N88-21846

Temperature-dependent conductivity of oxygen-depleted YBCO ceramics
[AD-A190340] 15 p2044 N88-22182

Developments in ceramic superconducting materials
15 p2052 N88-22229

RF properties of superconducting Pb electroplated onto Cu
[DE88-005918] 15 p2139 N88-22765

Superconductivity and the tailoring of lattice parameters of the compound YBa2Cu3O(sub x)
[DE88-005904] 15 p2140 N88-22769

Superconductivity in power engineering
[DE88-701414] 15 p2141 N88-22776

The Department of Defense Superconductivity Research and Development (DSRD) options. A study of possible directions for exploitation of superconductivity in military applications
[AD-A189747] 15 p2142 N88-22780

Thin superconducting film characterization by surface acoustic waves
[AD-A190417] 15 p2143 N88-22791

Magnetic anomalies in the rare earth oxide superconductors GdBa2Cu3O(7-x) and YbBa2Cu3O(7-x)
[AD-A190713] 15 p2144 N88-22793

Status of RF superconductivity at Argonne National Laboratory
[DE88-005913] 15 p2144 N88-22796

High-T(sub c) superconducting wire fabrication and testing
[DE88-005989] 15 p2144 N88-22798

High temperature superconductors in the La(sub 1+x)Ba(sub 2-x)Cu O(sub y system
[DE88-006367] 15 p2145 N88-22802

Synthesis and characterization of high-T(sub c) screen-printed Y-Ba-Cu-O films on alumina
[NASA-TM-100860] 15 p2146 N88-22805

The superconducting phase shifter in the development of a terahertz imaging radar system
[AD-A190866] 16 p2188 N88-23046

High temperature superconductivity
[AD-A190259] 16 p2281 N88-23655

Electrothermal instability in superconducting resonators
[DE88-701684] 16 p2282 N88-23664

Effects of 67.5 MeV electron irradiation on Y-Ba-Cu-O and Gd-Ba-Cu-O high-temperature superconductors
[AD-A191271] 16 p2283 N88-23669

Materials science with muon spin rotation
[NASA-CR-182891] 17 p2396 N88-24242

Systematic variation of magnetic-field penetration depth in high-T(c) superconductors studied by muon spin relaxation
17 p2396 N88-24243

Coexisting static magnetic ordering and superconductivity in CeCu2.1Si2 found by muon spin relaxation
17 p2396 N88-24245

Superconducting thin film vertex detector for SSC (Superconducting Super Collider) applications
[DE88-005951] 17 p2445 N88-24535

Method of producing high T(subc) superconducting NBN films
[NASA-CASE-NPO-16681-1-CU]
17 p2446 N88-24543

Crystalline metal-semiconductor superlattices
[DE88-007063] 18 p2581 N88-25332

A role for high frequency superconducting devices in free space power transmission systems
[NASA-TM-100971] 19 p2662 N88-25830

Superconductive analogue of spin glasses
[DE88-702059] 19 p2733 N88-26233

Effect of a weak magnetic field on high temperature superconductivity in Y-Ba-Cu-O ceramics
[DE88-702192] 19 p2733 N88-26235

Magnetization studies of multifilamentary Nb3Sn wires
[DE88-009103] 19 p2735 N88-26243

All-electron local density theory of electronic structure and superconductivity in YBa2Cu3O7 and YBa2Cu3O6
[DE88-009944] 19 p2735 N88-26246

Structural and magnetic properties of Fe impurities in YBa2Cu3O(sub 7-delta)
[DE88-009961] 19 p2735 N88-26247

Application of superconducting technology to earth-to-orbit electromagnetic launch systems
[NASA-TM-101134] 20 p2763 N88-26385

Application of superconducting technology to earth-to-orbit electromagnetic launch systems
[DE88-010022] 20 p2763 N88-26386

Superconducting rf and beam-cavity interactions
[DE88-008598] 20 p2852 N88-26936

Superconductivity of Cr/V superlattices
20 p2874 N88-27057

To the twinning plane superconductivity theory
[DE88-702195] 20 p2874 N88-27058

Effects of grain boundary composition on properties of YBa2Cu3O/sub 7-x/
[DE88-007679] 20 p2875 N88-27064

Superconductivity of heavy-electron uranium compounds
[DE88-007901] 20 p2875 N88-27065

The superconducting transition in oxygen deficient YBa2Cu3O(sub 7-Delta)
[DE88-009957] 20 p2877 N88-27079

Anisotropy of the lower critical field in YBa2Cu3O(sub 7-Delta)
[DE88-009971] 20 p2877 N88-27081

Preparation of high-T(sub)c Y1Ba2Cu3O(sub 7-Delta) superconducting thin films by MBE (Molecular-Beam-Epitaxy) techniques
[DE88-009999] 20 p2877 N88-27082

Oxygen vacancy ordering and superconductivity in YBa2Cu3O(sub 7-x)
[DE88-010005] 20 p2877 N88-27083

Superconducting electronic film structures
[AD-A192907] 20 p2879 N88-27091

On the chemistry of superconductivity
[DE88-010714] 20 p2880 N88-27096

Compilation of NRL publications on high temperature superconductivity
[AD-A189137] 21 p3019 N88-27921

Effect of high-amplitude high-frequency current on non-isothermal equilibrium of NS-boundary in innomogeneous superconductor
[DE88-701682] 21 p3019 N88-27922

Anharmonic model for high-Tc superconductors
[DE88-702196] 21 p3020 N88-27924

High-temperature superconductivity: An overview
DE88-702051] 21 p3020 N88-27925

Coupled even-parity superconducting states: Square lattice
[AD-A193432] 21 p3022 N88-27938

Properties of new low dimensional materials and mechanisms of high T(sub c) superconductivity
[DE88-012026] 21 p3024 N88-27951

Superconducting properties of LaBa2Cu3O(sub x) and YBa2Cu3O(sub y)
[DE88-012038] 21 p3024 N88-27952

X-ray studies of strain, interface and impurities in semiconductors
[DE88-012460] 21 p3025 N88-27954

High Tc superconducting HoBa2Cu(sub 1-x)Fe(sub x)3O(sub 7-y)
[DE88-008909] 22 p3155 N88-28768

Effect of neutron irradiation on critical magnetization current in single crystal YBa2Cu3O(sub 7-delta)
[DE88-009970] 22 p3156 N88-28775

Gravitation electromagnetic theory
22 p3158 N88-28790

SQUID (superconducting quantum interference device) arrays for simultaneous magnetic measurements: Calibration and source localization performance
[AD-A193815] 23 p3216 N88-29143

CryoSQUID: A SQUID-based magnetic field sensor
[AD-A194237] 23 p3239 N88-29275

Effects of metal substitutions (Fe and Ga) in YBa2Cu3O7 on its superconducting properties and microstructures
[DE88-007393] 23 p3287 N88-29572

Properties of strong coupled superconductors
[DE88-702050] 23 p3287 N88-29574

Possible mechanism for high-temperature superconductivity in the BaSr-La(Y)-CuO systems
[DE88-702060] 23 p3288 N88-29576

Electron microscopy of ceramic superconductors
[DE88-006446] 23 p3288 N88-29580

High-T(sub c) superconductor and its use in superconducting magnets
[DE88-008403] 23 p3289 N88-29581

An HVEM study of displacement cascade damage in Nb3Sn at 13 K
[DE88-009997] 23 p3289 N88-29584

Band electronic structures and crystal packing forces
[DE88-010247] 23 p3289 N88-29585

Stability experimental results of cable-in-conduit superconductor for fusion
[DE88-753424] 23 p3290 N88-29589

Development of Nb-Ti multifilamentar superconducting wires
[DE88-702324] 23 p3290 N88-29592

Study of superconducting properties in some many valley semiconductors
[DE88-702325] 23 p3291 N88-29596

Planar thin film SQUID with integral flux concentrator
[NASA-CASE-MFS-28282-1] 23 p3292 N88-29602

Dependence of high critical temperature of ceramic superconductors on the nominal Cu(sup 3+)Cu(sup 2+) ratio
[DE88-702734] 23 p3293 N88-29611

The thermal conductivity of dirty type 2 superconductors
[B8681488] 23 p3294 N88-29615

Theory of superconductivity in oxides
[AD-A195647] 24 p3433 N88-30432

Behaviour and hysteresis losses of irreversible type-2 superconducting cylindrical shell
[DE88-702708] 24 p3433 N88-30434

SUPERCONDUCTORS

NT HIGH TEMPERATURE SUPERCONDUCTORS

Simple instrumentation for testing of ceramic superconductors
[DE87-013849] 01 p0103 N88-10672

Abrikosov vortex motion and elementary pinning force in a SNS Josephson junction
[DE87-013607] 01 p0105 N88-10683

Multidimensional elemental analysis with the Sandia nuclear microprobe
[DE87-014158] 02 p0183 N88-11136

Properties of Nb3Sn superconductor wires with composite cores
[KFK-4263] 02 p0246 N88-11557

Consortium for Materials Development in Space Technical section
[NASA-CR-181308] 03 p0296 N88-11859

Powder-metallurgical preparation of A15 superconductors
[ETN-87-90584] 03 p0380 N88-12392

Topological aspects of infinite metal clusters and superconductors
[AD-A184104] 04 p0495 N88-13049

Magnetic field dependence of the specific heat of some high-T/sub c/ superconductors
[DE87-014078] 04 p0497 N88-13063

Anomalous phonon behavior of superconductor Y-Ba-Cu-O
[DE87-703401] 05 p0654 N88-14010

JPRS report: Science and technology. Japan
[JPRS-JST-87-023] 06 p0684 N88-14191

JPRS report: Science and technology. Japan
[JPRS-JST-87-027] 06 p0688 N88-14213

Hitachi develops ceramic superconducting device
06 p0688 N88-14214

Recent trends in superconductor development discussed
06 p0688 N88-14215

Superconducting material development
06 p0688 N88-14217

Study of some superconducting and magnetic materials on high T sub c oxide superconductors
[NASA-CR-182330] 06 p0785 N88-14813

The consequences of intergrain Josephson coupling in ceramic high-temperature superconductors
[DE87-013713] 06 p0785 N88-14816

Dynamic high pressure process for fabricating superconducting and permanent magnetic materials
[DE88-000848] 06 p0785 N88-14817

Superconducting switch program
[AD-A185682] 07 p0848 N88-15144

Fabrication of YBa2Cu3O7 superconducting ceramics
[DE88-003012] 07 p0938 N88-15701

Non-phonon mechanisms of superconductivity in high T/sub c/ superconducting oxides and other materials and their manifestation
[DE88-002708] 07 p0939 N88-15709

Localization of Cu 3d levels in the high Tc superconductor YBa2Cu3O approximately 7 by Cu2p X ray photoelectron spectroscopy
[NOTA-INTERNA-887] 07 p0939 N88-15710

Metal-oxide superconductor BaPbsub1-xBisubxO3: Unusual properties and new applications
08 p1077 N88-16494

Soft X-ray absorption and emission spectra and the electronic structure of the Ba2YCu3O/sub 7-x/ superconductor
[DE88-002609] 08 p1090 N88-16559

Coulomb interactions and effective strong coupling Hamiltonians in Cu-O superconductors
[DE88-002942] 08 p1090 N88-16561

Oxygen diffusion in high T/sub c/-superconductors
[DE88-002965] 08 p1090 N88-16562

Structural properties of high-T/sub c/ oxide superconductors
[DE88-002974] 08 p1090 N88-16563

Experimental aspects of high-T/sub c/ superconductors
[DE88-003019] 08 p1090 N88-16564

Interpretation of the temperature dependence of conductivity in superconducting oxides
[DE88-003028] 08 p1091 N88-16565

High T/sub c/ superconductor as a strongly correlated state
[DE88-003194] 08 p1091 N88-16569

Powder metallurgical preparation of A15 superconductors
[ETN-88-91072] 09 p1144 N88-16858

Mechanism of change of vortex structure orientation in type-2 superconductors 09 p1239 N88-17425

Magnetic properties of heavy fermion superconductors
[ETN-88-91078] 09 p1255 N88-17524

Forces on neutral atoms due to electromagnetic fields
[AD-A187461] 10 p1408 N88-18396

Spin disorder resistivity and bare Curie temperature in the ferromagnetic superconductor ErRh4B4
[DE88-003016] 10 p1415 N88-18445

High temperature processing of superconducting Y1Ba2Cu3O6.9
[DE88-003002] 10 p1416 N88-18449

Normal and superconducting state properties of La2-xSr/sub x/CuO4
[DE88-003013] 10 p1416 N88-18450

Superconducting and magnetic properties of Fe-doped oxide superconductors
[DE88-003024] 10 p1416 N88-18451

Positron-annihilation 2D-ACAR studies of disordered and defected alloys
[DE88-003118] 10 p1416 N88-18454

Improved magnetization for YBa2Cu3O/sub 7-delta annealed in oxygen above 1000 C
[DE88-003934] 10 p1418 N88-18469

The effect of magnetic impurities and barriers on the magnetization and critical current of fine filament NbTi composites
[DE88-004443] 10 p1419 N88-18472

Simulation and processing of high resolution images of defects and interfaces in superconducting YBa2Cu3O7
[DE88-003856] 10 p1420 N88-18480

Superconductivity of thin film intermetallic compounds
[AD-A187563] 10 p1421 N88-18489

Study of the production of some superconducting and magnetic materials by solidification in the drop tube and drop tower
[NASA-CR-182494] 11 p1461 N88-18708

Cryocooler systems demonstration
[AD-A188025] 11 p1467 N88-18745

Perturbation effects in the CEBAF beam transport system
[CEBAF-PR-87-010] 11 p1546 N88-19242

Atom probe microanalysis of superconducting YBa2Cu3O(sub 7-x)
[DE88-003203] 11 p1557 N88-19322

An electron spectroscopic investigation of high-temperature superconducting oxides
[DE88-003807] 11 p1558 N88-19325

Processing relationships in YBa2Cu3O(7-x) superconductors
[DE88-005137] 11 p1559 N88-19330

Proceedings of the First International Symposium on Physical and Technical Problems of Superconductivity Application in Power Generation
[DE88-700818] 11 p1559 N88-19332

Multipass beam breakup in recirculating linacs
[CEBAF-PR-87-007] 12 p1690 N88-20111

Artificially structured superconductors
[DE88-005345] 12 p1697 N88-20153

An overview of recent developments in high-temperature superconductivity
[DE88-005477] 12 p1697 N88-20155

Phase transitions in two-dimensional superconducting arrays in a transverse magnetic field
[INPE-4457-RPE/559] 12 p1697 N88-20157

Superconductors with structured surfaces: Fields and currents
[AD-A189353] 12 p1699 N88-20164

Large momentum pairing in one-dimensional systems
[AD A189226] 13 p1835 N88-20981

The relationship of the chemical bonding topology of high critical temperature copper oxide superconductors to that of the chevrel phases and the ternary lanthanide rhodium borides
[AD-A189255] 13 p1845 N88-21042

Discussion of radiation effects and high-temperature oxide superconductors
[DE88-001427] 13 p1846 N88-21046

A hydroxycarbonate route to superconductor precursor powders
[DE88-003638] 13 p1846 N88-21052

Superconducting superlattice structures
[DE88-005346] 13 p1847 N88-21058

A novel method for sputter-deposition of high T(sub c) superconductor films via a computer-controlled mass analyzed ion beam
[DE88-006001] 13 p1848 N88-21064

Superconducting transition temperature of Cu-Nb microcomposites 14 p1973 N88-21775

Thermal model describing development of normal region in superconductor film carrying electric current
14 p1973 N88-21776

Organic metal (ET)4Hg3Br8A quasi-two-dimensional superconductor 14 p1974 N88-21778

Properties of superconductors with strong electron-phonon interaction 14 p1974 N88-21779

Advances in applied superconductivity: A preliminary evaluation of goals and impacts
[DE88-006441] 14 p1986 N88-21844

Magnetic impurities in superconductors
[DE88-006917] 14 p1986 N88-21846

Temperature-dependent conductivity of oxygen-depleted YBCO ceramics
[AD-A190340] 15 p2044 N88-22182

Melt processing ceramic YBa2Cu3O(sub 6.9)
[DE88-007039] 15 p2047 N88-22199

Function of Japan Fine Ceramics Center described
15 p2052 N88-22227

Synthesis of metastable superconductors by high dynamic pressure
[DE88-005620] 15 p2139 N88-22764

Effective electron interactions due to virtual charge and spin excitations in an extended Hubbard model for Cu-O superconductors
[DE88-005971] 15 p2139 N88-22766

Superconductivity in power engineering
[DE88-701414] 15 p2141 N88-22776

Magnetic anomalies in the rare earth oxide superconductors GdBa2Cu3O(7-x) and YbBa2Cu3O(7-x)
[AD-A190713] 15 p2144 N88-22793

A sup 57 Fe Mossbauer study of the superconductor YBa sub 2 (Fe sub x Cu sub 1-x) sub 3 O sub y
[DE88-701543] 16 p2282 N88-23661

Effects of 67.5 MeV electron irradiation on Y-Ba-Cu-O and Gd-Ba-Cu-O high-temperature superconductors
[AD-A191271] 16 p2283 N88-23669

Materials science with muon spin rotation
[NASA-CR-182891] 17 p2396 N88-24242

Coexisting static magnetic ordering and superconductivity in CeCu2.1Si2 found by muon spin relaxation 17 p2396 N88-24245

Static magnetic ordering of CeCu2.1Si2 found by muon spin relaxation 17 p2396 N88-24246

Design of a superconducting alternator for space-based power generation 17 p2412 N88-24340

Lightweight power bus for a baseload nuclear reactor in space 17 p2438 N88-24505

Research work completed at the Naval Surface Warfare Center Solid State Group of the Radiation Division
[AD-A191627] 18 p2582 N88-25339

Vacancy ordering in the basal plane of YBa2Cu3O(sub)z
[DE88-004572] 18 p2583 N88-25348

Quench detection by fluid dynamic means in cable-in-conduit superconductors
[DE88-007269] 18 p2585 N88-25359

Workshop report and presentations from the Semiconductor Research Corporation-DOE Semiconductor Task Force Workshop
[DE88-007690] 19 p2733 N88-26232

Superconductive analogue of spin glasses
[DE88-702059] 19 p2733 N88-26233

RCL model for the development of hysteresis in superconductors
[DE88-702061] 19 p2733 N88-26234

Dimensional crossover in layered superconductors
19 p2734 N88-26237

Superfluidity of a two dimensional Boson Coulomb gas
[DE88-009827] 19 p2735 N88-26244

Theory of oxygen content, atomic ordering and oxygen diffusion in 1,2,3 superconducting oxides as a function of temperature and oxygen pressure
[DE88-007961] 19 p2735 N88-26248

Preparation of oxide superconductors
[DE88-009136] 20 p2875 N88-27063

Recent advances in atom-probe field ion microscopy
[DE88-008799] 20 p2876 N88-27070

HeFlow: A program for calculating pressure and temperature of helium in forced-flow superconductors. Part 1: Numerical solutions. Part 2: HeFlow user's manual
[DE88-008941] 20 p2876 N88-27071

Phenomenological approach to high T/sub c/ oxide superconductors
[DE88-701868] 20 p2876 N88-27074

Anisotropic characteristic lengths in single crystal YBa2Cu3O(sub 7-Delta)
[DE88-009959] 20 p2877 N88-27080

Ceramic processing of high-T(sub)c superconductors
[DE88-010090] 20 p2878 N88-27087

SIS (Superconductor-Insulator-Superconductor) mixer research
[AD-A192908] 20 p2879 N88-27092

Mitsubishi Electric Advance (R and D Edition), Volume 41
[PB88-194162] 21 p2929 N88-27388

Superconducting oxides with high critical temperatures
21 p2930 N88-27392

Effect of high-amplitude high-frequency current on non-isothermal equilibrium of NS-boundary in inhomogeneous superconductor
[DE88-701682] 21 p3019 N88-27922

Probing the electronic and defect structure of perovskite superconductors
[DE88-008349] 21 p3022 N88-27939

Thermodynamics of oxygen-vacancy ordering in YBa2Cu3O(sub z)
[DE88-009816] 21 p3022 N88-27940

Superconductor consolidation
[DE88-010938] 21 p3024 N88-27949

Study of the friction and wear-related properties of ceramic superconductors
[DE88-011844] 21 p3024 N88-27950

Ceramic fabrication technology for high-T(sub)c materials
[DE88-012060] 21 p3024 N88-27953

Materials research, superconductor and thin layer technology
[REPT-50/87] 21 p3025 N88-27955

Interactions between superconductivity and Kondo-grid properties in CeCu2Si2. Measurement results of specific heat under high pressure
[ETN-88-92377] 21 p3025 N88-27958

Modification of YBa2Cu3O(7-x) ceramics by adsorbed water and other gases
[DE88-011518] 22 p3057 N88-28140

Investigation of magnetic anisotropy and spin wave modes in transition metal multilayers
[DE88-009007] 22 p3154 N88-28765

Fabrication of bulk superconducting ceramics
[DE88-009956] • 22 p3155 N88-28773

Possible occurrence of band interplay in high Tc superconductor
[PREPRINT-593] 22 p3157 N88-28789

Gravitation control 22 p3158 N88-28795

Gravitational propulsion 22 p3158 N88-28796

Properties of strong coupled superconductors
[DE88-702050] 23 p3287 N88-29574

Electron microscopy of ceramic superconductors
[DE88-006446] 23 p3288 N88-29580

High-T(sub c) superconductor and its use in superconducting magnets
[DE88-008403] 23 p3289 N88-29581

Preparation of superconducting YBa2Cu3O(sub 7-x) films by magnetron sputtering
[DE88-009977] 23 p3289 N88-29583

Magnetic phase transitions in 90-K superconductors Ho1Ba2Cu3O(7-delta) and Gd1Ba2Cu3O(7-delta) observed by ZF-muon(+)SR
[DE88-752611] 23 p3290 N88-29588

Phase sensitive amplification with SIS (Superconductor-Insulator-Superconductor) quasiparticle mixers
[AD-A194594] 23 p3291 N88-29596

Fluctuations of order parameters in the high T(sub c) superconductors
[DE88-702549] 23 p3292 N88-29603

Anomalous dependence of the thermoelectric power on the temperature in YBaCuO high-T(sub c) superconducting samples
[DE88-702682] 23 p3292 N88-29605

SUPERCOOLING

NT CRYOGENIC COOLING

Structure and modification of winter mountain clouds in the Sierra Nevada: Nowcasting/forecasting the onset of supercooled liquid water 02 p0202 N88-11263

SUPERCRITICAL AIRFOILS

NT SUPERCRITICAL WINGS

A transonic model representation for two-dimensional wall interference assessment
[NLR-TR-86026-U] 01 p0001 N88-10006

Influence of the static deformation on a wing in the unsteady aerodynamic 05 p0551 N88-13357

Design and experimental evaluation of a swept supercritical Laminar Flow Control (LFC) airfoil
07 p0813 N88-14951

An aerodynamic comparison of blown and mechanical high lift airfoils 10 p1272 N88-17606

The NASA Langley Laminar-Flow-Control (LFC) experiment on a swept, supercritical airfoil: Design overview
[NASA-TP-2809] 14 p1861 N88-21117

Investigation of side-wall effects in wind tunnel with supercritical airfoil testing 15 p2054 N88-22241

Aerodynamic performance and pressure distributions for a NASA SC(2)-0714 airfoil tested in the Langley 0.3-meter transonic cryogenic tunnel
[NASA-TM-4044] 16 p2456 N88-24580

Calculation of 2-D unsteady transonic full potential flow about oscillating airfoils by two complementary approaches
[PB88-127519] 20 p2753 N88-26341

SUPERCRITICAL FLOW

Unsteady flow in a supercritical supersonic inlet
18 p2460 N88-24605

Electrochemistry in near-critical and supercritical fluids. 6: The electrochemistry of ferrocene and phenazine in acetonitrile between 25C and 300C
[AD-A192171] 18 p2482 N88-24723

SUPERCRITICAL FLUIDS

Supercritical fluid chromatography/supersonic jet spectroscopy
[DE88-000297] 03 p0282 N88-11774

Retention processes in supercritical fluid chromatography
[DE88-000079] 04 p0413 N88-12559

Thermodynamic properties of supercritical mixtures
[DE88-000809] 04 p0413 N88-12562

Supercritical fluid extraction-gas chromatography of Volatile Organic Compounds (VOC) from tenax devices
[PB88-124300] 10 p1298 N88-17759

Transport and relaxation processes in supercritical fluids
[DE88-004804] 10 p1419 N88-18474

Supercritical fluid chromatography/supersonic jet spectroscopy
[DE88-004436] 13 p1738 N88-20392

Development and evaluation of supercritical fluid chromatography-mass spectrometry
[DE88-005122] 13 p1738 N88-20394

Instrumental aspects of capillary supercritical fluid chromatography
[ETN-88-92242] 16 p2174 N88-22960

Electrochemistry in near-critical and supercritical fluids. 5: The dimerization of quinoline and acridine radical anions and dianions in ammonia from -70 C to 150 C
[AD-A190358] 16 p2175 N88-22967

Electrochemistry in near-critical and supercritical fluids. 6: The electrochemistry of ferrocene and phenazine in acetonitrile between 25C and 300C
[AD-A192171] 18 p2482 N88-24723

Supercritical fluid chromatography/supersonic jet spectroscopy
[DE88-007935] 19 p2614 N88-25511

SUPERCRITICAL WINGS

Investigations on a transonic airfoil with a 30 mm wide perforation/cavity arrangement
[ESA-TT-1072] 03 p0260 N88-11634

Static aeroelastic effects on the flutter of a supercritical wing 05 p0550 N88-13353

Testing of a schematic transport plane model in several European windtunnels
[PB87-170270] 09 p1113 N88-16671

Unsteady pressure and structural response measurements of an elastic supercritical wing
[NASA-TM-100591] 17 p2299 N88-23756

Analysis of experimental data for cast 10-2/DOA2 supercritical airfoil at high Reynolds numbers
[AD-A192827] 21 p2892 N88-27166

SUPERFLUID FLOW
U SUPERFLUIDITY

SUPERFLUIDITY

Superfluid He4 as a solar neutrino detector
[DE87-014477] 02 p0257 N88-11625

Design concepts for the ASTROMAG cryogenic system
[NASA-CR-181505] 04 p0497 N88-13060

Method of two-time Green functions in molecular hydrodynamics of superfluid liquid
06 p0771 N88-14735

Cryogenic acoustic microscopy
[AD-A187274] 10 p1299 N88-17767

Superfluid turbulence in He II at elevated pressures
10 p1422 N88-18493

Development of a motorized cryovalve for the control of superfluid liquid helium 14 p1925 N88-21477

Peculiarities of non-stationary heat transfer to superfluid helium
[DE88-701174] 16 p2200 N88-23124

Integrability of fermionic string in superfluid Hamiltonian approach
[DE88-701662] 16 p2284 N88-23678

Theoretical investigation of the development of the normal fluid and superfluid velocity distributions during spin-up for a He2-filled cylinder
[MPIS-6/1987] 18 p2510 N88-24892

Superfluid turbulence in counterflowing helium II
19 p2665 N88-25849

Superfluidity of a two dimensional Boson Coulomb gas
[DE88-008827] 19 p2735 N88-26244

Temperature rise in superfluid helium pumps
[NASA-TM-100997] 21 p2948 N88-27507

Superfluid Helium On-Orbit Transfer (SHOOT) operations
[NASA-TM-101009] 22 p3048 N88-28084

Stability experimental results of cable-in-conduit superconductor for fusion
[DE88-753424] 23 p3290 N88-29589

SUPERGIANT STARS

Basic properties and variability
02 p0252 N88-11593

Spectroscopy and nonthermal processes
02 p0252 N88-11594

Circumstellar shells, the formation of grains, and radiation transfer 02 p0252 N88-11596

Fifth Cambridge Workshop on Cool Stars, Stellar Systems and the Sun 04 p0502 N88-13092

The acceleration of winds by MHD waves in open magnetic structures 04 p0506 N88-13109

An analysis of the photospheric line profiles in F, G, and K supergiants 04 p0513 N88-13157

A flash spectrum of Cl I, C I, N I, and Ni II absorption in 31 Cygni: A direct observation of the reversing layer
04 p0513 N88-13158

Sensitivity of the H alpha line to expansion, geometrical extent and temperature gradient in the G and K supergiant chromospheres 04 p0514 N88-13159

Radio continuum emission from the ionized stellar winds of the cool supergiants in zeta Aurigae-like systems
04 p0514 N88-13160

Winds and shells around low-mass supergiants
04 p0514 N88-13164

Far infrared circumstellar debris shells of red supergiant stars 04 p0515 N88-13165

VLA observations of rapid 6 cm flux variations in alpha Ori 04 p0515 N88-13169

A comprehensive exploration of late-type stars in the far-ultraviolet 04 p0520 N88-13194

The EUV line flux variations and activity in Alpha Orionis 08 p1032 N88-16256

Evolutionary helium and CNO anomalies in the atmospheres and winds of massive hot stars
[NASA-CR-183254] 24 p3452 N88-30550

The kinematics of late-type supergiants
[SER-C-PREPUBL-FASC-28] 24 p3454 N88-30560

SUPERGRAVITY

Spontaneous symmetry breaking in N = 2 supergravity
[DE87-702749] 01 p0109 N88-10704

Spontaneous symmetry breaking in N = 3 supergravity
[DE87-702753] 01 p0109 N88-10705

New class of spherically symmetric interior solution with cosmological constant
[DE87-703095] 02 p0226 N88-11422

Our universe as an attractor in a superstring model
[DE87-703066] 02 p0251 N88-11585

Geometrization of Planck length in composite gravity and supergravity
[DE87-703085] 02 p0251 N88-11588

Chiral U(1) anomaly in D = 4 super Yang-Mills theory coupled to supergravity
[DE87-753022] 02 p0252 N88-11591

Research in theoretical physics: Results from last year 1986/87
[DE88-004922] 10 p1423 N88-18502

Freund-Rubin type solutions for different compactifications of the eleven-dimensional space
[DE88-700869] 12 p1686 N88-20082

Ten dimensional N = 1 supergravity coupled to supersymmetric Yang-Mills fields in superspace
[DE87-703033] 15 p2146 N88-22808

N = 2 supergravity in superspace: Solution to the constraints
[DE88-702135] 19 p2741 N88-26272

N = 2 supergravity in superspace: The invariant action
[DE88-702136] 19 p2741 N88-26273

N = 2 supergravity in superspace: different versions and matter couplings
[DE88-702137] 19 p2741 N88-26274

Lagrangian of the self-duality equation and d = 10, N = 2b supergravity
[DE88-701554] 24 p3455 N88-30563

SUPERHARMONICS

N = 2 supergravity in superspace: Solution to the constraints
[DE88-702135] 19 p2741 N88-26272

N = 2 supergravity in superspace: different versions and matter couplings
[DE88-702137] 19 p2741 N88-26274

SUPERHEATING

Development of creep resistant austenitic stainless steels for advanced steam cycle superheater application
[DE87-012929] 01 p0023 N88-10147

Microwave superheaters for fusion
[DE88-001656] 05 p0653 N88-14007

Review of nucleation and incipient boiling under pool and forced convection conditions
08 p0982 N88-15938

The effect of asymmetric current-supporting electron velocity distributions on second harmonic electron cyclotron resonance heating: A ray-tracing treatment for the compass tokamak
[INPE-4389-PRE/1209] 08 p1087 N88-16549

Kinetics of homogeneous nucleation in superheated F-11 and F-21 liquid freons
[NASA-TT-20286] 19 p2613 N88-25503

Solidification with natural circulation
[DE88-011197] 22 p3074 N88-28248

Initiation of explosive molten aluminum-water interactions at wet or underwater surfaces
[DE88-004686] 23 p3194 N88-29006

SUPERHETERODYNE RECEIVERS

Comparative investigation of heterodyne mixers at 1000 GHz
[FTL-068627] 09 p1158 N88-16940

SUPERHIGH FREQUENCIES

Phase 2 development of a 12 GHz MMIC FET amplifier
[IM-I86-1010] 01 p0038 N88-10240

Performance of high power S-band klystrons focused with permanent magnet
[DE87-753024] 02 p0167 N88-11053

X-band SAR for a European remote sensing payload
03 p0340 N88-12142

X-band uplink ground systems development: Part 2
04 p0436 N88-12703

Optically tuned MM-wave IMPATT source
[AD-A185250] 05 p0577 N88-13523

Results on the low elevation angle propagation experiment, part 1
[TUD-R-328] 06 p0693 N88-14250

GaAs MMIC yield evaluation --- monolithic microwave integrated circuits (MMIC)
[ESA-CR(P)-2470] 08 p0979 N88-15916

Investigation of the quantitative determination of two dimensional sea surface wave spectra from shipborne radar measurements
[GKSS-87/E/10] 09 p1195 N88-17163

X-band system performance of the very large array
11 p1473 N88-18789

DSS 14 64-meter antenna S- and X-band efficiency and system noise temperature calibrations, September 1987
11 p1473 N88-18790

Characterization of 6 soils in the X-band, through measurements of complex permittivity
[INPE-4376-TDL/302] 12 p1639 N88-19814

Preparation and execution of calibration measurements for handling of airborne SAR data (AGRISAR)
[ETN-88-92338] 17 p2333 N88-23926

Monolithic GaAs Ku-band one watt constant phase variable power amplifier
[DE88-006272] 18 p2506 N88-24866

An overview of the OmniTRACS: The first operational mobile Ku-band satellite communications
19 p2644 N88-25689

X-band resonant ring operation at 450 kW
22 p3064 N88-28181

X-band noise temperature near the Sun at a 34-meter high efficiency antenna 22 p3067 N88-28200

DSS 14 antenna calibrations for GSSR/VLA Saturn radar experiments 22 p3068 N88-28207

SUPERHYBRID MATERIALS
NT GRAPHITE-EPOXY COMPOSITES

SUPERIMPOSITION (MATHEMATICS)
U SUPERPOSITION (MATHEMATICS)

SUPERLATTICES

Metallic superlattices with monolayer modulation
[DE87-012724] 01 p0023 N88-10145

Superconducting properties of metallic superlattices
[DE87-012725] 01 p0023 N88-10146

Photoluminescence studies of GaAs/AlAs superlattices
[DE87-013817] 02 p0245 N88-11548

Interaction between defects and the formation of dissipative structures in irradiated impure crystals
[DE87-703125] 02 p0246 N88-11552

Non-lattice matched metallic superlattices
[DE87-011512] 04 p0497 N88-13062

MBE growth of InAsSb strained-layer superlattices
[DE88-000365] 05 p0654 N88-14011

Waves and vibrations in elastic superlattice composites 06 p0776 N88-14765

Structure of layered crystals studied by high energy ion beams
[DE88-001675] 06 p0786 N88-14822

Tailorable infrared sensing device with strain layer superlattice structure
[NASA-CASE-NPO-16607-1-CU]
06 p0788 N88-14836

The role of thermodynamic phase diagrams and lattice matching in superlattice growth
[DE88-003113] 08 p1091 N88-16568

Hydrogen in niobium-tantalum superlattices
09 p1146 N88-16867

Neutron and X-ray scattering studies of layered solids
09 p1246 N88-17469

Superlattice photodetectors
[AD-A186956] 09 p1253 N88-17511

Optical characterization of GaAs/sub 1-x/Sb/sub x/ and GaAs/sub 1-x/Sb/sub x/GaAs strained layer superlattices
[DE88-003393] 10 p1418 N88-18464

Magnetic rare earth superlattices
[DE88-003483] 10 p1418 N88-18465

MBE growth, characterization and electronic device processing of HgCdTe, HgZnTe related heterojunctions and HgCdTe-CdTe superlattices
[AD-A187456] 10 p1421 N88-18486

Theoretical studies of the interface electronic properties of tetrahedrally coordinated semiconductors
[AD-A187216] 11 p1555 N88-19306

MBE (Molecular Beam Epitaxial) growth characterization and electronic device processing of HgCdTe, HgZnTe related heterojunctions and HgCdTe-CdTe superlattices
[AD-A187416] 11 p1555 N88-19307
Atomic monolayer metallic superlattices
[DE88-005348] 12 p1607 N88-19612
Brillouin scattering from collective spin waves in magnetic superlattices
[DE88-005347] 12 p1697 N88-20154
Silicon-germanium heterostructures
13 p1844 N88-21034
Photon-controlled growth of multilayered structures
[DE88-005061] 13 p1847 N88-21054
Competing interactions in metallic superlattices
[DE88-005344] 13 p1847 N88-21057
Superconducting superlattice structures
[DE88-005346] 13 p1847 N88-21058
Dynamical aspects of carrier tunneling in semiconductor superlattices 14 p1977 N88-21799
The Shubnikov de Haas effect in narrow-gap semimagnetic semiconductors
[ETN-88-92249] 14 p1986 N88-21861
Experimental studies on electronic properties of HgTe/CdTe and Hg sub 1-z Cd sub x Te/CdTe heterostructures and superlattices
[AD-A189826] 15 p2142 N88-22783
Fundamental properties and devices applications of Ge(x)Si(1-x)/Si superlattices
[AD-A190129] 15 p2143 N88-22787
Neutron diffraction refinement of CsHSO4 superionic phase structure
[DE88-701496] 18 p2580 N88-25326
Crystalline metal-semiconductor superlattices
[DE88-007063] 18 p2581 N88-25332
Electronic structure, elementary excitations, optical and transport properties of semiconductor superlattices
[AD-A190795] 18 p2581 N88-25333
Magnetic superlattices
[AD-A191450] 18 p2581 N88-25334
Optical properties of heterostructures and superlattices
[AD-A191542] 18 p2581 N88-25335
An investigation of 2-6 superlattice deposition by laser photochemical techniques
[AD-A191547] 18 p2581 N88-25336
Molecular Beam Epitaxy (MBE) for high speed devices
19 p2656 N88-25770
Defects in high-mobility semiconductor systems
[AD-A191618] 19 p2732 N88-26224
Third International Conference on Superlattices, Microstructures and Microdevices
[AD-A191416] 20 p2861 N88-26995
Piezoelectric effects in strained layer superlattices
20 p2863 N88-27002
Control of carrier lifetime in PbTe nipi superlattices by external photoinjection 20 p2863 N88-27006
Metallic superlattices 20 p2864 N88-27012
Properties of synthetic magnetic superlattices
20 p2865 N88-27014
Superlattice doping interfaces
20 p2866 N88-27019
A 10 microns photoexcited avalanche gain due to electron impact ionization from GaAs quantum well superlattices 20 p2867 N88-27026
Transport study on Si/Si(1-x)Ge(x) superlattices selectively doped by secondary implantation of Sb
20 p2867 N88-27027
Electrical properties of p-type and n-type ZnSe-ZnTe strained-layer superlattices 20 p2868 N88-27029
MBE growth of HgTe/CdTe superlattices on Si(100) substrates 20 p2869 N88-27033
Growth of high quality CoSi2/Si superstructures on Si(111) 20 p2869 N88-27034
Phonons in semiconductor superlattices
20 p2869 N88-27035
Electronic structure of quantum-well states revealed under high pressures 20 p2870 N88-27038
On a-Si:H/a-SiN(x):H superlattices: Confinement or contamination 20 p2870 N88-27040
Extended and local plasmons in a lateral superlattice
20 p2870 N88-27041
Resonant tunneling in InGaAs-InP double-barrier structures and superlattices 20 p2871 N88-27047
Non-effective-mass matching in superlattices
20 p2872 N88-27049
Influence of interfaces on electronic and magnetic properties of MnSe/ZnSe superlattices near monolayer limit 20 p2872 N88-27050
Structural studies of (Ga,In)(As,P) alloys and (InAs) sub m (GaAs) sub n strained-layer superlattices by fluorescence-detected EXAFS 20 p2872 N88-27051
Type 3 - type 1 transition and strain effect in Hg(1-x)Cd(x)Te-CdTe and Hg(1-x)Zn(x)Te-CdTe superlattices 20 p2872 N88-27052
Ordering transitions of ternary alloys A(1-x)B(x)C
20 p2873 N88-27054
Aperiodic superlattices: Structured randomness
20 p2873 N88-27055
Characterization of structural and magnetic order of Er/Y superlattices 20 p2873 N88-27056
Superconductivity of Cr/V superlattices
20 p2874 N88-27057
Thermal conductivity of isotopically pure semiconductors, superlattices, semiconductor alloys and semiconductors as a function of temperature; control of the segregation coefficient in LEC crystal growth; and photo-Hall measurements of GaAs
21 p2927 N88-27375
Solar energy conversion through the interaction of plasmons with tunnel junctions. Part A: Solar cell analysis. Part B: Photoconductor analysis
[NASA-CR-183044] 21 p2967 N88-27621
Laser spectroscopy of quantum well and superlattice structures
[AD-A193336] 21 p3022 N88-27937
Investigations on the MBE (Molecular Beam Epitaxy) growth and properties of Al(sub y)Ga(sub y)In(sub 1-x-y)AsInP and InGaAs-InAlAs superlattices
[DE88-009105] 21 p3022 N88-27941
Meaning of energy diagrams used to describe hetero-structures
[DE88-702219] 21 p3023 N88-27943
Studies on strained (In,Ga)As/GaAs semiconductors and optical devices 23 p3287 N88-29575
Intrinsic and extrinsic energy states of semiconductors and heterostructures using novel techniques
[DE88-008560] 23 p3289 N88-29582
Electronic states in tunneling semiconductor superlattices
[DE88-011571] 23 p3290 N88-29587

SUPERMASSIVE STARS
Intermixing processes in massive stars and their influence on stellar evolution and nucleosynthesis
[ETN-88-91484] 11 p1568 N88-19388
IUE evidence on the nature of the innermost broad-line region in Seyfert 1 galaxies 17 p2450 N88-24552

SUPERNOVA REMNANTS
On the (lack of) proper motion of the Vela pulsar
01 p0097 N88-10635
Recent X-ray observations of supernova remnants and their interpretation
[MPE-PREPRINT-96] 09 p1262 N88-17563
A 23 hour EXOSAT observation of the X-ray pulsar 1E2259+586 and the associated supernova remnant G109.1-1.0
[MPE-PREPRINT-99] 14 p1994 N88-21882

SUPERNOVA 1987A
Data recorded by the Rome room temperature gravitational wave antenna, during the supernova SN 1987 A in the Large Magellanic Cloud
[NOTA-INTERNA-879] 06 p0806 N88-14922
A look at Supernova 1987A
[DE88-003411] 10 p1429 N88-18531
Particle physics and cosmology
[DE88-004944] 13 p1854 N88-21096
Astron observations of supernova 1987A in large magellanic cloud 24 p3445 N88-30504

SUPERNOVAE
NT SUPERNOVA 1987A
High explosive simulations of supernovae and the supernova shell fragmentation model of solar system formation
[DE87-014708] 02 p0251 N88-11584
Adiabatic supernova expansion into the circumstellar medium
[DE87-014241] 03 p0387 N88-12433
Neutrinos in supernovae
[DE87-014295] 03 p0387 N88-12434
Core bounce supernovae
[DE87-014910] 04 p0520 N88-13197
An automated supernova search and the design strategy
[DE88-001627] 05 p0660 N88-14051
Numerical modelling of the classical nova outburst
[NASA-TM-89707] 07 p0945 N88-15746
An introduction to nuclear astrophysics
[DE88-002761] 08 p1100 N88-16618
Onset of type 2 supernova in circumstellar envelope created by the stellar wind from presupernova
[DE88-700448] 10 p1428 N88-18526
Calculated late time spectra of supernovae
[DE88-003296] 10 p1428 N88-18530
Supernova mechanisms: Before and after SN1987a
[DE88-003489] 10 p1429 N88-18533
The type Ia supernova 1986G in NGC5128: Optical photometry and spectra
[INPE-4426-PRE/1230] 12 p1710 N88-20231
Hydrodynamical models of supernova SN 1987 A in the LMC
[DE88-701123] 15 p2151 N88-22837
Research and Technology, 1987, Goddard Space Flight Center
[NAS 1.15:101097] 17 p2453 N88-24572
Nuclear and astrophysical evidence on the equation of state
[DE88-007397] 18 p2572 N88-25279
Pre-supernova evolution of SN 1987A
[SER-C-PREPUBL-FASC-15] 18 p2593 N88-25409
To the opportunities of cluster analysis of light curves of supernovae
[DE88-701642] 21 p3030 N88-27982
Strange, quark and metastable neutron stars
[DE88-702404] 21 p3030 N88-27984
Resonant spin-flavor precession of solar and supernova neutrinos
[DE88-752604] 23 p3308 N88-29707
Gamma radiation expected from supernova 1987A in large magellanic cloud 24 p3445 N88-30505
Activities report in astronomy
[ISSN-0531-4496] 24 p3451 N88-30535

SUPERPLASTICITY
Superplastic deformation and post forming tensile properties of Ti-6Al-4V sheet
[RAE-TR-86015] 01 p0023 N88-10144
Tensile behavior of superplastic Al-Cu-Li-Zr alloy 2090 at cryogenic temperatures
[DE87-014084] 02 p0147 N88-10923
Investigation by differential scanning calorimetry of microstructure in a superplastic Al-Mg-Zr alloy
[AD-A184902] 05 p0564 N88-13439
Micromechanical and microstructural studies of ceramic superplasticity
[DE88-005793] 13 p1751 N88-20472
Superplastic flow of mullite-zirconia composites
[DE88-005905] 15 p2028 N88-22085
Superplasticity: A fundamental investigation on deformation mechanism and cavitation phenomena
[AD-A191548] 18 p2485 N88-24741
Optimizing superplastic response in lithium containing aluminum-magnesium alloys
[AD-A192217] 20 p2774 N88-26451
Thermomechanical processing of Al alloy 2090 for grain refinement and superplasticity
[AD-A192333] 21 p2912 N88-27281
Analysis of grain refinement and superplasticity in aluminum-magnesium alloys
[AD-A193029] 21 p2912 N88-27283
Equipment for the pressure welding of metals and alloys utilising the effects of superplasticity
[RAE-TRANS-2162] 22 p3055 N88-28129

SUPERPOSITION (MATHEMATICS)
A new method of calculating the boundary layer characteristics downstream of manipulators. Part 1: Boundary layer integral parameters
[PNR90455] 22 p3078 N88-28279

SUPERSATURATION
Microgravity nucleation and particle coagulation experiments support
[NASA-CR-181540] 04 p0423 N88-12618
Microgravity nucleation and particle coagulation experiments support
[NASA-CR-181541] 04 p0423 N88-12619
Precipitation in alumina-rich spinel: A transformation-toughened ceramic single crystal
[DE87-012380] 06 p0785 N88-14815
Nucleation in super-saturated products
[NASA-TT-20275] 15 p2037 N88-22134

SUPERSONIC AIRCRAFT
NT B-70 AIRCRAFT
NT CONCORDE AIRCRAFT
NT F-4 AIRCRAFT
NT F-14 AIRCRAFT
NT F-15 AIRCRAFT
NT F-16 AIRCRAFT
NT F-106 AIRCRAFT
NT F-111 AIRCRAFT
NT MIG AIRCRAFT
NT MIRAGE AIRCRAFT
NT RF-4 AIRCRAFT
NT SUPERSONIC TRANSPORTS
Experiences using the Mark IV supersonic hypersonic arbitrary body program 05 p0534 N88-13249
Time-temperature-stress capabilities of composite materials for advanced supersonic technology application
[NASA-CR-178272] 06 p0677 N88-14144
Aeropropulsion '87. Session 6: High-Speed Propulsion Technology
[NASA-CP-10003-SESS-6] 08 p0957 N88-15807
Shock structure and noise of supersonic jets in simulated flight to Mach 0.4
[NASA-TP-2785] 08 p1080 N88-16510
The design and use of a temperature-compensated hot-film anemometer system for boundary-layer flow transition detection on supersonic aircraft
[NASA-TM-100421] 13 p1723 N88-20304

Propulsion and airframe aerodynamic interactions of supersonic V/STOL configurations. Volume 1: Wind tunnel test pressure data report
[NASA-CR-177343-VOL-1] 16 p2157 N88-22866
Propulsion and airframe aerodynamic interactions of supersonic V/STOL configurations. Volume 2: Wind tunnel test force and moment data report
[NASA-CR-177343-VOL-2] 16 p2157 N88-22867
Propulsion and airframe aerodynamic interactions of supersonic V/STOL configurations. Volume 4: Summary
[NASA-CR-177343-VOL-4] 16 p2157 N88-22868
Parametric study of supersonic STOVL flight characteristics
[NASA-CR-177330] 16 p2161 N88-22893
PAN AIR analysis of the NASA/MCAIR 279-3: An advanced supersonic V/STOL fighter/attack aircraft
[NASA-TM-86836] 17 p2298 N88-23750
The challenges and opportunities of supersonic transport propulsion technology
[NASA-TM-100921] 17 p2307 N88-23806
Navier-Stokes analysis of transonic transport aircraft empennage 19 p2636 N88-25637
Low-speed wind-tunnel test of a STOL supersonic-cruise fighter concept
[NASA-TM-4050] 20 p2761 N88-26374
Supersonic transport/hypersonic transport (SST/HST) development
[REPT-881-111-101] 21 p2896 N88-27192
An analysis of lateral-directional handling qualities and Eigenstructure of high performance aircraft
[AD-A194874] 24 p3328 N88-29814

SUPERSONIC AIRFOILS
Supersonic aerodynamics of delta wings
[NASA-TP-2771] 10 p1273 N88-17615

SUPERSONIC BOUNDARY LAYERS
Supersonic boundary layer on a heated wall
[ETN-88-91617] 08 p0950 N88-15763
Fundamental aspects of the structure of supersonic turbulent boundary layers
[AD-A191494] 18 p2456 N88-24581

SUPERSONIC COMBUSTION
Interaction between two-dimensional sonic jets and supersonic flow to model heat addition in a supersonic combustor
[AD-A189572] 13 p1716 N88-20261
Turbulent reacting flows and supersonic combustion
[AD-A189690] 15 p2034 N88-22115
JPRS report: Science and technology. Japan
[JPRS-JST-88-005] 19 p2633 N88-25619
Basic research in supersonic combustion
19 p2634 N88-25623

SUPERSONIC COMBUSTION RAMJET ENGINES
SCRAM JET (Supersonic Combustion Ramjet) combustion experiments 04 p0404 N88-12512
Aerodynamics of Hypersonic Lifting Vehicles
[AGARD-CP-428] 05 p0529 N88-13219
Hypersonic airbreathing propulsion: Evolution and opportunities 05 p0531 N88-13231
Numerical analysis of flow through scramjet engine inlets 05 p0532 N88-13233
Ignition and flameholding in supersonic flow by injection of dissociated hydrogen 05 p0560 N88-13410
Advanced fabrication techniques for hydrogen-cooled engine structures
[NASA-CR-3949] 06 p0723 N88-14447
Analysis and performance prediction of scramjet inlets utilizing a three-dimensional Navier-Stokes code
07 p0811 N88-14936
Aeropropulsion '87. Session 6: High-Speed Propulsion Technology
[NASA-CP-10003-SESS-6] 08 p0957 N88-15807
Hypersonic propulsion research
08 p0958 N88-15812
An analytical study of the hydrogen-air reaction mechanism with application to scramjet combustion
[NASA-TP-2791] 08 p0966 N88-15846
An investigation into the feasibility of using a dual-combustion mode ramjet in a high Mach number tactical missile
[AD-A186906] 09 p1119 N88-16705
Investigations into shock-induced enhancement of mixing and combustion in supersonic burners
[AD-A189609] 12 p1607 N88-19609
Active cooling design for scramjet engines using optimization methods
[NASA-TM-100581] 13 p1783 N88-20669
Numerical and experimental investigation of multiple shock wave/turbulent boundary layer interactions in a rectangular duct
[AD-A190772] 15 p2066 N88-22320
Measurement data processing system based on personal computer: For scramjet combustion test
[DE88-751807] 16 p2174 N88-22959
Numerical simulation of scramjet inlet flow fields
[NASA-TP-2517] 17 p2296 N88-23735
Two-dimensional viscous flow computations of hypersonic scramjet nozzle flowfields at design and off-design conditions
[NASA-CR-182150] 19 p2603 N88-25459
Mach 2 combustion characteristics of hydrogen/hydrocarbon fuel mixtures
19 p2625 N88-25568

SUPERSONIC COMPRESSORS
Application of highly loaded single-stage mixed-flow compressors in small jet-engines
10 p1280 N88-17652
Design and testing of a front stage for an advanced high pressure compressor 10 p1283 N88-17679

SUPERSONIC CRUISE AIRCRAFT RESEARCH
Concept development of a Mach 3.0 high-speed civil transport
[NASA-TM-4058] 21 p2895 N88-27182

SUPERSONIC DRAG
Submunitions simulations, volume 2
[TR-CR-RD-SS-87-7-VOL-2] 19 p2641 N88-25669

SUPERSONIC FLIGHT
Time-temperature-stress capabilities of composite materials for advanced supersonic technology application
[NASA-CR-178272] 06 p0677 N88-14144
Wind tunnel investigation of wing and control panel loads at transonic and supersonic speeds on some schematic cruciform missile configurations
[FFA-TN-1986-43] 18 p2457 N88-24585

SUPERSONIC FLOW
Intergration effects of D-shaped, underwing, aft-mounted, separate-flow, flow-through nacelles on a high-wing transport
[NASA-TM-4018] 02 p0122 N88-10773
Numerical simulation of a supersonic chemically reacting mixing layer 02 p0143 N88-10900
Optical fiber interferometric sensor to measure temperature in gas flow
[ENST-87E006] 02 p0170 N88-11071
A supersonic potential gradient method for the calculation of unsteady aerodynamic pressures on harmonically oscillating wings
[ESA-TT-930] 03 p0259 N88-11631
Efficient numerical approaches for predicting supersonic flows with viscous/inviscid interaction
03 p0260 N88-11637
Supercritical fluid chromatography/supersonic jet spectroscopy
[DE88-000297] 03 p0282 N88-11774
A hybrid numerical technique for predicting the aerodynamic and acoustic fields of advanced turboprops
[NASA-CR-174926] 03 p0374 N88-12352
Experimental and theoretical study of condensation in multicomponent mixtures
[DE88-000897] 04 p0413 N88-12563
Conical wing with maximum lift-to-drag ratio in supersonic gas flow 04 p0425 N88-12633
Numerical study of supersonic flow around blunt bodies with extended needle nose 04 p0425 N88-12635
Combustion related shear-flow dynamics in elliptic supersonic jets 05 p0531 N88-13232
Solution of some 3-D viscous and inviscid supersonic flow problems by finite-volume space-marching schemes
05 p0532 N88-13235
The role of computation fluid dynamics in aeronautical engineering (4): The development and applications of implicit TVD finite volume code
05 p0536 N88-13259
Numerical analysis of supersonic flows using panel method 05 p0537 N88-13266
Interferometric data for a shock-wave/boundary-layer interaction
[NASA-TM-88227] 05 p0543 N88-13306
Ignition and flameholding in supersonic flow by injection of dissociated hydrogen 05 p0560 N88-13410
A Cartesian finite-volume method for the Euler equations 05 p0579 N88-13532
Investigation of the effect of laterally ejected gas jets on flows
[ISL-R-107/86] 05 p0581 N88-13545
Hot wire and laser velocimeter studies of turbulent flow at supersonic velocities
[ETN-88-91172] 05 p0585 N88-13566
Studies of supersonic turbulence and hot-wire response using Laser-Induced Fluorescence (LIF)
06 p0664 N88-14072
NASA supersonic STOVL propulsion technology program
[NASA-TM-100227] 06 p0668 N88-14093
Numerical study of chemically reacting flows using an LU scheme
[NASA-CR-180882] 06 p0668 N88-14094
Performance of supersonic impingement radial turbines 06 p0712 N88-14367
Aerodynamic design and test performance of supersonic turbines for the Vulcain rocket engine
06 p0713 N88-14373
Supersonic turbines for organic fluid Rankine cycles from 3 to 1300 kW 06 p0713 N88-14375
Raman spectra of adsorbed layers on space shuttle and AOTV thermal protection system surface
06 p0799 N88-14890
Application of a full potential method for analysis of complex aircraft geometries 07 p0809 N88-14930
Fundamental aspects of the structure of supersonic turbulent boundary
[AD-A186366] 07 p0815 N88-14959
Supersonic boundary layer on a heated wall
[ETN-88-91617] 08 p0950 N88-15763
The simulation of three-dimensional viscous supersonic flow past blunt bodies with a hybrid implicit/explicit finite difference method
[DFVLR-FB-87-32] 08 p0950 N88-15765
Supersonic throughflow fans for high-speed aircraft
08 p0958 N88-15810
New techniques in computational aerodynamics
[AD-A186719] 09 p1112 N88-16664
Application of highly loaded single-stage mixed-flow compressors in small jet-engines
10 p1280 N88-17652
Development and application of oxygen flow tagging for velocity measurements and flow visualization in turbulent three-dimensional supersonic flows
[AD-A187982] 10 p1289 N88-17714
On the interaction of Tollmein-Schlichting waves in axisymmetric supersonic flows
[NASA-CR-181619] 10 p1331 N88-17955
Experimental research on swept shock wave/boundary layer interactions
[AD-A187250] 10 p1331 N88-17957
The structure and control of three-dimensional shock wave turbulent boundary layer interactions
[AD-A187642] 10 p1332 N88-17961
Self-pumped phase conjugation in a supersonically flowing medium
[AD-A188281] 10 p1338 N88-17998
On the stability of the supersonic boundary layer
11 p1435 N88-18561
Nonaxisymmetric body supersonic, aerodynamic prediction
[AD-A189338] 13 p1716 N88-20259
Interaction between two-dimensional sonic jets and supersonic flow to model heat addition in a supersonic combustor
[AD-A189572] 13 p1716 N88-20261
Tests on the AFWAL 65 deg delta wing at NLR: A study of vortex flow development between Mach = 0.4 and 4
[NLR-MP-86058-U] 13 p1717 N88-20266
The international vortex flow experiment: A test case for compressible Euler codes
[NLR-MP-86076-U] 13 p1717 N88-20267
Supercritical fluid chromatography/supersonic jet spectroscopy
[DE88-004438] 13 p1738 N88-20392
Investigation of supersonic chemically reacting and radiating channel flow
[NASA-CR-182726] 14 p1862 N88-21125
Basic instability mechanisms in chemically reacting subsonic and supersonic flows
[AD-A190101] 15 p2034 N88-22120
JPRS report: Science and technology. China
[JPRS-CST-87-043] 15 p2053 N88-22233
Zero-lift drag predictions in supersonic flow for complex configurations 15 p2054 N88-22246
Numerical and experimental investigation of multiple shock wave/turbulent boundary layer interactions in a rectangular duct
[AD-A190772] 15 p2066 N88-22320
Analysis for high compressible supersonic flow in converging nozzle
[IPPJ-860] 16 p2157 N88-22869
An integral equation for the linearized supersonic flow over a wing
[AD-A191408] 16 p2158 N88-22875
User's manual for EULER3DS
[AD-A191048] 16 p2208 N88-23177
Multi-body aircraft with an all-movable center fuselage actively controlling fuselage pressure drag
[NASA-CASE-LAR-13511-1] 17 p2301 N88-23765
An efficient parallel algorithm for the simulation of three-dimensional compressible transition on a 20 processor Flex/32 multicomputer
[NASA-CR-178340] 17 p2337 N88-23943
Fundamental aspects of the structure of supersonic turbulent boundary layers
[AD-A191494] 18 p2456 N88-24581
Numerical simulations of the flat-plate laminar boundary layer in subsonic and supersonic flow
[PDR/CFDU/IC/36] 18 p2511 N88-24895

Numerical solutions of the complete Navier-Stokes equations
[NASA-CR-183023] 18 p2514 N88-24914
A characteristic method for calculating the generalized flat flutter aerodynamic forces
[NASA-TT-20300] 19 p2598 N88-25438
Aerodynamic focusing of particles and heavy molecules
[DE88-007145] 19 p2598 N88-25440
Cascades with harmonically oscillating blades in supersonic flow
[NASA-TT-20323] 19 p2599 N88-25446
Supercritical fluid chromatography/supersonic jet spectroscopy
[DE88-007935] 19 p2614 N88-25511
Dual Stokes cars measurements in supersonic combusting flow 19 p2625 N88-25569
Numerical simulation of supersonic free-jets
19 p2636 N88-25639
Relaxation scheme for compressible flows
19 p2640 N88-25663
Non equilibrium expansion of a radiating gas in a channel of varying section
[DE88-702063] 19 p2665 N88-25845
Navier-Stokes code NS3D for blunt bodies. Part 1: Analysis, results and verification
[DE88-010105] 19 p2666 N88-25855
Three-dimensional viscous flow computations of a circular jet in subsonic and supersonic cross flow
[NASA-CR-182153] 20 p2800 N88-26616
Nonaxisymmetric viscous lower branch modes in axisymmetric supersonic flows
[NASA-CR-181687] 21 p2891 N88-27164
Velocity measurements and flow visualization in turbulent three-dimensional supersonic flows using oxygen flow tagging
[AD-A192551] 21 p2892 N88-27165
Cryogenic free jets
[DFVLR-FB-88-16] 21 p2900 N88-27210
An improved version of NCOREL: A computer program for 3-D nonlinear supersonic potential flow computations
[NASA-CR-4165] 22 p3038 N88-28039
Chemically-produced N2(A) to NO(X) energy transfer in a supersonic flow
[AD-A192501] 22 p3082 N88-28302
NF (a 1 delta) production in a supersonic flow using N2F4+H2 in a BCL-16 nozzle
[AD-A194478] 22 p3082 N88-28304
An integral equation for the linearized unsteady supersonic flow over a wing
[AD-A193773] 23 p3172 N88-28887
Preliminary studies of NF3+H2 production of N2(A3 sigma(+)u) in a supersonic flow
[AD-A194479] 23 p3219 N88-29162
N2(A3epsilon u+) by reaction of N2F4+H2 in a supersonic flow
[AD-A194493] 23 p3219 N88-29163
Accuracy criteria for evaluating supersonic aerodynamic coefficient predictions 24 p3317 N88-29756
Compression pylon
[NASA-CASE-LAR-13777-1] 24 p3323 N88-29789

SUPERSONIC FLOW INLETS
U SUPERSONIC INLETS

SUPERSONIC FLUTTER
Detailed on-blade measurements on a transonic fan in unstalled supersonic flutter
[PNR90424] 22 p3039 N88-28043

SUPERSONIC INLETS
Unsteady flow in a supercritical supersonic inlet
18 p2460 N88-24605

SUPERSONIC JET FLOW
Numerical analysis of flow characteristics of supersonic free-jets 05 p0538 N88-13274
On the start up of supersonic underexpanded jets --- Mach disks 11 p1435 N88-18563
The thermal evolution of the jets in SS433 --- galactic object
[MPE-PREPRINT-107] 16 p2289 N88-23705
Velocity measurements and flow visualization in turbulent three-dimensional supersonic flows using oxygen flow tagging
[AD-A192551] 21 p2892 N88-27165

SUPERSONIC NOZZLES
Design of supersonic Coanda jet nozzles
10 p1270 N88-17599

SUPERSONIC SPEED
Aerodynamic sensitivities from subsonic, sonic and supersonic unsteady, nonplanar lifting-surface theory
[NASA-TM-100502] 04 p0394 N88-12459
The aerodynamics of supersonic parachutes
[DE87-014846] 04 p0395 N88-12464
Vortex formation over delta, double-delta and wave rider configurations at supersonic speeds
05 p0533 N88-13243
Design of wings and wing/body configurations for transonic and supersonic speeds
05 p0545 N88-13318
Supersonic beam observations of semiconductor clusters
[AD-A184991] 05 p0655 N88-14018
Supersonic aerodynamics of delta wings
[NASA-TP-2771] 10 p1273 N88-17615
Aerodynamic characteristics of wings designed with a combined-theory method to cruise at a Mach number of 4.5
[NASA-TP-2799] 12 p1575 N88-19420
Nonaxisymmetric body supersonic, aerodynamic prediction
[AD-A189338] 13 p1716 N88-20259
The structure of sonic underexpanded turbulent air jets in still air
[AD-A190656] 16 p2157 N88-22870
Submunitions simulations, volume 2
[TR-CR-RD-SS-87-7-VOL-2] 19 p2641 N88-25669
High speed and high angle of attack wind tunnel test results of the winged space vehicle C-2
[ISAS-RN-623] 20 p2751 N88-26329
Wind tunnel tests of elliptical missile body configurations at Mach numbers 0.4 to 5.0
[AD-A193525] 22 p3036 N88-28040
Wind tunnel investigation of wing and control panel loads at transonic and supersonic speeds on some schematic cruciform missile configurations
[FFA-TN-1986-43-SUPPL-1] 22 p3039 N88-28044

SUPERSONIC TRANSPORTS
NT CONCORDE AIRCRAFT
Propulsion challenges and opportunities for high-speed transport aircraft 08 p0958 N88-15809
Conceptual final paper on the preliminary design of an oblique flying wing SST
[NASA-CR-182679] 16 p2161 N88-22891
The challenges and opportunities of supersonic transport propulsion technology
[NASA-TM-100921] 17 p2307 N88-23806
Concept development of a Mach 3.0 high-speed civil transport
[NASA-TM-4058] 21 p2895 N88-27182

SUPERSONIC TURBINES
Design and test of a high blade speed, high work capacity transonic turbine 10 p1281 N88-17658
Numerical solutions of unsteady inviscid transonic turbine cascade flows
[AD-A196111] 24 p3316 N88-29748

SUPERSONIC WIND TUNNELS
The 0.6m x 0.6m trisonic test section (TMK) of DFVLR in Cologne-Porz, Federal Republic of Germany (status 1986)
[ESA-TT-1052] 03 p0267 N88-11681
Experimental investigation of the subsonic high-altitude operation of the NASA Lewis 10- by 10-foot supersonic wind tunnel
[NASA-TM-100214] 08 p0959 N88-15814
Design of a supersonic wind tunnel
[ETN-88-92078] 14 p1870 N88-21176
Numerical and experimental investigation of multiple shock wave/turbulent boundary layer interactions in a rectangular duct
[AD-A190772] 15 p2066 N88-22320
A comparative study of vortex flows in wind and water tunnels 16 p2204 N88-23151
Supersonic wall adaptation in the rubber tube test section of the DFVLR Goettingen
[IB-222-87-A-08] 24 p3330 N88-29824

SUPERSONICS
Planform effects on the supersonic aerodynamics of multibody configurations
[NASA-TP-2762] 04 p0393 N88-12454

SUPERSTRING THEORY
U STRING THEORY

SUPERSYMMETRY
Spontaneous symmetry breaking in N=2 supergravity
[DE87-702749] 01 p0109 N88-10704
New class of spherically symmetric interior solution with cosmological constant
[DE87-703095] 02 p0226 N88-11422
Anomalies in gauge theories
[DE87-014087] 02 p0229 N88-11444
Superconformal invariance and superstring in background fields
[DE87-703097] 02 p0247 N88-11561
Geometrization of Planck length in composite gravity and supergravity
[DE87-703085] 02 p0251 N88-11588
Chiral U(1) anomaly in D = 4 super Yang-Mills theory coupled to supergravity
[DE87-753022] 02 p0252 N88-11591
A supersymmetric Lagrangian for Poincare gauge theories of gravity
[DE88-001570] 04 p0500 N88-13078
Breaking of supersymmetry degeneracy and phenomenological conditions
[PREPRINT-559] 06 p0790 N88-14843
Instanton in supersymmetric theory with static disorder
[DE88-700357] 07 p0940 N88-15716
On the dynamical supersymmetry of atomic hydrogen
[DE88-700713] 10 p1422 N88-18495
Research in theoretical physics: Results from last year 1986/87
[DE88-004922] 10 p1423 N88-18502
SUSY anomaly in quantum-mechanical systems
[DE88-700890] 12 p1699 N88-20170
Summary of supersymmetric particle search with the CELLO detector at Petra (Italy)
[NOTA-INTERNA-898] 14 p1980 N88-21818
Gluino branching ratio effects on the search for supersymmetry
[PREPRINT-572] 14 p1981 N88-21821
Strings in four dimensions
[DE88-006435] 14 p1990 N88-21864
On the Hilbert space of supersymmetric quantum systems
[DE88-701648] 16 p2284 N88-23677
Introduction to covariant formulation of superstring (field) theory
[DE87-703038] 18 p2586 N88-25363
Comment on non-renormalization theorem in the four dimensional superstrings
[DE88-752551] 18 p2586 N88-25367
General relativity invariance and string field theory
[DE88-702045] 19 p2737 N88-26252
Superalgebras with Grassmann algebra-valued structure constants from superfields
[DE88-702239] 21 p3011 N88-27862
Research in the theory of condensed matter and elementary particles
[DE88-010180] 22 p3151 N88-28749
Lagrangian of the self-duality equation and d = 10, N = 2b supergravity
[DE88-701554] 24 p3455 N88-30563

SUPPLEMENTS
NASA thesaurus supplement: A four part cumulative supplement to the 1985 edition of the NASA Thesaurus
[NASA-SP-7053(SUPP-4)] 08 p1093 N88-16575

SUPPLYING
Prototype resupply scheduler
08 p1064 N88-16428
Steps toward lunar settlement
[DE88-009141] 21 p2900 N88-27213
Maintenance and supply options
[NASA-CR-172062] 24 p3332 N88-29837

SUPPORT SYSTEMS
NT CLOSED ECOLOGICAL SYSTEMS
NT GROUND SUPPORT SYSTEMS
NT LIFE SUPPORT SYSTEMS
Repulsive force support system feasibility study
[NASA-CR-178400] 04 p0402 N88-12497
The effect of mass, wind angle and erection technique on the aeroelastic behaviour of a cable-stayed bridge model
[NAE-AN-46] 04 p0455 N88-12819
Space station accommodations for lunar base elements: A study
[NASA-TM-100501] 06 p0804 N88-14907
A space transportation system operations model
[NASA-TM-100481] 07 p0823 N88-14999
Global meteorological data facility for real-time field experiments support and guidance
[NASA-TM-4023] 14 p1947 N88-21608
Engine component retirement for cause. Volume 1: Executive summary
[AD-A192730] 20 p2760 N88-26371
Inflight rearming
[AD-A193564] 23 p3176 N88-28909
Definition of common support equipment and space station interface requirements for IOC model technology experiments
[NASA-TM-100656] 24 p3336 N88-29856

SUPPORTS
NT PYLONS
A passive vibration-cancelling isolation mount
05 p0595 N88-13636
Strain gage sting balance 204-6. Calibration report --- wind tunnels
[F+W-FO-1836] 09 p1168 N88-17002
Dynamic response of a geared train of rotors subjected to random support excitations 09 p1181 N88-17073
Centaur G Prime modal test 09 p1181 N88-17075
Microgravity isolation mount
[ESA-CR(P)-2480] 11 p1443 N88-18604
Development of isostatic mounts and associated guidelines --- spacecraft payloads
[CASA-IM-WP-301] 13 p1731 N88-20354

Design of a sound neck in connection with the model-support system of a transonic wind tunnel test section
[ILR-MITT-186(1987)] 14 p1869 N88-21171

Kinematic support using elastic elements
14 p1926 N88-21481

Almond test body — for microwave anechoic chambers
[NASA-CASE-LAR-13747-1] 18 p2502 N88-24845

Thermal compensating mount
[NASA-CASE-LAR-13794-1] 18 p2519 N88-24942

FEB (Multifilter Electronics Box) lifting device analysis, revision A
[AD-A192313] 21 p2935 N88-27427

Method of forming dynamic membrane on stainless steel support
[NASA-CASE-MSC-18172-3] 23 p3201 N88-29052

SUPPRESSION
U RETARDING

SUPPRESSORS

Investigation of fuel additive effects on sooting flames
[AD-A186403] 07 p0829 N88-15026

Computation of LMS (Least-Mean-Square) and matched digital filters for optical clutter suppression
[AD-A188685] 12 p1687 N88-20093

Kinetic mechanisms for ionization and afterburning suppression
[AD-A189219] 13 p1737 N88-20383

SURFACE ACOUSTIC WAVE DEVICES

The design and implementation of surface acoustic wave devices for linear FM and a new non-linear FM pulse compression technique for radar applications
[AD-A186741] 08 p0980 N88-15922

The acoustic-electric field analysis of multilayered surface acoustic wave devices
[ETN-88-91592] 09 p1242 N88-17446

Surface acoustic wave deposition sensor
[DE87-006527] 09 p1243 N88-17452

Measuring thin film properties using SAW (Surface Acoustic Wave) devices: Diffusivity and surface area
[DE88-002216] 13 p1834 N88-20970

Isothermal measurement and thermal desorption using SAW devices 19 p2671 N88-25881

Thermodynamic study of hygroscopic polymers using surface acoustic waves 19 p2672 N88-25882

Surface acoustic wave gas sensor based on film conductivity changes 19 p2673 N88-25894

The covariance of scalar fields scattered by pressure-release randomly rough surfaces
[AD-A192489] 22 p3146 N88-28714

Large aperture multi-dimensional laser radar testbed
[AD-A193447] 23 p3218 N88-29155

The use of a surface acoustic wave technique to study the growth behavior of small cracks in a high strength steel alloy 23 p3225 N88-29193

A theoretical and experimental investigation into the use of SAW weighting techniques in optical diffraction gratings
[RSRE-MEMO-4128] 23 p3283 N88-29549

SURFACE COOLING

Transient cooling of a hot surface by droplets evaporation, March 1986 - March 1987
[PB88-153341] 10 p1330 N88-17950

Investigation of annular flow at high evaporation rates in view of liquid film cooling
[DFVLR-FB-88-08] 21 p2949 N88-27517

Studies of gas turbine heat transfer airfoil surface and end-wall cooling effects
[AD-A195165] 24 p3326 N88-29805

SURFACE CRACKS

Thermomechanical cracking in coated media due to high speed asperity excitation
[AD-A184176] 04 p0454 N88-12809

The effect of microstructure on the surface crack length: Crack depth relationship for short cracks
05 p0600 N88-13670

Summary of comparison between experimental and analytical (including empirical) results for initiation of crack growth for surface cracks
[DE88-001604] 06 p0721 N88-14433

Study on the correlation of polystyrene (PS) film craze to its fracture behaviour by TEM (Transmission Electron Microscopy)
[PB87-143343] 08 p0970 N88-15870

Nonlinear line-spring model for surface crack analysis with particular reference to work hardening materials
[PB87-144838] 08 p0994 N88-16016

Fracture-resistant characteristics of medium-strength plates with regard to the initiation, stable and unstable propagation of surface cracks
[PB87-144804] 08 p0996 N88-16025

Finite element analysis for the calculation of calibration curves of fracture mechanics specimen for semicircular surface cracks with several starting depths, for the crack depth measurement following the dc potential method
[GKSS-87/E/19] 09 p1183 N88-17086

Stress-intensity factors for small surface and corner cracks in plates
[NASA-TM-100599] 15 p2088 N88-22445

Surface crack analysis applied to impact damage in a thick graphite-epoxy composite
[NASA-TM-100600] 16 p2173 N88-22950

Fracture morphologies of carbon-black-loaded SBR (Styrene-Butadiene Rubber) subjected to low-cycle, high-stress fatigue
[DE88-006806] 16 p2181 N88-23002

On governing equations for crack layer propagation
[NASA-CR-182120] 16 p2223 N88-23272

The surface crack problem in an orthotropic plate under bending and tension
[NASA-CR-178281] 18 p2531 N88-25014

Boundary element method for contact heat transfer
[DE88-011013] 20 p2800 N88-26613

A critical review of IR drops and electrode potentials within pits, crevices and cracks
[AD-A192481] 21 p2935 N88-27431

Thermo-mechanical cracking in coated media with a cavity by a moving asperity friction
[AD-A193311] 21 p2961 N88-27586

Empirical fatigue crack growth data for a tension loaded threaded fastener
[AD-A194112] 22 p3088 N88-28334

SURFACE DEFECTS

Ultrasonic testing of near-surface zones using scattered signals
[ETN-88-90813] 07 p0929 N88-15642

Ultrasonic inspection of irregular surfaces
[AERE-R-12465] 13 p1780 N88-20648

Measurement of the elastic-plastic surface flaw back surface topology and its relation to constraint
[DE88-006765] 15 p2087 N88-22437

SURFACE DIFFUSION

De-alloying
[DE87-012488] 01 p0022 N88-10139

Studies of supported metal catalysts
[DE88-002546] 07 p0831 N88-15038

Numerical computations of natural convection heat transfer in irregular geometries
[DE88-002358] 07 p0852 N88-15178

Grain boundary and surface diffusion in oxides
[DE88-002348] 07 p0938 N88-15697

Laser-induced desorption determinations of surface diffusion on Rh(111)
[DE88-005159] 11 p1454 N88-18667

Depolarized infrared reflectance from dry and wetted surfaces
[AD-A188213] 11 p1492 N88-18903

On the global radiation incident variously orientated surfaces on the South Coast of Finland
[FMI-5] 20 p2823 N88-26746

SURFACE DISTORTION

Removal of out-of-plane distortion in mild steel panels using flame heating, volume 1
[AD-A187802] 11 p1457 N88-18684

Removal of out-of-plane distortion in mild steel panels using flame heating, volume 2
[AD-A187803] 11 p1457 N88-18685

Compensation of relector antenna surface distortion using an array feed
[NASA-TM-100286] 11 p1476 N88-18805

Case study of active array feed compensation with sidelobe control for reflector surface distortion
[NASA-TM-100287] 16 p2192 N88-23073

Thermal distortion analysis of the space station solar dynamic concentrator
[NASA-TM-100868] 19 p2606 N88-25475

Active feed array compensation for reflector antenna surface disturbions
[NASA-TM-100826] 19 p2654 N88-25762

SURFACE ENERGY

Estimating regional evapotranspiration from remotely sensed data by surface energy balance models
[NASA-CR-181400] 01 p0064 N88-10411

Evaluation of surface energy and radiation balance systems on the Konza Prairie
[NASA-CR-182534] 10 p1355 N88-18097

Surface free energy of laser-produced bond percolators
[PB88-130885] 11 p1493 N88-18913

SURFACE FINISHING

Surface treatment problems found in new aircraft designed using structural composites
[SNIAS-872-111-113] 05 p0558 N88-13397

The analysis of metal finishing solutions by ion chromatography
[AD-A184812] 05 p0561 N88-13414

Fatigue characteristics of ion treated surfaces
05 p0606 N88-13713

New application of transition metal carbides detailed
06 p0675 N88-14132

Ion-beam nitriding of steels
[NASA-CASE-LEW-14104-2] 06 p0682 N88-14179

Study of surface treatment before bonding of light alloys
[DCQ/L-48-287/F] 06 p0682 N88-14181

Surface modification using ion beams: Recent developments at ORNL
[DE88-000951] 06 p0786 N88-14819

Chemical cleaning of metal surfaces in vacuum systems by exposure to reactive gases
[AD-A188588] 12 p1606 N88-19616

Comparison of isopropyl alcohol and trichloroethylene in removing solder flux
[DE88-005556] 14 p1889 N88-21288

Specimen preperation techniques for the examination of ceramic and metal-matrix composites
[DE88-005157] 15 p2030 N88-22094

Auger electron spectroscopy of contrast-forming layers on metals
[NASA-TT-20182] 16 p2178 N88-22980

Surface conditioning products as tools for corrosion removal and corrosion prevention
17 p2320 N88-23856

Influence of carbon fiber surface treatment
[ETN-88-92536] 18 p2492 N88-24787

Evaluation of the chromium oxide arc spraying treatment on solar energy collectors
[ETN-88-92564] 18 p2537 N88-25053

The knowledge based automatic extraction of the machinable surfaces for automatic CAD-CAM system
[INPE-4542-PRE/1288] 20 p2836 N88-26824

Fabrication technology
[DE88-010598] 20 p2855 N88-26955

Study of surface treatments before adhesive bonding of light alloys — aircraft industry
[ETN-88-92743] 21 p2916 N88-27308

Optimization of fatigue and friction properties of titanium by means of surface treatments
[ECL-87-22] 22 p3056 N88-28133

Fractal surface finish
[DE88-007972] 22 p3057 N88-28137

SURFACE GEOMETRY

Approximation and representation of explicit surfaces in the presence of singularities
[ETN-88-92191] 16 p2258 N88-23496

Cylindrical surface profile and diameter measuring tool and method
[NASA-CASE-MFS-28287-1] 17 p2341 N88-23959

SURFACE INTERACTIONS
U SURFACE REACTIONS

SURFACE IONIZATION

Laser post-ionization secondary neutral mass spectroscopy
[DE88-002979] 09 p1172 N88-17027

SURFACE LAYERS
NT MONOMOLECULAR FILMS

Auger electron spectroscopy of oxidized titanium overlayers: Speciation of homogeneous and heterogeneous samples
[KFK-4221] 02 p0146 N88-10913

Bond character at a silicon/copper surface
[AD-A184167] 03 p0295 N88-11851

Far-infrared spectra of lithium deposited on a gold electrode: Interpretation using a cluster model
[AD-A184231] 04 p0495 N88-13050

Atomic and electronic structure of surfaces and chemisorbed layers
[DE87-014987] 04 p0498 N88-13065

Cosmological applications of singular hypersurfaces in general relativity 04 p0521 N88-13202

The effect of ion beam mixed Ni-Al surface layers on PSB extrusion morphology in fatigued nickel
05 p0598 N88-13652

Model Cu/ZnO catalysts for methanol synthesis: The role of surface structure
[DE88-002354] 07 p0830 N88-15037

Foam generation and air entrainment near a free surface
[AD-A185986] 07 p0848 N88-15149

Analysis of load-bearing capacity of nitrided layer
[PB87-144176] 08 p0968 N88-15857

Monolayer films prepared by the spontaneous self-assembly of symmetrical and unsymmetrical dialkyl sulfides from solution onto gold substrates: Structure, properties, and reactivity of constituent functional groups
[AD-A186717] 09 p1137 N88-16814

Geometric structure, pseudoband gaps, and surface vibrational resonances on metal surfaces
[AD-A187001] 09 p1143 N88-16851

Tactile sensing and inverse problems
[AD-A187464] 10 p1340 N88-18011

Cost 501 Project U.K.10. Part 4: The oxidation of fecralloy steel co-extruded onto strong steel substrates
[AERE-R-12432-PT-4] 11 p1456 N88-18679

Characterization of enhanced Schottky-barrier InGaAs/Al(1-x)As strained channel modulation-doped field-effect transistors
[AD-A188820] 12 p1698 N88-20162

Characterization of redox states of nickel hydroxide film electrodes by in-situ Raman spectroscopy
[AD-A189288] 13 p1741 N88-20411
Vertical turbulent transfer of matter in thin ocean surface layer during daytime heating 13 p1787 N88-20693
High-efficiency thin-film silicon-on-GaP solar cell for improved radiation resistance
[AD-A190268] 15 p2091 N88-22460
Studies of surfaces using optical sum-frequency generation
[DE88-006334] 15 p2131 N88-22715
Calculating depletion region carrier concentrations with capacitance-voltage measurements and etching
[AD-A189630] 15 p2141 N88-22777
On governing equations for crack layer propagation
[NASA-CR-182120] 16 p2223 N88-23272
Evaluating evaporation with satellite thermal data
[AD-A192042] 18 p2531 N88-25019
Surface phases and their influence on metal-oxide interfaces
[DE88-007938] 20 p2769 N88-26420
Fundamental optical studies of competitive adsorption and thin film phenomena
[DE88-008780] 20 p2875 N88-27068
Electronic and geometric structure of silver and palladium on aluminum (111) in monoatomic surface layers
[ETN-88-92120] 20 p2879 N88-27093
Thermo-mechanical cracking in coated media with a cavity by a moving asperity friction
[AD-A193311] 21 p2961 N88-27586
Elastic behavior of a rubber layer bonded between two rigid spheres
[AD-A193696] 23 p3198 N88-29030

SURFACE NAVIGATION
Dynamic image interpretation for autonomous vehicle navigation
[AD-A184043] 03 p0262 N88-11647
Autonomous Land Vehicle (ALV) planning and navigation system
[AD-A184243] 04 p0397 N88-12475
A computer simulation study of an expert system for walking machine motion planning
[AD-A187907] 11 p1438 N88-18577
A comparison of terrain association and resection as methods of position location
[AD-A189480] 13 p1790 N88-20710
Assessment of the differential technique for land navigation within 1000 km of Omega Australia
[AD-A191036] 16 p2160 N88-22885
The integration of digital maps in vehicle navigation systems 16 p2225 N88-23286
Joint University Program for Air Transportation Research, 1986
[NASA-CP-2502] 17 p2293 N88-23715
Navigation system for land vehicles
[NASA-CASE-LAR-13322-1] 18 p2462 N88-24620
Navigation using the Teldix fiber-optic gyroscope
18 p2517 N88-24933
Contribution of space to marine activities
19 p2700 N88-26057
Automatic omega station and LOP (Line Of Position) selection
[AD-A193302] 21 p2894 N88-27179
Measurement and interpretation of North Atlantic Ocean marine radar sea scatter
[AD-A196239] 24 p3364 N88-30036

SURFACE PRESSURE
U PRESSURE

SURFACE PROPERTIES
NT ADHESION
NT ADSORPTIVITY
NT COEFFICIENT OF FRICTION
NT INTERFACIAL TENSION
NT SKIN TEMPERATURE (NON-BIOLOGICAL)
NT SPECTRAL REFLECTANCE
NT SURFACE CRACKS
NT SURFACE DEFECTS
NT SURFACE ENERGY
NT SURFACE ROUGHNESS
NT SURFACE STABILITY
NT SURFACE TEMPERATURE
NT WALL TEMPERATURE
Recovery of vacuum gaps after arcing
[DE87-013852] 01 p0039 N88-10250
High-efficiency silicon solar cells: Numerical modeling, transient measurements, efficiency goals, and v-shaped grooves
[DE87-012842] 01 p0066 N88-10423
A surface science investigation of potential intermediates, catalysts, and promoters in the synthesis of higher alcohols by metals
[DE87-014188] 02 p0144 N88-10906
Field ion microscope studies of surface reconstructions
[DE87-014644] 02 p0147 N88-10924
Investigation of the structure of coatings of self fluxing alloys fused by laser energy
[BLL-M-37301-(5828.4)] 02 p0148 N88-10930
Surface topography and electrical response of metal-electrolyte interface
[DE87-013553] 02 p0166 N88-11046
Surface effects and low frequency noises in GaAs field effect transistors
[LAAS-87-179] 02 p0168 N88-11055
Analytical caustic surfaces
[NASA-TM-87805] 02 p0168 N88-11060
A preliminary taxonomy of visible surface algorithms
[DE87-013559] 02 p0220 N88-11386
Plasmon resonance absorption in layered structures of silver with periodic corrugation
[DE87-013183] 02 p0231 N88-11453
The structure and reactivity of heterogeneous surfaces and study of the geometry of surface complexes
[DE88-000158] 03 p0279 N88-11754
Materials preparation and longevity in hyperthermal atomic oxygen 03 p0297 N88-11862
The formation of optical membrane reflector surfaces using uniform pressure loading
[DE87-012275] 03 p0376 N88-12367
Characterization of catalysts with metal-support effects and of the species adsorbed on their surfaces
[DE87-014636] 04 p0414 N88-12564
Characterization of thin layers for optics
[PB87-217949] 04 p0490 N88-13017
Calibration on the Sun for stellar magnetic fields
04 p0506 N88-13113
The dynamics of solar magnetic flux tubes subjected to resonant foot point shaking 04 p0507 N88-13118
A complete linearized theory for the analysis and design of two-dimensional hydrofoils near a free surface
[UTIAS-TN-264] 05 p0579 N88-13531
Dynamical analysis of molecular decay at spherical surfaces
[AD-A184906] 05 p0647 N88-13964
Effect of metal surface properties on the fatigue crack growth behavior 06 p0716 N88-14390
Investigation of silicon surface passivation by silicon nitride film deposition
[NASA-CR-182350] 06 p0729 N88-14487
Automated satellite cloud analysis: A multispectral approach to the problem of snow/cloud discrimination
[AD-A185672] 06 p0746 N88-14591
A surface plasmon waveguide sensor: A new type of chemical transducer based on optical phenomena
[ETN-88-91322] 06 p0780 N88-14792
Extending the range of Low Energy Electron Diffraction (LEED) surface structure determination: Co-adsorbed molecules, incommensurate overlayers and alloy surface order studied by new video and electron counting LEED techniques
[DE88-001401] 06 p0786 N88-14820
Helium atom surface scattering apparatus for studies of crystalline surface dynamics
[DE88-002104] 06 p0787 N88-14826
Photon stimulated desorption from oxidized Al(110)
[DE88-002209] 06 p0787 N88-14828
A jet in a crossflow
[NASA-CR-182469] 09 p1113 N88-16674
Surface composition-reactivity relationships in heterogeneous catalysis
[DE87-003450] 09 p1140 N88-16834
Surface and interface electronic structure
[DE88-003363] 09 p1258 N88-17545
Monitoring interfacial dynamics by pulsed laser techniques
[DE88-003362] 10 p1335 N88-17976
Interactions of cultured human endothelial cells with polymeric surfaces
[PB88-112255] 10 p1369 N88-18178
Solving complex and disordered surface structures with electron diffraction
[DE88-003863] 10 p1418 N88-18467
Preliminary experiments on surface flow visualization in the cryogenic wind tunnel by use of condensing or freezing gases
[NASA-CR-181634] 11 p1442 N88-18602
In situ ultrahigh vacuum friction measurement and wear track analysis of ion implanted 304 stainless steel
[DE88-004537] 11 p1494 N88-18922
Scanning tunneling microscopy of silver, gold, and aluminium monomers and small clusters on graphite
[DE88-003871] 11 p1562 N88-19349
Some applications of surface Raman and infrared spectroscopies to mechanistic electrochemistry involved adsorbed species
[AD-A188777] 12 p1606 N88-19602
Measuring and modeling near surface reflected and emitted radiation fluxes at the FIFE site
[NASA-CR-182660] 12 p1640 N88-19818
Airborne electromagnetic sounding of sea ice thickness and sub-ice bathymetry
[AD-A188939] 12 p1649 N88-19879
Relationships between remotely-sensed surface properties and subsurface structure in the ocean
[AD-A189317] 12 p1650 N88-19881
Superconductors with structured surfaces: Fields and currents
[AD-A189353] 12 p1699 N88-20164
A study of the interaction of light with sub-micron metallic surfaces
[DE88-003138] 13 p1776 N88-20624
Computer aided surface representation
[DE88-005408] 13 p1817 N88-20854
Optics for large telescope 13 p1840 N88-21014
Hydrogen pumping and release by graphite under high flux plasma bombardment
[DE88-005860] 13 p1842 N88-21021
Advances in contact algorithms and their application to tires
[NASA-TP-2781] 14 p1922 N88-21456
Measurement from satellites of land surface parameters and fluxes in the thermal infrared bands: Problems and methods 14 p1937 N88-21557
Technical applications of solar energy. Project: Selective coatings
[BMFT-FB-T-86-213] 14 p1943 N88-21591
The nucleus of Comet Halley
14 p2004 N88-21947
Properties of the nucleus of P/Halley
14 p2004 N88-21952
Physical-mechanical properties of matrices on the comet nuclei surface models 14 p2010 N88-21987
Study of surface discharges
[ONERA-12/7236-PY] 15 p2026 N88-22073
Structure of sol-gel silica
[DE88-006870] 15 p2033 N88-22114
Measurement of emissivity of industrial surfaces using a simple method
[NASA-TT-20165] 15 p2036 N88-22130
The thermal radiative properties of metals at high temperature
[DE88-006625] 15 p2038 N88-22141
JPRS report: Science and technology. Japan
[JPRS-JST-88-002] 15 p2050 N88-22210
Material surface improvement by laser
15 p2051 N88-22217
First-principles calculations of quasiparticle energies at surfaces and interfaces: Semiconductor surface-state spectra and band offsets
[DE88-006340] 15 p2141 N88-22773
Experimental investigation of the hypersonic flow over a six finned configuration
[AD-A190870] 16 p2157 N88-22871
Surface and interfacial properties of carbon fibers
[NASA-CR-182890] 16 p2173 N88-22951
Method of digital surface photometry of galaxies and its application to the edge-on galaxy NGC 5907
16 p2287 N88-23695
Thematic mapping utilizing data from the Thematic Mapper sensor of the LANDSAT satellite
17 p2361 N88-24060
Analysis of the parameters responsible for the variations of the illumination conditions in the LANSAT data
17 p2362 N88-24070
Arc-textured metal surfaces for high thermal emittance space radiators
[NASA-TM-100894] 18 p2487 N88-24754
The electrokinetic behavior of calcium oxalate monohydrate in macromolecular solutions
[NASA-TM-101144] 18 p2493 N88-24791
Evidences for distributed combustion
19 p2628 N88-25586
How much do edges affect the ignition of a homogeneous reactive solid: Summary to date
19 p2631 N88-25606
Surface fatigue life of CBN and vitreous ground carburized and hardened AISI 9310 spur gears
[NASA-TM-100960] 19 p2677 N88-25916
X-ray and optical analysis of surface properties of metal optics
[DE88-004033] 19 p2727 N88-26195
Epitaxial iron films
[AD-A191815] 19 p2732 N88-26225
The catalytic reactivity of thin film crystal surfaces
[DE88-006387] 19 p2732 N88-26228
Production of powdered sodium hydride with large specific surface by the catalyzed reaction of molten sodium with hydrogen-1
[NASA-TT-20185] 20 p2776 N88-26462
Scattering patterns of dihedral corner reflectors with impedance surface impedances
[NASA-CR-183078] 20 p2789 N88-26545
Evaluation of surface energy and radiation balance systems for FIFE
[NASA-CR-183118] 20 p2826 N88-26778

Eigenmatrix representations of radiance distributions in layered natural waters with wind-roughened surfaces
[PB88-188701] 20 p2828 N88-26780
SEGMERGE: A scanline visible surface algorithm with adaptive span selection and inexpensive antialiasing
[DE88-009186] 20 p2836 N88-26826
Sound propagation over uneven ground and irregular topography
[NASA-CR-182956] 20 p2849 N88-26911
Fermi level dependent native defect formation: Consequences for metal-semiconductor and semiconductor-semiconductor interfaces
[DE88-008247] 20 p2875 N88-27066
Computer modeling for surface properties of carbon fibers 21 p2928 N88-27383
Analytical approximation of a distorted reflector surface defined by a discrete set of points
[NASA-TM-101323] 21 p2934 N88-27424
Methods of determining playa surface conditions using remote sensing
[AD-A192663] 21 p2965 N88-27612
Self-energies and the interactions of particles with surfaces
[DE88-010451] 21 p3014 N88-27885
Characterization of crystalline silicon by electrochemical and Raman spectroscopy at the frontier semiconductor/electrolyte
[ETN-88-92354] 21 p3025 N88-27956
Surface photometric investigations for spiral galaxies of large dimension structures in edge-on gemetry
[ETN-88-92126] 21 p3030 N88-27985
Fractal surface finish
[DE88-007972] 22 p3057 N88-28137
Modification of YBa2Cu3O(7-x) ceramics by adsorbed water and other gases
[DE88-011518] 22 p3057 N88-28140
Comparison of the bidirectional reflectance distribution function of various surfaces
[NASA-TM-101317] 22 p3153 N88-28760
Bulk plasmon enhanced photoemission from Nb(100) surface resonances
[AD-A192711] 22 p3154 N88-28767
Techniques for boundary layer tripping and control
23 p3168 N88-28863
Measure of hydrogen concentration profile in materials by resonant nuclear reactions
[DE88-702599] 23 p3193 N88-28999
Influence of local volume forces on surface relaxation of pure metals and alloys: Applications to Ni, Al, Ni3Al
[DE88-702718] 23 p3195 N88-29014
The mechanical behavior of surface modified ceramics
[DE88-010564] 23 p3196 N88-29022
Liquid thickness gauge
[NASA-CASE-LAR-13826-1] 23 p3217 N88-29150
Surface properties in electric discharge machining
[NASA-TT-20243] 23 p3223 N88-29182
Green's function approach to roughening transition of one-dimensional restricted solid on solid model
[DE88-702723] 23 p3278 N88-29512
Optical emission from surface waves supported in thin metal films 23 p3282 N88-29540
Potential induced structural transformations of the Au(100) and Au(111) surfaces
[DE88-005446] 23 p3287 N88-29571
Theoretical investigation of image states of the hydrogen covered Cu (100)
[DE88-702662] 23 p3292 N88-29604
System suitable for observing surface plasmon in a semi-infinite semiconductor superlattice
[DE88-702686] 23 p3293 N88-29606
Morphologic contrasts between Nirgal and Auqakuh Valles, Mars: Evidence of different crustal properties
23 p3304 N88-29681
Preliminary analysis of recent 2.2-4.2 micrometers telescopic observations of Elysium, Mars: Implications for crystallinity and hydration state of surface materials
23 p3306 N88-29692
Experimental determination of drag modifications due to elastic compliant surfaces using quantitative visual techniques
[AD-A194785] 24 p3372 N88-30082

SURFACE REACTIONS

Surface modification by metal deposition and laser irradiation 01 p0023 N88-10148
Gases released by surface flashover of insulators
[DE87-013851] 01 p0039 N88-10249
Silicon oxidation photoassisted with a continuous wave CO2 laser beam and contribution to the study of silica layers obtained
[LAAS-87-158] 02 p0179 N88-11115
Enhancement of surface-atmosphere fluxes by desert-fringe vegetation through reduction of surface albedo and of soil heat flux
[NASA-CR-181442] 02 p0197 N88-11231
Spacecraft surface exposure to atomic oxygen in low Earth orbit 03 p0273 N88-11715
Surface chemistry of transition metal carbides: A theoretical analysis
[AD-A184237] 03 p0291 N88-11829
Study of IR laser photoacoustic spectra of organic molecules adsorbed on metal surface
03 p0301 N88-11891
Deformation mechanisms of thermostructural materials
[AD-A184070] 03 p0338 N88-12128
Vectorial electron transfer on designed surfaces
[PB87-232229] 03 p0381 N88-12394
Surface catalytic degradation study of two linear perfluoropolyalkylethers at 345 C
[NASA-TP-2774] 04 p0410 N88-12543
Simulation studies for surfaces and materials strength
[NASA-CR-181535] 04 p0412 N88-12557
Influence of stratification in near-surface water layer on intensity of gas exchange between atmosphere and water 04 p0459 N88-12841
Reactions of porphyrins in surfactant assemblies, microemulsions and in solutions
[AD-A184797] 05 p0560 N88-13412
A study of the interaction of laser light with liquid propellant drops
[AD-A185117] 05 p0587 N88-13582
Pure dephasing of a vibrational adbond
[AD-A185222] 05 p0609 N88-13740
Energy dependence of ion-induced sputtering yields of monatomic solids in the low energy region
[IPPJ-AM-52] 05 p0651 N88-13988
Method for preparing hydride configurations and reactive metal surfaces
[DE88-000845] 06 p0679 N88-14161
Partial analysis of experiment LDEF A-0114
[NASA-CR-1792[illegible]] 06 p0780 N88-14787
Unified study of plasma-surface interactions for space power and propulsion
[AD-A186211] 07 p0825 N88-15007
Studies of metal/carbon surface chemistry
[DE87-009545] 07 p0829 N88-15029
Surface chemistry of chemically sensitive field effect transistors
[AD-A185917] 07 p0847 N88-15139
Phonon dispersion for several surfaces with ordered overlayers: A lattice dynamical study
07 p0876 N88-15315
Investigations in field of surface forces in metallurgy
[BLL-M-47406-(5828.4)] 08 p0969 N88-15860
Beneficial and detrimental effects of silica in the high temperature oxidation of 20Cr/25Ni/Nb stainless steel
[AERE-R-12667] 10 p1301 N88-17779
Apparatus for the study of silicon film deposition and silicon etching
[AD-A187616] 10 p1334 N88-17972
Nonmonotonic evolution and thermodynamic trends at metal/(Hg,Cd)Te interfaces: Yb/Hg0.78Cd0.22Te
[AD-A187591] 10 p1422 N88-18490
An application of active surface heating for augmenting lift and reducing drag of an airfoil
[NASA-TM-100563] 11 p1436 N88-18570
Theoretical studies of the potential surface for the F + H2 greater than HF + H reaction
[NASA-CR-182551] 11 p1557 N88-19319
FTIR (Fourier Transform Infrared) and FTNMR (Fourier Transform Nuclear Magnetic Resonance) study of organophosphorus surface reactions
[AD-A188337] 12 p1609 N88-19625
An interdisciplinary approach to predictive modeling of structural adhesive bonding: Factors affecting the durability of titanium/epoxy bonds
[AD-A189503] 12 p1611 N88-19636
Advanced electron optics for vibrational spectroscopy
[AD-A188469] 12 p1629 N88-19747
Photochemistry at structured surfaces: A classical electromagnetic approach
[AD-A189519] 13 p1737 N88-20387
Model catalyst studies of SMSI (Strong Metal/Support Interactions) and the role of D-electrons in chemisorption and catalysis
[DE88-004518] 13 p1738 N88-20393
Laser surface melting
[BMFT-FB-T-88-072] 14 p1914 N88-21435
Methods of measurement for the evaluation of monolayer properties. Development and applications — lung surfactants
[ETN-88-92229] 15 p2104 N88-22532
Surface enhanced Raman scattering applied to surface chemical kinetics
[AD-A191275] 16 p2176 N88-22969
A study of surface tension driven segregation in monotectic alloy systems
[NASA-CR-182894] 16 p2178 N88-22983
The application of Rutherford backscattering for analyzing multilayered structure change induced by pulsed ion beam bombardment 16 p2278 N88-23638
Microscopic control of semiconductor interface reactivity
[AD-A191193] 16 p2283 N88-23668
Surface interactions relevant to space station contamination problems 18 p2592 N88-25401
New instability phenomena in solid propellant combustion 19 p2628 N88-25591
Interactions of molecules with surfaces
[DE88-007950] 19 p2723 N88-26169
Laser induced surface emission of neutral species and its relationship to optical surface damage processes
[DE88-008035] 19 p2726 N88-26192
Numerical model for the computation of radiance distributions in natural waters with wind-roughened surfaces
[PB88-192703] 20 p2826 N88-26765
An IETS (Inelastic Electron Tunneling Spectroscopy) study of surface reactions applicable to adhesion
[AD-A192274] 21 p2909 N88-27261
Scanning tunneling microscopy as a surface chemical probe
[AD-A192710] 21 p2909 N88-27263
Self-energies and the interactions of particles with surfaces
[DE88-010451] 21 p3014 N88-27885
Initiation of explosive molten aluminum-water interactions at wet or underwater surfaces
[DE88-004686] 23 p3194 N88-29006
Quantitative surface temperature measurement using two-color thermographic phosphors and video equipment
[NASA-CASE-LAR-13740-1] 24 p3376 N88-30105
Cosmochemical trends of volatile elements in the solar system 24 p3451 N88-30542

SURFACE ROUGHNESS

Experience about the application and valuation of roughness strips for boundary layer transition control in wind tunnel tests in the high-speed range
[ESA-TT-1028] 01 p0044 N88-10278
The effect of size and surface on the lifetime prediction of StE 460 notched bars
[FD-6/1986] 01 p0058 N88-10374
Structure and grain coarsening during the processing of engineering ceramics
[NASA-TM-100235] 03 p0293 N88-11838
Roughness and waviness requirements for laminar flow surfaces 07 p0813 N88-14953
Wind tunnel model surface gauge for measuring roughness
[NASA-CR-182392] 07 p0822 N88-14996
Backscatter from a periodic rough surface at near grazing incidence
[NASA-CR-182397] 07 p0845 N88-15128
A new look at the use of linear methods to predict aircraft dynamic response to taxi over bomb damaged and repaired airfields 09 p1180 N88-17069
Propagation of creep waves around rough cylindrical surface 09 p1234 N88-17400
Comparison of the rough surface reflection coefficient with specularly scattered acoustic data
[AD-A187086] 09 p1242 N88-17444
Interferometric study of natural convection heat transfer from a vertical flat plate with transverse roughness elements 10 p1327 N88-17935
Comparison of methods for the calculation of thermal contact resistance of the first Brazilian satellite
[NASA-TT-20180] 14 p1880 N88-21239
Electromagnetic shadowing by an exponentially distributed rough surface
[AD-A189677] 14 p1906 N88-21391
Electromagnetic scattering by an exponentially distributed rough surface with the introduction of a rough surface generation technique
[AD-A189678] 14 p1906 N88-21392
Effect of freestream turbulence on a two dimensional cascade, with different surface roughness, at high Reynolds number
[AD-A190615] 15 p2065 N88-22316
Enhanced backscattering from rough surfaces
[AD-A190995] 16 p2190 N88-23063
Enhanced backscattering from rough surfaces
[AD-A191089] 16 p2274 N88-23610
Manufacturing requirements 17 p2297 N88-23745
An experimental study of the coherent under-ice reflectivity of sound in the Greenland Sea Marginal Ice Zone 18 p2548 N88-25125
Plastic deformation and roughness of free metal surfaces
[PB88-196621] 20 p2772 N88-26439
Numerical model for the computation of radiance distributions in natural waters with wind-roughened surfaces
[PB88-192703] 20 p2826 N88-26765
Eigenmatrix representations of radiance distributions in layered natural waters with wind-roughened surfaces
[PB88-188701] 20 p2828 N88-26780

Investigations of rough surface effects on friction factors in turbulent pipe flow
[AD-A193774] 22 p3075 N88-28255

Studies of internal stresses and surface roughness of sputtered Be and BeB films
[DE88-011737] 22 p3086 N88-28327

Analysis of soils using remote sensing information at the scale of the parcel 22 p3095 N88-28381

The covariance of scalar fields scattered by pressure-release randomly rough surfaces
[AD-A192489] 22 p3146 N88-28714

SURFACE ROUGHNESS EFFECTS

A preliminary demonstration of the use of boundary-layer models of flow in complex terrain for high resolution surface wind forecasting 02 p0212 N88-11330

Effects of enviromentally imposed roughness on airfoil performance 08 p0952 N88-15778

Adhesive bond strengths on aluminium alloys as a function of surface topographies and their wetting properties
[ARE-TM(UMM)-87403] 09 p1148 N88-16880

SURFACE STABILITY

Colloidal stability of oxidized silicon particles in ethanolic and aqueous media
[DE87-014783] 05 p0562 N88-13421

Microscopic control of metallization stability
[AD-A187553] 10 p1421 N88-18487

Computer Applications in Geotechnical Engineering (CAGE) and Geotechnical aspects of the Computer-Aided Structural Engineering (G-CASE) projects. User's guide. UTEXAS2 slope-stability package. Volume 1: User's manual
[AD-A187674] 11 p1511 N88-19025

The sensitivity of boundary layer instability growth rates to compliant wall properties
[AD-A190433] 15 p2064 N88-22309

Empirical flutter prediction method
[AD-A195699] 24 p3327 N88-29810

Mathematical problems of nonlinear wave propagation and of waves in heterogeneous media
[AD-A195970] 24 p3368 N88-30057

SURFACE TEMPERATURE

NT SKIN TEMPERATURE (NON-BIOLOGICAL)
NT WALL TEMPERATURE

Cooling effect of a single evaporating droplet on a hot semi-infinite metal body
[PB87-201802] 01 p0046 N88-10294

Estimating regional evapotranspiration from remotely sensed data by surface energy balance models
[NASA-CR-181400] 01 p0064 N88-10411

The use of satellite IR data in the enhancement of surface thermal fields 02 p0202 N88-11260

Use of time changes of surface data parameters in short range forecasting 02 p0206 N88-11291

Comparison of flight-measured and calculated temperatures on the space shuttle orbiter
[NASA-TM-88278] 03 p0321 N88-12029

Properties of the atmospheric boundary layer above a subtropical oceanic front
[AD-A184006] 03 p0351 N88-12215

An analytical soil thermodynamic model for the diurnal variation of ground surface temperature
[AD-A185366] 05 p0625 N88-13823

Role of anomalous currents in formation of ocean surface temperature field 06 p0727 N88-14474

Sea surface current estimates off central California as derived from enhanced AVHRR (Advanced Very High Resolution Radiometer) infrared images
[AD-A186867] 09 p1194 N88-17155

Relationships between remotely-sensed surface properties and subsurface structure in the ocean
[AD-A189317] 12 p1650 N88-19881

Radiative processes affecting ocean mixed-layer heat content and their monitoring from satellite
13 p1806 N88-20800

Monitoring ocean surface layer processes
13 p1806 N88-20801

Research sensors 15 p2085 N88-22430

Infrared radiometric technique in temperature measurement 17 p2330 N88-23913

Indentification of shallow groundwater regions in semi-arid Brazil by remote sensing methods
17 p2355 N88-24030

The potential impact on atmospheric ozone and temperature of increasing trace gas concentrations
[NASA-CR-182965] 17 p2373 N88-24112

Evaluating evaporation with satellite thermal data
[AD-A192042] 18 p2531 N88-25019

Surface temperature thermal fluxmeters for shock tubes
[NASA-TT-20319] 20 p2762 N88-26381

An empirical surface temperature model
[AD-A192737] 21 p2974 N88-27665

Surface energy balance of three general circulation models: Current climate and response to increasing atmospheric CO2
[DE88-010967] 21 p2975 N88-27673

Interannual variability in the Atlantic and Indian Oceans and its relationship to the southern oscillation
22 p3121 N88-28548

DERF forecasts of thickness
22 p3126 N88-28579

Measurement and interpretation of North Atlantic Ocean marine radar sea scatter
[AD-A196239] 24 p3364 N88-30036

Measurement of local high-level, transient surface heat flux
[NASA-TP-2840] 24 p3375 N88-30099

Energy budget and ground temperatures in hot regions
[AD-A196298] 24 p3404 N88-30268

SURFACE TENSION

U INTERFACIAL TENSION

SURFACE TO AIR MISSILES

A study of infrared missile seekers and the countermeasure techniques employed to defeat them
[ETN-87-90927] 02 p0131 N88-10822

Development of a computer model for missile simulation, or simulation of a kinetic coverage area for a target detection missile
[FOA-C-20666-2.5] 08 p1067 N88-16449

Development of a computer model for missile simulation, or simulation of a kinetic coverage area for a collimation guided missile
[FOA-C-20667-2.5] 08 p1067 N88-16450

The application of thermal imaging sensors and image processing techniques to a short range surface-to-air missile system
[ETN-88-92080] 14 p1982 N88-21829

The effect of a turbulent airstream on a vertically-launched missile at high angles of attack
[AD-A192408] 20 p2758 N88-26383

Future air-to-air training for the RF-4
[AD-A194363] 23 p3240 N88-29284

SURFACE TO SURFACE MISSILES

NT ANTITANK MISSILES
NT CRUISE MISSILES
NT MX MISSILE
NT TOMAHAWK MISSILES

The effects of data structure on total time on test plots
[AD-A187628] 10 p1389 N88-18296

LGM-30B stage 2 disected motor test report
[AD-A190771] 15 p2027 N88-22079

SURFACE TREATMENT

U SURFACE FINISHING

SURFACE VEHICLES

NT AIRCRAFT CARRIERS
NT AUTOMOBILES
NT ELECTRIC AUTOMOBILES
NT ELECTRIC MOTOR VEHICLES
NT MAGNETIC LEVITATION VEHICLES
NT MOTOR VEHICLES
NT ROADWAY POWERED VEHICLES
NT ROCKET PROPELLED SLEDS
NT ROVING VEHICLES
NT TANKS (COMBAT VEHICLES)
NT TRACKED VEHICLES
NT TRANSPORTER
NT TRUCKS
NT WALKING MACHINES

Correction of inertial navigation system drift errors for an autonomous land vehicle using optical radar terrain data
[AD-A184973] 05 p0544 N88-13311

Range imagery algorithms for the detection of obstacles by autonomous vehicles
[AD-A185421] 05 p0659 N88-14045

An overview of vision-based navigation for autonomous land vehicles 1986
[AD-A188186] 10 p1276 N88-17640

On the maneuvering of vehicles
[AD-A187632] 10 p1427 N88-18521

Low cost mobile robot
[AD-A188507] 12 p1633 N88-19776

Terrain classification from digital elevation data using slope and curvature information
[AD-A188940] 12 p1639 N88-19612

Feasibility report: Operation of light air cushion vehicle at McMurdo Sound, Antarctica
[AD-A189057] 13 p1755 N88-20494

Articulated suspension system
[NASA-CASE-NPO-17354-1-CU]
18 p2524 N88-24973

Local free-space mapping and path guidance for mobile robots
[AD-A192970] 20 p2810 N88-26674

Assessments of maneuverability with the TeleOperated Vehicle (TOV)
[AD-A191584] 21 p2993 N88-27751

SURFACE WATER

Influence of the Yukon River on the Bering Sea
[NASA-CR-182802] 17 p2376 N88-24126

SURFACE WAVES

NT BAROCLINIC WAVES
NT CAPILLARY WAVES
NT ELECTROMAGNETIC SURFACE WAVES
NT GRAVITY WAVES
NT RIPPLES

Effect of viscosity on a vertical cylinder due to surface waves
[ETN-87-90960] 02 p0171 N88-11075

Determination of fractal dimension, connection of space and temporal chaos and application to experimental results 03 p0313 N88-11977

Effect of plasma resonance on properties of surface waves 06 p0773 N88-14749

Materials for acceleration by surface electromagnetic waves
[DE88-700312] 07 p0846 N88-15133

Acoustic scattering from composite wind-wave surfaces 3: Forward scatter intensities and spatial coherence at low and high frequencies and small grazing angles for Bubble-free regimes
[AD-A185908] 07 p0881 N88-15345

Investigation of the quantitative determination of two dimensional sea surface wave spectra from shipborne radar measurements
[GKSS-87/E/10] 09 p1195 N88-17163

Surface acoustic wave deposition sensor
[DE87-006527] 09 p1243 N88-17452

Numerical studies of propagation of Lg waves across ocean continent boundaries using the Representation Theorem (RT) 10 p1353 N88-18085

Research and development of surface skimming bulk wave devices for sensor applications
[AD-A187504] 11 p1470 N88-18766

Lg wave excitation and propagation in the presence of one-, two-, and three-dimensional heterogeneities
[AD-A187364] 11 p1510 N88-19022

Applications and limitations of the spectral-analysis-of-surface-waves method
[PB88-136619] 11 p1513 N88-19036

Estimation of sea surface wave spectra using acoustic tomography
[AD-A187837] 11 p1516 N88-19057

Investigation of surface wave blindness in microstrip phased array antennas
[AD-A189326] 12 p1621 N88-19696

Energy and momentum fluxes through the sea surface
13 p1806 N88-20798

Hamiltonian description of the interaction of surface waves with mixed-layer currents
13 p1806 N88-20799

Thin superconducting film characterization by surface acoustic waves
[AD-A190417] 15 p2143 N88-22791

Surface wave accelerometer
[ETN-88-92000] 16 p2210 N88-23192

Investigation of the imaging of ocean surface waves using a synthetic aperture radar
[SER-A-WISS-ABHANDL-84] 16 p2236 N88-23357

Surface-wave model uncertainty assessment
[AD-A193094] 21 p2932 N88-27408

Nonlinear surface and internal waves on shear flow
[PREPRINT-584] 22 p3129 N88-28604

Optical emission from surface waves supported in thin metal films 23 p3282 N88-29540

SURFACE-ACTIVE AGENTS

U SURFACTANTS

SURFACES

Shear stress cleaning for surface departiculation
02 p0134 N88-10836

Aerodynamic sensitivities from subsonic, sonic and supersonic unsteady, nonplanar lifting-surface theory
[NASA-TM-100502] 04 p0394 N88-12459

Calculation of the distributed loads on the blades of individual multiblade propellers in axial flow using linear and nonlinear lifting surface theories
[NASA-TT-20173] 13 p1719 N88-20278

SURFACTANTS

Separation of anionic from nonionic alkoxy compounds using silica gel
[GB-PATENT-2-140-415-A] 01 p0020 N88-10122

Influence of surfactants on damping of gravity-capillary waves. 1: Frequency dependence
04 p0459 N88-12843

Reactions of porphyrins in surfactant assemblies, microemulsions and in solutions
[AD-A184797] 05 p0560 N88-13412

Precipitation of surfactants and surfactant mixtures in aqueous solutions
[DE88-003333] 10 p1298 N88-17763

A review of approaches to the study of turbulence modification by means of non-Newtonian additives
[AD-A188799] 12 p1627 N88-19734
Methods of measurement for the evaluation of monolayer properties. Development and applications --- lung surfactants
[ETN-88-92229] 15 p2104 N88-22532
Attenuated total reflectance FT-IR spectroscopy to measure interfacial reaction kinetics at silica surfaces
[AD-A196330] 24 p3344 N88-29906

SURGERY
Does the knife open perspectives for the myopic pilot?
[ETN-87-90166] 09 p1199 N88-17187

SURGES
Radio studies of large scale structures of the Sun's corona and transient activity 01 p0114 N88-10728
Was the eclipse comet of 1893 a disconnected coronal transient? 01 p0115 N88-10733
A numerical study of transient, thermally-conductive solar wind 01 p0115 N88-10738
Radiation-induced transient attenuation of optical fibers at 800 and 1300 nm
[DE87-013165] 02 p0235 N88-11485
Departmental report on program EMTP-machine windings surge transients: Travelling wave method
[PB87-123733] 04 p0438 N88-12719
Transient processes in the interaction between pulsed laser radiation and matter
[ISL-R-115/86] 05 p0588 N88-13586
Application of Vandermonde decomposition to directional and modal analysis of broadband transients
[AD-A185007] 05 p0646 N88-13956
A unified model for the WTS and the generation on Pi 2 pulsations --- Westward Traveling Surge (WTS)
08 p1096 N88-16593
Possibilities for on-line surge suppression by fast guide vane adjustment in axial compressors
10 p1283 N88-17674
Equipment test methods for externally produced electromagnetic transients
[RAE-TM-FS(F)-457] 14 p1865 N88-21140
Techniques for studying fast reactions in liquids
[DE88-005917] 14 p1888 N88-21265
Bloch oscillations in small Josephson junctions: Their manifestation in switching effects
14 p1969 N88-21756
Effects of emission energy transient in periodic-pulse XeCl excimer laser of approximately 400 W average power 14 p1971 N88-21763
Molecular dynamics of materials possessing high energy content
[AD-A190034] 15 p2034 N88-22118
Polarimetric ISAR imaging using either measured or calculated transient signatures
[AD-A190077] 15 p2056 N88-22259
Application of the reactivity constraint approach to the transient control of spacecraft reactors
17 p2406 N88-24305
EETAP (End-to-End Transient Analysis Program) for space nuclear power system simulation
17 p2418 N88-24381
Characterization of accelerating pipe flow
[AD-A193065] 21 p2943 N88-27481
Investigation of the quasi-steady approach used in transient two-phase flow analysis
[DE88-004303] 21 p2944 N88-27489

SURVEILLANCE
NT SPACE SURVEILLANCE (GROUND BASED)
NT SPACE SURVEILLANCE (SPACEBORNE)
Pyroelectric line scanner for remote IR imaging of vehicles
[DE87-012127] 02 p0235 N88-11484
Cooperative analysis expert situation assessment research 09 p1206 N88-17228
Terrestrial Propagation Characteristics in Modern Systems of Communications, Surveillance, Guidance and Control
[AGARD-CP-407] 12 p1614 N88-19653
Automatic knowledge acquisition for aerial image interpretation
[AD-A188616] 12 p1638 N88-19810
Specification for an infrared satellite surveillance system for the detection of aircraft
[AD-A189592] 13 p1797 N88-20746
A preliminary assessment of thunderstorm outflow wind measurement with airport surveillance radars
[AD-A189064] 13 p1799 N88-20757
The Effect of the Ionosphere on Communication, Navigation and Surveillance Systems Based on Ionospheric Effects Symposium held on 5-7 May 1987 in Springfield, Virginia
[AD-A191855] 18 p2541 N88-25081
Aerodynamics of seeing on large transport aircraft
[NASA-CR-183122] 23 p3174 N88-28896

SURVEILLANCE RADAR
NT AIRBORNE SURVEILLANCE RADAR
NT MULTISTATIC RADAR
Development of an airborne facility for advanced avionics research 17 p2307 N88-23801
Automated test device for FASR (Fixed Array Surveillance Radar) beam steering componentry
[AD-A191650] 18 p2500 N88-24829
Multi-target tracking algorithms for cluttered environments 20 p2789 N88-26543
Fine resolution errors in secondary surveillance radar altitude reporting
[RSRE-87019] 23 p3175 N88-28906
Evaluation of LISBON TAR SSR radar
[EEC/NOTE-5/87] 24 p3362 N88-30015

SURVEYING
U SURVEYS

SURVEYS
NT GEODETIC SURVEYS
NT GEOLOGICAL SURVEYS
NT SKY SURVEYS (ASTRONOMY)
Subjective probability, combination of expert opinion and probabilistic approaches to information retrieval
04 p0501 N88-13085
The Parkes radio survey of active chromosphere stars
04 p0511 N88-13141
A survey of existing hypersonic ground test facilities: North America 05 p0529 N88-13220
Survey state of the art: Electrical load management techniques and equipment
[AD-A184083] 05 p0577 N88-13517
Varifront 3 expedition data report (USNS DE STEIGUER CRUISE 1202-82). Bioluminescence, hydrographic, nutrient, and satellite data from the Gulf of California (November-December 1981)
[AD-A185011] 05 p0620 N88-13805
Survey of electronic measurement needs below 10 MHz
[PB88-110366] 07 p0844 N88-15121
NASA JSC neural network survey results
09 p1205 N88-17220
Environmental projects. Volume 4: Asbestos survey
[NASA-CR-182527] 10 p1353 N88-18083
Surveying with GPS in Australia
11 p1504 N88-18986
A study of technology transfer arrangements for national laboratories
[DE88-005423] 11 p1567 N88-19382
An evaluation of perceptions of form, fit, function (F3) standardization on the Standard Inertial Navigation Unit (STD INU) program
[AD-A188955] 12 p1579 N88-19446
A study on local level inertial surveying systems. Error model for the stationary system
[B8736714] 16 p2229 N88-23312
Study of reservoir water quality utilizing remote sensing techniques: Methodological concepts
17 p2364 N88-24076
Human performance issues arising from manned space station missions
[NASA-CR-3942] 18 p2553 N88-25156
Territorial management program
19 p2682 N88-25942
RRSAS (Robotic Radiation Survey and Analysis System) Project: A real time sensor driven robotic system
[DE88-006825] 20 p2808 N88-26661
Australian structures response evaluation. Ground shock and air blast measurements for site investigation survey
[MRL-TN-526] 20 p2813 N88-26685
Development of sensors for ceramic components in advanced propulsion systems: Survey and evaluation of measurement techniques for temperature, strain and heat flux for ceramic components in advanced propulsion systems
[NASA-CR-182111] 22 p3081 N88-28299
Signal processing software for ground penetrating radar, user's manual
[AD-A194266] 23 p3203 N88-29059
Seismic reflection experiments imaging the physical nature of crustal structures in southern California
23 p3232 N88-29235
The use of orbital remote sensing data for low cost ground-water survey
[INPE-4567-PRE/1318] 24 p3386 N88-30170
A dynamic analysis of piezoelectric strained elements
[AD-A196079] 24 p3432 N88-30430
A deep redshift survey of field galaxies. Comments on the reality of the Butcher-Oemler effect
[NASA-CR-183255] 24 p3454 N88-30558
Antarctic Meteorite Newsletter, Volume 11, Number 2, August 1988
[NASA-TM-89801] 24 p3457 N88-30573

SURVIVAL
Improved oil-off survivability of tapered roller bearings
[NASA-CR-180804] 02 p0182 N88-11135
The determination of nutritional requirements for Safe Haven Food Supply System (emergency/survival foods)
06 p0792 N88-14856
Survival analysis using additive risk models
[AD-A189053] 13 p1825 N88-20906
Validation of mathematical model predictions of immersion survival times
[IAM-652] 14 p1952 N88-21635
Radiation effects testing capabilities of the Texas A and M Nuclear Science Center 17 p2416 N88-24366
Survival analysis, or what to do with upper limits in astronomical surveys
[NASA-CR-182936] 17 p2449 N88-24551
Mobile robot survival
[DE88-009108] 20 p2809 N88-26665
Accidental hypothermia
[AD-A194967] 24 p3406 N88-30278

SUSCEPTIBILITY (MAGNETISM)
U MAGNETIC PERMEABILITY

SUSPENDING (HANGING)
NT MAGNETIC SUSPENSION
Comparative evaluation of stress repsonse of rats to different methods of simulating some effects of weightlessness 10 p1363 N88-18144
Morphological study of early changes in rat bones in simulated weightlessness 10 p1365 N88-18158
General equilibrium characteristics of a dual-lift helicopter system
[NASA-TP-2615] 12 p1573 N88-19407
Does 7-day hindquarters unloading simulate 7 days of weightlessness exposure in rat trabecular bone?
12 p1657 N88-19928
The suspended Japanese quail as an animal model for experiments related to microgravity
12 p1662 N88-19960
Oscillation damped movement of suspended objects
[DE88-005715] 15 p2086 N88-22433
Human response to prolonged motionless suspension in four types of full body harnesses
21 p2929 N88-27387

SUSPENDING (MIXING)
Optical instrumentation and study of gas-solid suspension flows
[DE88-000147] 04 p0442 N88-12744
Thematic mapper research in the earth sciences: Small scale patches of suspended matter and phytoplankton in the Elbe River Estuary, German Bight and Tidal Flats
[NASA-CR-182378] 08 p1019 N88-16180
Suspension cell culture in microgravity and development of a space bioreactor 09 p1196 N88-17169
Christiansen effect in infrared spectra of soil-derived atmospheric dusts
[AD-A187071] 09 p1248 N88-17479
Suspension of small metallic plates: A versatile sensor
[PB88-130901] 11 p1487 N88-18874
Velocity and concentration measurements in flowing suspensions by nuclear magnetic resonance
[DE88-006225] 13 p1770 N88-20589
LLNL Granular Solids Flow Project
[DE88-008023] 19 p2664 N88-25844

SUSPENSION SYSTEMS (VEHICLES)
Measurement of suspension and ride characteristics of the M1 main battle tank 05 p0596 N88-13637
The MBB propulsion concepts for magnetic suspension railways: Retrospective view and prospects
[MBB-Z-141/87] 10 p1316 N88-17865
Articulated suspension system
[NASA-CASE-NPO-17354-1-CU]
18 p2524 N88-24973
A review of gear housing dynamics and acoustics literature
[NASA-CR-183110] 20 p2811 N88-26675
Leaf spring
[GB-PATENT-2-192-689-A] 23 p3222 N88-29179

SWALLOWING
A simplified streamline swallowing procedure for the windward meridian of axisymmetric blunt bodies
[AD-A188413] 12 p1626 N88-19732

SWAMPS
U MARSHLANDS

SWASH
U SPLASHING

SWEAT COOLING
Polycythemia and hydration status: Effects on blood volume and thermoregulation during exercise-heat stress
[AD-A185946] 07 p0888 N88-15383
Temperature regulation at rest and exercise during the human menstrual cycle
[AD-A186461] 08 p1050 N88-16341
The effects of different combinations of inlet air conditions used for cooling as measured on a heated manikin
[AD-A191116] 18 p2552 N88-25151

SWEATING
U PERSPIRATION

SWEDEN
Esrange (Sweden): New installations, future plans and investments --- rocket range 08 p1029 N88-16235
Surface ozone measurements at a Swedish mountain site
[CM-72] 09 p1191 N88-17138
SWEDISH SPACE PROGRAM
Satimage and the Nordic SPOT market
03 p0340 N88-12145
Electric field measurements on Viking: First results
[TRITA-EPP-87-04] 05 p0625 N88-13826
Viking quick look plots: A short description --- Swedish satellite 06 p0692 N88-14243
The Swedish sounding rocket and balloon program
08 p1025 N88-16205
Viking: The first Swedish satellite
08 p1025 N88-16207
Global views of the aurora from the Viking satellite --- Swedish satellite 08 p1025 N88-16208
Instantaneous pictures of the high-latitude electrodynamics using Viking and DMSP/F7 observations --- Swedish satellite
08 p1025 N88-16209
First results from the Viking associated Aureld-VIP rocket and EISCAT campaign --- auroras; Swedish satellite
08 p1026 N88-16211
Small scale plasma density structures observed by the Viking double probe instrument --- Swedish satellite
08 p1098 N88-16604
Low frequency waves and small scale solitary structures observed by Viking --- Swedish satellite; auroras
08 p1099 N88-16611
Preliminary results from the dc electric field experiment on Viking --- Swedish satellite
[TRITA-EPP-87-03] 09 p1190 N88-17130
SWEEP ANGLE
NT LEADING EDGE SWEEP
NT SWEEPBACK
The effects of sweep and bluntness on a glancing shock wave turbulent boundary layer interaction
05 p0531 N88-13227
SWEEP EFFECT
Three-dimensional unsteady flow elicited by finite wings and complex configurations 04 p0395 N88-12468
SWEEP FREQUENCY
Material parameter measurements at high temperatures
[NASA-CR-182707] 13 p1739 N88-20397
SWEEPBACK
NT LEADING EDGE SWEEP
Structural Tailoring of Advanced Turboprops (STAT)
[NASA-CR-180861] 22 p3045 N88-28074
SWEEPBACK ANGLES
U SWEEPBACK
SWELLING
Swelling behavior of ferritic/martensitic steels
[DE88-001757] 06 p0682 N88-14177
Uranium nitride fuel swelling and thermal conductivity correlations 17 p2409 N88-24327
A comparison of uranium nitride and mixed carbide fuels swelling 17 p2435 N88-24485
SWEPT FORWARD WINGS
Wing divergence of trimmed aircraft
05 p0550 N88-13354
X-29A forward-swept-wing flight research program status
[NASA-TM-100413] 10 p1277 N88-17644
The aerodynamic design optimisation of a forward swept wing fighter aircraft
[CAR-87-18] 11 p1433 N88-18553
A correlation study of X-29A aircraft and associated analytical development
[NASA-CR-183103] 13 p1722 N88-20296
Development of a real-time aeroperformance analysis technique for the X-29A advanced technology demonstrator
[NASA-TM-100432] 14 p1866 N88-21151
Experiment investigation on longitudinal characteristics of the forward swept wing
[AD-A191553] 18 p2456 N88-24582
Current flight test experience related to structural divergence of forward-swept wings
[NASA-TM-100445] 18 p2464 N88-24633
High performance forward swept wing aircraft
[NASA-CASE-ARC-11636-1] 23 p3177 N88-28914
SWEPT WINGS
NT ARROW WINGS
NT DELTA WINGS
NT SWEPT FORWARD WINGS
NT SWEPTBACK WINGS
Investigations of separated flow states on wings of medium aspect ratio taking into account the wind tunnel interference problem
[ETN-87-90437] 01 p0003 N88-10016
Measurement techniques in low-speed turbulent flows: A report on EUROMECH 202
[NLR-MP-86038-U] 01 p0045 N88-10283
Three-dimensional unsteady flow elicited by finite wings and complex configurations 04 p0395 N88-12468
Calculation of three-dimensional stationary turbulent boundary layer on root section of wing ignoring compressibility 04 p0424 N88-12630
A swept wing panel in a low speed flexible walled test section
[NASA-CR-4106] 05 p0540 N88-13292
Static aeroelastic effects on the flutter of a supercritical wing 05 p0550 N88-13353
Flight research on natural laminar flow
07 p0813 N88-14950
Pressure distributions and oil-flow patterns for a swept circulation-control wing 10 p1270 N88-17596
Boundary-layer and wake measurements on a swept, circulation-control wing 10 p1270 N88-17597
Development of disturbances in swept wing flows
[NASA-CR-182675] 13 p1768 N88-20574
Preliminary in-flight boundary layer transition measurements on a 45 deg swept wing at Mach Numbers between 0.9 and 1.8
[NASA-TM-100412] 13 p1772 N88-20598
The NASA Langley Laminar-Flow-Control (LFC) experiment on a swept, supercritical airfoil: Design overview
[NASA-TP-2809] 14 p1861 N88-21117
Wave interactions in a three-dimensional attachment line boundary layer
[NASA-CR-181653] 14 p1910 N88-21414
Boundary-layer and wake measurements on a swept, circulation-control wing
[NASA-TM-89426] 15 p2014 N88-22013
Theoretical investigation of secondary instability of three-dimensional boundary-layer flows with application to the DFVLR-F5 model wing
[DFVLR-FB-87-44] 15 p2068 N88-22330
Nonlinear wave interactions in swept wing flows
[NASA-CR-4142] 16 p2206 N88-23160
A low speed wind tunnel investigation of Reynolds number effects on a 60-deg swept wing configuration with leading and trailing edge flaps
[NASA-CR-181684] 19 p2598 N88-25441
AGARD standard aeroelastic configurations for dynamic response. 1: Wing 445.6
[AGARD-R-765] 21 p2896 N88-27193
Method to predict external store carriage characteristics at transonic speeds
[NASA-CR-4170] 22 p3037 N88-28034
Techniques used in the F-14 variable-sweep transition flight experiment
[NASA-TM-100444] 24 p3374 N88-30093
SWEPTBACK WINGS
NT ARROW WINGS
NT DELTA WINGS
Variable sweep wings 10 p1309 N88-17823
SWIRLING
Numerical simulation of turbulent premixed combustion and decay of turbulent swirling flow
[DE87-014253] 03 p0284 N88-11787
An experimental and numerical investigation of swirling flows in a rectangular nozzle 06 p0700 N88-14295
Fuel-injector/air-swirl characterization
[NASA-CR-180864] 07 p0820 N88-14985
Numerical implementation and performance of Reynolds stress closures in finite volume computations of recirculating and strongly swirling flows
08 p0987 N88-15976
Calculation on film preparation and film motion of a swirl atomizer
[DFVLR-FB-87-25] 09 p1162 N88-16962
Numerical simulation of turbulent premixed combustion and decay of turbulent swirling flow
[DE88-006568] 14 p1886 N88-21284
Theoretical and experimental investigation of swirl flow phase separators for microgravity applications
17 p2411 N88-24335
Effect of initial tangential velocity distribution on the mean evolution of a swirling turbulent free jet
[NASA-TM-100934] 18 p2458 N88-24592
Development of a liquid-fed water resistojet
[NASA-TM-100927] 18 p2523 N88-24968
Turbulence structure of mixing swirling flows
[AD-A193063] 21 p2943 N88-27478
Euler analysis of a swirl recovery vane design for use with an advanced single-rotation propfan
[NASA-TM-101357] 24 p3320 N88-29771
Analysis of the flow through double swirl airblast atomizers 24 p3351 N88-29949
Development of a more general Reynolds stress closure for swirling flow
[AD-A195121] 24 p3374 N88-30092
SWIRLING WAKES
U TURBULENT WAKES
SWITCHES
NT ELECTRIC SWITCHES
NT SWITCHING CIRCUITS
NT VACUUM ARC SWITCHES
Switching devices used in the Lethality Test System
[DE87-011734] 01 p0011 N88-10062
New concepts for high current self-sustained diffuse discharge closing switches
[DE87-011678] 01 p0040 N88-10252
A high-voltage multistage laser-triggered gas switch
[DE87-011725] 01 p0040 N88-10253
Investigations into the design of multi-terawatt magnetic switches
[DE87-012014] 01 p0040 N88-10254
Characterization of surface discharge switches and high performance applications
[DE87-011763] 01 p0041 N88-10261
Toward pulsed power uses for photoconductive semiconductor switches: Closing switches
[DE87-012020] 01 p0041 N88-10262
A simple self-breaking 2 MV gas switch
[DE87-014346] 02 p0166 N88-11047
The design and construction of a thermally controlled single mode fiber switch
[ETN-87-90929] 02 p0236 N88-11491
Loss measurement of 3-port ferrite switches in the 90 GHz range
[ESA-TT-1054] 03 p0310 N88-11958
Low jitter laser-triggered high-voltage vacuum switch using low laser energies
[DE88-001922] 05 p0587 N88-13576
Program to development an optical transistor and switch
[AD-A185666] 06 p0637 N88-14278
Superconducting switch program
[AD-A185682] 07 p0848 N88-15144
Photoconductor switch and circuit analysis
[AD-A188168] 11 p1478 N88-18821
Analysis of anomalous resistivity during the conduction phase of the plasma erosion opening switch
[DE88-006382] 15 p2061 N88-22286
Repetitive opening switches using optically activated semiconductors
[AD-A190196] 15 p2143 N88-22790
Investigation of non-linear optical behavior of semiconductors for optical switching, volume 1
[AD-A191297] 16 p2274 N88-23611
A monolithic reduced-size Ku-Band SPDT (Single Pole Double Throw) FET switch
[DE88-006273] 18 p2505 N88-24858
The SRS (Segmented Rail Surface) railgun: A new approach to restrike control
[DE88-007907] 19 p2605 N88-25488
Picosecond electrical pulses for VLSI electronics characterization 19 p2655 N88-25780
Graphite as a picosecond laser activated opening switch 19 p2657 N88-25783
Investigation of photoconductive picosecond microstripline switches on self-implanted Silicon On Sapphire (SOS) 19 p2657 N88-25789
Fast GaAs photoconductive detectors with high sensitivity integrated in coplanar systems onto GaAs substrates 19 p2658 N88-25790
Picosecond optoelectronic switches using composite electronic materials 19 p2658 N88-25792
A new optoelectronic CW microwave source
19 p2660 N88-25818
Optical modulation above 20 GHz using a waveguide electrooptic switch 19 p2660 N88-25819
Electron-impact-ionization and electron-attachment cross sections of radicals important in transient gaseous discharges
[AD-A192248] 20 p2770 N88-26424
Development of liquid metal field-emission sources for use in fast repetitive opening switches
[AD-A192230] 20 p2795 N88-26583
Pseudospark switches
[DE88-702227] 23 p3207 N88-29085
Consideration of plasma opening switches from a wave propagation perspective
[AD-A195681] 24 p3431 N88-30421
SWITCHING
NT BEAM SWITCHING
NT MAGNETIC SWITCHING
NT MICROWAVE SWITCHING
NT OPTICAL SWITCHING
NT PACKET SWITCHING
Measuring technical and mathematical investigation of multiple reignitions at the switching of a motor using vacuum circuit breakers
[ETN-87-90406] 01 p0042 N88-10270
Contribution to the study of circuit switched networks: Modeling and numerical solutions
[LAAS-87-174] 02 p0162 N88-11017

Automatic antenna switching design for Extra Vehicular Activity (EVA) communication system
06 p0797 N88-14883
Experimental investigation of a three-stage railgun incorporating puff-switching
[MRL-R-1056] 09 p1130 N88-16785
Transient electromagnetic scattering from heterogeneous lossy spheres
[AD-A186669] 09 p1152 N88-16903
The characteristics of two broadband (2 MHz to 10 MHz) switched vee antennas
[AD-A187874] 11 p1471 N88-18770
New mode switching algorithm for the JPL 70-meter antenna servo controller 11 p1474 N88-18791
Fast switching of far infrared radiation by refractive index change in semiconductors using photoionization
[ETN-88-91490] 11 p1551 N88-19279
Two queues with alternating service and switching times
[CWI-OS-R8712] 13 p1831 N88-20949
Bloch oscillations in small Josephson junctions: Their manifestation in switching effects
14 p1969 N88-21756
Optical switching and control techniques using nonlinear optical wave mixing
[AD-A190467] 15 p2134 N88-22730
Experimental investigation of a three-stage railgun incorporating puff-switching
[AD-A191044] 16 p2166 N88-22918
Investigation of non-linear optical behavior of semiconductors for optical switching, volume 1
[AD-A191297] 16 p2274 N88-23611
Photoconductive generation of sub-picosecond electrical pulses and their measurement applications
19 p2656 N88-25778
Picosecond switching in Josephson tunnel junctions
19 p2657 N88-25780
High speed, high repetition rate, high voltage photoconductive switching 19 p2657 N88-25781
Generation and forming of ultrashort high voltage pulses 19 p2657 N88-25782
Energy variations in optical pulses from gain-switched AlGaAs diode lasers 19 p2658 N88-25796
Picosecond measurements of gain-switching in a semiconductor laser driven by ultrashort electrical pulses
19 p2658 N88-25800
Experiments applications guide: Advanced Communications Technology Satellite (ACTS)
[NASA-TM-100265] 22 p3048 N88-28082
Charge storage and switching phenomena in metal complexes
[AD-A193778] 23 p3192 N88-28996
Optics and symbolic computing
[AD-A195119] 24 p3360 N88-30004
Piezoelectric and electrostrictive materials for transducer applications, volume 2
[AD-A194956] 24 p3376 N88-30104
Use of depletion edge translation for high-speed modulation and switching of lightwaves
[AD-A195611] 24 p3430 N88-30417

SWITCHING CIRCUITS
Recent developments in opening photoconductive semiconductor switches
[DE87-012130] 01 p0041 N88-10263
Recording multiple signals on a single waveform recorder
[DE87-011632] 01 p0049 N88-10313
Progress toward a superconducting opening switch
[DE87-014170] 02 p0167 N88-11051
Evaluation of device figure of merit in microwave switching circuit design
[AD-A184898] 05 p0577 N88-13520
Digital control of a direct current converter for a hybrid vehicle
[LAAS-87-286] 05 p0578 N88-13527
Trip electrical circuit of the gyrotron
[INPE-4338-NTE/273] 12 p1622 N88-19701
RF-switches: Application and design --- satellite communication 14 p1877 N88-21215
The modeling, simulation and comparison of interconnection networks for parallel processing
[AD-A190571] 15 p2115 N88-22599
The bit-error rate performance of a satellite microwave matrix switch
[NASA-TM-100285] 16 p2167 N88-22920
Neutron effects on the electrical and switching characteristics of NPN bipolar power transistors
17 p2431 N88-24463
High speed opto-isolator for radar applications
19 p2658 N88-25795
Silicon pulse sharpening diodes-switching kilovolts in 10's of picoseconds 19 p2661 N88-25824
Extinction behavior of low voltage switching arc under consideration of cathodic coatings and dynamic arc column
[ETN-88-92384] 20 p2796 N88-26591

SWITCHING ELEMENTS
U SWITCHING CIRCUITS

SWITCHING THEORY
An exact analysis and performance of framed ALOHA with capture
[AD-A185006] 05 p0574 N88-13500

SWITZERLAND
Swiss scientific balloon and sounding rocket experiments 1985-1987 08 p1025 N88-16206
Research in Switzerland on ocean and inland-water colour monitoring 08 p1043 N88-16301

SYLLABLES
Motor theory of auditory perception
[AD-A192095] 18 p2550 N88-25136

SYMBIOSIS
The development of ODE methods: A symbiosis between hardware and numerical analysis
[DE87-014925] 03 p0370 N88-12325

SYMBOLIC PROGRAMMING
Petri nets as a support to symbolic execution of concurrent Ada programs
[REPT-87-007] 01 p0082 N88-10529
Integration of symbolic and algorithmic hardware and software for the automation of space station subsystems
[NASA-TM-89705] 07 p0907 N88-15497
Optical symbolic processor for expert system execution
[AD-A187494] 10 p1385 N88-18268
Deriving abstractions from a software object network
[AD-A187472] 10 p1389 N88-18294
Center for Supercomputing Research and Development
[DE88-003564] 10 p1418 N88-18466
Optical symbolic processor for expert system execution
[AD-A187882] 11 p1525 N88-19103
Integration of symbolic and algorithmic hardware and software for the automation of space station subsystems
17 p2387 N88-24190
Computer systems for the representation and manipulation of mathematical knowledge
[AD-A193547] 23 p3249 N88-29340
AI tools in computer based problem solving
23 p3263 N88-29424
MACSYMA program for the painleve test of nonlinear ordinary and partial differential equations
[AD-A194293] 23 p3270 N88-29458
Optics and symbolic computing
[AD-A195119] 24 p3360 N88-30004
Optical symbolic computing
[AD-A195690] 24 p3429 N88-30406

SYMBOLS
Symbolic, algebraic, and numeric solutions to heat conduction problems using Green's functions
09 p1165 N88-16987
Computer-assisted symbolization by raster data processing --- mapping 16 p2225 N88-23284
Extraction of texts and symbols from unstructured vector data --- mapping 16 p2225 N88-23287
Optical symbolic processor for expert system execution
[AD-A192005] 18 p2575 N88-25296

SYMMETRICAL BODIES
NT AXISYMMETRIC BODIES
NT BODIES OF REVOLUTION
NT CONCENTRIC SPHERES
NT CONICAL BODIES
NT CYLINDRICAL BODIES
NT ELLIPSOIDS
NT FAIRINGS
NT FALLING SPHERES
NT PARABOLIC BODIES
NT ROTATING CYLINDERS
NT ROTATING SPHERES
NT SLENDER CONES
NT SPHERES
NT TORUSES

SYMMETRY
NT BROKEN SYMMETRY
NT SUPERSYMMETRY
Observations of localized grain boundary dislocations in series of (001) and (110) symmetrical tilt boundaries in aluminum
[DE87-014011] 01 p0025 N88-10156
Summary and conclusions of the 6th Moriond workshop --- standard electroweak model
[USIP-87-11] 01 p0092 N88-10602
Systematic studies of molecular vibrational anharmonicity and vibration-rotation interaction by self-consistent-field higher derivative methods. Applications to asymmetric and symmetric top and linear polyatomic molecules
[DE87-014691] 02 p0232 N88-11465
Numerical experiments with a symmetric high-resolution shock-capturing scheme
[NASA-TM-88325] 03 p0370 N88-12332
Dynamics of atoms in low-symmetry systems
[AD-A184318] 03 p0375 N88-12361
Light scattering by oriented and randomly dispersed chiral particles
[DE87-014758] 03 p0376 N88-12368
The finite element method for electronic structure
[DE88-001708] 04 p0485 N88-12989
Conditional second order closure for turbulent shear flows
[AD-A185369] 05 p0581 N88-13542
RADSPHERE: A computer program for calculating the steady-state, axially symmetric, forced response and radiation field of a submerged spherical shell
[AD-A185025] 05 p0609 N88-13738
High energy molecules of high symmetry
[AD-A185385] 05 p0647 N88-13965
Buckling of braced monosymmetric cantilevers: Timoshenko energy approach
[PB87-133849] 06 p0723 N88-14445
On the work needed to factor a symmetric positive definite matrix
[AD-A185781] 06 p0759 N88-14660
Improved understanding of the loss-of-symmetry phenomenon in the conventional Kalman filter
[NASA-TM-100041] 06 p0766 N88-14709
Model of earlier stage of universe's evolution
06 p0775 N88-14758
Global bifurcation of periodic solutions with symmetry
[AD-A185881] 07 p0908 N88-15501
Nonsymmetric metrics in nonlinear field theory
[DE88-700509] 07 p0913 N88-15537
Calculation of symmetric and asymmetric vortex seperation on cones and tangent ogives based on discrete vortex models
[NASA-CR-4122] 08 p0950 N88-15768
Dynamical characteristics of weak turbulence
[AD-A186724] 09 p1161 N88-16957
An application of eigenspace methods to symmetric flutter suppression
[NASA-CR-181618] 10 p1284 N88-17684
The influence of small defects on tensile specimen ductility and symmetry of deformation
[AD-A187983] 10 p1346 N88-18044
Symmetries in nonlinear control systems and their applications 11 p1496 N88-18929
Symmetry and equivalence restrictions in electronic structure calculations
[NASA-TM-39252] 11 p1557 N88-19320
Symmetry problems in particle physics
[DE88-004927] 12 p1688 N88-20099
Chiral symmetry in the path-integral approach
[DE88-700833] 12 p1699 N88-20168
A symmetric set of Euler angles and oblique orientation space sections
[DE88-005317] 13 p1847 N88-21056
Symmetry and global bifurcation in nonlinear solid mechanics
[AD-A190521] 15 p2121 N88-22642
Ten dimensional N = 1 supergravity coupled to supersymmetric Yang-Mills fields in superspace
[DE87-703033] 15 p2146 N88-22808
Path integral, BRS symmetry, and string and membrane theories
[DE88-752300] 15 p2146 N88-22810
Local time displacement as a symmetry of nature in flat space-time
[NASA-TM-100610] 16 p2264 N88-23542
Rigid symmetries and BRST-invariance in gauge theories
[PB88-180948] 18 p2572 N88-25280
Symmetrized magnetic field configuration of low aspect ratio helical system
[IPPJ-869] 20 p2855 N88-26956
Nonlinear interaction between overall and local buckling of stiffened panels with symmetric cross-sections
[PB88-104054] 21 p2960 N88-27580
Closed string fields as parameters of extra gauge symmetry of open string field theory
[DE88-702046] 21 p3026 N88-27960
Symmetry problem of energy-momentum tensor and the creation of gravitational field
[DE88-702442] 21 p3026 N88-27964
Small scale mixing in the initial region of a jet
[AD-A193500] 23 p3192 N88-28994

SYMMETRY BREAKING
U BROKEN SYMMETRY

SYMPATHETIC NERVOUS SYSTEM
Individual functional typology of sympathoadrenal system as indicator of physiological status in adverse environments 12 p1665 N88-19979
Direct interaction between autonomic nerves and the immune system
[AD-A188576] 12 p1667 N88-19991

SYMPATHOMIMETICS
U ADRENERGICS

SYMPTOMS
U SIGNS AND SYMPTOMS

SYNAPSES
Large-scale neuronal circuits for selective storage and recognition of complex stimuli, a pilot study
[AD-A184134] 04 p0474 N88-12920
Biophysical and biochemical mechanisms in synaptic transmitter release
[AD-A187059] 09 p1199 N88-17184
Long term synaptic plasticity and learning in neuronal networks
[AD-A186834] 09 p1199 N88-17188
Synapses that compute motion
[AD-A190389] 15 p2116 N88-22607

SYNCHRONISM
NT BIT SYNCHRONIZATION
The navigation experiment NAVEX: Experimental results of clock synchronization
[DFVLR-MITT-87-05] 03 p0271 N88-11701
Comparing barrier algorithms
[NASA-CR-178377] 04 p0476 N88-12934
Asynchronous rotation in close binary systems with circular orbits 04 p0509 N88-13131
On detection of change points using mean vectors
[AD-A185581] 06 p0767 N88-14717
Super-short yttrium aluminate pulse generator with controlled resonator Q-factor 06 p0772 N88-14740
High repetition rate electron beam RF-acceleration and sub-millimeter wave generation via a free electron laser
[AD-A186066] 07 p0858 N88-15209
The navigation experiment NAVEX: Experimental results of clock synchronization
[ESA-TT-1084] 09 p1132 N88-16791
Parallel access to synchronization variables
[DE88-003570] 10 p1392 N88-18306
Frame synchronization performance and analysis
11 p1473 N88-18787
Electro-mechanical vibratory system
11 p1500 N88-18958
A neuronal model of classical conditioning
[AD-A188378] 12 p1670 N88-19999
On proving register atomicity
[CWI-CS-R8707] 13 p1818 N88-20862
A survey of provably correct fault-tolerant clock synchronization techniques
[NASA-TM-100553] 13 p1823 N88-20894
Approximate agreement
[AD-A191030] 16 p2251 N88-23455
Asynchronous optical sampling for laser-based combustion diagnostics in high pressure flames
[AD-A192920] 20 p2770 N88-26428
A modular proof of correctness for a network synchronizer
[AD-A192726] 21 p3002 N88-27802
Heating efficiency of beat wave excitation in a density gradient
[AD-A193066] 21 p3017 N88-27905
Synchronous response modelling and control of an annular momentum control device
[NASA-CR-4166] 24 p3358 N88-29995

SYNCHRONIZATION
U SYNCHRONISM

SYNCHRONIZED OSCILLATORS
Mode priming in an overmoded gyrotron oscillator
[AD-A189151] 13 p1772 N88-20602

SYNCHRONIZERS
A review of the semiconductor storage of television signals. Part 2: Applications 1975-1986
[BBC-RD-1987/6] 02 p0161 N88-11009
Interleaver design for trellis-coded differential 8-PSK modulation with non-coherent detection
19 p2648 N88-25719

SYNCHRONOUS DETECTORS
U CORRELATORS

SYNCHRONOUS MOTORS
The method of rigid armature flux orientation for the field-oriented control of highly dynamic drives with synchronous machines
[ETN-87-90405] 01 p0042 N88-10269
Contributions to fast-reacting and high-precision three-phase positioning systems --- machinery
[ETN-87-90427] 01 p0056 N88-10358
Computerized system for studies on creep of irradiated materials in the BR-10 reactor. Control system for electric motor
[DE87-702888] 03 p0310 N88-11952
The operational behavior of microprocessor-controlled and pulsed inverter-fed synchronous machines with permanent magnet excitation
[ETN-88-91479] 11 p1480 N88-18833
A high performance inverter-fed drive system of an interior permanent magnet synchronous machine
[DE88-006753] 15 p2061 N88-22288
Permanent magnet excitation of axial flow synchronous machines with high rotation moment
[ETN-88-92385] 20 p2796 N88-26592
Voltage directive drive with claw pole motor and control without rotor position indicator
[ETN-88-93120] 24 p3366 N88-30047

SYNCHRONOUS PLATFORMS
Communications payload concepts for geostationary facilities
[NASA-TM-100154] 05 p0576 N88-13513
Latitude coverage of observations of the middle atmosphere by solar absorption spectrometry from a heliosynchronous orbit
[AERONOMICA-ACTA-A-316-1987]
06 p0742 N88-14566
Coorbiting Platform Utilization Study (CPLUS), executive summary --- Columbus
[SN-WP-4000-DOC-6609/85/F]
09 p1133 N88-16796

SYNCHRONOUS SATELLITES
NT GOES SATELLITES
Low-g propellant gaging 08 p0982 N88-15937
Satellite assembly in geostationary orbit: A plug-and-socket concept 09 p1128 N88-16769
Investigations of high resolution imaging through the Earth's atmosphere using speckle interferometry
[AD-A189295] 12 p1692 N88-20121
Survey of the Air Force P78-2 (SCATHA) satellite plasma wave data during electron gun operations
[AD-A191014] 16 p2168 N88-22926
Construction of a 60 GHz Traveling Wave Tube (TWT) for intersatellite link on geostationary orbit (ISL/TWT)
[BMFT-FB-W-86-015] 16 p2192 N88-23076
On the collision hazard of colocated geostationary satellites
[DFVLR-FB-88-02] 23 p3184 N88-28952

SYNCHROTRON RADIATION
Brightness and coherence of radiation from undulators and high-gain free electron lasers
[DE87-011093] 02 p0177 N88-11102
Stratospheric particles: Synchrotron X-ray fluorescence determination of trace element contents
[DE87-012482] 02 p0198 N88-11234
Compact electron storage rings
[DE87-013301] 02 p0234 N88-11477
Resistor cooling in a vacuum
[DE88-000696] 04 p0440 N88-12733
Center for X-Ray Optics, 1986
[DE88-000715] 04 p0449 N88-12783
The generation and suppression of synchrotron sidebands
[DE88-000532] 04 p0449 N88-12787
The production of ultrasmall and superfine holographic diffraction gratings using synchrotron radiation and lithographic techniques
[AD-A185395] 05 p0585 N88-13562
Microwave superheaters for fusion
[DE88-001656] 05 p0653 N88-14007
JPRS report: Science and technology. Japan
[JPRS-JST-87-027] 06 p0688 N88-14213
HEAO-1 observations of gamma-ray bursts
07 p0947 N88-15756
The structure of the sideband spectrum in free electron lasers
[AD-A186952] 09 p1170 N88-17015
Grazing incidence X-ray scattering study of defect structures in MBE GaAs/Si using synchrotron radiation
[DE88-004556] 10 p1420 N88-18483
Initial operation of the Tevatron collider
[FNAL-TM-1449] 11 p1547 N88-19252
Multilayer-coated mirrors as power filters in synchrotron radiation beamlines
[DE88-003872] 11 p1550 N88-19276
Applications of the lateral shearing interferometer in measurement of synchrotron radiation optical elements
[DE88-005184] 13 p1840 N88-21011
Advances in geochemistry and cosmochemistry: Trace element microdistributions with the synchrotron X-ray fluorescence microprobe
[DE88-006355] 15 p2032 N88-22108
Transport simulations of ohmic ignition experiment: IGNITEX
[DE88-006055] 15 p2136 N88-22757
On bunch lengthening using the fourth harmonic cavity in the NSLS VUV ring
[DE88-007392] 18 p2574 N88-25288
An undulator radiation source for spin-polarized photoemission studies of novel magnetic materials
[AD-A193756] 22 p3083 N88-28307
Fourier transform of gravitational synchrotron radiation
[PREPRINT-588] 22 p3144 N88-28700
X-ray diffraction imaging (topography) of electroopticcrystals by synchrotron radiation
[NASA-CR-183266] 24 p3432 N88-30427
Diffraction imaging (topography) with monochromatic synchrotron radiation
[NASA-CR-183264] 24 p3433 N88-30431
Streaking images that appear only in the plane of diffraction in undoped GaAs single crystals: Diffraction imaging (topography) by monochromatic synchrotron radiation
[NASA-CR-183267] 24 p3433 N88-30437
Applications of synchrotron radiation to materials science: Diffraction imaging (topography) and microradiography
[NASA-CR-183265] 24 p3434 N88-30440

SYNCHROTRONS
NT STORAGE RINGS (PARTICLE ACCELERATORS)
National Synchrotron Light Source users manual: Guide to the VUV and X-ray beam lines
[DE88-001464] 04 p0490 N88-13020
Accelerators and Superconductivity: A Marriage of Convenience. Second John Adams Memorial Lecture
[DE88-700005] 07 p0931 N88-15656
A two-wavelength infrared interferometer/polarimeter system for CIT (Compact Ignition Tokamak)
[DE88-007681] 18 p2579 N88-25321
Optical guiding in the separable beam limit
[AD-A192452] 21 p2952 N88-27534

SYNCOPE
NT BLACKOUT (PHYSIOLOGY)

SYNDROMES
U SIGNS AND SYMPTOMS

SYNOPTIC MEASUREMENT
Analysis of winter season precipitation bands over the Southern Plains 14 p1947 N88-21609
The role of space borne imaging radars in environmental monitoring: Some shuttle imaging radar results in Asia
[NASA-TM-101175] 20 p2789 N88-26544
Meteorological features during the marginal ice zone experiment from 20 March to 10 April 1987
[AD-A193960] 23 p3235 N88-29251

SYNOPTIC METEOROLOGY
An illustrative example of the nowcasting challenge
02 p0199 N88-11243
Conceptual models of Baiu front and Baiu frontal disturbances in multiscale characteristics --- East Asia
02 p0203 N88-11271
A review of the analysis forecasting and research about severe local storms in Guangdong province (China)
02 p0207 N88-11298
Properties of the atmospheric boundary layer above a subtropical oceanic front
[AD-A184006] 03 p0351 N88-12215
Isentropic analysis and interpretation: Operational applications to synoptic and mesoscale forecast problems
[AD-A184814] 05 p0626 N88-13830
Global atmospheric circulation statistics: Four year averages
[NASA-TM-100690] 05 p0628 N88-13842
Synoptic perturbations and climate
08 p1016 N88-16158
Northern winter circulations for the period 1974-1983
[AD-A187779] 11 p1511 N88-19026
Dynamics of synoptic ocean eddies
13 p1786 N88-20689
Analysis of a six-component barotropic spectral model: Chaotic motion, predictability and vacillation --- atmospheric circulation
[CWI-AM-R8710] 18 p2542 N88-25090
Verification of regional climates of GISS GCM. Part 1: Winter
[NASA-TM-100695] 19 p2694 N88-26012
Synoptic patterns related to tropical cyclone recurvature
[AD-A192332] 20 p2827 N88-26771
Solar-geophysical data number 522, February 1988. Part 2: (Comprehensive reports). Data for August 1987 and miscellanea
[PB88-194741] 20 p2886 N88-27138
Some evidence for a Northern Hemispheric extratropic trigger mechanism of ENSO events
22 p3123 N88-28556

SYNTAX
NT SYLLABLES
NT WORDS (LANGUAGE)
Integrating syntax, semantics, and discourse DARPA (Defense Advanced Research Projects Agency) Natural Language Understanding Program
[AD-A184505] 03 p0364 N88- 2289
Ada (trade name) compiler validation summary report: Systems designers' PLC SD Ada-plus VAX/VMS x MC68020. Version 2B.00. Host: VAX 8600. Target: Motorola MC68020. Completion of on-site testing
[AD-A186571] 08 p1053 N88-16356
Substructure discovery in executed action sequences
[AD-A186446] 08 p1069 N88-16462
Experience with Omega: Implementation of a prototype programming environment, part 6
[AD-A187080] 10 p1385 N88-18270
KA-Prolog: Language definition
[GMD-249] 11 p1532 N88-19155

A parser generator for finitely ambiguous context-free grammars
[CWI-CS-R8712] 13 p1818 N88-20864
WORDNET: An electronic lexical reference system based on theories of lexical memory
[AD-A193086] 21 p3027 N88-27970
Unification and set-valued functions for functional and logic programming
[AD-A193643] 23 p3250 N88-29341
Experiments in automatic phrase indexing for document retrieval: A comparison of syntactic and non-syntactic methods 23 p3296 N88-29634
Exploiting lexical regularities in designing natural language systems
[AD-A195922] 24 p3423 N88-30375

SYNTHESIS
Reduced complexity structural modeling for automated airframe synthesis
[NASA-CR-177440] 04 p0393 N88-12453
A method for designing robust multivariable feedback systems
[NASA-CR-182459] 09 p1225 N88-17341
A methodology for the synthesis of robust feedback systems
[NASA-CR-182455] 09 p1225 N88-17342
Structural shape optimization in multidisciplinary system synthesis
[NASA-TM-100538] 12 p1614 N88-19650

SYNTHESIS (CHEMISTRY)
NT COPOLYMERIZATION
NT DIMERIZATION
NT POLYMERIZATION
Process for the preparation of acyl halides
[GB-PATENT-2-133-792-A] 01 p0020 N88-10124
Novel polymers and copolymers and production of poly(acetylene)
[EP-PATENT-0-173-473-A2] 01 p0026 N88-10161
A process for producing phenolic foams
[EP-PATENT-0-170-357-A1] 01 p0026 N88-10162
Novel conductive polymers
[EP-PATENT-0-182-548-A2] 01 p0026 N88-10163
Crosslinkable elastomeric materials
[EP-PATENT-0-181-735-A1] 01 p0026 N88-10165
Boronium complexes as polymer catalysts
[GB-PATENT-2-161-475-A] 01 p0026 N88-10166
Synthesis and characterization of processable polyimides with enhanced thermal stability
[NASA-CR-181447] 01 p0030 N88-10191
Synthesis of novel acid electrolytes for phosphoric acid fuel cells
[PB87-221305] 01 p0066 N88-10426
Preparation of polymer polyols
[EP-PATENT-0-162-589-A1] 01 p0102 N88-10665
Formation of amorphous alloys by solid state reactions
[DE87-013175] 02 p0146 N88-10918
Urea-polyurethane and polydimethylsiloxane mixtures: Morphology control using a block copolymer
[ISAL-ID11-87-05] 02 p0153 N88-10959
Wittig synthesis of conductive segmented block polymer compositions
[AD-A184018] 03 p0295 N88-11850
Synthesis and characterization of block copolymers
[AD-A184405] 03 p0295 N88-11855
Synthesis and characterization of block copolymers
[AD-A184406] 03 p0296 N88-11856
Highly Non-Linear Optical (NLO) organic crystals
03 p0297 N88-11865
Shock-induced chemical synthesis of phases similar to the high temperature superconductor oxides
[DE87-013725] 03 p0380 N88-12387
Ceramics thin film 04 p0403 N88-12505
Synthesis, NMR characterization and electrical properties of siloxane-based polymer electrolytes
[AD-A184184] 04 p0418 N88-12596
Conductive polymers via reactive aligomer
[AD-A184270] 04 p0419 N88-12597
Thermoplastic elastomers as LOVA (Low Vulnerability Ammunition) binders
[AD-A184350] 04 p0419 N88-12599
Proton abstraction as a route to conductive polymers
[AD-A184019] 04 p0421 N88-12612
Studies on syntheses of amine-carboxyboranes (boron analogues of amino acids) and derivatives
[AD-A184838] 05 p0557 N88-13386
Molecular-level synthesis and characterization of metal-polymer interfaces
[AD-A184956] 05 p0567 N88-13455
Preparation and characterization of members of the system (Zn,Se)1-xGaPx
[AD-A185073] 05 p0655 N88-14019
Method for preparing hydride configurations and reactive metal surfaces
[DE88-000845] 06 p0679 N88-14161
Model Cu/ZnO catalysts for methanol synthesis: The role of surface structure
[DE88-002354] 07 p0830 N88-15037
Biopolymers: Protein and nucleic acids
[AD-A185837] 07 p0835 N88-15066
The synthesis and characterization of some rare earth arsenides
[AD-A186445] 08 p0965 N88-15839
A 13C and 15N solid state NMR characterization of aramid-containing nylon-6 polymers synthesized by in situ polymerization of caprolactam with benzoyl caprolactam derivatives
[AD-A187067] 09 p1147 N88-16872
Thermoplastic elastomers as LOVA binders
[AD-A186563] 10 p1304 N88-17797
Electrically conducting polymer-copper sulphide composite films, preparation by treatment of polymer-copper (2) acetate composites with hydrogen sulfide
[NASA-TT-20204] 10 p1305 N88-17803
Effect of weightlessness on replicative function of rat hepatocyte DNA 10 p1360 N88-18129
RNA-synthesizing activity in rat liver following flight aboard Cosmos-1667 10 p1360 N88-18130
Electronic and ionic transport in polymers
[AD-A187253] 11 p1452 N88-18651
Synthesis and structure property studies of toughened epoxy resins via functionalized polysiloxanes: Friction and wear studies
[AD-A188258] 11 p1462 N88-18718
Preparation of thin film polyvinylidene fluoride shock wave pressure transducers
[PB88-156070] 11 p1490 N88-18893
Nonlinear optical waveguides containing a transition metal-based dye molecule
[DE88-003257] 11 p1550 N88-19275
The preparation of titanium nitride and titanium carbonitride by the preceramic polymer route
[AD-A188357] 12 p1610 N88-19626
Ordered polymers for space applications
[AD-A188460] 12 p1610 N88-19630
Synthesis and characterization of 1,2-cyclobutenedicarboxamides: Thermally generated polymers and Diels-Alder adducts
[AD-A188591] 12 p1611 N88-19633
A procedure for estimating the crystal densities of organic explosives
[AD-A189023] 12 p1613 N88-19646
Synthesis of energetic materials
[AD-A189115] 13 p1753 N88-20482
A hydroxycarbonate route to superconductor precursor powders
[DE88-003638] 13 p1846 N88-21052
The combustion synthesis of boride composites
[DE88-005474] 15 p2028 N88-22084
Research on stable processible conducting polymers for electronic applications
[AD-A190246] 15 p2044 N88-22180
New phosphorus based polymer systems
[AD-A190457] 15 p2045 N88-22186
A new approach to highly fluorinated lubricants
[AD-A190523] 15 p2045 N88-22188
Evaluation of direct methane conversion to higher hydrocarbons and oxygenates
[DE88-003812] 15 p2049 N88-22204
Synthesis of metastable superconductors by high dynamic pressure
[DE88-005620] 15 p2139 N88-22764
Remarks on solid state amorphizing transformations
[DE88-006452] 15 p2145 N88-22803
Synthesis and characterization of high-T(sub c) screen-printed Y-Ba-Cu-O films on alumina
[NASA-TM-100860] 15 p2146 N88-22805
Synthesis and properties of novel cluster phases
[DE88-006816] 16 p2175 N88-22964
Evaluation of a thermoplastic polyimide (422) for bonding GR/PI composite
[NASA-TM-100584] 16 p2182 N88-23003
Key problems and hydrogen atom formation
16 p2269 N88-23573
Improvements to Raney copper zinc methanol synthesis catalysts 17 p2318 N88-23844
Polymer precursors for SiC ceramic materials
17 p2326 N88-23889
Topological stereochemistry
[AD-A191867] 18 p2477 N88-24691
Aromatic cyclotriphosphazenes
[NASA-CASE-ARC-11428-3] 18 p2477 N88-24692
Proceedings of the American Society for Composites
[AD-A189861] 18 p2477 N88-24693
Current and future molecular structures of aerospace organic matrix resins 18 p2477 N88-24695
Industrial perspective on current and future needs in aerospace matrix resin chemistry
18 p2477 N88-24696
Applications of biotechnology to synthetic chemistry for aerospace matrix resins development
18 p2478 N88-24697
The application of hydrocarbon bioconversion technology to aerospace materials production
18 p2478 N88-24698
The synthesis of polyphenylene from a CIS-dihydrocatechol biologically produced monomer
18 p2478 N88-24699
Update of low temperature catalyst development
[DE88-007032] 18 p2480 N88-24715
Synthesis and characterization of new phosphazene polymers
[AD-A191508] 18 p2490 N88-24771
High strength/sigh modulus aromatic heterocyclic ABA block copolymers
[AD-A191666] 18 p2491 N88-24774
A cardiostimulant protein from the Australian Red Waratah Sea anemone, Actinia tenebrosa
18 p2550 N88-25138
Solid-state combustion synthesis of ceramics and alloys in reduced gravity
[NASA-CR-4163] 19 p2608 N88-25479
Improved structural polymer alloys and composites
[AD-A192092] 19 p2619 N88-25538
Substituted 1,1,1-Triaryl-2,2,2-Trifluoroethanes and processes for their synthesis
[NASA-CASE-LEW-14345-1] 20 p2767 N88-26404
Glass forming ranges of amorphous alloys
[DE88-007897] 20 p2772 N88-26438
Dual mechanism bifunctional polymers: Design, synthesis and application of a new category of metal ion complexing agents
[DE88-008233] 20 p2777 N88-26468
A study of solvent effects on the synthesis of pure component and composite ceramic powders by metal alkoxide hydrolysis
[DE88-008381] 20 p2777 N88-26470
Fundamental studies of elastomers
[DE88-009679] 20 p2778 N88-26471
Refractory Materials of Zirconate. Part 2: Synthesis and some properties of strontium, zirconate, calcium zirconate and barium zirconate
[NASA-TT-20186] 20 p2779 N88-26483
Cosmological helium production simplified
[DE88-009578] 20 p2885 N88-27130
Ionic conductive polymers based on crosslinked elastic siloxane-ethylene oxide copolymers
[DE88-011243] 21 p2917 N88-27311
Soluble metal chelate polymers of coordination numbers six, seven and eight
[AD-A192485] 21 p2917 N88-27314
Preparation and properties of high Q microwave dielectrics in the (CA, SR, BA) zirconate system
[AD-A193127] 21 p2918 N88-27317
Energy migration, motion and order in synthetic polymers
[AD-A193334] 21 p2918 N88-27320
New synthetic approaches to boron hydride transformations
[AD-A193872] 22 p3052 N88-28108
Super hydrides
[AD-A193710] 23 p3192 N88-28995
Polymerization of azaethylenes (imines) and aza-1,3-dienes: Potential reactive monomers
[AD-A194717] 23 p3197 N88-29028
Boron-containing organosilane polymers and ceramic materials thereof
[NASA-CASE-ARC-11649-1-SB]
23 p3199 N88-29040
Diamond film by hot filament CVD method
[NASA-TT-20335] 23 p3294 N88-29618
Novel ladder polymers for use as high temperature stable resins or coatings
[NASA-CASE-LEW-14203-1] 24 p3356 N88-29984

SYNTHESIZERS
Neural network based speech synthesizer: A preliminary report 08 p1064 N88-16429

SYNTHETIC APERTURE RADAR
NT SIDE-LOOKING RADAR
Study of a payload for Columbus Polar Platform Earth observation demonstration mission, executive summary
[ESA-CR(P)-2412] 01 p0014 N88-10079
X-band SAR for a European remote sensing paylcad
03 p0340 N88-12142
Inverse scattering analysis of diffraction limited SAR
[FOA-C-30459-3.2] 05 p0576 N88-13512
Arrays for discrete Fourier transform
[REPT-87-019] 05 p0632 N88-13861
Study of synthetic aperture radar data compression and encoding. Part 3: Performance evaluation of speckle suppression and data compression algorithms
[NLR-TR-85085-L-PT-3] 06 p0692 N88-14248
Study of synthetic aperture radar data compression and encoding. Part 4: Algorithm implementation aspects
[NLR-TR-85085-L-PT-4] 06 p0692 N88-14249

Texture study of Synthetic Aperture Radar (SAR) images of ocean surfaces
[AD-A186021] 07 p0841 N88-15101
Study of synthetic aperture radar data compression and encoding. Part 1: SAR image data analysis
[NLR-TR-85085-L-PT-1] 07 p0843 N88-15115
Study of synthetic aperture radar data compression and encoding. Part 2: SAR image speckle suppression and data compression algorithms
[NLR-TR-85085-L-PT-2] 07 p0843 N88-15116
SAR (Synthetic Aperture Radar). Earth observing system. Volume 2F: Instrument panel report
[NASA-TM-89701] 07 p0871 N88-15284
Earthnet's experience with Seasat SAR image processing 09 p1127 N88-16760
Radar backscatter from airports and surrounding areas 10 p1274 N88-17623
Rotor SAR (ROSAR): A new high-resolution all-weather vision method for helicopters
[MBB-UA-1046/87] 10 p1314 N88-17855
SAR (Synthetic Aperture Radar) imaging of ship wakes in the Gulf of Alaska
[AD-A186554] 10 p1317 N88-17872
Integrated optical synthetic aperture radar processor
[AD-A188019] 11 p1471 N88-18772
The complex point spread function of the RSRE SAR (Synthetic Aperture Radar)
[AD-A189011] 12 p1621 N88-19693
Synthetic-aperture radars viewed as interferometers with matched filter processing of the collected data
[AD-A190608] 15 p2057 N88-22262
Preliminary study of a coherent radar
[BCRS-86-03] 16 p2189 N88-23051
Investigation of the imaging of ocean surface waves using a synthetic aperture radar
[SER-A-WISS-ABHANDL-84] 16 p2236 N88-23357
Preparation and execution of calibration measurements for handling of airborne SAR data (AGRISAR)
[ETN-88-92336] 17 p2333 N88-23926
The role of space borne imaging radars in environmental monitoring: Some shuttle imaging radar results in Asia
[NASA-TM-101178] 18 p2502 N88-24844
Data volume reduction for imaging radar polarimetry
[NASA-CASE-NPO-17184-1-CU]
20 p2788 N88-26541
The role of space borne imaging radars in environmental monitoring: Some shuttle imaging radar results in Asia
[NASA-TM-101175] 20 p2789 N88-26544
Some characteristics in synthetic aperture radar (SAR) raw data and SAR images
[FOA-C-30483-3.2] 22 p3071 N88-28232
Effect of phase errors in stepped-frequency radar systems
[AD-A194476] 23 p3203 N88-29061
Acoustooptic processing of two-dimensional signals using temporal and spatial integration
[AD-A194803] 24 p3359 N88-29999
A submillimeter wavelength space-based imaging radar
[AD-A195846] 24 p3364 N88-30033
MIZEX (marginal ice zone experiment) 1987 SAR (Synthetic Aperture Radar) data summary
[AD-A195560] 24 p3364 N88-30035

SYNTHETIC APERTURES
High precision ultrasonic scanning system and SAFT-UT development
[DE87-010036] 01 p0006 N88-10044
Imaging of planar defects with synthetic aperture focusing technique (LSAFT) --- ultrasonic inspection
[VTT-466] 01 p0058 N88-10370
On the concept of resolution ellipse in aperture synthesis matched deconvolution with error analysis --- astronomical interferometry 01 p0095 N88-10621
OASIS: A mission concept --- Optical Aperture Synthesis Space Interferometry (OASIS) 01 p0095 N88-10622
Aperture synthesis in space: Technical problems
01 p0097 N88-10638
Holographically correcting synthetic aperture aberrations
[AD-A189510] 12 p1692 N88-20123

SYNTHETIC ARRAYS
ISIS: Image reconstruction experiments and comparison of various array configurations --- spaceborne interferometry 01 p0095 N88-10620
Fiber-linked telescope arrays on the ground and in space 01 p0095 N88-10626

SYNTHETIC FIBERS
NT CERAMIC FIBERS
NT GLASS FIBERS
NT NYLON (TRADEMARK)
Molecular composites: Processing, post-treatment and mechanics
[AD-A184458] 04 p0410 N88-12547
Structure of thermotropic polyesters with large substituents
[AD-A184086] 04 p0418 N88-12595
Solid state C-13 NMR characterization of textiles: Qualitative and quantitative analysis
[AD-A184349] 04 p0419 N88-12598
Development of test methods for the electrostatic properties of nonhomogeneous fabrics, phase 2
[AD-A190853] 18 p2489 N88-24767

SYNTHETIC FUELS
NT GASOHOL (FUEL)
Fifty years in synthetic fuels information: Have we lost a strategic national resource
[DE87-010902] 02 p0155 N88-10973
Emerging environmental constraints on the use of gasoline and diesel fuel and tradeoffs associated with the use of alternative fuels
[DE87-011504] 04 p0422 N88-12614
Combustion characteristics of gas turbine alternative fuels
[NASA-TM-100247] 05 p0548 N88-13338
Fuel nitrogen conversion in a supercharged spark ignition engine
[DE88-003739] 08 p0974 N88-15893
Engine testing for synfuel operation
[DE88-006044] 13 p1779 N88-20645
Production costs of hydrocarbon fuels from biomass
[DE88-006667] 18 p2495 N88-24804
Development of an equation of state for computation of supercompressibility factors, critical flow factors and other properties for wet, sour natural gases, synthetic gases and admixtures
[PB88-202676] 20 p2796 N88-26602
An outdoor test facility for the large-scale production of microalgae
[DE88-001146] 21 p2984 N88-27723
The behaviour of synthetic fuels in a small transparent combustor 24 p3351 N88-29950

SYNTHETIC RESINS
NT ACRYLIC RESINS
NT EPOXY RESINS
NT KEVLAR (TRADEMARK)
NT NYLON (TRADEMARK)
NT PEEK
NT PHENOLIC RESINS
NT POLYAMIDE RESINS
NT POLYETHER RESINS
NT POLYMETHYL METHACRYLATE
NT THERMOPLASTIC FILMS
NT THERMOPLASTIC RESINS
NT THERMOSETTING RESINS
NT VINYL COPOLYMERS
Flame retardation treatment of synthetic rubbers and synthetic resins
[NASA-TT-20285] 19 p2620 N88-25544

SYNTHETIC RUBBERS
NT BUNA (TRADEMARK)
NT ELASTOMERS
NT VULCANIZED ELASTOMERS
Flame retardation treatment of synthetic rubbers and synthetic resins
[NASA-TT-20285] 19 p2620 N88-25544
Development of a nitrile rubber for dynamic damping
[AD-A194060] 22 p3058 N88-28145

SYRIA
International manned flight, USSR-SAR
[NASA-TT-20260] 16 p2166 N88-22914

SYSTEM EFFECTIVENESS
Measurement of fault-tolerant parallel processors
[PB87-208328] 01 p0084 N88-10539
Experiments in fault tolerant software reliability
[NASA-CR-181554] 05 p0632 N88-13863
Field evaluation of interactive simulation for maintenance training: SH-3 helicopter electro-mechanical bladefold system
[AD-A185923] 07 p0821 N88-14991
Measurement and effects of transport delays in a state-of-the-art F-16C flight simulator
[AD-A187367] 11 p1441 N88-18599
The integration of artificial intelligence techniques to improve the effectiveness of electronic countermeasure strategies in a tactical environment
[AD-A189483] 12 p1682 N88-20056
A low cost automatic Earth observation satellite tracking ground receiving station 17 p2309 N88-23815
An enumeration of research to determine the optimal design and use of Army flight training simulators
[AD-A191242] 18 p2468 N88-24649
Vapor Compression Distillation Subsystem (VCDS) component enhancement, testing and expert fault diagnostics development, volume 1
[NASA-CR-172072] 22 p3134 N88-28634
The OFP (Operational Flight Program) update cycle needs you
[AD-A194910] 24 p3325 N88-29796
Controlled degradation of resolution of high-quality flight simulator images for training effectiveness evaluation
[AD-A196189] 24 p3330 N88-29823

SYSTEM FAILURES
Inadequacy of conventional dynamic recovery mechanisms in the presence of temporary failures
[AD-A186311] 07 p0866 N88-15251
Modelling of clustering effects in point processes: An application to failures in SPC-systems (stored program control-systems)
[PB87-149241] 07 p0904 N88-15480
Validation of a stochastic model to determine failure rates for communication-electronic systems
[AD-A186536] 08 p0960 N88-15920
Pattern-recognition software detecting the onset of failures in complex systems
[DE88-002861] 09 p1220 N88-17318
Airworthiness considerations
10 p1276 N88-17636
Failure mechanism of He-Ne lasers
14 p1902 N88-21362
On the danger of redundancies in some aerospace mechanisms 14 p1925 N88-21475
Orbiter processing facility service platform failure and redesign 14 p1928 N88-21494
Modeling failures of intermittently used machines
[AD-A190298] 15 p2074 N88-22367
Aircraft accident/incident summary reports: Modena, Pennsylvania, March 17, 1986; Redwater, Texas, April 4, 1986
[PB88-910403] 16 p2159 N88-22878
Expanded envelope concepts for aircraft control-element failure detection and identification
[NASA-CR-181664] 16 p2160 N88-22886
Design of the Detector 2: A CMOS gate array for the study of concurrent error detection techniques
[AD-A191247] 16 p2193 N88-23079
Compilation of preprints
[AD-A191245] 16 p2252 N88-23460
Modeling of functional specifications for onboard software: Experience with the Rafale avionics system
17 p2303 N88-23777
MTK: An AI tool for model-based reasoning
17 p2387 N88-24189
Applications of fault tree analysis to the design process
[DE88-007048] 18 p2525 N88-24982
Failure rate prediction of electronic components
[PB87-228953] 19 p2678 N88-25925
Electronic failure analysis-corrosion of avionics
22 p3054 N88-28122

SYSTEM IDENTIFICATION
Digital algorithms for the control and dynamic decoupling of industrial robot axes
[ETN-87-90441] 01 p0064 N88-10546
Effect of installation and calibration errors of sensors on system identification results of an aircraft
[ESA-TT-1059] 03 p0266 N88-11678
A system identification technique based on the random decrement signatures. Part 1: Theory and simulation
05 p0594 N88-13625
A system identification technique based on the random decrement signatures. Part 2: Experimental results
05 p0594 N88-13626
Lie algebraic method in filtering and identification
[CWI-PM-R8606] 08 p1072 N88-16467
A state space approach to the problem of adaptive pole assignment
[CWI-OS-R8704] 09 p1224 N88-17339
Identification of nonlinear output-affine systems using an orthogonal least squares algorithm
[RR-313] 14 p1958 N88-21679
Identification of nonlinear rational systems using a prediction-error estimation algorithm
[RR-317] 14 p1959 N88-21680
Application of the NARMAX method to nonlinear frequency response estimation
[RR-319] 14 p1964 N88-21721
Active control and system identification of rotordynamic structure 16 p2218 N88-23230
Identification of control structures --- expert systems
[REPT-87-66] 16 p2255 N88-23472
TVC (Thrust Vector Control) jet vane thermal modeling using parametric system identification
[AD-A191518] 18 p2474 N88-24678
System identification in vehicle dynamics
[DFVLR-MITT-87-22] 20 p2785 N88-26518
Flight vehicle system identification: Status and prospects 20 p2785 N88-26520
Vehicle dynamics: Identification in the frequency domain 20 p2785 N88-26523
Frequency domain identification of the dynamics of a scaled remotely-piloted helicopter
20 p2786 N88-26524
Multivariable identification of a flexible transport aircraft 20 p2786 N88-26525
A two-point aerodynamic model for identification
20 p2786 N88-26526

The identification of the direct lift control flap system of the research aircraft ATTAS
20 p2786 N88-26527
Identification methods for transport dynamical investigations 20 p2787 N88-26531
Utilization of identification methods in the time and frequency domain for the determination of the XV-15 (tilt-rotor) dynamics for lateral motion in hover flight
20 p2787 N88-26532
Identification of lateral operation dynamics of rail vehicles using roll test stand tests
20 p2787 N88-26534
Nonlinear identification of an aircraft for the direct calculation of an anticipatory control
20 p2787 N88-26535
Estimation of aircraft parameters using filter error methods and extended Kalman filter
[DFVLR-FB-88-15] 23 p3176 N88-28911

SYSTEMS ANALYSIS
NT SYSTEM IDENTIFICATION
Digital system bus integrity
[NASA-CR-181446] 01 p0006 N88-10030
A feasibility study of a hypersonic real-gas facility
[NASA-CR-180423] 01 p0008 N88-10043
Numerical predictions of EML system performance
[DE87-011727] 01 p0011 N88-10061
Spacecraft 2000
[NASA-CP-2473] 01 p0015 N88-10084
Space Assembly, Maintenance, and Servicing Study (SAMSS) 01 p0015 N88-10089
Spacecraft Systems Working Group report
01 p0015 N88-10091
System Development Working Group report
01 p0016 N88-10092
The periodic Lyapunov equations
[REPT-86-007] 01 p0087 N88-10567
Recent advances in structural dynamics of large space structures
[NASA-TM-100513] 02 p0138 N88-10867
Space lab system analysis
[NASA-CR-179207] 02 p0138 N88-10869
Direct Absorption Receiver (DAR) systems assessment
[DE87-012277] 02 p0196 N88-11222
Software reliability models for fault-tolerant avionics computers and related topics
[NASA-CR-181440] 02 p0220 N88-11382
Balloon track data analysis
[AD-A184750] 03 p0350 N88-12213
UNIX benchmark system
[AD-A184492] 03 p0367 N88-12308
Institute for Computational Mechanics in Propulsion (ICOMP) first year summary
[NASA-TM-100225] 03 p0370 N88-12330
Mathematical models for the S.D.I.
[AD-A184687] 03 p0373 N88-12345
Development and evaluation of a Monte Carlo code system for analysis of ionization chamber responses
[AD-A183970] 03 p0375 N88-12359
The impact of information technology on research in science and engineering
[DE88-000342] 03 p0385 N88-12417
CNET (Chief of Naval Education and Training) Program Automated Tracking System (CPATS). A comprehensive study
[AD-A184694] 03 p0385 N88-12418
An evaluation plan of bus architectures and protocols using the NASA Ames intelligent redundant actuation system
[NASA-CR-177458] 04 p0398 N88-12482
On dynamic loads in parallel shaft transmissions. 1: Modelling and analysis
[NASA-TM-100180] 04 p0451 N88-12797
PRAAGE: An interactive IBM-PC code for unreliability/aging analysis
[DE87-012124] 04 p0453 N88-12803
Extremum methods of structural analysis for system reliability assessment 04 p0456 N88-12824
Performance analysis of solar thermal power systems
[DE88-000583] 04 p0465 N88-12874
Applications of the hybrid automated reliability predictor
[NASA-TP-2760] 04 p0475 N88-12928
Software maintenance in scientific and engineering environments: An introduction and guide
[NASA-CR-177409] 04 p0479 N88-12954
Investigation, development and application of optimal output feedback theory. Vol. 4: Measures of eigenvalue/eigenvector sensitivity to system parameters and unmodeled dynamics
[NASA-CR-4108] 04 p0482 N88-12969
Propagation of random initial conditions in time
04 p0486 N88-12993
RSDIMU acceptance testing system: Overview of acceptance software and procedures
05 p0632 N88-13866
Post stall behavior in axial-flow compressors
[AD-A185712] 06 p0665 N88-14081
Controlled Ecological Life Support Systems (CELSS) physiochemical waste management systems evaluation
[NASA-CR-177422] 06 p0754 N88-14626
Characteristic trajectories of generalized Lanchester equations
[AD-A185762] 06 p0766 N88-14705
Summaries of FY 1987 engineering research
[DE88-002572] 07 p0840 N88-15096
How errors in component reliability affect system reliability
[AD-A186264] 07 p0865 N88-15249
Mathematical techniques for system realization and identification
[AD-A186352] 07 p0915 N88-15557
Risk analysis methodology survey
07 p0922 N88-15604
Orbital transfer vehicle studies overview
08 p0981 N88-15931
Adaptive exponential stabilization of a first order continuous-time system
[CWI-OS-R8705] 08 p1069 N88-16461
System analysis in rotorcraft design: The past decade
09 p1110 N88-16652
Dynamic analysis of multimesh-gear helicopter transmissions
[NASA-TP-2789] 09 p1176 N88-17045
Cooperative analysis expert situation assessment research 09 p1206 N88-17228
Approaches to the verification of rule-based expert systems 09 p1206 N88-17232
Building validation tools for knowledge-based systems
09 p1207 N88-17235
A performance comparison of the Cray-2 and the Cray X-MP
[NASA-CR-177461] 09 p1216 N88-17288
Concept of a programmable maintenance processor applicable to multiprocessing systems
[NASA-TM-100406] 09 p1223 N88-17333
A methodology for the synthesis of robust feedback systems
[NASA-CR-182455] 09 p1225 N88-17342
Latent failures and coverage in fault-tolerant systems. A VLSI CMOS circuit design technique to aid test generation
[AD-A187615] 10 p1325 N88-17921
Comprehensive analysis of helicopters with bearingless rotors
[NASA-CR-182537] 10 p1390 N88-18300
A two-stage isolated-word recognition system using discriminant analysis
[AD-A187425] 10 p1402 N88-18360
Linear prediction of stationary vector sequences
[NASA-TM-100069] 10 p1403 N88-18366
Multidimensional system analysis of electro-optic sensors with sampled deterministic output
[AD-A187083] 10 p1408 N88-18399
Development of tokamak reactor system analysis code NEW-TORSAC
[DE88-751067] 10 p1411 N88-18417
Orbiter transfer vehicle concept definition and system analysis study. Volume 4: Space station accommodations. Revision 1
[NASA-CR-179293] 11 p1444 N88-18609
Orbital transfer vehicle concept definition and system analysis study. Volume 4, Appendix A: Space station accommodations. Revision 1
[NASA-CR-179294] 11 p1444 N88-18610
Space station operating system study
[NASA-CR-179308] 11 p1446 N88-18619
Simulated performance of an order statistic threshold strategy for detection of narrowband signals
11 p1474 N88-18796
Design for performance enhancement in feedback control systems with multiple saturating nonlinearities
[NASA-CR-182614] 11 p1535 N88-19168
Generating the states of a probabilistic system
[AD-A187896] 11 p1540 N88-19208
Optimal arrangement of components via pairwise rearrangements
[AD-A187633] 11 p1541 N88-19213
ICF special studies
[DE88-004057] 11 p1551 N88-19281
Preliminary analysis of an integrated logistics system for OSSA payloads. Volume 2: OSSA integrated logistics support strategy 12 p1584 N88-19479
Motion simulation for in-orbit operations
12 p1589 N88-19514
Structural shape optimization in multidisciplinary system synthesis
[NASA-TM-100538] 12 p1614 N88-19650
Systems approach to energy quality and efficiency
[PB88-139506] 12 p1640 N88-19823
Analysis, estimation, and control for perturbed and singular systems and for systems subject to discrete events
[AD-A188496] 12 p1677 N88-20026
Knowledge-based system analysis and control
[AD-A188163] 12 p1681 N88-20049
Systems analysis and simulation techniques: Essential tools for balanced complex weapon system designs in terms of performance and cost
12 p1702 N88-20187
The TempIS Project: Performance analysis of temporal queries
[AD-A188354] 12 p1706 N88-20213
Study of the optimization of satellite system design for transfer orbit
[MBB-URV-135] 13 p1727 N88-20332
Solar dynamic power system definition study
[NASA-CR-180877] 13 p1733 N88-20361
Activities report of the Systems Department
[ETN-88-91987] 13 p1756 N88-20505
Coherent laser radar system theory
[AD-A188759] 13 p1774 N88-20612
On the sensitivity of complex, internally coupled systems
[NASA-TM-100537] 13 p1813 N88-20829
MacCAD (Macintosh Computer Aided Design), computer aided design tool for system analysis
[AD-A189241] 13 p1815 N88-20843
Further results on the McMillan degree and the Kronecker indices of ARMA models --- input-output relations of linear systems
[EUT-87-E-175] 13 p1827 N88-20925
MANPRINT handbook for RFP (Request For Proposal) development
[AD-A188321] 13 p1850 N88-21075
Advanced avionics system analysis. Modular avionics cost benefit study formulation
[AD-A189019] 14 p1867 N88-21158
Sensitivity of control-augmented structure obtained by a system decomposition method
[NASA-TM-100535] 14 p1954 N88-21647
Parametric methods of analysing linear and nonlinear systems
[RR-318] 14 p1967 N88-21741
A systems analysis of fire suppression alternatives for the US space station
[AD-A189847] 15 p2025 N88-22064
Comparative analysis
[AD-A190556] 15 p2065 N88-22313
Monitoring the usage of a computer system
[DE88-004310] 15 p2106 N88-22542
Fault tree analysis and synthesis
[ETN-88-92236] 16 p2261 N88-23521
Liquid droplet radiator development
17 p2424 N88-24415
MACRAD: A mass analysis code for radiators
17 p2424 N88-24418
Dynamic isotope power system critical component verification 17 p2425 N88-24421
Possibilities and limits for use of laser propulsion systems in interorbital space flight
[ILR-MITT-185] 18 p2475 N88-24683
Reliability of stochastically forced systems (extended version)
[CWI-AM-R8801] 18 p2526 N88-24985
Systems analysis of INTOR-like designs
[DE88-004422] 18 p2578 N88-25316
Diagnosing faults in autonomous robot plan execution
[NASA-CR-182480] 20 p2841 N88-26859
Finite-dimensional approximation for optimal fixed-order compensation of distributed parameter systems
[NASA-CR-181674] 20 p2843 N88-26873
The influence of weld metal properties, weld geometry and applied load on weld system performance
[AD-A193403] 21 p2961 N88-27588
Performability analysis: Measures, an algorithm and a case study
[AD-A192477] 21 p3001 N88-27800
Sources and nature of cost analysis data base reference manual
[AD-A193099] 21 p3028 N88-27976
Test and calibration system for monitoring the Advanced Technologies Testing Aircraft System (ATTAS) data acquisition system 22 p3037 N88-28029
Air Force Systems Command software independent verification and validation implementation analysis and guidance
[AD-A194309] 22 p3137 N88-28653
Combined and-or parallel execution of logic programs
[AD-A193648] 22 p3138 N88-28656
Modularity in the PASCAL model compiler
[NPL-DITC-111/88] 22 p3139 N88-28664
On the pseudo-linearization problem for nonlinear systems
[AD-A194021] 22 p3142 N88-28683

Use of Markov probability and reliability model generation methods in the analysis of reliability of a fault tolerant hardware and software based system with flexible repair policies
[PNR90467] 22 p3145 N88-28706
Analysis of the effect of faulty spares on the performance of diagnostic algorithms in reliable systems
[AD-A193526] 23 p3223 N88-29186
An analysis of heat transfer after loss of primary coolant in the SP-100 reactor systum
[AD-A194619] 23 p3261 N88-29539
Center for opto-electronic systems research instrumentation grant
[AD-A193711] 23 p3262 N88-29545
Knowledge based simulation: An artificial intelligence approach to system modeling and automating the simulation life cycle
[AD-A195838] 24 p3423 N88-30372
Center for opto-electronic systems research
[AD-A195159] 24 p3429 N88-30411

SYSTEMS COMPATIBILITY
Interoperability and integration of data relay satellite systems 03 p0339 N88-12134

SYSTEMS DESIGN
U SYSTEMS ENGINEERING

SYSTEMS ENGINEERING
NT COMPUTER SYSTEMS DESIGN
NT CONTROL SYSTEMS DESIGN
The ISA test system: A catalog of automatic support facilities 01 p0012 N88-10067
Preliminary study of a biotechnology research facility for microgravity, executive summary
[MATRA-EPT/AS/VT209/246/NT] 01 p0032 N88-10204
Prephase A study of a crystallization laboratory for Columbus, executive summary
[ESA-ITT/AO/1-1866/85F] 01 p0032 N88-10206
Robotic sensors and actuators for a service manipulator system. Volume 2: Service Manipulator System (SMS) handbook
[MATRA-EPT/DT/VT187/227] 01 p0053 N88-10342
A brief discussion of formally based approaches to rapid prototyping
[BAE-WAA-RP-RES-SWE-440] 01 p0079 N88-10508
Fiber optic engineering sensor system. Preliminary program management plan, phase 3 revision
[AD-A183663] 01 p0093 N88-10608
Aperture synthesis in space: Technical problems 01 p0097 N88-10638
AI expert system technology issues for guidance and control applications 02 p0128 N88-10808
Vacuum pumps and systems: A review of current practice 02 p0134 N88-10839
A modern space simulation facility to accommodate high production acceptance testing 02 p0134 N88-10841
Transient modeling of the thermohydraulic behavior of high temperature heat pipes for space reactor applications 02 p0136 N88-10857
A nondissipative Pyrotechnic Arming and Firing Unit (PAFU)
[CRA/REPO/8019] 02 p0155 N88-10974
A preliminary study of a fluid science laboratory for space station (Columbus). Part 4: Executive summary
[NLR-TR-87023-L-PT-4] 02 p0170 N88-11072
Study of closed loop control singularity in dynamic systems with a constraint on the final state
[LAAS-87-180] 02 p0223 N88-11405
Pinhole occulter experiment
[NASA-CR-179206] 02 p0235 N88-11481
Research simulators for helicopters 03 p0263 N88-11656
A129 advanced solutions for meeting today's combat helicopter requirement 03 p0265 N88-11669
The Avionics Flight Evaluation System (AFES) of the DFVLR
[ESA-TT-1037] 03 p0266 N88-11677
Mass spectroscopic facility 03 p0296 N88-11861
A design-philosophy for grounding and inter-unit wiring
[EMCR-20/85] 03 p0310 N88-11954
Discussions in support of the design-philosophy for grounding and inter-unit wiring
[EMCR-21/85] 03 p0310 N88-11955
The CNR/PSN Advanced Microwave Imaging Radiometer (AMIR) --- satellite-borne 03 p0340 N88-12141
Design and implementation of a debugger for an abstract machine
[AD-A184691] 03 p0363 N88-12283
The warp computer: Architecture, implementation, and performance
[AD-A184329] 03 p0363 N88-12286
Concepts and techniques for support of real time distributed operating systems
[AD-A184491] 03 p0367 N88-12307
National Science Foundation
[PB87-228375] 03 p0384 N88-12410
Multicast gateway design considerations
[PB87-219960] 04 p0430 N88-12663
Plant Growth Module (PGM) conceptual design 05 p0631 N88-13855
Carbon Dioxide observational platform system (CO-OPS) Feasibility Study
[NASA-CR-179225] 06 p0671 N88-14113
Objects architecture: A comprehensive design approach for real-time, distributed, fault-tolerant, reactive operating systems
[AD-A185476] 06 p0755 N88-14631
Design, production, and characterization of broadband optical waveguides
[DFVLR-FB-85-52] 06 p0780 N88-14791
Study of a Radio Relay Link (RRL). Cassini mission. Data package for final presentation
[ESA-CR(P)-2472] 07 p0847 N88-15138
SAR (Synthetic Aperture Radar). Earth observing system. Volume 2F: Instrument panel report
[NASA-TM-89701] 07 p0871 N88-15284
A software planning and development methodology with resource allocation capability
[AD-A186086] 07 p0902 N88-15462
Docking/Berthing Subsystem (DBS). Development part 1: Latching analysis --- Columbus
[ESA-CR(P)-2479] 08 p0962 N88-15825
Cryogenics program overview 08 p0981 N88-15926
Space Infrared Telescope Facility (SIRTF) design and thermal analysis 08 p0982 N88-15934
JPRS report. Science and technology. USSR: Space
[JPRS-USP-87-006] 08 p1001 N88-16063
Telescope design for Michelson Interferometer for Passive Atmospheric Sounding (MIPAS) B 08 p1017 N88-16167
A backscatter lidar proposed for the second German Spacelab mission 08 p1018 N88-16173
CLIPS: An expert system tool for delivery and training 08 p1056 N88-16368
Requirements and options for communications services in support of the Systems Autonomy Demonstration Project 08 p1057 N88-16374
Expert systems relations in space applications 08 p1059 N88-16391
FMEAssist: A knowledge-based approach to Failure Modes and Effects Analysis 08 p1060 N88-16395
LISP based simulation generators for modeling complex space processes 08 p1061 N88-16403
Knowledge-based simulation 08 p1061 N88-16404
Commonality analysis as a knowledge acquisition problem 08 p1062 N88-16413
Qualitative models for planning: A gentle introduction 08 p1062 N88-16414
Telemetry applications handbook
[AD-A186825] 09 p1132 N88-16789
Columbus feasibility studies. Volume 2: Element constituents, mechanical
[ETN-88-91074] 09 p1134 N88-16800
Columbus feasibility studies. Volume 3: Avionics, systems
[ETN-88-91075] 09 p1134 N88-16801
Design of a solid fuel combustion chamber
[VTH-LR-447] 09 p1141 N88-16837
A substructure method for dynamic simulation of flexible mechanical systems with geometric nonlinearities 09 p1176 N88-17044
Bioreactor design concepts 09 p1197 N88-17171
User engineering: A new look at system engineering 09 p1206 N88-17231
Design knowledge capture for the space station 09 p1206 N88-17239
CONFIG: Qualitative simulation tool for analyzing behavior of engineering devices 09 p1206 N88-17240
Evaluating software testing methods to reduce testing duplication in US Army communications equipment acquisition
[AD-A186961] 09 p1216 N88-17292
Application of a database system for inventory management of classified material
[AD-A186986] 09 p1261 N88-17558
Knowledge base refinement by monitoring abstract control knowledge, revision 1
[AD-A187502] 10 p1397 N88-18323
Multidimensional system analysis of electro-optic sensors with sampled deterministic output
[AD-A187083] 10 p1408 N88-18399
Plasma physics design and major specifications of candidate reactors for FER design studies. Conceptual design study of FY86 FER
[DE88-751066] 10 p1411 N88-18416
Development of the Extendable and Retractable Mast (ERM). Design phase 2. Volume 1 --- spacecraft payloads
[RP-2010-0000-DS/09] 11 p1467 N88-18750
A worked example of an application of the SAINT simulation program
[AD-A188198] 11 p1524 N88-19097
Evaluating expert system tools: A framework and methodology-workshops
[AD-A187190] 11 p1533 N88-19159
The design of the POSTGRES storage system
[AD-A187244] 11 p1564 N88-19365
UNIVERS product, phase 1
[AD-A187405] 11 p1564 N88-19367
Accessing hierarchical databases via SQL transactions in a multi-model database system
[AD-A187878] 11 p1565 N88-19369
The Hermes robot arm, its design and verification 12 p1588 N88-19508
Guidance and control of air-launched armaments: An aeroengineer's perspective 12 p1597 N88-19557
Alternative program approaches for the advanced satellite technology program
[AD-A188917] 12 p1600 N88-19576
An EHF telecommunication system engineering model 12 p1618 N88-19674
Emerging technologies program 3-5: Microelectronics Panel report
[AD-A189463] 12 p1624 N88-19716
Aspects of bioregenerative life support systems 12 p1655 N88-19917
Visual display representation of multidimensional systems: The effect of information correlation and display integrality
[AD-A188655] 12 p1672 N88-20010
Management information systems design implications: The effect of cognitive style and information presentation on problem solving
[AD-A188850] 12 p1705 N88-20205
A comparison of information system development methodologies
[AD-A188957] 12 p1707 N88-20219
Activities report of the Systems Department
[ETN-88-91987] 13 p1756 N88-20505
The acoustic-modeling problem in automatic speech recognition
[AD-A188529] 13 p1757 N88-20510
Design of a supersonic wind tunnel
[ETN-88-92078] 14 p1870 N88-21176
The development status of the strongback array --- spacecraft structure 14 p1875 N88-21201
System and concept design of the SSRMS latching end effector --- Space Station 14 p1875 N88-21204
Latching mechanisms for IOC --- EURECA 14 p1875 N88-21205
The EURECA antenna deployment and retraction mechanisms 14 p1878 N88-21225
Evolution of large momentum and reaction wheels 14 p1879 N88-21230
Development of an engineering model dynamic cooler --- spacecraft payloads
[F+W-TF-B-1885] 14 p1895 N88-21311
Continued design of a Pointing, Acquisition, and Tracking (PAT) subsystem for InterSatellite Laser links (ISL2)
[TELDIX-15-093-178] 14 p1905 N88-21384
DataViews: A personalizable, interactive, data display system for the decisionmaker
[AD-A188509] 14 p1991 N88-21868
Aluminum-air battery development
[DE88-006620] 15 p2061 N88-22287
Designs of profiles for cascades
[NASA-TT-20161] 15 p2067 N88-22326
Reliability analysis within a Computer Aided Engineering (CAE) infrastructure
[NLR-MP-86059-U] 15 p2074 N88-22369
Basic design studies for the realization of liquid crystal display systems in aircraft
[VA-87-001] 16 p2163 N88-22900
Toward a mathematical formalism of performance, task difficulty, and activation 16 p2239 N88-23372
The Design, Development and Testing of Complex Avionics Systems
[AGARD-CP-417] 17 p2302 N88-23767
Systems for the 21st century 17 p2302 N88-23769
Architecture and role of the Sensor Subsystem in future aircraft weapon systems 17 p2302 N88-23770
Rapid prototyping of complex avionic system architectures 17 p2302 N88-23771
The specification and design of a future maritime reconnaissance aircraft 17 p2303 N88-23772
A structured approach to weapon system design 17 p2303 N88-23773
Development of a generic architecture 17 p2303 N88-23774

Test philosophy of the EH101 integrated avionic 17 p2303 N88-23775

Systems engineering technique 17 p2303 N88-23776

A comparison of integrated and separate systems for flight control and navigation 17 p2303 N88-23779

Development and testing of a predictive methodology for optimization of man-machine interface in future avionics systems 17 p2304 N88-23780

A change in system design emphasis: From machine to man 17 p2304 N88-23782

Managing advanced avionic system design 17 p2304 N88-23783

Psychosensory cockpit ergonomics, advantages of intelligent information systems 17 p2304 N88-23784

Design for interoperability (interchangeability) 17 p2305 N88-23789

The integration, characterisation and trialling of a modern complex airborne radar 17 p2305 N88-23791

Experience in the integration of human engineering effort with avionics systems development 17 p2305 N88-23793

Developing systems using state-of-the-art CAD/CAM technology 17 p2306 N88-23795

Workshops for the design of avionics systems and the development of onboard software 17 p2307 N88-23802

Coherent functional development: Key to successful future system integration 17 p2307 N88-23803

Development of complex avionics systems: Experience from French military programs 17 p2307 N88-23804

Ariane 4 pyrotechnics system: Definition of the chains and pyrotechnic devices
[CNES-88/CT/DRT/TVE/IL/25] 17 p2310 N88-23816

Life Support Subsystem (LSS). Concept for the Botany Facility --- EURECA
[TN-RB524-107/86] 17 p2377 N88-24131

Botany Facility: Considerations and analyses of the balancing system philosophy proposed for the BF centrifuge
[SIRA-A/7373/WP110/PWF001] 17 p2378 N88-24139

Selection of a handling and maintenance option for the SP-100 ground engineering system test 17 p2402 N88-24285

The Curie point radiator 17 p2424 N88-24420

The high-throughput X-ray spectroscopy mission E6889478 MN513835 --- ESA program
[ESA-SP-1092] 17 p2450 N88-24554

Concepts for a laser gyroscope of the highest precision 18 p2517 N88-24929

A systems engineering based methodology for analyzing human electrocortical responses
[AD-A190809] 18 p2550 N88-25135

The ATF (Advanced Toroidal Facility) Data M Management System
[DE88-007265] 18 p2589 N88-25385

System capacity and economic modeling computer tool for satellite mobile communications systems 19 p2644 N88-25686

Development of the network architecture of the Canadian MSAT system 19 p2646 N88-25702

System architecture for the Canadian interim mobile satellite system 19 p2646 N88-25703

Design, development and trials of an airline passenger telephone system 19 p2646 N88-25704

Space cabin atmosphere and extracurricular sortie --- embolisms 19 p2696 N88-26023

Technical challenges in the development of a European space suit system and comparison with underwater suits 19 p2696 N88-26024

The SAGA highly autonomous assistance submarine 19 p2698 N88-26034

Safety aspects in design and operation practice of GKSS underwater simulation plant GUSI 19 p2698 N88-26037

Improvement of head-up display standards. Volume 1: Head-up display design guide, appendix
[AD-A192973] 20 p2834 N88-26809

An overview of the development of a linear broadband analog fiber-optic link
[DE88-008668] 20 p2854 N88-26945

Database design and management in engineering optimization
[AD-A193325] 21 p3003 N88-27813

New generation of integrated monitoring systems for modern aircraft 22 p3035 N88-28015

Artificial intelligence software acquisition program, volume 2
[AD-A194239] 22 p3141 N88-28680

Study of standard generic approach for spacecraft (S/C) autonomy and automation (phase 3). Book A: Autonomy concept description
[ESA-CR(P)-2555-VOL-1] 23 p3185 N88-28955

Study of standard generic approach for spacecraft (S/C) autonomy and automation (phase 3). Book B: Autonomy concept application example
[ESA-CR(P)-2555-VOL-2] 23 p3185 N88-28956

Study of standard generic approach for spacecraft (S/C) autonomy and automation (phase 3). Book C: Autonomy concept summary
[ESA-CR(P)-2555-VOL-3] 23 p3185 N88-28957

Computer aided filter design
[AD-A193959] 23 p3208 N88-29093

A proof of the Kahn principle for input/output automata
[AD-A194454] 23 p3248 N88-29333

Level 1 Ada/SQL (Structured Query Language) database language interface user's guide
[AD-A194480] 23 p3249 N88-29335

Computer systems for the representation and manipulation of mathematical knowledge
[AD-A193547] 23 p3249 N88-29340

Space station as a vital focus for advancing the technologies of automation and robotics
[IAF-86-62] 23 p3251 N88-29352

Artificial intelligence applied to process signal analysis 23 p3252 N88-29359

On recognizing ignorance 23 p3254 N88-29372

Strategic defense initiative architecture dataflow modeling technique version 1.5
[AD-A194356] 23 p3275 N88-29494

Dynamically reconfigurable distributed database systems
[AD-A194716] 23 p3297 N88-29636

Study of robotics spacecraft servicing and assembly in space. Volume 1: Executive summary
[ESA-CR(P)-2612-VOL-1] 24 p3333 N88-29839

Accommodation concept for fluid physics facilities, volume 2 --- Spacelab
[SG-TN-AI-027-VOL-2] 24 p3358 N88-29994

A detection theory analysis of visual display performance
[AD-A196291] 24 p3409 N88-30292

Study of human factors engineering criteria for extravehicular activity (EVA) systems, volume 1
[STF23-F87025-VOL-1] 24 p3410 N88-30298

Knowledge-based integrated information systems engineering: Highlights and bibliography. Knowledge-Based Integrated Information Systems Engineering (KBIISE) Project, volume 1
[AD-A195850] 24 p3435 N88-30449

Technical opinions regarding knowledge-based integrated information systems engineering, volume 8
[AD-A195857] 24 p3436 N88-30454

Knowledge-Based Integrated Information Systems Development Methodologies Plan. Knowledge-Based Integrated Information Systems Engineering (KBIISE) report, volume 2
[AD-A195851] 24 p3436 N88-30455

SYSTEMS FOR NUCLEAR AUXILIARY POWER

U SNAP

SYSTEMS INTEGRATION

Design principles and practices for implementation of MIL-STD-1760 in aircraft and stores
[AD-A183724] 01 p0005 N88-10027

Mid infrared LHS system packaging using flexible waveguides
[NASA-CR-181192] 01 p0093 N88-10607

Space station integrated propulsion and fluid system study: Fluid systems configuration databook
[NASA-CR-179215] 03 p0278 N88-11753

A modular BLSS simulation model 03 p0359 N88-12260

Methods for design and evaluation of integrated hardware/software systems for concurrent computation
[NASA-CR-181522] 04 p0479 N88-12953

GOLD: Integration of model-based control systems with artificial intelligence and workstations
[DE88-000706] 04 p0483 N88-12977

Small space reactor power systems for unmanned solar system exploration missions
[NASA-TM-100228] 05 p0660 N88-14054

Carbon Dioxide observational platform system (CO-OPS) Feasibility Study
[NASA-CR-179225] 06 p0671 N88-14113

Development of a graphical display on the DMS test bed 06 p0794 N88-14864

Space station software reliability analysis based on failures observed during testing at the multisystem integration facility 06 p0798 N88-14884

Fiber optics for controls 08 p0956 N88-15798

Servicer system demonstration plan and capability development
[NASA-CR-179246] 08 p0975 N88-15895

Rotorcraft flight-propulsion control integration 09 p1108 N88-16643

NASA/Army Rotorcraft Technology. Volume 3: Systems Integration, Research Aircraft, and Industry
[NASA-CP-2495-VOL-3] 09 p1110 N88-16650

Avionics systems integration technology 09 p1110 N88-16654

Integrated diagnostics 09 p1111 N88-16655

Systems integrated human engineering on the Navy's rapid acquisition of manufactured parts/test and integration facility 09 p1206 N88-17226

The IDEAL (Integrated Design and Engineering Analysis Languages) modeling methodology: Capabilities and Applications 09 p1206 N88-17227

Implementing clips on a parallel computer 09 p1211 N88-17259

Software for integrated manufacturing systems, part 1 09 p1211 N88-17261

Software for integrated manufacturing systems, part 2 09 p1211 N88-17262

Communication and control in an integrated manufacturing system 09 p1212 N88-17263

System integration of a Telerobotic Demonstration System (TDS) testbed 09 p1212 N88-17266

Columbus feasibility studies. Volume 4: Integration, test, and operations
[ETN-88-90576] 11 p1445 N88-18614

Interfacing of a microcomputer with a simultaneous atomic-emission spectrometer
[PB88-139571] 11 p1526 N88-19109

Workshop on the Integration of Finite Element Modeling with Geometric Modeling
[NASA-CR-182515] 11 p1526 N88-19111

Integration of finite element modeling with solid modeling through a dynamic interface 11 p1526 N88-19112

Integration of geometric modeling and advanced finite element preprocessing 11 p1526 N88-19114

Solid/FEM integration at SNLA
[SAND-87-0882A] 11 p1526 N88-19116

Workshop on Design Loads for Advanced Fighters
[AGARD-R-746] 12 p1579 N88-19449

Interaction between structural considerations and system design in advanced flight controls 12 p1580 N88-19458

Advanced propfan analysis for the family of commuter airplanes
[NASA-CR-182566] 12 p1582 N88-19468

A digital logic simulator with concurrent programming considerations
[AD-A188823] 12 p1678 N88-20032

Development cost reduction using integrated CAE-CAD-CAM techniques 12 p1701 N88-20182

Digital correlator for the portable channel prober measurement instrument
[AD-A189065] 14 p1904 N88-21377

Common database interface for heterogeneous software engineering tools
[AD-A189628] 14 p1991 N88-21870

AGARD Highlights 88/1 14 p2012 N88-22001

Supercomputer environment
[AD-A190633] 15 p2107 N88-22551

Integrated avionics reliability 17 p2294 N88-23723

Rule-based fault-tolerant flight control 17 p2294 N88-23725

The Design, Development and Testing of Complex Avionics Systems
[AGARD-CP-417] 17 p2302 N88-23767

A comparison of integrated and separate systems for flight control and navigation 17 p2303 N88-23779

Development and testing of a predictive methodology for optimization of man-machine interface in future avionics systems 17 p2304 N88-23780

Crewstation Information and Development System (CIDS) 17 p2304 N88-23781

Design for interoperability (interchangeability) 17 p2305 N88-23789

The electromagnetic threat to future avionic systems 17 p2305 N88-23790

The integration, characterisation and trialling of a modern complex airborne radar 17 p2305 N88-23791

Experience in the integration of human engineering effort with avionics systems development 17 p2305 N88-23793

A look toward the future of complex avionics systems development using the USAF Test Pilot School's avionics systems test training aircraft 17 p2306 N88-23797

Coherent functional development: Key to successful future system integration 17 p2307 N88-23803

Space vehicle/nuclear reactor thermal radiation integration issues 17 p2424 N88-24417

Dynamic resource allocation in a hierarchical multiprocessor system: A preliminary study
[NASA-CR-183177] 22 p3141 N88-28675

A relational data-knowledge base system and its potential in developing a distributed data-knowledge system 23 p3251 N88-29353

Coupling expert systems and simulation 23 p3252 N88-29360

Intelligent test integration system 23 p3254 N88-29371

Requirements for a tool to aid in the development of expert systems for space station applications
23 p3258 N88-29398

A methodology for multiple rule system integration and resolution within a singular knowledge base
23 p3261 N88-29413

Knowledge-based integrated information systems engineering: Highlights and bibliography. Knowledge-Based Integrated Information Systems Engineering (KBIISE) Project, volume 1
[AD-A195850]
24 p3435 N88-30449

Knowledge-Based Integrated Information Systems Development Methodologies Plan. Knowledge-Based Integrated Information Systems Engineering (KBIISE) report, volume 2
[AD-A195851]
24 p3436 N88-30455

Integrating information systems in a major decentralized international organization, volume 7
[AD-A195856]
24 p3439 N88-30468

SYSTEMS MANAGEMENT

Critical issues for establishment of a permanently-occupied lunar base
[AD-A187128]
09 p1263 N88-17567

The design and implementation of the Technical Facilities Controller (TFC) for the Goldstone deep space communications complex
11 p1474 N88-18794

UNIVERS product, phase 1
[AD-A187405]
11 p1564 N88-19367

National Informatics Centre: Profile of services
[PB88-134135]
12 p1706 N88-20211

Data management strategies in the industrial environment
[NLR-MP-87002-U]
16 p2286 N88-23684

Life-span knowledge engineering for space operations
23 p3259 N88-29401

A nonlinear filtering process diagnostic system for the Space Station
23 p3262 N88-29417

Real-time space system control with expert systems
23 p3262 N88-29419

SYSTEMS SIMULATION

Rivista Tecnica Selenia, volume 10, number 2
[ETN-87-90763]
01 p0011 N88-10064

The importance sampling and its application to radar simulation
01 p0012 N88-10065

System adaptivity and the modelling of stereotypes --- human-computer interaction
[NPL-DITC-91/87]
01 p0077 N88-10494

Study into a data relay satellite mission analysis tool
[ESA-CR(P)-2422]
02 p0220 N88-11384

Simulation of the perpendicular magnetic recording process
[B8713537]
05 p0586 N88-13570

An interactive-graphics method for dynamic system modelling, applying consistency rules
09 p1181 N88-17072

Reduction of time delays in Runge-Kutta integration methods --- systems simulation
[MBB/LKE-132/S/PUB/241/A]
09 p1229 N88-17363

Columbus Simulation Facility (CSF)
12 p1590 N88-19522

A comparative survey of mathematical models for dynamic simulation of in-orbit manipulation operations
12 p1592 N88-19533

AVSCOM'S modifications to Teledyne Systems Company's air-to-air fire control system simulation model
[AD-A189136]
13 p1722 N88-20294

SIMSAT: Simulation package for flexible systems. Beams in space
[TW-278]
13 p1730 N88-20348

Activities report of the Systems Department
[ETN-88-91987]
13 p1756 N88-20505

Model structure selection for multivariable systems by cross-validation methods
[EUT-87-E-176]
13 p1827 N88-20926

Numerical solution of multibody systems in space applications
14 p1875 N88-21200

An intelligent simulation model generator
[REPT-87-053]
15 p2109 N88-22562

Infrared simulation model Sensor Atmosphere Target (SENSAT)-2A
[DFVLR-FB-88-01]
16 p2165 N88-22910

On the computation of stationary deterministic behavior of nonlinear dynamic systems with applications to rotor-bearing structures
[ETN-88-92241]
16 p2214 N88-23213

The PROMISE simulation system: Software for the simulation of parallel processes
[NLR-MP-86077-U]
16 p2247 N88-23427

Tape versus queue and stacks: The lower bounds
[CWI-CS-R8752]
16 p2249 N88-23437

Monte Carlo analysis of lateral collection diode arrays
[RSRE-MEMO-4080]
17 p2335 N88-23938

Virtual interface environment
17 p2381 N88-24153

Recursive maximum likelihood identification of a nonlinear output-affine model
[RR-322]
18 p2569 N88-25257

Simulation of space manipulator operations (EUROSIM)
[NLR-MP-87017-U]
20 p2811 N88-26678

Study on NAVSAT system evaluation, phase 2. Part 1: Study results
[NLR-TR-87061-L-PT-1]
22 p3041 N88-28054

Study on NAVSAT system evaluation, phase 2. Part 2: Detailed simulation results
[NLR-TR-87061-L-PT-2]
22 p3041 N88-28055

Design and development of a refueling test bed
[FTMS-RP-ER-011]
24 p3357 N88-29986

Improvements of DCAP 1, phase 2-3/A
[D2-RP-AI-106]
24 p3414 N88-30325

SYSTEMS STABILITY

Closed-loop system analysis using Lyapunov stability theory
04 p0483 N88-12978

Robustness of linear systems
[PB87-220042]
05 p0639 N88-13909

Investigations of the equilibrium and stability of thin-walled double rings. A contribution to the solution of single-sided contact problems
[ETN-87-90044]
09 p1181 N88-17076

Modelling and control of an annular momentum control .device
[NASA-CR-4138]
13 p1754 N88-20491

Boundary stabilization of the reaction-diffusion equation with unilateral conditions
[RR-315]
14 p1964 N88-21720

Natural frequencies and stability of immiscible cylindrical z-independent liquid systems
[LRT-WE-9-FB-1(1987)]
22 p3053 N88-28112

Natural frequencies and stability of immiscible spherical liquid systems
[LRT-WE-9-FB-2(1987)]
22 p3053 N88-28113

SYSTOLIC ARRAYS

Implementation and performance of a complex vision system on a systolic array machine
[AD-A184331]
04 p0482 N88-12971

Correctness proofs for systolic algorithms: Palindromes and sorting
[PB88-106075]
07 p0912 N88-15534

SAGE: The Clemson University Systolic Array Generating Engine
10 p1379 N88-18235

Wafer scale implementation of a GaAs systolic signal processor cell
10 p1381 N88-18247

On systolic architectures for interpolation and integration
10 p1382 N88-18250

Systolic array adaptive beamforming
[AD-A187496]
10 p1385 N88-18269

Object recognition on a systolic array
[AD-A187726]
11 p1534 N88-19164

On the design of some systolic algorithms
[CS-8705]
14 p1957 N88-21666

Proposal for a parallel system with image processing applications
[INPE-4293-PRE/1164]
14 p1961 N88-21696

Systolic determination of absolute stability in feedback control systems
[OUEL-1704/87]
14 p1962 N88-21705

HIFI: A design method for implementing signal processing algorithms on VLSI processor arrays
[ETN-88-92238]
16 p2247 N88-23421

Synthesis and simulation of systolic algorithms
[ETN-88-92183]
16 p2247 N88-23423

Efficient bit-level, word-level and block-level systolic arrays for matrix-matrix multiplication
[DE88-011331]
20 p2841 N88-26856

A programmable systolic array for factorial analysis. Part 2: The symmetric eigenvalue problem
[AD-A192396]
21 p2995 N88-27762

A systolic array for efficient execution of the Faddeev algorithm
[DE88-011330]
22 p3135 N88-28635

Systolic array fault tolerance performance analysis
[AD-A193521]
23 p3244 N88-29306

Adaptive identification by systolic arrays
[AD-A193532]
23 p3266 N88-29444

T

T SHAPE

Two-phase flow forms and pressure drop in horizontal T tube joints with vertical branch
[GKSS-87/E/12]
09 p1163 N88-16969

Study of a water-steam two phase flow in a T-branch
[ETN-88-92306]
20 p2801 N88-26624

T TAURI STARS

Angular momentum evolution of young stars
04 p0504 N88-13099

Disk accretion during the early stages of stellar evolution
04 p0505 N88-13106

Pre-main sequence activity: How far is magnetis involved
04 p0517 N88-1317

The contribution of accretion luminosity to the infrare spectra of T Tauri stars: A possible test
04 p0518 N88-1318

Theoretical studies of mass loss and shock phenomen in cool star envelopes
[NASA-CR-182433]
08 p1099 N88-1661

T-33 AIRCRAFT

Access to microgravity: A technical description of the NAE T-33 microgravity facility
[NAE-AN-47]
04 p0405 N88-12518

TABLES (DATA)

Implementation of a digital optical matrix-vector multiplier using a holographic look-up table and residue arithmetic
[NASA-CR-180431]
01 p0078 N88-10496

TeXing the FORMULARY: A collection of examples of the use of TeX to produce ruled tables and displayed equations
[AD-A185920]
07 p0921 N88-15598

Bern solar observations. Solar data for January-December 1986
[REPT-53]
09 p1263 N88-17569

Evaluation and compilation of thermodynamic properties of high temperature chemical species
[AD-A187509]
11 p1452 N88-18654

Tabulation of Mie scattering calculation results for microwave radiative transfer modeling
[NASA-CR-4130]
14 p1947 N88-21612

Table of solar activity associated with coronal mass ejections observed by the SMM coronagraph/polarimeter in 1980
[PB88-170881]
14 p2011 N88-21998

The effects of inlet turbulence and rotor/stator interactions on the aerodynamics and heat transfer of a large-scale rotating turbine model. Part 4: Aerodynamic data tabulation
[NASA-CR-179469]
17 p2339 N88-23956

TABS (CONTROL SURFACES)

Analytic investigation of helicopter rotor blade appended aeroelastic devices
[NASA-CR-166525]
03 p0266 N88-11676

TACHISTOSCOPES

Mechanisms of early light and dark adaptations
12 p1663 N88-19972

TACHOMETERS

Design of a velocity and position control laboratory servo system
[AD-A186596]
06 p0990 N88-15997

TACHYCARDIA

Propranolol and the compensatory circulatory responses to orthostasis at high altitude
[AD-A192675]
22 p3131 N88-28618

TACTICS

An interactive computer graphics network monitor for a tactical communications network
[AD-A184131]
04 p0477 N88-12938

Impact of flying qualities on mission effectiveness for helicopter air combat, volume 1
[NASA-CR-166568]
06 p0669 N88-14100

Computer aided tactics for air combat
12 p1597 N88-19559

Aircrew training devices: Utility and utilization of advanced instructional features, phase 4
[AD-A188418]
12 p1670 N88-20000

Flight simulator: Field of view utilized in performing tactical maneuvers
[AD-A192412]
20 p2762 N88-26379

Biomedical aspects of military operations at high altitude
[AD-A192677]
22 p3132 N88-28619

Tactical air force night/adverse weather training
[AD-A194243]
22 p3133 N88-28625

TACTILE DISCRIMINATION

Optically coupled tactile sensor array for robotics
11 p1550 N88-19273

The rate of adaptation to altered g in the human centrifuge: Implications for simulations of mass-discrimination in space flight
12 p1659 N88-19941

Integrated polysilicon tactile sensor
19 p2669 N88-25863

Flexible tactile sensing arrays for robotics: Architectural robustness and yield considerations
19 p2671 N88-25878

TACTILE SENSATION
U TOUCH

TAGGING
U MARKING

TAIL ASSEMBLIES

Effect of empennage arrangement on single-engine nozzle/afterbody static pressures at transonic speeds
[NASA-TP-2753]
02 p0122 N88-10771

Base pressure measurements on a missile body with cruciform tail
[ESA-TT-1062] 03 p0270 N88-11695
Effect of permissible variations of center-of-gravity locations of cargo airplane on its mass
04 p0424 N88-12625
Navier-Stokes analysis of transonic transport aircraft empennage 19 p2636 N88-25637

TAIL MOUNTINGS
U TAIL ASSEMBLIES

TAIL ROTORS
NT HELICOPTER TAIL ROTORS
New aerodynamic design of the fenestron for improved performance 03 p0264 N88-11664
Aeroelastic characteristics of the AH-64 bearingless tail rotor 21 p2891 N88-27162

TAIL SURFACES
Effect of permissible variations of center-of-gravity locations of cargo airplane on its mass
04 p0424 N88-12625

TAILLESS AIRCRAFT
NT F-106 AIRCRAFT
Conceptual final paper on the preliminary design of an oblique flying wing SST
[NASA-CR-182879] 16 p2161 N88-22891

TAILS (ASSEMBLIES)
U TAIL ASSEMBLIES

TAIWAN
Observational analysis of the interaction between fronts and the orography in Taiwan during the late winter monsoon season 02 p0203 N88-11270
Taiwan area mesoscale experiment: P-3 aircraft operations summary
[PB88-169073] 18 p2544 N88-25098

TAKEOFF
NT VERTICAL TAKEOFF
Noise of a model high speed counterrotation propeller at simulated takeoff/approach conditions (F7/A7)
[NASA-TM-100206] 01 p0091 N88-10592
Optimum take-off run of aircraft on ground airfields
04 p0423 N88-12623
High speed propeller performance and noise predictions at takeoff/landing conditions
[NASA-TM-100267] 05 p0646 N88-13960
Flaps-up takoff performance of the OV-1D aircraft with YT53-L-704 engine installed
[AD-A185960] 07 p0819 N88-14979
Verification of obstacle accountability areas using a simple mathematical model. Part 1: Description of general model and application for a specific case --- engine failure at takeoff
[NLR-TR-85069-U] 09 p1115 N88-16683
Aerodynamic and acoustic characteristics of an advanced propeller under take-off and landing conditions
[NAL-TR-935] 09 p1243 N88-17453
Radar returns from ground clutter in vicinity of airports
10 p1274 N88-17624
Simulator investigation of wind shear recovery techniques 10 p1275 N88-17630
Changes in USAF structural loads requirements
12 p1580 N88-19452
Flight simulator experiments concerning take-off visibility minima
[NLR-TR-86050-U] 13 p1719 N88-20281
Advanced turboprop aircraft flyover noise: Annoyance to counter-rotating-propeller configurations with an equal number of blades on each rotor, preliminary results
[NASA-TM-100612] 16 p2265 N88-23547
Aircraft accident report: Air New Orleans, DBA continental express flight 962 British Aerospace 3101 (Jetstream 31), N331CY, New Orleans International Airport, Kenner, Louisiana, May 26, 1987
[PB88-910408] 19 p2601 N88-25450

TALKING
NT SYLLABLES
NT WORDS (LANGUAGE)

TANDEM MIRRORS
Massachusetts Institute of Technology Plasma Fusion Center: 1986-1987 Report to the President
[DE87-013518] 01 p0101 N88-10661
Fusion reactor physics and technology studies
[DE87-013691] 01 p0101 N88-10664
New methods of confinement and heating of plasma in magnetic fields
[DE88-701021] 15 p2135 N88-22738
Hot electron diagnostics using X-ray imaging on GAMMA10 17 p2443 N88-24530

ANDEM ROTOR HELICOPTERS
NT CH-46 HELICOPTER
Computer program for conceptual tandem rotor elicopter design
AD-A187832] 11 p1439 N88-18584

TANGENTS
Calculation of symmetric and asymmetric vortex seperation on cones and tangent ogives based on discrete vortex models
[NASA-CR-4122] 08 p0950 N88-15768

TANKS (COMBAT VEHICLES)
Weldability of 2219-T851 and 2519-T87 aluminum armor alloys for use in Army vehicle systems
[AD-A184296] 04 p0451 N88-12792
Measurement of suspension and ride characteristics of the M1 main battle tank 05 p0596 N88-13637
Failure of filament lamps subjected to vibration with special reference to the 26 volt 5 Watt tank lamp
[EL-135] 09 p1158 N88-16938
An investigation of steep descent guidance for terminally-guided sub-munitions
12 p1596 N88-19555
Armoured vehicle track elastomers: Research and development at MRL
[MRL-GD-0012] 19 p2620 N88-25541
Design guidelines for prevention of corrosion in combat and tactical vehicles
[AD-A194172] 22 p3055 N88-28126
Advanced development waste processing unit for combat vehicles, phase 2
[AD-A193793] 23 p3243 N88-29302

TANKS (CONTAINERS)
NT EXTERNAL TANKS
NT FUEL TANKS
NT PROPELLANT TANKS
NT SPHERICAL TANKS
NT STORAGE TANKS
NT WING TANKS
Evaluation of the thermal effectiveness of urethane foam and fiberglass as insulation systems for tank cars
[PB88-100797] 06 p0686 N88-14207
Use of water towing tanks for aerodynamics and hydrodynamics 16 p2204 N88-23149
Technical feasibility study of applying auto-control methods to plating process solutions
[DE88-008014] 19 p2641 N88-25670
Nonlinear oscillations in paraboloidal containers
[LRT-WE-9-FB-3(1988)] 22 p3078 N88-28275
Liquid oscillations in a prolate spheroidal container
[LRT-WE-9-FB-4(1988)] 22 p3078 N88-28276
Nonlinear hydroelastic vibrations in rectangular containers
[LRT-WE-9-FB-7(1987)] 22 p3088 N88-28340

TANTALUM
Metallic superlattices with monolayer modulation
[DE87-012724] 01 p0023 N88-10145
Superconducting properties of metallic superlattices
[DE87-012725] 01 p0023 N88-10146
Computer simulations of knock-on processes in bcc Ta crystal
[DE87-752980] 02 p0246 N88-11554
Use of nonporous metals membranes for the separation of hydrogen from gas mixtures
[BMFT-FB-T-86-206] 14 p1888 N88-21280
Rocket-propellant burn tests of silicide-coated niobium and tantalum
[DE88-010729] 20 p2781 N88-26496

TANTALUM ALLOYS
Reduced-activation ferritic steels: A comparison with Cr-Mo steels
[DE88-000332] 03 p0290 N88-11826

TANTALUM COMPOUNDS
NT TANTALUM OXIDES
Hydrogen in niobium-tantalum superlattices
09 p1146 N88-16867

TANTALUM OXIDES
On 1064 nm and 350 nm laser damage thresholds of high index oxide films deposited from organic solutions and sols
[DE88-001636] 07 p0859 N88-15217

TAPE RECORDERS
UARS spacecraft recorder
[NASA-CR-180768] 15 p2068 N88-22331
Mechanisms mediating perception of complex acoustic patterns
[AD-A189765] 15 p2102 N88-22520

TAPER
U TAPERING

TAPERED WINGS
U SWEPT WINGS

TAPERING
Improved oil-off survivability of tapered roller bearings
[NASA-CR-180804] 02 p0182 N88-11135
Taper sectioning to magnify the interface thickness of a dissimilar metal joint
[RFP-3890-REV] 03 p0333 N88-12099
Exact finite element method analysis of viscoelastic tapered structures to transient loads
05 p0595 N88-13632
Minimum weight design of rectangular and tapered helicopter rotor blades with frequency constraints
[NASA-TM-100561] 12 p1582 N88-19465
Inflow measurements made with a laser velocimeter on a helicopter model in forward flight. Volume 4: Tapered planform blades at an advance ratio of 0.15
[NASA-TM-100544] 16 p2156 N88-22863
Telescope illumination and beam measurements for submillimeter astronomy
[MPE-PREPRINT-88] 16 p2288 N88-23699
AGARD standard aeroelastic configurations for dynamic response. 1: Wing 445.6
[AGARD-R-765] 21 p2896 N88-27193

TAR SANDS
Aviation turbine fuels from tar sands bitumen and heavy oils. Part 2: Laboratory sample production
[AD-A185744] 06 p0687 N88-14211
Aviation turbine fuels from tar sands bitumen and heavy oils. Part 3: Laboratory sample production
[AD-A189278] 13 p1753 N88-20484
Turbine fuels from tar sands bitumen and heavy oil. Volume 2, phase 3: Process design specifications for a turbine fuel refinery charging San Ardo heavy crude oil
[AD-A190120] 16 p2183 N88-23011

TARE (DATA REDUCTION)
U DATA REDUCTION

TARGET ACQUISITION
Problems and possible solutions involved in hard target calibration of coherent Doppler lidar
07 p0922 N88-15602
Development of a computer model for missile simulation, or simulation of a kinetic coverage area for a target detection missile
[FOA-C-20666-2.5] 08 p1067 N88-16449
A piloted simulation investigating handling qualities and performance requirements of a single-pilot helicopter in air combat employing a helmet-driven turreted gun
[AD-A186878] 09 p1116 N88-16689
On the design of suboptimal matched filters for three-dimensional moving target detection
[AD-A188384] 12 p1619 N88-19682
Continued design of a Pointing, Acquisition, and Tracking (PAT) subsystem for InterSatellite Laser links (ISL2)
[TELDIX-15-093-178] 14 p1905 N88-21384
A study of Radar Cross Section (RCS) characteristics and their application in future weapon systems
[ETN-88-92081] 14 p1906 N88-21390
Strategic Defense Initiative Program: Status of space surveillance and tracking system
[PB88-150438] 14 p1967 N88-21739
Design and implementation of VLSI prime factor algorithm processor
[AD-A190483] 15 p2112 N88-22580
The superconducting phase shifter in the development of a terahertz imaging radar system
[AD-A190666] 16 p2188 N88-23046
Air-to-air radar flight testing
[AGARD-AG-300-VOL-7] 21 p2932 N88-27406
Interactive, networked moving platform simulators
[AD-A192374] 23 p3182 N88-28940
Evaluation of atmospheric effects for operational tactical decision aid
[AD-A194205] 23 p3232 N88-29236

TARGET PENETRATION
U TERMINAL BALLISTICS

TARGET RECOGNITION
Feature selection applied to radar target identification
[AD-A183880] 01 p0034 N88-10215
Detection of targets in the presence of clutter using target echo modulations caused by rotating structures
[REPT-12-86] 01 p0036 N88-10231
Independence in sonar observations
[ARE-TR-87102] 01 p0083 N88-10572
Scene simulation for passive IR systems
02 p0137 N88-10861
Theoretical Aspects of Target Classification
[AGARD-LS-152] 03 p0303 N88-11909
Input signal shaping: K-pulse
03 p0304 N88-11917
On the influence of false plots on tracking reliability. Simulations and preliminary analyses
[FOA-C-30443-3.2] 06 p0692 N88-14245
Investigation and implementation of an algorithm for computing optimal search paths
[AD-A185927] 07 p0902 N88-15461
Interaction of a vortex pair with a free surface
[AD-A186619] 08 p0988 N88-15988
Object detection in images from outdoor scenes using evidential reasoning
[FOA-C-30461-3.3] 08 p1020 N88-16183
Research on visual information processing with special reference to oculomotor behavior in the areas of exploration, recognition and search
[AD-A186598] 08 p1051 N88-16346

Visual attention effects on discrimination of line orientation and line arrangement
[AD-A187013] 09 p1200 N88-17190

Management Information and Downloader Interface System (MIDIS)
[AD-A186978] 09 p1261 N88-17557

Automated radar target recognition based on models of neural nets 11 p1476 N88-18804

On the design of suboptimal matched filters for three-dimensional moving target detection
[AD-A188384] 12 p1619 N88-19682

Position, scale, and rotation invariant target recognition using range imagery
[AD-A188828] 12 p1633 N88-19772

Human efficiency for visual detection of targets on CRT displays using a two-level multiple channel time history format
[AD-A188419] 12 p1670 N88-20001

An optimal branch-and-bound procedure for the constrained path, moving target search problem
[AD-A188962] 12 p1685 N88-20075

Analysis of spectral reflectance characteristics of targets under satellites and automatic cloud recognition
13 p1755 N88-20498

Passive autonomous infrared sensor technology
[AD-A188698] 13 p1839 N88-21005

Effect of friction and control parameters on the tracking accuracy of a target seeker
[AD-A190010] 15 p2056 N88-22257

Polarimetric ISAR imaging using either measured or calculated transient signatures
[AD-A190077] 15 p2056 N88-22259

Multi-disciplinary techniques for understanding time-varying space-based imagery
[AD-A190711] 15 p2117 N88-22610

Rigidity and smoothness of motion
[AD-A190555] 15 p2128 N88-22694

Method and device for the detection and identification of a helicopter
[NASA-TT-20251] 15 p2129 N88-22698

K-pulse estimation from incomplete multiple-frequency scattering data and target identification
[AD-A190827] 16 p2190 N88-23061

Parametric analysis of power requirements for space-based radar 17 p2399 N88-24260

Joint services electronics program
[AD-A191749] 18 p2504 N88-24853

Real-time optical multiple object recognition and tracking system and method
[NASA-CASE-NPO-17139-1-CU]
18 p2576 N88-25301

Multi-target tracking algorithms for cluttered environments 20 p2789 N88-26543

Optical data processing
[AD-A193024] 20 p2839 N88-26841

Outdoor sound propagation, its implications for unattended ground sensors
[FEL-1986-64] 20 p2850 N88-26917

An empirical surface temperature model
[AD-A192737] 21 p2974 N88-27665

Distributed algorithms for probabilistic solution of computational vision problems
[AD-A193150] 21 p2997 N88-27773

Autoregressive moving average modeling of radar target signatures
[AD-A194612] 22 p3069 N88-28218

Activities report of the Division of Reconnaissance and Seeker Systems
[FOA-C-30479-3.1/3.2/3.3/3.4]
22 p3116 N88-28513

Helicopter recognition using laser radars
22 p3149 N88-28736

Object discrimination via bulk temperature/velocity filtering, phase 1
[AD-A194533] 23 p3274 N88-29487

Modeling and performance of HF/OTH (High-Frequency/Over-the-Horizon) radar target identification systems
[AD-A196287] 24 p3365 N88-30038

TARGET THICKNESS

The Rayleigh-Taylor instability in ablatively accelerated targets with 1, 1/2 and 1/4 micrometers laser light
[AD-A185945] 07 p0858 N88-15208

TARGETS

NT LASER TARGETS
NT PARTICLE ACCELERATOR TARGETS
NT RADAR TARGETS

Shock-wave studies using plastic flyers driven by an electric gun for hypervelocity impact on selected materials
[DE87-012631] 01 p0008 N88-10046

Electron interactions with nuclei
[DE87-014587] 02 p0232 N88-11460

Helicopter fire control: Advantages of an automatic target tracker 03 p0264 N88-11667

Analysis of compressible flow on high-velocity jet penetration 03 p0302 N88-11898

Singularity expansion method: Target Resonances
03 p0303 N88-11912

Analytic model of an imploding Z-pinch plasma colliding inelastically with a thin-shelled cylindrical target
[DE88-000051] 03 p0378 N88-12379

Design and implementation of the ESL compact range underhung bridge crane
[NASA-CR-182396] 07 p0862 N88-15231

Effects of uniform target density on random search
[AD-A186468] 08 p1073 N88-16473

Target-reflectivity models for various terrain types
[DE88-005510] 11 p1505 N88-18992

Lower bounds on acceleration estimation accuracy
[AD-A188383] 12 p1619 N88-19681

Cramer-Rao bounds on the accuracy of location and velocity estimations using CCD optical sensors
[AD-A188481] 12 p1629 N88-19748

Sub-scaling of projectile/target system damaged by hypervelocity
[AD-A188683] 12 p1634 N88-19779

Properties of reactively sputtered WNx films Zhao, X.-A.
[AD-A188711] 13 p1835 N88-20976

An investigation of cruciform parachutes and towed targets
[BU-360] 14 p1862 N88-21122

Advanced guidance algorithms for homing missiles with bearings-only measurements
[AD-A190435] 15 p2017 N88-22026

A multiple model adaptive tracking algorithm against airborne targets
[AD-A190615] 15 p2057 N88-22263

TDWR (Terminal Doppler Weather Radar) clutter residue map generation and usage
[AD-A191148] 16 p2235 N88-23352

Numerical analysis of target implosion in LIB ICF
16 p2277 N88-23628

The application of Rutherford backscattering for analyzing multilayered structure change induced by pulsed ion beam bombardment 16 p2278 N88-23638

Self shielding of surfaces irradiated by intense energy fluxes
[DE88-007094] 18 p2579 N88-25318

High dose uranium ion implantation into silicon
[LBL-23509] 19 p2725 N88-26182

Analysis of the perforation of monolithic and simple laminate aluminium targets as a test of analytical deformation models
[MRL-R-1111] 20 p2813 N88-26686

Fiber-optics used to record high-speed photographs inside a pressurized tank during lethality testing
[DE88-011283] 21 p2951 N88-27529

HPM (High-Power Microwave) coupling into realistic targets
[DE88-011788] 23 p3207 N88-29084

Multi-sensory tracking mount control
[AD-A194675] 23 p3249 N88-29339

Comparative aspects of multiple processes of attention
[AD-A195805] 24 p3408 N88-30291

TASK COMPLEXITY

Examining the relative efficiency of Part- versus whole-task practice for multiple-task situations
[AD-A185056] 05 p0631 N88-13856

Artificial Intelligence (AI), Operations Research (OR), and Decision Support Systems (DSS): A conceptual framework 09 p1209 N88-17245

Cardiovascular and subjective measures of task demand in a low workload monitoring task
[REPT-8804] 10 p1368 N88-18176

Distraction and inhibition in continuous CRT performance: A replication and some new findings
[PB88-150941] 13 p1811 N88-20821

Toward a mathematical formalism of performance, task difficulty, and activation 16 p2239 N88-23372

Simultaneous multiple control force exertion capabilities of males and females versus helicopter control force design limits
[AD-A191653] 18 p2553 N88-25153

The relationship between system response time, working memory, and task complexity: An empirical investigation
[DE88-000976] 19 p2711 N88-26105

TASKS

Architecture for dynamic task allocation in a man-robot symbiotic system
[DE87-013872] 03 p0362 N88-12277

Some data processing requirements for precision Nap-Of-the-Earth (NOE) guidance and control of rotorcraft
[NASA-CR-177453] 04 p0401 N88-12493

The characterization of diagnostic tasks for engineering systems
[DE88-000093] 04 p0483 N88-12973

Taskomat, a task battery for information processing
[IZF-1987-2] 05 p0630 N88-13851

Examining the relative efficiency of Part- versus whole-task practice for multiple-task situations
[AD-A185056] 05 p0631 N88-13856

A study of the minority college programs at the NASA Johnson Space Center 06 p0798 N88-14887

Evoked brain activity and personnel performance
[AD-A185922] 07 p0897 N88-15436

Development of a task-level robot programming and simulation system 08 p1058 N88-16387

Crew procedures for microwave landing system operations
[NASA-CR-178359] 09 p1116 N88-16888

Dynamic function allocation in fighter cockpits
[AD-A185397] 09 p1201 N88-17199

Performance analysis of parallel branch and bound search with the hypercube architecture
09 p1206 N88-17229

Task-level robot programming: Integral part of evolution from teleoperation to autonomy
09 p1214 N88-17279

A note on the effect of preemptive policies on the stability of a priority queue
[AD-A186871] 09 p1227 N88-17345

Trends in the distribution of tasks between commercial pilots and flight control systems
[MBB-UT-008/87] 10 p1314 N88-17851

Investigation of effects of short-term exposure to high concentrations of carbon monoxide on operator's psychophysiological functions 10 p1361 N88-18133

On the number of task assignments in distributed computing systems 10 p 378 N88-18230

Deadlock prevention in processor self-scheduling for parallel nested loops
[DE88-003573] 10 p1393 N88-18313

Motor control in man and monkey
11 p1518 N88-19065

Brain activity during tactical decision-making. Part 2: Probe-evoked potentials and workload
[AD-A188688] 12 p1667 N88-19984

A representation for serial robotic tasks
12 p1681 N88-20048

Task allocation for efficient performance of a decentralized organization
[AD-A188699] 12 p1705 N88-20204

The space station assembly phase: Flight telerobotic servicer feasibility. Volume 2: Methodology and case study
[NASA-CR-182690] 13 p1731 N88-20352

Lifting and carrying capacities relative to physical fitness measures
[AD-A189305] 13 p1809 N88-20808

Proceedings of the Workshop on the Assessment of Crew Workload Measurements Methods, Techniques and Procedures. Volume 1: Preliminary Selection of Measures
[AD-A189004] 13 p1812 N88-20827

Method to evaluate image-recovery algorithms based on task performance
[DE88-005382] 13 p1816 N88-20853

POPEYE: A production rule-based model of multitask supervisory control (POPCORN)
16 p2240 N88-23384

Realization of natural language style robot task instruction by using the object oriented concept
16 p2257 N88-23487

NASA-Ames workload research program
17 p2380 N88-24151

Fault diagnosis in orbital refueling operations
17 p2381 N88-24154

Performance estimates for operations conducted while wearing individual protective equipment: User manual
[AD-A191871] 18 p2553 N88-25154

Lunar base surface mission operations. Lunar Base Systems Study (LBSS) task 4.1
[NASA-CR-172050] 18 p2594 N88-25415

Diagnosing faults in autonomous robot plan execution
[NASA-CR-182480] 20 p2841 N88-26859

TAURID METEOROIDS

On orbits and association of meteor streams with Comets P/Halley and P/Encke
14 p2003 N88-21945

TAXIING

A new look at the use of linear methods to predict aircraft dynamic response to taxi over bomb damaged and repaired airfields 09 p1160 N88-17069

Takeoff predictions for powered-lift aircraft
[NASA-CR-177491] 19 p2597 N88-25431

TAXONOMY

A preliminary taxonomy of visible surface algorithms
[DE87-013559] 02 p0220 N88-11386

A taxonomy of analytical computer performance models for computer design
[AD-A185561] 06 p0755 N88-14632

Developing a standard taxonomy or software engineering standards 10 p1379 N88-18234
A taxonomy for conjugate gradient methods
[DE88-008574] 21 p3004 N88-27817

TAYLOR INSTABILITY
A numerical and analytical investigation of Rayleigh-Taylor instability in a solid tungsten plate
[DE87-013593] 01 p0087 N88-10562
Numerical simulation of transient two-phase flow
[CFDU/87/4] 02 p0171 N88-11077
Computer modeling of two-phase flow
[CFDU/87/5] 02 p0171 N88-11078
Magnetic fields in the overshoot zone: The great escape 02 p0256 N88-11616
The dynamics of bubble growth for Rayleigh-Taylor unstable interfaces
[AD-A184752] 03 p0321 N88-12027
Rayleigh-Taylor instability in compressible fluids
[DE88-002473] 07 p0852 N88-15179
The Rayleigh-Taylor instability in ablatively accelerated targets with 1, 1/2 and 1/4 micrometers laser light
[AD-A185945] 07 p0858 N88-15208
Analytical and numerical analysis of finite amplitude Rayleigh-Taylor instability
[DE88-004056] 11 p1474 N88-18797
Rayleigh-Taylor instability in inertial confinement fusion
[DE88-701411] 15 p2137 N88-22750
Efficient shell implosion and target design
16 p2277 N88-23630
A comparison of analytical techniques for modeling the Rayleigh-Taylor response of elastic-plastic solids
[DE88-010372] 21 p2962 N88-27596

TAYLOR SERIES
Efficient method for structural optimization
15 p2054 N88-22240
Expressing mathematical subroutines constructively
[AD-A190559] 15 p2121 N88-22644

TAYLOR THEOREM
U TAYLOR SERIES

TAYLOR-GOERTLER INSTABILITY
U GOERTLER INSTABILITY

TDMA
U TIME DIVISION MULTIPLE ACCESS

TDR SATELLITES
Study on the suitability of a European data relay satellite to support a system of remote sensing satellites
[ESA-CR(P)-2400] 01 p0063 N88-10406
Data Relay Satellite antenna subsystem study
[ESA-CR(P)-2435-VOL-2] 02 p0162 N88-11014
Study of antenna configuration for Data Relay Satellite (DRS) user spacecraft
[A5/516/86] 02 p0162 N88-11018
DRS (Data Relay Satellite) antenna subsystem study
[ESA-CR(P)-2435-VOL-1] 02 p0162 N88-11019
Study into a data relay satellite mission analysis tool
[ESA-CR(P)-2422] 02 p0220 N88-11384
Interoperability and integration of data relay satellite systems 03 p0339 N88-12134
Ariane localization technique by Data Relay Satellite (DRS)
[SES/ENG/TN-548/86] 06 p0961 N88-15821
Operational aspects of a spacecraft planning/scheduling expert system
08 p1062 N88-16415
Study of dual beam antenna systems for the data relay satellite, volume 1
[S-272-02-VOL-1] 09 p1152 N88-16905
Study of dual beam antenna systems for the data relay satellite. Volume 2: Executive summary
[S-272-03-VOL-2] 09 p1153 N88-16906
Assessment of optical communications systems for Data Relay Satellite. Volume 1: Executive summary
[ESA-CR(P)-2488-VOL-1] 18 p2502 N88-24841
Assessment of optical communications systems for the Data Relay Satellite
[ESA-CR(P)-2488-VOL-2] 18 p2502 N88-24842
NOA: A Network Operator Assistant for scheduling Tracking and Data Relay Satellite System (TDRSS)
23 p3259 N88-29403
Optical multiple access intersatellite links
[BAE-TP-8502] 24 p3361 N88-300'3

TEA LASERS
TEA-TE: Powerful nitrogen-based laser system
07 p0919 N88-1558
Laser CO2/TEA frequency-stabilized by phase conjugation 22 p3082 N88-28303

TEACHING
U EDUCATION

TEACHING MACHINES
The associative memory ME7
[ESA-TT-1033] 01 p0079 N88-10506

TEAMS
Operational groups at the Aerospatiale Aircraft Division
[SNIAS-872-111-107] 05 p0658 N88-14036

TEARING
An investigation of fatigue crack growth in a ductile material at high growth rates 06 p0715 N88-14383

TEARING MODES (PLASMAS)
An unusual magnetopause encounter by AMPTE-UKS
08 p1097 N88-16602
A quadratic-form analysis of the collisionless tearing mode
[AD-A188886] 12 p1695 N88-20144

TECHNICAL WRITING
Role of the technical report in technological innovation
[PB87-232500] 05 p0658 N88-14040
Genie inference engine rule writer's guide
[AD-A185709] 06 p0762 N88-14675
Preliminary analysis of an integrated logistics system for OSSA payloads. Volume 3: OSSA integrated logistics support planning document 12 p1584 N88-19480
Directory of Japanese technical resources, 1987
[PB87-205258] 12 p1706 N88-20212
Text organization and comprehensibility in technical writing
[AD-A188913] 12 p1707 N88-20217
Computer-aided writing
[AD-A192516] 20 p2838 N88-26837
Technical communication in the computer industry: An information-development process to track, measure and ensure quality 23 p3297 N88-29635

TECHNIQUES
U METHODOLOGY

TECHNOLOGICAL FORECASTING
NT DELPHI METHOD (FORECASTING)
Spacecraft 2000 program overview
01 p0015 N88-10085
Military needs and forecast, 2
01 p0015 N88-10087
Propulsion Working Group report
01 p0016 N88-10098
Attitude Control Working Group report
01 p0016 N88-10099
New nowcasting opportunities using modern meteorological radar 02 p0199 N88-11245
Future directions in computer architecture and software workshop 10 p1383 N88-18258
Emerging supercomputer architectures
[DE88-003539] 10 p1384 N88-18262
TABLET: The personal computer of the year 2000
[NASA-CR-182528] 10 p1384 N88-18267
New generation imager system
[NASA-CR-180464] 10 p1408 N88-18398
AFGL (Air Force Geophysics Laboratory) fiscal year 1988 Air Force technical objectives document
[AD-A187701] 11 p1503 N88-18977
AFAL (Air Force Astronautics Laboratory) technical objective document FY89
[AD-A187861] 11 p1567 N88-19378
Study on long term evolution Towards European Autonomous Manned Spaceflight (STEAMS)
[SNIAS-SE/LS/AP-35-073] 13 p1727 N88-20330
European Progress on Space (EPOS): Participation in the creation of long term European space programs
[ILR-MITT-189] 14 p1871 N88-21180
Notes on artificial intelligence. Part 1: Technical forecast
[FOA-C-30448-3.3-PT-1] 17 p2390 N88-24208
Speculations on future opportunities to evolve Brayton powerplants aboard the space station
17 p2398 N88-24258
Possibilities and limits for use of laser propulsion systems in interorbital space flight
[ILR-MITT-185] 18 p2475 N88-24683
Air Force technical objective document, FY89
[AD-A193110] 21 p2896 N88-27194
Future trends in aviation propulsion
[PNR90443] 22 p3044 N88-28068

TECHNOLOGIES
NT BIOTECHNOLOGY
NT BUBBLE TECHNIQUE
NT ENERGY TECHNOLOGY
NT GEOTHERMAL TECHNOLOGY
NT MARINE TECHNOLOGY
NT MILITARY TECHNOLOGY
NT REACTOR TECHNOLOGY
JPRS report: Science and technology. China
[JPRS-CST-87-031] 03 p0299 N88-11880
JPRS report: Science and Technology. Europe and Latin America
[JPRS-ELS-88-002] 10 p1316 N88-17870
JPRS report: Science and technology. Europe and Latin America
[JPRS-ELS-88-003] 11 p1468 N88-18754
JPRS report: Science and technology. China
[JPRS-CST-87-029] 11 p1468 N88-18755
Conditions and mechanisms of the process of technological innovation in Brazil: The role of research institutes
[INPE-4175-TDL/274] 11 p1567 N88-19383
Science, technology and the Constitution: Background paper
[PB88-142534] 12 p1708 N88-20222
JPRS report: Science and technology. China
[JPRS-CST-88-003] 13 p1755 N88-20495
JPRS report: Science and technology. China
[JPRS-CST-87-030] 13 p1756 N88-20501
JPRS report: Science and technology. China
[JPRS-CST-88-009] 16 p2186 N88-23030
JPRS report: Science and technology. China
[JPRS-CST-88-001] 16 p2186 N88-23036
On-orbit technology experiment facility definition
[NASA-TM-100614] 17 p2311 N88-23824
Center for Electronics and Electrical Engineering technical publication announcements covering Center programs, July to September 1987
[PB88-196530] 20 p2793 N88-26572
Resources: NASA for entrepreneurs
[NASA-CR-182152] 20 p2883 N88-27119

TECHNOLOGY ASSESSMENT
Investigation of the suitability of the 8ft x 6ft transonic wind-tunnel for aeroacoustic research on propellers
[RAE-TM-AERO-2093] 01 p0008 N88-10041
Spacecraft 2000 program overview
01 p0015 N88-10085
Communication satellite technology trends
01 p0015 N88-10088
Spacecraft Systems Working Group report
01 p0015 N88-10091
System Development Working Group report
01 p0016 N88-10092
Electrical Power Working Group report
01 p0016 N88-10095
Propulsion Working Group report
01 p0016 N88-10098
Attitude Control Working Group report
01 p0016 N88-10099
Study on the suitability of a European data relay satellite to support a system of remote sensing satellites
[ESA-CR(P)-2400] 01 p0063 N88-10406
Practical limits to ground based interferometry and its impact on space interferometry
01 p0096 N88-10634
NASA's new technology reporting system: A review and future prospects
[NASA-CR-180954] 01 p0105 N88-10686
The British Technology Group
[ONRL-7-022-R] 01 p0107 N88-10698
A survey of aircraft integrated control technology
[AR-004-561] 02 p0126 N88-10794
Space technology to meet future needs
[NASA-CR-181473] 02 p0130 N88-10819
Center for Electronics and Electrical Engineering Technical Progress Bulletin covering center programs, October to December 1986 with 1987 CEEE events calendar
[PB87-226890] 02 p0168 N88-11058
Center for Electronics and Electrical Engineering technical publication announcements covering center programs, July to September 1986 with 1987 CEEE events calendar
[PB87-223442] 02 p0168 N88-11059
Transmission efficiency in advanced aerospace powerplant
[PNR90391] 02 p0182 N88-11133
Identifying areas of leading edge Japanese science and technology: Activity analysis using SIC (Standard Industrial Classes) categories and scientific subfields
[PB87-204087] 02 p0249 N88-11574
A critical assessment of wind tunnel results for the NACA 0012 airfoil
[NASA-TM-100019] 03 p0260 N88-11636
Comparative testing of wind measuring equipment. Part 1: Inventory and selection
[R-814-D-PT-1] 03 p0325 N88-12053
Laser sources today and tomorrow
[DE87-014247] 03 p0330 N88-12083
Potential applications of expert systems and operations research to space station logistics functions
[NASA-CR-180473] 03 p0372 N88-12342
Progress in improving weather forecasting viewed
04 p0458 N88-12533
The role of basic research in society
[DE88-000459] 04 p0502 N88-13090
Hypersonic airbreathing propulsion: Evolution and opportunities 05 p0531 N88-13231
The RAE experimental data-base for missiles at high Mach number and its use in assessing CFD methods
05 p0534 N88-13250
Hypersonic aerodynamics: Applications for HOTOL
05 p0535 N88-13252
A perspective of computational fluid dynamics
05 p0538 N88-13279
Fundamentals of fighter aircraft design
05 p0544 N88-13316

Progress toward the evolution of a Stirling space engine
[NASA-TM-100221] 05 p0659 N88-14046

Astronautics and aeronautics, 1978: A chronology
[NASA-SP-4023] 05 p0662 N88-14062

Radiation curing: Comparison of heat, UV, and radiation curing
[OEFZS-4393] 06 p0689 N88-14224

Selected aspects of microelectronics technology and applications: Numerically controlled machine tools. Technology trends series no. 2
[PB87-132973] 06 p0696 N88-14268

Interim review of the possibilities and opportunities for the ONR tropical cyclone motion research initiative
[AD-A185679] 06 p0746 N88-14592

Research and technology objectives and plans. Summary, Fiscal Year 1986
[NASA-TM-87504] 06 p0800 N88-14894

Wind tunnel wall interference
07 p0811 N88-14938

Survey of electronic measurement needs below 10 MHz
[PB88-110366] 07 p0844 N88-15121

The technology of centrifugal compressors: A design approach and new goals for research
07 p0850 N88-15163

Remote sensing of the biosphere
[NASA-CR-182382] 07 p0871 N88-15281

The results of the 1984/1985 Round-Robin Calibration of Reference Solar Cells for the Summit Working Group on Technology, Growth and Employment
[DE88-900215] 07 p0874 N88-15303

Risk analysis methodology survey
07 p0922 N88-15604

Expert system technology 07 p0926 N88-15628

Supersonic throughflow fans for high-speed aircraft
08 p0958 N88-15810

Advancing automation and robotics technology for the space station and for the US economy: Submitted to the United States Congress May 15, 1987
[NASA-TM-89811] 08 p0959 N88-15817

Advancing automation and robotics technology for the space station and for the US economy: Submitted to the United States Congress October 1, 1986
[NASA-TM-89190] 08 p0960 N88-15818

Advanced gyros in spacecraft control. Digital capture loops for dry tuned gyros
[LITEF-120046] 08 p0962 N88-15827

Summary record of presentations to the Federal Telecommunication Standards Committee/Fiber optics task group
[PB88-110853] 08 p0978 N88-15911

An overview of key technology thrusts at Bell Helicopter Textron 09 p1111 N88-16657

The wind tunnel as a yardstick for aircraft design
[NLR-MP-85032-U] 09 p1121 N88-16712

Electric propulsion: A controversial must for long-lived applications satellites 09 p1124 N88-16735

Satellite power systems under consideration by the United Nations 09 p1126 N88-16773

Microwave tubes: Literature study no. 8 comprising the year 1986
[FOA-C-30467-3] 09 p1159 N88-16944

Thermal energy storage by means of an absorption cycle
[ETN-88-91614] 09 p1166 N88-17106

Value-assessment of energy storage concepts in burst power systems
[DE87-013756] 09 p1167 N88-17115

An examination of the impact of potential advances in component technology for future military engines
10 p1279 N88-17650

Helicopter activities in Germany
[MBB-UD-487/86] 10 p1314 N88-17853

Future directions in computer architecture and software: The year 2000 10 p1377 N88-18218

Networking requirements and future alternatives
[NASA-TM-89711] 10 p1426 N88-18517

Technical-economical evaluation of a novel propfan concept in comparison with the turbofan for the nineties
[ETN-88-91022] 11 p1441 N88-18596

High performance composites research at NASA-Langley
[NASA-TM-100516] 11 p1450 N88-18642

Free-piston Stirling engine diaphragm-coupled heat-actuated heat pump component technology program, phase 1B
[DE88-003653] 11 p1483 N88-18854

Review of the state of the art and projected technology of low heat rejection engines
[PB88-131255] 11 p1496 N88-18934

Status of emerging technologies: An economic/technological assessment to the year 2000
[PB88-155775] 11 p1567 N88-19381

Assessment, development and application of combustor aerothermal models
[NASA-TM-100290] 12 p1582 N88-19469

Remote manipulation in orbital construction, servicing and repair missions: Is one arm enough? A comparative evaluation of the performance features of robots with one or more arms 12 p1588 N88-19509

Robotics servicing experiment --- European space programs 12 p1591 N88-19529

ROTEX: The Robotic Technology Experiment on Spacelab D-2 mission 12 p1592 N88-19530

Technology requirements for telerobotic satellite servicing in space 12 p1592 N88-19536

Space station accommodations for life sciences research facilities: Phase A conceptual design and programmatics studies for Missions SAAX0307, SAAX0302 and the transition from SAAX0307 to SAAX0302. Volume 1: Executive summary
[NASA-CR-179267] 12 p1599 N88-19571

Computer aided fast turnaround laboratory for research in VLSI (Very Large Scale Integration)
[AD-A189451] 12 p1624 N88-19715

Parametric study of the total cost of aircraft modernization in terms of development and equipment series costs 12 p1700 N88-20177

The increased time and cost of development: Causes and (some) remedies 12 p1701 N88-20178

Advanced Gas Turbine (AGT) technology development project
[NASA-CR-180891] 12 p1709 N88-20230

Workshop on Technology Development Issues for the Large Deployable Reflector (LDR)
[NASA-CP-2407] 12 p1710 N88-20235

A review of technologies applicable to low-speed flight of high-performance aircraft investigated in the Langley 14- x 22-foot subsonic tunnel
[NASA-TP-2796] 13 p1717 N88-20264

Spacecraft fire-safety experiments for space station: Technology development mission
[NASA-CR-182114] 13 p1731 N88-20353

A comparative assessment of US and UK explosives qualified as replacements for tetryl
[MRL-R-1094] 13 p1754 N88-20486

Cryogenic Fluid Management Technology Workshop. Volume 2: Roundtable Discussion of Technology Requirements
[NASA-CP-10009] 13 p1772 N88-20599

The evaluation of automatic barometers, illustrated by the Nakaasa barometer
[KNMI-TR-95] 13 p1774 N88-20610

Power from the sun: Principles of high temperature solar thermal technology
[DE87-001104] 13 p1795 N88-20736

Biophysical applications of solid state and tritium NMR
[DE88-005328] 13 p1808 N88-20806

The concept of intelligent integrated interactive CAD systems
[CWI-CS-R8717] 13 p1818 N88-20865

Energy loss of particles in dense matter-calorimetry
[NIKHEF-H/87-12] 13 p1836 N88-20988

Johnson Space Center's strategic game plan: Charting a course to the year 2000 and beyond
[NASA-TM-89733] 13 p1850 N88-21076

Development of a real-time aeroperformance analysis technique for the X-29A advanced technology demonstrator
[NASA-TM-100432] 14 p1866 N88-21151

Power systems for production, construction, life support and operations in space
[NASA-TM-100838] 14 p1883 N88-21254

Monolithic microwave integrated circuit technology for advanced space communication
[NASA-TM-100829] 14 p1906 N88-21389

X-ray lasers: State of art and prospect
[ETN-88-92003] 14 p1914 N88-21434

Laser technology: CO2 lasers and laser optics
[ETN-88-91469] 14 p1915 N88-21441

What has been done and what will be done by subnatural linewidth spectroscopy 14 p1978 N88-21807

Extension of free-electron lasers into the extreme ultraviolet
[DE88-005373] 15 p2070 N88-22341

Energy from the wind
[DE88-006897] 15 p2091 N88-22459

A method for estimating and controlling the cost of extending technology
[AD-A190717] 15 p2150 N88-22831

Development and qualification of an Augmented Electro-Thermal Hydrazine-Thruster (AEHT) with 0.1 to 0.2 N vacuum thrust
[BMFT-FB-W-86-012] 16 p2169 N88-22931

Status of CAD/CAM in medium-sized industries described 16 p2184 N88-23022

A 30 GHz monolithic receive module technology assessment
[NASA-CR-180825] 16 p2194 N88-23084

Microgravity robotics technology program
[NASA-TM-100898] 16 p2215 N88-23219

Soviet magnetic confinement fusion research
[PB88-152316] 16 p2279 N88-23644

Microelectronics the next fifteen years
17 p2305 N88-23792

Soviet spacecraft engineering research
[FASAC-TAR-3090] 17 p2311 N88-23823

Current stage of remote sensing system for cartographic application 17 p2366 N88-24090

Soviet remote sensing research and technology
[FASAC-TAR-3130] 17 p2369 N88-24108

Teleoperator human factors study
[NASA-CR-178930] 17 p2382 N88-24182

Applications of nuclear power to lunar and Mars missions 17 p2417 N88-24377

The dynamic isotope power system: Technology status and demonstration program 17 p2422 N88-24400

Assessment of nuclear reactor concepts for low power space applications 17 p2423 N88-24409

Value assessment of energy storage concepts in burst power systems 17 p2426 N88-24432

Low cross-section Mo-Nb thermocouples for nuclear application: The state-of-the-art
17 p2433 N88-24477

SNAP-DYN: Concepts for multikilowatt space power applications 17 p2435 N88-24486

Air Force ultrafast optical electronics center
[AD-A191491] 17 p2436 N88-24507

Proceedings of the American Society for Composites
[AD-A189861] 18 p2477 N88-24603

Industrial perspective on current and future needs in aerospace matrix resin chemistry
18 p2477 N88-24696

Differential technology in plastics industries differentiation in combination technology nonflammability technology
[NASA-TT-20256] 18 p2494 N88-24797

Assessment of optical communications systems for Data Relay Satellite. Volume 1: Executive summary
[ESA-CR(P)-2488-VOL-1] 18 p2502 N88-24841

Assessment of optical communications systems for the Data Relay Satellite
[ESA-CR(P)-2488-VOL-2] 18 p2502 N88-24842

Technical and economic evaluation of emerging biomass pyrolysis processes for gasoline production
18 p2536 N88-25046

Recent advances in low-thrust propulsion technology
[NASA-TM-100959] 18 p2569 N88-25260

Liquid Engine Jet Atomization Workshop report
19 p2627 N88-25584

Millimeter-wave integrated circuits
19 p2656 N88-25774

High performance quarter-micron-gate MODFETs
19 p2656 N88-25776

Remote sensing technique applied to vegetation as an aid to municipal planning 19 p2683 N88-25951

Man versus machine: The role of astronauts in extravehicular activity 19 p2699 N88-26045

Flight Mechanics Panel Symposium on Rotorcraft Design for Operations: Technical evaluation report
[AGARD-AR-243] 20 p2758 N88-26362

Pyrotechnic system failures: Causes and prevention
[NASA-TM-100633] 20 p2765 N88-26394

The outlook for ceramics in heat engines, 1990-2010: Results of a worldwide Delphi survey
[DE88-010075] 20 p2778 N88-26475

Photovoltaic concentrator technology: Recent results
[DE88-009586] 20 p2819 N88-26726

Design of booster wound structures --- spacecraft structures
[SNIAS-881-430-102] 21 p2903 N88-27228

Recent developments in nickel hydrogen technology
[DE88-011248] 21 p2939 N88-27456

Ceramic fabrication technology for high-T(sub)c materials
[DE88-012060] 21 p3024 N88-27953

Technology transfer for DOE's Office of Transportation Systems: Assessment and strategies
[DE88-010760] 21 p3029 N88-27977

Phase 1 results from the Stirling-powered vehicle project
[NASA-TM-100978] 21 p3029 N88-27980

The anatomy of the gyroscope
[AGARD-AG-313] 22 p3079 N88-28287

Recent advances in high-power microwave amplifiers
[DE88-007820] 23 p3206 N88-29083

Reliability assessment of Surface Mount Technology (SMT)
[AD-A193759] 23 p3208 N88-29089

Remotely Operated Vehicle (ROV) reliability study, phase 1
[AD-A194367] 23 p3222 N88-29177

Constitutive modeling for isotropic materials
[NASA-CR-182132] 24 p3327 N88-29811

Study on conceptual design of spacecraft using Computer Aided Engineering (CAE)
[SNIAS-920-CA/TS] 24 p3333 N88-29841
Study of the assembly, integration and verification programs of telecommunication satellites applicable to other satellite programs
[MATRA-100/CC/MLG/031/87]
24 p3334 N88-29847
Space structure (dynamics and control) theme development
[NASA-TM-100597] 24 p3335 N88-29850
Definition of common support equipment and space station interface requirements for IOC model technology experiments
[NASA-TM-100656] 24 p3336 N88-29856

TECHNOLOGY TRANSFER
NT AEROSPACE TECHNOLOGY TRANSFER
NASA's new technology reporting system: A review and future prospects
[NASA-CR-180954] 01 p0105 N88-10686
New technologies and intellectual property: An economic analysis
[N-2601-NSF] 01 p0107 N88-10695
The British Technology Group
[ONRL-7-022-R] 01 p0107 N88-10698
Using bibliographic databases in technology transfer
[NASA-CR-181403] 02 p0222 N88-11399
Assessment of the impacts of transferring certain nuclear reactor technologies to the Soviet Union and Eastern Europe
[DE87-014388] 02 p0249 N88-11576
Materials studies for magnetic fusion energy applications at low temperatures-X
[PB87-232575] 03 p0381 N88-12395
Spinoff
[NASA-TM-89651] 03 p0386 N88-12426
The attitudes of science policy, environmental, and utility leaders on US energy issues and fusion
[DE88-000784] 04 p0494 N88-13041
Technology transfer to China
[PB87-223418] 04 p0502 N88-13087
University research initiative research program summaries
[AD-A184876] 05 p0658 N88-14035
Tools and technologies for expert systems: A human factors perspective 06 p0797 N88-14882
Impressions, observations and comments on science and technology in Japan
[PB87-235743] 06 p0799 N88-14893
Research and technology objectives and plans. Summary, Fiscal Year 1986
[NASA-TM-87504] 06 p0800 N88-14894
Faraday cup characterization of electron beam welding parameters
[DE88-001896] 07 p0864 N88-15241
Biotechnology in western Europe
[PB88-105887] 07 p0883 N88-15360
Organizations of intermediation in technology transfer: Its role in technological innovation
[INPE-4354-TDL/297] 08 p1094 N88-16581
A study of federal technology transfer to the commercial sector
[AD-A187017] 09 p1262 N88-17560
Research and technology 1987
[NASA-TM-4021] 09 p1265 N88-17577
Mathematical modeling of two-state classification technology transfer summary and user's guide
[DE88-003849] 11 p1526 N88-19110
The status of R and D for superconducting power transmission systems
[DE88-003499] 11 p1561 N88-19346
AITI Test Report 87-002: Pratt and Whitney technical order transfer tests
[DE88-004045] 11 p1564 N88-19363
AITI Report 87-003: Honeywell technical order transfer tests
[DE88-004046] 11 p1564 N88-19364
A study of technology transfer arrangements for national laboratories
[DE88-005423] 11 p1567 N88-19382
JPRS report. Science and technology: Europe and Latin America
[JPRS-ELS-87-054] 12 p1573 N88-19406
JPRS report. Science and technology: Europe and Latin America
[JPRS-ELS-87-055] 12 p1686 N88-20086
Directory of Japanese technical resources, 1987
[PB87-205258] 12 p1706 N88-20212
NASA/UK TAP
[NASA-CR-180350] 12 p1708 N88-20223
A project to transfer technology from NASA centers in support of industrial innovation in the midwest
[NASA-CR-180360] 12 p1708 N88-20224
Development of a nationwide network for technology transfer
[NASA-CR-181058] 12 p1709 N88-20225
Technology transfer from US Federal laboratories: Report of a roundtable
[PB88-144803] 12 p1709 N88-20228
Technology '87: Research and Development Laboratory Technology Transfer Program
[DE88-003142] 13 p1852 N88-21084
Spin off businesses as mechanisms for transferring technologies
[DE88-005640] 13 p1852 N88-21085
Applicability of aerospace thermal insulation technologies to the civilian sector
[DE88-003717] 13 p1852 N88-21086
Technology transfer to China. Volume 2: Working papers, part 1
[PB88-158704] 14 p1992 N88-21872
Technology transfer to China. Volume 2: Working papers, part 2
[PB88-158712] 14 p1992 N88-21873
Recent advances in photovoltaic concentrator technology
[DE88-003948] 15 p2091 N88-22462
Small and medium power reactors 1987
[DE88-701435] 15 p2132 N88-22720
Developing systems using state-of-the-art CAD/CAM technology 17 p2306 N88-23795
The contribution of space to maritime activities
19 p2700 N88-26055
Workshop report and presentations from the Semiconductor Research Corporation-DOE Semiconductor Task Force Workshop
[DE88-007690] 19 p2733 N88-26232
Technology transfer, Sandia National Laboratories
[DE88-009790] 19 p2740 N88-26268
Wind Energy Technology: Generating power from the wind, a current awareness bulletin
[DE88-008292] 20 p2820 N88-26729
Thermal energy storage
[DE88-010753] 21 p2967 N88-27625
Technology transfer for DOE's Office of Transportation Systems: Assessment and strategies
[DE88-010760] 21 p3029 N88-27977
Argonne National Laboratory technology transfer report, FY87
[DE88-010091] 23 p3298 N88-29639
China's acquisition and use of foreign aviation technology
[AD-A194827] 24 p3440 N88-30471
Research and technology of the Lyndon B. Johnson Space Center
[NASA-TM-100463] 24 p3460 N88-30583

TECHNOLOGY UTILIZATION
Space station: Leadership for the future
[NASA-PAM-509/8-87] 01 p0013 N88-10072
Spacecraft 2000 program overview
01 p0015 N88-10085
Space station platforms 01 p0015 N88-10086
Military needs and forecast, 2
01 p0015 N88-10087
System Development Working Group report
01 p0016 N88-10092
Electrical Power Working Group report
01 p0016 N88-10095
Space station based interferometry
01 p0096 N88-10628
NASA's new technology reporting system: A review and future prospects
[NASA-CR-180954] 01 p0105 N88-10686
New technologies and intellectual property: An economic analysis
[N-2601-NSF] 01 p0107 N88-10695
The use of McIDAS as a Mesoscale forecasting tool during the Canadian Atlantic storms programs --- Man-computer Interactive Data Access System (McIDAS) 02 p0205 N88-11284
Spinoff, 1987
[NASA-TM-89652] 02 p0250 N88-11577
An examination of the Advanced Communications Technology Satellite (ACTS) and its application to the Defense Data Network (DDN)
[AD-A184003] 03 p0276 N88-11742
Optical laser technology, specifically CD-ROM (Compact Disc - Read Only Memory) and its application to the storage and retrieval of information
[AD-A184111] 03 p0330 N88-12086
Market potential for commercial remote sensing
03 p0339 N88-12137
Feasibility study of a range of products drawn from SPOT satellite imagery and specific to road-laying studies
03 p0342 N88-12157
Spinoff
[NASA-TM-89651] 03 p0386 N88-12426
Lasers measure atmosphere
04 p0461 N88-12849
Carbon-carbon composites and Aerospatiale. State of the art and prospects
[SNIAS-872-430-108] 05 p0559 N88-13401
A 40-kW fuel cell field test summary utilities activities report
[PB88-112800] 06 p0731 N88-14496
Artificial intelligence systems
06 p0761 N88-14670
Columbus pressurized module utilization study, executive summary
[CS-RP-AI-027] 07 p0825 N88-15005
Biotechnology in western Europe
[PB88-105887] 07 p0883 N88-15360
Advantages of manned lunar base
08 p1009 N88-16118
Technology developments to meet tomorrow's need for higher satellite frequencies 09 p1124 N88-16732
Introducing new technology into onboard handling systems 09 p1124 N88-16733
Heat pipes for space use 09 p1124 N88-16736
Parallel-processing computer systems and their possible applications in the agency 09 p1128 N88-16774
Microwave tubes: Literature study no. 8 comprising the year 1986
[FOA-C-30467-3] 09 p1159 N88-16944
The use of computer graphic simulation in the development of robotic systems
09 p1214 N88-17275
Study for history of technology developments in European space projects
[REPT-8518-1] 10 p1286 N88-17690
The NORSTAR Program: Space shuttle to space station 10 p1289 N88-17710
The prospects of space utilization
[MBB-UR-931/86] 10 p1314 N88-17856
Minutes of the meeting of the Indo-US Subcommission on Science and Technology (8th) held at Washington, D.C. on September 22-24, 1986
[PB88-130158] 10 p1423 N88-18503
Networking requirements and future alternatives
[NASA-TM-89711] 10 p1426 N88-18517
Science and technology in India
[PB88-134747] 11 p1564 N88-19362
Utilization of robotics and teleoperation for future in-orbit operations 12 p1591 N88-19527
NASA/UK TAP
[NASA-CR-180350] 12 p1708 N88-20223
A project to transfer technology from NASA centers in support of industrial innovation in the midwest
[NASA-CR-180360] 12 p1708 N88-20224
Development of a nationwide network for technology transfer
[NASA-CR-181058] 12 p1709 N88-20225
Johnson Space Center's strategic game plan: Charting a course to the year 2000 and beyond
[NASA-TM-89733] 13 p1850 N88-21076
Contemporary ceramics and the new technological revolution 14 p1902 N88-21363
Microprocessors in space instrumentation
[RR-321] 14 p1955 N88-21655
External tank gamma ray imaging telescope study. Final review, phase 2
[NASA-CR-179320] 15 p2150 N88-22834
Spectroradiometry in materials testing
16 p2273 N88-23601
Data management strategies in the industrial environment
[NLR-MP-87002-U] 16 p2286 N88-23684
Clinical applications of computerized thermography
17 p2330 N88-23915
The results of application studies for space nuclear power 17 p2398 N88-24259
P-Plus: Polar Platform utilization study, executive summary
[BAE-TP-8391] 18 p2469 N88-24653
Personal computer as a workstation in a cartographic automation system? 18 p2535 N88-25039
Different techniques for intervening under the sea: Possible links with space applications
19 p2697 N88-26030
Tasks foreseen for space robots and an example of an associated orbital infrastructure
19 p2699 N88-26044
The contribution of space to maritime activities
19 p2700 N88-26055
The role of aviation technology in the Caribbean Basin
[NASA-CR-183069] 20 p2745 N88-26289
Resources: NASA for entrepreneurs
[NASA-CR-182152] 20 p2883 N88-27119
High technology space flight orientation program: Overview and recommendations
[ETN-88-92332] 21 p3029 N88-27979
The use of AIMS data for operational and research purposes in atmospheric sciences
22 p3036 N88-28025
A 400 kV ion implanter: Operating principles and applications 22 p3069 N88-28213

Utilization of remote sensing for the observation of urban populations. Ongoing research in Quito (Ecuador)
22 p3098 N88-26399
China's acquisition and use of foreign aviation technology
[AD-A194827] 24 p3440 N88-30471

TECTONIC MOVEMENT
U TECTONICS

TECTONICS
Accuracy of GPS surveying technique and its possible application to the Wegener project --- Mediterranean tectonics
[REPT-85.3] 01 p0063 N88-10407
Tectonics of the Caroline Oceanic Step (southwestern Pacific Ocean) 06 p0725 N88-14462
Tectonics and magmatism of Walvis Ridge and Discovery Rise (Atlantic Ocean)
06 p0726 N88-14463
Tectonics of sedimentary cover and basement of Labrador Sea 06 p0726 N88-14468
Mid-tertiary volcano-tectonic development of the Southwestern Cordillera of North America
06 p0797 N88-14879
Geomechanical model of seismofocal zone of active continental margin 08 p1011 N88-16128
Comprehensive method for defining seismogenic zones 08 p1011 N88-16129
Thematic mapper study of Alaskan ophiolites
[NASA-CR-182554] 11 p1504 N88-18984
Experimental and theoretical constraints on the origin of mid-ocean ridge geothermal fluids
13 p1804 N88-20784
Tectonics and three-dimensional structure of spreading centers: Microearthquake studies and tomographic inversions
[PB88-163290] 14 p1945 N88-21602
Remote sensing and structural rupture: Application examples in the study of tectonics
17 p2359 N88-24050
Some geological aspects of the Pirapemas Lineament Belt 17 p2368 N88-24099
Specific features of emanation, temperature and hydrodynamic fields in the epicentral zone of tectonic earthquake
[DE88-701140] 17 p2373 N88-24114
Effects of a temperature-dependent rheology on large scale continental extension
[NASA-CR-183117] 20 p2825 N88-26759
SPOT imagery as an aid to understanding volcanism and tectonics: Examples from the Chilean Andes and the Tibetan Plateau 22 p3103 N88-28427
Analyzing the stratigraphy, tectonism, and mineralization at the Spanish side of the pyrite belt, Huelva province, Spain, using SPOT imagery 22 p3104 N88-28433
Analysis of the multispectral content and of SPOT subscenes in two regions of Burundi. Lithologic and tectonic interpretations 22 p3105 N88-28439
Effects of tectonic release on broadband regional distance bodywaves
[AD-A194247] 22 p3119 N88-28529
Documenting volcano-tectonic episodes in Mars' stratigraphic record 23 p3306 N88-29695
Workshop on the Growth of Continental Crust
[NASA-CR-183073] 24 p3392 N88-30201
Structure of Southwestern Michipicoten Greenstone Belt, Ontario: Evidence for Archean accretion
24 p3397 N88-30226
The tectonic setting of Archean anorthosites
24 p3397 N88-30231
Crustal growth in the Archean: The geochemical evidence 24 p3400 N88-30246
NASA MEVTV Program Working Group Meeting: Volcanism on Mars
[NASA-CR-183074] 24 p3442 N88-30487

TED
U TRANSFERRED ELECTRON DEVICES

TEDLAR (TRADEMARK)
U POLYVINYL FLUORIDE

TEE
U T SHAPE

TEFLON (TRADEMARK)
Sample decomposition in sealed teflon vessels
[NASA-TT-20189] 18 p2494 N88-24798

TELECHIRICS
U REMOTE HANDLING

TELECOMMUNICATION
NT AIRCRAFT COMMUNICATION
NT ALOHA SYSTEM
NT AUTOMATIC PICTURE TRANSMISSION
NT BIOTELEMETRY
NT BROADCASTING
NT CODE DIVISION MULTIPLE ACCESS
NT COMMUNICATION
NT DATA LINKS
NT DEMAND ASSIGNMENT MULTIPLE ACCESS
NT ELECTRONIC MAIL
NT FACSIMILE COMMUNICATION
NT FLEET SATELLITE COMMUNICATION SYSTEM
NT FREQUENCY DIVISION MULTIPLE ACCESS
NT LINE OF SIGHT COMMUNICATION
NT MULTICHANNEL COMMUNICATION
NT MULTIPLE ACCESS
NT OPTICAL COMMUNICATION
NT PACKET TRANSMISSION
NT PCM TELEMETRY
NT PULSE COMMUNICATION
NT RADIO COMMUNICATION
NT RADIO RELAY SYSTEMS
NT RADIO TELEMETRY
NT RADIOTELEPHONES
NT SATELLITE COMMUNICATION
NT SATELLITE TELEVISION
NT SINGLE CHANNEL PER CARRIER TRANSMISSION
NT SPACE COMMUNICATION
NT SPACECRAFT ANTENNAS
NT SPACECRAFT COMMUNICATION
NT TELEMETRY
NT TELEPHONY
NT TIME DIVISION MULTIPLE ACCESS
NT UNDERWATER COMMUNICATION
NT VIDEO COMMUNICATION
NT VOICE COMMUNICATION
NT WIDEBAND COMMUNICATION
ELF/VLF/LF propagation and system design
[AD-A183261] 01 p0033 N88-10212
Monitoring of harmful interference to the HF (High Frequency) broadcasting service. 3: Results of the June 1986 coordinated monitoring period
[PB87-210274] 01 p0036 N88-10229
HF (High Frequency) broadcasting planning model: A comparison of two versions
[PB87-210282] 01 p0036 N88-10230
An examination of the Advanced Communications Technology Satellite (ACTS) and its application to the Defense Data Network (DDN)
[AD-A184003] 03 p0276 N88-11742
Compilation of 1986 annual reports of the Navy ELF (Extremely Low Frequency) communications system ecological monitoring program, volume 3
[AD-A184563] 03 p0306 N88-11932
The design and testing of an analog optical communication link capable of the simultaneous transmission of four frequency division multiplexed audio signals
[AD-A184695] 03 p0307 N88-11936
The Black College satellite telecommunications network planning in support of energy-related collaborative research
[DE88-000182] 03 p0307 N88-11940
Heterogeneous multi-trunking queueing systems
[AD-A184255] 04 p0431 N88-12668
The Telecommunications and Data Acquisition Report
[NASA-CR-181546] 04 p0432 N88-12679
JPRS report: Science and technology. Japan
[JPRS-JST-87-023] 06 p0684 N88-14191
JPRS report: Science and technology. Japan
[JPRS-JST-87-027] 06 p0686 N88-14213
Status, outlook of optical technology in information equipment field 06 p0689 N88-14222
Channel access protocols for multihop packet radio networks
[AD-A186074] 07 p0842 N88-15105
Correctness proofs for systolic algorithms: Palindromes and sorting
[PB88-106075] 07 p0912 N88-15534
Summary record of presentations to the Federal Telecommunication Standards Committee/Fiber optics task group
[PB88-110853] 08 p0978 N88-15911
Team problem solving: Effects of communication and function overlap
[AD-A187010] 09 p1152 N88-16896
Crosstalk analysis of a broadband data communications system
[DE88-003652] 09 p1156 N88-16927
Communications patterns in a symbolic multiprocessor
[AD-A186896] 09 p1215 N88-17282
ELF (Extremely Low Frequency) communications system ecological monitoring program: Electromagnetic field measurements and engineering support, 1986
[AD-A188057] 11 p1509 N88-19017
Communication satellites: Guidelines for a strategic plan
[NASA-TM-89306] 12 p1599 N88-19569
JPRS report: Science and technology. Europe and Latin America
[JPRS-ELS-88-001] 12 p1614 N88-19649
Terrestrial Propagation Characteristics in Modern Systems of Communications, Surveillance, Guidance and Control
[AGARD-CP-407] 12 p1614 N88-19653
Envelope and phase statistics for non-Gaussian noise and resulting error probabilities for digital communications systems 12 p1617 N88-19672
A prototype for remotely shared textual workspaces
[AD-A188352] 12 p1679 N88-20040
Defending secrets, sharing data: New locks and keys for electronic information
[PB88-143185] 12 p1706 N88-20210
A simulation study of a parallel processor with unbalanced loads
[AD-A189573] 13 p1822 N88-20887
Near-real-time TOMS, telecommunications and meteorological support for the 1987 Airborne Antarctic Ozone Experiment
[NASA-CR-4133] 16 p2233 N88-23338
IPC for modular software requires a third party connect
[AD-A189199] 16 p2246 N88-23414
An algorithm for random access communication over a noisy channel
[AD-A191315] 16 p2252 N88-23461
Development of a generic architecture
17 p2303 N88-23774
An FSK (Frequency Shift Keying) telemetry module for vector measuring current meters
[AD-A192142] 18 p2470 N88-24861
Practical VLF/LF radio test system
[AD-A191768] 18 p2500 N88-24831
Information and stochastic systems
[AD-A192167] 18 p2501 N88-24838
The Effect of the Ionosphere on Communication, Navigation and Surveillance Systems Based on Ionospheric Effects Symposium held on 5-7 May 1987 in Springfield, Virginia
[AD-A191855] 18 p2541 N88-25081
Design, implementation and evaluation of an operating system for a network of transputers
[AD-A186593] 18 p2559 N88-25193
Selection and effects of channels in distributed communication and decision making tasks: A theoretica review and a proposed research paradigm
[AD-A191807] 18 p2587 N88-25375
Narrative compression coding for a channel with errors
[AD-A191577] 19 p2642 N88-25673
Extremely Low Frequency (ELF) communications system ecological monitoring program. Summary of 1986 progress
[AD-A192014] 19 p2642 N88-25676
Extremely Low Frequency (ELF) communications program: Non-ionizing electromagnetic radiation literature evaluation and assessment, 1986-1987 literature review
[AD-A192024] 19 p2642 N88-25677
Activities report of the Communications Department
[ENST-88D003] 21 p2931 N88-27401
An evaluation of two millimeter wave propagation models for horizontal atmospheric attenuation at 70-115 GHZ
[AD-A192699] 21 p2931 N88-27403
Experiments applications guide: Advanced Communications Technology Satellite (ACTS)
[NASA-TM-100265] 22 p3048 N88-28087
Basic research in electronics (JSEP) Joint Services Electronics Program
[AD-A193072] 23 p3206 N88-29079
Long haul communications in the HF spectrum utilizing high speed modems
[AD-A194683] 24 p3360 N88-30003
Design of a self-timed VLSI multicomputer communication controller
[AD-A194567] 24 p3361 N88-30014
A static scheduler for the computer aided prototyping system: An implementation guide
[AD-A194340] 24 p3414 N88-30322
Statistical analysis of the LMS (Last Mean Squares) and modified stochastic gradient
[AD-A195497] 24 p3424 N88-30376
Integrating images, applications, and communications networks, volume 5
[AD-A195854] 24 p3436 N88-30452
Information technology to facilitate group interaction
24 p3438 N88-30463
Using standards to break down information transfer barriers 24 p3439 N88-30467

TELECONNECTIONS (METEOROLOGY)
The atmosphere as a component of the climate system: Structure and variability 14 p1935 N88-21540

TELEGRAPH SYSTEMS
Fluxons and order in long Josephson junctions
[AD-A190879] 16 p2282 N88-236

TELEGRAPHY
U TELEGRAPH SYSTEMS

TELEMETERS
U TELEMETRY

TELEMETRY
NT BIOTELEMETRY
NT PCM TELEMETRY
NT RADIO TELEMETRY
TIROS-N/NOAA A-J space environment monitor subsystem
[PB87-203998] 01 p0015 N88-10083
Spacecraft 2000
[NASA-CP-2473] 01 p0015 N88-10084
Telemetry, Tracking, and Control Working Group report 01 p0016 N88-10096
Fiber optic engineering sensor system. Preliminary program management plan, phase 3 revision
[AD-A183663] 01 p0093 N88-10608
How we get pictures from space, revised edition
[NF-151/7-87-REV] 02 p0193 N88-11203
Detection of signals by weighted integrate-and-dump filter 04 p0435 N88-12696
Analysis of the ICE combiner for multiple antenna arraying 04 p0436 N88-12704
New approach to telemetry development will significantly increase productivity of Joint Test Assembly (JTA) teams
[DE88-001676] 05 p0554 N88-13373
A distributed architecture for intelligent monitoring and anomaly diagnosis of the Hubble Space Telescope
08 p1057 N88-16379
A knowledge-based system for monitoring the electrical power system of the Hubble Space Telescope
08 p1058 N88-16380
Exploring hypotheses in attitude control fault diagnosis
08 p1058 N88-16384
A multiprocessing architecture for real-time monitoring
08 p1059 N88-16390
Spacelab Data Processing Facility (SLDPF) quality assurance expert systems development
08 p1059 N88-16394
Telemetry applications handbook
[AD-A186825] 09 p1132 N88-16789
Concept, construction, and experimental testing of a polychromator for a Raman lidar for the simultaneous telemetering of carbon dioxide and water vapor, relative to oxygen
[GKSS-87/E/20] 09 p1191 N88-17134
POCC capabilities document. Payload support capabilities description: MCC, JSC POCC, remote POCC interface
[NASA-TM-89708] 09 p1260 N88-17555
Investigation of design considerations for Telemetry, Tracking and Command (TT and C) antenna system on Naval Postgraduate School Orion mini-satellite
[AD-A187130] 10 p1291 N88-17718
Digital bit error rate estimator for telemetry links
[INPE-4351-TDL/285] 12 p1598 N88-19563
Low cost telemetry and telecommand system for remote measurement of magnitude character
[INPE-4273-PRE/1145] 12 p1598 N88-19564
Estimating the solar irradiance of an intermountain region using GOES (Geostationary Operational Environmental Satellite) satellite data: A test of two statistical models
[AD-A188414] 12 p1642 N88-19834
The imaging of extra-galactic low-energy gamma-ray sources prospects, techniques, and instrumentation
[NASA-CR-182536] 12 p1713 N88-20251
Geometric restoration of satellite image data
[AD-A190462] 15 p2089 N88-22450
Survey of the Air Force P78-2 (SCATHA) satellite plasma wave data during electron gun operations
[AD-A191014] 16 p2168 N88-22926
Soviet remote sensing research and technology
[FASAC-TAR-3130] 17 p2369 N88-24108
TALOS: A distributed architecture for intelligent monitoring and anomaly diagnosis of the Hubble Space Telescope 17 p2386 N88-24193
An FSK (Frequency Shift Keying) telemetry module for vector measuring current meters
[AD-A192142] 18 p2470 N88-24661
Adaptive data acquisition multiplexing system and method
[NASA-CASE-MSC-21170-1] 18 p2471 N88-24662
A VLSI single-chip (225,223) Reed-Solomon encoder with interleaver
[NASA-CASE-NPO-17280-1-CU]
21 p2902 N88-27220
The Telecommunications and Data Acquisition Report
[NASA-CR-183131] 22 p3063 N88-28178
Telemetry SNR improvement using the DSN Advanced Receiver with results for Pioneer 10
22 p3064 N88-28184
Advanced Receiver tracking of Voyager 2 near solar conjunction 22 p3065 N88-28185
A new code for Galileo 22 p3065 N88-28186
The behavior of a Costas loop in the presence of space telemetry signals 22 p3067 N88-28198
Baseband assembly analog-to-digital converter board
22 p3067 N88-28201
Research and development objectives: Installation, startup, and test operation of a remote and program controlled measuring table for the calibration of EGRET experiment
[ETN-88-92105] 22 p3152 N88-28752
Multi-sensory tracking mount control
[AD-A194675] 23 p3249 N88-29339
An expert systems application to space base data processing 23 p3256 N88-29384
Long haul underwater fiber optic link
[AD-A194487] 23 p3282 N88-29542
Accuracy of satellite data navigation
[AD-A195877] 24 p3322 N88-29787
Mission telemetry system monitor: A real-time knowledge-based system 24 p3418 N88-30345
Automated cataloging and characterization of space-derived data 24 p3420 N88-30354
TELEOPERATOR MANEUVERING SYSTEM
U TELEOPERATORS
TELEOPERATORS
Telepresence work station system definition study, part 2
[NASA-CR-172006] 01 p0013 N88-10071
Telerobotics 01 p0015 N88-10090
Robotic sensors and actuators for a service manipulator system. Volume 3, phase A report and program plan
[MATRA-EPT/DT/VT187/229]
01 p0054 N88-10343
Traction-drive seven degrees-of-freedom telerobot arm: A concept for manipulation in space
[DE87-010895] 01 p0054 N88-10346
Teleoperation and control study --- orbital servicing
[BAE-TP-8268] 01 p0076 N88-10489
A methodology for dynamic task allocation in a man-machine system
[DE87-007373] 01 p0077 N88-10492
Evaluation of vision systems for teleoperated land vehicles
[DE87-013066] 03 p0333 N88-12100
Teleoperator and robotics system analysis
[NASA-CR-179220] 03 p0334 N88-12105
Operator multiple-tasking study for remotely operated platforms
[AD-A184487] 03 p0362 N88-12276
Experiences in teleoperation of land vehicles
[DE88-000429] 06 p0711 N88-14355
Experiences in teleoperation of land vehicles
[DE88-001695] 06 p0711 N88-14357
Issues associated with telerobotic systems in space
08 p1056 N88-16369
Telerobotic controller development
08 p1056 N88-16370
Software simulation of time delay in teleoperation
08 p1056 N88-16371
System integration of a Telerobotic Demonstration System (TDS) testbed 09 p1212 N88-17266
Manipulator arm design for the Extravehicular Teleoperator Assist Robot (ETAR): Applications on the space station 09 p1213 N88-17270
Crew interface with a telerobotic control station
09 p1213 N88-17273
NASA/NBS (National Aeronautics and Space Administration/National Bureau of Standards) standard reference model for Telerobot Control System Architecture (NASREM)
[PB88-124773] 10 p1338 N88-17999
Technology requirements for telerobotic satellite servicing in space 12 p1592 N88-19536
A teleoperated manipulator system concept for unmanned platforms --- Columbus
12 p1593 N88-19537
Multi-axis control of telemanipulators
12 p1593 N88-19539
The space station assembly phase: Flight telerobotic servicer feasibility, volume 1
[NASA-CR-182689] 13 p1731 N88-20351
The space station assembly phase: Flight telerobotic servicer feasibility. Volume 2: Methodology and case study
[NASA-CR-182690] 13 p1731 N88-20352
The 22nd Aerospace Mechanisms Symposium
[NASA-CP-2506] 14 p1924 N88-21468
Operational experience and design recommendations for teleoperated flight hardware
14 p1927 N88-21489
Design, development and evaluation of Stanford/Ames EVA prehensors
[NASA-CR-182688] 15 p2105 N88-22540
Teleoperator human factors study
[NASA-CR-178930] 17 p2382 N88-24162
A universal computer control system for motors
[NASA-CASE-NPO-17134-1-CU]
18 p2506 N88-24864
Underwater simulation for space teleoperation
19 p2698 N88-26040
Simulation of space manipulator operations (EUROSIM)
[NLR-MP-87017-U] 20 p2811 N88-26678
A demonstration of retro-traverse using a semi-autonomous land vehicle
[DE88-009851] 21 p2957 N88-27568
Assessments of maneuverability with the TeleOperated Vehicle (TOV)
[AD-A191584] 21 p2980 N88-27751
Mobile robotics R and D at the Savannah River Laboratory
[DE88-011665] 22 p3083 N88-28310
Concepts for robot motion primitives required for space station teleoperations 23 p3257 N88-29387
A teleoperated robotic manipulator system for materials processing experiment servicing
23 p3260 N88-29410
Low level image processing techniques using the pipeline image processing engine in the flight telerobotic servicer 24 p3418 N88-30346
The space station assembly phase: System design trade-offs for the flight telerobotic servicer
24 p3420 N88-30357
TELEPHONES
NT RADIOTELEPHONES
Land mobile satellite transmission measurements at 869 MHz: A comparison of error probabilities for various message block durations and fade margins as a function of vegetation shadowing
[NASA-CR-179929] 06 p0693 N88-14255
Inexpensive solution for the mass distribution of satellite images
[PB88-114038] 10 p1317 N88-17873
Design, development and trials of an airline passenger telephone system 19 p2646 N88-25704
MSAT mobile electronically steered phased array antenna development 19 p2647 N88-25711
TELEPHONY
Digital receiver structures and methods for the determination of the scanning frequency in modems for fast data transmission via telephone channels
[ETN-87-90429] 01 p0037 N88-10235
Digital to analog and analog to digital conversion using pulse duration modulation
[ETN-87-90415] 01 p0078 N88-10499
Study of a coding and modulation system for the V32 call of the CCITT
[ENST-87E007] 02 p0162 N88-11015
AUSSAT mobile satellite services
19 p2643 N88-25684
Development of the network architecture of the Canadian MSAT system 19 p2646 N88-25702
TELESCOPES
NT GAMMA RAY TELESCOPES
NT GERMAN INFRARED LABORATORY
NT HUBBLE SPACE TELESCOPE
NT INFRARED SPACE OBSERVATORY (ISO)
NT INFRARED TELESCOPES
NT PARTICLE TELESCOPES
NT RADIO TELESCOPES
NT SPACE INFRARED TELESCOPE FACILITY
NT SPACEBORNE TELESCOPES
NT SPECTROSCOPIC TELESCOPES
NT STRATOSCOPE TELESCOPES
NT ULTRAVIOLET TELESCOPES
NT VERY LARGE ARRAY (VLA)
NT X RAY ASTROPHYSICS FACILITY
NT X RAY TELESCOPES
An optoelectronic alignment telescope for straightness measurements
[ETN-87-90383] 01 p0093 N88-10609
Ground-based interferometry with the European Very Large Telescope (VLT) 01 p0096 N88-10632
Activities report in astronomy
[ISSN-0531-4496] 01 p0108 N88-10701
Automatic photometric monitoring of cool stars
04 p0504 N88-13103
Statistical properties of small high-velocity events in the solar transition region 04 p0506 N88-13112
Spectral analysis of APT RS CVn binary light curves
04 p0508 N88-13122
H alpha and Ca II emission line variability of FK comae 04 p0509 N88-13128
Automatic telescope operations
04 p0519 N88-13190
Optical photometer for the Tirgo telescope
[IFSI-87-5] 05 p0650 N88-13985
An automated supernova search and the design strategy
[DE88-001827] 05 p0660 N88-14051
Telescope design for Michelson Interferometer for Passive Atmospheric Sounding (MIPAS) B
08 p1017 N88-16167
Balloon-borne three-meter telescope for far-infrared and submillimeter astronomy
[NASA-CR-182310] 09 p1262 N88-17565

Optics for large telescope 13 p1840 N88-21014
Very high energy gamma ray astrophysics
[DE88-005821] 13 p1854 N88-21095
External tank gamma ray imaging telescope study. Final review, phase 2
[NASA-CR-179320] 15 p2150 N88-22834
Performance of the Los Alamos expanding telescope
[DE88-010924] 22 p3151 N88-28751
Martian surface analogs: Laboratory spectral studies in the mid infrared 23 p3307 N88-29699
Very high energy cosmic gamma rays from radio and X-ray pulsars 23 p3309 N88-29711
NASA Marshall Space Flight Center solar observatory
[NASA-TM-100339] 24 p3332 N88-29832
Binary star measurements using digital speckle interferometer of 6-m telescope
24 p3448 N88-30521
Activities report in astronomy
[ISSN-0531-4496] 24 p3451 N88-30535

TELESCOPING STRUCTURES
U FOLDING STRUCTURES

TELEVISION CAMERAS
Sensor fusion for robot navigation
[DE88-008383] 20 p2809 N88-26663

TELEVISION EQUIPMENT
NT IMAGE DISSECTOR TUBES
NT TELEVISION CAMERAS
NT TELEVISION RECEIVERS
A 1/2-inch high-definition baseband VCR
21 p2930 N88-27393

TELEVISION RECEIVERS
Receiver susceptibility measurements relating to interference between UHF (Ultra High Frequency) television and land mobile radio services
[PB87-228029] 06 p0690 N88-14228
Considerations concerning the basic bandwidth reduction of high definition television systems (HDTV) component signals, based on psychophysiological properties of the eye
[IRT-B-83/87] 09 p1153 N88-16909
An outdoor unit for Direct Broadcast Satellite (DBS) digital sound reception
[BMFT-FB-W-86-016] 16 p2189 N88-23050

TELEVISION RECEPTION
A review of the semiconductor storage of television signals. Part 2: Applications 1975-1986
[BBC-RD-1987/6] 02 p0161 N88-11009

TELEVISION SYSTEMS
NT SATELLITE TELEVISION
Lewis Information Network (LINK): Background and overview
[NASA-TM-100162] 03 p0305 N88-11925
Cineradiography
[DE87-013158] 03 p0324 N88-12045
Through-transmission/pulse-echo ultrasonic equipment evaluation
[AD-A186340] 07 p0929 N88-15641
Considerations concerning the basic bandwidth reduction of high definition television systems (HDTV) component signals, based on psychophysiological properties of the eye
[IRT-B-83/87] 09 p1153 N88-16909
Future television systems: Comparison of sequential and interlaced scanning
[BBC-RD-1987/18] 09 p1155 N88-16923
Optical data processing
[AD-A193024] 20 p2839 N88-26841
High definition television: Evaluation for remote task performance
[DE88-011573] 23 p3202 N88-29057

TELEVISION TRANSMISSION
A review of the semiconductor storage of television signals. Part 2: Applications 1975-1986
[BBC-RD-1987/6] 02 p0161 N88-11009
A digital audio link to the Channel Islands in the UHF television band: Protection of television signals from digitally modulated interference
[BBC-RD-1987/7] 02 p0161 N88-11010
A digital audio link to the Channel Islands in the UHF television band: Preliminary experimental results
[BBC-RD-1987/9] 02 p0161 N88-11011
Improvements to a UHF rebroadcast television link suffering tidal fading: Countisbury UHF relay station
[BBC-RD-1987/14] 05 p0573 N88-13495
Television motion measurement for DATV and other applications
[BBC-RD-1987/11] 05 p0573 N88-13496
Two-signal cross modulation effects, half-IF effects and interference criteria in land mobile sharing with UHF (Ultra High Frequency) television
[PB87-228037] 05 p0576 N88-13514
Future television systems: Comparison of sequential and interlaced scanning
[BBC-RD-1987/18] 09 p1155 N88-16923
The relationship between vision carrier-to-noise ratio and picture signal-to-noise ratio in a System I television receiver
[BBC-RD-1987/23] 10 p1318 N88-17877
Digital television routing systems: A survey of optical and electrical techniques
[BBC-RD-1988/3] 19 p2654 N88-25763
Organization of the TDF1/TDF2 program
22 p3161 N88-28827

TELLEGEN THEORY
U NETWORK ANALYSIS
U NETWORK SYNTHESIS

TELLURIDES
NT CADMIUM TELLURIDES
NT LANTHANUM TELLURIDES
NT LEAD TELLURIDES
NT MERCURY TELLURIDES
NT TIN TELLURIDES
NT ZINC TELLURIDES

TELLURIUM
Thermal expansion of some Ge-Se-Te glasses
[PD-MT-8722] 04 p0420 N88-12606
Studies on some Ge-Se-Te glasses
[PD-MT-8721] 04 p0420 N88-12607
Lattice-matched HgZnTe epitaxy development
[AD-A193677] 23 p3292 N88-29600

TELLURIUM ALLOYS
PbSnTe photovoltaic detectors for operation in the 2-14 micron band
[INPE-4252-PRE/1125] 11 p1508 N88-19008

TELLURIUM COMPOUNDS
NT CADMIUM TELLURIDES
NT LANTHANUM TELLURIDES
NT LEAD TELLURIDES
NT MERCURY TELLURIDES
NT TIN TELLURIDES
NT ZINC TELLURIDES

TEMPEL 2 COMET
Anisotropic emission from comets: Fans versus jets. 2: Periodic Comet Tempel 2 14 p2001 N88-21928
The comet rendezvous asteroid flyby mission
14 p2005 N88-21956

TEMPER (METALLURGY)
the influence of temper embrittlement on fatigue crack growth in hydrogen 05 p0605 N88-13709

TEMPERATE REGIONS
An analysis of apparent-motion vectors in, and the structure of, A mid-latitude sporadic E layer using a 2.66 MHz radar
[AD-A186126] 07 p0877 N88-15321
Preliminary analyses of SPOT HRV multispectral products for arid and temperate environments
22 p3099 N88-28407

TEMPERATURE
NT ABSOLUTE ZERO
NT AMBIENT TEMPERATURE
NT ATMOSPHERIC TEMPERATURE
NT AURORAL TEMPERATURE
NT BODY TEMPERATURE
NT BRIGHTNESS TEMPERATURE
NT COMBUSTION TEMPERATURE
NT CRITICAL TEMPERATURE
NT CRYOGENIC TEMPERATURE
NT CURIE TEMPERATURE
NT FLAME TEMPERATURE
NT FLASH POINT
NT GAS TEMPERATURE
NT GLASS TRANSITION TEMPERATURE
NT HIGH TEMPERATURE
NT IGNITION TEMPERATURE
NT INLET TEMPERATURE
NT ION TEMPERATURE
NT IONOSPHERIC TEMPERATURE
NT LOW TEMPERATURE
NT NOISE TEMPERATURE
NT OCEAN TEMPERATURE
NT OPERATING TEMPERATURE
NT PLASMA TEMPERATURE
NT ROOM TEMPERATURE
NT SATELLITE TEMPERATURE
NT SEA SURFACE TEMPERATURE
NT SKIN TEMPERATURE (BIOLOGY)
NT SKIN TEMPERATURE (NON-BIOLOGICAL)
NT SOLAR TEMPERATURE
NT SPIN TEMPERATURE
NT STELLAR TEMPERATURE
NT SURFACE TEMPERATURE
NT TRANSITION TEMPERATURE
NT WALL TEMPERATURE
NT WATER TEMPERATURE
Estimation from satellite imagery of summertime rainfall over varied space and time scales
[PB87-203246] 01 p0071 N88-10454
Estimating payload internal temperatures and radiator size for multimegawatt space platforms
[DE88-000244] 03 p0275 N88-11738
Temperature hysteresis and magnetic transitions in amorphous Fe-Ni-Zr alloys
[DE88-000228] 03 p0294 N88-11846
Scaling of size/time/temperature associated with dilatation and distortion in uniaxial specimens
03 p0336 N88-12117
Improper ferroelectricity: A theoretical and experimental study
[AD-A184614] 03 p0381 N88-12397
Studies of pressure-velocity coupling schemes for analysis of incompressible and compressible flows
[NASA-CR-181526] 04 p0443 N88-12748
Controlled ecological life support systems: Development of a plant growth module 05 p0630 N88-13854
Strength and structure of Ga sub 1-xIn sub xAs alloys
[AD-A188092] 10 p1303 N88-17795
Thermal analysis of transistor packages, part 2
[DE88-005091] 10 p1323 N88-17909
Calibration of a hot-wire/hot-film anemometer over a range of temperatures, velocities and pressures
[AD-A189717] 14 p1913 N88-21430
Calibration and processing of AVHRR data for temperature estimation
[INPE-4493-PRE/1257] 15 p2095 N88-22485
Monthly mean global climatology of temperature, wind, geopotential height, and pressure for 0 - 120 km
[NASA-TM-100697] 15 p2099 N88-22503
Physical, chemical and CTD (Conductivity/Temperature/Depth) data from the Marathon 2 expedition
[AD-A189930] 15 p2099 N88-22507
Global atmospheric circulation statistics, 1000-1 mb
[PB88-168240] 16 p2234 N88-23340
Analysis of crack-tip fields in a viscoplastic material
17 p2349 N88-23996
Theory of oxygen content, atomic ordering and oxygen diffusion in 1,2,3 superconducting oxides as a function of temperature and oxygen pressure
[DE88-007961] 19 p2735 N88-26246
Interfacial tension of immiscible polymer blends: Temperature and molecular weight dependence
[AD-A192463] 21 p2917 N88-27312
Object discrimination via bulk temperature/velocity filtering, phase 1
[AD-A194533] 23 p3274 N88-29487

TEMPERATURE COMPENSATION
Notes on transducer design based on resistance strain gages with applied temperature compensation
[FFA-MEMO-129] 01 p0050 N88-10319
Development of an electronically-scanned pressure module for operation at cryogenic temperatures
[NASA-CR-181610] 12 p1629 N88-19746
The design and use of a temperature-compensated hot-film anemometer system for boundary-layer flow transition detection on supersonic aircraft
[NASA-TM-100421] 13 p1723 N88-20304
Thermal compensating mount
[NASA-CASE-LAR-13794-1] 18 p2519 N88-24942
Further improvements relating to the temperature compensation of semiconductor strain gauge pressure transducers
[RAE-TR-87061] 22 p3081 N88-28298

TEMPERATURE CONTROL
Thermal Control Working Group report
01 p0016 N88-10094
Considerations concerning a thermal joint for a deployable or steerable battery radiator for the Columbus Polar Platform
[NLR-TR-86055-U] 03 p0276 N88-11739
Traveling-wave maser closed-cycle refrigerator data acquisition and display system 04 p0437 N88-12708
Two-watt, 4-Kelvin closed cycle refrigerator performance 04 p0437 N88-12709
Testing of heat pipes on SPAS-01
[BMFT-FB-W-86-014] 06 p0672 N88-14119
Orbital Replaceable Unit (ORU)/cold plate thermal interface study. Volume 1: Executive Summary
[BAE-TP-8430] 07 p0855 N88-15195
Development of an emulation-simulation thermal control model for space station application
[NASA-CR-182409] 08 p0962 N88-15823
Thermal structural control modelling techniques -- spacecraft
[FOK-TR-R-86-030] 08 p0962 N88-15826
MTK: An AI tool for model-based reasoning
08 p1056 N88-16372
Integration of symbolic and algorithmic hardware and software for the automation of space station subsystems
08 p1056 N88-16373
EUREX D: An expert system for failure diagnosis and recovery in the TCS of the European retrievable carrier EURECA 08 p1058 N88-16385
Heat pipes for space use 09 p1124 N88-16736

Analytical interactive approach for phenomena involving structures, thermal and control aspects. Volume 1: Theory --- spacecraft structures
[ESA-CR(P)-2503-VOL-1] 09 p1134 N88-16803
Analytical interactive approach for phenomena involving structures, thermal, and control aspects. Volume 2: Toward the solution --- spacecraft structures
[ESA-CR(P)-2503-VOL-2] 09 p1134 N88-16804
Analytical interactive approach for phenomena involving structures, thermal, and control aspects. Volume 3: Executive summary --- spacecraft structures
[ESA-CR(P)-2503-VOL-3] 09 p1134 N88-16805
TDAS: The Thermal Expert System (TEXSYS) data acquisition system 09 p1211 N88-17258
Moveable thermal joints for deployable or steerable spacecraft radiator systems
[NLR-MP-87016-U] 13 p1730 N88-20347
Feasibility demonstration of a sensor for high-quality two-phase flow --- Space Station
[NLR-TR-87009-U] 13 p1767 N88-20569
Development, manufacturing and testing of a gas-loaded variable conductance methanol heat pipe
[NLR-MP-87010-U] 13 p1767 N88-20571
High output paraffin actuators: Utilization in aerospace mechanisms 14 p1924 N88-21470
Advanced capacitor development
[AD-A189985] 15 p2059 N88-22276
Multi-color pyrometer for materials processing in space 17 p2329 N88-23905
The role of fiberoptics in remote temperature measurement 17 p2329 N88-23909
Real time thermal imaging of high temperature semiconductor melts 17 p2330 N88-23914
MTK: An AI tool for model-based reasoning
17 p2387 N88-24189
The effect of elevated temperature on irradiated MOS devices 17 p2406 N88-24308
Turbomachinery in space 17 p2408 N88-24321
Thermal management for multi-modal nuclear power plants 17 p2410 N88-24331
Silicon-on-insulator electronics for a space nuclear power system 17 p2431 N88-24461
Low gravity thermal management using dielectrophoretic forces 17 p2432 N88-24470
Method and apparatus for growing crystals
[NASA-CASE-MFS-28137-1] 17 p2446 N88-24544
Field experience with aquifer thermal energy storage
[DE88-007075] 18 p2538 N88-25058
Design and testing of a high power spacecraft thermal management system
[NASA-TM-4051] 20 p2764 N88-26389
Heat pump augmented radiators for spacecraft thermal management
[DE88-007890] 20 p2764 N88-26392
Modeling and thermal management of advanced batteries
[DE88-010023] 20 p2794 N88-26580
Thermal-sensation control: A new method of controlling cooled/heated environments 21 p2930 N88-27394
Biorack thermal performance during the D1 mission --- Spacelab 22 p3062 N88-28170
The heat pipe network of TDF-1/TV-SAT: Review of the development at completion
[SNIAS-881-440-103] 23 p3213 N88-29127
Testing degradation of a sample under thermal cycling
[GB-PATENT-2-188-163-A] 23 p3227 N88-29206
Reasoning about fault diagnosis for the space station common module thermal control system
23 p3258 N88-29395
Experimental and analytical study of two-phase flow in zero gravity
[AD-A195223] 24 p3358 N88-29993

TEMPERATURE DEPENDENCE
Hot-spot reaction in unsustained shocks
[DE87-011781] 01 p0044 N88-10277
Anelastic behaviour of materials under multiaxial strains. Part 3: Order-disorder transition, Snoek effect and Poisson's ratio in AISI-1080 steel
[DE87-703087] 02 p0191 N88-11193
Ignition and combustion of metals in oxygen
04 p0407 N88-12530
Retention processes in supercritical fluid chromatography
[DE88-000079] 04 p0413 N88-12559
Experimental perspectives on heavy electron metals
[DE87-014766] 04 p0416 N88-12583
Magnetic field dependence of the specific heat of some high-T/sub c/ superconductors
[DE87-014078] 04 p0497 N88-13063
Temperature dependent mechanical properties of an alumina fiber reinforced aluminum composite
06 p0677 N88-14147
Fatigue oxidation interaction in low cycle fatigue
06 p0719 N88-14420
Study of some superconducting and magnetic materials on high T sub c oxide superconductors
[NASA-CR-182330] 06 p0785 N88-14813
Effect of point defects on graphite lattice parameters
[DE88-700340] 07 p0827 N88-15019
Use of a local heat source for determining temperature of inlet heat section in ring channels
[DE88-700332] 07 p0854 N88-15187
Change of europium crystallographic symmetry at helicoidal magnetic ordering
[DE88-700559] 07 p0939 N88-15707
Study of the temperature dependence of the mechanical characteristics of the steels GX 5 CrNi 13 4 and GGG 40 in tensile and bending tests
[DE88-001469] 09 p1143 N88-16850
Hydrogen in niobium-tantalum superlattices
09 p1146 N88-16867
Structural relationships in high temperature superconductors
[DE88-002924] 09 p1257 N88-17534
Renormalization group analysis of the temperature dependent coupling constant in massless theory
[DE88-751059] 09 p1259 N88-17552
Flame propagation in the approximation of straight-line trajectories of burning products
[DE88-700675] 10 p1297 N88-17756
EXPLO: Explosives thermal analysis computer code
[DE88-001938] 10 p1307 N88-17814
Capacitor analysis for RF antennas
[DE88-004178] 10 p1318 N88-17883
Optical absorption in doped CdxHg1-xTe
[AD-A187434] 11 p1560 N88-19338
Increasing the rate at which ceramic castings undergo preliminary heat-treatment in an ultra-high frequency magnetic field 14 p1886 N88-21275
Data requirements to model creep in 9Cr-1Mo-V steel
14 p1931 N88-21512
Temperature-dependent conductivity of oxygen-depleted YBCO ceramics
[AD-A190340] 15 p2044 N88-22182
Strength and cracking resistance of ceramics. Report 3: SiC ceramics 16 p2180 N88-22994
Ultra high temperature direct propulsion
17 p2401 N88-24275
High-temperature thermal conductivity of a carbon-bonded carbon-fiber insulation
17 p2402 N88-24281
Temperature dependence of ultraviolet absorption cross sections of chlorofluoroethanes
[AERONOMICA-ACTA-A-325-1987]
18 p2482 N88-24726
Temperature-dependent tensile and shear response of graphite/aluminum
[NASA-CR-182914] 19 p2609 N88-25484
Anomalous temperature-dependent negative magnetoresistance in pregraphitic carbons
[AD-A191725] 19 p2619 N88-25535
Dimensional crossover in layered superconductors
19 p2734 N88-26237
Effects of a temperature-dependent rheology on large scale continental extension
[NASA-CR-183117] 20 p2825 N88-26759
Photoluminescence studies of InGaAlAs quaternary alloys
[DE88-007197] 20 p2874 N88-27062
Properties of strong coupled superconductors
[DE88-702050] 23 p3287 N88-29574
Intrinsic and extrinsic energy states of semiconductors and heterostructures using novel techniques
[DE88-008560] 23 p3289 N88-29582
Anomalous dependence of the thermoelectric power on the temperature in YBaCuO high-T(sub c) superconducting samples
[DE88-702682] 23 p3292 N88-29605
Influence of the temperature-dependence of recombination life-time of free carriers in amorphous semiconductors on thermostimulated photocurrent spectra
[DE88-702728] 23 p3293 N88-29609
Thermostimulated conductivity in amorphous semiconductors with non-exponential density of localized states
[DE88-702737] 23 p3293 N88-29612

TEMPERATURE DIFFERENCES
U TEMPERATURE GRADIENTS

TEMPERATURE DISTRIBUTION
Automatic seam welding with infrared sensor feedback
[DE87-013556] 01 p0055 N88-10352
Satellite and synoptic studies of chemical fronts in the California current and coastal upwelling zone
[AD-A183909] 01 p0073 N88-10466
An approximate solution to the problem of heating massive bodies by both radiation and convection
[BLL-M-37315-(5828.4)] 02 p0170 N88-11068
On the mixing of a row of jets with a confined crossflow 02 p0185 N88-11154
The use of satellite IR data in the enhancement of surface thermal fields 02 p0202 N88-11260
Finite element analysis of three-dimensional steady and unsteady temperature fields (computation of temperature distribution of turbine blade with composite cooling)
03 p0300 N88-11887
Numerical and experimental investigation of the unsteady temperature distribution in solar central receivers
[ESA-TT-1050] 03 p0347 N88-12193
Thermal analysis of electromagnetic launcher rails
[DE88-000166] 04 p0405 N88-12514
Microgravity nucleation and particle coagulation experiments support
[NASA-CR-181540] 04 p0423 N88-12618
Microgravity nucleation and particle coagulation experiments support
[NASA-CR-181541] 04 p0423 N88-12619
Resistivity of EuBa2(Cu/sub 1-y/Zn/sub y/)3O/sub x/ as a ffunction of temperature, magnetic field, pressure and Zn concentration
[DE87-014740] 04 p0499 N88-13069
Flux tube dynamics and solar/stellar redshift measurements 04 p0503 N88-13095
Occurance and growth of fatigue cracks in corrosion environment 05 p0604 N88-13704
Statistical structure of temperature field over South Pacific Ocean 06 p0726 N88-14465
Role of anomalous currents in formation of ocean surface temperature field 06 p0727 N88-14474
Structure-property relationships in thermoplastic elastomers 4: Dynamic mechanical relaxations in poly(dioxolane), poly(butyltrioxocane) and poly(propylene oxide) polyurethanes
[AD-A186278] 07 p0836 N88-15073
Supersonic boundary layer on a heated wall
[ETN-88-91617] 08 p0950 N88-15763
Determination of the heat conduction coefficient of the soil from the advance of the diurnal temperature wave
08 p1015 N88-16151
Observations and modeling of the prominence/corona transition region 08 p1094 N88-16585
Symbolic, algebraic, and numeric solutions to heat conduction problems using Green's functions
09 p1165 N88-16987
Approximate solutions of heat conduction in a medium with variable properties
[AD-A186933] 10 p1326 N88-17925
Influence of radiation and thermal conduction on temperature distribution in the thin wall of a hollow cylinder
[INPE-4428-TDL/308] 12 p1626 N88-19730
Retrieval of three-dimensional wind and temperature fields from single-Doppler radar data
12 p1646 N88-19858
Roys and radiosondes in the region
[INPE-4362-PRE/1186] 13 p1796 N88-20743
Arcs in cesium seeded noble gases resulting from a magnetically induced electric field
[EUT-87-E-177] 13 p1843 N88-21028
Comparison of methods for the calculation of thermal contact resistance of the first Brazilian satellite
[NASA-TT-20180] 14 p1880 N88-21239
Modeling growth of interdendritic silicon ribbons
14 p1897 N88-21322
Finite element explicit algorithm for solving temporal temperature fields 14 p1899 N88-21339
Thermal instability and heat transfer characteristics in water/ice systems
[AD-A189627] 15 p2062 N88-22297
Hydrographic observations in the northwestern Weddell Sea Marginal Ice Zone during March 1986
[PB88-173240] 16 p2237 N88-23359
Studies of heat and mass transfer during chemical vapor deposition 17 p2338 N88-23953
Tiros operational vertical sounder (TOVS) and radiosonding in the region 17 p2360 N88-24059
Specific features of emanation temperature and hydrodynamic fields in the epicentral zone of tectonic earthquake
[DE88-701140] 17 p2373 N88-24114
Observations of frontal instabilities on an upwelling filament
[AD-A191051] 17 p2375 N88-24122
Botany Facility: Test report on breadboard tests for the determination of the heat transfer at the glass disk and of the temperature distribution in the fluorescent tube
[BF-TN-ER-053] 17 p2378 N88-24136
A thermal equilibrium model for multi-megawatt space platforms 17 p2410 N88-24332
An irradiation performance data base for nitride fuels
17 p2427 N88-24438
Noncontact temperature pattern measuring device
[NASA-CASE-NPO-17024-1-CU]
18 p2519 N88-24943

Optical investigations of the thermal boundary layer in arc plasmas 18 p2578 N88-25313

Thermal distortion analysis of the space station solar dynamic concentrator
[NASA-TM-100868] 19 p2606 N88-25475

Coal particle behaviour in a counter-current combustor
[TAE-606] 19 p2612 N88-25498

Fuel droplet vaporization and temperature distributions of axisymmetric unsteady sprays
19 p2626 N88-25579

Energy dissipation in a rolling aircraft tire
[NASA-CR-182978] 19 p2676 N88-25913

A statistical treatment of accelerated life test data for copper-water heat pipes 20 p2783 N88-26509

Characteristics of long size thermosyphons made of corrugated tube 20 p2784 N88-26511

Study of temperature and stress fields of two sliding cylinders
[ETN-88-92134] 20 p2815 N88-26704

Cryogenic free jets
[DFVLR-FB-88-16] 21 p2900 N88-27210

A lubrication study of engine bearings
21 p2958 N88-27574

Analysis of lower hybrid current drive and rampup experiments on the JT-60 tokamak
[DE88-753136] 21 p3018 N88-27915

Effect of high-amplitude high-frequency current on non-isothermal equilibrium of NS-boundary in inhomogeneous superconductor
[DE88-701682] 21 p3019 N88-27922

Steady conduction of heat in prolate spheroidal systems
[LRT-WE-9-FB-16(1987)] 22 p3077 N88-28272

Heat transport in a parabolic tube of circular cross-section
[LRT-WE-9-FB-2(1988)] 22 p3078 N88-28274

Currents induced in a human being for electromagnetic fields to 10 kHz-50 MHz
[AD-A191977] 23 p3238 N88-29268

Reasoning about fault diagnosis for the space station common module thermal control system
23 p3258 N88-29395

The thermal behavior of film cooled turbulent boundary layers as affected by longitudinal vortices
[AD-A195155] 24 p3374 N88-30095

Theoretical modeling of accelerating arc plasmas
[AD-A195606] 24 p3432 N88-30426

TEMPERATURE EFFECTS

Stability relationship for water droplet crystallization with the NASA Lewis icing spray
[NASA-TM-100220] 02 p0125 N88-10790

Study of improved methods for predicting chemical equilibria
[DE87-014647] 02 p0145 N88-10908

The effect of temperature on fatigue crack initiation from aluminosilicate inclusions
[PNR90377] 02 p0154 N88-10962

Preparative electrophoresis for space
[NASA-TP-2777] 02 p0156 N88-10977

Qualification testing of General Electric 50 Ah nickel-cadmium cells with Pellon 2536 separator and passivated positive plates 02 p0165 N88-11036

Flight experience of solar mesosphere explorer's power system over high temperatures ranges
02 p0165 N88-11037

Reduction of temperature rise in high-speed photography
[NASA-TM-100222] 02 p0176 N88-11100

Creep-fatigue behavior of NiCoCrAlY coated PWA 1480 02 p0189 N88-11176

A one-dimensional model of thermally-driven coastal front evolution 02 p0204 N88-11274

Fracture mechanism of fine grain graphite under high heat fluxes
[IPPJ-842] 02 p0242 N88-11527

Processing and properties of SiC/Nicalon composites
[DE87-013885] 03 p0279 N88-11757

Stress corrosion cracking of high-strength steels in aqueous environments 03 p0289 N88-11818

A fundamental study of the mechanical and microstructural response of elevated temperature PM aluminum-titanium alloys 03 p0289 N88-11819

Investigation of structure-permeability relationships of silicone polymer membranes
[PB87-230181] 03 p0293 N88-11839

Estimations of gravitational effects on thermal denaturation process in a biopolymer
03 p0318 N88-12013

Kinetics of crack growth: Thermal/mechanical interaction 03 p0337 N88-12124

Structure of thermotropic polyesters with large substituents
[AD-A184086] 04 p0418 N88-12595

Effect of time and temperature on transformation toughened zirconias
[AD-A184356] 04 p0419 N88-12600

Pipe and bend erosion by pneumatic transport of solids at high temperature
[DE88-001345] 04 p0429 N88-12658

Combustion characteristics of gas turbine alternative fuels
[NASA-TM-100247] 05 p0548 N88-13338

The effect of temperature on the tensile properties of HSLA-100 steel
[AD-A184951] 05 p0565 N88-13441

Development of response models for the Earth Radiation Budget Experiment (ERBE) sensors. Part 1: Dynamic models and computer simulations for the ERBE nonscanner, scanner and solar monitor sensors
[NASA-CR-178292] 05 p0584 N88-13557

The initiation and growth of small fatigue cracks in copper at room and cryogenic temperatures
05 p0600 N88-13668

Effect of test temperature and frequency on fatigue crack propagation in PVC 05 p0606 N88-13715

Material design of high-purpose glass discussed
06 p0675 N88-14133

Pressure induced phase transitions, superconductivity of phosphorus described 06 p0675 N88-14134

Polymer material for heat sensors
06 p0676 N88-14142

Fractographic and microstructural aspects of fracture toughness testing in irradiated 304 stainless steel
[DE88-000795] 06 p0681 N88-14172

Mechanisms of rolling contact spalling
[NASA-CR-179243] 06 p0714 N88-14380

Cyclic deformation behaviour of cast irons with various graphite shapes in the temperature range 20 C less than or = T less than or = 500 C 06 p0715 N88-14384

Near-threshold fatigue 06 p0716 N88-14392

Near-threshold fatigue crack growth behavior at cryogenic temperature 06 p0718 N88-14409

Effect of temperature exposure on fatigue crack propagation 06 p0720 N88-14421

High temperature low cycle fatigue behavior and creep-fatigue interation of MA 6000 ODS alloy
06 p0720 N88-14425

The effect of temperature on fatigue crack initiation from aluminosilicate inclusions 06 p0720 N88-14427

An analysis of temperature effect on LCF crack growth rates in superalloy GH36 06 p0721 N88-14431

Thermomechanical fatigue of lead-base low tin solder
06 p0721 N88-14432

Daily dynamics of some physiological indicators of man under desert condition 06 p0750 N88-14605

Exercise in the heat: Effects of dinitrophenol administration
[AD-A185731] 06 p0752 N88-14622

Precipitation in alumina-rich spinel: A transformation-toughened ceramic single crystal
[DE87-012380] 06 p0785 N88-14815

The role of low temperature chemistry in the autoignition of n-butane
[DE88-002385] 07 p0829 N88-15031

Supersonic boundary layer on a heated wall
[ETN-88-91617] 08 p0950 N88-15763

Structural study of the impregnating resins of the type TGMDA/DDS — expoxy resins
[ETN-88-91616] 08 p0965 N88-15842

Kinetics and mechanism of thermal aging embrittlement of duplex stainless steels
[DE88-002987] 08 p0969 N88-15866

Description of tests run in the T2 cryogenic wind tunnel
[PB87-170296] 09 p1113 N88-16672

Mechanical properties of carbon fiber reinforced thermoplastic matrix composites
[NAL-TR-934] 09 p1139 N88-16827

Surface composition-reactivity relationships in heterogeneous catalysis
[DE87-003450] 09 p1140 N88-16834

Influence of post-anneal cooling treatments on suppression of cryogenic intergranular fracture in experimental Ni-free high-Mn austenitic steels
[DE88-002766] 09 p1145 N88-16863

Theory of transient thermal self-focusing of sound beams 09 p1234 N88-17401

Molecular dynamics study of high-temperature grain-boundary stability in a (100) sigma = 29 bicrystal model
[DE88-002955] 09 p1258 N88-17546

The influence of the heating procedure on the oxidation behaviour of NiAl studied by XPS
[AERE-R-12498] 10 p1300 N88-17776

A detailed microstructural examination of the cause of HAZ cracking in type 316 steel
[AERE-R-12428] 10 p1301 N88-17777

A review of pitting corrosion in high temperature aqueous solutions
[DE88-003547] 10 p1302 N88-17787

The measurement of stress in steels of varying microstructure by Barkhausen and magneto-acoustic emission
[AERE-R-12387] 10 p1343 N88-18027

Radiation and temperature effects on the time-dependent response of T300/934 graphite/epoxy
[NASA-CR-182603] 11 p1451 N88-18646

Gastric emptying during exercise: Effects of acute heat stress, acclimation and hypohydration
[AD-A188008] 11 p1519 N88-19073

MBE (Molecular Beam Epitaxial) growth characterization and electronic device processing of HgCdTe, HgZnTe related heterojunctions and HgCdTe-CdTe superlattices
[AD-A187416] 11 p1555 N88-19307

Convective heat transfer and its effect on inertial measurement units 12 p1578 N88-19442

Effects of moisture, elevated temperature, and fatigue loading on the behavior of graphite/epoxy buffer strip panels with center cracks
[NASA-TM-100558] 12 p1603 N88-19590

Thermal cracking and variable properties effects on free boundary layer diffusion flames
[NBS/GCR-88/542] 12 p1614 N88-19652

The fatigue behavior of ferritic and austenitic steels at elevated temperatures
[DE88-006304] 13 p1744 N88-20431

The calibration of photographic and spectroscopic films. Reciprocity failure and thermal responses of IIaO film at liquid nitrogen temperatures
[NASA-CR-181094] 13 p1773 N88-20606

A study of the dynamics of high temperature brittle intergranular fracture by acoustic emission
[AERE-R-12479] 13 p1780 N88-20650

Environmental effects on the post-impact compressive strength of CFC
[RAE-TM-MAT-STR-1088] 14 p1884 N88-21258

Influence of hydrogen on crack formation tendency in heat-affected zone with stress concentrator
14 p1887 N88-21276

Friction welding: Advanced method of producing and cutting tool 14 p1897 N88-21327

The effect of surface tension in the weld pool on seam formation when welding thin sheet with light rays
14 p1898 N88-21334

An internal variable constitutive model for the large deformation of metals at high temperatures
14 p1929 N88-21503

The effects of temperature and strain rate on the yielding behavior of the single crystal superalloy PWA 1480
14 p1931 N88-21517

An automated procedure for material parameter evaluation for viscoplastic constitutive models
14 p1932 N88-21520

Diversity of comets, synergic temperature effects and the stability of organic compounds in icy nuclei
14 p2005 N88-21955

Corrosion Research Center, University of Minnesota
[DE88-006681] 15 p2041 N88-22160

Influence of temperature on the tensile strength and toughness characteristics. Material 35NCD16 ESR. Test report M5-521800
[M5-521800] 15 p2041 N88-22163

Grain boundary oxidation and low-cycle fatigue at elevated temperatures 15 p2083 N88-22420

Examination of temperature effects on gate-to-drain avalanche breakdown in GaAs MESFETs (Metal-Semiconductor Field Effect Transistors) by measuring light emission under RF drive
[AD-A189634] 15 p214 N88-22776

Contribution to the study of modern materials for cutting tools
[ISAL-IDI1-87-17] 16 p2185 N88-23029

Analysis for fuel implosion in ICF target and pellet gain 16 p2276 N88-23620

Influence of fiber reinforcement on the vitreous transition temperature of M 10 matrix composites
[ONERA-RT-44/7086-M] 17 p2316 N88-23835

Polymer precursors for ceramic composites
17 p2326 N88-23890

SiC fiber analysis 17 p2326 N88-23891

The effect of elevated temperature on irradiated MOS devices 17 p2406 N88-24308

Analysis of thermal and radiation effects in materials using the GEMAT process 17 p2408 N88-24318

The effect of operating temperature on open multimegawatt space power systems
17 p2414 N88-24352

The response of selected semiconductor technologies to the combined environmental effects of high temperature and total dose gamma radiation
17 p2431 N88-24462

Effect of alloying, rapid solidification, and surface kinetics on the high temperature environmental resistance of niobium
[AD-A192093] 18 p2485 N88-24743

High temperature embrittleness of Cu-Cr alloy
[NASA-TT-20184] 18 p2488 N88-24759

Critical cooling rates on solution treatment of Cu-Cr and Cu-Be alloys
[NASA-TT-20163] 18 p2488 N88-24760

On the reversion phenomena of Cu-3 percent Ti alloys
[NASA-TT-20170] 18 p2488 N88-24762

Effect of size of precipitates on recrystallization temperatures in Cu-Cr, Cu-Zr, and Cu-Zr-Cr alloys
[NASA-TT-20166] 18 p2489 N88-24763

Rapidly solidified lightweight durable disk material
[AD-A191697] 18 p2491 N88-24775

Thermal distortion analysis of the space station solar dynamic concentrator
[NASA-TM-100868] 19 p2606 N88-25475

Pressure/temperature sensitive inorganic phosphors
19 p2627 N88-25583

Last spring frosts and first autumn frosts in Finland
[FMI-6] 19 p2693 N88-26008

RCL model for the development of hysteresis in superconductors
[DE88-702061] 19 p2733 N88-26234

Electron tunneling in junctions doped with semiconductors and metals 19 p2734 N88-26236

Critical point wetting drop tower experiment
[NASA-CR-183062] 20 p2798 N88-26603

Our climate in danger
[DE88-701824] 20 p2822 N88-26743

Photosynthetic water splitting
[DE88-007809] 20 p2830 N88-26791

Thermal inhibition by megagauss field due to variation of electron temperature in laser plasma
[DE88-701887] 20 p2859 N88-26977

Phase transformations and thermodynamic behavior of the YBa2Cu3O(sub)x system via EMF measurements
[DE88-010054] 20 p2878 N88-27086

Compilation of temperature factors of cubic elements
[PB88-108170] 21 p2906 N88-27260

Determination of lumped-mass thermal properties associated with autoclave curing of graphite/epoxy composites 21 p2925 N88-27364

Thermal stress and its effects on fine motor skill and decoding tasks 21 p2926 N88-27369

Temperature, moisture and strain rate effects on the compressive mechanical behavior of Nylon 6/6
[DE88-010734] 21 p2961 N88-27591

Photodiodes for optical communication in the near infrared
[ETN-88-92379] 21 p3016 N88-27900

Development and application of a finite element method to compute strongly heated turbulent flows
[ECL-88-02] 22 p3077 N88-28267

Marangoni convection in finite cylindrical liquid bridges
[LRT-WE-9-FB-5(1988)] 22 p3078 N88-28277

Effect of fuel burnup and cross sections on modular HTGR (High-Temperature Gas-cooled Reactor) reactivity coefficients
[DE88-006656] 22 p3151 N88-28748

Ultraviolet absorption cross sections of chloro- and chlorofluoromethanes at stratospheric temperatures
[AERONOMICA-ACTA-A-324-1988]
23 p3231 N88-29228

Intraplate deformation, stress in the lithosphere and the driving mechanism for plate motions
[NASA-CR-183121] 23 p3231 N88-29231

Thermodynamical, optical and X-rays studies of some thermotropic liquid crystals
[DE88-702301] 23 p3290 N88-29590

Temperature dependence of conductivity and of Hall coefficients for noble metal films
[ETN-88-92981] 23 p3294 N88-29616

Thermal stress analysis in PMR-15 carbon fibre laminates
[ETN-88-93123] 24 p3341 N88-29886

Effect of interfacial phenomena on contact line heat Transfer 3
[AD-A194941] 24 p3343 N88-29901

The thermal behavior of film cooled turbulent boundary layers as affected by longitudinal vortices
[AD-A195155] 24 p3374 N88-30095

Study of human factors engineering criteria for Extra Vehicular Activity (EVA) systems, volume 2
[STF23-F87025-VOL-2] 24 p3409 N88-30293

TEMPERATURE FIELDS
U TEMPERATURE DISTRIBUTION

TEMPERATURE GRADIENTS
NT THERMOCLINES

Icing detector with early warning capability
[AOA-4.1.0055] 03 p0325 N88-12050

Crack initiation and propagation due to cyclic thermal gradients — aircraft turbine blades
[ESA-TT-1023] 03 p0336 N88-12114

Nonlinear thermoviscoelastic analysis of metallic plane curved beams 03 p0336 N88-12119

Corrosion of ferritic steels by molten lithium: Influence of competing thermal gradient mass transfer and surface product reactions
[DE88-000334] 04 p0417 N88-12585

Influence of stratification in near-surface water layer on intensity of gas exchange between atmosphere and water 04 p0459 N88-12841

Thermophoresis of spherical aerosol particle at arbitrary Knudsen numbers 04 p0461 N88-12850

Evaluation of the Mellen EDG furnace for growth of large diameter GaAs single crystals in a horizontal configuration
[DE88-000463] 04 p0498 N88-13068

Sensitivity of the H alpha line to expansion, geometrical extent and temperature gradient in the G and K supergiant chromospheres 04 p0514 N88-13159

An analytical soil thermodynamic model for the diurnal variation of ground surface temperature
[AD-A185388] 05 p0625 N88-13823

Thin film and gradient-driven instability mechanisms
[PB88-101522] 07 p0853 N88-15182

A calorimeter for measuring the neutral beam power reaching the plasma
[DE88-001412] 07 p0937 N88-15691

Investigation of thermoacoustic heat transport using a thermoacoustic couple
[AD-A186689] 09 p1242 N88-17442

Side-by-side comparisons of evacuated compound parabolic concentrator and flat plate solar collector systems at temperatures of 90 to 100°C
[DE88-004717] 10 p1351 N88-18073

A neutral-beam diagnostic for fast confined alpha particles in a burning plasma: Applicatoin on CIT (Compact Ignition Tokamak)
[DE88-004890] 11 p1554 N88-19301

Remote sensing of meteorological parameters with the aid of a clear-air Doppler radar
[PB88-142518] 12 p1647 N88-19864

Vertical turbulent transfer of matter in thin ocean surface layer during daytime heating 13 p1787 N88-20693

The mixed layer of the western equatorial Pacific Ocean
[HIG-1861] 13 p1805 N88-20789

High output paraffin actuators: Utilization in aerospace mechanisms 14 p1924 N88-21470

Kinematic support using elastic elements
14 p1926 N88-21481

Two gimbal bearing case studies: Some lessons learned 14 p1927 N88-21487

Proceedings of the Seminar on Hydrodynamics and Crystal Growth
[ETN-88-92025] 14 p1987 N88-21853

Hydrodynamical regimes in molten metals under a horizontal temperature gradient
14 p1988 N88-21859

Experiments investigating advanced materials under thermomechanical loading 15 p2077 N88-22385

Ocean, Wave, and Tidal Energy Systems: Current abstracts
[DE88-008299] 19 p2687 N88-25973

The effects of gradients on boundary stability
[DE88-009592] 20 p2773 N88-26445

An experimental investigation of transient characteristics in a gravity-assisted heat pipe 20 p2783 N88-26506

HeFlow: A program for calculating pressure and temperature of helium in forced-flow superconductors. Part 1: Numerical solutions. Part 2: HeFlow user's manual
[DE88-008941] 20 p2876 N88-27071

Prediction of velocity and temperature profiles in thermally driven gravity currents applied to stratified thermal storage tanks
[DE88-004452] 21 p2946 N88-27496

An analysis of horizontal temperature gradients and heat content in the mixed layer and the surface forcing during PATCHEX
[AD-A192330] 21 p2976 N88-27678

TEMPERATURE INDICATORS
U INDICATING INSTRUMENTS
U TEMPERATURE MEASURING INSTRUMENTS

TEMPERATURE INSTRUMENTS
U TEMPERATURE MEASURING INSTRUMENTS

TEMPERATURE INVERSIONS

North Pacific Ocean, Gulf of Alaska, R/V Thomas G. Thompson 1 February - 8 March 1967. STD data report
[AD-A186569] 08 p1045 N88-16314

TEMPERATURE MEASUREMENT

Estimating regional evapotranspiration from remotely sensed data by surface energy balance models
[NASA-CR-181400] 01 p0064 N88-10411

A device for measuring fast temperature fluctuations — atmospheric temperature
[KNMI-TR-92] 01 p0070 N88-10449

Psychophysical considerations in measuring MRTD with staring arrays — minimum resolvable temperature difference (MRTD)
[RSRE-MEMO-4031] 01 p0076 N88-10487

The use of fiber optics in the determination of temperature and extent of reaction in detonating explosives
[DE87-012632] 01 p0094 N88-10612

Evaluation of the infrared test method for the olympus thermal balance tests 02 p0136 N88-10856

Optical fiber interferometric sensor to measure temperature in gas flow
[ENST-87E006] 02 p0170 N88-11071

Evaluating and testing thermographic phosphors for turbine-engine temperature measurements
[DE87-011772] 02 p0174 N88-11090

Further development of the dynamic gas temperature measurement system 02 p0184 N88-11141

Correlation of velocity and velocity-density turbulence in the exhaust of an atmospheric burner
02 p0185 N88-11147

Forecasting the kind of precipitation in winter
02 p0202 N88-11266

Time-resolved temperature and density measurements in ionizing, uniformly irradiated UV-laser-produced plasmas
[DE87-014649] 02 p0238 N88-11504

Comparison of flight-measured and calculated temperatures on the space shuttle orbiter
[NASA-TM-88278] 03 p0321 N88-12029

Comparison of measured temperatures, thermal stresses and creep residues with predictions on a built-up titanium structure
[NASA-TM-86814] 03 p0337 N88-12125

A simplified CARS measurement system for rapid determination of tamperature and oxygen concentration
[NASA-TM-100498] 03 p0374 N88-12353

Resistor cooling in a vacuum
[DE88-000696] 04 p0440 N88-12733

Noncontact temperature measurements of hot steel bodies using an electromagnetic acoustic transducer (EMAT)
[DE88-000560] 04 p0446 N88-12765

Calibration of a laser-pumped, thermographic phosphor remote thermometry system
[DE88-000452] 04 p0449 N88-12781

A mathematical model of high alloy nickel base high temperature alloys
[BLL-M-37381-(5828.4)] 05 p0564 N88-13436

October lower stratospheric Antarctic temperature and total ozone from 1979-1985 05 p0615 N88-13776

Development of a Doppler wind lidar system for atmospheric wind measurements
08 p1027 N88-16217

Aerosols in Martian Atmosphere and Natural Dust Observation (AMANDO). Proposal for the Mars orbiter balloon and rover to study the Martian atmosphere, its thermal content, and its interaction with the soil
[IFSI-87-9] 08 p1100 N88-16619

MARCE data evaluation 10 p1286 N88-17693

A reliable data collection/control system
10 p1289 N88-17708

CARS measurements of combustion. 1: Precision of thermometry
[NAL-TR-939] 10 p1299 N88-17769

NBS (National Bureau of Standards) measurement services: Platinum resistance thermometer calibrations
[PB88-135367] 10 p1333 N88-17967

Comparative evaluation of resistive and inductive techniques for measuring temperature of superconducting transition
[DE88-700603] 10 p1417 N88-18457

A noise-adding radiometer for the Parkes antenna
11 p1473 N88-18788

Measurement of velocity and temperature profiles in low-speed, turbulent non-isothermal flows
[PB88-155833] 11 p1486 N88-18872

Error evaluation of some practical thermocouple probes for gas turbine combustor tests
[NAL-TR-938] 11 p1489 N88-18886

A sky temperature survey at 19.2 GHz using a balloon borne Dicke radiometer for anisotropy tests of the cosmic microwave background 11 p1571 N88-19403

Vestibular response to caloric stimulation during orbital flight 12 p1658 N88-19939

Electron temperature measurements in an argon/cesium plasma diode
[AD-A188835] 12 p1695 N88-20141

Exhaust-gas pressure and temperature survey of F404-GE-400 turbofan engine
[NASA-TM-88273] 13 p1724 N88-20307

Measurement of detonation temperature of hydrogen-oxygen mixture by CARS (Coherent Anti-Stokes Raman Spectroscopy)
[NASA-TT-20227] 13 p1739 N88-20398

Remote fiber fluorometry techniques for pressure measurements
[DE88-004486] 13 p1773 N88-20604

Noncontact thermometry via laser pumped, thermographic phosphors: Characterization of systematic errors and industrial applications
[DE88-005599] 13 p1777 N88-20628

Phenomenological description of eddy registered in Gulf Stream 13 p1787 N88-20694

Monitoring ocean surface layer processes
13 p1806 N88-20801

On the structure of pulsed plasma jets
13 p1843 N88-21030

The astrophysics of nebulae and active galactic nuclear emission-line regions: New methods and applications
13 p1858 N88-21111

Tropic heat MR (Meteorological Recorder) meteorological data (April 1984 - June 1985)
[PB88-161286] 14 p1948 N88-21620

Temperature of the nucleus of Comet Halley
14 p2009 N88-21985

Measurement of emissivity of industrial surfaces using a simple method
[NASA-TT-20165] 15 p2036 N88-22130

Rocket measurements of ionospheric electron temperature over Natal
[INPE-4485-PRE/1250] 15 p2096 N88-22489

Validate algorithms for the determination of rainfall rates from SSM/I microwave satellite imagery
[AD-A188769] 16 p2233 N88-23337

Noncontact Temperature Measurement
[NASA-CP-2503] 17 p2327 N88-23895

Radiation thermometry: The measurement problem
17 p2328 N88-23896

The NBS scale of radiance temperature
17 p2328 N88-23897

Non-contact temperature measurement requirements for electronic materials processing
17 p2328 N88-23898

Noncontact temperature measurement: Requirements and applications for metals and alloys research
17 p2328 N88-23899

Noncontact temperature measurement in glass and other transparent materials 17 p2328 N88-23900

Noncontact temperature measurements in the microgravity fluids and transport phenomena discipline
17 p2328 N88-23901

Microgravity combustion discipline working group summary of requirements for noncontact temperature measurements 17 p2328 N88-23902

Requirements for temperature and species concentration measurements in microgravity combustion experiments 17 p2329 N88-23903

Non-contact temperature measurements for biotechnology discipline working group
17 p2329 N88-23904

Multi-color pyrometer for materials processing in space 17 p2329 N88-23905

Direct emissivity measurements on liquids and corrections to multi-color pyrometers
17 p2329 N88-23906

Common but unappreciated sources of error in one, two, and multiple-color pyrometry 17 p2329 N88-23907

Fast optical pyrometry 17 p2329 N88-23908

The role of fiberoptics in remote temperature measurement 17 p2329 N88-23909

Laser pyrometry 17 p2330 N88-23910

Noncontact true temperature measurement, 2
17 p2330 N88-23911

Laser Diagnostics for combustion temperature and species measurements 17 p2330 N88-23912

Infrared radiometric technique in temperature measurement 17 p2330 N88-23913

Real time thermal imaging of high temperature semiconductor melts 17 p2330 N88-23914

Clinical applications of computerized thermography
17 p2330 N88-23915

Summary report on the Japan-US Workshop on the Assessment of Spectroscopic Data for Temperature and Density Measurements --- plasma diagnostics
[IPPJ-861] 17 p2439 N88-24512

Effects of spatial resolution in CARS measurements
[PB88-121900] 18 p2482 N88-24727

Remote temperature-measurement instrumentation for a heated rotating turbine disk
[DE88-006456] 18 p2516 N88-24925

Special observations 18 p2545 N88-25108

Analysis of annular microstrip antennas for hyperthermic applicators
[PB88-151508] 19 p2643 N88-25679

Studies of error in temperature measurement with thermistors in the range between continual and free-molecule flows
[NASA-TT-20302] 19 p2674 N88-25900

Examination of the termalization of confined ions
[PB87-227815] 19 p2723 N88-26171

Evaluation of thermophosphor temperature technique
[DE88-007654] 20 p2805 N88-26638

Remote sensing of temperature profiles. Performance test of PASS
[DE88-753108] 20 p2826 N88-26768

Global-scale temperature changes to August 1987 and a comparison of satellite and conventional data
22 p3125 N88-28572

Energy conversion measurements in laser-sustained argon plasmas for application to rocket propulsion
[AD-A194931] 24 p3337 N88-29861

Measurement of local high-level, transient surface heat flux
[NASA-TP-2840] 24 p3375 N88-30099

Quantitative surface temperature measurement using two-color thermographic phosphors and video equipment
[NASA-CASE-LAR-13740-1] 24 p3376 N88-30105

Estimation of soil temperature profile from remote microwave and IR measurements
24 p3450 N88-30532

TEMPERATURE MEASURING INSTRUMENTS
NT BATHYTHERMOGRAPHS
NT OPTICAL PYROMETERS
NT PNEUMATIC PROBES
NT PYROMETERS
NT RADIATION PYROMETERS
NT RESISTANCE THERMOMETERS
NT THERMOMETERS

Realization of an instrument to measure temperature and concentration gradients in fluids --- microgravity
[CISE-3126] 09 p1168 N88-17003

Forward looking wind shear detection
10 p1275 N88-17629

Evaluation of a temperature remote sensing technique
[AD-A187885] 10 p1347 N88-18053

Boundary layer measurements using hot-film sensors
17 p2297 N88-23743

Noncontact Temperature Measurement
[NASA-CP-2503] 17 p2327 N88-23895

Measurement of local high-level, transient surface heat flux
[NASA-TP-2840] 24 p3375 N88-30099

TEMPERATURE PROBES
NT PNEUMATIC PROBES

TEMPERATURE PROFILES

Effect of NASA advanced designs on thermal behavior of Ni-H2 cells
[NASA-TM-100197] 01 p0021 N88-10132

Diagnosing short term changes in temperature and moisture profiles from single Doppler radar
02 p0200 N88-11251

Method for determining atmospheric temperature profiles from observations of astronomical refraction of stars 08 p1013 N88-16139

A study of finite difference and finite element vertical discretization schemes for baroclinic prediction equations
[AD-A186617] 08 p1040 N88-16291

GAS eleven node thermal model (GEM)
10 p1289 N88-17712

Suggested severe local storm operational scenario for GOES I-M
[NASA-TM-100688] 11 p1515 N88-19052

Editing master oceanographic observation data set 4
[AD-A188405] 12 p1649 N88-19876

Basic networks of TOGA: Determination of thermal profiles by XBT and of sea level by tide gage
14 p1939 N88-21568

Large ice masses: Characteristics, behaviour and relation to climate 14 p1939 N88-21569

Aerodynamic aspects of the Amazon Forest
[INPE-4445-TDL/313] 15 p2098 N88-22501

Antistokes coherent Raman diffusion of a nitriding plasma
[ONERA-RF-6/3644-PY] 16 p2175 N88-22962

Utilization of dense packed planar acoustic echosounders to identify turbulence structure in the lowest levels of the atmosphere
[AD-A191006] 16 p2233 N88-23335

Ion temperature profile measurement using charge exchange recombination spectroscopy on JIPP T-IIU
17 p2440 N88-24518

Spectroscopic measurements of ion temperature, rotation speed and beam deposition profile on DIII-D
17 p2440 N88-24519

Three-dimensional temperature fields in the atmosphere up to 50 km altitude
[ETN-88-92150] 18 p2542 N88-25089

Superthermal electron processes in the upper atmosphere of Uranus: Aurora and electroglow
[NASA-TM-101150] 18 p2594 N88-25417

Diurnal variations in optical depth at Mars: Observations and interpretations
[NASA-TM-100057] 18 p2595 N88-25420

Temperature and species profiles in propellant ignition and combustion 19 p2633 N88-25616

An arranging method on L/D of two-phase closed thermosyphons 20 p2783 N88-26508

Remote sensing of temperature profiles. Performance test of PASS
[DE88-753108] 20 p2826 N88-26768

Prediction of velocity and temperature profiles in thermally driven gravity currents applied to stratified thermal storage tanks
[DE88-004452] 21 p2946 N88-27496

Retrieval of temperature and concentration profiles from a limited number of absorption measurements
21 p2947 N88-27501

Temperature profile construction methods: An evaluation
[AD-A195919] 24 p3403 N88-30262

TEMPERATURE SCALES

The NBS scale of radiance temperature
17 p2328 N88-23897

TEMPERATURE SENSORS
NT THERMISTORS

Development of heat flux sensors for turbine airfoils
02 p0184 N88-11143

Icing detector with early warning capability
[AOA-4.1.0055] 03 p0325 N88-12050

Instrument for radiation testing/screening electronic devices over an extended temperature range
[AD-A184245] 03 p0326 N88-12060

Polymer material for heat sensors
06 p0676 N88-14142

Evaluation of a temperature remote sensing technique
[AD-A187885] 10 p1347 N88-18053

La Recherche Aerospatiale, bimonthly bulletin, number 1987-1, 236/January-February
[ESA-TT-1055] 11 p1433 N88-18549

Photonic temperature and pressure sensors for biosystems/pulsed microwave. Part 1: Interaction studies
[AD-A188887] 12 p1629 N88-19751

Characteristics of polysilicon layers and their application in sensors 19 p2669 N88-25861

Flexible tactile sensing arrays for robotics: Architectural robustness and yield considerations
19 p2671 N88-25878

Thermodynamic study of hygroscopic polymers using surface acoustic waves 19 p2672 N88-25882

Modulated-splitting-ratio fiber-optic temperature sensor
[NASA-TM-101332] 22 p3042 N88-28062

Development of sensors for ceramic components in advanced propulsion systems: Survey and evaluation of measurement techniques for temperature, strain and heat flux for ceramic components in advanced propulsion systems
[NASA-CR-182111] 22 p3081 N88-28299

TEMPERING

Partial substitution of vanadium by niobium in AISI H13 steel
[DE87-703548] 04 p0415 N88-12575

Study on substructures of martensite in steels containing rare earth metals
[PB87-143996] 07 p0833 N88-15050

Investigation of the auto-tempering of low-carbon martensite
[PB87-143970] 07 p0833 N88-15053

New mechanism of the high temperature (reversible) temper brittleness of alloy steels
[PB87-143954] 07 p0833 N88-15056

The measurement of stress in steels of varying microstructure by Barkhausen and magneto-acoustic emission
[AERE-R-12387] 10 p1343 N88-18027

TEMPLATES

Schwarz splitting and template operators
[AD-A187956] 10 p1404 N88-18370

Defect detection and classification in VLSI pattern inspection 18 p2507 N88-24871

TEMPORAL DISTRIBUTION

Optimization of explicit time-stepping algorithms and Stream-Function-Coordinate (SFC) concept for fluid dynamics problems 04 p0445 N88-12762

Convective wind fields as investigated with doppler lidar
[PB88-115472] 09 p1193 N88-17151

Evolution of acoustic gravity wave packet in spatially and temporally varying wind 11 p1469 N88-18760

Temporal evolution of ionospheric electric field driven by field-aligned current 11 p1469 N88-18761

Spatial and temporal distribution of precipitation chemistry across Maryland in 1984, volume 1
[PB88-148929] 14 p1943 N88-21595

Spatial and temporal distribution of precipitation chemistry across Maryland in 1984, volume 2
[PB88-148937] 14 p1944 N88-21596

The spatial and temporal variability of the arctic atmospheric boundary layer and its effect on electromagnetic (EM) propagation
[AD-A193958] 23 p3204 N88-29068

Mineralization through geologic time: Evolution of continental crust 24 p3400 N88-30250

TEMPORAL RESOLUTION

Estimation from satellite imagery of summertime rainfall over varied space and time scales [PB87-203246] 01 p0071 N88-10454

A CAMAC system controlled by an IBM AT computer for time-resolved spectroscopy [DE87-010111] 01 p0080 N88-10514

Evaluation of digital, multitemporal LANDSAT 5 thematic mapper data for the determination of the aerial snowcover extent and spectral separation of various surface types in the inner Cetztal (West Germany) with special regard to the significance of aerial snowcover information for water resources management [DFVLR-FB-86-46] 03 p0345 N88-12180

Visual evoked responses to sinusoidal gratings presented in central and right visual fields: 1 [DE87-014731] 04 p0473 N88-12919

Resolution limitations and optimization of the LLNL streak camera focus [DE88-001633] 05 p0586 N88-13572

Investigation of the evolution of the fusion processes in the plasma focus using time-resolved neutron spectroscopy [IPF-87-4] 09 p1251 N88-17493

Time-resolved spectroscopic measurement of anode plasma in magnetically-insulated diode 16 p2279 N88-23641

Applications of multitemporal compositions obtained from LANDSAT data in the study of urban growth [INPE-4480-PRE/1246] 16 p2287 N88-23692

Fast optical pyrometry 17 p2329 N88-23908

Electron device probing in the femtosecond time scale 19 p2660 N88-25821

TENDENCIES

Reference filters for electrostatic charging tendency measurements of fuels [AD-A191717] 18 p2495 N88-24803

TENSILE DEFORMATION

Polymer chain segment orientation during stress relaxation [DE87-013392] 01 p0027 N88-10174

An investigation of the high strain rate deformation of SiCw/2124 Al composite [OUEL-1675/87] 02 p0142 N88-10895

The effect of deformation rate on JBK-75 stainless steel forgings [DE88-001696] 07 p0834 N88-15061

Fatigue and uniaxial deformation behavior of Hastelloy XR at elevated temperatures [DE88-751058] 09 p1145 N88-16862

The influence of small defects on tensile specimen ductility and symmetry of deformation [AD-A187983] 10 p1346 N88-18044

An investigation of the influence of dislocation substructures on the deformation behavior of AK, DQ steel sheets [DE88-006337] 14 p1889 N88-21289

TENSILE PROPERTIES

Superplastic deformation and post forming tensile properties of Ti-6Al-4V sheet [RAE-TR-86015] 01 p0023 N88-10144

Tensile behavior of superplastic Al-Cu-Li-Zr alloy 2090 at cryogenic temperatures [DE87-014084] 02 p0147 N88-10923

A shape preserving interpolant which has tension controls [DE87-014615] 02 p0229 N88-11443

Effect of irradiation on the tensile properties of niobium-base alloys [DE87-002409] 03 p0285 N88-11790

The effect of strain rate on the yield behavior of iron-base LRO alloys at elevated temperatures [DE87-014893] 03 p0286 N88-11808

Carbon fiber reinforced glass matrix composites for space based applications [AD-A184355] 04 p0410 N88-12546

Molecular composites: Processing, post-treatment and mechanics [AD-A184458] 04 p0410 N88-12547

Mechanical behavior of a controlled rolled high-strength low alloy steeel plate, microalloyed with Nb and V [DE87-703507] 04 p0415 N88-12571

Welding and weldability of ductile intermetallic alloys [DE87-014061] 04 p0416 N88-12582

The accommodation of precipitate plates modelled as a tensile test [DE88-000207] 04 p0454 N88-12814

Small-diameter wire tensile testing [DE88-000835] 04 p0455 N88-12815

Influence of strain rate and notch depth on tensile properties of HITCO 6250 [DE88-001324] 04 p0455 N88-12816

The effect of temperature on the tensile properties of HSLA-100 steel [AD-A184951] 05 p0565 N88-13441

Tensile properties of extrusion consolidated Type 304 SS rapidly solidified powders [DE87-014875] 05 p0566 N88-13450

Basic energy sciences research in the Metals and Ceramics Division of Oak Ridge National Laboratory [DE87-013538] 06 p0681 N88-14171

The effect of neutron irradiation on the tensile properties and microstructure of several vanadium alloys [DE88-001755] 06 p0682 N88-14176

Electron microscopy studies of tensile cyclic fatigue-tested silicon nitride ceramics [DE88-001438] 06 p0685 N88-14196

Effect of hold time on fatigue of lead rich PbSn solder 06 p0715 N88-14387

High temperature low cycle fatigue behavior and creep-fatigue interation of MA 6000 ODS alloy 06 p0720 N88-14425

The relationship of tensile specimen size and geometry effects to unique constitutive parameters for ductile materials [AD-A186020] 08 p0994 N88-16012

Influence of post-anneal cooling treatments on suppression of cryogenic intergranular fracture in experimental Ni-free high-Mn austenitic steels [DE88-002766] 09 p1145 N88-16863

Effects of the neutron spectrum on mechanical property changes in low dose irradiations [DE88-003429] 10 p1302 N88-17786

Durability and damage tolerance of aluminum castings [AD-A186444] 10 p1341 N88-18013

Analysis and application of the constant tensile load test for polyethylene gas pipe materials [DE88-002868] 10 p1345 N88-18037

The effects of low doses of 14 MeV neutrons on the tensile properties of three binary copper alloys [DE88-003400] 11 p1458 N88-18691

Development of a constitutive equation for HSLA (High-Strength Low-Alloy)-100 at cryogenic temperatures [AD-A189243] 13 p1740 N88-20408

The effect of microstructure on the fatigue crack growth resistance of nickel base superalloys [AD-A189526] 13 p1741 N88-20414

Behaviour of fibre-reinforced composites under dynamic loading [AD-A191310] 16 p2174 N88-22955

Effects of natural environment on first generation solid rocket booster thermal protection system materials [NASA-TM-100329] 17 p2373 N88-24113

Creep behavior of tungsten/niobium and tungsten/niobium-1 percent zirconium composites 17 p2425 N88-24427

Dynamic consolidation of metal powders [AD-A192126] 18 p2485 N88-24744

Temperature-dependent tensile and shear response of graphite/aluminum [NASA-CR-182914] 19 p2609 N88-25484

The postirradiation tensile properties and microstructure of several vanadium alloys [DE88-007140] 19 p2615 N88-25515

Exploratory development in the system Al-Sc-X [DE88-008242] 19 p2618 N88-25529

Uniaxial tensile strain measurement for ceramic testing at elevated temperature: Requirements, problems and solutions [DE88-008090] 19 p2621 N88-25550

Initial development of high-temperature titanium silicide alloys [DE88-007860] 20 p2772 N88-26437

Helium induced degradation in the weldability of an austenitic stainless steel [DE88-009062] 20 p2773 N88-26443

Nickel aluminides: A new family of nickel + aluminum alloys featuring simple composition, low density, excellent oxidation resistance and high yield strength that increases with temperature [DE88-010692] 20 p2776 N88-26461

Thermomechanical processing of Al alloy 2090 for grain refinement and superplasticity [AD-A192333] 21 p2912 N88-27281

Some effects of nitrates on the tensile properties of Al 7075-T7351 [AD-A195118] 24 p3354 N88-29965

TENSILE STRENGTH

Gas tungsten arc welding of Al-10Fe-5Ce [AD-A184202] 03 p0334 N88-12104

Weldability of 2219-T851 and 2519-T87 aluminum armor alloys for use in Army vehicle systems [AD-A184296] 04 p0451 N88-12792

Fatigue strength of alloy A286 at cryogenic temperature 05 p0603 N88-13695

Effect of interface on mechanical properties of graphite/201 aluminum composites 05 p0606 N88-13717

Deformation, fatigue and fracture behavior of two cast anisotropic superalloys 05 p0608 N88-13732

Temperature dependent mechanical properties of an alumina fiber reinforced aluminum composite 06 p0677 N88-14147

Threshold stress intensity for stable crack growth in high strength steel at ambient temperature and below 06 p0718 N88-14407

Structural relaxation and mechanical properties of amorphous Fe-Zr alloys 07 p0840 N88-15094

Cavitation inception scale effects. 1. Nuclei distributions in natural waters. 2. Cavitation inception in a turbulent shear flow [AD-A186553] 08 p0988 N88-15987

Computation of the tensile and bending restraint intensities of welded specimens by finite element method [PB87-143798] 08 p0995 N88-16024

Investigation of microstructural factors that cause low fracture toughness in silicon carbide whisker/Al alloy composites [AD-A186443] 09 p1137 N88-16817

Long-term aging of cast stainless steels: Mechanisms and resulting properties [DE88-002888] 09 p1145 N88-16864

Aging degradation of cast stainless steels: Effects on mechanical properties [DE88-003053] 09 p1145 N88-16866

Materials Research Laboratory at Brown University [AD-A188006] 13 p1739 N88-20396

A direct correlation of strength with impact velocity [AD-A189251] 13 p1741 N88-20409

Use of reinforced inorganic cement materials for spark wire and drift chamber wire frames [NASA-CR-180759] 13 p1746 N88-20438

The statistical characterization of tensile strengths for a nuclear-type graphite 13 p1746 N88-20440

Statistical considerations of graphite strength for assessing design allowable stresses 13 p1746 N88-20441

High temperature Young's modulus of IG-110 graphite 13 p1746 N88-20443

Dynamic tensile cyclic fatigue of Si3N4 [DE88-003919] 13 p1781 N88-20658

The age hardening response of thermomechanically processed Al-Mg-Li alloys [AD-A189870] 15 p2039 N88-22147

Cracking tendencies of restrained welds in high strength low alloy steels under hyperbaric conditions [AD-A190255] 15 p2039 N88-22150

Influence of temperature on the tensile strength and toughness characteristics. Material 35NCD16 ESR. Test report M5-521800 [M5-521800] 15 p2041 N88-22163

Characterization of HYTUF steel. Semifinished product: 160 mm dia forging block. Processor: C3f. Test Report M3-434600 [M3-434600] 15 p2041 N88-22164

Strength and cracking resistance of ceramics. Report 3: SiC ceramics 16 p2180 N88-22994

Fracture morphologies of carbon-black-loaded SBR (Styrene-Butadiene Rubber) subjected to low-cycle, high-stress fatigue [DE88-006808] 16 p2181 N88-23002

High strength/sigh modulus aromatic heterocyclic ABA block copolymers [AD-A191666] 18 p2491 N88-24774

High temperature testing of C/C (Carbon/Carbon) composites [AD-A193012] 20 p2768 N88-26411

Development of a biaxial test system for thin-walled metal tubes using tensile-compressive axial load and internal-external pressure [DE88-011279] 21 p2962 N88-27592

A technique for measuring area under a curve [AD-A193559] 23 p3271 N88-29463

TENSILE STRESS

Constitutive modeling of superalloy single crystals with verification testing 02 p0188 N88-11169

Tensile mean stress effects on uniaxial fatigue behavior of 1045 HR steel 05 p0603 N88-13694

Mixed mode fatigue crack growth using the Brasilian disc 06 p0719 N88-14416

Effect of overload ratios on fatigue crack growth behavior in Ti-6Al-4V alloy [PB87-147062] 07 p0833 N88-15055

Deformation effects on microwave reflectivity [AD-A185684] 07 p0844 N88-15120

Shear failure in round bar tensile tests of Al-Zn-Mg-Cu alloys [PB87-143632] 07 p0869 N88-15271

Pressure and tension dependence of phase shift of polarization modes in birefringent single-mode fiber-optic waveguide 08 p1078 N88-16501

Elastoplastic response of unidirectional graphite/aluminum under combined tension-compression cyclic loading
[CCMS-88-01] 11 p1451 N88-18647
Fracture criterion of reactor graphite under multiaxial stresses 13 p1746 N88-20442
Environment effects on crack propagation with tensile stress
[GKSS-87/E/46] 16 p2223 N88-23267
Peak Acceleration Device (PAD)
[AD-A191639] 18 p2461 N88-24611
Stress corrosion cracking of A723 steel pressure vessels: Two case studies
[AD-A191741] 18 p2527 N88-24990
The surface crack problem in an orthotropic plate under bending and tension
[NASA-CR-178281] 18 p2531 N88-25014
Nonlinear stress-strain and inelastic rebound with exponential stiffness
[AD-A195667] 24 p3384 N88-30159

TENSILE TESTS
Cumulative fatigue and life prediction of fibre composites. Part 2: Experimental techniques and results
[BR101014] 02 p0142 N88-10894
An investigation of the high strain rate deformation of SiCw/2124 Al composite
[OUEL-1675/87] 02 p0142 N88-10895
Creep fatigue life prediction for engine hot section materials (isotropic): Third year progress review
02 p0188 N88-11173
Elevated temperature crack growth
02 p0188 N88-11174
The accommodation of precipitate plates modelled as a tensile test
[DE88-000207] 04 p0454 N88-12814
Test number 2 of propellant for rocket motor MK52
[PB87-226155] 05 p0571 N88-13480
Crack growth in contrasting titanium alloys under the conjoint action of high and low cycle fatigue
05 p0602 N88-13686
Device for measuring hole elongation in a bolted joint
[NASA-CASE-LAR-13453-1] 06 p0712 N88-14361
Shear failure in round bar tensile tests of Al-Zn-Mg-Cu alloys
[PB87-143632] 07 p0869 N88-15271
High temperature tensile testing of ceramic composites
[NASA-CR-180888] 08 p0990 N88-15996
Study of the temperature dependence of the mechanical characteristics of the steels GX 5 CrNi 13 4 and GGG 40 in tensile and bending tests
[DE88-001469] 09 p1143 N88-16850
High-temperature properties of ceramic fibers and insulations for thermal protection of atmospheric entry and hypersonic cruise vehicles
[NASA-TM-100059] 10 p1295 N88-17743
A study of the mechanical behavior of a 2-D carbon-carbon composite 11 p1449 N88-18638
Ethynylated aromatics as high temperature matrix resins
[NASA-TM-89829] 11 p1450 N88-18640
An experimental and numerical study of notch sensitivity of ARALL laminates
[CCMS-88-04] 11 p1450 N88-18644
Microstructural characterization of the heat affected zone of HSLA (High Strength Low Alloy)-100 steel GMA (Gas Metal Arc)-weldment
[AD-A187825] 11 p1457 N88-18686
Effects of moisture, elevated temperature, and fatigue loading on the behavior of graphite/epoxy buffer strip panels with center cracks
[NASA-TM-100558] 12 p1603 N88-19590
Development of a constitutive equation for HSLA (High-Strength Low-Alloy)-100 at cryogenic temperatures
[AD-A189243] 13 p1740 N88-20408
High temperature Young's modulus of IG-110 graphite
13 p1746 N88-20443
Notch sensitivity of graphite materials for VHTR
13 p1747 N88-20447
An investigation of the mechanical properties of improved carbon fibre composite materials
[RAE-TR-86021] 14 p1884 N88-21259
Materials testing at cryogenic temperatures
[BU-359] 14 p1923 N88-21462
The effective fracture toughness of aluminum at rapid heating rates
[AD-A189745] 15 p2036 N88-22146
A test for interfacial effects and stress transfer in ceramic matrix composites
[NASA-CR-182758] 15 p2046 N88-22194
A study of failure characteristics in thermoplastic composite material
[AD-A190613] 16 p2171 N88-22940
Test procedures and standards for mechanical property measurements on metal matrix composites
[NPL-DMA(A)-153] 16 p2172 N88-22944
Behaviour of fibre-reinforced composites under dynamic loading
[AD-A191310] 16 p2174 N88-22955
Mechanical and structural characterization of aluminum ceramic fibers
[ETN-88-92168] 17 p2323 N88-23870
Bearing-bypass material system test
[NASA-CASE-LAR-13458-1] 17 p2342 N88-23967
Fracture physics of delamination of composite materials
[AD-A192021] 19 p2609 N88-25482
High temperature testing of C/C (Carbon/Carbon) composites
[AD-A193012] 20 p2768 N88-26411
Investigation of structure and surface state effect on hydrogen embrittlement of steels, under consideration of acoustic emission analysis
[ETN-88-92350] 20 p2775 N88-26457
Cold worked reinforcing bars in tensile test under high loading rate and low temperatures
[DE88-752993] 21 p2964 N88-27610

TENSOR ANALYSIS
Nonlinear parametric least-squares adjustment
[AD-A184039] 03 p0371 N88-12336
Tensorial calibration. Part 1: First order tensorial calibration
[AD-A186708] 09 p1167 N88-16995
Relative chaos in stellar systems
[DE88-700148] 12 p1710 N88-20234

TENSOR FIELDS
U TENSORS

TENSORS
NT STRESS TENSORS
Direction dependent connections of complex manifolds and their submanifolds
[DE87-703073] 02 p0225 N88-11419
Fundamentals of turbulence for turbulence modeling and simulation 03 p0312 N88-11971
Lagrangian procedures for higher order field equations
[DE87-703365] 05 p0640 N88-13911
Eigenvalues and eigenvectors of field tensors and associated energy tensors
[DE88-001951] 06 p0763 N88-14662
Tensorial calibration. 2. Second order tensorial calibration
[AD-A186614] 09 p1167 N88-16994
Tensorial calibration. Part 1: First order tensorial calibration
[AD-A186708] 09 p1167 N88-16995
Estimates of green tensors for certain boundary value problems
[NASA-TT-20203] 11 p1535 N88-19172
Irreducible tensor operators and multiple-quantum NMR 11 p1542 N88-19217
Connection between general observers and Lanczos potential
[DE88-700139] 11 p1563 N88-19354
Body tensor formalism in finite deformation elasticity and application to the torsion of a circular cylinder
13 p1780 N88-20651
A piecewise quadratic strength tensor theory for composites
[AD-A190929] 16 p2173 N88-22952
Inflation in Einstein-Cartan theory with energy-momentum tensor with spin
[NASA-TM-101164] 17 p2447 N88-24547
Inevitable inflation in Einstein-Cartan theory with improved energy-momentum tensor with spin
[NASA-TM-101146] 18 p2586 N88-25365
Dissipative relativistic radiation hydrodynamics
[DE88-702092] 19 p2665 N88-25846
Symmetry problem of energy-momentum tensor and the creation of gravitational field
[DE88-702442] 21 p3026 N88-27964
On nonlinear equations admitting soliton solutions with a deBroglie phase
[DE88-702694] 23 p3277 N88-29506
Waves and instabilities in an electron-positron plasma in an ultra-strong magnetic field
23 p3283 N88-29551
New methods for nonlinear optimization
[AD-A195982] 24 p3412 N88-30313
The triangle: A multiprocessor architecture for fast curve and surface generation
[AD-A195882] 24 p3414 N88-30324

TERMINAL BALLISTICS
Mechanical property evaluation of a series of commercial tungsten alloys
[AD-A185440] 05 p0565 N88-13446
On the simulation of ballistic shock loads
05 p0593 N88-13615
Structural frequency functions for an impulsive, distributed forcing function 05 p0594 N88-13627
High-velocity reverse ballistic rocket sled testing at Sandia National Laboratories 09 p1179 N88-17059
Penetration theory for inclined and moving shaped charges
[MBB-UA-940/86] 10 p1315 N88-17861
A laboratory railgun for terminal ballistics and arc armature research studies
[AD-A187225] 11 p1442 N88-18603
Crack arrest fracture toughness of armor steels
[AD-A187711] 11 p1456 N88-18681
Splinter generator
[MBB-UA-1048/87] 11 p1491 N88-18897
Ballistic evaluation of applique armours: Presentation and interpretation of ballistic data
[MRL-TN-527] 19 p2635 N88-25629
Review of research concerning Solid Fuel Ramjet (SOFRAM) at the Research Institute of National Defence (FOA) 2
[FOA-C-20714-2.1] 24 p3327 N88-29813

TERMINAL FACILITIES
Issues in air transport and airport management
[PB87-204509] 02 p0124 N88-10782
FAA air traffic control operations concepts. Volume 2: ACF/ACCC (Area Control Facility/Area Control Computer Complex) terminal and en route controllers
[AD-A185980] 07 p0818 N88-14974
FAA air traffic control operations concepts. Volume 3: ISSS (Initial Sector Suite System) en route controllers
[AD-A185981] 07 p0818 N88-14975
FAA air traffic control operations concepts. Volume 4: TAAS (Terminal Advanced Automation System) terminal controllers
[AD-A185982] 07 p0818 N88-14976
FAA air traffic control operations concepts. Volume 5: ATCT/TCCC (Airport Traffic Control Tower/Tower Control Computer Complex) tower controllers
[AD-A185983] 07 p0818 N88-14977
A traveling-salesman-based approach to aircraft scheduling in the terminal area
[NASA-TM-100062] 12 p1576 N88-19424
Estimates of potential increases in airport capacity through ATC (Air Traffic Control) system improvements in the airport and terminal areas
[AD-A188533] 12 p1578 N88-19444

TERMINAL GUIDANCE
NT LASER GUIDANCE
An investigation of steep descent guidance for terminally-guided sub-munitions
12 p1596 N88-19555

TERMINAL VELOCITY
Efficiency aspects of short, low velocity railguns
[AR-004-847] 04 p0405 N88-12517
Phenomenological piercing characteristics of composite materials 14 p1895 N88-21315

TERMINATING
U STOPPING

TERMINOLOGY
Digital Name Data Base Antarctic as a component of a landscape data base of the Antarctic
01 p0065 N88-10419
Abregrams or deleweds: A forty-year view of acronyms
[DE87-010808] 01 p0106 N88-10690
Definitions as database records
[DE87-014057] 02 p0248 N88-11570
Energy Data Base: Subject Thesaurus
[DE87-008007] 03 p0384 N88-12414
NASA thesaurus supplement: A four part cumulative supplement to the 1985 edition of the NASA Thesaurus
[NASA-SP-7053(SUPP-4)] 08 p1093 N88-16575
NASA thesaurus: Astronomy vocabulary
[NASA-SP-7069] 17 p2450 N88-24553
NASA combined file postings statistics based on NASA thesaurus, Jan. 1968 - July 1988
[NASA-CR-182985] 18 p2589 N88-25384

TERMS
Radar descriptors for the classification of terrain features
[AD-A188145] 11 p1504 N88-18983
An assessment of index term ranking
21 p3026 N88-27974

TERNARY ALLOYS
NT ASTROLOY (TRADEMARK)
A geometrical model for determining the physicochemical properties of ternary metallic systems
[BLL-M-37303-(5826.4)] 02 p0149 N88-10931
CdTe(110)-Mn interface reaction and the formation of non-equilibrium ternary semimagnetic semiconductor alloys
[AD-A187593] 10 p1422 N88-18491
Ordering transitions of ternary alloys A(1-x)B(x)C
20 p2873 N88-27054

TERNARY SYSTEMS
Thermodynamic properties of supercritical mixtures
[DE88-000809] 04 p0413 N88-12582
Electronic structure calculations and binding analyses for selected binary and ternary metal hydrides
[ETN-88-91087] 09 p1256 N88-17527

TERNARY SYSTEMS (DIGITAL)
U DIGITAL SYSTEMS
TERPENES
NT AZULENE
TERRACES (LANDFORMS)
NT PIEDMONTS
NT PLATEAUS
TERRAIN
Evaluation of a scale-model experiment to investigate long-range acoustic propagation
[NASA-TP-2748] 02 p0230 N88-11450
The correspondence of surface climate parameters with satellite and terrain data
[NASA-CR-181515] 03 p0346 N88-12185
Disturbance and recovery of Arctic Alaskan tundra terrain. A review of recent investigations
[AD-A184442] 04 p0467 N88-12887
Large bandwidth ground scattering model --- radar scattering
[FOA-C-30458-3.2] 05 p0576 N88-13511
Electromagnetic wave probing of Earth's environment
[NASA-CR-182358] 06 p0690 N88-14232
Fast, colour displays of digital terrain elevation data
[AD-A185596] 06 p0729 N88-14485
Sound propagation over uneven ground and irregular topography
[NASA-CR-182352] 06 p0776 N88-14763
Academic course Space Methods for Studying Modern Landscapes of Continents 08 p1012 N88-16133
Radar returns from ground clutter in vicinity of airports
10 p1274 N88-17624
The digital landmass simulation production overview
[AD-A187978] 11 p1503 N88-18978
Three-dimensional image generation from an aerial photograph
[AD-A188039] 11 p1503 N88-18979
Contour-to-grid interpolation with nonlinear finite elements: A feasibility study
[AD-A188108] 11 p1503 N88-18980
Terrain Analyst Work Station (TAWS) demonstrations
[AD-A188139] 11 p1504 N88-18981
Radar descriptors for the classification of terrain features
[AD-A188145] 11 p1504 N88-18983
A digital terrain system for microcomputers
[INPE-4170-PRE/1067] 11 p1505 N88-18987
An investigation of terrain related variables for predicting the multipath fade depth distribution on terrestrial microwave lines 12 p1615 N88-19654
Development of a ground-conductivity map for the area of the Federal Republic of Germany from measured field-strength contours 12 p1615 N88-19656
Scattering and depolarization by random rough terrain and vegetation covered terrain-unified full wave approach 12 p1615 N88-19657
VHF/UHF propagation by diffraction: Calculation by numerical integration 12 p1615 N88-19659
Mono- and bistatic radar coverage diagrams including diffractive wave propagation 12 p1616 N88-19660
Development of a digital terrain modeling system for microcomputers
[INPE-4406-TDL/303] 12 p1639 N88-19816
Modification of the BLUEMAX 2 terrain following model to incorporate radar detection
[AD-A190594] 15 p2017 N88-22028
The visit problem: Visibility graph-based solution
[DE88-000343] 15 p2108 N88-22556
The use of LANDSAT-TM pictures for the detection of space-limiting elements for the benefit of landscape photomapping
[BCRS-87-02] 16 p2228 N88-23305
Visualization of digital terrain models
17 p2364 N88-24081
Terrain classification using SPOT images and the computer system GOP-300
[FOA-C-20677-2.7] 17 p2368 N88-24102
Digital monoplotting, part 1
[B8735122-PT-1] 17 p2369 N88-24106
Digital monoplotting, part 2
[B8735122-PT-2] 17 p2369 N88-24107
Land mobile satellite propagation results
19 p2645 N88-25698
Development of an atmospheric diffusion evaluation method incorporating topographical effects. Part 1: Literature review of atmospheric diffusion models incorporating terrain effects
[DE88-753104] 20 p2822 N88-26742
Sound propagation over uneven ground and irregular topography
[NASA-CR-182956] 20 p2849 N88-26911
Surface-wave model uncertainty assessment
[AD-A193094] 21 p2932 N88-27408
Army space systems for terrestrial applications
[AD-A192735] 21 p2965 N88-27613
Analysis of remotely sensed imagery using digital morphology
[AD A192738] 21 p2965 N88-27614
Active and passive remote sensing of ice
[AD-A193307] 21 p2966 N88-27617
Land use systems and rural landscapes in the center of Veracruz State (Mexico): First results
22 p3092 N88-28364
The suitability of SPOT imagery for monitoring landscape patterns 22 p3094 N88-28376
Digital terrain modelling with SPOT data and geological applications 22 p3110 N88-28474
Automatic production of orthophoto using SPOT images 22 p3112 N88-28487
Automatic creation of digital terrain models from SPOT image pairs 22 p3113 N88-28490
Constraints on the origin of fractured terrane, Northern Martian plains 23 p3304 N88-29684
Ridged and gullied terrains in the Martian uplands
23 p3307 N88-29700
Evolution of the Dharwar Craton: A terrain of early Archean crustal stability, long term orogenic cycles and large scale palaeobiological activity
24 p3399 N88-30241
Crustal growth in the Archean: The geochemical evidence 24 p3400 N88-30246
TERRAIN ANALYSIS
A Workshop on Desert Processes, September 24-28, 1984: Report on the conference
[AD-A184599] 03 p0345 N88-12184
A review of computer-assisted photo interpretation research at USAETL (US Army Engineer Topographic Laboratories)
[AD-A184034] 03 p0346 N88-12186
Correction of inertial navigation system drift errors for an autonomous land vehicle using optical radar terrain data
[AD-A184973] 05 p0544 N88-13311
An inexpensive real-time interactive three dimensional flight simulation system
[AD-A184868] 07 p0821 N88-14989
Determination of network attributes from a high resolution terrain data base
[AD-A186078] 07 p0870 N88-15279
Statistics of two-dimensional structure elements of mountainous ranges (mosaic model) for calculating three-dimensional reflection functions
[DFVLR-FB-87-33] 09 p1185 N88-17099
Target-reflectivity models for various terrain types
[DE88-005510] 11 p1505 N88-18992
Digital data dubbing capability
[AD-A188252] 11 p1525 N88-19105
Digital Topographic Support System (DTSS)
[AD-A188304] 12 p1638 N88-19808
Terrain classification from digital elevation data using slope and curvature information
[AD-A188940] 12 p1639 N88-19812
A comparison of terrain association and resection as methods of position location
[AD-A189480] 13 p1790 N88-20710
Remote sensing of earth terrain
[NASA-CR-182677] 13 p1790 N88-20711
Interpolation algorithms for digital terrain models
[INPE-4373-PRE/1196] 13 p1820 N88-20877
Modification of the BLUEMAX 2 terrain following model to incorporate radar detection
[AD-A190594] 15 p2017 N88-22028
Study of fracturing for groundwater research in the Sergipe state with remote sensing products
17 p2359 N88-24052
Updating of municipal official register of real estate through the geographical information system
19 p2684 N88-25952
Aerial photography as an instrument of atmospheric analysis: Maps of the middle atmosphere and its dynamics, Baixada Santista (SP) 19 p2684 N88-25955
Linear feature extraction from radar imagery. Phase 2: Base contract report
[AD-A192828] 21 p2931 N88-27404
Methods of determining playa surface conditions using remote sensing
[AD-A192663] 21 p2965 N88-27612
Research for reducing the labor intensive nature of high-resolution terrain analysis feature extraction
[AD-A192661] 22 p3089 N88-28345
Motion planning for legged locomotion systems on uneven terrain 23 p3221 N88-29170
Relief effect correction on LANDSAT imagery for forest applications using digital terrain models
[INPE-4611-PRE/1334] 24 p3388 N88-30179
A digital terrain model system for a microcomputer
[INPE-4610-PRE/1333] 24 p3413 N88-30316
TERRESTRIAL DUST BELT
The dust ring of the Earth
[RAE-TRANS-2163] 22 p3119 N88-28530
TERRESTRIAL MAGNETISM
U GEOMAGNETISM
TERRESTRIAL PLANETS
NT EARTH (PLANET)
NT MARS (PLANET)
NT VENUS (PLANET)
A bibliography of dunes: Earth, Mars, and Venus
[NASA-CR-4149] 20 p2885 N88-27134
TERRESTRIAL RADIATION
Radiation belts 03 p0272 N88-11707
Nimbus 7 Solar Backscatter Ultraviolet (SBUV) spectral scan solar irradiance and Earth radiance product user's guide
[NASA-RP-1199] 09 p1184 N88-17096
Net radiative flux at the Earth surface: Estimation from satellite observations 14 p1936 N88-21550
Results of radiation measurements in West Germany and from special measurement series in the Meteorological Observatory of Hamburg
[REPT-11] 18 p2542 N88-25088
Angular radiation models for Earth-atmosphere system. Volume 1: Shortwave radiation
[NASA-RP-1184] 21 p2976 N88-27677
Energy budget and ground temperatures in hot regions
[AD-A196298] 24 p3404 N88-30268
TEST BEDS
U TEST EQUIPMENT
TEST CHAMBERS
NT ANECHOIC CHAMBERS
NT HYPERBARIC CHAMBERS
NT PRESSURE CHAMBERS
NT REVERBERATION CHAMBERS
NT VACUUM CHAMBERS
Design, construction, activation, and operation of a high intensity acoustic test chamber
02 p0137 N88-10864
Man rating the b-1B molecular sieve oxygen generation system
[AD-A186275] 07 p0899 N88-15447
MBA payload testing by Compact Antenna Test Range (CATR)
[ESA-CR(P)-2473] 08 p0977 N88-15906
The ESTEC Mini Compact Antenna Test Range
[ESA-CR(P)-2475] 08 p0977 N88-15907
Environment test laboratory
[ETN-88-91885] 14 p1869 N88-21166
Study of mean free path effects on growth of ultrafine metallic aerosols
[AD-A190206] 15 p2039 N88-22149
Development of computer-controlled thermogravimetric instrumentation for measurement of environmental and high temperature volatilization and desorption of contaminants from polymeric materials
[AD-A195934] 24 p3343 N88-29900
TEST EQUIPMENT
Shielding effectiveness against electromagnetic interference
[DE88-003664] 07 p0846 N88-15131
Space station propulsion technology
[NASA-CR-179260] 08 p0964 N88-15835
Simulation test beds for the space station electrical power system
[NASA-TM-100786] 10 p1290 N88-17715
Construction aspects of testbeds for attitude control systems simulation of artificial satellites
[INPE-4283-PRE/1155] 11 p1445 N88-18616
Almond test body --- for microwave anechoic chambers
[NASA-CASE-LAR-13747-1] 18 p2502 N88-24845
Techniques utilized in the simulated altitude testing of a 2D-CD vectoring and reversing nozzle
[NASA-TM-100872] 19 p2604 N88-25464
AC power system breadboard
[NASA-CR-179369] 22 p3049 N88-28091
TEST FACILITIES
NT ANECHOIC CHAMBERS
NT BALLISTIC RANGES
NT BLOWDOWN WIND TUNNELS
NT CASCADE WIND TUNNELS
NT COMBUSTION WIND TUNNELS
NT CRYOGENIC WIND TUNNELS
NT ENVIRONMENTAL LABORATORIES
NT HOTSHOT WIND TUNNELS
NT HYDRAULIC TEST TUNNELS
NT HYPERSONIC WIND TUNNELS
NT HYPERVELOCITY WIND TUNNELS
NT LOW SPEED WIND TUNNELS
NT RECTANGULAR WIND TUNNELS
NT REVERBERATION CHAMBERS
NT ROCKET TEST FACILITIES
NT SHOCK TUNNELS
NT SLOTTED WIND TUNNELS
NT SUBSONIC WIND TUNNELS
NT SUPERSONIC WIND TUNNELS
NT TEST RANGES

NT TEST STANDS
NT TRANSIENT REACTOR TEST FACILITY
NT TRANSONIC WIND TUNNELS
NT TRISONIC WIND TUNNELS
NT WIND TUNNELS

High precision ultrasonic scanning system and SAFT-UT development
[DE87-010038] 01 p0008 N88-10044

Switching devices used in the Lethality Test System
[DE87-011734] 01 p0011 N88-10062

Anechoic Chamber test of the Electromagnetic Measurement System ground test unit
[DE87-012998] 01 p0035 N88-10226

Fourteenth Space Simulation Conference: Testing for a Permanent Presence in Space
[NASA-CP-2446] 02 p0132 N88-10829

Surveillance systems test and evaluation facilities
02 p0134 N88-10845

High intensity 5 eV O-atom exposure facility for material degradation studies 02 p0135 N88-10847

A digital control system for high level acoustic noise generation 02 p0138 N88-10865

Experiments: Test range facilities, part 2
03 p0305 N88-11921

The ac power system testbed
[NASA-CR-175068] 03 p0309 N88-11948

The LPX (Long Pulse Experiment) facility
[DE87-010493] 03 p0311 N88-11964

The LLNL 150-mm equation-of-state gun system
[DE88-000423] 04 p0405 N88-12519

Measured performance of the heat exchanger in the NASA icing research tunnel under severe icing and dry-air conditions
[NASA-TM-100116] 04 p0451 N88-12796

A survey of existing hypersonic ground test facilities: North America 05 p0529 N88-13220

High frequency data acquisition system for space shuttle main engine testing 05 p0595 N88-13630

An overview of the DOE/SANDIA/USDA vertical axis wind turbine Test Bed Project
[DE88-000604] 05 p0622 N88-13812

Feasibility study for gas-grain simulation facility
[NASA-CR-177468] 05 p0646 N88-13954

Atomic beam studies of the interaction of hydrogen with transition metal surfaces
[DE88-000208] 05 p0648 N88-13970

Aerodynamic testing of small turbines
06 p0713 N88-14371

Ground shock profiles for an accidental explosion at the proposed Large Rocket Test Facility at Arnold Engineering Development Center
[DE88-002652] 07 p0853 N88-15180

Long duration confinement of aquatic organisms in weightlessness (aquaspace) 07 p0887 N88-15380

Enhancement of computer system for applications software branch 07 p0923 N88-15610

Cavitation inception scale effects. 1. Nuclei distributions in natural waters. 2. Cavitation inception in a turbulent shear flow
[AD-A186553] 08 p0988 N88-15987

Calibration of the ARL (Aeronautical Research Laboratories) rain and icing facility
[AD-A186776] 09 p1121 N88-16710

ESA Bulletin No. 8
[ETN-87-90513] 09 p1122 N88-16718

Coordinated use of European test facilities
09 p1123 N88-16726

ESA Bulletin No. 10
[ETN-87-90514] 09 p1123 N88-16728

The European space battery test center
09 p1125 N88-16738

Major spacecraft hardware testing in Europe
09 p1125 N88-16740

Study on a double reflector compact range --- satellite antennas
[S-201-05] 09 p1153 N88-16908

The assessment of the sound insulation requirements for a large broadcasting studio, using a scale model: Theoretical considerations
[BBC-RD-1987/20] 09 p1155 N88-16921

NASDA's new test facilities for satellites and rockets
11 p1499 N88-18951

Robotics applications in the testing of inertial sensors
12 p1577 N88-19433

Cost effective development of a national test bed
[NASA-TM-100321] 12 p1601 N88-19585

Transient Pressure Test Article (TPTA) 1.1 and 1.1A, volume 1
[NASA-CR-179322-VOL-1] 12 p1603 N88-19588

Aircraft flight flutter testing at the NASA Ames-Dryden Flight Research Facility
[NASA-TM-100417] 13 p1723 N88-20301

Western aeronautical test range real-time graphics software package MAGIC
[NASA-TM-100425] 13 p1757 N88-20506

Overview of recent activities in the Heat Cycle Research Program
[DE88-005544] 13 p1795 N88-20738

Configuration management issues and objectives for a real-time research flight test support facility
[NASA-TM-100437] 13 p1813 N88-20832

Activities report of the Physics Department
[ETN-88-91985] 13 p1833 N88-20964

JPRS report: Science and technology. China
[JPRS-CST-87-038] 14 p1901 N88-21350

China constructing high-altitude test cell
14 p1901 N88-21351

Materials testing at cryogenic temperatures
[BU-359] 14 p1923 N88-21462

Test facilities of the structural dynamics branch of NASA Lewis Research Center
[NASA-TM-100800] 14 p1934 N88-21534

Procedures and requirements for testing in the Langley Research Center unitary plan wind tunnel
[NASA-TM-100529] 15 p2015 N88-22016

Small engine components test facility turbine testing cell
[NASA-TM-100887] 15 p2019 N88-22037

Investigation of aeroacoustic mechanisms by remote thermal imaging
[DE88-002612] 15 p2021 N88-22046

EMR (Electromagnetic Radiation) test facilities evaluation of reverberating chamber located at RADC (Rome Air Development Center), Griffiss AFB (Air Force Base), Rome, New York
[PB88-178827] 15 p2022 N88-22048

Investigations of test methodology for the stress loading facility
[PB88-166095] 15 p2022 N88-22049

Description of ground motion data processing codes, volume 2
[DE88-007137] 15 p2095 N88-22481

Requirements and cost considerations for a Combined Space Nuclear Reactor Test Facility
[DE88-006763] 15 p2132 N88-22719

Space directorate research and technology accomplishments for fiscal year 1987
[NASA-TM-100607] 15 p2153 N88-22854

Airworthiness and flight characteristics test of a ski assembly for the UH-60A Black Hawk helicopter
[AD-A191414] 16 p2162 N88-22895

Analysis and experiments concerning the performance and calibration of compact antenna-test ranges
[ISBN-9-09-001727-5] 16 p2188 N88-23048

Aerodynamic and Related Hydrodynamic Studies Using Water Facilities
[AGARD-CP-413] 16 p2200 N88-23125

Fast Algorithm Simulation and Test (FAST) facility
[AD-A191183] 16 p2252 N88-23457

Benefits of 20 kHz PMAD in a nuclear space station
17 p2398 N88-24256

Requirements and cost considerations for a combined space nuclear reactor test facility
17 p2401 N88-24277

Conceptual design of the SP-100 GES test site
17 p2402 N88-24284

Selection of a handling and maintenance option for the SP-100 ground engineering system test
17 p2402 N88-24285

SP-100 GES test site 17 p2417 N88-24375

Liquid metal testing at ETEC for the SP-100 program
17 p2428 N88-24446

SHaRE: Collaborative materials science research
[DE88-007175] 18 p2467 N88-24646

Safety aspects in design and operation practice of GKSS underwater simulation plant GUSI
19 p2698 N88-26037

Development of a model procedure for the determination of volume diffusion lengths by transient measurements on monocrystal silicon solar cells
[ETN-88-92119] 20 p2821 N88-26733

Vibrational impacts of hush house operation
[DE88-006983] 21 p2899 N88-27207

Development of a free electron laser user facility for the extreme ultraviolet
[DE88-007892] 21 p2953 N88-27541

Atmospheric turbulence research at DFVLR
[AGARD-R-752] 21 p2975 N88-27669

An outdoor test facility for the large-scale production of microalgae
[DE88-001146] 21 p2984 N88-27723

SP-100 Ground Engineering Systems: Test facility control systems
[DE88-009195] 21 p3015 N88-27895

Unsteady water channel
[AD-A194231] 23 p3171 N88-28884

Lewis Research Center space station electric power system test facilities
[NASA-TM-100924] 23 p3182 N88-28942

Testing degradation of a sample under thermal cycling
[GB-PATENT-2-188-163-A] 23 p3227 N88-29206

Development and design of windtunnel and test facility for RPV (Remote Piloted Vehicle) enhancement devices
[AD-A194842] 24 p3329 N88-29822

Design and development of a refueling test bed
[FTMS-RP-ER-011] 24 p3357 N88-29986

Numerical field model simulation of full scale fire tests in a closed spherical/cylindrical vessel
[AD-A195067] 24 p3359 N88-29998

Development and installation of an instrumentation package for GE F404 investigative testing
[AD-A196265] 24 p3376 N88-30107

The dynamics of transuranics and other radionuclides in natural environments, December 1985
[DE87-014456] 24 p3390 N88-30189

Maximum-likelihood multichannel deconvolution of P waves at seismic arrays
[AD-A194990] 24 p3391 N88-30191

TEST FIRING
NT STATIC FIRING

Results of the development motor 8 test firing
[GPO-78-692] 03 p0278 N88-11751

Failure control techniques for the SSME
[NASA-CR-179224] 04 p0409 N88-12537

Mechanical property evaluation of a series of commercial tungsten alloys
[AD-A185440] 05 p0565 N88-13446

Experimental investigation of a three-stage railgun incorporating puff-switching
[AD-A191044] 16 p2166 N88-22918

Orbital transfer vehicle 3000 LBF thrust chamber assembly hot fire test program
[NASA-CR-182145] 24 p3336 N88-29858

TEST PATTERN GENERATORS

Programmable Logic Arrays (PLA's) design for testability
[PB87-102935] 04 p0436 N88-12718

Short pseudorandom test sequences
[AD-A185883] 08 p1054 N88-16357

A new approach on test generation for array structures using the behavior of the system --- VLSI chips
[INF-87-27] 14 p1907 N88-21397

TEST RANGES
NT BALLISTIC RANGES

AFAR (Azores Fixed Acoustic Range) measurements of intensity and intensity moments
[AD-A184431] 03 p0355 N88-12237

The PC/AT compatible computer as a mission control center display processor at Ames-Dryden Flight Research Facility
[NASA-TM-100426] 14 p1955 N88-21654

Analysis and experiments concerning the performance and calibration of compact antenna-test ranges
[PB88-169263] 16 p2188 N88-23047

Radar cross section studies/compact range research
[NASA-CR-183124] 20 p2792 N88-26565

Development of procedures for performing end-to-end tests on the ERS-1 radar altimeter and AMI using a compact antenna test range --- Active Microwave Instrument (AMI)
[ESA-CR(P)-2558] 24 p3363 N88-30022

TEST STANDS

Requirements for a test stand for plastic rollers for the verification of nonequilibrium force laws
[ILR-MITT-176] 01 p0008 N88-10040

Description of an oscillating flow pressure drop test rig
[NASA-TM-100905] 16 p2170 N88-22933

Identification of lateral operation dynamics of rail vehicles using roll test stand tests
20 p2787 N88-26534

Beam optics test stand
[AD-A193901] 23 p3216 N88-29144

TEST VEHICLES

Vehicle dynamics: Identification in the frequency domain 20 p2785 N88-26523

TESTERS
U TEST EQUIPMENT

TESTES

Investigation of genetic structures of rat germ cells following flight aboard Cosmos-1514 biosatellite during their prenatal development 10 p1364 N88-18155

TESTING
U TESTS

TESTING MACHINES
U TEST EQUIPMENT

TESTS

Fire-related standards and testing
04 p0406 N88-12522

Announced United States nuclear tests: July 1945 through December 1986
[NVO-209-REV-7] 11 p1546 N88-19247

The design and fabrication of a Stirling engine heat exchanger module with an integral heat pipe
[NASA-TM-101296] 20 p2620 N88-26732

TETHERED SATELLITES
Research on Electrodynamic Tether Effects (RETE) experiment Electrical Ground Support Equipment (EGSE) --- tethered satellite
[IFSI-87-2] 05 p0555 N88-13378
RETE experiment Assembly, Integration, and Verification (AIV) activities
[IFSI-87-6] 05 p0555 N88-13380
Tethers in space handbook
[NASA-CR-181371] 06 p0673 N88-14123
Laboratory simulation of the electrodynamic interactions of a tethered satellite with an ionospheric plasma
[IFSI-86-3] 08 p0961 N88-15822
Tethers: An outline of a new concept for Earth observation 09 p1129 N88-16781
Kinetic isolation tether experiment
[NASA-CR-182458] 09 p1135 N88-16810
Deployable/retrievable boom: One application to tethered satellite 14 p1874 N88-21197
Analytical investigation of the dynamics of tethered constellations in earth orbit
[NASA-CR-179371] 23 p3184 N88-28950
TETHERING
Phase 3 study of selected tether applications in space. Volume 2: Study results
[NASA-CR-1791d6] 02 p0132 N88-10828
Electrodynamic tether system study
[NASA-CR-172024] 03 p0275 N88-11737
Hollow cathode plasma coupling study, 1986
[NASA-CR-171985] 03 p0309 N88-11949
Analytical investigation of the dynamics of tethered constellations in Earth orbit (phase 2)
[NASA-CR-179218] 04 p0408 N88-12533
Tethers in space handbook
[NASA-CR-181371] 06 p0673 N88-14123
Tether Elevator Crawler Systems (TECS)
07 p0927 N88-15631
Plasma contactors for use with electodynamic tethers for power generation
[NASA-CR-182424] 08 p1087 N88-16547
Kinetic isolation tether experiment
[NASA-CR-182458] 09 p1135 N88-16810
General equilibrium characteristics of a dual-lift helicopter system
[NASA-TP-2615] 12 p1573 N88-19407
Space plasma contactor research, 1987
[NASA-CR-182148] 16 p2280 N88-23649
Study of Plasma Motor Generator (PMG) tether system for orbit reboost
[NASA-CR-172074] 23 p3184 N88-28949
Analytical investigation of the dynamics of tethered constellations in earth orbit
[NASA-CR-179371] 23 p3184 N88-28950
TETHERLINES
Study of Plasma Motor Generator (PMG) tether system for orbit reboost
[NASA-CR-172016] 04 p0403 N88-12501
Tethers in space handbook
[NASA-CR-181371] 06 p0673 N88-14123
Power and charge dissipation from an electrodynamic tether 06 p0795 N88-14869
Theoretical investigation of EM wave generation and radiation in the ULF, ELF and VLF bands by the electrodynamic orbiting tether
[NASA-CR-182720] 13 p1760 N88-20529
Power transmission studies for tethered SP-100
[NASA-TM-100864] 14 p1883 N88-21251
Tethered diagnostic package for use from the space station
[DE88-006264] 16 p2167 N88-22921
Technologies applicable to space tethers
[NASA-CR-183055] 19 p2606 N88-25471
TETRAGONS
NT RECTANGLES
NT RHOMBOIDS
TETRANITROTETRAZACYCLOOCTANE
U HMX
TETRYL
A comparative assessment of US and UK explosives qualified as replacements for tetryl
[MRL-R-1094] 13 p1754 N88-20486
Recommended replacements for tetryl in Australian production fuzes and related ordnance
[MRL-R-1089] 13 p1754 N88-20489
TEXAS
Calendar year 1985 solar and weather data for Austin, Texas
[PB87-220174] 03 p0352 N88-12219
An overview of the DOE/SANDIA/USDA vertical axis wind turbine Test Bed Project
[DE88-000604] 05 p0622 N88-13812
TEXTBOOKS
Bibliography of textbooks on fibre reinforced plastics (212 books)
[PB87-146080] 07 p0827 N88-15017
TEXTILES
Solid state C-13 NMR characterization of textiles: Qualitative and quantitative analysis
[AD-A184349] 04 p0419 N88-12598
The role of textile material in clothing on thermoregulatory responses to intermittent exercise
[AD-A192599] 22 p3130 N88-28608
TEXTS
Stress effects and the optimum format of a scrolling seven-line VDT text window
[AD-A185559] 06 p0758 N88-14651
Extraction of texts and symbols from unstructured vector data --- mapping 16 p2225 N88-23287
TEXTURES
Cloud cover determination in polar regions from satellite imagery
[NASA-CR-181544] 04 p0471 N88-12908
The effect of texture on the crack growth resistance of alumina
[NASA-TM-100250] 06 p0686 N88-14206
The microstructure and texture of torsion-reverse torsion experiments
[DE88-001801] 06 p0721 N88-14434
Texture study of Synthetic Aperture Radar (SAR) images of ocean surfaces
[AD-A186021] 07 p0841 N88-15101
Textural features for image classification in remote sensing
[INPE-4169-PRE/1066] 08 p1020 N88-16181
A texture analysis approach to computer vision for identification of roads in aerial photographs
[AD-A189340] 12 p1639 N88-19815
Texture profile in thermomechanically processed 2-inch-thick 5 Ni-steel armor plate
[AD-A189275] 13 p1741 N88-20410
Micromechanical and microstructural studies of ceramic superplasticity
[DE88-005793] 13 p1751 N88-20472
A symmetric set of Euler angles and oblique orientation space sections
[DE88-005317] 13 p1847 N88-21056
Materials dependence of deformation texture development in various deformation modes
[DE88-004312] 14 p1922 N88-21457
Finding texture boundaries in images
[AD-A190554] 15 p2117 N88-22609
Investigation into the use of texturing for real-time computer animation
[AD-A191008] 16 p2251 N88-23454
Textural features for image classification in remote sensing 17 p2354 N88-24027
Remote sensing and structural rupture: Application examples in the study of tectonics
17 p2359 N88-24050
Shape from shading, occlusion and texture
[AD-A184840] 18 p2571 N88-25269
Texture perception and shape from texture
[AD-A192923] 21 p2996 N88-27771
Evaluation of automatic texture analysis for increased crop identification accuracy with SPOT data
22 p3094 N88-28373
TF-30 ENGINE
Fuel property effects on the US Navy's TF30 engine
24 p3345 N88-29911
TF-34 ENGINE
Knowledge based jet engine diagnostics
09 p1203 N88-17210
Noise assessment of unsuppressed TF-34-GE-100A engine at Warfield ANG, Baltimore, Maryland
[AD-A189966] 15 p2129 N88-22702
TFX AIRCRAFT
U F-111 AIRCRAFT
THAILAND
Thailand in maps. Application of the mapping system THEMAK2 for specific purpose atlas preparation
16 p2226 N88-23295
THALAMUS
The interaction of thalamo-cortical systems in the 40 Hz following response 21 p2979 N88-27694
THALLIUM ALLOYS
Studies of transverse phonon modes in premartensitic indium-thallium alloys
[DE88-003481] 13 p1744 N88-20428
THALLIUM COMPOUNDS
Non-linear materials (TAS)
[AD-A189197] 12 p1633 N88-19775
THAWING
U MELTING
THEMATIC MAPPERS (LANDSAT)
LANDSAT thematic mapper radiometric calibration study
[NASA-CR-182410] 07 p0872 N88-15287
Thematic mapper research in the earth sciences: Small scale patches of suspended matter and phytoplankton in the Elbe River Estuary, German Bight and Tidal Flats
[NASA-CR-182378] 08 p1019 N88-16180
Evaluation of the flooding areas of the Sao Goncalo Canal through LANDSAT 5 thematic mapper images
[INPE-4118-PRE/1039] 08 p1020 N88-16185
Detection of soil erosion with Thematic Mapper (TM) satellite data within Pinyon-Juniper woodlands
[NASA-CR-182476] 09 p1185 N88-17103
Land-use classification in a region north-west of Wuerzburg (Federal Republic of Germany) using digital, multispectral LANDSAT 5 Thematic Mapper data
[DFVLR-FB-87-37] 14 p1940 N88-21579
Method for restoration and resampling of TM sensor imagery
[INPE-4491-PRE/1255] 15 p2090 N88-22454
Turbidity patterns in the delta waters of southwest Netherlands on Thematic Mapper (TM) and multispectral scanner (MSS) satellite images
[BCRS-86-06] 16 p2227 N88-23303
The use of LANDSAT-TM pictures for the detection of space-limiting elements for the benefit of landscape photomapping
[BCRS-87-02] 16 p2228 N88-23305
Evaluation of an estimation system for an irrigated area in a tropical region through TM-LANDSAT imagery
17 p2363 N88-24075
Study of the Arachon (France) underwater delta using Thematic Mapper data 19 p2702 N88-26064
Digital and visual analysis of SPOT and TM data for crop discrimination in southern Brazil
22 p3096 N88-28385
A comparison between SPOT and LANDSAT TM for mapping of vegetation and bedrock outcrops
22 p3100 N88-28409
Accuracy of land use classification for SPOT image data 22 p3100 N88-28410
An evaluation of the utility of SPOT and Thematic Mapper data for providing forest inventory information
22 p3106 N88-28444
Evaluation of SPOT data for remote sensing of physical and biological properties of estuaries and coastal zones
22 p3108 N88-28458
TM/LANDSAT-5 data to evaluate wheat and bean percent soil cover and leaf area index
[INPE-4609-PRE/1332] 24 p3385 N88-30165
LANDSAT-TM data to map flooded areas
[INPE-4594-PRE/1324] 24 p3387 N88-30177
THEMATIC MAPPING
Remote sensing with LANDSAT 5 Thematic Mapper (TM) and its application to various planning levels: A case study from the Wuerzburg area, West Germany
[DFVLR-FB-86-62] 01 p0065 N88-10421
Development of a climatic map of rainfall attenuation for Europe
[REPT-372] 02 p0216 N88-11359
First assessment of processing and use of SPOT images by the Institut Geographique Nationale --- French National Geographic Institute 03 p0341 N88-12148
Evaluation of SPOT stereoscopic possibilities for cartography 03 p0342 N88-12156
Cartography and topography with SPOT
03 p0342 N88-12159
Vegetation classification, land systems and mapping using SPOT multispectral data: Preliminary results
03 p0342 N88-12160
The contribution of satellite data in drawing up maps used in rural development 03 p0343 N88-12167
A comparative thematic mapping analysis of SPOT data: The Vientiane Plain (Laos) 03 p0343 N88-12168
Applicability of SPOT for forest inventory, mapping and change monitoring 03 p0344 N88-12174
Evaluation of digital, multitemporal LANDSAT 5 thematic mapper data for the determination of the aerial snowcover extent and spectral separation of various surface types in the inner Oetztal (West Germany) with special regard to the significance of aerial snowcover information for water resources management
[DFVLR-FB-86-46] 03 p0345 N88-12180
New precipitation map of world ocean
04 p0458 N88-12834
Land cover/use classification of Cairns, Queensland, Australia: A remote sensing study involving the conjunctive use of the airborne imaging spectrometer, the large format camera and the thematic mapper simulator
05 p0612 N88-13759
Overview of Austrian Airborne Imaging Spectrometer (AIS) programme and first results
05 p0612 N88-13762
Mapping hydrothermally altered rocks in the Northern Grapevine Mountains, Nevada and California with the airborne imaging spectrometer 05 p0614 N88-13772
Use of space photographs for geomorphological studies in southwestern Tajikistan 08 p1008 N88-16109
Thematic mapper research in the earth sciences: Small scale patches of suspended matter and phytoplankton in the Elbe River Estuary, German Bight and Tidal Flats
[NASA-CR-182378] 08 p1019 N88-16180

Design and implementation of a data base system for Digital Land Mass System (DLMS) data
[FEL-IR-1987-19] 09 p1185 N88-17101

Mapping stellar surface features
09 p1262 N88-17564

Thematic mapper study of Alaskan ophiolites
[NASA-CR-182554] 11 p1504 N88-18984

An application of digital cartography updating middle and small scale thematic maps using orbital data
[INPE-4460-TDL/317] 12 p1637 N88-19805

Naval weapons center active fault map series
[AD-A188425] 12 p1643 N88-19835

Terrestrial gravity data and comparisons with satellite data 12 p1644 N88-19848

Inventory of topographic mapping and standardization of geographic names as the basis of a Geographic Information System (GIS) 16 p2225 N88-23281

Developments in the design of topographic maps in the Federal Republic of Germany: Activities and suggestions
16 p2226 N88-23290

The atlas of regional development
16 p2226 N88-23291

The use of LANDSAT-TM pictures for the detection of space-limiting elements for the benefit of landscape photomapping
[BCRS-87-02] 16 p2228 N88-23305

Latin American Symposium on Remote Sensing. 4th Brazilian Remote Sensing Symposium and 6th SELPER Plenary Meeting, volume 1 17 p2352 N88-24013

Utilization of TM/LANDSAT images in the implanted forests mapping in the Mogi-Guacu Region (SP-Brazil)
17 p2357 N88-24042

Thematic mapping utilizing data from the Thematic Mapper sensor of the LANDSAT satellite
17 p2361 N88-24060

Geometric image correction: An approach for the registration of LANDSAT-TM digital images supported by topographical maps of medium and great scales
17 p2361 N88-24061

Generation of thematic maps for updating aeronautical pilot charts utilizing LANDSAT-TM images
17 p2361 N88-24062

Utilization of LANDSAT-TM , for aiding in the localization of archeological sites in the state of Sao Paulo
17 p2362 N88-24069

Interpretation of MSS/LANDSAT data for evaluation of physical distribution of mangroves in Cananeia-Iguape (SP) 17 p2363 N88-24072

Utilization of LANDSAT-TM imagery in the hydroenergetic inventory of the Paraiba do Sul River Basin 17 p2364 N88-24077

Evaluation of a flood period (June, 1984) in the southern region of Laguna dos Patos, through remote sensing data, meteorological and oceanographic
17 p2365 N88-24083

Evaluation of the mangrove area at the Piaui River (SE) through remote sensing 17 p2365 N88-24086

Evaluation of TM false color composites for crop discrimination 17 p2367 N88-24096

Presentation of map information on a color display
[FOA-C-20687-2.7] 17 p2368 N88-24103

Mapping of land use in Sao Jose dos Campos municipality by remote sensing, an aid for the elaboration of its PDDI 19 p2681 N88-25940

Technique to obtain the agricultural ownership limits by satellite imagery, to approve control, and to accompany agricultural activity 19 p2682 N88-25943

The use of satellite imagery for municipal conditions in rural recording in Pereira Barreto (SP)
19 p2682 N88-25944

Use of remote sensing in the study of superficial formation certifying the development of integrated economy-case example: Rio Claro (SP) region
19 p2683 N88-25950

Canopy reflectance modeling in a tropical wooded grassland
[NASA-CR-182981] 19 p2685 N88-25961

Study of the Arachon (France) underwater delta using Thematic Mapper data 19 p2702 N88-26064

Development of automatic names placement software
[AD-A192786] 21 p2996 N88-27770

Mapping of streamflow and soil infiltration of a Sahelian catchment area by SPOT image interpretation: The Oursi pond catchment area in Burkino Faso
22 p3090 N88-28348

Comparison between the respective contributions of the TM LANDSAT-4 and HRV SPOT-1 data to the land use mapping of Mediterranean coastal zone
22 p3092 N88-28363

Delineation of ephemeral fluvial networks on low-relief Piedmont surfaces, Plutonium Valley, Nevada, USA
22 p3093 N88-28367

Use of SPOT imagery for vegetation/biomass mapping, geotechnical mapping, catchment area determination, and settlement location in the Turkana district, northern Kenya 22 p3096 N88-28384

A comparative thematic mapping analysis of SPOT data: The Vientiane Plain (Lao PDR)
22 p3096 N88-28386

Monitoring Tunisia's steppes with SPOT
22 p3097 N88-28390

Study of savannah formation in the Sudanian zone. Northwest sector of the La Comoe park, Ivory Coast
22 p3097 N88-28391

Agro-ecological mapping from SPOT 1 data in southern Thailand: New questions for an analysis of the farming-systems 22 p3097 N88-28394

A comparison between SPOT and LANDSAT TM for mapping of vegetation and bedrock outcrops
22 p3100 N88-28409

Thematic mapping of central Java (Indonesia)
22 p3100 N88-28412

Utilization of SPOT-1 multispectral data for mapping land cover and phytohygiene monitoring in the central zone of the Mercantour National Park (France)
22 p3100 N88-28413

Applications of SPOT data for urban real estate investment information systems
22 p3101 N88-28414

Mapping and urban multi-experimental assessment of SPOT: Urban results 22 p3101 N88-28415

SPOT imagery preliminary contribution to cartography and geodynamics in the Benue trough (Nigeria)
22 p3103 N88-28429

Forest mapping by visual interpretation of SPOT images 22 p3106 N88-28446

Contribution to the mapping of forests in an intensively divided area, with the help of SPOT image data
22 p3107 N88-28453

Contribution of SPOT satellite to qualitative and quantitative mapping of marine vegetation in the English Channel, North Altantic, western Mediterranean, and South Pacific 22 p3109 N88-28464

Relevance of a thematic map (SPOT data) with regards to the real flora and structure of the vegetation covering of salt marshes (Mont Saint Michel Bay, France)
22 p3109 N88-28468

The prospects for topographic mapping using SPOT data 22 p3110 N88-28470

The use of SPOT data for mapping and DEM production --- digital elevation model (DEM)
22 p3110 N88-28475

Evaluation of SPOT cartographic capabilities over the Aix Marseille area (France) 22 p3110 N88-28476

Assessment of SPOT imagery for topographic revision and vegetation mapping 22 p3111 N88-28477

SEP/VIPS 32 geographic information system. Processing and thematic analysis of images, maps, and associated data 22 p3114 N88-28499

Spectral characteristics and the extent of paleosols of the Palouse formation
[NASA-CR-180947] 23 p3228 N88-29210

THEODOLITES

Optical alignment of Centaur's inertial guidance system
[NASA-TM-88844] 04 p0405 N88-12515

THEOREM PROVING

A note on compactifications of products of semigroups
[CWI-PM-R8701] 08 p1072 N88-16469

A proof rule process creation
[CWI-CS-R8710] 13 p1822 N88-20691

About disequations simplification
[RR-645-I-IMAG-55-LIFIA] 15 p2119 N88-22624

Correctness proofs for systolic algorithms: A palindrome recognizer
[CWI-CS-R8747] 16 p2248 N88-23434

On a classification of problems on sets of bilinear forms by formal polynomials
[RR-642-I-IMAG-53-LIFIA] 17 p2392 N88-24219

Challenge problems focusing on equality and combinatory logic: Evaluating automated theorem-proving programs
[DE88-010057] 20 p2844 N88-26879

THEOREMS

NT BAYES THEOREM
NT BERNOULLI THEOREM
NT DUALITY THEOREM
NT EXISTENCE THEOREMS
NT GAUSS-MARKOV THEOREM
NT LAGRANGE SIMILARITY HYPOTHESIS
NT LEBESGUE THEOREM
NT LIOUVILLE THEOREM
NT POYNTING THEOREM
NT RECIPROCAL THEOREMS
NT RECIPROCITY THEOREM
NT SIMILARITY THEOREM
NT UNIQUENESS THEOREM

Homogeneous space-time of Goedel type in higher-derivate gravity
[DE87-703690] 04 p0500 N88-13077

Comment on the Adler-Bardeen theorem and related problems
[DE88-751051] 10 p1403 N88-18367

Nonlinear dynamic maximum power theorem
[AD-A187491] 11 p1477 N88-18810

A graph separator theorem and its application to Gaussian elimination to optimize Boolean expressions for parallel evaluation
[AD-A188527] 14 p1962 N88-21706

Decomposition of graphs on surfaces and a homotopic circulation theorem
[CWI-OS-R8719] 16 p2264 N88-23538

Comparison theorems and their use in the analysis of some nonlinear diffusion problems
[DE88-010032] 20 p2845 N88-26884

Challenge equality problems in lattice theory
[DE88-010094] 20 p2876 N88-27072

A Wong-Zakai type theorem for certain discontinuous semimartingales
[AD-A192713] 21 p3005 N88-27822

Ill-posed problems and integral equations
[AD-A193709] 22 p3143 N88-28691

THEORETICAL PHYSICS

NT BOHR THEORY
NT NEWTON THEORY
NT QUANTUM THEORY

Theoretical plasma physics
[DE88-001475] 04 p0492 N88-13029

Theoretical atomic and molecular physics
[DE88-001625] 05 pu649 N88-13974

JPRS report: Science and technology. USSR: Physics and mathematics
[JPRS-UPM-87-008] 06 p0769 N88-14727

Computers in theoretical physics
[DE88-700516] 07 p0941 N88-15720

Theoretical nuclear physics
[DE87-004504] 09 p1244 N88-17455

Activities report in nuclear physics
[ETN-88-91609] 09 p1245 N88-17458

Research in theoretical physics
[DE88-003201] 09 p1259 N88-17548

Research in theoretical physics: Results from last year 1986/87
[DE88-004922] 10 p1423 N88-18502

Theoretical studies in few-body intermediate energy physics
[DE88-004101] 12 p1669 N88-20106

Lie groups in prolongation theory
[B87217811] 14 p1967 N88-21743

On the Fefferman class of metrics associated with a 3-dimensional Cauchy-Riemann (CR)-space
[PREPRINT-579] 14 p1991 N88-21865

Theoretical plasma physics research of active space experiments
[AD-A192075] 18 p2577 N88-25309

Theoretical atomic and molecular physics
[DE88-007122] 19 p2724 N88-26175

Theoretical studies in elementary particle physics
[DE88-006929] 20 p2851 N88-26926

Research in theoretical particle physics
[DE88-008230] 20 p2851 N88-26927

Evidence for laser emission from the TICT exciplex of coumarin dyes
[DE88-702544] 23 p3220 N88-29167

Weak interaction physics: From its birth to the electroweak model
[DE88-702494] 23 p3260 N88-29531

Theoretical studies in high energy physics
[DE88-011606] 23 p3281 N88-29538

Theoretical particle physics
[DE88-011499] 23 p3295 N88-29621

Time travel in the homogeneous Som-Raychaudhuri universe
[DE88-702220] 23 p3295 N88-29622

Holomorphic geometry of interacting string
[DE88-702714] 23 p3295 N88-29627

Introduction to string theory
[DE88-702706] 24 p3435 N88-30445

THERAPY

NT CHEMOTHERAPY
NT RADIATION THERAPY

The effects of normal and therapeutic baths on the central vascular organs of persons with healthy hearts, as measured by X-ray
[NASA-TT-20252] 13 p1811 N88-20818

THERMAL ABSORPTION

Instability of strong-absorption domain in semiconductor 08 p1077 N88-16495

Isothermal measurement and thermal desorption using SAW devices 19 p2671 N88-25881

THERMAL AGITATION

U THERMAL ENERGY

THERMAL ANALYSIS
Effects of forced and free convections on structural temperatures of space shuttle orbiter during reentry flight
[NASA-TM-86800] 01 p0043 N88-10275
Evaluation of the infrared test method for the olympus thermal balance tests 02 p0136 N88-10856
Analysis of phase equilibria in NiTi-C system in high nickel regions
[BLL-M-37304-(5828.4)] 02 p0149 N88-10932
Flammability limits in cocurrent smoldering combustion
[DE87-014102] 03 p0284 N88-11785
Comparison of flight-measured and calculated temperatures on the space shuttle orbiter
[NASA-TM-88278] 03 p0321 N88-12029
Thermal analysis of electromagnetic launcher rails
[DE88-000166] 04 p0405 N88-12514
A two-dimensional finite difference program for thermal analysis of rocket thrust chambers
[NASA-TM-100191] 04 p0409 N88-12539
Synthesis of the monoclinic yttria by thermal plasma processing
[DE88-000496] 04 p0421 N88-12608
Light funnel concentrator panel for solar power
[NASA-CR-179223] 04 p0464 N88-12670
Space station systems: A bibliography with indexes
[NASA-SP-7056(05)] 05 p0556 N88-13382
Development of an integrated BEM approach for hot fluid structure interaction
[NASA-CH-181577] 05 p0556 N88-13384
Investigation by differential scanning calorimetry of microstructure in a superplastic Al-Mg-Zr alloy
[AD-A184902] 05 p0564 N88-13439
Thermal finite-element analysis of space shuttle main engine turbine blade
[NASA-TM-100117] 05 p0610 N88-13745
Modeling of thermal effects on TIBER 2 (Thermal Ignition/Burn Experimental Reactor) divertor during plasma disruptions
[DE88-001893] 06 p0783 N88-14805
A numerical thermal model of the rapid solidification parameters in the capacitor discharge welding process
[DE88-002206] 07 p0864 N88-15244
Development of an emulation-simulation thermal control model for space station application
[NASA-CR-182409] 08 p0962 N88-15823
Space Infrared Telescope Facility (SIRTF) design and thermal analysis 08 p0982 N88-15934
Thermal analysis for the Cryogenic Fluid Management Flight Experiment (CFMFE) 08 p0982 N88-15935
Analytical interactive approach for phenomena involving structures, thermal and control aspects. Volume 1: Theory --- spacecraft structures
[ESA-CR(P)-2503-VOL-1] 09 p1134 N88-16803
Analytical interactive approach for phenomena involving structures, thermal, and control aspects. Volume 2: Toward the solution --- spacecraft structures
[ESA-CR(P)-2503-VOL-2] 09 p1134 N88-16804
Analytical interactive approach for phenomena involving structures, thermal, and control aspects. Volume 3: Executive summary --- spacecraft structures
[ESA-CR(P)-2503-VOL-3] 09 p1134 N88-16805
Review of thermal properties of graphite composite materials
[NASA-TM-100049] 09 p1139 N88-16825
Thermal wave imaging
[AD-A186810] 09 p1177 N88-17046
EXPLO: Explosives thermal analysis computer code
[DE88-001938] 10 p1307 N88-17814
Thermal analysis of transistor packages, part 2
[DE88-005091] 10 p1323 N88-17909
Microcomputer analysis of regenerative heat exchangers for oscillating flow
[DE88-001773] 10 p1329 N88-17945
Simple renormalization group method for calculating thermal equations of states
[DE88-700143] 11 p1454 N88-18668
Effect of element size on the solution accuracies of finite-element heat transfer and thermal stress analyses of space shuttle orbiter
[NASA-TM-88292] 11 p1502 N88-18371
Thermal analysis in steady state conditions for satellites
[INPE-4429-TDL/309] 12 p1599 N88-19574
Thermal properties of soil: A case study
[INPE-4332-TDL/289] 12 p1637 N88-19803
Fluid-thermal-structural study of aerodynamically heated leading edges
[NASA-TM-100579] 13 p1783 N88-20666
Analysis of shell-type structures subjected to time-dependent mechanical and thermal loading
[NASA-CR-182705] 13 p1783 N88-20668
Investigation of Super*Zip separation joint
[NASA-TM-4031] 15 p2026 N88-22072
Thermal analysis of heat storage canisters for a solar dynamic, space power system
[DE88-004199] 15 p2027 N88-22075
Boundary shape identification problems in two-dimensional domains related to thermal testing of materials
[NASA-CR-181654] 15 p2105 N88-22541
Thermal remote anemometer system
[NASA-CASE-LAR-13508-1] 17 p2342 N88-23962
Application of integrated fluid-thermal-structural analysis methods
[NASA-TM-100625] 17 p2350 N88-24001
Cermet fuel thermal conductivity
17 p2410 N88-24329
HTPIPE: A steady state heat pipe analysis program
17 p2421 N88-24396
A scientific basis for an alternate cathode architecture
[AD-A191496] 18 p2481 N88-24717
Evaluating evaporation with satellite thermal data
[AD-A192042] 18 p2531 N88-25019
Nondestructive evaluation methods for determination of thermal history and mechanical properties of aluminum-lithium alloys
[DE88-007352] 19 p2615 N88-25516
MHD (magnetohydrodynamic) thermal hydraulic analysis of three-dimensional liquid metal flows in fusion blanket ducts
[DE88-009929] 19 p2731 N88-26219
Thermal and mechanical analysis of the Faraday shield for the compact ignition tokamak
[DE88-007855] 20 p2856 N88-26962
Transient thermal analysis of three latent heat storage configurations for rapid thermal charging
[DE88-008943] 20 p2881 N88-27104
Transient thermal analysis of three fast-charging latent heat storage configurations for a space-based power system
[DE88-009714] 23 p3186 N88-28960
Adaptive computational methods for aerothermal heating analysis
[NASA-CR-181636] 23 p3212 N88-29115
Free electron lasers with small period wigglers
[DE88-011627] 23 p3218 N88-29156
Construction of gallium arsenide solar concentrator for space use
[AD-A194658] 23 p3230 N88-29222
An analysis of heat transfer after loss of primary coolant in the SP-100 reactor system
[AD-A194619] 23 p3281 N88-29539
Principles of the optical differential thermal analysis
[AD-A195951] 24 p3429 N88-30408
Evolution of thermal structure of Benguela upswelling system according to satellite and shipboard data
24 p3449 N88-30525

THERMAL BARRIERS (PLASMA CONTROL)
First and second harmonic ECRH experience at gyrotron frequencies at LLNL
[DE88-003998] 10 p1413 N88-18430
Hot electron diagnostics using X-ray imaging on GAMMA10 17 p2443 N88-24530
Thrust chamber thermal barrier coating techniques
[NASA-TM-100933] 16 p2476 N88-24690

THERMAL BATTERIES
A case study of the development of a military specification - zirconium powder for thermal batteries
[AD-A188751] 13 p1792 N88-20717
Considerations and measurements of latent-heat-storage salts for secondary thermal battery applications
[DE88-011091] 23 p3228 N88-29213

THERMAL BLOOMING
Models of high spatial frequency thermal blooming instabilities
[DE87-014280] 01 p0052 N88-10330
High spatial frequency thermal blooming instability: A linear stability analysis
[DE88-010711] 20 p2807 N88-26655

THERMAL BOUNDARY LAYER
Optical investigations of the thermal boundary layer in arc plasmas 18 p2578 N88-25313
Thermal models pertaining to continental growth
24 p3397 N88-30230

THERMAL BUCKLING
A comparison of experimental and calculated thin-shell leading-edge buckling due to thermal stresses
[NASA-TM-100416] 17 p2349 N88-23999

THERMAL CONDUCTIVITY
A numerical study of transient, thermally-conductive solar wind 01 p0115 N88-10738
Thermal resistance of contacting metal surfaces at helium temperatures
[BLL-RISLEY-TR-5500-(9091.9F)]
02 p0148 N88-10929
Development of highly porous calcium silicate hydrate materials with extremely low thermal conductivity
[BMFT-FB-T-86-164] 02 p0150 N88-10941
LLE review
[DE87-014468] 02 p0178 N88-11110
A heat transfer model for a heated helium airship
[AD-A183786] 03 p0259 N88-11629
Characterization and thermal conductivity of hot-pressed silicon carbide
[DKG-25] 03 p0292 N88-11834
Pump assisted heat pipe 03 p0319 N88-12018
Development of response models for the Earth Radiation Budget Experiment (ERBE) sensors. Part 1: Dynamic models and computer simulations for the ERBE nonscanner, scanner and solar monitor sensors
[NASA-CR-178292] 05 p0584 N88-13557
Methods and first results of plasma non-isothermal parameters measurements in meteor trails
06 p0737 N88-14531
A calorimeter for measuring the neutral beam power reaching the plasma
[DE88-001412] 07 p0937 N88-15691
Characteristics of thermooptical sound excitation in metals 08 p1076 N88-16486
Bistable cellular flames
[DE88-003074] 09 p1142 N88-16848
Characterization of transparent insulation materials --- solar energy absorbers
[ETN-88-91052] 09 p1163 N88-16970
EXPLO: Explosives thermal analysis computer code
[DE88-001938] 10 p1307 N88-17814
Influence of radiation and thermal conduction on temperature distribution in the thin wall of a hollow cylinder
[INPE-4428-TDL/308] 12 p1626 N88-19730
Effects of high temperature neutron irradiation on the physical, chemical and mechanical properties of fine-grained isotropic graphite 13 p1747 N88-20444
A segmented calorimeter for low-energy particle beams in space
[DE88-001806] 13 p1838 N88-20997
Guidelines for estimation and characterization of the thermo-mechanical properties of new optical materials
[DE88-004359] 13 p1840 N88-21010
Thermal model describing development of normal region in superconductor film carrying electric current
14 p1973 N88-21776
Thermal conductivity of oxide ceramics
[DE88-005842] 15 p2042 N88-22169
Material surface improvement by laser
15 p2051 N88-22217
Thermal conductivity, electrical conductivity and specific heat of copper-carbon fiber composite
[NASA-TT-20172] 16 p2172 N88-22948
Some aspects of the unified model of non-ideal high-parameter plasmas: Electron EOS and conduction coefficients 16 p2277 N88-23632
Optimisation of the thermoelectric figure of merit of modified silicon germanium alloys
[AD-A191347] 16 p2283 N88-23670
High-temperature thermal conductivity of a carbon-bonded carbon-fiber insulation
17 p2402 N88-24281
Uranium nitride fuel swelling and thermal conductivity correlations 17 p2409 N88-24327
Cermet fuel thermal conductivity
17 p2410 N88-24329
Development of a lightweight structure with load bearing capability and high thermal conductance
17 p2420 N88-24393
Consistent transport coefficients in astrophysics
[NASA-TM-101154] 17 p2451 N88-24560
On the magnetic structure and energy balance of EUV-emitting plasma in the quiet Sun
17 p2452 N88-24567
Analytic and numerical modeling of heat and material transport in electrical hypervelocity guns
[AD-A192178] 18 p2469 N88-24655
Thermal conductivity of hard anodized coatings on aluminum
[AD-A191755] 18 p2492 N88-24784
Thermophysical properties of argon
[DE88-010376] 19 p2613 N88-25509
Ceramic substrates for semiconductor applications reported: AlN substrates 19 p2633 N88-25621
AlN substrate applications 19 p2634 N88-25622
Thermal management of integrated microsensors
19 p2670 N88-25875
Ion thermal conductivity and ion distribution function in the banana regime
[IPPJ-865] 19 p2729 N88-26208
Thermal conductivity of selected foams and systems from 100 to 300 K
[PB88-201553] 20 p2777 N88-26466
An experimental investigation of transient characteristics in a gravity-assisted heat pipe 20 p2783 N88-26506
Boundary element method for contact heat transfer
[DE88-011013] 20 p2800 N88-26613

Physical-chemical reactions at welding arc/molten pool interfaces
[DE88-007717] 20 p2808 N88-26662
Thermal conductivity of pure fluids in a large region around the critical point
[ETN-88-92135] 20 p2881 N88-27103
Thermal conductivity and thermal expansion of stainless steels D9 and HT9
[DE88-011973] 21 p2916 N88-27306
Ceramic technology for advanced heat engines project
[DE88-008945] 21 p2919 N88-27323
Studies of dynamic contact of ceramics and alloys for advanced heat engines
[DE88-008996] 21 p2919 N88-27324
Data compilation for radiation damage on ceramic insulators. Revised with updated data and reviews
[DE88-753426] 21 p2920 N88-27329
Determination of radiative properties of fiberglass and foam insulations
[DE88-007845] 21 p2920 N88-27331
Deformation, fracture and explosive properties of reactive materials
[AD-A193080] 21 p2923 N88-27348
Thermal conductivity of isotopically pure semiconductors, superlattices, semiconductor alloys and semiconductors as a function of temperature; control of the segregation coefficient in LEC crystal growth; and photo-Hall measurements of GaAs
21 p2927 N88-27375
Coupled thermal vibrations of beams with temperature-dependent properties
21 p2963 N88-27601
Measurement of the thermal conductivity of dielectric thin solid films with a thermal comparator
[DE88-008468] 21 p3016 N88-27898
The thermal conductivity of dirty type 2 superconductors
[B8881488] 23 p3294 N88-29615
Viking Landers and remote sensing
23 p3304 N88-29685

THERMAL CONTROL COATINGS
Thermal expansion mismatch and oxidation in thermal barrier coatings 02 p0189 N88-11182
The study of excited oxygen molecule gas species production and quenching on thermal protection system materials
[NASA-CR-172027] 02 p0233 N88-11470
Discharge prevention of geosynchronous orbit conductive thermal control materials and grounding systems 03 p0274 N88-11732
Low Earth orbit environmental effects on the space station photovoltaic power generation systems
[NASA-TM-100230] 03 p0387 N88-12429
Space environmental considerations for a long-term cryogenic storage vessel 08 p0981 N88-15933
Strength and failure rate of composite materials with carbon in ceramic matrix 16 p2180 N88-22995
Evaluation of ceramic thermal barrier coatings for gas turbine engine components
[ETN-88-91947] 16 p2181 N88-22998
Space vehicle/nuclear reactor thermal radiation integration issues 17 p2424 N88-24417

THERMAL CONVECTION
U FREE CONVECTION

THERMAL CURRENTS
U CONVECTIVE FLOW

THERMAL CYCLING TESTS
Contributions to the investigation of mechanical behavior of gamma/gamma NbC Cotac composites at medium and at high temperature
[ESA-TT-1031] 03 p0280 N88-11760
Effect of long-term thermal aging on coated Celion/LARC-160 composites
[NASA-TM-100495] 04 p0410 N88-12544
Stress intensity factors for cracking metal structures under rapid thermal loading, phase 1
[AD-A184112] 05 p0591 N88-13606
The effect of thermal shock on carbon fiber epoxy composites
[FOA-C-20675-2.6] 08 p0965 N88-15841
Cost 501 Project UK10 part 3: Thermal fatigue damage of Fecralloy steel-sprayed and co-extruded tubing
[AERE-R-12230] 10 p1343 N88-18026
Dynamic tensile cyclic fatigue of Si3N4
[DE88-003919] 13 p1781 N88-20658
Overview of recent activities in the Heat Cycle Research Program
[DE88-005544] 13 p1795 N88-20738
Effect of nonuniform state of thermal stress on resistance of EI826 alloy to thermal fatigue
14 p1895 N88-21313
Some structural aspects of crack propagation in heat-resistant steels under cyclic thermal and mechanical load 14 p1896 N88-21317
A fundamental understanding of the interfacial compatibility in hybrid material systems
[AD-A192921] 21 p2909 N88-27264
Thermal cycling tests on surface-mount assemblies
[DE88-007695] 21 p2939 N88-27453
Testing degradation of a sample under thermal cycling
[GB-PATENT-2-188-163-A] 23 p3227 N88-29206

THERMAL DECOMPOSITION
NT PYROLYSIS
Surface modification by metal deposition and laser irradiation 01 p0023 N88-10148
Low temperature reactivity of chars towards oxygen, appendix E2
[DE88-004088] 10 p1298 N88-17760
Kinetics of polymer decomposition
[DE88-005500] 13 p1749 N88-20460
Analytically modeling the carbothermic reduction of alumina in a thermal plasma
[DE88-005535] 13 p1841 N88-21020
Analysis of thermal and radiation effects in materials using the GEMAT process 17 p2408 N88-24318
Thermal decomposition studies of explosives for component applications
[DE88-007201] 18 p2495 N88-24805
Kinetic measurements of thermal decomposition of energetic materials at high pressures
[AD-A191612] 19 p2622 N88-25552
Pressure differential scanning calorimetry (DSC) evaluation of solid rocket propellant burn rate mod
19 p2631 N88-25606
Simultaneous thermogravimetric modulated beam mass spectrometry and time-of-flight velocity spectra measurements: Thermal decomposition mechanisms of RDX and HMX 19 p2632 N88-25612
Laser-RDX aerosol pyrolysis with matrix isolation of unstable intermediates 19 p2632 N88-25614
Theoretical studies of the chemical reactions involved in the ignition of nitramines 19 p2632 N88-25615

THERMAL DEFOCUSING
U THERMAL BLOOMING

THERMAL DEGRADATION
Behavior of graphites under intense heat loads
[DE87-012128] 01 p0028 N88-10179
Thermo-optical modeling of flashlamp-pumped zig-zag slabs
[DE87-011878] 01 p0051 N88-10326
Glassy GeO2 obtained by the gel process
[NASA-TT-20125] 06 p0685 N88-14201
Kinetics and mechanism of thermal aging embrittlement of duplex stainless steels
[DE88-002987] 08 p0969 N88-15866
Shelf life degradation of selected anaerobic threadlocking adhesives at various storage temperatures
[AD-A187712] 11 p1461 N88-18711
Degradations of thermal shock resistance and the fracture toughness of reactor graphite subjected to neutron irradiation 13 p1747 N88-20445
Interfacial chemistry-structure and fracture of ceramic composites
[DE88-005516] 13 p1750 N88-20461
On the use of thermal degradation data to predict cable ignition performance
[DE88-002276] 19 p2621 N88-25549
Antimisting kerosene: Low temperature degradation and blending
[NASA-CR-182725] 20 p2781 N88-26495
T55-L-714 engine development and qualification. Engine M11 low cycle fatigue test report. (0213-005-87)
[AD-A192765] 21 p2897 N88-27197
Aging of CFRP due to longterm storage in heated air
[DFVLR-FB-88-05] 21 p2922 N88-27345
Perfluoropolyalkylether lubricants under boundary conditions: Iron catalysis of lubricant degradation
[AD-A193241] 21 p2956 N88-27560
Testing degradation of a sample under thermal cycling
[GB-PATENT-2-188-163-A] 23 p3227 N88-29206

THERMAL DIFFUSION
Transient development of stratification in a partially divided enclosure
[DE87-011742] 05 p0572 N88-13490
Influence of fast alpha diffusion and thermal alpha buildup on Tokamak reactor performance
[DE88-003661] 09 p1251 N88-17496
Plasma confinement calculations for TIBER-2
[DE88-004044] 10 p1412 N88-18425
Interaction of a strong vortex with decaying turbulence
[DE88-007102] 14 p1911 N88-21420
Heating at a propagating crack tip in a viscoplastic material
[AD-A190952] 16 p2224 N88-23274
The structure and stability of spherically expanding flames 17 p2318 N88-23842
High spatial frequency thermal blooming instability: A linear stability analysis
[DE88-010711] 20 p2807 N88-26655
Numerical calculations of dopent diffusion involving flashlamp heating of silicon 21 p2929 N88-27384
Heat and mass transfer in a transport channel
[DE88-701968] 21 p2945 N88-27493
Time-dependent thermal convection of Earth mantle and double diffusive convection in magma chambers
[MITT-52] 21 p2974 N88-27663

THERMAL DIFFUSIVITY
Analysis of energy confinement of slideaway discharges
[DE87-753008] 02 p0240 N88-11515
Thermal wave imaging
[AD-A186810] 09 p1177 N88-17046
Effect of experimental variables on flash thermal diffusivity data analysis
[DE88-003631] 11 p1487 N88-18877
Thermophysical properties of argon
[DE88-010376] 19 p2613 N88-25509

THERMAL DISSOCIATION
Quantitative determination of a hydrogen impurity in a sodium coolant by hydride thermal dissociation
[NASA-TT-20239] 13 p1740 N88-20402

THERMAL EFFECTS
U TEMPERATURE EFFECTS

THERMAL EFFICIENCY
U THERMODYNAMIC EFFICIENCY

THERMAL EMISSION
NT THERMIONIC EMISSION
Thermal atmospheric models
02 p0253 N88-11599
Microwave observations of nonthermal phenomena in pre-main sequence stars 04 p0505 N88-13107
Unsteady heat transfer in turbine blade ducts: Focus on combustor sources
[NASA-TM-100815] 11 p1486 N88-18870
Stratospheric trace gas distributions from far infrared thermal emission spectroscopy
13 p1797 N88-20749
Arc-textured metal surfaces for high thermal emittance space radiators
[NASA-TM-100894] 18 p2487 N88-24754
Gamma rays from Cygnus X-1: Modeling and nonthermal pair production
[DE88-006830] 18 p2596 N88-25426
Anomalous emissivity from periodic micro-machined silicon surfaces 19 p2670 N88-25872
An objective technique for Arctic cloud analysis using multispectral AVHRR (Advanced Very High Resolution Radiometer) satellite imagery
[AD-A194732] 23 p3235 N88-29250

THERMAL ENERGY
Physical design of parameters of Nd:YAG disk laser
03 p0302 N88-11904
Heats of mixing for thermal energy storage systems. Phase 1: Selection of suitable liquid-liquid mixtures
[DE87-014971] 03 p0347 N88-12196
The numerical and analytical study of bifurcation and multicellular flow instability due to natural convection between narrow horizontal isothermal cylindrical annuli at high Rayleigh numbers 10 p1328 N88-17937
Determination of atmospheric moisture structure from high resolution MAMS radiance data
11 p1515 N88-19049
An assessment methodology for thermal energy storage evaluation
[DE88-004642] 13 p1794 N88-20732
Direct conversion of solar energy to thermal energy
[BMFT-FB-T-86-220] 14 p1943 N88-21592
Storage of thermal energy by means of an absorption cycle
[PB88-190814] 21 p2966 N88-27619
Thermal energy storage
[DE88-010753] 21 p2967 N88-27625

THERMAL ENERGY STORAGE
U HEAT STORAGE

THERMAL ENVIRONMENTS
Fourteenth Space Simulation Conference: Testing for a Permanent Presence in Space
[NASA-CP-2446] 02 p0132 N88-10829
Integration of symbolic and algorithmic hardware and software for the automation of space station subsystems
[NASA-TM-89705] 07 p0907 N88-15497
MARCE data evaluation 10 p1286 N88-17663
Characteristics of the thermal environment
[AD-A188359] 12 p1641 N88-19827
The role of water in the thermal balance of the coma
14 p1999 N88-21916
Integration of symbolic and algorithmic hardware and software for the automation of space station subsystems
17 p2387 N88-24190
Variability in intake and dehydration in young men during a simulated desert walk
[AD-A192654] 22 p3131 N88-28613
Experimental and analytical study of two-phase flow in zero gravity
[AD-A195223] 24 p3358 N88-29993

THERMAL EXPANSION
The effect of bromination of carbon fibers on the coefficient of thermal expansion of graphite fiber-epoxy composites
[NASA-TM-100236] 02 p0143 N88-10899
Carbon-fiber reinforced plastics
04 p0403 N88-12506
Study of zero CTE (Coefficients of Thermal Expansion) of graphite/epoxy composites
[DE87-013557] 04 p0412 N88-12554
Thermal expansion of some Ge-Se-Te glasses
[PD-MT-8722] 04 p0420 N88-12606
Advanced materials for solid oxide fuel cells
[DE88-002338] 10 p1350 N88-18071
The effects of various conductor components on Nb3Sn filament prestrain in cable-in-conduit conductors
[DE88-003956] 11 p1479 N88-18824
Determination of the equilibrium concentration of characteristic defects by the measurement of thermal expansion using neutron scattering and laser interferometry
[ETN-88-91489] 11 p1490 N88-18890
Properties fo seals made with Li2O-Al2O3-SiO2-glass ceramics and aluminum-containing austenitic stainless steels
[DE88-004688] 12 p1633 N88-19776
Effects of high temperature neutron irradiation on the physical, chemical and mechanical properties of fine-grained isotropic graphite 13 p1747 N88-20444
Guidelines for estimation and characterization of the thermo-mechanical properties of new optical materials
[DE88-004359] 13 p1840 N88-21010
Thermal deformation and strength of composite materials at high temperatures 14 p1885 N88-21263
Materials testing at cryogenic temperatures
[BU-250] 14 p1923 N88-21462
Thermally stable deployable structure
14 p1925 N88-21472
Thermal expansion behavior of randomly oriented short carbon fiber reinforced copper composites
[NASA-TT-20175] 15 p2031 N88-22099
Features and applications of the integrated composites analyzer (ICAN) code 15 p2078 N88-22391
Thermal stress in high temperature cylindrical fasteners
[NASA-TM-100611] 15 p2087 N88-22438
Thermal compensating mount
[NASA-CASE-LAR-13794-1] 18 p2519 N88-24942
Thermal conductivity and thermal expansion of stainless steels D9 and HT9
[DE88-011973] 21 p2916 N88-27306
Thin film-residual stress assessment
[AD-A193205] 23 p3196 N88-29018
High effectiveness contour matching contact heat exchanger
[NASA-CASE-MSC-20840-1] 23 p3214 N88-29132
Transverse expansion of individual carbon and graphite filaments
[AD-A195073] 24 p3342 N88-29891

THERMAL FATIGUE
Fatigue and thermal fatigue of Pb-Sn solder joints
[DE87-012881] 01 p0024 N88-10150
Determination of the fatigue strength of mechanically, thermally and corrosively loaded multilayer materials
[ETN-87-90375] 01 p0058 N88-10372
Fracture mechanical analysis of the initiation and propagation of matrix and surface cracks in thermally loaded fiber composite models
[ETN-87-90439] 01 p0062 N88-10400
The effect of temperature on fatigue crack initiation from aluminosilicate inclusions
[PNR90377] 02 p0154 N88-10962
Some new fatigue tests in high temperature water and liquid sodium environment
[DE87-753019] 02 p0192 N88-11197
Deformation mechanisms of thermostructural materials
[AD-A184070] 03 p0338 N88-12128
Thermal mechanical low cycle fatigue of 25CDV4-10 steel 06 p0721 N88-14429
Microstructural observations of the Sn-Pb solder/Cu system and thermal fatigue of the solder joint
[DE88-001392] 07 p0832 N88-15048
Creep and fatigue research efforts on advanced materials 09 p1119 N88-16701
Fatigue and uniaxial deformation behavior of Hastelloy XR at elevated temperatures
[DE88-751058] 09 p1145 N88-16862
Dynamic recrystallization during high temperature low cycle fatigue of nickel
[DE88-003224] 10 p1302 N88-17788
Cost 501 Project UK10 part 3: Thermal fatigue damage of Fecralloy steel-sprayed and co-extruded tubing
[AERE-R-12230] 10 p1343 N88-18026
Thermal fatigue of stainless steel
[DE88-004146] 11 p1458 N88-18694
Thermal-mechanical fatigue testing of a titanium-aluminide alloy
[AD-A189555] 12 p1609 N88-19620
Effect of nonuniform state of thermal stress on resistance of EI826 alloy to thermal fatigue
14 p1895 N88-21313
Effect of protective coatings on high-temperature fatigue of heat-resistant alloys 14 p1895 N88-21314
Effect of strain rate on high-temperature low-cycle fatigue behavior of Hastelloy X and Hastelloy XR
[DE88-752302] 15 p2037 N88-22140
Bithermal fatigue of a nickel-base superalloy single crystal
[NASA-TM-100885] 15 p2042 N88-22168
Unified constitutive model for single crystal deformation behavior with applications 15 p2078 N88-22388
Elevated temperature crack growth
15 p2084 N88-22421
Bithermal fatigue: A simplified alternative to thermomechanical fatigue 15 p2084 N88-22424
Analyses and experiments on the integrity and lifetime predictions of plasma-facing components in fusion reactors
[DE87-702957] 15 p2135 N88-22735

THERMAL GRAVIMETRY
U THERMOGRAVIMETRY

THERMAL INSTABILITY
Thermal instability and heat transfer characteristics in water/ice systems
[AD-A189627] 15 p2062 N88-22297

THERMAL INSULATION
Shear strength of the ASDEX upgrade Toroidal Field (TF) coil insulation: Rupture, fatigue and creep behavior --- tokamak
[IPP-1/230] 01 p0059 N88-10376
Thermal resistance of contacting metal surfaces at helium temperatures
[BLL-RISLEY-TR-5500-(9091.9F)]
02 p0148 N88-10929
Evaluation of the thermal effectiveness of urethane foam and fiberglass as insulation systems for tank cars
[PB88-100797] 06 p0686 N88-14207
Radiative heat transfer solutions in plane-parallel participating media: Application to multilayer insulations for space vehicles
[INPE-4221-PRE/1101] 08 p0962 N88-15824
Space environmental considerations for a long-term cryogenic storage vessel 08 p0981 N88-15933
Characterization of transparent insulation materials --- solar energy absorbers
[ETN-88-91052] 09 p1163 N88-16970
High-temperature properties of ceramic fibers and insulations for thermal protection of atmospheric entry and hypersonic cruise vehicles
[NASA-TM-100059] 10 p1295 N88-17743
Thermal analysis of transistor packages, part 2
[DE88-005091] 10 p1323 N88-17909
Ceramic-ceramic shell tile thermal protection system and method thereof
[NASA-CASE-ARC-11641-1] 11 p1448 N88-18628
Fire tests on loose-fill insulation materials
[DE88-751182] 11 p1467 N88-18746
Multilayer thermal insulation tests
[INPE-4475-PRE/1243] 12 p1626 N88-19729
Applicability of aerospace thermal insulation technologies to the civilian sector
[DE88-003717] 13 p1852 N88-21086
Fabric space radiators
[DE88-005569] 14 p1880 N88-21237
High-temperature thermal conductivity of a carbon-bonded carbon-fiber insulation
17 p2402 N88-24281
Development of refractory thermocouples for space nuclear power tests 17 p2434 N88-24478
Thermal conductivity of hard anodized coatings on aluminum
[AD-A191755] 18 p2492 N88-24784
Calculational model development for fibrous thermal insulation transient test procedures
[DE88-007843] 18 p2493 N88-24789
A monolithic gas flow sensor with polyimide as thermal insulator 19 p2669 N88-25864
Contribution to the development of coated fiber ceramic insolation material
[ETN-88-92361] 21 p2906 N88-27243
Determination of radiative properties of fiberglass and foam insulations
[DE88-007845] 21 p2920 N88-27331
The mechanical behavior of surface modified ceramics
[DE88-010564] 23 p3196 N88-29022

THERMAL MAPPING
Evaluation and certification of heater assemblies developed for thermal vacuum acceptance testing
02 p0136 N88-10853
Investigation of aeroacoustic mechanisms by remote thermal imaging
[DE88-002612] 15 p2021 N88-22046
Real time thermal imaging of high temperature semiconductor melts 17 p2330 N88-23914
Clinical applications of computerized thermography
17 p2330 N88-23915
Sky radiance distributions for thermal imaging backgrounds
[AD-A191135] 17 p2373 N88-24115
Noncontact temperature pattern measuring device
[NASA-CASE-NPO-17024-1-CU]
18 p2519 N88-24943
Image processing applied to quantitative numerical cartography of ocean circulation
19 p2702 N88-26065

THERMAL NEUTRONS
Defects in cubic silicon carbide on silicon
17 p2408 N88-24317
Interaction of slow neutrons with Ge74 single crystals
[DE87-703010] 17 p2445 N88-24536

THERMAL NOISE
Generating squeezed microwave radiation with a Josephson parametric amplifier
14 p1978 N88-21805

THERMAL PLASMAS
Synthesis of the monoclinic yttria by thermal plasma processing
[DE88-000496] 04 p0421 N88-12608
Analytically modeling the carbothermic reduction of alumina in a thermal plasma
[DE88-005535] 13 p1841 N88-21020
The effects of optical smoothing techniques on filamentation in laser plasmas
[AD-A188719] 16 p2275 N88-23614
Modelling of thermal plasma systems
18 p2578 N88-25314
Reconstruction of wave distribution functions in warm plasmas
[IRF-PREPRINT-104] 24 p3431 N88-30422

THERMAL POWER
U TURBOGENERATORS

THERMAL PROPERTIES
U THERMODYNAMIC PROPERTIES

THERMAL PROTECTION
Thermal barrier coating life prediction model development 02 p0190 N88-11183
Thermal barrier coating life prediction model development 02 p0190 N88-11184
Thermal barrier coating life prediction model development 02 p0190 N88-11185
The friction and wear of TPS fibers
[NASA-CR-181496] 03 p0291 N88-11830
Performance analysis of advanced spacecraft TPS
[NASA-CR-181532] 04 p0399 N88-12484
Space suit extravehicular hazards protection development
[NASA-TM-100458] 04 p0475 N88-12927
Advantages of internal thermal protection in a pyrotechnical plunger
[SNIAS-872-430-114] 05 p0571 N88-13478
National Aeronautics and Space Administration (NASA)/American Society for Engineering Education (ASEE) Summer Faculty Fellowship Program, 1987, Volume 2
[NASA-CR-172009-VOL-2] 06 p0796 N88-14874
Spectroscopic investigations and measurements of certain ARC jet parameters 06 p0796 N88-14877
Raman spectra of adsorbed layers on space shuttle and AOTV thermal protection system surface
06 p0799 N88-14890
Life modeling of thermal barrier coatings for aircraft gas turbine engines
[NASA-TM-100283] 07 p0834 N88-15060
In-flight rain damage tests of the shuttle thermal protection system
[NASA-TM-100438] 14 p1881 N88-21241
Aerothermal tests of quilted dome models on a flat plate at a Mach number of 6.5
[NASA-TP-2804] 15 p2067 N88-22325
Thermal stress minimized, two component, turbine shroud seal
[NASA-CASE-LEW-14212-1] 17 p2345 N88-23978
Effects of natural environment on first generation solid rocket booster thermal protection system materials
[NASA-TM-100329] 17 p2373 N88-24113

THERMAL RADIATION
NT BLACK BODY RADIATION
NT PHONON BEAMS
The effects of minor trace gases on the transfer of thermal infrared radiation through the Earth's atmosphere 04 p0468 N88-12893
Radiation curing: Comparison of heat, UV, and radiation curing
[OEFZS-4393] 06 p0689 N88-14224

Nonuniformity of electromagnetic field at Lambda = 10.6 micron wavelength inside atmospheric aerosol particles
06 p0772 N88-14743

Absorption, scattering, and thermal radiation by conductive fibers
[AD-A186105] 07 p0842 N88-15106

Commercial applications and scientific research requirements for thermal-infrared observations of terrestrial surfaces
[NASA-TM-89704] 08 p1019 N88-16179

Group 2A metastable collision complexes: Spectroscopy and behavior in intense radiation fields
[AD-A186737] 08 p1082 N88-16524

Thermal radiation from neutron stars
[MPE-203] 11 p1571 N88-19404

Fabric space radiators
[DE88-005569] 14 p1880 N88-21237

Combustion and fuels in gas turbine engines
[AGARD-CP-422] 24 p3345 N88-29910

Radiation from soot-containing flames
24 p3347 N88-29927

Flamelet chemistry modelling of soot formation for radiation 24 p3348 N88-29928

Radiation transfer in gas turbine combustors
24 p3348 N88-29929

Degradation of protective coatings on steel in corrosive environments 24 p3354 N88-29969

THERMAL REACTORS

Influence of fast alpha diffusion and thermal alpha buildup on Tokamak reactor performance
[DE88-003661] 09 p1251 N88-17496

THERMAL RESISTANCE

Polymers in solar technologies
[DE88-001102] 03 p0294 N88-11849

Technology development of a planar BiPolar transistor
[AD-A188761] 12 p1623 N88-19708

Degradations of thermal shock resistance and the fracture toughness of reactor graphite subjected to neutron irradiation 13 p1747 N88-20445

Comparison of methods for the calculation of thermal contact resistance of the first Brazilian satellite
[NASA-TT-20180] 14 p1880 N88-21239

High temperature testing of C/C (Carbon/Carbon) composites
[AD-A193012] 20 p2768 N88-26411

Heat transfer of mesh-wick heat-pipes (bottom heat mode) 20 p2783 N88-26507

THERMAL RESOURCES

NT GEOTHERMAL RESOURCES

THERMAL SHIELDING

U HEAT SHIELDING

THERMAL SHOCK

Rocket nozzle thermal shock tests in an arc heater facility 02 p0133 N88-10832

Comparison of high purity fine grain graphites from different suppliers with regard to physical, mechanical, and thermal properties --- Joint European Torus wall protection
[JUEL-SPEZ-401] 02 p0154 N88-10963

Performance of low upper-shelf material under pressurized-thermal-shock loading (PTSE-2)
[DE88-002297] 07 p0832 N88-15049

The effect of thermal shock on carbon fiber epoxy composites
[FOA-C-20675-2.6] 08 p0965 N88-15841

Photohydrodynamical processes near compact objects
11 p1569 N88-19390

Degradations of thermal shock resistance and the fracture toughness of reactor graphite subjected to neutron irradiation 13 p1747 N88-20445

Notch sensitivity of graphite materials for VHTR
13 p1747 N88-20447

Response of aluminum alloys to erosive particle impacts
[DE88-005910] 15 p2041 N88-22159

Fracture mechanics 17 p2324 N88-23877

Strength optimization of alpha-SiC by improved processing 17 p2324 N88-23880

Ceramic matrix composites 17 p2325 N88-23888

An analysis of the efficiency and directivity of the sound generated by a moving laser source
[AD-A192220] 20 p2849 N88-26914

Studies of dynamic contact of ceramics and alloys for advanced heat engines
[DE88-008996] 21 p2919 N88-27324

Evaluation of fracture models through pressurized-thermal-shock testing
[DE88-011834] 21 p2963 N88-27603

THERMAL SINKS

U HEAT SINKS

THERMAL STABILITY

Pressure effects on the thermal stability of SiC fibers
[NASA-TM-100146] 01 p0019 N88-10120

Viscosity measurements at high temperatures on a standard reference material supplied by BCR --- Bureau Communite de Reference (BCR) -
[NPL-DMA(A)-146] 01 p0020 N88-10126

Synthesis and characterization of processable polyimides with enhanced thermal stability
[NASA-CR-181447] 01 p0030 N88-10191

A numerical study of the thermal stability of solar loops 02 p0256 N88-11619

Thermally stable aromatic structures from acyclic precursors. 1: Para polyphenylene model compounds from 3-Dimethyl amino hex-5-EN-1-YNES
[AD-A185300] 05 p0568 N88-13462

High temperature stability of superconducting YBa2Cu3O subx as characterized by X-ray diffraction
[DE88-001856] 06 p0787 N88-14824

Development and applications of new technical advances to problems of fluid/electrolyte/mineral imbalance in military personnel
[AD-A186437] 07 p0889 N88-15388

Improved perfluoroalkylether fluid development
[NASA-CR-180872] 08 p0967 N88-15851

Self-lubricating coatings for high-temperature applications 09 p1119 N88-16703

Correlations of norbornenyl crosslinked polyimide resin structures with resin thermo-oxidative stability, resin glass transition temperature and composite initial mechanical properties
[NASA-TM-100791] 09 p1147 N88-16877

Polymerization of fluorinated diacetylenes
[AD-A188051] 11 p1462 N88-18716

A novel class of positive electrodes for rechargeable batteries
[DE88-004559] 13 p1763 N88-20545

Thermal deformation and strength of composite materials at high temperatures 14 p1885 N88-21263

Effect of nonuniform state of thermal stress on resistance of EI826 alloy to thermal fatigue
14 p1895 N88-21313

Effect of oxidation on strength and thermal stability of material based on Si3N4 14 p1896 N88-21319

Dependence of formation of radiative color centers in optical glass fibers on technological factors
14 p1896 N88-21321

Thermally stable deployable structure
14 p1925 N88-21472

High-performance polymeric materials
[AD-A190708] 15 p2046 N88-22190

Stability of the high-temperature G-16 primer composition
[DE88-006201] 15 p2049 N88-22206

Electronic structure and stability of small cation and anion hydrogen clusters 16 p2267 N88-23562

SiC fiber analysis 17 p2326 N88-23891

Current and future molecular structures of aerospace organic matrix resins 18 p2477 N88-24695

A thermally modified polymer matrix composite material with structural integrity to 371 C
[NASA-TM-100922] 19 p2609 N88-25483

Defect characterization of the redox behavior and stability of conducting oxides
[DE88-010799] 20 p2878 N88-27088

Reaction-theoretical aspects of the thermal behavior of lubricating oils and working fluids
[NASA-TT-20304] 23 p3199 N88-29041

THERMAL STRESSES

Thermal stress analysis of space shuttle orbiter subjected to reentry aerodynamic heating
[NASA-TM-88286] 01 p0061 N88-10389

Reinforced flexural elements for TEMP-STRESS Program
[DE87-012961] 01 p0061 N88-10391

Thermal testing by internal IR heating of the FEP module 02 p0136 N88-10854

Stress state of welded joints of dissimilar materials obtained by diffusion welding 03 p0286 N88-11799

Comparison of measured temperatures, thermal stresses and creep residues with predictions on a built-up titanium structure
[NASA-TM-86814] 03 p0337 N88-12125

Welding and weldability of ductile intermetallic alloys
[DE87-014061] 04 p0416 N88-12582

Thermal stress in the edge cladding of Nova glass laser disks
[DE88-000425] 04 p0448 N88-12780

Thermomechanical cracking in coated media due to high speed asperity excitation
[AD-A184176] 04 p0454 N88-12809

United States - Japan Workshop on Dielectric and Piezoelectric Ceramics (3rd) held in Toyama, Japan on November 9-12, 1986
[AD-A185113] 05 p0568 N88-13460

Fluid mass and thermal loading effects on the modal characteristics of space shuttle main engine liquid oxygen inlet splitter vanes 05 p0594 N88-13628

Fracture kinetics of corrosion fatigue
05 p0605 N88-13708

The effect of heat treatment on fatigue crack growth in polycarbonate 05 p0606 N88-13714

Thermo-mechanical behavior of high temperature fiber composites 06 p0678 N88-14149

Geometrically nonlinear analysis of stiffened panels
06 p0722 N88-14440

Thermoplastic elastomers as LOVA binders
[AD-A185864] 07 p0835 N88-15087

Thermal stress analysis of a cooled monochromator crystal
[DE88-002116] 07 p0937 N88-15696

Study of the mechanical behavior of a 2-D carbon-carbon composite
[NASA-CR-182594] 11 p1451 N88-18649

Oxidation and protection of fiberglass-epoxy composite masts for photovoltaic arrays in the low Earth orbital environment
[NASA-TM-100839] 11 p1465 N88-18734

The effects of various conductor components on Nb3Sn filament prestrain in cable-in-conduit conductors
[DE88-003956] 11 p1479 N88-18824

Effect of element size on the solution accuracies of finite-element heat transfer and thermal stress analyses of space shuttle orbiter
[NASA-TM-88292] 11 p1502 N88-18971

Monolithic nature of transversely reinforced composites 14 p1885 N88-21267

JPRS report: Science and technology. USSR: Materials science
[JPRS-UMS-87-007] 14 p1895 N88-21312

Thermally stable deployable structure
14 p1925 N88-21472

The viscoplasticity theory based on overstress applied to the modeling of a nickel base superalloy at 815 C
14 p1928 N88-21499

A unified creep-plasticity model suitable for thermo-mechanical loading 14 p1932 N88-21518

Constitutive response of Rene 80 under thermal mechanical loads 14 p1932 N88-21524

Thermal analysis of heat storage canisters for a solar dynamic, space power system
[DE88-004199] 15 p2027 N88-22075

Fundamental studies on high temperature deformation recrystallization, and grain growth of two-phase materials
[AD-A189725] 15 p2038 N88-22145

A test for interfacial effects and stress transfer in ceramic matrix composites
[NASA-CR-182758] 15 p2046 N88-22194

High-temperature combustor liner tests in structural component response test facility
15 p2077 N88-22383

Specialty three-dimensional finite element analysis codes 15 p2079 N88-22393

MHOST: An efficient finite element program for inelastic analysis of solids and structures
15 p2079 N88-22394

METCAN: The metal matrix composite analyzer
15 p2079 N88-22395

Structural tailoring of high-speed turbine blades (SSME/STAEBL) 15 p2080 N88-22398

Thermostructural analysis of simulated cowl lips
15 p2080 N88-22403

Thermal-structural analyses of Space Shuttle Main Engine (SSME) hot section components
15 p2081 N88-22404

Structural analyses of engine wall cooling concepts and materials 15 p2081 N88-22405

Elevated temperature crack growth
15 p2084 N88-22421

Thermal stress in high temperature cylindrical fasteners
[NASA-TM-100611] 15 p2087 N88-22438

JPRS report: Science and technology. USSR: Materials science
[JPRS-UMS-88-006] 16 p2179 N88-22988

Model study of thermal stresses in gas-turbine blades with protective coating 16 p2179 N88-22989

Thermal stress minimized, two component, turbine shroud seal
[NASA-CASE-LEW-14212-1] 17 p2345 N88-23978

A comparison of experimental and calculated thin-shell leading-edge buckling due to thermal stresses
[NASA-TM-100416] 17 p2349 N88-23999

Computational fluid dynamics applied to the prediction of the heat-transfer, mechanical and thermal-stress behavior of heat exchangers
[CFDU/87/7] 18 p2510 N88-24893

Advanced development of the boundary element method for elastic and inelastic thermal stress analyses
18 p2529 N88-25002

Study on the heat resisting and cooling property of the ceramics-metal hybrid stator vanes
[DE88-753117] 20 p2810 N88-26668

Thermal cycling tests on surface-mount assemblies
[DE88-007695] 21 p2939 N88-27453
Coupled thermal vibrations of beams with temperature-dependent properties
21 p2963 N88-27601
Stress intensity factors for cracked metallic structures under rapid thermal loading
[AD-A191219] 23 p3193 N88-29004
Thin film-residual stress assessment
[AD-A193205] 23 p3196 N88-29018
Analytical study of graphite-epoxy tube response to thermal loads
[NASA-CR-183215] 24 p3341 N88-29884
Thermal stress analysis in PMR-15 carbon fibre laminates
[ETN-88-93123] 24 p3341 N88-29886
Transverse expansion of individual carbon and graphite filaments
[AD-A195073] 24 p3342 N88-29891
Stress intensity factors for cracked metallic structures under rapid thermal loading
[AES-8609709F-1] 24 p3353 N88-29962

THERMAL VACUUM TESTS
Meeting today's requirements for large thermal vacuum test facilities 02 p0134 N88-10840
Mobile test fixture system for use in a thermal vacuum facility 02 p0134 N88-10843
Irradiation testing 03 p0274 N88-11727
Seven year thermal vacuum real life test of a medium speed (despin) mechanism manufactured by Dornier System
[ESA-ESTL-64] 09 p1175 N88-17038
Development of a slip-ring system for energy transfer in space conditions. Space flight qualification and extended life tests
[BMFT-FB-W-86-019] 16 p2169 N88-22932
Thermal vacuum sensors based on integrated silicon thermopiles
[ETN-88-92237] 16 p2210 N88-23190

THERMALIZATION (ENERGY ABSORPTION)
The role of hydrogen thermalization in shaping the Lyman-alpha coma — comets 14 p2007 N88-21971

THERMIONIC CATHODES
A synthetic plasma source
[TRITA-EPP-86-15] 05 p0652 N88-13995

THERMIONIC CONVERSION SYSTEMS
U THERMIONIC POWER GENERATION

THERMIONIC CONVERTERS
Irradiation test results on thermionic fuel element sheath insulators 17 p2402 N88-24280
MHW RTG performance during LES 8/9 and Voyager missions 17 p2405 N88-24300
A review of thermionic power conversion systems for SDI applications 17 p2407 N88-24310
Advanced thermionic converter technology for inductive output coupling 17 p2407 N88-24311
AMTEC electrode development
17 p2409 N88-24324
Sodium heat engine/AMTEC system experiments
17 p2409 N88-24325
Research and development of electrical insulators for thermionic applications 17 p2429 N88-24449
High power density alkaline fuel cell technology for MMW space burst power 17 p2429 N88-24451
Liquid metal thermal-electric converter electrode development
[DE88-009252] 23 p3230 N88-29221

THERMIONIC DIODES
Limiting efficiency of a thermionic diode
[DE88-700598] 11 p1479 N88-18830

THERMIONIC EMISSION
A scientific basis for an alternate cathode architecture
[AD-A191498] 18 p2481 N88-24717
Thermionic integrated circuit program
[DE88-010119] 19 p2662 N88-25833

THERMIONIC EMITTERS
A review of thermionic power conversion systems for SDI applications 17 p2407 N88-24310
Advanced thermionic converter technology for inductive output coupling 17 p2407 N88-24311

THERMIONIC POWER GENERATION
Energy storage for nuclear burst power systems
17 p2426 N88-24431
Candidate advanced energy storage concepts for multimegawatt burst power systems
17 p2426 N88-24434

THERMIONIC REACTORS
U ION ENGINES
U NUCLEAR ROCKET ENGINES

THERMIONICS
Physics and device design of vacuum integrated circuits 01 p0039 N88-10251
Thermionic Technology Program. A. Insulator test and evaluation
[DE88-004707] 13 p1795 N88-20735

THERMISTORS
Air temperature shield tests
[AD-A187459] 11 p1514 N88-19043
Studies of error in temperature measurement with thermistors in the range between continual and free-molecule flows
[NASA-TT-20302] 19 p2674 N88-25900
Effect of interfacial phenomena on contact line heat Transfer-3
[AD-A194941] 24 p3343 N88-29901

THERMOCHEMICAL PROPERTIES
NT HEAT OF COMBUSTION
NT HEAT OF FORMATION
NT HEAT OF FUSION
NT LATENT HEAT
The formation and thermochemical properties of multiligand complexes
[AD-A184935] 05 p0561 N88-13416
Phase diagrams in materials science and the use of the computer in their calculation
[PB88-155262] 18 p2586 N88-25364

THERMOCHEMISTRY
NT AEROTHERMOCHEMISTRY
NT COMBUSTION CHEMISTRY
Ultra-fine grained alloy material
[AD-A184500] 03 p0290 N88-11820
Application of solar technology to fuel production chemical processing, and thermochemical energy transport: Status and future
[DE87-014172] 03 p0346 N88-12189
The developmental status of solar thermochemical hydrogen production
[DE86-001778] 04 p0466 N88-12884
Phase diagram and thermochemical properties of the Al-Cu system
[ETN-88-91015] 05 p0566 N88-13447
A process study of the biothermal conversion of water hyacinths to methane
[DE88-000554] 06 p0730 N88-14488
Study of the vapor-liquid equilibria used in the fabrication process of hydrogen by thermochemistry
[DE88-900239] 07 p0830 N88-15035
A solar receiver-reactor with specularly reflecting walls for high-temperature thermoelectrochemical and thermochemical processes
[AD-A187612] 10 p1351 N88-18077
Evaluation and compilation of thermodynamic properties of high temperature chemical species
[AD-A187509] 11 p1452 N88-18654
Analysis of model fuels and their compatibility with selected elastomers, part 1
[AD-A188361] 12 p1612 N88-19639
Thermochemistry and high temperature thermodynamic properties of rare earth-alkaline earth-copper oxide superconductors
[DE88-005976] 15 p2140 N88-22770
An investigation of the crystalchemistry and thermochemistry of selected mineral systems
[AD-A189758] 15 p2142 N88-22781
Thermochemical analysis of mass transfer in a NB-1ZR-potassium heat pipe 17 p2412 N88-24346
Structure/property/reactivity relations among nitramine and other energetic materials
[AD-A190878] 18 p2481 N88-24716
Proceedings of the 1987 Biomass Thermochemical Conversion Contractors' Review Meeting
[DE88-006730] 18 p2535 N88-25041
Low-temperature thermochemical conversion of high moisture biomass feedstocks 18 p2536 N88-25047
Solid rocket motor performance: A workshop report
19 p2631 N88-25607
Chemical kinetics modeling of HMX combustion
19 p2633 N88-25617
Integrated solar reforming for thermochemical energy transport
[DE88-005010] 19 p2686 N88-25967
Kinetics of thermochemical gas-solid reactions important in the Venus sulfur cycle
[NASA-CR-182963] 19 p2742 N88-26280
Silicon oxidation studies: A review of recent studies on thin film silicon dioxide formation in the physics and chemistry of SiO2 and the Si-SiO2 interface
[AD-A193176] 21 p3021 N88-27932
Theoretical investigations of nitrocubane decomposition
[AD-A194556] 23 p3200 N88-29047
Chemical interactions between the present-day Martian atmosphere and surface minerals
23 p3305 N88-29689
Gas phase combustion chemistry of nitramine propellants
[AD-A195082] 24 p3344 N88-29902
Three-dimensional combustor predictors: A comparison of equilibrium and laminar flamelet chemistry models
24 p3350 N88-29940

THERMOCHROMATIC MATERIALS
Quasi-liquid crystalline materials with special electro-optic properties
[AD-A194579] 23 p3282 N88-29544

THERMOCLINES
Dynamics of isolated intrathermocline eddy
04 p0460 N88-12845
Effects of rainfall on the seasonal thermocline
[AD-A184432] 04 p0472 N88-12912
Intrathermocline lens of Mediterranean water in tropical North Atlantic 13 p1786 N88-20688
Dynamics of the Oceanic Surface Mixed Layer
[AD-A188348] 13 p1804 N88-20785
Structures and fluxes in a deep convecting mixed layer 13 p1804 N88-20786
Equatorial turbulence: Mixed layer and thermocline
13 p1804 N88-20787
Subduction 13 p1806 N88-20796
Wind forcing and observed oceanic wavenumber spectra 13 p1806 N88-20797
Monitoring ocean surface layer processes
13 p1806 N88-20801
The main ocean thermocline
14 p1938 N88-21563
An analysis of horizontal temperature gradients and heat content in the mixed layer and the surface forcing during PATCHEX
[AD-A192330] 21 p2976 N88-27678

THERMOCOUPLES
NT THERMOPILES
Temperature Metrology '86
[DE88-700236] 08 p0989 N88-15990
Investigation of thermoacoustic heat transport using a thermoacoustic couple
[AD-A186889] 09 p1242 N88-17442
Error evaluation of some practical thermocouple probes for gas turbine combustor tests
[NAL-TR-938] 11 p1489 N88-18886
Prototype thin-film thermocouple/heat-flux sensor for a ceramic-insulated diesel engine
[NASA-TM-100798] 11 p1490 N88-18892
Botany Facility. Thermal Control (TC) subsystem test report on experiment container of laboratory model and breadboard centrifuge
[BF-TN-ER-061/86] 17 p2378 N88-24135
Low cross-section Mo-Nb thermocouples for nuclear application: The state-of-the-art
17 p2433 N88-24477
Development of refractory thermocouples for space nuclear power tests 17 p2434 N88-24478
Thermocouple for heating and cooling of memory metal actuators
[NASA-CASE-NPO-17068-1-CU]
23 p3217 N88-29151

THERMODYNAMIC COUPLING
Specific heat of novel thin-film material systems
10 p1415 N88-18446
Predictions and studies with a one-dimensional ice/ocean model
[AD-A189158] 13 p1803 N88-20776
Advanced thermionic converter technology for inductive output coupling 17 p2407 N88-24311
Coupled even-parity superconducting states: Square lattice
[AD-A193432] 21 p3022 N88-27938

THERMODYNAMIC CYCLES
NT BRAYTON CYCLE
NT RANKINE CYCLE
NT STIRLING CYCLE
Analysis of shell-type structures subjected to time-dependent mechanical and thermal loading
[NASA-CR-181409] 01 p0060 N88-10388
Two-watt, 4-Kelvin closed cycle refrigerator performance 04 p0437 N88-12709
The application of liquid-metal MHD (magnetohydrodynamics) to renewable energy sources
[DE88-003083] 09 p1251 N88-17495
Nuclear electric propulsion system: Nuclear plant and thermomechanical conversion system
17 p2405 N88-24298
Studies for the definition of a Faraday converter for space nuclear systems 17 p2411 N88-24339
The liquid droplet radiator in space: A parametric approach 17 p2427 N88-24437

THERMODYNAMIC EFFICIENCY
Advanced natural gas fueled engine development. Part 1: Design and analyses
[PB87-224804] 03 p0331 N88-12087
Performance of highly concentrating mirror collectors and collector systems
[DFVLR-FB-87-29] 09 p1186 N88-17107
Nuclear electric propulsion system: Nuclear plant and thermomechanical conversion system
17 p2405 N88-24298

Preparation of improved PbSnTe thermoelectric alloys and evaluation of their figure of merit
[AD-A191346] 17 p2445 N88-24538

Computational study on thermal efficiency of ceramic gas turbine
[DE88-753114] 20 p2809 N88-26667

An analysis of the efficiency and directivity of the sound generated by a moving laser source
[AD-A192220] 20 p2849 N88-26914

THERMODYNAMIC EQUILIBRIUM

Evaluation of the infrared test method for the olympus thermal balance tests 02 p0136 N88-10856

Quasi-thermal models 02 p0253 N88-11600

Undercooling and nucleation in iron nickel alloys
[AD-A185500] 06 p0683 N88-14184

Review of nucleation and incipient boiling under pool and forced convection conditions
08 p0982 N88-15938

Spatial and temporal monitoring of the Jovian atmosphere 12 p1711 N88-20240

A thermal equilibrium model for multi-megawatt space platforms 17 p2410 N88-24332

THERMODYNAMIC PROPERTIES

NT CRITICAL POINT
NT CRITICAL TEMPERATURE
NT EMISSIVITY
NT ENTHALPY
NT ENTROPY
NT FREE ENERGY
NT GIBBS FREE ENERGY
NT HEAT OF COMBUSTION
NT HEAT OF FORMATION
NT HEAT OF FUSION
NT LATENT HEAT
NT MELTING POINTS
NT PYROELECTRICITY
NT SPECIFIC HEAT
NT SURFACE ENERGY
NT THERMAL CONDUCTIVITY
NT THERMAL DIFFUSION
NT THERMAL DIFFUSIVITY
NT THERMAL EXPANSION
NT THERMAL INSTABILITY
NT THERMAL STABILITY
NT THERMOCHEMICAL PROPERTIES
NT THERMOPHYSICAL PROPERTIES
NT VAPOR PRESSURE
NT VOLATILITY

The dissociation of dense liquid nitrogen and shock cooling
[DE87-013490] 01 p0022 N88-10136

Description of NCAR (National Center for Atmospheric Research) Community Climate Model (CCM1)
[PB87-203782] 01 p0072 N88-10462

Application of new conformal solution of theories
[PB87-214557] 01 p0105 N88-10684

Study of improved methods for predicting chemical equilibria
[DE87-014647] 02 p0145 N88-10908

The M-type stars
[NASA-SP-492] 02 p0252 N88-11592

Magnetic field morphology in the upper layers
02 p0255 N88-11610

Modelling and theories of alloy phase behavior
[DE87-014399] 03 p0287 N88-11804

The correlation between microstructure and thermomechanical properties of two-phase materials and porous sintered materials
[KFK-4205] 03 p0292 N88-11835

China report: Science and technology
[JPRS-CST-87-015] 03 p0298 N88-11873

Integrated 3-parameter diagram for determining thermodynamic properties of fluids
03 p0298 N88-11874

Study of IR laser photoacoustic spectra of organic molecules adsorbed on metal surface
03 p0301 N88-11891

Conjugated heat transfer from a radiating fluid in a rectangular channel 03 p0317 N88-12003

Effects of state recovery on creep buckling induced by thermomechanical loading 03 p0336 N88-12116

Phase transition of multifractals
[DE87-014344] 03 p0383 N88-12409

Research and development on high strength ceramic heaters discussed 04 p0404 N88-12508

Thermodynamic properties of supercritical mixtures
[DE88-000809] 04 p0413 N88-12562

Experimental study of thermocapillary flows in a thin liquid layer with heat fluxes imposed on the free surface
[NASA-TM-100252] 04 p0445 N88-12763

Thermodynamic properties for natural gas binaries
[PB87-226833] 04 p0500 N88-13074

Atmospheres of stars in the limits of thick and thin convection zones: M giants 04 p0505 N88-13105

An analytical soil thermodynamic model for the diurnal variation of ground surface temperature
[AD-A185388] 05 p0625 N88-13823

Molecular dynamics studies of aromatic hydrocarbon liquids
[DE88-001473] 05 p0648 N88-13973

Geochemistry of freezing brines, low-temperature properties of sodium chloride
[AD-A185751] 06 p0680 N88-14168

TMA-microrheological testing of polymers (thermomechanical analysis)
[PB87-228805] 06 p0683 N88-14187

Material design of high performance glasses discussed 06 p0688 N88-14216

Excess thermodynamic properties of aqueous electrolytes to high temperatures and pressures
[DE88-001768] 07 p0940 N88-15712

Determination of thermodynamic function of minerals at high temperatures
[DE88-001911] 07 p0940 N88-15713

Determination of thermodynamic function of minerals at high temperatures
[DE88-002311] 07 p0940 N88-15714

North Pacific Ocean. Subtropical front north of Hawaii. R/V Thomas G. Thompson: 7 January - 10 February 1974. CTD data report
[AD-A186565] 08 p1044 N88-16310

Thermodynamic and conductivity studies of nonstoichiometric cerium dioxide by Coulometric titration: A simultaneous measurement
[DE88-003054] 08 p1091 N88-16566

Analysis of the decomposition of transparent polymer materials (blocks) under the action of laser beams in free generation mode
[AD-A187090] 09 p1147 N88-16873

Numerical solutions of two moving boundary problems by both finite difference and finite element methods with applications
[DE88-002867] 09 p1230 N88-17374

Calculation and design of a ramjet missile
[REPT-TR-500] 10 p1311 N88-17832

Chemical activation of molecules by metals: Experimental studies of electron distributions and bonding
[DE88-004465] 10 p1407 N88-18393

Utilization of the JANAF (Joint Army Navy Air Force) database for chemical thermodynamic calculations
[DE88-004571] 10 p1423 N88-18501

Evaluation and compilation of thermodynamic properties of high temperature chemical species
[AD-A187509] 11 p1452 N88-18654

Documentation for computer code NACL
[LBL-21859] 11 p1531 N88-19145

Vibrational, mechanical and thermal properties of 3-5 semiconductors
[AD-A187569] 11 p1556 N88-19316

Hot corrosion in gas turbines: A new, unique and informative technique is EASE (Electronic Absorption Spectroscopy Experiments)
[AD-A188508] 12 p1583 N88-19470

Thermal properties of soil: A case study
[INPE-4332-TDL/289] 12 p1637 N88-19803

MOPAC manual: A general molecular orbital package, fourth edition
[AD-A188623] 13 p1733 N88-20362

High-temperature metal matrix composites
[AD-A189516] 13 p1734 N88-20367

Properties of molecular solids and fluids at high pressure and temperature
[DE88-004195] 13 p1738 N88-20391

Liquid alloys: New perspectives and challenges
[DE88-005935] 13 p1750 N88-20463

Thermodynamic theory of fluctuations and Rayleigh light scattering in solutions 13 p1785 N88-20681

The thermodynamic properties of organic oxygen compounds
[DE88-001208] 13 p1849 N88-21065

Rapid e-beam heating for measuring thermodynamics of metastable materials
[DE88-003565] 13 p1849 N88-21066

Review of selenium thermodynamic data
[DE88-006194] 13 p1849 N88-21068

Prediction of high-temperature thermodynamic properties of mixed electrolyte solutions including solubility equilibria, vapor pressure depression and boiling point elevation
[DE88-006344] 13 p1849 N88-21069

On the theory of the conversion of metallic mixed phases. 5: Fluctuations and nucleation in sub-cooled phases
[NASA-TT-20249] 14 p1890 N88-21296

Prediction of thermodynamic properties, including solubility equilibria and vapor pressures, for mixed aqueous electrolytes to high temperatures
[DE88-006317] 14 p1990 N88-21863

The thermal radiative properties of metals at high temperature
[DE88-006625] 15 p2038 N88-22141

Thermochemistry and high temperature thermodynamic properties of rare earth-alkaline earth-copper oxide superconductors
[DE88-005976] 15 p2140 N88-22770

Value of energy storage in pulsed space power systems
[AD-A191311] 16 p2170 N88-22938

TVC (Thrust Vector Control) jet vane thermal modeling using parametric system identification
[AD-A191518] 18 p2474 N88-24678

The thermodynamic properties of quinoline and isoquinoline
[DE88-001218] 18 p2484 N88-24735

Dynamic consolidation of metal powders
[AD-A192126] 18 p2485 N88-24744

An evaluation of some thermodynamic and transport properties of solid and liquid lithium over the temperature range 200 to 1700 K
[DE88-008947] 19 p2614 N88-25512

Mixing and thermodynamic critical phenomena of combusting monopropellant sprays
19 p2623 N88-25558

The development of a user friendly thermodynamic code for the personal computer 19 p2623 N88-25559

Dimensional analysis and experimental observation of the coupling phenomena between combustion and fracture of damaged propellant samples
19 p2630 N88-25603

On 3-5 transistors for MM-wave applications
[AD-A191580] 19 p2661 N88-25825

Radiative heat transfer and selective emission in planar slab coatings on hot emissive substrates
[AD-A193133] 21 p2918 N88-27319

An analysis of horizontal temperature gradients and heat content in the mixed layer and the surface forcing during PATCHEX
[AD-A192330] 21 p2976 N88-27678

Some theoretical considerations of the surface tension of liquid metals for metal matrix composites
[AD-A195999] 24 p3340 N88-29882

Thermomechanical computations for GAP: a high energy binder for composite propellants
[FOA-C-20718-2.1] 24 p3357 N88-29988

Particle trajectories and potentials in a plane sheath moving in a magnetoplasma
[AD-A196228] 24 p3390 N88-30190

The origin of the moon: Furthor studies of the giant impact 24 p3440 N88-30474

THERMODYNAMICS

NT AEROTHERMODYNAMICS
NT COMBUSTION PHYSICS
NT NONEQUILIBRIUM THERMODYNAMICS

Hot spot reaction in unsustained shocks
[DE87-011781] 01 p0044 N88-10277

Thermodynamics of interaction between nitrogen and molten nickel alloys
[BLL-M-37309-(5828.4)] 02 p0149 N88-10934

Energy changes in transforming solids
[DE87-011257] 02 p0191 N88-11194

Application of new conformal solution theories
[PB87-211934] 02 p0247 N88-11558

A heat transfer model for a heated helium airship
[AD-A183786] 03 p0259 N88-11629

The Proceedings of the Symposium on Mechanics for Space Flight
[ISAS-SP-5] 03 p0317 N88-12006

Retention processes in supercritical fluid chromatography
[DE88-000079] 04 p0413 N88-12559

Model for ultrasonic attenuation and elastic constant in chromium and its alloys
[DE87-703478] 04 p0415 N88-12570

Use of a thermodynamic analog for pneumatic transport in horizontal pipes
[AD-A184076] 04 p0441 N88-12740

Coupled acoustic and ocean thermodynamic model
[AD-A184357] 04 p0472 N88-12911

Non-lattice matched metallic superlattices
[DE87-011512] 04 p0497 N88-13082

Ionic transport and electrical relaxation in glass
[DE88-000887] 05 p0657 N88-14028

Calendar of selected aeronautical and space meetings
[AGARD-CAL-87/1] 05 p0657 N88-14033

Thermo-mechanical behavior of high temperature fiber composites 06 p0678 N88-14149

Reactions and bonding between glasses and titanium
[DE88-000603] 06 p0685 N88-14195

On the interconnection of dynamic processes in the lower thermosphere with meteorological phenomena in the tropostratosphere 06 p0734 N88-14512

The nonlinear thermodynamics of meteors, noctilucent clouds, enhanced airglow and global atmospheric circulation 06 p0738 N88-14538

Thermodynamic values from computer summation of group additivity data
[AD-A186131] 07 p0940 N88-15711

Investigations in field of surface forces in metallurgy
[BLL-M-47406-(5828.4)] 08 p0969 N88-15860

Zero-G thermodynamic vent system for shuttle/Centaur 08 p0983 N88-15943

Use of the thermodynamic evaporation formula of Hoffmann in energy balance models for flowing water
08 p1013 N88-16143

A study of the free energy of the Lenz-Ising model using the cluster variation method of Morita
[AD-A186023] 08 p1073 N88-16476

Thermodynamic and conductivity studies of nonstoichiometric cerium dioxide by Coulometric titration: A simultaneous measurement
[DE88-003054] 08 p1091 N88-16566

The role of thermodynamic phase diagrams and lattice matching in superlattice growth
[DE88-003113] 08 p1091 N88-16568

An analysis of the closure conditions for two-fluid models of two-phase flow
[DE88-003355] 09 p1164 N88-16982

Investigation of thermoacoustic heat transport using a thermoacoustic couple
[AD-A186889] 09 p1242 N88-17442

Metal hydrides
[DE88-005083] 10 p1299 N88-17766

A large strain thermomechanical forming model for elastic-viscoplastic behavior in metals
10 p1301 N88-17780

Collaborative studies of polar cap ionospheric dynamics
[AD-A187888] 10 p1355 N88-18098

Nonmonotonic evolution and thermodynamic trends at metal/(Hg,Cd)Te interfaces: Yb/Hg0.78Cd0.22Te
[AD-A187591] 10 p1422 N88-18490

Studies in finite time thermodynamics
[DE88-004531] 10 p1423 N88-18500

Utilization of the JANAF (Joint Army Navy Air Force) database for chemical thermodynamic calculations
[DE88-004571] 10 p1423 N88-18501

Velocity reversal and the arrows of time
[DE88-004237] 10 p1429 N88-18536

Analysis of shear-layer probe data for holes in hypersonic configurations
[DE88-003992] 11 p1435 N88-18564

Fundamental studies of corrosion of nonoxide structural ceramics
[PB88-141536] 11 p1461 N88-18709

Mechanisms in thermal mechanical forming of plates
[AD-A187797] 11 p1466 N88-18744

Thermodynamics of wetting by liquid metals
[DE88-003634] 11 p1563 N88-19360

A continuum damage model for viscoelastic materials
[AD-A189426] 12 p1637 N88-19800

Oxidation/sulfidation of materials in an SO3/SO2/O2 thermochemical-transport, distributed-receiver, solar-energy system
[DE88-005875] 13 p1795 N88-20739

Dynamical modeling of marine boundary layer convection 13 p1797 N88-20750

Predicting oscillatory finite difference solutions to the heat equation: A comparative study of the coefficient and matrix methods
[AD-A189591] 13 p1825 N88-20911

Two studies of nonlinear processes in irreversible thermodynamics
[DE88-005794] 13 p1849 N88-21067

Electrohydrodynamic migration of charged droplets in an insulating fluid
[NASA-TM-100849] 14 p1912 N88-21424

A viscoplastic theory applied to copper
[NASA-TM-100831] 14 p1928 N88-21497

Elements of sea ice dynamics and thermodynamics
14 p1939 N88-21571

Nucleation in super-saturated products
[NASA-TT-20275] 15 p2037 N88-22134

The age hardening response of thermomechanically processed Al-Mg-Li alloys
[AD-A189870] 15 p2039 N88-22147

Comparison of entropy generation and conventional design methods for heat exchangers
[AD-A190256] 15 p2064 N88-22306

Nondestructive evaluation of sintered ceramics
15 p2083 N88-22416

Sequential tests for the drift of a Wiener process with a smooth prior and the heat equation
[AD-A190322] 15 p2121 N88-22638

Advanced chemical heat pumps using liquid-vapor reactions
[DE88-006760] 16 p2205 N88-23159

Models in nonlinear thermomechanics. Finite element models and constitutive models for large deformation elastoplasticity
[ETN-88-92240] 16 p2222 N88-23262

Thermodynamic modeling of the no-vent fill methodology for transferring cryogens in low gravity
[NASA-TM-100332] 18 p2476 N88-24686

Isothermal and bithermal thermomechanical fatigue behavior of a NiCoCrAlY-coated single crystal superalloy
[NASA-TM-100907] 18 p2489 N88-24766

Advanced development of double-injection, deep-impurity semiconductor switches
[NASA-CR-182118] 18 p2583 N88-25346

Vacancy ordering in the basal plane of YBa2Cu3O(sub)z
[DE88-004572] 18 p2583 N88-25348

The morphological stability of continuous intergranular phases: Thermodynamic considerations
[DE88-006328] 18 p2584 N88-25350

Phase diagrams in materials science and the use of the computer in their calculation
[PB88-155262] 18 p2586 N88-25364

Study of data distributions and functions for the development of thermodynamic equations of state
[PB88-196365] 18 p2587 N88-25370

Mass spectrometric high temperature measurements of the barium oxide-zirconium dioxide system and the determination of thermodynamic data for barium zirconate. Clarification of the counter-stopping capacity of coated particles for solid fission products by zirconium dioxide addition
[NASA-TT-20187] 19 p2611 N88-25496

Next-generation fire extinguishing agent. Phase 1: Suppression concepts
[AD-A192279] 19 p2614 N88-25514

Initial value problems for nonlinear heat equations
[DE88-702021] 19 p2737 N88-26251

Thermo field dynamics and para statistical mechanics
[DE88-702057] 19 p2737 N88-26253

Thermostatistical estimations of vapor-state molecules affected by gravity in a heat pipe
20 p2783 N88-26505

Electrodynamic driver for the space thermoacoustic refrigerator (STAR)
[AD-A192337] 20 p2785 N88-26517

On microphysical principles of thermofluid dynamics
[ETN-88-92095] 20 p2801 N88-26620

Thermodynamic analysis of chemical heat storage system for heat pump
[DE88-753121] 20 p2820 N88-26728

Non-equilibrium phases and phase diagrams
[DE88-008896] 20 p2880 N88-27098

Thermomechanical processing of Al alloy 2090 for grain refinement and superplasticity
[AD-A192333] 21 p2912 N88-27281

Finite element methodology for integrated flow-thermal-structural analysis
[NASA-CR-183144] 21 p2964 N88-27606

Air-sea interaction in the vicinity of a land-sea boundary in the presence of upwelling 21 p2973 N88-27661

A study of tunneling phenomena in gallium arsenide-aluminum gallium arsenide heterostructures
21 p3023 N88-27946

The dynamics and thermodynamics of a 30-60 day oscillation 22 p3121 N88-28543

Thermodynamic data bases for multivalent elements: An example for ruthenium
[DE88-004395] 23 p3190 N88-28984

The construction of the thermoelasticity equations on the basis of contemporary notions of nonlinear continua mechanics
[NASA-TT-20307] 23 p3296 N88-29631

Experimental and analytical study of two-phase flow in zero gravity
[AD-A195223] 24 p3358 N88-29993

THERMOELASTICITY

A comparison of high damping shape memory alloys with Cu-Mn-based and Fe-Cr-based alloys
[AD-A184110] 04 p0414 N88-12566

A dissipation principle and its consequences for structured shock waves in thermoelastic materials
[DE87-013723] 04 p0454 N88-12813

On stress collapse in adiabatic shear bands
[AD-A187185] 11 p1498 N88-18942

Coupled thermal vibrations of beams with temperature-dependent properties
21 p2963 N88-27601

A transversely isotropic thermoelastic theory
[NASA-TM-101302] 22 p3087 N88-28332

The construction of the thermoelasticity equations on the basis of contemporary notions of nonlinear continua mechanics
[NASA-TT-20307] 23 p3296 N88-29631

Report on an overseas visit to USA relating to the thermoelastic measurement of stresses, 16-21 August 1987
[AD-A195313] 24 p3385 N88-30161

THERMOELECTRIC CONVERSION SYSTEMS

U THERMOELECTRIC POWER GENERATION

THERMOELECTRIC COOLING

Comparison of a thermoelectric cooling system and a groundwater heat pump
[DE88-001753] 08 p0984 N88-15950

THERMOELECTRIC GENERATORS

NT SNAP 19

General-Purpose Heat Source Safety Verification Test Program: Edge-on flyer plate tests
[DE87-006309] 03 p0376 N88-12362

Speculations on future opportunities to evolve Brayton powerplants aboard the space station
17 p2398 N88-24258

The Light-Weight Radioisotope Heater Unit (LWRHU): Development and application 17 p2405 N88-24299

Pioneer 10 and 11 RTG performance update
17 p2405 N88-24301

A review of thermionic power conversion systems for SDI applications 17 p2407 N88-24310

Optimization of SP-100 thermoelectric electromagnetic pump 17 p2418 N88-24382

Status of modular RTG technology
17 p2422 N88-24403

Weldability of general purpose heat source iridium capsules 17 p2426 N88-24429

Ceramic electrical insulator development for thermoelectric SACE power system
17 p2430 N88-24459

Study on iron disilicide thermoelectric generator
[AD-A193082] 22 p3116 N88-28517

THERMOELECTRIC MATERIALS

Improved GaP doped SiGe thermoelectric material
17 p2437 N88-24503

THERMOELECTRIC POWER GENERATION

Point defect structure of Cr2O3
[AD-A187620] 11 p1556 N88-19317

The results of application studies for space nuclear power 17 p2398 N88-24259

MHW RTG performance during LES 8/9 and Voyager missions 17 p2405 N88-24300

AMTEC electrode development
17 p2409 N88-24324

Sodium heat engine/AMTEC system experiments
17 p2409 N88-24325

A dynamic model for the aft accumulator in the TE SP-100 system 17 p2414 N88-24354

Parametric analyses of the TE SP-100 system performance 17 p2415 N88-24358

SP-100 system modeling: SNPSAM update
17 p2417 N88-24372

A nuclear powered space based multimegawatt MHD disc power system 17 p2432 N88-24471

Alkali metal thermoelectric converter design for space power systems applications 17 p2437 N88-24499

A capillary pumped SHE/AMTEC system
17 p2437 N88-24500

High power density electrodes for AMTEC
17 p2437 N88-24501

Performance of vapor-fed sodium heat engine/AMTEC systems 17 p2437 N88-24502

Preparation of improved PbSnTe thermoelectric alloys and evaluation of their figure of merit
[AD-A191346] 17 p2445 N88-24538

Liquid metal thermal electric converter theoretical and experimental studies
[DE88-008806] 19 p2688 N88-25974

Study on iron disilicide thermoelectric generator
[AD-A193082] 22 p3116 N88-28517

THERMOELECTRICITY

Effect of high-temperature annealing on the microstructure and thermoelectric properties of GaP doped SiGe
[NASA-TM-100164] 01 p0029 N88-10188

Thermoelectric power in disordered electronic systems near the Anderson transition
[PREPRINT-547] 06 p0731 N88-14494

Electrothermal instability in superconducting resonators
[DE88-701684] 16 p2282 N88-23664

Optimisation of the thermoelectric figure of merit of modified silicon germanium alloys
[AD-A191347] 16 p2283 N88-23670

Preparation of improved PbSnTe thermoelectric alloys and evaluation of their figure of merit
[AD-A191346] 17 p2445 N88-24538

Improved properties of SiGe/GaP alloys
[NASA-CASE-NPO-17259-1-CU]
18 p2585 N88-25358

Anomalous dependence of the thermoelectric power on the temperature in YBaCuO high-T(sub c) superconducting samples
[DE88-702682] 23 p3292 N88-29605

THERMOGRAMS

U RECORDING INSTRUMENTS
U TEMPERATURE MEASURING INSTRUMENTS

THERMOGRAPHY

Evaluating and testing thermographic phosphors for turbine-engine temperature measurements
[DE87-011772] 02 p0174 N88-11090

Calibration of a laser-pumped, thermographic phosphor remote thermometry system
[DE88-000452] 04 p0449 N88-12781

Measurement and control of damage in composite materials: Nondestructive controls by thermography, holography, and radiography
[SNIAS-872-430-110] 05 p0559 N88-13403

Geological evolution and analysis of confirmed or suspected gas hydrate localities. Volume 10: Basin analysis, formation and stability of gas hydrates of the Aleutian Trench and the Bering Sea
[DE88-001008] 10 p1346 N88-18048

Noncontact thermometry via laser pumped, thermographic phosphors: Characterization of systematic errors and industrial applications
[DE88-005599] 13 p1777 N88-20628

Clinical applications of computerized thermography
17 p2330 N88-23915

Thermographic detection of buried debonds
[AD-A192115] 18 p2475 N88-24680

Nondestructive testing using ultrahigh frequencies
[CERT-5/1333-MO] 18 p2526 N88-24984

Image processing applied to quantitative numerical cartography of ocean circulation
19 p2702 N88-26065

Stress analysis using infrared thermography
[ETN-88-92169] 20 p2816 N88-26705

Improvements in techniques of microwave thermography
[AD-A194613] 23 p3203 N88-29062

Improvements in techniques of microwave thermography
[AD-A193620] 23 p3239 N88-29276

THERMOGRAVIMETRY

Simultaneous TG/DSC (thermogravimetry/Differential Scanning Calorimetry) and TG/MS (thermogravimetry/Mass Spectrometry) analyses of polymeric and energetic materials
[DE88-000727] 04 p0413 N88-12561

Thermogravimetric analysis of polymeric materials for an intermediate temperature solid electrolyte
[DE88-004854] 10 p1306 N88-17809

Analysis of thermal and radiation effects in materials using the GEMAT process 17 p2408 N88-24318

Simultaneous thermogravimetric modulated beam mass spectrometry and time-of-flight velocity spectra measurements: Thermal decomposition mechanisms of RDX and HMX 19 p2632 N88-25612

Development of computer-controlled thermogravimetric instrumentation for measurement of environmental and high temperature volatilization and desorption of contaminants from polymeric materials
[AD-A195934] 24 p3343 N88-29900

THERMOHYDRAULICS

Low gravity fluid-thermal experiments
[DE88-000553] 04 p0423 N88-12620

A model for stationary and dynamic impression of undercooled boiling in coupled thermohydraulic and neutron physics calculations of nuclear reactors
[IKE-6-171] 09 p1247 N88-17472

Thermal-hydraulic considerations for particle bed reactors 17 p2400 N88-24266

ATHENA heat pipe transient model
17 p2412 N88-24344

Transient thermohydraulic heat pipe modeling
17 p2413 N88-24347

SP-100 control system modeling
17 p2414 N88-24356

ATHENA simulation of the 300 kW SP-100
17 p2414 N88-24357

Expert systems approach to modeling systems with the ATHENA thermal-hydraulics code
17 p2416 N88-24365

The THROHPUT code: Thermohydraulic heat pipe modeling 17 p2421 N88-24399

Study of a water-steam two phase flow in a T-branch
[ETN-88-92306] 20 p2801 N88-26624

THERMOMECHANICAL TREATMENT

NT HOT ISOSTATIC PRESSING
NT HOT PRESSING

Development of iron aluminides
[AD-A185190] 05 p0568 N88-13461

Interrelation and measurement of formability, strengthening, and thermomechanical processing under metalworking conditions
[DE88-002485] 08 p0967 N88-15850

Grain refinement during primary breakdown of alloy 718
[DE88-005193] 13 p1743 N88-20423

Simulation of thermo-mechanical forming processes: A mixed Eulerian-Langrangian finite element method
[PB88-155247] 14 p1933 N88-21530

Experiments investigating advanced materials under thermomechanical loading 15 p2077 N88-22385

METCAN: The metal matrix composite analyzer
15 p2079 N88-22395

THERMOMECHANICS

U THERMODYNAMICS

THERMOMETERS

NT RESISTANCE THERMOMETERS

Assessment of the reliability of a correction procedure for WGT (Wet Globe Thermometer) (Botsball) measurements of heat stress
[AD-A185193] 05 p0584 N88-13559

Temperature Metrology '86
[DE88-700236] 08 p0989 N88-15990

Johnson noise thermometer for high radiation and high temperature environments
[DE88-003770] 10 p1323 N88-17911

Air temperature shield tests
[AD-A187459] 11 p1514 N88-19043

Radiation thermometry: The measurement problem
17 p2328 N88-23896

Johnson noise thermometer for high-radiation and high-temperature environments
17 p2434 N88-24480

Evaluation of thermophosphor temperature technique
[DE88-007654] 20 p2805 N88-26638

THERMOMETRY

U TEMPERATURE MEASUREMENT

THERMONUCLEAR ENERGY

U THERMONUCLEAR POWER GENERATION

THERMONUCLEAR POWER GENERATION

Applications of neutral beam and rf technologies
[DE87-014936] 03 p0379 N88-12382

Study of Plasma Motor Generator (PMG) tether system for orbit reboost
[NASA-CR-172016] 04 p0403 N88-12501

THERMONUCLEAR PROPULSION

U NUCLEAR PROPULSION

THERMONUCLEAR REACTIONS

NT CONTROLLED FUSION
NT NUCLEAR FUSION

Fusion reactivity enhancement due to ion tail formation by beam and ion cyclotron heating
[DE87-753018] 02 p0240 N88-11518

A model for stationary and dynamic impression of undercooled boiling in coupled thermohydraulic and neutron physics calculations of nuclear reactors
[IKE-6-171] 09 p1247 N88-17472

Flame propagation in the approximation of straight-line trajectories of burning products
[DE88-700675] 10 p1297 N88-17756

Diffusion description of flame propagation due to the translational motion of burning reaction products
[DE88-700676] 10 p1297 N88-17757

Preliminary analysis on plasma equilibrium control. Conceptual design study of FY86 FER
[DE88-751441] 14 p1984 N88-21834

Rayleigh-Taylor instability in inertial confinement fusion
[DE88-701411] 15 p2137 N88-22750

BIFOLD: A dual-mode nuclear space power system
17 p2404 N88-24292

TIBER (Tokamak Ignition/Burn Experimental Reactor) 2 as a precursor to an international thermonuclear experimental reactor
[DE88-008906] 20 p2858 N88-26970

The classical nova outburst
[DE88-009138] 21 p3030 N88-27987

THERMOPHILIC PLANTS

NT BLUE GREEN ALGAE

THERMOPHORESIS

Thermophoresis of spherical aerosol particle at arbitrary Knudsen numbers 04 p0461 N88-12850

Atmospheric science 07 p0883 N88-15357

THERMOPHYSICAL PROPERTIES

NT CRITICAL POINT
NT CRITICAL TEMPERATURE
NT EMISSIVITY
NT HEAT OF FUSION
NT LATENT HEAT
NT MELTING POINTS
NT PYROELECTRICITY
NT SPECIFIC HEAT
NT THERMAL CONDUCTIVITY
NT THERMAL DIFFUSION
NT THERMAL DIFFUSIVITY
NT THERMAL STABILITY
NT VAPOR PRESSURE
NT VOLATILITY

PRMIXn: A computer program for thermophysical properties of real gases and gas mixtures
[GKSS-86/E/59] 01 p0020 N88-10125

Thermophysical Properties Measurement Facility (TPMF) --- Columbus space station
[ESA-CR(P)-2417] 02 p0157 N88-10981

Growth of solid solution single crystals
[NASA-TP-2787] 06 p0688 N88-14212

A theoretical and experimental study of the thermophysical properties of lithium hydride
[NASA-TT-20179] 16 p2175 N88-22965

Phase equilibria and density calculations in the critical region: A phenomenological correction for a classical equation of state
[PB88-185335] 19 p2723 N88-26167

THERMOPHYSICS

U THERMODYNAMICS

THERMOPILES

Thermal vacuum sensors based on integrated silicon thermopiles
[ETN-88-92237] 16 p2210 N88-23190

THERMOPLASTIC FILMS

Molecular composites: Processing, post-treatment and mechanics
[AD-A184458] 04 p0410 N88-12547

THERMOPLASTIC RESINS

NT PEEK
NT THERMOPLASTIC FILMS

Interfacial strength development in thermoplastic resins and fiber-reinforced thermoplastic composites
[NASA-CR-181525] 04 p0411 N88-12549

Thermoplastic elastomer compositions — cable jackets
[EP-PATENT-0-204-453-A1] 04 p0418 N88-12593

Thermoplastic elastomers as LOVA (Low Vulnerabilit Ammunition) binders
[AD-A184350] 04 p0419 N88-12599

Process for the production of a thermoplastic elastomer composition
[EP-PATENT-0-202-782-A2] 05 p0569 N88-13465

Flexibilized copolyimide adhesives
[NASA-TM-89303] 05 p0570 N88-13474

Development of an impact- and solvent-resistant thermoplastic composite matrix, phase 4
[NASA-CR-178413] 06 p0677 N88-14145

An investigation of physical properties of thermoplastic polyimides
[NASA-TM-100530] 06 p0678 N88-14151

Thermoplastic elastomers as LOVA binders
[AD-A185865] 07 p0835 N88-15068

Structure-property relationships in thermoplastic elastomers 4. Dynamic mechanical relaxations in poly(dioxolane), poly(butyltrioxocane) and poly(propylene oxide) polyurethanes
[AD-A186278] 07 p0836 N88-15073

Thermoplastic elastomers as LOVA binders
[AD-A186563] 10 p1304 N88-17797

The place for thermoplastic composites in structural components
[AD-A189149] 12 p1604 N88-19596

A continuum damage model for viscoelastic materials
[AD-A189426] 12 p1637 N88-19800

Reinforcing of thermoplastic polycarbonate and polysulfone with carbon fibers. Production and characteristics of UD-compound objects
[NASA-TT-20158] 13 p1735 N88-20374

Interlaminar fracture toughness of thermoplastic composites
[NASA-TM-100532] 15 p2030 N88-22097

Mechanical behaviour of particle filled thermoplastics
[PB88-169297] 15 p2047 N88-22196

A study of failure characteristics in thermoplastic composite material
[AD-A190613] 16 p2171 N88-22940

The adhesive bonding of thermoplastic composites
[AD-A190994] 16 p2173 N88-22953

The mechanical behavior of particle filled thermoplastics
[ETN-88-92234] 16 p2181 N88-22999

Evaluation of a thermoplastic polyimide (422) for bonding GR/PI composite
[NASA-TM-100584] 16 p2182 N88-23003

Loading rate sensitivity of open hole composites in compression
[NASA-TM-100634] 19 p2610 N88-25490

Thermoplastic coating of carbon fibers
[NASA-CR-183067] 20 p2767 N88-26407

Irreversible deformations during fracture in polymers
[W-7/86] 20 p2780 N88-26485

Characterization of elastic-plastic properties of AS4/APC-2 thermoplastic composite
[NASA-CR-183145] 21 p2906 N88-27242

Thermoplastic composite with continuous fibers
[FOA-C-20707-2.6] 22 p3051 N88-28103

An investigation of some basic properties of hybrid composite materials
[AD-A194136] 23 p3189 N88-28975

THERMOPLASTICITY

Constitutive modeling and thermoviscoplasticity
14 p1930 N88-21508

A unified creep-plasticity model suitable for thermo-mechanical loading 14 p1932 N88-21518

The adhesive bonding of thermoplastic composites
[AD-A190994] 16 p2173 N88-22953

The mechanical behavior of particle filled thermoplastics
[FTN-88-92234] 16 p2181 N88-22999
The crystallization of tough thermoplastic resins in the presence of carbon fibers
[NASA-CR-182984] 20 p2776 N88-26464

THERMOREGULATION

Microwave challenges to the thermoregulatory system
[AD-A185391] 05 p0629 N88-13847
Human thermoregulatory model for whole body immersion in water at 20 and 28 C
[AD-A185052] 05 p0629 N88-13849
Exercise in the heat: Effects of dinitrophenol administration
[AD-A185731] 06 p0752 N88-14622
Polycythemia and hydration status: Effects on blood volume and thermoregulation during exercise-heat stress
[AD-A185946] 07 p0888 N88-15383
Prediction of human thermoregulatory responses and endurance time in water at 20 and 24C
[AD-A186223] 08 p1048 N88-16326
Exercise thermoregulation after prolonged wakefulness
[AD-A186224] 08 p1048 N88-16327
Rational considerations for modelling human thermoregulation during cold water immersion
[AD-A186226] 08 p1048 N88-16329
Temperature regulation at rest and exercise during the human menstrual cycle
[AD-A186461] 08 p1050 N88-16341
Manipulation of muscle glycogen concentrations using high and low carbohydrate diets and exercise
[AD-A187732] 11 p1519 N88-19069
Validation of mathematical model predictions of immersion survival times
[IAM-652] 14 p1952 N88-21635
Further development of a mathematical model for the specification of immersion clothing insulation
[IAM-653] 14 p1954 N88-21644
Physiological responses to acute exercise-heat stress
[AD-A192606] 21 p2986 N88-27732
Plasma volume expansion in rats: Effects on thermoregulation and exercise
[AD-A192656] 22 p3130 N88-28606
The role of textile material in clothing on thermoregulatory responses to intermittent exercise
[AD-A192599] 22 p3130 N88-28608
Depressed sweating during exercise at altitude
[AD-A192603] 22 p3130 N88-28609
Accidental hypothermia
[AD-A194967] 24 p3406 N88-30278

THERMOSETTING RESINS

NT EPOXY RESINS
NT KEVLAR (TRADEMARK)
NT NYLON (TRADEMARK)
NT PHENOLIC RESINS
NT POLYAMIDE RESINS
Addition polyimide composition
[EP-PATENT-0-167-304-A1] 01 p0053 N88-10337
Study of the morphology of thermosetting matrices
[ONERA-RT-5/3346-M] 02 p0153 N88-10961
Composite structural materials
[NASA-CR-181416] 02 p0190 N88-11186
Cure and properties of thermosetting polymers
[AD-A184669] 03 p0293 N88-11843
High-temperature thermosets derived from the Diels-Alder polymerization of bisbenzocyclobutenes and bimaleimides
[AD-A188600] 13 p1747 N88-20449
Optimization of binary pigment coatings
[AD-A189103] 13 p1748 N88-20450
Correlation between dielectric and structural properties during epoxy cure
[AD-A190696] 16 p2181 N88-22997
Cellular thermosetting fluoropolymers and process for making them
[NASA-CASE-GSC-13008-1] 17 p2326 N88-23894
Injection compression for short fiber reinforced plastics
[SNIAS-881-430-118] 21 p2922 N88-27344

THERMOSIPHONS

Heat transfer of mesh-wick heat-pipes (bottom heat mode) 20 p2783 N88-26507
An arranging method on L/D of two-phase closed thermosyphons 20 p2783 N88-26508
Characteristics of long size thermosyphons made of corrugated tube 20 p2784 N88-26511

THERMOSPHERE

The climatic wind regime in the lower thermosphere from meteor radar observations 06 p0733 N88-14506
The lower thermosphere wind regime from simultaneous observations over Euroasia (Collm, Dushanbe, Frunze)
06 p0733 N88-14510
Wind regime peculiarities in the lower thermosphere in the winter of 1983/84 06 p0733 N88-14511
On the interconnection of dynamic processes in the lower thermosphere with meteorological phenomena in the tropostratosphere 06 p0734 N88-14512
Circulation in the mesosphere and lower thermosphere during the MAP (Middle Atmosphere Program)/WINE (Winter in the Northern Europe) period
06 p0734 N88-14514
Main results of atmospheric fine structure parameter observation in the lower thermosphere
06 p0735 N88-14518
On connection between evolution of troposphere fronts and changes of circulation regime in meteor zone
06 p0735 N88-14519
On the dependence of the lower thermospheric wind regime on the solar cycle 06 p0736 N88-14524
Longitudinal peculiarities of meridional circulation in lower thermosphere and mesosphere
06 p0736 N88-14525
Lower thermosphere wind regime according to radiometeor measurements in Kazan
06 p0736 N88-14526
Mesoscale density variability in the mesosphere and thermosphere: Effects of vertical flow accelerations
06 p0736 N88-14529
Some aspects of metallic ion chemistry and dynamics in the mesosphere and thermosphere
06 p0737 N88-14534
Monte Carlo modeling and meteor showers
06 p0740 N88-14549
Radar observations of high-latitude lower-thermospheric and upper-mesospheric winds and their response to geomagnetic activity 06 p0742 N88-14563
An analysis of apparent-motion vectors in, and the structure of, A mid-latitude sporadic E layer using a 2.66 MHz radar
[AD-A186126] 07 p0877 N88-15321
Solar tides in the upper equatorial thermosphere: A comparison between AE-E data and the NCAR thermospheric general circulation model
[AD-A186160] 08 p1023 N88-16196
TOTAL: A new instrument to study turbulent parameters in the mesosphere and lower thermosphere
08 p1029 N88-16234
The effects of a geomagnetic storm on thermospheric circulation
[AD-A186638] 09 p1190 N88-17128
The photons payload: G-494: A learning experience
10 p1288 N88-17701
Into the thermosphere: The atmosphere explorers
[NASA-SP-490] 10 p1353 N88-18084
USU (Utah State University) Center of Excellence in Theory and Analysis of the Geo-Plasma Environment
[AD-A187687] 11 p1511 N88-19026
Upper-thermospheric observations and neutral gas dynamics at high latitudes during solar maximum
[AD-A188058] 11 p1512 N88-19031
Effect of nitrogen dioxide release on thermosphere
13 p1789 N88-20704
The NASA Marshall engineering thermosphere model
[NASA-CR-179359] 20 p2825 N88-26760
Wave structures in thermospheric density from satellite electrostatic triaxial accelerometer measurements
[AD-A194134] 23 p3233 N88-29240
An improvement in the numerical integration procedure used in the NASA Marshall engineering thermosphere model
[NASA-CR-179389] 24 p3392 N88-30200

THERMOSTABILITY

U THERMAL STABILITY

THERMOTROPISM

U ANISOTROPY
U TEMPERATURE EFFECTS

THERMOVISCOELASTICITY

Nonlinear thermoviscoelastic analysis of metallic plane curved beams 03 p0336 N88-12119

THESAURI

Energy Data Base: Subject Thesaurus
[DE87-008007] 03 p0384 N88-12414
NASA thesaurus supplement: A four part cumulative supplement to the 1985 edition of the NASA Thesaurus
[NASA-SP-7053(SUPP-4)] 08 p1093 N88-16575
NASA thesaurus: Astronomy vocabulary
[NASA-SP-7069] 17 p2450 N88-24553
NASA combined file postings statistics based on NASA thesaurus, Jan. 1968 - July 1988
[NASA-CR-182985] 18 p2589 N88-25384
WORDNET: An electronic lexical reference system based on theories of lexical memory
[AD-A193086] 21 p3027 N88-27970
Capitalizing on experience with intelligence gateway software
[AD-A193362] 21 p3028 N88-27971
Exploiting lexical regularities in designing natural language systems
[AD-A195922] 24 p3423 N88-30375

THESES

Down-to-Earth approach for final projects in Karlsruhe (Federal Republic of Germany)
16 p2226 N88-23292

THETA PINCH

Steady state theta pinch concept for slow formation of FRC
[ISSN-0469-4732] 01 p0098 N88-10648
Experimental study of the initial plasma formation stage in a linear theta pinch of inverted field
[DE88-700010] 09 p1249 N88-17485

THICK FILMS

Elimination of subboundaries in 0.5-micron-thick Si-on-insulation films produced by ZMR
[AD-A184590] 03 p0381 N88-12396
Microstructure modifications of micron thick NbN films to improve J/sub c/ and H/sub c2/
[DE88-003078] 08 p1091 N88-16567
Synthesis and characterization of high-T(sub c) screen-printed Y-Ba-Cu-O films on alumina
[NASA-TM-100860] 15 p2146 N88-22805
The effects of thin compressive films on indentation fracture toughness measurements
[AD-A192243] 20 p2779 N88-26480
Superconducting electronic film structures
[AD-A192907] 20 p2879 N88-27091

THICK PLATES

Solution in vibration problems of rectangular plates with spline function
[PB87-143459] 08 p0996 N88-16029
Detection sensitivity in thick assemblies --- eddy currents, light alloys, aircraft construction materials
[REPT-48-912/F] 16 p2216 N88-23221

THICKNESS

Analysis of thickness fields retrieved from NOAA-7 observations through the 3I (improved Initialization Inversion) method: Interest for weather forecasting
02 p0201 N88-11255
Taper sectioning to magnify the interface thickness of a dissimilar metal joint
[RFP-3890-REV] 03 p0333 N88-12099
Microstructure modifications of micron thick NbN films to improve J/sub c/ and H/sub c2/
[DE88-003078] 08 p1091 N88-16567
Analysis of a turbulent premixed V-flame (influence of flame-thickening)
[NAL-TR-941] 10 p1299 N88-17770
Composition and thickness of multilayer foils using MeV ion-beam techniques
[DE88-004360] 11 p1448 N88-18629
Airborne electromagnetic sounding of sea ice thickness and sub-ice bathymetry
[AD-A188939] 12 p1649 N88-19879
Simulated impact damage in a thick graphite/epoxy laminate using spherical indenters
[NASA-TM-100539] 13 p1733 N88-20363
A new method of measuring multigrade oil shear elasticity and viscosity at high shear rates
[AD-A190145] 15 p2064 N88-22304
Surface crack analysis applied to impact damage in a thick graphite-epoxy composite
[NASA-TM-100600] 16 p2173 N88-22950
Gravity currents with heat transfer effects
[PB88-180047] 16 p2205 N88-23158
Thermal conductivity of hard anodized coatings on aluminum
[AD-A191755] 18 p2492 N88-24784
Heating and evaporation of turbulent liquid films: Measurement of film thickness and the onset of nucleate boiling
[DE88-006388] 18 p2512 N88-24905
Vibrations of rotating thick or thin rings
18 p2529 N88-25003
Forced motion of initially stressed shells and plates
18 p2529 N88-25005
Effect of thickness on downward flame spread over paper
[NASA-TT-20282] 19 p2612 N88-25501
Dimensional crossover in layered superconductors
19 p2734 N88-26237
GTAW characterization for weld penetration on 304L stainless steel
[DE88-010611] 20 p2810 N88-26672
Ice detector
[NASA-CASE-LAR-13776-1] 23 p3217 N88-29149
Liquid thickness gauge
[NASA-CASE-LAR-13826-1] 23 p3217 N88-29150
Thickness effects on the stability of shell like structures 23 p3224 N88-29192
Progress in determining the thickness and distribution of volcanic materials on Mars 23 p3302 N88-29670
Variation in the thickness of ejecta cover on Mars with increasing crater density 23 p3307 N88-29701
The use of hot-film technique for boundary layer studies on a 21 percent thick airfoil
[NAE-AN-45] 24 p3321 N88-29781

Predicting the durability of adhesives and coatings by remote detection of hidden defects and coating-thickness irregularities: A theoretical and numerical study
24 p3355 N88-29972

THICKNESS RATIO

Stress state of welded joints of dissimilar materials obtained by diffusion welding 03 p0286 N88-11799

THIN AIRFOILS

NT THIN WINGS

The effects of rotational flow, viscosity, thickness, and shape on transonic flutter dip phenomena
[NASA-TM-100811] 11 p1502 N88-18969

Technology for pressure-instrumented thin airfoil models
[NASA-CR-4173] 23 p3180 N88-28933

THIN FILMS

NT ENERGY ABSORPTION FILMS
NT MONOMOLECULAR FILMS

Use of sol-gels in the application of ceramic oxide thin films
[DE87-013610] 01 p0028 N88-10176

Direct formation of thin films and epitaxial overlayers at low temperatures using a low-energy (10-500 eV) ion beam deposition system
[DE87-012291] 01 p0103 N88-10675

Chemical vapor deposition of B6P and B6As films
[DE87-009288] 02 p0151 N88-10942

Stress measurements in sol-gel films
[DE87-014467] 02 p0153 N88-10955

The development of a new and novel Hadamard transform infrared spectrometer for analytical chemistry
[DE87-014804] 02 p0175 N88-11094

Multilayered foils as radiation entrance windows and spectral filters for image converters in the ultrasoft X-ray wavelength region
[MPE-PREPRINT-90] 02 p0176 N88-11099

The preparation of thin films for photovoltaic conversion by novel MOCVD techniques
[DE87-001185] 02 p0194 N88-11212

Preparation and properties of evaporated CdTe films
[DE87-012270] 02 p0195 N88-11216

CuInSe2 solar cell research by sputter deposition
[DE87-001184] 02 p0195 N88-11219

Wide bandgap passivation layers on silicon
[DE87-014307] 02 p0244 N88-11543

Ohmic contacting schemes to gallium arsenide devices
[DE87-014627] 02 p0244 N88-11544

Thin film microstructures: Simulation and theory
[DE87-014732] 02 p0246 N88-11553

Highly Non-Linear Optical (NLO) organic crystals
03 p0297 N88-11865

Highly Non-Linear Optical (NLO) organic crystals and films. Electrooptical organic materials
03 p0297 N88-11866

Ion plating: Fundamental processing studies and synthesis of high performance coatings
[AD-A184766] 03 p0303 N88-11908

Thin films for geothermal sensing
[DE88-000154] 03 p0326 N88-12061

Taper sectioning to magnify the interface thickness of a dissimilar metal joint
[RFP-3890-REV] 03 p0333 N88-12099

Investigation of hexagonal ferrite film growth techniques for millimeter-wave systems applications
[AD-A184335] 03 p0383 N88-12406

Experimental study of thermocapillary flows in a thin liquid layer with heat fluxes imposed on the free surface
[NASA-TM-100252] 04 p0445 N88-12763

Studies of thin surface films aim at seeing deep ocean processes 04 p0460 N88-12847

Theory and simulations of Zone 2 microstructures in thin films
[DE87-014752] 04 p0499 N88-13071

Influence of bonding shop moisture on metal-honeycomb junctions bonded with ultra-thin adhesive films
[SNIAS-872-422-112] 05 p0558 N88-13399

Raman microprobe characterization of dielectric films following high-energy pulsed laser irradiation
[DE88-000559] 05 p0568 N88-13[illegible]87

Tribology of thin film systems
[ETN-88-91365] 05 p0590 N88-13601

The effects of thin anodic films on the cyclic microstrain/macrostrain behavior of tungsten
05 p0597 N88-13650

Develop techniques for ion implantation of (lead-lanthanum-zirconate-titanate) for adaptive optics
[DE88-000642] 05 p0650 N88-13986

Structural characterization of ion implanted beta-SiC thin films
[DE87-014567] 05 p0656 N88-14027

Effects of hydrolysis on metallo-organic solution deposition of PZT films
[ATR-86(8443)-1] 06 p0679 N88-14160

Determination, by X-ray fluorescence, of platinum, palladium, ruthenium, iron and chromium in special steels
[PB87-132114] 06 p0683 N88-14183

An analysis of the effect of system variables on the quality of thin films and powders produced by laser-breakdown chemical vapor deposition
[DE88-001793] 06 p0708 N88-14342

Partial analysis of experiment LDEF A-0114
[NASA-CR-179236] 06 p0780 N88-14787

Structure of layered crystals studied by high energy ion beams
[DE88-001675] 06 p0786 N88-14822

Analytical investigations of bulk wave resonators in the piezoelectric thin film on gallium-arsenide configuration
[AD-A185716] 06 p0789 N88-14840

Very thin VLSI-layouts (Very Large Scale Integration-Layouts) of complete binary trees
[PB88-100847] 06 p0789 N88-14841

Microstructure and magnetic properties of cobalt-chromium alloys
[DE88-002762] 07 p0835 N88-15064

Superconducting switch program
[AD-A185682] 07 p0848 N88-15144

Radiation hardness evaluation of thin film ferroelectric capacitors
[DE88-001357] 07 p0848 N88-15147

Thin film and gradient-driven instability mechanisms
[PB88-101522] 07 p0853 N88-15182

Thin film electret boundary layer transition detector: A feasibility study
[AD-A18567[illegible]] 07 p0856 N88-15199

Contrast between the chemical, structural and electronic properties of thin films of Cu and Ni on the Ru(0001) surface
[DE88-002380] 07 p0938 N88-15698

Research sensors 08 p0955 N88-15795

TiN coatings on M2 steel produced by plasma assisted chemical vapor deposition
[DE88-003189] 08 p0970 N88-15867

Sputtered silver films to improve chromium carbide based solid lubricant coatings for use to 900 C
[NASA-TM-100783] 08 p0973 N88-15885

Depth of origin of sputtered atoms: Experimental and theoretical study of Cu/Ru(0001)
[DE88-002848] 08 p1082 N88-16520

Experimental aspects of high-T/sub c/ superconductors
[DE88-003019] 08 p1090 N88-16564

The role of thermodynamic phase diagrams and lattice matching in superlattice growth
[DE88-003113] 08 p1091 N88-16568

Monolayer films prepared by the spontaneous self-assembly of symmetrical and unsymmetrical dialkyl sulfides from solution onto gold substrates: Structure, properties, and reactivity of constituent functional groups
[AD-A186717] 09 p1137 N88-16814

The effect of varying sputtering parameters on the microstructure and mechanical properties of 10 percent Ni + TiB2 thin films
[DE88-002600] 09 p1254 N88-17517

Crystalline sulfur dioxide: Crystal field splittings, absolute band intensities and complex refractive indices derived from infrared spectra
[NASA-CR-182502] 09 p1258 N88-17547

Diffusion studies in amorphous NiZr alloys
[DE88-003009] 10 p1301 N88-17781

The migration of grain boundaries in ceramic materials with particular reference to the sintering process
[DE88-004065] 10 p1306 N88-17808

Adhesion of vapour phase deposited ultra-thin polyimide films on polycrystalline silver
[AD-A187930] 10 p1306 N88-17810

The soft/hard wet anodization of aluminum oxide and its use in a thin film multilayered capacitor
[AD-A187575] 10 p1325 N88-17919

Apparatus for the study of silicon film deposition and silicon etching
[AD-A187616] 10 p1334 N88-17972

Monitoring interfacial dynamics by pulsed laser techniques
[DE88-003362] 10 p1335 N88-17976

Optical measurements of surface oxide layer formation on metal films
[DE88-003163] 10 p1409 N88-18405

Specific heat of novel thin-film material systems
10 p1415 N88-18446

The physics of metallic superlattices: An experimental point of view
[DE88-003080] 10 p1416 N88-18452

Synthesis and characterization of thin films
[AD-A187335] 10 p1421 N88-18485

Superconductivity of thin film intermetallic compounds
[AD-A187563] 10 p1421 N88-18489

Evaluation of centrifugal barrel tumbling process for impregnation of molybdenum disulfide powder lubricant
[BDX-613-3698] 11 p1464 N88-18727

Ceramic decomposition under irradiation
[DE88-004327] 11 p1464 N88-18732

Cryocooler systems demonstration
[AD-A188025] 11 p1467 N88-18745

Prototype thin-film thermocouple/heat-flux sensor for a ceramic-insulated diesel engine
[NASA-TM-100798] 11 p1490 N88-18892

Preparation of thin film polyvinylidene fluoride shock wave pressure transducers
[PB88-156070] 11 p1490 N88-18893

Plasma deposition of silicon carbide thin films
[AD-A188093] 11 p1556 N88-19314

Proceedings of the Polycrystalline Thin Film Program Meeting
[DE87-001169] 11 p1557 N88-19321

Raman enhancement methods for molecular structure characterization of optical thin films
[DE88-003421] 11 p1558 N88-19324

Ion beam modification of film stress and the effectiveness of thin film encapsulants on GaAs
[DE88-004458] 11 p1558 N88-19328

Electrochromic thin films
[DE88-751099] 11 p1559 N88-19334

Preparation and characterization of thin films of alumina by metalorganic chemical vapor deposition
[AD-A188366] 12 p1608 N88-19614

Electrophoretically deposited styrene-acrylate coatings for suppression of internal electromagnetic pulse effects
[DE88-003820] 12 p1609 N88-19621

Polymeric materials for electro-optic testing
[AD-A188382] 12 p1610 N88-19627

The effects of thin polymeric surface films in reducing fretting corrosion and wear
[AD-A188633] 12 p1611 N88-19634

SiO2 film stress distribution during thermal oxidation of Si
[AD-A189552] 12 p1612 N88-19637

Artificially structured superconductors
[DE88-005345] 12 p1697 N88-20153

Characterization of redox states of nickel hydroxide film electrodes by in-situ Raman spectroscopy
[AD-A189268] 13 p1741 N88-20411

Improved methods for high resolution electron microscopy
[DE88-005731] 13 p1774 N88-20609

Research on high-efficiency, stacked, multijunction, amorphous silicon alloy thin-film solar cells
[DE88-001106] 13 p1793 N88-20723

CdZnTe as a wide-band-gap absorber for a tandem, thin-film solar cell
[DE88-001114] 13 p1793 N88-20724

Stable, high-efficiency, CuInSe2-based, polycrystalline thin-film tandem solar cells
[DE88-001116] 13 p1793 N88-20726

Cadmium sulfide/copper ternary heterojunction cell research
[DE88-001122] 13 p1793 N88-20727

Direct absorption receiver control studies
[DE87-013653] 13 p1795 N88-20737

Measurement of the properties of lossy materials inside a finite conducting cylinder
[NASA-CR-182664] 13 p1832 N88-20962

Measuring thin film properties using SAW (Surface Acoustic Wave) devices: Diffusivity and surface area
[DE88-002216] 13 p1834 N88-20970

Thin-film diffusion barriers for metal-semiconductor contacts
[AD-A188712] 13 p1844 N88-21035

Modulatable thin film field emission space gun
[AD-A189279] 13 p1845 N88-21043

Thin-film cadmium telluride solar cells
[DE88-001107] 13 p1846 N88-21050

X-ray diffraction study of a thin GaAs film on Si(100)
[DE88-005290] 13 p1847 N88-21055

Superconducting superlattice structures
[DE88-005346] 13 p1847 N88-21056

Initial stages of silicon growth on the (100) surface of silicon by localized laser CVD
[DE88-005420] 13 p1848 N88-21059

A novel method for sputter-deposition of high T(sub c) superconductor films via a computer-controlled mass analyzed ion beam
[DE88-006001] 13 p1848 N88-21064

The performance of thin solid films for satellite gears
14 p1876 N88-21209

Space station solar concentrator materials research
[NASA-TM-100862] 14 p1882 N88-21250

On the torque and wear behavior of selected thin film MOS2 lubricated gimbal bearings
14 p1926 N88-21485

Infrared reflection-absorption spectroscopy of hyperfine layers on surfaces of semiconductors and dielectrics
14 p1969 N88-21755

Giant Josephson signal in wide superconducting films 14 p1973 N88-21777

Femtosecond studies in hot carrier relaxation in GaAs and AlGaAs 14 p1977 N88-21801

Structure and properties of titanium nitride and zirconium nitride thin films prepared by reactive ion plating --- cutting tools [ETN-88-92218] 15 p2042 N88-22167

Vapor phase deposition and growth of polyimide films on copper [AD-A189969] 15 p2044 N88-22178

Development of a laboratory test for multiport injector deposits: Approaches 1 and 2 [AD-A190697] 15 p2048 N88-22203

Laser evaporation studies [AD-A189815] 15 p2071 N88-22346

High-efficiency thin-film silicon-on-GaP solar cell for improved radiation resistance [AD-A190268] 15 p2091 N88-22460

Fundamental studies of the mechanical behavior of microelectronic thin film materials [AD-A190038] 15 p2143 N88-22786

Thin superconducting film characterization by surface acoustic waves [AD-A190417] 15 p2143 N88-22791

Thin film research diagnostics instrumentation [AD-A191240] 16 p2213 N88-23207

Magnetic studies of iron-rare-earth-metalloid alloys [DE88-006801] 16 p2282 N88-23660

Boundary layer measurements using hot-film sensors 17 p2297 N88-23743

Superconducting thin film vertex detector for SSC (Superconducting Super Collider) applications [DE88-005951] 17 p2445 N88-24535

Micro-Raman analysis of dielectric optical thin films [AD-A191228] 17 p2445 N88-24537

Method of producing high T(subc) superconducting NBN films [NASA-CASE-NPO-16681-1-CU] 17 p2446 N88-24543

Electrical conduction in thin film carbons [AD-A191726] 18 p2491 N88-24780

Electron-Rayleigh wave interaction in thin film carbons [AD-A191727] 18 p2492 N88-24781

Joint services electronics program research in electronics [AD-A192206] 18 p2504 N88-24857

Magnetic superlattices [AD-A191450] 18 p2581 N88-25334

Molecular characterization of structure and bonding in thin film materials [DE88-006811] 18 p2584 N88-25351

Electrode films of porous agarose: The effects of physical structure on electron transport processes [DE88-007366] 19 p2611 N88-25493

Hydrogenated amorphous silicon-germanium alloys [DE88-001147] 19 p2620 N88-25546

Picosecond optoelectronic study of a thin film transmission line structure 19 p2661 N88-25823

The 1986 IEEE Solid-State Sensor Workshop [AD-A190922] 19 p2668 N88-25860

The structure and properties of RF reactive sputtered IrO2 films 19 p2672 N88-25884

Effect of process conditions on aluminum oxide thin film used in pH ISFET 19 p2673 N88-25892

Surface acoustic wave gas sensor based on film conductivity changes 19 p2673 N88-25894

Zinc-oxide thin films for integrated-sensor applications 19 p2673 N88-25896

Tin oxide microsensors on thin silicon membranes 19 p2673 N88-25897

The use of micromachined structures for the management of mechanical properties and adhesion of thin films 19 p2674 N88-25899

Systematics of excimer laser ablation: Thin film preparation of high T(sub c) material [DE88-010569] 19 p2675 N88-25909

Study of Staebler-Wronsky degradation effect in a Si:H based P-I-N solar cells [NASA-CR-182564] 19 p2687 N88-25970

Center for thin film studies [AD-A191996] 19 p2732 N88-26226

The catalytic reactivity of thin film crystal surfaces [DE88-006387] 19 p2732 N88-26228

The use of liquid films for spacecraft survivability to laser radiation [AD-A192954] 20 p2765 N88-26395

The effects of thin compressive films on indentation fracture toughness measurements [AD-A192243] 20 p2779 N88-26480

Preparation technology for thin film solid electrolyte fuel cells [PB88-131925] 20 p2821 N88-26735

Properties of multilayers for soft X-ray optics 20 p2867 N88-27025

Growth and characterization of thin films of ZnSnP(sub)2 [DE88-001164] 20 p2874 N88-27060

Fundamental optical studies of competitive adsorption and thin film phenomena [DE88-008780] 20 p2875 N88-27068

Characterization of the surface area and porosity of sol-gel films using saw devices [DE88-008794] 20 p2875 N88-27069

Preparation of high-T(sub)c Y1Ba2Cu3O(sub 7-Delta) superconducting thin films by MBE (Molecular-Beam-Epitaxy) techniques [DE88-009999] 20 p2877 N88-27082

Thin film and near-surface characterization using a mechanical properties microprobe [DE88-011399] 21 p2915 N88-27302

Equipment for building and testing superconductive flux flow electronic devices [AD-A192959] 21 p2936 N88-27436

Superconducting thin films, composites and junctions [AD-A193123] 21 p2937 N88-27440

Effects of surface tension and contact angle on sensible heating and boiling incipience in dielectric falling films [DE88-007057] 21 p2945 N88-27492

Chemical vapor deposition of TiO2 thin films at room temperature [DE88-008892] 21 p2953 N88-27542

Laser-heated CVD process for depositing thin films for low-cost solar-cell applications [DE88-001162] 21 p2967 N88-27623

Experimental fabrication of thin film single crystalline solar cells [PB88-131958] 21 p2967 N88-27627

Amorphous silicon solar cells using a metal substrate [PB88-131941] 21 p2968 N88-27628

Measurement of the thermal conductivity of dielectric thin solid films with a thermal comparator [DE88-008468] 21 p3016 N88-27898

Materials research, superconductor and thin layer technology [REPT-50/87] 21 p3025 N88-27955

Studies of internal stresses and surface roughness of sputtered Be and BeB films [DE88-011737] 22 p3086 N88-28327

Experimental fabrication of thin film single crystalline solar cells [PB88-131958] 22 p3116 N88-28516

Computer simulation of electromigration in thin films [AD-A194526] 22 p3157 N88-28782

Thin film coatings for space electrical power system applications [NASA-TM-101325] 23 p3187 N88-28966

Thin film-residual stress assessment [AD-A193205] 23 p3196 N88-29018

Dissolution rates of polymers and copolymers based on methyl, ethyl and butyl methacrylate [AD-A194713] 23 p3197 N88-29027

Theoretical investigation on heterojunction solar cell [DE88-701837] 23 p3229 N88-29219

Shear stress at a film-substrate interface due to mismatch strain [AD-A193461] 23 p3288 N88-29577

Preparation of superconducting YBa2Cu3O(sub 7-x) films by magnetron sputtering [DE88-009977] 23 p3289 N88-29583

Research on crystal and film ferroelectric materials for optoelectronic applications [AD-A193512] 23 p3291 N88-29597

High power storage system based on thin film solid ionics [AD-A193623] 23 p3291 N88-29598

New method for preparation of (Cd, Hg)Te thin films [DE88-702727] 23 p3293 N88-29608

Temperature dependence of conductivity and of Hall coefficients for noble metal films [ETN-88-92981] 23 p3294 N88-29616

Diamond film by hot filament CVD method [NASA-TT-20335] 23 p3294 N88-29618

Stress related failures causing open metallization [AD-A195061] 24 p3383 N88-30150

A review of melt and vapor growth techniques for polydiacetylene thin films for nonlinear optical applications [NASA-TM-100340] 24 p3430 N88-30412

Cluster beam studies [AD-A195182] 24 p3434 N88-30443

THIN PLATES

Generalized hybrid variational principle, corresponding finite element model 03 p0301 N88-11895

Models for penetration of thin plates [DE87-013727] 03 p0332 N88-12090

On the instability of thin circular shear layers 04 p0395 N88-12467

Fatigue failure of thin porous strips 04 p0426 N88-12640

The accommodation of precipitate plates modelled as a tensile test [DE88-000207] 04 p0454 N88-12814

Knot selection for least squares thin plate splines [AD-A185681] 06 p0759 N88-14657

Transient welding strain measurement by Moire technique: A comparison between experimental measurement and numerical analysis for strain-stress cycles during GTA spot-welding [PB87-143871] 07 p0868 N88-15269

Bending analysis of thin plates with openings [PB87-143400] 07 p0869 N88-15274

The nonlinear dynamic response of an elastic-plastic thin plate under impulse loading [AD-A182147] 08 p0994 N88-16013

Solution in vibration problems of rectangular plates with spline function [PB87-143459] 08 p0996 N88-16029

Integral equation method for the analysis of plates and shells [PB87-144788] 08 p0996 N88-16030

A note on the aerodynamic design of thin parallel-sided aerofoil sections [ARL-AERO-TM-388] 09 p1114 N88-16677

Investigation of thermoacoustic heat transport using a thermoacoustic couple [AD-A186889] 09 p1242 N88-17442

Transient sound radiation from infinite thin plate [ARE-TM(UHA)-87508] 09 p1243 N88-17449

Boundary stabilization of thin elastic plates [AD-A187123] 10 p1343 N88-18025

Numerical simulation of the perforation of thin plates [ISL-R-122/86] 11 p1495 N88-18926

Investigation into the operation of the new special drills for drilling holes in thin components made of composite materials --- aircraft components [LR-519] 16 p2215 N88-23215

Dynamic response of plates to moving loads: Structural impedance and finite element methods 18 p2528 N88-25000

Static analysis of thin plates using the finite strip-element method 19 p2679 N88-25931

An investigation of soft launch and instability breakup with a two-stage light gas gun [DE88-010371] 21 p2901 N88-27218

THIN WALLED SHELLS

Analysis of shell-type structures subjected to time-dependent mechanical and thermal loading [NASA-CR-181409] 01 p0060 N88-10388

Analytic model of an imploding Z-pinch plasma colliding inelastically with a thin-shelled cylindrical target [DE88-000051] 03 p0378 N88-12379

Integral equation method for the analysis of plates and shells [PB87-144788] 08 p0996 N88-16030

Successful mixed formulation for axisymmetric shell analysis employing discontinuous stress fields of the same order as the displacement field [DE88-700021] 09 p1178 N88-17052

Investigations of the equilibrium and stability of thin-walled double rings. A contribution to the solution of single-sided contact problems [ETN-87-90044] 09 p1181 N88-17076

Analysis of shell-type structures subjected to time-dependent mechanical and thermal loading [NASA-CR-182705] 13 p1783 N88-20668

Reversed field pinch operation with a thin shell [DE88-005521] 13 p1843 N88-21027

Topics in curved and flat space electromagnetism 13 p1854 N88-21100

A comparison of experimental and calculated thin-shell leading-edge buckling due to thermal stresses [NASA-TM-100416] 17 p2349 N88-23999

Nonlinear vibrations of imperfect thin walled cylindrical shells [ETN-88-92904] 23 p3227 N88-29205

Geometric and material nonlinear analysis of structures comprising rectangular hollow sections [CE-79] 24 p3382 N88-30141

THIN WALLS

Pulsed eddy-current inspection of thin-walled stainless steel tubing [DE88-001492] 04 p0457 N88-12830

Development on thin wall tubes of dispersion type [DE87-703384] 05 p0571 N88-13483

Distortional buckling formulae for thin-walled channel columns [PB87-124012] 06 p0722 N88-14437

Geometric nonlinear analysis of asymmetric thin-walled members [PB87-133856] 06 p0723 N88-14446

Influence of radiation and thermal conduction on temperature distribution in the thin wall of a hollow cylinder [INPE-4428-TDL/308] 12 p1626 N88-19730

The elastic analysis of a thin toroidal shell
[AD-A187801] 12 p1635 N88-19785

THIN WINGS
Calculation of aerodynamic heat transfer for blunt-nosed thin wings at different angles of attack at supersonic speeds
[NASA-TT-20127] 02 p0123 N88-10776
A supersonic potential gradient method for the calculation of unsteady aerodynamic pressures on harmonically oscillating wings
[ESA-TT-930] 03 p0259 N88-11631

THINNERS
U SOLVENTS

THIOLS
Reactions of some thiol collectors at noble-metal and pyrite electrodes
[PB88-138318] 11 p1455 N88-18674
Determination of low molecular weight thiols using monobromobimane fluorescent labeling and high-performance liquid chromatography
[NASA-CR-182932] 19 p2608 N88-25478
The evolution of glutathione metabolism in phototrophic microorganisms
[NASA-CR-182902] 19 p2695 N88-26015
Correlations between wettability and structure in monolayers of alkanethiols adsorbed on gold
[AD-A194348] 23 p3191 N88-28991

THIXOTROPIC PROPELLANTS
U GELLED ROCKET PROPELLANTS

THIXOTROPY
Thixotropic surface composition for phenolaldehyde resin laminates
[GB-PATENT-2-180-251-A] 04 p0410 N88-12545

THOMAS-FERMI MODEL
Semiclassical theory of the nuclear response function. Quasielastic electron scattering
[ETN-88-91082] 09 p1245 N88-17459

THOMAS-FERMI THEORY
U THOMAS-FERMI MODEL

THOMSON EFFECT
U THERMOELECTRICITY

THOMSON SCATTERING
Enhanced Thomson scattering from laser plasmas
[DE87-014463] 02 p0236 N88-11503
Feasibility of alpha particle measurement in a magnetically confined plasma by CO2 laser Thomson scattering
[DE88-000039] 02 p0241 N88-11522
Tangential Thomson scattering --- plasma diagnostics
[REPT-87-173] 08 p1067 N88-16548
Thomson scattering for determining electron concentrations and temperatures in an inductively coupled plasma. 1: Assessment of the technique for a low-flow, low-power plasma
[AD-A191323] 16 p2280 N88-23651
Measurement of time evolution of plasma electron component parameters on the Ogra-4 device by the Thomson scattering method
[DE88-701575] 16 p2282 N88-23662
Design and calibration of a two-channel low-noise heterodyne receiver for use in a CO2 laser Thomson scattering alpha particle diagnostic
[DE88-007866] 19 p2728 N88-26201
A CO2 laser Thomson scattering diagnostic for fusion product alpha particle measurement
[DE88-007683] 20 p2857 N88-26965
Multipoint Thomson scattering diagnostic for DIII-D
[DE88-008737] 20 p2857 N88-26969
Multi-mode optical fibers for simultaneous 13-position measurements Thomson scattering apparatus in the JFT-2M tokamak
[DE88-753133] 21 p3015 N88-27897

THORIUM
Phenomenological model of superconductivity of heavy fermions in U(sub 1-x)ThsubxBesub13
09 p1238 N88-17423
Effects of galactic chemical evolution on thorium/neodymium cosmochronology
[DE88-003829] 11 p1570 N88-19397

THORON
U RADON ISOTOPES

THREADS
Empirical fatigue crack growth data for a tension loaded threaded fastener
[AD-A194112] 22 p3088 N88-28334

THREAT EVALUATION
Military needs and forecast, 2
01 p0015 N88-10087
System for detecting objects that represent a threat
[NASA-TT-20244] 13 p1760 N88-20528
Investigations of test methodology for the stress loading facility
[PB88-166095] 15 p2022 N88-22049
Threat expert system technology advisor
[NASA-CR-177479] 24 p3328 N88-29816

THREE AXIS STABILIZATION
Country plans three-axis weather satellite
06 p0688 N88-14218
Control and stabilization of ESA satellites
09 p1124 N88-16734
Three axis attitude control system
[NASA-CASE-GSC-12970-1] 17 p2308 N88-23808
Wave structures in thermospheric density from satellite electrostatic triaxial accelerometer measurements
[AD-A194134] 23 p3233 N88-29240

THREE BODY PROBLEM
Asymptotics of the effective potentials and wave functions of a three-body problem in suitable coordinates
[DE87-703323] 03 p0370 N88-12326
Physics of few-body lambda hypernuclei
[DE87-014746] 03 p0375 N88-12357
Study on orbits near the triangular libration points in the perturbed restricted three body problem
[ESA-CR(P)-2440] 07 p0944 N88-15741
Limitation of spacecraft orbit near colinear libration center of limited elliptical three body problem
08 p1003 N88-16075
Periodic orbits of limited elliptical three body problem
08 p1004 N88-16081
Hyperspherical coordinate theory of two-electron processes: Future plans
[DE87-010653] 08 p1081 N88-16516
Adiabatic representation of three-body problem in hyperspherical coordinates. Statement of the problem
[DE88-701162] 15 p2126 N88-22678
A generic multibody simulation
[NASA-CR-182949] 17 p2388 N88-24198
Families of periodic solutions in problem of solid body rotation at triangular libration point in restricted three-body problem 24 p3446 N88-30508

THREE DIMENSIONAL BODIES
Problem and solution formulations for the generation of 3D block-structured grids --- aircraft design
[NLR-MP-86020-U] 01 p0005 N88-10028
A user's guide for BIE3D: A boundary integral equation computer program for three-dimensional elastostatic analysis
[RAE-TM-MAT-STR-1078] 01 p0079 N88-10509
Three dimensional reconstruction of optical microscope pictures using the three dimensional microscopic inverse point spread function
[ETN-87-90420] 01 p0098 N88-10646
The Green's function method for fully unsteady aerodynamics around three-dimensional bodies and its application to flutter analysis
[UTIAS-298] 03 p0260 N88-11639
The 3-D world modeling for an autonomous robot
[DE87-013878] 03 p0333 N88-12102
On the recognition of curved objects
[AD-A184441] 04 p0478 N88-12945
Finite-element method for three-dimensional electric and electromagnetic field problems
[PB87-138731] 06 p0696 N88-14274
Shuttle computational grid generation
06 p0794 N88-14863
A knowledge-based object recognition system for applications in the space station
[NASA-CR-182411] 08 p0989 N88-15991
Numerical analysis of motion of solid bodies in atmosphere 08 p1079 N88-16505
Self-adaptive analysis of three-dimensional structures using a p-version of finite element method
[FFA-TN-1987-31] 09 p1182 N88-17084
Boundary elements combined with singular fields for three-dimensional cracked solids
[RAE-TR-87038] 09 p1183 N88-17088
Solid modelling with faceted primitives
[ETN-88-91593] 09 p1218 N88-17305
Shape optimization of three-dimensional stamped and solid automotive components
[GMR-5168] 11 p1528 N88-19123
Measuring accuracy of 3-dimensional bodies by the GOMER-1 device
[DE87-703230] 12 p1625 N88-19744
Retrieval of three-dimensional wind and temperature fields from single-Doppler radar data
12 p1646 N88-19858
An interactive user-friendly approach to surface-fitting three-dimensional geometries
[NASA-CR-4126] 12 p1682 N88-20058
High-speed flow calculations past 3-D configurations based on the Reynolds averaged Navier-Stokes equations
[NASA-TM-100082] 14 p1911 N88-21421
Tectonics and three-dimensional structure of spreading centers: Microearthquake studies and tomographic inversions
[PB88-163290] 14 p1945 N88-21602
Definition and display of profiled sweep-objects --- computer graphics
[REPT-87-45] 14 p1957 N88-21665
A three-dimensional model for the elastic properties of a foam
[DE88-006197] 15 p2046 N88-22192
A 3-D solid rendering of NDT data
[DE88-006199] 15 p2076 N88-22373
On the geometric interpretation of image contours
[RR-647-I-IMAG-57-LIFIA] 15 p2109 N88-22563
Maximum likelihood parameter identification of flexible spacecraft
[LR-508] 16 p2168 N88-22924
Three-dimensional curved shell and solid-shell transition finite elements with temperature and temperature gradients as primary variables for steady state heat conduction
17 p2349 N88-23997
A survey of freeform solid modeling methods
[REPT-87-81] 20 p2839 N88-26847
The construction of composite grids for general three-dimensional regions 20 p2843 N88-26872
An aspect graph-based control strategy for 3-D object recognition 21 p2927 N88-27377
Creating aspect graphs for use in object recognition
21 p2928 N88-27379
Enhancement of modeling and image generation techniques for high-resolution 3-dimensional imagery
[DE88-008923] 21 p2998 N88-27782
Three-dimensional zonal grids about arbitrary shapes by Poisson's equation
[NASA-TM-101018] 22 p3039 N88-28042

THREE DIMENSIONAL BOUNDARY LAYER
Three-dimensional structure of boundary layers in transition to turbulence
[AD-A185466] 06 p0702 N88-14311
Unsteady behavior of three-dimensional vortices relevant to turbulent boundary layers
[AD-A186767] 09 p1161 N88-16958
Velocity measurements in a 3D (three dimensional) shock wave laminar boundary layer interaction
[AD-A187334] 10 p1332 N88-17959
The structure and control of three-dimensional shock wave turbulent boundary layer interactions
[AD-A187642] 10 p1332 N88-17961
General fuselage coordinates for the calculation of three-dimensional boundary layers
[MBB/LKE-122/S/PUB/244] 13 p1771 N88-20596
Wave interactions in a three-dimensional attachment line boundary layer
[NASA-CR-181653] 14 p1910 N88-21414
Theoretical investigation of secondary instability of three-dimensional boundary-layer flows with application to the DFVLR-F5 model wing
[DFVLR-FB-87-44] 15 p2068 N88-22330
Boundary layer transition
[CERT-OA-37/5018-AYD] 18 p2458 N88-24595
A documentation of two- and three-dimensional shock-separated turbulent boundary layers
[NASA-TM-101008] 21 p2949 N88-27519
Study of hypersonic boundary layers
[CERT-RSF-OA-17/5005-AYD]
23 p3213 N88-29121
User's manual for three dimensional boundary layer (BL3-D) code
[NASA-CR-174899] 24 p3369 N88-30063
Assessment of a 3-D boundary layer analysis to predict heat transfer and flow field in a turbine passage
[NASA-CR-174894] 24 p3370 N88-30066

THREE DIMENSIONAL COMPOSITES
Woven frameworks for three-dimensional reinforcement 14 p1884 N88-21262
Fracture behavior in multidimensional fiber-reinforced composites 22 p3051 N88-28099
An investigation of some basic properties of hybrid composite materials
[AD-A194136] 23 p3189 N88-28975

THREE DIMENSIONAL FLOW
NT SECONDARY FLOW
NASA-VOF3D: A three-dimensional computer program for incompressible flows with free surfaces
[DE87-011849] 01 p0045 N88-10286
Characteristics and boundary elements for three dimensional nonstationary Navier Stokes flows
[PREPRINT-1051] 02 p0172 N88-11086
Flow in a model turbine stator
02 p0187 N88-11163
IMPSOR: A fully vectorized FORTRAN code for three dimensional moving boundary problems with Dirichlet or Neumann boundary conditions
[DE87-014964] 02 p0226 N88-11427
On the onset of three-dimensionality and time-dependence in the Goertler vortex problem
[NASA-CR-178404] 03 p0260 N88-11638
Three-dimensional calculation in high subsonic axial compressor rotor and its comparison with L2F velocity measurement 03 p0300 N88-11[illegible]

Calculation of the three dimensional flow in the impeller of hydraulic turbomachines using a finite element method
[ETN-87-90612] 03 p0315 N88-11988
Theoretical analysis of primary instabilities in three dimensional boundary layer flows
[ESA-TT-1063] 03 p0315 N88-11992
On the scheme dependency of the three-dimensional Euler solutions 03 p0318 N88-12010
Development and application of computational aerothermodynamics flowfield computer codes
[NASA-CR-181534] 04 p0395 N88-12465
An analysis of the compressible-viscous flow field around a 3D-oscillating wing 05 p0535 N88-13254
Three-dimensional flow past a two-dimensional body
05 p0539 N88-13280
Computational study of three-dimensional wake structures
[REPT-2] 05 p0539 N88-13281
Time-marching finite-difference methods for the three-dimensional Euler equations of contravariant velocity components 05 p0539 N88-13285
Numerical simulation of transonic aircraft in comparison to wind tunnel test 05 p0540 N88-13289
A numerical study of the effects of curvature and convergence on dilution jet mixing
[NASA-TM-89878] 05 p0549 N88-13347
Displaying three-dimensional data
[AD-A185347] 05 p0560 N88-13541
The development and evaluation of three-dimensional models of cold flow in internal combustion engines
[DE88-900077] 05 p0589 N88-13594
Three-dimensional dynamic labyrinth seal analysis
[AD-A185353] 05 p0590 N88-13599
A system of three-dimensional complex variables
[NASA-TM-88318] 05 p0645 N88-13951
Numerical simulation of flight body circumference flow
06 p0676 N88-14137
Analysis of three-dimensional viscous internal flows
[AD-A186254] 07 p0849 N88-15155
Numerical calculation of appendage, flat plate junction flow
[AD-A186371] 07 p0850 N88-15158
Multitasked embedded multigrid for three-dimensional flow simulation
[NASA-CR-182398] 07 p0852 N88-15173
Acta Aerodynamica Sinica (selected articles)
[AD-A185723] 08 p0949 N88-15757
Unsteady three-dimensional flow separation
[NASA-CR-182412] 08 p0949 N88-15761
Consistent boundary conditions for Reduced Navier-Stokes (RNS) scheme applied to 3-dimensional internal viscous flows
[NASA-CR-180874] 08 p0950 N88-15762
The simulation of three-dimensional viscous supersonic flow past blunt bodies with a hybrid implicit/explicit finite difference method
[DFVLR-FB-87-32] 08 p0950 N88-15765
Turbomachinery 08 p0955 N88-15792
Finite Element Calculation Methods and Their Application to Turbomachinery, volume 2
[VKI-LS-1987-05-VOL-2] 08 p0985 N88-15965
Mesh generation 08 p0986 N88-15971
Active control of jet flowfields
[AD-A186736] 08 p0989 N88-15989
Numerical resolution of the equations of three-dimensional stable compressible transonic flows
[PB87-168415] 09 p1113 N88-16673
Techniques of flow visualization
[AGARD-AG-302] 09 p1164 N88-16977
Numerical modeling of multidimensional flow in seals and bearings used in rotating machinery
[NASA-TM-100779] 09 p1165 N88-16988
Numerical solutions of three-dimensional Navier-Stokes equations for closed-bluff bodies
[NASA-CR-1[illegible]2359] 09 p1166 N88-16990
Three dimensional Monte Carlo simulation of molecular movement and heat radiation in vacuum devices: Computer code MOVAK3D --- fusion reactors
[KFK-4292] 09 p1246 N88-17471
Development and application of oxygen flow tagging for velocity measurements and flow visualization in turbulent three-dimensional supersonic flows
[AD-A187982] 10 p1289 N88-17714
Three-dimensional Euler solutions for hypersonic Mach numbers
[MBB-UR-944/87] 10 p1315 N88-17859
An experimental investigation of pressure driven three-dimensional turbulent boundary layers
10 p1327 N88-17934
A three-dimensional dual potential procedure for rotational flows 10 p1329 N88-17942
Three-dimensional incompressible flowfield analysis for establishing rotor designs which optimize power extraction
10 p1329 N88-17943
Boundary-integral-equation method for computing the three-dimensional flow of groundwater
[PB88-126891] 10 p1330 N88-17951
Fluctuations and massive separation in three-dimensional shock-wave/boundary-layer interactions
[NASA-TM-89224] 11 p1434 N88-18559
Three-dimensional flow fields past reentry vehicles
11 p1484 N88-18858
Two and three dimensional elliptic flows
11 p1485 N88-18866
Topology and grid adaption for high-speed flow computations
[NASA-CR-182586] 11 p1487 N88-18875
Implementation of multigrid in SOLA algorithm --- fluid flow 11 p1538 N88-19191
Three-dimensional incompressible Navier-Stokes computations of internal flows
[NASA-TM-100076] 12 p1576 N88-19425
Numerical simulation of subsonic and transonic propeller flow
[NASA-TM-100163] 13 p1716 N88-20262
The construction of a three-dimensional finite volume grid generator for a wing in a wind tunnel with application to Navier-Stokes flow solvers
[FFA-TN-1987-58] 13 p1719 N88-20277
Three-dimensional shear layer experiments and their use as test cases for calculation methods
[NLR-MP-86036-U] 13 p1767 N88-20570
Development of disturbances in swept wing flows
[NASA-CR-182675] 13 p1768 N88-20574
Slip velocity method for three-dimensional compressible turbulent boundary layers
[NASA-TM-100586] 13 p1771 N88-20592
Numerical analysis of three-dimensional viscous internal flows
[NASA-TM-100878] 14 p1861 N88-21116
Problems appearing at interface balances --- flames
14 p1987 N88-21855
Experimental investigation of a spanwise forced mixing layer
[AD-A190136] 15 p2013 N88-22007
Trends in Computational Fluid Dynamics (CFD) for aeronautical 3D steady applications: The Dutch situation
[NLR-MP-86074-U] 15 p2015 N88-22017
Secondary instability of compressible boundary layer to subharmonic three-dimensional disturbances
[NASA-CR-4144] 16 p2200 N88-23122
Three-dimensional flow visualization using laser-sheet scanning 16 p2203 N88-23143
Application of high speed holography to aerodynamic and hydrodynamic three-dimensional velocimetry
16 p2203 N88-23144
Nonlinear wave interactions in swept wing flows
[NASA-CR-4142] 16 p2206 N88-23160
Accuracy versus convergence rates for a three dimensional multistage Euler code
[NASA-CR-181665] 16 p2261 N88-23519
Numerical simulation of scramjet inlet flow fields
[NASA-TP-2517] 17 p2296 N88-23735
An efficient parallel algorithm for the simulation of three-dimensional compressible transition on a 20 processor Flex/32 multicomputer
[NASA-CR-178340] 17 p2337 N88-23943
Development and improvement of a code to calculate small, three dimensional, unsteady transonic perturbations
[ONERA-RTS-31/3064-RY-062-R]
17 p2338 N88-23951
A variational finite element method for three-dimensional, steady, compressible, viscous flows
18 p2512 N88-24904
SOLA-DM: A numerical solution algorithm for transient three-dimensional flows
[DE88-007159] 18 p2514 N88-24913
Finite element solution of 3-D turbulent Navier-Stokes equations for propeller-driven slender bodies
18 p2515 N88-24919
Review of numerical methods for radionuclide transport in three-dimensional porous media, at high Peclet numbers
[CFDU/87/10] 18 p2538 N88-25061
Analysis of flow through pump of large rocket engine
19 p2637 N88-25646
Numerical analysis of three dimensional cascade flow by solving Navier-Stokes equations
19 p2638 N88-25650
Numerical analysis of duct flow using three-dimensional parabolized Navier-Stokes equation
19 p2638 N88-25652
On the stationary solutions of three-dimensional Euler equations by the TVD difference schemes
19 p2639 N88-25660
MHD (magnetohydrodynamic) thermal hydraulic analysis of three-dimensional liquid metal flows in fusion blanket ducts
[DE88-009929] 19 p2731 N88-26219
Use of direct solvers for multidimensional fluid flow computations
[DE88-010063] 20 p2799 N88-26611
Three-dimensional viscous flow computations of a circular jet in subsonic and supersonic cross flow
[NASA-CR-182153] 20 p2800 N88-26616
Improved 3-D turbomachinery CFD algorithm
[NASA-CR-179364] 20 p2801 N88-26619
Velocity measurements and flow visualization in turbulent three-dimensional supersonic flows using oxygen flow tagging
[AD-A192551] 21 p2892 N88-27165
Numerical methods for incompressible viscous flows with engineering applications
[NASA-CR-183143] 21 p2948 N88-27508
Study of three-dimensional transonic flow separations
[AD-A193018] 22 p3037 N88-28032
An improved version of NCOREL: A computer program for 3-D nonlinear supersonic potential flow computations
[NASA-CR-4165] 22 p3038 N88-28039
The application of the two-fluid model of turbulence to the 3-D simulation of turbulent combustion in reciprocating engines
[PDR/CFDU/IC/37] 22 p3052 N88-28110
Mass transport in flow of sources
[LRT-WE-9-FB-4(1987)] 22 p3077 N88-28268
Holographic flow visualization
[PNR30466] 22 p3079 N88-28283
Development of a hot-wire measurement technique for moderate intensity three-dimensional flows
22 p3080 N88-28289
Shock boundary layer interaction
23 p3170 N88-28873
Small scale mixing in the initial region of a jet
[AD-A193500] 23 p3192 N88-28994
Direct-solution techniques for viscous flows and their control
[AD-A194775] 23 p3211 N88-29114
Navier-Stokes calculations of transonic flows past cavities
[NASA-CR-180484] 23 p3212 N88-29116
Study of hypersonic boundary layers
[CERT-RSF-OA-17/5005-AYD]
23 p3213 N88-29121
Experience with three dimensional composite grids
23 p3247 N88-29324
Three-dimensional Navier-Stokes simulations of turbine rotor-stator interaction
[NASA-TM-100081] 24 p3316 N88-29750
Three-dimensional combustor predictors. A comparison of equilibrium and laminar flamelet chemistry models
24 p3350 N88-29940
An analysis of finite-difference and finite-volume formulations of conservation laws
[NASA-CR-177416] 24 p3370 N88-30071

THREE DIMENSIONAL MODELS
Three-dimensional adaptive grid generation for body-fitted coordinate system
[NASA-CR-182192] 21 p2950 N88-27520
The three-dimensional stress field around a cylindrical inclusion in a plate of arbitrary thickness
21 p2963 N88-27602
Prediction of regional pollutant dispersion using a nested-grid, three-dimensional numerical model
21 p2971 N88-27649
A three-dimensional model of the gas-cell atomic frequency standard
[AD-A193218] 21 p3011 N88-27868
A simple, analytic 3-dimensional downburst model based on boundary layer stagnation flow
[NASA-TM-100632] 22 p3042 N88-28058
Three-dimensional elliptic grid generation technique with application to turbomachinery cascades
[NASA-TM-101330] 24 p3372 N88-30078
Geometric modeling for computer aided design
[NASA-CR-183161] 24 p3413 N88-30320

THREE DIMENSIONAL MOTION
NT SECONDARY FLOW
NT THREE DIMENSIONAL FLOW
Three-dimensional transient electromagnetic modeling for exploration geophysics 10 p1346 N88-18047
On the design of suboptimal matched filters for three-dimensional moving target detection
[AD-A188384] 12 p1619 N88-19682
Simulation of measuring points for three dimensional measurements
[WPB-0115] 13 p1821 N88-20883
A three dimensional non-singular modelling of rigid manipulators
[AD-A189707] 15 p2116 N88-22604
Rigidity and smoothness of motion
[AD-A190555] 15 p2126 N88-22694

Minimal parameter solution of the orthogonal matrix differential equation
[NASA-TM-4043] 17 p2383 N88-24165
A generic multibody simulation
[NASA-CR-182949] 17 p2388 N88-24198
The avoidance of collisions for Newtonian bodies with hidden variables
[RSRE-87013] 22 p3041 N88-28053
Determining vehicle motion from stereo image sequences
[AD-A194371] 23 p3216 N88-29140

THRESHOLD CURRENTS
Total photoionization cross sections of atomic oxygen from threshold to 44.3A
[NASA-CR-182992] 17 p2397 N88-24252

THRESHOLD DETECTORS (DOSIMETERS)
Miniature radiation dosimeter for in vivo radiation measurements 19 p2672 N88-25889

THRESHOLD VOLTAGE
Development and experimental verification of a two-dimensional numerical model of piezoelectrically induced threshold voltage shifts in GaAs MESFETs
[AD-A193462] 23 p3206 N88-29080

THRESHOLDS (PERCEPTION)
Psychophysical considerations in measuring MRTD with staring arrays — minimum resolvable temperature difference (MRTD)
[RSRE-MEMO-4031] 01 p0076 N88-10487

THROTTLING
Integrated autopilot/autothrottle based on a total energy control concept: Design and evaluation of additional autopilot modes
[NASA-CR-4131] 13 p1724 N88-20308

THRUST
NT HIGH THRUST
NT JET THRUST
NT LOW THRUST
NT ROCKET THRUST
NT STATIC THRUST
High power ion thruster performance
[NASA-TM-100127] 04 p0409 N88-12542
An experimental investigation of an arcjet thruster exhaust using Langmuir probes
[NASA-TM-100258] 14 p1883 N88-21253
Development of a liquid-fed water resistojet
[NASA-TM-100927] 18 p2523 N88-24968
Low-speed wind-tunnel test of a STOL supersonic-cruise fighter concept
[NASA-TM-4050] 20 p2761 N88-26374
Iridium-coated rhenium thrusters by CVD
[NASA-TM-101309] 24 p3339 N88-29874

THRUST AUGMENTATION
Reduction of tilt rotor download using circulation control 10 p1271 N88-17605
Circulation control STOL aircraft design aspects
10 p1272 N88-17610
A computational study of thrust augmenting ejectors based on a viscous-inviscid approach
10 p1326 N88-17929
Augmentor performance of an F100 engine model derivative engine in an F-15 airplane
[NASA-TM-86745] 17 p2307 N88-23805

THRUST CHAMBER PRESSURE
Boundary layer development as a function of chamber pressure in the NASA Lewis 1030:1 area ratio rocket nozzle
[NASA-TM-100917] 19 p2664 N88-25841

THRUST CHAMBERS
A two-dimensional finite difference program for thermal analysis of rocket thrust chambers
[NASA-TM-100191] 04 p0409 N88-12539
MPD (magnetoplasmadynamic) thrust chamber flow dynamics
[AD-A189940] 15 p2137 N88-22751
Orbital transfer vehicle 3000 LBF thrust chamber assembly hot fire test program
[NASA-CR-182145] 24 p3336 N88-29858

THRUST CONTROL
NT THRUST VECTOR CONTROL

THRUST DISTRIBUTION
Low speed wind tunnel investigation of propeller slipstream aerodynamic effects on different nacelle/wing combinations. Part 1: Total forces and moments and pressure distributions on nacelle/wing at different angles of attack and yaw and at different thrust coefficients
[FFA-TN-1987-22] 05 p0542 N88-13302
Fixed wing CCW aerodynamics with and without supplementary thrust deflection
10 p1272 N88-17607
Development of circulation control technology for powered-lift STOL aircraft 10 p1272 N88-17608

THRUST FAULTS
U GEOLOGICAL FAULTS

THRUST MEASUREMENT
Space station propulsion technology
[NASA-CR-179260] 08 p0964 N88-15835

THRUST POWER
U THRUST

THRUST PROGRAMMING
The eivaN: A forward-looking interactive orbital trajectory plotting tool for use with proximity operations (PROX OPS) and other maneuvers: Description and user's manual
[NASA-CR-177490] 24 p3414 N88-30327

THRUST REVERSAL
Aerodynamics in ground effect and predicted landing ground roll of a fighter configuration with a secondary-nozzle thrust reverser
[NASA-TP-2834] 24 p3317 N88-29752

THRUST VECTOR CONTROL
Effects of the installation and operation of jet-exhaust yaw vanes on the longitudinal and lateral-directional characteristics of the F-14 airplane
[NASA-TP-2769] 04 p0393 N88-12455
An experimental and numerical investigation of swirling flows in a rectangular nozzle 06 p0700 N88-14295
Design of supersonic Coanda jet nozzles
10 p1270 N88-17599
Manoeuvres by default, by demand and by design
12 p1580 N88-19455
Static performance of an axisymmetric nozzle with post-exit vanes for multiaxis thrust vectoring
[NASA-TP-2800] 13 p1719 N88-20280
Optimal thrust vector control of coplanar orbital evasive maneuvers
[AD-A189544] 13 p1730 N88-20346
Static performance of nonaxisymmetric nozzles with yaw thrust-vectoring vanes
[NASA-TP-2813] 14 p1861 N88-21118
Pressure measurements of impinging jet with asymmetric nozzle
[NASA-CR-182753] 15 p2014 N88-22011
Heat transfer modeling of jet vane Thrust Vector Control (TVC) systems
[AD-A190106] 15 p2019 N88-22034
Experimental investigation of two-dimensional confined jet thrust vector control
[AD-A189845] 15 p2027 N88-22077
Method for prediction and determination of takeoff performance for vectored thrust vehicles
[AD-A191809] 18 p2463 N88-24626
Attitude control laws for gas-jet spacecraft
18 p2467 N88-24643
TVC (Thrust Vector Control) jet vane thermal modeling using parametric system identification
[AD-A191518] 18 p2474 N88-24678
The effects of RCS jet firing on the isolated Orbiter and mated coast phases of the glide return to launch site maneuver at Mach number 6 (IA302B)
[NASA-CR-180223] 20 p2766 N88-26403

THUNDERSTORMS
The physics of charge separation preceding lightning strokes in thunderclouds
[NASA-CR-178371] 01 p0071 N88-10452
Use of a 5 cm Doppler radar to detect and forecast severe thunderstorms in a real time forecast operation
02 p0200 N88-11247
Thunderstorm nowcasting using Doppler radar and soundings 02 p0200 N88-11248
The use of advanced data sets in the short-range forecasting of the development of a tornadic thunderstorm along a mesoscale convergence zone
02 p0200 N88-11250
VAS products as indices of thunderstorms and severe local storm potential — Visible and Infrared Spin Scan Radiometer Atmospheric Sounder (VAS)
02 p0201 N88-11253
Automated detection of severe thunderstorms using geosynchronous infrared data 02 p0201 N88-11257
Forecasting and nowcasting cumulus convection with soundings released from a storm-intercept vehicle
02 p0202 N88-11262
Mesoscale thunderstorm forecasting using RAOB data, surface mesonet observations, and an expert system
02 p0206 N88-11293
Cumulus and thunderstorm initiation by mountains
02 p0207 N88-11301
The importance of the lower level windshear profile in tornado/non-tornado discrimination
02 p0208 N88-11304
Short range forecasting of sea breeze generated thunderstorms at the Kennedy Space Center: A real-time experiment using a primitive equation mesoscale numerical model 02 p0211 N88-11324
Severe weather potential (SPOT) plotfile generator
[PB87-217717] 02 p0216 N88-11360
Definition and use of sensors for measuring electrical conductivity in thunderclouds
[ESA-TT-1047] 03 p0352 N88-12222
Experimental and analytic studies of the triggered lightning environment of the F106B
[NASA-CR-4104] 04 p0469 N88-12897
Atmospheric electricity
[NASA-CR-179239] 06 p0744 N88-14575
Radar observations of changes in precipitation size spectra associated with lightning
06 p0744 N88-14576
Thunderstorms with snow: A comprehensive, empirical study of their occurrence, development and structure
[AD-A185929] 07 p0879 N88-15329
Applicability of extremely low frequency global resonances for study of Venusian storm activity
08 p1005 N88-16093
Suggested severe local storm operational scenario for GOES I-M
[NASA-TM-100688] 11 p1515 N88-19052
Radio and radar holes and multipath zones: The global and local influences on atmospheric refractive structure and resulting adverse radio and radar performance
12 p1617 N88-19667
Pre-convective environmental conditions indicative of non-tornadic severe thunderstorm winds over Southeast Florida
[AD-A188679] 12 p1648 N88-19870
A preliminary assessment of thunderstorm outflow wind measurement with airport surveillance radars
[AD-A189064] 13 p1799 N88-20757
Wind shear as a predictor of severe weather for the eastern United States
[PB88-157144] 13 p1800 N88-20762
Upward propagating electric fields from thunderstorms and VLF transmitters 13 p1801 N88-20767
Stratospheric electric field and conductivity measurements over electrified convective clouds in the South American region, revised
[INPE-4046-PRE/1012-REV-3]
15 p2095 N88-22483
Atmospheric Science and Remote Sensing Laboratory
[NASA-CR-179290] 16 p2236 N88-23355
Analysis of lightning field changes during active thunderstorms in Florida 18 p2545 N88-25103
Satellite observed Mesoscale Convective System (MCS) propagation characteristics and a 3-12 hour heavy precipitation forecast index
[PB88-180161] 19 p2692 N88-26004
A radar study of the interaction between lightning and precipitation
[DE88-009120] 20 p2827 N88-26770
Investigations into the triggered lightning response of the F106B thunderstorm research aircraft
[NASA-CR-3902] 23 p3236 N88-29258

THYMINE
Survival and mutation induction of dehydrated yeast cells after UV exposure 12 p1657 N88-19932

THYRATRONS
Linear thyratron
[AD-A194111] 23 p3208 N88-29094

THYRISTORS
Study on the dynamics of executive electromechanism with thyristor commutator for cryogenic systems
[DE87-703209] 12 p1622 N88-19702

TIBET
SPOT imagery as an aid to understanding volcanism and tectonics: Examples from the Chilean Andes and the Tibetan Plateau 22 p3103 N88-28427

TIBIA
Changes in the status of the human tibia during antiorthostatic hypokinesia
[NASA-TT-20221] 13 p1810 N88-20813

TID
U TRAVELING IONOSPHERIC DISTURBANCES

TIDAL OSCILLATION
U TIDES

TIDE POWERED GENERATORS
Ocean, Wave, and Tidal Energy Systems: Current abstracts
[DE88-008299] 19 p2687 N88-25973

TIDEPOWER
Ocean, Wave, and Tidal Energy Systems: Current abstracts
[DE88-008299] 19 p2687 N88-25973
Survey on utility technology of a tidal and ocean current energy
[DE88-770148] 20 p2819 N88-26722

TIDES
NT ATMOSPHERIC TIDES
NT EARTH TIDES
Seasonal cycling of sulfur and iron in porewaters of a Delaware salt marsh
[NASA-CR-182385] 07 p0876 N88-15311
Tide- and wind-forced currents in Buzzards Bay, Massachusetts
[PB88-110580] 07 p0882 N88-15350
Infrared emission and tidal interactions of spiral galaxies 07 p0923 N88-15611
Tidal estimation in the Pacific with application to SEASAT altimetry
[NASA-TM-100694] 13 p1803 N88-20780

Fully implicit splitting method for accurate tidal computations
[PB88-183637] 20 p2828 N88-26781

TIG WELDING
U GAS TUNGSTEN ARC WELDING

TILES
Ceramic-ceramic shell tile thermal protection system and method thereof
[NASA-CASE-ARC-11641-1] 11 p1448 N88-18628
In-flight rain damage tests of the shuttle thermal protection system
[NASA-TM-100438] 14 p1881 N88-21241
Implementation of nonsquare tilings on an image processing system
[FOA-C-30487-3 3] 22 p3140 N88-28669

TILT
U ATTITUDE (INCLINATION)

TILT ROTOR AIRCRAFT
NT XV-15 AIRCRAFT
Rotorcraft designs for the year 2000
03 p0264 N88-11665
Rotorcraft aeroelastic stability
09 p1106 N88-16631
Reduction of tilt rotor download using circulation control 10 p1271 N88-17605
Frequency-response identification of XV-15 tilt-rotor aircraft dynamics 10 p1277 N88-17643
Improvements to tilt rotor performance through passive blade twist control
[NASA-TM-100583] 15 p2086 N88-22434
The role of aviation technology in the Caribbean Basin
[NASA-CR-183069] 20 p2745 N88-26289

TILT ROTOR RESEARCH AIRCRAFT PROGRAM
Flight research at NASA Ames Research Center: A test pilot's perspective
[NASA-TM-100025] 02 p0125 N88-10788
Hover performance tests of baseline metal and Advanced Technology Blade (ATB) rotor systems for the XV-15 tilt rotor aircraft
[NASA-CR-177436] 20 p2759 N88-26367

TILTING
U ATTITUDE (INCLINATION)

TILTING ROTORS
Using frequency-domain methods to identify XV-15 aeroelastic modes
[NASA-TM-100033] 10 p1277 N88-17646

TILTMETERS
Evaluation of a miniature horizontal pendulum tilt transducer 12 p1577 N88-19435

TIMBER INVENTORY
Stand based forest inventory from SPOT IMAGE: First experiments 03 p0344 N88-12173
Applicability of SPOT for forest inventory, mapping and change monitoring 03 p0344 N88-12174

TIME
NT EPHEMERIS TIME
NT FLIGHT TIME
NT MTBF
NT REACTION TIME
NT RELAXATION TIME
NT RESPONSE TIME (COMPUTERS)
NT TRANSIT TIME
Nonlinear techniques for detection and filtering of discrete-time signals 02 p0160 N88-11004
Modeling XV-15 tilt-rotor aircraft dynamics by frequency and time-domain identification techniques
03 p0263 N88-11657
Scaling of size/time/temperature associated with dilatation and distortion in uniaxial specimens
03 p0336 N88-12117
A multiple-time-scale turbulence model based on variable partitioning of turbulent kinetic energy spectrum
[NASA-CR-179222] 04 p0444 N88-12754
Propagation of random initial conditions in time
04 p0486 N88-12993
On-orbit frequency stability analysis of the GPS NAVSTAR 6 rubidium clock and NAVSTARs 9 and 10 cesium clocks
[AD-A184984] 05 p0544 N88-13312
Time domain electromagnetic waves in multilayered media
[AD-A185055] 05 p0574 N88-13502
Timing variation in dual loop benchmark
[AD-A185697] 06 p0707 N88-14338
Time characteristics of travelling wave lasing with two-photon picosecond optical pumping
07 p0918 N88-15578
Optical communication with semiconductor laser diodes
[NASA-CR-182464] 09 p1154 N88-16918
Time domain wave propagation in multilayered integrated circuits
[AD-A187462] 10 p1324 N88-17916
Time varying controller design for robot manipulator control
[AD-A188094] 11 p1494 N88-18919
Dynamics of production and oxidation of boranes
[AD-A188988] 12 p1606 N88-19605
Hypnosis: Possible applications for cosmonauts
12 p1665 N88-19984
An evaluation of historical algebras
[AD-A188350] 12 p1684 N88-20067
Flight Vehicle Development Time and Cost Reduction
[AGARD-CP-424] 12 p1700 N88-20173
The increased time and cost of development: Causes and (some) remedies 12 p1701 N88-20178
Reducing time required for the development of avionic systems 12 p1702 N88-20185
Minimizing development flight test time and cost in the US Air Force 12 p1703 N88-20192
The TEMPIS project: Current status
[AD-A188963] 12 p1707 N88-20220
Time characteristics of ultrashort light pulses from dye lasers with distributed feedback
14 p1970 N88-21759
CK-LOG system conversion (user's manual and user interface)
[AD-A190273] 15 p2111 N88-22577
State-of-the-art in true space-time finite element method 17 p2391 N88-24215
Optimal discrete-time LQR problems for parabolic systems with unbounded input: Approximation and convergence
[NASA-CR-181673] 18 p2567 N88-25247
Test of a prototype gate with fast opening equipping the shock tube 0 2 40 m at CEG
[PB87-227864] 19 p2604 N88-25465
A numerical study of the test time in a hypersonic shock tunnel
[AD-A194057] 23 p3172 N88-28888
A linear-time algorithm for finding a minimum spanning pseudoforest
[AD-A194029] 23 p3250 N88-29346
Improved time bounds for the maximum flow problem
[AD-A194034] 23 p3272 N88-29471
Time travel in the homogeneous Som-Raychaudhuri universe
[DE88-702220] 23 p3295 N88-29622

TIME CONSTANT
Measurements of the scintillation time constants of inorganic crystals for the development of a triple-Phoswich detector for high-energy X-ray quanta
[ETN-88-91501] 14 p1993 N88-21875

TIME DELAY
U TIME LAG

TIME DEPENDENCE
The analysis of moisture absorption in multi-layered media
[NPL-DMA(A)-147] 01 p0019 N88-10115
Analysis of shell-type structures subjected to time-dependent mechanical and thermal loading
[NASA-CR-181409] 01 p0060 N88-10388
3D inelastic analysis methods for hot section components 02 p0187 N88-11164
The impact on short-term precipitation forecast skill of time-dependent lateral and lower boundary conditions within a meso-beta numerical cloud prediction model
02 p0211 N88-11327
On the onset of three-dimensionality and time-dependence in the Goertler vortex problem
[NASA-CR-178404] 03 p0260 N88-11638
Effect of time and temperature on transformation toughened zirconias
[AD-A184356] 04 p0419 N88-12600
Alternating current circuit theory and pulsed NMR (Nuclear Magnetic Resonance)
[DE88-000641] 04 p0440 N88-12732
Canonical transformations and exact invariants for dissipative systems
[DE87-703663] 04 p0485 N88-12985
On the numerical simulation of three-dimensional hypersonic flow 05 p0532 N88-13237
Noise modelling in the time domain with the aid of Spice
[PB87-221941] 05 p0573 N88-13492
Numerical and analytical methods in nonlinear partial differential equations
[AD-A185210] 05 p0641 N88-13918
Time-dependent hypersonic viscous interactions
[AD-A185764] 06 p0665 N88-14082
Implicit time dependent methods for inviscid and viscous compressible flows 06 p0701 N88-14304
Photoionization of atoms and ions: Application of time-dependent response method within the density functional theory
[AD-A185686] 07 p0930 N88-15649
A new technique for rocket and space-borne investigations of time-dependant auroral morphology
08 p1030 N88-16241
Nonlinear diffusion in the presence of a time-dependent external electric field
[INPE-4378-PRE/1198] 08 p1085 N88-16533
Additional investigations in landing process of aircraft: Test distributions
[DFVLR-MITT-87-13] 09 p1115 N88-16686
A method for designing robust multivariable feedback systems
[NASA-CR-182459] 09 p1225 N88-17341
Explicit-implicit methods for time-dependent partial differential equations
[CWI-NM-R8703] 09 p1228 N88-17355
Time dependent degradation of energetic electrons in gaseous and condensed media
[DE88-002912] 09 p1246 N88-17465
Physics modeling support contract
[DE88-004039] 10 p1335 N88-17980
Scaling physiological pharmacokinetic models by physiological time
[DE88-000335] 10 p1368 N88-18173
Performance and optimization of direct implicit time integration schemes for use in electrostatic particle simulation codes
[DE88-003254] 10 p1406 N88-18381
Velocity reversal and the arrows of time
[DE88-004237] 10 p1429 N88-18536
Radiation and temperature effects on the time-dependent response of T300/934 graphite/epoxy
[NASA-CR-182603] 11 p1451 N88-18646
A new computational technique for generating algorithms, with application to the solution of the time-dependent incompressible Navier-Stokes equations
11 p1485 N88-18864
An adaptive grid finite difference method for time-dependent Magnetohydrodynamic (MHD) flows and its astrogeophysical applications
11 p1553 N88-19294
A discretization of the integral equation for the time dependent linearized subsonic potential flow over a wing
[AD-A188534] 12 p1574 N88-19411
Time-dependent Slow-Time-Scale theory of free-running and phase-locked gyrotron oscillators
[AD-A188910] 12 p1629 N88-19752
A representation for serial robotic tasks
12 p1681 N88-20048
Structural materials: The changing scene
12 p1703 N88-20190
Numerical model of the time independent mean flow in a rotating rocket motor 13 p1733 N88-20360
The calibration of photographic and spectroscopic films: Reciprocity failure and thermal responses of IIaO film at liquid nitrogen temperatures
[NASA-CR-181094] 13 p1773 N88-20606
Analysis of shell-type structures subjected to time-dependent mechanical and thermal loading
[NASA-CR-182705] 13 p1783 N88-20668
Applications of elastic-viscoplastic constitutive models in dynamic analyses of crack run-arrest events
14 p1930 N88-21507
Data requirements to model creep in 9Cr-1Mo-V steel
14 p1931 N88-21512
On the global/local time incrementing for viscoplastic analysis 14 p1932 N88-21519
Time dependent MHD models for the cometary magnetosphere 14 p1997 N88-21900
Short duration flow establishment on a profile in a Water-Ludwieg-Tunnel 16 p2201 N88-23134
Measurements of the time dependent velocity field surrounding a model propeller in uniform water flow
16 p2205 N88-23155
Nanosecond laser photolysis of opaque heterogeneous photosensitizers
[AD-A191424] 16 p2213 N88-23209
Study of mechanisms of time-dependent crack growth at elevated temperature
[DE88-006918] 16 p2223 N88-23271
Vectorization of the odd-even hopscotch scheme and the alternating direction implicit scheme for the two-dimensional Burgers' equations
[CWI-NM-R8720] 16 p2249 N88-23440
A multigrid approach for the solution of a nonlinear diffusion equation in a time-dependent area using Cartesian coordinates
[GMD-STUDIEN-122] 16 p2257 N88-23491
Measurement of time evolution of plasma electron component parameters on the Ogra-4 device by the Thomson scattering method
[DE88-701575] 16 p2282 N88-23662
Analysis of crack-tip fields in a viscoplastic material
17 p2349 N88-23996
Solving time-dependent two-dimensional eddy current problems
[NASA-TM-100875] 18 p2566 N88-25239
US participation in the TOGA (Tropical Ocean and the Global Atmosphere) Program: A research strategy
[DE88-010986] 19 p2681 N88-25938
Computer modeling of time dependent SBS (Stimulated Brillouin Scattering) in two and three dimensions
[DE88-008922] 19 p2720 N88-26150

Resistance of polyamide-6 against long time effects of various media at various temperatures
[NASA-TT-20297] 20 p2779 N88-26484

A new trajectory following polynomial-time algorithm for the linear programming problem
[REPT-87-87] 20 p2840 N88-26848

A nodal method for time-dependent transport equation
[DE88-004285] 20 p2844 N88-26876

The low-latitude auroral boundary: Steady-state and time-dependent representations
[AD-A193200] 21 p2972 N88-27656

Time-dependent thermal convection of Earth mantle and double diffusive convection in magma chambers
[MITT-52] 21 p2974 N88-27663

Staggered-grid finite element solution technique for the Maxwell's equations in the time domain
[DE88-011731] 21 p3007 N88-27838

The calculation of time dependent eddy currents in tokamaks
[REPT-206] 23 p3286 N88-29568

Chaotic behaviour in quantum dynamics
[AD-A193936] 23 p3295 N88-29623

Numerical methods: Euler time dependent solver
24 p3318 N88-29760

TIME DISCRIMINATION

Visual attention effects on discrimination of line orientation and line arrangement
[AD-A187013] 09 p1200 N88-17190

Comparative aspects of multiple processes of attention
[AD-A195805] 24 p3408 N88-30291

TIME DIVISION MULTIPLE ACCESS

Satellite ground-terminal user simulation
[NASA-TM-100234] 06 p0694 N88-14260

A 30/20 GHz multibeam array antenna suitable for future high rate TDMA European satellite networks
[ETN-88-93079] 24 p3365 N88-30037

TIME DIVISION MULTIPLEXING

Digital television routing systems: A survey of optical and electrical techniques
[BBC-RD-1988/3] 19 p2654 N88-25763

Rivista Tecnica Selenia, volume 10, no. 3, 1987
[ETN-88-92717] 22 p3068 N88-28210

The Frequency Division Multiple Access/Time Domain Multiplex (FDMA/TDM) system reviewed
22 p3069 N88-28214

TIME FUNCTIONS

Time accurate techniques using characteristic flux averaging with application to unsteady aerodynamics
08 p0985 N88-15957

Calculated late time spectra of supernovae
[DE88-003296] 10 p1428 N88-18530

Supporting valid time: An historical algebra
[AD-A187740] 11 p1565 N88-19368

Simple multireader registers using time-stamp schemes
[CWI-CS-R8758] 20 p2835 N88-26819

Study and temporal simulation of the electromagnetic susceptibility of interconnected systems
[ECL-87-19] 22 p3071 N88-28228

TIME LAG

Teleoperation and control study --- orbital servicing
[BAE-TP-8268] 01 p0076 N88-10489

Flap-lag equations of motion of rigid, articulated rotor blades with three hinge sequences
[NASA-TM-100023] 04 p0401 N88-12495

CGI delay compensation
[NASA-TM-86703] 04 p0476 N88-12932

The carbon dioxide chaperon efficiency for the reaction H + O2 + M yields HO2 + M from ignition delay times behind reflected shock waves
[NASA-TM-100125] 07 p0830 N88-15036

Multipath time-delay estimation via the EM algorithm
[PB88-106851] 07 p0845 N88-15124

Software simulation of time delay in teleoperation
08 p1056 N88-16371

Sojourn times in the M/G/1 queue with deterministic feedback
[CWI-OS-R8708] 08 p1074 N88-16479

Time delays and boundary feedback stabilization in one-dimensional viscoelasticity, appendices A through H
[AD-A187534] 10 p1401 N88-18353

Measurement and effects of transport delays in a state-of-the-art F-16C flight simulator
[AD-A187367] 11 p1441 N88-18599

Realtime pilot model parameter identification
[AD-A188873] 12 p1584 N88-19476

Sojourn times in feedback queues
[CWI-OS-R8710] 13 p1830 N88-20947

Radial track of moving objects determined by HF backscatter technique 14 p1901 N88-21354

Practical considerations for structural control: System uncertainty, system time delay and truncation of small control forces
[PB88-163738] 14 p1933 N88-21528

The effects of torque response and time delay on rotorcraft vertical axis handling qualities
[AD-A189873] 15 p2017 N88-22023

Loran-C monitor correlation over a 92-mile baseline in Ohio 17 p2293 N88-23720

Electro-optic sampling of high-speed, InP-based integrated circuits 19 p2655 N88-25769

Multigigahertz logic based on InP-MISFET's exhibiting extremely high transconductance
19 p2656 N88-25771

Concepts for robot motion primitives required for space station teleoperations 23 p3257 N88-29387

TIME MARCHING

Theoretical investigations of three turbine cascades using a two dimensional time marching procedure
[DFVLR-FB-87-02] 01 p0057 N88-10362

Application of Runge Kutta time marching scheme for the computation of transonic flows in turbomachines
[NASA-TM-86997] 04 p0394 N88-12461

Computation of flow past conical hypersonic wings using a second order Godunov method
05 p0533 N88-13241

Time-marching finite-difference methods for the three-dimensional Euler equations of contravariant velocity components 05 p0539 N88-13285

Electromagnetic scattering problem in the wave-vector-time domain
[PB88-106083] 06 p0694 N88-14263

Theoretical investigations of three turbine cascades using a 2-D time marching procedure
[ESA-TT-1077] 16 p2207 N88-23170

The 2-D and 3-D time marching transonic potential flow method for propfans 16 p2220 N88-23245

Reduced order models for nonlinear aerodynamics
16 p2220 N88-23248

TIME MEASUREMENT

Planning and execution of the NAVEX experiment in the Spacelab Mission D1
[DFVLR-FB-87-03] 01 p0010 N88-10056

Timing variation in dual loop benchmarks
[AD-A185697] 06 p0707 N88-14338

Electronics for the External Muon Detector (EMD) of ICARUS
[NOTA-INTERNA-880] 07 p0847 N88-15143

Chemical reactions in turbulent mixing flows
[AD-A186141] 07 p0849 N88-15153

Increasing time resolution of picosecond absorption spectrometer by selection of length of laser light pulses
07 p0919 N88-15579

The use of optical fibers for shock pressure and timing measurements at high pressures
[DE88-004012] 10 p1334 N88-17971

Electromechanical timing measurement technique
[DE88-005098] 11 p1489 N88-18889

Application of the Global Positioning System (GPS) time receivers to the fundamental station Wettzell
11 p1506 N88-18995

Results of one way transit time measuring in navigation experiment NAVEX
[DFVLR-MITT-87-17] 14 p1865 N88-21145

Securing the timescale of the NAVEX-reference clock and rate determinations by time comparisons with the help of the Global Positioning System (GPS) --- Spacelab D1 mission
[DFVLR-MITT-87-20] 16 p2159 N88-22879

Navigation experiment NAVEX. The reading differences between all ground station measuring clocks during each Spacelab pass of the D1 mission
[DFVLR-MITT-87-23] 16 p2159 N88-22880

The NAVEX experiment in the Spacelab D1 mission: Planning and execution
[ESA-TT-1078] 16 p2166 N88-22913

Timing for subnanosecond pulses
[DE88-701390] 16 p2192 N88-23074

A simulation analysis of errors in the measurement of standard electrochemical rate constants from phase-selective impedance data
[AD-A192739] 20 p2770 N88-26426

Quartz crystal resonators and oscillators for frequency control and timing applications
[AD-A193310] 21 p2937 N88-27443

TIME MEASURING INSTRUMENTS

NT ATOMIC CLOCKS
NT CLOCKS
NT TIMING DEVICES

TIME OF FLIGHT SPECTROMETERS

A program to study antiprotons in the cosmic rays: Arizona collaboration
[NASA-CR-180702] 01 p0120 N88-10764

Laser post-ionization secondary neutral mass spectroscopy
[DE88-002979] 09 p1172 N88-17027

High-voltage inverse-square function generator
[DE88-701109] 15 p2058 N88-22270

Ultrasonic Time-Of-Flight Diffraction (TOFD) measurements of crack depths in an acceleration reservoir of a high velocity research gun
[DE88-006544] 16 p2164 N88-22907

Timing for subnanosecond pulses
[DE88-701390] 16 p2192 N88-23074

Synopsis of a computer program designed to interface a personal computer with the fast data acquisition system of a time-of-flight mass spectrometer
[NASA-CR-177474] 21 p3001 N88-27798

Impurity analysis in SIMOX samples by high-efficiency resonance ionization time-of-flight mass spectrometry
[DE88-012061] 24 p3367 N88-30051

TIME OPTIMAL CONTROL

Optimal control, estimation compensation of linear discrete-time systems with stochastic parameters
[REPT-87-56] 16 p2255 N88-23478

Time-Optimal Adaptive Shaped Torque (TOAST) technical note
[AD-A192719] 20 p2843 N88-26869

Approximations and optimal control for the pathwise average cost per unit time and discounted problems for wideband noise driven systems
[AD-A192712] 21 p3008 N88-27847

TIME SERIES ANALYSIS

Time series infrared spectroscopy of long period variables 04 p0516 N88-13172

Quantile based unified distribution of extreme values and order statistics
[AD-A185171] 05 p0644 N88-13942

New approaches to some methodological problems of meteor science 06 p0741 N88-14557

On the least squares estimator in moving average models of order one
[AD-A186028] 07 p0909 N88-15508

Quasiperiodic variations in manifestations of solar activity 08 p1004 N88-16083

The linear dependency structure of covariance nonstationary time series
[AD-A186548] 09 p1232 N88-17383

Neutrino magnetic moment and time variation of solar neutrino flux
[DE88-700687] 10 p1430 N88-18542

Spectral measurements in a disturbed boundary layer over snow
[AD-A190217] 15 p2097 N88-22494

Simulation analysis of moored fluorometer time series from the Mid-Atlantic Bight
[DE88-006066] 15 p2099 N88-22505

Partial likelihood analysis of time series models with application to rainfall-runoff data
[AD-A191157] 16 p2261 N88-23516

Leave-K-Out diagnostics for time series
[AD-A191343] 16 p2261 N88-23518

Comparison of surface current determined from satellite-tracked buoy with shipboard wind data during the 4th Brazilian antarctic expedition, 10-14 March, 1986
17 p2354 N88-24024

Sea ice kinematics: Space and time scales
[AD-A191162] 17 p2376 N88-24128

Adaptive time series analysis using predictive inference and entropy
[AD-A191858] 18 p2560 N88-25199

Comparison of experimental rotor damping data-reduction techniques 21 p2891 N88-27159

Definition of long ocean wave slope for radar applications
[AD-A193198] 21 p2933 N88-27412

Solution to the compressible Navier-Stokes equations of motion by Chebyshev polynomials with implicit time stepping
[AD-A194119] 22 p3075 N88-28257

Tropospheric biennial variability and its relationship to the southern oscillation 22 p3121 N88-28549

A method to adjust climatological time series for discontinuous inhomogeneities
22 p3124 N88-28570

Atmospheric angular momentum and length of day
[AD-A194505] 23 p3233 N88-29238

TIME SHARING

IPC for modular software requires a third party connect
[AD-A189199] 16 p2246 N88-23414

Piecewise linear approach for timing simulation of VLSI (Very-Large-Scale-Integrated) circuits on serial and parallel computers
[AD-A191328] 16 p2252 N88-23462

Timesharing performance as an indicator of pilot mental workload
[NASA-CR-182807] 18 p2552 N88-25150

The emergence of multi-user expert systems
23 p3260 N88-29408

Networking and AI systems: Requirements and benefits 23 p3263 N88-29425

TIME TEMPERATURE PARAMETER
Effect of time and temperature on transformation toughened zirconias
[AD-A184356] 04 p0419 N88-12600
Time-temperature-stress capabilities of composite materials for advanced supersonic technology application
[NASA-CR-178272] 06 p0677 N88-14144
Finite element explicit algorithm for solving temporal temperature fields 14 p1899 N88-21339
The Time-Temperature-Transformation (TTT) diagram as a basis for relating the formation and properties of reactive coatings
[AD-A190872] 16 p2182 N88-23006
TIMERS
U TIMING DEVICES
TIMING
U TIME MEASUREMENT
TIMING DEVICES
Response of helical structures to high speed pulses or when can a helix be called an inductor
[DE87-014347] 01 p0090 N88-10587
Parallel binary and parallel coded decimal time code formats
[AD-A190126] 17 p2384 N88-24170
Timing control system
[NASA-CASE-NPO-16882-1-CU]
18 p2506 N88-2486
TIMOSHENKO BEAMS
Buckling of braced monosymmetric cantilevers: Timoshenko energy approach
[PB87-133849] 06 p0723 N88-14445
Boundary stabilization of thin elastic plates
[AD-A187123] 10 p1343 N88-18025
Behavior of a two-layered beam under impact loading
[OUEL-1716/87] 17 p2349 N88-23993
Refining finite element models. Numerical application to a lattice structure. Study of a macroelement of Timoshenko beam type
[ONERA-RT-8/3313-RY-070-R]
22 p3144 N88-28696
Analytical and experimental studies of beam waveguide absorbers for structural damping
[AD-A195085] 24 p3382 N88-30144
TIN
Effect of hold time on fatigue of lead rich PbSn solder
06 p0715 N88-14387
A laboratory study of tin whisker growth
[ESA-STR-223] 08 p1089 N88-16553
The effects of various conductor components on Nb3Sn filament prestrain in cable-in-conduit conductors
[DE88-003956] 11 p1479 N88-18824
Properties of reactively sputtered WNx films Zhao, X.-A.
[AD-A188711] 13 p1835 N88-20976
Photoionization dynamics and abundance patterns in laser vaporized tin and lead clusters
[AD-A191604] 18 p2482 N88-24722
Use of digital images as a mineral prospecting tool in the tin province of Goias, Brazil
[INPE-4537-PRE/1284] 24 p3387 N88-30173
TIN ALLOYS
Thermomechanical fatigue of lead-base low tin solder
06 p0721 N88-14432
PbSnTe photovoltaic detectors for operation in the 2-14 micron band
[INPE-4252-PRE/1125] 11 p1508 N88-19006
Fraction eutectic measurements in slowly cooled Pb - 15 wt percent Sn alloys
[NASA-CR-180830] 19 p2618 N88-25531
Magnetization studies of multifilamentary Nb3Sn wires
[DE88-009103] 19 p2735 N88-26243
An HVEM study of displacement cascade damage in Nb3Sn at 13 K
[DE88-009997] 23 p3289 N88-29584
TIN COMPOUNDS
NT NIOBIUM STANNIDES
NT TIN OXIDES
NT TIN TELLURIDES
The Moessbauer effect of SnI4 at high pressure
[DE87-014771] 04 p0495 N88-13048
TIN OXIDES
Steady state and transient behavior of the Pd-SnO(sub x) MIS oxygen sensors 19 p2672 N88-25890
Tin oxide microsensors on thin silicon membranes
19 p2673 N88-25897
TIN TELLURIDES
Analysis of the voltage-current characteristics of metal-isolator-tin-telluride sandwich structures
[ETN-88-91080] 09 p1256 N88-17528
TIP SPEED
Visualisation of the flow at the tip of a high speed axial flow turbine rotor
[AD-A189928] 15 p2063 N88-22300
Visualisation of the flow at the tip of a high speed axial flow turbine rotor: An assessment of flow visualisation techniques and the requirement of the experimental turbine
[AD-A189929] 15 p2063 N88-22301
TIPS
NT BLADE TIPS
NT CRACK TIPS
NT WING TIPS
TIRES
NT AIRCRAFT TIRES
Cornering characteristics of the main-gear tire of the space shuttle orbiter
[NASA-TP-2790] 11 p1438 N88-18583
Advances in contact algorithms and their application to tires
[NASA-TP-2781] 14 p1922 N88-21456
TIROS N SERIES SATELLITES
Assimilation of high resolution TOVS data into a mesoscale NWP model --- numerical weather prediction (NWP) 02 p0213 N88-11338
TIROS OPERATIONAL SATELLITE SYSTEM
Some problems with regard to the TOVS processing detected by using NOAA-HRPT data check program
17 p2351 N88-24009
TIROS SATELLITES
NT TIROS N SERIES SATELLITES
High-spatial-resolution TOVS observations for the FIRE/SRB Wisconsin experiment region from October 14 through November 2, 1986
[NASA-TM-100522] 06 p0747 N88-14593
TISSUES (BIOLOGY)
NT ADIPOSE TISSUES
NT ENDOTHELIUM
Space Bioreactor Science Workshop
[NASA-CP-2485] 09 p1196 N88-17168
Shear and mixing effects on cells in agitated microcarrier tissue culture reactors 09 p1197 N88-17173
Plant cell technologies in space: Background, strategies and prospects 09 p1198 N88-17177
Muscle preservation in the study of bioenergetic effects of hypokinesia 10 p1362 N88-18139
Lipid peroxidation in rat tissues with exposure to antiorthostatic hypokinesia, exercise and immobilization stress 10 p1365 N88-18159
Interactions of cultured human endothelial cells with polymeric surfaces
[PB88-112255] 10 p1369 N88-18178
Critical phenomena and electromagnetic effects in biological membranes
[AD-A188156] 11 p1518 N88-19064
Biophysical applications of solid state and tritium NMR
[DE88-005328] 13 p1808 N88-20806
Studies of model ion channels in defect-free multibilayers of phospholipids
[AD-A188740] 16 p2238 N88-23365
Leg volume change under Lower Body Negative Pressure (LBNP) in dependence on stratification
[DFVLR-FB-87-47] 16 p2238 N88-23367
Photochrome from green plants: Assay, purification and characterization
[DE88-007511] 19 p2702 N88-26067
Improvements in techniques of microwave thermography
[AD-A194613] 23 p3203 N88-29062
Improvements in techniques of microwave thermography
[AD-A193620] 23 p3239 N88-29276
TITAN
Parachute characteristics of Titan descent modules --- planetary probe
[BF-3/86-B] 02 p0122 N88-10774
Study of a Radio Relay Link (RRL). Cassini mission. Data package for final presentation
[ESA-CR(P)-2472] 07 p0847 N88-15138
New concepts for atmospheric braking deceleration in planetary atmosphere entry
[SNIAS-CAS-DECE-P003-DPAA]
16 p2168 N88-22923
Microwave instrument for planetary mission (Titan/CASSINI mission orbiter spacecraft)
[BAE-CS/TP-8359] 24 p3375 N88-30102
TITAN LAUNCH VEHICLES
Reduced flexibility in processing Titan 4 space launch vehicles at Cape Canaveral Air Force Station
[AD-A194908] 24 p3332 N88-29834
TITANATES
NT BARIUM TITANATES
NT LEAD TITANATES
NT LEAD ZIRCONATE TITANATES
NT PEROVSKITES
NT PIEZOELECTRIC CERAMICS
Modeling of irradiation-induced amorphization in a titanate ceramic
[DE87-014751] 03 p0292 N88-11833
Develop techniques for ion implantation of (lead-lanthanum-zirconate-titanate) for adaptive optics
[DE88-000642] 05 p0650 N88-13986
TITANIA
Hafnia-rich mixed oxide ceramics of the system HfO2-ZrO2-TiO2 for heaters and heat exchangers in electrothermal thrusters: The effects of titania on selected electrical and mechanical properties of Hafnia-rich mixed oxides in the system Hafnia-Zirconia-Titania, volume 1
[NASA-CR-182800-VOL-1] 15 p2047 N88-22197
TITANIUM
Comparison of measured temperatures, thermal stresses and creep residues with predictions on a built-up titanium structure
[NASA-TM-88814] 03 p0337 N88-12125
TiN coatings on M2 steel produced by plasma assisted chemical vapor deposition
[DE88-003189] 08 p0970 N88-15867
Tunable Al2O3:Ti3 + -laser with optical pumping
09 p1237 N88-17415
Effects of ion implantation on cavitation erosion of a cobalt based metal/carbide alloy
[AD-A187239] 10 p1303 N88-17793
Adhesion of PVD titanium coatings to beryllium substrates
[DE88-005147] 11 p1463 N88-18721
Optical waveguide formation by ion implantation of Ti or Ag
[DE88-004595] 11 p1551 N88-19278
Microprobe examination of composite materials produced by burning of Ti, Cr, C powders with powder of any one Fe-group metal 14 p1886 N88-21269
The effect of titanium reinforcement on the life of positive grids in lead-acid batteries 17 p2320 N88-23857
Stiffened titanium panels
[NASA-CASE-LAR-13814-1] 18 p2497 N88-24616
PLZT (Lead-Lathanium-Zirconium-Titanium) electro-optic photographic system
[AD-A193473] 23 p3215 N88-29137
Electrical properties of materials for elevated temperature resistance strain gage application
[NASA-CR-182214] 24 p3376 N88-30106
TITANIUM ALLOYS
NT NITINOL ALLOYS
Investigation of rapidly-solidified dispersion strengthened titanium alloys
[AD-A183882] 01 p0022 N88-10140
Contribution to the study of the Ti-Al phase diagram by conventional and high resolution electron microscopy
[ESA-TT-1021] 01 p0023 N88-10143
Superplastic deformation and post forming tensile properties of Ti-6Al-4V sheet
[RAE-TR 86015] 01 p0023 N88-10144
Structure of rapidly solidified Ni-Ti
[DE87-012252] 02 p0147 N88-10921
Strain rate effects in fast-gas-cooled uranium-titanium and uranium-niobium alloys
[OUEL-1683/87] 02 p0149 N88-10937
Corrosion-electrochemical and mechanical properties of composite graphite-carbide metal materials based on titanium and its alloys 03 p0285 N88-11794
A fundamental study of the mechanical and microstructural response of elevated temperature PM aluminum-titanium alloys 03 p0289 N88-11819
China report: Science and technology
[JPRS-CST-87-015] 03 p0298 N88-11873
Status of titanium alloys R and D described
03 p0298 N88-11876
The mechanical properties of solid state diffusion bonds between Ti-6Al-4V and 304L stainless steel
[BAJ-TR-113-1987] 03 p0332 N88-12093
The effect of microstructure on the surface crack length. Crack depth relationship for short cracks
05 p0600 N88-13670
Crack growth in contrasting titanium alloys under the conjoint action of high and low cycle fatigue
05 p0602 N88-13686
Characterization of the microstructures of various materials
[AD-A184961] 05 p0655 N88-14017
Reactions and bonding between glasses and titanium
[DE88-000603] 06 p0685 N88-14195
Effect of overload ratios on fatigue crack growth behavior in Ti-6Al-4V alloy
[PB87-147062] 07 p0833 N88-15055
The effect of varying sputtering parameters on the microstructure and mechanical properties of 10 percent Ni + TiB2 thin films
[DE88-002600] 09 p1254 N88-17517
Transmission electron microscopy studies of titanium-containing braze/alumina seals
[DE88-005243] 10 p1303 N88-17792
Structural analysis using X-ray scattering and neutron scattering on binary amorphous (Co,Cu)Ti alloys
[ETN-88-91487] 11 p1459 N88-18699

Elevated temperature crack growth studies of advanced titanium aluminides
[AD-A189025] 12 p1606 N88-19618
Thermal-mechanical fatigue testing of a titanium-aluminide alloy
[AD-A189555] 12 p1609 N88-19620
An interdisciplinary approach to predictive modeling of structural adhesive bonding: Factors affecting the durability of titanium/epoxy bonds
[AD-A189503] 12 p1611 N88-19636
Threshold fatigue crack growth in Ti-6Al-2Sn-4Zr-6Mo
[AD-A189560] 13 p1741 N88-20415
Phenomenological piercing characteristics of composite materials 14 p1895 N88-21315
Optimization of oxygen cutting process for titanium alloys 14 p1897 N88-21323
Characteristics of joint formation during friction welding of Ti alloys to Nb alloys 14 p1898 N88-21329
Growth and deformation mechanisms of refractory alloy hybrid materials
[AD-A190492] 15 p2039 N88-22152
Investigation of laser diagnostics of PACVD processes for depositing hard face coatings
[DE88-007083] 15 p2043 N88-22176
Titanium powder frit made during the transformation alpha-beta
[ETN-88-91999] 16 p2177 N88-22976
Deformation of rapidly solidified dispersion strengthened titanium alloys
[AD-A190793] 16 p2179 N88-22984
Fundamental studies of beta phase decomposition modes in titanium alloys
[AD-A191495] 18 p2485 N88-24740
On the reversion phenomena of Cu-3 percent Ti alloys
[NASA-TT-20170] 18 p2488 N88-24762
Optimization of mechanical/corrosion properties of TI-CODE 12 plate and sheet. Part 2: Thermomechanical processing effects
[DE88-007493] 19 p2616 N88-25517
Apparatus for pressure welding of titanium structures with a controlled rate of deformation
[RAE-TRANS-2161] 19 p2677 N88-25915
Study of probabilistic fatigue crack growth and associated scatter under constant-and-variable amplitude loading spectrum
[AD-A192027] 19 p2679 N88-25929
Prediction of fatigue life of notched specimens under aircraft loading and importance of the relative method in the case of local strain approach, part 2
[TAE-595-PT-2] 19 p2680 N88-25934
Initial development of high-temperature titanium silicide alloys
[DE88-007860] 20 p2772 N88-26437
Glass forming ranges of amorphous alloys
[DE88-007897] 20 p2772 N88-26438
A fundamental understanding of the interfacial compatibility in hybrid material systems
[AD-A192921] 21 p2909 N88-27264
Constant amplitude fatigue life data for notched and unnotched annealed Ti-6Al-4V sheet
[AD-A193420] 21 p2913 N88-27287
Influence of microstructure and microdamage processes on fracture at high loading rates
[AD-A192957] 21 p2960 N88-27583
Stress relaxation of a titanium (Ti-6Al-4V) threaded joint
[DE88-010102] 21 p2961 N88-27590
JTDE 1 XTE34 materials research and development report
[AD-A194268] 22 p3044 N88-28063
As-received microstructure of a SiC/Ti-15-3 composite
[NASA-TM-100938] 22 p3050 N88-28095
Optimization of fatigue and friction properties of titanium by means of surface treatments
[ECL-87-22] 22 p3056 N88-28133
Investigation of a SiC/Ti-24Al-11Nb composite
[NASA-TM-100956] 23 p3190 N88-28980
Influence of peak pressure on the substructure evolution and shock wave profiles of Ti-6Al-4V
[DE88-006458] 23 p3225 N88-29197
Development of Nb-Ti multifilamentar superconducting wires
[DE88-702324] 23 p3290 N88-29592

TITANIUM BORIDES
Carbon-fiber reinforced aluminum
04 p0403 N88-12507
Wire-cut electrical discharge machinability of ceramics
[AD-A186989] 09 p1146 N88-16870
The effect of varying sputtering parameters on the microstructure and mechanical properties of 10 percent Ni + TiB2 thin films
[DE88-002600] 09 p1254 N88-17517

TITANIUM CARBIDES
Analysis of phase equilibria in NiTi-C system in high nickel regions
[BLL-M-37304-(5828.4)] 02 p0149 N88-10932
Hadfield steels with Nb and Ti carbides
[DE87-703706] 04 p0416 N88-12579
New application of transition metal carbides detailed
06 p0675 N88-14132
Ball bearings with chemical vapor deposition (CVD)-TiC coated components 14 p1876 N88-21210
Titanium carbide coatings for aerospace ball bearings
14 p1927 N88-21486

TITANIUM COMPOUNDS
NT BARIUM TITANATES
NT LEAD TITANATES
NT LEAD ZIRCONATE TITANATES
NT PEROVSKITES
NT PIEZOELECTRIC CERAMICS
NT RUTILE
NT TITANATES
NT TITANIUM BORIDES
NT TITANIUM CARBIDES
NT TITANIUM NITRIDES
NT TITANIUM OXIDES
Optical frequency doubling in Ti:LiMbO3 waveguide resonators
[ETN-88-91486] 11 p1550 N88-19271
Muon motion in titanium hydride
17 p2396 N88-24247

TITANIUM DIOXIDE
U TITANIUM OXIDES

TITANIUM NITRIDES
Tin activated reactive ion plating and its application
[PB87-144036] 08 p0970 N88-15871
Bias, internal stress and substrate effects on the microstructure and properties of PVD-wear resistant coatings
[AERE-R-12360] 10 p1304 N88-17798
The preparation of titanium nitride and titanium carbonitride by the preceramic polymer route
[AD-A188357] 12 p1610 N88-19626
Structure and properties of titanium nitride and zirconium nitride thin films prepared by reactive ion plating --- cutting tools
[ETN-88-92218] 15 p2042 N88-22167

TITANIUM OXIDES
NT RUTILE
Auger electron spectroscopy of oxidized titanium overlayers: Speciation of homogeneous and heterogeneous samples
[KFK-4221] 02 p0146 N88-10913
Characterization of catalysts with metal-support effects and of the species adsorbed on their surfaces
[DE87-014636] 04 p0414 N88-12564
Titanium oxide absorption and spot sizes in II Peg, HR 1099 and UX An 04 p0508 N88-13126
On 1064 nm and 350 nm laser damage thresholds of high index oxide films deposited from organic solutions and sols
[DE88-001636] 07 p0859 N88-15217
Point defect structure of Cr2O3
[AD-A187620] 11 p1556 N88-19317
The influence of processing variables on physical properties of sol-gel derived TiO2 films
[DE88-005155] 11 p1559 N88-19331
Model catalyst studies of SMSI (Strong Metal/Support Interactions) and the role of D-electrons in chemisorption and catalysis
[DE88-004518] 13 p1738 N88-20393
Oxide-bound transition metal complexes for methane activation
[PB88-169719] 14 p1887 N88-21277
Chemical vapor deposition of TiO2 thin films at room temperature
[DE88-008892] 21 p2953 N88-27542
Al2O3-TiO2 and Al2TiO5 ceramic materials
[SNIAS-881-430-122] 23 p3199 N88-29038

TITRATION
Titrimetric analysis of HAN-based liquid propellants
[AD-A196225] 24 p3357 N88-29990

TNT (TRINITROTOLUENE)
U TRINITROTOLUENE

TOILETS
Evaluation of the Shasta Waterless System as a remote site sanitation facility
[AD-A186000] 07 p0898 N88-15442

TOKAMAK DEVICES
NT JOINT EUROPEAN TORUS
Behavior of graphites under intense heat loads
[DE87-012128] 01 p0028 N88-10179
Shear strength of the ASDEX upgrade Toroidal Field (TF) coil insulation: Rupture, fatigue and creep behavior --- tokamak
[IPP-1/230] 01 p0059 N88-10376
Millimeter wave tokamak heating and current drive with a high power free electron laser
[DE87-011324] 01 p0099 N88-10651
Massachusetts Institute of Technology Plasma Fusion Center: 1986-1987 Report to the President
[DE87-010518] 01 p0101 N88-10661
Thermally driven convective cells and tokamak edge turbulence
[DE87-014424] 02 p0238 N88-11499
On tokamak equilibrium
[DE87-014811] 02 p0239 N88-11507
System studies of compact ignition tokamaks
[DE87-014976] 02 p0239 N88-11508
Improvement of energy confinement of neutral beam heated plasma by lower hybrid current drive in JT-60
[DE87-752983] 02 p0239 N88-11509
Two dimensional neutral transport analysis in tokamak plasma
[DE87-752984] 02 p0239 N88-11510
Transport analysis of OH and NBI heated discharges in JT-60
[DE87-752985] 02 p0239 N88-11511
Spectrograms of the visible region in the JT-60 tokamak (wavelength range from 2210 A to 5250 A)
[DE87-753002] 02 p0240 N88-11513
Analysis of energy confinement of slideaway discharges
[DE87-753008] 02 p0240 N88-11515
Vectorization of MHD equilibrium and stability codes
[DE87-753013] 02 p0240 N88-11516
Planning for US ion cyclotron heating research relevant to the compact ignition tokamak and Alcator C-Mod
[DE88-000022] 02 p0241 N88-11520
Relative merits of size, field, and current on ignited Tokamak performance: A comparison of CITs and Super-JETs
[DE88-000038] 02 p0241 N88-11521
Fracture mechanism of fine grain graphite under high heat fluxes
[IPPJ-842] 02 p0242 N88-11527
Simulation of tokamak runaway-electron events. Study of the response of materials by use of an electron linear accelerator
[IPPJ-841] 02 p0242 N88-11528
Wavepacket propagation and current startup near the lower hybrid frequency in the torus
[IPPJ-840] 02 p0242 N88-11529
Limit of possible operation of crescent and bean shaped Tokamaks
[IPPJ-837] 02 p0242 N88-11532
Laser blow-off experiments on ASDEX --- tokamak
[IPP-III/119] 02 p0243 N88-11535
A microwave FEL (Free Electron Laser) code using waveguide modes
[DE88-000225] 03 p0330 N88-12084
Application of a two fluid theoretical plasma transport model on current Tokamak reactor designs
[DE87-013511] 03 p0377 N88-12373
Mathematical models of plasma discharge control in a tokamak
[DE87-702891] 03 p0378 N88-12377
Stability of low-shear Tokamaks
[DE88-000305] 03 p0379 N88-12383
Negative ion beams for heating and current-drive in NET
[AD-A184390] 04 p0489 N88-13012
Data base on the high heat flux behaviour of metals and carbon materials for plasma facing components. Experiments at the 10 MW neutral beam injection test stand of the IPP Nagoya
[IPPJ-AM-53] 04 p0492 N88-13031
Refueling and density control in the ZT-40M reversed field pinch
[DE88-000504] 04 p0493 N88-13040
Modular pump limiter systems for large tokamaks
[DE88-001487] 04 p0494 N88-13045
ICRF launcher studies
[DE88-001710] 04 p0495 N88-13046
ALT-1 pump limiter experiments
[DE88-000822] 05 p0651 N88-13989
Subcommittee for MHD theory
[DE88-000596] 05 p0653 N88-14003
Effect of plasma rotation in tokamak on stabilizing action of electrically conducting wall 06 p0773 N88-14748
Confinement of energy in tokamak-10 plasma during electron-cyclotron-resonance heating
06 p0773 N88-14750
TIBER 2 (Tokamak Ignition/Burn Experimental Reactor) parameters with neutral beams at high energies
[DE88-001891] 06 p0783 N88-14803
Overview of the TIBER 2 (Thermal Ignition/Burn Experimental Reactor) design
[DE88-001892] 06 p0783 N88-14804
Modeling of thermal effects on TIBER 2 (Thermal Ignition/Burn Experimental Reactor) divertor during plasma disruptions
[DE88-001893] 06 p0783 N88-14805
Slowing down tail enhanced, neoclassical and classical alpha particle fluxes in tokamak reactors
[DE88-001930] 06 p0783 N88-14806
Poloidal magnetics of compact ignition tokamaks
[DE88-001774] 07 p0934 N88-15672

Reversed field pinch experiments. Summary of progress report
[DE88-002367] 07 p0934 N88-15673
Method of plasma diagnostics by a heavy ion beam for the T-15 tokamak
[DE88-700342] 07 p0935 N88-15678
Study on the mechanical stresses in the elements of the model of a toroidal magnet of a tokamak with strong field
[DE88-700343] 07 p0935 N88-15679
Study on the model of a toroidal magnet for a tokamak with a strong field
[DE88-700346] 07 p0935 N88-15681
Gas feed system for the T-15 tokamak discharge chamber
[DE88-700351] 07 p0935 N88-15682
Simulation an experiment on plasma instability investigation in a tokamak with a divertor
[DE88-700352] 07 p0935 N88-15683
Model for plasma equilibrium configuration evolution in a tokamak with adiabatic compression
[DE88-700354] 07 p0936 N88-15684
Simple model for hot ion plasmas
[DE88-750045] 07 p0936 N88-15688
Conceptual design of a radio-frequency driven compact tokamak
[INPE-4364-PRE/1190] 08 p1085 N88-16535
A ray-tracing study of electron cyclotron resonance heating in tokamak plasmas with a superthermal electron tail
[INPE-4381-PRE/1201] 08 p1085 N88-16536
Shape of the plasma boundary in TBR
[INPE-4388-PRE/1208] 08 p1086 N88-16540
Absorption of electron cyclotron radiation in tokamak plasmas with a superthermal tail in the electron velocity distribution
[INPE-4391-PRE/1211] 08 p1086 N88-16541
Tangential Thomson scattering — plasma diagnostics
[REPT-87-173] 08 p1087 N88-16548
Nonlinear evolution of the internal kink mode in toroidal geometry for shaped tokamak plasmas
[DE88-003655] 08 p1087 N88-16550
Microwave system for the microwave Tokamak experiment (MTX)
[DE88-002391] 09 p1250 N88-17487
Influence of fast alpha diffusion and thermal alpha buildup on Tokamak reactor performance
[DE88-003661] 09 p1251 N88-17496
Two-dimensional analysis for a scrapeoff and divertor regions with an MHD model. Conceptual design study of FY86 FER
[DE88-751069] 09 p1251 N88-17497
Pump limiter experiments and analysis in the TEXTOR tokamak 09 p1252 N88-17506
Proceedings of the Energy Independence Conference. Fusion Energy and Plasma Physics
[DE88-700657] 09 p1253 N88-17507
Application of high temperature ceramic superconductors (CSC) to commercial tokamak reactors
[DE88-003973] 09 p1257 N88-17538
Tokamak with highly elongated cross-section of a plasma
[DE88-700356] 10 p1410 N88-18412
Plasma physics design and major specifications of candidate reactors for FER design studies. Conceptual design study of FY86 FER
[DE88-751066] 10 p1411 N88-18416
Development of tokamak reactor system analysis code NEW-TORSAC
[DE88-751067] 10 p1411 N88-18417
Toroidal confinement research concepts evaluation and tradeoff studies
[DE88-004277] 11 p1551 N88-19282
Magnetic and inertial fusion status and development plans
[DE88-004405] 11 p1552 N88-19288
Problems in modeling TF ripple loss of fast alphas from a tokamak reactor
[DE88-000612] 11 p1553 N88-19296
A neutral-beam diagnostic for fast confined alpha particles in a burning plasma: Applicatoin on CIT (Compact Ignition Tokamak)
[DE88-004890] 11 p1554 N88-19301
CIT (Compact Ignition Tokamak) fueling
[DE88-002709] 12 p1692 N88-20125
Plasma rotation in a tokamak
[DE88-700855] 12 p1693 N88-20128
FOM contributions to the 14th European Conference on Controlled Fusion and Plasma Physics
[REPT-87-174] 12 p1693 N88-20129
Microturbulent fluctuations in the TORTUR tokamak
12 p1693 N88-20131
Flux coordinate studies of elongated plasmas at high Beta
12 p1694 N88-20134
A high field launch for electron cyclotron heating using an external window
[DE88-005350] 13 p1838 N88-21000
Observations on energy transport in tokamaks: A new formula for turbulent transport
[DE88-005309] 13 p1841 N88-21019
Evolution of poloidal variation of impurity density and ambipolar potential in rotating tokamak plasma, part 1
[DE88-006263] 13 p1842 N88-21022
Potential off-normal events and associated radiological source terms for the compact ignition tokamak. Fusion Safety Program
[DE88-004112] 13 p1842 N88-21024
Consistency between current ramp-up/recharging scenario by non-inductive current drive and dense and cold divertor plasma. Conceptual design study of FY86 FER
[DE88-751438] 14 p1984 N88-21833
Preliminary analysis on plasma equilibrium control. Conceptual design study of FY86 FER
[DE88-751441] 14 p1984 N88-21834
Preparing the Alcator C bolometer system for use on MTX (Microwave Tokamak Experiment)
[DE88-006724] 15 p2134 N88-22733
Analyses and experiments on the integrity and lifetime predictions of plasma-facing components in fusion reactors
[DE87-702957] 15 p2135 N88-22735
Environmental assessment for the compact ignition Tokamak
[DE88-005633] 15 p2135 N88-22740
Long-time impurity confinement as a precursor to disruptions in ohmically heated tokamaks
[DE88-006183] 15 p2136 N88-22742
Current-drive on the Vers[illegible] tokamak with a slotted-waveguide fast wave coup[illegible]
[DE88-006261] 15 p[illegible]136 N88-22743
Improvement of plasma confinement due to electron Landau damping in tokamaks
[DE88-752339] 15 p2136 N88-22747
Transport simulations of ohmic ignition experiment IGNITEX
[DE88-006055] 15 p2138 N88-22757
Incorporating reliability into the design of experimental fusion facilities
[DE88-006767] 16 p2275 N88-23618
Soviet magnetic confinement fusion research
[PB88-182316] 16 p2279 N88-23644
Remote maintenance design activities and research and development accomplishments for the compact ignition tokamak
[DE88-006980] 16 p2279 N88-23645
Corpuscular plasma diagnostics complex on a tokamak with a strong field
[DE88-701576] 16 p2279 N88-23646
Ion temperature measurement with spectroscopy in JT-60 17 p2439 N88-24513
X-ray emission from tokamaks
17 p2439 N88-24514
X-ray spectroscopic diagnostics on JIPPT-IIU and HELIOTRON-E 17 p2440 N88-24515
Helium-like titanium spectra from tokamak plasmas
17 p2440 N88-24516
Spectroscopic results from JET: Some examples of data comparison and data needs 17 p2440 N88-24517
Tokamak studies of density sensitive line ratios
17 p2441 N88-24521
Flux density measurements of neutral iron in TEXTOR with laser induced fluorescence
17 p2442 N88-24528
Measurements of Z(sub eff) profile with a visible bremsstrahlung continuum detector array
17 p2443 N88-24529
Availability and quality of spectroscopic data and standards for tokamak studies 17 p2443 N88-24534
Systems analysis of INTOR-like designs
[DE88-004422] 18 p2578 N88-25316
A study of runaway electron confinement in the ASDEX tokamak
[DE88-007327] 18 p2579 N88-25319
A two-wavelength infrared interferometer/polarimeter system for CIT (Compact Ignition Tokamak)
[DE88-007681] 18 p2579 N88-25321
ECRH current drive in tokamak plasmas
[IPPJ-864] 19 p2729 N88-26209
Parallel gradient effects on ICRH (Ion Cyclotron Resonance Heating) in tokamaks
[DE88-009038] 19 p2730 N88-26216
Evolution of poloidal variation of impurity density and ambipolar potential in rotating tokamak plasma, part 2
[DE88-009882] 19 p2731 N88-26218
Thermal and mechanical analysis of the Faraday shield for the compact ignition tokamak
[DE88-007855] 20 p2856 N88-26962
Fusion programs in applied plasma physics and development and technology at GA Technologies, Inc.
[DE88-008406] 20 p2856 N88-26964
Multipoint Thomson scattering diagnostic for DIII-D
[DE88-008737] 20 p2857 N88-26969
TIBER (Tokamak Ignition/Burn Experimental Reactor) 2 as a precursor to an international thermonuclear experimental reactor
[DE88-008906] 20 p2858 N88-26970
Requirements for neutral beam current drive in tokamaks
[DE88-006180] 20 p2859 N88-26980
Impurity transport calculations for a drift-dependent tokamak scrape-off plasma
[DE88-010053] 20 p2859 N88-26984
Full-wave calculations in flux coordinates for toroidal geometry
[DE88-010131] 20 p2860 N88-26985
Toroidal and poloidal soft X-ray imaging system on the D3-D tokamak
[DE88-010585] 20 p2860 N88-26986
Vertical viewing ECE diagnostic for the D3-D tokamak
[DE88-010586] 20 p2860 N88-26987
MTX (Microwave Tokamak Experiment) plasma diagnostic system
[DE88-011326] 20 p2861 N88-26993
Multi-mode optical fibers for simultaneous 13-position measurements Thomson scattering apparatus in the JFT-2M tokamak
[DE88-753133] 21 p3015 N88-27897
Moment approach to neoclassical flows, currents and transport in auxiliary heated tokamaks
[DE88-008024] 21 p3016 N88-27901
Tokamak magnetic turbulence over the safety factor range 0.6 less than q less than 3
[DE88-008421] 21 p3017 N88-27904
ITER plasma equilibrium and poloidal field system design
[DE88-011005] 21 p3018 N88-27912
Global and local magnetohydrodynamic relaxations
[DE88-752602] 21 p3018 N88-27913
Design of divertor plate and measurements of double-null open divertor plasma in the JFT-2M tokamak
[DE88-753130] 21 p3018 N88-27914
Analysis of lower hybrid current drive and rampup experiments on the JT-60 tokamak
[DE88-753136] 21 p3018 N88-27915
Reactor applications of the Compact Fusion Advanced Rankine (CFAR) cycle for a D-T tokamak fusion reactor
[DE88-011351] 22 p3153 N88-28762
A survey of the current experimental database for lower hybrid current-drive and heating
[DE88-009830] 23 p3283 N88-29552
Numerical simulations of resistive magnetohydrodynamic instabilities in a poloidal divertor tokamak
[DE88-010768] 23 p3285 N88-29559
Bootstrap currents in radio-frequency-driven tokamak equilibria
[DE88-011136] 23 p3285 N88-29561
Tokamak plasma interaction with limiters
[UTIAS-325] 23 p3286 N88-29566
The calculation of time dependent eddy currents in tokamaks
[REPT-206] 23 p3286 N88-29568
Stability experimental results of cable-in-conduit superconductor for fusion
[DE88-753424] 23 p3290 N88-29589
The study of hydromagnetic waves and RF heating using the TORTUS tokamak, the development of diagnostic techniques based on submillimeter lasers and the gyrotron, and gas discharge 24 p3431 N88-30419

TOLERANCES (MECHANICS)
NT IMPACT TOLERANCES
Effects of barrel joints on hypervelocity projectiles
[DE87-013447] 02 p0157 N88-10983
Pinhole occulter experiment
[NASA-CR-179206] 02 p0235 N88-11481
Damage considerations in sizing aircraft cells. Life predictions
[SNIAS-872-111-116] 05 p0546 N88-13330
A study of damage tolerance in curved composite panels
[AD-A190617] 15 p2029 N88-22092
Manufacturing requirements 17 p2297 N88-23745
Fuel containment and damage tolerance in large composite primary aircraft structures. Phase 2: Testing
[NASA-CR-172519] 19 p2601 N88-25452
A comprehensive study on damage tolerance properties of notched composite laminates
[AD-A192952] 23 p3188 N88-28968

TOLERANCES (PHYSIOLOGY)
NT ACCELERATION TOLERANCE
NT ALTITUDE TOLERANCE
NT COLD TOLERANCE

NT HEAT TOLERANCE
NT HUMAN TOLERANCES
NT RADIATION TOLERANCE
Superoxide dismutase assays
[AD-A183972] 03 p0356 N88-12242
Microwave challenges to the thermoregulatory system
[AD-A185391] 05 p0629 N88-13847
Possible use of plasmids for study of effect of space flight factors on biological objects
08 p1046 N88-16319
Exercise thermoregulation after prolonged wakefulness
[AD-A186224] 08 p1048 N88-16327
Rational considerations for modelling human thermoregulation during cold water immersion
[AD-A186226] 08 p1048 N88-16329
Portable, ambient air microclimate cooling in simulated desert and tropic conditions
[AD-A186457] 08 p1050 N88-16338
Respiratory and cardiovascular responses to cold stress following repeated cold water immersion
[AD-A186460] 08 p1050 N88-16340
The role of hydration on peripheral response to cold
[AD-A186448] 09 p1199 N88-17186
Brain potentials and personality: A new look at stress susceptibility
[AD-A186931] 09 p1199 N88-17189
Annoyance caused by advanced turboprop aircraft flyover noise: Single-rotating propeller configuration
[NASA-TP-2782] 09 p1242 N88-17441
The precision of limits on bodily fluids when using beta-expectation inner tolerance limits
[AD-A187966] 10 p1369 N88-18185
Psychophysical, biochemical and histological studies of spectrally selective photic damage to primate retina
[AD-A188115] 11 p1517 N88-19063
Toxic effects of man-made mineral fibers with particular reference to ceramic fibers
[AD-A187949] 11 p1519 N88-19072
Interrelationship of heart rhythm indicators and resistance to hypoxia in Antarctic polar workers
12 p1664 N88-19974
Air quality and human performance, chapter 16
[AD-A188335] 12 p1666 N88-19988
Medical problems related to altitude in: Human performance physiology and environmental medicine at terrestrial extremes, chapter 14
[AD-A188340] 12 p1666 N88-19989
Direct interaction between autonomic nerves and the immune system
[AD-A188576] 12 p1667 N88-19991
Behavioral response of rats exposed to high-power microwave radiation
[AD-A192199] 18 p2548 N88-25128
Extremely Low Frequency (ELF) communications system ecological monitoring program: Summary of 1986 progress
[AD-A192014] 19 p2642 N88-25676
Assessment of cochlear damage after microwave irradiation
[AD-A193237] 21 p2987 N88-27737
Evaluation of the potential health hazards associated with the machining of carbon fiber composites
[AD-A194835] 24 p3408 N88-30286

TOLLMEIN-SCHLICHTING WAVES
Numerical simulation of Tollmien-Schlichting waves by use of a modified vortex particle-in-cell method
[IC-AERO-85-02] 02 p0171 N88-11079
Time-dependent hypersonic viscous interactions
[AD-A185764] 06 p0665 N88-14082
Computational design of natural laminar flow wings for transonic transport application 07 p0813 N88-14948
On the interaction of Tollmein-Schlichting waves in axisymmetric supersonic flows
[NASA-CR-181619] 10 p1331 N88-17955
Development of disturbances in swept wing flows
[NASA-CR-182675] 13 p1768 N88-20574
Ejection mechanisms in the sublayer of a turbulent channel 16 p2195 N88-23090
Wave-growth associated with turbulent spot in plane Poiseuille flow 16 p2199 N88-23116
Active control of 2-D instability waves on an axisymmetric body
[AD-A191578] 19 p2663 N88-25835
Variable Sweep Transition Flight Experiment (VSTFE)-parametric pressure distribution boundary layer stability study and wing glove design task
[NASA-CR-3992] 23 p3173 N88-28894
Nonlinear Tollmien-Schlichting/vortex interaction in boundary layers
[NASA-CR-181698] 24 p3311 N88-29715
The strong nonlinear interaction of Tollmien-Schlichting waves and Taylor-Goertler vortices in curved channel flow
[NASA-CR-181697] 24 p3311 N88-29716
On the generation of mean flows by the interaction of Goertler vortices and Tollmien-Schlichting waves in curved channel flows
[NASA-CR-181690] 24 p3315 N88-29743

TOLUENE
Detailed mechanism of toluene oxidation and comparison with benzene
[NASA-TM-100261] 05 p0563 N88-13428
Characterization of the dimensions of colloidal calcium carbonate dispersions in toluene with neutron small-angle scattering
[ECN-197] 06 p0680 N88-14167
Study of toluene stability for an Organic Rankine Cycle (ORC) space-based power system
[NASA-CR-180884] 24 p3337 N88-29863
Study of toluene rotary fluid management device and shear flow condenser performance for a space-based organic Rankine power system
[NASA-CR-180885] 24 p3338 N88-29872

TOMAHAWK MISSILES
Non-linear shipboard shock analysis of the Tomahawk missile shock isolation system 05 p0592 N88-13614

TOMOGRAPHY
NT COMPUTER AIDED TOMOGRAPHY
Model-based ultrasonic tomography
[DE87-013786] 01 p0058 N88-10369
A comparison of film based tomography and computed tomography for advanced ceramic materials
[DE88-003114] 07 p0837 N88-15079
A new technique for rocket and space-borne investigations of time-dependant auroral morphology
08 p1030 N88-16241
The Quick Response Multicolor Printer (QRMP) system
[AD-A188140] 11 p1504 N88-18982
Geophysical diffraction tomography for imaging isolated subsurface inclusions
[DE88-003918] 11 p1505 N88-18990
Estimation of sea surface wave spectra using acoustic tomography
[AD-A187837] 11 p1516 N88-19057
Three-dimensional image reconstruction in object space
[DE88-900279] 12 p1712 N88-20246
A study of satellite emission computed tomography
[AD-A189567] 13 p1797 N88-20745
Studies toward observing and modelling large energetic ocean regions
[AD-A189267] 13 p1803 N88-20778
Survey of acoustic techniques for monitoring El Nino
[PB88-157615] 13 p1804 N88-20783
Tectonics and three-dimensional structure of spreading centers: Microearthquake studies and tomographic inversions
[PB88-163290] 14 p1945 N88-21602
XDATAP
[DE88-007161] 20 p2837 N88-26827
The design of a digital Eprom oscillator for electrical impedance tomography
[DE88-012243] 21 p2940 N88-27462
Interferometric tomography of continuous fields with incomplete projections
[NASA-CR-183181] 22 p3081 N88-28295
Variation of carotid flow under load, studied by the Doppler echo method --- acceleration tolerance
[REPT-1149] 23 p3240 N88-29282
Positron emission tomography: A new technique for observing fluid behavior in engineering systems
[PNR90471] 24 p3374 N88-30091
Central adrenergic receptors as mediators of central response to stress: Study with Positron Emission Tomography (PET)
[AD-A194947] 24 p3407 N88-30284

TOMS
U TOTAL OZONE MAPPING SPECTROMETER

TONE
U PITCH

TONOMETRY
U PRESSURE MEASUREMENT

TONUS
U MUSCULAR TONUS

TOOLS
NT GRINDING MACHINES
NT LATHES
NT MACHINE TOOLS
NT MILLING MACHINES
NT SPACE TOOLS
Human engineering laboratory grounding analysis (HELGA)-2
[AD-A185367] 05 p0578 N88-13524
Interaction of microstructure and fatigue in tool steels
05 p0603 N88-13693
Tool and process for miniature explosive joining of tubes
[NASA-CASE-LAR-13662-1] 06 p0711 N88-14359
Proceedings of the DOD Workload Assessment Workshop on Workload Assessment Techniques and Tools held in Dayton, Ohio on 27-28 September 1986
[AD-A185650] 08 p1052 N88-16352
Friction welding: Advanced method of producing end cutting tool 14 p1897 N88-21327

TOPEX
Specifications and performance of ultrastable oscillators in the DORIS orbitography and positioning system
[ETN-88-92761] 24 p3331 N88-29831

TOPOGRAPHY
NT TERRAIN
Venusian surface and crust 01 p0010 N88-10054
The program DSMME: Digital Situation Model, Measurement --- mapping 01 p0065 N88-10418
Geoacoustic models of the Hudson Canyon area
[AD-A183535] 01 p0073 N88-10465
Surface topography and electrical response of metal-electrolyte interface
[DE87-013553] 02 p0166 N88-11046
On the role of snow in the redistribution of precipitation by small scale topography 02 p0203 N88-11267
Validation of a three dimensional numerical model of the sea breeze in complex terrain
02 p0211 N88-11325
Spherical harmonic expansion of the Levitus Sea surface topography
[NASA-CR-181448] 02 p0216 N88-11362
Cartography and topography with SPOT
03 p0342 N88-12159
Considering refraction in leveling with laser plane
04 p0462 N88-12857
Radial orbit error reduction and sea surface topography determination using satellite altimetry
04 p0462 N88-12861
The influence of the topography of fracture surfaces on crack closure 05 p0598 N88-13657
Sound propagation over uneven ground and irregular topography
[NASA-CR-182352] 06 p0776 N88-14763
Wind and temperature structure on the slopes of a mountain valley
[DE88-000080] 07 p0880 N88-15338
Laser system for automating topographic terrain survey 08 p1012 N88-16136
Estimation of gravity vector components from Bell gravity gradiometer and auxiliary data under consideration of topography and associated analytical upward continuation aspects
[AD-A188146] 10 p1355 N88-18099
NASA Oceanic Processes Program
[NASA-TM-4025] 10 p1357 N88-18109
Terrain Analyst Work Station (TAWS) demonstrations
[AD-A188139] 11 p1504 N88-18981
Digital data dubbing capability
[AD-A188252] 11 p1525 N88-19105
Silicon containing photoresists
[AD-A188666] 12 p1605 N88-19601
Influence of solar illumination conditions on TM/Landsat data
[INPE-4463-TDL/320] 12 p1638 N88-19806
Automatic knowledge acquisition for aerial image interpretation
[AD-A188616] 12 p1638 N88-19810
Research on the physical oceanography of the Gulf Stream
[AD-A188512] 12 p1649 N88-19877
Airborne electromagnetic sounding of sea ice thickness and sub-ice bathymetry
[AD-A188939] 12 p1649 N88-19879
A comparison of terrain association and resection as methods of position location
[AD-A189480] 13 p1790 N88-20710
Comparisons of global topographic/isostatic models to the Earth's observed gravity field
[NASA-CR-182696] 13 p1798 N88-20752
Planetary scale barotropic spectral model
13 p1801 N88-20766
Bathymetric hazard survey test
[AD-A189150] 13 p1803 N88-20775
Study of the dynamic topography of oceans by means of satellite altimetry 14 p1938 N88-21567
From satellite altimetry to ocean topography, a survey of data processing techniques
[ETN-88-91841] 14 p1939 N88-21575
Inventory of topographic mapping and standardization of geographic names as the basis of a Geographic Information System (GIS) 16 p2225 N88-23281
Mass digitization of topographic-cartographic information 16 p2226 N88-23288
Developments in the design of topographic maps in the Federal Republic of Germany: Activities and suggestions
16 p2226 N88-23290

The use of LANDSAT-TM pictures for the detection of space-limiting elements for the benefit of landscape photomapping
[BCRS-87-02] 16 p2228 N88-23305

Geometric image correction: An approach for the registration of LANDSAT-TM [illegible]tal images supported by topographical maps of medi[illegible] and great scales
17 p2361 N88-24061

Criteria for planimetric and altimetric correction of maps restituted from aerial photographs in 1:100,000 scale
17 p2367 N88-24097

The determination of gravity and topography from seismic velocities, accounting for dynamic behavior of the Earth's mantle
[ETN-88-92420] 17 p2374 N88-24117

Reports on cartography and geodesy. Series 1, no. 99
[ETN-88-92387] 18 p2533 N88-25025

West German Geodetic Working Group: Official topographic-cartographic information system (ATKIS), content description 18 p2533 N88-25026

West German Geodetic Working Group: Official topographic-cartographic information system (ATKIS), technical conception 18 p2533 N88-25027

Creation of digital topographic models with the ALK-GIAP. The DLM 25 as an example
18 p2534 N88-25031

Topographic data processing for environmental planning 18 p2534 N88-25032

State of development of ALK (October 1986)
18 p2534 N88-25035

Vectorization of raster algorithms for elevation data processing 18 p2534 N88-25036

Recent developments in software and hardware by Scitex Co. --- computer aided mapping
18 p2535 N88-25038

Use of remote sensing in the study of superficial formation certifying the development of integrated economy-case example: Rio Claro (SP) region
19 p2683 N88-25950

Updating of municipal official register of real estate through the geographical information system
19 p2684 N88-25952

Aerial photography as an instrument of atmospheric analysis: Maps of the middle atmosphere and its dynamics. Baixada Santista (SP) 19 p2684 N88-25955

Development of an atmospheric diffusion evaluation method incorporating topographical effects. Part 1: Literature review of atmospheric diffusion models incorporating terrain effects
[DE88-753104] 20 p2822 N88-26742

Influence of microstructure and microdamage processes on fracture at high loading rates
[AD-A192957] 21 p2960 N88-27583

X-ray studies of strain, interface and impurities in semiconductors
[DE88-012460] 21 p3025 N88-27954

Topography of an Antartic ice stream
22 p3092 N88-28361

Land use systems and rural landscapes in the center of Veracruz State (Mexico): First results
22 p3092 N88-28364

The suitability of SPOT imagery for monitoring landscape patterns 22 p3094 N88-28376

Topographic suppression and advances in classification for land cover mapping using SPOT-1 HRV imagery
22 p3099 N88-28404

The prospects for topographic mapping using SPOT data 22 p3110 N88-28470

Cartographic applications of SPOT imagery
22 p3110 N88-28472

The use of SPOT imagery for topographic mapping
22 p3110 N88-28473

The use of SPOT data for mapping and DEM production --- digital elevation model (DEM)
22 p3110 N88-28475

Assessment of SPOT imagery for topographic revision and vegetation mapping 22 p3111 N88-28477

Topographic mapping with SPOT 1 data. A practical approach by the Ordnance Survey
22 p3111 N88-28479

Extratropical response to tropical heating as a function of period of model integrations
22 p3125 N88-28577

Intraplate deformation, stress in the lithosphere and the driving mechanism for plate motions
[NASA-CR-183121] 23 p3231 N88-29231

Mars: Near-infrared comparative spectroscopy during the 1986 opposition 23 p3301 N88-29658

Topography of large craters on Mars: Implications for the highlands resurfacing history
23 p3306 N88-29691

Finite-difference simulations of Rayleigh-wave scattering by shallow heterogeneity
[AD-A194961] 24 p3402 N88-30259

X-ray diffraction imaging (topography) of electroopticcrystals by synchrotron radiation
[NASA-CR-183266] 24 p3432 N88-30427

Streaking images that appear only in the plane of diffraction in undoped GaAs single crystals: Diffraction imaging (topography) by monochromatic synchrotron radiation
[NASA-CR-183267] 24 p3433 N88-30437

Physical properties of surface materials on Martian volcanoes: Dust-covered lava and ash
24 p3443 N88-30493

Obligue metallogenic zones recognized by interpreting space photographs of southern Tien Shan
24 p3450 N88-30529

Structure of eastern Turkestan Ridge based on space photographs 24 p3450 N88-30530

TOPOLOGY

NT FIXED POINTS (MATHEMATICS)
NT HOMOTOPY THEORY
NT INVARIANT IMBEDDINGS
NT METRIC SPACE

Control of the German main triangulation network by macrometer measurement 1983-1985 (KONMAC)
[SER-B-282] 01 p0063 N88-10404

TIPS-1 user's manual: Cray-1 version
[DE87-013297] 01 p0081 N88-10522

Smooth dynamics on the interval (with an emphasis on unimodal maps)
[REPT-87-09] 01 p0086 N88-10555

Covariant Lorentz anomalies in higher dimensional space
[DE87-753021] 02 p0230 N88-11448

Topological aspects of infinite metal clusters and superconductors
[AD-A184104] 04 p0495 N88-13049

Topological equivalence of certain function spaces 2
[PB88-100904] 06 p0767 N88-14712

Embedding topological median algebras in products of dendrons
[PB88-100888] 06 p0767 N88-14713

Monte Carlo simulation of triangulated random surfaces in grand canonical ensemble
[DE88-700378] 07 p0941 N88-15718

The design of Impedance- matching networks for broadband antennas
[AD-A187600] 10 p1320 N88-17895

Topology and grid adaption for high-speed flow computations
[NASA-CR-182586] 11 p1487 N88-18875

Geometrical and topological issues in octree based automatic meshing 11 p1527 N88-19118

Finite octree meshing through topologically driven geometric operators 11 p1527 N88-19121

On exterior variational calculus
[DE88-700861] 12 p1683 N88-20062

Using design axioms and topology to model database semantics
[CWI-CS-R8711] 13 p1818 N88-20863

Measurement of the elastic-plastic surface flaw back surface topology and its relation to constraint
[DE88-006765] 15 p2087 N88-22437

Efficient, high resolution computations of projectile and missile flow fields
[AD-A191086] 16 p2158 N88-22873

Topological stereochemistry
[AD-A191867] 18 p2477 N88-24691

The determination of the topological structure of skin friction lines on a rectangular wing-body combination
[NASA-CR-4168] 20 p2753 N88-26343

Some remarks on geodesics in gauge groups and harmonic maps
[DE88-702665] 22 p3115 N88-28510

On the GKP and BS constructions of C-boundary
[DE88-702643] 22 p3159 N88-28799

Optimization-driven machine-oriented motion measurement 23 p3245 N88-29312

Monotone recurrence relations, their Birkhoff orbits and topological entropy
[AD-A193481] 23 p3276 N88-29504

TORCHES

Optimization of oxygen cutting process for titanium alloys 14 p1897 N88-21323

Studies of heat and mass transfer during chemical vapor deposition 17 p2338 N88-23953

Welding torch gas cup extension
[NASA-CASE-MFS-29252-1] 17 p2345 N88-23980

TORNADO AIRCRAFT

U MRCA AIRCRAFT

TORNADOES

The importance of the lower level windshear profile in tornado/non-tornado discrimination
02 p0208 N88-11304

The Windsor Locks, Connecticut tornado of 3 October 1979: An analysis of an intermittant severe weather event 02 p0208 N88-11305

Severe weather potential (SPOT) plotfile generator
[PB87-217717] 02 p0216 N88-11360

Tornado tracks in Southwestern Brazil, Eastern Paraguay, and Northwestern Argentina
17 p2362 N88-24071

TOROIDAL PLASMAS

Fast wave injection into high temperature tokamak plasmas in the lower-hybrid-density regime of JIPP T-IIU
[ISSN-0469-4732] 01 p0099 N88-10649

Nonlinear fluid equations for a low collisionality toroidal plasma
[DE87-013006] 01 p0100 N88-10655

Computational study of three-dimensional magnetohydrodynamic equilibria in toroidal helical systems
[DE87-753007] 02 p0240 N88-11514

Magnetohydrodynamic stability of spheromak plasma in toroidal flux conserver with rectangular cross section 3. Stability for symmetric modes
[IPPJ-845] 02 p0241 N88-11524

Limit of possible operation of crescent and bean shaped Tokamaks
[IPPJ-837] 02 p0242 N88-11532

A tapered poloidal gap for the reduction of field errors
[DE87-014750] 03 p0377 N88-12375

Interchange stability of noncircular reversed field pinches
[DE88-000177] 03 p0378 N88-12381

Ballooning modes or Fourier modes in a toroidal plasma?
[AD-A184299] 04 p0491 N88-13022

The role of stellarators in the advanced toroidal program
[DE87-014815] 04 p0491 N88-13025

A three-barrel repeating pneumatic pellet injector for plasma fueling of the Joint European Torus
[DE88-000330] 04 p0491 N88-13026

Transport simulations of the oscillating field current drive experiment in the ZT-40M reversed field pinch
[DE88-000538] 04 p0491 N88-13027

Dynamic processes in field-reversed-configuration compact toroids
[DE87-014756] 05 p0652 N88-13998

High midplane accessibility stellarator windings for high current toroidal accelerators
[AD-A186235] 07 p0933 N88-15665

A calorimeter for measuring the neutral beam power reaching the plasma
[DE88-001412] 07 p0937 N88-15691

Nonlinear evolution of the internal kink mode in toroidal geometry for shaped tokamak plasmas
[DE88-003655] 08 p1087 N88-16550

Evaluation of magnetic coordinates in finite-beta, asymmetric plasmas
[DE88-003665] 10 p1412 N88-18424

ATF experimental plans
[DE88-004177] 10 p1414 N88-18439

Toroidal confinement research concepts evaluation and tradeoff studies
[DE88-004841] 11 p1552 N88-19285

Improved confinement of screw pinch plasmas in SPICA 2 12 p1694 N88-20137

Effects of toroidal forces in current loops embedded in a background plasma
[AD-A188878] 12 p1695 N88-20143

Fully implicit three-dimensional MHD (magnetohydrodynamics) stability and evolution in toroidal geometry
[DE88-000624] 13 p1842 N88-21023

Theoretical studies of the heating of toroidal plasmas with radiofrequency electromagnetic radiation
[DE88-006913] 15 p2137 N88-22749

Ion thermal conductivity and ion distribution function in the banana regime
[IPPJ-865] 19 p2729 N88-26208

Full-wave calculations in flux coordinates for toroidal geometry
[DE88-010131] 20 p2860 N88-26985

Toroidal and poloidal soft X-ray imaging system on the D3-D tokamak
[DE88-010585] 20 p2860 N88-26986

Density fluctuations in currentless high beta plasmas in Heliotron E
[DE88-752310] 23 p3283 N88-29550

RFP (Revised Field Pinch) plasma experiment at INPE
[INPE-4613-PRE/1336] 24 p3431 N88-30420

TOROIDAL SHELLS

The elastic analysis of a thin toroidal shell
[AD-A187801] 12 p1635 N88-19785

TOROIDS

Shear strength of the ASDEX upgrade Toroidal Field (TF) coil insulation: Rupture, fatigue and creep behavior --- tokamak
[IPP-1/230] 01 p0059 N88-10376

A short introduction to the status and motivation for reversed field pinch and compact toroid research
[DE88-000487] 05 p0652 N88-13999
An introduction to poloidal and toroidal fields
[MITT-54] 17 p2394 N88-24232
TORPEDOES
Revised Impact Dynamic Design-Analysis Method (RIDDAM)
[AD-A190479] 16 p2217 N88-23225
TORQUE
Predictive momentum management for a space station measurement and computation requirements
[NASA-CR-172026] 02 p0138 N88-10866
Measurements and calculations of aerodynamic torques for a vertical-axis wind turbine
[DE88-001783] 04 p0465 N88-12876
Solar Dynamics and G-modes
[NASA-CR-180737] 06 p0805 N88-14911
Preliminary design of the ORION attitude control system
[AD-A187179] 10 p1292 N88-17729
Reaction wheel control through digital technique using reference models
[INPE-4220-PRE/1100] 12 p1599 N88-19570
Efficiency characteristics of speed modulated drives at predicted torque conditions for air-to-air heat pumps
[DE88-005846] 13 p1770 N88-20588
Models for steady and nonsteady Coulomb torque in ball bearings 14 p1876 N88-21208
On the torque and wear behavior of selected thin film MOS2 lubricated gimbal bearings
14 p1926 N88-21485
Two gimbal bearing case studies: Some lessons learned 14 p1927 N88-21487
The effects of torque response and time delay on rotorcraft vertical axis handling qualities
[AD-A189873] 15 p2017 N88-22023
Evaluation of a high-torque backlash-free roller actuator 16 p2219 N88-23239
Helicopter anti-torque system using fuselage strakes
[NASA-CASE-LAR-13630-1] 17 p2308 N88-23809
Time-Optimal Adaptive Shaped Torque (TOAST) technical note
[AD-A192719] 20 p2843 N88-26869
In-flight motor torque estimates for the second-stage Strypi 9 launch vehicle
[DE88-010833] 21 p2902 N88-27222
TORQUE MEASURING APPARATUS
U TORQUEMETERS
TORQUE MOTORS
A high performance inverter-fed drive system of an interior permanent magnet synchronous machine
[DE88-006753] 15 p2061 N88-22288
Study on design and control of torque-controlled manipulators
[NASA-TT-20197] 23 p3223 N88-29183
TORQUEMETERS
Analysis of free molecular effects on the attitude of satellites in geostationary transfer orbit. Part 2: Force and torque measurement in free molecular wind tunnel tests
[DFVLR-IB-222-86-A/07] 01 p0014 N88-10078
TORSION
Torsion as a source of expansion in a Bianchi type I universe in the self-consistent Einstein-Cartan theory of a perfect fluid with spin density
[AD-A184200] 03 p0322 N88-12037
Vibration and buckling of geometrically imperfect laminated cylindrical shells 04 p0456 N88-12822
Micromechanics of fatigue crack initiation under axial and torsional loadings 06 p0719 N88-14413
Multiaxial fatigue failure criterion: A new approach
06 p0719 N88-14418
The microstructure and texture of torsion-reverse torsion experiments
[DE88-001801] 06 p0721 N88-14434
Piezoelectric laminates for torsional and bending model control: Theory and experiment
10 p1343 N88-18029
An experimental investigation of the flap-lag-torsion aeroelastic stability of a small-scale hingeless helicopter rotor in hover
[NASA-TP-2546] 13 p1715 N88-20257
Development of a torsion balance for adhesion measurements
[NASA-TM-100799] 13 p1748 N88-20454
Coupled bending-torsion steady-state response of pretwisted, nonuniform rotating beams using a transfer-matrix method
[NASA-TM-100596] 15 p2086 N88-22435
Strain hardening at large strains in aluminum alloys
[DE88-007415] 18 p2484 N88-24737
The variation of torsional ductility of high-purity aluminum with temperature and strain rate
[DE88-005618] 18 p2487 N88-24755
TORSIONAL STRESS
Theory of deformation. Part 1: Kinematics
[DE88-003007] 08 p1001 N88-16062
TORSO
Analysis of head response to torso acceleration. Volume 1: Development of performance requirements
[PB88-156757] 14 p1953 N88-21640
TORUSES
Compact torus studies
[DE87-014254] 02 p0237 N88-11496
On meteor stream spatial structure theory
06 p0739 N88-14544
Unfoldings of quasi-periodic tori
[ZW-8706] 13 p1828 N88-20928
A high field launch for electron cyclotron heating using an external window
[DE88-005350] 13 p1838 N88-21000
Eigenmodes of a random walk on a 2-D lattice torus with one trap
[DE88-007830] 20 p2844 N88-26874
Unfoldings of quasi-periodic tori
[B8811118] 23 p3278 N88-29513
TOTAL ENERGY SYSTEMS
An analysis of gas-steam total power recovery energy system 20 p2784 N88-26512
TOTAL OZONE MAPPING SPECTROMETER
Scientific and Operational Requirements for TOMS Data
[NASA-CP-2497] 05 p0615 N88-13774
TOMS: The Antarctic ozone hole and ozone trends
05 p0615 N88-13775
Analysis of the breakdown of the Antarctic circumpolar vortex using TOMS ozone data
05 p0615 N88-13779
Insights into the general circulation of the lower stratosphere from TOMS 05 p0616 N88-13780
Lower-stratospheric/upper-tropospheric exchange processes associated with tropical cyclones as observed by TOMS 05 p0616 N88-13782
Tropical easterly jet located using TOMS data
05 p0616 N88-13783
The use of TOMS data for tropospheric ozone studies
05 p0616 N88-13784
TOMS as a monitor of the ultraviolet radiation environment: Applications to photobiology
05 p0617 N88-13785
Application of TOMS data to weather analysis models
05 p0617 N88-13787
Correlations of TOMS total ozone data (Nimbus-7 satellite) with tropopause height
05 p0617 N88-13788
TOMS ozone data compared at mesoscale resolution to tropopause heights from the AVE radiosonde network and to VAS radiances over the south-central United States 05 p0617 N88-13790
The use of TOMS-modified VAS data for large-scale NWP 05 p0618 N88-13791
Dobson-stations performance assessment using TOMS data 05 p0618 N88-13792
Volcanic eruption detection with TOMS
05 p0618 N88-13793
Analysis of SO2 signals in SBUV/TOMS data
05 p0618 N88-13794
Comparison of ground based and TOMS measurements of SO2 from volcanic emissions
05 p0618 N88-13795
TOMS and the NOAA/FAA volcano support plan
05 p0618 N88-13796
Observation guidelines for a Total Ozone Mapping Spectrometer (TOMS) in geosynchronous orbit
05 p0619 N88-13801
A geostationary imaging spectrometer TOMS instrument 05 p0619 N88-13802
The 1987 Airborne Antarctic Ozone Experiment: The Nimbus-7 TOMS data atlas
[NASA-RP-1201] 13 p1791 N88-20714
Near-real-time TOMS, telecommunications and meteorological support for the 1987 Airborne Antarctic Ozone Experiment
[NASA-CR-4133] 16 p2233 N88-23338
TOUCH
NT TACTILE DISCRIMINATION
Tactile sensing and inverse problems
[AD-A187464] 10 p1340 N88-18011
Integrated polysilicon tactile sensor
19 p2669 N88-25863
The interaction of thalamo-cortical systems in the 40 Hz following response 21 p2979 N88-27694
TOUGHNESS
NT NOTCH SENSITIVITY
Carbon fiber reinforced glass matrix composites for space based applications
[AD-A184355] 04 p0410 N88-12546
Interfacial strength development in thermoplastic resins and fiber-reinforced thermoplastic composites
[NASA-CR-181525] 04 p0411 N88-12549
The effect of temperature on the tensile properties of HSLA-100 steel
[AD-A184951] 05 p0565 N88-13441
Micromechanisms of fatigue crack growth and fracture toughness in metal matrix composites
[AD-A186941] 09 p1137 N88-16816
Strength and toughness of a brittle material
[VTT-RR-479] 09 p1183 N88-17089
Finite element substructuring methods for composite mechanics
[NASA-TM-100297] 10 p1296 N88-17745
The influence of small defects on tensile specimen ductility and symmetry of deformation
[AD-A187983] 10 p1346 N88-18044
Interaction of particulate and transformation toughening
[AD-A189321] 13 p1741 N88-20412
Degradations of thermal shock resistance and the fracture toughness of reactor graphite subjected to neutron irradiation 13 p1747 N88-20445
Fracture toughness testing of a ceramic matrix composite
[AD-A189846] 15 p2029 N88-22089
Influence of temperature on the tensile strength and toughness characteristics. Material 35NCD16 ESR. Test report M5-521800
[M5-521800] 15 p2041 N88-22163
Characterization of HYTUF steel. Semifinished product: 160 mm dia forging block. Processor: C3f. Test Report M3-434600
[M3-434600] 15 p2041 N88-22164
Transformation toughening of ceramics
[AD-A190399] 15 p2045 N88-22183
Determination of the toughness of a brittle material using strain gages
[ETN-88-92540] 18 p2527 N88-24993
Theoretical and experimental analysis of the toughening behavior of whisker reinforcement in ceramic matrix composites
[DE88-011841] 21 p2906 N88-27241
Development of high strength and toughness microcomposite HSLA Fe/Cr/Mn/C steel with and without Nb
[DE88-009813] 21 p2913 N88-27290
Effects of near interfacial microstructure on toughness and subcritical crack growth in ceramic/metal systems
[DE88-009842] 21 p2919 N88-27325
The influence of weld metal properties, weld geometry and applied load on weld system performance
[AD-A193403] 21 p2961 N88-27588
A technique for measuring area under a curve
[AD-A193559] 23 p3271 N88-29463
TOWED BODIES
Australian aerodynamic design codes for aerial tow bodies
[AD-A189048] 13 p1715 N88-20258
An investigation of cruciform parachutes and towed targets
[BU-360] 14 p1862 N88-21122
Bodies in unsteady flow
[AD-A190416] 15 p2064 N88-22308
TOWED TARGETS
U TARGETS
U TOWED BODIES
TOWERS
NT AIRPORT TOWERS
Build, install and demonstrate a variable stroke pump control and windmill system
[DE87-014656] 03 p0347 N88-12191
Facilities for research and weather observations on the 213 m tower at Cabauw (Netherlands) and at remote locations
[KNMI-WR-87-5] 06 p0746 N88-14587
TOWING
The use of a water towing tank for aerodynamic testing and methods for quantitative evaluation of photographs
16 p2202 N88-23140
Use of water towing tanks for aerodynamics and hydrodynamics 16 p2204 N88-23149
TOWNSEND DISCHARGE
NT GAS DISCHARGES
TOXIC HAZARDS
Hydride generation from the Exide load-leveling cells
[DE87-011361] 01 p0041 N88-10259
Opportunities for nowcasting air pollution episodes and accidental toxic and radioactive releases
02 p0210 N88-11317
Space station internal environmental and safety concerns 04 p0407 N88-12527
Investigation of the exposure to harmful compounds in the workshop of nondestructive materials testing at Gilze-Rijen (Netherlands)
[PML-1985-42] 05 p0623 N88-13816
Monitoring of space station life support systems with miniature mass spectrometry and artificial intelligence
08 p1057 N88-16376

Critical comparison of moving average and cumulative summation control charts for trace analysis data
[AD-A188312] 12 p1705 N88-20203

TOXICITY

Rapid toxicity detection in water quality control utilizing automated multispecies biomonitoring for permanent space stations 02 p0135 N88-10848

Aircraft fire safety research 04 p0406 N88-12526

Evaluation of the sensidyne toxic gas sensor for HF (Hydrogen Fluoride) vapor
[DE88-000647] 04 p0446 N88-12767

The toxicology and metabolism of nickel compounds
[DE87-014801] 04 p0474 N88-12921

Short-term in vitro screening studies related to the inhalation toxicology of potentially toxic aerosols
[AD-A184815] 05 p0629 N88-13845

Flammability, smoke and toxicity test on fire barrier fabric from the Porcher company --- Airbus aircraft
[ETN-88-91168] 06 p0666 N88-14085

Physiological and biochemical aspects of toxic effects of oxidants in man's environment (air, water)
07 p0890 N88-15391

Specific organic compounds in excreta
07 p0895 N88-15422

Kinetic toxic aspect of potential use of sulfur hexafluoride in closed environments 10 p1362 N88-18142

Toxic effects of man-made mineral fibers with particular reference to ceramic fibers
[AD-A187949] 11 p1519 N88-19072

Fibrous glass aerosols: A literature review
[AD-A188420] 12 p1672 N88-20008

Evaluation of the acute toxicity of a synthetic polyalphaolefin-based hydraulic fluid
[AD-A190412] 15 p2045 N88-22184

Reclamation of water contaminated with fuel system icing inhibitor. Phase 1: Literature review and information compilation
[DE88-006575] 16 p2183 N88-23013

Evaluation of the toxicity of products from the thermal degradation of materials
[ETN-88-91995] 18 p2549 N88-25130

Experimental study of protective effect of antioxidant enzymes-superoxide dismutase and catalase-when using intermittent toxic modes of hyperbaric oxygenation
19 p2707 N88-26094

National air toxics information clearinghouse: NATICH data base users guide for data viewing, February 1988
[PB88-197470] 21 p2970 N88-27645

TOXICITY AND SAFETY HAZARD

Investigation of the exposure to harmful compounds in the workshop of nondestructive materials testing at Gilze-Rijen (Netherlands)
[PML-1985-42] 05 p0623 N88-13816

Investigation of the nature and concentration of vapor and mist during the cleaning of aircraft
[PML-1985-29] 05 p0623 N88-13817

Waste destruction by plasma
[SNIAS-881-430-113] 21 p2971 N88-27651

TOXICOLOGY

JPRS report: Science and technology. USSR: Life sciences
[JPRS-ULS-87-012] 03 p0355 N88-12238

JPRS report: Science and technology. USSR: Life sciences
[JPRS-ULS-87-013] 06 p0750 N88-14608

Changes in functional parameters of animals during long-term inhalation of acetic acid
07 p0895 N88-15423

USSR report: Life sciences. Biomedical and behavioral sciences
[JPRS-UBB-87-010] 12 p1651 N88-19889

JPRS report: Science and technology. USSR: Life sciences
[JPRS-ULS-88-002] 12 p1665 N88-19982

JPRS report: Science and technology. USSR: Life sciences
[JPRS-ULS-88-009] 20 p2829 N88-26785

TOXINS AND ANTITOXINS

EURECA Botany Facility. Technical note: Removal of phytotoxins
[SIRA-A/7373/WP220/RJS/005]
17 p2379 N88-24143

TRACE CONTAMINANTS

First flight of the ATMOS instrument during the Spacelab 3 Mission, April 29 through May 6, 1985
[NASA-CR-182360] 06 p0728 N88-14482

Layered-capacitor method for dielectric bridge measurements. Algorithms for inversion and parameter fitting: Documentation, verification, data analysis
[PB88-131479] 11 p1505 N88-18989

High resolution infrared absorption spectra of various trace gases present in the upper atmosphere of the Earth
[NASA-CR-182590] 12 p1642 N88-19829

Critical comparison of moving average and cumulative summation control charts for trace analysis data
[AD-A188312] 12 p1705 N88-20203

A data acquisition system for atmospheric tracer studies
[DE88-006211] 14 p1991 N88-21869

Analytical Chemistry Division
[DE88-701236] 16 p2174 N88-22956

The potential impact on atmospheric ozone and temperature of increasing trace gas concentrations
[NASA-CR-182965] 17 p2373 N88-24112

Preliminary study of niobium alloy contamination by transport through helium 17 p2402 N88-24279

TRACE ELEMENTS

The effects of minor trace gases on the transfer of thermal infrared radiation through the Earth's atmosphere 04 p0468 N88-12893

Development of FTMS methods for the detection of trace chemical species and development of FTMS methods for the analysis of various chemical species
[AD-A185857] 07 p0828 N88-15023

Trace-element metabolism in man and animals in the presence of hypoxic states of diverse etiology
07 p0889 N88-15390

Long range reconnaissance of trace gases: A special aspect of emission spectroscopy
08 p1018 N88-16172

Trace element geochemistry of the South Atlantic Bight
[DE88-003515] 10 p1356 N88-18108

Stratospheric trace gas distributions from far infrared thermal emission spectroscopy
13 p1797 N88-20749

Advances in geochemistry and cosmochemistry: Trace element microdistributions with the synchrotron X-ray fluorescence microprobe
[DE88-006355] 15 p2032 N88-22108

A theoretical model of the washout of trace gases by raindrops in the atmosphere 17 p2375 N88-24125

Trace gas measurements in the troposphere using tunable diode lasers 18 p2540 N88-25072

Review of methods for remote sensing of atmospheric emissions from stationary sources
[PB88-190483] 20 p2821 N88-26739

Tracer water transport and subgrid precipitation variation within atmospheric general circulation models
[NASA-CR-182897] 20 p2823 N88-26745

Physical oceanography and tracer chemistry of the southern ocean
[DE88-006852] 20 p2828 N88-26779

Application of Auger electron spectroscopy to the study of trace element effects on weldability
[DE88-010457] 21 p2915 N88-27301

The 1985-86 measurements with the tunable diode laser absorption spectrometer
[PB88-214002] 23 p3231 N88-29226

Role of zircon in tracing crustal growth and recycling
24 p3394 N88-30211

Trace element differences between Archean, Proterozoic and Phanerozoic crustal components: Implications for crustal growth processes
24 p3399 N88-30243

TRACKED VEHICLES

Armoured vehicle track elastomers: Research and development at MRL
[MRL-GD-0012] 19 p2620 N88-25541

TRACKING (POSITION)

NT COMPENSATORY TRACKING
NT INFRARED TRACKING
NT MISSILE TRACKING
NT OPTICAL TRACKING
NT POLYSTATION DOPPLER TRACKING SYSTEM
NT PURSUIT TRACKING
NT RADAR TRACKING
NT RANGE AND RANGE RATE TRACKING
NT SATELLITE TRACKING
NT SATELLITE-TO-SATELLITE TRACKING
NT SPACECRAFT TRACKING
NT STAR TRACKERS

Tropical cyclone center locations from enhanced infrared satellite imagery
[PB87-213450] 01 p0071 N88-10455

Advanced dead reckoning navigation for mobile robots
03 p0262 N88-11646

Helicopter fire control: Advantages of an automatic target tracker 03 p0264 N88-11667

CNET (Chief of Naval Education and Training) Program Automated Tracking System (CPATS): A comprehensive study
[AD-A184694] 03 p0385 N88-12418

Effect of motion cues during complex curved approach and landing tasks: A piloted simulation study
[NASA-TP-2773] 04 p0398 N88-12480

A modern control theory based algorithm for control of the NASA/JPL 70-meter antenna axis servos
04 p0436 N88-12706

Supertracks: The building blocks of chaos
[DE88-001513] 04 p0522 N88-13207

Opportunities for tropical cyclone motion research in the Northwest Pacific region
[AD-A185068] 05 p0627 N88-13834

Boeing 727 MLS (Microwave Landing System) terminal instrument procedures (TERPS) approach data collection and processing, data report
[AD-A185523] 06 p0667 N88-14090

Optical seam tracking in robotic arc welding
[VTT-RR-463] 06 p0713 N88-14376

Experimental design of a piloted helicopter off-axis-tracking simulation using a helmet mounted display
[AD-A186228] 07 p0820 N88-14982

Tracking procedure for non-normally distributed measurement errors
[AD-A186287] 07 p0903 N88-15468

A piloted simulation investigating handling qualities and performance requirements of a single-pilot helicopter in air combat employing a helmet-driven turreted gun
[AD-A186878] 09 p1116 N88-16689

Role of optokinetic stimulation in vesibulospinal reflexes 10 p1360 N88-18131

Stable, robust tracking by sliding mode control
[AD-A188278] 10 p1401 N88-18358

An investigation of Doppler satellite positioning multi-station adjustment software
13 p1730 N88-20345

Robustifying the Kalman filter
[AD-A189240] 13 p1825 N88-20907

Multiple model parameter adaptive control for in-flight simulation
[AD-A190568] 15 p2021 N88-22044

Moving-bank multiple model adaptive estimation applied to flexible spacestructure control
[AD-A190761] 15 p2026 N88-22071

Effect of friction and control parameters on the tracking accuracy of a target seeker
[AD-A190010] 15 p2056 N88-22257

A multiple model adaptive tracking algorithm against airborne targets
[AD-A190619] 15 p2057 N88-22263

Comparison of surface current determined from satellite-tracked buoy with shipboard wind data during the 4th Brazilian antarctic expedition, 10-14 March, 1986
17 p2354 N88-24024

A system for determination of wind fields using geostationary meterological satellites
17 p2360 N88-24056

Near surface current determined from INPE's satellite-tracked buoy, during 6-26 November, 1985
17 p2360 N88-24058

Descriptions of HF and VHF Loran-C buoys and evaluations as potential datum marker buoys
[AD-A192069] 18 p2462 N88-24618

F-14 modeling study
[NASA-CR-4164] 19 p2603 N88-25462

MSAT mobile electronically steered phased array antenna development 19 p2647 N88-25711

Multi-target tracking algorithms for cluttered environments 20 p2789 N88-26543

A human factors evaluation of the Advanced Visual Technology System (AVTS) eye tracking oculometer
21 p2925 N88-27361

Passive multipath target tracking in an inhomogeneous acoustic medium
[AD-A193284] 21 p3012 N88-27873

Apparent brightness of stars and lasers
22 p3065 N88-28188

DSS 13 microprocessor antenna controller
22 p3066 N88-28192

A system for determination of wind fields from cloud tracks: INPE experiment
[INPE-4492-PRE/1256] 22 p3128 N88-28594

Interactive, networked moving platform simulators
[AD-A192374] 23 p3182 N88-28940

The gradient method for interface tracking
[AD-A194477] 23 p3248 N88-29334

Multi-sensory tracking mount control
[AD-A194675] 23 p3249 N88-29339

SSTS (Space Surveillance and Tracking System): The importance of early test and evaluation organizational participation
[AD-A193745] 23 p3276 N88-29499

Observed track-keeping performance of DC10 aircraft equipped with the Collins AINS-70 area navigation system: Karlsruhe and Masstricht UACs (Upper Area Control centres)
[EEC-202] 24 p3323 N88-29788

Analysis of environmental parameters from the Panama City tower radar experiment
[AD-A194994] 24 p3404 N88-30264

Dynamical systems and motion vision
[AD-A195932] 24 p3422 N88-30366

TRACKING AND DATA RELAY SATELLITES
U TDR SATELLITES
TRACKING ANTENNAS
U DIRECTIONAL ANTENNAS
TRACKING FILTERS
A multiple model adaptive tracking algorithm against airborne targets
[AD-A190619] 15 p2057 N88-22263
Object discrimination via bulk temperature/velocity filtering, phase 1
[AD-A194533] 23 p3274 N88-29487
TRACKING NETWORKS
NT DEEP SPACE NETWORK
NT POLYSTATION DOPPLER TRACKING SYSTEM
NT RADAR NETWORKS
Determination of TRANET (tracking station coordinates for tracking network) and SMTP (Special Mission Tracking Program) tracking station coordinates for use in the WGS (World Geodetic System) 84
[AD-A185863] 07 p0817 N88-14972
NASA (National Aeronsutics and Space Administration) ADP (Automated Data Processing) system: Information on the automated mission and the payload tracking system
[PB88-104989] 07 p0942 N88-15730
Horizontal estimation and information fusion in multitarget and multisensor environments
[AD-A186935] 09 p1224 N88-17336
Surface disturbances produced by low-level, subsonic B-1 aircraft
[AD-A192257] 20 p2824 N88-26752
An investigation of the uses of time domain capable vector network analyzers as a diagnostic for helix traveling-wave circuits
[AD-A192460] 21 p2935 N88-27430
TRACKING PROBLEM
Synthesizing controllers for uncertain systems by a quantitative pole-placement
[PB87-195590] 02 p0223 N88-11403
The robust tracking control of nonlinear systems with uncertain dynamics 21 p2999 N88-27788
TRACKING STATIONS
NT POLYSTATION DOPPLER TRACKING SYSTEM
Determination of TRANET (tracking station coordinates for tracking network) and SMTP (Special Mission Tracking Program) tracking station coordinates for use in the WGS (World Geodetic System) 84
[AD-A185863] 07 p0817 N88-14972
TRACKING STUDIES
U TRACKING (POSITION)
TRACTION
Traction model development
[AD-A188450] 15 p2073 N88-22359
Roller drive materials performance
16 p2219 N88-23241
A critical speed study for aircraft bias ply tires
[AD-A193616] 22 p3084 N88-28313
TRACTORS
NT TRACKED VEHICLES
TRACTS
U SITES
TRADEOFFS
Toroidal confinement research concepts evaluation and tradeoff studies
[DE88-004277] 11 p1551 N88-19282
On 3-5 transistors for MM-wave applications
[AD-A191580] 19 p2661 N88-25825
Array trade-off study using multilayer parasitic subarrays
[NASA-TM-101321] 22 p3070 N88-28222
TRADESCANTIA
Zero gravity and living organism
08 p1046 N88-16320
TRAFFIC
NT AIR TRAFFIC
Pyroelectric line scanner for remote IR imaging of vehicles
[DE87-012127] 02 p0235 N88-11484
Computer aided cartographic representation of traffic data: The traffic intensity maps of Baden-Wuerttemberg (Federal Republic of Germany)
16 p2225 N88-23282
Digital maps for an electronic traffic guide
18 p2534 N88-25033
TRAFFIC CONTROL
NT AIR TRAFFIC CONTROL
Simulation of an enhanced TCAS 2 system in operation
[NASA-CR-181545] 04 p0398 N88-12479
The estimation of basic matrices using travel intensity theorems
[REPT-87-13] 05 p0642 N88-13926
A traveling-salesman-based approach to aircraft scheduling in the terminal area
[NASA-TM-100062] 12 p1576 N88-19424
A three dimensional assignment method in the time space
[REPT-87-49] 16, p2287 N88-23690
Airport surface traffic automation study
[AD-A194553] 23 p3181 N88-28934
TRAILING EDGE FLAPS
Static aeroelastic considerations in the definition of design loads for fighter airplanes
05 p0550 N88-13351
Flight and wind-tunnel measurements showing base drag reduction provided by a trailing disk for high Reynolds number turbulent flow for subsonic and transonic Mach numbers
[NASA-TP-2638] 06 p0701 N88-14299
High-flaps for natural laminar flow airfoils
17 p2296 N88-23739
Pressure distributions from subsonic tests of an advanced laminar-flow-control wing with leading- and trailing-edge flaps
[NASA-TM-4040-PT-1] 17 p2300 N88-23758
A low speed wind tunnel investigation of Reynolds number effects on a 60-deg swept wing configuration with leading and trailing edge flaps
[NASA-CR-181684] 19 p2598 N88-25441
Pressure distributions from subsonic tests of an advanced laminar-flow-control wing with leading- and trailing-edge flaps
[NASA-TM-4040-PT-2] 24 p3321 N88-29776
TRAILING EDGES
A study of rotor broadband noise mechanisms and helicopter tail rotor noise 06 p0777 N88-14766
Navier-Stokes calculations and turbulence modeling in the trailing edge region of a circulation control airfoil
10 p1268 N88-17587
Investigations of a circulation control airfoil flowfield using an advanced laser velocimeter
10 p1269 N88-17589
Experimental investigation of the transonic flow at the leeward side of a delta wing at high incidence
[LR-518] 16 p2156 N88-22861
Structure of unsteady flows at leading- and trailing-edges: Flow visualization and its interpretation
16 p2205 N88-23154
Axisymmetric viscid-inviscid interaction by a frozen vorticity approximation
[AD-A191743] 18 p2509 N88-24885
Characteristics of merging shear layers and turbulent wakes of a multi-element airfoil
[NASA-TM-100053] 18 p2511 N88-24900
The influence of surface rounding on trailing edge noise
[AD-A193387] 21 p3012 N88-27876
Classical separation, trailing-edge flows and buffeting
23 p3170 N88-28874
Experiments on the dissipation of sound by separated flow at an edge
[ISVR-TR-151] 23 p3279 N88-29522
TRAINEES
U STUDENTS
TRAINERS
U TRAINING DEVICES
TRAINING
U EDUCATION
TRAINING AIRCRAFT
NT T-33 AIRCRAFT
A look toward the future of complex avionics systems development using the USAF Test Pilot School's avionics systems test training aircraft 17 p2306 N88-23797
TRAINING ANALYSIS
The construction of a pedagogy to promote meaningful learning of strategies and tactics for solving problems of elementary combinatorics
[AD-A187928] 11 p1542 N88-19216
Report of the participation in the International Training Course: Remote Sensing in Village Forestry
[INPE-4476-NTE/278] 12 p1637 N88-19802
Hypnosis: Possible applications for cosmonauts
12 p1665 N88-19984
TRAINING DEVICES
NT TEACHING MACHINES
Examining the relative efficiency of Part- versus whole-task practice for multiple-task situations
[AD-A185056] 05 p0631 N88-13856
Learning to program methodically. 3: The newly designed course of the elementary programming
[PB87-119871] 06 p0757 N88-14643
Application of the analysis phase of the instructional system development to the MK-105 magnetic minesweeping mission of the MH-53E helicopter
[AD-A186282] 07 p0822 N88-14994
Human performance data needed for training device design decisions
[AD-A185988] 07 p0898 N88-15441
Air Force Human Resources Laboratory technical reports and technical papers
[AD-A186830] 09 p1201 N88-17200
Space shuttle onboard navigation console expert/trainer system 09 p1203 N88-17208
Aircrew training devices: Utility and utilization of advanced instructional features, phase 4
[AD-A188418] 12 p1670 N88-20000
Parachute for in-flight training on parachute ejection
[REPT-87-11] 18 p2458 N88-24593
TRAINING EVALUATION
Investigation of pilot behavior in a training program for assessing handling qualities using a ground simulator
[ESA-TT-999] 03 p0357 N88-12247
Field evaluation of interactive simulation for maintenance training: SH-3 helicopter electro-mechanical bladefold system
[AD-A185923] 07 p0821 N88-14991
A validity study of a selection procedure for student airline pilots
[DFVLR-FB-87-34] 09 p1201 N88-17196
Measurement and effects of transport delays in a state-of-the-art F-16C flight simulator
[AD-A187367] 11 p1441 N88-18599
Visual recognition training: Effectiveness of computer graphics
[AD-A188302] 12 p1669 N88-19997
Utility NDE personnel qualification/certification: Enhanced personnel qualification requirements for ASME (American Society for Mechanical Engineers) Code Section 11 examinations
[DE88-006748] 16 p2216 N88-23222
Personality, attitudes, and pilot training performance: Preliminary analysis
[AD-A193102] 21 p2991 N88-27746
An expert system for a distributed real-time trainer
23 p3261 N88-29411
Controlled degradation of resolution of high-quality flight simulator images for training effectiveness evaluation
[AD-A196189] 24 p3330 N88-29823
Improvement of head-up display standards. Volume 3: An evaluation of head-up display safety
[AD-A195787] 24 p3410 N88-30300
TRAINING SIMULATORS
NT COCKPIT SIMULATORS
NT FLIGHT SIMULATORS
An enumeration of research to determine the optimal design and use of Army flight training simulators
[AD-A191242] 18 p2468 N88-24649
Development of training implying man-machine interface: From the aircraft to the spacecraft
19 p2700 N88-26052
Controlled degradation of resolution of high-quality flight simulator images for training effectiveness evaluation
[AD-A196189] 24 p3330 N88-29823
LANTIRN simulator training in the F-16C
[AD-A195201] 24 p3330 N88-29826
TRAJECTORIES
NT ABORT TRAJECTORIES
NT ASCENT TRAJECTORIES
NT BALLISTIC TRAJECTORIES
NT DESCENT TRAJECTORIES
NT ELECTRON TRAJECTORIES
NT HYPERBOLIC TRAJECTORIES
NT INTERPLANETARY TRAJECTORIES
NT MISSILE TRAJECTORIES
NT MOLECULAR TRAJECTORIES
NT PARTICLE TRAJECTORIES
NT REENTRY TRAJECTORIES
NT RENDEZVOUS TRAJECTORIES
NT ROUND TRIP TRAJECTORIES
NT SPACECRAFT TRAJECTORIES
NT UNDERWATER TRAJECTORIES
On the degree of generality of inflationary solutions in cosmological models with a scalar field
[DE87-703079] 02 p0251 N88-11586
A dissipation principle and its consequences for structured shock waves in thermoelastic materials
[DE87-013723] 04 p0454 N88-12813
Supertracks: The building blocks of chaos
[DE88-001513] 04 p0522 N88-13207
Trajectory control of robot manipulators with closed-kinematic chain mechanism
[NASA-TM-89305] 05 p0591 N88-13605
Cartesian path control of a two-degree-of-freedom robot manipulator
[NASA-CR-182331] 05 p0639 N88-13908
An evaluation of semianalytical satellite theory against long arcs of real data for highly eccentric orbits
[AD-A185825] 08 p0960 N88-15819
Heuristic search in robot configuration space using variable metric 08 p1059 N88-16389
POCC capabilities document. Payload support capabilities description: MCC, JSC POCC, remote POCC interface
[NASA-TM-89708] 09 p1260 N88-17555
Simulator investigation of wind shear recovery techniques 10 p1275 N88-17630

Orbital analysis of a STS (Space Transportation System) external tank in low earth orbit
[AD-A188829] 12 p1593 N88-19542
Base reaction optimization of manipulators with redundant kinematics 16 p2219 N88-23238
Microgravity manipulator demonstration
16 p2219 N88-23242
Comparison of surface current determined from satellite-tracked buoy with shipboard wind data during the 4th Brazilian antarctic expedition, 10-14 March, 1986
17 p2354 N88-24024
Tornado tracks in Southwestern Brazil, Eastern Paraguay, and Northwestern Argentina
17 p2362 N88-24071
A centered projective algorithm for linear programming
[AD-A192100] 18 p2557 N88-25178
Accelerator research studies
[DE86-007124] 18 p2574 N88-25290
A simulation of post boost vehicle deployment of multiple reentry vehicles
[DE88-009537] 20 p2764 N88-26391
Multi-target tracking algorithms for cluttered environments 20 p2789 N88-26543

TRAJECTORY ANALYSIS
Instrumentation package for a shrouded SWERVE/EPW rocket sled test
[DE87-014267] 01 p0008 N88-10045
Development and testing of an air-mass transformation trajectory model 02 p0209 N88-11309
Approach trajectory planning system for maximum concealment
[NASA-TM-88258] 02 p0227 N88-11435
Analysis of the motions and effects of hairpin vortices
03 p0316 N88-11997
Optoelectronic measurement methods for ballistic experiments
[PB87-110706] 05 p0583 N88-13554
Pattern recognition techniques for failure trend detection in SSME ground tests 07 p0924 N88-15614
An evaluation of semianalytical satellite theory against long arcs of real data for highly eccentric orbits
[AD-A185825] 08 p0960 N88-15819
Aircraft flight test trajectory control
[NASA-CR-179428] 09 p1120 N88-16707
Maneuverable reentry vehicle trajectory footprints: Calculation and properties
[DE88-004726] 10 p1292 N88-17726
Interplanetary mission design handbook. Volume 1, Part 5: Mars-to-Earth ballistic mission opportunities, 1992-2007
[NASA-CR-182525] 10 p1430 N88-18538
Three-dimensional trajectory analyses of two drop sizing instruments: PMS OAP and PMS FSSP
[NASA-CR-4113] 11 p1437 N88-18574
Store separation and missile firing from aircraft: Experimental methods for trajectory projection
[NASA-TT-20214] 11 p1439 N88-18589
Effect of transition aerodynamics on aeroassist flight experiment trajectories
[NASA-TM-100546] 11 p1446 N88-18620
The stress field surrounding the tip of a crack propagating in a finite body 11 p1500 N88-18962
Trajectory characteristics and heating of hypervelocity projectiles having large ballistic coefficients
[NASA-TP-2614] 12 p1574 N88-19412
Aeroassisted orbit transfer vehicle trajectory analysis
[NASA-TM-89138] 12 p1599 N88-19575
A method and measures to evaluate trackers for air traffic control
[NLR-TR-86072-U] 13 p1720 N88-20287
Trajectory code studies, 1987
[DE88-006218] 13 p1728 N88-20335
Linear programming along the trajectory of the problem
[REPT-87-41] 14 p1956 N88-21662
Distribution of neutral gas molecules at large distances from Halley's comet 14 p1999 N88-21914
Spacecraft trajectories
[ISBN-2-85-428166-7] 15 p2023 N88-22054
On the trajectory of a linear programming problem
[REPT-87-53] 16 p2250 N88-23442
Underwater optical trajectography and video image mosaics 19 p2700 N88-26051
A new trajectory following polynomial-time algorithm for the linear programming problem
[REPT-87-87] 20 p2840 N88-26848
A numerical simulation of side force effects by aerodynamic flight trajectory correction
[ISL-CO-211/87] 21 p2896 N88-27191
FORTRAN programs for computation of time dependent sea levels and trajectory errors from satellite altimeter data
[BONN-MITT-73] 21 p2901 N88-27216
A theoretical determination of the density at a traveling source that emitts particles
[ISAS-RN-351] 21 p3013 N88-27883
Asymptotic orders of reachability in perturbed linear systems
[AD-A192718] 22 p3143 N88-28688
Computational aerodynamic analysis for a range-limited 25mm training round
[AD-A185270] 24 p3320 N88-29772
Ascent guidance for a winged boost vehicle
[NASA-CR-172083] 24 p3334 N88-29846

TRAJECTORY CONTROL
NT TRAJECTORY OPTIMIZATION
Trajectory control using laterally ejected jets. Literature review
[ISL-R-117/85] 05 p0581 N88-13544
Cartesian path control of a two-degree-of-freedom robot manipulator
[NASA-CR-182331] 05 p0639 N88-13908
Optimal guidance of homing missiles
06 p0671 N88-14111
Real-time kinematic and dynamic analysis and adaptive model following control of manipulator arms
11 p1495 N88-18927
Aerodynamic possibilities for the realization of trajectory corrections
[ISL-CO-251/86] 14 p1862 N88-21120
A numerical simulation of side force effects by aerodynamic flight trajectory correction
[ISL-CO-211/87] 21 p2896 N88-27191
The VITE model: A neutral command circuit for a generating arm and articulator trajectories
[AD-A192715] 21 p2987 N88-27734
Time minimal computation of feedback control schemes for optimal guidance problems used in space flight
[ETN-88-92989] 23 p3184 N88-28953
The eivaN: A forward-looking interactive orbital trajectory plotting tool for use with proximity operations (PROX OPS) and other maneuvers: Description and user's manual
[NASA-CR-177490] 24 p3414 N88-30327

TRAJECTORY MEASUREMENT
Flightpath reconstruction and systematic radar error estimation from multiradar range-azimuth measurements
[NLR-MP-85064-U] 06 p0693 N88-14251
Determining trajectory of ground movement accompanying seismic phenomena
08 p1011 N88-16132
Spacecraft trajectories
[ISBN-2-85-428166-7] 15 p2023 N88-22054
A multiple model adaptive tracking algorithm against airborne targets
[AD-A190619] 15 p2057 N88-22263
Trajectory measurement of the Fokker 100 aircraft during autoland testing
[NLR-MP-86010-U] 20 p2758 N88-26366

TRAJECTORY OPTIMIZATION
Performance and optimization of direct implicit time integration schemes for use in electrostatic particle simulation codes
[DE88-003254] 10 p1406 N88-18381
Safe rendezvous approach to a space station by impulsive transfers and continuous thrust arcs
12 p1585 N88-19486
Safe and fuel minimum reference trajectories for closed loop controlled approaches --- space stations
12 p1585 N88-19488
Optimal thrust vector control of coplanar orbital evasive maneuvers
[AD-A189544] 13 p1730 N88-20346
Performance optimization of a cruise missile using dynamic-stall induced lift augmentation
[AD-A190497] 15 p2017 N88-22027
Periodic solutions in aircraft cruise-dash optimization
18 p2464 N88-24631
Optimum-Path-to-Go guidance of command adjusted trajectory projectiles
[AD-A193377] 22 p3040 N88-28051
The analysis and control of robotic manipulators operating at or near kinematically singular configurations
22 p3084 N88-28315
The eivaN: A forward-looking interactive orbital trajectory plotting tool for use with proximity operations (PROX OPS) and other maneuvers: Description and user's manual
[NASA-CR-177490] 24 p3414 N88-30327

TRANQUILIZERS
Carbamates, atropine, and diazepam: Effects on performance in the running rat
[AD-A188009] 11 p1517 N88-19062

TRANSATMOSPHERIC VEHICLES
Apollo Lightcraft project
[NASA-CR-182575] 11 p1445 N88-18615

TRANSCEIVERS
U TRANSMITTER RECEIVERS

TRANSCENDENTAL FUNCTIONS
NT COSINE SERIES
NT EXPONENTIAL FUNCTIONS
NT LOGARITHMS
NT PERIODIC FUNCTIONS
NT TANGENTS
NT TRIGONOMETRIC FUNCTIONS
High speed transcendental elementary function architecture in support of the Vector Wave Equation (VWE)
[AD-A189746] 15 p2119 N88-22627
Mahler's method in transcendence theory
17 p2393 N88-24227
General analytic solution of certain functional equations of addition type
[PREPRINT-583] 22 p3144 N88-28699

TRANSCONDUCTANCE
Characterization of enhanced Schottky-barrier InGaAs/Al(1-x)As strained channel modulation-doped field-effect transistors
[AD-A188820] 12 p1698 N88-20162

TRANSDUCERS
NT DIGITAL TRANSDUCERS
NT ELECTROACOUSTIC TRANSDUCERS
NT ELECTRONIC TRANSDUCERS
NT HYDROPHONES
NT IMAGE TRANSDUCERS
NT INTERDIGITAL TRANSDUCERS
NT MAGNETIC TRANSDUCERS
NT MICROPHONES
NT MODE TRANSFORMERS
NT PIEZOELECTRIC GAGES
NT PIEZOELECTRIC TRANSDUCERS
NT PIEZORESISTIVE TRANSDUCERS
NT PRESSURE SENSORS
NT QUARTZ TRANSDUCERS
NT SOUND TRANSDUCERS
NT THERMOPILES
NT ULTRASONIC WAVE TRANSDUCERS
Notes on transducer design based on resistance strain gages with applied temperature compensation
[FFA-MEMO-129] 01 p0050 N88-10319
Capacitive resonant transducer for the Frascati gravitational antenna
[IFSI-86-9] 05 p0578 N88-13528
A surface plasmon waveguide sensor: A new type of chemical transducer based on optical phenomena
[ETN-88-91322] 06 p0780 N88-14792
Statistical measures of clipped random signals
08 p1000 N88-16055
Investigation of thermoacoustic heat transport using a thermoacoustic couple
[AD-A186889] 09 p1242 N88-17442
Evaluation of a miniature horizontal pendulum tilt transducer 12 p1577 N88-19435
User's guide: Lower neck transducer for the Hybrid 3 dummy
[PB88-133319] 12 p1626 N88-19743
Evaluation tests of lower neck transducer for the Hybrid 3 Dummy
[PB88-133327] 12 p1626 N88-19745
Development of an electronically-scanned pressure module for operation at cryogenic temperatures
[NASA-CR-181610] 12 p1629 N88-19746
Computer grading of extensometers (BS 3846)
[NPL-DMA(A)-152] 15 p2108 N88-22560
Low power consumption current transducer
[NASA-CASE-NPO-16888-1-CU]
17 p2335 N88-23937
Characterization of noncontact piezoelectric transducer with conically shaped piezoelement
[NASA-CR-4151] 17 p2347 N88-23987
Single mode levitation and translation
[NASA-CASE-NPO-16675-1-CU]
17 p2395 N88-24241
Navigation system for land vehicles
[NASA-CASE-LAR-13322-1] 18 p2462 N88-24620
Thermodynamic study of hygroscopic polymers using surface acoustic waves 19 p2672 N88-25882
Air loading effects on a capacitively sensed membrane supported silicon accelerometer
19 p2672 N88-25886
Deposition techniques and properties of strain compensated LPCVD silicon nitride films
19 p2673 N88-25898
Acoustic emission calibration instrumentation
[DE88-010817] 21 p2951 N88-27528
Direct measurement of solids. High temperature sensing. Experimental development and testing of high temperature pulsed EMATs
[DE88-009859] 21 p2954 N88-27546
Piezoelectric and electrostrictive materials for transducer applications, volume 1
[AD-A194957] 24 p3374 N88-30096
Piezoelectric and electrostrictive materials for transducer applications, volume 2
[AD-A194956] 24 p3376 N88-30104
Piezoelectric and electrostrictive materials for transducer applications, volume 3
[AD-A194949] 24 p3377 N88-30112

TRANSEQUATORIAL PROPAGATION
Solar tides in the upper equatorial thermosphere: A comparison between AE-E data and the NCAR thermospheric general circulation model
[AD-A186160] 08 p1023 N88-16106

TRANSFER
U TRANSFERRING

TRANSFER FUNCTIONS
NT MODULATION TRANSFER FUNCTION
NT OPTICAL TRANSFER FUNCTION
Electromagnetic tests
[SNIAS-872-430-103] 05 p0575 N88-13508
Equivalence of input-output stability and exponential stability for infinite dimensional systems
[TW-276] 05 p0638 N88-13903
Asymptotically stable all-pass transfer functions: Canonical form, parametrization and realization
[PB87-123972] 06 p0763 N88-14684
Statistical analyses of measured directional wave and current data
[PB87-144523] 07 p0853 N88-15185
Characterization of all controlled invariant sub-spaces for spectral systems
[PB88-106638] 07 p0912 N88-15532
Frequency-response identification of XV-15 tilt-rotor aircraft dynamics 10 p1277 N88-17643
Dynamic modelling of an electromechanical valve using frequency response data
[AD-A187908] 11 p1494 N88-18918
Identification of microwave line-of-sight multipath components 12 p1616 N88-19665
Sensitivity reduction over a frequency band
[AD-A189123] 12 p1621 N88-19694
Multipass beam breakup in recirculating linacs
[CEBAF-PR-87-007] 12 p1690 N88-20111
Elimination of quantifiers of linear variables and corresponding transfer principles
[DE88-005692] 13 p1826 N88-20912
On a bound of the modeling errors of black-box transfer function estimates
[EUT-87-E-173] 14 p1963 N88-21708
Coupled bending-torsion steady-state response of pretwisted, nonuniform rotating beams using a transfer-matrix method
[NASA-TM-100596] 15 p2086 N88-22435
Method for restoration and resampling of TM sensor imagery
[INPE-4491-PRE/1255] 15 p2090 N88-22454
Experimental comparison of lightning simulation techniques to CV-580 airborne lightning strike measurements
[AD-A190576] 15 p2098 N88-22496
Development of a digital sun sensor for a spin-stabilized satellite
[INPE-4508-TDL/327] 16 p2169 N88-22929

TRANSFER OF TRAINING
National Aeronautics and Space Administration (NASA)/American Society for Engineering Education (ASEE) Summer Faculty Fellowship Program, 1987, Volume 1
[NASA-CR-172009-VOL-1] 06 p0792 N88-14855
Teaching artificial neural systems to drive: Manual training techniques for autonomous systems
09 p1207 N88-17238

TRANSFER ORBITS
Analysis of free molecular effects on the attitude of satellites in geostationary transfer orbit. Part 1: Theoretical analysis
[DFVLR-IB-222-86-A/08] 01 p0014 N88-10077
Analysis of free molecular effects on the attitude of satellites in geostationary transfer orbit. Part 2: Force and torque measurement in free molecular wind tunnel tests
[DFVLR-IB-222-86-A/07] 01 p0014 N88-10078
Single-burn transfer to nominally periodic orbit in the vicinity of point L2 of Earth-Sun system and related problems 08 p1006 N88-16100
Application of artificial intelligence to impulsive orbital transfers 08 p1066 N88-16439
Safe rendezvous approach to a space station by impulsive transfers and continuous thrust arcs
12 p1585 N88-19486
Cost-effective orbit transfer modes for satellite retrieval and servicing --- Space Station
12 p1586 N88-19489
Study of the optimization of satellite system design for transfer orbit
[MBB-URV-135] 13 p1727 N88-20332
Solar thermal propulsion for orbit transfer vehicles
17 p2428 N88-24445
Impact of ETO propellants on the aerothermodynamic analyses of propulsion components
[NASA-TM-101303] 24 p3374 N88-30094

TRANSFER TUNNELS
Modification of integrated partial payload lifting assembly
[NASA-CR-182573] 11 p1443 N88-18607

TRANSFERRED ELECTRON DEVICES
A planar IC-compatible transferred electron device for millimeter-wave operation
[AD-A192692] 21 p2936 N88-27433

TRANSFERRING
Personal computers and All-In-1: Document transfer and translation
[DE88-003760] 10 p1384 N88-18264
USAF hyperbaric animal transfer chamber system
[AD-A193633] 23 p3237 N88-29265

TRANSFORM INTEGRALS
U INTEGRAL TRANSFORMATIONS

TRANSFORMATION TENSORS
U TENSORS

TRANSFORMATIONS (MATHEMATICS)
NT COORDINATE TRANSFORMATIONS
NT FAST FOURIER TRANSFORMATIONS
NT FOURIER TRANSFORMATION
NT FOURIER-BESSEL TRANSFORMATIONS
NT HILBERT TRANSFORMATION
NT INTEGRAL TRANSFORMATIONS
NT LAPLACE TRANSFORMATION
NT LINEAR TRANSFORMATIONS
Theoretical aspects of target classification: Physical optics and radon transform methods
03 p0304 N88-11915
A theory for the articulation of robot manipulators
03 p0333 N88-12097
Frequency domain identification of structural dynamic systems with general damping matrices
03 p0337 N88-12120
Group analysis of equations arising in ocean acoustics
04 p0472 N88-12914
Canonical transformations and exact invariants for dissipative systems
[DE87-703663] 04 p0485 N88-12985
Darboux and Baecklund transformations for the Schroedinger equation
[PREPRINT-545] 06 p0763 N88-14685
Nonisospectral deformations and Darboux transformations for the 3rd order spectral problem
[PREPRINT-558] 06 p0764 N88-14690
Darboux transformation and special solutions for the two-dimensional Toda-lattice
[PREPRINT-562] 06 p0764 N88-14692
Loop coalescing: A compiler transformation for parallel machines
[DE88-003571] 10 p1392 N88-18307
The significance of orientation unknowns in station and net adjustments 11 p1506 N88-18994
Predicting transforms of stable noise and other Gaussian mixtures
[AD-A189280] 12 p1684 N88-20071
Introduction to classical mechanics of systems with constraints, part 1
[DE88-701055] 13 p1832 N88-20957
Introduction to classical mechanics of systems with constraints, part 2
[DE88-701056] 13 p1849 N88-21072
Introduction to classical mechanics of systems with constraints, part 3
[DE88-701057] 13 p1850 N88-21073
Iteration of transformation passes over attributed program trees --- compilers
[INF-87-28] 14 p1956 N88-21661
Recursion operator and Backlund Transformation for the Ruijsenaars-Toda lattice
[PREPRINT-577] 14 p1968 N88-21750
Utilization of space color transformation, linear contrast and filtration for enhancement of colored digital images
[INPE-4310-PRE/1176] 14 p1983 N88-21831
Remarks on the time transformation of path-integral measures
[DE87-703040] 15 p2118 N88-22617
Baecklund transformation and the Schwarzian derivative
[AD-A190277] 15 p2127 N88-22684
Space time processing, environmental-acoustic effects
[AD-A190764] 15 p2130 N88-22708
Reduced order models for nonlinear aerodynamics
16 p2220 N88-23248
Bogolyubov transformation in relativistic theory of gravitation
[DE88-701592] 16 p2232 N88-23329
New stable, vectorisable Kalman filter algorithms based on orthogonal transformations
[DFVLR-FB-87-52] 16 p2258 N88-23494
Mathematical morphology: An algebraic approach
[CWI-AM-R8707] 16 p2258 N88-23497
The 1 and 2D symmetric Helmert transformation: An exact nonlinear least squares solution
[REPT-87-1] 16 p2259 N88-23503
Application of its transformation in color enhancement of LANDSAT imagery 17 p2365 N88-24082
An analytic model for aerodynamic shapes
[AD-A191573] 18 p2456 N88-24583
Additive prophet inequalities for transforms of uniformly bounded pairwise independent random variables
[PB88-173513] 18 p2568 N88-25250
Numerical simulation of viscous flows over transonic aircraft configurations 19 p2637 N88-25642
Thermal inhibition by megagauss field due to variation of electron temperature in laser plasma
[DE88-701887] 20 p2859 N88-26977
Backlund transformations associated with a Riemann-Hilbert spectral problem
[PREPRINT-596] 22 p3146 N88-28712
DATATRAN: Datum transformation software
[AD-A195723] 24 p3397 N88-30175
Using primal sketch primitives as the basis for the Hough transform
[INPE-4564-PRE/1305] 24 p3412 N88-30310
Reconstruction of multidimensional signals from multiple level threshold crossings
[AD-A195561] 24 p3425 N88-30383

TRANSFORMERS
NT INSTRUMENT TRANSFORMERS
NT MODE TRANSFORMERS
NT VOLTAGE CONVERTERS (AC TO AC)
Analysis of the electromagnetic performance characteristics of stripline transformers
[DE87-012515] 01 p0042 N88-10264
The railgun and its power source
[MRL-R-1058] 09 p1130 N88-16786
Pulsed current transformer for low inductive loads
[AD-A187224] 10 p1324 N88-17913
Optimum transformer design for a pulsed power system
[DE88-006054] 13 p1760 N88-20525
The application of high temperature superconductors to space electrical power distribution components
[NASA-TM-100901] 16 p2171 N88-22939

TRANSFORMS
U TRANSFORMATIONS (MATHEMATICS)

TRANSIENT HEATING
NT PULSE HEATING
NT SHOCK HEATING
A numerical study of transient heat and mass transfer in crystal growth 07 p0925 N88-15619
Transient radiative energy transfer in incompressible laminar flows
[NASA-CR-182605] 11 p1488 N88-18883
Calculational model development for fibrous thermal insulation transient test procedures
[DE88-007843] 18 p2493 N88-24789
Transient thermal analysis of three latent heat storage configurations for rapid thermal charging
[DE88-008943] 20 p2881 N88-27104
Measurement of local high-level, transient surface heat flux
[NASA-TP-2840] 24 p3375 N88-30099

TRANSIENT LOADS
NT BLAST LOADS
NT GUST LOADS
NT IMPACT LOADS
NT LANDING LOADS
NT SHOCK LOADS
Exact finite element method analysis of viscoelastic tapered structures to transient loads
05 p0595 N88-13632
Boundary element analysis for dynamic loading of a circular plate on an elastic medium
[CI-86] 06 p0722 N88-14443
Transient dynamics of fibre reinforced composite plates
[IIT-B/CE/RR/87-1] 13 p1734 N88-20370
Transient analysis of a plate on an elastic foundation under a moving load 19 p2680 N88-25933

TRANSIENT OSCILLATIONS
An asymptotic theory for a class of initial-boundary value problems for weakly nonlinear wave equations with an application to a model of the galloping oscillations of overhead transmission lines
[REPT-87-12] 01 p0086 N88-10556
Asymptotics for a system of nonlinearly coupled wave equations with an application to the galloping oscillations of overhead transmission lines
[REPT-87-78] 17 p2348 N88-23991

TRANSIENT REACTOR TEST FACILITY
A novel plant protection strategy for transient reactors
17 p2425 N88-2442

TRANSIENT RESPONSE
A transient model for thermal detonation
[IKE-2-75] 03 p0314 N88-11984
Time domain electromagnetic waves in multilayered media
[AD-A185055] 05 p0574 N88-13502
Structuring data for concurrent vectorized processing in a transient dynamics finite element program
[DE87-013082] 05 p0636 N88-13890

The KIVA-2' computer program for transient multidimensional chemically reactive flows with sprays
[DE88-000502] 07 p0854 N88-15191

FABSTRAN: A computer program for frame and beam static and transient response analysis (nonlinear)
[ARE-TR-86205] 09 p1182 N88-17079

Experimental and mathematical investigation of response characteristics and aging phenomena in safety fuse elements
[ETN-88-91478] 11 p1480 N88-18832

Computational aspects of sensitivity calculations in transient structural analysis
[NASA-TM-100589] 14 p1924 N88-21467

Transient compressible flow in porous materials
[DE88-006685] 15 p2067 N88-22324

Progress in the computer modeling of the liquid phase behavior of a liquid metal heat pipe
17 p2412 N88-24342

Transient thermohydraulic heat pipe modeling
17 p2413 N88-24347

Thermal and power availability transient responses for the Argonne monolithic solid oxide fuel cell
17 p2419 N88-24384

The THROHPUT code: Thermohydraulic heat pipe modeling 17 p2421 N88-24399

Transient analyses of multimegawatt space reactors
17 p2430 N88-24456

SOLA-DM: A numerical solution algorithm for transient three-dimensional flows
[DE88-007159] 18 p2514 N88-24913

Steady state and transient behavior of the Pd-SnO(sub x) MIS oxygen sensors 19 p2672 N88-25890

An experimental investigation of transient characteristics in a gravity-assisted heat pipe 20 p2783 N88-26506

Techniques and instrumentation for transient characterization of metal-insulator-semiconductor diodes. Applications to metal-insulator InP system
[ECL-87-17] 21 p3025 N88-27959

Finite element analysis of steady and transiently moving/rolling nonlinear viscoelastic structure. Part 1: Theory
[NASA-CR-179886] 23 p3273 N88-29480

TRANSIENTS (SURGES)

U SURGES

TRANSISTOR AMPLIFIERS

Phase 2 development of a 12 GHz MMIC FET amplifier
[IM-I86-1010] 01 p0038 N88-10240

A 2.3-GHz cryogenically cooled HEMT amplifier for DSS 13 04 p0434 N88-12689

TRANSISTOR CIRCUITS

Formal multilevel hierarchical verification of synchronous MOS VLSI circuits
[AD-A187532] 10 p1324 N88-17918

Improved description of base dynamics in the modeling of bipolar transistors
[PB88-181516] 19 p2732 N88-26229

TRANSISTOR LOGIC

Development of a planar heterojunction bipolar transistor for very high speed logic
[AD-A188137] 11 p1478 N88-18820

Generating layouts for random logic: Cell generation schemes
[EUT-86-E-164] 14 p1956 N88-21658

TRANSISTORS

NT BIPOLAR TRANSISTORS
NT FIELD EFFECT TRANSISTORS
NT HIGH ELECTRON MOBILITY TRANSISTORS
NT JFET
NT JUNCTION TRANSISTORS
NT MODFETS
NT SILICON TRANSISTORS
NT SOS (SEMICONDUCTORS)

Chemically modified microelectrode arrays. New kinds of electronic devices
[AD-A184389] 04 p0439 N88-12724

Reevaluating the worst-case radiation response of MOS transistors
[DE87-014157] 04 p0497 N88-13059

Thermal analysis of transistor packages, part 2
[DE88-005091] 10 p1323 N88-17909

Numerical methods in the resolution of control electrovalve model
[INPE-4154-RPE/540] 13 p1764 N88-20554

Hot electron transistors grown by MOCVD
20 p2861 N88-26996

Excellent negative differential resistance of InGaAs/InAlAs resonant tunneling barrier structures and applications to a new functional device, RHET
20 p2872 N88-27048

Evaluation of silicon-on-insulator MOS (Metal-Oxide-Semiconductor) transistor response to 10-keV X-ray and cobalt-60 irradiation
[DE88-006102] 23 p3206 N88-29082

Metal grid base heterojunction transistor operating at 60 and 94 GHz
[AD-A194763] 23 p3207 N88-29087

TRANSIT TIME

A proposed Quantum Well Injection Transit Time device (QWITT) 19 p2657 N88-25785

TRANSITION

Temperature hysteresis and magnetic transitions in amorphous Fe-Ni-Zr alloys
[DE88-000228] 03 p0294 N88-11848

TRANSITION FLOW

Numerical study of the entrance flow and its transition in a circular pipe (2) 03 p0318 N88-12011

A numerical study of the effects of curvature and convergence on dilution jet mixing
[NASA-TM-89878] 05 p0549 N88-13347

Effect of transition aerodynamics on aeroassist flight experiment trajectories
[NASA-TM-100546] 11 p1446 N88-18620

The design and use of a temperature-compensated hot-film anemometer system for boundary-layer flow transition detection on supersonic aircraft
[NASA-TM-100421] 13 p1723 N88-20304

A new laminar water tunnel to study the transition process in a blasius layer and in a separation bubble and a new tool for industrial aerodynamics and hydrodynamic research 16 p2204 N88-23150

Simulation of laminar-turbulent transition in the vicinity of a wall
[AD-A191380] 16 p2208 N88-23180

An efficient parallel algorithm for the simulation of three-dimensional compressible transition on a 20 processor Flex/32 multicomputer
[NASA-CR-178340] 17 p2337 N88-23943

Modeling of cavitation phenomena in homogeneous flow in transitory regimes in pipes
[ISAL-IDI1-87-15] 17 p2337 N88-23948

Prediction of laminar and turbulent flows past single and twin airfoils 18 p2457 N88-24589

Turbulence transition in a circular pipe
20 p2782 N88-26503

Transition at hypersonic speeds
[NASA-CR-178315] 24 p3368 N88-30058

Transition mixing study empirical model report
[NASA-CR-182139] 24 p3371 N88-30076

Recent insights into instability and transition to turbulence in open-flow systems
[NASA-CR-181693] 24 p3372 N88-30079

TRANSITION LAYERS

Existence and stability of transition layers
[AD-A185806] 06 p0766 N88-14707

TRANSITION METALS

NT CADMIUM
NT CHROMIUM
NT COBALT
NT COBALT 60
NT GOLD
NT HAFNIUM
NT IRIDIUM
NT IRIDIUM ISOTOPES
NT IRON
NT IRON ISOTOPES
NT IRON 57
NT MANGANESE
NT MOLYBDENUM
NT NICKEL
NT NIOBIUM
NT NIOBIUM ISOTOPES
NT OSMIUM
NT PALLADIUM
NT PLATINUM
NT PLATINUM ISOTOPES
NT RHENIUM
NT RHENIUM ISOTOPES
NT RHODIUM
NT RUTHENIUM
NT SILVER
NT TANTALUM
NT TITANIUM
NT TUNGSTEN
NT VANADIUM
NT YTTRIUM
NT ZINC
NT ZIRCONIUM

Near-infrared dichroism of a mesogenic transition metal complex and its solubility in nematic hosts
[DE87-014471] 03 p0287 N88-11805

A theoretical analysis of the deactivation of metal surfaces upon carburization
[AD-A184556] 03 p0290 N88-11821

Surface chemistry of transition metal carbides: A theoretical analysis
[AD-A184237] 03 p0291 N88-11829

K-CO on transition metals: A local ionic interaction
[AD-A184342] 04 p0496 N88-13056

Atomic beam studies of the interaction of hydrogen with transition metal surfaces
[DE88-000208] 05 p0648 N88-13970

Cohesive energies of transition metal silicides and phosphides --- Knudsen effusion
[AD-A186691] 09 p1254 N88-17519

Nonlinear optical waveguides containing a transition metal-based dye molecule
[DE88-003257] 11 p1550 N88-19275

Gas phase reactions of electrons, negative ions and free-radicals with transition metal complexes
11 p1560 N88-19339

Transition metal cluster chemistry
[AD-A188731] 13 p1740 N88-20405

Clusters of transition metal atoms
[AD-A191265] 16 p2270 N88-23579

In situ spectroscopic studies of transition metal macrocycles as catalysts for the electrochemical reduction of oxygen
[PB88-203195] 20 p2769 N88-26416

Magnetic excitations in transition metal systems
[DE88-011022] 21 p2912 N88-27279

Investigation of magnetic anisotropy and spin wave modes in transition metal multilayers
[DE88-009007] 22 p3154 N88-28765

TRANSITION POINTS

On the search for experimentally observed grain boundary phase transitions
[DE87-012747] 02 p0244 N88-11539

Visible boundary layer transition points through flight tests 06 p0675 N88-14136

Nature of Western Pacific transition zone
08 p1010 N88-16122

Characterization of lubricants in terms of transition diagram data
[AD-A194264] 23 p3197 N88-29025

TRANSITION PROBABILITIES

Passage from two-parameters to infinite dimension
[ENST-87C002] 01 p0088 N88-10577

TRANSITION TEMPERATURE

Superconductivity of pseudobinary compounds Al5 (V-Cr)3Si, (V-MO)3Si, Mo3(Si-Re), bombarded with fast neutrons 03 p0285 N88-11792

Impact behavior of 9-Cr and 12-Cr ferritic steels after low-temperature irradiation
[DE88-000333] 03 p0291 N88-11827

Analytical treatment of the melting and solidification of latent heat store materials in finned tube geometries
[IKE-5-223] 03 p0314 N88-11985

Soliton twin boundaries of the cubic-tetragonal martensitic transformations in ferroelastic materials
[DE87-014741] 04 p0495 N88-13047

Metal-oxide superconductor BaPbsub1-xBisubxO3. Unusual properties and new applications
08 p1077 N88-16494

Study of the micromechanical properties of fluor glasses based on ZrF4
[ISAL-ITC1-87-03] 09 p1148 N88-16882

Study of molecular mobility of noncrystaline polymer alloys of different compatibility using mechanical spectrometry
[ISAL-87-0032] 09 p1149 N88-16883

High temperature superconductivity research at Argonne National Laboratory
[DE88-003055] 09 p1258 N88-17541

Superconductivity and phase stability in the heavy rare earth quaternary compounds RBa2Cu3O7 (R = Ho, Er, Tm, Yb, Lu)
[DE88-003478] 10 p1419 N88-18476

Rapid e-beam heating for measuring thermodynamics of metastable materials
[DE88-003565] 13 p1849 N88-21066

Superconducting transition temperature of Cu-Nb microcomposites 14 p1973 N88-21775

Properties of superconductors with strong electron-phonon interaction 14 p1974 N88-21779

Influence of fiber reinforcement on the vitreous transition temperature of M 10 matrix composites
[ONERA-RT-44/7086-M] 17 p2316 N88-23835

Method of producing high T(subc) superconducting NBN films
[NASA-CASE-NPO-16681-1-CU]
17 p2446 N88-24543

Crystalline metal-semiconductor superlattices
[DE88-007063] 18 p2581 N88-25332

The superconducting transition in oxygen deficient YBa2Cu3O(sub 7-Delta)
[DE88-009957] 20 p2877 N88-27079

High-temperature superconductivity: An overview
[DE88-702051] 21 p3020 N88-27925

Thermodynamics of oxygen-vacancy ordering in YBa2Cu3O(sub z)
[DE88-009816] 21 p3022 N88-27940

Properties of new low dimensional materials and mechanisms of high T(sub c) superconductivity
[DE88-012026] 21 p3024 N88-27951

Preparation and characterization of isotopic oxygen-enriched yttrium barium copper oxide
[DE88-010939] 22 p3154 N88-28766

High Tc superconducting HoBa2Cu(sub 1-x)Fe(sub x)3O(sub 7-y)
[DE88-008909] 22 p3155 N88-28768

Effect of neutron irradiation on critical magnetization current in single crystal YBa2Cu3O(sub 7-delta)
[DE88-009970] 22 p3156 N88-28775

High-T(sub c) superconductor and its use in superconducting magnets
[DE88-008403] 23 p3289 N88-29581

Thermodynamical, optical and X-rays studies of some thermotropic liquid crystals
[DE88-702301] 23 p3290 N88-29590

Fluctuations of order parameters in the high T(sub c) superconductors
[DE88-702549] 23 p3292 N88-29603

Dependence of high critical temperature of ceramic superconductors on the nominal Cu(sup 3+)Cu(sup 2+) ratio
[DE88-702734] 23 p3293 N88-29611

Theory of superconductivity in oxides
[AD-A195647] 24 p3433 N88-30432

Theoretical model of high temperature superconductors
[DE88-702707] 24 p3434 N88-30441

TRANSITS

NT THEODOLITES

TRANSLATING

NT MACHINE TRANSLATION

Errors associated with Russian name transliteration
[DE87-011717] 02 p0248 N88-11566

A data translation method for heterogeneous database systems 04 p0501 N88-13081

Programming language translation for multicomputers
10 p1381 N88-18244

Translations of scientific and technical literature: A guide to their location 16 p2286 N88-23686

Description of graphics translation software between Intergraph and Tektronix systems
[NASA-TM-100335] 17 p2389 N88-24202

The UMAC simulator 20 p2834 N88-26811

TRANSL: A PATRAN translator subroutine library
[DE88-010976] 21 p2996 N88-27784

Conversion of productions in OPS5 to their equivalent English
[ORNL/TM-10246] 24 p3411 N88-30306

TRANSLATIONAL MOTION

NT SECONDARY FLOW
NT THREE DIMENSIONAL FLOW
NT THREE DIMENSIONAL MOTION

Diffusion description of flame propagation due to the translational motion of burning reaction products
[DE88-700676] 10 p1297 N88-17757

Effects of translational and rotational nonequilibrium on CW (Continuous Wave) chemical laser performance
[AD-A191425] 16 p2214 N88-23210

A generic multibody simulation
[NASA-CR-182949] 17 p2388 N88-24198

Large planar maneuvers for articulated flexible manipulators
[NASA-CR-183079] 19 p2711 N88-26104

TRANSLUCENCE

Effect of translucence of engineering ceramics on heat transfer in diesel engines
[DE88-003732] 10 p1305 N88-17804

TRANSLUNAR SPACE

U INTERPLANETARY SPACE

TRANSMISSION

NT ACOUSTIC PROPAGATION
NT AERODYNAMIC HEAT TRANSFER
NT ALOHA SYSTEM
NT AUTOMATIC PICTURE TRANSMISSION
NT BIOTELEMETRY
NT CODE DIVISION MULTIPLE ACCESS
NT CONDUCTIVE HEAT TRANSFER
NT CONVECTIVE HEAT TRANSFER
NT DATA TRANSMISSION
NT DEMAND ASSIGNMENT MULTIPLE ACCESS
NT DIFFRACTION PROPAGATION
NT ELECTRIC POWER TRANSMISSION
NT ELECTROMAGNETIC WAVE TRANSMISSION
NT FREQUENCY DIVISION MULTIPLE ACCESS
NT FREQUENCY DIVISION MULTIPLEXING
NT GROUND WAVE PROPAGATION
NT HALOS
NT HEAT TRANSFER
NT HEAT TRANSMISSION
NT IONOSPHERIC PROPAGATION
NT LAMINAR HEAT TRANSFER
NT LIGHT SCATTERING
NT LIGHT TRANSMISSION
NT MICROWAVE ATTENUATION
NT MICROWAVE TRANSMISSION
NT MULTIPATH TRANSMISSION
NT MULTIPLE ACCESS
NT MULTIPLEXING
NT PACKET TRANSMISSION
NT PCM TELEMETRY
NT RADAR TRANSMISSION
NT RADIATIVE HEAT TRANSFER
NT RADIO TELEMETRY
NT RADIO TRANSMISSION
NT SATELLITE TRANSMISSION
NT SCATTER PROPAGATION
NT SHOCK WAVE PROPAGATION
NT SHORT WAVE RADIO TRANSMISSION
NT SIGNAL TRANSMISSION
NT SINGLE CHANNEL PER CARRIER TRANSMISSION
NT SOUND TRANSMISSION
NT SPREAD SPECTRUM TRANSMISSION
NT STRESS PROPAGATION
NT TELEMETRY
NT TELEPHONY
NT TELEVISION TRANSMISSION
NT TIME DIVISION MULTIPLE ACCESS
NT TIME DIVISION MULTIPLEXING
NT TRANSEQUATORIAL PROPAGATION
NT TURBULENT HEAT TRANSFER
NT WAVE PROPAGATION
NT WAVELENGTH DIVISION MULTIPLEXING

An analysis of simplified feed architectures for MMIC (Monolithic Microwave Integrated Circuit) T/R (Transmit/Receive) module arrays
[AD-A185474] 06 p0697 N88-14275

Parametric and experimental analysis using a power flow approach
[NASA-CR-182460] 09 p1116 N88-16693

Development of fiber optic systems for recording and transmitting holographic information
[AD-A189406] 13 p1773 N88-20603

Millimeter-wave integrated circuits
19 p2656 N88-25774

TRANSMISSION EFFICIENCY

Transmission efficiency in advanced aerospace powerplant
[PNR90391] 02 p0182 N88-11133

Developments in optical sensor technologies described 06 p0689 N88-14220

Land mobile satellite transmission measurements at 869 MHz. A comparison of error probabilities for various message block durations and fade margins as a function of vegetation shadowing
[NASA-CR-179929] 06 p0693 N88-14255

Designing variable-length codes with good error-recovery properties
[BBC-RD-1987/19] 10 p1317 N88-17876

Phase calibration generator 11 p1473 N88-18785

A concatenated coded modulation scheme for error control
[NASA-CR-182639] 12 p1621 N88-19697

Results of one way transit time measuring in navigation experiment NAVEX
[DFVLR-MITT-87-17] 14 p1865 N88-21145

Spatial distribution of traffic in a cellular mobile data network
[EUT-87-E-168] 14 p1904 N88-21378

TRANSMISSION LINES

NT BEAM WAVEGUIDES
NT CIRCULAR WAVEGUIDES
NT COAXIAL CABLES
NT COMMUNICATION CABLES
NT FLUID TRANSMISSION LINES
NT MICROSTRIP TRANSMISSION LINES
NT OPTICAL FIBERS
NT OPTICAL WAVEGUIDES
NT PLASMAGUIDES
NT POWER LINES
NT RECTANGULAR WAVEGUIDES
NT STRIP TRANSMISSION LINES
NT UNDERGROUND TRANSMISSION LINES
NT WAVEGUIDES

Crosstalk in braided shield coaxial cables
01 p0035 N88-10224

The development of diagnostic fuses
[SAND-86-0395] 03 p0311 N88-11963

Low-noise cryogenic transmission line
04 p0434 N88-12688

Departmental report on program EMTP-machine windings surge transients: Travelling wave method
[PB87-123733] 04 p0438 N88-12719

The use of coaxial transmission line elements in log-periodic dipole arrays
[AD-A184864] 05 p0574 N88-13499

Safety research of insulating materials of cable for nuclear power generating station
[NASA-TT-20202] 13 p1752 N88-20477

Harmonic and rectangular pulse reproduction through current transformers
[EUT-86-E-159] 14 p1907 N88-21395

The application of high temperature superconductors to space electrical power distribution components
[NASA-TM-100901] 16 p2171 N88-22909

A computer model investigation of a half square log-periodic array
[AD-A190955] 16 p2190 N88-23062

High frequency power distribution system
[NASA-CR-175071] 17 p2335 N88-23939

Space power radiation cooled dc transmission line analysis 17 p2438 N88-24506

Carrier lifetime versus ion-implantation dose in Silicon On Sapphire 19 p2658 N88-25791

Experimental investigation of simplest inhomogeneities in cylindrical slit line
[DE88-702388] 21 p2933 N88-27418

Multichannel data transmission through a fiber optic cable
[AD-A193842] 22 p3070 N88-28221

A fiber optic beamforming processor for wideband direction finding
[AD-A194862] 24 p3428 N88-30404

Ultra-wideband direction finding using a fiber optic beamforming processor
[AD-A194861] 24 p3430 N88-30413

TRANSMISSION LOSS

Loss measurement of 3-port ferrite switches in the 90 GHz range
[ESA-TT-1054] 03 p0310 N88-11958

Analysis of counting errors in the phase/Doppler particle analyzer
[NASA-TM-100231] 03 p0323 N88-12043

Photoinduced low-temperature changes in optical losses in fiber optics based on chalcogenide glasses
06 p0770 N88-14731

A diffraction based theoretical model for prediction of UHF path loss in cities 12 p1616 N88-19661

A program for the calculation of radio-wave transmission loss over the spherical earth and over obstacles
12 p1616 N88-19662

Low-loss, high-isolation, fiber-optic isolator
[NASA-CASE-NPO-17207-1-CU]
18 p2576 N88-25304

Surface-wave model uncertainty assessment
[AD-A193094] 21 p2932 N88-27408

TRANSMISSIONS (MACHINE ELEMENTS)

Transmission efficiency in advanced aerospace powerplant
[PNR90391] 02 p0182 N88-11133

Improved oil-off survivability of tapered roller bearings
[NASA-CR-180804] 02 p0182 N88-11135

The flight evaluation of an advanced engine display and monitoring system 03 p0264 N88-11659

A129 advanced solutions for meeting today's combat helicopter requirement 03 p0265 N88-11669

Multipath gear-friction planetary transmissions
04 p0424 N88-12629

On dynamic loads in parallel shaft transmissions. 1: Modelling and analysis
[NASA-TM-100180] 04 p0451 N88-12797

On dynamic loads in parallel shaft transmissions. 2: Parameter study
[NASA-TM-100181] 04 p0452 N88-12798

Efficiency testing of a helicopter transmission planetary reduction stage
[NASA-TP-2795] 07 p0861 N88-15224

Experimental investigation on the bending fatigue performance of gas carbonitrided and carburized gears
[PB87-147997] 08 p0992 N88-16003

Results of NASA/Army transmission research
09 p1108 N88-16640

Dynamic analysis of multimesh-gear helicopter transmissions
[NASA-TP-2789] 09 p1176 N88-17045

Advanced transmission studies
[NASA-TM-100867] 14 p1919 N88-21454

Computerized life and reliability modelling for turboprop transmissions
[NASA-TM-100918] 16 p2215 N88-23220

Magnetic drive coupling
[NASA-CASE-MSC-21171-1] 17 p2344 N88-23973

Design, manufacture and spin test of high contact ratio helicopter transmission utilizing Self-Aligning Bearingless Planetary (SABP)
[NASA-CR-4155] 18 p2524 N88-24975

Optimization of planetary gears
[ETN-88-92375] 21 p2958 N88-27573

Helicopter transmission research at NASA Lewis Research Center
[NASA-TM-100962] 24 p3379 N88-30128

TRANSMISSIVITY

National Aerospace Laboratory experiment
04 p0404 N88-12509

Determination of cloud base height and emissivity from downwelling angular radiances
[AD-A185985] 07 p0879 N88-15331

Experimental research on skin reflection, transmission, absorption of light rays 16 p2187 N88-23039

TRANSMISSOMETERS

Description of the MPTR system: Multi Path Transmissometer Radiometer
[FEL-1987-14] 20 p2855 N88-26954

TRANSMITTANCE

Distortion of wideband carbon dioxide laser radar waveforms due to atmospheric dispersion and absorption
[AD-A188687] 12 p1632 N88-19771

Enhancements to the atmospheric transmittance/radiance program FASCODE
[AD-A188863] 12 p1643 N88-19839

Spectral measurements for correcting LANDSAT data for atmospheric effects 17 p2362 N88-24066

Optical constants of minerals and other materials from the millimeter to the ultraviolet
[AD-A192210] 18 p2482 N88-24724

Development and validation of transmission measurements techniques of image contrast, utilizing existing IR imagers
[AD-A191471] 18 p2541 N88-25079

Filling of the atmospheric transmission window due to emission from very high rotational levels of NO and O3
[AD-A194670] 23 p3233 N88-29239

TRANSMITTER RECEIVERS

A laser communication experiment utilizing the ACT satellite and an airborne laser transceiver
[NASA-TM-100792] 11 p1492 N88-18910

The 2 FSK/QPSK (Frequency Shift Keying/Quadrature Phase Shift Keying) transmitter and receiver: Design and performance
[AD-A190028] 15 p2056 N88-22258

Picosecond photoconductive transceivers
19 p2656 N88-25777

Digital communication transmitter and receiver test procedures
[AD-A191218] 20 p2788 N88-26540

TRANSMITTERS

NT EMERGENCY LOCATOR TRANSMITTERS
NT IONOSONDES
NT RADAR TRANSMITTERS
NT RADIO BEACONS
NT RADIO TRANSMITTERS
NT RADIOSONDES
NT RADIOTELEPHONES
NT RAWINSONDES
NT REPEATERS
NT TRANSMITTER RECEIVERS

Ultrafast photoconductor detector-laser-diode transmitter
[DE87-013803] 03 p0329 N88-12082

Inductance effects in the high-power transmitter crowbar system 04 p0433 N88-12687

Receiver susceptibility measurements relating to interference between UHF (Ultra High Frequency) television and land mobile radio services
[PB87-228029] 06 p0690 N88-14228

A 104-km unrepeatered bidirectional fiber optic demonstration link
[AD-A190282] 15 p2134 N88-22728

Development of 20 GHz monolithic transmit modules
[NASA-CR-182134] 17 p2445 N88-24539

WIPP (Wave Induced Particle Precipitation) experiment logistic support
[AD-A191184] 18 p2499 N88-24824

Outer zone electron precipitation produced by a VLF transmitter
[AD-A191944] 19 p2691 N88-25993

TRANSMUTATION

Construction of approximations to acoustic Green's functions for nonhomogeneous oceans using transmutation
[PB88-185384] 18 p2548 N88-25126

TRANSOCEANIC FLIGHT

Desynchronization of heart rate and breathing frequency after transmeridional flight across three time zones
12 p1663 N88-19968

TRANSONIC AIRCRAFT

U SUPERSONIC AIRCRAFT

TRANSONIC COMPRESSORS

Radial compressor design using an Euler solver
10 p1283 N88-17675

Studies of unsteady axial-compressor functioning
24 p3380 N88-30129

TRANSONIC FLIGHT

Sensitivity of F-106B leading-edge-vortex images to flight and vapor-screen parameters
[NASA-TP-2818] 17 p2300 N88-23760

Wind tunnel investigation of wing and control panel loads at transonic and supersonic speeds on some schematic cruciform missile configurations
[FFA-TN-1986-43] 18 p2457 N88-24585

TRANSONIC FLOW

Transonic analysis and design of axisymmetric bodies in nonuniform flow
[NASA-CR-4101] 01 p0003 N88-10013

A method for the calculation of transonic flows for the control of adaptive wind tunnels
[ETN-87-90411] 01 p0003 N88-10015

A flow function method for the axisymmetric calculation of the transonic turbomachine flow taking into account the flow differences in circumferential direction
[ETN-87-90428] 01 p0056 N88-10359

Computation of transonic separated wing flows using an Euler/Navier-Stokes zonal approach
[NASA-TM-88311] 02 p0173 N88-11089

Investigations on a transonic airfoil with a 30 mm wide perforation/cavity arrangement
[ESA-TT-1072] 03 p0260 N88-11634

Fin gaps and body slots of guided projectiles: Effects, data correlation and modeling
[AD-A184440] 03 p0270 N88-11698

Application of the finite difference method to the solution of mixed partial differential equations for the case of transonic flow
[ETN-87-90760] 03 p0370 N88-12327

Application of Runge Kutta time marching scheme for the computation of transonic flows in turbomachines
[NASA-TM-86997] 04 p0394 N88-12461

Concepts for radically increasing the numerical convergence rate of the Euler equations
[NASA-CR-177456] 04 p0395 N88-12463

Solution of the two-dimensional Euler equations on unstructured triangular meshes
04 p0396 N88-12469

Some asymptotic modes of transonic vortex flow
04 p0425 N88-12632

The role of computation fluid dynamics in aeronautical engineering (4). The development and applications of implicit TVD finite volume code
05 p0536 N88-13259

Navier-Stokes simulation of transonic transportation aircraft configurations. 1: Flow-field simulation over wing-fuselage combinations 05 p0540 N88-13288

Numerical simulation of transonic aircraft in comparison to wind tunnel test 05 p0540 N88-13289

Study of the effect of mass transfer on a transonic boundary layer. Application to flow relaminarization
[ETN-88-91169] 05 p0541 N88-13296

Computation of transonic flows with nacelle simulation
[SNIAS-872-111-117] 05 p0542 N88-13300

Investigation of viscous/inviscid interaction in transonic flow over airfoils with suction 06 p0664 N88-14074

A zonal approach for the solution of coupled Euler and potential solutions of flows with complex geometries
[AD-A185465] 06 p0702 N88-14310

Finite-volume scheme for transonic potential flow about airfoils and bodies in an arbitrarily shaped channel
07 p0809 N88-14928

Breakdown of the conservative potential equation
07 p0809 N88-14929

Development of direct-inverse 3-D methods for applied aerodynamic design and analysis
[NASA-CR-182436] 08 p0950 N88-15767

Theoretical and experimental studies of the transonic flow field and associated boundary conditions near a longitudinally-slotted wind-tunnel wall
[NASA-CR-181169] 08 p0959 N88-15815

An initial investigation into methods of computing transonic aerodynamics sensitivity coefficients
[NASA-CR-182444] 09 p1112 N88-16663

Experimental investigation of shock-induced disturbances on transonic airfoils
[DFVLR-FB-87-28] 09 p1112 N88-16666

Numerical resolution of the equations of three-dimensional stable compressible transonic flows
[PB87-168415] 09 p1113 N88-16673

Mach number effects on transonic aeroelastic forces and flutter characteristics
[NASA-TM-100547] 09 p1113 N88-16675

Solution of the three-dimensional Navier-Stokes equations for transonic flow using a multigrid method
10 p1267 N88-17579

Navier-Stokes simulation of wind-tunnel flow using LU-ADI factorization algorithm
[NASA-TM-100042] 10 p1268 N88-17584

Navier-Stokes computations for circulation control airfoils 10 p1269 N88-17592

Wall jet analysis for circulation control aerodynamics. Part 2: Zonal modeling concepts for wall jet/potential flow coupling 10 p1269 N88-17593

A transonic-small-disturbance wing design methodology
[NASA-TP-2806] 10 p1273 N88-17614

The unsteady gas flow through stator and rotor of a turbomachine 10 p1281 N88-17660

The effects of rotational flow, viscosity, thickness, and shape on transonic flutter dip phenomena
[NASA-TM-100811] 11 p1502 N88-18969

A multigrid solver for two-dimensional transonic full potential flow calculations 11 p1538 N88-19189

A multigrid full potential transonic code for arbitrary configurations --- aircraft 11 p1539 N88-19195

Wing flutter calculations with the CAP-TSD unsteady transonic small disturbance program
[NASA-TM-100580] 12 p1575 N88-19419

Application of a flux vector splitting methodology towards the solution of unsteady transonic flows, with future emphasis on the blade flutter problem
[AD-A189500] 13 p1716 N88-20260

Numerical simulation of subsonic and transonic propeller flow
[NASA-TM-100163] 13 p1716 N88-20262

Tests on the AFWAL 65 deg delta wing at NLR: A study of vortex flow development between Mach = 0.4 and 4
[NLR-MP-86058-U] 13 p1717 N88-20266

The international vortex flow experiment: A test case for compressible Euler codes
[NLR-MP-86076-U] 13 p1717 N88-20267

Steady and unsteady transonic small disturbance analysis of realistic aircraft configurations
[NASA-TM-100557] 13 p1717 N88-20269

An L-U implicit multigrid algorithm to solve the Euler equations for transonic flow in rotating turbomachinery passages 13 p1718 N88-20270

An adaptive grid technique for solution of the Euler equations 13 p1768 N88-20579

Multigrid solution of the Euler equations
13 p1769 N88-20582

Wall interference assessment and corrections for transonic adaptive wall airfoil data
14 p1863 N88-21129

Transonic flow field analysis for real fuselage configurations 14 p1864 N88-21133

An experimental-computational investigation of transonic shock wave-turbulent boundary layer interaction in a curved test section
[CWI-NM-R8716] 14 p1909 N88-21408

Computational fluid dynamics drag prediction: Results from the Viscous Transonic Airfoil Workshop
[NASA-TM-100095] 15 p2014 N88-22009

Mixed direct-inverse problem of transonic cascade
15 p2054 N88-22244

A zonal approach for the solution of coupled Euler and potential solutions of flows with complex geometries
[AD-A189752] 15 p2114 N88-22595

A physically consistent model for artificial dissipation in transonic potential flow computations
[NASA-TM-100846] 15 p2122 N88-22652

Experimental investigation of the transonic flow at the leeward side of a delta wing at high incidence
[LR-518] 16 p2156 N88-22861

The 2-D and 3-D time marching transonic potential flow method for propfans 16 p2220 N88-23245

Development and improvement of a code to calculate small, three dimensional, unsteady transonic perturbations
[ONERA-RTS-31/3064-RY-062-R]
17 p2338 N88-23951

Accounting for the effects of unsteady, separated boundary layers in transonic two dimensional calculations
[ONERA-RT-30/3064-RY-063-R]
17 p2338 N88-23952

A transonic small disturbance wing design methodology 18 p2457 N88-24590

The calculation of transonic flow over the shuttle orbiter using slender body theory 18 p2460 N88-24606

Computational Fluid Mechanics
[NASA-CR-183022] 18 p2514 N88-24915

Navier-Stokes analysis of transonic transport aircraft empennage 19 p2636 N88-25637

Navier-Stokes code NS3D for blunt bodies. Part 1: Analysis, results and verification
[DE88-010105] 19 p2666 N88-25855

An initial investigation into methods of computing transonic aerodynamic sensitivity coefficients
[NASA-CR-183061] 20 p2752 N88-26332

Finite element approximation to a model problem of transonic flow
[DE88-701835] 20 p2752 N88-26333

Calculation of 2-D unsteady transonic full potential flow about oscillating airfoils by two complementary approaches
[PB88-127519] 20 p2753 N88-26341

A study of flow separation in transonic flow using inviscid and viscous computational fluid dynamics (CFD) schemes
[NASA-CR-183119] 20 p2801 N88-26618

Theoretical-numerical study of feasibility of use of winglets on low aspect ration wings at subsonic and transonic Mach numbers at reduce drag
[NASA-CR-4174] 21 p2892 N88-27168
Experimental determination of aerodynamic damping in a three-stage transonic axial-flow compressor
[NASA-TM-100953] 21 p2897 N88-27200
Investigation of viscous/inviscid interaction in transonic flow over airfoils with suction
[NASA-CR-183112] 21 p2945 N88-27490
Study of three-dimensional transonic flow separations
[AD-A193016] 22 p3037 N88-28032
Method to predict external store carriage characteristics at transonic speeds
[NASA-CR-4170] 22 p3037 N88-28034
Transonic blade-vortex interactions
22 p3037 N88-28035
Runge-Kutta finite-volume simulation of laminar transonic flow over the ONERA M6 wing using the Navier-Stokes equations
[FFA-TN-1987-06] 22 p3039 N88-28045
Boundary layer development and transition
23 p3169 N88-28871
The influence of numerical boundary conditions on transonic flow
[DFVLR-FB-88-06] 23 p3172 N88-28890
Navier-Stokes calculations of transonic flows past cavities
[NASA-CR-180464] 23 p3212 N88-29116
Three-dimensional elliptic grid generation for an F-16
23 p3246 N88-29315
A streamwise upwind algorithm for the Euler and Navier-Stokes equations applied to transonic flows
[NASA-TM-101019] 24 p3316 N88-29751
Application of unsteady aerodynamic methods for transonic aeroelastic analysis
[NASA-TM-100665] 24 p3317 N88-29754
Computational methods for the problems of the tip vortex
[NASA-CR-181438] 24 p3320 N88-29775
Theoretical aerodynamics, transonic flow
[AD-A196247] 24 p3321 N88-29777

TRANSONIC FLUTTER
Unsteady transonic algorithm improvements for realistic aircraft applications
[NASA-TM-100516] 08 p0949 N88-15760
Unsteady transonic small-disturbance theory including entropy and vorticity effects
[NASA-TM-100568] 12 p1575 N88-19418
Wing flutter calculations with the CAP-TSD unsteady transonic small disturbance program
[NASA-TM-100580] 12 p1575 N88-19419
Propagation of acoustic disturbances in transonic flow fields of lifting wings
[DFVLR-FB-88-13] 21 p3013 N88-27880

TRANSONIC INLETS
U SUPERSONIC INLETS

TRANSONIC NOZZLES
A research program on the aerodynamics of a highly loaded turbine stage 10 p1280 N88-17655

TRANSONIC SPEED
Comparison of wind tunnel and flight test afterbody and nozzle pressures for a twin-jet fighter aircraft at transonic speeds
[NASA-TP-2588] 02 p0121 N88-10765
Effect of empennage arrangement on single-engine nozzle/afterbody static pressures at transonic speeds
[NASA-TP-2753] 02 p0122 N88-10771
An experimental evaluation of advanced rotorcraft airfoils in the NASA Ames eleven-foot transonic wind tunnel
[NASA-CR-166587] 03 p0261 N88-11640
Design of wings and wing/body configurations for transonic and supersonic speeds
05 p0545 N88-13316
Development of transonic speed cascade design method using Euler code and inverse solution
06 p0676 N88-14139
Unsteady transonic algorithm improvements for realistic aircraft applications
[NASA-TM-100516] 08 p0949 N88-15760
Comparison of two transonic noise prediction formulations using the aircraft noise prediction program
[NASA-CR-181609] 12 p1688 N88-20095
Parametric flutter studies of an arrow-wing configuration: Some early results
[NASA-TM-100608] 19 p2599 N88-25444
Wind tunnel investigation of wing and control panel loads at transonic and supersonic speeds on some schematic cruciform missile configurations
[FFA-TN-1986-43-SUPPL-1] 22 p3039 N88-28044
Test results at transonic speeds on a contoured over-the-wing propfan model
[NASA-TM-88206] 23 p3177 N88-28918
Recent advances in transonic computational aeroelasticity
[NASA-TM-100663] 24 p3321 N88-29778

TRANSONIC TURBINES
U SUPERSONIC TURBINES

TRANSONIC WIND TUNNELS
A method for the calculation of transonic flows for the control of adaptive wind tunnels
[ETN-87-90411] 01 p0003 N88-10015
Investigation of the suitability of the 8ft x 6ft transonic wind-tunnel for aeroacoustic research on propellers
[RAE-TM-AERO-2093] 01 p0008 N88-10041
Wall interference tests of a CAST 10-2/DOA 2 airfoil in an adaptive-wall test section
[NASA-TM-4015] 02 p0122 N88-10772
Intergration effects of D-shaped, underwing, aft-mounted, separate-flow flow-through nacelles on a high-wing transport
[NASA-TM-4018] 02 p0122 N88-10773
The 0.6m x 0.6m trisonic test section (TMK) of DFVLR in Cologne-Porz, Federal Republic of Germany (status 1986)
[ESA-TT-1052] 03 p0267 N88-11681
Status of magnetic suspension technology
07 p0811 N88-14939
Preliminary calibration and test results from the National Transonic Facility 07 p0811 N88-14941
Effect of an optimized fiber orientation on transonic flutter characteristics of a high-aspect-ratio composite wing
[NAL-TR-930] 09 p1120 N88-16709
Transonic wind tunnel calibration 1986: Force measurements on three ONERA-C5 models and three half sphere cylinder calibration bodies in the F+W transonic test section
[F+W-FO-1854] 09 p1122 N88-16714
Influence of the wall boundary layer on force measurements on half models in the transonic wind tunnel
[F+W-TF-1876] 09 p1122 N88-16715
Pressure distributions from high Reynolds number transonic tests of an NACA 0012 airfoil in the Langley 0.3-meter transonic cryogenic tunnel
[NASA-TM-100526] 11 p1435 N88-18565
High Reynolds number transonic tests on a NACA 0012 airfoil in the Langley 0.3-meter transonic cryogenic tunnel
[NASA-TM-100527] 11 p1436 N88-18571
An evaluation in a modern wind tunnel of the transonic adaptive wall adjustment strategy developed by NPL in the 1940's
[NASA-CR-181623] 12 p1575 N88-19417
Design of a sound neck in connection with the model-support system of a transonic wind tunnel test section
[ILR-MITT-186(1987)] 14 p1869 N88-21171
Modifications to the Langley 8-foot transonic pressure tunnel for the laminar flow control experiment
[NASA-TM-4032] 15 p2021 N88-22047
Aerofoil testing in a self-streamlining flexible walled wind tunnel
[NASA-CR-4128] 16 p2156 N88-22865
The transonic wind tunnel (TWB) at DFVLR, Brunswick (Federal Republic of Germany)
[DFVLR-MITT-88-01] 16 p2164 N88-22909
Flow quality of NAL two-dimensional transonic wind tunnel. Part 1: Mach number distributions, flow angularities and preliminary study of side wall boundary layer suction
[NASA-TT-20209] 16 p2165 N88-22911
Design study. Manipulator systems for model handling in European transonic wind tunnels
[ETN-88-91944] 18 p2468 N88-24651
Empty test section streamlining of the transonic self-streamlining wind tunnel fitted with new walls
[NASA-CR-181680] 19 p2598 N88-25442
Wall interference assessment/correction of data from tests of a CAST 10-2/DOA 2 airfoil in the Langley 0.3-m transonic cryogenic tunnel 20 p2751 N88-26331
European transonic wind tunnel project: Assistanca to the design group
[ONERA-RSF-11/0694-GY-010-G]
21 p2900 N88-27208
Studies concerning the European transonic wind tunnel
[ONERA-RSF-10/0694-GY-010-G]
21 p2900 N88-27209
Hybrid procedure for dynamic measurements in transonic wind tunnels: Demonstrated by pitch oscillation
[DFVLR-FB-88-19] 21 p2900 N88-27211
Boundary layer simulation and control in wind tunnels
[AGARD-AR-224] 23 p3167 N88-28857

TRANSONICS
U TRANSONIC FLOW

TRANSPARENCE
Spatial characterization of acid rain stress in Canadian Shield Lakes
[NASA-CR-181136] 01 p0067 N88-10430
Spatial characterization of acid rain stress in Canadian Shield Lakes
[NASA-CR-180577] 01 p0067 N88-10431
Aluminum oxynitride spinel (ALON): A review
[AD-A184753] 03 p0294 N88-11845
Resistance of canopy materials against chemicals
[PML-1985-22] 05 p0569 N88-13466
Photoinduced low-temperature changes in optical losses in fiber optics based on chalcogenide glasses
06 p0770 N88-14731
Method for investigating the formation of crystals in a transparent material
[NASA-CASE-MFS-26008-1-CU]
06 p0788 N88-14835
Analysis of the decomposition of transparent polymer materials (blocks) under the action of laser beams in free generation mode
[AD-A187090] 09 p1147 N88-16873
Characterization of transparent insulation materials --- solar energy absorbers
[ETN-88-91052] 09 p1163 N88-16970
The interaction of small particles with laser beams
[AD-A190716] 15 p2072 N88-22354
Noncontact temperature measurement in glass and other transparent materials 17 p2328 N88-23900
Direct visualization of surfaces from computed tomography data
[AD-A193646] 22 p3153 N88-28758
Vision through aircraft transparencies
23 p3242 N88-29294
Maintenance of vision-related components
23 p3242 N88-29296
Precision measurement of the Fresnel drag coefficient using a ring laser
[AD-A196025] 24 p3366 N88-30043

TRANSPARENT MATERIALS
U TRANSPARENCE

TRANSPIRATION
A calculation method for the propulsive jet and its aerodynamic interaction with an afterbody
[ESA-TT-1039] 03 p0259 N88-11632
Study of the relationship between photosynthesis, respiration, transpiration, and mineral nutrition in wheat
03 p0360 N88-12268

TRANSPIRATION COOLING
U SWEAT COOLING

TRANSPONDERS
RF-switches: Application and design --- satellite communication 14 p1877 N88-21215
Refraction in underwater acoustics --- navigation systems
[B8735053] 17 p2395 N88-24236

TRANSPORT AIRCRAFT
NT A-300 AIRCRAFT
NT A-320 AIRCRAFT
NT BOEING 737 AIRCRAFT
NT BOEING 747 AIRCRAFT
NT C-130 AIRCRAFT
NT C-135 AIRCRAFT
NT CARGO AIRCRAFT
NT CH-46 HELICOPTER
NT CONCORDE AIRCRAFT
NT DC 9 AIRCRAFT
NT EUROPEAN AIRBUS
NT F-27 AIRCRAFT
NT SHORT HAUL AIRCRAFT
NT UH-60A HELICOPTER
NT VC-10 AIRCRAFT
Full-scale transport controlled impact demonstration program
[NASA-TM-89642] 01 p0004 N88-10021
Intergration effects of D-shaped, underwing, aft-mounted, separate-flow, flow-through nacelles on a high-wing transport
[NASA-TM-4018] 02 p0122 N88-10773
An aerodynamic performance evaluation of the NASA/Ames Research Center advanced concepts flight simulator
[NASA-TM-89659] 03 p0268 N88-11685
Investigation of pilot behavior in a training program for assessing handling qualities using a ground simulator
[ESA-TT-999] 03 p0357 N88-12247
Effect of permissible variations of center-of-gravity locations of cargo airplane on its mass
04 p0424 N88-12625
Computation of nacelle interference using boundary element method 05 p0537 N88-13267
Navier-Stokes simulation of transonic transportation aircraft configurations. 1: Flow-field simulation over wing-fuselage combinations 05 p0540 N88-13288
Aeroelastic analysis of modern transport aircraft
05 p0550 N88-13352

A study of the utilization of advanced composites in fuselage structures of commercial aircraft
[NASA-CR-172405] 06 p0679 N88-14157
Natural laminar flow nacelle for transport aircraft
07 p0813 N88-14949
Laminar flow integration: Flight tests status and plans
07 p0813 N88-14952
Handling qualities of a wide-body transport airplane utilizing Pitch Active Control Systems (PACS) for relaxed static stability application
[NASA-TP-2482] 07 p0821 N88-14987
Study on utilization of advanced composites in fuselage structures of large transports
[NASA-CR-172406] 07 p0827 N88-15014
Aeropropulsion '87. Session 6: High-Speed Propulsion Technology
[NASA-CP-10003-SESS-6] 08 p0957 N88-15807
Analysis of shock and vibration environments for cargo on C9B transport aircraft 08 p0999 N88-16051
Experimental study on the effect of fiber orientation on flutter characteristics of high-aspect-ratio transport wing
[NAL-TR-936] 09 p1120 N88-16708
Are windshear training aid recommendations appropriate for other than large jet transports? Pilot procedures: Shear models 10 p1275 N88-17635
Gear systems for advanced turboprops
10 p1282 N88-17667
Research and development. Technical-scientific publications (1956-1987): Retrospective view and prospects. Jubilee edition on the occasion of the 75th birthday of Dipl.-Engr. Dr.-Engr. E. H. Ludwig Boelkow
[ISSN-0931-9751] 10 p1309 N88-17819
High performance composites research at NASA-Langley
[NASA-TM-100518] 11 p1450 N88-18642
Application of hybrid laminar flow control to global range military transport aircraft
[NASA-CR-181638] 14 p1862 N88-21124
Trends in Computational Fluid Dynamics (CFD) for aeronautical 3D steady applications: The Dutch situation
[NLR-MP-86074-U] 15 p2015 N88-22017
KRASH parametric sensitivity study: Transport category airplanes
[AD-A189962] 15 p2017 N88-22024
Computational wing design studies relating to natural laminar flow 17 p2297 N88-23740
Integrated Application of Active Controls (IAAC) technology to an advanced subsonic transport project: Program review
[NASA-CR-3880] 17 p2301 N88-23762
Fuel containment concepts: Transport category airplanes
[AD-A189818] 18 p2494 N88-24799
Multivariable identification of a flexible transport aircraft 20 p2786 N88-26525
Application of complementary parameter identification techniques to flight test data of a transport aircraft
20 p2787 N88-26533
Concept development of a Mach 3.0 high-speed civil transport
[NASA-TM-4058] 21 p2895 N88-27182
Critical joints in large composite primary aircraft structures. Volume 1: Technical summary
[NASA-CR-3914] 23 p3190 N88-28983
Low-speed longitudinal flying qualities of modern transport aircraft 24 p3314 N88-29738

TRANSPORT COEFFICIENTS
U TRANSPORT PROPERTIES

TRANSPORT PROPERTIES
NT ATMOSPHERIC CONDUCTIVITY
NT CARRIER MOBILITY
NT DIFFUSION COEFFICIENT
NT EDDY VISCOSITY
NT ELECTRICAL RESISTIVITY
NT ELECTRON MOBILITY
NT GAS VISCOSITY
NT GASEOUS DIFFUSION
NT HOLE MOBILITY
NT IONIC MOBILITY
NT KONDO EFFECT
NT MAGNETORESISTIVITY
NT PHOTOCONDUCTIVITY
NT PLASMA CONDUCTIVITY
NT SUPERCONDUCTIVITY
NT THERMAL CONDUCTIVITY
NT THERMAL DIFFUSIVITY
NT VISCOSITY
Studies of transport processes in porous and ion exchahge membranes
[ISBN-951-99847-0-4] p0021 N88-10133
Aqueous-phase reactions in clouds
[DE86-005249] 01 p0069 N88-10445
Understanding the transport properties of silicon grain boundaries and how they relate to I.C. applications of polysilicon
[DE87-013809] 01 p0104 N88-10677
Conservation and transport properties of turbulence with large density variations
[LA-10911-MS] 03 p0321 N88-12032
Development and evaluation of a Monte Carlo code system for analysis of ionization chamber responses
[AD-A183970] 03 p0375 N88-12359
Novel macrocyclic carriers for proton-coupled liquid membrane transport
[DE88-000636] 04 p0413 N88-12560
Heat and moisture transport in the atmospheric boundary layer
[AD-A184222] 04 p0470 N88-12904
Numerical analysis of axisymmetric flow with H2-O2 reactions 05 p0538 N88-13272
Conditional second order closure for turbulent shear flows
[AD-A185369] 05 p0581 N88-13542
Monte Carlo photon transport on vector and parallel supercomputers
[DE88-002503] 07 p0905 N88-15486
Weak interactions and local order in strong turbulence
09 p1159 N88-16948
Transport delay compensation for computer-generated imagery systems
[NASA-TM-100084] 10 p1277 N88-17645
Models for ionic transport in glass
[DE88-002860] 10 p1304 N88-17799
Electronic and ionic transport in polymers
[AD-A187253] 11 p1452 N88-18651
High pressure electronic transport in semiconductors
[AD-A187428] 11 p1555 N88-19308
The physics of very small structures
[AD-A187672] 11 p1556 N88-19311
The influence of strain on hydrogen entry, transport, and embrittlement of a high strength steel in aqueous sodium chloride solution
[AD-A189302] 12 p1608 N88-19619
Transport properties of conductive polymers
[AD-A188411] 12 p1610 N88-19628
Competing interactions in metallic superlattices
[DE88-005344] 13 p1847 N88-21057
Electronic and ionic transport in polymers
[AD-A190434] 15 p2045 N88-22185
Noncontact temperature measurements in the microgravity fluids and transport phenomena discipline
17 p2328 N88-23901
Centrifugal acceleration of ions in the polar magnetosphere
[NASA-TM-101148] 17 p2374 N88-24120
An evaluation of energy-independent heavy ion transport coefficient approximations
[NASA-TM-101158] 17 p2397 N88-24251
Simplified curve fits for the transport properties of equilibrium air
[NASA-CR-178411] 18 p2513 N88-24911
Stochasticity in a Q-machine plasma
18 p2578 N88-25315
NASA research Program: The roles of fluid motion and other transport phenomena in the morphology of materials
[NASA-CR-182801] 18 p2580 N88-25327
Electronic structure, elementary excitations, optical and transport properties of semiconductor superlattices
[AD-A190795] 18 p2581 N88-25333
An evaluation of some thermodynamic and transport properties of solid and liquid lithium over the temperature range 200 to 1700 K
[DE88-008947] 19 p2614 N88-25512
Simulation of axisymmetric flow with H2O2 reactions
19 p2638 N88-25651
Longitudinally localized optical carrier injection for femtosecond transport studies 19 p2659 N88-25806
Ballistic transport and hot electron spectroscopy in Tunneling Hot Electron Transfer Amplifier (THETA)
19 p2659 N88-25808
Heavy ion fusion system assessment: Final focus and transport model
[LBL-23040] 19 p2725 N88-26183
Drift wave vortices and anomalous transport
[DE88-009562] 20 p2859 N88-26982
Impurity transport calculations for a drift-dependent tokamak scrape-off plasma
[DE88-010053] 20 p2859 N88-26984
Third International Conference on Superlattices, Microstructures and Microdevices
[AD-A191416] 20 p2861 N88-26995
Transport in GaAs heterojunction ring structures
20 p2864 N88-27011
Theoretical aspects of electron transport in modulated structures 20 p2865 N88-27016
Transport study on Si/Si(1-x)Ge(x) superlattices selectively doped by secondary implantation of Sb
20 p2867 N88-27027
Resonant tunneling in InGaAs-InP double-barrier structures and superlattices 20 p2871 N88-27047
Type 3 - type 1 transition and strain effect in Hg(1-x)Cd(x)Te-CdTe and Hg(1-x)Zn(x)Te-CdTe superlattices 20 p2872 N88-27052
Studies of HZE particle interactions and transport for space radiation protection purposes
[NASA-TM-101159] 20 p2886 N88-27142
Application of acoustic-Doppler current profiler and expendable bathythermograph measurements to the study of the velocity structure and transport of the Gulf Stream
[NASA-CR-183188] 22 p3129 N88-28605
A study of electronic transport and breakdown in SiO2
[AD-A194258] 22 p3156 N88-28780
Phenomena of the ionic transport in the stress corrosion of metals
[DE88-702502] 23 p3195 N88-29013
Transport of organic vapors in multiphase polymer system
[AD-A194097] 23 p3198 N88-29033
Development of computer-controlled thermogravimetric instrumentation for measurement of environmental and high temperature volatilization and desorption of contaminants from polymeric materials
[AD-A195934] 24 p3343 N88-29900
Experimental and analytical study of two-phase flow in zero gravity
[AD-A195223] 24 p3358 N88-29993
Models of cerebral-body perfusion and cerebral chemical transport
[AD-A194945] 24 p3407 N88-30283

TRANSPORT THEORY
NT MIXING LENGTH FLOW THEORY
Interactive Design of Accelerators (IDA)
[DE87-013298] 02 p0234 N88-11476
Computer models for kinetic equations of magnetically confined plasmas
[DE87-011571] 02 p0236 N88-11492
Two dimensional neutral transport analysis in tokamak plasma
[DE87-752984] 02 p0239 N88-11510
Transport analysis of OH and NBI heated discharges in JT-60
[DE87-752985] 02 p0239 N88-11511
Progress in stellarator/heliotron research, 1981-1986: Executive summary
[DE88-000017] 02 p0241 N88-11519
Nonequilibrium fluctuations and transport in sheared fluids 03 p0316 N88-11999
Momentum transport and particle dynamics in turbulent shear flows 03 p0317 N88-12002
Two layer stratified flow analysis of gravity currents and turbidity currents in lakes, reservoirs and the ocean
04 p0463 N88-12864
Development of the non-equilibrium reactive chemical transport code CHMTRNS
[DE88-000682] 04 p0481 N88-12964
Transport simulations of the oscillating field current drive experiment in the ZT-40M reversed field pinch
[DE88-000538] 04 p0491 N88-13027
Transport scaling in the collisionless-detrapping regime in stellarators
[DE88-001511] 05 p0653 N88-14006
Comparison of 2D memory SEU transport simulation with experiments
[ATR-86(8139)-2-REV-A] 05 p0656 N88-14025
Theoretical studies of multicomponent mixtures: Phase equilibrium and transport
[DE88-002717] 07 p0831 N88-15040
Use of back air trajectories in interpreting atmospheric chemistry data: A review and bibliography
[PB88-102108] 07 p0876 N88-15312
Particle transport in microdetonations --- inertial confinement fusion pellets
[OEFZS-4402] 09 p1164 N88-16976
Time dependent degradation of energetic electrons in gaseous and condensed media
[DE88-002912] 09 p1246 N88-17465
Two-dimensional analysis for a scrapeoff and divertor regions with an MHD model. Conceptual design study of FY86 FER
[DE88-751069] 09 p1251 N88-17497
Applied mathematics of transport theory
[DE88-004098] 10 p1404 N88-18369
Studies in finite time thermodynamics
[DE88-004531] 10 p1423 N88-18500
Boltzmann-Fokker-Planck calculations using standard discrete-ordinates codes
[DE88-005393] 11 p1537 N88-19185
Propagator solutions of partial differential equations applied to plasma transport
[DE88-006432] 13 p1816 N88-20852
Conservative finite volume solutions of a linear hyperbolic transport equation in two and three dimensions using multiple grids
[NASA-CR-182715] 13 p1828 N88-20934
FLOSIN: A fluid loop analyzer for SINDA
15 p2066 N88-22321

Transport simulations of ohmic ignition experiment: IGNITEX
[DE88-006055] 15 p2138 N88-22757
Analysis of reversible and irreversible hydrogen trapping in metals
[NPL-DMA(A)-154] 16 p2177 N88-22977
Modeling of turbulent transport as a volume process
16 p2196 N88-23099
A statistical investigation of the single-point pdf of velocity and vorticity based on direct numerical simulations 16 p2196 N88-23101
BRYNTRN: A baryon transport computer code, computation procedures and data base
[NASA-TM-4037] 16 p2290 N88-23714
Effects of space-dependent cross sections on core physics parameters for compact fast spectrum space power reactors 17 p2399 N88-24263
Consistent transport coefficients in astrophysics
[NASA-TM-101154] 17 p2451 N88-24560
A benchmark for galactic cosmic ray transport codes
[NASA-TM-101157] 17 p2453 N88-24571
Physical properties of f electron systems
[DE88-006886] 18 p2581 N88-25331
Electrode films of porous agarose: The effects of physical structure on electron transport processes
[DE88-007366] 19 p2611 N88-25493
Quantum transport calculation of resonant-tunneling response time 19 p2659 N88-25810
Multidimensional nodal transport methods for multiple-instruction multiple-data distributed memory machines
[DE88-004732] 19 p2713 N88-26108
Tracer water transport and subgrid precipitation variation within atmospheric general circulation models
[NASA-CR-182897] 20 p2823 N88-26745
Eigenmodes of a random walk on a 2-D lattice torus with one trap
[DE88-007830] 20 p2844 N88-26874
A nodal method for time-dependent transport equation
[DE88-004285] 20 p2844 N88-26876
Quantum transport theory of resonant-tunneling heterostructure devices 20 p2865 N88-27017
Quantum interference and transport in microstructures
20 p2866 N88-27022
Kinetic theory for plane flows of rough, inelastic, circular disks 21 p2946 N88-27499
Introduction to laser plasma diagnostics
[DE88-011056] 23 p3285 N88-29560
Bootstrap currents in radio-frequency-driven tokamak equilibria
[DE88-011136] 23 p3285 N88-29561

TRANSPORTATION
NT AIR TRANSPORTATION
NT RAIL TRANSPORTATION
NT RAPID TRANSIT SYSTEMS
NT SPACE TRANSPORTATION
NT SPACE TRANSPORTATION SYSTEM
NT URBAN TRANSPORTATION
Aircraft accident/incident summary reports: Unalaska, Alaska, September 25, 1985; Jenkinsburg, Georgia, September 29, 1985; Boston, Massachusetts, December 15, 1985; Dekalb, Texas, December 31, 1985; and Erie, Pennsylvania, February 21, 1986
[PB87-910408] 02 p0123 N88-10780
Spinoff, 1987
[NASA-TM-89652] 02 p0250 N88-11577
The development of laboratory vibration test schedules: Philosophies and techniques 08 p0999 N88-16049
The DFVLR-German Space Operations Center (GSOC) mobile rocket base 08 p1029 N88-16237
A lunar transportation system
[NASA-CR-182561] 11 p1567 N88-19379
A model of intrazonal trip distribution considering centrality index 16 p2257 N88-23486
A three dimensional assignment method in the time space
[REPT-87-49] 16 p2287 N88-23690
Technology transfer for DOE's Office of Transportation Systems: Assessment and strategies
[DE88-010760] 21 p3029 N88-27977

TRANSPORTATION NETWORKS
Study of the feasiblity of a satellite communication system for road transportation home office to vehicle communication. Volume 1: Conceptual analysis
[SC/87-E/6-VOL-1] 05 p0575 N88-13505
Study of the feasibility of a satellite communication system for road transportation home office to vehicle communication. Volume 2: Market study
[SC/87-E/6-VOL-2] 05 p0575 N88-13506
Determination of network attributes from a high resolution terrain data base
[AD-A186078] 07 p0870 N88-15279
Computer aided cartographic representation of traffic data: The traffic intensity maps of Baden-Wuerttemberg (Federal Republic of Germany)
16 p2225 N88-23282
From the extraction of linear networks towards following of them on SPOT images with the help of a knowledge-based interpretation system
22 p3113 N88-28494
Extraction of thin networks by an oriented following of ridges and valleys 22 p3113 N88-28495

TRANSPORTER
Space station mobile transporter
14 p1927 N88-21488

TRANSURANIUM ELEMENTS
NT LAWRENCIUM
NT NEPTUNIUM
NT PLUTONIUM ISOTOPES
NT PLUTONIUM 238

TRANSVERSE ACCELERATION
Determination of the drag of missiles with variable lateral acceleration possibility
[REPT-FM15] 10 p1310 N88-17831

TRANSVERSE OSCILLATION
NT H WAVES

TRANSVERSE WAVES
NT H WAVES
TE/TM (Transverse Electric/Transverse Magnetic) height profile measurements of transpolar VLF (Very Low Frequency) signals
[AD-A194503] 22 p3069 N88-28216

TRANSVERSELY EXCITED ATMOSPHERIC LASERS
U TEA LASERS

TRAPATT DIODES
U AVALANCHE DIODES

TRAPPED MAGNETIC FIELDS
Magnetic trapping of neutral atoms
[AD-A188473] 12 p1689 N88-20103
Comparison of analytic and full guiding center behavior at a trapped-passing interface in stellarators
[DE88-004174] 13 p1842 N88-21025
New methods of confinement and heating of plasma in magnetic fields
[DE88-701021] 15 p2135 N88-22738

TRAPPED PARTICLES
NT INNER RADIATION BELT
NT MAGNETICALLY TRAPPED PARTICLES
NT RADIATION BELTS
The free electron laser sideband instability reconsidered
[AD-A184269] 04 p0447 N88-12773
Forces on neutral atoms due to electromagnetic fields
[AD-A187461] 10 p1408 N88-18396
The JPL trapped mercury ion frequency standard
11 p1471 N88-18776
Toward a comprehensive theory for the sweeping of trapped radiation by inert orbiting matter
[NASA-CR-182584] 11 p1569 N88-19395
Theory of laser cooling and spectroscopy of harmonically trapped single atoms
[AD-A189576] 13 p1775 N88-20617
Comparison of analytic and full guiding center behavior at a trapped-passing interface in stellarators
[DE88-004174] 13 p1842 N88-21025
United States - Japan Seminar on Quantum Mechanical Aspects of Quantum Electronics
[AD-A186938] 14 p1974 N88-21781
Optical trapping of neutral atoms and dielectric particles by radiation pressure 14 p1974 N88-21783
Modeling the effects of heavy charged particles on MOSFETs (Metal-Oxide-Semiconductor Field Effect Transistors)
[AD-A190575] 15 p2143 N88-22792
Numerical simulation for particle acceleration and trapping by an electromagnetic wave
16 p2277 N88-23626
JFET/SOS (Junction Field-Effect Transistor/Silicon-on-Sapphire) devices: Gamma-radiation-induced effects
[AD-A193001] 20 p2795 N88-26586
Investigation of the potential impact of new photonic materials on optical processing systems
21 p2924 N88-27359
The dust ring of the Earth
[RAE-TRANS-2163] 22 p3119 N88-28530
Large area nuclear particle detectors using ET materials
[NASA-CR-180777] 23 p3215 N88-29136
Spontaneous force optical traps
[AD-A196103] 24 p3377 N88-30114
Research on a two-stage free electron laser oscillator
[AD-A195991] 24 p3377 N88-30115

TRAPPING
Conditions for geomagnetically trapping sub-micron lunar ejecta between L = 1.2 and L = 3.1
04 p0521 N88-13203
Propagation in longitudinally varying ducts, with emphasis on guiding to antiguiding transitions
12 p1615 N88-19658
MOSFET performance degradation due to hot carriers
13 p1848 N88-21063
Analysis of reversible and irreversible hydrogen trapping in metals
[NPL-DMA(A)-154] 16 p2177 N88-22977
Autoionization for lower level detrapping in X-ray lasers
[AD-A195845] 24 p3379 N88-30123

TRAPS
NT COLD TRAPS
NT ION TRAPS (INSTRUMENTATION)
Implications of the trapping-desorption and direct inelastic scattering channels on Dicke-narrowed lineshapes
[AD-A191410] 16 p2270 N88-23581

TRAVELING IONOSPHERIC DISTURBANCES
Interplanetary Magnetic Field (IMF) influence on the magnetic configuration and particle fluxes at geostationary orbit and on the substorm onset
08 p1031 N88-16247
A unified model for the WTS and the generation on Pi 2 pulsations --- Westward Traveling Surge (WTS)
08 p1096 N88-16593
Moving ionospheric perturbations induced by wave trains propagating through ocean 09 p1239 N88-17427
On the dynamics of the auroral ionosphere during the breakup of a substorm
[AD-A193368] 21 p2972 N88-27657

TRAVELING SALESMAN PROBLEM
Progress in mathematical programming
[AD-A185729] 06 p0759 N88-14658
A traveling-salesman-based approach to aircraft scheduling in the terminal area
[NASA-TM-100062] 12 p1576 N88-19424
Local search for constrained routing problems --- traveling salesman
[CWI-OS-R8711] 13 p1830 N88-20948
A concurrent neural network algorithm for the traveling salesman problem
[DE88-006981] 18 p2562 N88-25208
An extension of the Hopfield-Tank model for solution of the multiple traveling salesmen problem
[DE88-008377] 19 p2715 N88-26122

TRAVELING WAVE AMPLIFIERS
Solid-state travelling wave amplifiers based on multi-stream instability
[AD-A189566] 12 p1624 N88-19718
Construction of a 60 GHz Traveling Wave Tube (TWT) for intersatellite link on geostationary orbit (ISL/TWT)
[BMFT-FB-W-86-015] 16 p2192 N88-23076
Wide band gyrotron traveling wave amplifier analysis
[AD-A194269] 23 p3216 N88-29139

TRAVELING WAVE MASERS
A 2.3-GHz maser at Usuda, Japan, for TDRSS-orbiting VLBI experiment 11 p1472 N88-18779
A 2.3-GHz low-noise cryo-FET amplifier
22 p3066 N88-28195
An 8.4-GHz dual maser front end for Parkes reimplementation 22 p3066 N88-28197

TRAVELING WAVE MODULATION
A high frequency GaAlAs travelling wave electro-optic modulator at 0.82 micrometers
[NASA-TM-100970] 22 p3073 N88-28240

TRAVELING WAVE TUBES
Performance of a small, graphite electrode, multistage depressed collector with a 500-W, continuous wave, 4.8- to 9.6-GHz traveling wave tube
[NASA-TP-2788] 07 p0848 N88-15146
High efficiency, long life traveling wave tubes for future communications satellites
[NASA-TM-100837] 12 p1598 N88-19565
Construction of a 60 GHz Traveling Wave Tube (TWT) for intersatellite link on geostationary orbit (ISL/TWT)
[BMFT-FB-W-86-015] 16 p2192 N88-23076
Miniature traveling wave tube and method of making
[NASA-CASE-LEW-14520-1] 17 p2335 N88-23936
An investigation of the uses of time domain capable vector network analyzers as a diagnostic for helix traveling-wave circuits
[AD-A192460] 21 p2935 N88-27430
A millimeter-wave tunneLadder TWT
[NASA-CR-182184] 22 p3072 N88-28239

TRAVELING WAVES
NT SOLITARY WAVES
Intracavity absorption spectroscopy with ring traveling-wave dye laser 03 p0300 N88-11890
Determination of fractal dimension, connection of space and temporal chaos and application to experimental results 03 p0313 N88-11977
The 8.4-GHz low-noise maser pump source assembly
04 p0436 N88-12705
Traveling-wave maser closed-cycle refrigerator data acquisition and display system 04 p0437 N88-12706
Departmental report on program EMTP-machine windings surge transients: Travelling wave method
[PB87-123733] 04 p0438 N88-12719

Modeling and control of large flexible vehicles in the atmosphere and space
[AD-A185368] 05 p0555 N88-13377
Time characteristics of travelling wave lasing with two-photon picosecond optical pumping
07 p0918 N88-15578
Travelling waves and chaos in double-diffusive convection 11 p1484 N88-18857
Harmonic and rectangular pulse reproduction through current transformers
[EUT-86-E-159] 14 p1907 N88-21395
Squeezing via travelling-wave forward four-wave mixing in atomic vapors: Comparison with nondegenerate theory 14 p1978 N88-21804
Travelling wave concepts for the modeling and control of space structures
[AD-A191235] 17 p2310 N88-23819
Asymptotics for a system of nonlinearly coupled wave equations with an application to the galloping oscillations of overhead transmission lines
[REPT-87-78] 17 p2348 N88-23991
Electrical pulse compression by traveling-wave photoconductivity 19 p2661 N88-25822

TREADS
Armoured vehicle track elastomers: Research and development at MRL
[MRL-GD-0012] 19 p2620 N88-25541
A critical speed study for aircraft bias ply tires
[AD-A193616] 22 p3084 N88-28313

TREAT (TEST FACILITY)
U TRANSIENT REACTOR TEST FACILITY

TREES (MATHEMATICS)
NT FAULT TREES
File management using balanced trees
[ENST-87D001] 01 p0106 N88-10693
Subcritical branching processes in a two state random environment, and a percolation problem on trees
[PB87-230439] 06 p0762 N88-14677
Very thin VLSI-layouts (Very Large Scale Integration-Layouts) of complete binary trees
[PB88-100847] 06 p0789 N88-14841
A note on the partitioning shortest path algorithm
[CWI-OS-R8703] 08 p1067 N88-16451
An anlysis of the reliability of tree-structured interconnection networks 10 p1378 N88-18228
Improving battery reliability by using regression trees
[DE88-004539] 11 p1481 N88-18841
Finite octree meshing through topologically driven geometric operators 11 p1527 N88-19121
Iteration of transformation passes over attributed program trees --- compilers
[INF-87-28] 14 p1956 N88-21661
A comparison of supervised maximum likelihood and decision tree classification for crop cover estimation from multitemporal LANDSAT MSS data
17 p2352 N88-24014
Automatic routing in symbolic IC design environment
19 p2714 N88-26112

TREES (PLANTS)
NT CONIFERS
Effects of fire on composition, biomass, and nutrients in oak scrub vegetation on John F. Kennedy Space Center, Florida
[NASA-TM-100305] 08 p1020 N88-16182
Vegetation mapping using high resolution MSS (multispectral scanner) data: Canopy reflectance and shadow problems encountered and possible solutions
[DE88-004273] 14 p1939 N88-21574
Utilization of TM/LANDSAT images in the implanted forests mapping in the Mogi-Guacu Region (SP-Brazil)
17 p2357 N88-24042
Interpretation of MSS/LANDSAT data for evaluation of physical distribution of mangroves in Cananeia-Iguape (SP) 17 p2363 N88-24072
Evaluation of the mangrove area at the Piaui River (SE) through remote sensing 17 p2365 N88-24086
Stereoscopic photographs, ground and aerial, of trees used in the arborization of Curitiba (PR)
17 p2366 N88-24091
Propagation effects by roadside trees measured at JHF and L-band for mobile satellite systems
19 p2644 N88-25693
Attenuated direct and scattered wave propagation on simulated land mobile satellite service paths in the presence of trees 19 p2645 N88-25695
Propagation measurements for an Australian land mobile satellite system 19 p2645 N88-25697
Canopy reflectance modeling in a tropical wooded grassland
[NASA-CR-182981] 19 p2685 N88-25961
SPOT 1: Image utilization, assessment, results. A study of the Elburgon Forest area (Kenya) showing the spectral responses of different forest tree species
22 p3107 N88-28454

TRENDS
Communication satellite technology trends
01 p0015 N88-10088
Earth Radiation Budget Satellite (ERBS) orbiting profiles and Ni-Cd use 02 p0165 N88-11034
Technology transfer to China
[PB87-223418] 04 p0502 N88-13087
The technology of centrifugal compressors: A design approach and new goals for research
07 p0850 N88-15163
Long-term variation of total ozone
[INPE-4307-PRE/1173] 08 p1023 N88-16192
Trends in research and development in the Netherlands. The influence of national science policy between 1973 and 1986
[B8701588] 08 p1094 N88-16580
Lewis materials research and technology: An overview
09 p1119 N88-16699
Avionics acquisition, trends and future approaches
12 p1702 N88-20184
Function of Japan Fine Ceramics Center described
15 p2052 N88-22227
Marshall Space Flight Center 1960-1985: 25th anniversary report
[NASA-TM-100328] 15 p2153 N88-22852
Development of a multipurpose smart recorder for general aviation aircraft
[NASA-CR-168353] 18 p2465 N88-24637
The application of hydrocarbon bioconversion technology to aerospace materials production
18 p2478 N88-24698
Millimeter-wave integrated circuits
19 p2656 N88-25774
Trends in civil aircraft propulsion
[PNR90441] 22 p3044 N88-28067
Future trends in aviation propulsion
[PNR90443] 22 p3044 N88-28068

TRIANGLES
Solution of the two-dimensional Euler equations on unstructured triangular meshes
04 p0396 N88-12469
Non-rigid motion and Regge calculus
[AD-A190387] 15 p2121 N88-22640
The triangle: A multiprocessor architecture for fast curve and surface generation
[AD-A195882] 24 p3414 N88-30324

TRIANGULAR WINGS
U DELTA WINGS

TRIANGULATION
Control of the German main triangulation network by macrometer measurement 1983-1985 (KONMAC)
[SER-B-282] 01 p0063 N88-10404
Optimization of photogrammetric image adjustment
[SER-C-323] 07 p0872 N88-15289
Discovery and problem solving: Triangulation as a weak heuristic 08 p1062 N88-16412
Contour-to-grid interpolation with nonlinear finite elements: A feasibility study
[AD-A188108] 11 p1503 N88-18980
Adjustment in photogrammetry: Methods, programs and applications
[B8735130] 17 p2369 N88-24105
Adaptive mesh generation for viscous flows using Delaunay triangulation
[NASA-CR-181699] 24 p3316 N88-29749

TRIAXIAL STRESSES
A generalized least-squares determination of triaxial stress states by X-ray diffraction and the associated errors
[AD-A183851] 01 p0058 N88-10371
Periodic orbits around a satellite modelled as a triaxial ellipsoid
[AD-A190592] 15 p2022 N88-22051
Creep of carbon yarn and carbon-carbon composites at high temperatures and high stresses
[AD-A195224] 24 p3340 N88-29878

TRIAXIALITY
U TRIAXIAL STRESSES

TRIBOLOGY
Coatings for Advanced Heat Engines Workshop: Book of abstracts
[DE87-012623] 02 p0180 N88-11121
Boundary lubrication. Experiments with boundary lubrication and plain bearings at +60 -60 deg C temperatures
[DE87-752869] 02 p0180 N88-11124
Piston ring friction and vehicle fuel economy
[DE87-014536] 02 p0181 N88-11127
Double-effect absorption heat pump, phase 3
[PB87-232195] 03 p0317 N88-12005
Adiabatic diesel engine component development: Reference engine for on-highway applications
[NASA-CR-179531] 03 p0386 N88-12428
Calculation of the tribological properties of surfaces by semi-empirical methods
[AD-A184283] 04 p0450 N88-12791
Tribological properties of rf-sputtered MoS2 coatings
[DE88-000266] 04 p0452 N88-12802
Tribology of thin film systems
[ETN-88-91365] 05 p0590 N88-13601
Projects within the Center for Advanced Materials
[PB88-123054] 06 p0677 N88-14143
The tribological properties of MoS2 coatings in vacuum, low relative humidity and high relative humidity environments
[DE88-001611] 06 p0711 N88-14356
Tribological studies on high speed steel cutting tools
[DE88-002550] 07 p0864 N88-15246
The WAFTER: A versatile wear and friction tester
[MRL-TN-519] 09 p1169 N88-17012
Activities report in tribology
[ESA-ESTL-79] 09 p1174 N88-17037
Seven year thermal vacuum real life test of a medium speed (despin) mechanism manufactured by Dornier System
[ESA-ESTL-64] 09 p1175 N88-17038
Adhesion, friction and micromechanical properties of ceramics
[NASA-TM-100782] 10 p1305 N88-17801
Tribology of ceramics: Report of the Committee on Tribology of Ceramics
[NASA-CR-182506] 10 p1305 N88-17802
Tribological properties of alumina-boria-silicate fabric from 25 to 850 C
[NASA-TM-100806] 11 p1464 N88-18726
Overview of the DOE-ECUT Tribology Program
[DE88-002878] 13 p1778 N88-20637
Proceedings of the 3rd European Space Mechanisms and Tribology Symposium
[ESA-SP-279] 14 p1874 N88-21191
Models for steady and nonsteady Coulomb torque in ball bearings 14 p1876 N88-21208
Ball bearings with chemical vapor deposition (CVD)-TiC coated components 14 p1876 N88-21210
Separable electrical connectors for space: A tribological and electrical assessment 14 p1879 N88-21231
Towards a tribology information system: The results of a Planning Workshop held at the National Bureau of Standards, July-August 1985
[PB88-168604] 14 p1918 N88-21448
Structural Ceramics
[NASA-CP-2427] 17 p2323 N88-23872
Ceramics for turbine engines
17 p2323 N88-23873
Development of test methods for the electrostatic properties of nonhomogeneous fabrics, phase 2
[AD-A190853] 18 p2489 N88-24767
The lubricating properties of magnetron sputtered MoS2
[ESA-ESTL-76] 24 p3381 N88-30136

TRICHLORIDES
U CHLORIDES

TRIGGER CIRCUITS
Pseudospark switches
[DE88-702227] 23 p3207 N88-29085

TRIGGERS
U ACTUATORS

TRIGONOMETRIC FUNCTIONS
NT COSINE SERIES
NT TANGENTS
High speed transcendental elementary function architecture in support of the Vector Wave Equation (VWE)
[AD-A189746] 15 p2119 N88-22627

TRIM (BALANCE)
U AERODYNAMIC BALANCE

TRINITROTOLUENE
The viscosity of molten TNT
[MRL-R-1100] 19 p2622 N88-25553

TRINITROTRIAZOCYCLOHEXANE
U RDX

TRIPLE AXIS SPECTROMETERS
U NEUTRON SPECTROMETERS

TRIPLET EXCITATION
U ATOMIC ENERGY LEVELS

TRIPLET STATE
U ATOMIC ENERGY LEVELS

TRIPROPELLANTS
U LIQUID ROCKET PROPELLANTS

TRISONIC WIND TUNNELS
The 0.6m x 0.6m trisonic test section (TMK) of DFVLR in Cologne Porz, Federal Republic of Germany (status 1986)
[ESA-TT-1052] 03 p0267 N88-11681

TRITIUM
Magneto-Inertia Confinement Approach (MICA) to fusion in dynamic Z-pinch formed from a frozen deuterium-tritium tube
[IPPJ-856] 09 p1252 N88-17504
Weldability of tritium-charged 304L stainless steel
[DP-1740] 12 p1607 N88-19611

Biophysical applications of solid state and tritium NMR [DE88-005328] 13 p1808 N88-20806

Outlook for the fusion hybrid and tritium-breeding fusion reactors [PB88-149281] 13 p1843 N88-21029

Infrared spectroscopy of H3(+) 16 p2268 N88-23565

Analysis of containerless condensation of polyatomic hydrogen ions, with emphasis on H3(+,-) association channels and a future workshop to study related topics 16 p2269 N88-23576

Helium-3 fusion fuel resources for space power 17 p2410 N88-24330

The hole of a blanket tritium system on the fusion fuel cycle [DE88-010007] 20 p2859 N88-26983

TRITONS

Physics of few-body lambda hypernuclei [DE87 014746] 03 p0375 N88-12357

TROCHOIDS

U PIVOTS

TROPICAL METEOROLOGY

Annual tropical cyclone report, 1986 [AD-A184082] 04 p0470 N88-12903

Interactions between the Asian monsoons, the tropical Pacific and the southern hemisphere extratropics 04 p0470 N88-12907

A method to obtain a wind model for the boundary layer in a representative tropical region [R-818-D] 06 p0743 N88-14569

The effect of latitude on the development of tropical cyclones [AD-A185670] 06 p0746 N88-14590

US participation in the TOGA (Tropical Ocean and the Global Atmosphere) Program: A research strategy [DE88-010986] 19 p2681 N88-25938

Dynamic interaction of convective cumulus with large-scale environment [MITT-55] 20 p2827 N88-26773

Westward moving atmospheric wave disturbances over the African tropics: Dynamic and energetic aspects [MITT-57] 20 p2827 N88-26774

The patterns of tropical convection during the 1986-87 ENSO 22 p3120 N88-28537

Climatology of various synoptic systems over the tropical North Pacific 22 p3121 N88-28542

Complex EOF analysis of intraseasonal tropical wind fluctuations 22 p3121 N88-28544

On the impact of low-latitude anomalous forcing on local and remote circulation: Winters(DJF) 1978/79 to 1986/87 22 p3123 N88-28560

An observational study of interaction between large scale tropical cumulus convection and the equatorial circulation anomalies 22 p3124 N88-28564

The impact of the El Nino event on the ECMWF model performance 22 p3125 N88-28576

Extratropical response to tropical heating as a function of period of model integrations 22 p3125 N88-28577

Observed normal mode structure of low frequency oscillations 22 p3128 N88-28595

TROPICAL REGIONS

NT AMAZON REGION (SOUTH AMERICA)

The challenge of very short range forecasting in the tropics 02 p0205 N88-11287

Statistical relationships between the mesoscale organization of convection and the large-scale wind profiles during GATE --- GARP Atlantic Tropical Experiment (GATE) 02 p0208 N88-11302

The contribution of satellite data in drawing up maps used in rural development 03 p0343 N88-12167

On the interannual variability of South American climate and the Southern Oscillation 04 p0470 N88-12905

The use of TOMS data for tropospheric ozone studies 05 p0616 N88-13784

Modes of surface circulation and climate over the tropical Atlantic, Eastern Pacific, and Indian Oceans 06 p0742 N88-14564

A method to obtain a wind model for the boundary layer in a representative tropical region [R-818-D] 06 p0743 N88-14569

Tropical hydrology [WMO-655] 06 p0745 N88-14584

Geosat crossover analysis in the tropical Pacific. Part 1: Constrained sinusoidal crossover adjustment [NASA-CR-182391] 07 p0871 N88-15285

Variations of tropical circulation and associated rainfall anomalies, during 2 years of contrast [INPE-4359-TDL/300] 08 p1039 N88-16286

Corrosion and deterioration testing in humid tropic environments [AD-A186917] 10 p1302 N88-17783

Mapping of the mangroves of the Guanabarra Bay through the utilization of remote sensing techniques [INPE-3942-TDL/229] 12 p1637 N88-19804

JEDA (Joint Environmental Data Analysis) Center report on tropical Pacific subsurface thermal data management, 1986 [PB88-140090] 12 p1649 N88-19875

Perspectives in microclimate cooling involving protective clothing in hot environments [AD-A188370] 12 p1671 N88-20007

Basic networks of TOGA: Determination of thermal profiles by XBT and of sea level by tide gage 14 p1939 N88-21568

Ground-based column abundance measurements of atmospheric hydroxyl [NASA-CR-182676] 14 p1944 N88-21598

Tropical and monsoonal studies [AD-A188387] 14 p1947 N88-21611

Tropic heat MR (Meteorological Recorder) meteorological data (April 1984 - June 1985) [PB88-161286] 14 p1948 N88-21620

Current velocity and hydrographic observations in the Straits of Florida, the Caribbean Sea and offshore of the Antillean Archipelago: Subtropical Atlantic Climate Studies (STACS) 1986 [PB88-160767] 14 p1951 N88-21628

Tropical circulations and the associated rainfall anomalies during two contrasting years [INPE-4506-PRE/1261-REV] 15 p2098 N88-22502

A study of the dynamics of the Intertropical Convergence Zone (ITCZ) in a symmetric atmosphere-ocean model [NASA-TM-86220] 19 p2693 N88-26005

Following the seasonal evolution of a natural environment in a humid tropical region. Preliminary Evaluation of SPOT (PEPS) number 186: Bangui, Central Africa 22 p3093 N88-28368

Discrimination methods of traditional fields in a humid tropical region (Shaba Zaire) using digital classification on SPOT data 22 p3096 N88-28387

Assessment of SPOT satellite based system in humid tropical vegetation identification, classification and monitoring 22 p3100 N88-28408

Bibliography on tropical rain forests and the global carbon cycle. Volume 1: An introduction to the literature [DE88-010761] 22 p3118 N88-28523

The patterns of tropical convection during the 1986-87 ENSO 22 p3120 N88-28537

Some diagnostic results concerning the tropical 40-50 day oscillation 22 p3121 N88-28546

Evolution of thermal structure of Benguela upswelling system according to satellite and shipboard data 24 p3449 N88-30525

TROPICAL STORMS

NT HURRICANES

NT TYPHOONS

Tropical cyclone center locations from enhanced infrared satellite imagery [PB87-213450] 01 p0071 N88-10455

Summary of 1987 Atlantic tropical cyclone activity and verification of author's seasonal forecast 02 p0215 N88-11356

Opportunities for tropical cyclone motion research in the Northwest Pacific region [AD-A185068] 05 p0627 N88-13834

Environmental and convective influence on tropical cyclone development versus non-development [AD-A185231] 05 p0627 N88-13835

Estimation of rainfall rates in tropical cyclones by passive microwave radiometry 06 p0744 N88-14577

The effect of latitude on the development of tropical cyclones [AD-A185670] 06 p0746 N88-14590

Interim review of the possibilities and opportunities for the ONR tropical cyclone motion research initiative [AD-A185679] 06 p0746 N88-14592

Recent Colorado State University tropical cyclone research of interest to forecasters [AD-A185996] 07 p0879 N88-15332

Annual data summary and climatological evaluation CERC (Coastal Engineering Research Center) field research facility, 1985. Volume 1. Main text and appendixes A and B [AD-A186442] 08 p1039 N88-16289

Northern winter circulations for the period 1974-1983 [AD-A187779] 11 p1511 N88-19028

The role of vortex structure in tropical cyclone motion [AD-A190961] 16 p2235 N88-23351

Tropical cyclones, 1987: Central North Pacific [PB88-188081] 18 p2547 N88-25119

Tropical cyclone report [AD-A191883] 19 p2693 N88-26009

TROPICS

U TROPICAL REGIONS

TROPISM

NT GRAVITROPISM

TROPOPAUSE

Photochemical ozone overburden correction 05 p0615 N88-13778

Northwest Airlines flight experiments 05 p0617 N88-13786

Application of TOMS data to weather analysis models 05 p0617 N88-13787

Correlations of TOMS total ozone data (Nimbus-7 satellite) with tropopause height 05 p0617 N88-13788

An analysis of tropopause pressure and total ozone correlations 05 p0617 N88-13789

TOMS ozone data compared at mesoscale resolution to tropopause heights from the AVE radiosonde network and to VAS radiances over the south-central United States 05 p0617 N88-13790

The use of TOMS-modified VAS data for large-scale NWP 05 p0618 N88-13791

TROPOSPHERE

NT TROPOPAUSE

The importance of mesoscale waves in the upper troposphere for formation of cloud and precipitation areas 02 p0203 N88-11273

Scientific and Operational Requirements for TOMS Data [NASA-CP-2497] 05 p0615 N88-13774

Lower-stratospheric/upper-tropospheric exchange processes associated with tropical cyclones as observed by TOMS 05 p0616 N88-13782

Tropical easterly jet located using TOMS data 05 p0616 N88-13783

The use of TOMS data for tropospheric ozone studies 05 p0616 N88-13784

Numerical modeling of troposphere-induced gravity wave propagation 06 p0735 N88-14522

Observations of inertial period waves and vertical velocities in the tropical middle atmosphere using the MST radar technique 06 p0742 N88-14562

Investigation of OH reaction products. Excimer laser photolysis/slab laser fluorescence under tropospheric conditions [REPT-8] 09 p1191 N88-17137

Optical characterization of tropospheric aerosols [AD-A187839] 11 p1511 N88-19029

Initial results with the LLNL 2-D chemical-radiative-transport model of the troposphere and stratosphere [DE88-004355] 11 p1512 N88-19033

Photoacoustic measurements of atmospheric aerosol absorption coefficients at ultraviolet, visible and infrared wavelengths 11 p1512 N88-19036

A paper on horizontal deformation in the frontogenesis in south Brazil [INPE-4469-TDL/322] 12 p1647 N88-19867

Pre-convective environmental conditions indicative of non-tornadic severe thunderstorm winds over Southeast Florida [AD-A188679] 12 p1648 N88-19870

Computer simulation of tropospheric chemistry [JUEL-2144] 13 p1798 N88-20756

IREPS (Integrated Refractive Effects Prediction System) 3.0, user's manual [AD-A190398] 16 p2188 N88-23045

SAGE 1 and SAM 2 measurements of 1 micron aerosol extinction in the free troposphere [NASA-CR-182945] 17 p2374 N88-24121

A theoretical model of the washout of trace gases by raindrops in the atmosphere 17 p2375 N88-24125

Workshop on Atmospheric OH [BPT-7/87] 18 p2538 N88-25063

Effect of carbohydrate oxidation on the tropospheric HOx-system 18 p2539 N88-25067

Trace gas measurements in the troposphere using tunable diode lasers 18 p2540 N88-25072

Development of continuous wave laser frequency modulation of OH in tropospheric concentrations range 18 p2540 N88-25073

Tropospheric biennial variability and its relationship to the southern oscillation 22 p3121 N88-28549

Atmospheric deposition of nitrate to the ocean surface 23 p3231 N88-29227

Forty-eight-inch lidar aerosol measurements taken at the Langley Research Center, May 1974 to December 1987 [NASA-RP-1209] 23 p3232 N88-29234

Global vertical mass transport by clouds: A two-dimensional model study [CM-74] 24 p3391 N88-30192

TROPOSPHERIC RADIATION

Tropospheric ultraviolet radiation: Assessment of existing data and effect on ozone formation [PB88-130133] 10 p1354 N88-18095

TROPOSPHERIC SCATTERING

Results on the low elevation angle propagation experiment, part 1 [TUD-R-328] 06 p0693 N88-14250

Optical characterization of tropospheric aerosols [AD-A187839] 11 p1511 N88-19029

Corrections for differential scattering by aerosols in the measurement of ozone by DIAL --- differential absorption lidar (DIAL)
[NPL-QU-78]
14 p1945 N88-21603

TROPOSPHERIC WAVES
NT PLANETARY WAVES
The importance of mesoscale waves in the upper troposphere for formation of cloud and precipitation areas
02 p0203 N88-11273

TROUBLESHOOTING
U MAINTENANCE

TRUCKS
Adiabatic diesel engine component development: Reference engine for on-highway applications
[NASA-CR-179531]
03 p0386 N88-12428
Full scale and wind tunnel surface pressure measurements on the T.R.R.L. spray dispersion programme vehicles
[REPT-8623]
09 p1114 N88-16676
Ethanol as a fuel of a lorry. Use experience from a diesel engine modified to an otto engine
[DE88-752870]
21 p2958 N88-27569

TRUNCATION (MATHEMATICS)
U APPROXIMATION

TRUNCATION ERRORS
Spectral analysis in the linear geodetic boundary value problem
[B8735056]
16 p2259 N88-23502

TRUNKS (LINES)
U TRANSMISSION LINES

TRUNNIONS
U SHAFTS (MACHINE ELEMENTS)

TRUSSES
Simultaneous structural and control optimization via linear quadratic regulator eigenstructure assignment
05 p0594 N88-13622
Continuum modeling of large lattice structures: Status and projections
[NASA-TP-2767]
06 p0672 N88-14115
Buckling of braced monosymmetric cantilevers: Timoshenko energy approach
[PB87-133849]
06 p0723 N88-14445
Chromic acid anodizing of aluminum foil
[NASA-CR-178417]
07 p0837 N88-15077
Space station structures development
[NASA-CR-179261]
09 p1133 N88-16792
Optimized structure design using reanalysis techniques
09 p1180 N88-17067
Solar concentrator advanced development program, task 1
[NASA-CR-179489]
10 p1350 N88-18068
The integration of a mesh reflector to a 15-foot box truss structure. Task 3: Box truss analysis and technology development
[NASA-CR-178228]
11 p1497 N88-18941
Control augmented structural synthesis
[NASA-CR-4132]
13 p1721 N88-20290
A 60-meter erectable assembly concept for a control of flexible structures flight experiment
[NASA-TM-100497]
14 p1873 N88-21190
A sequentially deployable structure for space applications
14 p1875 N88-21202
Aerospatiale unfurlable reflector and associated mechanisms
14 p1875 N88-21203
Motion synchronization of a mechanism to deploy and restow a truss beam
14 p1925 N88-21474
Continuum modeling and dynamic analysis of large truss structures
17 p2349 N88-23995
Mobile remote manipulator system for a tetrahedral truss
[NASA-CASE-MSC-20985-1] 20 p2765 N88-26398
Collet lock joint for space station truss
[NASA-CASE-MSC-21207-1] 23 p3222 N88-29180
Clevis joint for deployable space structures
[NASA-CASE-LAR-13898-1] 24 p3380 N88-30130

RYPTAMINES
NT SEROTONIN

SUNAMI WAVES
Moving ionospheric perturbations induced by wave trains propagating through ocean 09 p1239 N88-17427

BE CATHODES
NT PHOTOCATHODES
NT THERMIONIC CATHODES
Improved cathode life testing
REPT-3189-T]
02 p0168 N88-11056
High-current density, high-brightness electron beams om large-area lanthanum hexaboride cathodes
AD-A187700]
11 p1477 N88-18813
Program to research laser-driven thermionic electron urces for free electron lasers
D-A190473]
15 p2072 N88-22353

E HEAT EXCHANGERS
Qualification of expansion and joint welding procedures tube-to-tubesheet joints for heat exchangers in nuclear wer plants
E87-703526]
05 p0589 N88-13592

Test methodology for infrared tubular heaters
[PB88-160916]
12 p1626 N88-19728
Development of protective coatings for ceramic tubular components
[PB88-197165]
20 p2776 N88-26463
Qualification of expansion and welding procedures of tube-to-tubesheet joints for heat exchangers in nuclear power plants
[DE88-701621]
23 p3221 N88-29174

TUBES
Studies of heat and mass transfer during chemical vapor deposition
17 p2338 N88-23953

TUBING
U PIPES (TUBES)

TUMORS
NT CANCER
NT NEOPLASMS

TUNABLE LASERS
Status, development of laser devices in China
03 p0303 N88-11907
NO2 heterodyne frequency measurements with a tunable diode laser, a CO laser transfer oscillator and CO2 laser standards
[NASA-CR-182393]
06 p0710 N88-14353
Dynamic restructuring of pulsed CO2 laser frequency and multiple-peak generation in a cell with IR-absorbing gas in the resonator
07 p0919 N88-15580
Effect of multiplication of spectral components of multi-frequency lasing of pulsed tunable laser
07 p0920 N88-15586
Characteristics of LKI-501 tunable dye laser with dyes in solid matrix
07 p0920 N88-15587
Dye laser for holographic interferometry
07 p0920 N88-15588
Tunable Al2O3:Ti3 + -laser with optical pumping
09 p1237 N88-17415
Continuously frequency-tunable high-pressure CC2-laser with plasmatic cathode
09 p1238 N88-17418
Growth and characteristics of materials for tunable lasers in the near infrared spectral region
[NASA-CR-182501]
11 p1491 N88-18901
Resonantly-enhanced, four-photon ionization of krypton at laser intensities exceeding 10(12) W/sq cm
[DE88-005038]
11 p1544 N88-19229
Projected performance of RF-linac-driven free-electron lasers in the VUV and soft X-ray regions
[DE88-004294]
13 p1776 N88-20625
A picosecond tunable ultrashort cavity dye laser
14 p1902 N88-21361
Nonlinearly tunable wideband emission of infrared radiation by Al2O3:Ti laser 14 p1970 N88-21758
Tunable condensed-media laser with antiresonant ring cavity
14 p1971 N88-21764
Diode laser spectroscopy of chemical moieties at surfaces
[AD-A190710]
15 p2036 N88-22127
Efficient narrow linewidth waveguide dye laser pumped by CuCl laser
16 p2187 N88-23038
Observation of synchronously transient pumped mode-locking dye laser under negative cavity detuning
16 p2187 N88-23041
Generation of tunable coherent radiation in 3 micrometers-5 micrometers region using semiconductor lasers in external cavities
[AD-A190860]
16 p2212 N88-23202
Isotope separation using tuned laser and electron beam
[NASA-CASE-NPO-16907-1-CU]
18 p2483 N88-24732
A new near-infrared tunable-room temperature solid state laser La3Ga5SiO14:Cr(3+)
[DE88-011341]
21 p2953 N88-27543
Initial testing of the tunable diode laser absorption spectrometer for measuring HNO3 in diesel engine exhaust, stage 2
[PB88-193073]
21 p2970 N88-27641
The 1985-86 measurements with the tunable diode laser absorption spectrometer
[PB88-214002]
23 p3231 N88-29226
Growth and characterization of materials for tunable lasers in the near infrared spectral region
[NASA-CR-183132]
24 p3377 N88-30113
Spectroscopic studies with multiple quantum well materials with applications to optical signal processing at room temperature
[AD-A194171]
24 p3429 N88-30409

TUNDRA
Disturbance and recovery of Arctic Alaskan tundra terrain. A review of recent investigations
[AD-A184442]
04 p0467 N88-12887

TUNGSTEN
Progress toward a crystal streak camera using tungsten bronze crystals for the electrooptic material
[DE87-013110]
03 p0323 N88-12044
The effects of thin anodic films on the cyclic microstrain/macrostrain behavior of tungsten
05 p0597 N88-13650
Anomalies in electromagnetic absorption of circularly polarized ultrasonic waves by tungsten within Doppler-shifted cyclotron resonance range
06 p0775 N88-14756
Shielding analysis of a small compact space nuclear reactor
[AD-A185566]
06 p0779 N88-14784
Growth and electronic properties of strained metal overlayers
[DE87-010956]
10 p1417 N88-18463
Creep behavior of tungsten/niobium and tungsten/niobium-1 percent zirconium composites
[NASA-TM-100804]
11 p1460 N88-18707
The effects of various conductor components on Nb3Sn filament prestrain in cable-in-conduit conductors
[DE88-003956]
11 p1479 N88-18824
Tungsten-carbon multilayer system studied with X-ray scattering
[DE88-005749]
13 p1735 N88-20373
Properties of reactively sputtered WNx films Zhao, X. -A.
[AD-A188711]
13 p1835 N88-20976
Compatibility in space reactor fuel systems
[DE88-005698]
13 p1839 N88-21004
Dynamic fracture toughness evaluation by measurement of CTOD
[WNS/ASD-88-02]
16 p2178 N88-22982
Creep behavior of tungsten/niobium and tungsten/niobium-1 percent zirconium composites
17 p2425 N88-24427
Irradiation effects on tungsten stabilized martensitic steels
[DE88-007074]
18 p2486 N88-24748
Low temperature film growth of the oxides of zinc, aluminum and vanadium (and related systems, oxides of gold and germanium, nitrides of aluminum and tungsten) by reactive sputter deposition
[AD-A193497]
23 p3191 N88-28986

TUNGSTEN ALLOYS
Equations for determining CVD tungsten-rhenium alloy composition and plating rate
[DE87-008831]
01 p0024 N88-10152
Reduced-activation ferritic steels: A comparison with Cr-Mo steels
[DE88-000332]
03 p0290 N88-11826
Mechanical property evaluation of a series of commercial tungsten alloys
[AD-A185440]
05 p0565 N88-13446
The effect of ion implantation on the corrosion behavior of a high-density sintered tungsten alloy
[AD-A185713]
06 p0683 N88-14185
Corrosion behavior of high density tungsten alloys
[AD-A187108]
09 p1143 N88-16852
Corrosion of tungsten alloys in marine environments
17 p2320 N88-23854
Irradiation effects on tungsten stabilized martensitic steels
[DE88-007074]
18 p2486 N88-24748
Low-chromium reduced-activation ferritic steels
[DE88-009060]
19 p2617 N88-25524
Formation of metastable structures and amorphous phases in Cu-W alloys using the triod sputtering technique
[DE88-009051]
21 p2915 N88-27298
Hot isostatic pressing of tungsten-nickel-iron composites
[FOA-C-20698-2.1]
22 p3056 N88-28135

TUNGSTEN CARBIDES
Surface chemistry of transition metal carbides: A theoretical analysis
[AD-A184237]
03 p0291 N88-11829

TUNGSTEN COMPOUNDS
NT TUNGSTEN CARBIDES
Improved cathode life testing
[REPT-3189-T]
02 p0168 N88-11056
Results from the melting of tungsten composites under microgravity (TEXUS 10 flight)
[FOA-C-20676-2.1]
05 p0571 N88-13482

TUNGSTEN INERT GAS WELDING
U GAS TUNGSTEN ARC WELDING

TUNING
Fast autotuning of a hydrogen maser by cavity Q modulation
04 p0436 N88-12707
Optically tuned MM-wave IMPATT source
[AD-A185250]
05 p0577 N88-13523
Tailorable infrared sensing device with strain layer superlattice structure
[NASA-CASE-NPO-16607-1-CU]
06 p0788 N88-14836
Simplified self-tuning control algorithms
[OUEL-1657/86]
07 p0907 N88-15494
Operation of electron-beam controlled CO2 laser at 6 atmospheres
11 p1468 N88-18758

Polarization effects in laser-pumped Nd:YAG lasers [DE88-004019] 11 p1492 N88-18904
Optimal placement of tuning masses for vibration reduction in helicopter rotor blades [NASA-TM-100562] 13 p1782 N88-20665
Development of aeroelastic analysis methods for turborotors and propfans, including mistuning 16 p2219 N88-23244
State of tuning [NASA-TT-20195] 18 p2561 N88-25205
Tuning a major part of a clustering algorithm [AD-A191446] 20 p2836 N88-26821
Aircraft interior noise reduction by alternate resonance tuning [NASA-CR-182540] 20 p2849 N88-26909
Visible tunable source [DE88-006442] 20 p2854 N88-26944
Prediction of the aeroelastic behavior of tuned blades. Application to aircraft engines [ISAL-87-0046] 21 p2897 N88-27199
An electronically tuned, stable 8415-MHz dielectric resonator FET oscillator for space applications 22 p3068 N88-28205
Experimental investigation of propfan aeroelastic response in off-axis flow with mistuning [NASA-TM-101320] 22 p3089 N88-28344

TUNING FORK GYROSCOPES
An analysis of DREO's (Defence Research Establishment Ottawa) analog rebalance loops for the CSG-2 (Canadian Strapdown Gyroscope) tuned-rotor gyroscope [AD-A188577] 12 p1629 N88-19749
A LQG regulator for the angular motion of the rotor at a tuned gyroscope [INPE-4280-PRE/1152] 12 p1631 N88-19759

TUNISIA
Monitoring Tunisia's steppes with SPOT 22 p3097 N88-28390

TUNNEL DIODES
Nanoelectronics [AD-A186969] 09 p1156 N88-16930
SIS (Superconductor-Insulator-Superconductor) mixer research [AD-A192908] 20 p2879 N88-27092

TUNNEL RESISTORS
U ELECTRON TUNNELING
U RESISTORS

TURBIDITY
Two-layer stratified flow analysis of gravity currents and turbidity currents in lakes, reservoirs and the ocean 04 p0463 N88-12864
Turbidity patterns in the delta waters of southwest Netherlands on Thematic Mapper (TM) and multispectral scanner (MSS) satellite images [BCRS-86-06] 16 p2227 N88-23303
Satellite remote sensing of turbidity and sediment concentration in Lagoa dos Patos 17 p2355 N88-24032

TURBINE BLADES
Modeling and measurement of heat transfer on turbine blade tips 01 p0006 N88-10032
Investigation of the excitation of turbine blade vibration in axial compressors in rotating stall [ETN-87-90377] 01 p0007 N88-10035
Experimental determination of the oscillatory forces on two turbine blade profiles [ETN-87-90417] 01 p0007 N88-10037
The effect of different packagings on the vibration behavior and the coupling factors of steam turbine blading [ETN-87-90425] 01 p0056 N88-10357
The influence of high free stream turbulence, intensive cooling and wake on the external heat transfer of convectively cooled gas turbine blades [ETN-87-90432] 01 p0056 N88-10360
Blade loss transient dynamics analysis, volume 1. Task 2: TETRA 2 theoretical development [NASA-CR-179632] 02 p0125 N88-10791
Blade loss transient dynamics analysis, volume 2. Task 2: TETRA 2 user's manual [NASA-CR-179633] 02 p0126 N88-10792
Comparison between numerical solutions and measurements for a high speed turbine blade [PNR90402] 02 p0172 N88-11082
Blade excitation criteria developed for aero derived engines in Arctic Alaska [PNR90368] 02 p0182 N88-11131
Turbine Engine Hot Section Technology, 1985 [NASA-CP-2405] 02 p0184 N88-11140
Development of heat flux sensors for turbine airfoils 02 p0184 N88-11143
Prediction of turbine blade heat transfer 02 p0187 N88-11162
3D inelastic analysis methods for hot section components 02 p0187 N88-11164
3-D inelastic analysis methods for hot section components 02 p0187 N88-11165
Component specific modeling 02 p0187 N88-11166
Constitutive modeling of superalloy single crystals with verification testing 02 p0188 N88-11169
Constitutive modeling for isotropic materials 02 p0188 N88-11171
Constitutive modeling for isotropic materials 02 p0188 N88-11172
Turbine airfoil deposition models and their hot corrosion implications 02 p0189 N88-11178
Experimental verification of vapor deposition rate theory in high velocity burner rigs 02 p0189 N88-11179
Thermal expansion mismatch and oxidation in thermal barrier coatings 02 p0189 N88-11182
Finite element analysis of three-dimensional steady and unsteady temperature fields (computation of temperature distribution of turbine blade with composite cooling) 03 p0300 N88-11887
Local heat/mass transfer and pressure drop in a two-pass rib-roughened channel for turbine airfoil cooling [NASA-CR-179635] 03 p0322 N88-12039
Crack initiation and propagation due to cyclic thermal gradients --- aircraft turbine blades [ESA-TT-1023] 03 p0336 N88-12114
National Aerospace Laboratory experiment 04 p0404 N88-12509
Simulated service test behavior of various internal and external coatings applied on CF6-50 first stage turbine blades [NLR-MP-86018-U] 05 p0549 N88-13343
Thermal finite-element analysis of space shuttle main engine turbine blade [NASA-TM-100117] 05 p0610 N88-13745
STAEBL/general composites with hygrothermal effects (STAEBL/GENCOM) [NASA-TM-100266] 05 p0611 N88-13754
Accurate rotor loads prediction using the FLAP (Force and Loads Analysis Program) dynamics code [DE88-001109] 05 p0623 N88-13815
Research on internal fluid mechanism between turbine blades 06 p0676 N88-14138
Development of transonic speed cascade design method using Euler code and inverse solution 06 p0676 N88-14139
Experimental study of secondary flow in the presence of two jet arrays on the wall of a turbine blade [ECL-87-11] 08 p0987 N88-15981
Creep and fatigue research efforts on advanced materials 09 p1119 N88-16701
VAWT (Vertical-Axis Wind Turbine) stochastic loads produced by atmospheric turbulence [DE88-001355] 09 p1187 N88-17110
A comparison of the predicted and measured gravitational stresses in VAWT (Vertical Axis Wind Turbine) blades [DE88-002113] 09 p1187 N88-17111
Advanced Technology for Aero Gas Turbine Components [AGARD-CP-421] 10 p1279 N88-17647
A research program on the aerodynamics of a highly loaded turbine stage 10 p1280 N88-17655
Advanced techniques employed in blade cooling research 10 p1281 N88-17659
Transonic blade design on rotational stream surfaces 10 p1282 N88-17671
Wake interaction effects on the transition process on turbine blades [AD-A188020] 10 p1332 N88-17962
Unsteady heat transfer in turbine blade ducts: Focus on combustor sources [NASA-TM-100815] 11 p1486 N88-18870
Testing of a one-bladed 30-meter-diameter rotor on the DOE/NASA Mod-O wind turbine [NASA-TM-100274] 11 p1509 N88-19014
Fatigue load measurements and evaluation of the 25m Horizontal Axis Wind Turbine (HAWT) at Petten, The Netherlands [NLR-MP-86054-U] 13 p1782 N88-20660
Nonlinear structural analysis of a turbine airfoil using the Walker viscoplastic material model for B1900 + Hf 14 p1932 N88-21522
New airfoil sections for straight bladed turbine [DE88-701075] 14 p1942 N88-21588
Aero/structural tailoring of engine blades (AERO/STAEBL) [NASA-CR-180805] 14 p1959 N88-21682
Structural tailoring of high-speed turbine blades (SSME/STAEBL) 15 p2080 N88-22398
Advanced probabilistic methods for quantifying the effects of various uncertainties in structural response 15 p2080 N88-22401
Model study of thermal stresses in gas-turbine blades with protective coating 16 p2179 N88-22989
Dependence of structure of stabilized ZrO2 coatings on condensation rate 16 p2180 N88-22990
Two-equation low-Reynolds-number turbulence modeling of transitional boundary layer flows characteristic of gas turbine blades [NASA-CR-4145] 16 p2209 N88-23185
Lewis Structures Technology, 1988. Volume 1: Structural Dynamics [NASA-CP-3003-VOL-1] 16 p2217 N88-23226
Low-cost optical data acquisition system for blade vibration measurement 16 p2219 N88-23240
SSME single-crystal turbine blade dynamics 16 p2221 N88-23257
Vanadic hot corrosion of gas turbine blade coating materials 17 p2321 N88-23864
The effect of operating temperature and turbine blade cooling on Brayton cycle space power systems 17 p2435 N88-24489
A 3 MW wood fired gas turbine at Red Boiling Springs, Tennessee 18 p2536 N88-25051
Recent advances in capacitance type of blade tip clearance measurements [NASA-TM-101291] 19 p2603 N88-25460
New super alloys used in turbochargers 19 p2634 N88-25628
Computational study on thermal efficiency of ceramic gas turbine [DE88-753114] 20 p2809 N88-26667
T55-L-714 engine development and qualification. Engine M11 low cycle fatigue test report. (0213-005-87) [AD-A192765] 21 p2897 N88-27197
Prediction of the aeroelastic behavior of tuned blades. Application to aircraft engines [ISAL-87-0046] 21 p2897 N88-27199
Advanced computational methods for turbomachinery blade design [PNR90438] 22 p3044 N88-28065
Structural Tailoring of Advanced Turboprops (STAT) [NASA-CR-180861] 22 p3045 N88-28074
Probabilistic structural analysis to quantify uncertainties associated with turbopump blades [NASA-TM-100278] 22 p3050 N88-28094
Thermal barrier coating life-prediction model development [NASA-CR-179507] 22 p3058 N88-28142
Optimization of nondestructive control of ceramic pieces for aeronautical turbines [ETN-88-92884] 22 p3059 N88-28149
Interaction of creep and fatigue damage in gas turbine blade material [PNR90440] 22 p3088 N88-28335
The mechanical behavior of surface modified ceramics [DE88-010564] 23 p3196 N88-29022
Dynamic response of a 330-kW horizontal axis wind turbine generator [DE88-001136] 23 p3228 N88-29212
Numerical solutions of unsteady inviscid transonic turbine cascade flows [AD-A196111] 24 p3316 N88-29748
User's manual for three dimensional boundary layer (BL3-D) code [NASA-CR-174899] 24 p3369 N88-30063
Impact of ETO propellants on the aerothermodynamic analyses of propulsion components [NASA-TM-101303] 24 p3374 N88-30094

TURBINE ENGINES
NT CONVERTIBLE FAN-SHAFT ENGINES
NT GAS TURBINE ENGINES
NT J-57 ENGINE
NT JET ENGINES
NT RAMJET ENGINES
NT SUPERSONIC COMBUSTION RAMJET ENGINES
NT TF-30 ENGINE
NT TURBOFAN ENGINES
NT TURBOJET ENGINES
NT TURBOPROP ENGINES
Blade loss transient dynamics analysis, volume 1. Task 2: TETRA 2 theoretical development [NASA-CR-179632] 02 p0125 N88-10791
Blade loss transient dynamics analysis, volume 2. Task 2: TETRA 2 user's manual [NASA-CR-179633] 02 p0126 N88-10792
Evaluating and testing thermographic phosphors for turbine-engine temperature measurements [DE87-011772] 02 p0174 N88-11090
Development of heat flux sensors for turbine airfoils 02 p0184 N88-11143
Film cooling heat transfer on a turbine airfoil 02 p0186 N88-11156
Thermal barrier coating life prediction model development 02 p0190 N88-11185
USSR report: Engineering and equipment [JPRS-UEQ-87-008] 04 p0423 N88-12621
Thermal finite-element analysis of space shuttle main engine turbine blade [NASA-TM-100117] 05 p0610 N88-13745

Recent advances in high temperature instrumentation for hot section applications
[NASA-TM-100282] 06 p0707 N88-14339
Creep-fatigue cracking in high temperature turbine rotors 06 p0720 N88-14426
Directions in propulsion control
08 p0956 N88-15799
Improved silicon nitride for advanced heat engines
[NASA-CR-175006] 08 p0973 N88-15886
Turbine engine monitoring systems: Can they benefit component improvement program management?
[AD-A186992] 09 p1120 N88-16706
Turbine flow meter with optical fiber pick-up
[NAL-TR-923] 09 p1169 N88-17009
Measurements of gas turbine combustor and engine augmentor tube sooting characteristics
[AD-A187831] 11 p1440 N88-18592
Utilization of parallel processing in solving the inviscid form of the average-passage equation system for multistage turbomachinery
[NASA-TM-89845] 14 p1868 N88-21160
NNEPEQ: Chemical equilibrium version of the Navy/NASA Engine Program
[NASA-TM-100851] 14 p1868 N88-21161
Aeropropulsive characteristics of isolated combined turbojet/ramjet nozzles at Mach numbers from 0 to 1.20
[NASA-TP-2814] 17 p2299 N88-23757
Ceramics for turbine engines
17 p2323 N88-23873
Thermal cyclic durability testing of ceramic materials for turbine engines 17 p2325 N88-23886
A high fidelity real-time simulation of a small turboshaft engine
[NASA-TM-100991] 20 p2761 N88-26378
JTDE 1 XTE34 materials research and development report
[AD-A194268] 22 p3044 N88-28063

TURBINE PUMPS
Seal technology for liquid oxygen (LOX) turbopumps
[NASA-CR-174866] 05 p0591 N88-13603
Incipient failure detection of space shuttle main engine turbopump bearings using vibration envelope detection
05 p0595 N88-13629
Thermal finite-element analysis of space shuttle main engine turbine blade
[NASA-TM-100117] 05 p0610 N88-13745
STAEBL/general composites with hygrothermal effects (STAEBL/GENCOM)
[NASA-TM-100266] 05 p0611 N88-13754
Evaluation of load tracks and wear of two sets of bearings from space shuttle main engine high pressure oxygen turbopumps
[NASA-CR-178969] 07 p0861 N88-15223
The determination of equivalent bearing loading for the BSMT that simulate SSME high pressure oxidizer turbopump conditions using the SHABERTH/SINDA computer programs 07 p0925 N88-15623
An expert system to analyze high frequency dependent data for the space shuttle main engine turbopumps
08 p1060 N88-16399
Disk pumping test
[AD-A187199] 11 p1440 N88-18591
Computer-aided design analysis of 57-mm, angular-contact, cryogenic turbopump bearings
[NASA-TP-2816] 11 p1496 N88-18933
Electromagnetic dampers for cryogenic applications
16 p2218 N88-23231
SSME single-crystal turbine blade dynamics
16 p2221 N88-23257
Rotor self-lubricating axial stop
[NASA-CASE-MFS-28273-1] 17 p2344 N88-23974
Analysis of flow through pump of large rocket engine
19 p2637 N88-25646
Probabilistic structural analysis to quantify uncertainties associated with turbopump blades
[NASA-TM-100278] 22 p3050 N88-28094
Evaluation of transfer films of Salox M on 440C for HPOTP bearing cage applications, task 119
[NASA-CR-179020] 23 p3223 N88-29184

TURBINE WHEELS
Determination of the critical crack length a (sub IC) in turbine discs
[PB87-144812] 07 p0820 N88-14986

TURBINES
NT AXIAL FLOW TURBINES
NT GAS TURBINES
NT SHROUDED TURBINES
NT STEAM TURBINES
NT SUPERSONIC TURBINES
NT WIND TURBINES
Performance of supersonic impingement radial turbines 06 p0712 N88-14367
Design and testing of a small radial turbine for auxiliary power units 10 p1281 N88-17661
Research on fluid dynamic energy separation
[DE88-002776] 10 p1339 N88-18001
A combined Rankine/Brayton pulse power cycle
17 p2435 N88-24490
Remote temperature-measurement instrumentation for a heated rotating turbine disk
[DE88-006456] 18 p2516 N88-24925
Extensive verification of blade-to-blade flow code based on Denton scheme 19 p2638 N88-25654
C-CAMP: A closed cycle alkali metal power system
[DE88-009715] 19 p2688 N88-25975
Numerical computation of three-dimensional turbulent flow in tightly curved ducts and spiral turbine casings
[ETN-88-92362] 21 p2948 N88-27511
Calibration of the portable wear metal analyzer
[AD-A192971] 21 p2950 N88-27524
The effects of inlet turbulence and rotor/stator interactions on the aerodynamics and heat transfer of a large-scale rotating turbine model. Volume 3: Heat transfer data tabulation 65 percent axial spacing
[NASA-CR-179468] 23 p3180 N88-28930
The effects of inlet turbulence and rotor/stator interactions on the aerodynamics and heat transfer of a large-scale rotating turbine model. Volume 2: Heat transfer data tabulation. 15 percent axial spacing
[NASA-CR-179467] 24 p3326 N88-29804
Studies of gas turbine heat transfer airfoil surface and end-wall cooling effects
[AD-A195165] 24 p3326 N88-29805
An investigation of constitutive models for predicting viscoplastic response during cyclic loading
[AD-A194875] 24 p3385 N88-30163

TURBOCHARGERS
U SUPERCHARGERS
U TURBOCOMPRESSORS

TURBOCOMPRESSORS
Modeling and measurement of heat transfer on turbine blade tips 01 p0006 N88-10032
Investigation of the excitation of turbine blade vibration in axial compressors in rotating stall
[ETN-87-90377] 01 p0007 N88-10035
Design verification tests for an axial gap permanent magnet compressor motor
[DE87-014360] 02 p0167 N88-11049
Three-dimensional calculation in high subsonic axial compressor rotor and its comparison with L2F velocity measurement 03 p0300 N88-11886
Automated design of controlled diffusion blades
[NASA-TM-100251] 05 p0542 N88-13304
Effects of free stream turbulence, Reynolds number and incidence angle on axial turbine cascade performance
05 p0548 N88-13339
Post stall behavior in axial-flow compressors
[AD-A185712] 06 p0665 N88-14081
Flow in labyrinth seals and its influence on rotor stability of turbocompressors 07 p0851 N88-15168
Technology developments for a compound cycle engine 09 p1107 N88-16637
Advanced Technology for Aero Gas Turbine Components
[AGARD-CP-421] 10 p1279 N88-17647
Optimisation of military compressors for weight and volume 10 p1279 N88-17649
Operation of gas turbine engines in dust-laden environments 10 p1280 N88-17654
Investigation of dihedral effects in compressor cascades 10 p1282 N88-17672
Possibilities for on-line surge suppression by fast guide vane adjustment in axial compressors
10 p1283 N88-17674
Design and development of an advanced F100 compressor 10 p1283 N88-17678
Experimental investigation of a supercritical compressor rotor blade section 10 p1284 N88-17680
Radial mixing in turbomachines
[AD-A188028] 11 p1482 N88-18847
Small engine components test facility turbine testing cell
[NASA-TM-100887] 15 p2019 N88-22037
Supersonic axial-flow fan flutter
16 p2221 N88-23255
Research on aero-thermodynamic distortion induced structural dynamic response of multi-stage compressor blading
[AD-A192169] 18 p2456 N88-24584
Servojet retrofit
[AD-A191075] 18 p2522 N88-24964
New super alloys used in turbochargers
19 p2634 N88-25628
Experimental determination of aerodynamic damping in a three-stage transonic axial-flow compressor
[NASA-TM-100953] 21 p2897 N88-27200
Modeling of large stall in axial compressors
[VKI-TN-164] 23 p3213 N88-29124

TURBOCONVERTERS
U TURBOGENERATORS

TURBOELECTRIC CONVERSION
U TURBOGENERATORS

TURBOFAN AIRCRAFT
NT BOEING 737 AIRCRAFT
NT CONCORDE AIRCRAFT
NT F-111 AIRCRAFT
Multiple-Purpose Subsonic Naval Aircraft (MPSNA): Multiple Application Propfan Study (MAPS)
[NASA-CR-175104] 23 p3177 N88-28917

TURBOFAN ENGINES
NT CONVERTIBLE FAN-SHAFT ENGINES
NT TF-30 ENGINE
NT TF-34 ENGINE
First article test noise survey of the A/F32T-9 large turbo fan engine enclosed noise suppressor system, Sky Harbor IAP (International Airport), Phoenix, Arizona
[AD-A183799] 01 p0090 N88-10588
The wide chord fan blade: A Rolls Royce first
[PNR90416] 02 p0125 N88-10789
Impact and promise of NASA aeropropulsion technology 09 p1118 N88-16698
Turbine engine monitoring systems: Can they benefit component improvement program management?
[AD-A186992] 09 p1120 N88-16706
Engine flow simulation for wind tunnel testing at NLR
[NLR-MP-87011-U] 13 p1723 N88-20305
Exhaust-gas pressure and temperature survey of F404-GE-400 turbofan engine
[NASA-TM-88273] 13 p1724 N88-20307
A microprocessor-based real-time simulator of a turbofan engine
[NASA-TM-100889] 14 p1868 N88-21163
Linear state space modeling of a turbofan engine
[AD-A190110] 15 p2019 N88-22035
Noise assessment of unsuppressed TF-34-GE-100A engine at Warfield ANG, Baltimore, Maryland
[AD-A189966] 15 p2129 N88-22702
Augmentor performance of an F100 engine model derivative engine in an F-15 airplane
[NASA-TM-86745] 17 p2307 N88-23805
Euler analysis of a swirl recovery vane design for use with an advanced single-rotation propfan
[NASA-TM-101357] 24 p3320 N88-29771
Developing the Rolls-Royce Tay
[PNR90447] 24 p3327 N88-29809
High performance turbofan afterburner systems
24 p3347 N88-29922
Contamination and distortion of steady flow field induced by discrete frequency disturbances in aircraft gas engines
[AD-A195440] 24 p3370 N88-30069
Development and installation of an instrumentation package for GE F404 investigative testing
[AD-A196265] 24 p3376 N88-30107

TURBOFANS
Technical-economical evaluation of a novel propfan concept in comparison with the turbofan for the nineties
[ETN-88-91022] 11 p1441 N88-18596
Measurement and analysis of the noise radiated by low Mach numbers centrifugal blowers
[AD-A189226] 13 p1833 N88-20966
Holographic interferometry for flow visualization studies in high speed fans
[PNR90459] 22 p3045 N88-28072

TURBOGENERATORS
Innovating systems and techniques for the diagnosis of materials and industrial plants
[CISE-3856] 08 p0976 N88-15901
Status of CEA design and simulation studies of a 200 KWe turboelectric space power system
17 p2400 N88-24268
Power source selection for neutral particle beam systems 17 p2407 N88-24314
Turbomachinery in space 17 p2408 N88-24321
Rotating-hoop, pulsed-energy converter
17 p2426 N88-24433

TURBOJET AIRCRAFT
U JET AIRCRAFT

TURBOJET ENGINE CONTROL
Testing of the engine compartment fire extinguishing system in the F/EF-111 aircraft
[AD-A188801] 12 p1576 N88-19423

TURBOJET ENGINES
NT J-57 ENGINE
NT TF-30 ENGINE
NT TURBOFAN ENGINES
NT TURBOPROP ENGINES
High-speed inlet research program and supporting analyses 08 p0958 N88-15811
The coming revolution in turbine engine technology
10 p1279 N88-17648
Numerical simulation of diffuser/combustor dome interaction 10 p1281 N88-17663
Development of vertical takeoff aircraft with turbojet engines in Germany 10 p1309 N88-17822
Aircraft emissions characterization: TF41-A2, TF30-P103 and TF30-P109 engines
[AD-A192053] 18 p2466 N88-24638

Vibrational impacts of hush house operation
[DE88-006983] 21 p2899 N88-27207
Air intake aerodynamics 24 p3318 N88-29762
Semiempirical methods for airbreathing missiles
24 p3318 N88-29763
Evaluation of the advanced air breathing propulsion concepts, executive summary
[ESA-CR(P)-2540] 24 p3325 N88-29802
Evaluation of advanced air breathing concepts. Volume 1: Executive summary
[ESA-CR(P)-2539] 24 p3326 N88-29806

TURBOMACHINE BLADES
NT COMPRESSOR BLADES
NT ROTOR BLADES (TURBOMACHINERY)
NT STATOR BLADES
NT TURBINE BLADES
A flow function method for the axisymmetric calculation of the transonic turbomachine flow taking into account the flow differences in circumferential direction
[ETN-87-90428] 01 p0056 N88-10359
The use of holographic interferometry for turbomachinery fan evaluation during rotating tests
[PNR90390] 02 p0176 N88-11098
The unsteady gas flow through stator and rotor of a turbomachine 10 p1281 N88-17660
High Reynolds number pump facility for cavitation research
[AD-A189310] 13 p1765 N88-20558
Calculation of displacement, constraints and eigenmodes of rotating blades
[ETN-88-92296] 16 p2224 N88-23277
Structural optimization of fiber composite turbomachine blades
[ETN-88-92351] 20 p2760 N88-26372
Coupled inviscid - boundary layer methods for turbomachinery blading design
[PNR90437] 22 p3076 N88-28260

TURBOMACHINERY
NT AXIAL FLOW TURBINES
NT CENTRIFUGAL COMPRESSORS
NT CENTRIFUGAL PUMPS
NT GAS TURBINES
NT SHROUDED TURBINES
NT STEAM TURBINES
NT SUPERSONIC TURBINES
NT TURBINE PUMPS
NT TURBINES
NT TURBOCOMPRESSORS
NT TURBOFANS
NT TURBOGENERATORS
NT WIND TURBINES
Navier-Stokes cascade analysis with a stiff Kappa-Epsilon turbulence solver
[NASA-TM-100218] 02 p0123 N88-10778
Optical flow diagnostic measurements in turbomachinery
[PNR90396] 02 p0172 N88-11081
Calculation of the three dimensional flow in the impeller of hydraulic turbomachines using a finite element method
[ETN-87-90612] 03 p0315 N88-11988
Application of Runge Kutta time marching scheme for the computation of transonic flows in turbomachines
[NASA-TM-86997] 04 p0394 N88-12461
Identification of perturbations in turbomachines by the analysis of pressure signals, vibrations and wavelike motions
[ETN-88-90602] 05 p0590 N88-13600
Numerical simulation of flows in axial and radial turbomachines using Euler solvers
06 p0713 N88-14372
Supersonic turbines for organic fluid Rankine cycles from 3 to 1300 kW 06 p0713 N88-14375
Blade vibration due to different flow excitation
07 p0851 N88-15166
Blade excitation due to unsteady flow phenomena
07 p0851 N88-15167
A multistage mesh generator for solving the average-passage equation system
[NASA-CR-179539] 08 p0951 N88-15769
Aeropropulsion '87. Session 3: Internal Fluid Mechanics Research
[NASA-CP-10003-SESS-3] 08 p0954 N88-15790
Turbomachinery 08 p0955 N88-15792
The Goddard Space Flight Center mechanical cooler program 08 p0983 N88-15944
Finite Element Calculation Methods and Their Application to Turbomachinery Flows, volume 1
[VKI-LS-1987-05-VOL-1] 08 p0985 N88-15960
Inviscid flows, part 1: Formulation of inviscid rotational flow problems by velocity potential and stream function methods. Applications to turbomachines
08 p0985 N88-15964
Inviscid flows, part 2 08 p0985 N88-15966
Viscous flows, part 1 08 p0986 N88-15967
Viscous flows, part 2 08 p0986 N88-15968
Modeling the unsteady flow found in axial turbomachinery
[ECL-87-07] 08 p0987 N88-15980
Numerical modeling of multidimensional flow in seals and bearings used in rotating machinery
[NASA-TM-100779] 09 p1165 N88-16988
The unsteady gas flow through stator and rotor of a turbomachine 10 p1281 N88-17660
Transonic blade design on rotational stream surfaces
10 p1282 N88-17671
An L-U implicit multigrid algorithm to solve the Euler equations for transonic flow in rotating turbomachinery passages 13 p1718 N88-20270
Numerical analysis of three-dimensional viscous internal flows
[NASA-TM-100878] 14 p1861 N88-21116
Utilization of parallel processing in solving the inviscid form of the average-passage equation system for multistage turbomachinery
[NASA-TM-89845] 14 p1868 N88-21160
Visualization of flows in turbomachinery
[AD-A189927] 15 p2063 N88-22299
Aeroelastic forced response analysis of turbomachinery 16 p2220 N88-23247
Forced response unsteady aerodynamics in a multistage compressor 18 p2512 N88-24903
Fluid dynamics of high performance turbomachines
[AD-A192073] 19 p2664 N88-25840
Improved method for stress and compatibility analysis of multicomponent rotating systems
[NASA-TM-100884] 19 p2680 N88-25935
A diagonally inverted LU implicit multigrid scheme
[NASA-TM-100911] 20 p2753 N88-26340
Improved 3-D turbomachinery CFD algorithm
[NASA-CR-179364] 20 p2801 N88-26619
Advanced computational methods for turbomachinery blade design
[PNR90438] 22 p3044 N88-28065
Investigation of the validity of Reynolds averaged turbulence models at the frequencies that occur in turbomachinery
[NASA-CR-182162] 22 p3048 N88-28087
Two-dimensional flow through a turbine cascade
[PDR/CFDU/IC/34] 22 p3076 N88-28264
Non-reflecting boundary conditions for computations of unsteady flows in turbomachines
[PNR90469] 22 p3079 N88-28284
The role of acoustic resonances in unsteady turbomachinery aerodynamics
[PNR90455] 22 p3147 N88-28720
Three-dimensional Navier-Stokes simulations of turbine rotor-stator interaction
[NASA-TM-100081] 24 p3316 N88-29750
An unconditionally stable Runge-Kutta method for unsteady flows
[NASA-TM-101347] 24 p3321 N88-29780
Three-dimensional elliptic grid generation technique with application to turbomachinery cascades
[NASA-TM-101330] 24 p3372 N88-30078

TURBOPROP AIRCRAFT
NT C-130 AIRCRAFT
NT F-27 AIRCRAFT
NT OV-1 AIRCRAFT
Noise of a model high speed counterrotation propeller at simulated takeoff/approach conditions (F7/A7)
[NASA-TM-100206] 01 p0091 N88-10592
A hybrid numerical technique for predicting the aerodynamic and acoustic fields of advanced turboprops
[NASA-CR-174926] 03 p0374 N88-12352
Noise of a model counterrotation propeller with reduced aft rotor diameter at simulated takeoff/approach conditions (F7/A3)
[NASA-TM-100254] 05 p0647 N88-13961
Are windshear training aid recommendations appropriate for other than large jet transports? Pilot procedures: Shear models 10 p1275 N88-17635
Sound transmission through the walls of light aircraft: An investigation of structure-borne noise in a Handley Page 137 Jetstream 3 aircraft
[NASA-CR-182509] 10 p1405 N88-18376
Analysis of in-flight acoustic data for a twin-engined turboprop airplane
[NASA-CR-178389] 11 p1543 N88-19220
NASA advanced turboprop research and concept validation program
[NASA-TM-100891] 16 p2163 N88-22902
NASA/industry advanced turboprop technology program
[NASA-TM-100929] 18 p2466 N88-24641
Multiple-Purpose Subsonic Naval Aircraft (MPSNA): Multiple Application Propfan Study (MAPS)
[NASA-CR-175104] 23 p3177 N88-28917

TURBOPROP ENGINES
Advanced turboprop wing installation effects measured by unsteady blade pressure and noise
[NASA-TM-100200] 01 p0002 N88-10008
Analysis and test evaluation of the dynamic stability of three advanced turboprop models at zero forward speed
[NASA-CR-175025] 06 p0668 N88-14095
Analysis and test evaluation of the dynamic response and stability of three advanced turboprop models at low forward speed
[NASA-CR-175026] 06 p0668 N88-14096
Flaps-up takoff performance of the OV-1D aircraft with YT53-L-704 engine installed
[AD-A185960] 07 p0819 N88-14979
Impact and promise of NASA aeropropulsion technology 09 p1118 N88-16698
Design and aerodynamic performance of a small mixed-flow gas generator turbine
10 p1281 N88-17662
Gear systems for advanced turboprops
10 p1282 N88-17667
Computerized life and reliability modelling for turboprop transmissions
[NASA-TM-100918] 16 p2215 N88-23220
Development of aeroelastic analysis methods for turborotors and propfans, including mistuning
16 p2219 N88-23244
Vibration and flutter analysis of the SR-7L large-scale propfan 16 p2221 N88-23254
Experimental and analytical evaluation of the effects of simulated engine inlets on the blade vibratory stresses of the SR-3 model prop-fan
[NASA-CR-174959] 23 p3179 N88-28927

TURBOPUMPS
U TURBINE PUMPS

TURBOROTORS
U TURBINE WHEELS

TURBOSHAFTS
The design of a turboshaft speed governor using modern control techniques
[NASA-CR-175046] 01 p0053 N88-10339
Test stand performance of a convertible engine for advanced V/STOL and rotorcraft propulsion
[NASA-TM-100211] 03 p0266 N88-11679
The convertible engine: A dual-mode propulsion system 09 p1108 N88-16639
A high fidelity real-time simulation of a small turboshaft engine
[NASA-TM-100991] 20 p2761 N88-26378

TURBULENCE
NT ATMOSPHERIC TURBULENCE
NT CLEAR AIR TURBULENCE
NT GUSTS
NT HOMOGENEOUS TURBULENCE
NT ISOTROPIC TURBULENCE
NT LOW LEVEL TURBULENCE
NT MAGNETOHYDRODYNAMIC TURBULENCE
NT PLASMA TURBULENCE
Study of pickup of cometary ions in turbulent solar winds 01 p0113 N88-10725
Impact of turbulence modeling on numerical accuracy and efficiency of compressible flow simulations
[NASA-TM-88333] 02 p0173 N88-11088
Prediction of turbine blade heat transfer
02 p0187 N88-11162
Flow in a model turbine stator
02 p0187 N88-11163
Thermally driven convective cells and tokamak edge turbulence
[DE87-014424] 02 p0238 N88-11499
Fundamentals of turbulence for turbulence modeling and simulation 03 p0312 N88-11971
A deterministic approach to turbulence: Chaos in Rayleigh-Benard convection 03 p0313 N88-11975
On helicity fluctuations and the energy cascade in turbulence
[NASA-CR-178403] 03 p0321 N88-12028
Conservation and transport properties of turbulence with large density variations
[LA-10911-MS] 03 p0321 N88-12032
Investigation of low-speed turbulent separated flow around airfoils
[NASA-CR-177450] 04 p0396 N88-12471
Fully developed turbulence via Feigenbaum's period-doubling bifurcations
[DE88-000242] 04 p0441 N88-12739
Optical instrumentation and study of gas-solid suspension flows
[DE88-000147] 04 p0442 N88-12744
A multiple-time-scale turbulence model based on variable partitioning of turbulent kinetic energy spectrum
[NASA-CR-179222] 04 p0444 N88-12754
Tracking through turbulence at the Tonopah Test Range
[DE88-001448] 04 p0446 N88-12766
Input turbulence features at a megawatt-size wind turbine, Medicine Bow, Wyoming
[DE88-000098] 04 p0464 N88-12873

Using a new characterization of turbulent wind for accurate correlation of wind turbine response with wind speed
[DE88-001453] 04 p0466 N88-12881

The velocity structure and turbulence at the center of the Orion Nebula 04 p0521 N88-13201

A perspective of computational fluid dynamics
05 p0538 N88-13279

Effects of free stream turbulence, Reynolds number and incidence angle on axial turbine cascade performance
05 p0548 N88-13339

Vortical Flows Research Program of the Fluid Dynamics Research Branch
[NASA-TM-88332] 05 p0582 N88-13549

Measurement of local convective heat transfer coefficients from a smooth and roughened NACA-0012 airfoil: Flight test data
[NASA-TM-100284] 05 p0582 N88-13552

Isentropic analysis and interpretation: Operational applications to synoptic and mesoscale forecast problems
[AD-A184814] 05 p0626 N88-13830

Chaos: Chto Delat? (What is to be done?)
[DE88-000513] 05 p0643 N88-13933

Studies of supersonic turbulence and hot-wire response using Laser-Induced Fluorescence (LIF)
06 p0664 N88-14072

Turbulence, turbulence control, and drag reduction
[AD-A185643] 06 p0665 N88-14080

The production of turbulence in boundary layers: The role of microscale coherent motions
[AD-A185568] 06 p0703 N88-14313

European reacting flow research: A final assessment
[AD-A185833] 07 p0828 N88-15022

Reynolds-stress and dissipation rate budgets in a turbulent channel flow
[NASA-TM-89451] 07 p0852 N88-15174

Numerical solution of turbulent flow past a backward facing step using a nonlinear K-epsilon model
[NASA-CR-178421] 07 p0854 N88-15189

Feasibility studies of optical processing of image bandwidth compression schemes
[AD-A186073] 07 p0932 N88-15660

Velocity and density measurements in a turbulent nonpremixed flame with comparison to numerical model predictions
[DE87-014695] 08 p0967 N88-15854

On the correlation of plume centerline velocity decay of turbulent acoustically excited jets
[NASA-TM-100193] 09 p1114 N88-16681

Numerical simulation of heat transfer turbulence, volume 1
[AD-A185132] 09 p1159 N88-16947

Analysis of a turbulent premixed V-flame (influence of flame-thickening)
[NAL-TR-941] 10 p1299 N88-17770

Universal power spectra for wave turbulence: Applications to wind waves, flicker noise, solar wind spectrum and classical second sound
10 p1318 N88-17879

One-dimensional leakage-flow vibration instabilities
[DE88-002875] 10 p1330 N88-17947

Remote sensing of atmospheric crosswinds by utilizing speckle-turbulence interaction and optical heterodyne detection
[AD-A187580] 10 p1347 N88-18052

Wake effects in a Fayette 95-IIS wind turbine array
[DE88-001103] 10 p1349 N88-18063

Turbulence loads on the Howden 26-m-diameter wind turbine
[DE88-001118] 10 p1351 N88-18075

Study of resistive pressure-gradient-driven turbulence
[DE88-005062] 10 p1414 N88-18441

Superfluid turbulence in He II at elevated pressures
10 p1422 N88-18493

An experimental investigation of straight and curved annular wall jets
[NASA-CR-182546] 11 p1434 N88-18557

Turbulence modeling in non-inertial frames of reference
[NASA-CR-181646] 11 p1488 N88-18880

Sound propagation through a turbulent atmosphere: Experimental techniques and data analysis
[AD-A188891] 12 p1688 N88-20094

Systems near the onset and in the well-developed regimes of turbulence
[DE88-005365] 13 p1766 N88-20565

Calculations of viscous flows with a multigrid method
13 p1769 N88-20580

Power spectral density analysis of wind-shear turbulence for related flight simulations
[NASA-CR-182721] 13 p1802 N88-20773

On the zonal momentum balance at the equator
13 p1805 N88-20788

Observations on energy transport in tokamaks: A new formula for turbulent transport
[DE88-005309] 13 p1841 N88-21019

The 30 x 30 inch wind tunnel
[IC-AERO-87-01] 14 p1869 N88-21168

Problems in fluid dynamics
[NASA-CR-182678] 14 p1909 N88-21410

The turbulent heat flux in low Mach number flows with large density variations
[DE88-006445] 14 p1911 N88-21419

Interaction of a strong vortex with decaying turbulence
[DE88-007102] 14 p1911 N88-21420

Effect of flow convergence on turbulence level in stream 14 p1973 N88-21773

Numerical simulation of turbulent flames using vortex methods
[AD-A189813] 15 p2034 N88-22116

Basic instability mechanisms in chemically reacting subsonic and supersonic flows
[AD-A190101] 15 p2034 N88-22120

Random processes, turbulence and disordering fields
[AD-A190123] 15 p2063 N88-22303

Film cooling effectiveness on a flat plate in high free-stream turbulence using a single row of 30 deg slant-hole injectors
[AD-A190500] 15 p2147 N88-22816

On the validation of a code and a turbulence model appropriate to circulation control airfoils
[NASA-TM-100090] 16 p2156 N88-22864

On local approximations of the pressure-strain term in turbulence models 16 p2197 N88-23102

Shear-layer structures in near-wall turbulence
16 p2198 N88-23110

Wave-growth associated with turbulent spot in plane Poiseuille flow 16 p2199 N88-23116

On the prediction of equilibrium states in homogeneous turbulence
[NASA-CR-181659] 16 p2207 N88-23174

Simulation of laminar-turbulent transition in the vicinity of a wall
[AD-A191380] 16 p2208 N88-23180

Random processes, turbulence and disordering fields
[AD-A191399] 16 p2209 N88-23181

Two-equation low-Reynolds-number turbulence modeling of transitional boundary layer flows characteristic of gas turbine blades
[NASA-CR-4145] 16 p2209 N88-23185

Experimental study of bypass transition in a boundary layer
[NASA-TM-100913] 16 p2209 N88-23186

A proposal for the establishment of a center of excellence in theoretical geoplasma research
[AD-A189742] 16 p2231 N88-23327

Measurements of edge turbulence with Langmuir probes in currentless Heliotron E plasmas
[DE88-752313] 16 p2275 N88-23617

Surface curvature and pressure gradient effects on turbulent flow: An assessment based on numerical solution of the Reynolds equations 17 p2336 N88-23954

The effects of inlet turbulence and rotor/stator interactions on the aerodynamics and heat transfer of a large-scale rotating turbine model. Part 4: Aerodynamic data tabulation
[NASA-CR-179469] 17 p2339 N88-23956

Generation of flux tube waves in stellar convection zones. 1: Longitudinal tube waves
[NASA-TM-101152] 17 p2451 N88-24561

Prediction of laminar and turbulent flows past single and twin airfoils 18 p2457 N88-24589

Cross stream differencing for integral boundary layer equations
[AD-A191744] 18 p2509 N88-24886

Fast algorithm development for large-eddy simulation of circular-jet turbulence
[AD-A192044] 18 p2509 N88-24887

Three dimensional spectral energy measurement on turbulence subjected to a high degree of plane deformation
[ETN-88-92537] 18 p2511 N88-24696

Computational Fluid Mechanics
[NASA-CR-183022] 18 p2514 N88-24915

Modelling of thermal plasma systems
18 p2578 N88-25314

Correlations of velocity and temperature fluctuations in the stagnation-point flow of circular cylinder in turbulent flow
[NASA-TM-100930] 19 p2597 N88-25435

Turbulence and flame propagation
[PB87-228912] 19 p2612 N88-25499

Noise generation by air bubbles in water: An experimental study of creation and splitting
[AD-A192063] 19 p2664 N88-25839

Scaling laws for homogeneous turbulent shear flows in a rotating frame
[NASA-CR-181672] 19 p2665 N88-25847

Wind flow study: July 1987 and November-December 1987
[DE88-008969] 20 p2828 N88-26776

Summary of discussions at the Tenth Meeting of the Sandia Cooperative Group on the Aerothermochemistry of Turbulent Combustion
[DE88-008467] 21 p2910 N88-27269

Coupled experimental and theoretical investigations of instability, chaos and turbulence in an axisymmetric jet flow
[AD-A192943] 21 p2942 N88-27476

Characterization of accelerating pipe flow
[AD-A193065] 21 p2943 N88-27481

Tokamak magnetic turbulence over the safety factor range 0.6 less than q less than 3
[DE88-008421] 21 p3017 N88-27904

Project wind, phase 4 (smoke test), Meadow Brook Valley, Red Bluff, California
[AD-A194742] 22 p3128 N88-28596

Aerodynamics of seeing on large transport aircraft
[NASA-CR-183122] 23 p3174 N88-28896

The effects of inlet turbulence and rotor/stator interactions on the aerodynamics and heat transfer of a large-scale rotating turbine model. Volume 3: Heat transfer data tabulation 65 percent axial spacing
[NASA-CR-179468] 23 p3180 N88-28930

The effects of inlet turbulence and rotor/stator interactions on the aerodynamics and heat transfer of a large-scale rotating turbine model. Volume 2: Heat transfer data tabulation. 15 percent axial spacing
[NASA-CR-179467] 24 p3326 N88-29804

Recent insights into instability and transition to turbulence in open-flow systems
[NASA-CR-181693] 24 p3372 N88-30079

Comparisons of solar nebula models
24 p3451 N88-30539

TURBULENCE EFFECTS

Vortex/boundary-layer interactions: Data report, volume 1
[NASA-CR-181462] 02 p0121 N88-10768

Turbulence generation in combustion
[AD-A184810] 05 p0561 N88-13413

Measurement in a wind tunnel of the modification of mean wind and turbulence characteristics due to induction effects near wind turbine rotors
[DE88-000249] 07 p0815 N88-14963

Effects of turbulence on stationary and non-stationary processes in C-systems
[AD-A186215] 07 p0849 N88-15154

Numerical simulation of heat transfer turbulence, volume 2
[AD-A185130] 08 p0983 N88-15947

Numerical simulation of turbulent spots in channel and boundary layer flows 08 p0983 N88-15948

Heat transfer from impinging flame jets
[ETN-88-91610] 09 p1162 N88-16964

Effect of freestream turbulence on a two dimensional cascade, with different surface roughness, at high Reynolds number
[AD-A190615] 15 p2065 N88-22316

High power, high frequency radiation from beam-plasma interactions
[AD-A190207] 15 p2137 N88-22752

Investigation of intensity and phase fluctuations of an acoustic wave after crossing thermal turbulence
[ETN-88-92542] 17 p2395 N88-24238

Design of a mechanism to control wind tunnel turbulence 21 p2926 N88-27370

Turbulence effects on the droplet distribution behind airblast atomizers 24 p3346 N88-29915

Radiation transfer in gas turbine combustors
24 p3348 N88-29929

TURBULENCE METERS

Flight test equipment for the on-board measurement of wind turbulence 24 p3311 N88-29719

A summary of atmospheric turbulence measurements with specially-equipped aircraft in the US
24 p3312 N88-29727

Measurement and analysis of low altitude atmospheric turbulence obtained using a specially instrumented Gnat aircraft 24 p3313 N88-29728

TURBULENCE MODELS

NT K-EPSILON TURBULENCE MODEL

Investigation of the validity of Reynolds averaged turbulence models at the frequencies that occur in turbomachinery
[NASA-CR-182162] 22 p3048 N88-28087

Turbulence modelling of flows with non-uniform density 22 p3075 N88-28256

TURBULENT BOUNDARY LAYER

Experimental study of three-dimensional turbulent jet-solid boundary interaction 01 p0046 N88-10293

Heat transfer with very high free stream turbulence
02 p0186 N88-11161

Computation of turbulent flows using an extended k-epsilon turbulence closure model
[NASA-CR-179204] 03 p0312 N88-11969

An experimental investigation of quasi-conical shock wave/turbulent boundary layer interactions
03 p0317 N88-12004

Visualization of the flow field around a generic destroyer model in a simulated turbulent atmospheric boundary layer
[AD-A184658] 03 p0320 N88-12023

Calculation of three-dimensional stationary turbulent boundary layer on root section of wing ignoring compressibility 04 p0424 N88-12630

An experimental investigation of unsteadiness in swept shock wave/turbulent boundary layer interactions
04 p0445 N88-12760

Heat and moisture transport in the atmospheric boundary layer
[AD A184222] 04 p0470 N88-12904

The effects of sweep and bluntness on a glancing shock wave turbulent boundary layer interaction
05 p0531 N88-13227

Development of the computer program for turbulent boundary layers 05 p0536 N88-13264

Interferometric data for a shock-wave/boundary-layer interaction
[NASA-TM-88227] 05 p0543 N88-13306

Experimental study of the fluid mechanics of unsteady turbulent boundary layers
[AD-A184856] 05 p0580 N88-13536

Asymptotic analysis of a turbulent boundary layer in a strong adverse pressure gradient
[AD-A185406] 05 p0581 N88-13543

Fluctuating pressure loads under high speed boundary layers
[NASA-TM-100517] 05 p0647 N88-13962

The production of turbulence in boundary layers: The role of microscale coherent motions
[AD-A185568] 06 p0703 N88-14313

Studies of unsteadiness in boundary layers
[AD-A185662] 06 p0703 N88-14315

Measurements of the free stream fluctuations above a turbulent boundary layer
[NASA-TM-100036] 06 p0704 N88-14321

Wall turbulence control 07 p0812 N88-14943

Airfoil large eddy breakup devices for turbulent drag reduction 07 p0814 N88-14956

Fundamental aspects of the structure of supersonic turbulent boundary
[AD-A186366] 07 p0815 N88-14959

Examination of the development of a compressible turbulent boundary layer on a rough and porous wall
[PB87-148266] 07 p0815 N88-14964

Mean velocities and Reynolds stresses in the juncture flow and in the shear layer downstream of an appendage
[AD-A185819] 08 p0980 N88-15923

Approximation of noncorrelated reflections in problem of sound propagation through waveguide with rough boundary 08 p1076 N88-16487

Unsteady behavior of three-dimensional vortices relevant to turbulent boundary layers
[AD-A186767] 09 p1161 N88-16958

Numerical simulation of the interaction of pressure waves with laminar and turbulent boundary layers
[DFVLR-FB-87-18] 09 p1161 N88-16960

A dynamical system/coherent structure approach to the fully developed turbulent wall layer
10 p1267 N88-17578

Burst vortex/boundary layer interaction
[NASA-CR-182510] 10 p1268 N88-17583

Boundary layer calculation using digital computers
[REPT-MM-4] 10 p1309 N88-17821

An experimental investigation of pressure driven three-dimensional turbulent boundary layers
10 p1327 N88-17934

An analysis of the motion and effects of hairpin vortices
[AD-A187261] 10 p1331 N88-17958

The structure and control of three-dimensional shock wave turbulent boundary layer interactions
[AD-A187642] 10 p1332 N88-17961

Shock wave/turbulent boundary layer interaction in high-Reynolds-number hypersonic flows
[AD-A188029] 11 p1434 N88-18555

Fluctuations and massive separation in three-dimensional shock-wave/boundary-layer interactions
[NASA-TM-89224] 11 p1434 N88-18559

Structure of shear flow turbulence and its control
[AD-A187909] 11 p1482 N88-18846

Changes in the turbulent boundary layer structure associated with net drag reduction by outer layer manipulators
[NASA-CR-178152] 11 p1483 N88-18853

A simplified streamline swallowing procedure for the windward meridian of axisymmetric blunt bodies
[AD-A188413] 12 p1626 N88-19732

Research on flow control
[AD-A189014] 12 p1627 N88-19736

Interaction between two-dimensional sonic jets and supersonic flow to model heat addition in a supersonic combustor
[AD-A189572] 13 p1716 N88-20261

Coherent structure-reflective turbulent viscous flow modeling
[AD-A188339] 13 p1765 N88-20556

Slip velocity method for three-dimensional compressible turbulent boundary layers
[NASA-TM-100586] 13 p1771 N88-20592

Research on turbulence in bottom boundary layer in ocean 13 p1788 N88-20697

Unsteady shallowing mixed layer
13 p1805 N88-20791

Flow/acoustic interaction in duct inflow
[AD-A189264] 13 p1833 N88-20967

JPRS report: Science and technology. China
[JPRS-CST-87-023] 14 p1863 N88-21130

Propagation of artificial disturbances immersed in thick turbulent boundary layer 14 p1864 N88-21136

An experimental-computational investigation of transonic shock wave-turbulent boundary layer interaction in a curved test section
[CWI-NM-R8716] 14 p1909 N88-21408

Enhanced viscous flow drag reduction using acoustic excitation
[NASA-CR-182734] 15 p2062 N88-22295

Bodies in unsteady flow
[AD-A190416] 15 p2064 N88-22308

Effect of freestream turbulence on a two dimensional cascade, with different surface roughness, at high Reynolds number
[AD-A190615] 15 p2065 N88-22316

Numerical and experimental investigation of multiple shock wave/turbulent boundary layer interactions in a rectangular duct
[AD-A190772] 15 p2066 N88-22320

Aerothermal tests of quilted dome models on a flat plate at a Mach number of 6.5
[NASA-TP-2804] 15 p2067 N88-22325

Studying Turbulence Using Numerical Simulation Databases. Proceedings of the 1987 Summer Program
[NASA-CR-182692] 16 p2194 N88-23086

Self similarity of two point correlations in wall bounded turbulent flows 16 p2195 N88-23089

Ejection mechanisms in the sublayer of a turbulent channel 16 p2195 N88-23090

Structure of turbulent shear flows
16 p2198 N88-23113

Coherent structures: Comments on mechanisms
16 p2199 N88-23118

Some visualization studies on turbulent boundary layers using multiwire hydrogen bubble generation
16 p2204 N88-23153

Laser Doppler anemometry
[NASA-TM 100072] 16 p2210 N88-23187

Technology Reports of Kyushu University, volume 61, no. 2
[ISSN-0023-2718] 16 p2256 N88-23485

Natural laminar flow and airplane stability and control
17 p2298 N88-23747

Unsteady flow about cambered plates
[AD-A191226] 17 p2337 N88-23945

Fundamental aspects of the structure of supersonic turbulent boundary layers
[AD-A191494] 18 p2456 N88-24581

Computation of the turbulent boundary layer downstream of vortex generators
[AD-A191544] 18 p2508 N88-24881

Theoretical investigation of 3-D shock wave-turbulent boundary layer interactions, part 6
[AD-A191546] 18 p2509 N88-24882

The behavior of drop-containing turbulent eddies
[AD-A191669] 18 p2509 N88-24883

Manipulation of the structure of a turbulent boundary layer 18 p2512 N88-24901

Hypersonic turbulent wall boundary layer computations
[NASA-CR-182147] 18 p2514 N88-24917

Correlations of velocity and temperature fluctuations in the stagnation-point flow of circular cylinder in turbulent flow
[NASA-TM-100930] 19 p2597 N88-25435

Study of the structure of turbulence in accelerating transitional boundary layers
[AD-A191698] 19 p2663 N88-25837

Comparison of the wall pressure fluctuations in artificially generated turbulent spots, natural transition and turbulent boundary layers
[AD-A191777] 19 p2663 N88-25838

Boundary layer development as a function of chamber pressure in the NASA Lewis 1030:1 area ratio rocket nozzle
[NASA-TM-100917] 19 p2664 N88-25841

Drag reduction of turbulent boundary layers by means of grooved surfaces
[ETN-88-92618] 20 p2802 N88-26630

Wind tunnel study of atmospheric diffusion in unstable stratified boundary layer. Part 2: Characteristic scale and diffusion
[DE88-753109] 20 p2823 N88-26749

The diffusion of vorticity from a plane boundary
[AD-A192706] 21 p2942 N88-27474

Experimental study of unsteady separating turbulent boundary layers
[AD-A192997] 21 p2943 N88-27477

The heat transfer and fluid dynamics of concave surface curvature
[AD-A193064] 21 p2943 N88-27479

A documentation of two- and three-dimensional shock-separated turbulent boundary layers
[NASA-TM-101008] 21 p2949 N88-27519

Plasma behavior in the boundary layer near a railgun surface
[DE88-008889] 21 p3017 N88-27909

The dynamic behavior of a turbulent boundary layer subjected to a shock-induced separation
[AD-A194164] 22 p3075 N88-28252

Coupled inviscid - boundary layer methods for turbomachinery blading design
[PNR90437] 22 p3076 N88-28260

A new method of calculating the boundary layer characteristics downstream of manipulators. Part 1: Boundary layer integral parameters
[PNR90455] 22 p3078 N88-28279

Development and analysis of turbulent non-equilibrium boundary layers 23 p3169 N88-28872

Environmental effects on transition and boundary layer characteristics 23 p3170 N88-28876

Stability and drag reduction in a boundary layer with microbubbles
[AD-A191975] 23 p3209 N88-29099

A mapping of the viscous flow behavior in a controlled diffusion compressor cascade using laser Doppler velocimetry and preliminary evaluation of codes for the prediction of stall
[AD-A194490] 23 p3211 N88-29112

A calculation of the turbulent boundary layer on a slender ellipsoid at low incidence
[FFA-TN-1988-02] 23 p3213 N88-29126

Studies of gas turbine heat transfer airfoil surface and end-wall cooling effects
[AD-A195165] 24 p3326 N88-29805

The effects of incoming boundary layer thickness on unsteady shock-induced turbulent separations induced by cylinders
[AD-A196190] 24 p3368 N88-30060

Numerical simulation of the interaction of pressure waves with laminar and turbulent boundary layers
[ESA-TT-1089] 24 p3371 N88-30075

Experimental and numerical investigation of the effect of distributed suction on oblique shock wave/turbulent boundary layer interaction
[NASA-TM-101334] 24 p3372 N88-30084

The thermal behavior of film cooled turbulent boundary layers as affected by longitudinal vortices
[AD-A195155] 24 p3374 N88-30095

Vortex formation and particle transport in a cross-field plasma sheath
[AD-A194838] 24 p3432 N88-30425

TURBULENT DIFFUSION

Experimental study of turbulent diffusion parameters in ocean 04 p0459 N88-12840

Active and passive plume distribution models in the convective boundary layer using a large eddy simulation model
[KNMI-TR-90] 05 p0581 N88-13546

Extinguishing diffusion flames with dry powder and halon at low Froude numbers
[PB87-111365] 06 p0679 N88-14159

Carbon monoxide and turbulence-chemistry interactions: Blowoff and extinction of turbulent diffusion flames
[AD-A186276] 07 p0828 N88-15025

Continuum theories for fluid-particle flows: Some aspects of lift forces and turbulence
[DE88-007038] 18 p2511 N88-24896

Turbulence and flame propagation
[PB87-228912] 19 p2612 N88-25499

Development of an atmospheric diffusion evaluation method incorporating topographical effects. Part 1: Literature review of atmospheric diffusion models incorporating terrain effects
[DE88-753104] 20 p2822 N88-26742

Wind tunnel study of atmospheric diffusion in unstable stratified boundary layer. Part 2: Characteristic scale and diffusion
[DE88-753109] 20 p2823 N88-26749

TURBULENT FLOW

NT CAVITATION FLOW

Reynolds number effects on the small scale structure of a turbulent channel flow 01 p0001 N88-10004

Measurement techniques in low-speed turbulent flows: A report on EUROMECH 202
[NLR-MP-86038-U] 01 p0045 N88-10283

Influence of a magnetic field on the diffusion of small particles in a turbulent flow
[DE87-702877] 01 p0046 N88-10291

Two-dimensional shear flow turbulence: A statistical theory of vortex filaments
[DE87-012234] 01 p0046 N88-10295

Mean flow structure of a turbulent junction vortex
[PB87-206231] 01 p0047 N88-10301

Numerical calculation of the turbulent flow about a cubic body
[ETN-87-90418] 01 p0047 N88-10302

Determination of the dynamic parameters of annular clearances with turbulent flow and incompressible media
[ETN-87-90434] 01 p0047 N88-10303

The influence of high free stream turbulence, intensive cooling and wake on the external heat transfer of convectively cooled gas turbine blades
[ETN-87-90432] 01 p0056 N88-10360

Navier-Stokes cascade analysis with a stiff Kappa-Epsilon turbulence solver
[NASA-TM-100218] 02 p0123 N88-10778

Radiative and free-convective heat transfer from a finite horizontal plate inside an enclosure
02 p0133 N88-10833

On the modelling of non-reactive and reactive turbulent combustor flows 02 p0169 N88-11061

Dimension densities for turbulent systems with spatially decaying correlation functions
[DE87-010119] 02 p0169 N88-11066

Large scale structures in turbulent pipe flow
[MPIS-MITT-83-1987] 02 p0172 N88-11085

The four spot time-of-flight laser anemometer
02 p0184 N88-11145

Correlation of velocity and velocity-density turbulence in the exhaust of an atmospheric burner
02 p0185 N88-11147

Improved numerical methods for turbulent viscous recirculating flows 02 p0185 N88-11148

Aerothermal modeling program, phase 2
02 p0185 N88-11149

Fuel-injector/air-swirl characterization
02 p0185 N88-11150

Measurement of airfoil heat transfer coefficients on a turbine stage 02 p0186 N88-11158

A calculation method for the propulsive jet and its aerodynamic interaction with an afterbody
[ESA-TT-1039] 03 p0259 N88-11632

Numerical simulation of turbulent premixed combustion and decay of turbulent swirling flow
[DE87-014253] 03 p0284 N88-11787

Computation of turbulent flows using an extended k-epsilon turbulence closure model
[NASA-CR-179204] 03 p0312 N88-11969

Special Course on Modern Theoretical and Experimental Approaches to Turbulent Flow Structure and its Modelling
[AGARD-R-755] 03 p0312 N88-11970

Turbulence modelling through one point closures-applications-enlightening by large eddy simulation 03 p0312 N88-11972

Homogeneous turbulence two-point closures and applications to one-point closures
03 p0312 N88-11973

Transition to turbulence via spatio-temporal intermittency 03 p0313 N88-11976

Determination of fractal dimension, connection of space and temporal chaos and application to experimental results 03 p0313 N88-11977

Stochastic model of the motion of suspended particles in turbulent flow
[HSBW-MITT-21/1987] 03 p0315 N88-11990

Analysis of the motions and effects of hairpin vortices
03 p0316 N88-11997

Numerical study of the entrance flow and its transition in a circular pipe (2) 03 p0318 N88-12011

Multidimensional modeling of convective heat transfer with application to I.C. engines
[DE87-014983] 03 p0322 N88-12036

Numerical simulation of internal combustion engine flows: Development and users guide for MAGIC radial-azimuthal version
[DE87-014453] 03 p0332 N88-12091

Optical instrumentation and study of gas-solid suspension flows
[DE88-000147] 04 p0442 N88-12744

Experiments on densely-loaded non-Newtonian slurries in laminar and turbulent pipe flows
[DE88-000719] 04 p0442 N88-12746

Theory of heat and moisture exchange between finely disperse storm-generated spray and turbulent air flow
04 p0461 N88-12851

Numerical analysis of flow through scramjet engine inlets 05 p0532 N88-13233

Numerical prediction of turbulent flows in dump diffusers 05 p0537 N88-13265

Delta wing in incompressible flow. Experimental study in F2
[ONERA-RT-36/1147-AN-249-G]
05 p0541 N88-13298

Interferometric data for a shock-wave/boundary-layer interaction
[NASA-TM-88227] 05 p0543 N88-13306

A numerical study of the effects of curvature and convergence on dilution jet mixing
[NASA-TM-89878] 05 p0549 N88-13347

Statistical theory of turbulent incompressible multimaterial flow
[DE88-000435] 05 p0579 N88-13535

Physical analysis and numerical simulation of coherent turbulent structures in mixed layers, jets, and wakes
[ETN-88-91183] 05 p0581 N88-13548

Hot wire and laser velocimeter studies of turbulent flow at supersonic velocities
[ETN-88-91172] 05 p0585 N88-13566

Analysis of internal flows relative to the space shuttle main engine
[NASA-CR-179240] 06 p0674 N88-14125

Visible boundary layer transition points through flight tests 06 p0675 N88-14136

Summary of discussions at the Ninth Meeting of the Sandia Cooperative Group on the Aerothermochemistry of Turbulent Combustion
[DE88-002281] 06 p0680 N88-14165

Experimental investigation of heterogeneous compressible shear layers 06 p0700 N88-14294

An experimental and numerical investigation of swirling flows in a rectangular nozzle 06 p0700 N88-14295

Extensions of the control volume based finite element method for fluid flow problems 06 p0700 N88-14296

Computation of turbulent flow of air through smooth and rough pipes using a two-equation turbulence model
06 p0700 N88-14298

Flight and wind-tunnel measurements showing base drag reduction provided by a trailing disk for high Reynolds number turbulent flow for subsonic and transonic Mach numbers
[NASA-TP-2638] 06 p0701 N88-14299

Approximate solutions for the momentum transport in turbulent flows in narrow rod array bundles using the finite element method
[ETN-88-90810] 06 p0701 N88-14306

On the subgrid-scale modeling of compressible turbulence
[NASA-CR-178420] 06 p0702 N88-14309

Three-dimensional structure of boundary layers in transition to turbulence
[AD-A185466] 06 p0702 N88-14311

The acoustic source created by turbulent flow over orifices and louvers
[REPT-97674] 06 p0776 N88-14764

A multistage time-stepping scheme for the thin-layer Navier-Stokes equations 07 p0810 N88-14932

Flow diagnostics and visualization in wind tunnels and flight 07 p0811 N88-14940

Overview of the Langley viscous drag reduction program 07 p0812 N88-14946

Natural laminar flow nacelle for transport aircraft
07 p0813 N88-14949

Fundamental aspects of the structure of supersonic turbulent boundary
[AD-A186366] 07 p0815 N88-14959

Turbulence in hypersonic flow
[AD-A185624] 07 p0815 N88-14961

High resolution simulation of turbulent flow in a channel
[AD-A186022] 07 p0848 N88-15150

Effects of turbulence on stationary and non-stationary processes in C-systems
[AD-A186215] 07 p0849 N88-15154

Identification and avoidance of instabilities in high performance turbomachinery 07 p0850 N88-15164

Reynolds-stress and dissipation rate budgets in a turbulent channel flow
[NASA-TM-89451] 07 p0852 N88-15174

Mixing in variable density, isothermal turbulent flows and implications for chemically reacting turbulent flows
[PB88-110044] 07 p0852 N88-15176

Numerical solution of turbulent flow past a backward facing step using a nonlinear K-epsilon model
[NASA-CR-178421] 07 p0854 N88-15189

Chemical reacting flows 08 p0955 N88-15793

Optical measurement systems
08 p0955 N88-15796

Viscous flows, part 1 08 p0986 N88-15967

Introduction to the Modeling of Turbulence
[VKI-LS-81-06] 08 p0986 N88-15972

Examples of turbulence-model applications
08 p0987 N88-15975

Direct and large eddy simulation of turbulence. Summary of the state of art 1987 08 p0987 N88-15977

Turbulence modeling for compressible flows
08 p0987 N88-15978

The effect of eddy distribution on momentum and heat transfer near the wall in turbulent pipe flow
[NASA-TM-100257] 08 p0988 N88-15984

Cavitation inception scale effects. 1. Nuclei distributions in natural waters. 2. Cavitation inception in a turbulent shear flow
[AD-A186553] 08 p0988 N88-15987

Fully turbulent internal flow excitation of pipe systems
08 p1000 N88-16056

Numerical calculation of turbulent recirculating flows
[TUM-LSM-84/29] 09 p1161 N88-16959

Numerical and physical aspects of large eddy simulation of turbulent flows
[ETN-88-91611] 09 p1162 N88-16965

The dynamics of heat transfer at a turbulent pipe flow
[OEFZS-4400] 09 p1164 N88-16975

Solution of the three-dimensional Navier-Stokes equations for transonic flow using a multigrid method
10 p1267 N88-17579

Numerical simulation of axisymmetric turbulent flow in combustors and diffusors
[NASA-CR-4115] 10 p1268 N88-17582

Navier-Stokes calculations and turbulence modeling in the trailing edge region of a circulation control airfoil
10 p1268 N88-17587

Wall jet analysis for circulation control aerodynamics. Part 1: Fundamental CFD and turbulence modeling concepts 10 p1269 N88-17588

Investigations of a circulation control airfoil flowfield using an advanced laser velocimeter
10 p1269 N88-17589

A theory for turbulent curved wall jets
10 p1269 N88-17590

Evaluation of a research circulation control airfoil using Navier-Stokes methods 10 p1269 N88-17591

Development and application of oxygen flow tagging for velocity measurements and flow visualization in turbulent three-dimensional supersonic flows
[AD-A187982] 10 p1289 N88-17714

Fully Lagrangian Renormalized Approximation theory of fluid turbulence
[DE88-004960] 10 p1330 N88-17952

An analysis of the motion and effects of hairpin vortices
[AD-A187261] 10 p1331 N88-17958

La Recherche Aerospatiale, bimonthly bulletin, number 1987-1, 236/January-February
[ESA-TT-1055] 11 p1433 N88-18549

Diagnostics for research in atomization and turbulent two-phase flows
[AD-A187338] 11 p1482 N88-18843

Structure of shear flow turbulence and its control
[AD-A187909] 11 p1482 N88-18846

Kinetic and turbulence models for granular and two-phase flows 11 p1484 N88-18862

A review of approaches to the study of turbulence modification by means of non-Newtonian additives
[AD-A188799] 12 p1627 N88-19734

Wavenumber - frequency structure of turbulent flow in a channel from a direct simulation
[AD-A189079] 12 p1627 N88-19737

Time-accurate simulations of a shear layer forced at a single frequency
[NASA-TM-100836] 12 p1628 N88-19740

Reynold stress closure in jet flows using wave models
[NASA-CR-182662] 12 p1628 N88-19741

Coherent structure-reflective turbulent viscous flow modeling
[AD-A188339] 13 p1765 N88-20556

Control of structure in turbulent flows: Bifurcating and blooming jets
[AD-A189607] 13 p1766 N88-20562

The influence of Mach number and heat transfer on the turbulent flow wall law
[NASA-TT-20230] 13 p1771 N88-20594

Research on flow around bluff bodies, flow induced vibrations 14 p1864 N88-21135

Numerical simulation of turbulent premixed combustion and decay of turbulent swirling flow
[DE88-006588] 14 p1888 N88-21284

Study on the burnout with variations of flow twisting over tube length
[DE87-703170] 14 p1909 N88-21405

Mean flow structure in the near wake of a turbulent junction vortex
[PB88-150115] 14 p1910 N88-21416

Accuracy requirements and benchmark experiments for CFD validation
[NASA-TM-100087] 14 p1911 N88-21423

Two-fluid turbulence models and reciprocating engines
[CFD/87/6] 14 p1918 N88-21449

Turbulent reacting flows and supersonic combustion
[AD-A189690] 15 p2034 N88-22115

An investigation of flow structure, mixing and chemical reaction in combusting turbulent flows
[AD-A189980] 15 p2034 N88-22117

Duct flow nonuniformities: Effect of struts in SSME HGM II(+)
[NASA-CR-179285] 15 p2062 N88-22296

Chemically reacting turbulent flow
[AD-A190522] 15 p2065 N88-22311

Experiments on densely-loaded non-Newtonian slurries in laminar and turbulent pipe flows
[DE88-006209] 15 p2067 N88-22323

Development of subminiature multi-sensor hot-wire probes
[NASA-TM-100052] 15 p2069 N88-22336

Describing the source created by turbulent flow over orifices and louvers
[AD-A190254] 15 p2130 N88-22706

Studying Turbulence Using Numerical Simulation Databases. Proceedings of the 1987 Summer Program
[NASA-CR-182692] 16 p2194 N88-23086

Stochastic estimation of conditional eddies in turbulent channel flow 16 p2194 N88-23087

A low dimensional dynamical system for the wall layer
16 p2194 N88-23088

Self similarity of two point correlations in wall bounded turbulent flows 16 p2195 N88-23089

Validation of EDQNM for subgrid and supergrid models 16 p2195 N88-23092

Angular distribution of turbulence in wave space
16 p2195 N88-23093

Big whorls carry little whorls 16 p2195 N88-23094

Study of one-dimensional spectral dynamic equations of the Reynolds stresses in homogeneous anisotropic turbulence: Application to split-spectrum modeling
16 p2196 N88-23095

Modeling scalar flux and the energy and dissipation equations 16 p2196 N88-23096

Direct numerical simulation of buoyantly driven turbulence 16 p2196 N88-23097

Premixed turbulent flame calculation
16 p2196 N88-23098

Modeling of turbulent transport as a volume process
16 p2196 N88-23099

Analysis of non-premixed turbulent reacting flows
16 p2196 N88-23100

A statistical investigation of the single-point pdf of velocity and vorticity based on direct numerical simulations 16 p2196 N88-23101

Local structure of intercomponent energy transfer in homogeneous turbulent shear flow
16 p2197 N88-23103

A general form for the dissipation length scale in turbulent shear flows 16 p2197 N88-23104

Test code for the assessment and improvement of Reynolds stress models 16 p2197 N88-23105

The decay of isotropic turbulence in a rapidly rotating frame 16 p2197 N88-23107

Evaluation of a theory for pressure-strain rate
16 p2198 N88-23108

Conditionally-averaged structures in wall-bounded turbulent flows 16 p2198 N88-23112

Structure of turbulent shear flows
16 p2198 N88-23113

Inflectional instabilities in the wall region of bounded turbulent shear flows 16 p2199 N88-23114

Active layer model for wall-bounded turbulence
16 p2199 N88-23115

Coherent structures: Comments on mechanisms
16 p2199 N88-23118

Coherent structures and dynamical systems
16 p2199 N88-23119

Coherent structures and modeling: Some background comments 16 p2199 N88-23120

Coherent structures --- in turbulent flows
16 p2199 N88-23121

Experimental studies of vortex flows
[NASA-CR-182674] 16 p2207 N88-23171

Random processes, turbulence and disordering fields
[AD-A191399] 16 p2209 N88-23181

Investigation of subgrid models in homogeneous incompressible turbulence
[ONERA-RSF-13/3419-AY-106-A]
16 p2209 N88-23183

Numerical simulation of scramjet inlet flow fields
[NASA-TP-2517] 17 p2296 N88-23735

Theoretical prediction of single phase turbulent flow distribution in particulate bed reactors
17 p2419 N88-24386

Fundamental aspects of the structure of supersonic turbulent boundary layers
[AD-A191494] 18 p2456 N88-24581

Wave growth associated with turbulent spots in plane Poiseuille flow
[FFA-TN-1988-08] 18 p2457 N88-24587

Application of Rayleigh scattering to turbulent flow with heat transfer and combustion
[AD-A191565] 18 p2481 N88-24720

Analysis of molecular mixing and chemical reaction in mixing layer
[AD-A191600] 18 p2482 N88-24721

Stagnating turbulent reacting flows
[AD-A191449] 18 p2508 N88-24877

Study of mixing and reaction in the field of a vortex
[AD-A191489] 18 p2508 N88-24878

Dynamics and control of turbulent shear flows
[AD-A191527] 18 p2508 N88-24879

Injection of drag reducing additives into turbulent water flows
[AD-A192072] 18 p2509 N88-24888

CFD benefits, goals, stepping-stones and techniques. Proposals for the scientific programme of the European Reserch Centre on flow, turbulence and combustion --- computational fluid dynamics
[CFDU/88/1] 18 p2510 N88-24894

Duct flow nonuniformities for Space Shuttle Main Engine (SSME)
[NASA-CR-179338] 18 p2511 N88-24899

Numerical solutions of the complete Navier-Stokes equations
[NASA-CR-183023] 18 p2514 N88-24914

Finite element solution of 3-D turbulent Navier-Stokes equations for propeller-driven slender bodies
18 p2515 N88-24919

Instrumentation for turbulent reacting flows
[AD-A191671] 18 p2515 N88-24923

Low frequency electrostatic turbulence in the polar cap E-region
[DRI-3-88] 18 p2540 N88-25077

Improved numerical methods for turbulent viscous recirculating flows
[NASA-CR-180852] 19 p2599 N88-25445

Coal particle behaviour in a counter-current combustor
[TAE-606] 19 p2612 N88-25498

Atomization in a turbulent shear layer: Preliminary measurements 19 p2624 N88-25565

Anatomy of group burning mode transitions in spray group combustion 19 p2626 N88-25578

Numerical simulation of transition to turbulence in plane Poiseuille flow by a spectral method
19 p2640 N88-25661

Numerical simulation of turbulent flow using the exponential expression of k-Epsilon equation
19 p2640 N88-25662

Superfluid turbulence in counterflowing helium II
19 p2665 N88-25849

Numerical simulation studies of laminar-turbulent transition in the plan channel 19 p2665 N88-25850

Pressure drop and heat transfer in turbulent non-Newtonian pipe flow of advanced energy transmission fluids
[DE88-010021] 19 p2666 N88-25853

Navier-Stokes code NS3D for blunt bodies. Part 1: Analysis, results and verification
[DE88-010105] 19 p2666 N88-25855

Direct simulations of chemically reacting turbulent mixing layers, part 2
[NASA-CR-180853] 19 p2667 N88-25857

Influence of rear body geometry on the velocity characteristics of the near wake
[ISL-R-113/87] 20 p2753 N88-26339

The effect of a turbulent airstream on a vertically-launched missile at high angles of attack
[AD-A192408] 20 p2758 N88-26363

An efficient computational tool for ramjet combustor research
[DE88-010034] 20 p2760 N88-26369

Heterogeneous diffusion flame stabilization
[AD-A193014] 20 p2771 N88-26429

Turbulence transition in a circular pipe
20 p2782 N88-26503

Nonlinear equation of state effects and the momentum-dilution trade-off in a turbulent buoyant jet
[DE88-701839] 20 p2799 N88-26610

Experiments on densely-loaded non-Newtonian slurries in laminar and turbulent pipe flows
[DE88-010579] 20 p2800 N88-26612

Experimental investigation of turbulent flow in smooth and longitudinal grooved tubes
[NASA-TM-77480] 20 p2800 N88-26615

Treatment of the separated flow around profiles (nonviscous, incompressible, two dimensional flow) by the singularities method
[ISL-R-106/87] 20 p2803 N88-26633

Evolution of hairpin vortices in a shear flow
[NASA-TM-100858] 20 p2845 N88-26885

Velocity measurements and flow visualization in turbulent three-dimensional supersonic flows using oxygen flow tagging
[AD-A192551] 21 p2892 N88-27165

The structure and stability of nonpremixed gas jet flames 21 p2908 N88-27257

Premixed turbulent flame propagation
[AD-A192955] 21 p2909 N88-27265

Summary of discussions at the Tenth Meeting of the Sandia Cooperative Group on the Aerothermochemistry of Turbulent Combustion
[DE88-008467] 21 p2910 N88-27269

Design of a mechanism to control wind tunnel turbulence 21 p2926 N88-27370

Predicting optical degradation of a laser beam through a turbulent shear layer 21 p2927 N88-27376

Numerical experiments on turbulent mixing
[AD-A192572] 21 p2942 N88-27473

Turbulence structure of mixing swirling flows
[AD-A193063] 21 p2943 N88-27478

Physical mechanisms in shock-induced turbulent separated flow
[AD-A193165] 21 p2944 N88-27484

Cavitation inception in a turbulent shear flow
[DE88-011486] 21 p2946 N88-27497

Laser-Doppler measurements of turbulence structures in free streams behind flat and rotation symmetrical profiles
[ETN-88-92336] 21 p2948 N88-27510

Numerical computation of three-dimensional turbulent flow in tightly curved ducts and spiral turbine casings
[ETN-88-92362] 21 p2948 N88-27511

Investigations on drag reduction in turbulent pipe flows by addition of ionic and nonionic high polymers
[ETN-88-92380] 21 p2949 N88-27515

Turbulent flow field visualization with integral interferometric imaging and computed tomography
21 p2950 N88-27521

Photon limited image processing in the space-time domain
[AD-A193142] 21 p2972 N88-27655

The influence of surface rounding on trailing edge noise
[AD-A193387] 21 p3012 N88-27876

The application of the two-fluid model of turbulence to the 3-D simulation of turbulent combustion in reciprocating engines
[PDR/CFDU/IC/37] 22 p3052 N88-28110

Interactions between coherent structures and premixed flame fronts
[ETN-88-92885] 22 p3053 N88-28111

Flow dynamics stimulated by hairpin-like vortices in initially laminar boundary layers
[AD-A194253] 22 p3075 N88-28254

Investigations of rough surface effects on friction factors in turbulent pipe flow
[AD-A193774] 22 p3075 N88-28255

Development and application of a finite element method to compute strongly heated turbulent flows
[ECL-88-02] 22 p3077 N88-28267

Calibration of a triple wire probe for turbulence measurements
[AD-A193956] 22 p3081 N88-28296

Small scale mixing in the initial region of a jet
[AD-A193500] 23 p3192 N88-28994

Three-dimensional laser Doppler velocimeter studies of flow in a 90 deg curved duct having a square cross-section 23 p3209 N88-29101

A numerical study of turbulent plane jets in still and flowing environments employing two-equation k-epsilon model 23 p3211 N88-29109

Modeling of momentum transport of axially parallel turbulent flows in rod cascades
[ETN-88-92978] 23 p3214 N88-29131

Aerodynamic heating of missiles
24 p3319 N88-29764

Flamelet modeling of turbulent premixed flames
24 p3350 N88-29942

Modeling the stability of a turbulent premixed flame, downstream from a step by a Lagrangian method
24 p3350 N88-29943

Modeling and experimental study of a reactive flow confined with well injection 24 p3351 N88-29946

Approximation of viscoelastic stresses from Newtonian turbulent kinematics
[AD-A194317] 24 p3371 N88-30077

Boltzmann equation approach to two-phase flow turbulence
[AD-A196153] 24 p3373 N88-30086

Analysis method for the production of Reynolds stresses in compressible turbulent flow (fluid mechanics) [NASA-TT-20330] 24 p3373 N88-30088
Development of a more general Reynolds stress closure for swirling flow [AD-A195121] 24 p3374 N88-30092

TURBULENT HEAT TRANSFER
The influence of high free stream turbulence, intensive cooling and wake on the external heat transfer of convectively cooled gas turbine blades [ETN-87-90432] 01 p0056 N88-10360
Heat and moisture transport in the atmospheric boundary layer [AD-A184222] 04 p0470 N88-12904
The development and evaluation of three-dimensional models of cold flow in internal combustion engines [DE88-900077] 05 p0589 N88-13594
Effects of turbulence on stationary and non-stationary processes in C-systems [AD-A186215] 07 p0849 N88-15154
Weak interactions and local order in strong turbulence 09 p1159 N88-16948
Heat transfer from impinging flame jets [ETN-88-91610] 09 p1162 N88-16964
Wake interaction effects on the transition process on turbine blades [AD-A188020] 10 p1332 N88-17962
Mixed turbulent convective heat transfer in vertical ducts 11 p1485 N88-18865
Turbulent transfer of momentum and heat in boundary layer of fluid beyond an obstacle. 1: Hydrodynamic characteristics 13 p1787 N88-20690
Vertical turbulent transfer of matter in thin ocean surface layer during daytime heating 13 p1787 N88-20693
Equatorial turbulence: Mixed layer and thermocline 13 p1804 N88-20787
Application of Rayleigh scattering to turbulent flow with heat transfer and combustion [AD-A191565] 18 p2481 N88-24720
Stagnating turbulent reacting flows [AD-A191449] 18 p2508 N88-24877
Turbulent heat transfer and fluid flow measurements downstream of abrupt expansions and in a cavity of a circular tube at a uniform wall temperature 18 p2515 N88-24920
Study of the structure of turbulence in accelerating transitional boundary layers [AD-A191698] 19 p2663 N88-25837
Multidimensional modeling of convective heat transfer with application to I.C. engines [DE88-007446] 19 p2738 N88-26257
The heat transfer and fluid dynamics of concave surface curvature [AD-A193064] 21 p2943 N88-27479
Studies of gas turbine heat transfer airfoil surface and end-wall cooling effects [AD-A195165] 24 p3326 N88-29805

TURBULENT JETS
Experimental study of three-dimensional turbulent jet-solid boundary interaction 01 p0046 N88-10293
Combustion in turbulent jets and buoyant flames [PB87-232674] 03 p0283 N88-11779
Laser Doppler measurements in a turbulent free jet [ESA-TT-1067] 03 p0315 N88-11994
Comparative studies in the near-field of turbulent transports of heated and unheated jets normal to a cross stream 04 p0444 N88-12756
Conditional second order closure for turbulent shear flows [AD-A185369] 05 p0581 N88-13542
A computational study of thrust augmenting ejectors based on a viscous-inviscid approach 10 p1326 N88-17929
Turbulence interactions in single- and multi-phase turbulent mixing and combustion processes [AD-A187505] 10 p1332 N88-17960
Active feedback interaction with a shear layer [AD-A188525] 12 p1573 N88-19410
Control of structure in turbulent flows: Bifurcating and blooming jets [AD-A189607] 13 p1766 N88-20562
The structure of sonic underexpanded turbulent air jets in still air [AD-A190856] 16 p2157 N88-22870
Noncondensing round turbulent gas jets in liquids [AD-A191191] 16 p2208 N88-23179
Effect of initial tangential velocity distribution on the mean evolution of a swirling turbulent free jet [NASA-TM-100934] 18 p2458 N88-24592
Particle-laden weakly swirling free jets: Measurements and predictions [NASA-TM-100920] 18 p2466 N88-24639
Hydroacoustic pulsating jet generator [MPIS-7/1987] 18 p2510 N88-24891
Coherent structures in the axisymmetric turbulent jet mixing layer 21 p2947 N88-27504

TURBULENT MIXING
Momentum transport and particle dynamics in turbulent shear flows 03 p0317 N88-12002
Blowup for a nonlinear evolution equation and self-reproducing strained shear layers 04 p0444 N88-12755
Turbulent mixing in a rotating, stratified fluid 04 p0445 N88-12759
Chemical reactions in turbulent mixing flows [AD-A186141] 07 p0849 N88-15153
On the pairing process in an excited, plane, turbulent mixing layer [AD-A186355] 07 p0850 N88-15157
Mixing in variable density, isothermal turbulent flows and implications for chemically reacting turbulent flows [PB88-110044] 07 p0852 N88-15176
Turbulence interactions in single- and multi phase turbulent mixing and combustion processes [AD-A187505] 10 p1332 N88-17960
Unsteady shallowing mixed layer 13 p1805 N88-20791
Radiative processes affecting ocean mixed-layer heat content and their monitoring from satellite 13 p1806 N88-20800
Coherent structure 16 p2199 N88-23117
Experimental studies of vortex flows [NASA-CR-182874] 16 p2207 N88-23171
The spreading and mixing of dense gas clouds in still air [KNMI-WR-87-12] 16 p2230 N88-23320
Study of mixing and reaction in the field of a vortex [AD-A191489] 18 p2508 N88-24878
Measurement of burning rates of NOSOL-363 propellants under cross-flow and strand burner conditions using real-time X-ray radiography 19 p2623 N88-25560
Direct simulations of chemically reacting turbulent mixing layers, part 2 [NASA-CR-180853] 19 p2667 N88-25857
Numerical experiments on turbulent mixing [AD-A192572] 21 p2942 N88-27473
Coherent structures in the axisymmetric turbulent jet mixing layer 21 p2947 N88-27504

TURBULENT WAKES
NT PROPELLER SLIPSTREAMS
NT SLIPSTREAMS
The influence of high free stream turbulence, intensive cooling and wake on the external heat transfer of convectively cooled gas turbine blades [ETN-87-90432] 01 p0056 N88-10360
A natural low frequency oscillation in the wake of an airfoil near stalling conditions [NASA-TM-100213] 02 p0123 N88-10779
Calculations of the turbulent wake behind a slender self-propelled double-body and comparisons with experiment [AD-A185661] 06 p0703 N88-14314
Investigation of large-scale structures in the near wake of a parallel flat plate [DFVLR-FB-87-31] 09 p1162 N88-16967
Coherent vortex structures in the wake of a stationary disk and of a disk excited to vibration [ESA-TT-994] 09 p1163 N88-16968
SAR (Synthetic Aperture Radar) imaging of ship wakes in the Gulf of Alaska [AD-A186554] 10 p1317 N88-17872
Wake interaction effects on the transition process on turbine blades [AD-A188020] 10 p1332 N88-17962
Structure of shear flow turbulence and its control [AD-A187909] 11 p1482 N88-18846
Active feedback interaction with a shear layer [AD-A188525] 12 p1573 N88-19410
Effect of freestream turbulence on a two dimensional cascade, with different surface roughness, at high Reynolds number [AD-A190615] 15 p2065 N88-22316
Characteristics of merging shear layers and turbulent wakes of a multi-element airfoil [NASA-TM-100053] 18 p2511 N88-24900
Numerical simulation and stability analysis of the absolutely and convectively unstable wake [DFVLR-FB-88-09] 21 p2949 N88-27518
Hot-wire measurements of compressor blade wakes in a cascade wind tunnel [AD-A194737] 23 p3181 N88-28936
Investigation of large-scale structures in the near wake of a parallel flat plate [ESA-TT-1100] 24 p3372 N88-30080

TURING MACHINES
Machine models and simulations [PB88-118690] 10 p1386 N88-18280
A labeling procedure for linear finite-state codes 11 p1472 N88-18781
Further results on finite-state codes 11 p1472 N88-18782
ESKISS: A program for optimal state assignment [EUT-87-E-167] 14 p1956 N88-21659
Tape versus queue and stacks: The lower bounds [CWI-CS-R8752] 16 p2249 N88-23437
Simple multireader registers using time-stamp schemes [CWI-CS-R8758] 20 p2835 N88-26819

TURKEY
Karst and submarine fresh water discharge in the Antalya area, southern Turkey 22 p3102 N88-28421

TVC (CONTROL)
U THRUST VECTOR CONTROL

TWENTY-SEVEN DAY VARIATION
Short term variability between 120 and 300 mm from Solar Mesosphere Explorer (SME) observations [AERONOMICA-ACTA-A-328-1988] 23 p3308 N88-29709

TWINNING
The structure and properties of twin boundaries in superconducting YBa2Cu3O7 [DE88-003864] 10 p1418 N88-18468
Single-crystal structural study of La2Cu/sub 0.95/Li/sub 0.05/O4 [DE88-003482] 11 p1554 N88-19302
Materials dependence of deformation texture development in various deformation modes [DE88-004312] 14 p1922 N88-21457
To the twinning plane superconductivity theory [DE88-702195] 20 p2874 N88-27058

TWISTING
Magnetic field twist driven by remote convective motions: Characteristics and twist rates 01 p0113 N88-10724
Twisted cube [PB87-162814] 09 p1220 N88-17316
Magnetization studies of multifilamentary Nb3Sn wires [DE88-009103] 19 p2735 N88-26243

TWO BODY ORBITS
U TWO BODY PROBLEM

TWO BODY PROBLEM
Propagation of random initial conditions in time 04 p0486 N88-12993
The avoidance of collisions for Newtonian bodies with hidden variables [RSRE-87013] 22 p3041 N88-28053

TWO DIMENSIONAL BODIES
A critical assessment of wind tunnel results for the NACA 0012 airfoil [NASA-TM-100019] 03 p0260 N88-11636
Development of the computer program for turbulent boundary layers 05 p0536 N88-13264
Rarefied gas numerical wind tunnel. 2: Two-dimensional and axially symmetric bodies 05 p0538 N88-13273
Three-dimensional flow past a two-dimensional body 05 p0539 N88-13280
Computation of flow around 2-D circular cylinder 05 p0539 N88-13284
Navier-Stokes analysis of laminar flow control of a two-dimensional airfoil 05 p0540 N88-13286
SUSIE reference manual [DE88-001462] 05 p0636 N88-13893
Potential flow around two-dimensional airfoils using a singular integral method [NASA-CR-182345] 06 p0664 N88-14070
Electromagnetic propagation in PEC and absorbing curved S-ducts [NASA-TM-100833] 12 p1621 N88-19698
Nonlinear resonance of two-dimensional ion layers [AD-A188890] 12 p1695 N88-20145
Organic metal (ET)4Hg3Br8A quasi-two-dimensional superconductor 14 p1974 N88-21778
Boundary shape identification problems in two-dimensional domains related to thermal testing of materials [NASA-CR-181654] 15 p2105 N88-22541
Two-dimensional graphics tools for a transputer based display board [NASA-TM-100820] 15 p2113 N88-22591
A finite-element alternating method for two-dimensional Mode-1 crack configurations [NASA-TM-100616] 16 p2224 N88-23276
Preliminary 2-D shell analysis of the space shuttle solid rocket boosters [NASA-TM-100515] 17 p2348 N88-23989

TWO DIMENSIONAL BOUNDARY LAYER
Prediction of turbine blade heat transfer 02 p0187 N88-11162
Numerical simulation of unsteady separated flows [AD-A184132] 04 p0442 N88-12741
An experimental investigation of the ignition and flammability limits of various hydrocarbon fuels in a two-dimensional solid fuel ramjet [AD-A184968] 05 p0549 N88-13342
Boundary layer calculation using digital computers [REPT-MM-4] 10 p1309 N88-17821

Experimental investigation of two-dimensional confined jet thrust vector control
[AD-A189845] 15 p2027 N88-22077

TWO DIMENSIONAL FLOW

NT COUETTE FLOW

A transonic model representation for two-dimensional wall interference assessment
[NLR-TR-86026-U] 01 p0001 N88-10006

An inviscid model of planar, separated flows of finite extent
[RAE-TR-86070] 01 p0044 N88-10279

Rayleigh-Benard convection in a Hele-Shaw cell: A numerical study
[KFK-4212] 01 p0044 N88-10280

Generation of body-fitted grids for two dimensional interior domains by the solution of a system of Poisson equations using multigrid techniques
[GMD-246] 01 p0044 N88-10281

Two-dimensional shear flow turbulence: A statistical theory of vortex filaments
[DE87-012234] 01 p0046 N88-10295

Locating parallel numerical tasks in the solution of viscous fluid flows
[DE87-013510] 02 p0169 N88-11064

Point vortex dynamics: Recent results and open problems
[DE87-014759] 03 p0314 N88-11982

Numerical calculation of two dimensional fluid flow with strong shocks
[KFK-4191] 03 p0314 N88-11986

Conjugated heat transfer from a radiating fluid in a rectangular channel 03 p0317 N88-12003

Solution of the two-dimensional Euler equations on unstructured triangular meshes
04 p0396 N88-12469

A free-Lagrange method for 2-D compressible flows
[DE88-000216] 04 p0442 N88-12745

Continuation finite element analysis of viscoelastic fluids 04 p0445 N88-12761

Computation of dynamic stall of NACA0012 airfoil by block pentadiagonal matrix scheme
05 p0535 N88-13255

Practical application of two-dimensional viscous flow computation 05 p0535 N88-13257

The role of computation fluid dynamics in aeronautical engineering (4). The development and applications of implicit TVD finite volume code
05 p0536 N88-13259

Numerical analysis of cascade flow solving Navier-Stokes equations 05 p0536 N88-13262

Inverse design method for two-dimensional transonic cascades 05 p0536 N88-13263

Numerical prediction of turbulent flows in dump diffusers 05 p0537 N88-13265

Three-dimensional structure of boundary layers in transition to turbulence
[AD-A185466] 06 p0702 N88-14311

Upwind relaxation algorithms for Euler/Navier-Stokes equations 07 p0810 N88-14931

An explicit method for the solution of the Euler equations, applied to unsteady two dimensional flows
[ETN-88-90807] 07 p0855 N88-15194

Parametric study of choke flutter with a linear theory
10 p1283 N88-17673

A numerical study of unsteady two-dimensional subsonic compressible base flow 10 p1327 N88-17931

Well-posedness and spectral estimation for infinite dimensional systems
[AD-A187621] 10 p1401 N88-18354

An experimental investigation of straight and curved annular wall jets
[NASA-CR-182546] 11 p1434 N88-18557

Experimental study of two-dimensional vortex patterns for impulsively started bodies in comparison with other configurations 11 p1435 N88-18562

Two and three dimensional elliptic flows
11 p1485 N88-18866

A generalisation of Hall's scheme for solving the Euler equations for two-dimensional flows
11 p1537 N88-19186

A multigrid solver for two-dimensional transonic full potential flow calculations 11 p1538 N88-19189

Application of a flux vector splitting methodology towards the solution of unsteady transonic flows, with future emphasis on the blade flutter problem
[AD-A189500] 13 p1716 N88-20260

Solution of two-dimensional Euler equations: Experience with a finite volume code
[DFVLR-FB-87-41] 13 p1767 N88-20572

An explicit method for the solution of the Euler equations applied to unsteady two-dimensional flows
[MBB/LKE-121/S/PUB/257] 14 p1910 N88-21411

Random-choice based hybrid methods for one and two dimensional gas dynamics
[CAR-88-01] 14 p1910 N88-21415

Flexiwall 3 SO: A second order predictive strategy for rapid wall adjustment in two-dimensional compressible flow
[NASA-CR-181662] 15 p2015 N88-22018

Effect of freestream turbulence on a two dimensional cascade, with different surface roughness, at high Reynolds number
[AD-A190615] 15 p2065 N88-22316

Application of a multigrid method for solving the Navier-Stokes equation in two-dimensional flow problems
[KU-SFB-210/T/32] 16 p2206 N88-23164

Accounting for the effects of unsteady, separated boundary layers in transonic two dimensional calculations
[ONERA-RT-30/3064-RY-063-R]
17 p2338 N88-23952

Surface curvature and pressure gradient effects on turbulent flow: An assessment based on numerical solution of the Reynolds equations 17 p2338 N88-23954

Prediction of laminar and turbulent flows past single and twin airfoils 18 p2457 N88-24589

Gas diffusion studies in steady and nonsteady cavities
18 p2512 N88-24902

A characteristic method for calculating the generalized flat flutter aerodynamic forces
[NASA-TT-20300] 19 p2598 N88-25438

Two-dimensional viscous flow computations of hypersonic scramjet nozzle flowfields at design and off-design conditions
[NASA-CR-182150] 19 p2603 N88-25459

One person's view of velocity-coupled instability
19 p2629 N88-25595

An initial investigation into methods of computing transonic aerodynamic sensitivity coefficients
[NASA-CR-183061] 20 p2752 N88-26332

Calculation of 2-D unsteady transonic full potential flow about oscillating airfoils by two complementary approaches
[PB88-127519] 20 p2753 N88-26341

Heterogeneous diffusion flame stabilization
[AD-A193014] 20 p2771 N88-26429

A numerical simulation of two-dimensional transient shear flow
[ISAS-RN-627] 20 p2797 N88-26600

Treatment of the separated flow around profiles (nonviscous, incompressible, two dimensional flow) by the singularities method
[ISL-R-106/87] 20 p2803 N88-26633

Implicit finite-difference simulation of an internal flow on a hypercube
[AD-A192474] 21 p2942 N88-27471

The calculation of the flow through a two-dimensional faired diffuser
[PNR90433] 22 p3076 N88-28259

Two-dimensional flow through a turbine cascade
[PDR/CFDU/IC/34] 22 p3076 N88-28264

Mass transport in flow of sources
[LRT-WE-9-FB-4(1987)] 22 p3077 N88-28268

Regular and chaotic motion of fluid particles in a two dimensional fluid
[PREPRINT-591] 22 p3078 N88-28278

Holographic flow visualization
[PNR90486] 22 p3079 N88-28283

Analyses and optimization of truncated scarf nozzles subject to external flow conditions
[NASA-TM-100955] 24 p3316 N88-29746

Numerical modelling of premixed flames in gaseous media 24 p3350 N88-29944

TWO DIMENSIONAL JETS

Techniques utilized in the simulated altitude testing of a 2D-CD vectoring and reversing nozzle
[NASA-TM-100872] 19 p2604 N88-25464

TWO DIMENSIONAL MODELS

Two-dimensional numerical modeling of the life cycle of fog 02 p0209 N88-11311

Two-dimensional static otolith model
10 p1367 N88-18167

Stability requirement FOT ignition and high gain implosion = 2-D simulation for high neutron yield experiment = 16 p2276 N88-23633

Theoretical study and numerical simulation of flame fronts
[PB88-122932] 22 p3051 N88-28104

TWO FLUID MODELS

A two-fluid model for solar wind fluid with higher order moments 01 p0116 N88-10739

International workshop on two-phase flow fundamentals
[DE88-001478] 06 p0699 N88-14287

Two-fluid turbulence models and reciprocating engines
[CFD/87/6] 14 p1918 N88-21449

ATHENA simulation of the 300 kW SP-100
17 p2414 N88-24357

Computer simulation of turbulent combustion in reciprocating engines
[CFDU/87/11] 18 p2482 N88-24725

The application of the two-fluid model of turbulence to the 3-D simulation of turbulent combustion in reciprocating engines
[PDR/CFDU/IC/37] 22 p3052 N88-28110

TWO PHASE FLOW

Thermal Control Working Group report
01 p0016 N88-10094

The numerical simulation of an idealised one-dimensional, steady monopropellant rocket
[PDR/CFDU/IC/31] 01 p0018 N88-10107

Research on one-dimensional two-phase flow: Theory on hydrodynamic balance in two fluid model and its application
[DE87-702615] 01 p0045 N88-10290

Two-phase non-Newtonian hydrodynamic modeling of slurries
[DE87-011519] 01 p0047 N88-10298

Problem specifications and collated solutions of the two-phase numerical-benchmark exercise 1986-7 — two phase flow
[CFDU/87/1] 01 p0047 N88-10300

Numerical simulation of transient two-phase flow
[CFDU/87/4] 02 p0171 N88-11077

Computer modeling of two-phase flow
[CFDU/87/5] 02 p0171 N88-11078

The dynamics of bubble growth for Rayleigh-Taylor unstable interfaces
[AD-A184752] 03 p0321 N88-12027

A study of two-phase flow in a reduced gravity environment
[NASA-CR-172035] 04 p0422 N88-12617

Geometric analysis of ensemble of solutions in two-phase flow and complete resolution of problem of choking
[DE88-001687] 04 p0445 N88-12764

Analysis of internal flows relative to the space shuttle main engine
[NASA-CR-179240] 06 p0674 N88-14125

International workshop on two-phase flow fundamentals
[DE88-001478] 06 p0699 N88-14287

Theoretical and numerical analysis of shock wave propagation through different dusty-gas mixture layers
06 p0699 N88-14292

An investigation into flow regimes for two-phase helium flow
[DE88-002834] 07 p0853 N88-15181

Influence of the friction coefficients, the power and the flowrate on the two-phase flow instabilities in natural circulation
[DE88-700036] 08 p0983 N88-15946

A review of two-phase flow-induced vibration
[DE88-001955] 09 p1160 N88-16955

Two-phase flow forms and pressure drop in horizontal T tube joints with vertical branch
[GKSS-87/E/12] 09 p1163 N88-16969

An analysis of the closure conditions for two-fluid models of two-phase flow
[DE88-003355] 09 p1164 N88-16982

An experiment to investigate Rankine cycle two-phase microgravity issues
[DE88-004197] 10 p1308 N88-17818

Boundary integral analysis of flow and deformation of long bubbles in capillaries
[DE88-002110] 10 p1326 N88-17927

Mechanistic model for void distribution in flashing flow
[DE88-002948] 10 p1326 N88-17928

Digital imaging techniques for single- and multi-phase reacting flowfields 10 p1327 N88-17933

A review of flow-induced vibration in two-phase flow
[DE88-002873] 10 p1329 N88-17946

Experimental investigation of low gravity two-phase flow behavior
[DE88-003779] 11 p1466 N88-18741

Diagnostics for research in atomization and turbulent two-phase flows
[AD-A187338] 11 p1482 N88-18843

Kinetic and turbulence models for granular and two-phase flows 11 p1484 N88-18862

To the problem of determining true volume steam content by measured values of mean density of a mixture in thermally unsteady two-phase flows
[DE88-700640] 12 p1626 N88-19728

Two-phase flows in the wake of in-cylinder projectiles
[AD-A189422] 13 p1765 N88-20559

Experimental and numerical study of liquid distribution in dispersive-annular flow
[DE88-700844] 14 p1909 N88-21406

Dense-spray structure and phenomena. Part 1: Turbulence/dispersed-phase interactions
[AD-A190606] 15 p2065 N88-22315

Noncondensing round turbulent gas jets in liquids
[AD-A191191] 16 p2208 N88-23179

Modeling of cavitation phenomena in homogeneous flow in transitory regimes in pipes
[ISAL-IDI1-87-15] 17 p2337 N88-23948

Pumped two-phase heat transfer loop
[NASA-CASE-MSC-20841-2] 17 p2339 N88-23958

Two-phase fluid management for a Rankine cycle isotope power system 17 p2405 N88-24303

An experiment to investigate Rankine cycle two-phase microgravity issues 17 p2409 N88-24322

ATHENA heat pipe transient model
17 p2412 N88-24344

Reduced-gravity two-phase flow experiments in the NASA KC-135 17 p2431 N88-24465

Analysis and interpretation of low gravity boiling experiments in the KC-135 17 p2432 N88-24466

Microgravity two-phase fluid flow pattern modeling
17 p2432 N88-24467

Experimental investigation of a microgravity separator for two phase mixtures containing small volumes of gas/vapor 17 p2432 N88-24468

Liquid phase decomposition in slurry fuels
19 p2624 N88-25564

Noise generation by air bubbles in water: An experimental study of creation and splitting
[AD-A192063] 19 p2664 N88-25839

An arranging method on L/D of two-phase closed thermosyphons 20 p2783 N88-26508

Characteristics of long size thermosyphons made of corrugated tube 20 p2784 N88-26511

Investigation of the quasi-steady approach used in transient two-phase flow analysis
[DE88-004303] 21 p2944 N88-27489

Mass flow rate influence on void fraction of two-phase helium flow
[DE88-702456] 21 p2945 N88-27495

Two phase flow in a rotating screw tube (screw tube pump). Investigation of the function and efficiency of the screw tube pump
[MPIS-16/1987] 23 p3222 N88-29178

Experimental and analytical study of two-phase flow in zero gravity
[AD-A195223] 24 p3358 N88-29993

Boltzmann equation approach to two-phase flow turbulence
[AD-A196153] 24 p3373 N88-30086

TWO PHASE SYSTEMS

U BINARY SYSTEMS (MATERIALS)

TWO PHOTON COHERENT STATES

U SQUEEZED STATES (QUANTUM THEORY)

TWO REFLECTOR ANTENNAS

Study of dual beam antenna systems for the data relay satellite, volume 1
[S-272-02-VOL-1] 09 p1152 N88-16905

Study of dual beam antenna systems for the data relay satellite. Volume 2: Executive summary
[S-272-03-VOL-2] 09 p1153 N88-16906

TWO-WAVELENGTH LASERS

Dye laser for holographic interferometry
07 p0920 N88-15588

Discussion of two-mode two-photon CW laser oscillation 16 p2187 N88-23042

TYPE 3 BURSTS

Small-scale structure in solar flare radio emission
08 p1097 N88-16598

TYPHOONS

Tropical cyclone intensity prediction based on empirical orthogonal function representation of wind and shear fields
[AD-A184699] 03 p0353 N88-12229

Annual tropical cyclone report, 1986
[AD-A184082] 04 p0470 N88-12903

Opportunities for tropical cyclone motion research in the Northwest Pacific region
[AD-A185068] 05 p0627 N88-13834

Typhoon structural evolution
[AD-A188090] 07 p0879 N88-15333

U

U BENDS

Laminar flow heat transfer downstream from U-bends
11 p1484 N88-1885

Numerical computation of three-dimensional turbulent flow in tightly curved ducts and spiral turbine casings
[ETN-88-92362] 21 p2948 N88-27511

U.S.S.R.

USSR report: Space
[JPRS-USP-87-003] 01 p0009 N88-10050

Errors associated with Russian name transliteration
[DE87-011717] 02 p0248 N88-11566

Assessment of the impacts of transferring certain nuclear reactor technologies to the Soviet Union and Eastern Europe
[DE87-014388] 02 p0249 N88-11576

USSR report: Engineering and equipment
[JPRS-UEQ-87-008] 04 p0423 N88-12621

USSR report: Earth sciences
[JPRS-UES-86-006] 04 p0458 N88-12831

Astrophysics observatory in Byurakan
[AD-A185144] 05 p0660 N88-14050

USSR report: Earth sciences
[JPRS-UES-87-004] 06 p0725 N88-14455

Polar Geophysical Institute's studies of magnetosphere, ionosphere 06 p0728 N88-14480

JPRS report: Science and technology. USSR: Life sciences
[JPRS-ULS-87-011] 06 p0749 N88-14601

USSR Space Life Sciences Digest index to issues 10-14
[NASA-CR-3922(17)] 07 p0883 N88-15361

Soviet state ergonomic standards (GOST)
[AD-A185537] 07 p0900 N88-15450

USSR report: Physics and mathematics
[JPRS-UPM-87-002] 07 p0918 N88-15575

USSR Space Life Sciences Digest, issue 14
[NASA-CR-3922(16)] 08 p1045 N88-16317

JPRS report: Science and technology. USSR: Physics and mathematics
[JPRS-UPM-87-009] 09 p1233 N88-17395

Proceedings of the First International Symposium on Physical and Technical Problems of Superconductivity Application in Power Generation
[DE88-700818] 11 p1559 N88-19332

Soviet high-technology restructuring drive: the MNTK network
[AD-A188138] 11 p1565 N88-19370

USSR report: Life sciences. Biomedical and behavioral sciences
[JPRS-UBB-87-010] 12 p1651 N88-19889

USSR report: Life sciences. Biomedical and behavioral sciences
[JPRS-UBB-87-008] 12 p1662 N88-19966

JPRS report: Science and technology. USSR: Life sciences
[JPRS-ULS-88-002] 12 p1665 N88-19982

Soviet military power, 1987 13 p1858 N88-21114

JPRS report: Science and technology. USSR: Materials science
[JPRS-UMS-87-009] 14 p1884 N88-21261

USSR Space Life Sciences Digest, issue 16
[NASA-CR-3922(19)] 15 p2101 N88-22515

Soviet remote sensing research and technology
[FASAC-TAR-3130] 17 p2389 N88-24108

Bibliography of Soviet laser developments, number 83, May - June 1986
[AD-A190969] 18 p2520 N88-24950

USSR space life sciences digest, issue 18
[NASA-CR-3922(21)] 19 p2707 N88-26096

Soviet dynamic fracture mechanics research
[FASAC-TAR-3140] 21 p2962 N88-27597

History of manned spaceflight
[CNES-NT-121] 21 p3032 N88-28000

Bibliography of Soviet laser developments, number 88, March - April 1987
[AD-A195978] 24 p3378 N88-30116

U.S.S.R. SPACE PROGRAM

Blagov commentary on Mir station, first manning
01 p0009 N88-10051

JPRS report: Science and technology. USSR: Life sciences
[JPRS-ULS-87-009] 04 p0473 N88-12915

JPRS report: Science and technology. USSR: Space
[JPRS-USP-87-006] 08 p1001 N88-16063

USSR Space Life Sciences Digest, issue 15
[NASA-CR-3922(18)] 10 p1368 N88-18175

Basic results of medical studies during prolonged manned flights on-board the Salyut-7/Soyuz-T orbital complex
[NASA-TT-20217] 10 p1369 N88-18182

Medilab: A project of a medical laboratory in space
12 p1660 N88-19946

JPRS report: Science and technology. USSR: Space
[JPRS-USP-88-002] 13 p1724 N88-20312

Soviet space transport systems
13 p1727 N88-20328

Features of Soyuz TM spacecraft
13 p1727 N88-20329

International manned flight, USSR-SAR
[NASA-TT-20260] 16 p2166 N88-22914

The USSR space systems for remote sensing of earth resources and the environment (sensor systems, processing techniques, applications)
17 p2356 N88-24035

USSR Space Life Sciences Digest, Issue 17
[NASA-CR-3922(20)] 17 p2381 N88-24155

Soviet space program handbook
[AD-A194332] 22 p3046 N88-28077

The Soviet MIR space station
[AD-A194040] 23 p3184 N88-28951

JPRS report: Science and technology. USSR: Space
[JPRS-USP-88-001] 24 p3444 N88-30498

U-2 AIRCRAFT

First results from the Airborne Visible/Infrared Imaging Spectrometer (AVIRIS) 06 p0707 N88-14335

UH-1 HELICOPTER

Preliminary airworthiness evaluation of a UH-1 equipped with a terrain mapping receiver antenna
[AD-A186274] 07 p0819 N88-14980

UH-60A HELICOPTER

Analytic investigation of helicopter rotor blade appended aeroelastic devices
[NASA-CR-166525] 03 p0266 N88-11676

Preliminary airworthiness evaluation of the UH-60A with Advanced Digital Optical Control System (ADOCS)
[AD-A190674] 15 p2018 N88-22030

Airworthiness and flight characteristics test of a ski assembly for the UH-60A Black Hawk helicopter
[AD-A191414] 16 p2162 N88-22895

UHTREX (NUCLEAR REACTORS)

U HIGH TEMPERATURE NUCLEAR REACTORS

UK SATELLITES

Validate algorithms for the determination of rainfall rates from SSM/I microwave satellite imagery
[AD-A191337] 16 p2236 N88-23353

Validate algorithms for the determination of rainfall rates from SSM/I microwave satellite imagery
[AD-A195428] 24 p3404 N88-30270

UK SPACE PROGRAM

Developments in ocean colour research in the United Kingdom 08 p1043 N88-16306

ULLAGE

Development and evaluation of an airplane fuel tank ullage composition model. Volume 2: Experimental determination of airplane fuel tank ullage compositions
[AD-A190408] 15 p2017 N88-22025

ULTRAHIGH FREQUENCIES

A digital audio link to the Channel Islands in the UHF television band: Protection of television signals from digitally modulated interference
[BBC-RD-1987/7] 02 p0161 N88-11010

A digital audio link to the Channel Islands in the UHF television band: Preliminary experimental results
[BBC-RD-1987/9] 02 p0161 N88-11011

Performance of high power S-band klystrons focused with permanent magnet
[DE87-753024] 02 p0167 N88-11053

A conformal aircraft phased array antenna for airplane-satellite communication in the L band
[ESA-TT-1057] 03 p0305 N88-11926

Atomic frequency standards for ultra-high-frequency stability 04 p0433 N88-12685

Improvements to a UHF rebroadcast television link suffering tidal fading: Countisbury UHF relay station
[BBC-RD-1987/14] 05 p0573 N88-13495

Two-signal cross modulation effects, half-IF effects and interference criteria in land mobile sharing with UHF (Ultra High Frequency) television
[PB87-228037] 05 p0576 N88-13514

VHF/UHF propagation by diffraction: Calculation by numerical integration 12 p1615 N88-19659

A diffraction based theoretical model for prediction of UHF path loss in cities 12 p1616 N88-19661

Increasing the rate at which ceramic castings undergo preliminary heat-treatment in an ultra-high frequency magnetic field 14 p1886 N88-21275

IREPS (Integrated Refractive Effects Prediction System) 3.0, user's manual
[AD-A190398] 16 p2188 N88-23045

The AMSC mobile satellite system
19 p2643 N88-25681

Propagation effects by roadside trees measured at UHF and L-band for mobile satellite systems
19 p2644 N88-25693

Development of a mobile satellite communication unit
19 p2646 N88-25701

Technical characteristics of the OmniTRACS: The first operation mobile Ku-band satellite communications system 19 p2647 N88-25709

Omni-directional L-band antenna for mobile communications 19 p2648 N88-25717

A microstrip array feed for MSAT spacecraft reflector antenna 19 p2652 N88-25747

ULTRAHIGH VACUUM

The effect of additives on the reactivity of palladium surfaces for the chemisorption and hydrogenation of carbon monoxide: A surface science and catalytic study
[DE87-014685] 02 p0145 N88-10909

Ceramics thin film 04 p0403 N88-12505

Calculated sputtering and atomic displacement cross-sections for applications to medium voltage analytical electron microscopy
[DE88-002904] 09 p1168 N88-17006

In situ ultrahigh vacuum friction measurement and wear track analysis of ion implanted 304 stainless steel
[DE86-004537] 11 p1494 N88-18922

best copy available

Mechanical design of a ultrahigh gravity UHV facility to launch and recover a low-speed projectile tested on board KC 135 14 p1877 N88-21216
Robotic joint experiments under ultravacuum
14 p1927 N88-21490
Analysis of the performance of the space ultravacuum research facility in attached and free-flyer mode
[NASA-TM-100325] 20 p2763 N88-26387

ULTRALIGHT AIRCRAFT
Structural and material testing of a composite microlite wing model
[BU-355] 14 p1923 N88-21461
Aeroacoustic investigation on the noise from ultralight aircraft
[DFVLR-FB-88-03] 21 p3013 N88-27879

ULTRALOW FREQUENCIES
U EXTREMELY LOW RADIO FREQUENCIES

ULTRALOW TEMPERATURE
U CRYOGENIC TEMPERATURE

ULTRAPURE METALS
Center for the Space Processing of Engineering Materials 07 p0838 N88-15083

ULTRASHORT PULSED LASERS
Dynamic restructuring of pulsed CO2 laser frequency and multiple-peak generation in a cell with IR-absorbing gas in the resonator 07 p0919 N88-15580
A picosecond tunable ultrashort cavity dye laser
14 p1902 N88-21361
SDIO/IST ultrashort wavelength laser: Novel experimental schemes for observing the Mossbauer effect in long-lived nuclear levels
[AD-A190275] 15 p2072 N88-22351
SDIO/IST ultrashort wavelength laser. Mossbauer effect in gamma-ray lasers
[AD-A190306] 15 p2072 N88-22352

ULTRASONIC FLAW DETECTION
Ultrasonic examination of high performance polymer composites
[DRIC-T-7862] 01 p0027 N88-10170
Nondestructive inspection of the pressure vessel in Stuttgart. ALOK part. Phase 1: ALOK combined with conventional probes
[REPT-860113-TW] 01 p0057 N88-10367
Stationary reconstruction method. Development, test and comparison in ultrasonic testing
[REPT-860125-TW] 01 p0057 N88-10368
Imaging of planar defects with synthetic aperture focusing technique (LSAFT) --- ultrasonic inspection
[VTT-468] 01 p0058 N88-10370
Method for the ultrasonic inspection of the soundness of the metal in weld joints in two-ply pipes
[BLL-CE-TRANS-8265-(9022.09)]
04 p0453 N88-12805
Ultrasonic method of inspecting austenitic weld joints in nuclear power station equipment
[BLL-CE-TRANS-8281-(9022.09)]
04 p0453 N88-12806
Nondestructive characterization of ceramic composite whiskers with neutron diffraction and ultrasonic techniques
[DE88-003075] 08 p0965 N88-15844
Scattering of longitudinal wave normally incident on discal cavity in elastic body 08 p1077 N88-16492
Ultrasonic inspection of advanced CFRP structures by computer-controlled, pulse-echo technique
[ETN-88-91665] 09 p1177 N88-17051
Focused ultrasonic backscatter technique for near-surface flaw detection in structural ceramics
[DE88-003112] 09 p1183 N88-17091
Institute for Materials Science and Engineering, nondestructive evaluation: Technical activities 1987
[PB88-153655] 10 p1342 N88-18020
Backscatter from flaws in fiber-reinforced composites
11 p1450 N88-18639
Reference standards for nondestructive tests
[AD-A187766] 11 p1497 N88-18936
STA-2A NDT testing
[NASA-CR-179301] 11 p1497 N88-18937
Comparison of ultrasonic flaw detection analysis for spherical composite test specimens using two data acquisition techniques
[DE88-005002] 12 p1634 N88-19782
Nondestructive testings of HTGR graphites
13 p1747 N88-20446
Ultrasonic inspection of irregular surfaces
[AERE-R-12465] 13 p1780 N88-20648
A system to measure damage in composite materials by the ultrasonic method
[ONERA-RT-2/7256-RY-061-R]
15 p2031 N88-22103
Ultrasonic characterization of ceramic joints
[DE88-005844] 15 p2043 N88-22173
Manufacturing of ultrasonic focused probes
[VTT-RR-487] 15 p2074 N88-22368
Nondestructive evaluation by acousto-ultrasonics
15 p2082 N88-22412
Characterization of sintered SiC by using NDE
15 p2082 N88-22413
Systems for ultrasonic scanning, analysis and imagery
15 p2082 N88-22414
Nondestructive testing using ultrahigh frequencies
[CERT-5/1333-MO] 18 p2526 N88-24984
Design and implementation of contact ultrasonic sensors to assess internal damage
[I-177/87] 21 p2906 N88-27247
Interface control using low frequency (3 to 20 MHz) acoustic microscopy
[REPT-48-411/F] 21 p2959 N88-27577
Ultrasonic method and apparatus for determining crack opening load
[NASA-CASE-LAR-13889-1] 24 p3385 N88-30160

ULTRASONIC RADIATION
Model for ultrasonic attenuation and elastic constant in chromium and its alloys
[DE87-703478] 04 p0415 N88-12570
Anomalies in electromagnetic absorption of circularly polarized ultrasonic waves by tungsten within Doppler-shifted cyclotron resonance range
06 p0775 N88-14756
Imaging subtle microstructural variations in ceramics with precision ultrasonic velocity and attenuation measurements
[NASA-TM-100129] 07 p0867 N88-15257
Ultrasonic testing of near-surface zones using scattered signals
[ETN-88-90813] 07 p0929 N88-15642
Attenuation of ultrasonic waves in nonmagnetized magnetic fluids 09 p1234 N88-17398

ULTRASONIC SCANNERS
Ultrasonic inspection of irregular surfaces
[AERE-R-12465] 13 p1780 N88-20648

ULTRASONIC TESTS
High precision ultrasonic scanning system and SAFT-UT development
[DE87-010038] 01 p0008 N88-10044
Ultrasonic examination of high performance polymer composites
[DRIC-T-7862] 01 p0027 N88-10170
Nonintrusive ultrasonic flow measurement techniques and their applications to BTU metering
[DE87-011390] 01 p0045 N88-10286
Evaluation of mechanical and technological parameters of different steel states by nondestructive micro- and macromagnetic measuring quantities as well as ultrasonic techniques
[MPA-810-079] 01 p0057 N88-10366
Stationary reconstruction method. Development, test and comparison in ultrasonic testing
[REPT-860125-TW] 01 p0057 N88-10368
Model-based ultrasonic tomography
[DE87-013786] 01 p0058 N88-10369
Needs assessment for NDT and characterization of ceramics: Assessment of inspection technology for green state and sintered ceramics
[DE87-013550] 02 p0151 N88-10947
Ultrasonic mechanized checking of weld joints of nuclear power plant equipment 02 p0158 N88-10987
Transply crack density detection by acousto-ultrasonics
[NASA-TM-100224] 03 p0279 N88-11758
Ultrasonic characterization of the nonlinear elastic properties of unidirectional graphite/epoxy composites
[NASA-CR-4100] 03 p0281 N88-11767
Flaw imaging and ultrasonic techniques for characterizing sintered silicon carbide
[NASA-TM-100177] 03 p0334 N88-12106
Real time analysis of the results from mechanized ultrasonic testing
[DE87-752511] 03 p0334 N88-12107
Elastodynamic ray theory and asymptotic methods for direct and inverse scattering problems
03 p0335 N88-12108
Improvement of deep resolution in ultrasonic echographic nondestructive evaluation using signal processing methods
[PB87-147658] 07 p0866 N88-15256
Ultrasonic testing of near-surface zones using scattered signals
[ETN-88-90813] 07 p0929 N88-15642
A-scan ultrasound measurement of ocular changes during accommodation
[AD-A186818] 09 p1198 N88-17181
Ultrasonic characterization of layered composite systems 10 p1404 N88-18374
Imaging methods for nondestructive materials testing
[ETN-88-91477] 11 p1497 N88-18940
Ultrasonic characterization of non-uniform porosity distributions in SiC ceramic
[DE88-004814] 13 p1749 N88-20459
Changes in the status of the human tibia during antiorthostatic hypokinesia
[NASA-TT-20221] 13 p1810 N88-20813
Detection of bonding delaminations in multilayer structures with lossy components
[NASA-CR-182716] 14 p1883 N88-21256
Nonlinear acoustic parameter and its application in ultrasonic imaging 14 p1902 N88-21364
A system to measure damage in composite materials by the ultrasonic method
[ONERA-RT-2/7256-RY-061-R]
15 p2031 N88-22103
Ultrasonic beam distortion in transversely isotropic media
[DE88-005937] 15 p2129 N88-22699
Ultrasonic Time-Of-Flight Diffraction (TOFD) measurements of crack depths in an acceleration reservoir of a high velocity research gun
[DE88-006644] 16 p2164 N88-22807
Nondestructive evaluation of large scale composite components
[AD-A190998] 16 p2173 N88-22854
Utility NDE personnel qualification/certification: Enhanced personnel qualification requirements for ASME (American Society for Mechanical Engineers) Code Section 11 examinations
[DE88-006748] 16 p2216 N88-23222
Acousto-ultrasonic input-output characterization of unidirectional fiber composite plate by SV waves
[NASA-CR-4152] 16 p2217 N88-23224
High frequency ultrasonic characterization of sintered SiC
[NASA-TM-100825] 17 p2347 N88-23985
Input-output characterization of fiber composites by SH waves
[NASA-CR-4153] 17 p2347 N88-23986
Characterization of noncontact piezoelectric transducer with conically shaped piezoelement
[NASA-CR-4151] 17 p2347 N88-23987
Interaction of ultrasonic waves with composite plates
[AD-A191879] 18 p2478 N88-24702
Knowledge based systems in nondestructive evaluation
[DE88-006653] 18 p2525 N88-24981
Direct and inverse diffraction problems for QNDE (Quantitative Non-Destructive Evaluation) applications
[AD-A194721] 22 p3085 N88-28322
Ultrasonic method and apparatus for determining crack opening load
[NASA-CASE-LAR-13889-1] 24 p3385 N88-30160

ULTRASONIC WAVE TRANSDUCERS
The application of group radiators for the determination of tension crack corrosion
[BAM-06264] 01 p0022 N88-10141
New wide-band transducer developed
14 p1901 N88-21353
In-flight measurement of ice growth on an airfoil using an array of ultrasonic transducers
[AIAA-PAPER-87-0178] 17 p2293 N88-23717

ULTRASONIC WAVES
U ULTRASONIC RADIATION

ULTRASONIC WELDING
Modeling of laser ultrasound generation in a weld pool
[DE88-005546] 13 p1834 N88-20871
Ultrasonic and video computerized data acquisition for automated welding
[DE88-006741] 19 p2677 N88-25018

ULTRASONICS
Experimental investigation in a wind tunnel of the stability and vorticity of the vortex breakdown phenomenon above delta wings, using the ultrasonic laser method
[DFVLR-FB-87-06] 01 p0003 N88-10017
High precision ultrasonic scanning system and SAFT-UT development
[DE87-010038] 01 p0008 N88-10044
Computerized certification of digital ultrasonic instrumentation
[DE88-000820] 04 p0488 N88-13008
Transport coefficients close to the mobility edge and nonlinear sigma model composite operators --- electron transport
[PREPRINT-541] 06 p0777 N88-14767
Wave propagation experiments on 22-bay lattice
[AD-A186140] 07 p0824 N88-15002
Through-transmission/pulse-echo ultrasonic equipment evaluation
[AD-A186340] 07 p0929 N88-15641
Low-g propellant gaging 08 p0982 N88-15937
A-scan ultrasound measurement of ocular changes during accommodation
[AD-A186818] 09 p1198 N88-17181
Durability and damage tolerance of aluminum castings
[AD-A186444] 10 p1341 N88-18013
Ultrasonic-velocity studies of composite and heterogeneous materials
[AD-A189000] 12 p1604 N88-19595
Ultrasonic measurements research: Progress in 1987
[AD-A188506] 12 p1687 N88-20062

A continued study of optical sound generation and amplification
[AD-A188362] 12 p1691 N88-20116

Ultrasonic physical modeling of seismic wave propagation from graben-like structures
[AD-A189066] 13 p1796 N88-20744

Ultrasonic oxygen sensor
[AD-A189723] 15 p2105 N88-22537

Acousto-ultrasonic input-output characterization of unidirectional fiber composite plate by P waves
[NASA-CR-4162] 19 p2678 N88-25923

Quantitative particle characterization by scattered ultrasound 20 p2848 N88-26908

Ultrasonic studies of stresses and plastic deformation in steel during tension and compression
[AD-A192308] 21 p2912 N88-27280

New acousto-ultrasonic techniques applied to aerospace materials
[NASA-TM-101299] 22 p3086 N88-28323

Theory of acoustoplasticity and ultrasonic measurements of residual stresses
22 p3087 N88-28328

Combustion studies of acoustically suspended liquid droplets
[AD-A193892] 23 p3192 N88-28998

An investigation of acoustic cavitation produced by pulsed ultrasound
[AD-A193523] 23 p3278 N88-29516

Ultrasonic detection of diffusion and adhesion loss
24 p3354 N88-29967

In situ fault detection by the hybrid ray mode method
[AD-A195226] 24 p3381 N88-30137

ULTRAVIOLET ABSORPTION

Laboratory measurements of the ozone absorption coefficient in the wavelength region 339 to 362 nm at different temperatures
[NOTA-INTERNA-862] 07 p0878 N88-15324

Soluble polysilane derivatives: Chemistry and spectroscopy
[AD-A187889] 11 p1461 N88-18713

Temperature dependence of ultraviolet absorption cross sections of chlorofluoroethanes
[AERONOMICA-ACTA-A-325-1987]
18 p2482 N88-24728

Precise ultraviolet absorbance study of the interaction of amino acids and mononucleosides in aqueous solution
[ISAS-RN-356] 21 p2908 N88-27256

Ultraviolet absorption cross sections of chloro- and chlorofluoromethanes at stratospheric temperatures
[AERONOMICA-ACTA-A-324-1988]
23 p3231 N88-29228

ULTRAVIOLET ASTRONOMY

Diagnostics of solar coronal loops at interferometric angular resolution 01 p0098 N88-10642

Ultraviolet observations of cataclysmic variables: The IUE archive
[MPE-PREPRINT-91] 02 p0250 N88-11580

Ultraviolet observations of AM Her — cataclysmic variable
[MPE-PREPRINT-92] 02 p0250 N88-11581

A comprehensive exploration of late-type stars in the far-ultraviolet 04 p0520 N88-13194

Optical photometer for the Tirgo telescope
[IFSI-87-5] 05 p0650 N88-13985

The EUV line flux variations and activity in Alpha Orionis 08 p1032 N88-16256

Solar ultraviolet spectrum obtained from a balloon gondola 08 p1032 N88-16258

Laser simulation of light and plasma action on comets and planets 09 p1237 N88-17413

Submillimeter and far infrared line observations of M17 SW: A clumpy molecular cloud penetrated by UV radiation
[NASA-CR-182866] 16 p2288 N88-23701

IUE evidence on the nature of the innermost broad-line region in Seyfert 1 galaxies 17 p2450 N88-24552

Detection of abundant molecular gas in the UV-excess quasar Mrk 1014 22 p3164 N88-28842

Beyond the visible: A decade of observations with the International Ultraviolet Explorer (IUE)
[ESA-F08] 24 p3331 N88-29828

ULTRAVIOLET DETECTORS
NT TOTAL OZONE MAPPING SPECTROMETER
NT ULTRAVIOLET SPECTROMETERS
NT ULTRAVIOLET SPECTROPHOTOMETERS

ULTRAVIOLET LASERS

JPRS Report: Science and Technology. China
[JPRS-CST-87-033] 03 p0326 N88-12062

Powerful picosecond ultraviolet laser output at 354.7 nanometers 03 p0327 N88-12063

Active medium formation in lasers using mixtures of inert gases and optical breakdown pumping
06 p0709 N88-14347

Efficiency of ionic noble gas and alkali metal molecules as ultraviolet and far-ultraviolet lasers
09 p1238 N88-17419

Research studies on extreme ultraviolet and soft X-ray lasers
[AD-A187506] 10 p1338 N88-17996

Research studies on extreme ultraviolet and soft X-ray lasers
[AD-A189163] 12 p1633 N88-19773

UV-Laser reactions of molecular adsorbates
[AD-A190796] 16 p2212 N88-23201

An investigation of 2-6 superlattice deposition by laser photochemical techniques
[AD-A191547] 18 p2581 N88-25336

A plasma ultraviolet source for short wavelength lasers
[AD-A192844] 21 p2952 N88-27537

ULTRAVIOLET LIGHT
U ULTRAVIOLET RADIATION

ULTRAVIOLET PHOTOGRAPHY

Global views of the aurora from the Viking satellite — Swedish satellite 08 p1025 N88-16208

The calibration of photographic and spectroscopic films. The response of 2aO film to small dosages of alpha particles from 3/10th's rad to 8 rads at energy levels 153 MeV, 79 MeV and 47 MeV
[NASA-CR-177830] 13 p1773 N88-20608

ULTRAVIOLET PHOTOMETRY

Satellite UV image processing
[AD-A190466] 15 p2089 N88-22451

ULTRAVIOLET RADIATION
NT EXTREME ULTRAVIOLET RADIATION
NT FAR ULTRAVIOLET RADIATION
NT LYMAN ALPHA RADIATION
NT NEAR ULTRAVIOLET RADIATION

The largest white light flare ever observed: 25 April 1984, 0001 UT 01 p0111 N88-10714

Mathematical modelling of solar ultraviolet radiation induced optical degradation in anodized aluminum
02 p0135 N88-10846

LLE (Laboratory for Laser Energetics) review, volume 31
[DE87-013732] 03 p0328 N88-12072

DNA damage and repair in human skin in situ
[DE87-014288] 03 p0356 N88-12241

The onset of chromospheric activity among the A- and F- type stars 04 p0511 N88-13144

VLA observations of rapid 6 cm flux variations in alpha Ori 04 p0515 N88-13169

TOMS as a monitor of the ultraviolet radiation environment: Applications to photobiology
05 p0617 N88-13785

Radiation curing: Comparison of heat, UV, and radiation curing
[OEFZS-4393] 06 p0689 N88-14224

UV radiation: Human exposure to ultraviolet radiation
[PB87-137410] 06 p0752 N88-14619

Studies on nonlinear mechanisms of excimer laser propagation in fused silica fibers
[AD-A186822] 09 p1156 N88-16929

Tropospheric ultraviolet radiation: Assessment of existing data and effect on ozone formation
[PB88-130133] 10 p1354 N88-18095

Charge exchange in low energy (keV) and hyperthermal energy (10-100 eV) ion scattering
[AD-A187643] 11 p1543 N88-19222

Polar mesospheric cloud experiment
[AD-A188936] 12 p1648 N88-19872

X-ray lithographic research: A collection of NRL contributions
[AD-A188313] 12 p1695 N88-20140

Research on absorption of UV radiation in Venusian atmosphere from Vega-1 and Vega-2 landing modules
13 p1725 N88-20316

Energy transfer and non-linear optical properties at near ultraviolet wavelengths: Rare earth 4f yields 5d transitions in crystals and glasses
[DE88-005403] 13 p1840 N88-21012

Extension of free-electron lasers into the extreme ultraviolet
[DE88-005373] 15 p2070 N88-22341

NOAA-ERL-ARL (National Oceanic and Atmospheric Administration-Environmental Research Laboratories-Air Resources Laboratory) solar UV radiation and climate research project: Program description
[PB88-169396] 16 p2233 N88-23339

Determination of tropospheric H concentrations by a double-pulsed UV laser method
18 p2539 N88-25070

Investigation of the diffuse ultraviolet background with DE data
[NASA-CR-182863] 19 p2741 N88-26271

Ultraviolet imaging of hydrogen flames
[DE88-009152] 20 p2769 N88-26422

A plasma ultraviolet source for short wavelength lasers
[AD-A192844] 21 p2952 N88-27537

International ultraviolet explorer spectral atlas of planetary nebulae, central stars, and related objects
[NASA-RP-1203] 22 p3164 N88-28843

ULTRAVIOLET SPECTRA

Relations between chromospheric and coronal structure, flux-flux correlations and convective zone properties
04 p0510 N88-13138

Satellite observations of extreme ultraviolet radiation
[AD-A185043] 05 p0661 N88-14059

Short-term temporal variations of Nimbus-7 measurements of the solar UV spectral irradiance
[PB88-102132] 07 p0946 N88-15753

Ultraviolet rocket-spectra of a sunspot
08 p1032 N88-16257

Solar ultraviolet spectrum obtained from a balloon gondola 08 p1032 N88-16258

Ultraviolet absorption cross sections of methylbromide at stratospheric temperatures
[AERONOMICA-ACTA-A-320-1987]
15 p2036 N88-22132

Observation of injected silicon in heliotron E
17 p2441 N88-24524

IUE evidence on the nature of the innermost broad-line region in Seyfert 1 galaxies 17 p2450 N88-24552

Optical constants of minerals and other materials from the millimeter to the ultraviolet
[AD-A192210] 18 p2482 N88-24724

An investigation of 2-6 superlattice deposition by laser photochemical techniques
[AD-A191547] 18 p2581 N88-25336

Ultraviolet spectra of subluminous objects found in the Kiso Schmidt survey and systematic reanalysis of the archived ultraviolet spectra of white dwarfs observed with the IUE satellite under the Astrophysics Data Program (ADP)
[NASA-CR-182976] 18 p2592 N88-25406

Ultraviolet spectra of two magnetic white dwarfs and ultraviolet spectra of subluminous objects found in the Kiso Schmidt survey
[NASA-CR-183051] 18 p2593 N88-25408

ULTRAVIOLET SPECTROGRAPHS
U ULTRAVIOLET SPECTROMETERS

ULTRAVIOLET SPECTROMETERS
NT TOTAL OZONE MAPPING SPECTROMETER

LLE review
[DE87-014468] 02 p0178 N88-11110

Lyman alpha SMM/UVSP absolute calibration and geocoronal correction
[NASA-TM-100314] 03 p0389 N88-12446

Use of satellite data in volcano monitoring
05 p0618 N88-13797

Selection of optimum wavelengths for ozone mapping from satellites 05 p0619 N88-13798

Determination of total ozone from HIRS2/MSU sounding data 05 p0619 N88-13799

Complementary information between UV and IR for remote sensing of total ozone 05 p0619 N88-13800

Satellite observations of extreme ultraviolet radiation
[AD-A185043] 05 p0661 N88-14059

An advanced visible-UV spectrometer for atmospheric composition measurements 08 p1029 N88-16231

Satellite UV image processing
[AD-A190466] 15 p2089 N88-22451

Ultraviolet radiometry: Radiation sources and measuring methods 16 p2272 N88-23596

ULTRAVIOLET SPECTROPHOTOMETERS

NBS (National Bureau of Standards) measurement services: Spectral reflectance
[PB88-109905] 06 p0779 N88-14785

ROCOZ-A (improved rocket launched ozone sensor) for middle atmosphere ozone measurements
08 p1029 N88-16233

ULTRAVIOLET SPECTROSCOPY

What's needed in the UV and EUV
02 p0255 N88-11612

Extreme ultraviolet beam-foil spectroscopy of highly ionized neon and argon
[AD-A185197] 05 p0561 N88-13418

Two-photon (VUV and visible) resonant ionization spectroscopy of atoms and molecules
[DE88-004332] 10 p1407 N88-18388

Spectral radiometry: Methods, measuring techniques, and applications — conference
[PTB-OPT-24] 16 p2271 N88-23585

Ion temperature measurement with spectroscopy in JT-60 17 p2439 N88-24513

Spectroscopic results from JET: Some examples of data comparison and data needs 17 p2440 N88-24517

Ion temperature profile measurement using charge exchange recombination spectroscopy on JIPP T-IIU
17 p2440 N88-24518

Spectroscopic measurements of ion temperature, rotation speed and beam deposition profile on DIII-D
17 p2440 N88-24519
Applications of charge transfer devices in spectroscopy
[AD-A194408] 23 p3192 N88-28992
High performance charge transfer device detectors
[AD-A194409] 23 p3192 N88-28993
ULTRAVIOLET TELESCOPES
International ultraviolet explorer observatory operations
[NASA-CR-180775] 22 p3145 N88-28708
ULYSSES MISSION
Media calibrations of the Doppler signal for a gravitational wave experiment --- interplanetary medium
[IFSI-86-13] 05 p0625 N88-13825
UMBRAS
A near-earth optical communications terminal with a corevolving planetary sun shield
04 p0434 N88-12693
UNCONSCIOUSNESS
NT BLACKOUT (PHYSIOLOGY)
UNDER SURFACE BLOWING
Wind tunnel studies of circulation control elliptical airfoils 10 p1270 N88-17598
Analysis of a fixed-pitch X-wing rotor employing lower surface blowing 10 p1271 N88-17602
Analysis of a fixed-pitch X-wing rotor employing lower surface blowing
[AD-A187379] 24 p3321 N88-29779
UNDERGROUND EXPLOSIONS
Analysis of photopole data reduction models
05 p0593 N88-13616
Characteristics of seismic sources of some Asian earthquakes and Soviet underground explosions from Gauribidanur array records
[DE88-701233] 15 p2093 N88-22472
An approximation technique for solving a system of Fredholm integral equations for asymmetric detector response functions
[AD-A190577] 15 p2121 N88-22645
Research and development activities of the Seismology Section
[DE88-701235] 16 p2231 N88-23323
Effects of tectonic release on broadband regional distance bodywaves
[AD-A194247] 22 p3119 N88-28529
UNDERGROUND STORAGE
Protecting old oil tanks made of steel against internal corrosion using organic coatings
[DE88-751089] 11 p1459 N88-18698
UNDERGROUND STRUCTURES
Reinforced cocnrete arches under blast and shock environments 09 p1180 N88-17065
Finite element analysis of an underground structure
[AD-A191747] 18 p2527 N88-24991
Signal processing software for ground penetrating radar, user's manual
[AD-A194286] 23 p3203 N88-29059
UNDERGROUND TRANSMISSION LINES
Technology survey for a robot which will investigate the condition of underground pipe
[PB87-209979] 01 p0055 N88-10351
UNDERWATER ACOUSTICS
Geoacoustic models of the Hudson Canyon area
[AD-A183535] 01 p0073 N88-10465
A new method for determining acoustic properties of the seabed from the ambient noise field in the ocean
[RAE-TR-86035] 01 p0090 N88-10590
Proceedings of Conference on Vibrodiagnostics discussed 02 p0158 N88-10990
Underwater acoustic backscatter from a model of arctic ice open leads and pressure ridges
[AD-A184693] 03 p0354 N88-12234
The effect of ocean fluctuations on sound transmission in the ocean
[AD-A184382] 03 p0355 N88-12236
AFAR (Azores Fixed Acoustic Range) measurements of intensity and intensity moments
[AD-A184431] 03 p0355 N88-12237
Coupled acoustic and ocean thermodynamic model
[AD-A184357] 04 p0472 N88-12911
Multipath time-delay estimation via the EM algorithm
[PB88-106851] 07 p0845 N88-15124
FOR3D: A computer model for solving the LSS (Lee-Saad-Schultz) three-dimensional, wide angle wave equation
[AD-A186649] 08 p1080 N88-16511
High frequency acoustic underwater communication with low probability of being traced
[REPT-4-87] 09 p1242 N88-17447
An application of dimensionless Eigenvalues to underwater acoustic ducts
[AD-A188167] 11 p1542 N88-19219
The temporal and spatial acoustical response of a point-driven fluid-loaded plate
[AD-A188504] 12 p1636 N88-19794
Observations of waves and Langmuir circulation with Doppler sonars 13 p1805 N88-20790
Mathematical models of sound waves in fluids
[AD-A189270] 13 p1834 N88-20968
New wide-band transducer developed
14 p1901 N88-21353
A computerized investigation using the method of images to predict the sound field in a fluid wedge overlying a slow fluid half-space
[AD-A190013] 15 p2130 N88-22704
Low frequency ocean ambient noise: Measurements and theory
[AD-A191188] 16 p2237 N88-23362
Refraction in underwater acoustics --- navigation systems
[B8735053] 17 p2395 N88-24236
Construction of approximations to acoustic Green's functions for nonhomogeneous oceans using transmutation
[PB88-185384] 18 p2548 N88-25126
Evaluation of the biot coefficients
[AD-A191643] 18 p2570 N88-25265
ELIT: An autonomous underwater observation robot
19 p2699 N88-26048
A modal approach to Arctic noise modelling with implied vertical coherence
[AD-A192966] 20 p2850 N88-26916
Robust methods for array signal processing
[AD-A192854] 21 p3012 N88-27871
Vertical directionality of ambient noise at 32 deg N as a function of longitude: Tape number 86180
[AD-A193228] 21 p3012 N88-27872
Numerical modeling results for mode propagation in a wedge
[AD-A193998] 22 p3147 N88-28718
Polynomials with restricted coefficients and their applications
[AD-A192589] 23 p3202 N88-29055
Reflection and scattering of acoustic rays computed for parabolic ice keel models
[AD-A193898] 23 p3278 N88-29517
Acoustic pressure distribution on the bottom of a wedge-shaped ocean
[AD-A193961] 23 p3278 N88-29518
UNDERWATER COMMUNICATION
High frequency acoustic underwater communication with low probability of being traced
[REPT-4-87] 09 p1242 N88-17447
Long haul underwater fiber optic link
[AD-A194487] 23 p3282 N88-29542
UNDERWATER ENGINEERING
The nature of metallurgical reactions in underwater welding
[AD-A184464] 04 p0414 N88-12568
Design and preliminary evaluation of an underwater [illegible]based imaging system
[DE88-010560] 19 p2675 N88-25908
UNDERWATER EXPLOSIONS
Validation of the Underwater Shock Analysis (USA) program. Part 1: Theoretical considerations --- ship design
[REPT-5073713-86-01] 06 p0702 N88-14308
UNDERWATER OPTICS
The analytical exponential decay coefficient of the submarine light field
[AD-A187215] 11 p1548 N88-19261
Activities report of the Division of Optical Technology
[FOA-C-30477-3] 18 p2576 N88-25299
Design and preliminary evaluation of an underwater laser-based imaging system
[DE88-010560] 19 p2675 N88-25908
Underwater optical trajectography and video image mosaics 19 p2700 N88-26051
Methods for processing satellite images and their application to underwater operations
19 p2702 N88-26066
UNDERWATER PHYSIOLOGY
Experience in occupational medicine, derived from 16 operational deep saturation trimix 5 dives in GUSI from 150 to 600 m 19 p2695 N88-26018
Life in a hyperbaric environment. A new O2-H2 breathing mixture for industrial diving 19 p2695 N88-26019
Decompression procedures and accidents in space and sea 19 p2698 N88-26035
Monitoring of divers/astronauts during missions
19 p2698 N88-26036
UNDERWATER RESOURCES
Karst and submarine fresh water discharge in the Antalya area, southern Turkey 22 p3102 N88-28421
UNDERWATER SOUND
U UNDERWATER ACOUSTICS
UNDERWATER STRUCTURES
Detection of defects on structures
[EP-PATENT-0-210-794-A2] 04 p0453 N88-12807
Design and test of high performance composite tubes for use in deep water drilling and production systems
[SNIAS-872-430-107] 05 p0572 N88-13487
High performance composite tubes for offshore applications
[SNIAS-872-430-116] 05 p0572 N88-13488
Validation of the Underwater Shock Analysis (USA) program. Part 1: Theoretical considerations --- ship design
[REPT-5073713-86-01] 06 p0702 N88-14308
Retarded potential technique applied for shock wave loading of doubly symmetric submerged structures
09 p1179 N88-17058
UNDERWATER TESTS
NT NEUTRAL BUOYANCY SIMULATION
Experimental studies on the tripping behavior of narrow T-stiffened flat plates subjected to hydrostatic pressure and underwater shock 05 p0592 N88-13613
HERMES Program: Airlock swimming pool tests
12 p1591 N88-19525
Underwater simulation for space teleoperation
19 p2698 N88-26040
Study of human factors engineering criteria for Extra Vehicular Activity (EVA) systems, volume 2
[STF23-F87025-VOL-2] 24 p3409 N88-30293
UNDERWATER TRAJECTORIES
A feasibility study in path planning using optimization techniques
[AD-A193030] 21 p2894 N88-27177
UNDERWATER VEHICLES
NT SUBMARINES
A conceptual design of an inertial navigation system for an autonomous submersible testbed vehicle
[AD-A188038] 11 p1438 N88-18578
Design features of small Brayton cycles for autonomous underwater vehicles
[AD-A187799] 11 p1506 N88-18999
A feasibility study in path planning using optimization techniques
[AD-A193030] 21 p2894 N88-27177
A conceptual design study of a hovering system controller for an autonomous underwater vehicle
[AD-A193423] 21 p2930 N88-27399
Estimation forces acting on an underwater vehicle with G.P.S. (Global Positioning System) and Kalman filtering
[AD-A194339] 23 p3175 N88-28901
Remotely Operated Vehicle (ROV) reliability study, phase 1
[AD-A194367] 23 p3222 N88-29177
UNIAXIAL STRAIN
U AXIAL STRAIN
UNIFIED FIELD THEORY
A supersymmetric Lagrangian for Poincare gauge theories of gravity
[DE88-00[illegible]0] 04 p0500 N88-13078
A review of two-phase flow-induced vibration
[DE88-001955] 09 p1160 N88-16955
Looking for new gravitational forces with antiprotons
[DE88-003154] 09 p1192 N88-17142
Ambiguity in determining the effective action for string-corrected Einstein gravity
[PB87-166153] 09 p1259 N88-17550
UNIFORM FLOW
NT BLASIUS FLOW
Conditions at infinity for theories of oscillating wings and propellers in subsonic flow
[NAL-TR-937] 11 p1434 N88-18556
UNIPHASE FLOW
U SINGLE-PHASE FLOW
UNIPOLAR TRANSISTORS
U FIELD EFFECT TRANSISTORS
UNIQUENESS THEOREM
On a class of similarity solutions of the equation u sub t = (absolute value of u sup m-1 u sub x) sub x with m greater than -1
[REPT-87-54] 14 p1963 N88-21713
UNITED KINGDOM
NT ENGLAND
NT SCOTLAND
Forecasting stratus over the British Isles
02 p0209 N88-11310
Time and cost reduction through computer integrated manufacture 12 p1703 N88-20191
A comparative assessment of US and UK explosives qualified as replacements for tetryl
[MRL-R-1094] 13 p1754 N88-20486
Managing and controlling change
[PNR90419] 22 p3159 N88-28601
UNITED KINGDOM SATELLITES
U UK SATELLITES
UNITED NATIONS
Current status of world weather service
06 p0725 N88-14459

Safety guidelines and procedures for bioscience-based industry and other applied microbiology
[PB87-140521] 08 p1045 N88-16316

System-wide medium-term environment programme for the period 1990-1995: Strategies of the United Nations system for the environment
[UNEP/GCSS.I/2] 12 p1641 N88-19826

United Nations deliberations of the use of nuclear power sources in space: 1978-1987 17 p2423 N88-24410

Discussions and agreements in the United Nations on important issues associated with nuclear power in space
17 p2423 N88-24411

UNITED STATES
NT ALABAMA
NT ALASKA
NT ARIZONA
NT CALIFORNIA
NT CONNECTICUT
NT DELAWARE
NT FLORIDA
NT HAWAII
NT ILLINOIS
NT KANSAS
NT KENTUCKY
NT MAINE
NT MASSACHUSETTS
NT MICHIGAN
NT MISSISSIPPI
NT NEVADA
NT NEW MEXICO
NT NEW YORK
NT NORTH CAROLINA
NT NORTH DAKOTA
NT TEXAS
NT WISCONSIN
NT WYOMING

Japanese industrial research on lean combustion: A case study: International Research Monitoring Program
[DE87-013839] 02 p0144 N88-10904

Assessment of the impacts of transferring certain nuclear reactor technologies to the Soviet Union and Eastern Europe
[DE87-014388] 02 p0249 N88-11576

Center for Electronics and Electrical Engineering Technical Progress Bulletin covering center programs, January to March 1987 with 1987 CEEE events calendar
[PB87-224648] 03 p0309 N88-11946

East coast gravity validation study
[AD-A184292] 03 p0351 N88-12217

Impacts of world development on selected characteristics of the atmosphere: An integrative approach. Volume 2: Appendices
[DE88-001496] 07 p0875 N88-15310

Aircraft accident reports: Brief format, US Civil and Foreign Aviation, Issue Number 5 of 1986 accidents
[PB87-916907] 08 p0952 N88-15780

Aircraft accident reports: Brief format, US Civil and Foreign Aviation, Issue Number 8 of 1986 accidents
[PB87-916910] 08 p0953 N88-15782

Advancing automation and robotics technology for the space station and for the US economy: Submitted to the United States Congress October 1, 1987
[NASA-TM-100777] 08 p0959 N88-15816

Advancing automation and robotics technology for the space station and for the US economy: Submitted to the United States Congress October 1, 1986
[NASA-TM-89190] 08 p0960 N88-15818

International role of US geoscience
[NASA-CR-182407] 08 p1035 N88-16281

Hurricane climatology for the Atlantic and Gulf coasts of the United States
[PB88-114657] 08 p1039 N88-16288

Recommendations for a US ice coring program
[PB88-115043] 09 p1185 N88-17102

America plans for space
[AD-A137465] 10 p1289 N88-17713

Proceedings of US-Japan Heliotron-Stellarator Workshop, volume 3
[DE88-004788] 11 p1554 N88-19299

Proceedings of US-Japan Heliotron-Stellarator Workshop, volume 2
[DE88-004789] 11 p1554 N88-19300

A comparative assessment of US and UK explosives qualified as replacements for tetryl
[MRL-R-1094] 13 p1754 N88-20486

Technology transfer to China. Volume 2: Working papers, part 1
[PB88-158704] 14 p1992 N88-21872

Technology transfer to China. Volume 2: Working papers, part 2
[PB88-158712] 14 p1992 N88-21873

Aircraft accident reports, brief format, US civil and foreign aviation, issue number 10 of 1986 accidents
[PB87-916912] 15 p2016 N88-22020

Monitoring space weaponry: Detection and verification issues
[DE88-008726] 20 p2847 N88-26900

Federal Council on Science, Engineering and Technology: Committee on Computer Research and Applications, Subcommittee on Science and Engineering Computing: The US Supercomputer Industry
[DE88-011262] 21 p2994 N88-27756

Potential use of SPOT satellite data for the national resources inventory 22 p3093 N88-28370

Factors influencing summer temperatures and precipitation in the southwest 22 p3124 N88-28565

On the modes of growing-season precipitation over central North America 22 p3124 N88-28567

Characteristics of regression equations for specifying monthly precipitation amounts over the United States from the field of concurrent mean 700 mb heights
22 p3127 N88-28591

UNITS OF MEASUREMENT
NT INTERNATIONAL SYSTEM OF UNITS

UNIVERSE

Our universe as an attractor in a superstring model
[DE87-703066] 02 p0251 N88-11585

Crucial cosmological observations
[DE87-703081] 02 p0251 N88-11587

Torsion as a source of expansion in a Bianchi type I universe in the self-consistent Einstein-Cartan theory of a perfect fluid with spin density
[AD-A184200] 03 p0322 N88-12037

Particle physics and cosmology
[DE87-005400] 03 p0387 N88-12432

Number count-redshift relation in universe models with nonzero cosmological constant
[DE87-703043] 03 p0388 N88-12435

New cosmological scenario
[DE87-703357] 04 p0520 N88-13198

Cosmological applications of singular hypersurfaces in general relativity 04 p0521 N88-13202

Galaxy formation by gravitational collapse in a universe dominated by cold dark matter 04 p0521 N88-13205

Laboratory and near-earth space plasma as a key to the plasma universe
[TRITA-EPP-87-09] 05 p0652 N88-13996

Cosmology in the plasma universe
[TRITA-EPP-87-07] 05 p0660 N88-14053

Model of earlier stage of universe's evolution
06 p0775 N88-14758

Evolution of perturbations in expanding universe
06 p0775 N88-14759

Number count-redshift relation in a perturbed Friedmann universe
[DE88-750302] 07 p0945 N88-15743

Post-Newtonian equations of motion in an expanding universe
[DE88-750303] 07 p0945 N88-15744

Evolution from pure states into mixed states in de Sitter space
[DE88-750316] 07 p0945 N88-15745

Existence of absolutely closed universe
08 p1080 N88-16509

The origin of the diffuse X-ray background and the formation of galaxies and voids
10 p1428 N88-18527

On the time delay of the ultrahigh energy radiation signal from the source Cygnus X-3
[DE88-700649] 10 p1431 N88-18547

Early reheating and cosmic strings
13 p1855 N88-21103

Rotation of universe --- metagalaxies
14 p1974 N88-21780

Density perturbations in a rotating universe
[DE87-703036] 15 p2151 N88-22840

Cosmology for high energy physicists
[DE88-005705] 15 p2151 N88-22842

On the dynamics of the metagalaxy
[TRITA-EPP-88-05] 22 p3166 N88-28852

Time travel in the homogeneous Som-Raychaudhuri universe
[DE88-702220] 23 p3295 N88-29622

Non-linear scale invariance in a cold-dark-matter universe
[DE88-011725] 23 p3299 N88-29644

UNIVERSITIES

The British Technology Group
[ONRL-7-022-R] 01 p0107 N88-10698

Experiments: Test range facilities, part 1
03 p0304 N88-11920

The Black College satellite telecommunications network planning in support of energy-related collaborative research
[DE88-000182] 03 p0307 N88-11940

Calendar year 1985 solar and weather data for Austin, Texas
[PB87-220174] 03 p0352 N88-12219

National Center for Atmospheric Research
[PB87-228391] 04 p0470 N88-12901

A national model at Howard University demonstrating private sector interrelationships that facilitate research in predominantly Black colleges and universities
[DE88-000160] 04 p0502 N88-13089

University research initiative research program summaries
[AD-A184876] 05 p0658 N88-14035

A study of the minority college programs at the NASA Johnson Space Center 06 p0798 N88-14887

Activities report of the Technical University of Twente
[ETN-88-90620] 06 p0799 N88-14802

Research reports: 1987 NASA/ASEE Summer Faculty Fellowship Program
[NASA-CR-179219] 07 p0922 N88-15601

TABLET: The personal computer of the year 2000
[NASA-CR-182528] 10 p1384 N88-18267

Cumulative reports and publications through December 31, 1987
[NASA-CR-181624] 11 p1524 N88-19099

Institute for Computational Mechanics in Propulsion (ICOMP)
[NASA-TM-100790] 11 p1540 N88-19202

Experimental elementary particle physics at the University of Pittsburgh
[DE88-003542] 11 p1545 N88-19234

Experience with Berkeley UNIX interprocess communications
[AD-A188353] 12 p1680 N88-20041

Basic research in ceramic and semiconductor science at selected Japanese laboratories, based on a September 1986 visit: Highlights, summary and overview and detailed notes from selected Japanese laboratories
[DOE/ER-0314] 12 p1696 N88-20150

A project to transfer technology from NASA centers in support of industrial innovation in the midwest
[NASA-CR-180360] 12 p1708 N88-20224

Microvax networked computer system
[AD-A190308] 15 p2114 N88-22596

Structural ceramics research
17 p2324 N88-23878

Fiber waveguide sensors for intelligent materials
[NASA-CR-183028] 17 p2343 N88-23968

Transactions of the Fifth Symposium on Space Nuclear Power Systems
[DE88-006165] 17 p2417 N88-24374

RLE progress report, January 1 to December 31, 1987
[RLE-PR-130] 21 p3011 N88-27869

UNIVERSITY PROGRAM

University program management information system, fiscal year 1985
[NASA-TM-88381] 06 p0790 N88-14846

UNLOADING

Dislocation free zone model of fracture under reverse loading
[DE88-002676] 07 p0869 N88-15276

UNMANNED SPACECRAFT
NT GALILEO PROBE
NT GALILEO SPACECRAFT
NT GIOTTO MISSION
NT HEAO 2
NT HELIOS 1
NT HELIOS 2
NT HOTOL LAUNCH VEHICLE
NT MARS OBSERVER
NT MARS PROBES
NT PIONEER VENUS SPACECRAFT
NT SPACE PROBES

Expected value analysis for an unmanned expendable launch vehicle payload escape system
[AD-A189494] 13 p1728 N88-20337

Arguments for manned or unmanned spacecraft activities
[REPT-46/87] 17 p2309 N88-23813

Review of past and current trials and uses of unmanned vehicles
[AD-A194527] 22 p3084 N88-28311

UNSTEADY AERODYNAMICS

A supersonic potential gradient method for the calculation of unsteady aerodynamic pressures on harmonically oscillating wings
[ESA-TT-930] 03 p0259 N88-11631

The Green's function method for fully unsteady aerodynamics around three-dimensional bodies and its application to flutter analysis
[UTIAS-298] 03 p0260 N88-11639

Numerical calculation in the Laplace domain for subsonic unsteady aerodynamic forces acting on a finite wing
05 p0535 N88-13256

Unsteady aerodynamics of an oscillating cascade in a compressible flow field
[NASA-TM-100219] 05 p0549 N88-13346

Influence of the static deformation on a wing in the unsteady aerodynamic 05 p0551 N88-13357

Integration of a supersonic unsteady aerodynamic code into the NASA FASTEX system
[NASA-CR-182329] 06 p0663 N88-14068

Unsteady transonic algorithm improvements for realistic aircraft applications
[NASA-TM-100516] 08 p0940 N88-15760
Time accurate techniques using characteristic flux averaging with application to unsteady aerodynamics
08 p0985 N88-15957
Computational unsteady aerodynamics for aeroelastic analysis
[NASA-TM-100523] 09 p1112 N88-16668
Investigation of dynamic stall using LDV (Laser Doppler Velocimetry): Mean flow studies
[AD-A187629] 10 p1272 N88-17611
Effectiveness of various control surfaces in quasi-steady and unsteady conditions
[AGARD-R-735] 10 p1284 N88-17682
A semianalytical technique for sensitivity analysis of unsteady aerodynamic computations
[NASA-TM-100810] 11 p1503 N88-18976
Calculated unsteady aerodynamics of wings
[AD-A189608] 12 p1574 N88-19415
Unsteady transonic small-disturbance theory including entropy and vorticity effects
[NASA-TM-100568] 12 p1575 N88-19418
Steady and unsteady transonic small disturbance analysis of realistic aircraft configurations
[NASA-TM-100557] 13 p1717 N88-20269
Unsteady aerodynamics of a Wortmann FX-63-137 wing in a fluctuating wind field
[AD-A190128] 15 p2013 N88-22006
Bifurcations in unsteady aerodynamics-implications for testing
[NASA-TM-100083] 15 p2015 N88-22014
Methodology for matching experimental and computational aerodynamic data
[NASA-TM-100592] 17 p2295 N88-23728
Unsteady pressure and structural response measurements of an elastic supercritical wing
[NASA-TM-10059] 17 p2299 N88-23756
Calculations of unsteady aerodynamics for a full aircraft configuration using boundary element method
19 p2637 N88-25643
Experimental determination of aerodynamic damping in a three-stage transonic axial-flow compressor
[NASA-TM-100953] 21 p2897 N86-27200
Investigation of oscillating cascade aerodynamics by an experimental influence coefficient technique
[NASA-TM-101313] 22 p3039 N88-28041
Program user's manual for an unsteady helicopter rotor-fuselage aerodynamic analysis
[NASA-CR-181701] 22 p3039 N88-28047
An unsteady helicopter rotor: Fuselage interaction analysis
[NASA-CR-4178] 23 p3171 N88-28880
Accurate solutions, parameter studies and comparisons for the Euler and potential flow equations
[NASA-TM-100664] 23 p3173 N88-28892
Application of unsteady aerodynamic methods for transonic aeroelastic analysis
[NASA-TM-100665] 24 p3317 N88-29754
History of aeroelasticity in Germany from the beginning to 1945
[ESA-TT-1082] 24 p3319 N88-29767
Recent advances in transonic computational aeroelasticity
[NASA-TM-100663] 24 p3321 N88-29778
Aeroelastic response of metallic and composite propfan models in yawed flow
[NASA-TM-100964] 24 p3326 N88-29807

UNSTEADY FLOW
NT OSCILLATING FLOW
Advanced turboprop wing installation effects measured by unsteady blade pressure and noise
[NASA-TM-100200] 01 p0002 N88-10008
ARSPNS: A method to calculate steady and unsteady potential flow about fixed and rotational lifting and nonlifting bodies
[NLR-TR-85114-U] 01 p0044 N88-10282
Calculation of stationary and low frequency unsteady flows in a steam turbine end stage
[MITT-23] 01 p0057 N88-1036
Personal Computer (PC) based image processing applied to fluid mechanics
[NASA-TM-100024] 02 p0172 N88-11067
On the prediction of the aeroelastic behavior of lifting systems due to flow separation
[ESA-TT-1043] 03 p0259 N88-11633
The Green's function method for fully unsteady aerodynamics around three-dimensional bodies and its application to flutter analysis
[UTIAS-298] 03 p0260 N88-11639
Aerodynamic sensitivities from subsonic, sonic and supersonic unsteady, nonplanar lifting-surface theory
[NASA-TM-100502] 04 p0394 N88-12459
Application of Runge Kutta time marching scheme for the computation of transonic flows in turbomachines
[NASA-TM-88987] 04 p0394 N88-12461
Three-dimensional unsteady flow elicited by finite wings and complex configurations 04 p0395 N88-12466
Numerical simulation of unsteady separated flows
[AD-A184132] 04 p0442 N88-12741
An experimental investigation of unsteadiness in swept shock wave/turbulent boundary layer interactions
04 p0445 N88-12760
Driving mechanism of unsteady separation shock motion in hypersonic interactive flow 05 p0530 N88-13226
Numerical calculation in the Laplace domain for subsonic unsteady aerodynamic forces acting on a finite wing
05 p0535 N88-13256
The development of a computer code (U2DIIF) for the numerical solution of unsteady, inviscid and incompressible flow over an airfoil
[AD-A185033] 05 p0541 N88-13293
Unsteady aerodynamics of an oscillating cascade in a compressible flow field
[NASA-TM-100219] 05 p0549 N88-13346
Influence of the static deformation on a wing in the unsteady aerodynamic 05 p0551 N88-13357
Experimental study of the fluid mechanics of unsteady turbulent boundary layers
[AD-A184856] 05 p0580 N88-13536
Physical analysis and numerical simulation of coherent turbulent structures in mixed layers, jets, and wakes
[ETN-88-91183] 05 p0581 N88-13548
A numerical model of unsteady, subsonic aeroelastic behavior
[NASA-TM-100487] 06 p0663 N88-14064
Development of an unsteady wake theory appropriate for aeroelastic analyses of rotors in hover and forward flight
[NASA-CR-182357] 06 p0664 N88-14075
Methods for reducing computational costs of typical finite element unsteady hydrodynamic models
[AD-A185499] 06 p0702 N88-14312
Studies of unsteadiness in boundary layers
[AD-A185662] 06 p0703 N88-14315
An explicit Runge-Kutta method for unsteady rotor/stator interaction
[NASA-TM-100787] 07 p0816 N88-14967
Analysis of three-dimensional viscous internal flows
[AD-A186254] 07 p0849 N88-15155
Flow in Centrifugal Compressors --- conference
[VKI-LS-1987-01] 07 p0850 N88-15160
Blade excitation due to unsteady flow phenomena
07 p0851 N88-15167
Numerical study of a centrifugal impeller response to a downstream static pressure perturbation
07 p0851 N88-15170
Programs for calculating transient Darcian flow through non-uniform materials
[DE88-001924] 07 p0852 N88-15177
An explicit method for the solution of the Euler equations, applied to unsteady two dimensional flows
[ETN-88-90807] 07 p0855 N88-15194
Unsteady three-dimensional flow separation
[NASA-CR-182412] 08 p0949 N88-15761
Three-dimensional unsteady flow elicited by finite wings and complex configurations
[AD-A186464] 08 p0951 N88-15770
Advanced propeller research
08 p0957 N88-15806
Time accurate techniques using characteristic flux averaging with application to unsteady aerodynamics
08 p0985 N88-15957
Modeling the unsteady flow found in axial turbomachinery
[ECL-87-07] 08 p0987 N88-15980
Computational unsteady aerodynamics for aeroelastic analysis
[NASA-TM-100523] 09 p1112 N88-16668
Mach number effects on transonic aeroelastic forces and flutter characteristics
[NASA-TM-100547] 09 p1113 N88-16675
Unsteady behavior of three-dimensional vortices relevant to turbulent boundary layers
[AD-A186767] 09 p1161 N88-16958
The unsteady gas flow through stator and rotor of a turbomachine 10 p1281 N88-17660
Parametric study of choke flutter with a linear theory
10 p1283 N88-17673
Ice-shelf response to ice-stream discharge fluctuation. Part 1: Unconfined ice tongues
[AD-A188147] 10 p1358 N88-18117
Well-posedness and spectral estimation for infinite dimensional systems
[AD-A187621] 10 p1401 N88-18354
Unsteady heat transfer in turbine blade ducts: Focus on combustor sources
[NASA-TM-100815] 11 p1486 N88-18670
Unsteady transonic small-disturbance theory including entropy and vorticity effects
[NASA-TM-100568] 12 p1575 N88-19418
To the problem of determining true volume steam content by measured values of mean density of a mixture in thermally unsteady two-phase flows
[DE88-700640] 12 p1626 N88-19726
Application of a flux vector splitting methodology towards the solution of unsteady transonic flows, with future emphasis on the blade flutter problem
[AD-A189500] 13 p1716 N88-20260
ARSPNSC: A method to calculate subsonic steady and unsteady potential flow about complex configurations
[NLR-TR-86122-U] 13 p1717 N88-20265
Discrete vortex analysis of unsteady flow about two-dimensional cambered plates
[DE88-006597] 14 p1909 N88-21407
An explicit method for the solution of the Euler equations applied to unsteady two-dimensional flows
[MBB/LKE-121/S/PUB/257] 14 p1910 N88-21411
Unsteady aerodynamics of a Wortmann FX-63-137 wing in a fluctuating wind field
[AD-A190128] 15 p2013 N88-22006
Oscillating airfoils: Achievements and conjectures
[AD-A190490] 15 p2014 N88-22008
Unsteady flow field measurements using LDV (Laser Doppler Velocimetry)
[AD-A189907] 15 p2063 N88-22298
Enhancement of data acquisition and numerical computation capabilities for unsteady fluid dynamics
[AD-A190115] 15 p2063 N88-22302
Bodies in unsteady flow
[AD-A190416] 15 p2064 N88-22308
Numerical study of unsteady viscous hypersonic blunt body flows with an impinging shock
[NASA-TM-100096] 15 p2122 N88-22650
Measurements of aerodynamic forces on unsteadily moving bluff parachute canopies
16 p2202 N88-23137
A non-invasive experimental technique for the measurement of unsteady velocity and vorticity fields
16 p2204 N88-23148
Structure of unsteady flows at leading- and trailing-edges: Flow visualization and its interpretation
16 p2205 N88-23154
Unsteady flow about cambered plates
[AD-A191226] 17 p2337 N88-23945
Development and improvement of a code to calculate small, three dimensional, unsteady transonic perturbations
[ONERA-RTS-31/3064-RY-062-R]
17 p2338 N88-23951
Accounting for the effects of unsteady, separated boundary layers in transonic two dimensional calculations
[ONERA-RT-30/3064-RY-063-R]
17 p2338 N88-23952
Research on aero-thermodynamic distortion induced structural dynamic response of multi-stage compressor blading
[AD-A192169] 18 p2456 N88-24584
Unsteady flow in a supercritical supersonic inlet
18 p2480 N88-24605
Forced response unsteady aerodynamics in a multistage compressor 18 p2512 N88-24803
Numerical simulation of nonlinear structural dynamics of large scale unsteady flow
[ETN-88-92156] 18 p2513 N88-24908
An implicit, high order accurate, upwind scheme for unsteady Euler equations 19 p2638 N88-25657
Pulsatile fluidic pump performance at elevated temperatures
[DE88-008046] 19 p2677 N88-25919
On the dynamic behavior of balloon during its launch, application of panel method and extension to unsteady problem
[ISAS-RN-622] 20 p2751 N88-26330
Calculation of 2-D unsteady transonic full potential flow about oscillating airfoils by two complementary approaches
[PB88-127519] 20 p2753 N88-26341
Control and use of unsteady flows: Insect use of various wing kinematics and related pressure measurements using a pitching airfoil 21 p2926 N88-27386
Coupled experimental and theoretical investigations of instability, chaos and turbulence in an axisymmetric jet flow
[AD-A192943] 21 p2942 N88-27476
Experimental study of unsteady separating turbulent boundary layers
[AD-A192997] 21 p2943 N88-27477
A computer model for the flow of a molten polymer in a narrow cavity
[NPL-DMA(A)-157] 22 p3058 N88-28146
Non-reflecting boundary conditions for computations of unsteady flows in turbomachines
[PNR90469] 22 p3079 N88-28284

The role of acoustic resonances in unsteady turbomachinery aerodynamics
[PNR90455] 22 p3147 N88-26720

An unsteady helicopter rotor: Fuselage interaction analysis
[NASA-CR-4178] 23 p3171 N88-28880

Unsteady water channel
[AD-A194231] 23 p3171 N88-28884

Unsteady flow past an NACA 0012 airfoil at high angles of attack
[AD-A194650] 23 p3172 N88-28886

An integral equation for the linearized unsteady supersonic flow over a wing
[AD-A193773] 23 p3172 N88-28887

Direct-solution techniques for viscous flows and their control
[AD-A194775] 23 p3211 N88-29114

Shock waves in unsteady flows
[NASA-TT-20329] 23 p3214 N88-29134

Numerical solutions of unsteady inviscid transonic turbine cascade flows
[AD-A196111] 24 p3316 N88-29748

An unconditionally stable Runge-Kutta method for unsteady flows
[NASA-TM-101347] 24 p3321 N88-29780

The effects of incoming boundary layer thickness on unsteady shock-induced turbulent separations induced by cylinders
[AD-A196190] 24 p3368 N88-30060

An analysis of finite-difference and finite-volume formulations of conservation laws
[NASA-CR-177416] 24 p3370 N88-30071

Numerical simulation of unsteady incompressible flow in a partially-filled rotating cylinder
[AD-A196001] 24 p3371 N88-30073

Numerical simulation of unsteady incompressible viscous flows in generalized coordinate systems
[NASA-TM-101016] 24 p3373 N88-30085

Studies of unsteady axial-compressor functioning
24 p3380 N88-30129

UNSTEADY STATE

Numerical and experimental investigation of the unsteady temperature distribution in solar central receivers
[ESA-TT-1050] 03 p0347 N88-12193

Aircraft dynamics: Aerodynamic aspects and wind tunnel techniques 05 p0545 N88-13320

Aircraft dynamics: Aerodynamic aspects and wind tunnel techniques 24 p3313 N88-29731

UP-CONVERTERS

Long duration coherent Lyman-alpha sources
16 p2268 N88-23571

UPDRAFTS

U VERTICAL AIR CURRENTS

UPGRADING

Effects of update and refresh rates on flight simulation visual displays
[NASA-TM-100415] 15 p2018 N88-22033

UPLINKING

A statistical rain attenuation prediction model with application to the advanced communication technology satellite project. Part 2: Theoretical development of a dynamic model and application to rain fade durations and tolerable control delays for fade countermeasures
[NASA-TM-100242] 03 p0308 N88-11945

X-band uplink ground systems development: Part 2
04 p0436 N88-12703

Tau ranging revisited 04 p0437 N88-12710

INPE position paper on the CCSDS standardized method of link budget computation
[INPE-4533-NTE/279] 15 p2148 N88-22820

Experimental radio frequency link for Ka-band communications applications
[NASA-TM-100824] 18 p2470 N88-24659

A statistical rain attenuation prediction model with application to the advanced communication technology satellite project. 1: Theoretical development and application to yearly predictions for selected cities in the United States
[NASA-CR-179498] 23 p3205 N88-29077

UPPER AIR

U UPPER ATMOSPHERE

UPPER ATMOSPHERE

NT D REGION
NT E REGION
NT EARTH IONOSPHERE
NT F REGION
NT F 2 REGION
NT LOWER IONOSPHERE
NT SPORADIC E LAYER
NT THERMOSPHERE
NT UPPER IONOSPHERE

Integrated systems with applications to the multi-phases of the ephemerides, physics and mathematics of the upper atmosphere
[AD-A185748] 06 p0743 N88-14570

Holes in OI 130 nm emission fields of upper atmosphere during day 08 p1004 N88-16082

Lidar metal density measurements in the upper atmosphere 08 p1027 N88-16219

The influence of atmospheric thermal tides on diurnal variations in chemical constituents in the mesosphere
11 p1512 N88-19035

High resolution infrared absorption spectra of various trace gases present in the upper atmosphere of the Earth
[NASA-CR-182590] 12 p1642 N88-19829

Quality control of upper air conventional data (TEMP and PILOT)
[INPE-4223-RPE/546] 12 p1647 N88-19862

Measurement of rate constants of elementary gas reactions of importance to upper atmosphere and combustion systems
[AD-A189432] 13 p1737 N88-20386

Study of polyatomic dynamics in the atmosphere
[AD-A190964] 16 p2233 N88-23334

Fog, rain and aerosol attenuation in the atmosphere
[AD-A190867] 16 p2235 N88-23350

The precipitation of energetic heavy ions into the upper atmosphere of Jupiter
[NASA-TM-101155] 17 p2452 N88-24565

Observations of wave number dependent spectral line ratio fluctuations in the atmospheric emissions
[IRF-PREPRINT-101] 18 p2542 N88-25085

Components of an atmospheric lidar system
[AD-A193366] 21 p2953 N88-27539

Design, development, fabrication and launch support for a high altitude release of neodymium vapor
[AD-A194196] 22 p3118 N88-28527

Present state of knowledge of the upper atmosphere 1988: An assessment report
[NASA-RP-1208] 23 p[illegible] N88-29233

Approximation of atmospheric density by Chebyshev polynomials in predicting motion of low artificial earth satellites 24 p3445 N88-30503

UPPER IONOSPHERE

NT F REGION
NT F 2 REGION

Experimental proof of quasilongitudinal propagation of low-frequency waves in middle latitudes in upper ionosphere 24 p3447 N88-30516

UPPER STAGE ROCKET ENGINES

Altitude simulation testing of Ariane's second-stage engine 09 p1126 N88-16747

The HM-7 engine of Ariane's third stage
09 p1126 N88-16753

Centaur G Prime modal test 09 p1181 N88-17075

LGM-30B stage 2 disected motor test report
[AD-A190771] 15 p2027 N88-22079

UPPER SURFACE BLOWING

On the effect of leading edge blowing on circulation control airfoil aerodynamics 10 p1270 N88-17595

A potential flight evaluation of an upper-surface-blowing/circulation-control-wing concept
10 p1272 N88-17609

UPPER SURFACE BLOWN FLAPS

A numerical investigation on wing/nacelle interferences 05 p0535 N88-13258

UPPER VOLTA

U BURKINA

UPSTREAM

Relaxation method for the compressible Navier-Stokes equations using upwind schemes
05 p0539 N88-13283

Upwind formulations for the Euler equations
08 p0984 N88-15952

A survey of upwind principles for the multidimensional Euler equations 08 p0984 N88-15953

UPWELLING

U UPWELLING WATER

UPWELLING WATER

Satellite and synoptic studies of chemical fronts in the California current and coastal upwelling zone
[AD-A183909] 01 p0073 N88-10466

Biogeochemical cycling in the ocean. Part 1: Introduction to the effects of upwelling along the west coast of North America
[NASA-TM-88230] 07 p0882 N88-15349

North Pacific Ocean: Gulf of Alaska, R/V Thomas G. Thompson: 1 February - 8 March 1967. STD data report
[AD-A186569] 08 p1045 N88-16314

Circulation and exchange processes on the South Atlantic Bight Continental Shelf
[DE88-003330] 13 p1804 N88-20781

Biological processes in the water column of the South Atlantic bight: Zooplankton responses
[DE88-004811] 14 p1951 N88-21630

Changes in the California current system observed off northern California during July-August 1986
[AD-A190027] 15 p2100 N88-22510

Numerical simulation of coastal upwelling phenomena in Cabo Frio (RJ) through a two layer finite element model
[INPE-4502-RPE/561] 16 p2237 N88-23361

Observations of frontal instabilities on an upwelling filament
[AD-A191051] 17 p2375 N88-24122

Stability of a coastal upwelling front over topography
[AD-A192354] 20 p2829 N88-26784

Evolution of thermal structure of Benguela upswelling system according to satellite and shipboard data
24 p3449 N88-30525

URACIL

Photochemical conversion of nucleic acid components catalyzed by lunar soil 06 p0750 N88-14604

URANIUM

NT URANIUM ISOTOPES
NT URANIUM 238

Relation between shock strength and strain-rate plasticity at maximum deviatoric stress
[DE87-011736] 01 p0061 N88-10390

Hydrogen retention and release from uranium dioxide
[DE88-002042] 07 p0829 N88-15030

Phenomenological model of superconductivity of heavy fermions in U(sub 1-x)ThsubxBesub13
09 p1238 N88-17423

An irradiation performance data base for nitride fuels
17 p2427 N88-24438

URANIUM ALLOYS

Strain rate effects in fast-gas-cooled uranium-titanium and uranium-niobium alloys
[OUEL-1683/87] 02 p0149 N88-10937

URANIUM COMPOUNDS

NT URANIUM FLUORIDES

Uranium nitride fuel swelling and thermal conductivity correlations 17 p2409 N88-24327

Evaluation of UN fuel pin failure modes and motion of fuel during severe accidents for reactors in space
17 p2425 N88-24424

Material property and irradiation performance correlations for nitride fuels 17 p2434 N88-24483

A comparison of uranium nitride and mixed carbide fuels swelling 17 p2435 N88-24485

URANIUM FLUORIDES

Neutronics conceptual design of a UF6-fueled gasesous laser system 17 p2422 N88-24405

URANIUM ISOTOPES

NT URANIUM 238

High dose uranium ion implantation into silicon
[LBL-23509] 19 p2725 N88-26182

URANIUM 238

Diffusion bonding depleted uranium to copper
[RFP-3783-REV] 03 p0333 N88-12098

URANUS (PLANET)

Electrical conductivity and equation of state measurements on planetary fluids at high pressures and temperatures
[DE87-013787] 01 p0110 N88-10708

IUE program SUGSD: Varability time scale of H Ly-alpha from Uranus
[NASA-CR-182706] 13 p1856 N88-21107

Ultraviolet geometric albedo of Uranus
[NASA-CR-183099] 20 p2885 N88-27136

URANUS ATMOSPHERE

The solar radiation incident at the top of the atmosphere of Uranus and Neptune
[AERONOMICA-ACTA-A-317-1987]
07 p0878 N88-15323

Magnetic field of planet Uranus: Predictions, measurements, interpretations 08 p1005 N88-16094

Superthermal electron processes in the upper atmosphere of Uranus: Aurora and electroglow
[NASA-TM-101150] 18 p2594 N88-25417

URANUS RINGS

Discovery by Voyager-2 of predicted satellites which determine resonance nature of Uranian rings
08 p1006 N88-16095

URANUS SATELLITES

NT TITANIA

Discovery by Voyager-2 of predicted satellites which determine resonance nature of Uranian rings
08 p1006 N88-16095

URBAN AREAS

U CITIES

URBAN DEVELOPMENT

Department of Housing and Urban Development, and Certain Independent Agencies Appropriations, 1988, Part 2
[S-HRG-100-106-PT-2] 03 p0385 N88-12423

Orbital remote sensing: An instrument for monitoring urban growth
[INPE-4456-PRE/1287] 15 p2150 N88-22833

Earth resources: A continuing bibliography with indexes (issue 57)
[NASA-SP-7041(57)] 16 p2229 N88-23314

Applications of multitemporal compositions obtained from LANDSAT data in the study of urban growth
[INPE-4480-PRE/1246] 16 p2287 N88-23692
Four urban heliport case studies
[DOT/FAA/PM-87/32] 19 p2604 N88-25463
Remote sensing techniques applied to the study of metropolitan regions: The west sector of the Sao Paulo metropolitan area 19 p2681 N88-25941
Remote sensing applied to the monitoring of mineral extraction in the proximity of urban areas: Pros and cons
19 p2684 N88-25954
SPOT imagery for detecting residential expansion on the rural-urban fringe of Toronto, Canada
22 p3098 N88-28397
Spread of large tropical conurbations
22 p3098 N88-28398
Applications of SPOT data for urban real estate investment information systems
22 p3101 N88-28414
Utilization of SPOT multispectral data for urban planning 22 p3101 N88-28418

URBAN PLANNING
Adaptation of numerical SPOT data to an urban environment 03 p0342 N88-12158
Orbital remote sensing: An instrument for monitoring urban growth
[INPE-4456-PRE/1267] 15 p2150 N88-22833
Analyses of heliport system plans
[DOT/FAA/PM-87/31] 17 p2308 N88-23810
Low altitude remote sensing data in the implementation of a mathematical model for the planning of urban equipment networks 17 p2363 N88-24074
Four urban heliport case studies
[DOT/FAA/PM-87/32] 19 p2604 N88-25463
National Meeting on Remote Sensing Applied to Municipal Planning 19 p2681 N88-25939
Mapping of land use in Sao Jose dos Campos municipality by remote sensing, an aid for the elaboration of its PDDI 19 p2681 N88-25940
The impact of disorganized occupation of urban sub-basins: Sub-basin of the Cabucu River, metropolitan area of Sao Paulo (SP) 19 p2682 N88-25945
Remote sensing technique applied to vegetation as an aid to municipal planning 19 p2683 N88-25951
Monitoring urban land cover changes at the urban fringe from SPOT HRV imagery in south-east England
22 p3099 N88-28406
Utilization of SPOT multispectral data for urban planning 22 p3101 N88-28418

URBAN RESEARCH
Urban cartography: A book review
16 p2227 N88-23297
SPOT imagery for detecting residential expansion on the rural-urban fringe of Toronto, Canada
22 p3098 N88-28397
Utilization of remote sensing for the observation of urban populations. Ongoing research in Quito (Ecuador)
22 p3098 N88-28399
Monitoring urban land cover changes at the urban fringe from SPOT HRV imagery in south-east England
22 p3099 N88-28406
Mapping and urban multi-experimental assessment of SPOT: Urban results 22 p3101 N88-28415
Comparison of SPOT, LANDSAT TM and combined data for urban studies 22 p3101 N88-28417
Radiometric analysis and potential of SPOT HRV imagery for applications in urban environments and geology 22 p3112 N88-28486

URBAN TRANSPORTATION
Adiabatic diesel engine component development: Reference engine for on-highway applications
[NASA-CR-179531] 03 p0386 N88-12428
Electric vehicle demonstration project
[DE88-004076] 11 p1566 N88-19376
Digital maps for an electronic traffic guide
18 p2534 N88-25033

UREAS
Validation of maximum permissible concentration of urea in reclaimed potable water and evaluation of its biological effect 19 p2705 N88-26086

URETHANES
Stressed fabric abrasion test procedure for urethane coated fabric fuel tanks
[AD-A196327] 24 p3356 N88-29982

URINE
Human adaptation to various hypercapnic conditions in relation to salivary electrolyte dynamics and renal function 12 p1664 N88-19977

USA (UNITED STATES)
U UNITED STATES

USER MANUALS (COMPUTER PROGRAMS)
Space station integrated wall design and penetration damage control
[NASA-CR-179169] 01 p0013 N88-10070
Hanford Meteorological Station computer codes. Volume 1: The GEN computer code
[DE87-012816] 01 p0071 N88-10456
A user's guide for BIE3D: A boundary integral equation computer program for three-dimensional elastostatic analysis
[RAE-TM-MAT-STR-1078] 01 p0079 N88-10509
Manual for GetData version 3.1: A FORTRAN utility program for time history data
[NASA-TM-88288] 01 p0081 N88-10520
TIPS-1 user's manual: Cray-1 version
[DE87-013297] 01 p0081 N88-10522
EVA reference manual
[DE87-014073] 01 p0082 N88-10526
NOSTRADAMUS programmable translator user's manual and programmer's manual
[DE87-013414] 01 p0083 N88-10533
Blade loss transient dynamics analysis, volume 2. Task 2: TETRA 2 user's manual
[NASA-CR-179633] 02 p0126 N88-10792
RANDOM NUMBER: A syntax-directed package to produce random numbers in user-specified, univariate distributions. User's guide
[DE87-014278] 02 p0228 N88-11436
Numerical simulation of internal combustion engine flows: Development and users guide for MAGIC radial-azimuthal version
[DE87-014453] 03 p0332 N88-12091
The user's guide to the BACK system --- knowledge representation
[KIT-42] 03 p0367 N88-12310
Competition Analysis Model (CAM). Volume 2: Computer manual
[AD-A184017] 03 p0384 N88-12411
IDMS application documentation made easy
[DE88-000199] 03 p0384 N88-12416
Digital-flight-control-system software written in automated-engineering-design language: A user's guide of verification and validation tools
[NASA-TM-88313] 04 p0401 N88-12494
NACHOS 2: A finite element computer program for incompressible flow problems. Part 2: User's manual
[DE88-001451] 04 p0443 N88-12750
User's guide to NCAR (National Center for Atmospheric Research) CCM1
[PB87-224386] 04 p0469 N88-12899
SDVS (State Delta Verification System) 5 users' manual
[AD-A184339] 04 p0478 N88-12943
PROVER: A first-order logic system in Ada
[DE88-000220] 04 p0479 N88-12951
Guidelines for preparing software user documentation
[NASA-CR-181550] 04 p0480 N88-12959
SUSIE reference manual
[DE88-001462] 05 p0636 N88-13893
Diagnostic emulation: Implementation and user's guide
[NASA-CR-178391] 06 p0756 N88-14638
User manual for ATILA, a finite-element code for modeling piezoelectric transducers
[AD-A185948] 07 p0847 N88-15141
GENLPLOT: An interactive program for display and analysis of data, user's manual
[DE88-002292] 07 p0905 N88-15485
Attitude dynamics for satellites stabilized through spin
[INPE-4403-NTE/275] 08 p0963 N88-15833
User's guide to DIANE: A microcomputer program for modeling battery performance in electric vehicles
[DE88-003713] 08 p1068 N88-16456
Numerical arc segmentation algorithm for a radio conference-NASARC, version 2.0: User's manual
[NASA-TM-100161] 09 p1156 N88-16928
Guide for the program EXACT-NL --- wave growth
[KNMI-TR-94] 09 p1163 N88-16971
Nimbus 7 Solar Backscatter Ultraviolet (SBUV) spectral scan solar irradiance and Earth radiance product user's guide
[NASA-RP-1199] 09 p1184 N88-17096
Voice technology using personal computers
[AD-A186743] 09 p1218 N88-17300
Handbook of the GEMS image processing system
[RAE-TR-86062] 09 p1219 N88-17310
General Rotorcraft Aeromechanical Stability Program (GRASP) version 1.03: User's manual
[NASA-TM-100043] 09 p1219 N88-17313
Operators manual for a computer controlled impedence measurement system
[AD-A187513] 10 p1324 N88-17917
MOAOPS and BOOM-MAP computer programs for sonic boom research, volume 1
[AD-A189548] 12 p1574 N88-19414
KREME (Knowledge Representation, Editing and Modeling Environment): A user's introduction, phase 1
[AD-A188906] 12 p1681 N88-20052
An interactive user-friendly approach to surface-fitting three-dimensional geometries
[NASA-CR-4126] 12 p1682 N88-20058
NFEARS (Nonlinear Finite Element Adaptive Research Solver): A nonlinear adaptive finite element solver. Part 2: User's manual
[AD-A189009] 12 p1684 N88-20070
Martian Clouds Data Workshop
[NASA-CR-182431] 12 p1711 N88-20238
Documentation and installation of the hypersonic arbitrary-body computer program (Mark 3 version) of A.E. Gentry on the IBM computer system
[MBB/LKE-127/S/PUB/256] 13 p1719 N88-20276
MOPAC manual: A general molecular orbital package, fourth edition
[AD-A188623] 13 p1733 N88-20362
MASPLT: A one-dimensional graphics post processor for wave propagation codes
[DE88-005506] 13 p1817 N88-20856
FLAP (Force and Loads Analysis Program) code development and validation
[DE88-001131] 15 p2075 N88-22371
Analysis of rotating flexible blades using MSC/NASTRAN 16 p2222 N88-23259
Integrated multidisciplinary analysis tool IMAT users' guide
[NASA-TM-100605] 16 p2223 N88-23273
COBOL Analysis System (CAS) users manual
[PB88-171442] 16 p2250 N88-23445
Fast Algorithm Simulation and Test (FAST) facility
[AD-A191183] 16 p2252 N88-23457
User's guide to the Fault Inferring Nonlinear Detection System (FINDS) computer program
[NASA-CR-178410] 18 p2462 N88-24619
SAM 2 data user's guide
[NASA-RP-1200] 18 p2543 N88-25094
Graphical Multiprocessing Analysis Tool (GMAT)
[DE88-008019] 19 p2715 N88-26116
A description of the reference frames and the coordinate transformations used in AMEER (Aero-Mechanical Equations Evaluations Routines)
[DE88-007960] 19 p2720 N88-26153
Axisymmetric liquid sloshing under low-g conditions. Numerical simulation method (reference manual)
[NLR-TR-86057-U] 20 p2802 N88-26627
PAX ECONOPACK economic analysis package users manual
[AD-A192949] 20 p2883 N88-27117
User's manual for C-HEMP: A two-dimensional wave propagation code. Volume 1: Description and derivations of the code
[AD-A193197] 21 p2944 N88-27486
DYNA3D (Nonlinear Dynamic Analysis of Structures in Three Dimensions) user's manual
[DE88-012242] 21 p2963 N88-27604
National air toxics information clearinghouse: NATICH data base users guide for data viewing, February 1988
[PB88-197470] 21 p2970 N88-27645
A PRELUDE (analysis and design of control systems-preliminary utilities depository). A data-based interactive system of control software, user's guide
[DFVLR-MITT-88-12] 21 p3000 N88-27795
User's manual for the two-dimensional transputer graphics toolkit
[NASA-TM-100974] 21 p3001 N88-27796
Program user's manual for an unsteady helicopter rotor-fuselage aerodynamic analysis
[NASA-CR-181701] 22 p3039 N88-28047
Walter user's manual (Version 1.0)
[AD-A192542] 22 p3136 N88-28644
Loglisp programming system users manual
[AD-A193933] 22 p3142 N88-28682
Finite Element Composite Analysis Program (FECAP) for a microcomputer
[NASA-TM-100670] 23 p3190 N88-28982
Signal processing software for ground penetrating radar, user's manual
[AD-A194286] 23 p3203 N88-29059
Level 1 Ada/SQL (Structured Query Language) database language interface user's guide
[AD-A194480] 23 p3249 N88-29335
User's manual for three dimensional boundary layer (BL3-D) code
[NASA-CR-174899] 24 p3369 N88-30063
Supermap for Cray FORTRAN: A user's guide
[NASA-CR-177410] 24 p3412 N88-30309
The eivaN: A forward-looking interactive orbital trajectory plotting tool for use with proximity operations (PROX OPS) and other maneuvers: Description and user's manual
[NASA-CR-177490] 24 p3414 N88-30327
An operations manual for the digital data system
[NASA-CR-181688] 24 p3415 N88-30329
Aircraft noise prediction program propeller analysis system IBM-PC version user's manual version 2.0
[NASA-CR-181689] 24 p3428 N88-30399

USER REQUIREMENTS
Space station platforms 01 p0015 N88-10086
Spacecraft Systems Working Group report
01 p0015 N88-10091

Electrical Power Working Group report
01 p0016 N88-10095
Development of methods for the analysis of the frequency and voltage statics of electricity users and electrical networks
[ETN-87-90412] 01 p0043 N88-10271
Battery development and testing at ESA
02 p0164 N88-11027
Applications and benefits of short period weather forecasts 02 p0199 N88-11240
Tutorial and hands-on demonstration of a fluent interpreter for CARE 3
[NASA-TM-4011] 02 p0220 N88-11383
A general approach to error propagation
[DE87-014287] 02 p0224 N88-11412
Orbital Spacecraft Consumables Resupply System (OSCRS). Volume 4: Extended study results Part 1: Executive Summary
[NASA-CR-172012] 03 p0268 N88-11686
Optical laser technology, specifically CD-ROM (Compact Disc - Read Only Memory) and its application to the storage and retrieval of information
[AD-A184111] 03 p0330 N88-12086
An overview of remote sensing users' requirements
03 p0340 N88-12139
SDVS (State Delta Verification System): Program verification system development fiscal year 1986
[AD-A184338] 03 p0366 N88-12302
Concepts and techniques for support of real time distributed operating systems
[AD-A184491] 03 p0367 N88-12307
Guidelines for preparing software user documentation
[NASA-CR-181550] 04 p0480 N88-12959
User interface for a partially incompatible system software environment with non-ADP users
[DE88-001518] 04 p0482 N88-12968
On the next generation of reliability analysis tools
[NASA-CR-178380] 04 p0487 N88-13000
Small reactor power systems for manned planetary surface bases
[NASA-TM-100223] 04 p0524 N88-13209
Orbital Spacecraft Consumables Resupply System (OSCRS). Volume 1: Executive summary
[NASA-CR-172010] 05 p0553 N88-13368
File usage analysis and resource usage prediction: A measurement-based study
[NASA-CR-181553] 05 p0633 N88-13867
Usage analysis of user files in UNIX
[NASA-CR-181561] 05 p0633 N88-13868
Window system: A toolbox for interactive computer graphics
[PB87-234282] 06 p0756 N88-14637
Using user models and automatic expertise acquisition in data base interactions
[PB87-234357] 06 p0791 N88-14848
Scientific data manipulation in a relational database system
[PB87-124400] 06 p0791 N88-14850
FAA air traffic control operations concepts. Volume 5: ATCT/TCCC (Airport Traffic Control Tower/Tower Control Computer Complex) tower controllers
[AD-A185983] 07 p0818 N88-14977
An approach to validation and verification of the communications load model with supporting user's guide
[AD-A185926] 07 p0840 N88-15098
A multi user random access communication system for users with different priorities
[AD-A186041] 07 p0841 N88-15102
Using multiple dialog modes in a user-system interface to accomodate different levels of user experience: An experimental study
[AD-A186115] 07 p0899 N88-15444
TeXing the FORMULARY: A collection of examples of the use of TeX to produce ruled tables and displayed equations
[AD-A185820] 07 p0921 N88-15598
User interface devices for mission control
09 p1205 N88-17224
User engineering: A new look at system engineering
09 p1206 N88-17231
POCC capabilities document. Payload support capabilities description: MCC, JSC POCC, remote POCC interface
[NASA-TM-89708] 09 p1260 N88-17555
Shared workspaces for real-time collaboration in distributed networks: Concepts, techniques, problems
[AD-A188150] 10 p1394 N88-18315
Presentation of flight control design and handling quality commonality by separate surface stability augmentation for the family of commuter airplanes
[NASA-CR-182567] 12 p1583 N88-19471
Customer concerns regarding satellite servicing
12 p1587 N88-19503
Conceptual design and programmatics studies of space station accommodations for Life Sciences Research Facilities (LSRF)
[NASA-CR-179270] 12 p1598 N88-19567
User perceptions of side-arm flight control in rotary-wing aircraft
[AD-A188519] 12 p1672 N88-20009
A digital logic simulator with concurrent programming considerations
[AD-A188823] 12 p1678 N88-20032
A prototype for remotely shared textual workspaces
[AD-A188352] 12 p1679 N88-20040
An interactive user-friendly approach to surface-fitting three-dimensional geometries
[NASA-CR-4126] 12 p1682 N88-20058
A directory of databases available through SearchMAESTRO
[AD-A188813] 12 p1706 N88-20214
Orbital transfer vehicle concept definition and system analysis study. Volume 2: OTV concept definition and evaluation. Book 1: Mission and system requirements
[NASA-CR-179321] 13 p1729 N88-20339
Online aiding for human-computer interfaces
[AD-A189239] 13 p1815 N88-20842
Investigation of European remote sensing user needs in accessing MOS-1 payload
[ESA-CR(P)-2535] 14 p1940 N88-21580
DataViews: A personalizable, interactive, data display system for the decisionmaker
[AD-A188509] 14 p1991 N88-21868
Real-time flight test data distribution and display
[NASA-TM-100424] 15 p2022 N88-22050
ECP (Electrical Circuitry Program): A proposed program for electrical circuitry analysis
[AD-A190494] 15 p2060 N88-22280
CK-LOG system conversion (user's manual and user interface)
[AD-A190273] 15 p2111 N88-22577
Maps for tourists. A systematic approach to tourist cartography 16 p2227 N88-23296
WMO Region 2/Region 5 Training Seminar on Climate Data Management and User Services
[WCP-133] 16 p2234 N88-23344
Concurrency efficiency user's manual
[AD-A190884] 16 p2251 N88-23450
PPDS compas-primer
[DE88-701589] 16 p2266 N88-23554
Data management strategies in the industrial environment
[NLR-MP-87002-U] 16 p2286 N88-23684
Solid Earth mission end-to-end data system study
[C04825.08/FR] 17 p2309 N88-23811
Practical image analysis using personal computers: The Canadian experience 17 p2356 N88-24037
The SAGE geographic analysis system
17 p2361 N88-24063
Multimegawatt power conditioning requirements study
17 p2438 N88-24504
P-Plus: Polar Platform utilization study, executive summary
[BAE-TP-8391] 18 p2469 N88-24653
CIMAG2: The computer program to generate color images
[AD-A191847] 18 p2557 N88-25175
Department of Defense statement on the X-ray Lithography Program to the Research and Development Subcommittee of the House Armed Services Committee of 100th Congress, second session
[AD-A191854] 18 p2582 N88-25341
Advanced development of double-injection, deep-impurity semiconductor switches
[NASA-CR-182118] 18 p2583 N88-25346
Mars rover/sample return mission requirements affecting space station
[NASA-CR-172046] 18 p2594 N88-25414
Ocean satellite data and the needs of designers and operators of marine units 19 p2701 N88-26061
Flight Mechanics Panel Symposium on Rotorcraft Design for Operations. Technical evaluation report
[AGARD-AR-243] 20 p2758 N88-26362
Direct manipulation and the design of user interfaces
[PB88-126354] 20 p2834 N88-26810
SIMS: Single Interface to Multiple Systems
[AD-A192264] 20 p2837 N88-26832
Interaction management in CAD systems with a history mechanism
[CWI-CS-R8756] 20 p2840 N88-26851
Programmer-friendly LL(1) parser generator
[PB88-126933] 20 p2841 N88-26857
Engineering data compendium. Human perception and performance. User's guide
[LC-87-19560] 21 p2993 N88-27749
Software engineering guidelines for RASP and ANDECS: Requirements and architectural design
[DFVLR-MITT-88-07] 21 p3000 N88-27793
Capitalizing on experience with intelligence gateway software
[AD-A193362] 21 p3028 N88-27971
The management of software in airborne recording systems 22 p3035 N88-28019
Engineering data compendium. Human perception and performance, volume 2
[LC-87-19560] 22 p3134 N88-28631
Engineering data compendium. Human perception and performance, volume 3
[LC-87-19560] 22 p3134 N88-28632
Loglisp programming system users manual
[AD-A193933] 22 p3142 N88-28682
ADP (Automated Data Processing) requirements definition and documentation through user-developed prototypes
[AD-A194407] 23 p3248 N88-29332
An adaptive overlapping local grid refinement method for two-dimensional parabolic systems
[AD-A193560] 23 p3271 N88-29464
Central user and browse service --- ERS-1 ground segment
[CU-PG-MDA-SY-0005] 23 p3297 N88-29637
MANIP --- spacecraft modeling program
[MANIP-217A] 24 p3335 N88-29855
A static scheduler for the computer aided prototyping system: An implementation guide
[AD-A194340] 24 p3414 N88-30322
Integrated resource scheduling in a distributed scheduling environment 24 p3417 N88-30342

USER-COMPUTER INTERFACE
U MAN-COMPUTER INTERFACE

UTILITIES
Methodology for control and operation of wind arrays in utility systems
[DE87-013129] 01 p0039 N88-10248
The Environment for Application Software Integration and Execution (EASIE) version 1.0. Volume 4: System installation and maintenance guide
[NASA-TM-100576] 17 p2386 N88-24185
Phosphoric acid electric utility fuel cell technology development
[DE88-010187] 20 p2795 N88-26582

UTILITY AIRCRAFT
NT BO-105 HELICOPTER
NT DO-28 AIRCRAFT
NT U-2 AIRCRAFT
NT UH-1 HELICOPTER
NT UH-60A HELICOPTER

UTILIZATION
NT GEOTHERMAL ENERGY UTILIZATION
NT LASER APPLICATIONS
NT LASER CUTTING
NT LASER FUSION
NT REUSE
NT WASTE ENERGY UTILIZATION
NT WASTE UTILIZATION
NT WINDPOWER UTILIZATION
Photocurrent generation from basic metals, utilizing a short pulsed ArF excimer laser
[AD-A184928] 05 p0587 N88-13579
Disuse condition stimulates bone resorption in organ culture 12 p1656 N88-19926

UV CETI STARS
U FLARE STARS

UV LASERS
U ULTRAVIOLET LASERS

V

V BAND
U EXTREMELY HIGH FREQUENCIES

V/STOL AIRCRAFT
NT AH-64 HELICOPTER
NT BO-105 HELICOPTER
NT CH-46 HELICOPTER
NT COMPOUND HELICOPTERS
NT HEAVY LIFT HELICOPTERS
NT HELICOPTERS
NT MILITARY HELICOPTERS
NT OH-58 HELICOPTER
NT RIGID ROTOR HELICOPTERS
NT ROTARY WING AIRCRAFT
NT ROTOR SYSTEMS RESEARCH AIRCRAFT
NT SHORT TAKEOFF AIRCRAFT
NT TANDEM ROTOR HELICOPTERS
NT TILT ROTOR AIRCRAFT
NT UH-1 HELICOPTER
NT UH-60A HELICOPTER
NT VERTICAL TAKEOFF AIRCRAFT
NT XV-15 AIRCRAFT
Flight research at NASA Ames Research Center: A test pilot's perspective
[NASA-TM-100025] 02 p0125 N88-10788

Civil applications of high-speed rotorcraft and powered-lift aircraft configurations
[NASA-TM-100035] 03 p0261 N88-11843
V/STOL aircraft configurations and opportunities in the Pacific Basin
[NASA-TM-100005] 03 p0261 N88-11644
Test stand performance of a convertible engine for advanced V/STOL and rotorcraft propulsion
[NASA-TM-100211] 03 p0266 N88-11679
Flight propulsion control integration for V/STOL aircraft
[NASA-TM-100226] 03 p0267 N88-11680
Integrated control and display research for transition and vertical flight on the NASA V/STOL Research Aircraft (VSRA)
[NASA-TM-100029] 05 p0551 N88-13359
Full-envelope aerodynamic modeling of the Harrier aircraft
[NASA-TM-88376] 05 p0552 N88-13363
NASA supersonic STOVL propulsion technology program
[NASA-TM-100227] 06 p0668 N88-14093
A jet in a crossflow
[NASA-CR-182489] 09 p1113 N88-16674
A flight-test methodology for identification of an aerodynamic model for a V/STOL aircraft
[NASA-TM-100067] 09 p1117 N88-16694
Application of empirical and linear methods to VSTOL powered-lift aerodynamics
[NASA-TM-100048] 10 p1267 N88-17581
Recommendations for ground effects research for V/STOL and STOL aircraft and associated equipment for large scale testing
[NASA-CR-177429] 10 p1268 N88-17585
A computational study of thrust augmenting ejectors based on a viscous-inviscid approach
10 p1326 N88-17929
A review of technologies applicable to low-speed flight of high-performance aircraft investigated in the Langley 14- x 22-foot subsonic tunnel
[NASA-TP-2796] 13 p1717 N88-20264
Propulsion and airframe aerodynamic interactions of supersonic V/STOL configurations. Volume 1: Wind tunnel test pressure data report
[NASA-CR-177343-VOL-1] 16 p2157 N88-22866
Propulsion and airframe aerodynamic interactions of supersonic V/STOL configurations. Volume 2: Wind tunnel test force and moment data report
[NASA-CR-177343-VOL-2] 16 p2157 N88-22867
Propulsion and airframe aerodynamic interactions of supersonic V/STOL configurations. Volume 4: Summary
[NASA-CR-177343-VOL-4] 16 p2157 N88-22868
A numerical study of the hot gas environment around a STOVL aircraft in ground proximity
[NASA-TM-100895] 17 p2295 N88-23729
PAN AIR analysis of the NASA/MCAIR 279-3: An advanced supersonic V/STOL fighter/attack aircraft
[NASA-TM-89838] 17 p2298 N88-23750
Flight testing a V/STOL aircraft to identify a full-envelope aerodynamic model
[NASA-TM-100996] 17 p2301 N88-23762

VACANCIES (CRYSTAL DEFECTS)
Interaction between defects and the formation of dissipative structures in irradiated impure crystals
[DE87-703125] 02 p0246 N88-11552
Simulation of the layer-growth dynamics in silver films: Dynamics of adatom clusters and vacancy clusters on Ag(100)
[DE87-014764] 03 p0380 N88-12390
Evolution of radiation-induced voids and dislocations at low temperature
[DE88-700350] 07 p0939 N88-15704
Effect of irradiation on the diffusion evolution of void ensemble in crystals
[DE88-700558] 07 p0939 N88-15706
Structural properties of high-T/sub c/ oxide super conductors
[DE88-002974] 08 p1090 N88-16563
Electron diffraction evidence for the ordering of excess nickel atoms by relation to stoichiometry in nickel-rich beta'-NiAl: formation of a nickel-aluminum (Ni2Al) superlattices
[NASA-TT-20177] 14 p1890 N88-21297
Abnormal diffusion of vacancies in metals
[DE88-701880] 20 p2773 N88-26441

VACUUM
NT HIGH VACUUM
NT LOW VACUUM
NT ULTRAHIGH VACUUM
Synergism of electroplating and vacuum processes
[DE87-013486] 01 p0033 N88-10211
Recovery of vacuum gaps after arcing
[DE87-013852] 01 p0039 N88-10250
Physics and device design of vacuum integrated circuits 01 p0039 N88-10251
Different ways of looking at the electromagnetic vacuum
[DE87-013150] 01 p0089 N88-10584
A new type of lamp and reflector for I.R. simulation
02 p0136 N88-10855
Vacuum ultraviolet electronic properties of liquids
[DE88-000165] 03 p0282 N88-11772
Cosmology with decaying vacuum energy
[DE88-000698] 03 p0389 N88-12443
Model of earlier stage of universe's evolution
06 p0775 N88-14758
Approximate method for predicting the permanent set in a beam in vacuo and in water subject to a shock wave 11 p1500 N88-18957
Molecular collision processes in gases and at surfaces
[AD-A189518] 13 p1836 N88-20982
A high field launch for electron cyclotron heating using an external window
[DE88-005350] 13 p1838 N88-21000
Vacuum-arc plasma centrifuge experiment
[INPE-4509-PRE/1263] 15 p2138 N88-22758
High frequency power distribution system
[NASA-CR-175071] 17 p2335 N88-23939
Propagation of neutralized ion beams
[AD-A191599] 18 p2574 N88-25289
Multiply stripped ion generation in the metal vapor vacuum arc
[DE88-008418] 19 p2725 N88-26179
A bibliography and author index for electrical discharges in vacuum (1897-1986)
[DE88-008744] 20 p2794 N88-26579
Theory and simulation of relaxed plasmoids
[AD-A192884] 21 p3032 N88-27997
Measurements of vacuum arc ion charge state distributions
[DE88-008249] 23 p3284 N88-29558

VACUUM APPARATUS
NT IONIZATION GAGES
NT VACUUM CHAMBERS
NT VACUUM GAGES
NT VACUUM PUMPS
Plasma centrifuge development at INPE
[INPE-4243-PRE/1117] 08 p1087 N88-16546
Three dimensional Monte Carlo simulation of molecular movement and heat radiation in vacuum devices: Computer code MOVAK3D --- fusion reactors
[KFK-4292] 09 p1246 N88-17471
Research and development of surface skimming bulk wave devices for sensor applications
[AD-A187504] 11 p1470 N88-18766
Planning, construction, and commissioning of a vacuum apparatus with a cold surface for the measurement of transistor functions at 20 K
[JUEL-SPEZ-397] 12 p1622 N88-19703
Low temperature storage container for transporting perishables to space station
[NASA-CASE-MFS-28248-1] 18 p2498 N88-24817
High temperature testing of C/C (Carbon/Carbon) composites
[AD-A193012] 20 p2768 N88-26411

VACUUM ARC SWITCHES
Measuring technical and mathematical investigation of multiple reignitions at the switching of a motor using vacuum circuit breakers
[ETN-87-90406] 01 p0042 N88-10270
Low-current behavior and current chopping of vacuum arcs
[ISBN-90-9001649-X] 05 p0578 N88-13529
The influence of ionization within a plasma opening switch
[AD-A193147] 21 p3017 N88-27906

VACUUM CHAMBERS
Meeting today's requirements for large thermal vacuum test facilities 02 p0134 N88-10840
Mobile test fixture system for use in a thermal vacuum facility 02 p0134 N88-10843
Test of the Hipparcos payload in the Liege vacuum facility focal 02 p0135 N88-10850
Evaluation and certification of heater assemblies developed for thermal vacuum acceptance testing
02 p0136 N88-10853
Thermal testing by internal IR heating of the FEP module 02 p0136 N88-10854
Chemical cleaning of metal surfaces in vacuum systems by exposure to reactive gases
[AD-A188588] 12 p1608 N88-19616
Ion generator and ion application system
[NASA-CASE-MFS-28122-1] 17 p2397 N88-24253
Conceptual design of the SP-100 GES test site
17 p2402 N88-24284

VACUUM DEPOSITION
Synthesis and characterization of thin films
[AD-A187335] 10 p1421 N88-18485
Deposition of device quality epitaxial layers of gallium nitride and indium nitride for electronic applications
[AD-A188001] 11 p1453 N88-18661
Design and demonstration of a system for the deposition of atomic-oxygen durable coatings for reflective solar dynamic power system concentrators
[NASA-CR-4158] 19 p2606 N88-25474
Laser measurement of particle velocities in vacuum plasma spray deposition
[DE88-007111] 19 p2728 N88-26198
Plasma deposition: Investigations on a new approach
[ETN-88-92619] 20 p2861 N88-26992
Growth and characterization of thin films of ZnSnP(sub)2
[DE88-001164] 20 p2874 N88-27060
Equipment for building and testing superconductive flux flow electronic devices
[AD-A192959] 21 p2936 N88-27436

VACUUM EFFECTS
Survival under space vacuum: Biochemical aspects
12 p1657 N88-19930
Ultraviolet (160 to 300 nm) action spectra for inactivation and DNA photoproduct formation of Bacillus subtilis spores under ultrahigh vacuum 12 p1657 N88-19931
Mechanical design of a ultrahigh gravity UHV facility to launch and recover a low-speed projectile tested on board KC 135 14 p1877 N88-21216

VACUUM GAGES
NT IONIZATION GAGES
Thermal vacuum sensors based on integrated silicon thermopiles
[ETN-88-92237] 16 p2210 N88-23190

VACUUM MELTING
Evaporation characteristics of elements during vacuum arc remelting of alloy A-286 15 p2055 N88-22248

VACUUM PUMPS
Vacuum pumps and systems: A review of current practice 02 p0134 N88-10839
Meeting today's requirements for large thermal vacuum test facilities 02 p0134 N88-10840
MPD (magnetoplasmadynamic) thruster advanced pumping system concepts
[AD-A190513] 15 p2138 N88-22756

VACUUM SYSTEMS
Meeting today's requirements for large thermal vacuum test facilities 02 p0134 N88-10840
Chemical cleaning of metal surfaces in vacuum systems by exposure to reactive gases
[AD-A188588] 12 p1608 N88-19616
Flotation processes
[PB88-180302] 18 p2540 N88-25075

VACUUM TESTS
NT THERMAL VACUUM TESTS
Outgassing data for selecting spacecraft materials
[NASA-RP-1124] 01 p0019 N88-10117
Altitude simulation testing of Ariane's second-stage engine 09 p1126 N88-16747
Robotic joint prototype for space applications
14 p1878 N88-21222
A test facility for the in-vacuo assessment of dry lubricants and small mechanisms at cryogenic temperatures 14 p1878 N88-21224
Separable electrical connectors for space: A tribological and electrical assessment 14 p1879 N88-21231

VACUUM TUBES
NT CATHODE RAY TUBES
NT CYCLOTRON RESONANCE DEVICES
NT KLYSTRONS
NT MAGNETRONS
NT MICROWAVE TUBES
NT TRAVELING WAVE TUBES

VACUUM ULTRAVIOLET RADIATION
U FAR ULTRAVIOLET RADIATION

VALENCE
Gaining control over rare earth valence fluctuations
[DE87-010116] 01 p0103 N88-10671
A quantum theoretical study of polyimides
[NASA-CR-181495] 03 p0292 N88-11831
The itinerant resonating-valence-bond model for superconductivity
[DE87-014794] 03 p0380 N88-12391
Superconductivity as a synchronous spatial alternation of valence bonds
[AD-A184208] 03 p0382 N88-12405
Valence bond theory and superconductivity
[AD-A184274] 04 p0496 N88-13052
Valence bond cluster studies of alkali metal/semiconductor bonding
[AD-A184276] 04 p0496 N88-13054
Atomic and electronic structure of surfaces and chemisorbed layers
[DE87-014987] 04 p0498 N88-13065
Electronic band structure and photoemission: A review and projection
[DE88-002236] 06 p0787 N88-14829
Electron Spin Resonance (ESR) measurements on intermediate-valence Cer compounds doped with paramagnetic ions: CeOs2:Gd ion and CePd3:Mn-ion
[ETN-88-91081] 09 p1256 N88-17526

Copper oxidation states, vacancy ordering and their ffect on high temperature superconductivity
DE88-003079] 09 p1258 N88-17542
Core-core and core-valence correlation
NASA-CR-182552] 11 p1544 N88-19226
On the bond distance in methane
NASA-CR-181436] 22 p3150 N88-28741
LIDATION
U PROVING
LKYRIE AIRCRAFT
U B-70 AIRCRAFT
LLEYS
A real-data numerical study and four-dimensional data ssimilation application for mesobeta-scale flow in complex terrain 02 p0212 N88-11329
Geological interpretation of a SPOT image over Kenya: The Gregory rift network of faults
03 p0343 N88-12164
Wind and temperature structure on the slopes of a ountain valley
DE88-000080] 07 p0880 N88-15338
Cross flow in the Alps and flat foehn during the xperiment MERKUR — mesoscale experiment
08 p1013 N88-16142
The role of anabatic winds in the heating of valleys
08 p1014 N88-16144
Simulation of a typical flow in a broad valley
08 p1015 N88-16154
Groundwater sapping valleys: Experimental studies, eological controls and implications to the interpretation f valley networks on Mars
NASA-CR-182718] 15 p2152 N88-22847
Application of remote sensing in the conservation of atural areas: Ribeira Valley 19 p2683 N88-25949
Intercrater plains deposits and the origin of Martian alleys 23 p3301 N88-29861
ALSALVA EXERCISE
The effect of orthostatic changes in central blood volume n the heart rate response to graded Valsalva aneuvers 12 p1652 N88-19904
ALSALVA MANEUVER
U VALSALVA EXERCISE
ALUE ENGINEERING
Value engineering — space projects
22 p3160 N88-28817
Value analysis 22 p3161 N88-28819
ALVES
NT CONTROL VALVES
NT PRESSURE REGULATORS
Advanced natural gas fueled engine development. Part 2: Materials investigation
[PB87-223160] 03 p0331 N88-12088
Development, construction and testing of a novel internal combustion engine with conical rotating slide valve
[DE88-900071] 05 p0589 N88-13533
Gas feed system for the T-15 tokamak discharge chamber
[DE88-700351] 07 p0935 N88-15682
Influence of magnetic material on the transient of a controle electrovalve
[INPE-4418-PRE/1223] 12 p1624 N88-19713
Numerical methods in the resolution of control electrovalve model
[INPE-4154-RPE/540] 13 p1764 N88-20554
AN ALLEN RADIATION BELTS
U RADIATION BELTS
AN DE GRAAFF ACCELERATORS
Particle beam alignment system for single event upset-Van de Graaf experiments
[AD-A189695] 15 p2132 N88-22721
AN DER WAAL FORCES
On the interaction of a planar metal surface with a charge and with a molecule
[DE87-703083] 02 p0147 N88-10920
The generalized van der Waals theory of pure fluids and mixtures
[DE88-002380] 07 p0855 N88-15192
Van der Waals clusters of aromatic molecules studied using supersonic molecular jet spectroscopy
[AD-A186087] 07 p0929 N88-15644
Half collision studies of inelastic energy transfer processes
[DE88-008096] 19 p2724 N88-26178
High resolution spectroscopy of dissociating molecules
[DE88-007959] 20 p2851 N88-26924
ANADIUM
Mechanical properties of an acicular ferrite steel microalloyed to niobium and vanadium
[DE87-703547] 04 p0415 N88-12574
Partial substitution of vanadium by niobium in AISI H13 steel
[DE87-703548] 04 p0415 N88-12575
Superconductivity and crystal structure of high-pressure phases in V-Ru-H system 09 p1239 N88-17426
Use of nonporous metals membranes for the separation of hydrogen from gas mixtures
[BMFT-FB-T-86-206] 14 p1888 N88-21280
Superconductivity of Cr/V superlattices
20 p2874 N88-27057
Constant amplitude fatigue life data for notched and unnotched annealed Ti-6Al-4V sheet
[AD-A193420] 21 p2913 N88-27287
VANADIUM ALLOYS
Investigation of creep crack growth in heat resistant tube steels
[ETN-87-90606] 03 p0288 N88-11813
Reduced-activation ferritic steels: A comparison with Cr Mo steels
[DE88-000332] 03 p0290 N88-11826
The effect of neutron irradiation on the tensile properties and microstructure of several vanadium alloys
[DE88-001755] 06 p0682 N88-14176
Effect of overload ratios on fatigue crack growth behavior in Ti-6Al-4V alloy
[PB87-147062] 07 p0833 N88-15055
Experimental method for investigating helium effects in irradiated vanadium
[DE88-002891] 08 p0969 N88-15865
Influence of neutron irradiation on the Charpy impact properties of V-15Cr-5Ti
[DE88-003430] 11 p1458 N88-18692
Vibration spectra of oxygen and vanadium atoms in vanadium-oxygen disordered interstitial alloys
[DE87-703166] 13 p1740 N88-20404
Effect of hydrogen, deuterium and oxygen on the anelastic properties of refractory alloys
[DE88-007349] 18 p2484 N88-24736
The postirradiation tensile properties and microstructure of several vanadium alloys
[DE88-007140] 19 p2615 N88-25515
Low-chromium reduced-activation ferritic steels
[DE88-009060] 19 p2617 N88-25524
Stress relaxation of a titanium (Ti-6Al-4V) threaded joint
[DE88-010102] 21 p2961 N88-27590
VANADIUM COMPOUNDS
NT VANADIUM OXIDES
VANADIUM OXIDES
The development of a new and novel Hadamard transform infrared spectrometer for analytical chemistry
[DE87-014804] 02 p0175 N88-11094
Vibration spectra of oxygen and vanadium atoms in vanadium-oxygen disordered interstitial alloys
[DE87-703166] 13 p1740 N88-20404
Vanadic hot corrosion of gas turbine blade coating materials 17 p2321 N88-23864
VANES
NT GUIDE VANES
NT JET VANES
Turbine Engine Hot Section Technology, 1985
[NASA-CP-2405] 02 p0184 N88-11140
Development of heat flux sensors for turbine airfoils
02 p0184 N88-11143
Component specific modeling
02 p0187 N88-11166
Constitutive modeling for isotropic materials
02 p0188 N88-11172
Turbine airfoil deposition models and their hot corrosion implications 02 p0189 N88-11178
Fluid mass and thermal loading effects on the modal characteristics of space shuttle main engine liquid oxygen inlet splitter vanes 05 p0594 N88-13628
Examination of the development of a compressible turbulent boundary layer on a rough and porous wall
[PB87-148266] 07 p0815 N88-14964
Experimental evaluation of a translating nozzle sidewall radial turbine 10 p1280 N88-17656
Static performance of an axisymmetric nozzle with post-exit vanes for multiaxis thrust vectoring
[NASA-TP-2800] 13 p1719 N88-20280
Study on the heat resisting and cooling property of the ceramics-metal hybrid stator vanes
[DE88-753117] 20 p2810 N88-26668
Euler analysis of a swirl recovery vane design for use with an advanced single-rotation propfan
[NASA-TM-101357] 24 p3320 N88-29771
VANS
U TRUCKS
VAPOR DEPOSITION
NT VACUUM DEPOSITION
Equations for determining CVD tungsten-rhenium alloy composition and plating rate
[DE87-008831] 01 p0024 N88-10152
Laser chemically vapor deposited silicon-carbide: Growth features, topography, microstructure, and composition
[DE87-013767] 01 p0029 N88-10184
Ceramic composites by chemical vapor infiltration
[DE87-009128] 01 p0029 N88-10185
Chemical vapor deposition of B6P and B6As films
[DE87-009288] 02 p0151 N88-10942
Experimental verification of vapor deposition rate theory in high velocity burner rigs 02 p0189 N88-11179
The preparation of thin films for photovoltaic conversion by novel MOCVD techniques
[DE87-001185] 02 p0194 N88-11212
Preparation and properties of evaporated CdTe films
[DE87-012270] 02 p0195 N88-11216
Laser spectroscopy and gas-phase chemistry in CVD
[DE87-013715] 03 p0281 N88-11770
Ion plating: Fundamental processing studies and synthesis of high performance coatings
[AD-A184766] 03 p0303 N88-11908
Excimer-laser-assisted deposition of GaAs, AlAs and (Al,Ga)As from Lewis acid-base adducts
[AD-A184588] 03 p0329 N88-12081
Inertial confinement fusion reactor cavity analysis
[DE88-000788] 04 p0492 N88-13028
Fabrication of composites by chemical vapor deposition
[DE87-014565] 05 p0559 N88-13408
Reactive sticking coefficients of silane on silicon
[DE88-000601] 05 p0570 N88-13473
Fundamental studies in the OM-CVD growth of Ga-In-As-Sb
[AD-A184822] 05 p0655 N88-14014
Bending properties of aluminum base composite with CVD-fiber
[PB87-130878] 06 p0678 N88-14156
An analysis of the effect of system variables on the quality of thin films and powders produced by laser-breakdown chemical vapor deposition
[DE88-001793] 06 p0708 N88-14342
Heteroepitaxial growth of 3-5 semiconductor compounds by metal-organic chemical vapor deposition for device applications
[NASA-CR-182346] 06 p0788 N88-14832
High-temperature electronics
08 p0956 N88-15797
TiN coatings on M2 steel produced by plasma assisted chemical vapor deposition
[DE88-003189] 08 p0970 N88-15867
Oxidation resistance of CVD coatings
[AD-A178337] 09 p1147 N88-16875
Superlattice photodetectors
[AD-A186956] 09 p1253 N88-17511
Microgravity research at the University of Mexico: Experiments in payload G-006 10 p1286 N88-17692
Metal modification for improved glass-ceramic to metal seals. 1: Auger results on ion implantation and vapor deposition films
[DE88-005244] 10 p1339 N88-18006
Fabrication and evaluation of transmissive multilayer optics for 8 keV X-rays
[DE88-003999] 10 p1409 N88-18402
Plasma deposition of silicon carbide thin films
[AD-A188093] 11 p1556 N88-19314
Preparation and characterization of Cu2Zn1-xMnxGeS4
[AD-A188113] 11 p1556 N88-19315
Feasibility studies of the growth of 3-5 compounds of boron by MOCVD
[NASA-CR-181622] 11 p1561 N88-19343
Preparation and characterization of thin films of alumina by metalorganic chemical vapor deposition
[AD-A188366] 12 p1608 N88-19614
Fundamental studies and device development in beta silicon carbide
[AD-A189540] 12 p1699 N88-20165
Research on mercury cadmium telluride
[AD-A189155] 13 p1845 N88-21039
Initial stages of silicon growth on the (100) surface of silicon by localized laser CVD
[DE88-005420] 13 p1848 N88-21059
Ball bearings with chemical vapor deposition (CVD)-TiC coated components 14 p1876 N88-21210
Chemical vapor deposited silica coatings for solar mirror protection
[NASA-TM-100834] 14 p1893 N88-21306
Measurements of optical nonlinearities in MOCVD-grown GaAs/GaAlAs multiple quantum wells
14 p1975 N88-21767
Numerical simulations of buoyancy driven flows in cylinders and cavities for vapor crystal growth
14 p1987 N88-21854
Oxide optical coatings prepared by metal organic vapor deposition
[DE88-006809] 15 p2043 N88-22175
Investigation of laser diagnostics of PACVD processes for depositing hard face coatings
[DE88-007083] 15 p2043 N88-22176
Vapor phase deposition and growth of polyimide films on copper
[AD-A189969] 15 p2044 N88-22178

JPRS report: Science and technology. Japan
[JPRS-JST-88-002] 15 p2050 N88-22210
Single crystal growth by laser CVD
15 p2050 N88-22213
Fine grain development by laser CVD
15 p2050 N88-22214
Hard ceramic film by laser PVD
15 p2051 N88-22216
Laser evaporation studies
[AD-A189815] 15 p2071 N88-22346
Beam assisted fabrication of 3-5/Si monolithic devices
[AD-A189979] 15 p2142 N88-22785
Limited reaction processing for semiconductor device fabrication
[AD-A190913] 16 p2283 N88-23666
SiC fiber reinforced reaction-bonded Si3N4 composites 17 p2326 N88-23892
Studies of heat and mass transfer during chemical vapor deposition 17 p2338 N88-23953
Fabrication of SP-100 fuel barrier structures by chemical vapor deposition 17 p2416 N88-24371
Joint services electronics program research in electronics
[AD-A192206] 18 p2504 N88-24857
An investigation of 2-6 superlattice deposition by laser photochemical techniques
[AD-A191547] 18 p2581 N88-25336
Optical nonlinearities in GaAs/GaAlAs multiple quantum wells fabricated by metalorganic chemical vapor deposition for use in optical signal processing
[AD-A191558] 18 p2582 N88-25337
Strong fibers
[DE88-007798] 19 p2610 N88-25486
Hydrogenated amorphous silicon-germanium alloys
[DE88-001147] 19 p2620 N88-25546
Fabrication of a flexible conductor by vapor deposition
[DE88-007500] 19 p2661 N88-25826
Deposition techniques and properties of strain compensated LPCVD silicon nitride films
19 p2673 N88-25898
Hot electron transistors grown by MOCVD
20 p2861 N88-26996
On the electrical properties of carbon/carbon composites densified by chemical deposit in vapor phase
[SNIAS-881-430-117] 21 p2907 N88-27252
Laser probes and numerical modeling as process diagnostics in chemical vapor deposition
[DE88-011622] 21 p2911 N88-27275
PECVD of amorphous nickel--phosphorus films
[DE88-011088] 21 p2915 N88-27299
Superconducting thin films, composites and junctions
[AD-A193123] 21 p2937 N88-27440
Chemical vapor deposition of TiO2 thin films at room temperature
[DE88-006892] 21 p2953 N88-27542
Laser-heated CVD process for depositing thin films for low-cost solar-cell applications
[DE88-001162] 21 p2967 N88-27623
Low-band-gap, amorphous-silicon-based alloys by photochemical vapor deposition
[DE88-001165] 21 p3023 N88-27944
Chemistry of adhesion at the polyimide-metal interface
[AD-A194647] 22 p3058 N88-28143
Ultrafine microstructure composites prepared by chemical vapor deposition
[AD-A193849] 23 p3189 N88-28973
Low temperature film growth of the oxides of zinc, aluminum and vanadium (and related systems, oxides of gold and germanium, nitrides of aluminum and tungsten) by reactive sputter deposition
[AD-A193497] 23 p3191 N88-28986
Metal grid base heterojunction transistor operating at 60 and 94 GHz
[AD-A194763] 23 p3207 N88-29087
Laser induced chemical vapor epitaxial growth of gallium arsenide films
[AD-A194254] 23 p3291 N88-29595
Diamond film by hot filament CVD method
[NASA-TT-20335] 23 p3294 N88-29618
Iridium-coated rhenium thrusters by CVD
[NASA-TM-101309] 24 p3339 N88-29874
Processing technology research in composites
[AD-A195693] 24 p3341 N88-29890
A review of melt and vapor growth techniques for polydiacetylene thin films for nonlinear optical applications
[NASA-TM-100340] 24 p3430 N88-30412

VAPOR GENERATORS
U VAPORIZERS

VAPOR LIQUID EQUILIBRIUM
U LIQUID-VAPOR EQUILIBRIUM

VAPOR PHASE EPITAXY
Epitaxial reactor development for growth of silicon-on-insulator devices
[AD-A184758] 03 p0382 N88-12399
Research on single-crystal CdTe solar cells
[DE88-001115] 13 p1793 N88-20725
Zone crystallization experiments in mirror heating facilities
[BMFT-FB-W-86-023] 16 p2184 N88-23016
Initial stages of molecular beam heteroepitaxial growth in GaAs-(Ca,Sr)F2 and GaAs/Si systems
[LAAS-87-355] 16 p2281 N88-23658
The VPE-hydride technique with alloy source: Equilibrium analysis
[AD-A194036] 22 p3157 N88-28784

VAPOR PHASES
Low temperature deposition by laser induced breakdown in the vapor phase
[DE87-007509] 01 p0024 N88-10151
Kinetics investigations of atmospheric chemical reactions
[PB87-213351] 01 p0069 N88-10439
Application of new conformal solution of theories
[PB87-214557] 01 p0105 N88-10684
Laser spectroscopy and gas-phase chemistry in CVD
[DE87-013715] 03 p0281 N88-11770
Phase behavior in the Li-Al-O-H system at intermediate temperatures
[AD-A185732] 06 p0697 N88-14280
The kinetics and dynamics of iodine monofluoride formation in gas-phase collisions
[AD-A185715] 06 p0709 N88-14352
Van der Waals clusters of aromatic molecules studied using supersonic molecular jet spectroscopy
[AD-A186087] 07 p0929 N88-15644
High-temperature photoelectron spectroscopy. An increased sensitivity spectrometer for studying vapor-phase species produced at furnace temperatures greater than 2000K
[AD-A186542] 09 p1140 N88-16835
Gas phase pulse radiolysis
[DE88-002981] 10 p1296 N88-17751
Adhesion of vapour phase deposited ultra-thin polyimide films on polycrystalline silver
[AD-A187930] 10 p1306 N88-17810
Investigation of real-time two-dimensional visualization of fuel spray liquid/vapor distribution via exciplex fluorescence
[AD-A188268] 10 p1307 N88-17816
Gas-phase photoelectron spectroscopy of metals and metal oxides of importance in the upper atmosphere
[AD-A187771] 11 p1511 N88-19027
Gas phase reactions of electrons, negative ions and free-radicals with transition metal complexes
11 p1560 N88-19339
An interpretation of the ethylenic, carbidic, and graphite auger lineshapes of chemisorbed carbon species
[AD-A189092] 13 p1736 N88-20379
Measurement of rate constants of elementary gas reactions of importance to upper atmosphere and combustion systems
[AD-A189432] 13 p1737 N88-20386
Chemical kinetics modeling of HMX combustion
19 p2633 N88-25617
Thermostatistical estimations of vapor state molecules affected by gravity in a heat pipe
20 p2783 N88-26505
On the electrical properties of carbon/carbon composites densified by chemical deposit in vapor phase
[SNIAS-881-430-117] 21 p2907 N88-27252
Electronic states of the Xe(sub n)HCl systems in gas and condensed phases
[AD-A193881] 23 p3192 N88-28997

VAPOR PRESSURE
Time-resolved measurements of shock-induced vapor-pressure profiles
[DE87-012972] 01 p0045 N88-10289
Prediction of high-temperature thermodynamic properties of mixed electrolyte solutions including solubility equilibria, vapor pressure depression and boiling point elevation
[DE88-006344] 13 p1849 N88-21069
Prediction of thermodynamic properties, including solubility equilibria and vapor pressures, for mixed aqueous electrolytes to high temperatures
[DE88-006317] 14 p1990 N88-21863
Study on shaft seals for potassium turbine
[EL-891] 15 p2074 N88-22364
The effect of weathering on octane quality for winter-grade and summer-grade gasolines
[AD-A190640] 16 p2183 N88-23012
Effects of moderate cold and heat stress on the potential work performance of industrial workers. Part 6: The effects of increasing vapour pressure at four air temperatures on the performance and physiology of white females
[PB88-124854] 18 p2550 N88-25137
Physical-chemical reactions at welding arc/molten pool interfaces
[DE88-007717] 20 p2808 N88-26862
Vapor Compression Distillation Subsystem (VCDS) component enhancement, testing and expert fault diagnostics development, volume 2
[NASA-CR-172078] 21 p2994 N88-27755

VAPORIZERS
NT EVAPORATORS
The design and development of mercury vaporisers for use with electron-bombardment ion engines
[RAE-TR-70042] 01 p0018 N88-10108
Evaluation of solder flux solvents in a vapor-degreasing application for hybrid microcircuits
[BDX-613-3638] 11 p1466 N88-18752
Development of a liquid-fed water resistojet
[NASA-TM-100927] 18 p2523 N88-24968
Flow characteristics of a model annular combustor
24 p3347 N88-29924

VAPORIZING
NT BOILING
NT EVAPORATION
NT EVAPOTRANSPIRATION
NT FILM BOILING
NT FLASHING (VAPORIZING)
NT NUCLEATE BOILING
NT SUBLIMATION
NT TRANSPIRATION
Energy balance in laser-irradiated vaporizing droplets
[DE88-000525] 04 p0449 N88-12782
Cohesive energies of transition metal silicides and phosphides — Knudsen effusion
[AD-A186691] 09 p1254 N88-17519
Liquid sprays and flow studies in the direct-injection diesel engine under motored conditions
[NASA-TM-100135] 11 p1440 N88-18594
Impact-induced devolatilization and hydrogen isotopic fractionation of serpentine: Implications for planetary accretion
[NASA-CR-182877] 16 p2175 N88-22966
Photoionization dynamics and abundance patterns in laser vaporized tin and lead clusters
[AD-A191604] 18 p2482 N88-24722
High-energy laser-assisted imaging through vaporizing aerosols
[DE88-007911] 18 p2521 N88-24957
Fuel droplet vaporization and temperature distributions of axisymmetric unsteady sprays
19 p2626 N88-25579
Vaporization studies of plasma interactive materials in simulated plasma disruption events
[DE88-010100] 19 p2731 N88-26222
Investigation of annular flow at high evaporation rates in view of liquid film cooling
[DFVLR-FB-88-08] 21 p2949 N88-27517
Design, development, fabrication and launch support for a high altitude release of neodymium vapor
[AD-A194196] 22 p3118 N88-28527
Simulation study of spraying, streaming and vaporization phenomena associated with fuel injection
24 p3345 N88-29914

VAPORS
NT MERCURY VAPOR
NT METAL VAPORS
NT SODIUM VAPOR
NT WATER VAPOR
Experimental and theoretical study of condensation in multicomponent vapors
[DE87-013663] 02 p0145 N88-10907
Detection of vapors of flammable liquids in air by atmospheric sampling mass spectrometry/mass spectrometry
[DE88-000030] 02 p0196 N88-11227
Application of new conformal solution theories
[PB87-211934] 02 p0247 N88-11558
Experimental and theoretical study of condensation in multicomponent mixtures
[DE88-000697] 04 p0413 N88-12563
Investigation of the nature and concentration of vapor and mist during the cleaning of aircraft
[PML-1985-29] 05 p0623 N88-13817
Safety implications of onboard refueling vapor recovery systems
[PB88-102603] 07 p0839 N88-15088
Summary and analysis of comments on the recommended practice for the measurement of refueling emissions
[PB88-101530] 07 p0876 N88-15313
Zero-G thermodynamic vent system for shuttle/Centaur 08 p0983 N88-15840
Some investigations of electrical discharges at the surfaces of solid cathodes immersed in aqueous electrolyte solutions
[PB87-168209] 09 p1159 N88-16846
Computer modeling for optical waveguide sensors
[AD-A187702] 11 p1549 N88-19283
Discharge excitation of dye vapors
[AD-A188428] 12 p1632 N88-19770

Heat pipe transient analysis: Vapor dynamics
[DE88-005132] 13 p1767 N88-20566
Infrared differential absorption lidar for vapor detection
[AD-A190600] 15 p2098 N88-22497
Sensitivity of F-106B leading-edge-vortex images to flight and vapor-screen parameters
[NASA-TP-2818] 17 p2300 N88-23760
Theoretical studies of Resonance Enhanced Stimulated Raman Scattering (RESRS) of frequency doubled Alexandrite laser wavelength in cesium vapor
[NASA-CR-182871] 17 p2317 N88-23841
Method of evaporation
[NASA-CASE-NPO-15609-2] 17 p2318 N88-23846
Transient analysis of heat pipe vapor dynamics
17 p2412 N88-24341
A compressible vapor flux model for transient heat pipe analysis 17 p2412 N88-24343
Transient thermohydraulic heat pipe modeling
17 p2413 N88-24347
Heat pipe transient analysis: Vapor dynamics
17 p2421 N88-24397
Photoconductivity in carbon fibers
[AD-A191728] 18 p2492 N88-24782
Molecular-beam, mass-spectrometric studies of wood vapor and model compounds over HZSM-5 catalyst
18 p2535 N88-25044
Upgrading pyrolysis vapors to aromatic gasoline with zeolite catalysis at atmospheric pressure
18 p2536 N88-25045
Effect of long-term inhalation of acetic acid vapor on some functional parameters of man
19 p2705 N88-26084
Transport of organic vapors in multiphase polymer system
[AD-A194097] 23 p3198 N88-29033

VARACTOR DIODE CIRCUITS
GaAs varactor diode MMIC fabrication technology — monolithic microwave integrated circuit (MMIC)
[RSRE-MEMO-4022] 09 p1158 N88-16943

VARIABILITY
A multiple-time-scale turbulence model based on variable partitioning of turbulent kinetic energy spectrum
[NASA-CR-179222] 04 p0444 N88-12754
Examination of the physical processes associated with the keyhole region of variable polarity plasma arc welds in aluminum alloy 2219 07 p0927 N88-15634
A method for designing robust multivariable feedback systems
[NASA-CR-182459] 09 p1225 N88-17341
Designing variable-length codes with good error-recovery properties
[BBC-RD-1987/19] 10 p1317 N88-17876
Implementing logical variables on a graph reduction architecture 10 p1382 N88-18252
Parallel access to synchronization variables
[DE88-003570] 10 p1392 N88-18306
A new algorithm for general multiobjective optimization
[NASA-TM-100536] 13 p1813 N88-20830
The atmosphere as a component of the climate system: Structure and variability 14 p1935 N88-21540
Wave propagation in locally isotropic turbulent medium with smoothly changing characteristics
[NASA-TT-20312] 20 p2800 N88-26617

VARIABLE AREA WINGS
U TRAILING EDGE FLAPS

VARIABLE GEOMETRY STRUCTURES
Test stand performance of a convertible engine for advanced V/STOL and rotorcraft propulsion
[NASA-TM-100211] 03 p0266 N88-11679
Solution of geometrically nonlinear problem for reinforced shell of revolution having arbitrary shape
04 p0426 N88-12637
Structurally tailorable non-linear snap-through spring system
[NASA-CASE-LAR-13729-1] 18 p2523 N88-24970
Techniques used in the F-14 variable-sweep transition flight experiment
[NASA-TM-100444] 24 p3374 N88-30093

VARIABLE LIFT
U LIFT

VARIABLE PITCH PROPELLERS
Analysis of possible transmission arrangements applicable for driving single or twin counterrotating fans on propfan engines 10 p1282 N88-17670
The effects of torque response and time delay on rotorcraft vertical axis handling qualities
[AD-A189673] 15 p2017 N88-22023
Structurally tailorable non-linear snap-through spring system
[NASA-CASE-LAR-13729-1] 18 p2523 N88-24970

VARIABLE STARS
NT CATACLYSMIC VARIABLES
NT CEPHEID VARIABLES
NT DWARF NOVAE
NT FLARE STARS
NT HERCULES NOVA
NT MIRA VARIABLES
NT NOVAE
NT SUPERNOVA 1987A
NT SUPERNOVAE
NT T TAURI STARS
Modes, masses, metallicities, and magnitudes of RR Lyrae variables
[DE87-013149] 01 p0109 N88-10703
The M-type stars
[NASA-SP-492] 02 p0252 N88-11592
Basic properties and variability
02 p0252 N88-11593
Differential B and V light curves of the bright BY Draconis star HD80715 04 p0509 N88-13130
Time series infrared spectroscopy of long period variables 04 p0516 N88-13172
A comprehensive exploration of late-type stars in the far-ultraviolet 04 p0520 N88-13194
The history and development of nonlinear stellar pulsation codes
[DE88-001828] 06 p0801 N88-14899
The distances and absolute magnitudes of RR Lyrae variable stars 11 p1568 N88-19386
A survey of the Ap stars for rapid variability
20 p2884 N88-27127
Analysis of emission features in IRAS LRS spectra
21 p2928 N88-27380
The ultrashort period dwarf nova SW Ursae Majoris
24 p3453 N88-30553

VARIABLE SWEEP WINGS
Variable sweep wings 10 p1309 N88-17823
Influence of unsteady aerodynamic forces on dynamic response of variable sweep aircraft
15 p2054 N88-22245
Pilot report: AFTI (Advanced Fighter Technology Integration) F-111
[AD-A192937] 21 p2895 N88-27184
Variable Sweep Transition Flight Experiment (VSTFE)-parametric pressure distribution boundary layer stability study and wing glove design task
[NASA-CR-3992] 23 p3173 N88-28894
Variable wing camber control systems for the future Airbus program
[MBB-UT-104/88] 23 p3180 N88-28932

VARIANCE (STATISTICS)
NT ANALYSIS OF VARIANCE
NT BIVARIATE ANALYSIS
NT COVARIANCE
NT MULTIVARIATE STATISTICAL ANALYSIS
NT REGRESSION ANALYSIS
A fully redundant double difference algorithm for obtaining minimum variance estimates from GPS observations
[NASA-CR-182363] 06 p0867 N88-14089
Nonparametric estimation of the generalized variance
[AD-A186029] 07 p0914 N88-15545
A note on extended quasi-likelihood
[AD-A186318] 07 p0915 N88-15555
Statistical evaluation of experimental results from fatigue strength tests on CFRP composite materials
11 p1449 N88-18635
Variances and higher order correlation coefficients: Continued
[RR-655-M] 18 p2563 N88-25219
Operational noise data for CH-47D and AH-64 army helicopters
[AD-A191059] 18 p2570 N88-25263
Definition of long ocean wave slope for radar applications
[AD-A193198] 21 p2933 N88-27412

VARIATION METHOD
U CALCULUS OF VARIATIONS

VARIATIONAL PRINCIPLES
Variational and nonvariational theory of frictionless adhesive contact between bodies
[REPT-87-11] 01 p0054 N88-10345
A mixed finite element method for the computation of stress in a composite with loaded holes
[ONERA-RT-34/4242-RY-054-R]
01 p0062 N88-10395
On the scheme dependency of the three-dimensional Euler solutions 03 p0318 N88-12010
A variational formulation of a hydrodynamic lubrication problem
[MEMO-642] 08 p0987 N88-15979
Transversely anisotropic curved optical fibres: Variational analysis of a nonstandard Eigenproblem
[PB88-112966] 08 p1083 N88-16526
Hypersonic blunt body computations including real gas effects
[NASA-TM-100074] 10 p1400 N88-18344
Flux coordinate studies of elongated plasmas at high Beta 12 p1694 N88-20134
Structural clearances and internal friction: Simulation by Eigen distortions
[ISSN-0208-5658] 13 p1779 N88-20640
Hamiltonian description of the interaction of surface waves with mixed-layer currents
13 p1806 N88-20799
A generalized variational method for solving stress intensity factors at cracks on the edge of holes in orthotropic plates
[IC-AERO-87-02] 17 p2348 N88-23992
Numerical simulation of the shock tube flows by TVD scheme 19 p2638 N88-25648
On the stationary solutions of three-dimensional Euler equations by the TVD difference schemes
19 p2639 N88-25660
Variational analysis of dielectrically loaded multidepth corrugated waveguides
[PB88-193602] 20 p2793 N88-26573
Theory and simulation of relaxed plasmoids
[AD-A192884] 21 p3032 N88-27997

VARIATIONS
NT ANNUAL VARIATIONS
NT DIURNAL VARIATIONS
NT GEOMAGNETIC MICROPULSATIONS
NT GEOMAGNETIC PULSATIONS
NT MAGNETIC VARIATIONS
NT NOCTURNAL VARIATIONS
NT PERIODIC VARIATIONS
NT SECULAR VARIATIONS
NT TWENTY-SEVEN DAY VARIATION
NT WIND VARIATIONS
The atomic weight and isotopic composition of nitrogen and their variation in nature
[DE87-012867] 02 p0144 N88-10902
Effects of pressure fluctuations on nickel electrodes
[AD-A184293] 03 p0311 N88-11967
The effect of ocean fluctuations on sound transmission in the ocean
[AD-A184382] 03 p0355 N88-12236
The atomic weight and isotopic composition of oxygen and their variation in nature
[DE87-014397] 04 p0413 N88-12558
Modes of surface circulation and climate over the tropical Atlantic, Eastern Pacific, and Indian Oceans
06 p0742 N88-14564
The EUV line flux variations and activity in Alpha Orionis 08 p1032 N88-16256
The advantage of variable geometry for turbine engines at low power 10 p1280 N88-17653
Ice-shelf response to ice-stream discharge fluctuation. Part 1: Unconfined ice tongues
[AD-A188147] 10 p1358 N88-18117
An investigation of terrain related variables for predicting the multipath fade depth distribution on terrestrial microwave lines 12 p1615 N88-19654
Evolution of poloidal variation of impurity density and ambipolar potential in rotating tokamak plasma, part 1
[DE88-006263] 13 p1842 N88-21022
The turbulent heat flux in low Mach number flows with large density variations
[DE88-006445] 14 p1911 N88-21419
Correlations of velocity and temperature fluctuations in the stagnation-point flow of circular cylinder in turbulent flow
[NASA-TM-100930] 19 p2597 N88-25435
Large-eddy simulations of concentration fluctuations
[DE88-009480] 21 p2973 N88-27660
On the estimation of a variance ratio
[AD-A193190] 21 p3009 N88-27854
The observed dynamical structure of low frequency variabilities 22 p3120 N88-28541
Climatology of various synoptic systems over the tropical North Pacific 22 p3121 N88-28542
Aspects of the 30-60 day oscillation in a GCM simulation 22 p3121 N88-28545
Modes of interannual climate variability and Sahel rainfall anomalies 22 p3121 N88-28547
Interannual variability in the Atlantic and Indian Oceans and its relationship to the southern oscillation
22 p3121 N88-28548
Low frequency variability of SST and its relationship to atmospheric forcing 22 p3122 N88-28554
Variations in the atmosphere associated with the 11-year solar cycle 22 p3122 N88-28557
The effects of changes in observation and data assimilation systems on CAC climate data sets
22 p3124 N88-28568
A method to adjust climatological time series for discontinuous inhomogeneities
22 p3124 N88-28570
Nonequilibrium flow of a radiating gas in a vertical channel with axial temperature variation
[DE88-702535] 23 p3212 N88-29120
Mathematical correlation between variations in solar radiation parameters. Part 1: Daily sums of global radiation and midday global radiation
[DE88-702742] 23 p3236 N88-29253
Improved time bounds for the maximum flow problem
[AD-A194034] 23 p3272 N88-29471

Fluctuations of order parameters in the high T(sub c) superconductors
[DE88-702549] 23 p3292 N88-29603
Nonequilibrium flow of a dissociating gas in a horizontal channel with axial temperature variation
[DE88-702536] 24 p3373 N88-30089
VARIOMETERS
NASA Marshall Space Flight Center solar observatory
[NASA-TM-100339] 24 p3332 N88-29832
VARISTORS
Metal oxide varistor polarization from an initial transient
[AD-A189012] 12 p1623 N88-19711
Electrical properties of medium field, chem-prep varistors
[DE88-006147] 13 p1762 N88-20540
Scale-up of a batch-type chemical powder preparation process for high field varistor fabrication
[DE88-006601] 13 p1762 N88-20541
The first synthesis of chem-prep varistor LAC (Lightning Arrestor Connector) granules
[DE88-008005] 21 p2936 N88-27438
VASCULAR SYSTEM
U CARDIOVASCULAR SYSTEM
VASOCONSTRICTION
The effects of acute cold exposure on exercise performance
[AD-A192650] 22 p3130 N88-28610
Alterations in cutaneous vasomotor regulation during acute and chronic hypoxia
[AD-A192653] 22 p3131 N88-28612
VASOCONSTRICTOR DRUGS
NT SEROTONIN
VASOMOTOR NERVOUS SYSTEM
U NERVOUS SYSTEM
VAX COMPUTERS
The VAXONLINE software system at Fermilab
[DE87-013565] 02 p0220 N88-11387
The MicroVAX-based data acquisition system for D0
[DE87-014475] 03 p0366 N88-12303
A new library of CAMAC routines for the control of the system CRATE by a microVAX in the VAXELN environment
[NOTA-INTERNA-893] 06 p0761 N88-14667
Introduction to the VMS (DEC) operating system
[ENST-87D006] 16 p2245 N88-23409
SAMS: The synchronization and monitoring system for ATF (Advanced Toroidal Facility) data acquisition provides unified data access for ATF data acquisition
[DE88-007268] 18 p2589 N88-25386
Effective communication between a microVAX and a specialized high-speed subprocessor
[DE88-007967] 19 p2714 N88-26115
VC-10 AIRCRAFT
A flight test investigation into flow separation and structural response for a transport aircraft at buffet onset
[RAE-TR-87006] 14 p1867 N88-21156
VCO
U VOLTAGE CONTROLLED OSCILLATORS
VECTOR ANALYSIS
NT COLLINEARITY
NT COPLANARITY
NT VORTICITY
Approximate polynomial preconditioning applied to biharmonic equations on vector supercomputers
[NASA-TM-100217] 01 p0087 N88-10563
Computational methods for problems in aerodynamics and large space structure using parallel and vector architectures
[AD-A185401] 05 p0541 N88-13294
Utilization of a high rate vector computer in computational fluid mechanics for aeronautics
[ETN-88-91171] 05 p0581 N88-13547
Asymptotic normality of poly-t densities with Bayesian applications
[AD-A185718] 06 p0768 N88-14719
A vectorized Poisson solver over a spherical shell and its application to the quasi-geostrophic omega-equation
[NASA-CR-4116] 08 p1039 N88-16285
Series representations of infinitely divisible random vectors and a generalized shot noise in banach spaces
[AD-A186502] 08 p1073 N88-16474
Tensorial calibration. 2: Second order tensorial calibration
[AD-A186614] 09 p1167 N88-16994
The linear dependency structure of covariance nonstationary time series
[AD-A186548] 09 p1232 N88-17383
Estimation of gravity vector components from Bell gravity gradiometer and auxiliary data under consideration of topography and associated analytical upward continuation aspects
[AD-A188146] 10 p1355 N88-18099
An efficient sparse matrix multiplication scheme for the CYBER 205 computer
[NASA-TM-4028] 10 p1390 N88-18302
Vector bundles over real algebraic varieties
[PB88-126677] 10 p1398 N88-18335
Overview of multi-input frequency domain modal testing methods with an emphasis on sine testing
11 p1499 N88-18949
Measurement and analysis of memory conflicts on vector multiprocessors
[AD-A188206] 11 p1525 N88-19104
Deep water mass circulation in the Alboran Basin. Measurements - January to April 1982: ALBORAN 2
[AD-A189205] 13 p1803 N88-20777
Instrumentation for the characterization and development of millimeter wave components compatible with monolithic integration
[AD-A189724] 15 p2059 N88-22275
Martingale representation and the Malliavin calculus
[AD-A189721] 15 p2119 N88-22626
High speed transcendental elementary function architecture in support of the Vector Wave Equation (VWE)
[AD-A189746] 15 p2119 N88-22627
An FSK (Frequency Shift Keying) telemetry module for vector measuring current meters
[AD-A192142] 18 p2470 N88-24661
Improving the performance of a finite element method using vector analysis on CRAY 1
[ETN-88-92153] 18 p2513 N88-24907
Gram-Schmidt implementation of a linearly constrained adaptive array
[AD-A191651] 18 p2560 N88-25196
An investigation of the uses of time domain capable vector network analyzers as a diagnostic for helix traveling-wave circuits
[AD-A192460] 21 p2935 N88-27430
Parallel solutions to geometric problems on the scan model of computation
[AD-A192321] 21 p3004 N88-27819
A note on vector bimeasures
[AD-A192841] 21 p3009 N88-27849
Object discrimination via bulk temperature/velocity filtering, phase 1
[AD-A194533] 23 p3274 N88-29487
Limiting distributions of non-linear vector functions of stationary Gaussian processes
[AD-A194569] 23 p3274 N88-29488
VECTOR CALCULUS
U VECTOR SPACES
VECTOR CONTROL
U DIRECTIONAL CONTROL
VECTOR CURRENTS
Quantization of axial electrodynamics
[DE88-701498] 15 p2147 N88-22813
An FSK (Frequency Shift Keying) telemetry module for vector measuring current meters
[AD-A192142] 18 p2470 N88-24661
VECTOR SPACES
NT ADJOINTS
NT BANACH SPACE
NT CANONICAL FORMS
NT EIGENVALUES
NT EIGENVECTORS
NT HESSIAN MATRICES
NT HILBERT SPACE
NT MATRICES (MATHEMATICS)
NT STATE VECTORS
NT STIFFNESS MATRIX
NT VECTORS (MATHEMATICS)
NT VORTICITY
Division algebras and sphere fibrations
[ETN-87-90677] 01 p0087 N88-10566
Electromagnetic scattering problem in the wave-vector-time domain
[PB88-106083] 06 p0694 N88-14263
Analysis and synthesis of the Earth's gravity field variable in space and time using vector surface spherical functions
[SER-C-325] 07 p0878 N88-15328
An application of eigenspace methods to symmetric flutter suppression
[NASA-CR-181618] 10 p1264 N88-17684
The existence of smooth densities for the prediction filtering and smoothing problems
[AD-A189865] 15 p2119 N88-22629
An introduction to poloidal and toroidal fields
[MITT-54] 17 p2394 N88-24232
Linearization along invariant manifolds and a generalization of the Hartman-Grobman theorems for degenerate singularities of vector fields in R cubed
[REPT-87-80] 20 p2845 N88-26886
Cosmology in an N-dimensional vector space
[DE88-702550] 23 p3277 N88-29507
VECTORS (MATHEMATICS)
NT EIGENVECTORS
NT STATE VECTORS
NT VORTICITY
Implementation of a digital optical matrix-vector multiplier using a holographic look-up table and residue arithmetic
[NASA-CR-180431] 01 p0078 N88-10496
Vectorization of MHD equilibrium and stability codes
[DE87-753013] 02 p0240 N88-11516
Solution of some 3-D viscous and inviscid supersonic flow problems by finite-volume space-marching schemes
05 p0532 N88-13235
Multidimensional least squares fitting of fuzzy models
[AD-A185148] 05 p0640 N88-13916
Least-squares for fuzzy vector data regression
[AD-A185156] 05 p0640 N88-13917
On detection of change points using mean vectors
[AD-A185581] 06 p0767 N88-14717
On hypercontractivity of alpha stable random variables, 0 less than alpha less than 2
[AD-A186425] 07 p0915 N88-15559
Vector performance of register-to-register vector computers
[DE88-004013] 10 p1384 N88-18265
Implementation and analysis of a Navier-Stokes algorithm on parallel computers
[NASA-CR-181614] 10 p1390 N88-18301
Straightening and the Stanley decomposition for the (2,n)-nilpotent vectorfield
[PB88-126685] 10 p1398 N88-18336
Linear prediction of stationary vector sequences
[NASA-TM-100069] 10 p1403 N88-18366
New representation for kinematics of manipulator
[DE88-751446] 14 p1917 N88-21445
Vectorization of the odd-even hopscotch scheme and the alternating direction implicit scheme for the two-dimensional Burgers' equations
[CWI-NM-R8720] 16 p2249 N88-23440
Systolic algorithm for matrix-vector multiplication
[PB88-165394] 16 p2256 N88-23484
Vector graphics and raster data processing for spatial information systems 18 p2533 N88-25028
Electric field measurement by S-520-9 sounding rocket using the time of flight technique of lithium ion beam
[ISAS-RN-367] 18 p2543 N88-2509
Robust vector quantization for noisy channels
19 p2653 N88-25754
Analysis and improvement of the vector quantization in SELP (Stochastically Excited Linear Prediction)
19 p2653 N88-25756
VEGA PROJECT
Final phase of Project Vega 01 p0009 N88-10053
Space missions to Comets Halley and Giacobini-Zinner 03 p0272 N88-11712
JPRS report: Science and technology. USSR Space
[JPRS-USP-88-002] 13 p1724 N88-20312
Vega-1 and Vega-2 automatic stations: Functioning of landing modules in Venusian atmosphere
13 p1725 N88-20313
Vega-1 and Vega-2 automatic stations: Functioning of flyby vehicles during encounter with Halley's comet
13 p1725 N88-20314
Thermal structure of Venusian Atmosphere determined from results of measurements from Vega-2 landing module 13 p1725 N88-20315
Research on absorption of UV radiation in Venusian atmosphere from Vega-1 and Vega-2 landing modules
13 p1725 N88-20316
Vertical structure of Venusian cloud layer at landing sites of Vega-1 and Vega-2 vehicles
13 p1725 N88-20317
Gas-chromatographic analysis of products of thermal reactions of aerosol in Venusian cloud layer on Vega-1 and Vega-2 automatic interplanetary stations
13 p1725 N88-20318
Roentgenoradiometric analysis of aerosol in Venusian clouds by Vega-1 and Vega-2 automatic interplanetary stations 13 p1726 N88-20319
Chemical composition and structure of Venusian clouds determined from results of roentgenoradiometric experiments carried out by landing modules of Vega-1 and Vega-2 automatic interplanetary stations
13 p1726 N88-20320
Determining chemical composition of aerosol in Venusian cloud layer on Vega-1 automatic interplanetary station using Malakhit mass spectrum analyzer
13 p1726 N88-20321
Elemental composition of Venusian rocks in northeastern part of Terra Aphrodite (determined using data from Vega-2 landing module)
13 p1726 N88-20322
Content of natural radioactive elements in Venusian rocks determined using data from Vega-1 and Vega-2 stations 13 p1726 N88-20323

Results of infrared spectrometer experiment 2: Infrared radiometry of nucleus of Halley's Comet
13 p1727 N88-20326

Analysis of hydrocarbon band 3.35 in spectrum of Halley's Comet using data from infrared spectrometer on Vega-1 spacecraft 13 p1727 N88-20327

Variability of Comet Halley's coma: VEGA-1 and VEGA-2 magnetic field observations 14 p1995 N88-21891

Physical processes in the vicinity of the cometopause interpreted on the basis of plasma, magnetic field and plasma wave data measured on board VEGA-2 spacecraft — Halley's comet 14 p1996 N88-21894

Some new features of plasma wave phenomena at Halley: APV-N observations — VEGA
14 p1996 N88-21895

A comparison between wave observations performed in the environments of Comets Halley and Giacobini-Zinner 14 p1996 N88-21896

Plasma phenomena in the vicinity of the closest approach of VEGA-1, 2 spacecraft to the Comet Halley nucleus 14 p1996 N88-21899

Water vapor and hydroxyl distributions in the inner coma of Comet Halley measured by the VEGA-2 three channel spectrometer TKS 14 p1998 N88-21910

Color fluctuations in the inner coma of Comet Halley as measured from VEGA-2 14 p2000 N88-21925

Dust photometry in the near nucleus region of Comet Halley from VEGA-2 observations
14 p2001 N88-21930

Image processing on VEGA pictures
14 p2009 N88-21983

Determination of the Venus flyby orbits of the Soviet Vega probes using VLBI techniques
22 p3067 N88-28203

VEGETABLES
NT POTATOES

VEGETATION
NT CANOPIES (VEGETATION)

Enhancement of surface-atmosphere fluxes by desert-fringe vegetation through reduction of surface albedo and of soil heat flux
[NASA-CR-181442] 02 p0197 N88-11231

Vegetation classification, land systems and mapping using SPOT multispectral data: Preliminary results
03 p0342 N88-12160

Vegetation studies in the national Park of Comoe (Ivory Coast) using SPOT 1 satellite data
03 p0343 N88-12166

Electromagnetic wave probing of Earth's environment
[NASA-CR-182358] 06 p0690 N88-14232

Effects of fire on composition, biomass, and nutrients in oak scrub vegetation on John F. Kennedy Space Center, Florida
[NASA-TM-100305] 08 p1020 N88-16182

Physiological and ecological implications of coupled heat- and water-transport mechanisms of endotherms and vegetation
[DE88-004170] 10 p1352 N88-18081

Scattering and depolarization by random rough terrain and vegetation covered terrain-unified full wave approach 12 p1615 N88-19657

Research in remote sensing of vegetation
[NASA-CR-182663] 12 p1639 N88-19817

Measuring and modeling near surface reflected and emitted radiation fluxes at the FIFE site
[NASA-CR-182660] 12 p1640 N88-19818

Mesoscale monitoring of the soil freeze/thaw boundary from orbital microwave radiometry
[NASA-CR-182659] 12 p1645 N88-19855

Subsurface morphology and geoarchaeology revealed by spaceborne and airborne radar
17 p2353 N88-24022

Anomalies in the vegetation in the Alto Xingu - MT
17 p2357 N88-24043

Temporal analysis of the changes in Parque Estadual de Jacupiranga vegetation through digital treatment of LANDSAT imagery 17 p2367 N88-24094

An update on remote measurement of soil moisture over vegetation using infrared temperature measurements: A FIFE perspective
[NASA-CR-182926] 17 p2370 N88-24109

Monitoring biological impacts of space shuttle launches from Vandenberg Air Force Base: Establishment of baseline conditions
[NASA-TM-100982] 18 p2549 N88-25133

Propagation modeling for land mobile satellite systems
19 p2645 N88-25694

Sources of scattering in vegetarian and other surfaces and objects
[NASA-CR-182975] 20 p2816 N88-26710

SPOT-1 HRV data and vegetation amount
22 p3095 N88-28379

Topographic suppression and advances in classification for land cover mapping using SPOT-1 HRV imagery
22 p3099 N88-28404

Assessment of SPOT satellite based system in humid tropical vegetation identification, classification and monitoring 22 p3100 N88-28408

A comparison between SPOT and LANDSAT TM for mapping of vegetation and bedrock outcrops
22 p3100 N88-28409

Evaluation of SPOT imagery for discriminating vegetation communities associated with surficial and bedrock geology and identifying anomalous and stressed vegetation associated with mineralization
22 p3103 N88-28426

Relevance of a thematic map (SPOT data) with regards to the real flora and structure of the vegetation covering of salt marshes (Mont Saint Michel Bay, France)
22 p3109 N88-28468

Assessment of SPOT imagery for topographic revision and vegetation mapping 22 p3111 N88-28477

Imaging instrument of the vegetation payload (SPOT 4)
[SNIAS-881-440-107] 24 p3386 N88-30169

Study of the spectral response of soybeans
[INPE-4592-PRE/1322] 24 p3387 N88-30174

Relief effect correction on LANDSAT imagery for forest applications using digital terrain models
[INPE-4611-PRE/1334] 24 p3388 N88-30179

VEGETATION GROWTH
NT CROP GROWTH

Controlled Ecological Life Support System: Regenerative Life Support Systems in Space
[NASA-CP-2480] 03 p0357 N88-12251

Progress in European CELSS activities
03 p0358 N88-12252

Design of an elemental analysis system for CELSS research 03 p0360 N88-12266

Study of the relationship between photosynthesis, respiration, transpiration, and mineral nutrition in wheat
03 p0360 N88-12268

Utilization of potatoes in bioregenerative life support systems 03 p0360 N88-12269

The effect of radiation on the long term productivity of a plant based CELSS 03 p0361 N88-12271

Mass balances for a biological life support system simulation model 03 p0361 N88-12272

Trickle water and feeding system in plant culture and light-dark cycle effects on plant growth
03 p0361 N88-12273

Disturbance and recovery of Arctic Alaskan tundra terrain. A review of recent investigations
[AD-A184442] 04 p0467 N88-12887

Comparative anatomic analysis of seedling organs of pisum sativum (fabaceae) cultivated under space flight conditions 06 p0749 N88-14603

Research on cotton plants grown in space
08 p1006 N88-16098

Species biology and potential for controlling four exotic plants (Ammophila arenaria, Carpobrotus edulis, Cortaderia jubata and Gasoul crystallinum) on Vandenberg Air Force Base, California
[NASA-TM-100980] 10 p1363 N88-18148

VEGETATIVE INDEX

Vegetation classification, land systems and mapping using SPOT multispectral data: Preliminary results
03 p0342 N88-12160

AIS-2 spectra of California wetland vegetation
05 p0613 N88-13763

Extension of the vegetation mission to thermal infrared spectral bands
[CNES-T-86/224-CT/DRT/TIT/IO]
16 p2227 N88-23299

Evaluation of a burned area and the vegetation regeneration affected by the burning in the Parque Nacional de Brazilia through TM/LANDSAT data
17 p2363 N88-24073

Use of LANDSAT images of vegetation cover to estimate effective hydraulic properties of soils
[NASA-CR-183185] 22 p3116 N88-28514

TM/LANDSAT-5 data to evaluate wheat and bean percent soil cover and leaf area index
[INPE-4609-PRE/1332] 24 p3385 N88-30165

LANDSAT TM and agrometeorological data for wheat yield estimation at the farm level
[INPE-4591-PRE/1321] 24 p3388 N88-30180

VEHICLE WHEELS

An investigation of the spray produced by a yawed wheel, including measurement of impact forces — aircraft wheels
[BU-363] 14 p1866 N88-21150

Finding wheels of vehicles in stereo images
[AD-A194372] 22 p3080 N88-28292

Frequency dependent sliding coefficients for general three-dimensional rolling contact in high frequency range
[ILR-MITT-192] 22 p3085 N88-28318

VEHICLES

An efficient representation of spatial information for expert reasoning in robotic vehicles
09 p1214 N88-17278

VEINS

Operation Everest 2: Comparison of four instruments for measuring blood oxygen saturation
[AD-A186456] 08 p1049 N88-16337

Leg volume change under Lower Body Negative Pressure (LBNP) in dependence on stratification
[DFVLR-FB-87-47] 16 p2238 N88-23367

VELOCITY
NT ACOUSTIC VELOCITY
NT AIRSPEED
NT ANGULAR VELOCITY
NT CRITICAL VELOCITY
NT FLOW VELOCITY
NT GROUP VELOCITY
NT HIGH SPEED
NT HYPERSONIC SPEED
NT LIGHT SPEED
NT LOW SPEED
NT ORBITAL VELOCITY
NT PHASE VELOCITY
NT PROPAGATION VELOCITY
NT RADIAL VELOCITY
NT RELATIVISTIC VELOCITY
NT ROTOR SPEED
NT SOLAR WIND VELOCITY
NT SUBSONIC SPEED
NT SUPERSONIC SPEED
NT TERMINAL VELOCITY
NT TIP SPEED
NT TRANSONIC SPEED
NT WIND VELOCITY

Exact solutions to the governing dynamic equations of plasma armature electromagnetic railguns
[DE87-014442] 01 p0011 N88-10063

Fronts propagating with curvature dependent speed: Algorithms based on Hamilton-Jacobi formulations
[NASA-CR-178382] 01 p0077 N88-10495

Analytical modeling of helicopter static and dynamic induced velocity in GRASP
[NASA-TM-100026] 02 p0123 N88-10777

Rarefaction velocities in shocked lead
[DE87-013141] 02 p0146 N88-10917

Effects of injection of free electron lasers on axial velocity spread of beams 03 p0299 N88-11878

Ultimate velocities for induction launchers
[DE87-012360] 04 p0404 N88-12513

Use of a thermodynamic analog for pneumatic transport in horizontal pipes
[AD-A184076] 04 p0441 N88-12740

The velocity structure and turbulence at the center of the Orion Nebula 04 p0521 N88-13201

Hydrogen and deuterium in the local interstellar medium 04 p0521 N88-13204

Time-marching finite-difference methods for the three-dimensional Euler equations of contravariant velocity components 05 p0539 N88-13285

Velocity scaled aeroelastic testing of an unducted fan
[GTL-191] 05 p0548 N88-13337

Wing divergence of trimmed aircraft
05 p0550 N88-13354

Imaging subtle microstructural variations in ceramics with precision ultrasonic velocity and attenuation measurements
[NASA-TM-100129] 07 p0867 N88-15257

Velocity measurements in a 3D (three dimensional) shock wave laminar boundary layer interaction
[AD-A187334] 10 p1332 N88-17959

Velocity reversal and the arrows of time
[DE88-004237] 10 p1429 N88-18536

Splinter generator
[MBB-UA-1048/87] 11 p1491 N88-18897

Cramer-Rao bounds on the accuracy of location and velocity estimations using CCD optical sensors
[AD-A188481] 12 p1629 N88-19748

Quantization of quadratic friction revisited
[DE88-700839] 12 p1686 N88-20081

Erosion in dual-phase microstructures
[DE88-004507] 13 p1743 N88-20421

Reduction of erosion in elbows due to flow modifications, phase 1
[DE88-001028] 13 p1769 N88-20584

Some effects of heating on the wind-driven velocity in the upper ocean 13 p1805 N88-20792

Calibration of a hot-wire/hot-film anemometer over a range of temperatures, velocities and pressures
[AD-A189717] 14 p1913 N88-21430

Current velocity and hydrographic observations in the Straits of Florida, the Caribbean Sea and offshore of the Antillean Archipelago: Subtropical Atlantic Climate Studies (STACS) 1986
[PB88-160767] 14 p1951 N88-21628

Continuous measurements of in-bore projectile velocity
[DE88-006841] 15 p2023 N88-22056

Analytic solutions to dynamic equations of plasma armature railguns
[DE88-005842] 15 p2023 N88-22057

On new solvable many-body dynamical systems with velocity dependent forces
[PREPRINT-581] 15 p2127 N88-22683

Railgun rail gouging by hypervelocity sliding contact
[DE88-006866] 16 p2166 N88-22916

Effect of mass-velocity on liquid jet atomization in Mach 1 gasflow
[NASA-TM-100813] 16 p2211 N88-23194

Analysis of crack-tip fields in a viscoplastic material
17 p2349 N88-23996

Electrical pulse compression by traveling-wave photoconductivity 19 p2661 N88-25822

Analysis of the electrical harmonic characteristics of a slip recovery variable speed generating system for wind turbine applications
[DE88-001140] 19 p2687 N88-25972

Laser measurement of particle velocities in vacuum plasma spray deposition
[DE88-007111] 19 p2728 N88-26198

On linear relationship between shock velocity and particle velocity
[DE88-701827] 20 p2880 N88-27099

Prediction of velocity and temperature profiles in thermally driven gravity currents applied to stratified thermal storage tanks
[DE88-004452] 21 p2946 N88-27496

A method for determining absolute velocities from hydrographic data: The numerical code
[AD-A193997] 22 p3129 N88-28603

Object discrimination via bulk temperature/velocity filtering, phase 1
[AD-A194533] 23 p3274 N88-29487

VELOCITY DISTRIBUTION

An application of L1 to astronomy --- stellar velocity
[REPT-87-10] 01 p0108 N88-10702

Personal Computer (PC) based image processing applied to fluid mechanics
[NASA-TM-100024] 02 p0172 N88-11087

Experimental study of interacting vortex rings
03 p0318 N88-12007

Solar magnetic and velocity fields
[AD-A184360] 03 p0390 N88-12449

Comparative studies in the near-field of turbulent transports of heated and unheated jets normal to a cross stream 04 p0444 N88-12756

Hydrogen and deuterium in the local interstellar medium 04 p0521 N88-13204

Model-based motion estimation and its application to restoration and interpolation of motion pictures
[AD-A185054] 05 p0584 N88-13558

The new CP3 06 p0691 N88-14237

Highlights from a research program on a very highly loaded axial gas generator turbine
06 p0713 N88-14369

Models of sporadic meteor body distributions
06 p0739 N88-14543

Meteor velocity distribution and an optimum monitoring mathematical model 06 p0739 N88-14546

Lift distribution and velocity field measurements for a three-dimensional, steady blade/vortex interaction
[NASA-TM-100013] 07 p0815 N88-14962

The single particle and collective descriptions of the anomalous Doppler resonance and the role of ion dynamics
[INPE-4390-PRE/1210] 08 p0976 N88-15904

Absorption of electron cyclotron waves by superthermal electron velocity distributions in tokamak plasmas
[INPE-4385-PRE/1205] 08 p1086 N88-16539

The effect of asymmetric current-supporting electron velocity distributions on second harmonic electron cyclotron resonance heating: A ray-tracing treatment for the compass tokamak
[INPE-4389-PRE/1209] 08 p1087 N88-16549

A review of some flow visualization experiments carried out at the Institut Franco-Allemand de Recherches (ISL) shock tubes
[ISL-CO-243/86] 09 p1163 N88-16974

Corrections for the pseudorapidity gap correlation method --- particle correlations
[USIP-87-12] 09 p1245 N88-17463

Investigations of a circulation control airfoil flowfield using an advanced laser velocimeter
10 p1269 N88-17589

Boundary-layer and wake measurements on a swept, circulation-control wing 10 p1270 N88-17597

Transonic blade design on rotational stream surfaces
10 p1282 N88-17671

Implicit solution of the incompressible Navier-Stokes equations in primitive variables on non-staggered grids
10 p1326 N88-17930

A velocity-pressure integrated, mixed interpolation, Galerkin finite element method for high Reynolds number laminar flows
[NASA-CR-179264] 11 p1486 N88-18868

Correction of the wind field measured by the NCAR electra during FASINEX (Frontal Air-Sea Interaction Experiment) for inertial navigation system drifts
[AD-A187780] 11 p1514 N88-19045

Return stroke velocities and currents using a solid state silicon detector system 11 p1515 N88-19050

Coherent structure-reflective turbulent viscous flow modeling
[AD-A188339] 13 p1765 N88-20556

Numerical simulations of buoyancy driven flows in cylinders and cavities for vapor crystal growth
14 p1987 N88-21854

Selective growth velocity in needle crystals
14 p1988 N88-21858

High Reynolds number, low Mach number, steady flow field calculations over a NACA 0012 airfoil using Navier-Stokes and interactive boundary layer theory
[AD-A189871] 15 p2013 N88-22005

Unsteady aerodynamics of a Wortmann FX-63-137 wing in a fluctuating wind field
[AD-A190128] 15 p2013 N88-22006

Boundary-layer and wake measurements on a swept, circulation-control wing
[NASA-TM-89426] 15 p2014 N88-22013

Stochastic estimation of conditional eddies in turbulent channel flow 16 p2194 N88-23087

Big whorls carry little whorls 16 p2195 N88-23094

A statistical investigation of the single-point pdf of velocity and vorticity based on direct numerical simulations 16 p2196 N88-23101

On local approximations of the pressure-strain term in turbulence models 16 p2197 N88-23102

A non-invasive experimental technique for the measurement of unsteady velocity and vorticity fields
16 p2204 N88-23148

Measurements of the time dependent velocity field surrounding a model propeller in uniform water flow
16 p2205 N88-23155

Effect of initial tangential velocity distribution on the mean evolution of a swirling turbulent free jet
[NASA-TM-100934] 18 p2458 N88-24592

Theoretical investigation of the development of the normal fluid and superfluid velocity distributions during spin-up for a He2-filled cylinder
[MPIS-6/1987] 18 p2510 N88-24892

A single streamwise vortical structure and its instability in shear flows 18 p2515 N88-24921

Coal particle behaviour in a counter-current combustor
[TAE-606] 19 p2612 N88-25498

Driving of axial acoustic fields by side-wall stabilized premixed flames 19 p2629 N88-25592

Observations of electron cyclotron harmonic emissions associated with field-aligned electron beams
[SD-TR-87-33] 19 p2724 N88-26173

The velocity field of the outer galaxy
[B8681472] 20 p2885 N88-27132

Prediction of velocity and temperature profiles in thermally driven gravity currents applied to stratified thermal storage tanks
[DE88-004452] 21 p2946 N88-27496

Mass transport in sector and annular sector tubes
[LRT-WE-9-FB-9(1987)] 22 p3077 N88-28269

Application of acoustic-Doppler current profiler and expendable bathythermograph measurements to the study of the velocity structure and transport of the Gulf Stream
[NASA-CR-183188] 22 p3129 N88-28605

Rotation symmetric inside flow with diametric expansion resolution
[ILR-MITT-193] 23 p3213 N88-29123

Application of Particle Image Displacement Velocimetry (PIDV) to complex flows: Velocity field measurements in front of a heavy gas cloud
[VKI-TN-166] 23 p3213 N88-29125

Clustering of galaxies and clusters of galaxies in a decaying-particle cosmological model with a massive decay product
[DE88-753434] 23 p3298 N88-29642

The dynamics of SBO galaxies. Part 1: The data
[SER-C-PREPUBL-FASC-22] 24 p3455 N88-30567

VELOCITY FIELDS

U VELOCITY DISTRIBUTION

VELOCITY MEASUREMENT

NT WIND VELOCITY MEASUREMENT

An observer approach to the estimation of helicopter airspeed
[DFVLR-FB-87-13] 01 p0005 N88-10029

Jet formation and characterization of a conical shaped charge
[DE87-012102] 02 p0155 N88-10969

Three-dimensional calculation in high subsonic axial compressor rotor and its comparison with L2F velocity measurement 03 p0300 N88-11886

Particle velocity and stress gage measurements in spherical diverging flow
[DE87-007333] 03 p0321 N88-12033

Single-periodic multilayer grating laser Doppler vibrometer 03 p0327 N88-12066

Comparative studies in the near-field of turbulent transports of heated and unheated jets normal to a cross stream 04 p0444 N88-12756

Flow diagnostics and visualization in wind tunnels and flight 07 p0811 N88-14940

Pressure and mass velocity measurements in solids subjected to dynamic loadings 07 p0921 N88-15595

Velocity and density measurements in a turbulent nonpremixed flame with comparison to numerical model predictions
[DE87-014695] 08 p0967 N88-15854

EISCAT measurements of ion velocities during Coordinated Auroral Experiment using Scatter And Rockets (CAESAR) campaign 08 p1031 N88-16251

Velocity interferometry in shock tubes and shock tunnels
[ISL-CO-203/87] 09 p1122 N88-16713

Flow field measurements using hotwire anemometry
[AD-A187029] 09 p1160 N88-16951

An integration test for accelerometer evaluation
09 p1178 N88-17054

Development and application of oxygen flow tagging for velocity measurements and flow visualization in turbulent three-dimensional supersonic flows
[AD-A187982] 10 p1289 N88-17714

Measurement of forces and moments on, and velocity about a body of revolution with an attached fin at angles of attack
[AD-A187796] 11 p1433 N88-18554

Fluctuations and massive separation in three-dimensional shock-wave/boundary-layer interactions
[NASA-TM-89224] 11 p1434 N88-18559

Production by pyrolysis of diffusion particles for velocimetry in shock tubes
[ISL-R-119/86] 11 p1455 N88-18671

Measurement of velocity and temperature profiles in low-speed, turbulent non-isothermal flows
[PB88-155833] 11 p1486 N88-18872

New monostatic balanced Doppler velocimeter using a polarization preserving fiber
[PB88-130869] 11 p1490 N88-18895

Experiments on the flow of viscoelastic fluids between eccentric rotating cylinders 12 p1625 N88-19723

Laser Doppler velocimetry primer
[NASA-CR-177386] 12 p1631 N88-19761

Velocity and concentration measurements in flowing suspensions by nuclear magnetic resonance
[DE88-006225] 13 p1770 N88-20589

Observations of waves and Langmuir circulation with Doppler sonars 13 p1805 N88-20790

Combined aerodynamic size, charge-to-mass, and velocity measurements of aerosol particles
[ST-REPT-VOL-5-NO-4] 14 p1944 N88-21599

Continuous measurements of in-bore projectile velocity
[DE88-006841] 15 p2023 N88-22056

Instruments for use in experimental studies of complex turbulent shear flow: Three component LDVs
[AD-A190526] 15 p2065 N88-22312

New measurements of radial velocities in clusters of galaxies
[INPE-4527-PRE/1277] 15 p2152 N88-22845

Application of high speed holography to aerodynamic and hydrodynamic three-dimensional velocimetry
16 p2203 N88-23144

A non-invasive experimental technique for the measurement of unsteady velocity and vorticity fields
16 p2204 N88-23148

Gravity currents with heat transfer effects
[PB88-180047] 16 p2205 N88-23156

Inflow measurement made with a laser velocimeter on a helicopter model in forward flight. Volume 5: Tapered planform blades at an advance ratio of 0.23
[NASA-TM-100545] 17 p2299 N88-23755

Laser measurement of particle velocities in vacuum plasma spray deposition
[DE88-007111] 19 p2728 N88-26198

Position and velocity determination using a Global Positioning System: An outline
[B8735052] 20 p2757 N88-26355

Heterogeneous diffusion flame stabilization
[AD-A193014] 20 p2771 N88-26429

Crosslinking of two vortex rings side by side
20 p2782 N88-26502

Development of advanced flow simulation system by water flow model. New method of velocity measurement using cross-correlation
[DE88-753120] 20 p2799 N88-26608

Velocity-pressure integrated versus penalty finite element methods for high Reynolds number flows
[NASA-CR-179357] 20 p2803 N88-26635
Velocity measurements and flow visualization in turbulent three-dimensional supersonic flows using oxygen flow tagging
[AD-A192551] 21 p2892 N88-27165
Velocity measurements downstream of a sudden expansion using the Laser Doppler Velocimeters (LDV) technique. Part 1: Method of measurement and experimental facility
[FOA-C-20700-2.1-PT-1] 22 p3076 N88-28262
Calibration of a triple wire probe for turbulence measurements
[AD-A193956] 22 p3081 N88-28296
Hot-wire measurements of compressor blade wakes in a cascade wind tunnel
[AD-A194737] 23 p3181 N88-28936
A mapping of the viscous flow behavior in a controlled diffusion compressor cascade using laser Doppler velocimetry and preliminary evaluation of codes for the prediction of stall
[AD-A194490] 23 p3211 N88-29112
Application of Particle Image Displacement Velocimetry (PIDV) to complex flows: Velocity field measurements in front of a heavy gas cloud
[VKI-TN-166] 23 p3213 N88-29125
Application of optical correlation techniques to particle imaging velocimetry
[NASA-TM-101306] 23 p3218 N88-29152
Radial velocity measurements of a sample of northern metal-deficient stars
[SER-C-PREPUBL-FASC-25] 24 p3455 N88-30564

VELOCITY PROFILES
U VELOCITY DISTRIBUTION

VENTILATION
Hydride generation from the Exide load-leveling cells
[DE87-011361] 01 p0041 N88-10259
A plethysmograph for measuring pulmonary ventilation in small animals
[AD-A184978] 05 p0629 N88-13846
Plant Growth Module (PGM) conceptual design
05 p0631 N88-13855
Life-cycle cost analysis of residential heat pumps and alternative HVAC (Heating, Ventilating and Air-Conditioning) systems
[DE88-003701] 07 p0839 N88-15090
Load carriage induced alterations of pulmonary function
[AD-A186227] 07 p0889 N88-15386
Proceedings of the 19th DOE/NRC Airborne Waste Management and Air Cleaning Conference
[NUREG/CP-0086-VOL-1] 11 p1509 N88-19018
Proceedings of the 19th DOE/NRC Airborne Waste Management and Air Cleaning Conference
[NUREG/CP-0086-VOL-2] 11 p1509 N88-19019
Testing of the engine compartment fire extinguishing system in the F/EF-111 aircraft
[AD-A188801] 12 p1576 N88-19423
Liquid ventilation: New data and possible use in space medicine 12 p1654 N88-19908
Impact of control errors on the volume/weight demand of the Ventilation and Dryer (VAD) concept --- EURECA Botany Facility
[TN-RB524-006/87] 17 p2377 N88-24132
Evaluation of the toxicity of products from the thermal degradation of materials
[ETN-88-91995] 18 p2549 N88-25130
Model test of air-exchange efficiency
[DE88-752862] 23 p3201 N88-29049

VENTILATORS
Computer code simulations of explosions in flow networks and comparison with experiments
[DE88-001946] 05 p0573 N88-13491

VENTING
Zero-G thermodynamic vent system for shuttle/Centaur 08 p0983 N88-15943
Payload bay atmospheric vent airflow testing at the Vibration and Acoustic Test Facility
[NASA-TM-100460] 11 p1437 N88-18572
Enhanced emergency smoke venting
[DOT/FAA/CT-88/22] 20 p2756 N88-26350

VENTS
Zero-G thermodynamic vent system for shuttle/Centaur 08 p0983 N88-15943
Experimental and theoretical constraints on the origin of mid-ocean ridge geothermal fluids
13 p1604 N88-20784
Modification and development of the external tank hydrogen vent umbilical system for the space shuttle vehicle 14 p1928 N88-21496

VENUS (PLANET)
Final phase of Project Vega 01 p0009 N88-10053
Comparative plasma tails of Venus and comets
01 p0116 N88-10742
Interplanetary magnetic field effects on the interaction of the solar wind with Venus 06 p0805 N88-14910
To what extent is mass loading responsible for the Venus bowshock procursor?
[NASA-TM-89307] 12 p1711 N88-20239
Vega-1 and Vega-2 automatic stations: Functioning of landing modules in Venusian atmosphere
13 p1725 N88-20313
Elemental composition of Venusian rocks in northeastern part of Terra Aphrodite (determined using data from Vega-2 landing module)
13 p1726 N88-20322
Engineering planetary lasers for interstellar communication
[NASA-CR-180780] 17 p2311 N88-23825
Kinetics of thermochemical gas-solid reactions important in the Venus sulfur cycle
[NASA-CR-182963] 19 p2742 N88-26280
The rate of volcanism on Venus
[NASA-CR-183039] 19 p2742 N88-26281
A bibliography of dunes: Earth, Mars, and Venus
[NASA-CR-4149] 20 p2885 N88-27134

VENUS ATMOSPHERE
NT VENUS CLOUDS
Venusian surface and crust 01 p0010 N88-10054
Preliminary estimation of color inhomogeneities on the surface of Venus according to the television images obtained by the VENERA-13 and VENERA-14 automated space probes
[NASA-TT-20114] 02 p0254 N88-11608
Mechanisms of cloud layer formation in Venusian atmosphere 08 p1004 N88-16087
Atmosphere of Venus in southern polar area
08 p1005 N88-16088
Atmosphere of Venus in south polar area based on radio transmission data 08 p1005 N88-16089
Atmosphere of Venus in north polar area based on radio transmission data from Venera-15 and Venera-16 spacecraft 08 p1005 N88-16090
Peculiarities of daytime ionosphere of Venus during years of low and high solar activity
08 p1005 N88-16091
Distribution of electron concentration in nighttime atmosphere of Venus based on radio transmission data
08 p1005 N88-16092
Applicability of extremely low frequency global resonances for study of Venusian storm activity
08 p1005 N88-16093
Vega-1 and Vega-2 automatic stations: Functioning of landing modules in Venusian atmosphere
13 p1725 N88-20313
Thermal structure of Venusian Atmosphere determined from results of measurements from Vega-2 landing module 13 p1725 N88-20315
Research on absorption of UV radiation in Venusian atmosphere from Vega-1 and Vega-2 landing modules
13 p1725 N88-20316
Vertical structure of Venusian cloud layer at landing sites of Vega-1 and Vega-2 vehicles
13 p1725 N88-20317
Gas-chromatographic analysis of products of thermal reactions of aerosol in Venusian cloud layer on Vega-1 and Vega-2 automatic interplanetary stations
13 p1725 N88-20318
Roentgenoradiometric analysis of aerosol in Venusian clouds by Vega-1 and Vega-2 automatic interplanetary stations 13 p1726 N88-20319
Chemical composition and structure of Venusian clouds determined from results of roentgenoradiometric experiments carried out by landing modules of Vega-1 and Vega-2 automatic interplanetary stations
13 p1726 N88-20320
Determining chemical composition of aerosol in Venusian cloud layer on Vega-1 automatic interplanetary station using Malakhit mass spectrum analyzer
13 p1726 N88-20321
Determination of the Venus flyby orbits of the Soviet Vega probes using VLBI techniques
22 p3067 N88-28203
Microphysical processes in cloud layers of Venus
24 p3448 N88-30522
Stability of Venusian ionopause
24 p3448 N88-30523

VENUS CLOUDS
Mechanisms of cloud layer formation in Venusian atmosphere 08 p1004 N88-16087
Roentgenoradiometric analysis of aerosol in Venusian clouds by Vega-1 and Vega-2 automatic interplanetary stations 13 p1726 N88-20319

VENUS RADAR ECHOES
Dike zones on Venus
[NASA-TT-20111] 02 p0254 N88-11607
Processing of radar images of Venus on the Magiscan-2 analyzer 08 p1009 N88-16117

VENUS SURFACE
Venusian surface and crust 01 p0010 N88-10054
Dike zones on Venus
[NASA-TT-20111] 02 p0254 N88-11607
Preliminary estimation of color inhomogeneities on the surface of Venus according to the television images obtained by the VENERA-13 and VENERA-14 automated space probes
[NASA-TT-20114] 02 p0254 N88-11608
Processing of radar images of Venus on the Magiscan-2 analyzer 08 p1009 N88-16117
Analysis of impact crater arrangement on the Venutian surface (from photographic materials of the Venera-15 and -16 spacecraft)
[NASA-TT-20211] 11 p1571 N88-19401
JPRS report: Science and technology. USSR: Space
[JPRS-USP-88-002] 13 p1724 N88-20312
Vega-1 and Vega-2 automatic stations: Functioning of landing modules in Venusian atmosphere
13 p1725 N88-20313
Elemental composition of Venusian rocks in northeastern part of Terra Aphrodite (determined using data from Vega-2 landing module)
13 p1726 N88-20322
Content of natural radioactive elements in Venusian rocks determined using data from Vega-1 and Vega-2 stations 13 p1726 N88-20323
Kinetics of thermochemical gas solid reactions important in the Venus sulfur cycle
[NASA-CR-182963] 19 p2742 N88-26280
The rate of volcanism on Venus
[NASA-CR-183039] 19 p2742 N88-26281

VERBAL COMMUNICATION
Training in time interval discrimination using verbal feedback 12 p1665 N88-19985
Activities report of the Department of Systems and Communications
[ENST-87D004] 16 p2189 N88-23053
The representational code of the internal model of dynamic systems: An individual differences and dual task approach
[AD-A190876] 16 p2244 N88-23403
A review of workload measurement in relation to verbal comprehension 21 p2925 N88-27360

VERIFICATION (PROVING)
U PROVING

VERMICULITE
Activities report in metal manufacturing
[ISSN-0524-7705] 07 p0839 N88-15086

VERTEBRATES
NT AMPHIBIA
NT BIRDS
NT CATS
NT CHICKENS
NT DOGS
NT FISHES
NT FROGS
NT HUMAN BEINGS
NT MAMMALS
NT MICE
NT MONKEYS
NT PRIMATES
NT RATS
NT WATERFOWL
Functional plasticity of the nervous system of vertebrates 01 p0074 N88-10474
Proceedings and program draft in Gravitational Biology in the Federal Republic of Germany --- Effects of Weightlessness on the Human Organism
[ESA-TT-988] 07 p0884 N88-15363

VERTICAL AIR CURRENTS
Mesoscale density variability in the mesosphere and thermosphere: Effects of vertical flow accelerations
06 p0736 N88-14529
A Lagrangian model of dry thermals
[DM-50] 09 p1193 N88-17150
NASA wind shear model: Summary of model analyses
10 p1273 N88-17617
Windshear detection effect of static air temperature bias 10 p1274 N88-17621
Are windshear training aid recommendations appropriate for other than large jet transports? Pilot procedures: Shear models 10 p1275 N88-17635
Global vertical mass transport by clouds: A two-dimensional model study
[CM-74] 24 p3391 N88-30192

VERTICAL DISTRIBUTION
NT STAR DISTRIBUTION
ECC (Electrochemical Concentration Cell) ozonesonde observations at South Pole, Antarctica during 1986
[PB87-207502] 02 p0197 N88-11228
Hydrochemical structure of Gulf Stream frontal zone waters 06 p0727 N88-14476
Effect of neutral wind on the latitudinal variation of nighttime F-layer vertical movements
08 p1030 N88-16244

A comparison of multi-layer meso-alpha MLAM model results with surface and aircraft observations from CAPTEX
[DE88-000549] 09 p1188 N88-17118
Measurement of vertical distributions of halogenated hydrocarbons in the stratosphere
[ETN-88-91065] 09 p1191 N88-17135
Model investigations of atmospheric ammonia scavenging
[DE88-002337] 09 p1194 N88-17153
Vertical structure of Venusian cloud layer at landing sites of Vega-1 and Vega-2 vehicles
13 p1725 N88-20317
Forty-eight-inch lidar aerosol measurements taken at the Langley Research Center, May 1974 to December 1987
[NASA-RP-1209] 23 p3232 N88-29234

VERTICAL FINS
U FINS

VERTICAL FLIGHT
Integrated control and display research for transition and vertical flight on the NASA V/STOL Research Aircraft (VSRA)
[NASA-TM-100029] 05 p0551 N88-13359
The impact of vertical axis characteristics on helicopter handling qualities
[AD-A188964] 12 p1583 N88-19474

VERTICAL JUNCTION SOLAR CELLS
Three-dimensional models of conventional and vertical junction laser-photovoltaic energy converters
[NASA-TM-4039] 17 p2370 N88-24111

VERTICAL LANDING
GPS vertical axis performance enhancement for helicopter precision landing approach
[NASA-CR-177443] 04 p0397 N88-12477
Parametric study of supersonic STOVL flight characteristics
[NASA-CR-177330] 16 p2161 N88-22893
A numerical study of the hot gas environment around a STOVL aircraft in ground proximity
[NASA-TM-100895] 17 p2295 N88-23729

VERTICAL MOTION
Vertical ship motions and sea loads considering nonlinear effects
[TAE-592] 20 p2784 N88-26515
Utilization of a single clear-air Doppler radar beam to measure vertical divergence
[AD-A195543] 24 p3405 N88-30271

VERTICAL MOTION SIMULATORS
Status of NASA/Army rotorcraft research and development piloted flight simulation
09 p1110 N88-16651

VERTICAL ORIENTATION
Investigation of vertical axis handling qualities for helicopter hover and NOE flight
03 p0263 N88-11653
Effects of combining vertical and horizontal information into a primary flight display
[NASA-TP-2783] 04 p0399 N88-12487
Data acquisition and analysis system for the Sandia 34-meter Vertical Axis Wind Turbine
[DE88-002417] 09 p1187 N88-17112
Relationships between remotely-sensed surface properties and subsurface structure in the ocean
[AD-A189317] 12 p1650 N88-19881
A polarization diversity meteorological radar system
[AD-A189291] 13 p1758 N88-20515
The effects of torque response and time delay on rotorcraft vertical axis handling qualities
[AD-A189873] 15 p2017 N88-22023
Deflection of a circular liquid jet on a flat plate perpendicular to the flow direction
[NASA-TT-20279] 16 p2207 N88-23173
Single phase liquid immersion cooling of discrete heat sources in a vertical channel
[AD-A191224] 17 p2337 N88-23944
Observations of frontal instabilities on an upwelling filament
[AD-A191051] 17 p2375 N88-24122
The effect of a turbulent airstream on a vertically-launched missile at high angles of attack
[AD-A192408] 20 p2758 N88-26363
Stability of a coastal upwelling front over topography
[AD-A192354] 20 p2829 N88-26784
A modal approach to Arctic noise modelling with implied vertical coherence
[AD-A192966] 20 p2850 N88-26916
Vertical viewing ECE diagnostic for the D3-D tokamak
[DE88-010586] 20 p2860 N88-26987
Vertical directionality of ambient noise at 32 deg N as a function of longitude: Tape number 86180
[AD-A193228] 21 p3012 N88-27872
Nonequilibrium flow of a radiating gas in a vertical channel with axial temperature variation
[DE88-702535] 23 p3212 N88-29120

Possibilities of determining vertical profiles of microphysical characteristics of stratospheric aerosol using space measurements of transparency and solar halo 24 p3449 N88-30526

VERTICAL STABILIZERS
U STABILIZERS (FLUID DYNAMICS)

VERTICAL TAILS
U STABILIZERS (FLUID DYNAMICS)
U TAIL ASSEMBLIES

VERTICAL TAKEOFF
The ability of modified pavement quality concrete to resist ground erosion caused by VTOL aircraft
[BAE-ARG-238] 03 p0267 N88-11683

VERTICAL TAKEOFF AIRCRAFT
Propulsion-induced effects caused by out-of-ground effects
[NASA-TM-100032] 06 p0666 N88-14088
Development of a plenum chamber burner system for an advanced VTOL engine 10 p1281 N88-17664
Development of vertical takeoff aircraft with turbojet engines in Germany 10 p1309 N88-17822

VERTICAL TAKEOFF AND LANDING
U VERTICAL LANDING
U VERTICAL TAKEOFF

VERTOL MILITARY HELICOPTERS
U BOEING AIRCRAFT

VERY HIGH FREQUENCIES
Future developments of auroral D-region research using the EISCAT VHF incoherent scatter radar
08 p1035 N88-16278
VHF/UHF propagation by diffraction: Calculation by numerical integration 12 p1615 N88-19659
Some measurements of height gain at V.H.F.
12 p1617 N88-19671
Descriptions of HF and VHF Loran-C buoys and evaluations as potential datum marker buoys
[AD-A192060] 18 p2462 N88-24618
Theoretical basis for an experimental test with regard to the origin of VHF (Very High Frequency) radiation from natural lightning
[DE88-007535] 18 p2544 N88-25102
Mini-station for VHF reception: Argos system simplified description
[INPE-4551-NTE/279] 19 p2655 N88-25764
The VHF experimental radar LARA. A long-wavelength radar for helicopter detection 22 p3149 N88-28738

VERY HIGH SPEED INTEGRATED CIRCUITS
U VHSIC (CIRCUITS)

VERY LARGE ARRAY (VLA)
VLA observations of the X-ray bright Hyades M-dwarfs
04 p0512 N88-13147
IUE/Optical/VLA flares on AD Leo
04 p0512 N88-13152
Microwave observations of red dwarf flare stars
04 p0513 N88-13153
A VLA survey of dMe flare stars
04 p0513 N88-13154
VLA observations of rapid 6 cm flux variations in alpha Ori 04 p0515 N88-13169
Mars: High resolution VLA observations at wavelengths of 2 and 6 cm and derived properties
06 p0804 N88-14909
X-band system performance of the very large array
11 p1473 N88-18789
DSS 14 antenna calibrations for GSSR/VLA Saturn radar experiments 22 p3066 N88-28207

VERY LARGE SCALE INTEGRATION
Contribution to the development of smart design techniques for VLSI integrated circuits --- CMOS
[LAAS-87-181] 02 p0221 N88-11395
The design plan of a VLSI single chip (255, 223) Reed-Solomon decoder 04 p0435 N88-12697
A simplified procedure for correcting both errors and erasures of a Reed-Solomon code using the Euclidean algorithm 04 p0435 N88-12698
On the VLSI design of a pipeline Reed-Solomon decoder using systolic arrays 04 p0436 N88-12700
A procedural method for the efficient implementation of full-custom VLSI designs 04 p0436 N88-12701
Research in VLSI (Very Large Scale Integration) systems
[AD-A184089] 04 p0438 N88-12721
A study of charged particles/radiation damage to VLSI device materials
[NASA-CR-172036] 05 p0577 N88-13518
New breakthrough in Chinese integrated circuits: Successful development of high-speed CMOS circuits
[AD-A185381] 05 p0578 N88-13525
Benchmarking and evaluation of hardware description languages for design of VLSI systems
[PB87-134557] 06 p0758 N88-14648
Very thin VLSI-layouts (Very Large Scale Integration-Layouts) of complete binary trees
[PB88-100847] 06 p0789 N88-14841

Correctness proofs for systolic algorithms: Palindromes and sorting
[PB88-106075] 07 p0912 N88-15534
Extraction of MOS VLSI (Very-Large-Scale-Integrated) circuit models including critical interconnect parasitics
[AD-A185847] 08 p0979 N88-15914
Application of parallel distributed processing to space based systems 08 p1059 N88-16393
High performance VLSI algorithms and architectures for digital signal processing 09 p1155 N88-16926
Formal multilevel hierarchical verification of synchronous MOS VLSI circuits
[AD-A187532] 10 p1324 N88-17918
Latent failures and coverage in fault-tolerant systems. A VLSI CMOS circuit design technique to aid test generation
[AD-A187615] 10 p1325 N88-17921
Signal processing studies program VLSI designs for unary functions
[AD-A188053] 10 p1325 N88-17922
The arithmetic cube and its associated algorithms
10 p1374 N88-18195
Wafer scale implementation of a GaAs systolic signal processor cell 10 p1381 N88-18247
A VLSI implementable block oriented data driven multiprocessor 10 p1381 N88-18249
On systolic architectures for interpolation and integration 10 p1382 N88-18250
Fuzzy logic inference processor for real time control: A second generation full custom design
[AD-A188155] 11 p1471 N88-18773
A comparison of VLSI architectures for time and transform domain decoding of Reed-Solomon codes
11 p1472 N88-18783
A simplified, general-purpose deep-space ranging correlator design 11 p1473 N88-18796
Description, analysis and simulation of a new realization of digital filters
[AD-A187763] 11 p1477 N88-18814
High bit rate serial input multipliers
[REPT-87-012] 11 p1530 N88-19140
On serial-input multipliers for two-complement numbers
[REPT-86-035] 11 p1536 N88-19181
Development of VLSI optical data link
[AD-A187883] 11 p1549 N88-19265
Development of VLSI optical data link
[AD-A187884] 11 p1549 N88-19266
Hercules: A power analyzer for MOS VLSI circuits
[AD-A188702] 12 p1623 N88-19706
VSLI design generators
[AD-A188706] 12 p1623 N88-19707
Computer aided fast turnaround laboratory for research in VLSI (Very Large Scale Integration)
[AD-A189451] 12 p1624 N88-19715
VLSI implementations for digital signal processing
[AD-A189612] 12 p1624 N88-19719
Gridless routing for generalized cell assemblies: Report and user manual
[EUT-87-E-180] 13 p1764 N88-20549
GM: A gate matrix layout generator
[EUT-87-E-179] 13 p1820 N88-20875
Applications of lasers to semiconductor studies
14 p1901 N88-21356
GADL: A gate array description language
[EUT-87-E-165] 14 p1907 N88-21396
Electron beam sensitive devices for controllability
[RR-658-I] 14 p1908 N88-21403
Higher levels of a silicon compiler
[EUT-86-E-163] 14 p1955 N88-21650
Generating layouts for random logic: Cell generation schemes
[EUT-86-E-164] 14 p1956 N88-21656
ESKISS: A program for optimal state assignment
[EUT-87-E-167] 14 p1956 N88-21659
Technology mapping from Boolean expressions to standard cells
[EUT-87-E-174] 14 p1963 N88-21708
Advanced packaging for VLSI/VHSIC (Very Large Scale Integrated Circuits/Very High Speed Integrated Circuits) applications: Electrical, thermal and mechanical considerations, an IR and D report
[AD-A189666] 14 p1965 N88-21724
An optimal CMOS structure for the design of a cell library
[EUT-87-E-166] 14 p1985 N88-21841
French Multiproject Chip (MPC) activity report, 1986
[RR-650-I] 15 p2059 N88-22273
Multiple-transform pipelines for image coding
[REPT-87-038] 15 p2108 N88-22561
Software structuring principles for VLSI CAD
[AD-A190386] 15 p2112 N88-22579
Design and implementation of VLSI prime factor algorithm processor
[AD-A190483] 15 p2112 N88-22580

Design of high yield microprocessors
ETN-88-92184] 16 p2245 N88-23410
Automatic layout generation of data processing sections
l VLSI microprocessor-like circuits
ETN-88-92185] 16 p2245 N88-23411
HIFI: A design method for implementing signal
rocessing algorithms on VLSI processor arrays
ETN-88-92238] 16 p2247 N88-23421
Silicon compilers: Application to the compilation of the
ontrol area
ETN-88-92188] 16 p2247 N88-23425
Correctness proofs for systolic algorithms: A palindrome
ecognizer
CWI-CS-R8747] 16 p2248 N88-23434
Piecewise linear approach for timing simulation of VLSI
Very-Large-Scale-Integrated) circuits on serial and parallel
omputers
AD-A191328] 16 p2252 N88-23462
A multigrid approach for the solution of a nonlinear
iffusion equation in a time-dependent area using
Cartesian coordinates
GMD-STUDIEN-122] 16 p2257 N88-23491
Microelectronics the next fifteen years
17 p2305 N88-23792
Interfacing and integrating hardware and software design
ystems 17 p2306 N88-23796
Evolution of a family of image processing systems at
NPE 17 p2361 N88-24065
Silicon-on-insulator electronics for a space nuclear
power system 17 p2431 N88-24461
Defect detection and classification in VLSI pattern
nspection 18 p2507 N88-24871
Some unsolved problems in modelling self-timed circuits
using Petri Nets, series B, number 2
PB88-181466] 18 p2507 N88-24872
SYMBL: A new Boolean compiler
18 p2554 N88-25160
An improved simulated annealing algorithm for standard
cell placement
NASA-CR-182952] 18 p2558 N88-25183
Mathematical models for VLSI device simulation
AD-A191125] 18 p2562 N88-25212
Progress and challenges in HEMT LSI technology
19 p2656 N88-25779
Effects of cosmic rays on single event upsets
NASA-CR-183053] 20 p2793 N88-26569
Research in VLSI computer systems
AD-A192915] 20 p2835 N88-26816
Digital carrier demodulation for the DSN Advanced
Receiver 22 p3064 N88-28183
Rule-based circuit optimization for CMOS VLSI
22 p3137 N88-28649
Performance analysis of k-ary n-cube interconnection
networks
AD-A195542] 24 p3361 N88-30010
Design of a self-timed VLSI multicomputer
communication controller
AD-A194567] 24 p3361 N88-30014

ERY LONG BASE INTERFEROMETRY
Extragalactic VLBI objects: Candidates for optical
interferometry? 01 p0094 N88-10616
EVN (European VLBI network) and MERLIN
observations of 5 superluminal radio sources
[PB87-110730] 04 p0520 N88-13193
Low-frequency VLBI in space and interstellar
refraction
[PB87-127643] 06 p0696 N88-14267
Low frequency VLBI in space using GAS-Can satellites:
Report on the May 1987 JPL Workshop
[NASA-CR-182362] 06 p0801 N88-14904
VLBI research on OH-maser IN W33
08 p1001 N88-16064
Crustal dynamics project data analysis, 1987. Volume
1: Fixed station VLBI geodetic results, 1979-1986
[NASA-TM-100682] 08 p1035 N88-16279
Crustal dynamics project data analysis, 1987. Volume
2: Mobile VLBI geodetic results, 1982-1986
[NASA-TM-100689-VOL-2] 08 p1035 N88-16280
Observation model and parameter partials for the JPL
VLBI parameter estimation software MASTERFIT-1987
[NASA-CR-182524] 10 p1427 N88-18523
Source and event selection for radio-planetary frame-tie
measurements using the Phobos Landers
11 p1471 N88-18775
A 2.3-GHz maser at Usuda, Japan, for TDRSS-orbiting
VLBI experiment 11 p1472 N88-18779
Phase calibration generator 11 p1473 N88-18785
Deformations in VLBI antennas
[NASA-TM-100696] 11 p1502 N88-18970
Geodetic positioning by employment of the
GPS-NAVSTAR satellites applying the techniques of VLBI
and sequential recursive optimal estimation
[INPE-4438-TDL/311] 12 p1594 N88-19547
Polarization properties of SiO masers
13 p1858 N88-21113
The Spring 1985 high precision baseline test of the JPL
GPS-based geodetic system
[NASA-CR-182686] 14 p1940 N88-21577
A 2.3-GHz low-noise cryo-FET amplifier
22 p3066 N88-28195
DSN very long baseline interferometry system Mark
IV-88 22 p3067 N88-28199
Determination of the Venus flyby orbits of the Soviet
Vega probes using VLBI techniques
22 p3067 N88-28203

VERY LOW FREQUENCIES
ELF/VLF/LF propagation and system design
[AD-A183261] 01 p0033 N88-10212
WAVFLD: A program to compute ionospheric height gain
functions and field strengths at VLF
[AD-A191159] 16 p2191 N88-23066
WIPP (Wave Induced Particle Precipitation) experiment
logistic support
[AD-A191184] 18 p2499 N88-24824
Outer zone electron precipitation produced by a VLF
transmitter
[AD-A191944] 19 p2691 N88-25993
Airborne measurement of low frequency atmospheric
noise ALFAN 1
[AD-A193056] 21 p2931 N88-27405
TE/TM (Transverse Electric/Transverse Magnetic)
height profile measurements of transpolar VLF (Very Low
Frequency) signals
[AD-A194503] 22 p3069 N88-28216
Influence of plasma parameters on VLF radiation in
near-rocket region 24 p3448 N88-30516

VESTIBULAR NYSTAGMUS
Role of optokinetic stimulation in vestibulospinal
reflexes 10 p1360 N88-18131

VESTIBULAR TESTS
Development of methods for the study of space motion
sickness 07 p0892 N88-15408
Vestibular response to caloric stimulation during orbital
flight 12 p1658 N88-19939
Facilitory effects of voluntary movements on
vestibulomotor reaction 12 p1664 N88-19976
Studies of the vestibulo-ocular reflex on STS 4, 5 and
6
[NASA-TM-100461] 12 p1666 N88-19987
Role of opioid peptides in pathogenesis of
vestibulovegetative disorders 19 p2704 N88-26079
Motion evoked vestibular potentials
21 p2982 N88-27712

VESTIBULES
Motion and space sickness 04 p0404 N88-12510
Vestibular integrated function and microgravity
12 p1658 N88-19937
Significance of sensory signal phase mismatch in
mechanisms of motion sickness development
20 p2830 N88-26787

VESTS
Fit evaluation of female body armor
[AD-A188721] 14 p1953 N88-21638

VFR (RULES)
U VISUAL FLIGHT RULES

VHSIC (CIRCUITS)
Interchange of electronic design through VHDL and
EIS 09 p1205 N88-17222
A production-quality UNIX Very High Speed Integrated
Circuit (VHSIC) Hardware Description Language (VHDL)
subset analyzer
[AD-A188832] 12 p1623 N88-19710
Advanced packaging for VLSI/VHSIC (Very Large Scale
Integrated Circuits/Very High Speed Integrated Circuits)
applications: Electrical, thermal and mechanical
considerations, an IR and D report
[AD-A189666] 14 p1965 N88-21724
Very High Speed Integrated Circuits (VHSIC)
[AD-A193225] 21 p2937 N88-27442

VIBRATION
NT BENDING VIBRATION
NT FLUTTER
NT FORCED VIBRATION
NT FREE VIBRATION
NT LATTICE VIBRATIONS
NT LINEAR VIBRATION
NT POGO EFFECTS
NT RANDOM VIBRATION
NT RESONANT VIBRATION
NT SELF INDUCED VIBRATION
NT STRUCTURAL VIBRATION
NT SUPERSONIC FLUTTER
NT TRANSONIC FLUTTER
Investigation of the excitation of turbine blade vibration
in axial compressors in rotating stall
[ETN-87-90377] 01 p0007 N88-10035
Activities report of the Institute of Sound and Vibration
Research
[ETN-87-90685] 01 p0090 N88-10589
The Shock and Vibration Digest, Volume 19, No. 11
03 p0265 N88-11673
The Shock and Vibration Digest, Volume 19, No. 10
03 p0335 N88-12112
Vibration and parametric excitation in rotating
asymmetric circular plates 04 p0456 N88-12823
Initial dynamic load estimates during configuration
design 05 p0593 N88-13621
The Shock and Vibration Digest, Volume 19, No. 12
05 p0610 N88-13746
Dynamics of cables and chains
05 p0610 N88-13747
Computation of natural frequencies of planar lattice
structure
[AD-A185387] 05 p0641 N88-13920
Influence of general vertical vibration on relationships
between mediators in various segments of brain
06 p0751 N88-14613
Vibrational properties of disordered solids: Far infrared
studies: Performance report
[DE88-001474] 06 p0786 N88-14821
Methods of improving compacting quality of intricately
shaped powder components
[BLL-M-37412-(5828.4)] 08 p0968 N88-15859
The Shock and Vibration Digest, Volume 20, No. 1
08 p0975 N88-15897
The Shock and Vibration Bulletin. Part 3: Isolation and
damping, vibration test criteria, and vibration analysis and
test
[AD-A186750] 08 p0997 N88-16040
The effects of rotor unbalance on the vertical response
of a soft-mounted block 08 p1000 N88-16057
Investigation of vibration problems with heterodyne
holographic interferometer 08 p1000 N88-16058
A summary of recent NASA/Army contributions to
rotorcraft vibrations and structural dynamics technology
09 p1105 N88-16628
Geometric structure, pseudoband gaps, and surface
vibrational resonances on metal surfaces
[AD-A187001] 09 p1143 N88-16851
Computational fluid dynamics and
aerothermodynamics
[NASA-CR-182490] 09 p1166 N88-16989
An analytical study of the effects of transverse shear
deformation and anisotropy on natural vibration
frequencies of laminated cylinders
[NASA-TM-100554] 10 p1295 N88-17739
One-dimensional leakage-flow vibration instabilities
[DE88-002875] 10 p1330 N88-17947
Vibration and flutter characteristics of the SR7L
large-scale propfan
[NASA-TM-100272] 10 p1344 N88-18036
Modal testing the EOLE
[DE88-003795] 10 p1350 N88-18066
Modal testing of a very flexible 110 m wind turbine
structure
[DE88-003796] 10 p1351 N88-18072
The Shock and Vibration Digest, volume 20, no. 2
10 p1417 N88-18459
Dynamic analysis of plane frames by microcomputer
11 p1531 N88-19143
Vibrational, mechanical and thermal properties of 3-5
semiconductors
[AD-A187569] 11 p1556 N88-19316
Study of the vibrational modes of subsurface oxygen
on Al (111) using diode laser infrared reflection-absorption
spectroscopy
[AD-A188322] 12 p1632 N88-19769
Vibrations of shells containing fluid
12 p1635 N88-19787
Vibration spectra of oxygen and vanadium atoms in
vanadium-oxygen disordered interstitial alloys
[DE87-703166] 13 p1740 N88-20404
Research on flow around bluff bodies, flow induced
vibrations 14 p1864 N88-21135
The buckling and vibration of composite plates using
the Levy method considering shear deformation and rotary
inertia
[AD-A189743] 15 p2076 N88-22374
Effect of vibrational excitation on rate parameters of
atmospheric reactions
[AD-A190464] 15 p2094 N88-22477
The nonlinear dynamics of a spacecraft coupled to the
vibration of a contained fluid
[DE88-007035] 16 p2168 N88-22925
Periodic response of nonlinear systems
16 p2217 N88-23228
Modal forced response of propfans in yawed flow
16 p2221 N88-23253
Computer simulation of a motor pump unit to aid in
interpreting vibration data
[DE88-004481] 16 p2223 N88-23270
The Shock and Vibration Digest, volume 20, no. 4
17 p2391 N88-24214
Low authority control of large space structures using a
constrained threshold control formulation
18 p2472 N88-24667

A dynamic analysis of piezoelectric strained elements
[AD-A191478] 18 p2503 N88-24851

Effects of Coriolis acceleration on the vibrations of spinning structures 18 p2522 N88-24966

Vibration protection of inelastic structures by means of active and passive control 19 p2526 N88-25001

Vibrations of rotating thick or thin rings
18 p2529 N88-25003

Bimolecular reactions and energy-transfer processes of highly vibrationally excited molecules related to energetic materials
[AD-A189013] 18 p2571 N88-25270

Para-ortho abundance ratio of molecular hydrogen in NGC2023
[ISAS-RN-352] 18 p2573 N88-25286

Spectroscopy and energy transfer kinetics of the interhalogens
[AD-A192103] 18 p2583 N88-25344

Aircraft accident report: Air New Orleans, DBA continental express flight 962 British Aerospace 3101 (Jetstream 31), N331CY, New Orleans International Airport, Kenner, Louisiana, May 26, 1987
[PB88-910408] 19 p2601 N88-25450

Rare Gas Halide (RGH) kinetics
[AD-A192352] 20 p2770 N88-26425

A review of gear housing dynamics and acoustics literature
[NASA-CR-183110] 20 p2811 N88-26675

Vibration frequencies of tapered bars with nonclassical boundary conditions
[NASA-CR-183059] 20 p2813 N88-26688

FEB structural analysis, revision H
[AD-A192302] 20 p2814 N88-26698

Low energy molecular collisions
[ISAS-RN-366] 20 p2850 N88-26919

Enhancement of volume H(-) production by vibrationally pre-exciting the hydrogen molecules
[DE88-010783] 20 p2853 N88-26937

Aperiodic superlattices: Structured randomness
20 p2873 N88-27055

Vibrational impacts of hush house operation
[DE88-006983] 21 p2899 N88-27207

Nonlinear vibrations of periodically stiffened plates
21 p2963 N88-27598

Wave propagation and vibration of fibre reinforced laminates
[AD-A194144] 22 p3051 N88-28101

Power flow analysis of two coupled plates with arbitrary characteristics
[NASA-CR-183165] 22 p3075 N88-28251

Overview of computational vibro acoustics. State of the art and future development
[FFA-TN-1988-17] 23 p3279 N88-29521

Vibration spectra induced by impurities in 3-5-compounds semiconductors
[DE88-702730] 23 p3293 N88-29610

Containment of a silicone fluid free surface in reduced gravity using barrier coatings
[NASA-TM-101314] 24 p3371 N88-30072

Intramolecular dynamics: A study of molecules at high levels of vibrational excitation
[AD-A195285] 24 p3428 N88-30400

VIBRATION DAMPERS
U VIBRATION ISOLATORS

VIBRATION DAMPING

The effect of different packagings on the vibration behavior and the coupling factors of steam turbine blading
[ETN-87-90425] 01 p0056 N88-10357

Test of the Hipparcos payload in the Liege vacuum facility focal 02 p0135 N88-10850

On the root locus method applied to flexural vibration control systems 03 p0320 N88-12022

Combined problem of slew maneuver control and vibration suppression
[NASA-CR-181537] 04 p0455 N88-12817

The 58th Shock and Vibration Symposium, volume 1
[NASA-CP-2488-VOL-1] 05 p0592 N88-13609

Viscous damped space structure for reduced jitter
05 p0594 N88-13623

A system identification technique based on the random decrement signatures. Part 1: Theory and simulation
05 p0594 N88-13625

A system identification technique based on the random decrement signatures. Part 2: Experimental results
05 p0594 N88-13626

An efficient frequency response solution for nonproportionally damped systems
05 p0595 N88-13634

Shape optimization of damping layers
05 p0595 N88-13635

Advanced joining concepts for passive vibration control 05 p0596 N88-13638

Active control of flexural vibrations in beams
06 p0794 N88-14866

Experimental investigation of damping characteristics of bolted structural connections for plates and shells
[AD-A186075] 07 p0867 N88-15259

Identification and feedback control of machine tool vibrations
[PB88-109715] 08 p0976 N88-15902

The Shock and Vibration Bulletin. Part 1: Welcome, Keynote Address, Invited Papers, Nondevelopment Items Workshop and Pyrotechnic Shock Workshop
[AD-A186748] 08 p0997 N88-16034

Dynamic testing: Seven years later
08 p0997 N88-16035

The Shock and Vibration Bulletin. Part 3: Isolation and damping, vibration test criteria, and vibration analysis and test
[AD-A186750] 08 p0997 N88-16040

Dynamic analysis of a structure with sliding base
08 p0998 N88-16045

Rotorcraft flight research with emphasis on rotor systems 09 p1111 N88-16656

Rotorcraft technology at Boeing Vertol: Recent advances 09 p1111 N88-16658

Recent Sikorsky R and D progress
09 p1111 N88-16659

Launch vehicle vibration: Measures taken to avoid pogo on ESA's Ariane launch vehicle
09 p1123 N88-16727

Kinetic isolation tether experiment
[NASA-CR-182458] 09 p1135 N88-16810

A review of two-phase flow-induced vibration
[DE88-001955] 09 p1160 N88-16955

The dynamics of an oscillating four-bar linkage
09 p1181 N88-17074

Using frequency-domain methods to identify XV-15 aeroelastic modes
[NASA-TM-100033] 10 p1277 N88-17646

Sensitivity of active vibration control to structural changes and model reduction 10 p1284 N88-17683

Suspension design for a satellite transport container
[INPE-4352-TDL/296] 12 p1600 N88-19578

Experimental and analytical investigation on a proposed embedded fiber optic displacement sensor
[AD-A189030] 12 p1630 N88-19756

The Shock and Vibration Digest, volume 20, no. 3
12 p1635 N88-19786

Active vibration control of a cantilevered beam with three elastic coordinates
[AD-A188824] 12 p1636 N88-19797

Optimal placement of tuning masses for vibration reduction in helicopter rotor blades
[NASA-TM-100562] 13 p1782 N88-20665

Investigations on higher harmonic blade pitch control at helicopters
[DFVLR-FB-87-38] 14 p1868 N88-21165

Vibration isolation system for the Stratospheric Observatory For Infrared Astronomy (SOFIA)
14 p1926 N88-21483

Investigation of boundary layer disturbances caused by periodic heating of a thin ribbon
[AD-A190572] 15 p2065 N88-22314

Instrumentation to provide an active control capability for distributed parameter systems
[AD-A190043] 15 p2076 N88-22375

Vibrations of structures with parametric uncertainties
[AD-A190400] 15 p2076 N88-22378

Vibration control of large structures
[AD-A191358] 16 p2168 N88-22928

Lewis Structures Technology, 1988. Volume 1: Structural Dynamics
[NASA-CP-3003-VOL-1] 16 p2217 N88-23226

Survey of impact damper performance
16 p2217 N88-23227

Piezoelectric pushers for active vibration control of rotating machinery 16 p2218 N88-23229

Active control and system identification of rotordynamic structure 16 p2218 N88-23230

The LDCM actuator for vibration suppression
[NASA-CR-182896] 17 p2335 N88-23940

Vibration and control of flexible rotor supported by magnetic bearings
[NASA-TM-100888] 17 p2345 N88-23977

Experimental vibration damping characteristics of the third-stage rotor of a three-stage transonic axial-flow compressor
[NASA-TM-100948] 18 p2466 N88-24642

Electromagnetic damping and vibration isolation of space structures
[AD-A191492] 18 p2471 N88-24665

Experimental study of active vibration control
[AD-A191454] 18 p2526 N88-24989

Technologies for antenna shape and vibration control
19 p2652 N88-25748

Design of a controller to reduce residual vibration in the positioning control of flexible robotic manipulators
20 p2806 N88-26658

Experimental and theoretical investigation of passive damping concepts for member forced and free vibration
[NASA-CR-183082] 20 p2814 N88-26693

Vibration response of constrained viscoelastically damped plates: Analyses and experiments
[AD-A192329] 20 p2815 N88-26699

Vibration control of large structures
[AD-A193317] 21 p2961 N88-27587

Dual adaptive control: Design principles and applications
[NASA-CR-177485] 22 p3038 N88-28038

The effects of moisture loss and elevated temperature upon the material damping of fibre reinforced polymer matrix composites
[UTIAS-324] 23 p3188 N88-28970

Passive damping concepts for free and forced member and grillage vibration
[NASA-CR-183114] 23 p3225 N88-29196

Experimental investigation of the effects of underwater exposure on the damping characteristics of bolted structural connections for plates and shells
[AD-A194486] 23 p3226 N88-29200

Anti-aliasing filters for dynamics and control experiments
[AD-A193758] 23 p3226 N88-29203

VIBRATION EFFECTS
NT POGO EFFECTS

Nonsteady-state vibrations in acoustic medium of elastic elliptical shell subjected to instantaneously applied uniform pressure 02 p0160 N88-11000

Incipient fault detection study for advanced spacecraft systems
[NASA-CR-172014] 02 p0183 N88-11138

Development of rotorcraft interior noise control concepts. Phase 2: Full scale testing, revision 1
• [NASA-CR-172594-REV-1] 06 p0777 N88-14769

Karyometric evaluation of neuronal reactions of rat cerebral cortex to the combined effect of ionizing radiation, longitudinal accelerations and vibration
07 p0890 N88-15396

Nystagmometric distinctions of individuals regularly exposed to vibration 07 p0891 N88-15401

A hybrid-stress finite element approach for stress and vibration analysis in linear anisotropic elasticity
[NASA-CR-179311] 12 p1634 N88-19784

Evaluation of chemical and atmospheric sciences research
[AD-A188468] 12 p1687 N88-20091

Vibration characteristics of pumped fluid systems (VCPFS) --- microgravity payloads
[ESA-CR(P)-2499] 14 p1895 N88-21310

Vibration testing of ACT fuselage
19 p2634 N88-25627

Effect of low-frequency whole-body vertical vibration on the serotoninergic system of the brain and spinal cord
19 p2704 N88-26081

Nonlinear hydroelastic vibrations in rectangular containers
[LRT-WE-9-FB-7(1987)] 22 p3088 N88-28340

VIBRATION ISOLATORS

Vibration-absorbing characteristics of metal-polymer shells 02 p0158 N88-10991

Controlling the dynamic environment during NOE flight
03 p0264 N88-11661

Modeling and control of large flexible vehicles in the atmosphere and space
[AD-A185368] 05 p0555 N88-13377

The 58th Shock and Vibration Symposium, volume 1
[NASA-CP-2488-VOL-1] 05 p0592 N88-13609

Optimal shock isolation with minimum settling time
05 p0595 N88-13633

A passive vibration-cancelling isolation mount
05 p0595 N88-13636

Microgravity isolation mount
[ESA-CR(P)-2480] 11 p1443 N88-18604

Suspension design for a satellite transport container
[INPE-4352-TDL/296] 12 p1600 N88-19578

Towards a practical microgravity environment --- isolation mount 14 p1878 N88-21223

The 22nd Aerospace Mechanisms Symposium
[NASA-CP-2506] 14 p1924 N88-21468

Vibration isolation system for the Stratospheric Observatory For Infrared Astronomy (SOFIA)
14 p1926 N88-21483

Development of a nitrile rubber for dynamic damping
[AD-A194060] 22 p3058 N88-28145

VIBRATION MEASUREMENT

USSR Report: Engineering and Equipment
[JPRS-UEQ-87-007] 02 p0157 N88-10985

Incipient fault detection study for advanced spacecraft systems
[NASA-CR-172014] 02 p0183 N88-11138

On the prediction of the aeroelastic behavior of lifting systems due to flow separation
[ESA-TT-1043] 03 p0259 N88-11633

Measurement of suspension and ride characteristics of the M1 main battle tank 05 p0596 N88-13637
Coupled elastic rotor/body vibrations with inplane degrees of freedom 05 p0596 N88-13643
Blade vibration problems in centrifugal compressors. Fundamental considerations 07 p0851 N88-15165
Modal analyses of the Kernville diagnostic canister [DE88-003268] 07 p0870 N88-15277
Parametric and experimental analysis using a power flow approach [NASA-CR-182460] 09 p1116 N88-16693
Spectral density estimates of coarsely quantized random vibration data 09 p1178 N88-17055
A reliable data collection/control system 10 p1289 N88-17708
Flaw identification from forced vibration testing [DE88-002641] 10 p1342 N88-18018
Low-cost optical data acquisition system for blade vibration measurement 16 p2219 N88-23240
Laboratory feasibility study of a composite embedded fiber optic sensor for measurement of structural vibrations [AD-A194270] 22 p3152 N88-28754
Use of holography in vibration and flutter study of fans [PNR90458] 24 p3375 N88-30098
Analytical and experimental studies of beam waveguide absorbers for structural damping [AD-A195085] 24 p3382 N88-30144
Vibrational power flow analysis of rods and beams [NASA-CR-183166] 24 p3383 N88-30151

VIBRATION METERS
NT SEISMOGRAPHS
Single-periodic multilayer grating laser Doppler vibrometer 03 p0327 N88-12066

VIBRATION MODE
Equivalent circuit consideration on the rotation of resonant modes of double resonant vibrators 07 p0839 N88-15092
Blade vibration due to different flow excitation 07 p0851 N88-15166
Modal analysis using frequency response measurement data 08 p0976 N88-15899
Overview of multi-input frequency domain modal testing methods with an emphasis on sine testing 11 p1499 N88-18949
A superelement component dynamic synthesis method 11 p1500 N88-18956
Method for finding principal modes of nonlinear vibration systems and their stabilities 14 p1899 N88-21340

VIBRATION PROTECTION
U VIBRATION ISOLATORS

VIBRATION SIMULATORS
NT VERTICAL MOTION SIMULATORS
Ultra-low frequency vibration data acquisition concerns in operating flight simulators [DE88-004795] 10 p1285 N88-17687

VIBRATION TESTING MACHINES
U VIBRATION SIMULATORS

VIBRATION TESTS
NT DAMPING TESTS
Surface scattering characteristics and the measurement of particulate contamination 02 p0137 N88-10862
Proceedings of Conference on Vibrodiagnostics discussed 02 p0158 N88-10990
Assessment of structural integrity from forced vibration testing [DE87-014642] 02 p0191 N88-11195
The Shock and Vibration Bulletin. Part 1: Welcome, Keynote Address, Invited Papers, Nondevelopment Items Workshop and Pyrotechnic Shock Workshop [AD-A186748] 08 p0997 N88-16034
Dynamic testing: Seven years later 08 p0997 N88-16035
Guidelines for qualifying non-development equipment to shock and vibration 08 p0997 N88-16036
Derivation of equipment vibration requirements for AV-8B 08 p0997 N88-16037
Designing electronics for pyrotechnic shock 08 p0997 N88-16038
TECOM's research efforts in the dynamic environments 08 p0999 N88-16048
The development of laboratory vibration test schedules: Philosophies and techniques 08 p0999 N88-16049
Laboratory vibration test schedules development beyond MIL-STD-810D 08 p0999 N88-16050
Comprehensive inflight vibration and acoustic testing 08 p0999 N88-16052
Evaluation of vibration specifications for acoustic environments 08 p0999 N88-16053
Fatigue effects of a swept sine test 08 p0999 N88-16054
Realization of the immediate objectives of the Aero-Gas Dynamics and Vibration Laboratory (LAGG) at the National Center for Research, Science and Technology (PUSPIPTEK) at Serpong, Java (Indonesia), Project TTA-79 [GG/QPR-10] 08 p1092 N88-16572
Failure of filament lamps subjected to vibration with special reference to the 26 volt 5 Watt tank lamp [EL-135] 09 p1158 N88-16938
Qualification by analysis of IUS plume deflectors 09 p1179 N88-17063
The dynamics of an oscillating four-bar linkage 09 p1181 N88-17074
Centaur G Prime modal test 09 p1181 N88-17075
Payload bay atmospheric vent airflow testing at the Vibration and Acoustic Test Facility [NASA-TM-100460] 11 p1437 N88-18572
NASDA's new test facilities for satellites and rockets 11 p1499 N88-18951
Design and dynamic testing of an instrumented spacecraft component 11 p1499 N88-18952
Random vibration (stress screening) of printed wiring assemblies 11 p1499 N88-18953
Development of a slip-ring system for energy transfer in space conditions. Space flight qualification and extended life tests [BMFT-FB-W-86-019] 16 p2169 N88-22932
Adjusting a finite element model using vibration type experimental data. Concept and error detection [ONERA-RT-7/3313-RY-060-R] 17 p2392 N88-24220
Vibration testing of ACT fuselage 19 p2634 N88-25627
Cross flow induced vibrations in tube bundle by displaced and misaligned tube configurations [ETN-88-92132] 20 p2801 N88-26621
Analytical and experimental studies of beam waveguide absorbers for structural damping [AD-A195085] 24 p3382 N88-30144

VIBRATIONAL FREQUENCIES (MOLECULAR)
U VIBRATIONAL SPECTRA

VIBRATIONAL FREQUENCIES (STRUCTURAL)
U RESONANT FREQUENCIES

VIBRATIONAL RELAXATION
U MOLECULAR RELAXATION

VIBRATIONAL SPECTRA
Picosecond CO2 laser interactions with polyatomic molecules [DE87-012072] 01 p0051 N88-10327
Diagnosis of flow channel in aircraft gas-turbine engines on basis of vibration spectrum characteristics 02 p0159 N88-10993
Kinetics of CO adsorption on nickel using time resolved vibration spectroscopy [ETN-87-90615] 03 p0289 N88-11814
Vibrational spectroscopy of shock-compressed fluid N2 and O2 [DE87-013138] 03 p0313 N88-11979
Ro-vibrational laser spectroscopy of ESD neutrals from chemisorbed species [DE87-013011] 04 p0447 N88-12770
Absorption of far IR-radiation by H2O-N2 complexes under atmospheric conditions 04 p0462 N88-12855
The delta upsilon = 1 fundamental bands of carbon monoxide in late-type stars 04 p0517 N88-13177
Pure dephasing of a vibrational adbond [AD-A185222] 05 p0609 N88-13740
Equilibrium retention in the nozzle of oxygen hydrogen propulsion systems 07 p0924 N88-15616
Fully turbulent internal flow excitation of pipe systems 08 p1000 N88-16056
Kinetic studies following state-selective laser excitation [DE88-004094] 10 p1335 N88-17981
Rovibrational spectroscopy of ArCO van der Waals complex [DE88-004291] 10 p1406 N88-18387
Coupling of vibrational modes of adsorbates: Application to field induced shifts for CO and CN on Cu(100) [AD-A187891] 11 p1453 N88-18659
In-situ vibrational spectroscopy of specifically adsorbed azide on silver electrodes [AD-A188511] 12 p1605 N88-19600
Advanced electron optics for vibrational spectroscopy [AD-A188469] 12 p1629 N88-19747
Stabilization and control problems in structural dynamics [AD-A190197] 15 p2073 N88-22361
Sequential excitation preparation of molecular energy levels with special structural and chemical properties [AD-A190041] 15 p2132 N88-22718
Time-resolved studies of free radicals and laser-initiated chain reactions [DE88-006569] 16 p2266 N88-23553
Vibrational spectroscopy of the hydrogen and hydrated hydronium cluster ions 16 p2268 N88-23566
Energy-transfer properties and mechanisms [DE88-007107] 18 p2571 N88-25272
Molecular characterization of structure and bonding in thin film materials [DE88-006811] 18 p2584 N88-25351
Polymeric electrolytes [AD-A193766] 23 p3198 N88-29031
Experimental investigation of the effects of underwater exposure on the damping characteristics of bolted structural connections for plates and shells [AD-A194466] 23 p3226 N88-29200
Measurements of XeF (Xenon Fluoride) ground state dissociation and vibrational equilibration [AD-A194611] 23 p3280 N88-29527
Analytical and experimental studies of beam waveguide absorbers for structural damping [AD-A195085] 24 p3382 N88-30144

VIBRATORY LOADS
Experimental determination of the oscillatory forces on two turbine blade profiles [ETN-87-90417] 01 p0007 N88-10037
Analytic investigation of helicopter rotor blade appended aeroelastic devices [NASA-CR-166525] 03 p0266 N88-11676
Resonant structures for integrated sensors 19 p2673 N88-25893

VIBROMETERS
U VIBRATION METERS

VICKERS VC-10 AIRCRAFT
U VC-10 AIRCRAFT

VICKERS 1100 AIRCRAFT
U VC-10 AIRCRAFT

VIDEO COMMUNICATION
Information technology to facilitate group interaction 24 p3438 N88-30463

VIDEO DATA
Fast, colour displays of digital terrain elevation data [AD-A185596] 06 p0729 N88-14485
A hybrid transform/DPCM encoder for data compression [DE88-003725] 09 p1154 N88-16919
Balance of X-ray radioscopy application to nondestructive tests of composite materials [SNIAS-881-430-110] 21 p2907 N88-27250
Use of optical disk technology at the Air Command and Staff College [AD-A192424] 21 p3027 N88-27969
More than a solar cycle of synoptic solar and coronal data: A video presentation [NASA-CR-181459] 23 p3308 N88-29708

VIDEO EQUIPMENT
Input devices for tasks using interactive video [NPL-DITC-87/87] 01 p0080 N88-10510
Health hazards of video display terminals: A comprehensive, annotated bibliography on a critical issue of workplace health and safety with sources for obtaining items and list of terminal suppliers [RSI-IAS-4] 03 p0355 N88-12240
Fiber optic video link [FOA-C-30444-3.1] 06 p0780 N88-14789
Issues associated with telerobotic systems in space 08 p1056 N88-16369
Reconfigurable work station for a video display unit and keyboard [NASA-CASE-MFS-26009-1-SB] 17 p2382 N88-24163
System overview: Teragon 4000, an image processing equipment at FOA 3 [FOA-C-30465-3.3] 18 p2557 N88-25179
Stereo and eye movement [AD-A193588] 22 p3142 N88-28681
Information technology to facilitate group interaction 24 p3438 N88-30463

VIDEO SIGNALS
Programmable real-time digital video image processing [PB87-104162] 04 p0430 N88-12661
Accommodating the residue of processed or computed digital video signals within the 8 bit CCIR recommendation 601 [BBC-RD-1987/12] 04 p0432 N88-12676
Digital video bit-rate reduction: DPCM for sub-Nyquist PAL [BBC-RD-1987/16] 05 p0573 N88-13494
Improvements to a UHF rebroadcast television link suffering tidal fading: Countisbury UHF relay station [BBC-RD-1987/14] 05 p0573 N88-13495
Two-signal cross modulation effects, half-IF effects and interference criteria in land mobile sharing with UHF (Ultra High Frequency) television [PB87-228037] 05 p0576 N88-13514
High-temperature photoelectron spectroscopy: An increased sensitivity spectrometer for studying vapor-phase species produced at furnace temperatures greater than 2000K [AD-A186542] 09 p1140 N88-16835

Limiting of YUV digital video signals
[BBC-RD-1987/22] 09 p1155 N88-16924
Simple high speed camera with CCD-sensor
[MPIS-8/1987] 18 p2518 N88-24940
Design and testing of a luminance and chrominance stabilization system for a computer-controlled color display
[AD-A191922] 18 p2554 N88-25159
Digital television routing systems: A survey of optical and electrical techniques
[BBC-RD-1988/3] 19 p2654 N88-25763
Underwater optical trajectography and video image mosaics 19 p2700 N88-26051
A 1/2-inch high-definition baseband VCR
21 p2930 N88-27393

VIDICONS
Characterization of new FPS (Focus Projection and Scale) vidicons for scientific imaging applications
[DE88-011213] 22 p3080 N88-28290

VIEW EFFECTS
Cloud cover determination in polar regions from satellite imagery
[NASA-CR-181544] 04 p0471 N88-12908
Surface reflectance factors derived from SPOT-1 HRV data at two view angles 22 p3113 N88-28492

VIEWING
NT FIELD OF VIEW
Vertical viewing ECE diagnostic for the D3-D tokamak
[DE88-010586] 20 p2860 N88-26987

VINEYARDS
Attempt to inventory vines using oblique SPOT images
22 p3095 N88-28380

VINYL COPOLYMERS
Group contribution analysis of the damping behavior of homopolymers, statistical copolymers and interpenetrating polymer networks based on acrylic, vinyl and styrenic mers
[AD-A185904] 07 p0836 N88-15070

VINYL CYANIDE
U ACRYLONITRILES

VINYL ETHYLENE
U BUTADIENE

VINYL POLYMERS
NT POLYVINYL FLUORIDE
NT VINYL COPOLYMERS
Novel conductive polymers
[EP-PATENT-0-182-548-A2] 01 p0026 N88-10163
Polyvinyl esters of omega-H-perfluoroacids and polyvinyl alcohol obtained from them
[AD-A184633] 03 p0279 N88-11755
High-molecular compounds (selected articles)
[AD-A184668] 03 p0293 N88-11842
Elementary fluorination of polymers
[ETN-88-90812] 07 p0836 N88-15075
Preparation of thin film polyvinylidene fluoride shock wave pressure transducers
[PB88-156070] 11 p1490 N88-18893
Piezoelectric polymer tactile sensor arrays for robotics
[AD-A188852] 12 p1634 N88-19780
Boundary layer measurements using hot-film sensors
17 p2297 N88-23743
Preferential surface adsorption in miscible blends of polystyrene and poly(vinyl methyl ether)
[AD-A191451] 18 p2490 N88-24769
Polymer-ceramic composites
[AD-A193244] 21 p2905 N88-27237
Alternative immersion accelerated testing of coating systems for Naval shoreline facilities
24 p3355 N88-29977

VINYLIDENE
Ferroelectric properties and impact behavior of the PVF2 polymer and the VF2/C2F3H polarized copolymers --- vinylidene polyfluorides
[ISL-CO-245/86] 08 p0971 N88-15876
NMR analysis of a fluorocarbon copolymer
[DE88-002364] 15 p2043 N88-22170
Interaction of vinylidene fluoride: Tetrafluoroethylene copolymer with ammonia
[NASA-TT-20292] 19 p2620 N88-25542

VIOLENCE
NT ATTACKING (ASSAULTING)

VIRGO GALACTIC CLUSTER
Molecular gas in Virgo cluster spiral galaxies
17 p2450 N88-24557

VIRGO STAR CLUSTER
U VIRGO GALACTIC CLUSTER

VIRIAL COEFFICIENTS
Optical determination of the virial coefficients of the gases C2H4, C2H6 and SF6
[ETN-87-90610] 03 p0282 N88-11776

VIRTUAL MEMORY SYSTEMS
Local concurrent error detection and correction in data structures using virtual backpointers
[NASA-CR-181432] 01 p0106 N88-10692
Memory systems for single bus multiprocessor architecture. Application to the SCOM system
[ENST-86E022] 02 p0219 N88-11379
Recovery using virtual memory
[AD-A187098] 09 p1217 N88-17296
Parallel garbage collection on a virtual memory system
[DE88-003567] 10 p1396 N88-18317

VIRTUAL PROPERTIES
Long-pulse, high-power vircator experiments
[DE88-011787] 21 p2940 N88-27458

VISCOELASTIC CYLINDERS
Buckling of viscoelastic columns
02 p0190 N88-11187
Calculation of rolling contact of two viscoelastic cylinders with application to the steady state normal contact problem
[ILR-MITT-188] 18 p2530 N88-25008

VISCOELASTIC DAMPING
Augmenting the control of a flexible manipulator with passive mechanical damping 01 p0055 N88-10350
Identification of linear structural models
03 p0337 N88-12121
Damping analysis of flexural waves in fluid-loaded single and constrained plates
[AD-A185116] 05 p0609 N88-13739
Investigation of constrained-layer technique using exact elasticity theory
[AD-A188664] 12 p1636 N88-19795
Feedback control of a hyperbolic partial-differential equation with viscoelastic damping
[AD-A192896] 21 p3003 N88-27810

VISCOELASTIC FLOW
U VISCOELASTICITY

VISCOELASTICITY
NT THERMOVISCOELASTICITY
Rheological behaviors of an elastomeric membrane
[DE87-013105] 01 p0061 N88-10392
Rheological and aging characterization of elastomers
[DE87-009598] 02 p0151 N88-10944
Interseismic deformation for normal fault earthquakes
03 p0349 N88-12207
Porosity influence on the strength and elasticity of first-year sea ice
[AD-A184493] 03 p0354 N88-12233
Explicit and implicit soil modelling for dynamic soil-structure interaction problems
04 p0428 N88-12650
Continuation finite element analysis of viscoelastic fluids 04 p0445 N88-12761
Exact finite element method analysis of viscoelastic tapered structures to transient loads
05 p0595 N88-13632
Bending of a bonded beam as a test method for adhesive properties
[AD-A184813] 05 p0609 N88-13736
Viscoelastic properties of EA951 adhesive: A source of creep deformations of a strongback
[DE88-001581] 06 p0685 N88-14197
Steady waves in a nonlinear theory of viscoelasticity
[AD-A185548] 06 p0723 N88-14448
The paradoxical asymptotic status of massless springs
[AD-A185625] 07 p0928 N88-15637
The properties of sound propagation in liquid constrained viscoelastic and polymeric structures
[AD-A185944] 07 p0929 N88-15640
Numerical solution methods for viscoelastic orthotropic materials
[NASA-CR-182381] 08 p0971 N88-15874
A finite element analysis of adhesively bonded composite joints including geometric nonlinearity, nonlinear viscoelasticity moisture diffusion and delayed failure
[AD-A187455] 10 p1296 N88-17747
Time delays and boundary feedback stabilization in one-dimensional viscoelasticity, appendices A through H
[AD-A187534] 10 p1401 N88-18353
A viscoelastic BEM (Boundary Element Method) for modeling oxidation
[AD-A187490] 11 p1452 N88-18653
Unstable elastic materials and the visco-elastic response of bars in tension
[AD-A187969] 11 p1498 N88-18946
Fracture characteristics of a viscoelastic polymer under constant load: Experiments and analysis
11 p1501 N88-18963
Experiments on the flow of viscoelastic fluids between eccentric rotating cylinders 12 p1625 N88-19723
On the energy release rate for dynamic transient anti-plane shear crack propagation in a general linear viscoelastic body
[AD-A188385] 12 p1635 N88-19791
On analysis of viscoelastic structures
[AD-A188445] 12 p1636 N88-19793
A continuum damage model for viscoelastic materials
[AD-A189426] 12 p1637 N88-19800
Viscoelastic behavior of a polyetheretherketone (PEEK) composite
[AD-A189545] 13 p1734 N88-20368
An analysis of large deformation axisymmetric inelastic problems by finite element and boundary element methods 13 p1782 N88-20664
Pressure induced ageing of polymers
14 p1929 N88-21504
Applications of elastic-viscoplastic constitutive models in dynamic analyses of crack run-arrest events
14 p1930 N88-21507
Thermoviscoelastic characterization and predictions of Kevlar/epoxy composite laminates
[NASA-CR-182878] 16 p2172 N88-22946
Effects of randomness of parameters on mean wave propagation in a viscoelastic medium
[REPT-87-60] 16 p2206 N88-23166
Effects of axial load on elastomeric isolation bearings
[PB88-179015] 16 p2223 N88-23269
Damage by creep fatigue: Influence of the visco-elasticity of the matrix
[PB88-124706] 18 p2528 N88-24998
Compression creep of filamentary composites
[NASA-CR-182550] 20 p2798 N88-26601
Vibration response of constrained viscoelastically damped plates: Analyses and experiments
[AD-A192329] 20 p2815 N88-26699
Thermo-viscoelastic analysis of composite materials, volume 1
[NASA-CR-183048-VOL-1] 21 p2904 N88-27230
Optimal design of viscoelastic structures
21 p2959 N88-27579
Finite element analysis of steady and transiently moving/rolling nonlinear viscoelastic structure. Part 1: Theory
[NASA-CR-179886] 23 p3273 N88-29480
Approximation of viscoelastic stresses from Newtonian turbulent kinematics
[AD-A194317] 24 p3371 N88-30077
Initial value problems in viscoelasticity
[AD-A196052] 24 p3382 N88-30145

VISCOMETERS
High intensity 5 eV O-atom exposure facility for material degradation studies 02 p0135 N88-10847

VISCOMETRY
Continual capillary viscosimetry using extrusiograph techniques
[PB88-166293] 15 p2046 N88-22195

VISCOPLASTIC FLOW
U VISCOPLASTICITY

VISCOPLASTICITY
Experimental determination of flow potential surfaces supporting a multiaxial formulation of viscoplasticity
02 p0187 N88-11167
Application of viscoplastic constitutive equations in finite element programs
[KFK-4254] 03 p0370 N88-12329
Ideal-viscoplastic extrusion model with application to deforming pistons in light-gas guns
[UTIAS-TN-266] 04 p0429 N88-12657
Steady shearing in a viscoplastic solid
[AD-A184341] 04 p0454 N88-12810
A critical review of the development of several viscoplastic constitutive theories
[AD-A185652] 07 p0867 N88-15262
A large strain thermomechanical forming model for elastic-viscoplastic behavior in metals
10 p1301 N88-17780
On stress collapse in adiabatic shear bands
[AD-A187185] 11 p1498 N88-18942
On the dissipative response due to discontinuous strains in bars of unstable elastic material
[AD-A188114] 11 p1498 N88-18947
Structure of a viscoplastic theory
[NASA-TM-100794] 11 p1501 N88-18968
Cyclic crack growth emanating at a round notch considering viscoplasticity
[AD-A189577] 13 p1781 N88-20655
A viscoplastic theory applied to copper
[NASA-TM-100831] 14 p1928 N88-21497
Nonlinear Constitutive Relations for High Temperature Applications, 1986
[NASA-CP-10010] 14 p1928 N88-21498
The viscoplasticity theory based on overstress applied to the modeling of a nickel base superalloy at 815 C
14 p1928 N88-21499
A viscoplastic constitutive theory for metal matrix composites at high temperature
14 p1929 N88-21500
Modeling the viscoplastic behavior of Inconel 718 at 1200 F 14 p1929 N88-21502
A simplified orthotropic formulation of the viscoplasticity theory based on overstress 14 p1929 N88-21505
Constitutive modeling and thermoviscoplasticity
14 p1930 N88-21506

A theory of viscoplasticity accounting for internal damage 14 p1930 N88-21508

Controlled-strain rate tests at very low strain rates of 2618 aluminum at 200 C 14 p1931 N88-21513

Cyclic uniaxial and biaxial hardening of type 304 stainless steel modeled by the viscoplasticity theory based on overstress 14 p1931 N88-21514

Some implications for cyclic plastic and viscoplastic equations based on nonproportional loading experiments 14 p1931 N88-21515

An experimental comparison of several current viscoplastic constitutive models at elevated temperature 14 p1931 N88-21516

On the global/local time incrementing for viscoplastic analysis 14 p1932 N88-21519

An automated procedure for material parameter evaluation for viscoplastic constitutive models 14 p1932 N88-21520

Nonlinear structural analysis of a turbine airfoil using the Walker viscoplastic material model for B1900 + Hf 14 p1932 N88-21522

Non-isothermal elastoviscoplastic analysis of planar curved beams 14 p1933 N88-21526

Effects of state recovery on creep buckling under variable loading 14 p1933 N88-21527

Evolution of hardening and damage during viscoplastic deformation
[AD-A190714] 15 p2077 N88-22381

Biaxial experiments supporting the development of constitutive theories for advanced high-temperature materials 15 p2078 N88-22386

Finite element (MARC) solution technologies for viscoplastic analyses 15 p2078 N88-22389

Heating at a propagating crack tip in a viscoplastic material
[AD-A190952] 16 p2224 N88-23274

Analysis of crack-tip fields in a viscoplastic material 17 p2349 N88-23996

Theory of viscoplasticity based on overstress with applications 18 p2529 N88-25007

Determination of multiaxial flow surfaces at elevated temperatures using the concept of dissipation potential
[ORNL/TM-10787] 24 p3383 N88-30149

An investigation of constitutive models for predicting viscoplastic response during cyclic loading
[AD-A194875] 24 p3385 N88-30163

ISCOSITY
NT EDDY VISCOSITY
NT GAS VISCOSITY

Viscosity measurements at high temperatures on a standard reference material supplied by BCR — Bureau Communite de Reference (BCR)
[NPL-DMA(A)-146] 01 p0020 N88-10126

Synthesis and characterization of processable polyimides with enhanced thermal stability
[NASA-CR-181447] 01 p0030 N88-10191

Two-phase non-Newtonian hydrodynamic modeling of slurries
[DE87-011519] 01 p0047 N88-10298

Effect of viscosity on a vertical cylinder due to surface waves
[ETN-87-90960] 02 p0171 N88-11075

The infiltration kinetics of aluminum in silicon carbide compacts
[AD-A184682] 03 p0290 N88-11823

Ion-matrix coupling in polymer electrolytes from relaxation time studies
[AD-A184632] 03 p0293 N88-11841

The axisymmetric sealing gap with variable viscosity. A variable hydraulic resistance
[ETN-87-90604] 03 p0314 N88-11987

In-situ characterization of the interface of glass reinforced composites
[AD-A185136] 05 p0557 N88-13391

Colloidal stability of oxidized silicon particles in ethanolic and aqueous media
[DE87-014783] 05 p0562 N88-13421

The effects of viscosity on resistive ballooning modes in line-tied coronal magnetic fields 08 p1097 N88-16599

Analysis of the spectral vanishing viscosity method for periodic conservation laws
[NASA-CR-181613] 09 p1231 N88-17378

Viscosity methods in optimal control of distributed systems
[AD-A188086] 10 p1401 N88-18357

Laser velocimeter measurements of solids in multiphase flow
[DE88-000196] 11 p1487 N88-18876

The effects of rotational flow, viscosity, thickness, and shape on transonic flutter dip phenomena
[NASA-TM-100811] 11 p1502 N88-18969

High shear rate rheometry of low-viscosity liquids
[AD-A188447] 12 p1627 N88-19733

Contrasting conductance/viscosity relations in liquid states of vitreous and polymer solid electrolytes
[AD-A189378] 13 p1748 N88-20452

A new method of measuring multigrade oil shear elasticity and viscosity at high shear rates
[AD-A190145] 15 p2064 N88-22304

A low dimensional dynamical system for the wall layer 16 p2194 N88-23088

Gravity currents with heat transfer effects
[PB88-180047] 16 p2205 N88-23158

Finite ion-relaxation and nonequilibrium radiation effects on laser-driven implosions 16 p2278 N88-23636

The viscosity of molten TNT
[MRL-R-1100] 19 p2622 N88-25553

Synthesis of model polymers and related structures in support of vinyl monomer grafting studies
[DE88-010245] 20 p2778 N88-26476

Optimal rheological characteristics in dynamic stability of polymer flow through porous media
[DE88-001225] 21 p2918 N88-27322

Fellowships in hypersonic aerodynamics
[AD-A194265] 23 p3172 N88-28885

A limiting viscosity approach to the Riemann problem for materials exhibiting change of phase
[AD-A193477] 23 p3210 N88-29103

Intraplate deformation, stress in the lithosphere and the driving mechanism for plate motions
[NASA-CR-183121] 23 p3231 N88-29231

Eruptive viscosity and volcano morphology 24 p3442 N88-30488

VISCOUS DAMPING
NT VISCOELASTIC DAMPING

Frequency domain identification of structural dynamic systems with general damping matrices 03 p0337 N88-12120

Viscous damped space structure for reduced jitter 05 p0594 N88-13623

Exact finite element method analysis of viscoelastic tapered structures to transient loads 05 p0595 N88-13632

VISCOUS DRAG

Viscous drag reduction of horizontal plates
[VKI-TN-159] 07 p0851 N88-15171

Boundary effects on the drag of a cylinder in axial motion at low Reynolds number 13 p1768 N88-20578

STARFIRE: Hypervelocity railgun development for high-pressure research
[DE88-008348] 19 p2605 N88-25469

Development and design of windtunnel and test facility for RPV (Remote Piloted Vehicle) enhancement devices
[AD-A194842] 24 p3329 N88-29822

VISCOUS FLOW
NT BOUNDARY LAYER FLOW
NT BOUNDARY LAYER SEPARATION
NT COUETTE FLOW
NT REATTACHED FLOW
NT SECONDARY FLOW
NT SEPARATED FLOW
NT STOKES FLOW

Locating parallel numerical tasks in the solution of viscous fluid flows
[DE87-013510] 02 p0169 N88-11064

FDM-FEM zonal method for viscous flow computations over multiple-bodies
[NAL-TR-925T] 02 p0170 N88-11069

Improved numerical methods for turbulent viscous recirculating flows 02 p0185 N88-11148

Mechanical and flow excited vibrations of elastic plates and cylindrical shells in dense fluids 03 p0316 N88-11996

Some experiences with the viscous-inviscid interaction approach
[NASA-TM-100015] 04 p0395 N88-12466

Total linearisation method for solving viscous free boundary flow problems by the finite element method
[PB87-222337] 04 p0441 N88-12737

Similar solutions for viscous hypersonic flow over a slender three-fourths-power body of revolution
[NASA-TM-100205] 04 p0443 N88-12752

Analytical studies of axially symmetric motion of an incompressible viscous fluid between two concentric rotating spheres 04 p0444 N88-12757

Low Reynolds number influence on aerodynamic performance of hypersonic lifting vehicles 05 p0531 N88-13230

Numerical simulation of the hypersonic flow around lifting vehicles 05 p0532 N88-13234

Numerical optimization of conical flow waveriders including detailed viscous effects 05 p0533 N88-13245

An analysis of the compressible-viscous flow field around a 3D-oscillating wing 05 p0535 N88-13254

Practical application of two-dimensional viscous flow computation 05 p0535 N88-13257

The role of computation fluid dynamics in aeronautical engineering (4). The development and applications of implicit TVD finite volume code 05 p0536 N88-13259

Computations of compressible viscous flows over multiple-bodies 05 p0539 N88-13262

A numerical study of the effects of curvature and convergence on dilution jet mixing
[NASA-TM-89878] 05 p0549 N88-13347

The simulation of the viscous flow around a cylinder by the random vortex method 05 p0579 N88-13534

Low thrust viscous nozzle flow fields prediction
[NASA-CR-182334] 05 p0582 N88-13551

Investigation of viscous/inviscid interaction in transonic flow over airfoils with suction 06 p0664 N88-14074

Implicit time dependent methods for inviscid and viscous compressible flows 06 p0701 N88-14304

Computation of free boundaries
[PB87-226023] 06 p0763 N88-14680

Rotation of magnetized particle in electrically conducting viscous medium 06 p0770 N88-14733

Viscous vortex flows 07 p0810 N88-14934

Wall turbulence control 07 p0812 N88-14943

Riblets for aircraft skin-friction reduction 07 p0814 N88-14955

Incompressible viscous flow simulations of the NFAC wind tunnel
[NASA-CR-177431] 07 p0816 N88-14969

Analysis of three-dimensional viscous internal flows
[AD-A186254] 07 p0849 N88-15155

Consistent boundary conditions for Reduced Navier-Stokes (RNS) scheme applied to 3-dimensional internal viscous flows
[NASA-CR-180874] 08 p0950 N88-15762

The simulation of three-dimensional viscous supersonic flow past blunt bodies with a hybrid implicit/explicit finite difference method
[DFVLR-FB-87-32] 08 p0950 N88-15765

Development of direct-inverse 3-D methods for applied aerodynamic design and analysis
[NASA-CR-182436] 08 p0950 N88-15767

Viscous flows, part 1 08 p0986 N88-15967

Viscous flows, part 2 08 p0986 N88-15968

Viscous flows. Part 3: Formulation of the Navier-Stokes equations by stream function vorticity methods 08 p0986 N88-15969

The viscous flow on surfaces with streamwise riblets
[DFVLR-FB-87-21] 09 p1162 N88-16961

Zonal solutions for viscous flow problems. Finite approximations in fluid mechanics
[MBB/LKE-122/S/PUB/226] 10 p1313 N88-17846

A three-dimensional dual potential procedure for rotational flows 10 p1329 N88-17942

Finite element methods of analysis for high speed viscous flows
[NASA-CR-182529] 11 p1483 N88-18852

Numerical analysis, computing and fundamental studies in fluid mechanics
[DE88-005343] 12 p1625 N88-19725

Mixing of viscous fluids: Behavior of microstructures and chaos
[DE88-006287] 13 p1766 N88-20566

Calculations of viscous flows with a multigrid method 13 p1769 N88-20580

Numerical analysis of three-dimensional viscous internal flows
[NASA-TM-100878] 14 p1861 N88-21116

Computational fluid dynamics drag prediction: Results from the Viscous Transonic Airfoil Workshop
[NASA-TM-100095] 15 p2014 N88-22009

Theoretical model and numerical solution for compressible viscous vortex cores 15 p2054 N88-22243

The numerical simulation of viscous flows with change of phase and chemical reaction
[DE88-003204] 15 p2062 N88-22292

Numerical study of unsteady viscous hypersonic blunt body flows with an impinging shock
[NASA-TM-100096] 15 p2122 N88-22650

High-resolution shock-capturing schemes for inviscid and viscous hypersonic flows
[NASA-TM-100097] 15 p2122 N88-22651

Coherent structures and dynamical systems 16 p2199 N88-23119

Numerical method for unsteady viscous-inviscid interaction to calculate buffeting
[ONERA-RSF-02/3617-AY-008-A] 17 p2309 N88-23949

Composite reduced Navier-Stokes procedures for flow problems with strong pressure interactions
[AD-A191127] 18 p2508 N88-24875

Theoretical investigation of 3-D shock wave-turbulent boundary layer interactions, part 6
[AD-A191546] 18 p2509 N88-24882

Axisymmetric viscid-inviscid interaction by a frozen vorticity approximation
[AD-A191743] 18 p2509 N88-24885

A variational finite element method for three-dimensional, steady, compressible, viscous flows
18 p2512 N88-24904

Development of a method of calculating unstable flows of cascades separated at the leading edge
[PB87-228714] 19 p2598 N88-25437

Improved numerical methods for turbulent viscous recirculating flows
[NASA-CR-180852] 19 p2599 N88-25445

Two-dimensional viscous flow computations of hypersonic scramjet nozzle flowfields at design and off-design conditions
[NASA-CR-182150] 19 p2603 N88-25459

Finite element analysis of incompressible viscous flow around multi-element aerofoils 19 p2635 N88-25634

Numerical calculation of supersonic flow by the PNS equations 19 p2636 N88-25636

Numerical simulation of viscous flows over transonic aircraft configurations 19 p2637 N88-25642

Numerical analysis of reconnection of vortex rings
20 p2782 N88-26500

Three-dimensional viscous flow computations of a circular jet in subsonic and supersonic cross flow
[NASA-CR-182153] 20 p2800 N88-26616

A study of flow separation in transonic flow using inviscid and viscous computational fluid dynamics (CFD) schemes
[NASA-CR-183119] 20 p2801 N88-26618

Spectral resolution of the Navier-Stokes equations in multi-domain curved complex geometries
[ONERA-NT-1987-2] 20 p2802 N88-26631

Nonaxisymmetric viscous lower branch modes in axisymmetric supersonic flows
[NASA-CR-181687] 21 p2891 N88-27164

Prediction of velocity and temperature profiles in thermally driven gravity currents applied to stratified thermal storage tanks
[DE88-004452] 21 p2946 N88-27496

A fast vortex code for computing 2-D flow in a box
[DE88-011732] 21 p2946 N88-27498

Numerical methods for incompressible viscous flows with engineering applications
[NASA-CR-183143] 21 p2948 N88-27508

Plasma behavior in the boundary layer near a railgun surface
[DE88-008889] 21 p3017 N88-27909

Field methods for computing high Reynolds number viscous flow
[FFA-TN-1988-01] 22 p3039 N88-28046

Numerical computation of space shuttle orbiter flow field
[NASA-CR-183193] 22 p3040 N88-28048

Boundary layer manipulation 23 p3170 N88-28877

Calculation of aerodynamic characteristics of airplane configurations at high angles of attack
[NASA-CR-4182] 23 p3172 N88-28891

A mapping of the viscous flow behavior in a controlled diffusion compressor cascade using laser Doppler velocimetry and preliminary evaluation of codes for the prediction of stall
[AD-A194490] 23 p3211 N88-29112

Direct-solution techniques for viscous flows and their control
[AD-A194775] 23 p3211 N88-29114

European research program on viscous flows
[DFVLR-AVA-IB-227-87-A-15] 23 p3214 N88-29129

Adaptive mesh generation for viscous flows using Delaunay triangulation
[NASA-CR-181699] 24 p3316 N88-29749

The viscous flow on surfaces with streamline riblets
[ESA-TT-1081] 24 p3370 N88-30067

Numerical simulation of unsteady incompressible viscous flows in generalized coordinate systems
[NASA-TM-101016] 24 p3373 N88-30085

VISCOUS FLUIDS

Effect of dissipation on propagation of spherical detonation shock wave 02 p0159 N88-10998

Locating parallel numerical tasks in the solution of viscous fluid flows
[DE87-013510] 02 p0189 N88-11064

Mechanical and flow excited vibrations of elastic plates and cylindrical shells in dense fluids
03 p0316 N88-11996

Numerical simulation of the interaction of vortex rings in viscous fluid 03 p0318 N88-12008

Dispersion equation for plane capillary-gravity wave on free surface of viscous incompressible fluid
04 p0459 N88-12842

Theoretical studies of multicomponent mixtures: Phase equilibrium and transport
[DE88-002717] 07 p0831 N88-15040

Properties of molecular solids and fluids at high pressure and temperature
[DE88-004195] 13 p1738 N88-20391

Implicit finite-difference simulation of an internal flow in a nozzle: An example of a physical application on a hypercube
[AD-A192475] 21 p2942 N88-27472

Heat transport in a parabolic tube of circular cross-section
[LRT-WE-9-FB-2(1988)] 22 p3078 N88-28274

Preliminary investigation of flow modeling during solid propellant processing
[AD-A196168] 24 p3357 N88-29987

Approximation of viscoelastic stresses from Newtonian turbulent kinematics
[AD-A194317] 24 p3371 N88-30077

VISIBILITY

NT LOW VISIBILITY

A preliminary taxonomy of visible surface algorithms
[DE87-013559] 02 p0220 N88-11386

Handling qualities criterion for very low visibility rotorcraft 03 p0263 N88-11654

ZEUS: A knowledge-based expert system that assists in predicting visibility at airbases
[AD-A184197] 05 p0626 N88-13829

Aerosol optical depth and ratios of diffuse-sky to total solar irradiance measured from aircraft following the eruption of El Chichon
[PB88-100789] 07 p0878 N88-15326

Visual evoked potentials
[AD-A187942] 11 p1519 N88-19071

The visioceilometer and its tactical applications
[AD-A188216] 12 p1647 N88-19866

Influence of hydrometeorological factors on visibility of objects detected by radar 13 p1790 N88-20707

Climatological data of the Netherlands lightvessels over the period 1949-1980 --- North Sea
[KNMI-WR-87-9] 14 p1947 N88-21613

VISIBLE INFRARED SPIN SCAN RADIOMETER

VISSR line number monitoring system
17 p2351 N88-24008

VISIBLE RADIATION

U LIGHT (VISIBLE RADIATION)

VISIBLE SPECTRUM

Visible free electron laser oscillator
[AD-A183871] 01 p0051 N88-10324

Spectrograms of the visible region in the JT-60 tokamak (wavelength range from 2210 A to 5250 A)
[DE87-753002] 02 p0240 N88-11513

An advanced visible-UV spectrometer for atmospheric composition measurements 08 p1029 N88-16231

Laser raman studies related to liquid propellants: Structural characteristics inferred from the nitrate anion spectra
[AD-A188462] 12 p1612 N88-19641

Synchronous measurements of effective photon path length in visible and near-IR spectral regions in real cloud systems 13 p1790 N88-20706

Global solar oscillations observed in the visible to near infrared continuum 13 p1858 N88-21110

On the interpretation of the 3 micron emission feature in the spectrum of Comet Halley: Abundances in Comet Halley and in interstellar matter
14 p2002 N88-21935

Comet P/Halley: Visual magnitude estimates and gas production 14 p2007 N88-21968

Spectrophotometric observations of Comet Halley
14 p2007 N88-21972

Laboratory amorphous carbon: A possible analog of cometary dust 14 p2009 N88-21981

VISION

NT BINOCULAR VISION
NT COLOR VISION
NT MONOCULAR VISION
NT NIGHT VISION
NT STEREOSCOPIC VISION

Vision of details in space and time
[B8711402] 06 p0753 N88-14624

Function-dependent plasticity in the nervous system
07 p0886 N88-15377

A directed method for locating the focus of expansion
[AD-A185840] 07 p0906 N88-15491

Solid modelling for the manipulative robot arm (power) and adaptive vision control for space station missions
08 p1061 N88-16409

A-scan ultrasound measurement of ocular changes during accommodation
[AD-A186818] 09 p1198 N88-17181

Image chunking: Defining spatial building blocks for scene analysis
[AD-A187072] 09 p1200 N88-17191

The relationship between vision carrier-to-noise ratio and picture signal-to-noise ratio in a System I television receiver
[BBC-RD-1987/23] 10 p1318 N88-17877

Hierachical object recognition using libraries of parameterized model sub-parts
[AD-A187476] 10 p1396 N88-18322

Computerised measurement of human horizontal smooth pursuit eye movements
13 p1811 N88-20819

Implementation of a visual servoing system for evaluation of robotic refueling applications
[AD-A189676] 14 p1954 N88-21645

A probabilistic approach to low-level vision
[AD-A189041] 15 p2107 N88-22553

Finding texture boundaries in images
[AD-A190554] 15 p2117 N88-22609

ROVER: A prototype active vision system
[AD-A189246] 15 p2133 N88-22722

Dissecting the visual and auditory pathways by means of the two-input technique 21 p2978 N88-27690

A study of sources in the human brain associated with stereopsis 21 p2979 N88-27695

Relation between VEP and visual function in lesions of the optic nerve and visual pathway
21 p2983 N88-27718

Vision research. A national plan: 1983-1987, 1987 evaluation and update
[PB88-192604] 21 p2985 N88-27726

A model for visual attention
[AD-A193061] 21 p2991 N88-27744

Distributed algorithms for probabilistic solution of computational vision problems
[AD-A193150] 21 p2997 N88-27773

Human performance and acute hypoxia, chapter 12
[AD-A192604] 23 p3238 N88-29270

Vision and visual protection in fast jet aircraft
23 p3241 N88-29292

Vision through aircraft transparencies
23 p3242 N88-29294

VISORS

Vision through aircraft transparencies
23 p3242 N88-29294

VISUAL ACCOMMODATION

Target size and luminance effects on accommodation and vergence
[AD-A185861] 08 p1051 N88-16343

Night Vision: Current Research and Future Directions, symposium proceedings
[PB88-132006] 11 p1550 N88-19274

VISUAL ACUITY

Eyesight trainer for pilots 03 p0355 N88-12239

The accommodative status in the dark of US Navy fighter pilots
[AD-A188188] 10 p1370 N88-18186

Laser flash effects on chromatic discrimination in monkeys
[AD-A187703] 11 p1517 N88-19061

Visual contrast sensitivity functions obtained from untrained observers using tracking and staircase procedures
[AD-A187715] 11 p1522 N88-19089

Measuring functional feasibility of human visual system 12 p1665 N88-19963

Laboratory equipment update
[AD-A189781] 15 p2102 N88-22522

Microesotropia patients performa well as military jet pilots 21 p2925 N88-27363

A model for visual attention
[AD-A193061] 21 p2991 N88-27744

A field study on soft contact lens wear in USAF military transport aircraft
[AD-A195962] 24 p3407 N88-30285

Functional assessment of laser irradiation
[AD-A195735] 24 p3408 N88-30287

VISUAL AIDS

Simulator evaluation of lineup visual landing aids for night carrier landing
[AD-A191212] 18 p2468 N88-24648

VISUAL DISCRIMINATION

Masking effects of fine and coarse grain pictorial noise
[IZF-1985-21] 01 p0076 N88-10485

Modulation transfer function --- SPOT
03 p0341 N88-12153

Latency differences and effects of selective attention to gratings in the central and right visual fields. 2
[DE87-014730] 04 p0473 N88-12918

Visual evoked responses to sinusoidal gratings presented in central and right visual fields. 1
[DE87-014731] 04 p0473 N88-12919

Visual attention effects on discrimination of line orientation and line arrangement
[AD-A187013] 09 p1200 N88-17180

Laser flash effects on chromatic discrimination in monkeys
[AD-A187703] 11 p1517 N88-19061

Visual contrast sensitivity functions obtained from untrained observers using tracking and staircase procedures
[AD-A187715] 11 p1522 N88-19089
Measuring functional feasibility of human visual system 12 p1665 N88-19983
Laboratory equipment update
[AD-A189781] 15 p2102 N88-22522
Perception of motion in statistically-defined displays
[AD-A193076] 21 p2991 N88-27745
Limits of pattern discrimination in human vision
[AD-A193449] 23 p3239 N88-29273
Functional assessment of laser irradiation
[AD-A195735] 24 p3408 N88-30287

VISUAL DISPLAYS
U DISPLAY DEVICES

VISUAL FIELDS
Latency differences and effects of selective attention to gratings in the central and right visual fields: 2
[DE87-014730] 04 p0473 N88-12918
Visual evoked responses to sinusoidal gratings presented in central and right visual fields: 1
[DE87-014731] 04 p0473 N88-12919
Target size and luminance effects on accommodation and vergence
[AD-A185861] 08 p1051 N88-16343
Influence of moving visual environment on saccadic eye movements and fixation 21 p2926 N88-27368

VISUAL FLIGHT
The role of adaptive supplemental visual cuing in flight simulation
[AD-A185932] 07 p0822 N88-14992
Task listing: Visually assisted and visually dependent tasks for fighter aircraft
[AD-A191041] 16 p2244 N88-23404

VISUAL FLIGHT RULES
Estimates of potential increases in airport capacity through ATC (Air Traffic Control) system improvements in the airport and terminal areas
[AD-A188533] 12 p1578 N88-19444

VISUAL OBSERVATION
Investigation of leaks in fiberglass-reinforced pressure vessels by direct observation of hollow fibers in glass cloth
[DE88-006936] 19 p2609 N88-25485

VISUAL PERCEPTION
NT SPACE PERCEPTION
NT VISUAL DISCRIMINATION
Computer-controlled testing of visual-spatial ability
[AD-A183971] 03 p0357 N88-12249
Effects of divided attention on identity and semantic priming
[AD-A184289] 03 p0357 N88-12250
An approach to object recognition: Aligning pictorial descriptions
[AD-A184462] 04 p0482 N88-12972
Learning a color algorithm from examples
[AD-A184385] 05 p0632 N88-13862
Interaction of different modules in depth perception: Stereo and shading
[AD-A185607] 06 p0759 N88-14655
The role of adaptive supplemental visual cuing in flight simulation
[AD-A185932] 07 p0822 N88-14992
Local versus global minima in visual pattern completion
[PB87-234803] 07 p0897 N88-15439
Image understanding by Image-Seeking Adaptive Networks (ISAN)
[AD-A186214] 07 p0906 N88-15492
Target size and luminance effects on accommodation and vergence
[AD-A185861] 08 p1051 N88-16343
Research on visual information processing with special reference to oculomotor behavior in the areas of exploration, recognition and search
[AD-A186598] 08 p1051 N88-16346
Considerations concerning the basic bandwidth reduction of high definition television systems (HDTV) component signals, based on psychophysiological properties of the eye
[IRT-B-83/87] 09 p1153 N88-16909
GAVID and ACQUIR, two Operations-Research (OR) models for visual detection
[FEL-1985-72] 09 p1200 N88-17194
Development of Moire machine vision
09 p1212 N88-17264
Perception and control of simulated self motion
[AD-A187444] 10 p1372 N88-18188
Measurement and effects of transport delays in a state-of-the-art F-16C flight simulator
[AD-A187367] 11 p1441 N88-18599
Visual contrast sensitivity functions obtained from untrained observers using tracking and staircase procedures
[AD-A187715] 11 p1522 N88-19089
Space vehicle approach velocity judgments under simulated visual space conditions
[NASA-TM-89437] 11 p1523 N88-19094
Night Vision: Current Research and Future Directions, symposium proceedings
[PB88-132006] 11 p1550 N88-19274
The visiocellometer and its tactical applications
[AD-A188216] 12 p1647 N88-19866
Neck receptor stimulation in 0 and 1 g
12 p1658 N88-19938
Mechanisms of early light and dark adaptations
12 p1663 N88-19972
Visual recognition training: Effectiveness of computer graphics
[AD-A188302] 12 p1669 N88-19997
Human efficiency for visual detection of targets on CRT displays using a two-level multiple channel time history format
[AD-A188419] 12 p1670 N88-20001
Computerised measurement of human horizontal smooth pursuit eye movements
13 p1811 N88-20819
Identification of visual evoked response parameters sensitive to pilot mental state
[NASA-CR-4140] 13 p1811 N88-20822
Mathematic modeling of visual perception problems
[INPE-4355-PRE/1186] 13 p1823 N88-20897
A comparison of visual evoked potential and behavioral measures of flashblindness in humans
[AD-A189757] 15 p2101 N88-22519
An evaluation of the effects of high visual taskload on the separate behaviors involved in complex monitoring performance
[AD-A190641] 15 p2105 N88-22538
Dynamic properties of human brightness perception
[ETN-88-92243] 16 p2238 N88-23366
Designing for design effectiveness of complex avionics systems 17 p2305 N88-23788
Image management research
17 p2380 N88-24150
Visual information processing in the perception of features and objects
[AD-A192026] 18 p2552 N88-25148
Shape from shading, occlusion and texture
[AD-A184840] 18 p2571 N88-25269
Biorhythms of binocular vision
20 p2830 N88-26788
The interaction of sensory and perceptual variables: Spatial, temporal and orientation response to figure and ground
[AD-A192897] 20 p2832 N88-26798
A new approach to machine-based perception of monocular images
[DE88-002418] 20 p2853 N88-26942
Three-dimensional scene analysis using stero based imaging
[AD-A193120] 21 p2894 N88-27178
Microesotropia patients performa well as military jet pilots 21 p2925 N88-27363
Assessments of maneuverability with the TeleOperated Vehicle (TOV)
[AD-A191584] 21 p2993 N88-27751
Models for motion perception
22 p3133 N88-28629
Natural object categorization
[AD-A194103] 22 p3139 N88-28662
Limits of pattern discrimination in human vision
[AD-A193449] 23 p3239 N88-29273
Visual motion perception and visual attentive processes
[AD-A193640] 23 p3241 N88-29288
Transformations of short-term visual memory
[AD-A193873] 23 p3241 N88-29290
Visual Effects in the High Performance Aircraft Cockpit
[AGARD-LS-156] 23 p3241 N88-29291
Visual related accidents/incidents
23 p3242 N88-29293
Multilevel computational theory of stereoscopic visual image processing
[AD-A195331] 24 p3408 N88-30288
Haptic exploration in humans and machines: Attribute integration and machine recognition/implementation
[AD-A193692] 24 p3410 N88-30299
Space station proximity operations windows: Human factors design guidelines
[NASA-TM-88233] 24 p3410 N98-30301
Dynamical systems and motion vision
[AD-A195932] 24 p3422 N88-30366

VISUAL PHOTOMETRY
Some ground-based optical observations of Comet Halley during its post-perihelion passage
08 p1033 N88-16259

VISUAL SIGNALS
Research on visual information processing with special reference to oculomotor behavior in the areas of exploration, recognition and search
[AD-A186598] 08 p1051 N88-16346
Helicopter external vision requirements and visual display characteristics: A report/bibliography, revision A
[AD-A187075] 10 p1276 N88-17641
A pyrotechnic delay ignition system for a submarine launched marine signal
[MRL-R-1079] 13 p1754 N88-20487
Analysis procedures and subjective flight results of a simulator validation and cue fidelity experiment
[NASA-TM-88270] 18 p2465 N88-24634

VISUAL STIMULI
Target size and luminance effects on accommodation and vergence
[AD-A185861] 08 p1051 N88-16343
Role of optokinetic stimulation in vesibulospinal reflexes 10 p1360 N88-18131
Visual contrast sensitivity functions obtained from untrained observers using tracking and staircase procedures
[AD-A187715] 11 p1522 N88-19089
Computerised measurement of human horizontal smooth pursuit eye movements
13 p1811 N88-20819
A systems engineering based methodology for analyzing human electrocortical responses
[AD-A190809] 18 p2550 N88-25135
Influence of moving visual environment on saccadic eye movements and fixation 21 p2926 N88-27368
Perception of motion in statistically-defined displays
[AD-A193076] 21 p2991 N88-27745
Human auditory and visual continuous evoked potentials 23 p3238 N88-29269
Visual motion perception and visual attentive processes
[AD-A193640] 23 p3241 N88-29288

VISUAL TRACKING
U OPTICAL TRACKING

VISUALIZATION OF FLOW
U FLOW VISUALIZATION

VITAMINS
NT NICOTINIC ACID

VITERBI DECODERS
The design plan of a VLSI single chip (255, 223) Reed-Solomon decoder 04 p0435 N88-12697
A simplified procedure for correcting both errors and erasures of a Reed-Solomon code using the Euclidean algorithm 04 p0435 N88-12698

VITREOUS MATERIALS
A-scan ultrasound measurement of ocular changes during accommodation
[AD-A186818] 09 p1198 N88-17181

VITRIFICATION
LFCM (Liquid-Fed Ceramic Melter) vitrification technology
[DE88-003441] 09 p1149 N88-16887
Remarks on solid state amorphizing transformations
[DE88-006452] 15 p2145 N88-22803
Influence of fiber reinforcement on the vitreous transition temperature of M 10 matrix composites
[ONERA-RT-44/7086-M] 17 p2316 N88-23835

VLASOV EQUATIONS
New directions in Vlasov plasma turbulence and anomalous transport
[DE87-014425] 02 p0238 N88-11500
Wave energy flow conservation for propagation in inhomogeneous Vlasov-Maxwell equilibria
[DE88-006705] 15 p2055 N88-22251

VLBI
U VERY LONG BASE INTERFEROMETRY

VLSI
U VERY LARGE SCALE INTEGRATION

VOCODERS
The design and performance of a real-time self excited vocoder 19 p2653 N88-25753
Development of an 8000 bps voice codec for AvSat
19 p2653 N88-25755

VOICE
Voice-stress measure of mental workload
16 p2240 N88-23381

VOICE COMMUNICATION
NT TELEPHONY
Integrated voice and visual systems research topics
[NASA-CR-177417] 03 p0356 N88-12246
Voice technology using personal computers
[AD-A186743] 09 p1218 N88-17300
Evaluating the performance of the LPC (Linear Predictive Coding) 2.4 kbps (kilobits per second) processor with bit errors using a sentence verification task
[AD-A188573] 12 p1620 N88-19686
Time-frequency representations for speech signals
[AD-A188661] 18 p2498 N88-24819

NASA's mobile satellite development program
19 p2643 N88-25682
Mobile satellite service for Canada
19 p2643 N88-25683
A satellite system for land-mobile communications in Europe 19 p2643 N88-25685
Developing a global aeronautical satellite system
19 p2644 N88-25687
World-wide aeronautical satellite communications
19 p2644 N88-25688
Satellite communications experiment for the Ontario air ambulance service 19 p2646 N88-25705
ACSB: A minimum performance assessment
19 p2649 N88-25731
A framework for implementing data services in multi-service mobile satellite systems
19 p2650 N88-25733
Speech coding at 4800 bps for mobile satellite communications 19 p2652 N88-25749
A 4.8 kbps code-excited linear predictive coder
19 p2652 N88-25750
Real-time speech encoding based on Code-Excited Linear Prediction (CELP) 19 p2653 N88-25751
Sinusoidal transform coding 19 p2653 N88-25752
The design and performance of a real-time self excited vocoder 19 p2653 N88-25753
Development of an 8000 bps voice codec for AvSat
19 p2653 N88-25755
Error performance of voice band data signals with an overloaded delta modulator
[FEL-1987-05] 20 p2792 N88-26562
A cockpit natural language study - selected transcripts
[AD-A192972] 20 p2834 N88-26808
Cockpit and cabin crew coordination
[AD-A192445] 21 p2993 N88-27752
A cockpit natural language study: Vocabulary and grammar analyses
[AD-A193289] 21 p2993 N88-27753
An overview of technology for spoken interaction with machines
[AD-A194153] 23 p3202 N88-29058

VOICE CONTROL
Integrated voice and visual systems research topics
[NASA-CR-177417] 03 p0356 N88-12246
Controlling robots with spoken commands
[DE88-000537] 04 p0452 N88-12801
Digital signal processing algorithms for automatic voice recognition 06 p0793 N88-14862
Voice/natural language interfacing for robotic control
[AD-A187765] 11 p1494 N88-18917

VOICE DATA PROCESSING
NT CEPSTRAL ANALYSIS
Activities report of the Department of Systems and Communications
[ENST-87D004] 16 p2189 N88-23053
Algorithms and architectures for acoustic phonetical detection of continuous speech
[ENST-87E016] 16 p2189 N88-23054
Experiments in isolated digit recognition using the multilayer perceptron
[RSRE-MEMO-4073] 17 p2333 N88-23927

VOICE OF AMERICA
Complementary satellite sound broadcasting systems: A NASA assessment for the Voice of America
[NASA-TM-100300] 10 p1321 N88-17899

VOID RATIO
Investigation of the inter-relationship between base pavement stiffness and asphalt overlay compaction
[DOT/FAA/ES-88/1] 14 p1869 N88-21170

VOIDS
The influence of microvoids on the electrical strength of glass fiber reinforced epoxy resins
[ETN-87-90443] 01 p0030 N88-10189
Effects of cure pressure on resin flow, voids, and mechanical properties
[AD-A184267] 03 p0295 N88-11853
Plastic strain localization between voids in shear deformation fields 04 p0427 N88-12648
A comparison of film-based tomography and computed tomography for advanced ceramic materials
[DE88-003114] 07 p0837 N88-15079
Evolution of radiation-induced voids and dislocations at low temperature
[DE88-700350] 07 p0939 N88-15704
Void formation in solidification
[DE88-003895] 11 p1452 N88-18650
A simulation of void lining during ductile fracture
[AD-A188404] 12 p1635 N88-19792
Material instabilities in solids
[AD-A189525] 13 p1738 N88-20398
Flaw characterization in structural ceramics using scanning laser acoustic microscopy
15 p2062 N88-22415
Vacancy ordering in the basal plane of YBa2Cu3O(sub)z
[DE88-004572] 18 p2583 N88-25348
Material void opening computation using particle method
[DE88-010950] 19 p2680 N88-25936
Mass flow rate influence on void fraction of two-phase helium flow
[DE88-702456] 21 p2945 N88-27495

VOLATILITY
Cost savings possible with Air Force conversion to JP-8 as its primary fuel
[AD-A183784] 01 p0030 N88-10192
Analysis of laser extracted volatiles in carbonaceous chondrites 06 p0793 N88-14861
Evaluation and prediction of Henry's law constants and aqueous solubilities for solvents and hydrocarbon fuel components. Volume 1: Technical discussion
[AD-A188571] 12 p1613 N88-19643
Martian geomorphology and its relation to subsurface volatiles
[NASA-CR-182428] 12 p1711 N88-20237
A mass spectrometer evolved gas analysis experiment for in-situ analysis of cometary dust volatiles
13 p1854 N88-21097
The effect of weathering on octane quality for winter-grade and summer-grade gasolines
[AD-A190640] 16 p2163 N88-23012
National ambient Volatile Organic Compounds (VOCs) data base update, documentation
[PB88-195631] 21 p2971 N88-27646

VOLATILIZATION
U VAPORIZING

VOLCANICS
U VOLCANOLOGY

VOLCANOES
NT MARS VOLCANOES
Solar Energy Meteorological Research and Training Site, Alaska
[DE87-013706] 01 p0069 N88-10440
Gravity and fault structures, Long Valley Caldera, California
[DE87-014117] 02 p0197 N88-11229
Volcanic eruption detection with TOMS
05 p0618 N88-13793
Analysis of SO2 signals in SBUV/TOMS data
05 p0618 N88-13794
Comparison of ground based and TOMS measurements of SO2 from volcanic emissions
05 p0618 N88-13795
TOMS and the NOAA/FAA volcano support plan
05 p0618 N88-13796
Use of satellite data in volcano monitoring
05 p0618 N88-13797
Interpretation of our present terrestrial climatic record
[DE88-000223] 06 p0744 N88-14573
Greatest volcanic eruptions in world during 17th-18th centuries and weather anomalies in Eurasian middle latitudes 08 p1012 N88-16134
Some evidence for a Northern Hemispheric extratropic trigger mechanism of ENSO events
22 p3123 N88-28558
Mars: Near-infrared comparative spectroscopy during the 1986 opposition 23 p3301 N88-29658
Early cratering rates and the nature of the Martian cratered uplands 23 p3306 N88-29694

VOLCANOLOGY
Volcanic eruption detection with TOMS
05 p0618 N88-13793
Mid-tertiary volcano-tectonic development of the Southwestern Cordillera of North America
06 p0797 N88-14879
Kinetics of thermochemical gas-solid reactions important in the Venus sulfur cycle
[NASA-CR-182963] 19 p2742 N88-26280
The rate of volcanism on Venus
[NASA-CR-183039] 19 p2742 N88-26281
SPOT imagery as an aid to understanding volcanism and tectonics: Examples from the Chilean Andes and the Tibetan Plateau 22 p3103 N88-28427
A review: Quantitative models for lava flows on Mars
23 p3301 N88-29656
Progress in determining the thickness and distribution of volcanic materials on Mars 23 p3302 N88-29670
Variability in spectral signatures of terrestrial volcanic rocks and implications for volcanology on Mars
23 p3303 N88-29672
The tectonic setting of Archean anorthosites
24 p3397 N88-30231
Physical processes in the growth of the continental crust 24 p3398 N88-30240
Volcanic contribution to crustal growth in the Central Andes: A new estimate and a discussion of uncertainties
24 p3401 N88-30255
NASA MEVTV Program Working Group Meeting: Volcanism on Mars
[NASA-CR-183074] 24 p3442 N88-30487
Eruptive viscosity and volcano morphology
24 p3442 N88-30488
Faulting and its relation to volcanism: Mars western equatorial region 24 p3443 N88-30489
Mars: Volcanism in the Valles Marineris overlooked
24 p3443 N88-30491
The Martian highland paterae: Evidence for explosive volcanism on Mars 24 p3443 N88-30492

VOLT-AMPERE CHARACTERISTICS
Analysis of the voltage-current characteristics of metal-isolator-tin-telluride sandwich structures
[ETN-88-91089] 09 p1256 N88-17528
Solid-state voltage standard performance and design guidelines
[PB88-123757] 10 p1322 N88-17905
Limiting efficiency of a thermionic diode
[DE88-700598] 11 p1479 N88-18830

VOLTAGE
U ELECTRIC POTENTIAL

VOLTAGE AMPLIFIERS
Arc lamp power supply using a voltage multiplier
[NASA-CASE-LAR-13202-1] 17 p2335 N88-23942

VOLTAGE BREAKDOWN
U ELECTRICAL FAULTS

VOLTAGE CONTROLLED OSCILLATORS
Spacecraft redesign to reduce microphonic response of a VCO component 11 p1499 N88-18955
Radio Frequency (RF) strain monitor
[NASA-CASE-LAR-13705-1] 18 p2530 N88-25011

VOLTAGE CONVERTERS (AC TO AC)
Voltage directive drive with claw pole motor and control without rotor position indicator
[ETN-88-93120] 24 p3366 N88-30047

VOLTAGE GENERATORS
Operation of the TEMPO machine
[DE87-011285] 01 p0038 N88-10241

VOLTAGE MEASUREMENT
U ELECTRICAL MEASUREMENT

VOLTAGE REGULATORS
Operation of multistage power supplies for electron beam welding installations 03 p0288 N88-11800

VOLTAGE VARIATION INDICATORS
U VOLTMETERS

VOLTERRA EQUATIONS
Experimental identification of nonlinear structural models
[DE88-001795] 09 p1184 N88-17094
New way to solve Volterra equations of the second kind
[PB88-148820] 13 p1828 N88-20931
Product-integrals and counting processes
[CWI-MS-R8707] 14 p1965 N88-21727
Computational sciences
[AD-A190826] 18 p2564 N88-25226
Numerical solution of a system of random Volterra integral equations. 1: Successive approximation method
18 p2564 N88-25227
Numerical solution to a system of random Volterra integral equations 18 p2565 N88-25230
Numerical solution of linear integral equations with random forcing terms 18 p2565 N88-25237

VOLTMETERS
Optical power line voltage and current measurement systems. Volume 1: Limits to the precision of electro-optic and magneto-optic sensors
[DE87-014556] 02 p0175 N88-11082

VOLUME
Evaluation of spare room in cerebrospinal system using noninvasive methods 10 p1361 N88-18137
Estimates of masses, volumes and densities of short-period comet nuclei 14 p2004 N88-21950
Mining volume measurement system
[NASA-CASE-LAR-13519-1] 17 p2342 N88-23963
A maximum entropy solution for the underdetermined electromagnetic field within a volume
[DE88-007020] 20 p2790 N88-26550
Progress in determining the thickness and distribution of volcanic materials on Mars 23 p3302 N88-29670

VOLUMETRIC ANALYSIS
On-line measurement of heat of combustion
[NASA-CR-183076] 19 p2738 N88-26255
Volumetric measurement of vorticity vectors by optical probe
[AD-A195997] 24 p3369 N88-30061

VOMITING
Gastric emptying assessment by echography after a stress (rotating chair) 12 p1661 N88-19955
Motion sickness: A study of its effects on human physiology
[AD-A188821] 12 p1667 N88-19995
Emetic mechanism in acute radiation sickness
[AD-A194102] 23 p3238 N88-29267

VON KARMAN EQUATION
Dynamics of the von Karman vortex street
03 p0316 N88-11998
Application of the Von Karman equation to the bifurcation theory
[NOTA-INTERNA-891] 05 p0642 N88-13927

Further study of relation of von Karman equation for elastic large deflection problem and Schrodinger equation for quantum eigenvalues problem
14 p1899 N88-21341

VON MISES THEORY
U STRESS FUNCTIONS

VORTEX ALLEVIATION
Computation of the turbulent boundary layer downstream of vortex generators
[AD-A191544] 18 p2508 N88-24881

VORTEX BREAKDOWN
Experimental investigation in a wind tunnel of the stability and vorticity of the vortex breakdown phenomenon above delta wings, using the ultrasonic laser method
[DFVLR-FB-87-06] 01 p0003 N88-10017
A note on the instability of a vortex sheet leaving a semi-infinite plate
[DFVLR-FB-87-16] 01 p0004 N88-10019
Breakdown of steady and unsteady interacting boundary layers
[NLR-MP-86047-U] 01 p0045 N88-10284
Analysis of the breakdown of the Antarctic circumpolar vortex using TOMS ozone data
05 p0615 N88-13779
A theory for the core flow of leading-edge vortices
07 p0810 N88-14935
Airfoil large eddy breakup devices for turbulent drag reduction 07 p0814 N88-14956
Control of vortical separation on conical bodies
10 p1267 N88-17590
Burst vortex/boundary layer interaction
[NASA-CR-182510] 10 p1268 N88-17583
Investigation on the movement of vortex burst position with dynamically changing angle of attack for a schematic deltawing in a watertunnel with correlation to similar studies in windtunnel 16 p2204 N88-23152
Rotation symmetric vortex in axiparallel flow
[ETN-88-92364] 21 p2948 N88-27512
Vortex flows 23 p3170 N88-28875

VORTEX COLUMNS
U VORTICES

VORTEX DISTURBANCES
U VORTICES

VORTEX FILAMENTS
Vortex filament simulation for the crosslinking rings
20 p2782 N88-26501

VORTEX FLAPS
On the pairing process in an excited, plane, turbulent mixing layer
[AD-A186355] 07 p0850 N88-15157

VORTEX FLOW
U VORTICES

VORTEX GENERATION
U VORTEX GENERATORS

VORTEX GENERATORS
The flow downstream of screens and the formation of longitudinal vortices in the stagnation point flow
[DFVLR-FB-87-27] 09 p1162 N88-16963
Burst vortex/boundary layer interaction
[NASA-CR-182510] 10 p1268 N88-17583
Transonic Navier-Stokes computations of strake-generated vortex interactions for a fighter-like configuration
[NASA-TM-100009] 15 p2014 N88-22010
Experimental studies of vortex flows
[NASA-CR-182874] 16 p2207 N88-23171
Computation of the turbulent boundary layer downstream of vortex generators
[AD-A191544] 18 p2508 N88-24881

VORTEX RINGS
The Proceedings of the Symposium on Mechanics for Space Flight
[ISAS-SP-5] 03 p0317 N88-12006
Experimental study of interacting vortex rings
03 p0318 N88-12007
Numerical simulation of the interaction of vortex rings in viscous fluid 03 p0318 N88-12008
Theory of dividing vortons 03 p0318 N88-12009
Numerical analysis of reconnection of vortex rings
20 p2782 N88-26500
Vortex filament simulation for the crosslinking rings
20 p2782 N88-26501
Crosslinking of two vortex rings side by side
20 p2782 N88-26502

VORTEX SHEDDING
A note on the instability of a vortex sheet leaving a semi-infinite plate
[DFVLR-FB-87-16] 01 p0004 N88-10019
The phenomenology of Karman vortex streets via sound in oscillatory flow
[MPIS-MITT-84-1987] 02 p0122 N88-10775
Vortex interaction with a leading-edge of finite thickness
[NASA-CR-182341] 05 p0543 N88-13307
Longitudinal mode combustion instabilities in air breathing engines 06 p0680 N88-14166
A study of rotor broadband noise mechanisms and helicopter tail rotor noise 06 p0777 N88-14766
Wall turbulence control 07 p0812 N88-14943
Meteosat tracks Karman vortex streets in the atmosphere 09 p1128 N88-16770
A numerical study of unsteady two-dimensional subsonic compressible base flow 10 p1327 N88-17931
On the prediction of highly vortical flows using an Euler equation model, part 2
[AD-A190245] 15 p2064 N88-22305
Bodies in unsteady flow
[AD-A190416] 15 p2064 N88-22308
Experiments to investigate the vortices shed from a submarine-like body of revolution
16 p2205 N88-23156
Stall flutter analysis of propfans
16 p2221 N88-23256
Theory of sound production by vortex-airfoil interaction
[AD-A193386] 21 p3012 N88-27875

VORTEX SHEETS
A note on the instability of a vortex sheet leaving a semi-infinite plate
[DFVLR-FB-87-16] 01 p0004 N88-10019
Coronal heating by means of helical magnetohydrodynamic turbulence
[AD-A187084] 10 p1410 N88-18413
Computational technique for compressible vortex flows using the integral equation solution
[NASA-CR-182695] 13 p1718 N88-20271
A multilifting line method and its application in design and analysis of nonplanar wing configurations
[DFVLR-FB-87-51] 16 p2155 N88-22860
Experimental study of vortex sheets in plane flow
16 p2203 N88-23142
A twin-mirrored galvanometer laser light sheet generator
[NASA-TM-100587] 19 p2674 N88-25901
Vortices on the world sheet and string's critical dynamics
[DE88-702116] 21 p3026 N88-27961
A study of the vortex sheet method for solving the Prandtl boundary layer equations
[DE88-011346] 22 p3074 N88-28249

VORTEX STREETS
NT KARMAN VORTEX STREET

VORTEX TUBES
U VORTICES

VORTEX-BLADE INTERACTION
U BLADE-VORTEX INTERACTION

VORTICES
NT WING TIP VORTICES
Mean flow structure of a turbulent junction vortex
[PB87-206231] 01 p0047 N88-10301
Vortex dynamics and transport to the wall in a crossed-field plasma sheath
[DE87-013286] 01 p0100 N88-10857
Vortex/boundary-layer interactions: Data report, volume 1
[NASA-CR-181462] 02 p0121 N88-10768
Vortex/boundary-layer interactions: Data report, volume 2
[NASA-CR-181463] 02 p0122 N88-10769
Numerical simulation of Tollmien-Schlichting waves by use of a modified vortex particle-in-cell method
[IC-AERO-85-02] 02 p0171 N88-11079
On the onset of three-dimensionality and time-dependence in the Goertler vortex problem
[NASA-CR-178404] 03 p0260 N88-11636
Analysis of the motions and effects of hairpin vortices
03 p0316 N88-11997
The diffusion-convection vortex method for solving two-dimensional incompressible Navier-Stokes equation
03 p0317 N88-12001
Momentum transport and particle dynamics in turbulent shear flows 03 p0317 N88-12002
Theory of dividing vortons 03 p0318 N88-12009
Structural characteristics of dean vortices in a curved channel
[AD-A184724] 03 p0320 N88-12024
Unsteady flow about cambered plates
[AD-A184725] 03 p0320 N88-12025
Numerical prediction of propeller performance by vortex lattice method
[UTIAS-TN-265] 04 p0400 N88-12489
Activities at government research laboratories reported 04 p0403 N88-12503
Some asymptotic modes of transonic vortex flow
04 p0425 N88-12632
Optical instrumentation and study of gas-solid suspension flows
[DE88-000147] 04 p0442 N88-12744
Blowup for a nonlinear evolution equation and self-reproducing strained shear layers
04 p0444 N88-12755
Equilibria, lattices and chaotic dynamics of point vortices 04 p0444 N88-12758
Turbulent mixing in a rotating, stratified fluid
04 p0445 N88-12759
Intensive synoptic eddies and quasigeostrophic approximation 04 p0460 N88-12844
Dynamics of isolated intrathermocline eddy
04 p0460 N88-12845
Influence of secondary eddy currents on scattering of admixture in zonal flow 04 p0460 N88-12846
Mesoscale eddy dynamics by the method of point vortices 04 p0463 N88-12863
Measurement of velocity and vorticity fields in the wake of an airfoil in periodic pitching motion
[NASA-TP-2780] 04 p0487 N88-13002
Vortex formation over delta, double-delta and wave rider configurations at supersonic speeds
05 p0533 N88-13243
The off-design performance of hypersonic waveriders
05 p0533 N88-13244
Application of discrete vortex method to analysis of separated flow around aerofoils
05 p0537 N88-13268
Three-dimensional flow past a two-dimensional body
05 p0539 N88-13280
Vortex interaction with a leading-edge of finite thickness
[NASA-CR-182341] 05 p0543 N88-13307
Nonlinear lift control at high speed and high angle of attack using vortex flow technology
05 p0545 N88-13319
Vortical Flows Research Program of the Fluid Dynamics Research Branch
[NASA-TM-88337] 05 p0582 N88-13549
Isentropic analysis and interpretation: Operational applications to synoptic and mesoscale forecast problems
[AD-A184814] 05 p0626 N88-13830
The production of turbulence in boundary layers: The role of microscale coherent motions
[AD-A185568] 06 p0703 N88-14313
Study of evolution of Gulf Stream cyclinic eddy
06 p0727 N88-14473
Viscous vortex flows 07 p0810 N88-14934
A theory for the core flow of leading-edge vortices
07 p0810 N88-14935
Vortex dynamics 07 p0812 N88-14945
Flow in volutes and the influence on the flow in centrifugal compressors 07 p0851 N88-15160
Typhoon structural evolution
[AD-A186090] 07 p0879 N88-15333
Acta Aerodynamica Sinica (selected articles)
[AD-A185723] 08 p0949 N88-15757
Calculation of symmetric and asymmetric vortex seperation on cones and tangent ogives based on discrete vortex models
[NASA-CR-4122] 08 p0950 N88-15768
Direct and large eddy simulation of turbulence. Summary of the state of art 1987 08 p0987 N88-15977
Computer program for the calculation of the profile-vortices interactions (two dimensional inviscid incompressible flow with point singularities)
[ISL-R-124/86] 08 p0987 N88-15982
The effect of eddy distribution on momentum and heat transfer near the wall in turbulent pipe flow
[NASA-TM-100257] 08 p0988 N88-15984
Cavitation inception scale effects. 1: Nuclei distributions in natural waters. 2: Cavitation inception in a turbulent shear flow
[AD-A186553] 08 p0988 N88-15987
Interaction of a vortex pair with a free surface
[AD-A188619] 08 p0988 N88-15988
Active control of jet flowfields
[AD-A186736] 08 p0989 N88-15989
Turbulence structure during high wind
08 p1014 N88-16149
A jet in a crossflow
[NASA-CR-182469] 09 p1113 N88-16674
Unsteady behavior of three-dimensional vortices relevant to turbulent boundary layers
[AD-A186767] 09 p1161 N88-16958
Numerical and physical aspects of large eddy simulation of turbulent flows
[ETN-88-91611] 09 p1162 N88-16965
Coherent vortex structures in the wake of a stationary disk and of a disk excited to vibration
[ESA-TT-994] 09 p1163 N88-16968
Mechanism of change of vortex structure orientation in type-2 superconductors 09 p1239 N88-17425
Investigation of the influence of wind shear on the aerodynamic characteristics of aircraft using a vortex-lattice method 10 p1274 N88-17619
Secondary flow measurements with L2F-technique in centrifugal compressors 10 p1283 N88-17676
Investigation of non-symmetric jets in cross flow
10 p1327 N88-17932
Instability and transition in curved channel flow
10 p1328 N88-17938

An analysis of the motion and effects of hairpin vortices
[AD-A187261] 10 p1331 N88-17958

Flow patterns induced by vortices
[NAL-TR-932] 10 p1332 N88-17963

Experimental study of two-dimensional vortex patterns for impulsively started bodies in comparison with other configurations 11 p1435 N88-18562

Structure of shear flow turbulence and its control
[AD-A187909] 11 p1482 N88-18846

The effects of rotational flow, viscosity, thickness, and shape on transonic flutter dip phenomena
[NASA-TM-100811] 11 p1502 N88-18969

Numerical analysis, computing and fundamental studies in fluid mechanics
[DE88-005343] 12 p1625 N88-19725

Rotational flow of rarefied gas between two coaxial cylinders with slip conditions
[INPE-4277-PRE/1149] 12 p1627 N88-19738

The international vortex flow experiment: A test case for compressible Euler codes
[NLR-MP-86076-U] 13 p1717 N88-20267

Control of structure in turbulent flows: Bifurcating and blooming jets
[AD-A189607] 13 p1766 N88-20562

An experimental investigation of decelerating flow about two-dimensional cambered plates
[DE88-006596] 13 p1766 N88-20567

Very large vortex calculations in two dimensions
[DE88-005748] 13 p1770 N88-20587

Mushroom-shaped currents (eddy dipoles) under rotation and stratification conditions
13 p1784 N88-20678

Dynamics of synoptic ocean eddies
13 p1786 N88-20689

Phenomenological description of eddy registered in Gulf Stream 13 p1787 N88-20694

Vortex flow over a delta wing with apex flaps using laser flow visualisation
[BU-356] 14 p1862 N88-21121

Incompressible theory of interaction between moving bodies and vorticity field: Force on moving bodies by vorticity field 14 p1863 N88-21132

Discrete vortex analysis of unsteady flow about two-dimensional cambered plates
[DE88-006597] 14 p1909 N88-21407

Mean flow structure in the near wake of a turbulent junction vortex
[PB88-150115] 14 p1910 N88-21416

Interaction of a strong vortex with decaying turbulence
[DE88-007102] 14 p1911 N88-21420

Ocean eddies 14 p1938 N88-21566

Alfven waves in plasma with finite ion temperatures
14 p1972 N88-21769

Experimental investigation of a spanwise forced mixing layer
[AD-A190136] 15 p2013 N88-22007

Transonic Navier-Stokes computations of strake-generated vortex interactions for a fighter-like configuration
[NASA-TM-100009] 15 p2014 N88-22010

Pressure measurements of impinging jet with asymmetric nozzle
[NASA-CR-182759] 15 p2014 N88-22011

Numerical simulation of turbulent flames using vortex methods
[AD-A189813] 15 p2034 N88-22116

Investigation of combustion in large vortices
[AD-A190406] 15 p2035 N88-22121

Theoretical model and numerical solution for compressible viscous vortex cores
15 p2054 N88-22243

Vortices in long Josephson junctions
[AD-A190338] 15 p2059 N88-22279

On the prediction of highly vortical flows using an Euler equation model, part 2
[AD-A190245] 15 p2064 N88-22305

Cavitation inception in rectangular two-dimensional slots
[AD-A190677] 15 p2066 N88-22318

The effects of time-dependent winds and ocean eddies on ice motion in a marginal ice zone
[AD-A190105] 15 p2100 N88-22511

A numerical model of unsteady, subsonic aeroelastic behavior
[NASA-TM-101126] 16 p2156 N88-22862

Stochastic estimation of conditional eddies in turbulent channel flow 16 p2194 N88-23087

Self similarity of two point correlations in wall bounded turbulent flows 16 p2195 N88-23089

EDQNM closure: A homogeneous simulation to support it. A quasi-homogeneous simulation to disprove it
16 p2195 N88-23091

Validation of EDQNM for subgrid and supergrid models 16 p2195 N88-23092

Big whorls carry little whorls 16 p2195 N88-23094

Conditionally-averaged structures in wall-bounded turbulent flows 16 p2198 N88-23112

Coherent structure 16 p2199 N88-23117

Coherent structures: Comments on mechanisms
16 p2199 N88-23118

Coherent structures and dynamical systems
16 p2199 N88-23119

Vortex breakdown and control experiments in the Ames-Dryden water tunnel 16 p2200 N88-23127

Flow visualization study of vortex manipulation on fighter configurations at high angles of attack
16 p2201 N88-23130

A comparative study of vortex flows in wind and water tunnels 16 p2204 N88-23151

Experimental studies of vortex flows
[NASA-CR-182874] 16 p2207 N88-23171

Random processes, turbulence and disordering fields
[AD-A191399] 16 p2209 N88-23181

The role of vortex structure in tropical cyclone motion
[AD-A190961] 16 p2235 N88-23351

Study of a system for reducing base drag by controlling vortices
[REPT-87/43] 17 p2295 N88-23730

Sensitivity of F-106B leading-edge-vortex images to flight and vapor-screen parameters
[NASA-TP-2818] 17 p2300 N88-23760

Unsteady flow around a profile subjected to pulsed motions
[ETN-88-92151] 18 p2458 N88-24594

Study of mixing and reaction in the field of a vortex
[AD-A191489] 18 p2508 N88-24878

The behavior of drop-containing turbulent eddies
[AD-A191669] 18 p2509 N88-24883

Fast algorithm development for large-eddy simulation of circular-jet turbulence
[AD-A192044] 18 p2509 N88-24887

Effects of Mach number on acoustic-vortex interactions in a ramjet 19 p2625 N88-25573

Numerical simulation of supersonic free-jets
19 p2636 N88-25639

Scaling laws for homogeneous turbulent shear flows in a rotating frame
[NASA-CR-181672] 19 p2665 N88-25847

Experimental and analytical studies of compressible vortices 19 p2665 N88-25848

Superfluid turbulence in counterflowing helium II
19 p2665 N88-25849

Numerical study of delta wing leading edge blowing
[NASA-CR-183101] 20 p2752 N88-26335

Vortex methods for separated flows
[NASA-TM-100068] 20 p2753 N88-26342

Evolution of hairpin vortices in a shear flow
[NASA-TM-100858] 20 p2845 N88-26885

Drift wave vortices and anomalous transport
[DE88-009562] 20 p2859 N88-26982

Theoretical and experimental investigations of a vortex drag behind a wing profile with spoiler
[ISL-PU-309/87] 21 p2892 N88-27169

A study of the interaction of diffusion flames with a vortex pair flowfield 21 p2908 N88-27258

Stream function-vorticity finite elements and the resolution of the Navier-Stokes equations
[DE88-702318] 21 p2945 N88-27494

A fast vortex code for computing 2-D flow in a box
[DE88-011732] 21 p2946 N88-27498

Higher order vortex methods with rezoning
[DE88-010777] 21 p2947 N88-27505

Rotation symmetric vortex in axiparallel flow
[ETN-88-92364] 21 p2948 N88-27512

Interactions between coherent structures and premixed flame fronts
[ETN-88-92885] 22 p3053 N88-28111

Flow dynamics stimulated by hairpin-like vortices in initially laminar boundary layers
[AD-A194253] 22 p3075 N88-28254

Vortex flows 23 p3170 N88-28875

Noise generation and boundary layer effects in vortex-airfoil interaction and methods of digital hologram analysis for these flow fields
[AD-A194191] 23 p3171 N88-28883

Unsteady flow past an NACA 0012 airfoil at high angles of attack
[AD-A194650] 23 p3172 N88-28886

Three-dimensional vortex interactions
[AD-A194066] 23 p3172 N88-28889

Vortex dynamics of coherent and chaotic structures (including algorithms for computer simulations and diagnosis)
[AD-A193580] 23 p3212 N88-29117

Construction of a laser Doppler anemometer and its use for the testing of a novel probe for the measurement of the variations of the lateral component of the vortex vector
[MPIS-13/1987] 23 p3217 N88-29147

Experiments on the dissipation of sound by separated flow at an edge
[ISVR-TR-151] 23 p3279 N88-29522

Vortex formation and particle transport in a cross-field plasma sheath
[DE88-008931] 23 p3284 N88-29553

Nonlinear Tollmien-Schlichting/vortex interaction in boundary layers
[NASA-CR-181698] 24 p3311 N88-29715

On the generation of mean flows by the interaction of Goertler vortices and Tollmien-Schlichting waves in curved channel flows
[NASA-CR-181690] 24 p3315 N88-29743

The present status and the future of missile aerodynamics
[NASA-TM-100063] 24 p3320 N88-29773

Computational methods for the problems of the tip vortex
[NASA-CR-181438] 24 p3320 N88-29775

The thermal behavior of film cooled turbulent boundary layers as affected by longitudinal vortices
[AD-A195155] 24 p3374 N88-30095

Vortex formation and particle transport in a cross-field plasma sheath
[AD-A194838] 24 p3432 N88-30425

VORTICITY

Description of NCAR (National Center for Atmospheric Research) Community Climate Model (CCM1)
[PB87-203782] 01 p0072 N88-10462

Measurement of velocity and vorticity fields in the wake of an airfoil in periodic pitching motion
[NASA-TP-2780] 04 p0487 N88-13002

Low-disturbance wind tunnels
07 p0811 N88-14937

The global balance of dynamic vorticity in relation to heat sources and sinks 07 p0876 N88-15316

Viscous flows. Part 3: Formulation of the Navier-Stokes equations by stream function vorticity methods
08 p0986 N88-15969

An introduction to single point closure methodology
08 p0986 N88-15973

Free-surface flow phenomena ahead of a two-dimensional body in a viscous fluid
10 p1329 N88-17944

Studies on homogeneous and heterogeneous reactive flows 11 p1484 N88-18861

Unsteady transonic small-disturbance theory including entropy and vorticity effects
[NASA-TM-100568] 12 p1575 N88-19418

Time-accurate simulations of a shear layer forced at a single frequency
[NASA-TM-100836] 12 p1628 N88-19740

Incompressible theory of interaction between moving bodies and vorticity field: Force on moving bodies by vorticity field 14 p1863 N88-21132

A low dimensional dynamical system for the wall layer
16 p2194 N88-23086

Ejection mechanisms in the sublayer of a turbulent channel 16 p2195 N88-23090

Direct numerical simulation of buoyantly driven turbulence 16 p2196 N88-23097

A statistical investigation of the single-point pdf of velocity and vorticity based on direct numerical simulations 16 p2196 N88-23101

Local structure of intercomponent energy transfer in homogeneous turbulent shear flow
16 p2197 N88-23103

Structure of turbulent shear flows
16 p2198 N88-23113

A non-invasive experimental technique for the measurement of unsteady velocity and vorticity fields
16 p2204 N88-23148

Crossflow vorticity sensor
[NASA-CASE-LAR-13436-1-CU]
17 p2300 N88-23759

Computation and characteristics of pulsatile multi-bifurcation flow 18 p2483 N88-24729

Axisymmetric viscid-inviscid interaction by a frozen vorticity approximation
[AD-A191743] 18 p2509 N88-24885

A single streamwise vortical structure and its instability in shear flows 18 p2515 N88-24921

The Proceedings of the Symposium on Mechanics for Space Flight 1987
[ISAS-SP-6] 20 p2782 N88-26499

The diffusion of vorticity from a plane boundary
[AD-A192706] 21 p2942 N88-27474

Cavitation inception in a turbulent shear flow
[DE88-011486] 21 p2946 N88-27497

Higher order vortex methods with rezoning
[DE88-010777] 21 p2947 N88-27505

Transonic blade-vortex interactions
22 p3037 N88-28035

On the energy source of 1982-83 ENSO episode simulated by the NCAR community climate model
22 p3122 N88-28556

Volumetric measurement of vorticity vectors by optical probe
[AD-A195997] 24 p3369 N88-30061

VORTICITY EQUATIONS
NT HELMHOLTZ VORTICITY EQUATION
Radial mixing in turbomachines
[AD-A188028] 11 p1482 N88-18847

VOYAGEUR HELICOPTER
U CH-46 HELICOPTER

VTOL
U VERTICAL LANDING
U VERTICAL TAKEOFF

VTOL AIRCRAFT
U VERTICAL TAKEOFF AIRCRAFT

VULCANIZATES
U VULCANIZED ELASTOMERS

VULCANIZED ELASTOMERS
Crosslinkable elastomeric materials
[EP-PATENT-0-181-735-A1] 01 p0026 N88-10165

VULCANIZING
Crosslinkable elastomeric materials
[EP-PATENT-0-181-735-A1] 01 p0026 N88-10165
Primerless RTV silicones
[BDX-613-3807] 24 p3356 N88-29980

VULNERABILITY
NT NUCLEAR VULNERABILITY
Performance evaluation of a half-wave resonant slot antenna over perfect ground using NEC (Numerical Electromagnetic Code)
[AD-A184004] 03 p0308 N88-11942
A methodology to assess the effects of high altitude electromagnetic pulse (HEMP) on electric power systems
[DE88-000338] 11 p1476 N88-18808
A computer graphics simulation of the endgame in aircraft combat survivability
[AD-A187826] 11 p1541 N88-19214
Defending secrets, sharing data: New locks and keys for electronic information
[PB88-143185] 12 p1706 N88-20210
The avionics software architecture impact on system architecture 17 p2303 N88-23778
The use of commercial off-the-shelf equipment and its impact on C3 (Command, Control and Communications EMP (electromagnetic pulse) survivability
[AD-A192614] 20 p2791 N88-26556
Fiber-optics used to record high-speed photographs inside a pressurized tank during lethality testing
[DE88-011283] 21 p2951 N88-27529
Defensive platform size and survivability
[DE88-011634] 23 p3184 N88-28948
Comparative analysis of passive communications satellites employing the SHF and HF spectrum for use in a strategic role
[AD-A194682] 24 p3362 N88-30019

W

W STARS
U WOLF-RAYET STARS

W WINGS
U VARIABLE SWEEP WINGS

W-R STARS
U WOLF-RAYET STARS

WAFERS
Hydrogen annealing of P(sub) b and E prime defect centers in oxidized silicon wafers
[DE87-014293] 02 p0152 N88-10951
Some 2-D WSI array architectures --- wafer scale integration (WSI)
[OUEL-1672/87] 02 p0219 N88-11381
Silicon microscale mechanisms from (110) oriented wafers
[DE88-002096] 06 p0787 N88-14825
Analytical investigations of bulk wave resonators in the piezoelectric thin film on gallium-arsenide configuration
[AD-A185716] 06 p0789 N88-14840
GaAs MMIC yield evaluation --- monolithic microwave integrated circuits (MMIC)
[ESA-CR(P)-2470] 08 p0979 N88-15916
Wafer scale implementation of a GaAs systolic signal processor cell 10 p1381 N88-18247
Corner compensation structures for (110) oriented silicon
[DE88-003300] 10 p1417 N88-18455
Fabrication and electrical characterization of multilevel aluminum interconnects used to achieve silicon-hybrid wafer-scale integration
[AD-A190519] 15 p2060 N88-22282
High-speed electron beam lithography devices discussed 16 p2185 N88-23023
A monolithic reduced-size Ku-Band SPOT (Single-Pole Double Throw) FET switch
[DE88-006273] 18 p2505 N88-24858
Determination of doping profiles in silicon from resistivity measurements via the four-point probe in combination with layer strippings via anodic oxidation
18 p2583 N88-25347
Chemical multisensors with selective encapsulation of ion-selective membranes 19 p2670 N88-25869
Stress modeling of microdiaphragm pressure sensors
19 p2670 N88-25873
Dissolution rates of polymers and copolymers based on methyl, ethyl and butyl methacrylate
[AD-A194713] 23 p3197 N88-29027

WAKEFULNESS
Sleep and wakefulness: Handbook for flight medical officers, second edition
[AGARD-AG-270(E)] 02 p0217 N88-11366
Effect of night watches and intermittent sleep on state of circadian rhythms of physiological functions of fishermen 06 p0750 N88-14610
Neurophysiological analysis of hypothalamic regulation mechanisms of primary sleep and hypobiosis
06 p0751 N88-14611
Pharmacological resetting of the Circadian sleep-wake cycle
[AD-A186194] 07 p0889 N88-15385
Exercise thermoregulation after prolonged wakefulness
[AD-A186224] 08 p1048 N88-16327
Role of adenosine analogs and growth hormone in waking and sleep
[AD-A187897] 11 p1519 N88-19070
Neurohumoral aspects of sleep
[AD-A188653] 12 p1667 N88-19992
Biological rhythms, sleep, and wakefulness in prolonged confinement 19 p2696 N88-26022

WAKES
NT AIRCRAFT WAKES
NT LAMINAR WAKES
NT NEAR WAKES
NT PROPELLER SLIPSTREAMS
NT SLIPSTREAMS
NT TURBULENT WAKES
Transverse focussing using plasma wake fields
[DE87-011503] 01 p0099 N88-10652
Investigations on a transonic airfoil with a 30 mm wide perforation/cavity arrangement
[ESA-TT-1072] 03 p0260 N88-11634
Unsteady flow about cambered plates
[AD-A184725] 03 p0320 N88-12025
The effect of object potentials on the wake of a flowing plasma
[AD-A184038] 03 p0379 N88-12385
A full potential flow analysis with realistic wake influence for helicopter rotor airload prediction
[NASA-CR-4007] 04 p0393 N88-12452
Measurement of velocity and vorticity fields in the wake of an airfoil in periodic pitching motion
[NASA-TP-2780] 04 p0487 N88-13002
An ultra-high-speed cinematographic method for the study of wakes in hypersonic ballistic ranges
05 p0531 N88-13228
Computational study of three-dimensional wake structures
[REPT-2] 05 p0539 N88-13281
Wakes of two dimensional bluff bodies in subsonic flow: Influence of a separating plate and of a pulsed injection of momentum
[IMFL-4200-86/75] 05 p0541 N88-13297
Development of an unsteady wake theory appropriate for aeroelastic analyses of rotors in hover and forward flight
[NASA-CR-182357] 06 p0664 N88-14075
Characteristics of a separating confluent boundary layer and the downstream wake
[NASA-TM-100046] 06 p0704 N88-14323
Observations of a midlatitude squall line boundary layer wake
[AD-A185609] 06 p0746 N88-14589
A qualitative study of wake fields for very short bunches
[DE88-002565] 09 p1164 N88-16980
Boundary-layer and wake measurements on a swept, circulation-control wing 10 p1270 N88-17597
SAR (Synthetic Aperture Radar) imaging of ship wakes in the Gulf of Alaska
[AD-A186554] 10 p1317 N88-17872
Emittance studies at the Los Alamos National Laboratory Free-Electron Laser (FEL)
[DE88-003146] 10 p1334 N88-17975
Wake effects in a Fayette 95-IIS wind turbine array
[DE88-001103] 10 p1349 N88-18063
Galileo probe parachute test program: Wake properties of the Galileo probe at Mach numbers from 0.25 to 0.95
[NASA-RP-1130] 11 p1488 N88-18884
Two-phase flows in the wake of in-cylinder projectiles
[AD-A189422] 13 p1765 N88-20559
Boundary-layer and wake measurements on a swept, circulation-control wing
[NASA-TM-89426] 15 p2014 N88-22013
Unsteady flow field measurements using LDV (Laser Doppler Velocimetry)
[AD-A189907] 15 p2063 N88-22298
Unsteady flow around a profile subjected to pulsed motions
[ETN-88-92151] 18 p2458 N88-24594
Supplements to the study of the wake of a Mirage G8 model at F2 --- wind tunnel
[CERT-RT-OA-20/5025-AYD] 18 p2458 N88-24596
Calibration of averaging total pressure flight wake rake and natural-laminar-flow airfoil drag certification
[NASA-CR-181630] 19 p2599 N88-25443
Analysis and modeling of complex non-stationary flows
[PB88-127188] 19 p2664 N88-25842
The diffusion of vorticity from a plane boundary
[AD-A192706] 21 p2942 N88-27474
A new method of calculating the boundary layer characteristics downstream of manipulators. Part 1: Boundary layer integral parameters
[PNR90455] 22 p3078 N88-28279
A new method of calculating the boundary layer characteristics downstream of manipulators. Part 2: Skin friction and net drag reduction
[PNR90456] 22 p3078 N88-28280
An examination of wake effects and power production for a group of large wind turbines
[DE88-009906] 22 p3117 N88-28518
Unsteady flow past an NACA 0012 airfoil at high angles of attack
[AD-A194650] 23 p3172 N88-28886

WALKING
Dynamics and stability of bipedal locomotion robots
03 p0333 N88-12096
Static standing and dynamic walking of a practical biped robot
[DE88-001367] 04 p0451 N88-12795
Determination of the effect of walking on the forced convective heat transfer coefficient using an articulated mannikin
[AD-A186452] 08 p1049 N88-16335
Morphological manifestations of primate adaptation to orthograde statics and walking erect
10 p1366 N88-18162
Force distribution and trajectory control for closed kinematic chains with applications to walking machines
13 p1779 N88-20642
Gastric emptying during walking and running: Effects of varied exercise intensity
[AD-A194025] 23 p3240 N88-29281

WALKING MACHINES
Correction of inertial navigation system drift errors for an autonomous land vehicle using optical radar terrain data
[AD-A184973] 05 p0544 N88-13311
A computer simulation study of an expert system for walking machine motion planning
[AD-A187907] 11 p1438 N88-18577
Space spider crane
[NASA-CASE-LAR-13411-1-SB]
17 p2312 N88-23828
Compliant robotic structures, part 3
[AD-A192426] 21 p2955 N88-27556

WALL FLOW
Wall interference tests of a CAST 10-2/DOA 2 airfoil in an adaptive-wall test section
[NASA-TM-4015] 02 p0122 N88-10772
Measurement of gas flow velocities near obstacles. Analysis and optimization of an optical barrier velocimeter. Associated signal processing
[ESA-TT-1056] 03 p0315 N88-11991
Analysis of the motions and effects of hairpin vortices
03 p0316 N88-11997
SCRAM JET (Supersonic Combustion Ramjet) combustion experiments 04 p0404 N88-12512
Time-dependent hypersonic viscous interactions
[AD-A185764] 06 p0665 N88-14082
A method for the approximate calculation of the skin friction coefficient of horizontal wavy plates
[VKI-TN-160] 07 p0851 N88-15172
Theoretical and experimental studies of the transonic flow field and associated boundary conditions near a longitudinally-slotted wind-tunnel wall
[NASA-CR-181169] 08 p0959 N88-15815
The effect of eddy distribution on momentum and heat transfer near the wall in turbulent pipe flow
[NASA-TM-100257] 08 p0988 N88-15984
Influence of the wall boundary layer on force measurements on half models in the transonic wind tunnel
[F + W-TF-1876] 09 p1122 N88-16715

A dynamical system/coherent structure approach to the fully developed turbulent wall layer
10 p1267 N88-17578

Navier-Stokes simulation of wind-tunnel flow using LU-ADI factorization algorithm
[NASA-TM-100042] 10 p1268 N88-17584

The influence of Mach number and heat transfer on the turbulent flow wall law
[NASA-TT-20230] 13 p1771 N88-20594

Wall interference assessment and corrections for transonic adaptive wall airfoil data
14 p1863 N88-21129

An efficient parallel algorithm for the simulation of three-dimensional compressible transition on a 20 processor Flex/32 multicomputer
[NASA-CR-178340] 17 p2337 N88-23943

Surface curvature and pressure gradient effects on turbulent flow: An assessment based on numerical solution of the Reynolds equations 17 p2338 N88-23954

Heat transfer from a negatively buoyant wall jet
[PB88-181953] 18 p2507 N88-24873

Hypersonic turbulent wall boundary layer computations
[NASA-CR-182147] 18 p2514 N88-24917

Wind tunnel wall interference (January 1980 - May 1988): A selected, annotated bibliography
[NASA-TM-4061] 19 p2604 N88-25466

Evolution of hairpin vortices in a shear flow
[NASA-TM-100858] 20 p2845 N88-26885

Supersonic wall adaptation in the rubber tube test section of the DFVLR Goettingen
[IB-222-87-A-08] 24 p3330 N88-29824

WALL JETS

Flow and heat transfer with impinging jets and rough surfaces
[DE87-014162] 02 p0169 N88-11065

Wall jet analysis for circulation control aerodynamics. Part 1: Fundamental CFD and turbulence modeling concepts 10 p1269 N88-17586

A theory for turbulent curved wall jets
10 p1269 N88-17590

Wall jet analysis for circulation control aerodynamics. Part 2: Zonal modeling concepts for wall jet/potential flow coupling 10 p1269 N88-17593

An experimental investigation of straight and curved annular wall jets
[NASA-CR-182546] 11 p1434 N88-18557

Heat transfer from a negatively buoyant wall jet
[NBS/GCR-88/541] 15 p2050 N88-22208

Variable Mach number wall jets for control/propulsion on hypervelocity projectiles/interceptors: Tests with an existing model
[AD-A192845] 21 p2892 N88-27167

Transition mixing study empirical model report
[NASA-CR-182139] 24 p3371 N88-30076

WALL PRESSURE

An engineering study of hybrid adaptation of wind tunnel walls for three-dimensional testing
[NASA-CR-178374] 07 p0814 N88-14957

Wavenumber - frequency structure of turbulent flow in a channel from a direct simulation
[AD-A189079] 12 p1627 N88-19737

Comparison of the wall pressure fluctuations in artificially generated turbulent spots, natural transition and turbulent boundary layers
[AD-A191777] 19 p2663 N88-25836

An experimental study of an adaptive-wall wind tunnel
[NASA-CR-183152] 24 p3329 N88-29821

The effects of incoming boundary layer thickness on unsteady shock-induced turbulent separations induced by cylinders
[AD-A196190] 24 p3368 N88-30060

WALL TEMPERATURE

Turbulent heat transfer and fluid flow measurements downstream of abrupt expansions and in a cavity of a circular tube at a uniform wall temperature
18 p2515 N88-24920

Plasma theory and simulation
[AD-A194674] 23 p3286 N88-29565

Radiative heat transfer to steady flow of a chemically reacting fluid in a horizontal porous channel with variable wall temperature
[DE88-702704] 24 p3372 N88-30081

WALLS

NT NOZZLE WALLS
NT POROUS WALLS
NT THIN WALLS
NT WIND TUNNEL WALLS

Space station integrated wall design and penetration damage control
[NASA-CR-179169] 01 p0013 N88-10070

Vortex dynamics and transport to the wall in a crossed-field plasma sheath
[DE87-013286] 01 p0100 N88-10657

A study of the optimal transition temperatue of PCM (Phase Change Material) wallboard for solar energy storage
[DE88-001522] 04 p0466 N88-12882

Aircraft interior noise reduction by alternate resonance tuning
[NASA-CR-181530] 04 p0486 N88-13005

The orientations of dipolar walls produced by cyclic deformation 05 p0598 N88-13655

Reversed field pinch plasmas with various boundary conditions
[DE88-000832] 05 p0653 N88-14004

The production of turbulence in boundary layers: The role of microscale coherent motions
[AD-A185568] 06 p0703 N88-14313

Geometrically nonlinear analysis of stiffened panels
06 p0722 N88-14440

Effect of plasma rotation in tokamak on stabilizing action of electrically conducting wall 06 p0773 N88-14746

Wall turbulence control 07 p0812 N88-14943

Examination of the development of a compressible turbulent boundary layer on a rough and porous wall
[PB87-148266] 07 p0815 N88-14964

Electromagnetic fields backscattered from an s-shaped inlet cavity with an absorber coating on its inner walls
[NASA-CR-182401] 07 p0845 N88-15130

Space station integrated wall damage and penetration damage control. Task 5: Space debris measurement, mapping and characterization system
[NASA-CR-179281] 10 p1285 N88-17688

One-dimensional leakage-flow vibration instabilities
[DE88-002875] 10 p1330 N88-17947

An analysis of the motion and effects of hairpin vortices
[AD-A187261] 10 p1331 N88-17958

Structural analyses of engine wall cooling concepts and materials 15 p2081 N88-22405

A low dimensional dynamical system for the wall layer
16 p2194 N88-23088

Self similarity of two point correlations in wall bounded turbulent flows 16 p2195 N88-23089

Conditionally-averaged structures in wall-bounded turbulent flows 16 p2198 N88-23112

Inflectional instabilities in the wall region of bounded turbulent shear flows 16 p2199 N88-23114

Active layer model for wall-bounded turbulence
16 p2199 N88-23115

Simulation of laminar-turbulent transition in the vicinity of a wall
[AD-A191380] 16 p2208 N88-23180

Research in electromagnetic shielding theory. Part1. Shielding by rectangular enclosures
[AD-A192881] 20 p2791 N88-26557

On the global radiation incident variously orientated surfaces on the South Coast of Finland
[FMI-5] 20 p2823 N88-26746

Aircraft interior noise reduction by alternate resonance tuning
[NASA-CR-182540] 20 p2849 N88-26909

Characterization of accelerating pipe flow
[AD-A193065] 21 p2943 N88-27481

Transverse resistive wall instability in a high-power, short-wavelength free-electron laser
[DE88-011730] 21 p2954 N88-27549

Solar energy absorption efficiency of an ellipsoidal receiver-reactor with specularly reflecting walls
[AD-A193726] 22 p3117 N88-28520

Experimental determination of drag modifications due to elastic compliant surfaces using quantitative visual techniques
[AD-A194785] 24 p3372 N88-30082

A parametric study of embedded cantilever retaining walls: The results of a finite element study
[RR-CE83] 24 p3383 N88-30152

WALSH FUNCTION

Estimation of multivariate binary density using orthonormal functions
[AD-A186386] 07 p0912 N88-15528

Solving singular systems using orthogonal functions
[AD-A190881] 16 p2260 N88-23512

WANKEL ENGINES

Performance and combustion characteristics of direct-injection stratified-charge rotary engines
[NASA-TM-100134] 04 p0400 N88-12490

WAR GAMES

Mapping a battlefield simulation onto message-passing parallel architectures
[NASA-CR-178396] 03 p0363 N88-12287

ADAM (Acquisition Deployment and Maneuvering): The space game
[AD-A189512] 12 p1685 N88-20078

Perfect knowledge and beyond --- chess endgames
[REPT-87-37] 14 p1967 N88-21738

WARFARE

NT ANTISUBMARINE WARFARE
NT CHEMICAL WARFARE
NT COMBAT
NT ELECTRONIC WARFARE
NT NUCLEAR WARFARE

Automation strategy and results for an airbase command and control information system
[NLR-MP-86031-U] 01 p0035 N88-10223

Performance evaluation of a half-wave resonant slot antenna over perfect ground using NEC (Numerical Electromagnetic Code)
[AD-A184004] 03 p0308 N88-11942

Assessment of physical activity intensity by heart rate during sleep limited military operations
[AD-A185913] 07 p0888 N88-15382

Relating service doctrine to space system requirements
[AD-A186620] 08 p1074 N88-16483

The evolution of naval warfare technology and the impact of space systems
[AD-A186900] 09 p1233 N88-17392

A strategy for space warfare
[AD-A186658] 09 p1233 N88-17394

Acta aeronautica et astronautica sinica (selected articles)
[AD-A191552] 18 p2455 N88-24575

Predicting Air Combat Maneuvering (ACM) performance: Fleet fighter ACM readiness program grades as performance criteria
[AD-A191605] 19 p2710 N88-26099

Computation of ECM (Electronic Counter-Measures) war reserve materiel spare requirements
[AD-A193301] 21 p2897 N88-27195

Proposal for a new aggressor aircraft
[AD-A194311] 22 p3041 N88-28056

Tactical air force night/adverse weather training
[AD-A194243] 22 p3133 N88-28625

The principles of mass and maneuver applied to space operations
[AD-A194037] 23 p3276 N88-29500

WARMING

U HEATING

WARNING DEVICES

U WARNING SYSTEMS

WARNING SIGNALS

U WARNING SYSTEMS

WARNING SYSTEMS

NT EARLY WARNING SYSTEMS

The flight evaluation of an advanced engine display and monitoring system 03 p0264 N88-11659

Techniques for fire detection
04 p0406 N88-12521

Annual tropical cyclone report, 1986
[AD-A184082] 04 p0470 N88-12903

Analytical study of the effect of early warning on optimal shock isolation 08 p0998 N88-16047

EUREX D: An expert system for failure diagnosis and recovery in the TCS of the European retrievable carrier EURECA 08 p1058 N88-16385

Airborne Wind Shear Detection and Warning Systems. First Combined Manufacturers' and Technologists' Conference
[NASA-CP-10006] 10 p1273 N88-17616

Response of wind shear warning systems to turbulence with implication of nuisance alerts
10 p1274 N88-17618

Windshear warning aerospatiale approach
10 p1274 N88-17620

Lidar windshear detection and avoidance: Performance and technical assessment 10 p1274 N88-17626

Infrared low-level wind shear work
10 p1275 N88-17628

Crew interface with windshear systems
10 p1275 N88-17631

Status of FAA terminal Doppler weather radar programs 10 p1275 N88-17632

The advanced low-level windshear alert system operational demonstration results, Summer, 1987, Denver Stapleton International Airport 10 p1275 N88-17633

Information transfer in the National Airspace System
10 p1275 N88-17634

Airworthiness considerations
10 p1276 N88-17636

Aviation weather: Status of FAA's (Federal Aviation Administration's) new hazardous weather detection and dissemination systems
[PB88-115910] 11 p1513 N88-19041

Rotorcraft TCAS (traffic alert and collision avoidance system) evaluation: Group 3 results
[AD-A191719] 18 p2461 N88-24614

An interagency working group on lightning threat warning
[DE88-009828] 20 p2826 N88-26767

Synoptic patterns related to tropical cyclone recurvature
[AD-A192338] 20 p2827 N88-26771
Helicopter Warning Sensor (HWS)
22 p3149 N88-28735

WASHING
NT BATHING
Analysis of water recovered after being used for washing by men and women 10 p1361 N88-18135

WASHOUT (RADIOACTIVITY)
U FALLOUT

WASTE DISPOSAL
NT HAZARDOUS MATERIAL DISPOSAL (IN SPACE)
The adaption and use of research codes for performance assessment
[DE88-000552] 06 p0756 N88-14639
Institute for Materials Science and Engineering, Metallurgy. Technical activities 1987
[PB88-157722] 11 p1460 N88-18702
Space reactor end of life issues
17 p2424 N88-24413
Review of numerical methods for radionuclide transport in three-dimensional porous media, at high Peclet numbers
[CFDU/87/10] 18 p2536 N88-25061
Optimization of mechanical/corrosion properties of Ti-CODE 12 plate and sheet. Part 2: Thermomechanical processing effects
[DE88-007493] 19 p2616 N88-25517
Waste destruction by plasma
[SNIAS-881-430-113] 21 p2971 N88-27651
Advanced development waste processing unit for combat vehicles, phase 2
[AD-A193793] 23 p3243 N88-29302

WASTE ENERGY UTILIZATION
Use of natural gas diesel engines in mechanical pulp production: A preliminary study
[DE87-753065] 02 p0181 N88-11129
Organic Rankine-cycle power systems working fluids study: Topical report No. 1: Fluorinol 85
[DE87-014604] 02 p0195 N88-11217
Application of Organic Rankine Cycles (ORCs) to decentralized power generation, preliminary study
[DE87-753331] 03 p0347 N88-12197
Open-cycle centrifugal vapor-compression heat pump
[PB88-157391] 11 p1488 N88-18885
Alternative Energy in the Midwest: Research and Applications. Conference Proceedings, Rosemont, Illinois, March 19-20, 1987
[PB88-142278] 11 p1509 N88-19015
Overview of 1987 moonlight project
15 p2052 N88-22231
Application and technology requirements for heat pumps at the process industries
[DE88-006740] 15 p2062 N88-22293
An analysis of gas-steam total power recovery energy system 20 p2784 N88-26512
A comparative economic evaluation of industrial heat pumps. Part 2: Addendum
[DE88-011701] 22 p3117 N88-28519
Absorption heat pumps
[DE88-752820] 23 p3229 N88-29218

WASTE HEAT
Space vehicle/nuclear reactor thermal radiation integration issues 17 p2424 N88-24417
Experimental demonstrations of organic Rankine cycle waste heat rejection systems 17 p2432 N88-24469
An analysis of gas-steam total power recovery energy system 20 p2784 N88-26512

WASTE TREATMENT
Catalytic processes for space station waste conversion
[NASA-CR-177423] 01 p0077 N88-10491
Innovative and alternative technology projects
[PB87-230165] 05 p0623 N88-13818
Controlled Ecological Life Support Systems (CELSS) physiochemical waste management systems evaluation
[NASA-CR-177422] 06 p0754 N88-14626
Electrochemical processing of solid waste
[NASA-CR-182413] 08 p0967 N88-15852
Proceedings of the 19th DOE/NRC Airborne Waste Management and Air Cleaning Conference
[NUREG/CP-0086-VOL-1] 11 p1509 N88-19018
JPRS report: Science and technology. Japan
[JPRS-JST-87-030] 16 p2185 N88-23026

WASTE UTILIZATION
Catalytic processes for space station waste conversion
[NASA-CR-177423] 01 p0077 N88-10491
Operation of an experimental algal gas exchanger for use in a CELSS 03 p0358 N88-12255
A review of recent activities in the NASA CELSS program 03 p0359 N88-12259
Preliminary experimental results of gas recycling subsystems except carbon dioxide concentration
03 p0359 N88-12261
Mass balances for a biological life support system simulation model 03 p0361 N88-12272

WASTE WATER
Innovative and alternative technology projects
[PB87-230165] 05 p0623 N88-13818
Reclamation of water contaminated with fuel system icing inhibitor. Phase 1: Literature review and information compilation
[DE88-006575] 16 p2183 N88-23013
Vapor Compression Distillation Subsystem (VCDS) component enhancement, testing and expert fault diagnostics development, volume 1
[NASA-CR-172072] 22 p3134 N88-28634

WASTES
NT HUMAN WASTES
NT INDUSTRIAL WASTES
NT LIQUID WASTES
NT MANURES
NT RADIOACTIVE WASTES
NT URINE
NT WASTE WATER
Technology '87: Research and Development Laboratory Technology Transfer Program
[DE88-003142] 13 p1852 N88-21084
Overview of the TITAN-2 reversed-field pinch aqueous fusion power core design
[DE88-008170] 20 p2857 N88-26966

WATCHES
U CLOCKS

WATER
NT COASTAL WATER
NT COLD WATER
NT DEEP WATER
NT FRESH WATER
NT GROUND WATER
NT INLAND WATERS
NT POTABLE WATER
NT SEA WATER
NT SHALLOW WATER
NT SURFACE WATER
NT WASTE WATER
Cooling effect of a single evaporating droplet on a hot semi-infinite metal body
[PB87-201902] 01 p0046 N88-10294
The water permeability of multi-layer coatings
[BLL-M-37252-(5828.4)] 02 p0148 N88-10927
Trickle water and feeding system in plant culture and light-dark cycle effects on plant growth
03 p0361 N88-12273
Technical evaluation of a solar-powered absorption cooling system (LiBr-H2O)
[PB87-108254] 04 p0463 N88-12867
RRS DISCOVERY cruise 160, 30 June-25 July, 1986. Geochemical sampling over the Madeira and Porcupine Abyssal Plains
[PB87-222030] 04 p0471 N88-12910
Phase purity of NiCo2O4, a catalyst candidate for electrolysis of water
[NASA-TM-100239] 05 p0556 N88-13385
Operating envelopes of particle sizing instrumentation used for icing research
[NASA-CR-180870] 05 p0586 N88-13573
Observing effect of laser radiation of low-frequency Raman scattering of light 06 p0772 N88-14742
Experimental and theoretical study of condensation in multicomponent mixtures
[DE88-002715] 07 p0830 N88-15033
Vapor condensation on a turbulent liquid interface
08 p0982 N88-15939
Evidence for human adaptive response to dehydration: Increase of circulating protein mass
[AD-A186225] 08 p1048 N88-16328
Analysis of water recovered after being used for washing by men and women 10 p1361 N88-18135
Approximate method for predicting the permanent set in a beam in vacuo and in water subject to a shock wave 11 p1500 N88-18957
Emission of gamma rays from various materials pulsed with 14-MeV neutrons
[DE88-003837] 11 p1544 N88-19227
Optically stimulated sound from gas bubbles in water
12 p1686 N88-20087
Numerical experiments on the stability of controlled boundary layers
[NASA-CR-181649] 13 p1771 N88-20591
An investigation of the spray produced by a yawed wheel, including measurement of impact forces --- aircraft wheels
[BU-363] 14 p1866 N88-21150
The role of water in the thermal balance of the coma
14 p1999 N88-21916
Determination of the content of CO(+) and H2O(+) ions in the tail of Comet Giacobini-Zinner and Comet Halley 14 p2006 N88-21964
Mass transfer mechanisms for water adsorbed on silica gel
[DE88-005993] 15 p2032 N88-22107
Noncondensing round turbulent gas jets in liquids
[AD-A191191] 16 p2208 N88-23179
Development of a liquid-fed water resistojet
[NASA-TM-100927] 18 p2523 N88-24968
Direct determination of part-per-billion levels of volatile organics in water and soil samples using glow discharge mass spectrometry
[DE88-011389] 21 p2910 N88-27272
Structure and function of the manganese complex involved in photosynthetic oxygen evolution determined by X-ray adsorption spectroscopy and electron paramagnetic resonance spectroscopy
[DE88-010360] 21 p2985 N88-27725
Finite-rate water condensation in combustion-heated wind tunnels
[NASA-TP-2833] 22 p3046 N88-28075
Initiation of explosive molten aluminum-water interactions at wet or underwater surfaces
[DE88-004686] 23 p3194 N88-29006
Sub-kilometer rampart craters in the equatorial region of Mars: Possible implications for the state and distribution of regolith H2O 23 p3302 N88-29666
How dirty is Mars' North Polar cap, and why isn't it black 23 p3303 N88-29677
Coadsorption of H2O and CO2 on the Martian surface
23 p3307 N88-29702
General equations for the motions of ice crystals and water drops in gravitational and electric fields
[NASA-CR-183229] 24 p3370 N88-30070

WATER BALANCE
The influence of space flight on water-salt homeostasis in man and animals 12 p1659 N88-19943
Changes in blood conductivity during immersion
12 p1663 N88-19969
Human adaptation to various hypercapnic conditions in relation to salivary electrolyte dynamics and renal function 12 p1664 N88-19977
Climatology and space observations
[ISBN-2-85-428179-9] 14 p1935 N88-21536
Continental surface processes and water cycle
14 p1937 N88-21555
Hydrological models 14 p1937 N88-21559
The Hapex-Mobilhy program 14 p1938 N88-21560
Measurement of the water content of soil from space and application to the regional water balance
14 p1938 N88-21561

WATER CIRCULATION
NT COASTAL CURRENTS
NT EL NINO
NT GULF STREAM
NT LOMONOSOV CURRENT
NT OCEAN CURRENTS
NT WATER CURRENTS
Ocean model processor for climate studies
[PB87-224713] 03 p0353 N88-12226
North Pacific Ocean. Northeast Pacific Transition Zone, R/V Thomas G. Thompson: 1 November - 6 December 1969. STD data report
[AD-A186574] 09 p1195 N88-17161
Numerical model of Rayleigh instability and spin-off eddies on fronts 13 p1788 N88-20696
Ocean eddies 14 p1938 N88-21566

WATER COLOR
The influence of yellow substances on remote sensing of sea water constituents from space. Volume 1: Summary
[ESA-CR(P)-2443-VOL-1] 07 p0872 N88-15292
The influence of yellow substances on remote sensing of sea water constituents from space. Volume 2: Appendices
[ESA-CR(P)-2443-VOL-2] 07 p0873 N88-15293
Ocean Colour Workshop --- conference
[ESA-SP-1083] 08 p1042 N88-16292
Europe's position concerning ocean colour activities
08 p1042 N88-16293
Overview of ESA's activities in ocean colour remote sensing 08 p1042 N88-16294
Update of NASA's ocean colour activities
08 p1042 N88-16295
Remote sensing of ocean colour for studies of biological productivity and biochemical cycles
08 p1042 N88-16296
Ocean colour applications in ocean dynamics and coastal processes 08 p1042 N88-16297
Technical aspects of future ocean colour remote sensing 08 p1042 N88-16298
Federal Republic of Germany's interests, activities and goals in remote sensing of ocean colour/fluorescence from space 08 p1043 N88-16302
French activities in ocean colour observations
08 p1043 N88-16303
Italian activities in ocean colour remote sensing
08 p1043 N88-16304

National Remote Sensing Program (NRSP) of the Netherlands 08 p1043 N88-16305
Developments in ocean colour research in the United Kingdom 08 p1043 N88-16306

WATER CONTENT
U MOISTURE CONTENT

WATER COOLED REACTORS
NT BOILING WATER REACTORS
NT LIGHT WATER REACTORS
NT PRESSURIZED WATER REACTORS
NT ZERO POWER REACTORS

WATER COOLING
U LIQUID COOLING

WATER CURRENTS
NT COASTAL CURRENTS
NT EL NINO
NT GULF STREAM
NT LOMONOSOV CURRENT
NT OCEAN CURRENTS
Tide- and wind-forced currents in Buzzards Bay, Massachusetts
[PB88-110580] 07 p0882 N88-15350
Use of the thermodynamic evaporation formula of Hoffmann in energy balance models for flowing water
08 p1013 N88-16143
Model of hydrodynamic adjustment of temperature, salinity and current fields 13 p1789 N88-20700
Circulation and exchange processes on the South Atlantic Bight Continental Shelf
[DE88-003330] 13 p1804 N88-20781
FORTRAN programs for computation of time dependent sea levels and trajectory errors from satellite altimeter data
[BONN-MITT-73] 21 p2901 N88-27216

WATER CYCLE (HYDROLOGY)
U HYDROLOGICAL CYCLE

WATER DEPTH
Sea level changes
[DE87-014357] 04 p0472 N88-12913

WATER FLOW
Experimental evidence for modifying the current physical model for ice accretion on aircraft surfaces
[NASA-TM-87184] 04 p0397 N88-12473
Evaluation of the magnetic induction conductivity method for detecting frazil ice deposits
[AD-A186940] 09 p1194 N88-17157
Boundary-integral-equation method for computing the three-dimensional flow of groundwater
[PB88-126891] 10 p1330 N88-17951
Changes in the California current system observed off northern California during July-August 1986
[AD-A190027] 15 p2100 N88-22510
Evaluation of the floodable area of the canal of Sao Goncalo through TM-LANDSAT 5 imagery
17 p2364 N88-24078
Injection of drag reducing additives into turbulent water flows
[AD-A192072] 18 p2509 N88-24888
Noise generation by air bubbles in water: An experimental study of creation and splitting
[AD-A192063] 19 p2664 N88-25839
Development of advanced flow simulation system by water flow model. New method of velocity measurement using cross-correlation
[DE88-753120] 20 p2799 N88-26608
Mapping of streamflow and soil infiltration of a Sahelian catchment area by SPOT image interpretation: The Oursi pond catchment area in Burkino Faso
22 p3090 N88-28348

WATER HAMMER
Hydroacoustic pulsating jet generator
[MPIS-7/1987] 18 p2510 N88-24891

WATER HEATING
Development of an innovative, low-cost solar collector
[PB87-206819] 02 p0194 N88-11210
Actual performance and economic feasibility of residential solar water heaters
[INPE-4399-RPE/555] 08 p1023 N88-16191
Application of the estimation method to parameter performance date of solar water heating systems
[INPE-4268-PRE/1141] 11 p1508 N88-19007

WATER IMMERSION
Human thermoregulatory model for whole body immersion in water at 20 and 28 C
[AD-A185052] 05 p0629 N88-13849
Changes in regional and central hemodynamics during seven-day water immersion 07 p0895 N88-15421
Prediction of human thermoregulatory responses and endurance time in water at 20 and 24C
[AD-A186223] 08 p1048 N88-16326
Rational considerations for modelling human thermoregulation during cold water immersion
[AD-A186226] 08 p1048 N88-16329
Rapid hypothermia subsequent to oral nicotinic acid and immersion in warm (30C) water
[AD-A186458] 08 p1050 N88-16339
Respiratory and cardiovascular responses to cold stress following repeated cold water immersion
[AD-A186460] 08 p1050 N88-16340
Role of body fat in the prediction of the metabolic response for immersion in cold water
[AD-A186914] 09 p1198 N88-17182
Comparative evaluation of orthostatic stability following immersion in horizontal and vertical positions
10 p1363 N88-18143
Influence of a 6 hr head-out water immersion on different tests of endurance performance capacity
12 p1653 N88-19903
Changes in blood conductivity during immersion
12 p1663 N88-19969
Validation of mathematical model predictions of immersion survival times
[IAM-652] 14 p1952 N88-21635
Further development of a mathematical model for the specification of immersion clothing insulation
[IAM-653] 14 p1954 N88-21644
Experimental investigation of Hover flowfields in water at the McDonnell Douglas Research Laboratories
16 p2202 N88-23135
Human hemodynamics during water immersion as related to position during submersion
19 p2703 N88-26071

WATER INJECTION
Dense-spray structure and phenomena. Part 2: Pressure-atomized sprays
[AD-A190312] 15 p2064 N88-22307
Turbulence and flame propagation
[PB87-226912] 19 p2612 N88-25499

WATER JETS
U HYDRAULIC JETS

WATER LANDING
NT DITCHING (LANDING)

WATER MANAGEMENT
The use of SPOT images for water resources surveys. The examples of the Kasserine area (Tunisia) and the Jebel Amour (Algeria) 03 p0345 N88-12179
The world's water resources: A major neglect. A study in remote sensing in hydrology and water management
[ESA-BR-40] 22 p3116 N88-28511

WATER MASERS
Water masers associated with 2 carbon stars: EU Andromedae and V778 Cygni 04 p0517 N88-13176
The distance to the center of the galaxy: H2O maser proper motions in Sgr B2(N)
[MPE-PREPRINT-104] 16 p2288 N88-23702

WATER POLLUTION
NT OIL POLLUTION
Influence of surfactants on damping of gravity-capillary waves. 1: Frequency dependence
04 p0459 N88-12843
Uses of airborne laser Chayka-1 for probing water, land surfaces 06 p0725 N88-14461
Trace element geochemistry of the South Atlantic Bight
[DE88-003515] 10 p1356 N88-18108
Environmental projects. Volume 5, part 1: Study of subsurface contamination. Part 2: Guide to implement environmental compliance programs
[NASA-CR-182691] 13 p1796 N88-20741
Global mixed-layer natural and anthropogenic fluxes
13 p1807 N88-20803
Feasibility study for a 2nd generation system for airborne maritime pollution surveillance
[ETN-88-92108] 15 p2092 N88-22466
Study of reservoir water quality utilizing remote sensing techniques: Methodological concepts
17 p2364 N88-24076
Hydrocarbon fuel spill dispersion on water: Literature review
[AD-A192486] 21 p2922 N88-27346

WATER PURIFICATION
U WATER TREATMENT

WATER QUALITY
Rapid toxicity detection in water quality control utilizing automated multispecies biomonitoring for permanent space stations 02 p0135 N88-10848
Investigation of effect of silver compounds on microflora in water reclaimed from atmospheric moisture condensate in a closed environment 07 p0892 N88-15407
Two decades of achievement in the ocean, 1968-1988
[PB88-167077] 16 p2236 N88-23356
Satellite remote sensing of turbidity and sediment concentration in Lagoa dos Patos
17 p2355 N88-24032
Study of reservoir water quality utilizing remote sensing techniques: Methodological concepts
17 p2364 N88-24076
Validation of maximum permissible concentration of urea in reclaimed potable water and evaluation of its biological effect 19 p2705 N88-26086
Use of SPOT HRV data in the US Army Corps of Engineers dredging program 22 p3109 N88-28466

WATER RECLAMATION
Reclamation of water contaminated with fuel system icing inhibitor. Phase 1: Literature review and information compilation
[DE88-006575] 16 p2183 N88-23013
Cardiac rhythm of animals consuming reclaimed water differing in concentration of sodium and potassium ions
19 p2705 N88-26085
Validation of maximum permissible concentration of urea in reclaimed potable water and evaluation of its biological effect 19 p2705 N88-26086
Liquid-phase oxidation of acetone with hydrogen peroxide on oxide catalysts 19 p2706 N88-26091

WATER RECOVERY
U WATER RECLAMATION

WATER RESOURCES
NT AQUIFERS
The use of SPOT images for water resources surveys. The examples of the Kasserine area (Tunisia) and the Jebel Amour (Algeria) 03 p0345 N88-12179
Study of fractures as subsidiary research of ground water in the Sergipe state: An approach through remote sensing data
[INPE-4319-TDL/286] 12 p1639 N88-19813
Botany Facility: Problems of water supply, plant nutrients and soil in the Botany Facility
[SIRA-A/ 373/WP220/RJS/003]
17 p2379 N88-24141
The use of SPOT images for water resources surveys in the Kasserine Basin (Tunisia)
22 p3090 N88-28349
Water resources and agricultural land use investigations in northeastern Gujarat (India) 22 p3091 N88-28355
Use of SPOT satellite in agrohydrology: Detection of spring water excess in a grassland region
22 p3091 N88-28357
The use of orbital remote sensing data for low cost ground-water survey
[INPE-4587-PRE/1318] 24 p3386 N88-30170

WATER RUNOFF
Groundwater sapping valleys: Experimental studies, geological controls and implications to the interpretation of valley networks on Mars
[NASA-CR-182718] 15 p2152 N88-22847
Reduce uncertainty in projection of future sea-level changes due to ice wastage
[DE88-009883] 22 p3129 N88-28601

WATER SPLITTING
DC conductivity studies in Li5AlO4 at intermediate temperatures and its possible application for the electrolysis of water
[AD-A185489] 06 p0697 N88-14276
Photosynthetic water splitting
[DE88-007809] 20 p2830 N88-26791

WATER TEMPERATURE
NT OCEAN TEMPERATURE
NT SEA SURFACE TEMPERATURE
Influence of stratification in near-surface water layer on intensity of gas exchange between atmosphere and water 04 p0459 N88-12841
Thermal instability and heat transfer characteristics in water/ice systems
[AD-A189627] 15 p2062 N88-22297
Observations of frontal instabilities on an upwelling filament
[AD-A191051] 17 p2375 N88-24122
Evaluating evaporation with satellite thermal data
[AD-A192042] 18 p2531 N88-25019
Study of human factors engineering criteria for Extra Vehicular Activity (EVA) systems, volume 2
[STF23-F87025-VOL-2] 24 p3409 N88-30293

WATER TREATMENT
Vapor compression distiller and membrane technology for water revitalization 03 p0359 N88-12262
An overview of Japanese CELSS research activities
03 p0360 N88-12267
Carbon dioxide treatment for scale removal and control in potable water systems
[AD-A184346] 04 p0412 N88-12556
Innovative and alternative technology projects
[PB87-230165] 05 p0623 N88-13818
Reverse osmosis treatment to remove inorganic contaminants from drinking water
[PB88-147780] 12 p1605 N88-19598
Review of selenium thermodynamic data
[DE88-006194] 13 p1849 N88-21088
Reclamation of water contaminated with fuel system icing inhibitor. Phase 1: Literature review and information compilation
[DE88-006575] 16 p2183 N88-23013
Vapor Compression Distillation Subsystem (VCDS) component enhancement, testing and expert fault diagnostics development, volume 1
[NASA-CR-172072] 22 p3134 N88-28634

WATER TUNNEL TESTS

Technical evaluation report on the Fluid Dynamics Panel Symposium on aerodynamic and related hydrodynamic studies using water facilities
[AGARD-AR-225] 03 p0312 N88-11968

High Reynolds number pump facility for cavitation research
[AD-A189310] 13 p1765 N88-20558

An experimental investigation of decelerating flow about two-dimensional cambered plates
[DE86-006598] 13 p1766 N88-20567

Water facilities in retrospect and prospect: An illuminating tool for vehicle design
16 p2200 N88-23126

Vortex breakdown and control experiments in the Ames-Dryden water tunnel 16 p2200 N88-23127

Qualification of a water tunnel for force measurements on aeronautical models 16 p2200 N88-23128

An experimental study to determine the flow and the subsonic static and dynamic stability characteristics of aircraft operating at high angles-of-attack
16 p2201 N88-23129

Oscillating flow over bluff bodies in a U-shaped water tunnel 16 p2201 N88-23131

The use of the NRC/NAE water facilities in Canadian aeronautical research and development
16 p2201 N88-23132

Short duration flow establishment on a profile in a Water-Ludwieg-Tunnel 16 p2201 N88-23134

Water tunnel measurements by an electrochemical method 16 p2203 N88-23146

Use of water towing tanks for aerodynamics and hydrodynamics 16 p2204 N88-23149

Investigation on the movement of vortex burst position with dynamically changing angle of attack for a schematic deltawing in a watertunnel with correlation to similar studies in windtunnel 16 p2204 N88-23152

Measurements of the time dependent velocity field surrounding a model propeller in uniform water flow
16 p2205 N88-23155

Unsteady water channel
[AD-A194231] 23 p3171 N88-28884

WATER TUNNELS

U HYDRAULIC TEST TUNNELS

WATER VAPOR

Millimeter-wave studies of moist air
[AD-A184681] 03 p0306 N88-11935

A method for remote sensing of precipitable water vapor and liquid in the atmosphere using a 22-ghz radiometer
[AD-A184204] 03 p0354 N88-12232

Absorption of far IR-radiation by H2O-N2 complexes under atmospheric conditions 04 p0462 N88-12855

Measurements of vapor flux, liquid water contents, precipitation rates and riming in a Utah mountain cloud system
[PB87-224945] 04 p0469 N88-12900

DC conductivity studies in Li5AlO4 at intermediate temperatures and its possible application for the electrolysis of water
[AD-A185489] 06 p0697 N88-14276

A critical review of measurements of water vapor absorption in the 840 to 1100 cm(-1) spectral region
[NASA-CR-182361] 06 p0742 N88-14565

Study of the vapor-liquid equilibria used in the fabrication process of hydrogen by thermochemistry
[DE88-900239] 07 p0830 N88-15035

Radiation absorption in the infrared spectral range: A comparison between laboratory measurements and theoretical calculation illustrated by a H2O 2.7 micrometer 08 p1018 N88-16170

In-situ stratospheric water vapor measurements on board long duration balloons 08 p1029 N88-16232

High-speed assembly language (80386/80387) programming for laser spectra scan control and data acquisition providing improved resolution water vapor spectroscopy
[NASA-CR-4117] 08 p1053 N88-16355

Concept, construction, and experimental testing of a polychromator for a Raman lidar for the simultaneous telemetering of carbon dioxide and water vapor, relative to oxygen
[GKSS-87/E/20] 09 p1191 N88-17134

Scattering of optical radiation by bursting water particles in fog 09 p1236 N88-17410

An experimental and theoretical study of the ice accretion process during artificial and natural icing conditions
[NASA-CR-182119] 14 p1865 N88-21143

Water vapor and hydroxyl distributions in the inner coma of Comet Halley measured by the VEGA-2 three channel spectrometer TKS 14 p1998 N88-21910

Mathematical modelling of the heat and water vapour transport in the human respiratory tract
17 p2382 N88-24160

Tracer water transport and subgrid precipitation variation within atmospheric general circulation models
[NASA-CR-182897] 20 p2823 N88-26745

Wavenumber spectra from THIR 6.7 micron water vapor data 20 p2824 N88-26756

Heat and mass transfer in laminar wavy film absorption with the presence of non-absorbable gases
21 p2947 N88-27502

On the energy source of 1982-83 ENSO episode simulated by the NCAR community climate model
22 p3122 N88-28556

WATER VEHICLES

NT AIRCRAFT CARRIERS
NT SHIPS
NT SUBMARINES
NT UNDERWATER VEHICLES

A comparative study of various electric propulsion systems and their impact on a nominal ship design
[AD-A187800] 11 p1477 N88-18816

WATER WAVES

Observations of wind waves on a reservoir
[IOS-234] 02 p0193 N88-11206

Breaking wave forces on vertical cylinders
[RR-CE71] 03 p0338 N88-12126

Studies of thin surface films aim at seeing deep ocean processes 04 p0460 N88-12847

Wave and wind data sources, environmental conditions committee report, International Ship and Offshore Structures Congress
[PB87-234902] 06 p0746 N88-14588

Far field of steady waves produced by local perturbation sources in stream of stratified fluid
06 p0771 N88-14736

Annual data summary and climatological evaluation, CERC (Coastal Engineering Research Center) field research facility, 1985, volume 2, appendix C
[AD-A185894] 07 p0881 N88-15344

Guide for the program EXACT-NL --- wave growth
[KNMI-TR-94] 09 p1163 N88-16971

Nearshore wave transformation study of sites near Port Canaveral Inlet, Florida
[AD-A186965] 09 p1195 N88-17159

Investigation of the quantitative determination of two dimensional sea surface wave spectra from shipborne radar measurements
[GKSS-87/E/10] 09 p1195 N88-17163

SAR (Synthetic Aperture Radar) imaging of ship wakes in the Gulf of Alaska
[AD-A186554] 10 p1317 N88-17872

Analysis of wind turbines on offshore support structures excited by random wind and random waves
[DE88-004772] 10 p1351 N88-18074

Variation of the wind stress related to frontal passages during FASINEX (Frontal Air-Sea Interaction Experiment) 1986
[AD-A187180] 11 p1514 N88-19042

Wave group analysis based on Kimura's method
[AD-A187610] 11 p1516 N88-19055

Effects of waves on the boundary layer of a surface-piercing flat plate: Experiment and theory
[AD-A188356] 12 p1626 N88-19731

Anisotropy of microstructural eddy motion in surface layer during calm 13 p1784 N88-20677

Numerical modeling of wave migration of seismic data
13 p1786 N88-20684

Invariant characteristics of acoustic field in stratified ocean 13 p1788 N88-20698

Study of spectra of sea waves on horizontally nonuniform current in rip zone 13 p1788 N88-20699

Dynamics of the Oceanic Surface Mixed Layer
[AD-A188348] 13 p1804 N88-20785

Wind forcing and observed oceanic wavenumber spectra 13 p1806 N88-20797

Energy and momentum fluxes through the sea surface
13 p1806 N88-20798

Hamiltonian description of the interaction of surface waves with mixed-layer currents
13 p1806 N88-20799

Evaluation of wave calculations using GONO in the period October 1985 - April 1986
[KNMI-TR-96] 13 p1807 N88-20804

Study of the dynamic topography of oceans by means of satellite altimetry 14 p1938 N88-21567

Climatological data of the Netherlands lightvessels over the period 1949-1980 --- North Sea
[KNMI-WR-87-9] 14 p1947 N88-21613

An improved wind input source term for third generation ocean wave modeling
[KNMI-WR-87-8] 14 p1950 N88-21624

Investigation of the imaging of ocean surface waves using a synthetic aperture radar
[SER-A-WISS-ABHANDL-84] 16 p2236 N88-23357

Research in nonlinear wave motion
[AD-A191686] 18 p2509 N88-24884

Definition of long ocean wave slope for radar applications
[AD-A193198] 21 p2933 N88-27412

Research on ocean forecasting and nonlinear wave propagation and numerical hydrodynamics in the ocean
[AD-A193363] 21 p2976 N88-27680

Nonlinear surface and internal waves on shear flow
[PREPRINT-584] 22 p3129 N88-28604

A singular perturbation analysis of the weakly nonlinear evolution of long and short water waves and waves in boundary layers 23 p3209 N88-29102

Mathematical problems of nonlinear wave propagation and of waves in heterogeneous media
[AD-A195970] 24 p3368 N88-30057

Impact force as a part of the total breaking wave force on a vertical cylinder
[RR-CE78] 24 p3384 N88-30154

A study of the feasibility of using sea and wind information from the ERS-1 satellite. Part 2: Use of scatterometer and altimeter data in wave modeling and assimilation
[ESA-CR(P)-2604-PT-2] 24 p3387 N88-30176

Analysis of environmental parameters from the Panama City tower radar experiment
[AD-A194994] 24 p3404 N88-30264

WATERFOWL

The suspended Japanese quail as an animal model for experiments related to microgravity
12 p1662 N88-19960

WATERPROOFING

Water disbondment characterization of organic Coating/metal substrate systems
[AD-A184847] 05 p0567 N88-13454

Improvement of the construction of protective clothing for better wearability and comfort --- rainwear
[IZF-1986-26] 07 p0899 N88-15448

WATERSHEDS

Surface hydrology, sediment transport dynamics and remote sensing of disturbed watersheds in a humid temperate region
[DE88-008719] 20 p2817 N88-26715

WATERWAVE ENERGY

Survey on utility technology of a tidal and ocean current energy
[DE88-770148] 20 p2819 N88-26722

WATERWAVE ENERGY CONVERSION

Ocean, Wave, and Tidal Energy Systems: Current abstracts
[DE88-008299] 19 p2687 N88-25973

WATTMETERS

NBS (National Bureau of Standards) wideband sampling wattmeter
[PB87-210324] 03 p0323 N88-12041

WAVE AMPLIFICATION

Production-process CO2 laser with amplified pulse-repetition operation 06 p0771 N88-14739

Performance of linear vertical antenna in refractive multimode waveguide 08 p1076 N88-16489

Simulation and modeling of whistler mode wave growth through cyclotron resonance with energetic electrons in the magnetosphere 10 p1353 N88-18089

WAVE ATTENUATION

NT ACOUSTIC ATTENUATION
NT RADIO ATTENUATION
NT SHOCK WAVE ATTENUATION

Influence of surfactants on damping of gravity-capillary waves. 1: Frequency dependence
04 p0459 N88-12843

Experimental studies on acoustic emission monitoring of crack propagation in offshore structures: A literature survey 05 p0610 N88-13748

Imaging subtle microstructural variations in ceramics with precision ultrasonic velocity and attenuation measurements
[NASA-TM-100129] 07 p0867 N88-15257

Radar reflectivity and attenuation of radio waves in the melting layer of precipitation
[PB88-121553] 10 p1318 N88-17882

Numerical studies of propagation of Lg waves across ocean continent boundaries using the Representation Theorem (RT) 10 p1353 N88-18085

Regional wave attenuation and seismic moment from the inversion of NORESS spectra
[AD-A187399] 11 p1510 N88-19023

Investigation of constrained-layer technique using exact elasticity theory
[AD-A188664] 12 p1636 N88-19795

Attenuated direct and scattered wave propagation on simulated land mobile satellite service paths in the presence of trees 19 p2645 N88-25695

WAVE DEGRADATION

Aircraft field degradation and electromagnetic compatibility
[PB88-183975] 19 p2602 N88-25456

WAVE DIFFRACTION

Observation of instabilities in time during dynamic self-diffraction of light in anisotropic nonhomogeneous medium 06 p0769 N88-14730

New description of Lau effect based on theory of raster image forming process 06 p0772 N88-14744

Diffraction of sound at junction of two waveguides 08 p1076 N88-16491

Plane wave diffraction by a thin dielectric wedge [RSRE-MEMO-4045] 09 p1153 N88-16912

Calculation of noise in spatial speckle-field holograms under conditions of saturated photoresponse 09 p1235 N88-17403

VHF/UHF propagation by diffraction: Calculation by numerical integration 12 p1615 N88-19659

A diffraction based theoretical model for prediction of UHF path loss in cities 12 p1616 N88-19661

Complex space monofiler approximation of diffraction currents on a conducting half plane [NASA-CR-182883] 16 p2273 N88-23605

Diffraction by a simple deep phase object --- integrated circuit measurement [RSRE-MEMO-4039] 22 p3070 N88-28224

WAVE DISPERSION

Method for single-shot measurement of picosecond laser pulse-lengths without electronic time dispersion [DE87-013171] 02 p0178 N88-11107

Dispersion equation for plane capillary-gravity wave on free surface of viscous incompressible fluid 04 p0459 N88-12842

Effect of plasma resonance on properties of surface waves 06 p0773 N88-14749

Geometric structure, pseudoband gaps, and surface vibrational resonances on metal surfaces [AD-A187001] 09 p1143 N88-16851

Betatron oscillations in a free electron laser [DE88-004859] 10 p1337 N88-17990

Slow waves in waveguide with elliptical cross section [DE88-700159] 13 p1757 N88-20508

Basic physics of laser-plasma interactions [ETN-88-92055] 14 p1984 N88-21838

Range determination of pulsars, taking into account H2 regions [ETN-88-91492] 14 p1993 N88-21877

Plasma wave radiative damping of a new type in a relativistic one-dimensional plasma [DE88-701191] 15 p2135 N88-22739

Beam waves in random inhomogeneous media [DE88-701631] 16 p2190 N88-23058

Dispersive spectral apparatus 16 p2271 N88-23587

Numerical research of dispersion properties of plasma cylindrical waveguides located in magnetic field [DE87-703009] 16 p2275 N88-23615

Elastic wave dispersion in laminated composite plate [AD-A192289] 23 p3188 N88-28967

Wide band gyrotron traveling wave amplifier analysis [AD-A194269] 23 p3216 N88-29139

Kinetic theory for electrostatic waves due to transverse velocity shears [AD-A193404] 23 p3284 N88-29557

WAVE DRAG

NT INTERFERENCE DRAG

WAVE EQUATIONS

NT DIRAC EQUATION

NT EIKONAL EQUATION

NT KORTEWEG-DEVRIES EQUATION

NT SCHROEDINGER EQUATION

Inhomogeneous conditions at open boundaries for wave propagation problems [AD-A183847] 01 p0033 N88-10214

The polarization field for pulsed Raman transitions [DE87-013118] 01 p0035 N88-10227

An asymptotic theory for a class of initial-boundary value problems for weakly nonlinear wave equations with an application to a model of the galloping oscillations of overhead transmission lines [REPT-87-12] 01 p0086 N88-10556

Different ways of looking at the electromagnetic vacuum [DE87-013150] 01 p0089 N88-10584

Fundamentals of numerical magnetohydrodynamics [DE87-011769] 01 p0100 N88-10656

Large-aperture high-efficiency frequency doubling using tandem KDP crystals 03 p0301 N88-11894

Four-wave mixing used in optical amplitude encoding 03 p0376 N88-12366

Pulse-mode expansions and refractive indices in plane-wave propagation [DE88-001326] 04 p0437 N88-12714

On the wave excitation in the turbulent meteor trace 06 p0737 N88-14530

Coherence, propagation and fluctuations of light: A generalized ray approach [DE88-001669] 06 p0780 N88-14786

Statistical analyses of measured directional wave and current data [PB87-144523] 07 p0853 N88-15185

Equation of acoustic and gravitational waves in stratified moving medium 08 p1077 N88-16493

Equation of gravitational-gyroscopic waves: Angular potential and its applications 08 p1079 N88-16504

FOR3D: A computer model for solving the LSS (Lee-Saad-Schultz) three-dimensional, wide angle wave equation [AD-A188649] 08 p1080 N88-16511

Relation of wave energy and momentum with the plasma dispersion relation in an inhomogeneous plasma [DE88-002305] 08 p1084 N88-16530

Exact image principle in electromagnetic field computation [EL-57] 09 p1153 N88-16907

A project to experimentally and theoretically examine fluid interfacial wave phenomena in a rotating cylindrical geometry: Current results and future plans [DE88-003738] 09 p1165 N88-16984

Feedback stabilization of distributed systems [AD-A187111] 09 p1222 N88-17328

Note on boundary stabilization of wave equations [AD-A187113] 09 p1227 N88-17348

Analiticity in fourth order wave equations [DE88-700837] 12 p1686 N88-20060

A finite-amplitude analysis of the buoyant instability of a highly viscous film over a less viscous half-space 13 p1769 N88-20581

WKB theory of wave tunneling for Hermitian vector systems of integral equations [DE88-005332] 13 p1831 N88-20951

High speed transcendental elementary function architecture in support of the Vector Wave Equation (VWE) [AD-A189746] 15 p2119 N88-22627

Pointwise stabilization for coupled quasilinear and linear wave equations [AD-A190031] 15 p2120 N88-22632

Effects of randomness of parameters on mean wave propagation in a viscoelastic medium [REPT-87-60] 16 p2206 N88-23166

Nonlinear wave and diffusion equations [AD-A191421] 16 p2265 N88-23544

Asymptotics for a system of nonlinearly coupled wave equations with an application to the galloping oscillations of overhead transmission lines [REPT-87-78] 17 p2348 N88-23991

Nonlinear waves [AD-A192148] 18 p2510 N88-24889

MHD bending waves in a current sheet [NASA-TM-101149] 18 p2579 N88-25323

High spatial frequency thermal blooming instability: A linear stability analysis [DE88-010711] 20 p2807 N88-26655

Propagation of inernio-acoustic gravity waves in a rotating and radiating opaque atmosphere [DE88-701866] 20 p2823 N88-26750

Wave equations for pulse propagation [DE88-011760] 21 p2954 N88-27548

Research on ocean forecasting and nonlinear wave propagation and numerical hydrodynamics in the ocean [AD-A193363] 21 p2976 N88-27680

A numerical treatment of the fluid/elastic interface under range-dependent environments [AD-A192476] 21 p3005 N88-27821

Initial boundary value problems of nonlinear wave equations in an exterior domain [DE88-701883] 21 p3026 N88-27962

The construction of implicit and explicit solitary wave solutions of nonlinear partial differential equations [AD-A193475] 23 p3269 N88-29452

Solution of large order Fourier-Bessel equations [ARE-TM(UHA)-88504] 23 p3272 N88-29475

WAVE EXCITATION

NT ACOUSTIC EXCITATION

NT HARMONIC EXCITATION

Self-consistent modification of a fast tail distribution by resonant fields in nonuniform plasmas [AD-A183790] 01 p0099 N88-10650

Ultrafast intrinsic bistable devices [PB87-109310] 05 p0649 N88-13978

Lg wave excitation and propagation in the presence of one-, two-, and three-dimensional heterogeneities [AD-A187364] 11 p1510 N88-19022

Beam waves in random inhomogeneous media [DE88-701631] 16 p2190 N88-23058

Heating efficiency of beat wave excitation in a density gradient [AD-A193066] 21 p3017 N88-27905

Three-dimensional vortex interactions [AD-A194066] 23 p3172 N88-28889

WAVE FRONT DEFORMATION

Wavefront error sensing [NASA-CR-181504] 03 p0321 N88-12030

Calculation of the spatial-temporal deformation of laser pulses in multiple scattering [MBB-Z-111/87] 10 p1311 N88-17837

WAVE FRONT RECONSTRUCTION

Stationary reconstruction method. Development, test and comparison in ultrasonic testing [REPT-860125-TW] 01 p0057 N88-10368

Lasers with wavefront-reversing mirrors (review article) 06 p0709 N88-14349

Holographic phase correction [RSRE-MEMO-4036] 09 p1167 N88-17000

Reconstruction of wave distribution functions in warm plasmas [IRF-PREPRINT-104] 24 p3431 N88-30422

WAVE FRONTS

NT SHOCK FRONTS

Thermo-optical modeling of flashlamp-pumped zig-zag slabs [DE87-011878] 01 p0051 N88-10326

Fronts propagating with curvature dependent speed: Algorithms based on Hamilton-Jacobi formulations [NASA-CR-178382] 01 p0077 N88-10495

Analytical caustic surfaces [NASA-TM-87805] 02 p0168 N88-11060

Nonconventional optical techniques for optical wavefront processing [AD-A185099] 05 p0650 N88-13982

Compensation of small-scale phase distortions by means of a Fourier phase corrector 06 p0708 N88-14345

On connection between evolution of troposphere fronts and changes of circulation regime in meteor zone 06 p0735 N88-14519

A raytrace method for a laterally heterogeneous environment [AD-A186525] 08 p0978 N88-15912

Color shadow methods of analyzing reconstructed wave front 09 p1236 N88-17407

Theoretical investigation of the wave shaping process in a section of ladder fracture tape [MRL-R-1081] 13 p1771 N88-20595

Nonlinear optical phase conjugation techniques to reduce the physical size of lasers [AD-A196170] 24 p3379 N88-30122

WAVE FUNCTIONS

NT MOLECULAR ORBITALS

NT PAULI EXCLUSION PRINCIPLE

Local spectra and wave distribution functions --- space plasma [KGI-PREPRINT-099] 01 p0100 N88-10659

Asymptotics of the effective potentials and wave functions of a three-body problem in suitable coordinates [DE87-703323] 03 p0370 N88-12326

The finite element method for electronic structure [DE88-001709] 04 p0485 N88-12989

Final (n,l) state-resolved electron capture by multiply charged ions from neutral atoms [IPPJ-AM-54] 04 p0492 N88-13030

Development of a new method of measuring the characteristic impedance and complex wave number of a porous acoustic material [AD-A185038] 05 p0646 N88-13957

Coherence, propagation and fluctuations of light: A generalized ray approach [DE88-001669] 06 p0780 N88-14786

Modified quantum mechanics of small composite systems [NIKHEF-H/87-1] 06 p0790 N88-14845

Wave functions for bound states of relativistic electrons in a crystal at electron movement along crystallographic planes [DE88-700563] 07 p0939 N88-15708

On exact solutions of multidimensional Schroedinger equation with polynomial potentials [DE88-700460] 09 p1230 N88-17373

Surface and interface electronic structure [DE88-003363] 09 p1258 N88-17545

An overview of the transactional interpretation of quantum mechanics [DE88-004236] 10 p1423 N88-18497

Polarization of electrons in an electromagnetic wave field in the presence of magnetic field [DE88-700169] 13 p1757 N88-20509

WKB theory of wave tunneling for Hermitian vector systems of integral equations [DE88-005332] 13 p1831 N88-20951

Numerical simulations of multiphoton processes in many electron atoms [DE88-003293] 13 p1837 N88-20990

Dynamic and spectral properties of semiconductor lasers with quantum well, quantum wire, and quantum box structures 14 p1975 N88-21788

To the field theory with a fundamental mass [DE88-701159] 15 p2146 N88-22807

On 1/n-expansion and wave functions
[DE88-701639] 16 p2260 N88-23509
Quantum transport in an electron waveguide
20 p2864 N88-27010
To the twinning plane superconductivity theory
[DE88-702195] 20 p2874 N88-27056
Phenomenological approach to high T/sub c/ oxide superconductors
[DE88-701868] 20 p2876 N88-27074
Cosmic wavefunction with induced gravity
[DE88-701873] 20 p2884 N88-27129
Passage of relativistic magnetic dipole moments through magnetic fields
[DE88-702640] 23 p3295 N88-29624

WAVE GENERATION
The generation of nearly isotropic turbulence by means of grids
[PNR90411] 02 p0172 N88-11084
Magnetic flux tubes as sources of wave generation
04 p0505 N88-13108
HF sidebands in the ionosphere
05 p0574 N88-13497
A study of the mechanism of internal gravity wave generation by quasigeostrophic meteorological motions
06 p0735 N88-14520
Study of internal gravity waves in the meteor zone
06 p0735 N88-14521
Far field of steady waves produced by local perturbation sources in stream of stratified fluid
06 p0771 N88-14736
Dependence of acoustical characteristics of laser-induced breakdown in dielectric materials on shape of inelastic region 06 p0774 N88-14753
High repetition rate electron beam RF-acceleration and sub-millimeter wave generation via a free electron laser
[AD-A186066] 07 p0858 N88-15209
Microwave tubes: Literature study no. 8 comprising the year 1986
[FOA-C-30467-3] 09 p1159 N88-16944
Theoretical investigation of EM wave generation and radiation in the ULF, ELF and VLF bands by the electrodynamic orbiting tether
[NASA-CR-182720] 13 p1760 N88-20529
Nonlinear acoustic parameter and its application in ultrasonic imaging 14 p1902 N88-21364
Millimeter wave generation by relativistic electron beams
[AD-A195683] 24 p3362 N88-30016

WAVE INTERACTION
NT SHOCK WAVE INTERACTION
Generation of IR stimulated radiation, UV visible violet coherent radiation by two-photon resonance pumping in K vapor 03 p0301 N88-11892
Breaking wave forces on vertical cylinders
[RR-CE71] 03 p0338 N88-12126
Numerical experiments with hypersonic flows beneath a cone-delta-wing combination 05 p0532 N88-13238
Computation of flow past conical hypersonic wings using a second order Godunov method
05 p0533 N88-13241
On the interconnection of dynamic processes in the lower thermosphere with meteorological phenomena in the tropostratosphere 06 p0734 N88-14512
Simulation of effect on biological systems of impact wave from heavy charged particle track
07 p0896 N88-15429
Interaction of acoustic and electromagnetic waves involved in anomalous skin effect
08 p1079 N88-16503
Studies of nonlinear and chaotic phenomena in solid state systems
[DE88-002330] 09 p1254 N88-17515
Universal power spectra for wave turbulence: Applications to wind waves, flicker noise, solar wind spectrum and classical second sound
10 p1318 N88-17879
On the interaction of Tollmein-Schlichting waves in axisymmetric supersonic flows
[NASA-CR-181619] 10 p1331 N88-17955
Velocity measurements in a 3D (three dimensional) shock wave laminar boundary layer interaction
[AD-A187334] 10 p1332 N88-17959
Flow/acoustic interaction in duct inflow
[AD-A189264] 13 p1833 N88-20967
Wave interactions in a three-dimensional attachment line boundary layer
[NASA-CR-181653] 14 p1910 N88-21414
Three-wave parametric resonance in plasma of relativistic electron flux 14 p1972 N88-21772
Basic physics of laser-plasma interactions
[ETN-88-92055] 14 p1984 N88-21838
Nonlinear wave interactions in swept wing flows
[NASA-CR-4142] 16 p2206 N88-23160
Interaction of solitons in single model optical fibres
17 p2439 N88-24511
Electron-Rayleigh wave interaction in thin film carbons
[AD-A191727] 18 p2492 N88-24781
Guided wave interactions in millimeter-wave integrated circuits
[AD-A193017] 21 p2936 N88-27437
Interactions between air and ground sound at the Earth surface 22 p3149 N88-28733
Three-dimensional vortex interactions
[AD-A194066] 23 p3172 N88-28869
Interactions between synoptic and planatery scales of motion
[AD-A192328] 23 p3234 N88-29246
On the degenerate Ferrari-ibanez solution for colliding plane gravitational waves
[MATH-REPT-209] 23 p3296 N88-29630
Nonlinear Tollmien-Schlichting/vortex interaction in boundary layers
[NASA-CR-181698] 24 p3311 N88-29715
The strong nonlinear interaction of Tollmien-Schlichting waves and Taylor-Goertler vortices in curved channel flow
[NASA-CR-181697] 24 p3311 N88-29716
Light-millimeter wave interactions in semiconductor devices
[AD-A195898] 24 p3432 N88-30428

WAVE MOTION
U WAVES

WAVE OSCILLATORS
U OSCILLATORS

WAVE PACKETS
Wavepacket propagation and current startup near the lower hybrid frequency in the torus
[IPPJ-840] 02 p0242 N88-11529
Quantum mechanics with spontaneous localization and the quantum theory of measurement
[DE87-703072] 02 p0247 N88-11559
A strategy to determine the transition state of an electron transfer reaction
[AD-A183976] 03 p0382 N88-12404
Evolution of acoustic gravity wave packet in spatially and temporally verying wind 11 p1469 N88-18760

WAVE PROPAGATION
NT ACOUSTIC PROPAGATION
NT DIFFRACTION PROPAGATION
NT GROUND WAVE PROPAGATION
NT HALOS
NT IONOSPHERIC PROPAGATION
NT LIGHT SCATTERING
NT SCATTER PROPAGATION
NT SHOCK WAVE PROPAGATION
NT TRANSEQUATORIAL PROPAGATION
Inhomogeneous conditions at open boundaries for wave propagation problems
[AD-A183847] 01 p0033 N88-10214
The polarization field for pulsad Raman transitions
[DE87-013118] 01 p0035 N88-10227
Geoacoustic models of the Hudson Canyon area
[AD-A183535] 01 p0073 N88-10465
Finite difference solution of a generic differential equation
[PB87-205878] 01 p0087 N88-10568
Fast wave injection into high temperature tokamak plasmas in the lower-hybrid-density regime of JIPP T-IIU
[ISSN-0469-4732] 01 p0099 N88-10649
Propagating shocks in the corona
01 p0112 N88-10718
Direct Absorption Receiver flow experiments
[DE87-014655] 02 p0196 N88-11221
Evaluation of a scale-model experiment to investigate long-range acoustic propagation
[NASA-TP-2748] 02 p0230 N88-11450
Wavepacket propagation and current startup near the lower hybrid frequency in the torus
[IPPJ-840] 02 p0242 N88-11529
Method estimating integral mean value of enhancement factor and path latitude for whistlers below magnetic latitude 10 deg 03 p0300 N88-11865
Target strength: An overview of some recent theoretical developments 03 p0303 N88-11910
Uniform guometrical theory of diffraction
03 p0303 N88-11911
A new method for measuring waveguide propagation losses
[DE87-011305] 03 p0307 N88-11938
Coupling and absorption phenomena in semiconductor-clad dielectric optical waveguides
[DE87-013446] 03 p0307 N88-11939
The effect of ocean fluctuations on sound transmission in the ocean
[AD-A184382] 03 p0355 N88-12236
General theory of radio propagation through a stratified atmosphere
[PB87-226197] 04 p0430 N88-12662
Pulse-mode expansions and refractive indices in plane-wave propagation
[DE88-001328] 04 p0437 N88-12714
High resolution finite volume methods on arbitrary grids via wave propagation
[NASA-CR-178397] 04 p0484 N88-12979
Boundary effects on the drag of an oscillating sphere: Applications to the magnetic sphere rheometer. Attenuation and dispersion of acoustic waves in nematic liquid crystals 04 p0488 N88-13007
The acceleration of winds by MHD waves in open magnetic structures 04 p0506 N88-13109
The dynamics of solar magnetic flux tubes subjected to resonant foot point shaking 04 p0507 N88-13118
Vortex interaction with a leading-edge of finite thickness
[NASA-CR-182341] 05 p0543 N88-13307
Measured characteristics of 800/900 MHz mobile radio channels with high-angle propagation through moderately dense foliage
[CRC-1398] 05 p0573 N88-13493
An investigation of millimeter wave propagation in the atmosphere: Measurement program
[AD-A184837] 05 p0574 N88-13498
Damping analysis of flexural waves in fluid-loaded single and constrained plates
[AD-A185116] 05 p0609 N88-13739
Theoretical and practical aspects of the functional absorber method of arranging sound absorbing panels
[BBC-RD-1987/15] 05 p0646 N88-13955
Propagation effects on satellite systems at frequencies below 10 GHz: A handbook for satellite systems design
[NASA-RP-1108/2] 06 p0690 N88-14226
Electromagnetic scattering problem in the wave-vector-time domain
[PB88-106083] 06 p0694 N88-14263
Tidal activity in the meteor zone over Budrio, Italy
06 p0734 N88-14517
Study of internal gravity waves in the meteor zone
06 p0735 N88-14521
Numerical modeling of troposphere-induced gravity wave propagation 06 p0735 N88-14522
Mesoscale density variability in the mesosphere and thermosphere: Effects of vertical flow accelerations
06 p0736 N88-14529
On the wave excitation in the turbulent meteor trace
06 p0737 N88-14530
A critical review of measurements of water vapor absorption in the 840 to 1100 cm(-1) spectral region
[NASA-CR-182361] 06 p0742 N88-14565
Effect of plasma resonance on properties of surface waves 06 p0773 N88-14749
Waves and vibrations in elastic superlattice composites 06 p0776 N88-14765
Coherence, propagation and fluctuations of light: A generalized ray approach
[DE88-001669] 06 p0780 N88-14786
Analytical investigations of bulk wave resonators in the piezoelectric thin film on gallium-arsenide configuration
[AD-A185716] 06 p0789 N88-14840
Solar-geophysical data number 515, July 1987. Part 1: (Prompt reports). Data for June 1987, May 1987 and late data
[PB87-233177] 06 p0805 N88-14912
Wave propagation experiments on 22-bay lattice
[AD-A186140] 07 p0824 N88-15002
Cage mode propagation experiments
[AD-A186019] 07 p0841 N88-15100
Microsecond beam propagation in air
[DE88-002221] 07 p0845 N88-15127
TRACKER: A 3-D radio ray tracing code
[DE88-003267] 07 p0847 N88-15137
Chapter 2: Threshold for Raman conversion of FEL laser pulses in the atmosphere
[DE88-002470] 07 p0859 N88-15215
Propagation of radiation along a constricting optical waveguide 07 p0920 N88-15590
Sound pressure distribution in front of a serrated boundary: Standing wave suppression and diffusion
07 p0928 N88-15639
Upwind formulations for the Euler equations
08 p0984 N88-15952
Fully turbulent internal flow excitation of pipe systems
08 p1000 N88-16056
Solar cosmic ray propagation in high-velocity solar wind stream 08 p1002 N88-16073
Interpretation of equatorial current meter data as internal waves
[PB88-108113] 08 p1044 N88-16309
Approximation of noncorrelated reflections in problem of sound propagation through waveguide with rough boundary 08 p1076 N88-16487
Mode pattern of field generated by parametric radiator in acoustic waveguide 08 p1076 N88-16488
Acoustic field in waveguide with sloping bed
08 p1076 N88-16490
Relativistic electromagnetic waves in an electron-ion plasma
[NASA-CR-182421] 08 p1085 N88-16532

Computational analysis of propagation properties of integrated-optical waveguides using a domain integral equation
[PB87-163358] 09 p1154 N88-16917

Guide for the program EXACT-NL --- wave growth
[KNMI-TR-94] 09 p1163 N88-16971

Induced turbulence in aerosol-loaded atmospheres, Jun. 1987
[DE87-014724] 09 p1192 N88-17141

Attenuation of ultrasonic waves in nonmagnetized magnetic fluids 09 p1234 N88-17398

Propagation of creep waves around rough cylindrical surface 09 p1234 N88-17400

Parametric interaction of optical modes in fiber-optic light guide 09 p1235 N88-17406

Statistics of breakdown centers appearing during propagation of laser radiation through turbulent atmosphere 09 p1236 N88-17411

Flame propagation in the approximation of straight-line trajectories of burning products
[DE88-700675] 10 p1297 N88-17756

Diffusion description of flame propagation due to the translational motion of burning reaction products
[DE88-700676] 10 p1297 N88-17757

Time domain wave propagation in multilayered integrated circuits
[AD-A187462] 10 p1324 N88-17916

Numerical studies of propagation of Lg waves across ocean continent boundaries using the Representation Theorem (RT) 10 p1353 N88-18085

Simulation and modeling of whistler mode wave growth through cyclotron resonance with energetic electrons in the magnetosphere 10 p1353 N88-18089

Evolution of acoustic gravity wave packet in spatially and temporally varying wind 11 p1469 N88-18760

Research and development of surface skimming bulk wave devices for sensor applications
[AD-A187504] 11 p1470 N88-18766

Numerical simulation of the propagation and absorption due to air breakdown of long microwave pulses
[DE88-005227] 11 p1475 N88-18798

Unsteady heat transfer in turbine blade ducts: Focus on combustor sources
[NASA-TM-100815] 11 p1486 N88-18870

Applications and limitations of the spectral-analysis-of-surface-waves method
[PB88-136619] 11 p1513 N88-19038

Coherent VUV source at 130 nm: Theory and modeling
[DE88-003874] 11 p1549 N88-19269

Wave propagation in laminated composite plates
[AD-A188999] 12 p1604 N88-19594

Ultrasonic-velocity studies of composite and heterogeneous materials
[AD-A189000] 12 p1604 N88-19595

Terrestrial Propagation Characteristics in Modern Systems of Communications, Surveillance, Guidance and Control
[AGARD-CP-407] 12 p1614 N88-19653

An investigation of terrain related variables for predicting the multipath fade depth distribution on terrestrial microwave lines 12 p1615 N88-19654

A review of the role of surface reflection in multipath propagation over terrestrial microwave links
12 p1615 N88-19655

Development of a ground-conductivity map for the area of the Federal Republic of Germany from measured field-strength contours 12 p1615 N88-19656

Propagation in longitudinally varying ducts, with emphasis on guiding to antiguiding transitions
12 p1615 N88-19658

VHF/UHF propagation by diffraction: Calculation by numerical integration 12 p1615 N88-19659

Mono- and bistatic radar coverage diagrams including diffractive wave propagation 12 p1616 N88-19660

A program for the calculation of radio-wave transmission loss over the spherical earth and over obstacles
12 p1616 N88-19662

A propagation campaign in a marine environment utilizing a digital system at 36 GHz 12 p1618 N88-19675

Two-dimensional electron fluid computer calculations of nanosecond pulse, low pressure microwave air breakdown in a rectangular waveguide and their verification by experimental measurement
[DE88-004407] 12 p1618 N88-19678

Historical electromagnetic propagation condition database description
[AD-A189157] 12 p1621 N88-19695

Electromagnetic propagation in PEC and absorbing curved S-ducts
[NASA-TM-100833] 12 p1621 N88-19698

The temporal and spatial acoustical response of a point-driven fluid-loaded plate
[AD-A188504] 12 p1636 N88-19794

Dynamical and photometric studies of Saturn's rings
12 p1711 N88-20241

Slow waves in waveguide with elliptical cross section
[DE88-700159] 13 p1757 N88-20508

Detonation velocity of the hydrazinum nitrate-hydrazine water system
[NASA-TT-20213] 13 p1770 N88-20590

Numerical modeling of wave migration of seismic data
13 p1786 N88-20684

Invariant characteristics of acoustic field in stratified ocean 13 p1788 N88-20698

Ultrasonic physical modeling of seismic wave propagation from graben-like structures
[AD-A189066] 13 p1796 N88-20744

Method for determination of the wind velocity and direction
[NASA-TT-20233] 13 p1802 N88-20769

MASPLT: A one-dimensional graphics post processor for wave propagation codes
[DE88-005506] 13 p1817 N88-20856

HISPLT: A history graphics post processor for wave propagation codes
[DE88-005507] 13 p1817 N88-20857

CSQPLT: A graphics post processor for multidimensional wave propagation codes
[DE88-005508] 13 p1817 N88-20858

Mathematical models of sound waves in fluids
[AD-A189270] 13 p1834 N88-20968

Method for determining artillery position
[NASA-TT-20238] 13 p1834 N88-20973

Nonlinear acoustic parameter and its application in ultrasonic imaging 14 p1902 N88-21364

Numerical modeling of divergent detonation wave
14 p1903 N88-21373

Millimeter-wave properties of the atmosphere: Laboratory studies and propagation modeling
[PB88-164215] 14 p1905 N88-21387

An improved wind input source term for third generation ocean wave modeling
[KNMI-WR-87-8] 14 p1950 N88-21624

AGARD Highlights 88/1 14 p2012 N88-22001

Wave propagation and dynamics of lattice structures
[AD-A190037] 15 p2025 N88-22066

Wave propagation and dynamics of lattice structures
[AD-A190611] 15 p2025 N88-22069

Numerical and experimental research on propagation of elastic stress waves in conical shell under axial impulsive loading 15 p2053 N88-22238

Wave energy flow conservation for propagation in inhomogeneous Vlasov-Maxwell equilibria
[DE88-006705] 15 p2055 N88-22251

Generation and propagation of sound waves in a collapsing or anti-collapsing star with uniform density
[DE87-703034] 15 p2151 N88-22839

Propagation of acoustic gravity wave spectrum through vertical wind shear region 16 p2186 N88-23035

Beam waves in random inhomogeneous media
[DE88-701631] 16 p2190 N88-23058

Effects of randomness of parameters on mean wave propagation in a viscoelastic medium
[REPT-87-60] 16 p2206 N88-23166

Acousto-ultrasonic input-output characterization of unidirectional fiber composite plate by SV waves
[NASA-CR-4152] 16 p2217 N88-23224

Numerical simulation for particle acceleration and trapping by an electromagnetic wave
16 p2277 N88-23626

Microinstabilities in ion beam propagation
16 p2277 N88-23631

Investigation of intensity and phase fluctuations of an acoustic wave after crossing thermal turbulence
[ETN-88-92542] 17 p2395 N88-24238

Wave growth associated with turbulent spots in plane Poiseuille flow
[FFA-TN-1988-08] 18 p2457 N88-24587

Nonlinear wave propagation
[AD-A192104] 18 p2501 N88-24835

Research in nonlinear wave motion
[AD-A191686] 18 p2509 N88-24884

Nonlinear waves
[AD-A192148] 18 p2510 N88-24889

Atmospheric propagation of laser beams
[AD-A191447] 18 p2520 N88-24952

Evaluation of the biot coefficients
[AD-A191643] 18 p2570 N88-25265

Light propagation through gravitationally perturbed Friedmann universes 18 p2577 N88-25307

Numerical investigation of acoustic energy exchange through flow turning 19 p2629 N88-25593

On the propagating speed in difference approximations for conservation laws 19 p2639 N88-25658

Propagation effects by roadside trees measured at UHF and L-band for mobile satellite systems
19 p2644 N88-25693

Propagation modeling for land mobile satellite systems
19 p2645 N88-25694

Attenuated direct and scattered wave propagation on simulated land mobile satellite service paths in the presence of trees 19 p2645 N88-25695

Mobile satellite propagation measurements and modeling: A review of results for systems engineers
19 p2645 N88-25696

Propagation measurements for an Australian land mobile satellite system 19 p2645 N88-25697

Propagation effects on spread-spectrum mobile satellite systems 19 p2645 N88-25699

Mobilestar field test program
19 p2646 N88-25707

Electro-optic sampling of high-speed, InP-based integrated circuits 19 p2655 N88-25769

Multigigahertz logic based on InP-MISFET's exhibiting extremely high transconductance
19 p2656 N88-25771

Acousto-ultrasonic input-output characterization of unidirectional fiber composite plate by P waves
[NASA-CR-4162] 19 p2678 N88-25923

Propagation of linear gravity waves in a relativistic atmosphere
[DE88-702062] 19 p2691 N88-25995

Proceedings of the Army Signal Processing Symposium. Treaty Verification Program
[DE88-008346] 20 p2790 N88-26548

Variational analysis of dielectrically loaded multidepth corrugated waveguides
[PB88-193602] 20 p2793 N88-26573

Wave propagation in locally isotropic turbulent medium with smoothly changing characteristics
[NASA-TT-20312] 20 p2800 N88-26617

The propagation of irradiance moments of an aberrated, apodized FEL beam
[DE88-008972] 20 p2806 N88-26648

Propagation of thermo-acoustic gravity waves in a rotating and radiating opaque atmosphere
[DE88-701866] 20 p2823 N88-26750

Westward moving atmospheric wave disturbances over the African tropics: Dynamic and energetic aspects
[MITT-57] 20 p2827 N88-26774

XDATAP
[DE88-007161] 20 p2837 N88-26827

On the self-focusing of electric helicons
[DE88-701870] 20 p2848 N88-26905

An evaluation of two millimeter wave propagation models for horizontal atmospheric attenuation at 70-115 GHZ
[AD-A192699] 21 p2931 N88-27403

User's manual for C-HEMP: A two-dimensional wave propagation code. Volume 1: Description and derivations of the code
[AD-A193197] 21 p2944 N88-27486

Simulation and analysis of wave propagation through random media 21 p2947 N88-27503

Wave equations for pulse propagation
[DE88-011760] 21 p2954 N88-27548

On the small signal gain of free electron lasers in the low-current regime
[DFVLR-FB-88-10] 21 p2955 N88-27552

Research on ocean forecasting and nonlinear wave propagation and numerical hydrodynamics in the ocean
[AD-A193363] 21 p2976 N88-27680

Ion Bernstein modes in current-carrying plasmas
21 p3017 N88-27903

Magnetohydrodynamic wave propagation in the solar wind
[DE88-702411] 21 p3032 N88-27995

Wave propagation and vibration of fibre reinforced laminates
[AD-A194144] 22 p3051 N88-28101

Rapid-scanning Fourier transform spectrometer for studies of propagation of near-millimeter-wave radiation through clear air and fog
[AD-A193752] 22 p3070 N88-28219

Activities report of the Electromagnetic Environment Division
[FOA-C-30484-3.2/3.3/4.1/4.2]
22 p3071 N88-28233

Time domain wave propagation in multilayered integrated circuits
[AD-A193821] 22 p3073 N88-28241

Nonlinear surface and internal waves on shear flow
[PREPRINT-584] 22 p3129 N88-28604

Wave structures in thermospheric density from satellite electrostatic triaxial accelerometer measurements
[AD-A194134] 23 p3233 N88-29240

The acoustic field scattered from some approximate pressure release materials
[AD-A194768] 23 p3278 N88-29515

Waves and instabilities in an electron-positron plasma in an ultra-strong magnetic field
23 p3283 N88-29551

Plasmoid propagation
[AD-A192378] 23 p3284 N88-29555

Wave propagation and remote sensing
24 p3364 N88-30029

Mathematical problems of nonlinear wave propagation and of waves in heterogeneous media
[AD-A195970] 24 p3368 N88-30057

Determination of the specific area of liquid gas and the velocity of weak pressure waves in aqueous foams
[NASA-TT-20347] 24 p3373 N88-30087

Rossby waves in mid-latitude oceans
24 p3405 N88-30273

Consideration of plasma opening switches from a wave propagation perspective
[AD-A195681] 24 p3431 N88-30421

Experimental proof of quasilongitudinal propagation of low-frequency waves in middle latitudes in upper ionosphere 24 p3447 N88-30516

AVE RADIATION
U ELECTROMAGNETIC RADIATION

AVE REFLECTION
NT MACH REFLECTION

Multichannel deconvolution of P waves at seismic arrays and three component stations
[AD-A184450] 04 p0467 N88-12888

Nonlinear reflection of sound wave in gas mixture
06 p0769 N88-14728

Approximation of noncorrelated reflections in problem of sound propagation through waveguide with rough boundary 08 p1076 N88-16487

Comparison of the rough surface reflection coefficient with specularly scattered acoustic data
[AD-A187086] 09 p1242 N88-17444

A review of the role of surface reflection in multipath propagation over terrestrial microwave links
12 p1615 N88-19655

Correcting ray field failures caused by focusing in an inhomogeneous duct: A critical look at the Gaussian beam method 12 p1616 N88-19663

A propagation campaign in a marine environment utilizing a digital system at 36 GHz 12 p1618 N88-19675

Input-output characterization of fiber composites by SH waves
[NASA-CR-4153] 17 p2347 N88-23986

Reflection of sound in open ended ducts
[PB88-103478] 21 p3012 N88-27870

Electromagnetic wave incoherent reflection by a half-space of weakly-ionized plasma with an absorbing boundary
[DE88-702413] 21 p3019 N88-27917

Wave and fracture phenomena in impacted ceramics
[AD-A192946] 23 p3196 N88-29020

AVE SCATTERING
NT ACOUSTIC SCATTERING
NT ATMOSPHERIC SCATTERING
NT ELECTROMAGNETIC SCATTERING
NT HALOS
NT LIGHT SCATTERING
NT MICROWAVE SCATTERING
NT MIE SCATTERING
NT RAMAN SPECTRA
NT RAYLEIGH SCATTERING
NT REVERBERATION
NT THOMSON SCATTERING
NT TROPOSPHERIC SCATTERING
NT X RAY SCATTERING

Parametrization in scattering models
03 p0304 N88-11916

Acoustic field in waveguide with sloping bed
08 p1076 N88-16490

Scattering of longitudinal wave normally incident on dieral cavity in elastic body 08 p1077 N88-16492

Backscatter from flaws in fiber-reinforced composites
11 p1450 N88-18639

Lg wave excitation and propagation in the presence of one-, two-, and three-dimensional heterogeneities
[AD-A187364] 11 p1510 N88-19022

An efficient numerical algorithm for solving scattering and inverse scattering problems of electromagnetic waves
[AD-A188479] 12 p1619 N88-19684

Three-dimensional scattering of impulsive acoustic waves by a semi-infinite crack in the plane interface of a half space and a layer
[PB88-146998] 12 p1687 N88-2008[illegible]

Transport and stability properties of free shear flows
13 p1768 N88-20577

Multiple scattering of waves in discrete random media
[AD-A191068] 18 p2499 N88-24823

Attenuated direct and scattered wave propagation on simulated land mobile satellite service paths in the presence of trees 19 p2645 N88-25695

Mobile satellite propagation measurements and modeling: A review of results for systems engineers
19 p2645 N88-25696

Staggered-grid finite element solution technique for the Maxwell's equations in the time domain
[DE88-011731] 21 p3007 N88-27838

Electromagnetic wave incoherent reflection by a half-space of weakly-ionized plasma with an absorbing boundary
[DE88-702413] 21 p3019 N88-27917

Mathematical problems of nonlinear wave propagation and of waves in heterogeneous media
[AD-A195970] 24 p3368 N88-30057

WAVEFORMS
NT PULSE AMPLITUDE
NT PULSE DURATION
NT SQUARE WAVES

Recording multiple signals on a single waveform recorder
[DE87-011632] 01 p0049 N88-10313

Computational methods and software for differential equations and their applications
[DE87-014601] 02 p0226 N88-[illegible]1424

Experimental and analytic studies of the triggered lightning environment of the F106B
[NASA-CR-4104] 04 p0469 N88-12897

High frequency periodic time domain waveform measurement system
[PB87-225256] 06 p0695 N88-14264

Waveform for short-dwell-time meteorological Doppler radars
[PB88-102199] 07 p0845 N88-15126

Digital control of high frequency pulse-width modulated inverters
[ETN-87-90711] 09 p1157 N88-16936

Air gap testing using Trailing Wire Antenna (TWA) waveform
[AD-A187639] 11 p1477 N88-18812

Distortion of wideband carbon dioxide laser radar waveforms due to atmospheric dispersion and absorption
[AD-A188687] 12 p1632 N88-19771

MOSFET performance degradation due to hot carriers
13 p1848 N88-21063

Electron device probing in the femtosecond time scale
19 p2660 N88-25821

Time-Optimal Adaptive Shaped Torque (TOAST) technical note
[AD-A192719] 20 p2843 N88-26869

A numerically efficient digital matched filter for periodic and windowed periodic radar waveforms
[AD-A193132] 21 p2932 N88-27410

Picosecond optoelectronic sampling of electrical waveforms produced by an optically excited field effect transistor
[AD-A192384] 21 p2935 N88-27428

A deconvolution technique using least-squares model-fitting and its application to optical pulse measurement
[NPL-DES-87] 22 p3144 N88-26694

Effect of phase errors in stepped-frequency radar systems
[AD-A194476] 23 p3203 N88-29061

The 1983 direct strike lightning data, part 1
[NASA-TM-86426-PT-1] 23 p3237 N88-29259

The 1983 direct strike lightning data, part 2
[NASA-TM-86426-PT-2] 23 p3237 N88-29260

The 1983 direct strike lightning data, part 3
[NASA-TM-86426-PT-3] 23 p3237 N88-29261

Waveform analysis on the IBM PC
[AD-A194249] 23 p3248 N88-29330

Wigner distribution function: Relation to short-term spectral estimation, smoothing and performance in noise
[AD-A193865] 23 p3275 N88-29492

Waveform relaxation applied to transient device simulation
[AD-A194992] 24 p3432 N88-30429

WAVEGUIDE ANTENNAS

The wavenumber: An alternative to the directional coupler for multimode analysis in oversized waveguides
[IPF-87-2] 01 p0037 N88-10237

Current-drive on the Versator-2 tokamak with a slotted-waveguide fast-wave coupler
[DE88-006261] 15 p2136 N88-22743

Investigation of radiating and guiding structures in microstrip patch antennas
[AD-A191445] 16 p2193 N88-23082

WAVEGUIDE FILTERS

A study of scattering from E-plane circuit elements
[AD-A184473] 04 p0431 N88-12[illegible]73

WAVEGUIDE LASERS

Investigation of BN CO2 wave guide laser
03 p0302 N88-11905

High power phased array and tailored gain semiconductor lasers 03 p0329 N88-12078

Coupled high power waveguide laser research
[AD-A189800] 15 p2071 N88-22345

Efficient narrow linewidth waveguide dye laser pumped by CuCl laser 16 p2187 N88-23038

UV-Laser reactions of molecular adsorbates
[AD-A190796] 16 p2212 N88-23201

Distributed feedback lasers
[NASA-CR-4154] 18 p2520 N88-24946

WAVEGUIDES
NT BEAM WAVEGUIDES
NT CIRCULAR WAVEGUIDES
NT OPTICAL FIBERS
NT OPTICAL WAVEGUIDES
NT PLASMAGUIDES
NT RECTANGULAR WAVEGUIDES

The wavenumber: An alternative to the directional coupler for multimode analysis in oversized waveguides
[IPF-87-2] 01 p0037 N88-10237

Design and analysis of a broadband TM(sub 01) mode generator in cylindrical waveguide
[DE87-011308] 01 p0038 N88-10243

Generalized coupled-mode equations, applications to fiber couplers 03 p0298 N88-11875

Coupling and absorption phenomena in semiconductor-clad dielectric optical waveguides
[DE87-013446] 03 p0307 N88-11939

Eigenmode analysis of parallel waveguide couplers
[PB87-132122] 06 p0693 N88-14254

ATF (Advanced Toroidal Facility) ECH (Electron Cyclotron Heating) waveguide component development and testing
[DE88-001432] 06 p0782 N88-14797

Propagation of radiation along a constricting optical waveguide 07 p0920 N88-15590

Low-g propellant gaging 08 p0982 N88-15937

Approximation of noncorrelated reflections in problem of sound propagation through waveguide with rough boundary 08 p1076 N88-16487

Mode pattern of field generated by parametric radiator in acoustic waveguide 08 p1076 N88-16488

Performance of linear vertical antenna in refractive multimode waveguide 08 p1076 N88-16489

Acoustic field in waveguide with sloping bed
08 p1076 N88-16490

Diffraction of sound at junction of two waveguides
08 p1076 N88-16491

Modeling of some coplanar waveguide discontinuities
[NASA-TM-100808] 10 p1318 N88-17880

Guided-wave approaches to spectrally selective energy absorption
[NASA-CR-182532] 10 p1320 N88-17892

First and second harmonic ECRH experience at gyrotron frequencies at LLNL
[DE88-003998] 10 p1413 N88-18430

Lg wave excitation and propagation in the presence of one-, two-, and three-dimensional heterogeneities
[AD-A187364] 11 p1510 N88-19022

Nonlinear optical waveguides containing a transition metal-based dye molecule
[DE88-003257] 11 p1550 N88-19275

Propagation in longitudinally varying ducts, with emphasis on guiding to antiguiding transitions
12 p1615 N88-19658

Two-dimensional electron fluid computer calculations of nanosecond pulse, low pressure microwave air breakdown in a rectangular waveguide and their verification by experimental measurement
[DE88-004407] 12 p1618 N88-19678

Transformation coefficient in wave-field acceleration scheme
[DE88-700158] 13 p1757 N88-20507

Slow waves in waveguide with elliptical cross section
[DE88-700159] 13 p1757 N88-20508

Multimode-waveguide laser beam deflector
[DE88-006222] 13 p1776 N88-20622

Low threshold ridge waveguide single quantum well lasers 13 p1777 N88-20631

Anisotropy of light absorption by color centers in waveguides produced on photochromic glasses by diffusion 14 p1896 N88-21320

Superconducting thin film vertex detector for SSC (Superconducting Super Collider) applications
[DE88-005951] 17 p2445 N88-24535

Nonlinear surface polaritons
[AD-A191046] 18 p2499 N88-24822

Signal processing with degenerate four-wave mixing
[AD-A191496] 18 p2499 N88-24825

Theoretical study of the folded waveguide
[DE88-007677] 19 p2654 N88-25759

Enhanced performance ultrabroadband distributed amplifiers 19 p2656 N88-25775

Characteristics and application of wideband guided-wave devices 19 p2660 N88-25817

Optical modulation above 20 GHz using a waveguide electrooptic switch 19 p2660 N88-25819

Variational analysis of dielectrically loaded multidepth corrugated waveguides
[PB88-193602] 20 p2793 N88-26573

Quantum transport in an electron waveguide
20 p2864 N88-27010

Experimental investigation of simplest inhomogeneities in cylindrical slit line
[DE88-702388] 21 p2933 N88-27418

Guided wave interactions in millimeter-wave integrated circuits
[AD-A193017] 21 p2936 N88-27437

An 8.4-GHz dual maser front end for Parkes reimplementation 22 p3068 N88-28197

Qualitative characteristics of open waveguide resonator spectra
[DE88-702387] 23 p3202 N88-29056

Confirmation of slow-waves in a crosstie overlay coplanar waveguide and its application to band-reject gratings and reflectors
[AD-A194981] 24 p3361 N88-30011

Dielectric millimeter waveguides: A feasibility study for a novel dielectric millimeter waveguide
[AD-A195104] 24 p3366 N88-30042

Analytical and experimental studies of beam waveguide absorbers for structural damping
[AD-A195085] 24 p3382 N88-30144

WAVELENGTH DIVISION MULTIPLEXING

Digital television routing systems: A survey of optical and electrical techniques
[BBC-RD-1988/3] 19 p2654 N88-25763

WAVELENGTHS

Spectrometric test of a linear array sensor
[NASA-TM-100676] 01 p0064 N88-10414

Selection of optimum wavelengths for ozone mapping from satellites 05 p0619 N88-13798

Collider constraints in the choices for wavelength and gradient scaling
[PB87-123691] 06 p0779 N88-14783

Modern pulsed wavemeters
[DE88-003875] 10 p1335 N88-17978

Study for the determination of general and specific properties of wide energy-band gap HgHdTe in the 1-2 micrometer wavelength range
[AD-A189177] 13 p1845 N88-21041

Theoretical studies of Resonance Enhanced Stimulated Raman Scattering (RESRS) of frequency-doubled Alexandrite laser wavelength in cesium vapor
[NASA-CR-182870] 15 p2036 N88-22133

SDIO/IST ultrashort wavelength laser. Mossbauer effect in gamma-ray lasers
[AD-A190308] 15 p2072 N88-22352

Dual wavelength holographic interferometry system
[NASA-CASE-MFS-28242-1] 17 p2341 N88-23960

Wavenumber spectra from THIR 6.7 micron water vapor data 20 p2824 N88-26756

WAVES

WKBJ method and strained coordinates for high frequency inertial wave filtering
[INPE-4214-PRE/1095] 11 p1537 N88-19186

Brunt-Doppler ducting of buoyancy waves in a temperature- and wind-stratified atmosphere
18 p2542 N88-25086

WEAK ENERGY INTERACTIONS

NT WEAK INTERACTIONS (FIELD THEORY)

Neutrinos in supernovae
[DE87-014295] 03 p0387 N88-12434

Few body hypernuclear systems: Weak decays
[DE87-014920] 04 p0488 N88-13010

The H5(+) potential energy hypersurface: Characterization of ten distinct energetically low-lying stationary points 16 p2267 N88-23561

Weak interaction physics: From its birth to the electroweak model
[DE88-702494] 23 p3280 N88-29531

WEAK INTERACTIONS (FIELD THEORY)

Summary and conclusions of the 6th Moriond workshop --- standard electroweak model
[USIP-87-11] 01 p0092 N88-10602

An introduction to charm and heavy quark physics
[DE87-013589] 02 p0231 N88-11455

The standard theory group: Summary and conclusions
[PREPRINT-551] 06 p0778 N88-14776

Determination of the neutral current chiral coupling constants u sublsq, u subrsq, d sublsq and d subrsq from an (anti)neutrino-deuterium experiment
[B8715857] 06 p0779 N88-14780

Theory of elementary particle studies in weak iteration and grand unification and studies in accelerator design
[DE88-004261] 11 p1545 N88-19238

Semileptonic weak interactions in nuclei: A relativistic analysis
[CEBAF-PR-87-024] 11 p1547 N88-19249

Searches for forces weaker than gravity
[DE88-003579] 13 p1832 N88-20959

Intermediate energy neutrino physics
[DE88-005378] 13 p1836 N88-20984

The response of a small liquid scintillation counter for low energy (gamma, p) experiments
[NOTA-INTERNA-901] 14 p1980 N88-21819

Lattice QCD calculation of K yields pi nonleptonic weak transition and other hadronic weak parameters
[PREPRINT-580] 15 p2132 N88-22717

Weak interaction physics: From its birth to the electroweak model
[DE88-702494] 23 p3280 N88-29531

WEAPON SYSTEM MANAGEMENT

Contribution of expert systems to avionics advance. Application on AS30 laser weapon system
[SNIAS-881-320-103] 23 p3267 N88-29449

WEAPON SYSTEMS

NT LASER WEAPONS

NT MISSILE SYSTEMS

Design principles and practices for implementation of MIL-STD-1760 in aircraft and stores
[AD-A183724] 01 p0005 N88-10027

Current status of high power microwave effects and simulation
[DE87-004112] 06 p0751 N88-14615

Integrated diagnostics 09 p1111 N88-16655

A piloted simulation investigating handling qualities and performance requirements of a single-pilot helicopter in air combat employing a helmet-driven turreted gun
[AD-A188878] 09 p1116 N88-16689

Neural network based architectures for aerospace applications 09 p1204 N88-17218

Research and development. Technical-scientific publications (1956-1987): Retrospective view and prospects. Jubilee edition on the occasion of the 75th birthday of Dipl.-Engr. Dr.-Engr. E. H. Ludwig Boelkow
[ISSN-0931-9751] 10 p1309 N88-17819

Investigation of several spread shot conditions
[REPT-TR-164] 10 p1310 N88-17830

Development savings through parametric modeling of program costs 12 p1700 N88-20175

Systems analysis and simulation techniques: Essential tools for balanced complex weapon system designs in terms of performance and cost
12 p1702 N88-20187

AGARD Highlights 88/1 14 p2012 N88-22001

The Design, Development and Testing of Complex Avionics Systems
[AGARD-CP-417] 17 p2302 N88-23767

Architecture and role of the Sensor Subsystem in future aircraft weapon systems 17 p2302 N88-23770

The specification and design of a future maritime reconnaissance aircraft 17 p2303 N88-23772

A structured approach to weapon system design
17 p2303 N88-23773

A change in system design emphasis: From machine to man 17 p2304 N88-23782

Advanced development of a cockpit automation design support system 17 p2304 N88-23785

The electromagnetic threat to future avionic systems
17 p2305 N88-23790

Coherent functional development: Key to successful future system integration 17 p2307 N88-23803

Flight testing under extreme environmental conditions
[AGARD-AG-300-VOL-8] 21 p2951 N88-27525

Can CNV amplitude predict ability to accomplish a demanding task? 21 p2980 N88-27700

Inflight rearming
[AD-A193564] 23 p3176 N88-28909

Computers in weapons systems: A look at the F-15
[AD-A194498] 23 p3178 N88-28920

WEAPONS

NT ARTILLERY

NT GUNS (ORDNANCE)

NT LASER WEAPONS

NT MINES (ORDNANCE)

NT NUCLEAR WEAPONS

NT SPACE WEAPONS

The impact of environmental factors on the performance of millimeter wave seekers in smart munitions
[DE87-014277] 03 p0270 N88-11697

The evolution of naval warfare technology and the impact of space systems
[AD-A186900] 09 p1233 N88-17392

Computational studies of wave-shaping in a blast simulator by perforated plates in the driver
[AD-A188200] 11 p1483 N88-18850

Soviet military power, 1987 13 p1858 N88-21114

Free electron lasers in strategic defense
[DE88-007024] 17 p2394 N88-24231

On 3-5 transistors for MM-wave applications
[AD-A191580] 19 p2661 N88-25825

Dependence effects in unique signal transmission
[DE88-010331] 21 p2933 N88-27419

A method for estimating the susceptibility of electronic systems to HPM (High Power Microwave)
[DE88-012246] 21 p2934 N88-27422

Fiber-optics used to record high-speed photographs inside a pressurized tank during lethality testing
[DE88-011283] 21 p2951 N88-27529

The Soviet Stealth fighter: Check or checkmate
[AD-A195200] 24 p3323 N88-29791

WEAPONS DELIVERY

The evolution of naval warfare technology and the impact of space systems
[AD-A186900] 09 p1233 N88-17392

Investigation of several spread shot conditions
[REPT-TR-164] 10 p1310 N88-17830

Implementation and performance analysis of parallel assignment algorithms on a hypercube computer
[AD-A190676] 15 p2115 N88-22600

WEAR

Endurance testing of a natural gas-fueled rotary engine
[PB87-215703] 01 p0055 N88-10356

Wear of iron and nickel in corrosive liquid environments
[NASA-TM-100246] 03 p0289 N88-11817

The friction and wear of TPS fibers
[NASA-CR-181496] 03 p0291 N88-11830

Wear of hard steel in rolling lubricated contact
[RP-699] 03 p0332 N88-12094

Real-time Raman detection of molecular changes in ceramics undergoing sliding friction
[DE88-000558] 04 p0421 N88-12809

Analysis of wear metals in engine oils using the atomic absorption spectrophotometric method
[NAL-TM-MT-8704] 05 p0564 N88-13435

Fretting wear and fretting fatigue damage
05 p0603 N88-13697

Sliding-wear properties of retained austenite in carburized layer
[PB87-149092] 07 p0833 N88-15054

Evaluation of load tracks and wear of two sets of bearings from space shuttle main engine high pressure oxygen turbopumps
[NASA-CR-178969] 07 p0861 N88-15223

Technology developments for a compound cycle engine 09 p1107 N88-16637

Characterization of the arc/spark excitation sources used in the spectrometric oil analysis program
[AD-A187131] 10 p1297 N88-17758

Friction and wear of monolithic and fiber reinforced silicon-ceramics sliding against IN-718 alloy at 25 to 800 C in atmospheric air at ambient pressure
[NASA-TM-100294] 10 p1304 N88-17796

Tribology of ceramics: Report of the Committee on Tribology of Ceramics
[NASA-CR-182506] 10 p1305 N88-17802

Mechanisms of wear in single- and two-phase materials
[DE88-003846] 10 p1305 N88-17806

Synthesis and structure property studies of toughened epoxy resins via functionalized polysiloxanes. Friction and wear studies
[AD-A188258] 11 p1462 N88-18718

Characterization and fundamental studies on CuO sorbent materials to determine attrition mechanisms on substrate gamma alumina
[DE88-003674] 13 p1749 N88-20456

Corrosion-wear process under rolling-sliding motion
[AD-A189603] 13 p1778 N88-20635

Overview of the DOE-ECUT Tribology Program
[DE88-002878] 13 p1778 N88-20637

On the torque and wear behavior of selected thin film MOS2 lubricated gimbal bearings
14 p1926 N88-21485

Friction and wear of ceramics
17 p2323 N88-23674

Ceramic technology for advanced heat engines project
[DE88-008945] 21 p2919 N88-27323

Studies of dynamic contact of ceramics and alloys for advanced heat engines
[DE88-008996] 21 p2919 N88-27324

Friction, wear and electrical contact resistance of precious metal alloys
[DE88-011244] 21 p2938 N88-27450

Calibration of the portable wear metal analyzer
[AD-A192971] 21 p2950 N88-27524

Influence of dispersed additives reinforcement on the wear reinforcement mechanisms of the alumina-steel couple. Macroscopic and structural aspects
[ECL-88-01] 22 p3059 N88-28148

An investigation of some basic properties of hybrid composite materials
[AD-A194136] 23 p3189 N88-28975

Static and dynamic metal-metal friction at plastic stress levels
[DE88-011281] 23 p3222 N88-29176

WEAR INHIBITORS

The performance of thin solid films for satellite gears
14 p1876 N88-21209

Ball bearings with chemical vapor deposition (CVD)-TiC coated components 14 p1876 N88-21210

Influence of dispersed additives reinforcement on the wear reinforcement mechanisms of the alumina-steel couple. Macroscopic and structural aspects
[ECL-86-01] 22 p3059 N88-28148

WEAR RESISTANCE
NT ABRASION RESISTANCE
Ceramic technology for advanced heat engines project
[DE88-001520] 04 p0420 N88-12605
Corrosion control by composite material substitution with application to the M-939 5-ton truck
04 p0428 N88-12654
The tribological properties of MoS2 coatings in vacuum, low relative humidity and high relative humidity environments
[DE88-001611] 06 p0711 N88-14356
Sliding-wear properties of retained austenite in carburized layer
[PB87-149092] 07 p0833 N88-15054
Modification of properties of metals by high-power ion beams 08 p1079 N88-16507
Bias, internal stress and substrate effects on the microstructure and properties of PVD-wear resistant coatings
[AERE-R-12360] 10 p1304 N88-17798
Institute for Materials Science and Engineering, Metallurgy: Technical activities 1987
[PB88-157722] 11 p1460 N88-18702
Synthesis and structure property studies of toughened epoxy resins via functionalized polysiloxanes
[AD-A187984] 11 p1462 N88-18715
Standardization of lubricity test
[AD-A187776] 11 p1465 N88-18736
The effects of thin polymeric surface films in reducing fretting corrosion and wear
[AD-A188633] 12 p1611 N88-19634
Reduction of erosion in elbows due to flow modifications, phase 1
[DE88-001028] 13 p1769 N88-20584
Titanium carbide coatings for aerospace ball bearings
14 p1927 N88-21486
Reciprocating sliding wear characteristics of copper-carbon fiber composites
[NASA-TT-20176] 15 p2031 N88-22100
High temperature solid lubrication by catalytically generated carbon
[AD-A190804] 16 p2182 N88-23004
The performance of perfluoropolyalkylether oils under boundary lubrication conditions
[AD-A191057] 17 p2323 N88-23869
Characterization of coating wear phenomena in nitride and carbide coated tool inserts
[DE88-011196] 20 p2779 N88-26478
Basic mechanisms of diesel lubrication correlation of bench and engine tests
[AD-A193360] 21 p2956 N88-27561
Development of high temperature, high pressure rotating shaft seals
[DE88-001029] 23 p3221 N88-29172

WEAR TESTS
Hot piston ring/cylinder liner materials: Selection and evaluation
[NASA-TM-100276] 08 p0971 N88-15872
The WAFTER: A versatile wear and friction tester
[MRL-TN-519] 09 p1169 N88-17012
Characterization of coating wear phenomena in nitride and carbide coated tool inserts
[DE88-011196] 20 p2779 N88-26478

WEATHER
NT COLD WEATHER
Hanford Meteorological Station computer codes. Volume 2: The PROD computer code
[DE87-014807] 02 p0215 N88-11355
Short reference year
[PB87-107470] 03 p0352 N88-12221
Study of microburst detection performance during 1985 in Memphis, Tennessee
[AD-A184013] 03 p0354 N88-12231
Drought, solar activity link established by Leningrad geophysicists 04 p0458 N88-12835
Application of TOMS data to weather analysis models
05 p0617 N88-13787
The use of TOMS-modified VAS data for large-scale NWP 05 p0618 N88-13791
Use of satellite data in volcano monitoring
05 p0618 N88-13797
The global climate system: Autumn 1984 to spring 1986
[CSM-R84/86] 06 p0745 N88-14563
Greatest volcanic eruptions in world during 17th-18th centuries and weather anomalies in Eurasian middle latitudes 08 p1012 N88-16134
Mariners Weather Log, Volume 31, Number 3, Summer 1987
[PB87-234894] 08 p1039 N88-16284
North Pacific Ocean. Subtropical front north of Hawaii, R/V Thomas G. Thompson: 7 January - 10 February 1974. CTD data report
[AD-A186565] 08 p1044 N88-16310
North Pacific Ocean. Subarctic front central Pacific, R/V Thomas G. Thompson: 8 September - 9 October 1975. CTD data report
[AD-A186567] 08 p1044 N88-16312
North Pacific Ocean. Northwest Pacific Transition Zone, R/V Thomas G. Thompson: 19 March - 1 May 1971. STD data report
[AD-A186568] 08 p1044 N88-16313
The Meteosat operational program
09 p1127 N88-16759
Revised uniform summary of surface weather observations. Parts A-F: Carswell AFB, Texas
[AD-A186820] 09 p1192 N88-17144
North Pacific Ocean. Central Pacific Transition Zone, R/V Thomas G. Thompson: 25 March - 3 May 1968. STD data report
[AD-A186570] 09 p1195 N88-17160
Continental shelf processes affecting the oceanography of the South Atlantic Bight
[DE88-004102] 09 p1196 N88-17166
The structure and dynamics of monsoon depressions
10 p1355 N88-18102
Proceedings of the Forest-Atmosphere Interaction Workshop
[CONF-8510250] 12 p1641 N88-19824
Revised Uniform Summary of Surface Weather Observations, Loring AFB, Maine, Parts A - F
[AD-A188201] 14 p1947 N88-21610
Mariners weather log, volume 32, number 1, Winter 1988
[PB88-173869] 18 p2544 N88-25097
Meteorological and Environmental Inputs to Aviation Systems
[NASA-CP-2498] 18 p2545 N88-25105
TDWR (Terminal Doppler Weather Radar) PRF (Pulse Repetition Frequency) selection criteria
[AD-A193089] 21 p2932 N88-27407
Withstand voltage of slightly polluted insulator chains in humid weather conditions
[DE88-752818] 22 p3072 N88-28237
Prolonged periods of above-normal temperatures in Canada, 1986/87 22 p3120 N88-28538
Typical weather months in the past (1973-1983) in Central Europe
[AD-A194701] 23 p3235 N88-29249
Basic causes of amplitude modulation in climatic/weather parameters
[DE88-702743] 23 p3236 N88-29254

WEATHER CHARTS
U METEOROLOGICAL CHARTS

WEATHER CONDITIONS
U WEATHER

WEATHER CONTROL
U WEATHER MODIFICATION

WEATHER FORECASTING
NT LONG RANGE WEATHER FORECASTING
NT NOWCASTING
NT NUMERICAL WEATHER FORECASTING
NT STATISTICAL WEATHER FORECASTING
Tropical cyclone center locations from enhanced infrared satellite imagery
[PB87-213450] 01 p0071 N88-10455
Hanford Meteorological Station computer codes. Volume 1: The GEN computer code
[DE87-012816] 01 p0071 N88-10456
Applications and benefits of short period weather forecasts 02 p0199 N88-11240
COST-73 and its application in very short range forecasting 02 p0199 N88-11242
Mesoscale forecasting today and tomorrow: Problems and opportunities. A position paper
02 p0199 N88-11244
Improved geostationary satellite soundings for the mesoscale weather analysis/forecast operation
02 p0200 N88-11252
Analysis of thickness fields retrieved from NOAA-7 observations through the 3I (Improved Initialization Inversion) method. Interest for weather forecasting
02 p0201 N88-11255
Operational cloud-clearing techniques of VAS radiance data --- Visible and Infrared Spin Scan Radiometer Atmospheric Sounder (VAS) 02 p0201 N88-11256
The combined use of diagnosed mesoscale frontogenesis and satellite imagery in forecasting squall line formation 02 p0201 N88-11258
The role of low-level cooling in a conceptual model of the Australian summertime cool change: Implications for very-short-range forecasting 02 p0204 N88-11275
Meteorological systems support to critical shuttle requirements on the Eastern Test Range --- STS
02 p0205 N88-11281
Evaluation of the Rainsat precipitation analysis system in real-time use 02 p0205 N88-11283
The use of McIDAS as a Mesoscale forecasting tool during the Canadian Atlantic storms programs --- Man-computer Interactive Data Access System (McIDAS) 02 p0205 N88-11284
A short-range forecasting experiment conducted during the Canadian Atlantic storms program
02 p0205 N88-11285
The challenge of very short range forecasting in the tropics 02 p0205 N88-11287
Simplified models for use in an operational short range forecasting system 02 p0206 N88-11289
Use of time changes of surface data parameters in short range forecasting 02 p0206 N88-11291
Mesoscale thunderstorm forecasting using RAOB data, surface mesonet observations, and an expert system
02 p0206 N88-11293
A review of the analysis forecasting and research about severe local storms in Guangdong province (China)
02 p0207 N88-11298
Short-term forecasting of lightning based on the surface wind field at Kennedy Space Center
02 p0208 N88-11306
Forecasting stratus over the British Isles
02 p0209 N88-11310
Short range forecast of the daily maximum temperature 02 p0209 N88-11313
Short range forecasting of sea breeze generated thunderstorms at the Kennedy Space Center: A real-time experiment using a primitive equation mesoscale numerical model 02 p0211 N88-11324
Summary of 1987 Atlantic tropical cyclone activity and verification of author's seasonal forecast
02 p0215 N88-11356
Severe weather potential (SPOT) plotfile generator
[PB87-217717] 02 p0216 N88-11360
Convective cross section analysis
[PB87-204566] 02 p0216 N88-11361
Kinds of bootstraps and kinds of jackknives, discussed in terms of a year of weather-related data
[AD-A184495] 03 p0353 N88-12227
Tropical cyclone intensity prediction based on empirical orthogonal function representation of wind and shear fields
[AD-A184699] 03 p0353 N88-12229
Progress in improving weather forecasting viewed
04 p0458 N88-12833
NWS (National Weather Service) watch/warning verification flash flood, winter storm and high wind, January 1980 - June 1986
[PB87-223053] 04 p0469 N88-12898
Annual tropical cyclone report, 1986
[AD-A184082] 04 p0470 N88-12903
Ozone, jet streaks and severe weather
05 p0616 N88-13781
ZEUS: A knowledge-based expert system that assists in predicting visibility at airbases
[AD-A184197] 05 p0626 N88-13829
Isentropic analysis and interpretation: Operational applications to synoptic and mesoscale forecast problems
[AD-A184814] 05 p0626 N88-13830
Mesoscale applications of high resolution imagery
[AD-A185039] 05 p0627 N88-13833
Opportunities for tropical cyclone motion research in the Northwest Pacific region
[AD-A185068] 05 p0627 N88-13834
USSR report: Earth sciences
[JPRS-UES-87-004] 06 p0725 N88-14455
Regional weather satellite data processing center opens in Tashkent 06 p0725 N88-14457
BARS-1M meteorological complex carried on IL-18 airplane 06 p0725 N88-14458
Current status of world weather service
06 p0725 N88-14459
Atmosphere dynamics in the equatorial meteor zone
06 p0733 N88-14508
Eighth Session of the Commission for Aeronautical Meteorology (abridged)
[WMO-673] 06 p0745 N88-14585
Verification of severe local storm forecasts issued by the National Severe Storms Forecast Center, 1986
[PB88-101407] 06 p0747 N88-14594
Objective prediction of monthly mean surface temperature and climatological relationships to mid-tropospheric heights
[DE88-000908] 07 p0880 N88-15340
Characterization of meteorological phenomena influencing aircraft operations 08 p0951 N88-15772
A study of finite difference and finite element vertical discretization schemes for baroclinic prediction equations
[AD-A186617] 08 p1040 N88-16291

Assessment of VAS-derived products created by a simultaneous algorithm on a convectively active day
[AD-A186158] 08 p1054 N88-16359
Numerical investigation of orographically enhanced instability
[AD-A186841] 09 p1189 N88-17125
Modification of a successive corrections objective analysis for improved higher order calculations
[NASA-CR-182467] 09 p1230 N88-17370
Prediction of polytomous events: Model description, algorithm development and methodological aspects, with an application
[AD-A186549] 09 p1232 N88-17384
Status of FAA terminal Doppler weather radar programs 10 p1275 N88-17632
AEV local verification for aviation, precipitation and temperature programs: AV, REL, TEM (September 1987 revision)
[PB88-115662] 10 p1355 N88-18101
Systematic errors of the FSU global spectral model
10 p1356 N88-18103
Aviation weather: Status of FAA's (Federal Aviation Administration's) new hazardous weather detection and dissemination systems
[PB88-115910] 11 p1513 N88-19041
Misty picture weather-watch and microbarograph project: Experiments 9412-14-18
[DE88-003949] 11 p1514 N88-19047
Optimal sampling to provide user-specific climate information 11 p1515 N88-19051
Model of limited area of 5 layers for numerical weather forcasting
[INPE-4324-RPE/551] 11 p1516 N88-19053
Effects of stress on judgement and decision making in dynamic tasks
[AD-A188203] 11 p1523 N88-19092
National Severe Storms Laboratory, fiscal year 1987
[PB88-140108] 12 p1647 N88-19863
Activities report in meteorology
[AR-86-87] 13 p1798 N88-20755
Wind shear as a predictor of severe weather for the eastern United States
[PB88-157144] 13 p1800 N88-20762
Adiabetic formation of large-scale models of the atmosphere 14 p1935 N88-21541
Baseline observing system experiments using the AFGL global data assimilation system
[AD-A188861] 15 p2024 N88-22062
Derivation of consistent surface fixed fields for use in a global NWP model
[AD-A190131] 15 p2083 N88-22475
Aircraft accident/incident summary reports: Modena, Pennsylvania, March 17, 1986; Redwater, Texas, April 4, 1986
[PB88-910403] 16 p2159 N88-22878
Very short range statistical forecasting of automated weather observations
[AD-A190803] 16 p2235 N88-23349
Fog, rain and aerosol attenuation in the atmosphere
[AD-A190867] 16 p2235 N88-23350
Spectroradiometry in meteorology
16 p2272 N88-23599
Adaptive grid refinement for numerical weather prediction
[AD-A192172] 18 p2544 N88-25101
Automation of surface observations program
18 p2545 N88-25106
Special observations 18 p2545 N88-25108
General-aviation's view of progress in the aviation weather system 18 p2546 N88-25110
National plans for aircraft icing and improved aircraft icing forecasts and associated warning services
18 p2546 N88-25113
Objective detection and forecasting of Clear-Air Turbulence (CAT): A status report
18 p2546 N88-25114
Denver ARTCC evaluation of PROFS (Prototype Regional Observations and Forecast System) mesoscale weather products 18 p2547 N88-25117
US participation in the TOGA (Tropical Ocean and the Global Atmosphere) Program: A research strategy
[DE88-010986] 19 p2681 N88-25938
ECMWF (European Centre for Medium Range Weather Forecasts) global analyses 1979-1986: Circulation statistics and data evaluation
[PB88-178165] 19 p2692 N88-26001
Suggested hurricane operational scenario for GOES I-M
[NASA-TM-89729] 19 p2692 N88-26002
Satellite observed Mesoscale Convective System (MCS) propagation characteristics and a 3-12 hour heavy precipitation forecast index
[PB88-180161] 19 p2692 N88-26004
BOLETIM: An expert system for weather forecasting
[INPE-4538-TDL/329] 19 p2693 N88-26011
Mariners weather log, volume 31, number 4, Fall 1987
[PB88-173851] 20 p2825 N88-26761
Synoptic patterns related to tropical cyclone recurvature
[AD-A192338] 20 p2827 N88-26771
Intercomparison of NMC (National Meteorological Center) and ECMWF (European Centre for Medium Range Weather Forecasts) global analyses: 1980-1986
[PB88-196548] 21 p2974 N88-27668
The Hanford meteorological data collection system and data base
[DE88-006632] 21 p2975 N88-27672
Modes of interannual climate variability and Sahel rainfall anomalies 22 p3121 N88-28547
Systematic behavior of NMC medium range forecasts and the effect of model changes 1985-87
22 p3125 N88-28575
The impact of the El Nino event on the ECMWF model performance 22 p3125 N88-28576
DERF forecasts of thickness
22 p3126 N88-28579
Analysis of the dynamic extended range forecast experiment 22 p3126 N88-28581
Investigations on the entropy of cloudy air
[ESA-TT-1060] 23 p3234 N88-29245
Typical weather months in the past (1973-1983) in Central Europe
[AD-A194701] 23 p3235 N88-29249
A study of the feasibility of using sea and wind information from the ERS-1 satellite. Part 1: Wind scatterometer data
[NASA-CR-182833] 24 p3386 N88-30167
A study of the feasibility of using sea and wind information from the ERS-1 satellite. Part 2: Use of scatterometer and altimeter data in wave modeling and assimilation
[ESA-CR(P)-2604-PT-2] 24 p3387 N88-30176
Temperature profile construction methods: An evaluation
[AD-A195919] 24 p3403 N88-30262

WEATHER FRONTS
U FRONTS (METEOROLOGY)

WEATHER MAPS
U METEOROLOGICAL CHARTS

WEATHER MODIFICATION
NT CLOUD DISPERSAL
NT CLOUD SEEDING
NT LIGHTNING SUPPRESSION
NT RAINMAKING
NT STORM ENHANCEMENT
NT STORM SUPPRESSION
Measurements of vapor flux, liquid water contents, precipitation rates and riming in a Utah mountain cloud system
[PB87-224945] 04 p0469 N88-12900
Altered and enhanced iodargyrite with bismuth triiodide for use in precipitation enhancement operations
[AD-A185229] 05 p0561 N88-13419
Electron acceleration by wave processes in the earth's ionosphere
[AD-A186110] 07 p0877 N88-15320
Cloud physics studies in SCPP (Sierra Cooperative Pilot Project) from 1977-87
[PB88-136924] 11 p1516 N88-19054
High altitude chemical release systems for project BIME (Brazilian Ionospheric Modification Experiments) project IMS (Ionospheric Modification Studies) project PIIE (Polar Ionospheric Irregularities Experiment) project polar arcs
[AD-A188299] 12 p1642 N88-19833
The Effect of the Ionosphere on Communication, Navigation and Surveillance Systems Based on Ionospheric Effects Symposium held on 5-7 May 1987 in Springfield, Virginia
[AD-A191855] 18 p2541 N88-25081

WEATHER RADAR
U METEOROLOGICAL RADAR

WEATHER STATIONS
NT AUTOMATIC WEATHER STATIONS
Hanford Meteorological Station computer codes. Volume 1: The GEN computer code
[DE87-012816] 01 p0071 N88-10456
Hanford Meteorological Station computer codes. Volume 2: The PROD computer code
[DE87-014807] 02 p0215 N88-11355
Calendar year 1985 solar and weather data for Austin, Texas
[PB87-220174] 03 p0352 N88-12219
A single-station weather forecasting expert system
[AD-A184889] 05 p0627 N88-13832
Inventory of weather stations. Climatological data from Dutch stations, no. 26
[KNMI-150-26] 05 p0628 N88-13841
Hanford Meteorological Station computer codes. Volume 5: The TOWER computer code
[DE88-001610] 05 p0628 N88-13843
Mariners Weather Log, Volume 31, Number 3, Summer 1987
[PB87-234694] 09 p1039 N88-16284
Automatic data acquisition system utilizing microcomputers: Automatic Meteorological Stations (AMS)
[INPE-4215-PRE/1096] 12 p1646 N88-19859
Climatic summaries of ocean weather stations
[PB88-162920] 14 p1948 N88-21617

WEATHERING
The distribution of evaporitic weathering products on Antarctic meteorites 06 p0798 N88-14888
Application of inverse gas chromatography to fluidity studies
[DE88-002896] 10 p1296 N88-17750
A five year weathering experiment with solar collectors
[DE88-900369] 13 p1796 N88-20740
The effect of weathering on octane quality for winter-grade and summer-grade gasolines
[AD-A190640] 16 p2183 N88-23012
Investigation of the long term effects of aging on carbon epoxy composites exposed naturally to the weather under cyclic loads. (Results of sampling after 2.5 years). Test report M1-641300
[CEAT-39/M/79-C-M1-641300]
17 p2316 N88-23834
Effects of natural environment on first generation solid rocket booster thermal protection system materials
[NASA-TM-100329] 17 p2373 N88-24113
A sedimentological and mineralogical study of the Koogah Formation, New South Wales
18 p2542 N88-25087
Selective weathering of shocked minerals and chondritic enrichment of the Martian fines
23 p3301 N88-29660
Weathering of sulfides on Mars
23 p3301 N88-29662
Variability in spectral signatures of terrestrial volcanic rocks and implications for volcanology on Mars
23 p3303 N88-29672
Aqueous alteration in S-N-C meteorites and implications for weathering products on Mars
23 p3303 N88-29673
Some probable characteristics of the Martian regolith
23 p3303 N88-29678
What SNC meteorites tell us about Martian magmatism 23 p3303 N88-29679
Preliminary analysis of recent 2.2-4.2 micrometers telescopic observations of Elysium, Mars: Implications for crystallinity and hydration state of surface materials
23 p3306 N88-29692
Photoacoustic Fourier transform infrared spectroscopy. An early detection technique for coatings degradation
24 p3354 N88-29968

WEAVING
Carbon-carbon composites and Aerospatiale: State of the art and prospects
[SNIAS-872-430-108] 05 p0559 N88-13401
Damage initiation and growth in sateen laminates under static and cyclic loading 11 p1449 N88-18634
An investigation of some basic properties of hybrid composite materials
[AD-A194136] 23 p3189 N88-28975

WEBS (MEMBRANES)
U MEMBRANES

WEDGE FLOW
Analytical investigation of reflection of a regular or mach reflection over a secondary wedge
[AD-A185690] 06 p0703 N88-14316
On the parabolized Navier-Stokes equations without sublayer assumptions
[AD-A186127] 07 p0649 N88-15152
Compressible flow in a pie-shaped cylinder rotating about the vertex 18 p2460 N88-24604
Navier-Stokes simulation of shock-tube flows over a wedge-type step by finite volume method
[ISAS-RN-628] 20 p2797 N88-26599

WEDGES
Eddy current density in wedge-shaped conducting cylinders with inhomogeneous conductivity
[ETN-87-90404] 01 p0042 N88-10268
Interior impedance wedge diffraction with surface waves
[NASA-CR-182405] 07 p0854 N88-15186
Plane wave diffraction by a thin dielectric wedge
[RSRE-MEMO-4045] 09 p1153 N88-16912
An interferometric investigation of the diffraction of planar shock waves over a half-diamond cylinder in air
[UTIAS-322] 13 p1768 N88-20575
Wind tunnel tests of the influence of airfoil-thickness on normal force and pitching moment of two slender wings at transonic and supersonic Mach numbers
[DFVLR-FB-88-17] 21 p2893 N88-27171
Experimental investigation of the reflection of a planar shock wave over a double wedge
[AD-A193078] 21 p2943 N88-27482

Numerical modeling results for mode propagation in a wedge
[AD-A193998] 22 p3147 N88-28718
Acoustic pressure distribution on the bottom of a wedge-shaped ocean
[AD-A193961] 23 p3278 N88-29518
WEIBULL DENSITY FUNCTIONS
A probabilistic model of brittle crack formation
[AD-A184423] 03 p0338 N88-12129
Static and dynamic determination of aluminum oxide toughness
[PB87-146999] 07 p0869 N88-15275
Statistical evaluation of experimental results from fatigue strength tests on CFRP composite materials
11 p1449 N88-18635
Tests for uniformity arising from a series of events
[AD-A189069] 13 p1828 N88-20935
Modeling failures of intermittently used machines
[AD-A190298] 15 p2074 N88-22367
Measurement and interpretation of North Atlantic Ocean marine radar sea scatter
[AD-A196239] 24 p3364 N88-30036
WEIERSTRASS FUNCTIONS
General solution of certain functional equations
[PREPRINT-554] 06 p0764 N88-14689
Mode 3 problems of doubly-periodic rhombic and rectangular array of equal cracks in an infinite plate
[PB87-144846] 08 p0996 N88-16031
WEIGHT
A class 2 weight assessment for the implementation of commonality and preliminary structural designs for the family of commuter airplanes
[NASA-CR-182565] 12 p1581 N88-19464
WEIGHT (MASS)
NT ATOMIC WEIGHTS
NT BIOMASS
NT BODY WEIGHT
NT STRUCTURAL WEIGHT
Shielding analysis of a small compact space nuclear reactor
[AD-A185566] 06 p0779 N88-14784
Alternative program approaches for the advanced satellite technology program
[AD-A188917] 12 p1600 N88-19576
Impact of control errors on the volume/weight demand of the Ventilation and Dryer (VAD) concept --- EURECA Botany Facility
[TN-RB524-006/87] 17 p2377 N88-24132
Ballistic evaluation of applique armours: Presentation and interpretation of ballistic data
[MRL-TN-527] 19 p2635 N88-25629
Spray automated balancing of rotors: Methods and materials
[NASA-CR-182151] 24 p3330 N88-29825
WEIGHT ANALYSIS
The initial calculation of range and mission fuel during conceptual design --- aircraft design
[LR-525] 16 p2161 N88-22889
WEIGHT FACTORS
U WEIGHT (MASS)
WEIGHT INDICATORS
Strain gage balance for half models 302-6. Calibration report --- wind tunnels
[F+W-FO-1803] 09 p1168 N88-17001
Strain gage sting balance 204-6. Calibration report --- wind tunnels
[F+W-FO-1838] 09 p1168 N88-17002
WEIGHT MEASUREMENT
Uniform laws and regulations as adopted by the National Conference on Weights and Measures (72nd), 1987
[PB88-123724] 06 p0689 N88-14225
Stability of uncapsulated weight cells with thin film elongation measurement bands under influence of humidity, temperature and operation voltage
[ETN-88-92383] 21 p2851 N88-27531
WEIGHT REDUCTION
The use of Kevlar on aero-engine fan containment casings
[PNR90410] 02 p0182 N88-11134
Rational reinforcement of cylindrical shells with variable stiffness frames subjected to external pressure
04 p0426 N88-12638
Corrosion control by composite material substitution with application to the M939 5-ton truck
04 p0428 N88-12654
Making space nickel/hydrogen batteries lighter and less expensive
[DE88-000168] 05 p0578 N88-13530
Study on utilization of advanced composites in fuselage structures of large transports
[NASA-CR-172406] 07 p0827 N88-15014
Composite/metal jointing technology for vehicle weight reduction
[DE88-900228] 08 p0992 N88-16005
Operation Everest 2: Nutrition and body composition
[AD-A186449] 08 p1049 N88-16333
Rotorcraft weight trends in light of structural material characteristics
[AD-A186578] 10 p1276 N88-17642
Lightsats and their attraction to budget oriented Federal agencies 10 p1289 N88-17711
Modern materials for light constructions --- aircraft
[MBB-Z-136/86] 10 p1312 N88-17839
Minimum weight design of rectangular and tapered helicopter rotor blades with frequency constraints
[NASA-TM-100561] 12 p1582 N88-19465
Minimum weight design of rotorcraft blades with multiple frequency and stress constraints
[NASA-TM-100569] 16 p2161 N88-22892
The application of high temperature superconductors to space electrical power distribution components
[NASA-TM-100901] 16 p2171 N88-22939
Development of a lightweight structure with load bearing capability and high thermal conductance
17 p2420 N88-24393
Weight savings in aerospace vehicles through propellant scavenging
[NASA-TM-100900] 19 p2605 N88-25470
Performance of lightweight nickel electrodes
[NASA-TM-100958] 20 p2771 N88-26430
High power pulse energy system concept
[AD-A192440] 21 p2935 N88-27429
Variability in intake and dehydration in young men during a simulated desert walk
[AD-A192654] 22 p3131 N88-28613
WEIGHTING FUNCTIONS
The criterion of equal integrated quality: An improved method of planning DBS systems
[BBC-RD-1987/10] 02 p0161 N88-11012
Weighted decoding of block codes and some topics on decoding complexity
[ENST-87E005] 02 p0221 N88-11394
Finite element techniques 06 p0701 N88-14303
A weighting sequence approach to the analysis and design of multivariable control systems
[AD-A186086] 07 p0917 N88-15570
Finite element fundamentals, part 2
08 p0985 N88-15962
Boundary elements combined with singular fields for three-dimensional cracked solids
[RAE-TR-87038] 09 p1183 N88-17088
Five-diagonal weighting scheme for geoidal profiles
[AD-A188033] 10 p1347 N88-18054
On the dynamic estimation of relative weights for observation and forecast in numerical weather prediction
[NASA-CR-182531] 10 p1356 N88-18106
Two dimensional uncorrelated bias in fix algorithms
[NASA-CR-182683] 13 p1815 N88-20847
Robustifying the Kalman filter
[AD-A189240] 13 p1825 N88-20907
Weighted averaging method for image smoothing reported 14 p1901 N88-21352
On 2-D versus 3-D: Sine of squared angular error and weighted perpendicular fixing
[NASA-CR-182899] 16 p2252 N88-23458
Asymptotic theory for weighted least squares estimators in Aalen's additive risk model
[AD-A191085] 18 p2562 N88-25210
Wigner distribution function: Relation to short-term spectral estimation, smoothing and performance in noise
[AD-A193865] 23 p3275 N88-29492
A theoretical and experimental investigation into the use of SAW weighting techniques in optical diffraction gratings
[RSRE-MEMO-4128] 23 p3283 N88-29549
WEIGHTLESSNESS
Aquarack: Aims and Possible Research Projects
[DFVLR-MITT-87-01] 01 p0073 N88-10469
Long term investigations of the growth, metabolism, and reproduction of fish under conditions close to weightlessness 01 p0074 N88-10473
The influence of weightlessness on the metabolism of the Biomphalaria glabrata 01 p0074 N88-10475
Life support systems for biological experiments under weightlessness in the German and European space programs 01 p0074 N88-10477
Testing of heat pipes on SPAS-01
[BMFT-FB-W-86-014] 06 p0672 N88-14119
Proceedings and program draft in Gravitational Biology in the Federal Republic of Germany --- Effects of Weightlessness on the Human Organism
[ESA-TT-988] 07 p0884 N88-15363
The role of the DFVLR project management life sciences in the space program of the Federal Republic of Germany 07 p0884 N88-15364
A theoretical concept for state changes and shape changes in weightlessness 07 p0884 N88-15365
Some remarks on gravitational biology
07 p0884 N88-15366
Investigations of Paramecium cells analyzed under microgravity conditions 07 p0884 N88-15367
The origin of the spicule skeleton of fresh water sponges (Spongillides) 07 p0885 N88-15368
Limb regeneration in amphibians, a suitable model for investigations of the effects of weightlessness as regards evolution and modifications 07 p0885 N88-15369
Investigations of the reproductive physiology of the rainbow trout (Salmo gairdneri Richardson)
07 p0885 N88-15370
Changes in the morphological and molecular biological processes during early embryo development in amphibians under micro-g conditions 07 p0885 N88-15371
Xiphophorus: A system to recognize radiation-induced mutations and to study the effects of zero-gravity environment on embryo development
07 p0885 N88-15372
Hypoxic hypoxia as a stimulus of erythropoiesis in vivo and in vitro 07 p0885 N88-15373
A learning model as a basis for investigations of the effects of gravity on the learning processes and memory formulation 07 p0886 N88-15374
Long-term adaptation of the otolith organs
07 p0886 N88-15375
Functional development of gravity receptors in insects and amphibians 07 p0886 N88-15376
Function-dependent plasticity in the nervous system
07 p0886 N88-15377
Questions on the evolution of the development program of the vertebrate inner ear under long term zero-g conditions 07 p0886 N88-15379
Long duration confinement of aquatic organisms in weightlessness (aquaspace) 07 p0887 N88-15380
Program draft for a special field: Gravitational biology
07 p0887 N88-15381
JPRS report: Science and technology. USSR: Space Biology and Aerospace Medicine, volume 21, no. 3, May - June 1987
[JPRS-USB-88-001] 07 p0889 N88-15389
Cardiac contractility in weightlessness according to spatial ballistocardiography 07 p0890 N88-15393
Cosmonauts' hormonal responses after brief spaceflights 07 p0890 N88-15394
Mother-fetus system as object for investigation of mechanisms of physiological effect of weightlessness
07 p0891 N88-15402
Investigation of energy metabolism of biological systems in weightlessness 07 p0893 N88-15409
Brain morphogenesis in rats developing in weightlessness 07 p0894 N88-15415
Circulatory response of males 45-52 years of age to antiorthostatic hypokinesia 07 p0894 N88-15416
The effect of microgravity on flame spread over a thin fuel
[NASA-TM-100195] 08 p0967 N88-15853
Results of research with biological satellites
08 p1006 N88-16097
Research on cotton plants grown in space
08 p1006 N88-16098
White blood cells in space: An experiment for the first Spacelab mission 09 p1127 N88-16757
JPRS Report: Science and Technology. USSR: Space Biology and Aerospace Medicine, volume 21, no. 5, September - October 1987
[JPRS-USB-88-003] 10 p1359 N88-18122
Embryonic development of guppy in weightlessness
10 p1360 N88-18127
Histomorphometric analysis of rat bones after spaceflight aboard Cosmos-1667 biosatellite
10 p1360 N88-18128
Isotope methods of determining distribution and movement of blood in the body
10 p1362 N88-18136
Comparative evaluation of stress response of rats to different methods of simulating some effects of weightlessness 10 p1363 N88-18144
Morphological study of early changes in rat bones in simulated weightlessness 10 p1365 N88-18158
New book on metabolic aspects of spaceflight stress
10 p1367 N88-18172
Genetic research in space
[NASA-TT-20216] 11 p1518 N88-19066
Ballistocardiography in weightlessness research
11 p1521 N88-19080
Central hemodynamics in antiorthostatic hypokinesia and immersion models of weightlessness
11 p1521 N88-19081
Summary of Payload Integration Plan (PIP) for Starlab-1 flight experiment, enclosure 3
[NASA-TM-89713] 11 p1522 N88-19086
Cytomorphology and ultrastructure of corn root meristem in weightlessness 12 p1651 N88-19891
The respiratory system under weightlessness
12 p1653 N88-19901
How does Physarum polycephalum perceive and use gravity? 12 p1655 N88-19918
Load and control of the cardiocirculatory system in weightlessness 12 p1656 N88-19922

Neck receptor stimulation in 0 and 1 g
12 p1658 N88-19938
Synopsis of the Spacelab D-1 frog statolith experiment STATEX 12 p1659 N88-19940
Cardiovascular effects of weightlessness and ground-based simulation
[NASA-TM-88314] 18 p2551 N88-25140
JPRS report: Science and technology. USSR: Space Biology and Aerospace Medicine, volume 22, no. 1, January - February 1988
[JPRS-USB-88-005] 19 p2702 N88-26069
Growth and differentiation of cells in organotypical rat embryo cerebellar culture developing in weightlessness
19 p2703 N88-26076
Axisymmetric liquid sloshing under low-g conditions. Numerical simulation method (reference manual)
[NLR-TR-86057-U] 20 p2802 N88-26627
Liquid motions in partially filled containers: Preliminary results of the D-1 mission --- Spacelab
[NLR-MP-86042-U] 20 p2802 N88-26629
Effect of weightlessness on brain development (results of flight of pregnant rats on Kosmos-1514 biosatellite and study of subsequent development of their progeny on earth 20 p2829 N88-26786
Nonlinear oscillations of an inviscid liquid column under zero-gravity
[LRT-WE-9-FB-8(1987)] 22 p3063 N88-28173
Nonlinear oscillations of axially independent liquid column under zero-gravity environment
[LRT-WE-9-FB-12(1987)] 22 p3063 N88-28174
Nonlinear oscillations of a nonviscous cylindrical liquid system in weightlessness condition
[LRT-WE-9-FB-14(1987)] 22 p3063 N88-28175

WEIGHTLESSNESS SIMULATION
NT NEUTRAL BUOYANCY SIMULATION
Access to microgravity: A technical description of the NAE T-33 microgravity facility
[NAE-AN-47] 04 p0405 N88-12518
Morphology and development of the inner ear of Anurans 07 p0886 N88-15378
Skylark sounding rocket development-Skylark 8
08 p1035 N88-16274
Dynamic testing of a docking system --- ground-based simulator 12 p1589 N88-19516
HERMES Program: Airlock swimming pool tests
12 p1591 N88-19525
Respiratory parameters aboard an aircraft performing parabolic flights 12 p1653 N88-19902
Influence of a 6 hr head-out water immersion on different tests of endurance performance capacity
12 p1653 N88-19903
Lung function in simulated microgravity
12 p1654 N88-19907
Neuro-reflex mechanisms of circulation regulation in simulated microgravity 12 p1656 N88-19923
Physiological reactions upon controlled changes of blood distribution in humans 12 p1656 N88-19924
P-31 Magnetic Resonance Spectroscopy (MRS) of limb muscles during bedrest with exercise countermeasures
12 p1656 N88-19925
An in vitro model system to study the effect of microgravity and loading conditions on the mineralization and resorption of skeletal tissues
12 p1657 N88-19927
Does 7-day hindquarters unloading simulate 7 days of weightlessness exposure in rat trabecular bone?
12 p1657 N88-19928
The suspended Japanese quail as an animal model for experiments related to microgravity
12 p1662 N88-19960
Some reflections on the standardization of bed-rest procedures for weightlessness simulation (cardiovascular and endocrine apsects) 12 p1662 N88-19961
Regulation of hemodynamics upon imitation of the transition to weightlessness (mathematical modeling)
13 p1810 N88-20817
The relationship between preflight underwater training and space motion sickness 19 p2696 N88-26025
Underwater simulation for space teleoperation
19 p2698 N88-26040
Marintek's ocean basin, a training facility for extravehicular activity? 19 p2698 N88-26041
The Marshall Space Flight Center KC-135 microgravity test program for FY84-86
[NASA-TM-4059] 22 p3056 N88-28136
Study of human factors engineering criteria for Extra Vehicular Activity (EVA) systems, volume 2
[STF23-F87025-VOL-2] 24 p3409 N88-30293

WELD STRENGTH
Reserach on microprocessor controller for spot welding
[PB87-143913] 07 p0863 N88-15240
Characteristics of joint formation during friction welding of Ti alloys to Nb alloys 14 p1898 N88-21329
Optimum duration of steady-state stage in friction welding of metals without artificial braking
14 p1898 N88-21330
Ensuring higher stability of immersed-arc welding of structural aluminum alloys and magnesium alloys
14 p1898 N88-21331
Diffusion welding of aluminomagnesium alloys to ceramics 14 p1898 N88-21333
Distribution of weld quality in thin section stainless steel tube attachment welds
[PB88-109632] 21 p2955 N88-27555
The influence of weld metal properties, weld geometry and applied load on weld system performance
[AD-A193403] 21 p2961 N88-27588

WELD TESTS
Ultrasonic mechanized checking of weld joints of nuclear power plant equipment 02 p0158 N88-10987
Resistance of welded joints in high temperature Hastelloy N-type nickel alloy to hot crack formation
03 p0286 N88-11798
The mechanical properties of solid state diffusion bonds between Ti-6Al-4V and 304L stainless steel
[BAJ-TR-113-1987] 03 p0332 N88-12093
Detection of defects on structures
[EP-PATENT-0-210-794-A2] 04 p0453 N88-12807
Study on the cryogenic toughness of stainless steel weld metals
[PB87-143830] 07 p0834 N88-15057
Characteristics of welds joining parts of high-strength pipe steels and produced by beam of continuous-wave CO2-laser 14 p1897 N88-21325
Structure and properties of welded joints produced between niobium parts in controllable helium atmosphere 14 p1897 N88-21326
Ensuring higher stability of immersed-arc welding of structural aluminum alloys and magnesium alloys
14 p1898 N88-21331
Principles of a nondestructive evaluation process for damage location, damage profile, and damage extension in welded joints by radiometric measurements
[MPA-86-02] 20 p2812 N88-26683
Distribution of weld quality in thin section stainless steel tube attachment welds
[PB88-109632] 21 p2955 N88-27555

WELDABILITY
Welding and weldability of ductile intermetallic alloys
[DE87-014061] 04 p0416 N88-12582
Weldability of 2219-T851 and 2519-T87 aluminum armor alloys for use in Army vehicle systems
[AD-A184296] 04 p0451 N88-12792
The effect of temperature on the tensile properties of HSLA-100 steel
[AD-A184951] 05 p0565 N88-13441
Weldability of a leaded carbon steel
[PB88-110341] 07 p0861 N88-15225
Effects of sulfur content on the plain strain fracture toughness of inertia welds in 4340 steel
[AD-A188192] 11 p1458 N88-18689
Weldability of tritium-charged 304L stainless steel
[DP-1740] 12 p1607 N88-19611
Properties fo seals made with Li2O-Al2O3-SiO2-glass ceramics and aluminum-containing austenitic stainless steels
[DE88-004688] 12 p1633 N88-19776
Inertia welding with variable magnitude of impact load
14 p1897 N88-21328
The weldability of consolidated rapidly solidified Type 304 SS powders
[DE88-006738] 16 p2178 N88-22978
Weldability of general purpose heat source iridium capsules 17 p2426 N88-24429
Helium induced degradation in the weldability of an austenitic stainless steel
[DE88-009062] 20 p2773 N88-26443
Application of Auger electron spectroscopy to the study of trace element effects on weldability
[DE88-010457] 21 p2915 N88-27301

WELDED JOINTS
NT SPOT WELDS
Ultrasonic mechanized checking of weld joints of nuclear power plant equipment 02 p0158 N88-10987
Process and equipment capabilities materials joining laboratory, 1987
[DE87-014534] 02 p0180 N88-11122
Resistance of welded joints in high temperature Hastelloy N-type nickel alloy to hot crack formation
03 p0286 N88-11798
Stress state of welded joints of dissimilar materials obtained by diffusion welding 03 p0286 N88-11799
Microstructural characterization of irradiated PWR steels using the atom probe field-ion microscope
[DE88-000341] 03 p0291 N88-11828
Gas tungsten arc welding of Al-10Fe-5Ce
[AD-A184202] 03 p0334 N88-12104
Welding and weldability of ductile intermetallic alloys
[DE87-014061] 04 p0416 N88-12582
Development of an acoustic emission monitor and monitoring techniques for long-term monitoring of U-0.8Ti electron-beam weldments for postweld cracking
[DE88-000819] 04 p0453 N88-12804
Method for the ultrasonic inspection of the soundness of the metal in weld joints in two-ply pipes
[BLL-CE-TRANS-8265-(9022.09)]
04 p0453 N88-12805
Ultrasonic method of inspecting austenitic weld joints in nuclear power station equipment
[BLL-CE-TRANS-8281-(9022.09)]
04 p0453 N88-12806
Qualification of expansion and joint welding procedures of tube-to-tubesheet joints for heat exchangers in nuclear power plants
[DE87-703526] 05 p0589 N88-13592
Welded joint fatigue of a AISI 304 L type stainless steel
[DE87-703530] 05 p0592 N88-13607
Fatigue strength of alloy A286 at cryogenic temperature 05 p0603 N88-13695
Development of research on fatigue of spot-weld in automobile structures in Japan
05 p0608 N88-13728
Basic energy sciences research in the Metals and Ceramics Division of Oak Ridge National Laboratory
[DE87-013538] 06 p0681 N88-14171
Study on fracture behaviour of a joint with a crack in transverse hard layer: Effect of hard layer width on COD
[PB87-143855] 07 p0868 N88-15267
Study on characteristics of SCC propagation da/dt for welded joint
[PB87-143640] 07 p0869 N88-15270
Effects of fabrication on the fatigue capacity of welded steel structures
[PB87-144226] 08 p0995 N88-16021
Study on the fracture behavior of 9 percent Ni steel welded joint
[PB87-143863] 08 p0995 N88-16023
Microstructural modification during laser welding
[DE88-002344] 09 p1144 N88-16860
The role of composition and microstructure gradients on weld metal properties and behavior
[DE88-004956] 10 p1303 N88-17791
The influence of small defects on tensile specimen ductility and symmetry of deformation
[AD-A187963] 10 p1346 N88-18044
Effects of sulfur content on the plain strain fracture toughness of inertia welds in 4340 steel
[AD-A188192] 11 p1458 N88-18689
Joining of dissimilar materials with the pulsed Nd-YAG laser
[DE88-003757] 11 p1458 N88-18692
Reduction of residual stresses and distortion in girth welded pipes
[AD-A187728] 11 p1494 N88-18920
Transformation, metallurgical response and behavior of the weld fusion zone and heat affected zone in Cr-Mo steels for fossil energy application
[DE88-006037] 13 p1744 N88-20430
Influence of hydrogen on crack formation tendency in heat-affected zone with stress concentrator
14 p1887 N88-21276
Characteristics of welds joining parts of high-strength pipe steels and produced by beam of continuous-wave CO2-laser 14 p1897 N88-21325
Structure and properties of welded joints produced between niobium parts in controllable helium atmosphere 14 p1897 N88-21326
Inertia welding with variable magnitude of impact load
14 p1897 N88-21328
Characteristics of joint formation during friction welding of Ti alloys to Nb alloys 14 p1898 N88-21329
Optimum duration of steady-state stage in friction welding of metals without artificial braking
14 p1898 N88-21330
Ensuring higher stability of immersed-arc welding of structural aluminum alloys and magnesium alloys
14 p1898 N88-21331
The effect of surface tension in the weld pool on seam formation when welding thin sheet with light rays
14 p1898 N88-21334
Joints in fiber-reinforced aluminum alloys
[NASA-TT-20160] 15 p2031 N88-22104
Cracking tendencies of restrained welds in high strength low alloy steels under hyperbaric conditions
[AD-A190255] 15 p2039 N88-22150
Reduced thermal input by proper selection of YAG laser welding parameters
[DE88-000730] 15 p2072 N88-22356
Microstructural characterization and properties of 3Cr-1.5Mo-0.1V thick section electron beam welds
[DE88-004330] 18 p2486 N88-24747
Apparatus for pressure welding of titanium structures with a controlled rate of deformation
[RAE-TRANS-2161] 19 p2677 N88-25915

Principles of a nondestructive evaluation process for damage location, damage profile, and damage extension in welded joints by radiometric measurements
[MPA-86-02] 20 p2812 N88-26683
Distribution of weld quality in thin section stainless steel tube attachment welds
[PB88-109632] 21 p2955 N88-27555
Determination of the residual stresses in welded structures using the elastoplastodynamic method
[ETN-88-92745] 22 p3087 N88-28330
Qualification of expansion and welding procedures of tube-to-tubesheet joints for heat exchangers in nuclear power plants
[DE88-701621] 23 p3221 N88-29174
Development of graded reference radiographs for aluminum welds, phase 1
[AD-A195594] 24 p3381 N88-30140

WELDED STRUCTURES
NT STEEL STRUCTURES
Advanced radiator concepts utilizing honeycomb panel heat pipes
[NASA-CR-172017] 04 p0443 N88-12747
Evaluation method of the brittle fracture strength in structurally stress-concentrated regions
[PB87-129490] 06 p0721 N88-14435
Study of combination type CO2 laser welding system
[PB87-143764] 08 p0992 N88-16002
Effects of fabrication on the fatigue capacity of welded steel structures
[PB87-144226] 08 p0995 N88-16021
Computation of the tensile and bending restraint intensities of welded specimens by finite element method
[PB87-143798] 08 p0995 N88-16024
Crack opening displacement test in tension
[PB87-143848] 08 p0996 N88-16026
Acoustic emission measurements of PWR weld materials with inserted defects
[AERE-R-12386] 10 p1341 N88-18016
Microstructural characterization of HSLA-100 GMA-weldments
[AD-A187782] 11 p1457 N88-18683
Removal of out-of-plane distortion in mild steel panels using flame heating, volume 1
[AD-A187802] 11 p1457 N88-18684
Removal of out-of-plane distortion in mild steel panels using flame heating, volume 2
[AD-A187803] 11 p1457 N88-18685
Microstructural characterization of the heat affected zone of HSLA (High Strength Low Alloy)-100 steel GMA (Gas Metal Arc)-weldment
[AD-A187825] 11 p1457 N88-18686
Fracture toughness of steel weldments containing lack of penetration defects 11 p1501 N88-18965
Hydrogen induced cracks in armor steel weldments fabricated with austenitic filler alloys
[AD-A188733] 13 p1740 N88-20406
Plasma joining of metal matrix composites
[AD-A193939] 22 p3051 N88-28100

WELDING
NT ARC WELDING
NT BRAZING
NT DIFFUSION WELDING
NT ELECTRON BEAM WELDING
NT EXPLOSIVE WELDING
NT FRICTION WELDING
NT FUSION WELDING
NT GAS TUNGSTEN ARC WELDING
NT GAS WELDING
NT LASER WELDING
NT PLASMA ARC WELDING
NT PRESSURE WELDING
NT ULTRASONIC WELDING
Automatic seam welding with infrared sensor feedback
[DE87-013556] 01 p0055 N88-10352
Materials studies for magnetic fusion energy applications at low temperatures-X
[PB87-232575] 03 p0381 N88-12395
Effects of stress-relieving on the mechanical properties and the structure of specimens of high-temperature fine-grained structural steels heat-treated to simulate welding
[BLL-CE-TRANS-8258-(9022.09)]
04 p0417 N88-12586
The modelling of orientation in planar polymer welding flows
[AD-A184404] 04 p0451 N88-12793
Alignment and assembly tool for very large diameter cylinders
[NASA-CASE-MFS-28001-2] 06 p0711 N88-14360
Sulfur-induced ductility-dip cracking in weld metal of low-carbon steel
[PB87-143814] 07 p0833 N88-15051
Welding in high pressure CO2 atmosphere — underwater welding
[PB87-144044] 07 p0862 N88-15232
Study on automatic detection and identification of defects in weld by microcomputer
[PB87-143897] 07 p0863 N88-15237
Reserach on microprocessor controller for spot welding
[PB87-143913] 07 p0863 N88-15240
Transient welding strain measurement by Moire technique. A comparison between experimental measurement and numerical analysis for strain-stress cycles during GTA spot-welding
[PB87-143871] 07 p0868 N88-15269
A large strain thermomechanical forming model for elastic-viscoplastic behavior in metals
10 p1301 N88-17780
The role of composition and microstructure gradients on weld metal properties and behavior
[DE88-004956] 10 p1303 N88-17791
A collaborative program of research in engineering sciences
[DE88-003383] 10 p1423 N88-18504
Fracture toughness of steel weldments containing lack of penetration defects 11 p1501 N88-18965
Investigation of the use of horizontally polarised shear waves for TOFD studies on austenitic steel
[AERE-R-12145] 13 p1780 N88-20649
JPRS report: Science and technology. USSR: Materials science
[JPRS-UMS-87-009] 14 p1884 N88-21261
Metals. Preliminary study for an Innovation-Oriented research Program (IOP)
[ETN-88-91317] 14 p1889 N88-21290
Innovation-Oriented research Program (IOP) metals. Annexes
[ETN-88-91318] 14 p1889 N88-21291
JPRS report: Science and technology. USSR: Materials science
[JPRS-UMS-87-007] 14 p1895 N88-21312
Segregation effects in welded stainless steels
[DE88-701224] 15 p2037 N88-22139
Weldability of general purpose heat source iridium capsules 17 p2426 N88-24429
Frequency Analysis of Acoustic Emission - Application to machining and welding
[DE88-701479] 18 p2570 N88-25262
Finite element welding computations using general purpose nonlinear analysis codes
[DE88-005398] 20 p2808 N88-26659
Milliwatt generator project
[DE88-011261] 20 p2853 N88-26939
High-speed, precision processing using an electron beam 21 p2929 N88-27391
The influence of weld metal properties, weld geometry and applied load on weld system performance
[AD-A193403] 21 p2961 N88-27588
Plasma joining of metal matrix composites
[AD-A193939] 22 p3051 N88-28100

WELDING MACHINES
Welding monitoring system
[NASA-CASE-MFS-29177-1] 06 p0712 N88-14362

WELLS
Status of the Magma Energy Project
[DE88-002413] 13 p1792 N88-20719
The use of orbital remote sensing data for low cost ground-water survey
[INPE-4587-PRE/1318] 24 p3386 N88-30170

WENTZEL-KRAMER-BRILLOUIN METHOD
WKB theory of wave tunneling for Hermitian vector systems of integral equations
[DE88-005332] 13 p1831 N88-20951

WEST COMET
Comet West: A view from the HELIOS zodiacal light photometers 01 p0117 N88-10749

WEST GERMANY
The history of aeroelasticity research in Germany from the beginning until 1945 — airframes
[DFVLR-MITT-86-25] 01 p0001 N88-10003
Observations of Earth tides by the German Geodetic Research Institute, division 1, in the period 1979-1985 at the Berchtesgaden and Wettzell stations
[SER-B-280] 07 p0872 N88-15291
The role of the DFVLR project management life sciences in the space program of the Federal Republic of Germany 07 p0884 N88-15364
German space policy on the threshold of the century. Analysis and proposals for the future
[ETN-88-90573] 07 p0943 N88-15734
The German scientific balloon and sounding rocket program 08 p1024 N88-16202
Federal Republic of Germany's interests, activities and goals in remote sensing of ocean colour/fluorescence from space 08 p1043 N88-16302
AZUR, the first German research satellite 625-A, 1964-1969 10 p1310 N88-17827
Protected areas with enhanced bird-aircraft collision risk in the Federal Republic of Germany
[GEOPHYSBDBW-FM-209] 11 p1437 N88-18576
Activities report in air traffic control
[ETN-88-91092] 11 p1438 N88-18581
Navigation experiment NAVEX. The reading differences between all ground station measuring clocks during each Spacelab pass of the D1 mission
[DFVLR-MITT-87-23] 16 p2159 N88-22880
Report on the cartographic activities of thc Federal Republic of Germany in the period 1984 - 1987
16 p2225 N88-23280
Computer-assisted cartography research and development report of the Federal Republic of Germany 1984 - 1986 16 p2226 N88-23289
The atlas of regional development
16 p2226 N88-23291
West German Geodetic Working Group: Official topographic-cartographic information system (ATKIS), content description 18 p2533 N88-25026
West German Geodetic Working Group: Official topographic-cartographic information system (ATKIS), technical conception 18 p2533 N88-25027
Creation of digital topographic models with the ALK-GIAP: The DLM 25 as an example
18 p2534 N88-25031
State of development of ALK (October 1986)
18 p2534 N88-25035
Results of radiation measurements in West Germany and from special measurement series in the Meteorological Observatory of Hamburg
[REPT-11] 18 p2542 N88-25088
Space policy of common sense and moderation
[REPT-49/87] 20 p2883 N88-27118
Economic impact of space flight activities in West Germany. Influence of allocations of Bundesministerium fuer Forschung und Technologie
[ETN-88-92106] 21 p2901 N88-27215
Atmospheric turbulence research at DFVLR
[AGARD-R-752] 21 p2975 N88-27669
Organization of the TDF1/TDF2 program
22 p3161 N88-28827
Investigation of the large-scale impact of air pollution components on forest ecosystems in Bavaria
[ESA-TT-1087] 24 p3390 N88-30187

WETLANDS
Correlation between aircraft MSS and LIDAR remotely sensed data on a forested wetland in South Carolina
[NASA-TM-89643] 02 p0193 N88-11204
Compilation of 1986 annual reports of the Navy ELF (Extremely Low Frequency) communications system ecological monitoring program, volume 3
[AD-A184533] 03 p0306 N88-11932
AIS-2 spectra of California wetland vegetation
05 p0613 N88-13763
Remote sensing of wetlands: Applications overview
[DE88-010895] 21 p2966 N88-27618
An evaluation of SPOT imagery for wetland monitoring
22 p3091 N88-28353

WETNESS
U MOISTURE CONTENT

WETTABILITY
Adhesive bond strengths on aluminium alloys as a function of surface topographies and their wetting properties
[ARE-TM(UMM)-87403] 09 p1148 N88-16880
Correlations between wettability and structure in monolayers of alkanethiols adsorbed on gold
[AD-A194348] 23 p3191 N88-28991

WETTING
The infiltration kinetics of aluminum in silicon carbide compacts
[AD-A184682] 03 p0290 N88-11823
Adhesive bond strengths on aluminium alloys as a function of surface topographies and their wetting properties
[ARE-TM(UMM)-87403] 09 p1148 N88-16880
Thermodynamics of wetting by liquid metals
[DE88-003634] 11 p1563 N88-19360
Critical point wetting drop tower experiment
[NASA-CR-183062] 20 p2798 N88-26603
Depressed sweating during exercise at altitude
[AD-A192603] 22 p3130 N88-28609

WHARVES
Impact force as a part of the total breaking wave force on a vertical cylinder
[RR-CE78] 24 p3384 N88-30154

WHEAT
Study of the relationship between photosynthesis, respiration, transpiration, and mineral nutrition in wheat
03 p0360 N88-12268
Wheat production in controlled environments
[UAES-PAPER-3324] 03 p0361 N88-12270
Optimal sampling to provide user-specific climate information 11 p1515 N88-19051
Closed system physiology: Role of oxygen in the development of wheat 12 p1655 N88-19916

Use of energy emission for detecting the necessity of irrigation in wheat in field conditions
[INPE-4461-TDL/318] 16 p2229 N88-23315
Estimation of an area cultivated with wheat from LANDSAT data through a two-phase sampling method
17 p2357 N88-24041
Application of SPOT multidate data to wheat yield estimation in Beauce (France) 22 p3094 N88-28374
TM/LANDSAT-5 data to evaluate wheat and bean percent soil cover and leaf area index
[INPE-4609-PRE/1332] 24 p3385 N88-30165
LANDSAT TM and agrometeorological data for wheat yield estimation at the farm level
[INPE-4591-PRE/1321] 24 p3388 N88-30180

WHEELS
NT FLYWHEELS
NT REACTION WHEELS
NT TURBINE WHEELS
NT VEHICLE WHEELS

WHIRL
U ROTATION

WHIRL INSTABILITY
U ROTARY STABILITY

WHIRLING
U ROTATION

WHISKER COMPOSITES
Investigation of microstructural factors that cause low fracture toughness in silicon carbide whisker/Al alloy composites
[AD-A186443] 09 p1137 N88-16817
Microstructures and properties of SiC whisker-reinforced mullite composites
[DE88-002611] 09 p1139 N88-16826
Micro-mechanisms of deformation in SiC/Al composites
[AD-A188282] 10 p1296 N88-17749
Composites strengthening
[AD-A189258] 13 p1734 N88-20364
Interfacial chemistry-structure and fracture of ceramic composites
[DE88-005516] 13 p1750 N88-20461
The effect of strain rate on the strength and ductility of SiCw/2124 Al composite
[OUEL-1692/87] 14 p1924 N88-21466
Whisker-reinforced ceramic composites for heat engine components 15 p2082 N88-22410
Factors influencing the toughening behavior of whisker reinforced ceramics
[DE88-011396] 20 p2779 N88-26479
Theoretical and experimental analysis of the toughening behavior of whisker reinforcement in ceramic matrix composites
[DE88-011841] 21 p2906 N88-27241

WHISKERS (CRYSTALS)
Production of metallic monocrystals described
03 p0286 N88-11796
Nondestructive characterization of ceramic composite whiskers with neutron diffraction and ultrasonic techniques
[DE88-003075] 08 p0965 N88-15844
A laboratory study of tin whisker growth
[ESA-STR-223] 08 p1089 N88-16553
An organometallic route to micron-sized whiskers of zinc sulfide
[AD-A195889] 24 p3430 N88-30414

WHISTLERS
JPRS report: Science and technology. China
[JPRS-CST-87-031] 03 p0299 N88-11880
Method estimating integral mean value of enhancement factor and path latitude for whistlers below magnetic latitude 10 deg 03 p0300 N88-11885
Simulation and modeling of whistler mode wave growth through cyclotron resonance with energetic electrons in the magnetosphere 10 p1353 N88-18089
Observations and analyses of summer whistlers at the Great Wall Station of Antarctica
11 p1469 N88-18759
An analysis of whistler-mode radiation from the Spacelab-2 electron beam, revision
[AD-A188228] 11 p1552 N88-19287
Electrostatic whistler mode conversion at plasma resonance
[AD-A192951] 20 p2860 N88-26989

WHITE BLOOD CELLS
U LEUKOCYTES

WHITE DWARF STARS
PG 0308 + 096: A short-period white dwarf + dM binary with strongly modulated H-alpha emission
04 p0509 N88-13132
BE Ursae Majoris: A detached binary with a unique reprocessing spectrum
[NASA-CR-182419] 08 p1083 N88-16526
The X-ray properties of AM Her stars
[MPE-PREPRINT-108] 16 p2289 N88-23704
Ultraviolet spectra of subluminous objects found in the Kiso Schmidt survey and systematic reanalysis of the archived ultraviolet spectra of white dwarfs observed with the IUE satellite under the Astrophysics Data Program (ADP)
[NASA-CR-182976] 18 p2592 N88-25406
Ultraviolet spectra of two magnetic white dwarfs and ultraviolet spectra of subluminous objects found in the Kiso Schmidt survey
[NASA-CR-183051] 18 p2593 N88-25408

WHITE LIGHT HOLOGRAPHY
Rainbow holographic image reconstructed by spatially extended white light source 15 p2055 N88-22249

WHITE NOISE
NT THERMAL NOISE
White noise calculus for two-parameter filtering
[ENST-87C003] 01 p0088 N88-10578
Detection of signals by the digital integrate-and-dump filter with offset sampling 04 p0435 N88-12695

WICKS
Heat transfer of mesh-wick heat-pipes (bottom heat mode) 20 p2783 N88-26507
Polymeric heat pipe wick
[NASA-CASE-GSC-13019-1] 23 p3214 N88-29133

WIDE ANGLE LENSES
Treatment of systematic errors in the processing of wide angle sonar sensor data for robotic navigation
[DE88-008961] 20 p2756 N88-26352

WIDEBAND
U BROADBAND

WIDEBAND COMMUNICATION
The characteristics of two broadband (2 MHz to 10 MHz) switched vee antennas
[AD-A187874] 11 p1471 N88-18770
The Effect of the Ionosphere on Communication, Navigation and Surveillance Systems Based on Ionospheric Effects Symposium held on 5-7 May 1987 in Springfield, Virginia
[AD-A191855] 18 p2541 N88-25081

WIGGLER MAGNETS
Brightness and coherence of radiation from undulators and high-gain free electron lasers
[DE87-011093] 02 p0177 N88-11102
Sideband suppression by an intracavity optical filter in the Los Alamos free-electron laser oscillator
[DE87-011740] 02 p0177 N88-11103
Center for X-Ray Optics, 1986
[DE88-000715] 04 p0449 N88-12783
A long electromagnetic wiggler for the paladin free-electron laser experiments
[DE88-000970] 05 p0588 N88-13589
Development of a strong electromagnet wiggler
[DE88-000971] 05 p0645 N88-13952
Development of a laced electromagnetic wiggler
[DE88-000972] 05 p0646 N88-13953
Tapered wiggler analysis of high gain free electron laser oscillators
[AD-A187997] 10 p1338 N88-17997
Wiggler taper optimization for free-electron-laser amplifiers with moderate space-charge effects
[DE88-003758] 13 p1775 N88-20618
Research on variable-period wiggler type free electron lasers 14 p1902 N88-21360
Pulsed magnet fields for free-electron lasers
14 p1903 N88-21367
The free-electron laser: Theoretical innovations and gas-loaded experiment 20 p2806 N88-26646
On the small signal gain of free electron lasers in the low-current regime
[DFVLR-FB-88-10] 21 p2955 N88-27552
Free electron lasers with small period wigglers
[DE88-011627] 23 p3218 N88-29156

WIGHTMAN THEORY
U FIELD THEORY (PHYSICS)
U QUANTUM THEORY
U RELATIVISTIC THEORY

WIGNER COEFFICIENT
Wigner distribution function: Relation to short-term spectral estimation, smoothing and performance in noise
[AD-A193865] 23 p3275 N88-29492

WILDERNESS
History of wildland fires on Vandenberg Air Force Base, California
[NASA-TM-100983] 18 p2549 N88-25134

WIND (METEOROLOGY)
NT GEOSTROPHIC WIND
NT GROUND WIND
NT GUSTS
NT JET STREAMS (METEOROLOGY)
NT MONSOONS
NT SEA BREEZE
NT SQUALLS
NT WINDS ALOFT
Analysis of the bivariate parameter wind differences between Jimsphere and Windsonde
[NASA-TM-4014] 01 p0072 N88-10461
Global positioning satellite-based automatic landing system and wind estimated feedback for the AH-64 helicopter 02 p0124 N88-10784
Direct Absorption Receiver flow experiments
[DE87-014655] 02 p0196 N88-11221
Mesoscale MOS forecast support for 1988 winter Olympics ski events --- model output statistics (MOS)
02 p0209 N88-11312
NWS (National Weather Service) watch/warning verification flash flood, winter storm and high wind, January 1980 - June 1986
[PB87-223053] 04 p0469 N88-12898
Tropical easterly jet located using TOMS data
05 p0616 N88-13783
Studies in Aeolian geology
[NASA-CR-182328] 05 p0625 N88-13828
Radar observations of high-latitude lower-thermospheric and upper-mesospheric winds and their response to geomagnetic activity 06 p0742 N88-14563
Wave and wind data sources, environmental conditions committee report, International Ship and Offshore Structures Congress
[PB87-234902] 06 p0746 N88-14588
Middle atmospheric wind measurements using a medium frequency radar
[AD-A185931] 07 p0879 N88-15330
Research work at the Meteorological Institute of the University of Munich (Federal Republic of Germany)
[MITT-56] 08 p1013 N88-16141
The role of anabatic winds in the heating of valleys
08 p1014 N88-16144
North Pacific Ocean: Tradewind region east of Hawaii, R/V Thomas G Thompson: 25 September - 1 November 1972. STD data report
[AD-A186566] 08 p1044 N88-16311
North Pacific Ocean: Northeast Pacific Transition Zone, R/V Thomas G. Thompson: 1 November - 6 December 1969. STD data report
[AD-A186574] 09 p1195 N88-17161
Airborne Doppler radar technology for wind shear detection 10 p1274 N88-17622
Radar backscatter from airports and surrounding areas 10 p1274 N88-17623
Universal power spectra for wave turbulence: Applications to wind waves, flicker noise, solar wind spectrum and classical second sound
10 p1318 N88-17879
Remote sensing of atmospheric crosswinds by utilizing speckle-turbulence interaction and optical heterodyne detection
[AD-A187580] 10 p1347 N88-18052
The structure and dynamics of monsoon depressions
10 p1355 N88-18102
Systematic errors of the FSU global spectral model
10 p1356 N88-18103
Evolution of acoustic gravity wave packet in spatially and temporally varying wind 11 p1469 N88-18760
Caribbean and Central America wind energy assessment
[DE88-005134] 11 p1507 N88-19002
Site effects on wind characteristics at a turbine rotor
[DE88-005135] 11 p1507 N88-19003
Upper-thermospheric observations and neutral-gas dynamics at high latitudes during solar maximum
[AD-A188058] 11 p1512 N88-19031
Numerical simulation of near-surface environments and particulate clouds generated by large-area fires
[AD-A188375] 12 p1641 N88-19828
Retrieval of three-dimensional wind and temperature fields from single-Doppler radar data
12 p1646 N88-19858
Simulating high-resolution vertical plane array wind characteristics using lower-spatial-resolution wind measurements
[DE88-005626] 13 p1800 N88-20761
Circulation and exchange processes on the South Atlantic Bight Continental Shelf
[DE88-003330] 13 p1804 N88-20781
Monthly mean global climatology of temperature, wind, geopotential height, and pressure for 0 - 120 km
[NASA-TM-100697] 15 p2099 N88-22503
Global atmospheric circulation statistics, 1000-1 mb
[PB88-168240] 16 p2234 N88-23340
Report on project WIND: Preliminary experiments with the UK Meteorological Office mesoscale model, September 1987
[AD-A19162] 18 p2544 N88-25099
Estimation of balloon position from wind data
[DE88-008968] 19 p2597 N88-25434
A radar study of the interaction between lightning and precipitation
[DE88-009120] 20 p2827 N88-26770
Wind flow study: July 1987 and November-December 1987
[DE88-008969] 20 p2828 N88-26776

Zonal wind observations at Christmas Island (2 deg N, 157 deg W) during the 1986-1987 El-Nino 22 p3120 N88-28539

The observed dynamical structure of low frequency variabilities 22 p3120 N88-28541

The dynamics and thermodynamics of a 30-60 day oscillation 22 p3121 N88-28543

Complex EOF analysis of intraseasonal tropical wind fluctuations 22 p3121 N88-28544

Some diagnostic results concerning the tropical 40-50 day oscillation 22 p3121 N88-28546

Recent secular changes in the wintertime circulation of the Southern Hemisphere 22 p3122 N88-28555

Variations in the atmosphere associated with the 11-year solar cycle 22 p3122 N88-28557

Extratropical response to tropical heating as a function of period of model integrations 22 p3125 N88-28577

Doppler radar analysis of coastal marine atmospheric boundary layer structure during a cold air outbreak [AD-A196023] 24 p3403 N88-30261

Analysis of environmental parameters from the Panama City tower radar experiment [AD-A194994] 24 p3404 N88-30264

WIND CIRCULATION

U ATMOSPHERIC CIRCULATION

WIND DIRECTION

Coastal winds of the southeast Alaska Peninsula [PB87-206173] 02 p0215 N88-11354

BARS-1M meteorological complex carried on IL-18 airplane 06 p0725 N88-14458

Remote sensing of atmospheric crosswinds by utilizing speckle-turbulence interaction and optical heterodyne detection [AD-A187580] 10 p1347 N88-18052

Method for determination of the wind velocity and direction [NASA-TT-20233] 13 p1802 N88-20769

Distribution of summertime lightning as a function of low-level wind flow in central Florida [PB88-160759] 14 p1948 N88-21619

Parameterization of horizontal wind velocity variability [AD-A190107] 15 p2097 N88-22493

The effects of time-dependent winds and ocean eddies on ice motion in a marginal ice zone [AD-A190105] 15 p2100 N88-22511

Geostrophic flow in the central Bering Sea, Fall 1986 and Summer 1987 [PB88-174354] 16 p2237 N88-23360

A system for determination of wind fields using geostationary meterological satellites 17 p2360 N88-24056

Project wind, phase 4 (smoke test), Meadow Brook Valley, Red Bluff, California [AD-A194742] 22 p3128 N88-28596

Analysis of environmental parameters from the Panama City tower radar experiment [AD-A194994] 24 p3404 N88-30264

WIND EFFECTS

The effect of wind and currents on gas exchange in an estuarine system [NASA-CR-181424] 01 p0073 N88-10468

Vertical profiles of wind-induced current --- North Sea [IOS-238] 02 p0193 N88-11207

Direct Absorption Receiver flow experiments [DE87-014655] 02 p0196 N88-11221

The application of divergence equation in the analysis of heavy rainfall 02 p0207 N88-11299

The effect of mass, wind angle and erection technique on the aeroelastic behaviour of a cable-stayed bridge model [NAE-AN-46] 04 p0455 N88-12819

Theory of heat and moisture exchange between finely disperse storm-generated spray and turbulent air flow 04 p0461 N88-12851

Environmental processes and spectral reflectance characteristics associated with soil erosion in desert fringe regions [NASA-CR-182332] 05 p0620 N88-13811

A comparison of the predicted and measured gravitational stresses in VAWT (Vertical Axis Wind Turbine) blades [DE88-002113] 09 p1187 N88- 7111

Site effects on wind characteristics at a turbine rotor [DE88-005135] 11 p1507 N88-19003

Mesoscale coastal ocean dynamics 11 p1517 N88-19060

Study of spectra of sea waves on horizontally nonuniform current in rip zone 13 p1788 N88-20699

Circulation and exchange processes on the South Atlantic Bight Continental Shelf [DE88-003330] 13 p1804 N88-20781

Dynamics of the Oceanic Surface Mixed Layer [AD-A188348] 13 p1804 N88-20785

On the zonal momentum balance at the equator 13 p1805 N88-20788

The mixed layer of the western equatorial Pacific Ocean [HIG-1861] 13 p1805 N88-20789

Unsteady shallowing mixed layer 13 p1805 N88-20791

Some effects of heating on the wind-driven velocity in the upper ocean 13 p1805 N88-20792

Mixed-layer shear related to wind stress in the central equatorial Pacific 13 p1805 N88-20793

Mixed-layer fronts in the California current 13 p1805 N88-20794

Horizontal scales of wind forced inertial motions 13 p1806 N88-20795

Wind forcing and observed oceanic wavenumber spectra 13 p1806 N88-20797

Energy and momentum fluxes through the sea surface 13 p1806 N88-20798

Hamiltonian description of the interaction of surface waves with mixed-layer currents 13 p1806 N88-20799

Monitoring ocean surface layer processes 13 p1806 N88-20801

An improved wind input source term for third generation ocean wave modeling [KNMI-WR-87-8] 14 p1950 N88-21624

Experimental study on the influence of wind on acoustic pressure sensors [ISL-R-121/86] 15 p2131 N88-22712

Use of energy emission for detecting the necessity of irrigation in wheat in field conditions [INPE-4461-TDL/318] 16 p2229 N88-23315

Numerical model for the computation of radiance distributions in natural waters with wind-roughened surfaces [PB88-192703] 20 p2826 N88-26765

Eigenmatrix representations of radiance distributions in layered natural waters with wind-roughened surfaces [PB88-188701] 20 p2828 N88-26780

An examination of wake effects and power production for a group of large wind turbines [DE88-009906] 22 p3117 N88-28518

Effects of precipitation on wind turbine performance [DE88-001144] 23 p3228 N88-29211

WIND ENERGY

U WINDPOWER UTILIZATION

WIND MEASUREMENT

NT WIND VELOCITY MEASUREMENT

Analyses and assessments of span wise gust gradient data from NASA B-57B aircraft [NASA-CR-178288] 01 p0002 N88-10007

Coastal winds of the southeast Alaska Peninsula [PB87-206173] 02 p0215 N88-11354

Comparative testing of wind measuring equipment. Part 1: Inventory and selection [R-814-D-PT-1] 03 p0325 N88-12053

Long-period variations of wind parameters in the mesopause region and the solar cycle dependence 06 p0733 N88-14509

Main results of atmospheric fine structure parameter observation in the lower thermosphere 06 p0735 N88-14518

Meteor detection on ST (MST) radars 06 p0740 N88-14554

Measurement in a wind tunnel of the modification of mean wind and turbulence characteristics due to induction effects near wind turbine rotors [DE88-000249] 07 p0815 N88-14963

Middle atmospheric wind measurements using a medium frequency radar [AD-A185931] 07 p0879 N88-15330

Development of a Doppler wind lidar system for atmospheric wind measurements 08 p1027 N88-16217

Project CONDOR: Middle atmosphere wind structure obtained with lightweight inflatable spheres near the equatorial electrojet 08 p1028 N88-16230

Wind measurements at high altitudes (150 m tower) [BMFT-FB-T-86-169] 09 p1193 N88-17149

Minimum Energy Routing through Interactive Techniques (MERIT) modeling [NASA-CR-182535] 10 p1356 N88-18105

Ground clutter processing for wind measurements with airport surveillance radars [AD-A187708] 11 p1514 N88-19044

Correction of the wind field measured by the NCAR electra during FASINEX (Frontal Air-Sea Interaction Experiment) for inertial navigation system drifts [AD-A187780] 11 p1514 N88-19045

A preliminary assessment of thunderstorm outflow wind measurement with airport surveillance radars [AD-A189064] 13 p1799 N88-20757

Mixed-layer shear related to wind stress in the central equatorial Pacific 13 p1805 N88-20793

Optical properties of Southern Hemisphere aerosols: Report of the joint CSIRO/NASA study [NASA-CR-179287] 14 p1945 N88-21605

Climatological data of the Netherlands lightvessels over the period 1949-1980 --- North Sea [KNMI-WR-87-9] 14 p1947 N88-21613

Solar wind observation at the time of closest encounter with Comet Halley 14 p1995 N88-21890

Prospects of satellite wind sensing systems in the years 1995-2000 17 p2350 N88-24004

Comparison of surface current determined from satellite-tracked buoy with shipboard wind data during the 4th Brazilian antarctic expedition, 10-14 March, 1986 17 p2354 N88-24024

Overview of wind behavior research in the US Wind Energy Program [DE88-005683] 18 p2537 N88-25057

Special observations 18 p2545 N88-25108

Aircraft/lidar turbulence comparison 18 p2546 N88-25111

The pneumatic wind shear sensor: A tool for meteorological investigations and flight management 22 p3036 N88-28024

A study of the feasibility of using sea and wind information from the ERS-1 satellite. Part 1: Wind scatterometer data [NASA-CR-182833] 24 p3386 N88-30167

A study of the feasibility of using sea and wind information from the ERS-1 satellite. Part 2: Use of scatterometer and altimeter data in wave modeling and assimilation [ESA-CR(P)-2604-PT-2] 24 p3387 N88-30176

Determining near-water wind speed using radar data from Cosmos-1500 artificial earth satellite 24 p3449 N88-30524

WIND PRESSURE

Typhoon structural evolution [AD-A186090] 07 p0879 N88-15333

Determination of the ultimate loads for corrugated-steel, barrel-type shell structures [AD-A187716] 11 p1498 N88-18944

WIND PROFILES

A real-time system for automatic single-Doppler wind field analysis 02 p0200 N88-11249

Statistical relationships between the mesoscale organization of convection and the large-scale wind profiles during GATE --- GARP Atlantic Tropical Experiment (GATE) 02 p0208 N88-11302

The importance of the lower level windshear profile in tornado/non-tornado discrimination 02 p0208 N88-11304

Short-term forecasting of lightning based on the surface wind field at Kennedy Space Center 02 p0208 N88-11306

Mesoscale surface field analysis from routine observations --- pressure, wind fields 02 p0209 N88-11315

High resolution determination of true surface winds at sea from wind and pressure data 02 p0210 N88-11316

A preliminary demonstration of the use of boundary-layer models of flow in complex terrain for high resolution surface wind forecasting 02 p0212 N88-11330

An improved method of analyzing surface geostrophic winds and pressure 02 p0212 N88-11334

Windfield simulations from a hierarchy of nested meso- and micrometeorological models 02 p0215 N88-11351

Middle Atmosphere Program. Handbook for MAP, volume 25 [NASA-CR-181571] 06 p0732 N88-14502

The climatic wind regime in the lower thermosphere from meteor radar observations 06 p0733 N88-14506

Meteor observation by the Kyoto meteor radar 06 p0733 N88-14507

Long-period variations of wind parameters in the mesopause region and the solar cycle dependence 06 p0733 N88-14509

The lower thermosphere wind regime from simultaneous observations over Euroasia (Colim, Dushanbe, Frunze) 06 p0733 N88-14510

Wind regime peculiarities in the lower thermosphere in the winter of 1983/84 06 p0733 N88-14511

On the interconnection of dynamic processes in the lower thermosphere with meteorological phenomena in the tropostratosphere 06 p0734 N88-14512

Tidal activity in the meteor zone over Budrio, Italy 06 p0734 N88-14517

On connection between evolution of troposphere fronts and changes of circulation regime in meteor zone 06 p0735 N88-14519

A study of the mechanism of internal gravity wave generation by quasigeostrophic meteorological motions 06 p0735 N88-14520

On the dependence of the lower thermospheric wind regime on the solar cycle 06 p0736 N88-14524

Lower thermosphere wind regime according to radiometeor measurements in Kazan 06 p0736 N88-14526

Some aspects of metallic ion chemistry and dynamics in the mesosphere and thermosphere
06 p0737 N88-14534

Observations of inertial period waves and vertical velocities in the tropical middle atmosphere using the MST radar technique
06 p0742 N88-14562

A method to obtain a wind model for the boundary layer in a representative tropical region
[R-818-D] 06 p0743 N88-14569

Improvements in profiler wind estimates using smoothed data in the spectrum finder algorithm
[PB88-102181] 07 p0881 N88-15342

Vertical sounding of th air layer close to a glacier on Mount Vernagferner in the Oetzal Alps, Tyrol (experiment LUZIVER 1983)
08 p1015 N88-16152

Simulation of a typical flow in a broad valley
08 p1015 N88-16154

Project CONDOR: Middle atmosphere wind structure obtained with lightweight inflatable spheres near the equatorial electrojet
08 p1028 N88-16230

Wind measurements at high altitudes (150 m tower)
[BMFT-FB-T-86-169] 09 p1193 N88-17149

Correction of the wind field measured by the NCAR electra during FASINEX (Frontal Air-Sea Interaction Experiment) for inertial navigation system drifts
[AD-A187780] 11 p1514 N88-19045

An analytical method for the determination of the average horizontal wind velocities across two-dimensional hills
[ISBN-3-923624-06-9] 11 p1515 N88-19048

Aerodynamic aspects of the Amazon Forest
[INPE-4445-TDL/313] 15 p2098 N88-22501

A system for determination of wind fields using geostationary meterological satellites
17 p2360 N88-24056

Special observations 18 p2545 N88-25108

Three-dimensional wind simulation
[DE88-009793] 21 p2975 N88-27671

Space shuttle natural environment analysis
[NASA-CR-179337] 21 p2976 N88-27676

A system for determination of wind fields from cloud tracks: INPE experiment
[INPE-4492-PRE/1256] 22 p3128 N88-28594

Wind measurements by electromagnetic probes
[NASA-TM-4066] 23 p3236 N88-29256

WIND SHEAR

Contributions to the modeling of wind shear for danger studies
[ETN-87-90442] 01 p0072 N88-10463

New nowcasting opportunities using modern meteorological radar 02 p0199 N88-11245

Nowcasting microbursts using Doppler radar in a forecaster-computer environment
02 p0200 N88-11246

The importance of the lower level windshear profile in tornado/non-tornado discrimination
02 p0208 N88-11304

Study of microburst detection performance during 1985 in Memphis, Tennessee
[AD-A184013] 03 p0354 N88-12231

Some aspects of metallic ion chemistry and dynamics in the mesosphere and thermosphere
06 p0737 N88-14534

Wind shear detection. Forward-looking sensor technology
[NASA-CP-10004] 07 p0817 N88-14970

Low altitude windshear threat to commercial aircraft
08 p0952 N88-15777

A comparison of multi-layer meso-alpha MLAM model results with surface and aircraft observations from CAPTEX
[DE88-000549] 09 p1188 N88-17118

Airborne Wind Shear Detection and Warning Systems: First Combined Manufacturers' and Technologists' Conference
[NASA-CP-10006] 10 p1273 N88-17616

NASA wind shear model: Summary of model analyses
10 p1273 N88-17617

Response of wind shear warning systems to turbulence with implication of nuisance alerts
10 p1274 N88-17618

Investigation of the influence of wind shear on the aerodynamic characteristics of aircraft using a vortex-lattice method 10 p1274 N88-17619

Windshear warning aerospatiale approach
10 p1274 N88-17620

Windshear detection effect of static air temperature bias 10 p1274 N88-17621

Airborne Doppler radar technology for wind shear detection 10 p1274 N88-17622

Radar backscatter from airports and surrounding areas 10 p1274 N88-17623

Wind shear radar simulation 10 p1274 N88-17625

Lidar windshear detection and avoidance: Performance and technical assessment 10 p1274 N88-17626

Airborne Doppler lidar detection of wind shear. Results of performance analysis 10 p1275 N88-17627

Infrared low-level wind shear work
10 p1275 N88-17628

Forward looking wind shear detection
10 p1275 N88-17629

Simulator investigation of wind shear recovery techniques 10 p1275 N88-17630

Crew interface with windshear systems
10 p1275 N88-17631

Status of FAA terminal Doppler weather radar programs 10 p1275 N88-17632

The advanced low-level windshear alert system operational demonstration results, Summer, 1987, Denver Stapleton International Airport 10 p1275 N88-17633

Are windshear training aid recommendations appropriate for other than large jet transports? Pilot procedures: Shear models 10 p1275 N88-17635

Airworthiness considerations
10 p1276 N88-17636

Windshear training aid. Volume 1: Overview, pilot guide, training program
[PB88-127196] 10 p1276 N88-17637

Variation of the wind stress related to frontal passages during FASINEX (Frontal Air-Sea Interaction Experiment) 1986
[AD-A187180] 11 p1514 N88-19042

Ground clutter processing for wind measurements with airport surveillance radars
[AD-A187708] 11 p1514 N88-19044

Wind shear as a predictor of severe weather for the eastern United States
[PB88-157144] 13 p1800 N88-20762

Power spectral density analysis of wind-shear turbulence for related flight simulations
[NASA-CR-182721] 13 p1802 N88-20773

Development and testing of the gust front algorithm
[AD-A189722] 14 p1949 N88-21622

Propagation of acoustic gravity wave spectrum through vertical wind shear region 16 p2186 N88-23035

Flight penetration of wind shear: Control strategies
17 p2294 N88-23727

The Federal Aviation Administration/Massachusetts Institute of Technology (FAA/MIT) Lincoln Laboratory Doppler weather radar program
18 p2547 N88-25118

Flight-management strategies for escape from microburst encounters
[NASA-TM-4057] 19 p2603 N88-25461

Influence of wind shear on the aerodynamic characteristics of airplanes
[NASA-TP-2827] 20 p2755 N88-26344

Intelligent guidance and control for wind shear encounter
[NASA-CR-183060] 20 p2755 N88-26347

The role played by FDRs in understanding the windshear phenomenon 22 p3036 N88-28023

The pneumatic wind shear sensor: A tool for meteorological investigations and flight management
22 p3036 N88-28024

Contributions to the modeling of wind shear for danger studies
[NASA-TT-20293] 23 p3174 N88-28900

Airborne radar technology for windshear detection
[NASA-CR-183203] 23 p3236 N88-29257

Cloud/mesoscale model development and application studies
[AFGL-TR-87-0219] 24 p3404 N88-30269

WIND TUNNEL APPARATUS

NT WIND TUNNEL DRIVES

A method for the calculation of transonic flows for the control of adaptive wind tunnels
[ETN-87-90411] 01 p0003 N88-10015

The generation of nearly isotropic turbulence by means of grids
[PNR90411] 02 p0172 N88-11084

Effect of a model support strut on measurement of aerodynamic longitudinal and lateral coefficients
[PB87-170288] 09 p1113 N88-16670

Strain gage balance for half models 302-6. Calibration report --- wind tunnels
[F+W-FO-1803] 09 p1166 N88-17001

Strain gage sting balance 204-6. Calibration report --- wind tunnels
[F+W-FO-1838] 09 p1166 N88-17002

Experimental evaluation of turning vane designs for high-speed and coupled fan-drive corners of 0.1-scale model of NASA Lewis Research Center's proposed altitude wind tunnel
[NASA-TP-2681] 10 p1285 N88-17686

Activities report of the Large Testing Facilities Department --- aircraft/spacecraft
[ETN-88-91982] 13 p1724 N88-20311

The 5.5 m low speed wind tunnel. Introduction to the facilities
[ARG-205] 14 p1870 N88-21172

Main features of Warton (United Kingdom) 2.7 x 2.1 m low speed wind tunnel
[AXM-124] 14 p1870 N88-21173

Details of low speed intake test facility at the Warton (United Kingdom) 2.7m x 2.1m wind tunnel
[AXM-127] 14 p1870 N88-21174

Design of a supersonic wind tunnel
[ETN-88-92078] 14 p1870 N88-21176

Equipment for mass flow measurements in the low-speed wind tunnel at DFVLR in Brunswick, West Germany
[DFVLR-MITT-88-02] 21 p2900 N88-27212

Computer programs for calculation of sting pitch and roll angles required to obtain angles of attack and sideslip on wind tunnel models
[NASA-TM-100659] 24 p3329 N88-29820

WIND TUNNEL BALANCES

U WEIGHT INDICATORS

U WIND TUNNEL APPARATUS

WIND TUNNEL CALIBRATION

Calibration of a five hole probe and testing of an evaluation method for flow field measurements
[ESA-TT-1051] 03 p0325 N88-12051

Transonic wind tunnel calibration 1986: Force measurements on three ONERA-C5 models and three half sphere cylinder calibration bodies in the F+W transonic test section
[F+W-FO-1854] 09 p1122 N88-16714

Strain gage balance for half models 302-6. Calibration report --- wind tunnels
[F+W-FO-1803] 09 p1166 N88-17001

Strain gage sting balance 204-6. Calibration report --- wind tunnels
[F+W-FO-1838] 09 p1166 N88-17002

Reynolds number effects and the wind tunnel environment 23 p3168 N88-28862

Flow visualization on a small scale
[AD-A194728] 23 p3181 N88-28935

Hot-wire measurements of compressor blade wakes in a cascade wind tunnel
[AD-A194737] 23 p3181 N88-28936

WIND TUNNEL DRIVES

Analysis of 7- X 10-foot high speed wind tunnel shaft loads in support of fan blade failure investigation
[NASA-TM-100504] 04 p0402 N88-12496

Experimental evaluation of turning vane designs for high-speed and coupled fan-drive corners of 0.1-scale model of NASA Lewis Research Center's proposed altitude wind tunnel
[NASA-TP-2681] 10 p1285 N88-17686

WIND TUNNEL MODELS

Possibilities for the modeling of dynamically loaded cylindrical structural parts in the wind tunnel
[KU-SFB-210/T/24] 01 p0001 N88-10005

A transonic model representation for two-dimensional wall interference assessment
[NLR-TR-86026-U] 01 p0001 N88-10006

Flutter suppression and gust load alleviation. Part 1: Results of phase 1 to 3. Part 2: Description of the Garteur model
[MBB/LKE-292/S/PUB/191] 01 p0007 N88-10038

Comparison of wind tunnel and flight test afterbody and nozzle pressures for a twin-jet fighter aircraft at transonic speeds
[NASA-TP-2588] 02 p0121 N88-10765

Static Aeroelastic Effects on High Performance Aircraft
[AGARD-CP-403] 05 p0550 N88-13348

The use of aeroelastic wind tunnel models to prove structural design 05 p0551 N88-13355

Aerodynamic and propeller performance characteristics of a propfan-powered, semispan model
[NASA-TM-86705] 06 p0667 N88-14092

Status of magnetic suspension technology
07 p0811 N88-14939

Preliminary calibration and test results from the National Transonic Facility 07 p0811 N88-14941

Effect of a model support strut on measurement of aerodynamic longitudinal and lateral coefficients
[PB87-170288] 09 p1113 N88-16670

Testing of a schematic transport plane model in several European windtunnels
[PB87-170270] 09 p1113 N88-16671

Wind tunnel modeling techniques
[KU-SFB-210/E/33] 09 p1121 N88-16711

Influence of the wall boundary layer on force measurements on half models in the transonic wind tunnel
[F+W-TF-1876] 09 p1122 N88-16715

Ariane 4, long version: Pressure distribution measurements on two models of different scale of the Ariane 4 nose fairings in the transonic tunnel of F+W Emmen (Switzerland) with varying tunnel configurations. Comparison with measurements taken at Modane (France) and with calculations after the Euler method
[F+W-TF-1878] 09 p1122 N88-16716

Strain gage balance for half models 302-6. Calibration report --- wind tunnels
[F+W-FO-1803] 09 p1168 N88-17001

Strain gage sting balance 204-6. Calibration report --- wind tunnels
[F+W-FO-1838] 09 p1168 N88-17002

Effects of winglets on a first-generation jet transport wing. 7: Sideslip effects on winglet loads and selected wing loads at subsonic speeds for a full-span model
[NASA-TP-2619] 11 p1436 N88-18567

Acoustic measurements from a rotor blade-vortex interaction noise experiment in the German-Dutch Wind Tunnel (DNW)
[NASA-TM-4024] 11 p1542 N86-19218

Design of an aeroelastic composite wing wind tunnel model
[AD-A188855] 12 p1582 N88-19466

A wind tunnel model with dynamic control
[BU-352] 13 p1724 N88-20310

Activities report of the Large Testing Facilities Department --- aircraft/spacecraft
[ETN-88-91982] 13 p1724 N88-20311

Surface flow visualization of separated flows on the forebody of an F-18 aircraft and wind-tunnel model
[NASA-TM-100436] 14 p1863 N88-21127

Inflow measurement made with a laser velocimeter on a helicopter model in forward flight. Volume 2: Rectangular planform blades at an advance ratio of 0.23
[NASA-TM-100542] 14 p1864 N88-21139

Design, simulation and laboratory testing of an inertial system for measuring the attitude and narrow-spaced motions
[DFVLR-FB-87-42] 14 p1912 N88-21426

Inflow measurement made with a laser velocimeter on a helicopter model in forward flight. Volume 3: Rectangular planform blades at an advance ratio of 0.30
[NASA-TM-100543] 15 p2015 N88-22015

Acoustic characteristics of 1/20-scale model helicopter rotors
[NASA-CR-177355] 16 p2265 N88-23548

Inflow measurement made with a laser velocimeter on a helicopter model in forward flight. Volume 5: Tapered planform blades at an advance ratio of 0.23
[NASA-TM-100545] 17 p2299 N88-23755

Control law parameterization for an aeroelastic wind-tunnel model equipped with an active roll control system and comparison with experiment
[NASA-TM-100593] 17 p2308 N88-23807

Inflow measurements made with a laser velocimeter on a helicopter model in forward flight. Volume 1: Rectangular planform blades at an advance ration of 0.15
[NASA-TM-100541] 18 p2460 N88-24607

Heterogeneous diffusion flame stabilization
[AD-A193014] 20 p2771 N88-26429

An experimental investigation of two 15 percent-scale wind tunnel fan-blade designs
[NASA-TM-88256] 22 p3046 N88-28076

Techniques for boundary layer tripping and control
23 p3168 N88-28863

Experimental tools: The tunnel and the model
23 p3168 N88-28864

Computational tools for simulation methodologies
23 p3168 N88-28865

Technology for pressure-instrumented thin airfoil models
[NASA-CR-4173] 23 p3180 N88-28933

Test of an 0.8-scale model of the AH-64 Apache in the NASA Langley full-scale wind tunnel
[AD-A196129] 24 p3319 N88-29768

Computer programs for calculation of sting pitch and roll angles required to obtain angles of attack and sideslip on wind tunnel models
[NASA-TM-100659] 24 p3329 N88-29820

WIND TUNNEL STABILITY TESTS

Effects of the installation and operation of jet-exhaust yaw vanes on the longitudinal and lateral-directional characteristics of the F-14 airplane
[NASA-TP-2769] 04 p0393 N89-12455

A wind tunnel model with dynamic control
[BU-352] 13 p1724 N88-20310

Investigation of boundary layer disturbances caused by periodic heating of a thin ribbon
[AD-A190572] 15 p2065 N88-22314

WIND TUNNEL TESTS

Wind-tunnel investigation of a full-scale general aviation airplane equipped with an advanced natural laminar flow wing
[NASA-TP-2772] 01 p0002 N88-10009

Investigations of separated flow states on wings of medium aspect ratio taking into account the wind tunnel interference problem
[ETN-87-90437] 01 p0003 N88-10016

Investigation of the suitability of the 8ft x 6ft transonic wind-tunnel for aeroacoustic research on propellers
[RAE-TM-AERO-2093] 01 p0008 N88-10041

Analysis of free molecular effects on the attitude of satellites in geostationary transfer orbit. Part 2: Force and torque measurement in free molecular wind tunnel tests
[DFVLR-IB-222-86-A/07] 01 p0014 N88-10078

Experience about the application and valuation of roughness strips for boundary layer transition control in wind tunnel tests in the high-speed range
[ESA-TT-1028] 01 p0044 N88-10278

Comparison of wind tunnel and flight test afterbody and nozzle pressures for a twin-jet fighter aircraft at transonic speeds
[NASA-TP-2588] 02 p0121 N88-10765

Wall interference tests of a CAST 10-2/DOA 2 airfoil in an adaptive-wall test section
[NASA-TM-4015] 02 p0122 N88-10772

Intergration effects of D-shaped, underwing, aft-mounted, separate-flow, flow-through nacelles on a high-wing transport
[NASA-TM-4018] 02 p0122 N88-10773

A critical assessment of wind tunnel results for the NACA 0012 airfoil
[NASA-TM-100019] 03 p0260 N88-11636

An experimental evaluation of advanced rotorcraft airfoils in the NASA Ames eleven-foot transonic wind tunnel
[NASA-CR-166587] 03 p0261 N88-11640

Experimental aerothermodynamic research of hypersonic aircraft
[NASA-CR-181533] 04 p0399 N88-12483

Results of the 1986 NASA/FAA/DFVLR main rotor test entry in the German-Dutch wind tunnel (DNW)
[NASA-TM-100507] 04 p0487 N88-13003

European hypersonic wind tunnels
05 p0530 N88-13221

Turbulence measurement in hypersonic flow
05 p0530 N88-13224

The drag of slender axisymmetric cones in rarefied hypersonic flow 05 p0531 N88-13229

Low Reynolds number influence on aerodynamic performance of hypersonic lifting vehicles
05 p0531 N88-13230

Vortex formation over delta, double-delta and wave rider configurations at supersonic speeds
05 p0533 N88-13243

The RAE experimental data-base for missiles at high Mach number and its use in assessing CFD methods
05 p0534 N88-13250

Tip aerodynamics from wind tunnel test of semi-span wing
[NASA-TM-88253] 05 p0540 N88-13290

A swept wing panel in a low speed flexible walled test section
[NASA-CR-4106] 05 p0540 N88-13292

Study of the effect of mass transfer on a transonic boundary layer. Application to flow relaminarization
[ETN-88-91169] 05 p0541 N88-13296

Delta wing in incompressible flow. Experimental study in F2
[ONERA-RT-36/1147-AN-249-G]
05 p0541 N88-13298

Low speed wind tunnel investigation of propeller slipstream aerodynamic effects on different nacelle/wing combinations. Part 1: Total forces and moments and pressure distributions on nacelle/wing at different angles of attack and yaw and at different thrust coefficients
[FFA-TN-1987-22] 05 p0542 N88-13302

Aircraft dynamics: Aerodynamic aspects and wind tunnel techniques 05 p0545 N88-13320

Fundamentals of fighter aircraft design: Engine intake and afterbody 05 p0545 N88-13322

The role of experimental investigation and computational fluid dynamics during fighter aircraft design
05 p0546 N88-13326

Requirements and recommendations for the development of theoretical codes and experimental facilities in the near future 05 p0546 N88-13327

Static Aeroelastic Effects on High Performance Aircraft
[AGARD-CP-403] 05 p0550 N88-13348

The use of aeroelastic wind tunnel models to prove structural design 05 p0551 N88-13355

Measurement of model deformation in wind tunnels
05 p0551 N88-13358

Measurement of local convective heat transfer coefficients from a smooth and roughened NACA-0012 airfoil: Flight test data
[NASA-TM-100284] 05 p0582 N88-13552

Assessment of the reliability of a correction procedure for WGT (Wet Globe Thermometer) (Botsball) measurements of heat stress
[AD-A185193] 05 p0584 N88-13559

Wind tunnel results for a high-speed, natural laminar-flow airfoil designed for general aviation aircraft
[NASA-TM-87602] 06 p0665 N88-14078

Analysis and test evaluation of the dynamic stability of three advanced turboprop models at zero forward speed
[NASA-CR-175025] 06 p0668 N88-14095

Dutch-German wind tunnel's tenth anniversary
[ETN-88-91350] 06 p0670 N88-14105

An investigation of the effects of the propeller slipstream on a wing boundary layer 06 p0700 N88-14293

Flight and wind-tunnel measurements showing base drag reduction provided by a trailing disk for high Reynolds number turbulent flow for subsonic and transonic Mach numbers
[NASA-TP-2638] 06 p0701 N88-14299

Flow diagnostics and visualization in wind tunnels and flight 07 p0811 N88-14940

Riblets for aircraft skin-friction reduction
07 p0814 N88-14955

An engineering study of hybrid adaptation of wind tunnel walls for three-dimensional testing
[NASA-CR-178374] 07 p0814 N88-14957

Measurement in a wind tunnel of the modification of mean wind and turbulence characteristics due to induction effects near wind turbine rotors
[DE88-000249] 07 p0815 N88-14963

Incompressible viscous flow simulations of the NFAC wind tunnel
[NASA-CR-177431] 07 p0816 N88-14969

Static force and moment test of the Holloman narrow-gage rocket sled at Mach numbers from 3.5 to 5.5
[AD-A186291] 07 p0822 N88-14995

Thin film electret boundary layer transition detector: A feasibility study
[AD-A185675] 07 p0856 N88-15199

Supersonic boundary layer on a heated wall
[ETN-88-91617] 08 p0950 N88-15763

Effects of aircraft deicing/antiicing fluids on airfoil characteristics 08 p0952 N88-15776

Supersonic STOVL propulsion technology program: An overview 08 p0957 N88-15808

Theoretical and experimental studies of the transonic flow field and associated boundary conditions near a longitudinally-slotted wind-tunnel wall
[NASA-CR-181169] 08 p0959 N88-15815

Wind tunnel investigations of periodic vortex separation on rough-surface circular cylinders using acoustic measuring methods
[DFVLR-FB-87-24] 09 p1112 N88-16665

Testing of a schematic transport plane model in several European windtunnels
[PB87-170270] 09 p1113 N88-16671

Description of tests run in the T2 cryogenic wind tunnel
[PB87-170296] 09 p1113 N88-16672

Full scale and wind tunnel surface pressure measurements on the T.R.R.L. spray dispersion programme vehicles
[REPT-8623] 09 p1114 N88-16676

Airplane load drop and missile firing: Experimental methods for predicting trajectories
[PB87-170494] 09 p1117 N88-16695

Wind tunnel modeling techniques
[KU-SFB-210/E/33] 09 p1121 N88-16711

The wind tunnel as a yardstick for aircraft design
[NLR-MP-85032-U] 09 p1121 N88-16712

Flow field measurements using hotwire anemometry
[AD-A187029] 09 p1160 N88-16951

Techniques of flow visualization
[AGARD-AG-302] 09 p1164 N88-16977

Investigations of a circulation control airfoil flowfield using an advanced laser velocimeter
10 p1269 N88-17589

Prediction of aeroelastic response of a model X-wing rotor 10 p1271 N88-17603

Analysis of highspeed propellers aerodynamics
10 p1282 N88-17669

Experimental investigation of a supercritical compressor rotor blade section 10 p1284 N88-17680

Effectiveness of various control surfaces in quasi-steady and unsteady conditions
[AGARD-R-735] 10 p1284 N88-17682

An experimental investigation of pressure driven three-dimensional turbulent boundary layers
10 p1327 N88-17934

A three-dimensional dual potential procedure for rotational flows 10 p1329 N88-17942

La Recherche Aerospatiale, bimonthly bulletin, number 1987-2, 237/March-April
[ESA-TT-1074] 11 p1433 N88-18550

Pressure distributions from high Reynolds number transonic tests of an NACA 0012 airfoil in the Langley 0.3-meter transonic cryogenic tunnel
[NASA-TM-100526] 11 p1435 N88-18565

High Reynolds number transonic tests on a NACA 0012 airfoil in the Langley 0.3-meter transonic cryogenic tunnel
[NASA-TM-100527] 11 p1436 N88-18571

Store separation and missile firing from aircraft: Experimental methods for trajectory projection
[NASA-TT-20214] 11 p1439 N88-18589
Space shuttle phase B wind tunnel test database
[NASA-CR-4121] 11 p1444 N88-18611
Changes in the turbulent boundary layer structure associated with net drag reduction by outer layer manipulators
[NASA-CR-178152] 11 p1483 N88-18853
Acoustic measurements from a rotor blade-vortex interaction noise experiment in the German-Dutch Wind Tunnel (DNW)
[NASA-TM-4024] 11 p1542 N88-19218
A review of technologies applicable to low-speed flight of high-performance aircraft investigated in the Langley 14- x 22-foot subsonic tunnel
[NASA-TP-2796] 13 p1717 N88-20264
Tests on the AFWAL 65 deg delta wing at NLR: A study of vortex flow development between Mach = 0.4 and 4
[NLR-MP-86058-U] 13 p1717 N88-20266
The international vortex flow experiment: A test case for compressible Euler codes
[NLR-MP-86076-U] 13 p1717 N88-20267
The construction of a three-dimensional finite volume grid generator for a wing in a wind tunnel with application to Navier-Stokes flow solvers
[FFA-TN-1987-58] 13 p1719 N88-20277
Engine flow simulation for wind tunnel testing at NLR
[NLR-MP-87011-U] 13 p1723 N88-20305
Activities report of the Large Testing Facilities Department --- aircraft/spacecraft
[ETN-88-91982] 13 p1724 N88-20311
Activities report of the Aerodynamics Department
[ETN-88-91979] 14 p1862 N88-21123
Wall interference assessment and corrections for transonic adaptive wall airfoil data
14 p1863 N88-21129
Propagation of artificial disturbances immersed in thick turbulent boundary layer 14 p1864 N88-21136
An experimental and theoretical study of the ice accretion process during artificial and natural icing conditions
[NASA-CR-182119] 14 p1865 N88-21143
Determination of canopy loads for a light aircraft by wind tunnel testing and computer modelling
[BU-353] 14 p1869 N88-21167
Design of a sound neck in connection with the model-support system of a transonic wind tunnel test section
[ILR-MITT-186(1987)] 14 p1869 N88-21171
The 5.5 m low speed wind tunnel. Introduction to the facilities
[ARG-205] 14 p1870 N88-21172
Main features of Warton (United Kingdom) 2.7 x 2.1 m low speed wind tunnel
[AXM-124] 14 p1870 N88-21173
An experimental-computational investigation of transonic shock wave-turbulent boundary layer interaction in a curved test section
[CWI-NM-R8716] 14 p1909 N88-21408
Quick actuating closure and handling system
14 p1925 N88-21476
Development of drive mechanism for an oscillating airfoil 14 p1926 N88-21482
Procedures and requirements for testing in the Langley Research Center unitary plan wind tunnel
[NASA-TM-100529] 15 p2015 N88-22016
Porous wind tunnel corrections for counterrotation propeller testing
[NASA-TM-100873] 15 p2015 N88-22019
Design of an integrated control system for flutter margin augmentation and gust load alleviation, tested on a dynamic windtunnel model
[PB88-149885] 15 p2020 N88-22038
JPRS report: Science and technology. China
[JPRS-CST-87-043] 15 p2053 N88-22233
Investigation of side-wall effects in wind tunnel with supercritical airfoil testing 15 p2054 N88-22241
FLAP (Force and Loads Analysis Program) code development and validation
[DE88-001131] 15 p2075 N88-22371
Langley aerospace test highlights, 1987
[NASA-TM-100595] 15 p2153 N88-22853
Space directorate research and technology accomplishments for fiscal year 1987
[NASA-TM-100607] 15 p2153 N88-22854
Aerofoil testing in a self-streamlining flexible walled wind tunnel
[NASA-CR-4128] 16 p2156 N88-22865
Propulsion and airframe aerodynamic interactions of supersonic V/STOL configurations. Volume 2: Wind tunnel test force and moment data report
[NASA-CR-177343-VOL-2] 16 p2157 N88-22867
Qualification of a water tunnel for force measurements on aeronautical models 16 p2200 N88-23128
Study of the boundary layer of a flow pulsed by acoustic waves
[ETN-88-91998] 16 p2206 N88-23163
Propfan model wind tunnel aeroelastic research results 16 p2220 N88-23246
Methodology for matching experimental and computational aerodynamic data
[NASA-TM-100592] 17 p2295 N88-23728
High Reynolds number tests of a Douglas DLBA 032 airfoil in the Langley 0.3-meter transonic cryogenic tunnel
[NASA-TM-87663] 17 p2296 N88-23734
Full potential methods for analysis/design of complex aerospace configurations
[NASA-CR-3982] 17 p2296 N88-23736
Wind tunnel testing of low-drag airfoils
17 p2297 N88-23741
PAN AIR analysis of the NASA/MCAIR 279-3: An advanced supersonic V/STOL fighter/attack aircraft
[NASA-TM-86838] 17 p2298 N88-23750
Wind-tunnel investigation of actuated forebody strakes for yaw control at high angles of attack
17 p2299 N88-23754
Pressure distributions from subsonic tests of an advanced laminar-flow-control wing with leading- and trailing-edge flaps
[NASA-TM-4040-PT-1] 17 p2300 N88-23758
Thermal remote anemometer system
[NASA-CASE-LAR-13508-1] 17 p2342 N88-23962
Sources and levels of background noise in the NASA Ames 40- by 80-foot wind tunnel
[NASA-TM-100077] 17 p2395 N88-24239
Aerodynamic performance and pressure distributions for a NASA SC(2)-0714 airfoil tested in the Langley 0.3-meter transonic cryogenic tunnel
[NASA-TM-4044] 18 p2456 N88-24580
Experiment investigation on longitudinal characteristics of the forward swept wing
[AD-A191553] 18 p2456 N88-24582
Passive shock wave-boundary layer control for the Bell FX69-H-098 airfoil 18 p2457 N88-24588
Unsteady flow around a profile subjected to pulsed motions
[ETN-88-92151] 18 p2458 N88-24594
Supplements to the study of the wake of a Mirage G8 model at F2 --- wind tunnel
[CERT-RT-OA-20/5025-AYD] 18 p2458 N88-24596
Summary of low-speed wind tunnel results of several high-speed counterrotation propeller configurations
[NASA-TM-100945] 18 p2458 N88-24597
High speed and high angle of attack aerodynamic characteristics of winged space vehicle
[ISSN-0285-6808] 18 p2459 N88-24599
The experimental verification of wall movement influence coefficients for an adaptive walled test section
[NASA-CR-181681] 19 p2598 N88-25439
Wind tunnel wall interference (January 1980 - May 1988): A selected, annotated bibliography
[NASA-TM-4061] 19 p2604 N88-25466
High speed and high angle of attack wind tunnel test results of the winged space vehicle C-2
[ISAS-RN-623] 20 p2751 N88-26329
Propfan test assessment testbed aircraft stability and control/performance 1/9-scale wind tunnel tests
[NASA-CR-182121] 20 p2757 N88-26360
Low-speed wind-tunnel test of a STOL supersonic-cruise fighter concept
[NASA-TM-4050] 20 p2761 N88-26374
Wind tunnel study of atmospheric diffusion in unstable stratified boundary layer. Part 2: Characteristic scale and diffusion
[DE88-753109] 20 p2823 N88-26749
Helicopter main-rotor noise: Determination of source contributions using scaled model data
[NASA-TP-2825] 20 p2848 N88-26907
Aeroelastic characteristics of the AH-64 bearingless tail rotor 21 p2891 N88-27162
Theoretical and experimental investigations of a vortex drag behind a wing profile with spoiler
[ISL-PU-309/87] 21 p2892 N88-27169
Wind tunnel tests of the influence of airfoil-thickness on normal force and pitching moment of two slender wings at transonic and supersonic Mach numbers
[DFVLR-FB-88-17] 21 p2893 N88-27171
Space shuttle phase B wind tunnel model and test information. Volume 2: Orbiter configuration
[NASA-CR-178415-VOL-2-PT-2]
21 p2893 N88-27172
Hybrid procedure for dynamic measurements in transonic wind tunnels: Demonstrated by pitch oscillation
[DFVLR-FB-88-19] 21 p2900 N88-27211
Design of a mechanism to control wind tunnel turbulence 21 p2926 N88-27370
Determination of the local heat-transfer characteristics on glaze ice accretions on a cylinder and a NACA 0012 airfoil 21 p2946 N88-27500
Laser-Doppler measurements of turbulence structures in free streams behind flat and rotation symmetrical profiles
[ETN-88-92336] 21 p2948 N88-27510
Hypersonic flight testing
[DE88-001655] 21 p3015 N88-27894
Wind tunnel tests of elliptical missile body configurations at Mach numbers 0.4 to 5.0
[AD-A193525] 22 p3038 N88-28040
Wind tunnel investigation of wing and control panel loads at transonic and supersonic speeds on some schematic cruciform missile configurations
[FFA-TN 1986-43-SUPPL-1] 22 p3039 N88-28044
Missiles, fuselage and similar bodies
23 p3167 N88-28858
High-aspect-ratio wings 23 p3167 N88-28859
Complex configurations 23 p3167 N88-28861
Reynolds number effects and the wind tunnel environment 23 p3168 N88-28862
Techniques for boundary layer tripping and control
23 p3168 N88-28863
Experimental tools: The tunnel and the model
23 p3168 N88-28864
Empirical tools for simulation methodologies
23 p3168 N88-28866
Introduction and critical flow phenomena
23 p3169 N88-28870
Environmental effects on transition and boundary layer characteristics 23 p3170 N88-28876
Boundary layer manipulation 23 p3170 N88-28877
Effects of independent variation of Mach and Reynolds numbers on the low-speed aerodynamic characteristics of the NACA 0012 airfoil section
[NASA-TM-4074] 23 p3170 N88-28879
Space shuttle phase B wind tunnel model and test information. Volume 2: Orbiter configuration
[NASA-CR-178415-VOL-2-PT-1]
23 p3171 N88-28881
Aerodynamic data accuracy and quality: Requirements and capabilities in wind tunnel testing
[AGARD-AR-254] 23 p3173 N88-28893
Steady and unsteady transonic pressure measurements on a clipped delta wing for pitching and control-surface oscillations
[NASA-TP-2594] 23 p3173 N88-28895
Test results at transonic speeds on a contoured over-the-wing propfan model
[NASA-TM-88206] 23 p3177 N88-28918
Experimental and analytical evaluation of the effects of simulated engine inlets on the blade vibratory stresses of the SR-3 model prop-fan
[NASA-CR-174959] 23 p3179 N88-28927
Space shuttle phase B wind tunnel model and test information. Volume 3: Launch configuration
[NASA-CR-178416-VOL-3-PT-2]
24 p3315 N88-29744
Space shuttle phase B wind tunnel model and test information. Volume 1: Booster configuration
[NASA-CR-178414-VOL-1-PT-1]
24 p3315 N88-29745
Test of an 0.8-scale model of the AH-64 Apache in the NASA Langley full-scale wind tunnel
[AD-A196129] 24 p3319 N88-29768
Space shuttle phase B wind tunnel model and test information. Volume 1: Booster configuration
[NASA-CR-178414-VOL-1-PT-2]
24 p3320 N88-29770
Pressure distributions from subsonic tests of an advanced laminar-flow-control wing with leading- and trailing-edge flaps
[NASA-TM-4040-PT-2] 24 p3321 N88-29776
An experimental study of an adaptive-wall wind tunnel
[NASA-CR-183152] 24 p3329 N88-29821
Supersonic wall adaptation in the rubber tube test section of the DFVLR Goettingen
[IB-222-87-A-08] 24 p3330 N88-29824

WIND TUNNEL WALLS

A transonic model representation for two-dimensional wall interference assessment
[NLR-TR-86026-U] 01 p0001 N88-10006
Wall interference tests of a CAST 10-2/DOA 2 airfoil in an adaptive-wall test section
[NASA-TM-4015] 02 p0122 N88-10772
An analysis of sound absorbing linings for the interior of the NASA Ames 80 x 120-foot wind tunnel
[NASA-CR-177396] 04 p0488 N88-13006
A swept wing panel in a low speed flexible walled test section
[NASA-CR-4106] 05 p0540 N88-13292
Wind tunnel wall interference
07 p0811 N88-14938
An engineering study of hybrid adaptation of wind tunnel walls for three-dimensional testing
[NASA-CR-178374] 07 p0814 N88-14957
Supersonic boundary layer on a heated wall
[ETN-88-91617] 08 p0950 N88-15763

Theoretical and experimental studies of the transonic flow field and associated boundary conditions near a longitudinally-slotted wind-tunnel wall

[NASA-CR-181169] 08 p0959 N88-15815

Influence of the wall boundary layer on force measurements on half models in the transonic wind tunnel

[F+W-TF-1876] 09 p1122 N88-16715

Predictive wall adjustment strategy for two-dimensional flexible walled adaptive wind tunnel: A detailed description of the first one-step method

[NASA-CR-181635] 12 p1573 N88-19409

An evaluation in a modern wind tunnel of the transonic adaptive wall adjustment strategy developed by NPL in the 1940's

[NASA-CR-181623] 12 p1575 N88-19417

Flexiwall 3 SO: A second order predictive strategy for rapid wall adjustment in two-dimensional compressible flow

[NASA-CR-181662] 15 p2015 N88-22018

Porous wind tunnel corrections for counterrotation propeller testing

[NASA-TM-100873] 15 p2015 N88-22019

Investigation of side-wall effects in wind tunnel with supercritical airfoil testing 15 p2054 N88-22241

Aerofoil testing in a self-streamlining flexible walled wind tunnel

[NASA-CR-4128] 16 p2156 N88-22865

Flow quality of NAL two-dimensional transonic wind tunnel. Part 1: Mach number distributions, flow angularities and preliminary study of side wall boundary layer suction

[NASA-TT-20209] 16 p2165 N88-22911

The experimental verification of wall movement influence coefficients for an adaptive walled test section

[NASA-CR-181681] 19 p2598 N88-25439

Empty test section streamlining of the transonic self-streamlining wind tunnel fitted with new walls

[NASA-CR-181680] 19 p2598 N88-25442

Wind tunnel wall interference (January 1980 - May 1988): A selected, annotated bibliography

[NASA-TM-4061] 19 p2604 N88-25466

Wall interference assessment/correction of data from tests of a CAST 10-2/DOA 2 airfoil in the Langley 0.3-m transonic cryogenic tunnel 20 p2751 N88-26331

An experimental study of an adaptive-wall wind tunnel

[NASA-CR-183152] 24 p3329 N88-29821

WIND TUNNELS

NT BLOWDOWN WIND TUNNELS
NT CASCADE WIND TUNNELS
NT COMBUSTION WIND TUNNELS
NT CRYOGENIC WIND TUNNELS
NT HOTSHOT WIND TUNNELS
NT HYPERSONIC WIND TUNNELS
NT HYPERVELOCITY WIND TUNNELS
NT LOW SPEED WIND TUNNELS
NT RECTANGULAR WIND TUNNELS
NT SHOCK TUNNELS
NT SLOTTED WIND TUNNELS
NT SUBSONIC WIND TUNNELS
NT SUPERSONIC WIND TUNNELS
NT TRANSONIC WIND TUNNELS
NT TRISONIC WIND TUNNELS

Possibilities for the modeling of dynamically loaded cylindrical structural parts in the wind tunnel

[KU-SFB-210/T/24] 01 p0001 N88-10005

Theoretical and experimental study of flow-control devices for inlets of indraft wind tunnels

03 p0268 N88-11684

Analysis of 7- X 10-foot high speed wind tunnel shaft loads in support of fan blade failure investigation

[NASA-TM-100504] 04 p0402 N88-12496

Measured performance of the heat exchanger in the NASA icing research tunnel under severe icing and dry-air conditions

[NASA-TM-100116] 04 p0451 N88-12796

Rarefied gas numerical wind tunnel. 2: Two-dimensional and axially symmetric bodies 05 p0538 N88-13273

Dutch-German wind tunnel's tenth anniversary

[ETN-88-91350] 06 p0670 N88-14105

Low-disturbance wind tunnels

07 p0811 N88-14937

Realization of the immediate objectives of the Aero Gas Dynamics and Vibration Laboratory (LAGG) at the National Center for Research, Science and Technology (PUSPIPTEK) at Serpong, Java (Indonesia). Project TTA-79

[GG/QPR-10] 08 p1092 N88-16572

Status of the special-purpose airfoil families

[DE88-001124] 11 p1506 N88-18998

Activities report of the Large Testing Facilities Department --- aircraft/spacecraft

[ETN-88-91982] 13 p1724 N88-20311

Quick actuating closure and handling system

14 p1925 N88-21476

Development of drive mechanism for an oscillating airfoil 14 p1926 N88-21482

Design and test of a new coaxial air joints

[DE88-751808] 16 p2164 N88-22906

Investigation on the movement of vortex burst position with dynamically changing angle of attack for a schematic deltawing in a watertunnel with correlation to similar studies in windtunnel 16 p2204 N88-23152

Sources and levels of background noise in the NASA Ames 40- by 80-foot wind tunnel

[NASA-TM-100077] 17 p2395 N88-24239

Rarefied gas numerical wind tunnel. 3. Universal code for three dimensional bouies 19 p2637 N88-25644

An experimental investigation of two 15 percent-scale wind tunnel fan-blade designs

[NASA-TM-88256] 22 p3046 N88-28076

Development and design of windtunnel and test facility for RPV (Remote Piloted Vehicle) enhancement devices

[AD-A194842] 24 p3329 N88-29822

WIND TURBINES

ARSPNS: A method to calculate steady and unsteady potential flow about fixed and rotational lifting and nonlifting bodies

[NLR-TR-85114-U] 01 p0044 N88-10282

Results of a wind turbine/sealed lead-acid battery experiment

[DE87-012720] 02 p0166 N88-11044

The physics and mathematical description of the Achilles heel of stationary wind turbine aerodynamics: The tip flow

[R-812-D] 03 p0260 N88-11635

Linearized aeroelastic analysis of a wind turbine with a two-bladed rotor

[ETN-87-90600] 03 p0347 N88-12192

Dynamic response of a 330 KW horizontal axis wind turbine generator

[DE87-014867] 03 p0347 N88-12195

Application of ray theory to propagation of low frequency noise from wind turbines

[NASA-CR-178367] 03 p0373 N88-12349

Input turbulence features at a megawatt-size wind turbine, Medicine Bow, Wyoming

[DE88-000098] 04 p0464 N88-12873

Measurements and calculations of aerodynamic torques for a vertical-axis wind turbine

[DE88-001783] 04 p0465 N88-12876

Using a new characterization of turbulent wind for accurate correlation of wind turbine response with wind speed

[DE88-001453] 04 p0466 N88-12881

Variability of wind power near Oklahoma City and implications for siting of wind turbines

[DE88-000444] 04 p0470 N88-12902

An overview of the DOE/SANDIA/USDA vertical axis wind turbine Test Bed Project

[DE88-000604] 05 p0622 N88-13812

Accurate rotor loads prediction using the FLAP (Force and Loads Analysis Program) dynamics code

[DE88-001109] 05 p0623 N88-13815

Performance measurements of the Kolibrie and FACT rotor blades without tip vanes on the full-scale experimental wind turbine

[IW-R518] 06 p0665 N88-14077

Measurement in a wind tunnel of the modification of mean wind and turbulence characteristics due to induction effects near wind turbine rotors

[DE88-000249] 07 p0815 N88-14963

Data on existing wind energy converters in Denmark

[DE88-900199] 07 p0874 N88-15300

Realization and demonstration of a wind turbine of 200 kW demonstration project

[DE88-900207] 07 p0874 N88-15302

Collecting of new data on existing wind energy converters

[DE88-900221] 07 p0875 N88-15305

A proposed metric for assessing the potential of community annoyance from wind turbine low-frequency noise emissions

[DE88-001113] 08 p1022 N88-16187

Data acquisition and analysis system for the Sandia 34-meter Vertical Axis Wind Turbine

[DE88-002417] 09 p1187 N88-17112

Wind turbine acoustics research bibliography with selected annotation

[NASA-TM-100528] 09 p1243 N88-17450

Cape Blanco wind farm feasibility study

[DE88-003749] 10 p1349 N88-18060

Wake effects in a Fayette 95-IIS wind turbine array

[DE88-001103] 10 p1349 N88-18063

Modal testing the EOLE

[DE88-003795] 10 p1350 N88-18066

Preliminary results from the dynamic response testing of the Westinghouse 600-kW wind turbine

[DE88-001123] 10 p1350 N88-18070

Modal testing of a very flexible 110 m wind turbine structure

[DE88-003796] 10 p1351 N88-18072

Analysis of wind turbines on offshore support structures excited by random wind and random waves

[DE88-004772] 10 p1351 N88-18074

Turbulence loads on the Howden 26-m-diameter wind turbine

[DE88-001118] 10 p1351 N88-18075

Status of the special-purpose airfoil families

[DE88-001124] 11 p1506 N88-18998

Site effects on wind characteristics at a turbine rotor

[DE88-005135] 11 p1507 N88-19003

Testing of a one-bladed 30-meter-diameter rotor on the DOE/NASA Mod-O wind turbine

[NASA-TM-100274] 11 p1509 N88-19014

Fatigue load measurements and evaluation of the 25m Horizontal Axis Wind Turbine (HAWT) at Petten, The Netherlands

[NLR-MP-86054-U] 13 p1782 N88-20660

New airfoil sections for straight bladed turbine

[DE88-701075] 14 p1942 N88-21588

The 25 m horizontal-axis turbine as a test case for standard Dutch aerodynamic calculation methods for high-speed rotors

[R-762-D] 14 p1942 N88-21589

Comparison of pressure distributions on model and full-scale NACA 64-621 airfoils with ailerons for wind turbine application

[NASA-TM-100802] 14 p1943 N88-21593

FLAP (Force and Loads Analysis Program) code development and validation

[DE88-001131] 15 p2075 N88-22371

Lewis Structures Technology, 1988. Volume 3: Structural Integrity Fatigue and Fracture Wind Turbines HOST

[NASA-CP-3003-VOL-3] 15 p2081 N88-22408

Large-scale wind turbine structures

15 p2085 N88-22429

Lewis Structures Technology, 1988. Volume 1: Structural Dynamics

[NASA-CP-3003-VOL-1] 16 p2217 N88-23226

Variable speed optimal control of a wind turbine generator

[LAAS-87-358] 16 p2229 N88-23316

Aerodynamic noise of wind turbines

[PB88-165188] 16 p2265 N88-23546

Yaw dynamics of horizontal axis wind turbines

[DE88-001137] 18 p2537 N88-25055

The MOD-2 wind turbine: Aeroacoustical noise sources, emissions, and potential impact

[DE88-001132] 19 p2687 N88-25971

Analysis of the electrical harmonic characteristics of a slip recovery variable speed generating system for wind turbine applications

[DE88-001140] 19 p2687 N88-25972

Analysis of the electrical characteristics of a Westinghouse variable speed generating system for wind turbine applications

[DE88-001139] 20 p2818 N88-26721

Modal testing in the design evaluation of wind turbines

[DE88-010374] 21 p2968 N88-27632

Three-dimensional wind simulation

[DE88-009793] 21 p2975 N88-27671

Electromagnetic interference to radar and radio link systems caused by large scale wind turbines

[FOA-C-30486-3.2] 22 p3071 N88-28234

An examination of wake effects and power production for a group of large wind turbines

[DE88-009906] 22 p3117 N88-28518

Effects of precipitation on wind turbine performance

[DE88-001144] 23 p3228 N88-29211

Dynamic response of a 330-kW horizontal axis wind turbine generator

[DE88-001136] 23 p3228 N88-29212

WIND VARIATIONS

Parameterization of horizontal wind velocity variability

[AD-A190107] 15 p2097 N88-22493

Variable speed optimal control of a wind turbine generator

[LAAS-87-358] 16 p2229 N88-23316

Atmospheric angular momentum and length of day

[AD-A194505] 23 p3233 N88-29238

WIND VELOCITY

NT SOLAR WIND VELOCITY

Coastal winds of the southeast Alaska Peninsula

[PB87-206173] 02 p0215 N88-11354

A model for the convective atmospheric boundary layer during the winter in the Khartoum Region (Sudan)

[R-822-A] 03 p0353 N88-12225

Study of microburst detection performance during 1985 in Memphis, Tennessee

[AD-A184013] 03 p0354 N88-12231

Using a new characterization of turbulent wind for accurate correlation of wind turbine response with wind speed

[DE88-001453] 04 p0466 N88-12881

Variability of wind power near Oklahoma City and implications for siting of wind turbines

[DE88-000444] 04 p0470 N88-12902

The climatic wind regime in the lower thermosphere from meteor radar observations 06 p0733 N88-14506
Atmosphere dynamics in the equatorial meteor zone 06 p0733 N88-14508
The lower thermosphere wind regime from simultaneous observations over Euroasia (Collm, Dushanbe, Frunze) 06 p0733 N88-14510
Characteristics of atmospheric disturbances with a quasi-two day period 06 p0734 N88-14515
Tidal activity in the meteor zone over Budrio, Italy 06 p0734 N88-14517
Longitudinal peculiarities of meridional circulation in lower thermosphere and mesosphere 06 p0736 N88-14525
Atmosphere dynamic processes structure at 80-105 km altitude 06 p0736 N88-14527
Observations of inertial period waves and vertical velocities in the tropical middle atmosphere using the MST radar technique 06 p0742 N88-14562
Mean and peak wind load reduction on heliostats
[DE87-012281] 07 p0873 N88-15296
Wind and temperature structure on the slopes of a mountain valley
[DE88-000080] 07 p0880 N88-15338
Improvements in profiler wind estimates using smoothed data in the spectrum finder algorithm
[PB88-102181] 07 p0881 N88-15342
Turbulence structure during high wind 08 p1014 N88-16149
Extrapolation of extremum values of the wind velocity 08 p1015 N88-16150
NASA wind shear model: Summary of model analyses 10 p1273 N88-17617
Caribbean and Central America wind energy assessment
[DE88-005134] 11 p1507 N88-19002
Site effects on wind characteristics at a turbine rotor
[DE88-005135] 11 p1507 N88-19003
Air temperature shield tests
[AD-A187459] 11 p1514 N88-19043
Correction of the wind field measured by the NCAR electra during FASINEX (Frontal Air-Sea Interaction Experiment) for inertial navigation system drifts
[AD-A187780] 11 p1514 N88-19045
An analytical method for the determination of the average horizontal wind velocities across two-dimensional hills
[ISBN-3-923624-06-9] 11 p1515 N88-19048
Determining Langmuir circulation parameters on basis of similarity theory 13 p1785 N88-20680
Wind velocity measurement data. Zimbabwe, 4 measuring stations
[R-845-D] 13 p1802 N88-20770
Study of passages of cross-equatorial current during southern monsoon 14 p1900 N88-21347
Unsteady aerodynamics of a Wortmann FX-63-137 wing in a fluctuating wind field
[AD-A190128] 15 p2013 N88-22006
Parameterization of horizontal wind velocity variability
[AD-A190107] 15 p2097 N88-22493
Describing the source created by turbulent flow over orifices and louvers
[AD-A190254] 15 p2130 N88-22706
A system for determination of wind fields using geostationary meterological satellites 17 p2360 N88-24056
Overview of wind behavior research in the US Wind Energy Program
[DE88-005683] 18 p2537 N88-25057
Wind flow study: July 1987 and November-December 1987
[DE88-008969] 20 p2828 N88-26776
Three-dimensional wind simulation
[DE88-009793] 21 p2975 N88-27671
Project wind, phase 4 (smoke test), Meadow Brook Valley, Red Bluff, California
[AD-A194742] 22 p3128 N88-28596
A review of measured gust responses in the light of modern analysis methods 24 p3312 N88-29724
A summary of atmospheric turbulence measurements with specially-equipped aircraft in the US 24 p3312 N88-29727
Re-assessment of gust statistics using CAADRP data 24 p3313 N88-29732
Analysis of environmental parameters from the Panama City tower radar experiment
[AD-A194994] 24 p3404 N88-30264
A digital simulation technique for the Dryden atmospheric model
[NASA-TT-20342] 24 p3404 N88-30266
Determining near-water wind speed using radar data from Cosmos-1500 artificial earth satellite 24 p3449 N88-30524

WIND VELOCITY MEASUREMENT
A 15 cm aperture LED scintillometer for C(n) squared and crosswind measurements
[KNMI-WR-87-3] 01 p0070 N88-10448
A real-time system for automatic single-Doppler wind field analysis 02 p0200 N88-11249
Middle Atmosphere Program. Handbook for MAP, volume 25
[NASA-CR-181571] 06 p0732 N88-14502
A statistical study of variations of internal gravity wave energy characteristics in meteor zone 06 p0735 N88-14523
On the dependence of the lower thermospheric wind regime on the solar cycle 06 p0736 N88-14524
The Cyclone meteor radar system for routine wind measurements in the lower thermosphere 06 p0741 N88-14555
Collecting of new data on existing wind energy converters
[DE88-900221] 07 p0875 N88-15305
Limiting accuracy of scatterometer determination of wind speed over ocean from satellite 08 p1007 N88-16107
Vertical sounding of th air layer close to a glacier on Mount Vernagferner in the Oetzal Alps, Tyrol (experiment LUZIVER 1983) 08 p1015 N88-16152
Remote measurement of aerosol stream velocity with continuous-wave CO2-laser 08 p1079 N88-16506
Convective wind fields as investigated with doppler lidar
[PB88-115472] 09 p1193 N88-17151
Method for determination of the wind velocity and direction
[NASA-TT-20233] 13 p1802 N88-20769
Wind velocity measurement data. Zimbabwe, 4 measuring stations
[R-845-D] 13 p1802 N88-20770
Wind measurements by electromagnetic probes
[NASA-TM-4066] 23 p3236 N88-29256

WINDING
NT FILAMENT WINDING
NT HELICAL WINDINGS
Tape wrapping apparatus and method
[EP-PATENT-0-181-747-A2] 01 p0053 N88-10336
Departmental report on program EMTP-machine windings surge transients: Travelling wave method
[PB87-123733] 04 p0438 N88-12719
High midplane accessibility stellarator windings for high current toroidal accelerators
[AD-A186235] 07 p0933 N88-15665
Thermoplastic composite with continuous fibers
[FOA-C-20707-2.6] 22 p3051 N88-28103

WINDMILLS (WINDPOWERED MACHINES)
Build, install and demonstrate a variable stroke pump control and windmill system
[DE87-014656] 03 p0347 N88-12191

WINDOWS
Space station proximity operations windows: Human factors design guidelines
[NASA-TM-88233] 24 p3410 N88-30301

WINDOWS (APERTURES)
Multilayered foils as radiation entrance windows and spectral filters for image converters in the ultrasoft X-ray wavelength region
[MPE-PREPRINT-90] 02 p0176 N88-11099
A high field launch for electron cyclotron heating using an external window
[DE88-005350] 13 p1836 N88-21000
Space station proximity operations and window design 17 p2380 N88-24149
Determination and application of bidirectional solar-optical properties of fenestration systems
[DE88-010364] 20 p2820 N88-26727

WINDOWS (INTERVALS)
NT LASER WINDOWS

WINDPOWER UTILIZATION
Methodology for control and operation of wind arrays in utility systems
[DE87-013129] 01 p0039 N88-10248
Variability of wind power near Oklahoma City and implications for siting of wind turbines
[DE88-000444] 04 p0470 N88-12902
An overview of the DOE/SANDIA/USDA vertical axis wind turbine Test Bed Project
[DE88-000604] 05 p0622 N88-13812
Wind measurements at high altitudes (150 m tower)
[BMFT-FB-T-86-169] 09 p1193 N88-17149
Cape Blanco wind farm feasibility study
[DE88-003748] 10 p1348 N88-18059
Caribbean and Central America wind energy assessment
[DE88-005134] 11 p1507 N88-19002
8th Wind Energy Symposium
[DE88-770028] 11 p1507 N88-19004
Alternative Energy in the Midwest: Research and Applications. Conference Proceedings, Rosemont, Illinois, March 19-20, 1987
[PB88-142278] 11 p1509 N88-19015
Wind energy resource survey of New Zealand: National resource assessment
[PB88-139365] 12 p1640 N88-19822
Wind velocity measurement data. Zimbabwe, 4 measuring stations
[R-845-D] 13 p1802 N88-20770
Activities report in flight and space travel
[ISSN-0070-3966] 14 p2012 N88-22000
Energy from the wind
[DE88-006897] 15 p2091 N88-22459
Overview of wind behavior research in the US Wind Energy Program
[DE88-005683] 18 p2537 N88-25057
Analysis of the electrical characteristics of a Westinghouse variable speed generating system for wind turbine applications
[DE88-001139] 20 p2818 N88-26721
Wind Energy Technology: Generating power from the wind, a current awareness bulletin
[DE88-008292] 20 p2820 N88-26729

WINDPOWERED GENERATORS
Methodology for control and operation of wind arrays in utility systems
[DE87-013129] 01 p0039 N88-10248
Results of a wind turbine/sealed lead-acid battery experiment
[DE87-012720] 02 p0166 N88-11044
Data on existing wind energy converters in Denmark
[DE88-900199] 07 p0874 N88-15300
Realization and demonstration of a wind turbine of 200 kW demonstration project
[DE88-900207] 07 p0874 N88-15302
Optimal control of windpowered plants
[FOA-C-20610-2.7] 08 p1022 N88-16188
Study on a rotor speed control system for a horizontal axis windmill
[NAL-TR-931] 10 p1349 N88-18062
Wind energy resource survey of New Zealand: National resource assessment
[PB88-139365] 12 p1640 N88-19822
Variable speed optimal control of a wind turbine generator
[LAAS-87-358] 16 p2229 N88-23316
Overview of wind behavior research in the US Wind Energy Program
[DE88-005683] 18 p2537 N88-25057
Analysis of the electrical characteristics of a Westinghouse variable speed generating system for wind turbine applications
[DE88-001139] 20 p2818 N88-26721

WINDPOWERED PUMPS
Linear and nonlinear theories of flow through an actuator disk --- windpowered pumps
[R-803-A] 03 p0316 N88-11995
Pump rod forces due to hydrodynamic effects in piston pumps
[PB88-164850] 16 p2214 N88-23212

WINDS ALOFT
NT GEOSTROPHIC WIND
NT JET STREAMS (METEOROLOGY)
Effect of neutral wind on the latitudinal variation of nighttime F-layer vertical movements 08 p1030 N88-16244

WINDSCREENS
U WINDSHIELDS

WINDSHIELDS
The deviation of light rays passing through a curved windscreen --- aircraft
[BAE-MSC.115] 01 p0093 N88-10610
Fracture study of windshield glass panes 06 p0799 N88-14891
Vision through aircraft transparencies 23 p3242 N88-29294

WING CAMBER
Variable wing camber control systems for the future Airbus program
[MBB-UT-104/88] 23 p3180 N88-28932

WING FLAPS
NT LEADING EDGE FLAPS
NT TRAILING EDGE FLAPS
NT VORTEX FLAPS
Investigation into the effects of flap end modifications on the performance of a wing with a single slotted flap
[BU-357] 14 p1866 N88-21148

WING LOADING
The RAE experimental data-base for missiles at high Mach number and its use in assessing CFD methods 05 p0534 N88-13250
Reduction of tilt rotor download using circulation control 10 p1271 N88-17605

Shape sensitivity analysis of wing static aeroelastic characteristics [NASA-TP-2808] 15 p2018 N88-22031

Methodology for matching experimental and computational aerodynamic data [NASA-TM-100592] 17 p2295 N88-23728

A summary of methods for establishing airframe design loads from continuous gust design criteria 24 p3312 N88-29721

WING NACELLE CONFIGURATIONS

A numerical investigation on wing/nacelle interferences 05 p0535 N88-13258

Computation of nacelle interference using boundary element method 05 p0537 N88-13267

Nacelle-wing interactions (studies 1986) development of a finite element code in a multi-domain version [ONERA-RTS-10/3417-AY-308A] 08 p0950 N88-15764

WING OSCILLATIONS

An analysis of the compressible-viscous flow field around a 3D-oscillating wing 05 p0535 N88-13254

Computation of dynamic stall of NACA0012 airfoil by block pentadiagonal matrix scheme 05 p0535 N88-13255

Influence of the static deformation on a wing in the unsteady aerodynamic 05 p0551 N88-13357

ARSPNSC: A method to calculate subsonic steady and unsteady potential flow about complex configurations [NLR-TR-86122-U] 13 p1717 N88-20265

Optimal control of the wing rock phenomenon 21 p2927 N88-27373

WING PANELS

Factors affecting the sticking of insects on modified aircraft wings [NASA-CR-182451] 09 p1148 N88-16878

Accuracies of southwell and force/stiffness methods in the prediction of buckling strength of hypersonic aircraft wing tubular panels [NASA-TM-88295] 09 p1183 N88-17090

Computational wing design studies relating to natural laminar flow 17 p2297 N88-23740

Fuel containment, lightning protection and damage tolerance in large composite primary aircraft structures [NASA-CR-3875] 17 p2317 N88-23839

WING PLANFORMS

NT ARROW WINGS
NT DELTA WINGS
NT SWEPT FORWARD WINGS
NT SWEPTBACK WINGS
NT VARIABLE SWEEP WINGS

A discretization of the integral equation for the time dependent linearized subsonic potential flow over a wing [AD-A188534] 12 p1574 N88-19411

Design of an aeroelastic composite wing wind tunnel model [AD-A188855] 12 p1582 N88-19466

An integral equation for the linearized supersonic flow over a wing [AD-A191408] 16 p2158 N88-22875

Computational wing design studies relating to natural laminar flow 17 p2297 N88-23740

Computational design of low aspect ratio wing-winglet configurations for transonic wind-tunnel tests [NASA-CR-183021] 18 p2464 N88-24630

An integral equation for the linearized unsteady supersonic flow over a wing [AD-A193773] 23 p3172 N88-28887

WING PROFILES

NT WING SPAN

Three-dimensional unsteady flow elicited by finite wings and complex configurations 04 p0395 N88-12468

Conical wing with maximum lift-to-drag ratio in supersonic gas flow 04 p0425 N88-12633

A numerical procedure for conformal mapping of the exterior of a circle onto the exterior of a wing profile with a spoiler [ISL-R-110/86] 11 p1536 N88-19180

Wing flutter calculations with the CAP-TSD unsteady transonic small disturbance program [NASA-TM-100580] 12 p1575 N88-19419

Shape sensitivity analysis of wing static aeroelastic characteristics [NASA-TP-2808] 15 p2018 N88-22031

Improved potential flow computational methods with Euler corrections for airfoil and wing/body design [AD-A192303] 20 p2752 N88-26334

Theoretical and experimental investigations of a vortex drag behind a wing profile with spoiler [ISL-PU-309/87] 21 p2892 N88-27169

WING SPAN

Investigation of side-wall effects in wind tunnel with supercritical airfoil testing 15 p2054 N88-22241

WING TANKS

Fuel containment and damage tolerance in large composite primary aircraft structures. Phase 2: Testing [NASA-CR-172519] 19 p2601 N88-25452

WING TIP VORTICES

Dispersion in the wake of aircraft: An investigation of the effects of a ground plane on trailing vortices. Literature survey [IC-AERO-REP-86-04] 01 p0003 N88-10014

A study of rotor broadband noise mechanisms and helicopter tail rotor noise 06 p0777 N88-14766

Tip vortices of isolated wings and helicopter rotor blades [AD-A191336] 16 p2158 N88-22874

Wave growth associated with turbulent spots in plane Poiseuille flow [FFA-TN-1986-08] 18 p2457 N88-24587

WING TIPS

Analytic investigation of helicopter rotor blade appended aeroelastic devices [NASA-CR-166525] 03 p0266 N88-11676

Tip aerodynamics from wind tunnel test of semi-span wing [NASA-TM-88253] 05 p0540 N88-13290

WINGLETS

Effects of winglets on a first-generation jet transport wing. 7: Sideslip effects on winglet loads and selected wing loads at subsonic speeds for a full-span model [NASA-TP-2619] 11 p1436 N88-18567

Investigation into the effects of flap end modifications on the performance of a wing with a single slotted flap [BU-357] 14 p1866 N88-21148

Computational design of low aspect ratio wing-winglet configurations for transonic wind-tunnel tests [NASA-CR-183021] 18 p2464 N88-24630

Theoretical-numerica study of feasibility of use of winglets on low aspect ration wings at subsonic and transonic Mach numbers at reduce drag [NASA-CR-4174] 21 p2892 N88-27168

WINGS

NT AEROELASTIC RESEARCH WINGS
NT ARROW WINGS
NT BEARINGLESS ROTORS
NT CAMBERED WINGS
NT CIRCULATION CONTROL ROTORS
NT CRUCIFORM WINGS
NT DELTA WINGS
NT FIXED WINGS
NT LOW ASPECT RATIO WINGS
NT OBLIQUE WINGS
NT RIGID ROTORS
NT ROTARY WINGS
NT SLENDER WINGS
NT SUPERCRITICAL WINGS
NT SWEPT FORWARD WINGS
NT SWEPT WINGS
NT SWEPTBACK WINGS
NT THIN WINGS
NT TILTING ROTORS
NT VARIABLE SWEEP WINGS
NT X WING ROTORS

Advanced turboprop wing installation effects measured by unsteady blade pressure and noise [NASA-TM-100200] 01 p0002 N88-10008

Wind-tunnel investigation of a full-scale general aviation airplane equipped with an advanced natural laminar flow wing [NASA-TP-2772] 01 p0002 N88-10009

Computation of transonic separated wing flows using an Euler/Navier-Stokes zonal approach [NASA-TM-88311] 02 p0173 N88-11089

AGARD standard aeroelastic configurations for dynamic response. Candidate configuration I -wing 445.6 [NASA-TM-100492] 02 p0192 N88-11202

On the prediction of the aeroelastic behavior of lifting systems due to flow separation [ESA-TT-1043] 03 p0259 N88-11633

On the scheme dependency of the three-dimensional Euler solutions 03 p0318 N88-12010

Reduced complexity structural modeling for automated airframe synthesis [NASA-CR-177440] 04 p0393 N88-12453

Calculation of aerodynamic characteristics of three-dimensional finite span wings in potential incompressible flow 04 p0425 N88-12631

Numerica calculation in the Laplace domain for subsonic unsteady aerodynamic forces acting on a finite wing 05 p0535 N88-13256

Numerical analysis of supersonic flows using panel method 05 p0537 N88-13266

Navier-Stokes simulation of transonic transportation aircraft configurations. 1: Flow-field simulation over wing-fuselage combinations 05 p0540 N88-13288

Design of wings and wing/body configurations for transonic and supersonic speeds 05 p0545 N88-13318

An examination of coating failure on wing pivot fittings of f111 aircraft [AD-A185028] 05 p0546 N88-13328

Nonlinear aerodynamic wing design [NASA-CR-3950] 06 p0665 N88-14079

Design verification and fabrication of active control systems for the DAST ARW-2 high aspect ratio wing, part 1 [NASA-CR-177959-PT-1] 06 p0669 N88-14101

Design verification and fabrication of active control systems for the DAST ARW-2 high aspect ratio wing. Part 2: Appendices [NASA-CR-177959-PT-2] 06 p0669 N88-14102

An investigation of the effects of the propeller slipstream on a wing boundary layer 06 p0700 N88-14293

Insect contamination protection for laminar flow surfaces 07 p0814 N88-14954

Unsteady stall penetration experiments at high Reynolds number [AD-A186120] 07 p0814 N88-14958

Development of direct-inverse 3-D methods for applied aerodynamic design and analysis [NASA-CR-182436] 08 p0950 N88-15767

Three-dimensional unsteady flow elicited by finite wings and complex configurations [AD-A186464] 08 p0951 N88-15770

Effects of wing simulated ground frost on aircraft performance 08 p0952 N88-15775

Effect of an optimized fiber orientation on transonic flutter characteristics of a high-aspect-ratio composite wing [NAL-TR-930] 09 p1120 N88-16709

Computational fluid dynamics and aerothermodynamics [NASA-CR-182490] 09 p1166 N88-16989

Solution of the three-dimensional Navier-Stokes equations for transonic flow using a multigrid method 10 p1267 N88-17579

A transonic-small-disturbance wing design methodology [NASA-TP-2806] 10 p1273 N88-17614

The intelligent wing. Aerodynamic development direction for future passenger aircraft [MBB-UT-006/87] 10 p1313 N88-17848

Conditions at infinity for theories of oscillating wings and propellers in subsonic flow [NAL-TR-937] 11 p1434 N88-18556

A discretization of the integral equation for the time dependent linearized subsonic potential flow over a wing [AD-A188534] 12 p1574 N88-19411

Factors affecting the sticking of insects on modified aircraft wings [NASA-CR-182615] 12 p1575 N88-19421

Computer aided deflection measurement of an aircraft wing [AD-A187778] 12 p1581 N88-19461

Crack distribution and growth rates for critical fastener holes in Mirage wing RH79 [AD-A189080] 13 p1722 N88-20293

Constructing Gloved wings for aerodynamic studies [NASA-TM-100440] 14 p1863 N88-21128

Scale model development for aeroelasticity studies [ETN-88-91887] 14 p1868 N88-21164

Structural and material testing of a composite microlite wing model [BU-355] 14 p1923 N88-21461

Control of laminar flow around of the wing in free-air conditions [AD-A187479] 15 p2013 N88-22004

Unsteady aerodynamics of a Wortmann FX-63-137 wing in a fluctuating wind field [AD-A190128] 15 p2013 N88-22006

A multilifting line method and its application in design and analysis of nonplanar wing configurations [DFVLR-FB-87-51] 16 p2155 N88-22860

A numerical model of unsteady, subsonic aeroelastic behavior [NASA-TM-101126] 16 p2156 N88-22862

Propulsive performance of a lifting flapping wing 17 p2296 N88-23733

Sensitivity of F-106B leading-edge-vortex images to flight and vapor-screen parameters [NASA-TP-2818] 17 p2300 N88-23760

High speed and high angle of attack aerodynamic characteristics of winged space vehicle [ISSN-0285-6808] 18 p2459 N88-24599

Applications of the Navier-Stokes equations to wings and complex configurations using a zonal approach [NASA-TM-100080] 18 p2459 N88-24602

Investigation of the effect of minimum loads and compression of load spectra on the prediction capacities of the ONERA crack model — wings [ONERA-RTS-33/7169-RY-064-R] 18 p2527 N88-24994

On the stationary solutions of three-dimensional Euler equations by the TVD difference schemes 19 p2639 N88-25660

Numerical simulation of turbulent flow using the exponential expression of k-Epsilon equation
19 p2640 N88-25662

Development of direct-inverse 3-D methods for applied transonic aerodynamic wing design and analysis
[NASA-CR-183127] 22 p3037 N88-28033

Runge-Kutta finite-volume simulation of laminar transonic flow over the ONERA M6 wing using the Navier-Stokes equations
[FFA-TN-1987-06] 22 p3039 N88-28045

Transport-type configurations
23 p3169 N88-28867

An integral equation for the linearized unsteady supersonic flow over a wing
[AD-A193773] 23 p3172 N88-28887

Critical joints in large composite primary aircraft structures. Volume 2: Technology demonstration test report
[NASA-CR-172587] 23 p3177 N88-28915

Critical joints in large composite primary aircraft structures. Volume 3: Ancillary test results
[NASA-CR-172588] 23 p3177 N88-28916

Test results at transonic speeds on a contoured over-the-wing propfan model
[NASA-TM-88206] 23 p3177 N88-28918

Development of a glass fiber wing following the construction regulation FAR Part 23
[ETN-88-92966] 23 p3189 N88-28979

Critical joints in large composite primary aircraft structures. Volume 1: Technical summary
[NASA-CR-3914] 23 p3190 N88-28983

WINTER

Nowcasting rain/snow transitions and freezing rain
02 p0202 N88-11265

Forecasting the kind of precipitation in winter
02 p0202 N88-11266

Observational analysis of the interaction between fronts and the orography in Taiwan during the late winter monsoon season 02 p0203 N88-11270

A model for the convective atmospheric boundary layer during the winter in the Khartoum Region (Sudan)
[R-822-A] 03 p0353 N88-12225

NWS (National Weather Service) watch/warning verification flash flood, winter storm and high wind, January 1980 - June 1986
[PB87-223053] 04 p0469 N88-12898

Wind regime peculiarities in the lower thermosphere in the winter of 1983/84 06 p0733 N88-14511

Circulation in the mesosphere and lower thermosphere during the MAP (Middle Atmosphere Program)/WINE (Winter in the Northern Europe) period
06 p0734 N88-14514

The sodium layer at 69 N latitude in wintertime
08 p1027 N88-16218

Observational evidence for saturation of gravity waves and the production of turbulence in the mesosphere
08 p1028 N88-16229

Biorhythmic aspects of intercontinental Antarctic adaptation 08 p1046 N88-16321

Systematic errors of the FSU global spectral model
10 p1356 N88-18103

Aircraft and ground vehicle friction correlation test results obtained under winter runway conditions during joint FAA/NASA Runway Friction Program
[NASA-TM-100506] 11 p1438 N88-18582

Northern winter circulations for the period 1974-1983
[AD-A187779] 11 p1511 N88-19028

Estimates of ocean-atmosphere thermal interaction in Gulf Stream energy-active test range in winter of 1984
13 p1785 N88-20679

Analysis of winter season precipitation bands over the Southern Plains 14 p1947 N88-21609

Verification of regional climates of GISS GCM. Part 1: Winter
[NASA-TM-100695] 19 p2694 N88-26012

Recent secular changes in the wintertime circulation of the Southern Hemisphere 22 p3122 N88-28555

On the impact of low-latitude anomalous forcing on local and remote circulation: Winters(DJF) 1978/79 to 1986/87 22 p3123 N88-28560

Interannual variability of 850 mb temperatures during the Northern Hemisphere winter
22 p3123 N88-28562

Some screening experiments in objective prediction of monthly mean temperature over the United States during the winter season 22 p3127 N88-28589

One equatorial anomaly in nighttime ionospheric F region 24 p3447 N88-30517

WIRE

NT ELECTRIC WIRE

NT GUY WIRES

Wire interconnection reliability and moisture levels in hybrid microcircuits with epoxy-attached components
[DE87-012987] 01 p0039 N88-10247

Composite bearing materials containing solid lubricant in filamentary form, stages 3 and 4
[IRD-87/2] 01 p0054 N88-10344

Carbon-fiber reinforced aluminum
04 p0403 N88-12507

Small-diameter wire tensile testing
[DE88-000835] 04 p0455 N88-12815

Fracture analysis of drawn composite dual-phase steel wire
[DE88-001396] 06 p0681 N88-14173

Single wire drift chamber design
[DE87-011002] 07 p0857 N88-15205

MIG welding with pulsed wire feed
[PB87-143582] 07 p0863 N88-15234

Single-layer wire routing
[AD-A186990] 09 p1157 N88-16932

Composite ceramic superconducting filaments for superconducting cable
[AD-A187833] 11 p1556 N88-19312

High-T(sub c) superconducting wire fabrication and testing
[DE88-005989] 15 p2144 N88-22798

Corrosion and fatigue properties of FeCrB/Si metallic glass wires in aqueous environments
17 p2320 N88-23855

Magnetization studies of multifilamentary Nb3Sn wires
[DE88-009103] 19 p2735 N88-26243

A model for insulated wires in the method of moments code NEC (Numerical Electromagnetics Code)
[DE88-008920] 20 p2794 N88-26577

Performance study of a unipole antenna with conventional and elevated radial wire ground screens
[AD-A193283] 21 p2933 N88-27413

Development of Nb-Ti multifilamentar superconducting wires
[DE88-702324] 23 p3290 N88-29592

WIRE CLOTH

Fatigue failure of regenerator screens in a high frequency Stirling engine 17 p2436 N88-24491

WIRE MESH

U WIRE CLOTH

WIRING

A design-philosophy for grounding and inter-unit wiring
[EMCR-20/85] 03 p0310 N88-11954

Discussions in support of the design-philosophy for grounding and inter-unit wiring
[EMCR-21/85] 03 p0310 N88-11955

Assessment of existing specifications against the design-philosophy for grounding and inter-unit wiring (EMCR 20/85)
[EMCR-22/85] 03 p0310 N88-11956

Alternatives to the techniques implicit in the design philosophy, and the penalties in performance associated with them --- grounding and wiring
[EMCR-31/85] 03 p0310 N88-11957

Summary record of presentations to the Federal Telecommunication Standards Committee/Fiber optics task group
[PB88-110853] 08 p0978 N88-15911

Gridless routing for generalized cell assemblies: Report and user manual
[EUT-87-E-180] 13 p1764 N88-20549

Locality, communication and interconnect length in multicomputers
[CWI-CS-R8706] 13 p1822 N88-20890

Characteristics of LSI-wiring expert system discussed
15 p2052 N88-22226

An improved simulated annealing algorithm for standard cell placement
[NASA-CR-182952] 18 p2558 N88-25183

WIRING SYSTEMS

U WIRING

WISCONSIN

GOES observations for the FIRE/SRB Wisconsin experiment region from October 11 through November 2, 1986
[NASA-TM-100485] 01 p0071 N88-10453

WKB APPROXIMATION

U WENTZEL-KRAMER-BRILLOUIN METHOD

WOLF-RAYET STARS

Grids of evolutionary models of massive stars with mass loss and overshooting. Properties of Wolf-Rayet stars sensitive to overshooting
[PUBL-SER-C-FASC-12] 03 p0388 N88-12437

The effects of rotation on the winds from hot stars
11 p1569 N88-19393

Colliding stellar winds in the eclipsing Wolf-Rayet binary V444 Cygni
[NASA-CR-182937] 17 p2451 N88-24563

Review of the theoretical changes of surface chemistry during massive star evolution
[SER-C-PREPUBL-FASC-17] 18 p2593 N88-25411

WOLFRAM

U TUNGSTEN

WOMEN

U FEMALES

WOOD

Use of natural gas diesel engines in mechanical pulp production: A preliminary study
[DE87-753065] 02 p0181 N88-11129

Method of radiographic inspection of wooden members
[NASA-CASE-LAR-13724-1] 17 p2346 N88-23983

Proceedings of the 1987 Biomass Thermochemical Conversion Contractors' Review Meeting
[DE88-006730] 18 p2535 N88-25041

An advanced extruder-feeder biomass liquefaction reactor system 18 p2535 N88-25042

Low pressure entrained flow pyrolysis of biomass to produce liquid fuels 18 p2535 N88-25043

Molecular-beam, mass-spectrometric studies of wood vapor and model compounds over HZSM-5 catalyst
18 p2535 N88-25044

Research on hydrotreating catalysts to hydrodeoxygenate biocrude oils
18 p2536 N88-25046

Bench-scale studies on fluid-bed pyrolysis of wood using different contact gases 18 p2536 N88-25049

A 3 MW wood fired gas turbine at Red Boiling Springs, Tennessee 18 p2536 N88-25051

WORD PROCESSING

An evaluation of WPS-Plus word processing software for the IBM PC and compatibles
[DE87-011972] 01 p0081 N88-10518

Electronic authoring tools
[DE87-011797] 02 p0248 N88-11567

WORDS (LANGUAGE)

NT SYLLABLES

Abregrams or deleweds: A forty-year view of acronyms
[DE87-010808] 01 p0106 N88-10690

Studies of the processing of single words using positron tomographic measures of cerebral blood flow change
[AD-A184058] 03 p0356 N88-12244

A two-stage isolated-word recognition system using discriminant analysis
[AD-A187425] 10 p1402 N88-18360

Auditory perception of complex sounds
[AD-A190528] 15 p2103 N88-22529

WORDNET: An electronic lexical reference system based on theories of lexical memory
[AD-A193086] 21 p3027 N88-27970

Exploiting lexical regularities in designing natural language systems
[AD-A195922] 24 p3423 N88-30375

Words: Keys or barriers to information transfer
24 p3438 N88-30464

WORK

NT PHYSICAL WORK

A comparison of plastic work energy and external input for fatigue crack propagation 05 p0607 N88-13722

Software-implemented fault insertion: An FTMP example
[NASA-CR-178423] 06 p0761 N88-14668

Risk of hypertension and functional cerebral laterality in oil expedition works in far north
12 p1665 N88-19980

Subsea approach to work systems development
17 p2379 N88-24146

WORK CAPACITY

Prediction of physical workload in reduced gravity environments 06 p0794 N88-14867

Cardiovascular and subjective measures of task demand in a low workload monitoring task
[REPT-8804] 10 p1366 N88-18176

Development of a coping strategies questionnaire to assess endurance performance
[AD-A188010] 11 p1520 N88-19074

Heat acclimatization under controlled hyperthermia
12 p1665 N88-19981

Hypnosis: Possible applications for cosmonauts
12 p1665 N88-19984

Efficiency of human workers and means to increase it
12 p1666 N88-19986

Psychophysical load of glider pilots on long-duration flights
[DFVLR-FB-87-38] 14 p1953 N88-21642

Experience in occupational medicine, derived from 16 operational deep saturation trimix 5 dives in GUSI from 150 to 600 m 19 p2695 N88-26018

A review of workload measurement in relation to verbal comprehension 21 p2925 N88-27360

Thermal stress and its effects on fine motor skill and decoding tasks 21 p2926 N88-27369

WORK FUNCTIONS

Question on the measurement of the metal work function in an electron spectrometer by the secondary-electron emission threshold method
[NASA-TT-20190] 16 p2178 N88-22979

WORK HARDENING

NT STRAIN HARDENING

Hardening of metal during production of bent shapes
[BLL-M-37250-(5828.4)] 02 p0148 N88-10928

Cyclic uniaxial and biaxial hardening of type 304 stainless steel modeled by the viscoplasticity theory based on overstress 14 p1931 N88-21514

WORK-REST CYCLE

Implications of shiftwork in space for human physiology experiments 12 p1659 N88-19942

Performance effectiveness and the work/rest cycle
[AD-A191448] 18 p2551 N88-25145

WORKING FLUIDS

Organic Rankine-cycle power systems working fluids study. Topical report No. 1: Fluorinol 85
[DE87-014604] 02 p0195 N88-11217

Pump assisted heat pipe 03 p0319 N88-12018

Working fluids for sorption heat pumps
[DE88-900203] 07 p0874 N88-15301

Design of a high-power-density Ljungstroem turbine using potassium as a working fluid
17 p2409 N88-24323

Low gravity thermal management using dielectrophoretic forces 17 p2432 N88-24470

Pressure drop and heat transfer in turbulent non-Newtonian pipe flow of advanced energy transmission fluids
[DE88-010021] 19 p2666 N88-25853

Heat transfer of mesh-wick heat-pipes (bottom heat mode) 20 p2783 N88-26507

The heat transfer and fluid dynamics of concave surface curvature
[AD-A193064] 21 p2943 N88-27479

Reaction-theoretical aspects of the thermal behavior of lubricating oils and working fluids
[NASA-TT-20304] 23 p3199 N88-23041

Radiative heat transfer to steady flow of a chemically reacting fluid in a horizontal porous channel with variable wall temperature
[DE88-702704] 24 p3372 N88-30081

WORKLOADS (PSYCHOPHYSIOLOGY)

Effect of motion cues during complex curved approach and landing tasks: A piloted simulation study
[NASA-TP-2773] 04 p0398 N88-12480

Research papers and publications (1981-1987): Workload research program
[NASA-TM-100016] 04 p0474 N88-12924

Taskomat, a task battery for information processing
[IZF-1987-2] 05 p0630 N88-13851

Prediction of physical workload in reduced gravity environments 06 p0794 N83-14867

Stability, reliability and cross-mode correlations of tests in a recommended 8-minute performance assessment battery
[NASA-CR-172039] 08 p1052 N88-16351

Proceedings of the DOD Workload Assessment Workshop on Workload Assessment Techniques and Tools held in Dayton, Ohio on 27-28 September 1986
[AD-A185650] 08 p1052 N88-16352

Helicopter human factors research
09 p1109 N88-16644

Identification and proposed control of helicopter transmission noise at the source
09 p1109 N88-16647

An integrated approach to rotorcraft human factors research 09 p1110 N88-16653

Crew procedures for microwave landing system operations
[NASA-CR-178359] 09 p1116 N88-16688

Measuring mental workload: A performance battery
[AD-A187118] 09 p1200 N88-17192

Trends in the distribution of tasks between commercial pilots and flight control systems
[MBB-UT-008/87] 10 p1314 N88-17851

Second All-Union Conference on Physiology of Extreme States and Individual Protection of Man
10 p1363 N88-18147

Cardiovascular and subjective measures of task demand in a low workload monitoring task
[REPT-8804] 10 p1368 N88-18176

Electromagnetic metrics of mental workload
[AD-A188205] 11 p1523 N88-19093

Identification of visual evoked response parameters sensitive to pilot mental state
[NASA-CR-4140] 13 p1311 N88-20822

Proceedings of the Workshop on the Assessment of Crew Workload Measurements Methods, Techniques and Procedures. Volume 1: Preliminary Selection of Measures
[AD-A189004] 13 p1812 N88-20827

A comparison of two chord keyboard coding systems for alphanumeric data entry
[AD-A189230] 13 p1813 N88-20834

Psychophysical load of glider pilots on long-duration flights
[DFVLR-FB-87-38] 14 p1953 N88-21642

Mental-State Estimation, 1987
[NASA-CP-2504] 16 p2239 N88-23370

Toward a mathematical formalism of performance, task difficulty, and activation 16 p2239 N88-23372

Predicting operator workload during system design
16 p2239 N88-23375

Pupil measures of alertness and mental load
16 p2239 N88-23378

Voice-stress measure of mental workload
16 p2240 N88-23381

Primary task event-related potentials related to different aspects of information processing
16 p2240 N88-23382

Defining and measuring pilot mental workload
16 p2240 N88-23383

POPEYE: A production rule-based model of multitask supervisory control (POPCORN)
16 p2240 N88-23384

Estimating the cost of mental loading in a bimodal divided-attention task: Combining reaction time, heart-rate variability and signal-detection theory
16 p2241 N88-23385

Information processing deficits in psychiatric populations: Implications for normal workload assessment 16 p2241 N88-23390

C3 generic workstation: Performance metrics and applications 16 p2242 N88-23397

NASA-Ames workload research program
17 p2380 N88-24151

An evaluation of three linear scale radar altimeter displays
[AD-A192173] 18 p2465 N88-24636

Timesharing performance as an indicator of pilot mental workload
[NASA-CR-182807] 18 p2552 N88-25150

Simultaneous multiple control force exertion capabilities of males and females versus helicopter control force design limits
[AD-A191653] 18 p2553 N88-25153

Proceedings of the Workshop on the Assessment of Crew Workload Measurement Methods, Techniques and Procedures. Volume 2: Library references
[AD-A191209] 19 p2710 N88-26101

Method for observing changes in functional state of human operator 20 p2830 N88-26789

A review of workload measurement in relation to verbal comprehension 21 p2925 N88-27360

Event-related brain potentials as indices of mental workload and attentional allocation
21 p2979 N88-27696

Event-related and steady potential changes in the brain related to workload during tracking
21 p2981 N88-27705

Behavioral effects of exposure to the tempo high-power microwave system
[AD-A193305] 21 p2987 N88-27738

Determinants of dual-task interference and resource theories in cognitive psychology
[DFVLR-FB-88-14] 21 p2992 N88-27748

Threat expert system technology advisor
[NASA-CR-177479] 24 p3328 N88-29816

WORKSTATIONS

A work station for EXELFS data acquisition and analysis
[USIP-87-10] 01 p0078 N88-10498

The use of McIDAS as a Mesoscale forecasting tool during the Canadian Atlantic storms programs --- Man-computer Interactive Data Access System (McIDAS) 02 p0205 N88-11284

The challenge of very short range forecasting in the tropics 02 p0205 N88-11287

A scientific workstation operator-interface for accelerator control
[DE87-014689] 03 p0362 N88-12278

Some performance comparisons for a fluid dynamics code
[PB88-113709] 07 p0852 N88-15175

Facility design validation of the information systems laboratory
[AD-A186309] 07 p0906 N88-15488

An innovative workstation 08 p1063 N88-16421

Foundation: Transforming data bases into knowledge bases 08 p1063 N88-16423

A learning apprentice for software parts composition
08 p1065 N88-16436

MPAD MCC workstation system: ADDAM and EEVE
09 p1203 N88-17209

Development of a comprehensive software engineering environment 09 p1203 N88-17211

Simplifying the construction of domain-specific automatic programming systems: The NASA automated software development workstation project
09 p1204 N88-17212

Signal processing studies program VLSI designs for unary functions
[AD-A188053] 10 p1325 N88-17922

Shared workspaces for real-time collaboration in distributed networks: Concepts, techniques, problems
[AD-A188150] 10 p1394 N88-18315

Terrain Analyst Work Station (TAWS) demonstrations
[AD-A188139] 11 p1504 N88-18981

A prototype for remotely shared textual workspaces
[AD-A188352] 12 p1679 N88-20040

GM: A gate matrix layout generator
[EUT-87-E-179] 13 p1820 N88-20875

GADL: A gate array description language
[EUT-87-E-165] 14 p1907 N88-21336

Higher levels of a silicon compiler
[EUT-86-E-163] 14 p1955 N88-21650

Generating layouts for random logic: Cell generation schemes
[EUT-86-E-164] 14 p1956 N88-21658

ESKISS: A program for optimal state assignment
[EUT-87-E-167] 14 p1956 N88-21659

Software quality assurance workstation
[P-1124/RT-14791] 14 p1957 N88-21670

Technology mapping from Boolean expressions to standard cells
[EUT-87-E-174] 14 p1963 N88-21709

An optimal CMOS structure for the design of a cell library
[EUT-87-E-166] 14 p1985 N88-21841

Sigma system: Overview, prospects
15 p2052 N88-22230

Mental-State Estimation, 1987
[NASA-CP-2504] 16 p2239 N88-23370

Point accessibility and primary workspace of simple six-link robots 17 p2345 N88-23976

The geometric workstation, a new approach for geometric corrections of remotely sensed data
17 p2352 N88-24017

Reconfigurable work station for a video display unit and keyboard
[NASA-CASE-MFS-26009-1-SB]
17 p2382 N88-24163

Ergonomy and interior furnishing of the cabins of deep diving manned submarines: The Nautile example --- couch 19 p2697 N88-26032

The high speed local area network
19 p2717 N88-26133

The MELCOM PSI 2 AI workstation
21 p2930 N88-27395

Assessing and enhancing human performance: Utility of a workstation network
[AD-A192840] 21 p2991 N88-27743

Research on wide area workstations
[AD-A192529] 22 p3136 N88-28643

Automated software development workstation
23 p3263 N88-29423

WORLD

U EARTH (PLANET)

WORLD DATA CENTERS

Wave and wind data sources, environmental conditions committee report, International Ship and Offshore Structures Congress
[PB87-234902] 06 p0746 N88-14588

WORLD METEOROLOGICAL ORGANIZATION

Current status of world weather service
06 p0725 N88-14459

Wave and wind data sources, environmental conditions committee report, International Ship and Offshore Structures Congress
[PB87-234902] 06 p0746 N88-14588

The World Climate Research Program
14 p1935 N88-21538

Activities report of the World Meteorological Organization
[WMO-689] 24 p3404 N88-30265

WRAPAROUND CONTACT SOLAR CELLS

U SOLAR CELLS

WRINKLING

Contribution to the study of wrinkling in metal stamping
[ISAL-IDI1-87-08] 08 p0976 N88-15900

WRIST

Causes and prevention of occupational Repetition Strain Injuries (RSI) 11 p1521 N88-19083

Real-time implementation of a kinematic optimization scheme for seven-degree-of-freedom redundant robots with spherical wrists
[DE88-006785] 18 p2524 N88-24974

Kinematics of Hooke universal joint robot wrists
[NASA-TM-100567] 20 p2843 N88-26870

WU-2 AIRCRAFT

U U-2 AIRCRAFT

WYOMING

Geological characterization and statistical comparison of outcrop and subsurface facies: Shannon Shelf sand ridges
[DE87-001243] 03 p0348 N88-12202

X

X BAND
U SUPERHIGH FREQUENCIES

X RAY ABSORPTION
L2,3 XANES of the high T sub c superconductor YBa2Cu3O7 with variable oxygen content
[NOTA-INTERNA-888] 06 p0788 N88-14837
Soft X-ray absorption and emission spectra and the electronic structure of the Ba2YCu3O/sub 7-x/ superconductor
[DE88-002609] 08 p1090 N88-16559
Variable spectra of active galaxies
[NASA-CR-182694] 13 p1853 N88-21091
EXAFS studies of the microstructure of semiconductor alloys, defects and semiconductor-metal interfaces
20 p2868 N88-27031
Structural studies of (Ga,In)(As,P) alloys and (InAs) sub m (GaAs) sub n strained-layer superlattices by fluorescence-detected EXAFS 20 p2872 N88-27051

X RAY ANALYSIS
NT X RAY SPECTROSCOPY
X-ray studies of strain, interface and impurity in semiconductors
[DE87-013856] 01 p0104 N88-10678
Cooperative analysis of zirconium and zirconium alloys by fluorescent X-ray method
[DE87-753011] 02 p0148 N88-10926
X-ray emission from high-Z spherical laser plasmas: Implications for plasma dynamics
[DE87-014722] 02 p0239 N88-11506
Flaw imaging and ultrasonic techniques for characterizing sintered silicon carbide
[NASA-TM-100177] 03 p0334 N88-12106
The Einstein survey of the young stars in the Orion Nebula 04 p0518 N88-13182
X-ray analysis of polycrystalline aluminium subjected to fatigue cycling
[NAL-TM-MT-8706] 05 p0564 N88-13434
X-ray fatigue failure prediction based on plasticity response to microcracks 05 p0607 N88-13725
X-ray structure analyses and molecular mechanics analyses of dense energetic materials
[AD-A185462] 06 p0779 N88-14781
X-ray microfluorescence analysis of thin- and thick-sectioned geologic materials
[DE87-009803] 09 p1189 N88-17126
High-resolution X-ray microstructural study of single crystals of YBa2Cu3O/sub 7-y/
[DE88-004856] 10 p1421 N88-18484
Advances in X-ray line profile analysis to determine microstructure information about ceramics
[DE88-003938] 13 p1750 N88-20465
The effects of normal and therapeutic baths on the central vascular organs of persons with healthy hearts, as measured by X-ray
[NASA-TT-20252] 13 p1811 N88-20818
Advances in geochemistry and cosmochemistry: Trace element microdistributions with the synchrotron X-ray fluorescence microprobe
[DE88-006355] 15 p2032 N88-22108
Detecting delaminations in CFRP specimens using X-ray techniques
[FFA-TN-1988-04] 18 p2479 N88-24704
Electrochemistry in liquid crystals
[AD-A191554] 18 p2481 N88-24719
On the reversion phenomena of Cu-3 percent Ti alloys
[NASA-TT-20170] 18 p2488 N88-24762
X-ray and optical analysis of surface properties of metal optics
[DE88-004033] 19 p2727 N88-26195
Photoconducting X-ray detectors for Z-pinch experiments
[DE88-007118] 19 p2728 N88-26199
X-ray response of GaAlAs/GaAs radiation hardened double: Heterostructure photodiode compared to SiPIN photodiodes
[DE88-007425] 19 p2733 N88-26231
Development of an automated X-ray gauge for nondestructive quantitative analysis
[DE88-008633] 20 p2812 N88-26681
X-ray studies of strain, interface and impurities in semiconductors
[DE88-012460] 21 p3025 N88-27954
ZT imaging system for layered thin wall structures
[AD-A195466] 24 p3352 N88-29954
A method for the quantitative determination of crystalline phases by X-ray
[NASA-TT-20324] 24 p3434 N88-30444

X RAY APPARATUS
NT X RAY TUBES
LLE Review, volume 30
[DE87-014469] 02 p0178 N88-11109
MAXIE-1 (Magnetospheric Atmospheric X-ray Imaging Experiment)
[AD-A192846] 21 p2902 N88-27221

X RAY ASTRONOMY
NT X RAY BINARIES
NT X RAY SOURCES
USSR report: Space
[JPRS-USP-87-003] 01 p0009 N88-10050
X-ray astronomy instruments to operate on Mir station
01 p0009 N88-10052
Multilayered foils as radiation entrance windows and spectral filters for image converters in the ultrasoft X-ray wavelength region
[MPE-PREPRINT-90] 02 p0176 N88-11099
The hard X-ray eclipse in the intermediate polar EX Hydrae
[MPE-PREPRINT-95] 02 p0251 N88-11582
Hard X-ray telescope HAPI-1 and its observation of Crab pulsar 03 p0269 N88-11692
A re-examination of the corona-wind dividing line: Diagnostics of non-coronal atmospheres
04 p0504 N88-13101
Recent X-ray observations of supernova remnants and their interpretation
[MPE-PREPRINT-96] 09 p1262 N88-17563
AXAF: The Advanced X-ray Astrophysics Facility
[NASA-EP-251(M)] 10 p1292 N88-17725
Investigation of nuclei of active galaxies as well as sources in the Large Magellanic Cloud using the X-ray astronomy satellite EXOSAT
[ETN-88-91494] 11 p1570 N88-19399
MAXIE 1
[AD-A189688] 14 p1882 N88-21247
Further development of a stellar camera following the rotation-modulation-collimator principle for balloon-borne observations in the X-ray range
[ETN-88-91496] 14 p1913 N88-21428
Measurements of the scintillation time constants of inorganic crystals for the development of a triple-Phoswich detector for high-energy X-ray quanta
[ETN-88-91501] 14 p1993 N88-21875
Data analysis of an observation of the quasar 3C 273 in the high-energy X-ray range, and the significance for astrophysical models
[ETN-88-91493] 14 p1993 N88-21878
EXOSAT observations of active galaxies in the medium-energy X-ray domain
[ETN-88-91499] 14 p1993 N88-21879
The X-ray properties of AM Her stars
[MPE-PREPRINT-106] 16 p2289 N88-23704
The thermal evolution of the jets in SS433 --- galactic object
[MPE-PREPRINT-107] 16 p2289 N88-23705
SW UMa and V426 Oph: EXOSAT surprises
19 p2740 N88-26269
EXOSAT observations of Hercules X-1
[MPE-PREPRINT-119] 22 p3164 N88-28841
The high-throughput X-ray spectroscopy mission: The mission-science report
[ESA-SP-1097] 24 p3453 N88-30557

X RAY ASTROPHYSICS FACILITY
The Goddard Space Flight Center mechanical cooler program 08 p0983 N88-15944
AXAF: The Advanced X-ray Astrophysics Facility
[NASA-EP-251(M)] 10 p1292 N88-17725

X RAY BINARIES
EXOSAT guest observer program: Binary parameters of the X-ray Pulsar 4U1626-67
[NASA-CR-182374] 06 p0802 N88-14905
A 23 hour EXOSAT observation of the X-ray pulsar 1E2259+586 and the associated supernova remnant G109.1-1.0
[MPE-PREPRINT-99] 14 p1994 N88-21882
Spectral classification of Low Mass X-ray Binaries (LMXB) energy spectra with color-color diagrams
[MPE-PREPRINT-111] 22 p3163 N88-28837
The evolution of low-mass X-ray binaries
[MPE-PREPRINT-118] 22 p3165 N88-28851

X RAY DIFFRACTION
A generalized least-squares determination of triaxial stress states by X-ray diffraction and the associated errors
[AD-A183851] 01 p0058 N88-10371
The production of ultrasmall and superfine holographic diffraction gratings using synchrotron radiation and lithographic techniques
[AD-A185395] 05 p0585 N88-13562
Two digital X-ray imaging systems for applications in X-ray diffraction
[PB87-123683] 06 p0669 N88-14103
X-ray structure analyses and molecular mechanics analyses of dense energetic materials
[AD-A185462] 06 p0779 N88-14781
High temperature stability of superconducting YBa2Cu3O subx as characterized by X-ray diffraction
[DE88-001856] 06 p0787 N88-14824
X-ray diffraction study of thermotropic liquid crystalline polyesters and diester model compounds
[AD-A186788] 09 p1255 N88-17521
High-temperature charge-density studies of CeO/sub 2-x/ using X-ray and neutron diffraction techniques
[DE88-002988] 09 p1257 N88-17536
High resolution electron and ion microscopy
[AERE-R-12502] 10 p1297 N88-17754
Novel analytical X-ray Non-Destructive Evaluation (NDE) tool for quality control of energetic materials
[AD-A187737] 11 p1497 N88-18935
Advances in X-ray optics, 1987
[DE88-003296] 11 p1549 N88-19268
The synthesis, characterization and structural studies of In(C5H4Me) by X-ray diffraction and electron diffraction techniques and a reinvestigation of the crystalline state of In(C5H5) by X-ray diffraction studies
[AD-A189110] 13 p1844 N88-21038
X-ray diffraction study of a thin GaAs film on Si(100)
[DE88-005290] 13 p1847 N88-21055
Analysis of explosives. 1: Computer programs for processing of X-ray powder deffraction data
[PB88-156896] 14 p1894 N88-21309
An investigation of the crystalchemistry and thermochemistry of selected mineral systems
[AD-A189758] 15 p2142 N88-22781
The structural analysis of some crystalline and semi-crystalline substances using X-ray and neutron diffraction 17 p2445 N88-24540
Equation of state of solid neon from X-ray diffraction measurements to 110 GPa
[DE88-008723] 19 p2734 N88-26241
Precise rotational alignment of X-ray transmission diffraction gratings
[DE88-010599] 21 p2911 N88-27273
Superconducting oxides with high critical temperatures
21 p2930 N88-27392
Short pulse X-ray diffraction studies of shocked and annealed crystals using the JANUS research laser
[DE88-011329] 23 p3286 N88-29579
X-ray diffraction imaging (topography) of electroopticcrystals by synchrotron radiation
[NASA-CR-183266] 24 p3432 N88-30427
Applications of synchrotron radiation to materials science: Diffraction imaging (topography) and microradiography
[NASA-CR-183265] 24 p3434 N88-30440
Crystal structure and density of helium to 232 kbar
24 p3441 N88-30481

X RAY FLUORESCENCE
Cooperative analysis of zirconium and zirconium alloys by fluorescent X-ray method
[DE87-753011] 02 p0148 N88-10926
Stratospheric particles: Synchrotron X-ray fluorescence determination of trace element contents
[DE87-012482] 02 p0198 N88-11234
Development of an X-ray fluorescence microprobe at the National Synchrotron Light Source, Brookhaven National Laboratory: Early results: Comparison with data from other techniques
[NASA-CR-181468] 02 p0236 N88-11486
Determination, by X-ray fluorescence, of platinum, palladium, ruthenium, iron and chromium in special steels
[PB87-132114] 06 p0683 N88-14183
X-ray microfluorescence analysis of thin- and thick-sectioned geologic materials
[DE87-009803] 09 p1189 N88-17126
Advances in geochemistry and cosmochemistry: Trace element microdistributions with the synchrotron X-ray fluorescence microprobe
[DE88-006355] 15 p2032 N88-22108

X RAY IMAGERY
X-ray tomography and nuclear magnetic resonance imaging applications for advanced ceramic materials
[DE87-011534] 01 p0027 N88-10171
Time-resolved ablation measurements of imploding targets
[DE87-014464] 02 p0178 N88-11111
Time-resolved absorption measurements on OMEGA
[DE87-014465] 02 p0179 N88-11112
Cineradiography
[DE87-013158] 03 p0324 N88-12045
Computer-aided X-ray image system design and evaluation
[DE88-000997] 04 p0481 N88-12965
X-ray imaging: Status and trends
[DE88-000756] 05 p0649 N88-13980
Two digital X-ray imaging systems for applications in X-ray diffraction
[PB87-123683] 06 p0669 N88-14103
Use of spherical optics in high resolution soft X-ray grating monochromators
[PB87-125191] 06 p0780 N88-14788
MAXIE 1 (Magnetospheric Atmospheric X-ray Imaging Experiment) Program
[AD-A185876] 07 p0877 N88-15317
Auroral X-ray images during a pulsation event
08 p1026 N88-16214

AURIO: A proposal for flying auroral imaging observatory on the Polar Platform in the Space Station/Columbus program 08 p1034 N88-16268
Recent X-ray observations of supernova remnants and their interpretation
[MPE-PREPRINT-96] 09 p1262 N88-17563
MAXIE 1
[AD-A189688] 14 p1882 N88-21247
Hot electron diagnostics using X-ray imaging on GAMMA10 17 p2443 N88-24530
The XRD (X-Ray Diode) array, the grazing incidence spectrometer and the X-ray imaging camera on PBFA 2
[DE88-007282] 19 p2728 N88-26200
Toroidal and poloidal soft X-ray imaging system on the D3-D tokamak
[DE88-010585] 20 p2860 N88-26986
MAXIE-1 (Magnetospheric Atmospheric X-ray Imaging Experiment)
[AD-A192846] 21 p2902 N88-27221
X-ray diffraction imaging (topography) of electroopticcrystals by synchrotron radiation
[NASA-CR-183266] 24 p3432 N88-30427

X RAY INSPECTION
Aviation security: FAA (Federal Aviation Administration) needs preboard passenger screening performance standards
[PB87-216800] 02 p0124 N88-10783
A comparison of film-based tomography and computed tomography for advanced ceramic materials
[DE88-003114] 07 p0837 N88-15079
Nondestructive testings of HTGR graphites
13 p1747 N88-20448
Damage in a perforated graphite-epoxy plate under monotonic, cyclic biaxial loading
[ONERA-NT-1987-5] 20 p2816 N88-26708
Balance of X-ray radioscopy application to nondestructive tests of composite materials
[SNIAS-881-430-110] 21 p2907 N88-27250
Optimization of nondestructive control of ceramic pieces for aeronautical turbines
[ETN-88-92884] 22 p3059 N88-28149

X RAY IRRADIATION
Variations in semiconductor device response in a medium-energy x-ray dose-enhancing environment
[DE87-012400] 02 p0243 N88-11538
The development of diagnostic fuses
[SAND-86-0395] 03 p0311 N88-11963
Late radiation damage in bone, bone marrow and brain vasculature, with particular emphasis upon fractionation models
[DE87-753039] 08 p1048 N88-16330
Practical constraints on sources for pulsed beam lithographies
[DE88-006594] 13 p1776 N88-20623
X-ray production in low energy proton stopping
[NASA-TM-100619] 16 p2270 N88-23582
The ratio of microwaves to X-rays in solar flares: The case for the thick target model
[NASA-CR-183102] 19 p2743 N88-26287

X RAY LASERS
XUV emission features from the Livermore soft X-ray laser experiments
[DE88-000420] 04 p0448 N88-12779
J = O Task Force
[DE88-001326] 04 p0450 N88-12788
The gamma-ray laser project
[AD-A184824] 05 p0587 N88-13578
Lawrence Livermore National Laboratory Soft X-ray Laser Program
[DE88-001888] 07 p0859 N88-15218
The application of photoconductive detectors to the measurement of X-ray production in laser produced plasmas
[DE88-001630] 07 p0934 N88-15671
Spatially resolved X-ray laser spectra and demonstration of gain in nickel-like systems
[DE88-003957] 10 p1335 N88-17979
Research studies on extreme ultraviolet and soft X-ray lasers
[AD-A187506] 10 p1338 N88-17996
Soft X-ray beamsplitters and highly dispersive multilayer mirrors for use as soft X-ray laser cavity components
[DE88-004003] 11 p1549 N88-19270
Research studies on extreme ultraviolet and soft X-ray lasers
[AD-A189163] 12 p1633 N88-19773
Wavelength scaling of lithium-like recombination scheme for X-UV gain production --- X-ray lasers
[ETN-88-92002] 13 p1778 N88-20634
X-ray lasers: State of art and prospect
[ETN-88-92003] 14 p1914 N88-21434
Progress in X-ray laser experiments
[ETN-88-92004] 14 p1915 N88-21442
Review of X-ray laser studies at the GRECO: Laser-matter interaction
[ETN-88-92005] 14 p1915 N88-21443
An elliptical spectrograph/gated microchannel plate detector for time-resolved spectral measurements in the X-ray region
[DE88-007590] 20 p2856 N88-26961
Target designs for plasma-implosion-driven, photoionization-pumped soft X-ray lasers
[DE88-011278] 21 p2954 N88-27547
LLE (Laboratory for Laser Energetics) review
[DE88-008065] 23 p3219 N88-29158
Modeling of atomic processes in X-ray laser plasmas
[AD-A194118] 23 p3286 N88-29567
Autoionization for lower level detrapping in X-ray lasers
[AD-A195845] 24 p3379 N88-30123

X RAY SCATTERING
Neutron- and X-ray-small angle scattering with Fe-base metallic glasses
[DE88-002538] 09 p1147 N88-16876
Neutron and X-ray scattering studies of layered solids
09 p1246 N88-17469
Grazing incidence X-ray scattering study of defect structures in MBE GaAs/Si using synchrotron radiation
[DE88-004556] 10 p1420 N88-18483
Structural analysis using X-ray scattering and neutron scattering on binary amorphous (Co,Cu)Ti alloys
[ETN-88-91487] 11 p1459 N88-18699
Tungsten-carbon multilayer system studied with X-ray scattering
[DE88-005749] 13 p1735 N88-20373

X RAY SOURCES
NT X RAY BINARIES
Soft X-ray observations of pre-main sequence stars in the chamaeleon dark cloud
[NASA-CR-181457] 02 p0250 N88-11579
A search for X-ray luminous late type stars in NIPSS data 04 p0511 N88-13143
Characteristics of laser-plasma X-radiation source (review) 09 p1239 N88-17428
Advances in X-ray optics, 1987
[DE88-003298] 11 p1549 N88-19268
Variable spectra of active galaxies
[NASA-CR-182694] 13 p1853 N88-21091
A model for the X-ray binary 4U1820-30
[NASA-TM-101143] 17 p2451 N88-24562
A coded mask telescope for observations of X and gamma ray sources in the southern sky
[INPE-4580-PRE/1314] 24 p3453 N88-30551
Activities in astrophysics
[INPE-4582-PRE/1316] 24 p3456 N88-30570

X RAY SPECTRA
Electron beam requirements for soft X-ray/XUV free-electron lasers
[DE87-011750] 01 p0051 N88-10325
Generating soft X-ray spectra using the SPEED pentaxial diode
[DE87-013591] 01 p0098 N88-10647
Fast wave injection into high temperature tokamak plasmas in the lower-hybrid-density regime of JIPP T-IIU
[ISSN-0469-4732] 01 p0099 N88-10649
Semiconductor detector performance for low-energy X-rays
[DE87-014132] 02 p0244 N88-11542
Relations between chromospheric and coronal structure, flux-flux correlations and convective zone properties
04 p0510 N88-13138
VLA observations of the X-ray bright Hyades M-dwarfs
04 p0512 N88-13147
Exosat results on the dMe flare Star Wolf 630AB and on VB 8 04 p0512 N88-13151
Singularities in X-ray spectra of metals
[DE88-001440] 06 p0681 N88-14174
Spatially resolved X-ray laser spectra and demonstration of gain in nickel-like systems
[DE88-003957] 10 p1335 N88-17979
Variable spectra of active galaxies
[NASA-CR-182694] 13 p1853 N88-21091
Smoothing technique to resolve X-ray spectra in laser nuclear fusion 15 p2053 N88-22235
Observation of injected silicon in heliotron E
17 p2441 N88-24524
Inner-shell X-ray line spectra of highly ionized titanium, chromium, iron and nickel and their appliation to laboratory plasmas
[PB87-225181] 19 p2730 N88-26212
The properties of solar coronal active regions deduced from X-ray line spectra
[AD-A193026] 20 p2886 N88-27141
Detection of absorption lines in the spectra of X-ray bursts from X1608-52
[ISAS-RN-360] 20 p2887 N88-27143

X RAY SPECTROGRAPHY
U X RAY SPECTROSCOPY

X RAY SPECTROMETRY
U X RAY SPECTROSCOPY

X RAY SPECTROSCOPY
Center for X-Ray Optics, 1986
[DE88-000715] 04 p0449 N88-12783
Review of X-ray spectroscopy from laser-produced plasmas
[DE88-000755] 04 p0494 N88-13043
Area detectors for X-ray spectroscopy
[DE88-001429] 06 p0679 N88-14163
Determination, by X-ray fluorescence, of platinum, palladium, ruthenium, iron and chromium in special steels
[PB87-132114] 06 p0683 N88-14183
First results of balloon-borne X-ray and electric field observations near the footprint of the Viking satellite
08 p1026 N88-16215
Application of a simple rotational spherical grating mounting to high resolution soft X-ray spectroscopy
[PB87-164836] 09 p1142 N88-16845
Recent X-ray observations of supernova remnants and their interpretation
[MPE-PREPRINT-96] 09 p1262 N88-17563
Durability and damage tolerance of aluminum castings
[AD-A186444] 10 p1341 N88-18013
S-glass analysis by X-ray spectroscopy
[DE88-004636] 11 p1454 N88-18666
UHV (Ultra-High Vacuum) double crystal monochromator design
[DE88-003904] 11 p1456 N88-18676
Ion temperature measurement with spectroscopy in JT-60 17 p2439 N88-24513
X-ray emission from tokamaks
17 p2439 N88-24514
X-ray spectroscopic diagnostics on JIPPT-IIU and HELIOTRON-E 17 p2440 N88-24515
Spectroscopic results from JET: Some examples of data comparison and data needs 17 p2440 N88-24517
The high-throughput X-ray spectroscopy mission E6889478 MN513835 --- ESA program
[ESA-SP-1092] 17 p2450 N88-24554
The XRD (X-Ray Diode) array, the grazing incidence spectrometer and the X-ray imaging camera on PBFA 2
[DE88-007282] 19 p2728 N88-26200
Time-resolved doubly bent crystal X-ray spectrometer
[DE88-007899] 20 p2805 N88-26637
The high-throughput X-ray spectroscopy mission: The mission-science report
[ESA-SP-1097] 24 p3453 N88-30557

X RAY STARS
The 35 day cycle of Hercules X-1
[MPE-204] 11 p1571 N88-19405

X RAY TELESCOPES
NT X RAY ASTROPHYSICS FACILITY
X-ray astronomy instruments to operate on Mir station
01 p0009 N88-10052
Hard X-ray telescope HAPI-1 and its observation of Crab pulsar 03 p0269 N88-11692
Some highlights on ROSAT mechanisms
14 p1874 N88-21195
Design, construction and performance of the ROSAT high resolution X-ray mirror assembly
[MPE-PREPRINT-101] 15 p2150 N88-22836

X RAY TUBES
Stabilized X-ray generator power supply
[DE88-700297] 07 p0830 N88-15034

X RAYS
NT COSMIC X RAYS
NT SOLAR X-RAYS
Saturn: A large area X-ray simulation accelerator
[DE87-012021] 02 p0233 N88-11472
X-ray pulsars: Accretion flow deceleration
03 p0390 N88-12451
The X-ray orbital lightcurves of AR Lac and TY Pyx
04 p0509 N88-13129
Solar-geophysical data number 515, July 1987. Part 2: (Comprehensive reports). Data for January 1987 and miscellanea
[PB87-233185] 06 p0805 N88-14913
Characterization of microstructure in metallic and composite materials
[AD-A186193] 07 p0826 N88-15012
Stabilized X-ray generator power supply
[DE88-700297] 07 p0830 N88-15034
Fabrication techniques used in the construction of a high resolution X-ray framing camera
[DE88-002653] 07 p0856 N88-15200
X-ray measurements of phason distortion in ion-implanted Al-Mn
[DE87-014566] 07 p0937 N88-15694
Energetics and dynamics of simple impulsive solar flares
[NASA-TM-87816] 07 p0947 N88-15755
Emission angles for soft X-ray coherent transition radiation
[AD-A186851] 09 p1151 N88-16896

The ISO narrow spectrum series of filtered X-radiations at NPL
[NPL-RS(EXT)-92] 09 p1245 N88-17462

The measurement of chemical compositon with high spatial resolution using a dedicated scanning transmission electron microscope
[AERE-R-12317] 10 p1297 N88-17753

Suppression of X-rays generated by runaway electrons in ATF
[DE88-004179] 10 p1414 N88-18440

Effects of X irradiation and high field electron injection on the electrical properties of rapid thermal oxides
[DE88-002642] 10 p1417 N88-18461

The origin of the diffuse X-ray background and the formation of galaxies and voids
10 p1428 N88-18527

An experimental measurement of metal multilayer X-ray reflectivity degradation due to intense X-ray flux
[LA-10989-T] 11 p1547 N88-19255

Advances in X-ray optics, 1987
[DE88-003298] 11 p1549 N88-19268

X-ray lithographic research: A collection of NRL contributions
[AD-A188313] 12 p1695 N88-20140

X-rays from z-pinches
[AD-A188911] 12 p1696 N88-20146

The imaging of extra-galactic low-energy gamma-ray sources prospects, techniques, and instrumentation
[NASA-CR-182536] 12 p1713 N88-20251

Solar-geophysical data number 519, November 1987. Part 2: (Comprehensive reports). Data for May 1987 and miscellanea
[PB88-158910] 14 p2011 N88-21997

Theory of interactions of intense light with nonlinear, inhomogeneous and periodic structures and its applications to optical bistability, optic gyroscopes, nonlinear spectroscopy, radiation protection, X-ray emission and related fields
[AD-A190040] 15 p2133 N88-22725

Computing X-ray effects in optics
[DE88-006722] 15 p2134 N88-22732

Preparing the Alcator C bolometer system for use on MTX (Microwave Tokamak Experiment)
[DE88-006724] 15 p2134 N88-22733

A model for the X-ray binary 4U1820-30
[NASA-TM-101143] 17 p2451 N88-24562

Progress toward a soft X-ray FEL
[DE88-007669] 19 p2675 N88-25905

Generation of coherent soft X-rays using a single-pass free-electron laser amplifier
[DE88-009137] 19 p2675 N88-25907

The solar flare of 18 August 1979. Incoherent scatter radar data and photochemical model comparisons
[DE88-007616] 19 p2743 N88-26286

Microfocus X-ray techniques for flaw location
[DE88-008636] 20 p2812 N88-26680

In-situ reactive of X-ray optics by glow discharge
[DE88-009840] 20 p2854 N88-26947

Properties of multilayers for soft X-ray optics
20 p2867 N88-27025

The hard X-ray burst spectrometer event listing 1980-1987
[NASA-TM-4036] 20 p2887 N88-27144

X- and gamma-ray background observations in Antarctic
[INPE-4583-PRE/1317] 24 p3459 N88-30578

X WING ROTORS

Rotorcraft designs for the year 2000
03 p0264 N88-11665

Proceedings of the Circulation-Control Workshop, 1986
[NASA-CP-2432] 10 p1268 N88-17586

Analysis of a fixed-pitch X-wing rotor employing lower surface blowing
10 p1271 N88-17602

Prediction of aeroelastic response of a model X-wing rotor
10 p1271 N88-17603

X-wing potential for Navy applications
10 p1271 N88-17604

Analysis of a fixed-pitch X-wing rotor employing lower surface blowing
[AD-A187379] 24 p3321 N88-29779

X-29 AIRCRAFT

An integrated study of structures, aerodynamics and controls on the forward swept wing X-29A and the oblique wing research aircraft
[NASA-CR-181548] 04 p0399 N88-12486

X-29A forward-swept-wing flight research program status
[NASA-TM-100413] 10 p1277 N88-17644

A correlation study of X-29A aircraft and associated analytical development
[NASA-CR-183103] 13 p1722 N88-20296

Development of a real-time aeroperformance analysis technique for the X-29A advanced technology demonstrator
[NASA-TM-100432] 14 p1866 N88-21151

Operational viewpoint of the X-29A digital flight control system
[NASA-TM-100434] 14 p1866 N88-21152

X-30 VEHICLE

National aero-space plane: A technology development and demonstration program to build the X-30
[GAO/NSIAD-88-122] 17 p2301 N88-23764

XANTHINES

NT CAFFEINE

Role of adenosine analogs and growth hormone in waking and sleep
[AD-A187897] 11 p1519 N88-19070

XB-70 AIRCRAFT

U B-70 AIRCRAFT

XENON

State parameters of pulse-discharge plasma in xenon-filled closed tube 06 p0773 N88-14747

Low-power photolytically pumped lasers
[DE88-002448] 08 p0991 N88-15998

Electron stimulated desorption and coherent electron scattering
[AD-A189091] 13 p1835 N88-20978

Theoretical calculations of XeF ground state kinetics
[AD-A191398] 16 p2270 N88-23580

Rare Gas Halide (RGH) kinetics
[AD-A192352] 20 p2770 N88-26425

Performance of 10-kW class xenon ion thrusters
[NASA-TM-101292] 22 p3049 N88-28088

Electronic states of the Xe(sub n)HCl systems in gas and condensed phases
[AD-A193881] 23 p3192 N88-28997

XENON CHLORIDE LASERS

XeCl excimer laser induced multiphoton ionization of ammonia molecule 03 p0299 N88-11883

Operational performance of repetitive KrF, XeCl excimer lasers 03 p0327 N88-12068

Gas flow effects in pulse avalanche discharge XeCl excimer lasers 03 p0328 N88-12070

Minimum necessary intensity of source of preionization for stabilization of a self-sustaining laser discharge with mean power raised by electron beam or X-rays
[PB87-178158] 09 p1171 N88-17024

Direct solar-pumped iodine laser amplifier
[NASA-CR-182674] 13 p1777 N88-20630

Folded long-pulse XeCl excimer laser described
14 p1901 N88-21357

XeCl laser-pumped nanosecond dye lasers
14 p1902 N88-21359

Emission characteristics of XeCl-laser excited by electron beam of microsecond duration
14 p1970 N88-21762

Effects of emission energy transient in periodic-pulse XeCl excimer laser of approximately 400 W average power 14 p1971 N88-21763

Controlling XeCl-laser by means of external signal with less than 2 W/cm (sup)2 intensity
14 p1972 N88-21768

Pulse duration control of XeCl*-laser by means of plasma shutter 14 p1973 N88-21774

Realization of an XeCl laser producing 100W on average
[ETN-88-92541] 17 p2344 N88-23970

Dynamics of a plasma produced under effect of the XeCl-laser radiation on metallic surface
[DE88-701983] 21 p3017 N88-27902

XENON FLUORIDE LASERS

XeF excimer laser pumped by high-intensity relativistic electron beam 14 p1901 N88-21355

Discharge excitation of the XeF C to A transition
[DE88-006448] 15 p2070 N88-22339

Optical coatings for high average power XeF lasers
[DE88-011356] 20 p2807 N88-26656

Measurements of XeF (Xenon Fluoride) ground state dissociation and vibrational equilibration
[AD-A194611] 23 p3280 N88-29527

XEROGRAPHY

Application of magnification xeroradiography to advanced ceramics
[DE88-009965] 20 p2778 N88-26473

XV-15 AIRCRAFT

Modeling XV-15 tilt-rotor aircraft dynamics by frequency and time-domain identification techniques
03 p0263 N88-11657

Using frequency-domain methods to identify XV-15 aeroelastic modes
[NASA-TM-100033] 10 p1277 N88-17646

Hover performance tests of baseline metal and Advanced Technology Blade (ATB) rotor systems for the XV-15 tilt rotor aircraft
[NASA-CR-177436] 20 p2759 N88-26367

Utilization of identification methods in the time and frequency domain for the determination of the XV-15 (tilt-rotor) dynamics for lateral motion in hover flight
20 p2787 N88-26532

Y

YAG (GARNET)

U YTTRIUM-ALUMINUM GARNET

YAG LASERS

JPRS report: Science and technology. China
[JPRS-CST-87-034] 03 p0301 N88-11897

Saturable absorbers for colliding pulse-locked Nd:YAG lasers 03 p0302 N88-11902

Physical design of parameters of Nd:YAG disk laser
03 p0302 N88-11904

Investigations of solid state slab lasers
[ETN-88-91055] 09 p1171 N88-17022

High-power periodic-pulse YAG:Nd3+ -laser system with telescopic unstable resonator and two-stage amplifier
09 p1237 N88-17414

Airborne Doppler lidar detection of wind shear. Results of performance analysis 10 p1275 N88-17627

Diode pumped fiber laser
[AD-A187694] 11 p1491 N88-18902

Polarization effects in laser-pumped Nd:YAG lasers
[DE88-004019] 11 p1492 N88-18904

Radiation absorption in neodymium glasses during passage of strong laser pulse 14 p1969 N88-21757

Solid-state ring laser with acoustooptical phase nonreciprocity of opposing waves
14 p1970 N88-21761

Nonlinear stage of ultrashort-pulse formation in solid-state laser 14 p1971 N88-21765

Laser processing status, perspectives
15 p2050 N88-22211

Reduced thermal input by proper selection of YAG laser welding parameters
[DE88-000730] 15 p2072 N88-22356

Observation of synchronously transient pumped mode-locking dye laser under negative cavity detuning
16 p2187 N88-23041

Process control improvements in pulsed Nd:YAG laser closure welding of electromechanical relays
[DE88-006275] 21 p2957 N88-27564

YANG-MILLS FIELDS

Ten dimensional N = 1 supergravity coupled to supersymmetric Yang-Mills fields in superspace
[DE87-703033] 15 p2146 N88-22808

YANG-MILLS THEORY

Chiral U(1) anomaly in D = 4 super Yang-Mills theory coupled to supergravity
[DE87-753022] 02 p0252 N88-11591

YARNS

Creep of carbon yarn and carbon-carbon composites at high temperatures and high stresses
[AD-A195224] 24 p3340 N88-29878

YAW

Low speed wind tunnel investigation of propeller slipstream aerodynamic effects on different nacelle/wing combinations. Part 1: Total forces and moments and pressure distributions on nacelle/wing at different angles of attack and yaw and at different thrust coefficients
[FFA-TN-1987-22] 05 p0542 N88-13302

An investigation of the spray produced by a yawed wheel, including measurement of impact forces -- aircraft wheels
[BU-363] 14 p1866 N88-21150

Modal forced response of propfans in yawed flow
16 p2221 N88-23253

Actuated forebody strakes
[NASA-CASE-LAR-13983-1] 18 p2464 N88-24628

Yaw dynamics of horizontal axis wind turbines
[DE88-001137] 18 p2537 N88-25055

Aeroelastic response of metallic and composite propfan models in yawed flow
[NASA-TM-100964] 24 p3326 N88-29807

YAWING MOMENTS

A comparison between theory and experiment for the yaw moment induced by a loose internal part
[AD-A187053] 09 p1131 N88-16787

Cornering characteristics of the main-gear tire of the space shuttle orbiter
[NASA-TP-2790] 11 p1438 N88-18583

Wind-tunnel investigation of actuated forebody strakes for yaw control at high angles of attack
17 p2299 N88-23754

YAWMETERS

U ATTITUDE INDICATORS

U YAW

YEAST

Survival and mutation induction of dehydrated yeast cells after UV exposure 12 p1657 N88-19932

Cellular effects of heavy ions: Experimental results and theoretical approaches -- space radiation
12 p1658 N88-19933

YEMEN

Topographic mapping with SPOT 1 data: A practical approach by the Ordnance Survey
22 p3111 N88-28479

YHU-1 HELICOPTER
U UH-1 HELICOPTER
YIELD
GaAs MMIC yield evaluation -- monolithic microwave integrated circuits (MMIC)
[ESA-CR(P)-2470] 08 p0979 N88-15916
YIELD POINT
Dugdale solutions for strain hardening materials
[FD-6/1985] 01 p0059 N88-10380
Long-range pulselength scaling of 351nm laser damage thresholds
[DE87-014754] 04 p0448 N88-12777
A finite element procedure for interference-fit and cold-working problems with limited yielding
[AR-004-517] 04 p0485 N88-12992
Fiber composite structural durability and damage tolerance: Simplified predictive methods
[NASA-TM-100179] 05 p0580 N88-13409
Optimized approach to damage tolerance --- spacecraft
[FOK-FSS-R-87-024] 09 p1134 N88-16806
Database of average-power damage thresholds at 1064 nm
[DE88-004352] 13 p1776 N88-20626
GARTEUR TP-037: Impact damage tolerance of carbon fiber and hybrid laminates
[RAE-TR-87057] 17 p2316 N88-23837
An experimental study of biaxial yield in modified 9Cr-1Mo steel at room temperature
[NASA-CR-175012] 24 p3385 N88-30164
YIELD STRENGTH
Face compression yield strength of the copper-inconel composite specimen
[DE87-011974] 01 p0019 N88-10116
Wire interconnection reliability and moisture levels in hybrid microcircuits with epoxy-attached components
[DE87-012987] 01 p0039 N88-10247
Need for composites, new materials discussed
02 p0160 N88-11001
Corrosion-electrochemical and mechanical properties of composite graphite-carbide metal materials based on titanium and its alloys 03 p0285 N88-11794
The effect of strain rate on the yield behavior of iron-base LRO alloys at elevated temperatures
[DE87-014893] 03 p0288 N88-11808
Small-diameter wire tensile testing
[DE88-000835] 04 p0455 N88-12815
Analysis of end stresses in glass-metal bimaterial strips
[DE87-007848] 05 p0610 N88-13750
Effect of metal surface properties on the fatigue crack growth behavior 06 p0716 N88-14390
The relationship of tensile specimen size and geometry effects to unique constitutive parameters for ductile materials
[AD-A186020] 08 p0994 N88-16012
An experimental and numerical study of notch sensitivity of ARALL laminates
[CCMS-88-04] 11 p1450 N88-18644
Properties fo seals made with Li2O-Al2O3-SiO2-glass ceramics and aluminum-containing austenitic stainless steels
[DE88-004688] 12 p1633 N88-19776
A direct correlation of strength with impact velocity
[AD-A189251] 13 p1741 N88-20409
The effects of temperature and strain rate on the yielding behavior of the single crystal superalloy PWA 1480
14 p1931 N88-21517
Rapidly solidified lightweight durable disk material
[AD-A191697] 18 p2491 N88-24775
Geometric and material nonlinear analysis of structures comprising rectangular hollow sections
[CE-79] 24 p3382 N88-30141
YOUNG MODULUS
U MODULUS OF ELASTICITY
YTTERBIUM
Ytterbium monolayer diffusion barriers at Hg(1-x)Cd(x)Te/Al junctions
[AD-A188013] 10 p1299 N88-17768
YTTRIUM
Magnetic anomalies in the rare earth oxide superconductors GdBa2Cu3O(7-x) and YbBa2Cu3O(7-x)
[AD-A190713] 15 p2144 N88-22793
Synthesis and characterization of high-T(sub c) screen-printed Y-Ba-Cu-O films on alumina
[NASA-TM-100860] 15 p2146 N88-22805
Effects of 67.5 MeV electron irradiation on Y-Ba-Cu-O and Gd-Ba-Cu-O high-temperature superconductors
[AD-A191271] 16 p2283 N88-23669
Characterization of structural and magnetic order of Er/Y superlattices 20 p2873 N88-27056
Pure metallic bridge and point-contact tunneling into single- and polycrystal YBa2Cu3O(sub 7-y)
[DE88-010030] 20 p2878 N88-27084
The high temperature creep deformation of Si3N4-6Y2O3-2Al2O3
[NASA-CR-183204] 23 p3190 N88-28961
YTTRIUM COMPOUNDS
NT YTTRIUM OXIDES
NT YTTRIUM-ALUMINUM GARNET
400-nm photoluminescence of a color center in undoped YAG grown under reducing atmosphere
[DE88-001760] 07 p0858 N88-15213
Growth and characteristics of materials for tunable lasers in the near infrared spectral region
[NASA-CR-182501] 11 p1491 N88-18901
A sup 57 Fe Mossbauer study of the superconductor YBa sub 2 (Fe sub x Cu sub 1-x) sub 3 O sub y
[DE88-701543] 16 p2282 N88-23661
Effect of a weak magnetic field on high temperature superconductivity in Y-Ba-Cu-O ceramics
[DE88-702192] 19 p2733 N88-26235
All-electron local density theory of electronic structure and superconductivity in YBa2Cu3O7 and YBa2Cu3O6
[DE88-009944] 19 p2735 N88-26246
Anharmonic model for high-Tc superconductors
[DE88-702196] 21 p3020 N88-27924
Superconducting properties of LaBa2Cu3O(sub x) and YBa2Cu3O(sub y)
[DE88-012036] 21 p3024 N88-27952
YTTRIUM OXIDES
Synthesis of the monoclinic yttria by thermal plasma processing
[DE88-000496] 04 p0421 N88-12608
High temperature stability of superconducting YBa2Cu3O subx as characterized by X-ray diffraction
[DE88-001856] 06 p0787 N88-14824
Atomic-level studies of superconducting YBa2Cu3O sub 7-x
[DE88-002522] 06 p0788 N88-14831
Low field characterization of YBa2Cu3O sub 7-delta single crystals
[DE88-002895] 07 p0938 N88-15700
Fabrication of YBa2Cu3O7 superconducting ceramics
[DE88-003012] 07 p0938 N88-15701
Soft X-ray absorption and emission spectra and the electronic structure of the Ba2YCu3O/sub 7-x/ superconductor
[DE88-002609] 08 p1090 N88-16559
Advanced materials for solid oxide fuel cells
[DE88-002338] 10 p1350 N88-18071
The structure and properties of twin boundaries in superconducting YBa2Cu3O7
[DE88-003864] 10 p1418 N88-18468
Improved magnetization for YBa2Cu3O/sub 7-delta annealed in oxygen above 1000 C
[DE88-003934] 10 p1418 N88-18469
Freestanding films of YBa2Cu3O/sub 6.9/
[DE88-003995] 10 p1419 N88-18471
Grain boundaries, planar defects and superconducting properties of YBa2Cu3O7
[DE88-003477] 10 p1419 N88-18475
Superconducting properties and structural characterization of high T/sub c/ oxides
[DE88-003479] 10 p1420 N88-18477
Penetration depth measurements of YBa2Cu3O/sub 7-delta/ at 4 MHz
[DE88-003493] 10 p1420 N88-18478
The electronic structure of YBa2Cu3O/sub 7-delta/ above and below T/sub c/
[DE88-003495] 10 p1420 N88-18479
Simulation and processing of high resolution images of defects and interfaces in superconducting YBa2Cu3O7
[DE88-003856] 10 p1420 N88-18480
High-resolution X-ray microstructural study of single crystals of YBa2Cu3O/sub 7-y/
[DE88-004856] 10 p1421 N88-18484
The YAlO(sub 3):Er laser
[PB88-130877] 11 p1493 N88-18911
Atom probe microanalysis of superconducting YBa2Cu3O(sub 7-x)
[DE88-003203] 11 p1557 N88-19322
Processing relationships in YBa2Cu3O(7-x) superconductors
[DE88-005137] 11 p1559 N88-19330
Mass transport and chemical demixing of Y-Ba-Cu-O compounds during sintering in temperature gradients
[DE88-004887] 12 p1696 N88-20151
Ordered structures in YBa2Cu3O/sub 7-y/, La2Cu3O/sub 7-y/, La/sub 2-x/Sr/sub x/CuO/sub 4-par delta/ and related perovskites
[DE88-006461] 14 p1987 N88-21851
Melt processing ceramic YBa2Cu3O(sub 6.9)
[DE88-007039] 15 p2047 N88-22199
Superconductivity and the tailoring of lattice parameters of the compound YBa2Cu3O(sub x)
[DE88-005904] 15 p2140 N88-22769
Vacancy ordering in the basal plane of YBa2Cu3O(sub)z
[DE88-004572] 18 p2583 N88-25348
Effects of grain boundary composition on properties of YBa2Cu3O/sub 7-x/
[DE88-007679] 20 p2875 N88-27064
The superconducting transition in oxygen deficient YBa2Cu3O(sub 7-Delta)
[DE88-009957] 20 p2877 N88-27079
Anisotropic characteristic lengths in single crystal YBa2Cu3O(sub 7-Delta)
[DE88-009959] 20 p2877 N88-27080
Anisotropy of the lower critical field in YBa2Cu3O(sub 7-Delta)
[DE88-009971] 20 p2877 N88-27081
Preparation of high-T(sub)c Y1Ba2Cu3O(sub 7-Delta) superconducting thin films by MBE (Molecular-Beam-Epitaxy) techniques
[DE88-009999] 20 p2877 N88-27082
Oxygen vacancy ordering and superconductivity in YBa2Cu3O(sub 7-x)
[DE88-010005] 20 p2877 N88-27083
Electron irradiation effects in YBa2Cu3O7-Delta single crystals
[DE88-010050] 20 p2878 N88-27085
Phase transformations and thermodynamic behavior of the YBa2Cu3O(sub)x system via EMF measurements
[DE88-010054] 20 p2878 N88-27086
Ceramic processing of high-T(sub)c superconductors
[DE88-010090] 20 p2878 N88-27087
Compilation of NRL publications on high temperature superconductivity
[AD-A189137] 21 p3019 N88-27921
Thermodynamics of oxygen-vacancy ordering in YBa2Cu3O(sub z)
[DE88-009816] 21 p3022 N88-27940
Preparation and characterization of isotopic oxygen-enriched yttrium barium copper oxide
[DE88-010939] 22 p3154 N88-28766
Superconducting properties of oxygen deficient YBa2Cu3O(sub 7-delta)
[DE88-009969] 22 p3155 N88-28774
Effect of neutron irradiation on critical magnetization current in single crystal YBa2Cu3O(sub 7-delta)
[DE88-009970] 22 p3156 N88-28775
Effects of metal substitutions (Fe and Ga) in YBa2Cu3O7 on its superconducting properties and microstructures
[DE88-007393] 23 p3287 N88-29572
Preparation of superconducting YBa2Cu3O(sub 7-x) films by magnetron sputtering
[DE88-009977] 23 p3289 N88-29583
YTTRIUM-ALUMINUM GARNET
Characterization of yttrium aluminum garnet/YAG/using 14 MeV neutron activation
[AD-A191925] 18 p2582 N88-25342
YUH-1 HELICOPTER
U UH-1 HELICOPTER
YUH-60A HELICOPTER
U UH-60A HELICOPTER

Z

ZEEMAN EFFECT
Laser induced fluorescent study of relativistic electron beams
[AD-A184456] 04 p0447 N88-12774
Measurements of stellar magnetic fields
04 p0503 N88-13093
Exploring the IR: Solar and stellar spectroscopy in the IR 04 p0504 N88-13102
Magnetic fields on K and M stars
04 p0510 N88-13137
Observations and analysis of the photospheric magnetic fields on dwarf G, K and M stars
04 p0520 N88-13196
Nature of gigantic resistance fluctuations in metal-oxide-semiconductor wires
[DE88-002905] 09 p1256 N88-17533
ZENER DIODES
U AVALANCHE DIODES
ZEOLITES
Preliminary market analysis for large zeolite crystals
[NASA-CR-182882] 15 p2049 N88-22207
Upgrading pyrolysis vapors to aromatic gasoline with zeolite catalysis at atmospheric pressure
18 p2536 N88-25045
Studies of photochemically and electrochemically driven electron transport in zeolites
[DE88-008644] 22 p3155 N88-28769
ZERO CROSSINGS
U ROOTS OF EQUATIONS
ZERO GRAVITY
U WEIGHTLESSNESS
ZERO LIFT
Planform effects on the supersonic aerodynamics of multibody configurations
[NASA-TP-2762] 04 p0393 N88-12454

ZERO POWER REACTORS
Benchmark physics experiments for SP-100
17 p2429 N88-24453
ZETA PINCH
Analytic model of an imploding Z-pinch plasma colliding inelastically with a thin-shelled cylindrical target
[DE88-000051] 03 p0378 N88-12379
Magneto-Inertia Confinement Approach (MICA) to fusion in dynamic Z-pinch formed from a frozen deuterium-tritium tube
[IPPJ-856] 09 p1252 N88-17504
On selfsimilar thermonuclear ignition of a plasma in necks of zeta devices
[DE88-701640] 16 p2280 N88-23647
Photoconducting X-ray detectors for Z-pinch experiments
[DE88-007118] 19 p2728 N88-26199
Zero-dimensional calculation for ZT-H
[DE88-009175] 19 p2731 N88-26217
ZETA THERMONUCLEAR REACTOR
Zero-dimensional calculation for ZT-H
[DE88-009175] 19 p2731 N88-26217
ZIMBABWE
Wind velocity measurement data. Zimbabwe, 4 measuring stations
[R-845-D] 13 p1802 N88-20770
ZINC
Preparation and characterization of Cu2Zn1-xMnxGeS4
[AD-A188113] 11 p1556 N88-19315
Technology base research on zinc/air battery systems
[DE88-004893] 13 p1763 N88-20546
Influence of alternating magnetic fields on Zn-67 Moessbauer resonance in ZnO
[PB88-186432] 18 p2584 N88-25352
Laser fluorescence spectroscopy of zinc neutrals originating from laser-irradiated and ion-bombarded zinc sulfide and zinc surfaces
[DE88-008037] 20 p2769 N88-26418
Lattice-matched HgZnTe epitaxy development
[AD-A193677] 23 p3292 N88-29600
An electrochemical impedance spectroscopy study of reactions at the metal/coating interface
24 p3355 N88-29975
Zinc filled coatings 24 p3355 N88-29978
ZINC ALLOYS
Effect of Zr or Cr content on the fracture toughness of the high purity Al-Zn-Mg alloys
[NASA-TT-20294] 19 p2616 N88-25518
ZINC COATINGS
Adhesion properties of polyelectrolyte-chemisorbed zinc phosphate conversion coatings
[DE87-012489] 01 p0029 N88-10186
Studies on hot-dip zinc-aluminum coated sheet steels
[ETN-88-92217] 15 p2042 N88-22166
Polyacrylic acid electrolyte-modified zinc phosphate conversion coatings for corrosion protection of steel
[DE88-004878] 19 p2617 N88-25527
ZINC COMPOUNDS
NT ZINC OXIDES
NT ZINC SELENIDES
NT ZINC SULFIDES
NT ZINC TELLURIDES
Grace DAKASEP alkaline battery separator
02 p0164 N88-11031
Studies on estimation of nickel in zinc base die casting by D.C. polarography
[PD-MT-8729] 04 p0417 N88-12588
Resistivity of EuBa2(Cu/sub 1-y/Zn/sub y/)3O/sub x/ as a ffunction of temperature, magnetic field, pressure and Zn concentration
[DE87-014740] 04 p0499 N88-13069
ZINC NICKEL BATTERIES
U NICKEL ZINC BATTERIES
ZINC OXIDES
Sintering and densification of particulate composites: Inclusion size and clustering
[DE88-002230] 06 p0685 N88-14199
Model Cu/ZnO catalysts for methanol synthesis: The role of surface structure
[DE88-002354] 07 p0830 N88-15037
High temperature solar electrothermal processing-3. Zinc from zinc oxide at 1200-1675K using a non-consumable anode
[AD-A186600] 09 p1141 N88-16836
Improvements to Raney copper zinc methanol synthesis catalysts 17 p2318 N88-23844
Influence of alternating magnetic fields on Zn-67 Moessbauer resonance in ZnO
[PB88-186432] 18 p2584 N88-25352
Zinc-oxide thin films for integrated-sensor applications
19 p2673 N88-25896
The first synthesis of chem-prep varistor LAC (Lightning Arrestor Connector) granules
[DE88-008005] 21 p2936 N88-27438
Low temperature film growth of the oxides of zinc, aluminum and vanadium (and related systems, oxides of gold and germanium, nitrides of aluminum and tungsten) by reactive sputter deposition
[AD-A193497] 23 p3191 N88-28986
ZINC SELENIDES
Blue-green laser diode research program
[AD-A183517] 01 p0051 N88-10323
Physical vapor transport crystal growth
03 p0296 N88-11860
Preparation and characterization of members of the system (Zn,Se)1-xGaPx
[AD-A185073] 05 p0655 N88-14019
Inadequacies of EMI-seal material: A corrosion study
17 p2319 N88-23852
Growth and characterization of thin films of ZnSnP(sub)2
[DE88-001164] 20 p2874 N88-27060
Atomic layer epitaxy of ZnS and ZnSe
[AD-A192307] 21 p3020 N88-27928
Blue-green laser diode research program
[AD-A191980] 23 p3218 N88-29153
ZINC SULFIDES
Laser fluorescence spectroscopy of zinc neutrals originating from laser-irradiated and ion-bombarded zinc sulfide and zinc surfaces
[DE88-006033] 13 p1776 N88-20620
Laser fluorescence spectroscopy of zinc neutrals originating from laser-irradiated and ion-bombarded zinc sulfide and zinc surfaces
[DE88-008037] 20 p2769 N88-26418
Atomic layer epitaxy of ZnS and ZnSe
[AD-A192307] 21 p3020 N88-27928
The optical spectroscopy of copper-blue luminescence in zinc sulfide crystals. Zero-phonon line spectra under the influence of magnetic field, temperature and excitation intensity
[ETN-88-93122] 24 p3344 N88-29903
An organometallic route to micron-sized whiskers of zinc sulfide
[AD-A195889] 24 p3430 N88-30414
ZINC TELLURIDES
MBE (Molecular Beam Epitaxial) growth characterization and electronic device processing of HgCdTe, HgZnTe related heterojunctions and HgCdTe-CdTe superlattices
[AD-A187416] 11 p1555 N88-19307
CdZnTe as a wide-band-gap absorber for a tandem, thin-film solar cell
[DE88-001114] 13 p1793 N88-20724
ZINC-BROMIDE BATTERIES
Extended abstracts: Eighth Battery and Electrochemical Contractors' Conference
[DE88-000960] 06 p0730 N88-14489
ZINC-OXYGEN BATTERIES
Zinc-redox battery: A technology update
[DE87-010737] 01 p0040 N88-10256
A new concept in an electrically rechargeable zinc-air alkaline battery
[DE88-003858] 13 p1762 N88-20539
ZIRCONATES
Develop techniques for ion implantation of (lead-lanthanum-zirconate-titanate) for adaptive optics
[DE88-000642] 05 p0650 N88-13986
Refractory Materials of Zirconate. Part 2: Synthesis and some properties of strontium, zirconate, calcium zirconate and barium zirconate
[NASA-TT-20186] 20 p2779 N88-26483
Preparation and properties of high Q microwave dielectrics in the (CA, SR, BA) zirconate system
[AD-A193127] 21 p2918 N88-27317
ZIRCONIUM
Cooperative analysis of zirconium and zirconium alloys by fluorescent X-ray method
[DE87-753011] 02 p0148 N88-10926
The effect of sulfur and zirconium Co-doping on the oxidation of NiCrAl
[NASA-TM-100209] 02 p0150 N88-10940
Investigation by differential scanning calorimetry of microstructure in a superplastic Al-Mg-Zr alloy
[AD-A184902] 05 p0564 N88-13439
Creep behavior of tungsten/niobium and tungsten/niobium-1 percent zirconium composites
[NASA-TM-100804] 11 p1460 N88-18707
A case study of the development of a military specification - zirconium powder for thermal batteries
[AD-A188751] 13 p1792 N88-20717
A dense and strong ceramic material made from zirconium dioxide 14 p1886 N88-21274
Ion-beam mixing and amorphization in Au/Zr bilayers
[DE88-005999] 15 p2140 N88-22767
Characterization of precipitates in a niobium-zirconium-carbon alloy
[NASA-TM-100848] 16 p2178 N88-22981
Creep behavior of tungsten/niobium and tungsten/niobium-1 percent zirconium composites
17 p2425 N88-24427
Effect of Zr or Cr content on the fracture toughness of the high purity Al-Zn-Mg alloys
[NASA-TT-20294] 19 p2616 N88-25518
PLZT (Lead Lathanium-Zirconium-Titanium) electro-optic photographic system
[AD-A193473] 23 p3215 N88-29137
Electrical properties of materials for elevated temperature resistance strain gage application
[NASA-CR-182214] 24 p3376 N88-30106
ZIRCONIUM ALLOYS
Cooperative analysis of zirconium and zirconium alloys by fluorescent X-ray method
[DE87-753011] 02 p0148 N88-10926
Microstructure of amorphous and crystalline zirconium alloys rapidly solidified
[DE87-703700] 05 p0564 N88-13432
Structural relaxation and mechanical properties of amorphous Fe-Zr alloys 07 p0840 N88-15094
Diffusion studies in amorphous NiZr alloys
[DE88-003009] 10 p1301 N88-17781
Crystallization and glass formation in electron and laser beam irradiated Cu-Zr alloys
[DE88-003390] 11 p1464 N88-18729
The precipitation processes of Cu-Zr-Cr alloys
[NASA-TT-20168] 18 p2488 N88-24758
Oxidation behavior and microstructural studies of melt-spun glassy Fe-Al-Zr metal
[DE88-009964] 19 p2617 N88-25526
ZIRCONIUM COMPOUNDS
NT ZIRCONATES
NT ZIRCONIUM NITRIDES
NT ZIRCONIUM OXIDES
Study of the micromechanical properties of fluor glasses based on ZrF4
[ISAL-ITC1-87-03] 09 p1148 N88-16882
Role of zircon in tracing crustal growth and recycling
24 p3394 N88-30211
The early archaean crustal history of West Greenland as recorded by detrital zircons 24 p3395 N88-30221
Growth of early archaean crust in the ancient Gneiss complex of Swaziland and adjacent Barberton Greenstone Belt, Southern Africa 24 p3396 N88-30223
ZIRCONIUM NITRIDES
Structure and properties of titanium nitride and zirconium nitride thin films prepared by reactive ion plating --- cutting tools
[ETN-88-92218] 15 p2042 N88-22167
ZIRCONIUM OXIDES
Effect of time and temperature on transformation toughened zirconias
[AD-A184356] 04 p0419 N88-12600
Studies of alumina additions in zirconia - magnesia
[DE87-703500] 04 p0419 N88-12602
Internal reforming development for solid oxide fuel cells
[DE87-006518] 04 p0464 N88-12871
On 1064 nm and 350 nm laser damage thresholds of high index oxide films deposited from organic solutions and sols
[DE88-001636] 07 p0859 N88-15217
Advanced materials for solid oxide fuel cells
[DE88-002338] 10 p1350 N88-18071
Perturbed angular correlations in zirconia ceramics
[DE88-004117] 11 p1464 N88-18731
The elastic properties of monoclinic ZrO2
[DE88-005920] 14 p1986 N88-21847
Stability limits in the monoclinic-tetragonal transformations of zirconia
[DE88-005924] 14 p1986 N88-21849
Superplastic flow of mullite-zirconia composites
[DE88-005905] 15 p2028 N88-22085
High-strength ceramic based on tetragonal ZrO2 with Al2O3 admixture 16 p2180 N88-22996
Mass spectrometric high temperature measurements of the barium oxide-zirconium dioxide system and the determination of thermodynamic data for barium zirconate. Clarification of the counter-stopping capacity of coated particles for solid fission products by zirconium dioxide addition
[NASA-TT-20187] 19 p2611 N88-25496
Preparation and characterization of ceramic materials based on Al2O3 reinforced with a ZrO2 dispersion
[ISAL-87-0041] 21 p2922 N88-27340
Comparison of sol-gel procedures for zircon and alumina
[REPT-881-430-108] 21 p2922 N88-27342
Preparation of superconducting YBa2Cu3O(sub 7-x) films by magnetron sputtering
[DE88-009977] 23 p3289 N88-29583
ZODIACAL DUST
Interaction mechanisms of comets with the zodiacal dust cloud 14 p2008 N88-21977
ZODIACAL LIGHT
Comet West: A view from the HELIOS zodiacal light photometers 01 p0117 N88-10749

Interaction mechanisms of comets with the zodiacal dust cloud 14 p2008 N88-21977
Doppler distortion of solar Fraunhofer lines in zodiacal light by reflection from interplanetary dust
19 p2740 N88-26270

ZONAL CIRCULATION
U ZONAL FLOW (METEOROLOGY)

ZONAL FLOW (METEOROLOGY)
Atmosphere dynamics in the equatorial meteor zone
06 p0733 N88-14508
Wind regime peculiarities in the lower thermosphere in the winter of 1983/84 06 p0733 N88-14511
Circulation in the mesosphere and lower thermosphere during the MAP (Middle Atmosphere Program)/WINE (Winter in the Northern Europe) period
06 p0734 N88-14514
A statistical study of variations of internal gravity wave energy characteristics in meteor zone
06 p0735 N88-14523
Lower thermosphere wind regime according to radiometeor measurements in Kazan
06 p0736 N88-14526
Atmosphere dynamic processes structure at 80-105 km altitude 06 p0736 N88-14527
JPRS report: Science and technology. China
[JPRS-CST-87-042] 14 p1899 N88-21338
Physical processes for maintaining mean meridional and zonal circulation of atmosphere in middle latitudes, volume 1 14 p1900 N88-21343
Numerical simulation of generation of mesoscale convective systems in large-scale environment
14 p1900 N88-21344
Physical process for maintenance of mean meridional and zonal circulation of atmosphere in middle latitudes, volume 2 14 p1900 N88-21345
On regime selection in global atmospheric flow
17 p2374 N88-24119

ZONAL HARMONICS
The contraction of satellite orbits under the influence of air drag. Part 8: Orbital lifetime in an oblate atmosphere, when perigee distance is perturbed by odd zonal harmonics in the geopotential
[RAE-TR-86069-PT-8] 01 p0010 N88-10058

ZONE MELTING
Elimination of subboundaries in 0.5-micron-thick Si-on-insulation films produced by ZMR
[AD-A184590] 03 p0381 N88-12396

ZONE REFINING
U ZONE MELTING

ZONES
U REGIONS

ZOOM LENSES
A high-speed, eight-frame image intensified electro-optic camera with 200-800mm zoom objective capability
[DE88-000229] 03 p0326 N88-12059
Zoom versus full-field sensitivity at the ETS (Experimental Test System)
[AD-A188162] 12 p1628 N88-19742

ZPR REACTORS
U ZERO POWER REACTORS

VOLUME 26 NUMBERS 1-6

Scientific and Technical Aerospace Reports

Abstracts **January—March 1988**

TABLE OF CONTENTS

STAR Issue *Page*

1 1
2 121
3 259
4 393
5 529
6 663

VOLUME 26 NUMBERS 7-12

Scientific and Technical Aerospace Reports

Abstracts **April—June 1988**

TABLE OF CONTENTS

STAR Issue	*Page*
7	**809**
8	**949**
9	**1105**
10	**1267**
11	**1433**
12	**1573**

VOLUME 26 NUMBERS 13-18

Scientific and Technical Aerospace Reports

Abstracts **July—September 1988**

TABLE OF CONTENTS

STAR Issue *Page*
13 1715
14 1861
15 2013
16 2155
17 2293
18 2455

VOLUME 26 NUMBERS 19-24

Scientific and Technical Aerospace Reports

Abstracts October—December 1988

TABLE OF CONTENTS

STAR Issue	Page
19	2597
20	2745
21	2889
22	3033
23	3167
24	3311

*U.S. GOVERNMENT PRINTING OFFICE:1989-230-323

National Aeronautics and
Space Administration
Code NTT-4
Washington, D.C.
20546

Official Business
Penalty for Private Use, $300

SPECIAL FOURTH CLASS RATE
POSTAGE & FEES PAID
NASA
PERMIT No. G-27

POSTMASTER: If Undeliverable (Section 158
Postal Manual) Do Not Return